Proceedings of
The Fifth International Symposium
on the
Chemistry of Cement
Tokyo, 1968

PART I
CHEMISTRY OF CEMENT CLINKER
(Volume I)

Proceedings of
The Fifth International Symposium
on the
Chemistry of Cement
Tokyo, 1968

PART I
CHEMISTRY OF CEMENT CLINKER
(Volume I)

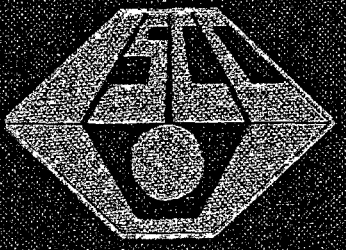

The Organizing Committee
for the Fifth International Symposium
on the Chemistry of Cement
The Cement Association of Japan

Proceedings of
The Fifth International Symposium
on the
Chemistry of Cement
Tokyo, 1968

PART I

CHEMISTRY OF CEMENT CLINKER

(Volume I)

Symposium held October 7–11, 1968 at the
Tokyo Metoropolitan Festival Hall, Tokyo

Proceedings published in 4 volumes December 31, 1969

Proceedings of The Fifth International Symposium
on the Chemistry of Cement Tokyo, 1968

ERRATA

	page	line	wrong	right
VOLUME I	40	left column 22	Hans E. Schmiete	Hans E. Schwiete
	277	5	Fudamentals on Belite	Fundamentals on Belite
VOLUME II	210	22	Reactivites of Cement	Reactivities of Cement
	212	right column 6	Through Rolution Seaction	Through Solution Reaction
VOLUME III	iii	33	Yu. M. Butt V. M. Kolbasov	Yu. M. Butt, V. M. Kolbasov
	138	29	Experimental Prodecure	Experimental Procedure
	268	31	Discuion of Test Result-Part II	Discussion of Test Result-Part II
	503	3	John Jessing	Jørn Jessing
	521	right column 12	John Jessing	Jørn Jessing
VOLUME IV	135	2	artificial puzzolans	artificial puzzolanas
	228	2	and Maganese	and Manganese

Preface

Though more than a half century ago meetings covering various materials including cements were held among researchers, it was not before 1918 in London where an international meeting was held to discuss the setting of cements under the sponsorship of the Faraday Society that the chemistry of cements was dealt with independently and systematically in such a magnitude worth a title of an international symposium. Hence, this international gathering became more and more accustomed to be called as the First International Symposium on the Chemistry of Cement, though not so called at the beginning.

Just as the famous ancient Olympics in Greece which in their earliest stage were celebrated for one day only, the First International Symposium on the Chemistry of Cement dawned on January 14, 1918 in London was closed on the same day, with the presentation of 10 papers followed by 12 discussions. The Proceedings consisting of 69 pages were published in the Transactions of the Faraday Society, Volume XIV, 1918–19, thus leaving the first footprints and pattern to the later Symposia.

The Second Symposium on the Chemistry of Cement took place from July 6 to 8, 1938, in Stockholm, sponsored by the Royal Swedish Institute for Engineering Research and the Swedish Cement Association. With the participation of 47 persons from 13 countries, 52 discussions were made on 13 papers presented thereto. The Proceedings consisting of 578 pages were published in Stockholm in 1939 by the Royal Swedish Institute for Engineering Research.

The devastation of World War II could not nip the Symposium in the bud. On the contrary, it called for a Post-War program of reconstruction everywhere on a scale never before attempted, in which the cement was destined to play an important role all around. With this background, the Third International Symposium on the Chemistry of Cement was held in London in September, 1952. It was a five-day meeting in which 260 persons took part and 23 papers were presented. The number of discussions amounted to 102. The Proceedings consisting of 870 pages were published in London in 1954 by the Cement and Concrete Association, who cosponsored this Symposium with Department of Scientific and Industrial Research of the United Kingdom.

The host country of the Fourth Symposium was the United States of America. Under the sponsorship of the National Bureau of Standard and the Portland Cement Association, the Fourth International Symposium on the Chemistry of Cement was held at Washington, D. C., October 2–7, 1960. Among 362 persons who accepted the invitations, 271 persons were in attendance from various countries including the host country. The number of papers presented thereto amounts to 66 of which 18 were Principal Papers and 48 were Supplementary Papers, and they were followed by 87 Discussions.

As the Post-Symposium event, a travel to Skokie (Illinois) was organized and many Symposium members took part in it. The participants visited the laboratories of the Portland Cement Association and attended a series of seminars. The Proceedings consisting of 1125 pages were published in Washington, D.C., in 1962 by the National Bureau of Standards.

It was during the Fourth Symposium in Washington that the Japanese cement circles were asked to assume a task of organizing the Fifth Symposium. Encouraged by elder authorities of many participating countries, the representatives of the Japanese cement circles finally accepted to hold in Japan the Fifth International Symposium on the Chemistry of Cement. In 1964, a provisional organizing committee was formed in the bureau of Japan Cement Engineering Association and preparation work started right away. In 1966, Japan Cement Engineering Association was merged in the organization of the Cement Association of Japan, and the proper Organizing Committee and Secretariat were settled in the office of the latter.

Since then, the Organizing Committee and the Secretariat coped with the colossal work for staging the Symposium in Tokyo, and preparation works went on smoothly thanks to the cooperations of the Symposium members in Japan and abroad. Thus, on October 6, 1968, the Fifth International Symposium on the Chemistry of Cement, sponsored by the Cement Association of Japan, dawned with a cocktail party celebrating the 50th anniversary of this Symposium, under the auspices of the Science and Technology Agency and the Ministry of International Trade and Industry, and supported by the Science Council of Japan, the Ceramic Association of Japan, Japan Society of Civil Engineers, the Architectural Institute of Japan and the Chemical Society of Japan.

All the sessions of the Symposium were held, from October 7 to 11, at the Tokyo Metropolitan Festival Hall, Ueno Park, Tokyo. The whole day of October 12 was devoted to technical visits to laboratories and cement works in and around Tokyo.

The Symposium members regularly registered amounted to 606 persons including 325 from Japan and 281 from 42 other countries. But number actually in attendance was 485 including 307 from Japan and 178 from 34 other countries. Accompanying persons from abroad amounted to 40 persons.

An opening ceremony was held on Monday morning, October 7, at the Tokyo Metropolitan Festival Hall before calling to order proper working sessions. The addresses of welcome were given by Mr. H. Inouye, President of the Organizing Committee and by Mr. N. Nabeshima, Minister of State and Director of Science and Technology Agency of Japan. Mr. J. H. Walker, Vice President of the Portland Cement Association, U.S.A., responded on behalf of the members of the Symposium.

The first formal speech entitled "On the Contribution of Chemical Studies to Japanese Cement Industry" was made by Dr. S. Nagai, Professor Emeritus of the University of Tokyo. In succession, Sir F. M. Lea, former Director of the Building Research Station of the United Kingdom, made a speech entitled "Cement Research —Some Views for the Future".

Succeeding working sessions are devoted to technical papers submitted to this Symposium, which amounted to 172 including 20 Principal Papers, 124 Supplementary Papers and 28 Written Discussions. In consideration of too short period of this Symposium to allow each author of Supplementary Papers to present paper in person, the Organizing Committee adopted General Report System where each group of Supplementary Papers under each specific topic was digested systematically by a General Reporter and presented in summarized version at each corresponding session. Thus, time for oral discussions getting available, 69 oral discussions were made throughout five day working sessions.

The themes of the Fifth Symposium consisted of four Parts, and each Part had a categorical topic of its own to which specific subjects treated by Principal and Supplementary Papers were attributed. Each working session covered a group of these specific subjects.

Preprints of Principal Papers in full text and Supplementary Papers in abstract were distributed to enrolled members before the Symposium. Preprints of Written Discussions and General Reports both in full text were distributed at the Symposium site to the attending members.

Technical visits to laboratories and cement plants on October 12 (Saturday) were carried out with the participation of many Symposium members, divided into three groups. The first group visited the cement plant in Saitama Pref. of Nihon Cement Co. Ltd., the second inspected the cement plant of Chichibu Cement Co. Ltd. in Kumagaya city and the Central Research Laboratory of Onoda Cement Co. Ltd. in Tokyo, and the third made a tour of inspection to Kajima Institute of Construction Technology, the Research Laboratory of Engineering Materials of Tokyo Institute of Technology and the Central Research Laboratory of Onoda Cement Co. Ltd, all the three in Tokyo metropolis.

The Proceedings of the Fifth International Symposium on the Chemistry of Cement contain all the written contributions in full text except General Reports, all the oral discussions made on Principal and Supplementary Papers together with their closing discussions and two inauguration speeches at the Opening Ceremony. Being English the official language of this symposium, the Proceedings have been published in English only.

A survey of this Symposium can be made by referring to the annexed table of general program.

General Program of the Fifth International Symposium on the Chemistry of Cement

Parts & Topics	Dates	Sessions and Subjects	Authors of P. P.	Chairmen & Co-Chairmen	Number of S. P.	General Reporters of S. P.
Part I Chemistry of Cement Clinker	Oct. 7 Afternoon	I-1 Structure of Portland Cement Minerals	A. Guinier M. Regourd (France)	I-1 & 2 F. M. Lea (U.K.) T. Yamauchi (Japan)	6	Th. Hahn (W. Germany)
		I-2 Phase Equilibria and Formation of Portland Cement Minerals	R. W. Nurse (U.K.)		9	Y. Suzukawa (Japan)
	Oct. 8 Morning	I-3 Analysis of Portland Cement Clinker	G. Yamaguchi S. Takagi (Japan)	I-3 & 4 R. W. Nurse (U.K.) G. Yamaguchi (Japan)	12	A. E. Moore (U.K.)
		I-4 Chemistry of Calcium Aluminates and their Relating Compounds	T. D. Robson (U.K.)		2	P. E. Halstead (U.K.)
Part II Hydration of Cements	Oct. 8 Afternoon	II-1 Crystal Structures and Properties of Cement Hydration Prodocuts (Calcium Silicate Hydrates)	H. F. W. Taylor (U.K.)	II-1, 2 & 3 H. F. W. Taylor (U.K.) R. Kondo (Japan)	0	
		II-2 Crystal Structures and Properties of Cement Hydration Products (Hydrated Calcium Aluminates and Ferrites)	H. E. Schwiete U. Ludwig (W. Germany)		7 (Structures) 5 (Properties)	W. Locher (W. Germany) M. H. Roberts (U.K.)
		II-3 Phase Equilibria of Cement-Water	P. Seligmann N. R. Greening (U.S.A.)		0	
	Oct. 9 Morning	II-4 Kinetics of Hydration of Cements	R. Kondo S. Ueda (Japan)	II-4 & 5 H. zur Strassen (W. Germany) S. Nagai (Japan)	6 (Mechanism) 8 (Kinetics)	H. Mori (Japan) H. N. Stein (Netherlands)
		II-5 Hydration of Portland Cement	L. E. Copeland D. L. Kantro (U.S.A.)		7	H. zur Strassen (W. Germany)
Part III Properties of Cement Paste and Concrete	Oct. 10 Morning	III-1 Structures and Physical Properties of Cement Paste	G. J. Verbeck R. A. Helmuth (U.S.A.)	III-1 & 2 G. J. Verbeck (U.S.A.) M. Kokubu (Japan)	8 (Fundamental) 7 (Application)	W. C. Hansen (U.S.A.) W. L. Dolch (U.S.A.)
		III-2 Durability of Concrete	O. Valenta (Czech)		10	Imre Biczok (Hungary)
		III-3 Carbonation of Concrete	M. Hamada (Japan)	III-3, 4 & 5 R. H. Mills (Canada) T. Nishi (Japan)	3	H. G. Smolczyk (W. Germany)
	Oct. 10 Afternoon	III-4-a Hydration of Portland Cement Paste at High-Temperature under Atmospheric Pressure	G. M. Idorn (Denmark)		3	P. J. Sereda (Canada)
		III-4-b High-Temperature Curing of Concrete under Atmospheric Pressure	Yu. M. Butt V. M. Kolbasov V. V. Timashev (U.S.S.R.)			
		III-5 High-Temperature Curing of Concrete under High Pressure	G. Kalousek (U.S.A.)		3	H. E. Vivian (Australia)
Part IV Admixtures and Special Cements	Oct. 11 Morning	IV-1 Use of Surface Active Agents in Concrete	R. Mielenz (U.S.A.)	IV-1 & 2 N. Stutterheim (S. Africa) M. Okushima (Japan)	5	K. Okada (Japan)
		IV-2 Fly Ash and Fly Ash Cement	M. Kokubu (Japan)		4	A. Joisel (France)
	Oct. 11 Afternoon	IV-3 Slags and Slag Cements	F. Schröder (W. Germany)	IV-3, 4 & 5 J. H. Walker (U.S.A.) K. Chujo (Japan)	9 (Slag) 3 (High-Sulphate Slag)	R. Sersale (Italy) S. K. Chopra (India)
		IV-4 Expansive Cement	P. P. Budnikov I. V. Kravchenko (U.S.S.R.)		7	G. J. Verbeck (U.S.A.)
		IV-5 By-product Gypsum from Various Chemical industries, as a Retarder for the Setting of Cement	K. Murakami (Japan)		0	
Total		20 sessions	20 papers	16 persons	124 papers	20 persons

List of the Symposium Regular Members

ABE, Hirotoshi
Central Research Institute of Electric Power Industry ..... Japan
AGO, Shunji
Onoda Cement Co., Ltd. ..... Japan
AHN, Kyu Young ..... Rep. of Korea
AKAIWA, Shigeo
Chichibu Cement Co., Ltd. ..... Japan
AKATSU, Takeshi
Yawata Chemical Industry Co., Ltd. ..... Japan
†AKGERMAN, Bedri ..... Turkey
AKIYAMA, Keiichi
Shibaura Institute of Technology ..... Japan
AKUTSU, Kenji
Taisei Construction Co., Ltd. ..... Japan
†ALEXANDER, Kenneth M.
Commonwealth Scientific & Industrial Research Organization ..... Australia
AMAFUJI, Morio
Onoda Cement Co., Ltd. ..... Japan
AMEMIYA, Masashi
Sumitomo Cement Co., Ltd. ..... Japan
AOKI, Shigeki
Nihon University ..... Japan
AONO, Masashi
Chubu Electric Co., Inc. ..... Japan
AONO, Takeo
Denki Kagaku Kogyo Kabushiki Kaisha ..... Japan
ARDJANGGI, Sotion
P. N. Semen Gresik ..... Indonesia
ARAMAKI, Kikuo
Toyo Soda Manufacturing Co., Ltd. ..... Japan
ARIIZUMI, Akira
Kajima Construction Co., Ltd. ..... Japan
ASAHARA, Kinpei
Chichibu Cement Co., Ltd. ..... Japan
ARSOY, Orhan
Cimento Fabrikasi Müdürü ..... Turkey
ASANO, Masakazu
Daiichi Cement Co., Ltd. ..... Japan
ASANO, Tadashi
Naigai Consultant Co., Ltd. ..... Japan
ASAOKU, Shunichiro
Onoda Cement Co., Ltd. ..... Japan
ASO, Taro
Aso Cement Co., Ltd. ..... Japan
AYSAN, Sevki Mehmet ..... Turkey
BAK'R, Tahsin N.
State Organization for Industry ..... Iraq
BANNAI, Hideo
Denki Kagaku Kogyo Kabushiki Kaisha ..... Japan
†BARTOSCH, Eberhardt
Gebr. Leube, Portlandzementwerk ..... Austria
†BATES, Allan A.
National Bureau of Standards ..... U.S.A.
†BAUSET, René J.
Hydro-Quebec ..... Canada
BECKER, Fridolin
Technical Center Holderbank ..... Switzerland
BERGER, Richard L.
American Cement Corporation ..... U.S.A.
BERNAL, Rufo B.
Marinduque Mining & Industrial Corporation ..... Philippines
†BESSEY, George E.
Building Materials Consultant ..... United Kingdom
BICZÓK, Imre
Institute of Geodesy and Geotechnics ..... Hungary
†BLAINE, Raymond L.
National Bureau of Standards ..... U.S.A.
†BLAKEY, Frank A.
Commonwealth Scientific & Industrial Research Organization ..... Australia
BLANK, Alton J.
Cementos Atoyac, S.A. ..... Mexico
BOIKOVA, Alexandra
Grebenshchikov Institute of Silicate Chemistry, the Academy of Science ..... U.S.S.R.
BROCARD, Jacques
Centre Expérimental de Recherches de Batiment et des Trauaux Publics ..... France
BROWN, Arthur W.
The Associated Portland Cement Manufacturers, Ltd. ..... United Kingdom
BROWN, Owen E.
Marquette Cement Manufacturing Company ..... U.S.A.
BUCCHI, Renato
Italcementi S.p.A. ..... Italy
BUDNIKOV, Peter P.
Moscow Academy of Science ..... U.S.S.R.
BUTED, Jose
Bacnotan Cement Industries, Inc. ..... Philippines
BUTT, Yuri M.
The Moscow Mendeleev's Institute of Chemical Technology ..... U.S.S.R.
†BUZZI, Sandro
F.lli Buzzi Cementi S.p.A. ..... Italy
CALLEJA, José
Instituto "Eduardo Torroja" de la Construccion y del Cemento ..... Spain
†CASSIDY, J. E.
Imperial Chemical Industries Limited ..... United Kingdom
CATANI, Antonio
Italcementi S.p.A. ..... Italy
CATTINI, Luigi
Grace Italiana S.p.A. ..... Italy
†CELANI, Adriano
Soc. Calci e Cementi di Segni ..... Italy
†CESARENI, Cesare
Cementir-Cementerie del Tirreno S.p.A. ..... Italy
CHANG, Ching-Chi ..... Rep. of China
†CHATTERJI, Susanta Kumar
Birkbeck College ..... United Kingdom
CHEN, Nai-Neng
Chien Tai Cement Corp. Ltd. ..... Rep. of China
CHEN, Ying-Nan
Building Materials Research Laboratory .... Rep. of China
†CHERON, Marcel L. E.
Cimenteries CBR ..... Belgium
CHOI, Sang-Heul
Hanyang University ..... Rep. of Korea
CHOI, Yung Kook
Tong Yang Cement Mfg. Co., Ltd. ..... Rep. of Korea
†CHOPRA, Surinder K.
Central Building Research Institute ..... India
CHUDO, Akira
Osaka Cement Co., Ltd. ..... Japan
CHUJO, Kimbe
Nihon Cement Co., Ltd. ..... Japan
†CLAUSEN, Carl F.
Cement Research Institute of India ..... India
COLLIS, Henry C.
Cembureau, The European Cement Association ..... France
COPELAND, Llewellyn E.
Portland Cement Association ..... U.S.A.
CORONAS, Juan-Maria R.
Universidad de Barcelona ..... Spain
†COVA, Fedele
Cementir-cementerie del Tirreno S.p.A. ..... Italy
†CUSSINO, Luciano
Laboratorio Centrale-Unione Cementi Marchino & C. ..... Italy
†CZERNIN, Wolfgang

Daggers indicate persons who did not attend the Symposium.

Vorstandsmitglied der Perlmooser Zementwerke A.G. ..... Austria
DALMIA, Mridu Hari
Orissa Cement, Ltd. ..... India
†DAUGHERTY, Kenneth E.
American Cement Corporation ..... U.S.A.
DAVIES-GRAHAM, Lewis R.
North Australian Cement, Ltd. ..... Australia
†De KEYSER, Walter L.
Centre National de Recherches Scientifiques et Techniques pour Industrie Cimentiére ..... Belgium
DELARYD, Bengt
Swedish Embassy ..... Sweden
DEMIRMAN, Çetin Hüsnü
Çimento Fabrikasi Müdürü ..... Turkey
†DIAMOND, Sidney
Purdue University ..... U.S.A.
DOLCH, W. L.
Purdue University ..... U.S.A.
†DOSCH, Werner
Mineralogisches Institut der Universität ..... West Germany
DUNCAN, Raymond A.
Adelaide Cement Co., Ltd. ..... Australia
†DUNGAN, Claude K.
United Portland Cement Co., Ltd. ..... Rhodesia
†DUTRON, P.
Centre National de Recherches Scientifiques et Techniques pour Industrie Cimentière ..... Belgium
†DYCKERHOFF, Walter
Tyngatu S.A. Industrial & Comercial ..... Argentina
†DYCZEK, Jerzy R.
Akademia Górniczo Hutnicza, Katedra Technologii Materialów Wiazacych ..... Poland
ELSNER von GRONOW, Harald
Firma Bauwesen ..... West Germany
ESENWEIN, Paul
Eidg. Materialprüfungs und Versuchsanstalt ..... Switzerland
ETOH, Tetsuo
Asahi Glass Co., Ltd. ..... Japan
FEHNEL, Charles D.
Lone Star Cement Corporation ..... U.S.A.
FELDMAN, Rolf F.
National Research Council ..... Canada
FELICIANO, Lupo V.
Republic Cement Corporation ..... Philippines
FORSS, Bengt U.
Paragas Kalkbergs Aktiebolag ..... Finland
FOREST, Jean
Etablissements Poliet & Chausson ..... France
†FRANK, Peter J.
General Electric Research and Development Center ..... U.S.A.
FROHNSDORFF, Geoffrey J.
American Cement Corporation ..... U.S.A.
FUJII, Kinjiro
The Government Chemical Industrial Research Institute ..... Japan
FUJII, Yoshio
Tokuyama Soda Co., Ltd. ..... Japan
FUKUDA, Nobue
Tokuyama Soda Co., Ltd. ..... Japan
FUKUDA, Yoshiharu
Onoda Cement Co., Ltd. ..... Japan
FUKUSHIMA, Yaroku
Meiji University ..... Japan
FUKUWATARI, Tadashi
Japan Siporex Inc. ..... Japan
†FULTON, F. S.
Portland Cement Institute ..... South Africa
FUNAOKA, Masao
Asahi Glass Co., Ltd. ..... Japan
†FUNK, Herbert B.
Freie Universität Berlin ..... West Germany
GALLAGHER, Rodger E.
HI Cement Corporation ..... Philippines
†GASKIN, Arthur J.
Commonwealth Scientific & Industrial Research Organization ..... Australia
GERBER, Andre P.
W. R. Grace Ltd. ..... Hong Kong
†GHANI, Mohamed Abdul
West Pakistan Industrial Development Corporation ..... Pakistan
†GHARPUREY, M. K.
The Associated Cement Cos, Ltd. ..... India
GÖKSALTIK, Suat X.
Türk çimentosu ve kireci, çimento fabrikasi-Zeytinburna ..... Turkey
†GOOSSENS, Pierre J.
N. V. Portland Cement J. Van Den Heuvel ..... Belgium
†GORIA, Carlo
Politecnico di Torino ..... Italy
GOTO, Kikuji
Nihon Cement Co., Ltd. ..... Japan
GOTO, Masaki
Kanda Cement Co., Ltd. ..... Japan
GOTTLIEB, Steven
Gorresen's Pty. Ltd. ..... Australia
GREENING, Nathan R.
Portland Cement Association ..... U.S.A.
GREENHILL, Edgar B.
Australian Portland Cement, Ltd. ..... Australia
†GRUENWALD, Ernst ..... U.S.A.
GUINIER, André
Université de Paris ..... France
GÜNEL, Tahsin
Aslan ve Eskihisar Müttehit Çimento ve Su Kireci Fabrikalari ..... Turkey
GÜNGÖR, Yilmaz ..... Turkey
GUTMANN, Phillip W.
Medusa Portland Cement Company ..... U.S.A.
†GUTT, Witold
Building Research Station ..... United Kingdom
HAHN, Theodor
Institut für Kristallographie ..... West Germany
HALSTEAD, Philip E.
Cement and Concrete Association ..... United Kingdom
HAMADA, Minoru
Tokyo University of Science ..... Japan
HANADA, Mitsuo
Yawata Chemical Industry Co., Ltd. ..... Japan
†HANSEN, Waldemar C.
Consulting Chemist ..... U.S.A.
HARADA, Tamotsu
Kanagawa University ..... Japan
HASEBE, Atsushi
Sika Company Ltd. ..... Japan
HASEGAWA, Sachio
Chubu Electric Power Co., Inc. ..... Japan
HASHIMOTO, Hirokazu
Taisei Construction Co., Ltd. ..... Japan
HASHIMOTO, Kenichi
Government Chemical Industrial Research Institute ..... Japan
HASHIZUME, Yutaka
Aso Cement Co., Ltd. ..... Japan
HATA, Seiichiro
Nihon Cement Co., Ltd. ..... Japan
HATTIANGADI, R. R.
The Associated Cement Cos., Ltd. ..... India
HATTORI, Kenichi
Kao Soap Co., Ltd. ..... Japan
HATTORI, Takashige
Hokkaido University ..... Japan
HAYASHI, Masamichi
Hokkaido Development Bureau ..... Japan
HAYASHI, Ryosuke
Sumitomo Cement Co., Ltd. ..... Japan
HAYASHI, Shigeru
Hokoku Cement Co., Ltd. ..... Japan
HEDGES, C. Roland
New Zealand Cement Holdings Ltd. ..... New Zealand
†HEDIN, Rune V.
Cement-och Betonginstitutet ..... Sweden

†HEDVALL, Arvid
Chalmers Tech. Institute ..... Sweden
†HEILMANN, Thorbjørn
F. L. Smidth & Co. A/S ..... Denmark
HELLINGS, Robert F.
Pretoria Portland Cement Co., Ltd. ..... South Africa
HELMUTH, Richard A.
Portland Cement Association ..... U.S.A.
HESAKA, Tsuneo
Ube Industries, Ltd. ..... Japan
HIGUCHI, Yoshiro
Railway Technical Research Institute ..... Japan
HIRAGA, Kenichi
Taisei Construction Co., Ltd. ..... Japan
HIRAOKA, Genzo
Chuo University ..... Japan
HIRAOKA, Takeshi
Osaka Cement Co., Ltd. ..... Japan
HISASHIGE, Michio
Nihon Cement Co., Ltd. ..... Japan
HISHIYA, Kentaro
W. R. Grace Kabushiki Kaisha ..... Japan
†HÖGBERG, Erik A.
Cement-och Betonglaboratoriet ..... Sweden
HOKINOUE, Yoshikazu
Sumitomo Cement Co., Ltd. ..... Japan
HOKUGO, Tadanobu
Hitachi Cement Co., Ltd. ..... Japan
HONGO, Kozo
Daiichi Cement Co., Ltd. ..... Japan
HONMA, Eigoro
Nihon Cement Co., Ltd. ..... Japan
HORI, Genya
Kobe Material Co., Ltd. ..... Japan
HOSOI, Junzo
Nihon Cement Co., Ltd. ..... Japan
HSU, Mau Lin
Universal Cement Corporation ..... Rep. of China
HUMMEL, Christoph
Dyckerhoff-Zementwerke A. G. ..... West Germany
IDORN, Gunnar M.
Concrete Research Laboratory ..... Denmark
IKEDA, Tadao
Osaka Cement Co., Ltd. ..... Japan
INOUE, Giichi
Osaka Cement Co., Ltd. ..... Japan
INOUE, Kiyoshi
Hitachi Cement Co., Ltd. ..... Japan
INOUE, Yuji
Chichibu Cement Co., Ltd. ..... Japan
†ISHAI, Ori
Israel Institute of Technology ..... Israel
ISHII, Mineo
Nihon Cement Co., Ltd. ..... Japan
ISHIKAWA, Hiroyasu
Mitsubishi Cement Co., Ltd. ..... Japan
†ISH-SHALOM, Moshe
Israel Ceramic and Silicate Institute ..... Israel
ISOGAI, Jun
Denki Kagaku Kogyo Kabushiki Kaisha ..... Japan
ITO, Hiroshi
Onoda Cement Co., Ltd. ..... Japan
ITO, Shigetomi
Public Works Research Institute ..... Japan
ITO, Tomizo
Sumitomo Cement Co., Ltd. ..... Japan
ITO, Yoji
Hokkaido Development Bureau ..... Japan
IWABUCHI, Toshitsugu
Fuji Cement Co., Ltd. ..... Japan
IWAI, Tohru
Kajima Construction Co., Ltd. ..... Japan
JACK, Orville E.
Kaiser Cement & Gypsum Corporation ..... U.S.A.
JAMBOR, Jaromir
Institute of Construction and Architecture, Slovak Academy of Sciences ..... Czechoslovakia
†JAMES, A. N.
The Cementation Co., Ltd. ..... United Kingdom
†JANSSENS, Paul F.
Société des Ciments d'Outremer ..... Belgium
†JASPERS, Michel
S. A. Compagnie des Ciments Belges ..... Belgium
JECKS, Peter M.
Australian Portland Cement, Ltd. ..... Australia
JEEVARATNAM, Jeevarajah
Kankesan Cement Works ..... Ceylon
†JENSEN, Ib J.
Dundee Cement Company ..... U.S.A.
JESSING, Jørn
Danmarks Ingeniørakademi, Bygningsafdelingen ..... Denmark
JOHANSEN, Vagn C.
F. L. Smidth & Co. A/S ..... Denmark
JOISEL, Albert
Centre d'Etudes et de Recherches de l'Industrie des Liants Hydrauliques ..... France
KADOMOTO, Joji
Hokoku Cement Co., Ltd. ..... Japan
KAISER, Herman
Compañía Anónima Venezolana de Cementos ..... Venezuela
KAJII, Motohiko
Ube Industries, Ltd. ..... Japan
†KALOUSEK, George L.
Bureau of Reclamation, Denver Federal Center ..... U.S.A.
KAMATA, Wataru
Nihon Cement Co., Ltd. ..... Japan
KAMEDA, Yasuhiro
Building Research Institute ..... Japan
KAMIMURA Katsuro
Building Research Institute ..... Japan
KAMIURA, Masao
Railway Technical Research Institute ..... Japan
KANEISHI, Ryuma
Toyo Soda Manufacturing Co., Ltd. ..... Japan
KANTRO, David L.
Portland Cement Association ..... U.S.A.
KARASUDA, Sensuke
Shimizu Construction Co., Ltd. ..... Japan
KASAHARA, Minoru
Chichibu Cement Co., Ltd. ..... Japan
KASAI, Junichi
Nihon University ..... Japan
KASAI, Koichi
Onoda Cement Co., Ltd. ..... Japan
KASAI, Yoshio
Nihon University ..... Japan
KASE, Tsutomu
Tokuyama Soda Co., Ltd. ..... Japan
KATO, Akihisa
Tsuruga Cement Co., Ltd. ..... Japan
KATO, Mutsumi
Tokyo Institute of Technology ..... Japan
KAWADA, Naoya
Nihon Cement Co., Ltd. ..... Japan
KAWAI, Zenzaburo
Chichibu Cement Co., Ltd. ..... Japan
KAWAKAMI, Hideo
Fukui University ..... Japan
KAWAKAMI, Seiichiro
Hokoku Cement Co., Ltd. ..... Japan
KAWAMURA, Shigeo
Onoda Cement Co., Ltd. ..... Japan
KEN, Yong
Taiwan Cement Corporation ..... Rep. of China
KENBER, Ercüment
Aslan ve Eskihisar Müttehit Çimento ve Su Kireci Fabrikalari Anonim Sirketi ..... Turkey
†KENNERLEY, Roy A.
Department of Scientific and Industrial Research ..... New Zealand
KERMAN, Guy M.
Aberthaw & Bristol Channel Portland Cement Co., Ltd. ..... United Kingdom
KIKKAWA, Motoji
Kanda Cement Co., Ltd. ..... Japan

KIKUCHI, Hiroshi
Onoda Cement Co., Ltd. ..... Japan
KIM, Jin Won
Hanil Cement Mfg. Co., Ltd. ..... Rep. of Korea
KIMURA, Shigeo
Mitsubishi Cement Co., Ltd. ..... Japan
KIMURA, Takanori
Yawata Chemical Industry Co., Ltd. ..... Japan
KINCH, William M.
W. R. Grace & Co. ..... U.S.A.
KINJO, Takayuki
Ryukyu Cement Co., Ltd. ..... Japan
KIRA, Kinichi
Mitsubishi Cement Co., Ltd. ..... Japan
KIRIYAMA, Ryoichi
Osaka University ..... Japan
KISHITANI, Koichi
The University of Tokyo ..... Japan
KITAGAWA, Kinichi
Osaka Cement Co., Ltd. ..... Japan
KITSUGI, Kyoichi
Onoda Cement Co., Ltd. ..... Japan
†KLEIN, Alexander
University of California ..... U.S.A.
†KLIEGER, Paul
Portland Cement Association ..... U.S.A.
KOBAYASHI, Waichi
Ube Industries, Ltd. ..... Japan
KODAMA, Kazumi
Nisso Master Builders Co., Ltd. ..... Japan
KOELLIKER, Emil
Technische Forschungs und Beratungs-
stelle der Schweiz. Zementindustrie ..... Switzerland
KOH, Yoshiro
Hokkaido University ..... Japan
KOHTA, Taichi
Nihon University ..... Japan
KOIDE, Shigeaki
Seikei University ..... Japan
KOIDE, Yoshiharu
Sumitomo Cement Co., Ltd. ..... Japan
KOIKE, Michio
Hokkaido University ..... Japan
KOJIMA, Yuji
Osaka Cement Co., Ltd. ..... Japan
KOKUBU, Masatane
The University of Tokyo ..... Japan
KOMATSUBARA, Masashi
Nippon Asbestos Co., Ltd. ..... Japan
KONDO, Maretaka
Mitsubishi Cement Co., Ltd. ..... Japan
KONDO, Minoru
Nihon Cement Co., Ltd. ..... Japan
KONDO, Motoki
Takenaka Komuten Co., Ltd. ..... Japan
KONDO, Osamu
Public Works Research Institute ..... Japan
KONDO, Renichi
Tokyo Institute of Technology ..... Japan
KONDO, Wakichi
Government Chemical Industrial Research
Institute ..... Japan
KONO, Hisashi
Ube Industries, Ltd. ..... Japan
KOYANAGI, Katsuzo
Chiba Institute of Technology ..... Japan
†KREIJGER', Pieter C.
Institute TNO for Building Materials and
Building Structures ..... Netherlands
KUBO, Kazuhiko
Osaka Packing Mfg. Co., Ltd. ..... Japan
KUNTZE, Richard A.
Ontario Research Foundation ..... Canada
KUNUGI, Masanaga
Kyoto University ..... Japan
KURAMOTO, Toru
Hokoku Cement Co., Ltd. ..... Japan
KURIBAYASHI, Hiroshi
Sugai Chemical Industry Co., Ltd. ..... Japan
KUROKAWA, Naohiro
Ube Industries, Ltd. ..... Japan
KUSAKAWA, Shintaro
Mitsui Cement Co., Ltd. ..... Japan
KUZEL, Hans J.
Institut für Kristallographie der Univer-
sität Frankfurt ..... West Germany
†LAUER, Kenneth R.
University of Notre Dame ..... U.S.A.
LEA, Frederick M. ..... United Kingdom
LEE, Whee-Soo
Tokyo Institute of Technology ..... Japan
Le BEL, François
Ciments Lafarge ..... France
Le BOURRE, François
Centre Expérimental de Recherches de
Batiment et des Trauaux Publics ..... France
LEKATOMPESSY, Junus D.
P. N. Semen Gresik ..... Indonesia
†Le SAR, Dennis
Cape Portland Cement Co., Ltd. ..... South Africa
LIEBER, Werner
Portland-Zementwerke Heidelberg
A.G. ..... West Germany
LIEBAU, Friedrich
Mineralogische-Petrographisches Institut
der Universität Kiel ..... West Germany
LIN, Li-Chuan
Chien Tai Cement Corp. Ltd. ..... Rep. of China
LOCHER, Friedrich W.
Forschungsinstitut der Zementindustrie .... West Germany
LOESCHE, E. Guenter
Loesche Hartzerkleinerungs und Zement
Maschinen K.G. ..... West Germany
†LONGUET, Paul
Centre d'Études et de Recherches de l'In-
dustrie des Liants Hydrauliques ..... France
LOZADA, R. Faustino
Fillipinas Cement Corporation ..... Philippines
LUDWIG, Udo
Institut für Gesteinshüttenkunde ..... West Germany
LYON, Charles A.
Nisso Master Builders Co., Ltd. ..... U.S.A.
†McFARLANE, John D.
Simon Carves, Ltd. ..... United Kingdom
MacINNIS, Cameron
The University of Windsor ..... Canada
MACHIDA, Atsuhiko
Saitama University ..... Japan
MAEJIMA, Shoichi
Asahi Asbestos Co., Ltd. ..... Japan
MAEKAWA, Shizuo
Hokkaido Development Bureau ..... Japan
†MALINOWSKI, Roman
Chalmers University of Technology ..... Sweden
MANABE, Toshio
Nihon Kenki Co., Ltd. ..... Japan
MANTEL, Dirk G.
White's South African Portland Cement
Co., Ltd. ..... South Africa
MARCHESE, Bernardo
Università di Napoli ..... Italy
MARSHALL, Samuel M.
Southern Portland Cement, Ltd. ..... Australia
MARTINEZ, Joaquin Angel F.
Marinduque Mining & Industrial Corpora-
tion ..... Philippines
MASSAZZA, Franco
Italcementi S.p.A. ..... Italy
MATHER, Bryant
U.S. Army Engineer Waterways Experi-
ment Station ..... U.S.A.
MATHER, Katharine
U.S. Army Engineer Waterways Experi-
ment Station ..... U.S.A.
MATSUDA, Keisuke
Ube Industries, Ltd. ..... Japan
MATSUEDA, Akira
Mitsubishi Cement Co., Ltd. ..... Japan

MATSUI, Motohiro
Nihon Cement Co., Ltd. ..... Japan
MATSUI, Yoshitaka
Nihon University ..... Japan
MATSUMOTO, Katsumi
Kogakuin University ..... Japan
MATSUMOTO, Shigeji
Denki Kagaku Kogyo Kabushiki Kaisha ..... Japan
MATSUNAGA, Minoru
Tokyo University of Agriculture & Technology ..... Japan
MATSUNAGA, Tetsuo
Ube Industries, Ltd. ..... Japan
MATTIJK, Kiagus
P. N. Semen Padang ..... Indonesia
MAU, Kong Tong ..... U.S.A.
McCOY, Walter J.
Lehigh Portland Cement Company ..... U.S.A.
MCHEDLOV-PETROSYAN, Otar P.
Railway Engineering Institute ..... U.S.S.R.
MEHTA, Povindar Kumar
The University of California ..... U.S.A.
MEINTRUP, Ernst Mei
Polysius G.m.b.H. ..... West Germany
MEYER, Adolf
Portland-Zementwerke Heidelberg AG ..... West Germany
MEYERS, Bernard L.
The University of Iowa ..... U.S.A.
†MIDGLEY, Henry G.
Building Research Station ..... United Kingdom
MIELENZ, Richard C.
Master Builders Co. ..... U.S.A.
MIKATA, Masayuki
Fujisawa Pharmaceutical Co., Ltd. ..... Japan
MILLS, Ronald H.
The University of Calgary ..... Canada
MINATO, Hideo
The University of Tokyo ..... Japan
MINEGISHI, Keiichi
Chichibu Cement Co., Ltd. ..... Japan
MINEYAMA, Takashi
Osaka Cement Co., Ltd. ..... Japan
MISHIMA, Kiyotaka
Asahi Glass Co., Ltd. ..... Japan
MIYADAI, Toshimitsu
Sumitomo Cement Co., Ltd. ..... Japan
MIYAKAWA, Tsugio
Nihon University ..... Japan
MIZOGUCHI Yoshiro
Osaka Cement Co., Ltd. ..... Japan
MIZUTA, Kyozo
Chichibu Cement Co., Ltd. ..... Japan
MOCHIZUKI, Mitsuo
Sumitomo Cement Co., Ltd. ..... Japan
MOORE, Alice E.
Cement and Concrete Association ..... United Kingdom
MOORE, Murray Ira
Adelaide Cement Co., Ltd. ..... Australia
MORI, Hitoaki
Chichibu Cement Co., Ltd. ..... Japan
MORI, Shigejiro
Onoda Cement Co., Ltd. ..... Japan
MORI, Toru
Kajima Construction Co., Ltd. ..... Japan
MORITA, Kengo
Onoda Cement Co., Ltd. ..... Japan
MUGURUMA, Hiroshi
Kyoto University ..... Japan
MURAKAMI, Keiichi
Tohoku University ..... Japan
MURAKAMI, Yoshikazu
Chichibu Cement Co., Ltd. ..... Japan
MURAMATSU, Chiaki
Takemoto Oil and Fat Co., Ltd. ..... Japan
MURATA, Jiro
Tokyo Metropolitan University ..... Japan
MURATA, Yoshio
Ube Industries, Ltd. ..... Japan
NAGAHIRO, Akio
Asahi Glass Co., Ltd. ..... Japan
NAGAI, Shoichiro
The University of Tokyo (Prof. Emeritus) ..... Japan
NAGANO, Takuzo
Onoda Cement Co., Ltd. ..... Japan
NAGASE, Tatsuo
Sumitomo Cement Co., Ltd. ..... Japan
NAGASHIMA, Noriyuki
Onoda Cement Co., Ltd. ..... Japan
NAGATAKI, Shigeyoshi
Tokyo Institute of Technology ..... Japan
NAGAYAMA, Kiichi
Asahi Glass Co., Ltd. ..... Japan
NAKAGAWA, Koji
Denki Kagaku Kogyo Kabushiki Kaisha ..... Japan
NAKAGAWA, Masaichi
W.R. Grace Kabushiki Kaisha ..... Japan
NAKAHARA, Manjiro
Nihon University ..... Japan
NAKAJIMA, Koji
Sanyo Pulp Co., Ltd. ..... Japan
NAKAJIMA, Yukio
Nihon Cement Co., Ltd. ..... Japan
NAKAMA, Yasuo
Ryukyu Cement Co., Ltd. ..... Japan
NAKAMURA, Atsushi
Nihon Cement Co., Ltd. ..... Japan
NAKAMURA, Kiyoshi
Pneumoconiosis Research Institute, Pulverized Coal Burnt Ash Research Institute ..... Japan
NAKAMURA, Masuo
Yawata Chemical Industry Co., Ltd. ..... Japan
NAKAMURA, Takanori
Chichibu Cement Co., Ltd. ..... Japan
NAKAMURA, Takashi
Nihon Cement Co., Ltd. ..... Japan
†NEGRO, Alfredo
Politecnico di Torino ..... Italy
NAKAMURA, Yukio
Mitsui Cement Co., Ltd. ..... Japan
NEVILLE, Adam M.
The University of Leeds ..... United Kingdom
†NERENST, Poul
H+H-Industri A/S ..... Denmark
NIËL, Egide M.M.G.
Eerste Nederlandse Cement Industrie N.V. ..... Netherlands
NISHI, Tadao
The University of Tokyo ..... Japan
NISHIBAYASHI, Shinzo
Tottori University ..... Japan
NISHIDA, Tadasu
Onoda Cement Co., Ltd. ..... Japan
NISHIOKA, Shiro
Nihon Cement Co., Ltd. ..... Japan
NIWA, Yunosuke
Mitsubishi Cement Co., Ltd. ..... Japan
NOGUCHI, Katsuhisa
Nihon Cement Co., Ltd. ..... Japan
NURSE, Ronald W.
Building Research Station ..... United Kingdom
OBATA, Masatsugu
Hitachi Cement Co., Ltd. ..... Japan
ODA, Seiichi
Mitsui Cement Co., Ltd. ..... Japan
OGASAWARA, Takenori
Yamaso-Kagaku Co., Ltd. ..... Japan
OGAWA, Akira
The Fujita General Construction Co., Ltd. ..... Japan
OGAWA, Tadashi
Sumitomo Cement Co., Ltd. ..... Japan
OHAMA, Yoshihiko
Building Research Institute ..... Japan
OHASHI, Toshio
Tokuyama Soda Co., Ltd. ..... Japan
OH-SANG, Kwan
Chungbuk Cement Mfg. Co., Ltd. ..... Rep. of Korea
OHSAWA, Junichi
Sumitomo Cement Co., Ltd. ..... Japan

OHSAWA, Shigenari
Tokyo Institute of Technology ..... Japan
OHSHIMA, Hisaji
Chiba Institute of Technology ..... Japan
†OHTA, Chisato
Shin Nihon Chemical Industry Co., Ltd. ..... Japan
OHTSUBO, Masasuke
Aso Cement Co., Ltd. ..... Japan
OJIRI, Kozo
Asahi Glass Co., Ltd. ..... Japan
OKADA, Keiko
Seikei University ..... Japan
OKADA, Kiyoshi
Kyoto University ..... Japan
OKAMURA, Hajime
The University of Tokyo ..... Japan
OKUMA, Rokuro
Daiichi Cement Co., Ltd. ..... Japan
OKUNO, Chiko
Asano Concrete Co., Ltd. ..... Japan
OKUSHIMA, Masaichi
Osaka University ..... Japan
OLIVER, Russel N.
Australian Portland Cement, Ltd. ..... Australia
OMURA, Toshio
Mitsubishi Cement Co., Ltd. ..... Japan
ONO, Isao
Asahi Glass Co., Ltd. ..... Japan
ONO, Koh-hei
Asahi Glass Co., Ltd. ..... Japan
ONO, Mikiya
Mitsubishi Cement Co., Ltd. ..... Japan
ONO, Yoshio
Kanda Cement Co., Ltd. ..... Japan
ONO, Yoshio
Onoda Cement Co., Ltd. ..... Japan
ONO, Yoshizo
Denki Kagaku Kogyo Kabushiki Kaisha ..... Japan
†ORSINI, Paolo G.
Universitá di Napoli ..... Italy
†OSTBERG, Werner
Dundee Cement Company ..... U.S.A.
OTOUMA, Takashi
Nippon Asbestos Co., Ltd. ..... Japan
†OTTO, Peter A.
Institut für Gesteinshüttenkunde ..... West Germany
†PAI, V. N.
The Associated Cement Cos. Ltd. ..... India
PALMER, Kenneth E.
Ideal Cement Co. ..... U.S.A.
PALOMAR, Patricio
Compañía Catalana de Cementos Portland S.A. ..... Spain
PAO, L. Y.
Asia Cement Plant ..... Rep. of China
PARKER, Cecil D.
Water Science Laboratories ..... Australia
PARMAN, Cemil
Anadolu Çimentolari Türk Anonim Şirketi ..... Turkey
PAULIN, William T. H.
New Zealand Cement Holdings, Ltd. ..... New Zealand
PESENTI, Carlo
Italcementi S.p.A. ..... Italy
PESENTI, Giampiero
Italcementi S.p.A. ..... Italy
PEUKERT, Karl G. H.
Didier-Werke A.G. ..... West Germany
PHILLEO, Robert E. ..... U.S.A.
†PIERSON, Charles U.
The M. W. Kellogg Company ..... U.S.A.
†PIKE, Robert G.
Bureau of Public Roads ..... U.S.A.
POHL, Günther
Rheinisch-Westrälische Kalkwerke AG ..... West Germany
POLLITT, Harry W. W.
The Associated Portland Cement Manufacturers, Ltd. ..... United Kingdom
†POPOVICS, Sandor
Auburn University ..... U.S.A.
RAVID, Shlomo Ami ..... Israel
REGOURD, Micheline
Centre d'Études et de Recherches de l'Industrie des Liants Hydrauliques ..... France
REVENTAR, Rolando E.
Filipinas Cement Corporation ..... Philippines
REYES, R. Rodrigo
Republic Cement Corporation ..... Philippines
RICHARTZ, Werner
Forschungsinstitut der Zementindustrie ..... West Germany
†RIO, Arturo
Soc. Calci e Cementi di Segni ..... Italy
RITZMANN, Horst Rz
Polysius G.m.b.H. ..... West Germany
†ROBERTS, Melville H.
Building Research Station ..... United Kingdom
ROBSON, Thomas D.
The Lafarge Organisation, Ltd. ..... United Kingdom
†ROPER, Harold
Commonwealth Scientific & Industrial Research Organization ..... Australia
ROSALES, Guillermo
Cementos Asland ..... Spain
ROWE, Kenneth C.
Goliath Portland Cement Co., Ltd. ..... Australia
ROY, Della M.
The Pennsylvania State University ..... U.S.A.
RUMYANTSEV, P. F.
Institute of Silicate Chemistry of the Academy of Science ..... U.S.S.R.
RUTLE, John
Betongkjemisk A/S ..... Norway
†SADRAN, G.
Centre de Recherches de la Jonchère-Côte de la Jonchère Ciments Lafarge ..... France
SAITO, Chokui
Fuji Cement Co., Ltd. ..... Japan
SAITO, Minoru
Hitachi Cement Co., Ltd. ..... Japan
SAITO, Tsuruyoshi
Onoda Cement Co., Ltd. ..... Japan
SAJI, Kenjiro
Nihon Cement Co., Ltd. ..... Japan
SAJI, Taiji
Kyushu University ..... Japan
SAKAI, Toru
Asahi Glass Co., Ltd. ..... Japan
SAKATA, Motoki
Kobe Material Co., Ltd. ..... Japan
SAKURAI, Toshio
Nihon Cement Co., Ltd. ..... Japan
SANADA, Yoshiaki
Sumitomo Cement Sales Co-operative Association ..... Japan
SANADA, Yukitoshi
Sumitomo Cement Co., Ltd. ..... Japan
SANDLER, Robert
Anglo-Alpha Cement Ltd. ..... South Africa
SASAKI, Ayao
Onoda Cement Co., Ltd. ..... Japan
SASAKI, Takaharu
Ube Industries, Ltd. ..... Japan
SATA, Toshiyuki
Tokyo Institute of Technology ..... Japan
SATARIN, V. I.
Institute Yuzhgiprocement ..... U.S.S.R.
SATO, Hajime
Sumitomo Cement Co., Ltd. ..... Japan
SATO, Masao
Sumitomo Cement Co., Ltd. ..... Japan
SATO, Nagamitsu
Onoda Cement Co., Ltd. ..... Japan
SATO, Takeshi
Nihon Cement Co., Ltd. ..... Japan
ŠAUMAN, Zdeněk
Research Institute of Building Materials ..... Czechoslovakia
SCHRODER, Ernest M.
Adelaide Cement Co., Ltd. ..... Australia

SCHRÖDER, Fritz J.
Forschungsinstitut für Hochofenschlacke ..West Germany
SCHRÄMLI, Werner
Technical Center Holderbank .....Switzerland
†SCHWIETE, Hans E.
Institut für Gesteinshüttenkunde .....West Germany
†SEAGER, Edmund S.
The Rugby Portland Cement Co., Ltd. ..United Kingdom
SEKI, Shingo
Central Research Institute of Electric Power Industry .....Japan
SEKIYA, Michio
Kogakuin University .....Japan
†SELIGMANN, Paul
Portland Cement Association .....U.S.A.
SEREDA, Peter J.
National Research Council.....Canada
SERSALE, Riccardo
Università di Napoli.....Italy
SETOYAMA, Katsumi
Kogakuin University .....Japan
†SHARMA, Lakshman Swaroop
Dalmia Cement (Bharat) Ltd. .....India
†SHALON, Rahel
Israel Institute of Technology .....Israel
SHEN, Hsung Lung
China Products Company .....Rep. of China
SHIBUYA, Yoichi
Sumitomo Cement Co., Ltd. .....Japan
SHIINA, Sadao
Ube Industries, Ltd. .....Japan
†SHIIRE, Toyokazu
Tokyo Institute of Technology .....Japan
SHIKAMI, Gunji
Osaka Cement Co., Ltd. .....Japan
SHIMA, Ikuo
Osaka Cement Co., Ltd. .....Japan
SHIMADA, Yutaka
Ube Industries, Ltd. .....Japan
SHIMODA, Akio
Tokyo Institute of Technology .....Japan
SHINOHARA, Kinji
Kyushu University .....Japan
SHIODA, Masatoshi
Nihon Cement Co., Ltd. .....Japan
SHIOTA, Masatoshi
Asahi Glass Co., Ltd. .....Japan
SHIOYA, Youichi
Tokuyama Soda Co., Ltd. .....Japan
SHIRAYAMA, Kazuhisa
Building Research Institute .....Japan
†SIMEONOV, Lordan
Bulgarian Academy of Science .....Bulgaria
SIMPSON, John
James Hardie & Co. Pty., Ltd. .....Australia
SKJOLDBORG, Poul A.
Cementfabrikken Rørdal .....Denmark
SLATE, Floyd O.
Cornell University .....U.S.A.
SMOLCZYK, Heinz G.
Forschungsinstitut für Hochofenschlacke ..West Germany
SODA, Takao
Nihon Cement Co., Ltd. .....Japan
SONODA, Hiraki
Ube Industries, Ltd. .....Japan
SOROKA, Itzhak
Israel Institute of Technology .....Israel
SOSHIRODA, Tomozo
Shibaura Institute of Technology .....Japan
SPOHN, Eberhard
Portland Zementwerke Heidelberg .....West Germany
†STAGG, Rawson F.
The Ketton Portland Cement Co., Ltd. .....United Kingdom
STEIN, Hans N.
Technological University Eindhoven .....Netherlands
STUTTERHEIM, Niko
South African Council for Scientific & Industrial Research .....South Africa
SUDOH, Giichi
Chichibu Cement Co., Ltd. .....Japan
SUGANUMA, Takehiko
Asahi Glass Co., Ltd. .....Japan
†SUGAYA, Yasushi
Japanese National Committee on Large Dams.....Japan
SUGIKI, Rokuro
Nippon Concrete Industry Co., Ltd. .....Japan
SUGIMORI, Toshio
Denki Kagaku Kogyo Kabushiki Kaisha .....Japan
SUGIURA, Kozo
Nihon Cement Co., Ltd. .....Japan
SUGO, Eisuke
Onoda Cement Co., Ltd. .....Japan
†SULIKOWSKI, Jerzy
Academy of Mining and Metallurgy .....Poland
SUZUKAWA, Yuichi
Ube Industries, Ltd. .....Japan
SUZUKI, Hiromasa
Onoda Cement Co., Ltd. .....Japan
SUZUKI, Kazutaka
Nagoya Institute of Technology .....Japan
SUZUKI, Setsuzo
Onoda Cement Co., Ltd. .....Japan
SUZUKI, Sueo
Chichibu Cement Co., Ltd. .....Japan
†TABIKH, Ali A.
Marquette Cement Manufacturing Co. .....U.S.A.
TACHIBANA, Shiro
Hitachi Cement Co., Ltd. .....Japan
TAGAI, Hideo
Tokyo Institute of Technology .....Japan
†TAKADA, Akira
Hazama-Gumi, Ltd. .....Japan
TAKAGI, Nobutaro
Takenaka Komuten Co., Ltd. .....Japan
TAKAGI, Shigehide
The University of Tokyo .....Japan
TAKAGI, Yozo
Sumitomo Metal Mining Co., Ltd. .....Japan
TAKAHASHI, Hisao
Ohbayashi-Gumi Ltd.....Japan
TAKAHASHI, Kozo
Koken Sangyo Kabushiki Kaisha .....Japan
TAKAMI, Takashi
Aso Cement Co., Ltd. .....Japan
TAKASHIMA, Saburo
Osaka Cement Co., Ltd. .....Japan
TAKEDA, Osamu
Sumitomo Cement Co., Ltd. .....Japan
TAKEMOTO, Kunihiro
Onoda Cement Co., Ltd. .....Japan
†TAMÁS, Ferenc
Central Research and Design Institute for Silicate Industry .....Hungary
TANAKA, Akira
Sika Company Ltd.....Japan
TANAKA, Hirobumi
Tohoku University .....Japan
TANAKA, Iwao
Osaka Cement Co., Ltd. .....Japan
TANAKA, Masaki M.
The Ken Mayor Engineering Corp. .....Japan
TANAKA, Taro
Science University of Tokyo .....Japan
TANAKA, Mitsuo
Chichibu Cement Co., Ltd. .....Japan
†TANIKAWA, Kiyoyuki
Rigaku Denki Co., Ltd. .....Japan
TAO, Heng Sheng
Tasek Cement Berhad .....Malaysia
TAPLIN, John H.
Commonwealth Scientific & Industrial Research Organization .....Australia
TASHIRO, Yoshifumi
Sumitomo Cement Co., Ltd. .....Japan
TATENO, Tamotsu
Sumitomo Cement Co., Ltd. .....Japan
TAYLOR, Harry F. W.

University of Aberdeen ..... United Kingdom
†TAZAWA, Eiichi
Taisei Construction Co., Ltd. ..... Japan
TENOUTASSE, Nemat
Centre National de Recherches Scientifiques et Techniques pour Industrie Cimentière ..... Belgium
TERADA, Akira
Onoda Cement Co., Ltd. ..... Japan
TERAMOTO, Hideo
Nihon Cement Co., Ltd. ..... Japan
TERANO, Atsuyoshi
Denki Kagaku Kogyo Kabushiki Kaisha ..... Japan
†TERRIER, Pierre
Centre d'Etudes et de Recherche de l'Industrie des Liants Hydrauliques ..... France
TEZEL, Behçet
Çimento Fabrikasi Müdürü ..... Turkey
†THOMAS, George H.
United Steel Co., Ltd. ..... United Kingdom
TOGASAKI, Yoshio
Hitachi Cement Co., Ltd. ..... Japan
TOGAWA, Eiji
Japan Siporex Inc. ..... Japan
†TOGNON, Giampietro
Italcementi S.p.A. ..... Italy
TOKI, Takashi
Onoda Cement Co., Ltd. ..... Japan
TOKUNE, Yoshio
Nihon Cement Co., Ltd. ..... Japan
TOMITA, Kinzo
Sumitomo Cement Co., Ltd. ..... Japan
†TOROPOV, Nikita, A.
(The defunct) ..... U.S.S.R.
†TORRES, Ary Frederico ..... Brazil
†TOUBEAU, Georges
S. A. Ciments D'obourg ..... Belgium
TOYABE, Ryo
Onoda Cement Co., Ltd. ..... Japan
TSAI, En-Ching
Southeast Cement Corporation ..... Rep. of China
TSUBOI, Tatsuaki
Sumitomo Cement Co., Ltd. ..... Japan
TSUCHIYA, Michiyo
Denki Kagaku Kogyo Kabushiki Kaisha ..... Japan
TSUKAYAMA, Ryuichi
Nihon Cement Co., Ltd. ..... Japan
TSUTSUMI, Kenji
Sumitomo Cement Co., Ltd. ..... Japan
†UCHIDA, Hiroshi
Rigaku Denki Co., Ltd. ..... Japan
UCHIKAWA, Hiroshi
Onoda Cement Co., Ltd. ..... Japan
UEDA, Megumu
Onoda Cement Co., Ltd. ..... Japan
UEDA, Shunro
Nihon Cement Co., Ltd. ..... Japan
UEMURA, Jiro
Osaka Cement Co., Ltd. ..... Japan
UENO, Takashi
Myojo Cement Co., Ltd. ..... Japan
UNO, Tatsujiro
Onoda Cement Co., Ltd. ..... Japan
URAGAMI, Taro
Ube Industries, Ltd. ..... Japan
URANO, Teruo
Murakashi Lime Industry Co., Ltd. ..... Japan
USUI, Koji
Ube Industries, Ltd. ..... Japan
VALENTA, Oldřich
Building Research Institute Technical University ..... Czechoslovakia
VALORE, Jr., Rudolph C.
Valore Research Association ..... U.S.A.
Van AARDT, J. H. P.
South African Council for Scientific and Industrial Research ..... South Africa
Van HAUTE, André A.
University of Louvain ..... Belgium
VERBECK, George J.
Portland Cement Association ..... U.S.A.
VILLAVECCHIA, Jorge
Cementos Asland ..... Spain
†VIRELLA, Albert B.
Companhia Portuguesa de Cimentos Brancos "CIBRA" ..... Portugal
VISVESVARAYA, Hoshagrahar C.
Cement Research Institute of India ..... India
VIVIAN, Harald E.
Commonwealth Scientific & Industrial Research Organization ..... Australia
VULKOV, Vasil V.
НИИСМ ..... Bulgaria
†VYRODOV, Ivan Petrowitsch
Krasnodar Polytechnical Institute ..... U.S.S.R.
†WAGNER, L. R. ..... U.S.A.
WALKER, Joseph H.
Portland Cement Association ..... U.S.A.
WALZ, Kurt P. O.
Forschungsinstitut der Zementindustrie .... West Germany
WANG, Clarence Chong-Chien
Taiwan Cement Corporation ..... Rep. of China
WANG, Wen-Bing
Southeast Cement Corporation ..... Rep. of China
WANG, Yeuh Huei
Universal Cement Corporation ..... Rep. of China
†WARD, Michael A.
The University of Calgary ..... Canada
WARRIS, Birger
Swedish Cement and Concrete Research Institute ..... Sweden
WATANABE, Kosaburo
Ube Industries, Ltd. ..... Japan
WATANABE, Tsunemasa
Nippon Asbestos Co., Ltd. ..... Japan
WATANABE, Yoshika
Onoda Cement Co., Ltd. ..... Japan
†WEBER, Paul Pw
Polysius G.m.b.H. ..... West Germany
†WESCHE, Karlhans
Institute für Bauforschung Technische Hochschule Aachen ..... West Germany
†WHITE, Clifford A.
Associated Portland Cement Manufacturers, Ltd. ..... Australia
†WIEKER, W.
Institut für Anorganische Chemie, Deutsche Akademie der Wissenschaften zu Berlin .... East German
†WIERIG, Hans-Joachim
Zement-u. Beton-Laboratorium Beckum GmbH u. Co. KG ..... West Germany
†WILLIAMS, Peter P.
Department of Scientific and Industrial Research ..... New Zealand
WILSON, Brian
Goliath Portland Cement Co., Ltd. ..... Australia
WOERMANN, Eduard
Institut für Petrologie ..... West Germany
YAMADA, Hideo
Daiichi Cement Co., Ltd. ..... Japan
YAMADA, Junji
Nihon Cement Co., Ltd. ..... Japan
YAMAGUCHI, Goro
The University of Tokyo ..... Japan
YAMAGUCHI, Taro
Onoda Cement Co., Ltd. ..... Japan
YAMAHASHI, Takeshi
Nihon Cement Co., Ltd. ..... Japan
YAMAMOTO, Takaaki
Tsuruga Cement Co., Ltd. ..... Japan
YAMAMOTO, Yasuhiko
The University of Tokyo ..... Japan
YAMANE, Shigeru
Kogakuin University ..... Japan
YAMANE, Sho
Takenaka Komuten Co., Ltd. ..... Japan
YAMASHITA, Keisuke
Mitsui Cement Co., Ltd. ..... Japan

YAMAUCHI, Toshiyoshi
National Institute for Researches in Inorganic Materials ..... Japan
YAMAZAKI, Kanji
Nihon Cement Co., Ltd. ..... Japan
YANG, Julie C.
Johns-Manville Products Corp. ..... U.S.A.
YASUFUKU, Tadayoshi
Kobe Material Co., Ltd. ..... Japan
YOKOMICHI, Hideo
Hokkaido University ..... Japan
†YOKOYAMA, Kiyoshi
Nihon University ..... Japan
YONEYAMA, Koichi
Tokyo Institute of Technology ..... Japan
YOSHIDA, Kozaburo
Ube Industries, Ltd. ..... Japan
YOSHIDA, Sensuke
Sumitomo Cement Co., Ltd. ..... Japan
YOSHIOKA, Takashi
Nihon Cement Co., Ltd. ..... Japan
†YOUNG, James Francis
Department of Scientific and Industrial Research ..... New Zealand
ZEYTINOGLU, Mesut ..... Turkey
†ZIPELLI, Cesare
Società Cementi Segni, Istituto Chimica Industriale ..... Italy
Zur STRASSEN, Heinrich
Dyckerhoff-Zementwerke A.G. ..... West Germany

Inauguration Speeches at the Opening Ceremony of the Fifth International Symposium

Cement Research—Some Views for the Future

Frederick M. Lea*

It is just fifty years since the Faraday Society arranged an international meeting in London to discuss the setting of cements. Though not so-called at the time, we count this as the first international symposium on the chemistry of cements. It was, however, the symposium held in Stockholm in 1938 which first reviewed the main fields of cement chemistry and set the pattern for the later symposia in London in 1952, in Washington in 1960 and now here in Tokyo. These symposia have all been held in countries where research in cement chemistry has been vigorously pursued. In meeting here in Japan we continue that same tradition and pay tribute to the many contributions to the subject that have come from research workers in this country.

There can be only a few of us here today who were present at the Stockholm Symposium in 1938. At that time our knowledge of the phase equilibria between the various oxides present in cements was well advanced and the constitution of Portland cement had been established in terms of the four major clinker compounds. The properties of cements had been broadly linked with their constitution, though much still remained to be resolved on the influence of the minor constituents. The main features of the chemistry of the hydrated cement compounds and of the reactions of cements with water were clearer for the aluminate than the silicate compounds, for which the existing techniques of investigation were not sufficiently powerful to resolve some of the problems involved. We had only just started to probe into the crystal structure of the cement compounds, anhydrous or hydrated, and our knowledge of the physical structure of set cement was lacking in depth. We saw at Stockholm that wide fields still awaited investigation, but nevertheless we felt that the basic foundations of cement chemistry had been well laid. Indeed I remember my old friend, the late Dr. Lennart Forsén of Sweden, saying to me at the end of the Stockholm Symposium—'the main questions are now solved, what remains is detail.' That was I think a legitimate expression of gratification at the way in which the Stockholm Symposium had shown how existing knowledge fitted together, even if in hindsight one would add to the word 'detail' some such phrase as—'and new principles of which we are as yet unaware.' I recently came across a quotation from Goethe which said—'Every solution of a problem is a new problem.' It is characteristic of science that the introduction of new concepts and new techniques opens new fields for investigation and the ensuing years have shown that the chemistry—and physics—of cement is no exception to this rule.

I would like in passing to recall that it was to Lennart Forsén that we really owe the concept of these symposia. If one further recollection may be permitted, as a matter of history, I have never forgotten how the plans for the 1938 Stockholm Symposium were worked out during discussions between Dr. Forsén, Mr. Giertz-Hedström, also of Sweden, Dr. Robert Bogue and myself when we all met in the USA in 1936.

The symposia in 1952 and 1960 showed how much our subject had advanced, thanks to the introduction of new and improved techniques. The crystal structures of cement compounds, the physical structure and properties of set cement paste and the chemistry of cement hydration can be mentioned as examples. The London Symposium of 1952 was widened to include various special types of cements, the durability of concrete and some questions relevant to cement manufacture. If the Stockholm Symposium was devoted solely to science, the London Symposium introduced also technology. This process was continued in 1960 in Washington when we added to our discussions such problems as volume change in concrete, admixtures, cement-aggregate reaction and frost resistances of concrete.

The reports presented to the present symposium

*Former Director of Building Research Station, United Kingdom.

again introduce some new subjects and show how notable have been the advances in the older ones. I cannot attempt in the time available to survey these in detail. Rather would I use them as a starting point for some comments on fields which seem potentially fruitful for future research.

Let me start with cement constitution. We are accustomed to calculate the compound content of Portland cement from its composition, or to estimate it by X-ray and microscopic methods. Much effort has been devoted to reducing the imperfections of these methods. Phase equilibrium studies have yielded much information on the limits of solid solution of other oxides in the silicate, aluminate and ferrite compounds. We now have in the electron probe a powerful new method for analysis of the clinker minerals as present in Portland cement. Already reliable results are available on the silicate phases, but to obtain equal reliability with the interstitial material in clinker either the instrument must be improved or some selection and heat processing of the clinker may be necessary. From electron probe analysis on clinker compounds we may be able to reach agreement on certain average formulae for the composition of the clinker minerals and to use these in calculating the compound content of a cement from its chemical analysis. The results will still be approximate since some minor constituents will not be present in sufficient quantity to saturate the clinker compounds, but we should obtain a closer approximation to the true values than is given by the simple Bogue calculation. The general availability of computer services will facilitate such calculations. A complementary study lies in the effect of the composition of the clinker components on strength development. It is well established that the strength of dicalcium silicate can be controlled by solid solution and to some extent the early, if not the final, strength of tricalcium silicate. Electron probe analysis will tell us how a given minor constituent is partitioned between the main phases of the clinker and provide a basis for more systematic study on the influence of solid solution on strength development.

On the chemistry of hydrated cement we still need to know more about the properties of the calcium silicate hydrates. It is well known that other oxides can be taken up in the tobermorite lattice and we have an indication that this may influence both strength and shrinkage. Can we control this solid solution in a favourable way? Is it related solely to the composition of the anhydrous clinker components or is it determined by the particular equilibria, or lack of equilibria, associated with the hydration process? Electron probe analysis of the composition of the calcium silicate hydrates in set cements is likely to be more difficult than on cement clinker, but if it proves possible it may provide data to help us link physical properties with the composition of the hydrates. Perhaps we have looked too much at clinker composition as the determinant of strength and not enough at how it is influenced by the vagaries of the hydration process.

The last two decades have seen notable advances in our knowledge of the physical structure of set cement, but how wide are still the fields of ignorance. Can we remain satisfied while we still lack an adequate understanding of bonding and strength, of fracture, of shrinkage and creep, an understanding that might help us to do more to control these properties. We have various rival theories based on particular models and mechanisms. They give us only descriptions, often, it is true, capable of mathematical formulation, but not real understanding of phenomena. We shall not get that understanding until we can base the theories on a fundamental knowledge of the way in which hydrated cement particles bond to each other and to the aggregate particles. Attempts have been made to account for the mechanical properties of cement paste by reference to the morphology and crystal structure of the constituents, but we know little of the real nature of the bonds formed between them. The crucial experiments have still to be devised.

High surface area is a common characteristic of set cements of different kinds, but it is not essential for strength as is shown by the properties of autoclaved products. The strength of all materials is much lower than theory would indicate. In materials such as metal or glass we explain this by theories such as the Griffith's crack theory, but how far this is applicable to concrete is still open to question. We may speculate that the low strength of set cement, as compared with theoretical calculation based on the strength of the crystals, may reflect not so much a low strength of the individual bonds—physical or chemical—but to the bonds being too few in number. Most of our present data and theories come from studies on Portland cement. Many studies have been made on the specific surface, crystal size and physical properties of set Portland cement. These studies need to be extended to other cements and to crystalline hydrates to help to elcuidate the mechanism of bonding.

The strength tests we use are adequate for structural purposes but they are crude as measures of the parameters we need to investigate in developing theories of fracture mechanics. Most of the strength

data we have refer only to wet or dry concrete with little information over the intermediate range. We know little about the effect of other polar liquids on any of the physical properties of concrete. Such information could well increase our understanding of the role played by water in set cement.

The development of high voltage electron microscopy with 500 or 1000 kV electrons combined with the developments of skill in making very thin sections is making possible high resolution photography and diffractometry while at the same time reducing damage to the specimen while under observation. The scanning electron microscope provides stereographic images at lower resolution but giving a more global picture of the structure and in greater depth facilitating the study of fracture cracking and porosity in great detail. We might for instance resolve such an apparently simple problem as the part played by calcium hydroxide crystals in the strength of Portland cement and learn more of the nature of the cement-aggregate bond.

An increase in the strength of concrete would be valuable, but the outstanding problem is shrinkage and cracking. We see one attack on this problem in the development of expansive cements, but, though these may eliminate or reduce the initial drying shrinkage, the reversible wet-dry movement still remains. If we could find means of reducing the elastic modulus of concrete without reducing the tensile strength more deformation would be possible without cracking. This would be of major importance in many uses of concrete, but no practicable solution is in sight. I have mentioned earlier that solid solution of other oxides in the tobermorite lattice may influence shrinkage. The field for study of this phenomenon is wide. It is also surprising, in view of its importance, how few are the published papers on the nature of the bond between cement paste and aggregate.

There are many other problems which I can do no more than mention which have much practical significance in the use of cement and concrete. There is no reason to believe that we have yet found the optimum solutions in the use of admixtures and particularly in the development of water-reducing agents, and of plasticising agents less sensitive to the cement composition. We are beginning to understand the physical chemistry of the action of admixtures but there is still scope for basic studies. Acceleration of hardening both in precast concrete manufacture and for in-situ work has much economic significance. The effect of temperature on the physical structure of the set cement paste and the way in which it is built up needs clarification.

The durability of concrete has been much studied both by field surveys and trials and by laboratory tests and experiments. We cannot say, however, that we know enough about the basic mechanism of the various chemical and physical destructive processes that lead to deterioration of concrete, nor can we express durability sufficiently in quantitative terms. With the trend in structural engineering to limit state design, which depends on estimates of the probability that a structure will not become unfit for its intended purpose during its lifetime, it would be an added gain if one of the parameters considered was more directly related to durability. Deterioration, not collapse, is the normal determinant of the life of a structure.

The role of the minor components in a cement clinker and their influence on the properties of the resulting cement and the burning process should continue to occupy a place in research. The influence on burning appears to have particular significance with the more unusual processes or raw materials as in the cement-sulphuric acid process or when unusual amounts of components such as phosphorus pentoxide or fluorine are present in the raw materials. The chemical and physical problems of manufacture, and indeed those of the use of cement, have received less attention than they warrant in our symposia.

I do not wish to suggest that there are not still many outstanding problems in the chemistry of cements other than Portland, such as pozzolanic cement, slag-containing cements and high alumina cement, and it is evident that expansive cements are still a developing material with scope for further investigation. Nor would I imply that there is not a good deal of detail to work out on the hydration of cements generally. My purpose in this address, however, has been to stress what seem to me to be some major areas which call for new and imaginative approaches.

On the Contribution of Chemical Studies to Japanese Cement Industry

Shoichiro Nagai*

Mr. President, Ladies and Gentlemen;

It is a great pleasure and honor for me to present this lecture on this occasion.

The Third International Symposium was held in London in 1952 when many nations had gone through a period of reconstruction following World War II. Three delegates from Japan attended this Symposium. Eight years later, in 1960, the Fourth Symposium was held in Washington D.C. with the participation of fifteen delegates from Japan. It was on the occasion, that I, being the senior Japanese delegate, proposed that the Fifth Symposium be held in Tokyo. This proposal was unanimously accepted during the course of the grand banquet. Thus, the first symposium on the cement chemistry ever to be held in Asia became a reality.

With your permission I would like to confine my talk to chemical studies which have contributed to the development of the Japanese cement industry in the following three progressive stages.

The first stage began about 95 years ago with the establishment of the first cement industry in Japan in the form of a public enterprise. In 1883, after ten years later, the management was transferred from public to private. From 1881 to 1883, a few other factories were established. Together they contributed to the gradual development of the cement industry. After the Sino-Japanese War and the Russo-Japanese War, Japanese industries as a whole became prosperous and the cement industry was no exception. It made particularly remarkable progress up to 1913, just before the outbreak of World War I.

During this first stage of fourty years, research and experimentation on quality improvement in cement factories, as well as studies on mortar and concrete, in relation to the establishment and revisions of the Japanese Engineering Standards (JES) of cement, were extensively carried out. In this connection, exceptionally important contributions were made in the chemical field by Dr. S. Kasai, Mr. M. Fujii, Mr. T. Taniguchi, Mr. M. Okada, Prof. Dr. S. Kondo, Mr. S. Nagaya, Mr. K. Otomo, Mr. S. Kano, Mr. M. Komuro, Mr. S. Asaeda, and others.

The scale of the Annual General Meeting of the then Portland Cement Association grew larger each year. Those of us who were in the middle age group (now senior group) profited from the learning and were greatly influenced by the great scholars just mentioned, and we participated in joint research and experimentation.

The prosperity of the cement industry from 1913 to 1917 (just during World War I) owed much to the contribution made by chemical studies on cement, and its production. In those days, researches and tests on Portland cement, Portland blast-furnace slag cement, slag and the relevant pozzolan were carried out very frequently. The strength of cement and mortar, as specified in the Japanese Engineering Standards, was based on the standard sand-cement dry or so-called non-plastic mortar method. Efforts to perform comparative tests were made and several revisions of standards were sought concerning standard sand and testing apparatus. Consequently, the quality of cement rapidly improved.

During the early second stage which involved World War I period, the cement industry did not suffer from that war, and made great strides, together with other industries. During the ensuing 24 to 25 years, i.e., until World War II, annual cement production in Japan increased continuously to reach its highest peak of about 6.2 million tons in 1939.

In this second stage, those who studied under or collaborated with the forerunners of the first stage, became independent, and those who returned from studying in Europe became leading researchers. For example, Dr. K. Koyanagi, Mr. Y. Tokune, Prof. Dr. T. Yamauchi, Mr. T. Ando, Dr. T. Tanaka, Dr. Y. Sanada, Mr. J. Hosoi, Mr. T. Asano, Dr. T. Yoshii, Dr. M. Nakahara and many others (including ourselves) indefatigably conducted studies on cement. Results of detailed and fundamental chemical, microscopic and X-ray researches made on cement minerals were presented in both national and foreign scientific journals and are frequently referred to in technical documents.

*Professor Emeritus of the University of Tokyo
Vice-President of the Organizing Committee for the Fifth International Symposium.

At the same time, a number of younger researchers were developing, forming a solid cadre of cement chemical researchers who would become active in the present time.

The third stage commenced at the end of World War II and spans the last approximately 23 years to the present day. All Japanese industries were destroyed during World War II, including the cement industry. Thus cement production in 1946, the year following the end of the war, was at its lowest with only about 930,000 tons, dropping below 1 million tons. However, since cement, together with steel, was regarded as an indispensable building material in the national reconstruction program, production increased very rapidly. As a consequence, six years later, in 1951, annual production exceeded 6.7 million tons, and three years later, in 1954, it exceeded 11 million tons. Again, six years later, in 1960, annual production was over 22.7 million tons, while three years later, in 1963, it reached over 31.1 million tons. In 1967, production figures of over 42.6 million tons were obtained. The population also has steadily increased, to reach 100 million. Thus, annual production is 426 kg per capita, which is still inferior to the highest European level of 600–650kg per capita, but it is expected to reach over 500–550kg per capita before long.

Remarkable fact during this third stage is that research was conducted on the fifth and sixth components magnesia and alkali, in addition to research started in the second stage, that is, studies on clinker minerals by the four component system lime, silica, alumina and ferric oxide. The relation between magnesia and ferric oxide and the color of cement was also studied, as the tint of mortar and concrete is of much importance. In this connection, reports of studies on the five component system, lime, silica, alumina, ferric oxide, magnesia, and on the importance of alkali were also presented at the Third London Symposium.

The next fact worthy of special mention is the research on hydration products of cement—the synthetic research concerning calcium silicate hydrates and calcium aluminate hydrates which were found largely in natural form or in hardened cement. From 1930 to 1932, I made synthetic studies at the former Kaiser Wilhelm Institut für Silikat-forschung in Berlin, under Prof. Dr. W. Eitel and reports on calcium silicate hydrates and calcium aluminate hydrates obtained by a hydrothermal synthetic process in autoclaving of the ternary systems of lime-silica-water and lime-alumina-water. Those were presented in German, English and Japanese chemical journals. Furthermore, at the Fourth Symposium held in Washington D. C., in 1960, many reports on tobermorite as the principal product of cement hydration were presented. Moreover, concerning this hydrothermal reaction of lime-silica-water system, there are many reports on the hardening test for autoclaved lightweight concrete (ALC) in prefabricated building materials.

As to the types of cement, basic researches on high early strength Portland cement and low heat or moderate heat Portland cement were carried over from the second stage, and production and utilization of high quality products were supplied as essential building and construction materials. These research programs of the second and third stages were conducted by many young prominent researchers, such as the chairman of Program Committee of this Fifth International Symposium, Dr. K. Chujo, the chairman of Arrangements Committee, Dr. T. Yamaguchi, and the authors of the principal papers of this symposium, Prof. Dr. K. Murakami, Prof. Dr. G. Yamaguchi, Dr. R. Kondo and many other younger researchers who will present many supplementary papers. It is a great joy to see so many of these cement researchers here today.

Around 1948 or 1949, when the cement industry was about to arise from wartime destruction, the former JES became the JIS (Japan Industrial Standards). After that, new standards were set concerning blended cements in terms of A, B and C, according to the proportion of admixture in Portland blast-furnace slag cement, silica cement and fly ash cement. As to the strength test for mortar, after about ten years of research and tests, the wet or so-called plastic mortar method was introduced, to replace the conventional dry method. Thus, in Japan, mortar strength of high early strength Portland cement and that of normal Portland cement and of A grade blended cements of all three types are extremely good, being among the best quality in the world. It seems only natural that Japan should lead the world in cement exports.

In regard to special cement, that is, in 1937 high aluminous (53 to 55% alumina content) cement and alumina began to be produced simultaneously. This led to research and development of hydraulic refractory mortar, and now it is known as castable refractories. Research and utilization of low expansive or non-contractive cement, making use of the expansive nature of calcium sulpho-aluminate hydrate was also started in Japan. Three supplementary papers on this subject will be presented at this symposium.

Before concluding, I would like to touch upon the

following two points.

(a) The first is that annual production of natural gypsum in Japan is only 600,000~700,000 tons, and its quality is so poor that it can scarcely be used only for cement. On the other hand, with production of cement increasing yearly, reaching 46~47 million tons this year, about 3 percents, of that figure (about 1.5 million tons/year) of gypsum is necessary. We have to seek the source of supply of half the necessary amount in byproduct gypsum from various chemical industries. Production of phosphoric acid solution by reacting sulphuric acid to phosphate rock yields a particularly large amount (about 2 million tons this year) of phospho-gypsum as a byproduct, and half that amount goes successfully into cement production. One principal paper will be presented by Prof. Dr. K. Murakami's research group concerning this special point.

(b) The next point I wish to mention is the treatment of papers on the subject of concrete at this symposium. In Japan, more than half the papers presented at the Annual General Meeting on Cement Engineering, held every year by the Cement Association of Japan, were related to concrete. In view of these facts, both principal papers and supplementary papers on concrete based on the chemistry of cement are dealt with in Parts III and IV, ranking with Parts I and II where papers on the chemistry of cement will be presented. Supplementary papers being so numerous, they will be presented by general reporters in the form of summarized report. This system is something new in our international symposium, but I hope this solution proves to be highly successful.

I have spoken of the development of research and experimentation in cement chemistry in Japan, and I very much appreciate the kind attention you have paid me. Thank you.

Explanatory Notes

Abbreviations.

The following symbols, which have been universally recognized by cement chemists for formulating more complex compounds, are used interchangeably with the respective oxide formulas throughout this book:

$C = CaO$, $S = SiO_2$, $A = Al_2O_3$, $F = Fe_2O_3$,
$M = MgO$, $N = Na_2O$, $K = K_2O$, $H = H_2O$,

Less common abbreviations of this type are defined as they occur.

Commonly used abbreviations of more general nature are as follows:

DTA = differential thermal analysis
EPMA = electron probe micro analysis
IR = infrared
NMR = nuclear magnetic resonance
psi (or p s.i.) = pounds per square inch
rh (or RH) = relative humidity
w/c (or W/C) = water — cement ratio
XRD = X-ray diffraction

Identification Number of Supplementary Papers

Example: Supplementary Paper III—50, III is session III and 50 is the arrival number of contribution. This number coincides with the number used in the preprint of papers distributed in advance of the symposium.

Contents

Volume I

Session I-3 Analysis of Portland Cement Clinker

SESSION I-1 STRUCTURE OF PORTLAND CEMENT MINERALS

Principal Paper Structure of Portland Cement Minerals

André Guinier and Micheline Regourd*

Synopsis

In portland cement clinker, the four principal constituents are found in the form of solid solutions. The polymorphic variations of these solid solutions being numerous and ill-defined, we have first dealt with the structure and polymorphism of the pure compounds.

Pure C_3S, passes through six allotropic forms between ambient temperature and 1100°C, all very close to the trigonal high-temperature form. A pseudo-structure which is a good approximation to the real structure has been proposed by Jeffery. Alites usually crystallize in the monoclinic and trigonal forms of C_3S.

On the other hand, the five forms of C_2S are different. Their crystal lattices are distinct and the stacking of silicate tetrahedra differs from one to another. Only the structures of β and γ have been determined. Belites usually crystallize in modified β forms, more rarely as the γ' form.

The cubic structure of C_3A has not been determined. Tricalcium aluminate forms solid solutions with the aluminoferrites of the interstitial phase. This can occur as a glassy phase when clinkering temperature is high, quenching rapid and the A/F ratio >1.

The hydraulic properties of the clinker constituents are linked to their crystal structure, particularly the irregular Ca co-ordination, and the presence of holes in the structure. All the forms of C_3S show comparable reactivity whereas the forms of C_2S differ in their hydraulic properties.

Introduction

This is a study of the four minerals which are the principal constituents of all portland cement clinkers and are designated, following the classical abbreviations, as C_3S, C_2S, C_3A and C_4AF.

In fact, each of these abbreviations represents a group comprising the pure phase and the solid solutions having a crystal lattice with identical or very similar lattice dimensions. The alites and belites which correspond respectively to C_3S and C_2S are the solid solutions formed by the addition of impurities which are present in all commercial cement clinkers and are principally the ions or oxides of Al, Mg, Fe, Na, K, Cr, Ti, Mn, P, et cetera. Even when no impurities are present, the aluminoferrite, "C_4AF", can have a variable composition $C_2(A_pF_{1-p})$ where p varies from 0 to 0.7.

On a polished clinker surface, the microscope clearly distinguishes the different phases. C_3S appears in the form of well-defined crystalline grains varying in size from 10μ to 40μ. C_2S occurs as rounded crystals or twinned polyhedra, with a smooth or striated surface.

Between these grains there lies an interstitial phase in which it is sometimes possible to identify well-formed crystals of C_3A but often the interstitial phase is so finely crystallized that the individual grains are not visible.

The object of this paper is to describe the crystal structure of each of the phases listed above and how the structure varies with temperature and with additions to the pure stoichiometric composition.

*Centre d'Etudes et de Recherches de l'Industrie des Liants Hydrauliques, Paris, France

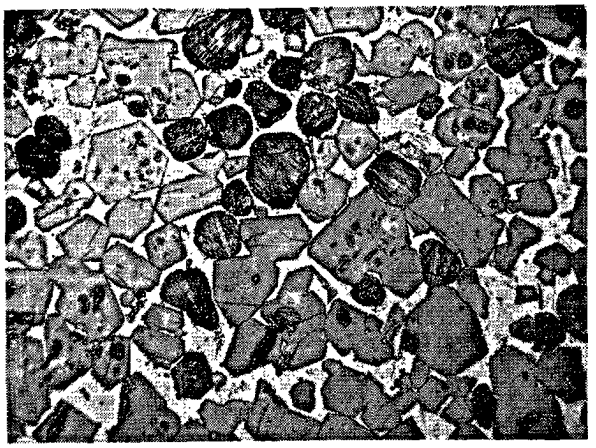

Fig. 1. *Photomicrograph of portland cement clinker: the alite crystals are pseudo-hexagonal, the belite grains rounded and striated. The interstitial phase lies between the C_3S and C_2S crystals. Terrier and Hormain (105).*

The whole system presents a difficult field of study because, with certain exceptions, one cannot obtain the clinker phases in the form of single crystals of sufficient size to permit a structure determination by classical methods. In general, one is reduced to characterising a phase solely by its lattice, deduced from powder diagrams. But even this technique is difficult to use in this field because of the low symmetry or large unit cell of certain phases and above all because the variations which one is trying to detect as a function of temperature or of additions are very small. Furthermore, it has only recently become possible to obtain high quality powder patterns at temperatures up to 1500°C. In his paper of 1960, F. Ordway (1) insisted upon the necessity for developing special high temperature techniques adapted to the study of clinker minerals.

The results obtained by X-ray diffraction must obviously be checked with those given by other techniques such as microscopy, infra-red absorption, spectroscopy, electron-probe microanalysis, etc., and especially differential thermal analysis.

Numerous papers have appeared on problems in this field. Not all of these are based upon the use of the most sophisticated techniques and contradictions exist between the results reported. However, on the whole, certain facts emerge which clarify the problem. A general review must naturally emphasize the points on which there is agreement but one must also mention other observations even where they are contradictory.

In order to resolve these two incompatible demands, we have chosen not to follow the chronological order in reporting successive papers. In each chapter of this article, dealing respectively with tricalcium silicate, dicalcium silicate and the interstitial phase (calcium aluminoferrite and tricalcium aluminate), we begin by giving what we ourselves regard as the most complete and satisfactory solution to the structural problem. Next, we group the studies which make a partial contribution to the preceding results, or contradict them. We try then, in the latter case, to discuss the possible origin of these differences with what we consider to be the most probable soultions.

In the conclusion, we discuss the general character of the polymorphism of the calcium silicates and hence the relations between the crystal structures and clinker properties.

Tricalcium Silicate

It is the tricalcium silicate phase which has the most numerous allotropic forms. We have shown that there are six between ambient temperature and 1100°C. One can find all the same forms in the solid solutions but all have lattices extremely close to trigonal, the simplest form.

The X-ray powder diffraction patterns are indistinguishable except for slight movements of certain lines or their separation into very close multiplets; but the relative intensities do not vary. This shows that the structure of the least symmetrical forms remains, to a very good approximation, that of the most symmetrical.

Jeffery's Structure (2)

The structure of C_3S has been determined by Jeffery on a single crystal of sufficient size, which was isolated from a blast-furnace slag. In this work, which dates from 1950, Jeffery, on the basis of the visually estimated intensities of the diffracted spots (without Lorentz-polarization correction), determined a trial structure which is a good approximation to the true structure. O' Daniel, Hahn and Müller (3, 4) have confirmed these results by a Patterson synthesis. No other structure has been proposed.

The pseudo-structure, proposed by Jeffery, is trigonal, with $a = 7$, $c = 25$ Å (hexagonal notation), space group R3m. It is composed of independent tetrahedra; three SiO_4 tetrahedra and three oxygen ions lie on the trigonal axes (5). The calcium ions link the tetrahedra and are octahedrally co-ordinated to the three oxygen ions which are not linked to Si^{4+} (see Fig. 2). Identical columns are found on each

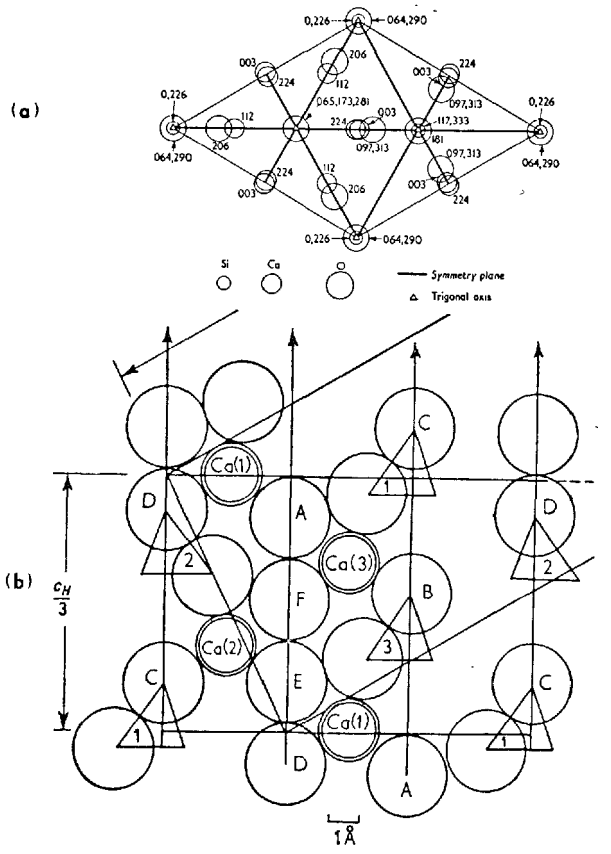

Fig. 2. *Tricalcium silicate: Jeffery's structure.*
a) basal plane
b) vertical section through the long diagonal of the hexagonal cell. The relationship of the monoclinic axes to the hexagonal cell is shown. (Taylor: Chemistry of Cements, pp. 149–150).

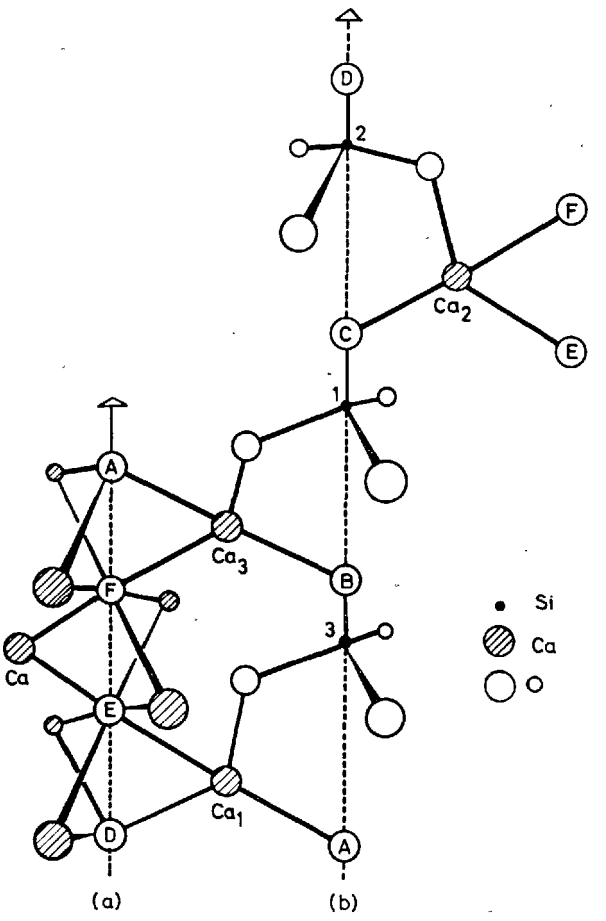

Fig. 3. *Tricalcium silicate Jeffery's structure.*
Two adjacent columns of tetrahedra and single 0 atoms, surrounded by Ca atoms. A complete column is obtained if (b) is placed on top of (a) and the labelling of the various atoms corresponds to that of Figure 2b). (Taylor: Chemistry of Cements, p. 148).

trigonal axis, but at different heights (see Fig. 3). These form irregular octahedra of atoms around the calcium ions and leave holes large enough to accommodate other atoms.

It is the irregular co-ordination of the Ca ions (the bonds vary from 2.54 to 3.24 Å) and the holes adjacent to these ions that give C_3S its hydraulicity.

Nevertheless, Jeffery's structure is certainly only approximate. The lattice of the lower temperature forms is not the simple trigonal. We have tried to grow crystals from molten $CaCl_2$ (6). From a number of crystals between 4 and 10μ, we chose a 7μ pseudo-hexagonal crystal. An oscillation photograph shows superlattice lines corresponding to a = 14 Å (7). Construction of the reciprocal lattice from a Weissenberg photograph gives approximate values for b and c of 14 and 25 Å. The parameters may be obtained more accurately by indexing powder photographs on a pseudo-hexagonal lattice.

Study of Polymorphic Transformations of C_3S by DTA

The results of differential thermal analysis are the most straightforward and a definitive list of the transition points can be established (see Table 1). Four reversible DTA peaks at 600°, 920°, 980° and 990°C characterize C_3S (see Fig. 4). Due to the powerful resolution of micro DTA (8), the peaks at 980°C and 990°C are well resolved. The thermal effects of these transitions are very weak, smaller than the $\alpha - \beta$ transformation of quartz (1.4 cal/g) (9). The transformation point at 990°C was discovered both by Boikova and Toropov (10) in pure C_3S, and by Woermann, Hahn and Eysel (11) in both C_3S and in the solid solutions.

Boikova and Toropov (10) cross-checked the

Table 1. *Characteristic properties of D.T.A. peaks of pure C_3S*

Temperature of transformation (beginning of the signal during heating, °C)	Shape of the peaks—hysteresis	Estimated thermal effect related to the transformation (cal/g)	
		D.T.A.*	direct ** calorimetry
585 ± 5	Broad peak up to 30° width depending on heating rate and strong hysteresis (20–40°C) upon cooling		0.6
917 ± 3	Sharp, strong peak, weak hysteresis (10°C)	1	1.3
975 ± 3	Sharp, strong peak without appreciable hysteresis	0.5	0.6
990 ± 2	Sharp, very small peak without appreciable hysteresis	0.05	

* From area of the peaks and comparison with the area of the peak obtained in high-low quartz transition. For this last thermal effect 1.4 cal/g was admitted as given by R. ROY(9).
**In this set of experiments(13) the thermal effect of the quartz transition was found to be 2 cal/g.

DTA results by a study of a small crystal on a high-temperature microscope. The transformations at 620°, 920° and 980°C could be observed and were found to be reversible, but the authors do not indicate whether the crystal transforms without change of habit.

Study of the Polymorphic Transformations of C_3S by X-ray Diffraction (XRD)

At high temperature, the lattice is trigonal. On cooling, the lowering of the symmetry causes splitting of the hexagonal reflexions into groups of lines whose number and spacing permit the determination of the true lattice (7).

At 1100°C the lattice is trigonal, with hexagonal parameters a = 7.15, c = 25.56 Å. The 30 lines of the powder pattern (up to 1.48 Å) show the extinctions corresponding to space-group R3m: $-h + k + l = 3n$.

Our results are in good agreement with Jeffery's predictions, deduced from the trial structure.

With decreasing temperature, the transformations are clearly visible on three hexagonal spacings $\bar{2}01$, $\bar{2}04$ and 220, which become successively doublets and triplets (see Fig. 5).

In the range of temperatures used, the 009 reflexion does not show any splitting at all and its relative intensity remains constant relative to the other reflexions. The stacking of planes perpendicular to c, about 8.4 Å apart, therefore remains the same. A sliding of these planes in the direction perpendicular to the c axis takes place.

The principal characteristics of the transformations are:

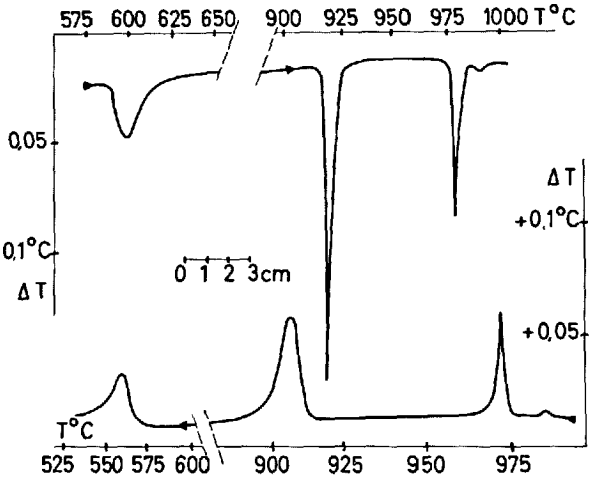

Fig. 4. *Tricalcium silicate. DTA diagram, heating rate 13°C/min. Mazières (8).*

1) *1050°C: change of symmetry from rhombohedral→ monoclinic* ($R \rightarrow M_{II}$). The transformation is continuous and only the hexagonal basal plane is deformed (see Fig. 6).

The pseudo-hexagonal cell deduced from the reduced cell chosen according to Donnay (14) is defined by the parameters a = b = 7.130 Å, c = 25.43 Å, $\alpha = \beta = 90°$, $\gamma = 119.88°$. This can be considered as an orthorhombic cell with parameters a = 12.342, b = 7.143, c = 25.434 Å (7).

Nevertheless, the structure cannot be anything but monoclinic: the small but continuous deformation of the trigonal lattice does not permit of the formation of an orthorhombic structure; there is no orthorhombic sub-group of the trigonal space group. The transformation is probably of the second order, the structure can only be monoclinic (M_{II}) (11).

2) *990°C: discontinuous transformation of the unit cell without change of symmetry:* $M_{II} \rightarrow M_I$. The components of the doublets $\bar{2}01$, $\bar{2}04$ and 220 are clearly separated (see Fig. 5).

As well as the deformation of the hexagonal basal plane, there is now added an inclination of the c axis to this plane ($\beta = 89.88°$) (see Fig. 6).

The stability region of the M_I phase is only 10°. We suspected the presence of this form from the small signal given by μDTA at 990°C. We therefore took a series of photographs between 970°C and 990°C and found a diagram characteristic of M_I. The components of the doublets are, indeed, less well defined than in the other forms but this variety has been confirmed in solid solutions of $C_3S + Al_2O_3$ by both Bigaré (12) and Woermann, Hahn and Eysel (15). These authors have all observed an increase in the zone of stability of M_I to 60° for the solid solution $C_3S + 1\%\ Al_2O_3$.

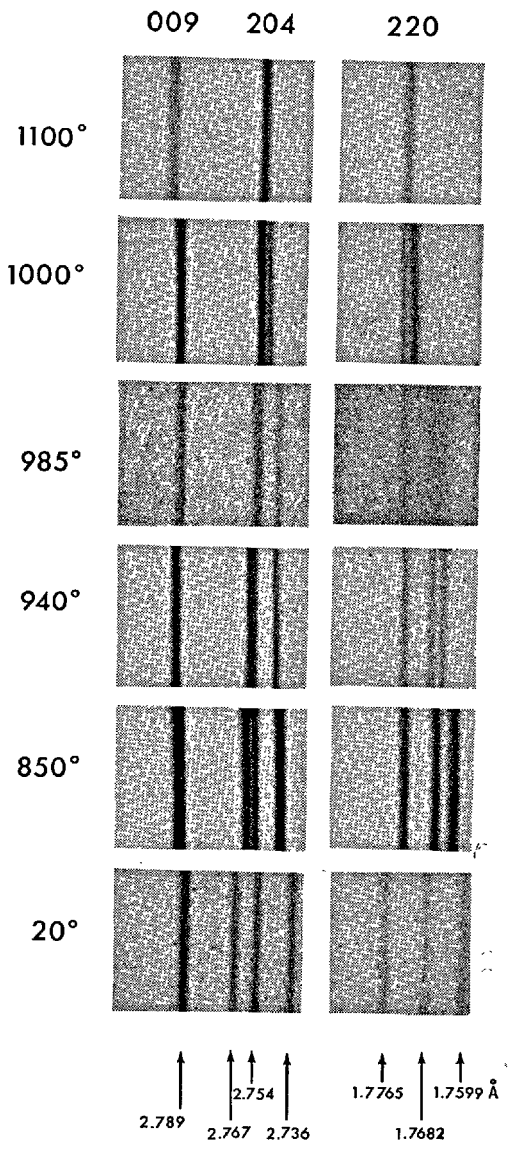

Fig. 5. *Tricaliium silicate. Evolution of the hexagonal reflexions 009, 204, 220 from 1100°C to ambient temperature. The powder patterns are obtained with a high temperature Guinier camera. At 1000°C the components of the 220 doublet are separated by* 3×10^{-3} *Å, 220 → 1.786, 1.783 Å, and 204 → 2.780, 2.776 Å Regourd (32).*

3) *980°C: change of symmetry* $M_I \rightarrow T_{III}$. The characteristic doublets become triplets and the lattice is now triclinic; in the hexagonal basal plane the three axis a, b and d are different. A diagram taken at 940°C shows about 100 lines which can not be indexed without doubling the pseudo-hexagonal parameters a and b to 14 Å. The superlattice in the basal plane only involves a change of orientation of the rhombohedron in which obverse becomes inverse. If one retains the orientation of the original unit cell, the extinction rule

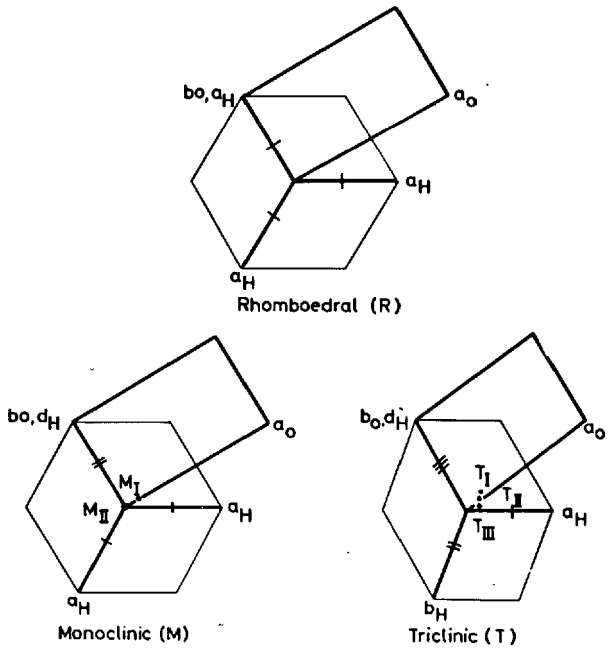

Fig. 6. *Tricalcium silicate: deformation of basal plane of the hexagonal cell. H = (pseudo-) hexagonal, O = (pseudo-) orthohexagonal. Dots indicate the projections of vectors [001] on the (001) plane. Regourd (11, 32).*

is not the same: it becomes $+ h - k + 1 = 3n$ (11). At 940C°, the pseudo-hexagonal cell has the parameters a = 14.229, b = 14.249, c = 25.412 Å, $\alpha = 90.10°$, $\beta = 89.85°$, $\gamma = 119.76°$.

4) *920°C.* Although DTA gives a strong signal, we observe *no change of symmetry , nor any change in volume of the unit cell.* The components of the triplets, arising from the hexagonal reflexions $\bar{2}01$, $\bar{2}04$ and 220 separate progressively from 980° until 620°.

5) *600°C. No change of symmetry* is observed but a slight discontinuity in the splitting of the characteristic triplets.

6) *20°C.* On a photograph exposed for 40 hours (6 mA, 30 KV, Cu Kα), we detected two very weak reflexions ($I/I_o < 1/100$) with long spacings 14 and 8.2 Å. These are hk0 reflexions and would imply the doubling of parameters a and b. The new unit cell would be defined thus:

a = 28.160	b = 28.294	c = 25.103 Å
$\alpha = 90.30°$	$\beta = 89.77°$	$\gamma = 119.53°$

The variations in the pseudo-hexagonal parameters from ambient temperature to 1100°C are shown in Table 2.

Nature of C_3S Transformations

The characteristic properties of the transformations

Table 2. *Lattice constants of the modifications of pure* C_3S (*Average errors: a, b, c;* $\pm 2 \times 10^{-3}$ Å; *α, β, γ:* $\pm 3 \times 10^{-2}$ *degree*) Pseudo-hexagonal lattice constants

Temperature °C	Allotropic form	$a_{(Å)}$	$b_{(Å)}$	$c_{(Å)}$	$\alpha_{(°)}$	$\beta_{(°)}$	$\gamma_{(°)}$
1100	Rhombohedral R	7.150	7.150	25.560	90	90	120
1000	Monoclinic M_{II}	7.130	7.130	25.434	90	90	119.88
985	Monoclinic M_I	7.125	7.125	25.420	90.13	89.88	119.84
940	Triclinic T_{III}	14.229	14.249	25.412	90.10	89.85	119.76
				Possibly doubling of a and b			
680	Triclinic T_{II}	14.169	14.209	25.289	90.22	89.80	119.62
20	Triclinic T_I	14.080	14.147	25.103	90.30	89.77	119.53

Table 3. *Characteristic properties of the transitions in pure* Ca_3SiO_5

Transition temperatures (°C)	Characteristic effects		Type of* transition	Allotropic form	Space group
	X-Ray	D.T.A.			
1050	Change of symmetry, continuous deformation of the cell	No peak	Type a continuous	Rhombohedral (R) Monoclinic II (M_{II})	R3m C1m1
990	No change of symmetry, change of cell volume	Very small reversible peak	Type a discontinuous	Monoclinic I (M_I)	C1m1
980	Change of symmetry, change of cell volume; superstructure: doubling of *a* and *b* to 14Å	Strong reversible peak	Type a + b discontinuous	Triclinic III (T_{III})	C1
920	No change of symmetry, no change of subcell volume; (possibly second superstructure)	Strong reversible peak	Type b discontinuous	Triclinic II (T_{II})	C1
600	No change of symmetry, small deformation of the cell; possibly second superstructure	Broad reversible peak	Type a discontinuous	Triclinic I (T_I)	C1

*Type a: with decreasing temperature the degrees of freedom of the thermal vibrations are reduced thus leading to discontinuous or continuous changes in cell volume. The structural groups are slightly deformed but their periodicity is unaffected.

Type b: upon cooling, in the arrangement of the groups, regular stacking faults perpendicular to the c axis are produced, leading to the formation of superstructures but not affecting appreciably the volume of the subcell.

of C_3S are collected in Table 3 (11).

DTA and X-ray have established 5 reversible transformations between six allotropic forms. Three of these transitions (990°, 980° and 600°C) have been observed by both DTA and X-ray methods.

The transformation $R - M_{II}$, found by X-ray, gives no DTA signal. The transition, which is continuous and weak, extends over 60°C, beginning at about 1050°C. Possibly it is a second order transition.

The transition $T_{III} - T_{II}$, at 920°C, undetectable by X-rays, is characterised by a strong DTA signal. The unit cell is triclinic up to 980°C and the Debye-Scherrer pattern maintains the same relative intensities. The strong thermal effect is perhaps due to a second superstructure which, while leaving the fundamental spacings unchanged, modifies the long spacings which are too weak to be detected under normal conditions. The superstructure found for T_I could exist equally in T_{II} (we have not verified this hypothesis because of the very long exposures which would be required at high temperature). A re-arrangement of the hexagonal groups in the lattice could vary the energy of the structure appreciably and this would explain the thermal effect.

To conclude, C_3S undergoes numerous small amplitude transformations around a constant atomic arrangement. All the transformations are of the "displacive" type (16). They are produced by small movements of the atoms from their positions in the original structure, without any alteration of the general arrangement of the chemical bonds.

We have shown evidence of two types of transition: change of symmetry and superstructure:

—the hexagonal structure, advanced by Jeffery (2), is constructed of independent SiO_4 tetrahedra. At high temperature, the atoms of the SiO_4 tetrahedra are vibrating freely; the hexagonal unit cell shows a corresponding symmetry. As the temperature decreases, the degrees of freedom diminish and the departures from symmetry appear. They reveal themselves by changes in the X-ray powder diagram, that is to say, by the splitting of characteristic reflexions;

—the structure of C_3S is a stacking of hexagonal groups. With decreasing temperature the stacking faults give rise to a superstructure which is revealed by weak reflexions at low angles.

Certain of our results (the superstructure in T_{II}), not being directly proved, may be open to discussion. The powder patterns which we have studied permit determination of lattice dimensions and symmetry but give no other information on the structure. We are unable to distinguish a pseudo-orthorhombic form from a true orthorhombic structure. The superstructure in T_I is only indicated by the presence of two very

weak Debye-Scherrer lines at long spacings. However, in an oscillating crystal photograph of alite (with the hexagonal axis parallel to the axis of rotation) Jeffery (2) has shown evidence for the existence of superlattice lines corresponding to a = 40 Å. Thus, in the T_I form of pure C_3S, it seems more likely that a = 42 Å than 28 Å.

The study of the polymorphism of C_3S demands experimental techniques with great powers of resolution. Only the combination of X-ray and DTA has given complete results. To elucidate the structural relations of the different polymorphs completely, it will be necessary to prepare single crystals of sufficient size.

Tricalcium silicate, being of type A_3BX_5, is isomorphous with tricalcium germanate, Ca_3GeO_5 (17, 18) and sodium fluoberyllate, Na_3BeF_5 (19).

Other Studies on Tricalcium Silicate

All the transitions which have been described in the preceding paragraphs have not been detected by the first workers in the field either because they did not use DTA or because they had no X-ray equipment of sufficient resolution. On the other hand, transitions which proved to be due to an impurity (such as a small amount of C_2S) have been attributed to C_3S.

Thus Nurse and Welch (20) found 6 transformation points, at 464°, 622°, 750°, 923°, 980°, 1465°C. An interpretation of this thermogram was proposed by Jeffery (21). The first transformation corresponds to the dehydration of free lime. The peaks at 622°, 750°, 1465°C are characteristic of the $\beta - \alpha'$, $\gamma - \alpha'$, and $\alpha' - \alpha$ transformations of C_2S. The only peaks, due to C_3S are those at 923°C and 980°C, characteristic of three forms following this scheme:

$$\text{Triclinic} \xrightarrow{923} \text{Monoclinic} \xrightarrow{980} \text{Trigonal}$$

Yamaguchi and Miyabe (22) repeated, in 1960, Jeffery's work, and defined the same polymorphic transformations. A triclinic, pseudo-orthorhombic unit cell, calculated by these authors, has the parameters

$a = 12.195$	$b = 7.104$	$c = 25.069$ Å
$\alpha = 90°$	$\beta = 89°44'$	$\gamma = 89°44'$

The transformation at 990°C was not detected in a recent study by Miyabe and Roy (23). These authors, on the other hand, attribute to C_3S a broad signal at 675°C, which is characteristic of the $\beta \rightarrow \alpha'$ transformation of C_2S. Boikova and Toropov (10) have shown evidence for the existence of this thermal effect when the tricalcium silicate synthesis is incomplete. We ourselves have verified that, in DTA, traces of βC_2S give a thermal effect at 675°C.

The polymorphism of C_3S has been studied, in 1964, with the help of powder patterns, by Miyabe and Roy (23), who used a high temperature diffractometer, as we ourselves were using a high temperature Guinier camera (24) (see Fig. 7).

Fig. 7 shows the diffractometer traces of Miyabe and Roy at 600°C and 650°C, together with one of our double-exposure Guinier photographs taken at 600°C and 625°C (1962) (24). Miyabe and Roy found a mixture of phases T_α and T_β; we observed only, in accordance with the phase rule, T_I at 600°C and T_{II} at 625°C.

The resolution of the focussing camera (25) is better because we are operating with rigorously monochromatised (Cu $K\alpha_1$) radiation and we eliminate variations of intensity and apparent displacements of certain lines due to crystal growth at transformation points. The sample temperature is more difficult to measure than in the diffractometer but it is sufficiently uniform and well-controlled to give lines at high temperature which are as sharp as those produced at ambient. We have established a temperature scale using known transition points. This calibration curve between the heating current and the temperature of the sample-holder is re-adjusted with the help of the temperatures of the DTA peaks of C_3S. We can thus obtain a set of high-resolution photographs at selected temperatures which show the progress of the transformations.

Our results are in disagreement with those of Miyabe and Roy. The differences are as follows:

1) Miyabe and Roy found only the rhombohedral form (R) above 970°C; we detected three modifications (R, M_{II}, M_I) above 980°C (Fig. 8).

2) According to Miyabe and Roy, the stable form between 980°C and 920°C is monoclinic. We have shown evidence, in the splitting of the 620 reflexion (620, $\bar{6}20$), for the presence of a triclinic form, T_{III}. The separation of the lines is 0.003 Å, which was not resolved by previous workers.

3) Miyabe and Roy obtained a considerable contraction of the unit cell of T_β between 600°C and 700°C (Fig. 9) suggesting a new transition, $T_\beta \rightarrow T\gamma$, at about 700°C. We consider that some of the lines for T_β, T_γ and M are incorrectly indexed. If the spacings in Miyabe and Roy's diagrams are correctly indexed and the parameters recalculated, the contraction disappears (see Fig. 10). The curve showing variation of pseudo-orthohexagonal parameters is then similar to ours (Fig. 11).

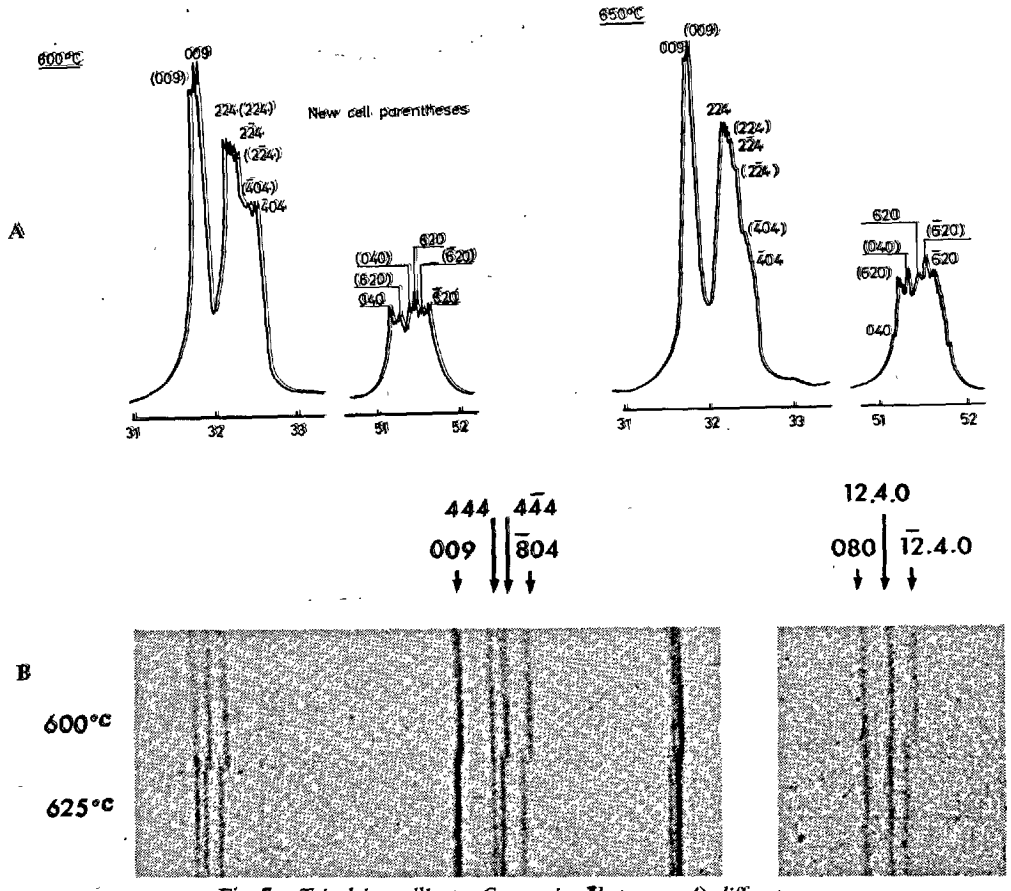

Fig. 7. *Tricalcium silicate. Comparison between: A) diffractometer traces by Miyabe and Roy (23) taken at 600°C and 650°C, showing a mixture of α and β phases; B) a pair of high temperature Guinier photographs showing T_I at 600°C and T_{II} at 625°C. Yannaquis, Regourd, Mazières, Guinier (24).*

Solid Solutions of Tricalcium Silicate

The transformations of C_3S occur rapidly at well-defined temperatures, and without noticeable hysteresis. One cannot stabilize, by quenching, any of the high temperature forms.

On the other hand, if one introduces small amounts of foreign ions into the C_3S lattice, one obtains, at ambient temperature, phases which have the same lattice as one of the phases of pure C_3S. There is thus, by additions, stabilization at ambient temperature of forms which in the pure compound only exist in narrow ranges of temperature. One might say that the disorder introduced by foreign ions is playing a role analogous to the disorder of thermal vibration.

Table 4 (11) indicates the nature of the phases observed by different additions, as a function of their concentration. The different solid solutions have been prepared by synthesis from pure materials. In clinker, the solid solutions must be more complex. Table 4 shows how one addition will not, in general, stabilize all the forms. The highest symmetry phase is stabilized by ZnO but not by any other single oxide. Nevertheless, it is observed in certain clinkers which contain insufficient ZnO but a very large number of other impurities (Al_2O_3, Fe_2O_3, MgO, Cr_2O_3, TiO_2, Na_2O, K_2O etc.). These complex mixtures have not been reproduced by synthesis. The studies of the solid solutions as a function of temperature have been made only on the simplest synthetic products and we will begin with the addition of ZnO which stabilizes the most complete range of phases.

Solid solutions of C_3S + ZnO. Zinc oxide stabilizes, at ambient temperature, the forms T_I, T_{II}, M_I, M_{II}, R of C_3S (11); Zn^{2+} replaces Ca^{2+} in the C_3S lattice. The variations in the parameters as a function of percentage of ZnO show clearly the different varities stabilized (Fig. 12). The DTA results confirm the stability ranges. The transformation temperatures are decreased by the addition of ZnO. At 0.75% ZnO

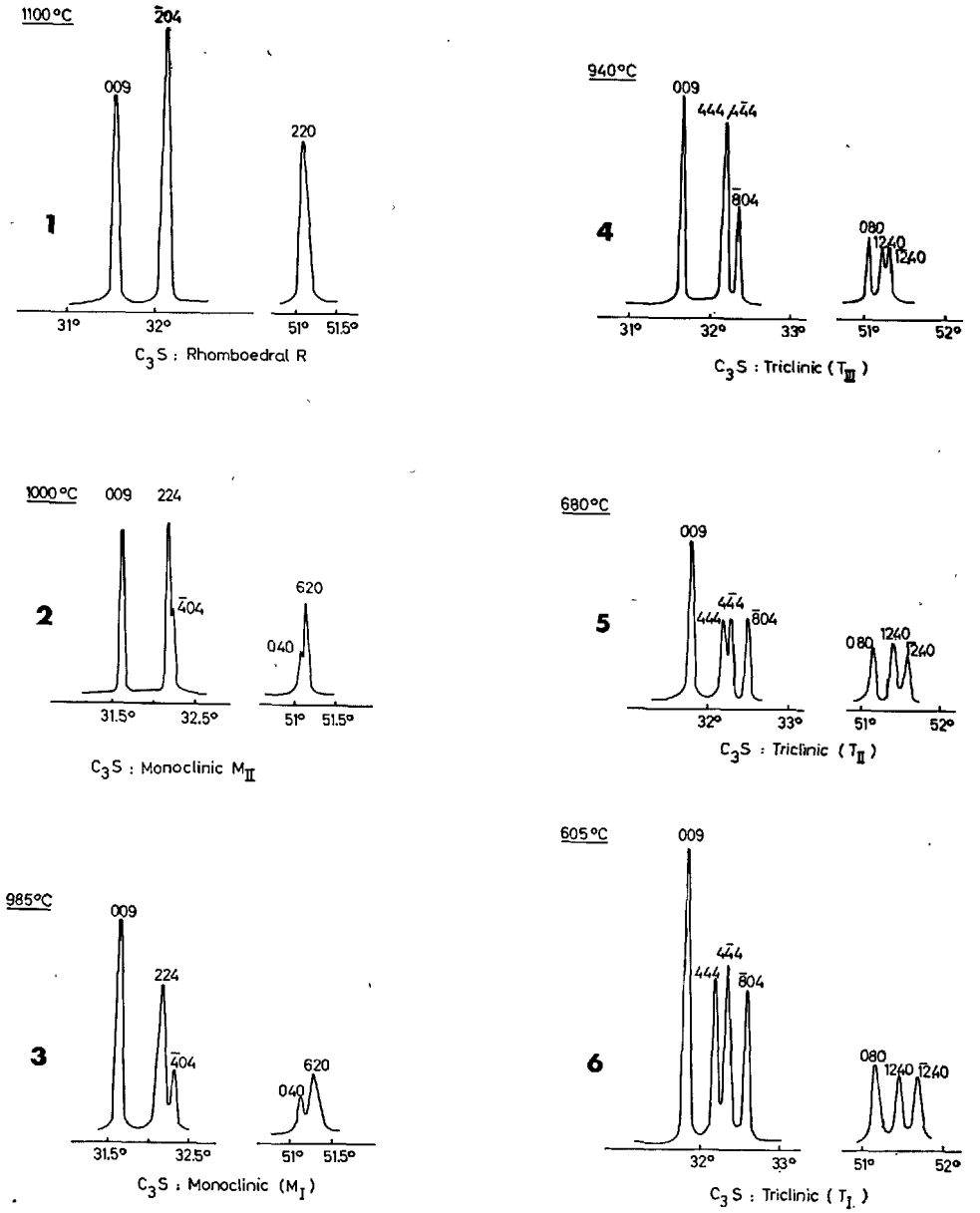

Fig. 8. *Tricalcium silicate. Characteristic reflexion groups in the powder patterns of the various modifications.*
A) Microdensitometer tracings of high-temperature focussing film patterns, Regourd (32);

Table 4. *Stabilization of high-temperature allotropic forms by various oxides*

Oxide	Composition ranges of allotropic forms quenched to room temperature, weight % added oxide					Limit of solid solution at 1550°C, weight % added oxide
	T_I	T_{II}	M_I	M_{II}	R	
Cr_2O_3	0–1.4	—	—	—	—	1.4
Fe_2O_3	0–0.9	0.9 –1.1	—	—	—	1.1
Ga_2O_3	0–0.9	0.9 –1.9	—	—	—	1.9
Al_2O_3	0–0.45	0.45–1.0	—	—	—	1.0
MgO	0–0.55	0.55–1.45	1.45–2.0	—	—	2.0
ZnO	0–0.8	0.8 –1.8	1.8 –2.2	2.2–4.5	4.5–5.0	5.0 (1400°C)

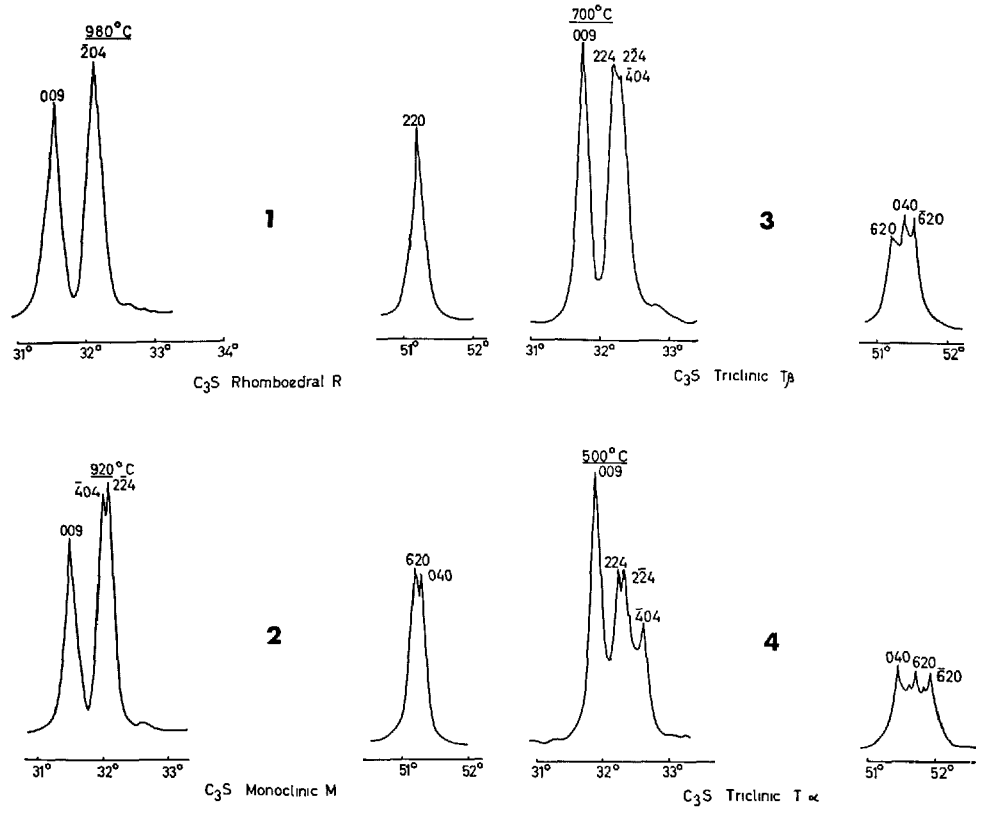

Fig. 8.
B) high-temperature diffractometer tracings Miyabe and Roy (23).

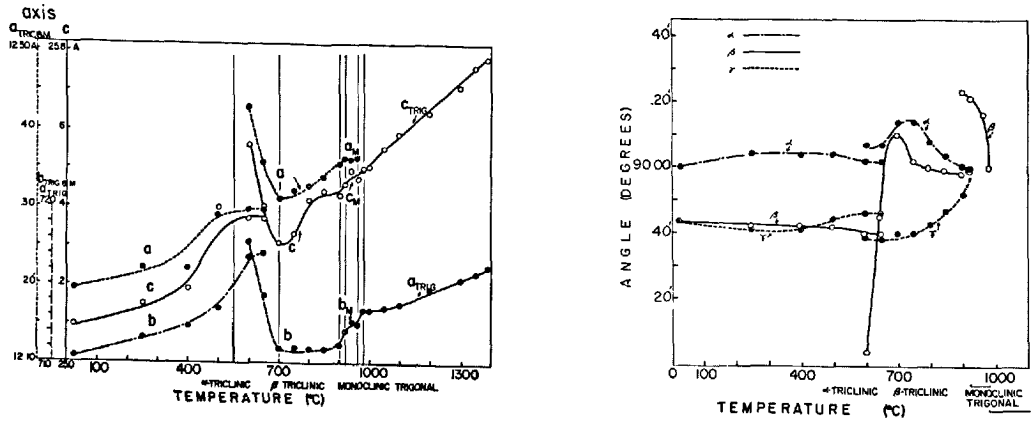

Fig. 9. *Tricalcium silicate: variation of pseudo-orthohexagonal lattice constants with temperature, Miyabe and Roy.*

the thermal effects at 920°C and 980°C marge into one with addition of their intensities. The stability zone of T_{III} disapears. Above 0.75% ZnO, M_I transforms directly to T_{II}. The fusion of the two DTA peaks implies a change of symmetry from monoclinic to triclinic, with the formation of two superstructures, simultaneously.

The temperature of the small signal at 990°C does not vary and the thermal effect persists above 2.25% ZnO, into the region where, according to X-rays, M_{II} and R appear to be stabilized. This is a new example of a phase-change detected by DTA but imperceptible by XRD. Above 2.25% ZnO, the solid solutions C_3S + ZnO would again be monoclinic but of a form approaching so closely to rhombohedral that XRD cannot resolve the symmetry.

There is one difference between the monoclinic

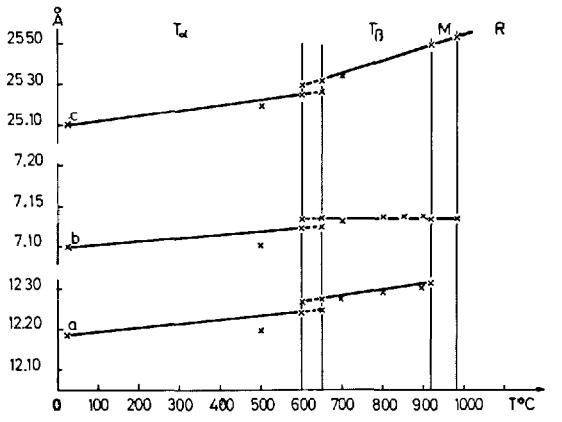

Fig. 10. *Tricalcium silicate. Variation of pseudo-orthohexagonal lattice constants with temperature, recalculated (11) from data of Miyabe and Roy.*

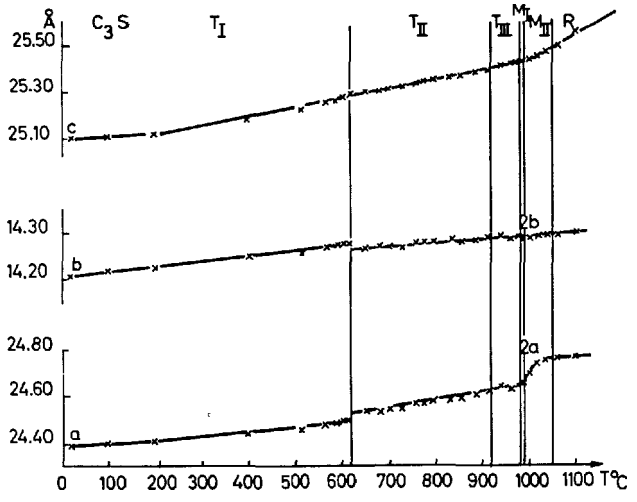

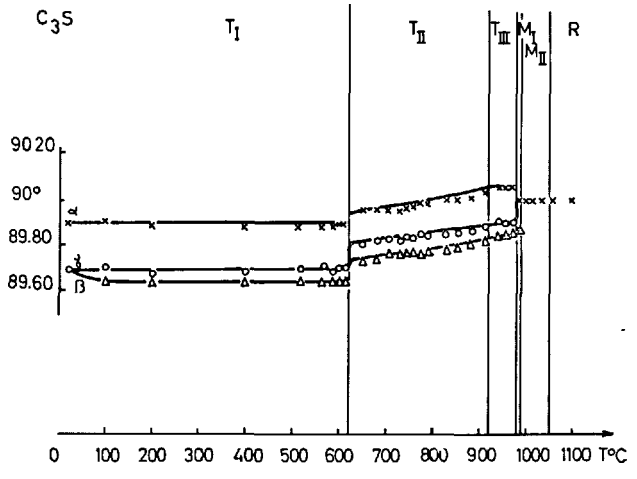

Fig. 11. *Tricalcium silicate. Variation of pseudo-orthohexagonal lattice constants with temperature. Regourd (11, 32).*

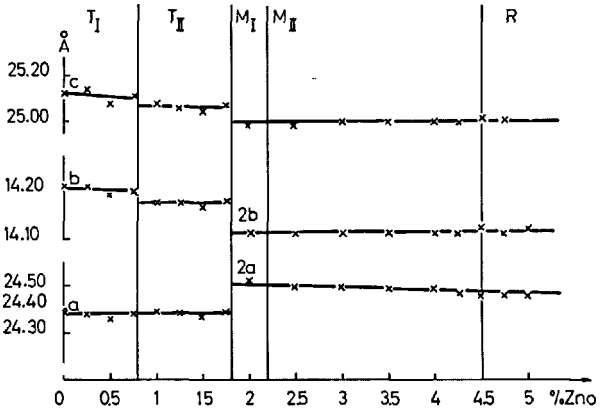

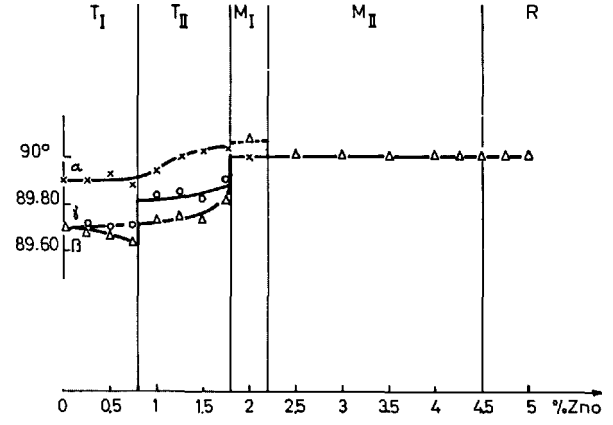

Fig. 12. *Ca_3SiO_5-ZnO solid solutions. Variation of pseudo-orthohexagonal lattice constants with composition at room temperature in the Ca_3SiO_5-ZnO solid solution series. Woermann, Hahn and Eysel (11).*

forms M_I and M_{II} of pure C_3S and the solid solutions $C_3S + ZnO$. The characteristic reflexions 224, $\bar{4}04$ and 620, 040 are reversed (Fig. 13).

This inversion has already been observed by Yamaguchi and Miyabe (22) and interpreted in a study of the solid solutions $3CaO\text{-}SiO_2\text{-}Al_2O_3\text{-}MgO$ by Yamaguchi and Kato (26). It corresponds to a different a/b ratio of the pseudo-orthohexagonal parameters and a different β angle. In the case of pure C_3S at 985°C: $a/b < \sqrt{3}$, $\beta \leq 90°$, in the solid solution $C_3S + 2\%$ ZnO: $a/b > \sqrt{3}$, $\beta > 90°$. The monoclinic forms of the solid solutions reverse at high temperature to the monoclinic forms of pure C_3S. The intermediate form with $a/b = \sqrt{3}$ and $\beta = 90°$ has an orthohexagonal unit cell even though the symmetry is not rhombohedral.

Ono, Uno and Kanai (27) have also stabilized the trigonal form of C_3S by the addition of 6.3% ZnO. Furthermore, a solid solution $C_3S + 15\%\ C_3A + 5\%\ CaF_2$, prepared by the same authors, is reported as rhombohedral with hexagonal parameters $a = 7.088$, $c = 25.115$ Å, but the optic axial angle 2V is not 0 as in the case of $C_3S + 6.3\%\ Zn_3SiO_5$; it is less than 15°(−). Presumably, this solid solution is not truly hexagonal.

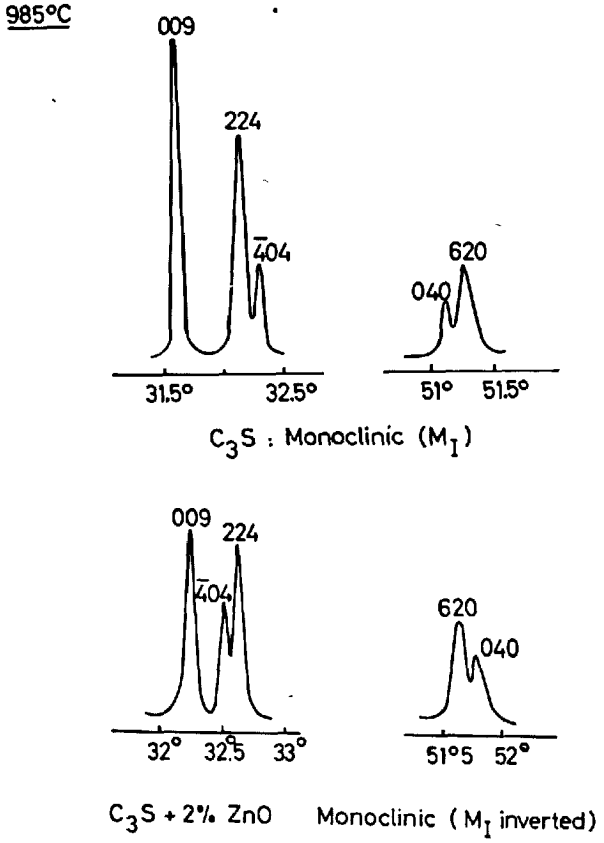

Fig. 13. *Comparison of densitometer records showing characteristic reflexions of monoclinic forms of pure C_3S at 985°C and $C_3S + 2\%\ ZnO$ at ambient temperature. In the solid solution ($C_3S + 2\%\ ZnO$) the 224, $\bar{4}04$ and 620, 040 reflexions are inverted.*

Solid solutions $C_3S + MgO$. Woermann, Hahn and Eysel (15) have proposed, for the solid solutions $C_3S + MgO$, the following formula: $(Ca_{1-x}Mg_x)_3SiO_5$, where $0 \leq x \leq 0.0125$ at 1550°C. The Mg^{2+} ions replace an equal number of Ca^{2+} ions in the C_3S lattice (28). The solubility limit is 2% MgO but this depends on the temperature (15, 26, 29). In addition, CaO dissolves small quantities of MgO (30). Thus crystals of the solid solutions Ca_3SiO_5 — "Mg_3SiO_5" and (Ca, Mg)O (31) can co-exist. The forms of C_3S which are stabilized are T_I (up to 0.55% MgO), T_{II} (0.55 to 1.45% MgO) and M_I (from 1.45 to 2.0% MgO). Above 2%, periclase appears, identified both optically and by the lines in the X-ray powder diagram. In the monoclinic form, the characteristic lines are again inverted: in the solid solution $C_3S + 2\%$ MgO, $a/b = 1.737$ and $\beta = 90.12°$ (32).

Solid solutions $C_3S + Al_2O_3$. The alumina incorporated in the lattice of C_3S can be either in the form of Al_2O_3 or C_3A. The solid solutions are characterized by a field in the system $CaO\text{-}Al_2O_3\text{-}SiO_2$. This implies that the solid solution is formed by CaO and Al_2O_3 (31). Woermann, Hahn and Eysel (15) have distinguished two types of solid solution:

a) *between 0 and 0.45% Al_2O_3*

Al^{3+} replaces Si^{4+} in the tetrahedra but occupies the free octahedral sites also, thus maintaining the electrostatic neutrality of the lattice. The formation of the solid solution, by both addition and substitution, is expressed by the formula:

$$Ca_3^{IV}Al_{x/4}^{VI'}(Si_{1-3x/4}Al_{3x/4})^{IV}O_5$$

where $0 \leq x \leq 0.02$, IV′ being a vacant octahedral site. The only form of C_3S stabilized is T_I (12, 15).

b) *between 0.45 and 1% Al_2O_3*

above 0.4% Al_2O_3, the incorporation of Al_2O_3 may be: —either the result of two linked substitutions: Si-Al (tetrahedral sites), Ca-Al (octahedral sites), following the formula:

$$(Ca_{3-x/2}Al_{x/2})^{VI}(Si_{1-x/2}Al_{x/2})^{IV}O_5$$

—or the continuous balanced replacement of Si by Al for the most part in the octahedral sites occupied by Ca(VI) and to a very small extent in the vacant octahedral sites (VI′).

These interpretations appear more probable than that of Locher (28) in which the loss of the oxygens which are not bonded to the tetrahedra permits the neutralization of the charge after substitution of Al for Si.

The form which is stabilized is T_{II} (10, 15, 29).

DTA shows the decrease in transformation temperatures of the forms stabilized by Al_2O_3, up to 1%, the limit of solubility. Above the solubility limit the lines of C_3A appear in X-ray powder patterns (12). The solubility limit is independent of temperature. Midgley and Fletcher (29) found the same results, but maintain that the substitution of Al in the lattice is not due to insertion of C_3A in C_3S but to a solid solution of the series C_3S — "$C_{4.5}A$".

The presence of Al does not change the type of substitution of Mg, but, on the other hand, Mg does affect the substitution scheme of Al (31).

Solid solutions $C_3S + Fe_2O_3$. The limit of solubility of Fe_2O_3 in C_3S is 1.1% (15). Only the triclinic forms T_I (from 0 to 0.8% Fe_2O_3) and T_{II} (from 0.8 to 1.1% Fe_2O_3) are stabilized. According to Fletcher (33), the solid solutions are of the type C_3S — "C_3F": $3Ca^{2+}$ are replaced by $3Fe^{3+}$, $6Si^{4+}$ by $6Fe^{3+}$, and the charge is compensated by one Fe^{3+} ion in an interstitial position.

Other solid solutions of C_3S. Tricalcium silicate also forms solid solutions with the following additions: $La_2O \cdot SiO_2$ (34), $Y_2O_3 \cdot SiO_2$ (35), SO_3 (36), Co_2O_3 (37) and Na_2O(38).

Na_2O substitutes for CaO in the C_3S lattice. Above 0.3% Na_2O, the structure is monoclinic with parameters $a = 12.262$, $b = 7.053$, $c = 25.086$ Å, $\beta = 90°07'$ (39).

CaF_2 (40) enters into solid solution in C_3S. At 0.74% CaF_2, the X-ray powder diagram is similar to that of alite in clinker. Above 0.74% there is a decomposition of C_3S into α' C_2S.

It seems equally probable that C_3S can take up to 1% P_2O_5 into solid solution (40), involving more a distortion of the lattice than true polymorphism.

Constitution and Structure of Alites in Clinker

In alites, one can find triclinic, monoclinic and trigonal forms (41, 42). In Fig. 14, we show the patterns of two clinkers in which the alite is in the forms M_{II} (inverse) and R.

The alite grains in portland cement clinker appear to have trigonal symmetry and to be practically uniaxial. However, each grain is an assembly of numerous crystallites of lower symmetry, twinned at 120°. As Jeffery (2) has suggested, these crystals are thus paramorphs of the high temperature form.

A recent study by Yamaguchi and Ono (43) shows evidence for two types of alite crystal: regular hexagons corresponding to the 0001 face and hexagonal sections elongated in the characteristic planes $1\bar{1}02$ and $10\bar{1}1$ (Fig. 15).

The transition form rhombohedral → monoclinic is a small energy change: the monoclinic a axis coincides effectively with the rhombohedral c axis and the monoclinic b axis with one of the rhombohedral

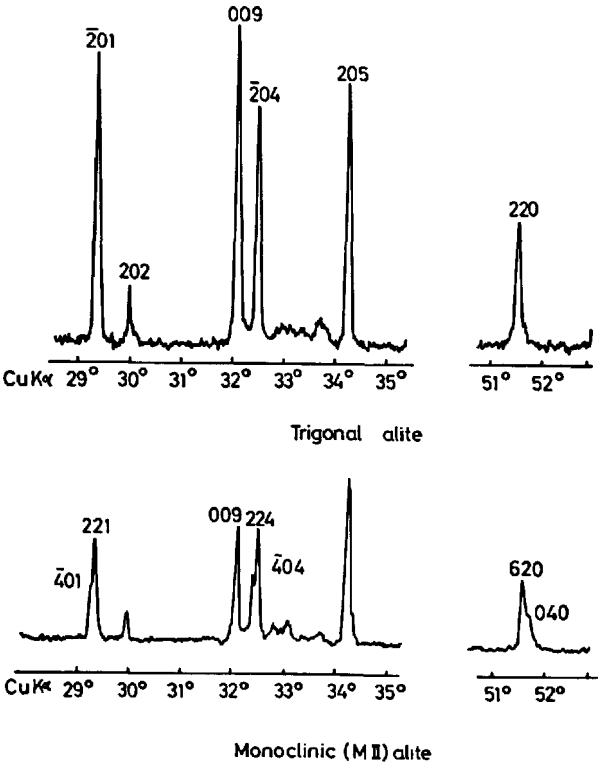

Fig. 14. *Densitometer records of powder patterns (Guinier camera) of two clinkers, in which the alite is respectively trigonal and inverse monoclinic.*

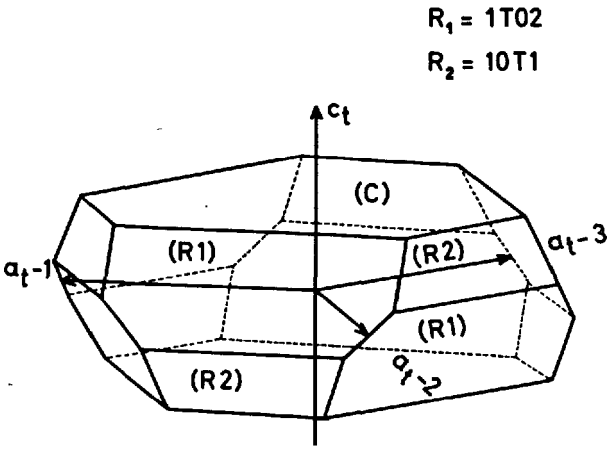

Fig. 15. *Relation between the trigonal axes $a_t - 1$, $a_t - 2$, $a_t - 3$, c_t and the crystal habit of a clinker alite. Yamaguchi and Ono (43).*

a_1, a_2, a_3 such that the twinning of the transformation is triple.

Jeffery (2) has considered alite as a definite composition with additional atoms in fixed lattice sites. In alite of formula $54CaO \cdot MgO \cdot Al_2O_3 \cdot 16SiO_2$ there is replacement of Ca by Mg, of 2Si by 2Al, and the addition of one Mg ion in a vacant hole, to maintain neutrality of the lattice.

The structure of this alite is monoclinic, with parameters a = 33.08, b = 7.07, c = 18.56 Å, $\beta = 94°10'$, space group Cm. One of the 3 true mirror planes of the trigonal structure is preseved in monoclinic structure, two become pseudo mirror planes (Fig. 2). The oscillation and Weissenberg photographs show a large number of satellite spots, which could be interpreted to give a "c" spacing of 150 Å.

The existence of different types of C_3S solid solutions shows that alite is a true solid solution. The introduction of foreign ions and balancing of charges are continuous and statistical. Alite is not a compound with a definite composition like the stoichiometric formula given by Jeffery. As early as 1958, Von Euw (44) showed that this composition contains C_3A as an impurity.

From powder diagrams, Yamaguchi and Miyabe (22) calculated the monoclinic unit cell of Jeffery's alite and found the parameters a = 12.246, b = 7.045, c = 24.975 Å, $\beta = 90°04'$. Ordway (1) re-calculated the unit cell to a = 12.248, b = 7.045, c = 24.972 Å, $\beta = 90°06'$, an elementary cell which allows the indexing of all the lines visible in the powder diagram. Only Jeffery studied a single crystal of alite and was able to find the true larger unit cell.

Toropov and Volkonskii (45) (1960) and Chromy (46) (1964) observed only two forms of C_3S in clinker: β and α, the α form being trigonal and the transformation $\beta \rightarrow \alpha$ taking place at 1375°C.

Stability of Tricalcium Silicate and Alites

Several methods of preparation of tricalcium silicate have been reported (47, 48, 49, 50, 51). Mineralizers such as NaF, Na_2SiF_6 (47), LiCl (52), CaF_2, CO_2 (53) accelerate the formation of C_3S. Complete synthesis of tricalcium silicate is difficult. Boikova and Toropov (10) detected, by DTA and by microscopy, C_2S in contact with C_3S. If this C_2S is saturated with CaO, the CaO/SiO_2 ratio becomes equal to 3.02 — 3.04 in tricalcium silicate.

On the other hand, a chemical and optical study by Woermann, Hahn and Eysel (31) has shown that tricalcium silicate is a definite compound, with the stoichiometric formula $3CaO \cdot SiO_2$ (CaO = 73.68%, SiO_2 = 26.32%). In samples with a lime content higher than 73.68%, C_3S co-exists with free CaO; there is no C_2S.

C_3S is stable between 1250°C and 2070°C, the temperature at which it melts incongruently to form CaO and a liquid phase (54). Below 1250°C, pure C_3S does not decompose (55, 22) or its decomposition is so slow that it can only be detected by the analysis of trace quantities of free lime (54).

Alite will decompose into belite and free lime in the presence of certain minor elements (K_2O, CaF_2). A considerable decomposition of alite occurs at 1180°C in metallurgical clinkers. The Fe^{2+} ions replace the Ca^{2+} in the C_3S lattice (56).

Dicalcium Silicate

It is necessary to note first of all the differences that exist between the polymorphisms of C_2S and C_3S. The lattices of the different C_2S form are known and their parameters are quite distinct. At the moment, only the structures of the β and γ forms have been determined; they are completely different. It seems equally certain that the α and α' structures show small but distinct differences. In addition, there is complete agreement between the transition points revealed by DTA and by XRD crystal analysis. In the case of C_2S we have the usual types of transformations, whereas in C_3S we have a very special case because all the forms can be derived from a single structure by slight variations.

Structure of the 5 Forms of C_2S

αC_2S. Of all the forms of C_2S, the α form, which exists only between 1425°C and its melting point, at 2130°C, has been least studied because of the difficulties of carrying out high temperature experiments.

The most recent work is that of Yamaguchi, Ono, Kawamura and Soda (57) who used diffractometry at 1500°C to determine the trigonal lattice (space group P $\bar{3}$m 1) with parameters a = 5.527, c = 7.311 Å (hexagonal notation). These results agree with those of Bredig (58) (a = 5.45, c = 7.19 Å) obtained from high temperature powder photographs taken by Van Valkenburg and McMurdie (59). The space group is

C $\bar{3}$m (P $\bar{3}$m 1) by analogy with glaserite, $NaK_3(SO_4)_2$.

The other determinations have been made on stabilized phases but with additions of such large proportions that one ought to consider whether the lattice has been substantially altered. Thus a α form "stabilized" by 2.5% Al_2O_3 + 2.5% Fe_2O_3 + 6% Na_2O has parameters a = 5.419, c = 7.022 Å (57).

A.M.B. Duglas (60) observed a small amount of a trigonal phase, with parameters a = 5.46, c = 6.76 Å, similar to α C_2S, in the 'single' crystals of bredigite extracted from vugs in blast furnace slag. These composite crystals, of composition $Ca_{1.59}Ba_{0.08}Mg_{0.31}Mn_{0.09}SiO_4$, always contained the trigonal and orthorhombic phases in fixed relative orientation.

The crystals of nagelschmidtite $2Ca_2SiO_4 \cdot Ca_3(PO_4)_2$, also extracted from a vug in slag (61), have a hexagonal lattice defined by unit cell parameters which are multiples of those given above: a = 21.80, c = 21.54 Å. Likewise, Yamaguchi, Miyabe, Amano and Komatsu (62) in 1957, have suggested that the lattice of glaserite cannot be applied to α C_2S unless a is multiplied by 4 (a = 21.8 Å) and c by 3 (21.50 Å). The unit cell of α C_2S would, in this case, be more complex, but these results were not retained by Yamaguchi, Ono, Kawamura and Soda (57) in 1963.

$\alpha'C_2S$. There exist two forms of $\alpha'C_2S$: α'_H and α'_L whose stability regions are respectively 1420° — 1160°C and 1160° — 675°C (63). The parameter variation curves calculated by Niesel and Thormann (63) from diffractometer traces of pure C_2S, show a reversible change of slope at 1160°C. We ourselves, with the help of high-temperature powder photographs, have confirmed the existence of two different forms of α' C_2S at 1145°C and 1200°C. Our results form the subject of a Supplementary paper to this Symposium.

Smith, Majumdar and Ordway (64) have already observed on diffractometer charts a variety $C_2S\alpha'_L$, obtained by heating γ C_2S, slightly different from $C_2S\alpha'_H$, obtained by cooling the α form. Similarly, Yamaguchi, Ono, Kawamura and Soda (57) have detected differences of intensity in the lines of α' prepared from α on the one hand and from γ on the other. This intensity difference disappears towards 1100°C. At 1300°C, the orthorhombic unit cell of α'_HC_2S, calculated by Yamaguchi, Ono, Kawamura and Soda (57) from powder patterns, has parameters a = 6.883, b = 5.600, c = 9.543 Å (space group Pnma).

Determinations have been made on stabilized α' forms. Thus, for a phase containing 10% $CaMgSiO_4$ and 4% K_2O, Yamaguchi, Ono, Kawamura and Soda (57) found the following parameters: a = 6.748, b = 5.494, c = 9.261 Å. The form stabilized corresponded to the form α'_HC_2S above, described by the same authors. In this case, the differences are not due solely to thermal expansion, but also to distortion of the lattice by the impurities.

Douglas (60), working on the natural mineral bredigite, usually considered identical with $\alpha'C_2S$, and on the composite crystals referred to above, calculated a cell which has the a and b parameters doubled: a = 10.91, b = 19.41, c = 6.76 Å (space group Pmnn) and she found a similar cell by indexing Trömel's powder data (65) taken at 750°C; certain weak lines necessitate the doubled cell. Ordway (1) points out that the powder patterns of pure $\alpha'C_2S$ and Douglas's material are significantly different though the structures are probably closely related.

The $\alpha'C_2S$ structure is unknown. Bredig (58) has proposed the hypothesis that it is analogous to that of βK_2SO_4. Majumdar, Smith and Ordway (66) give a model founded upon the analogy between βC_2S and βK_2SO_4 but without justification by intensity measurements.

βC_2S. The most precise determination of the parameters was obtained by Yannaquis (55) using a synthetic preparation of pure βC_2S. The lattice is monoclinic with parameters a = 5.507, b = 6.754, c = 9.317 Å, β = 94°38′ (A.S.T.M. card 9–351), space group $P2_1/n$.

From a powder diagram of βC_2S at 550°C ,Yamaguchi, Ono, Kawamura and Soda (57) have proposed a monoclinic unit cell with parameters a = 5.558, b = 6.823, c = 11.261 Å, β = 123°11′, space group $P2_1/c$, which is identical to the Yannaquis's lattice (see Fig. 16).

Lattice determinations have also been made on stabilized βC_2S phases: C_2S + 0.5% B_2O_3 is defined by the parameters a = 5.48, b = 6.76, c = 9.28 Å, β = 94°33′, (space group $P2_1/n$) (61) and βC_2S + 0.25% Cr_2O_3 by parameters a = 5.514, b = 6.757, c = 11.197 Å, β = 123°59′ (57). These results show that the distortions introduced by foreign ions, though not negligible, are very small.

The structure of monocrystals of βC_2S stabilized by 0.5% B_2O_3 is monoclinic (61), and is constructed from independent SiO_4 tetrahedra and two sorts of Ca atoms. Four of these 8 Ca atoms (Ca_I) are placed alternately above and below the SiO_4 tetrahedra in the direction of the b axis. The structure can be described as columns of alternating tetrahedra and Ca atoms, linked together by the other four Ca atoms (Ca_{II}) placed in the holes between the tetrahedra (21). The pseudo-trigonal arrangement of the SiO_4 tetrahedra around the Ca_{II} atoms is shown in Fig. 16.

The co-ordination of Ca_I is irregular: 6 neighbours

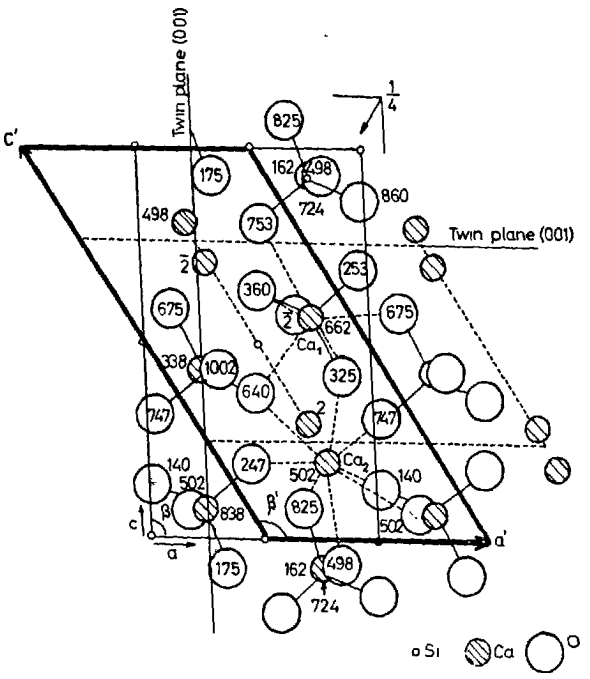

Fig. 16. *Dicalcium silicate. The projection of β C_2S structure on a plane perpendicular to the b-axis Midgley (61). The pseudo-hexagonal cell, axes a′ and b′, is shown Yamaguchi, Ono, Kawamura and Soda (57).*

lie at distances between 2.30 and 2.75 Å and six others between 2.98 and 3.56 Å. If the co-ordination is equal to 9, the contribution of each of the six nearest neighbours being 2/9 and that of the other six 1/9, Pauling's rule is approximately satisfied. The co-ordination of Ca_{II} is equally irregular. The eight neighbours belonging to six neighbouring tetrahedra lie at distances between 2.36 and 2.80 Å.

This structure, determined by Midgley (61) from 200 h01, 0k1 and hk0 reflexions, has a "reliability" factor of 19%, the R factor being reduced to 9% by McIver (67). McIver suggests that the space group $P2_1/n$ is incorrect, the true space group being one of: $P2_1$, Pn, $P\bar{1}$ or P1. Furthermore, Midgley notes that slight displacements of the atoms transform this sturcture to an orthorhombic structure of the βK_2SO_4 type, and somewhat larger changes give a trigonal structure (αC_2S). The polysynthetic twinning occurs on the (100) and (001) planes (Fig. 16) which become the planes of symmetry in the structure of $\alpha' C_2S$.

The unit cell of Yamaguchi, Ono, Kawamura and Soda (57) defined by the parameters a′, b′, c′ (Fig 16) is deduced from that of Midgley (a, b, c) by the following relations:

$$\vec{a'} = \vec{a}, \quad \vec{b'} = \vec{b}, \quad \vec{c'} = \vec{c} - \vec{a}$$

γC_2S. The unit cell has been determined from

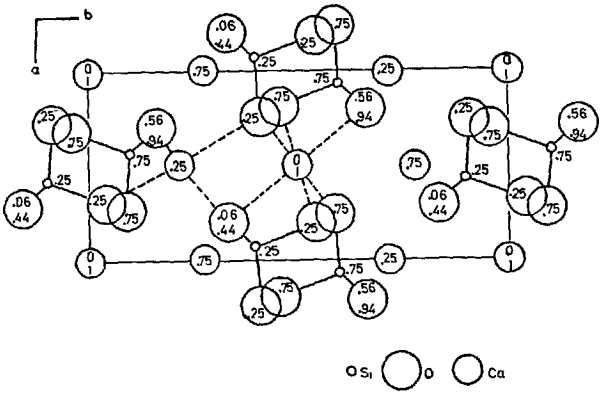

Fig. 17. *Dicalcium silicate. The projection of γC_2S structure on a plane perpendicular to the c-axis. Smith, Majumdar and Ordway (66).*

powder data by several authors. Their results are in agreement:

a = 5.076 b = 6.756 c = 11.230 Å (space group Pmcn) A.S.T.M. card 9-369 (55);

a = 11.232 b = 6.773 c = 5.083 Å (57) (space group Pnma);

a = 5.091 ± 0.010 b = 11.371 ± 0.020 c = 6.782 ± 0.010 Å (66) (space group Pbnm).

The volume expansion during the $\beta - \gamma$ transformation on cooling, shatters the crystals into fragments too small ($1 - 100\mu$) for single crystal study. Smith, Majumdar and Ordway (54) prepared C_2S from ethyl orthosilicate hydrolysed by a solution of $Ca(NO_3)_2$. The mixture was dried at 100°C, denitrated at 400°C, heated to 1500°C and quenched in air. Several single crystals were isolated and their complete structure was determined. This structure is of the olivine type Mg_2SiO_4 (55, 56). The Ca^{2+} ions replace the Mg^{2+} but, being larger, expand the unit cell of Mg_2SiO_4 but without altering the general regular arrangement (21). The SiO_4 tetrahedron is irregualr (Fig. 17). The Si-O distances vary from 1.589 to 1.725 Å. This irregularity is probably due to the distortions in the hexagonal arrangement of the oxygen ions. All the Ca ions are octahedrally co-ordinated; the low co-ordination of Ca explains the greater molar volume of the low temperature phase.

There is also a structural analogy between C_2S and Na_2BeF_4 (68, 69) on the one hand, and C_2S and Ca_2GeO_4 (70) on the other.

Other Studies on C_2S

Apart from these five phases which are universally agreed and well defined, some authors have claimed

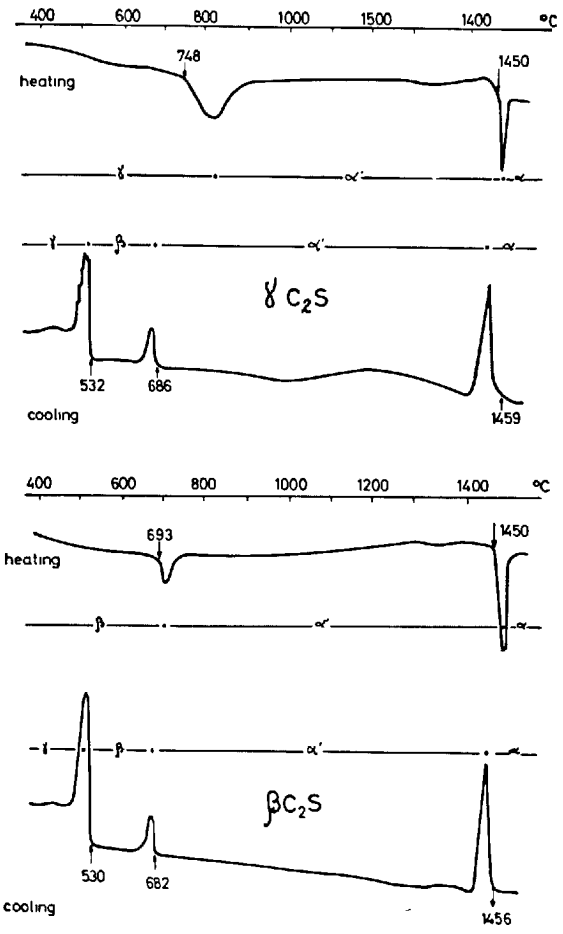

Fig. 18. *Dicalcium silicate. DTA diagram of γC_2S and βC_2S (Courtault) The temperatures of transformations seem higher than usual.*

the existence of other modifications.

1) A modification of β, called β', has been detected by Vasenin (71) in a DTA study. This phase, as described by Toropov, Volkonskii and Sadkov (72), has a pattern similar to that of α' ,and is stable from 900 to 1230°C. Its existence seems to be confirmed by a DTA signal at 1230°C, found by Schlaudt and Roy (73) in a study of the system Ca_2SiO_4–$CaMgSiO_4$. The β' phase has not been confirmed by Welch and Gutt (40) nor by ourselves.

2) Kurdowski (74) reported a new phase produced at 600°C from a β form stabilized by excess silica, which was very close to β'. This phase appears doubtful because excess silica does not stabilize βC_2S but favours the transformation $\beta \rightarrow \gamma$ (30).

3) A cubic form stable at 1600°C has been reported by Saalfeld (75). His high temperature patterns show an absence of 110 reflexion and enhanced intensity of 102. This behaviour, wihch is reversible, could be due either to a variation of the hexagonal axial ratio c/a resulting from the rotation of the anions or to the formation of a cubic phase (a = 5.8 Å). The trigonal 102 reflexion would become the cubic 200. Since 1953, this phase has not been reported by other research workers. However, a solid solution $C_2S + Na_2O$ reported by Ono (76) is perhaps a superstructure of Saalfeld's cubic form stabilized at room temperature. The mineral obtained in the CaO–SiO_2–Al_2O_3–Fe_2O_3 system by an equimolar substitution of Na_2O for CaO is isotropic with a = 17.769 Å $\fallingdotseq$ 3 × 5.8.

Study of the Transformations of C_2S

To describe the processes of change from one phase to another, we will consider the transformations observed first with decrease and then with increase in temperature.

1) *With decreasing temperature.* We start with the α phase, stable at high temperature (t > 1420°C):

$\alpha - \alpha'_H$: the transformation is reversible without hysteresis (Fig. 18). The structural changes of the $\alpha - \alpha'_H$ inversion cannot be characterized with certainty. Smith, Majumdar and Ordway (66) suggest that "half the SiO_4 tetrahedra rotate so that their apices point in opposite directions at the phase change. The rapidity of the transformation is certainly facilitated by the elevated temperature, even though the change may require a structural re-arrangement". Niesel and Thormann (63) have found at 1160°C, a DTA peak, corresponding to the $\alpha'_H - \alpha'_L$ transformation.

$\alpha' \rightarrow \beta$: 650°C. The transformation is reversible with a hysteresis of 25°C (Roy (77) found a hysteresis of 50°C); it occurs at a well-defined temperature. According to Smith, Majumdar and Ordway (66) the transformation involves a rotation of the SiO_4 tetrahedra and a change in the Ca ion co-ordination. From 8-fold in the α', the Ca co-ordination becomes variable, 8 or 9 fold, in the β form.

$\beta \rightarrow \gamma$: the β phase forms the γ by the process $\alpha' \rightleftarrows \beta \rightarrow \gamma$ This monotropic transition involves a considerable change in volume (dusting). From the structural point of view, the $\beta \rightarrow \gamma$ transition is a transformation of primary co-ordination (78). According to Smith, Majumdar and Ordway (66) the transition involves a rotation of the SiO_4 tetrahedron and should be considered as semi-reconstructive because of the large movements of some of the Ca atoms. The sluggish nature of the transformation is perhaps due to the complexity of the bond re-adjust-

ments.

The $\beta \rightarrow \gamma$ transformation has certain peculiar characteristics: in effect, it has been observed at different temperatures by different authors, 525°C (79), 450°C (71), 400°C (74), 375°C (80), 300°C (81, 82), and in addition it is incomplete. One usually obtains a mixture of β and γ but in variable proportions; one can obtain anything from nearly pure γ to nearly pure β. These phenomena will be the subject of a later paragraph.

2) *With increasing temperature.* At ambient temperature, one may start with either β or γ:

a) βC_2S: the transformation $\beta \rightarrow \alpha'_L$ takes place at 675°C then $\alpha'_L \rightarrow \alpha'_H$ at 1160°C (63) and $\alpha'_H \rightarrow \alpha$ at 1420°C. The transformations are visible on DTA and are confirmed by XRD.

b) γC_2S: starting with the γ phase, α'_L forms slowly between 725°C and 860°C. The DTA peak is elongated (spread out). Guinier camera photographs (see Fig. 19) taken at 750°C and 850°C show the co-existence of the two forms γ and α'_L.

One can explain the different characters of the $\beta \rightarrow \alpha'_L$ and $\gamma \rightarrow \alpha'_L$ transformations by structural considerations. If the α'_L structure is only slightly different from β, it is very different from γ. The $\gamma \rightarrow \alpha'_L$ transformation is semi-reconstructive. According to Smith, Majumdar and Ordway (66) this implies a rotation of the SiO_4 tetrahedra, a change in Ca coordination from 6 to 8, and an appreciable displacement of one type of Ca atom. Like the $\beta \rightarrow \gamma$ transformation, its sluggishness is perhaps due to the complexity of the bond changes.

The whole group of C_2S transformations is shown schematically by Niesel and Thormann (63) (see Fig. 20).

The energy diagram proposed by Bredig (58) now requires to be completed.

The different form of C_2S can also be identified by infra-red absorption spectra (83, 84).

Stabilization of Different Forms of C_2S

As indicated on Bredig's diagram, it is the γ phase which is most stable at ambient temperature. However, one can succeed instabilizing α and α', and one can obtain β at ambient temperature.

Certain oxides, such as MgO, Al_2O_3, Fe_2O_3, BaO, K_2O, P_2O_5 and Cr_2O_3, stabilize both α' and α forms (85, 86, 87, 88, 89, 90). A phase previously considered to be a definite compound of composition $K_2O \cdot 23CaO \cdot 12SiO_2$ was shown by Suzukawa (91) to be a solid solution of K_2O in the α' form of C_2S. However, Welch and Gutt (40) could not obtain this form at ambient temperature, finding that it trans-

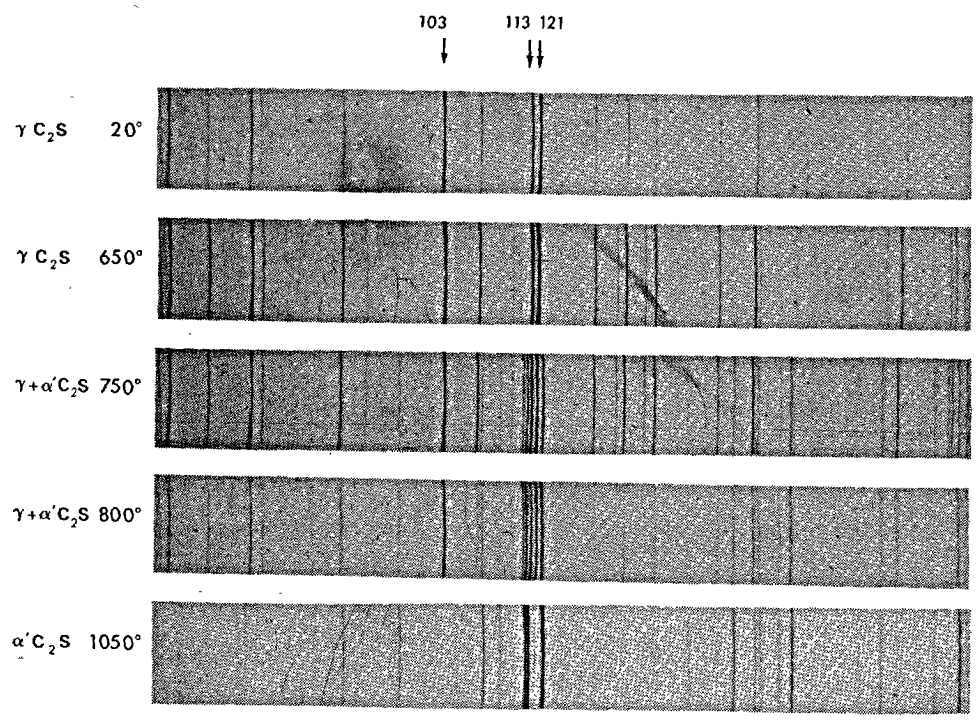

Fig. 19. *Dicalcium silicate. $\gamma \rightarrow \alpha'_L$ transformation investigated by high-temperature X-ray powder patterns. At 750° and 850°C, the γ and α'_L forms coexist.*

formed rapidly to β. On the other hand, merwinite does not seem to be solid solution of MgO in $\alpha'C_2S$ (5), as was proposed by Bredig (58). Yamaguchi and Suzuki (92) have prepared crystals of $3CaO \cdot MgO \cdot 2SiO_2$ of stoichiometric composition, and with a monoclinic structure ($a = 9.336$, $b = 5.301$, $c = 13.286$ Å, $\beta = 92°8'$, space group $P2_1/c$). Furthermore, Gutt (93) reports the existence of a still higher Ca compound, $CaO_{1.7}\ MgO_{0.3}SiO_2$, which is stated to co-exist with the C_2S polymorphs. The most interesting problems are those of the $\beta \rightarrow \gamma$ transformation and the conditions of stabilization of the β form.

a) *Influence of nucleation.* Even with pure synthetic products, considerable variation can be observed in the conditions for the $\beta \rightarrow \gamma$ transformation. Yannaquis and Guinier (78) have reported the influence which crystallite size has upon the stability of β: this phase is more stable the smaller the crystals. Microscope observations show that grains of β which are stable at ambient temperature are never larger than 5μ, although grains of γ which have been derived from β are in general 10 to 100μ in size. These observations are confirmed by XRD patterns. The reflexions from a stationary sample of γC_2S are spotty, while, under the same conditions, those of βC_2S are continuous, (Fig. 21).

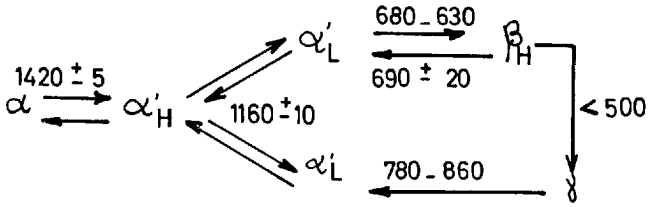

Fig. 20. *Dicalcium silicate. Schematic diagram of C_2S transformations. Niesel and Thormann (63).*

This behaviour may be explained by the mechanism of the $\beta \rightarrow \gamma$ transformation, which operates by nucleation and growth. Let us suppose that nucleation is difficult; in these circumstance a grain of β, whatever its size, will transform entirely if it contains at least one nucleus of γ. If after the $\alpha' \rightarrow \beta$ transformation the crystals of the latter are sufficiently large, the probability that each grain will contain a nucleus of γ is high, and one obtains, at ambient temperature, a high proportion of γ. If, on the other hand, the crystals of β are very small, many of them will not contain γ nuclei and cannot transform during cooling.

One can thus predict that if one can succeed in preparing α' in very small grains, stabilization of the β form may be achieved. This condition is realized if C_2S is prepared by solid state reaction between CaO and SiO_2 at 1200°C (94). In the stability range of the α' phase, the ratio rate of growth/rate of nucleation is low or nearly zero. In the same way, a smaple of C_2S heated to 1550°C, in the α zone, gives 90% of β on quenching because the passage through the $\alpha \rightarrow \alpha'$ transition is very rapid and the crystals remain small. On the other hand, the same smaple cooled slowly from 1550° to 1400°C and then quenched, gives 95% γ. The slow passage through the $\alpha \rightarrow \alpha$ transformation allows time for crystal growth and in spite of quenching the transition $\beta \rightarrow \gamma$ is practically complete. This explains also the role of the temperature of 1420°C in the stabilization of β or γ, which has been remarked by several authors (64, 95). According to Niesel and Thormann (63) it seems that 1160°C should be the optimum growth temperature for crystals of $\alpha'C_2S$; if C_2S is synthesized below 1160°C, one obtains β, while a sample prepared at a temprature above

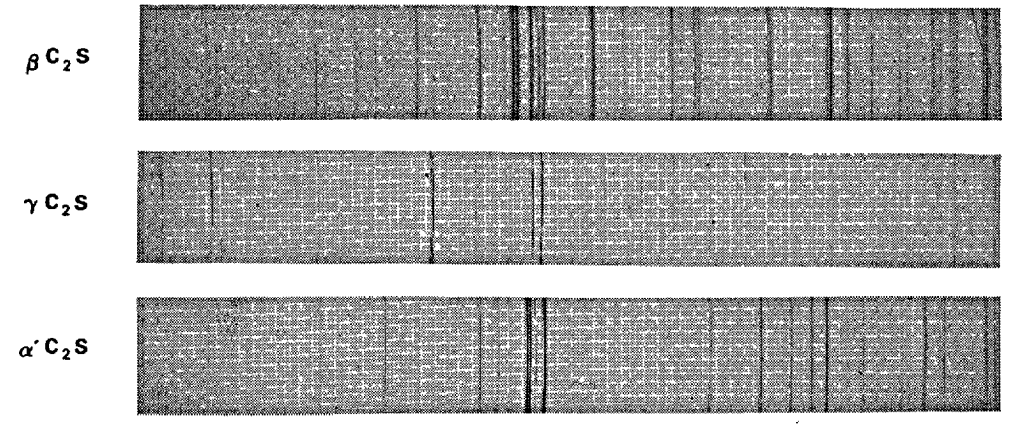

Fig. 21. *Dicalcium silicate. X-ray powder patterns of high-temperature Guinier camera with a stationary sample. The lines of γC_2S are spotty while, under the same conditions, those of βC_2S are continuous.*

1160°C gives a mixture of β and γ. One should point out that Chromy (96) has also shown, by optical methods, the effect of crystallite size of C_2S.

Again, the analogy between the structure of γC_2S and $NaBeF_4$ is to be found in the nature of their transformations. The process of nucleation (97) is the determining factor in the transition $\gamma \rightarrow \alpha'$ of Na_2BeF_4.

b) *Influence of pressure.* The nature of the phenomenon of apparent stability of βC_2S has been more precisely defined (98). It is possible to provoke a partial transformation from β to γ even at room temperature. Percussion of pellets of βC_2S will induce a transformation to γ of as much as 30%. Crushing between the platens of an hydraulic press may give up to 50% γ. The transformation is activated by the creation of nuclei of γ as the crystals are sheared under compression. On the other hand, if powdered β is submitted to hydrostatic pressure, even very high (9 tonnes/cm^2 $= 8.8 \times 10^5$ KN/M^2), no transformation occurs; the γ phase is less dense than the β phase, and increase of pressure does not favour the transformation (99). High pressures give β a stability region which does not exist at atmospheric pressure (77). Thus, the β phase is stable at ambient temperature under 2 atmospheres and it would be possible to transform γ to β under 17 bars (100).

c) *stabilization by additions of forign ions and by departures from stoichiometry.* The effect of grain size is, according to the theory presented above, merely statistical; but other factors are certainly involved in the stabilization of β, in particular the presence of impurities or of excess CaO or SiO_2 over the stoichiometric ratio:

Effect of excess CaO: it is possible to introduce an excess of CaO (1%) into C_2S. The form obtained at ambient temperature is β, yet the crystals are quite large (10μ). The specific effect of CaO is thus independent of that of size (78).

These results may be relevant to the work of Roy (77) who, having prepared large crystals of βC_2S from the hydrates, seemed to disagree with the theory of Yannaquis and Guinier. It is possible that these crystals were stabilized by an excess of CaO present in the hydrates (54).

Effect of an excess of SiO_2: the solubility of SiO_2 in C_2S lies between 1.5 and 2%, and the form obtained is γ. Crystals of C_2S–SiO_2 solid solutions range in size from 5 to 250μ. The addition of silica modifies the distribution of growth rates in the C_2S crystal and favours the transformation $\beta \rightarrow \gamma$ (78).

The effect of an excess of SiO_2 can be seen in the dusting of badly quenched clinkers or slags. Microscopic examination shows that the sources of the dusting lie round the grains of quartz; the crystals of belite which are to rich in silica transform to γ.

Effect of foreign ions: B_2O_3 is the classical stabilizer for β C_2S (61, 55). Using less than 0.5% B_2O_3, the lattice of βC_2S is not significantly altered (Fig. 22).

Yannaquis and Guinier (98) suggest that holes are formed by the elimination of Si^{4+} ions (probably in the form of silica) necessary to balance the charges of the higher valency $(BO_4)^{5-}$ groups. At 0.5% B_2O_3, there is one Si vacancy in 160 molecules of C_2S. Such holes seem a more likely site for additional Ca^{2+} ions than do interstitial positions in a lattice as compact as that of C_2S.

The solid solutions of $C_2S + B_2O_3$ are well crystallized. The lattice of C_2S + 2% B_2O_3 is monoclinic with parameters a = 5.475, b = 6.770, c = 9.290 Å, $\beta = 93°42'$. One can regard this solid solution as a limit structure and refer to it as a model.

Na_2O and K_2O also stabilize the β form (101) which is then formed as large crystals (78). Na_2O seems to diminish, even more than CaO, the probability of nucleation of γ C_2S. Very small numbers of Na atoms

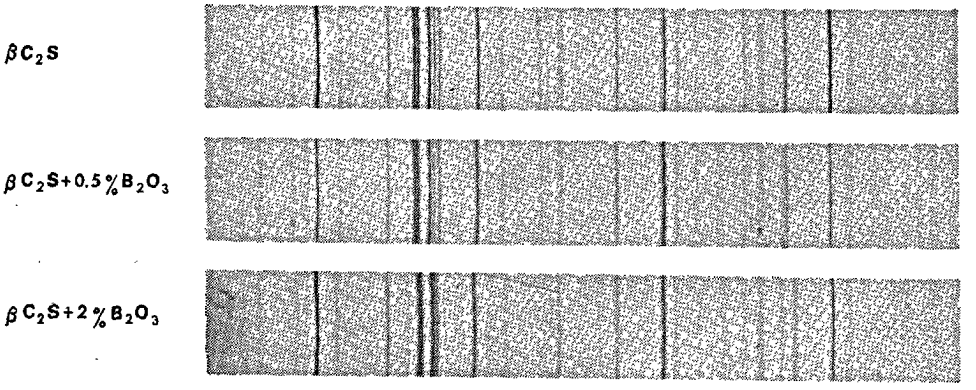

Fig. 22. *Dicalcium silicate and its solid solutions with B_2O_3. The lattice of $\beta C_2S + 0.5\% B_2O_3$ is not significantly altered.*

are sufficient to inhibit completely the $\beta \rightarrow \gamma$ inversion. The threshold of effectiveness seems to lie between 0.17 and 0.27% Na_2O but, contrary to Thilo and Funk's views, Yannaquis and Guinier (98), Niesel and Thormann (63) have shown that the alkalis are not essential for the stabilization of βC_2S.

Niesel and Thormann (63) have studied the solid solutions $C_2S + MoO_3$, $C_2S + C_3A$. Observations on the reaction products with the electron micro-probe have shown that there is formation of an envelope of $CaMoO_4$ or of an aluminous layer which hinders the $\beta \rightarrow \gamma$ transformation during rapid cooling (1000°C/minute) but which breaks up during slow cooling (10°C/minute) to permit the formation of grains of γC_2S.

Yannaquis and Guinier (98) have reported, during the Fourth Symposium, the influence of pressure on the stabilization of the β form of C_2S. The $\beta \rightarrow \gamma$ transformation occurs more readily when the C_2S lattice is not modified, as is the case with the solid solution $C_2S \cdot P_2O_5$ (1% $CaNaPO_4$). On the other hand, the silicates with a modified lattice, $C_2S + 0.5\%$ B_2O_3 or larnite (natural dicalcium silicate containing traces of Al_2O_3 or Fe_2O_3) give rise to no $\beta \rightarrow \gamma$ transformation under the influence of pressure. Either the crystals deform less or the formation of nuclei of γ is more difficult.

Belites in Clinker

In clinker, belite corresponds to a βC_2S with a lattice slightly modified by the addition of foreign ions. The XRD pattern of crystals of belite extracted from portland cement clinker (55) is in general that of βC_2S. It shows, however, some reflexions which are broader and certain others slightly displaced. Belite is thus a product of imperfect crystallization and apparently a non-equilibrium composition. In the lattice of C_2S, Ca^{2+} can be substituted by Mg^{2+}, K^+, Na^+, Ba^{2+}, Cr^{3+}, Mn^{2+} and the $(SiO_4)^{4-}$ group by $(PO_4)^{3-}$ or $(SO_4)^{2-}$ (79).

If β C_2S is stabilized by an ion substituting for Si, it is stable when fired in reducing conditions (102). On the other hand, under these conditions the $\beta \rightarrow \gamma$ inversion is easily produced in Ca-substituted pre parations (102, 73). In a reducing atmosphere, Fe^{2+} can replace Ca^{2+} or another stabilizing ion, to form a solid solution $FeO + C_2S$ and provoke dusting of the clinker.

The XRD pattern of belite is different from that of the solid solutions $C_2S + B_2O_3$. The theory of Mircea (103) that in clinker B_2O_3 reacts with C_3S to form CaO and a solid solution saturated with C_2S and C_5BS must be regarded as untenable.

Belite usually occurs as rounded, striated grains, with markedly laminated structure. The striations appear at the moment of the α—α' transformations (Type I: singly orientated)and the α'—β (type II: doubly orientated) (104). The usual form is β, and only occasionally does one find α' (105, 106) or α (107).

The composition of belite is unknown; syntheitc studies, by substitution for Ca (V, Ti, Na, K) or by addition of Al_2O_3, Fe_2O_3 to C_2S, have not given positive results.

Forest (108) has been able to prepare belites similar to those in clinker. These are oxygen-defective solid solutions with substituted Si of general formula $Ca_2M_xSi_{1-x}O_{4-x/2}$. The synthesis and crystallographic character of these belites form the subject of a communication to this Symposium.

Interstitial Phase

The interstitial phase, visible between the C_2S and C_3S in micrographs of clinker (Fig. 1) consists of two crystalline phases, generally referred to as C_3A and C_4AF. In reality, each of these phases can differ from the stoichiometric composition either by variation in the proportions of A and F or by the introduction of impurities in solid solution.

Tricalcium Aluminate

Structure of C_3A. Tricalcium aluminate is a definite composition which shows no polymorphic transformations (109). It melts incongruently at 1542°C to form CaO and a liquid phase. The crystal lattice is cubic with a = 15.262 Å (110) but the structure is still unknown.

Büssem (111) proposes a structure based on measurements of the strontium isomorph. The structure is a lattice of planar AlO_4 groups and octahedra of both AlO_6 and CaO_6; but as shown by Ordway (112) the oxygen atoms all lie at x, y, z = 0 or $\frac{1}{2}$, and the sub-cell ($\frac{1}{8}$ the true cell) contains 8 calcium *and no other* ions inside the faces. Ordway (112) succeeded in growing a C_3A crystal and determined, using Laue and Weissenberg photographs, the unit cell and

space-group ($T_h^6 - Pa_3$) which agree with Büssem's structure.

Schroeder and Lyons (113) have proposed a structure in which the AlO_6 groups are present as elongated octahedra, but Tarte (114) disagrees with this structure because it requires unusually large Al–O distances (2.6 Å). Further studies of C_3A by both infra-red absorption and X-ray fluorescence (115, 116) suggest that the aluminium/oxygen co-ordination is probably all tetrahedral.

A structure which is based on Al_6O_{18} rings of six tetrahedra has been proposed by Moore (117) with 64 Ca at the corners of the a/4 lattice and a further 16 positions to be occupied by 8 Ca or 16 Na. Using diffractometer powder intensities and some of Ordway's single crystal data, least squares refinement has not given values of R below 40%.

Solid solutions of C_3A: solid solutions $C_3(A_{1-x}F_x)$. Schlaudt and Roy (118), Tarte (119), Majumdar (120) and Moore (117) have reported the existence of solid solutions $C_3(A_{1-x}F_x)$. The limits of composition obtained for the solid solutions are different.

Fig. 23 represents the variations of cell parameter a as a function of the molar percentage $C_3F/C_3A + C_3F$.

These results show great differencies. Although the methods and temperatures of preparation were different, Majumdar and Moore found that the parameter continued to increase slowly with iron content beyond the limiting compositions. These compositions have thus not reached their equilibrium state. In Tarte's work, on the other hand, the parameter is constant when the ratio Fe/Al + Fe exceeds 10%. Furthermore, the isomorphous replacement Al–Fe is accompanied, in the IR absorption spectra, by a change of position of bands, a more or less profound alteration in band profiles and the appearance of a new band which suggests the presence of tetrahedral FeO_4 groups.

Other solid soultions. In the lattice of C_3A, CaO can be replaced by Na_2O. Brownmiller and Bogue (121) found the composition $Na_2O \cdot 8CaO \cdot 3Al_2O_3$ in the Na_2O–CaO–Al_2O_3 system. Conwicke and Day (122), Fletcher, Midgley and Moore (123) proposed a limiting composition 91% C_3A, 9% N_3A (mol) which is close to NC_8A_3. The parameter a decreases with addition of Na_2O. At 3% (mol) Na_2O there is a discontinuous change of symmetry from cubic to orthorhombic (123).

A composition $K_2O \cdot 8CaO \cdot 3Al_2O_3$ (91), isomorphous with $Na_2O \cdot 8CaO \cdot 3Al_2O_3$, exists in the presence of SiO_2; the K atom has a large ionic radius, 1.33 Å, (Na = 0.95 Å), and some Si ($\tau = 0.41$ Å) would replace the larger Al ions ($\tau = 0.50$ Å) (114).

The limit of solubility of MgO in C_3A is 2.5% (by weight) according to Muller-Hesse and Schwiete (124). MgO substitutes for CaO, and the parameter a decreases (117). Examination of portland cement clinker in the electron-probe suggests that MgO concentrates preferentially in the C_3A (125), at least when the C_3A is in the orthorhombic form.

In the solid solution $C_3A + SiO_2$, Si replaces Al. If one considers that the number of oxygen atoms remains constant, there atoms of Si replace four of Al, creating vacant sites (117). The parameter a decreases and the limit of solubility is 5–6% Si/Al + Si (atom %).

Table 5.

Author	Experimental method	Temp. °C	x
Schlaudt and Roy	Optical examination of nature of phases	1389	0.035
		1300	0.02
Tarte	Exact measurements of dimensions of lattice of the solid solution by X-ray diffraction	1310	0.10
Majumdar		1325	0.07
Moore		1350	0.04

Alumino-Ferrite Phase

Hansen, Brownmiller and Bogue (126) showed that complete miscibility exists between C_2F and a hypothetical "C_2A "up to C_4AF.

(a)—*C_2F: structure.* Bertaut, Blum and Sagnières (127) have determined the structure of C_2F. The unit cell is orthorhombic with parameters a = 5.64, b = 14.68, c = 5.39 Å and space group Pcmn, and contains 4 molecules of C_2F.

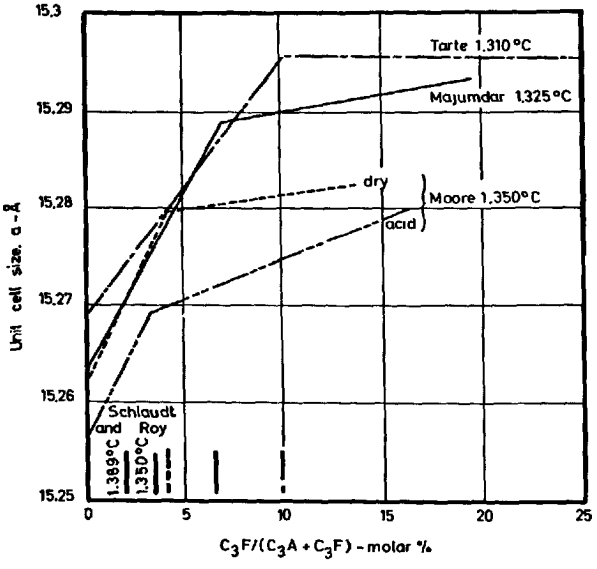

Fig. 23. *Tricalcium aluminate. Change in lattice parameter of C_3A with replacement of Al^{3+} by Fe^{3+}. Moore (117).*

The structure is pseudo-tetragonal. Projections along a and c are very similar (Fig. 24).

Along the b axis, a layer of FeO_6 octahedra alternates with a layer of FeO_4 tetrahedra; these tetrahedra and octahedra do not share oxygens. Ca is lodged in large cavities in the lattice of oxygen atoms and its co-ordination is very irregular; there are 9 neighbours, of which one is rather distant (3.3 Å), to share the bonding. Cirilli and Burdese (128) and Malquori and Cirilli (129) proposed the space group Imma for the whole series of alumino-ferrite solid solutions. Bertaut, Blum and Sagnières (127) found weak reflexions which could not be indexed except in the space group Pcmn; the layers of octahedra have the symmetry Imma but slight changes in the tetrahedral layers and in the Ca atom positions reduce the symmetry to Pnma (130), (≡ Pcmn in Bertaut's orientation).

—*Allotropic transformations of C_2F:* Differential thermograms of C_2F give two signals, at 430°C and 690°C, with a very flat region between the two peaks (131). The transformations are reversible with about 10° hysteresis.

We have attempted to determine the nature of these two allotropic transformations with the help of high-temperature X-ray diagrams. The transformation at 430°C is linked with a discontinuity in unit-cell volume. At 690°C, the curve of parameter variation shows a slight change of slope, the expansion being slower above 690°C. The number of reflexions does not change and there seems to be no change of lattice.

(b) *C_4AF.* C_4AF or brownmillerite has the same lattice as C_2F. The orthorhombic parameters are a = 5.428, b = 14.760, c = 5.596 Å (130) but the space group is Imma. The complete structure, especially the role of A and F, has not yet been determined. Brownmillerite is one member of the solid solution series C_2F + "C_2A" and seems the most stable. Hansen, Brownmiller and Bogue considered C_4AF to be a definite compound.

(c) *Aluminoferrite solid solutions.* Solid solutions $C_2F_{1-p}A_p$: In C_2F, some of the Fe ions can be replaced by Al ions; these solid solutions are of the form $C_2F_{1-p}A_p$.

A study of these solid solutions by X-ray powder disgrams has enabled Woermann, Hahn and Eysel (131) to detect two discontinuities in the variation of parameters as a function of p, the molar fraction of Al ions (see Fig. 25).

But these discontinuities correspond to very slight changes of slope. The limit of solubility is reached at p = 0.70. Examination of differential thermograms shows that the temperature of the first signal at 430°C decreases, as a function of alumina content, to 200°C and disappears at p = 0.30. The temperature of the signal at 690°C decreases similarly up to p = 0.2.

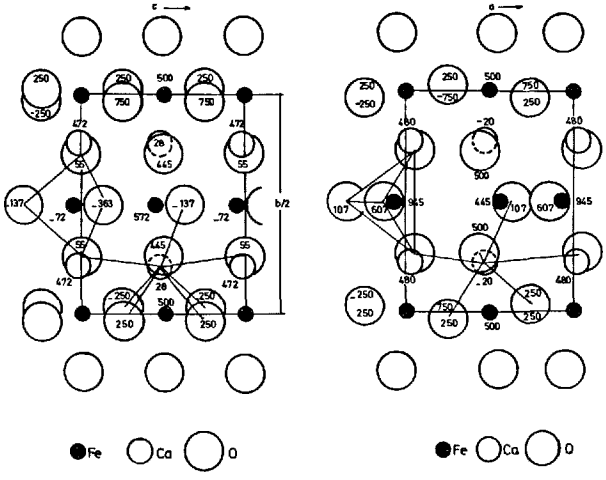

Fig. 24. *Dicalcium ferrite. Structure of C_2F. The projections along a and c axes are very similar. Bertaut, Blum and Sagnièrer (127).*

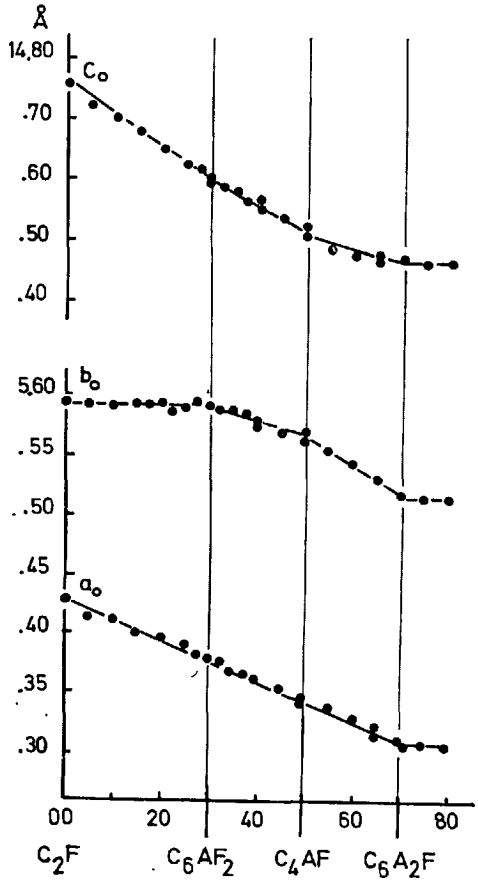

Fig. 25. *C_2F solid solutions: variation of C_2F lattice constants a_0, b_0, c_0 with composition in the C_2F—"C_2A" solid solutions series. Woermann, Hahn and Eysel (131).*

From $p = 0.2$ to $p = 0.5$, two peaks are observed which disappear at $p = 0.5$. It is difficult to draw precise conclsuions from this work; only the disappearance of the first signal at $p = 0.30$ seems to be linked with the change of symmetry from Pnma to Imma found by Smith (130) in his study of single crystals of composition $C_2F_{1-p}A_p$.

From the variations in intensity of characteristic h01 and 0k0 reflexions as a function of Al content, Smith (130) deduced that initially Al replaces tetrahedral Fe. When about half the tetrahedral sites are filled, Al enters both types of site equally. At about $p = 0.33$ the change of space group Pnma → Imma occurs. This change involves a contraction and rotation of the tetrahedra, and displacement of the Ca atoms. The Al atoms are distributed about equally in tetrahedral and octahedral sites. The variation of parameters a, b and c as a function of p is continuous. In brownmillerite, $C_2A_{0.5}F_{0.5}$, approximately 75% of the Al atoms are substituted for tetrahedral Fe and 25% for octahedral.

At the same time, Majumdar (120), in studying the phases in the pseudo-system $CaO–CaO\cdot Al_2O_3–2CaO\cdot Fe_2O_3$, found that the equidus temperatures for mixes on the hypothetical line C_2F–"C_2A" varied continuously as a function of the substitution Al^{3+}–Fe^{3+} in the ferrite lattice. C_3A and $C_{12}A_7$ appear when p is greater than 0.70.

In a study by infra-red spectra, of solid solutions $C_2A_pF_{1-p}$, Tarte (119) observed an increase in wave number and then, above $C_2A_{0.7}F_{0.3}$, no change, until at higher alumina contents, up to $C_2A_{0.85}F_{0.15}$, the position of certain lines changes again apparently due to the apperance of new phases such as C_3A and $C_{12}A_7$.

On the other hand, according to P. Longuet (132), the rate of reduction of C_4AF in a hydrogen atmosphere is regular as in the case of a definite composition. It seems that brownmillerite is the most stable member of the solid solution series $C_2A_pF_{1-p}$.

MgO-ferrite solid solutions: Magnesia enters into the ferrite lattice; normally red-brown, the latter becomes grey-black in the presence of MgO. It has been assumed for a long while that Mg substitutes for Ca but Woermann, Hahn and Eysel (131) have detected two types of solid solution. These authors used a precise analytical method to determine the free or uncombined CaO: the samples contained a small quantity of excess CaO; after the addition of a given percentage of MgO, the quantity of free CaO was determined and from the resultant curve, the type and the limit of solid solution were deduced.

The solid solution MgO-ferrite takes up more lime than the ferrite. According to the slope of the curve representing the change in free lime content as a function of added MgO, it appears that for 3 parts of MgO, 2 parts (molar equivalent) of CaO are combined; the limit of solid solution corresponds to the formation of periclase. The formula of the hypothetical end-member of the solid solution series is $Ca_2Mg_3O_5$ and the solid solution of Mg in C_2F is thus a substitution of Mg^{2+} for Fe^{3+}. Electroneutrality is maintained by the addition of an Mg ion in an interstitial position for every two Mg ions substituting for Fe. Hence, the type I solid solution:

$$Ca_2(Fe_{1-2x/3}Mg_x)_2O_5 \quad O < x < 0.023 \text{ at } 1400°C$$

At about $p = 0.50$, only one part of CaO is combined to 3 parts of MgO. Woermann, Hahn and Eysel proposed a superposition of a type I solid solution upon a normal Ca–Mg substitution. In type II, 1/5 of the Mg is substituing for Ca, while 4/5 is in type I solid solution (8/15 replacing the trivalent Fe_2, 4/15 in interstitial positions). Hence the formula:

$$(Ca_{1-x/5}Mg_{x/5})_2(R_{1-8x/15}Mg_{4x/5})_2O_5, \; x=0.049 (1300°C)$$

The change from type I to type II occurs at about $p = 0.49$. The discontinuity in the substitution of MgO can be established in the crystal structure, suggesting a discontinuity in the ferrite solid solution series. The aluminoferrites $C_2A_pF_{1-p}$ corresponding to $p > 0.5$ are unstable in the presence of free CaO. For this reason, Woermann, Hahn and Eysel did not extend their work to the whole solid solution series.

The MgO-ferrite solid solutions have also been studied by Kato (133), who finds that SiO_2 and MgO substitute for $(Al,Fe)_2O_3$ up to about 10% (molar). The substitution is of the melilite type.

SiO_2 alone can also enter into the ferrite lattice. The mechanism of SiO_2 solubility could be explained by the same type of substitution.

(d) *Interactions between the phases C_3A and $C_2(A,F)$.* C_3A and $C_2(A, F)$ constitute the interstitial phase of clinker. It is of interest to see whether, in synthetic preparations, these two phases can react to give solid solutions. This work, undertaken by Tarte (119) has shown the following results:

(1) Fe–Al exchange: in a mixture of $C_3A + C_4AF$, there is formed after heating to 1300°C a solid solution $C_3(A, F)$ resulting from the passage of a certain amount of iron from the C_4AF to the C_3A, this being compensated by the transfer of the equivalent Al from the C_3A to the C_4AF. The solid solution $C_3(A, F)$ has the limiting composition $C_3(A_{0.90}F_{0.10})$;

(2) Formation of poorly-crystalline phases: besides the displacements of characteristic XRD reflexions, Tarte (119) has observed in the solid solutions a simultaneous broadening of some of the high angle XR

reflexions and of the infra-red absorption bands, when comparing a mixture of the two phases before thermal treatment with the same mixture after treatment. This effect is more marked when the mixture already treated at 1300°C is taken to 1340°C.

Yet the same phases treated separately at the same temperature retain their IR spectra and XRD patterns perfectly sharp.

Tarte (119) has deduced that the state of crystallization of the phases obtained by mutual reaction is incomplete. This alteration of the crystallization is more marked at 1340°C, this being the temperature at which the majority of the mixture undergoes a partial fusion;

(3) Formation of a glassy phase: when the solid solutions have a high alumina content, a vitreous phase appears, the IR absorption spectrum of a sample of composition $C_2(A_{0.8}F_{0.2})$ taken to 1340°C is diffuse (Fig. 26) and shows no XRD lines whatever. On the other hand, the crystallization is complete when the Al/Fe ratio is colse to 1.

The Interstitial Phase in Clinker

In portland cement clinker, one finds tricalcium aluminate, the aluminoferrites and their respective solid solutions.

(1) *C_3A.* The tricalcium aluminate extracted from clinker has the lattice parameter a smaller than that

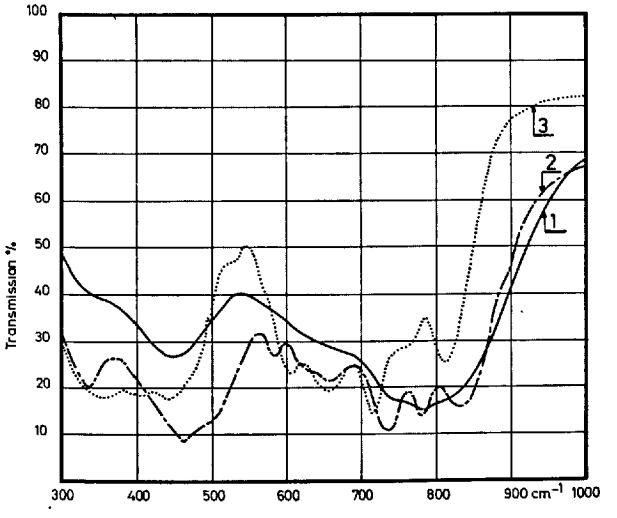

Fig. 26. *C_2F solid solutions. Infra-red absorption spectra Tarte (119):*
(1) of the vitreous phase formed from a composition $C_2(A_{0.80}F_{0.20})$;
(2) of the cryrtalline phases formed from the same composition as (1);
(3) of C_4AF.

of C_3A (117). It is thus in the form of solid solutions due to the addition of impurity oxides such as Na_2O, K_2O, MgO, Fe_2O_3, SiO_2 but the concentration limits of these different additions are not known.

(2) *Aluminoferrites.* The composition of the ferrite phase in commercial cements depends as much on the thermal treatment as on the A/F ratio, in all cases where equilibrium is not reached (134).

Midgley (135) has observed broad lines in the diffraction patterns of clinker ferrites and attributes this broadening to the fact that equilibrium could not be established in the course of cooling. Yamaguchi and Kato (136), Satou, Takashima and Kato (137) have both obtained less well-defined lines in patterns from clinker than in those from pure synthetic compositions.

The IR absorption bands of C_3A and $C_2(A, F)$ in clinker, easily observed in a smaple synthesized at 1200°C, become more and more diffuse as the sample is taken up to 1300–1400°C. In certain clinkers, there exists a very diffuse absorption band which seems to be linked with the alumina content, and hence with the existence of a glassy phase (119).

Hansen, Brownmiller and Bogue (126) have shown that complete miscibility exists between C_2F and "C_2A" up to C_4AF. Numerous studies (138 to 142) thereafter have established that the ferrite phase in clinker is not necessarily of the composition C_4AF but may extend to the solid solutions richer in alumina, in which the ratio Al_2O_3/Fe_2O_3 reaches 2.2 to 2.3 ($p \simeq 0.70$ in the series $C_2A_pF_{1-p}$).

Midgley (135) has studied the composition of the ferrite phase in fifteen English clinkers: 2 had the composition C_4AF, 2 had C_6AF_2, 4 an intermediate composition and the remainder an ill-defined composition (broadened XRD lines) but always lying between C_6AF_2 and C_6A_2F.

In American clinkers, Copeland, Brunauer, Kantro, Schultz and Weise (143) found that the compositions of the ferrites lay between $C_6A_{1.22}F_{1.78}$ and $C_6A_{1.77}F_{1.23}$. The mean value $C_6A_{1.47}F_{1.53}$ is very close to brownmillerite.

Gourdin (144) has analysed by XR diffraction the ferrite phase from 15 French cements; four clinkers contained the composition C_4AF, one contained C_6AF_2, and the other 8 an intermediate composition very close to C_4AF.

Schwartz (145) separated out the aluminoferrite phase from 66 French clinkers, by the salicylic acid in methanol method of Takashima (146). The aluminoferrite phases separated out had a chemical composition much more complex than the interstitial phase calculated by the Bogue method. The analyses,

by X-ray fluorescence spectrometry, revealed a stoichiometric defect in CaO which reached as much as 5%. This lime definiency increased if one included K_2O, Na_2O and MgO and diminished if one included SiO_2. The solubility limits of the minor elements in the interstitial phase were determined as 3% K_2O, 4% MgO, 7% SiO_2.

To conclude, C_3A and $C_2(A, F)$ cannot co-exist as such in clinker. Exchange of Al_2O_3 and Fe_2O_3 occur easily in the aluminates and aluminoferrites. Furthermore, at 1300°C, a small amount of iron will convert from the ferric to the ferrous state (120, 147). The presence of ferrous oxide noticeably modifies the stability regions of the solid solutions (148). The solid solutions $2CaO\,(Al, Fe)_2O_3$ decompose in the presence of CaF_2 and $CaCl_2$ (149).

Conclusion

Properties of the Clinker Minerals

We have considered the structures of the various polymorphs of the principal clinker components and there is a correlation between the crystalline structures of these components and the hydraulic properties of the clinker.

1) *C_3S.* Of all the phases in clinker, it is the tricalcium silicate which is the most significant and important from the point of view of the hardening of cements (150). The hydraulic cementing properties of C_3S are associated with the poor co-ordination of calcium ions and the presence of 'holes' in the crystal lattice (21). We have shown that the crystal structures of the different forms of C_3S and its solid solutions are very close to that of the trigonal form of pure C_3S stable at high temperatures. On the other hand, differences in the relative intensities of the diffracted rays are scarcely noticeable. The different crystalline forms are thus constructed from the same atomic groupings. These are only very slightly displaced or distorted. The polymorphic transformations are 'displacive', they bring into play only weak forces and do not appreciably alter the chemical combinations (151). This results in all the forms having a similar reactivity. Nurse, Midgley, Gutt and Fletcher (152) have found that the transformations $T_I \rightarrow T_{II} \rightarrow M$ of the synthetic solid solutions $C_{156-x}M_xS_{52}$ have no effect on the strengths developed when these materials hydrate. In the same manner, the strength of commercial cements containing trigonal alite does not differ significantly from that of cements in which the alite is in the monoclinic form. Yamaguchi, Shirasuka and Ota (153) have compared the properties of monoclinic and trigonal alite. Monoclinic alite (inverse) hydrates more rapidly. It is obtained by rapid cooling and seems to be thermodynamically unstable. If subjected to gentle heating it is converted into the triclinic form which by contrast gives greater early strength (154). Verbeck (155) has shown that the introduction of alumina and magnesia into tricalcium silicate brings about a significant increase in early strength but the effect does not persist beyond 70–80 days. The introduction of other foreign ions such as P_2O_5 (156), SO_3 (157), $CaSO_4 \cdot 2H_2O$ and $CaCl_2$ (158), Cr_2O_3 (159), can modify the properties of C_3S but the changes in reactivity do not seem to correlated with changes instructure (160). An increase in size of the alite crystals is generally observed.

2) *C_2S.* The five forms of C_2S have, on the other hand, quite different structures. The lattices are different and the ionic groupings change from one form to another. One can therefore reasonably presuppose that the five forms will have different hydraulic properties.

In the β form, the polyhedral co-ordination of the Ca ions is irregular and the extra-long Ca-O bonds facilitate the hydration reaction. Similarly, because of its predisposition to undergo a major structural rearrangement (64), metastable βC_2S is more readily hydratable. The γ form of C_2S is known to be inert (79) or feebly hydraulic (161). This poor reactivity is associated with the symmetrical co-ordination of the calcium ions (21) and the strong Ca–O bonds arising from the low co-ordination number of the Ca ions (64).

The α' forms should be only hydrated with difficulty and seem to possess no hydraulic cementive power (79).

The minor consistuents of clinker which stabilize the different forms of C_2S can affect the relationship between the hydraulic cementive characteristics of belite (40, 162, 163) and its other properties (164).

3) *Interstitial phase.* Tricalcium aluminate reacts rapidly with water. Calcium auminoferrite is only feebly hydraulic.

However, during the clinkering process, the burning temperature, the method of clinker cooling, the interaction of C_3A with the ferrite phase, the presence of foreign ions and the formation of a vitreous phase all alter the phase equilibrium conditions and so change the properties of the clinker in respect of the kinetics of its reactivity towards water (119).

Acknowledgments

We gratefully acknowledge the assistance of the many research-workers who have communicated their results to us, and especially those who have allowed us to read their papers before publication:

M. Dr. J. Forest
M. P. Gourdin
Prof. Th. Hahn
M. H. C. de Saint-Chamant
M. J. Schwartz
Prof. P. Tarte
Prof. G. Yamaguchi

and also to Miss A.E. Moore who both assisted in the preparation of the paper and translated it into English.

References

References to the previous Symposia on the Chemistry of Cement are abbreviated as follows:—for example, papers from the Proceedings of the Fourth International Symposium on the Chemistry of Cement, Washington 1960, published by the National Bureau of Standards as Monograph No. 43, Volume I or II, pages .... (1962), will be given throughout as "Washington, 1960, Vol. I (or II), pp. ...."

1. F. Ordway, "Crystal structures of clinker constituents", Washington, 1960, Vol. I, pp. 39–58.
2. J.W. Jeffery, "The crystal structure of tricalcium silicate", PhD Thesis, University of London (1950). Acta Cryst. **5**, 26–35 (1952).
3. H. O'Daniel, Th. Hahn and H. Müller, "The structure of $3CaO \cdot SiO_3$: investigation with Patterson syntheses" (in German), Neues Jahrb. Mineral. Monatsh, 1–15 (1953).
4. Th. Hahn, "New determination of structure of tricalcium silicate Ca_3SiO_5" (in German), Silikattechnik **113**. 96–397 (1960).
5. The Chemistry of Cements, Vol. I (Academic Press, London, England, and New York, U.S.A., 1964), Edited by H.F.W. Taylor. See chapter by J.W. Jeffery entitled "The crystal structures of the anhydrous compounds", pp. 131–164.
6. R.W. Nurse, "Summarized proceedings of conference on X-ray analysis, London, April 1948", J. Sci. Instr. **26**, 102 (1949).
7. M. Regourd, "Determination of the lattices of microscopic crystals. Application to the different forms of tricalcium silicate" (in French), Bull. Soc. Franc. Minèral. Crist. **87**, 2, 241–272 (1964). C.E.R.I.L.H. Technical Paper No. 152.
8. C. Mazières, "Micro and semimicro differential thermal analysis (μ DTA)", Anal. Chem. **36**, 602–605 (1964).
9. R. Roy, "Reactivity of solids", 4th International Symposium on the Reactivity of Solids, Amsterdam 1960, p. 225 (Elsevier NV Uitgeversmij, Amsterdam, Netherlands, 1961).
10. A. I. Boikova and N. A. Toropov, "Stoichiometry and polymorphism of tricalcium silicate" (in Russian), Dokl. Akad. Nauk. SSSR. **156**, No. 6, 1428–1431 (1964). Chem. Abstr. **61**, 7917f (1964).
11. M. Bigaré, A. Guinier, C. Mazieres, M. Regourd, N. Yannaquis (France) and W. Eysel, Th. Hahn, E. Woermann (Germany) "Polymorphism of tricalcium silicate and its solid solutions". J. Am. Ceram. Soc., Vol. **50**, No. 11, 609–619 (1967).
12. M. Bigaré, "Development of a high-temperature X-ray camera with controlled atmosphere. Investigation of Al_2O_3–Ca_3SiO_5 solid solutions" (in French), Rev. des Matériaux de Construct., **598–599**, 325–334 (1965) and **600**, 394–404 (1965). C.E.R.I.L.H. Technical Paper No. 166.
13. P. Gregorie, Private communication (1967) reported in 15.
14. J.D.H. Donnay, Crystal data: determinative tables, 2nd ed., p. 2, (Monograph No. 5, American Crystallographic Association, Washington, U.S.A., 1963).
15. E. Woermann, Th. Hahn and W. Eysel, "Chemical and structural investigations of the solid solutions of tricalcium silicate" (In German), Zement-Kalk-Gips. **16**, 370–375 (1963).
16. M. J. Buerger, "Crystallographic aspects of phase transformations", Phase Transformations in Solids (Symposium held at Cornell University 1948), pp. 183–211 (John Wiley and Sons Inc., New York, U.S.A. 1951).
17. Th. Hahn and W. Eysel, "Structure, polymorphism and solid solution of germanates and silicates of types A_2BX_4 and A_3BX_5", Paper 4·74, International Congress of Crystallography, Rome (1963). Acta Cryst., Special Issue, p. A45 (1963).
18. Th. Hahn and W. Eysel, "Structure and polymorphism of tricalcium germanate" (in German), Naturwissenschaften, **50**, No. 13, 471 (1963).
19. Th. Hahn, "Models relations between silicates and fluoberyllates" (in German), Neues. Jahrb. Mineral. Abhandlungen **86**, 1–65 (1953): Zement-Kalk-Gips No. 1, 385–391 (1967).
20. R. W. Nurse and J. H. Welch, Private communication (1951) reported by J. W. Jeffery, London, 1952, p. 44.
21. J. W. Jeffery, "The tricalcium silicate phase", London, 1952, pp. 30–48.
22. G. Yamaguchi and H. Miyabe, "Precise determination of the $3CaO \cdot SiO_2$ cells and interpretation of their X-ray diffraction patterns", J. Am. Ceram. Soc., **43**, 219–224 (1960).
23. H. Miyabe and D. M. Roy, "A re-examination of the polymorphism of Ca_3SiO_5", J. Am. Ceram. Soc. **47**, 318–319 (1964).
24. N. Yannaquis, M. Regourd, C. Mazières and A. Guinier, "On the polymorphism of tricalcium silicate" (in French), Bull. Soc. Franc. Mineral. Crist. **85**, 271–281 (1962).
25. A. Guinier, "X-ray crystallography theory and practice", (in French), p. 196–212, (Ed. Dunod, Paris, 1964), 3rd edition.
26. G. Yamaguchi and K. Kato, "$3CaO \cdot SiO_2$–Al_2O_3–MgO solid solution" (in Japanese), Semento Gijutsu Nenpo, **XVI**, 28–32 (1962).

27. Y. Ono, T. Uno and Y. Kanai, "Synthesis of five polymorphic modifications of C_3S" (in Japanese), Semento Gijutsu Nenpo, **XIX,** 36–41 (1965).
28. F. W. Locher, "Solid solution of alumina and magnesia in tricalcium silicate", Washington, 1960, Vol. I, pp. 99–106.
29. H. G. Midgley and K. E. Fletcher, "The role of alumina and magnesia in the polymorphism of tricalcium silicate", Trans. Brit. Ceram. Soc. **62,** 11, 917–937 (1963).
30. F. Trojer and K. Konopicky, "The system calcium oxide—magnesium oxide" (in German), Radex-Rundschau, No. 4, pp. 161–162 (1949).
31. E. Woermann, Th. Hahn and W. Eysel, "Chemical and structural investigations on the formation of solid solutions of tricalcium silicate. 2: phase relations in the system $CaO–MgO–SiO_2$ and $CaO–Al_2O_3–SiO_2$" (in German), Zement-Kalk-Gips, No. **9,** 385–391 (1967).
32. M. Regourd, "Polymorphic transformations of tricalcium silicate" (in French), Rev. des Matériaux de Construct., **620,** pp. 167–176 (1967). C. C.E.R.I.L.H. Technical Paper no. 182.
33. K. E. Fletcher, "The effect of Fe^{3+} and Al^{3+} on the polymorphism of tricalcium silicate", Trans. Brit. Ceram. Soc. **64,** 8, 377–385 (1965).
34. A. I. Boikova and N. A. Toropov, "Investigations on the C_3S solid solutions with the rare earth orthosilicates" (in Russian), Experiment and Technical Mineralogy and Petrography (Eksperiment v Tekhnicheskoy Mineralogii i Petrographii), 7th Colloquium on Experimental and Technical Mineralogy and Petrography (Po Materialam VII Coveshchaniya po Eksperimental'noy i Teknicheskoy Mineralogii u Petrographii), Moscow (1966). Chem. Abstr. **65,** 11956a.
35. N. A. Toropov and A. I. Boikova, "Solid solutions of tricalcium silicate with yttrium oxyorthosilicate" (in Russian), Dokl. Akad. Nauk. SSSR, **151,** No. 5, 114–117 (1963).
36. H. Lafuma, "Cement: scientific, technical, economic Problems", C.E.R.I.L.H. Information Note No. 17 (1961).
37. A. P. Khashkovskaya, M. M. Sychev and V. I. Korneev, "Composition and characteristics of the crystallization of $3CaO·SiO_2$ in the presence of admixtures" (in Russian), Tr. Gos. Vses. Inst. po. Proektir. i. Nauchn.-Issled. Rabotam v Tsementn. Prom. No **29,** 13–20 (1964).
38. G. Yamaguchi, H. Uchikawa and S. Kawamura, "Influence of sodium oxide upon the formation and the crystal structure of tricalcium silicate solid solution in the system $CaO–SiO_2–Al_2O_3–Fe_2O_3$" (in Japanese), J. Ceram. Assoc. Japan, **70,** 7, 209–220 (1962).
39. G. Yamaguchi and H. Uchikawa, "Investigations on the mixed crystals in the system $3CaO·SiO_2–Na_2O$" (in German), Zement-Kalk-Gips, **14,** No. 11, 497–504 (1961).
40. J. H. Welch and W. Gutt, "The effect of minor components on the hydraulicity of the calcium silicates", Washington, 1960, Vol. I, pp. 59–68.
41. H. G. Midgley, K. E. Fletcher and A. G. Cooper, "The identification and determination of Alite in portland cement clinker", Analysis of Calcareous Materials, pp. 363–371 (Monograph No. 18, Society of Chemical Industry, London, 1964).
42. G. Yamaguchi and H. Uchikawa, "On the Alite phase in portland cement clinker with varying alkali contents", Semento Gijutsu Nenpo, **XVI,** 23–28 (1962).
43. G. Yamaguchi and Y. Ono. "Microscopic study on Alite in portland cement clinker" (in German), Zement-Kalk-Gips, **20,** No. 9, 390-394 (1966).
44. M. Von Euw, "Quantitative X-ray analysis of portland cement clinkers" (in French), Silicates Industriels, **23,** 643–649 (1958).
45. N. A. Toropov and B. V. Volkonskii, "Polymorphic transformations of $3CaO·SiO_2$ and the influence of ferrous oxide on $3CaO·SiO_2$ and other clinker minerals" (in Russian), Tsement, **26,** No. 6, 17–20 (1960).
46. S. Chromy, "Notes on the petrography of fused cement", Silikaty, **8,** (1) 45–52, (1954).
47. W. Kurdowski, "C_2S and C_3S formation at 1300°C", Silicates Industriels, **30,** No. 9, 500–506 (1965).
48. P. P. Budhnikov, I. M. Petrovich and V. G. Savelev, "New method of synthesis of tricalcium silicate and studies on the properties of the obtained product", Cement-Wapno-Gips, **17,** No. 4, pp. 91–93 (1962).
49. M. Polivka, A. Klein and C. H. Best, "laboratory preparation of high-purity tricalcium silicate", Mater. Res. Standards, (A.S.T.M.), **1,** 7, 524–528 (1961).
50. L. A. Kroichuk and V. A. Shteerman, "Thermodynamic probability of formation of tricalcium silicate in calcium oxide-pseudowollastonite", Zh. Vses. Khim. Obshchestva im. D. I. Mendeleeva, **8,** (5), 581–582 (1963).
51. B.V.S. Subba Rao, Safia Mehdi, S. D. Datar and Abde Ali, "Formation of tricalcium silicate by the interaction of calcium carbonate and silica at 840°C", J. Sci. Ind. Res., Vol. 21D, 249–250 (1962).
52. A. Bereczky, "Reaction kinetics of the system $CaO–SiO_2$ in presence of catalysts", Silikattechnik, **11,** 474–475 (1960).
53. B. Courtault, "Study of solid state reactions up to 1600°C, with DTA: applications to cement chemistry" (in French), Rev. des Matériaux de Construct., **571,** 110–124 (1963). C.E.R.I.L.H. Technical Paper No. 140.
54. J. H. Welch and W. Gutt, "Tricalcium silicate and its stability within the system $CaO–SiO_2$", J. Am. Ceram. Soc. **42,** No. 1, 11–15 (1959).
55. N. Yannaquis, "X-ray studies of silicates in clinker" (in French), Rev. des Matériaux de Construct., **480,** 213–228 (1955). C.E.R.I.L.H. Technical Paper No. 74.
56. E. Woermann, "Decomposition of Alite in technical portland cement clinker", Washington, 1960, Vol. I, pp. 119–129.
57. G. Yamaguchi, Y. Ono, S. Kawamura and Y. Soda, 1. "Syntheses of the various modifications of Ca_2SiO_4 and the determination of their powder X-ray diffraction patterns" (in Japanese), English

summary, J. Ceram. Assoc. Japan, **71,** no. 2, 21–26 (1963); 2. "Differential thermal analysis and high temperature X-ray diffraction studies of $2CaO \cdot SiO_2$" (in Japanese), English summary, J. Ceram. Assoc. Japan, **71,** No. 1, 9–12 (1963).
58. M. A. Bredig, "Polymorphism of calcium orthosilicate", J. Am. Ceram. Soc., **33,** 6, 188–192 (1950).
59. A. Van Valkenburg, Jr., and H. F. McMurdie, "High-temperature X-ray diffraction apparatus", J. Res. Natl. Bur. Standards, **38,** 415–418 (1947).
60. A.N.B. Douglas, "X-ray investigation of bredigite", Mineral. Mag., **29,** 875–884 (1952).
61. C. M. Midgley, "Crystal structure of β dicalcium silicate", Brit. J. Appl. Phys., 3, 277–282 (1951). Acta Cryst. **5,** Part 3, 307–312 (1952).
62. G. Yamaguchi, H. Miyabe, K. Amano and S. Komatsu, "Synthesis of each modification of $2CaO \cdot SiO_2$ and their certification", J. Ceram. Assoc. Japan, **65,** 99–104 (1957).
63. K. Niesel and P. Thormann, "The stability fields of dicalcium silicate modifications" (in German), Tonind. Zeitung, **91,** 9, 362–369 (1967).
64. D. K. Smith, A. J. Majumdar and F. Ordway, "Re-examination of the polymorphism of dicalcium silicate", J. Am. Ceram. Soc., **44,** 8, 405–411 (1961).
65. G. Trömel, "The calcium orthosilicate Ca_2SiO_4 modifications" (in German), **36,** 88 (1949).
66. D. K. Smith, A. J. Majumdar and F. Ordway, "The crystal structure of γ-dicalcium silicate", Acta Cryst., **18,** 787–795 (1965).
67. E. J. McIver, "Rievew of the dicalcium silicate phase", Private communication (1960).
68. H. O'Daniel and L. Tscheischwili, "On the γ C_2S structure" (in German), Z. Kryst., **104,** 124–141 (1942).
69. E. Thilo and F. Liebau, "Silicate models. III. Modifications of Na_2BeF_4 and their relation to those of Ca_2SiO_4" (in German), Z. physik. Chem., **199,** 125–141 (1952).
70. W. Eysel and Th. Hahn, "Polymorphism in the system Ca_2GeO_4–Ca_2SiO_4", Neues Jahrb. Mineral. Monatsh. (6), 137–139 (1963).
71. F. I. Vasenin, "Polymorphic inversions of calcium orthosilicate" (in Russian), Zh. Priklad. Khim. SSSR, **21,** 10–17 (1948).
72. N. A. Toropov, B. V. Volkonskii and V. I. Sadkov, "The polymorphism of dicalcium silicate" (in Russian), Dokl. Akad. Nauk. SSSR, **112,** 467–469 (1957).
73. C. M. Schlaudt and D. M. Roy, "The join Ca_2SiO_4–$CaMgSiO_4$", J. Am. Ceram. Soc., **49,** No. 8, 430–432 (1966).
74. W. Kurdowski, "Polymorphic transformation of dicalcium silicate at low temperatures", Proceedings of the 6th Conference on the Silicate Industry, Budapest, 1961. Akadémiai Kiadó, Budapest, ed. B. Beke and F. Tamás, pp. 263–272 (1963).
75. H. Saalfeld, "Structure of dicalcium silicate (C_2S)" (in German), Ber. Deut. Keram. Ges., **30,** 185–189 (1953).
76. Y. Ono, "Cubic mineral derived from Ca_2SiO_4", Semento Gijutsu Nenpo, **XI,** 18 (1957).
77. R. Roy, Discussion of Nurse's Paper "Phase equilibria and constitution of portland cement clinker", Washington, 1960, Vol. I, pp. 29–32.
78. N. Yannaquis and A. Guinier, "Polymorphic $\beta - \gamma$ transition of calcium orthosilicate" (in French), Bull. Soc. Franc. Mineral. et Crist., **82,** 126–136 (1959).
79. R. W. Nurse, "The dicalcium silicate phase", London, 1952, pp. 56–77.
80. H. Funk, "On the stabilization of high-temperature modifications of α, α', (β) dicalcium silicate" (in German), Silikattechnik, 5, 186–189 (1955).
81. F. Wolf and J. Hille, "Stabilization of β-Ca_2SiO_4 by elementary carbon" (in German), Silikattechnik, **10,** 530–536 (1959).
82. T. Sasaki and Y. Suzukawa, "Effect of ferrous oxide on $\beta - \gamma$ inversion temperature of dicalcium silicate" (in German), Zement-Kalk-Gips, **17,** 5, 196–198 (1964).
83. N. A. Toropov, N. F. Fedorov and A. M. Shevyakov, "Infrared absorption spectra of polymorphic modifications of dicalcium silicate" (in Russian), Zh. Neorgan. Khim, **8,** 69–71 (1962).
84. H. Lehmann and H. Dutz, "Infrared spectroscopy studies on the hydration of clinker minerals and cements", Washington, 1960, Vol. I, pp. 513–518.
85. G. Yamaguchi, Y. Ono, S. Kawamura and Y. Soda, "The mortar strength of each modification of Ca_2SiO_4", Semento Gijutsu Nenpo, **XVII,** 39–43 (1963).
86. G. Yamaguchi, Y. Ono, S. Kawamura and Y. Kanai, "Solid solubility of Al_2O_3, Fe_2O_3 and Na_2O in Belite", Semento Gijutsu Nenpo, **XVII,** 37–41 (1963).
87. N. F. Fedorov and E. R. Brodkina, "Solid solutions in the $2CaO \cdot SiO_2$–$K_2O \cdot CaO \cdot SiO_2$ system" (in Russian), Izvest. Akad. Nauk SSSR, Neorgan. Materialy, **2** (4), 745–748 (1966).
88. C. Brisi and P. Appendino, "Solid state equilibria in the CaO–BaO–SiO_2 system" (in Italian), Ann. di Chim., **55,** (5), 461–468 (1965).
89. R. W. Nurse, J. H. Welch and W. Gutt, "High-temperature phase equilibria in the system dicalcium silicate-tricalcium phosphate", J. Chem. Soc., **220,** 1077–1083 (1959).
90. R. Kondo and S. Goto, "A study of the system CaO–SiO_2–Cr_2O_5–Al_2O_3", Semento Gijutsu Nenpo, **XIX,** 42–44 (1965).
91. Y. Suzukawa, "The alkali phases in portland cement: II. The potassium phase" (in German), Zement-Kalk-Gips, 9, 390–396 (1956).
92. G. Yamaguchi and K. Suzuki, "Structural analysis of merwinite", J. Ceram. Assoc. Japan, **75,** No. 7, 221–229 (1967).
93. W. Gutt, "The system dicalcium silicate-merwinite", Nature, **207,** no. 4993, 184–185 (1965).
94. A. Guinier and N. Yannaquis, "Polymorphism of Ca_2SiO_4" (in French), Compt. Rend., **244,** 2623–2625 (1957).
95. J. Grzymek and J. Skalny, "On the polymorphism of C_2S" (in German), Tonind. Ztg., **91,** No. 4, 128–130 (1967).
96. S. Chromy, "Optical relations between modifications of Ca_2SiO_4", (in Czech), Silikaty, 4, 338–349

(1966).
97. A. Bielanski, J. Nedoma and W. Turowa, "Dilatometric studies of polymorphic transformations of sodium floroberyllate", 5th International Symposium on the Reactivity of Solids, Munich 1964, pp. 90–99 (Elsevier NV Uitgeversmij, Amsterdam, Netherlands, 1965).
98. N. Yannaquis and A. Guinier, Discussion of Nurse's Paper "Phase equilibria and constitution of portland cement clinker", Washington, 1960, Vol. I, pp. 21–23.
99. F. Dachille and R. Roy, "High pressure phase transformations in laboratory mechanical mixers and mortars", Nature, **186**, 34–35 (1960).
100. D. Roy, "Studies in the system CaO–Al_2O_3–SiO_2–H_2O: III. New data on the polymorphism of Ca_2SiO_4 and its stability in the system CaO–SiO_2–H_2O", J. Am. Ceram. Soc., **41**, No. 8, 293–299 (1958).
101. E. Thilo and H. Funk, "Effect of small amounts of alkalis on the $\beta - \gamma$ inversion of C_2S", (in German), Z. Anorg. Allgem. Chem., **273**, 1–2, 28–40 (1953).
102. T. Sasaki, a) "X-ray study of the inversion of the crystal form of dicalcium silicate", J. Sci. Hiroshima Univ. Ser. A, **23**, no. 3, 425–444 (1960); b) "X-ray study on the inversion of the crystal form of dicalcium silicate, especially on the effect of stabilizing agents", Semento Gijutsu Nenpo, **XIV**, 22–23 (1960).
103. S. Mircea, "Decomposition of tricalcium silicate with boric oxide" (in Czech), Silikaty, **9**, 1, 34–42 (1965).
104. G. Yamaguchi and Y. Ono, "Microscopic studies on the textures of Belite in portland cement clinker", Semento Gijutsu Nenpo, **XVI**, 32–34 (1962).
105. P. Terrier and H. Hornain, "The application of mineralogical methods at the industry of hydraulic binders" (in French), Rev. des Matériaux de Construct., **619**, pp. 123–140 (see p. 135) (1967). C.E.R.I.L.H. Technical Paper No. 180.
106. A.A.T. Metzger, "The occurrence of bredigite (α' Ca_2SiO_4) in portland cement clinkers" (in German), Zement-Kalk-Gips, **6**, 269–270 (1953).
107. Y. Ono and Y. Soda, "Effect of the crystallographic properties of Alite and Belite on the strength of cement", Semento Gijutsu Nenpo, **XIX**, 78–82 (1965).
108. J. Forest, Study of local encrustation in cement rotary-kilns and belites. Silicates Industriels, 32, No. 11, I, 373–384, No. 12, II . . . (1967).
109. B. V. Volkonskii, "Studies of C_3S and C_3A in the range of high temperatures" (in Russian). Reports of a Symposium on the Chemistry of Cements, pp. 83–92. (State Publications of Literature on Structural Materials, Moscow 1956).
110. H. E. Swanson, N. T. Gilfrich and G. M. Ugrinic, "Data for 45 inorganic substances: (tricalcium aluminate, $3CaO \cdot Al_2O_3$ (cubic))" Standard X-Ray Diffraction Powder Patterns, NBS Circular 539, Vol. V, pp. 10–13 (1955), reprinted with corrections 1963. (U. S. Department of Commerce, U.S. Government Printing Office, Washington).
111. W. Büssem, "X-ray and cements chemistry", Stockholm 1938, pp. 141–168.
112. F. Ordway, "Tricalcium aluminate", London 1952, pp. 91–111.
113. R. A. Schroeder and L. L. Lyons, "Infrared spectra of the crystalline inorganic aluminates", J. Inorg. Nucl. Chem., **28**, 2, 1155–1163 (1966).
114. P. Tarte, "Infrared spectra of inorganic aluminates and characteristic vibrational frequencies of AlO_4 tetrahedra and AlO_6 octahedra", Spectrochimica Acta, **23A**, 2127–2143 (1967).
115. D. E. Day, "Determining the co-ordination number of aluminium ions by X-ray emission spectroscopy", Nature, **200**, No. 4907, 649–651 (1963).
116. V. L. Burdick and D. E. Day, "Co-ordination of aluminium ions in tricalcium aluminate", J. Am. Ceram. Soc., **50**, 2, 97–101 (1967).
117. A. E. Moore, "Tricalcium aluminate and related phases in portland cement", Mag. Concrete Res., **18**, No. 55, 59–64 (1966).
118. C. M. Schlaudt and D. M. Roy, "Crystalline solution in $3CaO \cdot Al_2O_3$ on the join $Ca_3Al_2O_6$–'$Ca_3Fe_2O_6$", Nature, **206**, No. 4986, p. 819 (1965).
119. P. Tarte, "Al-Fe isomorphous substitution in $3CaO$–Al_2O_3 and $2CaO \cdot Fe_2O_3$ and interactions between the so-called C_3A and C_4AF phases", Nature, **207**, No. 5000, 973–974 (1965); "Structural investigations of cement minerals—study of interactions between C_3A and C_4AF" (in French), Silicates Industriels, **31**, 343–352 (1965).
120. A. J. Majumdar, "The ferrite phase in cements", Trans. Brit. Ceram. Soc., **64**, 2, 105–119 (1965).
121. L. T. Brownmiller and R. H. Bogue, "The system CaO–Na_2O–Al_2O_3", Am. J. Sci., **23**, 501–524 (1932).
122. J. A. Conwicke and D. E. Day, "Crystalline solubility of soda in tricalcium aluminate", J. Am. Ceram. Soc., **47**, 12, 654–655 (1964).
123. K. E. Fletcher, H. G. Midgley and A. E. Moore, "Data on the binary system $3CaO \cdot Al_2O_3$–$Na_2O.8CaO.3Al_2O_3$ within the system CaO–Al_2O_3–Na_2O," Mag. Concrete Res., **17**, No. 53, 171–176 (1965).
124. H. Müller-Hesse and H. E. Schwiete, "On the solid solution of MgO in some cement clinker minerals", Zement-Kalk-Gips, **9**, 9, 386–389 (1956).
125. A. E. Moore, "Examination of a portland cement clinker by electron probe micro-analysis", Silicates Industriels, **30**, 8, 445–450 (1965).
126. W. C. Hansen, L. T. Brownmiller and R. H. Bogue, "Studies on the system calcium oxide—alumina—ferric oxide", J. Am. Chem, Soc., **50**, 396–406 (1928).
127. E. F. Bertaut, P. Blum and A. Sagnières, "Structure of dicalcium ferrite and Brownmillerite" (in French), Acta Cryst. **12**, 149–159 (1959).
128. V. Cirilli and A. Burdese, "On dicalcium ferrite and ternary solid solution in lime-alumina-ferric oxide system" (in Italian), Ric. Sci, 21, 1185–1191 (1951).
129. G. Malquoria dn V. Cirilli, "The ferrite phase", Londong 1952, pp. 120–136.

130. D. K. Smith, "Crystallographic changes with the substitution of aluminium for iron in dicalcium ferrite", Acta Cryst., **15,** 11, 1146–1152 (1962).
131. E. Woermann, Th. Hahn and W. Eysel, "Solid solution of Mg in $Ca_2Fe_2O_5$ and Ca_2FeAlO_5", Am. Ceram. Soc. Bull, **44,** 299 (1965).
132. P. Longuet, "Note on the behaviour of tetracalcium aluminoferrite in an atmosphere of hydrogen", Washington 1960, Vol. I, pp. 131–133.
133. A. Kato, "The possibility of the entry of SiO_2 into the clinker ferrite phase to form a solid solution", Semento Gijutsu Nenpo, **XIII,** 1–2 (1959).
134 A. Van Bemst, "Contribution to the study of reactions between the constituents of portland cement pastes during their burning" (in French), Silicates Industriels, 26, No. 6, 290–296 (1961).
135. H. G. Midgley, Discussion on Malquori and Cirilli's paper "The ferrite phase", London 1952, pp. 140–143.
136. G. Yamaguchi and A. Kato, "X-ray investigation of the ferrite phase", Semento Gijutsu Nenpo, **XI,** p. 19 (1957).
137. S. Satou, S. Takashima and M. Kato, "Studies on the compositions of ferrite in the industrial portland cements and clinkers", Semento Gijutsu Nenpo, **XVI,** 36–39 (1962).
138. N. A. Toropov, L. D. Merkov and N. A. Shishakov, "The binary system $5CaO \cdot 3Al_2O_3$–$4CaO \cdot Al_2O_3 \cdot Fe_2O_3$ (in Russian), Tsement, No. 1, 28 (1937).
139. T. Yamauchi, "The system $CaO \cdot Fe_2O_3$", J. Japan. Ceram. Assoc., 45, 279 (1937).
140. M. A. Swayze, "A report on studies of (1) the ternary system CaO-C_5A_3-C_2F, (2) the quaternary system CaO-C_5A_3-C_2F-C_3S", Am. J. Sci., **244** (1) p. 1–30; (2) p. 65–94 (1946).
141. N. A. Toropov and A. I. Boikova, "Composition and conditions of crystallization of celite in clinker portland cement" (in Russian), Izvest., Academy of Sciences, USSR, (Chemical Series), No. 6, 972–980, (1955).
142. T. F. Newkirk and R. D. Thwaite, "Pseudo-ternary system calcium oxide—monocalicum aluminate—dicalcium ferrite", J. Res. Nat. Bur. Standards, **61,** 4, 233–245 (1958).
143. L. E. Copeland, S. Brunauer, D. L. Kantro, E. G. Schultz and C. H. Weise, "Quantitative determination of the four major phases of portland cement by combined X-ray and chemical analysis", Anal. Chem., **31,** 1521–1530 (1959).
144. P. Gourdin, "Mineralogical composition and properties of portland clinker" (in French), Thesis C.N.A.M., Paris (1967). To be published in Rev. des Matériaux de Construct.
145. J. Schwartz, "Contribution to the investigation of aluminous ferrite phase in portland cement clinkers", Thesis C.N.A.M., Paris (1967). For possible publication in Rev. des Matériaux de Construct.
146. S. Takashima, "Systematic dissolution of calcium silicate in commercial portland cement by organic acid solution", Semento Gijutsu Nenpo, **XII,** 12–13 (1958).
147. R. R. Dayal, "The system CaO-Al_2O_3-FeO-Fe_2O_3", Thesis, University of Aberdeen, (1966).
148. H. C. de Saint-Chemant, "Recent study of the diagram "CaO-Al_2O_3-Fe_3O_4-FeO" (in French), paper presented to the "Journées d'Etudes' of the Association Belge pour Favoriser l'étude des verres et des composés siliceux", Brussels, 28 February to 4 March 1966. To be published in Silicates Industriels.
149. C. Brisi and P. Rolando, "The influence of CaF_2 and $CaCl_2$ on the solid solutions 2 CaO (Al, Fe)$_2O_3$" (in Italian), Ind. Ital. del Cemento, 1, 37–40 (1967).
150. F. Trojer, "The present state of knowledge of the phase composition of portland cement clinker" (in German), Zement-Kalk-Gips, 5, 207–215 (1966).
151. H. Lafuma, "French basic research in the cement industry", (in French), Rev. des Matériaux de Construct., **603,** 545–550 (1965). C.E.R.I.L.H. Technical Note no. 18.
152. R. W. Nurse, H. G. Midgley, W. Gutt and K. E. Fletcher, "Effect of polymorphism of tricalcium silicate on its reactivity", Symposium on Structure of Portland Cement Paste and Concrete. Special Report 90, pp. 258–262. (Highway Research Board, Washington, USA, 1966).
153 G. Yamaguchi, K. Shirasuka and T. Ota, "Comparison of hydration properties between monoclinic and inverted triclinic Alite", Symposium on Structure of Portland Cement Paste and Concrete, Special Report 90, pp. 263–268, (Highway Research Board, Washington, USA, 1966).
154. Y. Ono and Y. Soda, "Effect of the crystallographic properties of Alite and Belite on the strength of cement", J. Res. Onoda Cement Company, **XVII,** No. 65, 24–38 (1965).
155. G. Verbeck, "Cement hydration reactions at early ages," J. PCA Res. Development Lab., USA, **7,** No. 3, 57–63 (1965).
156. M. Musialik and A. Gruszczy'nska, "Some observations concerning P_2O_5 influence on the mineral structure of portland cement", Cement Wapno Gips, **XVI,** 1, 1–5 (1961).
157 R. Kondo, "Effect of special components on the mineral compositions of portland cement clinker", Semento Gijutsu Nenpo, **XVII,** 31–32 (1963).
158. A. Celani, M. Collepardi and A. Rio, "Influence of gypsum and calcium chloride on C_3S hydration" (in Italian), Ind. Ital. del Cemento, 7, 669–678 (1966).
159. V. A. P'jacev and Z. V. Tikhonenkova, "The processus of lime fixation in the synthesis of clinker minerals and in the burning of clinkers with additions Cr_2O_3, B_2O_3, P_2O_5, V_2O_5", (in Russian), Izvest. Vyss Uchebn. Zav. SSSR. Khim. i. khim. Tekn'n, No. 5, 802–806 (1966).
160. Yu. M. Butt and V. V. Timashev, "Dependence of the binding properties of the clinker minerals on their burning temperature and crystal structure", (in Russian), Tsement, **27,** 2, 17–22 (1961).
161. G. D. Uryvaeva, "On the hydraulic properties of γ dicalcium silicate" (in Russian), Izvest. Sibirsk. Akad. Nauk SSSR, Series Khim, No. 7, 2, 113–118 (1965).

162. G. V. Kukolev and M. T. Mel'nik, "Effect of solid solutions with C_2S on the properties of portland cement clinkers" (in Russian), Tsement, 22, 16–19 (1956).
163. A. E. Sheikin and S. A. Slobodchikova, "The hydraulic activity of Belite in relation to the conditions of its formation and the type of stabilizer" (in Russian), Nauchn. Soobshch. Vses. Nauch. Issled. Inst. Tsementa, **43**, 12, 8–13 (1961).

Written Discussion

Jean Forest

It is important to emphasize that alite is formed by pseudomorphosis (1) in what is at that time a tridimensionnal space (time, temperature, physical, chemical and mineralogical nature of the components of the raw meal).

Two cases can be envisaged:

The sintering reaction takes place in the solid state. Only the diffusion mechanisms must be considered, CaO in Al_2O_3, Fe_2O_3, SiO_2 (2) then in α C_2S.

The mineralogy and especially the granularity of the components of the raw meal, quartz in particular, affect the reaction fundamentally. Under certain conditions which we have studied, it is possible at 1300°C to combine completely the oxides present.

The sintering reaction continues with the liquidus. It becomes heterogeneous, once again, this is a diffusion process which permits the combining of CaO, although the physico-chemical properties of the liquidus—which may be impaired by minor elements either naturally present or added (3), influence the kinetics of the process.

However, as α C_2S has been transformed into belite, part of the latter produces alite, simultaneously liberating aluminates (4).

According to well established data it appears that the most symmetrical forms of alite are obtained at room temperature by replacing Ca by more polarizing atoms. If the substitution concerns Si, an atom with less polarizing power will have to be introduced, although its effect will not permit the symmetry T_{II} to be surpassed. Finally if the substitution concerns Ca and Si, the form M_{II} is obtained. The group Mg, Al stabilizes an inverse monoclinic alite. With the group Al, Ti one can obtain all forms from Ti to M_{II} as we verified by sintering at 1550°C, to a degree of accuracy of one supplementary molecule of CaO, a mixture corresponding to the composition of a belite saturated with alumina in which 0.02 moles of SiO_2 are replaced by TiO_2.

The insertion of Mg^{2+}, Al^{3+}, Ti^{4+}, produces the form R (5), whereas that of P^{5+} produces no modification at least in our experimental context.

It is also essential to recall that the symmetry deduced from the X-rays spectrum is sometimes superior to that which the interpretation of the DTA thermogram furnishes.

The sum of the data is assembled in Table I. It is conceivable therefore that the alite of industrial clinkers generally presents the forms M(inverse) and R. This situation, in the first case at least, can be modified as we shall see further on.

It is now opportune to generalize the notion of paragenesis into the chemistry of cement. It is possible to group under this heading intermediate substances which although not necessary to the fabrication of clinker. $CaSO_4$; $(C_2S)_2CaSO_4^*$; $2CaSO_4$, K_2SO_4; $(C_2S)_2$ $CaCO_3$, modify the normal course of reactions, often facilitating them and sometimes disturbing certain of their properties.

Table 1.

Composition	Burning: Time in hour	Burning: Temperature in °C	Symmetry of the alite	Free CaO %	Observations
$Ca_3Al_{0.06}Si_{0.92}Ti_{0.02}O_{4.97}$	6 +4 +16	1540 1500 1550	T forms M_I M_{II}	presence traces	presence of C_3A
Clinker α 100%	15	1300	inverse M_I	0.65	Blaine fineness of the quartz: 12000 cm^2g^{-1}
Clinker α 99.5% $Ca_3(PO_4)_2$ 0.5%	15 4	1300 1450	inverse M_I	0.18 —	
Clinker α 99.4% $CaSO_4$ 0.6%	15	1300	R	0.98	
Clinker α without MgO	15	1300	T_{II}	11.72	
Clinker α without MgO 99.5% $Ca_3(PO_4)_2$ 0.5%	15	1300	T_{II}	3.71	
Clinker α without MgO 99.4% $CaSO_4$ 0.6%	15	1300	T forms	5.82	

"Dusting" is observed with all these products and γC_2S is caracterized by X-rays. Heating rate 500°C h^{-1}. The time of 15 hours has been chosen for the sakes of convenience, but the reaction is finished a long time before.

α Clinker composition:

SiO_2	21.3%
Al_2O_3	7.0%
Fe_2O_3	2.5%
TiO_2	0.3%
MgO	1.8%
CaO	67.1%

*Experiment shows that $3C_2S \cdot 2CaSO_4$, in fact is a mixture of $(C_2S)_2CaSO_4$ and $CaSO_4$.

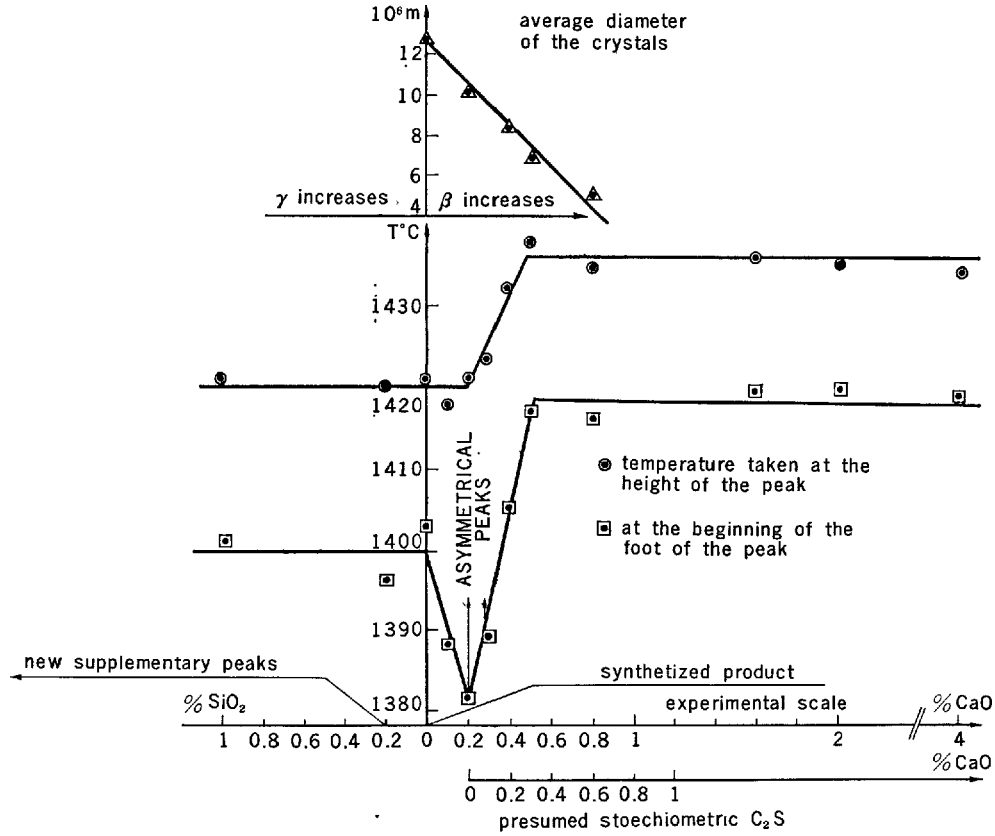

Fig. 1 *Synthesis made with 14.0176g of* SiO_2 *impurity 0.26% determined by chemical analysis 46.4895g of* $CaCO_3$, *rate of purity: more than 99% Prolabo RP. loss of weight at 100°C 0.094% 1000°C 43.89%*

That is why we consider that generally the dynamic process of sintering takes place in a quadridimensionnal space. In fact it is fitting to add to the preceding dimensions the sintering capacity of the substance during the sintering process which more or less disturbed leads to the fabrication of light even pulverulent clinkers without γ form of dicalcium silicate.

The technical literature is regularly enriched by new examples of paragenesis and the matter is treated in certain papers at this symposium.

The rotary cement kiln acts like a phase separator. Each phase may appear in a given temperature range and may be deposited on the inner surfaces inasmuch as it participates directly in the formation of a liquidus or that it is the final evolutionnary stage of the latter.

The use of the unitary scale and of Gygi's temperature curves constitutes an instrument which is useful for the comprehension of these phenomena (6).

Various thermic treatments were undertaken to determine the effect of CaO on C_2S for rates up to 6 per cent. It was found that the $\alpha'_H \rightleftharpoons \alpha$ inversion temperature is displaced from 1420°C to 1437°C for 100% C_2S to 99.7% C_2S–0.3% CaO.** Simultaneously the amo unt of βC_2S increases.

Between 0.6 and 1.4 per cent of CaO the X-rays spectrum obtained with Guinier de Wolff's camera equipped with a monochromator permits one to induce that there is a strong probability of the presence of C_3ST_I. With 6 per cent of the oxide, C_3S is particularly evident.

Finally the D.T.A. thermograms specify that the passage from $\alpha'_H \leftrightarrows \alpha$ takes place approximately at the same temperature as that of CaO–C_2S limit solid solution for the three independent series of trials undertaken. The entirety of the data which conflicts with that presented by V. I. Korneev and E. B. Bygalina (7) is grouped in Table 2.

This preliminary which needed developping is

**A more complete development about this problem will be published as soon as possible.

Table 2. *First set of experiments: independent synthesis*

Number	Theoretical composition	Observations	T°C $\alpha'_H \rightleftarrows \alpha$ by D.T.A.	X-rays data concerning C_2S (dÅ-hkl)
1	γC_2S	Synthesis made by M. Regourd	1440°C	
2	99%C_2S 1%CaO	Burning at 1450°C during 1 hour. Homogenization and burning: 1450°C 2 hours	1441°C	
3	98.4%C_2S 1.6%CaO		1445°C	
4	C_2S	Burning at 1450°C during 11 hours. Homogenization + 12 h at 1060°C + 2 h at 1200°C	1449°C	Like 5 but very weak lines. Not exactly stoechiometric
5	C_2S 2%CaO		1444°C	Spotty lines at 6Å 021 1.776Å 080 3.01Å 401
		Second set of experiments		
4	As previously	Matters pressed in a cylindrical form burning 1410°C 16h.	1420°C*	Like 5 but very weak lines
5			1435°C	Lines at 6Å 021 1.776Å 080 2.755Å $0\bar{4}4$
New experiments: here the mixture of $CaCO_3$ and pure fused SiO_2 was strongly homogenized, then divided in three parts				
6	C_2S	Burning at 1200°C 15 hours.	1432°C	
		As previously +6.5 hours at 1500°C	1428°C	Lines at near the stoechiometry 3.01Å 401 2.767Å $0\bar{4}4$ 2.776Å 445 1.776Å 080
7	98%C_2S 2%CaO	Burning at 1200°C 15 hours	1430°C	
		As previously +6.5 hours at 1500°C	1425°C	Lines at 3.01Å 2.767Å 2.61Å borded line 1.776Å
8	94%C_2S 6%CaO	Burning at 1550°C 19 hours	1424°C	Lines at: 5.97Å 021 3.041Å 441 3.01Å 401 2.97Å $4\bar{4}2$ 2.767Å $0\bar{4}4$ 2.612Å $4\bar{4}5$ 1.776Å 080 1.76Å $\bar{1}240$

Note: $CaCO_3$ High purity grade free of alkalies.
SiO_2 Pure fused Blaine fineness first set: 6400g cm^{-2} second set: 12000g cm^{-2}
Purity 99.7%
Ball mill in tungstene carbure and calcination at 1100°C before use. (Purity 99.55%)
*Use of a new thermocouple for T°C measurement probably not strictly identical to the preceding.

Table 2. (Cont.) *Third set of experiments*

Number	Theoretical composition	Observations	T°C $\alpha'_H \rightleftarrows \alpha$ by D.T.A.	X-rays data concerning C_2S (dÅ-hkl)
10	C_2S Synthetized product see Fig. N'1	Burning at 1500°C 9 hours	1421°C	
11	99.2%C_2S + 0.8%CaO	4 hours at 1500°C	1432°C	2.76Å v.w. $0\bar{4}4$
12	98.4%C_2S + 1.6%CaO	4 hours at 1500°C	1436°C	2.76Å $0\bar{4}4$ 1.776Å 080
13	98%C_2S + 2%CaO	4 hours at 1500°C	1435°C	3.01Å 401 1.776Å 080 2.76Å $0\bar{4}4$ 1.76Å $\bar{1}240$
14	96%C_2S + 4%CaO	4 hours at 1500°C	1434°C	3.01Å 401 1.776Å 080 2.76Å $0\bar{4}4$ 1.76Å $\bar{1}240$

not in complete disagreement with the hypothesis of the compact structure of β C_2S and facilitates the considerations which follow.

The establishment of a closed cycle of SO_2 in the rotary kiln can lead to various disorders in the regular working order and provoke the blocking of a section by the thickening of a ring formed primarily by sulfatic spurrite and by β C_2S (8).

Generally, self-destructive deposits are formed. The mixture of their fragments with the raw-material more or less affects the sintering capacity. Finally, the clinker can contain variable rates of SO_3 according to the thermic rhythm. When the latter contains K_2SO_4, measurable by the thermogravimetric method of P. Longuet (9), the cement may lump rapidly in humid air as the result of the formation of a tangle

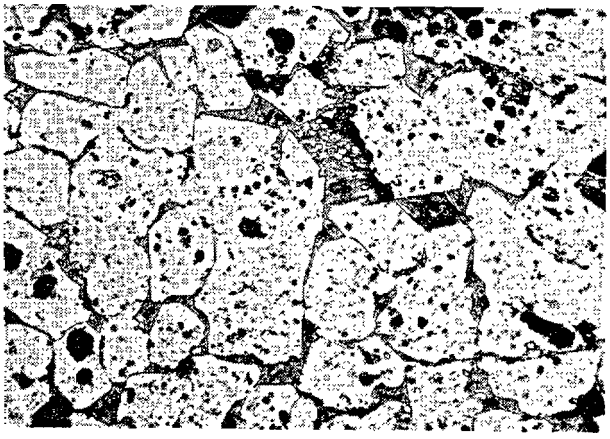

Fig. 2. $(Ca_2SiO_4)_2$ $CaSO_4$ *completed with* CaO *to give* C_3S (T_I *Alite*) × *62* — NO_3H *etching.*

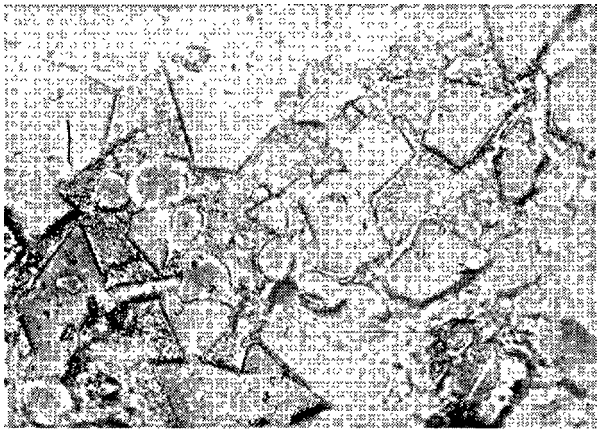

Fig. 3 *2* $(Ca_2Al_{0,065}Fe_{0,015}Si_{0,92}O_{3,96})$, $Ca_2K_2(SO_4)_3$ *completed with* CaO *to give* C_3S (*R. Alite*) × *180* — NO_3H *etching.*

of syngenite needles, $K_2Ca(SO_4)_2 \cdot H_2O$ (10).

In the presence of sulfates, silicates are capable of forming solid solutions.

An equimolecular mixture of sulfatic spurrite and of CaO burned for one hour at 1450°C gives alite crystals of the form T_I (D.T.A. gives peaks at 636°C, 882°C, 930°C, 978°C) attaining 300 μ on an average, by means of the well known mineralizing effect of SO_3 (Fig. 2).

Conversely, the global composition: $2(Ca_2Al_{0.065}$ $Fe_{0.015}$ $Si_{0.92}$ $O_{3.96})$, Ca_2 K_2 $(SO_4)_3$, 2 CaO forms R alite under the same thermic treatment as previously explained (Fig. 3).

Similarly the heating of the mixture corresponding to 99.4 per cent clinker and 0.6 per cent $CaSO_4$ (Table 1) gives an R alite. The same observation can be made in sintering, in a confined atmosphere with a model which permits heating at real time temperature, raw cement material enriched by $CaSO_4$ and Ca_2K_2 $(SO_4)_3$ as may be produced for example in the cyclones of the Humboldt kiln.

The percentage of SO_3 which produces the transition from the inverse form M to R seems to fall between 0.24 and 0.45 per cent for an amount of potential C_3S in the neighbourhood of 55 per cent. Inasmuch as all the SO_3 is combined with the alite, the result is in close accordance with that which H. Lafuma indicates (11).

Taking in account the hypothesis concerning the compacity of the β C_2S structure, one can easily predict that the formula for the constitution of the sulfate belites can be written:

$$Ca_{2-x}Si_{1-x}S_xO_4$$
$$Ca_{2-2x}K_{2x}Si_{1-x}S_xO_4$$

The solubility limits were determined by D.T.A. during the second heating cycle, from mixtures corresponding to various values of x, previously heated for two hours at 900°C then for 3 hours at 1180°C.***

In this way we verified that with $CaSO_4$, $x = 0.06$, and with K_2SO_4, $x = 0.02$ (Fig. 4 and 5).

Moreover it appears in the second case that the insertion takes place in the form α'_L, whereas it is necessary to go beyond the inversion temperature $\alpha'_L \rightleftarrows \alpha'_H$ in the presence of $CaSO_4$. The X-rays spectra reveal that a β_1 belite (12) corresponding to a weak variation of the constants of the lattice, is stabilized. K_2SO_4 is discernable from the point $x = 0.05$ onwards, and is detected by the peak of transition at 560°C for $x = 0.04$ in D.T.A.

$CaSO_4$ is partly combined in the form of sulfatic spurrite between 900°C and 1150°C, and at 1180°C $CaSO_4$, $Ca(OH)_2$ are additionally present along with β C_2S, the reaction not yet being complete. Heating for 10 minutes at 1450°C followed by quenching, produces mixtures where γ C_2S is found, with the exception of the $CaSO_4$ synthesis which on the contrary contain a form α' for high values of x.

Belites are of the β_1 type slightly modified. 2 hour plateau at the same temperature increases the modification of the crystalline cell when SO_3 is introduced as $CaSO_4$. Slow cooling accentuates the instability in a manner similar to that of the belites Ca_2 M_x Si_{1-x} $O_{4-x/2}$

The same is true for the K_2O belites all of which have the form β_1, and which seem to correspond to the composition formula $Ca_{2-x}K_xSiO_{4-x/2}$.

The solubility limit $x = 8 \cdot 10^{-2}$ was deduced from

***This temperature has been chosen in order to avoid the risks of volatilization.

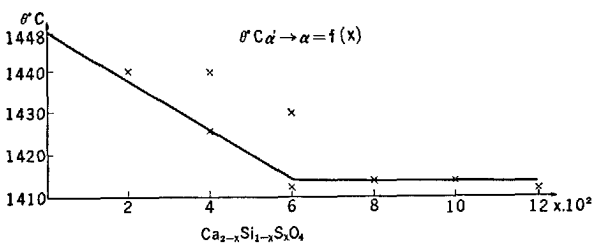

Fig. 4. *The two experimental points figuring on the graph for $x = 0.04$ and $x = 0.06$ results from the observation of a double peak.*

Note: *During the first heating cycle, an endothermic peak is noticed about 1360°C, which characterizes $(C_2S)_2CaSO_4$, increasing with x, and which disappears during the second heating.*

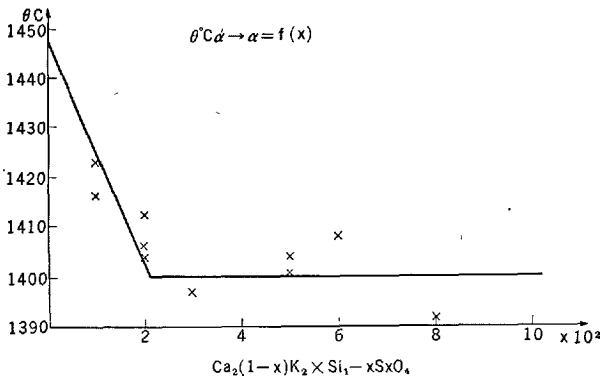

Fig. 5. *The different points which are represented for the same value of x have been obtained with several experiments and distinct synthesis.*

the D.T.A. (Fig. 6) during the second heating cycle as precedently on products heated for 3 hours at 1180°C,* although the peak $\alpha'_H \rightleftarrows \alpha$ was very flat. For $0.07 < x < 0.12$, a temporary phase—giving at approximately 1250°C endothermic peak which increases in size with x—appears during the course of the first heating.

Moreover, with $K_2CO_3 \cdot 23\ CaCO_3 \cdot 12\ SiO_2$ heated at 950°C this effect is observed:

The result of the heating at 950°C gives an X-rays spectrum which corresponds to an imperfectly crystallized α' configuration. After a 3 hour plateau at 1180°C the X-rays spectrum resembles that of $Ca_{1.88}\ K_{0.12}\ SiO_{3.94}$ where one perceives β C_2S and some supplementary equidistances in the neighbourhood of 2.705 Å and 1.99 Å.

The diverse synthesis expressible by the formula $Ca_{2-x}K_xSiO_{4-x/2}$ brought to a temperature of 1180°C for 3 hours contain percentages of γ C_2S which decrease when x increases. The reaction not yet being complete it is possible to detect CaO and cristobalite.

Heating at 1450°C for 10 minutes followed by

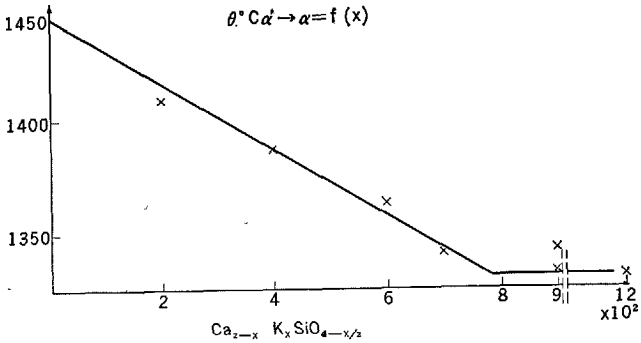

Fig. 6. *Two synthesis have been made for $x = 0.09$.*

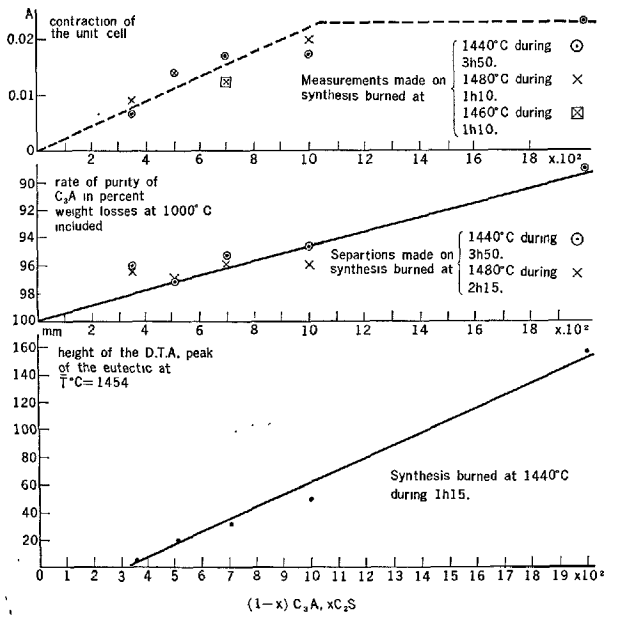

Fig. 7. *The spectra of powder containing silicium as an internal standard of reference were obtained with Guinier de Wolff's focalisation chamber equipped with a monochromator. The contraction of the crystalline unit cell was determined by applying the statistical method to approximately 35 reticular distances, which were calculated after being corrected by comparison with the silicium, and whoss bragg angles are located in the domain of achromatization $\alpha_1\alpha_2$ of Kα Cu. (C.V.% = 18)*

Note: *A broadening of the lines is observed when x rises. Blaine fineness of SiO_2 used for the synthesis: 12000 cm^2g^{-1} when $x = 0.1$, it seems that the intensity of the lines 440 and 008 is about 10%, lower than those observed with C_3A.*

intense quenching leads to β_1 belites and stabilizes an α' form for $x \geq 0.07$.

These observations, as N. F. Fedorov and E. R. Brodkina have already demonstrated, therefore seem to contradict the accepted fact that the formula $KC_{23}S_{12}$ represents K_2O belite (14).

Finally, the study of the process of inserting Si

into C_3A which we are continuing to study and which is included in the framework of the activities of C.E.T.I.C. (14) concerning the diffractometric measurement of this phase was based on the publication of A. E. Moore (15).

Considering the movement of the figurative point of the Rankin diagram along the C_3A–C_2S line, experience shows that the saturation corresponding to a contraction of the crystalline cell of 0.02 Å is obtained for 0.1 C_2S–0.9 C_3A with a purity rate of 95 per cent determined by the salicylic acid method of S. Takashima (16) (Fig. 7 groups all the observations).

References

1. J. Grzymek, "Influences on the formation of the alite in the clinker of portland cement" (in German). Silikattechnik 28–1–6 1959.
2. W. L de Keyser, "Studies on the solid state reactions between: SiO_2, Al_2O_3, MgO, CaO, Fe_2O_3, ZrO_2." Proceedings of the Eight Conference on the Silicate Industry Akademiai Kiado—Budapest 1966.
3. M. M. Sichov, Problem of admixtures" (Present symposium).
4. J. Forest, "Study of local encrustation in rotary kilns for cement and belite" (in french) Silicates Industriels No. 11. 373–384 November 1967 No. 12. 427–441 Décember 1967.
5. R. Kondo and K. Yoshida, "Miscibilities of special elements in tricalcium, silicate and alite and the hydratation." Properties of resulted solid solutions (present symposium).
6. J. Forest, "Contribution to the study of some rings" (in french) Technical Publication No. 173 of the C.E.R.I.L.H.
7. V. I. Korneev and E. B. Bygalina, "Thermal stabilization of β C_2S" (present symposium).
8. E. Demoulian, "Coatings in the rotary kilns in the wet process" (in French) Colloquy 1967 upon the problems of fabrication organized by the C.E.R.I.L.H.
9. P. Longuet, "The use of thermogravimetric measurements in cement chemistry" (present symposium).
10. J. Forest Research on the clodding of some cements (in French) R.M.C. 557 35–41 Février 1962.
11. H. Lafuma, "Cement—scientific, technical, economic problems" (in French) C.E.R.I.L.H. Information Note No. 17 (1961).
12. M. Regourd, M. Bigare, J. Forest and A. Guinier, "Synthesis and crystallographic investigation of some belites" (present symposium).
13. N. R. Fedorov and E. R. Brodkina, "Solid solutions in the system 2 $CaO \cdot SiO_2$–$K_2O \cdot CaO$–SiO_2" (in Russian) Neorganicheskie materialy 1966 Vol II No. 47–45–8.
14. C.E.T.I.C. Committee of Technical studies of the Cement Industry.
    Private organism grouping members of following cement societies. C.B.R. (Cimenteries et Briqueteries Réunies) (Belgium) ENCI (Eerste Nederlandsche Cement Industrie) (Holland) Holder-Bank (Cement Fabrik Holderbank) (Swiss) Italcementi (Fabbriche riunite cemento) (Italy) Lafarge (France) Ciments Luxe Bourgeois (Luxembourg) Ciments D'Ob-ourg (Belgium) Poliet et Chausson (France).
15. A. E. Moore, "Tricalcium aluminate and related phases in portland cement" Mag. of Concrete Research 18–55–64 June 1966.
16. S. Takashima "Systematic dissolution of calcium silicate in commercial portland cement by organic acid solution", Semento Gijutsu Nenpo, XII, 12–13 (1958).

Oral Discussion

Theodor Hahn, W. Eysel, P. Brenner and Eduard Woermann

Structures of α'-and α-Ca_2SiO_4

At this symposium, Regourd et al. (1) reported the existence of two α'–Ca_2SiO_4 forms: α'_H and α'_L (transformation temperature 1160°C). The high-form is *isotypic*, the low-form *homeotypic* to low-K_2SO_4. The structure of α'_L represents a small deformation of the α'_H structure, involving doubling of *a* and *b*. This is clearly evident from the structure determination of Suzuki and Yamaguchi (2). The space group of α'_H is Pmcn. For α'_L, however, it is not yet certain whether all the space groups listed in Table 1 actually occur (for instance in different solid solutions) but in all of these space groups structures homeotypic to low-K_2SO_4 may be attained.

For the high-temperature α-form only little data exist: On the basis of crystal-chemical considerations and by comparison of powder patterns. Bredig (5) suggested that this modification is trigonal and isotypic to high-K_2SO_4 (space group $P\bar{3}ml$). This result is supported by single crystal studies by Douglas (3).

Recent single crystal investigations, however, indicate that the symmetry of α-Ca_2SiO_4 and α-Ca_2GeO_4 is not trigonal but hexagonal (Table 2): For all three crystals the Laue symmetry 6/mm was clearly established. For two crystals a *c*-glide was found. Packing considerations exclude a mirror plane perpendicular to the six-fold axis. Therefore, of the three possible space groups, $P\bar{6}2c$, $P6_3/mmc$ and $P6_3mc$, the first two can be rejected and the last one appears to be the most probable space group

Table 1. *Lattice constants and space groups of* α'_L *and* α'_H-Ca_2SiO_4

Author	Type	a[Å]	b[Å]	c[Å]	Space group	Temperature of pattern	Material
Regourd et al. (1)	α'_L	11.184	18.952	6.837	Pmcn or Pbcn or Pmnn	1000°C	Powder, pure Ca_2SiO_4
Douglas (3)	α'_L	11.08	18.55	6.76	Pmnn (?)	750°C	Powder, pure Ca_2SiO_4
"	α'_L	10.91	18.41	6.76	Pmnn	20°C	Single crystals, bredigite
Suzuki and Yamaguchi (2)	α'_L	11.07	18.80	6.85	$Cmc2_1$	20°C	Single crystals, stabilized with BaO
" " "	α'_L	11.02	18.69	6.83	$Cmc2_1$	20°C	Single crystals, stabilized with SrO
" " "	α'_L	10.96	18.43	6.86	$Cmc2_1$	20°C	Single crystals stabilized with B_2O_3
" " "	α'_L	Cell similar to stabilized crystals				1000°C	Powder, pure Ca_2SiO_4
Regourd et al. (1)	α'_H	5.593	9.535	6.860	Pmcn	1250°C	Powder, pure Ca_2SiO_4
Yamaguchi et al. (4)	α'_H	5.605	9.543	6.883	Pmcn	1300°C	Powder, pure Ca_2SiO_4

Table 2. *Crystallographic data of single crystals of* α-Ca_2SiO_4

Material (Stabilizer)	a[Å]	c[Å]	Extinctions	Probable space group
α-Ca_2SiO_4(6) (V_2O_5)	5.45	3 × 7.20	hhl with l odd	$P6_3mc$
α-Ca_2GeO_4(7) (Al_2O_3)	5.52	7.16	hhl with l odd	$P6_3mc$
α-Ca_2SiO_4(8) ($Na_4P_2O_7$)	5.47	7.23	None	(P6mm)

of hexagonal α-Ca_2SiO_4.*

If the new results are correct, the structures of α-Ca_2SiO_4 and α-Ca_2GeO_4 can not be isomorphous to high-K_2SO_4: In the hexagonal structure the apices of all tetrahedra are aligned in one direction (along the *c*-axis) while in the trigonal structure they are alternately oriented. Regardless whether the symmetry of α-Ca_2SiO_4 is hexagonal or trigonal, the transformation α'_H-α involves a structural rearrangement: Half of the tetrahedra must rotate but in each case different tetrahedra are involved.

Isotypism of Na_3BeF_5, Ca_3SiO_5 and Ca_3GeO_5

Structure and polymorphism of Ca_3SiO_5 and Ca_3GeO_5 are very similar (9). One of the present authors (10) showed that Na_3BeF_5 is the fluoride "model" of Ca_3SiO_5. Recent investigations revealed that at room temperature Na_3BeF_5 occurs in a triclinic modification, which is very similar to modification T_I of Ca_3SiO_5 and Ca_3GeO_5 (Table 3).

In this table the doubling of the *a*- and *b*-axes, as found for Ca_3SiO_5 (11), has been neglected. The close analogy of all three compounds is apparent. As expected, the fluoride has a smaller cell. We have indications that for Na_3BeF_5 also a monoclinic modification exists.

*Even if twinning is assumed, a hexagonal space group with a *c*-glide can not be derived from the trigonal space group $P\bar{3}ml$.

Table 3. *Lattice parameters of* Ca_3SiO_5, Ca_3GeO_5 *and* Na_3BeF_5 (*Modification* T_I)

	a[Å]	b[Å]	c[Å]	α[°]	β[°]	γ[°]
Ca_3SiO_5(11)	12.199	7.106	25.103	89.91	89.69	89.69
Ca_3GeO_5(9)	12.429	7.237	25.467	89.84	89.76	89.78
Na_3BeF_5	11.827	6.908	24.481	89.81	89.93	89.64

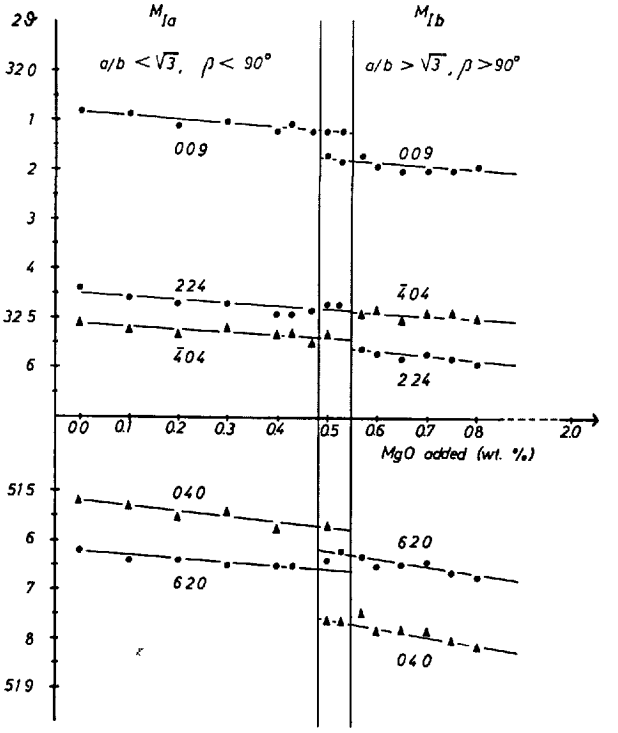

Fig. 1. *Variation of some characteristic 2θ-values of* Ca_3SiO_5 *solid solutions. Constant concentrations of* Al^{3+} *and* Fe^{3+} *(0.9%*Al_2O_3 *+ 0.5%*Fe_2O_3*) and variable amounts of* MgO.

Modification M_I of Ca_3SiO_5

The monoclinic form M_I of Ca_3SiO_5 occurs in two types: Pure C_3S, between 980 and 990°C, has a mono-

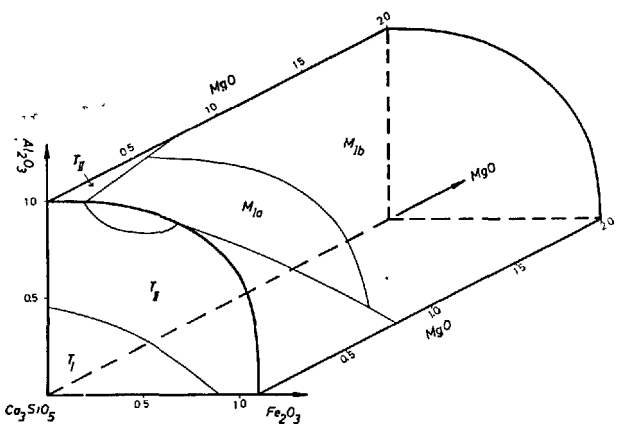

Fig. 2. *Body of solid solutions of* Ca_3SiO_5 *with* MgO, Al_2O_3 *and* Fe_2O_3 *(weight %). The domains of the stabilized modifications* T_I, T_{II}, M_{Ia} *and* M_{Ib} *on the surface of this body are indicated by thin lines.*

clinic cell with $a/b < \sqrt{3}$ and $\beta < 90°$ (11). For solid solutions at room temperature, however, only $a/b > \sqrt{3}$ and $\beta > 90°$ have been reported thus far. We have recently found that *both* types can be stabilized by incorporation of $MgO + Al_2O_3 + Fe_2O_3$. In Fig. 1 characteristic 2θ-values are plotted. The difference between both types is evident.

Previously (11), it was assumed that the two types represent different metrices of the unit cell of M_I. The *discontinuous* change with composition (Fig. 1), however, suggests the existence of two distinct forms: M_{Ia} with $a/b < \sqrt{3}$, $\beta < 90°$ and M_{Ib} with $a/b > \sqrt{3}$, $\beta > 90°$.

The composition region of the monoclinic Ca_3SiO_5 solid solutions with MgO, Al_2O_3 and Fe_2O_3 is subdivided into domains of M_{Ia} and M_{Ib} as shown in Fig. 2.

Further details will be reported in Zement-Kalk-Gips.

References

1. M. Regourd, M. Bigaré, J. Forest and A. Guinier, "Synthesis and crystallographic investigation of some belites", This Symposium, Paper 1–10.
2. K. Suzuki and G. Yamaguchi, "A structural study on α'-Ca_2SiO_4", This Symposium, Paper 1-92.
3. A.M.B. Douglas, "X-ray investigations of bredigite", Min. Mag. **29**, 875–84 (1952).
4. G. Yamaguchi, Y. Ono, S. Sawamura and Y. Soda, "Differential thermal analysis and high temperature powder X-ray diffraction of $2CaO \cdot SiO_2$", (in Japanese, English abstract) J. Ceram. Assoc. Japan **71**, 9–12 (1963).
5. M. A. Bredig, "Polymorphism of calcium orthosilicate", J. Americ. Ceram. Soc. **71**, 188–192 (1950).
6. H. Saalfeld, "Contributions to the crystal chemistry of dicalcium silicate, Ca_2SiO_4" (in German) Ber. Deutsche Keram. Ges. **44**, 279–283 (1967) and personal communication (1968).
7. W. Eysel and Th. Hahn, "Polymorphism and solid solutions of germanates and silicates. II. Ca_2GeO_4 and Ca_2SiO_4", In preparation.
8. M. Siegert, "Contribution to the structure of dicalcium silicate" (in German), Diploma thesis, Institut für Gesteinshüttenkunde, Technische Hochschule Aachen (1968).
9. W. Eysel and Th. Hahn, "Polymorphism and solid solution of germanates and silicates. I. Ca_3GeO_5 and Ca_3SiO_5", In press.
10. Th. Hahn, "Model relations between silicates and fluoberyllates" (in German) Neues Jahrb. Mineral. Abh. **86**, 1–65 (1953).
11. M. Bigaré, A. Guinier, C. Mazières, M. Regourd, N. Yannaquis, W. Eysel, Th. Hahn and E. Woermann, "Polymorphism of tricalcium silicate and its solid solutions," J. Amer. Ceram. Soc. **50**, 609–619 (1967).

Oral Discussion

Kinzo Tomita

Guinier and Regourd show that α'-C_2S hardly reacts to water, that is, it may have no hydraulic property.

Ono, Kawamura and Soda (1), however, have reported on the α'-C_2S stabilization by MgO and K_2O, and Suzuki, Morita and Sugiyama (2) also have reported on the α'-C_2S stabilization by BaO, SrO and other additives. Both of these have shown that these α'-C_2S have a higher hydraulic strength than β-C_2S.

References

1. Y. Ono, S. Kawamura and Y. Soda, Microscopic observations of alite and belite and hydraulic strength of cement, Tokyo, Supplementary Paper No. I–79 (1968).
2. K. Suzuki, M. Morita and H. Sugiyama, α-Ca_2SiO_4 stabilized by Ba, Sr and Mg. Semento Gijutsu Nenpo XXI, 43 (1967).

Oral Discussion

Yoshio Ono

In your study, M-II phase of alite is monoclinic after space group, but the three angles between the

orthohexagonal crystal axes are kept to be 90°, against variation of temperature and solid solution, and the inversion from R to M-II takes place continuously without detective heat change.

On our microscopic study, alite in portland cement clinker seems optically as if orthorhombic, e.g. $2V = 20° - 60°$ and X II c (3-fold axis of trigonal outer shape). The optical axial angle and birefringence are varied widely according as the variation of minute component and burning condition, but the parallelism between X and c is kept rigidly against the above variations.

I suppose that there is substantial relationship between your X-ray crystallographic result and my optical observation. Though these phenomena can not be explained by the symmetry of space group, these must not be accidental on view point of phenomenon.

I should be very much obliged if you would give me your opinion.

Oral Discussion

Hans E. Schmiete, W. Krönert and K. Deckert

According to our investigations the crystal chemical stabilization of C_2S is determined by three factors:

1. by the size of the stabilizing impurity ions or ion complexes
2. by the amount of stabilizer added
3. by the presence of a non-stabilizing substance, which may replace the stabilizer within certain limits

The Size of the Stabilizing Ion

According to the hypothesis of A. Dietzel and L. Tscheischwili (1), stability can be achieved in two different ways.

a) The Ca^{2+}-ions are replaced by a corresponding amount of larger cations, or
b) a part of $(SiO_4)^{4-}$-groups, is replaced by a smaller anion complex.

Our results for oxides of chrome and manganese can also be explained by this theory. We found in these experiments a relationship between the partial pressure of oxygen present and the stabilizing effect of C_2S, as follows:

At a pressure of ≥ 75 Torr O_2 for chrome and ≥ 150 Torr O_2 for manganese, the impurity ions will oxydize. Cr^{6+} with a radius of 0, 35 Å and M^{6+} with ~ 0.4 Å radius exist, so that the specified conditions for stability are fulfilled.

Quantity of Stabilizing Ion

With regard to the added stabilizers, H. Funk (2) found out, that the substances which stabilize α–C_2S as well as α'–C_2S, also supply β–C_2S when added in very small quantities. This is made clear in the case of Na_3BO_3, in which the quantities of 200, 100, and 1 mol per 1000 mol C_2S clearly showed the X-ray results: α-, α'-and β-forms respectively.

The Interchangeability of Stabilizing Ion

By our experiments we are able to show that stabilizers could be exchanged partly by iron, manganese and magnesium silicates. This is evident from X-ray diffraction diagrams of C_2S with a constant quantity of 3 mol% Ba_2SiO_4 and with variable admixture of Mg_2SiO_4, shown in Fig. 1.

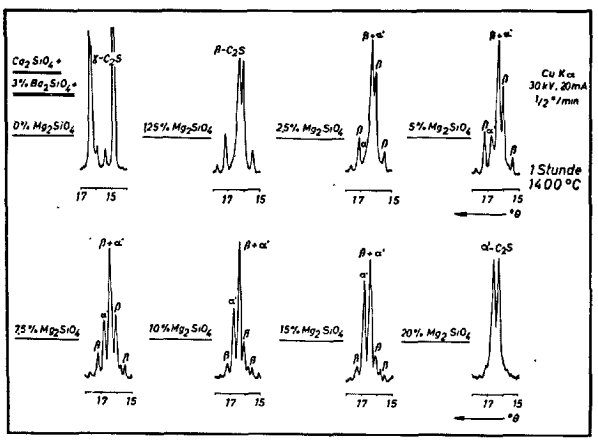

Fig. 1.

For the stability condition we propose the following hypothesis: According to the findings of M. Volmer (3), I. N. Stranski and co-workers (4, 5) on nucleation regarding the modifications of polymorphic transformation, there is below the transformation point for each temperature a critical nucleus size for the new phase. All the smaller nuclei return to the old phase, whilst all the larger nuclei grow and build up new modifications. As the rate of undercooling in-

creases the critical nucleus size decreases. The transformation of a sample into the new modification is more probable when cooled.

If one considers a substance stabilized by crystal chemical means, it can be deduced, that the nucleus growth will be interrupted by the stabilizing ions. But when these impurity ions are present in the sample in such quantities that no nucleus exceeds the critical size, than the old phase remains stable.

With this theory it is possible to explain the small amounts which are necessary for the stabilization in the case the change of phase is determined by spatial nuclei. Then by statistical division of the stabilizing ions, the substance is subdivided into small blocks whose corners are each occupied by an impurity ion. Because a stabilized ion belongs simultaneously to 8 adjoining blocks, it follows that one impurity ion is necessary for the stabilization of each block. But this would mean that at room temperature the amount of 0.1% for the prevention of β-γ-transformation of C_2S, would be required. So that a cube of C_2S of $10 \times 10 \times 10$ formula units could be stabilized by one stabilizing ion, and would correspond to a critical nucleus radius of ~ 15 Å.

According to the hypothesis of A. Dietzel and L. Tscheischwili (1), only those substances whose size allows them to fit well into the C_2S-lattice, act as stabilizers. Beside that certain substances, which because of their ion radii should not be structural effective, can replace the stabilizers within certain limits. This process may be explained by the higher degree of disorder, so that the incorporation of stabilizers into the C_2S-lattice is facilitated.

Because for α-C_2S as well as for α'-C_2S at room temperature the degree of supercooling correspondingly increases, a greater number of impurity ions is necessary for the stabilization of these modifications, compared with β-C_2S.

References

1. A. Dietzel and L. Tscheischwili: Ber. Deutsch. Keram. Ges. 30 (1953). 151–154.
2. H. Funk: Silikattechnik 6 (1955), 186–189.
3. M. Volmer: Kinetik der Phasenbildung. Verlag Th. Steinkopff, Dresden (1939).
4. R. Kaischew and I. N. Stranski: Z. phys. Chem. (B) 26 (1934), 317–326.
5. O. Knacke and I. N. Stranski: Ergebn. exakt. Naturwiss. 26 (1952). 383–427.

Authors' Closure

André Gunier and Micheline Regourd

Reply to J. Forest

Dr Forest's contribution establishes a link between the behaviour of the pure components and the reactions actually taking place during the clinkerisation of industrial products: synthesis of belites and alites have been carried out in presence of minor oxides MgO, Al_2O_3, TiO_2, K_2O and sulfates $CaSO_4$, K_2SO_4.

Another important and new result is the evaluation of the maximum content of CaO which can be introduced in βC_2S (0.5%): these additions of CaO cause an increase of the $\alpha'_H \rightarrow \alpha$ transition temperature. However one must note that the accuracy of the chemical analysis is of the order of 0.2%. Furthermore the state and location in the lattice of the excess Ca ions is not known. Perhaps CaO is simply dissolved in the lattice or its introduction is accompanied by imperfections like oxygen vacancies for instance.

Dr. Forest's reports that "the symmetry deduced from the X-ray spectrum is sometimes superior to that which the interpretation of the DTA thermogram furnishes". G. Yamaguchi, K. Shirasuka and T. Ota have shown that the monoclinic alite in the system C_3S–Al_2O_3–MgO is thermodynamically instable. During a slow heating, the monoclinic form inverts to the stable triclinic form. In agreement with these results, Th. Hahn, E. Woermann and W. Eysel have found that the M_I forms in the C_3S–MgO solid solutions, during heating, transforms first into T_{II} at about 700°C, the temperature being dependent on the amount of MgO. Further heating causes the usual endothermic transformation T_{II}–M_I at about 900°C.

Reply to Th. Hahn, W. Eysel. P. Brenner and E. Woermann

Phase transformation of $\alpha \rightarrow \alpha'$ Ca_2SiO_4

It seems difficult to characterize surely the nature of the $\alpha \rightarrow \alpha'_H$ C_2S transformation. Perhaps this transition is not purely displacive as indicated by the sharp and reversible DTA signal or the α C_2S structure is not trigonal as suggested by Bredig but hexagonal.

Stabilized crystals of α C_2S have an hexagonal structure, however the space groups are different. In the solid solutions, the nature and amount of the stabilizer, the burning and cooling of the sample can modify substantially the structure of α C_2S. Further

studies would be necessary.

Modification M_I of Ca_3SiO_5

The discontinuous change of the two C_3S monoclinic forms M_{Ia} and M_{Ib} in Al_2O_3, Fe_2O_3, MgO, C_3S solid solutions is very interesting.

We had also found two types of M_I modification in synthesized MgO-C_3S solid solutions: M_{Ia} for $C_3S + 1.25$ MgO and M_{Ib} for $C_3S + 2\%$MgO (we had called it inverted form). The last form is metastable: M_{Ia} is obtained, at room temperature, after 4 hours at 650°C.

Reply to K. Tomita

We thank Mr. K. Tomita for his contribution on hydrated $\alpha'C_2S$ strength.

In our paper, we had reported Dr. Nurse's results: $\alpha'C_2S$ stabilized by P_2O_5 hardly reacts to water. However, another stabilizers such as MgO, K_2O, BaO, SrO ... can modify the C_2S lattice and give better hydraulic properties.

Reply to Y. Ono

The M_{II} form of pure C_3S is monoclinic with $\beta = 90°$. The lattice parameters have been obtained accurately by indexing powder patterns on a pseudo-hexagonal lattice.

The shape of the crystal lattice is orthorhombic. Dr. Ono's microscopic observations show the parallelism between the optical axis X and the axis $\vec{c}$. However, the stacking of the structural groups does not permit the orthorhombic symmetry: there is no orthorhombic subgroup of the R 3 m trigonal space-group and the $R \rightarrow M_{II}$ transformation is small and continuous. However, we have not exactly proved this result. Only Laue and oscillation photographs of a single crystal would distinguish a pseudo-orthorhombic form from a true orthorhombic structure.

Another examples of monoclinic structures with $\beta = 90°$ exist. For instance, the W V_2O_7 crystals are monoclinic (1) with the parameters $a = 12.20$, $b = 3.72$, $c = 3.95$ Å, $\beta = 90°$.

References

1. S. Mondet A. Rimsky, J. Borene, W. Freundlich. "Crystal structure of W V_2O_7 phase" (in french). C. R. Acad. Sci., Paris, Série C, *266*, 1145–1148, April 1968.

Reply to H. E. Schwiete, W. Krönert and K. Decket

According to the working hypothesis of A. Dietzel and L. Tscheischwili on the size of the stabilizing ions, H. E. Schwiete, W. Krönert and K. Deckert have given two examples showing that, in the C_2S lattice, the Ca^{2+} ions (0.99 Å) may be replaced only by a respective amount of bigger cations or a part of $(SiO_4)^{4-}$ groups (Si = 0.39 Å) is replaced by a smaller anion complex.

But our own experiments do not verify this criteria. J. Forest (1) has been able to synthesize some belites $Ca_2\ M_x\ Si_{1-x}\ O_{4-x/2}$ in which. M = Al^{3+} (0.50 Å) and Fe^{3+} (0.64 Å) are out of the precedent limits, however the β form is obtained.

References

1. M. Regourd, M. Bigaré, J. Forest and A. Guinier. "Synthesis and crystallographic investigations of some belites". This Symposium, Supplementary Paper 1–10.

Closure

The Supplementary Papers and Discussions permit to clarify some problems and to propose further studies on the structures of portland cement minerals.

C_3S The results of C_3S studies are the most complete. The list of the transition points and the various phases is definitively established. The identification of any alite form is possible and sure with high resolution X-ray diffraction and DTA. However, the DTA diagrams must be interpreted with care in the case of inverted monoclinic forms M_{Ib} and M_{IIb} which are decomposed above 600°C. Some alites, similar to those found in clinkers have been synthesized: they are solid solutions with Al_2O_3, Fe_2O_3, MgO, Cr_2O_3, TiO_2, MnO_2. It shall be possible to classify all the alites of clinker with the combined use of electron probe microanalysis which identifies the foreign ions and X-ray diffraction which characterizes the crystalline structure.

The six forms of C_3S have very close crystal structures and present a similar reactivity. Only the early strength can be increased in presence of some foreign ions as Cr_2O_3 but these effect does not persist.

C_2S A new transformation $\alpha'_L \overset{1170°C}{\rightleftarrows} \alpha'_H$ C_2S has been detected by DTA and X-ray diffraction. The α'_L form is a superstructure of the orthorhombic α'_H structure (a and b doubled).

The structures of the α' and α forms are not well known. Stabilized crystals of these forms have different space groups. Further studies would be necessary about the following topics:

—the nature of the $\alpha \rightarrow \alpha'_H$ transition

—the space group of the α and α'_L forms

—the formation of α' and α belites

—the introduction of CaO in βC_2S

The five forms of C_2S have different structures and present different hydraulic properties. The minor oxides, present in the clinker, can modify the crystal lattice of C_2S and affect the cementive properties of belites.

C_3A The structure of C_3A is not known. In the cubic lattice, the aluminium/oxygen coordination is probably all tetrahedral. A new paper (1) on isomorphous replacement in tricalcium aluminate indicates that the aluminium ions are not in AlO_6 octahedra and the Ca^{2+} ions occupy two types of reticular sites.

In C_3A, it is possible to replace the group Ca–Al by Na–Si, K–Si. Orthorhombic C_3A solid solutions with alkalis would be more reactive at early ages than cubic forms.

C_4AF Solid solutions of $C_2(A_pF_{1-p})$ with MgO, Cr_2O_3, Mn_2O_3 have been synthesized. Microcrystalline ferrite phase has been observed in industrial clinkers by X-ray diffraction (broad powder lines); the Mössbauer spectra (2) of Fe^{57} of the ferrite present in portland cement can be understood assuming that the volumes of some of the ferrite particles are small enough to show superparamagnetism instead ferromagnetism.

References

1. P. Tarte "Structural investigations of cement minerals. II isomorphous replacement phenomena in tricalcium aluminate" (in French) Silicates Industriels, XXXIII, No. 11, 333–339 (1968).
2. F. Wittmann "Mesures of the Mössbauer effect in the system 2 CaO $(Al_2O_3)_x(Fe_2O_3)_{1-x}$" (in German) Silicates Industriels, 32, 393–94, Nov 1967.

Supplementary Paper I-10 Synthesis and Cyrstallographic Investigation of Some Belites

Micheline Regourd,* Michel Bigaré,* Jean Forest and André Guinier*****

Belites in clinker are solid solutions of dicalcium silicate. Their X-ray diagrams are, usually, similar to that of the βC_2S form, more rarely to that of the $\alpha' C_2S$ forms.

Dicalcium Silicate

The structure of the five C_2S forms is described in the Principal Paper entitled "Structure of Portland Cement Minerals" (1).

At high temperature ($t > 1420°C$) the αC_2S form is hexagonal. We have calculated the lattice constants from powder pattern: $a = 5.526$, $c = 7.307$ Å at 1500°C. These results agree with those of Yamaguchi, Ono, Kawamura and Soda (2): $a = 5.527$, $c = 7.311$ Å, space group $P\bar{3}m1$.

With decreasing temperature, the α variety gives the α' form. By X-rays and D.T.A., Niesel and Thormann (3) have proved the existence of two α' forms: α'_H and α'_L whose stability domains are respectively 1420–1165°C and 1165–650°C. We have confirmed the existence of these two $\alpha' C_2S$ forms.

At 1250°C the parameters of the orthorhombic $\alpha'_H C_2S$ unit cell are $a = 5.593$, $b = 9.535$, $c = 6.860$ Å, space group Pmcn (Table 1).

Yamaguchi, Ono, Kawamura and Soda (2) have found the same unit cell $a = 6.883$, $b = 5.606$, $c = 9.543$ Å, space group Pnma at 1300°C.

We have determined the lattice of the α'_L form, at 1000°C.

The orthorhombic parameters are $a = 11.184$, $b = 18.952$, $c = 6.837$ Å, space group Pmcn (Table 2).

Table 1. $\alpha'_H C_2S$ (1250°C)

hkl	I/I_1	$d_{observed}$	$d_{calculated}$
011	3	5.574	5.569
110	1	4.830	4.824
020	5	4.766	4.767
111	9	3.945	3.946
021	9	3.916	3.915
002	19	3.430	3.430
012	8	3.226	3.227
121	25	3.209	3.207
102	37	2.924	2.924
031	22	2.8842	2.8837
200 112	100	2.7960	2.7964 2.7954
022	20	2.7842	2.7842
130	90	2.7632	2.7632
131	3	2.5632	2.5631
211	3	2.4988	2.4990
122	4	2.4927	2.4925
220	21	2.4128	2.4121
032	36	2.3311	2.3313
221	28	2.2755	2.2759
041	23	2.2513	2.2516
013	53	2.2226	2.2230
202	7	2.1674	2.1674
212	12	2.1136	2.1135
141	28	2.0087	2.0887
113	7	2.0657	2.0663
023	15	2.0613	2.0617
231	18	2.0078	2.0075
222	25	1.9734	1.9730
042	11	1.9572	1.9574
033	2	1.8565	1.8562
142	3	1.8479	1.8475
051	7	1.8376	1.8373
150	4	1.8043	1.8049
232	20	1.7911	1.7906
213	15	1.7407	1.7404
004	7	1.7148	1.7150
014	4	1.6876	1.6879
321	3	1.6830	1.6832
052	6	1.6670	1.6667
302	7	1.6387	1.6380
114 312	14	1.6151	1.6159 1.6143
330	15	1.6091	1.6080
242	5	1.6041	1.6036
152	3	1.5910	1.5913
143	11	1.5827	1.5827
124	7	1.5501	1.5505
251	6	1.5357	1.5355
034	4	1.5094	1.5093
161	2	1.4926	1.4920
204	1	1.4629	1.4620
134	2	1.4572	1.4571
214	5	1.4453	1.4451

* C.E.R.I.L.H., Paris, France
** Etablissements Poliet et Chausson, Paris, France
***Laboratoire de Physique des Solides, Faculté des Sciences Unversité de Paris, Orsay, France

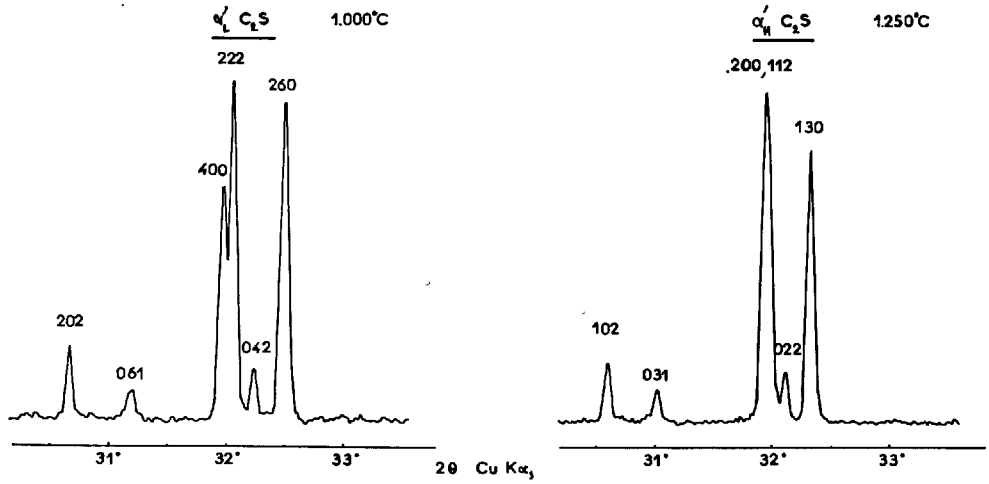

Fig. 1. *Microdensitometer tracings of α'_L- and α'_H- C_2S, Guinier camera pat.*

Table 2 α'_LC_2S (1000°C)

hkl	I/I_1	$d_{observed}$	$d_{calculated}$
021	1	5.542	5.545
220	4	4.826	4.816
040	1	4.736	4.738
221	5	3.938	3.937
041	6	3.895	3.894
231	2	3.565	3.571
002	12	3.420	3.419
022	5	3.217	3.216
241	17	3.195	3.196
122	2	3.088	3.090
202	24	2.918	2.917
061	13	2.8672	2.8675
400	70	2.7969	2.7961
222	100	2.7881	2.7878
042	18	2.7730	2.7724
260	83	2.7496	2.7503
341	3	2.6993	2.6931
350	2	2.6583	2.6579
261	1	2.5514	2.5516
421	2	2.4953	2.4966
242	2	2.4837	2.4839
440	12	2.4076	2.4081
062	21	2.3202	2.3200
441 / 162	16	2.2714	2.2714 / 2.2717
081	12	2.2375	2.2385
023	32	2.2157	2.2160
123	2	2.1764	2.1737
402	4	2.1643	2.1644
422 / 530	7	2.1095	2.1101 / 2.1086
281	15	2.0774	2.0782
043	6	2.0531	2.0539
461 / 233	9	2.0011	2.0019 / 2.0018
442	28	1,9683	1.9687
082	6	1.9463	1.9472
063	1	1.8488	1.8483
282	4	1.8380	1.8389
0.10.1	3	1.8259	1.8264
462	12	1.7848	1.7854
423	8	1.7368	1.7367
004	3	1.7097	1.7094
641	3	1.6814	1.6814
363 / 443	4	1.6566	1.6559 / 1.6553
204	4	1.6354	1.6347
622	6	1.6119	1.6127
660	10	1.6046	1.6054
482	3	1.5968	1.5979
523 / 283	8	1.5751	1.5743 / 1.5759
244	4	1.5450	1.5453
4.10.1	3	1.5280	1.5291
652	4	1.5024	1.5025
2.12.1	2	1.4830	1.4837
0.10.3	1	1.4527	1.4572
264	3	1.4512	1.4518
424	4	1.4408	1.4415
681	2	1.4318	1.4324

The doubling of a and b parameters is required by the presence of five weak lines which cannot be indexed with a cell similar to α'_H cell ($d_{231} = 3.565$ Å, $d_{122} = 3.088$ Å, $d_{341} = 2.699$ Å, $d_{350} = 2.658$ Å, $d_{123} = 2.176$ Å).

A.M.B. Douglas (4) using a natural mineral, bredigite $Ca_{1.59}$ $Ba_{0.08}$ $Mg_{0.31}$ $Mn_{0.09}$ SiO_4 usually considered identical with $\alpha'C_2S$ has found an analogous cell a = 10.91, b = 19.41, c = 6.76 Å space group Pmnn and on the other hand she indexed Trömel's (5) powder data taken at 750°C with an orthorhombic cell of parameters a = 11.08, b = 18.55, c = 6.76 Å.

The $\alpha'_H \rightarrow \alpha'_L$ transition corresponds therefore to a superstructure and beside to a small change of parameters.

The Fig. 1 shows the microdensitometer tracings of α'_H and α'_L focussing film patterns. At 1250°C, the calculated components of the doublet 220, 112 being only separated by 1×10^{-3} Å (Table 1) are not resolved on the powder pattern but it is obvious that the 200 line is broader than the single line 130.

The transition $\alpha'_L \rightarrow \beta$ takes place at 650°C. The β structure is monoclinic (6). The new parameters of pure β C_2S, calculated from powder Guinier camera pattern, at room temperature, are a = 5.506, b = 6.749, c = 9.304 Å, $\beta = 94.62°$, space group $P\,2_{1/n}$.

Yannaquis and Guinier (7) have suggested that the βC_2S, B_2O_3 solid solutions correspond to a partial substitution of $(SiO_4)^{4-}$ by $(BO_4)^{5-}$ groups and to the formation of tetrahedric vacancies in order to maintain electroneutrality in the lattice by the elimination of Si^{4+} ions (probably in the form of silica). The insertion of supplementary ions seems difficult in a lattice as compact as that of βC_2S. Sasaki (8), Schlaudt and Roy (9) have shown that β form is not stabilized in Ca substituted preparations.

Forest (10) has been able to prepare some belites similar to those found in clinker. These belites are oxygen-defective solid solutions with Si substituted, with general formula $Ca_2M_xSi_{1-x}O_{4-x/2}$. In the C_2S crystal lattice, the exchange reaction $2Si^{4+} + O^{2-} \rightarrow 2M^{3+}$ forms the solid solutions at temperatures higher than $\alpha'_H \rightarrow \alpha$ inversion.

The limits of solubility of Al, Fe, B in C_2S have been determined by D.T.A., through the decrease of the $\alpha'_H \rightarrow \alpha$ transition temperature (Fig. 2). The microscopic examination shows that the belite generally bistriated by the quenching contains a very small amount of interstitial phase located at the grain boundaries (Fig. 3 (a)).

Belite is apparently a non-equilibrium phase. In a belite containing alumina, synthesized at 1550°C, a very rapid quenching from 1550°C stabilizes a large part of α' type form, quenching from 1450° gives a mixture of α' and β forms and from 1000°C the β form with C_3A (Fig. 4). Furthermore, the microscopic examination of slowly cooled belites reveals the presence of solutes within the β grain which is spotty (Fig. 3 (b)).

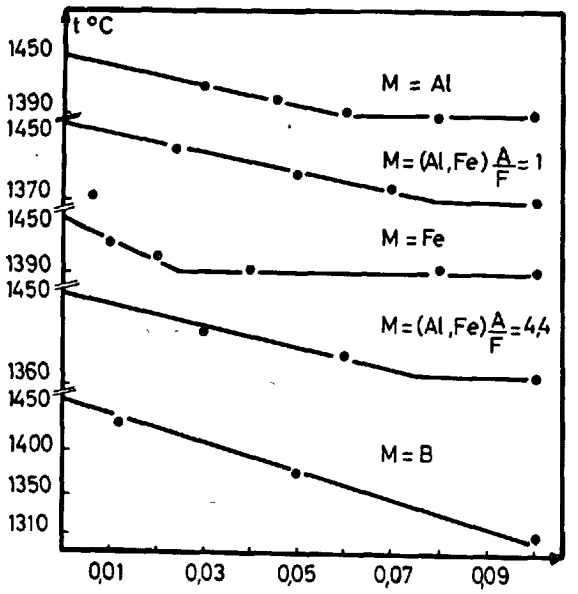

Fig. 2. *Limits of solubility of Al, Fe, B in* C_2S *through the decrease of the* $\alpha'_H \rightarrow \alpha$ *transition temperature.*

(*a*)

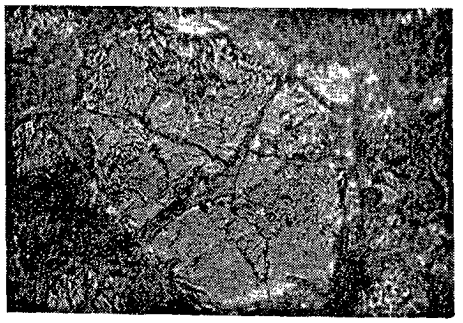

(*b*)

Fig. 3. *Belite* $Ca_2Al_{0.03}Fe_{0.03}Si_{0.94}O_{3.97}$ *(3h at 1450°C, 3 grindings).*
(*a*) *quenched from 1450°C: striated.*
(*b*) *slowly cooled from 1450°C: partly spotty.*

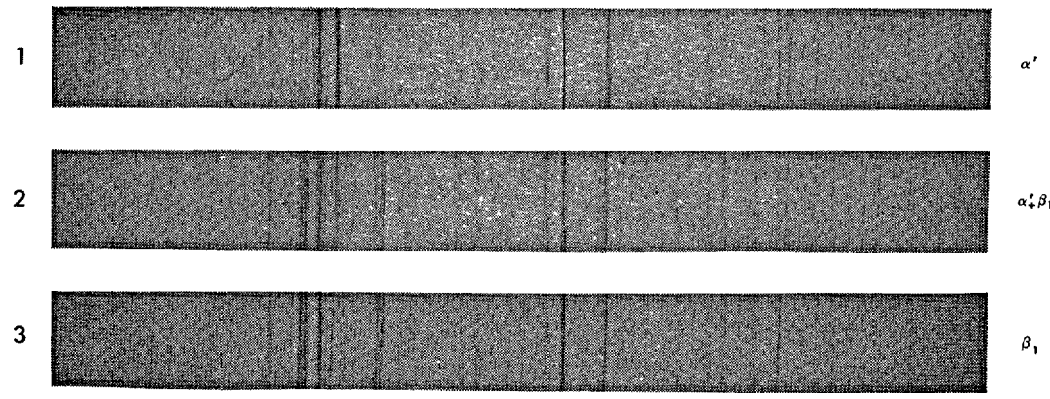

Fig. 4. *Belite* $Ca_2Al_{0.10}Si_{0.90}O_{3.95}$ *synthesized at 1550°C.*
1. rapid quenched from 1550°C: large part of α form
2. quenched from 1450°C: β + α' forms
3. quenched from 1000°C: β form + C_3A

Crystallographic investigation of some β Belites

Powder patterns of four β belites $Ca_2M_xSi_{1-x}O_{4-x/2}$ in which M = B, Al = Fe, and the C_2S–C_2F mixture are reproduced in Fig. 5. The comparison with the βC_2S diagram shows the displacement of some lines,

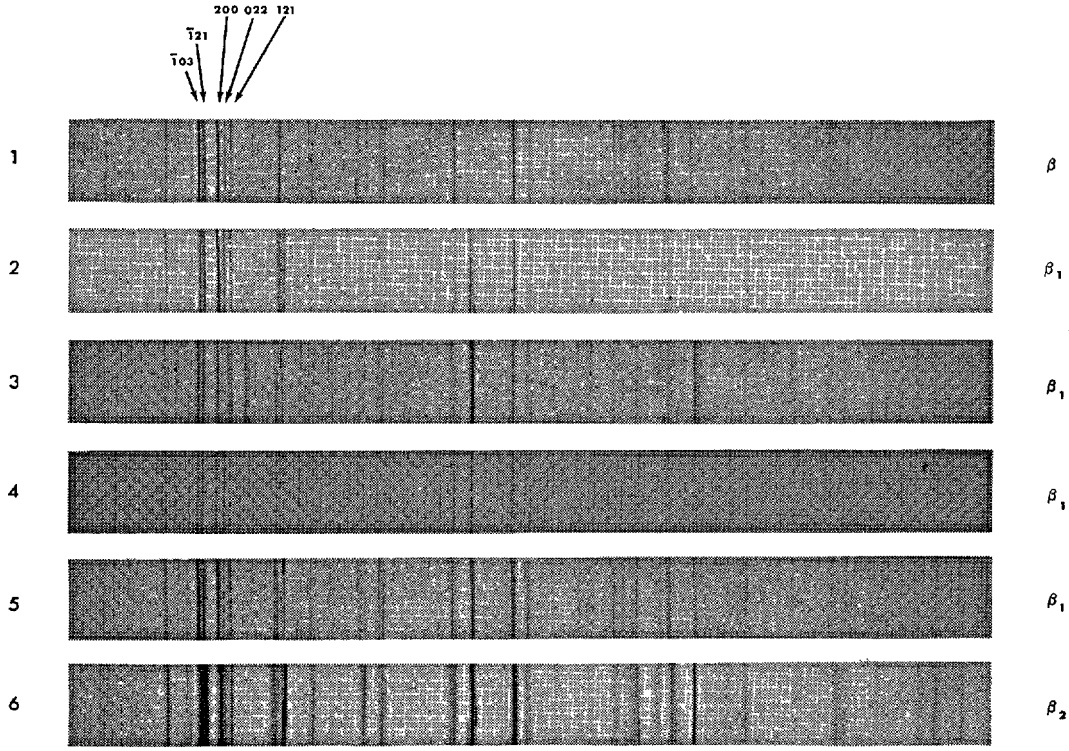

Fig. 5. *X-ray diagrams of some β belites (Guinier camera, Cu K* α_1 *radiation).*
1. βCa_2SiO_4
2. $Ca_2B_{0.01}Si_{0.99}O_{3.995}$
3. Ca_2SiO_4(70%) + Ca_2FeO_5(*30%*) (*presence of* C_2F)
4. $Ca_2Fe_{0.012}Al_{0.012}Si_{0.976}O_{3.988}$ (*prerence of* γC_2S)
5. $Ca_2Fe_{0.035}Al_{0.035}Si_{0.930}O_{3.965}$
6. $Ca_2Fe_{0.050}Al_{0.050}Si_{0.900}O_{3.950}$

in particular $\bar{1}03$, $\bar{1}21$ and 200, 022, 121.

Belite is a product of imperfect crystallisation. With increasing proportion of foreign ions, reflections are broader and broader (see in Fig. 5, M = Al, Fe, in 4, 5, 6).

The lattice constants of five β belites have been calculated, the results being collected in Table 3. The βC_2S lattice is slightly altered, the symmetry remaining monoclinic. We have called β_1 the type of belites in which the βC_2S lattice is not significantly modified and β_2 a belite such as $Ca_2Fe_{0.05}Al_{0.05}Si_{0.90}O_{3.95}$ in which the powder pattern presents broad lines and a modification more important of the triplet 200, 022, 121, corresponding to a larger variation of c and β parameters.

Table 3. *Lattice constants of some β belites*

Type of belite	Constitution Formula	$a_{(Å)}$	$b_{(Å)}$	$c_{(Å)}$	$\beta_{(°)}$
	$\beta\ Ca_2SiO_4$	5.506	6.749	9.304	94.62
β_1	$Ca_2Al_{0.10}Si_{0.90}O_{3.95}$ (quenched at 1000°C)	5.499	6.745	9.318	94.53
β_1	$Ca_2B_{0.01}Si_{0.99}O_{3.995}$	5.503	6.749	9.302	94.51
β_1	$Ca_2Fe_{0.035}Al_{0.035}Si_{0.930}O_{3.965}$	5.502	6.750	9.316	94.45
β_1	Ca_2SiO_4(70%) + Ca_2FeO_5(30%)	5.507	6.755	9.325	94.45
β_2	$Ca_2Fe_{0.050}Al_{0.050}Si_{0.900}O_{3.950}$	5.502	6.753	9.344	94.19

Synthetic belites of β_1 type with M = Al, Fe are similar to some belites extracted from industrial clinkers (10) but are different from solid solutions C_2S, B_2O_3 (11) wich approach β_2 belites.

Conclusion

The X-ray diagrams of belites are similar to those of β and $\alpha'C_2S$ forms.

The precise parameters of $\beta, \alpha'_L, \alpha'_H, \alpha C_2S$ have been calculated from powder Guinier camera patterns. Our observations on pure dicalcium silicate confirm the previous data obtained with bredigite, C_2S solid solution. The α'_H—α'_L transition, at 1170°C, corresponds to a superstructure (a and b doubled) and a very small change of lattice which remains orthorhombic.

In the C_2S crystal lattice, the reaction $2Si^{4+} + O^{2-} \rightarrow 2M^{3-}$ forms belites at temperatures higher than $\alpha'_H \rightarrow \alpha$ inversion. These solid solutions, oxygen-defective compositions $Ca_2M_xSi_{1-x}O_{4-x/2}$, synthesized at 1500°C, are metastable in the case of M = Al, Fe. Furthermore, a decrease of foreign ions solubility in C_2S is observed after a long heating at high temperature.

The crystal lattice of stabilized belites, similar to some belites extracted from industrial clinkers is monoclinic, corresponding to a slightly altered βC_2S lattice. However belites are products of imperfect crystallization.

It seems to exist one form of $\alpha'C_2S$ type, its lattice constants shall be calculated.

Other β belites may be synthesized in the presence of sulphates and alkalis. Their powder patterns are similar to those of precedent belites.

References

1. A. Guinier and M. Regourd, "Structure of portland cement minerals" Principal Paper. This Symposium.
2. G. Yamaguchi, Y. Ono, S. Kawamura and Y. Soda, "Differential thermal analysis and high temperature X-ray diffraction studies of 2 $CaO \cdot SiO_2$" (in Japanese, English Summary). J. Ceram. Assoc. Japan, **71**, No. 1, 9–12 (1963).
3. K. Niesel and P. Thormann, "The stability fields of dicalcium silicate modifications" (in German). Tonind. Zeitung, **91**, 362–369 (1967).
4. A.M.B. Douglas, "X-ray investigation of bredigite", Mineral Mag., **29**, 875–884 (1952).
5. G. Trömel, "The calcium orthosilicate Ca_2SiO_4 modifications" (in German). Naturwissenschaften, **36**, 88 (1949).
6. C. M. Midgley, "Crystal structure of β dicalcium silicate". Brit. J. Appl. Phys. 3, 277–82 (1951). Acta Cryst. **5**, Part 3, 307–312 (1952).
7. N. Yannaquis and A. Guinier, Discussion of Nurse's Paper, "Phase equilibria and constitution of portland cement clinker". Washington 1960, National Bureau of Standards, Monograph 43, Vol. 1, p. 21–23.
8. T. Sasaki, "X-ray study on the inversion of the crystal form of dicalcium silicate, especially on the effect of stabilizing agents", Semento Gijutsu Nenpo, XIV, 22–23 (1960).
9. C. M. Schlaudt and D. M. Roy, "The join Ca_2SiO_4–Ca Mg SiO_4", J. Am. Ceram. Soc. **49**, No. 8, 430–432 (1966).
10. J. Forest, "Study of local encrustation in cement rotary-kilns and belites" (in French). Silicates Industriels **32**, No. 11, 373–384, No. 12, 427–441 (1967).
11. H. G. Midgley, "The formation and phase composition of portland cement clinker", The chemistry of cements, edited by H.F.W. Taylor, Vol. 1, p. 93, Academic Press, London (1964).

Supplementary Paper I-36 Cation and Anion Replacements in the Structure of Tricalcium Silicate

Nikita A. Toropov*

Synopsis

This article contains the results of experimental work by the author and his collaborators establishing numerous cases of formation of solid solution between different constituents of portland cement clinker. The authors have established the dissolution of rare-earth oxyorthosilicates in tricalcium silicate, the formation of continuous solid solution between Ba_2GeO_4–Ba_2SiO_4, between Ca_3SiO_5–Ca_3GeO_5 etc. These studies were accomplished with the aid of the polarizing microscope, X-rays, and thermal analysis.

Crystal Lattice of Tricalcium Silicate

The anionic part of the structure of tricalcium silicate is treated usually as constructed by silicon-oxygen tetrahedra SiO_4^{4-} and by additional oxygen ions which do not participate in the formation of tetrahedra. The cationic part of the structure is formed by calcium ions characterized by two kinds of oxygen coordination polyhedra.

The accurate determination of the crystal structure of tricalcium silicate using direct diffraction methods is rather complicated. The main difficulties are connected with large single cell parameters, existence of superstructure and with complexity of the mutual coordination of atoms composing this structure. And this is why other methods of crystal chemistry are of great importance. The study of compounds isostructural (or isomorphous) to tricalcium silicate is especially promising. Equally important are the investigations of solid solutions produced by tricalcium silicate and its structural components with some other radicals.

The most useful and effective is the studying of the crystals of chemical compounds isostructural to C_3S.

Solid Solutions of Tricalcium Silicate

Particular investigations of the solid solutions formed by C_3S or its separate structural radicals and various structural constituents are of special value. A waste number of isovalence or hetervalence type substitutions are possible as well as partial penetration of some atoms and ions in the lattice of tricalcium silicate.

These solid solutions may be confined by certain limits of possible replacements or may be quite continuous. However the second type of solid solutions formed by C_3S has not yet been described in literature.

Contrarily, all examples studied up to date have been characterized by small concentrations of replacements in the matrix lattice of C_3S (0.5 to 5.0 weight %).

Only recently in our laboratory the possibility of the full replacement of one of the structural units has been demonstrated in the system $3CaO \cdot SiO_2$–$3CaO \cdot GeO_2$ by Boikova, Toropov and Vavilonova (1). Nonlimited substitution of SiO_4^{4-} radicals by isomorphous radicals GeO_4^{4-} takes place in this system. It is worth mentioning that in the case of the system $2BaO \cdot SiO_2$–$2BaO \cdot GeO_2$ there occurs only a very narrow region of interruption according to

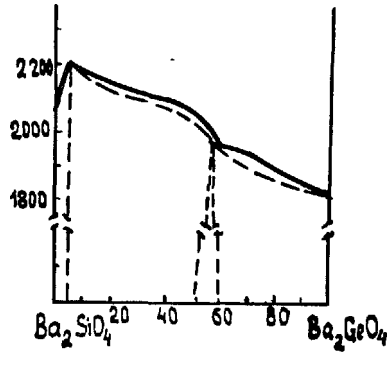

Fig. 1. *Phase diagram of the system* Ba_2SiO_4–Ba_2GeO_4

*The Academy of Science of the USSR, Institute of Silicate Chemistry, Leningrad, U.S.S.R.

Grebenschikov, Toropov (2).

The possibility of the synthesis of C_3S single-crystals where one of the structural components–SiO_4^{4-} is fully replaced by other component with larger atomic weight is of great importance for the further X-ray investigations of the initial crystal and its structural analog.

In our recent investigations special attention has been paid to the structural transitions between the states with different degree of ordering of the atomic arrangement in the structure of tricalcium silicate.

These transformations for the case of pure tricalcium silicate have been previously examined by X-ray and DTA methods by Regourd (3, 4). Only a few data are available concerning such transformations in solid solutions of this compound.

Nonstoichiometry of the Composition of Tricalcium Silicate

The synthesis of nonstoichiometric forms of C_3S and of solid solutions of C_3S with the excess of CaO is considered to be very important. The possibility of the penetration of some additional amounts of calcium oxide into the lattice of tricalcium silicate has been found in our laboratory in the course of the examination of the solid solutions between $Ca_3O \cdot SiO_4$ and $Y_2O \cdot SiO_4$.

The choice of yttrium silicate as a component of this new type of the solid solutions was made by various reasons. One of them is the closeness of the ionic radii $Ca^{2+} = 0.96$ Å and $Y^{3+} = 0.99$ Å (according to Pauling's data). The other one is concerned with the similarity in chemical structure of both silicates. The differencies between these compounds in optical properties, density and other characteristics provide the use of yttrium oxyorthosilicate and some other rare-earth silicates as a kind of crystal chemicals indicators. The determination of concentration limits for solid solutions, and the study of complex polymorphism of them are considerably simplified when using such indicators.

For example, only the use of this method enables us to succeed in the determination of the possible entering of some excess calcium atoms into the lattice of C_3S and its solid solutions.

Microscopical (in transmitted and in reflected light) and X-ray analyses of the samples with 6–7 weight % of yttrium oxyorthosilicate proved the homogeneity of this solid solution. At higher concentrations this silicate separates into a second crystalline phase.

From these data follows the formation of a limited series of solid solutions between $Ca_3O \cdot SiO_4$ and $Y_2O \cdot SiO_4$.

All samples of solid solutions contained some amounts of β–Ca_2SiO_4 and γ–Ca_2SiO_4 crystals.

The amounts of these crystals increased with increasing yttrium oxyorthosilicate contents and reached the value of 10-15%. The increase in the number of the vacant positions in the structure caused by the heterovalent replacement $3Ca^{2+} \rightleftarrows 2Y^{3+}$ is the cause of this phenomenon. The filling of these vacancies causes formation of the solid solutions of oxyorthosilicates with the excess CaO according to the stoichiometric ratio 3: 1.

The chemical analysis data given in Table 1 confirmed these predictions and showed that the excess of chemically bonded CaO increased from 0.5 weight % in pure $Ca_3O \cdot SiO_4$ to 2.5–3.0 weight % in the solid solution. The accuracy of the determinations amounted $\pm 0.3\%$ for CaO and $\pm 0.2\%$ for SiO_2 and Y_2O_3.

These results were checked up additionally using the C_3S samples obtained by sintering $CaCO_3$ precipitated from $Ca(NO_3)_2$ and $(NH_4)_2CO_3$ of high purity and by sintering rock crystal.

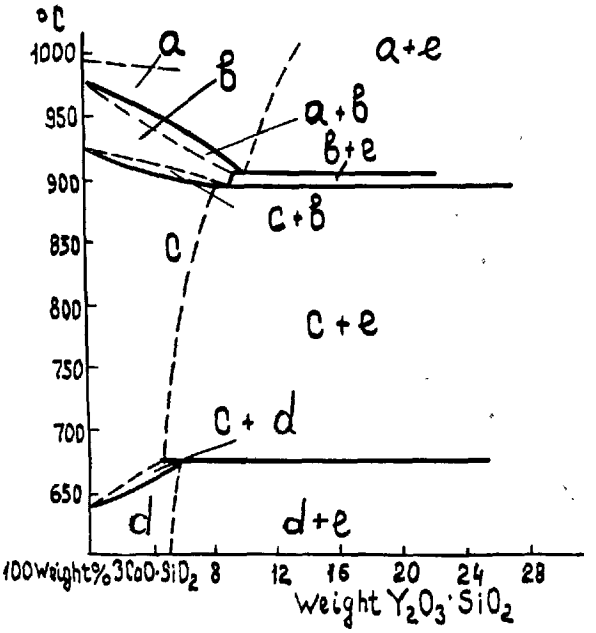

Fig. 2. *Phase diagram of the system* Y_2SiO_5–Ca_3SiO_5
a—Monoclinic solid solutions
b—Triclinic " " (III)
c—Triclinic " " (II)
d—Triclinic " " (I)
e—$Y_2O_3 \cdot SiO_2$

Our data concerning C_3S polymorphism are well correlated with polymorphism of its crystal chemistry analog—tricalcium germanate, and region of solid solutions in the phase diagram for the system $3CaO \cdot SiO_2$–$3CaO \cdot GeO_2$.

DTA data (Fig. 4) show that increasing germanate concentration in the solid solution primarily causes slight decrease in the temperatures of endothermic effects. Then these temperatures begin to increase and approach those for germanate. According to Regourd (4) phase transitions of C_3S are as follows:

$$\text{triclinic I} \overset{620^\circ C}{\rightleftarrows} \text{triclinic II} \overset{920^\circ C}{\rightleftarrows} \rightleftarrows \text{triclinic III} \overset{970^\circ C}{\rightleftarrows} \text{monoclinic} \overset{990^\circ C}{\rightleftarrows} \rightleftarrows \text{orthorhombic} \overset{1050^\circ C}{\rightleftarrows} \text{hexagonal.}$$

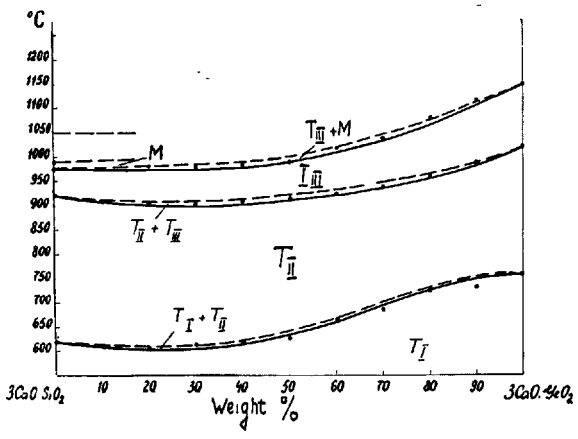

Fig. 3. *Phase diagram of the system* Ca_3SiO_5–Ca_3GeO_5
M—Monoclinic solid solutions
T_I—Triclinic " " (I)
T_{II}— " " " (II)
T_{III}— " " " (III)

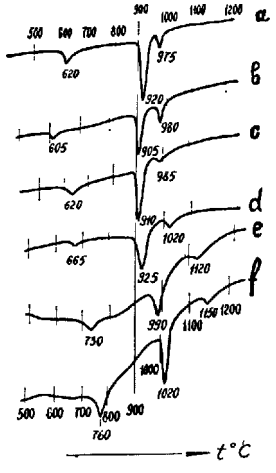

Fig. 4. *DTA-curves of solid solutions* Ca_3SiO_5-Ca_3GeO_5

These transitions of $3CaO \cdot GeO_2$ take place according to our data at 750°, 1020°, 1150°C and are as follows:

$$\text{triclinic I} \overset{750^\circ C}{\rightleftarrows} \text{triclinic II} \overset{1090^\circ C}{\rightleftarrows} \rightleftarrows \text{tricilinic III} \overset{1150^\circ C}{\rightleftarrows} \text{monoclinic}$$

It was previously shown by Toropov, Boikova (5)(6) that C_3S can contain some amount of the excess CaO according to the stoichiometric ratio 3: 1.

This content of nonstoichiometric CaO can be increased with increasing firing temperature. Deviations from stoichiometry were also observed in $3CaO \cdot GeO_2$.

Chemical analysis of $3CaO \cdot GeO_2$ carried out for the composition containing excess CaO proved that the excess CaO in germanate can achieve 1.5 weight %. The presence of free lime was not observed.

Fig. 5 gives infrared absorption spectra of the solid

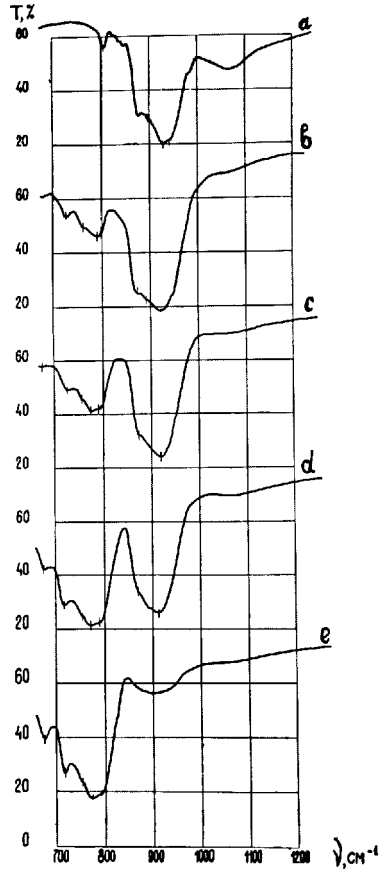

Fig. 5. *YR-spectra of solid solutions* $Ca_3Si \cdot O_5$–Ca_3GeO_5
a—Ca_3SiO_5
b—30%Ca_3SiO_5 + 70%Ca_3GeO_5
c—50%Ca_3SiO_5 + 50%Ca_3GeO_5
d—80%Ca_3SiO_5 + 20%Ca_3GeO_5
e—Ca_3GeO_5

Table 1. *Chemical analyses of samples of nonstoichiometric solid solutions tricalcium silicate*

NN	Chemical analysis after recalculation to dehydrated material. weight %				$CaO:SiO_2$ in calcium silicate	Excess of CaO in solid solution above stoichiometry.
	CaO	SiO_2	Y_2O_3	Σ		
1	68.96	25.64	5.40	100.0	3.05:1	1.20
2	67.79	25.64	6.57	100.0	3.04:1	0.97
3	67.90	25.64	6.45	100.0	3.04:1	0.97
4	67.37	25.06	7.57	100.0	3.13:1	3.09
5	67.07	25.10	7.83	100.0	3.12:1	2.86

Table 2. *Nonstoichiometric tricalcium silicate*

NN	Chemical analysis weight %				Amount of free CaO weight %	$CaO:SiO_2$ in final product	Excess of CaO above stoichiometry
	CaO	SiO_2	Losses on heating	Σ			
1	73.35	25.50	0.94	99.79	0.9	3.04:1	0.97
2	73.28	25.98	0.89	100.15	—	3.02:1	0.50
3	73.63	26.10	0.37	100.10	—	3.02:1	0.50
4	73.83	26.17	—	100.0		3.02:1	0.50

solutions recorded in the interval 700–1200 cm^{-1}. They are in agreement with other data indicating the formation of continuous solid solutions. Some shift of Si–O stretching bands to lower wave numbers corresponding to the increasing $3CaO \cdot GeO_2$ content is typical of orthosilicate-orthogermanate solid solutions. On the other hand, Ge–O stretching bands between 700 and 800 cm^{-1} move to slightly higher wave numbers when the content of the silicate increases. This concentration dependence is another straightforward indication of continuous series of solid solutions in this system.

The above-mentioned system $3CaO \cdot SiO_2$–$Y_2O_3 \cdot SiO_2$ is an example of C_3S solid solutions with limited solubility of another component. Phase diagram for its subsolidus region is shown in Fig. 2 according to Boikova and Toropov (7).

Electron Microscopic Investigations

Studies of solid solutions of C_3S with various oxides have been carried out in our laboratory with the aid of electron microscope. The main points of this investigation are:

1. Morphological study of crystals of solid solutions.
2. Observations of some defects of crystal surface with various minor components.
3. One of the first tasks of this investigation is connected with refinements in sample preparations and conditions of etching. Figs. 6 and 7 give the obtained photomicrographs which show different forms of etching figures, their interorientation and emergences of dislocations.

Fig. 6. *Etching figures of crystals* C_3S-*Magn.* × *15000*

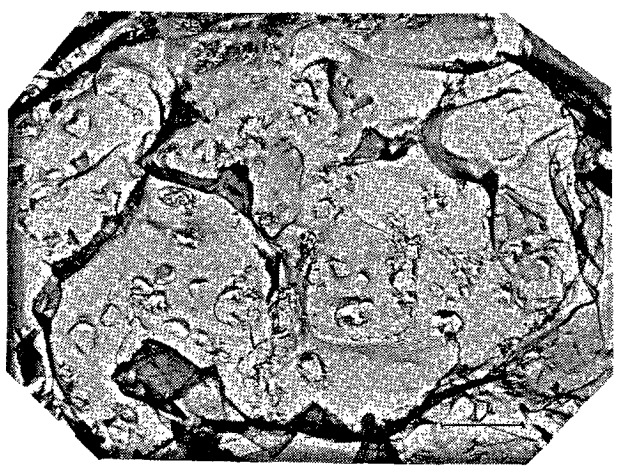

Fig. 7. *Etching figures of crystals solid solutions* $Ca_3SiO_5 + 1\%P_2O_5$

References

1. A. I. Boikova, N. A. Toropov and V. T. Varilonova, "On the analogy and solid solutions between tricalcium silicate and tricalcium germanate" (in Russian), Doklady Akad. Nauk SSSR, Chem. Ser., **175**, 654–657 (1967).
2. R. G. Grebenschikov, N. A. Toropov and V. I. Shitova, "Solid solutions Ba_2SiO_4–Ba_2GeO_4" (in Russian), Izv. Akad. Nauk SSSR, Neorgan. Materialy, 1, 121–125 (1965).
3. Research Centre of the Industry of Hydraulic Cements (Paris) Techn. Bubl. N182. M. Regourd, "Polymorphous transformations of tricalcium

silicate" (in French), Commun. presented at the meeting of the French Association of Crystallography on 1 st May 1967.
4. M. Regourd, "Determination of the lattice of microscopic crystals. Application to different forms of tricalcium silicate" (in French), Bull. Soc. Franc. Miner. Crist., **87**, 241–272 (1964).
5. N. A. Toropov and A. I. Boikova, "Solid solutions of yttrium oxyorthosilicate in tricalcium silicate" (in Russian), Doklady Akad. Nauk SSSR, **151**, 1114–1117 (1963).
6. A. I. Boikova and N. A. Toropov, "Stoichiometry and polymorphism of tricalcium silicate" (in Russian), Doklady Akad. Nauk SSSR, **156**, 1428–1431 (1964).
7. Experiment in Technical Mineralogy and Petrography. Materials of the 7th Conference (Nauka, Moscow, USSR, 1966) See article by A. I. Boikova and N. A. Toropov entitled "Investigation of solid solutions of tricalcium silicate with rare-earth oxyorthosilicates" (in Russian).

Supplementary Paper I-54 Polymorphism and Solid Solution of the Ferrite Phase

Eduard Woermann, Walter Eysel and Theodor Hahn*

Synopsis

In the ferrite solid solution $Ca_2(Fe_{1-p}Al_p)_2O_5$ with $0 \leq p \leq 0.70$ magnesium is incorporated according to two different substitution schemes. For $0 \leq p < 0.50$ the substitution ratio Ca/Mg = 2/3 is verified (limit of solid solution 1.6 mol. % MgO), while for $p \geq 0.50$ the ratio is Ca/Mg = 1/3 (solubility limit 3.0 mol.% MgO).

The curves of the lattice parameters as a function of p indicate two discontinuities at $p \approx 0.30$ and $p \approx 0.50$.

DTA-investigations of $Ca_2Fe_2O_5$ revealed two polymorphic transformations of very small enthalpies. High-temperature X-ray patterns showed that the three modifications are very similar.

DTA-results on samples with varying p support the discontinuities at $p \approx 0.30$ and at $p \approx 0.50$.

Introduction

Since the publication by Hansen, Brownmiller and Bogue (1) on the system $CaO–Al_2O_3–Fe_2O_3$ the ferrite solid solution series $Ca_2Fe_2O_5$–"$Ca_2Al_2O_5$" has been the subject of many detailed investigations. The present paper deals with the polymorphism of the ferrite series and its solid solution with MgO.

The ferrites are represented by the chemical formula $Ca_2(Fe_{1-p}\ Al_p)_2O_5$ where, (Majumdar (2)), $0 \leq p \leq 0.70$ (line C_2F–L in Fig. 1). According to Swayze (3), in equilibrium with free CaO the solid solution terminates slightly below $p = 0.50$, according to Newkirk and Thwaite (4) and Majumdar (2) slightly above this value. In agreement with the latter we found $p = 0.52$ for the limiting composition of ferrites in equilibrium with free CaO and aluminate at 1300°C (point B in Fig. 1).

Substitution of Magnesium in Ferrite

The fact that the ferrites take up MgO in solid solution is well known. Fujii and Asaoka (6) as well as Schwiete and zur Strassen (7) observed that a normally reddish-brown ferrite acquires a greenish-black colour in the presence of MgO. The latter authors found that upon incorporation of MgO into the ferrite structure no CaO is liberated. They concluded that Mg cannot substitute for Ca. On the other hand, Kato (8) as well as Sanada and Miyazawa (9, 10) assume replacement of Ca by Mg. The limits of solid solution are given by Sanada and Miyazawa to be < 1.0 wt.% MgO in $Ca_2Fe_2O_5$ ($p = 0$) and 1.5% in Ca_2FeAlO_5 ($p = 0.50$).

We have investigated the modes and limits of substitution of Mg by means of the "lime deviation method": The original ferrite sample was synthesized with a small excess of free CaO which was analytically determined using the method of Franke (11). Subsequently, a definite amount of MgO was added to the sample and after equilibration at 1300°C the free CaO was analyzed again. From the gain or loss of free CaO the type and limit of substitution of MgO in the structure can be derived. This procedure is of high accuracy (maximum error ±0.05% CaO). It should be noted, however, that it can only be applied to phase assemblages containing free CaO in equilibrium.

*Institut für Kristallographie der Technischen Hochschule Aachen, Aachen, West Germany.

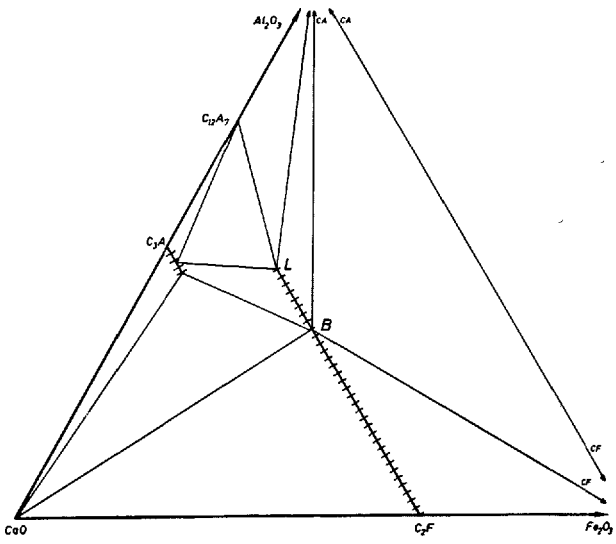

Fig. 1. *Subsolidus phase relations in the ternary system* $CaO–Fe_2O_3–Al_2O_3$ *after Newkirk and Thwaite (4a) (4) and Tarte (4b) (5). The diagram is based on mol. %.*

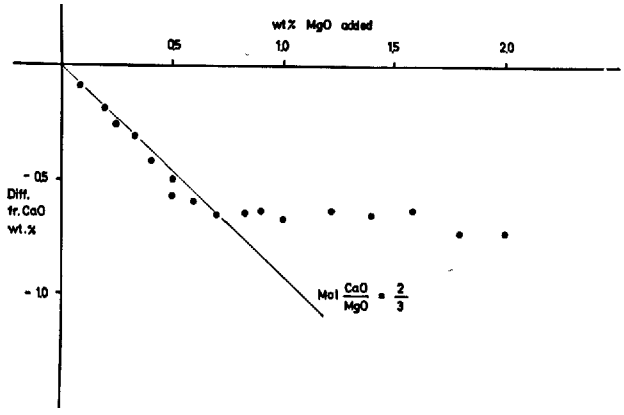

Fig. 2. *Decrease in free* CaO *as a function of incorporation of* MgO *in* $Ca_2Fe_2O_5$. *Temperature of ignition 1300°C.*

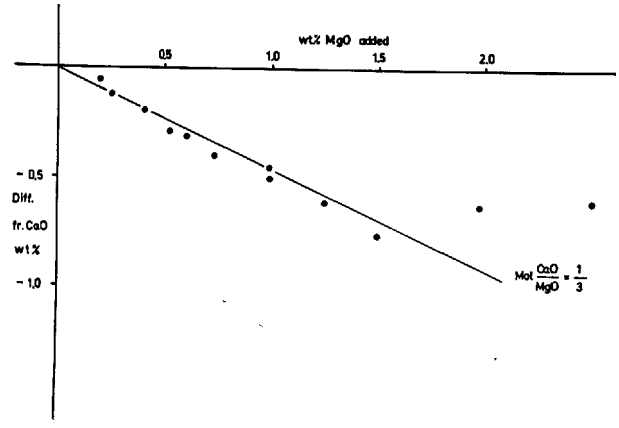

Fig. 3. *Decrease in free* CaO *as a function of incorporation of* MgO *in* Ca_2FeAlO_5 *(p = 0.50). Temperature of ignition 1300°C.*

Fig. 2 represents the results for $Ca_2Fe_2O_5$: Upon addition of MgO the amount of free CaO is reduced, i.e. additional CaO is combined by the ferrite. Beyond 0.7% MgO the amount of free CaO remains constant. Surplus MgO forms periclase without reacting with the ferrite phase. Thus the bend in the curve represents the limit of solid solution.

The slope of the curve corresponds to an atomic ratio Ca/Mg = 2/3. This indicates that incorporation of three Mg atoms causes two additional Ca-atoms to enter the structure, resulting in a solid solution of $Ca_2Fe_2O_5$ with the hypothetical end member "$Ca_2Mg_3O_5$". This implies that two out of three Mg^{2+} ions replace two Fe^{3+} ions, while the third Mg^{2+} ion occupies one of the interstitial sites, according to the formula:

$$Ca_2^{2+}Mg_{\frac{x}{3}}^{2+}[Fe_{1-\frac{1}{3}x}^{3+}Mg_{\frac{1}{3}x}^{2+}]_2O_5 \qquad (1)$$

with $0 \leq x \leq 0.045$ at 1300°C.

Similar investigations on Ca_2FeAlO_5 (p = 0.50) gave somewhat different results (Fig. 3): Again, additional CaO is combined by incorporation of MgO (solubility limit 1.5% MgO). The atomic substitution ratio, however, is changed to Ca/Mg = 1/3, i.e. with three Mg atoms one additional Ca atom is incorporated. This leads to another solid solution with the hypothetical end-member "$CaMg_3O_4$" = "$Ca_5Mg_{15}O_{20}$".

This end-member can be compared with the pure ferrite $Ca_2R_2O_5$:

$$[Ca_8] \qquad [R_8]O_{20}$$
$$[Ca_5Mg_3] \quad Mg_4 \quad [Mg_8]O_{20}$$

where $R = Fe^{3+}, Al^{3+}$

Thus, the solid solution involves simultaneous Mg-substitution in three different structural sites: Replacement of Ca, replacement of R and occupation of interstitial positions. This effect can be described as superposition of the two simple substitution types

$[Mg_8]$		$[R_8]O_{20}$	Ca/Mg = −1 (Ca/Mg-substitution)
$[Ca_8]$	Mg_4	$[Mg_8]O_{20}$	Ca/Mg = +2/3 (end-member of (1))

in the fixed ratio 1: 4, resulting in formula (2) for Mg-incorporation into a ferrite with p = 0.50.

$$[Ca_{1-\frac{x}{10}}Mg_{\frac{x}{10}}]_2Mg_{\frac{4}{15}x}[R_{1-\frac{4}{15}x}Mg_{\frac{4}{15}x}]_2O_5 \qquad (2)$$

with $0 \leq x \leq 0.100$.

Figs. 4 and 5 represent the solid solutions of the ferrites with p = 0 and p = 0.50 resp. in the respective "ternary" systems.

The question arises on whether the change from the

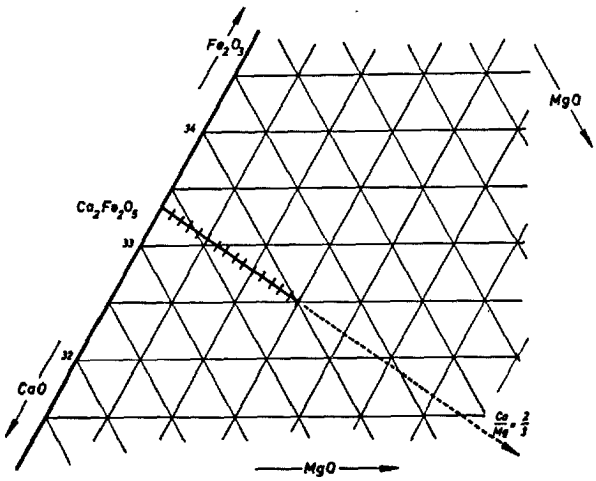

Fig. 4. *Solid solution of* $Ca_2Fe_2O_5$ *in the ternary system* CaO–MgO–Fe_2O_3 *at 1300°C; concentration lines in intervals of 0.5 mol. %.*

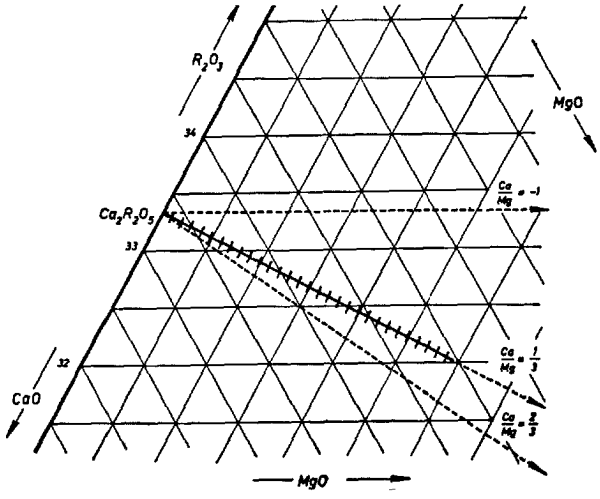

Fig. 5. *Solid solution of* Ca_2FeAlO_5 *in the "ternary" system* CaO–MgO–R_2O_3 *with* $R_2O_3 = (Fe_{0.5}Al_{0.5})_2O_3$ *at 1300°C.*

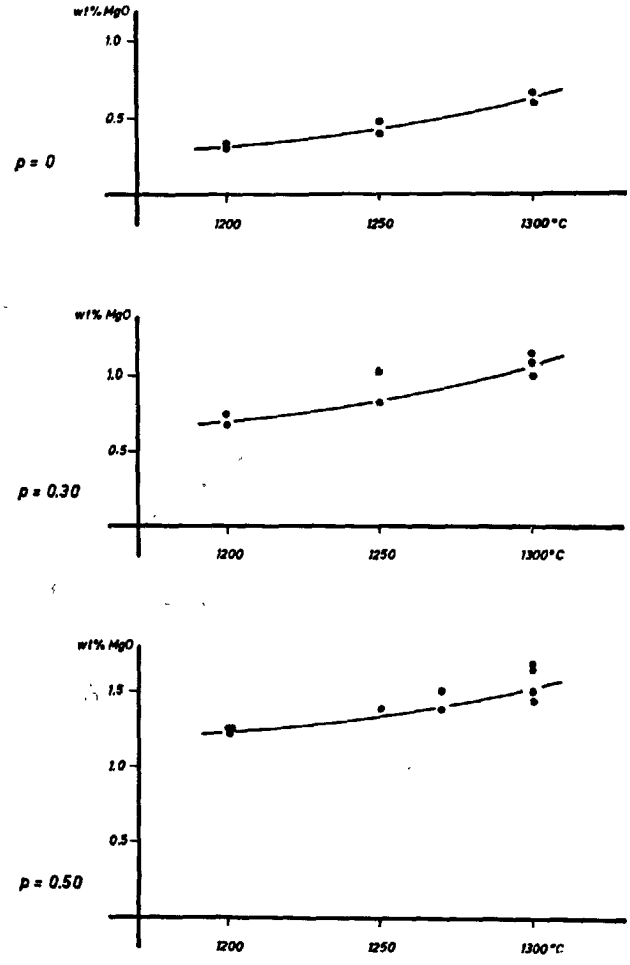

Fig. 6. *Solubility of MgO in several ferrites as a function of temperature.*

substitution ratio Ca/Mg = 2/3 to Ca/Mg = 1/3 is gradual or whether occurs as a discontinuous step. Experiments show that Mg is substituted according to formula (1) in ferrites with $0 \leq p \leq 0.48$, and according to formula (2) in ferrites with $0.50 \leq p \leq 0.52$. The composition p = 0.49 gave somewhat scattering results. Members with $p > 0.52$ cannot be investigated by the lime-deviation method since they are not stable in equilibrium with free CaO (see Fig. 1). Therefore, it could not be ascertained whether formula (2) is valid up to p = 0.70.

These results indicate an abrupt change in the mode of substitution of MgO near p = 0.49 to 0.50. Since all specimens were quenched rapidly, a transformation of one type into the other during cooling can be excluded, particularly in view of the structural rearrangements involved. The observed substitution type of Mg, therefore, corresponds to that of the temperature of synthesis (1300°C).

The solubility limit of MgO increases with the Al-concentration as well as with temperature (Fig. 6). At 1300°C, the limits are 0.7 wt.% MgO for $Ca_2Fe_2O_5$ and 1.5 wt.% MgO for Ca_2FeAlO_5, corresponding to 1.6 mol.% MgO and 3.0 mol.% MgO resp. These data are in good agreement with those of Sanada and Miyazawa (9, 10).

X-ray Investigations

X-ray investigations of the ferrite series have been carried out by various authors. Smith (12) has established a structural discontinuity around $p = 0.30$. For $p < 0.30$ the space group is Pnma, in agreement with the structure determination by Bertaut, Blum and Sagnieres (13). Above $p = 0.33$ the higher-symmetrical space group Imma exists. The change of the structure is gradual as indicated by the continuous decrease of the intensities of certain reflexions and their final disappearance at $p \approx 0.30$. In $Ca_2Fe_2O_5$ half of the Fe atoms occupy octahedral, the other half tetrahedral positions. Smith assumes that in the Pnma-phase the tetrahedral Fe are preferentially replaced by Al, while above $p = 0.33$ the rate of Al-substitution in both positions is nearly equal. This assumption has been confirmed by Tarte (14) with the aid of infrared absorption spectra and by Pobell and Wittmann (15) by means of the Mößbauer technique.

The discontinuity at $p \approx 0.30$ is reflected in Smith's curves of lattice constants: The *b*- and *c*-axes show changes of slope, while the *a*-axis remains straight. This confirms the results of Newkirk and Thwaite (2) who found slight bends in the curves of all three lattice constants at $p \approx 0.33$.

We have investigated the lattice parameters as a function of composition for two ferrite solid solution series, one without MgO and one saturated with MgO. The samples were prepared in the subsolidus region at 1300°C, and investigated by powder diffractometry using FeK_α-radiation and NaCl as internal standard.

The results for the MgO-free ferrites are given in

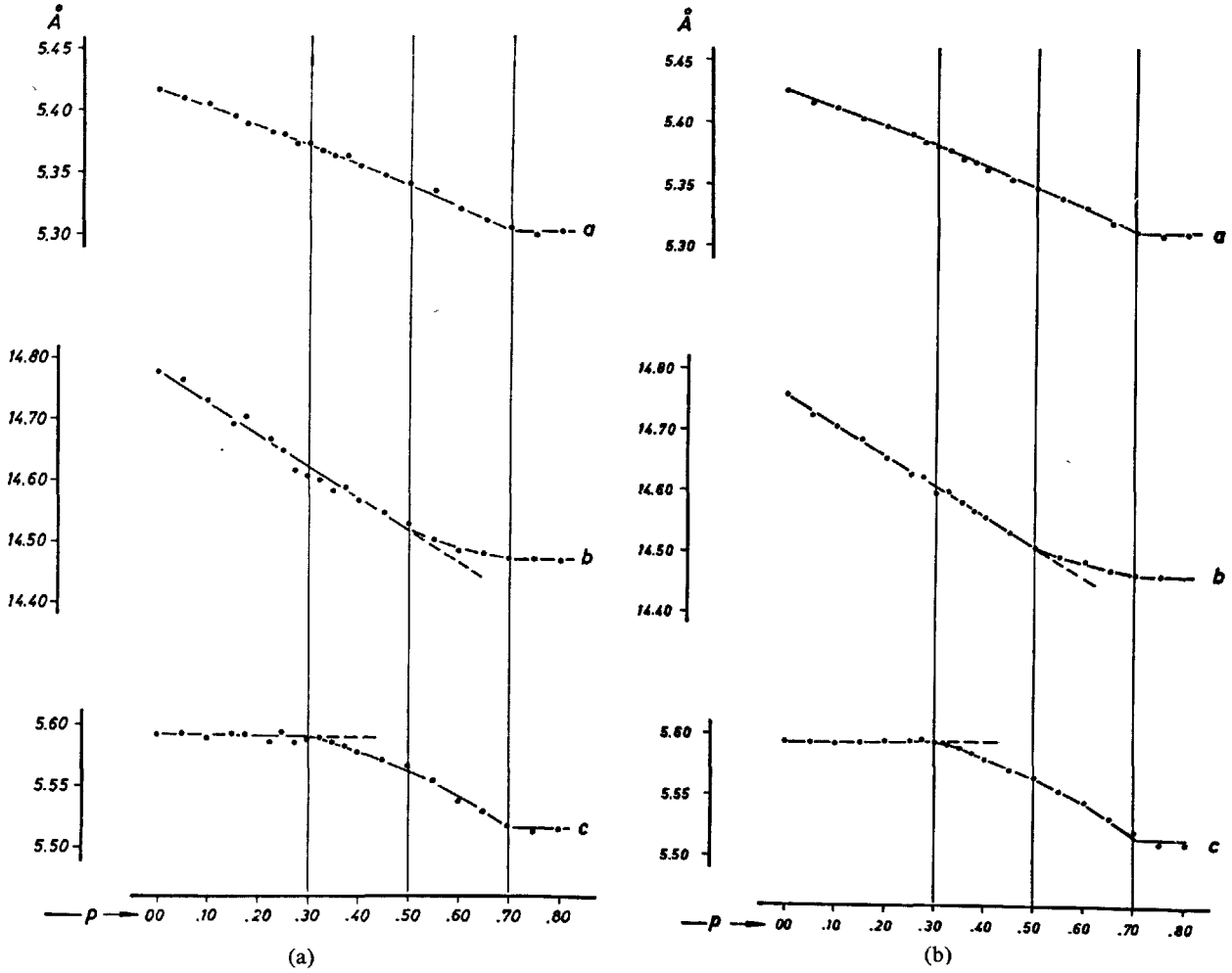

Fig. 7. *Variation of lattice parameters of ferrites as a function of the Al-content, a) MgO-free samples, b) samples saturated with MgO.*

Table 1. *Lattice constants of ferrite solid solutions* $Ca_2(Fe_{1-p}Al_p)_2O_5$ *(Average standard deviations for* a *and* c: *0.003Å, for* b: *0.005Å)*

		p = 0				p = 0.30	p = 0.50	p = 0.70
		Bertaut et al. (13)	Smith (12)	Yannaquis et al. (17)	This paper	This paper	This paper	This paper
Without MgO	*a*	5.39	5.42	5.432	5.427	5.380	5.346	5.309
	b	14.68	14.76	14.760	14.758	14.606	14.508	14.463
	c	5.64	5.60	5.600	5.594	5.592	5.564	5.514
Saturated with MgO	*a*				5.417	5.374	5.341	5.303
	b				14.778	14.623	14.520	14.470
	c				5.591	5.590	5.565	5.516

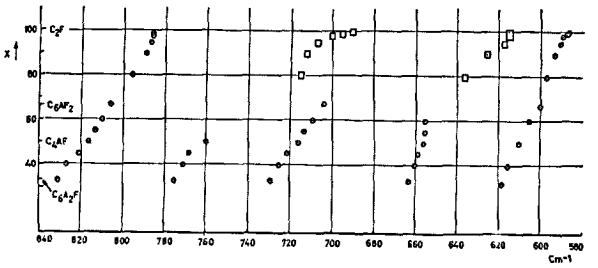

Fig. 8. *Position of infrared absorption bands in the ferrite series after Tarte (Fig. 6 in ref. 13); p = 1 − x/100.*

Fig. 7. The cell-dimensions decrease with increasing substitution of the smaller Al ion for the larger Fe ion. The plot of the *a*-axis is nearly a straight line without any discontinuity. The curves for the *b*- and the *c*-axes, however, exhibit one bend each. The *c*-axis plot shows a dinstinct inflection at $p \approx 0.30$, thus confirming the discontinuity discussed above. The *b*-axis curve is straight up to $p \approx 0.50$. At this value the slope changes distinctly.

Similar effects are observed in the samples saturated with MgO, thus confirming again the two discontinuities at $p \approx 0.30$ and $p \approx 0.50$ (Fig. 7b). A comparison of the lattice constants in Table 1 demonstrates that the incorporation of MgO causes the *a*-axis to increase and the *b*-axis to decrease while it has no effect on *c*.

Indications of a discontinuity at $p = 0.50$ have been described previously by two authors: Swayze (3) found that the composition $p = 0.50$ "acts as a definite compound so far as its influence on melting temperature along the C_3A–$C_6A_xF_y$ phase boundary line is concerned". Tarte's (14) diagram of infrared absorption spectra (Fig. 8) shows the occurrence of a new absorption band at 780–760 cm^{-1}. According to the author, no explanation of this effect can yet be given (16).

High-Temperature Investigations

Several members of the ferrite solid solution series were investigated by differential thermal analysis.

The end-member $Ca_2Fe_2O_5$ shows two weak (order of magnitude 0.1 cal./g) but distinct signals at 430°C and 690°C resp. (Fig. 9). Both are reversible without any measurable hysteresis. This implies that $Ca_2Fe_2O_5$ occurs in three different polymorphic forms. Yannaquis & Regourd (17) have kindly investigated the nature of these phase transformations by means of high-temperature X-ray measurements (Fig. 10): The transformation at 430°C is accompanied by a sudden shrinkage of the cell in all dimensions ($\Delta V = 0.7\%$), while the 690°C-transformation involves a slight decrease of thermal expansion. No systematic extinctions of X-ray diffraction lines occur up to 900°C, thus proving that the space group Pnma persists in the entire temperature range. All experiments indicate that the differences between the three polymorphic forms are very small and that the transformations are of the displacive type.

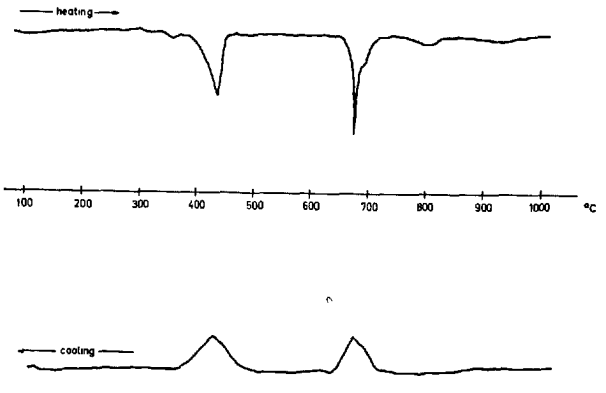

Fig. 9. *DTA-diagram of* $Ca_2Fe_2O_5$*(5°C/min).*

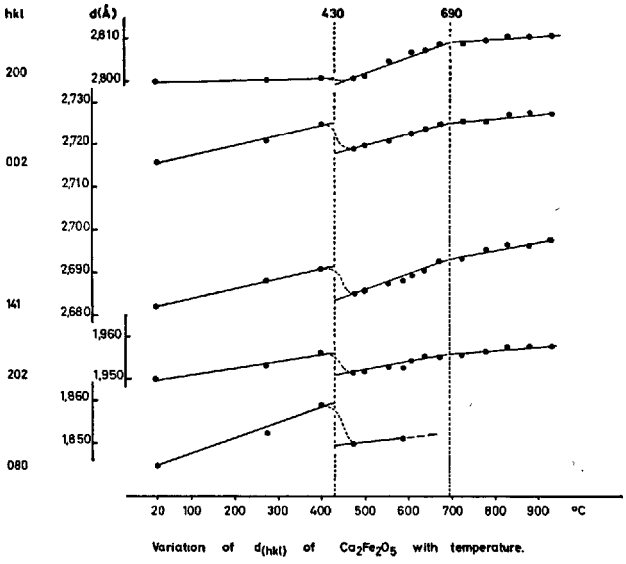

Fig. 10. *High-temperature X-ray results: Variation of spacings of several lines with temperature. (After Yannaquis & Regourd 17).*

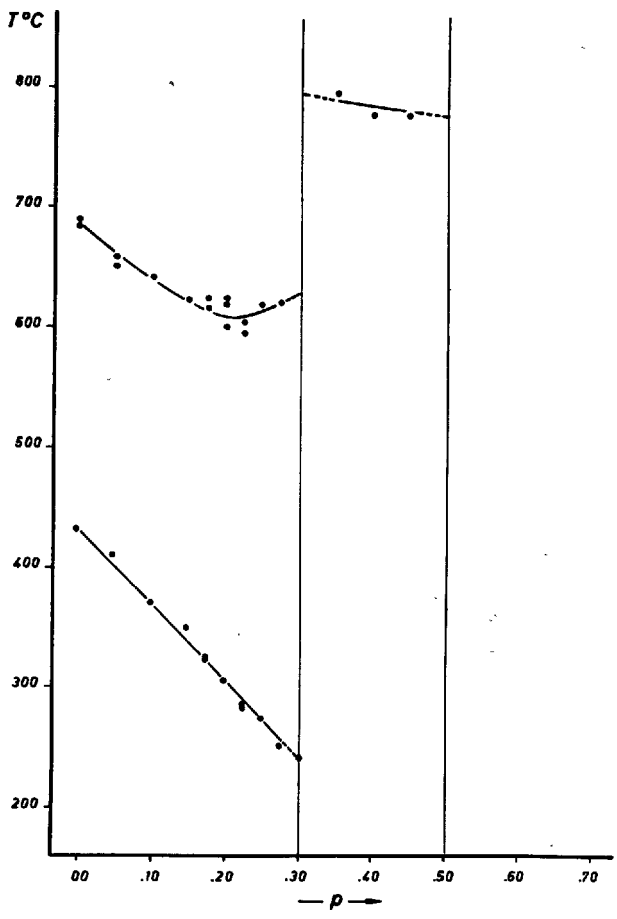

Fig. 11. *Variation of transition temperatures in the ferrite series as determined by DTA.*

According to Fig. 11 both DTA-peaks are shifted to lower temperatures with increasing amount of Al, at the same time decreasing in intensity and finally disappearing around $p = 0.30$ at temperatures of 220°C and 630°C resp. There is an indication that the latter peak is splitting into a doublet just before its disappearance (17). For compositions $0.30 < p < 0.50$ a very weak and indistinct thermal effect occurs in the region 780°–800°C. For solid solutions with $p > 0.50$ no DTA-signals have been observed.

The DTA signals of $Ca_2Fe_2O_5$ saturated with MgO occur at slightly lower temperatures (365°C and 670°C resp.). With increasing p the signals again shift to lower temperatures and finally disappear. Here, too, very weak thermal effects are observed around 800°C for samples with $p = 0.35$, 0.40 and 0.45. The thermal behaviour of magnesia-free and magnesia-saturated ferrites thus is quite similar.

Conclusion

The investigations offer evidence for two discontinuities in the ferrite solid solution series $Ca_2(Fe_{1-p}Al_p)_2O_5$ at $p \approx 0.30$ and $p \approx 0.50$. Of these only the first one has been described before.

The discontinuity at $p \approx 0.30$ is indicated by the following effects:

1. Change of space group from Pnma to Imma (Smith, 12)
2. Bend in the curve of the *c*-axis
3. Disappearance of the two DTA signals at 220°C and 630°C
4. Infrared-absorption spectra (Tarte, 14).

The new discontinuity at $p \approx 0.50$ is supported by the following evidence:

1. Bend in the plot of the *b*-axis
2. Disappearance of the weak DTA signal at 800°C
3. Appearance of an additional IR absorption band (Tarte, 14)
4. Change of the substitution type of MgO.

The discontinuity at $p \approx 0.50$ has been established for MgO-free samples. This suggests that the discontinuity is inherent in the ferrite series and thus is the reason for the change in the substitution type of MgO.

Smith (12) has explained the discontinuity at $p \approx 0.30$ as the transition from predominant Al-incorporation in tetrahedral sites to nearly equal rates of replacement in both tetrahedral and octahedral positions. It seems reasonable to interpret the effect at $p \approx 0.50$ as the beginning of preferential Al-substitution into octahedral sites.

Acknowledgement

We are indebted to the "Deutsche Forschungsgemeinschaft" and the "Verein Deutscher Zementwerke e.V." for support of this work.

References

1. W. C. Hansen, L. T. Brownmiller and R. H. Bogue, "Studies on the system calcium oxide-alumina-ferric-oxide", Journ. Amer. Chem. Soc. **50**, 396–408 (1928).
2. A. J. Majumdar, "The ferrite phase in cements", Trans. Brit. Ceram. Soc. **64**, 105–119 (1965).
3. M. A. Swayze, "A report on studies of 1. The ternary system $CaO–C_5A_3–C_2F$ 2. The quaternary system $CaO–C_5A_3–C_2F–C_2S$ 3. The quaternary system as modified by 5% MgO", Amer. Journ. Sci. **244**, 1–30, 65–94 (1946).
4. T. F. Newkirk and R. D. Thwaite, "Pseudoternary system calcium oxide-monocalcium aluminate ($CaO \cdot Al_2O_3$)—dicalcium ferrite ($2CaO \cdot Fe_2O_3$)", Journ. Research N.B.S. **61**, 233–245 (1958).
5. P. Tarte, "Structural investigations of cement minerals—study of interactions between C_3A and C_4AF" (in French), Silicates Industrielles **31**, 343–352 (1965).
6. M. Fujii and K. Asaoka, "About the influence of MgO slightly contained in cement on the colour and formation of alite" (in Japanese) Rev. Assoc. Jap. Portland Cement Engineers **20**, 133–150 (1931).
7. H. E. Schwiete and H. zur Strassen, "On the combination of magnesia in portland cement" (in German) Zement **23**, 113–116 (1934).
8. A. Kato, "A study on the solubility of Mg in the ferrite phase of portland cement clinker by X-ray investigations", Rev. Meeting Jap. Cem. Eng. Assoc. **12**, (1958).
9. Y. Sanada and K. Miyazawa, "On the behaviour of MgO against cement clinker minerals", Rev. Gen. Meeting Jap. Cem. Eng. Assoc. **11**, (1957).
10. Y. Sanada and K. Miyazawa, "On the behaviour of MgO against cement clinker minerals", Rev. Gen. Meeting Jap. Cem. Eng. Assoc. **13**, (1959).
11. B. Franke, "A new method for the determination of calcium oxide and calcium hydroxide in the presence of anhydrous and hydrous calcium silicate" (in German), Zement **30**, 401 (1941).
12. D. K. Smith "Crystallographic changes with the substitution of aluminium for iron in dicalcium ferrite", Acta Cryst. **15**, 1146–1152 (1962).
13. E. F. Bertaut, P. Blum and A. Sagnières, "The structure of dicalcium ferrite and brownmillerite" (in French), Acta Cryst. **12**, 149–159 (1959).
14. P. Tarte, "Infrared investigation of dicalcium ferrite $2CaO \cdot Fe_2O_3$ and of the solid solutions $2CaO \cdot (Al, Fe)_2O_3$" (in French), Rev. Chimie Minérale **1**, 425–438 (1964).
15. F. Pobell and F. Wittmann, "Replacement of Fe^{3+} by Al^{3+} in calcium aluminate ferrite", Physics Letters **19**, 175–176 (1965).
16. P. Tarte, Personal Communication (1968).
17. N. Yannaquis and M. Regourd, Personal Communication (1964).

Supplementary Paper 1-55 Crystal Chemisty of Tricalcium Silicate Solid Solutions

Theodor Hahn, Walter Eysel and Eduard Woermann*

Synopsis

The incorporation of various atoms into Ca_3SiO_5 has been investigated with respect to the types of substitution, the limits of solubility and the stabilization of high-temperature modifications. In particular, the effects of the following oxides have been studied: MgO, ZnO, GeO_2, Fe_2O_3, Al_2O_3.

The combined substitutions of MgO and Al_2O_3, MgO and Fe_2O_3, Al_2O_3 and Fe_2O_3 correspond to three-dimensional bodies in the appropriate quaternary systems. From these results conclusions about the alite phase in the quinary system CaO–MgO–Al_2O_3–Fe_2O_3–SiO_2 have been drawn.

Introduction

Solid solutions of Ca_3SiO_5, called alite, are the main constituents of cement clinker. Confusion existed about the nature of the alite phase until in 1933 Guttmann and Gille (1) were able to prove that alite is Ca_3SiO_5, modified by slight solid solution. In 1952 Jeffery (2) determined the structure of Ca_3SiO_5. Later work confirmed his results (3). The structure consists of Ca ions, isolated SiO_4 tetrahedra and additional oxygens, the latter being coordinated to Ca only. The oxygen coordination around calcium is very irregular and the structure contains voids. These features are considered to be the main reasons for the hydraulic properties of this substance (4).

Jeffery postulated three modifications for C_3S. Recent detailed investigations, however, revealed six polymorphs (5): three triclinic (T_I, T_{II}, T_{III}), two monoclinic (M_I, M_{II}) and the rhombohedral high-temperature form (R). The structures of all these modifications are extremely similar. The five transformations represent small distortions of the structural framework (displacive transformations) and their enthalpies are minute.

Of particular interest, both for the crystal chemistry and the technical role of Ca_3SiO_5, are the modes and limits of incorporation of foreign atoms into the structure and the stabilization of the different polymorphs.

Pure Ca_3SiO_5 is unstable with respect to Ca_2SiO_4 and CaO below ~1200°C. In solid solutions this temperature is shifted slightly; the principal situation, however, remains unchanged. This necessitates that Ca_3SiO_5 and its solid solutions can be prepared only above 1200°C, i.e. in the stability range of the rhombohedral modification (R).

Fortunately, the solid solutions can be quenched and investigated at room temperature. Depending on the composition of the solid solution, some of the transformations are suppressed, thus causing the stabilization of high-temperature modifications. In particular, ZnO is unique in stabilizing all polymorphs except T_{III} (5). It should be noted that all transformations occur in the temperature range in which Ca_3SiO_5 is metastable.

We have studied the incorporation of various oxides into Ca_3SiO_5 (6, 7, 8, 9, 10). In particular, the combined substitution of MgO, Al_2O_3 and Fe_2O_3 resembles very closely the alite phase in clinker; accordingly, the results reveal several aspects of the nature of this phase.

Our investigations established that pure tricalcium silicate possesses no compositional range, but represents a stoichiometric compound of composition $3CaO \cdot SiO_2$ (7). This disagrees with results by Boikova and Toropov (11), who found an excess of 0.5—1.0 wt.% CaO in pure tricalcium silicate, corresponding to ratios CaO: SiO_2 of 3.02—3.04.

*Institut für Kristallographie der Technischen Hochschule, Aachen, West Germany.

Individual Substitution of Foreign Atoms

Replacement of Ca in 6-coordinated (VI) positions:

$$(Ca_{1-x}Me_x)_3^{VI}SiO_4 \quad (Ca/Me = 1.0) \qquad (1)$$

with Me = Zn, Mg

The limits of solid solution for MgO and ZnO are strongly dependent on temperature. At 1550°C up to 2.0 wt.% MgO and at 1400°C up to 5.0 wt.% ZnO can be incorporated into Ca_3SiO_5.

For MgO, very similar results have been obtained by Locher (12) and by Midgley and Fletcher (13).

Replacement of Si in tetrahedral (IV) sites by Ge:

$$Ca_3^{VI}(Si_{1-x}Ge_x)^{IV}O_5 \quad (Ca/Ge = 3.0) \qquad (2)$$

Our results (14) are in good agreement with those of Boikova et al. (15). Ca_3GeO_5 exhibits the same structures and polymorphism as Ca_3SiO_5; unlimited solid solution exists between both compounds. In analogy to Ca_3SiO_5, germanate-alites can be prepared and high-temperature modifications can be stabilized. Likewise, Ca_3GeO_5 is metastable at lower temperatures (below 1335°C) but the rate of decomposition into Ca_2GeO_4 and CaO is much higher than that of the silicate. Thus the investigations on Ca_3GeO_5 support the results obtained for the silicate.

The incorporation of the trivalent ions Fe and Al is more complicated:

Substitution of Fe^{3+} takes place in two structural sites. Half of the Fe-ions substitute for Si, the other half for Ca:

$$(Ca_{1-\frac{x}{6}}Fe_{\frac{x}{6}})_3^{VI}(Si_{1-\frac{x}{2}}Fe_{\frac{x}{2}})^{IV}O_5 \quad (Ca/Fe = 1.0) \qquad (3)$$

Accordingly, the solid solution is represented on the line Ca_3SiO_5–"$Ca_2Fe_2O_5$" in the system CaO–Fe_2O_3–SiO_2. Contrary to these results, Fletcher (16) found a solid solution along the line Ca_3SiO_5–"$Ca_3Fe_2O_6$". The limit of solid solution at 1550°C is 1.1 wt.% Fe_2O_3, in good agreement with Fletcher's value of 1.05% Fe_2O_3.

Substitution of Al: Aluminum atoms can enter into three different positions in the structure of Ca_3SiO_5: Substitution for Si (IV), substitution for Ca (VI) and occupation of 6-coordinated voids (VI'). The distribution of Al among these three sites is variable and controlled by the amount of Ca-atoms available.

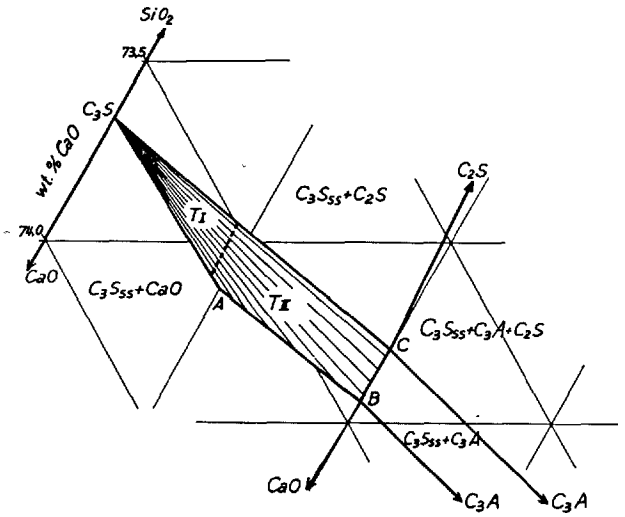

Fig. 1. *Field of* Ca_3SiO_5 *solid solution in the ternary system* CaO–Al_2O_3–SiO_2 *at 1550°C. The regions of the stabilized modifications* T_I *and* T_{II} *apply to room temperature.*

Thus, Al as well as Ca take part in the solid solution and the substitution must be described by two parameters, i.e. in the system CaO–Al_2O_3–SiO_2 the C_3S-phase is represented by an area and not by a line. This area has a small but well defined "CaO-width" (up to 0.14% CaO at B–C in Fig. 1).

All solid solutions can be described by superposition of the two formulae:

$$(Ca_{1-\frac{y}{6}}Al_{\frac{y}{6}})_3^{VI}(Si_{1-\frac{y}{2}}Al_{\frac{y}{2}})^{IV}O_5 \quad (Ca/Al = 1.0) \qquad (4)$$

$$Ca_3^{VI}Al_{\frac{z}{4}}^{VI'}(Si_{1-\frac{3}{4}z}Al_{\frac{3}{4}z}^{3})^{IV}O_5 \quad (Ca/Al = 2.25) \qquad (5)$$

These substitution types correspond to the hypothetical end-members "$Ca_2Al_2O_5$" and "$Ca_3Al_{4/3}O_5$" respectively. Midgley and Fletcher (13) found substitution type (5) only, while Locher (12) assumed replacement of Si by Al, the balance of charges being maintained by removal of oxygen atoms from the structure. Both models correspond to lines in the ternary diagram but not to areas. The limit of solubility of Al_2O_3 in Ca_3SiO_5 is independent of temperature and amounts to 1.0 wt.% Al_2O_3.

Combined Substitution of Mg and Al in Ca_3SiO_5

So far the solid solutions of Ca_3SiO_5 with individual oxides have been described. In the following chapters the results of the combined substitution of MgO, Al_2O_3 and Fe_2O_3 will be presented. The object of the investigations has been to establish the one-phase regions of the alites in the respective quaternary sys-

Table 1. *Coexisting phases on the faces of the bodies of Fig. 2, 3 and 4 at 1550°C*
(On cooling the liquids crystallize to the phases given in brackets)

System $CaO–MgO–Al_2O_3–SiO_2$		System $CaO–MgO–Fe_2O_3–SiO_2$		System $CaO–Al_2O_3–Fe_2O_3–SiO_2$	
Face	Coexisting phases	Face	Coexisting phases	Face	Coexisting phases
C_3S–B–B′–L*	C_3S + CaO	C_3S–M–M′–L	C_3S + CaO	C_3S–B–S–M	C_3S + CaO
B–C–C′–B′	C_3S + liq.(C_3A)	M–M′–N′	C_3S + liq.(C_2F)	B–C–S–T	C_3S + liq.(aluminate)
C_3S–C–C′–L	C_3S + C_2S	C_3S–M–N′–L	C_3S + C_2S	C_3S–C–T–M	C_3S + C_2S
L–B′–C′	C_3S + MgO	L–M′–N′	C_3S + MgO	S–T–M	C_3S + liq.(ferrite)

*The line A–A′ in Figure 2 represents a bend in this face which is of no significance for the phase relations.

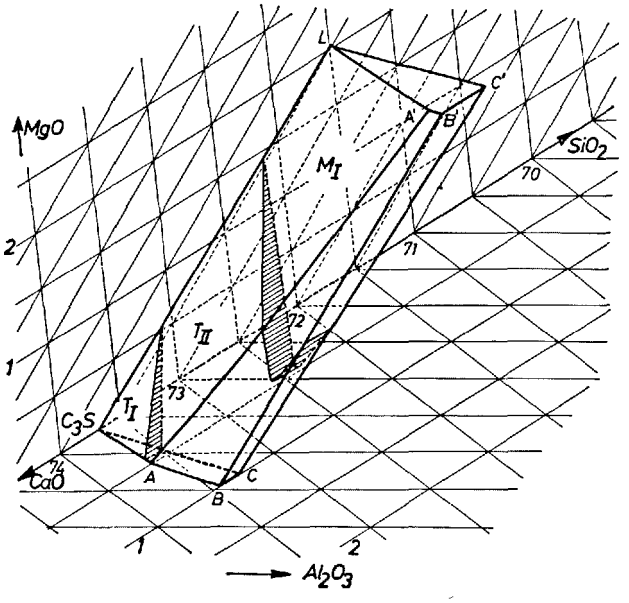

Fig. 2. *Body of* Ca_3SiO_5 *solid solution in the quaternary system* $CaO–MgO–Al_2O_3–SiO_2$ *at 1550°C.*

tems.

Fig. 2 shows that the solid solutions of Ca_3SiO_5 with MgO and Al_2O_3 in the quaternary system $CaO–MgO–Al_2O_3–SiO_2$ are represented by a nearly prismatic body. This implies that not only MgO and Al_2O_3 but also CaO participate in the solid solution. The basis C_3S–A–B–C corresponds to the Al-substitution in the system $CaO–Al_2O_3–SiO_2$ (Fig. 1). The edge C_3S–L corresponds to the Mg-substitution in the system $CaO–MgO–SiO_2$. The phases which coexist on the different faces of the body are given in Table 1.

The "CaO-width" B–C (0.14% CaO) is enlarged to B′–C′ (0.34% CaO) due to the influence of Mg. Upon combined substitution the individual limits of solid solution of MgO and Al_2O_3 remain unchanged and amount to 2.0% MgO and 1.0% Al_2O_3 at 1550°C. This is in good agreement with the results of Midgley and Fletcher (13). The limit for Al_2O_3 is independent of temperature, while the MgO-solubility decreases with falling temperature (e.g. 1.5% at 1420°C). No accurate data exists about the temperature-dependence of the CaO-width.

The solid solutions with Al_2O_3 are described above as superpositions of formulae (4) and (5), while the incorporation of MgO is represented by formula (1). Upon combined incorporation of MgO and Al_2O_3 the individual substitution types remain valid. Accordingly, the solid solution can be described by superposition of formulae (6) and (7):

$$(Ca_{1-x-\frac{y}{6}}Mg_xAl_{\frac{y}{6}})_3{}^{IV}(Si_{1-\frac{y}{2}}Al_{\frac{y}{2}})^{IV}O_5 \qquad (Ca/Al = 1.0) \qquad (6)$$

$$(Ca_{1-x}Mg_x)_3{}^{VI}Al_{\frac{z}{4}}{}^{VI'}(Si_{1-\frac{3}{4}z}Al_{\frac{3}{4}z})^{IV}O_5 \qquad (Ca/Al = 2.25) \qquad (7)$$

Independence of substitution types was already proposed by Midgley and Fletcher (13). Their model, however, corresponds to formula (7) only, i.e. to one of the limiting faces of the body in Fig. 2. Jeffery's alite (2, 4) $Ca_{54}MgAl_2Si_{16}O_{90}$ as well as the line connecting this composition with the point of pure Ca_3SiO_5 are entirely outside of this body.

Fig. 2 also shows the regions of the various modifications which can be quenched to room temperature. The stabilized forms depend upon the amount of MgO and Al_2O_3 but are independent of the CaO-concentration. The stabilization effects were also investigated by Yamaguchi and Kato (17) and by Midgley and Fletcher (13).

Combined Substitution of Mg and Fe in Ca_3SiO_5

The combined substitution of MgO and Fe_2O_3 in Ca_3SiO_5 is represented in the system $CaO–MgO–Fe_2O_3–SiO_2$ by the body of Fig. 3, which is less complicated than that of Fig. 2. While the individual solid solutions with MgO and with Fe_2O_3 (lines C_3S–L and C_3S–M resp.) exhibit no "CaO-width", combined

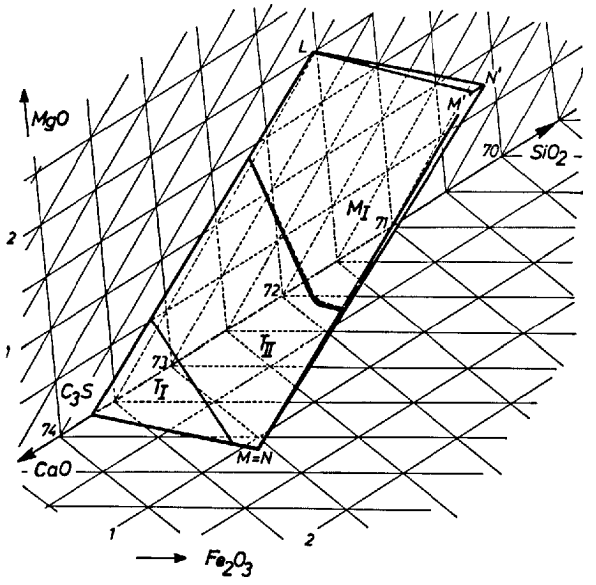

Fig. 3. *Body of* Ca_3SiO_5 *solid solution in the quaternary system* $CaO–MgO–Fe_2O_3–SiO_2$ *at 1550°C.*

substitution results in a very small width with a maximum value at M'–N'. The coexisting phases are compiled in Table 1.

From the shape of the body it can be deduced that the individual limits of solid solution of both oxides (2.0% MgO and 1.1% Fe_2O_3 at 1550°C) do not influence each other. The substitution types are analogous to those for combined Mg–and Al–substitution (formulae (6) and (7)).

The regions of the stabilized modifications T_I, T_{II} and M_I are also indicated in Fig. 3.

Combined Substitution of Al and Fe in Ca_3SiO_5

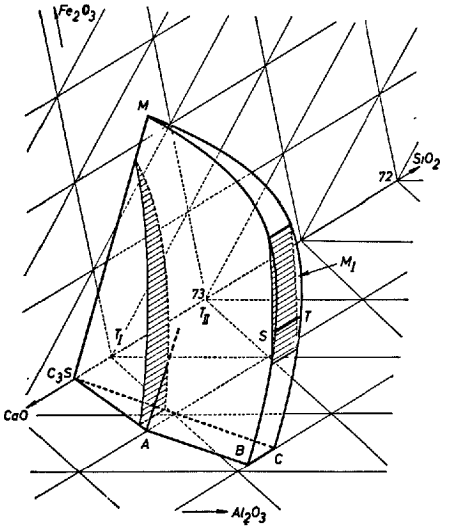

Fig. 4. *Body of* Ca_3SiO_5 *solid solution in the quaternary system* $CaO–Al_2O_3–Fe_2O_3–SiO_2$ *at 1550°C. The points S and T apply to subsolidus temperatures (< 1340°C).*

For the tricalcium silicate phase in the system $CaO–Al_2O_3–Fe_2O_3–SiO_2$ the body of Fig. 4 has been found. It is again characterized by a CaO–width, which in this case is predominantly a function of the Al_2O_3–concentration. The coexisting phases are given in Table 1.

In contrast to the two cases discussed above, the limits of solid solution of Al_2O_3 and Fe_2O_3 are not independent. The interaction causes the face B–C–M to be curved. This can be accounted for by the fact that Fe and Al atoms compete for the same positions in the structure. Fletcher (16), however, reports independent limits of solid solution.

In this system the modifications T_I and T_{II} occur at room temperature (Fig. 4). In addition, a small region of form M_I has been found.

Combined Substitution of Mg, Al and Fe in Ca_3SiO_5

On the basis of the results in the three quaternary systems and of additional experiments in the quinary system $CaO–MgO–Al_2O_3–Fe_2O_3–SiO_2$ the following conclusions on the tricalcium silicate phase in the latter system can be drawn (10):

1. Since the Ca_3SiO_5 phases in the various quater-

nary systems are represented by three-dimensional bodies, it follows that in the quinary system a four-dimensional "body" occurs. The bodies in Figs. 2 to 4 represent limiting "faces" of the latter.

2. The independence of the limits of solubility, for the atoms Mg and Al as well as Mg and Fe resp. and the interaction between Al and Fe, observed in the quaternary systems, have been found to persist in the quinary system. The CaO-concentration does not influence the solubility limits of the other atoms.

3. The "CaO-width" of the tricalcium silicate phase saturated with ($Al_2O_3 + Fe_2O_3$) is increased by addition of MgO.

4. No "higher" modification than M_I has been obtained in the quinary system at room temperature.

5. Tricalcium silicate in the quinary system CaO–MgO–Al_2O_3–Fe_2O_3–SiO_2 closely resembles the alite phase in technical clinker. Thus our results may safely be extended to technical alite (10).

Discussion

The investigations established that alites are true solid solutions of Ca_3SiO_5 which are represented by definite phase regions in the appropriate multi-component systems. The ranges of these solid solutions are very small, except for the unlimited substitution Si–Ge.

The different modes of incorporation of foreign ions are based on simple substitution types which are well known in crystal chemistry, for example the distribution of Al^{3+} or Fe^{3+} among tetrahedral and octahedral sites in silicates.

Mutual interactions of Mg, Al and Fe influence the stabilization of the high-temperature modifications T_I, T_{II} and M_I: Figs. 2 to 4 demonstrate that the amount of one oxide which is necessary to obtain a "higher" form is decreased with increasing amounts of the other oxide. These results as well as those of Ono, Uno and Kanai (18) indicate that by addition of further suitable atoms also the modifications M_{II} and R can be stabilized., thus explaining the occurrence of these forms in some clinkers.

Acknowledgement

We gratefully acknowledge support of this work by the "Verein Deutscher Zementwerke e.V." and the "Deutsche Forschungsgemeinschaft".

References

1. A. Guttmann and F. Gille, "A final statement on the Alite problem" (in German) Zement **20**, 144–147 (1931).
2. J. W. Jeffery, "The crystal structure of tricalcium silicate", Acta Cryst. **5**, 26–35 (1952).
3. a. H. O'Daniel, Th. Hahn and H. Müller, "The structure of $3CaO \cdot SiO_2$: Investigations with Patterson syntheses" (in German), Neues Jahrb. Mineral. Monatsh. 1–15 (1953).
   b. Th. Hahn, "New determination of the structure of tricalcium silicate, Ca_3SiO_5" (in German), Silikattechnik **11**, 396–397 (1960).
4. J. W. Jeffery, "The tricalcium silicate phase", Proc. 3. Int. Symp. Chem. Cements, London 1952, Cement and Concrete Assoc., London (1954), p. 30–55.
5. M. Bigaré, A. Guinier, C. Mazières, M. Regourd, N. Yannaquis, W. Eysel, Th. Hahn and E. Woermann "Polymorphism of tricalcium silicate and its solid solutions", J. Am. Ceram. Soc. **50**, 609–619 (1967).
6. E. Woermann, Th. Hahn and W. Eysel, "Chemical and structural investigations on the solid solutions of tricalcium silicate. I" (in German) Zement-Kalk-Gips **16**, 370–375 (1963).
7. E. Woermann, W. Eysel and Th. Hahn "Chemical and structural investigations on the solid solutions of tricalcium silicate. II: Phase relations in the systems CaO–MgO–SiO_2 and CaO–Al_2O_3–SiO_2" (in German), Zement-Kalk-Gips **20**, 385–391 (1967).
8. E. Woermann, W. Eysel and Th. Hahn, "Chemical and structural investigations on the solid solutions of tricalcium silicate. III: Combined substitution of MgO and Al_2O_3 in Ca_3SiO_5" (in German) Zement-Kalk-Gips **21**, 241–251 (1968).
9. E. Woermann, W. Eysel and Th. Hahn, "Chemical and structural investigations on the solid solutions of tricalcium silicate. IV: Combined substitution of Fe_2O_3, Al_2O_3 and MgO in Ca_3SiO_5" (in German) Zement-Kalk-Gips, in press.
10. E. Woermann, W. Eysel and Th. Hahn, "Chemical and structural investigations on the solid solutions of tricalcium silicate. V: The alite phase in the

quinary system $CaO–MgO–Al_2O_3–Fe_2O_3–SiO_2$ and in cement clinker" (in German), Zement-Kalk-Gips, to be published.
11. a. A. I. Boikova and N. A. Toropov, "Stoichiometry and polymorphism of tricalcium silicate", (in Russian), Dokl. Akad. Nauk. SSSR **156,** 1428–1431 (1964).
    b. N. A. Toropov, "Cation and anion replacements in the structure of tricalcium silicate", Paper 1–36 of this symposium (1968).
12. a. F. W. Locher, "Solid solution of Al_2O_3 and MgO in tricalcium silicate" (in German), Zement-Kalk-Gips **13,** 389–394 (1960).
    b. F. W. Locher, "Solid solution of alumina and magnesia in tricalcium silicate", Proc. 4. Int. Symp. Chem. Cements, Washington (1960), Nat. Bur. Standards, Washington (1962), Vol. I, p. 99–106.
13. H. G. Midgley and K. E. Fletcher, "The role of alumina and magnesia in the polymorphism of tricalcium silicate", Trans. Brit. Ceram. Soc. **62,** 917–937 (1963).
14. a. Th. Hahn and W. Eysel, "Structure and polymorphism of tricalcium germanate" (in German), Naturwissensch. **50,** 471 (1963).
    b. W. Eysel and Th. Hahn, "Crystal chemistry, polymorphism and solid solutions of silicates and germanates. I: Ca_3GeO_5 and Ca_3SiO_5", in course of preparation.
15. A. I. Boikova, N. A. Toropov and V. T. Vavilonova, "Structural relations and solid solutions of tricalcium silicate and tricalcium germanate" (in Russian), Doklady Akad. Nauk. USSR **175,** 653–658 (1967).
16. K. E. Fletcher, "The effect of Fe^{3+} and Al^{3+} on the polymorphism of tricalcium silicate", Trans. Brit. Ceram. Soc. **64,** 377–385 (1965).
17. G. Yamaguchi and K. Kato, "$3CaO \cdot SiO_2–Al_2O_3–MgO$ solid solution", Rev. Gen. Meeting Japan. Cement Engin. Assoc. **16,** 28–32 (1962).
18. Y. Ono, T. Uno and Y. Kanai, "Synthesis of five polymorphic modifications of C_3S", Rev. Gen. Meeting Japan. Cement Engin. Assoc. **19,** 36–41 (1965).

Supplementary Paper 1-92 A Structural Study on α'-Ca_2SiO_4

Kazutaka Suzuki* and Goro Yamaguchi**

Synopsis

The α'-C_2S is synthesized by substituting Ba, Sr for Ca and substituting B for Si. The authors synthesized the single crystal of α' form and analyzed the structure of it by optical observation, Laue method, rotating crystal method and X-ray goniometry. The lattice parameters of the α' form with Ba, Sr and B were obtained about as follows; $a = 11.07$Å, $b = 18.80$Å, $c = 6.85$Å in Ba stabilized, $a = 11.02$Å, $b = 18.69$Å, $c = 6.83$Å in Sr stabilized and $a = 10.96$Å, $b = 18.43$Å, $c = 6.86$Å in B stabilized. Among them the lengths of a- and b-axes are 2 times as long as so far authorized ones ($a = 5.49$Å, $b = 9.26$Å, $c = 6.75$Å). The 152 diffraction which could be interpreted only by these large lattice was also observed in pure α'-C_2S by the high temperature X-ray diffraction. The crystal structure of α'-C_2S stabilized by Ba was analyzed and the atomic parameters were determined.

Introduction

As to the crystal structure of C_2S polymorphs, only that of β-C_2S is reliable because it has been analyzed by the single crystal method (1). The structures of other polymorphs have been estimated by Yamaguchi et al. (2), but they cannot but be said to be approximation. Suzuki (3) investigated the substitution amount and the sort of the ion which can stabilize each form and obtained α' form by Ba, Sr and B, α form by Ba, V, P and β form by a small quantity of each ion when the preparations were carried out by quenching from about 1500°C. According to the above mentioned experiments, the authors succeeded to obtain single crystals of α'–C_2S so that they attempted to analyze a true crystal structure.

Preparation of α'-C_2S Stabilized by Ba, Sr and its X-ray Analysis

The mixtures of raw materials of C_2S whose CaO is substituted by 0.15–0.30 mole of BaO or SrO were burned at 1500°C about 20 minutes and quenched, thus α'–C_2S was formed distinctly containing single crystals of fairly good size. In more substitution of BaO, about 0.7 mole, α type was formed by quenching, but by substitution of SrO none of α type was formed. The composition of single crystal was 56.12 per cent CaO, 11.21 per cent BaO and 32.67 per cent SiO_2 and that stabilized by Sr was 57.84 per cent CaO, 8.65 per cent SrO and 33.51 per cent SiO_2. Optical observation revealed the crystals have no twinning and the refraction indices are $n_g = 1.741$, $n_p = 1.726$ in Ba stabilized one and $n_g = 1.737$ and $n_p = 1.721$ in Sr stabilized one. Laue's photographs of these α'–C_2S are really same one another, namely, the symmetries along X, Y are that with perpendicularly crossed mirror planes, but along Z is pseudo 3 fold. The reciprocal lattice projections on $b^* - c^*$ plane and rotating crystal photographs about a-axis show that the length of a-, b-axis are about 2 times as long as those of Tromel's α'–C_2S (4); $a = 11.07$Å, $b = 18.80$Å, $c = 6.85$Å in Ba stabilized one and $a = 11.02$Å, $b = 18.69$Å, $c = 6.83$Å in Sr stabilized one. These Laue's photographs, rotating crystal photograph and reciprocal projections are shown in Fig. 1, Fig. 2 and Fig. 3. The systematic absence of this projections are as follows:

hkl	$h + k = 2n$	h00	$h = 2n$
0kl	$k = 2n$	0k0	$k = 2n$
h0l	$1 = 2n$	00l	$1 = 2n$
hk0	$h + k = 2n$		

*Nagoya Institute of Technology, Nagoya, Japan.
**Faculty of Engineering, The University of Tokyo, Japan.

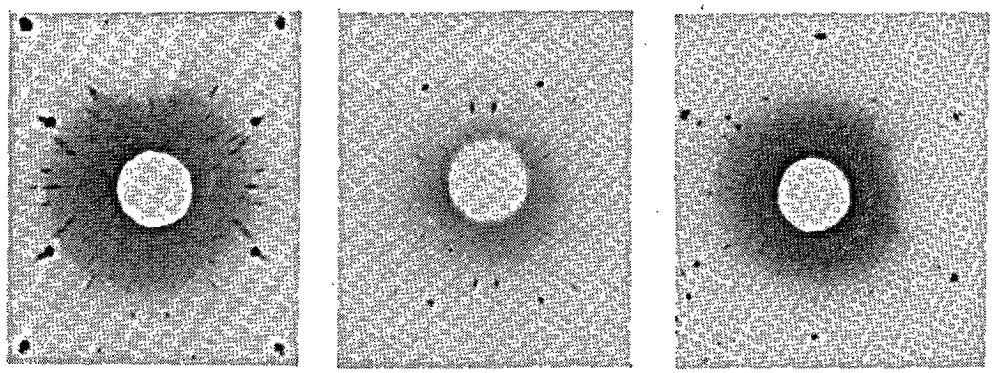

Along a-axis Along b-axis Along c-axis

Fig. 1. *Laue's photographs of α′-C_2S stabilized by Ba*

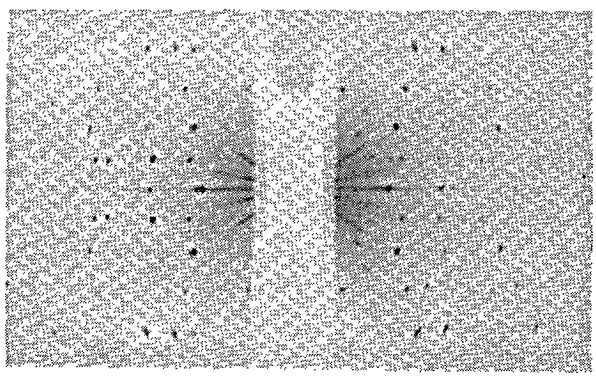

Fig. 2. *Rotating crystal photograph of α′-C_2S stabilized by Ba (about a-axis)*

Thus the space group of this α′ form was decided as $Cmc2_1$. The X-ray powder diffraction figures were indexed and the lattice parameters were calculated as shown in Table 1 and Fig. 4.

Table 1-1. *Powder diffraction data of α′-C_2S stabilized by Ba* $a = 11.07$Å, $b = 18.80$Å, $c = 6.85$Å

hkl	observed			calculated	
	2θ(CuKα)	d	I/I_o	2θ(CuKα)	d
040	18.98	4.67	5	18.94	4.69
002	25.94	3.43	3	25.91	3.45
112	27.56	3.23	3	27.56	3.23
022, 311	27.65	3.22	3	27.63	3.22
				27.75	3.21
241	28.08	3.17	10	28.08	3.17
202	30.59	2.919	11	30.56	2.922
132	30.78	2.903	8	30.74	2.906
331	30.85	2.896	4	30.92	2.891
061	31.51	2.838	5	31.45	2.842
222	32.06	2.789	65	32.05	2.790
400, 042	32.19	2.778	74	32.21	2.777
				32.28	2.770
260	32.88	2.721	100	32.88	2.721
152	36.35	2.469	3	36.36	2.468
440	37,67	2,386	10	37,62	2,389
062	38.95	2.310	8	38.95	2.310
441	40.00	2.252	13	39.92	2.256
113, 023	40.56	2.222	11	40.45	2.228
				40.51	2.225
081	40.72	2.214	15	40.68	2.216
422	42.93	2.105	5	42.93	2.105
223	43.83	2.064	5	43.78	2.056
281, 043	44.00	2.056	7	43.97	2.058
				43.97	2.058
461	45.75	1.982	4	45.65	1.986
191, 442	46.30	1.959	16	46.26	1.960
				46.27	1.960
082	46.92	1.935	3	46.92	1.935
153	47.09	1.928	3	47.10	1.928

Table 1-2. *Powder diffraction data of α′-C_2S stabilized by Sr* $a = 11.02$Å, $b = 18.69$Å, $c = 6.83$Å

hkl	observed			calculated	
	2θ(CuKα)	d	I/I_o	2θ(CuKα)	d
040	19.01	4.66	4	18.98	4.67
002	26.05	3.418	2	26.07	3.41
112				27.72	3.21
022, 311	27.81	3.21	2	27.79	3.20
				27.81	3.20
241	28.16	3.17	15	28.16	3.17
202	30.73	2.907	10	30.72	2.907
132, 331	30.88	2.893	5	30.91	2.891
				31.00	2.882
061	31.51	2.837	7	31.55	2.833
222	32.22	2.776	75	32.21	2.776
400, 042	32.25	2.773	95	32.26	2.773
				32.45	2.757
260	32.96	2.715	100	32.96	2.715
152	36.50	2.460	4	36.52	2.458
440	37.69	2.384	8	37.69	2.384
062	39.22	2.301	15	39.22	2.301
441	40.05	2.249	17	40.02	2.251
113, 023	40.73	2.213	19	40.71	2.214
				40.76	2.212
081	40.76	2.212	24	40.80	2.210
422	43.09	2.098	7	43.09	2.098
223, 281	44.05	2.054	5	44.04	2.054
				44.08	2.053
043	44.16	2.050	9	44.22	2.046
461	45.87	1.977	7	45.92	1.974
191, 442	46.41	1.955	15	46.40	1.955
				46.41	1.955
082	47.12	1.931	3	47.11	1.928
153	47.20	1.924	2	47.23	1.923

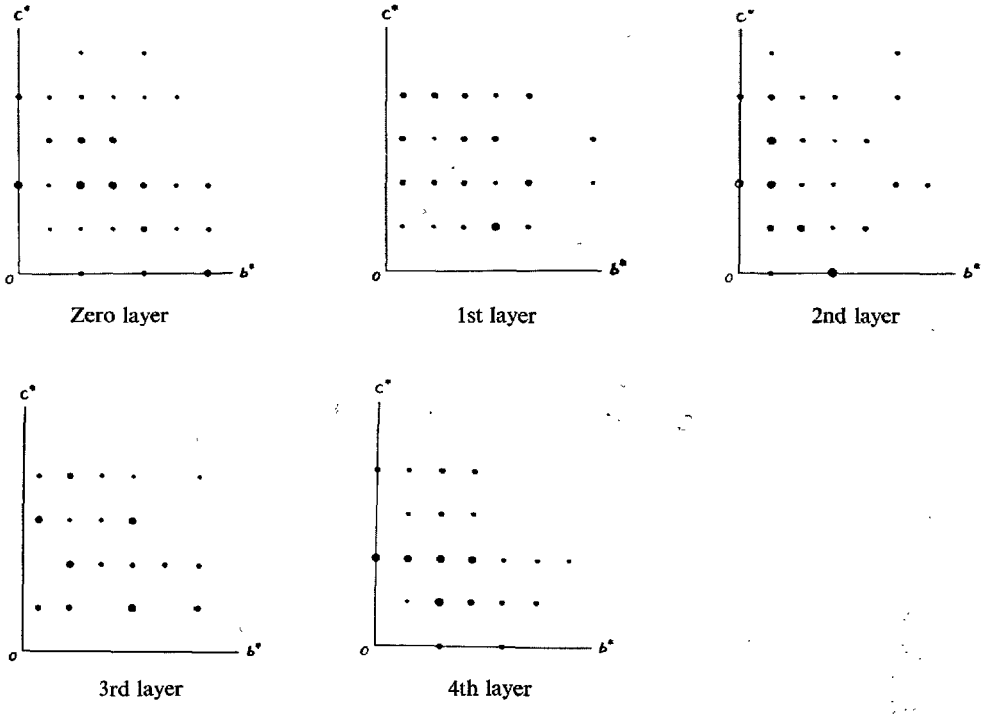

Fig. 3. *Reciprocal lattice projections of α′-C_2S stabilized by Ba (about a-axis)*

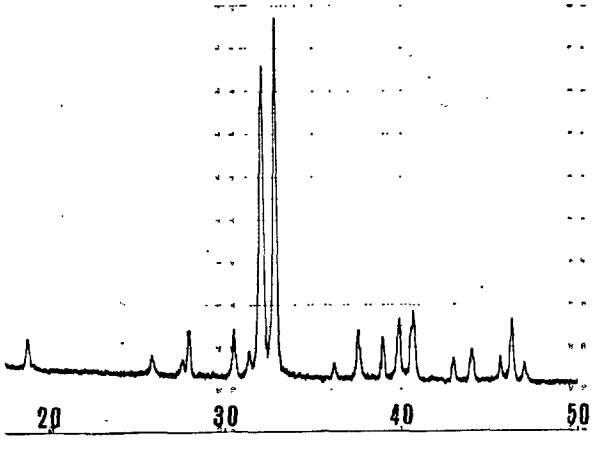

Fig. 4-1. *X-ray powder diffraction pattern of α′-C_2S stabilized by Ba*

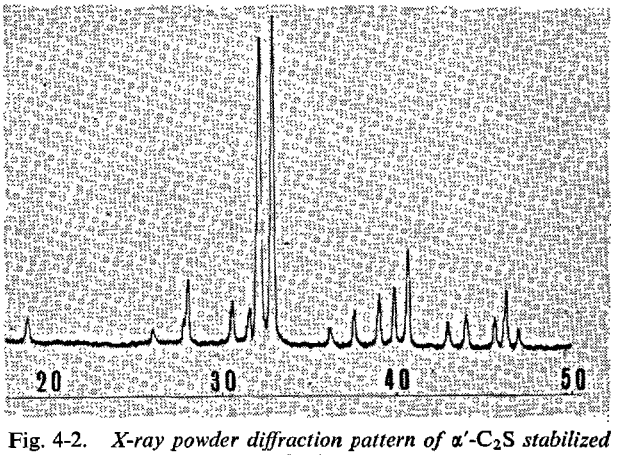

Fig. 4-2. *X-ray powder diffraction pattern of α′-C_2S stabilized by Sr*

Preparation of α′-C_2S Stabilized by B and its X-ray Analysis

The raw materials mixtures were prepared supposing the substitution of B for Si. The most proper composition to get α′ form was 67.88 per cent CaO, 31.17 per cent SiO_2, 0.95 per cent B_2O_3. This mixture was heated and quenched from the temperature of 1450–1500°C and the single crystal was picked up from the products whose composition was analyzed to have about the same composition as the raw materials mixture; 67.91 per cent, CaO, 31.18 per cent SiO_2, 0.91 per cent B_2O_3. Optical properties are the same as that of Ba stabilized one and the refraction indices were $n_g = 1.732$ and $n_p = 1.709$. The symmetry of Laue's photographs and the projection data by Weissenberg goniometry are nearly the same as those of

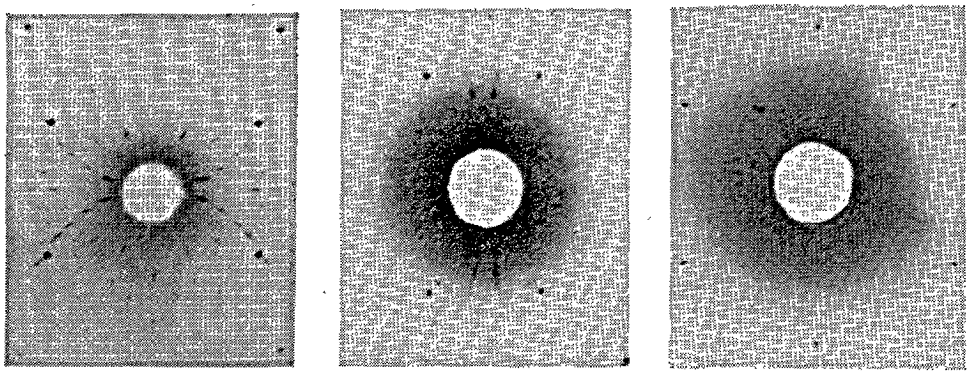

Fig. 5. *Laue's photographs of α′-C_2S stabilized by B*

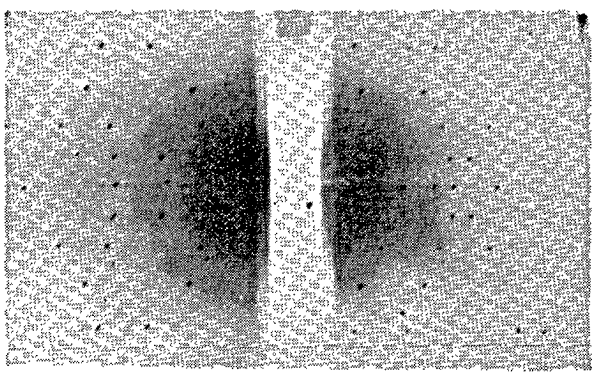

Fig. 6. *Rotating crystal photograph of α′-C_2S stabilized by B (about a-axis)*

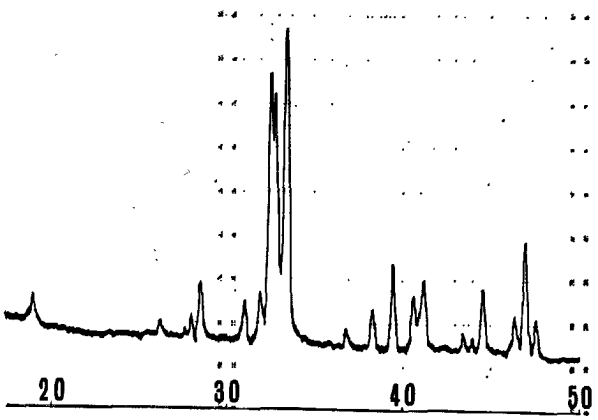

Fig. 7. *X-ray powder diffraction pattern of α′-C_2S stabilized by B*

Table 2. *Powder diffraction data of α′-C_2S stabilized by B $a = 10.96$Å, $b = 18.43$Å, $c = 6.86$Å*

hkl	observed			calculated	
	2θ(CuKα)	d	I/I_0	2θ(CuKα)	d
040	18.93	4.61	8	19.25	4.61
002	25.94	3.43	6	25.96	3.42
112	27.57	3.23	1	27.66	3.22
022	27.87	3.20	7	27.74	3.21
311	28.10	3.17	7	28.06	3.18
241	28.41	3.14	17	28.43	3.14
202	30.79	2.901	5	30.73	2.907
132	30.98	2.884	13	30.93	2.888
331	31.33	2.853	18	31.30	2.856
061	31.87	2.806	1	31.90	2.803
222	32.36	2.764	38	32.26	2.774
042	32.54	2.749	83	32.52	2.751
400	32.64	2.741	79	32.64	2.741
260	33.42	2.679	100	33.42	2.679
152	36.76	2.443	6	36.69	2.447
440	38.25	2.351	13	38.17	2.356
062	39.34	2.288	26	39.35	2.288
441	40.49	2.226	12	40.45	2.228
113	40.59	2.221	17	40.57	2.222
023				40.63	2.219
081	41.24	2.187	22	41.31	2.183
422	43.38	2.084	3	43.35	2.085
223	44.03	2.055	4	43.99	2.057
043	44.24	2.046	4	44.19	2.048
281	44.61	2.029	19	44.63	2.028
461	46.35	1.957	13	46.29	1.960
442	46.92	1.934	36	46.75	1.942
191	47.24	1.922	8	47.15	1.931
153	47.50	1.912	13	47.49	1.913
082				47.51	1.912

α′ form substituted by Ba and Sr. Thus, it was clarified that this crystal has the same structure as those synthesized by Ba, Sr. Laue's photographs and rotating crystal photograph are shown in Fig. 5 and Fig. 6, and X-ray powder diffraction data and figure are shown in Fig. 7 and Table 2. Lattice lengths of it are listed as $a = 10.96$Å, $b = 18.43$Å, $c = 6.86$Å.

Lattice Parameters of Pure α′-Ca_2SiO_4

The lattice parameters of α′ form stabilized by Ba, Sr and B have all the same periodicity along each axis, and this is based on the same stacking of Ca and SiO_4 packing. But these periodicity seems unlikely

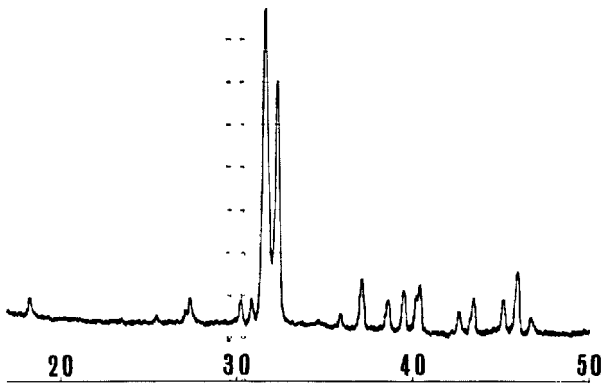

Fig. 8. *High temperature X-ray diffraction pattern of pure* α'-C_2S *(at 1000°C)*

due to the substutution of Ba, Sr or B ion at the symmetrical place such as to make these periodicity along each axis. For example, in the calculation of the structure factor of α' form stabilized by Ba, an assumption that Ba is substituted for the special position of Ca gives less agreement than an assumption that Ba enters to the position of Ca at random. In the former assumption, the atomic scattering factor of Ba and Ca were adopted for each atom respectively in calculation, but in the latter, mean values according to the composition ratio of Ba and Ca were adopted. The synthesis of a single crystal of pure α'-C_2S is unable, so that the high temperature X-ray diffraction method should be taken as the only method to confirm the periodicity. Pure γ-C_2S was employed for this experiment. It inverts into α' at about 890°C and to α at 1450°C. In the range of temperature where α' form is stable, the characteristic peak such as to suggest the lattice parameters appears in the diffraction pattern; this was confirmed by 152 diffraction. This diffraction pattern is shown in Fig. 8.

The Crystal Structure of α'-C_2S Stabilized by Ba

Determination of atomic parameters of α'-C_2S and their refining by Fourier synthesis were carried out. The α' form stabilized by Ba was used because its X-ray powder diffraction figure is most similar to that of pure α'-C_2S. Approximately cylindrical crystal having average radius of 0.2 mm, was used for collecting intensity data. The intensity data were recorded on equi-inclination Weissenberg photographs by the multiple-film technique with Cu Kα radiation. Five layers 0k*l*–4k*l* were collected about the *a*-axis. Absorption effect was so small that it was neglected and the extinction effect was also negligible. The structure factors were caluculated using the temperature factor 1.1, and the parameters that was made by piling the Yamaguchi's unit cell (2) gave a reliability index $R = 0.42$. This shows that Yamaguchi's data are fairly reliable. But about the structure of stabilized by Ba, the pile are not constructed by parallel moving of the Yamaguchi's cell but are constructed with small shift. This is explained by the fact that if the pile is made by parallel moving of the unit cell, the diffraction such as $h + k = 2n$ disappeared when h and k are both odd, but if the pile is constructed with small shift, the upper diffraction appears and its structure factors are not usually zero. Thus the slight moving of Ca, Si or O atom can make the structure factors to have more good agreement with observed structure factors. For this purpose two-dimensional or three-dimensional Fourier summations were carried out on the computer. Form the symmetry of the space group it is understood that the projection is sufficient to be limited in $a/2 \times b/2 \times c$. The former was carried out to obtain a projection on *b*-*c* plane deviding $b/2$ into 30 parts and *c* into 20 parts and calculating the summation of F(0k*l*) in a range of $k = 0 - 8$, $l = 0 - 4$. The latter was carried out to obtain bounded projections on *a*-*c* plane limited bound of *b*-axis 0.0–0.25, 0.25–0.50, deviding $a/2$ into 20 parts and *c* into 20 parts and calculating the summation of F(hk*l*) in a range of $h = 0 - 4$, $k = 0 - 8$, $l = 0 - 4$. Thus the atomic parameters in the step of the present time, the bond lengths and angles were obtained as shown in Table 4 and Table 5. The structure factor calculated showed fairly good agreement with those observed. Thus the R index was reduced to 0.11 for both 0k*l* and kh*l* reflexions. A list of observed and calculated

Table 4. *Atomic parameters of* α'-C_2S *stabilized by Ba*

	x	*y*	*z*
Ca 1	0.00	−0.095	0.382
Ca 2	0.00	0.405	0.367
Ca 3	0.25	0.17	0.113
Ca 4	0.00	0.271	0.00
Ca 5	0.00	0.228	0.50
Ca 6	0.25	0.022	0.50
Si 1	0.25	0.16	−0.28
Si 2	0.00	0.105	0.28
Si 3	0.00	0.395	−0.22
O 1	0.125	0.20	−0.16
O 2	0.375	0.20	−0.16
O 3	0.25	0.08	−0.17
O 4	0.25	0.155	−0.54
O 5	0.125	0.065	0.16
O 6	0.00	0.185	0.17
O 7	0.00	0.11	0.54
O 8	0.125	0.435	−0.34
O 9	0.00	0.315	−0.33
O 10	0.00	0.39	0.04

structure factors is given in Table 3, and the electron-density maps are shown in Fig. 9.

Table 5. *Chief bond lengths and angles*

Ca1–01	2.42Å	06–Ca1–05	64°13′
Ca1–03	2.81	06–Ca1–01	63 37
Ca1–05	2.40	07–Ca1–01	89 2
Ca1–06	2.56	07–Ca1–03	82 14
Ca1–07	2.32	05–Ca1–05′	70 53
		05–Ca1–03	60 00
Ca6–03	2.47	05–Ca1–05′	130 10
Ca6–03′	2.23	01–Ca1–01′	70 1
Ca6–05	2.79		
Ca6–08	2.40		
		03–Ca7–08	84 12
Si1–01	1.77	08–Ca7–05	70 48
Si1–02	1.77	08–Ca7–05	69 41
Si1–03	1.67	03–Ca7–08	80 21
Si1–04	1.75	08–Ca7–08′	105 40
		08–Ca7–05	146 6
01–02	2.78	03–Ca7–08	127 27
01–03	2.64		
01–04	3.02		
03–04	2.86		

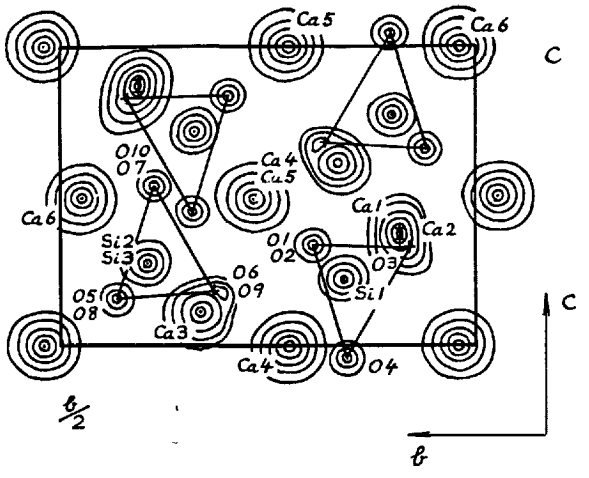

Fig. 9-1. *Section of the electron density map on b-c plane*

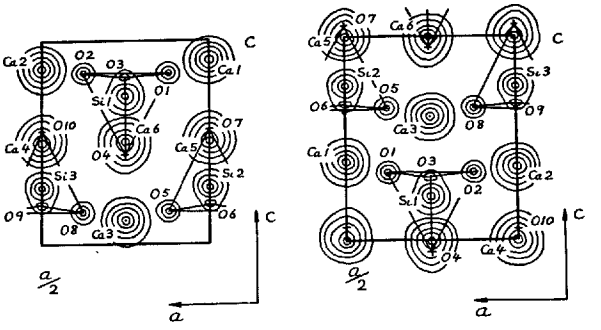

0.25–0.50 0.00–0.25

limited bound of *b*-axis

Fig. 9-2. *Sections of the electron density maps on a-c plane*

Table 3. *Observed and calculated structure factors of α′-C_2S*

hkl	Fo	Fc	hkl	Fo	Fc	hkl	Fo	Fc	hkl	Fo	Fc	hkl	Fo	Fc
001	0	0	101	0	0	201	0	0	301	0	0	401	0	0
2	141	149	2	0	0	2	330	334	2	0	0	2	402	392
3	0	0	3	0	0	3	0	0	3	0	0	3	0	0
4	76	78	4	0	0	4	121	120	4	0	0	4	340	356
010	0	0	110	0	0	210	0	0	310	0	0	410	0	0
1	0	0	1	9	7	1	0	0	1	13	7	1	0	0
2	0	0	2	21	19	2	0	0	2	0	18	2	0	0
3	0	0	3	19	17	3	0	0	3	42	16	3	0	0
4	0	0	4	25	30	4	0	0	4	36	28	4	0	0
020	80	145	120	0	0	220	202	244	320	0	0	420	12	73
1	186	185	1	0	0	1	102	68	1	0	0	1	92	113
2	70	64	2	0	0	2	411	425	2	0	0	2	476	504
3	660	676	3	0	0	3	603	620	3	0	0	3	247	204
4	35	24	4	0	0	4	404	394	4	0	0	4	401	376
030	0	0	130	0	0	230	0	0	330	0	0	430	0	0
1	0	0	1	23	12	1	0	0	1	9	11	1	0	0
2	0	0	2	20	5	2	0	0	2	25	4	2	0	0
3	0	0	3	18	29	3	0	0	3	32	27	3	0	0
4	0	0	4	25	7	4	0	0	4	48	7	4	0	0
040	282	278	140	0	0	240	0	0	340	0	0	440	350	327
1	65	60	1	0	0	1	325	318	1	0	0	1	467	500
2	457	469	2	0	0	2	220	237	2	0	0	2	466	480
3	402	418	3	0	0	3	212	223	3	0	0	3	463	439
4	335	310	4	0	0	4	180	171	4	0	0	4	350	328
050	0	0	150	0	0	250	0	0	350	0	0	450	0	0
1	0	0	1	45	32	1	0	0	1	0	2	1	0	0
2	0	0	2	10	21	2	0	0	2	42	20	2	0	0
3	0	0	3	29	4	3	0	0	3	16	4	3	0	0
4	0	0	4	16	33	4	0	0	4	7	31	4	0	0
060	0	13	160	0	0	260	940	985	360	0	0	460	0	89
1	81	64	1	0	0	1	138	20	1	0	0	1	302	345
2	275	413	2	0	0	2	245	283	2	0	0	2	590	639
3	593	551	3	0	0	3	163	204	3	0	0	3	167	126
4	139	175	4	0	0	4	188	154	4	0	0	4	249	227
070	0	0	170	0	0	270	0	0	370	0	0	470	0	0
1	0	0	1	180	154	1	0	0	1	42	9	1	0	0
2	0	0	2	29	48	2	0	0	2	26	9	2	0	0
3	0	0	3	131	153	3	0	0	3	46	22	3	0	0
4	0	0	4	103	58	4	0	0	4	43	15	4	0	0

Conclusion

From the result of high temperature X-ray diffraction of pure C_2S, we acknowledged that 152 peak appears in many case in the temperature range where α' form is stable. This shows that the pure C_2S has perhaps the same periodicity as that of α' solid solution phase. But the intensity of this diffraction is not strong and it does not appear immediately after α' inversion. When the specimen is kept in its stable temperature more than 20 minutes, the peak appears perhaps according to the good rearrangement of atom packing The other diffractions which prove the doubling of *a*- and *b*-axes, lie overlapping upon another diffractions, so we cannot confirm the doubling of *a*-, *b*-axis by them. This 152 diffraction appears also in other α' forms stabilized by V and P. Four Si–O distances of the SiO_4 tetrahedra are significantly different. And this is caused by the combination of each O to two types of Ca ion. As to 32 Ca ions, 16 of them (Ca 1, 2, 3) are positioned alternately above and below SiO_4 tetrahedra in the *z* direction and the remaining 16 (Ca 4, 5, 6) are accommodated in the holes between the tetrahedra. The co-ordination number of Ca, 1, 2, 3 are eight and of Ca 4, 5, 6 are six. The positions of Ca 1, 2, 3 are perhaps easily substituted by other ions but in the structure of α' form the stabilizing ion does not enter into the special position of Ca or Si but enters at random.

References

1. C. M. Midgley, Acta Crystallographica, **5,** 307 (1952).
2. G. Yamaguchi, Y. Ono, S. Kawamura and Y. Soda, "Synthesis of the modifications of Ca_2SiO_4 and the determination of their powder X-ray diffraction patterns" J. Ceram. Assoc. **71,** 21–26 (1963).
3. K. Suzuki and M. Tsujita, "Influence of the minute quantity of impurities on the transformation of dicalcium silicates" J. Ceram. Assoc. **69,** 241–257 (1961).
4. G. Tromel, Naturwissenschaften **36,** 3 88 (1949).

Oral Discussion

Yoshio Ono

As I understand, you have determined the space-group of the low-temperature form of α'–C_2S being $Cmc2_1$. Could you tell me how you did it? What is the correlation between this and the high-temperature form?

Authors' Closure

K. Suzuki and G. Yamaguchi

The space group and the structure of α'_H was suggested by us.* Its space group is Pnma and in another setting Pmcn as shown in the figure. While the X-ray powder diffraction pattern of α'_L is very similar to that of α'_H, so that α'_L has a very similar atomic arrangement to α'_H. It was interpreted that the unit cell of α'_H is piled toward *a*- and *b*-directions by two times slightly changing symmetries as shown in the figure. Thus the space group of α'_L was determined as $Cmc2_1$.

* J. Ceram. Assoc. Japan, 71, 21-26 (1963)

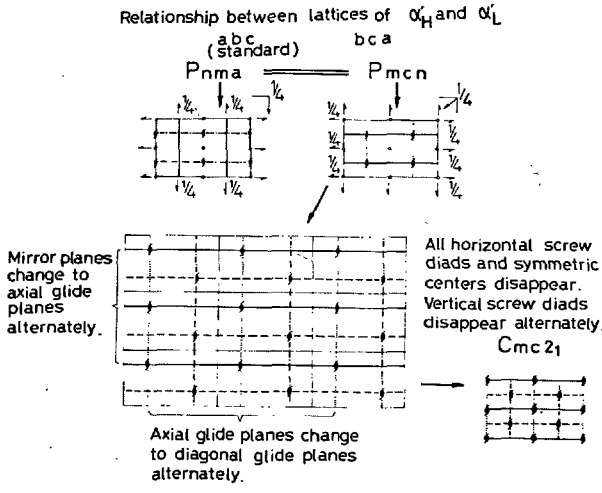

Supplementary Paper 1-127 New Crystallographic Data of Some Calcium Silicate Phases

Friedrich K. F. Liebau*

Synopsis

Attempts to prepare material of Ca_2SiO_4 and Ca_3SiO_5 for hydration studies yielded besides others single crystals which by X-ray methods gave crystallographic data different from those given in the literature for calcium silicates.

1) Ca_2SiO_4: For one phase lattice constants similar but definitely $CaCl_2$ small amounts of slightly hygroscopic needle-like crystals were formed. X-ray single crystal studies and crystal optical studies revealed two different but structurally related phases. Lattice constants show no relation to other known calcium-silicates. Crystals of both phases show diffuse OD-structure diffraction effects. The chemical composition could not yet been determined but chloride ions were not detectable in them.

Lattice constants of all these phases will be given and other results of investigations in progress will be discussed.

Introduction

Experiments for the synthesis of material of Ca_2SiO_4 and Ca_3SiO_5 for hydration studies yielded a large number of crystals which were large enough for single crystal X-ray work. Many of these gave lattice constants in agreement with values given in the literature by various authors. A number of crystals, however, gave crystal data different from those given before. These new results only are described in this paper.

Ca_2SiO_4

A mixture of polycrystalline Ca_3SiO_5, Ca_2SiO_4 and a large excess of $CaCl_2$ was heated to 1500°C for 4 1/2 hours in a platinum vessel and slowly cooled in the furnace. After dissolution of the calcium chloride with methanol twinned crystals of γ-Ca_2SiO_4 ($\leq 400\ \mu$) and some platy crystals of up to 100 μ were found in the sample. One of the latter gave lattice constants which are compared with those given for α'-Ca_2SiO_4 by Bredig (1) and Douglas (2) and for merwinite $Ca_3Mg[SiO_4]_2$ by Nurse (3) in Table 1.

Although the cell dimensions of our crystal are similar to the values of Douglas' α'-Ca_2SiO_4 our crystal is certainly not identical with Douglas' α' because

$$^{a}\text{Liebau} < {}^{a}\text{Douglas}$$

while

$$^{b}\text{Liebau} > {}^{b}\text{Douglas}.$$

Only hk0 reflexions with $h + k = 2n$ and h00 reflexions with $h = 4n$ were observed in the Weissenberg diagram.

This and some other observations suggest that, depending on the amount and kind of impurities as well as the heating and cooling history of the Ca_2SiO_4 sample, the structure of the α' phase may be somewhat different. These structural differences are probably small at temperatures in the stability range of the α' phase and become more pronounced below this temperature range.

Table 1. *Cell dimensions of various* α'-Ca_2SiO_4 *varieties*

Phase	a[Å]	b[Å]	c[Å]
α', 20°C, Liebau (this paper)	$10.80 = 2 \times 5.40$	$18.92 = 2 \times 9.46$	6.79
α', 750°C, Douglas (1)	$11.08 = 2 \times 5.54$	$18.55 = 2 \times 9.28$	6.76
α', 700°C, Bredig (2)	5.30	9.55	6.78
merwinite, Nurse (3)	$10.77 = 2 \times 5.38$	9.20	$13.62 = 2 \times 6.36$

*Mineralogisch-petrographisches Institut der Universität Kiel, Kiel, West Germany.

Pseudowollastonite α-$CaSiO_3$

The low-temperature form β–$CaSiO_3$ is known as wollastonite. It is an inosilicate in which the [SiO_4] tetrahedra are joined to long chains. Due to different stacking sequences, there are at least three polytypes of this phase:

1) ordered triclinic wollastonite (4)
2) ordered monoclinic wollastonite (5)
3) disordered wollastonite (6, 7)

The high-temperature modification α-$CaSiO_3$ is called pseudowollastonite. It is a cyclosilicate containing [Si_3O_9] rings. So far three stacking modifications of this phase have been reported.

A fourth one has been found in this investigation.

From polycrystalline Ca_3SiO_5 heated with small amounts of $Ca(OH)_2$ and CaF_2 in a sealed quartz tube to 1300°C for 18 hours, dendritic pseudowollastonite crystals were formed by transport reactions. On Weissenberg photographs these crystals gave diffuse streaks parallel c* with intensity maxima for which $\zeta = n1\frac{l}{2}$ (related to c = 9.72 Å). No deviations from hexagonal symmetry were observed for the intensities. This disordered form of α–$CaSiO_3$ is, therefore, analogous to the disordered forms of $Sr_3Si_3O_9$ and $Ba_3Si_3O_9$ described by Hilmer (11) and Dornberger-Schiff (12).

Table 2. *Cell dimensions of the polytypes of pseudowollastonite*

	a[Å]	b[Å]	d_{000l}[Å]
Mc Geachin (8)	~6.9	~11.8	~9.8
Jeffery and Heller (9)	6.90	11.78	19.65 = 2 × 9.83
Smith (10)	~6.9	~11.8	~3 × 9.8
Liebau (this paper)	6.90	11.95	9.72

Phases of Unknown Chemical Compositions

An equimolar mixture of polycrystalline Ca_2SiO_4 and CaO was heated to 1500°C with an excess of $CaCl_2$ until the calcium chloride was almost evaporated. After treatment with methanol the resulting material was found containing a small amount of slightly hygroscopic needles. Microanalytically no chloride ions were detectable in them.

Single crystal diagrams revealed two different but structurally related phases with [010] as needle axes. The lattice constants of these two phases are given in Table 3.

They show no simple relations to the cell dimensions of any of the known calcium silicate phases.

For both phases reflexions with k = 2n + 1 are extremely weak and diffuse so that rotation photographs about [010] look similar to those of disordered β-wollastonite.

Due to the small amount and the failure to seperate these phases their chemical compositions could not yet be determined. Attempts to study these two phases in more detail are going on.

Table 3. *Cell dimensions of two new calcium silicate phases of unknown chemical composition*

	Phase LI	Phase LII
a[Å]	16.08	18.36
b[Å]	7.56	7.75
c[Å]	7.62	12.63
α[°]	90.0	90
β[°]	104.4	90.0
γ[°]	~90	90
V[Å³]	897	1797
Symmetry	triclinic	orthorhombic or monoclinic

References

1. A. M. B. Douglas, "X-ray investigation of bredigite", Miner. Mag. **29**, 875–884 (1952).
2. M. A. Bredig, "Polymorphism of calcium orthosilicate", J. Amer. Ceram. Soc. **33**, 188–192 (1950).
3. R. W. Nurse, "The dicalcium silicate phase", Proc. 3rd Internat. Sympos. Chemistry of Cement, London 1952, p. 56–90.
4. M. J. Buerger, "The arrangements of atoms in crystals of the wollastonite group of metasilicates", Proc. Nat. Acad. Sci. **42**, 113–116 (1956).
5. J. Tolliday, "Crystal structure of β-wollastonite", Nature **182**, 1012–1013 (1958).
6. J. W. Jeffery, "Unusual X-ray diffraction effects from a crystal of wollastonite", Acta Cryst. **6**, 821–825 (1953).
7. K. Dornberger-Schiff, F. Liebau and E. Thilo. "Über die Kristallstruktur des $(NaAsO_3)_x$, des Maddrellschen Salzes und des β-Wollastonits", Acta Cryst. **8**, 752–754 (1955).
8. H. McGeachin, private communication in "The chemistry of cements", editor H.F.W. Taylor, Academic Press, London 1964, Vol. 1, p. 139.
9. J. W. Jeffery and L. Heller, "Preliminary X-ray investigation of pseudowollastonite", Acta Cryst. **6**, 807–808 (1953).
10. G. W. Smith, private communication in "The chemistry of cements", editor H.F.W. Taylor, Vol. 1, p. 138.
11. W. Hilmer, "An X-ray investigation of strontium germanate, $SrGeO_3$", Soviet Physics-Crystallogr. **7**, 573–576 (1963).
12. K. Dornberger-Schiff, "The symmetry and structure of strontinum germanate $Sr(GeO_3)$ as a structure model for α-wollastonite, $Ca(SiO_3)$", Soviet Physics-Crystallogr. **6**, 694–700 (1962).

SESSION I-2 PHASE EQUILIBRIA AND FORMATION OF PORTLAND CEMENT MINERALS

Principal Paper Phase Equilibria and Formation of Portland Cement Minerals

Ronald W. Nurse*

Synopsis

A review is made of new or revised phase diagrams or associated data published since the Washington Symposium. Crystalline solutions of the main clinker phase are considered; insufficient attention has been paid to the dependence of solubility on temperature and to the precise composition of the solute. Systems between CaO, SiO_2 or CaO, Al_2O_3 and volatile components such as SO_3 and water vapour are described and also systems with fluxing agents such as fluorides. Deviations from equilibrium and especially the question of glass content are discussed. Some reference is made to kinetics of reactions occurring during the formation of the clinker minerals.

The conclusion is drawn that phase studies are a valuable aid to understanding clinker constitution, but that it is not warranted to try to obtain very great accuracy in calculating constitution from the chemical analysis. If very precise estimates of constitution are required each clinker must be individually studied by chemical, microscopie, X-ray and electron beam microprobe methods.

Introduction

In the course of this paper the constitution of clinker will be considered solely from the point of view of phase studies. Questions of mineral structure and direct estimation of consititution will be dealt with by other authors. Papers earlier than the Washington (1960) Symposium will rarely be referred to, and in order to avoid a too lengthy list of references it will be assumed that detailed references to the Washington and earlier symposia are unnecessary.

Cement Quaternary System, with MgO

System $CaO–SiO_2$

The currently accepted melting point diagram and stability relations in the pure system are given as diagram 237 in reference (1) and incorporate the revised melting behaviour of C_3S described by Welch and Gutt (2). Gutt has since revised the temperature of incongruent melting of C_3S to 2150°C with concomitant rise in the liquidus temperature (Fig. 1). From the viewpoint of cement technology the effects of solid solutions in the system on the silicate phases are of major interest and these will be discussed next.

The Solid Solutions of $3CaO \cdot SiO_2$

As has been shown in the previous paper, the pure substance C_3S can exist in many polymorphic forms.

*Building Research Station, Ministry of Public Building and Works, Garston, Watford, Herts., United Kingdom.

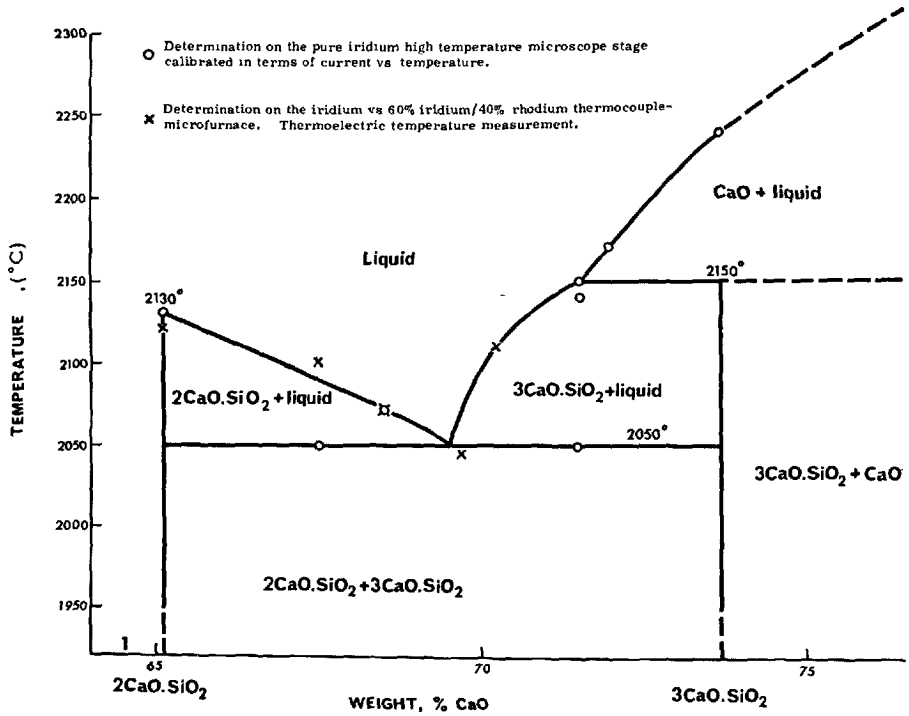

Fig. 1. *Revised phase diagram for lime-rich portion of system* $CaO–SiO_2$ *(Ref. 12)*

In theory, when C_3S is in equilibrium with other compounds and crystalline solutions are a possibility, the solubility/temperature curve for a given impurity will be different for each of the modifications, and the trend of this curve towards higher or lower temperatures will determine whether the presence of the impurity will stabilize the given polymorph or vice versa. In practice, the inversions all take place below 1050°C at a temperature where solution and exsolution will be very slow, and where they are metastable (because of the decomposition of C_3S at about 1275°C); therefore the matter of principal concern is the solid solubility of impurities in the trigonal form of C_3S stable at clinkering temperatures. This is the so-called alite of portland cement, although it may have inverted to a lower symmetry on cooling. The interval between first liquid formation and clinkering temperature is several hundred degrees, so that it is possible for a range of alite compositions to be found even in the same clinker, corresponding to the solubility levels of impurities at the different temperatures of formation.

We have to consider whether in these circumstances the phase diagram, being necessarily drawn for equilibrium conditions, is helpful.

An examination of recent investigations into alite shows that in many cases the results become clearer when the phase diagram is taken into account. Thus one frequently reads that the solubility of Al_2O_3 in C_3S has been determined. Such a crystalline solution must fall within the diagram C–A–S and since Al_2O_3 is not in equilibrium with C_3S in that system, it is extremely unlikely that a solid solution of these two components would form without side reactions involving the formation of C_2S in order to make extra calcium available for the solid solution. Midgley and Fletcher (3) have shown that this is the case and that 4.5 moles of CaO must accompany each mole of Al_2O_3 taken into solution in C_3S. An enlarged part of the phase diagram would appear as in Fig. 2. Below 1475°C, the temperature of the $C_3S–CaO–C_3A$ invariant point, the C_3S solid solution will be in equilibrium with C_3A and CaO; above, it will be in equilibrium with CaO and liquid. If now we consider the results of Woermann, Hahn and Eysel (4), we note that their preparations were made up with up to 4% excess CaO, and were processed at 1550°C. The inflections in their curves of CaO absorbed do not therefore indicate a change in the nature or composition of the solid solution but are to be expected as the composition of the starting material leaves the triangle $CaO–C_3S–C_3S$ (Solid Solution) and begins to form liquid at point "A". Considering only the compositions which do not melt, their results confirm exactly

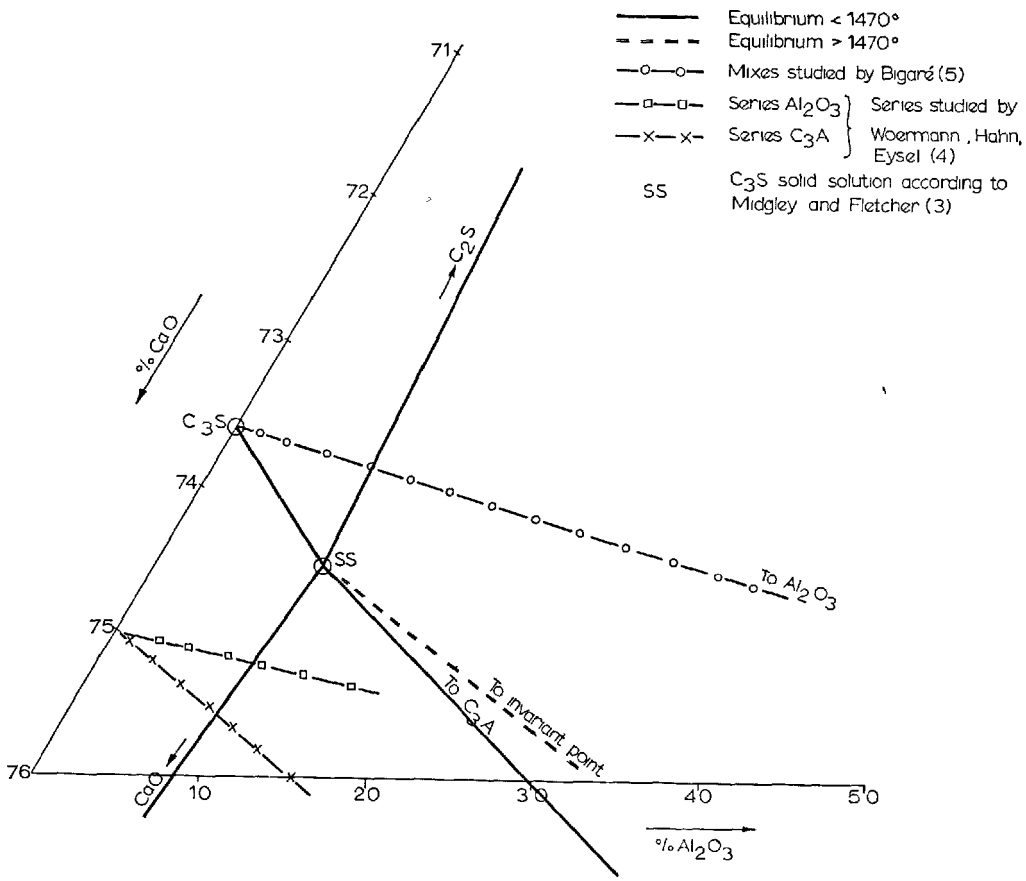

Fig. 2. *Part of system* $CaO–Al_2O_3–SiO_2$ *(Diagrammatic only)*

Midgley and Fletcher's ratio of 4.5 for the C/A in solid solution. Similarly Bigaré (5) calculates an "expected" C_3A content although his mixes were processed at 1650°C; the C_3A he found must have formed during the cooling of his specimens. Midgley and Fletcher also processed their mixes at a temperature where liquid formation is expected, but their solid solution composition was calculated after substraction of all other solid phases present including C_2S and C_3A and although the results are variable they should be free from consistent error. Locher (6) recognised that melting was occurring in those mixes between C_3S and C_3A containing more than 2% C_3A, but he assumed without proof that the solid solution lies on this join.

Midgley and Fletcher, and Woermann, Hahn and Eysel agree that each Al incorporated requires 2.25 Ca and a structural explanation can be found for this (3). Since the lines solid solution—CaO and solid solution—C_2S are essentially parallel to the $CaO–SiO_2$ side of the ternary system, the results of all authors can be compared as to the approximate percentage of Al_2O_3 taken up at the temperature of synthesis. About 1% by weight of Al_2O_3 is taken up at 1500°C, accompanied by enough CaO to maintain a C/A ratio of 4.5. There is some indication that the solubility falls off with increasing temperature but this tentative conclusion requires checking by further experiments. If it proved to be correct, it would explain why synthetic preparations based on Jeffery's (7) formula for alite are found to contain C_3A when processed at 1400–1450°C. Microprobe analyses of alite in clinker give Al_2O_3 contents from 0.2–1.1%.

By contrast, the solid solution of MgO in C_3S is a simple substitution of MgO for CaO. A phase diagram is suggested by Schlaudt and Roy (8) (Fig.3) and by Schlaudt (9). Woermann, Hahn and Eysel (4) show the increase in solubility with temperature (Fig. 4); their results are in fair agreement with others but probably underestimate the solubility somewhat, since they studied the join C_3S–MgO and not C_3S–"M_3S"; according to Fig. 3 their estimate represents the composition on the line from CaO towards the solid solution in equilibrium with CaO and MgO. Most

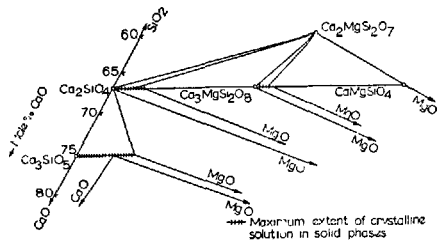

Fig. 3. *Revised solidus compatibility relations in part of system* $CaO–MgO–SiO_2$ *(Ref. 8)*

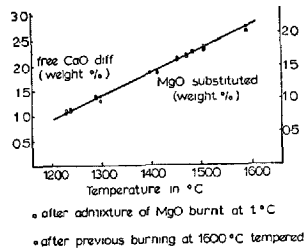

Fig. 4. *Increase in free* CaO *and consequent substitution of* MgO-*oversaturated* C_3S *samples (3% or 5%* MgO*) in relation to the reaction temperature (Ref. 4)*

authors agree that the solubility of MgO is little affected by Al_2O_3 and vice versa. Fletcher (10) found that Fe_2O_3 dissolved in C_3S to the extent of 1% by weight at 1400–1500°C in the form of a hypothetical $3CaO \cdot Fe_2O_3$. This conclusion was little changed by the simultaneous presence in solution of Al_2O_3 or MgO.

Solid Solutions of $2CaO \cdot SiO_2$

The position in this case is simpler, since the inversions in C_2S take place over a temperature range where the parent phase is stable. Most of the data reported by the present author at the 1952 Symposium remain valid, and most authors of new work have recognized the need to establish the nature of the new phase in equilibrium with the C_2S solid solution studied.

Yamaguchi, Ono and Kawamura state that in the presence of 2% MgO, C_2S is stable in content with C_3A and C_4AF when Al_2O_3 and Fe_2O_3 are added. The solubility of Al_2O_3 is between 2–3% by weight in the α-form (1400–1500°C) and less than 1% in the α′-form (1300°–1350°C); the solubility of Fe_2O_3 is 1.5% in the α-form at 1400°C, 2.5% in the α-form at 1500°C, and less than 1% in the α′-form at 1300–1350°C.

The solubility of MgO in C_2S according to Schlaudt and Roy is shown in Fig. 3. Gutt (12) also investigated the system $C_2S–C_3MS_2$; he noted some solubility of merwinite in α-C_2S but did not give a limit; Schlaudt and Roy give the equivalent of 1.5% MgO in α-C_2S at 1600°C. For α′C_2S at 1400°C Gutt gives 2% as against Schlaudt and Roy's 1.0% of MgO, but his diagram shows the solid solution in contact with phase $T(C_{1.7}M_{0.3}S)$, not merwinite.

System $CaO–Al_2O_3$

This system was revised (13) by Nurse, Welch and Majumdar, using high temperature microscopy and X-ray studies. That portion of special interest in portland cement was studied in more detail by the same

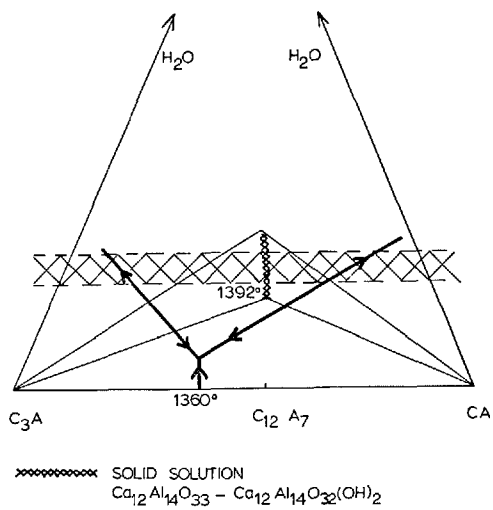

Fig. 5. *Hypothetical diagram* $CaO–Al_2O_3–H_2O$

authors (14), who showed the important effect of water in the furnace atmosphere on the equilibria observed. It appears probable that in a completely dry atmosphere a eutectic is formed between C_3A and CA, but at normal laboratory humidities a compound intermediate between $Ca_{12}Al_{14}O_{33}$ and $Ca_{12}Al_{14}O_{32}(OH)_2$ intervenes, melting into homogenous liquid at 1392°C with expulsion of water vapour. In the presence of products of combustion in rotary kilns, the formation of a '$C_{12}A_7$' phase in appropriate circumstances can be assumed.

No work appears to have been done to establish the effect of water vapour on the temperatures or positions of the invariant points involving $C_{12}A_7$ in such systems as C–A–S, C–A–S–F. Since the water vapour counts as an additional component, such invariant points will be one phase higher in rank and the additional phase will be in equilibrium.

Fig. 5 is a hypothetical representation of the phase equilibria in the system $CaO–Al_2O_3–H_2O$ at high temperatures. Preparations processed in moist laboratory air will fall within the shaded band, giving a '$C_{12}A_7$' phase which will expel water as the tempera-

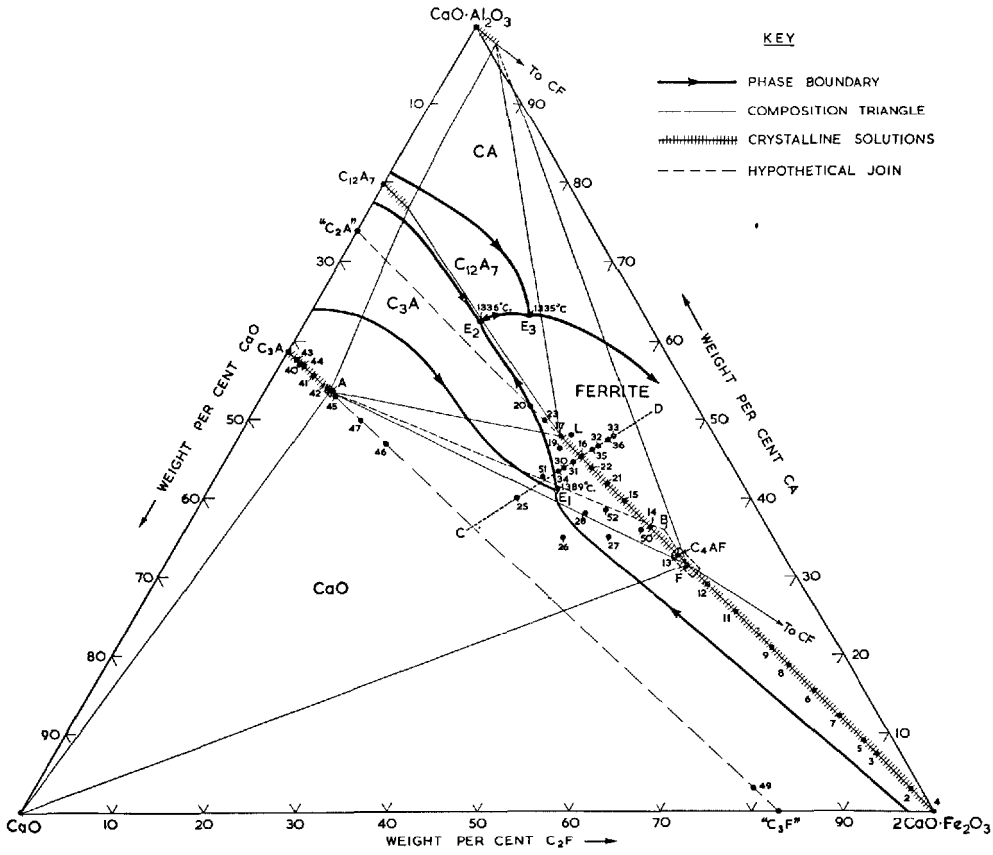

Fig. 6. *Amended phase-diagram for* $CaO–CaO \cdot Al_2O_3–2CaO \cdot Fe_2O_3$ *system.*

ture is raised so that '$C_{12}A_7$' disappears at the constant temperature 1392°C as reported in (14).

Solid Solutions of Calcium Aluminates

Miyazawa and Tomita (15) quote various determinations of the maximum solubility of MgO in C_3A but finally redetermine it as 0.4% MgO replacing CaO at 1410°C, Majumdar (16) found 4.5% of Fe_2O_3 present in C_3A as "C_3F" at 1325°C and Lister and Glasser (17) 4.2% Fe_2O_3 as "C_3F" at 1180°C. The latter authors find 4.9% Fe_2O_3 as C_2F in $C_{12}A_7$ at 1180°C.

System $CaO–Al_2O_3–Fe_2O_3$

This system has been re-investigated by Lister and Glasser (17) and the portion of interest to cement technology by Majumdar (16). The latter's diagram is reproduced as Fig. 6. The principal conclusions were that, although the solid solutions C_2F–'C_2A' are continuous from 70% mol% 'C_2A', the ferrite phase compatible with C_3A(SS) and CaO is 48 mol% C_2A, i.e. very close to C_4AF. The C_3A(SS)–C–Ferrite invariant point was judged to be peritectic. To obtain exact phase relations Majumdar carried out his preparations in pure oxygen atmosphere, in air some slight reduction occurred. Lister and Glasser worked at controlled partial pressures of oxygen in a specially constructed furnace. Schlaudt obtained very similar results (9).

System $CaO–MgO–SiO_2$

The high MgO region of this system has been further studied by Gutt (12) and Roy (8) (9). Both groups record the occurrence of a new compound "T" described by Gutt (18) with the composition $C_{1.7}M_{0.3}S$, stable in contact with C_2S at sub-solidus temperatures. Schlaudt and Roy thought that it decomposed at 1381°C and was therefore unstable with respect to α-C_2S, but Gutt shows α-C_2S and T in co-existence, T decomposing at 1460°C. This discrepancy could be of some importance since according to Gutt's diagram T might form in portland cement clinkers in contact with liquid. Schlaudt and Roy also show a lower

decomposition limit for T at 979°C, but Gutt considers it stable at room temperature.

System $CaO–Al_2O_3–MgO–SiO_2$

Two new compounds in the system C–M–A were described by Welch (19); $C_{25}A_{17}M_8$ exists at the liquidus and CAM is metastable. While not of direct importance to portland cement they could occur in high alumina cement and Majumdar (20) has pointed out their relationship to the quaternary phase of high alumina cement. Majumdar considers the stable ternary phase to be C_3A_2M, but he was unable to resolve the discrepancy between X-ray and phase equilibrium results on the quaternary compound; the composition must be close to the C_6A_4MS of Parker. Welch's view that it is a solid solution was not upheld.

The sections $C_2S–M_2S–A$ and $C_3MS_2–MA–C_2AS$ have been delineated by Gutt (21, 22) and Christie (23) has reviewed the melilite series as a whole. Schlaudt (9) records significant solid solution of CaO and SiO_2 in MgO at 1750°C; if such solution takes place at clinkering temperature it could be highly significant in cement technology.

The Alkali Systems

The latest work confirms that in the system C_2S–KCS solid solutions are formed, and not the compound $KC_{23}S_{12}$; at 1300°C. and air quenching β C_2S is stable up to 5% KCS, at 10% α'-C_2S is stabilized and at 25% α-C_2S (24). Yamaguchi and Ono give a diagram (Fig. 7) showing C_2S solid solutions of Na_2O together with Al_2O_3 and Fe_2O_3 (25). According to Yamaguchi and Uchikawa (26), Na substitutes for Ca and/or Mg in Jeffery's alite structure. The solubility in material processed at 1200–1400°C is 0.3 to 6.7% Na_2O.

Brownmiller and Bogue reported temperature maxima on the boundary curves "C_5A_3"–CA and 'C_3A_3'–C_3A which they interpreted as indicating solid solution in "C_5A_3" of one or more of the calcium sodium aluminates. The extent of this solid solution would be about 1% of Na_2O.

The relation between C_3A and C_8NA_3 has been re-investigated (27). Lattice changes were observed in C_3A up to 2% replacement of CaO by Na_2O. The results for greater amounts of Na_2O could be interpreted as mixtures of C_3A(SS) and C_8NA_3(SS) or as showing polymorphic behaviour in C_3A with extensive solid solution. The system $CaO–Na_2O–Al_2O_3$ close to the C–A boundary system should be re-investigated in a water-free atmosphere.

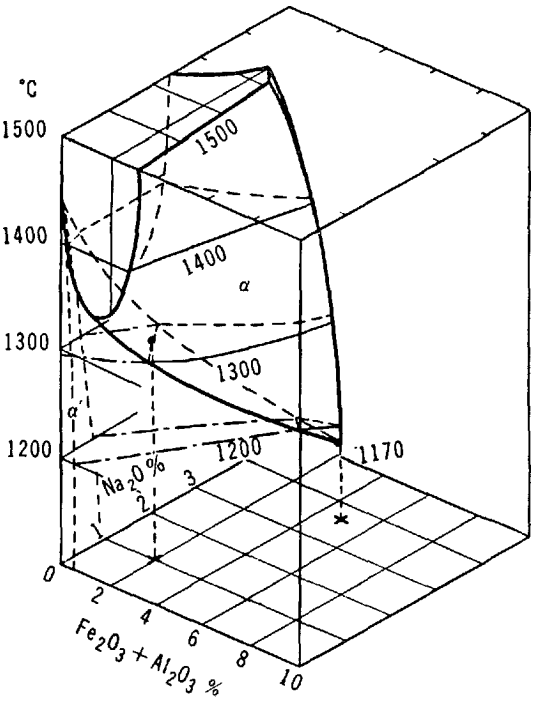

Fig. 7. *Solid solution region of* α-Ca_2SiO_4 *in the system* $2CaO \cdot SiO_2$–$(2CaO(Al_2O_3 \cdot Fe_2O_3))$–$Na_2O$–5% MgO; $Al_2O_3/Fe_2O_3 = 1$.

Sulphates, Fluorides, Phosphates

A technique of studying systems with volatile components using sealed capsules has been described (28), and used in studying part of the system $CaO–SiO_2–CaSO_4$ (29)(30). A new silico-sulphate, $2(2CaO \cdot SiO_2) \cdot CaSO_4$, was described, decomposing at 1298°C into α'-C_2S and $CaSO_4$. The maximum content of SO_3 in α'-C_2S at 1200°C is 0.4%.

Halstead and Moore confirm the composition of the expansive component of certain expanding cements as $3CaO \cdot 3Al_2O_3 \cdot CaSO_4$ and give a suggested structure (31). Budnikov, Kuznetsova and Savelev discuss the formation of this compound from the

aluminates in the presence of SO_3 (32).

A new version of the system $CaO–CaF_2–2CaO \cdot SiO_2$ has been produced by Mukerji (33). A much larger field of C_2S is shown compared with the earlier version of Eitel. No solid solution in the various forms of C_3S or C_2S was discovered. Similar results at the liquidus were reported by Gutt and Osborne (34) but they found an intermediate compound $2(2CaO \cdot SiO_2) \cdot CaF_2$, the fluoride analogue of calcio-chondrondite. The new compound decomposes at 1040°C into α'-C_2S and CaF_2. It seems likely that $2(2CaO \cdot SiO_2) \cdot CaF_2$ is 'phase B' described by Bereczky (35), who also found another compound in the system, 'phase A', related to C_3S. Akaiwa, Sudoh and Tanaka (36) identify this as $11CaO \cdot 4SiO_2 \cdot CaF_2$. The same authors also show changes in the X-ray spacings of β-C_2S up to 3% of added CaF_2.

In the system $CaO–Al_2O_3–CaF_2$, Leary (37) found $3CaO \cdot 3Al_2O_3 \cdot CaF_2$ and Jeevarathnam (38) $11CaO \cdot 7Al_2O_3 \cdot CaF_2$ ($Ca_{12}Al_{14}O_{32}F_2$, analogous with $Ca_{12}Al_{14}O_{32}(OH)_2$).

The system $CaO–P_2O_5–SiO_2$ in the high lime region has been described by Gutt (12), Fig 8. Schlaudt (9) also did some work on this system, and accepted Gutt's liquidus data. He interprets the solid solution equilibria rather differently, guided in part by an assumed structural interpretation. The conclusions for cement technology are not materially affected by the discussion.

Fig. 9 shows the section $3CaO \cdot SiO_2–3(3CaO \cdot P_2O_5)$ CaF_2 (fluorapatite) after Schlaudt (9), and Fig. 10 the system $CaO–C_2S$–fluorapatite. These systems were investigated in order to clarify the effect of fluorspar additions to phosphate-containing cement. Schlaudt concludes that since C_3S disappears from the system $CaO–C_3S–C_3P$ at 3 molecular percentage of C_3P and from the $CaO–C_3S$–fluorapatite system at 4 molecular percentage of fluorapatite, the "tolerance for combined fluoride and phosphate impurity in cement raw materials is seen not to be substantially different from the tolerance for phosphate alone." This does not however allow for the much higher molecular weight of apatite compared with tricalcium phosphate. In fact, the addition of fluorspar to the system according to Schlaudt's data increases the tolerance for phosphate in terms of the weight of P_2O_5 about $3\frac{1}{2}$ times. Fig. 10 also indicates that fluorapatite will not appear as a phase until all C_3S has been decomposed. This is in agreement with the mineralogical examination of cement clinkers containing these impurities.

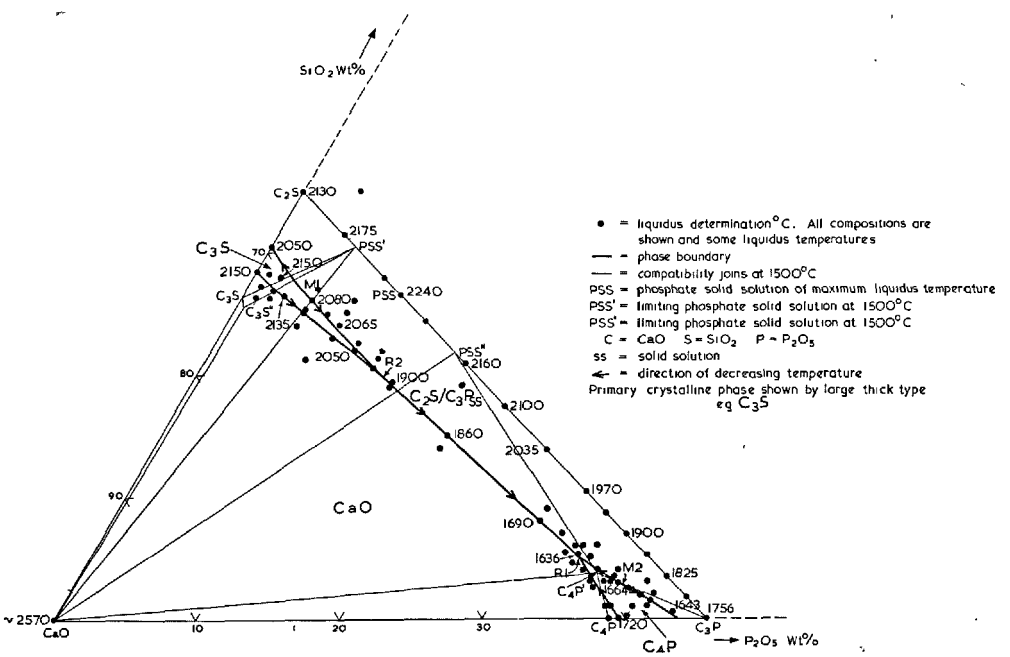

Fig. 8. *Phase diagram of the system* $C_2S–C_3P–CaO$ (Ref. 12)

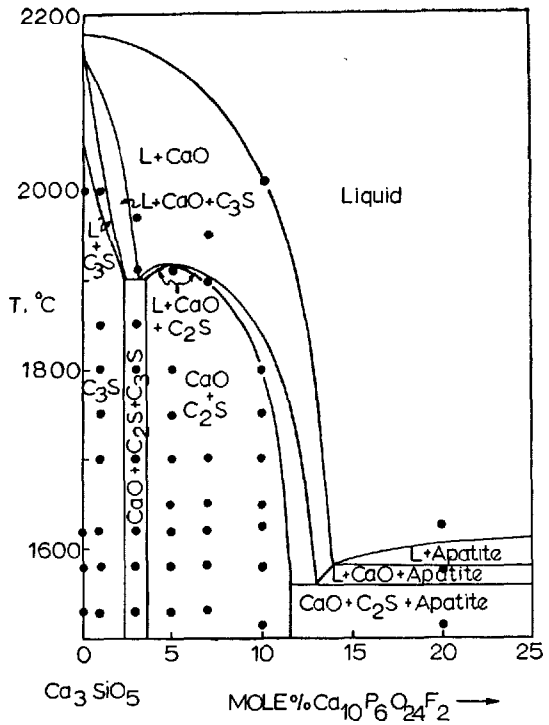

$C_3S = Ca_3SiO_5$ Crystalline solutions

$C_2S = Ca_2SiO_4$ Crystalline solutions

L = Liquid Apatite = fluorapatite • indicates critical quenching runs

Fig. 9. *Condensed phase equilibrium diagram for the join* $3CaO \cdot SiO_2$–$3C_3P \cdot CaF_2$ *through the system* CaO–$2CaO \cdot SiO_2$–$3C_3P \cdot CaF_2$ *(Ref. 9)*

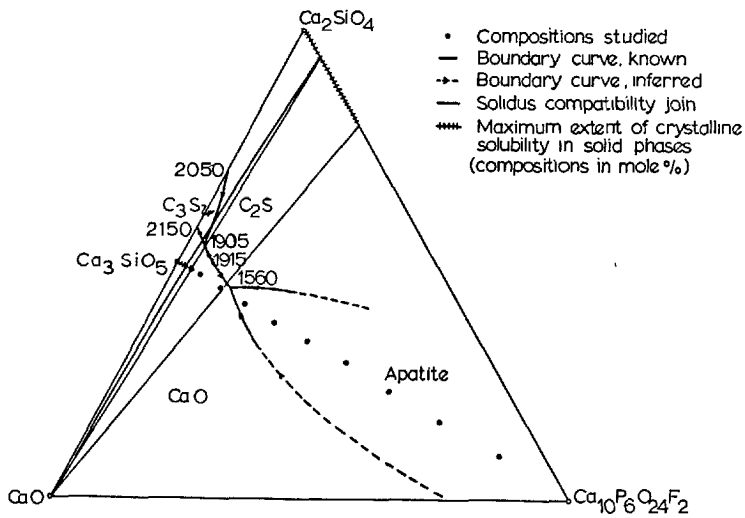

$C_2S = Ca_2SiO_4$ Crystalline solutions Apatite = fluorapatite

$C_3S = Ca_3SiO_5$ Crystalline solutions Compatibility data for solidus temperatures

Fig. 10. *Condensed phase equilibrium diagram for the system* Ca_2SiO_4–$Ca_{10}P_6O_{24}F_2$ *(Ref. 9)*

Reducing Conditions

Several contributions at the Washington Symposium dealt with this question, and in particular the role of FeO. It was shown that formation of FeO in large quantities results in dusting of the clinker and an acceleration of the low-temperature decomposition of C_3S. Woermann determined the solubility of FeO in C_3S at 1500–1600°C as 2.6 per cent, substituting for CaO. Phillips, Somiya and Muan's (39) studies on MgO-iron oxide in air atmosphere indicate that extensive solid solution of FeO in MgO may occur at clinkering temperatures; earlier work (40) indicated solid solution of FeO in CaO (10 per cent maximum) which slowed down the rate of hydration.

The reduction of Cr_2O_3 and its effect on C_2S were studied by Glasser and Osborn (41), and Kondo and Goto have described a new compound $7CaO \cdot Cr_2O_5 \cdot 2SiO_2$ (42). In the system $2CaO \cdot SiO_2$–$2MnO \cdot SiO_2$ Glasser (43) measured maximum solid solubility of 19 and 31.5% Mn_2SiO_4 in α and α' C_2S, respectively.

Other Minor Components

The solid solutions of the orthosilicates of alkaline earth oxides were described by Toropov at the Washington Symposium, and a new study with Fedorov (44) concerns the system $2BaO \cdot SiO_2$–$2CaO \cdot SiO_2$. The same authors (45) find that 'complex' crystals as previously described by Douglas at the London 1952 Symposium occur in the system $2CaO \cdot SiO_2$–$2Nd_2O_3 \cdot 3SiO_2$ (neodymium orthosilicate). Four new compounds in the system $2BaO \cdot SiO_2$–$2CaO \cdot SiO_2$–$2MgO \cdot SiO_2$ were found by Nadchovski and Grylicki (46). Reference (4) quotes solubility (at 1550°C) of Cr_2O_3 (1.4%) and Ga_2O_3 (0.9%) in C_3S. Sychov and Korneev (47) state that Cr substitutes for Si in C_3S up to a weight percentage of 2% Cr_2O_3. Larger additions of oxide decompose the C_3S. See also (41). Part of the quaternary system CaO–ZnO–Al_2O_3–SiO_2 was investigated by Segnit (48). Willemite, $2Zno \cdot SiO_2$, does not co-exist with C_2S; the latter forms a join with ZnO and no solid solution was observed.

Glass Formation

Since the development of improved methods of X-ray analysis, in particular quantitative diffractometry, doubts have been expressed as to the possibility of a glassy phase existing in portland cement clinker. For instance it has been considered that such differences as do exist between clinkers cooled at different rates are "textural" rather than qualitative. Nevertheless, quicker cooling of clinker is accepted in practice as improving strength and particularly soundness with regard to MgO and resistance to sulphate attack.

All the observations on which opinions regarding the absence of glass are based have been made on commercial clinkers as received from the kiln and rely on the fact that the totals of C_3S, C_2S, C_3A and ferrite phases are reasonably close to that expected on the assumption of complete crystallinity, having regard to the known fairly high errors in diffractometry of clinker. It could be asked whether the method is accurate enough to detect the small quantities of glass which might be expected in commercially prepared clinkers. Jeffery and Chatterji (49) prepared quenched and annealed clinkers from plant clinkers, but although some changes in X-ray pattern were noted did not detect glass either by difference or by a diffuse X-ray reflection. It was therefore decided at the Building Research Station to look for glass in laboratory clinkers, cooled under controlled conditions. The clinkers chosen were repetitions of some of the compositions studied by Parker (50). The compositions chosen are given in Table 1 and the results obtained in Table 2. Methods of preparation and cooling were as described by Parker.

The quantities of glass calculated from the diffraction results are almost certainly significant and varied from 10–20% as compared with calculated values of 31–32% assuming perfect quenching. Looking at the results from a different angle, the reduction in C_3A brought about by quenching is from 15 to 5% for composition 15; 17–13 for composition 17 and 17–5 for composition 18. This correlates well with Parker's observations that the alkali– and magnesia-free clinker 17 was difficult to quench, and that this clinker differed little in sulphate resistance whether

Table 1. *Composition of synthetic portland cement clinkers (Original preparations from Parker (50))*

Sample	Original	CaO	Free CaO	SiO_2	Al_2O_3	Fe_2O_3	MgO	K_2O	Na_2O
15X	Original preparation	63.96	0.30	22.26	7.78	2.93	1.97	0.36	0.75
Annealed	New preparation*	63.77	0.17	22.17	7.97	3.59	1.99	0.09	0.42
15G	Original preparation	63.78	0.30	22.04	8.20	3.41	1.89	0.11	0.24
Quenched	New preparation	63.70	0.06	22.14	7.96	3.59	1.99	0.11	0.52
17X	Original preparation	67.42	0.60	20.86	8.08	3.33	—	—	—
Annealed	New preparation	67.55	0.07	20.93	8.18	3.35	—	—	—
17G	Original preparation	67.22	0.60	20.86	8.26	3.36	—	—	—
Quenched	New preparation	67.55	0.13	20.93	8.18	3.35	—	—	—
18X	Original preparation	66.00	0.20	20.22	8.06	3.32	1.93	0.13	0.27
Annealed	New preparation	65.85	0.30	20.24	8.05	3.31	2.00	0.09	0.49
18G	Original preparation	65.97	0.20	20.36	8.04	3.30	2.00	0.16	0.34
Quenched	New preparation	55.87	0.09	20.25	8.05	3.31	2.00	0.08	0.46

*The new preparations were analysed only for K_2O, Na_2O, and free CaO. The analysis is deduced from the original composition.

Table 2. *Constitution of synthetic clinkers*

Sample		C_3S	C_2S	C_3A	C_4AF	Form of C_3S	Form of C_3A	Ferrite composition mol.% C_2F	*Estimated glass by difference, %
15X	Bogue calculation	32	40	15	11				
Annealed	X-ray diffraction	43	36	15	10	Monoclinic	Cubic	59–70 mostly 59	—
	Microscopy	41	36	20					
15G	Bogue calculation	32	39	15	11				
Quenched	X-ray diffraction	56	15	5	5	Monoclinic or Trigonal	Cubic, some orthorhombic	50	20
	Microscopy	52	26	22					
17X	Bogue calculation	56	18	16	10				
Annealed	X-Ray diffraction	63	10	17	10	Monoclinic	Cubic	53	—
	Microscopy	54	22	22					
17G	Bogue calculation	56	18	16	10				
Quenched	X-ray diffraction	63	11	13	5	Monoclinic	Cubic	64	10
	Microscopy	65	14	19					
18X	Bogue calculation	54	17	16	10				
Annealed	X-ray diffraction	59	12	17	10	Monoclinic	Cubic	54	—
	Microscopy	70	10	19					
18G	Bogue calculation	55	17	16	10				
Quenched	X-ray diffraction					Trigonal	Cubic and orthorhombic	Peak too weak	20
	Microscopy								

*Rounded to nearest 10.

quenched or crystallized. Clinkers 15 and 18 increased markedly in sulphate resistance when quenched.

It is worth while noting some other indications brought out in this study. In general the C_3S/C_2S ratio found by diffractometry or microscopy is higher than calculated from Bogue's formula. It is higher also than the raised values obtained by the modified Lea and Parker's formulae. Nurse and Parker reporting on the microscopy of Parker's clinkers found fair agreement with Bogue's formula for annealed clinkers but raised C_3S/C_2S ratios in better agreement with Lea and Parker's formulae for quenched clinkers. Lea in his book gives a table of factors all tending to raise the C_3S/C_2S ratio above that given by the simple Bogue formula.

Clinkers 15 and 18 when quenched gave a trigonal form of C_3S. It might be queried whether this could have affected the properties of the quenched series as compared with the crystalline. Parker's original tables indicate that such an effect if present is overshadowed by the effect of cooling rate.

It appears that glass cannot be ignored as a possible phase in cement. Present accuracy in diffractometry means that it cannot be detected unless present in large amounts. The effect of cooling rate on clinker warrants further study, both in regard to the factors affecting the glass stability and the effect of cooling rate on the C_3S/C_2S ratio (51).

Other recent studies of the liquid phase have not attempted to estimate changes in constitution with heating rate (49) (52).

Kinetics

The departures from equilibrium which have so far been considered are those arising from the range of the clinkering temperature and the rate of cooling. A very important deviation is caused by lack of homogeneity in the clinker, either by insufficient grinding, poor mixing, segregation or absorption of foreign material such as ash or volatile matter in the kiln; phase studies can be of only minor help in solving these problems. Studies with synthetic systems can be useful when carefully blended raw materials are processed according to a known temperature schedule and the progress towards equilibrium is measured. Alternatively the interface between reactants may be studied.

The author pointed out at the Washington Symposium the importance of free CaO as a clinker constituent, and the possible effect it may have on the composition of the liquid at the clinkering temperature. It is not unusual for British cements to have free CaO as high as 4%. Free CaO may be present as relict, unreacted matter; may have formed at equilibrium either in the absence of C_2S or in contact with C_3S and C_2S solid solutions; may have been formed by high temperature decomposition reactions, or may result from low temperature decomposition of C_3S. The composition of the clinker liquid at various stages of time and temperature and its viscosity are highly important factors in the kinetics of clinker formation. During the preheating and cooling stages solid/solid reactions are important.

A review of the contribution of the Brussels group to the subject of solid state reactions was published in 1956 (53). Andouze (54) showed that CA is the primary compound formed at 900°C in the system CaO–Al_2O_3, the rate-controlling process of formation of other aluminates being diffusion; on the other hand Uchikawa, Tsumagari and Koike found a preferential formation of C_3A in the early stages (55). In the system CaO–SiO_2 Schrämli and Becher (56) demonstrated the importance of the physical condition of the silica phase, the low rate of reaction of pure crystalline quartz is a severe problem in cement burning. The extension of DTA. methods to high temperatures has opened up new possibilities of studying the process of clinker formation (57).

It has always been recognized that the low temperature decomposition of C_3S represents a hazard in processes, such as shaft kiln burning, which involve slow cooling. Formation of FeO or presence of other oxides which lower the decomposition temperature increases these difficulties. On the other hand, in the presence of these substances there is a longer temperature range for the formation of C_3S in the heating cycle. Butt and Timashev show that C_3S forms already at 900–1000°C in the presence of $CaSO_4$ or CaF_2 (58). Under atmospheric conditions favouring the formation of spurrite $2(2CaO \cdot SiO_2)CaCO_3$, C_3S is formed at 1050°C (57) (59). The discovery of new silicofluorides, silicosulphates and the recognition of the possibility of transient formations of silicocarbonates throws new light on the possible use of mineralisers in cement burning. By further studying the kinetics and phase equilibria in these systems it might be possible to invent new methods of cement burning using a large excess of volatile flux at intermediate temperatures which could be driven off at a higher temperature, recovered and returned to the kiln. It seems important in each case to establish the phase equilibria precisely. This information is also required to follow processes using impure raw materials such as by-product gypsum.

Mineralizers affect not only the silicate phases but the aluminates, and it is important to study them in combination (60) (61). Also many minor components have a disproportionate effect on the composition of the ferrite phase.

Discussion and Conclusions

With the greater precision now attempted, the accuracy of chemical analysis needs to be questioned; e.g. recent changes in specifications have introduced a more direct estimation of Al_2O_3, of practical importance in defining sulphate-resistant cements.

The merits of phase studies as a means of elucidating clinker constitution are (1) the number of independent variables is reduced and trends emerge much more clearly (2) there is the possibility of calculating clinker constitution from the bulk analysis.

It is now becoming apparent that too close a limitation of the number of constituents will lead to errors of two kinds; an incorrect estimation of the nature and quantity of the phases present and the obscuring of variability that may exist among the physical and chemical properties of these phases. For instance, while the addition of MgO to the C–A–S–F system is fairly simply dealt with as in Swayze's classical work, when the C_3S and C_2S contain minor oxides in solid solution, the addition of MgO to the system often

materially changes the solid solubility. Even larger disturbances are created by some of the 'fluxing' substances such as fluorides, sulphates, carbonates and FeO. In each case it is necessary to work out the phase diagrams accurately. Some classification may then be possible e.g. between those minor components that form extensive C_2S solid solutions in equilibrium with C_3S and CaO, and those which either themselves enter into equilibrium with CaO and C_3S or form definite compounds which do so. The sub-solidus reactions of C_3S must be investigated in each case.

Attempts are made to introduce more accurate computations of phase constitution than the Bogue formula. For instance Schlaudt (9) has set up a computer programme which aims to take into account a number of minor constituents. Miyazawa (15) suggests allowing for MgO present in liquid and in solid solution in C_3S: Free MgO = Total MgO − (0.77 + $0.12C_3S$). It is doubtful if these formulae will be of much practical use until a more accurate allowance can be made for the composition of the ferrite phase. For most purposes the Bogue calculation is sufficient; otherwise the composition of the ferrite may be determined by X-rays and the "modified Bogue" composition calculated. For any more detailed estimation of clinker constitution a combination of optical microscopy, X-ray analysis, phase calculation, microprobe analysis and DTA. is desirable. Nevertheless proper and rigorous phase studies among clinker components remain a fruitful and necessary region of study.

References

1. E. M. Levin, C. R. Robbins and H. F. Mc'Murdie, "Phase Diagrams for Ceramists," The American Ceramic Society, Columbus, Ohio, 1964.
2. J. H. Welch and W. Gutt, "Tricalcium silicate and its stability within the system $CaO–SiO_2$" J. Am. Ceram. Soc. **42**, No. 1, 11–15, 1959.
3. H. G. Midgley and K. E. Fletcher "The role of alumina and magnesia in the polymorphism of tricalcium silicate," Trans. Brit. Ceramic Soc. **62**, No. 11 917–937, 1963.
4. E. Woermann, Th. Hahn and W. Eysel, "Chemical and structural investigations on the solid solutions of tricalcium silicate" (in German), Zement-Kalk-Gips **16**, No. 9, 370–5, 1963.
5. M. Bigaré, "Study of a series of solid solutions of alumina in tricalcium silicate" (in French), Publication Technique No. 166, Centre d'Etudes et de Recherches de l'Industrie des Liants Hydrauliques, Paris, 1965.
6. F. W. Locher, "The intercalation of Al_2O_3 and MgO into tricalcium silicate" (in German), Zement-Kalk-Gips **13**, No. 9, 389–94, 1960.
7. J. W. Jeffery "The crystal structure of tricalcium silicate," Acta Cryst. **5**, 26–35, 1952.
8. C. M. Schlaudt and D. M. Roy, "The join Ca_2SiO_4–$CaMgSiO_4$", J. Am. Ceram. Soc. **49**, No. 8, 430–432, 1966.
9. C. M. Schlaudt, "Phase equilibria and crystal chemistry of cement and refractory phases in the system $CaO–MgO–Al_2O_3–Fe_2O_3–CaF_2–P_2O_5–SiO_2$," Ph. D. Thesis Pennsylvania State Univ. 1964.
10. K. E. Fletcher, "The polymorphism of tricalcium silicate, a comparison of the effect of Fe^{3+} and Al^{3+} ions," Trans; Brit. Ceram. Soc. **64**, (8), 372–385, 1965.
11. G. Yamaguchi, Y. Ono and S. Kawamura, "The solid solution ranges of Al_2O_3 and Fe_2O_3 in the high temperature modifications of $2CaO·SiO_2$", Review of 16th General Meeting, Japan Cement Engineering Assoc. May 1962 Tokyo. 35–36.
12. W. Gutt, "High temperature equilibria in polycomponent silicate systems," Ph. D. Thesis, London, 1966.
13. R. W. Nurse, J. H. Welch and A. J. Majumdar, "The $CaO–Al_2O_3$ system in a moisture free atmosphere," Trans. Brit. Ceram. Soc. 64 (9), 409–18, 1965.
14. R. W. Nurse, J. H. Welch, and A. J. Majumdar, "The $12CaO·7Al_2O_3$ phase in the $CaO–Al_2O_3$ system," Trans. Brit. Ceram. Soc. **64** (6), 323–32, 1965.
15. K. Miyazawa and K. Tomita, "The influence of MgO on the properties of portland cement" (in German), Zement-Kalk-Gips, **55** (2), 82–5, 1966.
16. A. J. Majumdar, "The ferrite phase in cements," Trans. Brit. Ceram. Soc. **64** (2), 105–119, 1965.
17. D. H. Lister and F. P. Glasser, "Phase relations in the system $CaO–Al_2O_3$-Iron oxide," Trans. Brit. Ceram. Soc. **66** (7), 293–305, 1967.
18. W. Gutt, "A new calcium magnesiosilicate," Nature **190** (4773), 339–40, 1961.
19. J. H. Welch, "Ternary compound formation in the system $CaO–Al_2O_3–MgO$", Nature **191** (4788) 559, 1961.
20. A. J. Majumdar, "The quaternary phase in high-alumina cement," Trans. Brit. Ceram. Soc. **63** (7), 347–64, 1964.
21. W. Gutt, "High temperature phase equilibria in the partial system $2CaO·SiO_2–2MgO·SiO_2–Al_2O_3$," J. Iron and Steel Institute, **201** (6) 532–6, 1963.
22. W. Gutt, "High temperature phase equilibria for the partial system $3CaO·MgO·2SiO_2–MgO·Al_2O_3–2CaO·Al_2O_3·SiO_2$."
23. O.H.J. Christie, "A contribution to the mineralogy of the melilite group," Universitets forlaget, Oslo, 1964.
24. N. F. Federov and E. R. Brodinka, "Solid solutions in the system $2CaO·SiO_2–K_2O·CaO·SiO_2$" (in Russian), Neorganicheskie Materialiy **2** (4), 7458, 1966.
25. G. Yamaguchi and Y. Ono, "The solid solution regions of the high temperature modifications of Ca_2SiO_4 for Al_2O_3, Fe_2O_3 and Na_2O," Review of 17th Gen. Meeting. Japan Cement Engineering

Assoc. Tokyo, 1963, 28–30.
26. G. Yamaguchi and H. Uchikawa, "Investigations into the solid solutions in the system $3CaO \cdot SiO_2$–Na_2O" (in German), Zement-Kalk-Gips **14** (11), 497–503, 1961.
27. K. E. Fletcher, H. G. Midgley and A. E. Moore, "Data on the binary system $3CaO \cdot Al_2O_3$–$Na_2O \cdot 8CaO \cdot Al_2O_3$ within the system CaO–Na_2O–Al_2O_3," Mag. Concr. Res. **17** (12), 171–6, 1965.
28. A. D. Russell, "Differential thermal analysis of materials with very volatile components", J. Sci. Instr. **44**, 399–400, 1967.
29. W. Gutt and M. A. Smith, "The α-form of $CaSO_4$", Trans. Brit. Ceram. Soc. **66** (8), 337–345, 1967.
30. W. Gutt and M. A. Smith, "Studies of the sub-system CaO–$CaO \cdot SiO_2$–$CaSO_4$," Trans. Brit. Ceramic Soc.
31. P. E. Halstead and A. E. Moore, "The composition and crystallography of an anhydrous calcium aluminosulphate occurring in expanding cement," J. App. Chem. **12**, 413–417, 1965.
32. P. P. Budnikov, I. P. Kuznetsova and V. G. Savelev, Silikattechnik **16**, 414–417, 1965.
33. J. Mukerji, "Investigation of the phase diagram of the ternary system CaO–$2CaO \cdot SO_2$–CaF_2," Mem. Sci. Rev. Metallurg. **60** (II) 785–96, 1963.
34. W. Gutt and G. J. Osborne, "The system $2CaO \cdot SiO_2$–CaF_2", Trans. Brit. Ceram. Soc. **65** (9), 521–534, 1966.
35. E. Bereczky, "The accelerated formation and stabilisation of tricalcium silicate (Part II)" (in Hungarian), Epitoanyag **16** (12), 441–448, 1964.
36. S. Akaiwa, G. Sudoh and M. Tanaka, "Studies on mineralizing effect of CaF_2 and a ternary compound in the system CaO–SiO_2–CaF_2," Review of 20th General Meeting, The Cement Association of Japan, 1966, 34–8.
37. J. K. Leary, "New compound in the system CaO–Al_2O_3–CaF_2", Nature, **194** (4823), 79–80, 1912.
38. J. Jeevaratham, F. P. Glasser and L. Dent-Glasser, "Anion substitution and structure of $12CaO \cdot 7Al_2O_3$", J. Am. Ceram. Soc. **47** (2), 105–6, 1964.
39. B. Phillips, S. Somiya and A. Muan, "Melting relations of magnesium oxide-iron oxide mixtures in air", J. Am. Ceram. Soc. **44** (4), 167–169, 1961.
40. W. C. Allen and R. B. Snow, "The orthosilicate-iron oxide portion of the system CaO–FeO–SiO_2", J. Am. Ceram. Soc. **38** (8) 264–280, 1955.
41. F. P. Glasser and E. F. Osborn, "Phase equilibrium studies in the system CaO–Cr_2O_3–SiO_2", J. Am. Ceram. Soc. **41** (9) 358–67, 1958.
42. R. Kondo and S. Goto, "A study of the system CaO–SiO_2–Cr_2O_3–Al_2O_3", review of Nineteenth General Meeting, Cement Assoc. of Japan 42–44, 1965.
43. F. P. Glasser, "The system Ca_2SiO_4–Mn_2SiO_4", Am. J. Sci. 259 (1), 46–59, 1961.
44. N. A. Toropov and N. F. Federov, "The Ba_2SiO_4–Ca_2SiO_4 system" (in Russian), Zh. Neorg. Khim **9** (8), 1939–44, 1964.
45. N. A. Toropov and N. F. Federov, "Solid solutions in the calcium orthosilicate-neodymium orthosilicate" (in Russian), Zh. Neorg. Khim **9** (1), 156–63, 1964.
46. F. Nadachowski and M. Grylicki, "Phase equilibria in the system $2BaO \cdot SiO_2$–$2CaO \cdot SiO_2$–$2MgO \cdot SiO_2$" (in German), Silikattechnik **10** (2), 77–80, 1959.
47. M. M. Sychev and V. I. Korneev, "Chromalite of portland cement clinkers" (in Russian), Zh. Prikl. Khim. 38, 2642–47, 1965.
48. E. R. Segnit, "Three planes in the quaternary system CaO–ZnO–Al_2O_3–SiO_2", J: Am. Ceram. Soc. 45 (12), 600–7, 1962.
49. S. Chatterji and J. W. Jeffery, "The effect of various heat treatments of the clinker on the early hydration of cement pastes," Mg. Concr. Res. 16 (46), 3–10, 1964.
50. T. W. Parker, "Influence of the heat treatment of portland cement clinker on the properties of cement," J. Soc. Chem. Ind. 58 (6), 203–213, 1939.
51. V. N. Yung, Yu. M. Butt and V. V. Timashev, "The influence of cooling rate on the properties of cement" (in Russian), Trudy Moskov. Khim-teknol. Inst. im. Mendeleeva (24), 25–35, 1957.
52. P. Terrier, "The liquid phase during firing" (in French), Journées Régionales du Ciment, Oct. 1963. Centre d'Etudes et de Recherches de L'Industrie des Liants Hydrauliques, Publication Technique 155, 34–37.
53. W. L. de Keyser, "Reactivity in the solid state between oxides of the cement system," IVA 26 (1955) (7) 292–308, Royal Swedish Academy of Engineering Sciences, Stockholm, 1956.
54. B. Andouze, "Contribution to the study of solid-state reaction between lime and alumina" (in French), Silicates Industriels, **26** (4) 179–190, 1961.
55. H. Uchikawa, A. Tsumagari and H. Koike, "On the formation of calcium aluminates in the system CaO–Al_2O_3", Procs. 17th General Meeting Japan Cement Eng. Assoc., Tokyo, 1963, 32–37.
56. W. Schramli and F. Becker, "The reactions between lime and silica of different activity below 1100°C" (in German), Zement-Kalk-Gips **13** (6), 265–269, 1960.
57. B. Courtault, "Study of reactions in the solid state up to 1600°C" (in French), Centre d'Etudes et de Recherches de l'Industrie des Liants Hydrauliques, Pub. Tech. 140, 1963.
58. Yu. M. Butt and V. V. Timashev, "Dependence of the binding properties of clinker minerals on their burning temperature and crystal structure" (in Russian), Tsement **27** (2), 17–27, 1961.
59. P. Longuet and B. Courtault, "Ease of clinkering of cement raw meal" (in French), Journées Régionales du Ciment. Oct. 1963. Centre d'Etudes et de Recherches de l'Industrie des Liants Hydrauliques, Publication Technique 155, 20–33.
60. S. D. Okorov, S. L. Golynko-Volfson and T. N. Yarkina, "Influence of fluorides on mineral formation in the system CaO–Al_2O_3–SiO_2" (in Russian), Tsement **29** (1), 7–9, 1963.
61. C. Kroger and G. Fulop, "Formation of calcium silicate and aluminate from carbonate and oxides in the presence of foreign fluxes" (in German), Zement-Kalk-Gips **50** (12), 545–8, 1961.

Written Discussion

J. A. Hedvall

I have the impression that reactions in the solid state, taking place at temperatures as low as 500–600 degr. centigrade have not, as yet, been sufficiently investigated. Such reactions, whether the formation of more or less complex compounds or solid solutions, influence the reactions and sintering processes or the formation of molten phases at the higher temperatures in the kiln.

Many industries, especially cement factories, start with very heterogeneous raw materials. Many years ago it was established that calcium silicate (first C_2S) and aluminates are formed already at about 500 degr. and that the compositions of limestone and clay do not exactly correspond to the ideal formulae of calcium carbonate or kaolin. We have to take into consideration the influence of many factors, admixtures of other substances, lattice distortions in the form of guest particles and the formation of a number of unstable reactive phases formed during thermal decomposition processes. At our institute we have studied such reactivity effects. I am leaving out the great but very little investigated influence of dissolved inert gases on the properties of surfaces.

In order to complete our knowledge many problems are still left more or less unanswered about the properties of single substances, binary or more complex systems and the behaviour of such systems at different temperatures, especially the processes at relatively low temperatures.

Oral Discussion

E. Woermann and D. Knoefel

Non-Equilibrium Crystallization of Free Lime

In the ternary system CaO–Al_2O_3–SiO_2 the "lime limit" (1) of white portland cement clinker—i.e. the maximum amont of CaO which can be combined without the formation of free lime—is given by the straight line through the points C_3S and invariant point D ($CaO + C_3S + C_3A$ + liq; 1470°C). The equation of this line is: $CaO = 2.80\ SiO_2 + 1.18\ Al_2O_3$.

It has been found, however, that free lime can also appear upon quick cooling of certain mixtures in which equilibrium crystallization of free lime is

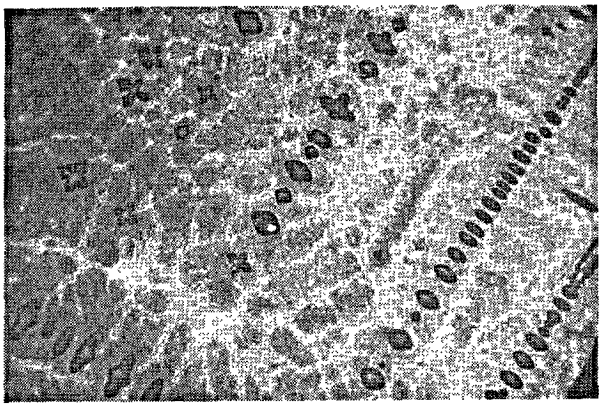

Fig. 1. *Quench growth of free lime (dark grey) in a sample corresponding to the composition of the invatriant point D (2), after rapid cooling (5°C/sec.) from above the liquidus temperature. Enlarged: 500x; etched with dist. water.*

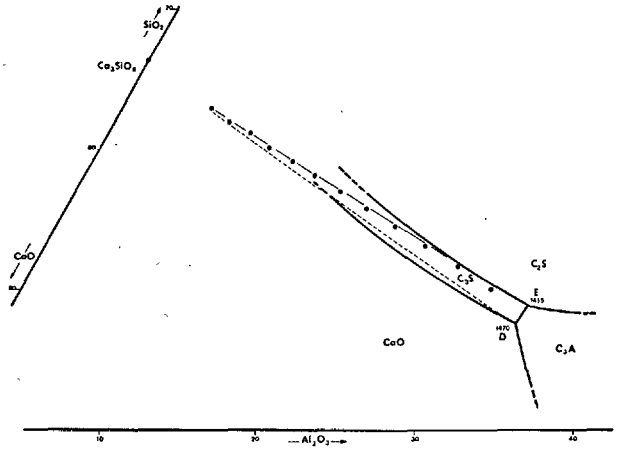

Fig. 2. CaO-*rich corner of the ternary system* CaO–Al_2O_3–SiO_2. *Experimental data on the "lime-limit" of samples cooled at a rate of 10°C/sec. The dashed line corresponds to the theoretical lime limit assuming quenched high-temperature equilibrium.*

excluded (Fig. 1). Thus the practical lime limit is shifted to lower CaO-concentrations (Fig. 2).

The possibility that the position of the invariant point D with: $CaO = 58.2\%$, $Al_2O_3 = 33.1\%$ and $SiO_2 = 8.7\%$ (2) is incorrect, can be excluded. Therefore the surprising appearance of free lime beyond the line C_3S–D must be due to non-equilibrium crystallization or quench growth, effected by the high viscosity of the liquid phase and the sluggish crystallization of the aluminate.

The amount of free lime is dependent on composition and cooling rate of the sample: Fig. 3 shows that for the sample-composition of the invariant point D a maximum value of about 4.5% free CaO is attained for a cooling rate of about 1°C/sec.

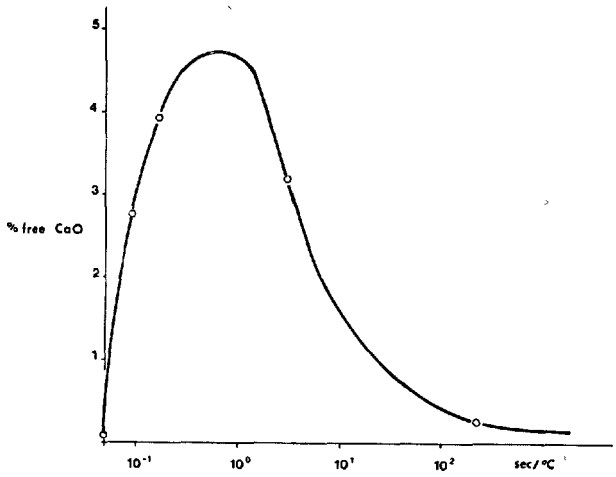

Fig. 3. *Formation of non-equilibrium free lime in a sample corresponding to composition D as a function of cooling rate. (The abscissa represents the reciprocal value of the cooling rate in an arbitrary spacing.)*

This effect may be important to manufacturers of white cement. In iron-containing systems, however, the viscosity of the liquid phase is lower and the ferrite phase crystallizes quite rapidly. Accordingly, non-equilibrium crystallization of free lime is not observed in normal portland cement clinker.

References

1. E. Spohn, "The lime-limit of portland cement" (in German), Zement **21**, (1932), 702–706, 717–723, 731–736.
2. M. A. Swayze, "A report on studies of: 1. The ternary system CaO–C_5A_3–C_2F 2. The quaternary system CaO–C_5A_3–C_2F–C_2S 3. The quaternary system as modified by 5% magnesia Am. Journ. Sci. **244**, (1946), 1–30, 65–94.

Oral Discussion

Della M. Roy

Dr. Nurse has emphasized the point that one must consider the effect of temperature when describing the limits of crystalline solution of a particular component in a given phase. A good example of this was found in our studies of C_3S–"M_3S" crystalline solutions, where we have found that up to 9 mole percent "M_3S" may be incorporated in C_3S at high temperatures in equilibrium with liquid. These crystalline solutions are, however, metastable at lower temperatures. Slow cooling, or re-cycling, such as under the conditions present in DTA experiments results in exsolution to produce a phase containing relatively little Mg. Such changes in the character of the crystalline solutions are reflected in the temperature of the DTA peaks of the resultant phase.

Author's Closure

Ronald W. Nurse

Since the preparation of the Principal Paper, Woerman, Hahn and Eysel have published two more papers (1) (2) on the question of MgO and Al_2O_3 in C_3S. Their first paper described a chemical investigation by the free lime method and used starting mixtures stated to contain 2–4% free CaO. The final limit of solution of Al_2O_3 at 1% was said to be determined microscopically. The second and third papers started in addition with mixes originating with C_3S or its solid solution, without excess free CaO, and relied also on microscopic determinations by reflected light. These investigations are therefore more rigorous than the original one and suggest that a range of solid solutions is possible, giving rise to a solid volume in the quaternary system CaO–MgO–Al_2O_3–SiO_2. The high CaO limit of this volume is in agreement with Midgley and Fletcher (loc.cit) in respect of CaO/Al_2O_3 ratio, but not in the Al_2O_3 value, which shows an inflexion at 0.5%, terminating at 1%. Both Woermann, Hahn and Eysel and Midgley and Fletcher chose to process their mixes above the eutectic temperature rather than wait long periods for equilibrium to be attained by solid state sintering. This may well account for the discrepancy between their results, for the appearance of C_3A on subsequent heat treatment will depend very markedly on time and temperature. It has been noted by all the early workers on the quaternary system that it is almost impossible to re-absorb free CaO formed by decomposition of C_3A. Nevertheless, if only those points in Woermann, Hahn and Eysel's diagram showing a homogenous crystalline solution of C_3S are noted, the evidence for solutions of varying C/A ratio is strong, and the authors have given a crystallographic interpretation of what happens.

Foster (3) has pointed out an error in the presentation of phase diagrams for pure C_2S. Regourd, Bigaré, Forest and Guinier (this Symposium) confirm the existence of the α'_H and α'_L forms. The difference in structure appears to be small and there may not therefore be much difference in the solubility of other

ions in the two α' forms. This could be checked by determining the variation of the $\alpha'_H \rightleftharpoons \alpha'_L$ inversion temperature in the presence of added ions. The same authors determined the effect of added ions on the $\alpha \rightleftharpoons \alpha'_H$ inversion and from this deduced the solubility in the α phase. Since the lowered inversion points are lower than the usual clinkering temperature of cement, this is the appropriate solubility to be considered. Inversion to β on cooling may produce exsolution, according to the cooling rate and the nature of the dissolved ions.

The various vlaues suggested for the solubility of MgO, Al_2O_3, Fe_2O_3 in alite and belite are in good agreement and approximate to what has been found in microprobe analysis. The "partition" of foreign ions between alite and belite will depend on the direction of the tie lines in the appropriate ternary system, or on the intersection of bounding planes in higher systems. For Mg, Al and Fe solutions these are almost parallel to the CaO–SiO_2 axis and so only a small range of the "partition coefficient" is found (Midgley, this Symposium). The relative proportions of K_2O and Na_2O in the silicate phase as found by microprobe analysis and by chemical separation (Pollitt and Brown, this Symposium) are not in good agreement. Some further work on this is required.

In the ferrite system Woermann, Eysel and Hahn (this Symposium) have again used their very accurate free CaO determinations to investigate the solid solutions with MgO for those ferrites in equilibrium with CaO. They propose polymorphic inversions in the ferrite phase.

The very interesting work by Pollitt and Brown reinforces the need to study further the phase relations of the orthorhombic calcium aluminate, especially in respect to K_2O. The new paper by Gutt and Smith (4) summarises data on the effect of Mg and SO_4 ions on the system CaO–Al_2O_3–SiO_2, but without alkalies. As Brown and Pollitt show, alkalies must always be considered together with SO_3 in clinker constitution. Compounds richer in SO_3 may form transiently during the burning process.

The new compound described as $Ca_{12}Si_4O_{19}F_2$ by Tanaka, Sudoh and Akaiwa (this Symposium) is identical with the $3(3CaO \cdot SiO_2) \cdot CaF_2$ of Gutt and Osborne (5), and phase II appears to be the $2(2CaO \cdot SiO_2) \cdot CaF_2$ of Gutt and Osborne. Tanaka et al. found a primary phase field for the incongruently melting $Ca_{12}Si_4O_{19}F_2$. Further study is required to settle the exact composition of this compound.

The possibility of glass formation has become of increased interest because of the renewed study of high-magnesia cements. Rapid cooling reduces the amount of free periclase, but whether this is due to glass formation or to retention of magnesia in crystalline solutions is not clear. Some Stereoscan photographs of clinker, appear to show glassy envelopes on silicate grains.

I am grateful to Prof. Hedvall for emphasising the importance of kinetics of reaction in the solid state, which was dealt with interestingly by a number of supplementary papers. Mrs. D.M. Roy underlines the importance of controlling the temperature when studying solid solubility.

The new reason advanced by E. Woermann for formation of free CaO in clinker mixes emphasizes the need for continuing study of the liquid formed at clinkering temperatures, and its crystallization independently of the silicate phases. At temperatures below 1250° the lime will form under equilibrium conditions.

I thank all those who have contributed to the discussion which emphasises the need to use a combination of crystallographic, synthetic and analytical methods in studying clinker.

References

1. E. Woermann, Th. Hahn, and W. Eysel, Zement-Kalk-Gips (in German) **20** (9) 435–439, 1967.
2. Ibid, **21** (6) 241–251, 1968.
3. W. R. Foster, J. Am. Ceram, Soc. **51** (6) 353–354, 1968.
4. W. Gutt and M. A. Smith, Trans. Brit. Ceramic Society **67** (10) 1968.
5. W. Gutt and J. Obsorne, Trans. Brit. Ceramic Society **67** (4) 125–133, 1968.

Supplementary Paper I-9 Manufacture of Portland Cement from Phosphatic Raw Materials

Witold Gutt*

Synopsis

The importance of the minor constituents in modifying the major phases of portland cement clinker was emphasized by Welch and Gutt at the 4th International Symposium on the chemistry of cement. The present paper deals with the manufacture of portland cement from materials containing one such impurity, phosphate.

After discussing the possible mode of action of the minor constituents an account is given of studies by Nurse which led to the utilization of phosphatic limestone deposits at Totoro, Uganda, for cement manufacture. This work was followed by detailed studies at the Building Research Station of phase equilibria in the system $CaO–SiO_2–P_2O_5$, their objective being to provide a fundamental basis for the understanding of the effect of phosphate. Phase diagrams of the systems $2CaO \cdot SiO_2–3CaO \cdot P_2O_5$ and $2CaO \cdot SiO_2–3CaO \cdot P_2O_5–CaO$ have resulted from this work. The practical significance of these phase equilibria in relation to manufacture of portland cement from phosphatic limestone and other phosphatic raw materials is explained in the present paper.

Since fluorspar is in practice sometimes added to phosphatic cement raw meal to facilitate manufacture, the role of fluorine in the process is also considered. In the course of periodic examination of plant produced phosphatic cements it has been found that fluorine and sulphate may in some circumstances have a combined controlling influence on the hydration and therefore early strength of phosphatic portland cements. Examples of this are given.

The influence of sulphate and of fluorine is being studied systematically by examining the systems $CaO–SiO_2–CaF_2$ and $CaO–SiO_2–SO_3$. Some data is given in the present paper on the strength of tricalcium silicate containing sulphate and fluorine.

Introduction

The importance of the minor components in modifying the major clinker phases, a role in which their influence is far greater than their quantitative representation in the clinker might suggest, was emphasized by Welch and Gutt (1) at the 4th Symposium. The presence of these minor components may influence the formation of the principal cement compounds, their proportion in the clinker and their quality as cementing compounds. Generally, minor components can affect the properties of the cement in three main ways:

a) They can lead to different phase relations and therefore to different reaction products at the temperature at which cement clinker is made in the kiln. This effect may include the stabilization of high temperature polymorphs of the cement compounds. They may differ in their reactivity towards water.
b) They may alter the reactivity of the main cementing compounds towards water by forming solid solutions of different properties.
c) Minor components could produce compounds soluble in water which influence the process of setting and hardening.

Phosphate combined in the clinker has influence under categories (a) and (b). The nature of its influence, and the measures taken in the manufacture of portland cement from phosphatic raw materials to take account of this influence, and the side effects of these measures, are the subject of the present paper.

*Ministry of Public Building and Works, Building Research Station, Garston, Herts, United Kingdom.

The Effect of Phosphate on the Constitution and Hardening of Portland Cement

Work Leading to the Establishment of the Uganda Cement Industry

While in most portland cements the phosphate level is of the order of 0.2% expressed as P_2O_5, phosphate occurs in significant amounts in various limestone deposits. In Uganda, for instance, the only limestone available for cement manufacture, until recently, was a carbonatite containing up to 6% P_2O_5. Phosphate in such amounts was known from experience to be deleterious in the cement making process but the nature of its action was not understood until Nurse (2) began to investigate it in 1950 in connection with the possible utilization of the Uganda phosphatic limestone for cement manufacture. This had been considered before, in 1940, and was rejected because of the phosphate, (3) but the intention to build the Owen Falls dam which controls the outflow of the river Nile from Lake Victoria lent special importance to the investigations in 1950.

Nurse (2) made experimental portland cement clinkers containing known amounts of CaO, SiO_2, Al_2O_3, Fe_2O_3 and P_2O_5 and studied their mineralogical content. He found that their tricalcium silicate content decreased as their P_2O_5 content grew and became nil at 7% P_2O_5 by weight. It was established that phosphate was present in the clinker in solid solution with dicalcium silicate and that the maximum solid solution had the approximate composition 66.5% CaO, 26.5% SiO_2, 7% P_2O_5. The practical recommendations made by Nurse (2) were that to obtain a satisfactory portland cement, phosphate should be kept below 2.25% P_2O_5 and a process was devised for reducing the phosphate content of the limestone by a three stage process consisting of ignition, hydration of the resulting CaO and elutriation of the lime hydrate. By elutriation the coarse fraction containing phosphatic material could be removed and the phosphate in the lime hydrate diluted.

On the basis of his findings Nurse (2) provided proportioning formulae for the manufacture of cement from phosphatic limestone. These formulae were based on the assumption that in a portland cement containing phosphate, all the phosphate would be combined as the previously mentioned solid solution, or if the cement is not lime-saturated, a solid solution lying between $2CaO \cdot SiO_2$ and the composition given above. He showed that for each 1% P_2O_5 added the content of $3CaO \cdot SiO_2$ is lowered by 9.9% and that of the dicalcium silicate phase is raised by 10.9%. Nurse (2) tested the validity of these equations by making experimental cements and comparing their compound content based on these equations with that obtained by microscopic point counts of crystals seen in polished and etched sections of clinker viewed in reflected light. These were found to be in agreement. Nurse stressed two other points, firstly the need to maintain the saturation of lime, and secondly, the lower water requirements in mixing phosphatic cement. In a dry mix (0.5% water) phosphatic cements gave better results than ordinary portland cements.

Nurse's work provided the basis for the establishment of the Uganda Cement Industry who commenced manufacture at Tororo in 1953. Over 17,000 tons of the cement was used in the building of the Owen Falls dam maintaining supply when it would have been impossible to obtain sufficient cement via the port of Mombasa.

Phase Equilibria in the System $CaO–SiO_2–P_2O_5$

Phase studies of the system dicalcium silicate—tricalcium phosphate by Nurse, Welch and Gutt (4) and of the system $2CaO \cdot SiO_2–3CaO \cdot P_2O_5–CaO$ by Gutt (5–6) have consolidated and extended the interpretations which followed from the earlier work. The system $2CaO \cdot SiO_2–3CaO \cdot P_2O_5$ presents at high temperature a continuous series of solid solutions with a liquidus maximum at 2240°C. A new high temperature form of $3CaO \cdot P_2O_5$ designated $\bar{\alpha}$ was discovered (4–7) which does not survive quenching to room temperature but is completely miscible with the α form of $2CaO \cdot SiO_2$. Since the discovery of the superalpha form ($\bar{\alpha}$) of tricalcium phosphate by Nurse, Welch and Gutt (4) Trömel and Fix (8) and Berak (9–10) repeated some of their earlier studies and published confirmations of the new polymorph. It is of practical importance that β, α' and α dicalcium silicates can in turn be stabilized by increasing phosphate additions. At lower temperatures two compounds are formed by solid state reactions, the long-known silicocarnotite stable below 1450°C and a new phase denoted 'A' stable below 1125°C of the approximate composition $7CaO \cdot P_2O_5 \cdot 2SiO_2$. The latter compound will not therefore be a compatibility product relevant to the clinkering temperature of portland cement. The phase diagram of the system $2CaO \cdot SiO_2–3CaO \cdot P_2O_5$ is reproduced in Fig. 1.

Gutt (5–6) studied the system $2CaO \cdot SiO_2–3CaO \cdot P_2O_5–CaO$ and delineated the liquidus surface. Four

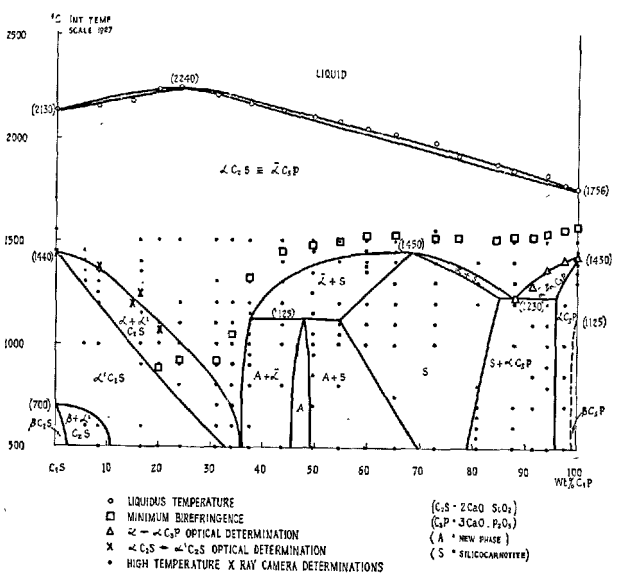

Fig. 1. *The system* $C_2S \cdot C_3P$

solid phases were individually recognisable at the liquidus, tricalcium silicate, lime. tetracalcium phosphate and dicalcium silicate/tricalcium phosphate solid solution.

The primary crystallisation fields of these phases were delineated by the examination of 68 compositions by high temperature microscopy. For these compositions the liquidus temperature and the primary phase were established and, where possible, the crystallisation path was followed and the second phase and its dissolution temperature were also determined. Some compositions selected for examination lay on two-phase boundaries and the composition of the reaction point where the three phases C_2S/C_3P_{SS}, CaO and C_4P coexist with liquid where also located experimentally. All the individual compositions studied and the observations relating to each of them together with an account of the melting behaviour and characteristics of crystal growth of the solid phases encountered in this system were given by Gutt (6) In accordance with the study of $3CaO \cdot SiO_2$ by Welch and Gutt (11) which established that this compound melts incongruently, $3CaO \cdot SiO_2$ has a primary crystallisation field in the system $2CaO \cdot SiO_2$–$3CaO \cdot P_2O_5$–CaO which extends to the binary system CaO–SiO_2. In the system $2CaO \cdot SiO_2$–$3CaO \cdot P_2O_5$–CaO this field extends to 13% P_2O_5.

There are two reaction points. The first of these R_1 between lime, C_4P and C_2S/C_3P_{SS} occurs at the composition 34.5 P_2O_5, 60.75 CaO, 4.75 SiO_2 (weight %) and has a liquidus temperature of 1636°C. The simultaneous presence of the three phases at the liquidus temperature in this composition was established by high temperature microscopy. R_1 is a ternary eutectic point. The boundary between the primary crystallisation fields of C_4P and the C_2S/C_3P_{SS} passes through a liquidus temperature maximum M_2 before reaching R_1. The maximum M_2 occurs at the point where the C_4P–C_2S/C_3P_{SS} boundary is intersected by the Alkemade line C_4P'–C_3P. The formula C_4P' represents a solid solution of C_4P with calcium and silicate ions.

The second reaction point between C_3S, CaO and C_2S/C_3P_{SS} occurs at the composition 67.2 CaO, 19.8 SiO_2, 13 P_2O_5 (wt %) and its liquidus temperature is 1970°C. The liquidus temperature maximum M_1 on the C_3S–C_2S/C_3P_{SS} field boundary is at the point where the Alkemade line C_2S–PSS' intersects this boundary although some displacement of PSS' towards C_3P is expected as the temperature rises.

The liquidus temperatures along the C_3S/CaO primary field boundary rise from the reaction point R_2 and reach 2150°C as this boundary approaches the CaO–SiO_2 system. This seemed to be in conflict with the liquidus temperature of 2070°C reported by Welch and Gutt (11) for the composition 71.5% CaO, 28.5% SiO_2 (wt %) where the incongruent boundary with lime occurs. In view of this the lime rich region of the system CaO–SiO_2 was re-examined leading to the revised diagram (5–6) in Fig. 2. It will be seen that the work of Welch and Gutt (11) is confirmed in every respect with the exception of the liquidus temperatures between the eutectic, between C_2S and C_3S and lime.

The phase diagram of the system C_2S–C_3P–CaO is reproduced (5–6) in Fig. 3. In comparing it with earlier phase diagrams proposed by Barret and McCaughey (12) and of Trömel, Harkort and Hotop (13) it should be remembered that their work preceded successful delineation of the equilibria in the binary system $2CaO \cdot SiO_2$–$3CaO \cdot P_2O_5$ (4), the detection of $\bar{\alpha}$ tricalcium phosphate (7) and the demonstration that $3CaO \cdot SiO_2$ melts incongruently (11). These earlier studies failed to detect the primary crystallisation field of $3CaO \cdot SiO_2$ in the system $2CaO \cdot SiO_2$–$3CaO \cdot P_2O_5$. Barret and McCaughey included in their proposed diagram a primary crystallisation field for silicocarnotite a phase which does not exist at liquidus temperatures as it inverts above 1450°C without decomposition into a $\bar{\alpha}$ tricalcium phosphate solid solution (see Fig. 1).

Compatibility relations were examined for the system C_2S–C_3P–CaO that apply at 1500°C since this is the temperature of particular importance in portland cement manufacture. While considering the division of the system into compatibility triangles a hypothe-

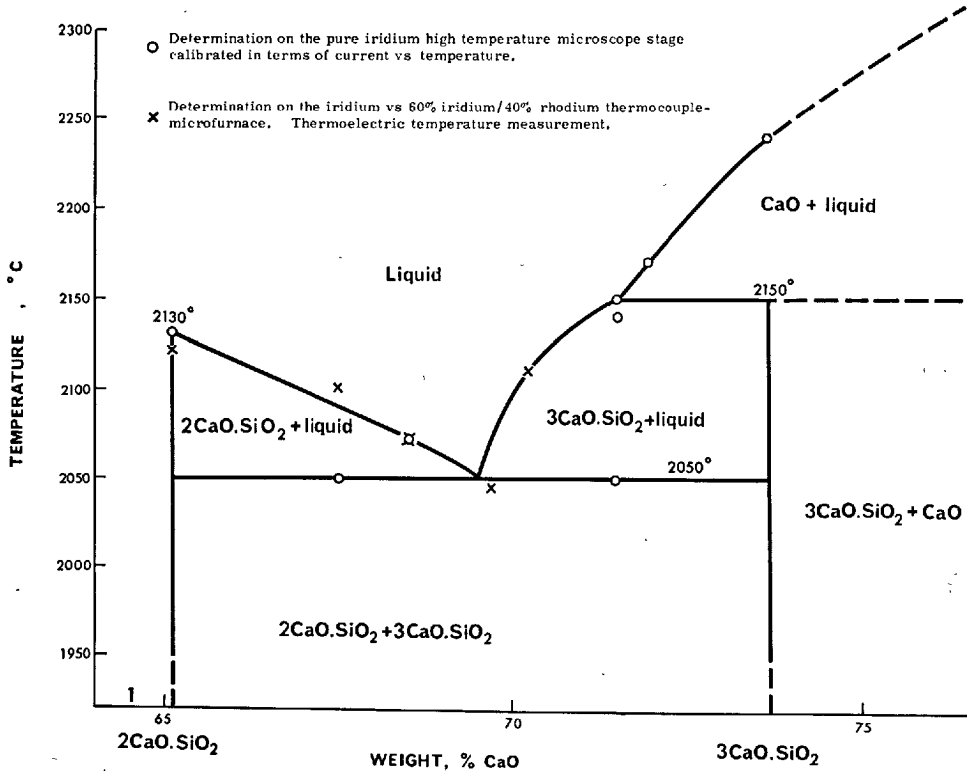

Fig. 2. *Revised phase diagram for lime rich portion of system* $CaO–SiO_2$

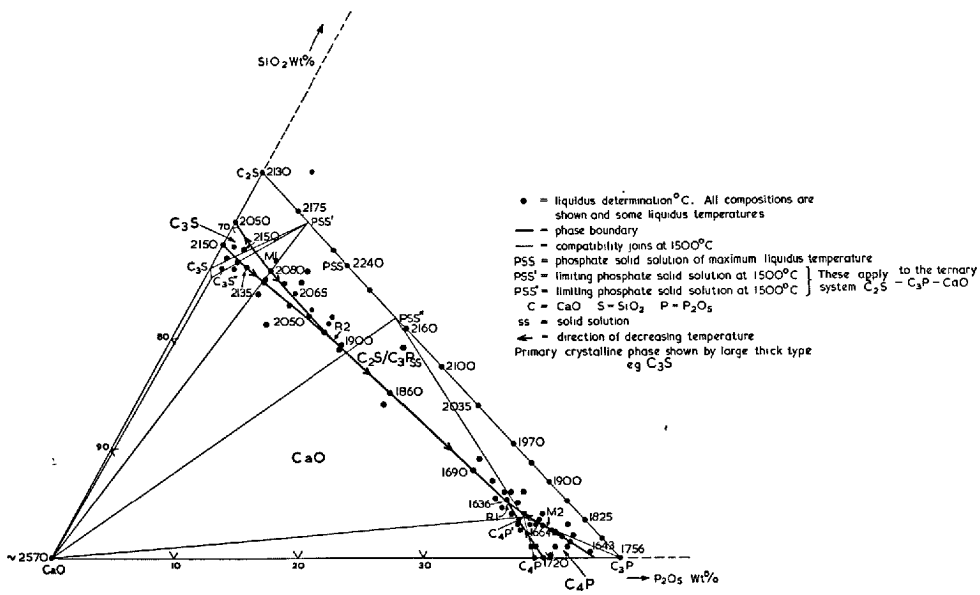

Fig. 3. *Phase diagram of the system* $C_2S–C_3P–CaO$

tical join was studied between C_3S and PSS the composition of maximum liquidus temperature on the C_2S–C_3P join (PSS = 75.9% C_2S, 24.1% C_3P wt). Examination of fully reacted compositions showed, however, that lime was present in compositions on the side of this join nearer to the system CaO–SiO_2 indicating that the true join led to a point on the C_2S–C_3P join poorer in C_3P than PSS. The method then adopted for the location of the true joins consisted of free lime analysis of selected compositions in the system in which CaO is one of the three stable phases at 1500°C. Subtraction of free lime gave the corresponding two phase compositions on the join.

The joins

	PSS′	—	C_3S''
	C_3S	—	C_3S''
	C_4P	—	C_4P'
and	C_4P	—	PSS″

where thus established.

The whole scheme was tested by examining by X-ray analysis the phases present in 40 selected compositions, which are plotted in Fig. 4, and further, by examining equilibria at 1650°C. The full details were given by Gutt (5–6), but the compatibility diagram is reproduced in Fig. 4.

Schlaudt (14) studied the system CaO–SiO_2–P_2O_5 with reference to C_3S crystalline solutions and examined experimentally 19 compositions on the joins $Ca_{19}Si_5O_{29}$–C_4P and C_3S–C_4P. For other parts of the system Schlaudt (14) accepted the liquidus data published by Gutt (5) and he also accepted the validity of the phase diagram of the system C_3S–C_3P provided by Nurse, Welch and Gutt (4). Since all the compositions studied experimentally by Schlaudt lie inside the primary crystallization field of lime and provide no data on phase boundaries, Schlaudt, in effect, assumed the validity of the whole of the liquidus surface of the system C_2S–C_3P–CaO due to Gutt (5) and reproduced here in Fig. 3. Schlaudt's work therefore produced no modification of the phase diagram at liquidus temperatures. Schlaudt further stated that "he disregarded subsolidus reactions in phase identification and that higher temperature assemblages were determined by observation of textures". He stated also however, that "crystal growth during the quenching process was so rapid throughout the system that the appearance of several quench phases often masked the true high-temperature equilibrium assemblages". In these circumstances, the interpretation of Schlaudt's observations by the methods he adopted must indeed have been difficult and the advantages of high temperature microscopy and X-ray analysis used by Gutt (5–6) are manifest.

While accepting Gutt's liquidus surface for the system C_2S–C_3P–CaO, Schlaudt suggested minor modifications to the compatibility diagram for the subsolidus. These included, firstly, a preferred composition for the tricalcium silicate solid solution with calcium and phosphate ions, i.e. 98.2 C_3S, 1.8 C_5P mole% = 73.4 CaO, 25.5 SiO_2, 1.1 P_2O_5 wt% for

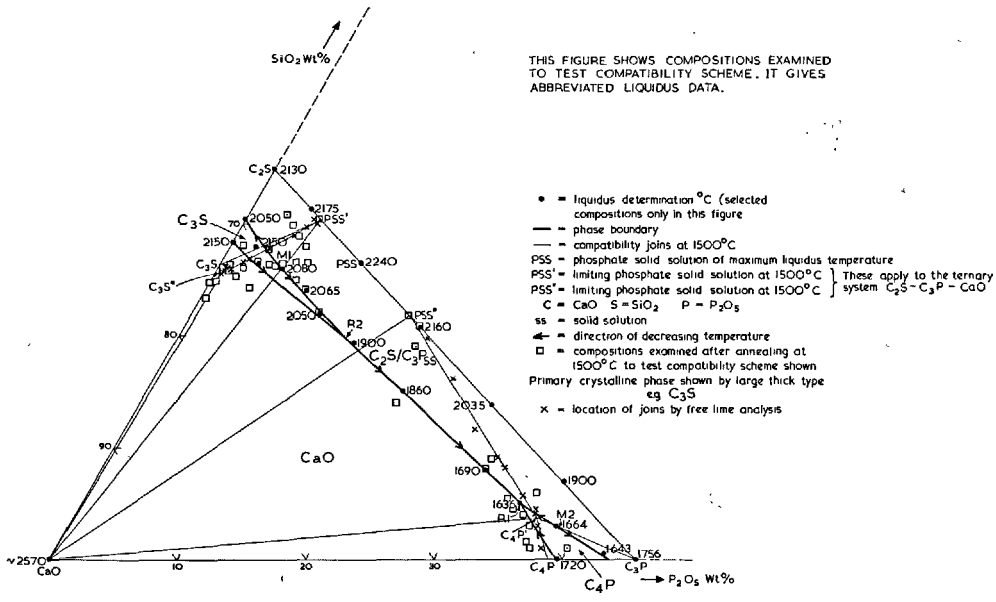

Fig. 4. *Phase diagram of the system* C_2S–C_3P–CaO

$C_{3.11}SP_{0.01}$ = 74 CaO, 25.5 SiO_2, 0.5 P_2O_5, wt%, on the grounds that it is theoretically more fitting. Secondly, Schlaudt arrived at the composition 58 mole% C_2S, 42 mole% C_3P as preferable to PSS'' which is equivalent to 75 mole% C_2S, 25 mole% C_3P. This preference does not appear to be borne out by Schlaudt's experimental results. Thirdly, Schlaudt would prefer the composition 94.8 C_2S, 5.2 C_3P mole% = 91 C_2S, 9 C_3P wt% = 64.1 CaO, 31.8 SiO_2, 4.1 P_2O_5, wt% to Gutt's point PSS' given at the composition 92.65 C_2S, 7.35 C_3P mole% = 87.5 C_2S, 12.5 C_3P wt%.

It should furthermore be noted that Schlaudt's compatibility triangles apply to unspecified solidus temperatures and cannot be directly compared with Gutt's (5–6) compatibility scheme for the system C_2S–C_3P–CaO applicable at 1500°C and checked at 1650°C. Further theoretical speculations were also made by Schlaudt (14) on compatibility in the region of C_4P but these were not based on any experimental data.

On p. 58 of his thesis Schlaudt (14) attributes to Welch and Gutt the assertion that αC_2S cannot be stabilized to room temperature by 'phosphorus' alone. These authors have, in fact, earlier shown (4) that αC_2S can be stabilized by calcium phosphate in the region of 34 C_3P (wt%) in the system C_2S–C_3P as shown in Fig. 1, reproduced here. Welch and Gutt (1) have also used the same composition to assess the hydraulicity of αC_2S stabilized as phosphate. The modifications suggested by Schlaudt to the system C_2S–C_3P–CaO do not affect significantly the practical considerations which follow in which Gutt's (5–6) original phase diagram for the system C_2S–C_3P–CaO is used and all subsolidus reactions (4) are taken into account.

Practical Significance of the Phase Data in Relation to the Cement Making Process

Before the publication of Nurse's paper in 1952 (2) it was believed that tricalcium silicate, the most important compound in portland cement clinker did not occur in the system CaO–SiO_2–P_2O_5 and that the phases formed in phosphate containing cement would be CaO, $2CaO \cdot SiO_2$ and Nagelschmidtite ($7CaO \cdot P_2O_5 \cdot 2SiO_2$) or $2CaO \cdot SiO_2$, $3CaO \cdot 2SiO_2$ and Nagelschmidtite. If this had been true it would have been impossible to make portland cement from phosphatic raw materials. Nurse showed by making cements containing tricalcium silicate with raw material having up to 7% P_2O_5 that the earlier phase diagrams of the system CaO–SiO_2–P_2O_5 could not be correct in relation at least to tricalcium silicate. The present work has shown directly that $3CaO \cdot SiO_2$ has a primary crystallization field extending to 13% P_2O_5 and that at 1500°C $3CaO \cdot SiO_2$ or $(3CaO \cdot SiO_2)''$ (see Figs. 3–4) would be present as compatibility products in compositions of low P_2O_5 concentration.

The second point in order of importance is that in addition to limiting the quantity of $3CaO \cdot SiO_2$ due to preferential formation of a phosphatic dicalcium silicate solid solution, the presence of phosphate may lead to stabilization of dicalcium silicate in the non-hydraulic α or the weakly hydraulic α' form. This adverse effect of phosphate is counter-balanced by the fact that β dicalcium silicate stabilized by phosphate may be of high cementing quality (15). The cementing quality of the four polymorphs of dicalcium silicate stabilized with calcium phosphate was assessed by Welch and Gutt (1).

The maximum solid solution of phosphate with $2CaO \cdot SiO_2$ at 1500°C would be in weight per cent PSS' (87.5% $2CaO \cdot SiO_2$, 12.5% $3CaO \cdot P_2O_5$) or PSS'' (62.4% $2CaO \cdot SiO_2$, 37.6% $3CaO \cdot P_2O_5$) not the composition suggested by Nurse (66.5% CaO, 26.5% SiO_2, 7% P_2O_5). This, however, applied to the ternary system. Nurse's (2) composition for this solid solution originates from studies of five component mixtures containing also Fe_2O_3 and Al_2O_3 and this difference must represent the effect of Fe and Al on the phase relations.

The tricalcium silicate solid solution with Ca^{++} and PO_4^{---} ions (C_3S'') has been tested for strength. The cementing quality of the composition (C_3S'') is not much different from that of pure $3CaO \cdot SiO_2$ apart from slightly lower one day strength.

The polymorphism of $3CaO \cdot SiO_2$ has been studied by Nurse and Welch (16) who found transformations at 923°C and 980°C respectively. These transformations have been confirmed and further studied by Yamaguchi and Miyabe (17). More recently further complexities of the polymorphism of this compound have been studied and (18–19) the question whether the cementing quality of the different structural modifications differs has received attention (20). The existing evidence indicates that the influence of polymorphism on hydraulicity of tricalcium silicate is small but in this connection it should be stated that both the phases $3CaO \cdot SiO_2$ and $(3CaO \cdot SiO_2)''$ identified in the system CaO–$2CaO \cdot SiO_2$–$3CaO \cdot P_2O_5$ were in the triclinic form.

The Role of Fluorine in Portland Cement Manufacture

It is necessary to consider next the effect of fluorine on the reactions occurring in the formation of portland cement clinker since CaF_2 may be added to the raw meal to improve the quality of phosphatic cement. The phosphatic cement made at Tororo, Uganda, contains approximately 1% fluorine.

Welch and Gutt (1) reported at the previous symposium that fluorine ions enter the crystal lattice of tricalcium silicate changing the structure from triclinic in the direction of the monoclinic form. The addition of fluorine increased the rate of formation of $3CaO \cdot SiO_2$ but its cementing quality was reduced. Fluorine did not stabilize high temperature forms of C_2S. Nurse, Midgley, Gutt and Fletcher (20) explored the effect of polymorphism of C_3S on the reactivity of this compound towards water. They used preparations in the series $C_{156-x}M_xS_{52}$ in which x took the values 0, 1, 2, 5, 6. A second series of preparations of the same composition was made with addition of CaF_2 and subtraction of CaO so that 0.5% fluorine remained in the mix. In this way various polymorphs of C_3S were stabilized. It was concluded that the T_{II}–T_I–Mono structural changes do not have a strong influence on reactivity towards water as meausred by strength of mortars. The effect of the change to the trigonal structure remained in doubt since Gutt (21) had found that a trigonal (or possibly orthorhombic M_{II}) preparation of C_3S containing 2.9% MnO and 0.7% F give very low strength. Fluorine had a predominant effect independent of structural form leading to lowered strength for T_{II} structures.

Since then the practical importance of the role of fluorine enhanced by world interest in fluorophosphatic materials had warranted renewed study of the system CaO–SiO_2–CaF_2. Gutt and Osborne (22) established the phase diagram of the system C_2S–CaF_2 showing that C_2S polymorphs do not form solid solutions with fluorine ions alone (1,22). These authors (22) characterized two calcium silico fluorides $(C_2S)_2 \cdot CaF_2$ and $(C_3S)_3 \cdot CaF_2$ which are believed to be intermediates in the formation of C_2S and C_3S when fluorine is present in the cement raw materials. The following reaction sequences have been identified:

This sequence of reactions was observable in compositions in the ternary system containing 2% fluorine. The formation of C_3S in the presence of fluorine occurs at 1170°C in agreement with previous work (1).

Evidence is available from two sources that the proposed mechanisms based on studies of the system

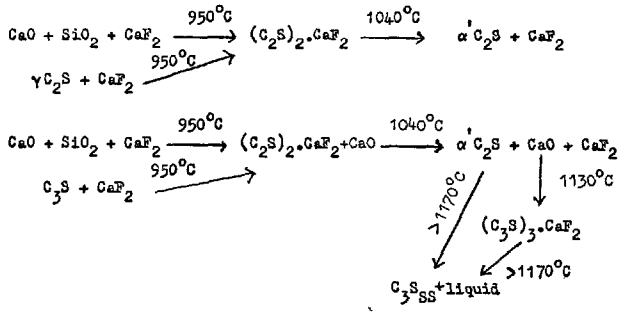

CaO–SiO_2–CaF_2 are applicable to cement clinker. Firstly, Bereczky (23) reported two calcium silicofluoride phases, which he named A and B, as present in ignited mixtures of C_3S and calcium fluoride. He did not assign compositions to these phases but they are identical with the compounds $(C_3S)_3 \cdot CaF_2$ and $(C_2S)_2 \cdot CaF_2$ respectively, both of which were characterized by Gutt and Osborne (22). Bereczky also identified phases A and B in cement compositions during ignition of cement raw meal containing fluorine and he proposed that C_3S was formed by the following mechanism:

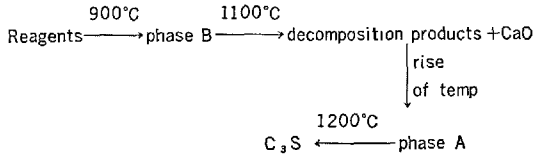

Secondly, Akaiwa, Sudoh and Tanaka (24) have reported a calciumsilico-fluoride of the composition $11CaO \cdot 4SiO_2 \cdot CaF_2$. Comparison of their X-ray diffraction pattern for this compound shows that it is identical with the compound $(C_3S)_3 \cdot CaF_2$ reported by Gutt and Osborne (22a) and with phase A reported by Bereczky (23). Akaiwa et al.* found that the compound $11CaO \cdot 4SiO_2 \cdot CaF_2$ formed by decomposition of C_3S_{SS} and was especially prominent in slow cooled clinkers. They also stated that at 2% CaF_2, C_3A lines were no longer detectable and preferential formation of $11CaO \cdot 4SiO_2 \cdot CaF_2$ occurred in the clinker. Ignition of $11CaO \cdot 4SiO_2 \cdot CaF_2$ above 1190°C gave monoclinic C_3S.

The formation of the compounds $(C_2S)_2 \cdot CaF_2$ and $(C_3S)_3 \cdot CaF_2$ in the quaternary system CaO–SiO_2–P_2O_5–CaF_2 is being studied but there is no reason to suppose that the reaction sequences proposed above do not apply similarly to phosphatic cement.

*approximate formula.

*Sudoh and Tanaka.

Table 1. *Compositions in the system* $CaO–SiO_2–P_2O_5–CaF_2$ (*wt %*)

CSPF	CaO	P_2O_5	SiO_2	F
1	70.99	1.98	26.03	1.04
2	71.99	0.99	26.04	1.04
3	69.99	2.97	26.04	1.07
4	72.34	1.00	26.17	0.51
5	71.34	1.99	26.17	0.50
6	68.31	3.17	27.52	1.00
7 ≡ (PSS′ with 1%F)	63.16	5.64	30.20	1.00

The System $CaO–SiO_2–P_2O_5–CaF_2$

In considering the effect of fluorine in the specific case of phosphatic cement the system $CaO–SiO_2–P_2O_5–CaF_2$ is especially relevant.

The compositions which have been examined are given in Table 1 below. They were all ignited at 1450°C for $1\frac{1}{4}$ hr and air-quenched. The fluorine figures are derived from chemical analysis after heat treatment.

X-ray analysis of compositions 1 to 6 in Table 1 showed as the main phase, tricalcium silicate modified towards the monoclinic form in the same way as reported by Welch and Gutt (1) for C_3S containing fluorine alone.

The 7th preparation was the solid solution designated PSS′ (see Figs 3–4)with 1% added fluorine and ignited to nil free time. In this $\alpha'C_2S$ was the phase identified. The compressive strength of 1 : 3 half inch mortar cubes made from this preparation and 4% gypsum was 20 psi at 1 day and nil at later ages indicating that $\alpha'C_2S$ stabilized with phosphate in the presence of fluorine was even less hydraulic than phosphatic α' in the absence of fluorine (1).

Schlaudt (14) studied the system $CaO–C_2S–Ca_{10}P_6O_{24}F_2$ (fluorapatite) and proposed a phase diagram for the system $C_3S–Ca_{10}P_6O_{24}F_2$. α dicalcium silicate was stabilized to room temperature. A tricalcium silicate solid solution with fluorapatite was found on the join $C_3S–Ca_{10}P_6O_{24}F_2$ up to slightly more than 2 mole% at 1905°C, the invariant temperature for coexistence of liquid, C_3S, CaO and C_2S. On the basis of his work on this join a phase diagram was also proposed for the system $CaO–C_2S–Ca_{10}P_6O_{24}F_2$.

In this diagram a very small primary field is shown for C_3S extending to 3 mole% of $Ca_{10}P_6O_{24}F_2$ which is equivalent to 5.08% P_2O_5 whereas Gutt (5–6) has shown that in the system $C_2S–C_3P–CaO$ the C_3S field extends to 13% (wt) P_2O_5. It is considered that the existing data on the extent of the C_3S primary field in the system $CaO–SiO_2–CaF_2$ is still imprecise. Eitel (25) reported that this field in the system $CaO–C_2S–CaF_2$ ended at 43% CaF_2 and Mukerji (26–27) that it extends to 44% CaF_2 but the diagrams proposed by these authors differ substancially in the proposed stable phase assemblages in this region and include different phase grouping at invariant points. The discovery of the compound $(C_3S)_3 \cdot CaF_2$ means that the primary field of this compound may intrude in the ternary system. An important feature in Schlaudt's results for the join $C_3S–Ca_{10}P_6O_{24}F_2$ is that fluorapatite does not appear in mixtures containing less than 10% (mole%) of this compound.

This is equivalent to 1.2% fluorine (wt%) and this compound need not be expected therefore in detectable amounts in phosphatic-fluorinated portland cements which normally contain no more than 1.4% fluorine. Schlaudt stated that 3 mole% of C_3P or 4 mole% of fluorapatite would be needed to eliminate C_3S from the compatibility products. He argued that "the tolerance for combined fluoride and phosphate impurity in cement raw materials is not substantially different from the tolerance for phosphate alone (11). This interpretation must be questioned since 3 mole% of C_3P in the composition $97C_3S$, $3C_3P$ (mole%) is equivalent to 4.03 wt% C_3P or 1.84 wt% P_2O_5, whereas 4 mole% of $3C_3P \cdot CaF_2$ in the composition $96C_3S$, $4C_3P \cdot CaF_2$ (mole%) is equivalent to 15.75 wt% $3C_3P \cdot CaF_2$ or to 6.55 wt% P_2O_5. It follows that the tolerance for phosphate is substantially greater in the presence of fluoride and this is compatible with practical experience in cement manufacture.

The Role of Sulphate in the Manufacture of Phosphatic Portland Cement

Practical evidence exists from studies of Uganda cements that the amount of SO_3 in the clinker influences the quality of phosphatic portland cements. For this reason the systems $CaO–SiO_2–SO_3$ and $CaO–SiO_2–SO_3–F$ are being studied and a logical extension of this work would include the systems $CaO–SiO_2–P_2O_5–SO_3$ and $CaO–SiO_2–F–SO_3$.

The System $CaO–SiO_2–SO_3$

The volatility of sulphate causes considerable experimental difficulty in the study of this system being examined by Gutt and Smith. These authors have delineated the stable phase assemblages in the subsystem $CaO–CS–CaSO_4$ at 1000°C and 1200°C

(28). They also detected a new compound $(C_2S)_2 \cdot CaSO_4$ which takes part in stable assemblages at these temperatures. This compound is analogous to silicocarnotite C_5PS in the system C_2S–C_3P (4). The only solid solution detected in the 1000°–1200°C temperature range was between $\alpha' C_2S$ and Ca^{2+} and SO_4^{2-} ions giving 98.9 C_2S, 1.1 $CaSO_4$ mole% as the maximum solid solution at 1200°C and 98.3 C_2S, 1.7 $CaSO_4$ mole% at 1000°C. The C_3S primary crystallization field has not been delineated as yet. The compound $(C_2S)_2 \cdot CaSO_4$ appears to be incompatible with C_3S and the decomposition temperature for $(C_2S)_2 \cdot CaSO_4$ on the join C_2S–$CaSO_4$ is 1300°C. To study the behaviour of C_3S it is necessary to treat at above 1300°C where liquid is also present in the system CaO–CS–$CaSO_4$ as a stable phase. The presence of liquid complicates the diagram of the isothermal section at 1310°C which has been studied.

If it is assumed that the $CaSO_4$ present in preparations annealed at 1310°C and water quenched has crystallized from the glass and has not been exsolved from the C_3S_{ss} then compatibility triangles can be drawn for the system at 1310°C. The results based on this procedure give the maximum solid solution of C_3S and Ca^{2+} and SO_4^{2-} ions as 92% C_3S, 8% $2CaSO_4 \cdot SiO_2$ mole%, which is equivalent to 2.9 wt% SO_3. The substitution assumed was 1 sulphur ion for $2Ca^{2+} + 0.5Si^{4+}$. Tricalcium silicate was detected after this heat treatment at 1310°C, in the presence of 38 wt% SO_3, a much higher figure then the equivalent for phosphate.

Many workers (28, 30) have reported stabilization of the β form of C_2S by very small amounts of $CaSO_4$ and Okorokov, Golynko-Wolfson and Korneyev (30) claimed high strength for βC_2S so stabilized. It has also been claimed (31) that $CaSO_4$ accelerates formation of C_3S in the temperature range 1300°C–1450°C and improves its crystalline form. Sychev and Korneyev (32) reported that at 1500°C formation of C_3S was hindered by the presence of SO_3. The questions whether $(C_2S)_2 \cdot CaSO_4$ has a primary field in the ternary system and whether this compound is an intermediate in the formation of C_2S and C_3S solid solutions in cement clinker if the SO_3 content is substantial remain unanswered. It has been shown, however, that $(C_2S)_2 \cdot CaSO_4$ is compatible with $3CA \cdot CaSO_4$ at 1200°C. The effect of iron on the stability of $(C_2S)_2 \cdot CaSO_4$ was tested by prolonged heating of a mixture of reagents of the composition 33.3% $(C_2S)_2 \cdot CaSO_4$, 33.3% $3CA \cdot CaSO_4$, 33.3% C_4AF at 1200°C and air-quenching. The compound $(C_2S)_2 \cdot CaSO_4$ was also stable after this heat treatment.

Strength Test of Preparations on the Join C_3S–SO_3

Preparations of compositions on the join C_3S–SO_3 were ignited at 1400°C in covered platinum boats until free lime was less than 1%. Some of these preparations contained glass and they were annealed at 1300–1350°C to crystallize the glass phase. In Fig. 5 the time taken to obtain combination less than 1% free lime is plotted against % SO_3 added, showing a rapid fall in the time needed between 1 and 3% SO_3, a region in which SO_3 clearly aids the formation of C_3S; the effect of fluorine is as expected from earlier work. The heat treatment and phase composition of the preparations are shown in Table 2. These preparations were ground to 3700–4000 sq.cm/g mixed with 4% gypsum and tested for compressive strength on half inch 1 : 3 mortar cubes. The strength results are given in Fig. 6.

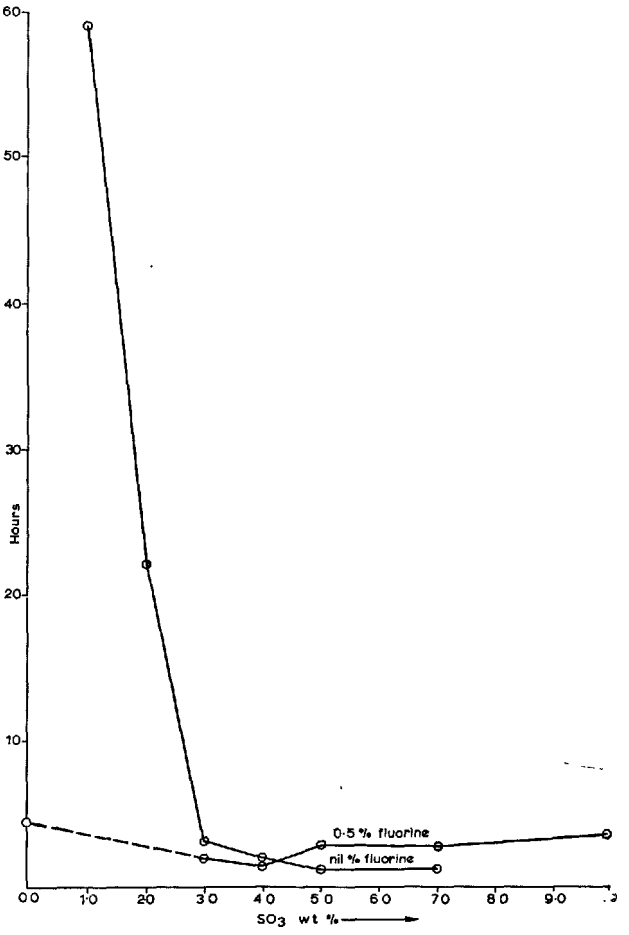

Fig. 5. *Time to obtain free lime ≤ 1.0% against added* SO_3 %

Results and Discussion

The phases identified in the preparations tested for strength are listed in Table 2. Tricalcium silicate was present in the triclinic form and there were no detectable changes towards the monoclinic structures such as reported by Welch and Gutt (1) for C_3S with added fluorine. The only marked change, probably connected with SO_4^{2-} solid solution, was that the intensity of the reflection at 32.1° 2θ increased relatively to that of the reflection at 34.4° 2θ. Dicalcium silicate was present in the β form.

The strength results (Fig. 6) show that up to 3% SO_3 there is a decline in strength followed by a very sudden drop just above 3% SO_3 as shown by the strengths of the preparation with analysed SO_3 figure of 3.035%. This SO_3 level is almost identical with the maximum solid solution limit for SO_3 in C_3S at 1310°C beyond which $CaSO_4$ appears.

The effect of sulphate ions is similar to that of phosphate ions (see Fig. 2 of ref. 1) in producing at low SO_3 concentrations a C_3S_{ss} of low strength but the analogy ends here since continued addition of sulphate, unlike that of phosphate, does not lead to enhanced hydraulicity of the C_3S_{ss}. Between 3 and 6.5% SO_3 the strength rises and this can be attributed to the entry of βC_2S_{ss} of high cementing quality (30). The slow decline in strength beyond 6.5% SO_3 is connected with the increased quantity and possibly also specific action of $CaSO_4$.

The System $CaO–SiO_2–SO_3–CaF_2$

Compositions on the join $C_3S–SO_3$ with 0.5% added fluorine were also studied. The details of the preparations used are shown in Table 3. The entry of βC_2S and of $CaSO_4$ occurs at a lower SO_3 content in the presence of fluorine indicating a C_3S_{ss} of lower SO_4^{2-} content. The strength results in Fig. 7 show that the features found in the presence of SO_3 without fluorine are reproduced, but largely at lower strengths. The strength minimum occurs again in the region of 3% SO_3. The most significant feature is presented by the 1 day strength curve. This has become isolated from the curves for later ages and it lies at very low strength with a minimum at 300 psi at 3.2(4)% SO_3 and 0.45% fluorine. Furthermore, the strength recovery seen in the 1 day strength curve for preparations containing SO_3 but not fluorine is not reproduced. It will be seen from a discussion of phosphatic cements

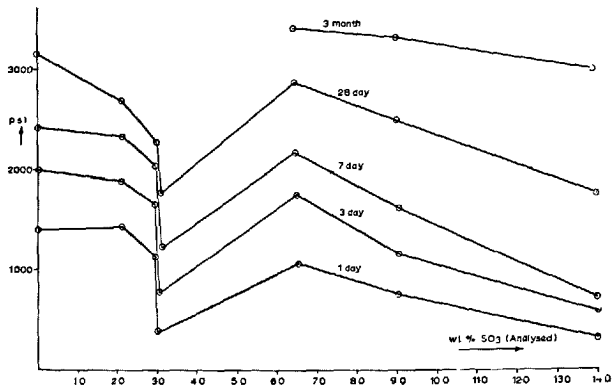

Fig. 6. *Compressive strengths of 1: 3 mortar, ½″ cubes of* C_3S *with* SO_3 *only. (Cement fineness 3700 to 4000* cm^2/g)

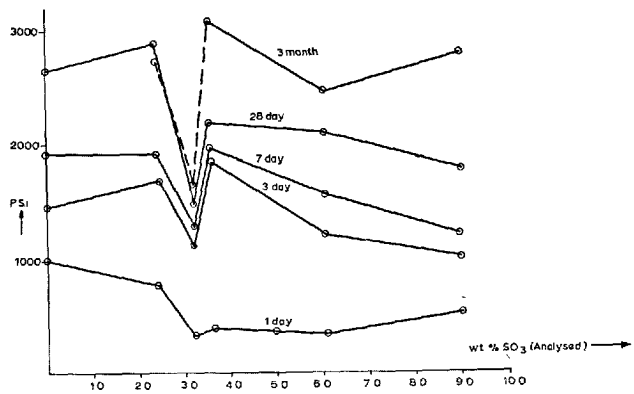

Fig. 7. *Compressive strengths of 1: 3 mortar, ½″ cubes of* C_3S *with* SO_3 *and 0.5%F. (Cement fineness 3700 to 3900* cm^2/g)

Table 2. *The system* $CaO–SiO_2–SO_3$

Mix	Initial SO_3 (wt %)	Composition of ignited mix (wt %)			Heat treatment at 1400°C	Free lime (wt %)	X-ray analysis phase composition
		Analysed SO_3	Recalculated				
			CaO	SiO_2			
13	1	Nil	73.68	26.32	59 hours	0.78	triclinic C_3S only
12	2	Nil	73.68	26.32	22.5 "	0.56	do.
3	3	2.14	72.11	25.75	3.0 "	0.30	triclinic C_3S, $CaSO_4$ tr.
4	4	3.00	71.47	25.53	1.75 "	Nil	do.
1	5	3.03(5)	71.45	25.52	1.0 "	0.79	triclinic C_3S, CaO, tr. $CaSO_4$
17A	7	6.55	68.86	24.59	1.3 "	0.16	do.
10	10	9.08	66.99	23.93	1.0 "	0.50	triclinic C_3S, βC_3S & $\beta CaSO_4$ tr.
11(a)	15	14.08	63.31	22.61	1.5 "	0.56	triclinic C_3S, βC_2S, $\beta CaSO_4$

tr = trace

Table 3. *The system* $CaO–SiO_2–SO_3–CaF_2$

Mix	Initial composition wt %		Composition after ignition wt %				Heat treatment hrs. 1400°C	Free lime wt %	X-rays analysis
	SO_3	F	SO_3 (analysed)	F	CaO (calculated)	SiO_2			
5	3.0	0.5	2.43	0.48	71.54	25.55	1.75	<1.00	C_3S, βC_2S & $\beta CaSO_4$ trace
8	4.0	0.5	3.64	0.43	70.68	25.25	1.50	1.35	C_3S do CaO
2	5.0	0.5	3.24	0.45	70.96	25.35	2.75	1.06	C_3S
18	7.0	0.5	6.09	0.40	68.90	24.61	3.00	0.93	C_3S, $CaSO_4$, βC_2S, CaO trace
9	10.0	0.5	9.06	0.40	66.75	23.84	2.25	1.05	C_3S, $CaSO_4$, βC_2S

Note: The C_3S found in these mixes was triclinic modified towards monoclinic as described for C_3S with fluorine alone[1]

in the final section of this paper that the strength behaviour of C_3S with SO_3 and fluorine offers vital evidence for the theory that the combined influence of SO_3 and fluorine superimposed on the effects of phosphate can in certain circumstances decide the early strength of phosphatic cements especially at 1 day. In the region of nil to 2% SO_3 the effect of 0.5% fluorine is not great but it is expected that the position of the strength minimum on the SO_3 ordinate varies with the fluorine content and that it may occur at a lower SO_3 figure than 3.2(4)%.

Examination of Cements

In the preceding sections of this paper the various systems relevant to the manufacture of portland cement from phosphatic materials were considered in turn and the links between them and the manufacturing process have been indicated. The final section of this paper will be devoted to observations on phosphatic cements which may add to the information previously published (1, 2, 6).

The cements made by the Uganda Cement Industry have continued to be made at the rate of approximately 100,000 tons per annum and to pass B.S.12 Portland Cement in every respect. The P_2O_5 level has generally been near 2%. An important special feature of the process in Uganda is the addition of fluorspar to the raw meal in a quantity leading to approximately 0.9% fluorine in the clinker. The lime saturation factor calculated by the modified equations put forward by Nurse (2) is kept very near one. The alite present in Uganda cements is very often present in the trigonal form (20) whereas monoclinic alite is the predominant form in other portland cements. No correlation was found, however, between the strengths of Uganda cements and the polymorphic form of the alite present. Welch and Gutt (1) found $\alpha'C_2S$ in Uganda clinkers and the presence of this polymorphic has continued to be a feature of these cements. The C_3A content of Uganda cements is low and their low heat of hydration makes them suitable for use in massive concrete constructions as low heat cement. For the same reason their sulphate resistance is expected to be good.

Whereas the blended Uganda cement is satisfactory in every respect 'spot' samples of clinkers taken from the plant and examined individually have at times given low early strength at one day. Groups of such samples have been examined and examples are given below in Table 4 of their minor component content and other properties.

Welch and Gutt (1) argued at the previous symposium that strength measurements must be made in conjunction with microscopic estimates of phase present to assess cementing quality of clinkers and that the latter alone may mislead. The figures in Table 4 give further evidence of this. Cements containing alite

Table 4a. *Details of low strength cements prepared from special clinkers (compositions are in wt %)*

No.	F	SO_3	MgO	P_2O_5	K_2O	Na_2O	Strength psi			Free CaO
							1d	3d	7d	
*										
B 95	0.87	1.19	0.56	2.23	0.80	0.62	840	4390	6140	2.2
B 97	1.11	1.35	0.96	2.29	1.18	0.80	nil	4150	5170	0.5
B102	1.44	1.75	1.01	2.57	1.04	0.65	nil	4090	5530	0.2
B121	0.62	1.39		2.66	1.08	1.05	nil	2530	3370	1.8

*control sample
BS12 mortar cubes

Table 4b. *Phase composition wt % by microscopy*

	Alite	Belite	Interstitial
B 97	55	25	20
B102	67	13	20
	67	14	19
	72	9	19
B121	53	35	12

in quantities from 53 to 72% can be seen to give nil strength at 1 day.

The early hydration of cement B 121 was studied by X-ray diffractometry (33). Cement B 119 which gave 1505 psi at 1 day was used as a control. The low strength cement showed a much lower rate of production of calcium hydroxide and a lower rate of disappearance of alite than the high strength cement.

The rate of hydration of clinker B102 was followed by the method described by Lea and Jones (34) in which the development of strength is taken as proportional to the rate of hydration. The clinker was ground and a paste with 32% of water was sealed and stored at 64°F for varying periods of time. At 1, 3 and 7 days samples were removed, ground, dried at 110°C and heated to 900°C. Lea and Jones found that the corrected weight loss between 110°C and 550°C was a useful criterion of the degree of hydration and they obtained a smooth curve of compressive strength versus this weight loss. The loss for clinker B102 was at 5.5% low and corresponded to a strength of 300 psi for 1 : 2 : 4 concrete.

It is believed that these slow hydrating clinkers contain low strength alite of the type encountered in the studies of fluorinated C_3S and of phosphatic clinkers reported by Welch and Gutt (1), and in the present work especially in the case of C_3S containing fluorine and sulphate at certain levels. It is not argued that the fluorine and sulphate figures in Table 4 give the precise numerical position of the minimum strength region in all clinkers since it is known that other minor components such as K_2O, Na_2O and MgO exert additional influence. It is argued that the results derived from the examination of C_3S containing SO_3 and F together with the observations on the cements having nil one day strength show that a controlling influence by SO_3 and fluorine is at times probable and indicates how a pessimum in the cement strength may arise due to low strength alites or C_3S solid solutions.

The possibility that phosphate may produce compounds soluble in water which influence the process of setting and hardening of portland cement was explored. Two cements were selected from plant production of markedly different early strength but the same chemical and phase composition. A paste of high water cement ratio was made up with the weaker cement and after two hours the liquid was separated by centrifuging. This solution was then used as mixing water for the high strength cement. The strength of the latter was unaffected indicating absence of influence through the solution phase.

Acknowledgements

Parts of this work, indicated in the text, originate from the author's, London University PhD Thesis.

The work described formed a part of the programme of the Building Research Station and the paper is published by permission of the Director.

References

1. J. H. Welch and W. Gutt. 'The effect of minor components on the hydraulicity of the calcium silicates'. Chemistry of Cement, Proceedings of the Fourth International Symposium, Washington, 1960, **1**, pp. 59–68 (U.S. Dept. of Commerce, National Bureau of Standards, Monograph 43, 1962).
2. R. W. Nurse. 'The effect of phosphate on the constitution of portland cement'. J. Appl. Chem., **2**, 708–716 (1952).
3. K. A. Davies. 'Cement manufacture in Uganda'. Colonial Geological and Mineral Resources, **4**, (4), 366–372 (1954).
4. R. W. Nurse, J. H. Welch and W. Gutt. 'High temperature phase equilibria in the system dicalcium silicate—tricalcium phosphate'. J. Chem. Soc., No. 220, 1077–1083 (1959).
5. W. Gutt. 'High temperature phase equilibria in the system $2CaO \cdot SiO_2$–$3CaO \cdot P_2O_5$–CaO'. Nature, **197**, (4863), 142–143 (1963).
6. W. Gutt. 'High temperature phase equilibria in polycomponent silicate systems'. Ph. D. Thesis, London University (1966).
7. R. W. Nurse, J. H. Welch and W. Gutt. 'A new form of tricalcium phosphate'. Nature, **182**, 1230 (1958).
8. G. Trömel and W. Fix. 'Studies of the system CaO–P_2O_5'. Archiv. Eisenhüttenwesen, **32**, 209–13 (1961).
9. J. Berak. 'The system CaO–$3CaO \cdot P_2O_5$–CaF_2,. Roczniki Chemii, **35**, 69 (1961).
10. J. Berak. 'Possibilities of substitution of oxygen for fluorine in apatite'. Chemia Stosowana, **4**, 565 (1961).
11. J. H. Welch and W. Gutt. 'Tricalcium silicate and its stability within the system CaO–SiO_2'. J. Amer. Ceram. Soc., **42**, 11–15 (1959).
12. R. L. Barret and W. J. McCaughey. 'The system CaO–SiO_2–P_2O_5'. Amer. Mineralogist, **27**, 680–95 (1942).

13. G. Trömel, H. J. Harkort and W. Hotop. 'Investigation of the system $CaO–SiO_2–P_2O_5$'. Z. Anorg. Chem. **256**, 253–272 (1948).
14. C. M. Schlaudt. 'Phase equilibria and crystal chemistry of cement and refractory phases in the system $CaO–MgO–Al_2O_3–Fe_2O_3–CaF_2–P_2O_5–SiO_2$'. Ph. D. Thesis, Pennsylvania State University (1964).
15. R. W. Nurse. 'The dicalcium silicate phase'—Proceedings of the Third International Symposium on the Chemistry of Cement, 1952, p. 56–90. (Cement and Concrete Association, London, 1954).
16. R. W. Nurse and J. H. Welch. (see Nurse, Ref. 15).
17. G. Yamaguchi and H. Miyabe. 'Precise determination of the $3CaO \cdot SiO_2$ cells and interpretation of their X-ray diffraction pattern'. J. Amer. Ceram. Soc. **43**, 219–224 (1960).
18. M. Regourd. 'Determination of unit cells: Application to the polymorphs of tricalcium silicate'. Bull. Soc. Mineral Crist., France, **87**, 241–272 (1964).
19. E. Woerman, Th. Hahn and W. Eysel. 'Chemical and structural investigations on the solid solutions of tricalcium silicate'. Zement-Kalk-Gips, **16**, 370–75 (1963).
20. R. W. Nurse, H. G. Midgley, W. Gutt and K. Fletcher. 'Effect of polymorphism of tricalcium silicate on its reactivity'. Special Report 90, p. 258–62 (Highway Research Board, U.S. National Research Council, Washington, D.C., 1966).
21. W. Gutt. See R. W. Nurse, 'The effect of some minor components on cement setting and hardening'. Proc. 7th Conference on the Silicate Industry 1963, Akademiaj, Kiado Budapest (1965).
22. W. Gutt and G. J. Osborne. 'The system $2CaO \cdot SiO_2–CaF_2$'. Trans. Brit. Ceram. Soc., **65**, 521–534, (1966).
22a. W. Gutt and G. J. Osborne, 'The calcium silicofluoride of tentative composition $(3CaO \cdot SiO_2)_3 \cdot CaF_2$' Trans. Brit. Soc. **67** 125–133 (1968).
23. E. Bereczky. 'Acceleration in the formation and stabilisation of tricalcium silicate, II'. Epitoanyag, **16**, 441–448 (1964).
24. S. Akaiawa, G. Sudoh and M. Tanaka. 'Studies on the mineralising effect of CaF_2 and a ternary compound in the system $CaO–SiO_2–CaF_2$'. p. 34–8. Review of 20th General Meeting of the Cement Association of Japan (Tokyo, 1966).
25. W. Eitel. 'The system $CaO–CaF_2–Ca_2SiO_4$'. Z. Angew. Min., **1**, 269 (1938).
26. J. Mukerji. 'Phase equilibrium diagram $CaO–CaF_2–2CaO \cdot SiO_2$'. J. Amer. Ceram. Soc., **48**, 210–213 (1965).
27. J. Mukerji. 'Diagrams of the ternary system $CaO–CaF_2–2CaO \cdot SiO_2$'. D. Sc. Thesis Serie A, No. 3955 (Univ. of Paris, 1962).
28. W. Gutt and M. A. Smith. 'Studies of the subsystem $CaO–CaO \cdot SiO_2–CaSO_4$'. Trans. Brit. Ceram. Soc., **66**, (1967). 557–67.
29. W. Gutt and M. A. Smith. 'A new calcium siliconsulphate'. Nature, **210**, 408–9, (1966).
30. S. D. Okorokov, S. L. Golynko-Wolfson and V. I. Korneyev. 'Change in the strength of C_2S as a function of the nature of the stabilising admixture'. Tr. Leningr. Tekhnol. Inst. in Lensoveta, **1960** (56) 93–98 (1960).
31. T. A. Ragozina and M. A. Akhmedo. 'The effect of $CaSO_4$ on the phase composition of calcium silicates and aluminates on firing'. Uzbek. Khim. Zh. **6**, 5–11 (1962).
32. M. M. Sychev and V. I. Korneyev. 'Effect of raw material admixtures and alloying additives on the technical properties of C_3S'. Tr. Gos. Vses Inst. po Proektir i Nauchn-Issled. Rabotam v Tsementn Prom., **29**, 3–12 (1964).
33. H. G. Midgley, K.E. Fletcher and L. Hjorth. Private Communication.
34. F. M. Lea and F. E. Jones. 'The rate of hydration of portalnd cement and its relation to the rate of development and strength'. J. Soc. Chem. Indsut., **54**, 63T–70T, (1935).

Supplementary Paper I-18 Burnability of Raw Mixes

Jerzy P. Sulikowski*

Synopsis

The work constitutes an attempt to elaborate a laboratory method to enable the quantitative, if only relative, definition of the burnability of a raw mix.

The suggested test consists in determining the changes in the content of uncombined CaO in the mix within the temperature range from 900°C to 1400°C and in measuring the temperatures at which the cylindrical specimens prepared from calcined mix undergo a definite deformation under a constant load.

The results of the above mentioned parallel tests serve for the calculation of three values which may serve as the basis for a comparative estimation of the behaviour of the raw mix during its burning in a rotary kiln.

Four industrial raw mixes of various origins were tested by means of the suggested method.

Observations were carried out during a long period on the behaviour of the mix during burning, its effect upon the refractory lining, and the length of the burning zone. These observations were carried out in the rotary kilns of the cement plants from which the four mixes tested originated.

The observations proved the possibility of applying the three suggested values for a comparative evaluation of the burnability of the raw mixes.

The results of the investigations also confirmed the known fact that the burnability of raw mixes cannot be assessed on the basis of their chemical composition.

Introduction

Observations of the material in the burning zone of industrial rotary kilns testify that raw mixes of various origin behave in a different way during burning.

In practice it is said that the mixes prepared for the production of portland clinker, but blended of components of different geologic origin, have a different burnability.

Some of these mixes sinter at a lower temperature and in a shorter time, others require higher temperature and a longer time for the synthesis of alite and thus a longer sintering zone in the rotary kiln.

The differences in burnability mentioned above may be estimated by observation of the differences in consistency of the whole mass of grains in motion in the hot zone of the rotating kiln. It should be mentioned here that a raw material mix of a given cement plant, i.e. a mix always blended with the same raw materials components also shows variations in burnability. This is caused by the natural chemical variation of the raw material deposit, that is, by the fluctuations in the content of such components as for example SiO_2 and Fe_2O_3.

Moreover, intentional changes in the degree of saturation with lime, which is sometimes applied for technical reasons, clearly influence the burnability of the mix.

It should be stressed that the burnability of mixes has also an evident influence on the refractory lining of the kiln and very often decrease in the burnability of the mix is decisive in the shortening of the lining life.

Thus the problem of burnability is of great importance in industrial practice. A correct, and if possible, quantitative determination of burnability will enable a more exact technological characterization of the raw material deposit and facilitate the selection of the suitable type of rotary kiln and kind of refractory material.

*Academy of Mining and Metallurgy, Kraków, Poland.

Discussion of the Problem

As mentioned in the previous chapter, the specific consistency of the whole mass of clinker grains in the burning zone of the rotary kiln is characterized by the fact that this material as a whole cannot be defined as bulk materials.

The separate grains of this material are lifted in consequence of the kiln rotations, but reaching their highest position they do not roll freely and individually on the slope of the material. The rotating kiln carries up the whole mass of material, which, though an agglomeration of separate granules, when considered as a whole, displays a certain compactness. This material has a dictinct adhesiveness occurring on the interferences of the individual granules.

This phenomenon is explained by the fact that each clinker grain while remaining in the high temperature zone is imbibed with a liquid phase.

In these circumstances it may be concluded that in the temperature range in which the said phase is liquid each clinker grain is not only sticky on the outside, but also deformable under the influence of mechanical static load.

Both the above mentioned adhesiveness and deformability of the clinker grains while in the high temperature zone depend on the amount of the liquid phase and its viscosity and both these features change in turn with temperature.

There exist, moreover, justified grounds for stating that the deformability of hot clinker granules depends also on the amount, size and habit of the crystals glued with the above mentioned liquid phase. This calls to mind an analogy with the macrostructure of fireclay bricks.

It should be also mentioned that in the case of portland clinker the dimensions and the crystal habit of the calcium silicate crystals and their distribution in a clinker granule depend to a great extent on the natural structure of the raw materials. Such a statement is the more justified as it is shown in practice, that the burnability of cement raw materials does not depend merely on their chemical composition.

The total result of the co-operation of all the above presented factors and phenomena is conclusive as regards the burnability of raw materials for cement plants. The burnability can be quantitatively and comparatively assessed visually by observing the differences in the consistency of the material in the burning zone of the rotary kiln.

The Idea of the Present Investigation

The present investigation is an attempt to elaborate a laboratory method which would enable a quantitative, though only a relative, determination of the burnability of the raw material mix.

The idea of the suggested method lies in the quantitative determination of the changes of one of the chemical features of a sample heated in given conditions and in the measurement of temperature at which appropriately shaped specimens of raw mix undergo defined physical changes.

Thus each raw material mix is tested in parallel in two different ways, two series of tests being carried out.

The first series is the determination of the changes in the content of uncombined calcium oxide in the mix in the temperature range from 900°C to 400°C.

The second series of investigation consists in the measurement of temperature at which the specimen formed of the tested mix undergoes further defined deformations during heating under the influence of a constant static load.

Investigated Materials

The idea of investigating the raw mix in the two different ways presented in the previous chapter was applied to several raw mixes of industrial origin.

The mixes originated from four cement plants working with the wet method. Each of these plants has its own deposit of raw materials and the deposits differ from each other as to geologic and petrographic characteristics.

The A cement plant exploits the raw material from cretaceous deposits. Soft chalk of great natural dispersion, easily forming slurries with water is the carbonate component of this raw material. In general the argillaceous component is distributed uniformly thoughout the whole mass of the deposit.

The B cement plant exploits Jurassic limestones, having a high $CaCO_3$ content and the mix has to be

prepared with additional component, i.e. bituminous shales.

The C cement plant also bases its production on its own deposit of raw material of Jurassic origin built of rather hard limestone interbedded with marls of various $CaCO_3$ content.

The D cement plant blends its mix for the production of portland clinker from marls with relatively low $CaCO_3$ content and from very hard crystal Devon limestones of high purity.

It should be added that in the four cement plants from which mixes were sampled, bituminous coal with a rather high ash content is burned in their rotary kilns. For this reason the mixes are adjusted to a rather high CaO content.

The portions of the mixes designed for the tests were not submitted to preliminary grinding to powder and they remained in the state in which they were supplied from the plants. The omission of the preliminary grinding of these samples is justified by the fact that the burnability of the raw mix is not only influenced by numerous factors such as chemical composition and textures of the raw material components, but also by the degree of grinding of the mix which is characteristic in each of the given plants.

The chemical composition of the raw mixes used is given in Table 1.

Table 1. *Chemical composition of mixes*

	Raw mixes			
	A	B	C	D
Loss of ign.	35.60	36.04	37.92	35.51
SiO_2	15.52	13.12	12.50	13.66
Al_2O_3	3.86	3.75	3.72	4.10
Fe_2O_3	1.20	2.07	2.08	2.10
CaO	42.94	43.56	42.48	43.96
MgO	—	0.50	1.08	0.52
Total	99.12	99.04	99.78	99.85
	Calcined mixes			
SiO_2	24.48	20.82	20.25	21.24
Al_2O_3	6.02	5.94	6.02	6.36
Fe_2O_3	1.90	3.25	3.37	3.25
CaO	67.60	69.20	68.60	68.29
MgO	—	0.79	1.76	0.86

Methods of Investigation

Determination of Uncombined Lime

A sample of raw material mix was pressed by hand so as to give it the shape of a cylinder of the dimensions $\phi 20 \times 20$ mm.

The specimen thus shaped was placed in a cold electric furnace on a platinum plate and heated to a definite temperature. The measurement of temperature was carried out by means of a Pt-PtRh thermocouple.

Heating up to 1000°C was carried out at the rate of 10°C/min and above 1000°C at the rate of 5°C/min.

After the desired temperature has been reached, the specimen was removed from the furnace and after cooling in dessicator it was ground and the content of uncombined CaO was determined by the glycol method.

Deformation of the Samples During Heating under a Static Load

Cylindrical specimens of sizes $\phi 20 \times 20$ mm were pressed from the mixes and placed in a vertical electric furnace under a constant load of 0.02 kg/cm². The heating rate was the same as in the test described previously.

The readings of the value of the deformations of a cylindrical specimen squeezed during heating under a static load given above were taken by means of a gauge as accurate to within 0.01 mm. Changes in the sample height were transmitted directly to the gauge by means of a refractory bar. The terminal elongation of the bar during heating the furnace was predetermined experimentally, which made it possible to introduce a suitable correction to the measurements of the deformation of the specimen.

Results

Detailed numerical data are not presented in tables and only a graphic presentation of the results is given in Fig. 1 and Fig. 2.

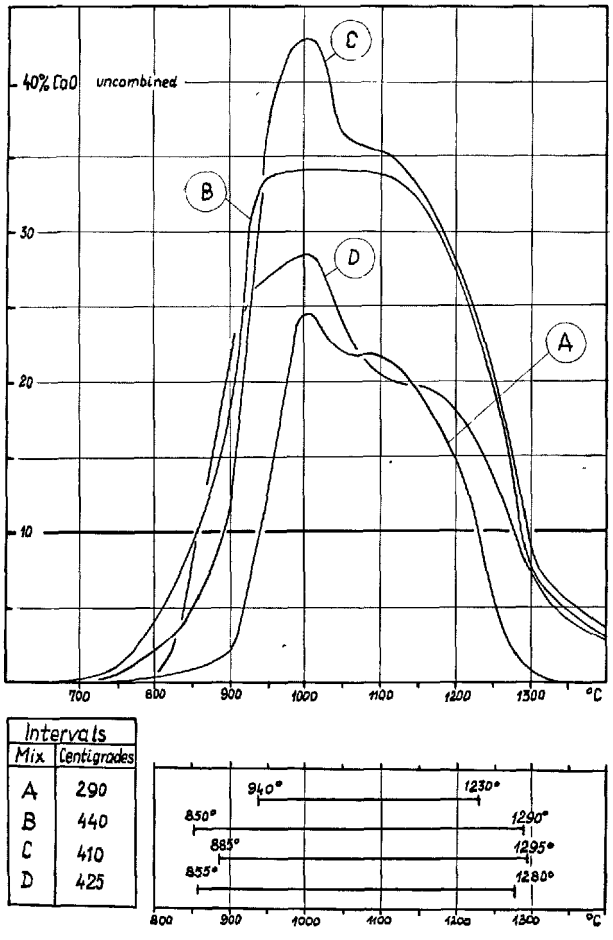

Intervals	
Mix	Centigrades
A	290
B	440
C	410
D	425

Fig. 1. *Changes of free* CaO

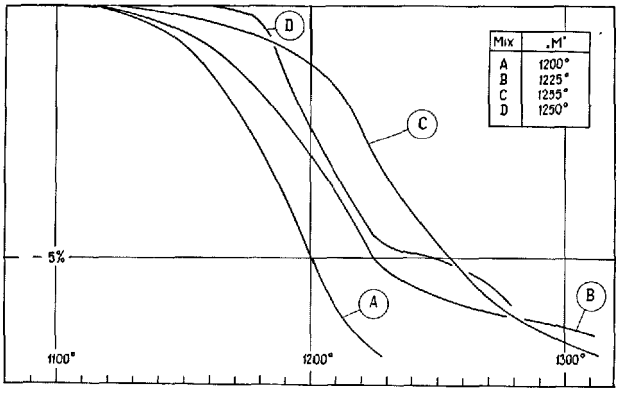

Fig. 2. *Deformations under load*

Discussion of the Results

All the four raw mixes tested were blended for the production of normal standard portland clinker and differed only relative slightly as regards their chemical composition.

Even a superficial comparison of the results obtained allows to state that the four mixes tested behave in a markedly different way during burning.

There are different temperature intervals in which, during burning of these mixes, a considerable amount of uncombined CaO exists.

Maximum amounts of free CaO which appear during the heating of each mix differ greatly.

The deformation of the specimens prepared from different mixes has a different course during burning.

The differences described above and observed during the tests confirm the comparative observations made during a long period in the cement plants from which the four raw mixes tested are supplied. As might be expected the attempt to establish a relationship between the chemical composition of the mixes and the numerical results of the tests did not indicate any regularity which would make it possible to assess the burnability of the mixes on the basis of their chemical composition.

The known fact that the burnability of a mix depends on many factors acting simultaneously which are difficult to formulate quantitatively, was confirmed by this.

The Suggested Quantitative Characterization of Burnability

On the basis of the results of the tests presented above the author suggests the characterization of the

burnability of raw mixes by means of the following three values: "K"—The ratio of the CaO content in the calcined raw mix to the maximum free lime content which occurs during the burning of the mix,
"L"—The temperature range in which the burned mix contains the free lime content in amounts exceeding 10%,
"M"—The temperature at which the cylindrical specimen of the pressed mix is sqeezed in its height by 5% under a static load of 0.02 kg/cm².

Table 2 illustrates the values of K, L and M calculated and measured for all the four mixes tested.

Table 2. *Characteristics of burnability*

	Mix			
	A	B	C	D
"K"	2.74	2.03	1.59	2.40
"L"	290°	440°	410°	425°
"M"	1200°	1225°	1255°	1250°

Conclusions

During a long period observations were carried out on the behaviour of the raw mixes in the burning zone of the rotary kilns of four cement plants from which the tested mixes were sampled. It was proved that in each of these cement plants the observed mix behaved differently. In other words, it was proved that each cement plant has at its disposal a raw material with a specific burnability for the given deposit.

The differences in burnability were considerable and it was impossible to explain them univocally by comparative analyses of the chemical composition of the mixes. It was impossible to establish neither any correlation nor any functional relationship between the chemical composition of the material and its burnability.

However the three values characterizing the burnability introduced in the present work make it possible to assess comparatively the raw mixes as regards their behaviour during burning.

Value "K" indicates the reactivity of the mix components and the degree of the chemical aggressiveness of the mix toward the refractory lining of the rotary kiln.

Value "L" enables to a certain degree a comparative estimation of the length of the burning zone and the time the burned material remains in the calcining and clinkering zones.

Value "M" may constitute an intermediate measure of viscosity of the liquid phase of the clinker and this value makes it possible to assess comparatively the tendency of the clinker granules to adhere to one another.

Supplementary Paper I-38 On Kinetics of Formation of Portland Cement Clinker

P. F. Rumyantsev*

Synopsis

Investigation of portland cement clinker burning as a single process and derivation of a general kinetic equation are connected with inconceivable difficulties. Therefore, it is worth while to study the mechanism and the rates of separate stages of clinker formation.

Formation of cement clinker is accomplished by physico-chemical processes in the liquid phase appearing as a result of partial melting of cement raw mix on heating.

Kinetics of these processes has been studied at the Institute of Silicate Chemistry for several years.

Data on kinetics of dissolution of CaO, $3CaO \cdot SiO_2$, $2CaO \cdot SiO_2$ clinker minerals and SiO_2 (quartz) in the clinker liquid phase have been obtained. These data confirm the determining role of the dissolution rates of CaO and $2CaO \cdot SiO_2$ in formation of $3CaO \cdot SiO_2$. Kinetic equation which adequately describes the dissolution functions got experimentally, may be used in the converted form as a kinetic equation of clinker formation.

Crystallization of the clinker liquid phase in the temperature range 850–1450°C proceeds very quickly disregarding the fact whether one phase or a eutectic is crystallizing.

In the case of the crystallization of one phase the process is mainly determined by the linear velocity of the crystal growth, while on the simultaneous crystallization of two and more phases the process is to a greater extent determined by the rate of the crystal nuclei formation.

Glasses obtained from the clinker liquid phase are stable up to 800°C. Above this temperature intense crystallization of the glasses is observed.

Introduction

Kinetics of the portland cement clinker formation is a very important and difficult problem.

The importance of its decision is determined by the necessity of further development of scientific views on the processes occurring in clinker formation. Evolution of these ideas is necessary for automatization and intensification of the existing cement technology and its progress.

The difficulties in the decision of this problem consist of a series of physico-chemical processes occurring on clinker formation, for it appears impossible to express the rates of these processes by common parameters. In addition, in studying the kinetics of some processes there arise difficulties due to the lack of the reliable methods and the impossibility of experimental modeling of the separate processes apart from the other processes.

The rate of CaO interactions with other constituents of cement raw mixture may serve as a general and most significant parameter for a series of physico-chemical processes occurring on cement burning. Usually a figured and graphical expression of the free CaO content is used for characterization of the given parameter. This parameter is common for the limestone decomposition, the majority of the solid state reactions, and the sintering process.

Using the available experimental material on the changes of free CaO in the burning process, it appears possible even at present to derive a kinetic equation for the given parameter. Such equation will be very complicated and formal because the constants will be deprived of physical sense, and the functional characteristics on different stages of burning will not reveal the mechanism of the processes taking place during the burning.

But it seems more difficult to derive a kinetic equation revealing the intrinsic nature and the character of the interaction between the elementary particles on burning. For derivation of such equation it is necessary to study the kinetics of separate processes, and on the base of the joining of kinetic equations for these

*Institute of Silicate Chemistry of the Academy of Science, Leningrad, U.S.S.R.

separate processes, to get more general kinetic characteristics and equations of clinker formation.

On Kinetics of Cement Clinker Sintering

Basing on the considerations given in introduction, kinetics of the processes occurring on cement clinker sintering (namely the final and less studied stage of sintering) has been under study at the Institute of Silicate Chemistry of the Academy of Science of the USSR for several years.

Sintering of clinker is considered to be a complex of three interdependent physico-chemical processes:

1. Dissolution of the minerals of raw mixture and the products of solid state reactions in the liquid phase of clinker.
2. Diffusion of Ca^{2+} and SiO_4^{4-} ions from the sites of their migration into the melt to the crystallization regions of new phases.
3. Crystallization of new phases.

The mutual connection and the chain character of the above processes stipulate the determining role of that process in the sintering which proceeds at the minimum rate.

Analysis of many literature data permitted us to assume that the dissolution process has the minimum rate.

The works by Toropov, Rumyantsev and Filipovich (1) and those by Toropov and Rumyantsev (2) give the results of the studies on dissolution kinetics of clinker minerals CaO, $3CaO \cdot SiO_2$, $2CaO \cdot SiO_2$ and SiO_2 (quartz) in the liquid phase of cement clinker.

Two equations have been derived to describe the dependence of the dissolution time (τ) on temperature (T) and diameter of the dissolving particles (D):

Experimentally

$$\tau = \frac{D}{A} \cdot e^{E/RT} \qquad (1)$$

and theoretically

$$\tau = \frac{N\bar{D}}{2\delta\nu_0} \cdot e^{(E+\Delta E)/RT} \qquad (2)$$

where E = activation energy of dissolution, R = gas constant, A = constant value, $\bar{D} < D$ = certain effective size of the grain, ΔE = activation energy of the block separated from the grain (for example, the activation energy of the crack emergence in crystals), N = multiplication factor considering that $10^9 - 10^{10}$ particles separated as a whole block fit for one molecularly separated particle, δ = diameter of the elementary particle, ν_0 = frequency of elastic vibrations of the elementary particle in the solid state.

Analogous appearance of two equations describing one and the same process but obtained in different ways confirms, to a certain extent, their accuracy.

Moreover, it can be imagined that $A = N/2\delta\nu_0$, and E of equation (1) is equal to $E + \Delta E$ of equation (2).

Thus both equations turn into one.

Establishment of the molecular-dispersion character of the dissolution is considered to be an important result of the presented works. This means that the dissolution of clinker minerals in the liquid phase doesn't proceed through migration of the elementary particles (atoms, ions, molecules) into melt, but it proceeds by means of separation of individual blocks with sizes to 1 micron from dissolving crystals and polycrystals.

Derived functions are analogous to temperature dependence of the rate of tricalcium silicate formation obtained by Kondo (3), but the activation energies of CaO and $2CaO \cdot SiO_2$ dissolution (150 kcal/mol) approach to the activation energy of the $3CaO \cdot SiO_2$ formation (200 kcal/mol).

The determining role of the dissolution and not that of the diffusion in silicate melts was shown by Cooper and Kingery (4).

The established time for the grain dissolution of CaO and $2CaO \cdot SiO_2$ about 0.1–0.01 mm in size is of the same order as the time for the assimilation of free CaO obtained by Toropov and Luginina (5).

The indicated conformities as well as the experimental confirmation of the determining role of dissolution given by Rumyantsev and Kozlov (6) permit us to convert equations (1) and (2) into kinetic equations for clinker formation of the following type:

$$V_k = \frac{A}{D} \cdot e^{-E/RT} \qquad (3)$$

$$V_k = \frac{2\delta\nu_0}{ND} \cdot e^{-(E+\Delta E)/RT} \qquad (4)$$

Where it is taken into consideration that $Vp = 1/\tau$ and $Vp = V_k$, V_k = rate of clinker formation, Vp = rate of dissolution of CaO or $2CaO \cdot SiO_2$ in the liquid phase of clinker; the values of the other letters are the same as in formulas (1) and (2).

On Kinetics of Crystallization of Clinker Liquid Phase

The final stage of clinker sintering—the liquid phase crystallization—is of interest from the view-point of clinker formation kinetics because it appears possible to obtain from here data on the mechanism and the rate of crystallization under conditions where participate diffusion and crystallization without overlap of the dissolution process.

Data on kinetics of crystallization of the liquid phase is also useful for the progress of crystallization theory in complex silicate systems. For our investigation a liquid clinker phase with alumina modulus $p = 1$ was synthesized at 1450°C. Its composition (in wt%) was as follows:

6.7 SiO_2; 18.5 Al_2O_3; 18.5 Fe_2O_3; 56.3 CaO.

The observation on the crystallization was accomplished with the aid of the high-temperature microscope.

On cooling the melt pre-heated up to 1500°C at the rate of 20° per second, there was observed the growth of one (sometimes two) crystal of tetra-calcium aluminoferrite, and the rate of its growth almost doesn't fall behind the rate of decreasing temperature.

Fig. 1a, represents photomicrographs of the melt at 1400°C where one can see such crystal.

Fig. 1b, shows an increase in the crystal size with decreasing temperature up to 1360°C.

The same photomicrograph also shows that crystallization of other phases is taking place at 1360°C. At the same time their crystallization is of different character, that is, it doesn't proceed through the linear crystal growth but it is due to the formation of a great amount of fine crystals.

With further decrease in temperature up to 1330°C the growth of tetra-calcium aluminoferrite crystal ceases and the formation of fine crystals continues down to the full crystallization of the sample shown in Fig. 1c.

Small samples of glass were obtained by rapid cooling of a fully fused liquid phase. At slow heating of these samples of glass quick crystallization was observed as soon as temperature exceeds 820°C, whereupon for this period of time crystals grew up to 20–30 microns. Photomicrographs of such crystals are given in Fig. 1d.

With fast heating and stoppings at higher temperatures (850–1250°C), still quicker crystallization was observed.

During seconds and parts of seconds crystallization from the melt on its fast cooling till 850–1250°C is also taking place.

In Fig. 1e, are shown crystals of 60–80 microns in size grown for 1 second at 1200°C.

The quenching method appears to be ineffective for determining crystallization rates, because a considerable crystal growth inhibiting to record the sample state at the temperature of the experiment occurs on cooling. In Fig. 1f, is given a photomicrograph of the sample quenched from 1390°C.

A crystal of $4CaO \cdot Al_2O_3 \cdot Fe_2O_3$ is seen here. It consists of two parts. The central part is a crystal which exists at temperature 1390°C, and the outer part is that formed during quenching.

The presented actual data indicate that crystallization processes in the clinker liquid phase proceed very intensively if they are not connected with the dissolution process. The latter is one more proof for the determining role of the dissolution of raw mixture minerals and products of solid state reactions on burning of cement clinker.

Quick crystallization, the rate of which is impossible to calculate because of the overlap of the crystal growth on determining the experimental temperature, doesn't permit to approximate with acceptable precision kinetic rules of the liquid phase crystallization with the aid of the existing methods of investigation.

Conclusions

Burning of cement at the stage connected with the process of CaO and $2CaO \cdot SiO_2$ dissolution in the liquid phase is depends upon by the rate of the dissolution. Therefore the formulas describing the dissolution process may be used as kinetic equations of clinker formation.

The principal conclusions on kinetics of crystallization of clinker liquid phase at the given stage of investigation may result in the following:

Crystallization of clinker liquid phase in the temperature range 820–1450°C proceeds very quickly.

In the case when one phase is crystallizing, the rate of crystal growth is predominant, while in the case of crystallization of two and more phases the rate of crystal nuclei formation appears to be prevailing.

There is also observed quick crystallization of glasses obtained from the liquid phase at temperatures above 800°C.

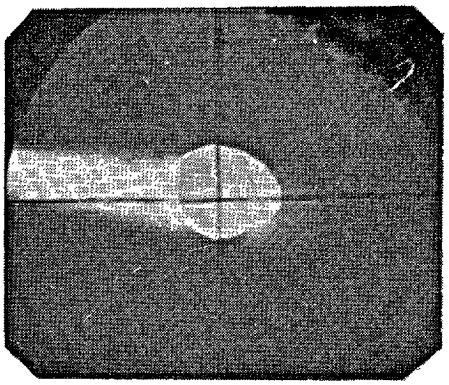

a

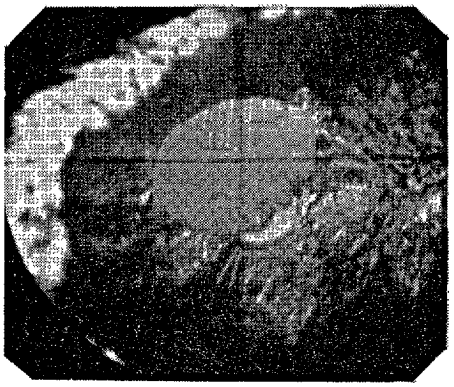

b

c

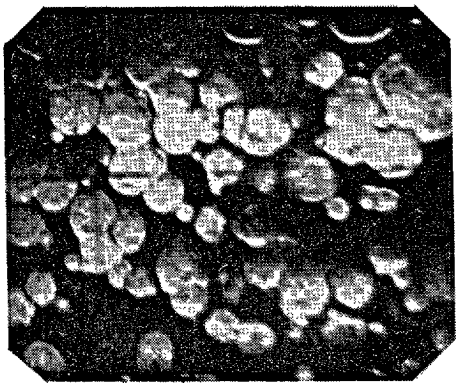

d

e

f

Fig. 1. *Crystallization of the liquid phase of cement clinker preheated up to* 1500°C. a—*at* 1400°C, b—*at* 1360°C, c—*at* 1330°C, d—quenched and heated to 820°C e—*at* 1200°C, f—*quenched at* 1390°C.

References

1. N. A. Toropov, P. F. Rumyantsev and V. N. Filipovich, "On kinetics of dissolution of CaO, $3CaO \cdot SiO_2$, $2CaO \cdot SiO_2$ and SiO_2 in the liquid phase of clinker" (in Russian), Zhurn. Fiz. Khimii, **33**, 974–977 (1964).
2. N. A. Toropov and P. F. Rumyantsev, "On kinetics of clinker formation" (in German), Silikattechn., **10**, 322–326, 349–354 (1967).
3. Chemistry of Cement. Proc. Fourth Intern. Symposium. Washington, 1960, vol. 1. See article by R. Kondo entitled "Reaction velocity in portland cement clinker formation".
4. A. R. Cooper and W. D. Kingery, "Dissolution in ceramic systems: 1. Molecular diffusion, natural convection and forced convection studies of sapphire dissolution in calcuim aluminium silicate", J. Am. Ceram. Soc., **47**, 37–43 (1964).
5. N. A. Toropov and I. G. Luginina, "On the influence of sintering on formation of cement clinker" (in Russian), Zement, No. 1, 4–8 (1953).
6. Siliconf, 1967. The Ninth Conference on the Silicate Industry. Budapest, 21–15. XI. 1967. See article by P. F. Rumyantsev and G. V. Kozlov entitled "Effect of CdO and CuO additives on the kinetics of formation and properties of cement clinker" (in Russian).

Supplementary Paper I-49 Clinker Burning in Fluidized Bed

Yuichi Suzukawa, Hisashi Kono, Haruhiko Miyazaki and Sigeyuki Nakai*

Synopsis

The burning of cement clinker in a fluidized bed has already been known as the Pyzel process. (1–4)

The purpose of this paper consists in establishing the basic chemical process designs on this process through the operation of a pilot plant, particularly on the combustion of fuel oil in the fluidized bed, control of the size distribution of solid particles in the bed, and heat-recovery installations of the exit gas and of the red hot clinker from the bed.

Through these studies, it has been found that this process makes it easy to control the burning temperature and makes it possible to manufacture clinker containing low alkalis and free lime of uniform and superior quality.

Introduction

The chemical process designs of clinker burning by the fluidized-bed process were studied by using the pilot plant.

The basic chemical process design of the combustion of fuel oil in the bed was established, and the particle size distribution of solid particles in the bed was controlled by charging a suitable amount of the seed pellets into the bed and simultaneously by selective discharge of coarse clinker particles from the bed.

The agglomeration of solid particles with each other and the adhesion of solid particles to the inside wall or the bottom of the bed were prevented by the injection of gas jet stream which is used for selective discharge of coarse clinker particles and does not pass the gas distributor of the bed. This gas jet stream was not only effective for the improvement of the flow and motion of solid particles in the bed, but also for the dispersion of fuel oil throughout the bed, thus the complete combustion of fuel oil being attained.

The heat-recovery systems for the exit gas at the high temperature and for the red hot clinker from the bed were also established.

Tests of the resulting clinker showed that the quality is good and is comparable with that of the clinker of rotary kiln.

Experimental

The schematic diagram of the fluidized-bed parts and the flow sheet of the pilot plant are shown in Figs. 1 and 2, respectively.

Powdered cement raw mix and seed pellets were fed into fluidized-bed reactor (1) together with preheated air through the injection opening of solid materials (10).

On the other hand, the fuel oil injected through injection nozzle of fuel oil (6) was burnt by the aid of the gas jet streams injected through the injection opening of gas jet stream (8) and the selective discharge pipe opening (12) so as to maintain the bed at the temperature required for burning cement clinker.

Into fluidized-bed reactor (1) was also introduced the fluidizing air through gas distributor (4) so as to maintain solid particles in the bed in a good fluidizing state.

Solid particles in the bed at a temperature of approximately 1450°C reacted with powdered raw mix and grew in size, simultaneously cement clinkering reaction being promoted.

The sintered coarse clinker particles which has grown in size larger than a definite diameter, e.g., approximately 2 mmϕ, were selectively discharged from the bed through the selective discharge pipe (11)

*Central Research Laboratory, Ube Industries, Ltd., Ube, Japan.

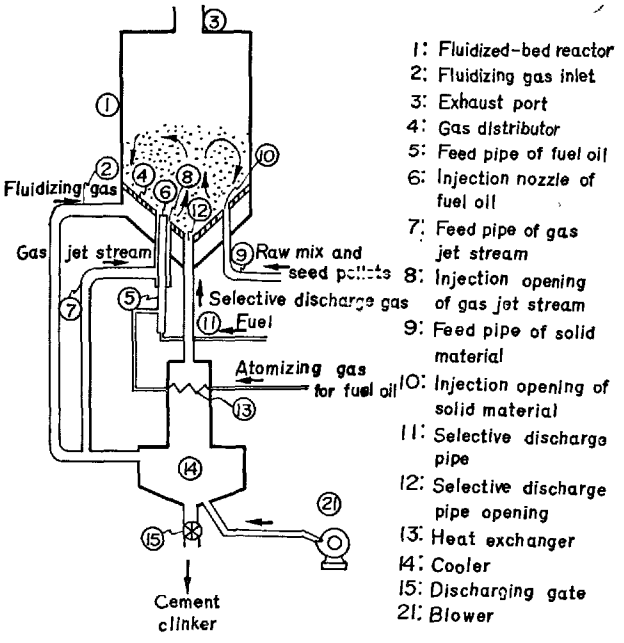

Fig. 1. *Schematic diagram of the fluidized-bed parts of the pilot plant.*

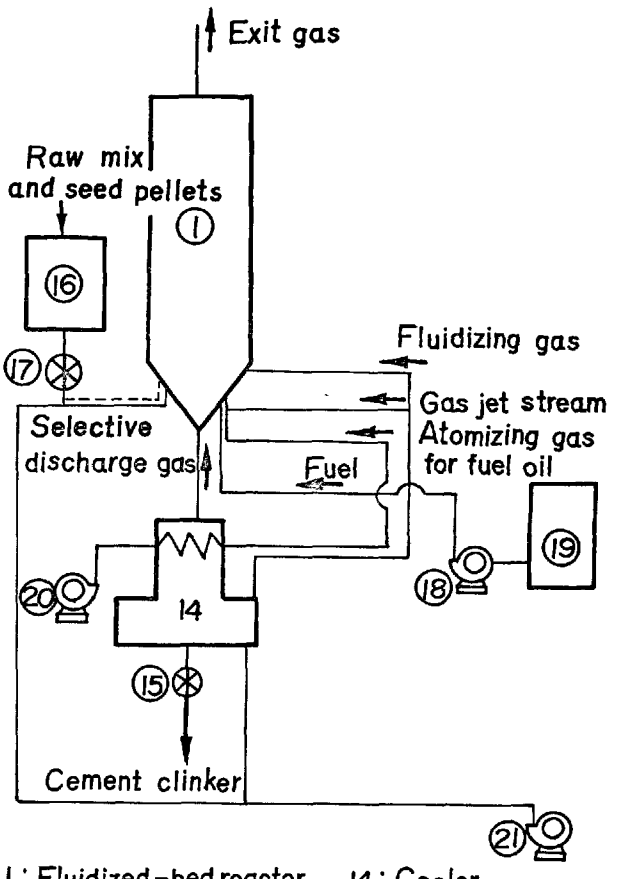

Fig. 2. *Flow sheet of the pilot plant.*

by means of the preheated air through heat exchanger (13), transferred to the clinker cooler (14) and then discharged as the final product by means of discharge gate (15). The gas velocity at selective discharge pipe opening (12) was adjusted at approximately 20 m/sec.

Further, in the present fluidized-bed reactor of cement clinker, funnel-shaped portion of gas distributor (4) is indispensable.

The solid particles in the bed which liquid fuel was blown on their surface, were dispersed from the vicinity of the injection nozzle of fuel oil (4) by gas jet stream injected through the injection opening of gas jet stream (8) around injection nozzle of fuel oil (6) and further dispersed throughout the bed by a forced circulation flow caused by the gas jet stream for use to discharge selectively the coarse clinker particles. Consequently the dispersion of fuel oil in the bed is very good, and the complete combustion of fuel oil in the bed is accomplished.

In order to cool the clinker discharged from the reactor, the cooler (14) shown in Fig. 1 was installed. The red hot clinker discharged from the bed and the air contact countercurrently with each other, and the resulting preheated gas was introduced into the bed through three pipes (2), (7) and (11) respectively. Thus the enthalpy of the hot clinker can be recovered efficiently, and the discharged clinker is cooled as low as 200°C.

To recover the enthalpy of the exit gas from the fluidized-bed reactor, a new hot cyclone system was developed. In the ordinary hot cyclone system used for cement kiln such as Humboldt system (5), the hot exit gas at higher than 1000°C could not be used directly for calcining and preheating cement raw mix, because the adhesion of raw mix to the inside wall of the cyclone is liable to occur. This adhesion phenomenon was prevented by contacting the hot gas at 1400–1450°C with lime and clay mix components separately as shown in Fig. 3.

The example of the chemical analysis of cement raw mix was shown in Table 1.

As a controlling factor of the size distribution of solid particles in the fluidized bed, seed pellets of 1.0–1.6 mm ϕ made with cement raw mix were used. The chemical composition was also shown in Table 1. These seed pellets were prepared with the fluidized-bed pelletizer developed in this laboratory (6).

In order to maintain the temperature of the bed at

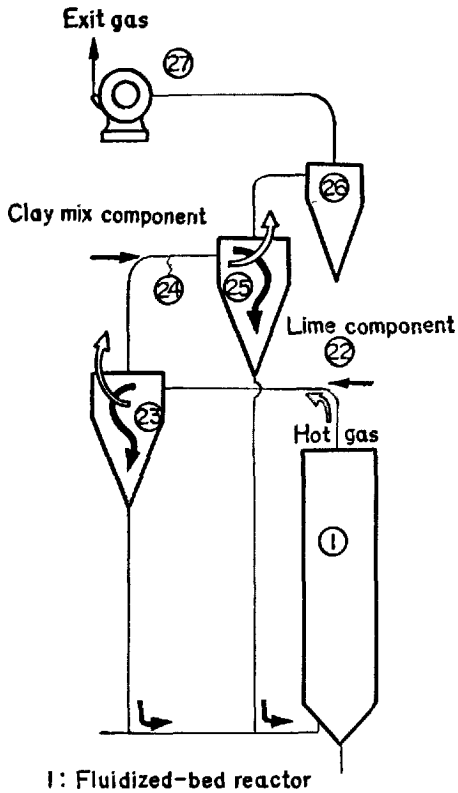

1: Fluidized-bed reactor
22: Inlet of lime component
23: Hot cyclone for heating lime component
24: Inlet of clay mix component
25: Hot cyclone for heating clay mix component
26: Dust collector
27: Suction blower

Fig. 3. *Heat-recovery system of hot exit gas from the fluidized-bed reactor.*

Table 1. *Chemical composition of powdered raw mix and seed pellets*

	Powdered raw mix	Seed pellets
Ig. loss	35.1	35.0
SiO_2	14.3	14.6
Al_2O_3	3.5	3.7
Fe_2O_3	2.1	2.1
CaO	43.8	43.3
MgO	0.6	0.6
SO_3	0.03	0.03
Na_2O	0.20	0.19
K_2O	0.45	0.45
Total	100.08	99.97

approximately 1450°C., heavy oil (JIS C-heavy oil corresponding to ASTM D396–48T No. 6) was used.

Results and Discussion

Operating Condition of the Pilot Plant and Quality of the Cement Clinker

The pilot plant was operated under the condition shown in Table 2.

The quality of the clinker is shown in Table 3.

As shown in Table 3, the quality of the clinker is as good as that of the clinker of rotary kiln. It is characteristic of the clinker that it has low alkalis and free lime.

Combustion of Fuel Oil in the Fluidized Bed

It is very difficult to realize a complete combustion of fuel oil with a high load in the ordinary fluidized bed. In the pilot plant, however, the fuel oil could effectively be burnt with a combustion load as high as 6,000,000 Kcal./m.^{3} hr. so as to maintain the bed at a temperature required for burning cement clinker, and the temperature of the bed was controlled within a range of 10°C. Such a precise temperature control could have never been attained in the other burning processes of cement clinker.

Control of the Size Distribution of Solid Particles

To operate the pilot plant continuously for a long

Table 2. *Operating conditon of the pilot plant*

Gas velocities:
Superificial velocity in the fluidized bed U_0 = 6 m./sec. (at 1450°C.)
Velocity of the gas jet stream U_j = 25 m./sec. (at 600°C.)
Velocity of the selective discharges gas U_s = 20 m./sec. (at 1000°C.)

Ratios of volume flow rate of the gases:
$V_j/V_0 = 0.25$ $V_{rm}/V_0 = 0.10$ $V_F/V_0 = 0.50$ $V_s/V_0 = 0.10$ $V_c/V_0 = 0.05$

Temperature:
Burning temperature in the fluidized-bed reactor = 1450°C.
Temperature of clinker discharged from the cooler = 200°C.
Temperature of exit gas from the fluidized-bed reactor = 1400°C.
Specific combustion load = approx. 6,000,000 (Kcal./m³.hr.)

Feed ratio of seed pellets to powdered raw mix: $F_s/F_r = 0.15$

Size distribution:
Seed: 1.0–1.6 mmϕ Final cement clinker: 2–4 mmϕ

where,
V_c: Volume flow rate of the atomizing gas (N.m.³/hr.)
V_F: Volume flow rate of the fluidizing gas (N.m.³/hr.)
V_j: Volume flow rate of the gas jet stream (N.m.³/hr.)
V_0: Volume flow rate of the whole gas (N.m.³/hr.)
V_{rm}: Volume flow rate of the gas for feeding solid material (N.m.³/hr.)
V_s: Volume flow rate of the selective discharge gas (N.m.³/hr.)
F_s: Amount of seed pellets (Kg/hr.)
F_r: Amount of powdered raw mix (Kg/hr.)

Table 3. *Quality of the resulting cement clinker*

Chemical composition		Physical property	
Ig. loss	0.2	Amount of gypsum as SO_3 1.7%	
Insol.	0.2	Specific surface 3350 (cm²/g.) (Blaine)	
SiO_2	21.5		
Al_2O_3	6.2		
Fe_2O_3	3.7	*Time of setting	
CaO	67.0	Initial	2—46 (hr.—min.)
MgO	0.9	Final	4—48 (hr.—min.)
SO_3	0.2		
Na_2O	0.07	**Compressive strength	
K_2O	0.10	3 days	2420 (psi)
Total	100.07	7 days	3300 (psi)
		28 days	5650 (psi)
Free CaO	0.1		
H.M.	2.13	**Tensile strength	
S.M.	2.22	3 days	371 (psi)
I.M.	1.7	7 days	412 (psi)
L.S.R.	0.96	28 days	461 (psi)

* Time of setting are the valves of ASTM C266-65 (Gillmore).
**Compressive and tensile strength are the values of ASTM C109-64 and C190-63, respectively.

time, it is indispensable to control the size distribution of solid particles in the bed. For this purpose, the gas velocity for the selective discharge of clinker was adjusted, and also the size and amount of the seed pellets were controlled. The selective discharge efficiency of the clinker η_s was defined as shown in Fig. 4.

In Fig. 5, the relation between mean diameter of solid particles D_p mean and η_s is given.

In Fig. 6, the relation is shown between η_s, gas velocity of selective discharge U_s, and mean retention time of solid particles in the bed $\bar{\theta}$.

In Fig. 7, the relation between mass velocity of the discharged clinker F_c and gas velocity of selective discharge U_s is given, in which the amount of seed pellets F_s is used as a parameter.

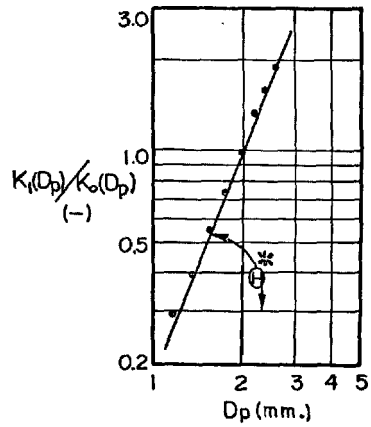

Dp: Diameter of solid particle (mm.)
$K_1(D_p)$: Particle size distribution of clinker particles discharged from the fluidized-bed reactor (−)
$K_0(D_p)$: Particle size distribution of solid particles in the fluidized-bed reactor (−)
* Selective discharge efficiency $\eta_s = \tan\theta$

Fig. 4. *Definition of the selective discharge efficiency η_s.*

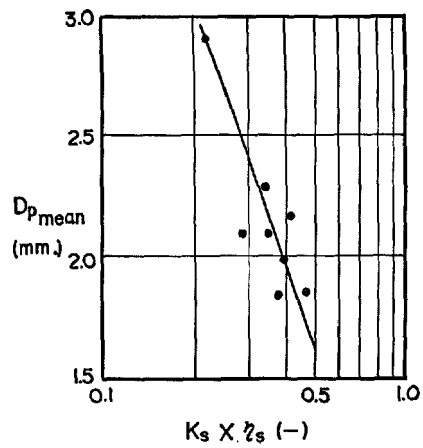

$D_{p_{mean}}$: Average diameter of the solid particles in the fluidized-bed reactor (mm.)
K_s: Feed ratio seed pellets to discharged clinker: F_s/F_c (−)
η_s: Selective discharge efficiency (−)

Fig. 5. *Relation between mean diameter of solid particles in the bed selective discharge efficiency.*

By using these relations the process design for the control of the size distribution of solid particles in the bed was achieved.

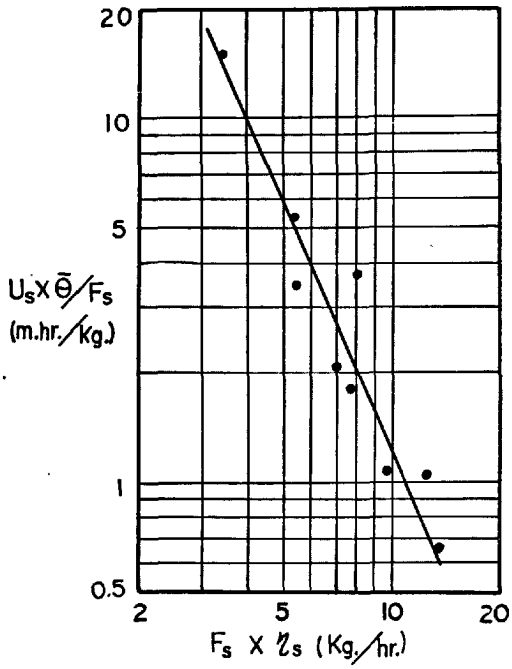

F_s : Amount of seed pellets (Kg./hr.)

U_s : Gas velocity of selective discharge (m./hr.)

η_s : Selective discharge efficiency (–)

$\bar{\theta}$: Mean retention time of solid particles in the fluidized-bed reactor (hr.)

Fig. 6. *Relation between gas velocity of selective discharge and selective discharge efficiency.*

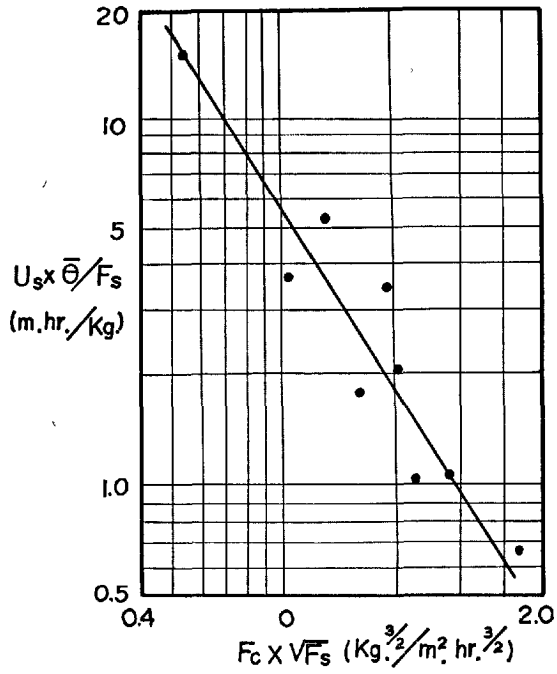

F_c: Mass velocity of the discharged clinker (Kg./m^2.hr.)

F_s: Amount of the seed pellets (Kg./hr.)

U_s: Gas velocity of the selective discharge gas (m./hr.)

$\bar{\theta}$: Average retention time of solid particles in the fluidized-bed reactor (hr.)

Fig. 7. *Relation between mass velocity of the discharged clinker and gas velocity of selective discharge.*

Conclusion

The burning of cement clinker in the fluidized-bed reactor was studied by using the pilot plant, and the basic chemical process designs were established. The characteristic points are summarized as follows;
(a) The fluidized bed in which solid particles were circulated forcedly by the gas jet streams, fuel oil such as heavy oil can efficiently be burnt with a combustion load as high as 6,000,000 Kcal./m.^{3}hr.
(b) The temperature of the bed can be controlled within a range of 10°C.
(c) The size distribution of solid particles in the bed can be controlled by the gas velocity of selective discharge and also the size and amount of the seed pellets. These seed pellets are efficiently prepared in the fluidized-bed pelletizer developed in this laboratory.
(d) The heat-recovery systems for the exit gas and the red hot clinker discharged from the bed were studied.
(e) The resulting clinker has low alkalis and free lime and shows a uniform and superior quality.

References

1. "Pyzel fluid-bed cement process", Chem. Week p. 108 & 110, Feb. 16 (1957).
2. R. Pyzel, "Hydraulic cement process", U.S. Patent 3,022,989 (1962).
3. C. Goes, "Eindrücke eines Studienaufenthaltes in den USA", Zement-Kalk-Gips **13**, 23–7 (1963).
4. A. M. Sadler, "A high temperature fluidized bed process for the production of portland cement compounds", Preprint Am. Inst. Chem. Eng. Meeting

in New York, Nov. 30 (1967).
5. E. Bomke, "Die Entwicklung der ersen Neuanlage des Homboldtschwebegaswärmeaustauscher von 1953 bis 1958". Zement-Kalk-Gips **9**, 377–81 (1958).
6. H. Kono, "Fluidized-bed pelletizer" (in Japanese), Proc. 1st. Chem. Plant Eng. Conf., Soc. Chem. Eng., Japan, pp. 1–3, Session 6 (1966).

Oral Discussion

Hitoaki Mori

I am much interested in the burning of cement clinker in a fluidized bed. In your paper, the gas jet streams are injected into the fluidized bed in addition to the fluidizing gas which passes through the gas distributor.

Could the authors explain the effects of these gas jet streams on the burning process in the fluidized bed? Why the fuel oil could effectively be burnt with a high combustion load?

Author's Closure

Hisashi Kono

I should like to answer for the question presented by Mr. Mori.

As is shown in our paper, in addition to the fluidizing gas, which passes through the gas distributor, the gas jet streams are injected into the reactor in order to realize the forced circulation flow of solid particles in the bed.

The forced circulation flow of solid particles in the bed can be controlled by the gas velocity and volume flow rates of said gas jet streams. Through these circulation flows, the dispersion of atomized fuel oil in the bed can easily be controlled.

In this way, the complete combustion of fuel oil with a high combustion load in the bed can be attained, which have never been realized by the conventional fluidized bed.

Supplementary Paper I-75 New Compound $Ca_{12}Si_4O_{19}F_2$ in the System CaO–SiO_2–CaF_2 and the Role of CaF_2 in the Burning of Cement Clinker

Mitsuo Tanaka, Giichi Sudoh and Shigeo Akaiwa*

Synopsis

By finding the presence of a new ternary compound of the system CaO–SiO_2–CaF_2 and explicating its properties, a new interpretation was given to the mineralizing mechanism of CaF_2 in the burning of cement clinker.

The chemical formula of this phase was determined to be $Ca_{12}Si_4O_{19}F_2$ and it was considered that this phase takes up, when formed in the clinker, small amounts of Na_2O and Al_2O_3 in solid solution. The form of pure $Ca_{12}Si_4O_{19}F_2$ was orthorhombic (pseudo-hexagonal) with $a = 12.29$, $b = 7.09$, $c = 5.69$Å. Its observed density was 3.13 g/cm³ and the number of formula unit was 1. Under the microscope, it looked granular and colorless in thin section, being biaxial ($2V \simeq 0$) negative with the refractive indices $\alpha = 1.676 \pm 0.002$, $\gamma = 1.684 \pm 0.002$. The heat of hydration was low, approximately 7, 39, and 51 cal/g at the age of 7, 28, and 56 days, showing little hydraulic activity. The synthetic phase was stable in a temperature range of about 1110° to 1185°C if held in a closed state, and over 1185 ± 2°C it melted incongruently into trigonal C_3S, α'-C_2S, and a liquid phase. The primary crystallization field of $Ca_{12}Si_4O_{19}F_2$ in the phase diagram CaF_2–SiO_2–$2CaO \cdot SiO_2$ was determined.

In the burning of a raw mix with addition of CaF_2, formation of this phase was conspicuous at about 1050°C and it transformed into an alite phase and probably a belite phase, too, between 1100° and 1150°C. Namely, one of the important role of CaF_2 as a mineralizer is thought to be intermediate formation of the new phase $Ca_{12}Si_4O_{19}F_2$ solid solution, which mainly transforms into an alite phase at a low temperature level. Even in the cooling process after burning, $Ca_{12}Si_4O_{19}F_2$ solid solution was formed again while covering the alite phase when fluorine remained in the liquid phase. This peritectic structure was considered to be one cause of decline in the mechanical strength of cement.

In fluorine-containing clinker generally, the amounts of alite and belite phases tended to decrease, and formation of the aluminate phase was obstructed while the ferrite phase grew Al_2O_3—rich in composition as the fluorine content increased. Surplus fluorine became concentrated mainly in the liquid phase.

Introduction

Many investigations have been made concerning various effects of fluorite, a mineralizer actually in use for production of portland cement. In order to explicate the effects of fluorine component on the formation and structure of clinker minerals, we have also tried detailed studies on clinker burned with addition of CaF_2.

The studies revealed the presence of a new compound based on the system CaO–SiO_2–CaF_2 in the clinker (1) (2). The properties of this compound were investigated precisely, and at the same time the mineralizing mechanism of CaF_2 as well as the cement-chemical significance of this compound was discussed.

Moreover, the fine structure of clinker containing fluorine is explained in the present paper.

*Chichibu Cement Co., Ltd., Tokyo, Japan.

Experimental

Burning Conditions of CaF_2—Containing Raw Mix

Table 1 shows the chemical composition of the raw mix used in the present experiment. To this raw mix was added reagent-grade CaF_2 in varying amounts 0.0–5.0 wt-% and the burning temperature was varied from 800° to 1400°C. The variation of the raw mix moduli due to the addition of CaF_2 was corrected by simultaneous admixing of calculated amounts of powder reagents SiO_2, Al_2O_3, and Fe_2O_3 so that they might be equalized to the initial raw mix moduli. All burnings were carried out in an electric furnace. The clinker was immediately taken out of the furnace after burning and quenched in air or mercury.

Selective Dissolution and X-ray Diffraction Analysis of Clinker Minerals

In order to identify the new compound phase or determine its content in the clinker, a solution of salicylic acid in methanol (3) was used for selective dissolution and removal of silicate phases and free CaO. Namely, 7g of clinker powder was dispersed in 300 cc of the 10% salicylic acid methanol solution, and agitated for 2 hours with a magnetic stirrer. After separation of the liquid and solid by filtrating, the insoluble residue left on the filter paper was sufficiently washed with methanol and dried at 105°C. These conditions permitted an almost complete removal of the alite phase, belite phase, and free CaO.

The insoluble residue consisted mainly of the ferrite phase, new phase, and glass phase, and contained also an aluminate phase and CaF_2 depending upon the burning conditions. Meanwhile, the synthetic new compound that will be discussed later was hard to dissolve in the salicylic acid methanol solution, and 5 g in fine powder of the compound as put in 100 cc of the same solution dissolved no more than about 2 wt-% under the condition mentioned above. Therefore this method of selective dissolution was considered to satisfy the intended purposes. X-ray investigation and chemical analysis were carried out on the insoluble residue of clinker.

Synthesis of New Compound

Based on the results of X-ray powder diffraction and chemical analyses on findings of the clinker residue from selective dissolution, the various mixtures of pure chemicals were burned for X-ray diffraction and chemical analyses. The fluorine component of the synthetic compound was repeatedly analyzed by means of quantitative colorimetric determination with Neo Thorine. (4)

Studies on Crystallographic Property

The oscillating-crystal and powder X-ray diffraction methods were employed to determine the crystal system and lattice constants of the synthetic compound. The single crystals tested, measuring about 0.1–0.2 mm in size, were prepared from pre-synthesized fine crystals by heating them in a closed platinum capsule for 150 hours at 1140 $\pm$ 20°C.

Studies on Thermal Property

The thermal properties were studied by DTA, high-temperature X-ray diffraction analysis, and electron probe microanalysis methods. The starting materials used for DTA were the synthetic new compound and also the compositions which, in the phase equilibrium diagram CaF_2–SiO_2–$2CaO \cdot SiO_2$ of J. Mukerji (5), were included mainly in the primary crystallization field of C_3S, and moreover have a liquidus temperature range of 1200–1450°C. In order to minimize the loss of fluorine, the starting materials were sealed in platinum capsules. The DTA heating and cooling rates were 10°C/min, the synthetic new compounds and mixtures being held for 30 minutes at 1250°C and at a higher temperature than the expected liquidus before they were cooled. The heating rate of high-temperature X-ray analysis applied to the synthetic new compound was 0.94°C/min.

As the samples for electron probe microanalysis, pellets made of the pre-synthetized new compound of about 0.1 mm size were heated again at specified temperatures and then quenched in air. For selection

Table 1. *Chemical composition and fineness of starting raw mix.*

Chemical composition (%)										Fineness	
ig. loss	SiO_2	Al_2O_3	Fe_2O_3	CaO	MgO	SO_3	Na_2O	K_2O	Total	88μ residue (%)	Blaine surface area (cm^2/g)
34.4	14.8	3.4	2.0	43.5	1.1	tr	0.52	0.48	100.2	7.2	5,430

of the field to be examined, slight etching was provided with a solution of 1% HNO_3 in alcohol. The etched surface was carbon spattered for conductive coating. The conditions for microanalysis were: acc. voltage, 15kV; sample current, 0.1 μA; X-rays, CaKα, SiKα, FKα; crystals, LiF, ADP, KAP; detectors, Kr-Exatron, Ne-Exatron, FPC; X-ray spot size, 1.5 $\mu\phi$; sample scan. speed, 8 μ/min; chart speed, 20 mm/min.

Studies on Solubility of Al_2O_3 and Na_2O in Pure $Ca_{12}Si_4O_{19}F_2$

The new compound phase formed in the clinker differed somewhat in lattice constants from pure synthetic compound. To explain this, studies were made. To the pure compound were added specified amounts of reagent-grade α-Al_2O_3 and Na_2CO_3 as Al_2O_3 and Na_2O, sufficiently mixed and finely ground in an agate mortar, and molded under pressure into pellets. After drying, the pellets were sealed in a platinum capsule and held at specified temperatures. With Al_2O_3 added, the pellets were heated at 1130°C for 3 hours, and with Na_2O added, they were heated for 2 hours with the temperature lowered from 1130°C at the rate of 30°C with every 1% increase in the dosage up to 8% because the temperature of transformation into C_3S declined depending on the Na_2O dosage. After being heated, they were quenched in air. The lattice constants were measured by X-ray powder diffraction analysis using silicon (99.99% purity) as an internal standard and compared with those of the phase existing in the clinker.

Results and Discussion

Identification of New Compound Phase in Clinker and Determination of Chemical Composition by Pure Synthesis

Table 2 shows the result of X-ray diffraction analysis for the cement clinker completely freed of silicate phases and free CaO by the solution of salicylic acid in methanol. In the clinker with addition of over 2% CaF_2, a total of 9 unknown peaks were identified over an angle range 10° to 70° 2θ CuKα. Especially, the 2.70Å peak (33.1° 2θ CuKα) in the diffraction pattern agreed well with the peaks of C_3A (the 440), α'-C_2S (the 130), and α-C_2S (the 110) (6) in position, but the presences of those compounds were denied because no other characteristic peaks of them were detected.

Table 2. *X-ray powder data of synthetic* $Ca_{12}Si_4O_{19}F_2$ *and insoluble residue of clinker burned with 5%* CaF_2 *addition.*

Insoluble residue			Pure $Ca_{12}Si_4O_{19}F_2$			
d(Å) obs.	Int.	Mineral	d(Å) obs.	Int.	hkl	d(Å) cal.
7.31	m	F	6.14	w	110, 200	6.14
6.17	vw	NC	4.17	vw	111, 201	4.17
3.65	m	F	3.55	w	020, 310	3.55
3.153	vs	CaF_2	3.31	vw		
3.087	s	NC	3.071	s	220, 400	3.071
2.929	w	?	2.844	vs	002	2.844
2.800	s	NC	2.703	vs	221, 401	2.703
2.770	s	F	2.471	w		
2.704	s	NC	2.434	vw		
2.663	m	F	2.361	vw		
2.644	vs	F	2.326	w	130, 420, 510	2.322
2.582	w	F	2.218	w	022, 312	2.219
2.202	w	F	2.149	w	131, 421, 511	2.150
2.152	w	F	2.087	s	222, 402	2.087
2.074	m	NC	1.927	w	331, 601	1.927
2.053	m	F	1.851	w		
1.931	s	CaF_2	1.773	m	040, 620	1.773
1.917	s	F	1.703	vw	240, 530, 710	1.704
1.852	w	F	1.683	w		
1.823	w	F	1.663	w	332, 602	1.662
1.780	w	NC	1.614	m	223, 403	1.614
1.721	vw	F	1.537	vw	440, 800	1.536
1.647	m	CaF_2	1.504	m	042, 622	1.505
1.596	w	NC	1.484	w	441, 801	1.482
1.571	w	F	1.421	w	004	1.422
1.502	w	NC	1.390	vw	333, 603	1.391
1.488	vw	NC	1.352	w	442, 802	1.351
			1.292	vw	224, 404	1.291
			1.194	w	443, 803	1.193
			1.162	vw	840, 10.2.0, 260	1.161
			1.138	w	841, 10.2.1, 261	1.137
			1.110	w	044, 624	1.109

Notation of mineral: F = Calcium aluminoferrite; NC = New compound phase.

Checks by the synthesis on pure chemicals showed the unknown phase to be a ternary compound based on the system CaO–SiO_2–CaF_2, and experiments with open burning in a platinum boat disclosed that the synthetic which was composed of (8.0–8.1) CaO, $3SiO_2$, and (1.0–9.0) CaF_2 and burned 2 times at 1130°C for 3 hours, most easily gave only the unknown peaks detected in the insoluble residue of clinker. X-ray data of this compound did not correspond to those of various CaO–SiO_2 compounds or of cuspidine $Ca_4Si_2O_7F_2$ (7) (8) previously described in the system CaO–SiO_2–CaF_2.

The result of chemical analysis on the synthetic compound which was regarded as a single phase in X-ray diffraction and microscopic observation is given in Table 3, which tentatively shows the unknown

Table 3. *Chemical analysis of new compound*

	CaO	F	SiO_2	Chemical formula
Found (%)	71.2	3.99	(26.5)	11.1 CaO·4.2 SiO_2·CaF_2
Theoretical (%)	71.95	4.07	26.70	11 CaO·4 SiO_2·CaF_2 –

compound to be $Ca_{12}Si_4O_{19}F_2$. Because an accurately determined value can not be expected of silicon which easily combines with fluorine and volatilizes during chemical analysis, the percentage of SiO_2 given in Table 3 indicates the value obtained by subtracting the contents of CaO and F from the entire amount. Table 2 also shows the X-ray powder data of the synthetic $Ca_{12}Si_4O_{19}F_2$ compared with those of the phase detected in clinker.

Crystallographic and Optical Properties

Fig. 1 shows an oscillating-crystal photograph of the synthetic $Ca_{12}Si_4O_{19}F_2$. Analyses of the photographs and the X-ray powder data revealed its unit cell to be orthorhombic (pseudo-hexagonal) with $a = 12.28_6$, $b = 7.09_2$ $c = 5.68_9$Å. Its density was observed to be 3.13 g/cm³ and its number of formula unit Z was determined to be 1. Although the axial ratio a/b was equal to $\sqrt{3}$, the diffraction spots on the photograph showed no hexagonal symmetry. Thus, the indexing of the X-ray powder data given in Table 2 is based on the orthorhombic cell. Meanwhile oscillating-crystal photographs disclosed the presence of vertical oblique pairs of weak diffraction spots being centered on strong diffraction spots and forming weak layer lines above and below the strong layer lines. No definite interpretation is still available as to this pattern as well as to the weak peaks which could not be indexed in Table 2.

Under the microscope, the new compound when well developed usually looks granular, being colorless in thin section. Cleavage also is observed but few show twins. It is biaxial negative ($2V \simeq 0$) with refractive indices $\alpha = 1.676 \pm 0.002$, $\gamma = 1.684 \pm 0.002$, and its birefringence is weak. In the clinker, it could be identified as a phase of indeterminate form surrounding an alite phase.

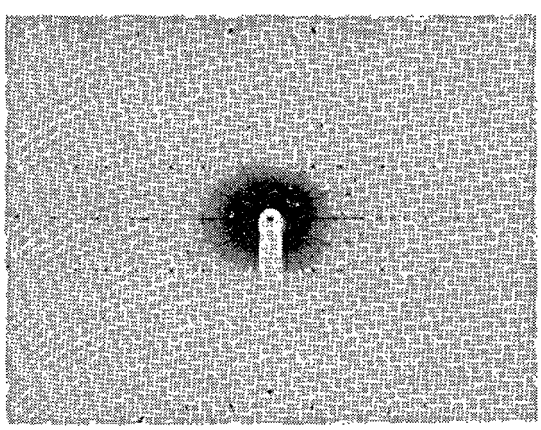

Fig. 1. *Oscillating-crystal photograph of* $Ca_{12}Si_4O_{19}F_2$. *(b-oscillation)*

Thermal Property and Determination of Primary Crystallization Field in Phase Equilibrium Diagram CaF_2–SiO_2–$2CaO \cdot SiO_2$

Fig. 2 shows the results of DTA and high-temperature X-ray diffraction analysis on the synthetic $Ca_{12}Si_4O_{19}F_2$. This compound was stable in a temperature range of about 1110° to 1185°C and metastable at room temperature. When cooled slowly or when held in an open state for many hours even in the stable temperature range, it had a tendency to dusting.

When being heated, it showed no particular decomposition temperature, began to decompose gradually at 500–600°C, and while liberating CaO and small amounts of C_2S, changed into a different unknown compound phase containing fluorine. In the present paper, this unknown phase is referred to tentatively as Phase II. The endothermic peak, at 825°C in the DTA curve shows an inversion of formed C_2S. Phase II decomposed at about 1040°C into C_2S, CaF_2, and probably CaO, too. The two phases A and B reported by E. Bereczky (9) seem, from their thermal proper-

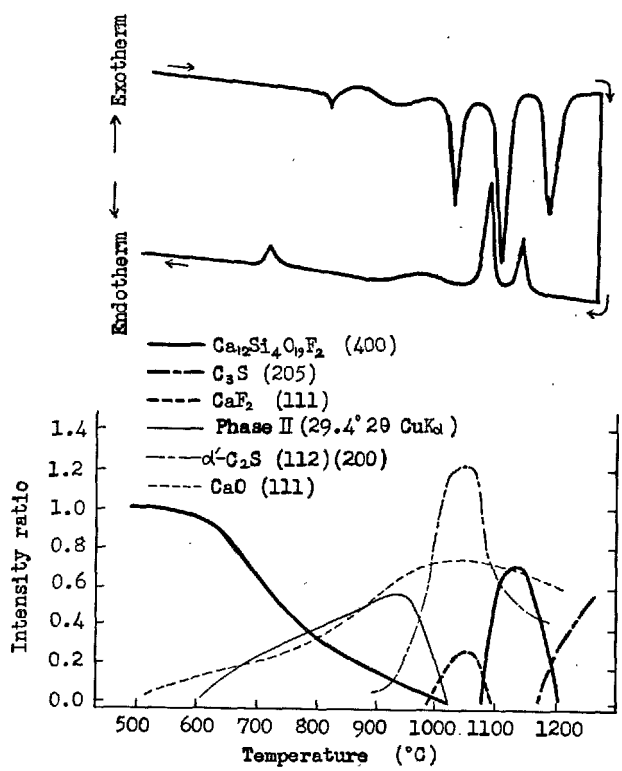

Fig. 2. *DTA and high-temperature X-ray diffraction analysis on* $Ca_{12}Si_4O_{19}F_2$.

ties, to correspond respectively with our $Ca_{12}Si_4O_{19}F_2$ and with Phase II. If Phase II is a single phase, it is a compound with considerably less CaO content than $Ca_{12}Si_4O_{19}F_2$ and showing 3.80, 3.31, 3.04, 2.95, 2.89 Å and so forth as its main interplanar spacings.

The prominent endothermic peak beginning at 1113°C indicates an initial formation of liquid or a solidus. At this temperature, an intial thin liquid layer was expected to form between CaF_2 and the grains aorund it, facilitating movement of atoms and allowing $Ca_{12}Si_4O_{19}F_2$ to crystallize rapidly here. The formed $Ca_{12}Si_4O_{19}F_2$ melted incongruently to crystallize C_3S and C_2S, together with a liquid phase when it reached 1185 ± 2°C by heating. In the burning of the raw mix, formation of such a liquid phase will accelerate diffusion of atoms and the alite phase crystallized by incongruent melting will also serve as a germ promoting the subsequent growth of alite crystals.

A large part of the C_3S crystallized by incongruent melting showed parallel growths. Alite phase of clinker burned with a relatively high CaF_2 dosage was also observed to present this elongated form. The C_3S crystallized here belonged to the trigonal system, its lattice constants a and c being 7.06 and 25.05 Å, respectively. When quenched in air, it showed a tendency to inversion into a monoclinic form. The lattice constants of this monoclinic C_3S were determined as $a = 12.26$, $b = 7.05$, $c = 25.09$ Å, and $\beta = 90°07'$. Both the trigonal and monoclinic forms of C_3S took lower values than their lattice constants previously reported (10), and this was thought to be due to containing some fluorine being contained in solid solution.

$$Ca_{12}Si_4O_{19}F_2 \xrightarrow[(1185\pm2°C)]{} \text{trigonal } C_3S + \alpha'\text{-}C_2S + \text{liquid}$$

Fig. 3–1 shows a representative form of synthetic $Ca_{12}Si_4O_{19}F_2$, and Figs. 3–2 to 3–5 illustrate the processes of incongruent melting indicated in the order of the numbers given. Namely, Fig. 3–2 represents the earliest stage of incongruent melting where $Ca_{12}Si_4O_{19}F_2$ began to transform. Fig. 3–3 shows C_3S beginning to develop in strip form with the progress of incongruent melting where the formation of a liquid phase and globular C_2S grains can be identified. Figs. 3–4 and 3–5 show completion of the melting with disappearance of $Ca_{12}Si_4O_{19}F_2$ and C_3S beginning to develop. The amount of liquid phase increases and C_3S grows in prismatic or rectangular form. Fig. 3–6 shows a characteristic structure due to the development of much grown trigonal C_3S and α'-C_2S.

In the cooling process, an exothermic peak was observed at 1145°C in addition to a major exothermic peak for the solidus. Quenching experiments showed this exothermic peak to mean an energy change due to peritectic reaction and not an exothermic peak for the liquidus. Namely, it indicated the presence of a ternary peritectic point where peritectic reaction took place on the surface of contact between C_3S and the liquid phase containing great amounts of fluorine, decomposing C_3S and at the same time absorbing C_2S to crystallize $Ca_{12}Si_4O_{19}F_2$. Microscopic observation revealed that the peritectic reaction did not proceed completely at the relatively rapid cooling from the above peritectic temperature, and the peritectic structure covering the periphery of C_3S with $Ca_{12}Si_4O_{19}F_2$ was formed as shown in Fig. 4. The cause for the peritectic temperature given by DTA being considerably lower than the decomposition temperature of $Ca_{12}Si_4O_{19}F_2$, 1185°C, is probably thermal hysteresis.

There are phase diagrams proposed by W. Eitel (11) and J. Mukerji (5) as typical of the system CaF_2–SiO_2–$2CaO \cdot SiO_2$. Despite the well-known presence of cuspidine $Ca_4Si_2O_7F_2$ as a compound of this system, none of the diagrams carries a ternary compound as the primary crystal phase. Because preparation of a phase equilibrium diagram for this system involves the difficulty of fluorine being easily volatilized in high temperature range, no complete diagram has yet been established. C. Brisi (7) stated that cupsidine was a eutectic stable compound melting congruently above 1400°C, if heated in welded containers. Our $Ca_{12}Si_4O_{19}F_2$ is a stable compound melting incongruently. DTA investigation of the cooling process down to 1090°C for the compositions contained in the various primary crystallization fields of C_3S, C_2S, CaO, and CaF_2 on the diagram of J. Mukerji disclosed mainly the compositions in the C_3S primary crystallization field to produce an exothermic peak at around 1145°C in addition to peaks for the liquidus and the solidus. Based on the results obtained, the primary crystallization field for $Ca_{12}Si_4O_{19}F_2$ has been established on the phase equilibrium diagram. It is shown in Fig. 5.

Result of Examination by Electron Probe X-ray Microanalyzer

The results of electron probe microanalysis are indicated in Fig. 6. These reveal the density distribution of elements and also phases present in the incongruent melting process of $Ca_{12}Si_4O_{19}F_2$ and the process of peritectic reaction that occurs during cooling.

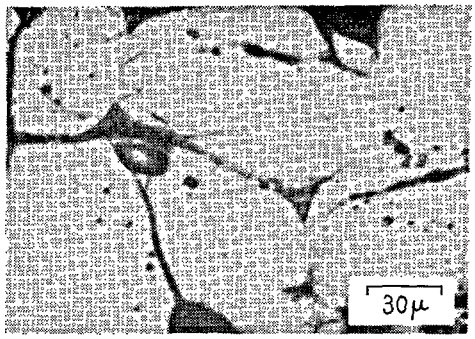

1

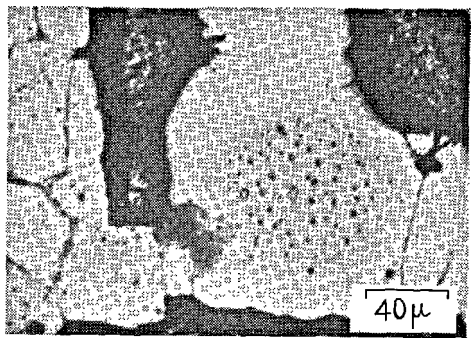

2

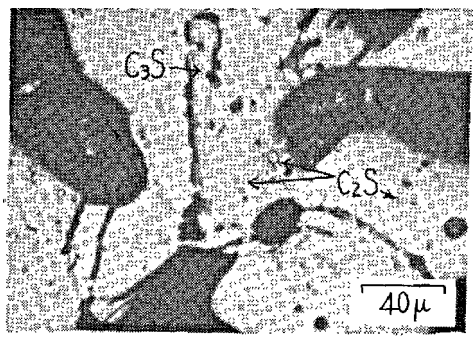

3

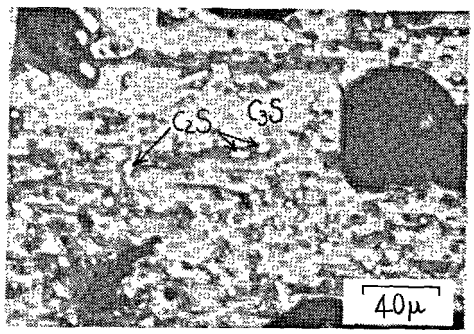

4

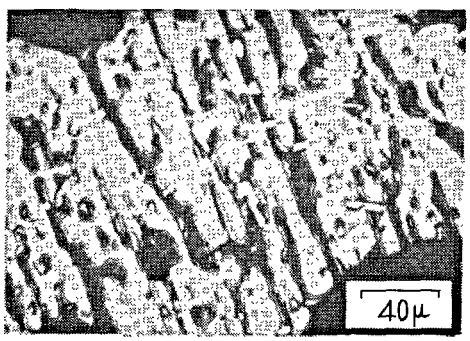

5

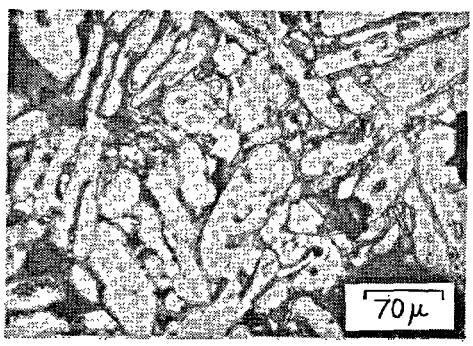

6

Fig. 3. *Synthetic* $Ca_{12}Si_4O_{19}F_2$ *and its incongruent melting. Optical micrograph, reflected light.* 1. *Typical form of* $Ca_{12}Si_4O_{19}F_2$; 2. *Earliest stage of melting;* 3. *Formations of* C_3S, C_2S, *and liquid phase with progress of melting;* 4. *Completion of melting;* 5. *Development of* C_3S *crystal after completion of melting;* 6. *Characteristic structure provided by well-developed* C_3S *and fine* C_2S.

Fig. 4. $Ca_{12}Si_4O_{19}F_2$ *formed by peritectic reaction. Optical micrograph, transmitted light.* 1. $Ca_{12}Si_4O_{19}F_2$ *covering* C_3S; 2. *Same field as 1. Crossed nicols.*

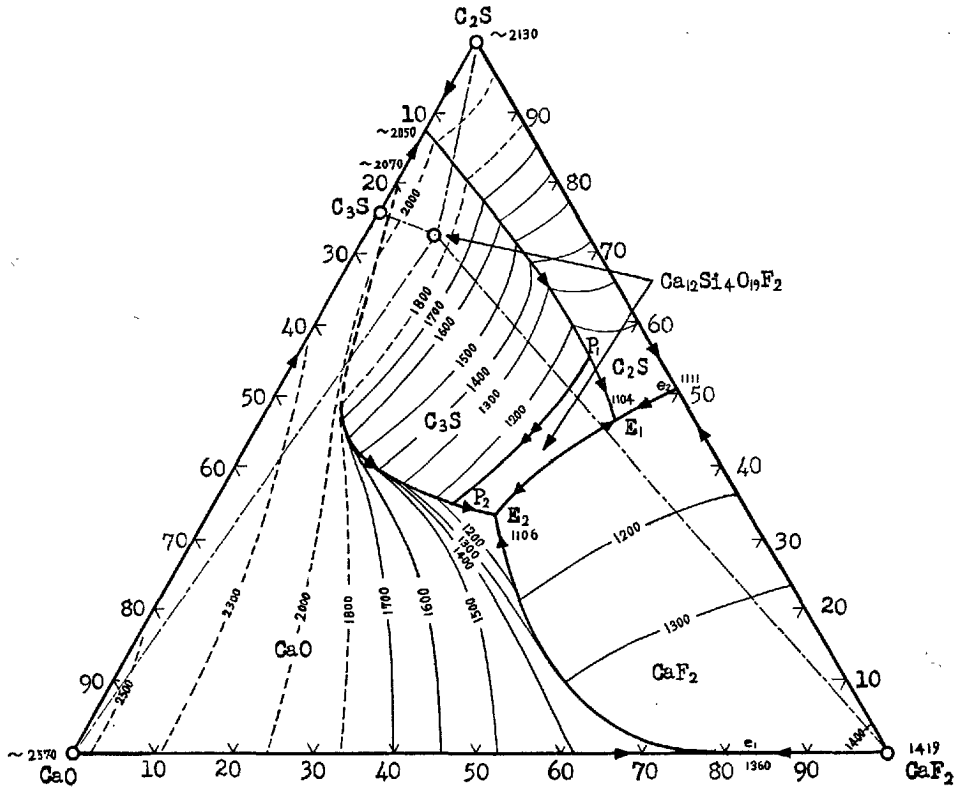

Fig. 5. *Primary crystallization filed of* $Ca_{12}Si_4O_{19}F_2$ *in the phase diagram* CaF_2–SiO_2–$2CaO \cdot SiO_2$.

Fig. 6–1 indicates the texture of coarse C_3S crystals, fine C_2S crystals, and liquid phase formed with the progress of incongruent melting as well as of the still remaining $Ca_{12}Si_4O_{19}F_2$. Fig. 6–2 indicates the incongruent melting completed, $Ca_{12}Si_4O_{19}F_2$ extinct, and all transformed into C_3S, C_2S, and liquid phase. Fig. 6–3 shows the structure of $Ca_{12}Si_4O_{19}F_2$ formed by peritectic reaction to cover C_3S in the process of cooling from above the peritectic temperature. The presence of $Ca_{12}Si_4O_{19}F_2$ enclosing C_3S was proved by the stepped curve of fluorine distribution on the periphery of C_3S as seen in the line analysis of Fig. 6–3. Figs. 6–1 to 6–3 disclose surplus fluorine concentrated mainly in the liquid phase, and in the cooling process, very fine CaF_2 crystals are easily crystallized secondarily from this liquid phase. Little silicon was

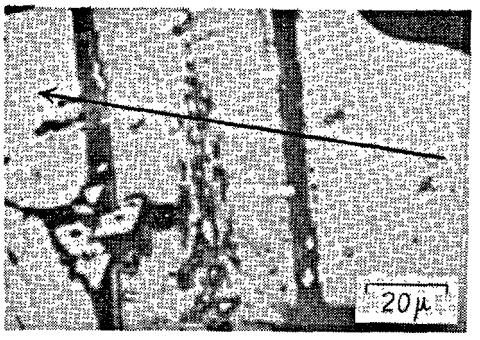

1

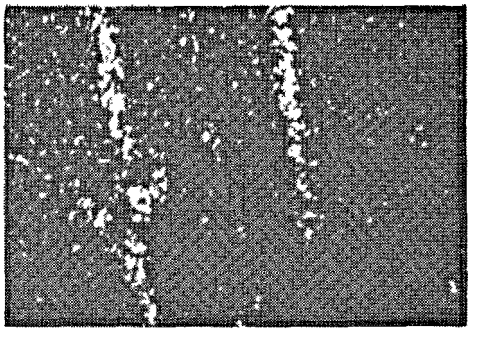

2

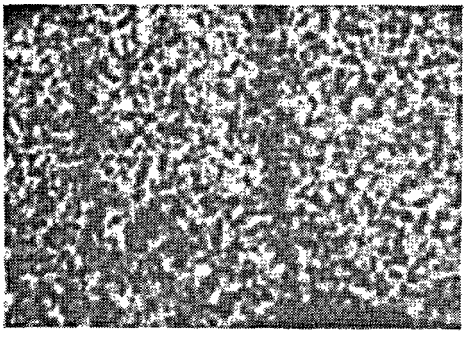

3

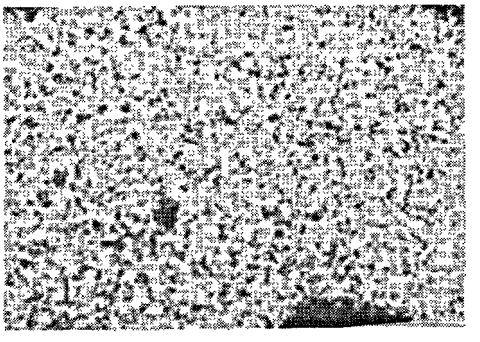

4

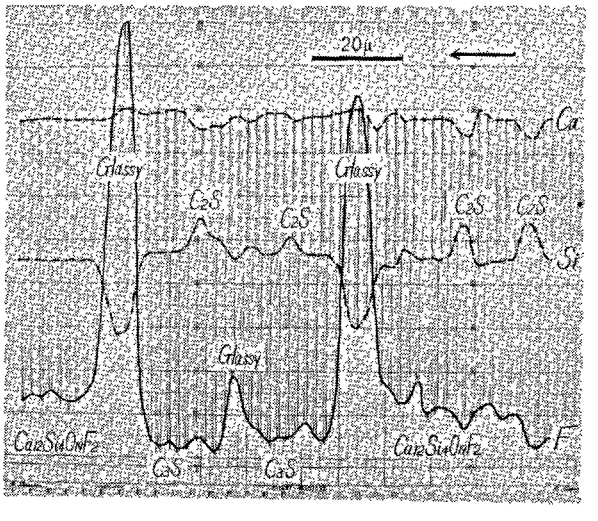

5

Fig. 6-1. *Transformation of* $Ca_{12}Si_4O_{19}F_2$ *by incongruent melting. Electron probe microanalysis.* 1. *Optical micrograph;* 2. FKα *characteristic X-ray image;* 3. SiKα *characteristic X-ray image;* 4. CaKα *characteristic X-ray image;* 5. *Line analysis following on the arrow head in the optical micrograph.*

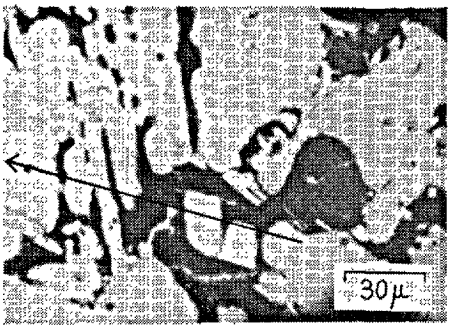

1

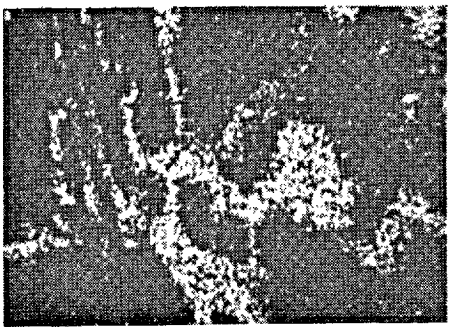

2

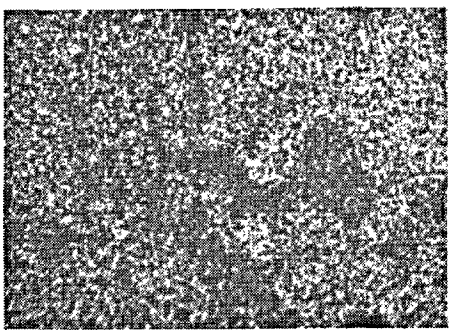

3

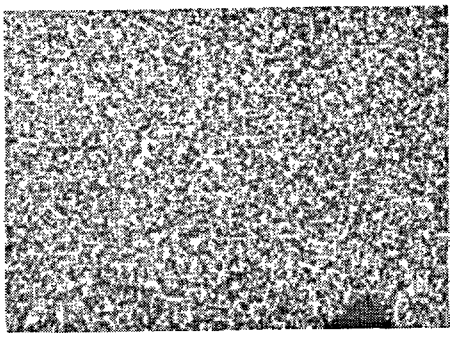

4

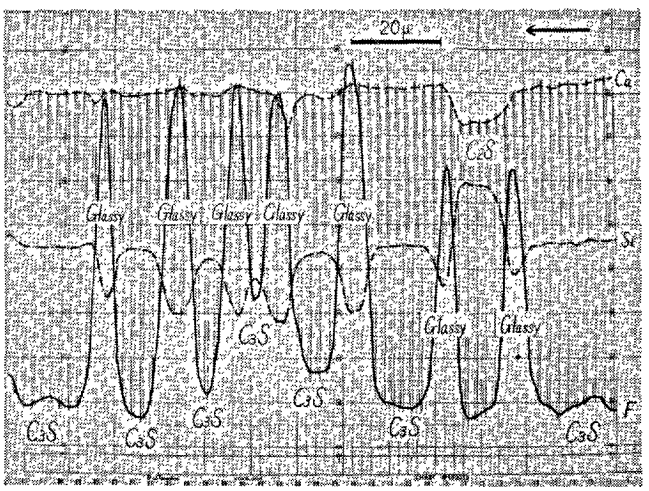

5

Fig. 6-2. C_3S, C_2S, *and liquid phase formed by incongruent melting. Electron probe microanalysis.* 1. *Optical micrograph:* 2. FKα *characteristic X-ray image;* 3. SiKα *characteristic X-ray image;* 4. CaKα *characteristic X-ray image;* 5. *Line analysis following on the arrow head in the optical micrograph.*

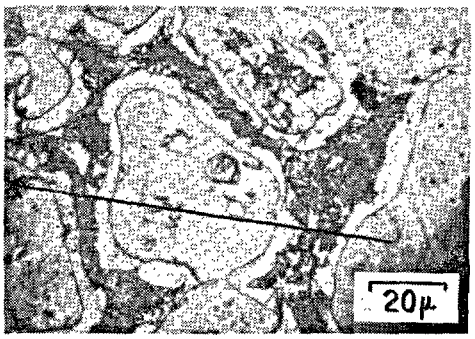

1

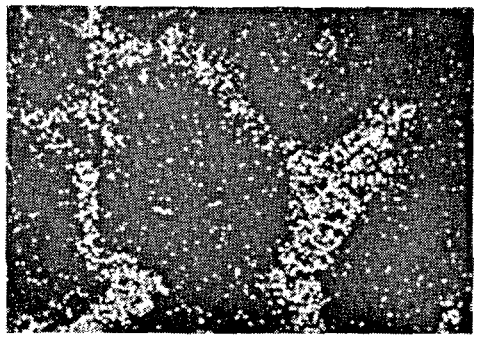

2

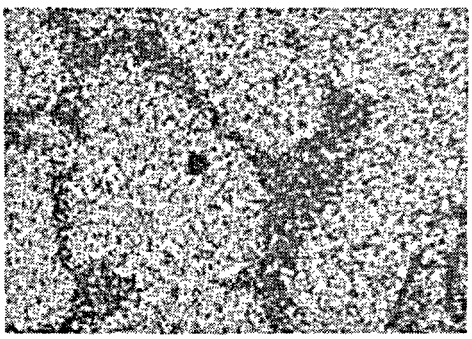

3

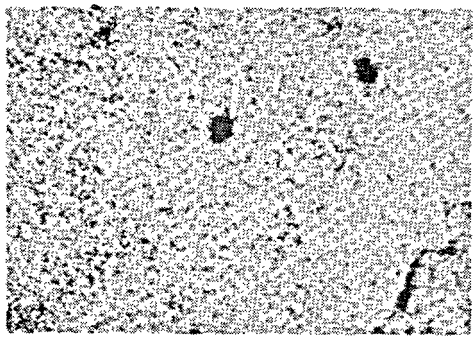

4

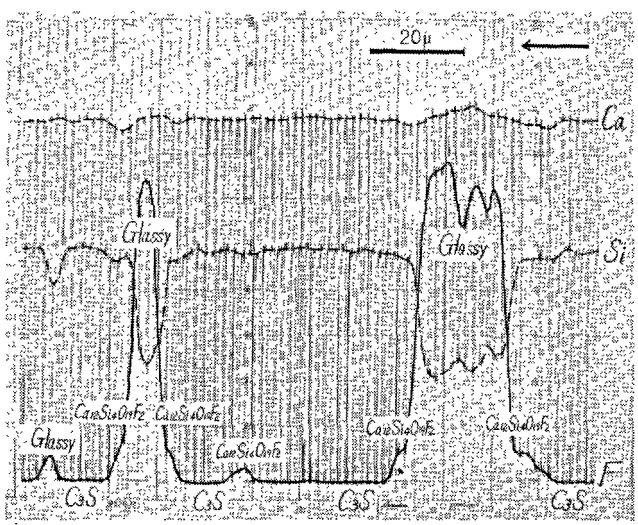

5

Fig. 6-3. *Peritectic structure produced in cooling process. Electron probe microanalysis.* 1. *Optical micrograph;* 2. FKα *characteristic X-ray image;* 3. SiKα *characteristic X-ray image;* 4. CaKα *characteristic X-ray image;* 5. *Line analysis following on the arrow head in the optical micrograph.*

identified in the liquid phase.

The electron micrograph carried in Fig. 7 shows very fine stripes of CaF_2 grain crystallized from the liquid phase and also some $Ca_{12}Si_4O_{19}F_2$ formed on the surface of C_3S crystal even in the case of immediate quenching from above the peritectic temperature.

Heat of Hydration and Hydraulicity of $Ca_{12}Si_4O_{19}F_2$

As Table 4 shows, the heat of hydration measured for synthetic $Ca_{12}Si_4O_{19}F_2$ was only somewhat higher than that of β-C_2S. A twin-type conduction calorimeter was used for measurement at the age of one hour. With the progress of hydration, $Ca_{12}Si_4O_{19}F_2$ transformed gradually into fibrous tobermorite phase with liberating $Ca(OH)_2$ and showed some cementation at the age of 28 days, but this compound after all proved to be poor in hydraulicity.

R.W. Nurse et al (12) reported a low hardening property of C_3S holding fluorine in solid solution. But attention must be paid to the effect of $Ca_{12}Si_4O_{19}F_2$ which is frequently present together with C_3S solid solution containing fluorine. Our measurement on the insoluble residue from a salicylic acid methanol solution treatment of C_3S synthesized by adding fluorine in the form of CaF_2 gave the value of the residue as 18.7% with 1.64% fluorine, as 0.31% with 0.82% fluorine, and as 0.03% with 0.55% fluorine. On the other hand, the pure C_3S without addition of fluorine dissolved completely. This suggested these insoluble residues to be $Ca_{12}Si_4O_{19}F_2$.

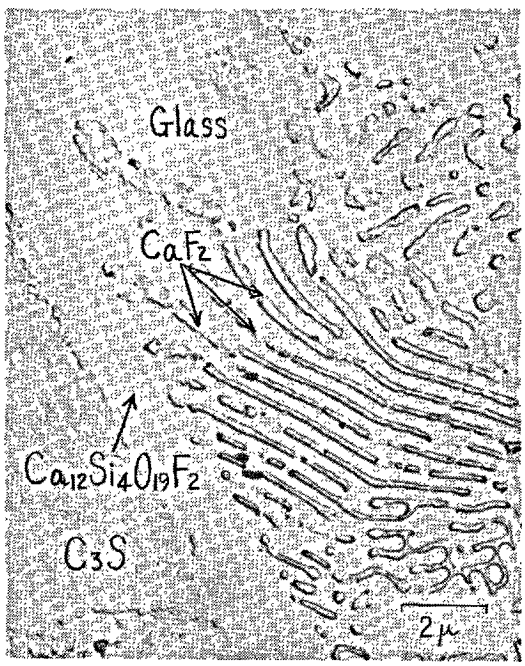

Fig. 7. *Secondary-formed fine* CaF_2 *in the glass phase. Electron micrograph.*

Solubility of Al_2O_3 and Na_2O in Pure $Ca_{12}Si_4O_{19}F_2$

As already shown in Table 2, there is some difference in interplanar spacing and peak intensity in X-ray diffraction patterns between synthetic $Ca_{12}Si_4O_{19}F_2$ and the phase existing in the clinker. Further investigation in this respect revealed the difference to be due mainly to the solubility of Al_2O_3 and Na_2O in $Ca_{12}Si_4O_{19}F_2$. Fig. 8 shows the lattice constants of the

Table 4. *Heat of hydration of* $Ca_{12}Si_4O_{19}F_2$ *(w/s = 40%)*

Heat of solution (cal/g)	Heat of hydration (cal/g)			
	1 hr	7 days	28 days	56 days
546.3	(0.27)	7.3	39.1	50.9

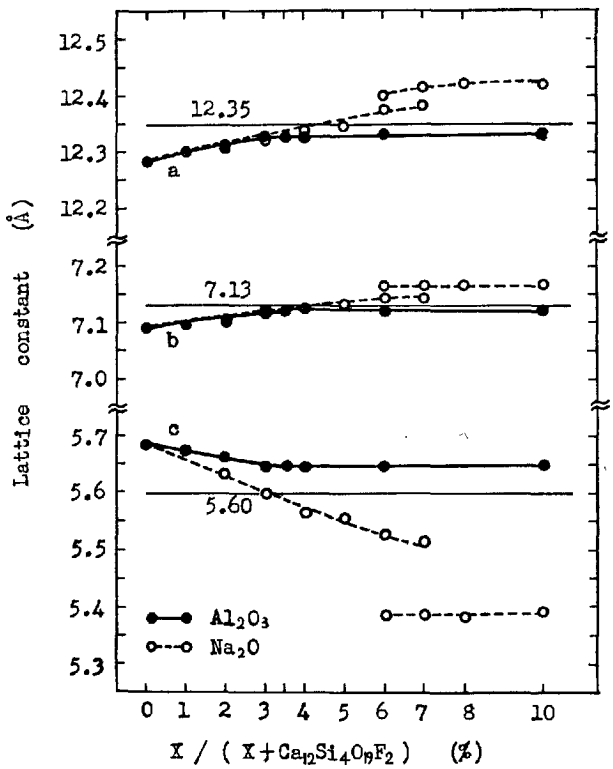

Fig. 8. *Variation of lattice constant of* $Ca_{12}Si_4O_{19}F_2$ *with take-up of* Al_2O_3 *and* Na_2O.

Notes: 1. X denotes the amount of Al_2O_3 or Na_2O added.
2. The numerals on the chart indicate the lattice constants of the phase existing in clinker.

phase actually identified in the clinker and the variation of lattice constants with take-up of Al_2O_3 and Na_2O in $Ca_{12}Si_4O_{19}F_2$.

In the case of Al_2O_3, the interplanar spacings changed successively up to 3.0–3.5% addition, and above that level, $C_{12}A_7$ ($\bar{F}$) formed. When heated with addition of Na_2O, the synthetic compound encouraged liberation of CaO, and in a dosage range of 6–7%, developed a structural change to become an unknown phase having hexagonal lattice constants $a = 14.34$ and $c = 5.39$ Å which appeared to be a ternary compound based on the system CaO–SiO_2–NaF. CaO was liberated at the rate of 2 moles for 1 mole of Na_2O added—a unique phenomenon—and the content of free CaO became constant (12.7%) over 7% addition.

The dosages of Al_2O_3 and Na_2O with which the compound became most similar to the phase present in the clinker were 3.5 wt-% and 3.0–4.0 wt-%, respectively. The amount of C_2S liberated by heating with addition of Al_2O_3 and the amount of CaO liberated by heating with addition of Na_2O were quantitatively determined and calculated to be equivalent to about 4.0–5.0 wt-% of Al_2O_3 and about 3.5–4.5 wt-% of Na_2O held in solid solution. In this case, Al_2O_3 was assumed not to be contained in C_2S with heating at about 1100°C.

Formation Condition and Amount of New Compound Formed in Burning of Raw Mix

Fig. 9 shows the relationship between burning temperature and amount of mineral present in the clinker, and Fig. 10 shows the relationship between CaF_2 dosage and amount of mineral present in the clinker. At 800°C, $CaCO_3$ still remained in a considerable amount so that there also was much insoluble residue resulting from the treatment with the solution of salicylic acid in methanol, but at 850°C, decomposition of $CaCO_3$ was almost over and a $Ca_{12}Si_4O_{19}F_2$ solid solution began to form. The maximum amount of $Ca_{12}Si_4O_{19}F_2$ solid solution occurred at around 1050°C, and in this region free CaF_2 was absent. If this phase is of pure $Ca_{12}Si_4O_{19}F_2$ even when formed in the clinker, and moreover, if added CaF_2 entirely takes part in the formation of this phase, then:

$$\%\ Ca_{12}Si_4O_{19}F_2 = \%\ CaF_2\ \text{Added} \times (Ca_{12}Si_4O_{19}F_2\ \text{mol. weight})/(CaF_2\ \text{mol. weight})$$

Since the content of ignition loss of raw mix is 34.4% in the present experiment, the maximum amount of $Ca_{12}Si_4O_{19}F_2$ to be formed is calculated at 54.8 wt-% with addition of 3 wt-% CaF_2 (dry base) if the above-mentioned assumption is followed. Actually, however, the amount of it lessens because the fluorine is contained in other compounds, and also because it inevitably volatilizes out of the system. As Fig. 10 shows, with less than 1% CaF_2, $Ca_{12}Si_4O_{19}F_2$ solid solution could not be identified by X-ray investigation even at 1050°C where it was most stable.

In the raw mix system, $Ca_{12}Si_4O_{19}F_2$ soild solution transformed into an alite phase and probably a belite phase, too, at 1100–1150°C. Therefore, formation of the alite phase was started at a temperature 150–200°C lower than in the case of a raw mix not containing CaF_2. With an initial CaF_2 addition of over 2%, meanwhile, the presence of a $Ca_{12}Si_4O_{19}F_2$ solid solution was recognized even in the clinker burned over 1150°C. This was a product of secondary crystallization in the cooling process. Formation of a $Ca_{12}Si_4O_{19}F_2$ solid solution is considered as one cause of decline in the mechanical strength of cement, and it is practically supported by a sharp decline in

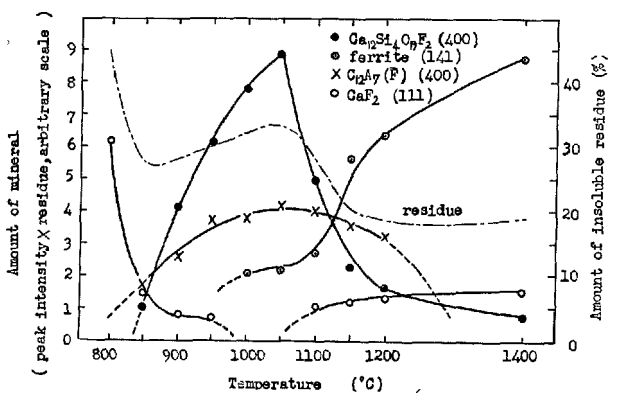

Fig. 9. *Burning temperature and amount of mineral existing in clinker (with 3.0% CaF_2 addition)*

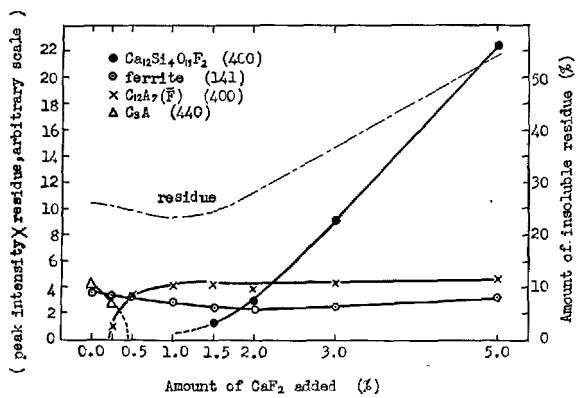

Fig. 10. *Amount of CaF_2 added and amount of mineral existing in clinker (burning temperature: 1050°C)*

the mechanical strength of cement burned with over 2% CaF_2 (2).

Influence of Burning with CaF_2 on Other Clinker Minerals

Among the alite, belite, aluminate, and ferrite phases that constitute portland cement clinker, most affected by the addition of CaF_2 is the aluminate phase. In the clinker burned at 1400°C with over 2% CaF_2, no aluminate phase whatever could be identified by X-ray examination. Instability of C_3A arising from fluorine has already been reported by W. Eitel (13), and it has been disclosed by J. Jeevaratnam et al (14) that the $C_{12}A_7(\bar{F})$ made stable instead of C_3A is a solid solution $Ca_{24}Al_{28}O_{64}F_4$ which has substituted 4 fluorine atoms for 2 oxygen atoms not definitely located but statistically distributed in the unit cell and whose lattice constant a is 11.964 Å, about 0.02 Å less than that of pure $C_{12}A_7$. In the present experiment, too, $C_{12}A_7(\bar{F})$ could be definitely identified in the clinker burned below 1250°C, but its formation could not be recognized in the clinker burned above 1300°C. It will remain to be studied why $C_{12}A_7(\bar{F})$ is absent in clinkers burned at high tempertures.

In contrast to the sharp decrease in the aluminate phase caused by fluorine, a quantitative increase and a shrinkage of interplanar spacing (the 141) were observed in the ferrite phase. Measurements on the 141 reflection revealed its intensity to be maximum with 3% CaF_2 addition, about 1.4 times its value in the case of burning without CaF_2. Likewise, with 3% CaF_2, the interplanar spacing (the 141) was minimum. Fig. 11 shows the variation of molar Al_2O_3/Fe_2O_3 ratio of the ferrite phase as calculated by the methods of L.E. Copeland et al, D.K. Smith, or H.G. Midgley (15).

The variations of interplanar spacings of alite phase at 30.1°, and belite phase at 31.0° 2θ CuKα are also indicated in Fig. 11. In the clinker burned without CaF_2, the composition of ferrite phase was approximate to that of $C_{10}A_2F_3$ in the present experiment. With an increased dosage of CaF_2, however, it became Al_2O_3-rich and almost equal to the composition of C_4AF with 3.0% addition. This phenomenon is interpreted to mean that part of the alumina content to form aluminate entered into the ferrite phase to make this Al_2O_3-rich and at the same time to increase its amount. With over 3.0% CaF_2, however, the alumina content in the ferrite phase began to decrease again because of formation of a great deal of the $Ca_{12}Si_4O_{19}F_2$ solid solution holding Al_2O_3 in it.

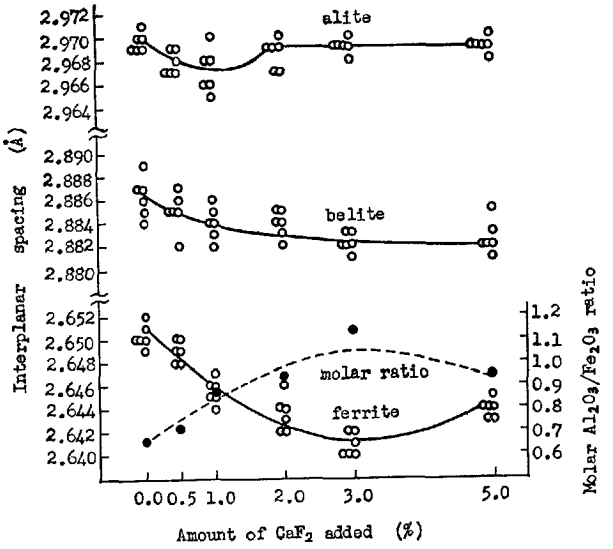

Fig. 11. *Amount of* CaF_2 *added and interplanar spacing of clinker mineral.*

The intensity of alite reflection at 30.1° 2θ CuKα began to decline appreciably and decrease in amount with addition of 2% CaF_2, and that of belite reflection at 31.0° 2θ CuKα, with 3% addition. With 5% CaF_2, they were 0.65 and 0.88 times respectively the intensities of them in the clinker burned without CaF_2. These decreases in amount both came probably from peritectic crystallization of $Ca_{12}Si_4O_{19}F_2$ solid solution in the cooling process of clinker. The interplanar spacing of alite phase at 30.1° 2θ CuKα shrank up to 1.0% CaF_2 addition, but beyond that, it again expanded. The interplanar spacing of belite phase at 31.0° 2θ CuKα contracted unilaterally with an increased addition of CaF_2. Generally, surplus fluorine occurred mainly in the glass phase, and fine free CaF_2 produced secondarily was frequently identified in the clinker burned with over 2% CaF_2.

Acknowledgements

We sincerely thank Professor S. Iwai of Tokyo Institute of Technology for his invaluable advice, and one of us (G.S.) wishes to express his profound gratitude to Professor G. Yamaguchi of Tokyo University for his continuing guidance. Thanks are also due to President T. Ohtomo and Vice-president M. Horiguchi of the Chichibu Cement Co., Ltd., for their interest and encouragement.

Notation

Chemical compositions were expressed by abbreviation symbols based on the usage of cement chemistry, but fluorine contained in solid solution was distinguished as $\bar{F}$ and parenthesized at the end of chemical formula.

References

1. S. Akaiwa, G. Sudoh and M. Tanaka, "Studies on mineralizing effect of CaF_2 and a ternary compound in the system CaO–SiO_2–CaF_2" (in Japanese), Semento Gijutsu Nenpo **20,** 26–31 (1966).
2. S. Akaiwa, G. Sudoh and M. Tanaka, "On the properties of a ternary new compound $11CaO \cdot 4SiO_2 \cdot CaF_2$" (in Japanese), Semento Gijutsu Nenpo **21,** 22–28 (1967).
3. S. Takashima and F. Amano, "On the content of tricalcium aluminate in portland cement" (in Japanese), Semento Gijutsu Nenpo **13,** 50–54 (1959).
4. K. Emi and T. Hayami, "Colorimetric determination of small amounts of flouride with Neo Thorin" (in Japanese), J. Chem. Soc. Japan **76,** 1291–1293 (1955).
5. J. Mukerji, "Phase equilibrium diagram CaF_2–SiO_2–$2CaO \cdot SiO_2$", J. Am. Ceram. Soc. **48,** 210–213 (1965).
6. G. Yamaguchi, H. Miyabe, K. Amano and S. Komatsu, "Synthesis of each modification of $2CaO \cdot SiO_2$ and their certification" (in Japanese), J. Ceram. Assoc. Japan **65,** 99–104 (1957).
7. C. Brisi, "Role of cuspidine ($3CaO \cdot 2SiO_2 \cdot CaF_2$) in the system CaO–SiO_2–CaF_2", J. Am. Ceram. Soc. **40,** 174–178 (1957).
8. ASTM Powder Diffraction File, Section 13, No. 410 (Philadelphia, U.S.A., 1963).
9. E. Bereczky, "Kutatások a trikalciumszilikát keletkezésének gyorsítására és stabilizálására II", Építőanyag **16,** 441–448 (1964); cf. Chem. Abstr. **65,** 11953 f (1966).
10. M. Bigaré, A. Guinier, C. Mazières, M. Regourd, N. Yannaquis, W. Eysel, Th. Hahn and E. Woermann, "Polymorphism of tricalcium silicate and its solid solutions", J. Am. Ceram. Soc. **50,** 609–619 (1967).
11. W. Eitel, "Die Wirkung der Fluoride als Mineralisatoren beim Klinkerbrand", Zement **27,** 469–472 (1938).
12. R. W. Nurse, H. G. Midgley, W. Gutt and K. Fletcher, "Effect of polymorphism of tricalcium silicate on its reactivity", Symposium on Structure of Portland Cement Paste and Concrete, Highway Research Board, Special Report 90, Washington, D.C., p. 258–262 (1966).
13. W. Eitel, "Untersuchungen über das System CaO–$5CaO \cdot 3Al_2O_3$–CaF_2 und über die Stabilität des Tricalciumaluminats", Zement **30,** 17–21 (1941); **30,** 29–32 (1941).
14. J. Jeevaratnam, F. P. Glasser and L. S. Dent Glasser, "Anion substitution and structure of $12CaO \cdot 7Al_2O_3$", J. Am. Ceram. Soc. **47,** 105–106 (1964).
15. The Chemistry of Cements, Vol. I, p. 115 (Academic Press Inc., London, England, and New York, U.S.A., 1964), Edited by H.F.W. Taylor. See Chapter 3 by H. G. Midgley entitled "The formation and phase composition of portland cement clinker".

Supplementary Paper I-82 Formation of Double Salt in Cement Burning

Morio Amafuji and Akira Tsumagari*

Synopsis

We have undertaken an investigation concerning the mineral composition of ring in cement kiln in order to expose the cause of the formation of ring.

Through this investigation we found in the texture of ring a few kinds of double salt minerals, $2Ca_2SiO_4 \cdot CaCO_3$, $3Ca_2SiO_4 \cdot 2CaSO_4$** and $2CaSO_4 \cdot K_2SO_4$ etc., besides single salt minerals, $CaCO_3$, $CaSO_4$ and $(K, Na)_2SO_4$.

Two double salt minerals, except $2Ca_2SiO_4 \cdot CaCO_3$, have not been produced yet in natural world, they were synthetized in laboratory.

$2Ca_2SiO_4 \cdot CaCO_3$, named spurrite in mineralogy, is rarely found in geological metamorphic calcite rock zone.

We assumed that these salt minerals in cement kiln were formed by gas-solid reaction between CO_2 or SO_2 of fuel gas and raw material or clinker in cement burning. Thereupon, we made an experiment for verifying this gas-solid reaction under current of CO_2 or SO_2 gas by electric furnace in laboratory.

The results of this burning experiment determined clearly the forming condition of these double salt minerals in the burning of raw material or clinker under current of CO_2 or SO_2 gas.

We were able to conclude that even a small quantity of SO_2 gas by far predominates a large quantity of CO_2 gas at the reaction with raw material and clinker at high temperature.

Moreover, we found by the original experiment that the burned pieces bearing a large quantity of double salt minerals have great coagulative strength.

The results obtained from these experiments are expected to give some important suggestions to the research both about the cause of the generation of ring and about the temperature condition at each inner part of kiln where ring adheres.

Introduction

Since long ago, many reports of the research about ring adhered in cement kiln have been published (1, 2, 3, 4, 5, 6, 7, 8, 9, 10). Almost all of them have not dealt with the texture of the ring body, but generally with the various operating conditions of kiln or the chemical properties of clinker which were supposed to have an principal effect upon the generation of the ring.

It is natural that the burning condition of cement kiln is strongly influenced by the ring adhered to the inner wall. The ring is always an obstacle in the burning operation of kiln. It is especially affected in case of excess charge of raw material or in case of long period operation. Naturally, generation of the ring has attracted attentions of many investigators.

Fortunately, we had many chances to observe directly the state of formation of the ring in kiln and pick pieces of sample for test purposes from each part of the body of ring from surface to bottom.

Each sample picked up systematically from the each part of ring as shown Fig. 1 was tested for making

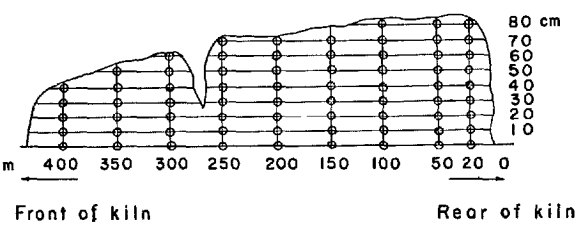

Fig. 1. *The position in ring where the samples were picked.*

* Central Research Laboratory, Onoda Cement Co., Ltd., Tokyo, Japan.

** The chemical formula of this silicosulphate is postulated from the chemical analysis of this mineral occuring in ring. The theoretical formula should be detected by crystalographic study.

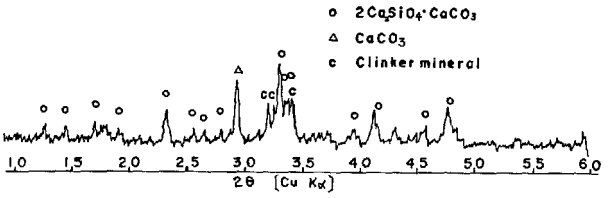

Fig. 2. *The X-ray diffraction pattern of a ring material principally composed of* $2Ca_2SiO_4 \cdot CaCO_3$.

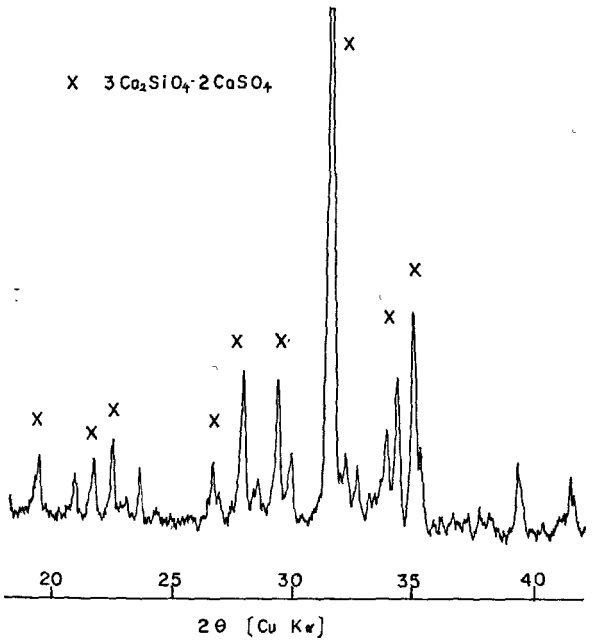

Fig. 3. *The X-ray diffraction pattern of a ring material principally composed of* $3Ca_2SiO_4 \cdot 2CaSO_4$.

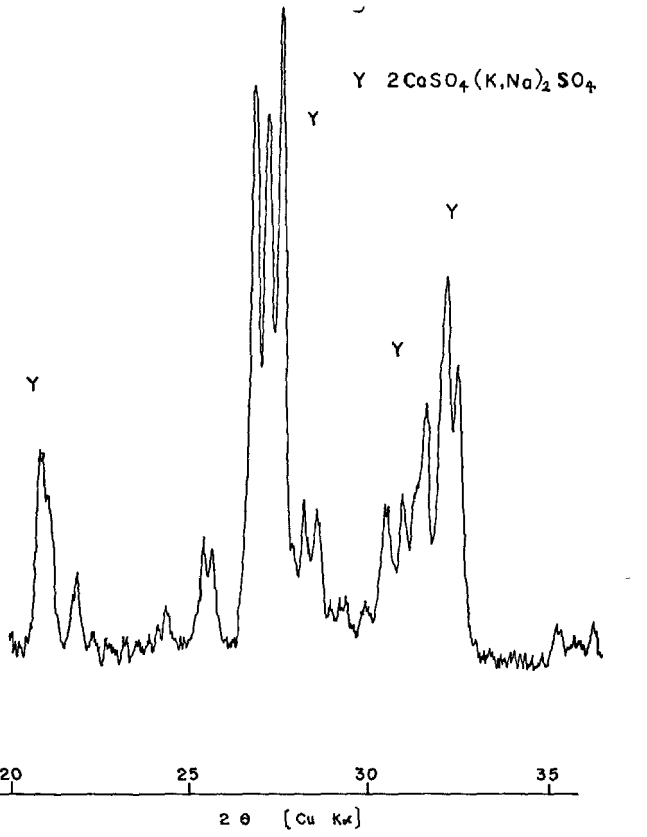

Fig. 4. *The X-ray diffraction pattern of a ring material principally composed of* $2CaSO_4 \cdot (K, Na)_2SO_4$.

clear mineralogical composition by simple chemical treatment, chemical analysis, microscopic observation, X-ray diffraction, and differential thermal analysis etc.

We found a few kinds of mineral which were not expected to be formed in cement kiln. They are double salt minerals composed of Ca_2SiO_4 or $CaSO_4$.

$2Ca_2SiO_4 \cdot CaCO_3$ was frequently found in the ring adhered to the wall not far from burning zone (11). On the other hand, $3Ca_2SiO_4 \cdot 2CaSO_4$ (12, 13) and $2CaSO_4 \cdot (K, Na)_2SO_4$ were found in the ring adhered to the wall of calcing zone or the one near the upper end of kiln.

When we used grate chamber or disused gas utilized boiler directly connecting to the upper end of kiln, the pile that adhered to the wall or to water tubes was principally composed of $3Ca_2SiO_4 \cdot 2CaSO_4$ or $2CaSO_4 \cdot (K, Na)_2SO_4$. We regard the piles as ring in this paper.

These double salt minerals are generally formed accompanied by Ca_2SiO_4, $CaSO_4$, $CaCO_3$ or $(K, Na)_2SO_4$ respectively.

Fig. 2, Fig. 3 and Fig. 4 which show the results of X-ray diffraction of the ring are principally composed of $2Ca_2SiO_4 \cdot CaCO_3$, $3Ca_2SiO_4 \cdot 2CaSO_4$ or $2CaSO_4 \cdot (K, Na)_2SO_4$ respectively. Table 1 shows the difference in chemical and mineralogical characters between the double salt minerals and the already known clinker minerals.

$2Ca_2SiO_4 \cdot CaCO_3$ is rarely formed in geological metamorphic calcite rock region in natural world (14, 15). It is supposed that CO_2 gas at a certain temperature range plays an important part in forming $2Ca_2SiO_4 \cdot CaCO_3$. $3Ca_2SiO_4 \cdot 2CaSO_4$ and $2CaSO_4 \cdot (K, Na)_2SO_4$ were synthesized by J. J. Rowe, G. W. Morey and C. C. Silber through solid-solid reaction using of reagents of sulphates (16).

We supposed that these double salt minerals in the ring were formed by gas-solid reaction between CO_2 or SO_2 of fuel gas and raw material or clinker in cement burning.

Table 1. *The difference in chemical and mineralogical characters between the double salts minerals and the clinker minerals.*

		C_3S			C_2S		C_3A	C_4AF	Spurrite		Calcium langbeinite
Chemical formula		Ca_3SiO_5			Ca_2SiO_4		$Ca_3Al_2O_6$	$Ca_4Al_2Fe_2O_{10}$	$2Ca_2SiO_4 \cdot CaCO_3$	$3Ca_2SiO_4 \cdot 2CaSO_4$	$K_2SO_4 \cdot 2CaSO_4$
Chemical	CaO	73.7			65.1		62.3	46.2	63.1	56.9	25.1
	SiO_2	26.3			34.9				27.0	22.8	
	Al_2O_3						37.7	21.0			
	Fe_2O_3							32.8			
Analysis	CO_2								9.9		
	SO_3									20.3	53.8
	K_2O										21.1
Polymorphism			α	α'	β	γ					
Specific gravity		3.15	3.035	3.31	3.28	2.974	3.04	3.77	3.014		
Refractive index	$\alpha(\omega)$	1.718	1.652	1.712	1.717	1.642			1.640	1.628	1.52
	β			1.716		1.645	1.710	2.05	1.674		
	$\gamma(\epsilon)$	1.723	1.661	1.725	1.735	1.654			1.679	1.636	
Birefringence		0.005	0.009	0.013	0.018	0.012		0.10	0.039	0.008	1.53
Optical character		uniaxial (−)			biaxial (+)	biaxial (−)	isotropic	uniaxial (−)	uniaxial (−)		biaxial
2V, degrees		small	0–20°	30°	large	60°		medium	40°	large	

Thereupon, we made an experiment for verifying the above mentioned gas-solid reaction under current of CO_2 or SO_2 gas by electric furnace in laboratory.

The Manner of an Experiment of the Gas-Solid Reaction

For the experiments of the gas-solid reaction we used a horizontally laid electric furnace, made of about 5cm in diameter mullite tube surrounded with six heat elements of SiC. Two end sides of the tube are tightly closed by plugs which have openings for passages of both gas and thermocouple.

The material was laid in the center of the tube and the top of the thermocouple was laid very closely to the material in order to measure the accurate temperature of it. The temperature controller was employed.

The gas drawn from the gas bomb was led to passing through the bin for regulation of gas pressure filled with conc H_2SO_4, and then through the flow-meter. The bin of conc H_2SO_4 was used for the purpose of dehydration of gas. The disused gas that passed through the furnace was led into the bin of conc NH_4OH for the purpose of absorption of wasted SO_2 gas and then was sucked out by aspirater. In the experiment by the mixed gas we used the bin for mixing of gases.

The whole apparatus of experiment is shown in Fig. 5.

The actual disused gas of the upper end of cement kiln contains about 0.05 percent SO_2 gas and about 20 percent CO_2 gas. Even very small quantity of SO_3 was supposed to have strong reactivity.

We made an experiment with saturated CO_2 or SO_2 gas in the first step. Next we used the mixed gas component which is similar to the actual disused gas located at the upper end of kiln. The gas was let flow at room temperature with a constant quantity of 150 cc per minute, except in special cases.

As the material cement clinker we used ordinary one. As the material cement raw material we used the one in which calcined calcite was mixed as CaO component. Their chemical analysis are shown in Table 2.

After the material was burned in rising temperature with constant speed of 15°C per minute it was kept for an hour at a certain aimed temperature. Then the mineral constituent of the burning pieces was investigated mainly by means of X-ray diffraction.

Table 2. *The Chemical Analysis of the materials for the test under current of saturated gas.*

Chemical composition	Ig. loss	SiO_2	Al_2O_3	Fe_2O_3	CaO	MgO	Na_2O	K_2O	SO_3	Total
Clinker	0.30	22.52	4.16	3.50	65.75	2.77	0.38	0.47	0.03	99.88
Raw material	4.80	21.60	3.10	62.60	1.70	0.40	0.53			99.33

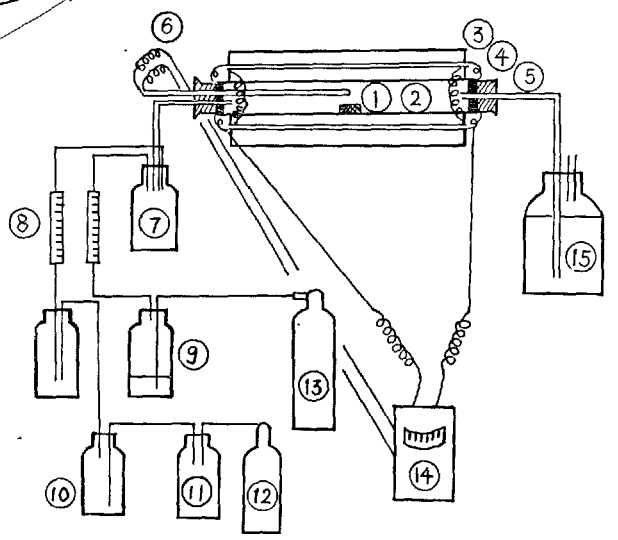

Fig. 5. *Outline of the apparatus for experiment of the gas-solid reaction.*

The Reaction between CO_2 Gas and Raw Material or Clinker

By the pre-experiment we ascertained the phenomenon that $2Ca_2SiO_4 \cdot CaCO_3$ could be synthesized by the gas-solid reaction between CO_2 gas and β-Ca_2SiO_4, γ-Ca_2SiO_4 or β-$CaSiO_3$ with $CaCO_3$ in the range of temperature from 800°C to 900°C.

In this experiment, by the improved apparatus, we studied details in regard to the formation of $2Ca_2SiO_4 \cdot CaCO_3$ by the gas-solid reaction. The result of X-ray diffraction of the burned pieces of raw material under the current of CO_2 gas is omitted here as it does not show special phenomenon.

Fig. 6 and Table 3 show the result of X-ray diffraction of the burned pieces of clinker under the current of CO_2 gas. By these results we came to the conclusion described below.

Re-crystalized $CaCO_3$ was formed and no $2Ca_2SiO_4 \cdot CaCO_3$ was formed in the reaction between CO_2 gas and raw material. On the other hand, $2Ca_2SiO_4 \cdot CaCO_3$ was remarkably formed in the reaction between CO_2 gas and clinker.

In case of the former, $CaCO_3$ was remarkably formed at temperature above 600°C and de-carbonized mostly in the range of temperatures between 900°C and 1,000°C, then $2Ca_2SiO_4$ was formed at 1,100°C.

Table 3. *The mineral composition of the burned pieces of clinker under current of CO_2 gas.*

Burning temperature °C	Forming mineral					Penetrative degree*
	$Ca_3Si_2O_5$	β-Ca_2SiO_4	$CaCO_3$	CaO	$2Ca_2SiO_5 \cdot CaCO_3$	
Room temp.	+++	++				0
600	+++	++				71
700	+++	++				497
750		+++	+++		+++	792
800		+++	+++		+++	1440
850		+++	++		+++	
900		+++	+	++	+++	1568
950		+++	−	++		1505
1000		+++	−	++		1393
1100		+++		++		1757

+++ Very much ++ Much + Moderate − A little
*Later mention.

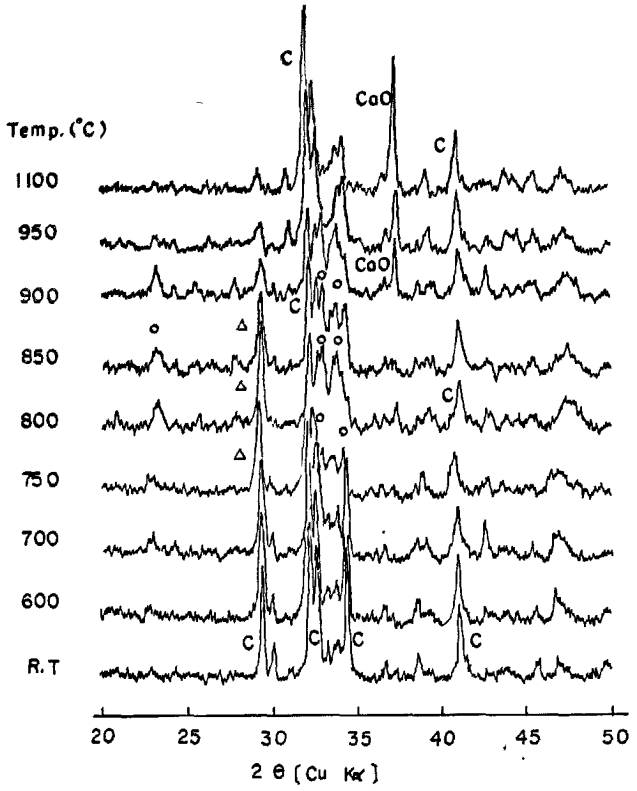

Fig. 6. *The X-ray diffraction patterns of the burned pieces of clinker under current of CO_2 gas.*

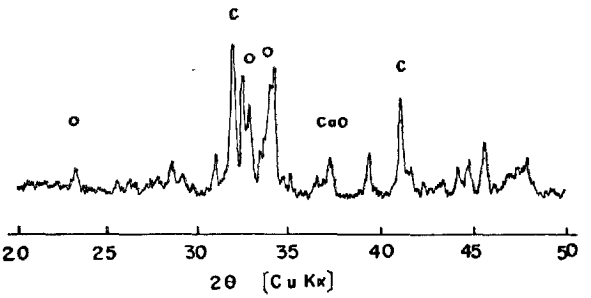

Fig. 7. *The X-ray diffraction pattern of the burned piece mixing β-Ca_2SiO_4 and $CaCO_3$ under current of CO_2 gas. (Keeping temperature at 850°C)*

In case of the latter, we found a decrease in intensity of X-ray diffraction peak of alite, Ca_3SiO_5, as increase in $2Ca_2SiO_4 \cdot CaCO_3$. The diffraction peak of $2Ca_2SiO_4 \cdot CaCO_3$ showed the strongest intensity in the range of temperatures between 800°C and 900°C and mostly disappeared at 950°C, while the diffraction peak of β-Ca_2SiO_4 and CaO showed the strongest intensity at temperature above 950°C.

The following chemical reaction was noted with the increase in the temperature.

$$\underset{\text{Alite}}{Ca_3SiO_5} + \underset{\text{Belite}}{Ca_2SiO_4} + CO_2 \xrightarrow{750°C \sim 900°C}$$

$$2Ca_2SiO_4 \cdot CaCO_3 \xrightarrow{\text{above } 900°C} 2Ca_2SiO_4 + CaO$$

Fig. 7 shows the result of X-ray diffraction of the burning piece which was made by the reaction of pure β-Ca_2SiO_4, $CaCO_3$ and CO_2 gas. We also found clearly the formation of $2Ca_2SiO_4 \cdot CaCO_3$ in this case.

At any rate, the evidence thus obtained supports the suggestion that the formation of $2Ca_2SiO_4 \cdot CaCO_3$ is influenced by the control of density of CO_2 gas, the quantity of clinker mineral and the temperature of reaction. Therefore we can know why $2Ca_2SiO_4 \cdot CaCO_3$ was not formed from raw material which does not change to clinker mineral at temperature under 900°C. The existence of Ca_3SiO_5 is presumed to accelerate the production of $2Ca_2SiO_4 \cdot CaCO_3$.

In both cases of the gas-solid reaction with raw material and the one with clinker, $CaCO_3$ was clearly re-crystalized as shown in Fig. 6 and Table 3.

The Reaction between SO_2 Gas and Raw Materal or Clinker

We made an experiment of the gas-solid reaction between SO_2 gas and raw material or clinker at a

Table 4. *The mineral composition of the burned pieces of raw material under current of SO_2 gas.*

Burning temperature °C	Forming mineral						Penetrative degree
	Ca_3SiO_5	β-Ca_2SiO_4	CaO	α-Quartz	$CaSO_4$	$3Ca_2SiO_4 \cdot 2CaSO_4$	
Room temp.			+++	++			0
500			+++	++			
550			+++	++			
600			+++	++	++		217.5
700			+++	++	++		
800			+++	+	+++		
900			++	+	++		
950			++	+	+++		426
1000			++	+	+++		
1050		−			+++	+	
1070					+++	++	2165
1100					+++	+++	>2800
1125					+++	++	>2800
1150					+++	++	>2800

Table 5. *The mineral composition of the burned pieces of clinker under current of SO_2 gas.*

Burning temperature °C	Forming mineral					Penetrative degree
	Ca_3SiO_5	β-Ca_2SiO_4	CaO	$CaSO_4$	$3Ca_2SiO_4 \cdot 2CaSO_4$	
Room temp.	+++	++				0
500	+++	++		−		60
550	+++	++		+		474
600	+++	++		++		>2800
700	+	+		++		>2800
800		++		++		
900		++		++		
950		++		+++		
1000		++		+++		
1050		++		+++	+	
1070		−		+++	+++	2800
1100				+++	+++	2800
1125		−		++	++	2800

fixed condition, 15°C per minute speed of rising temperature, keeping the aimed temperature constant for an hour and a 150 cc per minute speed of SO_2 flow.

Fig. 8 and Table 4 show the result of X-ray diffraction of the burned pieces by the reaction between SO_2 gas and raw material. Fig. 9 and Table 5 show the burned pieces of clinker under current of SO_2 gas. We can notice by these that there is a remarkable formation of $CaSO_4$ or $3Ca_2SiO_4 \cdot 2CaSO_4$ in both cases by the reaction of raw material and the one by clinker.

In case of the former, $CaSO_4$ is first formed at 600°C and $3Ca_2SiO_4 \cdot 2CaSO_4$ is formed when β-Ca_2SiO_4 begins to appear at 1,050°C. This double salt mineral grows and increases at 1,100°C. In case of the latter, the condition of the formation of $CaSO_4$ and $3Ca_2SiO_4 \cdot 2CaSO_4$ is similar to the former one. $CaSO_4$ is first formed at 550°C and $3Ca_2SiO_4 \cdot 2CaSO_4$ is formed at 1,050°C and this double salt mineral grows and increases at 1,100°C.

No doubt the formation of $CaSO_4$ is due to the decomposition of clinker minerals with the attack of SO_2 gas and the formation of $3Ca_2SiO_4 \cdot 2CaSO_4$ is due to the reaction between formed $CaSO_4$ and Ca_2SiO_4 in clinker. The SO_2 gas itself plays a very important part in the reaction as a catalyzer. Furthermore the existance of H_2O vapour may remarkably affect the reaction.

In reference to the result of the gas-solid reaction we show the result of the solid-solid reaction in Fig. 10. This shows the result of X-ray diffraction of the burned pieces which are products of the experiment of the reaction between the powder of synthesized belite ($2Ca_2SiO_4$) and the reagent of anhydrite ($CaSO_4$), in a proportion of 3: 2 at temperature over 1,100°C. It was found that $3Ca_2SiO_4 \cdot 2CaSO_4$ is rarely formed at 1,100°C and a little quantity of $3Ca_2SiO_4 \cdot 2CaSO_4$ is formed at 1,150°C.

Fig. 11 shows the relation between SO_3 content and burning temperature concerning the burned pieces formed by the reaction between SO_2 gas and raw material or clinker.

E. Vogel performed a similar experiment as ours (17). Fig. 12 shows the result of the experiment by him. The results of Vogel's experiment the condition of which are probably different from ours in the equipment, the quantity of gas-flow and the way of keeping of temperature etc., is almost similar to ours in case of raw material. However, there is a remarkable difference in the results between his experiment and our one in case of clinker.

In both experiments, Vogel's and ours, the quantity of absorbed SO_3 increases slowly as the temperature increases to 1,000°C. It decreases slowly as the temperature increases over 1,000°C in Vogel's experiment. In our experiment it increases rapidly as the temperature increases to 1,100°C and reaches to the maximum quantity at 1,100°C.

The increase of absorbed SO_3 between 500°C and 1,000°C means the formation of $CaSO_4$, while the rapid increase of absorbed SO_3 between 1,070°C and

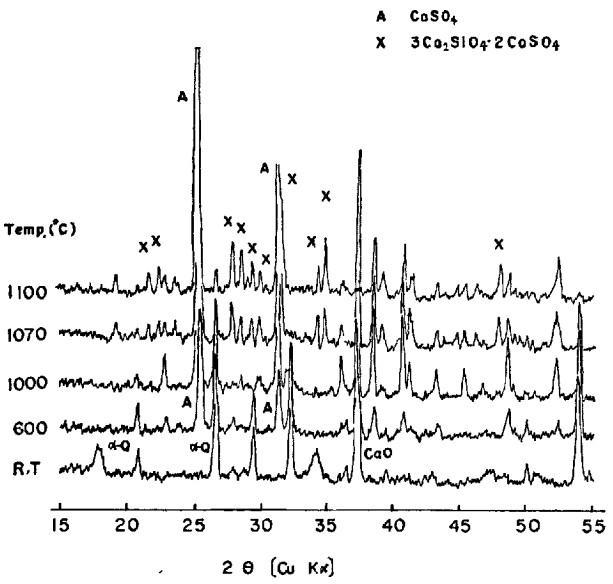

Fig. 8. *The X-ray diffraction patterns of the burned pieces of raw material under current of* SO_2 *gas.*

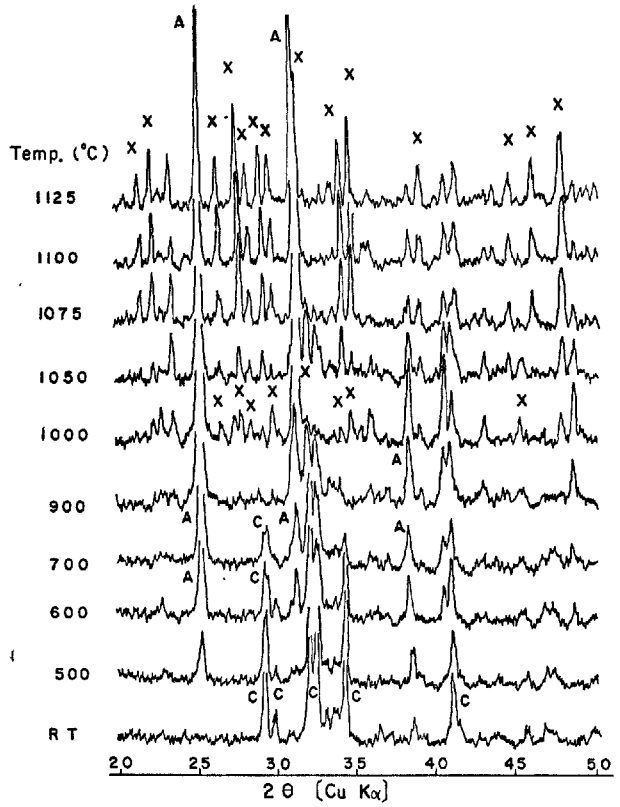

Fig. 9. *The X-ray diffraction patterns of the burned pieces of clinker under current of* SO_2 *gas.*

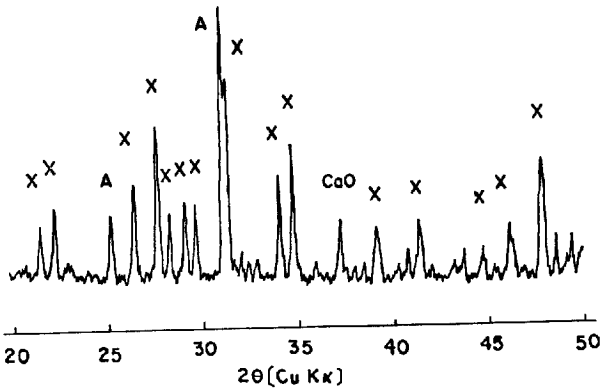

Fig. 10. $3Ca_2SiO_4 \cdot 2CaSO_4$ *synthesized from the solid-solid reaction between* β-Ca_2SiO_4 *and the reagent of* $CaSO_4$.

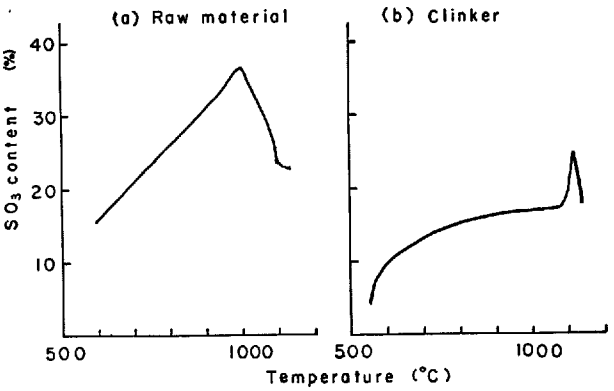

Fig. 11. *The relation between* SO_3 *content and burning temperature concerning the burned pieces of raw material or clinker under current of* SO_2 *gas.*

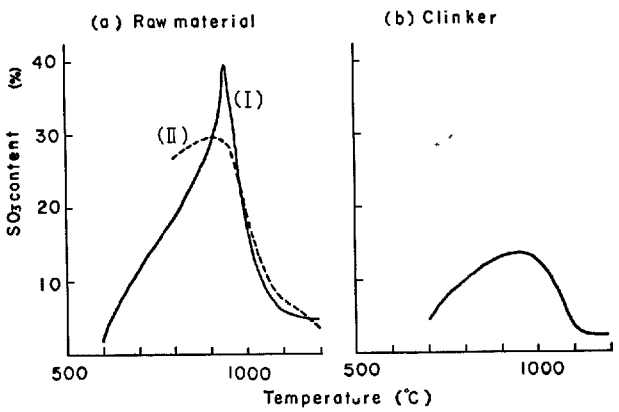

Fig. 12. *The relation between* SO_3 *content and burning temperature concerning the burned pieces of raw material or clinker under current of* SO_2 *gas.* (By E. Vogel)

1,100°C means the formation of $3Ca_2SiO_4 \cdot 2CaSO_4$. The earlier investigator did not find the phenomenon of the extraordinary absorption of SO_2 gas by clinker caused by the formation of $3Ca_2SiO_4 \cdot 2CaSO_4$.

The Reaction under Current of Mixed Gas

By the results of the above mentioned experiment we know that cement clinker is very easily decomposed by CO_2 gas or SO_2 gas.

It is presumed that general fuel gas consists of about 80 percent N_2 gas, less than 20 percent CO_2 gas and less than 1 percent SO_2 gas. Naturally, if we want to study about the gas-solid reaction in cement kiln, we must consider the effect of the mixed gas consisting mainly of N_2, CO_2 and SO_2, especially the effect of SO_2 as change of density of it.

We made the same experiment of gas-solid reaction as mentioned above using the mixed gas the composition of which is shown in Table 6. The apparatus for this experiment is the same as that used in the foregoing experiment.

The value of chemical analysis of raw material and clinker used here is shown in Table 7. No. 1 raw material is chosen as one of a little more alkali component, but No. 2 raw material as one of a little less alkali component. The clinker is the same as used in the foregoing experiment.

Each gas was passed into the burning tube of the furnace through the bin for mixing gas after it was dehydrated by conc H_2SO_4 solution and was measured by flow meter.

The conditions of experiment, speed in rising temperature, timing of the aimed temperature and the speed of gas flow etc., were the same as the above.

Tables 8, 9, 10 and 11 show the result of this experiment. The tables show the mineral composition of burned pieces after the reaction at each temperature. Data is derived from the result of X-ray diffraction. In these tables two signs are shown in each mineral component. The upper sign shows the quantity of the mineral component of the upper part of the pieces, from the surface down to the 3 cm, while the lower sign shows the lower part of the pieces, from the 3 cm to the bottom.

It was unavoidable that there was a few difference of the mineral component between the upper part and the lower one of the burned pieces, because the length of time of the aimed temperature was not enough for uniform reaction through the body in case of mixed gas. These tables, however, undoubtedly show the general tendency of the reaction in case of the mixed gas.

Table 8 and Table 9 show the results of the examinations of two kinds of raw material. The former shows the result for No. 1 raw material and the latter for No. 2 raw material. This experiment indicates that we can not find the double salt minerals derived from the gas-solid reaction between CO_2 or SO_2 gas and raw material, but find the single salt minerals, $CaCO_3$ and $CaSO_4$.

In contrast to this result, we found evidently the double salt minerals, $2Ca_2SiO_4 \cdot CaCO_3$ and $3Ca_2SiO_4 \cdot 2CaSO_4$ in the reaction by clinker as shown in Table 10 and Table 11. Table 10 shows the result of the reaction keeping the aimed temperature for one hour and Table 11 when the temperature is keeped for two hours.

The range of the producing temperature of each double salt minerals is clearly distinguishable: $2Ca_2SiO_4 \cdot CaCO_3$ is produced in range of temperatures from 800°C to 850°C, and $3Ca_2SiO_4 \cdot 2CaSO_4$ is from 900°C to 1,100°C. At 850°C $2Ca_2SiO_4 \cdot CaCO_3$ is decomposed to Ca_2SiO_4, CaO and CO_2.

In the reaction with the raw material the formation of $CaCO_3$ is dominant at temperature below 800°C and $CaSO_4$ above 700°C. In the reaction with the clinker the formation of $CaCO_3$ is barely seen in range of whole temperature and that of $CaSO_4$ is dominant at temperature above 700°C. By these results it seems reasonable to assume that even a small quantity of SO_2 gas by far predominates a large quantity of CO_2 gas at the reaction with raw material and clinker at high temperature.

Table 6. *The composition of the mixed gas.*

	Quantity of flow cc/min	Volume percent
N_2	960	79.5
CO_2	240	19.9
SO_2	7	0.6

Table 7. *The Chemical analysis of the materials for the test under current of the mixed gas. (Value of dry base.)*

	SiO_2	Al_2O_3	Fe_2O_3	CaO	Na_2O	K_2O	Total
No. 1 Raw material	22.76	5.60	3.48	66.91	0.15	0.36	99.26
No. 2 Raw material	22.52	5.38	3.36	66.01	0.42	0.59	98.28

Table 8. *The mineral composition of the burned pieces of No. 1 raw material under current of the mixed gas. (In case of keeping in 1 hour at the aimed temperature.)*

Burning temperature °C	Tested part	Forming mineral						Penetrative degree
		Ca_3SiO_5	β-Ca_2SiO_4	CaO	$CaSO_4$	$CaCO_3$	α-Quartz	
800	Upper				++	++++	+++	40
	Lower				+	++++	+++	
950	Upper			++++	+++		+++	47
	Lower			++++	+		+++	
1050	Upper		++	++++	++		+++	40
	Lower			++++			+++	
1150	Upper		++	++++	+		++	196
	Lower		++	++++			++	
1200	Upper		+++	+++				760
	Lower		+++	+++				

Table 9. *The mineral composition of the burned pieces of No. 2 raw material under current of the mixed gas. (In case of keeping for 1 hour at the aimed temperature.)*

Burning temperature °C	Tested part	Forming minerals						Penetrative degree
		Ca_3SiO_5	β-Ca_2SiO_4	CaO	$CaSO_4$	$CaCO_3$	α-Quartz	
600	Upper					++++	+++	17
	Lower					++++	+++	
700	Upper				+	++++	+++	10
	Lower				−	++++	++	
800	Upper				++++	++++	+	70
	Lower				−	++++	++	
900	Upper			+++	++	++	+	30
	Lower			++++	+		++	
950	Upper			++++	+++		+	35
	Lower			++++	−		+	
1000	Upper		−	++++	+		+	30
	Lower		−	++++			+	
1050	Upper		++	++++				52
	Lower		++	++++				
1100	Upper		+++	+++				52
	Lower		+++	+++				
1150	Upper		+++	+++				190
	Lower		+++	+++				
1200	Upper		+++	+++				740
	Lower		+++	+++				

++++ Remarkably much +++ Very much ++ Much + Proper − A little

Table 10. *The mineral composition of the burned pieces of the clinker under current of the mixed gas. (In case of keeping for 1 hour at the aimed temperature.)*

Burning temperature °C	Tested part	Forming minerals							Penetrative degree
		Ca_3SiO_5	β-Ca_2SiO_4	CaO	$CaSO_4$	$3Ca_2SiO_4 \cdot 2CaSO_4$	$2Ca_2SiO_4 \cdot CaCO_3$	$CaCO_3$	
500	Upper	+++	+++						27
	Lower	+++	+++						
600	Upper	+++	+++						45
	Lower	+++	+++						
700	Upper	++	+++		+++				156
	Lower	++	+++	−					
800	Upper	++	+++	−	+++				285
	Lower	+	++				++	++	
850	Upper	−	+++	++	+++		++	−	562
	Lower	+	+++	++			++		
900	Upper	−	+++		+++				300
	Lower	+	+++	++					
950	Upper		++	++	+++	++			1000
	Lower	−	+++	+++					
1000	Upper	−	+++	+++	+				152
	Lower	−	+++	+++					
1050	Upper	+	+++	+++	−				215
	Lower	+	+++	+++	−				
1100	Upper	−	+++	+++	−				215
	Lower	+	+++	+++					
1150	Upper	+	+++	+++	−				265
	Lower	−	+++	+++					
1200	Upper	+	+++	++					415
	Lower	++	+++	++					

Effect by Alkali Component upon the Gas-Solid Reaction

In the foregoing experiment of the gas-solid reaction we used both raw material and clinker of a small quantity of alkali component, not more than 1 percent of R_2O.

It is widely known that the flying dust at the end side of the kiln contains a large quantity of alkali sulphate. As it is apt to condense at the end part of the kiln, alkali sulphates are presumed to be one of the cause of the generation of the ring (18, 19, 20, 21).

Therefore, we made an experiment of the gas-solid reaction using the raw material and the clinker consisting of a great deal of alkali components.

The manner of the experiment is the same as above. We selected K_2CO_3 as alkali component as its vapor pressure is moderate, and added it to the raw material or the clinker, which were used in the foregoing experiment under current of saturated gas, so as to K_2O is calculated 3, 6 and 9 weight percent for the

Table 11. *The mineral composition of the burned pieces of the clinker under current of the mixed gas. (In case of keeping for 2 hours at the aimed temperature.)*

Burning temperature °C	Tested part	Forming minerals							Penetrative degree
		Ca_3SiO_5	β-Ca_2SiO_4	CaO	$CaSO_4$	$3Ca_2SiO_4 \cdot 2CaSO_4$	$2Ca_2SiO_4 \cdot CaCO_3$	$CaCO_3$	
700	Upper	+	+++		+++				210
	Lower		++		++				
800	Upper	−	++		+++				490
	Lower		++				+++		
850	Upper		++		+++				275
	Lower	+	+++	++					
900	Upper		++		+++	++			725
	Lower	−	+++	+					
950	Upper		++	−	+++	+			210
	Lower	++	+++	++					
1000	Upper		+++	+++	−	+			325
	Lower	+	+++	+++					
1050	Upper	−	+++	+++		+			255
	Lower	+	+++	+++					
1100	Upper		++	++	+	++			255
	Lower		+++	+++					
1150	Upper		+++	+++					325
	Lower		+++	+++					
1200	Upper	−	+++	+++					505
	Lower	−	+++	+++					

raw material or the clinker. The values of chemical analysis of the raw material and clinker are much the same as in the foregoing experiment.

The mineral components of the burned pieces after the gas-solid reaction were made clear by X-ray diffraction. Table 12, Table 13 and Table 14 show the mineral components of the burned pieces of raw material with K_2O added. Table 15, Table 16 and Table 17 show mineral components of the burned pieces of clinker with K_2O added. Fig. 13, Fig. 14 and Fig. 15 show parts of the results of X-ray diffraction of the burned pieces.

We found both single salt mineral and double salt mineral $CaCO_3$, $CaSO_4$ and $2Ca_2SiO_4 \cdot CaCO_3$ in the foregoing experiments, at the proper temperature, and also found K_2SO_4 which had not been found in the foregoing experiments. We found an unknown mineral Y also.

This unknown mineral could be found remarkably well in the samples picked up from the pile that adhered to the surface of the water tube of the wasted gas boiler. Fig. 4 shows the result of X-ray diffraction of the sample obtained from one place in the gas boiler.

We presumed that this unknown mineral Y must be a double salt mineral consisting of $CaSO_4$ and $(K, Na)_2SO_4$. In order to ascertain this assumption we made the experiment of gas-solid reaction among K_2CO_3, $CaCO_3$ and SO_2 gas. The manner of the experiment for the reaction is the same as the one in the foregoing experiment. Two kinds of solid material, K_2CO_3 and $CaCO_3$ were inserted into the center of the tube of the furnace.

Fig. 16 shows the result of X-ray diffraction of the burned sample in range of temperatures from 600°C to 900°C. $CaCO_3$ and K_2CO_3 were mixed in the pro-

Table 12. *The mineral composition of the burned 3% K_2O pieces mixing raw material and K_2CO_3 under current of the mixed gas. (In case of keeping for 1 hour at the aimed temperature.)*

Burning temperature °C	Tested part	Forming minerals								Penetrative degree
		β-Ca_2SiO_4	CaO	$CaSO_4$	$2Ca_2SiO_4 \cdot CaCO_3$	$CaCO_3$	Y	K_2SO_4	α-Quartz	
800	Upper	+		+++		+++			+	15
	Lower	+				+++			+	
900	Upper	++	+++							15
	Lower	++	+++							
950	Upper	++	+++							15
	Lower	++	+++							
1000	Upper	++	+++							15
	Lower	++	+++							
1100	Upper	+++	+++					++		20
	Lower	+++	+							

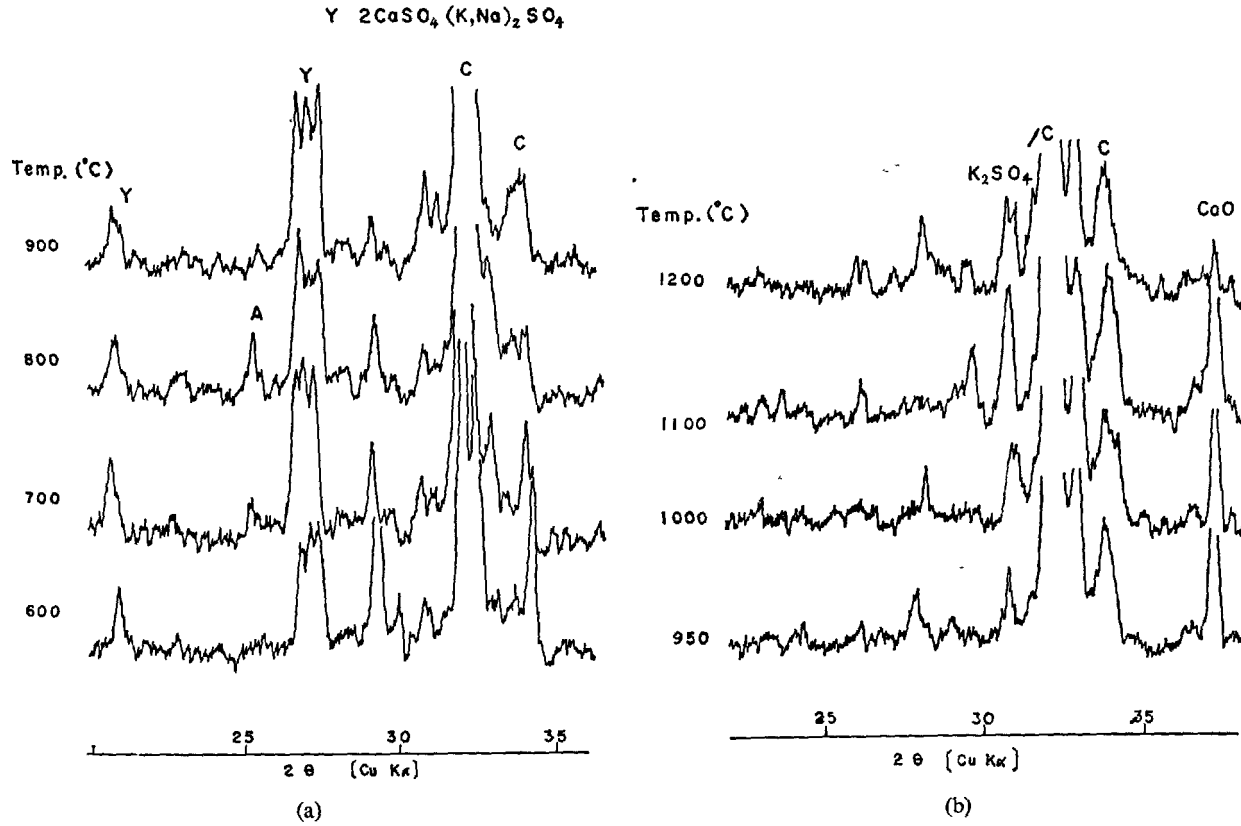

Fig. 13. *'The X-ray diffraction patterns of the burned 6% K_2O pieces mixing clinker and K_2CO_3 under current of SO_2 gas. (The ones of upper side of the pieces)*

Table 13. *The mineral composition of the burned 6% K_2O pieces mixing raw material and K_2CO_3 under current of the mixed gas. (In case of keeping for 1 hour at the aimed temperature.)*

Burning temperature °C	Tested past	Forming minerals								Penetrative degree
		β-Ca_2SiO_4	CaO	$CaSO_4$	$2Ca_2SiO_4 \cdot CaCO_3$	$CaCO_3$	Y	K_2SO_4	α-Quartz	
800	Upper	+			+	+++	+		−	55
	Lower	+				+++			+	
900	Upper	+++	+++				+	+		455
	Lower	+++	+++					+		
950	Upper	+++	+++					+		270
	Lower	+++	+++							
1000	Upper	+++	+++					+		210
	Lower	+++	+++							
1100	Upper	+++	+++					+		340
	Lower	+++	+++					+		
1200	Upper	+++	++					+		90
	Lower	+++	++					+		

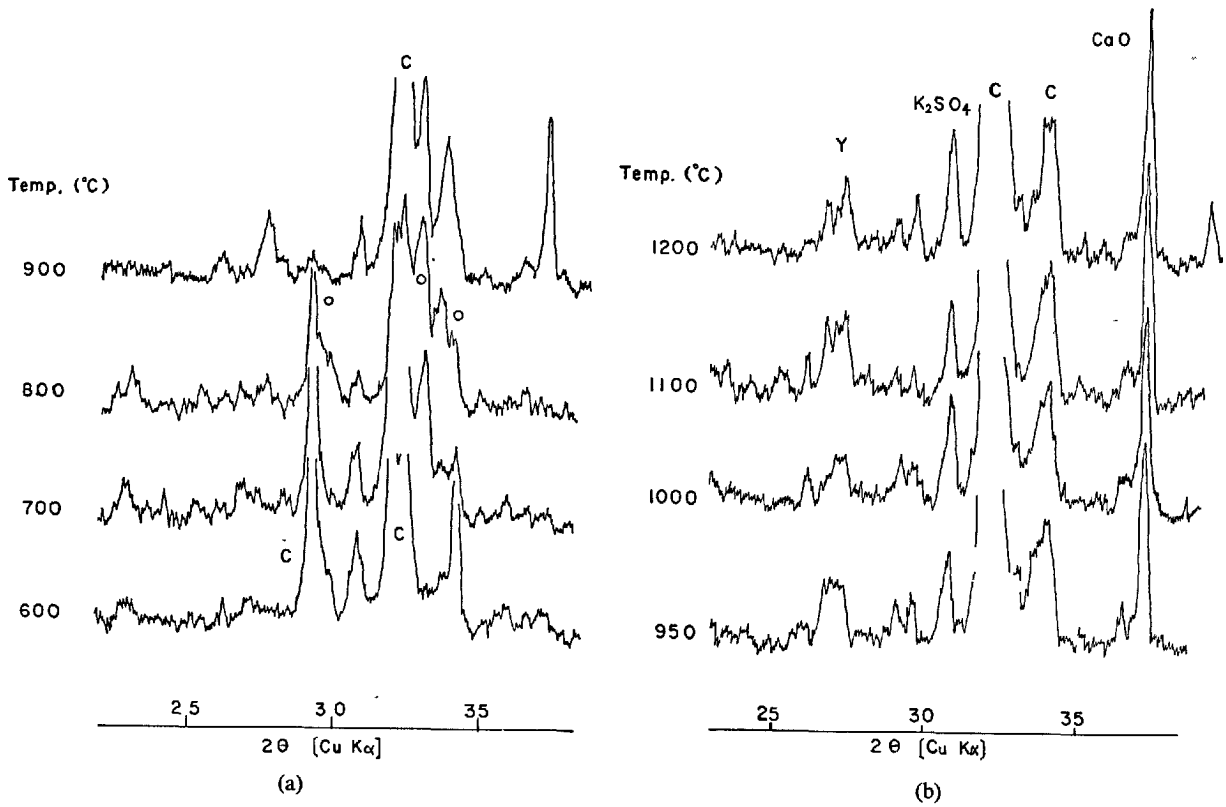

Fig. 14. *The X-ray diffraction patterns of the burned 6% K_2O pieces mixing clinker and K_2CO_3 under current of SO_2 gas. (The ones of lower side of the pieces)*

Table 14. *The mineral composition of the burned 9% K_2O pieces mixing raw material and K_2CO_3 under current of the mixed gas. (In case of keeping for 1 hour at the aimed temperature.)*

Burning temperature °C	Tested past	Forming minerals								Penetrative degree
		β-Ca_2SiO_4	CaO	$CaSO_4$	$2Ca_2SiO_4 \cdot CaCO_3$	$CaCO_3$	Y	K_2SO_4	α-Quartz	
800	Upper	+++		−	+++	+++	+++			340
	Lower	++			+++	+++				
900	Upper	+++	+++				++		++	1460
	Lower	+++	+++						++	
950	Upper	+++	+++						++	970
	Lower	+++	+++							
1000	Upper	+++	+++						++	680
	Lower	+++	+++						++	
1100	Upper	+++	+++						++	1110
	Lower	+++	+++						++	

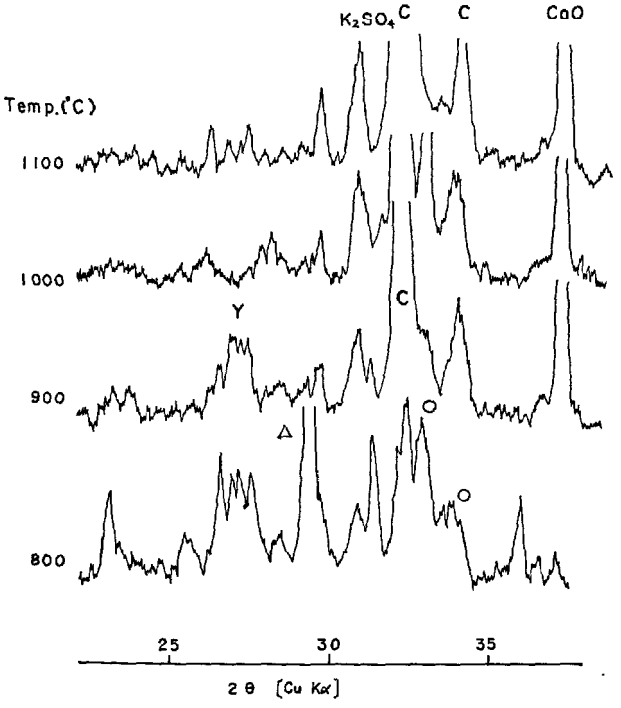

Fig. 15. *The X-ray diffraction patterns of the burned 6% K_2O pieces mixing raw material and K_2CO_3 under current of SO_2 gas. (The ones of upper side of the pieces)*

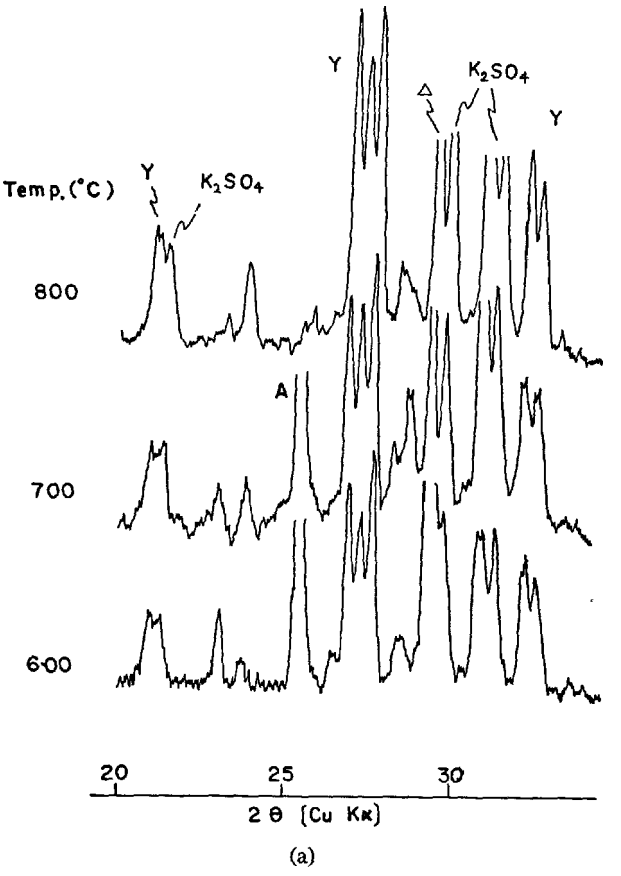

Fig. 16. *The X-ray diffraction patterns of the burned pieces mixing K_2CO_3 and $CaCO_3$ in the proportion of 1: 2 under current of SO_2 gas.*

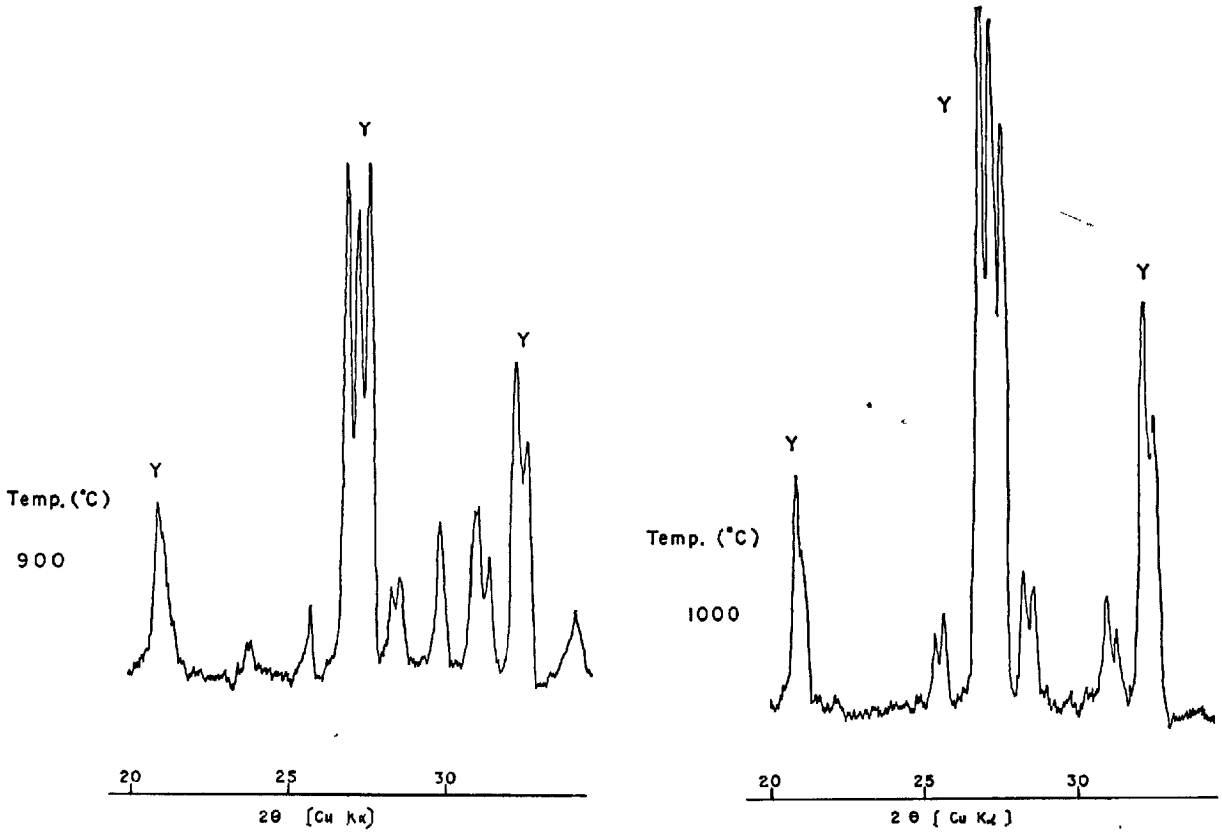

Fig. 16

Table 15. *The mineral composition of the burned 3% K_2O pieces mixing clinker and K_2CO_3 under current of the mixed gas. (In case of keeping for 1 hour at the aimed temperature.)*

Burning temperature °C	Tested past	Forming minerals							Penetrative degree
		Ca_3SiO_5	β-Ca_2SiO_4	CaO	$CaSO_4$	$2Ca_2SiO_4 \cdot CaCO_3$	$CaCO_3$	Y	
700	Upper	++	+++		++			+	250
	Lower	++	+++		−		−	+	
800	Upper	++	+++		+++			−	2110
	Lower		++			+++	+++		
900	Upper		+++	++				+	1310
	Lower		+++	+++					
950	Upper		+++	++				++	1200
	Lower		+++	+++					
1000	Upper		+++	++				+	610
	Lower		+++	++					
1100	Upper		+++	+++				−	570
	Lower		+++	+++					
1200	Upper		+++	++					540
	Lower		+++	++					

Table 16. *The mineral composition of the burned 6% K_2O pieces mixing clinker and K_2CO_3 under current of the mixed gas. (In case of keeping for 1 hour at the aimed temperature.)*

Burning temperature °C	Tested past	Forming minerals								Penetrative degree
		$Ca_3Si_2O_5$	β-Ca_2SiO_4	CaO	$CaSO_4$	$2Ca_2SiO_4 \cdot CaCO_3$	$CaCO_3$	Y	K_2SO_4	
600	Upper	++	+++					++		95
	Lower	+++	+++							
700	Upper	+	+++					++		120
	Lower	+	++				+++	+		
800	Upper	+	+++		+			++		350
	Lower		+			+++				
900	Upper		+++					++		2180
	Lower		+++	++						
950	Upper		+++	++				+	+	2150
	Lower		+++	+++						
1000	Upper		+++	++				−	+	1110
	Lower		+++	++						
1100	Upper		+++	++				+	+	930
	Lower		+++	++					+	
1200	Upper		+++	++				+	+	300
	Lower		+++	++					+	

portion of 2: 1. We could detect three characteristic diffraction peak in a row from 27° to 28° in 2θ as shown in Fig. 16. These three characteristic diffraction peaks coincide with the characteristic peaks of the unknown mineral Y.

Other experiment for the solid-solid reaction between $CaSO_4$ and K_2SO_4 in proportion 2: 1, 1: 1 and 3: 1 at each temperature proved that the three characteristic diffraction peaks stood in a row from 27° to 28° in 2θ must be of $2CaSO_4 \cdot K_2SO_4$.

The burned pieces mixed in 2: 1 proportion have neither diffraction peaks of $CaSO_4$ nor ones of K_2SO_4, but have only several characteristic lines that is attributed to the synthesized double salt mineral. The burned pieces mixed in 1: 1 proportion have the refractive lines of unreacted K_2SO_4 in addition to the ones of the synthesized double salt mineral, and the burned pieces mixed in 3: 1 proportion have the refractive lines of unreacted $CaSO_4$ in addition to the synthesized double salt mineral. It seems most reasonable to conclude that this synthesized double salt mineral is $2CaSO_4 \cdot K_2SO_4$. Fig. 17 shows one part of the result of X-ray analysis of the burned pieces in this experiment of solid-solid reaction.

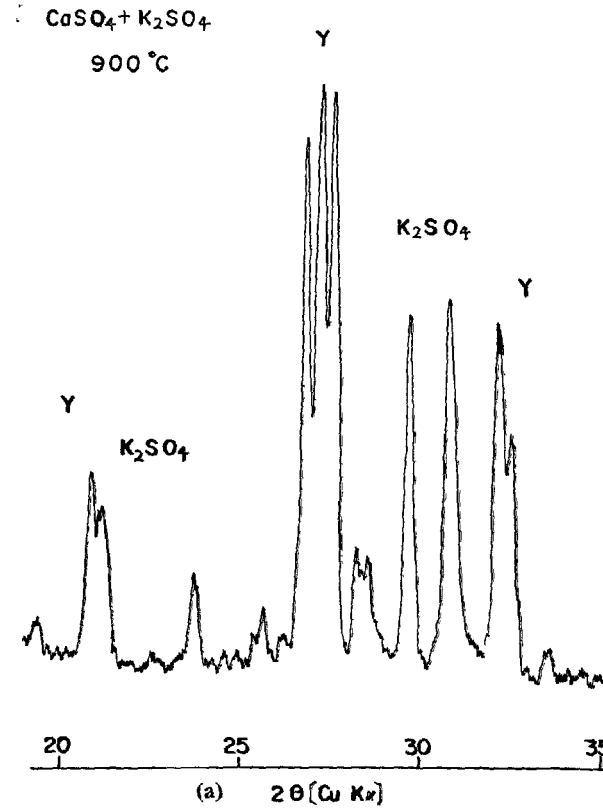

Fig. 17. *Some of the X-ray diffraction patterns of the burned pieces mixing $CaSO_4$ and K_2SO_4.*

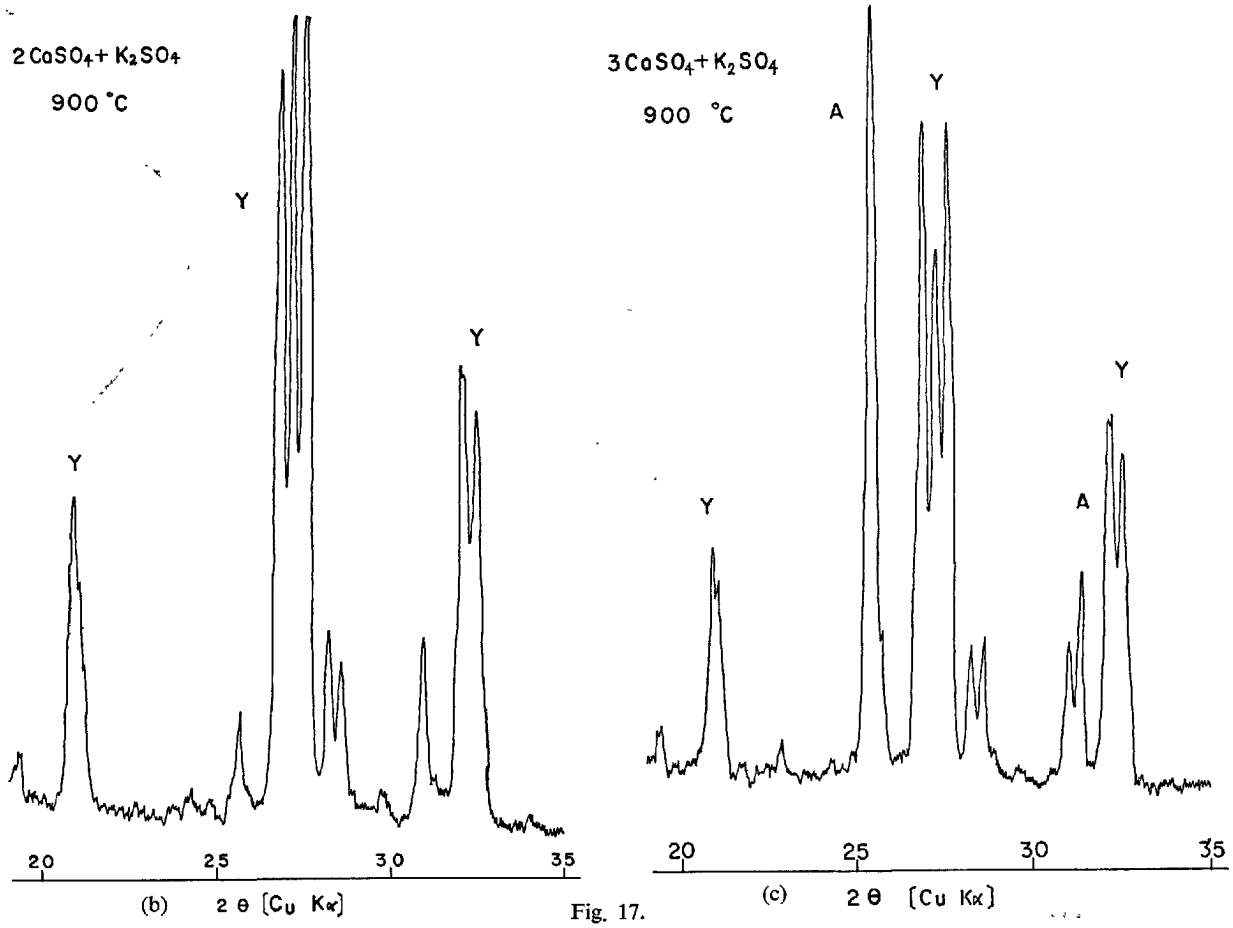

Fig. 17.

Table 17. *The mineral composition of the burned 9% K_2O pieces mixing clinker and K_2CO_3 under current of the mixed gas. (In case of keeping for 1 hour at the aimed temperature.)*

Burning temperature °C	Tested past	Forming minerals								Penetrative degree
		Ca_3SiO_5	β-Ca_2SiO_4	CaO	$CaSO_4$	$2Ca_2SiO_4 \cdot CaCO_3$	$CaCO_3$	Y	K_2SO_4	
700	Upper	++	+++		++			−		160
	Lower	++	+++				++			
800	Upper	++	+++		+			+		2500
	Lower		+++			+++				
900	Upper		+++	++				+	++	2500
	Lower		+++	++						
950	Upper		+++	++					++	2500
	Lower		+++	+++						
1000	Upper		+++	++					++	2500
	Lower		+++	++						
1100	Upper		+++	+++					+	2080
	Lower		+++	+++						
1200	Upper		+++	++					++	980
	Lower		+++	+++					++	

Recently we chanced to read the paper "The Ternary System K_2SO_4–$MgSO_4$–$CaSO_4$" by J. J. Rowe, G. W. Morey and C. C. Silber. We got the information of the binary system K_2SO_4 from it and knew that $2CaSO_4 \cdot K_2SO_4$ was already named "calcium langbeinite" (16).

The index of optic refraction of our synthesized double salt mineral shows about 1.550, while the double salt mineral show about 1.553 which is a component of the sample picked from the pile in the gas boiler. This little difference is supposed to be caused by other chemical elements which are soluble in very small quantity.

In view of the above facts it was made clear that a great quantity of alkali component condensed at the end part of the kiln easily reacts with SO_2 gas forming the double salt mineral, $2CaSO_4 \cdot K_2SO_4$, in addition to the single salt mineral, K_2SO_4, and both salt minerals are contained in abundance in the pile or the ring.

One of Physical Properties of Double Salt Minerals

We could find a few double salt minerals, $2Ca_2SiO_4 \cdot CaCO_3$, $3Ca_2SiO_4 \cdot 2CaSO_4$ and $2CaSO_4 \cdot K_2SO_4$ in addition to re-crystallized single salt minerals, $CaCO_3$, $CaSO_4$ and K_2SO_4 both in the ring and in the pile at end part of the kiln.

On the other hand we could succeed in synthesizing those double salt minerals by means of the gas-solid reaction between raw material or clinker and CO_2 or SO_2 gas.

Furthermore we found the character of strong coagulation of those double salt minerals in the course of the gas-solid reaction.

We show the result of the experiment of coagulation by the following data. We are sure that this data gives important suggestion to the elucidation of the cause of generation of the ring.

Hitherto various kinds of means have been devised concerning measurement of the strength of adhesion or coagulation of solid grains at lower or room temperature, but it has been hard to apply a higher temperature for industrial purposes.

We devised an original apparatus for the measurement of the strength of coagulation of the burned pieces in the gas-solid reaction. Outline of the apparatus is shown in Fig. 18. It was changed from the Vicker's cement-setting test apparatus.

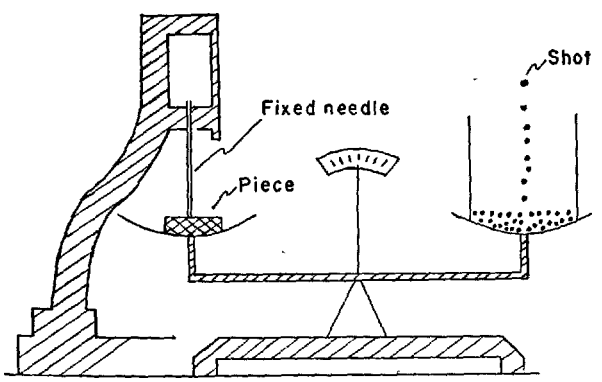

Fig. 18. *Outline of the apparatus for the measurement of the strength of coagulation.*

We regarded the penetrative degree of the fixed needle as the strength of coagulation of the burned pieces on the one side of dish of the balance. The penetrative degree was measured by the weight of shot on the other side of the dish just when the fixed needle penetrated into the bottom of the piece. The figure of the penetrative degree of the fixed needle is written down in each foregoing table which show the mineral composition of the burned pieces at the gas-solid reaction, Tables 3, 4, 5, 8, 9, 10, 11, 12, 13, 14, 15, 16, 17.

Figs. 19, 20, 21, 22 show graphs of the temperature and the penetrative degree of the needle obtained from the result of the experiment of each foregoing

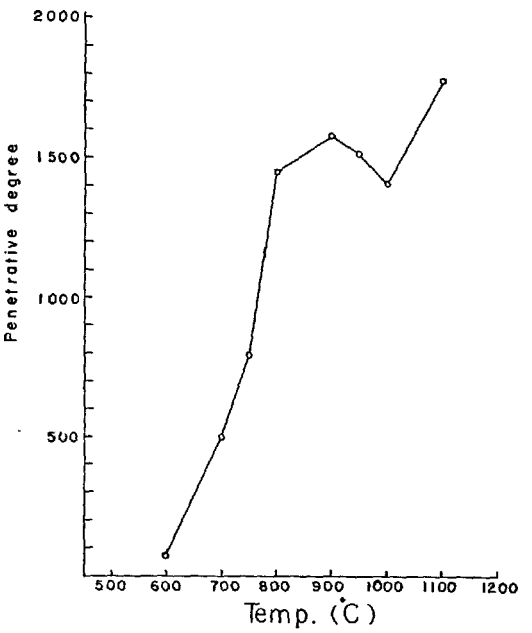

Fig. 19. *The relation between the burning temperature and the penetrative degree of the burned pieces of clinker under current of saturated* CO_2 *gas.*

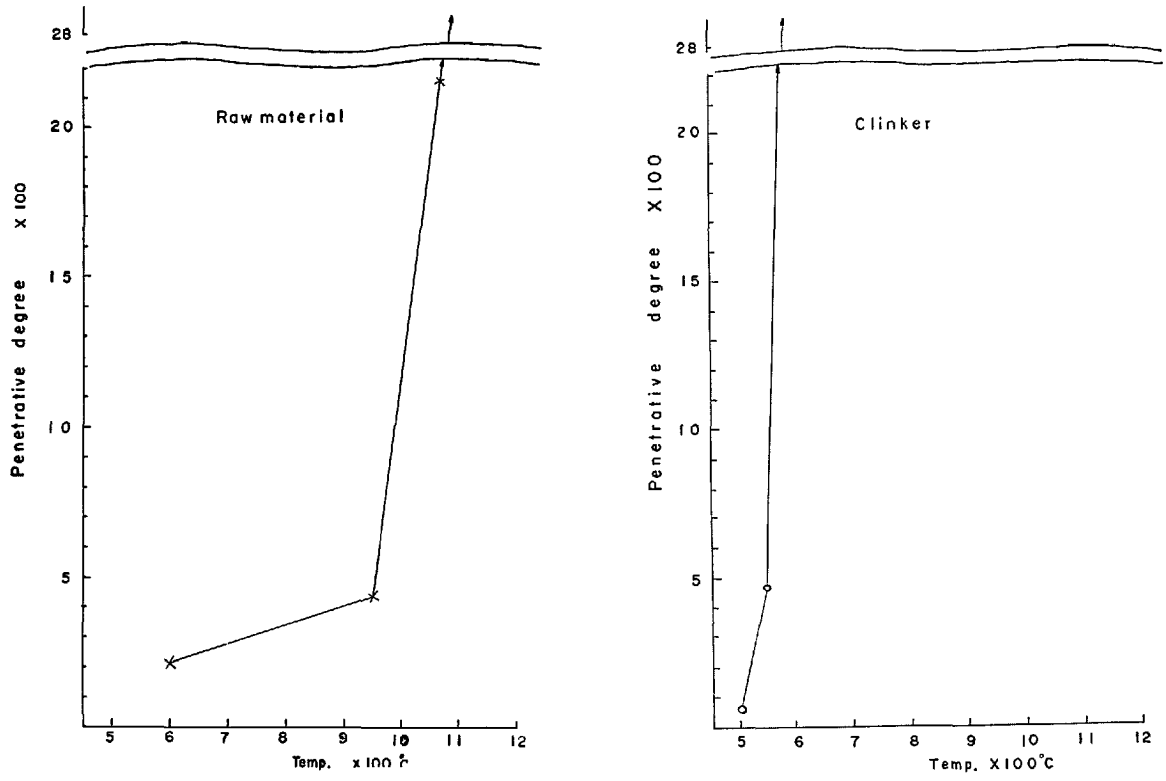

Fig. 20. *The relation between the burning temperature and the penetrative degree of the burned pieces of raw material and clinker under current of saturated* SO_2 *gas.*

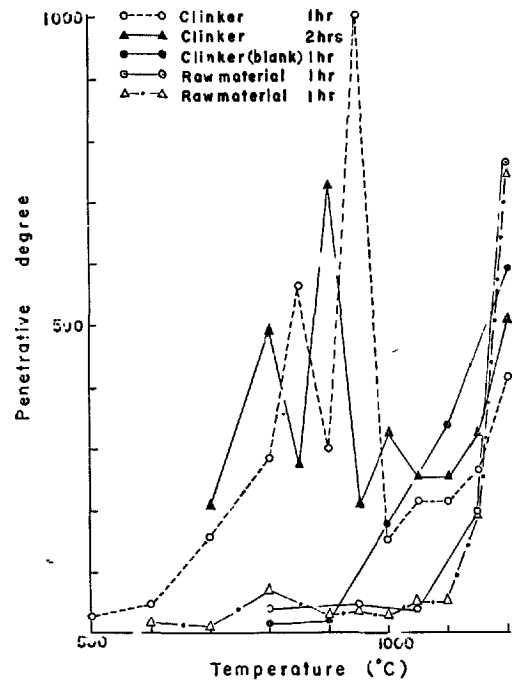

Fig. 21. *The relation between the burning temperature and the penetrative degree of the burned pieces of raw material or clinker under current of the mixed gas.*

gas-solid reaction.

Fig. 19 shows graph of the burning temperature and the penetrative degree of the burned pieces in the gas-solid reaction between saturated CO_2 gas and raw material or clinker. Fig. 20 shows the one in the reaction between saturated SO_2 gas and raw material or clinker. Fig. 21 shows the one in the reaction between the mixed gas and raw material or clinker. Fig. 22 shows the one in the reaction between the mixed gas and the clinker to which a little quantity of K_2O are added.

From Fig. 19 we know that the penetrative degree of burned pieces in the reaction with clinker increases remarkably at 800°C as the quantity of $2Ca_2SiO_4 \cdot CaCO_3$ increases. On the other hand, there shows very small quantity of the penetrative degree of pieces at each burning temperature in the reaction with raw material, because $2Ca_2SiO_4 \cdot CaCO_3$ is barely formed from raw material unable to produce $2Ca_2SiO_4$ easily.

From Fig. 20 we know that a very rapid increase of the penetrative degree is shown at 1,050°C as $3Ca_2SiO_4 \cdot 2CaSO_4$ is formed in the reaction with raw material. In the reaction with clinker, however,

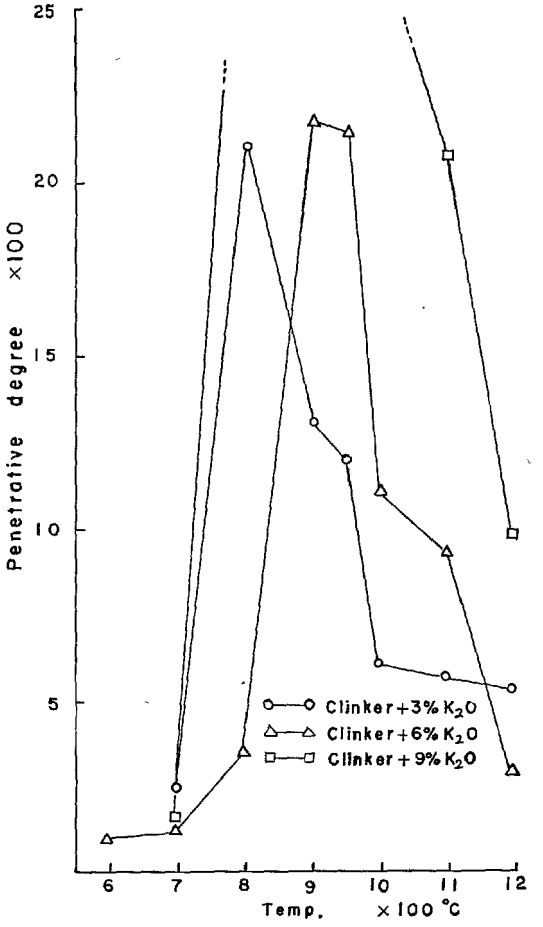

Fig. 22. *The relation between the burning temperature and the penetrative degree of the burned pieces of clinker* K_2O *added under current of the mixed gas.*

very rapid increase of the penetrative degree is shown at 600°C as $CaSO_4$ is formed. The piece burned at 1,070°C forming $3Ca_2SiO_4 \cdot 2CaSO_4$ shows very strong coagulation in appearance. Its penetrative degree is far over the limit of measurement.

From Fig. 21 we know that extraordinary increase of the penetrative degree is shown at the range of temperatures from 800°C to 1,000°C in the reaction between the mixed gas and clinker. On the contrary no increase of the penetrative degree is shown in the reaction with raw material and sintering appears at 1,200°C. It is surprising that even a very small quantity of SO_2 gas gives considerable effect on the penetrative degree of burned pieces producing $3Ca_2SiO_4 \cdot 2CaSO_4$.

From Fig. 22 we know that an extraordinary increase of the penetrative degree is shown at the range of the temperatures from 800°C to 1,000°C in the reaction between the mixed gas and clinker with addition of K_2O. It is probably caused by the formation of $2K_2SO_4 \cdot CaSO_4$. The increase of the penetrative degree in the reaction with raw material with addition of K_2O is far less than the one in the reaction with clinker by addition of K_2O.

Conclusion

From the investigation for the detail of mineral composition of ring we found ordinarily some kind of double salt minerals, $2Ca_2SiO_4 \cdot CaCO_3$, $3Ca_2SiO_4 \cdot 2CaSO_4$ and $2CaSO_4 \cdot K_2SO_4$ besides single salt minerals, $CaCO_3$, $CaSO_4$ and $(K, Na)_2SO_4$, in the texture of ring.

As we assumed that these salt minerals found in cement kiln were formed by gas-solid reaction between CO_2 or SO_2 of fuel gas and raw material or clinker in cement burning, we tried to make an experiment to verify the existence of this reaction.

The experiment was made by burning raw material or clinker in the electric furnace at each temperature under the current of CO_2 or SO_2 gas.

The results of this experiment led to determine exactly the forming condition of these salt minerals in burning of raw material or clinker under current of CO_2 or SO_2 gas.

In the reaction between saturated CO_2 gas and clinker, $CaCO_3$ was newly formed at the range of temperatures from 700°C to 900°C and $2Ca_2SiO_4 \cdot CaCO_3$ was formed remarkably well from 750°C to 900°C, but in the reaction between CO_2 gas and raw material $2Ca_2SiO_4 \cdot CaCO_3$ was not observed. It is supposed that gas density, temperature condition and volume of clinker minerals, especially volume of Ca_3SiO_5 play an important role in the formation of $2Ca_2SiO_4 \cdot CaCO_3$.

In the reaction between saturated SO_2 gas and raw material or clinker, $CaSO_4$ was newly formed well in the range of temperatures from 550°C to 1,150°C and $3Ca_2SiO_4 \cdot 2CaSO_4$ was formed well from 1,050°C to 1,150°C. It is probable that SO_2 gas has the action of catalyzer for acceleration of the formation of $3Ca_2SiO_4 \cdot 2CaSO_4$.

On the other hand, in the reaction between the

mixed gas, N_2 of 79.5 vol. percent, CO_2 of 19.9 vol. percent and SO_2 of 0.6 vol. percent, and clinker $CaCO_3$ was not newly formed in the range of temperatures used, but $CaSO_4$ was dominant above 700°C. In this case $2Ca_2SiO_4 \cdot CaCO_3$ was formed in the range of temperatures from 800°C to 850°C and $3Ca_2SiO_4 \cdot 2CaSO_4$ was formed from 900°C to 1,100°C. We could conclude that even a small quantity of SO_2 gas by far predominates than a large quantity of CO_2 gas in the reaction with raw material and clinker at high temperature. In the reaction between the mixed gas and raw material we could synthesize $CaCO_3$ and $CaSO_4$, however could not do the double salt minerals at each temperature.

In the reaction between the mixed gas and raw material and clinker to which K_2O of 3, 6 and 9 wt. percent was added, $2CaSO_4 \cdot K_2SO_4$ was formed at 600°C and remarkably well in the range of temperatures from 600°C to 900°C. From this fact we assumed that after clinker minerals, especially alite (Ca_3SiO_5), was dissociated to belite (Ca_2SiO_4) and CaO, $CaSO_4$ was formed by the reaction between CaO and SO_2 gas and K_2SO_4 was formed from K_2O, then the double salt mineral ($2CaSO_4 \cdot K_2SO_4$) was formed by the reaction between $CaSO_4$ and K_2SO_4.

Furthermore we found that the double salt minerals show greater strength of coagulation than clinker minerals. We verified this fact by the original experiment.

The results obtained from these experiments should give important suggestions to the research about the cause of the generation of the ring and also about the temperature condition of each inner part of kiln where the ring adheres.

References

1. D. R. Zollinger, "Der Einfluss der Rohmaterial komponenten auf die Zementart und auf den Brennprozess", Zement **21,** 419–424 (1932).
2. G. Mussgung, "Ansatzbildung in Zementdrehöfen und Futterhaltbarkeit", Zement-Kalk-Gips **1,** 41–46 (1948).
3. K. Konopicky, "Beitrag zur Frage der Ansatzbildung in Drehrohröfen", Zement-Kalk-Gips **4,** 240–245 (1951).
4. H. zur Strassen, "Auskleidung der Sinterzone von Zementdrehöfen", Zement-Kalk-Gips **5,** 356–361 (1952).
5. F. Matouschek, "Ansatzringe im Zementdrehöfen", Tonind. Ztg. **77,** 160–162 (1953).
6. J. Slegten, "Beitrag zum Studium der Ringbildung in Zement-Drehöfen", Zement-Kalk-Gips **9,** 397–402 (1956).
7. G. Witols, "Die Bekämpfung von Sulfatringen im Drehöfen", Zement-Kalk-Gips **12,** 18–20 (1959).
8. G. Witols, "Die Bekämpfung von Sulfatringen im Drehöfen", Zement-Kalk-Gips **15,** 205–207 (1962).
9. A. Majadic and H. E. Schwiete, "Über die Ansatzbildung im Drehöfen", Zement-Kalk-Gips **12,** 89–101 (1959).
10. A. Majadic and H. E. Schwiete, "Haftfestigkeit des Zementklinkeransatzes auf basischen feuerfesten Steinen", Zement-Kalk-Gips **15,** 45–51 (1962).
11. M. Amafuji, "Occurance of spurrite in the cement manufacture process" (in Japanese), Jour. Miner. Soc. Japan **6,** 285–316 (1964).
12. N. Sundius and O. Peterson. "Doppelvereinigung von Sulfat und Silikat aus Sogenannten Sulfatringen in den Zementöfen in Limhamn", Radex-Rundschau **2,** 100–103 (1960).
13. Y. Ono, M. Amafuji and T. Okumura, "Double salt from sulfate rings adhered to the wall of rotary kiln" (in Japanese), Jour. Research Onoda Cement Company **17,** 1–15 (1966).
14. C. E. Tilley, "Tricalcium disilicate (rankinite), A new mineral from scawt hill, Co. Antrim", Mineralog. Mag. **26,** 190–196 (1942).
15. N. L. Bowen, "Progressive metamorphism of siliceous limestone and dolomite", Jour. Geol. **48,** 225–274 (1940).
16. J. J. Rowe, G. W. Morey and C. C. Silber, "The ternary system K_2SO_4–$MgSO_4$–$CaSO_4$" Jour. Inorg. Nucl. Chem. **29,** 925–942 (1967).
17. E. Vogel, "Zum Problem der Stauringbildung in Zementdrehöfen (I, Teil)", Silikattechnik **9,** 361–364 (1958).
18. H. E. Schwiete, "Der einfluss der Tonminerale auf die Staubbildung beim Klinkerbrand", Zement-Kalk-Gips **9,** 351–357 (1956).
19. E. Vogel, "Zum Problem der Stauringbildung in Zementdrehöfen (II, Teil)", Silikattechnik **9,** 449–452 (1958).
20. E. Vogel, "Zum Problem der Stauringbildung in Zementdrehöfen (III, Teil)", Silikattechnik **9,** 502–505 (1958).
21. H. Carisen, "Behavior of alkalies during the burning process", Rock Products **69,** 87 (1966).

Supplementary Paper I-94 Problem of Admixtures

Maxim M. Sichov*

Synopsis

The influence of raw material admixtures and alloying additions on the properties of the liquid are considered in the paper, (viscosity, electrical conductivity, surface tension) as well as the peculiarities of clinker sintering and the microstructure in the presence of admixtures. The influence of admixtures and alloying additions on the properties of cement is also discussed. The role of BaO, SrO, Cr_2O_3, R_2O, P_2O_5, B_2O_3, SO_3, TiO_2, Mn_2O_3 in the formation of tricalcium silicate has been found. It has been shown that in the presence of P_2O_5 and B_2O_3 the passivation of SiO_2 and CaO takes place, which results in the difficulties of the reaction of CaO + SiO_2. It has been found that the formation of C_3S in the presence of certain admixtures goes not only according to the scheme of C_2S + CaO but also by means of the interaction of C_2S supersaturated with CaO and C_3S. It is shown that the hydraulic activity of C_3S increases when the concentration of P_2O_5 and Cr_2O_3 are low. It occurs if the concentration of P_2O_5 and Cr_2O_3 in the solid solution does not exceed the solubility limit.

The modifying action of P_2O_5 and Cr_2O_3 is the reason of increasing the hydraulic activity of cement in the presence of P_2O_5 and Cr_2O_3 which appeared to be surface active substances and they affect the conditions of the crystallization of the minerals from the liquid. The action of the raw material admixtures is seen not only on the surface tension but also on the viscosity. So, there is a miximum on the viscosity curves for concentration of the liquid containing MgO. In contrast to the generally recognized ideas, alkalies increase the viscosity of the liquid which is the result of increasing the basicity of the melt and the fact that aluminium and iron ions show more expressed acidic properties. The connection has been found between the physicochemical properties of the liquid in the presence of admixtures and the peculiarities of clinker sintering in the case of contamination of the raw material by MgO and R_2O. It has been shown that the raw material admixtures and the alloying additions may be mineralizers and the mineralizers may become alloying components. It has been suggested, therefore, to single out the problem of admixtures and additions into a special section of the chemistry of cement.

Introduction

The minor components of portland-cement clinker have been investigated mainly with concentrations of 1–3 per cent. (1, 2, 3, 4). When the works of L.D. Ershov appeared (5) who introduced the idea of alloying action of admixtures, it became necessary to pay greater attention to admixtures when their concentration is less than 1–0.5 per cent.

From the author's point of view the role of minor components of raw materials in clinker sintering has not been considered quite fully.

The present work carried out by V. I. Korneev, P. V. Zozulia and G. I. Kopina under the guidance of the author, at the chair of chemical technology of cement, Leningrad Lensoviet Institute of Technology, USSR, is dedicated to the role of admixtures in sintering and to the influence of low concentration of admixtures and additions on the properties of cement.

*Leningrad Lensoviet Institute of Technology, Leningrad, U.S.S.R.

Influence of Admixtures on Hydraulic Activity of C_3S and Cements

To find out the influence of admixture components upon the formation and the properties of C_3S it was necessary to elaborate the method of obtaining pure monomineral C_3S during one burning since the existing methods require repeated sintering which leads to the passivation of the mineral. For this it was necessary to secure great fineness of the raw materilas ($CaCO_3$ and SiO_2) while retaining the purity of the latter.

It was realized by grinding the raw materials in a jet mill (particle size 0.5–3 micron, specific surface 11,500 sq.cm per g.) After a single burning at the temperature of 1500°C (during 6 or 7 hrs) there was no free CaO in the product. The preparation, however, contained several per cent of C_2S, it being the result of supersaturating of C_3S with excess CaO.

Thus, to obtain monomineral C_3S the raw mixture should be prepared with the greater molar ratio than 3. As a result, a sufficiently pure preparation containing 99 per cent of C_3S can be obtained.

Further, on the basis of physico-chemical and petrographic analysis the influence of admixtures (K_2O, Na_2O, P_2O_5, SO_3, TiO_2, Mn_2O_3) on the formation and composition of tricalcium silicate has been found. Beside the admixtures of raw materials, BaO, SrO, B_2O_3, Cr_2O_3 have been considered which are analogous to the raw materials components. A number of interesting peculiarties of C_3S formation in the presence of admixtures have been discovered. Below is given the information about the admixtures for which the new data were received.

In the presence of P_2O_5 the preparation contained free CaO the amount of which required approximately 13 per cent of C_3S; However, with regard to the presence of about 40–45 per cent of low-basic compounds in the sintered material, the author explains from the fact that CaO forms solid solutions with $2CaO \cdot SiO_2$ and $3CaO \cdot SiO_2$. Quartz was also present in the sinter material in the shape of grains which were like those of the original raw silicic acid. Thus, if concentration P_2O_5 exceeds its solubility limit in C_3S, it leads not only to the dissociation of C_3S but also brings about the passivation of CaO and SiO_2. The same picture may be noticed in the presence of B_2O_3. The reason for such a course of synthesis can be explained by the difficulty of the reaction of $CaO + SiO_2$ in the presence of B_2O_3 and P_2O_5 rather than of the reaction of $2CaO \cdot SiO_2 + CaO$ as it is usually thought.

Therefore, the formation of C_3S in the presence of admixtures goes not only according to the scheme of $C_2S + CaO$, but also by means of the interaction of C_2S (supersaturated with CaO) and tricalcium silicate. This fact indicates to the importance of studying the phase relations in the system of C_2S–C_3S in greater detail than the author and his collaborators are now doing.

Further, it was necessary to find out the influence of additions on the technical properties of C_3S. For this purpose the physico-mechanical properties of sintered materials of C_3S have been determined with regard to compressive strength and grindability as well as its hydraulic activity, the latter containing 0.25, 0.5 and 1.0 per cent of additives. It was found that TiO_2, Mn_2O_3 and Cr_2O_3 decrease the strength of sintered materials and improves the grindability. P_2O_5, SrO, Cr_2O_3, TiO_2, Mn_2O_3, La_2O_3, CeO_2, and Na_2O_3 increase the hydraulic activity of C_3S, the latter changing in the presence of admixtures more often during the first three days of hardening. Thus, the admixture effect depends both upon its nature and upon the concentration.

As a result of this, it became clear that most of the raw material admixtures affect the composition and the formation of the alit crystals that points to the alloying role of certain admixtures (natural alloying) and also to the possibility of employing a number of materials for the artificial alloying of the clinker. As it was mentioned above, the action of admixtures is determined not only by their nature but also by their concentration. Therefore, a number of oxides, the presence of which in the raw material is generally considered to be harmful, may be thought of as prospective alloying components if proper concentration, lower than the solubility limit in C_3S is provided. Taking this into consideration, P_2O_5, Cr_2O_3, TiO_2 and SrO present greatest interest as alloying components. To confirm this statement it was necessary to study the formation of solid solutions of the alloying oxides in C_3S and their properties in greater detail. From the systems C_3S–alloying oxide, it was decided to consider C_3S–Cr_2O_3 system, as far as the solid solutions of P_2O_5 and SrO have been already studied (1, 6, 7).

The physico-chemical investigations give reason to think that chrome plays the same role in chromalite as aluminium in alite, i.e. it substitutes a silicon atom. The maximum solubility of Cr_2O_3 in C_3S may be estimated at 2 per cent and it corresponds to the data of A. I. Boikova (8). When the concentration of Cr_2O_3 is more than 2 per cent, solid solution dissociates as a result of chemical interaction with Cr_2O_3. In the presence of TiO_2 alite is formed in the shape of short

prismatic crystals, their refractive indices being higher than those of C_3S. This indicates the formation of the solid solution of TiO_2 in $3CaO \cdot SiO_2$.

The hydraulic activity of solid solutions of TiO_2 in C_3S appeared to be higher than that of the pure C_3S. Therefore, one should consider titanium-containing clays as a raw material which is suitable for obtaining natural alloying clinkers.

Further, it was important to define more exactly the allowable content of P_2O_5, TiO_2, Cr_2O_3 in the clinker and to find the materials suitable for use as alloying additions. It appeared that, at a certain concentration of Cr_2O_3, free CaO is found in the clinker, the amount of which is connected with the CS value (CS-coefficient of saturation). The permitted Cr_2O_3 amount in the clinker depends upon the CS value. It is 2.6% when CS = 0.85; 1.6% when CS = 0.90; 1.4% if CS = 0.95.

The concentration of Cr_2O_3 resulting in the improvement of cement properties (approximately 0.25 per cent) is five or six times lower than the permitted Cr_2O_3 content in the clinker that allows proportioning of chrome—containing materials in a usual way. The permitted P_2O_5 content in the clinker is equal to 0.10–0.20%. For this purpose it is advisable to deal with materials having low content of P_2O_5, and in certain cases it is necessary to dilute the phosphorus—containing material with limestone. The utmost permissible TiO_2 content is estimated at 2–2.5 per cent to obtain high alite cements.

The Reasons for Increasing the Hydraulic Activity of Cements in the Presence of Raw Material Admixtures or Alloying Additions

It was stated above that the formation of the solid solutions of admixtures in C_3S increases the hydraulic activity if the concentration of the admixture is lower than the solubility limit in C_3S. If the concentration of an admixture or an alloying addition is lower than it is necessary for the depolymerization of the structure, its presence leads to the formation of defects and vacancies in the lattice of $3CaO \cdot SiO_2$ which explains the higher hydraulic activity of solid solutions in comparison to pure C_3S. If the concentration of admixtures or additions is sufficient to form the overstructure, the increase of the hydraulic activity is explained by increasing the energy of the lattice, by breaking the bonds and by lowering the density of the high—temperature form. It should be taken into account that the hydraulic activity of C_3S containing admixtures depends upon the nature of an ion which is a part of the structure of $3CaO \cdot SiO_2$. (basic or acidic character, valency, ion radius).

In 1955—56 the works of E. Grzhimek and V. N. Young (9, 10) appeared in which it was stated that the increase of the hydraulic activity of cement may be realized by the modification of the microstructure.

E. Grzhimek showed, in particular, that the modification may be realized by introducing certain admixtures into the alite lattice and in this way may be obtained the alite having the ratio of axes up to 1 : 7. Later, U. M. Butt and V. V. Timashov (11) developed those works and at present modification showed to be a recognized method of improving cement quality.

The raw material admixtures affect the physico-chemical properties of the liquid. As far as the greatest amount of C_3S is crystallized from the clinker liquid (liquid phase) and aluminates and aluminoferrites are crystallized when the melt solidifies, the presence of admixtures or alloying and mineralizing additions cannot but affect the crystallization conditions and therefore the clinker microstructure. There appeared the idea whether the increase of the hydraulic activity of cement in the presence of admixtures and alloying additions is connected not only with the formation of solid solutions but also with the modification of the clinker microstructure at the expense of surface—active action of admixtures.

From the point of view of adsorption theory, the modification should lead to the change of shape, since when adsorbing a surface-active substance the relation of the crystallization speed is changed on different faces. Thermo-dynamic description of the phenomena taking place during modification was given by P. A. Rebinder and M. S. Lipman (12). According to P. A. Rebinder, if the surface activity of $d\sigma/dc$ is less than zero (the gradient of surface tension in concentration) i.e. if the surface tension decreases when the concentration increases, the positive adsorption takes place and the dissolved substance should be considered a surface-active one. And, on the contrary, if the surface tension increases when the concentration is raised ($d\sigma/dc$ is greater than 0) a negative adsorption takes place and the dissolved substance should be considered as a surface-inactive one. Therefore, the surface activity of substances is determined by changing the surface tension of the melt and the estimation of the modifier may be based on the information about the influence of additions upon the surface tension of the melt. That is why P. V. Zozulia and G. I. Kopina studied the influence

Table 1.

alumina modulus P	Composition in per cent			
	CaO	SiO_2	Al_2O_3	Fe_2O_3
1.0	55.2	7.1	18.85	18.85
2.5	57.0	8.0	25.0	10.0

of Cr_2O_3, P_2O_5 and TiO_2 on the surface tension of the liquid.

To measure the surface tension the method of determining the shape of drops of fluid was used. The measurement was done at the temperature of 1400°C. The measurement of the parameters of the melted drops on the negative was made by means of a microscope. The surface tension was calculated with the help of the tables of Bashfort and Adams (13) according to the formula:

$$\sigma = a^2 \rho g$$

where

a—is a capillary constant
ρ—the density of the melt
g—the acceleration of the gravitational force.

There have been two melts chosen the composition of which was determined according to Lea and Parker (14), the former corresponding to the composition of the melt at 1450°C formed from the readily sintered raw mixture having alumina modulus p = 1.0, the latter corresponding to the melt at 1450°C formed from hard sintered raw mixture having alumina modulus p = 2.5. The chosen compositions are given in Table 1.

The additions were introduced into the original mixtures in the amount providing in the melt 0.25, 0.5, 2.05, and 4.0 per cent. The results of determination of the surface tension are given in Table 2.

The analysis of the data given in Table 2 shows that when Cr_2O_3 and P_2O_5 are introduced a considerable decrease of the surface tension of the liquid is observed. The isotherms of dependability of surface tension on the concentration of the addition have the appearance of the curve convex to the X-axis which is characteristic, according to V. K. Semchenko, for the surface active substances. Cr_2O_3 has the greatest surface activity: when the content of Cr_2O_3 is four per cent in the melt, $\Delta\sigma = \sigma_0 - \sigma$ reaches 70–100 erg per sq.cm.

One should note the similarity of the values of surface tension of the melts having different alumina modulus and containing either Cr_2O_3 or P_2O_5. Therefore, Cr_2O_3 and P_2O_5 are typical modifiers, the introduction of which favours the microstructure of the clinker, particularly when burning hard-sintered raw material.

And indeed, when alloying additions are introduced into the raw mixture in amounts providing the maximum increase of hydraulic activity of cement (0.25% of Cr_2O_3, 0.15% of P_2O_5 in the clinker), the size of the crystals and the habit of alite and belite are changed (the elongated alite and split belite appear) i.e. the modification of the clinker with the compounds of chrome in particular takes place which is one of the reasons for increasing the hydraulic activity of cements.

Table 2.

alumina modulus P		σ erg per sq. cm											
		concentration of additions in per cent											
	without additions	Cr_2O_3					P_2O_5					TiO_2	
		0.12	0.62	1.25	2.37	3.89	0.10	0.43	0.81	1.80	3.65	2.0	4.0
1.0	562	519	499	486	450	425	561	540	551	533	510	575	562
2.5	608	565	517	486	471	420	555	566	550	520	493	600	548

The Role of Admixtures in the Process of Sintering

It was shown by the author above that the peculiarities of sintering raw mixtures of different compositions are determined by the properties of the liquid during the final period that allows the use of physico-chemical analysis as the basis of optimization of raw mixtures composition. The presence of admixtures in the raw materials, however, cannot but affect the properties of the liquid and their viscosity in the first instance. That is why P.V. Zozulia made an experimental determination of viscosity of the clinker liquid containing

MgO and R_2O in the laboratory of the chair.

According to the data of Kholin and Entin (15) and Mgjdic and Schwiete (16) the greater the decrease of the viscosity and of the eutectic melt, the greater the content of MgO in the raw material. According to the determinations made by P. V. Zozulia, the viscosity decrease in the presence of MgO is particularly noticable at the temperatures approaching the eutectic one. Such viscosity decrease is connected with the destruction of the prenucleous groups in the preliquid area (group P according to Augustinik (17)) and by lowering the eutectic temperature at the expence of making the melt composition more complex. If MgO concentration in the melt is brought to 5–6 per cent (1.5–2.0% in the clinker) the viscosity of the liquid is again raised. At first the introduction of Mg^{2+} cations having greater field of force than Ca^{2+} (greater electronegativity and smaller radius) promotes the transformation of Al^{3+} and Fe^{3+} from tetrahedral coordination to the octahedral one is accompanied by the viscosity decrease. With greater Mg^{2+} concentration the ion bridge can be formed between the tetrahedrons of SiO_4 which is possible only when MgO content in the melt becomes comparable to the silica amount that takes place when the MgO concentration in the melt is increased up to 5 or 6 per cent.

In contrast to the generally recognized views it appeared that the introduction of alkalies into the clinker liquid leads to the viscosity increase. Such a mechanism of alkalies action is connected with the basicity increase of the melt the result of which is that aluminium and iron ions acquire acidic properties that leads to the tetrahedral coordination of aluminium and iron in relation to oxygen. The complexes $[AlO_4]$ are able to replace tetrahedrons isomorphously, $[SiO_4]$ forming alumino—silicon—oxygen frame that increases the viscosity. In the light of the data obtained the generally accepted explanation of the peculiarities of sintering in the presence of R_2O needs to be corrected.

In the system C–S–A–F–R–M the viscosity is lower than that of the clinker liquid of the like composition without MgO. Therefore, it is assumed that in the raw material containing alkalies, the presence of a small amount of MgO (up to 1 per cent in the clinker) or the intensional introduction of such amounts of magnesia additions may be favourable for the clinker formation, that is confirmed by the investigators (18). When there are alkalies and a great amount of MgO (more than 1.5% in the clinker) in the raw material the raw mixtures will sinter with greater difficulties.

Since the eutectic melts in the system C_3S–C_2S–C_3A–C_4AF refer to the associated liquids, the Frenkel equation cannot be used for the description of the temperature dependence of their viscosity. The temperature dependence of viscosity may be well described by means of the Evstropiev equation (19). MgO effect on the viscosity of the clinker melt brings to the changes in the crystallization character as well. So, for clinkers containing one per cent of MgO the more distinct crystallization of silicates is typical, the crystal sections have more regular shapes, greater uniformity of size, it referring particularly to alite, the uniformity of the distribution of all phases and negligible content of joints and aggregates of alite and belite. When MgO content is increased up to two per cent in the clinker the deterioration of crystallization takes place. For clinkers containing alkalies (1% of R_2O) zonal structure of the grains is typical—in a thin layer on the surface of a grain greater crystals of alite are formed—up to 300 micron and in the centre their size is up to 50–70 microns. When introducing magnesium oxide into alkali-containing raw mixtures the weakening of alkalies influence upon the character of silicates crystallization takes place.

The cited information shows that most raw material admixtures affect the composition and formation of alite crystals that indicates the alloying role of certain admixtures (natural alloying) as well as the possibility of using a number of materials for the artificial alloying of the clinker. It is the alloying action of natural admixtures that explains the differences in the activity of cements produced at the mills having the same kind of equipment and similar clinker composition.

The action of admixtures and additions is seen also during the solid phase stage of clinker minerals formation, the admixtures and alloying additions producing mineralizing and inhibiting effect. Thus, there is a direct connection between admixtures and alloying and mineralizing additions. Mineralizing additions should not be considered only from the point of view of catalytic effect. The influence of mineralizers upon the properties of the liquid phase of sintering clinker may bring about the modification of clinker minerals. Besides, mineralizers may affect the peculiarities of structure of clinker minerals. Therfore, mineralizers often have alloying effect. Meaning by alloying the artificially introduced additions, one should not forget that many admixture additions may be considered as natural alloying materials, rendering proper effect if their concentration is low enough. The raw material admixtures having high concentration produce harmful effect on technology and properties of cement.

Taking into account the facts stated above, the author suggests to single out the problem of admix-

tures and additives including admixtures, as well as alloying and mineralizing components into a separate section of the chemistry of cements.

References

1. R. W. Nurse. "Gen. Appl. Chem." No 2, 708–716 (1962).
2. R. E. Simanovskaja and Z. V. Vodzinskaya "Cement" (in Russian) No. 5, Moscow, USSR (1955).
3. G. H. Welch and W. Gutt, "The influence of small additions on the hydraulic properties of calcium silicates". p. 56. Proceedings of the Fourth Intern. symp. on the Chem. of Cem,., Washington (1960).
4. F. M. Lea, "The chemistry of cement and concrete". p. 75, London (1956).
5. L. D. Ershov, "High quality cements" (in Russian) Gostekhizdat. Kiev. USSR (1952).
6. N. A. Toropov and M. I. Borisenko. "Cement" (in Russian) No. 6, Moscow, USSR (1959).
7. N. A. Toropov and A. I. Boikova. "Reports academy of sciences" (in Russian) Vol. 137, No. 4, Moscow, USSR (1962).
8. A. I. Boikova, M. A. Toropov, M. M. Purutko and C. V. Grum-Grzhimailo "Inorganic materials". (in Russian) Vol. II, No. 10, Moscow, USSR (1966).
9. E. Gzhimek. Proceeding of the Symposium on Chemistry of Cement (in Russian) Promstroiizdat, p. 27, Moscow, USSR (1956).
10. V. N. Young "Cement" (in Russian), No. 6, Moscow, USSR (1955).
11. U. M. Butt and V. V. Timashev. "Technology and properties of special cements". (in Russian) Stroiizdat. p. 52, Moscow, USSR (1967).
12. P. A. Rebinder and M. S. Lipman, "Research in the field of surface phenomena" (in Russian) p. 8. Moscow, USSR. (1936).
13. F. Basnforth and G. C. Adams "An attempt to test the theories of capillary action". Cambridge (1883).
14. F. M. Lea, T. W. Parker, Build. Research Station Technical. Paper No. 16 (1935).
15. I. I. Kholin and Z. B. Entin "New in the chemistry and technology of cement" (in Russian) Gosstroiizdat p. 7 Moscow. USSR. (1962).
16. A. Mgjdic and H. E. Schwiete "Zement-Kalk-Gips". (in German) No. 3 (1959).
17. A. I. Augustinik "Glasslike condition" (Proc of III Sym. Acad. Sciences. USSR) p. 13. (1960).
18. S. Kakitani and M. Fujisaka "Zement-Kalk-Gips" (in German) No. 12 (1960).
19. K. S. Evstropiev and N. A. Toropov "Chemistry of silicon and physical chemistry of silicates". (in Russian) Promstroiizdat, p. 98. Moscow. USSR (1956).

Supplementary Paper I-98 Mechanisms and Kinetics of Portland Cement Clinker Formation for an Example of the Solid State Reaction in the Presence of a Liquid Phase

Renichi Kondo* and San-Heul Choi**

Synopsis

The mechanism and kinetics of the solid state reaction between CaO and C_2S to form C_3S, in the presence of a melt, was investigated.

In order to make clear the mechanism of reaction the sandwich method was employed, powdered glassy phase is sandwiched between the compact disk of CaO and β-C_2S. After where heating, studies were carried out with the aid of X-ray diffraction, microscopic observation, and electron probe micro analysis. The results show dissolution and diffusion of CaO and C_2S into the melt. The melt is supersaturated on these components, and C_3S crystallizes out from the melt.

The viscosities were measured by the ball pulling-up device for the melt containing various amounts of CaO, γ-C_2S, and C_3S. The relationship between η vs. 1/T could not be acccpted as linear in a wide temperature range.

Furthermore the kinetics of the solid state reaction in the presence of a liquid phase has been developed. The reaction is thought to be controlled mainly by the diffusion in the liquid phase. On the same assumption, a Jander's type of equation is derived where dissolution is considered in spite of the inward diffusion being assumed by Jander. This equation is found to express the experimental data most appropriately.

Finally, diffusion coefficient was calculated from the results on the rate of reaction and the concentration difference estimated in the phase diagram. Calculated value was lower than those obtained by viscosity and tracer experiments. As these discrepancies are in such a magnitude to be compensated by the effects of a limited amount of melt and the tortuosity of diffusion path, the assumptions on the kinetics in this study seem to be reasonable.

Introduction

On the solid state reaction a number of studies which dealt with the mechanisms and kinetics have appeared since the early works of Tamman and Jander. So far as a melt is concerned, however, it has not been investigated owing to the difficulties experienced.

There are also a few studies on the mechanisms and kinetics of the formation of portland cement clinker. One of the present authors, Kondo (1) in his studies on the kinetics of this reaction found it necessary to simplify the experimental conditions in order to obtain accurate results. Yamaguchi, Uchikawa, and Kawamura (2), on the other hand, observed by microscope that the formation of alite took place in the liquid phase. Further, the rate of dissolution of CaO, C_2S, C_3S, and silica in a melt was studied by Toropov, Rumyantsev, and Filipovich (3) using a high-temperature microscope.

In this paper, the solid state reaction in the presence of a liquid phase in the formation of portland cement clinker is dealt with.

* Research Laboratory of Engineering Materials, Tokyo Institute of Technology, Tokyo, Japan.
** Hanyang University, Seoul, Republic of Korea.

Experimental Methods and Results

Starting Materials

Starting materials except silica used for synthesis were special grade reagents. As the source of silica, quartz with high purity was selected and ground. It was then purified by acid washing and elutriated to cut off coarser particles of more than 10 μ in radius. Synthesis of γ-C_2S, C_3S and the glassy phase were made. The composition of the glassy phase was chosen the invariant point (4) in which C_3S, C_2S, C_3A, and C_4AF are coexisted at 1338°C. Its chemical composition corresponds to 54.8 CaO 22.7 Al_2O_3 6.0 SiO_2 and 16.5 Fe_2O_3. The particles of synthetics of limited size were then isolated by the Bahco type classifier.

The Reaction on the Boundary Layer

In order to investigate the mechanism of reactions on the boundaries of CaO–melt and C_2S–melt, a sandwich method was designed. A powdered glassy phase is sandwiched between the specimens which consists of two compact disks of CaO and β-C_2S each. After heating in an electric furnace, the specimen was air quenched, and then examined by X-ray diffraction, microscopic observation and electron probe micro analysis.

X-ray Diffraction

The heat-treated specimen was cut at the position of interfaces of CaO and C_2S each in parallel with the boundary of the two disks and investigated by X-ray diffraction on each surface. In consequence, the formation of C_3S was clarified in the melt of the boundary surface. Fig. 1 shows the diffraction patterns of each part before heating (A) and after heating for 120 min. at 1450°C (B).

Microscopic Observation

The heat-treated specimen was cut vertically at the boundary of disks and the thin sections were utilized, so that it can be observed through the reflection and transparent polarizing microscopes. The formation of C_3S crystals was confirmed in the melt of the boundary surface. Fig. 2 shows the appearances forming C_3S by heat treatment of for 120 min. at 1450°C. The crystals of C_3S tended to elongate to the parallel with the boundary.

Concentration Distribution of Components in the Boundary Layer

Since the analysis of the chemical composition of micro area of solid surface became possible by electron probe micro analysis, it has been applicable to the analysis of cement clinker. The concentration distribution of Ca, Si, Al, and Fe on the boundary layer was investigated by electron probe micro analysis

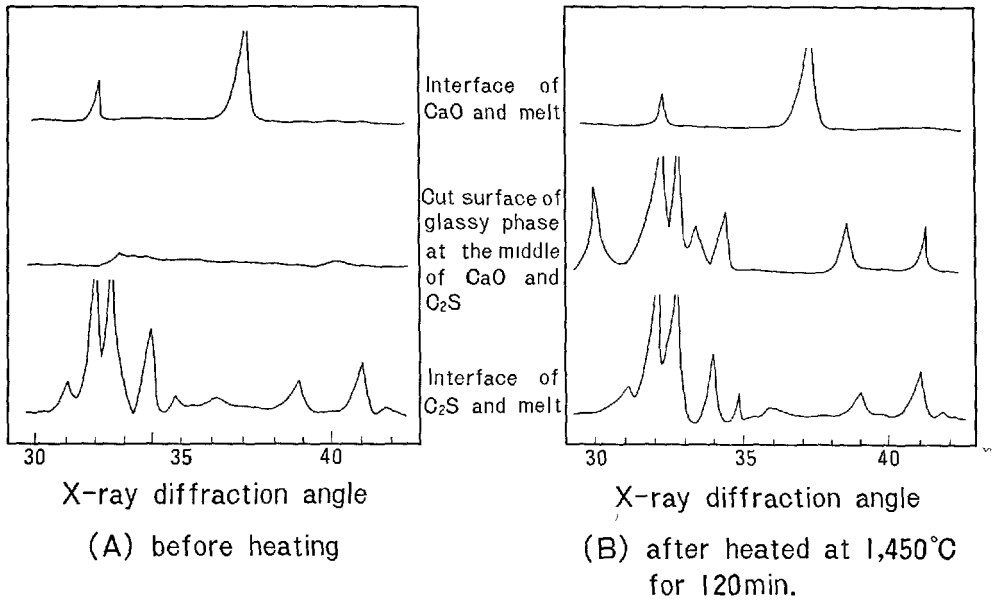

Fig. 1. *X-ray diffraction patterns of sandwich specimen.*

with the results as shown in Fig. 3.

The concentrations of various chemical components on the boundary layer were corresponding to the theoretical value of mineral components. Nearly the same amount of Al and Fe seems to be incorporated in both C_2S and C_3S, more in the former, to form solid solutions. The reason for the higher concentration of Si at the holes, is attributed to carborundum intermixed at polishing (5).

From the experimental results it is considered that, when the sandwiched specimen is heat-treated, the glassy phase melts above 1338°C, and dissolves CaO and C_2S, and then after the melt is supersaturated on these components, C_3S crystallizes out from the melt.

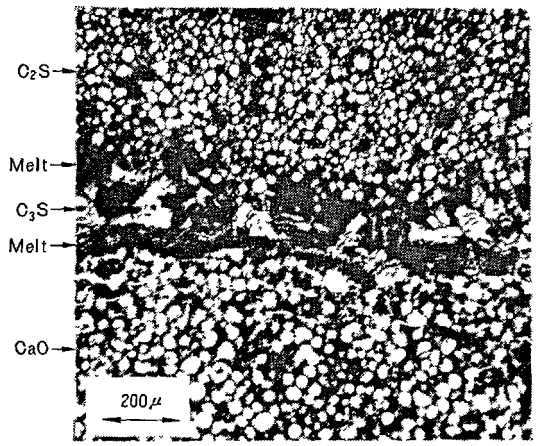

Fig. 2. C_3S *formed in the melt heated at 1450°C for 120 min. (Open nicol)*

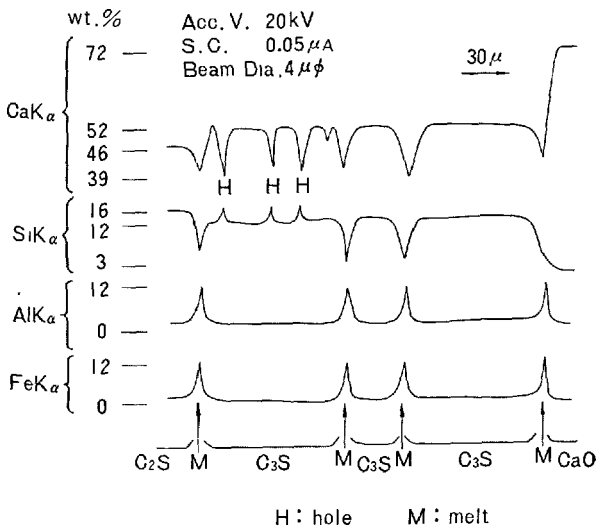

Fig. 3. *Concentration distribution in sandwich specimen by line analysis of EPMA.*

Viscosity of the Melt

On the viscosity of the melt assumed to exist at the time of portland cement clinker formation, Vysotskii, Butt and Timashev (6) studied the effect of temperature and chemical composition, and Sychev, Zozulya, Shtefan, and Ivantsova (7) studied the influence of raw admixture and additional agents such as Cr_2O_3, TiO_2, MgO, P_2O_5, and $K_2O + Na_2O$.

In this study, the viscosities were measured with the ball pulling-up device (8) for the melt containing various amount of CaO, γ-C_2S and C_3S in the temperature range from 1360°C to 1550°C. Fig. 4 shows the relationship between the viscosity (η) and reciprocal absolute temperature ($1/T$). The relationship could not be accepted as linear, in a wide temperature range. The values of activation energy for the viscous flow were calculated from the following equation, on the assumption that the linear relationship holds within a narrow temperature range.

$$\log \eta = \log A + 0.4343 \frac{E\eta}{RT} \qquad (1)$$

A marked decrease in the activation energy is observed with increasing temperature which may result from the structural change.

Fig. 5 shows the influence of the addition of CaO, γ-C_2S, and C_3S respectively on the viscosity of the melt. The viscosity increases with the amount of C_3S or C_2S and decreases with the amount of CaO, but the effect of composition on the activation energy of viscosity affects reversely.

Determination of the Reaction Rate

The raw mixtures consisting of the particles of CaO,

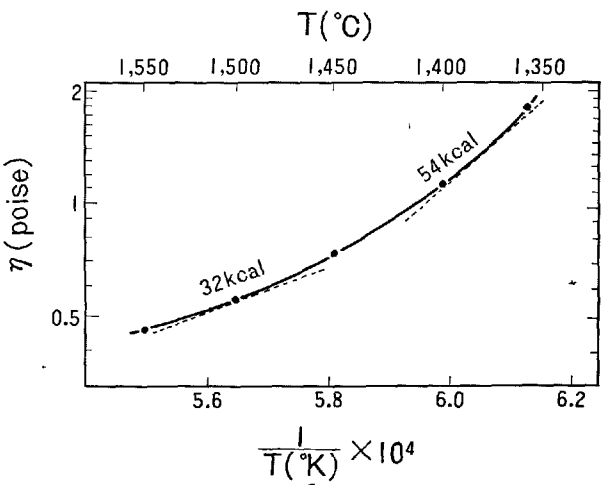

Fig. 4. *Temperature dependence of the viscosity of the melt.*

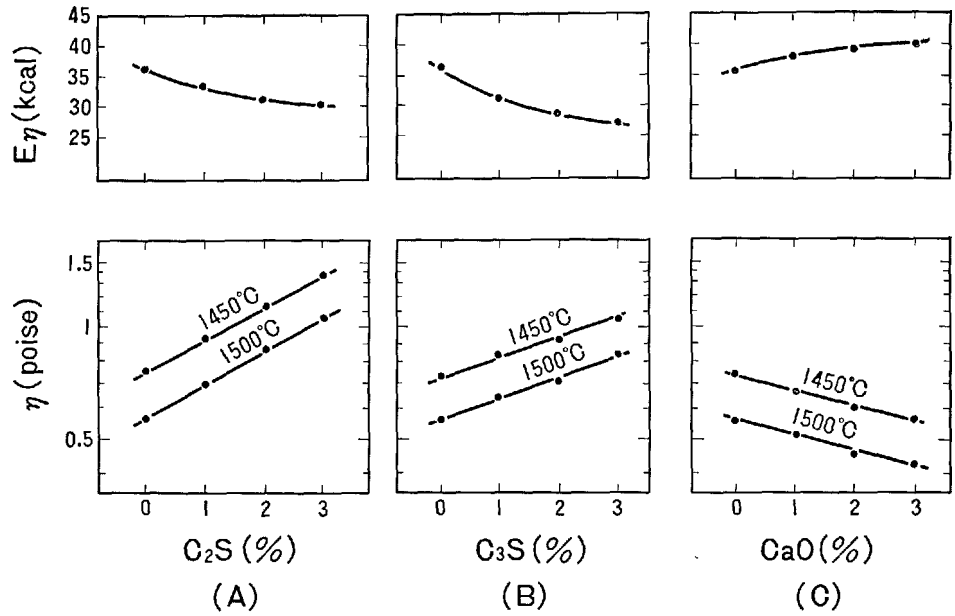

Fig. 5. *Viscosity isotherms and energy of activation for viscous flow.*

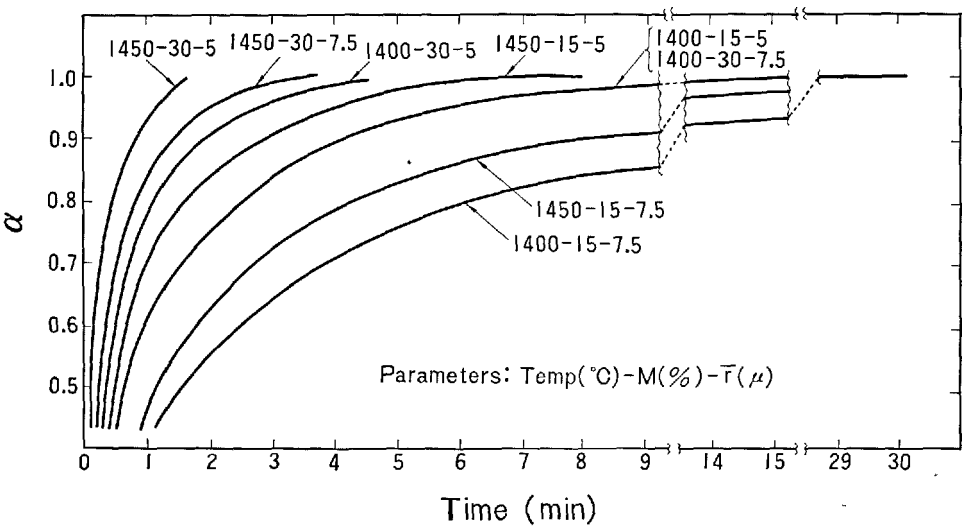

Fig. 6. *Fraction of reacted part vs. reaction time.*

γ-C_2S and the glassy phases were pressed at a pressure of 100 kg/cm² to form disk of an area of 1 cm² and weight of 1 gr. Determinations of the free CaO were made on these disks after they were heat-treated and air quenched. For the simplification in the theoretical treatment, uniform size of particles were used. The chemical composition and fineness of the raw mixtures and the burning conditions in this experiment are as follows:

CaO: γ-C_2S = 1: 1 (molar ratio)

amount of the glassy phase = 15%, 30% (in wt% of CaO and C_2S)

particle size $\bar{r} = 5\mu, 7.5\mu$

heating temperature = 1400°C, 1450°C

heating time = 2, 4, 8, 15, 30, 60 min.

The heating was done in a vertical electric furnace with an automatic temperature controller. The specimen was put into a small container made of platinum foil and suspended with platinum wire for the convenience of rapid heating and quenching.

The free CaO content of the heat-treated specimen was determined by modified Franke's method, using a mixture of isoprophyl alcohol and ethyl aceto acetate as the extraction solvent.

The reaction ratio are calculated from the value of free CaO as shown in Fig. 6. The rate of C_3S formation increases with the content of the glassy phase, fineness of the particle of reactants, and temperature. And the degree of these effect is approximately in this order.

Discussion

Mechanism of the Reaction

On the reaction of CaO and C_2S in the presence of the melt, the composition change accompanied with dissolution is considered. The phase diagram of the system CaO–C_2S–C_4AF (4) is selected for simplification and used for consideration. Fig. 7 is a part of the diagram of above system. The course and composition of dissolutions of CaO and C_2S in the melt indicated by point T will be examined. In the process of dissolution, if the boundary reaction is sufficiently rapid compared with transport, the interface composition has the value of the liquid composition and if the boundary reaction is sufficiently slow, the interface composition is identical with that of the bulk. We shall now consider the mechanism of the formation of C_3S in making use of Fig. 7. It is expected that the concentration path would be along the straight lines T–CaO and T–C_2S when CaO and C_2S are separately dissolved in the melt marked as T. In the concentration path, however, the interface compositions are not always located on the straight line but shifts as indicated by the dotted line, because of the difference in the relative rates of diffusions of the components. This effect has been described by Cooper and Kingery; Samaddar, Kingery, and Cooper; Oishi, Cooper, and Kingery (9) in their studies on the dissolution mechanisms in a ceramic system.

If we suppose the temperature is 1450°C, the composition of melts at the interfaces of CaO and C_2S should be C_1 and D_1 respectively. According to the counter diffusion between the melts C_1 and D_1, the compositions of melts move with the isotherms towards M beyond C_2 and D_2 which indicate the solubility of C_3S in coexistence with CaO or C_2S respectively. For the supersaturated solution with compositions beyond C_2 and D_2, C_3S is crystallized out. After a steady state is reached, the concentration of the interface of CaO and C_2S are indicated as C_3 and D_3, the melt is in this range, as a result of counter diffusion between the interfaces. Accompanied with increasing temperature, the rate of formation of C_3S is accelerated because of increasing the amount of melt, decreasing of the viscosity and increasing of the diffusion coefficient.

Kinetics of the Reaction

Since Jander the kinetics of the solid state reaction have been studied by many investigators. The effect of a melt coexist with reactants has never been considered in the solid state reactions, especially when they are in powder. In the presence of a melt,

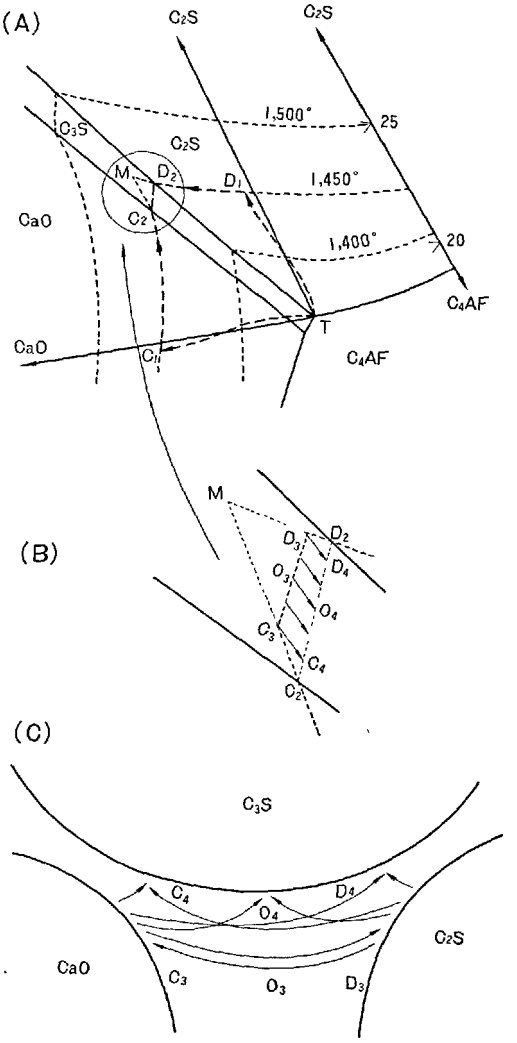

Fig. 7. *Detail of the high* C_4AF *portion of the system* CaO–C_2S–C_4AF [4] *(A) (B) and schematic illustration of the concentration difference and diffusion paths in the melt (C).*

the starting material are dissolved and diffuse each other in a melt from which a product is formed.

Depth of Dissolved Layer

On the assumption that the dissolution begins from the surface of a spherical particle of radius r_0, the volume of the substance unreacted after the time t is

$$V = \frac{4}{3}\pi(r_0 - \xi)^3 \tag{2}$$

or

$$V = \frac{4}{3}\pi r_0^3(1 - \alpha) \tag{3}$$

from Eq. (2) and Eq. (3), Eq. (4) is obtained

$$\xi = r_0(1 - \sqrt[3]{1 - \alpha}) \tag{4}$$

where ξ is the depth of the dissolved layer and α is the reaction ratio.

Fig. 8 shows the relationship between the depth of dissolution and heating time obtained by author in comparison with the results obtained by Cooper and Kingery (9), and Toropov, Rumyantsev, and Filipovich (3). Within the limits of experimental error, the depth of the dissolved layer does not depend upon the particle size. The plots of the depth of dissolution ξ versus the root time treated $t^{1/2}$ can be taken as linear in a certain range. It is observed some shift from the straight line at the later stage of reaction, and this seems to be due to the effect of distribution of the particle size, however the powder of reactants was elutriated. Above mentioned facts suggest that the particle dissolution is diffusion-controlled.

Similar results were obtained by Cooper and Kingery (9). However, they employed an alumina rod dipped in molten slag. On the other hand, Toropov, Rumyantsev, and Filipovich (3) presents somewhat different results from those above mentioned, and this discrepancy seems to have a relation with their experimental conditions in which they used different sizes of reactant particles. As the big particle may not be a single crystal, it disperses before dissolution so that it may be eliminated in a shorter time than expected.

Rate of Reaction

The rate of solid state reaction is accelerated by the presence of a melt, in which the solid reactants are dissolved and counter diffused. The composition of the melt is supersaturated with the product which crystallizes out from the melt. Assuming that the rate is proportional to the concentration gradient across the diffusion layer formed around the dissolving particle, as the amount of the melt is limited, the

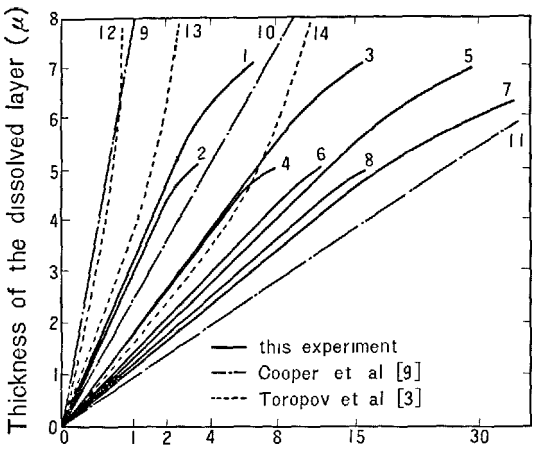

	T°C	glassy phase%	r̄μ		T°C
(1)	1,450	30	7.5	(9)	1,480
(2)	1,450	30	5	(10)	1,410
(3)	1,400	30	7 5	(11)	1,350
(4)	1,400	30	5		
(5)	1,450	15	7 5	(12)	1,450
(6)	1,450	15	5	(13)	1,400
(7)	1,400	15	7.5	(14)	1,350
(8)	1,400	15	5		

Fig. 8. *Thickness of dissolved layer vs. time of heat-treatment.*

area of diffusion is regarded as corresponding to the surface of dissolving particle. The following equations are derived from Fick's first law.

$$\frac{d\alpha}{dt} = -AD\frac{\Delta C}{\Delta X} \tag{5}$$

or

$$\frac{dr}{dt} = -D\frac{\Delta C}{\xi} \tag{6}$$

where $A = 4\pi r^2$, $\xi = r_0 - r$, and

$$d\xi = -dr \tag{7}$$

and hence

$$\frac{\xi^2}{2} + c = D \cdot \Delta C \cdot t \tag{8}$$

and $c = 0$ which the initial condition $\xi = 0$ when $t = 0$ therefore

$$\xi^2 = 2D \cdot \Delta C \cdot t \tag{9}$$

from Eq. (4) and Eq. (9)

$$(1 - \sqrt[3]{1 - \alpha})^2 = \frac{2D \cdot \Delta C}{r_0^2}t = Kt = F(\alpha) \tag{10}$$

Thus a Jander's type of equation is derived with a clear physical meaning where dissolution is considered in this paper in spite of the inward diffusion being assumed by Jander. This equation is found to express the experimental results with better accordance than

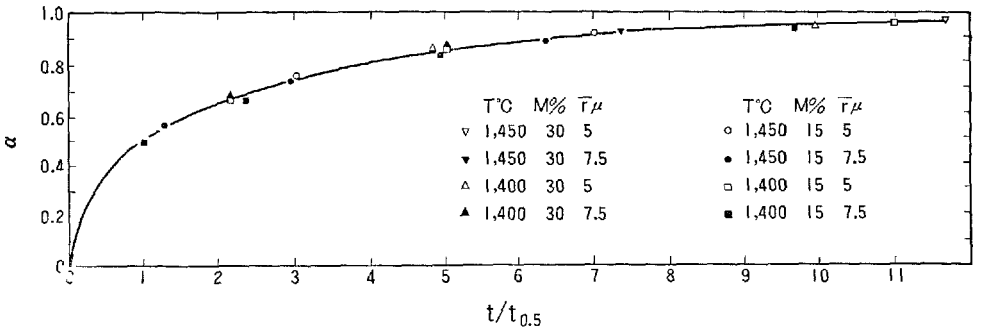

Fig. 9. *Fraction of reacted part vs. reduced time.*

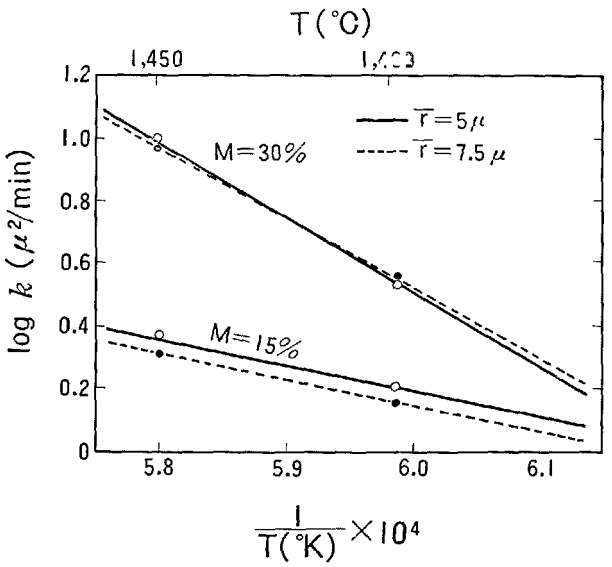

Fig. 10. *Temperature dependence of the reaction constant.*

the other kinetic formulas such as the one reported by Ginstling.

It is convenient in comparing experimental data with Eq. (10) to use a reduced time scale, such as $t/t_{0.5}$ where $t_{0.5}$ corresponds to $\alpha = 0.5$. Then

$$F(0.5) = 0.0426 = Kt_{0.5} \tag{11}$$

combining Eq. (10) and Eq. (11) gives

$$F(\alpha) = 0.0426\left(\frac{t}{t_{0.5}}\right) \tag{12}$$

From Eq. (12), a single curve can be drawn on α versus $t/t_{0.5}$. This single curve represents all the data obtained in various conditions including temperature, particle size, and content of the melt as shown in Fig. 9.

The apparent activation energy E can be obtained by Arrhenius' equation;

$$\log K = \log A - \frac{E}{4.574T} \tag{13}$$

Table 1. *Apperent activation energy*

Glassy phase M (%)	Particle size $\bar{r}(\mu)$	E (kcal/mol)	A
30	5	123	$10^{16.5}$
30	7.5	121	$10^{15.5}$
15	5	42	$10^{6.7}$
15	7.5	42	$10^{5.8}$

As shown in Table 1 the activation energy depends upon the content of the melt, so that, the activation energy increases with amount of the melt.

Further research will be carried out to examine the relation between the rate of reaction and the relevant surface area or the tortuosity or the situation of the phases.

Activiation Energy

The temperature dependence of the reaction constant K on each experimental condition was calculated from Eq. (10) and plotted in Fig. 10. The slopes of $\log k$ ($k = \bar{r}^2K$) versus $1/T$ show different tendencies according to the content of melt, that is, the temperature dependence becomes greater with the content of the melt, and point of intersection of the lines coincide with the melting point of the melt.

The value of activation energy in a low amount of the melt coincides with the one from viscosity measurement. On the other hand, the value obtained with a large amount of the melt is in the same order with the value reported by Toropov, Rumyantsev, and Filipovich (3). The similarity in order obtained by the dissolution of various oxides in a melt imply that the counter diffusion in the melt is directly related with activation energy. There are unexpectedly greater values which doesn't seem to be a real activation energy on the material transfer in the melt but contains other effects such as dispersion or a change of tortuosity of the path for diffusion.

Diffusion Coefficient

The diffusion coefficient of each species could be calculated from Eq. (10) in which α is given experimentally, r_0 and t are known, and ΔC is approximated to one half of the concentration difference between C_2 and D_2 in Fig. 7(B).

As the diffusion of silicon in the melt is regarded as the slow step in the reaction, calculated results on silicon are shown in Fig. 10 as M-line.

Next, the diffusion coefficient is also calculated from the following equation,

$$D = \frac{RT}{6\pi\eta\delta N} \tag{14}$$

where η is experimentally obtained in this study and δ is the radius of diffusing species and assumed to be Si^{4+} ion with 0.4 Å. Result is shown in Fig. 11 as V-line, however, the values must be somewhat lowered if the silicate ions are the diffusing species.

On the other hand, tracer diffusion coefficient for Si^{31} in a molten slag has been measured by Towers and Chipman (10). In consideration of the melt, however, diffusion coefficient must be corrected on the basis of the effect of viscosity. Following relation must hold good, when T and δ are the same.

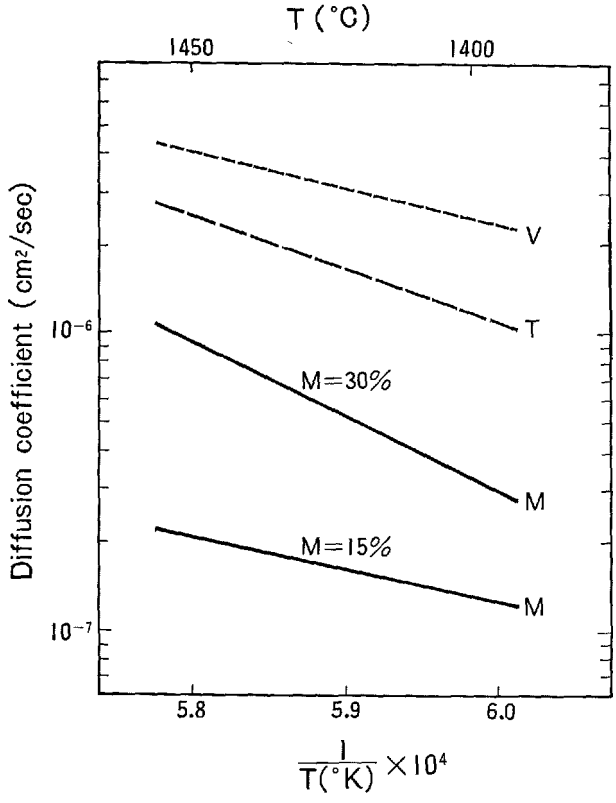

Fig. 11. *Diffusion coefficients of silicon in the melt.*

$$D\eta = D'\eta' \tag{15}$$

where D and D' are diffusion coefficients of the melt and the slag. η and η' are viscosities of the melt and the slag (11). The corrected result is shown in Fig. 10 as T-line.

In comparison between various results, V and T are in good accordance, however M is lower than the formers. This discrepancy is considered to be due to the effects of the amount of melt and tortuosity of the diffusion paths.

Thus, the assumption on the kinetics in this study seem to be reasonable as such result on diffusion coefficient was obtained from the rate of reaction.

The authors are indebted to Mr. M. Kobayashi and his co-workers for electron probe micro analysis.

One of the present authors, S. Choi is studying abroad from Korea at the Japanese Governments expense. Thanks are due to the authorities concerned of both countries.

References

1. R. Kondo, "Reaction velocity in portland cement clinker formation", Fourth International Symposium on the Chemistry of Cement, Washington, (1960), 107–112 (1962).
2. G. Yamaguchi, H. Uchikawa and S. Kawamura, "Influence of sodium oxide upon the formation and crystal structure of tricalcium silicate solid solution in the system CaO–SiO_2–Al_2O_3–Fe_2O_3" (in Japanese), J. Ceram. Assoc. Japan. **70**, 209–220, (1962).
3. N. A. Toropov, P. F. Rumyantsev and V. N. Filipovich, "Kinetics of the dissolution of CaO, $3CaO \cdot SiO_2$, $2CaO \cdot SiO_2$, and SiO_2 in a molten cement clinker", J. Phys. Chem. USSR, **38**, 528–530, (1964). N. A. Toropov and P. F. Rumyantsev, "The kinetics of formation of portland cement clinker", J. Appl. Chem. USSR, **38**, 658–660, 1106–1108, 1576–1578, 1810–1812, 1813–1814, 2066–2067, 2068–2069. (1965). N. A. Toropov and P. F. Rumyantsev, "The kinetics of formation of cement clinker" (in German), Silikattechnik, **18**, 322–323, 349–354, (1967).
4. F. M. Lea and T. W. Parker, "Investigations of a portion of the quaternary system CaO–C_2S–C_5A_3–C_4AF", Phil. Trans. Royal Soc. **234A**, 1–41, (1934).
5. H. Tagai, H. Suzuki and T. Iseki, "Application of X-ray micro-analyzer to study of refractories" (in Japanese), Refractories, **19**, 605–609, (1967).
6. D. A. Vysotskii, Yu. M. Butt and V. V. Timashev, "Viscosity of clinker melt at 1300–1700°" (in Russian), Tr. Mosk. Khim. Technol. Inst., No. 45, 30–33, (1964).
7. M. M. Sychev, P. V. Zozulya, M. Shtefan and S. M. Ivantsova, "Influence of raw admixture and addi-

tional agents on the viscosity of portland cement in the fluid phase" (in Russian), Tsement, **32**, 5–7, (1966).
8. I. Sawai, M. Kunugi, and T. Yamate, "Studies on the viscosity of glass in molten state (I) viscosity measurement of glass by a ball pulling-up method" (in Japanese), J. Japan Soc. Testing Materials, **8**, 615–618, (1959).
9. A. R. Cooper, Jr., and W. D. Kingery, "Dissolution in ceramic systems I", J. Am. Ceram. Soc., **47**, 37–43, (1964). B. N. Samaddar, W. D. Kingery, and A. R. Cooper, Jr., "Dissolution in ceramic systems II", J. Am. Ceram. Soc., **47**, 249–254, (1964). Y. Oishi, A. R. Cooper, Jr., and W. D. Kingery, "Dissolution in ceramic systems III", J. Am. Ceram. Soc., **48**, 88–95, (1965).
10. H. Towers and J. Chipman, "Diffusion of calcium and silicon in a lime-alumina-silica slag", J. Metals, **9**; Trans AIME **209**, 769–773, (1957).
11. J. S. Machin and T. B. Yee, "Viscosity studies of system CaO–MgO–Al_2O_3–SiO_2: II, CaO–Al_2O_3–SiO_2", J. Am. Ceram. Soc., **31**, 200–204, (1948).

Supplementary Paper I-133 A Refinement of the Lime Standard Formula

Eberhard Spohn,* Eduard Woermann, and Dietbert Knoefel**

Synopsis

The lime standard formula I was postulated by Kühl on the basis of investigations by Spohn. Its modification by Lea and Parker has served for more than 30 years as a valuable tool in calculating the raw mix composition. Together with the

$$\text{Silica Ratio (Silikatmodul)} \frac{SiO_2}{Al_2O_3 + Fe_2O_3} \text{ and the}$$

$$\text{Alumina Ratio (Tonerdemodul)} \frac{Al_2O_3}{Fe_2O_3}$$

cement properties can be well judged. The following refined Lime Standard Formula is now proposed.

$$\text{LSt III} = \frac{100(CaO + 0.75\ MgO)}{2.80\ SiO_2 + 1.18\ Al_2O_3 + 0.65\ Fe_2O_3}$$

where the values for MgO shall not exceed 2.0.

The complete analysis data of a cement clinker expressed in the oxides CaO, SiO_2, Al_2O_3 etc. are not very convenient for the purpose of recognizing the phase composition from which the cement properties can be deduced. The cement manufacturer cannot judge directly, whether the mixture has an optimum lime content, or whether some lime deficiency will lead to poor strength, or excess of lime to expansion of the cement product.

A number of manufacturers use Spohn's lime deviation method (1) to measure directly the deviation from the optimum lime content. The result can be obtained in approximately one hour. Today, however, a complete analysis can be made by X-ray fluorescence-method within a few minutes. Here again, we look for a method to transform the analysis data to some figures which meet our purpose.

For many years, two such methods have been in use: One is connected with the name of Bogue, the other one with the name of Kühl. Since the time of their origin, our knowledge of the chemistry of cement clinker has been enlarged. Let us have a look at these two methods from the point of view we have today.

The classical research of Bogue and the other scientists is still the foundation of our cement industry. From the investigation of phase relationships in the ternary system $CaO–Al_2O_3–SiO_2$ and the quaternary system $CaO–Al_2O_3–Fe_2O_3–SiO_2$ Bogue devised a method to calculate the theoretical amounts of the cement minerals C_3S, C_2S, C_3A and C_4AF. This calculation seems to be ideal for the classification of cement, if we suppose that the cement properties can be deduced from the mineral composition. This helped to spread the Bogue-formula (2) all over the world.

Some disadvantages, however, have to be taken account of:

1. The formula does not indicate the optimum amount of lime in a technical clinker and
2. some errors are introduced by neglecting the mutual solid solutions of the clinker minerals as well as the fact that the calculated amount of C_2S partially is not present as a mineral itself at sintering temperature but makes up part of

* Portlandzementwerke Heidelberg A.-G., Heidelberg, West Germany.

** Institut für Kristallographie der Technischen Hochschule Aachen, West Germany.

the liquid phase. Upon cooling the high-temperature equilibrium will be quenched.

The mineral composition calculated according to Bogue, has been called "potential composition" in the English language. The word "potential" is easily forgotten, especially when translating into languages which have no corresponding expression. After the "potential composition" has been incorporated into the standards of some countries, this expression has been shifted from the use of the chemists to the use of salesmen and cement consumers. They readily ignore the word "potential" and even take the calculated phase composition for actual or approximately so. By the time this formula was borne, one could not probably think of the actual size of descrepancies which were faintly suggested by that word "potential". Meanwhile, it became evident that in a clinker not the pure compounds C_3S, C_2S etc. are present but quite complex solid solutions, and the old names of alite, belite and ferritic phase were taken up again.

In order to obtain a comparison between the "real" phase composition and the calculated "potential" composition according to Bogue's formula 52 technical clinkers from 9 cement plants were analyzed by standard wet-chemical methods for the oxides as well as by microscopic point-counting methods for their respective phase compositions. The data obtained by point-counting methods were transformed to weight-percent data by multiplication with the corresponding density factors:

alite	$d = 3.22$ g/cm³
belite	$d = 3.28$ "
aluminate	$d = 3.04$ "
ferrite	$d = 3.76$ "

The data obtained by these methods are compared graphically in Fig. 1.

It appears that the alite content is higher than the calculated amount of C_3S throughout, in some cases by as much as 20%. Conversely, the belite content is lower than the potential C_2S-content. The differences between calculated and measured values for the aluminate and the ferrite phases are sometimes positive, sometimes negative, but generally small by comparison. It can be expected that the latter deviations will be more serious in the range of a smaller C_3A-content than in our samples. Analogous effects have been observed by other authors, and they are discussed in detail by Lea (3). According to Krämer and zur Strassen (4), the MgO-content is a predominant factor in controlling the deviation of the alite content from the potential C_3S-value. The presumptive advantage that cement properties can be estimated with sufficient accuracy from the potential composition proves to be an illusion.

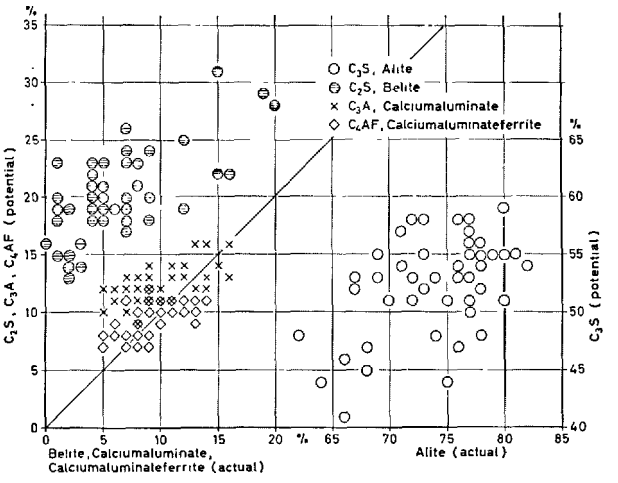

Fig. 1. *Comparison of the potential composition of technical portland cement clinker and their actual phase composition determined by microscopical point counting method.*

Another method to transform the analysis data has been given by Kühl (5). His consideration is based on the comparison of the actual lime content of a clinker with the maximum amount of lime to be combined under technical conditions, the "Standard Lime" (Standardkalk). Taking the Standard Lime as 100, the ratio of the lime content of a technical clinker to its Standard Lime will be the "Lime Standard" (Kalkstandard). Together with the Silica Ratio (Silikatmodul) $S/(A+F)$ and the Alumina Ratio (Tonerdemodul) A/F an expert has a clear concept of the composition of a cement and its properties. For the layman the figures are not as temptingly demonstrative as the "potential composition"—we would say fortunately they are not.

Kühl's lime standard formula was based on a paper by Spohn (6) who found that the "*lime limit*" of a clinker is controlled by equilibrium conditions at sintering temperature. Upon cooling this equilibrium is quenched. The formula suggested by Kühl (5) was

$$\text{LSt I} = \frac{100\text{CaO}}{2.8\text{SiO}_2 + 1.1\text{Al}_2\text{O}_3 + 0.7\text{Fe}_2\text{O}_3}$$

Basing on the work of Lea and Parker (7) the formula was later modified to

$$\text{LSt II} = \frac{100\text{CaO}}{2.80\text{SiO}_2 + 1.18\text{Al}_2\text{O}_3 + 0.65\text{Fe}_2\text{O}_3}$$

In the British Standards (8) the so-called Lime Saturation-Factor of a cement is defined as

$$\text{LSF} = \frac{\text{CaO} - 0.7\text{SO}_3}{2.8\text{SiO}_2 + 1.2\text{Al}_2\text{O}_3 + 0.65\text{Fe}_2\text{O}_3}$$

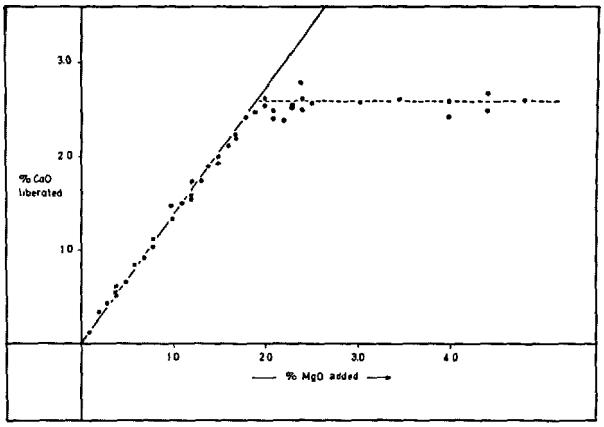

Fig. 2. CaO *liberated from* C_3S *as a function of additions of* MgO. (*11*)

(thus taking consideration of the gypsum content of cement by the SO_3-factor.)

Kühl's as well as Lea and Parker's formulas, however, are functions of CaO, SiO_2, Al_2O_3 and Fe_2O_3 only. Minor components, such as MgO, Na_2O, K_2O, SO_3, P_2O_5, TiO_2 and others are not being considered although some of them may be present in measurable amounts and accordingly exert influences on the lime-limit of a clinker. Both formulas, therefore, do contain a certain error. It is known for a long time, indeed, that with some raw materials lime standard values of approximately 100 can be attained, while with some other materials the practical limit is lower, sometimes, even as low as 96.

In this paper it is attempted to refine the lime standard formula by including a factor for MgO. Investigations of the solid solution of Ca_3SiO_5 with MgO (9, 10, 11) (Fig. 2) proved that MgO is replacing CaO up to a limit which, being temperature dependent, is 1.6% MgO at 1450°C the normal firing temperature of portland cement clinker.

Since in lime-saturated clinker C_3S is a major compound and, at sintering temperature, the only solid phase in equilibrium with liquid, it is evident that the liberation of lime by incorporation of MgO in C_3S must be a measurable quantity in clinker, too.

In the ternary system $CaO–Al_2O_3–SiO_2$ the formula

$$CaO = 2.80SiO_2 + 1.18Al_2O_3$$

is the analytical expression for the straight line connecting the point of C_3S and the invariant point $C_3S + C_3A + CaO +$ liquid. It must be kept in mind, however, that the C_3S-phase contains some Al_2O_3 in solid solution, and the point representing the composition of the alite-phase is shifted accordingly.

Any MgO added to this phase assemblage is distributed among the coexisting phases alite + liquid according to a defined distribution scheme. A set of tielines exists, until finally both the C_3S-phase and the liquid are saturated with MgO and periclase appears. Accordingly the lime-limit is to be defined as surface between the points:

1. Alite (saturated with respect to CaO and Al_2O_3)
2. Invariant point $C_3S + CaO + C_3A +$ liquid
3. Invariant point $C_3S + CaO + C_3A + MgO +$ liquid
4. Alite (saturated with respect to CaO, Al_2O_3 and MgO)

The line through the latter two points at the same time is the magnesia-limit.

These four points do not lie in one plane, however, and the surface connecting these points is slightly contorted. Its analytical expression is complicated and not suitable for quick calculations on clinker analyses.

It is more convenient to select a certain sector of this surface around "normal" clinker compositions, treating the latter as a plane by approximation.

Analogous problems arise on defining the lime-limit in the quinary system $CaO–MgO–Al_2O_3–Fe_2O_3–SiO_2$, requiring the same limitations to "normal" compositional ranges.

Preliminary experiments were conducted to prove the assumption, that CaO is liberated by addition of MgO to clinkers.

A laboratory clinker with composition:

CaO	69.69%
Al_2O_3	5.46%
Fe_2O_3	3.64%
SiO_2	21.21%
Alumina Ratio	1.50
Silica Ratio	2.33

—thus representing a "normal" portland cement clinker-composition—was carefully mixed from r.g. reagents and heated to a temperature of 1500°C, rapidly cooled and analysed for free CaO after the method of Franke (12)*. Subsequently this finely ground homogeneous clinker was subdivided into equal portions of 3 grams each, and different, well defined amounts of MgO were added to each sample which was finally heated for a second time for two hours at 1500°C to accomplish equilibrium. After cooling the free lime was determined. The sample's increase in free lime above that of the magnesia-free charge was entered into a graph (Fig. 3) against the corresponding addition of MgO.

*In preliminary experiments, the method after Schlaepfer-Bukowski (13) was applied. This method, however, introduces analytical errors by attacking the C_3S-phase.

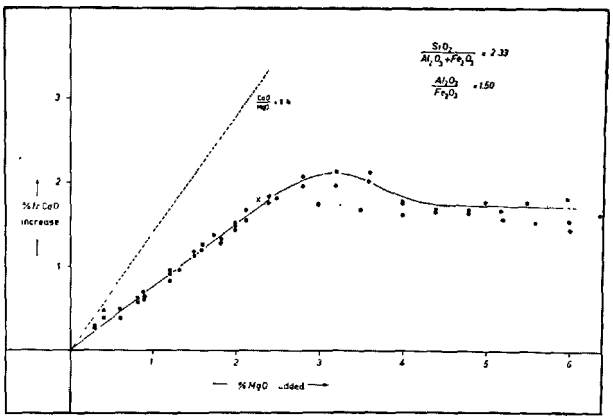

Fig. 3. *Increase in free* CaO *by additions of* MgO *to a laboratory clinker with "normal" clinker composition.*

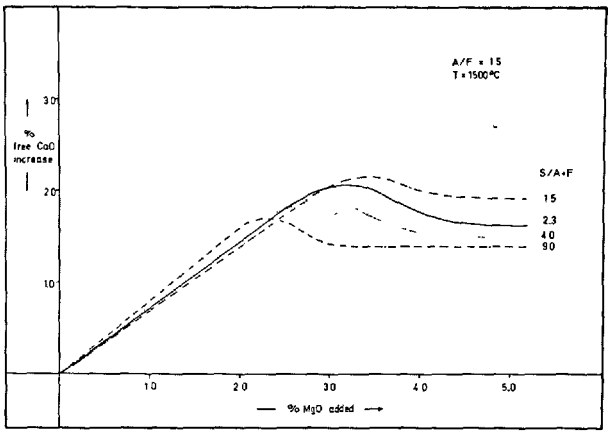

Fig. 4. *Influence of variable silica-ratio on the combination of* MgO *and liberation of* CaO *in laboratory clinkers.*

The curve in Fig. 3 may be subdivided into three sections:

In section I (low magnesia-contents) a steady increase in free lime, proportional—but not equivalent—to the MgO-additions is observed. This is due partly to the solid solution of MgO in alite, thus causing a liberation of free lime as demonstrated in Fig. 2 and partly to the solution of MgO in the liquid phase at sintering temperature, thus causing a change of its composition to lower CaO–contents. No periclase has been observed during microscopical investigation of these samples. Thus all MgO is present in the combined form.

In section II the free lime content with a smooth curve passes through a maximum and then decreases with higher MgO–contents to lower free CaO–values. No satisfactory explanation so far is given for the maximum of the curve. It may be due to supersaturation of the sample with respect to MgO. The first periclase is observed on the descending part of the curve.

In section III (high magnesia-contents) the curve is straight again and practically parallel to the abscissa. Further additions of MgO do not exert any influence on the lime-limit of the clinker. They result in formation of periclase which can be observed microscopically.

The following information is gained from the curve:

1. The relationship between liberated CaO and combined MgO–the "C/M–ratio"—is given by the slope of the curve in section I.
2. For the limiting amount of MgO to be combined, the maximum of the curve should be representative. Since, however, the data in section II of the curve were less reliable and were, moreover, influenced by the cooling rate, the intersection of the two straight portions of the curve—sections I and III (point "X" in Fig. 3)—was preferred to define the magnesia-limit. In addition, this point makes it possible to determine the amount of CaO liberated by MgO, regardless of higher MgO–concentrations.

The above model clinker was selected to have a normal clinker-composition. It is necessary, however, to investigate whether

1. the C/M–ratio and
2. the magnesia-limit

are influenced by a change of composition or of temperature. For the purpose a series of laboratory clinkers was investigated by analogous methods.

Fig. 4 presents graphically the results of these experiments on some clinker with constant alumina-ratios A/F but changing silica ratio $S/(A + F)$. With increasing silica ratio there is a shift towards higher C/M–ratios of the first section of the curve, but a decrease of combined MgO. In the range of normal clinker compositions, however, this shift is small.

Fig. 5 shows the results of experiments on clinker with constant silica ratio but varying alumina-ratios: The C/M–ratio remains essentially unchanged, but the total amount of combined MgO increases with increasing Al_2O_3–content and decreases with increasing Fe_2O_3–content.

Fig. 6 shows the influence of the firing temperature on the solution of MgO in the solid and liquid clinker-phases: Again the C/M–ratio remains unchanged while the total amount of MgO combined is temperature dependent.

From the above data the following deductions are made:

1. The C/M–ratio is independent of temperature

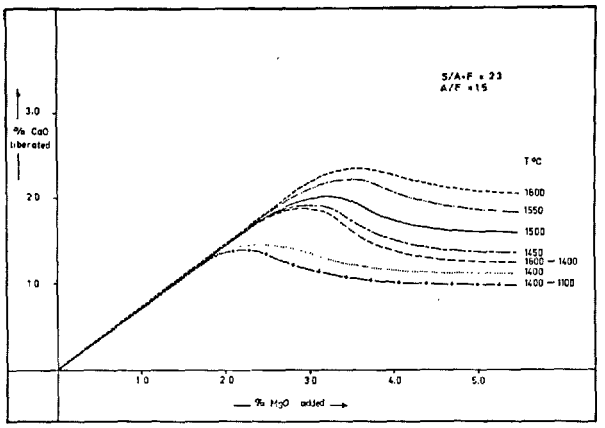

Fig. 5. *Influence of variable alumina ratio on the combination of* MgO *and liberation of* CaO.

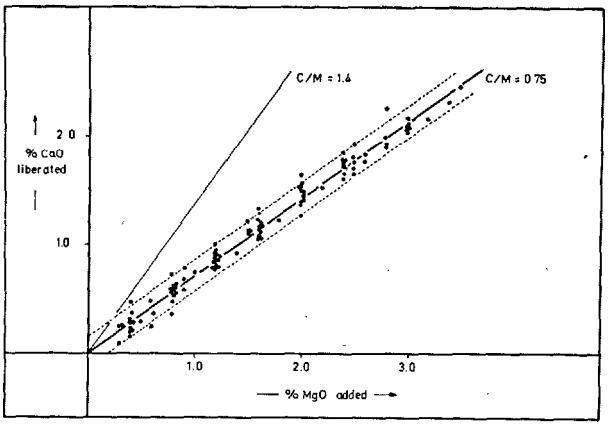

Fig. 7. *Experimental data on the C/M-ratio of all clinker samples investigated in the range of silica ratio 1.5–4.0*

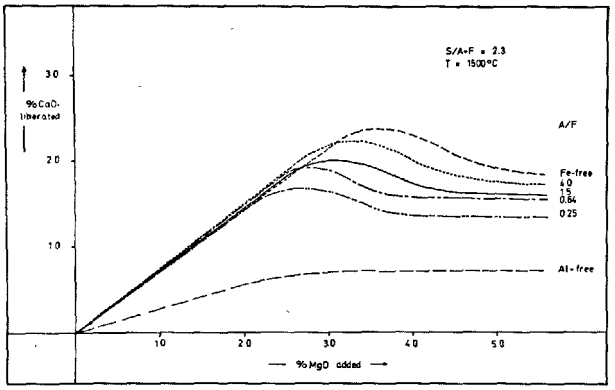

Fig. 6. *Influence of temperature on the combination of* MgO *and liberation of* CaO *from a laboratory clinker. The curves marked 1600°–1400° and 1400°–1100°C show the corresponding results on clinker samples heated to the higher temperature indicated and cooled slowly—within 1 hour—to the lower temperature.*

and of the alumina-ratio of the clinker, but it is slightly shifted with the silica ratio. This shift, however, is small, being hardly greater than the experimental error if only normal cement compositions with silica ratio = 1.5 — 4.0 are considered. Fig. 7 contains all experimental data within this range. The weighted average of these points lies on a line representing a C/M–ratio of 0.75. Accordingly, it may be concluded that MgO is distributed among the solid and liquid clinker phases in such a way that as a resultant effect for each weight unit of MgO dissolved 0.75 units of CaO are liberated. This distribution factor is independent of temperature in the investigated temperature range.

2. The total amount of MgO combined is influenced by a greater variety of factors:

Table 1. *The magnesia-limit at various clinker compositions*

$\frac{S}{A+F}$	1.50	1.86	2.33	3.0	4.0
$\frac{A}{F}$					
0.64	(2.5)*	(2.3)	2.1	(2.0)	(1.9)
1.50	2.6	(2.4)	2.2	(2.1)	2.0
4.0	(2.7)	(2.5)	2.3	(2.2)	(2.1)

*numbers in brackets are interpolations

The increase of the MgO–limit with temperature (±0.6%/100°C according to Fig. 6) is in agreement with the higher solubility of magnesia in the liquid phase at higher temperatures, and at the same time with the temperature dependence of the solid solution of MgO in C_3S.

Since the concentration of MgO in alite (1.8% MgO at 1500°C) is considerably lower than the magnesia content of the Mg–saturated liquid (5.5% MgO at the invariant point $C_3S + CaO + C_3A + MgO +$ liq. (14) and ±5.0% MgO at the invariant point $C_3S + CaO + C_3A +$ ferrite $+ MgO +$ liquid (15)) an increase in the liquid content will result in a corresponding increase of the magnesia-limit. Since the concentration of the silicates (i.e. of C_3S at the lime limit) and of liquid are controlled by the silica-ratio, and since, moreover, with constant silica-ratio a clinker with higher alumina-ratio contains a higher amount of liquid, the influence of these factors on the total amount of combined MgO is explained.

The following data for the magnesia-limit in clinker in equilibrium at 1500°C are taken from Figs. 4 and 5.

Thus for compositions of technical portland cement clinker (inside the frame in the table) about 2.1–2.5%

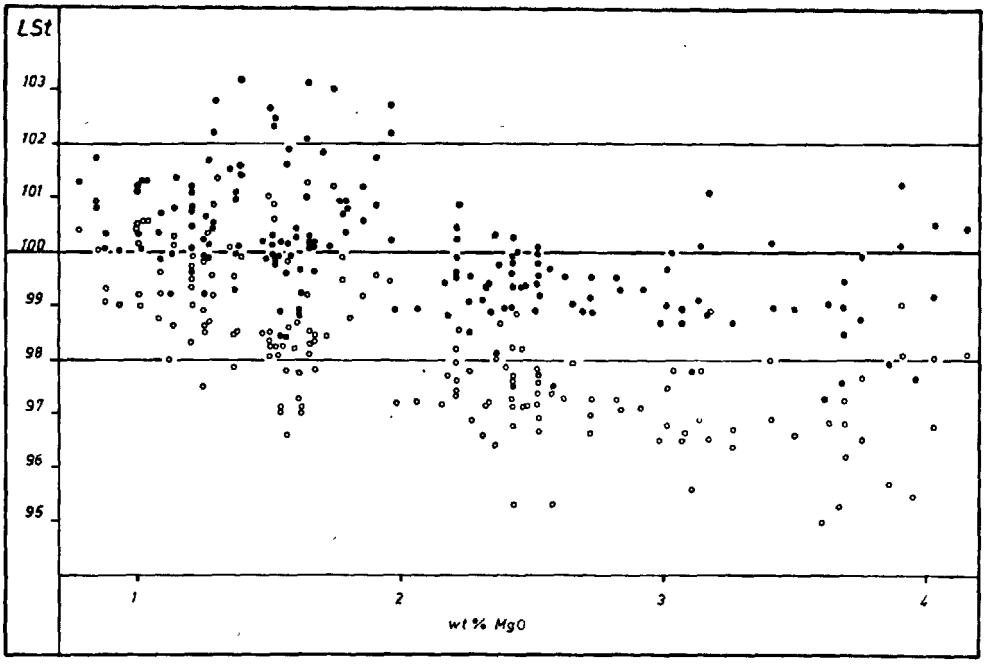

Fig. 8. *Comparison of the formulas LSt II (open circles) and LSt III (black dots) as applied to technical clinker from nine different cement plants. The lime limit of these clinkers has been determined by the lime deviation method. The straight lines at LSt = 98 and 102 define the total error tolerated in wet-chemical routine-analyses.*

MgO are combined by alite and the liquid phase at 1500°C. Assuming a temperature dependance of 0.6% MgO/100°C (see Fig. 6), this range will be shifted to 1.8–2.2% MgO at 1450°C, or, in the average, to 2.0% MgO.

The magnesia-limit at 2.0% MgO is supported by microscopical investigation of technical clinker: With considerable regularity periclase is observed in clinker with more than about 2.0% MgO. There are exceptions, however. In some cases clinker with MgO–contents of up to 2.5% did not show periclase, or, on the other hand, clinker with lower MgO–concentration contained periclase. Mostly the latter case, however, may be due to inhomogenities of the raw mix.

In order to apply these results successfully to technical conditions they may be simplified as follows:

A maximum of 2.0% MgO can be combined in clinker at a CaO/MgO–ratio of 0.75.

Based on these data a factor for MgO may be included into the formula LSt II. Since MgO is equivalent to CaO, this factor must be added to the amount of CaO.

The modified formula will be:

$$\text{LSt III} = \frac{100(\text{CaO} + 0.75\text{MgO})}{2.80\text{SiO}_2 + 1.18\text{Al}_2\text{O}_3 + 0.65\text{Fe}_2\text{O}_3}$$

for all compositions with $\text{MgO} \leqq 2.0\%$ and

$$\text{LSt III} = \frac{100(\text{CaO} + 1.50)}{2.80\text{SiO}_2 + 1.18\text{Al}_2\text{O}_3 + 0.65\text{Fe}_2\text{O}_3}$$

for clinker compositions with $\text{MgO} > 2.0\%$.

In order to check whether the new formula is an improvement for the calculation of the lime limit under technical conditions, carefully analysed clinkers from nine different cement plants were tested: They were finely ground and according to Spohn's lime deviation method mixed with a well defined addition of $CaCO_3$, then subsequently heated for 30 minutes to 1450°C. Free lime was determined and subtracted from the bulk composition. The results were calculated according to LSt II and LSt III. Under ideal conditions now the lime standard should be equal to 100. The experimental results are compared graphically in Fig. 8. Here the open circles represent the calculations after LSt II while the black dots show corresponding data for LSt III.

From Fig. 8 it follows that the points calculated after LSt II are, in the average, distinctly too low.

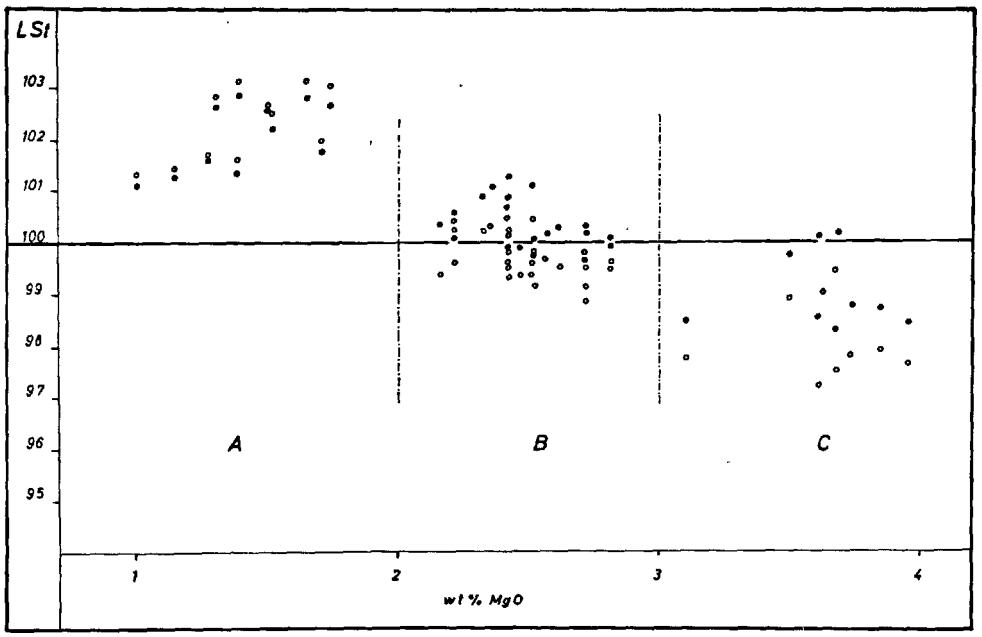

Fig. 9. *Standard Lime for clinker of three different cement works (A, B and C)*
Open circles: heated for 30 minutes at 1450°C
Black dots: heated for 15 hours at 1500°C

Calculated after LSt III the points are shifted to higher values. For the greater part of the investigated clinkers they now fall within a range between LSt = 98 — 102, which is set by tolerance limits of wet-chemical analyses in plant laboratories.

It may be noted that still some of the points are too low, but some distinctly too high. On comparing the clinkers of single plants seperately, it is demonstrated that a certain high or low deviation is typical for each cement plant. These deviations are due to the influence of further minor components in clinker. Some clinkers, containing more alkalies than their equivalent of SO_3 will have the tendency to shift the points to lower LSt values, while others containing more SO_3 will shift the points to higher LSt values. Expelling these components by heating the sample for a few hours at 1500°C helped to shift these points closer to the line of LSt = 100 (Fig. 9). Here we find an indication that the formula LSt III still can be improved by further investigations.

In consideration, however, of the fact that our values are within the range of analytical error, the formula LSt III seems to be accurate enough for most practical purposes.

References

1. E. Spohn, "Die Kalkfehlermethode bei der Zementrohmehleinstellung." Zement-Kalk-Gips, **12,** (1959), 560–566.
2. R. H. Bogue, "Calculation of compounds in portland cement," Ind. Eng. Chem. Anal. Ed. **1,** (1929), 192–197.
3. F. M. Lea, The Chemistry of Cement and Concrete. 2nd Ed., Arnold Publishers, London, (1956,) 140–143.
4. H. Krämer and H. zur Strassen, Discussion Proc. 4th Int. Symposium on the Chemistry of Cement, Washington, 1960, 32–33.
5. H. Kühl, "Der Kalkstandard der Portlandzemente," Tonindustrie-Zeitung, **57,** (1933), 460–464.
6. E. Spohn, Die Kalkgrenze des Portlandzements. Zement 21, (1932), 702–706, 717–723, 731–736.
7. F. M. Lea and T. W. Parker, "The quaternary system CaO–Al_2O_3–SiO_2–Fe_2O_3 in relation to cement technology," Building Research Techn. Paper **16,** (1935), 1–51.
8. British Standards: Standard 12:1958.
9. F. W. Locher, "Solid solution of alumina and magnesia in tricalcium silicate," Proc. 4th int. Symposium on the Chemistry of Cement, Washington, (1960), 99–103.
10. E. Woermann, Discussion Proc. 4th Int. Symposium

on the Chemistry of Cement, Washington, (1960), 104–106.
11. E. Woermann, Th. Hahn and W. Eysel, "Chemische und strukturelle Untersuchungen der Mischkristallbildung von Tricalciumsilikat," 1. Bericht: Zement-Kalk-Gips, **16,** (1963), 370–375. 2. Bericht: Phasenbeziehungen in den Systemen $CaO–MgO–SiO_2$ und $CaO–Al_2O_3–SiO_2$ Zement-Kalk-Gips, **20,** (1967), 385–391. 3. Bericht: Kombinierter Einbau von MgO und Al_2O_3 in Ca_3SiO_5. Zement-Kalk-Gips, **21,** (1968), 241–251.
12. B. Franke, "Ein neues Verfahren zur Bestimmung von Calciumoxyd und Calciumhydroxyd neben wasserfreiem und wasserhaltigem Calciumsilikat," Zement, **30,** (1941), 401.
13. P. Schlaepter and R. Bukowski, Ber Eidgen. Mater. Prüf. Anst., **109,** (1937).
14. H. E. McMurdie and H. Insley, "Studies on the quaternary system $CaO–MgO–2CaO·SiO_2–5CaO–3Al_2O_3$," Journ. Res. National Bureau of Standards, **16,** (1936), 467–474.
15. M. A. Swayze, "A report on studies of: 1. The ternary system $CaO–C_5A_3–C_2F$ 2. The quaternary system $CaO–C_5A_3–C_2F–C_2S$ 3. The quaternary system as modifies by 5% magnesia," Amer. Journ. Sci., **244,** (1946), 1–30, 65–94.

SESSION I-3 ANALYSIS OF PORTLAND CEMENT CLINKER

Principal Paper I-3 The Analysis of Portland Cement Clinker

Goro Yamaguchi and Shigehide Takagi*

Synopsis

The identification study in the cement chemistry by the X-ray powder diffraction method has been developed immensely since diffraction patterns of the cement minerals became able to be interpreted precisely. Circumstances of the development are described.

As to the separation of the cement minerals from clinker, physical separation and chemical separation were employed. Any separation method was not perfect alone but combination of treatments was useful for clarifying the nature of the minerals.

Analysis of the chemical composition of the minerals and the mineral composition of clinker was attempted using a combination method of separations and chemical analysis.

Transmitted light and reflected light microscopy are both useful for analyzing the texture of clinker, especially the former is indispensable for clarifying it completely. Using these methods the inversion texture was interpreted.

Using an electron microscope fine textures of inverted belite were analyzed and photographs are presented.

Application of an electron probe microanalyzer to the clinker analysis is explained. Photographs of reflected light microscopy and electron probe microanalysis in the same field of clinker are presented and explained in order to clarify alite, belite, ferrite and aluminate textures.

The chemical composition of the minerals and the mineral composition of clinker obtained by several methods are discussed.

Introduction

It is so long since portland cement has been invented and it seems that the improvement has been already at a top level. In spite of the scientific researches performed by many investigators, the analysis from the standpoint of the modern materials science is not enough and delicate properties of cement are still left not clear.

The first problem is about the nature of the clinker minerals. What are true chemical compositions of alite phase, belite phase, ferrite phase and aluminate phase? What are their crystal structures? What relationship is there between properties of cement such as hydration, hardening etc. and the natures of mineral phases? About those problems there exist many questions.

The second problem is how do those minerals exist and make textures in clinker. Although the development of measuring and observing equipments made some successful answers possible, many questions are yet left as future problems.

The third problem is how their textures are produced in sintering and cooling processes of manufacturing. The process and the result of solid state reaction, crystal growth and modification transition have many insolvable points.

At this circumstance a project of this thesis is to attempt to systematize an analytical method of cement clinker. In order to approach to the project many analytical procedures conducted by former investiga-

*Faculty of Engineering, The University of Tokyo, Tokyo, Japan.

tors were practiced, considered and improved and new procedures were developed using several Japanese clinkers as testing samples.

Mineral phases mainly objected in this experiment are four major components of clinker, that is, alite phase, belite phase, ferrite phase and aluminate phase, and minor components are treated in a necessary case. Clinkers employed in the experiment are ten kinds from Japanese factories denoted N_1, N_2, N_3, N_4, N_5, R, M_1, M_2, W_1 and W_2. N means normal cement, R rapidly hardening cement, M moderate heat cement and W white cement.

Identification by the X-ray Diffraction

The identification of the cement minerals by the X-ray powder diffraction method has been carried out since so long time. However, the correct interpretation of diffraction patterns has not been done before the development of a recording X-ray diffractometer. The same subject was dealt with in the last symposium but this time it will be described on the standpoint of clarifying circumstances.

The X-ray powder diffraction data before the development of a recording X-ray diffractometer were less reliable, because many diffraction lines were not indexed and some times wrongly indexed. The development of the apparatus resulted in correct measurement to separate and index multiplets and to revise wrong indexings. Those studies were conducted by many investigators by means of synthesizing and examining clinker and its component minerals in pure state and solid solution state.

A recording X-ray diffractometer caused splendid progress in a field of the identification of the cement minerals. However, its weak point is that it cannot resolve an extremely close multiplet because of adjoining of α_1 and α_2 diffractions although it has a higher resolution power than an ordinary diffraction camera. For this purpose an application of a focusing diffraction camera caused the wonderful results.

The following is description about respective minerals. Through this experiment a diffraction angle is expressed in 2θ by Cu Kα radiation.

Alite and Relating Minerals

R. Naito, Y. Ono and T. Iiyama (1957) (1) described examining characteristic powder diffraction patterns of pure C_3S and C_3S solid solution that a diffraction pattern of pure C_3S mentioned as triclinic seemed more complex and lower symmetric than that of C_3S solid solution mentioned as monoclinic and that indexing of the powder diffraction patterns seemed nearly impossible.

However, G. Yamaguchi, H. Miyabe and K. Tanaka (1959) (2) successfully attempted to index the main diffractions of pure C_3S and C_3S solid solution using a pseudo-orthorhombic provisional lattice based upon the result of the structure analysis done by J. W. Jeffery (1952) (3). Moreover, G. Yamaguchi, H. Miyabe (1960) (4) measured precisely and indexed the diffraction patterns of the triclinic and the monoclinic lattices, and succeeded in an interpretation of the diffraction patterns and a calculation of the lattice parameters, and presented useful data for the identification of the minerals.

The characteristics of the diffraction pattern of C_3S minerals are diffractions of 221, 401, 222 and 402 at 29°–30°, 009, 224, $\bar{4}04$, $\bar{2}25$ and 405 at 31°–34°, $\bar{2}28$ and 319 at 41°, and 620 and 040 at 51°–52°. These indexes are after the provisional pseudo-orthorhombic lattice of Yamaguchi et al. Among these diffractions 620 and 040 diffractions are most important because they are independent from other minerals and remarkably changeable according to lattice deformation.

N. Yannaquis, M. Regourd, Ch. Mazieres and A. Guinier (1962) (5) mentioned there exist six kinds of polymorphs in pure C_3S, and they denoted T_I, T_{II} and T_{III} in triclinic, M_I and M_{II} in monoclinic and R in trigonal according to an experiment using a focusing camera. They did not agree with the indexing of Yamaguchi et al. but it seems misunderstanding as well as a description in "The Chemistry of Cement" by J. W. Jeffery (1964) (6). M. Regourd (1964) (7), however, adopted the principle of Yamaguchi et al. and connected her result with that principle using a pseudo-hexagonal lattice based on the trigonal lattice instead of the pseudo-orthorhombic lattice of Yamaguchi et al. She suggested T_I and T_{II} have large lattices because of some extra diffractions of long spacings and M_{II} might be orthorhombic. According to the author's opinion, it is more convenient to use the pseudo-orthorhombic lattice as a provisional lattice, anyway it is no more than a convenient one.

H. Miyabe and D. M. Roy (1964) (8) studied that problem using a recording X-ray diffractometer and recognized polymorphs corresponding to T_I and T_{II} but not T_{III} and M_{II}. This disagreement seems due to the lower resolution power of a recording diffractometer than a focusing camera.

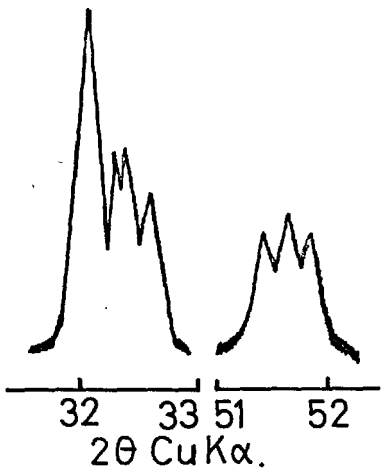

Fig. 1. *Characteristic diffraction pattern of triclinic* C_3S

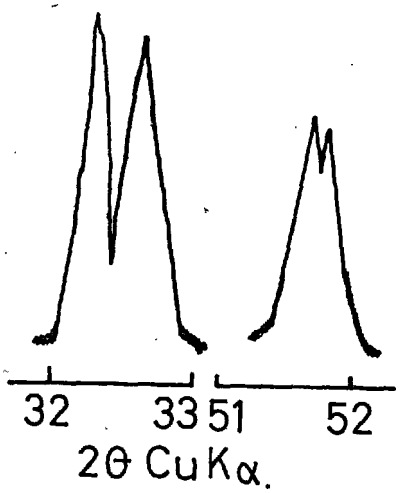

Fig. 2. *Characteristic diffraction pattern of monoclinic* C_3S

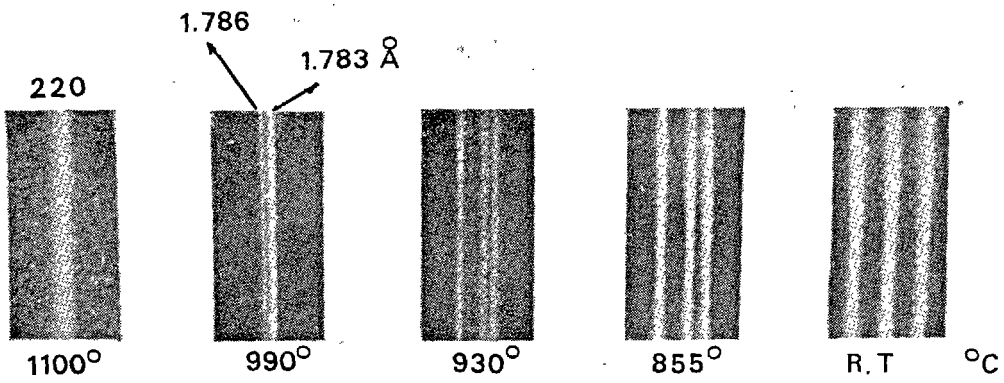

Fig. 3. *Fine structure of diffraction pattern of* C_3S *polymorphs* (7)

Besides thermal polymorphism of C_3S, studies of lattice deformation caused by impurity solid solution were carried out. G. Yamaguchi and H. Uchikawa (1960–1) (9), (1961–2) (10) described that a triplet diffraction at 51°–52° of triclinic C_3S solid solution with Na_2O gets closer in proportion to an amount of Na_2O and inverts into monoclinic having a doublet diffraction with 040 shifted to high angle side.

G. Yamaguchi, H. Uchikawa, S. Takagi and H. Koike (1962) (11) and G. Yamaguchi, H. Uchikawa and S. Kawamura (1961) (12), (1962) (13) recognized the same phenomena in C_3S solid solution system with Al_2O_3, Fe_2O_3 and Na_2O. G. Yamaguchi and H. Uchikawa (1962) (14) traced that lattice deformation concerning to alite in commercial clinkers. G. Yamaguchi and K. Kato (1962) (15) studied a lattice deformation in the solid solution system with MgO and Al_2O_3. E. Woermann, Th. Hahn and W. Eysel (1963) (16) and H. G. Midgley and K. E. Fletcher (1963) (17) performed the same investigation more minutely. Especially Woermann et al. found out a discontinuity of spacing shift among triclinic forms with gradiently different amount of impurities and denoted them T_{I} and T_{II} corresponding to pure C_3S polymorphs.

Y. Ono, T. Uno and Y. Kanai (1965) (18) synthesized triclinic C_3S solid solutions with various impurities having different features of diffractions. These phases seem to be discontinuous one another, but it remains as a problem to define them as different polymorphs until the certification of the phase discontinuity or another certification would be done.

G. Yamaguchi and K. Kato (1964) (19) and G. Yamaguchi, K. Shirasuka and T. Ohta (1966) (20) examined that monoclinic C_3S solid solution inverts into triclinic by reheating.

Recently M. Bigaré, A. Guinier, M. Regourd, N. Yannaquis, W. Eysel, Th. Hahn and E. Woermann (1967) (21) summarized this C_3S polymorphs problem

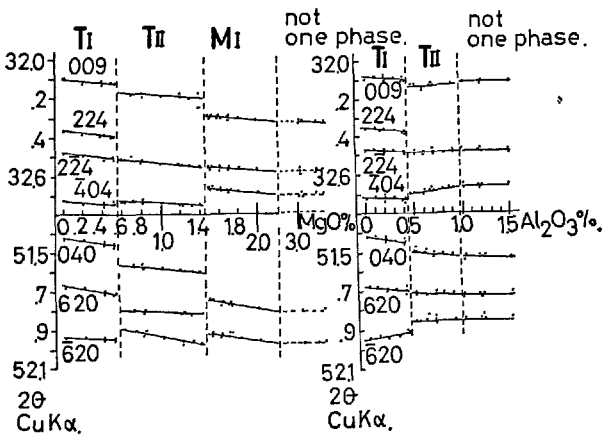

Fig. 4. *Shift of diffraction of* C_3S *solid solution with* MgO *and* Al_2O_3(16)

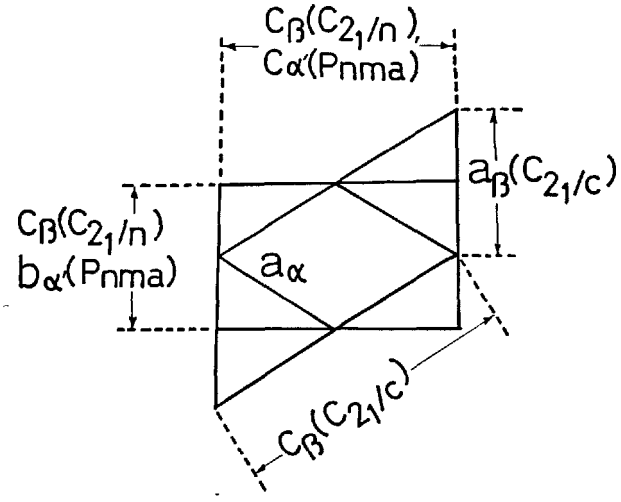

Fig. 5. *Relation of* C_2S *lattices among* βP2 1/c, βP2 1/n, α' Pnma *and* αP$\bar{3}$c1

Table 1. *Relation of equistructural indexes of* C_2S

α P$\bar{3}$c1	α' Pnma	β P2 1/c	β P2 1/c
101	111	110	111
		11$\bar{2}$	11$\bar{1}$
		012	012
	102	12$\bar{2}$	12$\bar{1}$
		121	121
102	211		
	202	022	022
	013	10$\bar{4}$	10$\bar{3}$
110		102	103
	020	200	200
	122	21$\bar{4}$	21$\bar{2}$
201		210	212
	104	014	014
		22$\bar{4}$	22$\bar{2}$
202	222	220	222
	204	024	024

and confirmed the correspondency of T_I, T_{II} and T_{III} in the pure system to those of the solid solution system from the standpoint of the spacing discontinuity and the differential thermal analysis.

The classification and the identification of polymorphs among those which have only such very small gaps of physico-chemical continuity as seen in the C_3S system are delicate problem and it needs much more experiments to systematize the problem. Any way, since Yamaguchi et al. have succeeded in interpretation of the X-ray powder diffraction through Bigaré et al. have summarized the problems, a splendid progress has been brought in this field.

As to relating minerals, S. Akaiwa, G. Sudoh and M. Tanaka (1966) (22) found and analyzed a new mineral $11CaO \cdot 4SiO_2 \cdot CaF_2$ which resembles C_3S structurally.

Belite and Relating Minerals

G. Yamaguchi, H. Miyabe, K. Amano and S. Komatsu (1957) (23) and G. Yamaguchi, Y. Ono, S. Kawamura and Y. Sohda (1963–1) (24), (1963–2) (25) interpreted and indexed X-ray powder diffraction patterns of C_2S polymorphs at high temperature and stabilized by several impurities, using a provisional lattice based on the monoclinic lattice obtained by C. M. Midgley (1952) (26) and presented useful data for identification. The lattice of β–C_2S should be P2 1/c after International Table for X-ray Crystallography (27) but P2 1/n is more convenient to compare with the α'–C_2S lattice (Pnma). The indexes will be shown in P2 1/n followed by those in P2 1/n as hkl (h'k'l').

Characteristic diffractions of β–C_2S are 10$\bar{4}$(10$\bar{3}$), 12$\bar{2}$(12$\bar{1}$), 20$\bar{2}$(200), 022(022) and 120(121) at 32°–33°, 102(103) at 34° and 014(014) and 031(031) at 41°. However, all these diffractions overlap to those of C_3S, so that these diffractions are not convenient for identification. For that purpose 12$\bar{1}$(120) diffraction at 31° is independent and convenient though it has somewhat weak intensity.

As to α–C_2S, 110 diffraction at 33° is the strongest and characteristic one though it situates rather near by diffractions of others.

The strongest diffraction of α'–C_2S, 020, 211, 202 at 32°–33° overlaps to others then 013 diffraction near by 110 of α–C_2S is characteristic. Suggestions of a slight inversion in α'–C_2S, $\alpha'_L \rightleftarrows \alpha'_H$, were presented by D. K. Smith, A. J. Majumdar and F. Ordway (1961) (28) and K. Niesel and P. Thormann (1967) (29), although confirmation by the X-ray diffraction was not carried out.

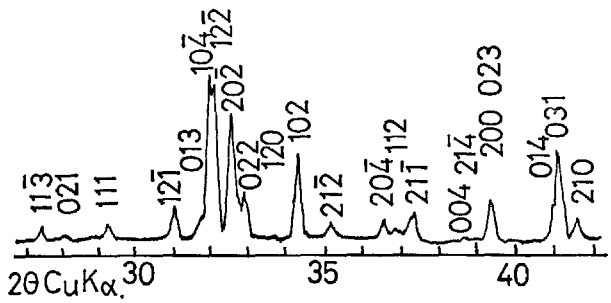

Fig. 6. *Diffraction pattern of* βC_2S (P2 1/c)

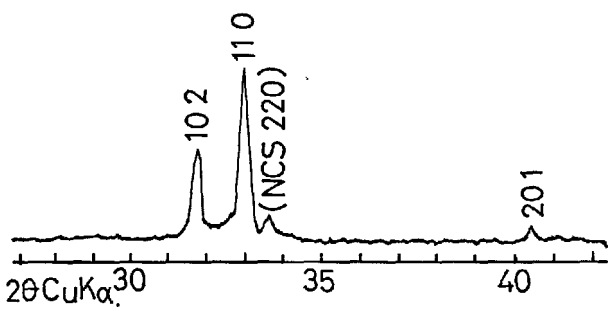

Fig. 7. *Diffraction pattern of* αC_2S

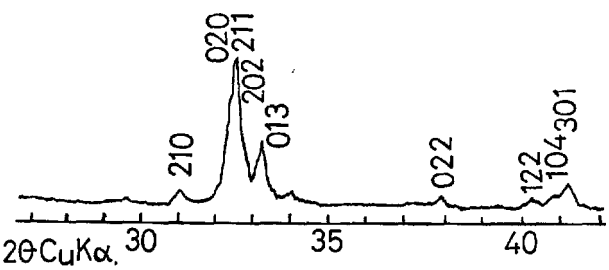

Fig. 8. *Diffraction pattern of* $\alpha' C_2S$ (P_{nma})

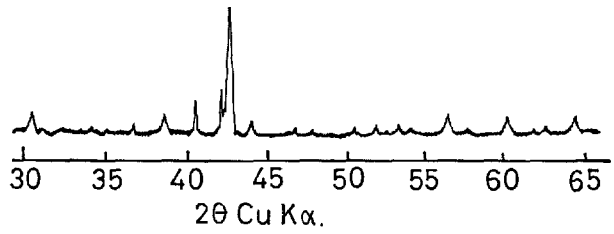

Fig. 9. *Diffraction pattern of* C_4AF

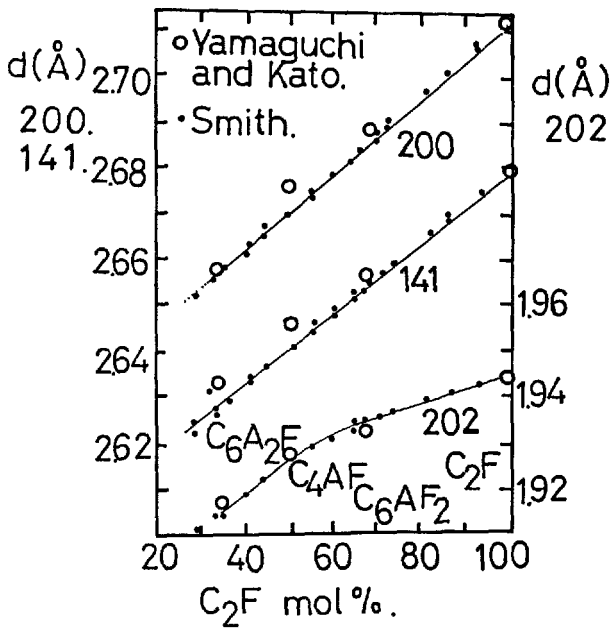

Fig. 10. *D-spacing of* C_4AF *solid solution of* C_2F–C_2A *system*

The lattice parameters and the situations of diffractions of polymorphs of pure C_2S can not be obtained because pure C_2S inverts into γ–C_2S at room temperature. The shift of the lattice parameters and diffractions of polymorphs of C_2S solid solutions according to impurity amount cannot also be determined because each polymorph is not able to be stabilized by any kind and any amount of impurities. However, the fact that a shift of diffractions of C_2S is caused by impurity is shown in data of G. Yamaguchi, Y. Ono, S. Kawamura and Y. Sohda (1962) (30).

As to relating minerals, a precise interpretation of X-ray powder diffraction of $KC_{23}S_{12}$ was done by Y. Ono (1963) (31), a diffraction of merwinite, C_3MS_2, was correctly determined from powder diffractions and single crystal data by G. Yamaguchi and K. Suzuki (1967) (32) although questionable data of M. A. Bredig (1945) (33) (34) had been so far quoted, and a intermediate mineral, $(C_2S)_{5.6}(C_3MS_2)_{4.4}$, between C_2S and C_3MS_2 was reported by W. Gutt (1961) (35).

Ferrite and Relating Minerals

The lattice parameters of C_4AF solid solution had been determined by the single crystal analysis but the analysis of powder diffraction patterns for identification had been incorrect, for instance, diffractions of 141 and 200 had been misindexed. G. Yamaguchi and A. Kato (1957) (36) correctly analyzed it followed by E. F. Bertaut, P. Blum and A. Sagieres (1959) (37) who determined the atomic parameters also. Relation between compositions of solid solutions and d-spacings has been measured somewhat differently according to investigators. Fig. 10 shows data of G. Yamaguchi et al. and D. K. Smith (1962) (38).

A. Kato (1958) (39), (1959) (40) studied the solid

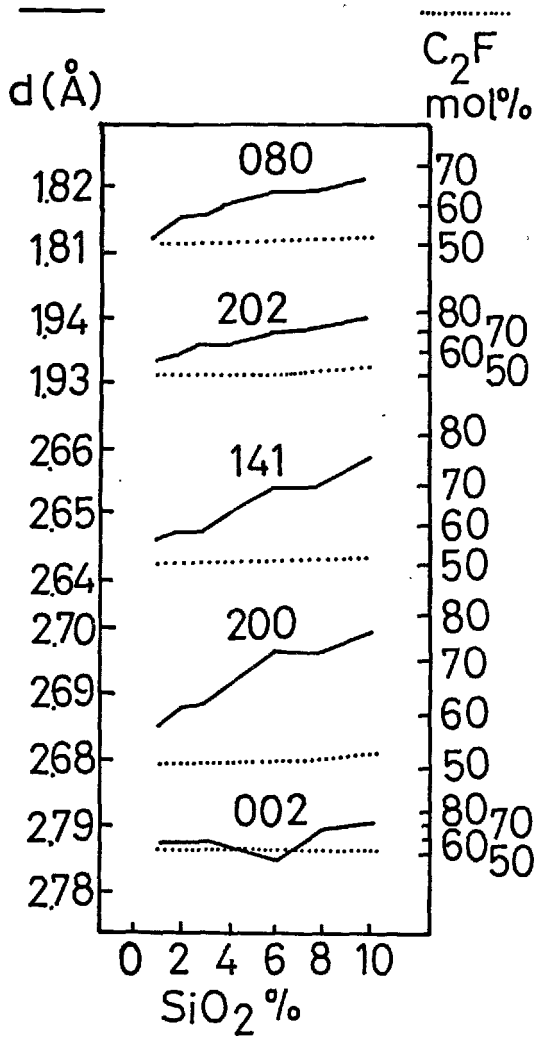

Fig. 11. *D-spacing of* C_4AF *solid solution with* SiO_2, *right scale side corresponds to* C_2F *mol %*

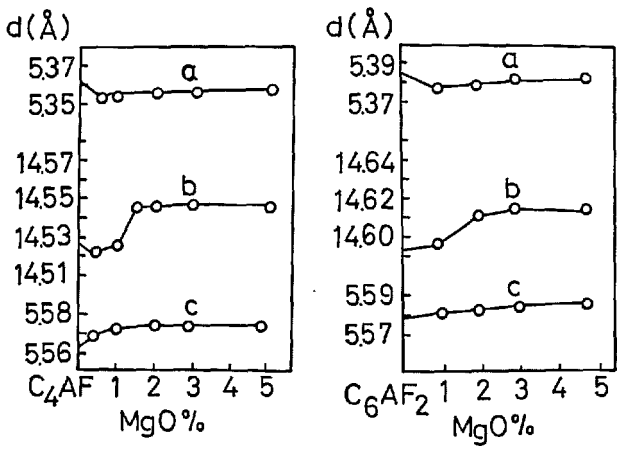

Fig. 12. *Lattice parameters of* C_4AF *solid solution with* MgO

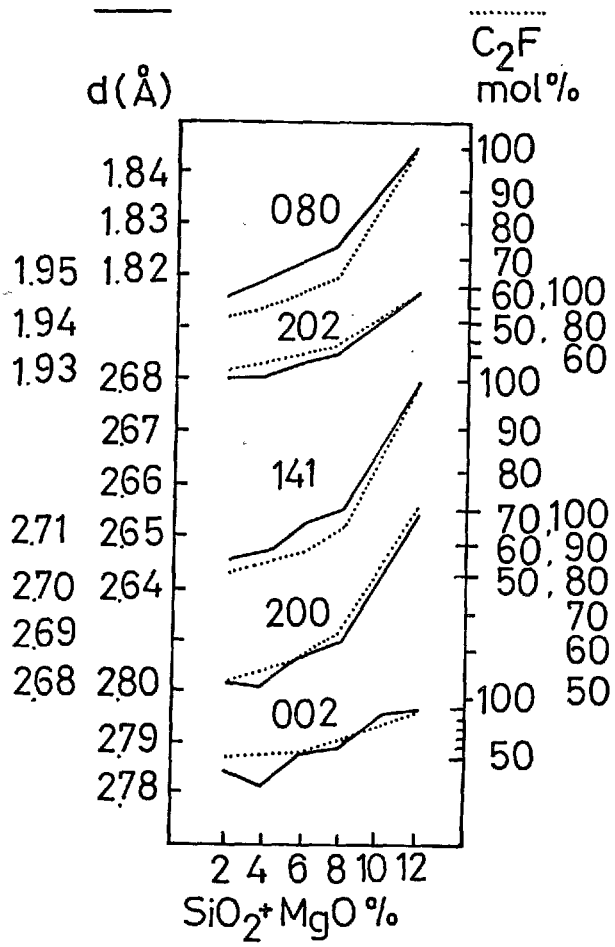

Fig. 13. *D-spacing of* C_4AF *solid solution with* MgO *and* SiO_2, *right side scale corresponds to* C_2F *mol %*

solution system of C_4AF with MgO and SiO_2 and found out the fact that some spacings and crystal axes expand according to the dissolution of MgO and SiO_2.

Aluminate and Relating Minerals

Pure C_3A and its solid solution with small amount of impurities are cubic having diffractions analyzed already but the splitting of cubic diffractions has been recognized by many investigators in the case of solid solution with some amount of Na_2O, especially NC_8A_3. A. E. Moore (1963) (41) interpreted the splitting as a formation of an orthorhombic lattice. J. A. Conwicke and D. E. Day (1964) (42) dealt with the same problem and K. E. Fletcher, H. G. Midgley and A. E. Moore (1965) (43) summarized well this problem.

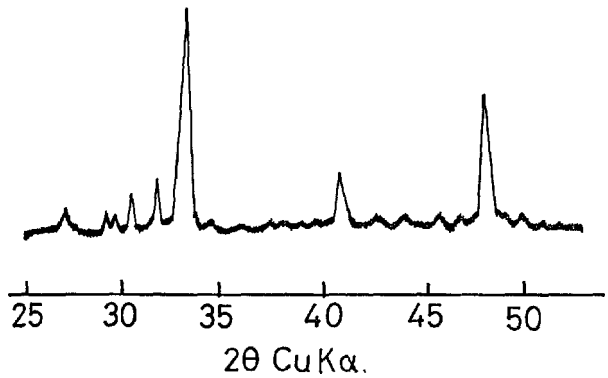

Fig. 14. *Diffraction pattern of cubic* C_3A

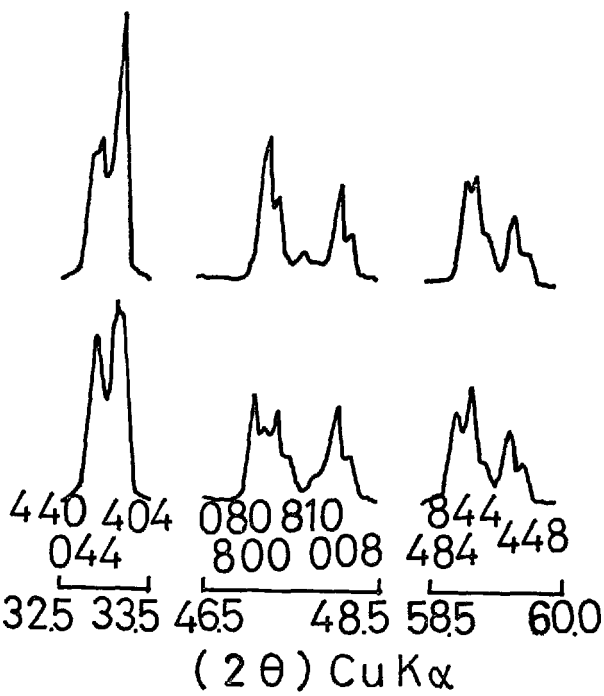

Fig. 15. *Diffraction pattern of orthorhombic* C_3A

A shift of diffractions caused in cubic C_3A by small amount of impurities such as Na_2O, MgO, SiO_2 and Fe_2O_3 was investigated by C. M. Schlaut, D. M. Roy (1965) (44), A. J. Majumdar (1965) (45), P. Tarte (1965) (46) and A. E. Moore (1966) (47) and it was clarified that Na_2O, MgO and SiO_2 cause shrinking of a lattice while Fe_2O_3 causes expanding.

Commercial Clinker

Fig. 17 is a typical X-ray powder diffraction pattern of a commercial clinker. In general the pattern of alite is dominant because of its large amount and high

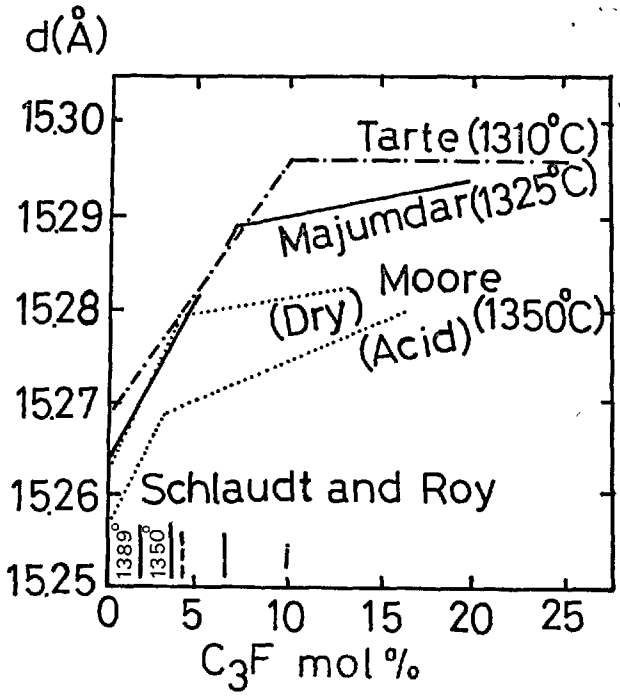

Fig. 16. *Lattice parameter of* C_3A-C_3F *solid solution*

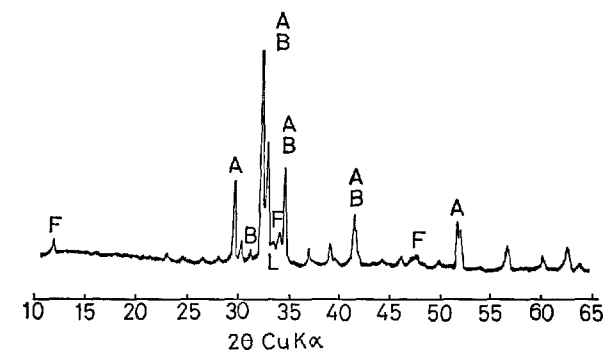

Fig. 17. *Typical diffraction pattern of commercial clinker*

crystallinity.

At 51°–52°, 610 and 040 diffractions of alite (A) appear as a doublet in the case of monoclinic but a triplet in the case of tricilnic, so that a question which is dominant whether monoclinic or triclinic is detectable. At 41°–42°, $\bar{2}28$ and 319 diffractions of alite and 014(014) and 031(031) diffractions of belite (B) as β-C_2S are overlapping. At high angle side of 34°, $\bar{2}25$ and 405 diffractions of alite are dominant but 102(103) diffraction of belite is overlapping. At low angle side of 34°, 141 diffraction of ferrite (F) solid solution appears. Its 200 diffraction appears at about 1/2° lower from 141 in the case of pure C_4AF but in the case of commercial clinker it usually overlaps to a low angle side of 141 diffraction with clearance about

1/4°. Other diffractions of ferrite solid solution appear at 47° overlapping to high angle side of $\bar{4}0,10$ and $2\bar{2},10$ diffractions of alite and at 12° independently. The former diffraction is 202 and the latter 020.

A diffraction at 33.3° is 440 of aluminate (L) but this is somehow overlapping to 220 of C_4AF in the case of pure minerals. However, in the case of commercial clinker the overlapping does not realize. If a part of belite is the form of α–C_2S or α'–C_2S, 110 diffraction of the former or 013 diffraction of the latter appears near 33°. At 32°–33°, 009, 224 and $\bar{4}04$ diffractions of alite and $10\bar{4}(10\bar{3})$, $12\bar{2}(12\bar{1})$, $20\bar{2}(200)$, 022(022) and 120(121) diffractions of belite as β–C_2S appear overlapping and forming two peaks. A diffraction at 31° is $12\bar{1}(120)$ of belite as β–C_2S and diffractions at 29°–30° are 221, 401, 222 and 402 of alite. Figs. 18 a–j are diffraction patterns of Japanese commercial clinkers.

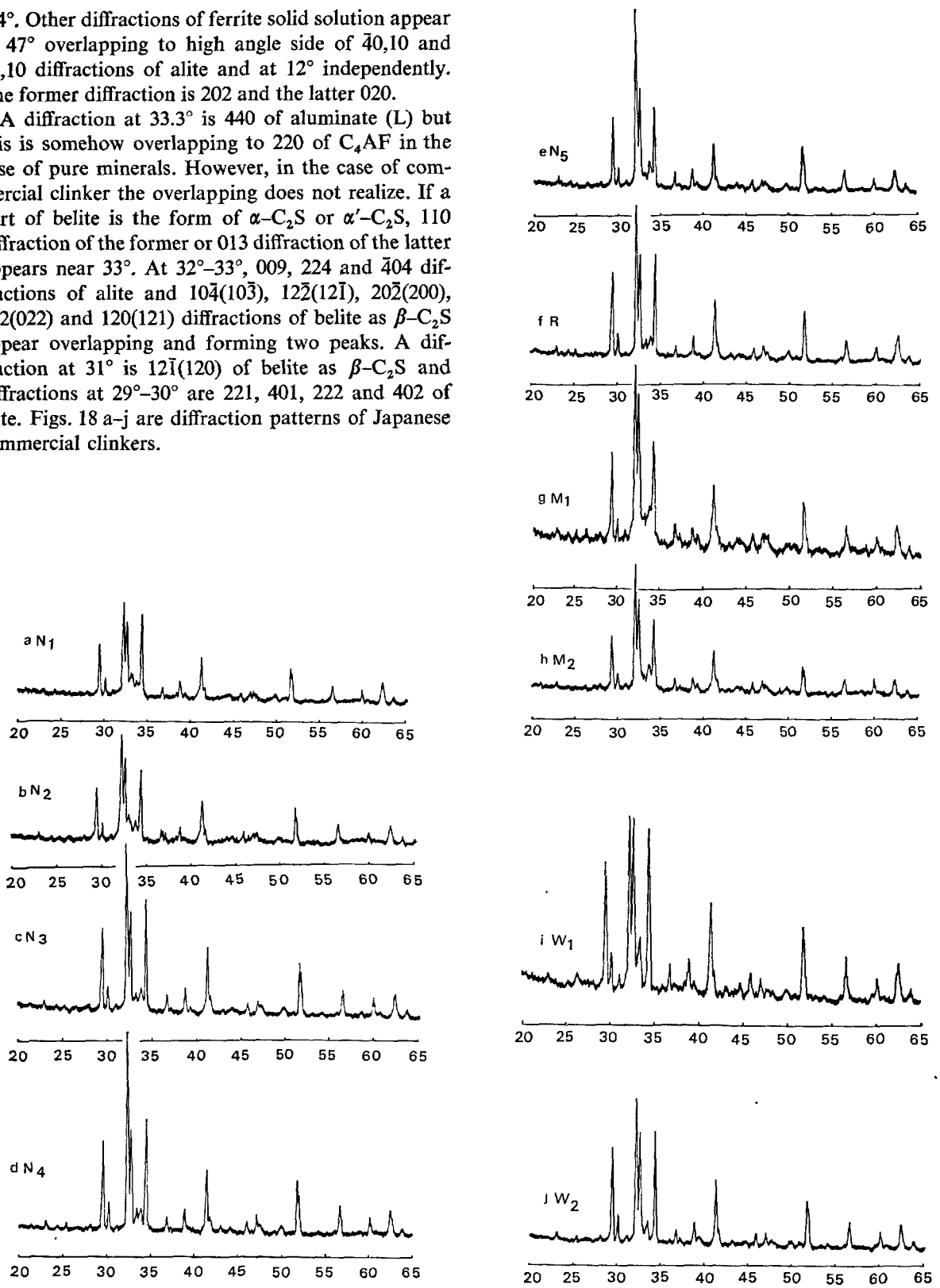

Fig. 18. *Diffraction pattern of commercial clinker*

Monoclinic alite is dominant in all clinkers and belite is β–C_2S except diffractions at 33° in N_1 and N_2 seem belonging to α–C_2S. In W_1 and W_2 there exists little amount of ferrite but a large amount of aluminate.

Heavy Liquid Separation

The heavy liquid separation study of the cement minerals has been carried out since long time but perfect separation is very difficult. On the other hand a separation yield is so small that there is a fear whether or not a gathered sample may represent a whole lot. The method of separation employed in this experiment to gather average samples as far as possible was as follows:

Clinker were pulverized into particles all passable through a 4900 mesh (88μ) sieve. Then 10 kg of them were suspended in absolute alcohol and particles smaller than 20μ were removed by sedimentation. Next, 3 kg of them were treated with a magnetic separator repeatedly until 300 g of sample with low ferrite content remained. At last, the centrifugal separation by heavy liquid of a definite specific gravity was employed to gather alite part and belite part. The liquid was made from methylene iodide-benzene mixture. Proper ranges of specific gravity were 3.13–3.17 for alite and 3.18–3.26 for belite. Figs. 19a–j are X-ray diffraction patterns of separated alite parts and Figs. 20a–j are those of belite parts.

Difficulty of the separation is differrent according to kind of clinkers. In general, alite is separated easily but belite is not and has a tendency of being accompanied with ferrite and alite.

The belite parts of N_1 and N_2 show strong diffractions at 33° and they seem to be 110 diffractions of

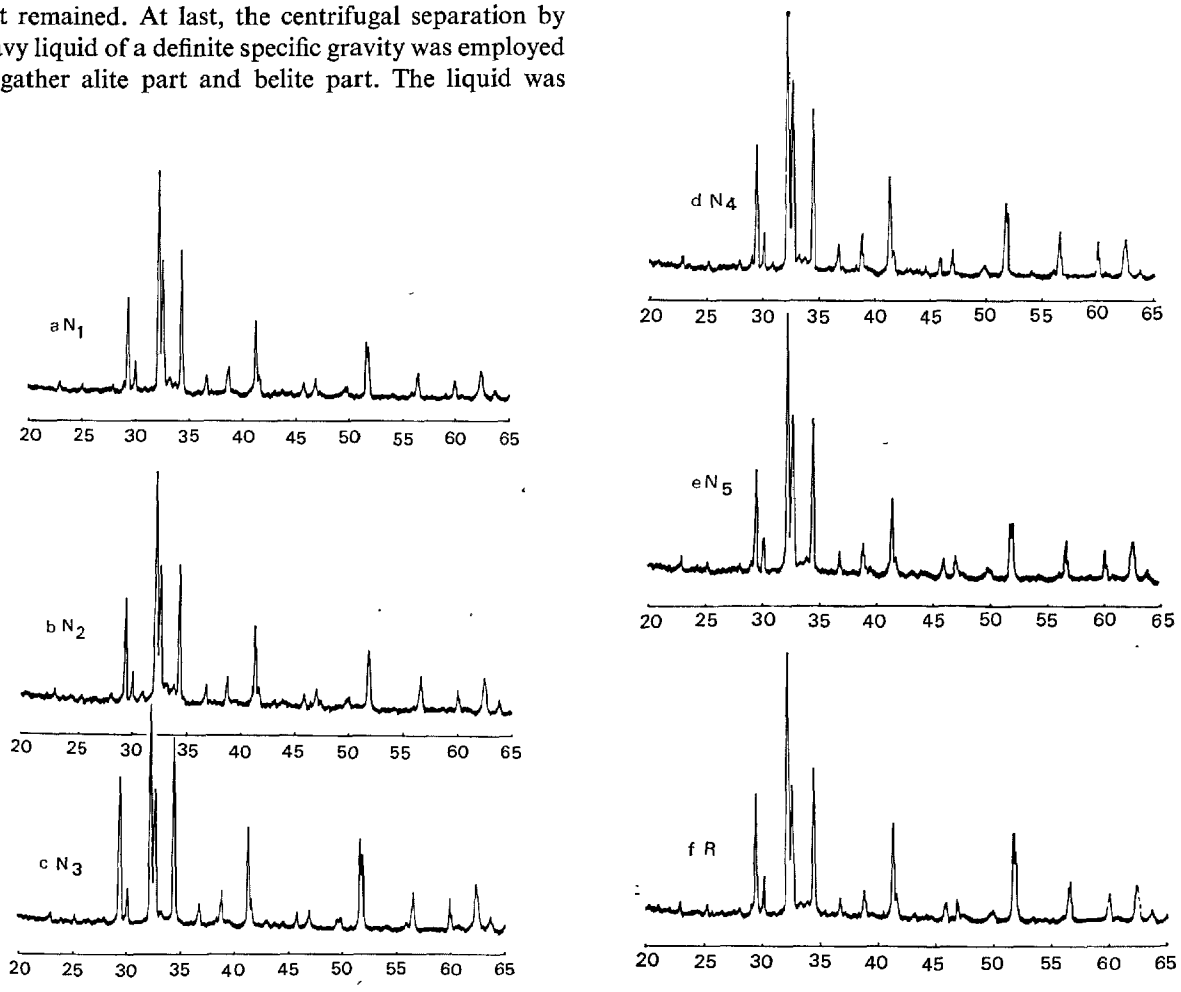

Fig. 19. *Diffraction pattern of alite part*

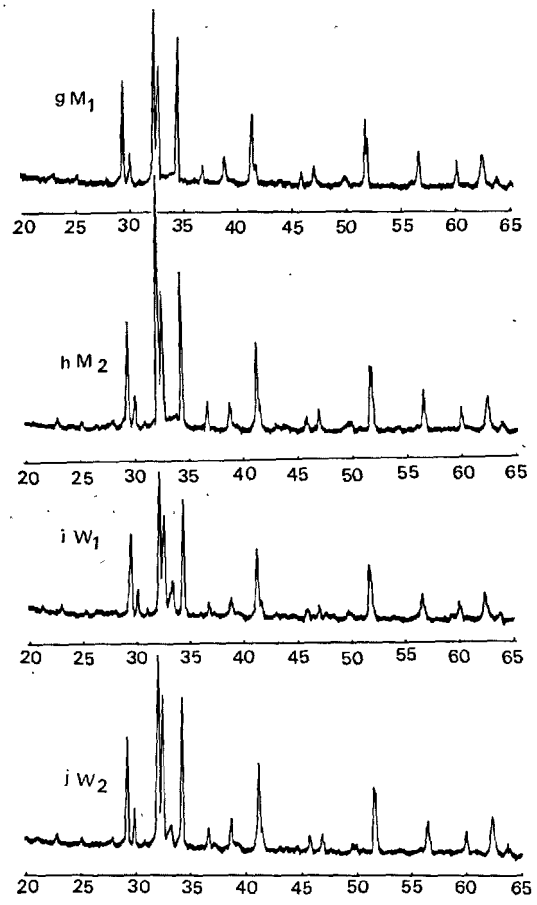

Fig. 19. *continued*

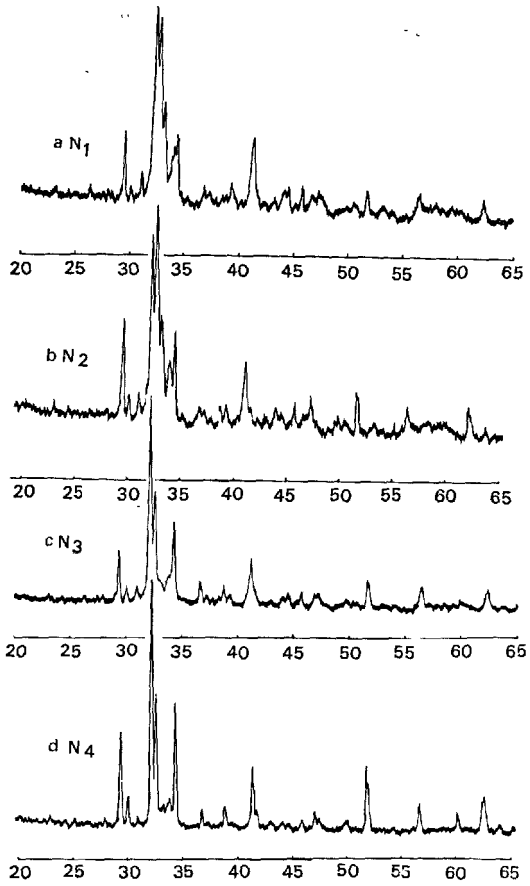

Fig. 20. *Diffraction pattern of belite part*

Table 2. *Comparison of 110 diffraction of* α-C_2S *and 013 diffraction of* α'-C_2S

	110 diffraction of α-C_2S		013 diffraction of α'-C_2S			
Stabilizer	P_2O_5	Al_2O_3, Fe_2O_3 and Na_2O	B_2O_3	MgO and K_2O	N_1	N_2
Literature	(23)	(25)	(23)	(25)		
2θ	33.00	33.02	33.27	33.28	33.00	32.97

α–C_2S. However, 013 diffraction of α'–C_2S is expected to appear near by, so that a careful checking is needed to confirm that the diffraction is whether α or α'. Table 2 shows the checking data of them.

These data show α–C_2S is probable. If the diffraction were 013 of α'–C_2S the strongest diffraction of 020 and 211 would appear together at 33.5° and a shape of diffraction peak would change immensely. As a further evidence for α–C_2S, nearly pure α–C_2S was gathered by careful separation of N_1 clinker as shown in Fig. 21. This problem will be reported separately (48).

It was not until the precise interpretation of X-ray powder diffraction patterns of cement minerals could be established that a discussion of this kind became possible.

A principle of the separation method mentioned above is an equal weight sampling from all parts of clinker, so that it does not contain such a pretreatment that ferrite-less parts in clinker are selected. Therefore, the interstitital phase is apt to adhere to alite and belite, and a perfect separation is nearly impossible.

Another experiment of separation including a pretreatment of selecting ferrite-less parts was performed, although it might be a problem in an equal weight sampling. X-ray diffraction patterns of those samples are shown in Figs. 22 and 23. Both of these samples seem fairly pure and it is interesting that diffractions of belite are broader than those of alite.

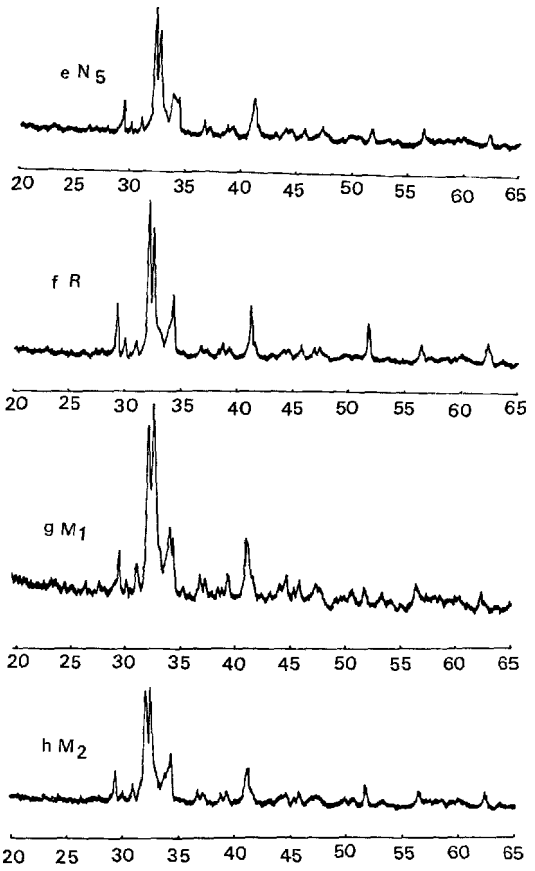

Fig. 20-2.

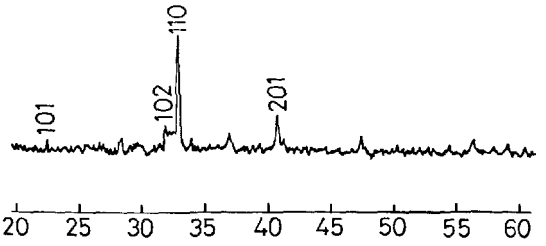

Fig. 21. *Diffraction pattern of separated* αC_2S

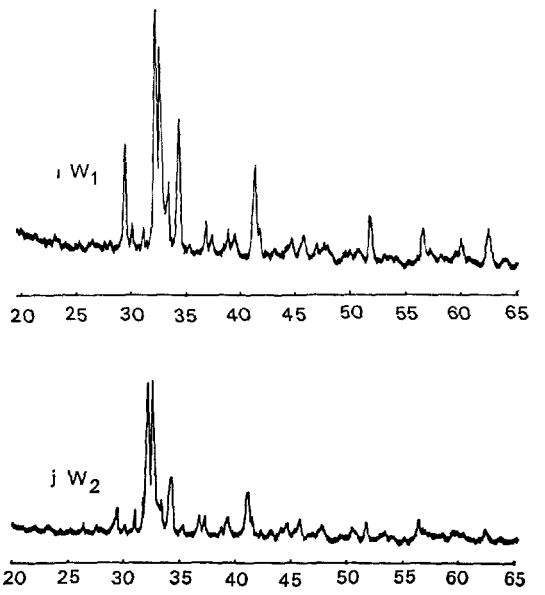

Fig. 20-3.

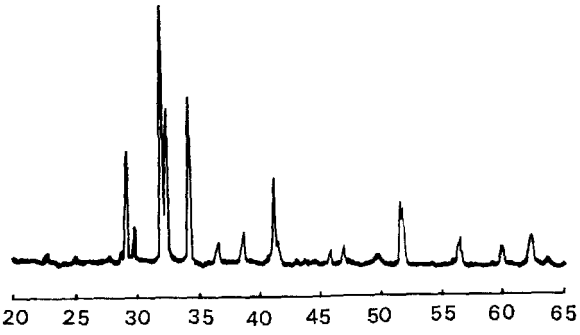

Fig. 22. *Diffraction pattern of well separated alite*

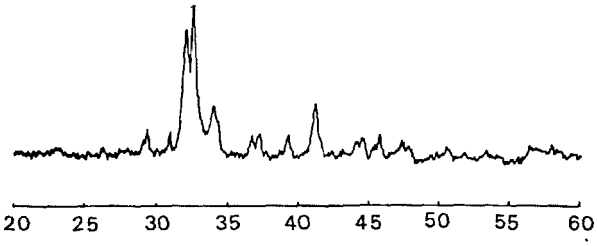

Fig. 23. *Diffraction pattern of well separated belite*

Chemical Separation

A separation between alite and belite is nearly impossible because they have very close chemical property. Various methods of separating the interstitial phase were tested and it was found that salicylic acid methanol solution method studied by S. Takashima (1958) (49) is the best and quantitative method.

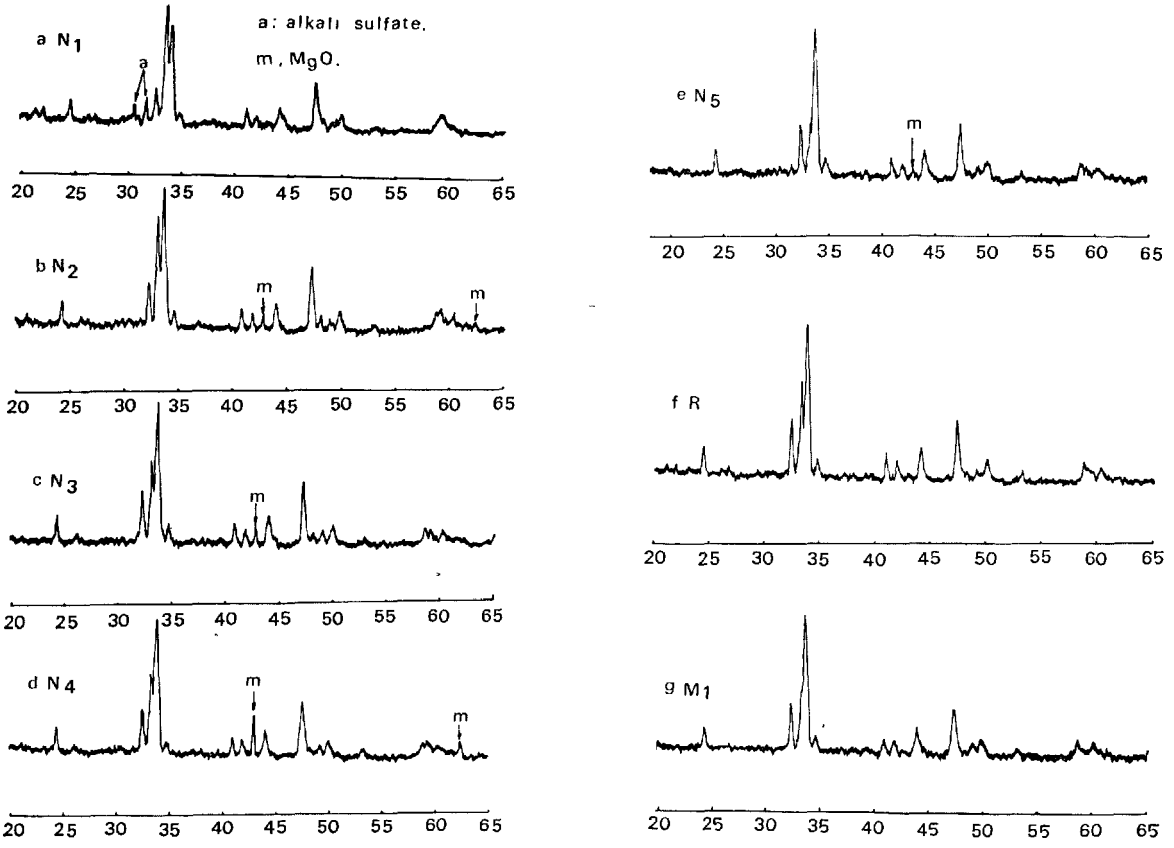

Fig. 24. *Diffraction pattern of separated interstitial phase*

The residue of this treatment was again treated with 1 N acetic acid aqueous solution and after this treatment all of aluminate and a part of ferrite were dissolved into solution and the major part of ferrite was left as a residue. The glass phase is also hardly dissolved. Figs. 24a–j are X-ray diffraction patterns of the interstitial phases and Fig. 25 is characteristic patterns of the interstitial and the ferrite phase of N_3 clinker. Amounts of the interstitial phase determined by this method are shown in Table 10 (line C).

The interstitial phase of N_1 contains fairly large amount of alkali sulphate and the aluminate phase. Those of N_2, N_3 and N_4 contain free MgO. Those of M_1 and M_2 consist almost only of ferrite. Those of W_1 and W_2 contain no ferrite. The 440 diffraction of all aluminate show splitting, so that all aluminates consist of or contain orthorhombic one.

The diffraction of 141 and 200 of ferrite appear very closely. The former lies at about 33.8° and the latter at about 1/4° low angle side. In the case of pure C_4AF, 141 is at almost the same situation but 200 is at about 1/2° low angle side.

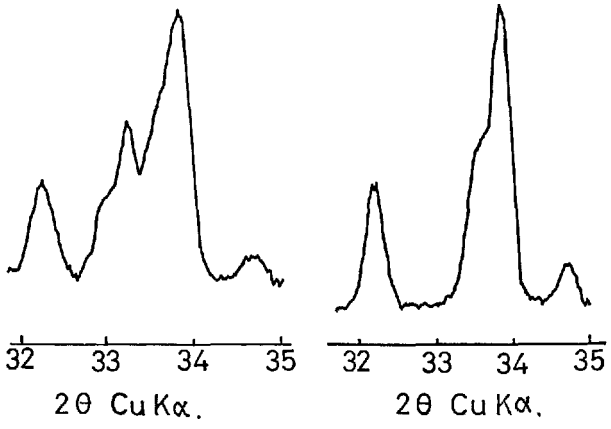

Fig. 25. *Characteristic diffraction patterns of separated interstitial and ferrite phase from* N_3 *clinker*

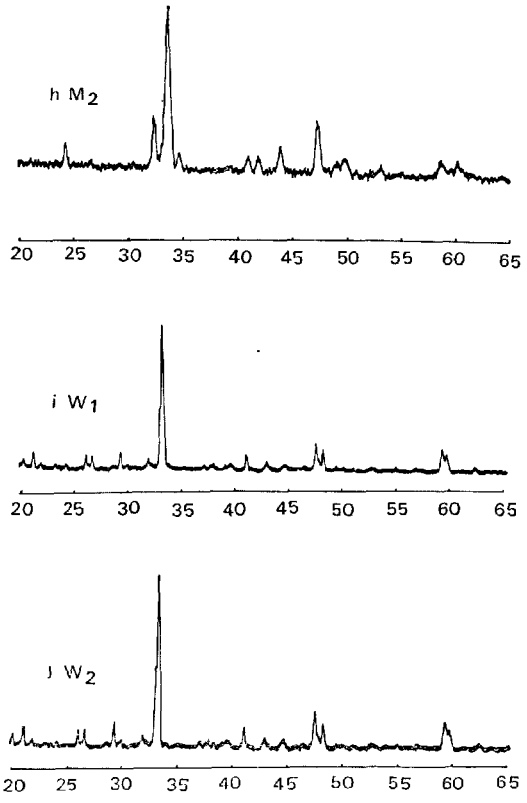

Fig. 24. *continued*

Chemical Analysis

As to wet chemical analysis there are many studies and regulations in every country. The chemical analysis was conducted applying Japanese Industrial Standard, JIS R 5202. Table 3 shows results of wet chemical analysis.

Chemical analysis of the separated alite part (A), the belite part (B), the residue of the salicylic acid treatment (R) and the residue of the acetic acid treatment (F) were conducted.

If the glass phase does not exist in (F), its chemical composition is that of the ferrite phase. Mixed ratio of ferrite and aluminate in (R) was determined by the X-ray quantitative analysis. Then chemical composition of the aluminate phase was determined considering free MgO and free alkali sulphate.

(A) and (B) were treated with salicylic acid methanol solution, and chemical compositions of alite-belite mixtures in (A) and (B) were obtained. Contents of alite and belite in (A) and (B), α_A, β_A, α_B and β_B, were determined by the X-ray quantitative

Table 3. *Chemical composition of clinkers*

Clinker	Ig. loss	Insol.	SiO_2	Al_2O_3	Fe_2O_3	CaO	MgO	SO_3	Na_2O	K_2O	Free CaO
N_1	0.43	0.01	22.66	5.03	2.96	64.31	1.40	1.18	0.55	1.07	0.65
N_2	0.73	0.01	22.93	5.87	3.35	64.10	1.85	0.54	0.44	0.79	0.08
N_3	0.77	0.01	23.11	4.73	3.17	65.76	1.67	0.39	0.44	0.98	0.00
N_4	0.44	0.22	21.15	5.55	3.17	65.31	3.36	0.46	0.21	0.53	0.31
N_5	0.93	0.02	23.14	5.65	3.22	64.60	1.68	0.64	0.17	0.61	0.12
R	0.70	0.03	22.41	5.28	2.74	67.33	1.32	0.06	0.07	0.21	0.30
M_1	0.78	0.02	23.41	4.92	3.72	64.97	1.41	0.45	0.16	0.32	0.02
M_2	0.75	0.01	23.36	5.02	3.60	65.10	1.57	0.33	0.17	0.34	0.03
W_1	1.34	0.05	23.27	5.33	0.29	66.31	1.44	0.26	0.48	0.11	0.67
W_2	1.65	0.04	23.15	4.93	0.23	66.24	1.41	0.30	0.33	0.14	1.71

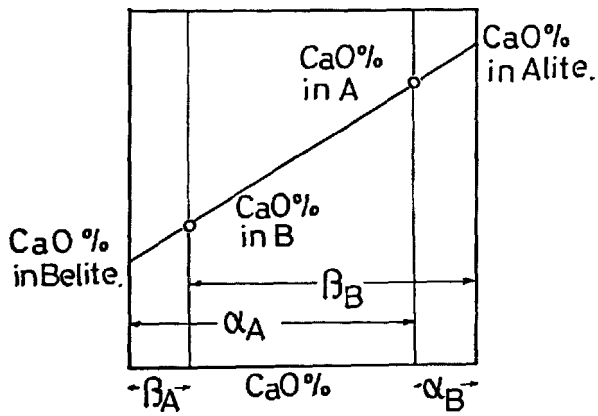

Fig. 26. *Calculation chart of chemical composition of component from mixture.*

analysis. From these values, chemical compositions of alite and belite were determined. This calculation was performed following Fig. 26, an example of CaO.

Chemical compositions of the salicylic acid dissolved parts of the clinkers are values of alite and belite mixtures in clinkers. Then using these values and CaO contents in alite and belite, which were most reliable and had sufficient gradient, contents of alite and belite in the original clinkers could be calculated. Details will be reported separately (50).

Transmitted Light Microscopic Observation

Transmitted light microscopic observation has been established as the mineralogical optics. Nevertheless, the application of this method to the cement minerals is not so frequently conducted because its technique is more difficult than that of reflected light microscopic observation. This technique, however, is indispensable in order to investigate the nature of minerals and should be applied more frequently. The measurement of optical properties and the observation of stereographic structure cannot be done by a reflected light microscopy. The systematization of both microscopy of cement clinker was almost established by H. Insley and V. D. Frechette (1955) (51).

Almost no study using the transmitted light microscopic technique has been carried out since the last symposium with some exception. G. Yamaguchi and Y. Ono (1966) (52) studied the alite phase. They measured precisely angles of two characteristic shapes of alite and correctly interpreted that these shapes are trigonal own shapes formed at high temperature. Moreover, they recognized two kinds of twins whose twinning planes are a basal plane and an R_1 plane, characteristic optical properties such as wavy extinction caused by trigonal-monoclinic inversion twinning and a polysynthetic twinning parallel to c axis caused by monoclinic-triclinic inversion.

As to the type I and type II structure of belite, it had been interpreted that the type I structure is a polysynthetic twinning of α-α' inversion and the type II structure is that of α'-β inversion. But no more detail of twinning structure had not been clarified.

G. Yamaguchi and Y. Ono (1962) (53) mentioned that the type I and type II structures can be seen without nicol and in almost all cases neighboring parallel lamellas have the same extinction position, and therefore lamella structures are not always polysynthetic twinnings but dominantly simple flake structures. Their further results are as follows:

Parallel lamella structure of the type I is a simple flake structure and not parallel polysynthetic twinning structure, but as it will be mentioned later, sometimes α–C_2S phase is being sandwiched between main lamellas which have already inverted into β–C_2S but remain as α'–C_2S skeletons. However, the intersecting parts of lamellas show usually complex wavy extinction and seem probably having twinning structure whose twinning plane should be $\alpha'\{013\}$ as will be shown later.

Yamaguchi et al. measured the orientation of lamellas using microscope with universal stage and found out that there exist six directions of lamellas in one grain at maximum and that angles between lamellas and the X-Y plane $33 \pm 5°$. The angle between {102} and c plane in α–C_2S is theoretically 36°, so that the type I lamellas seem to be $\alpha'\{101\}$ planes which are equistructural to the $\alpha\{102\}$ plane and developed topotaxitically on that plane. Fig. 27 shows the orientation of the type I lamellas of belite corresponding to {102} of α–C_2S.

In Fig. 28 the type II lamellas of belite can be observed also without nicol. They lie nearly parallel to the Y-Z plane (b-c plane in P2 1/n) and can be observed distinctly from Y direction but imperfectly from Z direction. When the lamellas are observed with crossed nicols from Y direction extinction position of every parallel lamella is same, but from Z direction polysynthetic twinning structure parallel to lamellas can be seen. Therefore lamellas observed without

nicol are flake structure of {101} in P2 1/n or {100} in P2 1/n which topotaxially developed on {010} plane of α'–C_2S(Pnma) and polysynthetic structures of the same direction can be observed only from Z direction with crossed nicols.

The orientation of lamellas and twinning planes can be clearly explained in the following interpretation in which the structure of α'–C_2S is treated as α'_H and Pnma same as the above description.

In α–C_2S($P\bar{3}cl$), {110}, {$\bar{1}$20} and {2$\bar{1}$0} are mirror planes, so that when it inverts topotaxially into α'–C_2S (Pnma), these mirror planes change into twinning planes or remain as a mirror plane of α'. In Fig. 29, if α'{101} lamella grows topotaxitically on α{102}, in this α' lamella crystal α{110} and {2$\bar{1}$0} change into twinning planes as α'{013} and {0$\bar{1}$3} respectively and α{1$\bar{2}$0} remains as a mirror plane α'{010}.

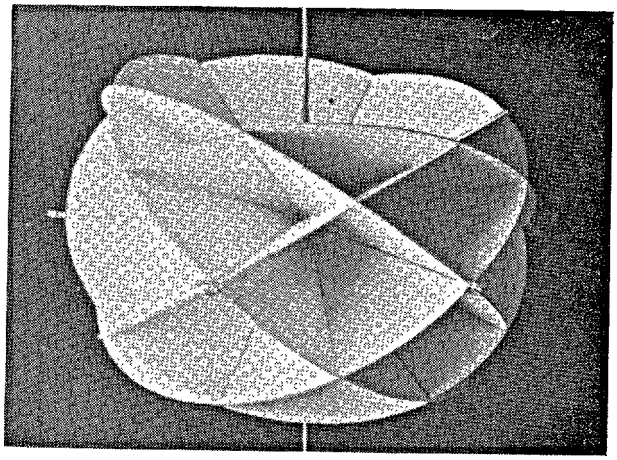

Fig. 27. *Orientation of type I lamellas*

Then, when α'–C_2S inverts topotaxitically into β–C_2S(P2 1/n), mirror plane {010} of α'–C_2S changes into a twinning plane {100} of β–C_2S.

The type I lamella in belite and the type III belite which have already inverted into β–C_2S should have a structure like type II. However, that structure can not be observed so easily. They might have extremely fine flake structure and polysynthetic structure.

A. Metzger (1953) (54) mentioned that α'–C_2S was found by the optical observation at a drop like inclusion in C_3S. In the present experiment α'–C_2S was never found in any of Japanese clinkers but in N_1 and N_2 clinker many grains containing α–C_2S could be found.

Fig. 30 shows a belite grain of N_1 clinker having the type I structure in which lamellas of two directions can be seen. A reason why only lamellas of two directions are distinct is that only those lamellas are nearly perpendicular to a stage. In a space between lamellas

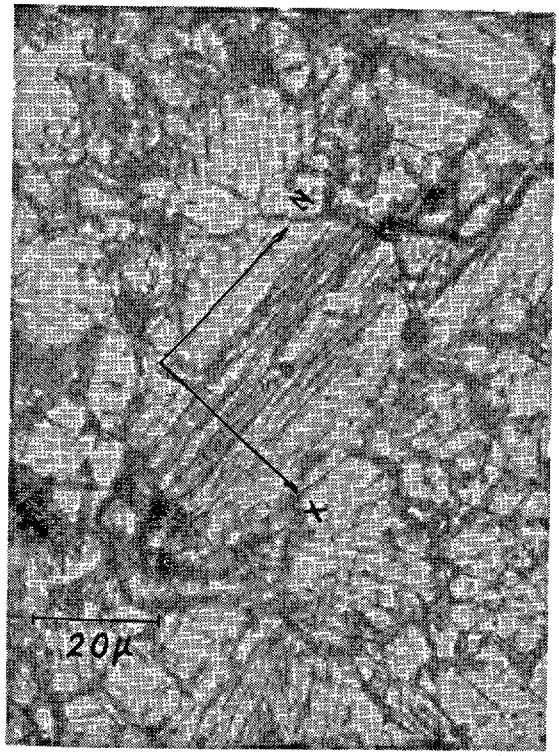

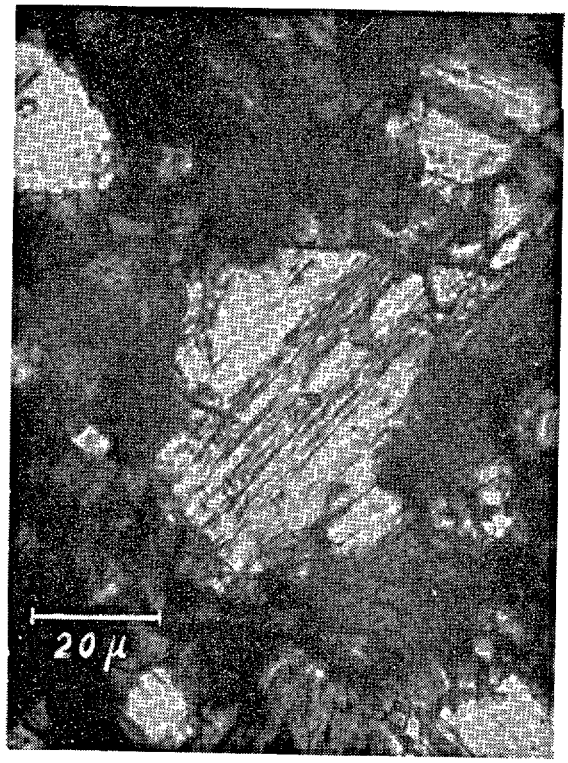

• Fig. 28. *Type II lamella and optical axes in belite*

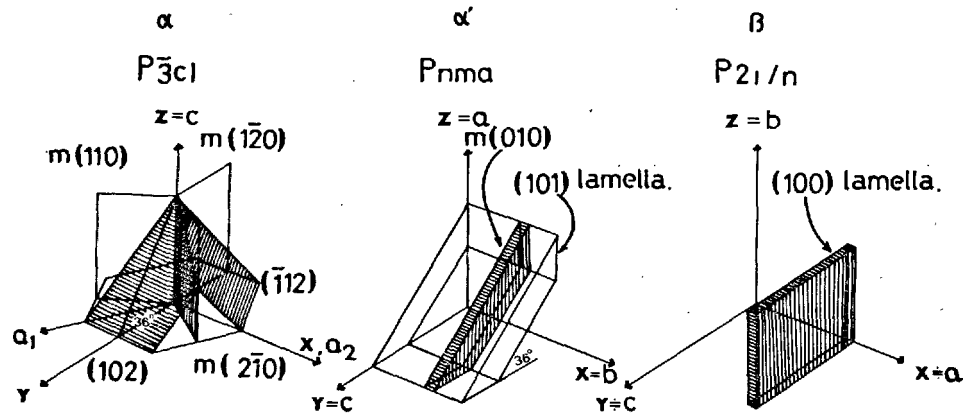

	α	α'	β
Relation of lamella.	{102}.....{101}		
		{010}.....{100}	
Relation of mirror	m{2$\bar{1}$0}.....t	{01$\bar{3}$}.....{10$\bar{3}$}	
plane and twinning	m{1$\bar{2}$0}.....m{010}.....t	{100}	
plane.	m{110}.....t	{013}.....{103}	

Fig. 29. *Relation among lamellas, mirror planes and twinning planes in* C_2S *polymorphs*

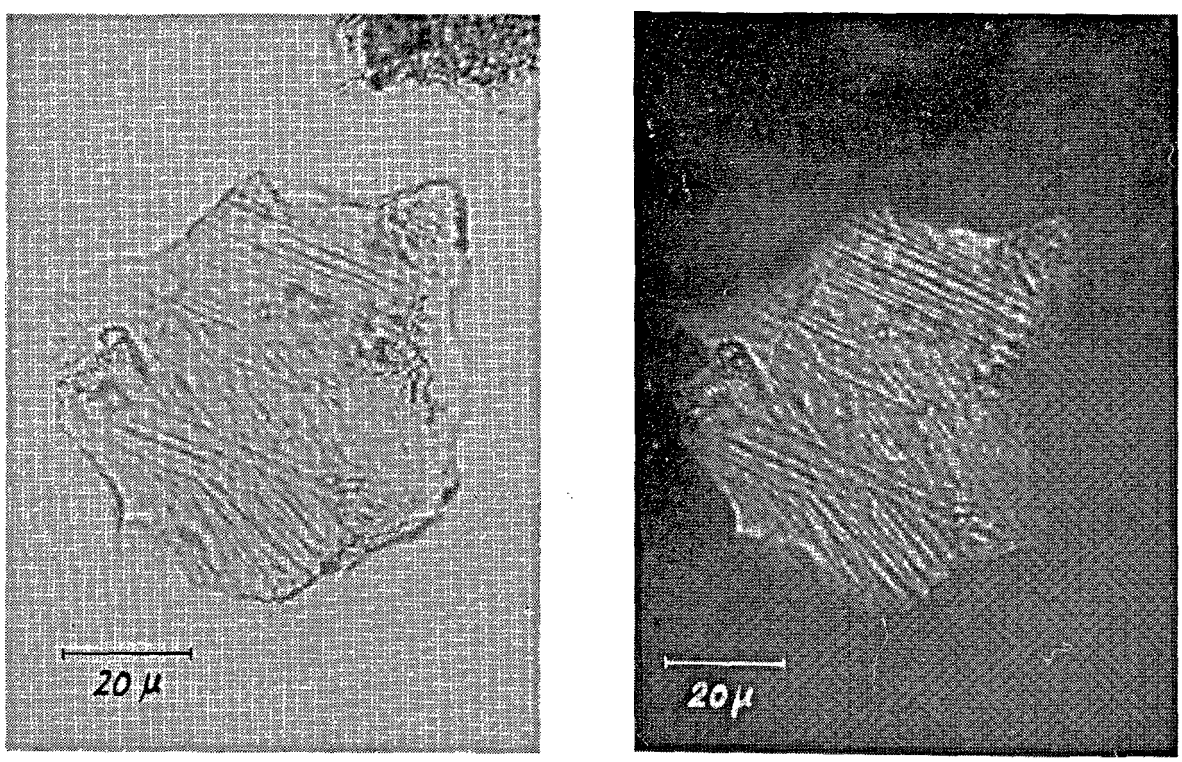

Fig. 30. *Transmitted light microscopic photograph of belite grain containing* αC_2S

a matter of low refractive index and low birefringence is sandwiched. This structure is liable to be misunderstood as a polysynthetic twinning structure. If α–C_2S had inverted into α'–C_2S to make polysynthetic twinning structure and α'–C_2S had remained as it was or reinverted into β–C_2S, it would be possible that extinction positions are different one another, but it would be impossible that lamellas have so dif-

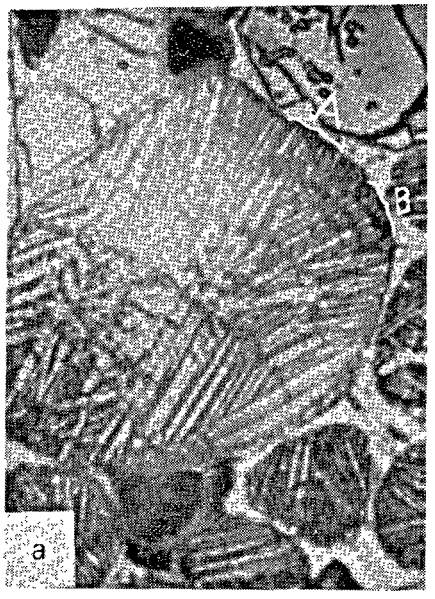

a reflected light photograph of etched surface

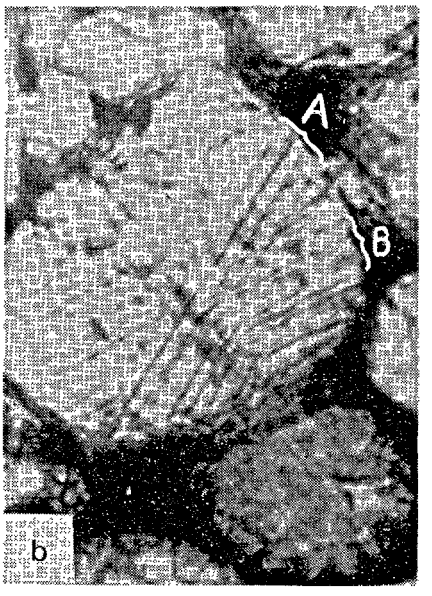

b transmitted light photograph of thin-sectioned specimen (a) without nicol

c with crossed nicols at the extinction position of B lamellas

d with crossed nicols at the extinction position of A lamellas

Fig. 31. *Reflected and transmitted light microscopic photograph of type I belite grain.*

ferent birefringence from the stand point of topotaxitic inversion. Moreover, the sandwiched matter has low refractive index, considering all those facts it is nearly unquestionable that the matter should be α–C_2S.

In Fig. 31 a reflected light microscopic photograph of an etched surface and transmitted light microscopic photographs of the thin sectioned same field are shown. A large belite grain has two parallel lamella groups A and B. Both groups can be recognized even in parallel nicols. Each group has almost the same extinction position and the difference of angle between extinction position of A and B groups is only about 4°. Although, the α'–β inversion structure cannot be seen in this figure.

Reflected Light Microscopic Obeservation

Reflected light microscopic observation has been systematized also by Insley et al. Investigations applying this method are being conducted as a daily work, especially a point counting quantitative analysis of the mineral composition. The essential point of this method is a polishing and etching technique. Table 4 shows usual etching techniques.

The interpretation about informations observed from a polished and etched surface of clinker is established. Recently F. Trojer (1966) (55) described this problem clearly. Figs. 32–36 are typical photographs of clinkers of the present experiment.

Table 4. *Some examples of etching technique*

Etching reagent	Etching period		Reaction effect to;
1–5% HNO_3 alcohol solution	10 sec	Alite	Uniformly etched, out line is cleared.
		Belite	Inner texture and out line is cleared.
		Ferrite	Unetched, looks light.
		Aluminate	Etched, looks dark.
1–5% NH_4Cl aqueous solution	10 sec	Alite	Same as above
		Belite	Same as above
Salicylic acid saturated methanol solution	4 sec	Alite	Same as above
		Belite	Same as above
		Ferrite and aluminate	Unetched, looks light
HF vapor	properly	Alite	Etched, colored brown
		Belite	Etched, colored bluish
		Ferrite and aluminate	Unetched, looks light

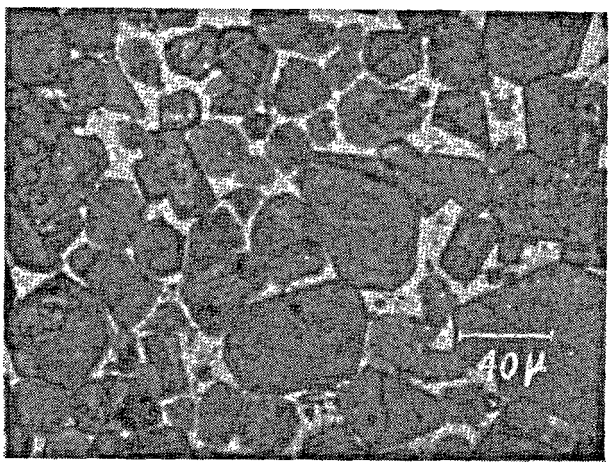

Fig. 32. *Reflected light microscopic photograph of alite group etched with* HNO_3*-alcohol.*

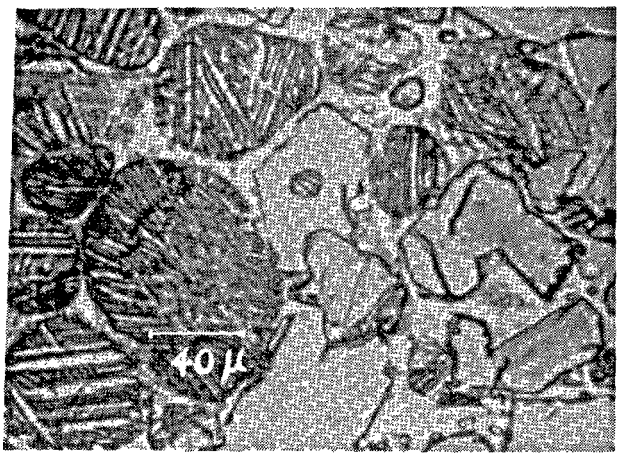

Fig. 33. *Reflected light microscopic photograph of alite and type I belite etched with* HNO_3*-alcohol.*

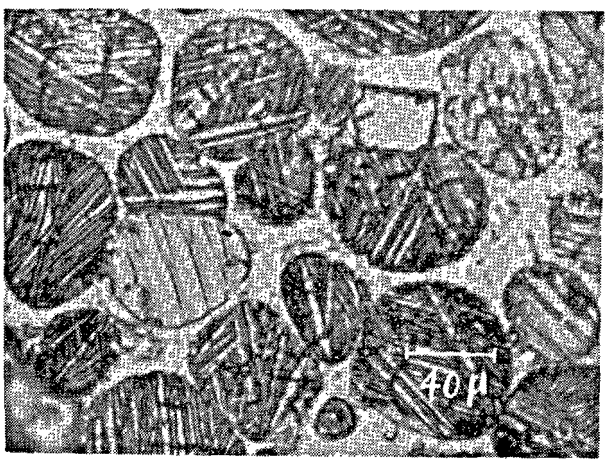

Fig. 34. *Reflected light microscopic photograph of type I and type II belite etched with* HNO_3*-alcohol.*

Fig. 35. *Reflected light microscopic photograph of type III belite etched with* HNO_3*-alcohol.*

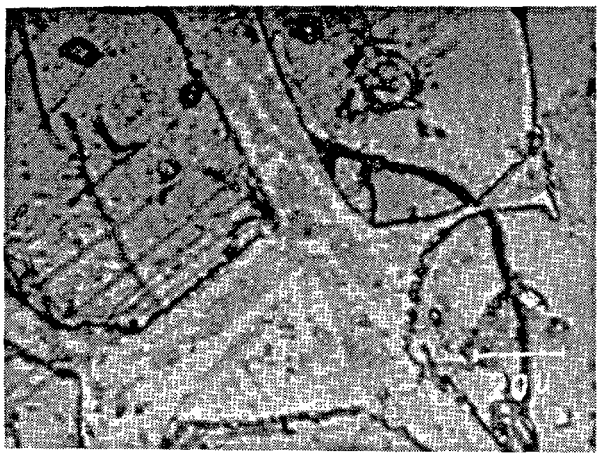

Fig.36. *Reflected light microscopic photograph of dark interstitial and light interstitial etched with* HNO_3*-alcohol.*

Electron Microscopic Observation

A few investigations into cement clinker using an electron microscope have been reported since the last symposium. G. Yamaguchi and Y. Ono (1962) (53) observed very fine type II structure in the type III belite and lamella of the type I belite. P. Brunner (1965) (56) explained electron microscopic photographs of clinker comparing to reflected light microscopic photographs. F. Trojer (1966) (55) presented a photograph taken by the ion etching technique. The photograph shows the very fine type II structure in

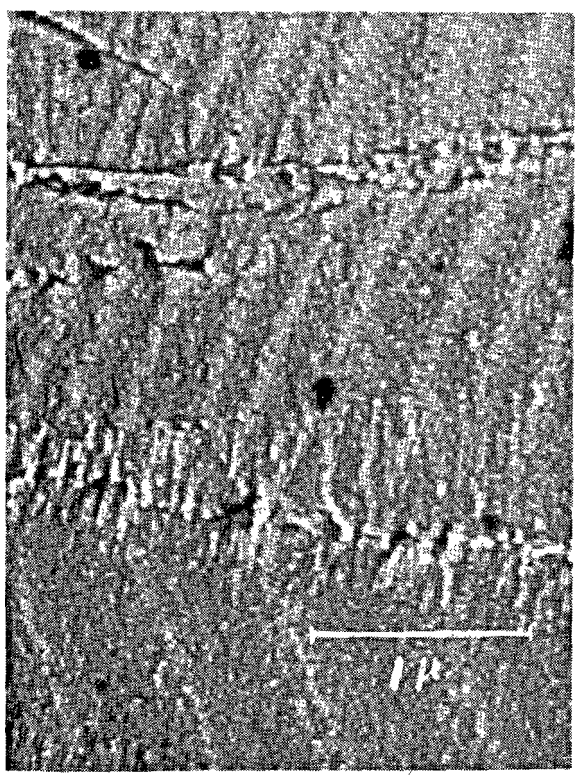

Fig. 37. *Electron microscopic photograph of type II structure in type III belite.*

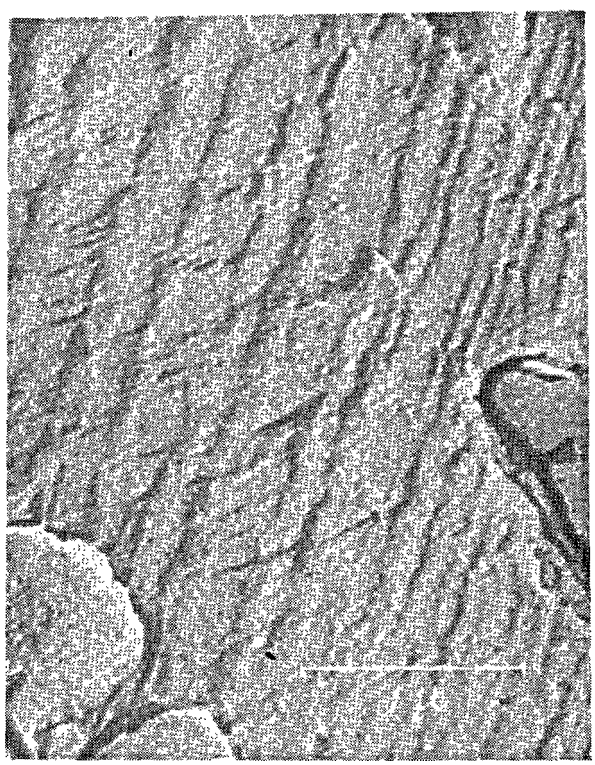

Fig. 38. *Electron microscopic photograph of type II structure in type I lamella of belite.*

lamellas of the type I belite.

It is necessary to use the electron microscopic technique in order to clarify fine textures which cannot generally be observed with an ordinary optical microscope. The $\alpha'-\beta$ inversion in belite is not always observed even with an electron microscope, so that improved observation techniques are needed to confirm this structure. Some photographs taken with an electron microscope in this experiment are presented in Figs. 40–42 in which whether or not a fine structure in belite is due to the $\alpha'-\beta$ inversion is not clear.

The scanning type electron microscopic observation will become useful in future. Some photographs are shown in Figs. 43 and 44.

Fig. 39. *Electron microscopic photograph of type II structure in type I lamella of belite* (55).

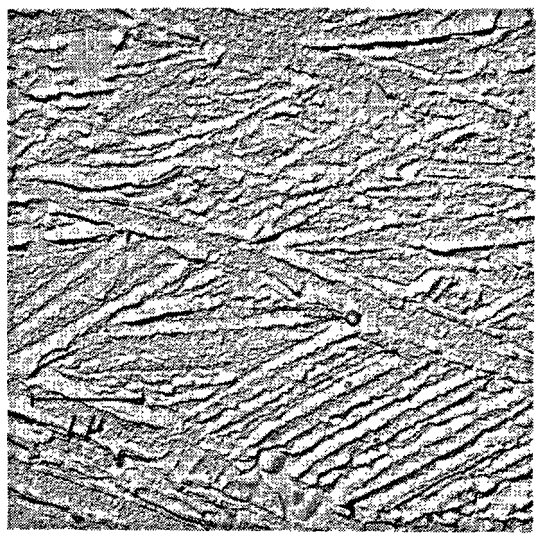

Fig. 40. *Electron microscopic photograph of type I belite*

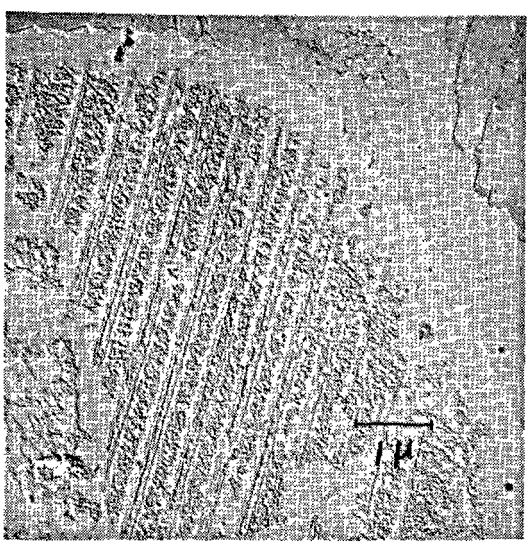

Fig. 41. *Electron microscopic photograph of type II belite*

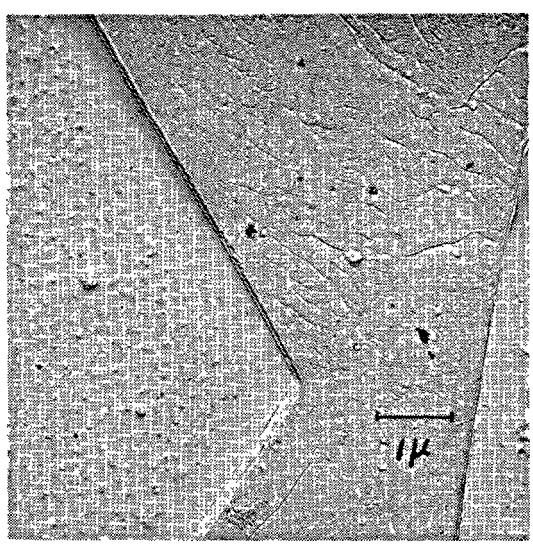

Fig. 42. *Electron microscopic photograph of alite*

Fig. 43. *Scanning electron microscopic photograph of etched surface of* N_2 *clinker.*

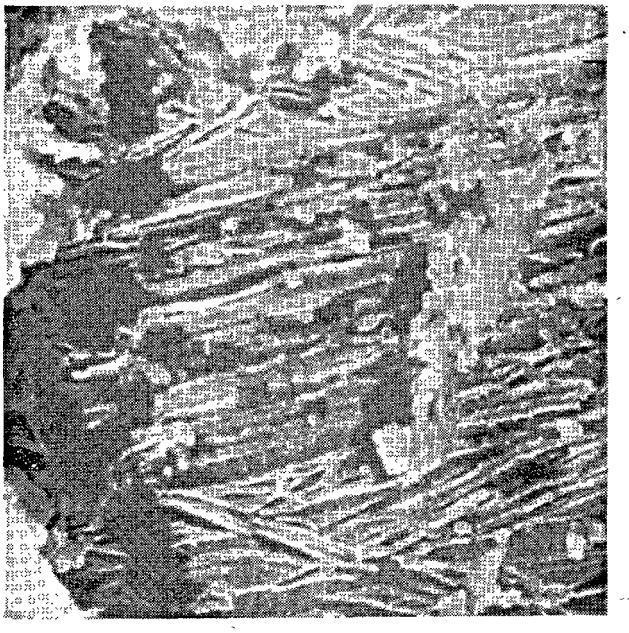

Fig. 44. *Scanning electron microscopic photograph of belite of* N_5 *clinker etched with* HNO_3*-alcohol.*

Differential Thermal Analysis

The differential thermal analysis (DTA) has been applied as a testing technique of experimentally synthesized clinker. Especially it is useful for a supplementary method to identify a polymorph of minerals. For instance, it is not reasonable to maintain that some C_3S solid solution should be classified into the same polymorph of pure C_3S such as T_{II} from only a reason of resemblance of 620 and 040 diffractions. But if there is resemblance of DTA feature, the reliability of the classification increases.

The fact that two phases belong to the same polymorph means thermodynamical parameters (atomic parameter, lattice parameter, lattice enthalpy, lattice entropy etc.) of those phases are varying with no gap according to conditions such as temperature, chemical composition etc. In other words, the fact that two phases belong to different polymorphs means there exists a gap between two continuous series of parameters of those phases. That gap is sometimes so small that its detection is not so easy and even impossible as in the case of some polymorph of C_3S.

In an experiment of comparing polymorphs of pure C_3S and C_3S solid solution, the continuity between T_I of pure C_3S and that of C_3S solid solution can be proved by an experiment, but the continuity between T_{II} of pure C_3S and that of C_3S solid solution cannot be proved. Therefore there is nothing useful but DTA experiment to increase the reliability to maintain those classification, so far as today's experimental technique.

A problem of clarifying a relation among polymorphs of minerals in clinker, those of pure minerals at several temperatures and those of solid solution phases is very important. For this project DTA method will act an important role as well as the X-ray method etc. Moreover, a study of thermal change in the cooling process of the manufacturing should be an essential problem.

Electron Probe Micro Analysis

An application of the electron probe micro analysis (EPMA) to an investigation of cement clinker developed after the last symposium. Some results have been reported. H. G. Midgley (1964) (57) presented EPMA

photographs of clinker in "The Chemistry of Cement". K. E. Fletcher, H. G. Midgley and A. E. Moore (1965) (58) applied this technique to determine the chemical composition of a phase of Na_2O–Al_2O_3–CaO system. G. Yamaguchi, H. Uchikawa and S. Takagi (1965) (59) discussed the method of the application, took photographs and performed the quantitative analysis of Al and Fe in alite and belite. G. Yamaguchi, S. Takagi, M. Yoshizumi and T. Ohta (1966) (60) analyzed the ferrite phase and obtained such a result that its composition is in a range between C_4AF and C_6A_2F containing special elements such as Zn, Cu, Co etc. At the same time they reported that a back scattered electron image (BSEI) has very good resolution power. G. Yamaguchi, S. Takagi and M. Yoshizumi (1967) (61) analyzed MgO, Na_2O and K_2O quantitatively in alite and belite. S. Akaiwa, G. Sudoh and M. Tanaka (1966) (22), (1967) (62) reported a new mineral $11CaO \cdot 4SiO_2 \cdot CaF_2$ analyzing with EPMA. I. Peterson (1967) (63) analyzed Al_2O_3, K_2O and MgO in clinker.

An application of EPMA to cement clinker has some difficulties comparing to that to metals because it consists of light metal oxides and has very fine textures. Details will be reported separately (64) but essential points are as follows; they are preparation methods of specimens such as grinding and coating, and setting of experimental conditions such as voltage, current, beam diameter, diffraction crystal, counter and pulse hight analyzer system.

Specimen Preparation

Grade of grinding should be the same as microscopy specimens but more flat surface is needed so that it is desirable to use fine diamond powder paste whose diameter is less than 0.2μ at finishing. Carbon coating and beryllium coating are both useful for giving electric conductivity but the latter is better.

Resolution Power

The texture of clinker is so fine that the resolution power is important to decide a limit of the application. An ability expected to EPMA is to analyze the composition of every texture quantitatively, therefore, not only in that analysis but also in measuring a qualitative distribution of elements the check of resolution power is essential. Because clinker consists of light metal oxides, there exist such several causes which decrease the resolution power as an electron penetration effect and a secondary X-ray effect. Among several setting conditions which cause to decrease the resolution power are too high voltage, unsuitableness of coating and too large diameter of electron beam. However, decreasing the exitation voltage causes decrease of signal intensity and results badly in a signal noise ratio, so that it has naturally a limit to decrease the voltage. In general, a proper range of the exitation voltage is 15–35 KV. Even when the exitation voltage is 15 KV the resolution power of the X-ray image is about 5μ. Therefore, a matter having a diameter or thickness less than 5μ can not be reliably detected. On the contrary BSEI has a good resolution power which can be expected less than 1μ.

X-ray Image

The X-ray image has a demerit of lower resolution power but a merit of conveniency to look over the distribution of elements. Its essential points are to set a proper voltage, to cut a noise well enough by pulse hight analyzer and to give a long exposure in order to gain an enough density of light points, but so small beam size is not necessary. The X-ray image of any element can make the contrast between a low content part and a high content part, but can not make so good contrast between parts in which difference of contents is not so large.

Back Scattered Electron Image

The BSEI has high resolution power and it can resolve less than 1μ. That image has the contrast caused by difference of the electron scattering power, so that difference of composition can be detected.

Figs. 45–49 are photographs taken in this experiment. Photographs (a) are reflected light microscopic figures in which the alite phase, the belite phase, the dark interstitital phase and the light interstitial phase are clear. These photographs were taken by such a procedure that after EPMA test specimens were repolished and etched. Photographs (b) are BSEI which can detect all phases distinctly with high resolution. Photographs (c) are Fe X-ray image (XRI), photographs (d) are Al XRI, photographs (e) are Si XRI, photographs (f) are Ca XRI and photographs (g) are Mg XRI. Those EPMA photographs have non linear deformations which result in shortening of longitudinal size.

In Fig. 49 correspondency of (b) to (a) is very good because careful polishing has been conducted, but in other figures images are somewhat changed. Photographs (c) and (d) reveal that Fe_2O_3 and Al_2O_3 distribute nearly uniformly in the interstitial phase but only at some parts which are ferrite phases of large size

a

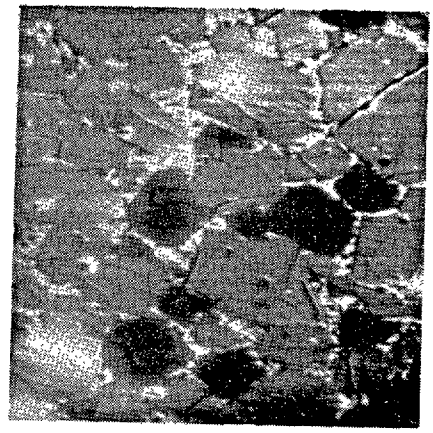

b

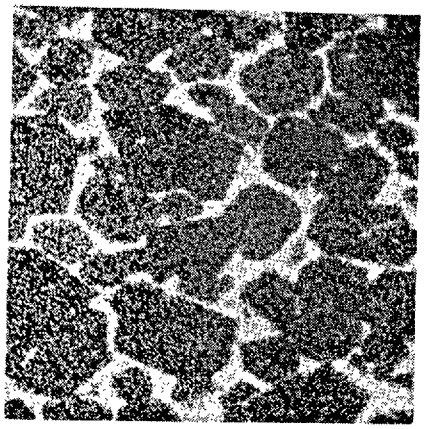

c

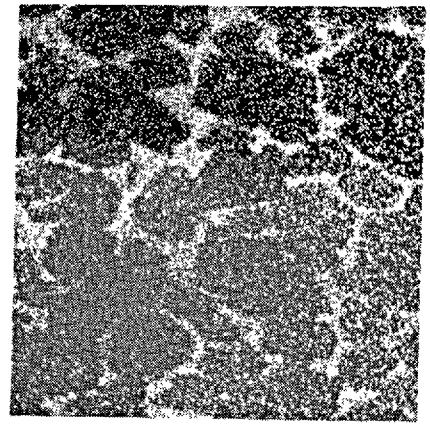

d

100 μ

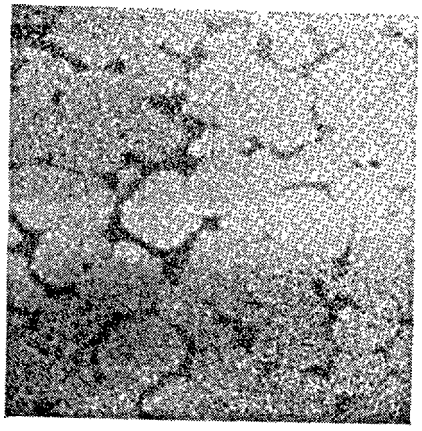

e

Fig. 45. *EPMA photograph of clinker.*

a

b

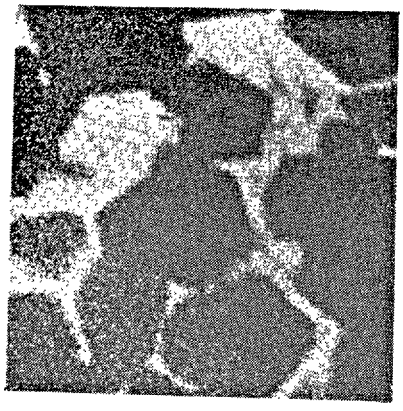

c

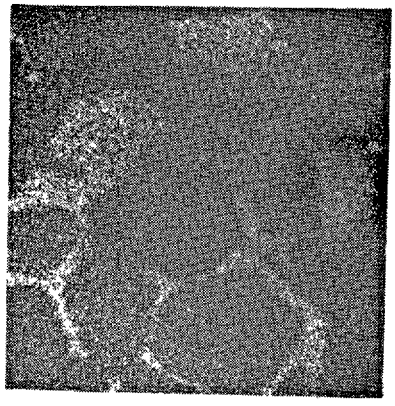

d

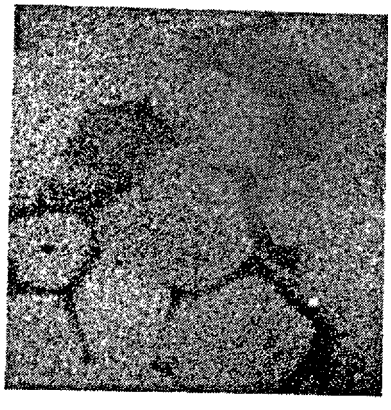

e

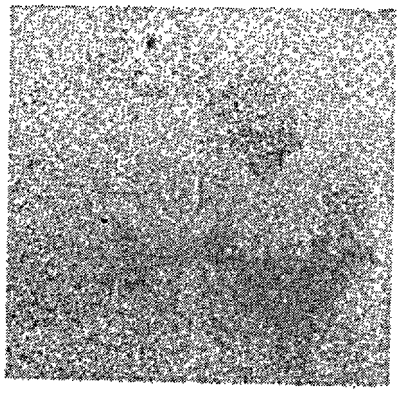

f

20μ

Fig. 46. *EPMA photograph of clinker.*

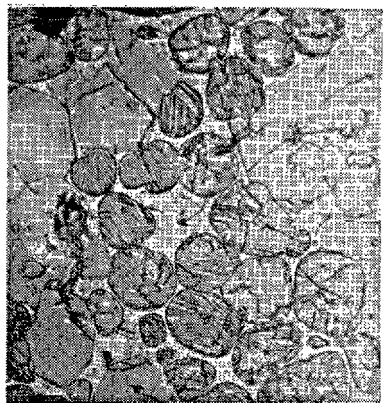

a

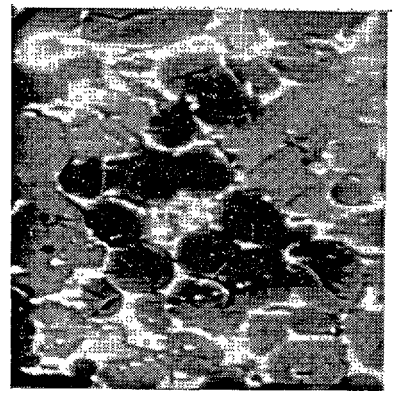

b

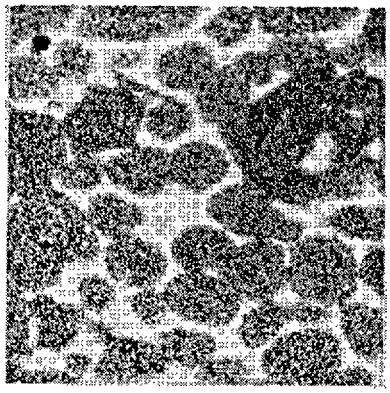

c

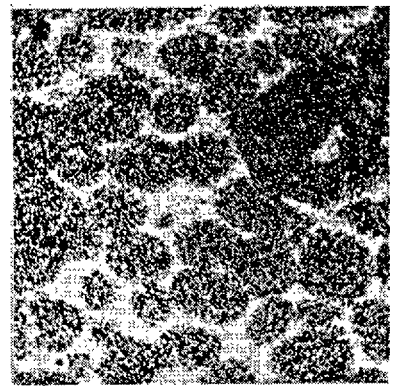

d

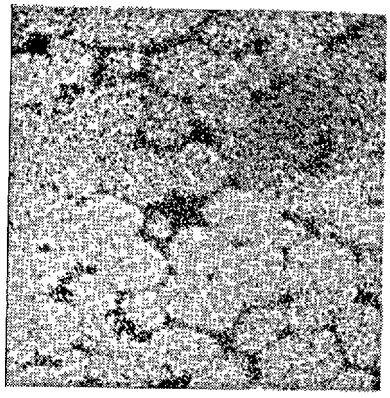

e

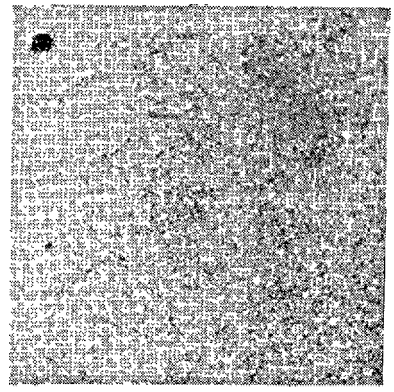

f

100μ

Fig. 47. *EPMA photograph of clinker.*

left (h) is an explanatory figure
(A) alite (B) belite
(L) light interstitial
(D) dark interstitial

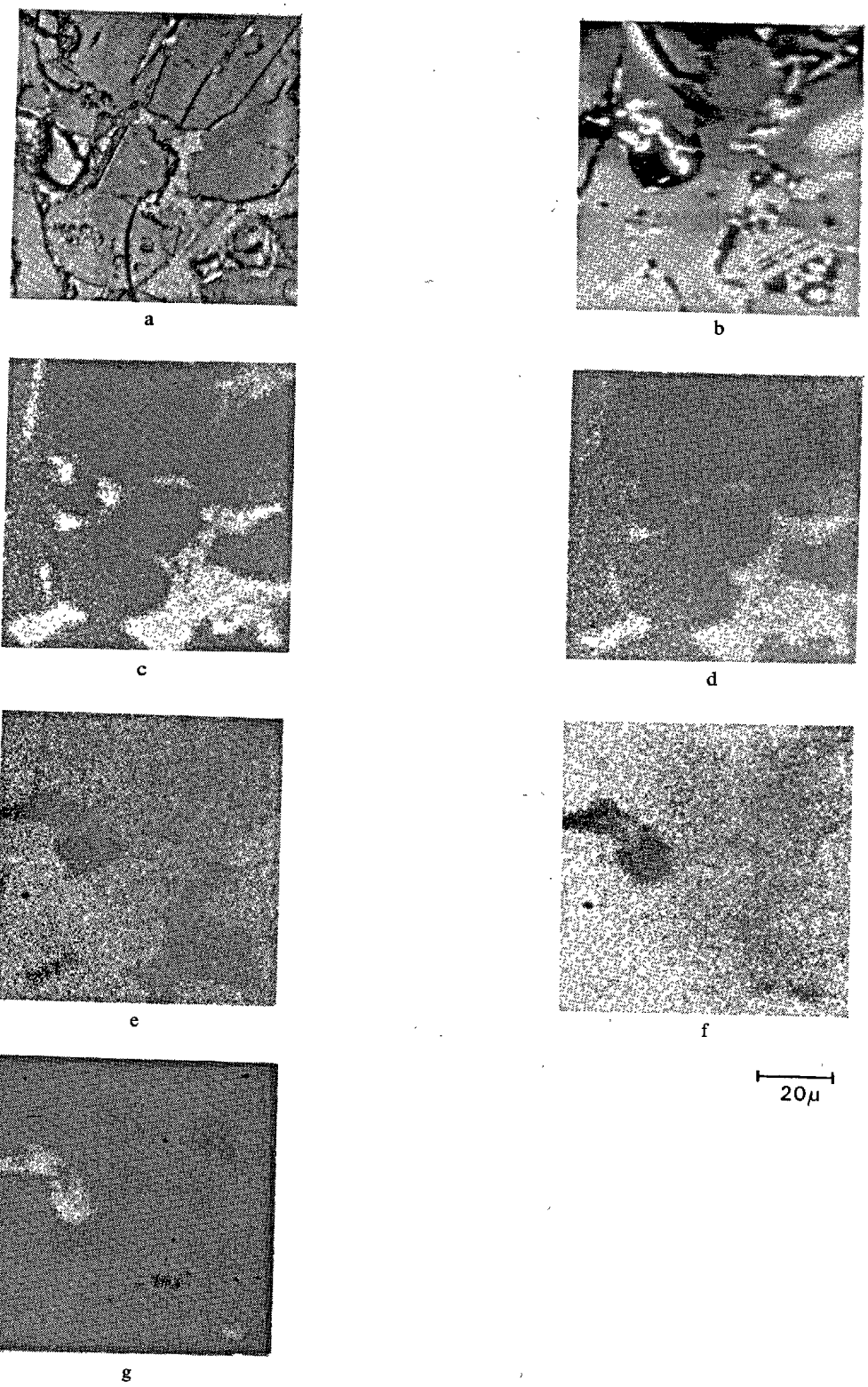

Fig. 48. *EPMA photograph of clinker.*

left (g) shows an MgO rich spot which makes a hole by polishing.

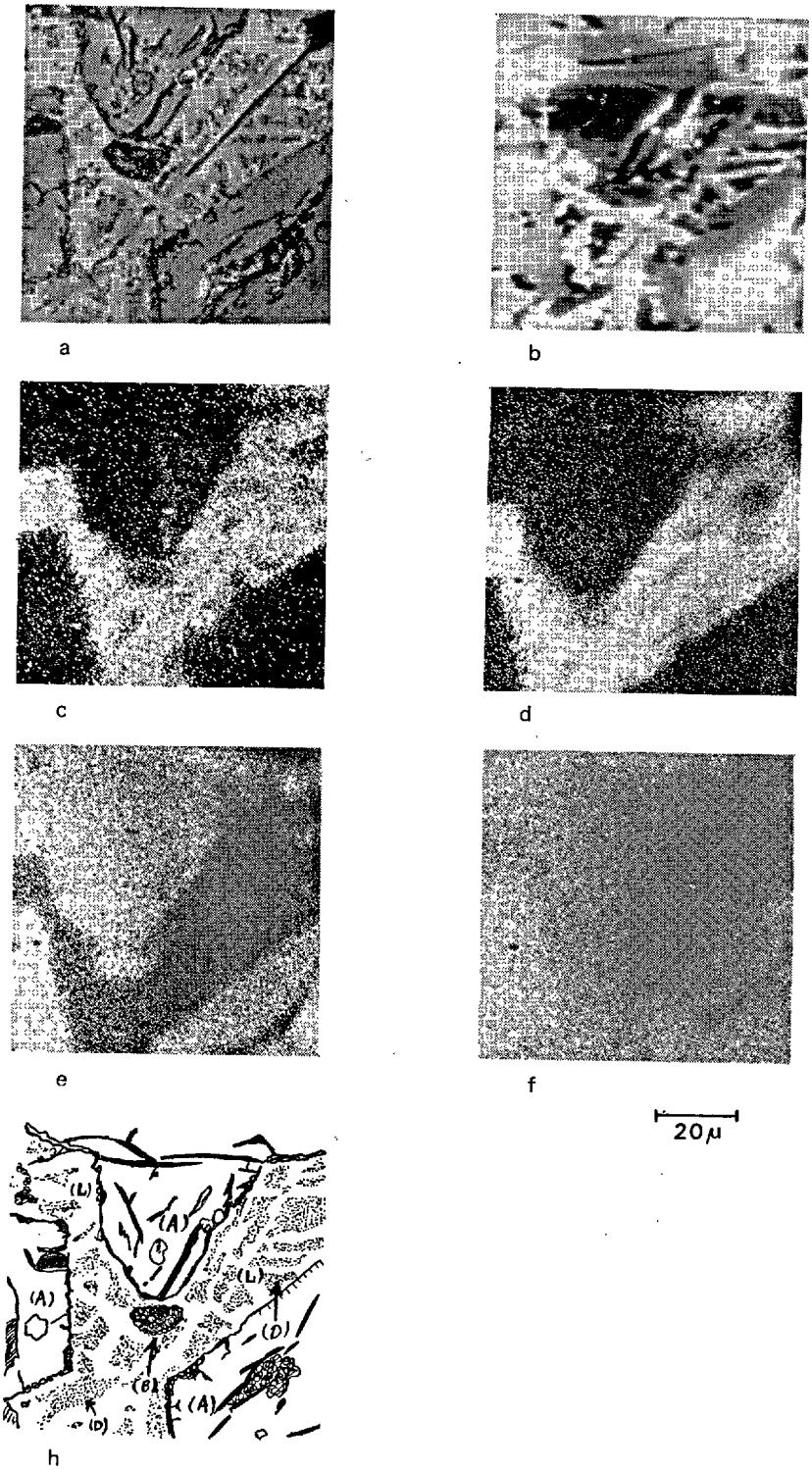

Fig. 49. *EPMA photograph of clinker.*

left (h) is an explanatory figure
(A) alite (a) belite
(L) light interstitial
(D) dark interstitial

high concentration of Fe can be vaguely seen. This fact is due to low resolution power of the XRI.

Photographs (f) show nearly uniform intensities of Ca in the alite phase, the blite phase and the interstitial phase, but according to an experimental condition some difference can be given. Photographs (e) show Si is rich in alite and belite and also show existence of some Si in the interstitial phase.

The order of whiteness in photographs (b) is as follows; light interstitial, alite, dark interstitial, then belite. This phenomenon corresponds to the fact that light interstitial is the ferrite phase and dark interstitial is the aluminate phase.

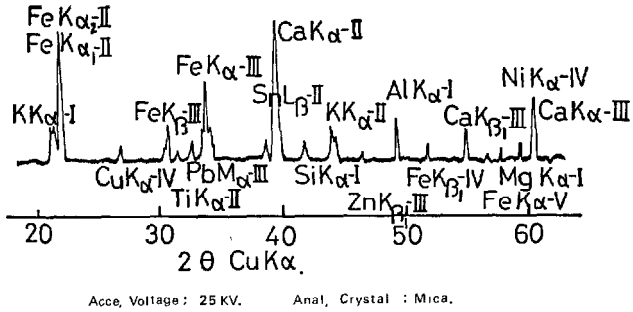

Fig. 50. *EPMA qualitative analysis of interstitial phase.*

Table 5. *Result of EPMA quantitative analysis*

	Al_2O_3	Fe_2O_3	MgO	Na_2O	K_2O
N_1 alite	0.88–1.40	0.40–1.20	0.11–0.98	0.01–0.12	0.01–0.10
N_1 belite	0.80–3.10	0.63–1.55	0.21–1.05	0.01–0.20	0.10–0.42
M_1 alite	0.45–2.50	0.51–1.31	0.32–0.65	0.01–0.02	0.03–0.09
M_1 belite	0.60–3.51	0.40–1.51	0.36–1.11	0.01–0.06	0.11–0.33

Point Analysis

The resolution power of the point analysis is also not so high. The information seems to come from a range of several microns diameter from the center of a beam though signal intensity is weighted average about the center. The point qualitative analysis is conducted simply by rotating a diffraction crystal. Fig. 50 is a result of the qualitative analysis of the interstitial phase showing the existence of many heavy metals.

As to the quantitative analysis, the first problem is also the resolution power. In the case of a small crystal, a thin crystal or an inclusion containing crystal, the determination of the true chemical composition is difficult. Therefore, it is impossible by this method to obtain the reliable chemical composition of minerals in cement clinker except it contains fairly large crystals.

The second problem is a procedure of the quantitative treatment. In the case of metals it is well known that the calculation is not so hard to conduct, but in the case of light metal oxides such as cement clinker, the quantitative calculation is nearly impossible. So that a method using standard samples is the only way of conducting the quantitative analysis. The

Table 6. *Flow chart of clinker analysis*

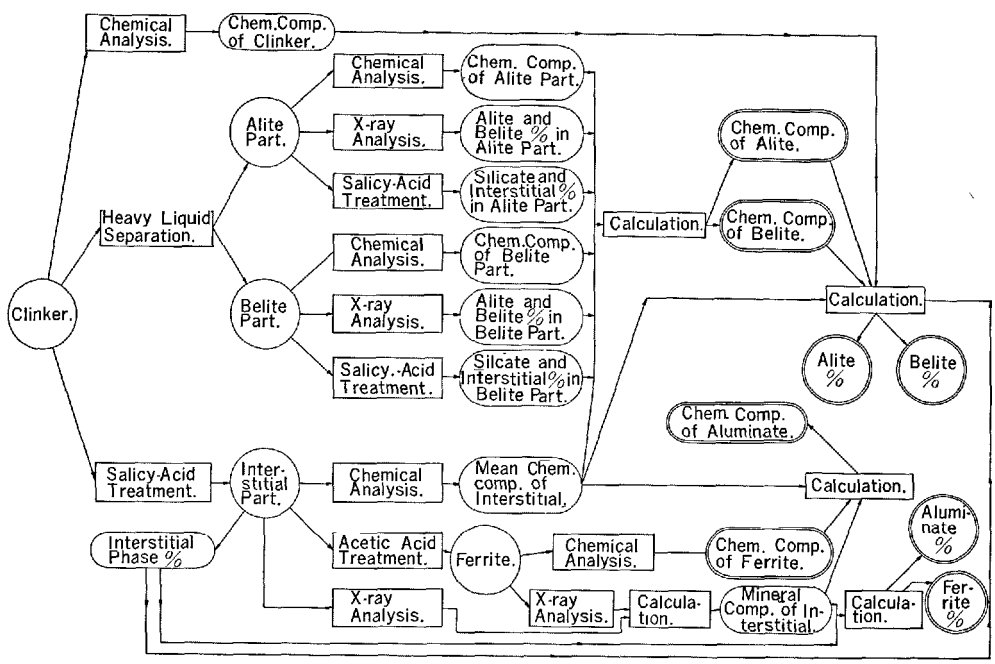

best standard samples are experimentally synthesized alite, belite, ferrite and aluminate crystals which contain definite amount of impurities and have large sizes, but to make those samples is impossible. Therefore, instead of true base crystals, lithium borate glasses containing 50 weight % of constituents of each base crystal were employed as standard bases. Definite amounts of several impurities were dissolved into base glasses to make standard samples. These standard samples were tested by the point analysis and calibration curves were drawn in intensity ratio to Ca and Si. Values of EPMA analysis were so variable according to conditions that calibration curves had to be drawn by a test conducted together with unknown samples at the same time and on the same sample holder.

Results of quantitative analysis are shown in Table 5.

Chemical Composition of Minerals

Chemical composition of the cement minerals has not yet been determined precisely because of experimental difficulties, nevertheless it is one of the most important problems in the chemistry of cement. Therefore, this problem was considered from all directions as a main project.

X-ray Diffraction Method

The chemical composition of a solid solution can be determined by measuring the d-spacing if the solid solution system is simple.

L. E. Copeland, S. Brunauer, D. L. Kantro, E. D. Schulz and C. H. Weise (1959) (65) and M. G. Midgley, D. Rosaman and K. E. Fletcher (1960) (66) reported results of employing this method to the ferrite phase. S. Sato, S. Takashima and M. Kato (1962) (67) reported the same kind of result. This method is effective when a shift of some diffraction caused by solid solution formation is remarkable but if a complex solid solution is formed this method is unapplicable.

In the case of the ferrite phase, 141 diffraction shifts to low angle side according to the substitution of Al by Fe while it shifts to high angle side according to the substitution of Fe by Al. However, A. Kato (1958) (39), (1959) (40) clarified that the ferrite solid solution with Si and Mg have a shift of 141 diffraction to low angle side as shown in Figs. 11–13.

The former three reports mentioned above show that the ferrite phase in clinker is generally C_4AF composition and sometimes shifts to Fe_2O_3 rich side. However, this conclusion has disregarded the effect of Si and Mg, so that the true composition should be at C_6A_2F side. In this experiment, 141 diffraction of the ferrite phase appears at about 33.8° as shown in Figs. 23 and 24 and this situation is that of pure C_4AF. Therefore, if the system were pure C_2F–C_2A, the composition would be C_4AF, but in fact the ferrite phase contains some amount of Si and Mg, so that the true composition seems surely to be at C_6A_2F side.

This method cannot be employed in the polycomponent system. But, in this experiment, it was applied successfully to the determination of alkali sulphate composition in the interstitial phase. According to Fig. 51, the composition of alkali sulphate in N_1 clinker was determined to be at slightly K rich side of $3K_2SO_4 \cdot Na_2SO_4$.

EPMA Method

A result of EPMA method is not reliable unless a

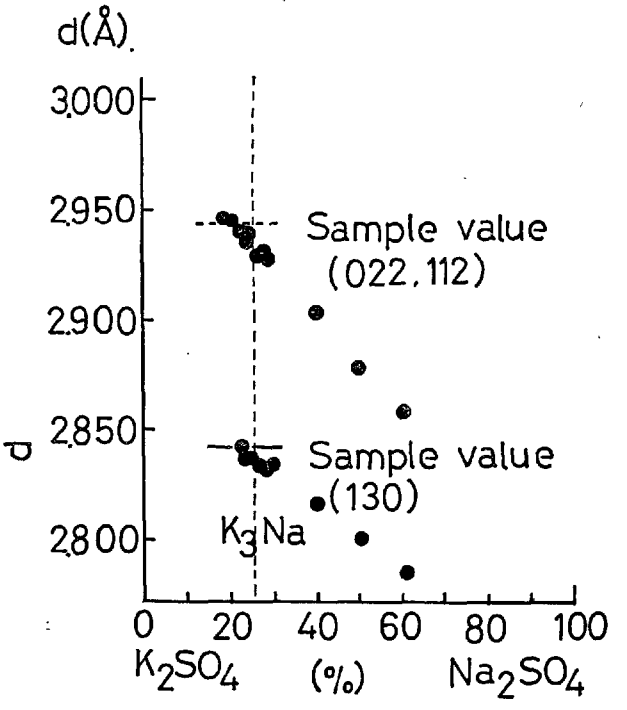

Fig. 51. *X-ray quantitative analysis of composition of alkali sulphate.*

tested point is more than 10μ far from another phase from the standpoint of the resolution power. On the other hand, from the standpoint of the technique, a reliable analysis seems not to be easily realized. In this experiment, it was successful result that the solid solution composition of alite and belite was roughly estimated and the composition of the ferrite phase was obtained to be at rather C_6A_2F side.

Chemical Analysis

A method combining the chemical treating separation, the heavy liquid separation, the X-ray analysis and the chemical analysis was already mentioned above. A combination flow chart is shown as Table 6. Results of that calculation are shown in Table 7. The chemical formulas of them are expressed as a standardized form having 90 oxygen atoms as shown in Table 8. Moreover, the standard chemical formulas having 180 oxygen atoms and the theoretical chemical compositions of cement minerals contained in Japanese clinkers are obtained and shown in Table 9. Details will be reported separately (68).

Table 7. *Chemical composition of minerals in clinkers*

Clinker	SiO_2	Al_2O_3	Fe_2O_3	CaO	MgO	SO_3	Na_2O	K_2O
Alite								
N_1	24.15	1.30	0.66	72.76	1.10	0.00	0.03	0.00
N_2	25.13	1.17	0.61	71.46	1.40	0.00	0.05	0.18
N_3	24.10	1.20	0.61	72.74	1.16	0.05	0.09	0.05
N_4	difficult to separate							
N_5	23.95	1.49	0.47	72.54	1.16	0.25	0.03	0.11
R	24.10	1.38	0.41	73.05	0.94	0.05	0.02	0.05
M_1	24.72	1.36	0.77	71.85	1.01	0.16	0.05	0.08
M_2	25.66	0.59	0.45	71.98	1.23	0.00	0.03	0.06
W_1	25.71	0.37	0.28	72.53	0.93	0.07	0.11	0.00
W_2	25.52	1.16	0.24	71.94	1.00	0.11	0.00	0.03
Belite								
N_1	31.85	2.68	1.25	62.53	0.74	0.27	0.36	0.32
N_2	33.17	1.61	1.05	62.38	0.79	0.05	0.46	0.49
N_3	31.62	1.99	0.78	63.86	0.60	0.26	0.40	0.49
N_4	difficult to separate							
N_5	31.52	2.38	1.43	63.51	0.89	0.00	0.16	0.11
R	31.68	2.99	1.03	62.65	1.02	0.08	0.08	0.49
M_1	30.66	2.41	1.29	63.79	0.72	0.52	0.22	0.39
M_2	31.36	2.81	1.63	62.35	0.60	0.50	0.25	0.50
W_1	32.92	0.49	0.16	65.09	0.53	0.32	0.33	0.16
W_2	31.80	1.94	0.10	64.33	0.62	0.50	0.58	0.13
Ferrite								
N_1	4.3	25.1	20.0	45.5	4.2	0.0	0.6	0.3
N_2	3.0	24.6	22.2	44.9	4.3	0.0	0.6	0.5
N_3	4.3	24.3	22.1	44.5	4.2	0.0	0.3	0.3
M_1	4.2	22.7	21.9	46.4	4.5	0.0	0.2	0.1
Aluminate								
N_1	4.6	27.2	11.4	53.0	2.2	0.0	1.5	0.1
N_2	7.1	27.5	6.0	53.4	2.2	0.0	2.0	1.8
N_3	5.8	28.7	5.3	54.8	2.2	0.0	1.7	0.8
M_1	5.0	21.4	16.0	54.2	2.2	0.0	0.3	0.9

Table 8. *Chemical formula of minerals in clinker*

Clinker	Si	Al	Fe	Ca	Mg	S	Na	K	O
Alite									
N_1	16.59	1.04	0.34	53.58	1.13	0.00	0.04	0.00	90
N_2	17.15	0.94	0.30	52.29	1.41	0.00	0.06	0.16	90
N_3	16.57	0.98	0.32	53.46	1.19	0.02	0.12	0.04	90
N_5	16.49	1.20	0.24	53.48	1.19	0.13	0.04	0.10	90
R	16.74	1.12	0.22	54.37	0.97	0.03	0.02	0.04	90
M_1	16.93	1.10	0.40	52.72	1.03	0.48	0.06	0.06	90
M_2	17.71	0.48	0.24	53.13	1.26	0.00	0.04	0.04	90
W_1	17.57	0.30	0.14	53.11	0.95	0.04	0.14	0.00	90
W_2	17.37	0.94	0.12	52.45	1.01	0.06	0.00	0.02	90
Belite									
N_1	21.52	2.06	0.60	43.48	0.72	0.13	0.46	0.26	90
N_2	20.44	1.22	0.52	43.21	0.76	0.02	0.58	0.26	90
N_3	20.64	1.54	0.38	44.67	0.58	0.12	0.52	0.40	90
N_5	20.49	1.82	0.70	44.23	0.86	0.00	0.20	0.10	90
R	20.63	2.28	0.50	43.49	0.98	0.04	0.10	0.40	90
M_1	20.10	1.86	0.64	44.80	0.71	0.26	0.28	0.32	90
M_2	20.43	2.16	0.80	43.51	0.58	0.24	0.32	0.42	90
W_1	20.73	0.38	0.08	45.47	0.51	0.16	0.42	0.14	90
W_2	20.74	1.48	0.04	44.95	0.60	0.24	0.74	0.10	90
Ferrite									
N_1	2.95	18.52	10.31	33.41	4.29	0.00	0.80	0.26	90
N_2	2.99	20.09	11.53	33.34	4.45	0.00	0.81	0.44	90
N_3	2.96	19.68	11.43	32.78	4.31	0.00	0.40	0.26	90
M_1	2.92	18.51	11.41	34.44	4.65	0.00	0.27	0.09	90
Aluminate									
N_1	3.2	21.9	5.8	38.7	2.3	0.0	2.4	0.1	90
N_2	4.8	21.8	3.1	38.6	2.2	0.0	3.1	1.6	90
N_3	3.9	22.7	2.7	39.5	2.9	0.0	2.7	0.7	90
M_1	3.5	17.6	8.4	40.6	2.3	0.0	0.5	0.8	90

Alkali sulphate in N_1 is about $K_3Na(SO_4)_2$

Table 9. *Standard chemical formulas of cement minerals and their compositions*

Alite	$Ca_{106}Mg_2(Na_{1/4}K_{1/4}Fe_{1/2})O_{36}(Al_2Si_{34}O_{144})$
Belite	$Ca_{87}Mg\ AlFe(Na_{1/2}K_{1/2})(Al_2Si_{42}O_{180})$
Ferrite	$Ca_{66}Mg_4(Na_{1/2}K_{1/2}Fe)(Al_{40}Fe_{22}Si_5Mg_5O_{180})$
Aluminate	$Na_6K_8Ca_{78}Mg_4(Al_{44}Fe_8Si_8O_{180})$

	SiO_2	Al_2O_3	Fe_2O_3	CaO	MgO	Na_2O	K_2O
Alite	24.83	1.24	0.49	72.23	0.98	0.09	0.14
Belite	32.50	2.63	1.03	62.83	0.52	0.20	0.30
Ferrite	3.61	24.51	22.08	44.50	4.36	0.37	0.57
Aluminate	5.88	27.43	7.81	53.49	1.97	2.27	1.15

Texture of Interstitial Phase

It seems a reasonable interpretation that the light interstitial corresponds to the ferrite phase and the dark interstitial to the aluminate phase in the etched figure of the interstitial phase. However, a perfect

certification of the fact from many experimental standpoints has never been carried out. In the figure of the interstitial in Fig. 49, correspondency of the reflected light microscopic figure to the back scattered electron image is very good, while the X-ray images are not so clear because of the low resolution for too small crystals. One of the best methods to identify the ferrite phase and the aluminate phase is to combine the transmitted light microscopic observation in a thin section. This combined technique was attempted and the result is shown in Fig. 52. In this figure, correspondency among two reflecting (reflected light and back scattered electron) images and two transmitting (open nicols and crossed nicols) images is fairly good about silicate crystals but not so good, though somehow detactable, about ferrite crystals which show yellow-colored high birefringence. The reason is that the section is not so thin that crystals lie one upon another in the vertical direction especially in the case of small crystals.

Therefore, a synthesis of the interstitial phase of large crystals were attempted with experimental composition from the residue of the salicylic acid methanol treatment. The texture of thus synthesized interstitial phase resembled that of commercial clinker but consisted in more than ten times larger crystals, and the specimen could be polished into a thin section easily. Ferrite crystals are sectioned longitudinally in Fig. 53, and transversely in Fig. 54. In both figures, correspondency among light and dark

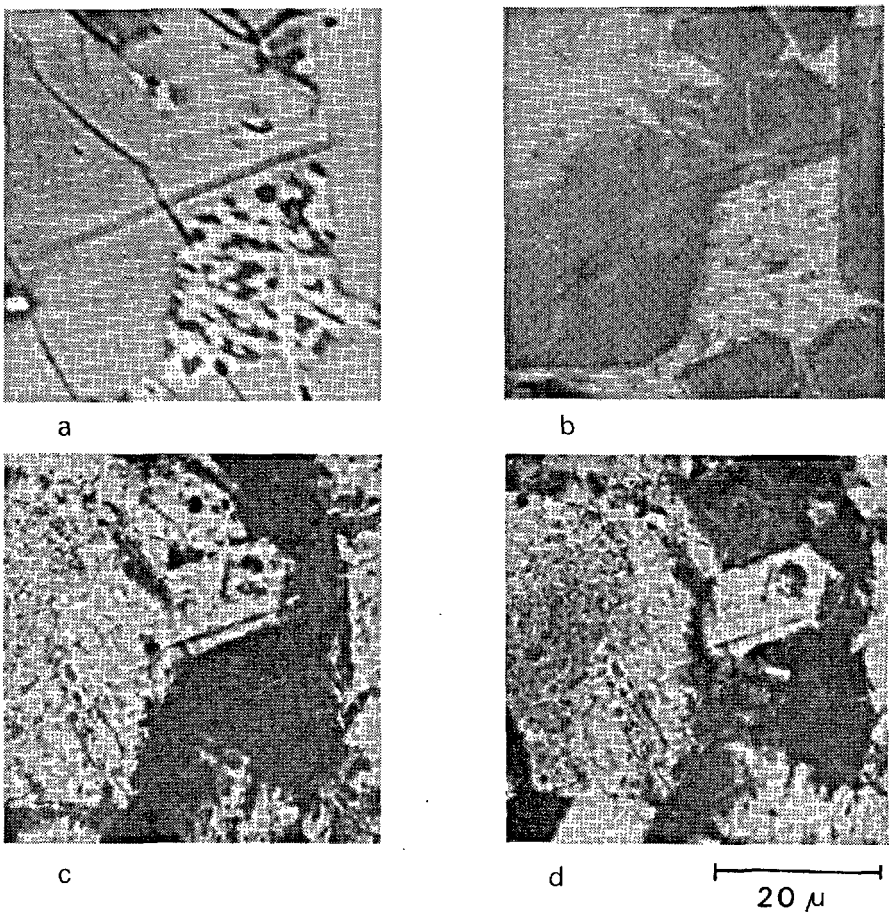

a) EPMA back scattered electron image
b) Reflected light microscopic image
c) Open nicols microscopic image
d) Crossed nicols microscopic image

Fig. 52. *EPMA and optical microscopic photograph of interstitial in commercial clinker.*

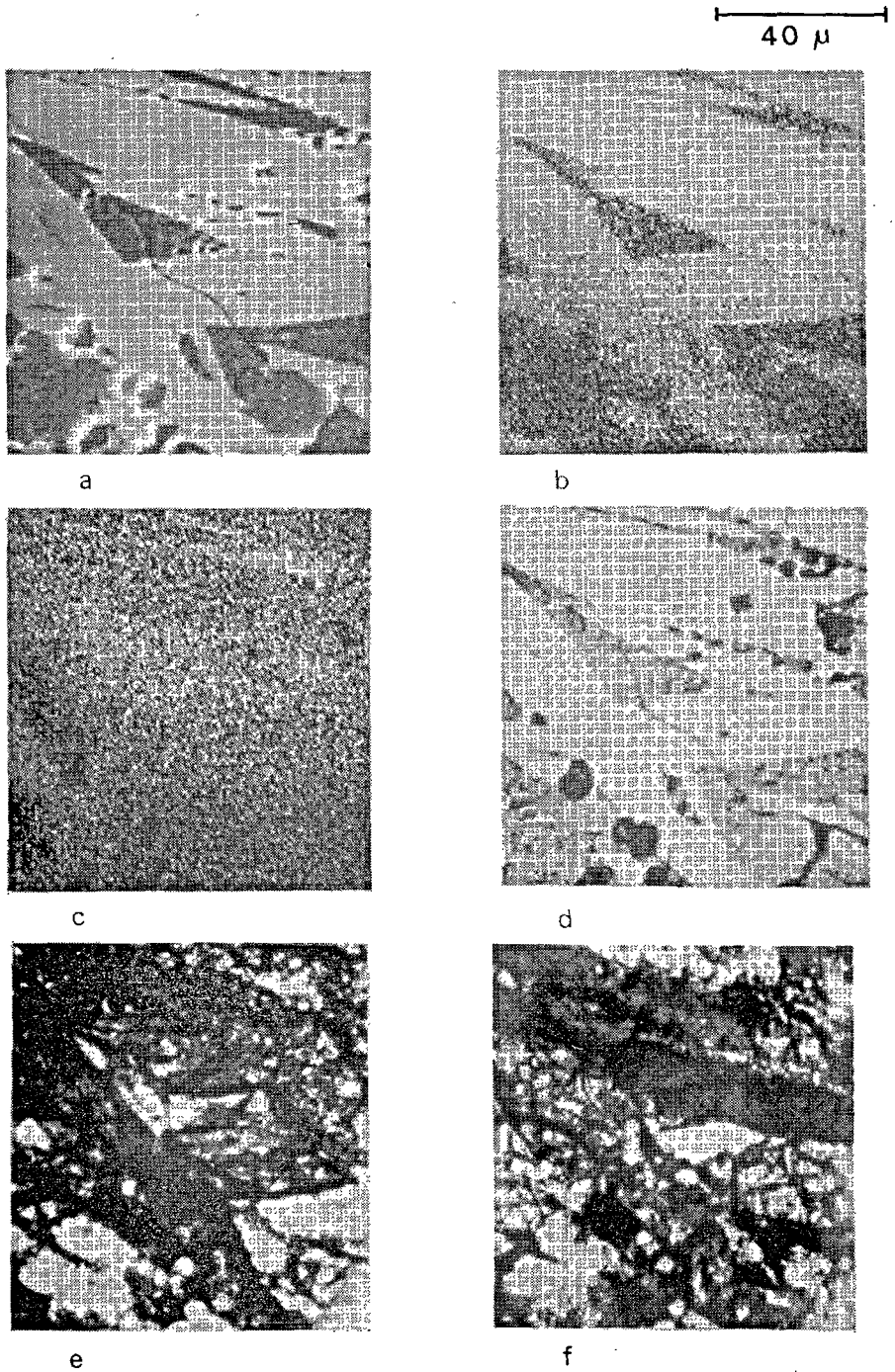

a) EPMA back scattered electron image
b) EPMA Fe image
c) EPMA Al image
d) Reflected light microscopic image
light part—ferrite
dark part—aluminate
e) Open nicols microscopic image
f) Crossed nicols microscopic image

Fig. 53. *EPMA and optical microscopic photograph of synthetic interstitial.*

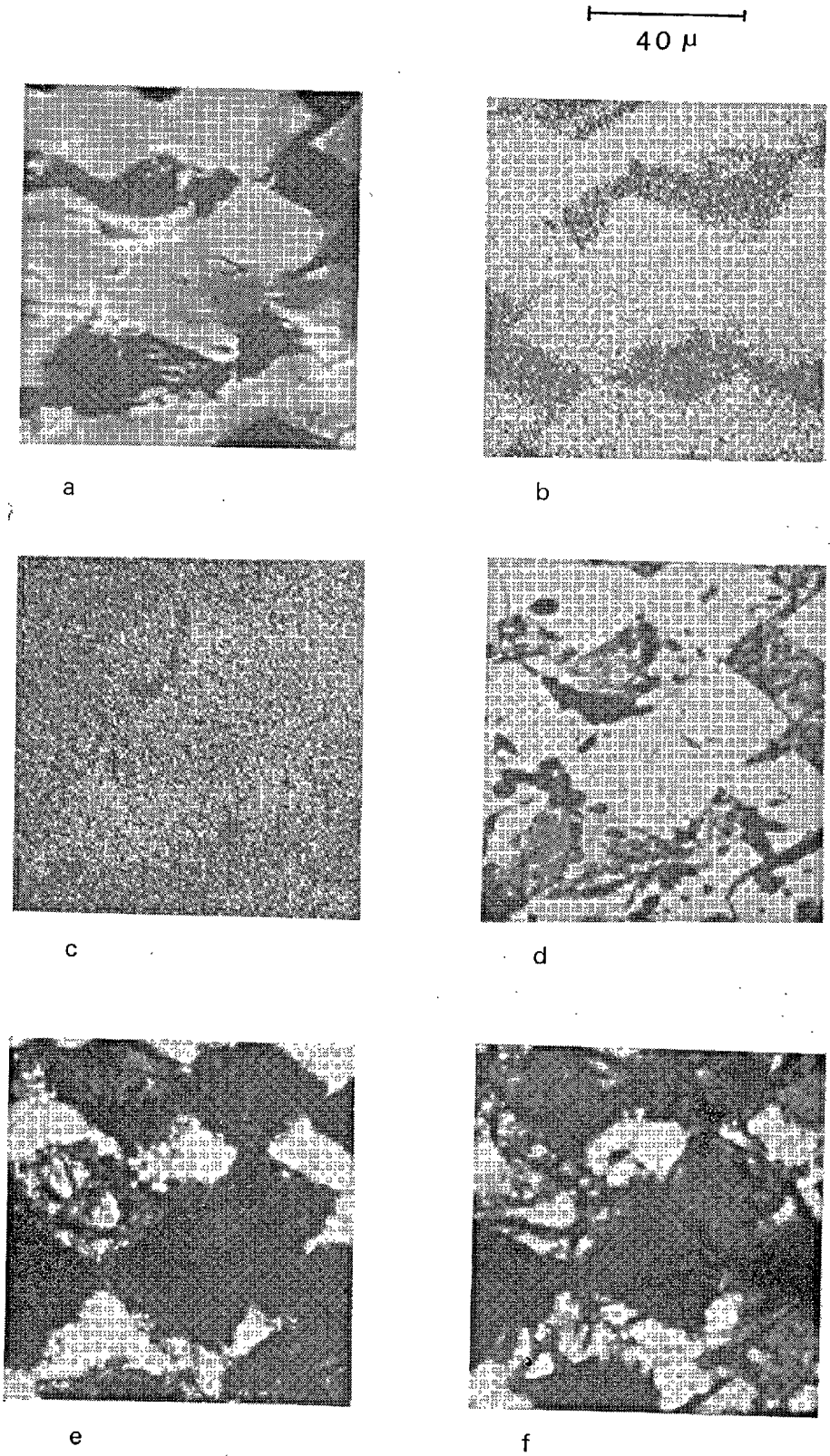

Fig. 54. *EPMA and optical microscopic photograph of synthetic interstitial.*

Texture of Interstitial Phase (P.P. I-3)

Open nicols

Crossed nicols

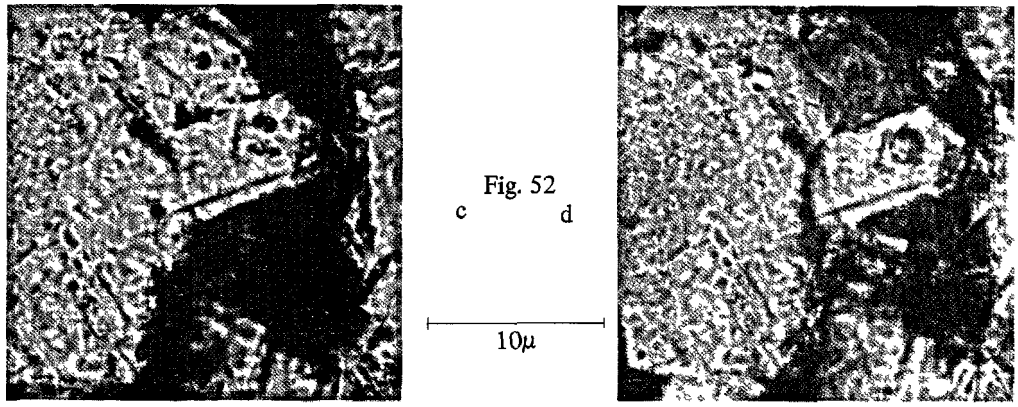

Fig. 52
c d

10μ

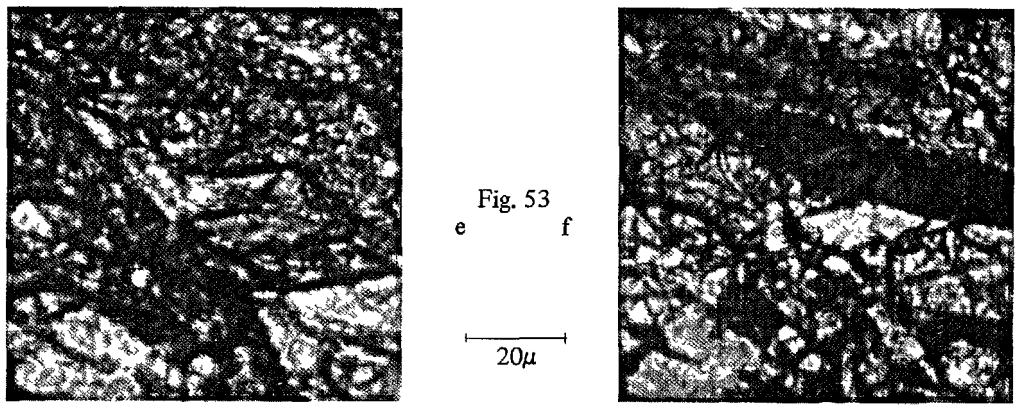

Fig. 53
e f

20μ

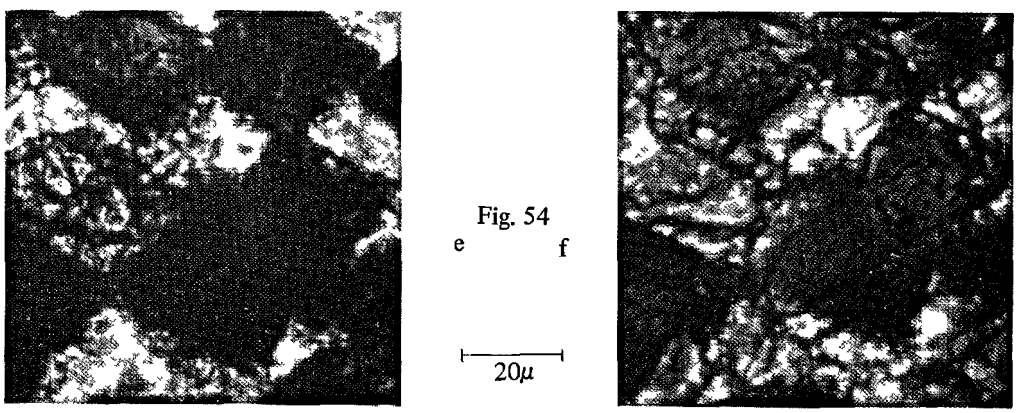

Fig. 54
e f

20μ

Fig. 52 Silicate part is alite. Interstitial seems dark because of its complex structure rich in Fe_2O_3. Ferrite seems strongly anisotropic with yellow polarization color in crossed nicols.

Fig. 53 Ferrite seems strongly anisotropic with yellow polarization color while aluminate seems weakly anisotropic with dark bluish color in crossed nicols.

Fig. 54 Ferrite seems anisotropic with yellow polarization color and dark brown own color. Aluminate seems weakly anisotropic. (This photo-plate was contributed by the authors).

interstitials, electron scattering power, Fe and Al distribution and optical properties of crystals is reasonable.

Especially it is characteristically stressed that Al distribution is nearly uniform, ferrite has strong birefringence and aluminte is somewhat anisotropic. The anisotropy of aluminate agrees with the X-ray diffraction data showing orthorhombic. This analysis will be reported separately (68).

Mineral Composition of Clinker

Bogue's Method

Mineral compositions were calculated by the conventional Bogue's method. It is well known that Bogue's calculation is fairly practical in spite of neglecting the solid solution phenomena. This fact is explained as follows: The composition of the ferrite phase has lower Fe_2O_3 than C_4AF but Bogue's calculation is conducted applying the composition C_4AF, so that the fact that Fe_2O_3 content is lower is compensated by its distribution other phases. The composition of the aluminate phase has also lower Al_2O_3 than C_3A, but this fact is compensated by substitution with Fe_2O_3 etc., and the calculation value becomes rather reasonable. In the silicate phases, CaO contents are lower than the simple theoretical value but the same phenomenon takes place and rather reasonable values are obtained. Results are shown in Table 10.

Point by Point Counting Method

The counting method has been already established. The reliability depends technically on the etching method and theoretically on the distribution character. The relation among content, accuracy, reliability and count number is informed from values of the binominal distribution shown in Table 11.

However, the distribution uniformity should be taken into account for measurement. If the distribution is uniform enough, the distance between one counted point and a next point must not be so long, on the contrary if the uniformity is not enough, for instance, when there exist nests of some phase, the distance must be long. Therefore employing the same counting system independently to the uniformity is not reasonable, and a measuring method of the uniformity and a proper counting distance suitable to that should be established. Counted results are shown in Table 10.

Calculation from Chemical Composition

According to the method of calculation of the

Table 10. *Mineral composition determined by several method*

Clinker	Method	Alite	Belite $\alpha+\beta$, (α)	Ferrite	Aluminate	Others
N_1	Bogue	52	26	8	9	
	Microscopy	52	30	10	9	
	Chemical	51	32	8	7	2{$K_3Na(SO_4)_2$ 1.4, CaO 0.6 MgO 0.03
	X-ray	55	26 (8)	9	9	
	New method	54	28	13	5	
N_2	B	42	34	10	10	
	M	52	32	11	5	
	C	59	23	10	6	2{$K_3Na(SO_4)_2$ 0.7, CaO 0.08 MgO 0.6
	X	55	26 (6)	11	7	
	N	49	31	13	7	
N_3	B	57	24	10	7	
	M	65	20	7	8	
	C	61	22	10	6	1{$K_3Na(SO_4)_2$ 0.2, MgO 0.7
	X	58	24 (0)	11	7	
	N	61	23	13	2	
N_4	B	63	13	10	9	
	M	69	17	9	6	
	C	72	10			{MgO 1.05, CaO 0.31
	X					
	N	65	13	14	7	
N_5	B	45	33	10	10	
	M	50	36	8	6	
	C	50	36			{CaO 0.12
	X					
	N	52	30	12	7	
R	B	64	16	9	8	
	M	65	18	9	8	
	C	67	19	14		{CaO 0.03
	X					
	N	73	11	8	8	
M_1	B	48	31	11	7	
	M	48	32	10	10	
	C	51	33	9	2	5{CaO 0.02
	X	49	33 (0)	14	3	
	N	58	27	14	0	
M_2	B	49	30	11	7	
	M	55	26	10	9	
	C	56	27	17		{CaO 0.03
	X					
	N	58	26	14	1	

Table 11. *Values of binominal distribution*

Accuracy $\pm\varepsilon\%$	Reliability $\pm\lambda\sigma$	Composition % 10 90	20 80	30 70	40 60	50 50
ε	λ	n				
1	1	900	1600	2100	2400	2500
	2	3600	6400	8400	9600	10000
	3	8100	14400	18900	21600	22500
2	1	225	400	525	600	625
	2	900	1600	2100	2400	2500
	3	2025	3600	4725	5400	5625
3	1	100	178	233	267	278
	2	400	712	932	1068	1112
	3	900	1602	2097	2403	2502

mineral composition from chemical analysis, the mineral compositions were calculated as shown in Table 10 (line C). Moreover, if the standard chemical compositions of the minerals shown in Tables 8 and 9 are reliable, the mineral compositions can be obtained by solving the following equations applying the least square method. Solutions of this method obtained using an automatic computor are shown in Table 10 (line N).

Equation	Main notation	Suffix
$C_ax + C_by + C_fz + C_lu = C_c$	C CaO%	a alite
$S_ax + S_by + S_fz + S_lu = S_c$	S SiO_2%	b belite
$F_ax + F_by + F_fz + F_lu = F_c$	F Fe_2O_3%	f ferrite
$A_ax + A_by + A_fz + A_lu = A_c$	A Al_2O_3%	l aluminate
$x + y + z + u = 100$		c cement

X-ray Quantitative Analysis

The X-ray quantitative analysis has been studied by many investigators. This method concerning to the cement chemistry employed first to the analysis of $Ca(OH)_2$. G. Yamaguchi and A. Kato (1956) (69) and L. E. Copeland and R. H. Bragg (1958) (70) conducted such an analysis. The analysis of clinker in the early stage was studied by G. Yamaguchi, H. Miyabe and K. Tanaka (1958) (71), M. Euw (1958) (72), G. Yamaguchi, K. Tanaka and M. Kajii (1959) (73), L. E. Copeland, S. Brunauer, D. L. Kantro, E. G. Schulz and C. H. Weise (1959) (74), G. Yamaguchi, K. Takemoto, H. Uchikawa and S. Takagi (1959) (75), H. G. Midgley, D. Rosaman, K. E. Fletcher (1960) (76), G. Yamaguchi, K. Takemoto, H. Uchikawa and S. Takagi (1960–1) (77), (1960–2) (78) and H. G. Smolzyk (1961) (79). As the latest one, R. L. Berger, G.J.C. Erohnsdorff, P. H. Harris and P. D. Johnson (1966) (80) reported a routine method using an automatic computor. Principles of these methods are almost the same and there would be no trouble if the diffraction patterns of minerals were always constant. But the fact is not so simple and there are habits of patterns according to clinkers. Some problems are shown as follows:

a. What are the best for standard samples?
b. A pattern of alite always appears dominantly. Therefore, what is the best way to determine belite? To use the diffraction at 31° or what?
c. At the valley between 33° and 34°, there appear diffractions of ferrite, aluminate and α–C_2S. How are they treated?

After some considerations in this experiment the following conclusion was obtained. Details will be reported separately (68).

a. The separated minerals are the best for standards.
b. The intensity of diffraction is measured as total counts through a proper angular range.
c. The determination of alite can be conducted by counting only two doublet diffractions, 620 and 040 at 51°–52°, and 221 and 401 at 29° more reliably than by counting other diffractions together.
d. The determination of belite can be conducted by counting only two diffractions, 014 and 031 at 41°, and $12\bar{1}$ at 31° more reliably than by counting other diffractions together.
e. The primary approximate contents of ferrite, aluminate and α–C_2S are calculated from those peak-point intensities, and each overlapping total count is estimated and used as correction value to others.

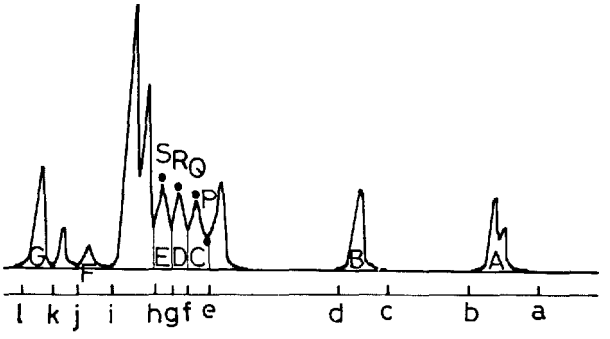

Point.	Angle.	Notation of total count.	Notation of peak point intensity.
a	52.25		
b	51.22	A	
c	41.75		
d	40.50	B	
e, P	34.00		P
Q	33.75	C	Q
f	33.50		
R	33.25	D	R
g	33.00		
S	32.90	E	S
h	32.75		
i	31.25		
j	30.50	F	
k	29.75		
l	28.75	G	

Fig. 55. *Counting program of X-ray diffraction quantitative analysis of cement clinker.*

Counting ranges, counting points and their notations are shown in Fig. 55. Calculation formulas are as follows and results are shown in Table 10.

Alite %	$\alpha = xA/A_0 + (1-x)G/G_0$		minerals
Belite %	$\beta = yF/F_0 + (1-y)(B - \alpha B\alpha_0)/B\beta_0$ as β-C_2S	x, y	Coefficients owing to clinker
		P_0, Q_0, R_0, S_0	Differction peak point intensities of pure minerals
Ferrite %	$\gamma = (C - pp/p_0 - r'R/P_0)/C_0$		
Aluminate %	$\delta = (D - qQ/Q_0 - s'S/S_0 - k\beta)/D_0$	p, q, r, r', s'	Coefficients of intensity effect to neighbours
α-C_2S %	$\varepsilon = (E - rR/R_0 - k'\beta)/E_0$		
$A_0, B\alpha_0, B\beta_0, C_0, D_0, E_0, F_0, G_0$,	Diffraction intensities of pure	k, k'	Coefficients of β-C_2S effect

Discussion of Compositions

As to the chemical compositions of alite and belite, if the formulas keep the structural stoichiometry, they may be described as follows respectively referring to the experimental ones:

$$Ca_{104}Mg_2Al(Na_{1/4}K_{1/4}Fe_{1/2})O_{36}(AlSi_{35}O_{144})$$

and

$$Ca_{85}MgAl_2Fe(Na_{1/2}K_{1/2})(Al_2Si_{43}O_{180}).$$

However, these formulas result in lower CaO and higher SiO_2 values than experimental ones in both minerals. On the contrary the following experimental formulas,

$$C_{106}Mg_2(Na_{1/4}K_{1/4}Fe_{1/2})O_{36}(Al_2Si_{34}O_{144})$$

and

$$Ca_{87}MgAlFe(Na_{1/2}K_{1/2})(Al_3Si_{42}O_{180}),$$

are slightly out of the structural stoichiometry and have cations occupied excess lattice points.

Alite has little impurity except MgO and Al_2O_3, so that the simplified typical formula is described as $Ca_{105}Mg_2AlO_{36}(AlSi_{35}O_{144})$. This corresponds to Jeffery's alite formula which may be described as $Ca_{108}Mg_2O_{36}(Al_4Si_{32}O_{144})$ but has a half of Al_2O_3. Less Al_2O_3 content in alite has been recognized and mentioned by many investigators.

The formulas of ferrite and aluminate may have some errors because the existence of glass phase was neglected, but in general they show the tendency of the chemical compositions of those minerals, so that several crystallochemical phenomena can be interpreted from these compositions. The mineral compositions of clinkers calculated from the simultaneous equation are fairly reasonable, this fact shows a reliability of these chemical compositions of the minerals. However, about these problems it needs further investigation to obtain the perfect solution.

As to the quantitive analysis of the mineral composition of clinker, of course the X-ray analysis is a direct and desirable method, but still it has many problems and establishment of that system is expected.

This experiment was carried out by the following members besides the authors:
Motohiko Yoshizumi, Takeshi Ohta, Shunji Takeda, Eiichi Miyao and Akio Kawashima.

References

1. R. Naito, Y. Ono and T. Iiyama, Ann. Rept. Japan Cement Eng. Assoc. (in Japanese) **11,** 20–27 (1957).
2. G. Yamaguchi, H. Miyabe and K. Tanaka, Ann. Rept. Japan Cement Eng. Assoc. (in Japanese) **12,** 16–17 (1958).
3. J. W. Jeffery, Acta Cryst., **5,** 26–35 (1952).
4. G. Yamaguchi and H. Miyabe, J. Amer. Ceram. Soc., **43,** 219–224 (1960).
5. N. Yannaguis, M. Regourd, Ch. Mazeres and A. Guinier, Bull. Soc. Franc. Miner. Crist. (in French) **85,** 271–281 (1962).
6. J. W. Jeffery, The Chemistry of Cement, Vol. I, 131–161, Academic Press, London and New York, Composed by H. F. W. Taylor (1964).
7. M. Regourd, Bull. Soc. Franc. Miner. Crist. (in French) **87,** 241–272 (1964).
8. H. Miyabe and D. M. Roy, J. Amer. Ceram. Soc., **47,** 318–319 (1964).
9. G. Yamaguchi and H. Uchikawa, Bull. Chem. Soc. Japan, **34,** 1536–1537 (1961).
10. G. Yamaguchi and H. Uchikawa, Zement-Kalk-Gips, (in German) **50,** 497–504 (1961).
11. G. Yamaguchi, H. Uchikawa, S. Takagi and H. Koike, J. Ceram. Assoc. Japan (in Japanese) **70,** 147–164 (1962).
12. G. Yamaguchi, H. Uchikawa and S. Kawamura, Research Rept. Onoda Cement Company (in Japanese) **13,** 191–204 (1961).
13. G. Yamaguchi, H. Uchikawa and S. Kawamura, J. Ceram. Assoc. Japan (in Japanese) **70,** 209–219 (1962).
14. G. Yamaguchi and H. Uchikawa, Ann. Rept. Japan Cement Eng. Assoc. (in Japanese) **16,** 21–26 (1962).
15. G. Yamaguchi and K. Kato, Ann. Rept. Japan Cement Eng. Assoc. (in Japanese) **16,** 27–29 (1962).
16. E. Woermann, Th. Hahn and W. Eysel, Zement Kalk Gips (in German) **52,** 370–375 (1963).
17. H. G. Midgley and K. E. Fletcher, Trans. Brit.

Ceram. Soc., **62,** 917–937, (1963).
18. Y. Ono, T. Uno and Y. Kanai, Ann. Rept. Japan Cement Eng. Assoc. (in Japanese) **19,** 33–37 (1965).
19. G. Yamaguchi and K. Kato, Ann. Rept. Japan Cement Eng. Assoc., **18,** 43–44 (1964). (in Japanese).
20. G. Yamaguchi, K. Shirasuka and T. Ohta, Symp. Structure of Portland Cement Paste and Concrete, 234–253 (1966).
21. M. Bigare, A. Guinier, M. Regourd, N. Yannaquis, W. Eysel, Th. Hahn and E. Woermann, J. Amer. Ceram. Soc., **50,** 609–619 (1967).
22. S. Akaiwa, G. Sudoh and M. Tanaka, Ann. Rept. Japan Cement Eng. Assoc. (in Japanese) **20,** 26–31 (1966).
23. G. Yamaguchi, H. Miyabe, K. Amano and S. Komatsu, J. Ceram. Assoc. Japan (in Japanese) **65,** 99–104 (1957).
24 G. Yamaguchi, Y. Ono, S. Kawamura and Y. Sohda, J. Ceram Assoc. Japan (in Japanese) **71,** 9–12 (1963).
25. G. Yamaguchi, Y. Ono, S. Kawamura and Y. Sohda, J. Ceram. Assoc. Japan (in Japanese) **71,** 21–26 (1963).
26. C. M. Midgley, Acta Cryst., **5,** 307 (1952).
27. International Table for X-ray Crystallography, The Kynoch Press, Birmingham, England.
28. D. K. Smith, A. J. Majumdar and F. Ordway, J. Amer. Ceram. Soc. **44,** 405–411 (1961).
29. K. Niesel and P. Thormann, Tonind.-Ztg., **91,** 362–369 (1967).
30. G. Yamaguchi, Y. Ono, S. Kawamura and Y. Sohda, Ann. Rept. Japan Cement Assoc., (in Japanese) **16,** 34–40 (1962).
31. Y. Ono, Doctor Thesis of University of Tokyo (1963).
32. G. Yamaguchi and K. Suzuki, J. Ceram. Assoc. Japan, **75,** 220–229 (1967).
33. M. A. Bredig, J. Phys. Chem., **49,** 537–553 (1945).
34. ASTM Powder Diffraction Data File
35. W. Gutt, Nature, **190,** 339–340 (1961).
36. G. Yamaguchi and A. Kato, Ann. Rept. Japan Cement Assoc., **11,** 35–41 (1957) (in Japanese).
37. E. F. Bertaut, P. Blum and A. Sagieres, Acta Cryst., (in French) **12,** 149–159 (1959).
38. D. K. Smith, Acta Cryst., **15,** 1146–1152 (1962).
39. A. Kato, Ann. Rept. Japan Cement Eng. Assoc., **12,** 17–25 (1958) (in Japanese).
40. A. Kato, Ann. Rept. Japan Cement Eng. Assoc., **13,** 27–31 (1959) (in Japanese).
41. A. E. Moore, Nature, **199,** 480–481 (1963).
42. J. A. Conwicke and D. E. Day, J. Amer. Ceram. Soc., **47,** 654–655 (1964).
43. K. E. Fletcher, H. G. Midgley and A. E. Moore, Mag. Concrete Res., **53,** 171–176 (1965).
44. C. M. Schlaut and D. M. Roy, Nature, **207,** 819 (1965).
45. A. J. Majumdar, Trans. Brit. Ceram. Soc., **64,** 105–119 (1965).
46. P. Tarte, Nature, **207,** 973–974 (1965).
47. A. E. Moore, Mag. Concrete Res., **55,** 59–64 (1966).
48. G. Yamaguchi, will be submitted to J. Ceram. Assoc. Japan.
49. S. Takashima, Ann. Rept. Japan Cement Eng. Assoc., **12,** 49–55 (1958).
50. G. Yamaguchi, will be submitted to J. Ceram. Assoc. Japan.
51. H. Insley and V. D. Frechette, Microscopy of Ceramics and Cements, Academic Press Inc., New York (1955).
52. G. Yamaguchi and Y. Ono, Zement-Kalk-Gips, (in (German) **55,** 390–394 (1966).
53. G. Yamaguchi and Y. Ono, Ann. Rept. Japan Cement Eng. Assoc., **16,** 30–34 (1962) (in Japanese).
54. A. Metzger, Zement-Kalk-Gips, (in German) **42,** 269–270 (1953).
55. F. Trojer, Zement-Kalk-Gips (in German) **55,** 207–215 (1966).
56. P. Brunner, Zement-Kalk-Gips, (in German) **54,** 247–252 (1965).
57. H. G. Midlgey, The Chemistry of Cement, Vol. I, 89–130, Academic Press, London and New York, Composed by H. F. W. Taylor (1964).
58. K. E. Fletcher, H. G. Midgley and A. E. Moore, Mag. Concrete Res., **53,** 171–176 (1965).
59. G. Yamaguchi, H. Uchikawa and S. Takagi, Ann. Rept. Japan Cement Eng. Assoc. (in Japanese) **19,** 29–32 (1965).
60, G. Yamaguchi, S. Takagi, M. Yoshizumi and T. Ohta, Ann. Rept. Japan Cement Eng. Assoc. (in Japanese) **20,** 32–36 (1966).
61. G. Yamaguchi, S. Takagi and M. Yoshizumi, Ann. Rept. Japan Cement Eng. Assoc. (in Japanese) **21,** 123–129 (1967).
62. S. Akaiwa, G. Sudo and M. Tanaka, Ann. Rept. Japan Cement Eng. Assoc. (in Japanese) **21,** 22–28 (1967).
63. I. Peterson, Zement-Kalk-Gips (in German) **56,** 61–64 (1967).
64. G. Yamaguchi, will be submitted to J. Ceram. Assoc. Japan.
65. L. E. Copeland, S. Brunauer, D. L. Kantro, E. D. Schulz and C. H, Weise, Analyt. Chem., **31,** 1521–1530 (1959).
66. H. G. Midgley, D. Rosaman and K. E. Fletcher, Proceedings of 4th Intern. Symp. Chem. of Cement, 69–74 (1960).
67. S. Sato, S. Takashima and M. Kato, Ann. Rept. Japan Cement Eng. Assoc. (in Japanese) **16,** 41–45 (1962).
68. G. Yamaguchi, will be submitted to J. Ceram. Assoc. Japan.
69. G. Yamaguchi and A. Kato, Ann. Rept. Japan Cement Eng. Assoc. (in Japanese) **10,** 214–221 (1956).
70. L. E. Copeland and R. H. Bragg, Analyt. Chem., **30,** 196–201 (1958).
71. G. Yamaguchi, H. Miyabe and K. Tanaka, Ann. Rept. Japan Cement Assoc. (in Japanese) **12,** 16–17 (1958).
72. N. Euw, Silicates Ind. (in French) **23,** 643–649 (1958).
73. G. Yamaguchi, K. Tanaka and M. Kajii, Ann. Rept. Japan Cement Eng. Assoc. (in Japanese) **13,** 31–33 (1959).
74. L. E. Copeland, S. Brunauer, D. L. Kantro, E. G.

Schulz and C. H. Weise, Analyt. Chem., **31**, 1521–1530 (1959).
75. G. Yamaguchi, K. Takemoto, H. Uchikawa and S. Takagi, Ann. Rept. Japan Cement Eng. Assoc. (in Japanese) **13**, 62–74 (1959).
76. H. G. Midgley, D. Rosaman and K. E. Fletcher, Proceedings of 4th Intern. Symp. Chem. of Cement, 69–74 (1960).
77. G. Yamaguchi, K. Takemoto, H. Uchikawa and S. Takagi, Proceedings of 4th Intern. Symp. Chem. of Cement, 495–499 (1960).
78. G. Yamaguchi, K. Takemoto, H. Uchikawa and S. Takagi, Zement-Kalk-Gips (in German) **49**, 467–478 (1960).
79. H. G. Smolzyk, Zement-Kalk-Gips, (in German) **50**, 391–399 (1961).
80. R. L. Berger, G. J. C. Erohnsdorff, P. H. Harris and P. D. Johnson, Symp. Structure of Portland Cement Paste and Concrete, 234–253 (1966).
Note 1. Ann. Rept. Japan Eng. Assoc., English synopsis is published separately.
Note 2. J. Ceram. Assoc. Japan, always with English synopsis and sometimes written in English.

Written Discussion

Pierre Terrier

When different methods lead independently to the same result, they strengthen this result. It is the case for the Fe_2O_3 content of alite crystals of clinker.

Our results, obtained from the electron microprobe indicate that the Fe_2O_3 content of the alite crystals is variable, it depends on the Fe_2O_3 content of the clinker (Table 1). Your results (Table 3 and Table 6 of the principal paper: The analysis of portland cement clinker) obtained from a different manner agree with this observation. We can group these data on Fig. 1, showing as an average

$$Fe_2O_{3\ \text{ALITE}} = 0.2Fe_2O_{3\ \text{CLINKER}}$$

Our operating conditions are as follows:
—MS 46 CAMERA electron microprobe
—diamond polishing of embedded clinker
—nickel metallization of the polished face
—Fe K_α radiation analysis
—crystal analyzer quartz 10^{-}II
—accelerating tension of the electrons 20 kV
—standard = S_2Fe pyrite
—corrected concentration from TONG formula

Table 1. Fe_2O_3 *in alite crystals (by EPMA) and* Fe_2O_3 *content of clinkers (chemical analysis)*

Fe_2O_3 Alite	Fe_2O_3 Clinker
0.35	0.51
0.47	2.25
0.48	2.61
0.53	2.55
0.63	3.02
0.66	3.42
0.73	2.81
1.04	5.09
1.36	5.42

Table 2. MgO *in alite crystals (by EPMA) T or M, and* MgO *content of clinkers (chemical analysis)*

Form	MgO Alite	MgO Clinker
trigonal	0.23	0.41
trigonal	0.30	0.91
trigonal	0.33	0.30
trigonal	0.37	1.02
monoclinic	0.55	1.81
trigonal	0.58	1.44
monoclinic	1.00	1.61
monoclinic	1.04	2.11
monoclinic	1.10	2.32

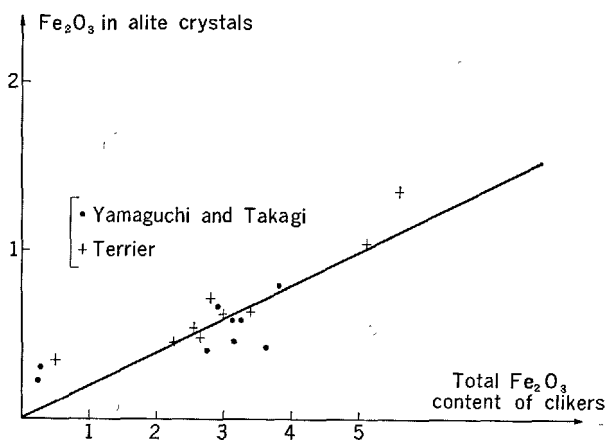

Fig. 1. *Relation between* Fe_2O_3 *in Alite crystals and total* Fe_2O_3 *content of clinkers*

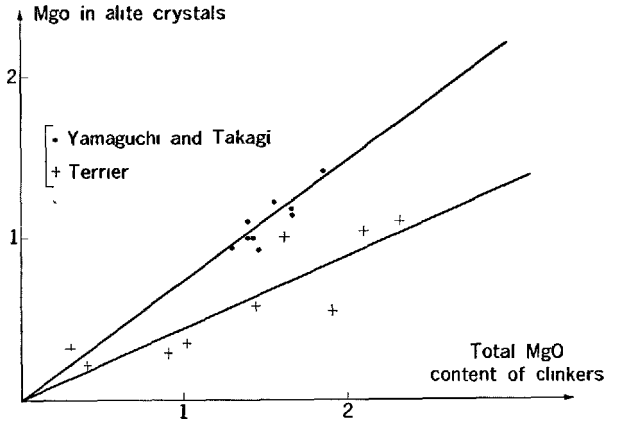

Fig. 2. *Relation between* MgO *in Alite crystals and total* MgO *content of clinkers*

On the other hand, your results (Table 3 and Table 6 of principal paper: The analysis of portland cement clinker) and ours (Table 2) indicate that the MgO content of alite crystals is variable, depending on the MgO content of the clinker.

But, whilst your results organize about the right line with a 0.74 slope, ours do about 0.45 slope line (Fig. 2).

Here is a problem, the importance of which will not escape to us, so much the more that the X-ray diffratometers have shown that the low MgO content alites were trigonals and the high content ones were monoclinic.

Our operating conditions are as follows:
—Mg K_α radiation analysis
—crystal analyser KAP
—accelerating tension of the electrons 12 kV
—standard: MgO, periclase
Contributions:
M. Venuat sampling
M. Regourd X-ray diffractometer
P. Longuet chemical analysis
P. Terrier, H. Hornain, G. Socroun E.P.M.A.

Written Discussion

Kenneth E. Palmer and Kenneth T. Greene

The authors have indicated the applicability of the electron probe microanalyzer in the analysis of portland cement clinker and have described several of the techniques which may be used with this instrument. Another method which they did not mention is the line scan, which gives an X-ray intensity profile for an element of interest along a preselected line on the surface of the specimen. Such scans, while not highly quantitative, provide data for a qualitative and semiquantitative correlation of the various elements present in the phases occurring along the line of scan.

Line scan analyses of several portland cement clinkers were performed for us by the Applications Laboratory of Applied Research Laboratories, Dearborn, Michigan, U.S.A. The instrument used was an AMX microprobe, and scanning was done by the electron beam scanning method. This instrument has a take-off angle of 52½°. Operating parameters were: 15 kV excitation potential and 0.1 μA sample current. The beam diameter was 1 μm or less.

Data on two clinkers are presented in Figs. 1–4. These specimens received a final polish with 1 μm diamond paste and were coated with an evaporated carbon film. Clinker A was a failry normal U.S.A. Type II clinker. Clinker B was of U.S.A. Type I composition but was laboratory prepared from relatively pure natural raw materials and contained 0.21 percent chlorine by chemical analysis as a result of interburning with a small addition of $CaCl_2$. In these figures the zero positions of the traces for some of the elements have been adjusted in a vertical direction to avoid confusing overlap.

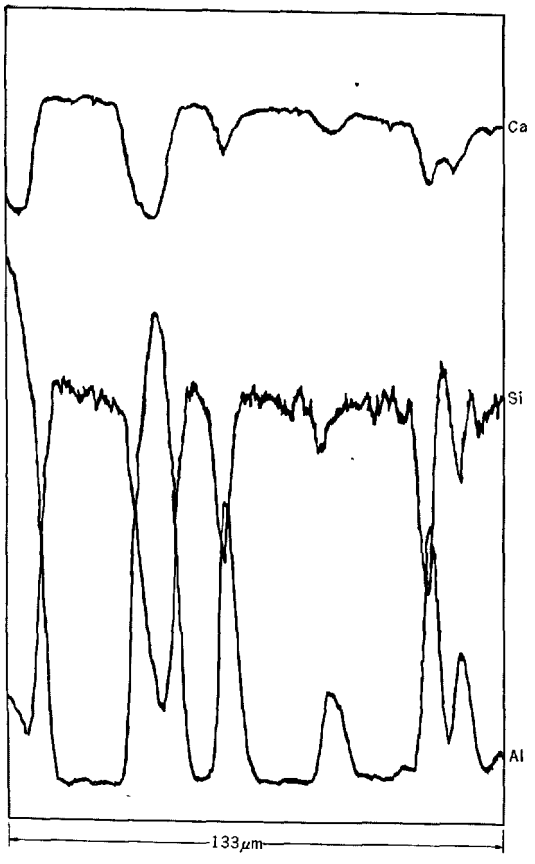

Fig. 1. *X-ray line scans across clinker A. Counts per second full scale;* Ca 30,000; Si 3000; Al 10,000.

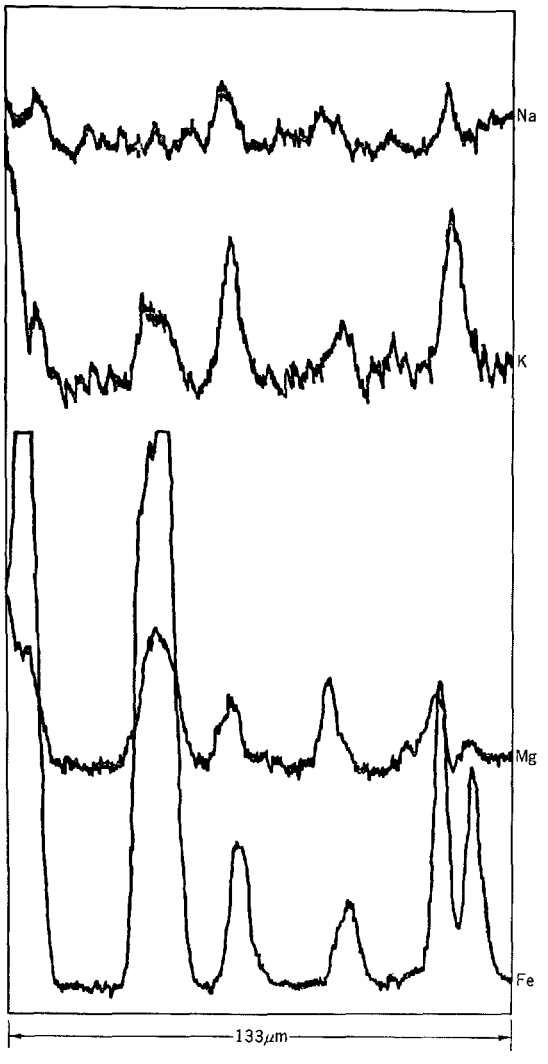

Fig. 2. *X-ray scans along same line on clinker A as in Fig. 1. Counts per second full scale:* Na 300; K 1000; Mg 3000; Fe 3000.

Figs. 1 and 2 show line scans taken along the same line on Clinker A. Of particular interest is the strong direct correlation of Mg with Fe and Al (ferrite phase) and the partial direct correlation of Na and K. There is some indication that part of the Na and K is concentrated in the belite phase (direct correlation with Si), whereas part—particularly K—may be in the ferrite phase. It appears from Fig. 1 that the silicate grains along this traverse line on Clinker A are essentially all alite, except for a small belite grain near the right side of the figure.

Of primary interest in Figs. 3 and 4 is the distribution of Cl relative to the other elements. It appears that Cl generally correlates directly with Al when Fe and Mg are low but not when they are high. This suggests that Cl is present in an aluminate phase such as $C_{11}A_7 \cdot CaCl_2$ or possibly an impure C_3A, but is absent or of much lower concentration in the ferrite phase. One exception may be noted where, about midway across Fig. 4, a Cl peak appears to correlate directly with moderate-sized Al and Fe peaks and a small Mg peak. The silicate grains along this line on Clinker B are also mainly alite. However, the higher Si and somewhat lower Ca concentrations located at about 30 μm from the left side of Fig. 3 indicate the presence of a small belite grain.

In these experiments we observed that the instrument was able to reproduce an X-ray scan rather accurately on repeated traverses along the same line. Small peaks no more than 1 or 2 μm broad were reproduced quite faithfully.

Obviously, these observations are of a preliminary nature, but they serve to illustrate further the potentialities of the electron probe microanalyzer in cement research.

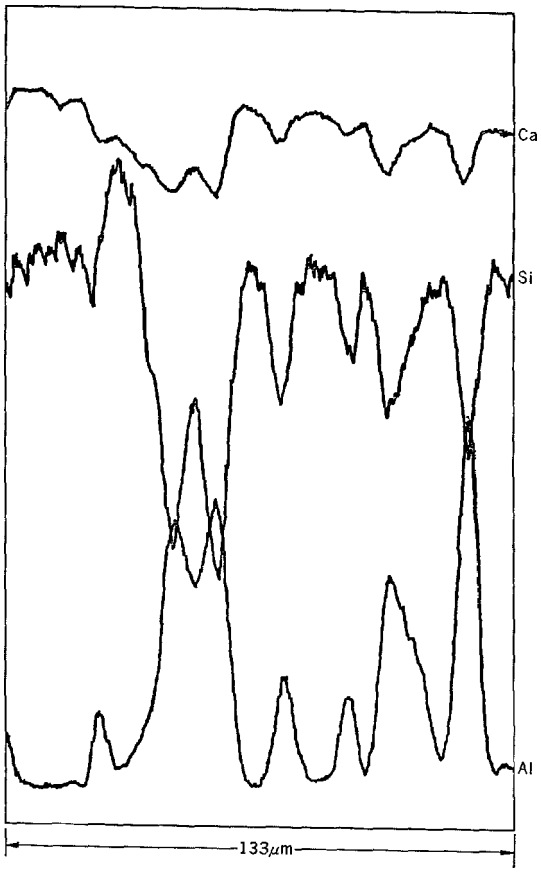

Fig. 3. *X-ray line scans across clinker B. Counts per second full scale:* Ca 30,000; Si 3000; Al 10,000.

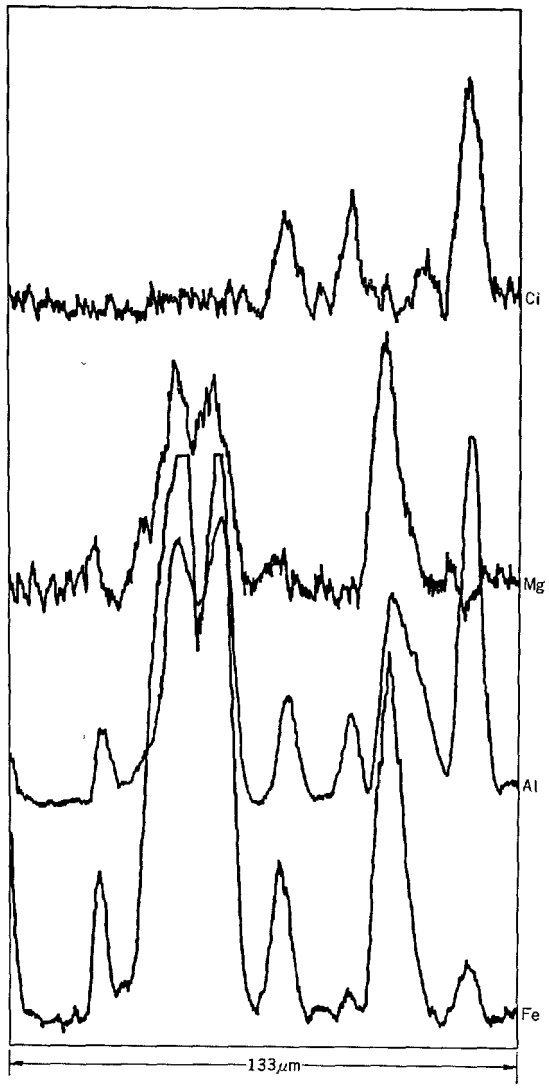

Fig. 4. *X-ray scans along same line on clinker B as in Fig. 3. Counts per second full scale:* Cl 1000; Mg 1000; Al 10,000; Fe 3000.

Written Discussion

Toshio Sakurai and Takeshi Sato

Introduction

The purpose of this discussion is to report the results of some studies on an application of X-ray fluorescent spectrometry to a solid state analysis of minor components, such as chromium oxide, in portland cement minerals.

Although an analysis of solid state of minor components is very important in order to explain the physical and chemical properties of clinker minerals, it is, nevertheless, very difficult to separate the solid state of minor components from that of their mothers.

From this viewpoint the authors think that an application of X-ray fluorescent spectrometry on an solid state analysis of chromium oxide in clinker minerals is very effective.

Experimental

The Philips' vacuum spectrometer was used in

this work with a special receiving slit of 10 cm long. Excitation condition was fixed at voltage of 50 KV, used with 36 mA. Topaz crystal was used for chromium lines $K\beta_{1,3}$. The step scanning method was adopted at the fixed time of 20 seconds in every 0.01 degree (2θ) step. And this method was repeated 10 times on each sample.

In order to detect the direct relation between 2 and valency of chromium in the crystal field, chromium $K\beta_{1,3}$ line of Cr_2O_3, CrO_2, Cr_3O_8 and CrO_3 was measured.

Each spectral curve was analyzed as follows; as this spectral curve can be regarded as Gaussian distribution function:

$$S = \frac{A}{\sqrt{2\pi}\,\sigma} \quad e \times p\left[\frac{-(x-\mu)^2}{2\sigma^2}\right]$$

where S is intensity, σ the standard deviation of each curve, μ the average value, x the degree (2θ) and A the coefficient determined by the chromium concentration in each sample. At the region of $x \approx \mu$, this function can be written as:

$$S = -\frac{A}{2\sqrt{2\pi}\,\sigma^3}x^2 + \frac{A\mu}{\sqrt{2\pi}\,\sigma^3}x + \frac{A}{2\sqrt{2\pi}\,\sigma^3}(2\sigma^2 - \mu^2)$$

In this equation, each coefficient σ, μ and A can be calculated from the measured data by the simultaneous equations using the least mean square method. simultaneous equations.

Experimental Results

Listed in Table 1 are the terms σ, μ and A calculated from the coefficients of each spectral curve equation. Fig. 1 shows three examples of the spectral curves. Fig. 2 shows a calibration curve correlating each 2θ with the valency of each standard chromium.

Although each point has some deviation from the calibration curve, this linear relation is very significant.

The average valencies gained by interpolating the measured values in this linear relation are listed in Table 2. In this table the average valencies of dissolved chromium obtained by chemical analysis (1) are also listed in contrast with the former.

For tri-calcium silicate solid solutions, these pairs of values agree fairly well with each other. For di-

Table 1. *The term σ, μ and A calculated from the coefficients of each chromium $K\beta_{3,1}$ spectral curves.*

Sample	$\mu(2\theta)$	σ	A
Cr (met.)	100.5089	0.1092	−18936.7031
Cr_2O_3	100.4980	0.1078	−17890.6116
CrO_2	100.5015	0.1102	−14867.9246
Cr_3O_8	100.5223	0.1136	−16943.2391
CrO_3	100.5229	0.1133	−17101.9860
$K_2Cr_2O_7$	100.5189	0.1141	−4766.2096
C_2F + 0.05mol C_3Cr	100.5026	0.1133	−409.2528
C_2F + 0.10mol C_3Cr	100.5034	0.1124	−739.0879
C_4AF + 0.05mol C_3Cr	100.5018	0.1278	−262.9488
C_4AF + 0.20mol C_3Cr	100.5024	0.1151	−771.5176
C_3S + 0.75wt% Cr_2O_3	100.5113	0.1423	−155.2836
C_3S + 1.75wt% Cr_2O_3	100.5143	0.1291	−257.3000
C_3S s.s. ($Ca_{30}Si_9Al_6Fe_2Cr_5O_\lambda$)	100.5121	0.1306	−228.1802

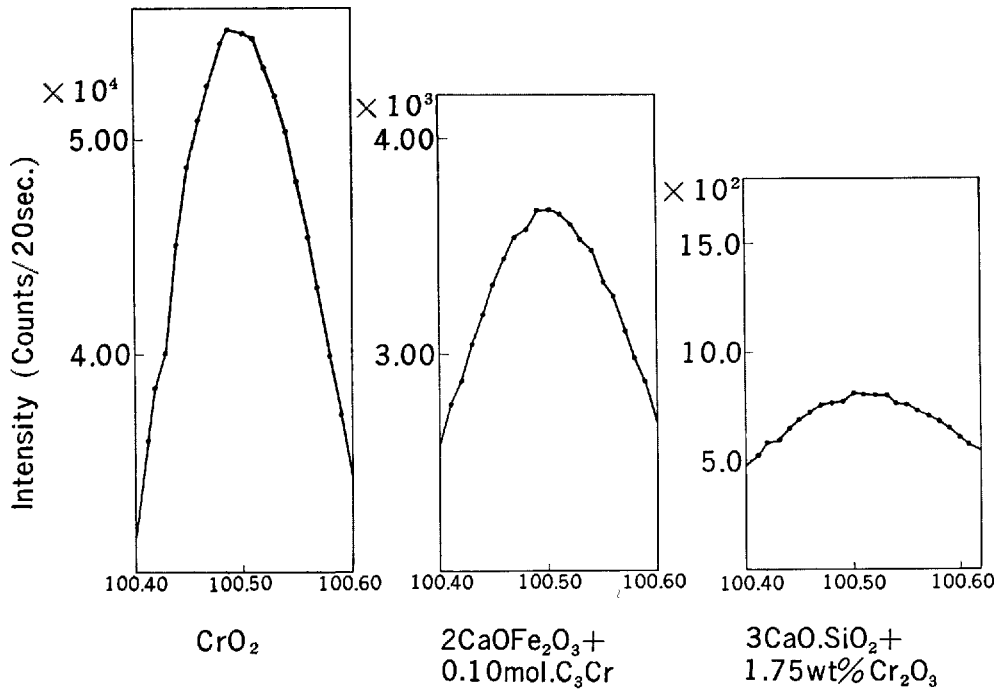

Fig. 1. *Three examples of the chromium $K\beta_{1,3}$ spectral curve.*

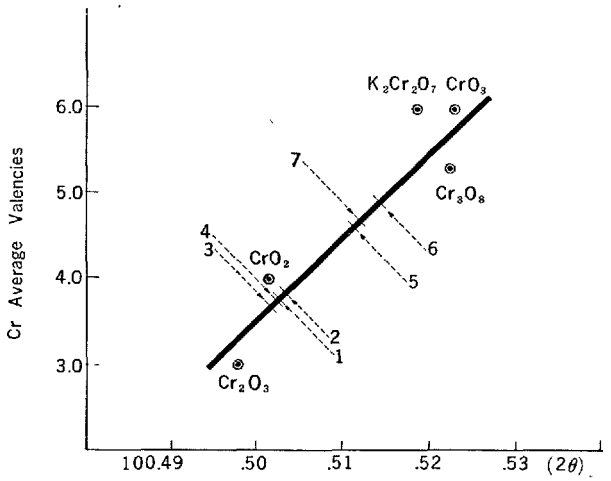

Fig. 2. *The calibation curve showing 2θ against the valencies of dissolved chromium.*

Table 2. *Comparison of a pair of average valencies between* (A) *and* (B).
(A) by X-ray fluorescent spectrometry
(B) by chemical analysis

Sample	Cr average valencies	
	X-ray spectrometry	Chemical analysis
$C_2F + 0.05^{mol}C_3Cr$	3.8	3.2
$C_2F + 0.10^{mol}C_3Cr$	3.8	3.6
$C_4AF + 0.05^{mol}C_3Cr$	3.7	3.1
$C_4AF + 0.20^{mol}C_3Cr$	3.7	3.2
$C_3S + 0.75^{wt\%}Cr_2O_3$	4.9	4.6
$C_3S + 1.75^{wt\%}Cr_2O_3$	4.6	4.4
C_3S solid solution ($Ca_{300}Si_{94}Al_6Fe_2Cr_5O_x$)	4.7	4.8

calcium ferrite solid solutions and for tetra-calcium alumino ferrite solid solutions, however, the values by chemical analysis are considerably smaller than those by X-ray spectrometry. This may be because, in chemical analysis, chromium in these solid solutions reduces to the more stable valence state, Cr^{3+}, during dissolving of these solid solution into H_2SO_4 solvent. Therefore, these values obtained by X-ray spectrometry show the truer valence state in solid solutions.

In Fig. 2, chromium in these ferrites takes the average valencies of 3.7~3.8 which are corresponding to the valency of chromium in CrO_2.

CrO_2 has the structure of rutile TiO_2 of 6 : 3 coordination. Every chromium atom is surrounded by six oxygen atoms approximately at the corners of a regular octahedron, and every oxygen atom by three chromium atoms approximately at the corners of an equilateral triangle.

The structure of $2CaO \cdot Fe_2O_3$ determined by Bertaut et al. is composed of one layer of octahedral groups of oxygen atoms around iron atom connected with another layer of tetrahedral groups of oxygen atoms around iron atom.

On the other hand, chromium trioxide, CrO_3, has an arrangement composed of CrO_3 chains held together only by van der Waals forces within which each chromium atom has four oxygen neighbors. Every two of these four oxygens is combined with only one chromium atom and every other two is surrounded by two chromium atoms.

Considering these structures, the structure of CrO_2 octahedra is far similar to the iron octahedra in $2CaO \cdot Fe_2O_3$ than the structure of CrO_3 tetrahedra is.

Therefore, it may be sure that chromium in the ferrites substitutes for octahedral iron or aluminum ion. The similarity of the standard deviation σ of the chromium spectral curves of the ferrites to those of the standard samples also proves that chromium in ferrite substitutes only for octahedral iron or aluminum ion.

Fig. 2 also shows that chromium in tri-calcium silicate solid solutions take the average valencies of 4.6~4.9.

In this case, these average valencies are situated about in the middle between those of CrO_2 and CrO_3.

In Table 1, the standard deviation σ from the chromuim spectral curves of tri-calcium silicate solid solutions is obviously a little larger than the standard deviation from the chromium spectral curves of the ferrites and of the standard chromium oxides.

This result means that these spectral curves of tricalcium silicate solid solutions are composed of two or more curves.

In other words it may be sure that chromium in tri-calcium silicate solid solutions has two or more kinds of valence states and coordination numbers.

In order to clarify the details of these considerations, however, the study of X-ray absorption-edge spectrometry for chromium in these tricalcium silicate solid solutions must be performed.

Conclusion

As mentioned above, solid state of minor compo-

nent, chromium oxide, dissolved in portland cement clinker minerals can be clarified failry well by X-ray spectrometry using the proper standard samples.

This method can be, of course, applied to the other transition elements dissolved as minor components.

The key to a significant resolution of the problem is to find the most profitable standard samples for a coming minor element and to improve the analytical accuracy of X-ray spectrometer.

Acknowledgement

The authors thank Dr. Asada of the Government Chemical Indiustrial Research Institute, Tokyo for his kind instruction and for preparations of the standard chromium oxides.

References

1. T. Sakurai; T. Sato and E. Asada, will be submitted to J. Ceram. Assoc, Japan.

Oral Discussion

Hiroshi Uchikawa

I should like to ask you about the calculation of the mineral compositions.

Although you did not refer to it today, in your principal paper you have put forward a method for it, that is, solutions of simultaneous equations by the least square method. May I ask, to what extent we can count on the accuracy of this method?

Author's Closure

Goro Yamaguchi

Reply to Terrier

It seems reasonable that the contents of minor constituents in clinker minerals depend to their total contents in clinker. In our study, however, we could not confirm this phenomenon because there is little dispersion of contents of minor constituents in Japanese clikers.

Mr. Terrier's and our results about Fe_2O_3 content in alite are coincident, so that the values seem highly reliable. As to MgO content in alite our result and his are somewhat different. It is not clear whether or not the contents are essentially different between Japanese clinkers and others.

I would like to check the reliability of our results. We also attempted to determine minor constituents in clinker minerals by the electron probe microanalysis. However, we could not obtain a reliable result because of the low resolution of the microanalysis. I would like to know many details and error problem of his experiment such as resolution, standard specimen and calculation.

Reply to Palmer and others

We also carried out the line scanning analysis of the electron probe microanalyzer but did not describe it in our principal paper. I think that analysis is valuable to find some special elements at some points. In their results a behavior of chroline is especially interesting. If whole data had been presented together with reflected light microscopic images they would be more valuable.

I think spectrum of line scanning analysis should show nearly rectangular shape. In their case, however, as well as our experiment a fact that the spectrum does not show rectangular shape seems due to low resolution of the microanalysis. I can not estimate sizes of ferrite and aluminate of their clinker. In our clinkers texture of ferrite and aluminate is very fine and complex as shown in our principal paper. Therefore, I can not exectly discuss the descrimination between ferrite and aluminate in the interstitial phase of their clinker and the descrimination seems not so clear as well as in our clinkers.

Reply to Sakurai and others

I also think that X-ray florescent study is useful to investigate states of elements in solid phase if uniform samples can be provided as in the case of synthesized samples.

We applied an electron probe microanalyzer to obtain such an information from fine minerals in clinker, especially an information of iron. We have recognized that the diffraction of Fe Kα radiation from ferrite in clinker shifts to slightly higher angle side than that from a metalic iron. As to Fe radiation from other mineral phases in clinker, such an observation has not been accomplished because of very low intensity.

Reply to Uchikawa

The simultaneous equations consist of four varia-

bles and five equations. If analytical data of chemical composition of minerals were exact it would be able to solve the mineral composition from upper four equations. However, because some errors are inevitable, the fifth equation become necessary in order to apply the least square method. The calculation was carried out using an automatic computer giving some proper weight to equations.

The calculation did not become possible until fairly exact chemical compositions of minerals could be obtained. However, a little deviation of the chemical composition of minerals affects a value of the mineral composition, so that as much as possibly exact chemical compositions are needed. Especially, ratios of $CaO: SiO_2$ in alite and belite affect the results. Moreover, exactly saying, chemical compositions of minerals are slightly different according to a kind of clinkers, especially in white cement, so that we can not obtain exact mineral composition unless using special data according to a kind of clinkers.

At the todays' step, errors have not become so small but I think it is valuable to use this analyzing system in each factory according to its own clinker.

Supplementary Paper I-12 The Minor Elements in Alite (Tricalcium Silicate) and Belite (Dicalcium Silicate) from Some Portland Cement Clinkers as Determined by Electron Probe X-ray Microanalysis

Henry G. Midgley*

Synopsis

The minor elements present in tricalcium silicate (alite) and dicalcium silicate (belite) from four portland cement clinkers have been determined quantitatively by electron probe X-ray micro analysis.

The following elements were detected in alite: calcium, silicon, iron, aluminium, potassium, magnesium with traces of cobalt and sulphur; and in belite, calcium, silicon, iron, aluminium, potassium, phosphorous, chromium, titanium and traces of cobalt, sulphur and magnesium.

It has been found that magnesium, aluminium and iron are present as important additions in alite, and that alkalies, iron and aluminium are important constituents of belite, and these have been determined quantitatively. The ranges of each substituting element have been investigated for the clinkers and compared.

Introduction

Midgley (1) referred to the use of electron probe X-ray micro analysis, gave an analysis for alite and published a series of elemental distribution photographs of portland cement clinker in 1964, but the first serious work on the subject published seems to be that by A.E. Moore (2) in 1965. Peterson (3) has presented some values for Al_2O_3, K_2O, Na_2O and SO_3 in alite and belite crystals in portland cement clinkers. Midgley (4) has investigated the composition of alite in one portland cement clinker and Fletcher (5) has investigated the composition of belite in two portland cement clinkers.

Experimental

The technique of electron probe X-ray micro analysis has been dealt with extensively in the literature; for a recent compendium of the methods and a review of mineralogical applications Adler (6) should be consulted.

In the present work a "Geoscan" microprobe manufactured by the Cambridge Instrument Co. Ltd. of Cambridge, United Kingdom was used. This instrument is capable of resolving an electron "spot" of 1μ m. in size. The take-off angle is 75° for X-rays and the spectrometer is of the fully focussing type. A flow proportional counter using argon-carbon dioxide gas mixture is used as the X-ray sensing device and the output is capable of pulse height analysis. The high take-off angle has a major advantage in that it minimizes the effect of surface relief and at the same time reduces the need for large adsorption corrections. One of the few disadvantages of the geometry is that the instrument is thus capable of receiving X-rays generated at a comparatively great depth below the surface. The presence of shallowly lying artefacts beneath the surface can thus give rise to erroneous results. Such results can usually be checked by moving the sample in relation to the static probe. In the event of an artefact giving rise to a signal the count rate would significantly change in the vicinity, the exception being where the boundary of the

*Ministry of Public Building and Works, Building Research Station, Garston, Herts, United Kingdom.

two phases lies parallel to the surface of the sample. The likelihood of this occurring is statistically small when compared with the probability of the phase boundary making a significant angle to the specimen surface.

An accelerating voltage of 20 kV was used for all elements and a specimen current of about 100 mμ amps was found to give the best compromise between stability and counter rates. The diffracting crystals used were mica for sodium, magnesium and aluminium K alpha X-radiation; quartz for potassium K alpha X-radiation and lithium fluoride for titanium, manganese, and iron K alpha X-radiation.

The specimens were prepared by standard methods used for optical microscopy of polished sections, Midgley and Taylor (7). The clinkers were embedded in a resin (araldite) and the specimen surface ground flat using a rotating steel lap with 120 grade silicon carbide powder. The specimen surface was then polished by using successively 6μ, 1μ, and $\frac{1}{4}\mu$ diamond paste on nylon bolting cloths. Following polishing the specimens were given a conducting coating with about 200 Å layer of graphite deposited in a vacuum shadow casting unit.

Since the electron probe had co-axial visual and electron optics the specimen could be examined microscopically with the same instrument.

The method of analysis depended upon the nature and size of the mineral grains. Where the minerals were sufficiently large (alite and belite) at least two local spot analyses were made on each grain. Where the minerals were present as complex intergrowths in the ground mass recourse was made to a scanning method by which the sample was moved very slowly, 3μm per min., under a stationary probe, the ratemeter readings being used to activate the pen of a chart recorder. Ratemeter readings had a much lower precision than those obtained by counting but interference of phases could be readily assessed and therefore the overall accuracy was better for this type of specimen.

For quantitative analysis standards were prepared by synthesizing minerals with bulk compositions near those to be analysed and spanning the range of elemental content encountered in the unknowns.

The composition of C_3S and the introduction of elements into its lattice has been studied in detail by various workers and preparations based on these studies were made with magnesium, aluminium, potassium, titanium, sodium and iron in C_3S. These preparations were also used as standards for C_2S with appropriate corrections for absorption and enhancement. One of the major advantages of using C_3S or other mineral of similar matrix as a standard for C_2S instead of the pure metals is that the corrections due to matrix differences are very small and this minimizes the errors introduced by uncertainty of values for mass absorption coefficients. The homogeneity of all standards was checked by X-ray diffractometry and by optical microscopy. The standards used are listed in Table 1.

A melt corresponding to the invariant point in the system $CaO—Al_2O_3—Fe_2O_3—SiO_2$, Lea and Parker (8) was also made; this was useful in estimating small quantities of aluminium and iron.

Absorption corrections were made following the general formula given by Philibert (9) and fluorescence enhancement corrections were made by the formula given by Castaing (10).

The sensitivities of the method for various elements are given in Table 2.

A considerable amount of information can be obtained by deflecting the electron beam to describe a raster over the surface of the clinker. The outputs of the counterrecording the reflected electrons and the countermeasuring the X-ray output can then be used to modulate a cathode ray tube. Typical "pictures" for certain elements are shown in Fig. 1 which illustrates element distribution in a part of a cement clinker, (P.1012/3), showing alite, belite and interstitial minerals.

Table 1. *Standards used for electron probe micro analysis*

Sodium	C_3A containing 3%Na_2O
Magnesium	C_3S containing 1.02% 0.67% and 0.32%MgO
Aluminium	C_3A, C_4AF, and C_3S containing 0.80%Al_2O_3
Silicon	C_3S, C_2S and C_3S_2 (Rankinite)
Potassium	$C_{12}A_7$ melt containing 1%K_2O
Calcium	C_3A, C_3S, C_2S, C_4AF
Titanium	C_3S containing 0.61 and 0.31%TiO_2
Manganese	C_3S containing 0.73%MnO_2
Iron	C_3S with varying small amounts of Fe_2O_3, C_4AF

Table 2. *Sensitivity i.e. 3 × standard deviation of background for 200 sec. counting times, for minor and trace elements in calcium silicate matrices. This is the minimum quantity detectable.*

Element	Sensitivity wt. per cent
Na	0.01
Mg	0.04
Al	0.05
K	0.02
Ti	0.02
Mn	0.01
Fe	0.01

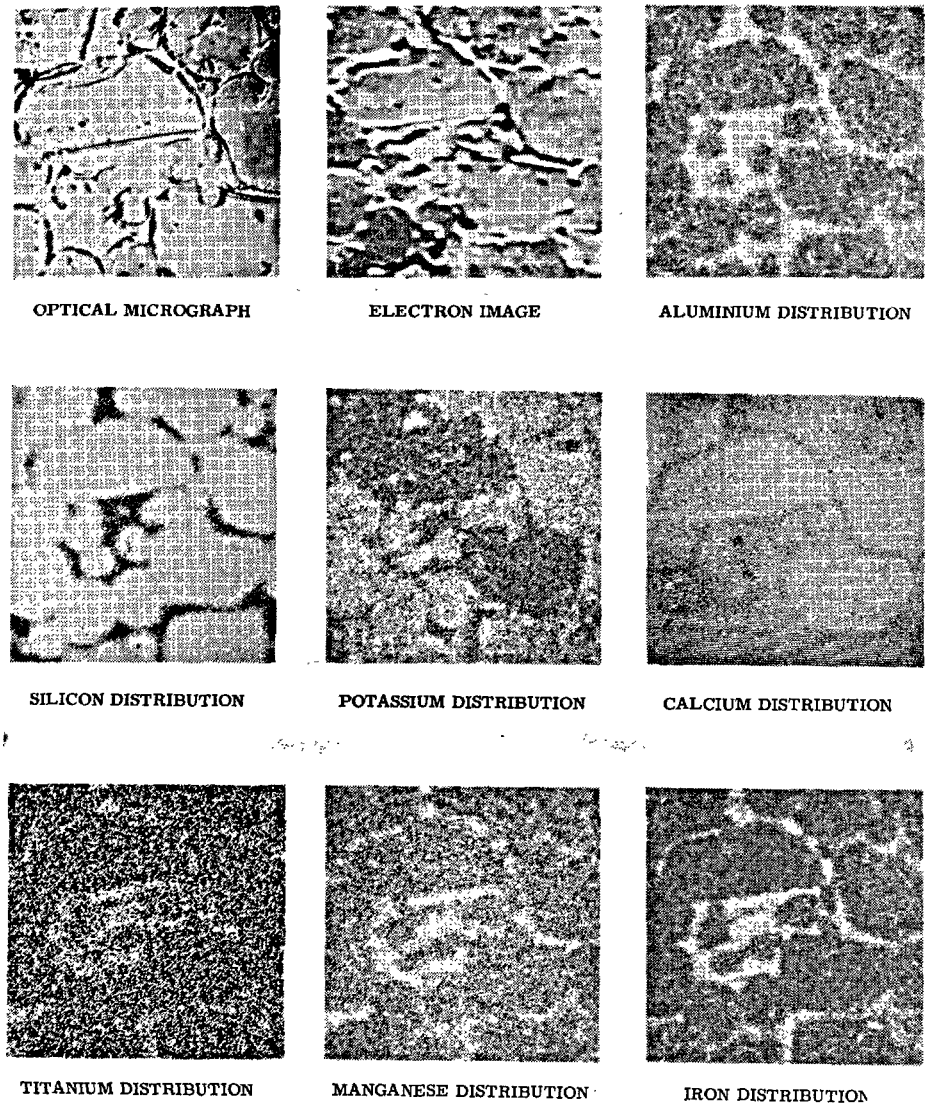

Fig. 1. *Elemental distribution in minerals in a portland cement clinker. The hexagonal shaped outlines are of alite* (C_3S), *rounded belite* (C_2S) *and the rest interstitial. It is quite evident from these pictures that the aluminium is concentrated in the interstitial, which is also deficient in silicon.*

Cement Clinkers Examined

Four samples of portland cement clinker, P 1012/3, P 1017/2, P 1018/1 and P 1020/1 of the collection of the Mineralogy Laboratory, Building Research Station, were examined. Table 3 is a summary of the chemical and mineralogical compositions. The mineralogical composition was determined by the quantitative X-ray diffraction analysis (Q.X.R.D.) method proposed by Midgley, Fletcher and Cooper (11). Clinkers No. P 1012/3 and P 1017/2 are of the sulphate resisting type, having a C_3A content of less than 3.5 per cent (S.R.P.C.). The other two are ordinary portland cements (O.P.C.).

Table 3. *Chemical and mineralogical composition of portland cement clinkers used*

	P1012/3	P1017/2	P1018/1	P1020/1
SiO_2	23.06	21.90	23.56	21.39
Al_2O_3	4.23	3.89	4.83	6.00
Fe_2O_3	6.33	6.69	2.55	3.09
TiO_2	0.28	0.26	0.24	0.34
P_2O_5	0.24	0.20	0.20	0.19
CaO	64.08	64.35	65.75	65.47
MgO	0.88	0.86	0.96	1.34
SO_3	0.24	0.64	0.19	0.73
Loss	0.11	0.41	0.06	0.32
K_2O	0.40	0.62	0.21	0.86
Na_2O	0.28	0.20	0.51	0.20
Mineralogical composition by Q.X.R.D.				
alite	41.6	52.9	53.4	56.0
belite	31.1	27.4	25.8	23.0
C_3A	3.8	2.6	7.8	11.8
f.ss.	14.4	14.2	6.9	8.7
Composition of ferrite solid solution in mol per cent C_2F				
	56	64	51	52
Mineral composition according to Bogue calculation				
C_3S	47.3	50.6	47.7	57.4
C_2S	30.2	24.7	31.3	17.3
C_3A	6.5	nil	8.5	10.7
C_4AF	19.3	19.6	7.8	9.4

*All the alites were monoclinic by X-ray diffraction (X.R.D.)

Composition of Alite

The following elements were detected by the probe in alite crystals in various clinkers: calcium, silicon, iron, aluminium, potassium, manganese, magnesium, with traces of cobalt and sulphur. It was found that sodium, magnesium, aluminium, potassium, titanium, manganese and iron were the more important and so these were determined quantitatively. The resulting alite compositions are given in Table 4 where the elements have been calculated as being present as the oxides. It is clear from the coefficients of variation 'c' that the difference in composition between individual alite grains with some clinker is real since the 'c' values for most elements present should be much lower, in the range of 0.5 per cent to 10.0 per cent. Fletcher (5) using the same instrument as the present author has given the standard deviations (Table 5) for determination of the same elements in similar cements. The coefficient of variation 'c' has also been calculated assuming average oxide contents for alite. It must be noted here that the large values for the coefficient of variation for sodium determinations (Table 4) may be due to the inaccuracies of the estimation.

Examination of the results for the minor elements

Table 4. *Summary of minor element contents in alite* (C_3S)

Oxide	Clinker	Average wt % of oxide in phase $\bar{x}$	n	s	c	Range
Na_2O	P1012/3	0.3	6	0.0(5)	16.7	0. —0.5
	P1017/2	0.2	2			0. —0.3
	P1018/1	0.2(5)	6	0.1	40	0.1 —0.4
	P1020/1	0.2(5)	4	0.2	80	0.1 —0.4
MgO	P1012/3	0.86	6	0.16	18.5	0.67—1.03
	P1017/2	0.61	5	0.07	11.5	0.52—0.68
	P1018/1	0.90	7	0.16	17.7	0.61—1.10
	P1020/1	1.01	4	0.17	16.8	0.81—1.20
Al_2O_3	P1012/3	1.19	6	0.09	7.6	0.87—1.57
	P1017/2	0.92	3			0.83—1.05
	P1018/1	1.26	6	0.20	15.6	0.91—1.45
	P1020/1	1.68	4	0.50	29.8	1.03—2.24
K_2O	P1012/3	0.10	9	0.02	20	0.08—0.12
	P1017/2	0.25	2			0.23—0.26
	P1018/1	0.06(2)	10	0.01(4)	23.0	0.04(5)—0.08(5)
	P1020/1	0.13	12	0.02(5)	19.4	0.10—0.17
TiO_2	P1012/3	0.11	2			0.09—0.13
	P1017/2	0.16(5)	1			
	P1018/1	0.12	6	0.05(3)	44	0.06—0.19
	P1020/1	0.15	7	0.06	25	0.08—0.25
MnO_2	P1012/3	0.02	8	0.01	50	0.01—0.04(5)
	P1017/2	0.03	4	0.02	67	n.d.—0.05
	P1018/1	0.02	4	0.01	50	n.d.—0.03
	P1020/1	0.02	8	0.01	50	0.01—0.04
Fe_2O_3	P1012/3	1.39	11	0.29	21	0.92—1.94
	P1017/2	1.62	2			1.51—1.73
	P1018/1	0.43	2			0.30—0.56
	P1020/1	0.72	11	0.09	13	0.47—1.44

$\bar{x}$ = arithmetical mean
n = number of determinations
s = standard deviation
c = coefficient of variation, $\frac{s \times 100}{\bar{x}}$

Table 5. *Standard deviation of determination of elements in portland cement clinker minerals on the electron probe microanalyser at the Building Research Station.*

Element, as oxide	Standard deviation	Coefficient of variation, per cent†
CaO	0.25	3.3
SiO_2	0.25	9.4
K_2O	0.025	10.0
Na_2O	0.05	15.0
MgO	0.025	2.5
Fe_2O_3	0.05	5.0
TiO_2	0.025	25.0
Al_2O_3	0.05	5.0

†The coefficient of variation has been calculated using approximate values for the contents of the oxides in alite.

present in alites from the four clinkers show that for sodium, magnesium, potassium, titanium, and manganese, the difference between clinkers is less than the differences expected between individual crystals in a single clinker. The greatest difference between clinkers occurs with aluminium and iron, the ratio of Fe_2O_3–Al_2O_3 in the alite being governed by the ratio in the whole clinker. Table 3 gives the analyses of the clinkers used; Table 6 gives the Fe_2O_3–Al_2O_3 ratios for alite and for clinker. It must be noted here that it is the iron content of the alite which varies most; Al_2O_3 varies from 0.92 to 1.68 per cent, difference 0.76 per cent while the Fe_2O_3 varies from 0.43 to 1.62 per cent, difference 1.19 per cent. If the molar contents of the alites are calculated for the three clinkers P 1012/3, P 1017/2 and P 1020/1 the sums for Fe_2O_3 and Al_2O_3 are very similar, respectively 0.020, 0.022 and 0.021. Clinker P 1018/1 is different, having a molar percentage of Al_2O_3 plus Fe_2O_3 of 0.015. It is not clear why this should be so, except that the original material is exceptionally low in iron, 2.55 per cent Fe_2O_3, as compared with 3.09, 6.33 and 6.99 per cent for the other clinkers.

Table 6. Fe_2O_3–Al_2O_3 *ratios in alite and in cement clinker*

Sample number	P1012/3	P1017/2	P1018/1	P1020/1
Alite	1.17	1.76	0.34	0.43
Clinker	1.50	1.72	0.53	0.51

The analyses of the alites expressed as molar contents are Na_2O : 0.004; K_2O: 0.002; MgO: 0.020; TiO_2: 0.002; $Al_2O_3 + Fe_2O_3$: 0.020.

These results may be compared with one alite crystal thoroughly analyzed by Midgley (4); with Na_2O: 0.005; K_2O: 0.001; MgO: 0.020; TiO_2: 0.001; Al_2O_3: 0.010; Fe_2O_3: 0.009; $Al_2O_3 + Fe_2O_3$: 0.019.

One the basis of a cell content of 180 oxygens the composition is $Ca_{165.54}Fe_{1.43}Al_{1.92}Na_{0.80}K_{0.18}Mn_{0.02}Ti_{0.11}Si_{34.48}O_{180}$.

In one special clinker, B.R.S. sample No. B102, the following elements were also detected in the alite; phosphorus and strontium, equivalent to P_2O_5: 2.0; SrO: 0.5 per cent by weight. This result shows that the average composition for alite only applies to raw materials that contain similar elemental compositions.

Composition of Belite

Table 7. *Summary of minor element contents in belite* βC_2S

Oxide	Clinker	Average wt % of oxide in phase $\bar{x}$	n	s	c	Range
Na_2O	P1012/3	0.9	6	0.2(5)	27.8	0.6 —1.2
	P1017/2	0.5	3			0.1 —0.9
	P1018/1	1.0	6	0.3(5)	35.0	0.4 —1.3
	P1020/1	0.5	4	0.3	60	0 —0.9
MgO	P1012/3	0.56	6	0.16	28.6	0.17—0.75
	P1017/2	0.24	5	0.03	12.5	0.17—0.28
	P1018/1	0.50	7	0.15	30.0	0.27—0.76
	P1020/1	0.42	4	0.08	19.0	0.32—0.49
Al_2O_3	P1012/3	1.19	6	0.28	23.5	0.87—1.57
	P1017/2	1.25	5	0.18	14.4	0.97—1.43
	P1018/1	2.04	6	0.31	15.2	1.65—2.57
	P1020/1	2.58	5	0.47	18.2	1.96—3.28
K_2O	P1012/3	0.75	14	0.07	9 3	0.62—0.87
	P1017/2	0.95	9	0.20	21.0	0.66—1.25
	P1018/1	0.50	13	0.14	27.9	0.27—0.88
	P1020/1	0.70	7	0.12	17.1	0.53—0.87
TiO_2	P1012/3	0.18	2			0.15—0.21
	P1017/2	0.14	2			0.12—0.15
	P1018/1	0.12	10	0.04	33	0.07—0.18
	P1020/1	0.17	7	0.04	23.5	0.11—0.24
MnO_2	P1012/3	0.06	7	0.02	33	0.05—0.07
	P1017/2	0.01(2)	5	0.00(7)	58	n.d.—0.02
	P1018/1	0.03	5	0.01	33	0.02—0.04
	P1020/1	0.02	2	0.00(7)	35	0.02—0.03
Fe_2O_3	P1012/3	2.16	16	0.65	30.0	1.34—3.76
	P1017/2	1.79	10	0.20	11.3	1.49—2.10
	P1018/1	0.69	9	0.27	39.0	0.36—1.23
	P1020/1	0.86	14	0.16	18.6	0.48—2.50

n = }
s = } See key at end of Table 4
c = }
$\bar{x}$ = Average wt % of oxide present in belite in clinker.

The following elements were detected by the probe in belite crystals in the clinker samples: calcium, silicon, iron, aluminium, potassium, magnesium, phosphorus, chromium, titanium, and traces of cobalt and sulphur. The same elements were determined quantitatively for belite as for alite. Results are given in Table 7, calculated as oxides. It is noticeable that the coefficient of variation, c, is of the same order as for alite, but that Na_2O, Al_2O_3, K_2O and Fe_2O_3 contents are higher in belite than in alite, MgO is less and TiO_2 about the same. Again the greatest difference between belite in different clinkers is in the Fe_2O_3 and Al_2O_3 contents, the ratio being governed by the Fe_2O_3–Al_2O_3 ratio of the original clinker. The results are given in Table 8.

The average molar compositions of the belites can be represented by Na_2O: 0.008; K_2O: 0.008; MgO: 0.010; TiO_2: 0.002; $Al_2O_3 + Fe_2O_3$: 0.026. The ranges in compositions are given in Table 7.

Table 8. Fe_2O_3–Al_2O_3 *ratios in belite and in cement clinker*

Sample number	P1012/3	P1017/2	P1018/1	P1020/1
Belite	1.81	1.43	0.34	0.33
Clinker	1.50	1.72	0.53	0.51

Distribution of Elements between Co-Existing Alite and Belite Crystals

The partition of minor elements between alite and belite crystals has been determined by experimentally estimating the elements in adjacent grains of alite and belite; the results are given in Tables 9 and 10.

The factors influencing partitioning of the trace elements between co-existing mineral phases in portland cement clinker are many and complex. There is some evidence to indicate that there is a considerable lack of homogeneity in the sample populations. Tables 9 and 10 show that the values of minor elements in the host minerals may differ by a factor of 4 within the same sample.

Generally speaking, however, the partition coefficients, here defined as the ratio of element concentration in belite to alite, do not depart from each other to the same degree. This, of course, may only reflect gross inhomogeneities within the initial raw material, and that the mainly solid state reactions have not been sufficiently energetic or have not continued for a sufficiently long time to average out these differences. It is thus likely that areas initially high in potassium, for example, would favour the nucleation and growth of belite. Belite is often concentrated around vesicles in the clinker, which may have contained gaseous potassium ions, flue gases are often rich in this constituent. However, owing to the difficulty of obtaining reliable analyses for the interstitial clinker phases it

Table 9. *Partition of elements between juxtaposed pairs of alite and belite*

Oxide	Sample	Wt % of oxide in phase		$\frac{C_2S}{C_3S}$
		C_3S	C_2S	
Na_2O	P1012/3	0.38	1.00	2.6
		0	0.45	>4.5
		0.4	0.9	2.25
		0.1	1.1	11.0
		0.5	1.2	2.4
		0.3	0.6	2.0
	P1017/2	0	0.1(5)	1.5
		0.3	0.9	3.0
	P1018/1	0.2	0.4	2.0
		0.4	1.1	1.7
		0.2	0.7	3.5
		0.2	1.1	5.5
		0.4	1.3	3.3
		n.d.	0.4	4.0
	P1020/1	0.4	0.7	1.7(5)
		0.4	0.9	2.2(5)
		0	0.4	—
		0	0	—
MgO	P1012/3	1.03	0.62	0.60
		0.93	0.58	0.62
		0.94	0.75	0.80
		0.92	0.63	0.68
		0.68	0.52	0.76
		0.67	0.27	0.40
	P1017/2	0.68	0.24	0.35
		0.63	0.17	0.27
		0.62	0.23	0.37
		0.52	0.28	0.54
		0.61	0.26	0.43
	P1018/1	0.83	0.41	0.49
		1.10	0.61	0.55
		0.86	0.27	0.31
		0.88	0.76	0.86
		0.61	0.47	0.77
		1.06	0.46	0.43
		0.95	0.50	0.53
	P1020/1	1.10	0.32	0.29
		0.93	0.47	0.51
		1.20	0.49	0.40
		0.81	0.39	0.46
Al_2O_3	P1012/3	1.40	1.80	1.3
		0.94	1.40	1.5
		1.32	1.65	1.2(5)
		1.03	1.32	1.3
		0.87	1.70	1.9(5)
	P1017/2	0.87	1.43	1.6(5)
		1.05	1.17	1.1
		0.83	1.28	1.5(5)
		0.97	1.39	1.4(5)
	P1018/1	1.28	2.10	1.6(5)
		1.39	2.57	1.8(5)
		0.91	2.08	2.3
		1.35	1.94	1.4(5)
		1.45	1.64	1.1(5)
		1.16	1.88	1.6
	P1020/1	2.24	2.59	1.1(5)
		1.03	2.49	2.4
		1.64	1.96	1.2
		1.81	2.58	1.8

Teble 9. (Cont'd)

Oxide	Sample	Wt % of oxide in phase		$\frac{C_2S}{C_3S}$
		C_3S	C_2S	
K_2O	P1012/3	0.08	0.75	9.4
		0.12	1.10	9.2
		0.11	0.72	6.5
		0.11	0.73	6.7
		0.10	0.76	7.6
		0.08	0.81	10.1
		0.09	0.87	9.7
		0.07	0.80	11.5
	P1017/2	0.26	0.92	3.5
		0.23	0.70	2.7
	P1018/1	0.04	0.88	19.6
		0.06	0.70	11.7
		0.05	0.45	9.0
		0.08(5)	0.62	7.3
	P1020/1	0.17	0.71	4.2
		0.12	0.64	5.3
		0.12	0.75	6.3
		0.16	0.53	3.3
		0.14	0.60	4.3
		0.13	0.87	6.7
	B102	0.18	0.75	4.2
		0.11	0.91	8.3
		0.11	0.73	6.6
		0.10	0.64	6.4
		0.15	0.52	3.5
		0.17	0.70	4.1
		0.17	0.82	4.8

is not possible to give a quantitative expression for this inhomogeneity. No data is available for the temperature of formation and the differences in partition coefficients, although generally small, are nevertheless significantly greater than would be expected, were the clinkers all brought to equilibrium at the same temperature. In many cases, however, the distributions are distinctly different between clinkers and the minor differences within the clinkers could be attributed to differences in the temperatures at which parts of the clinker achieved equilibrium.

Table 9. (Cont'd)
Partition of elements between juxtaposed pairs of alite and belite

Oxide	Sample	Wt % of oxide in phase		$\frac{C_2S}{C_3S}$
		C_3S	C_2S	
TiO_2	P1012/3	0.09	0.21	2.3
		0.13	0.15	1.3
	P1017/2	0.16(5)	0.12(5)	0.76
	P1018/1	0.19	0.18	0.95
		0.18	0.11	0.60
		0.07	0.07	1.00
		0.08	0.10	1.20
		0.14	0.16	1.11
		0.06	0.07(5)	1.33
	P1020/1	0.16	0.22	1.4
		0.17	0.15	0.88
		0.16	0.10	0.6
		0.25	0.24	0.9(5)
		0.08	0.12(5)	1.55
		0.10	0.15	1.50
		0.12	0.17	1.4
MnO_2	P1012/3	0.02	0.05	2.5
		0.04	0.03	0.75
		0.02	0.07	3.5
		0.04(5)	0.07	1.75
		0.02	0.05	2.5
		0.02(5)	0.05(5)	2.6
		0.02(5)	0.06(5)	2.6
	P1017/2	0	0.05	—
		0.02	0	—
		0.05	0	—
		0	0	—
	P1018/1	0.02	0.02	1
		0	0.04	—
		0	0.02	—
		0.01(5)	0.02(5)	1.7
	P1020	0.02	0.03	1.5
		0.02	0.02	1
		0.02(5)	0.03	1.2
		0.01	0.02	2.0
		0.03(5)	0.03	0.8(5)
		0.00(5)	0.01(5)	3
		0.01(5)	0.02	1.3
Fe_2O_3	P1012/3	1.28	2.00	1.56
		1.23	2.23	1.82
		0.92	1.38	1.56
		1.39	2.04	1.47
		1.15	1.04	1.78
		1.18	1.71	1.45
		1.53	2.72	1.78
		1.76	3.76	2.15
		1.34	3.27	2.34
		1.94	2.27	1.17
	P1017/2	1.52	1.74	1.16
		1.73	1.73	1.00
	P1018/1	0.56	0.92	1.64
		0.30	0.58	1.94
	P1020/1	0.47	2.51	5.30
		0.61	0.77	1.27
		0.85	1.05	1.24
		0.52	0.61	1.09
	P1012/8	0.44	0.58	1.32
		0.49	0.50	1.02
		0.48	0.66	1.38
		0.45	0.86	1.91

Acknowledgements

The author would like to thank his colleague Dr. T.K. Ball who carried out much of the experimental work reported here.

This paper deals with work forming part of the programme of the Building Research Station, and is published by permission of the Director.

Table 10. *Summary of data for partition coefficients of oxides present in* C_3S *and* C_2S

Oxide	Sample	$\bar{x}$	n	s	c
Na_2O	P1012/3	4.1	6	3.5	85
	P1017/2	2.2	2		—
	P1018/1	3.3	6	1.7(5)	53
	P1020/1	2.2(5)	4	1.1(5)	51
MgO	P1012/3	1.63	6	0.42	26
	P1017/2	2.69	5	0.66	24
	P1018/1	1.95	7	0.67	34
	P1020/1	2.48	4	0.66	27
Al_2O_3	P1012/3	1.46	5	0.29	20
	P1017/2	1.44	4	0.24	17
	P1018/1	1.67	6	0.39	23
	P1020/1	1.53	4	0.57	37
K_2O	P1012/3	8.9	8	1.9	21
	P1017/2	3.1	2		—
	P1018/1	11.9	4	5.4(5)	45
	P1020/1	5.0	6	1.3	26
	B102	5.4	7	1.7	31
TiO_2	P1012/3	1.80	2	—	—
	P1017/2	0.76	1	—	—
	P1018/1	1.03	6	0.08	8
	P1020/1	1.18	7	0.37	31
MnO_2	P1012/3	2.31	7	0.81	35
	P1017/2	<0.5	4	—	—
	P1018/1	>2.2	4	—	—
	P1020/1	1.55	7	0.74	48
Fe_2O_3	P1012/3	1.70	10	0.11	6.5
	P1012/8	1.41	4	0.37	26
	P1017/2	1.08	2	—	—
	P1018/1	1.79	2	—	—
	P1020/1	2.22	4	2.04	92

$\bar{x}$ = arithmetical mean of partition coefficient for mineral pairs.
n = number of determinations
s = standard deviation
c = coefficient of variation

References

1. H. G. Midgley, "The chemistry of cement, Volume 1." Academic Press, London 1964. Ed, H.F.W. Taylor, "The formation and phase composition of portland cement clinkers," Chapter 3, p. 89.
2. A. E. Moore, "Examination of a portland cement clinker by electron probe micro analyses." Revue Silicates Industries, 30, August 1965 p. 455.
3. O. Peterson "Investigation of portland cement clinkers with the microprobe." Zement-Kalk-Gips., 2, 1967. p. 61–64.
4. H. G. Midgley, "The composition of alite (tricalcium silicate) in a portland cement clinker." Mag. Concrete. Res., in the press.
5. K. E. Fletcher, "The composition of belite (dicalcium silicate) in portland cement clinker." To be published.
6. I Adler, "X-ray emission spectrography in geology." Elseiver Publishing Company 1966.
7. H. G. Midgley and H.F.W. Taylor. "The chemistry of cement, Volume 2." Academic Press, London 1964. Ed. H.F.W. Taylor "Optical microscopy" Chapter 20 p. 223.
8. F. M. Lea and T. W. Parker, Building Research Technical Paper, No. 16, H.M.S.O. London.
9. J. Philibert, "3rd international symposium X-ray optics, X-ray microanalysis". Academic Press, London, 1963.
10. R. Castaing, Advances in electron physics. **13**, 1960, p. 317.
11. H. G. Midgley, K. E. Fletcher and A. G. Cooper, "The identification and determination of alite in portland cement clinker." Analysis of calcareous materials, S.C.I. Monograph. No. 18. Society of Chemical Industry, 1964, p. 362.

Supplementary Paper I-37 The Effect of Chromium Oxide on the Structural Transformations in Tricalcium Silicate

A. I. Boikova*

Synopsis

Solid solutions between $3CaO \cdot SiO_2$ and Cr_2O_3, and $3CaO \cdot SiO_2$, Cr_2O_3 and MgO have been investigated. It has been shown that at Cr_2O_3 concentration higher than 1.5 wt % decomposition of solid solutions with formation of new phases takes place. MgO as a component of solid solutions prevents this decomposition.

The effect of oxidation-reduction conditions on the oxidation degree of Cr_2O_3 in solid solutions has been studied. Solid solutions of yellow, green and blue color have been obtained under various conditions. Chromium valence has been determined in the samples by chemical analysis.

Spectroscopic investigation has shown that solid solutions of yellow, green and blue color have different spectra characteristic for each of them. Theoretical interpretation of the absorption spectra has been considered.

Assumptions on Cr^{3+} and Cr^{6+} positions in the structure of the solid solutions have been proposed.

X-ray method was used to show disordering of the solid solutions. Solid solutions can be triclinic and monoclinic depending on chemical nature of addition, its amount and heat-treatment conditions.

Introduction

The main cementing mineral of commercial clinkers-$3CaO \cdot SiO_2$-always contains some amount of additions occurring in the lattice in the form of solid solution. Chemical nature of the addition, its amount and heat-treatment conditions considerably change the structure of the silicate and consequently, its chemical and technical properties.

Among the studied solid solutions of $3CaO \cdot SiO_2$ with other components, chromium solid solutions are of special interest because of the presence of a cation of variable valence in the lattice.

Experiment

The tested samples were obtained by annealing in air in a Pt–Rh furnace at temperatures 600–1500°C and in argon at 1600–1800°C using a tungsten vacuum microfurnace.

The synthesis of the samples was realized according to the method described by Boikova and Toropov (1). Solid solutions of the yellow (at 600°C in air), green (at 1500°C in air), and blue (at 1600–1800°C in argon) color were obtained.

Most of the tests were carried out at temperatures 1450–1500°C in air under conditions near to practical ones.

Methods of Investigation and Results

The preference was given to the study of the solid solutions of the green color. The blue and the yellow solid solutions were examined in connection with the question of the influence of oxidation-reduction conditions on the chromium valence.

By means of optical, X-ray, DTA and chemical (determination of free CaO) methods it was found that

*Grebenshchikov Institute of Silicate Chemistry of the Academy of Science, Leningrad, U.S.S.R.

the limiting solid solution contained only 1.5 wt % Cr_2O_3, had light green color and refractive indices higher than those of pure $3CaO \cdot SiO_2$:

$Ng_{Na} = 1.726 \pm 0.003$ and $Np_{Na} = 1.722 \pm 0.003$

Characteristic property of the solid solutions with Cr_2O_3 is their instability. If Cr_2O_3 content in the mixture exceeds 2 wt %, there occurs the decomposition of the solid solutions with formation of free CaO and crystals of the green color brighter than the solid solution itself and representing one of the high-temperature forms of dicalcium silicate stabilized by Cr_2O_3. Their refractive indices are as follows:

$Ng_{Na} = 1.767 \pm 0.003$ and $Np_{Na} = 1.754 \pm 0.003$.

With increasing Cr_2O_3 content in the mixture the amount of the solid solution $3CaO \cdot SiO_2$ with Cr_2O_3 decreases, and at more than 5 wt % Cr_2O_3 no formation of the solid solution is observed.

Differential Thermal Analysis

DTA curves in Figs 1 and 2 show polymorphous transformations most characteristic of pure $3CaO \cdot SiO_2$, where two brightly expressed effects are observed at 920° and 980°C (Fig. 2, a).

One of the interesting phenomena detected in the DTA curves is the splitting effect of the curves for solid solutions with 1.5 and 2 wt % Cr_2O_3 (Fig. 1, c, d).

The DTA curves also show that with increasing Cr_2O_3 content in the samples, the amount of $3CaO \cdot SiO_2$ solid solution with Cr_2O_3 decreases while in the samples with 5 %Cr_2O_3 and 95% $3CaO \cdot SiO_2$ the solid solution does not form. Endothermic effects in the temperature regions 700–800°C, 1000–1100°C and 1200–1300°C characterize the phases developed as a result of the decomposition (Fig. 1, e, f, g). The splitting of endothermic effects is characteristic of the state preceding the decomposition.

In the study of the solid solutions between $3CaO \cdot SiO_2$, Cr_2O_3 and MgO, the presence of magnesium in the lattice was found to prevent the decomposition. DTA curves for the solid solutions with MgO (Fig. 2) allow to observe the phenomenon opposite to that characteristic of the curves for the solid solutions without MgO. With increasing MgO content in the solid solution two endothermic effects converge, and in the sample curves two endothermic effects fuse into a single effect (Fig. 2, d, e, f).

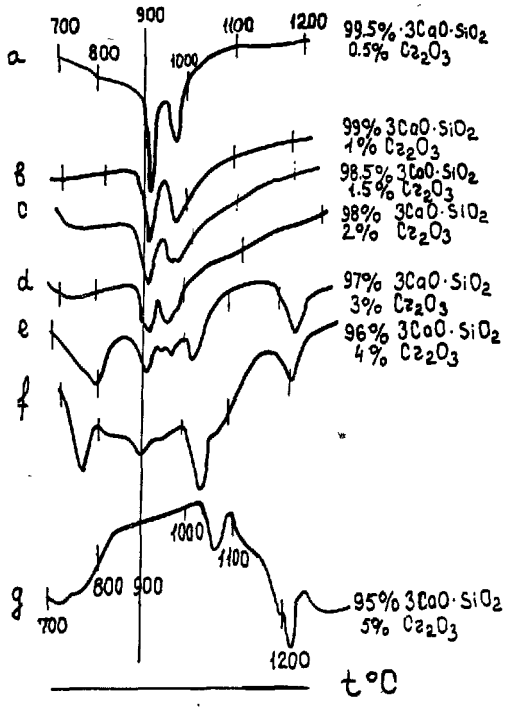

Fig. 1. *DTA curves of the solid solutions with* Cr_2O_3.

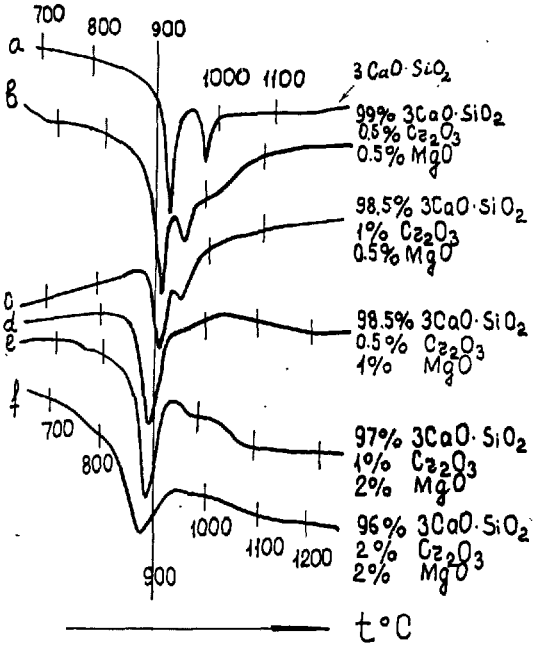

Fig. 2. *DTA curves of the solid solutions with* Cr_2O_3 *and* MgO.

X-ray Analysis

X-ray diffraction patterns of pure $3CaO \cdot SiO_2$ represent complicated lines changing their shape and intensity in relation to certain factors: chemical nature of the addition, its amount and heat-treatment conditions. In Figs. 3 and 4 are given most characteristic areas of X-ray diffraction pattern for the solid solutions at the angles 2θ 32–34° and 51–53°.

Analysis of the diffraction effects show that depending on the nature of the addition (Fig. 3, b, c) and heat-treatment conditions (Fig. 4, b, c, d), distances between the effects change, splitting or fusing of some of them and redistribution of the intensities are observed. These factors indicate the disordering of the solid solution lattice. Solid solutions may be both triclinic and monoclinic depending on the nature of the addition, its amount and heat-treatment conditions.

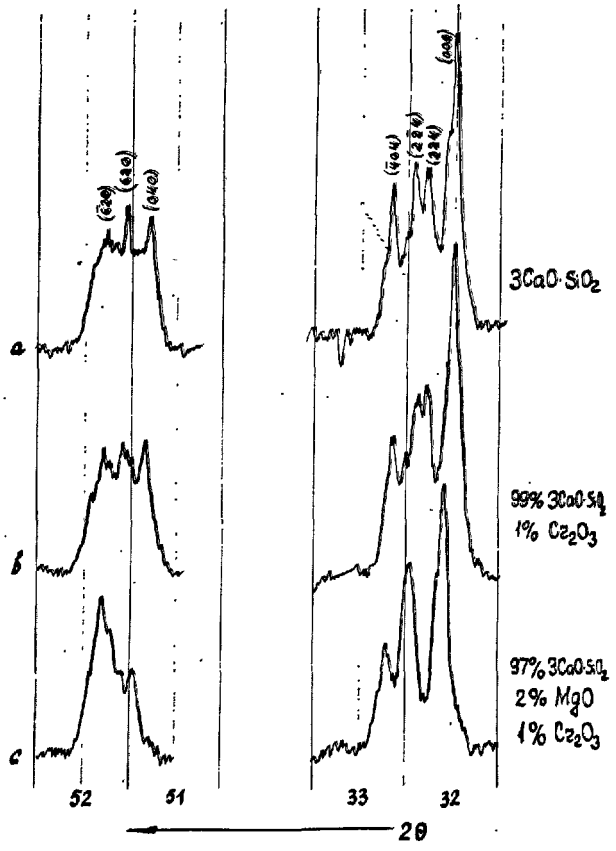

Fig. 3. *X-ray diffraction patterns of the solid solutions with* Cr_2O_3 *and with* Cr_2O_3 *and* MgO.

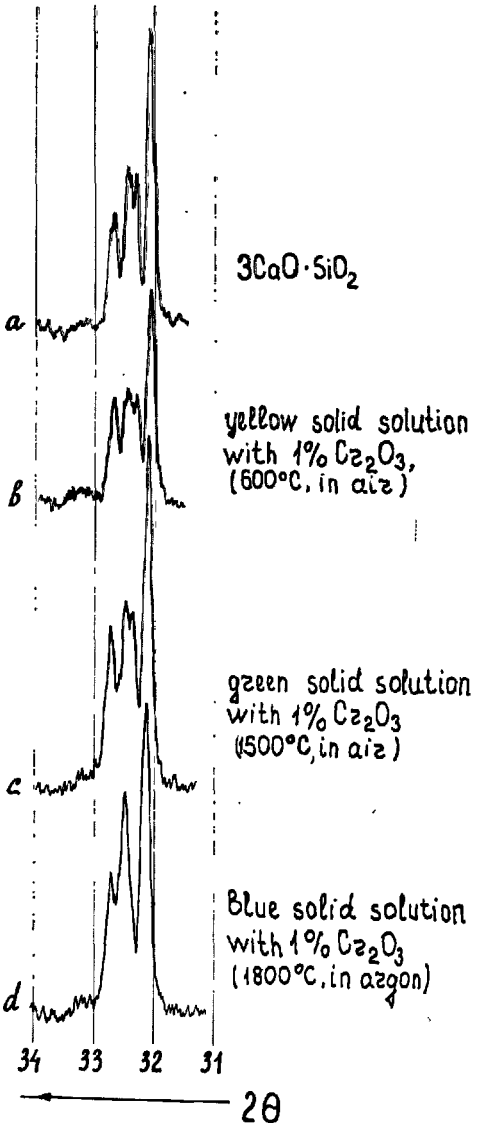

Fig. 4. *X-ray diffraction patterns of the yellow (b), green (c), and blue (d) solid solutions.*

Chemical Analysis

Depending on the change in the oxidation-reduction conditions of the experiment, the oxidation degree of chromium altered, too. Thus, it was found by chemical analysis that solid solutions of the yellow color obtained in air at 600°C contained mainly Cr^{6+}. Solid solutions heated in air at 1500°C got green color and

showed the presence of both Cr^{6+} and Cr^{3+}. Heating in vacuum in argon under gas pressure of about 7–8 psi at 1600–1800°C produced solid solutions of blue color. According to the chemical analysis data, these samples contained mainly Cr^{6+}.

Table 1 represents results of the chemical analysis of the solid solutions with Cr_2O_3.

Table 1. *Results of chemical analysis of solid solutions with* Cr_2O_3

Initial composition of samples	Experimental conditions	Color	Components content according to analysis (wt %)					
			CaO	SiO_2	Cr_2O_3	CrO_3	Losses on heating	Sum(Σ)
99%3CaO·SiO_2 1%Cr_2O_3	600°C in air	yellow	72.69	25.36	—	1.32	0.78	100.15
99%3CaO·SiO_2 1%Cr_2O_3	550°C in air	yellow	73.30	24.66	—	1.06	0.99	100.01
98%3CaO·SiO_2 2%Cr_2O_3	550°C in air	yellow	70.84	25.40	—	2.39	1.09	100.32
98.5%3CaO·SiO_2 1.5%Cr_2O_3	1450°C in air	green	72.75	25.05	0.41	1.05	1.03	100.28
99%3CaO·SiO_2 1%Cr_2O_3	1500°C in air	green	72.52	25.37	0.42	0.56	0.62	99.49
98%3CaO·SiO_2 2%Cr_2O_3	1500°C in air	green	71.71	25.73	0.62	1.54	0.49	100.09
99%3CaO·SiO_2 1%Cr_2O_3	1800°C in argon	blue	73.61	25.77	0.84	—	—	100.22
99%3CaO·SiO_2 1%Cr_2O_3	1600°C in argon	blue	72.71	26.02	0.82	0.22	—	99.77

Optical Investigations

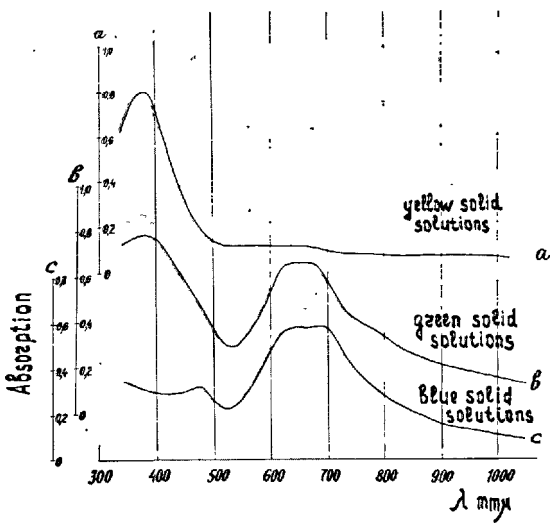

Fig. 5. *Absorption spectra curves of the yellow (a), green (b), and blue (c) solid solutions.*

Fig. 5 shows the absorption spectra curves obtained on a spectrograph SF-4 for polycrystalline samples in the region 340–1100mmμ under reflected light. The absorption spectrum curve for the yellow sample represents one band in the shortwave range with a maximum at 380 mmμ. The absorption spectrum of the green solid solution exhibits two bands (Fig. 5, b): one corresponding to the intense band of the yellow sample with a maximum at 380 mmμ and the other-to the broad band of the blue sample with a flat maximum in the wavelength range 640–700 mmμ. The blue crystal spectrum displays two absorption bands: an intense broad band with a flat maximum in the wavelength range 640–700 mmμ and a considerably more narrow weak band with a maximum at 470 mmμ (Fig. 5, c).

Discussion

According to the chemical analysis data for the yellow solid solutions and to the conditions of the synthesis providing the maximum degree of Cr oxidation, the absorption band at 380 mmμ characterizes Cr^{6+}. The blue solid solutions contain mainly Cr^{3+}. Two absorption bands—a broad one with a maximum at the wavelength region 640–700 mmμ and a narrow weak band with a maximum at 470 mmμ-characterize Cr^{3+}. Though in the samples heated in vacuum there was chiefly found Cr^{3+}, nevertheless conditions of vacuum could provide formation of chromium with lower valence, namely Cr^{2+}, as a result of partial reduction or possible disproportionation of Cr^{3+}. But according to the method of chemical analysis

used by Boikova, Toropov, Grum-Grzimailo and Piryutko (2), it was impossible to determine Cr^{2+} in the presence of Cr with valence higher than three. Theoretical interpretation of the absorption spectra given by Sviridov and Boikova (3) permits to suppose the occurrence of Cr^{2+} in the blue solid solutions, too.

The absorption spectrum of the green solid solutions seems to represent a summary curve of two spectra: one—for the yellow sample (with Cr^{6+}) and the other —for the blue one (with Cr^{3+}). Chemical analysis data for the green solid solutions show that crystals really contain both Cr^{6+} and Cr^{3+}.

In the lattice of $3CaO \cdot SiO_2$ additions may occupy three positions: to substitute isomorphously Ca^{2+} and Si^{4+} and to be placed in the holes whose occurrence was stated by Jeffery (4) in studying the fine structure. Cr^{6+} ($\tau_k = 0.35$Å) probably substitutes Si^{4+} ($\tau_k = 0.39$Å) in tetrahedral coordination. The substitution proceeds with formation of vacancies according to the scheme $3Si^{4+} \rightleftarrows 2Cr^{6+} + \square$.

In case of Cr^{3+} ions, the octahedral coordination is most advantageous, and in our opinion, isomorphous substitution of Ca^{2+}($\tau_k = 1.04$Å) by Cr^{3+} in octahedral coordination takes places in the structure of the solid solutions: $3Ca^{2+} \rightleftarrows 2Cr^{3+} + \square$.

References

1. N. A. Toropov and A. I. Boikova, "Solid solutions of tricalcium silicate with yttrium oxyorthosilicate" (in Russian), Doklady Akad. Nauk SSSR, **151,** 1114–1117 (1963).
2. A. I. Boikova, N. A. Toropov, M. M. Piryutko and S. B. Grum-Grzimailo, "Effect of chromium oxide on structural transformations of tricalcium silicate" (in Russian), Izv. Akad. Nauk SSSR, Neorgan. Materialy, **2,** 1796–1802 (1966).
3. D. T. Sviridov and A. I. Boikova, "On the question of chromium valence in solid solutions of tricalcium silicate" (in Russian), Izv. Akad. Nauk SSSR, Neorgan. Materialy, **4,** (1968).
4. J. W. Jeffery, "The crystal structure of tricalcium silicate", Acta Cryst., **5,** 26–35 (1952).

Supplementary Paper I-42 The Use of Thermogravimetric Measurements in Cement Chemistry

Paul Longuet*

Synopsis

In this paper the contribution of the thermogravimetry to the chemistry of cements is reported with a particular mention of the works carried out at the CERILH (Centre d'Etudes et de Recherches de l'Industrie des Liants Hydrauliques).

After a short map of generalities the characteristics of the thermogravimetric measure are specified and the essential contribution of the quantitative ponderable balance to the interpretation of thermograms is shown.

Next it is suggested to present the bibliographical analysis of the works starting from the principal thermoponderable reactions met in the chemistry of cements, particularly the heterogeneous equilibria solid-gas, in presence or no of the equilibrium gas, of the type hydration-dehydration, carbonation-decarbonation, oxidation-reduction, adsorption-desorption.

In this summary, two examples will only be quoted:

1. In the scope of the general reaction hydration-dehydration the use of the equilibrium:

$$\underset{\text{(solid)}}{Ca(OH)_2} \qquad \underset{\text{(solid) (gas)}}{CaO + H_2O}$$

for the investigation and the determination of "free" CaO and $Ca(OH)_2$, for the reactivity of $Ca(OH)_2$ in complex systems and for the hydration in the vapor phase of the system $C_3S + C$.

2. In the scope of the general reaction carbonation-decarbonation, the use of the equilibrium:

$$\underset{\text{(solid)}}{CO_3Ca} \qquad \underset{\text{(solid) (gas)}}{CaO + CO_2}$$

for the measurements of reactivity in the systems calling into action CO_3Ca (synthetic mixes, raw mixes), for the study of C_3S behaviour in CO_2 and its determination in the complex powdered mixtures and for the evolution of the system CO_3Ca–SiO_2–CO_2 under atmospheric pressure in presence of mineralizers with the showing and the synthesis of spurrite $Ca_5(SiO_4)_2CO_3$.

The conclusion shows the research possibilities given by the thermoponderable analysis and the continuous weighing applied to the chemistry of cements.

Thermogravimetry allows one to measure in a constant way the changes in weight, as a function, either of temperature or of time, of a sample undergoing a given thermic treatment in a definite atmosphere.

The conception of continuous weighing goes back to the beginning of the century. The first reference to it seems to be that of Nernst and Riesenfeld (1) and the thermobalance was invented by Honda (2). Reference can be made to an excellent historical summary of the question in the book of Clement Duval (3).

*Centre d'Etudes et de Recherches de l'Industrie des Liants Hydrauliques, Paris, France.

Apparatus

Thermogravimetry may be used, as a rule, to study all the physico-chemical systems the evolution of which occurs with a ponderable change. This highly general use of the method is the source of an impressive number of laboratory devices and various commercial applications. In the present work, only the general principles will be quickly commented on, in referring to notes 3 and 5 for the essential descriptions and the drawing up of a fairly complete list of the different models we put forward.

A thermobalance has 3 essential components: the balance, the thermal and the recording components.

The Balance Component

This component may be divided into two large sections according as the change in weight is measured either by a deviation (deflection balances) or by the value of the restoring force to return to the original null-point (compensation or null-point balances).

In both cases the same weighing arrangements are used in the laboratory apparatus: conventional analytical balance, more or less modified, wire suspension balance, torsion balance, helical springs in silica glass or in invar, strain gauges... These instruments can weight from one milligram to one hundred grams, the sensitivity being of about 10^{-6} times the weight.

In the deflection balances, the deviation generally in proportion to the change in weight, can be measured with an optical collector (a turning mirror), electric collector (feeler with mechanical deviation), a magnetic, photo-electric, ionizing collector.

In case the collector should exert no stain on the deviation, the initial properties of the balance which is used remain entirely the same. One may reproach this type of instrument with having an area of measures relatively narrow bound to the sensitivity. Moreover, the deviation may binder direct actions on the sample (simultaneous measures, magneto chemistry...)

In the null-point, any change in balance is at once counterbalanced. This compensation entails, first, the detection of the lack of balance (electric, electrostatic, magnetic, photo-electric and ionizing collectors). This detection must have a sensitivity higher than that of the weighing arrangements which are used. The feed-back force may either have a mechanical origin (deviation of a chain bound to the beam, torque, electro deposit, hydrostatic pull on a diver), or be of an electric nature (action of a magnetic field on a permanent magnet, an iron core, or a mobile coil). Sometimes, the same arrangement provides for both the detector and the compensation. With the null-point the sample keeps a fixed position, which increases the number of possible measurements (connector without feed-back torque permitting electric connections or direct gas admission, sedimentometric analysis....).

The Thermal Component

As a rule, it is the thermal resistance of the sample holder which limits the temperature of thermogravimetric measurements which can be effected either in constant temperature, or according to a definite thermal cycle.

For low temperatures, one uses liquefied gases or refrigerating machines (from about −80° C), around the room temperature the thermostats or conventional drying ovens, and, at last, electric ovens for higher temperatures (nichrome resistor up to 1,200°C, platinum, alloy of platinum or rhodium, from 1,200 to 1,700°C, graphite or tungsten (under vacuum up to 3,000°C (16),). One must secure, first, a homogeneous thermal area around the sample, then in the case of the thermal cycle, carry out a continuous temperature change vs time in a determined programme, (generally linear). These requirements set delicate problems in the designing of ovens, problems of regulation and of planning which have been rightly resolved, in several different ways mainly up to 1,600°C.

The Recording Component

This component must ensure the recording of changes in weight and that of temperature. The recording of these two variables vs time on a same diagram is preferred to the recording in X—Y in order to allow the immediate examination of the incidence of a casual thermal anomaly on the weighing curve.

The type of balance and the method of regulation of temperature make one decide on the type(s) of recorders to be used.

Additional Devices

Most of the apparatus, to-day, permit one to work either under vacuum or in a controlled atmosphere by atmospheric pressure, whilst higher pressures need very special apparatus.

The gases evolved during the reaction may often be collected quantitatively. Many thermobalances

permit one to associate differential thermal analysis (DTA) to thermogravimetry (TGA) so as to complete understanding of the thermal effects occuring in the studied system, although it often happens that the ideal thermal conditions for each technique are not simultaneously fulfilled. Many commercial thermobalances now put on the market offer this possibility which often leads to make easier the comparison between the curves, to draw also, on the same diagram, the derivated thermogravimetric curve (DTGA) achieved by electric or electronic treatment of the direct TGA information. Densitometric (gas and liquids), tensiometric, magnetochemical, sedimentometric, chromatographic measurements... can as well be effected with the thermogravimetric apparatus (8).

Thermogravimetric Measurement

The use and interpretation of the experimental values achieved with a thermogravimetric apparatus must take into account the conditions which are peculiar to the measurement. The problems having been raised lead to a lot of published works we referred to in the general articles already quoted (3) to (15). In this study we will only give the essential points of the problems.

The Thermogramme

The changes in weight plotted against temperature, as showed in Fig. 1, represent the most commonly faced aspects. A plateau shows that there is no weighing change. An isolated weighing change—A—shows a continuous loss of weigh $\Delta\omega$ characterized by an initial temperature t_i and a final temperature t_f (the value of $\frac{d\omega}{dt}$ which starts from zero, goes up to a maximum and goes down to zero, generally allows a strict definition of t_i, t_f and also t_m corresponding to a maximum). In the case of simultaneous weighing changes (chosen with opposed signs in B part) $\frac{d\omega}{dt}$ is not reduced to zero. These reflections show the advantage of the simultaneous recording of the TGA and DTGA values.

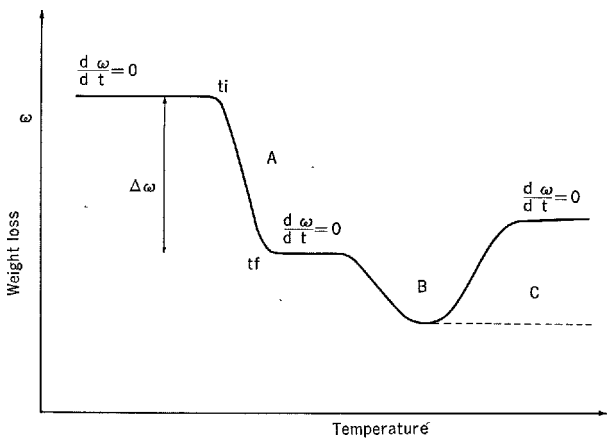

Fig. 1. *Schematic thermogramme.*

Measurement of Temperatures

Any influence preventing the instantaneous homogeneous distribution of temperature alters the real value.

Influence of the Collector

The measurement of temperature depends on the position of the collector (usually a thermo-electric torque). The optimum position enabling one to obtain the real value is the center of the sample. This condition is now often fulfilled, in the apparatus specially in those achieving simultaneously TGA and DTA.

Influence of the Studied System

Weight, volume, calorific capacity, thermal conductivity, reaction heat, state of subdivision, compactness, sintering, apparition of a liquid phase and any other cause which can be the start of a temperature gradient disturbs the measurement.

Influence of the Crucible or Sample Container

In addition to its own thermal inertia, this fitting determines the importance of the interface system-wall and marks the limits of the free area of the sample (catalytic effects—gaseous exchanges).

Influence of the Thermal Cycle

All the other conditions remaining the same, a more rapid heating rate strengthens the heterogeneity of the temperatures due to the previous influences. The deviation can reach tens of centigrade degrees for a sample of about one milligram, under requested conditions of temperature, with a speed varying from one to three.

Influence of the Gaseous Environment

This influence has an effect on the conditions of the

balance gas-solid and must be considered as an influencial factor, and not as a disturbing factor.

Measurement of Weights

Any influence liable to exert an action on the balance of the weighing devices apart from the changes in weight of the system must be either taken into account, or suppressed.

Influence of the Gaseous Buoyancy

The gaseous atmosphere surrounding the sample container, the crucible and its content, exerts on the whole a pressure function of temperature, nature of the gas and gas flow too, in the case of a renewed atmosphere. In spite of the different trials of a priori calculation, the rectification is most often effected by achieving a blank test in the expected conditions. This rectification is almost always indispensable.

A lowering of pressure permits the buoyancy to be reduced but phenomena of molecular pressure occur when the average molecular courses reach the value of the chamber dimensions.

A dependent shell reduces this effect but hinders the gaseous exchanges. Devices also exist allowing to act in presence of corrosive gases.

Influence of Convection

The crucible must be at best protected by shields against the turbulence resulting from the overheating of the gaseous atmosphere.

Various Influences

The distortions obtained by expansion of the weighing system must be avoided by keeping isotherm the balance housing.

In microthermogravimetry (weighing at a 10^{-9} g.) radiometric and electrostatic effects are to be taken into consideration.

Standardization of the Thermogramme

The buoyancy rectification being most often enough to achieve correct variations in weight, the exact values of the reaction temperatures are the most difficult to reach, and a certain number of thermogravimetric standards allowing interesting comparisons, have been proposed (18).

Anyway, it is advisable, when issuing a thermogramme, to state precisely as much as possible the experimental conditions and especially to indicate clearly which thermal cycle is used.

Interpretation of the Thermogravimetric Data

Thermogravimetry presents the fundamental advantage to obtain the weight balance of the studied reactions. This sound quantitative element has lead numerous authors to attempt the reckoning, from the thermogrammes, of a certain number of kinetic constants: the speed of polymerization, the order of the reactions, the activating energy (4), (5), (8). The evaluations are often long and delicate, but the expansion of the calculations, using an electronic computer, will certainly make this kind of application easier.

Present Tendencies in Thermogravimetry

The critical study of the disturbing causes in thermogravimetric measurement shows the advantage of working with very small quantities of substance.

The evolution will certainly go that way up to a compromise taking into account the easiness of measurements and the limits of representativity of the studied sample. Moreover, the simultaneous TGA, DTGA and DTA measurements on the same apparatus will be generalized.

Fundamental Reactions

The heterogeneous solid-gas systems, or, more rarely, liquid-gas systems, under the general decarbonation-carbonation, dehydration-hydration, oxidation-reduction and desorption-adsorption forms, are at the origin of the main thermogravimetric studies concerning he cement chemistry. It is thus necessary to start with the study of basic reactions before dealing with the applications often involving several simple reactions (19).

Decarbonation-Carbonation

The CO_2 combinations take an important part, as well in the production as in its use and they deserve a detailed study.

Equilibrium $CO_3Ca \rightleftharpoons CaO + CO_2$

It has been the subject of numerous theoretical studies apart from the programme of the present work;

the Fig. 2 gathers the essential thermogravimetirc conclusions:

—In a current of gas, inert towards the system (air without H_2O and CO_2, nitrogen, argon, etc. . .) the plot of the curve (in dotted lines) is fixed by the variation of dissociation pressures, vs temperature, the evolved CO_2 being continuously withdrawn.

—In a current of CO_2 equilibrated with the atmospheric pressure there is no reaction up to the dissociation temperature at this pressure. Over that stage, the decomposition is quite rapid. During the cooling cycle, a rapid recarbonation, always incomplete and variable, is noticed. No compound of the $CO_3Ca \cdot CaO$ type, pointed out by Raoult (20) could be revealed.

Equilibrium $CO_3Mg \rightleftarrows MgO + CO_2$

Under the same conditions as those achieved for CO_3Ca the pure giobertite (CO_3Mg) gives the same curves as in Fig. 3.

CO_2 at the atmospheric pressure fairly changes the dissociation temperature of CO_3Mg and the resulting MgO does not fix CO_2 during the cooling. The reaction is practically irreversible.

Dehydration-Hydration

The process of the thermal elimination of water depends on its type of binding in the studied compound. The association of water with solids assumes very different forms and the numerous types of classification which are offered (21) do nothing else but stress the complexity of the problem. Bader's proposition (22) concerning the fixed water in a continuous way, and the water fixed in a discontinuous way fits perfectly with the thermogravimetric studies of the hydrated compounds of the cement chemistry for which a superposition of the different types of binding of water are often noticed. The thermogrammes must be achieved in well-controlled experimental conditions (well-defined law of the heating rate and definite water-vapor pressure) in order to allow an interpretation. The water-vapor adds a further difficulty during the treatment of the atmosphere by condensing on every "cool-point" for which it becomes saturing. To avoid this trouble, many devices have been proposed (23) (24). We will quote as the main basic reactions, those referring to the well-defined crystalline structured hydrates. For the hydrated phases imperfectly crystallized and sometimes unstable requiring the setting of a network of isobaric and isothermal curves, so as to state precisely the different equilibria of hydration, the excellent study by Lavanant on hydrated calcium aluminates will be referred to (24).

Equilibrium $Ca(OH)_2 \rightleftarrows CaO + H_2O$

The loss of water is bound to the disparition of the OH^- groups. The thermogravimetric study (23) is summarized in Fig. 4.

—In a current of gas, inert towards the system (air without H_2O and CO_2, nitrogen and argon. . .) the plot of the curve is the dotted one. The weight balance often shows an incomplete hydration and a light carbonation. The pressures of dissociation varying rapidly with temperature, the slope changes are quite clearly marked.

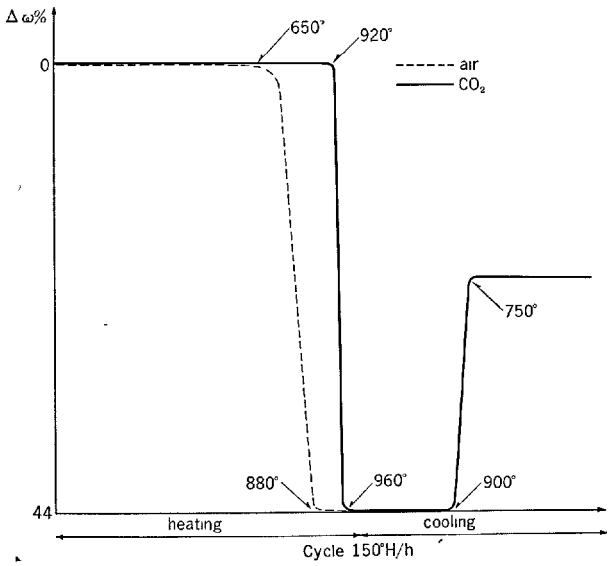

Fig. 2. $CO_3Ca \rightleftarrows CaO + CO_2$

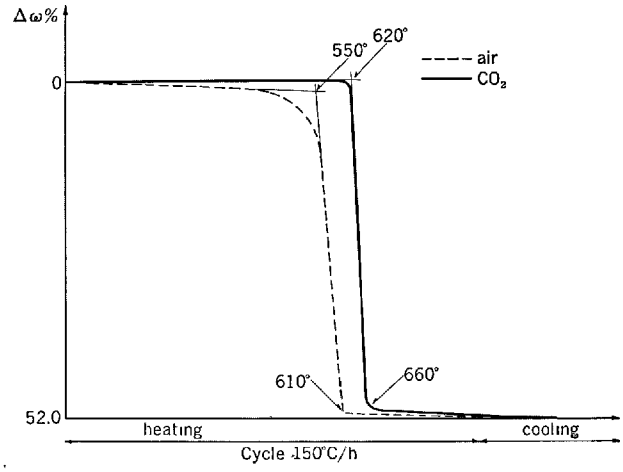

Fig. 3. $CO_3Mg \rightleftarrows MgO + CO_2$

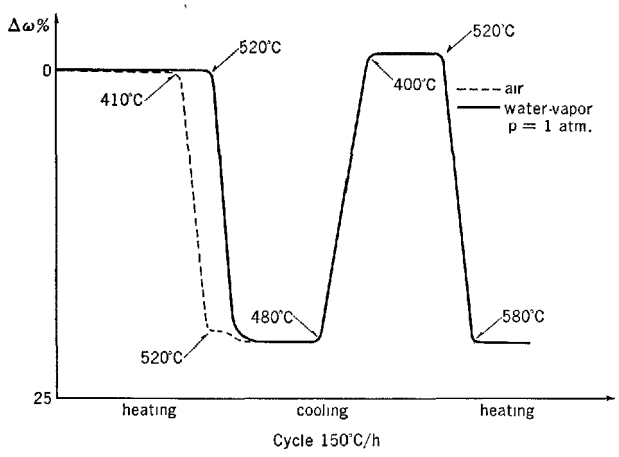

Fig. 4. $Ca(OH)_2 \rightleftarrows CaO + H_2O$

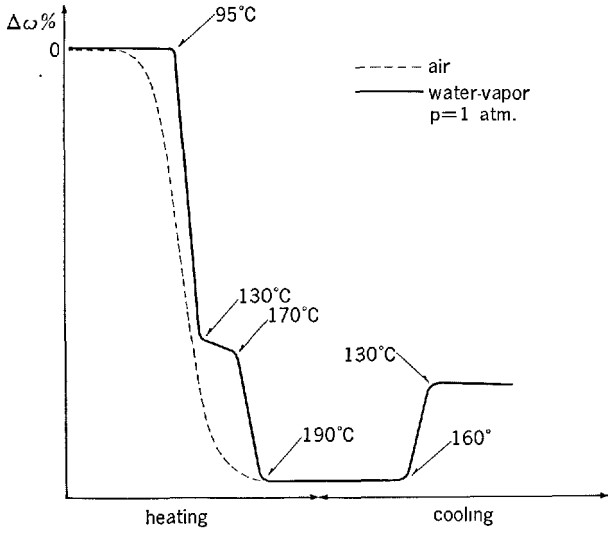

Fig. 5. $SO_4Ca \cdot 2H_2O \rightleftarrows SO_4Ca + 2H_2O$

—In a water-vapor saturated atmosphere, at the ambient pressure, (curve drawn in thick line), the dissociation temperature is clearly stressed. A series of hydration-dehydration cycles points out the previous remark about the weight balance by achieving a total rehydration after the loss of CO_2 and shows the perfect reversibility of the system.

Equilibrium $SO_4Ca \cdot 2H_2O \rightleftarrows SO_4Ca + 2H_2O$ (23)

In conditions similar to those achieved for $Ca(OH)_2$, SO_4Ca, $2H_2O$ provides the curves shown in Fig. 5.

The water-vapor saturated atmosphere makes clear the formation of hemihydrate. At this moment the rehydration is incomplete and variable according to the nature of the sample.

Oxidation-Reduction

Carbon, iron and sulphur elements or their compounds are mainly at the origin of the auto-reducing phenomena met in cement chemistry. The nature of the gaseous environment encompassing the sample gives rise to the different simple reactions liable to occur (19, 25).

Oxidizing Atmosphere

It is the most frequent case, the reactions occurring, most often, in presence of air. The action can be strengthened by the use of pure oxygen.

$C + O_2 \longrightarrow CO_2$

$SCa + 2O_2 \longrightarrow SO_4Ca$

$4Fe + 3O_2 \longrightarrow 2Fe_2O_3$ This reaction may occur from 400°C in CO_2 atmosphere with the oxygen resulting from the dissociation: $2CO_2 \rightleftarrows 2CO + O_2$

Neutral or Inert Atmosphere

Oxidation is hindered. Nitrogen, argon, helium and vacuum too, are used. However, the present reducers may then react with other components of the system during the increase of temperature. The reduction of sulphates by the carbon is a frequent example (19):

$SO_4Ca + 2C \longrightarrow 2CO_2 + SCa$

$SO_4K_2 + 2C \longrightarrow 2CO_2 + SK_2$ (the resulting alkali sulphide is volatile above 800°C and can be eliminated).

The relative initial concentrations of the reactants fix the reaction balance.

Reducing Atmosphere

Hydrogen is often used. The three reactions:

$SO_4Ca + 4H_2 \longrightarrow SCa + 4H_2O$

$SO_4K_2 + 4H_2 \longrightarrow SK_2 + 4H_2O$

(same reaction with $SO_3\ Na_2$)

$Fe_2O_3 + 3H_2 \longrightarrow 2Fe + 3H_2O$

are very important in cement industry. The reductant being in excess, the reactions are complete. The disadvantage comes from the secondary reaction of the possible interaction between the watervapor and the resulting sulphides (25).

Adsorption-Desorption

These phenomena are mainly used in the specific surface area measurements by gaseous adsorption for which the sluggish balancing and the very small changes in weight require special techniques (from 9 to 14). In the conventional measurements, disturbing effects are bound to changes of gaseous environment

(passage from H_2 to CO_2, for instance) during the same determination. They specially appear with systems of noticeable surface (from m^2/g.)

Real Systems

A real system is most often the site of several simple reactions. The following general cases may occur.

Distinct Reactions

It is the most simple case. Each reaction is marked by its characteristic temperatures and its importance measured by the corresponding change in weight.

Simultaneous Reactions

The curves are more or less mingled together and directly uninterpretable. One tries thus to make the balance factors varying in order to diversify the two reactions. A conventional example is given by the dolomite $(CO_3)_2Ca$, Mg which forms in the air, a continuous carbonation curve parting in two stages in a CO_2 atmosphere (see Figs. 2 and 3).

Competitive Reactions

There are simultaneous reactions with interaction.

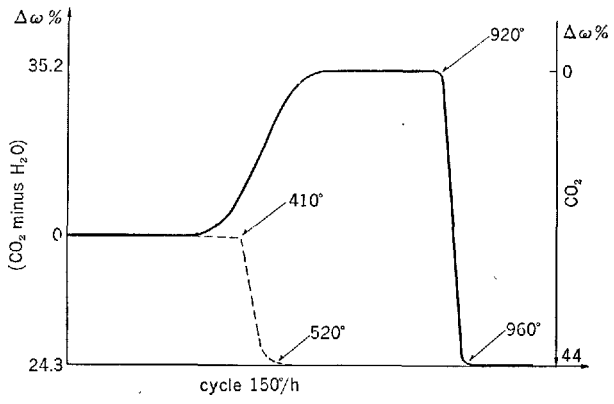

Fig. 6. —$Ca(OH)_2$ *in* CO_2 *atmosphere*
----$Ca(OH)_2 \rightarrow CaO + H_2O$ *in air*

The interpretation is delicate and additional measurements are often necessary (X-rays, diffraction, analysis of the gaseous compounds eventually evolving). Fig. 6 relative to the dehydration of $Ca(OH)_2$ in CO_2 atmosphere at the atmospheric pressure (19) illustrates a case of carbonation-dehydration competition. The weight balance and the thermogramme in inert atmosphere allow the complete understanding.

Applications

The applications will be introduced by following the conventional order of the different chapters of cement chemistry; the most characteristic researches will be stated if necessary for each of them.

Raw Materials

Clays

In cement chemistry the "clay-phase" is often wrongly defined and raises delicate problems of characterization (26). This is the reason why basic studies dealing with the thermogravimetric behaviour of definite mineral species (from 27 to 35), the influence of the particle sizes in same particular cases (36, 37), the grinding effects (38) or the formation of clay organometallic complex (39, 40) will certainly allow one to make the problem clearer.

Limestones

The determination of the CO_3Ca content does not generally present difficulties. The case of the simultaneous presence of CO_3Ca and CO_3Mg has been examined (19). Calcareous substances are often thermogravimetrically studied (41, 42, 43).

Raw Mixtures—Formation and Synthesis of the Spurrite

In this area, the problem of reactivity is raised. The principle of the thermogravimetric measurement utilizes the $CO_3Ca \rightleftarrows CaO + CO_2$ balance under a CO_2 pressure of one atmosphere. In such conditions a system containing CO_3Ca, does not show any loss of weight before the dissociation temperature (about 900°C) is reached, except if stable combinations with the present CO_3Ca occur. In the latter case the loss of weight before 900°C permits to estimate the "reactivity" of the system at this temperature (Fig. 7). On this basis, numerous studies have been carried out at the CERILH either on the technological level for calcareous pastes (45), raw mixes with or without mineralizers (46, 47) or in the fundamental research level, where the study of the CO_2–CaO–SiO_2 system in presence of small quantities of F_2Ca, has proved that the stable phase was the spurrite $(SiO_2 \cdot 2CaO)_2$ CO_3Ca which offers the thermogravimetric peculiarity of decomposing at about 980°C under CO_2 at

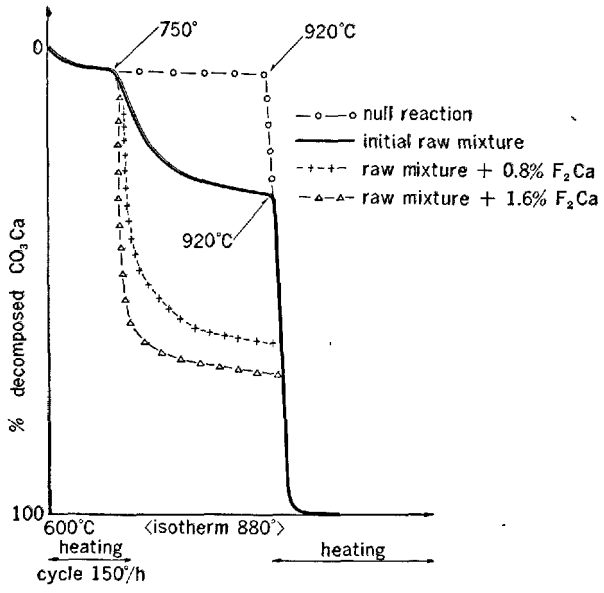

Fig. 7. *Reactivity of raw mixtures.*

the atmospheric pressure (48, 49). The compound synthesis has been described, with its main properties (50). The CO_2–CaO–Al_2O_3 system has been also partly studied in the same conditions and a compound of empirical formula $7\,Al_2O_3 \cdot 12\,CaO \cdot 2.5\,CO_3Ca$ pointed out (48).

Fuels

The fact of working either in an inert atmosphere (argon, nitrogen...) or in an oxidizing atmosphere permits and easy study and determination of the humidity, of the volatile substances and of the coal ashes (19 and 51).

Clinkers

The basic studies refer more specially to the pure clinker components (C_3S, C_2S, C_3A, C_4AF...).

Determination of C_3S

The systematic study of the behaviour of these components in CO_2 atmosphere allows to state that C_3S only (after the possible elimination of free lime) binds CO_2 according to the theoretical equation $SC_3 + CO_2 \rightarrow CO_3Ca + SC_2$. The importance of the binding allows one to estimate the SC_3 content. In reality, the reaction is more complex (19) and it really results in a mixture of spurrite and CO_3Ca. An addition of F_2Ca leads more rapidly to the compelte equilibrium (48, 53). This determination offers the advantage of being liable to be achieved on ground cement

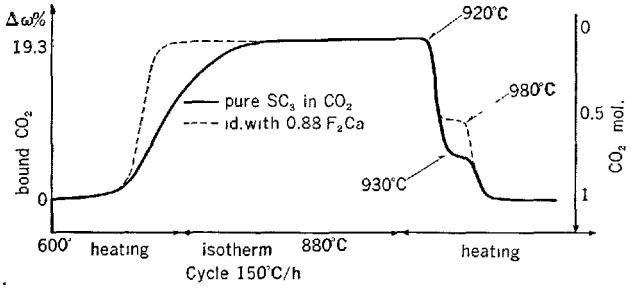

Fig. 8. *Reactions between* CO_2 *and* SC_3
—Pure SC_3 fixes one mole CO_2 per mole SC_3. A mixture of variable composition is formed. This binding allows the determination of SC_3 in clinkers.
----With fluoride, the reaction is faster and reproducible. Spurrite $Ca_5(SiO_4)_2CO_3$ is quantitatively formed as per equation $2SC_3 + 2CO_2 \rightarrow CO_3Ca + (SC_2)_2CO_3Ca$ (spurrite).

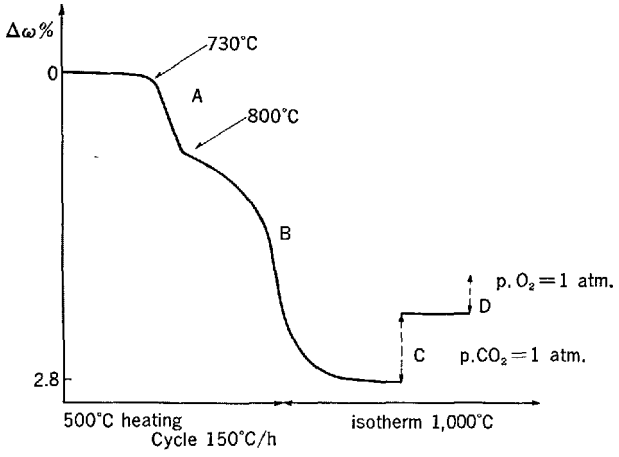

Fig. 9. *Oxide-reducing study of a clinker.*
A. Reduction of SO_4K_2 or SO_4Na_2
B. Reduction of SO_4Ca and C_4AF } by H_2 atm.
Distillation of SNa_2 and SK_2
C. Oxidation of Fe at 1,000°C by CO_2 atm.
D. Oxidation of SCa 1,000°C by O_2 atm.

and of being of a precision comparable with the methods of determination by X-ray diffraction. (Fig. 8).

Oxidoreduction Reactions

The behaviour of the alumino ferrite phase and sulphated combination in hydrogen atmosphere, already mentioned (25) allows one to indicate the quantity of iron having reacted and the nature of sulphated phases existing by the action at 1,000°C, after reduction and elimination by volatilization of alkali sulphide, of CO_2 first oxidizing of reduced iron) then O_2 (oxidizing of SCa into SO_4Ca) (Fig. 9).

Preparation of Pure Compounds

The checking of the reactivity of the initial mixtures intended to the preparation of calcium silicates or aluminates has led to recommend the general method of coprecipitation from homogeneous solutions of the components (calcium nitrate, aluminium nitrate, colloidal silica gel. . . .) in order to obtain the close contact of the reagents (19). The fact that the weight balance is known enables one to verify the compound formula from the changes in weight: thus the $4\,CaO_3 \cdot Al_2O_3 \cdot SO_3$ compound has been made clear in the CaO, Al_2O_3, SO_3 system (54), the reactions of CO_3Ca with SO_2 in oxidizing environment have been stated (55) and the simple or composite ferrite stoichiometry has been better defined (56).

Addition Products

Calcium Sulphates

Before addition to the clinker, the nature of the sulphate ($SO_4Ca \cdot 2H_2O$, generally) and its purity are of easy determination. After grinding, the more delicate problem of the state of hydration is raised. Solutions have been offered for the mixtures of pure components, as plasters, for instance (57, 58) but the low relative sulphate content of cement makes the determination more complex.

Blast-Furnace Slags

The slags contain reductant substances and show a gain in weight after the roasting above 700°C in air environment. In inert atmosphere takes place the real loss (19). To the roasting, a devitrification is joined, and so the thermal analysis of a slag cement often uses both the two techniques DTA and TGA (48, 59, 60).

Thermic Power Station Ashes

No marked characterization for these products except the determination of the unburnt substances, made easier, if necessary, by a pure oxygen environment.

Cements

The Problem of Free Lime

The free calcium oxide of the clinker hydrates more or less completely during the making of cement and may, if noticeable quantities are left, cause prejudicial swellings after use. The usual chemical methods give the sum: $CaO + Ca(OH)_2$, the thermogramme measures $Ca(OH)_2$ and free CaO is deducted by difference. In order to avoid the uncertainties of the chemical titration, it is possible, by starting from Bied's observations (61) to achieve a preferential hydration of free CaO at 250°C in the water-vapor, at the atmospheric pressure. The comparison between the thermogramme, after the hydration and the thermogramme of the initial sample, allows an easy estimation of free CaO which may be corrected of a casual carbonation (Fig. 10). This method (62, 19) has been compared with the chemical or physical methods (63 and 64).

Aeration of Cements (19)

The hydraulic properties of a cement are altered when left for a long time in air environment. Thermogravimetry contributes to the study of this phenomenon (Fig. 11). The small variation of $Ca(OH)_2$ content seems to prove a superficial attack of the anhydrous components by atmospheric water and CO_2 with a cumulative formation of CO_3Ca and rather loose bindings of water which are shown by the dotted curve obtained after alcohol treatment according to Hayden (65). Besides the determination of C_3S which has already been described (19) shows the decrease of the content of this phase. Let us remark, too, a formation of syngenite $(SO_4)_2\ K_2Ca \cdot H_2O$ in a study on the clodding during aeration (66).

Loss on Ignition of Cements

When oxidizable compounds are lacking, the thermogramme differenciates the loss on ignition into three areas (Fig. 11). The first one corresponds to water fixed on SO_4Ca and eventually aeration water, the

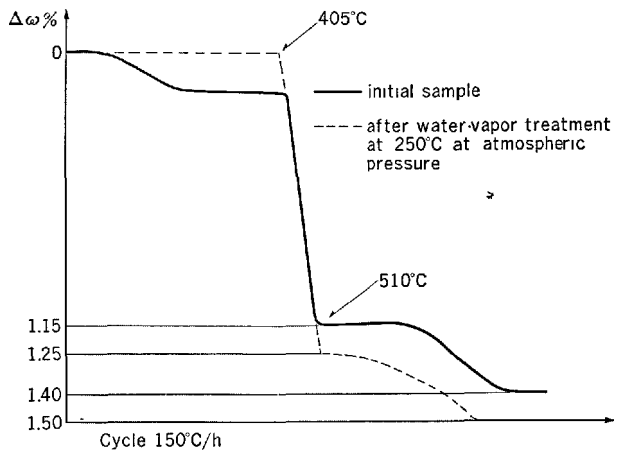

Fig. 10. *Determination of free* CaO *and* $Ca(OH)_2$. *Water loss due to the free* CaO *hydration:* $1.25 - 1.05 = 0.15\%$ *or in* CaO *content:* $\frac{0.15 \times 56}{18} = 0.46$

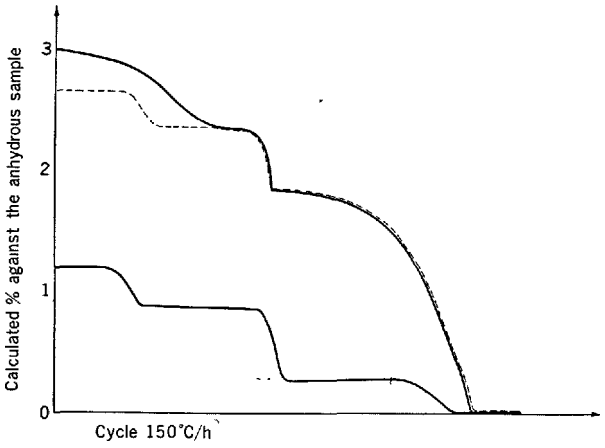

Fig. 11. *Aeration of a CPA.*
A. initial sample
B. after aeration
C. aerated cement treated by Hayden method.

second one to water fixed on $Ca(OH)_2$ and the third on to CO_2 fixed on CO_3Ca. In presence of reductors (slags, unburnt substances) an inert environment enables one to avoid the oxidizing but secondary reactions may be observed (62,19).

Hydrated Products

Hydration forms an important fundamental part of cement chemistry liable to have numerous thermogravimetric applications

Pure Compounds

The first study on the hydrates of cement chemistry appears to be Lefol's thesis (67). Since then the method has been often used to measure the stage of progress of the hydration reaction by evaluating the quantity of released $Ca(OH)_2$, (68, 69). As this quantity does not perhaps represent all the released lime (70) the DTGA brings some precisions (71, 72). The beginning of a thermogramme of an hydrated product depends on the evolution of the different existing hydrated phases; according to the heating rate and the water vapor pressure which are in the shell. Numerous checkings are necessary to definite the system, we have already referred to the study on the calcium aluminates (24). The zeolithic water may also be indicated in certain cases (73).

Cement Pastes, Mortars, Concretes

The technological studies are numerous. They use almost exclusively the changes of the $Ca(OH)_2$ content to follow the different studied phenomena: setting and hardening (74, 75), influence of thermal treatments (76, 77, 78, 79), resistance to corrosion (80) action of accelerators and retarders (81). The action of CO_2 under pressure on $Ca(OH)_2$ and the concretes have been subject to a particular examination (82). The pozzolanic activity of an addition can be evaluated by comparing the quantities of released $Ca(OH)_2$ during the hydration, in comparable conditions, for the same binder, either with an addition of pozzolane, or of an equal quantity of inert substance (19).

Various Considerations

We shall only mention, in this chapter, a certain number of references regarding articles issued from the previous headings but which have a general interest for cement chemistry. Application of thermogravimetric analysis to building materials, to the study of soils (83, 84), to refractory rocks (from 85 to 88), to different minerals: asbestos (89, 90), brucite (91), siderite (92), oxidized compounds (93), zeolites (94), phosphate cements (95) and at last to fundamental problems: action of fluoride on kaolin (96), dehydroxilation of kaolinite (97), study of Fe-Mg spinel (98), evaporation and dehydration (99) and on adsorbed water (100).

References

1. W. Nernst, E. H. Riesenfeld, Chem. Ber, **36**, 2.086 (1903).
2. K. Honda, Sci. Repts Tohoku Imp. Univ. **4**, 97 (1915); C.A., 2.610 (1915).
3. C. Duval, Inorganic Thermogravimetric Analysis, 2nd ed. (Elsevier Publ. Comp., Amsterdam, London, New-York, 1963).
4. A. W. Coats and J. P. Redfern, "Thermogravimetric analysis", Analyst, **88**, 906–24 (1963).
5. C. B. Murphy, "Thermal analysis", Anal. Chem. **36**, No. 5, part **1**, 347 R-354 R (1964).
6. P.F.S. Cartwright and D.W. Wilson, "Analytical chemistry", Annu, Rep. Progr. Chem. **57**, 410–61 (1960).
7. H. Saito, "Developments of the thermobalance during the past fifty years and description of a new apparatus for simultaneous D.T.A. and T.G.A. measurements", (in Japanese), Jap. Analyst. **13**, No. 9, 941–9 (1964).
8. C. B. Murphy, "Thermal analysis", Anal. Chem. **38**, No. 5, 443 R-451 R (1966).
9. M. J. Katz, Vacuum Microbalance Techniques, **1** (Plenum Press, New-York 1960).

10. R. F. Walker, Vacum Microbalance Techniques, **2** (Plenum Press, New-York 1961).
11. K. H. Behrndt, Vacuum Microbalance Techniques, **3** (Plenum Press, New-York 1963).
12. P. M. Waters, Vacuum Microbalance Techniques, **4** (Plenum Press, New-York 1965).
13. K. H. Behrndt, Vacuum Microbalance Techniques, **5** (Plenum Press, New-York 1966).
14. A. W. Czanderna, Vacuum Microbalance Techniques, **6** (Plenum Press, New-York 1967).
15. C. Eyraud, M. Cronenberger and M. Cogniat, "Thermogravimetry", (in French), Tech. Ing. 880.1–880.13 (1962).
16. P. F. Woerner and G. F. Wakefield, "High temperature thermobalance", Rev. Sci. Instrum. **33,** No 12, 1.456–7 (1962).
17. P. W. Selwood, Magnetochemistry, (Inters. Publis. New-York 1956).
18. C. J. Keattch, "Thermal standards in thermogravimetry", Talanta 14, No 1, 77–83 (1967).
19. P. Longuet, "Applications of the thermogravimetry to the cement chemistry", (in French), Revue des Matériaux de Construction No 537, 140–8: No 538–9, 183–9; No 540, 233–43 (1960).
20. Raoult, Scientia, No 13, 13 (Oct. 1901).
21. Pascal, Nouveau Traité de Chimie Minérale, vol. 1 (Masson Publisher, Paris 1956) Edited by P. Pascal. "Water association systems and compounds" (in French) 526–564.
22. E. Bader, Zentralbl. Miner. Geol. 96 (1940).
23. P. Longuet, "Thermogravimetric studies with vaporous water saturated atmosphere", (in French), Congr. of Industrial Chemistry, Bordeaux, France 1961.
24. F. Lavanant, "Contribution to the study of some hydrated calcium aluminates", (in French), Revue des Matériaux de Construction No. 592–3–4–6–5–7 (1965).
25. P. Longuet, "Study of some oxido-reduction reactions in cement chemistry", (in French), Silicates Industriels, Bruxelles, **26,** No. 10, 463–6 (1961).
26. Ch. Kiefer, "Stability and classification of phyllitic minerals-applications to cementry clays", (in French), Revue des Matériaux de Construction No. 422 to 432 (1951).
27. S. Shimoda, "Mineralogical studies on the garnierite and aquacreptite", Clay Sci. Jap. **2,** No. 1, 8–21 (1964).
28. L. Stoch, "Thermal dehydroxilation of minerals of the kaolinite group", Bull. Acad. Polon. Sci., Ser. Sci. Geol. Geogr. **12,** No. 3, 173–80 (1964).
29. H. Micheelsen, "Thermal analysis of three Danish flint types", Thermal Analysis-Proc. 1st intern. Congress Aberdeen, MacMillan, London, p. 230 (1965).
30. H. Minato, "Dehydration curves of kaolin minerals, especially in hydrated halloysite", Thermal Analysis-Proc. 1st intern. Congress Aberdeen, MacMillan, London, p. 199 (1965).
31. G. Fiedler and R. Wagner, "Results of examinations of different montmorillonites with the derivatograph", (in German), Thermal Analysis-Proc. 1st intern. Congress Aberdeen, MacMillan, London, p. 204 (1965).
32. T. Takats, "Thermal investigations in the silicate industry"—Proc. of the 7th Conference on the Silicate Industry 1963, Akademiai Kiado, Budapest, p. 87–113 (1965).
33. M. Boros, "Derivatographic investigation of clay mineral rehydrability"—Proc. of the 7th Conference on the Silicate Industry 1963, Akademiai Kiado, Budapest, p. 119–135 (1965).
34. M. H. Grange and G. Watelle-Marion, "Pressure-temperature diagram of the water-heulandite system and heulandite-metaheulandite transformation pattern", (in French), C. R. Acad. Sci. C., **263** No. 7, 517–20 (1966).
35. J. B. Holt, I. B. Cutler and M. E. Wadsworth, "Kinetics of the thermal dehydration of hydrous silicates", Amer. Chem. Soc. Abstr, Papers, No. 144, 28 B (1963).
36. C. H. Horte and J. Wiegmann, "Thermal investigations of different kaolinites samples", (in German), Silikat Technik, No. 1, 16–20 (1967).
37. R. Pampuch, "Influence of particle size on the mechanism of thermal decomposition reactions of layer-lattice silicates and hydroxides", Siliconf 1967, 9th Conference on the Silicate Industry, Budapest, p. 24–29 (1967).
38. W. Lodding and H. P. Vaughan, "Determination of strain energy in muscovite by simultaneous differential thermal analysis-thermogravimetric analysis", Thermal Analysis—Proc. 1st intern. Congress Aberdeen, MacMillan, London, p. 191 (1965).
39. W. Bodenhelmer, B. Kirson and S. Yariv, "Organo metallic clay complexes", Israel J. Chem. 1 No. 2 69–78 (1963).
40. V. S. Ramachandran and K. P. Kacker "The thermal decomposition of dye-clay mineral complexes", J. Appl. Chem. G. B. **14,** No. 10, 455–60 (1964).
41. J. R. Wright, I. Hoffman and M. Schnitzer, "Application of thermogravimetry to the analysis of carbonate occuring in soils", J. Sci. Food Agric. G. B., **11,** No. 3, 163–72 (1960).
42. T. Takats and M. Boros, "Investigations of the raw-materials in the silicate industry with the derivatograph", (in German), Silikat Technik, **14,** No. 1/2, 1–8 (1963).
43. L. Erdey, F. Paulik and J. Paulik, "Newer results of thermoderivatography", Mikrochim. Acta No. 4–5, 699–712 (1966).
44. P. Longuet, "Thermogravimetric study of limestones pastes in carbon dioxide atmosphere", (in French), Congrès de Céramique 1960, Bulletin de la Société Française de Céramique No. 48.
45. B. Courtault, "Reactivity of the raw-materials in cement industry", (in French), Silicates Industriels No. 3 (1962).
46. B. Courtault, "Reactivity of $CaCO_3$ with SiO_2 and Al_2O_3 in presence of alkaline and alkaline-earth halogenated compounds", (in French), 33th Congrès Chimie Industrielle, Bordeaux (1961).
47. P. Longuet and B. Courtault, "Clinkerisation of the cement raw materials", (in French), Journées Régionales du Ciment, Marseille 1963, Publ. Tech. du

CERILH, Paris, No. 155, p. 20.
48. B. Courtault, "Investigation of solid state reactions up to 1,600°C, by differential thermal analysis—applications to the cement chemistry", (in French), Revue des Matériaux de Construction No. 569 to 573, (1963).
49. B. Courtault, "Study of the mineralisation by calcium fluoride-particularly in the SiO_2–CaO–CO_2 system", (in French), Techniques et Economie Industrielles No. 2, (1965).
50. B. Courtault, "Synthesis of spurrite", (in French), Bull. Soc. Franc. Mineral. Crist. No. 4, 527 (1964).
51. A. Deudosz and A. Karcz, "Thermogravimetric study of coal degasification", Zesz. Nauk. Akad. Gorn. Hutn. Krakovie Metal. Odlew, **6**, 121–136 (1966).
52. P. Longuet, "Compounds thermogravimetric study in CO_2 of the pure clinker components", (in French), 31e Congrès de Chimie, Liège, Belgique, (1958).
53. P. Longuet and B. Courtault, "Thermal analysis in cement chemistry", Journées Internationales des Silicates—Bruxelles (1961).
54. J. A. Forrester, "Two examples of thermogravimetric applications to the cement chemistry", Thermal Analysis—Proc. of the 1st intern. Congress Aberdeen 1965, MacMillan, London, p. 258 (1965).
55. Pechkovsky, Ketov, Malceva and Pridatchenkov, "Thermogravimetric study of the reaction between SO_2 and $CaCO_3$ in oxidising atmosphere", Izvest. Vyssh. Luchebn Zabel. Khim Tekhnol. SSSR, **6**, No. 6, 991–6 (1963).
56. E. D. Macklen, "Thermogravimetric investigations of the preparation of ferrites from metal oxalates", Thermal Analysis—Proc. 1st intern. Congress Aberdeen 1965, MacMillan, London, p. 244 (1965).
57. C. J. Keattch, "Determination of the hydrates of calcium sulphate by thermogravimetric analysis", Thermal Analysis—Proc. 1st intern. Congress Aberdeen 1965, MacMillan, London (1965).
58. C. J. Keattch, "Analysis of gypsum plasters and minerals by thermogravimetry", J. Appl. Chem. London, **17**, No. 1, 27–8 (1967).
59. O. P. Mtschedlow-Petrossian, N. A. Lewtschuk and I. S. Sstrelkowa, "Thermal determination of slags quality and quantity introduced in cements", (in German), Silikat Technik, **13**, No. 5, 153–156 (1962).
60. J. E. Krüger, "The study of blast furnace slag by means of thermal analysis", Thermal Analysis—Proc. 1st intern. Congress Aberdeen 1965, MacMillan, London, p. 269 (1965).
61. Bied, "Industrial investigations on the limes, cements and plasters", (in French), Dunod, Paris (1926).
62. P. Longuet, "Thermogravimetric study of the loss on ignition of cements", (in French), 29 ème Congrès de Chimie Industrielle, Paris (1956).
63. R. Sierra, A. Bernard and J. Louvrier, "Free lime in cement: its determination" (in French), Chimie Analytique, **49**, No. 7, 363–70 (1967).
64. T. Gacesa, "Methods for determination of free $Ca(OH)_2$ in cement clinker and hydrated cement" Cement (Zagreb), **10**, No. 1 12–18, (1966).
65. R. Hayden, "New research for the determination of free lime in portland cement", "The water bound by cement", "The setting of portland cement", (in German) Zement-Kalk-Gips No. 2, 36, (1950); No. 3, 120 (1956); No. 1, 16, (1957).
66. J. Forest, "Investigation on the clodding of some cements", (in French), Revue des Matériaux de Construction, No. 557, 35–41 (1962).
67. J. Lefol, "Hydration of aluminates, double salts, calcium silicate and sulphate", (in French), Soc. Gen. Imprimerie et Edition, Sens, France (1937).
68. A. Nicol, "Development of crystallized calcium silicates and aluminates with little but enough water to make paste", (in French). Revue des Matériaux de Construction, No. 477–478–479, (1955).
69. Z. Adonyi, G. Y. Gyarmathy, Y. Kilian and I. Szekely, "Thermogravimetric examination of the hydration process in tricalcium aluminate and tricalcium aluminate + gypsum" (in Hungarian), Siliconf 1967, 9th Conference on the Silicate Industry, Budapest, p. 50–54 (1967).
70. S. Brunauer and S. A. Greenberg, "The hydration of tricalcium silicate and β dicalcium silicate at room temperature" 4ème Symposium International de la Chimie du Ciment, Washington, (1960).
71. A. Van Bemst, "Study on hydration of pure calcium silicates" (in French), Bull. des Soc. Chim. Belges, No. 64, 333–351, (1955).
72. W. L. de Keyser, R. Derie and A. Van Bemst, "Application of differential thermogravimetry to the study of the hydration of cements", Symp. Struct. Portland Cement Paste Concrete, Washington D. C., p. 398–405, (1966).
73. M. H. Grange, "Identification test of zeolitic water in hydrates, in D.T.A. and thermogravimetry", (in French) C.R. Acad. Sci. **259**, No. 19, 3, 277–80 (1964).
74. F. Paulik, G. Liptay and L. Erdey, "Derivatographic study of hydration in cement", Thermal Analysis. Proc. 1st Intern. Congress Aberdeen, MacMillan, London, p. 267 (1965).
75. G. V. Topil'skij, J. M. Butt and V. M. Kolbasov, "Influence of the water-cement ratio on the hardening process, the structure and properties of the cements, at low temperatures", (in Russian), Moskov. khim. tekhnol. Inst. D. I. Mende Leeva Trudy, No. 50 107–12, (1966).
76. J. Kilian and I. Skekely, "Structure of cement and concrete stones after vaporous treatment", (in Hungarian), Epitoanyag, Magyar, **19**, No. 2, 41–8, (1967).
77. R. Kovacs, "Thermal analysis of set cements", Proc. 7th Conf. Silicate Industry, Budapest 1963, Akademiai Kiado, Budapest, (1965).
78. Z. Sauman, "Study of the hydration of 3 $CaO \cdot SiO_2$ and β 2 $CaO \cdot SiO_2$ under hydrothermal conditions", (in Czech.) Silikaty, Czeskoslo, **8**, No. 3, 185–195, (1964).
79. J. Gebauer and I. Odler, "Hydration of the cement during thermal treatment", (in German), Zement-Kalk-Gips, **55**, No. 6–7, (1966).
80. R. Greschuchna and M. Boros, "Influence of special ferrari cement clinker composition on the corrosion resistance of mortars and concretes", (in German), Siliconf 1967, 9th Conf. on the Silicate Industry Budapest, p. 279–283, (1967).
81. F. Tamas and G. Liptay, "A thermoanalytical investi-

gation of accelerators and retarders and their mechanism", Proc. of the 8th Conf. on the Silicate Industry, Budapest, Akademiai Kiado Budapest, p. 299–305, (1965).
82. C. Chauvel-Trepier and M. Murat, "Application of thermogravimetry with pressure to the study of carbonation of calcium hydroxide and concrete", (in French), Revue des Matériaux de Construction, No. 625, 369–72, (1967).
83. R. Sierra and A. Bernard, "Thermogravimetric analysis —applications to the study of soils, clays and cements", (in French), Bull. Liaison Lab. Rout. Fr., No. 5, 1–12, (1964).
84. C. J. Keattch, "The application of thermogravimetric analysis to the study of building materials", 35th Intern. Congress of Indust. Chemistry, Warsaw, (1964).
85. V. Locsei, "Thermogravimetric study of mullite formation in aluminium fluoride-laolinite system", (in Russian), Acta. Chim. Acad. Sci. Hungar. **40** No. 1, 79–97, (1964).
86. T. Földi, "Heat conductivity of monolithic refractories" (in Hungarian), Siliconf 1967, 9th Conference on the Silicate Industry, Budapest, p. 73–77 (1967).
87. J. Albert, "The chemical and mineral composition and the technological characteristics of brick 'clays" (in Hungarian), Siliconf 1967, 9th Conference on the Silicate Industry, Budapest, p. 322–327, (1967).
88. M. Revay, "Production and quality testing of high-alumina refractory cement manufactured in Hungary", (in Hungarian), Siliconf 1967, 9th Conference on the Silicate Industry, Budapest, p. 272–278, (1967).
89. J. C. Themier, "Study of asbestos chrysotile for industral use", Thesis, Ing. C.N.A.M., Paris, (1959).
90. D. J. O'Connor and J. H. Patterson, "The solid-state reaction of the thermal decomposition of Australian crocidolite in vacuum", Proc. of the 8th Conference on the Silicate Industry, Budapest, Akademiai Kiado, Budapest, p. 181–188, (1965).
91. H. Minato, "A thermogravimetric curve of brucite", Chem. Abstr. **66**, No. 26. 117–748d (1967).
92. E. A. Prodan, M. M. Pavlyuchenko, S. A. Slyshkina and V. A. Boiko, "Self disintegration and thermal decomposition of Bakalsk siderite in carbon dioxide atmosphere", (in Russian), Vestsi Akad. Navuk Belarus. SSSR. Ser. Khim. Navuk, No. 1, 23–7, (1967).
93. H. Uwents, "Analysis of oxide compounds by thermogravimetric methods", Intern. Symp. on Thermal Analysis, Northern Polytechnic, London (1965).
94. R. Otsuka, "Thermographs of some zeolites", Thermal Analysis, Proc. 1st Intern. Congress Aberdeen, MacMillan, London, p. 210, (1965).
95. J. Forest, "Research on cements bound with orthophosphoric acid and study of some aluminium phosphates", (in French), Revue des Matériaux de Construction, No. 580, 581, 582, 583, (1964).
96. A. Bien and W.L. de Keyser "The effects of aluminium fluoride on the thermal behaviour of kaolin", Clay Miner, Bull. G.B., **5**, No. 28, 80–9, (1962).
97. F. Toussaint and J. J. Fripiat, "Dehydroxilation of kaoli-nite", J. Phys. Chem. USA, **67**, No. 1, 26–30, (1963).
98. H. Schröder, "Fe^{2+} content and network defects concentration of Mg–Fe spinelles by thermogravimetric measurements" (in German), Monalslerich, dtsch. Akad. Wissenschaf, Berlin **4**, No. 2, 141–2 (1962).
99. Z. Adonyi, "Differential thermogravimetry for distinguishing between evaporation and decomposition in thermogravimetric analysis", Period Polytechni Chem. Enging, Hungary, **10**, No. 3, 325–34, (1966).
100. K. R. Lange, "Activation energy studies of the physically absorbed water on SiO_2 surface". Amer. Chem. Soc. Abstr. Papers, No. 147, 29–34, (1964);

Supplementary Paper I-64 On the Color Change of Portland Cement

Kiyoshi Miyazawa and Kinzo Tomita*

Synopsis

The cause of the color change of portland cement in presence of a small amount of MgO is studied by measuring the electrical specific resistance of synthesized C_4AF–MgO solid solution. The result obtained shows that lightness L and specific resistance tend to decrease with increasing of MgO content in analogous inclination.

The experiment may suggest that C_4AF–MgO solid solution contains, in its structure, somewhat free electrons or positive holes, which would increase the conductivity and as well respond to any wave length of the visible spectrum; thus leading to color change in black.

In addition, the color change of portland cement with the increase of rate of cooling is studied by measuring the color, strength, and heat of hydration of the prepared cements. These clinkers are cooled from 1450°C in following methods: that is, slow cooling, quenching in air, and quenching in water. When the clinker is quenched in air, the color of cement is more darkened than that of the clinker cooled slowly. If the clinker is quenched in water, the color of cement becomes yellow with the highest lightness. Strength test shows maximum strength can be obtained when the clinker is cooled slowly from 1450°C to 1250°C or above and then quenched in air.

X-ray diffraction of the interstitial materials of these clinkers shows that the change of d-spacings with the increase of rate of cooling gives different inclination from that with the increase of C_2F content in system C_2A–C_2F.

When quenched in nitrogen, the color of the clinker becomes as yellow as that of the clinker quenched in water. X-ray diffraction patterns of the interstitial material of the clinker quenched in nitrogen agree with those of the clinker quenched in air. This fact may suggest that light color of the clinker quenched in water is not due to freezing the iron-containing liquid to glass, but to the absence of oxygen.

Introduction

Color of portland cement is changeable with innumerable factors. In this report, effect of MgO contained in clinker, and that of cooling rate were studied.

Effect of MgO on the Color of Portland Cement

The Color of the Prepared Cement (1)

It is well-known that portland cement is darkened by small amounts of MgO. K. Fujii and K. Asaoka (2) have took the lead in this subject. Practically, MgO is useful not only for obtaining a slate-gray color, but also for promoting a strength of the cement. However, the reason of the above color change has not been clarified yet.

Three kinds of original raw mixes of portland cement, i.e. normal type (type N), high early strength type (type H), and moderate heat type (type M) were made from pure chemical reagents to which magnesium carbonate were added so as to contain MgO 0 to 3% on nonvolatile basis. The chemical compositions of the clinkers resulting from original raw mixes are shown in Table 1. These raw mixes were burnt at 1450°C for half an hour. Produced clinkers were

Table 1. *The chemical compositions of the prepared clinkers resulting from original raw mixes*—(%)

	Loss	SiO_2	Al_2O_3	Fe_2O_3	CaO	MgO	Na_2O	K_2O	HM	SM
Type N	0.2	23.4	5.3	3.4	67.4	0.08	0.03	0.02	2.10	2.7
Type H	0.4	22.3	5.3	3.2	68.6	0.07	0.05	0.02	2.23	2.6
Type M	0.2	24.4	4.8	4.2	66.4	0.06	0.01	0.02	1.99	2.7

*Sumitomo Cement Co., Ltd, Tokyo, Japan.

ground with adequate amounts of natural gypsum as shown in Table 2.

The color of the prepared cement was measured by means of the photo-electric color difference meter. The prepared cement was packed into a capsule made by transparent glass. The light beam was reflected at the capsule and the reflected light was converted to electric current by the photo-cells which were fitted in three windows with color filter. The color was measured reading the current and indicated L, a, and b color scale values (3). L indicates lightness, and $+a$, $-a$, $+b$ and $-b$ indicates degree of red, green, yellow and blue respectively (Fig. 1).

The color of the prepared portland cement was given in Fig. 2 as function of MgO content.

As to value L, all types of the cement have a minimum point in the range of 1 to 2% in weight of MgO.

The Color of Ferrite Phase (1)

The color of ferrite phase, which may principally dominate the color of cement, was examined. Raw mixes composed of the formula $4\{(1-x)\mathrm{CaO}\cdot$

Table 2. *Properties of the prepared cement*

	SO_3(%)	Specific surface (cm²/g)	F. CaO(%)
Type N	1.6	3200 ± 100	< 0.2
Type H	2.3	4300 ± 100	< 0.6
Type M	1.6	3200 ± 100	< 0.3

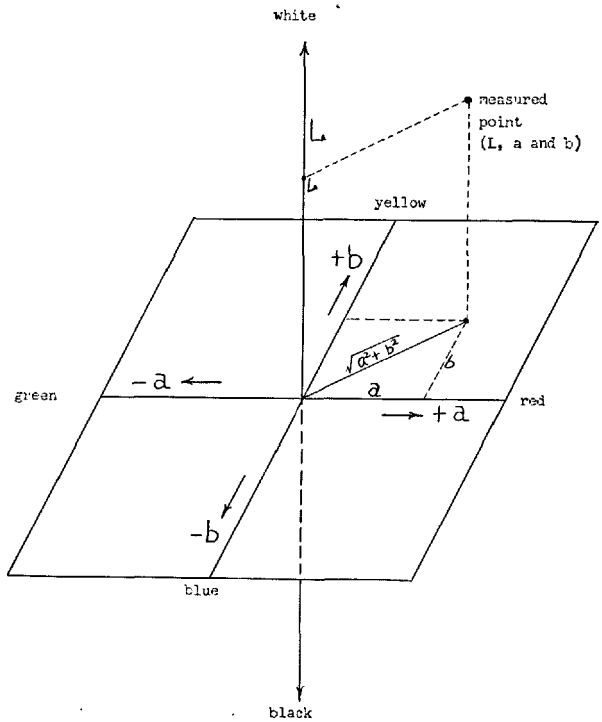

Fig. 1. *Color diagram of L, a and b color scale system.*

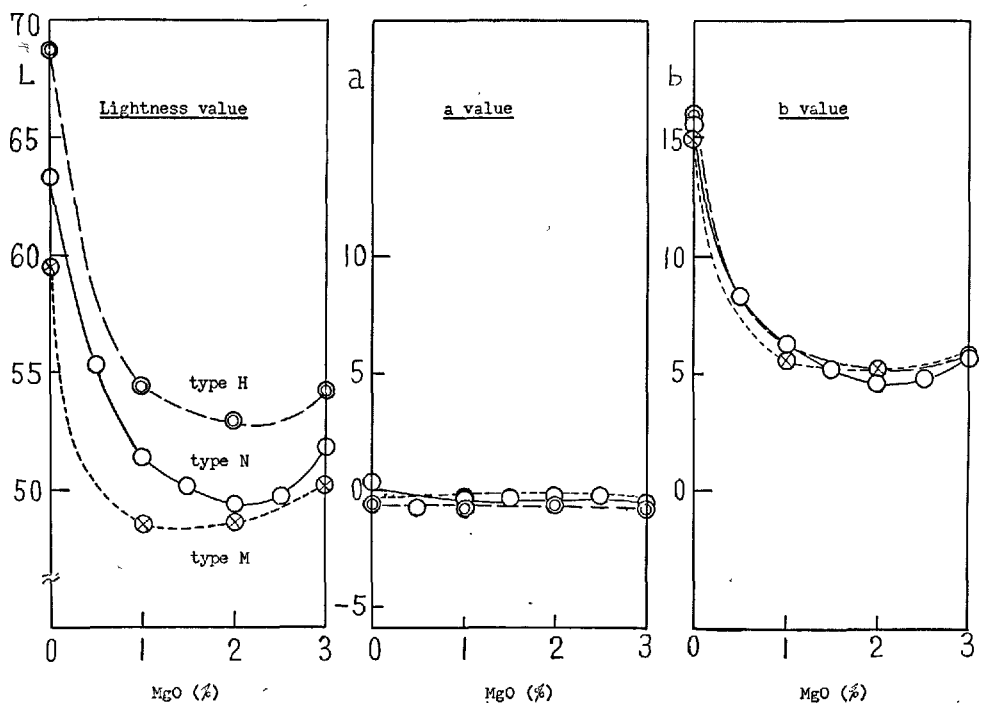

Fig. 2. *The color of the prepared cement.*

$xMgO\}Al_2O_3 \cdot Fe_2O_3$ were made from pure chemical reagents and burnt somewhat below their melting point and cooled quickly. The chemical compositions of the ground clinkers are shown in Table 3 and the lightness values of them are shown in Fig. 5.

Lightness L of the ferrite decreases with the increase of MgO content and has the minimum at 4.5 to 6 moles % of MgO, in agreement with the solubility limit of MgO in C_4AF, as clarified in our previous report (4).

Electrical Specific Resistance of Ferrite Phase

The ferrite shown in Table 3 were examined by X-ray diffractometer. In this study, it is found that d-spacing for (141) expands with the increase of MgO content and becomes unchangeable at 4.5 to 6 moles % of MgO; however, intensity of the reflection lines of X-ray diffraction is almost unchangeable. Therefore, cause of the color change cannot be explained by the slight change of crystal structure of ferrite phase directly.

In this report, the cause of above color change was studied by measuring the electrical specific resistance of synthesized C_4AF–MgO solid solution.

The specimens were made by compressing the synthesized ferrites in a steel mold under a pressure of 300 kg/cm², to form disks of 40 mm in diameter, about 5 mm in thickness and by reheating at 1200, 1250 and 1300°C respectively. The specimens were coated by the conductive silver coating material as shown in Fig. 3 and put between electrode as shown in Fig. 4.

Each of the specific resistance values of the specimens, as shown in Fig. 5, was measured by the microamperemeter at 50 volts and calculated from following formulas.

ρ: specific resistance (Ω-cm) $= A \cdot R/d$
A: available area of specimen (cm²) $= \pi \cdot r_0^2$, $r_0 = (r_1 + r_2)/2$
d: thickness of specimen (cm)
R: Resistance (Ω) = voltage/current

The bulk specific gravities of the specimens depended on the reheating temperature as shown by following results: — about 2.3 g/cm³, 2.5 g/cm³ and 3.2 g/cm³ at 1200°C, 1250°C, and 1300°C respectively; however, they did not depend on the MgO content. The result obtained showed that lightness L and specific resistance tended to decrease with the increase of MgO content in analogous inclination (Fig. 5).

Somewhat higher resistance of the specimens reheated at 1200°C may be affected with the insufficiency of

Table 3. *The chemical compositions of the prepared C_4AF–MgO system*

Comp. No.	Replaced MgO (moles %)	Oxide analysis—(%)			
		CaO	Al_2O_3	Fe_2O_3	MgO
Co	0	46.16	20.98	32.86	0.00
$C_{1.5}$	1.5	45.56	21.02	32.92	0.50
$C_{3.0}$	3.0	44.95	21.06	32.99	1.00
$C_{4.5}$	4.5	44.34	21.11	33.05	1.50
$C_{6.0}$	6.0	43.73	21.14	33.12	2.01
$C_{9.0}$	9.0	42.50	21.23	33.25	3.02

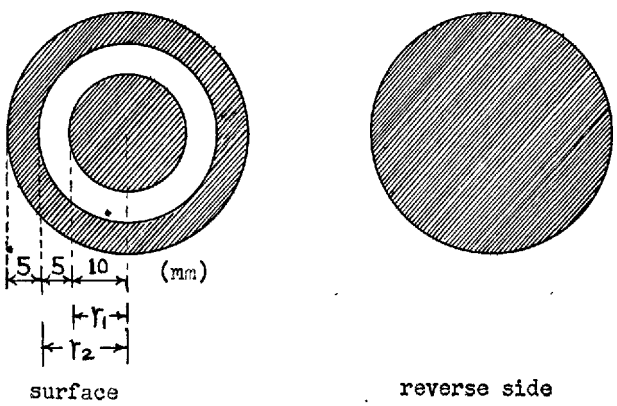

Fig. 3. *Specimen coated by silver coating material:—coated part is indicated by shading.*

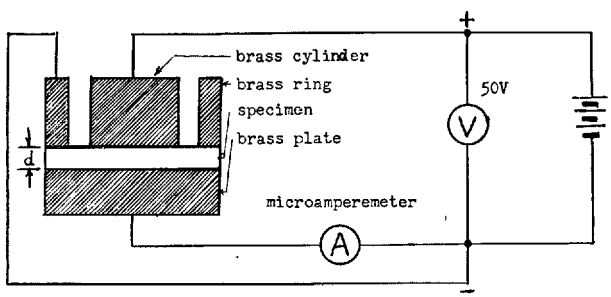

Fig. 4. *Circuit diagram for specific resistance measurement.*

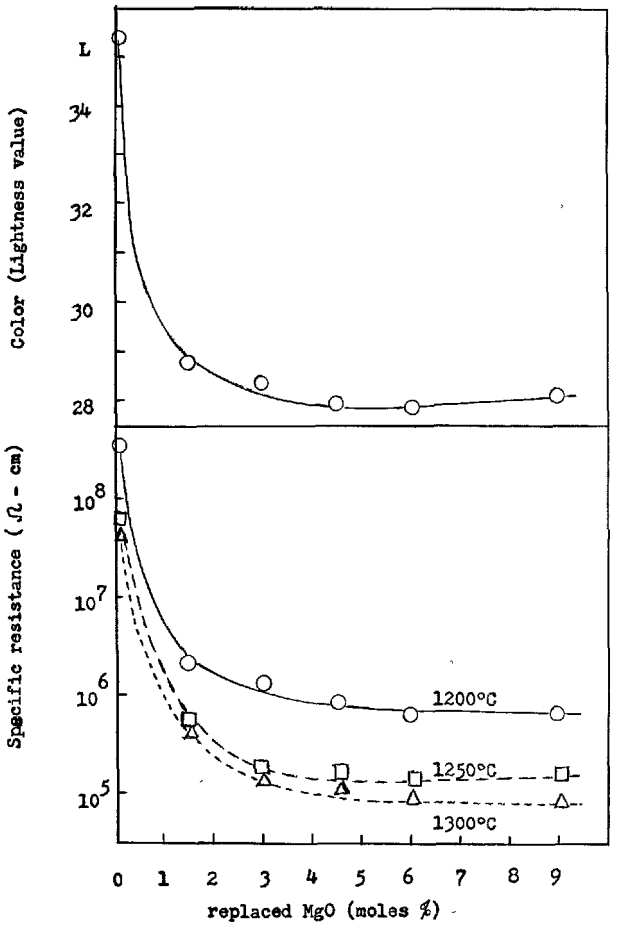

Fig. 5. *The color and the electrical specific resistance of* C_4AF *as a function of* MgO *moles %.*

sintering. The curve of the specimens burnt at 1250°C almost agreed with that of the specimens burnt at 1300°C in spite of considerable difference of bulk specific gravities.

Discussion on the Color Change of Ferrite Phase by Small Amount of MgO

Because the color of C_4AF–MgO becomes darkest when MgO ranges from 4.5 to 6 mol. % (1.5 to 2% by weight), in agreement with the solubility limit of MgO in C_4AF, the above color change may be due to incorporation of MgO into ferrite phase. However, it is considered that the color change cannot be explained by a slight change of some spacings of C_4AF–MgO solid solution.

As mobility of ions increases at high temperature, specific resistance at high temperature may be affected by ionic conduction; however, above measuring being carried out at room temperature, the increase in the electrical conductivity was considered to be caused by the increase in electrons playing as carrier.

The experiment may suggest that C_4AF solid solution with MgO contains, in its structure, somewhat free electrons or positive holes, which would increase the conductivity and as well respond to any wave length of the visible spectrum; thus leading to color change in black (5). As an example, it is possible that positive holes are brought about by substitution of Mg^{2+} ions for Fe^{3+} ions.

Effect of Rate of Cooling on the Color of Portland Cement

Effect of Cooling Rate on the Properties of Portland Cement

In cement clinker burning, effect of cooling rate is more important for strength and heat of hydration of cement than the matter of color. On the color, it is said that the color of clinker quenched in air is darkened than that of the clinker cooled slowly. Light color of the clinker quenched in water takes advantageous to white cement production.

Two kinds of industrial raw mixes used in A or B works, were put into a electric furnace and heated at a rate of 180°C/hour and held at 1450°C for half an hour. After burning, they were cooled by five following methods:—

a) cooled slowly: the clinkers were cooled at a rate of 100°C/hour up to 1000°C; and then cooled with the furnace to room temperature.
b) quenched in air (1250): the clinkers were cooled at a rate of 200°C/hour up to 1250°C; and then taken out from the furnace to air.
c) quenched in air: immediately, the clinkers were taken out from the furnace to air.
d) quenched in water (1250): the clinkers were cooled at a rate of 200°C/hour up to 1250°C; and then the clinkers taken out from the furnace were put into water and dried.
e) quenched in water: immediately, the clinkers taken out from the furnace were put into water and dried.

The chemical compositions of the clinkers quenched in air are shown in Table 4.

Produced clinkers were ground with adequate amounts of natural gypsum containing 44.6% of SO_3 as shown in Table 5. The color of the prepared cement was shown in Table 6.

When the clinker is quenched in air, the color of cement is more darkened than that of the clinker cooled slowly. If the clinker is quenched in water, the color of cement becomes yellow with the highest lightness as shown in Table 6. The difference of color between A and B is small because the specific surface, and Fe_2O_3 or MgO content of the cement A are almost equal to the cement B.

In addition, the color of the cement almost depends on the color of its ground clinker containing no gypsum. At same finesnes, the color of the cement is almost equal to its ground clinker.

The strength of these cement mortars was measured by means of JIS R 5201 and heat of hydration was tested also by means of JIS R 5203. The result obtained is shown in Table 7 and Table 8.

Table 4. *The chemical compositions of the clinkers (Quenched in air)*—(%)

	Loss	SiO_2	Al_2O_3	Fe_2O_3	CaO	MgO	SO_3	Na_2O	K_2O	HM	SM
A	0.1	23.4	5.1	3.3	65.9	1.2	0.1	0.36	0.32	2.07	2.8
B	0.1	22.0	5.8	3.2	66.5	1.4	0.1	0.32	0.30	2.15	2.4

Table 5. *Properties of the prepared cement*

	SO_3(%)	Specific surface (cm^2/g)	F. CaO(%)
A	1.6	3200 ± 100	< 0.7
B	1.6	3200 ± 100	< 0.9

Table 6. *The color of the prepared cement*

Cooling condition	Cement A			Cement B		
	L	a	b	L	a	b
Cooled slowly	52.8	−0.6	+6.2	53.0	−0.6	+7.0
Quenched in air (1250)	48.0	−0.3	+6.6	49.4	−0.3	+7.1
Quenched in air	47.0	−0.1	+6.6	48.4	−0.3	+7.1
Quenched in water (1250)	63.5	+0.3	+15.0	66.2	+0.2	+15.2
Quenched in water	67.4	+0.6	+16.1	67.3	+0.3	+15.9
Industrial cement*	48.1	±0.0	+7.3	50.4	−0.3	+7.3

*These industrial cements are produced by A or B works. Chemical composition and fineness are somewhat different from the prepared cement.

It is well-known that the higher strength of cement is obtained when a clinker is cooled slowly from the sintering temperature to about 1250°C, and then quenched in air. As shown in Table 7, this result agrees with this experience. Moreover, maximum strength is obtained when clinker is quenched from higher temperature above 1250°C. The cement prepared from clinker of water quenching shows retardation of setting and lower strength at 3 days; but the strength of 28–91 days approaches to that of air quenching.

Heat of hydration may tend to increase correspondingly with their strength; however, the difference of heat of hydration with the increase of cooling rate is so small that the ratio of heat of hydration to strength for higher strength cement is smaller than that for lower strength cement.

The color of hydrated cement paste was measured also. The color of hydrated cement may be considerably changeable depending upon its hydrating conditions.

In this test, the cement prepared above was mixed with water (W/C = 0.30), spread on glass plate and then cured in damp closet for 24 hours, and then the specimens were put into boiling water for 90 minutes, and dried in air.

The surface color of the prepared specimens was measured and the results were shown in Table 9.

In roughly speaking, the color of hydrated cement paste depends on the color of dry cement; however, the difference in the lightness values of hydrated cement is smaller than that of dry cement and the lightness values of cement cooled slowly are rather lower than that of cement quenched in air. The lightness values of the hydrated cement B containing high calcium are higher than those of the hydrated cement A containing low calcium.

Table 7. *The strength of the prepared cement mortar**

	Flow	Bending strength (kg/cm^2)				Compressive strength (kg/cm^2)			
		3d	7d	28d	91d	3d	7d	28d	91d
A cooled slowly	228	29.4	41.7	52.2	62.9	104	185	282	384
quenched in air (1250)	238	28.5	48.6	66.3	77.2	105	215	380	488
quenched in air	242	27.5	49.1	78.9	81.9	108	218	425	508
quenched in water (1250)	230	26.9	41.6	65.4	77.0	99	176	364	455
quenched in water	225	26.4	39.3	61.8	74.8	94	158	342	436
B cooled slowly	237	37.2	50.4	66.8	72.5	151	251	342	419
quenched in air (1250)	232	32.3	54.3	72.7	75.8	139	255	430	475
quenched in air	246	30.3	53.7	69.1	75.8	132	258	438	498
quenched in water (1250)	232	31.4	46.4	71.5	79.1	127	230	412	474
quenched in water	230	29.1	42.8	70.2	78.9	119	200	398	464

*Mixing ratio 1:2, water—cement ratio 0.65

Table 8. *Heat of hydration of the prepared cement*

	Heat of solution of dry cement (cal/g)	Heat of hydration (cal/g) 1d	3d	7d	28d
A cooled slowly	614.8	41.4	57.6	76.7	90.5
quenched in air	618.3	40.8	57.4	74.8	96.8
quenched in water	617.1	38.7	47.8	69.1	91.0
B cooled slowly	620.5	45.7	61.7	77.9	91.4
quenched in air	624.2	41.9	56.2	76.5	97.8
quenched in water	624.0	41.1	54.9	70.6	94.0

Table 9. *The surface color of the hydrated cement paste specimens*

	Cement A L	a	b	Cement B L	a	b
Cooled slowly	35.2	+1.0	+3.8	38.8	+0.8	+4.2
Quenched in air (1250)	37.8	+0.8	+3.4	38.3	+0.8	+3.3
Quenched in air	38.1	+0.8	+3.4	41.4	+0.5	+2.9
Quenched in water (1250)	45.2	+1.3	+9.8	46.2	+1.0	+8.8
Quenched in water	47.7	+1.9	+11.9	49.5	+1.8	+11.3

X-ray Diffraction of the Residue after Salicylic Acid Treatment of the Clinkers

The color change of portland cement with the increase of cooling rate was studied by means of X-ray diffraction of the residue after salicylic acid treatment of the clinkers shown in Table 6. Since X-ray diffraction of clinker is not enough to provide information of ferrite or interstitial materials, which may principally dominate the color of clinker, ferrite enriched residue was prepared by means of treatment with salicylic acid proposed by Satō, Takashima and Katō (6).

The residue was prepared as follows:—5 g of clinker was treated with 35 g of salicylic acid and 200 ml of methanol, stirred for 30 minutes, filtered and dried. The typical chemical composition of the residues is shown in Table 10. No appreciable difference of composition between A and B or among cooling rate was observed.

FeO was determined by titrimetric method with dichromate as titrant proposed by Ishii, Einaga and Watanuki (7). Loss of ignition and FeO content of water quenching specimens are somewhat greater than others.

X-ray diffraction patterns of the residue resulting from the clinker A are shown in Fig. 6. As internal standard, α-Al_2O_3 was used. Both the residues resulting from A and B clinkers showed almost the same X-ray patterns and d-spacings, except for difference of relative intensity of C_3A and ferrite.

The patterns of ferrite phase become broader and smaller with the increase of rate of cooling. It may show an increase of vitrified part. The d-spacings also change with the increase of the rate of cooling as shown in Fig. 7.

As the cooling rate is increased, d-spacing for (141) reflection expands, but d-spacings for (002) and (202) reflections shrink. This shrinking phenomena gives contrary inclination comparing with that the spacings for (002) and (202) reflections expand with the increase of C_2F content in system C_2A–C_2F.

The result of Fig. 7 suggests that crystalline ferrite

Table 10. *The typical chemical composition of the residues after salicyclic acid treatment of clinker—(%)*

Loss	SiO_2	Al_2O_3	Fe_2O_3	CaO	MgO	FeO	
1.0	10.4	23.0	13.9	45.8	4.0	Cooled slowly:	0.12—0.19
						Quenched in air:	0.15—0.19
						Quenched in water:	0.26—0.30
						Industrial clinker:	0.10—0.20

in the clinker deforms by rapid cooling as well as its partial vitrification. When the lattice parameters are calculated from d-spacings for (141), (002) and (202), *a* is almost unchangeable, *b* expands and *c* shrinks with the increase of rate of cooling; however, somewhat different *a*, *b* and *c* values are given, when they are calculated from other d-spacings values. The cause of the crystal deformation cannot be clarified yet. Perhaps the change of co-ordination of some atoms may occur.

Above experiments indicate that the expansion of d-spacing for (141) does not always mean the increase of iron content in ferrite.

X-ray diffraction patterns and d-spacings for the residue resulting from the industrial clinkers (A and B works) almost coincide with those of the clinker quenched in air.

However, above experiments do not make clear the reason for the color change with the increase of the cooling rate.

Study of Clinker Quenched in Nitrogen

A raw mix from the same cement works as shown in Table 4-A was burnt at same process (1450°C–30 minutes) and quenched in a cylindrical vessel which had been filled with nitrogen. Comparative test was carried out, quenching this clinker in the above vessel which had been filled with air instead of nitrogen. The color of the ground cl nkers (specific surface: 3200 cm^2/g) is shown in Table 11.

The color of the clinker quenched in nitrogen agrees with that of the clinker quenched in water as shown in Table 6. Of course, the color of the clinker

Table 11. *The color of the ground clinkers quenched in nitrogen or in air*

	L	a	b
Clinker quenched in nitrogen	65.9	+0.1	+15.6
Clinker quenched in air	50.1	−0.5	+7.3

quenched in the vessel which is filled with air instead of nitrogen agrees with that of the clinker quenched in air as already shown in Table 6.

The residue after salicylic acid treatment of both clinkers gives similar X-ray diffraction patterns and d-spacings, which are almost equal to those of the clinker quenched in air (Fig. 8).

FeO content of the residue resulting from the clinker quenched in nitrogen and in air was 0.39 and 0.15 % respectively.

Thermal Gravimetrical Analysis and Differential Thermal Analysis

Both of the residues resulting from the clinkers shown in Fig. 6 and from the clinker quenched in nitrogen were tested by means of thermal gravimetrical analysis and differential thermal analysis. During operating temperature up to 1000°C, the color of the residues resulting from both the clinkers quenched in water and in nitrogen changed from yellow to black;

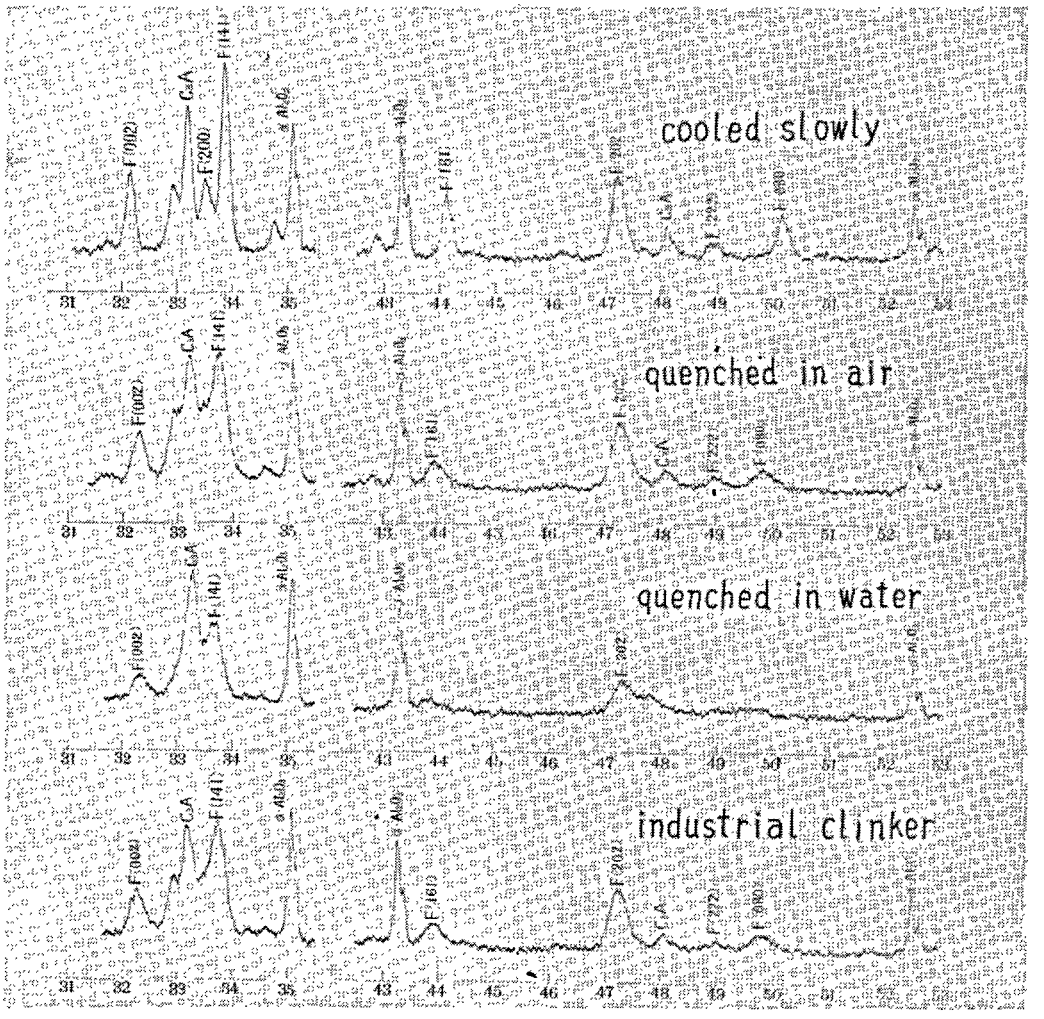

Fig. 6. *X-ray diffraction patterns of the residue after salicylic acid treatment of the clinkers.*
Target: Cu, Filter: Ni, Voltage: 40 KVP, Current: 16 mA, Time constant: 4 sec., Scanning speed: 0.25°/min., Divergence slit: 1°, Receiving slit: 0.15 mm, Internal standard: α-Alumina.

however, no appreciable thermal change was observed.

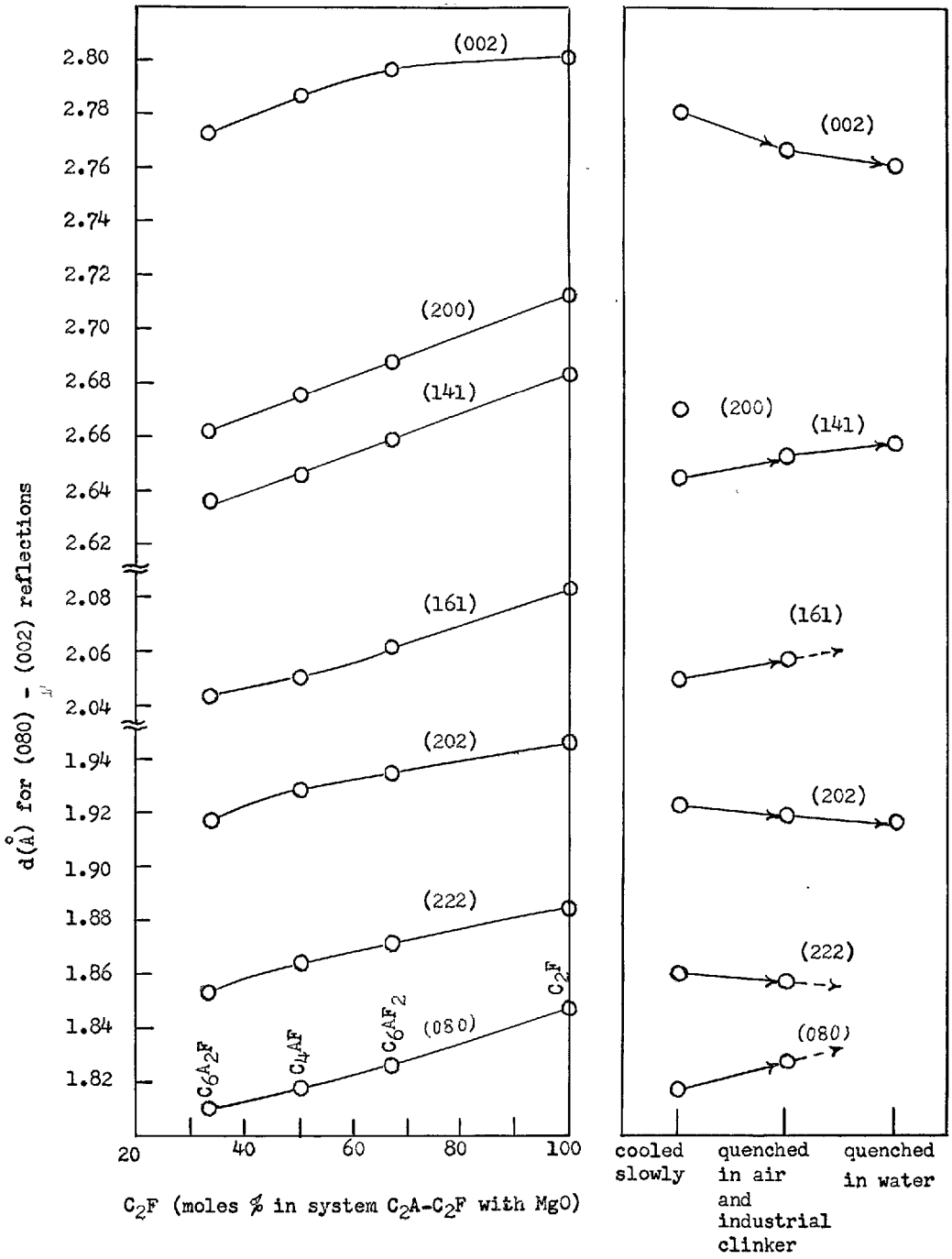

Fig. 7. *X-ray powder spacings for* C_2A-C_2F *(with* MgO*) system and for the residue after salicylic acid treatment of the clinkers.*

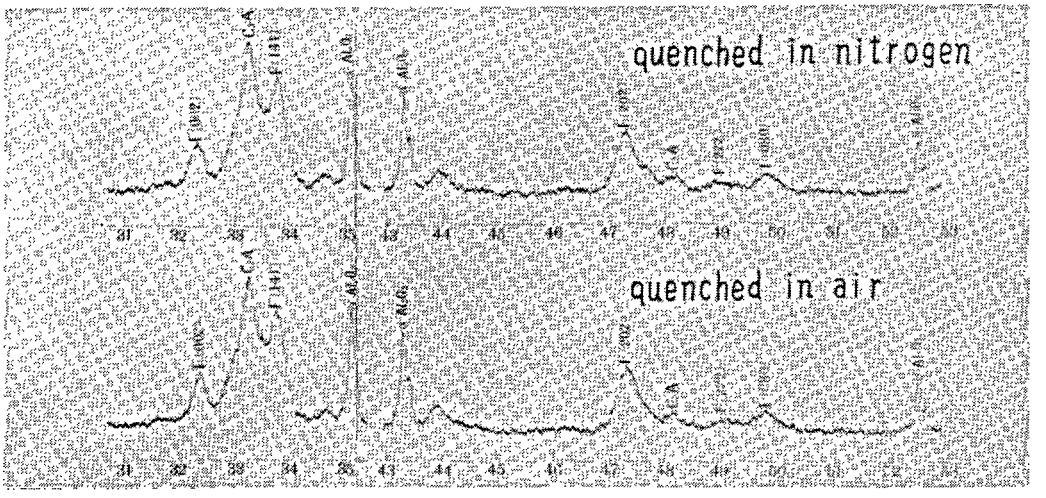

Fig. 8. *X-ray diffraction patterns of the residue after salicylic acid treatment of the clinker quenched in nitrogen and those of the clinker quenched in air instead of nitrogen.*
Operating condition of X-ray diffractometer is the same as Fig. 6.

Discussion on the Color Change of Portland Cement with the Increase of the Cooling Rate

There is a concept that the color change of portland cement with the increase of rate of cooling is due to the decrease of the amount of crystalline iron compound present and its replacement by glass (8). Generally, it may be considered that, in rapid cooling, MgO comprised in ferrite solid solution is released and dissolves in the liquid phase, and as a result the absence of MgO in crystalline ferrite leads to the light color of clinker.

However, the color of the clinker quenched in nitrogen became as yellow as that of the clinker quenched in water. This result suggests that the color change of the clinker quenched in water may not depend on freezing the iron-containing liquid to glass, but on the absence of oxygen in cooling process. Both in the water quenching and nitrogen quenching, the clinkers did not contact with oxygen in cooling process.

Though the color of the clinker quenched in nitrogen is considerably different from that of the clinker quenched in air, the X-ray diffraction patterns of their residues are almost equal as shown in Fig. 8. This fact suggests that the reason for the color change of the clinker with the increase of the cooling rate does not largely depend on the crystal structure of ferrite, but on the distribution of electrons which surround the ions constituting the crystal, as in the case of the C_4AF–MgO as shown in above. These information may rather be determined by electrical or magnetic methods.

The effect of oxygen to ferrite could not be clarified. Both by the fact that little FeO is present in the residues and by the results of thermal gravimetrical analysis and differential thermal analysis, it is suggested that no simple oxydation occurs.

It is doubtful that oxygen can diffuse into clinker grain within a few seconds. Peculiar mechanism of oxygen to ferrite phase may be concerned.

It could not also be clarified why the color of the clinker quenched in air is darkened than that of the clinker cooled slowly. Although a part of this may be due to the properties of C_2S, it may be chiefly due to the slight color change of the ferrite itself.

Moreover, microscopic or electron microscopic examination also should be carried out besides above testing methods.

The authors wish to express their gratitude for guidance and encouragement received from Dr. Eiji Anbo, Professor of Gumma University. We would like to thank Mr. Etuzō Kato, Chief of first section of ceramics department, Government Industrial Research Institute, Nagoya, for valuable information. Acknowledgement is also due to Mr. Hiroshi Narahashi, director of Sumitomo Cement Co., Ltd. for permission to publish this paper.

References

1. K. Miyazawa and K. Tomita, "The effect of MgO on the properties of portland cement" (in German) Zement-Kalk-Gips **19** (2) 82–85 (1966).
2. K. Fujii and K. Asaoka, "The effect of MgO on the color and on Alite formation of cement" (in Japan) J. Ceram. Assoc. Japan **40** 148, 291 (1932).
3. ASTM D 2244–64T "Instrumental evaluation of color differences of opaque materials."
4. Y. Sanada and K. Miyazawa, "On the behaviour of MgO against cement clinker mineral" Japan Cement Engineering Association, Review of the Eleventh General Meeting (11) 20 (1957).
5. Leonidas Tcheichivili and Woldemar A. weyl, "The synthesis of ceramic pigments" The Glass Industry 24, 25, 49 (Jan. 1963).
6. S. Satō, S. Takashima and M. Katō, "Studies on the compositions of ferrite in the industrial portland cement and clinker", Japan Cement Engineering Association, Review of the Sixteenth General Meeting (16) 36–39 (1962).
7. H. Ishii, H. Einaga and T. Watanuki, "Determination of ferrous iron in portland cement clinker" Japan Cement Engineering Association, Review of the Nineteenth General Meeting (19) 87–89 (1965).
8. F. M. Lea and C. H. Desch, "The chemistry of cement and concrete" p. 146–147, Edward Arnold Ltd., London (1956).

Oral Discussion

Kinjiro Fujii

I should like to make two questions. First, did you measure the photoconductivity of your material? Secondly, what is the temperature coefficient of the electrical conductivity? As I understand, these measurements will help you to interpret the mechanism of the electrical conduction of the material.

Authors' Closure

Kiyoshi Miyazawa and Kinzo Tomita

Neither of these properties you mentioned has been determined yet. I agree with you in that such measurements are necessary for understanding the mechanism of the electric conductivity more accurately. Since these are the iron-containing compounds, the partial pressure of oxygen should be taken into consideration in order to clarify the relationship between the temperature and the electric conductivity.

Supplementary Paper I-76 Miscibilities of Special Elements in Tricalcium Silicate and Alite and the Hydration Properties of C_3S Solid Solutions

Renichi Kondo* and Kozaburo Yoshida**

Synopsis

The purposes of this study are, firstly, to determine the miscibilities of special elements such as Ti and Mn in C_3S and alite and, secondly, to elucidate the hydraulic properties of these solid solutions.

The compositions lay in the hypothetical systems, C_3S–$3CaO \cdot TiO_2$, C_3S–$3CaO \cdot MnO_2$, alite-$3CaO \cdot TiO_2$ and alite-$3CaO \cdot MnO_2$. To synthesize the sample, each mixture was heated at 1500°C or 1600°C and air-quenched.

The limit of miscibility and the modification of the synthesized solid solution were examined by means of chemical analysis, X-ray diffraction, microscopic observation and electron probe X-ray microanalysis.

It was found that Ti can substitute for 0.13 mole Si both in C_3S and alite and that their crystal lattice expands and their modifications change into the high-temperature forms through its substitution. In the case of dissolution of Mn, it was also found that Mn dissolves up to 0.06 mole in C_3S and up to 0.08 mole in alite. Their crystal lattice contracts very slightly and the modification of C_3S changes into the high-temperature form and that of alite changes into the low-temperature form through its dissolution.

Moreover, the effects of Ti and Mn on the hydraulic properties of C_3S and alite were studied. The samples used were C_3S, alite, and their solid solutions containing 0.07 mole Ti or 0.05 mole Mn. As shown formerly, these samples were prepared by heating at 1500°C.

The hydration on paste was investigated by means of calorimetry, X-ray diffraction and chemical analysis, and the mortar strength was also tested. It was found that the hydration characteristics of C_3S and alite are affected by the dissolution of Ti or Mn. In the Ti bearing solid solutions, the degree of hydration is lowest at early stage, but, after 3 days' curing, it becomes highest and the mortar strength also becomes highest. In the Mn bearing solid solutions, the degree of hydration and the mortar strength become higher at later stage. These results seem to be due to the chemical composition rather than to the change in the modification of C_3S or alite.

Introduction

An investigation on the behavior of additional special elements in cement compounds is considered not only interesting scientifically but also as enabling us to expect therefrom some technological advancement.

Above all, as alite is the most important hydraulic mineral in portland cement, many reports have been found on the miscibilities of Al and Mg, both and individual, and on the polymorphism of alite by Woermann, Hahn and Eysel (1–2), Yamaguchi and Kato (3), Locher (4) and Midgley and Fletcher (5).

Yamaguchi, Shirasuka and Ota (6), Nurse, Midgley, Gutt and Fletcher (7) and Ono, Uno and Soda (8) recently reported on the effects of the polymorphism on the hydration and mechanical strength of C_3S. However, no clear conclusion has yet been obtained, partly because this is due to the greater effects of some foreign elements added.

The miscibilities of minor or special elements such as Ti, Mn, P, S and Cr in C_3S or alite were studied by Kondo (9). The effects of these elements on the properties of cement had been studied in order to improve the hardening ability or utilize special raw materials for cement manufacture (10–12). Moreover, studies

* Research Laboratory of Engineering Materials, Tokyo Institute of Technology, Tokyo, Japan.
**Central Research Laboratory, Ube Industries Ltd., Ube, Japan.

were made on the effect of F and P by Welch and Gutt (13), on Ti by Ershov (12) and on Mn by Sakurai (14). However, systematical studies on the limit of miscibility, type of dissolution, rate of hydration and mechanical strength have been scarcely made. The effects of additional special elements on the properties of alite containing Al and Mg, have not yet been reported.

The purpose of this study is to elucidate the miscibilities of Ti or Mn in C_3S and alite as well as their effects on the hydraulic properties such as the rate of hydration and the mortar strength.

The Miscibility of Ti or Mn in C_3S and Alite

Experimental Procedure

In order to clarify the limits of miscibily of Ti or Mn in C_3S and alite, the hypothetical systems, C_3S–$3CaO \cdot TiO_2$, C_3S–$3CaO \cdot MnO_2$, alite-$3CaO \cdot TiO_2$ and alite-$3CaO \cdot MnO_2$ were examined, on the assumption that Ti^{4+} or Mn^{4+} substitutes for the Si^{4+} in C_3S or alite up to a certain amount and that when the special element added exceeds this limit, the other low-lime compound will be formed, accompanying with the liberation of free CaO. According to the report by Woermann, Hahn and Eysel (1), the chemical composition of alite used in this experiment was CaO 71.08, MgO 2.14, Al_2O_3 1.01 and SiO_2 25.77%.

All these preparations were made by using guarantee grade reagents in Japanese industrial standards and quartz powder of high purity and smaller than 10μ in radius. Each mixture was ground, mixed thoroughly and then formed into granules of 3 mm in radius with water and dried at 110°C. The granules were placed in a platinum crucible and heated at 1500°C for 5 hours in an automatically controlled electric furnace and then air-quenched. This process was repeated three times to approach to the equilibrium state. The heating was made also at 1600°C on samples in hypothetical systems, C_3S–$3CaO \cdot TiO_2$ and C_3S–$3CaO \cdot MnO_2$.

The samples obtained were then examined by means of chemical analysis, X-ray diffraction, microscopic observation and electron probe X-ray microanalysis. Free CaO was determined by a modified Franke's method, the solution consisting of 80 parts isopropanol and 12 parts acetoacetic ethylester being used as the extraction solvent. X-ray diffraction was made in the region of 15–55° (2θ, CuKα). In order to identify the modification of solid solutions of C_3S and alite containing Ti or Mn, accurate determination was made by using quartz as an internal standard. Selected peaks are those of (009), (224), ($2\bar{2}4$), ($\bar{4}04$), (040), ($\bar{6}20$) and (620). The identification was made with reference to the shape of these peaks which had been studied by Bigaré, Guinier, Mázières, Regourd, Yannaquis, Eysel, Hahn and Woermann (15). Especially in the case of Mn, an electron probe X-ray microanalyzer was also used to determine the limit of miscibility in C_3S or alite.

Experimental Results

The results of free CaO determination on the samples in the systems, C_3S–$3CaO \cdot TiO_2$ and C_3S–$3CaO \cdot MnO_2$ heated at 1500°C or 1600°C are shown in Fig. 1. Fig. 2 shows free CaO on the samples in the systems alite-$3CaO \cdot TiO_2$ and alite-$3CaO \cdot MnO_2$ at 1500°C.

The changes in the d-values of (040), (620) and ($\bar{6}20$) on the samples in the system C_3S–$3CaO \cdot TiO_2$ are shown in Fig. 3; those in the system C_3S–$3CaO \cdot MnO_2$ in Fig. 4; and those in systems alite-$3CaO \cdot TiO_2$ and alite-$3CaO \cdot MnO_2$ in Fig. 5, respectively.

The X-ray diffraction patterns of the samples in which the miscibility is approximately above or below its maximum value are shown in Figs. 6–7.

The characteristic X-ray images by CaKα, by SiKα and by MnKα on the sample containing 3CaO.

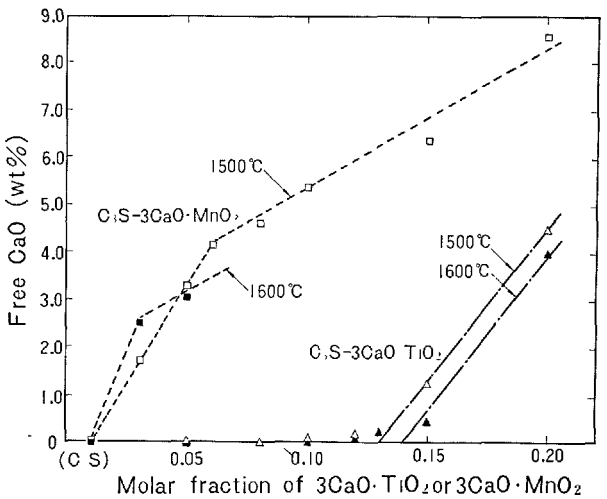

Fig. 1. *Free CaO content on sample in the systems,* C_3S–$3CaO \cdot TiO_2$ *and* C_3S–$3CaO \cdot MnO_2$ *heated at 1500°C or 1600°C and quenched.*

MnO_2 0.08 mole in the system C_3S–$3CaO \cdot MnO_2$ and these images on the sample containing $3CaO \cdot MnO_2$ 0.10 mole in the system alite-$3CaO \cdot MnO_2$ are shown in Figs. 8 and 9, respectively,

Discussion

It is convenient to discuss the miscibilities case by case on the combinations of components.

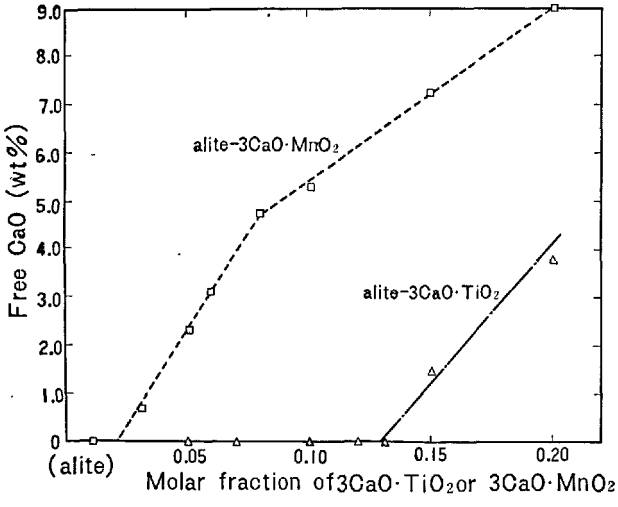

Fig. 2. *Free* CaO *content on sample in the systems, alite–*$3CaO \cdot TiO_2$ *and* C_3S–$3CaO \cdot MnO_2$ *heated at 1500°C and quenched.*

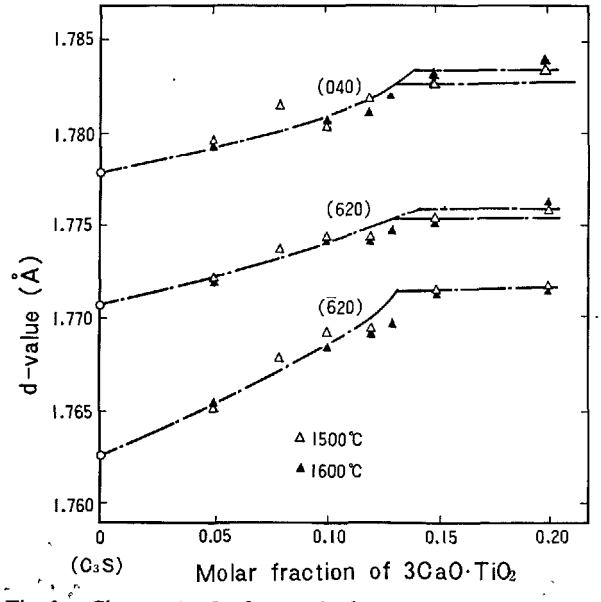

Fig. 3. *Changes in d-values with the content of* $3CaO \cdot TiO_2$ *in* C_3S.

Miscibility of Ti in C_3S

It is concluded from the facts described below, that the Si^{4+} in C_3S is substituted by Ti^{4+} up to 0.13 mole at 1500°C and up to 0.14 mole at 1600°C, and that the triclinic lattice of C_3S expands slightly with increasing amount of dissolved Ti^{4+}.

First of all, free CaO is hardly found in the samples

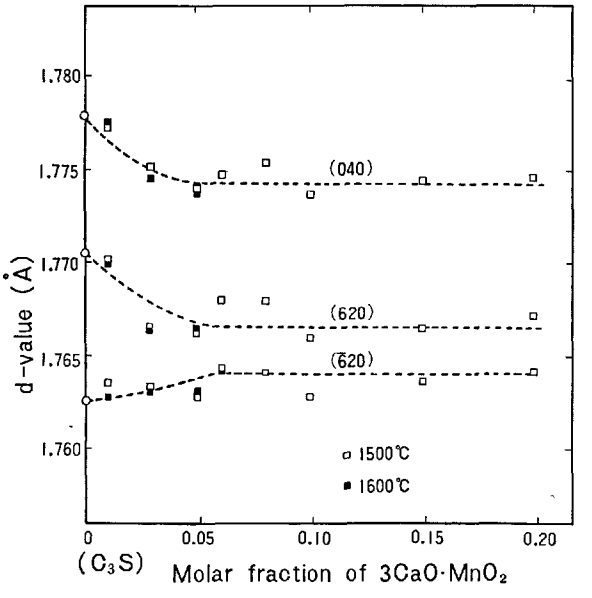

Fig. 4. *Changes in d-values with the content of* $3CaO \cdot MnO_2$ *in* C_3S.

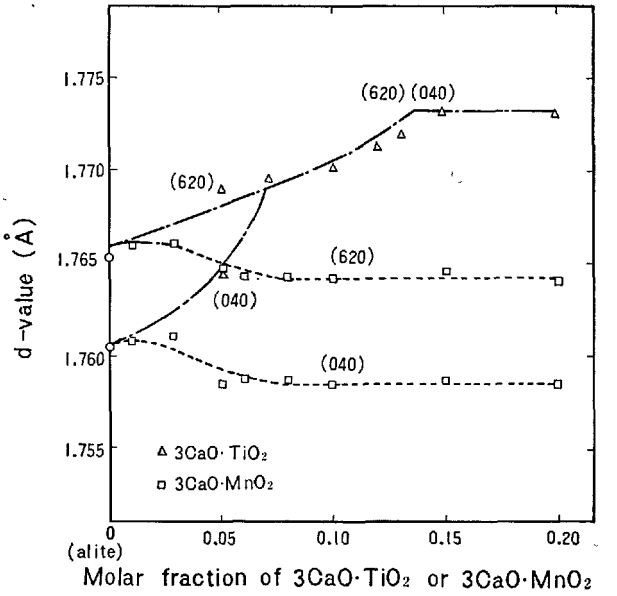

Fig. 5. *Changes in d-values with the content of* $3CaO \cdot TiO_2$ *or* $3CaO \cdot MnO_2$ *in alite at 1500°C.*

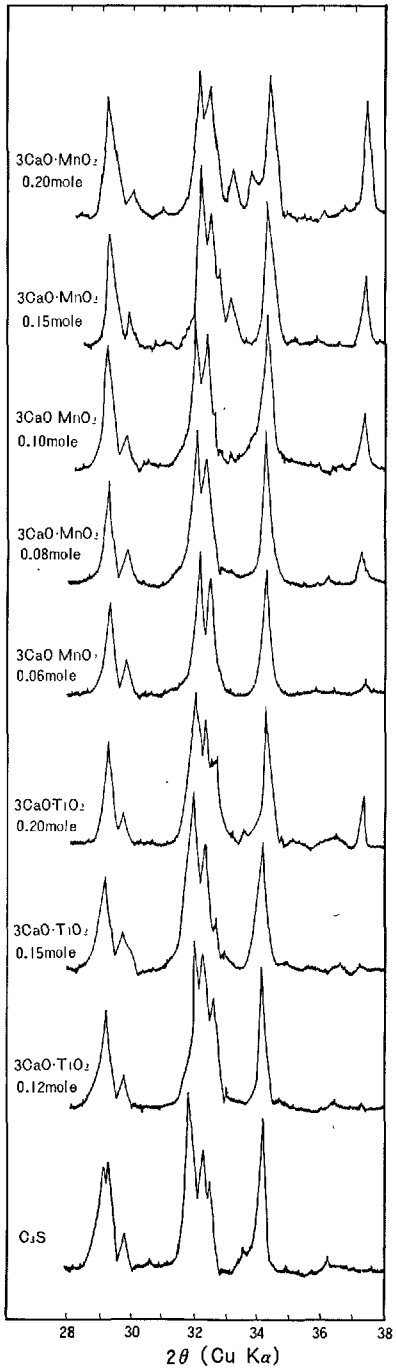

Fig. 6. *X-ray diffraction diagram of* C_3S, C_3S–$3CaO \cdot TiO_2$ *and* C_3S–$3CaO \cdot MnO_2$.

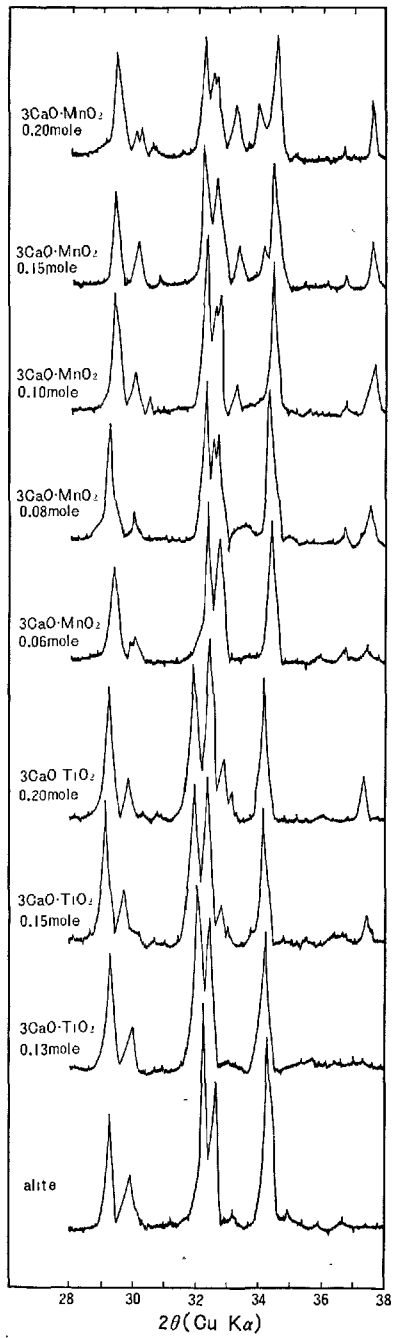

Fig. 7. *X-ray diffraction diagram of alite, alite*–$3CaO \cdot TiO_2$ *and alite*–$3CaO \cdot MnO_2$

containing up to 0.13 mole $3CaO \cdot TiO_2$ and heated at 1500°C and up to 0.14 mole and heated at 1600°C. The d-values of (040), (620), ($\bar{6}20$) expand slightly with increasing amount of replaced $3CaO \cdot TiO_2$ up to 0.13 mole at 1500°C and up to 0.14 mole at 1600°C. However, in the case exceeding these value, they become constant. Moreover, the X-ray diagram of each sample containing 0.15 or 0.20 mole $3CaO \cdot TiO_2$ indicates the existence of $3CaO \cdot 2TiO_2$ or $CaO \cdot TiO_2$. As an evidence, a peak is found at approximately $2\theta =$

(A) Ca-Kα Image

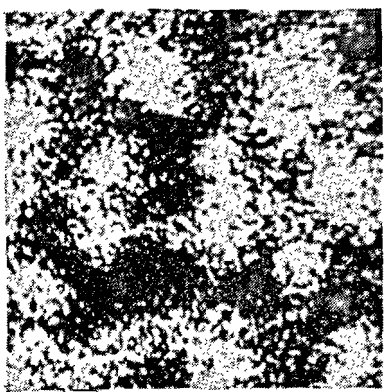

(B) Si-Kα Image

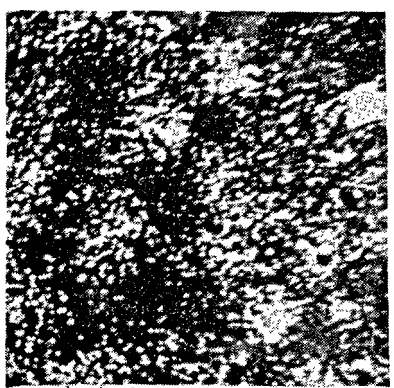

(C) Mn-Kα Image

Fig. 8. *Characteristic X-ray images on the sample containing 0.08 mole* $3CaO \cdot MnO_2$ *in the system* C_3S–$3CaO \cdot MnO_2$ (×500)

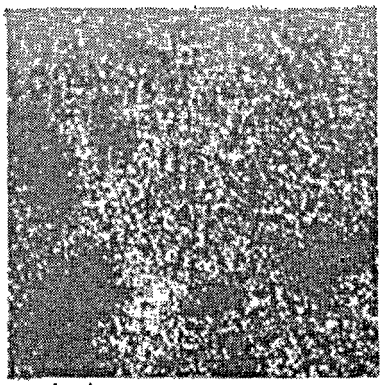

(A) Ca-Kα Image

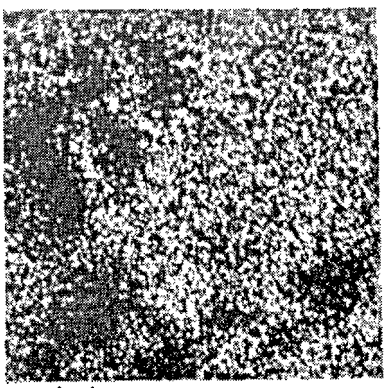

(B) Si-Kα Image

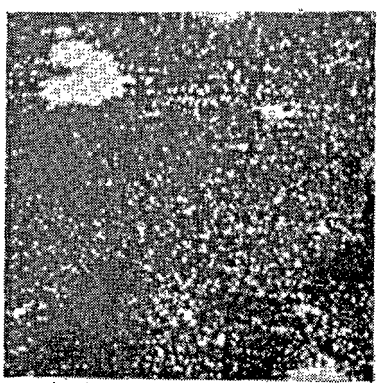

(C) Mn-Kα Image

Fig. 9. *Characteristic X-ray images on the sample containing 0.10 mole* $3CaO \cdot MnO_2$ *in the system alite*–$3CaO \cdot MnO_2$ (×500)

33° (CuKα). The sample containing 0.20 mole $3CaO \cdot TiO_2$ was treated with a salithylic acid-methanol solution to remove CaO and C_3S phases (16), and then the residue was examined by X-ray diffraction. And the result showed that the residue is most likely $CaO \cdot TiO_2$. Attention must be paid, however, to the fact that $CaO \cdot TiO_2$ precipitated also from the Ti dissolved solution with lapse of time by this method.

The modification of C_3S solid solution changes from triclinic T_I to triclinic T_{II} through the dissolution

of Ti under 0.05 mole.

The lattice expansion due to the dissolution of Ti in C_3S seems to be related with the difference of ionic radii between Si^{4+} and Ti^{4+}, Ionic radii are reported as 0.40Å for Si^{4+} and 0.68Å for Ti^{4+}, and a little smaller value is expected for the 4-fold co-ordinated ion, Ti^{4+}.

Miscibility of Mn in C_3S

On the miscibility of Mn in C_3S, it is found that the hypothetical compound, $3CaO \cdot MnO_2$, dissolves at 1500°C congruently in C_3S up to 0.01 mole and incongruently from 0.01 to 0.06 mole with the liberation of free CaO. When the amount of Mn extends over 0.06 mole, free CaO and $2CaO \cdot MnO_2$ are formed.

As for the evidence, free CaO was not liberated up to 0.01 mole $3CaO \cdot MnO_2$ in the system C_3S–$3CaO \cdot MnO_2$ at 1500 or 1600°C, and the liberation of free CaO occurs, when the amount of $3CaO \cdot MnO_2$ extends over 0.01 mole. The amount of free CaO in sample increases sharply in propertion to the amount of $3CaO \cdot MnO_2$ in the range from 0.01 to 0.06 mole and less sharply in the range exceeding 0.06 mole. The molar ratio of free CaO to Mn can be calculated from the curve in Fig. 1. This ratio is 0 for the amount of Mn up to 0.01 mole, approximately 3 for its amount from 0.01 to 0.06 mole and approximately 1 for its amount over 0.06 mole.

The d-values of (040) and (620) of C_3S decrease very slightly with increasing amount of mixed $3CaO \cdot MnO_2$ up to 0.06 mole, and become almost constant over this value. The d-value of $(\bar{6}20)$, however, increases very slightly, and both values of (620) and $(\bar{6}20)$ approach each other, with increasing amount of mixed $3CaO \cdot MnO_2$ up to approximately 0.06 mole.

The peaks at $2\theta(CuK\alpha) = 32 - 33°$ in Fig. 6 are found on the samples containing not less than 0.10 mole $3CaO \cdot MnO_2$, and these peaks seem to be due to the existence of $2CaO \cdot MnO_2$. Under a polarization microscope, this phase was an opaque crystal, identified as $2CaO \cdot MnO_2$ and also detected in the sample containing 0.08 mole $3CaO \cdot MnO_2$. Moreover, the electron probe microanalysis revealed that Mn is distributed uniformly in C_3S on the sample containing $3CaO \cdot MnO_2$ not more than 0.06 mole. On the other hand, the mass concentration of Mn occurs on the sample containing $3CaO \cdot MnO_2$ at 0.08 mole, as shown in Fig. 8.

It may be considered from the results described above that the Si^{4+} in C_3S is substituted by Mn^{4+} up to 0.01 mole, and that when the amount of Mn extends over 0.01 mole, the simultaneous substitution of Ca^{2+} and Si^{4+} with Mn^{2+} and Mn^{4+} occurs in the ratio of 3:1, or all Mn, regardless of valencies, is introduced in the interstitial positions of C_3S, up to 0.06 mole. The ionic radii of Ca^{2+} and Si^{4+} are 0.99 and 0.40Å, respectively and those of Mn^{2+} and Mn^{4+} are 0.80 and 0.60Å respectively. The last value is that for the 6-fold co-ordinated ion, and a little samller value is expected for the 4-fold co-ordinated ion. The lattice of C_3S will expand slightly, if Si^{4+} is substituted by Mn^{4+}, and the lattice will contract slightly, if Ca^{2+} is substituted by Mn^{2+}. As the lattice are found to be contracted in this experiment, the substitution for Si^{4+} is probably superseded by the substitution for Ca^{2+}. The modification of C_3S solid solution changes from triclinic T_I to triclinic T_{II} through the dissolution of Mn under 0.01 mole and changes from triclinic T_{II} to triclinic T_{III} through its dissolution above approximately 0.06 mole. According to Yamaguchi and Uchikawa (17), the modification of C_3S has a tendency to change from triclinic to monoclinic through the substitution of Ca^{2+} with other ion.

Miscibility of Ti in Alite

It is obvious from the data in Figs. 2, 5 and 7 that the Si^{4+} in alite is also substituted by Ti^{4+} to the extent of 0.13 mole at 1500°C in accordance with the case of C_3S, nevertheless alite is already saturated with Al^{3+} and Mg^{2+}. The modification of alite changes from monoclinic M_{II} to rhombohedral R through the dissolution of Ti above approximately 0.07 mole. The d-values of alite expand slightly with increasing amount of replaced $3CaO \cdot TiO_2$ up to 0.13 mole. But, when the amount of $3CaO \cdot TiO_2$ is beyond this value, free CaO and calcium titanate are formed. The composition of this titanate is suggested to be $CaO \cdot TiO_2$ by the X-ray diagram in Fig. 7 and also by the chemical analysis, in which the molar ratio of combined CaO to excessive TiO_2 is approximately 1, as shown in Fig. 2. An additional evidence of the formation of $CaO \cdot TiO_2$ is the result of X-ray analysis of the residue from which CaO and C_3S or alite phases were separated by the treatment of the sample containing 0.20 mole $3CaO \cdot TiO_2$ with the salithylic acid-methanol solution.

Miscibility of Mn in Alite

It is estimated from Figs. 2 and 7, that the hypothetical compound $3CaO \cdot MnO_2$ dissolves congruently in alite up to 0.02 mole at 1500°C and incongruently from 0.02 to 0.08 mole with the liberation of free CaO. The molar ratio of free CaO to Mn reaches to 3, when $3CaO \cdot MnO_2$ from 0.02 to 0.08 mole is contained (Fig. 2). $2CaO \cdot MnO_2$ was detected in the sample containing $3CaO \cdot MnO_2$ not less than 0.10 mole by

X-ray diffraction (Fig. 7) and also by microscopic observation. Moreover, the characteristic X-ray images on the samples containing $3CaO \cdot MnO_2$ not more than 0.08 mole showed that Mn is distributed uniformly in alite. Meanwhile, the mass concentration of Mn occurs on the sample containing $3CaO \cdot MnO_2$ at 0.10 mole, as shown in Fig. 9.

These results probably indicate that the Si^{4+} in alite is substituted by Mn^{4+} up to 0.02 mole, and that the simultaneous substitution of Ca^{2+} and Si^{4+} with Mn^{2+} and Mn^{4+} occurs in the ratio 3:1 up to 0.08 mole, when the amount of Mn extends over 0.02 mole. It may also be concluded that the excessive amount of $3CaO \cdot MnO_2$ forms free CaO and calcium manganate. From the fact that the molar ratio of combined CaO to excessive Mn is not 2 but 1.5, it seems that the composition of the manganate is $2CaO \cdot MnO_2$, and C_2S is not formed appreciably.

The d-values of (040) and (620) decrease very slightly with increasing amount of dissolved Mn. The modification of alite changes from monoclinic M_{II} to monoclinic M_I through the dissolution of Mn above approximately 0.03 mole.

The Hydraulic Properties of C_3S, Alite and Their Solid Solutions Containing Ti or Mn

Experimental Procedure

Preparation of Samples

The samples used for hydration experiment were C_3S, 0.07 mole Ti bearing C_3S (hereafter abbreviated as C_3S (Ti 0.07)), C_3S (Mn 0.05), alite, alite (Ti 0.07) and alite (Mn 0.05), all of which were synthesized by heating three times at 1500°C for 5 hours as described previously. It was confirmed that the samples thus obtained contain no free CaO and other foreign phases. The chemical compositions of them are shown in Table 1. The modifications were identified as triclinic T_I for C_3S, triclinic T_{II} for C_3S (Ti) and C_3S (Mn), monoclinic M_{II} for alite and alite (Mn) and rhombohedral R for alite (Ti).

The sintered products were crushed to pass through a sieve with 2 mm openings and pulverized in a pot mill of sintered corundum. The particle size distributions of the final samples were determined with Bahco particle classifier.

As shown in Fig. 10, the particle size distributions showed no difference in the samples of C_3S series and those in alite series, respectively. Blaine surface area of C_3S series was $3{,}220 \pm 20$ cm²/g and that of alite series was $3{,}420 \pm 20$ cm²/g, respectively.

Tests on Hydration

Neat paste of each sample with a water-cement

Table 1. *Chemical compositions of synthesized samples for hydration experiment*

Sample	SiO_2	TiO_2	MnO_2	Al_2O_3	CaO	MgO
C_3S	26.32	—	—	—	73.68	—
C_3S (Ti 0.07)	24.33	2.43	—	—	73.24	—
C_3S (Mn 0.05)	25.10	—	1.91	—	70.20	—
alite	25.77	—	—	1.01	71.08	2.14
alite (Ti 0.07)	23.80	2.45	—	0.93	70.75	1.97
alite (Mn 0.05)	24.30	—	1.91	0.96	68.44	2.02
			Estimated chemica' formulas			
C_3S	Ca_3SiO_5					
C_3S (Ti 0.07)	$Ca_3Si_{0.93}Ti_{0.07}O_5$					
C_3S (Mn 0.05)	$(Ca_{2.97}Mn^{II}_{3.03})(Si_{0.98}Mn^{IV}_{0.02})O_5$					
alite	$(Ca_{2.879}Mg_{0.112}Al_{0.0093})Al_{0.0056}(Si_{0.971}Al_{0.029})O_5$					
alite (Ti 0.07)	$(Ca_{2.879}Mg_{0.112}Al_{0.0093})Al_{0.0056}(Si_{0.903}Al_{0.027}Ti_{0.070})O_5$					
alite (Mn 0.05)	$(Ca_{2.851}Mg_{0.117}Al_{0.0093}Mn^{II}_{0.023})Al_{0.0058}(Si_{0.942}Al_{0.029}Mn^{IV}_{0.029})O_5$					

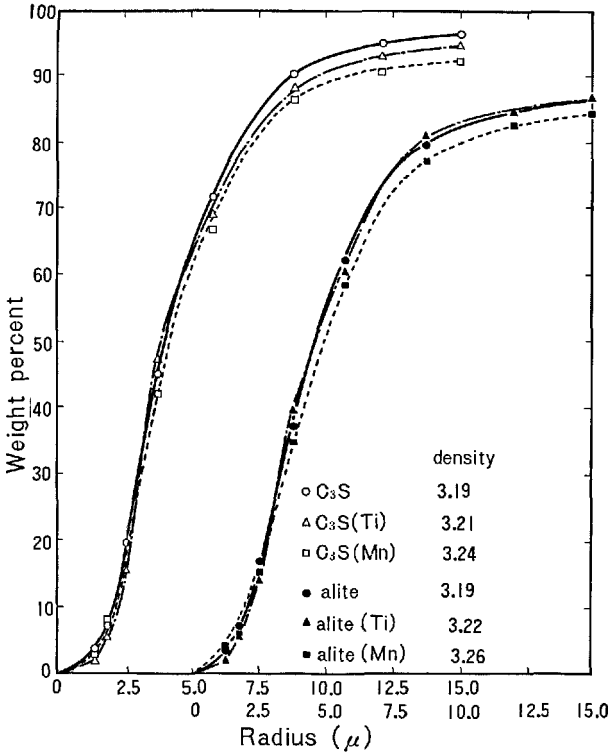

Fig. 10. *Particle size distribution of sample for hydration experiment.*

ratio of 0.50 was prepared and, after sealing in a plastics bottle, cured at 20 ± 1°C. After reaching a certain period, hardened paste was crushed, stopped the hydration, and subjected to "D-drying" reported by Copeland and Hayes (18). The free $Ca(OH)_2$ and loss on ignition of each dried sample were determined, and the unhydrated part was determined quantitatively by X-ray diffraction.

Free $Ca(OH)_2$ was determined by a modified Franke's method and loss on ignition was determined by heating at 1000°C and its amount was regarded as the amount of combined water. In the quantitative determination by X-ray diffraction, periclase powder from 2 to 5μ in radius was used as the internal standard. On the same sample, five new compacted specimens were used and its determination was repeated twice. The intensities of peaks, $2\theta(CuK\alpha) = 42.9°$ (200) of periclase and $2\theta(CuK\alpha) = 41$–$42°$(319 etc.) of C_3S or alite, were used for this determination.

The hydration at early stage was also examined with a conduction calorimeter at 20°C on paste with a water-cement ratio of 0.50.

Mortar Test

Mortar strength was determined according to the RILEM method on each sample without gypsum. The sand-cement-water ratio was 3–1–0.5. The test pieces of 2 × 2 × 8 cm were cured in water at 20 ± 1°C.

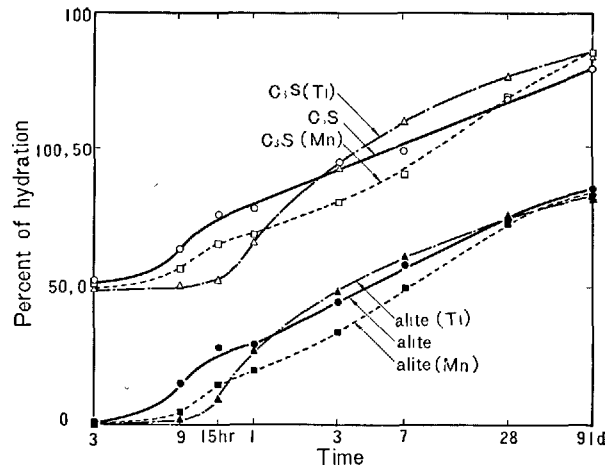

Fig. 11. *Degree of hydration of C_3S, alite and their solid solutions determined by X-ray determination ($w/c = 0.5$, at 20°C).*

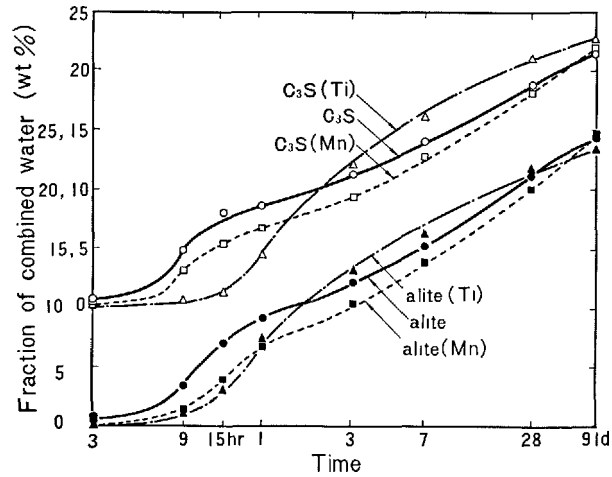

Fig. 12. *Combined water content in D-dried paste with C_3S, alite and their solid solutions represented on ignited base ($w/c = 0.5$, at 20°C)*

Experimental Results and Discussion

Hydration Characteristics

The degree of hydration determined by X-ray dif fraction, the content of combined water and free $Ca(OH)_2$ are shown in Figs. 11–13, respectively. All of the data were determined on D-dried paste and represented on ignited base.

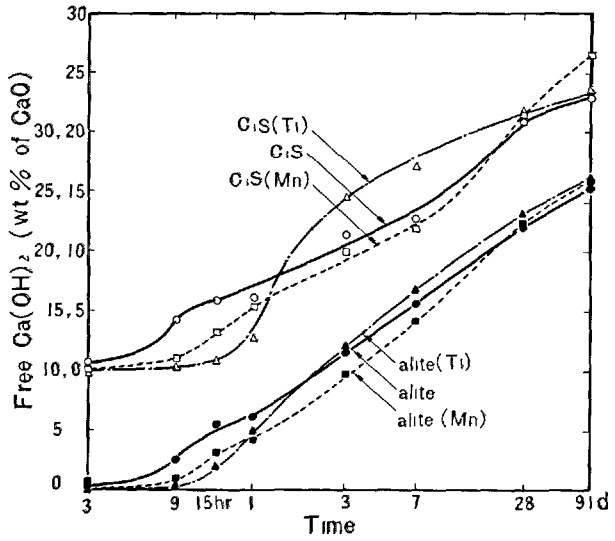

Fig. 13. *Free* $Ca(OH)_2$ *in D-dried paste with* C_3S, *alite and their solid solutions represented on ignited base* ($w/c = 0.5$, *at 20°C).*

Table 2-A. CaO/SiO_2 *molar ratio on calcium silicate hydrates*

Sample	Curing time (hours or days)						
	9h	15h	1d	3d	7d	28d	91d
C_3S	1.5	2.1	2.1	1.9	1.9	1.8	1.8
C_3S (Ti)	—	—	2.2	1.6	1.8	1.8	1.8
C_3S (Mn)	2.0	2.2	1.7	1.6	1.8	1.7	1.7
alite	2.2	2.2	2.1	1.9	1.9	1.8	1.8
alite (Ti)	—	2.0	2.2	2.0	1.8	1.7	1.7
alite (Mn)	2.1	2.0	2.0	1.8	1.8	1.7	1.7

Table 2-B. H_2O/SiO_2 *molar ratio on calcium silicate hydrates*

Sample	Curing time (hours or days)						
	9h	15h	1d	3d	7d	28d	91d
C_3S	3.1	2.9	3.1	2.1	2.6	2.4	2.4
C_3S (Ti)	—	—	3.3	2.2	2.3	2.4	2.3
C_3S (Mn)	6.1	3.7	3.4	2.6	2.6	2.0	2.0
alite	2.9	2.2	2.7	2.4	2.2	2.4	2.4
alite (Ti)	—	3.1	2.4	2.5	2.3	2.4	2.2
alite (Mn)	4.2	2.4	3.3	3.3	2.3	2.3	2.5

As Figs. 11–13 show the similar tendency, the data in Fig. 11 are used as the representing ones to discuss the degree of hydration. But the data are accompanied inevitably with experimental errors in the intensity of X-ray diffraction. In addition, the chemical composition of calcium silicate hydrate seems to change during the progress of reaction as shown in Table 2.

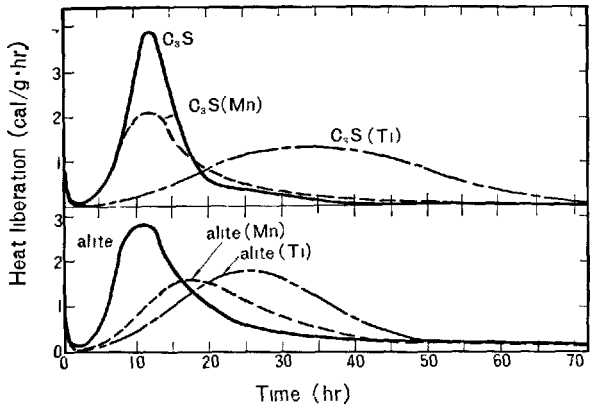

Fig. 14. *Heat of liberation on paste with* C_3S, *alite and their solid solutions* ($w/c = 0.5$, *at 20°C).*

The rate of heat liberation was determined with the conduction calorimeter, and the results are shown in Fig. 14.

As shown in Figs. 11–14 except from a very rapid hydration immediately after contact with water, the progress of hydration can be divided into the following three stages:

(1) At the induction period the rate of hydration is extremely low;
(2) At the acceleratory period the rate of hydration increases and then reaches to a maximum value;
(3) At the decay period the rate of hydration decreases.

The induction period of C_3S and alite is over within 2 hours and the maximum rate is observed at 11 hours. The maximum rate of C_3S and alite is higher than those of their solid solutions, (Fig. 14). In the case of C_3S (Mn) and alite (Mn), the induction period is a little longer and the acceleratory period is a little shorter than those of C_3S and alite, respectively. The hydration behaviors of C_3S (Ti) and alite (Ti) differ extremely from those of the other samples.

Rate of Hydration

To compare the rate of hydration, the thickness of reacted layer was calculated from the data of the particle size distribution (Fig. 10) and of the degree of hydration (Fig. 11). In this calculation, it was assumed that the individual reactant particles were spherical and the thickness of the reacted layer is always uniform. Although the thickness of the reacted layer is not the same with that of the layer of hydration product, it can be regarded equal to the thickness

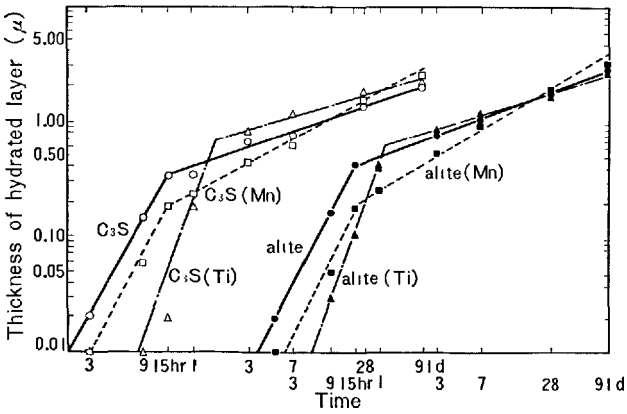

Fig. 15. *Thickness of hydrated layer calculated from degree of hydration and particle size distribution (w/c = 0.5, at 20°C)*

of the layer of inner product. In Fig. 15, the relationship between thickness of reacted layer (y) and the curing time (t) is expressed on logarithmic scale.

In the figure, the degree of hydration is expressed by two-straight lines with a crook point, and the rate corresponds to the slope of these lines. The reaction time required for reaching the crook point corresponds to that required for reaching the maximum rate of hydration on each sample (Fig. 14). The inclinations of the lines before the crook points are approximately 1.7, 1.9, 1.9, and 2.0 for C_3S, C_3S (Mn), alite and alite (Mn), respectively. As these are all approximately 2, the following equation is derived,

$$\frac{d\log y}{d\log t} = 2. \tag{1}$$

Therefore,

$$\log y = 2\log t + \log k_1 \text{ or } y = k_1 t^2 \tag{2}$$

The differentiation with respect to t, one obtains

$$\frac{dy}{dt} = 2K_1 t = K_1' t \tag{3}$$

In this equation, K_1' is the rate constant which is calculated from the thickness of hydrated layer at a certain unit of time.

Thus, in the acceleratory period, the rates of hydration of C_3S, alite and their solid solutions of Mn increase with time. The hydration during this stage may be considered to be a kind of autocatalytic reaction. In connection with this process, further discussion will be presented by one of the authors in the other paper at this symposium (19).

On the other hand, the inclinations of the lines before the crook points are approximately 2.7 for C_3S (Ti) and approximately 2.8 for alite (Ti). When these values approach to 3, the rate of this reaction can be expressed as follows;

$$\frac{dy}{dt} = K_2' t^2. \tag{4}$$

In this equation, K'_2 is the rate constant which can be calculated from the thickness of reacted layer at a certain unit of time. Thus, this type of hydration may also be considered to be a kind of autocatalytic reaction. This type of reaction will also be discussed by one of the authors in the other paper at this symposium.

The inclinations of lines after the crook points are 0.39 for C_3S, 0.32 for C_3S s.s. (Ti), 0.57 for C_3S. (Mn), 0.40 for alite, 0.37 for alite (Ti), 0.62 for alite (Mn). If they are approximated as 0.5, the following equation is derived,

$$\frac{d\log y}{d\log t} = 0.5. \tag{5}$$

Therefore,

$$\log y = 0.5\log t + \log k_3 \text{ or } y = k_3 t^{0.5} \tag{6}$$

Differentiation with respect to t, one obtains

$$\frac{dy}{dt} = 0.5k_3^2\frac{1}{y} = K_3'\frac{1}{y}, \tag{7}$$

where K_3' is the rate constant which can be calculated from the apparent thickness of the reacted layer obtained by extrapolating the lines straightly to a certain unit of time.

Thus, the rate of hydration at this stage changes in inverse proportion to the thickness of the hydrated layer. It can be considered that the thickness of the hydration product layer is in proportion to that of the hydrated layer, so that the rate of hydration during this decay period is controlled by diffusion through the layer of hydration product formed around the particle of reactant. As described previously, all the inclinations obtained on C_3S, alite and their solid solutions of Ti are smaller than 0.5, so their hydration products may become denser with the progress of reaction.

Finally, the hydration process of the samples used in this experiment is outlined as follows:

In the hydration of C_3S and alite, the induction period is shorter, so that the acceleratory hydration begins earlier. After the thickness of hydrated layer reaches to 0.3μ, the rate of hydration is affected mainly by the diffusion through the layer of hydration product and the value is decreased gradually. In the cases of Ti bearing C_3S and alite, on the contrary, the induction period is exceedingly prolonged, but the degree of hydration at 1–3 days is high, because the rapid autocatalytic hydration continues until the hydration product layer reaches to 0.6μ. In the hydration of the Mn bearing C_3S and alite, the induction period is prolonged a little at early stage. After the

thickness of the hydrated layer reaches to 0.2μ, the rate of hydration is affected mainly by the diffusion phenomenon through the layer of the hydration product and the value is decreased gradually. After 28 days, however, the degree of hydration is highest in comparison with that of the other samples, because the layer of hydration product is not so dense compared with the other samples.

Mortar Test

It was observed that the setting of mortar made with C_3S and alite occurs within a few hours after mixing. The setting of C_3S (Mn) and alite (Mn) were a little slower and that of C_3S (Ti) and alite (Ti) occurred after approximately 10 hours.

Mortar strength is shown in Fig. 16. On 1 day strength, the highest value is obtained by C_3S and alite, followed by C_3S (Mn) and alite (Mn) and the lowest by C_3S (Ti) and alite (Ti). However, the strength of the samples containing Ti was increased, extremely between 1 day and 7 days, C_3S (Ti) showing the highest strength at 3, 7, 28 and 91 days among the samples of C_3S series. Alite (Ti) showed also the highest strength at 3, 7, and 28 days among the samples of alite series. The increases in the strength development of C_3S and alite are a little greater at early stage and a little smaller at later stage than those of C_3S (Mn) and alite (Mn). The strength development of alite is a little greater than that of C_3S and the strength development of alite (Mn) is also a little greater than that of C_3S (Mn).

The significant effects of Ti, Mn or Mg and Al on mortar strength of C_3S may be mainly due to the chemical effects of the elements rather than to the changes of the modification.

Relations between the Degree of Hydration and the Mortar Strength

The relationship between the degree of hydration and the mortar strength is shown in Fig. 17.

The effects of the degree of hydration on the strength, both compressive and bending, are similar in the series C_3S solid solution and alite series. The effects of Ti or Mn are also observed similarly in both series.

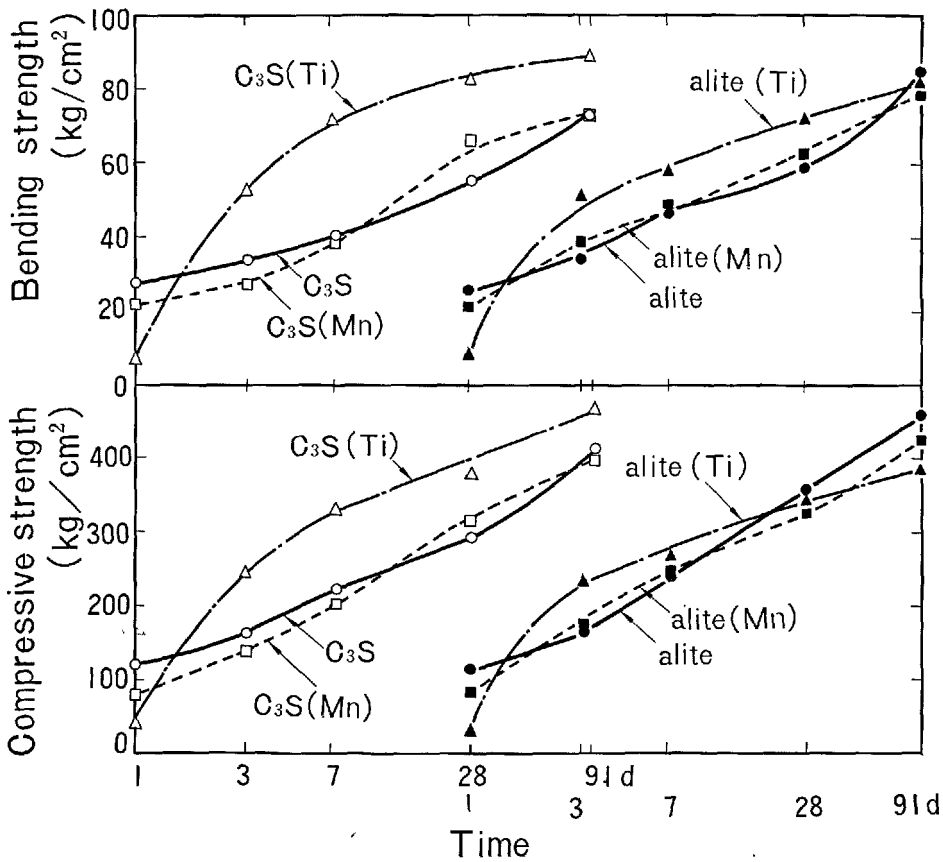

Fig. 16. *Mortar strength on C_3S, alite and their solid solutions (c: s: w = 1: 3: 0.5, at 20°C)*

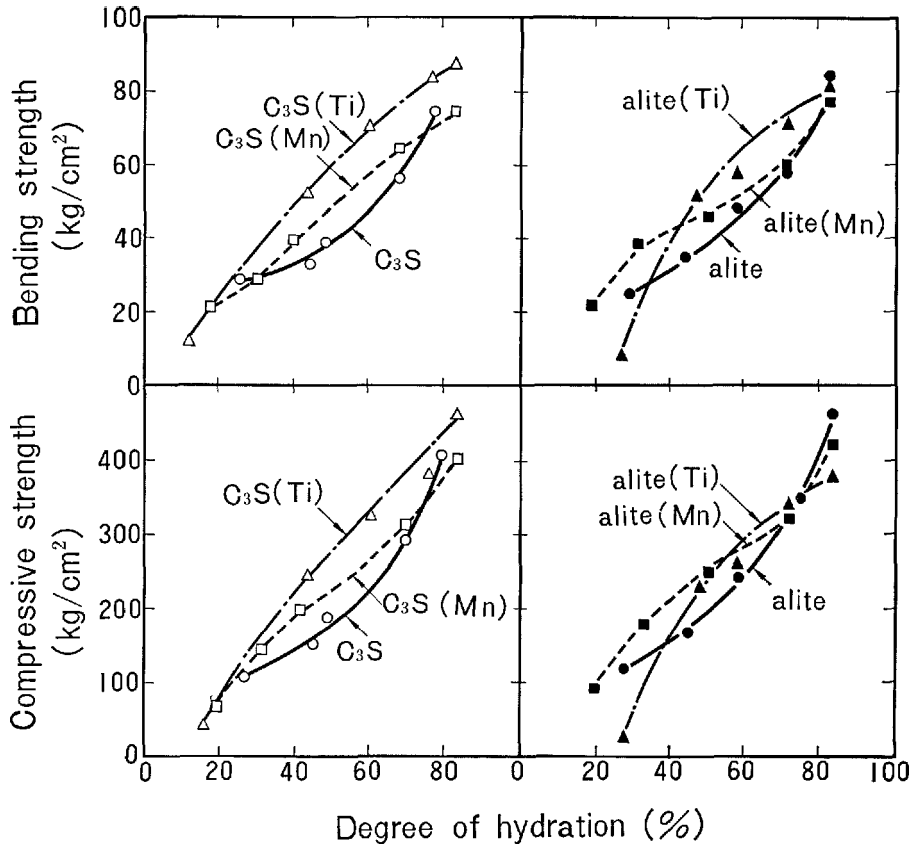

Fig. 17. *Relationship between degree of hydration and mortar strength.*

The ratio of the strength to the degree of hydration is higher for the Mn bearing solid solutions at early age of hydration, but the ratio decreases at later ages. The strength of the Ti bearing solid solutions shows highest value at later above middle ages of hydration. These facts suggest that mortar strength is affected greatly by the change in property of hydration product which occurs by the addition of the special elements.

The authors wish to thank Dr. Y. Suzukawa of the Central Research Laboratory of Ube Industries, Ltd. for his encouragement. Thanks are also due to Mr. M. Kobayashi in charge of Tokyo Institute of Technology for his assistance in using the electron probe X-ray microanalyzer.

References

1. E. Woermann, Th. Hahn and W. Eysel, "Chemical and structural investigation on the solid solution of tricalcium silicate" (in German), Zement-Kalk-Gips **16,** 370–375, (1963).
2. E. Woermann, W. Eysel and Th. Hahn, "Chemical and structural investigations with the formation of solid solutions of tricalcium silicate" (in German), Zement-Kalk-Gips **20,** 385–391, (1967).
3. G. Yamaguchi and K. Kato, "$3CaO \cdot SiO_2$–Al_2O_3–MgO solid solution" (in Japanese), Semento Gijutsu Nenpo **16,** 27–29, (1962). Rev. 16th Meeting Japan Cement Eng. Assoc., Tokyo, 1962. p. 28–32. (1962).
4. F. W. Locher, "Solid solution of alumina and magnesia in tricalcium silicate", Proc. 4th Intern. Symp. Chemistry of Cement, Washington, 1960, p. 99–106, (U. S. Dept. of Commerce, 1962).
5. H. G. Midgley and K. E. Fletcher, "The role of alumina and magnesia in the polymorphism of tricalcium silicate", Trans. Brit. Ceram. Soc, **62,** 917–937, (1963).
6. G. Yamaguchi, K. Shirasuka and T. Ota, "Comparison of hydration properties between monoclinic and inverted triclinic alite", Sympo. Structure of

Portland Cement Paste and Concrete, Highway Research Board, Washington, U.S.A., p. 263–268, (1966).
7. R. W. Nurse, H. G. Midgley, W. Gutt and K. Fletcher, "Effect of polymorphism of tricalcium silicate on its reactivity" Symp. Structure of Portland Cement Paste and Concrete, Highway Research Board, Washington, U.S.A., p. 258–262, (1966).
8. Y. Ono, T. Uno and Y. Soda, "The mortar strength of each polymorphic form of Ca_3SiO_5" (in Japanese), Semento Gijutsu Nenpo **20,** 54–59 (1966). Rev. 20th General Meeting, Tech. Ses., Cement Assoc. Japan, Tokyo, 1966 p. 53–57 (1966).
9. R. Kondo, "Effects of special components on the mineral compositions of portland cement clinker" (in Japanese), Semento Gijutsu Nenpo **17,** 42–49, (1963). Rev. 17th General Meeting, Japan Cement Eng. Assoc. Tokyo, 1963, p. 31–32, (1963).
10. F. M. Lea and C. H. Desch, revised by F. M. Lea. The Chemistry of Cement and Concrete, p. 147–150, (Edward Arnold Publishers Ltd., London, England, 1956).
11. R. H. Bogue, The Chemistry of Portland Cement, 2nd ed., p. 365–375, (Reinford Publishing Co., New York, U.S.A., 1955).
12. W. Eitel, Silicate Science, Vol. V, Ceramic and Hydraulic Binders, p. 325–338, (Academic Press Inc., New York, U,S.A., and London, England, 1966).
13. J. H. Welch and W. Gutt, "The effect of minor components on the hydraulicity of the calcium silicates", Proc. 4th Internatl. Symp. Chemistry of Cement, Washington, 1960, p. 59–67, (U. S. Dept. of Commerce, 1962).
14. T. Sakurai, "The behavior of manganese in cement clinker minerals", (in Japanese), Semento Gijutsu Nenpo **14,** 32–35 (1960). Rev. 14th General Meeting, Japan Cement Eng. Assoc., Tokyo, 1960, p. 23–24, (1960).
15. M. Bigaré, A. Guinier, C. Mazières, M. Regourd, N. Yannaquis, W. Eysel, Th. Hahn and E. Woermann, "Polymorphism of tricalcium silicate and its solid solutions", J. Am. Ceram. Soc. **50,** 609–619, (1967).
16. S. Takashima and M. Kato, "Preparation of standard alite" (in Japanese), Semento Gijutsu Nenpo **15,** 19–23, (1961). Rev. 15th General Meeting, Japan Cement Eng. Assoc., Tokyo, 1961, p. 33–34, (1961).
17. G. Yamaguchi and H. Uchikawa, "On the alite phase in portland cement clinker with varying alkali contents" (in Japanese), Semento Gijutsu Nenpo **16,** 21–26, (1962).
18. L. E. Copeland and J. C. Hayes, "Determination of non-evaporable water in the hardened portland cement paste", ASTM Bull., No. 194 70–74, (Dec., 1953).
19. R. Kondo and S. Ueda, "Kinetics and mechanisms of the hydration of cements", 5th Internatl. Sympo, Chem. Cement, Tokyo, 1968.

Supplementary Paper I-79 Microscopic Observations of Alite and Belite and Hydraulic Strength of Cement

Yoshio Ono, Shigeo Kawamura and Yoshiaki Soda*

Synopsis

The external forms and the inner texture of alite and belite occurring in clinker are studied, referring to the crystal structures and inversion of the temperature modifications. And the facial indexes and the orientation of optical axes are determined.

Relationships between the microscopic figure of alite and belite, the conditions of cement burning and the hydraulic strength are given.

The microscopic exermination is effective to the daily control of clinker burning in manufacture. For this purpose, observation of the crystallization and the inversion textures of alite and belite, birefringence of alite, color of belite and content of α-phase in belite, is light and effective.

Introduction

For a long time, many microscopic investigations were made on the clinker minerals, and were in detail. But the analysis and the interpretations on the crystal form and the inner texture remained incomplete, since the microscopic measurement of the minute and complex textures is very difficult.

A. E. Törnebohm (1) showed by poralizing microscopic examination that clinker was composed of "Alit", "Belit", "Celit", "Felit" and "isotrop Substanz", "Alite" was psendo-hexagonal orthorhombic. E. S. Shepherd and G. A. Rankin (2) and N. Sundius (3) found more complex and minute textures in clinker minerals. B. Tavasci (4), H. Insley (5) and W. C. Taylor (6) presented precise reflecting microphotographs of the clinker minerals, and explained the minute texture of belite in relation to the burning condition. C. E. Tilley (7) (8) examined on larnite (β-C_2S) and bredigite (α'-C_2S) occurring in natural rock and slag, and it was concluded that the former was monoclinic and the latter was pseudo-hexagonal orthorhombic. In recent year, the former microscopic studies on clinker minerals were compiled by F. Trojer, (9) P. Terrier and H. Hornain (10).

Through the advance of X-ray crystallographic studies on synthetic single crystals of clinker minerals, the crystal structure and polymorphism of Alite were made clear by A. Guttmann and F. Gille (11) and J. W. Jeffery (12) and those of belite by M. A. Bredig (13), C. M. Midgley (14), D. K. Smith et al.

In this paper, the microscopic figure, texture and optical property of alite and belite are examined (16), (17), (18) by polarizing microscope and explained from the crystal structure and the polymorphism, and the relationships between burning condition, crystallographic property and hydraulic strength are given.

Microscopy on Clinker Minerals

In this study, polarizing microscope, X400, with universal stage was used. For precise observation, the thin section must be polished perfectly, to be free from irregular dispersion of light, and the thickness of thin section must be fit for each purposes, e.g. for the optics of alite: 25μ, for the fine texture of belite: 10μ.

*Central Research Laboratory, Onoda Cement Co., Ltd, Tokyo, Japan.

The direction of the acute bisectrix, X, of alite can be determined most accurately, and is suitable for the basis of goniometry of the crystal faces and the textures.

The horizontal section, X being perpendicular to the section, shows a regular hexagonal shape with 3-fold symmetry, and the side planes bounding the hexagon are inclined against X. The birefringence of this section is very weak.

The vertical section, X being parallel to the section, shows a elongate hexagonal shape. The elongate sides are normal to X, and the faces are perpendicular to the section. Rotating the section about X, the another four faces can be brought to vertical position. At this position, the all six faces are parallel to view line, and the elongate hexagonal outline shows 2-fold symmetry.

Above observation shows that the external form of alite is bounded by a set of basal planes (c), and two sets of rohmbohedrons, (r1) and (r2), and may belong to D_{3d}. The angles between the rohmbohedrons and X are measured as (r1) $\wedge$ X = 26.2°, (r2) $\wedge$ X = 13.5°, therefor

$$\{c\}:\{0001\},\ \{r1\}:\{01\bar{1}2\},\ \{r2\}:\{10\bar{1}1\}.$$

These observations are in good agreement with the results obtained by Guttmann, who could measure accurately the facial angles of alite, grown in a large crystal in basic slag, using reflective goniometer.

Guttmann showed the facial indises as $\{r1\}:\{10\bar{1}2\}$ and $\{r2\}:\{1\bar{1}01\}$. The difference in the notation of facial indices comes from differing in setting of crystallographic axes, and is not substantial.

In this paper the crystal axes are set as, $-h + k + 1 = 3n$, after International Table for X-ray Crystallography, for the benefit of comparison with the X-ray diffraction data.

Jeffery concluded from the X-ray crystallographic study that the high temperature modification of alite belonged to C_{3v}. D_{3d} is made by adding point of symmetry to C_{3v}. From the careful observation on the difference in growth of crystal faces, no indication is found which shows lack of point of symmetry.

The form of alite changes extremely by the paragenetic twin due to the trigonal symmetry. These twin crystals are abundant in clinker. The twin planes are (c) and (r1).

In twin crystal, twin plane being (c), the difference in extinction position of each twins cannot be detected by polarizing microscope, and the twin crystal seems as if single crystal having horizontal symmetry and being D_{3h}. When alite inverts to triclinic form, inversion polysynthetic twin of triclinic system occurs and the textures are discontinuous at the twin plane, and it becomes evident that the crystal is not single crystal but twin crystal.

The twin crystal of which twin plane is (r1), shows frequently hexagonal outline in thin section, and the diagonal of the hexagon is coincident with the twin plane (r1). In these sections, the twin method was frequently mistaken for $(10\bar{1}0)$ of pseude-hexagonal system. When a twin plane (r1) inclines to the section, remarkable wavy extinction appears on the contact zone.

No other paragenetic twin of the symmetry in trigonal system, except (c) and (r1), occurs in alite in commercial cement.

The external form of alite occurring in cement clinkers shows the trigonal symmetry of its high temperature polymorph, but almost all of the diffractometer traces of alite are monoclinic and those of trigonal and triclinic are very rare.

Alite of which diffractometer traces are trigonal of the high temperature polymorph is uniaxial negative or its optic angle is very small:

$$2V = 0 - 20°\mathrm{X}\|\mathrm{c(trigonal)}$$

Alite of which diffractmeter traces are monoclinic of the medium temperature polymorph (metastable) is biaxial negative, 2V = 20 — 60°, X||c (trigonal): This relation is accurately established. Y||a (trigonal), Z$\perp$a (trigonal): The accuracy in the determination is less than in that of the direction of the X axis.

In the horizontal section, the extinction position differs locally, and irregular patches of triple cryclic twin can be observed. On the contrary, in the vertical section, the crystal extincts at the same time exactly, and the twin structure can not be detected. This cyclic twin is paragenetric twin through R $\rightarrow$ M inversion, so the twins must be orientated geometrically with 3-fold symmetry of R. Therefore, it is concluded that X of monoclinic form exactly coincides with 3-fold axis, c, of trigonal form. Through R $\rightarrow$ M inversion, 3-fold axis changes to oblique axis of monoclinic form. It is unnatural that an optical elastic axis coincides with an oblique axis of monoclinic form. These properties are those of pseudo-hexagonal orthorhombic crystal, and may be caused by the remarkable likeness of crystal structure between the trigonal form and the monoclinic form or existence of submicroscopic twin.

Alite of which diffractometric traces are triclinic of low temperature polymorph is biaxial negative,

$2V = 20 - 60°$. X axis inclines to c (trigonal) :X $\wedge$ c (trigonal) $= 0 - 15°$.

In the horizontal section of the crystal the extinction is very obscure. In the vertical section, indistinct stripes parallel to c axis like the polysynthetic twins are observed.

The presence of (0001) twin is clear from the discontinuous stripes in two crystals.

Fudamentals on Belite

H. Insley classified belite into the types of I, Iα, II and III from the observations of clinkers by the reflecting microscope.

Belite of type I and Iα is obtained by heating up to the stability temperature region of α-form.

Belite of these types has the complex inversion textures due to the transitions of $\alpha \rightarrow \alpha'$ and $\alpha' \rightarrow \beta$. Belite of type I$\alpha$ separates its impurities along the inversion texture of $\alpha \rightarrow \alpha'$ inversion and has the textures as well as type I.

Belite of type II crystallizes at the α' phase region of temperature and is cooled to room temperature having the inversion textures due to $\alpha' \rightarrow \beta$ inversion.

Belite of type III belongs to type I or type II having the indistinct inversion textures which are so minute as not to be determined by the optical microscope or not to be observed in some sections.

Thus belite is then classified into type I and II from its inversion textures. Törnebohm called the former "Belit" and the latter "Felit".

Belite of Type 1

Type I crystallizes in a rounded grain having indistinct crystal faces. It has a complicatedly crossed lamellar structure and a set of lamellae, in two directions crossing in about 60° each other, is usually observed distinctly. The acute bisectrixes, Z, of all lamellae in a grain are parallel each other, and can be accurately determined.

In horizontal section, Z being perpendicular to the section, the birefringence is very weak and the extinction are indistinct. The section is divided into minute patches by the difference of the extinction positions.

In the vertical section, Z being parallel to the section, the birefringence is highest and it extincts at the same time. Rotating the vertical section around Z, a set of lamellae, in two directions crossing about 60° each other, can be brought to vertical position, the crystal faces of the lamellae being parallel to view line. At this position, the set of lamellae makes a symmetry extinction, and the obtuse bisectrix of angle of the lamellae is coincident with Z. The angle between the lamellae and X–Y plane is about 33°. Then the section is further rotated 60° form the vertical position around Z, a new set of lamellae becomes prominent and the crystal faces of the lamellae become parallel to view line.

Above observation shows that belite is composed of 3 sets of lamellae and the sets are orientated with 3-fold symmetry around Z.

Usually, the lamellae do not rigidly connect each other, but there are some spaces between the lamellae. The spaces are filled with glassy phase. The refractive index and birefringence of the lamellae with high birefringence are shown as follows: $N = 1.720$, $B = 0.015 - 0.018$.

Those of the glassy phase with low birefringence are shown as follows:

$$N = 1.700 - 1.710 \quad B = 0.000 - 0.003$$

The very minute polysynthetic twins are often observed in the lamellae with high birefringence and its twin planes are parallel to Z.

Above shows that the high birefringence phase is β and the low birefringence phase is α.

The complex lamellar structure with 3-fold symmetry must be skeleton structure through $\alpha \rightarrow \alpha'$ inversion with remainder of α-phase, The minute polysynthetic twin structure of lamella must be inversion twin structure through $\alpha' \rightarrow \beta$ inversion.

Because of the resemblance of crystal structure between α, α' and β-forms, the crystal axes of each modifications keep in same direction through the inversions, and 3-fold axis, c, of α form is transformed to unique axis, b, of β-form.

The facial indexes of the lamellae of the skeleton structure are calculated, from the facial angle obtained by microscopic measurement and the lattice constants obtained by X-ray diffraction. The facial indexes are as follows:

α-form $(10\bar{1}2) \rightarrow \alpha'$-form (112),

$(022) \rightarrow \beta$-form $(1\bar{1}2)(112)(022)$

For the convenience of comparison, the crystal axes of α'- and β-form are set after the ortho-hexagonal axes of α-form.

Belite of Type II

This type of Belite crystallizes in a irregular grain with the distinct parallel striations whose directions are in Z'.

In the horizontal section, Z being perpendicular to the section, the striations are incomplete and observed as cleavage or parting parallel to X and Z. The minute polysynthetic twins, i.e. (100) and (010) approximately parallel to X and Y, are clearly observed and the difference of their extinction positions is from 10° to 20°.

In the vertical section, Z being parallel to the section, striations are observed as complete cleavage or parting parallel to Z. The section extincts at the same time, and the polysynthetic twin structure cannot be observed. Though never abundant, the lamellae parallel to Z and inclined to the optic plane in 60°, i.e. to (110), and those of nearly parallel to X and inclined X-Y plane in 35°, i.e. (011), are observed. These are important to determine the directions of the crystal axes.

Following may be concluded from the aboves. X ||a (approx.), Y||b (approx.), Z||c and X $\wedge$ a = 10°. (In this case, the monoclinic acute bisectrix is c.)

It is evident that the polysynthetic twin structure of (100) and (010) can not occur in orthorhombic system (α') but in $\alpha' \rightarrow \beta$ inversion. The polysynthetic twins observed in the lamellae in belite of type I may be the same ones in belite of type II.

Effects of the Burning Condition of Clinker on the Microscopic Textures of Clinker Minerals

The minerals in clinkers and cements being examined in detail by the microscope, the clear differences will be found in their microscopic textures. This comes from the differences in the conditions of producing: For examples, in kinds, fineness and minor components of raw mixtures or in heat treatments. Thus the conditions of producing may be analyzed from the microscopic textures of minerals.

Many factors exist in the conditions of cement producing. They can be simplified in terms of the crystallization velocity and the recrystallization of minerals, their solution and exsolution of impurities and polymorphic transformation.

Textures of Alite

Effects of the Crystallization Velocity

Since alite crystallizes as precipitation from the liquid phase in which Ca^{2+} and SiO_4^{4-} diffuse and mix and supersaturate for C_3S, the crystallization velocity will be effective on the shape and size of crystals.

When the crystallization is rapid, the crystals will be in small and thin grains of developing in (0001). The slow crystallization will result in the formation of large and thick crystals of well developing in rohmbohedrons of $(01\bar{1}2)$ and $(10\bar{1}1)$.

In the early state of formation of alite, at the temperature of 1250–1300°C, CaO and C_2S are very minute, as 1–2μ, and in contact with each other. The reaction between CaO and C_2S proceeds rapidly and alite is crystallized in minute and thin crystal. As the coming reaction brings about the consumption and the crystal growth of CaO and C_2S, the resulting long distance between them in the reaction and the down of the crystallization velocity result in the formation of the moderate size of alite (15–30μ).

Since it is considerable of decreasing in amount of CaO, as less than 5%, in the late period of reaction, the further long distance between CaO and C_2S and

the delay in the reaction velocity result in the formation of thick and large size of alite (30–60μ).

The crystallization reaction of alite going on through the liquid in which Ca^{2+} and SiO_4^{4-} diffuse, and the diffusing velocity of Ca^{2+} is regarded higher than SiO_4^{4-}, alite crystallizes in a large crystal near the nest of belite, because of the reaction occurring near the nest of belite.

Alite occurring near the nest of belite has often a periodic zonal structure. The width of the zones coming broad near belite. The zoning structure of alite shows that alite grews toward belite.

It may be concluded that the minute alite flocking in a region, in which often small grains of CaO are dispersed, crystallizes in the early state.

Even in a piece of clinker alite distributes differing is shape and grain size, according to the varying period of reaction.

When clinkers are burnt quickly to a high temperature, the amount of the small alite increases and that of large one decreases.

When clinkers are burnt slowly at a medium low temperature, amount of the small alite decreases and amount of the thick and moderate size alite increases with accompanying considerable amount of large alite.

When the raw mixture is fine, the small alite occurs. The raw mixture being coarse, large alite increases. These all come from the difference in the crystallization velocity of alite.

The components of Na_2O, K_2O and SO_3 restrain the crystallization of alite. When these components are contained considerablely in clinkers, alite becomes extremely thick and large, as up to 100–200μ.

Effects of Recrystallization

Alite being treated at a high temperature for a long time, it recrystallizes and grows, but the rate of recrystallization is very slow: It requires 20 hours at 1450°C for 10μ alite to grow to 20μ. Therefore, effects of the recrystallization of alite are practically negligible in a clinker burnt by rotary kiln and its shape and size are considered to be kept as it is at the state of crystallizing.

Alite of moderate size is generally abundant in the well-burnt clinkers, and alite in the half-burnt clinkers is small. These phenomena are not caused by the length of time in treatment at a high temperature, but by the following: In the former case, a raw mixture comes into the burning zone after limestone has already been decomposed and silica has been spent to form C_2S and CaO and C_2S grow to some crystal size in decarbonating zone. In the latter, since a raw mixture containing the half decomposed limestone and free silica comes into the igniting zone, the decarbonation of limestone, C_2S formation and one of C_3S all occurs at the same time to crystallize C_3S explosively.

Effects of the Solid Solution

Birefringence of pure C_3S is in 0.002–0.003. That of alite in clinkers is generally in 0.004–0.007, but comes up to 0.010 in clinkers rich in Na_2O, SO_3 and MgO and burnt at a high temperature.

In general, birefringence of alite is low in clinkers burnt at a low temperature, and that is high when clinkers are burnt sufficiently at a high temperature. These may be caused by the high solubility of impurities in alite at a high temperature and the poor one at a low temperature.

A zoning alite whose birefringence is lower in the inner part of the crystal than in its outer zone is often found in clinkers burnt slowly to a high temperature. This may shows the process that alite with low birefringence crystallized at a low temperature absorbs the impurities from the liquid in the course of its heating up to a high temperature.

Effects of Polymorphic Transformation

Alite is usually monoclinic and rarely trigonal and triclinic in clinkers. Trigonal C_3S, containing some stabilizer, shows a high birefringence and triclinic C_3S, being pure, shows a low birefringence. It is difficult to determine whether the above tendency exists on the three forms of alite with the same chemical composition in the same quantity or trigonal alite is cooled absorbing a large quantity of impurities and triclinic alite is in the comparatively high purity.

When alite is cooled slowly in the temperature range of 1250–1300°C, its birefringence often comes to be remarkably low in spite of the absence of the decomposition of $C_3S(C_3S \rightarrow CaO + C_2S)$ and its being monoclinic optically and in the diffractometric traces. In this case, the texture of alite always departs into many small parts with the different extinction positions and the extinction in whole is indistinct. It may be reasonable that the indetectable decomposition of alite at 1250–1300°C makes the crystal structure into disorder, and this disorder acts as a nucleus in the trigonal → monoclinic inversion.

Textures of Belite

Effects of Crystallization Velocity

Belite crystallizes mostly in the very minute crystals of 1–4μ below 1300°C through the dry solid-solid reaction. The crystals of 20–40μ found in clinkers is formed by recrystallization in the course of the heat treatment at a high temperature. The direct relation cannot be found between the size of belite and its formation velocity.

Effects of Recrystallization

The liquid being formed in the course of the rising of temperature, belite begins to recrystallize quickly to a large crystal. The growth of belite in clinkers is due to the recrystallization. The grain size of belite is related to the period of the heat treatment at a high temperature after the liquid formation.

Since the large grains of feldspar or clay and CaO always react to form the liquid with a low melting point, belite contacting to the liquid crystallizes quickly to form a crust of belite crystals around the liquid. Thus these crystals are then larger than those usual.

Effects of the Solution and Separation of Impurities

Belite crystallizes at first in α'-form which is almost pure. In the previous investigation (20) the solubility of Al_2O_3, Fe_2O_3 and Na_2O are less than 1% in total. After $\alpha' \rightarrow \alpha$ inversion belite begins to absorb the impurities.

Belite separate the impurities according to the difference in their solubility during $\alpha \rightarrow \alpha'$ inversion on cooling. When belite is cooled quickly, the separation of impurities cannot be observed optically and crystals are colorless. Being cooled in a medium velocity, crystals are pale yellow. A slow cooling makes belite muddy yellow. In a extremely slow cooling, it can be observed the minute dots of impurities separated to be despersing.

Yellow or muddy of belite is more remarkable in outer zone of the crystal than in its inner part. This may be attributed to the fact that the inner part of the crystal has scarcely absorbed impurities in $\alpha' \rightarrow \alpha$ inversion and its outer part has overgrown on the former absorbing plenty of impurities by the recrystallization in $\alpha' \rightarrow \alpha$ inversion.

The half-burnt clinker burnt at a remarkably low temperature easily brings about "dusting", because belite is cooled in a pure α'-form.

Effects of Polymorphic Transformation

When clinkers are burnt below the temperature of the stable α–C_2S and cooled from the stability temperature of α'–C_2S, belite is cooled in type II with the monoclinic polysynthetic twins due to $\alpha' \rightarrow \beta$ inversion. But belite of type II is scarcely found in the commercial cements.

When clinkers are burnt at the stability temperature of α–C_2S, belite is cooled in type I with both of the skeletal structure due to $\alpha \rightarrow \alpha'$ inversion and the monoclinic polysynthetic twins due to $\alpha' \rightarrow \beta$ inversion.

The quantity of α phase of belite being contained among skeletons varys in the range of 0–30% with differing clinkers.

For α phase of belite being cooled to room temperature, it is necessary to be rich in Al_2O_3, Fe_2O_3 and Na_2O in clinkers and to cool clinkers quickly.

When clinkers are kept for a sufficiently long time at a high temperature and cooled quickly from near the lower limit of stability temperature of α–C_2S, the quantity of α phase of belit increases. This shows that the crystallinity of α–C_2S rises to restrain $\alpha \rightarrow \alpha'$ inversion under the above condition.

When clinkers are cooled very slowly, α–C_2S inverts completely to α'–C_2S. The skeletal structure occurred in three directions disappears entirely to alter into a single crystal of α'–C_2S taking a texture recrystallized in one direction, which inverts immediately to β–C_2S taking a texture of type II.

It can be easily determined whether belite of type II is one formed by the burning at a low temperature or one by the very slow cooling, because the former is taking a small round shape and the latter is a large irregular shaped grain.

Strength of Cement and Burning Condition

Hydraulic modulus, free lime and fineness of cement are known as important factors for the strength of

cement, and these are always controled by cement makers to be optimum values. But the considerable difference of the strength of cement, such as the compressive strength at the age of 28 days is 300–450 kg/cm², is usually examined. These must be due to the difference of properties of clinker minerals, such as polymorphism, crystallinity and solid solution.

Alite in commercial clinkers is almost monoclinic form, and exsolution of solutes from solid solution through cooling period cannot be detected. The difference of crystallinity can be deduced from the difference of the birefringence and of the intensity of X-ray diffraction.

Belite in commercial clinker consists of α and β-phase, and the difference of solid solution and of crystallinity also can be detected.

The compressive strength of each modifications of belite stabilized by usual components of commercial cement is examined, and the compressive strength of α-form is found to be about 3 times, that of β-form.

The chemical composition of each modifications is as follows:

	SiO_2	Al_2O_3	Fe_2O_3	CaO	MgO	K_2O	Na_2O
α-form	30.4	2.4	2.5	59.1	—	—	5.8
α'-form	33.8	—	—	60.0	2.3	3.8	—
β-form	31.4	2.5	2.5	63.1	—	—	0.5

(%)

The compressive strength of each modifications is as follows:

	7 days	28 days	91 days
α-form	47	80	169
α'-form	11	41	86
β-form	11	38	51

(kg/cm²)

In commercial cement, α'-form cannot be detected. Even if α'-form is contained in cement, the crystallinity may be exceedingly imperfect, and may be practically regarded as warped β-form, the compressive strength of both modifications is about the same.

The content of α-form in belite is varied according to the cooling condition. Belite quickly cooled from a high temperature contains α-form abundantly, and gives high strength. Belite slowly cooled to a low temperature scarcely contains α-form, and gives very low strength.

The relationship between the content of α-form and the strength of belite, saturated with Al_2O_3, Fe_2O_3 and Na_2O, is examined.

The chemical composition of belite is as follows:–

SiO_2	Al_2O_3	Fe_2O_3	CaO	MgO	Na_2O
32.3	1.5	1.5	62.3	0.5	2.0

(%)

The samples of belite are burnt at 1450°C for 0.5, 1.0, 2.0 and 3.0 hours, and cooled under several conditions. The content of α-form is determined by X-ray diffraction method, and the strength of the cement is examined.

The results are shown as follows:

The relationship between the content of α-form and the compressive strength of belite, burnt under several burning conditions.

Burning period at 1450°C (hr)	Quickly cooled from the temp. (°C)	α-form (%)	Compressive strength* (kg/cm²) 7d.	28d.	91d.
0.5	1400	20	42	102	183
	1300	24	57	132	231
	1200	29	42	126	251
	1100	0	26	50	138
1.0	1400	35	66	116	231
	1300	32	71	141	268
	1200	40	48	120	245
	1100	0	25	50	175
2.0	1400	19	69	146	268
	1300	26	53	138	262
	1200	20	45	101	204
	1100	0	26	53	142
3.0	1400	4	46	116	253
	1300	22	47	132	265
	1200	17	32	89	206
	1100	0	19	53	172

*Test pieces of 1 × 1 × 7cm—1/2 Mortar (W/C = 0.65)

The effect of colling condition on the strength of cements prepared from raw materials used in plant is examined.

The chemical composition and the mineral composition of the clinker are as follows:

	SiO_2	Al_2O_3	Fe_2O_3	CaI	MgO	Na_2O	K_2O (%)
MC	24.5	4.2	4.3	65.7	1.7	0.33	0.41
NC	22.7	5.1	3.3	66.2	1.6	0.30	0.54
HC	21.9	5.1	3.0	67.3	1.7	0.28	0.45

Free CaO	C_3S	C_2S	C_3A	C_4AF	Alite	Belite	Matrix (%)
0.0	46.3	35.5	3.9	13.1	46	36	18
0.5	56.2	22.9	8.0	10.0	64	16	20
1.4	63.7	14.9	8.4	9.0	76	2	22

Note: MC; Moderate heat cement, NC; Normal cement
HC; High early strength cement
C_3S—C_4AF; Calculated by Bogue's equation
Alite—matrix; Measured by microscopic method.

The moderate heat cements and the normal cements were burnt at 1450°C for 30 minutes, and the high early strength cements were burnt at 1500°C for 45 minutes, and each cements were cooled under four conditions, shown as (Q), (M), (S) and (VS).

(Q): Quickly cooled from burning temperature.
(M): → 1200°C for 15 mins., → 500°C for 10 mins.
(S): → 1000°C for 25 mins., → 500°C for 15 mins.
(VS): → 1000°C for 25 mins., → 500°C for 35 mins.
The compressive strength of cements are as follows:

Cement	Cooling condition	3d	7d	(kg/cm²) 28d
MC	Q	57	93	215
	M	60	83	172
	S	62	94	157
	VS	59	89	158
NC	Q	99	153	259
	M	97	210	273
	S	97	193	239
	VS	87	187	230
HC	Q	102	188	293
	M	142	267	333
	S	102	210	292
	VS	91	181	279

The strength of moderate heat cement at the ages of 3 days and 7days is scarcely varied by cooling condition. At the age of 28 days, the slower is the cooling, the lower is the strength.

The strength of high early strength cement, at all ages, moderately cooled is strongest.

The situation of normal cement is medium for the above two types cements. From these facts, the following is induced.

1) When clinker is cooled quickly, belite contains α-form abundantly, and the compressive strength becomes stronger.
2) When clinker is cooled moderately, the crystallinity of R-form of alite may rise at the lower part in the stable temperature reagion of the R-form, and inversion of modifications may be disturbed, and alite is cooled in active state.
3) The compressive strength of cement is additive for that of alite and belite.

The burning condition and strength of cement are now inferable from the optical and X-ray diffraction test, and the faults in burning can be pointed out to reform the quality of clinker.

Normal portland cements sold in Japan in 1962 and 1963 were examined. Some of them are omitted, having the obvious faults on chemical composition, free lime, fineness and storage.

The properties of the 45 cements used in this examination were as follows:
Specific gravity: 3.12–3.18 specific surface (Blaine) 3010–3430 cm²/g., ig. loss: 0.5–1.5%, SM: 2.5–3.0, HM: 2.02–2.11, free lime: 0.2–1.1%.

Among the several properties obtained by microscopic observation and X-ray diffraction, content of α-form in belite, color of belite and birefringence of alite were most characteristic.

Compressive strength at 28 days (kg/cm²)	Number of cement	α-form(%) Max.–Min.(Mean)	Color of belite (No. of cement) Color-less	Yellow	Amber
(455)— 410	14	36—13(22.4)	14	0	0
410 — 360	19	30— 8(18.2)	0	18	1
300 —(298)	12	24— 0(9.7)	0	3	9

birefringence of alite (number of cement)	
$B \geqq 0.007$	$B < 0.007$
13	1
3	16
0	12

Occurrance of alite with high birefringence and belite containing α-form abundantly and being colorless in high strength cement shows that the cement was burnt at a high temperature and quickly cooled. Low temperature burning and slow cooling almost go together in cement burning, and take the greater parts of faults in cement burning.

Conclusion

The authors studied the microscopic figures and inner textures of the minerals occurring in clinkers, referring to the fundamental knowledges about the crystal structures and the polymorphisms. And the meaning of the figures and the textures were ascertained.

The conclusions are as follows:

a–1 The external figure of alite is that of trigonal form with the symmetry of D3d.

a–2 The crystal faces are indexed, setting the crystal axes as $-h + k + 1 = 3n$, as tabular basal planes {c}:{0001}, rhombohedral planes {r1}: $\{01\bar{1}2\}$ and rhombohedral planes {r2}:$\{10\bar{1}1\}$.

a–3 Acute bisectrix, X, is exactly parallel to the 3-fold axis, c, of trigonal form and perpendicular to basal plane, (c), except triclinic form. X is used as most sure datum line.

a–4 The external figure of alite is deformed by paragenetic twin. The twin planes, (c) and (r1), are common.

a–5 The optical property of alite is disordered by metagenetic twin. Triple cyclic twin occurres by trigonal → monoclinic inversion, polysynthetic twin occurres by monoclinic → triclinic inversion.

b–1 Belite in clinker is crystallized in irregular rounded grain.

b–2 Belite is classified into two types, named "Type I" and "Type II"

b–3 Type I has a skeleton structure and a polysynthetic structure. Type II has only a polysynthetic twin structure. The skeleton structure is observed as complexed lamellae structure. The polysynthetic twin structure of Type I is very minute. The polysynthetic twin structure of Type II, substantially same as that of Type I, is observed as parallel striations.

b–4 The skeleton structure occurres by $\alpha \rightarrow \alpha'$ inversion. Through this process, α'-phase grows into skeleton crystal, following the crystal structure and symmetry of α-form, and a part of α-form remains between the lamellae of skeleton crystal.

The crystal faces of the lamellae of skeleton crystal are indexed as follows:

α-form $\{10\bar{1}2\} \rightarrow \alpha'$-form $\{112\}$,

$\{022\} \rightarrow \beta$-form $\{1\bar{1}2\}$, $\{112\}$, $\{022\}$

b–5 The polysynthetic twin structure occurres by $\alpha' \rightarrow \beta$ inversion. The conjugate planes of the twin structure are as follows: (100) and (010) are dominant, (110) and (011) are rare.

b–6 The acute bisectiox, Z, of β-form is exactly parallel to the 3-fold axis, c, of α-form, and is used as most sure datum line.

Burning condition of cement clinker and hydraulic strength of cement can be deduced from the microscopic observations of clinker minerals. In this examination, immersed powder preparation of clinker or cement may be used for thin section. This technique is effective to the daily control of clinker burning in manufacture.

Distinct features of clinker minerals varied with burning conditions are as follows:

c–1 When raw mixture is heated slowly, at low temperature C_2S and CaO grow to coarse grains, and velocity of C_3S formation at high temperature decreases, and alite in clinker crystallizes in large and thick form.

c–2 When clinker is burnt up to a high temperature, birefringence of alite becomes higher. This phenomenon may depend on the crystallinity of alite and the content of impurities in alite.

c–3 When clinker is burnt for a long period, alite and belite recrystallize into large crystals.

c–4 When clinker is cooled slowly, value of birefringence of alite decreases and that of belite increases, and α–C_2S content of belite decreases and belite exsolutes the solid solute and the color of belite grains turns from colorless to yellow or amber. These phenomena are related to transformation of temperature modifications of alite and belite.

The quality of alite and belite is a dominant factor affecting the compressive strength of cement. Generally, high temperature modification of crystals is more active than low temperature modification.

In order to obtain a high strength cement, (1) clinker must be burnt at a high temperature for a sufficiently long period to raise crystallinity of high temperature modification and (2) cooled quickly from moderately high temperature to stop the inversion.

References

1. A. E. Törnebohm, "Uber die Petrographie des Portland Cement, Internationalen Verband für die Materialprüfungen der technik", Stockholm, (1897).
2. E. S. Shepherd and G. A. Rankin, "Preliminary report on the ternary system CaO–Al_2O_3–SiO_2. A study on the constitution of portland cement". J. Ind. Eng. Chem., 3–, **4** (1911).
3. N. Sundius, "Uber die Eigenschaften von α-und β-Dicalciumsilikat und die Dicalciumsilikate des Portlandzement-klinkers", **213**, 343–352, (1933).
4. B. Tavasci, "Untersuchungen über die Tonstitution des Portlandzement-kilnkers", Tonid. Ztg., **44**, 487–490 (1937).
5. H. Insley, "Structural characteristics of some constituents of portland cement clinker", J. Res. NBS., **17**, 353–361, (1936).
6. W. C. Taylor, "Nature of the prismatic dark interstitial material in portland cement clinker", J. Res. NBS., **30**, 329–346 (1943).
7. C. E. Tilley, "On larnite (calcium orthosilicate, a new mineral) and its associated minerals from the limestone contact-zone of Scawt Hill, Co. Antrim., J. Mineral, Soc., **22** (125), 77–86 (1929).
8. C. E. Tilley and H. C. G. Vinecnt, "The occurrence of an orthorhombic high-temperature form of Ca_2SiO_4 (bredigite) in scawt hill contactzone and as a constituent of slags"., Mineral. Mag., **28** (200), 255–271 (1948).
9. F. Trojer, "Die oxydischen Kristallphasen der anorganischen Industrieprodukte", E. Schweizerbart'sche Verlagsbuchhandlung (1963).
10. P. Terrier et H. Hornain, "Sur l'application des mé-

thodes mineralogiques á l'industrie des liants hydrauliques", Revue des matériaux de construction, **618** 79–96, **619** 123–140, **620** 177–187. (1967).
11. A. Guttmann und F. Gille, "Zemmenttechnische Bedeutung und Feinbau des Trikalziumsilikats", Zement-Kalk-Gips. **22** 383–388, 402–405 (1933).
12. J. W. Jeffery, "The crystal structure of tricalcium silicate", Acta Cryst., **5** 26–35 (1952).
13. M. A. Bredig, "Isomorphism and allotropy in compounds of the type A_2XO_4", J. Phys, Chem. **46** 747–764 (1942).
14. C. M. Midgley, "The crystal structure of β-dicalcium silicate," Acta Cryst., **5** 307–312 (1952).
15. D. K. Smith, A Majumdar and F. Ordway, "The crystal structure of dicalcium silicate", Acta Cryst. **18**, 787–795 (1965).
16. G. Yamaguchi und Y. Ono, "Mikroskopische Untersunchungen am Alit des Portlandzementklinkers", Zement-Kalk-Gips, **9** 390–394 (1966).
17. G. Yamaguchi and Y. Ono, "Microscopic study on the texture of belite in portland cement clinker", Review of XVI General Meeting, Japan Cement Engineering Association, 32–34 (1962).
18. Y. Ono and T. Shimoda,"Microscopic studies on the texture of ferrite phase", Review of XXI General Meeting, Japan Cement Engineering Association (1967).
19. Y. Ono and Y. Soda, "Effect of the crystallographic properties of alite and belite on the strength of cement", Review of XIX General Meeting, Japan Cement Engineering Association, 78–82 (1965).
20. G. Yamaguchi, Y. Ono and S. Kawamura, "The solid solution region of Al_2O_3 and Fe_2O_3 in the high temperature modification of $2CaO \cdot SiO_2$". Review of XVI General Meeting, Japan Cement Engineering Association (1962). G. Yamaguchi, Y. Ono, S. Kawamura and Y. Kanai, "The solid solution region of the high temperature modifications of Ca_2SiO_4 for Al_2O_3, Fe_2O_3 and Na_2O." Review of XVII General Meeting, Japan Cement Engineering Association. (1963).

Supplementary Paper I-95 Thermal Stabilization of β-2CaO, SiO_2

Valentin I. Korneev and Elysaveta B. Bygalina*

Synopsis

The conditions of transformation of γ–2CaO·SiO_2 into the β-form due to heat treatment without introducing the additions—stabilizers have been studied. The degree of transformation of γ–β–C_2S depends upon the temperature and upon the duration of heat treatment (reheating in the range of 900–1500°C). Thermally stabilized β–C_2S has the refractive indices, X-ray data and differential thermal analysis corresponding to the β-form, and it preserves the shape of the grains, the cleavage, the extinction and the elongation which is typical of the original γ–C_2S. The formation of solid solutions of CaO in dicalcium silicate promotes the stabilization of the β-form. β–2CaO·SiO_2 has been obtained which contains up to 6 per cent of excess CaO in a solid solution. The availability of binding properties of γ–C_2S containing CaO in a solid solution has been determined. The dependence of the hydraulic activity of the β-form of dicalcium silicate upon the concentration of CaO in a solid solution has been found.

Introduction

It is considered that dicalcium silicate which is one of the main minerals of portland-cement clinker may exist in four polymorphous modifications: γ, β, α' and α, from which only γ–C_2S is stable at room temperature (1, 2). The existence of high temperature modifications of Ca_2SiO_4 in industrial products is connected with crystallochemical stabilization (the presence of additions-stabilizers). The attempts to obtain β, α' or α–C_2S without introducing stabilizers were not successful.

In the works of the chair of chemical technology of cement, Leningrad Lensoviet Institute of Technology, the Soviet Union, the possibility to obtain β–C_2S without stabilizers by means of thermal stabilization (by annealing) has been considered. The problems of thermal stabilization of β–C_2S depending upon the formation and the concentration of solid solutions of calcium oxide in dicalcium silicate (with the ratio of $\frac{CaO}{SiO_2} \leqslant 2$) are discussed in the present paper.

Experimental Part

The raw mixture of $\frac{CaCO_3}{SiO_2} = \frac{2}{1}$ was prepared from the calcium carbonate of high purity and anhydrous spectrally pure silicic acid. The raw mixture was ground in a jet mill until the fineness of 1–3 microns was reached, in conditions excluding contamination. On the basis of such a raw mixture, after its having been mixed according to the chemical analysis, the mixtures of the following compositions have been prepared: $\frac{CaO}{SiO_2} = 2.00$, 2.10, 2.20, 2.22 and 2.24. The burning of the samples was carried out in the laboratory kiln with carborundum heaters at the temperature of 1500°C and rapidly cooled in air.

The petrographic analysis of sinter materials (not containing CaO) did not show the presence of any other phases but dicalcium silicate up to the ratio of $\frac{CaO}{SiO_2} = 2.20$. Only with greater CaO content the phases different from those of C_2S appear in the sinter material.

As far as the authors were interested in the stage where dicalcium silicate appeared, the work was further carried on with the following compositions of $\frac{CaO}{SiO_2} = 2.00$, 2.10, and 2.20, which contained 0.3 and 6 per cent of excess CaO respectively in comparison

*Leningrad Lensoviet Technological Institute, U.S.S.R.

with the stoichiometric dicalcium silicate. The immersion analysis has shown that the sinter material of $\frac{CaO}{SiO_2} = 2.0$ composition, which crumbled on cooling, consists completely of γ-C_2S, where $Ng' = 1.656$ and $Np' = 1.642$ ($Ng' - Np' = 0.014$). The crystals of γ-C_2S are prismatically elongated in shape, have perfect cleavage and great 2V, positive optical sign and negative elongation; they are also biaxial. The extinction is parallel to the prism.

The sinter materials which $\frac{CaO}{SiO_2}$ is higher than 2.0, except γ-form, have a certain amount of β-C_2S ($Ng' = 1.739$, $Np' = 1.718$); it amounts to 10–15 per cent for $\frac{CaO}{SiO_2} = 2.10$ and 15–20 per cent for $\frac{CaO}{SiO_2} = 2.20$. γ-$2CaO \cdot SiO_2$ in those sinter materials has $Ng' = 1.662$; $Np' = 1.642$; $Ng' - Np' = 0.020$. The shape of the grains is prismatically elongated, with perfect cleavage. The elongation is negative, 2V is great, the optical sign is negative, the grains are biaxial. The extinction is parallel to the cleavage.

The durable burning at the temperature of synthesis did not change the phase relationships (the relation between γ-β forms), only the dimensions of the grains of $2CaO \cdot SiO_2$ were altered. Thus, the difference of sinter materials having $\frac{CaO}{SiO_2}$ more than 2.0 from stoichometric composition is in the appearance of β-form, which is connected with the excess lime stabilization. The stabilization, however, takes place only partially (up to 20 per cent). γ-$2CaO \cdot SiO_2$ in sinter materials which $\frac{CaO}{SiO_2}$ is more than 2.0 has higher refractive index than the normal ones, greater birefringence and it changes the optical sign of the crystals from positive to the negative one, which indicates the formation of solid solution of CaO in γ-dicalcium silicate. This conclusion is confirmed by the X-ray analysis and the infra-red spectroscopy.

The compositions burned at 1500°C and having molar ratio of $\frac{CaO}{SiO_2} = 2.00$; 2.10; 2.20 were annealed (reheated) within the temperature range of 800–1400°C during the time from 5 to 240 min. The degree of thermal stabilization (the content of β-$2CaO \cdot SiO_2$) was determined by the immersion method for all samples (See Table 1).

It follows from the table that 90–95 per cent β-C_2S can be obtained as a result of thermal stabilization, by means of annealing γ-C_2S. The degree of γ-β transformation during thermal stabilization (annealing) depends upon the composition of the original γ-$2CaO \cdot SiO_2$. The most favourable conditions for stabilizing β-C_2S are obtained at a maximum level of supersaturation γ-dicalcium silicate with $CaO\left(\frac{CaO}{SiO_2} = 2.20\right)$.

For C_2S having $\frac{CaO}{SiO_2} = 2.00$ and 2.10, β-C_2S is thermally stabilized only at the temperature of 1000°C. For the composition having $\frac{CaO}{SiO_2} = 2.20$, β-form is stabilized within the temperature range of 1000–1400°C. For each annealing temperature there is a most favourable time period, giving the maximum yield of β-$2CaO \cdot SiO_2$.

To avoid possible stabilization of β-C_2S by the materials sublimed out of refractories, coatings, and heaters of the furnace, the control experiments were made with annealing of γ-C_2S in a closed platinum crusible sealed in quartz tube. Under those conditions the stabilization of β-$2CaO \cdot SiO_2$ also took place, that gives reason to consider the process of stabilization from the point of view of annealing exclusively.

Petrographically, in β-C_2S, stabilized by the annealing of the γ-form and having the ratio of $\frac{CaO}{SiO_2} = 2.00$, the shape of the grains, the cleavage, the extinction, the elongation, which are characteristic for the γ-dicalcium silicate are retained. At the same time the optical sign of the crystals is changed and the refractive indices are found, which are characteristic for β-$2CaO \cdot SiO_2$ $Ng' = 1.734$, $Np' = 1.716$ ($Ng' - Np' = 0.018$). The crystals of β-C_2S, obtained from

Table 1. *Thermal stabilization of* β-$2\,CaO \cdot SiO_2$

The ratio of $\frac{CaO}{SiO_2}$ in dicalcium silicate	The degree of thermal stabilization (content of β-C_2S in %)														
	800°C			1000°C			1100°C			1200°C			1400°C		
	Time of annealing in minutes														
	5	30	90	5	30	90	5	30	90	5	30	90	5	30	90
2.00	0	0	0	75	85	70	0	0	0	0	0	0	0	0	0
2.10	0	0	0	55	80	80	0	0	0	0	0	0	0	0	0
2.20	0	0	0	70	80	95	75	85	95	80	90	95	90	95	95

γ–$2CaO \cdot SiO_2$, which contains in the lattice 3 and 6 per cent of excess lime respectively are characterised by the prismatically elongated shape, perfect cleavage, greater 2V value, negative optical sign and $Ng' = 1.739$; $Np' = 1.716$. $(Ng' - Np' = 0.023)$

The X-ray patterns of the annealed products with variable ratio of $\frac{CaO}{SiO_2}$ show the difraction maximums of the β-form of C_2S (in the samples, where $\frac{CaO}{SiO_2} = 2.00$ and 2.10, γ-C_2S is also present). Particularly clearly the thermal stabilization of β–$2CaO \cdot SiO_2$ is determined by the method of differential thermal analysis (Fig. 1). Thus, for the curves 5, 3 and 1 corresponding to γ–C_2S, having the ratio of $\frac{CaO}{SiO_2} = 2.00$; 2.10 and 2.20 respectively, the transformation of γ-α' is typical at the temperatures 750–760°C. The curves 6, 4, 2 correspond to the same products in the annealed state. In the curves 6 and 4 the endothermal effects are shown which are characteristic of the β to α' (at 660°C) and γ to α' (at 745°C) transformations.

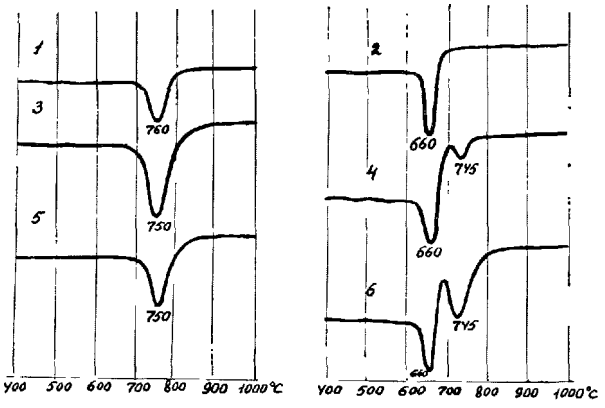

Fig. 1. *Differential thermal analysis of* $2CaO \cdot SiO_2$.
1, 3, 5 are the curves of heat treatment of γ-C_2S obtained from the raw material and having $CaO/SiO_2 = 2.20$, 2.10 and 2.00 respectively.
2, 4, 6 are the curves of heat treatment of the annealed materials of γ–C_2S having the same ratio of CaO/SiO_2 (respectively).

β-from thermally stabilized from γ–C_2S, where $\frac{CaO}{SiO_2} = 2.20$ (curve 2) does not contain γ–C_2S and so it gives only one endothermal effect (at 660°C) which is characteristic for the β to α' transformation.

As far as non-stoichiometric γ–C_2S or β–C_2S which did not contain the additions-stabilizers were not known, it was interesting to study the properties of these phases and especially their hydraulic activity. The compressive strength of samples (1 : 3 mortar) kept under humid condition is determined after 7,28 days and three months curing. Moreover, the compressive strength of specimens autoclaved under the pressure of 8 atm. is determined (See Table 2). The binding properties of the compounds received by the authors have been compared with those of γ–C_2S and β-form stabilized by boric anhydride (Table 2). Two points should be considered (Table 2):

1. The appearance of binding properties of γ–C_2S containing CaO in solid solution.
2. The influence of CaO concentration in solid solution $\left(\text{the ratio of } \frac{CaO}{SiO_2}\right)$ on the hydraulic activity of β–$2CaO \cdot SiO_2$.

The hydraulic activity of γ–C_2S (having $\frac{CaO}{SiO_2} = 2.20$) is of the same order as that of the β-form stabilized by B_2O_3 and on the same level as β–C_2S thermally stabilized and having $\frac{CaO}{SiO_2} = 2.00$.

While increasing the ratio of $\frac{CaO}{SiO_2}$ up to 2.20 (6 per cent of CaO in solid solution) the hydraulic activity of C_2S increases twice during 28 days, and four times when autoclaving. γ–$2CaO \cdot SiO_2$ with the molar ratio of $\frac{CaO}{SiO_2} = 2.00$ has no binding properties. One should think that when excess CaO is dissolved in dicalcium silicate, the regular olivine structure of γ–C_2S is changed into the one having irregular coordination of calcium with oxygen that is supposed to be the reason of the appearance of binding properties.

Table 2. *Binding properties of synthesized forms of dicalcium silicate*

Composition of the product	Molar relation of $\frac{CaO}{SiO_2}$	Compressive strength in kgs. per sq. cm			
		after 7 days	after 28 days	after 3 months	after autoclaving under 8 atm.
γ–C_2S	2.00	0	0	0	not determined
γ–C_2S	2.20	10	15	not determined	40
β–C_2S stabilized by B_2O_3	2.00	15	15	not determined	15
β–C_2S	2.00	10	15	not determined	10
β–C_2S	2.10	10	20	40	55
β–C_2S	2.20	10	15	140	250

Summary

1. The authors have the conditions of stabilizing β–$2CaO \cdot SiO_2$ not containing additions-stabilizers, due to annealing γ–C_2S. The formation of solid solutions CaO in C_2S propmotes the stabilization of the β-form of dicalcium.

2. γ and β–$2CaO \cdot SiO_2$ have been synthesized which contain up to six per cent of excess calcium oxide in a solid solution.

3. The binding properties of γ–C_2S has been given when it contained CaO in a solid solution.

The dependence of the hydraulic activity of β–C_2S upon concentration in a solid solution of calcium oxide has been shown.

References

1. R. Nurse, "The phase of dicalcium silicate" Intern. Cong. on the Chem. of Cem. Moscow (in Russian) Gosstroiizdat. p. 27 (1958).

2. M. M. Sichov, V. I. Korneev and N. F. Fedorov. "Alite and belite in portland cement clinker". Leningrad (in Russian) Gosstroiizdat, p. 30 (1965).

Supplementary Paper I-101 Properties of Substituted Dicalcium Silicate and Alumino-Ferrite

M. K. Gharpurey and V. N. Pai*

Synopsis

It is known that ionic substitutions can occur in portland cement clinker minerals, and that such substitutions can materially alter their properties including the rate of hydration.

In this study β–C_2S was prepared in which some of the Si^{4+} ions were substituted with tetrahedral Al^{3+}, by using lime-soda felspar (bytownite) and potash soda felspar (microcline), in which all the Al^{3+} ions are tetrahedrally coordinated as the main siliceous material.

The bytownite-based products required boric acid for stabilization of the β–C_2S phase, while the microcline-based preparations did not require boric acid. The products contained some C_3A, those with larger attempted substitution containing more C_3A.

The larger was the attempted substitution of Si^{4+} by Al^{3+}, the faster was the rate of hydration. The bytownite-based products released much more $Ca(OH)_2$ during hydration.

In the $C_6A_xF_{3-x}$ series, in C_4AF with Fe partly or wholly substituted with Mn and/or Ca partly substituted with Mg and in C_6AF_2 with half of Fe substituted by Mn, the rates and the products of hydration were studied, and differences observed.

On admixing with water, some of these started hydrating immediately while the others exhibited induction periods of at least 1 1/2–2 hours before the start of hydration.

Introduction

The main phases of portalnd cement clinker, viz. the two calcium silicates, and calcium aluminate and alumino-ferrite are not pure in that other ions such as aluminium and magnesium are known to enter e.g. the silicate lattice. The presence of such foreign ions may modify the structure and stabilize certain phases, or make the compound more or less hydraulic.

Thus e.g. a number of oxides besides B_2O_3 stabilize the β–C_2S structure by substitution for SiO_4^{4-} other groups such as BO_4^{5-}, PO_4^{3-} where B^{3+}, P^{5+} are smaller than Si^{4+} ions, or by replacing some of the Ca^{2+} ions with larger cations Ba^{2+}, K^+ etc. (1). Stabilization due to larger size ions such as of chromium and manganese substituting for Si^{4+} has also been reported (2). Incorporation of P_2O_5, V_2O_5, BaO makes β–C_2S chemically more active to the hydration reactions (3), and it is thought that in the extreme case β–C_2S can be made to approach C_3S in the development of early strength (4). Therefore, a study of the formation of such substituted compounds and their hydration behaviour should prove to be of interest.

One of the possible significant modifications of β–C_2S is the substitution of some of the Si^{4+} ions with tetrahedrally coordinated Al^{3+} ions with the charge neutralization being obtained with interstitial cations or in some other way. Towards this end members of the felspar series were chosen as the main siliceous material since in these all the Al^{3+} ions are tetrahedrally coordinated with the oxygens and form part of the silicate network, the charge balance being effected by cations such as Na^+, K^+, Ca^{2+} in intermediate lattice positions (5). The felspar together with lime and silica to give varying degrees of substitution of Si^{4+} by Al^{3+} was heated to high temperatures to give the β–C_2S.

The calcium alumino-ferrite in portland cement is a member of the solid solution series from C_2F to alumina-rich $C_6A_{2.1}F_{0.9}$. The rate of hydration as well as the nature of hydrated products in this series are known to depend on the A/F ratio of the material (6). Further changes in the properties of these compounds on replacing the Fe_2O_3 partly or wholly by Mn_2O_3 as also on replacing CaO partly by MgO should prove of interest. The manganite analogue of C_4AF, viz. C_4AM' ($M' = Mn_2O_3$) is known, and a complete solid solution range between C_4AF and

*The Associated Cement Cos'. Central Research Station, Thana, India.

C_4AM' has been observed (7). However, the hydration behaviour of the manganese-containing compounds does not appear to have been reported.

Experimental

The finely powdered −90 microns materials were blended, pelletized at 30 tons/sq. inch pressure, and heated for 2–4 hours at temperatures around 1250°–1450°C at which the pellets showed slight softening. After powdering the pellets the free lime of the product was determined, and in case it was above 1.0 per cent, the pelletizing and the heat treatment were repeated. The pellets were now pulverized to −44 microns and used for further hydration studies. The powdered material as such or after admixing 4.3% $CaSO_4 \cdot 2H_2O$ (2.0% SO_3) was used for further hydration studies.

1. The specific gravity of the samples was determined. The different substituted β–C_2S preparations were assumed to have the same monoclinic symmetry as β–C_2S, and the various ferrites and manganites to have the same orthorhombic symmetry as brownmillerite. From the X-ray spacings of four and three lines respectively the unit cell dimensions were calculated and, in the case of ferrite-manganite series, the density as determined in this manner from the X-ray data was compared with the above value. Cu KαX-radiation was used for the diffraction studies.
2. The different powders (with and without $CaSO_4 \cdot 2H_2O$) were mixed with water to have a W/C ratio of 0.4–0.5 for the β–C_2S preparations and 0.5 for the ferrite-manganites (0.75 was required for C_6A_2F in order to avoid undue stiffening during mixing) and left hydrating in sealed test tubes. At the end of 1- (for ferrite-manganites only), 3-, 7-, 14-, 28- and 56- (for β–C_2S preparations only) day hydration the material was powdered to −592 microns, washed twice with acetone and ether, filtered, further powdered to −75 microns, and taken up for D.T.A. and X-ray diffraction examination as well as for fixed water (loss on ignition). It was found that the loss due to any uncombined water, acetone and ether still remaining in the sample was less than 1 per cent so that prior drying of the sample before ignition was not resorted to. For D.T.A. 125 mg of the sample was mixed with equal mass of finely powdered calcined alumina and the whole material was packed in the sample holder. For X-ray examination 0.5 g of the unhydrated material or 0.45 g of the hydrated material was packed in the standard size diffractometer specimen holder.
3. In some case 100 ml of water were added to 0.4 g of the sample along with 0.15 g of $CaSO_4 \cdot 2H_2O$, and the flask was shaken continuously. The pH of the suspension was periodically determined. At the end of 1 and 3 days the suspension were filtered and the residue examined by D.T.A.
4. In the case of the ferrites-manganites the sample was mixed with water (W/C = 0.5), packed in the X-ray diffractometer specimen holder, covered with a thin polythene film, the diffractometer adjusted to the top of the most intense ferrite peak, and the X-ray count taken periodically to determine the initial rate of hydration according to the method described by Tsumura (8).

The results for the β–C_2S and the alumino-ferrites are discussed separately in the following.

Substituted β-C_2S

Materials

There were two felspars used for the following experiments, a lime-soda felspar and a potash-soda felspar called bytownite and microline respectively in the following:

In calculating the compositions of the felspars the following assumptions were made:

i) Al^{3+} went into tetrahedral positions along with Si^{4+} to the extent that other charge neutralizing cations were available;

ii) In the case of bytownite, where there was an excess of the charge neutralizing cations, these were present in the felspar lattice in proportion to their molar concentration in the sample.

On these assumptions, these samples were supposed to be composed of the following:

Bytownite $Na_{0.51}K_{0.05}Ca_{0.96}Mg_{0.19}Al_{2.85}Si_{5.15}O_{16}$		94.46%
	Excess Fe_2O_3	4.20
	CaO	0.16
	MgO	0.02
	Na_2O	0.19
	K_2O	0.03
	Loss	0.50
	Total	99.56
Microcline $K_{1.34}Na_{0.47}Al_{1.81}Si_{6.19}O_{16}$		94.94%
	Excess Al_2O_3	3.67
	Loss	0.63
	Total	99.24

Thus, in bytownite, the Al^{3+} had substituted for Si^{4+} in 5.70 positions out of 16 and, in microcline, the substitution was in 3.62 positions in 16.

This tetrahedrally coordinated aluminium was regarded as equivalent to silicon and the felspar was regarded as equivalent to SiO_2 with some charge neutralizing interstitial cations. Silica and lime were added to the felspar so that in the β–C_2S finally produced the Al^{3+} should substitute for Si^{4+} in 4, 2,1 positions in 16. (The microcline did not require any silica addition for approximate 4 in 16 substitution).

Silica gel (B.D.H) and dehydrated amorphous silicic acid were used for silica additions. The lime used was obtained by calcining $CaCO_3$ of better than 99.5% purity.

The following observations were made:

i) The microcline-based preparations required heating at 1460°–1480°C, while the bytownite-based preparations reacted at 1380°–1400°C only.

ii) The two preparations with 4 in 16 Al substitution required two heating cycles, while the remaining four required a single heating cycle only for bringing down the free lime.

iii) The bytownite-based preparations required 0.5 % B_2O_3 added to the raw mix to prevent conversion of the product to γ–C_2S and consequent dusting. On the other hand, the microcline-based preparations did not require a stabilizer for the β–C_2S phase. The 4 in 16 substitution product did not dust at all. The 2 in 16 product showed slight dusting tendency and the 1 in 16 product dusted to the extent of 10% only, and was examined free of dust.

The bytownite-based 4 in 16 product was analyzed for ferrous iron since Fe^{2+} has been reported to promote the conversion of β–C_2S to γ–C_2S (2). However, all the iron in it was found to be in the ferric state.

For comparison, synthetic C_3S and boric acid stabilized β–C_2S were also used.

Results

The six products were chemically analyzed. The design and the actual values of the alkalis are given in the following:

Bytownite-based preparations

Desired replacement of Si *by* Al:	*4 in 16*		*2 in 16*		*1 in 16*	
	Actual	*Design*	*Actual*	*Design*	*Actual*	*Design*
Na_2O	0.81%	0.77%	0.49%	0.39%	0.32%	0.20%
K_2O	Nil	0.10	Nil	0.05	Nil	0.03

Microcline-based preparations:

Desired replacement of Si *by* Al:	*4 in 16*		*2 in 16*		*1 in 16*	
	Actual	*Design*	*Actual*	*Design*	*Actual*	*Design*
Na_2O	0.54%	0.96%	0.32%	0.57%	0.26%	0.28%
K_2O	0.19	4.18	0.19	2.43	0.58	1.24

The analyses show that from the microcline-based preparations a large proportion of the potash as well as some soda also had evaporated during the heat treatment. From the bytownite-based preparations also the minor quantities of potash volatilized completely.

The X-ray diffraction analysis also showed these samples to be composed of β–C_2S as the main phase along with some C_3A, the proportion of C_3A increasing in the higher substituted compounds. Obviously some of the aluminium ions had come out of the β–C_2S lattice so that the actual substitution of Si^{4+} by Al^{3+} was less than the attempted 4, 2 and 1 in 16. For convenience, however, these samples will be referred to as 4, 2 and 1 in 16 substitution products.

In addition to the above, the two 4 in 16 products contained some C_3S. (In the microcline-based sample a little more lime than needed was already present in the raw mix).

The 4 in 16 bytownite-based product showed, in addition, the presence of some α–C_2S from the 32.4° 2θ line between the 32.1° and 32.6° β–C_2S lines as well as from the fact that the 33.2° 2θ line (due to C_3A) did not disappear completely at 3-day hydration, but rather went down to a small peak at 33.0° 2θ, which corresponds to α–C_2S and which had earlier merged in the strong C_3A line.

Unit Cell Dimensions

The X-ray diffractometer records of these six products were taken with silicon metal as internal standard, and the positions of the (020), (210), (031) and (202) peaks of β–C_2S accurately determined. Assuming these products to have the same monoclinic

symmetry as boric acid stabilized β–C_2S, the lattice constants of these modified β–C_2S products were determined.

Attempted substitution	β–C_2S *Bytownite-based*	*Microcline-based*
4 in 16	$a = 5.50$Å	$a = 5.51$Å
	$b = 6.79$	$b = 6.78$
	$c = 11.06$	$c = 11.00$
	$\beta = 123°28'$	$\beta = 123°47'$
2 in 16	$a = 5.50$Å	$a = 5.50$Å
	$b = 6.77$	$b = 6.76$
	$c = 11.22$	$c = 11.18$
	$\beta = 123°40'$	$\beta = 123°45'$
1 in 16	$a = 5.50$Å	$a = 5.51$Å
	$b = 6.77$	$b = 6.77$
	$c = 10.98$	$c = 11.04$
	$\beta = 123°39'$	$\beta = 123°46'$

These values may be compared with the literature values for β–C_2S (9)

$a = 5.514$Å
$b = 6.757$
$c = 11.197$
$\beta = 123°59'$

The differences are thus not very significant.

Specific Gravity

The specific gravity of these products was found to be:

Design substitution	*Bytownite-based*	*Microcline-based*
4 in 16	3.19	3.23
2 in 16	3.24	3.25
1 in 16	3.24	3.29

The literature values of the specific gravity of a few of the substances concerned are as follows (9):

β–C_2S	3.28
γ–C_2S	2.97
α–C_2S	3.04
α'–C_2S	3.40
C_3S	3.12–3.25
CaO	3.345
C_3A	3.03

The 4 in 16 products contained the largest C_3A, besides some C_3S. In addition, the bytownite-based product showed some α–C_2S also. Thus, these products showed lowest specific gravity.

One may add that, if there is 4 in 16 substitution of Si^{4+} by Al^{3+} with lime alone as the charge neutralizing cation, the formula for C_2S would be:

Table 1. *Fixed water of samples hydrated for varying periods/days (Unhydrated basis)* (%)

	Hydrated as such					Hydrated with 2.0%SO_3*				
Preparation	3	8	14	28	56	3	8	14	28	56
Bytownite-based										
4 in 16	16.7	24.5	28.5	31.6	36.0	18.3	24.2	28.2	32.4	34.8
2 in 16	8.7	13.8	18.1	25.5	28.7	10.2	15.2	18.3	24.5	25.8
1 in 16	4.2	7.4	12.2	19.0	28.9	7.1	9.2	12.6	17.0	23.8
Microcline-based										
4 in 16	19.8	23.3	24.2	25.3	30.6	18.1	23.5	24.4	25.5	30.4
2 in 16	6.2	7.9	8.0	10.9	18.5	8.3	18.9	10.5	12.0	13.8
1 in 16	4.7	5.9	5.9	10.7	19.0	7.5	7.8	10.4	14.7	21.2
β-C_2S (Boric acid stabilized)	3.7	9.5	13.9	18.8	—					
C_3S	16.0	19.3	24.1	29.0	—					

*The fixed water of unhydrated material will be 0.9% due to 4.3% gypsum.

$16CaO \cdot CaAl_2Si_6O_{16}$ instead of $16CaO \cdot Si_8O_{16}$. Assuming no change in the lattice dimensions, the specific gravity would increase from 3.28 to 3.37 only.

Fixed water

The water fixed at 3 days is, to non-inconsiderable extent, due to the hydration of C_3A. Since the higher substitution products contained more C_3A, their higher fixed water contents are partly due to the C_3A hydration.

The difference in the water fixed at 3 days and at 8 days can be, for a given series of products, a measure of the rate of hydration of the β–C_2S. The higher substitution products thus appear to hydrate faster.

The water fixed by the bytownite-based products is higher than that by the microcline-based products. This is, to some extent, due to more $Ca(OH)_2$ being released by the former during hydration, as will be presently seen.

Hydration Studies with X-ray Diffraction and D.T.A.

Bytownite-Based Products:
4 in 16:

Almost all the C_3A had hydrated at 3 days giving C_4AH_{13} when hydrated as such, and monosulphate with a trace of ettringite when hydrated with gypsum. The ettringite disappeared at later ages while the C_4AH_{13} and monosulphate respectively remained at the same level as examined both by X-rays as well as by D.T.A.

The small quantity of C_3S had of course hydrated at 3 days.

The amount of $Ca(OH)_2$ formed was large com-

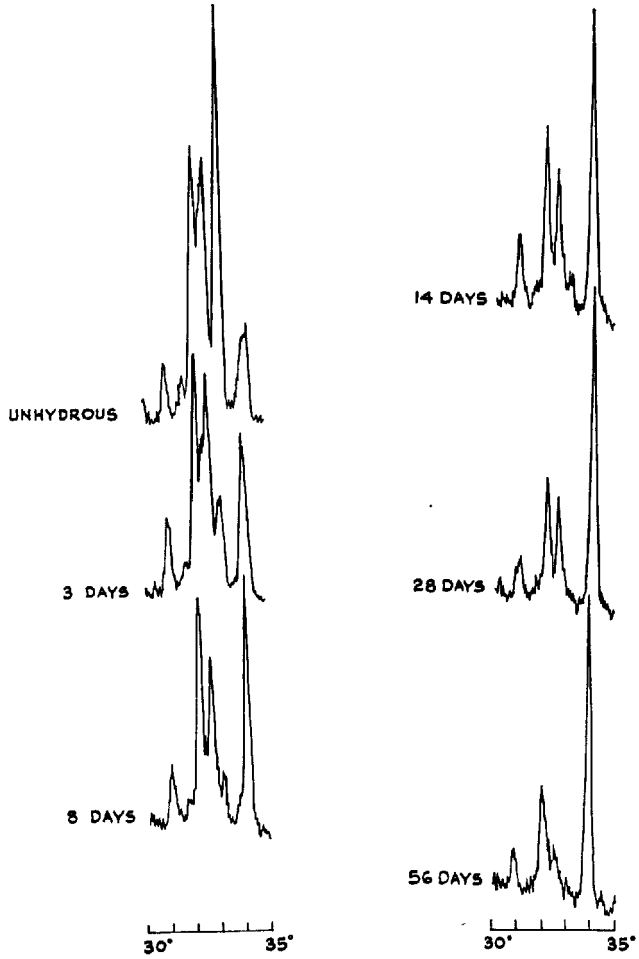

Fig. 1. *X-ray diffractometer trace between 30° and 35° 2θ of bytownite-based "4 in 16" substituted β-C_2S hydrated for different periods.*

pared to that formed by pure β–C_2S at 3 days, and this increased with age along with the endothermic dip due to tobermorite gel, while at the same time the X-ray lines due to the unhydrated β–C_2S went down in intensity (Fig. 1). The lime was obviously coming out of the β–C_2S lattice.

A small tobermorite peak at 50.0° 2θ appeared at 14-day hydration only as with C_3S, and a further low angle 8.1° peak appeared at 28 days.

On hydrating with SO_3, α–C_2S also appeared to hydrate by 2 months.

The X-ray lines due to the β–C_2S went down in intensity considerably by 56 days.

2 in 16 and 1 in 16:

These products contained, besides β–C_2S, lower and lower amounts of C_3A as compared with 4 in 16, the C_3A formed decreasing with the attempted substitution of Si by Al. As a result, on hydrating without SO_3 less and less of C_4AH_{13} was formed, the low angle X-ray peak of which became much diffused and smaller at 28 days.

On hydrating with SO_3, the 2 in 16 gave monosulphate and ettringite, while the 1 in 16 gave ettringite only. These sulpho-aluminates remained constant at later ages except that in 1 in 16 the ettringite peak at 8.9° split up into two (9.0°, 9.2°) at 28 days.

The lower the attempted substitution, the less was the $Ca(OH)_2$ formed, and the tobermorite D.T.A. endothermic peak was less strong at a given age with lower substitution products. Under X-rays the 50.0° 2θ peak also appeared later at 28 days with the 2 in 16 product hydrated with SO_3, and with the 1 in 16 products.

The higher substitution products thus appeared to hydrate faster.

Microcline-Based Products:

4 in 16:

At 3 days the small quantity of C_3S and the C_3A hydrated completely, the latter yielding C_4AH_{13} on hydration without SO_3, and monosulphate and C_4AH_{13} when hydrated with SO_3. These compounds remained at a constant level throughout further period of hydration.

There was only a trace of $Ca(OH)_2$ at 3 days. Of course some of the lime released must have been taken up to form C_4AH_{13} from C_3A. The $Ca(OH)_2$ increased with age.

A prominent endotherm due to tobermorite was seen at 3 days, comparable to that due to C_3S (Figs. 2 & 3). However, the 50.0° 2θ X-ray peak due to tobermorite was noticeable at 28–56 days only.

If the tobermorite gel formed by the substituted β–C_2S contained some Al^{3+} ions, the associated endothermic effect could be a little higher since the heat of hydration of aluminates (e.g. C_3A) is higher.

2 in 16 and 1 in 16:

These gave C_4AH_{13} at 3 days on hydrating without SO_3, the quantity of C_4AH_{13} being less the lower the substitution. In fact the 1 in 16 substitution products gave only a trace of C_3A.

On hydrating with SO_3 the 2 in 16 gave monosulphate with a trace of ettringite. The latter disappeared at 8 days while the monosulphate increased, and then remained constant at later ages, showing a sharp low angle peak.

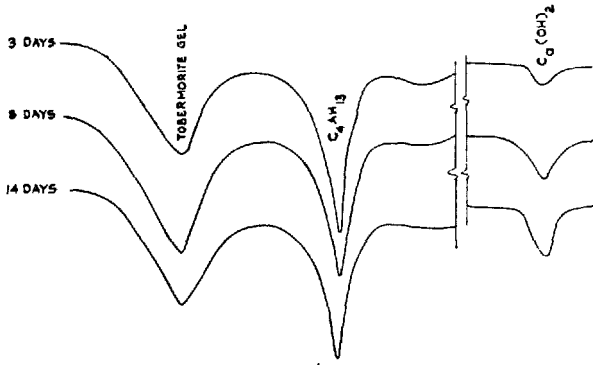

Fig. 2. *D.T.A. curves of microcline-based "4 in 16" substituted β-C_2S hydrated for different periods.*

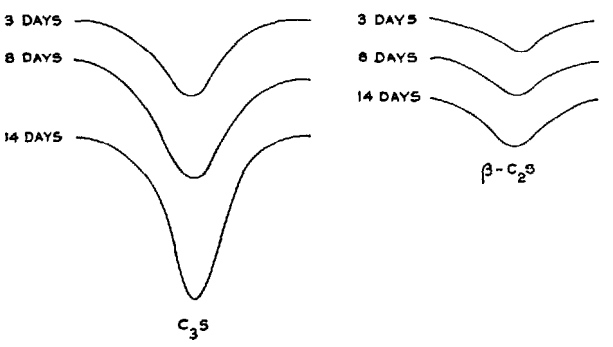

Fig. 3. *D.T.A. endotherms due to tobermorite gel formed by C_3S and boric acid stabilized β-C_2S hydrated for different periods.*

The 1 in 16, surprisingly enough, gave ettringite and C_4AH_{13} at 3 days. Both remained constant till 14 days. At 28 days, the 9.05° 2θ ettringite peak split up into two (8.95° and 9.25°) and the C_4AH_{13} went down.

The lower the substitution products, lesser $Ca(OH)_2$ was formed, which nevertheless increased with duration of hydration.

The tobermorite endotherm also developed slower with lower substitution products, and the 50.0° 2θ X-ray peak also appeared at 28–56 days.

From the fall in the unhydrate β–C_2S peak intensities it was estimated that the 2 in 16 microcline-based product hydrated less in 2 months than the 1 in 16 bytownite-based product.

It was, however, felt that the microcline-based products started hydrating earlier. In order to check this 0.5 g of C_3S, and the products were kept shaking in 100 ml water for 3 days, filtered and the residue examined by D.T.A. The microcline-based 4 in 16 product showed a much stronger endotherm of tobermorite than even C_3S, while the corresponding 2 in 16 exhibited only a trace of the same. The bytownite-based 4 in 16 and 2 in 16 products also showed only a trace of tobermorite endotherm. Nevertheless at later ages, the bytownite-based products appeared to have hydrated to a greater extent (as seen from the X-ray intensities) as compared with the corresponding microcline-based preparations.

Discussion

In the above, attempts were made to prepare β–C_2S with varying degrees of substitution of Si^{4+} with Al^{3+} tetrahedrally coordinated. However, the substitution was not complete as seen from the formation of C_3A in all cases, the quantity of C_3A being larger, the larger the attempted substitution. Even then, the products with larger attempted substitution appeared to hydrate faster.

The usual stabilizers of β–C_2S such as B_2O_3 act by forming BO_4^{5-} groups replacing SiO_4^{4-}, where the B^{3+} ions are smaller in size than Si^{4+} and where these ions are small enough so that the size of the RO_4 group is almost entirely determined by the O–O distances, the substitution not involving a significant change in lattice dimensions (1). It is further believed that the substitution of Si^{4+} by Al^{3+} or Fe^{3+} would increase the size of the tetrahedral group and would favour the α or γ forms. The self-stabilization of the microcline-based products is contrary to the above.

As regards charge balancing, it has been suggested that when BO_4^{5-} groups are inserted, extra Ca^{2+} ions must be introduced in the holes in C_2S since a sample of β–C_2S containing 0.3% B_2O_3 had a $CaO:SiO_2$ molar ratio of 2.1:1(1). As an alternative, since β–C_2S is a compact structure the stabilization by B_2O_3 is again explained as due to BO_4^{5-} replacing SiO_4^{4-}, the charge being balanced by missing Si^{4+} ions, probably in the form of silica (10)—although for charge neutralization it has to be missing SiO_4^{4-}.

The stabilization of β–C_2S by excess lime has also been suggested as due to the excess Ca^{2+} and O^{2-} ions occupying interstitial positions (1). Again, however, doubts have been expressed if there would be room for the large O^{2-} ions in the β–C_2S structure and, as an alternative, it has been proposed that the Ca^{2+} occupy normal lattice positions and that some of the Si^{4+} sites are vacant for charge balancing (11).

In the case of the bytownite-based products, with Al^{3+} substituting for some of the Si^{4+}, one may explain the charge balancing in one of the two alternate ways: (i) with the charge balancing Ca^{2+} ions occupying interstitial positions as in the bytownite itself; or (ii) with some of the SiO_4^{4-} groups missing from the lattice. If the latter were the case, then these SiO_4^{4+} groups which are released and the Ca^{2+} ions

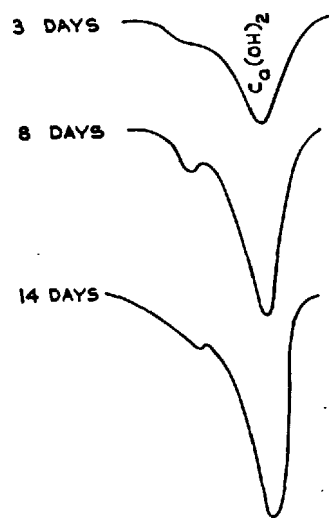

Fig. 4. *D.T.A. endotherms due to* $Ca(OH)_2$ *formed during the hydration of bytownite-based " 4 in 16" substituted* β-C_2S *hydrated for different periods.*

which acted as charge neutralizers in the bytownite and which also are released now would from some more β–C_2S. In this case, the lime released as $Ca(OH)_2$ during hydration would be the same as that released during the hydration of boric acid stabilized β–C_2S.

However, since during the course of hydration, while the unhydrated material went down, both the tobermorite and the $Ca(OH)_2$ were on the increase, and since this $Ca(OH)_2$ was definitely more than in the case of boric acid stabilized β–C_2S, or the microcline-based β–C_2S (Figs. 2 and 4), this lime may well have come from interstitial Ca^{2+}. Again, the more $Ca(OH)_2$ was released, the larger was the attempted substitution confirming this hypothesis.

In the case of microcline-based products, since most of the potash and half of soda, which are the charge neutralizers in this felspar network, evaporated off, either the lime added during the preparation of β–C_2S may have served the purpose of charge neutralizing cations by replacing K^+ or the charge balance may have been effected say by missing SiO_4^{4-}. In this case, if Ca^{2+} had replaced the alkalis as charge neutralizing cations, then these products would have had properties similar to the bytownite-based products. However, these two products are different in at least three ways:

i) Boric acid had to be added to the bytownite-based raw mixes in order to stabilize the β–C_2S, while the microcline-based products were self-stabilized.

ii) A Larger amount of lime was released from the bytownite-based products.

iii) The bytownite-based products hydrated to a larger extents during the course of, say, 28 days. However, the microcline-based products started hydrating early and started showing tobermorite endotherms at earlier ages.

It is thus possible that in the microcline-based products the charge compensation may be effected in a way different from that in the bytownite-based products.

Substituted Alumino-Frerrite

Materials

Finely powdered oxides Al_2O_3, Fe_2O_3, MgO, CaO (calcined $CaCO_3$), and MnO_2 were taken. MnO_2 reduces to Mn_2O_3 at 535°C, which further reduces to Mn_3O_4 at 933°C (12). However, the second stage reduction was inhibited since the compounds containing manganese also had their X-ray diffraction patterns resembling C_4AF. In some cases, e.g., in an attempt to prepare $2CaO \cdot Mn_2O_3$, the compound actually formed was $2CaO \cdot 2MnO_2$ ($CaMnO_3$) showing that in this case MnO_2 had not reduced at all.

The temperatures of heat treatment for synthesis of the different compounds are given in the following:

1220–1240°C: C_6AF_2, $C_{3.7}M_{0.3}AF$, $C_{3.7}M_{0.3}AF_{0.85}M'_{0.15}$;

1280–1300°C: $C_4AF_{0.85}M'_{0.15}$, C_6AFM';

1310–1330°C: C_6A_2F, C_4AF, $C_4AF_{0.5}M'_{0.5}$, C_4AM';

1370–1390°C: C_2F.

($M = MgO$, $M' = Mn_2O_3$)

Results

X-ray diffractometer records of the different samples were taken with silicon metal as internal standard. From the positions of three lines the unit cell dimensions and the density were calculated. All these data are given in Table 2, from which the X-ray calculated density values may be compared with those obtained directly.

Fixed Water

The values of the fixed water given in Table 3 give

Table 2.

Compound	Molecular wt.	Unit cell dimensions				Density g/cc	
		$a_{Å}$	$b_{Å}$	$c_{Å}$	$v = abc_{Å^3}$	From X-ray data	Measured
C_6A_2F(13)	700.10	5.52	14.39	5.30	420.99	3.66	—
C_4AF(9)	485.98	5.34	14.50	5.58	432.06	3.73	—
C_6AF_2	757.83	5.41	14.78	5.59	447.21	3.73	3.46
C_2F(9)	271.86	5.43	14.76	5.60	448.82	4.00	
$C_4AF_{0.85}M'_{0.15}$	485.70	5.34	14.64	5.56	434.76	3.69	3.70
$C_4AF_{0.5}M'_{0.5}$	485.07						3.72
C_4AM'(14)	484.16	5.23	14.68	5.44	417.74	3.82	3.78
$C_{3.7}M_{0.3}AF$	481.25	5.36	14.59	5.57	435.60	3.65	3.54
$C_{3.7}M_{0.3}AF_{0.85}M'_{0.15}$	480.97	5.35	14.62	5.56	435.05	3.65	3.69
C_6AFM'	756.01	5.37	14.75	5.51	436.55	3.81	3.86

(M = MgO, M′ = Mn_2O_3)

Note: The X-ray data of four of the compounds were taken from literature to which references are made.

Table 3. (%) *Fixed water of samples hydrated for varying periods/days (Unhydrated basis).*

Compound	Hydrated as such					Hydrated with 2% SO_3*				
	1	3	7	14	28	1	3	7	14	28
C_6A_2F	28.7	34.7	35.5	—	38.3	—	37.4	39.4	—	56.0
C_4AF	22.1	26.4	26.9	28.5	32.5	15.0	20.8	20.9	24.1	25.6
C_6AF_2	31.2	36.8	38.7	—	37.3	11.5	34.0	37.6	35.5	39.1
C_2F	13.7	17.7	22.1	27.2	26.6	4.0	4.2	3.0	4.0	5.9
$C_4AF_{0.85}M'_{0.15}$	22.4	26.4	33.1	34.4	37.9	27.4	33.9	34.0	—	40.4
$C_4AF_{0.5}M'_{0.5}$	16.8	25.3	25.2	—	26.9	8.7	9.9	—	11.0	12.2
C_4AM'	18.6	23.6	22.5	30.0	29.0	22.2	29.5	28.9	—	33.3
$C_{3.7}M_{0.3}AF$	30.0	33.0	33.3	34.6	32.0	29.5	—	34.0	—	35.5
$C_{3.7}M_{0.3}AF_{0.85}M'_{0.15}$	20.2	26.1	31.6	33.7	—	19.6	—	28.5	29.4	—
C_6AFM'	12.3	17.4	26.9	27.4	30.2	6.6	12.6	24.7	26.7	34.2

M = MgO, M′ = Mn_2O_3

*The fixed water of unhydrated material will be 0.9% due to 4.3% gypsum.

an idea of the rate at which the different compounds hydrated. These results are discussed at the relevant places along with the D.T.A. and X-ray diffraction results.

Hydration Studies with X-ray Diffraction and D.T.A.

The results are discussed separately for the different series of compounds.

C_6A_2F–C_4AF–C_6AF_2–C_2F

A number of workers have studied the hydration behaviour of these compounds. On hydrating C_4AF at 25°C (W/C = 0.7) Kalousek and Adams (15) found cubic hydrogarnets with some hexagonal C_4AF_{13} type phase at 7 days. The hydrogarnets decreased with age, while the hexagonal phase increased, and the product was the hexagonal hydrate at 180 days. On hydrating with gypsum, ettringite was formed at 7 days which slowly changed over to the solid solution $3C(A, F)\cdot CaSO_4\cdot 12H_2O$–$3C(A, F)\cdot Ca(OH)_2\cdot 12H_2O$. Jones (16), summarizing the earlier work, concluded that $C_4A\cdot aq$–$C_4F\cdot aq$ was formed as a first step towards $C_3A\cdot aq$–$C_3F\cdot aq$. Dekeyser (6) reported that among these, C_6A_2F hydrated fastest, and that the rate of hydration decreased with the decreasing alumina content. He also reported, in agreement with Jones, that all these formed the hexagonal phase which changed over to the cubic hydrogarnets in due course, except with C_2F in which case this transformation did not occur unless C_2F was hydrated with lime.

In the present work, in conformity with the loss on ignition data, both C_6A_2F and C_6AF_2 hydrated rather fast, as was seen by X-ray diffraction and D.T.A., and substantial amounts of these were hydrated at 24 hours. C_4AF did not hydrate as fast, and C_2F even slower. Thus, at 28 days, quite some C_4AF and a larger quantity of C_2F were still unhydrated.

C_6A_2F, C_4AF and C_6AF_2 all gave the cubic hydrogarnets at 1 day along with some hexagonal hydrate. While C_6A_2F showed the C_2AH_8 type in some small quantity, the other two gave only trace of C_4AH_{13} type. The cubic hydrate increased with age. The hexagonal hydrate disappeared at 3 days in the case of C_4AF, but the latter two gave the hexagonal

hydrates at later ages also, although to lesser extent. C_4AF gave, in addition, some $Ca(OH)_2$.

C_2F gave only the hexagonal hydrate C_4FH_{13} at all ages.

On hydrating with SO_3, C_4AF did not react fast enough so that some gypsum was still left at 24-hour hydration, and a 740°C exotherm was present presumably due to a gel. Both the gypsum and this endotherm disappeared at 3 days. The small ettringite and monosulphate peaks at 8.9° and 9.7° 2θ disappeared at 3 days into broad diffuse area. The monosulphate-$C_4(A, F)H_{13}$ solid solution was shown up at later ages. The hydrogarnets appeared at 7 days and later.

Most of the C_6A_2F had hydrated at 3 days giving C_2AH_8 type hexagonal phase, ettringite and monosulphate. The ettringite disappeared at 28 days giving monosulphate-$C_4(A, F)_{13}$ solid solution along with the C_2AH_8 type hexagonal phase. The hydrogarnets were absent.

A large part of C_6AF_2 hydrated at 7 days after which the hydration was relatively slow as judged from the X-ray line intensities and from the fixed water (Table 3). It showed ettringite at 1 day, and monosulphate and solid solution at later ages.

C_2F did not hydrate to an appreciable extent in 28 days, and showed a trace of ettringite. The fixed water data (in Table 3) confirmed this observation as also that C_6AF_2 hydrated faster than C_4AF.

In order to see if the relatively high rate of hydration of C_6AF_2 was due to the finer pulverization of this compound, the specific surface of undermentioned compounds was measured with the Blaine apparatus.

Compound	*Specific surface* (cm^2/g)
C_6A_2F	1700
C_4AF	2050
C_6AF_2	2590
C_2F	1640

Thus the C_6AF_2 was finer ground. However, as will be seen later, the initial rate of hydration also of C_6AF_2 was found to be higher.

C_4AF–$C_4AF_{0.85}M'_{0.15}$–$C_4AF_{0.5}M'_{0.5}$–C_4AM' ($M' = Mn_2O_3$)

This series was studied with a view to studying the effect of progressive replacement of iron by manganese on the hydration behaviour.

The main products on hydrating without SO_3 were the hydrogarnets besides some hexagonal hydrates shown at early ages (especially at 1 day) by all except $C_4AF_{0.5}M'_{0.5}$. Unlike C_4AF, the other two gave C_2AH_8 type, C_4AM' giving the same in larger quantity.

At 28 days $C_4AF_{0.85}M'_{0.15}$ had substantially hydrated while $C_4AF_{0.5}M'_{0.5}$ showed probably the largest unhydrated material. The fixed water data (Table 3) confirmed that on replacing a small part of Fe by Mn the compound hydrated faster than C_4AF, while with 50:50 replacement the hydration was slowed down, C_4AM' again hydrating faster.

The 720–740°C endotherm present in the products of the two compounds containing both Fe and Mn may be ascribed to Fe-Mn hydroxide gel.

On hydrating with SO_3, $C_4AF_{0.5}M'_{0.5}$ hydrated rather slowly, showing only ettringite and the presence of gypsum even at 28 days. (Please see Table 3 also). The others (except C_4AF) had consumed gypsum at 1 day.

Both $C_4AF_{0.85}M'_{0.15}$ and C_4AM' showed broad prominent ettringite-monosulphate low angle X-ray peak. The peak decreased till 7 days after which the monosulphate rose up and other monosulphate peaks also showed up. These monosulphate peaks were sharper in the case of C_4AM', and diffuse in the case of $C_4AF_{0.85}M'_{0.15}$. This was in marked contrast with C_4AF. All these three gave the cubic hydrate at later ages.

The pH studies of $C_4AF_{0.85}M'_{0.15}$ hydrated with SO_3 showed erratic pH changes at early ages.

C_4AF–$C_{3.7}M_{0.3}AF$–$C_4AF_{0.85}M'_{0.15}$–$C_{3.7}M_{0.3}AF_{0.85}M'_{0.15}$ ($M = MgO$, $M' = Mn_2O_3$)

This series was studied with a view to seeing the effect of partial replacement of CaO with MgO and/or of Fe_2O_3 with Mn_2O_3.

On hydrating without SO_3, C_4AF, $C_4AF_{0.85}M'_{0.15}$ and $C_{3.7}M_{0.3}AF_{0.85}M'_{0.15}$ all gave the cubic hydrate at one day with a little hexagonal hydrate. The latter two, unlike C_4AF, gave the lime-poor C_2AH_8 type hexagonal hydrate, the last one giving it in a slightly larger quantity. Again at later ages only the cubic hydrate was found and in larger quantities.

$C_{3.7}M_{0.3}AF$ formed C_2AH_8 type hydrate in large quantity by 1 day. This came down only slowly up to 28 days. The cubic hydrate was noticed at 7 days only and it increased with age. A trace of $Mg(OH)_2$ was detected from 3 days onwards.

Manganese thus accelerated the formation of the cubic hydrate while magnesia gave rise to the lime-poor C_2AH_8 type hydrate and delayed the formation of the cubic hydrate phase.

On hydrating with gypsum, the products formed by C_4AF and $C_4AF_{0.85}M'_{0.15}$ are already discussed in the

earlier sections.

$C_{3.7}M_{0.3}AF_{0.85}M'_{0.15}$ also gave ettringite and monosulphate at early ages and a fairly strong monosulphate peak which had grown up at 28 days.

$C_{3.7}M_{0.3}AF$ gave strong low angle ettringite and monosulphate peaks at early ages, which went down, and showed a broad solid solution area at 28 days resembling the behaviour of C_4AF. These peaks, however, appeared to be displaced somewhat in this case.

C_6AF_2–C_6AFM' ($M' = Mn_2O_3$)

Unlike C_6AF_2 which had substantially hydrated in 3 days, C_6AFM' remained partly unhydrated even at 28 days. Thus, in this case also, replacement of half of Fe_2O_3 by Mn_2O_3 gave a slower hydrating compound. (See Table 3 also).

C_6AFM' gave the cubic hydrate only and showed a 740°C exothermic peak ascribed to Fe-Mn hydroxide gel.

On hydrating with SO_3, less of C_6AFM' had hydrated even by 28 days. Although C_6AF_2 had substantially hydrated by 7 days.

As mentioned earlier, C_6AF_2 gave ettringite at 1 day, monosulphate-solid solution at later ages.

C_6AFM' gave ettringite at 1 day which decreased and disappeared at 7 days. Strong monosulphate and some C_4AH_{13} type phase appeared at 3 days. The latter went down later, while the monosulphate remained very strong even at 28 days, thus showing lesser tendency of Mn containing compounds to form monosulphate-$C_4(A, F, M')H_{13}$ type solid solutions. The cubic hydrate appeared at 7 days and increased with age.

Initial Rate of Hydration

From a knowledge of the specific surface of the compound, and from the rate at which the height of a prominent X-ray peak falls down, the initial rate of hydration (as depth of hydration, microns/hour) can be calculated according to Tsumura's method (8). The values found for hydration without SO_3 are:

Compound	*Depth of hydration (microns/hr)*
C_6A_2F	2.4
C_4AF	2.1
C_6AF_2	3.2
C_2F	1.0
$C_4AF_{0.85}M_{0.15}$	1.6

The remaining compounds, even though they did hydrate appreciably at 24 hours, had not hydrated at all in the first two hours and thus exhibited initial induction period of at least 2 hours, and did not start appreciable hydration in this time.

C_6AF_2 again showed the largest initial rate of hydration, contrary to the earlier finding that its rate of hydration is intermediate to that of C_4AF and C_2F.

Again $C_4AF_{0.85}M'_{0.15}$ hydrated to a larger extent at 28 days than C_4AF. However, its initial rate of hydration was less than that of C_4AF.

It may be mentioned that these initial rates of hydration fell off to much lower values within a matter of 10–15 minutes probably as the thickness of the hydrated layer increased so that further hydration was governed by the rate of diffusion through the hydrated layer.

The value of the rate of hydration for C_4AF may be compared with the value obtained by Tsumura of 1.65 microns/hr who took the density of C_4AF as 3.89 g/cc.

Conclusions

1) The rate of hydration of the C_2F–$C_6A_{2.1}F_{0.9}$ series is thus found to depend on the A/F ratio in agreement with the previous workers. However, C_6AF_2 appeared to hydrate faster than C_4AF.
2) If in C_4AF a small part of the Ca was replaced by Mg and/or a small part of Fe was replaced by Mn, then the resulting product hydrated faster.
3) Replacing half of the Fe in C_4AF and in C_6AF_2 by Mn gave compounds which hydrated considerably slower. With complete substitution in C_4AF of Fe by Mn, the resulting product viz. C_4AM' hydrated faster than $C_4AF_{0.5}M'_{0.5}$.
4) On hydration with water, all the compounds tended to give the hexagonal phase at early ages (along with the cubic hydrate) which changed over to the cubic phase. C_2F gave only the hexagonal phase.
5) C_4AF and the two compounds C_6AF_2 and C_2F gave the $C_4(A, F)H_{13}$ type hydrate. The iron oxide poorer C_6A_2F gave the lime-poor C_2AH_8 type hydrate phase.
6) Replacing the iron oxide in C_4AF either partly or wholly by Mn_2O_3 or the lime partly by magnesia gave compounds which on hydration again

gave the lime-poor hexagonal hydrate of the C_2AH_8 type.

7) On hydration with SO_3 compounds containing Mn generally gave a large monosulphate peak at 28 days indicating that these did not form the monosulphate-$C_4(A, F, M')H_{13}$ solid solution readily.

8) Some of these compounds started hydrating immediately on admixture with water, while others exhibited induction periods, before the start of hydration, of 1 1/2–2 hours.

Acknowledgements

Thanks are due to Dr. R. R. Hattiangadi for his kind interest and to Mr. A. D. Kilpadikar and Mr. S. Viswanathan for the experimental work.

References

1. R. W. Nurse, "The dicalcium silicate phase", Proc. 3rd Internatl. Symp. on the Chemistry of Cement, London 1952, 56–77.
2. Y. Suzukawa and T. Sasaki, "Influence of reducing atmosphere on the constitution of clinker", Proc. 4th Internatl. Symp. on the Chemistry of Cement, Washington 1960, 83–85.
3. G. V. Kukolev and M. T. Mel'nik, "The effect of admixture of Cr_2O_3, P_2O_5, V_2O_5 and BaO on the microstructure of portland cement clinker" (in Russian), Doklady AN SSSR **132,** 168–171 (1960).
4. R. W. Nurse, "The effect of some minor components on cement setting and hardening", Proc. 7th Conf. on Silicate Ind. Budapest 1965, 179–285.
5. A. F, Wells, Structural Inorganic Chemistry, 3rd ed., p. 808 (Clarendon Press, Oxford, England, 1962).
6. W. L. De Keyser, "Work executed under the guidance of the committee on fundamental research of C.R.I.C. (Belgium)", (in French) "The chemistry of cement" Meeeting on 17th March 1965, 46–61.
7. T. W. Parker, Discussion, Proc. 3rd Internatl. Symp. on the Chemistry of Cement, London 1952, 143–149.
8. S. Tsumura, "Rates and mechanisms of hydration of clinker minerals in paste form" (in German), Zement-Kalk-Gips **55,** 511–518 (1966).
9. H. F. W. Taylor, "Tabulated crystallographic data", The Chemistry of Cements, Vol. 2, Ed. H.F.W. Taylor, 347–404 (Academic Press, London, U. K. and New York U.S.A. 1964).
10. N. Yannaquis and A. Guinier, Discussion, Proc. 3rd Internatl. Symp. on the Chemistry of Cement, London 1952, 21–23.
11. A.M.B. Douglas, Discussion, Proc. 3rd Internatl. Symposium on the Chemistry of Cement, London 1952, 78–82.
12. C. Duval, Inorganic thermogravimetric analysis, 2nd ed. p. 313, (Elsevier Publishing Co., Amsterdam, Netherlands, London, U. K. and New York, U.S.A., 1963).
13. H. G. Midgley, "A compilation of X-ray powder diffraction data of cement minerals", Mag. Concr. Res., **9,** 17–24 (1957).
14. T. W. Parker, Discussion, Proc. 3rd International Symposium on the Chemistry of Cement, London 1952, 143–149.
15. G. L. Kalousek and M. Adams, "Hydration products formed in cement pastes at 25 to 175°C", Proc. Amer. Conc. Inst., **48,** 77–90 (1952).
16. F. E. Jones, "Hydration of calcium aluminates and ferrites", Proc. 4th Internatl. Symp. on the Chemistry of Cement, Washington 1960, 204–242.

Supplementary Paper I-105 The Effect of Minor Components on the Early Hydraulic Activity of the Major Phases of Portland Cement Clinker

Toshio Sakurai, Takeshi Sato and Atushi Yoshinaga*

Synopsis

Solid state physics is well applicable to the effect of minor components on the early hydraulic activity of C_3S and calcium aluminoferrite.

C_3S can take 1.7 wt. % Cr_2O_3. With addition of 0–1.4% Cr_2O_3, modification T_I is obtained and T_{II} with addition of 1.4–1.7%.

C_2F and C_4AF can dissolve 4.8% and 5.4% Cr_2O_3 respectively in ordinary atmosphere. These introductions of Cr_2O_3 increase enormously the early hydraulic activity of both C_3S and calcium aluminoferrite.

C_3S with Cr_2O_3 is a P-type semiconductor, of which the electric conductivity and the dielectric constant increase with Cr_2O_3.

Dislocations are found on the C_3S crystal surfaces electronmicroscopically.

The density of dislocation etch pits increases with introduction of Cr_2O_3 and it attains to the maximum $10^8/cm^2$.

These dislocations have been thought to be a key to the hydraulic activity of clinker minerals. For this case, however, not all dislocations are sensitive to hydration. It is the screw dislocation at the centre of growth spiral that is vigorously active at hydration.

The early hydration reaction starts both at the point of emergence of screw dislocations and at the grain boundaries. The reaction then progresses along the step and deepens the crystal surface step by step until the depth of one thousand several hundred angstrom of the surface layer is dissolved out.

The early hydration reaction is explainable as the dissolution of Ca^{++} ions on the surface of a P-type semiconductor. The case of calcium alumino ferrite is similarly explainable.

Introduction

The minor components, their incorporated state and the clinkering condition affect the hydraulic activity and the strength of the major phases of portland cement clinker. Jander (1) suggested that the strength produced by the alite in a cement might depend not only on the presence of ions in solid solution but also on the occurrence of structural defect and of cracks and irregularities of colloidal dimensions. These three factors are nevertheless not to be independent individually but related closely to one another.

In this report, the authors will try from the viewpoint of both crystal chemistry and solid state physics to explain systematically how minor components affect crystal structure and structural imperfections of C_3S, calcium alumino-ferrite, and also how minor components affect their hydraulic activity.

The minor components used are Cr_2O_3 (Cr ions as a cationic minor component), CaF_2 (F ions as an anionic minor component) and P_2O_5.

The role which Cr_2O_3 plays in the early strength of portland cement clinkers has been discussed by various researchers. Of such studies, notable were those by K. Akiyama (2), M.M. Sychov and V. I. Korneev (3).

The influence of fluorine on C_3S hydration was reported by J. H. Welch and W. Gutt (4) and P_2O_5 by W. Gutt (4) and M.M. Sychov and V. I. Korneev (3).

Many reports have supposed the effect of minor components at the early hydration and the early strength of clinker minerals, connecting with the formation of crystal imperfections or defects (5), but no details of these mechanisms have been clarified.

*Research Laboratory, Nihon Cement Co., Ltd, Tokyo, Japan.

The Effect of Cr_2O_3 on C_3S

Solid Solution of C_3S with Cr_2O_3

In this series the solid solubility of Cr_2O_3 is investigated by using guaranteed chemical reagents, $CaCO_3$, SiO_2 and Cr_2O_3 as starting materials. Synthesis is performed at 1550°C for 3 hours in air for each cycle, with the SiC furnance, and five cycles of burning are repeated for each sample to obtain desired solid solutions.

C_3S can take up to 1.7 wt. % Cr_2O_3 instead of 1.4 wt. % reported by E. Woermann et al (6). With addition of 0–1.4% Cr_2O_3, modification T_I is obtained at room temperature and T_{II} are obtained with addition of 1.4–1.7%.

The lattice parameters are plotted by using Yamaguchi's indices (7) in Fig. 1.

The discontinuity at 1.4% is the opposite nature to that of the transition T_I–T_{II} in C_3S with Al_2O_3 reported by M. Bigaré et al (8). The lattice parameters shrink continuously during 0–1.4%, 1.4%–1.7% Cr_2O_3, while the discontinuity at 1.4% is far larger than that at Al_2O_3 0.45%.

The X-ray powder patterns near this transition region are shown in Fig. 2.

The average valencies of Cr ion in this series are measured by chemical analysis and +4.6 is gained which is constant in all this series. This fact shows Cr ion can dissolve in the same way in all this series.

With addition of more than 1.8% Cr_2O_3, C_3S decomposes into C_2S and CaO.

Solid Solution of C_3S with Cr_2O_3, Al_2O_3 and Fe_2O_3

In this series, solid solubility of a mixture of Cr_2O_3, Al_2O_3 and Fe_2O_3 in C_3S is studied.

In Table 1 each chemical composition of the clinkers of C_3S–C_3A–C_4AF–Cr_2O_3 system is shown.

Table 1. *Clinker composition in the* C_3S–C_3A–C_4AF–Cr_2O_3 *system*

Sample No.	SiO_2	Al_2O_3	Fe_2O_3	CaO	Cr_2O_3	Total
1	21.78	5.21	2.83	70.18	0.00	100.0
2	21.67	5.19	2.81	70.08	0.25	100.0
3	21.55	5.15	2.81	70.00	0.50	100.0
13	21.44	5.12	2.79	69.90	0.74	100.0
4	21.32	5.10	2.77	69.82	0.99	100.0
14	21.10	5.05	2.75	69.63	1.47	100.0
5	20.88	5.00	2.71	69.46	1.95	100.0
15	20.66	4.95	2.69	69.28	2.43	100.0

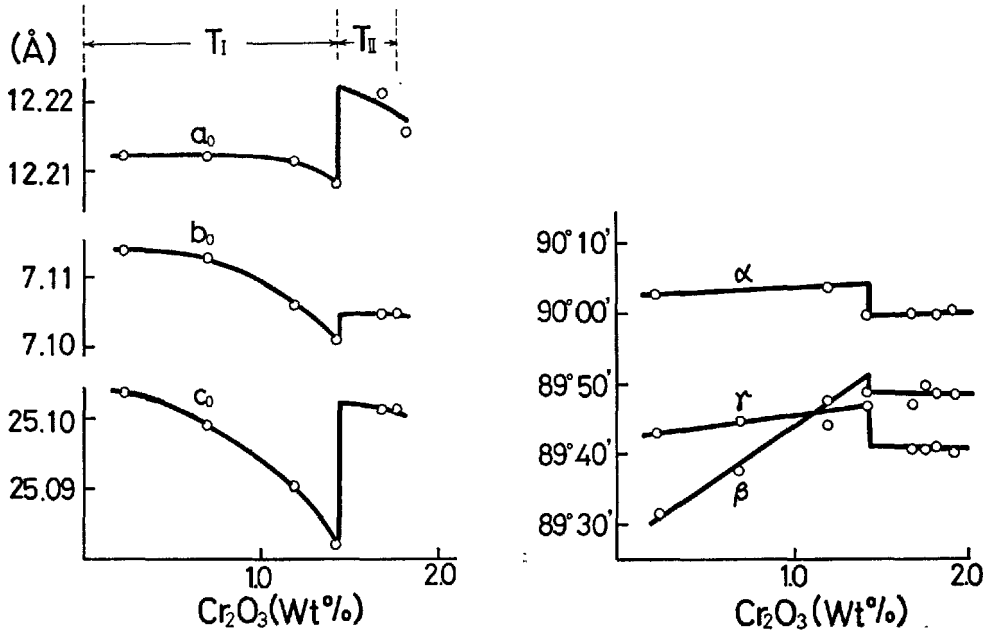

Fig. 1. *Variation of pseudo-orthorhombic lattice constants at room temperature in the* C_3S–Cr_2O_3 *solid solution series.*

Solid solubility of Cr_2O_3, Al_2O_3 and Fe_2O_3 in C_3S is determined by the fractional dissolution method with salicylic acid in methyl alcohol (9). In order to confirm these compositions obtained, the C_3S solid solutions are synthesized based on the chemical compositions obtained.

In Fig. 3, the chemical composition of each C_3S_{ss} is illustrated in comparison with the early hydraulic activity of C_3S_{ss} which will be discussed in the subsequent section.

C_3S can introduce 1.7% Cr_2O_3, 1.3% Al_2O_3 and 0.7% Fe_2O_3 altogether. With no Cr_2O_3, C_3S can take up to 1.1% Al_2O_3 and 0.9% Fe_2O_3. With dissolution of Cr_2O_3, solid solubility of Al_2O_3 increases, while that of Fe_2O_3 decreases. The limit of solid solubility of Cr_2O_3 1.7% in this series is quite the same with the limit of solubility of Cr_2O_3 alone in C_3S studied in the above section. This fact means that Cr_2O_3 can be taken in C_3S independently of Al_2O_3 and Fe_2O_3 in a mixture.

The average charge of Cr ion of each C_3S in this series is constantly +4.6 which is also the same value with the case of Cr_2O_3 alone in C_3S.

In this case C_3S takes the modification of T_{II} at room temperature. In Table 2 the ionic mole ratio of C_3S_{ss} in this series is shown standardizing Ca^{++} ionic mole number as 3000.

With addition of Cr_2O_3, Al^{3+} increases while Si^{4+} and iron ion decrease instead.

These changes suggest that Cr ions and Al ions are substituting for Si ions in tetrahedra. The increased mole number of $Cr^{4.7+}$ is much more than two times of the decreased mole number of Si^{4+}. Moreover, it is impossible for Cr ions to neutralize the charge +4.7 only by ordinary substitution for Si^{4+} or for Ca^{++}.

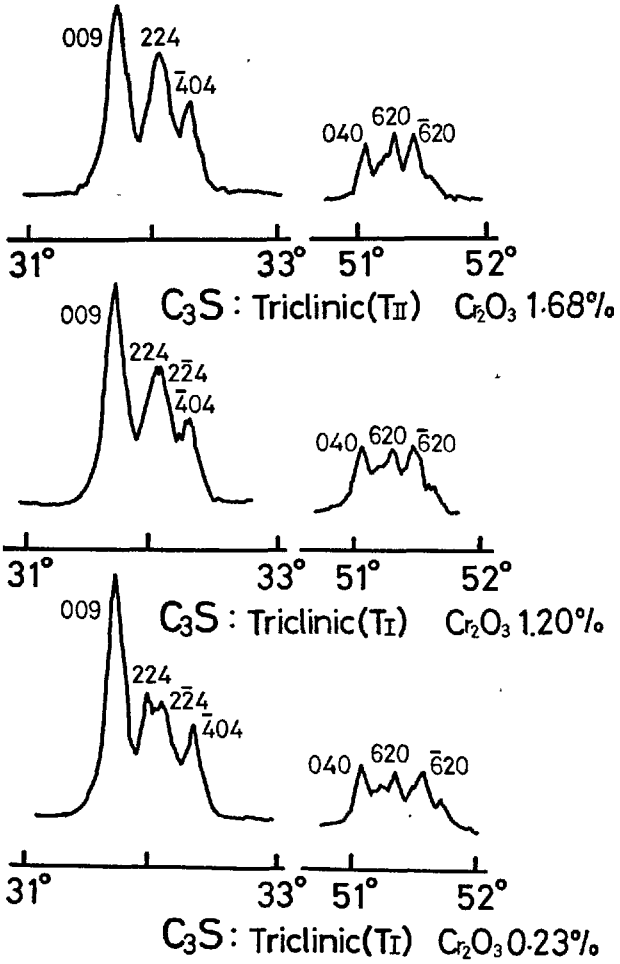

Fig. 2. *Characteristic reflection groups in the powder patterns of modifications T_I and T_{II} of C_3S with Cr_2O_3 at room temperature.*

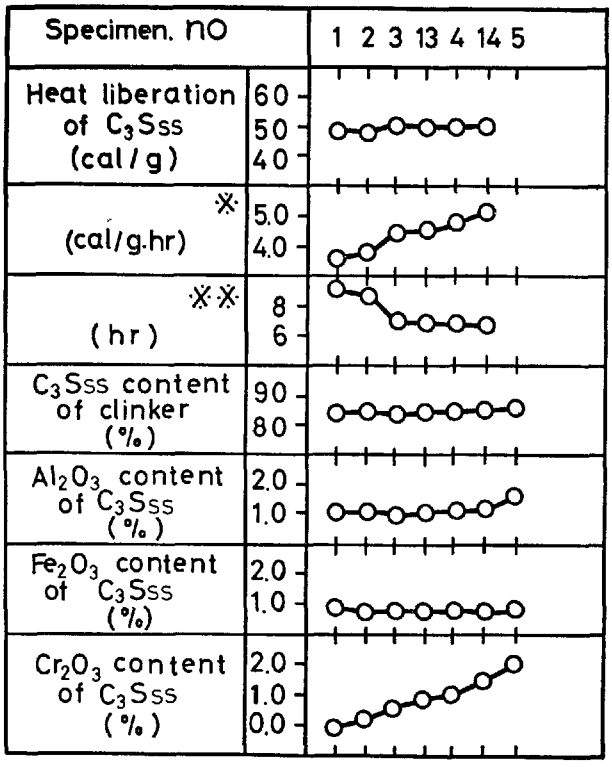

※ Maximum rate of heat liberation of C_3S_{ss}.

※※ Time from just after contact with water to maximum rate of heat liberation.

Fig. 3. *Effect of minor components on early hydraulic activity of C_3S_{ss} in the C_3S–Cr_2O_3–Al_2O_3–Fe_2O_3 solid solution series.*

Table 2. *Ionic mole ratios of each composition in the* C_3S–Cr_2O_3–Al_2O_3–Fe_2O_3 *solid solution series, converting each ionic mole number to 3000 basis of* Ca^{++} *ionic mole number.*

	$[Ca^{2+}]$	[Cr ion]		$[Al^{3+}]$		$[Fe^{3+}]$		$[Si^{4+}]$	
Sample No.	Ionic mole ratio in C_3S_{ss}	Ionic mole ratio	Average charge	Ionic mole ratio	$[\Delta Al^{3+}]$	Ionic mole ratio	$[\Delta Fe^{3+}]$	Ionic mole ratio	$[\Delta Si^{4+}]$
1	3000	0	—	50	0	26	0	963	0
2	3000	8.9	4.6	50	0	21	−5	968	5
3	3000	17.0	4.6	50	0	24	−2	959	−4
13	3000	25.0	4.8	55	5	22	−4	957	−6
4	3000	33.6	4.8	55	5	21	−5	950	−13
14	3000	50.0	4.8	60	10	21	−5	942	−21

The D.C. Conductivity of C_3S with Cr_2O_3

As mentioned in the preceding section there will be electron holes or vacancies in C_3S crystal, if Cr ions of positive charge 4.6 are substituting for cations in the lattices. In order to study the property of such the lattices doped with transition element, Cr, it may be available to measure the d.c. conductivity of the crystal.

There have been few studies about the electroconductivity of cement clinker minerals (10).

Samples for measurement are prepared from the synthesized C_3S with Cr_2O_3 and some other minor components. Some examples of composition of the samples are listed in Table 2.

Samples are pressed to 50 mm ϕ × 20 mm disks at the pressure of 1 ton/cm², and then sintered at 1550°C until the desired density is obtained.

These sintered samples are then cut to the disks of 45 mm ϕ × 3 mm, coated with the silver paste as electrodes. The insulation resistor is used to measure the d.c. conductivity of samples.

Some of the results are shown in Fig. 4.

As the d.c. conductivity of these specimens is in the region of 10^{-11}–10^{-12} [Ω-cm] at room temperature, these C_3S with Cr_2O_3 are in the region of semiconductor. As the conductivity increases with additon of Cr ions, this conductivity is caused by the migration of electrons and/or holes between Cr ions in the different charges.

Considering that Cr ions can exist as Cr^{2+}, Cr^{3+}, Cr^{4+}, Cr^{5+} and Cr^{6+} among which Cr^{2+} and Cr^{6+} are unstable in this experimental condition (11), (12) and that the average charge of Cr ions in C_3S_{ss} is +4.6, Cr^{3+}, Cr^{4+} and Cr^{5+} must play part in this conduction.

The d.c. conductivity of $Cr^{3+} - O^{2-} - Cr^{4+}$ has been studied by many researchers. G.H. Jonker (13) proved $Cr^{3+} \rightarrow Cr^{4+}$ is prior to $Fe^{3+} \rightarrow Fe^{4+}$. F. Kanamaru and R. Kiriyama (14) measured the activation energy of Cr^{3+}–O^{2-}–Cr^{4+} conduction in solid

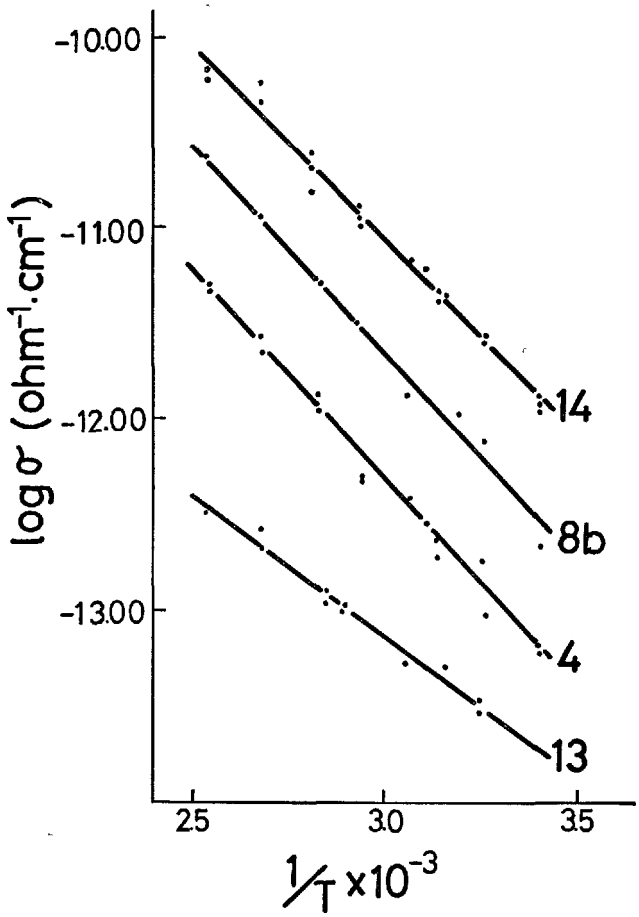

Fig. 4. *D. C. conductivity of* C_3S_{ss} *in the* C_3S–Cr_2O_3–Al_2O_3–Fe_2O_3 *solid solution series, sintered at 1550°C in air.*

solution of $CaFeO_4$ with Cr_2O_3. This activation energy is 0.16–0.27 eV.

The activation energy of the d.c. conductivity calculated from the incline of $\log \sigma - \frac{1}{T}$ curves is between 0.25 eV and 0.38 eV, which is a little larger than the activation energy of Cr^{3+}–Cr^{4+}, Fe^{2+}–Fe^{3+}, Fe^{3+}–Fe^{4+} and Mn^{3+}–Mn^{4+} measured by many researchers. Therefore, the mechanism of this d.c. conduction in these solid solutions may surely consist of Cr^{3+}–O^{2-}–Cr^{4+} and/or Cr^{4+}–O^{2-}–Cr^{5+} and/or Cr^{3+}–O^{2-}–Cr^{5+}. From these results, Cr ions in C_3S solid solution may be in charges of Cr^{3+}, Cr^{4+} and Cr^{5+}.

Dielectric Property of C_3S with Cr_2O_3

In order to study more about the situation of Cr ions in C_3S solid solution, the dielectric constant of C_3S_{ss} is used. The C_3S_{ss} disks used are the same specimens used in the measurement of the d.c. conductivity.

In an electric field, dielectric polarization of an insulator may be generated in the following mechanisms; (a) shift of electron distribution of atoms or molecules in an electric field; (b) relative migration of foreign atoms or ions; (c) orientation of molecules which have the permanent dipole moment along with the direction of an electric field.

To a dielectric substance in an electric field, the Calusius—Mosotti equation is applicable;

$$\frac{\epsilon - 1}{\epsilon + 2} \cdot \frac{M}{d} = \frac{4\pi}{3} N\bar{\alpha} \qquad (1)$$

where ϵ is the dielectric constant of the substance, d is the density, M is the molecular weight, N is the Avogadro's number and $\bar{\alpha}$ is the polarizability of a substance. For a polar substance, which has a permanent dipole moment, the term $\mathrm{Po} = \frac{4}{3}\pi N \cdot \frac{\mu^2}{3\kappa T}$ must be inserted to the equation (1), that is;

$$P_G = \frac{\epsilon - 1}{\epsilon + 2} \cdot \frac{M}{d} = \frac{4}{3}\pi N\bar{\alpha} + \frac{4}{3}\pi N \cdot \frac{\mu^2}{3\kappa T} \qquad (2)$$

where P_G is the total polarization, μ is the permanent dipole moment and κ is the Boltzmann constant. From the equation (2), there comes a linear relationship between P_G and $\frac{1}{T}$, so that μ can be calculated from the incline of the $P_G - \frac{1}{T}$ curves obtained experimentally.

Though this equation is well applicable to gas phases, there are some problems in applying this to solid phases. However, the approximate tendencies may be able to be obtained.

The dielectric constant of each specimen is measured with the Q-metre at 20°C, 60°C, 70°C and 90°C in a thermostat. The frequency used is 100 KC.

In Table 3 the results are listed.

In this Table, $(\epsilon - 1)/(\epsilon + 2)$ is a fraction of the molar polarization in the equation (1). Because M/d in this equation may be nearly constant in this series of solid solution and within this temperature condition, it is used instead of the molar polarization P_G. The relation between a fraction of the molar polarization $(\epsilon - 1)/(\epsilon + 2)$ and $1/T$ is shown in Fig. 5.

The curves rise with temperature from 20°C to 70°C. From the equation (2), P_G falls at the higher temperature, while these curves in Fig. 5 rise at the higher temperature. It is very difficult to explain this inclination, but it may be considered that C_3S with Cr_2O_3 have no permanent dipole moment.

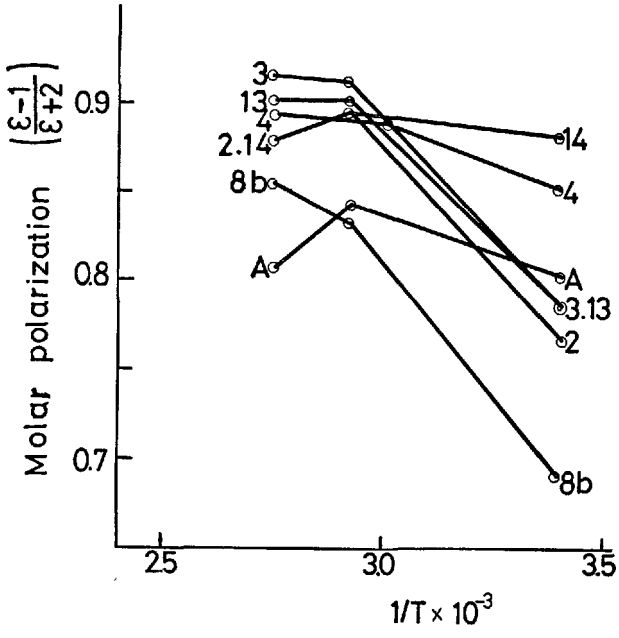

Fig. 5. *Variation of a fraction of molar polarization* $(\epsilon - 1)/(\epsilon + 2)$ *with* $1/T$ *in the* C_3S–Cr_2O_3–Al_2O_3–Fe_2O_3 *series.*

Table 3. *Electric conductivity and dielectric property of C_3S_{ss}, each specimen equal to that at Table 1.*

Sample	Cr_2O_3 content of C_3S_{ss} (%)	Specific electric conductivity $[\Omega^{-1}cm^{-1}]$ at 30°C	Activation energy of electric conductivity (eV)	Dielectric constant at 20°C	Molar polarization $\frac{\epsilon-1}{\epsilon+2}$ at 20°C
No. 2	0.25	$<10^{-14}$	—	11.0	0.77
3	0.50	$<10^{-14}$	—	12.1	0.79
13	0.75	3.0×10^{-13}	0.25	12.1	0.79
4	1.10	1.0×10^{-13}	0.38	12.7	0.85
14	1.62	3.6×10^{-12}	0.36	11.9	0.78
C_3S with Cr_2O_3 only, (8b)	1.70	1.4×10^{-12}	0.38	(8.6)	0.79

Mechanism of Dissolution of Cr Ions in C_3S_{ss}

As mentioned in the preceding section, the number of Cr ions dissolved in C_3S is much more than the number of Si^{4+} which is replaced by Cr ions. Therefore, it is natural to assume that Cr ions may substitute not only for Si^{4+} but also for Ca^{++}. Measuring the activation energy of the d.c. conductivity, Cr ions in C_3S are confirmed to stay as Cr^{3+}, Cr^{4+} and Cr^{5+}. And the average charge of Cr ions in C_3S is constantly +4.6. Therefore, 80% of the total Cr ions would be Cr^{5+} and the rest Cr^{3+}, if these Cr ions could be classified into Cr^{5+} and Cr^{3+}.

Considering all the information obtained, the following formulas for substitution of Cr ions could be suggested;

$$Si^{4+} + Ca^{2+} \rightarrow Cr^{5+} + Ca\square^{--} + Cr^{3+} \quad (1)$$

$$2Si^{4+} + (Ca^{2+} + Ca\square^{--}) \rightarrow 2Cr^{5+} + Ca\square^{--} \quad (2)$$

$$Si^{4+} \rightarrow Cr^{4+} \quad (3), \qquad 2Si^{4+} \rightarrow Cr^{5+} + Cr^{3+} \quad (4)$$

where $Ca\square^{--}$ is a Ca ion vacancy with minus two charge.

In these formulas the equation (4) would seldom occur. Referring the model of Na dissolution in C_3S proposed by G. Yamaguchi and H. Uchikawa (15) a Ca ion vacancy or $Ca\square^{--}$ in the formula (1), may generate at the site between the Cr^{5+} tetrahedra and Cr^{3+} in the Ca^{++} site. Oxygen ions surrounding the $Ca\square^{--}$ site may be then attracted toward the adjacent Cr^{5+} and Cr^{3+}, and their charges may be neutralized. In the formula (2), a Ca ion vacancy may generate at the Ca^{++} site where is adjacent to two Cr^{5+} tetrahedra. Oxygen ions surrounding $Ca\square^{--}$ may be neutralized by these two Cr^{5+}.

Considering these substitution and vacancies, the lattice shrinkage of C_3S with Cr_2O_3 may be well explained.

In this model the increase of the molar plarization of C_3S_{ss} in the electric field may be also explained as follows; Cr^{3+} of which ionic radius is 0.67 angstrom by Goldschmidt may have room for self-polarization in the electric field, when it substitutes for Ca^{++} of which ionic radius is 1.05 angstrom.

Otherwise, oxygen ions surrounding $Ca\square^{--}$ may cause the polarization in the electric field.

These dissolved Cr^{5+} and Cr^{3+} may exert the strong polarizing power on the adjacent oxygens and may polarize the surrounding oxygens. Therefore Ca ions in the vicinity of polarized field may not be screened enough by oxygen ions and may stay rather unstable.

C_3S_{ss} with Cr_2O_3 is, therefore, a P-type semiconductor.

Lattice Imperfections on Crystals of C_3S with Cr_2O_3

It has long been deducted by many cement researchers that lattice imperfections in cement clinker minerals may probably have a great influence on their hydraulic activity (5). This deduction, however, has not yet been realized, because no actual examination or observation of lattice imperfections has been successful.

The authors have tried the various methods of examination to verify lattice imperfections on C_3S crystals. Among them are the measurement of the lattice strain from the powder diffraction patterns, the X-ray topographical observation of lattice imperfections and the observation of dislocations with the electronmicroscope. The authors, however, have not

succeeded in obtaining the satisfactory results except in the observation of dislocation by E. M. method on C_3S crystals in an aggregate.

In the following study these observations will be described. Lattice imperfections are generally classified into

(a) point defects (Frenkel type and Schottky type)
(b) line imperfections (edge and screw dislocation)
(c) boundary dislocations and stacking faults
(d) lattice distortion.

The details of these classifications were summarized in the preceding Symposium by F. Ordway (16).

Among these imperfections the existence of point defects are mentioned in the above section by defining C_3S with Cr_2O_3 to be a P-type semiconductor.

There are two keys in the observation of dislocation etch pits on C_3S_{ss} aggregate with the electronmicroscope.

The one is how to make up the most smooth fracture surfaces, and the other is to find the most suitable etchant.

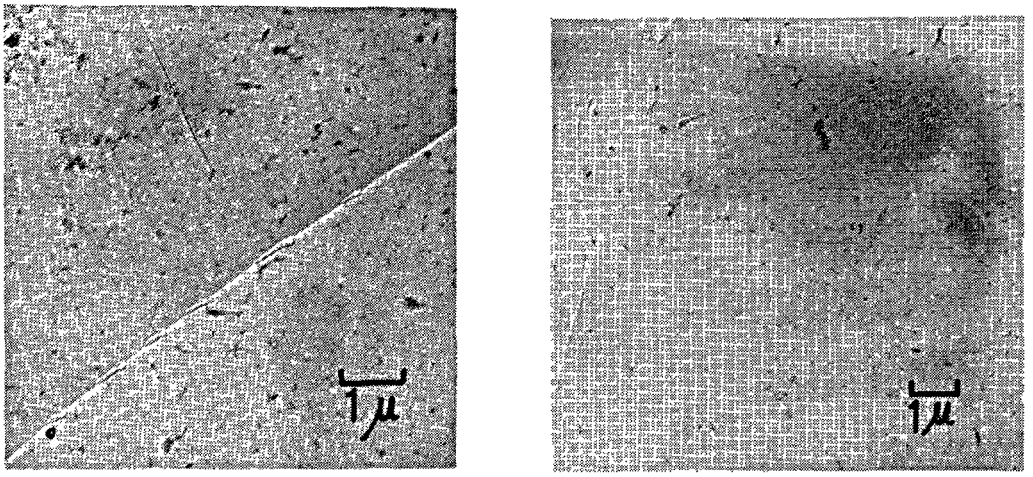

Fig. 6. *Unetched fracture surfaces of* C_3S_{ss} *crystals in the* C_3S–Cr_2O_3–Al_2O_3–Fe_2O_3 *solid solution series.*

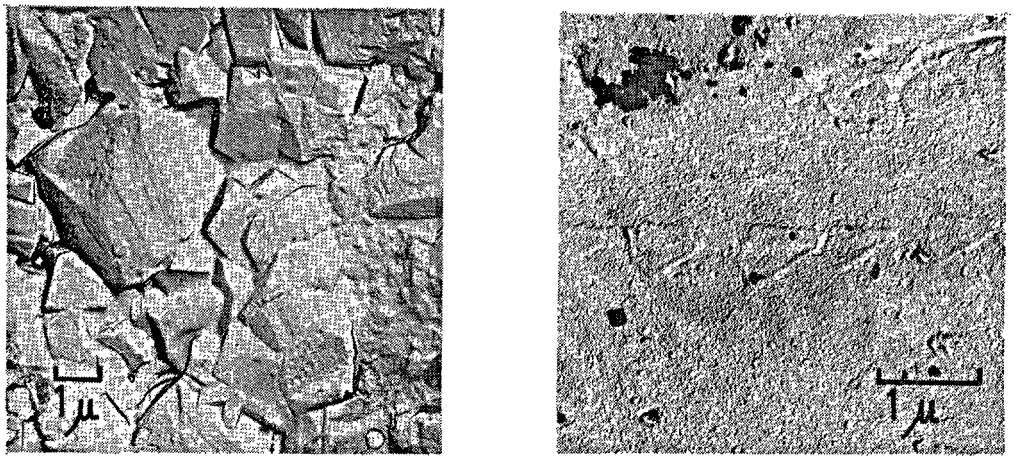

Fig. 7. *Etch pit shapes that reflect crystal symmetry.*

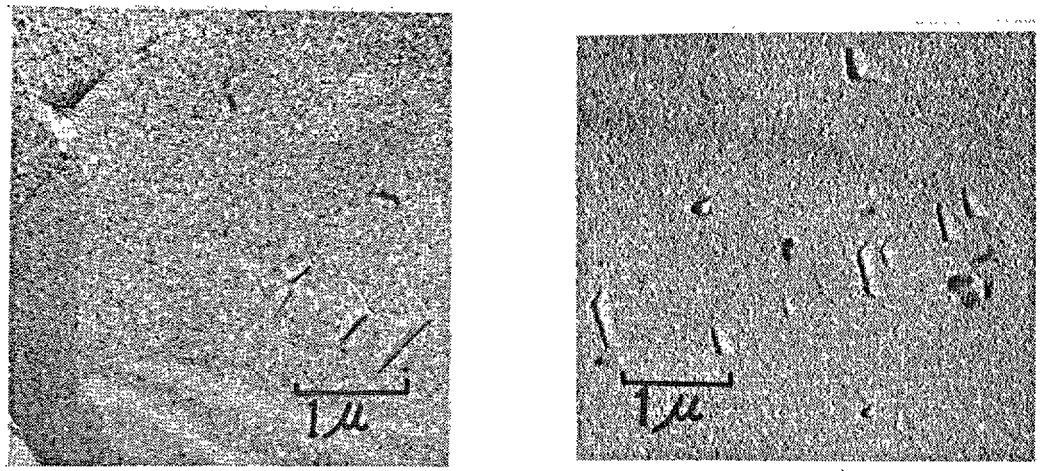

Fig. 8. *Variation of etch pit density with* Cr_2O_3 *content of* C_3S_{ss}. *Etch pit density about* $10^6/cm^2$ *in* C_3S_{ss} *with 0.25 wt. %* Cr_2O_3.
Etchant : 0.4% HF with 0.6% HNO_3 in ethyl alcohol
Etching time: 1 minute

As for the etching specimens, the C_3S_{ss} in Fig. 3 are used. These are pressed at 1 ton/cm², and sintered enough at 1550°C until the desired density is obtained. The specimens are then gradually cooled down and quenched at 1200°C in open air. Thereby the smooth fracture surfaces of single crystals are created in these dense aggregate by the rapid volume change and the cracking. In Fig. 6 the nonetched fracture surfaces are shown.

As for the etchant, 0.4% HF with 0.6% HNO_3 in C_2H_5OH solution, and 0.4% HF with 0.3% HNO_3 in H_2O are successfully used.

In the following figures the dislocation etch pits are shown comparing the etch pit density with Cr_2O_3 content of C_3S_{ss}.

Etch pits observed are trigons, hexagons and their pseudo-morphs which may reflect their crystal symmetry.

There have been few studies about the morphology or the crystal habits of C_3S in which the study of Grzymek (17) is evident.

These etch pit shapes in this observation are, however, very difficult to connect with morphology, because the crystal axis cannot be determined.

In Fig. 7, the general shapes of dislocation etch pits are exhibited.
Some surfaces have dense etch pits, while some others have rare ones. Grain boundary dislocations are also observed.

Figs. 8, 9, and 10 show that the etch pit density increases depending upon the addition of Cr_2O_3 in C_3S_{ss}. These relation will be discussed in the subsequent section.

Figs. 11–18 show the changes of the surface behavior of C_3S_{ss} at the initial stage of hydration. In this case, the etchant used is distilled water containing 0.4% HF with 0.3% HNO_3. The etchant-C_3S_{ss} ratio is about 200 %. Fig. 11 shows the spiral etch pits formed at the points of emergence of the screw dislocations. These spiral etch pits are enlarged concentrically along the steps. This corrosion proceeds further and, then, eliminates the corrosion front from the surface and no more corrosion occurs at the point of screw dislocation. However, the vicinity of the screw dislocation becomes selectively rough. These changes are shown in Fig. 12.

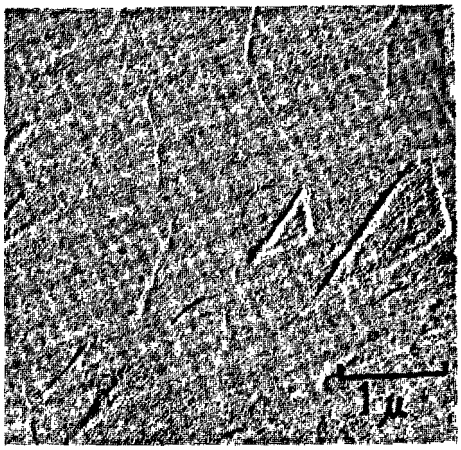

Fig. 9. *Variation of etch pit density with* Cr_2O_3 *content of* C_3S_{ss}. *Etch pit density about* $10^7/cm^2$ *in* C_3S_{ss} *with 0.50 wt. %* Cr_2O_3.
Etchant : 0.4% HF with 0.6% HNO_3 in ethyl alcohol.
Etching time: 1 minute

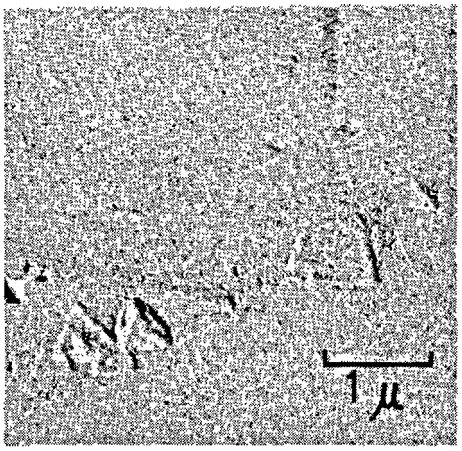

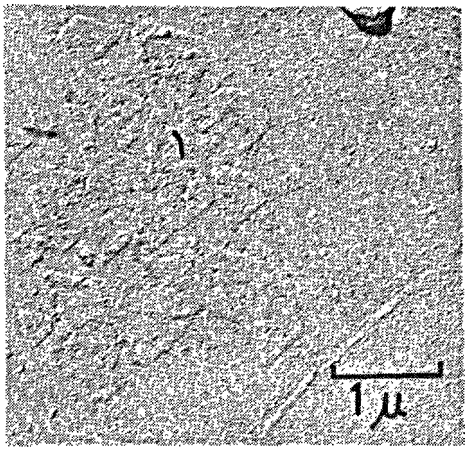

In Figs. 13–16 the changes of the surfaces at the later stage of hydration are shown. In Fig. 17, exhibited is corrosion at the surface contacted with the interstitial phases which have already been eliminated.

Fig. 18 shows the surface behavior after continuous contact with the etchant for one hour. The surfaces have been covered with the gel like skin, so that morphology of the surfaces becomes obscure.

These hydration reactions on C_3S surfaces at the initial stage of hydration can be schematically drawn in Fig. 19.

This dissolution mechanism would be in reverse to that of the crystal growth.

In summary, the violent dissolution reaction on C_3S surfaces at the initial stage of hydration occurs (a) at the point of emergence of screw dislocations, (b) at the grain boundaries and the edges of a crystal, (c) at the surfaces contacting with the interstitial phases. Through this initial dissolution reaction, the surfaces of a C_3S_{ss} crystal are dissolved to the depth of about one thousand several hundred angstrom.

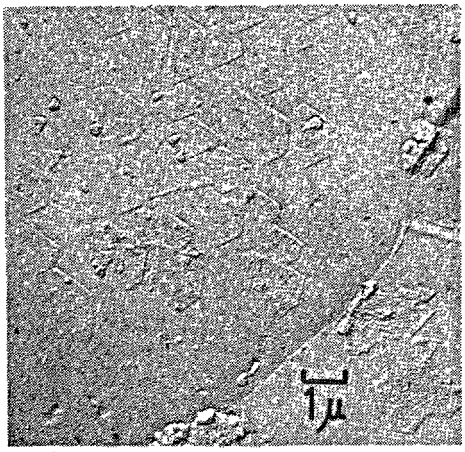

Fig. 10. *Variation of etch pit density with* Cr_2O_3 *content of* C_3S_{ss}. *Etch pit density about* $10^8/cm^2$ *in* C_3S_{ss} *with 1.1 wt. %* Cr_2O_3.
Etchant : 0.4% HF with 0.6% HNO_3 in ethyl alcohol.
Etching time: 1 minute

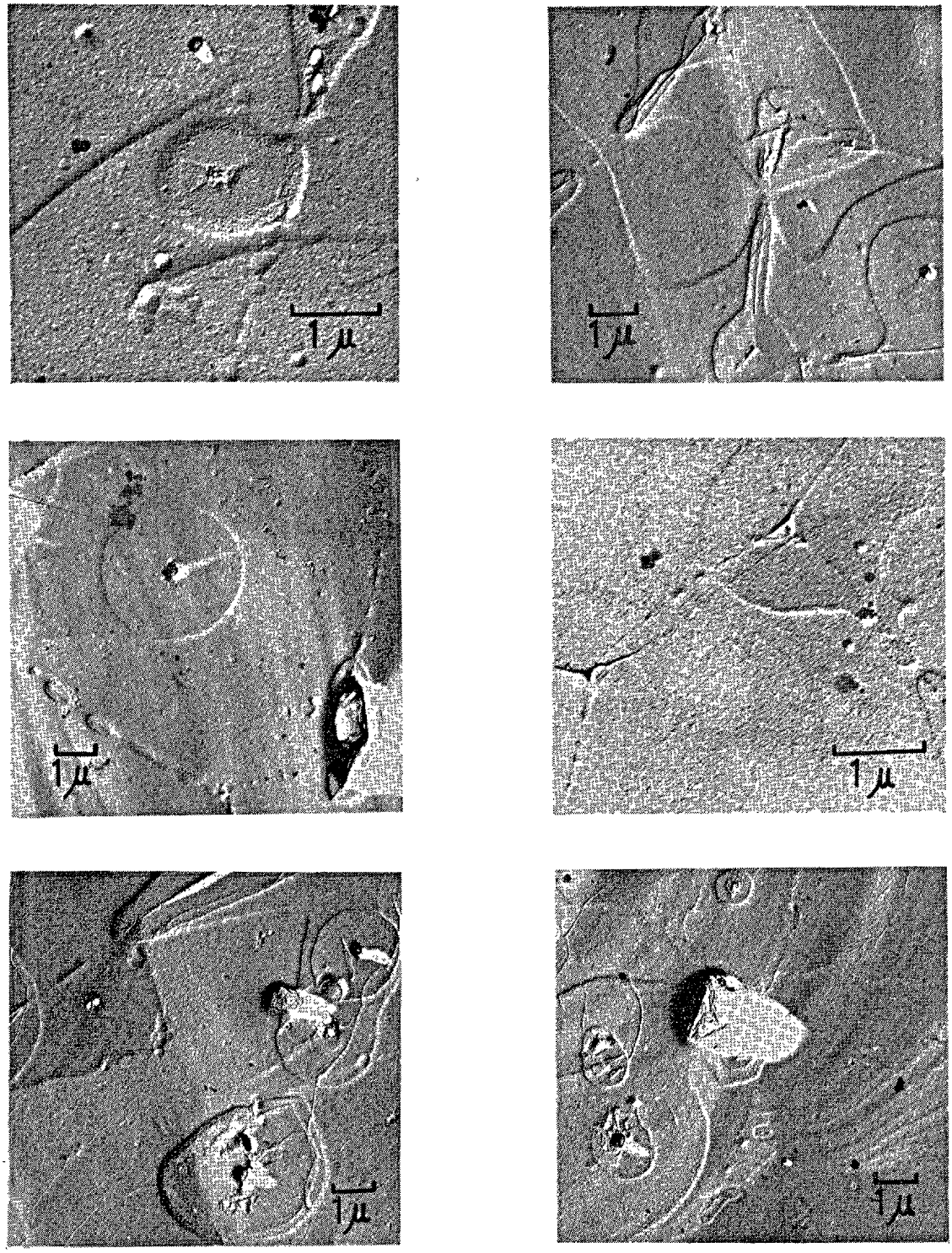

Fig. 11. *Dissolution reaction of C_3S_{ss} crystal surfaces at the initial stage of hydration. Dissolution starts from spiral etch pit formed at the point of emergence of a screw dislocation. Dissolution also occurs at crystal edges and grain boundaries.*
Etchant : 0.4% HF with 0.3% HNO_3 in distilled water.
Etching time: 30 sec.
Specimen : C_3S_{ss} with 1.1 wt. % Cr_2O_3.

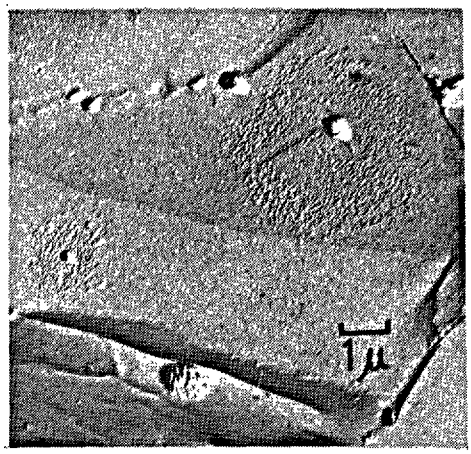

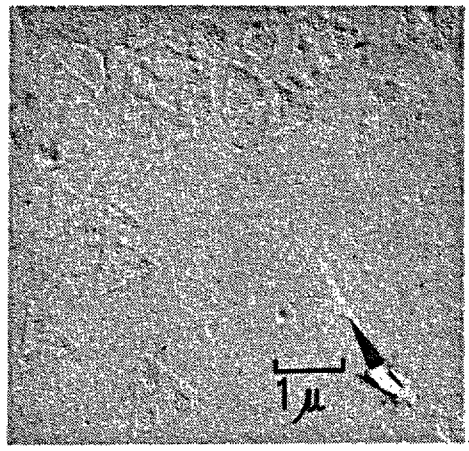

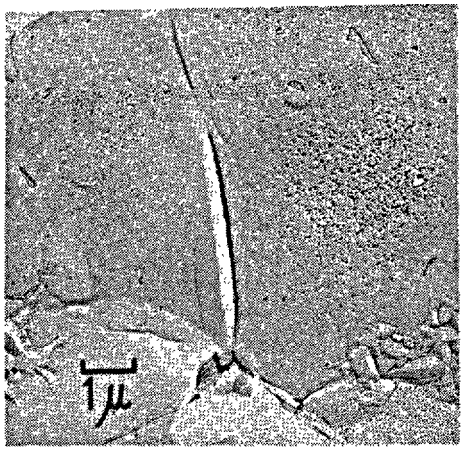

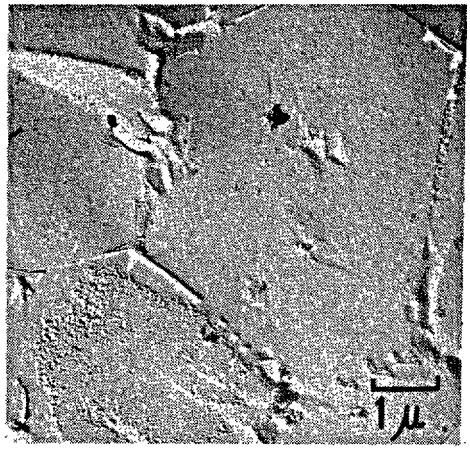

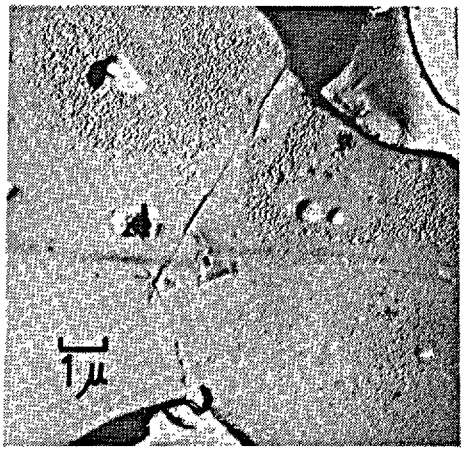

Fig. 12. *Changes of crystal surfaces after 1 minute in etchant.* Specimen: C_3S_{ss} with 1.1 wt. % Cr_2O_3.

Fig. 13. *Changes of crystal surfaces after 3 minutes in etchant.*

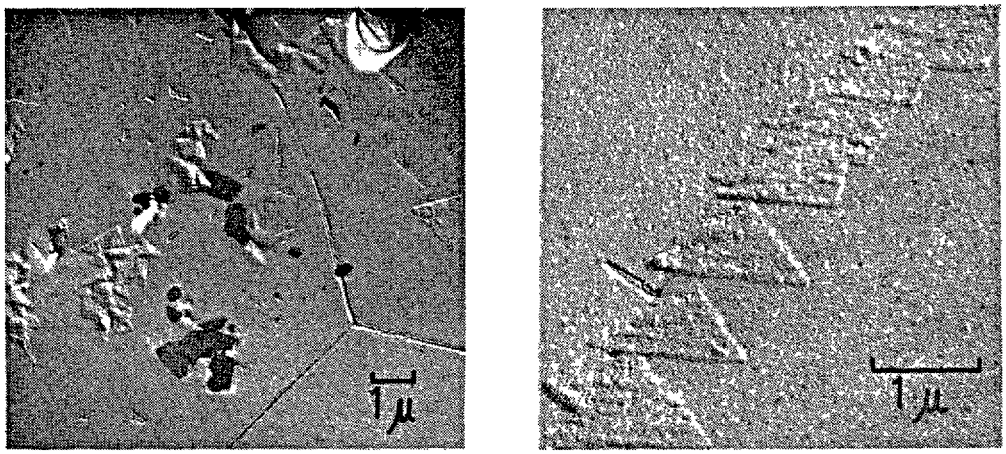

Fig. 14. *Changes of crystal surfaces after 5 minutes in etchant.*

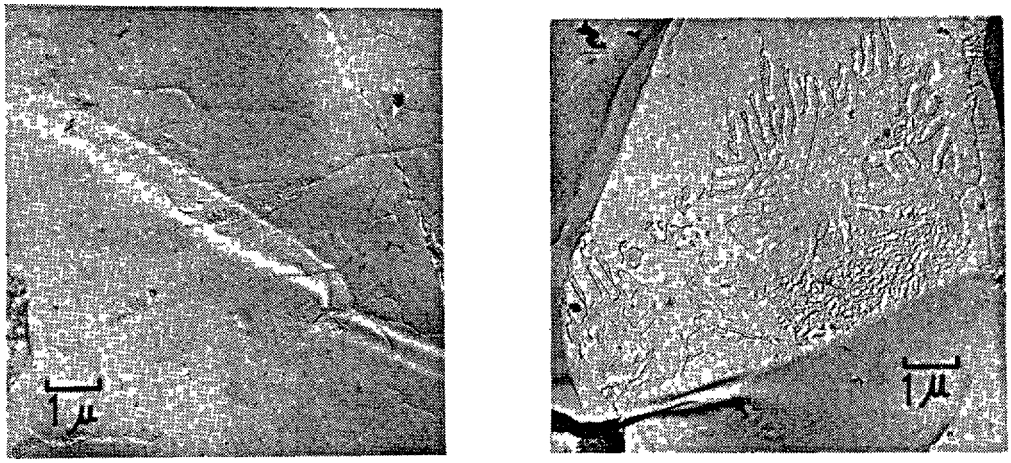

Fig. 15. *Changes of crystal surfaces after 7 minutes in etchant.*

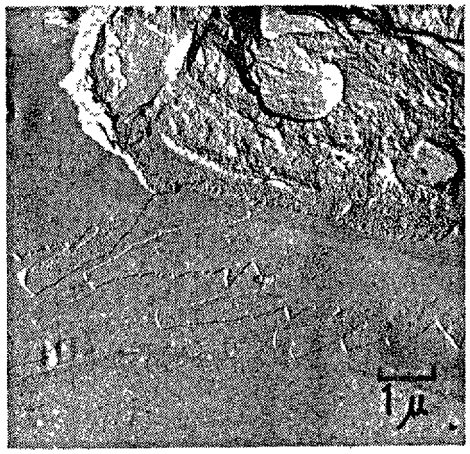

Fig. 16. *Changes of crystal surfaces after 10 minutes in etchant.*

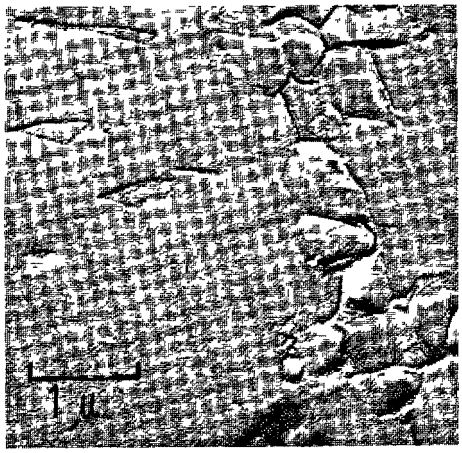

Fig. 17. *Dissolution at the surface contacted with interstitial phases.*

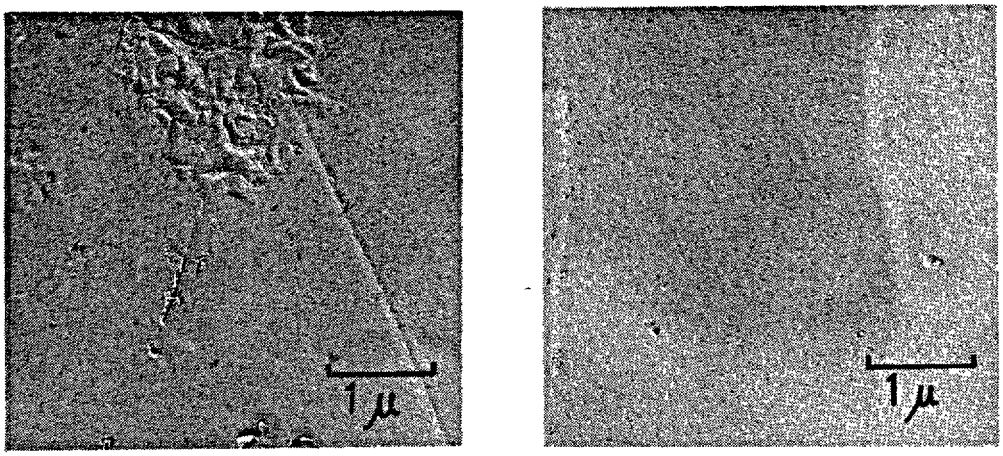

Fig. 18. *Crystal surfaces after one hour in etchant. Surfaces are covered with gel like phases.*

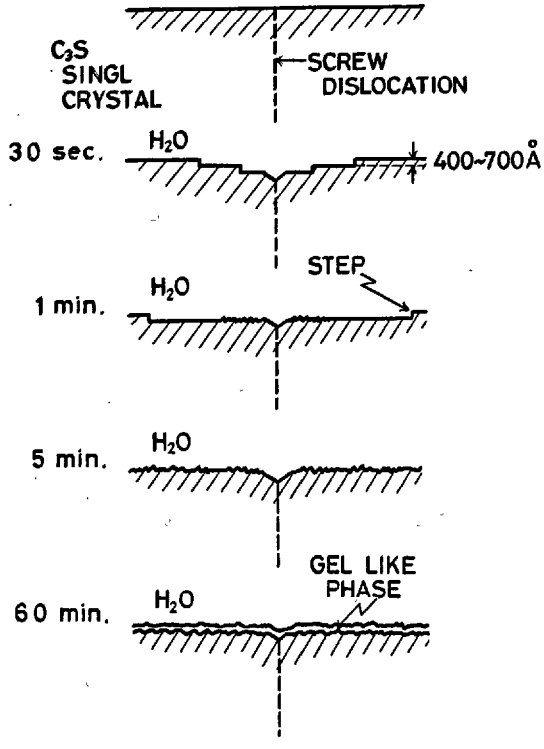

Fig. 19. *Schematic drawings of early dissolution process on C_3S_{ss} crystal surfaces.*

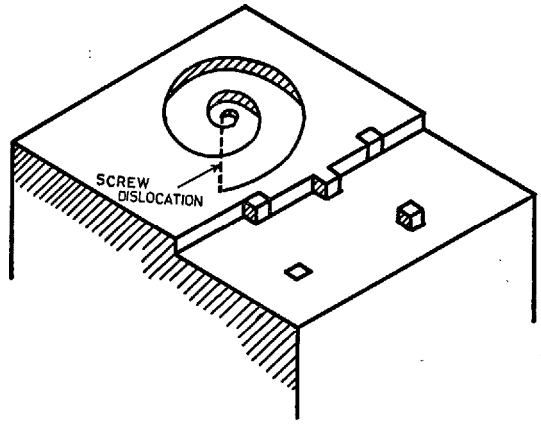

Fig. 20. *Sketch of features on a crystal surface at early dissolution reaction. Dissolution process may be a reverse of the crystal growth process.*
(After J. E. Burke,)

The Early Hydraulic Activity of C_3S with Cr_2O_3, Al_2O_3 and Fe_2O_3 altogether

In this section, the effect of minor components, Cr_2O_3, Al_2O_3 and Fe_2O_3 on the early hydraulic activity of C_3S is studied. This early hydraulic activity of C_3S_{ss} is discussed based on the heat liberation curve obtained with a twin type micro conduction calorimetre (18).

Specimens used are those which are listed in Table 1, in the section of solid solution of C_3S with Cr_2O_3, Al_2O_3 and Fe_2O_3 altogether.

The early hydration reaction of C_3S_{ss} is defined on

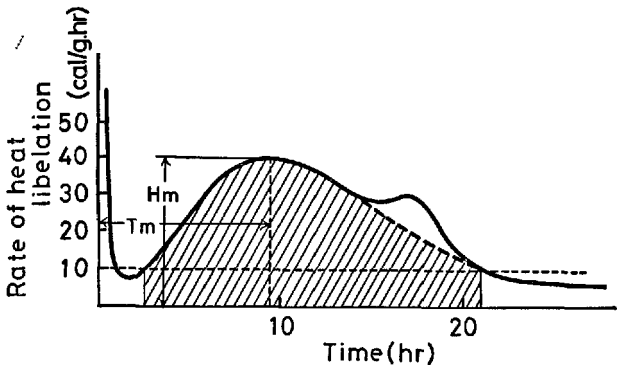

Fig. 21. *The definition of early hydraulic activity of* C_3S_{ss} *on a heat liberation curve of a clinker.*
The shaded portion: The early heat liberation of C_3S_{ss} *(cal/g)*
Hm: The maximum rate of heat liberation (cal/g. hr)
Tm: The time interval from just after contact with water to the maximum rate of heat liberation. (hour)

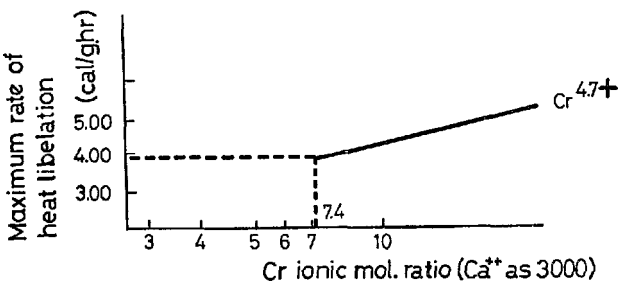

Fig. 22. *Relation between* Cr_2O_3 *content and the maximum rate of heat liberation of* C_3S_{ss}.

the heat liberation curve divided between at the point of 1 cal/g.hr. of heat liberation on the rising curve and at the point of 1 cal/g.hr. of heat liberation on the falling curve. If a third peak which corresponds to hydration reaction of the unhydrated C_3A appears on the heat liberation curve, it is eliminated as shown in Fig. 21.

The early hydraulic activity is defined by the following terms; the early heat liberation which corresponds to the total heat liberation in the above region; the maximum rate of heat liberation; and the time interval of from just after contact with water to the maximum rate of heat liberation. But the direct definition of the early hydraulic activity is represented by the latter two terms.

All the specimens are powdered to 4000 cm^2/g exactly, and 4.0 % SO_3 is added as gypsum to each specimen. The water cement ratio is 50 per cent.

In Fig. 3, illustrated are the heat liberation, the maximum rate of heat liberation and the time just after contact with water to the maximum rate of heat liberation comparing to the C_3S content of clinker, Cr_2O_3, Al_2O_3 and Fe_2O_3 in C_3S_{ss}. The heat liberation of each specimen is about 50 cal/g and is nearly constant independently of minor components. On the other hand both the maximum rate of heat liberation and the time interval have a direct relation with Cr_2O_3 content of C_3S_{ss}. The former increases and the latter is shortened with addition of Cr_2O_3. Between the maximum rate of heat liberation and Cr_2O_3 content, there exists a formula; $Hm = A \log(Cr^{+4.7}) + B$, where Hm is the maximum rate of heat liberation, A and B are the positive constans and $(Cr^{+4.7})$ means the ionic mole ratio of $Cr^{+4.7}$ comparing to the Ca^{++} mole number in C_3S_{ss} standardized as 3000 in Table 2.

Al_2O_3 and Fe_2O_3 seem to have no serious effect on the early hydraulic activity of C_3S_{ss}.

Solid Solution of C_3S with Fluorine and P_2O_5

In order to confirm the effect of Cr_2O_3 in a mixture of Cr_2O_3, Fe_2O_3, Al_2O_3, and also to confirm the effect of fluorine and phosphate on C_3S_{ss} with Al_2O_3, Fe_2O_3, fluorine and P_2O_5, solid solutions of C_3S with Al_2O_3, Fe_2O_3, fluorine and phosphate altogether are studied.

This experiment is performed in the same way as described in the study of C_3S_{ss} with Cr_2O_3, Al_2O_3 and Fe_2O_3. Fluorine is added as CaF_2 and phosphate is added as $3CaO \cdot P_2O_5$. In Table 4 each chemical composition of the clinkers of the C_3S–C_3A–C_4AF–CaF_2–$3CaO \cdot P_2O_5$ system is shown. Solid solubility of flourine, Al_2O_3, Fe_2O_3 and P_2O_5 in C_3S_{ss} is determined by the fractional dissolution method with salicyclic acid in methyl alcohol (14)(15). In order to confirm these compositions obtained, the C_3S solid solutions are synthesized based on the above results obtained.

The solid solubility of each in a mixture of Al_2O_3, Fe_2O_3, fluorine and P_2O_5 in C_3S_{ss} is shown in Fig. 23. The ionic mole ratios of cations, fluorine and phosphor in C_3S_{ss} in this series are listed in Table 5, where the Ca^{++} ionic mole ratio is defined as 3000.

Al^{3+} ionic mole ratio increases proportionately to fluorine in C_3S_{ss}, while Fe^{3+} decreases instead. As Al^{3+} increases, Si^{4+} decreases in a reciprocal proportion.

Therefore, it may be assumed that Al^{3+} will substitute for the Si^{4+} tetrahedra $(SiO_4)^{4-}$ in the form of $(AlO_3F)^{4-}$ accompanying with fluorine.

Table 4. *Clinker compositions in the* C_3S–C_3A–C_4AF–CaF_2–P_2O_5 *system.*

Sample No.	SiO_2	Al_2O_3	Fe_2O_3	CaO	P_2O_5	F	Total
1	21.5	5.4	2.8	70.0	0.00	0.00	99.7
2	21.5	5.4	2.8	69.4	0.24	0.04	99.4
3	21.5	5.4	2.8	69.5	0.24	0.04	99.5
4	21.5	5.4	2.7	69.6	0.24	0.10	99.5
5	21.5	5.4	2.7	69.6	0.24	0.14	99.6
6	20.9	5.4	2.7	69.6	0.24	0.54	99.4
7	21.1	5.4	2.7	69.7	0.24	0.54	99.7
8	20.8	5.5	2.7	69.8	0.24	1.02	100.1
9	20.5	5.3	2.6	69.7	0.24	1.10	99.4
10	20.2	5.2	2.6	69.5	0.25	1.61	99.4
11	20.6	5.3	2.9	70.1	0.44	0.00	99.3
12	20.7	5.4	2.8	70.0	0.48	0.01	99.4
13	20.6	5.3	2.8	70.1	0.49	0.08	99.4
14	20.6	5.5	2.8	70.1	0.48	0.09	99.6
15	20.3	5.6	2.8	70.0	0.49	0.20	99.4
16	20.1	5.4	2.7	70.1	0.48	0.46	99.2
17	19.9	5.4	2.7	70.2	0.47	0.86	99.5
18	19.6	5.4	2.7	70.0	0.49	0.90	99.1
19	19.1	5.0	2.6	69.8	0.49	1.51	98.5

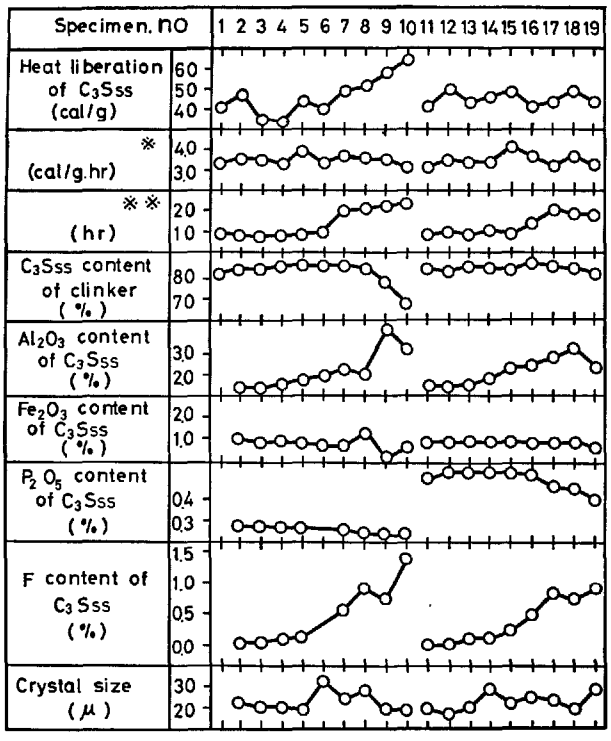

※ Maximum rate of heat liberation of C_3S_{ss}.

※※ Time from just after contact with water to maximum. rate of heat liberation.

Fig. 23. *Effect of minor components on early hydraulic activity of* C_3S_{ss} *in the* C_3S–Al_2O_3–Fe_2O_3–*fluorine*–P_2O_5 *solid solution series.*

Table 5. *Ionic mole ratios of each composition in the* C_3S–Al_2O_3–Fe_2O_3–CaF_2–P_2O_5 *solid solution series, converting each ionic mole number to 3000 basis of* Ca^{++} *ionic mole number.*

	$[Ca^{2+}]$	$[Al^{3+}]$		$[Fe^{3+}]$		$[Si^{4+}]$		$[P^{5+}]$	$[F^-]$
Sample No.	Ionic mole ratio in C_3S_{ss}	Ionic mole ratio	$[\Delta Al^{3+}]$	Ionic mole ratio	$[\Delta Fe^{3+}]$	Ionic mole ratio	$[\Delta Si^{4+}]$	Ionic mole ratio	Ionic mole ratio
1	3000	50	0	28	0	984	0	0	0
2	3000	56	6	28	0	981	17	8	5
3	3000	56	16	28	0	972	8	8	4
4	3000	66	16	28	0	964	0	8	13
5	3000	80	30	22	−6	956	−10	8	17
6	3000	86	36	16	−12	921	−43	—	—
7	3000	106	56	16	−12	905	−59	8	71

The Effect of Fluorine on the Early Heat Liberation of C_3S_{ss}

In Fig. 23 shown are the early heat liberation, the maximum rate of heat liberation, the time interval comparing with fluorine, Al_2O_3, Fe_2O_3 and P_2O_5 dissolved in C_3S solid solution. In these series, the maximum rate of heat liberation and the time interval are invariable with addition of Al_2O_3, fluorine, Fe_2O_3 and P_2O_5. On the other hand, the early heat liberation increases with addition of Al_2O_3 and fluorine. In Figs.

24–27 the relations between heat liberation of C_3S_{ss} and minor components are illustrated. These results mean that the dissolution of Al_2O_3 and fluorine in C_3S_{ss} increases the early heat liberation, but does not accelerate the early hydration reaction.

This is a remarkable feature of Al_2O_3 and fluorine in C_3S compared with Cr_2O_3 in C_3S.

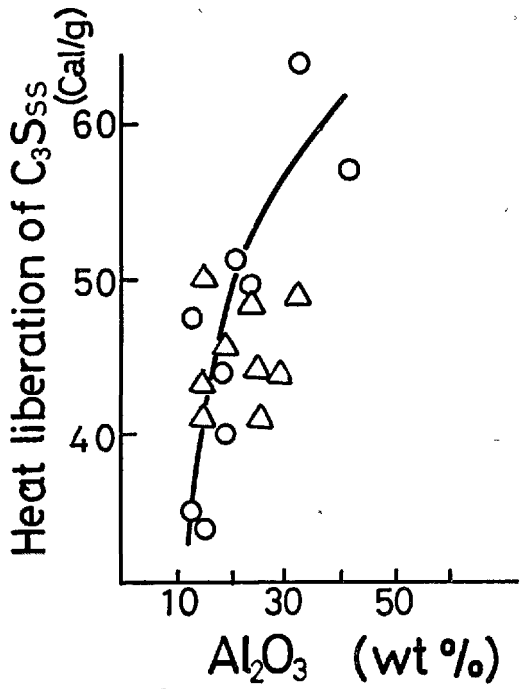

Fig. 24. *Relation between Al_2O_3 content and the early heat liberation of C_3S_{ss} in Fig. 23.*

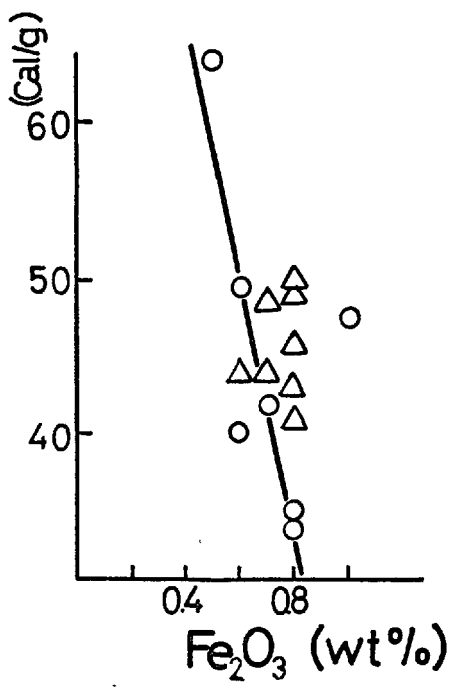

Fig. 25. *Relation between Fe_2O_3 content and the early heat liberation of C_3S_{ss} in Fig. 23.*

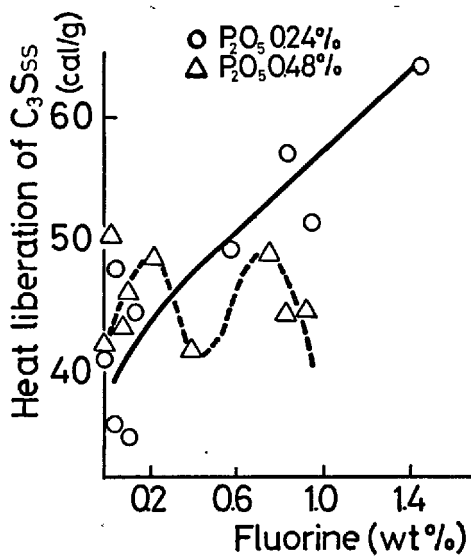

Fig. 26. *Relation between fluorine content and the early heat liberation of C_3S_{ss} in Fig. 23.*

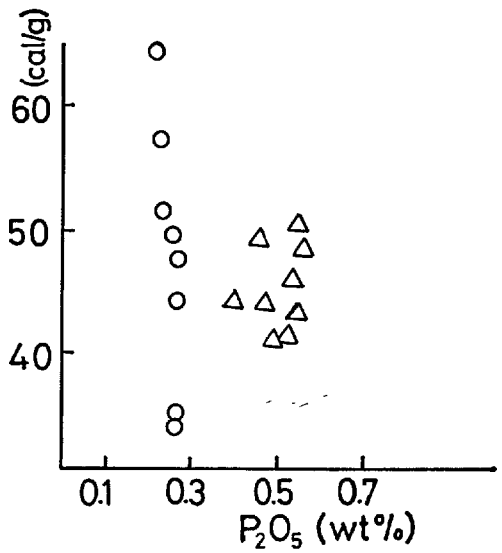

Fig. 27. *Relation between P_2O_5 content and the early heat liberation of C_3S_{ss} in Fig. 23.*

Effect of Cr_2O_3 on the Ferrite Phase

In portland cement, the calcium alumino ferrite phases are always present with several major constituents. It is, therefore, of importance to examine the effect of Cr_2O_3 on the ferrite phase as well as the above examination of Cr_2O_3 on C_3S_{ss}.

Solid Solution of Ferrite (C_2F, C_4AF) with Cr_2O_3

In this study, the C_4AF-hypothetical "C_2Cr" system as well as the C_2F–"C_2Cr" system has been examined in air and in O_2. Mixes (in Table 6) were prepared in a horizontal externally heated tube furnace by solid state sintering at 1300°C. Mixes were then cooled at the rate of 50 degree per hour. The limit of Cr substitution in C_2F and C_4AF at 1300°C in air were determined by means of X-ray, optical and chemical techniques. The variation of the lattice constants with Cr_2O_3 are shown in Figs. 28 and 29.

The limits of Cr substitution are 4.8 wt. % of C_2F_{ss} and 5.3 wt. % of C_4AF_{ss}, which correspond to 9.1 mole % "C_2Cr" and 8.4 mole % "C_2Cr" respectively.

The average charges of Cr ions in the ferrite phases are +3.2 which were obtained by chemical analysis. The excess Cr ions, if present, coexist with the ferrite phases in the form of calcium chromate, $3CaO \cdot Cr_2O_5$.

The shrinkage of the C_2F_{ss} lattice constants is in good proportion to the difference of Cr^{3+} (0.64Å) from Fe^{3+} (0.67Å). Now, it is the variation of the C_4AF_{ss} lattices with Cr_2O_3 that deviates from the

Table 6. *Chemical compositions of ferrite with* Cr_2O_3.

Sample	Al_2O_3%	Fe_2O_3%	Cr_2O_3%	CaO%
C_2F	—	58.7	—	41.3
C_2F + 0.05 C_3Cr	—	55.5	2.6	41.9
C_2F + 0.08 C_3Cr	—	53.7	4.1	42.2
C_2F + 0.10 C_3Cr	—	52.6	5.0	42.4
C_2F + 0.15 C_3Cr	—	49.9	7.1	43.0
$C_2A_{1/2}F_{1/2}$	21.0	32.9	—	46.2
$C_2A_{1/2}F_{1/2}$ + 0.05C_3Cr	19.7	30.8	2.9	46.6
$C_2A_{1/2}F_{1/2}$ + 0.08 C_3Cr	19.0	29.7	4.5	46.8
$C_2A_{1/2}F_{1/2}$ + 0.10 C_3Cr	18.5	29.0	5.5	46.9
$C_2A_{1/2}F_{1/2}$ + 0.15 C_3Cr	17.5	27.4	7.8	47.2

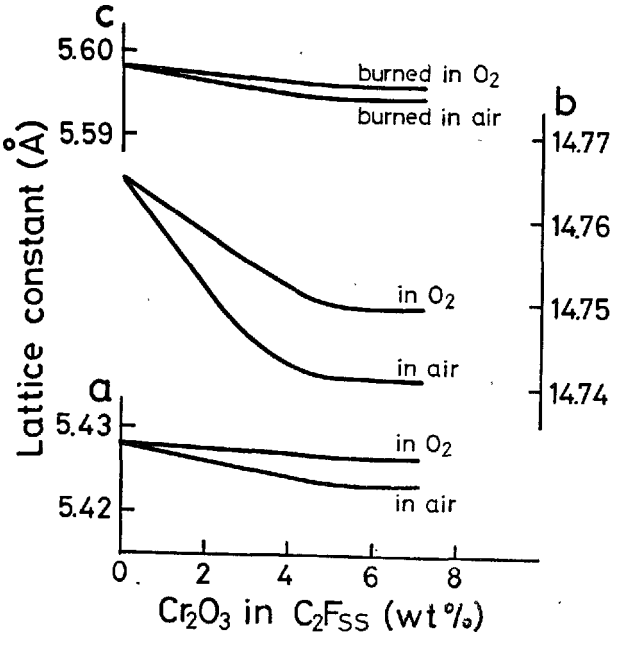

Fig. 28. *Variation of orthorhombic lattice constants with composition in* $2CaO \cdot xFe_2O_3(1-x)Cr_2O_3$.

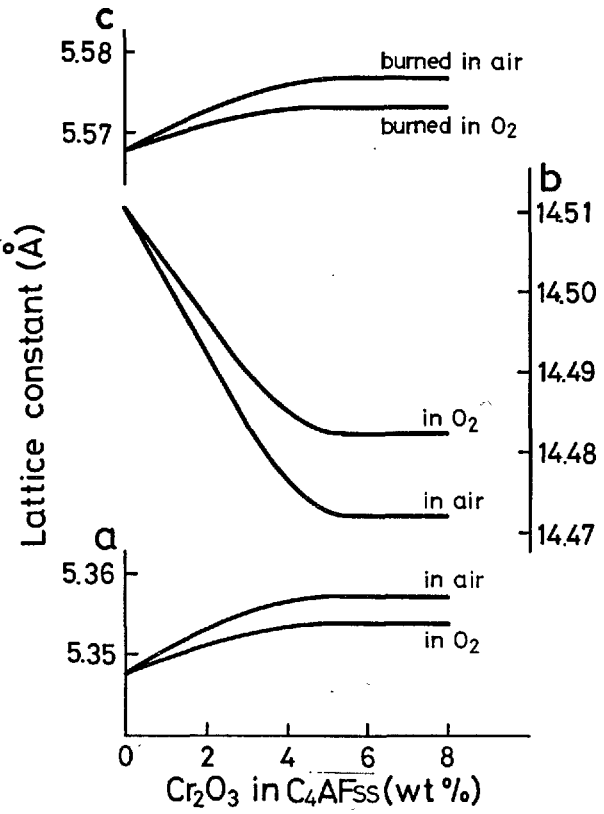

Fig. 29. *Variation of orthorhombic lattice constants with composition in* $4CaO \cdot xFe_2O_3 \cdot xAl_2O_3 \cdot (1-2x)Cr_2O_3$.

calculated values; the *b* axis shrinks beyond the calculated values, while the *a,c* axes expand unexpectedly.

These kinds of unexplainable variations of the ferrite lattices have been, however, reported by several researchers; among them, Sakurai (19) has observed in the C_4AF–C_4AM solid solution series, the *b* axis expands with addition of Mn_2O_3, while the *a,c* axes shrink instead; Kato (20) has found the similar irregular changes in the C_2F–MgO system, the C_4AF–MgO system and the C_2F–CaO system. Furthermore, Kato's cases are accompanied by the unusual increase in the intensity of the 020 reflection. If the ferrite structure proposed by Bertaut et al (21) and Smith (22) is correct, these lattice variation must be considered to result from the special characters of the doped transition metal ion Cr^{3+} in the ferrite ligand field.

These lattice variations, however, is recovered to some extent, by re-sintering these ferrite phases in O_2. This is partly because Cr^{3+} ions in the lattices are oxidized into the higher charges and eliminated from the lattices.

The early hydraulic activity of C_2F_{ss} with Cr_2O_3 was determined in the same way as in C_3S_{ss}. As a result, it was proved that Cr_2O_3 can activate the early hydraulic activity of C_2F, although the total heat liberation is invariable. Addition of Cr_2O_3 beyond the limit of substitution, however, decreases the early hydraulic activity of C_2F.

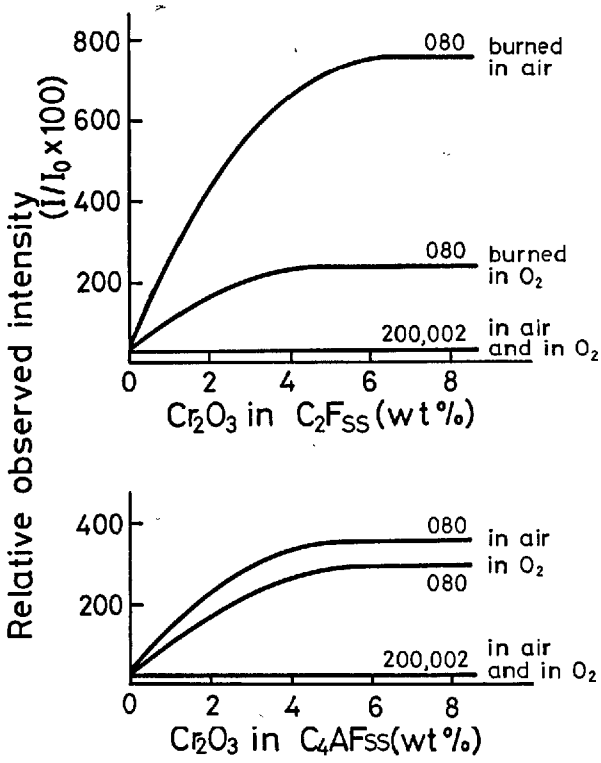

Fig. 30. *The increase of intensity for* 0k0 *reflections with increasing* Cr *content in ferrite solid solutions. Relative observed intensity;* $I/I_0 \times 100$.
I: Intensity for hkl reflections of each sample.
I_0: Intensity for 141 reflections of C_2F and C_4AF.

Abnormal Properties of the Ferrite Phase with Cr_2O_3

It was observed that the ferrite with Cr_2O_3 causes an abnormal increase in the diffraction intensity of 0k0 reflection. As some instances shown in Fig. 30, the diffraction intensities of 080, 040 and 020 plane in the ferrite phases prepared in air increase by more than 30 times in C_2F_{ss} and 15 times in C_4AF_{ss}, whereas no intensity change occurs in the other planes. In C_2F_{ss}, however, this intensity decreases if the C_2F_{ss} is sintered in O_2, whereas the intensity in C_4AF_{ss} shows no changes.

To analyse these phenomena, the infrared absorption spectra of these ferrites were studied.

The absorption curves obtained are shown in Figs. 31, 32 and 33.

In the infrared absorption spectra of the ferrite in the C_2F–"C_2Cr" system, the absorption peaks at 1160 cm^{-1}, 950 cm^{-1} and 710 cm^{-1} become stronger

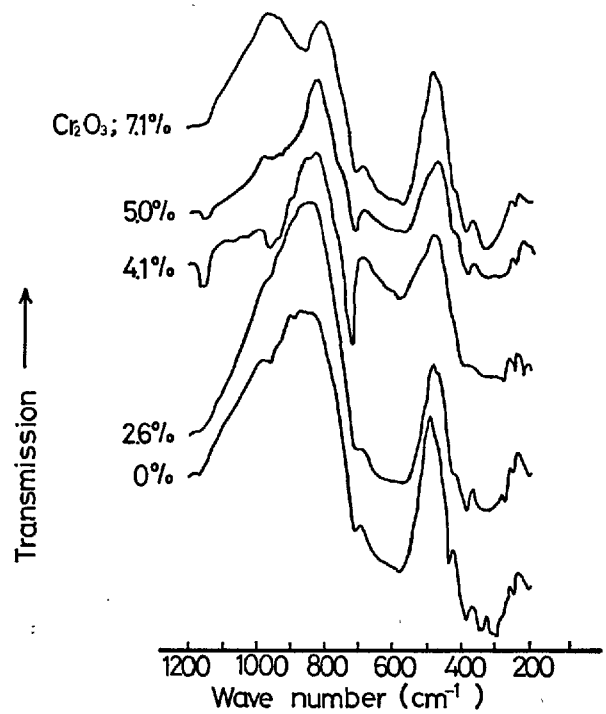

Fig. 31. *Infrared absorption spectra of samples of composition* $2CaO \cdot xFe_2O_3 \cdot (1-x) \cdot Cr_2O_3$.

with increasing substitutions of Cr_2O_3, but the absorption bands in the 640 cm^{-1}–580 cm^{-1} region become weaker instead.

In the infrared absorption spectra of the ferrite in the C_4AF–"C_2Cr" system, the absorption peaks at 1160 cm^{-1} and 720 cm^{-1}, which are also observed in the C_2F–"C_2Cr" system, become stronger, too, with increasing substitution of Cr_2O_3, whereas the strong absorption spectra at 780 cm^{-1} and 430 cm^{-1} become weaker.

After Koresova (23), the frequency of the band in the 720 cm^{-1}–780 cm^{-1} region in the silicate crystals whose lattices contain Al atoms is determined by the fraction of its covalency. An increase in the ionic character of the band, i.e. transfer of Al atoms from anion shell into cation state, eliminates the 720 cm^{-1}–780 cm^{-1} band from the spectrum.

As these spectra at 780 cm^{-1} and 430 cm^{-1}, which are observed in the C_4AF–"C_2Cr" system and in the C_2F–"C_2A" system, cannot be observed in the C_2F–"C_2Cr" system, they may be caused by AlO_4 tetrahedra, and then the spectra in the lower frequency region 660 cm^{-1}–610 cm^{-1} may be caused by the FeO_4 tetrahedra.

In these cases, the above spectra are weakened by increasing substitution of Cr_2O_3. As described above, this decrease of absorption may correspond to an increase in the ionic character of the bonding. Therefore, the substituted Cr_2O_3 seems to increase the ionic character of AlO_4 and FeO_4 tetrahedra.

The strong absorption band in the 710–730 region which is observed in these three phases is subject to no effect by substitution of Cr_2O_3. This absorption peak may belong to a bond of the high symmetry, but is difficult to be indexed.

The above unusual diffraction intensity can be influenced by an adsorption and a desorption of H_2O on the ferrite surfaces.

This is a reversible variation which accompanies no structural change. Therefore this phenomenon may be caused by an electrostatic effect of H_2O.

This reduction of intensity is also caused by mechanical crushing of the ferrite crystals.

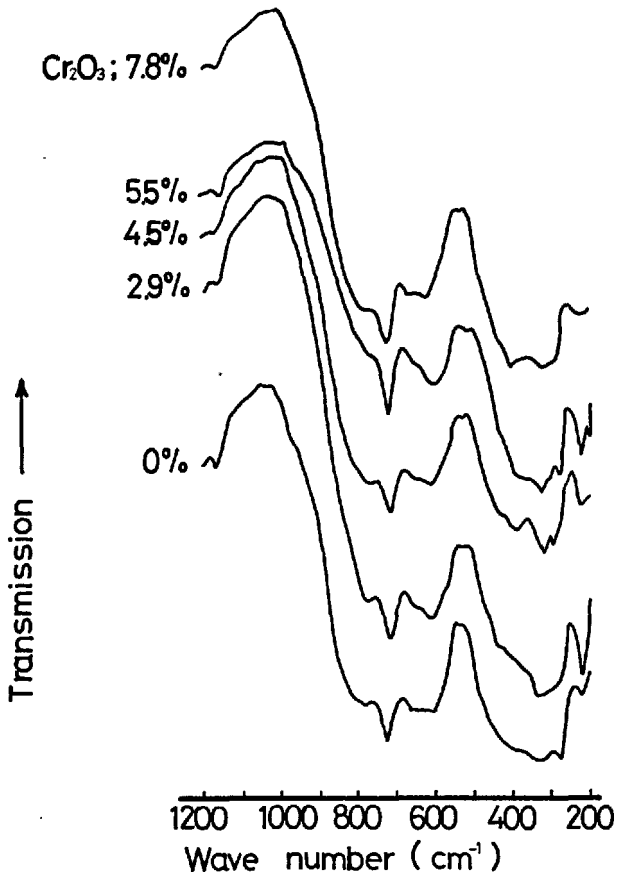

Fig. 32. *Infrared absorption spectra of samples of composition* $4CaO \cdot xFe_2O_3 \cdot xAl_2O_3 \cdot (1 - 2x)Cr_2O_3$.

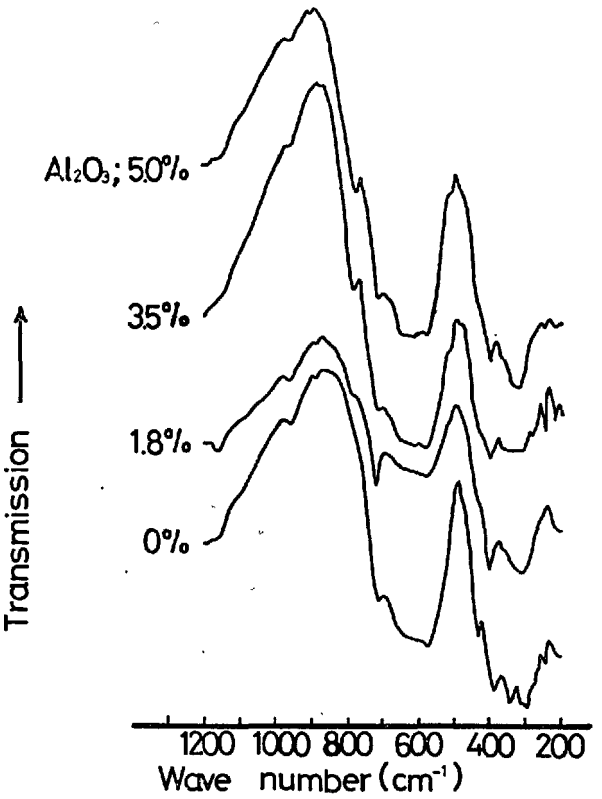

Fig. 33 *Infrared absorption spectra of samples of composition* $2CaO \cdot xFe_2O_3 \cdot (1 - x)Al_2O_3$.

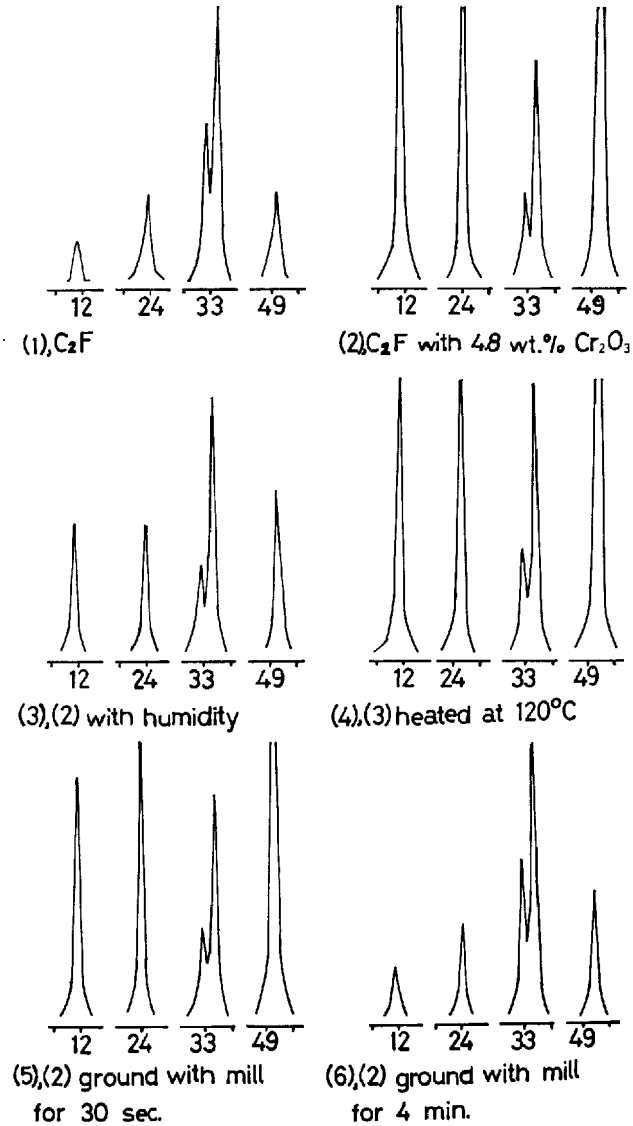

Fig. 34. *Abnormal variation of intensity for* 0k0 *reflections of ferrite solid solutions with* Cr_2O_3.
Sample 1; C_2F sintered at 1300°C in O_2.
Sample 2; C_2F with 4.8 wt% Cr_2O_3 sintered at 1300°C in O_2.

This change is irreversible and cannot be recovered even if the crushed ferrite be heated at 1000°C or at the higher temperature.

The phenomenon caused by an adsorption of H_2O is directly relative to the effect of Cr_2O_3 on the early hydraulic activity of ferrite.

The Mechanism of the Early Hydraulic Action of C_3S with Cr_2O_3

It may be clear from the results in the preceding sections that C_3S with Cr_2O_3 promotes its early hydraluic activity, whereas C_3S with fluorine and Al_2O_3 in the form of $(AlO_3F)^{4-}$ does not, though it increases the early heat liberation.

This difference may be based on semiconductivity of C_3S with Cr_2O_3.

Chatterji and Phatak (10) studied the semiconductivity of normal portland cement. They reported that the clinker material was behaving as a P-type semiconductor, and that the hydraulic action of portland cement clinker was N-type reaction on P-type semiconductor. Hansen (22) reported that the reaction between lime and water might be a N-type reaction on P-type semiconductor. As mentioned above, C_3S with Cr_2O_3 is a P-type extrinsic semiconductor.

Though the hydration reaction of C_3S with Cr_2O_3 starts at the point of emergence of screw dislocation, the later process of hydration may be affected rather by semiconductivity of C_3S solid solution than by

dislocations of C_3S solid solution.

In another words, in the early hydration, the hydration velocity on the surface of C_3S solid solution is accelerated multiplicatively both by the density of screw dislocations and by semiconductivity of C_3S solid solution.

When a P-type semiconductor, C_3S solid solution is in contact with water, the contact surface may be surrounded by a diffuse double layer of water. By screening theory, Si^{4+} is screened enough by the oxygen tetrahedra even on the surface of C_3S_{ss}. Ca^{++} on the surface, however, may not be screened enough by oxygen so that H_2O molecules may be able to attain Ca^{++}, and combine with Ca^{++} as follows;

$$Ca_{lattice} + 2H_2O = Ca(OH)_2 + 2H^+ + Ca\square^{--}$$

In this case, the corrosion theory of semiconductor of germanium (23) may be applicable.

During this combination action, $2e^-$ from $Ca\square^{--}$ may be carried out to the other places by electron holes, where they may recombine with H^+. This reaction may be, however, considerably slow, because of the relaxation effect of the C_3S surface.

That is to say, for the hydraulic action on the C_3S surface, it postulates the operation of two half-cell reactions, the oxidation of Ca and the reduction of H^+. These reactions may be assumed to proceed independently, as if they were the two half-reactions of a short circuited battery.

This oxidation-reduction reaction may be remarkable in the weathering of natural rocks. Therefore the hydraulic action of C_3S may be able to regard as a violent weathering action.

Conclusion

The early hydraulic activity of C_3S is remarkably promoted by addition of Cr_2O_3. This unique effect of Cr_2O_3 must be based on semiconductivity of C_3S with Cr_2O_3. Among imperfections in C_3S solid solution, electron holes and vacancies may help Ca ions being released from the lattice sites. Screw dislocations observed are the starting points of dissolution reaction on C_3S surfaces, while the other dislocations seem to give no obvious effect on the hydration reaction of C_3S_{ss}. These effect of promotion of the early hydraulic activity of C_3S may be also found in some other transition elements which have the similar properties with Cr.

Calcium aluminoferrite also has its hydraulic activity promoted by Cr_2O_3. This case may be also explained by semiconductivity of ferrite with Cr_2O_3.

As everybody know, there remain so many problems of clinkers unsolved. These are the effect of rapid cooling or quenching, the effect of overburning, the effect of minor components on cement clinker minerals and so on. If studies of clinkers are developed from the two viewpoints both of solid state physics and of crystal chemistry, these problems may be easily solved and the properties of clinkers may be improved further.

In order to proceed with a study of the hydration reaction of cement clinker minerals, it may be also very useful to know the weathering mechanism of the natural rocks.

Acknowledgements

The authors would like to thank Dr. K. Chujo (a Managing Director of Nihon Cement Company) Dr. J. Yamada (the Chief Manager of this Research Laboratory) for their kind suggestions. The authors would also like to thank Dr. N. Kawada for his kind advise, and thank the collegue of the authors, Messrs. M. Hashimoto, T. Matsu, and M. Fukungaga for their kind assistance during this work.

References

1. W. Jander, Angew, Chem. **51**, 696 (1938).
2. K. Akiyama, "Research of special portland cement, (I)" (in Japanese), Kogyo Kagaku Zasshi, **37**, 1297 (1934).
3. M. M. Sychov and V. I. Korneev, "Alloying additive improve the properties of cement" (In Russ.), Tsement, **30**, 3 (1964).
4. J. H. Welch and W. Gutt, "Effect of minor components on hydraulicity of the calcium silicates", Proc. 4th International Symposium Chem. of

Cement, Washington, 59 (1962).
5. Y. Ono and Y. Soda, "Effect of the crystallographic properties of Alite and Belite on the strength of cement" (in Japanese), Semento Gijutsu Nenpo, **19,** 93 (1965).
6. E. Woermann, Th. Hahn and W. Eysel, "Chemical and structural investigations on the solid solutions of tricalcium silicate" (in German), Zement-Kalk-Gips, **9,** 370 (1963).
7. G. Yamaguchi and H. Miyabe, "Precise determination of the $3CaO \cdot SiO_2$ cells and interpretation of their X-ray diffraction patterns", J. Am. Ceram. Soc., **43,** 219 (1960).
8. M. Bigaré, A. Guinier, C. Mazieres, M. Regourd, N. Yannaquis, W. Eysel, Th. Hahn and E. Woermann, "Polymorphism of tricalcium silicate and its solid solutions", J. Am. Ceram. Soc., **50,** 604 (1967).
9. S. Takashima, "Systematic dissolution of calcium silicate in commercial portland cement by organic acid solution" (in Japanese), Semento Gijutsu Nenpo, **12,** 49 (1958).
10. A. K. Chatterji and T. C. Phatak, "Reaction between portland cement clinker and water", Nature, **203,** 138 (1964).
11. F. P. Glasser and E. F. Osborn, "Phase equilibrium studies in the system $CaO–Cr_2O_3–SiO_2$", J. Am. Ceram. Soc. **41,** 358 (1958).
12. T. Nishino and T. Sakurai, "On the reaction between CaO-bearing compound and Cr_2O_3" (in Japanese), Yogyo-Kyokai-Shi, **25,** 259 (1967).
13. G. H. Jonker, "Semiconducitng properties of mixed crystals with perovskite structure", Physica, **20,** 1118 (1954).
14. F. Kanamaru and R. Kiriyama, "Crystal structure and electromagnetic properties of calcium ferrite-calcium chromate solid solution" (in Japanese), Kogyo Kagaku Zasshi, **85,** 463 (1964).
15. G. Yamaguchi and H. Uchikawa, "Investigations on the mixed crystals in the system $3CaO \cdot SiO_2–Na_2O$" (in German), Zement-Kalk-Gips, **14,** 497 (1961).
16. F. Ordway, "Crystal structures of clinker constituents" Proc. 4th International Symposium Chem. of Cement, Washington, 39 (1962).
17. J. Grzymek, "Significance of the exterior crystal habit of alite for the production of super-portland cements", (in German) Silikattechnik, **6,** 296 (1955).
18. K. Fujii and T. Watanabe, "Immediate heat liberation of portland cement as mixed with water" (in Japanese), Semento Gijutsu Nenpo, **8,** 120 (1964).
19. T. Sakurai, "The behaviour of magnanese in cement clinker minerals", (in Japanese), Semento Gijutsu Nenpo, **14,** 32 (1960).
20. A. Kato, "A study on the solubility of Mg in the ferrite phase of portland cement clinker by X-ray investigation", Semento Gijutsu Nenpo, **12,** 17 (1958).
21. E. F. Bertaut, P. Blum and A. Sagnieres, "Structure of dicalcium ferrite and brownmillerite", Acta Cryst., **12,** 149 (1959).
22. Deane K. Smith, "Crystallographic changes with the substitution of aluminum for iron in dicalcium ferrite", Acta Cryst., **15,** 1146 (1962).
23. V. A. Kolesova, "Infrared absorption spectra of aluminum-containing silicates and some crystalline aluminates", Opt. i Spektroskopiya, **6(1),** 38 (1959); Opt Specty. (USSR) (English Transl.) **6,** 20 (1959).
24. W. C. Hansen, "Solid liquid reactions in portland cement pastes", Materials Research & Standards, **2,** 490 (1962).
25. J. F. Dewald, "Semiconductors", p. 727, (Reinhold Publishing Co. N.Y., U.S.A., 1959).

Supplementary Paper I-126 The Distribution of Alkalis in Portland Cement Clinker

Harry W. W. Pollitt and Arthur W. Brown*

Synopsis

The distribution of alkalis in portland cement clinker has been studied using X-ray diffraction and selective solvent extraction and hydrolysis of clinkers.

Alkalis occur in clinker in the form of sulphates outside the four main crystalline components, and as substitution compounds within these crystalline components.

If sufficient SO_3 is available the alkalis occur as sulphates rather than as substitution compounds. Increasing quantities of SO_3 produce more calcium sulphate. Potassium sulphate is the preferred form of alkali sulphate; the molar ratio of potash/soda in sulphate form can be twice that in the alkalis as a whole. There is evidence of a series of double alkali sulphates and of a specific compound $2CaSO_4 \cdot K_2SO_4$ frequently found in clinker. Potassium sulphate is shown to have an important bearing on cement storage properties.

At least half the alkalis not accounted for as sulphate occur in the C_3A and ferrite in quantities determined by the alumina contents of those two compounds. The crystal form of C_3A is modified by potash as well as by soda.

In the silicates the quantitative distribution of alkalis is as yet less clear. Certainly soda as well as potash is capable of modifying belite. It is considered probable that both potash and soda exist in alite in small quantities, probably associated with alumina in solid solution. The association of alkalis with alumina may relate to that proved in the C_3A and ferrite phases.

Introduction

The Research Department of the Associated Portland Cement Manufacturers, Ltd. took a special interest in the distribution of alkalis in clinker following an investigation of the storage properties of ordinary portland cement. This investigation showed that potassium sulphate in cement could influence air-setting or pack-setting through its capacity to react with the gypsum component to form syngenite, $K_2SO_4 \cdot CaSO_4 \cdot H_2O$, during storage. Forest (1) reached a different conclusion in respect of blastfurnace cements.

X-ray diffraction studies of cement composition had also produced evidence that the "split-peak" orthorhombic form of C_3A reported by Moore (2) was not exclusively confined to cements with significant soda contents.

The present paper describes work that has been done by the Department to throw more light on the location of the alkalis in portland cement clinker. Whilst the more advanced techniques have proved invaluable, much has been learned by differential solvent extraction and by microscopic studies.

Separation of Alkali Sulphates in Clinker

In the course of the study of storage properties of cement already referred to, micro-electron probe techniques revealed a close association between the elements potassium and sulphur in what appeared to be deposits sited in the celite (C_3A + ferrite). Improved microscopic techniques permitted the identification of alkali sulphate (Photo 1) and attempts were made to estimate them quantitatively by wet chemical methods.

It was found that alkali sulphates as such could be extracted by hot ethylene glycol using the normal technique for free lime determination. Analysis of the extract and the residual clinker showed that alkali and sulphate in some form remained in the clinker. Further controlled extraction by water was shown to

*Research Department, the Associated Portland Cement Manufacturers, Limited, Kent, United Kingdom.

⊢⊣ 10 μ ×800

Photo 1. *This shows alkali sulphate, arrowed A, infilling irregular pores in the clinker and is thus clearly one of the last phases to crystallise. It occurs here as small oriented crystals, etched a dark colour with hydrofluoric acid vapour. Interpenetration of the embedding plastic resin, arrowed B, used during specimen preparation, indicates volume changes during cooling.*
Characteristically the alkali sulphate is surrounded by a halo of unetched clinker.

remove from the clinker further alkali and calcium sulphate, the quantity of the latter suggesting that it was in a highly soluble form. The remaining sulphate in the clinker was later shown to be β-calcium sulphate.

Thus differential extraction separated simple alkali sulphates on the one hand from some other form of alkali and calcium sulphates on the other leaving relatively insoluble β-calcium sulphate in the clinker. The whole of the sulphate could be accounted for in this way. It was also found that no significant quantity of alkali remaining in forms other than as sulphate (or in two cases as free alkali) was removed by the extraction process.

A water extraction alone of course removes the simple alkali sulphates as well as the other water-soluble form of alkali and calcium sulphate. The totals of alkalis and sulphates so extracted are referred to as the water-soluble alkalis and sulphates respectively.

Forms of Calcium Sulphate

As mentioned above, calcium sulphate was shown to occur in a very water-soluble form.

Initial examination by X-ray diffraction of clinkers containing this form of calcium sulphate did not

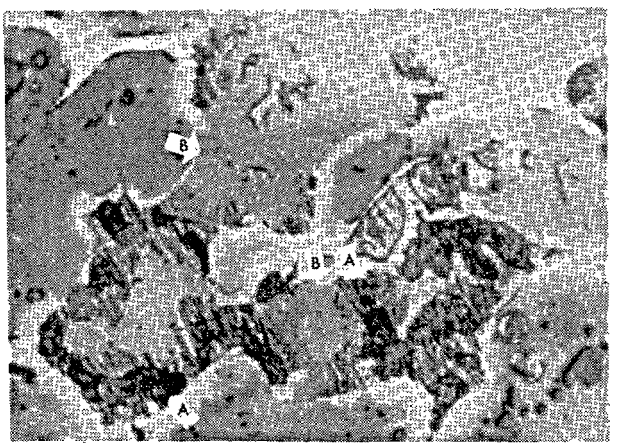

⊢⊣ 10 μ ×800

Photo 2. *The coexistence of alkali sulphate, arrowed A, and* $2CaSO_4 \cdot K_2SO_4$, *arrowed B, in clinker is shown here.*
Clearly the original composition of the alkali and calcium sulphate melt lay to the potassium sulphate side of the eutectic composition and crystallisation of the small needles of alkali sulphate took place as the temperature fell. The composition of the liquidus moved towards $2CaSO_4 \cdot K_2SO_4$, *which finally crystallised encasing the earlier formed alkali sulphate. The characteristic halo appears on both the sulphates although it is narrower around the* $2CaSO_4 \cdot K_2SO_4$.

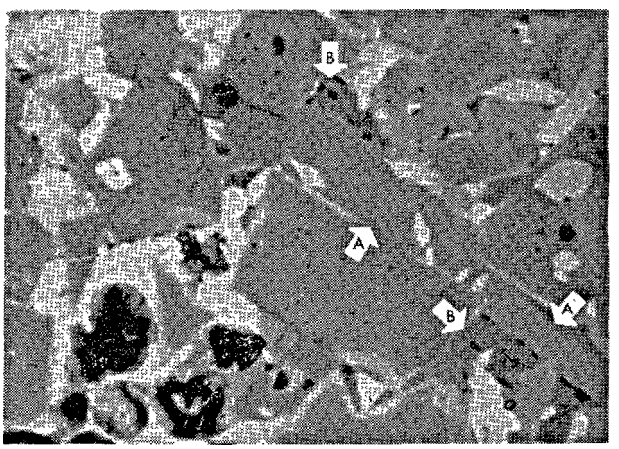

⊢⊣ 10 μ ×800

Photo 3. *In this photomicrograph the coexistence of calcium sulphate, arrowed A, with* $2CaSO_4 \cdot K_2SO_4$, *arrowed B, is illustrated. In this case the alkali sulphate is not present and it is apparent that the composition of the melt lay towards the calcium sulphate side of the eutectic composition. The initial crystallisation of calcium sulphate was followed by that of the* $2CaSO_4 \cdot K_2SO_4$.

reveal anything identifiable against the background radiation, but further examination of fine fractions of ground clinker, separated in a Bahco air-separator, in which the sulphate content was considerably concentrated resulted in the appearance of a triple peak between 26.5 and 28° 2θ CuKα. This, see Fig. 1, was identified as being due to the double sulphate $2CaSO_4 \cdot K_2SO_4$, which was found to be produced by heating together any form of calcium sulphate with potassium sulphate. Subsequent work showed that this compound can form with an excess of either alkali sulphate or calcium sulphate indicating that it is a preferred mode of occurrence in this system. The presence of sodium sulphate can, however, modify this conclusion.

In some clinkers with high sulphate alkali ratios, β-calcium sulphate remained after water extraction and has been identified by its main diffraction peak at 25.4° 2θ CuKα. Clinkers containing a relatively large amount of soda were also found to contain β-calcium sulphate, and this will be referred to again. These forms have been observed microscopically, and Photo 2 and 3 illustrate their co-existence in clinker.

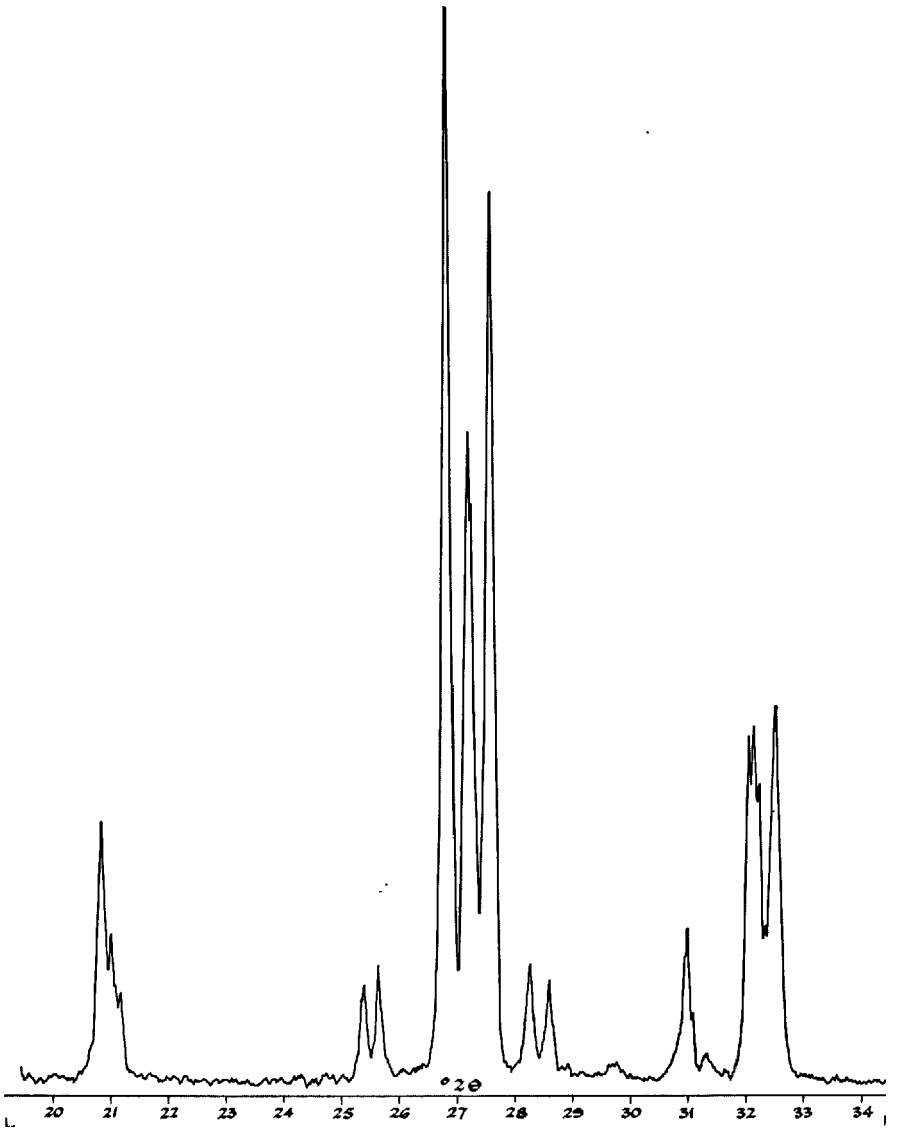

Fig. 1. *X-ray diffraction pattern for the double sulphate.* $2CaSO_4 \cdot K_2SO_4$

In order to examine whether any systematic relationship exists between the clinker sulphate and alkali content, and the proportion of the sulphate which is present as alkali sulphate, works clinkers were examined together with a series of laboratory-prepared clinkers for which the relative amounts of alkali and sulphate in the raw materials were varied over a wide range. On these clinkers the total alkalis and sulphates were determined together with the corresponding water-soluble alkalis and sulphates.

Table 1. *Total and soluble, alkali and sulphate contents of eleven laboratory prepared clinkers*

Sample	Total			Soluble			$\frac{\bar{S}_{Tot}}{\equiv K}$	$\frac{\bar{S}_{Alk}}{\bar{S}_{Tot}}$
	K_2O %	Na_2O %	SO_3 %	K_2O %	Na_2O %	SO_3 %		
A	1.05	0.20	0.71	0.74	0.06	0.71	0.52	1.00
B	1.64	0.22	1.41	1.36	0.09	1.28	0.71	0.91
C	1.06	0.17	0.99	0.95	0.07	0.90	0.75	0.91
D	2.16	0.26	2.36	1.93	0.11	2.05	0.92	0.76
E	1.30	0.22	1.73	1.25	0.11	1.77	1.05	0.70
F	1.92	0.21	2.57	1.78	0.10	1.85	1.14	0.64
G	0.72	0.18	1.28	0.68	0.09	0.80	1.28	0.55
H	2.04	0.20	3.07	1.90	0.11	2.32	1.31	0.57
J	2.12	0.24	3.56	2.00	0.12	2.86	1.43	0.52
K	1.50	0.23	3.82	1.34	0.10	2.78	2.07	0.34
L	1.01	0.23	3.67	0.80	0.11	2.03	2.70	0.23

Table 2. *Total and soluble, alkali and sulphate contents of 30 works clinkers from 20 different works*

Sample	Total			Soluble			$\frac{\bar{S}_{Tot}}{\equiv K}$	$\frac{\bar{S}_{Alk}}{\bar{S}_{Tot}}$
	K_2O %	Na_2O %	SO_3 %	K_2O %	Na_2O %	SO_3 %		
1	0.52	0.26	0.15	0.13	0.03	0.15	0.16	1.00
2	0.99	0.16	0.22	0.24	0.02	0.22	0.18	1.00
3	0.64	0.29	0.26	0.24	0.05	0.26	0.24	1.00
4	0.51	0.42	0.30	0.19	0.08	0.30	0.26	0.87
5	0.85	0.19	0.32	0.31	0.05	0.32	0.28	1.00
6	0.56	0.50	0.40	0.32	0.11	0.40	0.30	1.00
7	0.84	0.22	0.42	0.42	0.05	0.42	0.36	1.00
8	0.67	0.15	0.34	0.36	0.03	0.34	0.38	1.00
9	0.79	0.15	0.43	0.44	0.04	0.43	0.42	0.98
10	0.62	0.17	0.39	0.34	0.05	0.39	0.45	0.90
11	0.73	0.20	0.48	0.42	0.06	0.44	0.46	0.92
12	0.78	0.35	0.62	0.50	0.11	0.60	0.47	0.92
13	1.26	0.26	0.88	0.89	0.09	0.88	0.53	1.00
14	0.51	0.35	0.56	0.34	0.11	0.43	0.54	0.77
15	0.73	0.17	0.55	0.48	0.06	0.54	0.56	0.87
16	0.91	0.26	0.74	0.71	0.11	0.74	0.56	1.00
17	0.61	0.16	0.49	0.42	0.06	0.49	0.56	0.90
18	1.36	0.24	1.02	0.98	0.08	1.00	0.59	0.91
19	0.95	0.25	0.88	0.72	0.10	0.88	0.66	0.84
20	1.04	0.31	0.99	0.77	0.12	0.96	0.66	0.83
21	0.90	0.33	0.94	0.73	0.13	0.93	0.67	0.84
22	0.96	0.25	0.96	0.82	0.11	0.95	0.72	0.87
23	1.04	0.63	1.57	0.96	0.35	1.57	0.79	0.81
24	0.97	0.50	1.46	0.90	0.36	1.42	0.84	0.84
25	1.43	0.25	1.53	1.12	0.10	1.49	0.85	0.71
26	0.71	0.27	1.50	0.51	0.18	0.99	1.34	0.45
27	0.66	0.12	0.96	0.54	0.05	0.90	1.13	0.54
28	0.53	0.10	1.00	0.39	0.04	0.81	1.47	0.38
29	0.76	0.16	1.59	0.67	0.07	1.13	1.57	0.42
30	0.55	0.09	1.18	0.38	0.03	0.75	1.71	0.31

Table 1 shows the results for 11 laboratory prepared clinkers, and Table 2 the corresponding results for 30 works clinkers representing clinker produced in 20 different works by a variety of processes.

In these tables the relative quantities of sulphate and alkalis are expressed by the ratios $\bar{S}_{Tot}/\equiv K$, in which $\bar{S}_{Tot}$ is the total sulphate, and $\equiv K$ is the total alkali content expressed as equivalent potash. (Potash is the predominant alkali in most of the clinkers studies). The proportion of the total sulphate which is present as alkali sulphate is expressed by the ratio $\bar{S}_{Alk}/\bar{S}_{Tot}$, where $\bar{S}_{Alk}$ is the sulphate equivalent to the soluble alkalis. In Fig. 2 values of $\bar{S}_{Alk}/\bar{S}_{Tot}$ are plotted against the corresponding values of $\bar{S}_{Tot}/\equiv K$. The points for the laboratory-prepared clinkers show a good relationship. The works clinkers follow a similar trend but are in general below the drawn curve. This is considered to reflect the fact that as regards CaO, K_2O and SO_3, equilibrium conditions are not fully attained or uniformly approached in a kiln, so that works clinkers tend to contain more calcium sulphate than do laboratory clinkers.

Study of the relationship between total potash and soda and that present as sulphate indicates that there

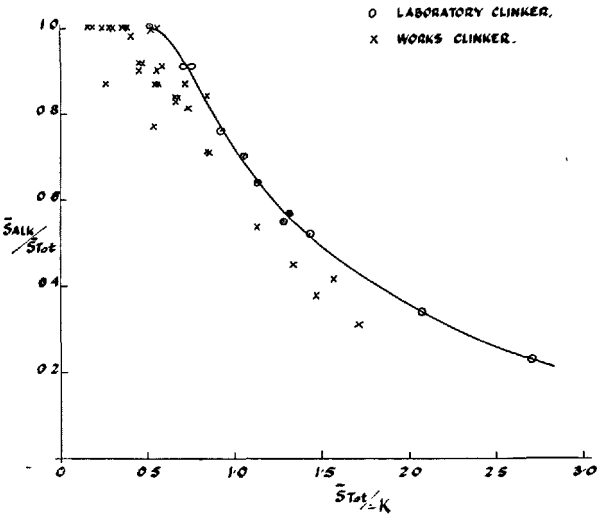

Fig. 2. *Proportion of total sulphate combined with alkalis* ($\bar{S}_{Alk}/\bar{S}_{Tot}$) *as a function of the ratio total sulphate to total alkali as equivalent potash* ($\bar{S}_{Tot}/\equiv K$)

is a marked preference for potash to form sulphate. Table 3 and Fig. 3 show the comparison of corresponding molar ratios for 43 works clinkers. In general the molar ratio of potash to soda as sulphate is about twice the molar ratio of potash to soda in the clinker as a whole.

X-ray diffraction studies of heated mixtures of potassium and sodium sulphates showed that they form a continuous series of double sulphates between molar ratios of 3:1 and 1:3 K_2SO_4/Na_2SO_4 giving characteristic diffraction patterns differing essentially only in changing peak positions with changing molar ratio. The X-ray diffraction patterns of the extremes and centre of this system are shown in Fig. 4. While at the level of occurrence this double sulphate has not yet been directly detected in cement clinkers, it has been found in flue dusts and kiln deposits with a sufficiently high alkali sulphate content. It, therefore, seems probable that within the above molar range any sodium sulphate present in clinker with potassium sulphate will be as a double alkali sulphate.

Where potash, soda and lime are all available it is possible, as has previously been remarked, that the double alkali sulphate may affect the production of $2CaSO_4 \cdot K_2SO_4$. In some clinkers, of which 15A in Table 4 is one, the considerable quantity of calcium sulphate present is in the β-form only. In these clinkers there is sufficient Na_2SO_4 to form the double alkali sulphate with the whole of the K_2SO_4 present, and it would appear likely that the stability or order of crystallisation of the double alkali sulphate is such as to preclude the formation of $2CaSO_4 \cdot K_2SO_4$. This suggestion remains to be confirmed by further study.

Summing up, it appears that K_2SO_4 is likely to occur either alone or in one of two double sulphate forms according to the available quantities of Na_2SO_4 and $CaSO_4$, the preference probably being for the double alkali sulphate. Na_2SO_4 may occur alone but in the clinkers examined is more probably as the double alkali sulphate. It does not form a double sulphate with calcium sulphate. Calcium sulphate occurs alone or as $2CaSO_4 \cdot K_2SO_4$ subject to the prior formation of double alkali sulphate. Overall, potash is twice as likely to produce soluble sulphate as soda.

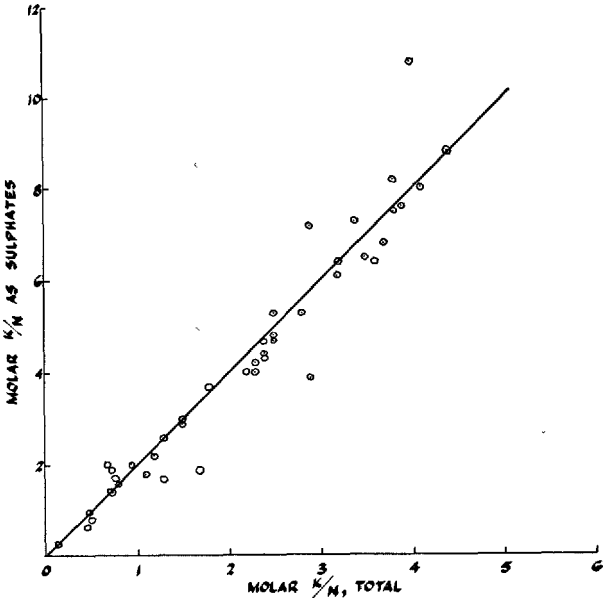

Fig. 3. *Molar ratio of potash and soda, total and as sulphates, in works clinkers*

Table 3. *Comparison of the molecular ratios of potash and soda in clinker, as a whole and as sulphates*

Total alkalis molar ratio $\frac{K_2O}{Na_2O}$	Soluble alkalis molar ratio $\frac{K_2O}{Na_2O}$	Total alkalis molar ratio $\frac{K_2O}{Na_2O}$	Soluble alkalis molar ratio $\frac{K_2O}{Na_2O}$
1.3	2.6	1.1	1.8
4.1	8.0	1.3	1.7
1.5	3.0	3.8	7.5
0.80	1.6	1.7	1.9
2.9	3.9	3.7	6.8
0.74	1.9	3.5	6.5
2.5	5.3	3.2	6.1
2.9	7.2	3.9	7.6
3.4	7.3	0.47	0.67
2.4	4.3	2.3	4.0
2.4	4.7	0.13	0.29
1.5	2.9	3.6	6.4
3.2	6.4	0.77	1.7
0.96	2.0	2.4	4.4
2.8	5.3	1.2	2.2
2.3	4.2	0.50	1.0
2.5	4.7	4.4	8.8
3.8	8.2	0.70	2.0
2.5	4.8	0.73	1.4
2.2	4.0	0.52	0.80
1.8	3.7	4.0	10.8
2.5	4.8		

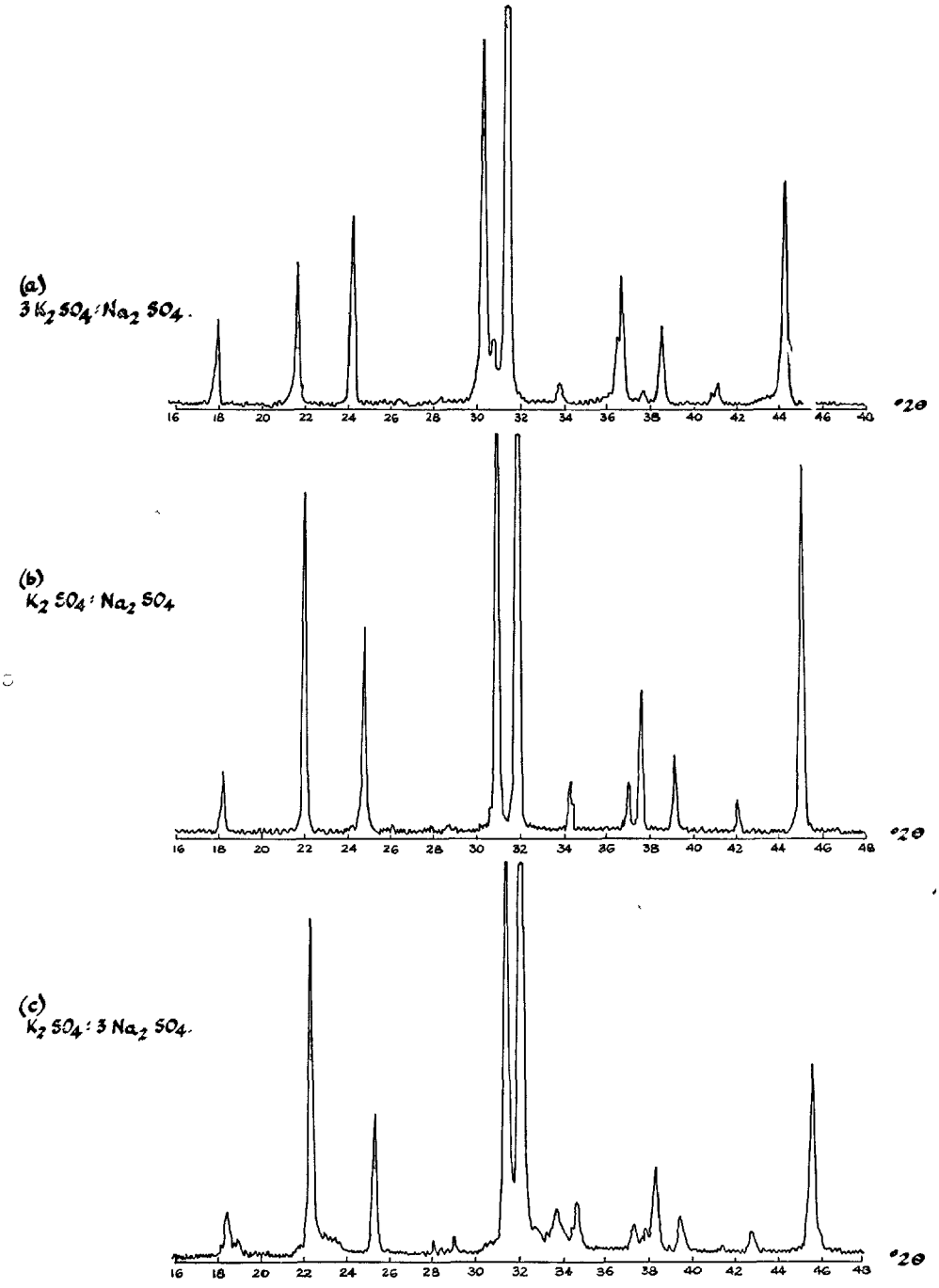

Fig. 4. *X-ray diffraction patterns for the sodium/potassium double sulphate system.*

Determination of Alkali in the Main Phases

The distribution of the alkalis within the four crystalline phases; tricalcium aluminate, calcium aluminoferrite and the two calcium silicates has been studied by a process of progressive solution to remove the phases stepwise and determine the alkalis in the undissolved residues. Following the removal of the

Table 4. *Chemical analysis, compound composition and alkali distribution for 16 works clinkers*

	1A %	2A %	3A %	4A %
SiO_2	22.49	22.46	22.06	20.69
I.R.	0.22	0.08	0.04	0.09
Al_2O_3	4.82	5.28	4.66	6.14
Fe_2O_3	1.95	2.65	3.54	3.30
Mn_2O_3	0.14	0.03	0.04	0.08
TiO_2	0.35	0.32	0.26	0.23
P_2O_5	0.23	0.16	0.05	0.07
CaO	67.69	66.32	65.35	66.14
MgO	0.89	1.56	1.17	1.81
SO_3	0.09	0.10	0.11	0.12
L.O.I.	0.50	0.30	0.44	0.41
K_2O	0.49	0.37	0.72	0.85
Na_2O	0.17	0.52	0.63	0.08
	100.03	100.15	100.07	100.01
Free CaO	2.1%	2.6%	2.6%	2.0%
Ferrite Comp.				
Mol % C_2F	55	56	59	54
Alite	65.3	58.8	63.0	69.7
Belite	17.3	19.8	15.0	6.0
C_3A	8.7	10.5	9.3	11.4
Ferrite	5.7	7.4	9.4	9.6
	97.0	96.5	96.7	96.7

Alkalis	K_2O	Na_2O	K_2O	Na_2O	K_2O	Na_2O	K_2O	Na_2O
As sulphates	0.09	0.01	0.05	0.05	0.09	0.02	0.13	0.01
Free alkali	—	—	—	—	0.11	0.06	0.10	0.02
In aluminate	0.14	0.05	0.13	0.19	0.22	0.25	0.30	0.02
In ferrite	0.05	0.03	0.04	0.06	0.10	0.10	0.13	0.01
In silicates	0.21	0.08	0.15	0.22	0.21	0.20	0.19	0.02
	0.49	0.17	0.37	0.52	0.72	0.63	0.85	0.08

	5A %	6A %	7A %	8A %
SiO_2	23.14	21.64	19.87	21.99
I.R.	0.11	0.20	0.08	0.06
Al_2O_3	5.56	5.54	7.88	5.08
Fe_2O_3	2.25	4.20	2.41	3.50
Mn_2O_3	0.06	0.05	0.09	0.06
TiO_2	0.34	0.72	0.33	0.19
P_2O_5	0.15	0.17	0.19	0.07
CaO	66.27	63.60	65.95	65.74
MgO	0.79	2.35	1.07	1.42
SO_3	0.19	0.29	0.32	0.38
L.O.I.	0.33	0.34	0.53	0.28
K_2O	0.67	0.16	0.98	0.61
Na_2O	0.19	0.79	0.18	0.52
	100.05	100.05	99.88	99.90
Free CaO	1.7%	0.5%	3.2%	1.5%
Ferrite Comp.				
Mol % C_2F	54	61	54	58
Alite	50.9	59.3	55.3	62.3
Belite	30.5	19.6	17.9	16.8
C_3A	9.3	8.3	15.8	8.5
Ferrite	6.8	10.4	6.6	9.8
	97.5	97.6	95.6	97.4

Alkalis	K_2O	Na_2O	K_2O	Na_2O	K_2O	Na_2O	K_2O	Na_2O
As sulphates	0.18	0.03	0.06	0.14	0.32	0.03	0.29	0.11
In aluminate	0.19	0.07	0.04	0.24	0.36	0.08	0.16	0.20
In ferrite	0.04	0.03	0.01	0.12	0.07	0.02	0.07	0.09
In silicates	0.23	0.06	0.05	0.29	0.23	0.05	0.09	0.12
	0.67	0.19	0.16	0.79	0.98	0.18	0.61	0.52

Table 4 (*Continued*)

	9A %	10A %	11A %	12A %
SiO_2	21.67	21.58	21.39	22.30
I.R.	0.26	0.07	0.05	0.40
Al_2O_3	5.77	5.68	4.99	6.16
Fe_2O_3	1.70	2.49	2.80	2.03
Mn_2O_3	0.07	0.06	0.05	0.08
TiO_2	0.27	0.33	0.35	0.35
P_2O_5	0.17	0.19	0.11	0.17
CaO	67.44	66.67	68.00	64.97
MgO	0.91	1.29	1.40	1.09
SO_3	0.34	0.38	0.39	0.42
L.O.I.	0.60	0.46	0.08	0.92
K_2O	0.78	0.55	0.22	0.88
Na_2O	0.21	0.31	0.29	0.13
	100.19	100.06	100.12	99.90
Free CaO	2.6%	2.1%	0.9%	2.0%
Ferrite comp.				
Mol % C_2F	56	57	55	53
Alite	65.2	64.5	81.0	49.8
Belite	16.2	15.1	3.3	29.7
C_3A	9.7	10.0	6.0	9.9
Ferrite	5.1	7.1	8.0	6.1
	96.2	96.7	98.3	95.5

Alkalis	K_2O	Na_2O	K_2O	Na_2O	K_2O	Na_2O	K_2O	Na_2O
As sulphate	0.35	0.05	0.31	0.09	0.12	0.08	0.44	0.03
In aluminate	0.22	0.08	0.10	0.08	0.04	0.08	0.13	0.03
In ferrite	0.04	0.02	0.03	0.02	0.02	0.05	0.03	0.01
In silicates	0.17	0.06	0.11	0.10	0.04	0.08	0.28	0.06
	0.78	0.21	0.55	0.31	0.22	0.29	0.88	0.13

	13A %	14A %	15A %	16A %
SiO_2	22.71	23.07	20.80	20.30
I.R.	0.03	0.06	0.08	0.12
Al_2O_3	5.38	4.69	4.48	6.67
Fe_2O_3	3.32	2.56	5.62	2.72
Mn_2O_3	0.04	0.05	0.31	0.13
TiO_2	0.27	0.31	0.31	0.30
P_2O_5	0.12	0.12	0.16	0.10
CaO	64.91	66.02	65.41	65.11
MgO	1.15	1.33	1.32	1.54
SO_3	0.50	0.84	0.87	0.89
L.O.I.	0.25	0.19	0.08	0.34
K_2O	0.72	0.52	0.29	1.56
Na_2O	0.68	0.47	0.37	0.26
	100.08	100.23	100.10	100.04
Free CaO	0.5%	1.9%	0.8%	1.2%
Ferrite comp.				
Mol % C_2F	58	57	60	53
Alite	58.3	58.3	71.7	68.6
Belite	18.8	25.2	9.0	10.2
C_3A	13.0	5.8	1.0	10.7
Ferrite	8.3	7.1	15.4	8.5
	98.4	96.4	97.1	98.0

Alkalis	K_2O	Na_2O	K_2O	Na_2O	K_2O	Na_2O	K_2O	Na_2O
As sulphate	0.40	0.13	0.42	0.19	0.24	0.20	0.97	0.06
In aluminate	0.15	0.28	0.03	0.08	0.01	0.01	0.22	0.09
In ferrite	0.05	0.09	0.02	0.05	0.02	0.06	0.09	0.04
In silicates	0.12	0.18	0.05	0.15	0.02	0.10	0.28	0.07
	0.72	0.68	0.52	0.47	0.29	0.37	1.56	0.26

alkali sulphates and double sulphates by aqueous extraction as described above, the remaining alkalis were determined. The silicates were next removed by selective hydrolysis using a solution of salicylic acid in methanol and the residual alkalis in the celite were determined. Finally, the ferrite was isolated using

aqueous acetic acid as the solvent for the other phases with a final pH of 3.5–3.8, and the alkali content of the ferrite residue was determined.

At each stage it was confirmed by chemical analysis and X-ray diffraction examination that the residues used for alkali determinations were in the one case a mixture of C_3A and ferrite uncontaminated with alite or belite and in the second case ferrite containing neither silicates nor C_3A.

From these results the alkali content of the combined silicates, of the C_3A and of the ferrite were obtained and in Table 4 these results are shown for 16 clinkers together with their chemical analyses and compound compositions as determined by X-ray diffraction.

Alkali in Tricalcium Aluminate and Ferrite

Examination of the results shown in Table 4 for the alkali content of the C_3A and ferrite, related to the quantity of each of these phases in the clinkers suggests that the distribution of alkalis between C_3A and ferrite is dependent on the quantities of alumina in these compounds. In Table 5 the alkali content of both C_3A and ferrite is shown expressed as a percentage of the alumina present in those phases. The same results are plotted in Fig. 5. The fit of the points to the line is considered good in relation to possible experimental error and provides evidence that the alkalis are associated with alumina equally in the two phases.

Also in Table 5 the alkali content of the C_3A expressed as a percentage of the C_3A present is shown relative to the crystal form of the C_3A, whether as the normal cubic form or as the alkali-modified orthorhombic form (Photo 4) showing the peak splitting at about 33° 2θCuKα and in the regions 46.5 to 48.5° 2θ and 59.5 to 60° 2θCuKα. The highest level of alkali consistent with the cubic form is just below 2.7% equivalent potash, whereas the lowest level of alkali consistent with the orthorhombic form is at 2.9% equivalent potash, suggesting a critical level at about 2.8% equivalent potash or 1.8% of soda. This is lower than the level (2.25% soda) reported by Conwicke and Day (3) in their investigation of the system C_3A–NC_8A_3, or indeed that (2.1% soda) suggested by Fletcher, Midgley and Moore (4), which strengthens their suggestion that the production of orthorhombic C_3A in clinker need not be due solely to soda.

That this modification can be caused by potash as well as by soda is also indicated by these results, and is particularly well illustrated by clinker 4A in which the total soda content of the clinker only represents

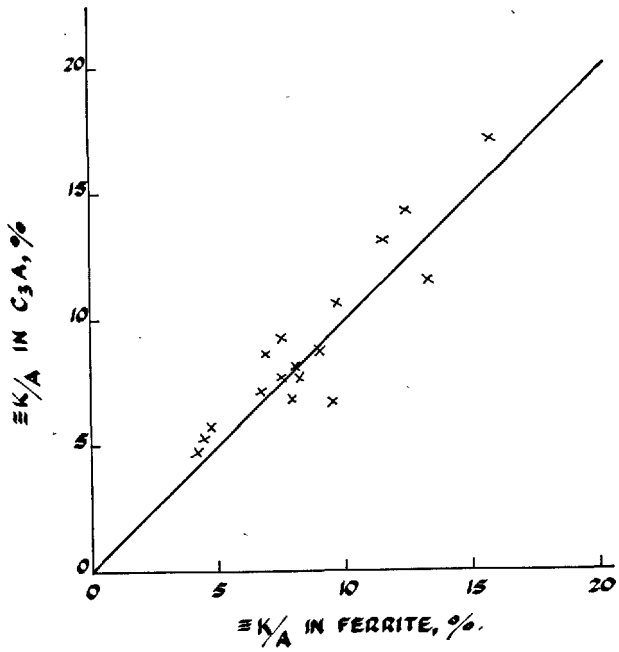

Fig. 5. *Relationship of the alkali/alumina ratios (≡K/A) in C_3A and ferrite respectively.*

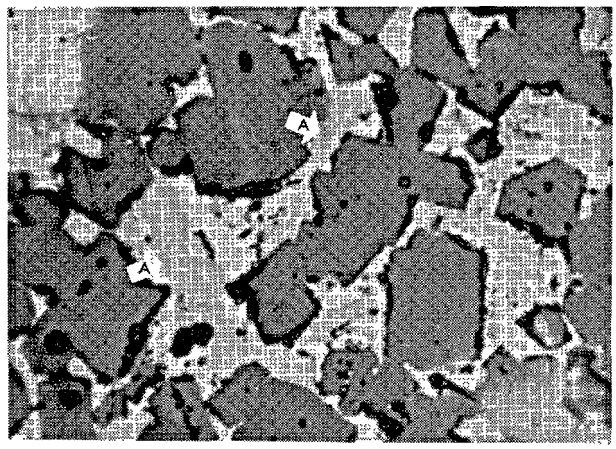

10 μ ×800

Photo 4. *Alkalis in excess of that required to form alkali sulphates are available for incorporation in other crystal phases. In the clinker shown here excess K_2O has been taken up by the C_3A resulting in the formation of the typical lath shaped alkali modified C_3A, arrowed A, which crystallises in the orthorhombic system.*

Table 5. *Alkali contents of tricalcium aluminate and ferrite phases for 16 clinkers*

Sample	Alkali in C_3A		Form of C_3A	As % of Al_2O_3 in C_3A	Alkali in ferrite	
	% $\equiv K_2O$	As % of C_3A			% $\equiv K_2O$	As % of Al_2O_3 in ferrite
1A	0.22	2.53	cubic	6.7	0.10	9.5
2A	0.42	4.00	orthorhombic	10.6	0.13	9.7
3A	0.60	6.45	orthorhombic	17.1	0.25	15.7
4A	0.33	2.89	orthorhombic	7.7	0.15	8.2
5A	0.30	3.23	orthorhombic	8.6	0.09	6.9
6A	0.41	4.94	orthorhombic	13.1	0.19	11.5
7A	0.48	3.04	orthorhombic	8.1	0.10	8.0
8A	0.46	5.41	orthorhombic	14.3	0.21	12.4
9A	0.34	3.50	orthorhombic	9.3	0.07	7.5
10A	0.22	2.20	cubic	5.8	0.06	4.7
11A	0.16	2.67	cubic	7.1	0.10	6.7
12A	0.18	1.82	cubic	4.8	0.05	4.2
13A	0.57	4.38	orthorhombic	11.6	0.19	13.3
14A	0.15	2.59	cubic	6.9	0.10	7.9
15A	0.02	2.00	cubic	5.3	0.11	4.4
16A	0.36	3.36	orthorhombic	8.9	0.15	9.0

0.7% of the C_3A present and where less than 10% of the alkali determined in the C_3A is soda, but which nevertheless shows the characteristic change in X-ray pattern and characteristic appearance under microscopic examination as illustrated by the photomicrograph of this clinker (Photo 4).

Clinkers 7A and 9A also show these same features, the soda in the C_3A being 0.5% and 0.4% respectively. In these cases the potash is mainly responsible for the orthorhombic C_3A.

We have been unable so far to synthesise C_3A in the orthorhombic form using potash as the sole alkali present. It is believed that when potash is the sole or predominant alkali involved, the inclusion of silica and additional lime in the structure may be necessary to produce the orthorhombic crystal form of C_3A. In this connection lime and silica are known to occur in C_3A in works clinkers.

Alkalis in the Silicates

The distribution of alkalis in the silicates is still being studied. We have not yet succeeded in isolating the two silicates separately to permit direct analysis, nor have we obtained firm evidence using the micro-electron probe technique.

Nevertheless, Table 4 shows the potash and soda contained in the silicates in the 16 clinkers on which Table 5 was based. Newkirk (5) suggested that potash, other than as sulphate, appeared in belite as $KC_{23}S_{12}$. In Fig. 6 the equivalent potash in the silicates is plotted against belite content for the 16 clinkers. Also plotted is a line indicating Newkirk's alkaline belite composition.

It will be seen that four points lie reasonably close to the Newkirk line, but that the remainder lie well below that line. An immediate interpretation is that in only 4 cases are the quantities of alkali and belite both consistent with Newkirk's composition, whereas in the other 12 cases there is insufficient alkali to convert more than a part of the available belite.

Photo 5 illustrates the coexistence of normal belite and alkali stabilised belite, while Photo 6 shows unstable belite inverting to the γ-form in a clinker in which the alkali content of the silicates was known to be extremely low.

The above interpretation may well be the only one necessary in many cases, but it has occurred to us that some of the alkali may also be found in the alite. Alite is known to contain alumina in solid solution to an extent influenced by the magnesia present. Furthermore, it was shown earlier that the distribution of alkali between C_3A and ferrite is well related to their alumina contents.

Following this line of thought the clinker (11A) closest to the Newkirk composition in Fig. 6 was

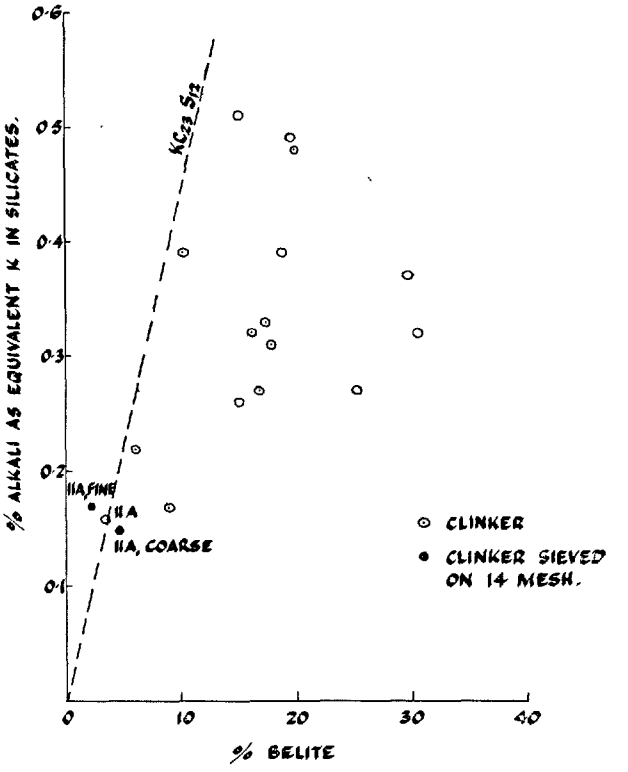

Fig. 6. *Alkali (equivalent potash) in silicates as function of belite quantity in works clinkers*

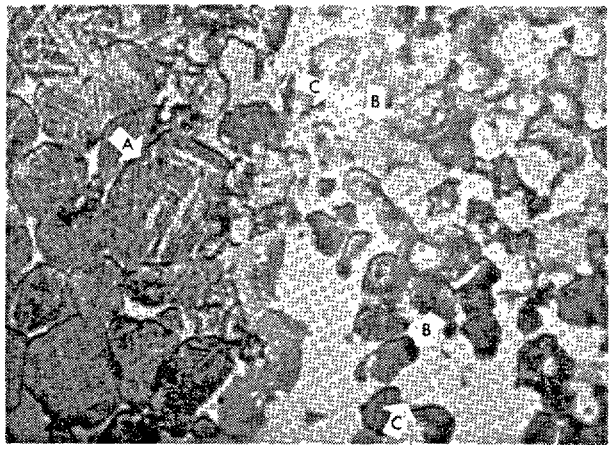

⊢⊣ 10 μ ×800

Photo 5. *Both the normal belite, arrowed A, and the alkali stabilised belite, arrowed B, are illustrated here. The coexistence of alkali modified belite in contact with free lime crystals, arrowed C, indicates the considerable stability of the alkaline belite inhibiting its assimilation of further lime to form alite.*

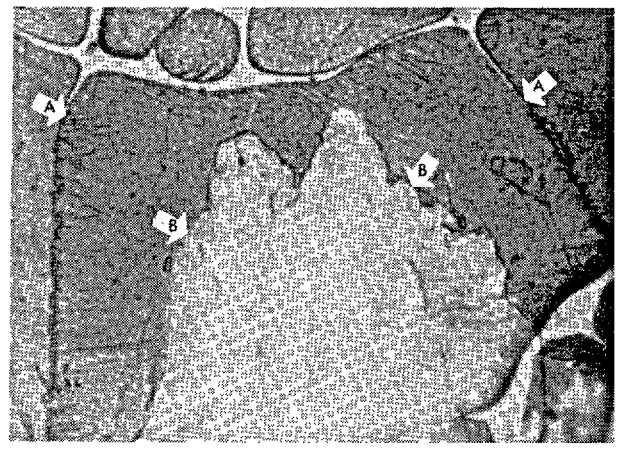

⊢⊣ 10 μ ×800

Photo 6. *In clinker of very low alkali content the β-C_2S may exhibit considerable instability and tend to invert to its more stable γ-phase. This is illustrated here where a single crystal of β-C_2S, arrowed A, is undergoing inversion to the γ form, arrowed B. This inversion is accompanied by a 10% volume increase and the resulting microcracking can be seen radiating away from the inverted area.*

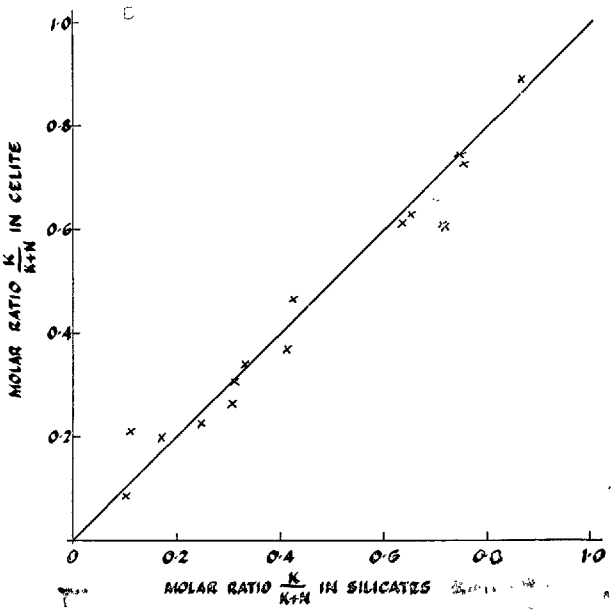

Fig. 7. *Proportion of potash in alkalis in celite as a function of that in silicates.*

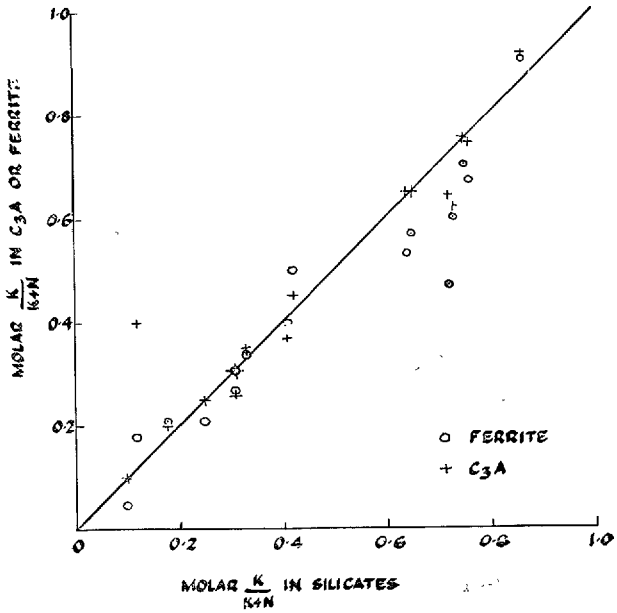

Fig. 8. *Proportion of potash in alkalis in* C_3A *or ferrite as a function of that in silicates.*

fractionated by sieving on a 14 mesh sieve, in order to vary the alite/belite proportions, and the coarse and fine components analysed. The resulting data are plotted adjacent to the point for the clinker as a whole. Clearly the fine fraction contains more alkali in the silicates than can be explained by Newkirk's alkaline belite. This, in itself, does not prove that the alkali is not in the belite, but since between the three relevant points an increase in belite appears to be associated with, if anything, a decrease in alkali, there is a good case for suggesting that there is alkali in the alite. The estimated alkali/alumina ratio in the silicates in clin-

ker 11A is 11%. This figure compares with approximately 7% for the C_3A and ferrite in that clinker. This could suggest that part of the alkali is in the alite, associated with alumina, the remainder being in the belite and not associated with alumina.

It is worth adding that, while the remaining points in Fig. 5 are consistent with partial conversion of the belite to Newkirk's form, this does not mean that all the alkali available to the silicates is in fact in the belite.

It was shown above that the molar ratio of potash to soda as sulphate was about twice that for total potash and soda. Fig. 7 shows the molar proportion of potash in the alkalis in the celite plotted against that in the silicates. Fig. 8 is a similar graph for the C_3A and ferrite separately. These Figs. indicate no tendency for potash to prefer the silicates and soda the aluminates, but rather that in works clinkers potash and soda are equally likely to be found in the phases in proportion to their residual concentrations in the clinker after sulphate formation.

Free Alkali

In two clinkers out of 43 the water-soluble alkalis exceeded the water soluble sulphates equivalent to alkali. The excess of alkali represents so-called free alkali, probably in the form of carbonate. The presence of free alkali is associated with low $\bar{S}_{Tot}/\equiv K$ ratios and high alkali content, but in the two clinkers concerned the crystal phases contain less alkali than is possible. It is considered that the explanation must lie in the mechanisms of dissociation and formation of alkali compounds in the clinkering process.

Conclusions and Discussion

The main points which emerge from the work are:

1. Alkalis occur in clinker as sulphates and double sulphates and as substitution components of the crystal phases. In a few cases free alkali may also be found.
2. The evidence suggests that the sulphate content of the clinker makes the prior demand on the alkalis. The resulting quantity of alkali sulphate is determined by the ratio of total clinker sulphate to total alkali. The remaining sulphate is calcium sulphate either as a soluble double sulphate or as β-calcium sulphate. At this stage potash has twice the affinity of soda for sulphate.
3. After allocating alkali to sulphate as in 2, the remainder appears to be distributed between the silicates, the C_3A and the ferrite, with no evidence of a preference of the silicates for potash or of the aluminates for soda.
4. The quantity of alkalis in the C_3A and ferrite respectively is well related to the alumina contents of those phases.
5. The orthorhombic form of C_3A is formed with a minimum alkali content of 2.8% equivalent potash or 1.8% equivalent soda.
6. The proportion of potash in the alkali is broadly the same in the silicates, C_3A and ferrite respectively.
7. The basis for the quantitative division of alkalis between silicates on the one hand and C_3A and ferrite on the other is not yet clear, although the latter generally take about half or more of the available alkali. There is evidence that alite may contain alkali.
8. Overall, potash and soda appear to be interchangeable in the crystal phases, but potash is distinguished in that it has a much greater affinity than soda for sulphate and a capacity, which soda has not, to form two double sulphates with lime: $2CaSO_4 \cdot K_2SO_4$ in clinker and $K_2SO_4 \cdot CaSO_4 \cdot H_2O$ in cement.

Further work will be done to elucidate the distribution of alkali in silicates. In the meantime the vairous forms of alkali shown to occur in clinker may well behave differently during hydration. In practice, therefore, it may be important to distinguish the alkalis more precisely. The specific influence of potassium sulphate on cement storage properties has been referred to.

Perhaps the most important practical interest in alkalis arises from the limitation imposed by certain standards on total alkali as equivalent dosa where alkali-aggregate reaction is feared. The literature in this field contains enough anomalous or controversial information to suggest that a closer definition of the forms in which the alkalis occur in a clinker may lead to a more precise understanding of its capacity to promote alkali-aggregate reaction.

The same closer definition may also be important

in the wider field of the setting, workability and strength characteristics of cements.

References

1. J. Forest, "Research on the air-setting of certain cements" (In French). Revue des Materiaux **557**, 35–41 (1962).
2. A. E. Moore, "Evidence for new phase occurring in portland cements", Nature, Vol 199, No. 4892, 480–481 (1963).
3. J. A. Conwicke and D. E. Day, "Crystalline solubility of soda in tricalcium aluminate", Journ. Amer. Ceram. Soc. **47**, 654–655, (1964).
4. K. E. Fletcher, H. G. Midgley and A. E. Moore, "Data on the binary system $3CaO \cdot Al_2O_3$–$Na_2O \cdot 8CaO \cdot 3Al_2O_3$ within the system CaO–Al_2O_3–Na_2O". Magazine of Concrete Research **17**, 171–176, (1965).
5. T. F. Newkirk, "The alkali phases in portland cement clinker", Proceedings of the 3rd International Symposium on the Chemistry of Cement 1952. 151–167.

Supplementary Paper I-131 Cement Surface Area Determination by Gas Adsorption near Room Temperature

Ali A. Tabikh*

Synopsis

An apparatus to determine the specific surface areas of hydrated and unhydrous cements has been developed employing gas flow techniques and thermistor detectors. The specific surface area of a sample is determined by measuring the desorbed organic molecules. The adsorption equilibrium is maintained at 30°C. and the desorption temperature used is 200°C. The adsorbate used is either benzene, acetone, or methyl alchohol. Helium is used as a carrier, but also serves as a diluent to obtain the desired relative pressure (P/P_0).

The determination is rapid since a single point measurement, at a given P/P_0, is required. However, if one wishes to make measurements at several P/P_0 points, the BET equation may be applied to calculate the surface area.

The results of adsorption studies using this method on two hydrated and several unhydrated cements are discussed.

Introduction

The measurements of surface area of cement are usually made by air permeability methods or calculated from turbidimeter data. Both procedures are inadequate for providing detailed information about surface properties, particularly with regard to internal surfaces and porosity.

Continuous flow methods have been developed which greatly simplify nitrogen adsorption measurements (1, 2). Other more recent papers have been published which describe flow methods using various organic vapors as adsorbates (3, 4).

The present study was undertaken to develop the equipment and methods for a simple and rapid procedure of surface area measurement. Therefore, emphasis was placed on adsorption near ambient temperature, minimum handling of the sample, and the ability to measure a wide range of surface areas (.01 m^2 and up) accurately. The instrument which has been developed appears to fulfill the objectives of the project.

The data presented here have been derived from a current investigation being conducted on hydrated as well as unhydrated cements using various vapor pressures in order to evaluate the surface properties. These data are intended to illustrate the capabilities of the apparatus and the methods of studying these surface properties. In addition, some of the properties related to the specific surface of a cement particle are pointed out.

Apparatus

The schematic diagram of Fig. 1 illustrates the apparatus which has been developed. The carrier gas used is helium. A sensitive pressure regulating system is necessary to obtain uniform and accurate flow rates. All tubing in the flow system is one-eighth inch diameter nylon or copper tubing.

The carrier gas flows through two calibrated flowmeters H and V, where the portion going through H supplies the diluent, and that going through V becomes the vapor-saturated gas. The two streams are mixed in a mixing tube M where the desired partial vapor pressure P/P_0 of the adsorbate is obtained. The tube M feeds the two identical flow channels from this point on to the vent. In regard to the forward flow, tube M acts as a back-pressure damper, thus there is no cross channel interference during the sudden heating of desorption. The vapor saturating arrangement, in-

*Marquette Cement Mfg., Co., Illinois, U.S.A.
Formerly California Portland Cement Co., California, U.S.A.

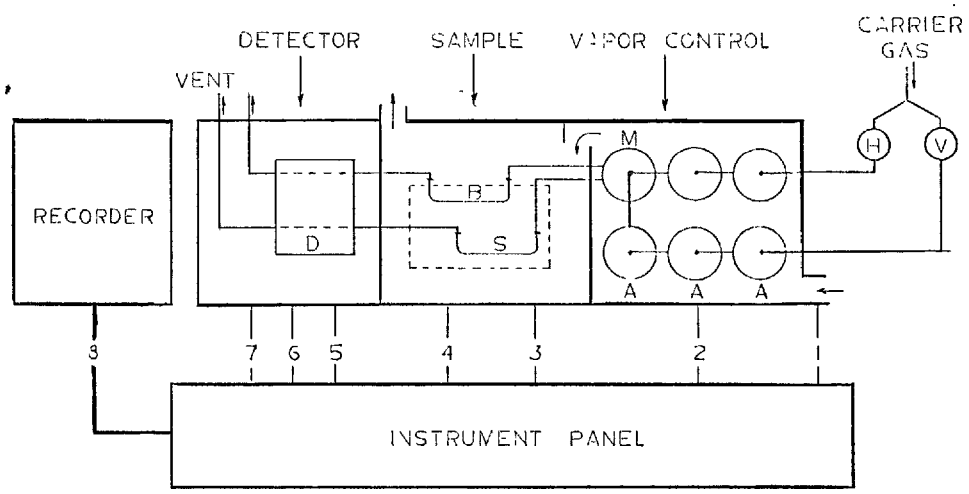

Fig. 1. *Diagram illustrating the surface area apparatus. H and V are flowmeters. The cells A contain the liquid adsorbate. M is the mixing tube and back pressure damper. S and B are the sample tubes; B is the blank in the reference channel. The dotted area is the high temperature enclosure. D is the thermal conductivity cell. The instrument panel provides the following controls: (1) air heater, (2) temperature sensing and control, (3) high temperature power supply, (4) high temperature regulator, (5) constant temperature source, (6) power supply to detector, (7) signal output balance, and (8) signal output to recorder.*

cluding tube *M*, is made up of a series of vacuum trap-type tubes. The tubes A containing liquid adsorbate are connected in series and are lined inside with filter paper to assure a vapor saturated atmosphere. The vapor control chamber is held at 30°C ± .01 using a thermister controlled circuit. The temperature setting, however, is variable from a potentiometer.

In the test chamber one of the gas streams flows through a blank sample tube *B*. The other stream flows through the sample tube *S* which contains the specimen. These sample tubes are constructed from glass tubing 0.6 cm I.D. They form a broad U, 10 cm long, and are equipped with tapered glass joints for quick connecting.

The sample tubes are mounted into an aluminum rack which is equipped with a heating unit capable of bringing the temperature of the sample up to 200°C in 2 minutes. With this arrangement it is possible to degas the sample prior to making the adsorption measurements in the apparatus itself. This rapid, controlled heating also provides the means to measure the desorption peaks for determinations of the surface area.

The adsorption temperature is nomrally the same as the temperature in the vapor control chamber (30°C ± .01).

The thermal conductivity cell *D* was developed in this research laboratory. It employs two matched thermisters which are mounted in the paths of the two gas streams. They are powered by a well regulated D.C. voltage source (normal operating voltage is about 17 volts). The output signals, 0–125 millivolts, from the two thermistors are balanced by a bridge circuit and sent to a recorder.

In addition to operating the apparatus near room temperature, its design allows studies to be made at either extremely low or higher than ambient temperatures. Both are achieved with minor modifications and/or auxiliary equipment.

Procedure

All samples are oven-dried at 105°C before weighing. The required sample weight varies from .01 to .5 g depending on the surface area of the sample. In the case of unhydrated cement, 0.0500 g is used.

The *U*-tube containing the sample is connected to the apparatus, and the flowmeter *H* is adjusted to deliver 30 cc per minute. Then, the high heat is turned on and the sample is purged at the preset temperature

(200°C is used in this study) until a steady output signal is received. The high heat is turned off at this time and the sample is allowed to cool down to the adsorption temperature, usually 30°C. At the same time the flowmeters are adjusted to give the desired vapor pressure.

The partial vapor pressure calculations are made in normal manner with corrections for slight volume changes when the carrier gas is saturated with the organic vapor. The necessary saturation vapor pressure data are taken from Jordan (5).

The total flow rates are kept constant for all the points of the very isotherm. These are, in cc per minute, 32 for benzene, 70 for acetone, 37.5 for alcohol, and 30 cc for nitrogen. Half of each quantity flows through the sample, the other half through the blank channel. When a steady signal is received from the detector, indicating a steady state between the sample surface and the vapor phase of the gas stream, it is time to desorb and mesure the desorption peak. This is accomplished by turning the high heat on. The time required to degas a cement sample is 15 to 20 minutes, and an adsorption-desorption cycle takes about 15 minutes.

The organic liquids used are all Mallinkrodt spectrophotometric grade reagents. The carrier gas is atomic grade helium. The nitrogen is a Matheson prepurified grade.

The recorder used in this study is a Sargent model SR equipped with a Disc integrator and an output range of 0–125 millivolts. The desorption peaks are usually sharply defined and are sometimes over 100 millivolts high with tails of 1 to 4 minutes duration depending on the nature of the sample being tested.

The detector response is linear within the normal surface area range of cements, when the single point method of determination is used, i.e., at any single vapor pressure setting. However, its sensitivity decreases as the vapor pressure of the adsorbate is raised. So, it becomes necessary to establish a correction curve in order to convert all peak areas to a common reference point, as illustrated in Fig. 2. The descending curve in this figure shows the decrease in sensitivity when 0.2 ul increments of benzene are injected into the sample gas stream at increasing partial vapor pressures. The ascending curve gives the correction factors at similar vapor pressure levels which would convert the counts to values comparable to those taken at $P' = 0.1$. For example, at $P' = 0.6$ (point A in Fig. 2) the peak counts are 492 and the correction factor is 1.768 (point B), and their product is 870 which is what the counts would be if no decrease in sensitivity would take place.

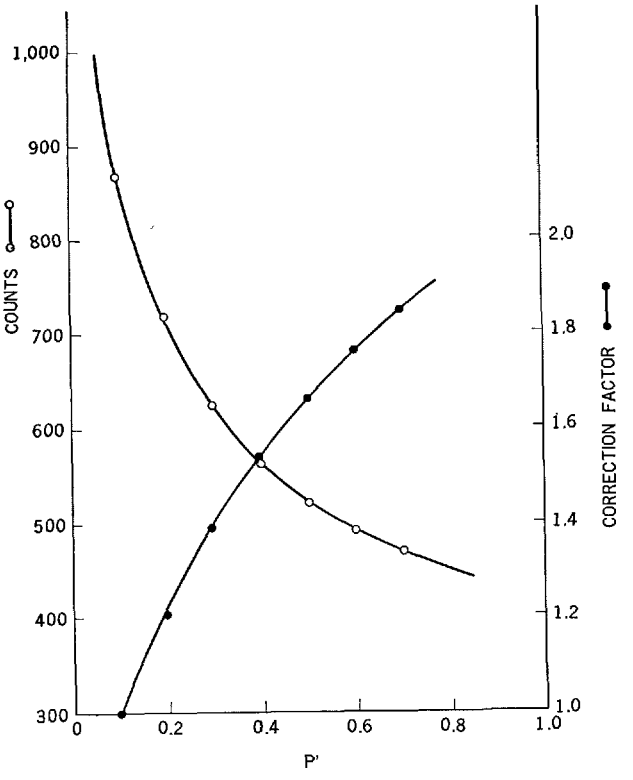

Fig. 2. *Change of detector response to benzene increments as the vapor pressure of benzene in the gas stream approached saturation, and the correction curve to change the output counts to $P = 0.10$ basis.*

The desorption peak areas are expressed in integrator counts at one millivolt in all calculations and plotting. The final values which represent the monolayer are converted to Cm^2 or m^2 by using the equation $A = fc$ where f is a calibration factor and c is counts at one millivolt per gram. The factor f is obtained by comparing the peaks from nitrogen adsorption versus, say, benzene for a given cement sample.

In the case of nitrogen adsorption, 0.5 cc increments of the gas are injected into the sample stream and the resulting counts are taken. From the known weight of nitrogen injected these are expressed as counts per unit area by use of the equation:

$$S = \frac{G}{M} N \cdot A_{mx}\, 10^{-20}$$

where S is the specific surface in $m^2/g.$, G is the nitrogen used in grams, M is the molecular weight of nitrogen, N is Avogadro's number, and A_m is the molecular cross-sectional area of nitrogen. The value 16.2 Å^2 is used for A_m in the calculations. Since the desorption peaks of organic vapors have been calibrated with samples whose nitrogen adsorption values are known, there is no need to know the mole-

cular cross-sectional surface areas of the organic adsorbate. This is a safe approach since these areas vary widely (7) because the packing arrangement of the adsorbed molecules is influenced by the energetic properties of the solid surface.

When a complete adsorption isotherm is made the calculations are based on the BET equation (6), written in the following form:

$$\frac{P''}{X} = \frac{1}{X_m C} + \frac{C-1}{X_m C} P'$$

where P' is the partial pressure P/P_0, P'' is the term $\frac{P}{P_0 - P}$, X is the quantity of vapor adsorbed, X_m the portion of vapor equivalent to the monolayer coverage, and C is a constant related to the net heat of adsorption. From the slope and intercept of the BET curve X_m can be expressed as follows:

$$X_m = \frac{1}{s+i}$$

where s = the slope, and i = the intercept.

The hydrated cements tested have been treated in the following manner: Oven dried samples weighing 0.25 g are placed in 3 cc size polyethylene tubes. The tubes are stoppered after adding 2 cc of CO_2 free distilled water and shaken in a rotary mixer for the desired interval of time. The slurry is centrifuged and the supernatant liquid is replaced by methyl alchohol. The solids are dispersed and shaken in the alcohol for one minute. Following centrifugation the alcohol wash is repeated once more. The solids are transferred into a tared polyethylene weighing dish. After oven drying the final weight of the hydrated cement is determined. Carefully weighed samples equivalent to .0125 g of the original unhydrated cement are weighed and used for the surface area determination.

The unhydrated cements tested are all Type II. At the time of testing cements 1 and 4 were several weeks old, cement 2 was one day old, cement 3 was fresh from the mill, and cement 5 was from the same clinker as cement 3 but ground coarser. All of these, except cement 4, are the products of one cement plant.

The samples of C_2S and C_3S were furnished by the Engineering Materials Laboratory of the University of California in Berkeley.

Discussion

Three methods have thus far been used to measure surface area with the apparatus described here. Nitrogen adsorption at liquid nitrogen temperature is made by pouring liquid nitrogen into a modified sample tube holder and recording the adsorption peaks. By repeating this at several vapor pressure levels sufficient data are obtained to draw the adsorption isotherm curve and calculate the monolayer area by the BET equation. This is done to establish a basis for comparison between organic vapor and nitrogen adsorption on various materials. The other two methods of measurement employ benzene, methyl alcohol, or acetone. They are the single point method and the complete adsorption isotherm determination. The latter is especially necessary for a completely unknown sample, while the former approach is satisfactory for samples of similar surface properties. A recent abstract of a paper (in Russian) by Gavrilova and Kiselev (8) indicates they are using a similar approach, measuring near P/P_0 of 0.05.

Preliminary results indicate dry cements are similar in their overall surface adsorption behavior. Fig. 3 shows the BET curve for cements from two different plants to be practically identical. Calculations from these and several other cements show the monolayer coverage to fall between vapor pressure values of 0.07 and 0.1.

The values of the specific surface determined for unhydrated samples are given in Table 1. In comparison to the Blaine surfaces which fall between 3100 and 4100 cm² per gram, the higher values, by a factor approximately of 10, have been verified by nitrogen

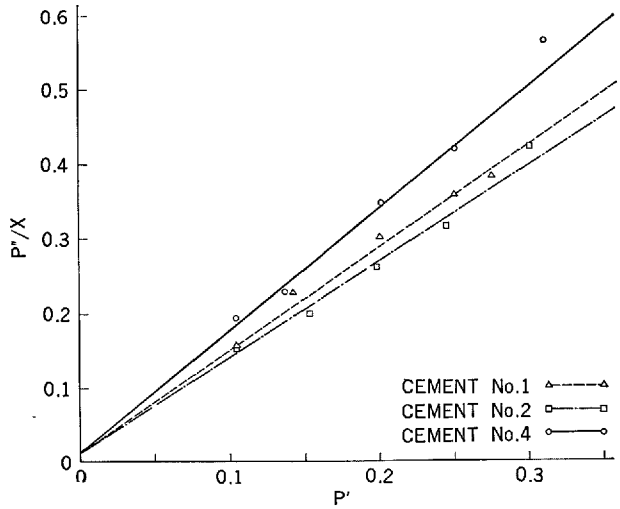

Fig. 3. *B.E.T. curves for three cements to illustrate the similarity between their surface adsorption properties.*

Table 1. *Specific surface area as determined by the adsorption of nitrogen and other organic liquids*

Sample	Surface area—m^2/g				
	BET method		Single point		
	Nitrogen	Benzene	Benzene	Acetone	Methyl alcohol
1	4.39	4.40	4.40	4.34	4.47
2	4.65	4.35	4.79	—	4.84
3	5.06	—	4.84	—	5.48
4	3.43	3.46	3.44	3.22	3.46
5	1.63	—	1.70	—	—
C_3S	—	—	0.57	—	—
C_2S	—	—	0.23	—	—

adsorption and are accepted as the true total solid surfaces. The explanation which has been offered (9) attributing such differences between air permeability and gas adsorption results to hydration during the normal handling of a sample, does not appear valid at least in the samples examined here. Age differences of these dry cements do not seem to have a measurable influence on their specific surface areas. As indicated in Table 1, a fresh-from-the mill cement (No. 3) has the largest area. We know with certainty that it has had no air hydration of any extent. Therefore, it looks like the larger adsorption areas reported here being indicative of the extent of crevaces and micropores on the particles.

Sample No. 5 lends support to the foregoing argument. It is made from the same clinker as No. 3; it was produced only three days later in the same mill, but ground coarser. Its Blaine area is 3100 cm^2 per gram against 4070 cm^2 per gram for No. 3. Therefore, by grinding finer the air permeability area increases about 30 percent, whereas the adsorption area increases by about 200 percent. Since the air permeability results are primarily influenced by the external surface properties it becomes evident that as the particles are broken up into smaller fragments they must be exposing many new pores and cracks in order to cause the internal surface area to increase at such a faster rate. This suggests, at least in this instance, that the cement particles possess a microcellular structure.

The older cements (No. 1 and 4) were stored in metal containers under optimum atmospheric conditions, however, some hydration was anticipated. If this does occur, evidently it produces no significant change in the adsorption surface area. Of course, exposure to an atmosphere of high relative humidity will ultimately cause sufficient hydration to impart a measurable increase of the cement surface.

Cements 1 and 4 were hydrated as described earlier for intervals of time from 5 minutes to 7 days. The surface development is presented in Fig. 4. A few

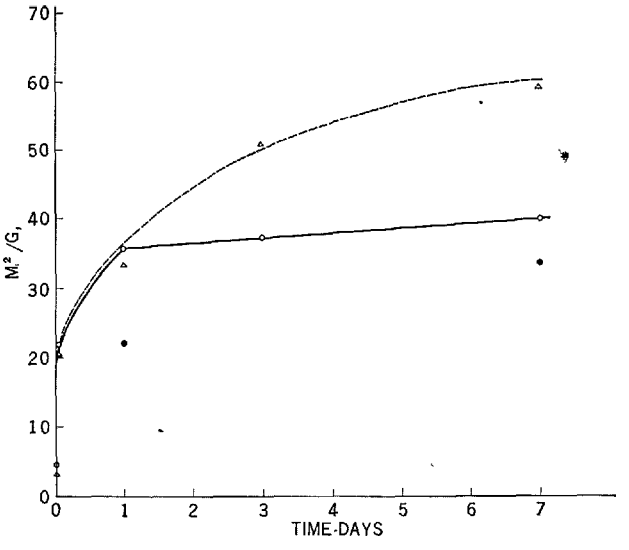

Fig. 4. *The surface area development of two different cements hydrated up to 7 days.*

other hydrated specimens give values between 50–70 m^2 which are comparable to some of the results given by Hunt, Tomes, and Blaine (10) and somewhat lower than those presented by Powers and Brownyard (9). As pointed out by Powers (11), the nitrogen adsorption values are usually 20 to 50 percent of the specific surfaces measured with water. Furthermore, the hydration procedure used here and the degassing at 200°C are likely to cause a contraction of the crystal lattice structure. This might render a considerable portion of the surface area inaccessible to the nitrogen or benzene molecules; whereas, the penetration of the highly polar and smaller water molecules might be affected to a lesser extent.

The points below the curve in Fig. 4 are hydrated samples of cement 1 which are not centrifuged but taken to dryness at 105°C. The lower surface areas shown are probably caused by higher lime content than in the centrifuged samples. This seems to be consistent with the discussion of Kantro, Brunauer, and Weise (12) that the higher the lime content is in tobermorite, the lower the surface area, which could be attributed to the cementing effect of lime on the crystals of tobermorite.

The foregoing discussion illustrates some of the results which can be obtained by this new technique. It would be feasible to study the surface properties of cement pastes by water adsorption without change or addition to the apparatus. In addition, it would be possible to study the porosity by measuring adsorption at high vapor pressures ($P' = 0.8$ to 1.0). At thse higher vapor pressures the desorption peaks of unhy-

drous cements start splitting and forming patterns characteristics of the sample, and may represent fractions of the adsorbate which have been adsorbed at different energy levels.

Acknowledgement

The author is indebted to Robert Miller for his assistance in the design and construction of the electrical circuits.

References

1. F. M. Nelsen, and F. T. Eggertsen, "Determination of surface area-adsorption measurements by a continuous flow method", Anal. Chem. **30,** 1387–90 (1958).
2. H. W. Daeschner, and G. H. Stross, "An efficient dynamic method for surface area determination", Anal. Chem. **34,** 1150–55 (1962).
3. E. Smolkova, L. Kristofikova, L. Feltl, and O. Grubner, "Determination of the surfaces of powder substances by the method of thermal desorption using organic vapors as the sorbates", Collection Czeck. Chem. Commun., **31,** No. 2, 450–6 (1966).
4. J. J. Jurinak, and T. S. Inouye, "Measurement of vapor adsoprtion and surface area of soils by a flow technique", Soil Sci., **99,** 289–94 (1965).
5. T. E. Jordan, "Vapor pressures of organic compounds", Interscience Pub., New York, 1954.
6. S. Brunauer, P. H. Emmett, and E. Teller, "Adsorption of gases in multimolecular layer", J. A . Chem. Soc., **60,** 309, 1938.
7. S. J. Gregg, and K. S. Sing, "Adsorption, surface area and porosity", p. 116. Academic Press, Inc., London England, and New York, U.S.A., 1967.
8. T. B. Gavrilova, and A. V. Kiselev, "Isotherms of adsorption and rapid determination of the specific surface area by gas-chromatographic method of thermal desorption", Zh. Fiz. Khim, **39,** No. 9, 2582–5 (1965) (in Russian).
9. T. C. Powers, and T. L. Brownyard, "Studies of the physical properties of hardened portland cement paste", Proc. Am. Concrete Inst. **43,** 469–504 (1946).
10. C. M. Hunt, L. A. Tomes, and R. L. Blaine, "Some effects of aging on the surface area of portland cement paste", J. Res. Nat. Bur. Stand., **64A,** No. 2, 163–9 (1960).
11. T. C. Powers, "Physical properties of cement paste", Proc. fourth Int. Symp. on the Chem. of Cement, Washington, D. C., 577–609 (1960).
12. D. L. Kantro, S. Brunauer, and C. H. Weise, "Development of surface in the hydration of calcium silicates", Advances in Chem. Ser., No. 33, 199–219 (1961).

Supplementary Paper I-136 The Crystallization of Compounds in the Presence of Cr_2O_3, P_2O_5 or SO_3 and the Properties of the Resultant Cement

Yuri M. Butt, Vladimir V. Timashev and Ludmila I. Malozohn*

Synopsis

The influences of Cr_2O_3, P_2O_5 or SO_3 on the crystallic lattice of clinkers having high (1) and low (0.67) saturation factors at various technological conditions were studied. Also were studied the properties of cements made on these clinkers. The amounts of the said oxides introduced amounted to 0.5, 1.0, 1.5, 2.0 and 3 per cent respectively.

The presence of 0.5 per cent of an oxide in the raw mix rather increases the clearness of the clinker crystallic lattice. The amount of an admixture over 1.0 per cent brings about the formation of imperfect forms of crystals. The crystals of belite had strong hatching, had splitted edges or disintegrated into separate "blocks"; the number of inclusion into alite crystals increased. In the presence of SO_3 some alite crystals assumed an indefinite form.

The occlusion of the modifying agents into the lattice was accompanied, in case of Cr_2O_3—with an increase, and in case of SO_3 or P_2O_5—with a decrease of alite and belite refringence data.

The time of grinding in the presence of Cr_2O_3, P_2O_5 or SO_3 decreases–especially in clinkers of high saturation factor.

The presence of Cr_2O_3 or SO_3 in cement having SF = 1 contributes to rapid gain of strength during the initial period of the cement paste hardening. In the presence of P_2O_5 the rate of cement hardening decreases.

Introduction

Crystallization of alite and belite in clinkers was studied—depending on the amount of Cr_2O_3, P_2O_5 or SO_3. Features of resultant cements were studied.

The composition of raw mixes was so designed as to obtain clinkers with saturation factors (SF) 1 and 0.67. The flux content amounted to 20 per cent (14 per cent of C_4AF and 6 per cent of C_3A). The admixture investigated were added in the form of Cr_2O_3, P_2O_5 and $CaSO_4 \cdot 2H_2O$ in amounts of 0.5, 1.0, 1.5, 2.0 and 3.0 per cent—expressed as SO_3 content. Specimens pressed with 400 kg/cm² force were burnt in silit furnace at 1450°C. The retention time at this temperature was 1 and 4 hours for clinkers having SF values 0.67 and 1 respectively (excluding alite clinkers with 3 per cent admixture—these being burnt for 1 hour). The clinkers resulted were air quenched and slowly cooled in the furnace at the rate of 5° approximately per minute. In addition, the clinkers with 3 per cent admixture suffered three-times burning—in order to obtain more complete assimilation of the lime.

The presence of 0.5–3.0 per cent of Cr_2O_5, P_2O_5 or SO_3 in the raw mix having saturation factor of 0.67, does not adversely influence the forming of clinker: the amount of free CaO in clinker did not exceed some

*The Moscow Mendeleev's Institute of Chemical Technology, Moscow, U.S.S.R.

tenth of per cent (2, 4, 5). In clinkers having saturation factor 1 and with 0.5–2.0 per cent of SO_3 or P_2O_5 the content of free CaO does not exceed 1 per cent while in those with the addition of Cr_2O_3 the free CaO content is 2 per cent.

During the burning partial and rather uneven volatilization of oxide admixtures was observed (Table 1).

Table 1. *The amount of* P_2O_5, SO_3 *or* Cr_2O_3 *in clinkers, per cent, as to the chemical analysis data*

The designed amount of an oxide into the raw mix, per cent	P_2O_5		SO_3		Cr_2O_3	
	SF = 0.67	SF = 1	SF = 0.67	SF = 1	SF = 0.67	SF = 1
0.5	0.44	0.47	no	0.17	0.35	0.63
1.0	1.37	0.98	no	0.33	0.51	0.57
1.5	1.34	0.92	no	0.12	0.82	0.82
2.0	1.62	1.32	0.84	0.14	1.14	1.45

Crystallic Structure of Clinkers

The presence of 0.5 per cent of P_2O_5, Cr_2O_3 or SO_3 in a raw mix having saturation factor of—0.67 (Belite clinker) brings about some more distinct crystallization of the clinkering minerals and to more distinct forming of crystals as to compare with the clinkers without admixtures—though the microscopic figures of both these clinkers are very similar. The crystals of belite in these clinkers are of rounded or almost polygonal form with even edges and with smooth or weakly hatched surface. The clinker forming compounds (except alite and belite) are heterogenous with a disordered location of light and dark crystals of shapeless form.

In a raw mix the increasing of the concentrations of: P_2O_5 up to 2–3 per cent, Cr_2O_3 up to 1.5–3.0 per cent or SO_3 over 1.0 per cent brought about the appearing of not properly formed crystals, when seen under the microscope. The defects of these crystals reveal in the form of appearing of the sharp hatching of the crystals of belite (Fig. 1), full or partial splitting of the crystals for separate "blocks" in the marginal zone and in the form of stains of various colours during the etching of crystals. To add, that in the presence of SO_3 there occur belite crystals of an indefinite form; these crystals are of an increased microporic structure.

The refractive index of belite in the presence of P_2O_5 and SO_3 lowers (Table 2), when 0.5–2.0 per cent of SO_3 is introduced into the raw mix, belite in clinker stabilizes into the form of β–C_2S, when 3.0

Table 2. *The sizes of alite and belite crystals in the presence of* P_2O_5, Cr_2O_3 or SO_3 *and their refractive index.*

The amount of the oxide, %	Cooling pattern	P_2O_5						Cr_2O_3						SO_3					
		SF = 0.67			SF = 1			SF = 0.67			SF = 1			SF = 0.67			SF = 1		
		belite crystals, size, microns	Ng	Np	alite crystals, size, microns	Ng	Np	belite crystals, size, microns	Ng	Np	alite crystals, size, microns	Ng	Np	belite crystals, size, microns	Ng	Np	alite crystals, size, microns	Ng	Np
0.0		5–50 (25–35)	1.740	1.724	8–30	1.728	1.724	5–50 (20–30)	1.740	1.724	8–30	1.728	1.724	5–50 (20–30)	1.740	1.724	8–30	1.728	1.724
0.0*		5–15	1.732	1.714	10–70 (25)	1.720	1.716	5–15	1.732	1.714	10–70	1.720	1.716	5–15	1.732	1.714	10–70	1.720	1.716
0.5		5–55 (15–35)	1.732	1.718	5–60 (20)	1.724	1.720	5–50 (20–30)	1.735	1.718	15–100 (35–45)	1.724	1.720	5–40	1.732	1.720	10–45	1.724	1.720
0.5*		15–35	1.735	1.716	15–30	1.720	1.716	1–20 (5–10)	1.737	1.720	5–40	1.728	1.724	5–40	1.735	1.717	10–50	1.722	1.717
1.0*	rapid	10–35	1.728	1.714	15–70 (35)	1.720	1.716	1–10	1.737	1.720	5–40	1.728	1.724	5–40	1.735	1.717	5–50	1.722	1.717
1.5*		5–40	1.728	1.714	10–70 (40)	1.720	1.716	10–50	1.745	1.722	5–50	1.732	1.728	5–40	1.735	1.717	10–70	1.722	1.717
2.0*		5–40	1.728	1.714	30–80 (40–50)	1.717	1.714	5–40	1.745	1.722	10–50	1.732	1.728	5–35	1.735	1.717	50–500	1.722	1.717
3.0		15–40	1.722	1.707	—	1.720	1.716	30–40	1.740	1.720	—	—	—	15–60 (20–40)	1.726	1.707	—	—	—
Three-times burning		10–70 (40)	1.726	1.712	—	—	—	30–60	1.745	1.728	—	—	—	5–80 (40)	1.728	1.712	5–40	1.726	1.722
0.0		20–170 (40–120)	1.735	1.718	5–40	1.724	1.720	20–170 (40–120)	1.735	1.718	5–40	1.724	1.720	20–170 (40–120)	1.735	1.718	5–40	1.724	1.720
3.0	slow	15–45 (35)	1.718	1.704	—	—	—	20–150	1.740	1.724	—	—	—	30–150 (30–65)	1.726	1.707	150–450	—	—

*Clinkers having SF = 1 were cured at the temperature 1450°C during 4 hours.

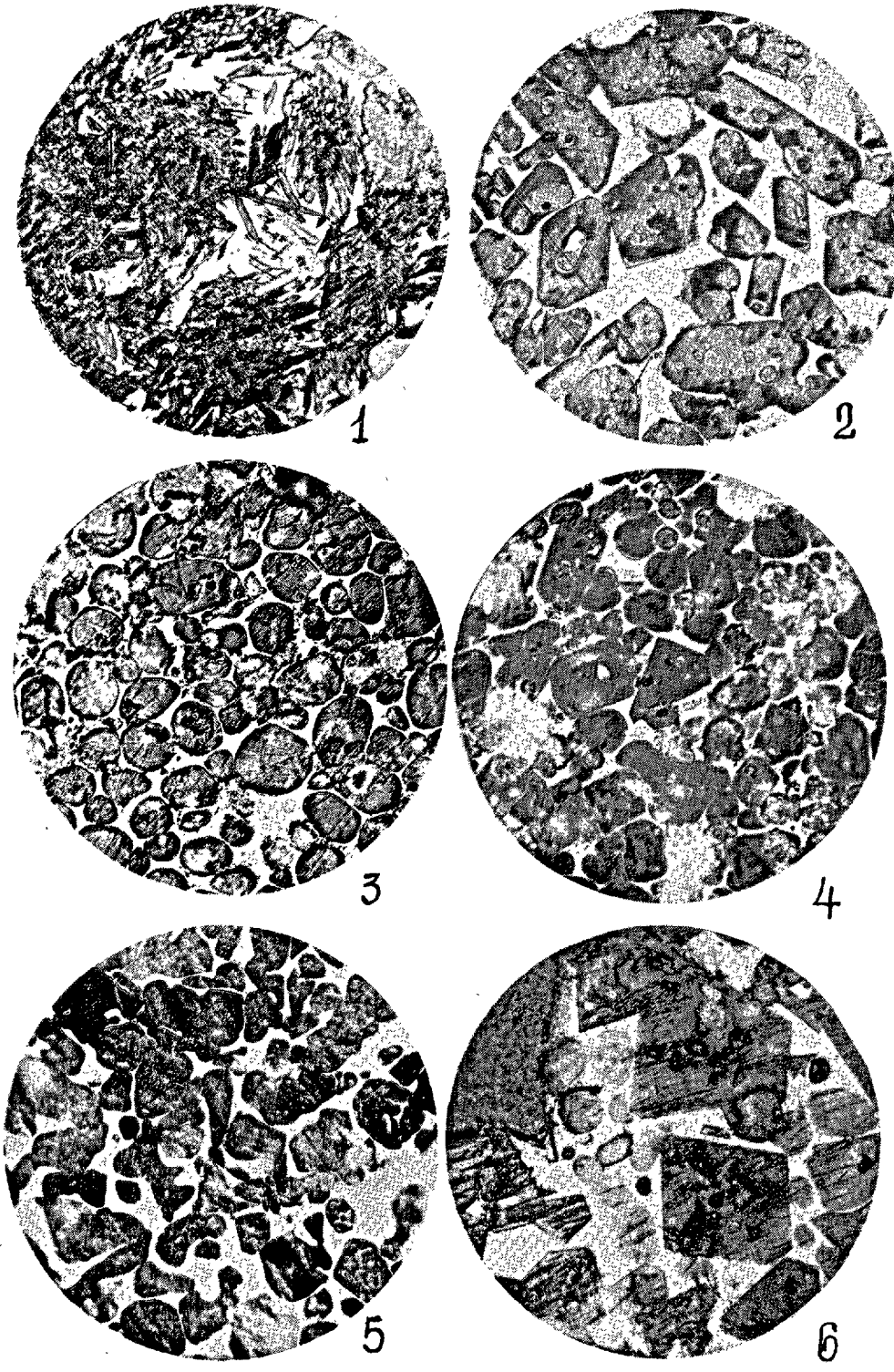

Fig. 1. *Microscopic structures of clinkers containing* Cr_2O_3, P_2O_5 *or* SO_3. *Specific macrodefects. Reflected light* $\times 400$.

1—belite clinker, 3 per cent of Cr_2O_3
2—alite clinker, 0.5 per cent of Cr_2O_3
3—belite clinker, 3 per cent of P_2O_5
4—alite clinker, 2 per cent of P_2O_5
5—belite clinker, 1.5 per cent of SO_3
6—alite clinker, 2 per cent of SO_3

per cent of SO_3 is introduced, the refractive index correspond to that of α'–C_2S. In the presence of 0.5 per cent of P_2O_5, the refractive index becomes near to β–C_2S; when increasing the content of phosphorus pentoxide up to 1.0–2.0 per cent, the refractive index becomes lower up to the data, specified to α'–C_2S, while 3.0 per cent of this pentoxide lowers the refractive index even a little bit more. The refractive index of belite crystals in the presence of Cr_2O_3 increases—and the more of this oxide is introduced into the raw mix, the higher these data are. The change of the refractive index of the crystals proves the occlusion of ions into the crystallic lattice of C_2S. However, this occlusion did not bring about a pronounced influence on the character of analytic lines of belite on the X-ray patterns of respective clinkers. Clinkers having 5 per cent admixture of either Cr_2O_3 or SO_3 reveal some amount of γ–C_2S, which disappeared with the increase of the admixture content.

The composition of aluminoferrous phase in clinker having 0.5 and 1.0 per cent of SO_3 and 0.5, 1.5 and 2.0 per cent of Cr_2O_3 is near to C_4AF, while in clinkers having 0.5–2.0 per cent of P_2O_5, 1.0 per cent of Cr_2O_3 or 1.5–2.0 per cent of SO_3 the composition of this phase approaches to C_6A_2F. Slow cooling of clinkers, containing 3 per cent of P_2O_5, SO_3 or Cr_2O_3 contributed both to the increasing of dimensions of belite crystals and to the formation of crystals of an indefinite form, these crystals being partly coalescent.

Refractive index of belite in a slowly cooled clinkers in the presence of P_2O_5 and SO_3 lowered down compared with quenched clinkers; The presence of Cr_2O_3 did not bring about the change of refractive index with the alteration of the cooling process. The three-times burning of clinkers having 3 per cent admixture contributed to the splitting of crystals for separate "blocks" and to the increase of the refractive idex compare with the single burning.

The introduction in the raw mix having SF = 1 (alite clinker) of 0.5 per cent P_2O_5, Cr_2O_3 or SO_3 as well, as in clinkers having low saturation factor, does not bring to any considerable change into the way of the crystallization of the clinkering minerals, but it makes the crystal structure more distinct. The crystals of alite have the form of elongated (1:1.5; 1:2) hexagonal plates. The inclusions of belite grains and of the phase, containing clinker forming compounds (except alite and belite) into the crystals of alite are not numerous and the edges of the crystals are quite distinct and smooth. The increase of Cr_2O_3, P_2O_5 and SO_3 over 0.5 per cent contributes to enlargement of the dimensions of alite crystals in the mass, to the alteration of a long-prismatic form of crystals for a shortprismatic, polyhedral one and to the increasing of the number of crystals coalescences (Fig. 1). The amount of inclusions of the intermediate phase and especially of belite into the crystals of alite increases as well. Very sharp alterations are observed in the clinkers resulted from raw mix with 2 and 3 per cent of oxide introduced. The crystals of alite in clinker having 2 per cent of SO_3 are of high microporous structure. The dimensions of some alite crystals amount to 500 microns, i.e. 10–15 times greater of a middle dimension of alite crystals in a clinker having 0.5 per cent of SO_3.

In the presence of 2–3 per cent of the admixture in clinkers, the amount of belite in alite clinkers and of CaO increases. The crystals of belite in alite clinkers, as to be judged by both X-ray and refractive index have the form of β–C_2S. In the presence of 3 per cent of the admixture in the raw mix, the synthesis of alite, for obtaining of which the raw mix had been designed, performed, as to be judged by the amount of free CaO, just as much as 20–30 per cent.

In polished microsections of this clinker the crystals of alite were not identified—but in the clinker with the addition of SO_3, where separate alite crystals of 450–500 microns size were seen. Therefore, the synthesis of high alite crystals is hard to perform in the presence of P_2O_5, Cr_2O_3 and SO_3.

The refractive index of the crystals of alite in the presence of Cr_2O_3 increase, while in the presence of P_2O_5 or SO_3 the refractive index decreases. However, the variation of the refractive index of the said crystals, depending on the amount of the admixture is a little or somewhat lesser than the variation of these data for the crystals of belite (Table 2). In the presence of 3 per cent of each admixture in clinkers having SF = 1, a crystallic phase was observed, this might be referred to as α-quartz; its amount does not exceed 3 per cent. The change of the rapid cooling for a slow cooling did not bring the pattern of crystallization of minerals in clinkers having SF = 1 and with 3 per cent of the addition. As a result of the three-times burning of the clinker with SF = 1 and with 3 per cent of SO_3, resulted in the full assimilation of lime. The crystallic pattern of the clinker with 3 per cent of P_2O_5 or Cr_2O_3, as a result of a three-times burning, was, in comparison with a single burning, negligible.

As seen from the X-ray structural analysis, the introduction of 0.5, 1.0, 1.5 and 2.0 per cent of Cr_2O_3 does not influence the pattern of analytical lines of alite, while the introduction of the similar amounts of P_2O_5 and SO_3 rather decreases the half width of the said lines of alite, without changing their position.

In addition, in the presence of 0.5 per cent of P_2O_5 some asymmetry of the profile of C_3S line is observed (620 + 040); this asymmetry in the case of 2 per cent addition of P_2O_5, turns into a poorly resulting twin reflection.

Aluminoferrous phase in clinkers having SF = 1 and with admixtures of Cr_2O_3, P_2O_5 and SO_3 up to 2 per cent, is of C_4AF compound composition. In microscopic observation, the intermediate phase in clinkers with the admixture of Cr_2O_3 and P_2O_5 is seemed as light and dark crystals having an indefinite form, while in the presence of SO_3 the dark crystals are distinct ones in the form of short prisms.

The Properties of Cements

The cements studied were made by grinding clinkers having 5.1 per cent of $CaSO_4 \cdot 2H_2O$ to specific area of 3,000 cm^2/g. From the cements obtained were made specimens of 1.41 × 1.41 × 1.41 cm. size (paste = 1:0), which were tested for compression strength after 0.5, 1, 3 and 28 days and 3, 6, 12 and 36 months of air-humid curing. Every age was represented by 12 twin-samples.

The time necessary to grind clinkers with SF = 1 and containing either P_2O_5, Cr_2O_3 or SO_3, decreases by 35–60 per cent as compared with that required for grinding (up to the same specific area) a clinker without these admixtures.

However, the introduction of but P_2O_5 considerably increases the grindability of the clinker and the maximum effect is attained when 0.5 per cent of this oxide is introduced, while the least effect is attained when 2.0 per cent is introduced (Fig. 2).

The grindability of clinkers with low saturation factor (0.67), which contain either P_2O_5 or SO_3, is near to that without the admixtures. The grindability of clinkers containing 0.5 and 1.0 per cent of chromium oxide is by 40–50 per cent higher while that of clinkers containing 1.5 and 2.0 per cent is 30–10 per cent lower compared with clinkers without admixtures.

Normal consistency of the cement paste containing P_2O_5, Cr_2O_3 and SO_3 increases by 1–6 per cent (absolutely). Initial and final setting times of the cement paste of clinkers having P_2O_5, Cr_2O_3 and SO_3 increase, except for the paste of clinker with SO_3 and having SF = 1; initial setting time of this clinker is about the half of that of the clinker without this admixture.

The setting time of the cement paste also increases, except in the case of cement paste resulted from the clinker having 0.5 per cent of P_2O_5 and SF = 0.67; for this paste the setting time is a minimum one–6 min.

According to the X-ray data (Table 3) the biggest influence on the rate of hydration process is shown by Cr_2O_3, P_2O_5 and SO_3 during the initial period of the cement paste hardening, i.e. during 12 hours after the cement has been mixed with water.

0.5, 1.0, 1.5 and 2.0 per cent of SO_3 and 0.5, 1.0 and 1.5 per cent of Cr_2O_3 increase the hydration rate of alite by 1.5–2 times compared with the cements without admixtures. Phosphorus pentoxide shows a delaying effect on the hydration process of alite during the initial period, but at 3 days the hydration rate of alite both in cement without admixtures and in cements containing one of the oxide, assumes common rate and, in 28 days of hardening in air-humid conditions, it amounts nearly 80 per cent in all the specimens studied.

The hydration process of the aluminoferrite phase is accelerated by minor traces of the admixtures considered: 0.5 per cent of Cr_2O_3 and of SO_3 and 0.5–1.0 per cent of P_2O_5. These oxides in more quantities retard the hydration process of the aluminoferrite phase.

Chromium oxide does not show significant influ-

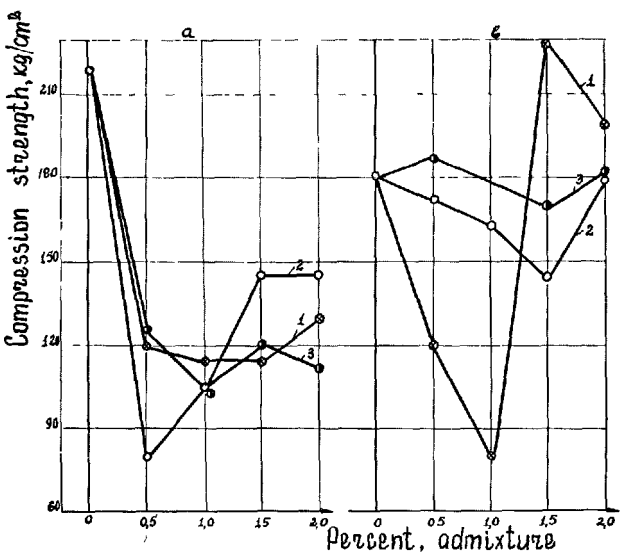

Fig. 2. *The influence of* Cr_2O_3, P_2O_5 *and* SO_3 *on the grindability of clinker.*
a) clinker having SF = 1 (as designed);
b) clinker having SF = 0.67 (as designed)

Table 3. *Hydration rate (per cent) of separate compounds in a hardened cement paste, having admixtures of* Cr_2O_3, P_2O_5 *or* SO_3

Hardened cement paste, age	Name of an oxide added	Oxide added, per cent	C_3S	C_2S	C_3A	C_4AF
12 hours	No oxide added		19	1	20	20
	Cr_2O_3	0.5	32	1	22	31
		1.0	37	1	21	11
		1.5	46	1	9	21
		2.0	10	1	21	10
	P_2O_5	0.5	10	1	1	38
		1.0	8	1	5	58
		1.5	3	1	1	23
		2.0	2	1	12	12
	SO_3	0.5	33	1	1	36
		1.0	32	1	9	15
		1.5	40	1	8	13
		2.0	38	1	17	12
3 days	No oxide added		59	8	53	79
	Cr_2O_3	0.5	64	5	56	74
		1.0	63	6	57	76
		1.5	78	4	40	69
		2.0	60	5	57	59
	P_2O_5	0.5	44	4	19	52
		1.0	49	5	32	63
		1.5	48	8	22	69
		2.0	49	5	42	62
	SO_3	0.5	60	5	36	78
		1.0	60	2	35	10
		1.5	56	5	30	20
		2.0	63	5	40	69
28 days	No oxide added		80	14	68	80
	Cr_2O_3	0.5	78	7	71	78
		1.0	78	8	71	79
		1.5	87	7	51	75
		2.0	76	11	69	70
	P_2O_5	0.5	75	24	48	65
		1.0	77	20	60	71
		1.5	80	8	53	77
		2.0	85	9	63	74
	SO_3	0.5	72	37	63	90
		1.0	71	14	63	73
		1.5	72	19	58	76
		2.0	71	22	60	82

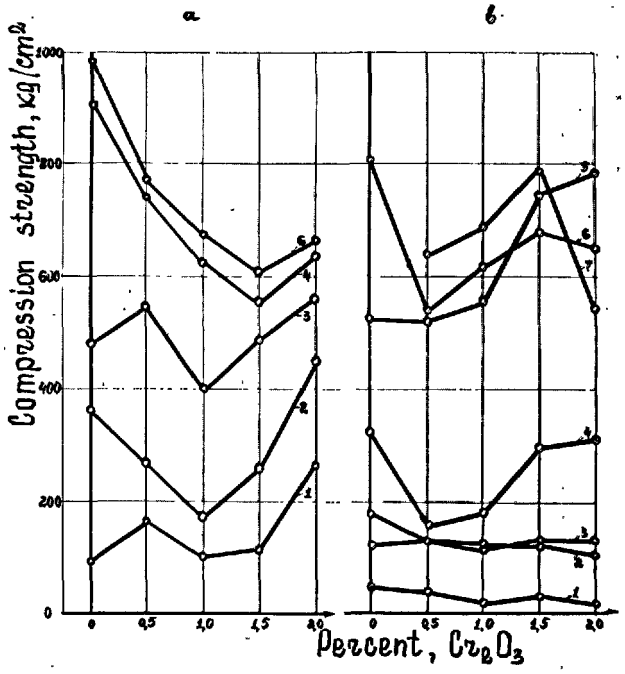

Fig. 3. *The change of strength of the hardened cement paste made with cement containing chrome.*
a) SF = 1 (as designed)
b) SF = 0.67 (as designed)
1–0.5 day; 2–1 day; 3–3 days; 4–28 days; 5–3 months; 6–6 months; 7–1 year

ence on the hydration process of calcium aluminates, while phosporus pentoxide and sulphur trioxide retard their hydration process.

It is impossible to trace the influence of the admixtures on the hydration process of belite in an early age (up to 3 days) due to the low rate of the process of this age. At the age of 28 days the tendency of an accelerated hydration process of C_2S appears by the addition of SO_3 and rather a retarded one by the addition of P_2O_5 and Cr_2O_3.

According to the X-ray data, the products of hydration of calcuim silicates are $Ca(OH)_2$ and tobermorite-like silicate hydrate of C_2SH_2 type while the products of hydration of alumina-bearing compounds is a high-sulphate form of calcium sulphoaluminate hydrate (ettringite) ($d = 9.8$; 5.6Å)—this probably containing some ferric oxide. Gradually ettringite transforms into a low sulphate form of sulphoaluminate hydrate ($d = 9$Å), which, at the age of 28 days, becomes a prevailing form. In samples of hardened cement paste on resulted from cement containing either phosphor or sulphur and having SF = 0.67, and at 28-day hydration of cement pastes resulted from cement containing either phosphor or sulphur and having SF = 0.57, C_4AH_{13} and α-C_4AH_{13} are also observed and they form mixed crystals in a phospho-containing cement paste with the low sulphate form of calcium aluminate sulphate.

There is a definite dependence between the rate of hydration of tricalcium silicate hydrate and of aluminoferrous phase contained in the hardened cement paste, and the strength of the said paste.

The presence of Cr_2O_3 in cements having high saturation factor contributes to a quick gain of strength, in an initial period of hardening, this strength increasing with the increase of the amount of Cr_2O_3 (Fig. 3). However, at the age of over 28 days, the com-

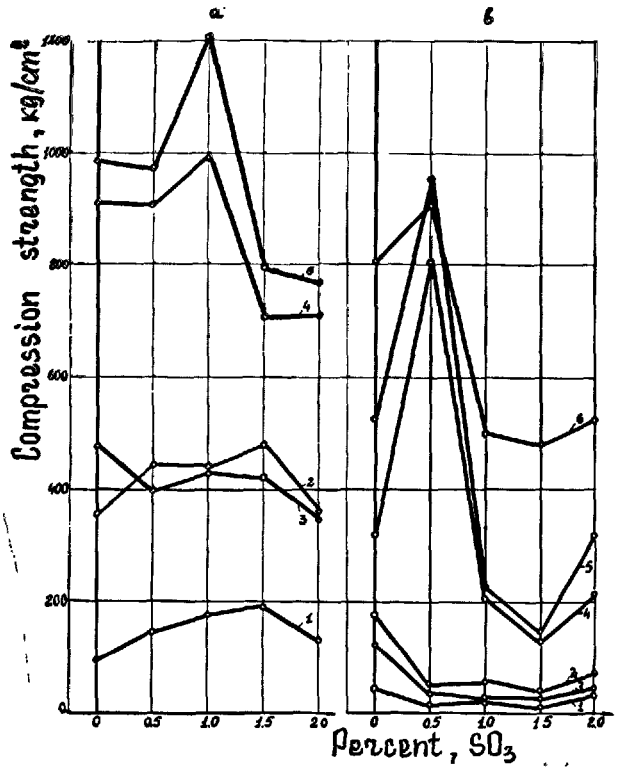

Fig. 4. *The change of strength of the hardened cement paste made with cement containing sulfur*
a) SF = 1 (as designed)
b) SF = 0.67 (as designed)
1–0.5 day; 2–1 day; 3–3 days; 4–28 days; 5–3 months; 6–6 months

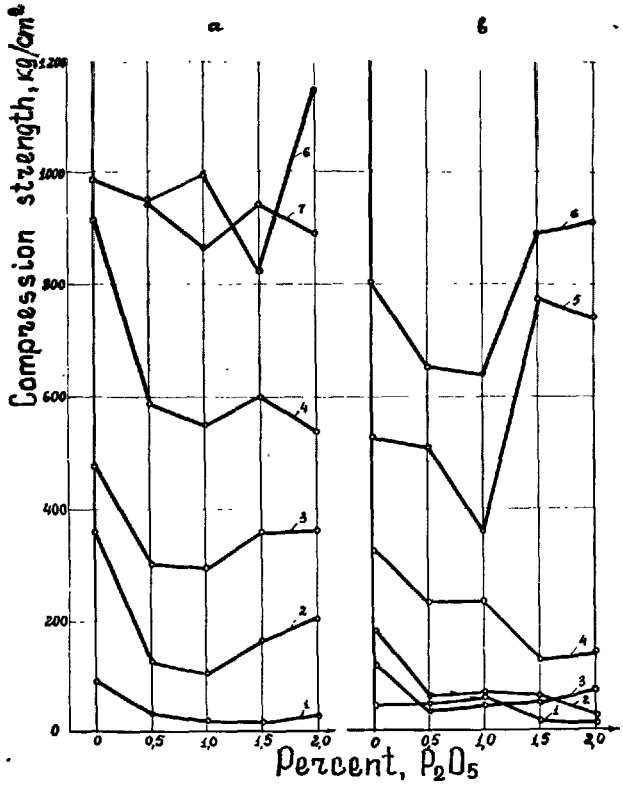

Fig. 5. *The change of the strength of the hardened cement paste made with cement containing phosphorus.*
a) SF = 1 (as designed)
b) SF = 0.67 (as designed)
1–0.5 day; 2–1 day; 3–3 days; 4–28 days; 5–3 months; 6–6 months

pressive strength of the chrome containing hardened cement paste is lower than that of the paste without the admixture. And there is an inverse dependence between the compressive strength of a clinker and the amount of the admixture.

The presence of Cr_2O_3 in cement with SF = 0.67 brings to the strength increase during neither initial nor subsequent periods of hardening.

The presence of SO_3 in cement with SF = 1 also contributes to the quick strength gain of the cement paste during its initial period of the hardening. And, up to 3-day age of the hardening cement paste no definite relation is observed between the strength of the paste and the amount of the admixture. During the period of 28 days–3 months, the maximum strength is obtained in the samples of the hardening cement paste made on clinker resulting from the raw mix with 1 per cent of SO_3 introduced (Fig. 4). 0.5 per cent of SO_3 is an optimum one for the cement having SF = 0.67. The compressive strength of 28 days samples was higher than that of the cement without the admixture approximately by 100 and 500 kg/cm² in cements having saturation factor 1 and 0.67 respectively.

The compressive strength of the hardening cement paste made with phosphor-containing clinker samples is—up to 28-day age and irrespective of P_2O_5 content —considerably lower compared with the samples made from cements without the admixture (Fig. 5). Only in later age the strength values of various cements level off.

Conclusion

Minor amounts of Cr_2O_3, SO_3 and P_2O_5 (0.–0.5 per cent) do not delay the formation of clinkering compounds during the manufacture of clinker, though, with an increasing of the solid oxides in the range 0.5–

2.0 per cent, the reaction of C_3S formation greatly retards and completely performs for a 4-hour burning at 1450°C. The crystallic structure of clinker having 0.5 per cent of the said oxides is near to that of common clinkers. However, when the concentration of the oxides is raised up to 1.5–2.0 per cent, the crystals of alite and belite show the defects, specific to the presence of a modifying element. The occlusion of modifying elements into the lattice is accompanied with the increase (Cr_2O_3) or the decrease (P_2O_5, SO_3) of the refractive index of the compound. The microhardness of crystals increases in the presence of Cr_2O_3 and SO_3 and decreases in the presence of P_2O_5.

The grindability of alite clinkers having 0.5–2.0 per cent of the said oxides increases.

The presence of SO_3 accelerates the setting of cement, while the presence of Cr_2O_3 and P_2O_5 retards it. Both SO_3 and Cr_2O_3 contribute to a quicker hardening of cements up to 28 days, while P_2O_5 retards the strength gain.

References

1. L. Ya. Lopatnikowa "Petrologic method of the quality control of cement" (Russian) "Transactions of NIICEMENT", **18**, 75–86, (1963).
2. Technology and properties of special cements (Stroyizdat, Moscow, USSR, 1967), Yu. M. Butt and V. V. Timashev "The processes of crystallization running at the burning of portland cement raw mixes". 52–88.

3' "New in the chemistry and technology of cement" (Gosstroyizdat, Moscow, USSR, 1962) S. D. Okorokov and S. L. Golynko–Wolfson "The improvement of technical properties of cements by means of directed change of the process of clinkering compounds formation at the burning", 82–93.

4. M. M. Sychev and V. I. Korneev "Alloying admixtures improve the cement properties" (Russian), "Cement", **5**, 3–5 (1964).
5. N. A. Toropov "The chemistry of cements", 263 (Gosstroyizdat, Moscow, USSR, 1956).
6. A. E. Sheikin and S. A. Slobodchikowa, "The structure and hydration activity of alite depending both on the conditions of its obtaining and on the phosphorus content in it" (Russian) "Scientific publication of NIICEMENT" **14**, 1–9 1962.

SESSION I-4 CHEMISTRY OF CALCIUM ALMINATES AND THEIR RELATING COMPOUNDS

Principal Paper The Chemistry of Calcium Aluminates and Their Relating Compounds

Thomas D. Robson*

Synopsis

A survey is made of the compounds present in the $CaO–Al_2O_3$ system, including their historical background, properties and cell structure. Confirmation of the existence and stoichiometry of CA_6, the incongruent melting of CA and CA_2, and doubts about the stability of $C_{12}A_7$ when entirely free from hydroxyl ion, represent the main developments in this system in recent years. Certain changes at the high-alumina end of the $CaO–Al_2O_3–SiO_2$ phase diagram are also reported. These changes result mainly from a re-allocation of the anorthite—CA_6—corundum invariant point thus increasing the area of the corundum field at the expense of the CA_6 field.

Aluminous cements are classified here into four types on the basis of analysis and method of manufacture and a short account is given of the various processes by which the clinkers are obtained industrially. The calcium aluminates, as they appear in aluminous cement clinker are then further discussed, and details are reported of two related compounds ($3CA \cdot CaF_2$ and $C_{11}A_7 \cdot CaF_2$) both of which have probably been identified in clinkers made by one particular process. Very considerable progress has recently been made in elucidating the constitution of the pleochroic compound found in some clinkers and the latest ideas on its structure are described. It is now clear that this material is definitely a quaternary compound (but with a formula different from that previously allocated) and a cell structure has been proposed. The calcium alumino-ferrite solid solutions which form an important part of certain types of clinker have also received attention and a report is given of work (as yet unpublished) which indicates a clear correlation between reflectivity values and the degree of substitution of ferric oxide by titania.

The ternary compound $4CaO \cdot 3Al_2O_3 \cdot SO_3$ (or $3CA \cdot CaSO_4$), which has been discovered in the $CaO–Al_2O_3–SO_3$ system is now important in the manufacture of expansive cements. It is treated in this survey as a compound related to the calcium aluminates and its history, properties and structure are dealt with.

In conclusion a brief summary is made of proposed uses for calcium aluminates in fields outside those of hydraulic cements.

Introduction

Practical interest in calcium aluminates (other than C_3A) results mainly from the presence of certain members of this series in aluminous or high-alumina cements (calcium aluminate cements). The following survey of the anhydrous calcium aluminates, and of some related compounds, has therefore been written with this particular interest predominantly in mind, although other possible applications are mentioned where appropriate. Tricalcium aluminate, which is not thought to be a normal constituent of aluminous cement, receives no detailed treatment since the importance of this compound to the portland cement chemist guarantees further discussion elsewhere.

The relative activities of the compounds during

*The Lafarge Organization Ltd, London, United Kingdom.

hydration and the resulting cementitious properties will be compared but the scope of this account is otherwise limited to the anhydrous compounds and the hydration products are not discussed.

The Pure Calcium Aluminates

The compounds occurring in the binary CaO–Al_2O_3 phase system are normally given as C_3A, $C_{12}A_7$, CA, CA_2 and CA_6. The formulae of $C_{12}A_7$ and CA_2 have been agreed only after much investigation, and even the existence of CA_6 has been questioned until relatively recently. It will be seen later that the inclusion of $C_{12}A_7$ in this system is subject to an interesting controversy but, apart from this, and perhaps a small residual doubt concerning the exact stoichiometry of CA_6, all the above calcium aluminate formula are now widely accepted. The existence of the metastable orthorhombic C_5A_3 phase has also been confirmed.

The lattice structure of CA is known in fair detail but many of the structures proposed for the other aluminates are only partially resolved, and all require various degrees of refinement.

Tricalcium Aluminate, $3CaO \cdot Al_2O_3$

This compound is cubic and often forms rounded or spherical grains although rectangular, hexagonal or octagonal tablet forms are also reported. It has a hardness of about 6, a density of 3.03 g/cc. and a refractive index $n = 1.710$.

At 1539° ± 5°C it melts incongruently to CaO and a liquid of composition 57.2% CaO, 42.8% Al_2O_3 by weight (1), the liquidus temperature being about 1700°C.

There is only one form of C_3A but, in spite of numerous investigations, the structure has not yet been acceptably defined. The stronger lines of the powder pattern originally indicated a cubic unit cell having $a = 7.6$Å but the true cell edge is approximately double this length and has been given as $a = 15.262$Å (2). The unit cell (with space-group T_h^6–Pa3) is therefore composed of eight similar pseudocells. The aluminium ions appear to have 4-fold (tetrahedral) co-ordination with the oxygens and according to Burdick and Day (3) there is no evidence of 6-fold co-ordination.

C_3A hydrates more rapidly than any other calcium aluminate but, by itself, produces little or no hydraulic strength in mortars.

The $12CaO \cdot 7Al_2O_3$ Phase

The stable cubic "C_5A_3" compound of Rankin and Wright (4) was shown to have the formula $C_{12}A_7$ by Büssem and Eitel (5) who originally gave the following data:

$a = 11.95$Å. $Z = 2$.

Probable space-group T_d^6 Density 2.69.

The lattice was envisaged as a framework of distorted AlO_4 tetrahedra, partially linked by oxygen atoms, but leaving two of the 64 oxygen atoms to be distributed statistically. The calcium ions were in 6-fold co-ordination with oxygen and the lattice contained large structural "holes" which might account for the rapid hydration observed in practice. Analogies with the structures of C_3AH_6 and lime-alumina garnet were noted (6). The space-group is now thought to be $I\bar{4}3d$.

Although other C/A ratios were subsequently proposed for this compound, several workers have since confirmed the $C_{12}A_7$ formula and this ratio is now accepted generally. Nevertheless difficulty has long been experienced in delineating that portion of the binary C–A phase diagram which is adjacent to the $C_{12}A_7$ composition, and indeed this region appeared to have ternary characteristics (7). The refractive index of $C_{12}A_7$ had previously been found to be lower than that of quenched glass of the same composition and other peculiarities in density and in melting behaviour were evident.

Welch (8) noted that the compound absorbed atmospheric moisture at high temperatures and that the presence of water in the crystal was responsible for variations in cell volume, density and refractive index. Similar observations were made by Roy and Roy (9) who concluded that, in atmospheric air, $C_{12}A_7$ was not an anhydrous phase but a hydrate near in composition to $C_{12}A_7H$. Because of the reversible absorption of water over a wide temperature range (without major change of structure) $C_{12}A_7$ could be termed a zeolitic phase.

Jeevaratnam, Glasser and Dent Glasser (10) also noted that water was retained at about 1100°C, but crystals prepared from compositions by heating at 1200°C then at 1390°C for several days, were con-

sidered anhydrous, and would subsequently take up water only when heated to 400°–500°C. As a result of later work (11) they again judged that $C_{12}A_7$ could definitely exist in essentially anhydrous form and that the water was present in the crystal as OH^-. However, Nurse, Welch and Majumdar (12) found that when a $C_{12}A_7$ composition was melted at 1500°C, annealed at 1000°C, and cooled in a dry oxygen-free nitrogen atmosphere, traces of hydroxyl ion could still be detected by infra-red spectroscopy and a small weight loss was observed when a sample was re-heated to 950°C–1375°C in the nitrogen atmosphere. Although agreeing that the constitutional formula for the fully saturated compound is best represented as $Ca_{12}Al_{14}O_{32}(OH)_2$, they were therefore not convinced that completely anhydrous $C_{12}A_7$ could be prepared.

The $12CaO \cdot 7Al_2O_3$ compound is customarily given a small stable field between those of C_3A and CA. As shown in Fig. 1, it has a congruent melting-point at about 1392°C and the binary eutectics $C_{12}A_7$–C_3A and $C_{12}A_7$–CA are both at about 1360°C (13).

However, the congruent melting of $C_{12}A_7$ has been questioned for several reasons, including the fact that two endotherms at about 1370°C and 1395°C have been observed in D.T.A. work (12). Nurse, Welch and Majumdar found that the liquidus temperature of $C_{12}A_7$ in moist air was certainly at 1392°C ± 3°C but this remained substantially constant for compositions with a range of C/A ratios on either side of that of $C_{12}A_7$, and, in dry argon, $C_{12}A_7$ melted incongruently to CA and liquid at 1374°C.

If hydroxyl ions remain in the lattice of $C_{12}A_7$ the compound cannot strictly be included in the binary C–A diagram and a possible representation of this part of the system under anhydrous conditions has been given by Nurse, Welch and Majumdar (Fig. 2).

The stable field of $C_{12}A_7$ disappears and is replaced by a eutectic between C_3A and CA at 50.7% Al_2O_3 (wt.) and 1360°C ± 5°C. Thermodynamic calculations (although not yet conclusive) indicate that the C_3A + CA assemblage may indeed be more stable than $C_{12}A_7$ at the latter composition (12).

The reversible equilibrium between $C_{12}A_7$ and water vapour at high temperatures can be briefly summarised as follows: Between 950°–1350°C, weight is lost on the heating cycle and gained on the cooling cycle, but this process becomes irreversible if the crystals are allowed to melt or, of course, if the cooling cycle takes place under anhydrous conditions. The maximum uptake of water occurs at 950°–100°C corresponding to an increase in weight (over that of the "anhydrous" compound) of about 1.3% (12). In this condition the compound corresponds to $C_{12}A_7H$ and, with hydroxyl ions present in the lattice, the constitutional formula is believed to be $Ca_{12}Al_{14}O_{32}(OH)_2$.

When the compound is prepared by fusion and cooling to room temperature (always under anhydrous conditions) the formula $C_{12}A_7$ is correct or nearly correct but it is not certain that a completely anhydrous material has yet been prepared.

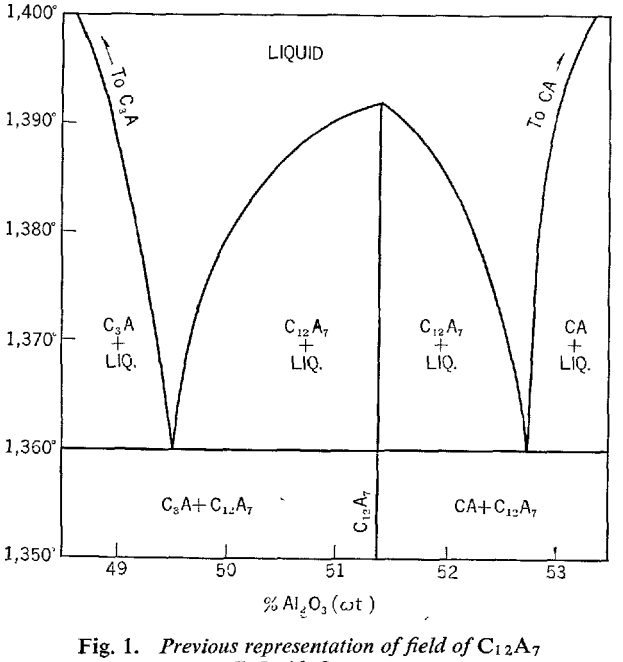

Fig. 1. *Previous representation of field of* $C_{12}A_7$ *in* CaO–Al_2O_3 *system*

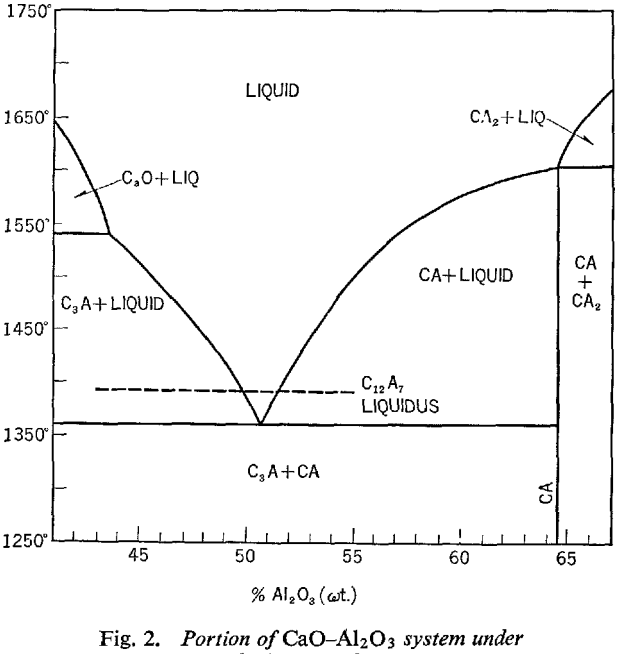

Fig. 2. *Portion of* CaO–Al_2O_3 *system under anhydrous conditions*

Table 1. *Properties of* $C_{12}A_7$ *and* $C_{12}A_7H$

Property	Compound	A	B	C
Density g/cc	$C_{12}A_7$	2.68	2.68	—
	$C_{12}A_7H$	2.72	2.73	—
Refractive index	$C_{12}A_7$	1.611	1.609	1.616
	$C_{12}A_7H$	1.620	1.619 ±0.001	1.610 ±0.002
Unit cell length Å	$C_{12}A_7$	11.983	11.9880	11.978
	$C_{12}A_7H$	11.977	11.9747 ±0.0002	11.982

The effect of water in the lattice on density, refractive index, and cell dimensions is shown in Table 1 where A, B and C are the results respectively of Jeevaratnam, Glasser and Dent Glasser, (11) Nurse, Welch and Majumdar (1) and D. M. Roy and R. Roy (9).

On passing from $C_{12}A_7$ to $C_{12}A_7H$ there is an increase in density and two of the above teams indicate an increase in refractive index and a decrease in cell volume. Roy and Roy reported a reduction in refractive index and a slight increase in cell volume. The values shown for cell dimension under C in Table 1 are those calculated by Jeevaratnam, Glasser and Dent Glasser from the original data of Roy and Roy who gave results for the d_{642} spacing.

$C_{12}A_7$ can form halogenated derivatives and it has been proposed that this occurs by the complete or partial replacement of two oxygen atoms per cell by up to four univalent ions (11). In this work Jeevaratnam, Glasser and Dent Glasser noted the attraction of equating the replaceable oxygens with those which (according to the Büssem and Eitel structure) require to be distributed statistically. Reaction between calcium fluoride or chloride and $C_{12}A_7$ at 900°–1000°C gave isotropic products identified as $C_{11}A_7 \cdot CaF_2$ and $C_{11}A_7 \cdot CaCl_2$. On the other hand calcium bromide did not react. The new compounds appear to be based on the $C_{12}A_7$ structure with cell contents $C_{24}Al_{28}O_{64}X_4$ where X is F or Cl (the cell contents of $C_{12}A_7H$ by analogy are consequently $C_{24}A_{28}O_{64}(OH)_4$). Substitution of oxygen by halogen in the $C_{12}A_7$ lattice caused progressive increase in cell volume until the equivalent of two oxygen atoms per cell had been replaced. Further investigation of $C_{11}A_7 \cdot CaCl_2$ and $C_{12}A_7$ led these workers to doubt the Büssem and Eitel structure for the latter compound, serious discrepancies arising during the preparation of Patterson maps of both compounds.

It is certainly clear that $C_{12}A_7$ is an unusually interesting compound in which the lattice may be under considerable strain. Birefringent inclusions found in crystals of $C_{12}A_7$ (particularly when prepared under anhydrous conditions) may possible be visual evidence of this (12). The 6-oxygen co-ordination shell of the calcium atoms is evidently extremely irregular and the large structural holes together with the presence of several vacant sites in the lattice (which can be filled by suitable univalent ions) may be responsible for the rapid hydration characteristics and for the uptake of hydroxyl ion at high temperatures.

Pentacalcium Trialuminate, $5CaO \cdot 3Al_2O_3$

Rankin and Wright (4) reported two polymorphs of C_5A_3 in the $CaO–Al_2O_3$ system. The stable cubic form has since been assigned the formula $C_{12}A_7$ but the other "unstable" form, originally described as possibly orthorhombic, has later been the subject of much confusion.

It is now reasonably certain that a metastable C_5A_3 compound with the properties described by Rankin and Wright does exist; it is not the pleochroic material which appears as fibres or laths in certain aluminous cements, and it is not a high-temperature polymorph of $C_{12}A_7$ (14).

An examination by Aruja (15) of single crystals prepared on a hot-wire microscope confirmed the C_5A_3 formula (18) and the orthorhombic symmetry. The until cell contained four molecules and had the following parameters.

$a = 10.975$, $b = 11.250$, $c = 10.284$ (±0.005Å)

Probable space-group $C\,222_1$ Density 3.06–3.03 g/cc.

The structure was not further determined but Aruja noted points of similarity to gehlenite, C_2AS. The latter compound has $Si_2O_7^{6-}$ groups in the lattice while orthorbombic C_5A_3 may be based on $Al_2O_7^{8-}$ groups.

Majumdar (16), in work on ternary $CaO–Al_2O_3–MgO$ compounds, noted that the *a* dimensions of the cells were all simple multiples of about 5.5Å. Since the *b* and *c* dimensions were almost identical, the unit cell of the relevant compounds appeared to be built up of blocks having the approximate volume $5.5 \times 10.75 \times 5.13$Å.

A possible similarity in basic structure can be noted in the case of orthorhombic C_5A_3 and Midgley (17) has suggested that this compound is best represented by the constitutional formula $Ca_5Al_2(Al_2O_7)_2$ with the cell containing two layers viz:

A A ⟶ *a* (doubled)
A A *b*

The structure could therefore be represented by

$$\begin{array}{cccc} A & Y & Z & A \\ A & Y & Z & A \end{array} \begin{array}{l} \longrightarrow a \\ \downarrow b \end{array}$$

where A = Al_2O_7, Y = Ca and Z = vacant site. Three calcium atoms lie between the Al_2O_7 groups and four calcium atoms between the layers.

Majumdar and Smith (14) were not able to form C_5A_3 from melts having compositions between C_5A_3 and $C_{12}A_7$, by cooling slowly to 1000°C and then quenching, but they were able to grow C_5A_3 crystals by the hot-wire technique of Welch as described by Aruja. They never obtained orthorhomic C_5A_3 alone, or from melts of C_5A_3 composition, although it could be grown from a $C_{12}A_7$ melt. Melts with compositions bordering the $C_{12}A_7$ composition may yield orthorhombic C_5A_3 essentially, when cooling takes place in an anhydrous atmosphere (12).

C_5A_3 melts incongruently in air at 1361°C and at 1352°C in dry argon. The corresponding melting-points of $C_{12}A_7$ are 1392°C and 1374°C and it would seem that orthorhombic C_5A_3 must be metastable to $C_{12}A_7$ near its melting-point. It crystallises from melts in tabular form and the refractive indices are

$$\alpha = 1.680,\ \beta = 1.682,\ \gamma = 1.685 \text{ (17)}$$

Monocalcium Aluminate, $CaO \cdot Al_2O_3$

The structure of CA was investigated by Heller (19) but, as she had to work with a twinned crystal, the resolution of crystal structure was only partial. Further examination by Dougill (20) of fragments cut from large single-crystals gave initial data reasonably similar to those reported by Heller.

The cell dimensions were $a = 8.69$, $b = 8.09$, $c = 15.21 \pm 0.02$Å, $\beta = 90°8'$. Space-group $P2_1/n$. Slightly amended dimensions have since appeared (21). The observed density was 2.96 g/cc. against a calculated density of 2.94 g/cc. indicating Z = 12.

CA is structurally related to β-tridymite by substituting all the silicon atoms of the latter with aluminium atoms. This produces an unusual three-dimensional arrangement of linked tetrahedra which was illustrated in this work by the pseudo-hexagonal b-axis projection. The general β-tridymite framework is strongly distorted by the large calcium ions which are accommodated in cavities. While two of the three types of calcium ions are co-ordinated by six oxygens in an octahedron (Ca–O distances 2.31–2.72Å) the third calcium is surrounded by nine oxygens (Ca–O distances 2.36–3.17Å). The earlier structure of Heller had proposed 6-co-ordination for two of the calciums but 7-co-ordination for the third type. Of the nine oxygens just mentioned, six (each shared by two calciums) from an elongated octahedron giving a continuous chain in the b-direction. The remaining three oxygens lie in the plane at right-angles to the chain at greater Ca–O distances, and Al–O–Al angles in the pseudo-hexagonal direction have an average value of 132°, others being about 120°. The atomic co-ordinates for CA have been reported by Jeffery (21).

Pure CA forms prismatic or irregular grains which, although monoclinic are frequently pseudo-hexagonal. It is biaxial negative, 2V = 36°, the refractive indices being

$$\alpha = 1.643,\quad \beta = 1.655,\quad \gamma = 1.663$$

Uniaxial interference figures previously reported have not been fully confirmed and such anomalous figures may possibly be due to spherulitic quench growths (1). Twinning is very frequent, indeed characteristic, and an example of multiple twinning is shown in Fig. 3 (22).

The melting-point of Ca was thought to be congruent but high-temperature microscopy by Welch and by Auriol, Hauser and Wurm has revealed that it melts just incongruently at 1602° ± 5°C to CA_2 and liquid (1).

Pure, well crystallised, CA hydrates more slowly than the more basic calcium aluminates and produces high mortar or concrete strengths. Taylor (23) has noted that in CA there are no "free" oxide ions linked only to calcium, since every oxygen is bonded to two aluminium ions as well as to calcium. The reactivity to water cannot therefore be so explained but, as with all the other more basic calcium aluminates CA appears to exhibit irregular cation co-ordination, leading no doubt to high lattice energy.

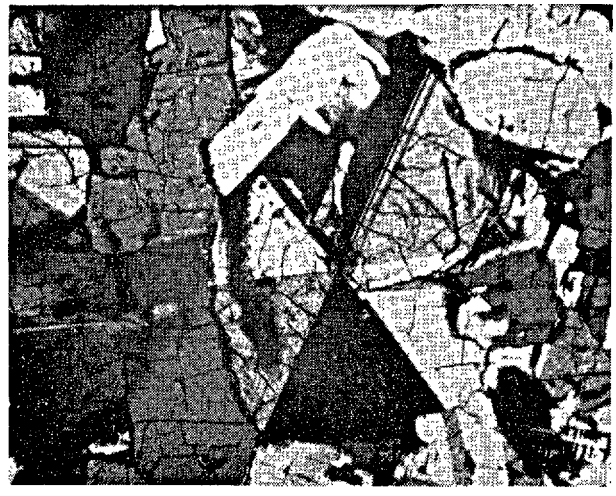

Fig. 3. *Monocalcium aluminate hexa-twin (22) (crossed nicols. ×60)*

Calcium Dialuminate, $CaO \cdot 2Al_2O_3$

Of the two polymorphs of C_3A_5 described by Rankin and Wright (4) the unstable form has never since been confirmed. The stable form of C_3A_5 was given the formula CA_2 in 1935 by Tavasci (24) who found the same optical properties as Rankin and Wright. This C/A ratio was confirmed by Lagerqvist, Wallmark and Westgren, and by several workers in Russia, Japan, Italy, U.S.A. and England.

Lagerqvist, Wallmark and Westgren (25) determined that the compound was monoclinic with $a = 12.82$ Å, $b = 8.84$ Å, $c = 5.42$ Å and similar values for the cell dimensions were found by Goria and Burdese (26) who placed CA_2 in the space-group C_2^6H.

Up to this time most investigators had to report that CA_2 was uniaxial positive but, after a detailed study of CA_2 and the isomorphous SrO_2, Boyko and Wisnyi (27) found that it was biaxial positive with $\alpha = 1.6178$, $\beta = 1.6184$, $\gamma = 1.6516$, $2V = 12°$. The negligible difference between α and β explained why this had not been previously resolved. For the unit cell, Boyko and Wisnyi gave $a = 12.897$ Å, $b = 8.879$ Å, $c = 5.454$ Å, $\beta = 107°3'$. The density of 2.86 g/cc. was rather lower than that of earlier studies. The space-group is $C2/c$, $Z = 4$.

In CA_2 the Al atoms are again tetrahedrally co-ordinated by oxygen. Three tetrahedra share one oxygen at the common corner and the Ca atoms are asymmetrically co-ordinated with five Ca–O bonds much shorter than the other four.

CA_2 grows from melts as strongly birefringent needles or laths but can also appear as rounded grains. There has been little agreement in the past over melting-point, the values having varied from 1720°–1790°C, and opinion has been equally divided on whether the melting-point was congruent or incongruent. The most recent work indicates that it is definitely incongruent giving CA_6 and liquid. Welch (28), Rolin and Pham Huu Thanh (29), Auriol, Hauser and Wurm (30) and Nurse, Welch and Majumdar (1) have reported values of 1789°, 1780°, 1770° and 1762° ± 5°C respectively, and in Fig. 4 CA_2 is shown to melt incongruently at about 1765°C.

CA_2 hydrates very slowly and it was considered that it might be hydraulically inert at ordinary temperatures if completely pure. Buttler and Taylor (31) showed that CA_2 did react slowly with water even at 5°C and the reaction is faster at higher temperatures and at higher pH values. At ordinary temperatures the reaction, once started, may therefore become self-accelerating.

The presence of very small amounts of alkali metal ion in this compound could obviously have a very marked effect on the rate of reaction with water at atmospheric temperatures and it remains doubtful whether CA_2 has yet been prepared in a form sufficiently free from Na^+ to allow one to be certain about the behaviour of the "pure" compound.

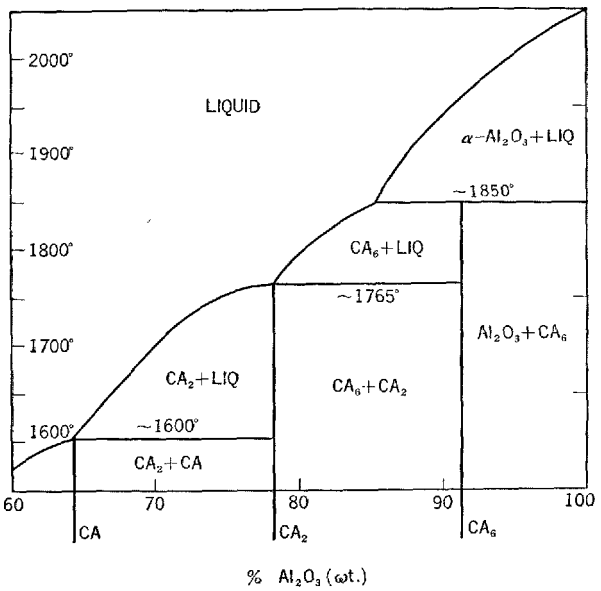

Fig. 4. *High alumina part of* $CaO–Al_2O_3$ *system*

Calcium Hexa-Aluminate $CaO \cdot 6Al_2O_3$

Lagerqvist, Wallmark and Westgren (25) first reported a new compound at the higher alumina end of the $CaO–Al_2O_3$ system and assigned the formula C_3A_{16}. The compound was hexagonal and appeared isomorphous with β-alumina (NA_{11}).

Adelskold (32) supported by Toropov and Stukalova (33) confirmed the cell dimensions given by the above workers ($a = 5.536$, $c = 21.825$ Å) but considered that the compound was CA_6 and that it was isomorphous with magneto-plumbite ($PbO \cdot 6Fe_2O_3$). In 1949 Filonenko confirmed the existence of CA_6 in the $CaO–Al_2O_3$ system and, in further work with Lavrov the same year (34), amended the $CaO–Al_2O_3–SiO_2$ phase-diagram to include a stable field for this compound.

However, as late as 1963, Gentile and Foster (35) pointed out that acceptance of Filonenko's work was by no means general on the part of American investigators—some of whom regarded CA_6 as a metastable phase and failed to allot any stable field. Mohanty (36) and others (30) had also reverted to the original formula C_3A_{16}, claiming that free alumina could be

found in melts having the composition CA_6. Nevertheless, the work of Gentile and Foster confirmed the existence of a stable compound CA_6 and, in general, confirmed the findings of Filonenko and Lavrov.

The compound has hexagonal symmetry with the cell parameters as given above. There are two molecules in the unit cell, the space-group being $P6_3/mmc$. The structure has strong similarities to that of β-alumina (NA_{11}) and magnetoplumbite but details remain to be agreed.

The optical properties are sufficiently close to those of corundum to cause confusion since it crystallises as perfect hexagonal plates, uniaxial negative, $\omega = 1.759$, $\epsilon = 1.667$ (34) Buist (37) has recently given $\omega = 1.755$, $\epsilon = 1.763$ (in white light) for pure CA_6 prepared by sintering for an hour in argon at 1850°C.

The melting-point of CA_6 has been found incongruent by all investigators, but considerable differences exist between the actual values which range from 1833° ± 15°C (1) to 1870° ± 10°C (37). In Fig. 4, CA_6 is shown to melt incongruently at about 1850°C, but although the general form of this diagram is probably correct in showing incongruent melting of CA, CA_2 and CA_6, further re-examination of the exact melting points of CA_2 and CA_6 is called for. The melting-point of α-alumina has been placed at 2050°C but again there remains much controversy about the exact value, which may be as high as 2070°C or as low as 2040°C.

CA_6 is harder than any other calcium aluminate and does not appear to hydrate in water.

Aluminous Cement Clinker

Before proceeding to an examination of the aluminates and related compounds which may be present in a clinker, it is necessary to give some account of the various manufacturing processes, and of the different raw materials used, since these can have a very marked effect on the constitution of the product.

The major cementitious component in clinker is always the monocalcium aluminate, CA, but the commercial cements from various countries show a remarkably wide range of chemical composition. In certain cases additions to the clinker (during or after grinding) may contribute to this diversity but, even without this, the clinker analyses still cover a much broader range than is usual in the portland cement field.

Types of Cement and Their Manufacture

Nearly all the cements in commercial manufacture today can be included in one or other of the four categories given in Tabe 2, where the classification is based on chemical analyses and methods of manufacture. The variable appearance and chemical composition of these types are due either to the nature of the raw materials (in particular the source of the alumina required for the formation of CA) or to the method of clinker manufacture. In general, the final composition of the clinker is always arranged to produce the maximum amount of CA.

Type 1. By far the largest proportion of world production consists of this type, the raw materials being limestone and red ferruginous bauxite, which is the most widely distributed economic source of alumina. A fusion process is almost invariably used to manufacture Type 1 clinkers and they contain all the non-volatile constituents of the raw materials. The variable Al_2O_3/Fe_2O_3 and Al_2O_3/SiO_2 ratios in diverse, but suitable, red bauxites is therefore responsible for the range of total iron oxide and silica contents found in the clinkers.

During fusion, part of the Fe_2O_3 present is reduced to FeO and the ferrous compounds impart to Type 1 clinkers their characteristic dark colour. The precise colour shade depends on the total iron oxide content and the Fe_2O_3/FeO ratio and, to some extent, the lime content. The small amount of Type 1 cement which is made by sintering these raw materials remains more highly oxidised and therefore may have a brown-rust colour.

Table 2. *Main types of high-alumina cement*

Type	Colour	Al_2O_3 %	Iron oxides as % Fe_2O_3	SiO_2 %	CaO %	Source of alumina	Process of manufacture
1	Grey to black	37–40	11–17	3–8	36–40	Red bauxite	Fusion
2	Light-grey	48–51	1–1.5	5–8	39–42	Red bauxite	Reductive fusion with removal of Fe metal
3	Cream or light-grey	51–60	1–2.5	3–6	30–40	'White' bauxite	Sintering clinkering fusion
4	White	72–80	0–0.5	0–0.5	17–27	Alumina	Sintering clinkering

Type 2. Such cements are made from essentially the same raw materials as Type 1 but during fusion the iron oxide in the bauxite is reduced to metallic iron which is then separated. The residual iron oxide (FeO) content of the clinker is low, although a small amount of residual iron metal is also found. Clinkers in this category may be produced in a blast furnace (38) or in a cupola (39) using coke as the reducing agent.

Type 3. The natural distribution of "white" bauxite is much more restricted than that of red bauxite but its much lower Fe_2O_3 content allows the production of low-iron Type 3 clinker by direct fusion, sintering or clinkering with a pure limestone. The sintering or clinkering process (40) is more common when, as in this case, the clinker contains less than about 5% Fe_2O_3, but completely fused cements of this type are also produced.

Type 4. Analysis of these cements reveals little apart from lime and alumina. The raw materials are pure limestone and alumina of (at least) Bayer-process purity. The high melting-point of the clinker usually imposes a sintering or clinkering method of manufacture but fusion in an electric furnace may be justified in certain countries. The virtual absence of titania from the analysis distinguishes this type from all the others—which employ some kind of bauxite as a raw material. The clinkers produced in this group differ mainly in the proportion of CA_2 which may be present with the CA.

Manufacture from Other Raw Materials or by Other Processes

A full appraisal of methods of manufacture and of possible raw materials has been given elsewhere (41) but some continuing interest has been shown in the simultaneous manufacture of calcium aluminate clinker and yellow phosphorus.

In the electric-furnace reduction process for phosphorus, a mixture of aluminium phosphate, calcium phosphate or lime, and coke has been substituted for the normal furnace charge (42) and this resulted in the production of an aluminous cement slag. Ablichenkov and Postnikov (43) similarly investigated an electric-furnace reduction method employing phosphate rock, or apatite concentrate, together with bauxite or titania-alumina slags (derived from the production of ferro-titanium). The use of apatite concentrate and a titania-alumina slag appeared to give greater productivity and saving in electricity.

Other claims have recently been made for the reductive fusion of bauxite and phosphates (44) and

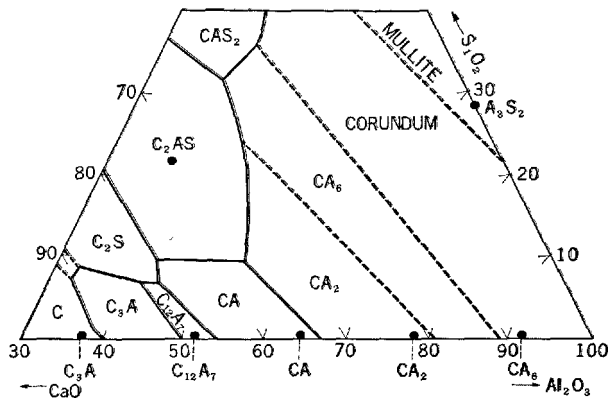

Fig. 5. *Part of* $CaO–Al_2O_3–SiO_2$ *phase diagram*

for the use of a rotary kiln in treating a mixture of calcareous and aluminous materials containing phosphates (45). However, it seems that there has been little or no commercial manufacture by any of the above processes.

In the U.S.S.R. aluminous cement compositions have also been made by adding more alumina to the molten lime-alumina slag used in steel-refining (46). The aluminous materials added to the converter for this purpose are bauxite or the titania-alumina slag mentioned above (47). The latter material has also been directly fused with limestone (instead of steel slag) in order to yield an aluminous cement clinker (48).

Clinker produced by many of the above processes would contain constituents not present to any significant extent in those made by usual methods (e.g. chromium, vanadium, manganese, fluorine etc.). In other cases greatly increased percentages of titania and alkali might result and therefore the properties of such cements need not be similar in all respects to those of the customary types. However, advantages have been claimed (48) for cements containing substantial proportions of certain metal ions such as Cr^{3+}, Mn^{3+} and Ti^{3+}.

Calcium Aluminates in Clinker

The $CaO–Al_2O_3–SiO_2$ phase diagram, which is relevant for aluminous cements containing little or no iron oxide, has undergone some change in recent years. The general outlines of the necessary part of this diagram are as shown in Fig. 5 which represents the position after the inclusion of a stable field for CA_6 but before it was accepted that CA and CA_2 melted incongruently.

Further work by Gentile and Foster (35) on CA_6

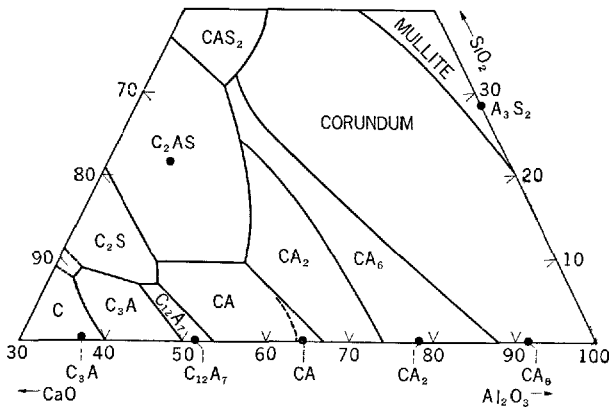

Fig. 6. *Part of* $CaO–Al_2O_3–SiO_2$ *phase diagram (as amended by Gentile and Foster)*

in this system led to a considerable reduction in the area of the CA_6 field since they placed the anorthite—CA_6—corundum invariant point at 28% CaO, 39.7% Al_2O_3, 32.3% SiO_2 and at a temperature of 1405° ± 5°C. Filonenko and Lavrov (34) (to whom Fig. 5 is largely due) had previously located this point at 23% CaO, 41% Al_2O_3, 36% SiO_2 and at 1495° ± 5°C.

The altered character of the diagram produced by Gentile and Foster is shown in Fig. 6 and this requires a small further change (indicated by the dotted line amendment of the CA field) to allow for the incongruent melting of CA.

It will be seen that the field of $C_{12}A_7$ has been retained in the ternary diagram although Fig. 2 omits it from the $CaO–Al_2O_3$ system. In the furnaces used for clinker manufacture the atmosphere is always humid and the anhydrous conditions represented by Fig. 2 do not apply. Accordingly the phase assemblages found in practice agree more closely with those indicated by the ternary diagram or by Fig. 1. An additional reason for this is the great rapidity of crystal growth of $C_{12}A_7$. The maximum linear rate of growth found by Scholze and Kumm (49) was 8700 μ per minute and, although 1% additions of CaO, Al_2O_3, K_2O, SiO_2 or Fe_2O_3 decreased this rate by varying extents, it is clear that crystal growth is much faster with $C_{12}A_7$ than with any other calcium aluminate in comparable conditions. When nucleation occurs it is therefore probable that $C_{12}A_7$ will precipitate rapidly and may exclude the formation of other phases which might be more stable.

Consequently, C_3A is not a normal constituent of aluminous cements—especially those which have been completely fused and whose raw materials have been correctly compounded. However, in sintering or clinkering processes of manufacture, it is conceivable that some C_3A might be produced locally in the clinker or sinter, for example in any unusually large particle of lime. Particles of lime or alumina which are too large to reach chemical equilibrium under the specific kiln conditions may have a zoned structure after passage through the kiln and may contain aluminates other than those desired. Because of the number of different calcium aluminates, careful control of the maximum particle size of raw materials is a particularly vital factor in maintaining the correct mineralogical composition of sinters or of clinkers not wholly fused.

The solid-state reaction between lime and alumina has been studied by numerous investigators without final agreement on its mechanism. Adouze (50) and de Keyser (51) included unstable C_5A_3 among the reaction products and this renders their work difficult to interpret since it is no longer thought that this compound is formed in these conditions. Adouze found that CA was first formed at 900°C and $C_{12}A_7$ at 950°C, while de Keyser also concluded that CA had a tendency to form as first product. Mchedlov-Petrosyan and Babushkin (52) predicted that $C_{12}A_7$ will form preferentially at temperatures below 1000°C, but that it ceases to be an important non-equilibrium product above 1100°C. They also believed that C_3A will not form directly from lime and alumina but only by reaction of $C_{12}A_7$ with lime, while CA will form only by reaction of $C_{12}A_7$ with alumina. These conclusions were not confirmed to any substantial extent by Williamson and Glasser (53) who investigated compositions corresponding to all the calcium aluminates and who showed the critical effect of particle size upon the time taken to reach equilibrium. The most recent work on this reaction seems to lend support to the findings of Uchikawa, Tsumagari and Koike (54) who found that C_3A was formed preferentially at 800°–1000°C, whatever the initial proportions of lime and alumina. However, until there is more standardisation of the particle size of raw materials, differences in interpretation of results will continue. Somewhat different conclusions may also be reached according to whether the materials are heated in a static condition or in motion (as in a rotary kiln).

The proportion of $C_{12}A_7$ in a normal aluminous cement clinker is usually kept low since more than about 10% may cause unduly fast setting-times, and this effect is accentuated if, for any reason, the clinker contains more alkali ions than is customary. Like all other calcium aluminates, $C_{12}A_7$ can take Fe^{3+} ions into the lattice and therefore it is rarely found in a substantially pure form in the clinker. On the other hand Ti^{4+} enters the lattice in insignificant amounts.

Fig. 7. $C_{12}A_7$ (*probably* $C_{11}A_7 \cdot CaF_2$) *in calcium aluminate slag* (22) (*Plane polarised light.* ×22)

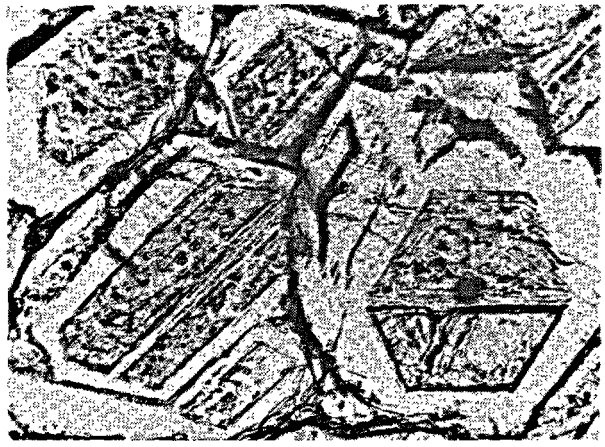

Fig. 8. *The compound* $3CaO \cdot 3Al_2O_3 \cdot CaF_2$ (22) (*Plane polarised light.* ×100)

When made by the process which simultaneously yields phosphorus, aluminous cement clinkers normally contain an appreciable proportion of fluorine, and refractive index determinations suggest that any "$C_{12}A_7$" in such clinkers may in fact be present as the $C_{11}A_7 \cdot CaF_2$ compound described by Jeevaratnam, Glasser and Dent Glasser (11). The refractive index of $C_{11}A_7 \cdot CaF_2$, as found by the latter, was $n = 1.601$ which must be compared with $n = 1.611$ for $C_{12}A_7$ and $n = 1.620$ for $C_{12}A_7H$. An investigation by Leary (22) of "$C_{12}A_7$" in aluminous slag from the phosphorus process showed that its refractive index was 1.602 ± 0.002 (see Fig. 7).

CA crystallises readily from the fused clinker composition and, even when the cooling process is relatively rapid, the compound appears as quite large prismatic crystals, often in a dendritic arrangement and inter-grown. Twinned crystals with opposite extinctions are very frequent and, when a comparison is made with the pure compound, an increase in refractive index and a reduction in axial angle are usual. If the clinker contains any appreciable amount of iron oxide, some is always taken up by the CA. In any given clinker the amount taken up by CA is remarkably constant throughout, but in different clinkers the degree of substitution by iron varies directly with the ferric oxide content (55), lending support to the belief that it is primarily Fe^{3+} which is involved. In many Type 1 clinkers (which have high iron oxide contents) the substitution in CA approaches the limit concentration of 4.5% Fe found by Dayal (56) in work on the CaO–Al_2O_3–FeO–Fe_2O_3 system. It is therefore clear that CA may take up a considerable part of the total ferric oxide present in Type 1 clinkers. In addition, an examination of CA crystals in commercial clinker by the scanning micro-probe has revealed the presence of many small inclusions of the ironbearing interstitial material (55). Micro-probe images of the clinker itself have been shown by Crussard (57) and these reveal the general distribution of Al, Si, Ca, Ti and Fe across the surface of a clinker fragment.

An interesting new compound (believed to be $3CaO \cdot 3Al_2O_3 \cdot CaF_2$) has been identified by Leary (58) in calcium aluminate slag produced in the phosphorus process. The compound has hexagonal symmetry with

$$a = b = 17.29, \quad c = 7.01 \text{ Å}$$

Experimental density 2.96 g/cc. Theoretical 3.03 g/cc.

The X-ray diffraction data were also determined by Leary. The crystals, uniaxial negative with refractive indices $\omega = 1.628$, $\epsilon = 1.618$, are shown in Fig. 8.

The fluorine in this compound is quite labile at high temperatures and subsequent attempts to repeat the synthesis by heating CaO, Al_2O_3 and CaF_2 at 1340°C for four hours were not successful, the product being $C_{12}A_7$, CA and some CA_2 (59). However other workers found that $3CA \cdot CaF_2$ (together with some $C_{12}A_7$) could be produced by heating the appropriate composition for a much shorter time (30 mins.–1 hour) at 1400°C. Longer heating at higher temperatures released fluorine; for example after heating for 6 hours at 1450°C the composition retained only 2% fluorine whereas $3CA \cdot CaF_2$ should contain 6.38% (60). After adapting a high-temperature D.T.A. technique to deal with systems containing a volatile constituent, Gutt (61) found that the compound appears to melt congruently at $1505° \pm 2°C$ which confirms the original value of $1507° \pm 2°C$ given by Leary. When $3CA \cdot CaF_2$ was ground to cement fineness, Leary found that it set and hardened giving

excellent mortar strengths at one day. The setting-time was greatly affected by water-cement ratio and there was always a very long delay between initial and final sets. This behaviour is possibly what would be expected if the compound progressively dissociates into CA and CaF_2 during hydration.

The presence of CA_2 in Type 1 and Type 2 clinkers is not general and is usually due to non-equilibrium conditions existing locally in the melt, for example in the vicinity of a bauxite-lump residue. On the other hand, CA_2 may be a common constituent of some Type 3 and Type 4 clinkers. Dayal (56) found that CA_2 could take up iron oxide to a limit of 5.7% Fe, but this limit is apparently not closely approached in the CA_2 occurring in commercial clinkers. The hydration of CA_2 is accelerated when it takes place in company with that of CA but, even then, it is not sufficiently rapid to make any appreciable contribution to 1-day mortar or concrete strengths at atmospheric temperatures. It has been claimed that the inclusion in the lattice of certain trivalent ions (such as Cr^{3+}, Mn^{3+}, Ti^{3+}, and Fe^{3+}) increases the rate of hydration to the extent that CA_2 no longer behaves essentially as inert material during the earlier stages of concrete hardening (48). It would certainly appear that the hydration of CA containing Fe^{3+} is rather faster than that of the pure compound, and the same may apply to CA_2. The effect of "alien" ions in the lattice on hydration rate, and on the concrete strength produced by calcium aluminates, is a subject requiring much further investigation. The possibilities include not only some increase in the activity of compounds such as CA_2 but also (possibly by retardation of hydration) an increase in the hydraulic strength given by compounds such as $C_{12}A_7$.

Complete hydration of CA_2 can be achieved quite rapidly in the autoclave and investigators, chiefly in the U.S.S.R., have found that under such conditions it yields higher strengths than CA (62). It has been suggested that the superior properties of hydrated CA_2 are due to the relief of internal stresses through the agency of the boehmite which is produced during hydration (63). However, Robson (64) has given a different explanation, based on the relative void-filling capacities of the products of hydration of CA and CA_2, and has predicted that refractory castables, made with a CA_2 cement and then autoclaved, will retain a particularly high strength after firing to furnace temperatures.

Calcium hexa-aluminate (CA_6) is not found as a constituent of aluminous cement. The solid-state reaction of lime and alumina to form this compound is slow to reach equilibrium, particularly if much Na^+ ion is present in the raw materials. The synthesis of CA_6 in this way may therefore require more than one firing with intermediate re-grinding. It can be formed *in situ* when refractory castables, compounded of Type 4 cements and alumina aggregate, are heated to high temperatures in service, and Buist (37) has detected it in the immediate hot-face zone of high-alumina bricks serving in electric-arc furnace roofs. In this case a 12–13% atomic replacement of Al^{3+} by Fe^{3+} had occurred in the CA_6, giving an increased refractive index, reflectivity, and hardness. Dayal and Glasser (65), in a study of the CaO–Al_2O_3–Fe_2O_3 system, have shown that up to 40% replacement of Al^{3+} by Fe^{3+} can occur in CA_6.

The compound does not hydrate in water at ordinary temperature and is probably still inert at higher temperatures, although the behaviour of impure forms in the autoclave does not appear to have been fully investigated.

Some Other Clinker Phases

The Quaternary Compound

In cements such as those of Type 1, which contain substantial quantities of ferrous as well as ferric oxide, a strongly pleochroic material in the form of fibres or long laths is frequently observed. Although the amount present in a normal clinker should be small, special conditions of composition and furnace atmosphere may produce clinkers in which this material occurs to the exclusion of nearly all the CA.

As early as 1924 Dyckerhoff (66) noted its appearance in clinker and believed that it might be the unstable C_5A_3 compound reported by Rankin and Wright (4). At the Stockholm Symposium (1938), Sundius gave the results of work on crystals which had been carefully separated from a suitable clinker and analysis showed that oxides other than lime and alumina still remained in, or on, the crystals (67). Sundius treated such oxides as impurities in a calcium aluminate, but Parker (1952) stated that the pleochroic phase was definitely not the "unstable C_5A_3" and that it probably was a compound containing CaO, Al_2O_3, FeO and SiO_2 (68) Parker and Ryder had found a quaternary compound, of probable composition C_6A_4MS, with a primary phase field in the CaO–Al_2O_3–MgO–SiO_2 system and, by analogy, the pleochroic material in aluminous cement clinker might be C_6A_4fS (where f = FeO).

The magnesian compound and its ferrous "analogue" were crystallographically very similar but later work by Midgley and Gross (1952) (17) showed that

it was impossible to reconcile the C_6A_4MS formula with the unit cell volume and experimental density of a powder of that composition. High-temperature microscopy by Welch of C_6A_4MS compositions also failed to confirm that they yielded a single phase but he did discover two new ternary compounds (which had optical properties similar to C_6A_4MS) in the CaO–Al_2O_3–MgO system (69), and deduced that C_6A_4MS might really be a solid solution of one of these ternary compounds and gehlenite. However, later work by members of the same group including Nurse, Welch, and Majumdar indicated that "C_6A_4MS" was indeed a separate compound but again proved that it could not have that particular formula.

Majumdar (16), as was noted when previously discussing orthorhombic C_5A_3, found that the quaternary magnesian compound, the two ternary magnesian compounds, orthorhombic C_5A_3, and gehlenite all had cells which appeared to be composed of subcells of approximate volume $5.5 \times 10.75 \times 5.13$ Å, although he stressed that no evidence of such subcells was revealed by single-crystal X-ray photography. Although the orthorhombic C_5A_3 contained $Al_2O_7^{-8}$ groups the ternary and quaternary magnesian compounds were expected to have mixed groupings i.e., not exclusively X_2O_7 groups.

The most recent work by Midgley (17), who has examined the pleochroic compound from clinker (as well as the magnesian compounds) with the X-ray electron microprobe analyser, has given much further understanding of the nature of these compounds and has led to a proposed structure for the quaternary compound in clinker.

The sample of the latter material used in this work consisted of needles with straight extinction, negative elongation, refractive indices $\alpha = 1.676$, $\gamma = 1.680$, $2V = 40°$ positive, strong dispersion $v > r$. Experimental density $= 3.14$ g/cc. $a = 33.1$, $b = 11.0$, $c = 5.14$ Å.

Midgley determined a constitutional formula of $Ca_{22}Al_{35}Fe_3^{+}Si_2O_8$ (Molecular weight = 3302.41) with one formula unit to the cell. This formula can be written $Ca_{22}Fe_3^{+}Al_{14}(Al_2O_7)_8(AlO_4)_4(SiO_4)_2$ and the structure can be visualised as four layers of $2(Al_2O_7)$ groups and two layers of $3(XO_4)$ groups (where X is either Al or Si). The resulting six layers bring the a axis to $6 \times 5.5 = 33.0$ Å which is very close to the observed 33.1 Å. The packing arrangement is represented as follows:

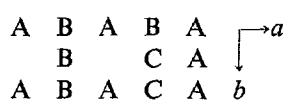

where $A = Al_2O_7$, $B = AlO_4$ and $C = SiO_4$.

Rows of three calcium atoms fit between each layer of Al_2O_7 and XO_4 groups while rows of aluminium atoms occur between the Al_2O_7 and XO_4 groups. Four calcium atoms and three iron atoms fill alternate spaces between the Al_2O_7 groups leaving one vacant site.

All the magnesian compounds were also found to be mixed layers of $2(Al_2O_7)$ groups and $3(XO_4)$ groups, and the formula of the quaternary "C_6A_4MS" compound could be given as $CA_{35}Mg_4Al_{24}(Al_2O_7)_8(AlO_4)_{13}(SiO_4)_5$.

It is clearly not a magnesian analogue of "pleochroite"—the quaternary compound occurring in aluminous cement clinker.

The Iron-Bearing Phases

The mineralogical constitution of the clinker of aluminous cements which contain little iron oxide can often be deduced with satisfactory accuracy from the Al_2O_3–CaO–Fe_2O_3 phase diagram. In such cases the manufacturing process employed evidently allows a

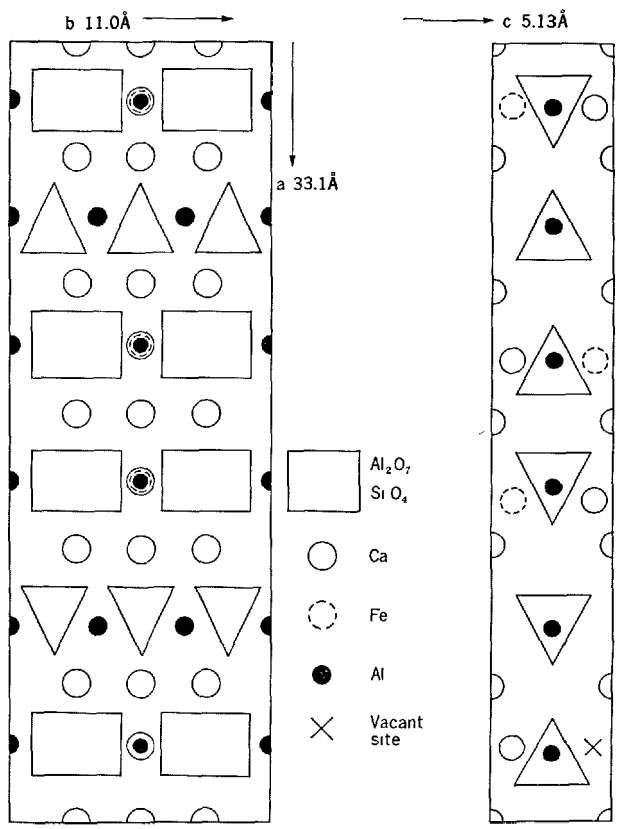

Fig. 9. *Possible structure of "Pleochroite" (after H. G. Midgley (17))*

close approach to equilibrium conditions. However, in the more general Type 1 cements, the nature and distribution of the iron-bearing phases (which are an important part of the whole) have not been known with reasonable certainty. Accordingly, calculation of the compounds present (from the chemical analysis) has never been consistently successful.

Parker (68) pointed out that FeO (wüstite) can be a final crystallization product in such cements and that the ratio Fe_2O_3/FeO cannot be predicted accurately. He suggested an analytical procedure followed by a method of calculation intended to allow for the presence of FeO as a separate phase and also for the presence of the pleochroic quaternary compound (at that time considered to be C_6A_4fS). It has been found with many clinkers that this method gives greatly exaggerated values of the amount of quaternary compound (70) and the search for a suitable method, applicable to a fairly wide variety of clinker types, still continues.

In the manufacture of Type 1 clinkers by fusion of limestone and red bauxite, process control is directed towards achieving a "standard" clinker and it is of interest to examine the constitution of such a clinker resulting from the successful application of certain manufacturing principles. Microscopic examination would show a "standard" clinker to consist of well-defined crystals of CA, a small amount of β-C_2S (usually as small rounded granules) and an appreciable quantity of iron-bearing interstitial material. $C_{12}A_7$ is not detectable or is present in small amount. Pleochroic needles or laths are similarly absent or exist in minimal quantities since their formation is avoided as far as possible during manufacture. Limits placed on the silica content of the melt prevent the formation of much C_2AS and CA_2 is normally absent. When the clinker is cooled fairly slowly there is very little true glass present.

Thus the constitution of the "standard" clinker is superficially simple and the interstitial matter can be broadly sub-divided into three types according to reflectivity capacity. The least abundant type, with the greatest reflectivity, is essentially wüstite but variable amounts of Fe_2O_3 may be present and it may be quite strongly magnetic. Areas of least reflectivity occur in the greatest abundance and the other areas are of intermediate reflectivity and abundance. The two latter types of material are classified as calcium aluminoferrite solid solutions with compositions on the join between C_2F and "C_2A", and X-ray diffraction studies indicate that, in this clinker, both have the general composition $C_{10}A_4F$ (55). This implies a higher concentration of C_2F in the solid solutions than had previously been accorded, but confirms the postulation of Cirilli and Abbatista (71).

A study of the two calcium aluminoferrite solid solutions in clinker has recently been made with the scanning electron micro-probe and several interesting observations resulted (55). It was found that, although the two phases contained substantially the same content of Al, Si and Ca, the difference in reflectivity was paralleled by a difference in Ti content.

In effect one molecule of Fe_2O_3 could be substituted by two molecules of TiO_2 and the solid solutions could be represented as (1) iron-rich $C_{10}A(0.9F \cdot 0.2T)_4$ and (2) titania-rich $C_{10}A(0.4F \cdot 1.2T)_4$. Substantially all the titania in this clinker was present in the calcium aluminoferrite solid solution and no perovskite was detected. It will be remembered that Sundius (67) found perovskite only in high-silica low-iron aluminous cements. An appreciable part of the SiO_2 also enters the aluminoferrite solid solution thus reducing the visible C_2S content of the clinker.

A comparison of an iron-free aluminous cement with one which contains a relatively high iron content demonstrates that the iron-containing clinker phases can make a substantial contribution to mortar and concrete strengths. Butt, Timashev and Paramonova (72), in an examination of several calcium aluminoferrite compositions, found that those possessing the greatest hydraulic activity were $C_{7.4}AF_{2.3}$, and $C_{4.9}AF_{1.3}$, which does not strongly support the idea that the hydraulic activity of the solid solution series increases with alumina content. These workers investigated the effect on various calcium aluminoferrite compositions of reduction in a hydrogen atmosphere and found that complete decomposition into CaO $3C_3A$, FeO and Fe occurred at high temperatures (1400°–1500°C). On the other hand incomplete reduction at 400°C, with much substitution of Fe^{2+} for Fe^{3+}, gave increased hydraulic activity which, it was suggested, might be due to the appearance of lattice defects and vacant sites.

Many manufacturing processes for aluminous cement allow reduction of Fe^{3+} to Fe^{2+} but it is not known whether this could occur at the time of formation of the calcium aluminoferrite phases. However it is interesting to speculate whether this action could be responsible for creating a more active solid-solution in the clinker.

The System CaO–Al_2O_3–SO_3

Zinsen (73) in 1943 suggested that the break-down of boiler-slag was due to the hydration of a compound

$C_3A \cdot 3CaSO_4$. However the existence of a ternary anhydrous compound in the system $CaO–Al_2O_3–SO_3$ was not generally accepted until very much later, e.g. in 1952 it was reported (74) that no ternary compound had been found in the clinker prepared as the expansive component for the cements developed by Lossier (75).

Ragozina (1957) claimed to have isolated a ternary compound in this system and, as a result of later work with Ahmedov (1962) finally assigned to it a formula corresponding to $3CA \cdot CaSO_4$ (76). In the interim period Klein and Troxell (77) examined clinkers prepared by firing aluminous and calcareous materials with gypsum and deduced from the X-ray diffraction pattern that an anhydrous calcium sulpho-aluminate was present. They estimated, from the oxide compositions, that the new compound might be $C_4A_2 \cdot CaSO_4$ or $C_8A_4 \cdot CaSO_4$, but Fukuda (78) in 1961 gave the formula $3CA \cdot CaSO_4$ to a ternary anhydrous compound which was found as the major constituent in clinkers obtained by firing mixtures of lime, bauxite and gypsum at 1350°C.

The work of Halstead and Moore (79) confirmed that the compound was $3CA \cdot CaSO_4 (4CaO \cdot 3Al_2O_3 \cdot SO_3)$ and that it seemed to be the only ternary compound in the system $CaO–Al_2O_3–SO_3$ below 1350°C. Crystallographic data indicated that it was identical with the compound detected by Kelin and Troxell, and by Fukuda. It could be synthesised by heating the appropriate chemical composition in air for several hours at 1350°–1400°C.

The compound was isotropic with refractive index 1.57 and the cell was cubic, body-centred ($a = 18.39$ Å). The calculated density for cell contents of $16(Ca_4Al_6O_{12}SO_4)$ agreed with the experimental density of 2.61 g/cc. All the strong reflections could be indexed on a cubic cell with $a = 9.195$ Å which therefore indicated that the structure contained a prominent pseudo-cell with contents $2(Ca_4Al_6O_{12}SO_4)$. This pseudo-cell is comparable in size to the cells of sodalite and haüynite and it seems that the ternary compound could be regarded as an end-member of the sodalite-noselite-haüynite series in which all Si is replaced by Al and all Na by Ca atoms. Its constitutional formula would thus be $Ca_4(Al_6O_{12})(SO_4)$, and the space-group $I\bar{4}3m$ is compatible with the structure of the pseudo-cell.

The structure is made up of a three-dimensional continuous framework of polyhedra whose vertices are all occupied by Al replacing the Si present in the sodalite series. Oxygen atoms lie at about the centres of edges and those projecting from the vertices form part of adjacent units. The SO_4 tetrahedra are situated at the centre of each unit, possibly stabilising the $CaO–Al_2O_3$ lattice, and the calcium atoms lie at the centres of the hexagonal faces.

The melting-point of the compound in an open system was in the region of 1590°–1600°C and the stability of the structure at elevated temperatures is quite high since Halstead and Moore found that the loss of SO_3 from $CaSO_4$ at 1350°C was about thirty times that of SO_3 from $Ca_4(Al_6O_{12})(SO_4)$ at the same temperature. This suggested that it might be formed and retained in portland cement or aluminous cement clinkers when a high-sulphur fuel is used during manufacture, but the presence of the anhydrous ternary compound has not yet been reported in aluminous cement clinkers even when made by a sintering or clinkering process.

The compound reacts with water readily to give mainly calcium aluminate hydrates and the expansive component required for addition to portland cement clinker (to produce expansive cements) must contain additional lime and calcium sulphate (80). Mehta and Klein (81) for example showed that the molar composition which hydrates completely to give only ettringite is $6CaO \cdot Al_2O_3 \cdot 3SO_3$ and this would consist of 30% ternary compound, 53.5% $CaSO_4$ and 16.5% CaO. Clinkers containing $Ca_4(Al_6O_{12})(SO_4)$ together with additional lime and sulphate are ground with portland cement clinker (low C_3A content) to form the shrinkage-compensated cements which have been commercially manufactured for some time (82).

An interesting possible application for the ternary compound follows from the claim by Mehta (83) that its presence in a calcium aluminate cement will prevent the conversion of the hydrate CAH_{10} into the cubic C_3AH_6, under hot-wet conditions. Mehta found that monocalcium aluminate, mixed with 5% (wt.) of $Ca_4(Al_6O_{12})(SO_4)$ and initially hydrated at low temperature, contained only a small amount of C_3AH_6 even after prolonged storage under water at 38°C.

Possible Uses of Calcium Aluminates other than in Cements

For cements, monocalcium aluminate is made in considerable tonnages; in most cases the product is very impure but in others the clinker consists of relatively pure material. However very few industrial uses outside the cement field have yet been developed for any of the calcium aluminates.

Some interest has been shown in the properties of calcium aluminate glasses (84) which have been found to have a high refractive index and high infra-red transmittance. Such glasses can be stabilized against devitrification by the incorporation of alkali and iron ions and the transmittance value is further increased in such material by the addition of other elements such as manganese or copper (85). The resistance to moisture remains lower than that of normal optical glass but some protection can be gained by "blooming" the glass with MgF_2. Optical and physical properties have been reported (86) and several patents have been granted. A crystalline ceramic material has also been made by melting a composition containing 65–100 mol. % of $CA_{1.5}$, cooling below the liquidus temperature to form a glass, and then reheating above the annealing temperature to allow crystallization (87). A powdered calcium aluminate glass may be useful in preventing atmospheric hydration of shapes pressed from pure calcium oxide. The glass and granular lime were mixed and hot-pressed in a graphite mould at 1250°–1450°C (88).

Cookayne (89) has described a technique for the preparation of very large optically transparent single crystals of $C_{12}A_7$ and CA_2 and such crystals may be useful as host lattices for laser ions, particularly those of CA_2 (90).

It would appear that CA_6 is of interest for microwave applications. A small proportion of CA_6 in alumina increases the ambient temperature microwave permittivity and loss tangent (91). The use of CA_6 as an aggregate for refractory castables has also been proposed. The aggregate is prepared by firing a 6:1 molar ratio of lime and alumina at 1150°–1815°C and crushing the product to form a grog (92).

References

1. R. W. Nurse, J. H. Welch and A. J. Majumdar. "The $CaO–Al_2O_3$ system in a moisture-free atmosphere", Trans. Brit. Ceram. Soc. **64,** No. 9, 409–418 (1965).
2. H. E. Swanson, N. T. Gilfrich and G. M. Ugrinic. Standard X-ray Diffraction Powder Patterns. Nat. Bur. Stand. Circ. 539, **5,** 10–13 (1955). U. S. Govt. Printing Office, Washington, D.C.
3. V. L. Burdick and D. E. Day. "Co-ordination of aluminium ions in tricalcium aluminate", J. Am. Ceram. Soc. **50,** No. 2, 97–101 (1967).
4. G. A. Rankin and F. E. Wright. "The ternary system $CaO–Al_2O_3–SiO_2$", Am. J. Sci. (4) **39,** No. 229, 1–79 (1915).
5. W. Büssem and A. Eitel. "The structure of pentacalcium trialuminate" (in German), Z. Kritst., **95,** No. 3–4, 175–188 (1936).
6. Symposium on the Chemistry of Cements, Stockholm (1938). Ingeniörsvetenskapsakademien, Stockholm (1939). W. Büssem. "On X-rays and cement chemistry", 141–167.
7. R. W. Nurse. "Chemical laws and chemical lawbreaking", J. Brit. Ceram. Soc., **4,** No. 3, 387–400 (1967).
8. Fourth International Symposium on the Chemistry of Cement, Washington (1960). Nat. Bur. Stand. (U. S.) Monograph No. 43 (1962). R. W. Nurse reporting work of J. H. Welch Vol. **1,** 36.
9. D. M. Roy and R. Roy. Reference No. 8, Vol **1,** 307–314.
10. J. Jeevaratnam, L. S. Dent Glasser and F. P. Glasser. "Structure of calcium aluminate, $12CaO·7Al_2O_3$," Nature, Lond., **194,** No. 4830, 764–765 (1962).
11. J. Jeevaratnam, F. P. Glasser and L. S. Dent Glasser. "Anion substitution and structure of $12CaO·7Al_2O_3$," J. Am. Ceram. Soc., **47,** No. 2, 105–106 (1964).
12. R. W. Nurse, J. H. Welch and A. J. Majumdar. "The $12CaO·7Al_2O_3$ phase in the $CaO–Al_2O_3$ system," Trans. Brit. Ceram. Soc., **64,** No. 6, 323–332 (1965).
13. The Chemistry of Cements, (Academic Press, London & New York, 1964). Edited by H. F. W. Taylor. J. H. Welch, Vol. **1,** Chapter 2, 49–88.
14. A. J. Majumdar and D. K. Smith. Reference No. 8, Vol. **1,** 24–25.
15. E. Aruja. "The unit cell of orthorhombic pentacalcium trialuminate $5CaO·3Al_2O_3$", Acta Cryst., **10,** 337–339 (1957).
16. A. J. Majumdar. "The quaternary phase in high-alumina cement", Trans. Brit. 3. Ceram. Soc., **63,** No. 7, 347–364 (1964).
17. H. G. Midgley, Building Research Station, England. Private communication (1966).
18. F. Ordway. Reference No. 8 Vol. **1,** 53.
19. L. Heller. "The structure of calcium aluminate and dicalcium silicate α-hydrate", Thesis, Univ. of London (1951).
20. M. W. Dougill. "Crystal structure of monocalcium aluminate", Nature, Lond., **180,** (4580), 292–293 (1957).
21. J. W. Jeffery. References 13, Vol. **1.** "The crystal structures of the anhydrous compounds," Chapter 4, 131–164.
22. J. K. Leary. Albright & Wilson (Mfg) Ltd. Oldbury, England. Private communication (1967).
23. H. F. W. Taylor. The Chemistry of Cements. Research, **14,** 154–158 (1961).
24. B. Tavasci. "Research on the constitution of aluminous cements" (in Italian), Chim. e l'Industr., **17,** 461–471 (1935).
25. K. Lagerqvist, S. Wallmark and A. Westgren. "X-ray study of the systems $CaO–Al_2O_3$ and $SiO_2–Al_2O_3$" (in German), A. Anorg. Chem., **234,** 1–16 (1937).
26. C. Goria and Z. Burdese. "Lime-alumina system. X-

ray studies on monocrystals of $CaO \cdot 2Al_2O_3$ produced from aluminous cement" (in Italian), Ric. Sci., **21**, 1613–1632 (1951).
27. E. R. Boyko and L. G. Wisnyi. "The optical properties and structures of CA_2 and SrA_2," Acta Cryst., **11**, No. 6, 444–445 (1958).
28. J. H. Welch. Reference No. 13 Vol. 1, Chapter 2, 57.
29. M. Rolin and Pham Huu Thanh. "Phase diagrams of mixtures that are nonreactive with molybdenum" (in French), Rev. Hautes Temp. Refractaires. **2**, No. 2, 175–179 (1965).
30. A. Auriol, G. Hauser and J. G. Wurm. Phase Diagrams for Ceramists. The American Ceramic Soc. Inc. (1964). Fig. 232.
31. F. G. Buttler and H. F. W. Taylor. "Action of water and lime solutions on anhydrous calcium aluminates at 5°C", J. Appl. Chem., **9**, 616 (1959).
32. V. Adelsköld. "X-ray studies on magneto-plumbite $PbO \cdot 6Fe_2O_3$, and other structures resembling beta-alumina, $Na_2O \cdot 11Al_2O_3$," Ark. Kemi Min. Geol. **12A**, No. 29, 1–9 (1938).
33. N. A. Toropov and M. M. Stukalova. "Replacement of sodium in crystals of beta-alumina with Ca, Sr, Ba," (in Russian), C. R. Acad. Sci. USSR, **27** 974–977 (1940).
34. N. E. Filonenko and I. V. Lavrov. "Calcium hexaaluminate in the system $CaO–Al_2O_3–SiO_2$" (in Russian), C. R. Acad. Sci. USSR, **66**, No. 4, 673–676 (1949).
35. A. L. Gentile and W. R. Foster. "Calcium hexaluminate and its stability relations in the system $CaO–Al_2O_3–SiO_2$", J. Am. Ceram. Soc., **46**, No. 2, 74–76 (1963).
36. G. H. Mohanty. "An investigation of the characteristics of high alumina castables," Thesis, Univ. of Missouri (1954).
37. D. S. Buist. "A study of calcium hexaluminate", Min. Mag (To be published in 1968).
38. United States Steel Corp. U. S. Patent 3052534 (1962). British Patent 957094 (1964).
39. Ciments Lafarge. French Patent 1283331 (1961). U. S. Patent 3130041 (1964).
40. United States Steel Corp. French Patent 1462103 (1966).
41. "High-alumina cements and concretes," T. D. Robson. Contractors Record Ltd. London, John Wiley & Sons Inc. New York (1962).
42. Albright and Wilson (Mfg) Ltd. British Patents 747016 (1956); 919322 (1960), 980764 (1962). U. S. Patent 2859124 (1958).
43. I. I. Ablichenkov and N. N. Postnikov. "The simultaneous production of yellow phosphorus and aluminous cement" (in Russian), Khim. Prom., No. 6, 431–436 (1964).
44. Virginia-Carolina Chemical Corp. British Patent 889263 (1962), Socony Mobil Oil Co. German Patent 1188501 (1965), Mobil Oil Corp. U. S. Patent 3262798 (1966).
45. A. Klein. U. S. Patent 3257219 (1966).
46. V. F. Krylov. "New types of high-alumina cement", (in Russian) Tsement **28**, No. 1, 8 (1962).
47. V. F. Krylov and V. K. Pomyan. "Manufacture of high-alumina cement in Russia", (in Russian), Tsement **26**, No. 2, 1–6 (1960).
48. Steinwerke Feuerfest Karl Albert G. m. b. H. French Patent 1255963 (1961). British Patent 908073 (1962). German Patent 1150612 (1963).
49. H. Scholze and K-A. Kumm. "The kinetics of crystallization of $C_{12}A_7$" (in German), Tonindustr. Ztg., **90**, No. 12, 559 (1966).
50. B. Adouze. "Contribution to the study of solid-state reaction between lime and alumina" (in French), Silicates Industr., **26**, No. 4, 179–190 (1961).
51. W. L. de Keyser. "Reactions in the solid state between lime and alumina" (in French), Bull. Soc. Chim. Belge, **60**, 516–541 (1952).
52. O. P. Mchedlov-Petrosyan and V. I. Babushkin. "Thermodynamic investigation of the solid state reactions in silicate systems", Silikattech., **9**, No. 5, 205–212 (1958).
53. J. Williamson and F. P. Glasser. "Reactions in heated lime-alumina mixtures", J. Appl. Chem., **12**, No. 12, 535–538 (1962).
54. H. Uchikawa, A. Tsumagari and H. Koike. "Mechanism of formation of calcium aluminates" (in Japanese), Semento Gijutsu Nenpo, **17**, 50–59 (1963).
55. M. Jeanne and G. Sadran, Ciments Lafarge. Private communication. (1967).
56. R. R. Dayal. "The system $CaO–Al_2O_3–FeO–Fe_2O_3$," Thesis, Univ. of Aberdeen (1965).
57. C. Crussard. "Metals, battlefield between order and disorder" (in French), Ann. des Mines, 37–48 (June 1962).
58. J. K. Leary. "New compound in the system $CaO–Al_2O_3–CaF_2$," Nature, Lond., **194**, No. 4823, 79–80 (1962).
59. F. P. Glasser, Univ. of Aberdeen. Private Communication (1963).
60. W. Gutt and J. Jeevaratram. Building Research Station, England. Private communication (1963).
61. W. Gutt. Private communication (1967).
62. M. T. Mel'nik and N. N. Shapovalova. "The effect of autoclave hardening on the properties of calcium aluminates" (in Russian), Tsement, **28**, No. 4, 9–10 (1962).
63. M. T. Mel'nik, N. N. Shapovalova, L. D. Berkhoer and L. N. Filatova. "Formation of boehmite in the hydration of CA_2" (in Russian), Zh. Prikl. Khim., **40**, 904–906 (1967).
64. Materials Technology in Steam Reforming Processes (Proceedings of Symposium held at Billingham, England 1964). Pergamon Press, London, New York, Paris, Frankfurt (1965). T. D. Robson. "Some principles governing the performance of refractory concretes" p. 295–304.
65. R. R. Dayal and F. P. Glasser. Science of Ceramics Vol. 3. To be published.
66. W. Dyckerhoff. "Petrography of the high-alumina cement melts" (in German), Zement, **13**, 386–388, 399–402 (1924).
67. N. Sundius, References No. 6 p. 395.
68. Proceedings Third International Symposium on the Chemistry of Cement, London (1952). Cement and Concrete Association, London (1964) T. W. Parker. The Constitution of Aluminous Cement p.

485–515.
69. J. H. Welch. "Ternary compound formation in the system $CaO–Al_2O_3–MgO$" Nature, Lond., **191,** No. 4788, 559–560 (1961).
70. T. D. Robson. Reference No. 68. p. 522.
71. V. Girilli and F. Abbatista. L'Ind. Ital. Cementi **10,** 769–776 (1963).
72. Yu. M. Butt, V. V. Timashev and V. A. Paramonova. "Effect of reducing atmosphere on the stability and hydration activity of calcium aluminoferrites" (in Russian), Tsement, No. 4, 8–11 (1967).
73. A. Zinsen, "Fuel ash in industrial firing" (in German), Forschung auf dem Gebiet des Ingenieurwesens, **14,** 89 (1943).
74. H. Lafuma. Reference No. 68. p. 587–597 (1952).
75. H. Lossier and A. Caquot, "Expanding concretes and their application" (in French), Genie Civil, **121,** No. 8, 61–65 (1944).
76. P. E. Halstead. Reference No. 13, Nol. **2,** 87–99 (1964).
77. A. Klein and G. E. Troxell. "Studies of calcium sulfoaluminate admixtures for expansive cements," Am. Soc. Testing Materials Proc., **58,** 986–1008 (1958).
78. N. Fukuda. "Composition of sulpho-aluminous cement" (in Japanese), Yogyo Kyokai Shi, **69,** No. 786, 187–191 (1961).
79. P. E. Halstead and A. E. Moore. "The composition and crystallography of an anhydrous calcium alumino-sulphate occuring in expanding cement", J. Appl. Chem., **12,** No. 4, 413–417 (1962).
80. S. Aroni, M. Polivka and B. Bresler. "Expansive cements and expanding concretes," Univ. of California. Report No. 66–7, Dept. of Civil Engineering (1966).
81. P. K. Mehta and A. Klein. "Formation of ettringite by hydration of a system containing an anhydrous calcium sulfoaluminate," J. Am. Ceram. Soc., **48,** No. 8, 435–436. (1965).
82. A. Klein and Chemically Prestressed Concrete Corp. U. S. Patents 3155526 (1964), 3251701 (1966), 3303037 (1967).
83. P. K. Mehta. U. S. Patent application (1966).
84. S. A. Lindroth. "Formation of glass in the system $CaO–Al_2O_3$" (in German), Glastech. Ber., **23,** No. 9, 241–247 (1950).
85. R. A. Weidel. "Influence of some transition elements on visible and infra-red transmission of calcium aluminate glasses", J. Am. Ceram. Soc., **42,** No. 9, 408–412 (1959).
86. H. C. Hafner, N. J. Kreidl and R. A. Weidel. "Optical and physical properties of calcium aluminate glasses", J. Am. Ceram. Soc., **41,** No. 8, 315–323 (1958).
87. Bausch and Lomb (N. J. Kreidl and R. A. Weidel). U. S. Patent 3,007,804 (1962).
88. S. A. Long and T. D. McGee, "Stabilisation of lime with a protective glass coating", Proc. Iowa Acad. Sci., **71,** 166–172 (1964).
89. B. Cockayne. "Observation and control of deviations in molar composition in single-crystal growth of mixed oxides", J. Am. Ceram. Soc., **49,** No. 4, 204–207 (1966).
90. B. Cockayne and D. S. Robertson. "Single crystals of calcium aluminate, cell and transmittance parameters", Solid State Comm., **2,** No. 11, 359–360 (1964).
91. G. S. Perry. Paper presented to the Eighth Electromagnetic Window Symposium, Georgia Inst. of Technology, June 1966.
92. Harbison-Walker Refractories Co. (E. D. Miller Jr.). U. S. Patent 3269849 (1966).

Oral Discussion

Kiyotaka Mishima

Among various alumina cements, there are some in which plenty of gehlenite crystals is formed. How does this crystal influence upon cement hydration?

The new applications of calcium aluminates other than cement were very interesting. Are there any other applications in the modern technical fields such as space technology, atomic energy and so forth?

Author's Closure

Thomas D. Robson

An increasing proportion of gehlenite usually appears in high-alumina cement clinkers as the silica content rises (particularly above 5% SiO_2). Since the gehlenite is practically non-hydraulic at ordinary temperatures (and since it utilises alumina which otherwise could be present as calcium aluminate) the effect is to reduce the cement strength—especially the early strength. It is also usual for the setting-time of the cement to be delayed when the clinker contains higher percentages of silica.

Among the applications (actual or proposed) for calcium aluminate cements in modern technologies the following can be mentioned:

Castable refractories for forming the pads on which vertical-take-off aircraft are tested, for constructing flame-deflectors in tests on large rocket engines, and for constructing the inner wall of concrete pressure-vessels serving as the whole (or part) of the radiation shield of nuclear reactors. A mix of calcium aluminate and fused silica aggregate has been patented for casting rocket nozzles and a similar mix has been tested for infilling a stainless-steel honeycomb acting as protection to missiles during atmospheric re-entry.

Supplementary Paper I-78 The Crystal Structure of $11CaO, 7Al_2O_3, CaF_2$

Perter P. Williams*

Synopsis

The crystal structure of the material obtained by replacing two O^{2-} ions in the unit cell of $C_{12}A_7$ by four F^- ions has been determined. The structure previously deduced by Büssem and Eitel for $C_{12}A_7$ has been shown to be substantially correct, and the fluoride ions have been found to be randomly distributed on 12-fold positions. The calcium atoms have been found to be coordinated either to six oxygens in a very asymmetric manner, or to six oxygens and one fluorine, in an arrangement similar to octahedral coordination. The single position parameter of the calcium atoms may assume one of two values, depending upon whether an adjacent site is occupied by a fluoride ion. It is suggested that the affinity that $C_{12}A_7$ shows for water at high temperatures can be ascribed to the requirement that the coordination sphere about the calcium atoms be more or less regular.

Introduction

The observations by Roy and Roy (1) and by Nurse (2) that the compound $C_{12}A_7$ absorbs one mole of water from air of normal humidity at temperatures up to 1100°C reawakened interest in the crystal structure of this material. Büssem and Eitel (3) had previously deduced an approximate structure, but later work by Jeevaratnam, Glasser and Glasser (4, 5) failed to give definite confirmation of the structure. Jeevaratnam, Glasser and Glasser (5) also showed that by heating anhydrous $C_{12}A_7$ or $C_{12}A_7H$ with calcium fluoride or chloride, compounds of the type $C_{11}A_7 \cdot CaX_2$ could be formed, with structures closely related to those of $C_{12}A_7$ and $C_{12}A_7H$. These observations suggested that the hydrate contains replaceable OH^- groups, and can be formulated $C_{11}A_7 \cdot Ca(OH)_2$. The cubic unit cell contains two formula weights of the compound, i.e. $Ca_{24}Al_{28}O_{66}$ for the anhydrous material, and for the hydrate, or the halides, $Ca_{24}Al_{28}O_{64}X_4$. The space group chosen by Büssem and Eitel (3) for the anhydrous material, $I\bar{4}3d$, cannot accommodate 66 oxygen atoms in the normal equipoint sets, and the suggested structure accounted only for the cell contents $C_{24}Al_{28}O_{64}$, leaving two oxygen atoms per unit cell to be accounted for. It has been suggested (5) that it is these oxygen atoms that are used in forming hydroxyl groups in the hydrate.

It was clearly of interest to determine accurately the crystal structure of this material in order to locate the extra oxygen atoms, and, if possible, to find a reason for the unusual hydration behaviour of $C_{12}A_7$. Since, if Büssem and Eitel's (3) structure is correct, the unlocated oxygen atoms must be disordered, it was felt that there was a better chance of locating the extra atoms in the hydrate, or a halide analogue, in which there are four extra atoms per unit cell, than in the anhydrous material, which has only two, The very great similarity in the X-ray patterns of all the compounds make it seem likely that the extra atoms occupy the same types of position in the anhydrous material, the hydrate and the halides. However, it was realised that results obtained from the hydrate or a halide may not be applicable to the anhydrous material. Nevertheless, when crystals of the fluoride became available through the courtesy of Dr J. K. O'Leary, of Albright and Wilson Ltd, the structure determination was commenced.

*Chemistry Division, Department of Scientific and Industrial Research, Petone, New Zealand.

Experimental

Three-dimensional diffraction data from a small equant single crystal were collected on a Hilger Linear automatic diffractometer within a sphere of radius approximately 1.2 r.l.u., using Mo radiation and balanced fitters. Data were collected over four quadrants, so that general reflections hkl were observed up to 24 times. All reflections were reduced to structure amplitudes independently, and the root mean square averages of sets of equivalent structure amplitudes obtained. A total of 213 independent structure amplitudes were used in the structure analysis.

A critical examination was made of the diffractometer output, and of Weissenberg and precession photographs to verify the systematic absences previously reported, and to check for the absence of superlattice reflections. No reflections apart from those expected for a cubic structure, space group $I\bar{4}3d$ were observed, the reflections expected to be absent gave integrated intensities not greater than the standard deviation of the measurements, and equivalent reflections gave intensities agreeing to within two standard deviations. Thus, no experimental evidence could be found to contradict the conclusions formed by previous workers.

The cell dimension was measured from a powder diffractometer pattern calibrated with silicon powder. The value obtained, $a = 11.970$Å is in fair agreement with the published (5) value of 11.964Å.

An unsharpened Patterson synthesis computed from the full set of data appeared to indicate a structure in which the atoms occupy positions strictly analogous to those occupied in the similar compound C_3AH_6, i.e., calcium atoms in positions 24d (of $I\bar{4}3d$) with $x = 1/8$, and aluminium atoms in positions 16c with $x = 0$. Twelve other aluminium atoms were placed on the fixed positions 12a, and 64 oxygen atoms on 16c with $x = .07$ and on 48e, with $x = .19$, $y = .29$, $z = .10$. Structure factors computed with these parameters gave an R-factor of about 0.35. When refinement was attempted, the atoms moved towards the positions deduced by Büssem and Eitel. Consequently, Büssem and Eitel's parameters were used as a starting point for refinement. The R-factor, initially about 0.2 dropped to 0.12 after two cycles of block diagonal least squares refinement. A difference synthesis at this point indicated that the calcium atoms were very anisotropic, being elongated along the 2-fold axes on which they lie. Peaks occurred in the synthesis in the positions 12b, each peak corresponding approximately to one-third of a fluorine atom. Two more cycles of block diagonal least squares refinement in which an anisotropic temperature factor was refined for the calcium atoms indicated that the anisotropy of the calciums was much greater than could be expected for ordinary thermal vibrations. Two cycles of full matrix least squares refinement were carried out, in which occupancy factors, and position parameters of two fractional calcium atoms, and the occupancy factor of the fluorine atom were allowed to vary. This refinement resulted in an R-factor of .097. Since the essential features of the structure were clear at this stage, no further refinement was performed.

Discussion of the Structure

The final atomic parameters are given in Table 1.

The general features of the structure are as described by Büssem and Eitel (3). It is composed of a three dimensional network of linked AlO_4 tetrahedra, each oxygen (O(2)) in the general 48-fold position being bonded to an aluminium on a 16-fold position (Al(2), symmetry 3) and to an aluminium on a 12-fold position (Al(1), symmetry $\bar{4}$). The other 16 oxygens (O(1)) are bonded only to the neighbouring Al(2) atoms. The AlO_4 tetrahedra are slightly distorted, those for the Al(1) atoms being extended slightly in the direction of the 2-fold axis, and those for the Al(2) atoms being extended in the direction of the 3-fold axis. Bond lengths are shown in Table 2.

All Al–O bond lengths are within the normal range, except for the Al(2)–O(1) bond, which is longer than normal. However, the O(1) atom had not clearly reached its optimum position when refinement was stopped, and further refinement would probably reduce this bond length.

The calcium and Al(1) atoms lie in rows on the 2-fold axes, as shown in Fig. 1.

The arrangement of the atoms lying on the 2-fold axis is:

—Ca Al Ca hole Ca Al Ca hole—

In the crystals studied, roughly 24% of the holes are occupied by fluoride ions, and a corresponding frac-

Table 1. *Final coordinates of the atoms, and the fractional occupancy factors of the calcium atoms in each of the two sites, and of the fluorine atoms.*

	x	y	z	B	Occupancy factor
Ca (1)	0.10824	0	1/4	0.90	0.744
Ca (2)	0.06738	0	1/4	0.90	0.254
Al (1)	3/8	0	1/4	0.37	
Al (2)	0.98089	0.98089	0.98089	0.33	
O (1)	0.06977	0.06977	0.06977	0.79	
O (2)	0.19091	0.28616	0.09919	0.94	
F	7/8	0	1/4	1.29	0.238

Table 2. *Interatomic distances in the structure*

Al—O distances:			
Al(1)—O(2)	1.744Å	(4 equivalent bonds)	
Al(2)—O(1)	1.843Å		
Al(2)—O(2)	1.775Å	(3 equivalent bonds)	
Ca—O distances:			
Ca(1)—O(1)	2.359	(2 equivalent bonds)	"Square plane"
Ca(1)—O(2)	2.328	(" " ")	
	2.539	(" " ")	
Ca(2)—O(1)	2.314	(2 equivalent bonds)	"Square plane"
Ca(2)—O(2)	2.357	(" " ")	
	2.961	(" " ")	
Ca(2)—F	2.303		

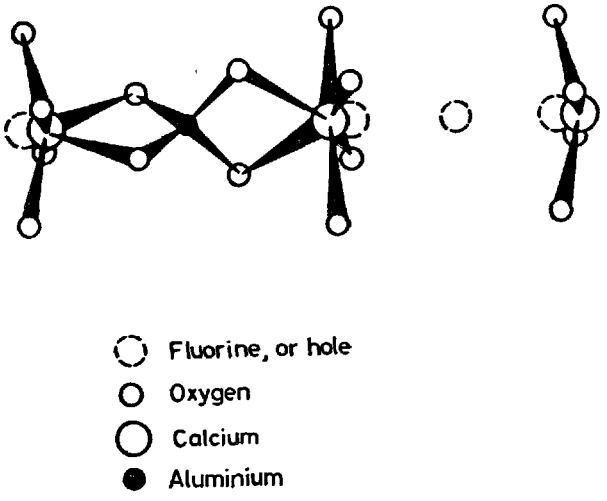

Fig. 1. *The coordination of the calcium atoms.*

tion of the calcium atoms, 25%, lie closer to the holes than the remaining 75%. It seems fairly certain, therefore, that if a hole is occupied by a fluoride ion, both the adjacent calcium atoms are displaced towards the fluoride ion by about 0.5Å from the positions they normally occupy.

In Fig. 1, it can be seen that the coordination of oxygens to the calcium is rather unusual if the adjacent hole is not occupied by fluorine. Six oxygens lie within 2.54Å of the calcium, four of them lying at the corners of a distorted square centred approximately on the calcium atom, and oriented at right angles to the 2-fold axis. This square planar coordination group has Ca–O distances of about 2.34Å. The two remaining oxygen atoms lie on the same side of the square planar group, at a distance of about 2.54Å from the calcium. If the neighbouring hole is occupied by a fluorine atom, the calcium atom occupies a different position, still near the centre of the square planar arrangement, but about 2.96Å away from the other two oxygen atoms. The calcium-fluorine distance is about 2.30Å. In this situation, therefore, the coordination of the calcium is 7-fold, and the arrangement approximately octahedral, there being two weak Ca–O interactions trans to the Ca–F bond.

If the results of this analysis are applied directly to anhydrous $C_{12}A_7$ and to the hydrate, it would appear that the unusual hydration characteristics of $C_{12}A_7$, can be explained in terms of the unsatisfactory coordination of five-sixths of the calcium atom in the anhydrous phase. Hydration or reaction with calcium fluoride or chloride allows one-third of the calcium to adopt an approximately octahedral coordination, leading to a more satisfactory structure. However, it may be noted that in the hydrate and the halides, two-thirds of the calcium atoms remain poorly coordinated, and it may be possible to introduce neutral ligands into the remaining holes in the structure, and so satisfy the coordination requirements of all the calcium atoms.

The results of this analysis suggest that in the particular sample studied, fewer than one-third of the holes are occupied by fluoride ions, and that if charge balance is to be preserved, the formula of the material must be approximately $11.56CaO \cdot 7Al_2O_3 \cdot 0.44CaF_2$. The good agreement between the fractional occupancy parameters for the Ca(2) and the fluorine atoms indicates that this is a real effect, and has not been introduced by the adoption of an unsatisfactory scattering curve for fluorine. The length of the cell edge for the material studied is slightly greater than that reported (5) for the fluoride, as would be expected for the composition given above.

Jeevaratnam, Glasser and Glasser (5) reported the lengths of the cell edges for the anhydrous phase, the hydrate, and the halides. The cell edges, according to their figures, increase in the order fluoride < hydrate (hydroxide) < anhydrous phase < chloride. These authors note that the results of Roy and Roy (1) indicate that the cell volume increases with hydration, whereas their own figures show a decrease. Since the calcium-aluminium—hole (or anion) chains indicated in Fig. 1 lie parallel to the cell edge, it is reasonable to

suppose that the length of the cell edge can be correlated with the extent of occupation of holes by anions, and by the calcium-anion distance. If values are adopted of 2.30Å for the Ca–F bond (as measured in this work), of 2.43Å for a typical Ca–OH bond, and of 2.73Å for a Ca–Cl bond, and these are plotted against the cell dimensions for the appropriate compounds, a straight line results, as shown in Fig. 2.

This result suggests, firstly, that the assumption that the anions occupy the same sites in these three compounds is justified, and secondly, that the reduction in cell size upon hydration observed by Jeevaratnam, Glasser and Glasser (5) is real, since the average size of the holes in the chains becomes smaller upon hydration.

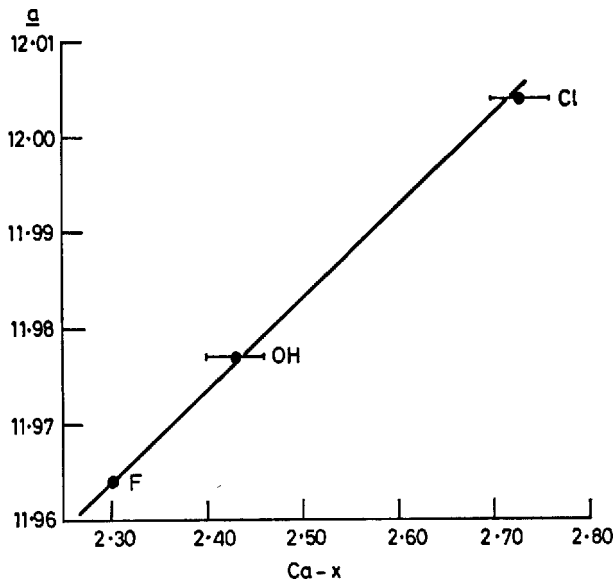

Fig. 2. *Variation of the unit cell parameter with expected calcium—anion distances.*

Conclusions

The structure reported by Büssem and Eitel (3) for $C_{12}A_7$ is substantially correct. However, in this phase, and in the hydrate, and the halide analogues, the anions which cannot be accommodated in a fully ordered structure are randomly distributed on a 12-fold equipoint of point symmetry $\bar{4}$. These anions contribute to a modified octahedral coordination of up to one-third of the calcium atoms. Large holes occur in the structure where sites in this equipoint remain unfilled, and adjacent calcium atoms have an unbalanced coordination shell. The cell dimensions of the hydrate and halide analogues can be correlated with the calcium-anion distances to be expected in the structures.

Acknowledgements

The work described herein was performed while the author was working in the Chemistry Department of the University of Aberdeen. Support was provided by a Commonwealth Travelling Fellowship awarded by the Niffield Foundation. Grateful thanks is offered to all those who supported and encouraged this work.

References

1. D. M. Roy and Rustum Roy, "Crystalline solubility and zeolitic behaviour in garnet phases in the system $CaO–Al_2O_3–SiO_2–H_2O$", Chemistry of Cement: Proc. 4th Internatl. Symp., Washington, Oct. 1960 Nat. Bur. Std. (U. S.) Monograph No. 43, p. 307–314 (1962).
2. R. W. Nurse, "Phase equilibria and constitution of portland cement", Chemistry of Cement: Proc. 4th Internatl. Symp., Washington, Oct. 1960. Nat. Bur. Std. (U. S.) Monograph No. 43 p. 9–37 (1962).
3. W. Büssem and A. Eitel, "Die Struktur des Pentakalziumtrialuminats", Z. Krist, **95**, 175–188 (1936).
4. J. Jeevaratnam, L. S. Dent Glasser and F. P. Glasser, "Structure of calcium aluminate, $12CaO·7Al_2O_3$", Nature, **194**, 764–765 (1962).
5. J. Jeevaratnam, F. P. Glasser and L. S. Dent Glasser, "Anion substitution and structure of $12CaO·7Al_2O_3$", J. Am. Ceram. Soc. **47**, 105–106 (1964).

Supplementary Paper I-90 The Solid Solution in the System C_2AS (Gehlenite) —CA_2 and a New Ternary Phase

Kozo Sugiura and Takashi Yoshioka*

Synopsis

Studies were made on the crystal phase obtained by heating, at different temperatures, the glasses of the system C_2AS–CA_2, having several different chemical compositions.

As a result, it was found that the melilite crystallizing on the C_2AS side of the said system could form a metastable solid solution. This solid solution is in most cases metastable, but it may possibly be stable as for the glass having the composition quite near to C_2AS end member. The amount of the CA_2 taken up in solid solution, as far as determined by this experiment, is 16.6% by weight at the maximum, and when this solid solution is heated under a certain condition it separates CA_2 crystal. This solid solution has its lattice constant changed not only by the amount of its CA_2 but also by the heating condition.

When the glass of the said system having a certain composition was heated at 1000°C, a new crystal phase which has not been known heretofore was crystallized. This crystal phase, by heating glass granules having C_2AS, CA_2 equi-mole composition (C_3A_3S composition) at 1000°C for 4 – 48 hours, can be obtained as a monophase. By further studies it was disclosed that this phase has a relatively wide field of solid solubility. That is, under the heating condition of 1000°C for 48 hours, this phase can crystallize as a monophase inside the triangle having anorthite, CA and CA_2 as the vertices, and also in a composition range of SiO_2 extending from approximately 11–27%. Under differential thermal analysis, this phase shows an exothermic reaction at about 1100°C and decomposes into stable minerals. Therefore, this crystal phase can be considered as metastable.

The Melilite Solid Solution in the System C_2AS–CA_2

H. G. Midgley (1) analyzed the melilite, separated from marketed high alumina cement, and noted that its Al_2O_3 content is unusually greater than the ordinary gehlenite, and indicated that the solid solution must be generated between C_2AS and CA_2. J. R. Goldsmith (2) made a study on the system $CaAl_2Si_2O_8$–$Ca_2Al_2SiO_7$–$NaAlSiO_4$ and noted that the refractive indices of the melilite originating within this system are substantially lower than those of the pure gehlenite, and this, he thought, may have been caused by the gehlenite's solid solutioning of CA_2. H. J. Christie (3) studied the ionic substitutions of melilite by the synthetic method and stated that it may be possible to make Al completely replace the Si positions of gehlenite. The authors, while studying the high alumina cement clinker minerals, discovered that the melilite crystallizing from the glass of the system C_2AS–CA_2 could take up a certain amount of CA_2 to form a solid solution.

Homogeneous glasses having various compositions of the system C_2AS–CA_2 were obtained from pure quartz powder, pure reagent of $CaCO_3$ and Al_2O_3, by flame fusioning with oxygen-acetylene burner. However, when the CA_2 component is more than 70% by weight (hereinafter all % is by weight), even with the rapid quenching process perfect glass could not be obtained, the formation of C_2A crystal being inevitable. The glass granules (1–3 mm. ϕ) thus obtained were kept for 6 hours in an electric furnace at the temperatures of 900–1450°C. The phases were identified mainly by the X-ray powder method together with the microscopy. The lattice constant a_0 of the melilite thus formed was obtained from the d-values of 400, 330 and 420 for an measurement metallic germanium powder being used as the standard. The diffraction condition was as follows:

Target Cu, Filter Ni, Voltage 40 KV, Current 20 mA, Count Full Scale 200 C/S,
Time Constant 4 sec., Scanning Speed 1/8°/min., Receiving Slit 0.1 mm.

The refractive indices of this melilite were also measured by the oil immersion method.

The results of the identification of the formed phases

*Research Laboratory, Nihon Cement Co., Ltd. Tokyo, Japan.

are shown in Table 1. This melilite is monophase up to 5.7% CA_2 content at 1450°C, and monophase up to 16.6% CA_2 content at 1100°C. At the temperature below 1000°C, an unknown crystal, which will be described in the next section, was found to occur within the ranges of 16.6% to 63.0% CA_2 content. The glass phase remains at 900°C.

The lattice constant a_0 of the crystallized melilite is shown in Fig. 1. The richer was the CA_2 component in the glass composition, the greater was the a_0 of melilite crystallizing therefrom. The lower the heating temperature, the more eminent was this tendency. In spite of the fact that the melilite is monophase up to 16.6% CA_2 at 1100°C, the change of a_0 value is small in comparison with the component change. At 1200°C and at 1300°C, the melilite is monophase up to 11.2% CA_2 content in both cases, but the a_0 change is still smaller.

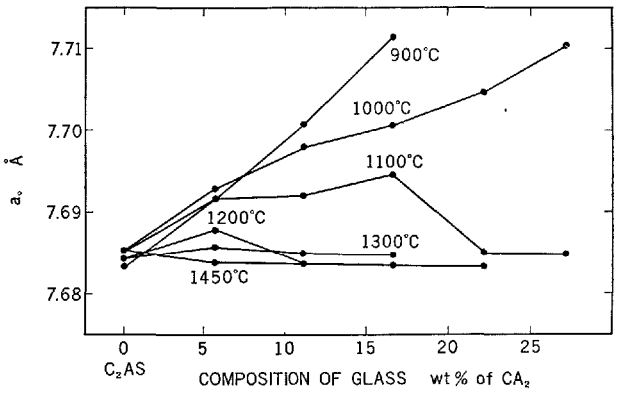

Fig. 1. *Lattice constant* a_0 *of melilites crystallized from the glasses of* C_2AS–CA_2 *composition at several temperatures.*

Taking the mixtures with 16.6% CA_2 content as an example, melilite crystallized and glass phase remained at 900°C; unknown crystal was also found to be formed at 1000°C; and, it became melitlie monophase only at 1100°C. The melilites crystallizing at the temperatures of 900–1100°C may probably have CA_2 in solid solution, and the size of the lattice dimensions became smaller with the rise of the temperature. Even at the low temperature, the lattice dimension shrinked when kept for long hours (Fig. 2). At 1200°C, CA_2 was found to be formed and the lattice dimension of the melilite became equal to that of the ordinary gehlenite. In the melilite having CA_2 in solid solution, it is assumed that a part of Si in the ordinary gehlenite is replaced by Al, and a part of Ca is also replaced by Al as follows: $(Ca_{2-x}Al_x)Al$ $Al(Si_{1-x}Al_x)O_7$. In the case of 16.6% CA_2 content, $X = 0.174$. These substitutions may probably take place, resulting in the formation of rather unstable substance, and if a sufficient thermal energy is given

Table 1. *Phases formed by heating the glasses of* C_2AS–CA_2 *composition.*

Comp. wt % of CA_2	Temperature °C					6 hours heating	
	900	1000	1100	1200	1300	1450	1530
0	*m*	*m*	*m*	*m*	*m*	*m*	*m*
5.7	*m*	*m*	*m*	*m*	*m*	*m*	*m*, CA_2
11.2	*m*, *g*	*m*	*m*	*m*	*m*	*m*, CA_2	*m*, CA_2
16.6	*m*, *g*	*m*, *x*	*m*	*m*, CA_2	*m*, CA_2		
22.1	*m*, *g*	*m*, *x*	*m*, CA_2	*m*, CA_2			
27.3	*m*, *g*	*m*, *x*	*m*, CA_2				
32.5	*m*, *x*, *g*	*m*, *x*	*m*, CA_2				
37.7	*m*, *x*, *g*	*m*, *x*	*m*, CA_2				
42.9	*m*, *x*, *g*	*m*, CA_2, *x*	*m*, CA_2				
53.1	*m*, CA_2, *x*	*m*, CA_2, *x*	*m*, CA_2				
63.0	*m*, CA_2, *x*	*m*, CA_2, *x*	*m*, CA_2				
72.6	*m*, CA_2	*m*, CA_2	*m*, CA_2				
81.9	*m*, CA_2	*m*, CA_2	*m*, CA_2				
91.0	*m*, CA_2	*m*, CA_2	*m*, CA_2				
100.0	CA_2	CA_2	CA_2				

m: melilite *x*: unknown ternary phase *g*: glass

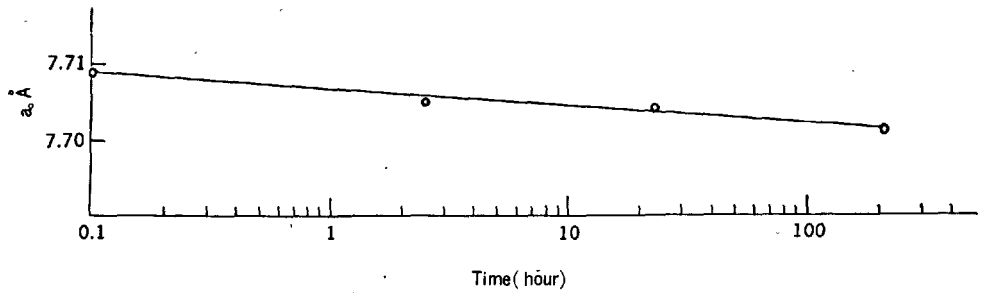

Fig. 2. *Lattice constantt* a_0 *of melilites crystallized from the glass of 16.6% CA_2 composition at 1000°C held for various periods.*

the solid solution will be decomposed into C_2A and gehlenite. The fact, that the melilite having CA_2 in solid solution shows the change of lattice dimension subjected to temperatures must have some bearing on the instability of the structure. Such fact is not recognized in C_2AS end member. The D.T.A. curve of the glass with 16.6% CA_2 content is shown in Fig. 3. Exothermic peaks were seen at 995°C, 1020°C and 1120°C. It was confirmed by the use of X-ray analysis that the first peak (lower temperature side) is caused by the melilite crystallization and the second peak by the formation of unknown crystal. The third peak must be caused by the reaction of the decomposition of unknown crystal and the formation of melilite monophase as a whole. Because the specimen obtained by rapidly quenching from 1200°C is mostly composed of the melilite, a minute quantity of the unknown crystal remains, but CA_2 does not exist.

As to the glasses with 11.2% and 5.7% CA_2 contents, a_0 of the melilite decreases with the rise of the temperature, but when shrinked to the size exactly equal to a_0 of ordinary gehlenite, the melilite still contains CA_2 component in solid solution. Even when the specimen glass is used in powder form CA_2 does not segregate by 6 hours heating at 1300°C, up to 11.2% CA_2 content. The glass with 5.7% CA_2 content still does not segregate CA_2 by 6 hours heating at 1450°C, but it segregated CA_2 when heated at 1530°C for 6 hours.

It seems that the change of the lattice dimension of melilite has little effect upon the refractive indices. (Fig. 4 A, B.)

From the above facts, melilite having CA_2 in solid solution and also having large a_0 can be considered as metastable phase. The formation of the melilite containing CA_2 up to 11.2% at 1200°C and at 1300°C, and up to 5.7% at 1450°C and having lattice constant a_0 nearly equal to that of ordinary gehlenite shows a strong possibility of the existence of a range of solid solubility on the gehlenite side of this system, even under an equilibrium state. However, this is not confirmed yet.

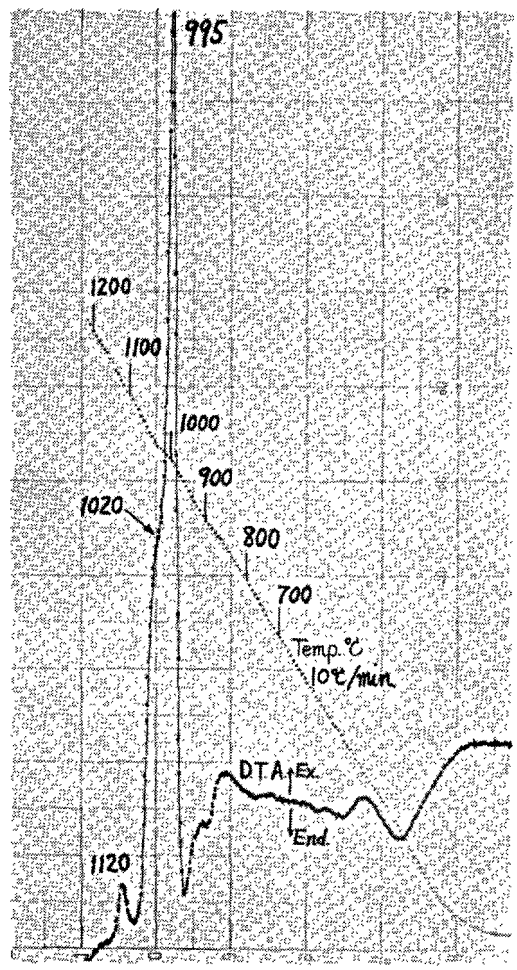

Fig. 3. *DTA curve of the glass of 16.6% CA_2 composition.*

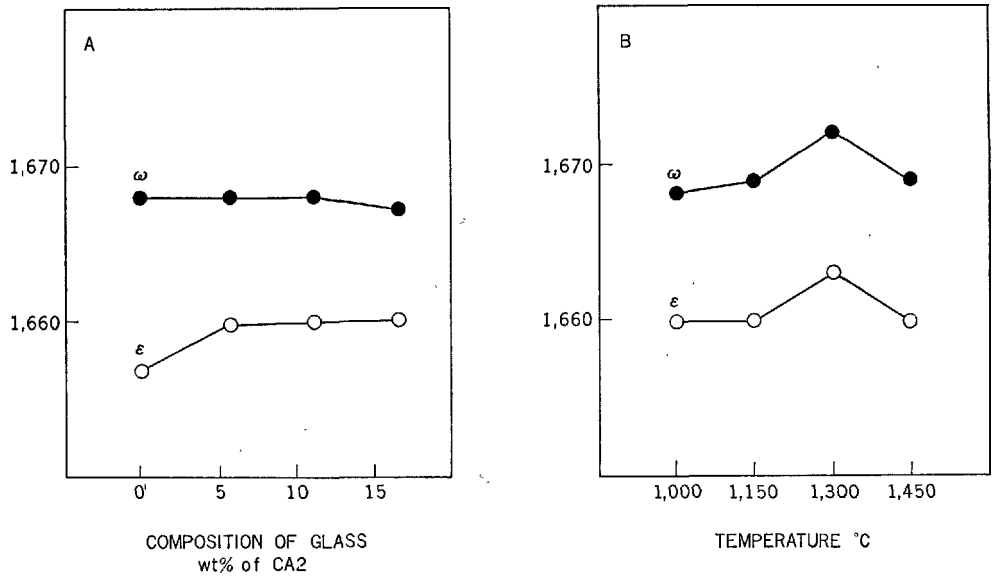

Fig. 4. *Refractive indices of melilites crystallized from the glasses*
A. crystallized at 1000°C.
B. crystallized from the glass of 11.2% CA_2 composition.

New Ternary Phase in the System CaO–Al_2O_3–SiO_2

As shown in Table 1, when the glass granules of the system C_2AS–CA_2 were heated at the temperature below 1000°C, an unknown crystal was obtained in 15–60% CA_2 components ranges. By heating drop-

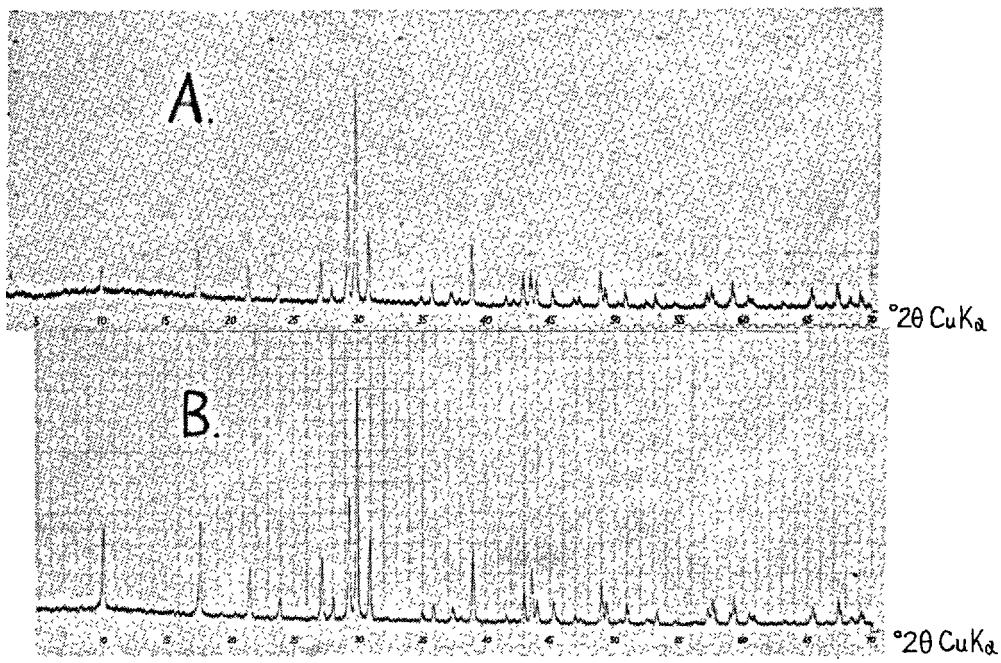

Fig. 5. *X-ray diffraction diagrams of the new ternary phase*
A. C_3A_3S composition
B. $C_3A_3S_2$ composition

lets (3–8 mm. ϕ) of the glass with C_2AS, CA_2 equimole, that is C_3A_3S composition, for 4 – 48 hours at 1000°C it was obtained in a monophase form. These droplets were prepared by flame fusioning as already mentioned.

Under microscopic observation this crystal shows straight extinction, it is uniaxial positive, has negative elongation, $n \fallingdotseq 1.626$ and its special property is that it has an extraordinary weak birefringence. Specific gravity = 2.86. X-ray powder diffraction diagram is shown in Fig. 5–A and Table 2. As shown in Table 2, indexing it as hexagonal system is possible. The D.T.A. curve of this crystal is given in Fig. 6–A. At about 1200°C it shows an exothermic reaction, decomposes and forms a stable mineral assemblage, which is composed of C_2AS and CA_2.

Result of the study of this phase, conducted on still wider range of chemical composition, is shown in Fig. 7. This shows the phase or the combination of the phases obtained when granules of glasses having various components were heated for 48 hours at 1000°C. Inside the triangle having anorthite, CA, CA_2 as vertices, only the new crystal phase alone forms in a relatively broad range, approximately 11–27%, of SiO_2.

All of the X-ray power diffraction diagrams of the new crystal phase formed are exceedingly similar but by compositions the peak positions were found shifted slightly. Taking the example of the new crystal phase forming on the connecting line of CA–anorthite, d values change linearly with the compositions, but the lines break at the point $C_3A_3S_2$, as shown in Fig. 8, which gives the result of the values measured, using quartz as standard. Studies were made on the new crystal phase formed on other composition lines and the same inflections were seen when crossing over the connecting line $C_3A_3S_2$–$C_2A_3S_2$. The above-mentioned crystal of C_3A_3S composition has a weak birefringence, but it becomes stronger as it nears the anorthite. A microscopic photo of the crystal with $C_3A_3S_2$ composition is presented in the Photo 1.

Although the new crystal phase is a solid solution belonging to the ternary system CaO–Al_2O_3–SiO_2, strictly it might be classified into two different phases somewhere in a vicinity of the connecting line $C_3A_3S_2$–$C_5A_6S_4$–$C_2A_3S_2$.

According to the differential thermal analysis, the new crystal phase when heated above a set temperature will decompose with an exothermic reaction into a stable mineral assemblage. The peak temperatures and the minerals formed by decomposition of course will differ with compositions. The D.T.A. curve of the new crystal phase with $C_3A_3S_2$ composition is given

Table 2. *X-ray powder data of the uew ternary phase of C_3A_3S composition*

CuKα radiation

Observed		Calculated as hexagonal with $a = 10.005$Å, $c = 8.235$Å.		
d(Å)	I	Qobs.	Qcale	hkl
8.67	17	.0133	.0133	10,0
5.00	33	.0400	.0400	11.0
4.117	23	.0590	.0590	00.2
3.717	12	.0724	.0723	10,0
(3.30)	20.2Kβ			
3.276	30	.0931	.0932	21.0
3.175	8	.0992	.0989	11.2
3.040	64	.1082	.1080	21.1
2.981	100	.1125	.1123	20.2
2.884	46	.1202	.1199	30.0
2.561	7	.1525	.1522	21.2
2.493	17	.1609	.1599	22.0
2.403	12	.1732	.1732	31.0
2.364	5	.1789	.1789	30.2
2.305	46	.1882	.1849	31.1
2.164	7	.2135	.2131	40.0
2.134	4	.2196	.2188	22.2
2.103	22	.2261	.2260	21.3
2.075	27	.2323	.2322	31.2
2.059	19	.2359	.2359	00.4
2.003	13	.2493	.2492	10.4
1.932	7	.2679	.2678	32.1
1.917	8	.2721	.2721	40.2
1.860	28	.2891	.2892	20.4
1.842	16	.2947	.2945	41.1
1.791	12	.3118	.3120	32.2
1.720	8	.3380	.3387	41.2
1.677	3	.3556	.3558	30.4
1.606	12	.3877	.3877	42.1
1.598	17	.3916	.3920	50.2
1.564	8	.4088	.4086 .4090	11.5 31.4
1.558	20	.4120	.4124	41.3
1.530	10	.4272	.4276	51.1
1.522	7	.4317	.4319	42.2
1.432	7	.4877	.4885	30.5
1.426	15	.4918	.4923	33.3
1.388	18	.5191	.5195	52.0
1.373	7	.5305	.5308	00.6
1.359	13	.5415	.5417	31.5

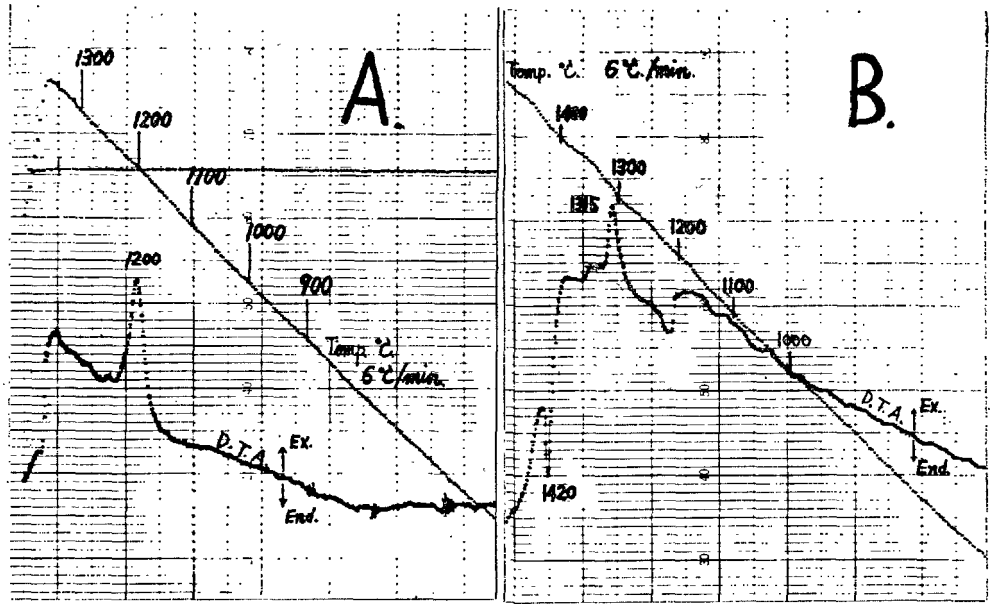

Fig. 6. *DTA curves of the new ternary phase.*
A. C_3A_3S composition.
B. $C_3A_3S_2$ composition.

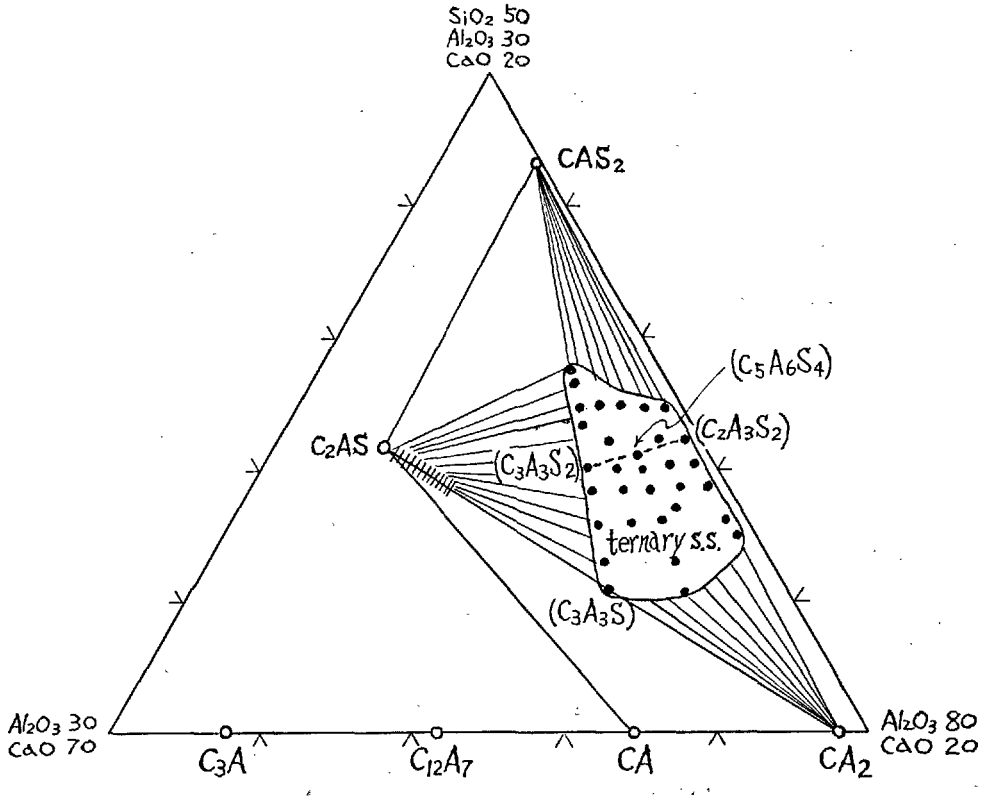

Fig. 7. *Phase assemblages formed by heating the glasses of the ternary compositions at 1000°C for 48 hours.*

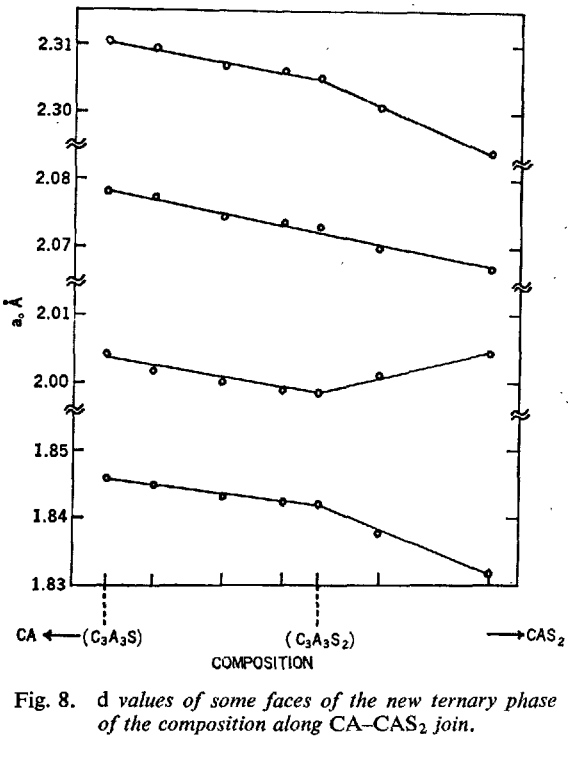

Fig. 8. d *values of some faces of the new ternary phase of the composition along* CA–CAS_2 *join.*

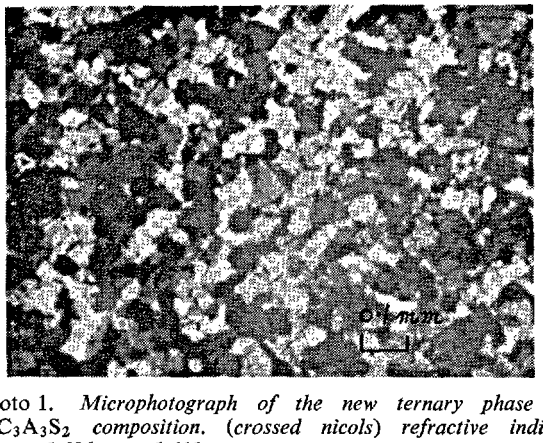

Photo 1. *Microphotograph of the new ternary phase of* $C_3A_3S_2$ *composition. (crossed nicols) refractive indices* $\omega = 1.606$, $\epsilon = 1.611$.

in Fig. 6–B. In this case, it decomposes into gehlenite, anorthite and CA_6 by an exothermic reaction of 1315°C.

From the above facts, the new crystal phase can be considered as the metastable solid solution of the ternary system CaO–Al_2O_3–SiO_2.

The authors are especially grateful to Dr. K. Chujo, Managing Director and to Dr. J. Yamada, Director of the Laboratory, Nihon Cement Co., Ltd., for the permission to publish this report.

References

1. H. G. Midgley "Melilite from high-aluminous cement" Proc. 3rd International Symposium on the Chemistry of Cement, London 1952, Cement and Concrete Association, London, p. 515–516.
2. J. R. Goldsmith "The system $CaAl_2Si_2O_8$–$Ca_2Al_2SiO_7$–$NaAlSiO_4$." Jour. Geology LV Nr. 5 pp. 381–404 (1947).
3. Olav H. J. Christie "On sub solidus relations of silicates. III. A contribution to the chemistry of melilites" Norsk Geologisk Tidsskrift **42,** See p. 26 (1962).

Oral Discussion

Yoshio Ono and Kinjiro Fujii

I would like to ask about the new compound C_3A_3S. The optical properties as well as the specific gravity of C_3A_3S resemble those of melilite. The lattice constants a and *c*, however, are very close to those of feldspars.

Is it not possible that C_3A_3S has similar structure to anorthite, the composition of anorthite $CaAl_2Si_2O_8$ being partially replaced by monocalcium aluminate $Ca_2Al_4O_8$?

Author's Closure

Kozo Sugiura and Takashi Yoshioka

We have not attached much importance to the facts that the refractive indices and the specific gravity of the new crystal resemble those of gehlenite and that the lattice constants are close to those of anorthite. It seemed to us however that these facts have no any special meaning, because the new crystal phase seems to be one of the stuffed derivatives of silica structures (1). We give on reasoning as follows:

Further studies were made by T. Yoshioka on the

systems $3CaO \cdot 3Al_2O_3 \cdot 2SiO_2$–$NaAlSiO_4$ and $3CaO \cdot 3Al_2O_3 \cdot 2SiO_2$–$KAlSiO_4$ by the same method as described in the main paper. In the former system the new crystal single phase was obtained up to 3% $NaAlSiO_4$ composition. In 3~10% $NaAlSiO_4$ compositions the specimens were composed of two phases; one was the new crystal and the other the nepheline solid solution which resembles that of $NaAlSiO_4$–$CaO \cdot Al_2O_3$ system described by J. R. Goldsmith (1949) (2). In the compositions of more than 12% $NaAlSiO_4$ the nepheline solid solution was obtained as a single phase. The solid solution was optically positive up to 70% $NaAlSiO_4$ composition but at about 80% $NaAlSiO_4$ composition it was isotropic and above 80% it was negative, accompanying small amount of carnegieite. In the latter system the new crystal was obtained as a single phase up to 5% $KAlSiO_4$ composition. In the composition of more than 5% $KAlSiO_4$ the new crystal was found existing with the other crystal phase which was obtained as a single phase in the compositions of 13~50% $KAlSiO_4$. It was optically uniaxial positive and its X-ray powder pattern was almost identical with that of the nepheline solid solution above mentioned. It can be considered as K, Ca-nepheline solid solution.

It was observed that the new crystal resembled the nepheline solid solutions in its X-ray powder pattern. Therefore the powder data of the new crystals were re-examined to certify that they had hexagonal symmetry. In this case, a more acceptable match was obtained between Q-values observed and calculated and most of the reflections of the new crystal had the same indices with those of the nepheline solid solutions. On the assumption that the new crystal had a similar lattice with that of nepheline, a_0 of $3CaO \cdot 3Al_2O_3 \cdot 2SiO_2$ crystal was indentical with that extrapolated from the nepheline solid solutions, but rather different as to c_0. For example,*

nepheline s. s. of 88 $C_3A_3S_2$12$NaAlSiO_4$
composition . . . a_0 10.002 Å, c_0 8.410 Å
nepheline s. s. of 86.8 $C_3A_3S_2$13.2$KalSiO_4$
composition . . . a_0 10.036 Å, c_0 8.432 Å
new crystal of $100C_3A_3S_2$
composition . . . a_0 10.008 Å, c_0 8.224 Å

In this way we believe that the structure of the new crystal has a close relation to that of nepheline, a stuffed derivative of high temperature-tridymite.

It is also expected that some interesting relations can be found between the structures of the new crystal and that of $CaO \cdot Al_2O_3$ which is also a stuffed derivative of high temperature-tridymite.

*These were calculated from the d-values of 21.0, 21.1, 20.2, 30.0 of the nepheline and nepheline-type solid solutions observed by using Si as a standard.

References

1. Buerger, M. J. (1954), The stuffed derivatives of the silica structures: Am. Min., **39**, 600–614.
2. Goldsmith, J. R. (1949), Some aspects of the system $NaAlSiO_4$–$CaO \cdot Al_2O_3$: Am. Min., **34**, 471–493.

Author Index

For Volume I

Subject Index

For Volume I

V-ISCC
PRINCIPAL PAPER

SESSION—1

STRUCTURE OF PORTLAND CEMENT MINERALS

1968
TOKYO

By
André Guinier and Micheline Regourd
(France)

On Preprint of Principal Papers and Other Information

Dear Sirs:

Please find enclosed herewith Preprint of Principal Papers (Full texts) covering 16 Principal Papers, which is distributed to each enrolled member of the Symposium as announced in Preliminary Program. Other 4 Principal Papers will be distributed in the same way as soon as we receive them.

Preprints in full text is prepared for Principal Papers only, so Written Discussions will be made only in connection with Principal Papers. (Please refer to Page 13 of "Circular No. 2"). Those who want to present Written Discussions will send their Paper in conformity with the instructions of "Guide for Authors of Supplementary Papers and Written Discussions" to the Organizing Secretariat so that they may arrive thereto not later than the end of June 1968.

After the example of Supplementary Papers, application of Written Discussions will be allowed at the rate of one Discussion per person, and for regular member only. Abstracts in 1000 Words of Written Discussions will be distributed at the Symposium site.

ORGANIZING SECRETARIAT
FOR
V — ISCC
c/o THE CEMENT ASSOCIATION OF JAPAN
HATTORI BLDG. NO. 1, 1-CHOME,
KYOBASHI, CHUO-KU, TOKYO, JAPAN

Corrigenda: "Structure of Portland Cement Minerals" by André Guinier and Micheline Regourd (France)

Page	Line	Errors in the text	Corrections
23	23	lime content lower than 73.68 %	lime content higher than 73.68 %
40	22	the $(SiO_4)^{4-}$ group by $(SO_4)^{3-}$ or $(SO_3)^{2-}$	the $(SiO_4)^{4-}$ group by $(PO_4)^{3-}$ or $(SO_4)^{2-}$
Figure captions 2 8 (fig.7)		taken at 680° and 650°C	taken at 600° and 650°C
3 27 (fig.19)		$\gamma \longrightarrow \alpha'_H$ transformation	$\gamma \longrightarrow \alpha'_L$ transformation

STRUCTURE OF PORTLAND CEMENT MINERALS

André Guinier and Micheline Regourd

(France)

CONTENTS

SYNOPSIS

In Portland cement clinker, the four principal constituents are found in the form of solid solutions. The polymorphic variations of these solid solutions being numerous and ill-defined, we have first dealt with the structure and polymorphism of the pure compounds.

Pure C_3S, passes through six allotropic forms between ambient temperature and 1100°C, all very close to the trigonal high-temperature form. A pseudo-structure which is a good approximation to the real structure has been proposed by Jeffery. Alites usually crystallise in the monoclinic and trigonal forms of C_3S.

On the other hand, the five forms of C_2S are different. Their crystal lattices are distinct and the stacking of silicate tetrahedra differs from one to another. Only the structures of β and γ have been determined. Belites usually crystallize in modified β forms, more rarely as the γ' form.

The cubic structure of C_3A has not been determined. Tricalcium aluminate forms solid solutions with the aluminoferrites of the interstitial phase. This can occur as a glassy phase when clinkering temperature is high, quenching rapid and the A/F ratio > 1.

The hydraulic properties of the clinker constituents are linked to their crystal structure, particularly the irregular Ca co-ordination, and the presence of holes in the structure. All the forms of C_3S show comparable reactivity whereas the forms of C_2S differ in their hydraulic properties.

INTRODUCTION

This is a study of the four minerals which are the principal constituents of all portland cement clinkers and are designated, following the classical abbreviations, as C_3S, C_2S, C_3A and C_4AF.

In fact, each of these abbreviations represents a group comprising the pure phase and the solid solutions having a crystal lattice with identical or very similar lattice dimensions. The alites and belites which correspond respectively to C_3S and C_2S are the solid solutions formed by the addition of impurities which are present in all commercial cement clinkers and are principally the ions or oxides of Al, Mg, Fe, Na, K, Cr, Ti, Mn, P, et cetera. Even when no impurities are present, the aluminoferrite, "C_4AF", can have a variable composition $C_2(A_pF_{1-p})$ where p varies from 0 to 0·7.

On a polished clinker surface, the microscope clearly distinguishes the different phases. C_3S appears in the form of well-defined crystalline grains varying in size from 10μ to 40μ. C_2S occurs as rounded crystals or twinned polyhedra, with a smooth or striated surface.

Figure 1

Between these grains there lies an interstitial phase in which it is sometimes possible to identify well-formed crystals of C_3A but often the interstitial phase is so finely crystallised that the individual grains are not visible.

The object of this paper is to describe the crystal structure of each of the phases listed above and how the structure varies with temperature and with additions to the pure stoichiometric composition.

The whole system presents a difficult field of study because, with certain exceptions, one cannot obtain the clinker phases in the form of single crystals of sufficient size to permit a structure determination by classical methods. In general, one is reduced to characterising a phase solely by its lattice, deduced from powder diagrams. But even this technique is difficult to use in this field because of the low symmetry or large unit cell of certain phases and above all because the variations which one is trying to detect as a function of temperature or of additions are very small. Furthermore, it has only recently become possible to obtain high quality powder patterns at temperatures up to 1500°C. In his paper of 1960, F. Ordway[1] insisted upon the necessity for developing special high temperature techniques adapted to the study of clinker minerals.

The results obtained by X-ray diffraction must obviously be checked with those given by other techniques such as microscopy, infra-red absorption, spectroscopy, electron-probe microanalysis, etc., and especially differential thermal analysis.

Numerous papers have appeared on problems in this field. Not all of these are based upon the use of the most sophisticated techniques and contradictions exist between the results reported. However, on the whole, certain facts emerge which clarify the

problem. A general review must naturally emphasise the points on which there is agreement but one must also mention other observations even where they are contradictory.

In order to resolve these two incompatible demands, we have chosen not to follow the chronological order in reporting successive papers. In each chapter of this article, dealing respectively with tricalcium silicate, dicalcium silicate and the interstitial phase (calcium aluminoferrite and tricalcium aluminate), we begin by giving what we ourselves regard as the most complete and satisfactory solution to the structural problem. Next, we group the studies which make a partial contribution to the preceding results, or contradict them. We try then, in the latter case, to discuss the possible origin of these differences with what we consider to be the most probable solutions.

In the conclusion, we discuss the general character of the polymorphism of the calcium silicates and hence the relations between the crystal structures and clinker properties.

TRICALCIUM SILICATE

It is the tricalcium silicate phase which has the most numerous allotropic forms. We have shown that there are six between ambient temperature and 1100°C. One can find all the same forms in the solid solutions but all have lattices extremely close to trigonal, the simplest form.

The X-ray powder diffraction patterns are indistinguishable except for slight movements of certain lines or their separation into very close multiplets; but the relative intensities do not vary. This shows that the structure of the least symmetrical forms remains, to a very good approximation, that of the most symmetrical.

Jeffery's Structure[2]

The structure of C_3S has been determined by Jeffery on a single crystal of sufficient size, which was isolated from a blast-furnace slag. In this work, which dates from 1950, Jeffery, on the basis of the visually estimated intensities of the diffracted spots (without Lorentz-polarization correction), determined a trial structure which is a good approximation to the true structure. O'Daniel, Hahn and Müller[3,4] have confirmed these results by a Patterson synthesis. No other structure has been proposed.

The pseudo-structure, proposed by Jeffery, is trigonal, with a = 7, c = 25 Å (hexagonal notation), space group R3m. It is composed of independent tetrahedra; three SiO_4 tetrahedra and three oxygen ions lie on the trigonal axes.[5] The calcium ions link the tetrahedra and are octahedrally co-ordinated to

the three oxygen ions which are not linked to Si^{4+} (see Figure 2).

Figure 2

Identical columns are found on each trigonal axis, but at different heights (see Figure 3). These form irregular octahedra

Figure 3

of atoms around the calcium ions and leave holes large enough to accommodate other atoms.

It is the irregular co-ordination of the Ca ions (the bonds vary from 2·54 to 3·24 Å) and the holes adjacent to these ions that give C_3S its hydraulicity.

Nevertheless, Jeffery's structure is certainly only approximate. The lattice of the lower temperature forms is not the simple trigonal. We have tried to grow crystals from molten $CaCl_2$[6]. From a number of crystals between 4 and 10 μ, we chose a 7 μ pseudo-hexagonal crystal. An oscillation photograph shows superlattice lines corresponding to a = 14 Å [7]. Construction of the reciprocal lattice from a Weissenberg photograph gives approximate values for b and c of 14 and 25 Å. The parameters may be obtained more accurately by indexing powder photographs on a pseudo-hexagonal lattice.

Study of Polymorphic Transformations of C_3S by DTA

The results of differential thermal analysis are the most straightforward and a definitive list of the transition points can be established (see Table 1). Four reversible DTA peaks at

Table 1

600°, 920°, 980° and 990°C characterise C_3S (see Figure 4).

Figure 4

Due to the powerful resolution of micro DTA[8], the peaks at 980° and 990° are well resolved. The thermal effects of these transitions are very weak, smaller than the α - β transformation of quartz (1·4 cal/g)[9]. The transformation point at 990° was discovered both by Boikova and Toropov[10] in pure C_3S, and by Woermann, Hahn and Eysel[11] in both C_3S and in the solid solutions.

Boikova and Toropov[10] cross-checked the DTA results by a study of a small crystal on a high-temperature microscope. The transformations at 620°, 920° and 980° could be observed and were found to be reversible, but the authors do not indicate whether the crystal transforms without change of habit.

Study of the Polymorphic Transformations of C_3S by X-ray Diffraction (XRD)

At high temperature, the lattice is trigonal. On cooling, the lowering of the symmetry causes splitting of the hexagonal reflexions into groups of lines whose number and spacing permit the determination of the true lattice[7].

At 1100°C the lattice is trigonal, with hexagonal parameters a = 7·15, c = 25·56 Å. The 30 lines of the powder pattern (up to 1.48 Å) show the extinctions corresponding to space-group R3m: $-h + k + l = 3n$.

Our results are in good agreement with Jeffery's predictions, deduced from the trial structure.

With decreasing temperature, the transformations are clearly visible on three hexagonal spacings $\bar{2}01$, $\bar{2}04$ and 220, which become successively doublets and triplets (see Figure 5).

Figure 5

In the range of temperatures used, the 009 reflexion does not show any splitting at all and its relative intensity remains constant relative to the other reflexions. The stacking of planes perpendicular to c, about 8·4 Å apart, therefore remains the same. A sliding of these planes in the direction perpendicular to the c axis takes place.

The principal characteristics of the transformations are:

1) 1050°C: change of symmetry from rhombohedral → monoclinic ($R \rightarrow M_{II}$). The transformation is continuous and only the hexagonal basal plane is deformed (see Figure 6).

Figure 6

The pseudo-hexagonal cell deduced from the reduced cell chosen according to Donnay[14] is defined by the parameters a = b = 7·130 Å, c = 25·43 Å, $\alpha = \beta = 90°$, $\gamma = 119.88°$. This can be considered as an orthorhombic cell with parameters a = 12·342, b = 7·143, c = 25·434 Å [7].

Nevertheless, the structure cannot be anything but monoclinic: the small but continuous deformation of the trigonal lattice does not permit of the formation of an orthorhombic structure; there is no orthorhombic sub-group of the trigonal space group. The transformation is probably of the second order, the structure can only be monoclinic (M_{II})[15].

2) 990° C: discontinuous transformation of the unit cell without change of symmetry: $M_{II} \rightarrow M_I$. The components of the doublets $\bar{2}01$, $\bar{2}04$ and 220 are clearly separated (see Figure 5).

As well as the deformation of the hexagonal basal plane, there is now added an inclination of the c axis to this plane ($\beta = 89.88°$) (see Figure 6).

The stability region of the M_I phase is only 10°. We suspected the presence of this form from the small signal given by μ-DTA at 990°C. We therefore took a series of photographs between 970° and 990°C and found a diagram characteristic of M_I. The components of the doublets are, indeed, less well defined than in the other forms but this variety has been confirmed in solid solutions of $C_3S + Al_2O_3$ by both Bigaré[12] and Woermann, Hahn and Eysel[11]. These authors have all observed an increase in the zone of stability of M_I to 60° for the solid solution C_3S + 1% Al_2O_3.

3) 980°C: change of symmetry $M_I \rightarrow T_{III}$. The characteristic doublets become triplets and the lattice is now triclinic; in the hexagonal basal plane the three axes a, b and d are different. A diagram taken at 940° shows about 100 lines which cannot be indexed without doubling the pseudo-hexagonal parameters a and b to 14 Å. The superlattice in the basal plane only involves a change of orientation of the rhombohedron in which obverse becomes inverse. If one retains the orientation of the original unit cell, the extinction rule is not the same: it becomes $+ h - k + l = 3n$[15]. At 940°, the pseudo-hexagonal cell has the parameters a = 14·229, b = 14·249, c = 25·412 Å, α = 90.10°, β = 89.85°, γ = 119.76°.

4) 920°C. Although DTA gives a strong signal, we observe no change of symmetry, nor any change in volume of the unit cell. The components of the triplets, arising from the hexagonal reflexions $\bar{2}01$, $\bar{2}04$ and 220 separate progressively from 980° until 620°.

5) 600°C. No change of symmetry is observed but a slight discontinuity in the splitting of the characteristic triplets.

6) 20°C. On a photograph exposed for 40 hours (6 mA, 30 Kv, Cu K α), we detected two very weak reflexions ($I/I_o < \frac{1}{100}$) with long spacings 14 and 8·2 Å. These are hk0 reflexions and would imply the doubling of parameters a and b. The new unit cell would be defined thus:

$$a = 28{\cdot}160 \qquad b = 28{\cdot}294 \qquad c = 25{\cdot}103 \text{ Å}$$

$$\alpha = 90.30^\circ \qquad \beta = 89.77^\circ \qquad \gamma = 119.53^\circ$$

The variations in the pseudo-hexagonal parameters from ambient temperature to 1100° are shown in Table 2.

Table 2

Nature of C_3S Transformations

The characteristic properties of the transformations of C_3S are collected in Table 3[15].

Table 3

DTA and X-ray have established 5 reversible transformations between six allotropic forms. Three of these transitions (990°, 980° and 600°) have been observed by both DTA and X-ray methods.

The transformation R - M_{II}, found by X-ray, gives no DTA signal. The transition, which is continuous and weak, extends over 60°, beginning at about 1050°. Possibly it is a second order transition.

The transition T_{III} - T_{II}, at 920°, undetectable by X-rays, is characterised by a strong DTA signal. The unit cell is triclinic up to 980° and the Debye-Scherrer pattern maintains the same relative intensities. The strong thermal effect is perhaps due to a second superstructure which, while leaving the

fundamental spacings unchanged, modifies the long spacings which are too weak to be detected under normal conditions. The superstructure found for T_I could exist equally in T_{II} (we have not verified this hypothesis because of the very long exposures which would be required at high temperature). A re-arrangement of the hexagonal groups in the lattice could vary the energy of the structure appreciably and this would explain the thermal effect.

To conclude, C_3S undergoes numerous small amplitude transformations around a constant atomic arrangement. All the transformations are of the "displacive" type[16]. They are produced by small movements of the atoms from their positions in the original structure, without any alteration of the general arrangement of the chemical bonds.

We have shown evidence of two types of transition: change of symmetry and superstructure:

- the hexagonal structure, advanced by Jeffery[2], is constructed of independent SiO_4 tetrahedra. At high temperature, the atoms of the SiO_4 tetrahedra are vibrating freely; the hexagonal unit cell shows a corresponding symmetry. As the temperature decreases, the degrees of freedom diminish and the departures from symmetry appear. They reveal themselves by changes in the X-ray powder diagram, that is to say, by the splitting of characteristic reflexions;

- the structure of C_3S is a stacking of hexagonal groups. With decreasing temperature the stacking faults give rise to a superstructure which is revealed by weak reflexions at low angles.

Certain of our results (the superstructure in T_{II}), not being directly proved, may be open to discussion. The powder patterns which we have studied permit determination of lattice dimensions and symmetry but give no other information on the structure. We are unable to distinguish a pseudo-orthorhombic form from a true orthorhombic structure. The superstructure in T_I is only indicated by the presence of two very weak Debye-Scherrer lines at long spacings. However, in an oscillating crystal photograph of alite (with the hexagonal axis parallel to the axis of rotation) Jeffery[2] has shown evidence for the existence of superlattice lines corresponding to a = 40 Å. Thus, in the T_I form of pure C_3S, it seems more likely that a = 42 Å than 28 Å.

The study of the polymorphism of C_3S demands experimental techniques with great powers of resolution. Only the combination of X-ray and DTA has given complete results. To elucidate the structural relations of the different polymorphs completely, it will be necessary to prepare single crystals of sufficient size.

Tricalcium silicate, being of type A_3BX_5, is isomorphous with tricalcium germanate, Ca_3GeO_5[17,18] and sodium fluoberyllate, Na_3BeF_5[19].

Other Studies on Tricalcium Silicate

All the transitions which have been described in the preceding paragraphs have not been detected by the first workers in the field either because they did not use DTA or because they had no X-ray equipment of sufficient resolution. On the other hand, transitions which proved to be due to an impurity (such as a small amount of C_2S) have been attributed to C_3S.

Thus Nurse and Welch[20] found 6 transformation points, at 464°, 622°, 750°, 923°, 980°, 1465°. An interpretation of this thermogram was proposed by Jeffery[21]. The first transformation corresponds to the dehydration of free lime. The peaks at 622°, 750°, 1465° are characteristic of the β - α', γ - α', and α' - α transformations of C_2S. The only peaks due to C_3S are those at 923° and 980°, characteristic of three forms following this scheme:

$$\text{Triclinic} \xrightarrow{923} \text{Monoclinic} \xrightarrow{980} \text{Trigonal}$$

Yamaguchi and Miyabe[22] repeated, in 1960, Jeffery's work, and defined the same polymorphic transformations. A triclinic, pseudo-orthorhombic unit cell, calculated by these authors, has the parameters

$$a = 12{\cdot}195 \qquad b = 7{\cdot}104 \qquad c = 25{\cdot}096 \text{ Å}$$

$$\alpha = 90 \qquad \beta = 89°44' \qquad \gamma = 89°44'$$

The transformation at 990° was not detected in a recent study by Miyabe and Roy[23]. These authors, on the other hand, attribute to C_3S a broad signal at 675°, which is characteristic of the $\beta \rightarrow \alpha'$ transformation of C_2S. Boikova and Toropov[10] have shown evidence for the existence of this thermal effect when the tricalcium silicate synthesis is incomplete. We ourselves have verified that, in DTA, traces of β C_2S give a thermal effect at 675°.

The polymorphism of C_3S has been studied, in 1964, with the help of powder patterns, by Miyabe and Roy[23], who used a high temperature diffractometer, as we ourselves were using a high temperature Guinier camera[24] (see Figure 7).

Figure 7

Figure 7 shows the diffractometer traces of Miyabe and Roy at 600° and 650°C, together with one of our double-exposure Guinier photographs taken at 600° and 625°C (1962)[24]. Miyabe and Roy found a mixture of phases T α and T β; we observed only, in accordance with the phase rule, T_I at 600° and T_{II} at 625°.

The resolution of the focussing camera[25] is better because we are operating with rigorously monochromatised ($Cu\ K\alpha_1$) radiation and we eliminate variations of intensity and apparent displacements of certain lines due to crystal growth at transformation points. The sample temperature is more difficult to measure than in the diffractometer but it is sufficiently uniform and well-controlled to give lines at high temperature which are as sharp as those produced at ambient. We have established a temperature scale using known transition points. This calibration curve between the heating current and the temperature of the sample-holder is re-adjusted with the help of the temperatures of the DTA peaks of C_3S. We can thus obtain a set of high-resolution photographs at selected temperatures which show the progress of the transformations.

Our results are in disagreement with those of Miyabe and Roy. The differences are as follows:

1) Miyabe and Roy found only the rhombohedral form (R) above 970°; we detected three modifications (R, M_{II}, M_I) above 980° (Figure 8).

Figure 8

2) According to Miyabe and Roy, the stable form between 980° and 920° is monoclinic. We have shown evidence, in the splitting of the 620 reflexion (620, $\bar{6}20$), for the presence of a triclinic form, T_{III}. The separation of the lines is 0·003 Å, which was not resolved by previous workers.

3) Miyabe and Roy obtained a considerable contraction of the unit cell of T_β between 600 and 700° Figure 9) suggesting a new transition, $T_\beta \rightarrow T_\gamma$, at about 700°. We consider that

Figure 9

some of the lines for T_β, T_γ and M are incorrectly indexed. If the spacings in Miyabe and Roy's diagrams are correctly indexed and the parameters recalculated, the contraction disappears (see Figure 10). The curve showing variation of pseudo-orthohexagonal

Figure 10

parameters is then similar to ours (Figure 11).

Figure 11

Solid Solutions of Tricalcium Silicate

The transformations of C_3S occur rapidly at well-defined temperatures, and without noticeable hysteresis. One cannot stabilize, by quenching, any of the high temperature forms.

On the other hand, if one introduces small amounts of foreign ions into the C_3S lattice, one obtains, at ambient temperature, phases which have the same lattice as one of the phases of pure C_3S. There is thus, by additions, stabilisation at ambient temperature of forms which in the pure compound only exist in narrow ranges of temperature. One might say that the disorder introduced by foreign ions is playing a role analogous to the disorder of thermal vibration.

Table 4

Table 4[15] indicates the nature of the phases observed by different additions, as a function of their concentration. The different solid solutions have been prepared by synthesis from pure materials. In clinker, the solid solutions must be more complex. Table 4 shows how one addition will not, in general, stabilize all the forms. The highest symmetry phase is stabilized by ZnO but not by any other single oxide. Nevertheless, it is observed in certain clinkers which contain insufficient ZnO but a very large number of other impurities (Al_2O_3, Fe_2O_3, MgO, Cr_2O_3, TiO_2, Na_2O, K_2O etc.). These complex mixtures have not been reproduced by synthesis. The studies of the solid solutions as a function of temperature have been made only on the simplest synthetic products and we will begin with the addition of ZnO which stabilizes the most complete range of phases[19].

Solid solutions of C_3S + ZnO. Zinc oxide stabilizes, at ambient temperature, the forms T_I T_{II}, M_I, M_{II}, R of C_3S[15]; Zn^{2+} replaces Ca^{2+} in the C_3S lattice. The variations in the parameters as a function of percentage of ZnO show clearly the different varities stabilized (Figure 12). The DTA results confirm the stability

Figure 12

ranges. The transformation temperatures are decreased by the addition of ZnO. At 0·75% ZnO the thermal effects at 920 and 980° merge into one with addition of their intensities. The stability zone of T_{III} disappears. Above 0·75% ZnO, M_I transforms directly to T_{II}. The fusion of the two DTA peaks implies a change of symmetry from monoclinic to triclinic, with the formation of two superstructures, simultaneously.

The temperature of the small signal at 990° does not vary and the thermal effect persists above 2·25% ZnO, into the region where, according to X-rays, M_{II} and R appear to be stabilized. This is a new example of a phase-change detected by DTA but imperceptible by XRD. Above 2·25% ZnO, the solid solutions C_3S + ZnO would again be monoclinic but of a form approaching so closely to rhombohedral that XRD cannot resolve the symmetry.

There is one difference between the monoclinic forms M_I and M_{II} of pure C_3S and the solid solutions C_3S + ZnO. The characteristic reflexions 224, $\bar{4}04$ and 620, 040 are reversed (Figure 13).

Figure 13

This inversion has already been observed by Yamaguchi and Miyabe[22] and interpreted in a study of the solid solutions $3CaO\text{-}SiO_2\text{-}Al_2O_3\text{-}MgO$ by Yamaguchi and Kato[26]. It corresponds to a different a/b ratio of the pseudo-orthohexagonal parameters and a different β angle. In the case of pure C_3S at 985°: $a/b < \sqrt{3}$, $\beta \leq 90°$, in the solid solution C_3S + 2% ZnO: $a/b > \sqrt{3}$, $\beta > 90°$. The monoclinic forms of the solid solutions reverse at high temperature to the monoclinic forms of pure C_3S. The intermediate form with $a/b = \sqrt{3}$ and $\beta = 90°$ has an orthohexagonal unit cell even though the symmetry is not rhombohedral.

Ono, Uno and Kanai[27] have also stabilized the trigonal form of C_3S by the addition of 6·3% ZnO. Furthermore, a solid solution C_3S + 15% C_3A + 5% CaF_2, prepared by the same authors, is reported as rhombohedral with hexagonal parameters a = 7·088, c = 25·115 Å, but the optic axial angle 2V is not 0 as in the case

of C_3S + 6·3% Zn_3SiO_5; it is less than 15°(-). Presumably, this solid solution is not truly hexagonal.

Solid solutions C_3S + MgO. Woermann, Hahn and Eysel[11] have proposed, for the solid solutions C_3S + MgO, the following formula: $(Ca_{1-x}Mg_x)_3SiO_5$, where $0 \leq x \leq 0{\cdot}0125$ at 1550°C. The Mg^{2+} ions replace an equal number of Ca^{2+} ions in the C_3S lattice[28]. The solubility limit is 2% MgO but this depends on the temperature[26,29]. In addition, CaO dissolves small quantities of MgO[30]. Thus crystals of the solid solutions Ca_3SiO_5 - "Mg_3SiO_5" and (Ca, Mg)O[31] can co-exist. The forms of C_3S which are stabilized are T_I (up to 0·55% MgO), T_{II} (0·55 to 1·45% MgO) and M_I (from 1·45 to 2·0% MgO). Above 2%, periclase appears, identified both optically and by the lines in the X-ray powder diagram. In the monoclinic form, the characteristic lines are again inverted: in the solid solution C_3S + 2% MgO, $a/b = 1{\cdot}737$ and $\beta = 90.12°$[32].

Solid solutions C_3S + Al_2O_3. The alumina incorporated in the lattice of C_3S can be either in the form of Al_2O_3 or C_3A. Woermann, Hahn and Eysel[11] have distinguished two types of solid solution:

a) between 0 and 0·45% Al_2O_3

Al^{3+} replaces Si^{4+} in the tetrahedra but occupies the free octahedral sites also, thus maintaining the electrostatic neutrality of the lattice. The formation of the solid solution, by both addition and substitution, is expressed by the formula:

$$Ca_3^{IV}\ Al_{\frac{x}{4}}^{VI'}\left(Si_I - \frac{3x}{4}\ Al_{\frac{3x}{4}}\right)^{IV}\ O_5$$

where $0 \leq x \leq 0{\cdot}02$, VI' being a vacant octahedral site. The only form of C_3S stabilized is T_I[11,12].

b) <u>between 0·45 and 1% Al_2O_3</u>

above 0·4% Al_2O_3, the incorporation of Al_2O_3 may be:

- either the result of two linked substitutions: Si-Al (tetrahedral sites), Ca-Al (octahedral sites), following the formula:

$$\left(Ca_3 - \frac{x}{2}\ Al_{\frac{x}{2}}\right)^{VI}\quad\left(Si_I - \frac{x}{2}\ Al_{\frac{x}{2}}\right)^{IV}\ O_5$$

- or the continuous balanced replacement of Si by Al for the most part in the octahedral sites occupied by $Ca^{(VI)}$ and to a very small extent in the vacant octahedral sites (VI').

These interpretations appear more probable than that of Locher[28] in which the loss of the oxygens which are not bonded to the tetrahedra permits the neutralisation of the charge after substitution of Al for Si.

The form which is stabilized is T_{II}[10,11,29].

DTA shows the decrease in transformation temperatures of the forms stabilized by Al_2O_3, up to 1%, the limit of solubility. Above the solubility limit the lines of C_3A appear in X-ray powder patterns[12]. The solubility limit is independent of temperature. Midgley and Fletcher[29] found the same results, but maintain that the substitution of Al in the lattice is not due to insertion of C_3A in C_3S but to a solid solution of the series C_3S - "$C_{4\cdot5}A$".

The presence of Al does not change the type of substitution of Mg, but, on the other hand, Mg does affect the substitution scheme of Al[31].

Solid solutions $C_3S + Fe_2O_3$. The limit of solubility of Fe_2O_3 in C_3S is 1·05%[11]. Only the triclinic forms T_I (from 0 to 0·8% Fe_2O_3) and T_{II} (from 0·8 to 1·05% Fe_2O_3) are stabilized. According to Fletcher[33], the solid solutions are of the type C_3S - "C_3F": $3Ca^{2+}$ are replaced by $3Fe^{3+}$, $6Si^{4+}$ by $6Fe^{3+}$, and the charge is compensated by one Fe^{3+} ion in an interstitial position.

Other solid solutions of C_3S. Tricalcium silicate also forms solid solutions with the following additions: $La_2O.SiO_2$[34], $Y_2O_3.SiO_2$[35], SO_3[36], Co_2O_3[37] and Na_2O[38].

Na_2O substitutes for CaO in the C_3S lattice. Above 0·3% Na_2O, the structure is monoclinic with parameters a = 12·262, b = 7·053, c = 25·086 Å, $\beta = 90°07'$[39].

CaF_2[40] enters into solid solution in C_3S. At 0·74% CaF_2, the X-ray powder diagram is similar to that of alite in clinker. Above 0·74% there is a decomposition of C_3S into α' C_2S.

It seems equally probable that C_3S can take up to 1% P_2O_5 into solid solution[40], involving more a distortion of the lattice than true polymorphism.

Constitution and Structure of Alites in Clinker

In alites, one can find triclinic, monoclinic and trigonal forms[41,42]. In Figure 14, we show the patterns of two clinkers in which the alite is in the forms M_{II} (inverse) and R.

Figure 14

The alite grains in portland cement clinker appear to have trigonal symmetry and to be practically uniaxial. However, each grain is an assembly of numerous crystallites of lower symmetry,

twinned at 120°. As Jeffery[2] has suggested, these crystals are thus paramorphs of the high temperature form.

A recent study by Yamaguchi and Ono[43] shows evidence for two types of alite crystal: regular hexagons corresponding to the 0001 face and hexagonal sections elongated in the characteristic planes $1\bar{1}02$ and $10\bar{1}1$ (Figure 15).

Figure 15

The transition from rhombohedral → monoclinic is a small energy change: the monoclinic a axis coincides effectively with the rhombohedral c axis and the monoclinic b axis with one of the rhombohedral a_1, a_2, a_3 such that the twinning of the transformation is triple.

Jeffery[2] has considered alite as a definite composition with additional atoms in fixed lattice sites. In alite of formula $54CaO.MgO.Al_2O_3.16SiO_2$ there is replacement of Ca by Mg, of 2Si by 2Al, and the addition of one Mg ion in a vacant hole, to maintain neutrality of the lattice.

The structure of this alite is monoclinic, with parameters a = 33·08, b = 7·07, c = 18·56 Å, $\beta = 94°10'$, space group Cm. One of the pseudo mirror planes of the trigonal structure becomes a true mirror plane (Figure 2). The oscillation and Weissenberg photograph show a large number of satellite spots, which could be interpreted to give a "c" spacing of 150 Å.

The existence of different types of C_3S solid solutions shows that alite is a true solid solution. The introduction of foreign ions and balancing of charges are continuous and statistical. Alite is not a compound with a definite composition like the stoichiometric formula given by Jeffery. As early as 1958, Von Euw[44] showed that this composition contains C_3A as an impurity.

From powder diagrams, Yamaguchi and Miyabe[22] calculated the monoclinic unit cell of Jeffery's alite and found the parameters a = 12·246, b = 7·045, c = 24·975 Å, β = 90°04'. Ordway[1] re-calculated the unit cell to a = 12·248, b = 7·045, c = 24·972 Å, β = 90°06', an elementary cell which allows the indexing of all the lines visible in the powder diagram. Only Jeffery studied a single crystal of alite and was able to find the true larger unit cell.

Toropov and Volkonskii[45] (1960) and Chromy[46] (1964) observed only two forms of C_3S in clinker: β and α, the α' form being trigonal and the transformation $\beta \rightarrow \alpha'$ taking place at 1375°C.

Stability of Tricalcium Silicate and Alites

Several methods of preparation of tricalcium silicate have been reported[47,48,49,50,51]. Mineralisers such as NaF, Na_2SiF_6[47], LiCl[52], CaF_2, Co_2[53] accelerate the formation of C_3S. Complete synthesis of tricalcium silicate is difficult. Boikova and Toropov[10] detected, by DTA and by microscopy, C_2S in contact with C_3S. If this C_2S is saturated with CaO, the CaO/SiO_2 ratio becomes equal to 3·02 - 3·04 in tricalcium silicate.

On the other hand, a chemical and optical study by Woermann, Hahn and Eysel[31] has shown that tricalcium silicate is a definite compound, with the stoichiometric formula $3CaO.SiO_2$ (CaO = 73·68%, SiO_2 = 26·32%). In samples with a lime content lower than 73·68%, C_3S co-exists with free CaO; there is no C_2S.

C_3S is stable between 1250° and 2070°, the temperature at which it melts incongruently to form CaO and a liquid phase[54]. Below 1250°, pure C_3S does not decompose[55,22] or its decomposition is so

slow that it can only be detected by the analysis of trace quantities of free lime[54].

Alite will decompose into belite and free lime in the presence of certain minor elements (K_2O, CaF_2). A considerable decomposition of alite occurs at 1180° in metallurgical clinkers. The Fe^{2+} ions replace the Ca^{2+} in the C_3S lattice[56].

DICALCIUM SILICATE

It is necessary to note first of all the differences that exist between the polymorphisms of C_2S and C_3S. The lattices of the different C_2S forms are known and their parameters are quite distinct. At the moment, only the structures of the β and γ forms have been determined; they are completely different. It seems equally certain that the α and α' structures show small but distinct differences. In addition, there is complete agreement between the transition points revealed by DTA and by XRD crystal analysis. In the case of C_2S we have the usual types of transformations, whereas in C_3S we have a very special case because all the forms can be derived from a single structure by slight variations.

Structure of the 5 Forms of C_2S

α C_2S. Of all the forms of C_2S, the α form, which exists only between 1425° and its melting point, at 2130°C, has been least studied because of the difficulties of carrying out high temperature experiments.

The most recent work is that of Yamaguchi, Ono, Kawamura and Soda[57] who used diffractometry at 1500° to determine the trigonal lattice (space group P $\bar{3}$m 1) with parameters a = 5·527, c = 7·311 Å (hexagonal notation). These results agree with those of Bredig[58] (a = 5·45, c = 7·19 Å) obtained from high temperature powder photographs taken by Van Valkenburg and McMurdie[59]. The space group is C $\bar{3}$m (P $\bar{3}$m 1) by analogy with glaserite, $NaK_3(SO_4)_2$.

The other determinations have been made on stabilized phases but with additions of such large proportions that one ought to consider whether the lattice has been substantially altered. Thus a α form "stabilized" by 2·5% Al_2O_3 + 2·5% Fe_2O_3 + 6% Na_2O has parameters a = 5·419, c = 7·022 Å[57].

A.M.B. Douglas[60] observed a small amount of a trigonal phase, with parameters a = 5·46, c = 6·76 Å, similar to α' C_2S, in the 'single' crystals of bredigite extracted from vugs in blast furnace slag. These composite crystals, of composition $Ca_{1·59}Ba_{0·08}Mg_{0·31}Mn_{0·09}SiO_4$, always contained the trigonal and orthorhombic phases in fixed relative orientation.

The crystals of nagelschmidtite $2Ca_2SiO_4.Ca_3(PO_4)_2$, also extracted from a vug in slag[61], have a hexagonal lattice defined by unit cell parameters which are multiples of those given above: a = 21·80, c = 21·54 Å. Likewise, Yamaguchi, Miyabe, Amano and Komatsu[62] in 1957, have suggested that the lattice of glaserite cannot be applied to α C_2S unless a is multiplied by 4 (a = 21·8) and c by 3 (21·50). The unit cell of α C_2S would, in this case, be more complex, but these results were not retained by Yamaguchi, Ono, Kawamura and Soda[57] in 1963.

α' C_2S. There exist two forms of α' C_2S: α'_H and α'_L whose stability regions are respectively 1420° - 1160°C and 1160° - 675°C[63]. The parameter variation curves calculated by Niesel and Thormann[63] from diffractometer traces of pure C_2S, show a reversible change of slope at 1160°C. We ourselves, with the help of high-temperature powder photographs, have

confirmed the existence of two different forms of α' C_2S at 1145° and 1200°C. Our results form the subject of a Supplementary paper to this Symposium.

Smith, Majumdar and Ordway[64] have already observed on diffractometer charts a variety $C_2S\,\alpha'_L$, obtained by heating γ C_2S, slightly different from $C_2S\,\alpha'_H$, obtained by cooling the α form. Similarly, Yamaguchi, Ono, Kawamura and Soda[57] have detected differences of intensity in the lines of α' prepared from α on the one hand and from γ on the other. This intensity difference disappears towards 1100°C. At 1300°C, the orthorhombic unit cell of $\alpha'_H C_2S$, calculated by Yamaguchi, Ono, Kawamura and Soda[57] from powder patterns, has parameters a = 6·883, b = 5·600, c = 9·543 Å (space group Pnma).

Determinations have been made on stabilized α' forms. Thus, for a phase containing 10% $CaMgSiO_4$ and 4% K_2O, Yamaguchi, Ono, Kawamura and Soda[57] found the following parameters: a = 6·748, b = 5·494, c = 9·261 Å. The form stabilized corresponded to the form $\alpha'_H C_2S$ above, described by the same authors. In this case, the differences are not due solely to thermal expansion, but also to distortion of the lattice by the impurities.

Douglas[60], working on the natural mineral bredigite, usually considered identical with α' C_2S, and on the composite crystals referred to above, calculated a cell which has the a and b parameters doubled: a = 10·91, b = 19·41, c = 6·76 Å (space group Pmnn) and she found a similar cell by indexing Trömel's powder

data[65] taken at 750°C; certain weak lines necessitate the doubled cell. Ordway[1] points out that the powder patterns of pure α' C_2S and Douglas's material are significantly different though the structures are probably closely related.

The α' C_2S structure is unknown. Bredig[58] has proposed the hypothesis that it is analogous to that of β K_2SO_4. Majumdar, Smith and Ordway[66] give a model founded upon the analogy between β C_2S and β K_2SO_4 but without justification by intensity measurements.

_β C_2S. The most precise determination of the parameters was obtained by Yannaquis[55] using a synthetic preparation of pure β C_2S. The lattice is monoclinic with parameters a = 5·507, b = 6·754, c = 9·317 Å, β = 94°38' (A.S.T.M. card 9-351), space group $P2_{1/n}$

From a powder diagram of β C_2S at 550°C, Yamaguchi, Ono, Kawamura and Soda[57] have proposed a monoclinic unit cell with parameters a = 5·558, b = 6·823, c = 11·261 Å, β = 123°11', space group $P2_{1/c}$, which is identical to the Yannaquis's lattice (see figure 16)

Lattice determinations have also been made on stabilized β C_2S phases: C_2S + 0·5% B_2O_3 is defined by the parameters a = 5·48, b = 6·76, c = 9·28 Å, β = 94°33', (space group $P2_{1/n}$)[61] and β C_2S + 0·25% Cr_2O_3 by parameters a = 5·514, b = 6·757, c = 11·197 Å, β = 123°59'[57]. These results show that the distortions introduced by foreign ions, though not negligible, are very small.

The structure of monocrystals of β C_2S stabilized by 0·5% B_2O_3 is monoclinic[61], and is constructed from independent SiO_4 tetrahedra and two sorts of Ca atoms. Four of these 8 Ca atoms (Ca_I) are placed alternately above and below the SiO_4 tetrahedra in the direction of the b axis. The structure can be described as columns of alternating tetrahedra and Ca atoms, linked together by the other four Ca atoms (Ca_{II}) placed in the holes between the tetrahedra[21]. The pseudo-trigonal arrangement of the SiO_4 tetrahedra around the Ca_{II} atoms is shown in Figure 16.

Figure 16

The co-ordination of Ca_I is irregular: 6 neighbours lie at distances between 2·30 and 2·75 Å and six others between 2·98 and 3·56 Å. If the co-ordination is equal to 9, the contribution of each of the six nearest neighbours being $^2/_9$ and that of the other six $^1/_9$, Pauling's rule is approximately satisfied. The co-ordination of Ca_{II} is equally irregular. The eight neighbours belonging to six neighbouring tetrahedra lie at distances between 2·36 and 2·80 Å.

This structure, determined by Midgley[61] from 200 h0l, 0kl and hk0 reflexions, has a "reliability" factor of 19%, the R factor being reduced to 9% by McIver[67]. McIver suggests that the space group $P2_1/n$ is incorrect, the true space group being one of: $P2_1$, Pn, $P\bar{1}$ or P1. Furthermore, Midgley notes that slight displacements of the atoms transform this structure to an orthorhombic structure of the β K_2SO_4 type, and somewhat

larger changes give a trigonal structure (α C_2S). The polysynthetic twinning occurs on the (100) and (001) planes (Figure 16) which become the planes of symmetry in the structure of α' C_2S.

The unit cell of Yamaguchi, Ono, Kawamura and Soda[57] defined by the parameters a', b', c' (Figure 16) is deduced from that of Midgley (a, b, c) by the following relations:

$$\vec{a'} = \vec{a}, \quad \vec{b'} = \vec{b} \quad \vec{c'} = \vec{c} - \vec{a}$$

γ C_2S. The unit cell has been determined from powder data by several authors. Their results are in agreement:

a = 5·076 b = 6·756 c = 11·230 Å (space group Pmcn) A.S.T.M. card 9-369[55];

a = 11·232 b = 6·773 c = 5·083 Å[57] (space group Pnma);

a = 5·091 ± 0·010 b = 11·371 ± 0·020 c = 6·782 ± 0·010[66] (space group Pbnm).

The volume expansion during the β - γ transformation on cooling, shatters the crystals into fragments too small (1 - 100 μ) for single crystal study. Smith, Majumdar and Ordway[54] prepared C_2S from ethyl orthosilicate hydrolysed by a solution of $Ca(NO_3)_2$. The mixture was dried at 100°, denitrated at 400°, heated to 1500° and quenched in air. Several single crystals were isolated and their complete structure was determined. This structure is of the olivine type Mg_2SiO_4[55,56]. The Ca^{2+} ions replace the Mg^{2+} but, being larger, expand the unit cell of Mg_2SiO_4 but without altering the general regular arrangement[21]. The SiO_4 tetrahedron is irregular (Figure 17). The Si-O distances

Figure 17

vary from 1·589 to 1·725 Å. This irregularity is probably due to the distortions in the hexagonal arrangement of the oxygen ions. All the Ca ions are octahedrally co-ordinated; the low co-ordination of Ca explains the greater molar volume of the low temperature phase.

There is also a structural analogy between C_2S and Na_2BeF_4[68,69] on the one hand, and C_2S and Ca_2GeO_4[70] on the other.

Other Studies on C_2S

Apart from these five phases which are universally agreed and well defined, some authors have claimed the existence of other modifications.

1) A modification of β, called β', has been detected by Vasenin[71] in a DTA study. This phase, as described by Toropov, Volkonskii and Sadkov[72], has a pattern similar to that of α', and is stable from 900 to 1230°C. Its existence seems to be confirmed by a DTA signal at 1230°, found by Schlaudt and Roy[73] in a study of the system Ca_2SiO_4 - $CaMgSiO_4$. The β' phase has not been confirmed by Welch and Gutt[40] nor by ourselves.

2) Kurdowski[74] reported a new phase produced at 600° from a β form stabilized by excess silica, which was very close to β. This phase appears doubtful because excess silica does not stabilize β C_2S but favours the transformation $\beta \rightarrow \gamma$ [30].

3) A cubic form stable at 1600° has been reported by Saalfeld[75]. His high temperature patterns show an absence of 110 reflexion and enhanced intensity of 102. This behaviour, which is reversible, could be due either to a variation of the hexagonal axial ratio c/a resulting from the rotation of the anions or to the formation of a cubic phase (a = 5·8 Å). The trigonal 102 reflexion would become the cubic 200. Since 1953, this phase has not been reported by other research workers. However, a solid solution $C_2S + Na_2O$ reported by Ono[76] is perhaps a superstructure of Saalfeld's cubic form stabilized at room temperature. The mineral obtained in the $CaO - SiO_2 - Al_2O_3 - Fe_2O_3$ system by an equimolar substitution of Na_2O for CaO is isotropic with a = 17·769 Å ≠ 3 x 5.8.

Study of the Transformations of C_2S

To describe the processes of change from one phase to another, we will consider the transformations observed first with decrease and then with increase in temperature.

1) With decreasing temperature. We start with the α phase, stable at high temperature (t > 1420°):

$\alpha - \alpha'_H$: the transformation is reversible without hysteresis (Figure 18). The structural changes of the $\alpha - \alpha'_H$ inversion

Figure 18

cannot be characterized with certainty. Smith, Majumdar and Ordway[66] suggest that "half the SiO_4 tetrahedra rotate so that their apices point in opposite directions at the phase change. The rapidity of the transformation is certainly facilitated by the elevated temperature, even though the change may require a structural

re-arrangement". Niesel and Thormann [63] have found at 1160°, a DTA peak, corresponding to the α'_H —— α'_L transformation.

$\alpha' \rightarrow \beta$: 650°. The transformation is reversible with a hysteresis of 25° (Roy[77] found a hysteresis of 50°); it occurs at a well-defined temperature. According to Smith, Majumdar and Ordway[66] the transformation involves a rotation of the SiO_4 tetrahedra and a change in the Ca ion co-ordination. From 8-fold in the α', the Ca co-ordination becomes variable, 8 or 9 fold, in the β form.

$\beta \rightarrow \gamma$: the β phase forms the γ by the process $\alpha' \rightleftarrows \beta \rightarrow \gamma$ This monotropic transition involves a considerable change in volume (dusting). From the structural point of view, the $\beta \rightarrow \gamma$ transition is a transformation of primary co-ordination[78]. According to Smith, Majumdar and Ordway[66] the transition involves a rotation of the SiO_4 tetrahedron and should be considered as semi-reconstructive because of the large movements of some of the Ca atoms. The sluggish nature of the transformation is perhaps due to the complexity of the bond re-adjustments.

The $\beta \rightarrow \gamma$ transformation has certain peculiar characteristics: in effect, it has been observed at different temperatures by different authors, 525°[79], 450°[71], 400°[74], 375°[80], 300°[81,82], and in addition it is incomplete. One usually obtains a mixture of β and γ but in variable proportions; one can obtain anything from nearly pure γ to nearly pure β. These phenomena will be the subject of a later paragraph.

2) <u>With increasing temperature</u>. At ambient temperature, one may start with either β or γ :

a) βC_2S: the transformation $\beta \rightarrow \alpha'_L$ takes place at 675° then $\alpha'_L \rightarrow \alpha'_H$ at 1160°[63] and $\alpha'_H \rightarrow \alpha$ at 1420°C.

The transformations are visible on DTA and are confirmed by XRD.

b) γ C_2S: starting with the γ phase, α'_L forms slowly between 725° and 860°C. The DTA peak is elongated (spread out). Guinier camera photographs (see Figure 19) taken at 750° and 850°

Figure 19

show the co-existence of the two forms γ and α'_L.

One can explain the different characters of the $\beta \rightarrow \alpha'_L$ and $\gamma \rightarrow \alpha'_L$ transformations by structural considerations. If the α'_L structure is only slightly different from β, it is very different from γ. The $\gamma \rightarrow \alpha'_L$ transformation is semi-reconstructive. According to Smith, Majumdar and Ordway[66] this implies a rotation of the SiO_4 tetrahedra, a change in Ca co-ordination from 6 to 8, and an appreciable displacement of one type of Ca atom. Like the $\beta \rightarrow \gamma$ transformation, its sluggishness is perhaps due to the complexity of the bond changes.

The whole group of C_2S transformations is shown schematically by Niesel and Thormann[63] (see Figure 20).

Figure 20

The energy diagram proposed by Bredig[58] now requires to be completed.

The different forms of C_2S can also be identified by infra-red absorption spectra[83,84].

Stabilization of Different Forms of C_2S

As indicated on Bredig's diagram, it is the γ phase which is most stable at ambient temperature. However, one can succeed in stabilizing α and α', and one can obtain β at ambient temperature.

Certain oxides, such as MgO, Al_2O_3, Fe_2O_3, BaO, K_2O, P_2O_5 and Cr_2O_3, stabilize both α' and α forms[85,86,87,88,89,90]. A phase previously considered to be a definite compound of composition $K_2O.23CaO.12SiO_2$ was shown by Suzukawa[91] to be a solid solution of K_2O in the α' form of C_2S. However, Welch and Gutt[40] could not obtain this form at ambient temperature, finding that it transformed rapidly to β. On the other hand, merwinite does not seem to be a solid solution of MgO in $\alpha' C_2S$[5], as was proposed by Bredig[58]. Yamaguchi and Suzuki[92] have prepared crystals of $3CaO.MgO.SiO_2$ of stoichiometric composition, and with a monoclinic structure (a = 9·336, b = 5·301, c = 13·286 Å, β = 92°8', space group $P2_1/c$). Furthermore, Gutt[93] reports the existence of a still higher Ca compound, $CaO_{1.7}MgO_{0.3}SiO_2$, which is stated to co-exist with the C_2S polymorphs. The most interesting problems are those of the $\beta \rightarrow \gamma$ transformation and the conditions of stabilization of the β form.

a) Influence of nucleation. Even with pure synthetic products, considerable variation can be observed in the conditions for the $\beta \rightarrow \gamma$ transformation. Yannaquis and Guinier[78] have reported the influence which crystallite size has upon the stability of β: this phase is more stable the smaller the crystals. Microscope observations show that grains of β which are stable at ambient temperature are never larger than 5 μ, although grains of γ which have been derived from β are in general 10 to 100 μ in size. These observations are confirmed by XRD patterns. The reflexions from a stationary sample of γ C_2S are spotty, while, under the same conditions, those of β C_2S are continuous.

Figure 21

(Figure 21).

This behaviour may be explained by the mechanism of the $\beta \rightarrow \gamma$ transformation, which operates by nucleation and growth. Let us suppose that nucleation is difficult; in these circumstances a grain of β, whatever its size, will transform entirely if it contains at least one nucleus of γ. If after the $\alpha' \rightarrow \beta$ transformation the crystals of the latter are sufficiently large, the probability that each grain will contain a nucleus of γ is high, and one obtains, at ambient temperature, a high proportion of γ. If, on the other hand, the crystals of β are very small, many of them will not contain γ nuclei and cannot transform during cooling.

One can thus predict that if one can succeed in preparing α' in very small grains, stabilization of the β form may be achieved. This condition is realised if C_2S is prepared by solid state reaction between CaO and SiO_2 at 1200°(94). In the stability range of the α' phase, the ratio rate of growth/rate of nucleation is low or nearly zero. In the same way, a sample of C_2S heated to 1550°C, in the α zone, gives 90% of β on quenching because the passage through the $\alpha \rightarrow \alpha'$ transition is very rapid and the crystals remain small. On the other hand, the same sample cooled slowly from 1550° to 1400° and then quenched, gives 95% γ. The slow passage through the $\alpha \rightarrow \alpha$ transformation allows time for crystal growth and in spite of quenching the transition $\beta \rightarrow \gamma$ is practically complete. This explains also the role of the temperature of 1420° in the stabilization of β or γ, which has been remarked by

several authors[64,95]. According to Niesel and Thormann[63] it seems that 1160° should be the optimum growth temperature for crystals of α' C_2S; if C_2S is synthesized below 1160°C, one obtains β, while a sample prepared at a temperature above 1160° gives a mixture of β and γ. One should point out that Chromy[96] has also shown, by optical methods, the effect of crystallite size of C_2S.

Again, the analogy between the structure of γ C_2S and $NaBeF_4$ is to be found in the nature of their transformations. The process of nucleation[97] is the determining factor in the transition $\gamma \rightarrow \alpha'$ of Na_2BeF_4.

b) Influence of pressure. The nature of the phenomenon of apparent stability of β C_2S has been more precisely defined[98]. It is possible to provoke a partial transformation from β to γ even at room temperature. Percussion of pellets of β C_2S will induce a transformation to γ of as much as 30%. Crushing between the platens of an hydraulic press may give up to 50% γ. The transformation is activated by the creation of nuclei of γ as the crystals are sheared under compression. On the other hand, if powdered β is submitted to hydrostatic pressure, even very high (9 tonnes/cm^2 = 8.8×10^5 KN/M^2), no transformation occurs; the γ phase is less dense than the β phase, and increase of pressure does not favour the transformation[99]. High pressures give β a stability region which does not exist at atmospheric pressure[77]. Thus, the β phase is stable at ambient temperature under 2 atmospheres and it would be possible to transform γ to β under 17 bars (100).

c) Stabilization by additions of foreign ions and by departures from stoichiometry. The effect of grain size is, according to the theory presented above, merely statistical; but other factors are certainly involved in the stabilization of β, in particular the presence of impurities or of excess CaO or SiO_2 over the stoichiometric ratio:

Effect of excess CaO: it is possible to introduce an excess of CaO (1%) into C_2S. The form obtained at ambient temperature is β, yet the crystals are quite large (10 μ). The specific effect of CaO is thus independent of that of size[78].

These results may be relevant to the work of Roy[77] who, having prepared large crystals of β C_2S from the hydrates, seemed to disagree with the theory of Yannaquis and Guinier. It is possible that these crystals were stabilized by an excess of CaO present in the hydrates[54].

Effect of an excess of SiO_2: the solubility of SiO_2 in C_2S lies between 1·5 and 2%, and the form obtained is γ. Crystals of C_2S - SiO_2 solid solutions range in size from 5 to 250 μ. The addition of silica modifies the distribution of growth rates in the C_2S crystal and favours the transformation $\beta \rightarrow \gamma$ [78].

The effect of an excess of SiO_2 can be seen in the dusting of badly quenched clinkers or slags. Microscopic examination shows that the sources of the dusting lie round the grains of quartz; the crystals of belite which are too rich in silica transform to γ.

Effect of foreign ions: B_2O_3 is the classical stabilizer for β C_2S[61,55]. Using less than 0·5% B_2O_3, the lattice of

β C_2S is not significantly altered (Figure 22).

Figure 22

Yannaquis and Guinier[98] suggest that holes are formed by the elimination of Si^{4+} ions (probably in the form of silica) necessary to balance the charges of the higher valency $(BO_4)^{5-}$ groups. At 0·5% B_2O_3, there is one Si vacancy in 160 molecules of C_2S. Such holes seem a more likely site for additional Ca^{2+} ions than do interstitial positions in a lattice as compact as that of C_2S.

The solid solutions of C_2S + B_2O_3 are well crystallized. The lattice of C_2S + 2% B_2O_3 is monoclinic with parameters a = 5·475, b = 6·770, c = 9·290 Å, $\beta = 93^{\circ}42'$. One can regard this solid solution as a limit structure and refer to it as a model.

Na_2O and K_2O also stabilize the β form[101] which is then formed as large crystals[78]. Na_2O seems to diminish, even more than CaO, the probability of nucleation of γ C_2S. Very small numbers of Na atoms are sufficient to inhibit completely the $\beta \rightarrow \gamma$ inversion. The threshold of effectiveness seems to lie between 0·17 and 0·27% Na_2O but, contrary to Thilo and Funk's views, Yannaquis and Guinier[98], Niesel and Thormann[63] have shown that the alkalis are not essential for the stabilization of β C_2S.

Niesel and Thormann[63] have studied the solid solutions C_2S + MoO_3, C_2S + C_3A . Observations on the reaction products with the electron micro-probe have shown that there is formation of an envelope of $CaMoO_4$ or of an aluminous layer which hinders the $\beta \rightarrow \gamma$ transformation during rapid cooling (1000°C/minute)

but which breaks up during slow cooling ($10^{\circ}C$/minute) to permit the formation of grains of γ C_2S.

Yannaquis and Guinier[98] have reported, during the Fourth Symposium, the influence of pressure on the stabilization of the β form of C_2S. The $\beta \rightarrow \gamma$ transformation occurs more readily when the C_2S lattice is not modified, as is the case with the solid solution $C_2S.P_2O_5$ (1% $CaNaPO_4$). On the other hand, the silicates with a modified lattice, C_2S + 0·5% B_2O_3 or larnite (natural dicalcium silicate containing traces of Al_2O_3 or Fe_2O_3) give rise to no $\beta \rightarrow \gamma$ transformation under the influence of pressure. Either the crystals deform less or the formation of nuclei of γ is more difficult.

Belites in Clinker

In clinker, belite corresponds to a β C_2S with a lattice slightly modified by the addition of foreign ions. The XRD pattern of crystals of belite extracted from Portland cement clinker[55] is in general that of β C_2S. It shows, however, some reflexions which are broader and certain others slightly displaced. Belite is thus a product of imperfect crystallization and apparently a non-equilibrium composition. In the lattice of C_2S, Ca^{2+} can be substituted by Mg^{2+}, K^{+}, Na^{+}, Ba^{2+}, Cr^{3+}, Mn^{2+} and the $(SiO_4)^{4-}$ group by $(SO_4)^{3-}$ or $(SO_3)^{2-}$ [79].

If β C_2S is stabilized by an ion substituting for Si, it is stable when fired in reducing conditions[102]. On the other hand, under these conditions the $\beta \rightarrow \gamma$ inversion is easily produced in Ca-substituted preparations[102,73]. In a reducing atmosphere, Fe^{2+} can replace Ca^{2+} or another stabilizing ion, to form a solid solution FeO + C_2S and provoke dusting of the clinker.

The XRD pattern of belite is different from that of the solid solutions $C_2S + B_2O_3$. The theory of Mircea[103] that in clinker B_2O_3 reacts with C_3S to form CaO and a solid solution saturated with C_2S and C_5BS must be regarded as untenable.

Belite usually occurs as rounded, striated grains, with markedly laminated structure. The striations appear at the moment of the $\alpha - \alpha'$ transformations (Type I: singly orientated) and the $\alpha' - \beta$ (type II: doubly orientated)[104]. The usual form is β, and only occasionally does one find α'[105,106] or α[107].

The composition of belite is unknown; synthetic studies, by substitution for Ca (V, Ti, Na, K) or by addition of Al_2O_3, Fe_2O_3 to C_2S, have not given positive results.

Forest[108] has been able to prepare belites similar to those in clinker. These are oxygen-defective solid solutions with substituted Si of general formula $Ca_2M_xSi_{1-x}O_{4-x/2}$. The synthesis and crystallographic character of these belites form the subject of a communication to this Symposium.

INTERSTITIAL PHASE

The interstitial phase, visible between the C_2S and C_3S in micrographs of clinker (Figure 1) consists of two crystalline phases, generally referred to as C_3A and C_4AF. In reality, each of these phases can differ from the stoichiometric composition either by variation in the proportions of A and F or by the introduction of impurities in solid solution.

Tricalcium Aluminate

Structure of C_3A. Tricalcium aluminate is a definite composition which shows no polymorphic transformations[109]. It melts incongruently at 1542°C to form CaO and a liquid phase. The crystal lattice is cubic with a = 15·262 Å[110] but the structure is still unknown.

Büssem[111] proposes a structure based on measurements of the strontium isomorph. The structure is a lattice of planar AlO_4 groups and octahedra of both AlO_6 and CaO_6; but as shown by Ordway[112] the oxygen atoms all lie at x, y, z = 0 or $\frac{1}{2}$, and the sub-cell ($\frac{1}{8}$ the true cell) contains 8 calcium and no other ions inside the faces. Ordway[112] succeeded in growing a C_3A crystal and determined, using Laue and Weissenberg photographs, the unit cell and space-group (T_h^6 - Pa_3) which agree with Büssem's structure.

Schroeder and Lyons[113] have proposed a structure in which the AlO_6 groups are present as elongated octahedra, but Tarte[114] disagrees with this structure because it requires unusually large Al - O distances (2·6 Å). Further studies of C_3A by both

infra-red absorption and X-ray fluorescence[115,116] suggest that the aluminium/oxygen co-ordination is probably all tetrahedral.

A structure which is based on Al_6O_{18} rings of six tetrahedra has been proposed by Moore[117] with 64 Ca at the corners of the $a/_4$ lattice and a further 16 positions to be occupied by 8 Ca or 16 Na. Using diffractometer powder intensities and some of Ordway's single crystal data, least squares refinment has not given values of R below 40 %.

Solid solutions of C_3A: solid solutions $C_3(A_{1-x}F_x)$. Schlaudt and Roy[118], Tarte[119], Majumdar[120] and Moore[117] have reported the existence of solid solutions $C_3(A_{1-x}F_x)$. The limits of composition obtained for the solid solutions are different.

TABLE 5

Author	Experimental method	Temp. °C	x
Schlaudt and Roy	Optical examination of	1389	0·035
	nature of phases	1300	0·02
Tarte	Exact measurements of	1310	0·10
Majumdar	dimensions of lattice of	1325	0·07
Moore	the solid solution by	1350	0·04
	X-ray diffraction		

Figure 23

Figure 23 represents the variations of cell parameter a as a function of the molar percentage $\frac{C_3F}{C_3A + C_3F}$

These results show great differencies.

Although the methods and temperatures of preparation were different, Majumdar and Moore found that the parameter continued to increase slowly with iron content beyond the limiting compositions. These compositions have thus not reached their equilibrium state. In Tarte's work, on the other hand, the parameter is constant when the ratio $\frac{Fe}{Al + Fe}$ exceeds 10%.

Furthermore, the isomorphous replacement Al-Fe is accompanied, in the IR absorption spectra, by a change of position of bands, a more or less profound alteration in band profiles and the appearance of a new band which suggests the presence of tetrahedral FeO_4 groups.

Other solid solutions. In the lattice of C_3A, CaO can be replaced by Na_2O. Brownmiller and Bogue[121] found the composition $Na_2O.8CaO.3Al_2O_3$ in the Na_2O-CaO-Al_2O_3 system. Conwicke and Day[122], Fletcher, Midgley and Moore[123] proposed a limiting composition 91% C_3A, 9% N_3A (mol) which is close to NC_8A_3. The parameter a decreases with addition of Na_2O. At 3% (mol) Na_2O there is a discontinuous change of symmetry from cubic to orthorhombic[123].

A composition $K_2O.8CaO.3Al_2O_3$[91], isomorphous with $Na_2O.8CaO.3Al_2O_3$, exists in the presence of SiO_2; the K atom has a large ionic radius, 1·33 Å, (Na = 0·95 Å), and some Si (τ = 0·41 Å) would replace the larger Al ions (τ = 0·50 Å)[114].

The limit of solubility of MgO in C_3A is 2·5% (by weight) according to Muller-Hesse and Schwiete[124]. MgO substitutes for CaO, and the parameter a decreases[117]. Examination of Portland cement clinker in the electron-probe suggests that MgO

concentrates preferentially in the C_3A[125], at least when the C_3A is in the orthorhombic form.

In the solid solution $C_3A + SiO_2$, Si replaces Al. If one considers that the number of oxygen atoms remains constant, three atoms of Si replace four of Al, creating vacant sites[117]. The parameter a decreases and the limit of solubility is 5-6% $\frac{Si}{Al + Si}$ (atom %).

Alumino-Ferrite Phase

Hansen, Brownmiller and Bogue[126] showed that complete miscibility exists between C_2F and a hypothetical "C_2A" up to C_4AF.

(a) - C_2F : structure Bertaut, Blum and Sagnières[127] have determined the structure of C_2F. The unit cell is orthorhombic with parameters a = 5·64, b = 14·68, c = 5·39 and space group Pcmn, and contains 4 molecules of C_2F.

The structure is pseudo-tetragonal. Projections along a and c are very similar (Figure 24).

Figure 24

Along the b axis, a layer of FeO_6 octahedra alternates with a layer of FeO_4 tetrahedra; these tetrahedra and octahedra do not share oxygens. Ca is lodged in large cavities in the lattice of oxygen atoms and its co-ordination is very irregular; there are 9 neighbours, of which one is rather distant (3·3 Å), to share the

bonding. Cirilli and Burdese[128] and Malquori and Cirilli[129] proposed the space group Imma for the whole series of alumino-ferrite solid solutions. Bertaut, Blum and Sagnières[127] found weak reflexions which could not be indexed except in the space group Pcmn; the layers of octahedra have the symmetry Imma but slight changes in the tetrahedral layers and in the Ca atom positions reduce the symmetry to Pnma[130], (≡ Pcmn in Bertaut's orientation).

– Allotropic transformations of C_2F: Differential thermograms of C_2F give two signals, at 430°C and 690°C, with a very flat region between the two peaks[131]. The transformations are reversible with about 10° hysteresis.

We have attempted to determine the nature of these two allotropic transformations with the help of high-temperature X-ray diagrams. The transformation at 430° is linked with a discontinuity in unit-cell volume. At 690°, the curve of parameter variation shows a slight change of slope, the expansion being slower above 690°. The number of reflexions does not change and there seems to be no change of lattice.

(b) C_4AF. C_4AF or brownmillerite has the same lattice as C_2F. The orthorhombic parameters are a = 5·428, b = 14·760, c = 5·596 Å[130] but the space group is Imma. The complete structure, especially the role of A and F, has not yet been determined. Brownmillerite is one member of the solid solution series C_2F + "C_2A" and seems the most stable. Hansen, Brownmiller and Bogue considered C_4AF to be a definite compound.

(c) Aluminoferrite solid solutions. Solid solutions $C_2F_{1-p}A_p$: In C_2F, some of the Fe ions can be replaced by Al ions; these solid solutions are of the form $C_2F_{1-p}A_p$.

A study of these solid solutions by X-ray powder diagrams has enabled Woermann, Hahn and Eysel[131] to detect two discontinuities in the variation of parameters as a function of p, the molar fraction of Al Ions (see Figure 25).

Figure 25

But these discontinuities correspond to very slight changes of slope. The limit of solubility is reached at p = 0·70. Examination of differential thermograms shows that the temperature of the first signal at 430° decreases, as a function of alumina content, to 200° and disappears at p = 0·30. The temperature of the signal at 690° decreases similarly up to p = 0·2. From p = 0·2 to p = 0·5, two peaks are observed which disappear at p = 0·5. It is difficult to draw precise conclusions from this work; only the disappearance of the first signal at p = 0·30 seems to be linked with the change of symmetry from Pnma to Imma found by Smith[130] in his study of single crystals of composition $C_2F_{1-p}A_p$.

From the variations in intensity of characteristic h0l and 0k0 reflexions as a function of Al content, Smith[130] deduced that initially Al replaces tetrahedral Fe. When about half the tetrahedral sites are filled, Al enters both types of site equally. At about p = 0·33 the change of space group Pnma $\longrightarrow$ Imma occurs. This change involves a contraction and rotation of the tetrahedra, and displacement of the Ca atoms. The Al atoms are distributed about equally in tetrahedral and octahedral sites. The variation of parameters a, b and c as a function of p is continuous. In brownmillerite, $C_2A_{0·5}F_{0·5}$, approximately 75% of the Al atoms are substituted for

tetrahedral Fe and 25% for octahedral.

At the same time, Majumdar, in studying the phases in the pseudo-system CaO - $CaO.Al_2O_3$ - $2CaO.Fe_2O_3$, found that the liquidus temperatures for mixes on the hypothetical line C_2F - "C_2A" varied continuously as a function of the substitution Al^{3+} - Fe^{3+} in the ferrite lattice. C_3A and $C_{12}A_7$ appear when p is greater than 0·70.

In a study by infra-red spectra, of solid solutions $C_2A_pF_{1-p}$, Tarte[119] observed an increase in wave number and then, above $C_2A_{0.7}F_{0.3}$, no change, until at higher alumina contents, up to $C_2A_{0.85}F_{0.15}$, the position of certain lines changes again apparently due to the appearance of new phases such as C_3A and $C_{12}A_7$.

On the other hand, according to P. Longuet[132], the rate of reduction of C_4AF in a hydrogen atmosphere is regular as in the case of a definite composition. It seems that brownmillerite is the most stable member of the solid solution series $C_2A_pF_{1-p}$.

MgO-ferrite solid solutions: Magnesia enters into the ferrite lattice; normally red-brown, the latter becomes grey-black in the presence of MgO. It has been assumed for a long while that Mg substitutes for Ca but Woermann, Hahn and Eysel[131] have detected two types of solid solution. These authors used a precise analytical method to determine the free or uncombined CaO: the samples contained a small quantity of excess CaO; after the addition of a given percentage of MgO, the quantity of free CaO was determined and from the resultant curve, the type and the limit of solid solution were deduced.

The solid solution MgO-ferrite takes up more lime than the ferrite. According to the slope of the curve representing the change in free lime content as a function of added MgO, it appears that for 3 parts of MgO, 2 parts (molar equivalent) of CaO are combined; the limit of solid solution corresponds to the formation of periclase. The formula of the hypothetical end-member of the solid solution series is $Ca_2Mg_3O_5$ and the solid solution of Mg in C_2F is thus a substitution of Mg^{2+} for Fe^{3+}. Electroneutrality is maintained by the addition of an Mg ion in an interstitial position for every two Mg ions substituting for Fe. Hence, the type I solid solution:

$$Ca_2(Fe_{1-\frac{2}{3}x}Mg_x)_2O_5 \qquad o < x < 0{\cdot}023 \text{ at } 1400^{\circ}C$$

At about p = 0·50, only one part of CaO is combined to 3 parts of MgO. Woermann, Hahn and Eysel proposed a superposition of a type I solid solution upon a normal Ca - Mg substitution. In type II, $^1/_5$ of the Mg is substituting for Ca, while $^4/_5$ is in type I solid solution ($^8/_{15}$ replacing the trivalent Fe_2, $^4/_{15}$ in interstitial positions). Hence the formula:

$$(Ca_{1-\frac{x}{5}}Mg_{\frac{x}{5}})_2\,(R_{1-\frac{8x}{15}}Mg_{\frac{4x}{5}})_2\,O_5$$

The change from type I to type II occurs at about p = 0·49. The discontinuity in the substitution of MgO can be established in the crystal structure, suggesting a discontinuity in the ferrite solid solution series. The aluminoferrites $C_2A_pF_{1-p}$ corresponding to $p > 0{\cdot}5$ are unstable in the presence of free CaO. For this reason, Woermann, Hahn and Eysel did not extend their work to the whole solid solution series.

The MgO-ferrite solid solutions have also been studied by Kato[133], who finds that SiO_2 and MgO substitute for $(Al, Fe)_2O_3$ up to about 10% (molar). The substitution is of the melilite type.

SiO_2 alone can also enter into the ferrite lattice. The mechanism of SiO_2 solubility could be explained by the same type of substitution

(d) Interactions between the phases C_3A and $C_2(A,F)$.

C_3A and $C_2(A, F)$ constitute the interstitial phase of clinker. It is of interest to see whether, in synthetic preparations, these two phases can react to give solid solutions. This work, undertaken by Tarte[119] has shown the following results:

(1) Fe-Al exchange: in a mixture of $C_3A + C_4AF$, there is formed after heating to 1300°C a solid solution $C_3(A, F)$ resulting from the passage of a certain amount of iron from the C_4AF to the C_3A, this being compensated by the transfer of the equivalent Al from the C_3A to the C_4AF. The solid solution $C_3(A, F)$ has the limiting composition $C_3(A_{0.90}F_{0.10})$;

(2) Formation of poorly-crystalline phases: besides the displacements of characteristic XRD reflexions, Tarte[119] has observed in the solid solutions a simultaneous broadening of some of the high angle XR reflexions and of the infra-red absorption bands, when comparing a mixture of the two phases before thermal treatment with the same mixture after treatment. This effect is more marked when the mixture already treated at 1300° is taken to 1340°C.

Yet the same phases treated separately at the same temperature retain their IR spectra and XRD patterns perfectly sharp.

Tarte[119] has deduced that the state of crystallization of the phases obtained by mutual reaction is incomplete. This alteration of the crystallization is more marked at 1340°C, this being the temperature at which the majority of the mixture undergoes a partial fusion;

(3) Formation of a glassy phase: when the solid solutions have a high alumina content, a vitreous phase appears, the IR absorption spectrum of a sample of composition $C_2(A_{0.8}F_{0.2})$ taken to 1340°C is diffuse (Figure 26) and shows no XRD lines whatever. On the other hand, the crystallization

Figure 26

is complete when the Al/Fe ratio is close to 1.

The Interstitial Phase in Clinker

In Portland cement clinker, one finds tricalcium aluminate, the aluminoferrites and their respective solid solutions.

(1) C_3A. The tricalcium aluminate extracted from clinker has the lattice parameter a smaller than that of C_3A[117]. It is thus in the form of solid solutions due to the addition of impurity oxides such as Na_2O, K_2O, MgO, Fe_2O_3, SiO_2 but the concentration limits of these different additions are not known.

(2) Aluminoferrites. The composition of the ferrite phase in commercial cements depends as much on the thermal treatment as on the A/F ratio, in all cases where equilibrium is not reached[134].

Midgley[135] has observed broad lines in the diffraction patterns of clinker ferrites and attributes this broadening to the

fact that equilibrium could not be established in the course of cooling. Yamaguchi and Kato[136], Satou, Takashima and Kato[137] have both obtained less well-defined lines in patterns from clinker than in those from pure synthetic compositions.

The IR absorption bands of C_3A and $C_2(A, F)$ in clinker, easily observed in a sample synthesized at 1200°C, become more and more diffuse as the sample is taken up to 1300-1400°C. In certain clinkers, there exists a very diffuse absorption band which seems to be linked with the alumina content, and hence with the existence of a glassy phase[119].

Hansen, Brownmiller and Bogue[126] have shown that complete miscibility exists between C_2F and "C_2A" up to C_4AF. Numerous studies[138 to 142] thereafter have established that the ferrite phase in clinker is not necessarily of the composition C_4AF but may extend to the solid solutions richer in alumina, in which the ratio Al_2O_3/Fe_2O_3 reaches 2·2 to 2·3 ($p \simeq 0{\cdot}70$ in the series $C_2A_pF_{1-p}$).

Midgley[135] has studied the composition of the ferrite phase in fifteen English clinkers: 2 had the composition C_4AF, 2 had C_6AF_2, 4 an intermediate composition and the remainder an ill-defined composition (broadened XRD lines) but always lying between C_6AF_2 and C_6A_2F.

In American clinkers, Copeland, Brunauer, Kantro, Schultz and Weise[143] found that the compositions of the ferrites lay

between $C_6A_{1.22}F_{1.78}$ and $C_6A_{1.77}F_{1.23}$. The mean value $C_6A_{1.47}F_{1.53}$ is very close to brownmillerite.

Gourdin[144] has analysed by XR diffraction the ferrite phase from 15 French cements; four clinkers contained the composition C_4AF, one contained C_6AF_2, and the other 8 an intermediate composition very close to C_4AF.

Schwartz[145] separated out the aluminoferrite phase from 66 French clinkers, by the salicylic acid in methanol method of Takashima[146]. The aluminoferrite phases separated out had a chemical composition much more complex than the interstitial phase calculated by the Bogue method. The analyses, by X-ray fluorescence spectrometry, revealed a stoichiometric defect in CaO which reached as much as 5%. This lime deficiency increased if one included K_2O, Na_2O and MgO and diminished if one included SiO_2. The solubility limits of the minor elements in the interstitial phase were determined as 3% K_2O, 4% MgO, 7% SiO_2.

To conclude, C_3A and $C_2(A, F)$ cannot co-exist as such in clinker. Exchange of Al_2O_3 and Fe_2O_3 occur easily in the aluminates and aluminoferrites. Furthermore, at 1300°, a small amount of iron will convert from the ferric to the ferrous state[120,147]. The presence of ferrous oxide noticeably modifies the stability regions of the solid solutions[148]. The solid solutions $2CaO\ (Al,Fe)_2O_3$ decompose in the presence of CaF_2 and $CaCl_2$[149].

CONCLUSION

Properties of the Clinker Minerals

We have considered the structures of the various polymorphs of the principal clinker components and there is a correlation between the crystalline structures of these components and the hydraulic properties of the clinker.

1) C_3S. Of all the phases in clinker, it is the tricalcium silicate which is the most significant and important from the point of view of the hardening of cements[150]. The hydraulic cementing properties of C_3S are associated with the poor co-ordination of calcium ions and the presence of 'holes' in the crystal lattice[21]. We have shown that the crystal structures of the different forms of C_3S and its solid solutions are very close to that of the trigonal form of pure C_3S stable at high temperatures. On the other hand, differences in the relative intensities of the diffracted rays are scarcely noticeable. The different crystalline forms are thus constructed from the same atomic groupings. These are only very slightly displaced or distorted. The polymorphic transformations are 'displacive', they bring into play only weak forces and do not appreciably alter the chemical combinations[151]. This results in all the forms having a similar reactivity. Nurse, Midgley, Gutt and Fletcher[152] have found that the transformations $T_I \rightarrow T_{II} \longrightarrow M$ of the synthetic solid solutions $C_{156-x}M_xS_{52}$ have no effect on the strengths developed when these materials hydrate. In the same manner, the strength of commercial cements

containing trigonal alite does not differ significantly from that of cements in which the alite is in the monoclinic form. Yamaguchi, Shirasuka and Ota[153] have compared the properties of monoclinic and trigonal alite. Monoclinic alite (inverse) hydrates more rapidly. It is obtained by rapid cooling and seems to be thermodynamically unstable. If subjected to gentle heating it is converted into the triclinic form which by contrast gives greater early strength[154]. Verbeck[155] has shown that the introduction of alumina and magnesia into tricalcium silicate brings about a significant increase in early strength but the effect does not persist beyond 70 - 80 days. The introduction of other foreign ions such as P_2O_5[156], SO_3[157], $CaSO_4.2H_2O$ and $CaCl_2$[158], Cr_2O_3[159], can modify the properties of C_3S but the changes in reactivity do not seem to correlated with changes in structure[160]. An increase in size of the alite crystals is generally observed.

2) $\underline{C_2S}$. The four forms of C_2S have, on the other hand, quite different structures. The lattices are different and the ionic groupings change from one form to another. One can therefore reasonably presuppose that the four forms will have different hydraulic properties.

In the β form, the polyhedral co-ordination of the Ca ions is irregular and the extra-long Ca-O bonds facilitate the hydration reaction. Similarly, because of its predisposition to undergo a major structural re-arrangement[64], metastable β C_2S is more readily hydratable. The γ form of C_2S is known to be inert[79] or feebly hydraulic[161]. This poor reactivity is

associated with the symmetrical co-ordination of the calcium ions[21] and the strong Ca-O bonds arising from the low co-ordination number of the Ca ions[64].

The α' form of C_2S is only hydrated with difficulty and seems to possess no hydraulic cementive power[79].

The minor constituents of clinker which stabilize the different forms of C_2S can affect the relationship between the hydraulic cementive characteristics of belite[40,162,163] and its other properties[164].

3) Interstitial phase. Tricalcium aluminate reacts rapidly with water. Calcium aluminoferrite is only feebly hydraulic.

However, during the clinkering process, the burning temperature, the method of clinker cooling, the interaction of C_3A with the ferrite phase, the presence of foreign ions and the formation of a vitreous phase all alter the phase equilibrium conditions and so change the properties of the clinker in respect of the kinetics of its reactivity towards water[119].

Acknowledgments

We gratefully acknowledge the assistance of the many research-workers who have communicated their results to us, and especially those who have allowed us to read their papers before publication :

M. J. Forest
M. P. Gourdin
Prof. Th. Hahn
M. H.C. de Saint-Chamant
M. J. Schwartz
Prof. P. Tarte
Prof. G. Yamaguchi

and also to Miss A.E. Moore who both assisted in the preparation of the paper and translated it into English.

REFERENCES

References to the previous Symposia on the Chemistry of Cement are abbreviated as follows:- for example, papers from the Proceedings of the Fourth International Symposium on the Chemistry of Cement, Washington 1960, published by the National Bureau of Standards as Monograph No. 43, Volume I or II, pages ..... (1962), will be given throughout as "Washington, 1960, Vol. I (or II), pp. ....."

1. F. Ordway, "Crystal Structures of Clinker Constituents", Washington, 1960, Vol. I, pp. 39-58.

2. J.W. Jeffery, "The Crystal Structure of Tricalcium Silicate", PhD Thesis, University of London (1950). Acta Cryst. 5, 26-35 (1952).

3. H.O'Daniel, Th. Hahn and H. Müller, "The Structure of $3CaO.SiO_2$: Investigation with Patterson Syntheses" (in German), Neues Jahrb. Mineral. Monatsh. 1-15 (1953).

4. Th. Hahn, "New Determination of Structure of Tricalcium Silicate Ca_3SiO_5" (in German), Silikattechnik 11, 396-397 (1960).

5. The Chemistry of Cements, Vol. I (Academic Press, London, England, and New York, U.S.A., 1964), Edited by H.F.W. Taylor. See chapter by J.W. Jeffery entitled "The Crystal Structures of the Anhydrous Compounds", pp. 131-164.

6. R.W. Nurse, "Summarized Proceedings of Conference on X-ray Analysis, London, April 1948", J. Sci. Instr. 26, 102 (1949).

7. M. Regourd, "Determination of the Lattices of Microscopic Crystals. Application to the Different Forms of Tricalcium Silicate" (in French), Bull. Soc. Franc. Mineral. Crist. 87, 2, 241-272 (1964). C.E.R.I.L.H. Technical Paper No. 152.

8. C. Mazières, "Micro and Semimicro Differential Thermal Analysis (μDTA)", Anal. Chem. 36, 602-605 (1964).

9. R. Roy, "Reactivity of Solids", 4th International Symposium on the Reactivity of Solids, Amsterdam 1960, p. 255 (Elsevier NV Uitgeversmij, Amsterdam, Netherlands, 1961).

10. A.I. Boikova and N.A. Toropov, "Stoichiometry and Polymorphism of Tricalcium Silicate" (in Russian), Dokl. Akad. Nauk. SSSR, 156, no. 6, 1428-1431 (1964). Chem. Abstr. 61, 7917f (1964).

11. E. Woermann, Th. Hahn and W. Eysel, "Chemical and Structural Investigations of the Solid Solutions of Tricalcium Silicate" (in German), Zement-Kalk-Gips 16, 370-375 (1963).

12. M. Bigaré, "Development of a High-temperature X-ray Camera with Controlled Atmosphere. Investigation of Al_2O_3-Ca_3SiO_5 Solid Solutions" (in French), Rev. des Matériaux de Construct., 598-599, 325-334 (1965) and 600, 394-404 (1965). C.E.R.I.L.H. Technical Paper No. 166.

13. P. Gregoire, Private Communication (1967) reported in 15.

14. J.D.H. Donnay, Crystal Data: Determinative Tables, 2nd ed., p. 2, (Monograph No. 5, American Crystallographic Association, Washington, U.S.A., 1963).

15. M. Bigaré, A. Guinier, C. Mazières, M. Regourd, N. Yannaquis (France) and W. Eysel, Th. Hahn and E. Woermann (Germany), "Polymorphism of Tricalcium Silicate and its Solid Solutions", to be published in J. Am. Ceram. Soc. (1967).

16. M.J. Buerger, "Crystallographic Aspects of Phase Transformations", Phase Transformations in Solids (Symposium held at Cornell University 1948), pp. 183-211 (John Wiley and Sons Inc., New York, U.S.A. 1951).

17. Th. Hahn and W. Eysel, "Structure, Polymorphism and Solid Solution of Germanates and Silicates of Types A_2BX_4 and A_3BX_5", Paper 4·74, International Congress of Crystallography, Rome (1963). Acta Cryst., Special Issue, p. A45 (1963).

18. Th. Hahn and W. Eysel, "Structure and Polymorphism of Tricalcium Germanate" (in German), Naturwissenschaften, 50, no. 13, 471 (1963).

19. Th. Hahn, W. Eysel and E. Woermann, "A_3BO_5 Compounds: Polymorphism and Solid Solution", Am. Ceram. Soc. Bull. 44, 299 (1965).

20. R.W. Nurse and J.H. Welch, Private Communication (1951) reported by J.W. Jeffery, London, 1952, p.44.

21. J.W. Jeffery, "The Tricalcium Silicate Phase", London, 1952, pp. 30-48.

22. G. Yamaguchi and H. Miyabe, "Precise Determination of the $3CaO.SiO_2$ Cells and Interpretation of their X-ray Diffraction Patterns", J. Am. Ceram. Soc., 43, 219-224 (1960).

23. H. Miyabe and D.M. Roy, "A Re-examination of the Polymorphism of Ca_3SiO_5", J. Am. Ceram. Soc. 47, 318-319 (1964).

24. N. Yannaquis, M. Regourd, C. Mazières and A. Guinier, "On the Polymorphism of Tricalcium Silicate" (in French), Bull. Soc. Franc. Mineral. Crist. 85, 271-281 (1962).

25. A. Guinier, "X-Ray Crystallography Theory and Practice", (in French), p. 196-212, (Ed. Dunod, Paris, 1964), 3rd edition.

26. G. Yamaguchi and K. Kato, "$3CaO.SiO_2$-Al_2O_3-MgO Solid Solution" (in Japanese), Semento Gijutsu Nenpo, XVI, 28-32 (1962).

27. Y. Ono, T. Uno and Y. Kanai, "Synthesis of Five Polymorphic Modifications of C_3S" (in Japanese), Semento Gijutsu Nenpo, XIX, 36-41 (1965).

28. F.W. Locher, "Solid Solution of Alumina and Magnesia in Tricalcium Silicate", Washington, 1960, Vol. I, pp. 99-106.

29. H.G. Midgley and K.E. Fletcher, "The Role of Alumina and Magnesia in the Polymorphism of Tricalcium Silicate", Trans. Brit. Ceram. Soc. 62, 11, 917-937 (1963).

30. F. Trojer and K. Konopicky, "The System Calcium Oxide - Magnesium Oxide" (in German), Radex-Rundschau, no. 4, pp. 161-162 (1949).

31. E. Woermann, Th. Hahn and W. Eysel, "Chemical and Structural Investigations on the Formation of Solid Solutions of Tricalcium Silicate. 2: Phase Relations in the System $CaO-MgO-SiO_2$ and $CaO-Al_2O_3-SiO_2$" (in German), to be published in Zement-Kalk-Gips (1967).

32. M. Regourd, "Polymorphic Transformations of Tricalcium Silicate" (in French), Rev. des Matériaux de Construct., 620, pp. 167-176 (1967). C.E.R.I.L.H. Technical Paper no. 182.

33. K.E. Fletcher, "The Effect of Fe^{3+} and Al^{3+} on the Polymorphism of Tricalcium Silicate", Trans. Brit. Ceram. Soc. 64, 8, 377-385 (1965).

34. A.I. Boikova and N.A. Toropov, "Investigations on the C_3S Solid Solutions with the Rare Earth Orthosilicates" (in Russian), Experiment and Technical Mineralogy and Petrography (Eksperiment v Teknicheskoy Mineralogii i Petrographii), 7th Colloquium on Experimental and Technical Mineralogy and Petrography (Po Materialam VII Coveshchaniya po Eksperimental'noy i Teknicheskoy Mineralogii u Petrographii), Moscow (1966). Chem. Abstr. 65, 11956a.

35. N.A. Toropov and A.I. Boikova, "Solid Solutions of Tricalcium Silicate with Yttrium Oxyorthosilicate" (in Russian), Dokl. Akad. Nauk. SSSR, 151, no. 5, 114-117 (1963).

36. H. Lafuma, "Cement: Scientific, Technical, Economic Problems", C.E.R.I.L.H. Information Note no. 17 (1961).

37. A.P. Khashkovskaya, M.M. Sychev and V.I. Korneev, "Composition and Characteristics of the Crystallization of $3CaO.SiO_2$ in the Presence of Admixtures" (in Russian), Tr. Gos. Vses. Inst. po. Proektir. i. Nauchn.-Issled. Rabotam v Tsementn. Prom. no. 29, 13-20 (1964).

38. G. Yamaguchi, H. Uchikawa, S. Kawamura, "Influence of Sodium Oxide upon the Formation and the Crystal Structure of Tricalcium Silicate Solid Solution in the System $CaO-SiO_2-Al_2O_3-Fe_2O_3$" (in Japanese), J. Ceram. Assoc. Japan, 70, 7, 209-220 (1962).

39. G. Yamaguchi and H. Uchikawa, "Investigations on the Mixed Crystals in the System $3CaO.SiO_2-Na_2O$" (in German), Zement-Kalk-Gips, 14, no. 11, 497-504 (1961).

40. J.H. Welch and W. Gutt, "The Effect of Minor Components on the Hydraulicity of the Calcium Silicates", Washington, 1960, Vol. I, pp. 59-68.

41. H.G. Midgley, K.E. Fletcher and A.G. Cooper, "The Identification and Determination of Alite in Portland Cement Clinker", Analysis of Calcareous Materials, pp. 363-371 (Monograph No. 18, Society of Chemical Industry, London, 1964).

42. G. Yamaguchi and H. Uchikawa, "On the Alite Phase in Portland Cement Clinker with Varying Alkali Contents", Semento Gijutsu Nenpo, XVI, 23-28 (1962).

43. G. Yamaguchi and Y. Ono, "Microscopic Study on Alite in Portland Cement Clinker" (in German), Zement-Kalk-Gips, 20, no. 9, 390-394 (1966).

44. M. Von Euw, "Quantitative X-Ray Analysis of Portland Cement Clinkers" (in French), Silicates Industriels, 23, 643-649 (1958).

45. N.A. Toropov and B.V. Volkonskii, "Polymorphic Transformations of $3CaO.SiO_2$ and the Influence of Ferrous Oxide on $3CaO.SiO_2$ and Other Clinker Minerals" (in Russian), Tsement, 26, no.6, 17-20 (1960).

46. S. Chromy, "Notes on the Petrography of Fused Cement", Silikaty, 8, (1), 45-52, (1964).

47. W. Kurdowski, "C_2S and C_3S Formation at 1300°C", Silicates Industriels, 30, no. 9, 500-506 (1965).

48. P.P. Budnikov, I.M. Petrovich and V.G. Savelev, "New Method of Synthesis of Tricalcium Silicate and Studies on the Properties of the Obtained Product", Cement-Wapno-Gips, 17, no. 4, pp. 91-93 (1962).

49. M. Polivka, A. Klein and C.H. Best, "Laboratory Preparation of High-Purity Tricalcium Silicate", Mater. Res. Standards, (A.S.T.M.), 1, 7, 524-528 (1961).

50. L.A. Kroichuk and V.A. Shteerman, "Thermodynamic Probability of Formation of Tricalcium Silicate in Calcium Oxide-Pseudowollastonite", Zh. Vses. Khim. Obshchestva im. D.I. Mendeleeva, 8, (5), 581-582 (1963).

51. B.V.S. Subba Rao, Safia Mehdi, D.S. Datar and Abde Ali, "Formation of Tricalcium Silicate by the Interaction of Calcium Carbonate and Silica at 840°C", J. Sci. Ind. Res., Vol. 21D, 249-250 (1962).

52. A. Bereczky, "Reaction Kinetics of the System $CaO-SiO_2$ in Presence of Catalysts", Silikattechnik, 11, 474-475 (1960).

53. B. Courtault, "Study of Solid State Reactions up to 1600°C, with DTA:Applications to Cement Chemistry" (in French), Rev. des Matériaux de Construct., 571, 110 - 124 (1963). C.E.R.I.L.H. Technical Paper no. 140.

54. J.H. Welch and W. Gutt, "Tricalcium Silicate and its Stability Within the System $CaO.SiO_2$", J. Am. Ceram. Soc. 42, no. 1, 11-15 (1959).

55. N. Yannaquis, "X-Ray Studies of Silicates in Clinker" (in French), Rev. des Matériaux de Construct., 480, 213-228 (1955). C.E.R.I.L.H. Technical Paper no. 74.

56. E. Woermann, "Decomposition of Alite in Technical Portland Cement Clinker", Washington, 1960, Vol. I, pp. 119-129.

57. G. Yamaguchi, Y. Ono, S. Kawamura and Y. Soda, 1."Syntheses of the Various Modifications of Ca_2SiO_4 and the Determination of Their Powder X-Ray Diffraction Patterns" (in Japanese), English summary, J. Ceram. Assoc. Japan, 71, no. 2, 21-26 (1963);

2. "Differential Thermal Analysis and High Temperature X-Ray Diffraction Studies of $2CaO.SiO_2$" (in Japanese), English summary, J. Ceram. Assoc. Japan, 71, no. 1, 9-12 (1963).

58. M.A. Bredig, "Polymorphism of Calcium Orthosilicate", J. Am. Ceram. Soc., 33, 6, 188-192 (1950).

59. A. Van Valkenburg, Jr., and H.F. McMurdie, "High-Temperature X-Ray Diffraction Apparatus", J. Res. Natl. Bur. Standards, 38, 415-418 (1947).

60. A.M.B. Douglas, "X-Ray Investigation of Bredigite", Mineral. Mag., 29, 875-884 (1952).

61. C.M. Midgley, "Crystal Structure of β Dicalcium Silicate", Brit. J. Appl. Phys., 3, 277-282 (1951). Acta Cryst. 5, Part 3, 307-312 (1952).

62. G. Yamaguchi, H. Miyabe, K. Amano and S. Komatsu, "Synthesis of Each Modification of $2CaO.SiO_2$ and Their Certification", J. Ceram. Assoc. Japan, 65, 99-104 (1957).

63. K. Niesel and P. Thormann, "The Stability Fields of Dicalcium Silicate Modifications" (in German), Tonind. Zeitung, 91, 9, 362-369 (1967).

64. D.K. Smith, A.J. Majumdar and F. Ordway, "Re-examination of the Polymorphism of Dicalcium Silicate", J. Am. Ceram. Soc., 44, 8, 405-411 (1961).

65. G. Trömel, "The Calcium Orthosilicate Ca_2SiO_4 Modifications" (in German), 36, 88 (1949).

66. D.K. Smith, A.J. Majumdar and F. Ordway, "The Crystal Structure of γ -dicalcium Silicate", Acta Cryst., 18, 787-795 (1965).

67. E.J. McIver, "Review of the Dicalcium Silicate Phase", Private Communication (1960).

68. H. O'Daniel and L. Tscheischwili, "On the γ C_2S Structure" (in German), Z. Kryst., 104, 124-141 (1942).

69. E. Thilo and F. Liebau, "Silicate Models. III. Modifications of Na_2BeF_4 and Their Relation to Those of Ca_2SiO_4" (in German), Z. physik. Chem., 199, 125-141 (1952).

70. W. Eysel and Th. Hahn, "Polymorphism in the System Ca_2GeO_4-Ca_2SiO_4", Neues Jahrb. Mineral. Monatsh. (6), 137-139 (1963).

71. F.I. Vasenin, "Polymorphic Inversions of Calcium Orthosilicate" (in Russian), Zh. Priklad. Khim. SSSR, 21, 10-17 (1948).

72. N.A. Toropov, B.V. Volkonskii and V.I. Sadkov, "The Polymorphism of Dicalcium Silicate" (in Russian), Dokl. Akad. Nauk. SSSR, 112, 467-469 (1957).

73. C.M. Schlaudt and D.M. Roy, "The join Ca_2SiO_4-$CaMgSiO_4$", J. Am. Ceram. Soc., 49, no. 8, 430-432 (1966).

74. W. Kurdowski, "Polymorphic Transformation of Dicalcium Silicate at Low Temperatures", Proceedings of the 6th Conference on the Silicate Industry, Budapest, 1961. Akadémiai Kiadó, Budapest, ed. B. Beke and F. Tamas, pp. 263-272 (1963).

75. H. Saalfeld. "Structure of Dicalcium Silicate (C_2S)" (in German), Ber. Deut. Keram. Ges., 30, 185-189 (1953).

76. Y. Ono, "Cubic Mineral Derived from Ca_2SiO_4", Semento Gijutsu Nenpo, XI, 18 (1957).

77. R. Roy, Discussion of Nurse's Paper "Phase Equilibria and Constitution of Portland Cement Clinker", Washington, 1960, Vol. I, pp. 29-32.

78. N. Yannaquis and A. Guinier, "Polymorphic $\beta - \gamma$ Transition of Calcium Orthosilicate" (in French), Bull. Soc. Franc. Mineral. et Crist., 82, 126-136 (1959).

79. R.W. Nurse, "The Dicalcium Silicate Phase", London, 1952, pp. 56-77.

80. H. Funk, "On the Stabilization of High-Temperature Modifications of α , α', (β) Dicalcium Silicate" (in German), Silikattechnik, 5, 186-189 (1955).

81. F. Wolf and J. Hille, "Stabilization of β-Ca_2SiO_4 by Elementary Carbon" (in German), Silikattechnik, 10, 530-536 (1959).

82. T. Sasaki and Y. Suzukawa, "Effect of Ferrous Oxide on $\beta - \gamma$ Inversion Temperature of Dicalcium Silicate" (in German), Zement-Kalk-Gips, 17, 5, 196-198 (1964).

83. N.A. Toropov, N.F. Fedorov and A.M. Shevyakov, "Infrared Absorption Spectra of Polymorphic Modifications of Dicalcium Silicate" (in Russian), Zh. Neorgan. Khim, 8, 69-71 (1962).

84. H. Lehmann and H. Dutz, "Infrared Spectroscopy Studies on the Hydration of Clinker Minerals and Cements", Washington, 1960, Vol. I, pp. 513-518.

85. G. Yamaguchi, Y, Ono, S. Kawamura and Y. Soda, "The Mortar Strength of Each Modification of Ca_2SiO_4", Semento Gijutsu Nenpo, XVII, 39-43 (1963).

86. G. Yamaguchi, Y. Ono, S. Kawamura and Y. Kanai, "Solid Solubility of Al_2O_3, Fe_2O_3 and Na_2O in Belite", Semento Gijutsu Nenpo, XVII, 37-41 (1963).

87. N.F. Fedorov and E.R. Brodkina, "Solid Solutions in the $2CaO.SiO_2$ - $K_2O.CaO.SiO_2$ System" (in Russian), Izvest. Akad. Nauk SSSR, Neorgan. Materialy, 2 (4), 745-748 (1966).

88. C. Brisi and P. Appendino, "Solid State Equilibria in the $CaO-BaO-SiO_2$ System" (in Italian), Ann. di Chim., 55, (5), 461-468 (1965).

89. R.W. Nurse, J.H. Welch and W. Gutt, "High-Temperature Phase Equilibria in the System Dicalcium Silicate-Tricalcium Phosphate", J. Chem.Soc., 220, 1077-1083 (1959).

90. R. Kondo and S. Goto, "A Study of the System $CaO-SiO_2-Cr_2O_5-Al_2O_3$", Semento Gijutsu Nenpo, XIX, 42-44 (1965).

91. Y. Suzukawa, "The Alkali Phases in Portland Cement: II. The Potassium Phase" (in German), Zement-Kalk-Gips, 9, 390-396 (1956).

92. G. Yamaguchi and K. Suzuki, "Structural Analysis of Merwinite", J. Ceram. Assoc. Japan, 75, no. 7, 221-229 (1967).

93. W. Gutt, "The System Dicalcium Silicate -Merwinite", Nature, 207, no. 4993, 184-185 (1965).

94. A. Guinier and N. Yannaquis, "Polymorphism of Ca_2SiO_4" (in French), Compt. Rend., 244, 2623-2625 (1957).

95. J. Grzymek and J. Skalny, "On the Polymorphism of C_2S" (in German), Tonind. Ztg., 91, no. 4, 128-130 (1967).

96. S. Chromy, "Optical Relations between Modifications of Ca_2SiO_4", (in Czech), Silikaty, 4, 338-349 (1966).

97. A. Bielanski, J. Nedoma and W. Turowa, "Dilatometric Studies of Polymorphic Transformations of Sodium Fluoroberyllate", 5th International Symposium on the Reactivity of Solids, Munich 1964, pp. 90-99 (Elsevier NV Uitgeversmij, Amsterdam, Netherlands, 1965).

98. N. Yannaquis and A. Guinier, Discussion of Nurse's Paper "Phase Equilibria and Constitution of Portland Cement Clinker", Washington, 1960, Vol. I, pp. 21-23.

99. F. Dachille and R. Roy, "High Pressure Phase Transformations in Laboratory Mechanical Mixers and Mortars", Nature, 186, 34-35 (1960).

100. D. Roy, "Studies in the System $CaO-Al_2O_3-SiO_2-H_2O$: III. New Data on the Polymorphism of Ca_2SiO_4 and its Stability in the System $CaO-SiO_2-H_2O$", J. Am. Ceram. Soc., 41, no. 8, 293-299 (1958).

101. E. Thilo and H. Funk, "Effect of Small Amounts of Alkalis on the $\beta - \gamma$ Inversion of C_2S", (in German), Z. Anorg. Allgem. Chem., 273, 1-2, 28-40 (1953).

102. T. Sasaki, a) "X-Ray Study of the Inversion of the Crystal Form of Dicalcium Silicate", J. Sci. Hiroshima Univ. Ser.A, 23, no.3, 425-444 (1960); b) "X-Ray Study on the Inversion of the Crystal Form of Dicalcium Silicate, Especially on the Effect of Stabilizing Agents", Semento Gijutsu Nenpo, XIV, 22-23 (1960).

103. S. Mircea, "Decomposition of Tricalcium Silicate with Boric Oxide" (in Czech), Silikaty, 9, 1, 34-42 (1965).

104. G. Yamaguchi and Y. Ono, "Microscopic Studies on the Textures of Belite in Portland Cement Clinker", Semento Gijutsu Nenpo, XVI, 32-34 (1962).

105. P. Terrier and H. Hornain, "The Application of Mineralogical Methods at the Industry of Hydraulic Binders" (in French), Rev. des Matériaux de Construct., 619, pp. 123-140 (see p. 135) (1967). C.E.R.I.L.H. Technical Paper no. 180.

106. A.A.T. Metzger, "The Occurrence of Bredigite ($\alpha'Ca_2SiO_4$) in Portland Cement Clinkers" (in German), Zement-Kalk-Gips, 6, 269-270 (1953).

107. Y. Ono and Y. Soda, "Effect of the Crystallographic Properties of Alite and Belite on the Strength of Cement", Semento Gijutsu Nenpo, XIX, 78-82 (1965).

108. J. Forest, Study of local encrustation in cement rotary-kilns and belites. Silicates Industriels, 32, n° 11, I, 373-384, n° 12, II...(1967).

109. B. V. Volkonskii, "Studies of C_3S and C_3A in the Range of High Temperatures" (in Russian). Reports of a Symposium on the Chemistry of Cements, pp. 83-92. (State Publications of Literature on Structural Materials, Moscow 1956).

110. H.E. Swanson, N.T. Gilfrich and G.M. Ugrinic, "Data for 45 Inorganic Substances: (tricalcium aluminate, $3CaO.Al_2O_3$(cubic))" Standard X-Ray Diffraction Powder Patterns, NBS Circular 539, Vol. V, pp.10-13 (1955), reprinted with corrections 1963. (U.S. Department of Commerce, U.S. Government Printing Office, Washington).

111. W. Büssem, "X-Rays and Cement Chemistry", Stockholm 1938, pp. 141-168.

112. F. Ordway, "Tricalcium Aluminate", London 1952, pp. 91-111.

113. R.A. Schroeder and L.L. Lyons, "Infra-red Spectra of the Crystalline Inorganic Aluminates", J. Inorg. Nucl. Chem., 28, 2, 1155-1163 (1966).

114. P. Tarte, "Infra-red Spectra of Inorganic Aluminates and Characteristic Vibrational Frequencies of AlO_4 Tetrahedra and AlO_6 Octahedra", Spectrochimica Acta, 23A, 2127-2143 (1967).

115. D.E. Day, "Determining the Co-ordination Number of Aluminium Ions by X-Ray Emission Spectroscopy", Nature, 200, no. 4907, 649-651 (1963).

116. V.L. Burdick and D.E. Day, "Co-ordination of Aluminium Ions in Tricalcium Aluminate", J. Am. Ceram. Soc., 50, 2, 97-101 (1967).

117. A.E. Moore, "Tricalcium Aluminate and Related Phases in Portland Cement", Mag. Concrete Res., 18, no. 55, 59-64 (1966).

118. C.M. Schlaudt and D.M. Roy, "Crystalline Solution in $3CaO.Al_2O_3$ on the Join $Ca_3Al_2O_6$ - '$Ca_3Fe_2O_6$'", Nature, 206, no. 4986, p. 819 (1965).

119. P. Tarte, "Al-Fe Isomorphous Substitution in $3CaO-Al_2O_3$ and $2CaO.Fe_2O_3$ and Interactions Between the So-Called C_3A and C_4AF Phases", Nature, 207, no. 5000, 973-974 (1965); "Structural Investigations of Cement Minerals - Study of Interactions Between C_3A and C_4AF" (in French), Silicates Industriels, 31, 343-352 (1965).

120. A.J. Majumdar, "The Ferrite Phase in Cements", Trans. Brit. Ceram. Soc., 64, 2, 105-119 (1965).

121. L.T. Brownmiller and R.H. Bogue, "The System $CaO-Na_2O-Al_2O_3$", Am. J. Sci., 23, 501-524 (1932).

122. J.A. Conwicke and D.E. Day, "Crystalline Solubility of Soda in Tricalcium Aluminate", J. Am. Ceram. Soc., 47, 12, 654-655 (1964).

123. K.E. Fletcher, H.G. Midgley and A.E. Moore, "Data on the Binary System $3CaO.Al_2O_3$ - $Na_2O.8CaO.3Al_2O_3$ Within the System CaO - Al_2O_3 - Na_2O, " Mag. Concrete Res., 17, no. 53, 171-176 (1965).

124. H. Muller-Hesse and H.E. Schwiete, "On the Solid Solution of MgO in Some Cement Clinker Minerals", Zement-Kalk-Gips, 9, 9, 386-389 (1956).

125. A.E. Moore, "Examination of a Portland Cement Clinker by Electron Probe Micro-Analysis", Silicates Industriels, 30, 8, 445-450 (1965).

126. W.C. Hansen, L.T. Brownmiller and R.H. Bogue, "Studies on the System Calcium Oxide - Alumina - Ferric Oxide", J. Am. Chem. Soc., 50, 396-406 (1928).

127. E.F. Bertaut, P. Blum and A. Sagnières, "Structure of Dicalcium Ferrite and Brownmillerite" (in French), Acta Cryst. 12, 149-159 (1959).

128. V. Cirilli and A. Burdese, "On Dicalcium Ferrite and Ternary Solid Solution in Lime-Alumina-Ferric Oxide System" (in Italian), Ric. Sci, 21, 1185-1191 (1951).

129. G. Malquori and V. Cirilli, "The Ferrite Phase", London 1952, pp. 120-136.

130. D.K. Smith, "Crystallographic Changes with the Substitution of Aluminium for Iron in Dicalcium Ferrite", Acta Cryst., 15, 11, 1146-1152 (1962).

131. E. Woermann, Th. Hahn and W. Eysel, "Solid Solution of Mg in $Ca_2Fe_2O_5$ and Ca_2FeAlO_5", Am. Ceram. Soc. Bull, 44, 299 (1965).

132. P. Longuet, "Note on the Behaviour of Tetracalcium Aluminoferrite in an Atmosphere of Hydrogen", Washington 1960, Vol. I, pp. 131-133.

133. A. Kato, "The Possibility of the Entry of SiO_2 into the Clinker Ferrite Phase to Form a Solid Solution", Semento Gijutsu Nenpo, XIII, 1-2 (1959).

134. A. Van Bemst, "Contribution to the Study of Reactions Between the Constituents of Portland Cement Pastes During Their Burning" (in French), Silicates Industriels,26, no.6, 290-296 (1961).

135. H.G. Midgley, Discussion on Malquori and Cirilli's paper "The Ferrite Phase", London 1952, pp. 140-143.

136. G. Yamaguchi and A. Kato, "X-Ray Investigation of the Ferrite Phase", Semento Gijutsu Nenpo, XI, pl 19 (1957).

137. S. Satou, S. Takashima and M. Kato, "Studies on the Compositions of Ferrite in the Industrial Portland Cements and Clinkers", Semento Gijutsu Nenpo, XVI, 36-39 (1962).

138. N.A. Toropov, L.D. Merkov and N.A. Shishakov, "The Binary System $5CaO.3Al_2O_3$-$4CaO.Al_2O_3.Fe_2O_3$ (in Russian), Tsement, no. 1, 28 (1937).

139. T. Yamauchi, "The System $CaO.Fe_2O_3$", J. Japan. Ceram. Assoc., 45, 279 (1937).

140. M.A. Swayze, "A Report on Studies of (1) The Ternary System $CaO.C_5A_3.C_2F$, (2) The Quaternary System $CaO.C_5A_3.C_2F.C_3S$", Am. J. Sci., 244 (1) p. 1-30; (2) p. 65-94 (1946).

141. N.A. Toropov and A.I. Boikova, "Composition and Conditions of Crystallization of Celite in Clinker Portland Cement" (in Russian), Izvest., Academy of Sciences, USSR, (Chemical Series), no. 6, 972 - 980, (1955).

142. T.F. Newkirk and R.D. Thwaite, "Pseudo-Ternary System Calcium Oxide - Monocalcium Aluminate - Dicalcium Ferrite", J. Res. Nat. Bur. Standards, 61, 4, 233-245 (1958).

143. L.E. Copeland, S. Brunauer, D.L. Kantro, E.G. Schultz and C.H. Weise, "Quantitative Determination of the Four Major Phases of Portland Cement by Combined X-Ray and Chemical Analysis", Anal. Chem., 31, 1521-1530 (1959).

144. P. Gourdin, "Mineralogical Composition and Properties of Portland Clinker" (in French), Thesis C.N.A.M., Paris (1967). To be published in Rev. des Matériaux de Construct.

145. J. Schwartz, "Contribution to the Investigation of Aluminous Ferrite Phase in Portland Cement Clinkers", Thesis C.N.A.M., Paris (1967). For possible publication in Rev. des Materiaux de Construct.

146. S. Takashima, "Systematic Dissolution of Calcium Silicate in Commercial Portland Cement by Organic Acid Solution", Semento Gijutsu Nenpo, XII, 12-13 (1958).

147. R.R. Dayal, "The System $CaO.Al_2O_3.FeO.Fe_2O_3$", Thesis, University of Aberdeen, (1966).

148. H.C. de Saint-Chamant, "Recent Study of the Diagram "$CaO.Al_2O_3.Fe_3O_4.FeO$"" (in French), Paper presented to the "Journées d'Etudes' of the Association Belge pour Favoriser l'étude des verres et des composes siliceux", Brussels, 28 February to 4 March 1966. To be published in Silicates Industriels.

149. C. Brisi and P. Rolando, "The Influence of CaF_2 and $CaCl_2$ on the Solid Solutions 2 CaO (Al, Fe)$_2O_3$" (in Italian), Ind. Ital. del Cemento, 1, 37-40 (1967).

150. F. Trojer, "The Present State of Knowledge of the Phase Composition of Portland Cement Clinker" (in German), Zement-Kalk-Gips, 5, 207-215 (1966).

151. H. Lafuma, "French Basic Research in the Cement Industry", (in French), Rev. des Matériaux de Construct., 603, 545-550 (1965). C.E.R.I.L.H. Technical Note no. 18.

152. R.W. Nurse, H.G. Midgley, W. Gutt and K.E. Fletcher, "Effect of Polymorphism of Tricalcium Silicate on its Reactivity", Symposium on Structure of Portland Cement Paste and Concrete. Special Report 90, pp. 258-262. (Highway Research Board, Washington, USA, 1966).

153. G. Yamaguchi, K. Shirasuka and T. Ota, "Comparison of Hydration Properties between Monoclinic and Inverted Triclinic Alite", Symposium on Structure of Portland Cement Paste and Concrete, Special Report 90, pp. 263-268, (Highway Research Board, Washington, USA, 1966).

154. Y. Ono and Y. Soda, "Effect of the Crystallographic Properties of Alite and Belite on the Strength of Cement", J. Res. Onoda Cement Company, XVII, no. 65, 24-38 (1965).

155. G. Verbeck, "Cement Hydration Reactions at Early Ages," J. PCA Res. Development Lab., USA, 7, no. 3, 57-63 (1965).

156. M. Musialik and A. Gruszczy'nska, "Some Observations Concerning P_2O_5 Influence on the Mineral Structure of Portland Cement", Cement Wapno Gips, XVI, 1, 1-5 (1961).

157. R. Kondo, "Effect of Special Components on the Mineral Compositions of Portland Cement Clinker", Semento Gijutsu Nenpo, XVII, 31-32 (1963).

158. A. Celani, M. Collepardi and A. Rio, "Influence of Gypsum and Calcium Chloride on C_3S Hydration" (in Italian), Ind. Ital. del Cemento, 7, 669-678 (1966).

159. V.A. P'jacev and Z.V. Tikhonenkova, "The Processus of Lime Fixation in the Synthesis of Clinker Minerals and in the Burning of Clinkers with Additions Cr_2O_3, B_2O_3, P_2O_5, V_2O_5", (in Russian), Izvest. Vyss Uchebn. Zav. SSSR. Khim. i. khim. Tekn'n, no.5, 802-806 (1966).

160. Yu. M. Butt and V.V. Timashov, "Dependence of the Binding Properties of the Clinker Minerals on Their Burning Temperature and Crystal Structure", (in Russian), Tsement, 27, 2, 17-22 (1961).

161. G.D. Uryvaeva, "On the Hydraulic Properties of γ Dicalcium Silicate" (in Russian), Izvest. Sibirsk. Akad. Nauk SSSR, Series Khim, no. 7, 2, 113-118 (1965).

162. G.V. Kukolev and M.T. Mel'nik, "Effect of Solid Solutions with C_2S on the Properties of Portland Cement Clinkers" (in Russian), Tsement, 22, 16-19 (1956).

163. A.E. Sheikin and S.A. Slobodchikova, "The Hydraulic Activity of Belite in Relation to the Conditions of its Formation and the Type of Stabilizer" (in Russian), Nauchn. Soobshch. Vses. Nauch. Issled. Inst. Tsementa, 43, 12, 8-13 (1961).

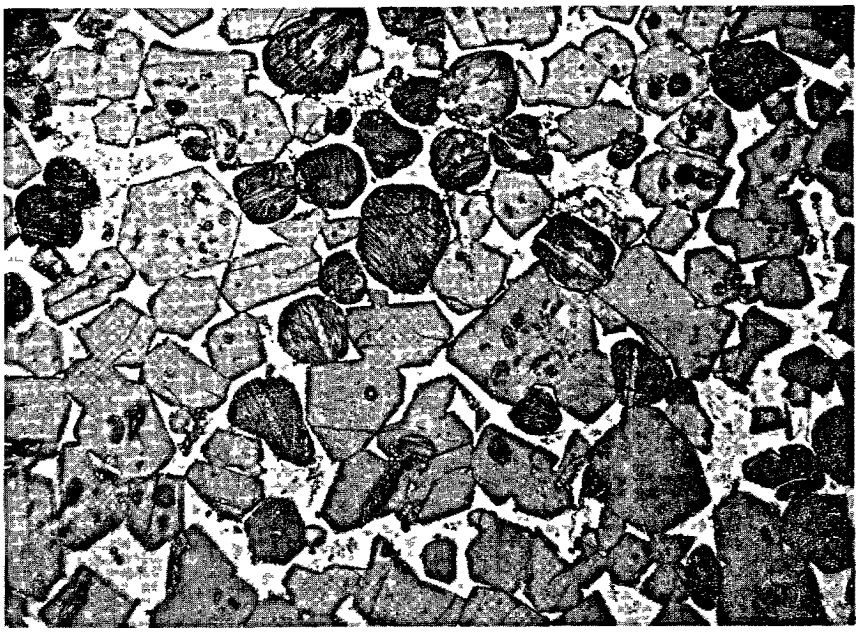

Figure 1

Photomicrograph of Portland cement clinker: the alite crystals are pseudo-hexagonal, the belite grains rounded and striated. The interstitial phase lies between the C_3S and C_2S crystals.(Terrier).

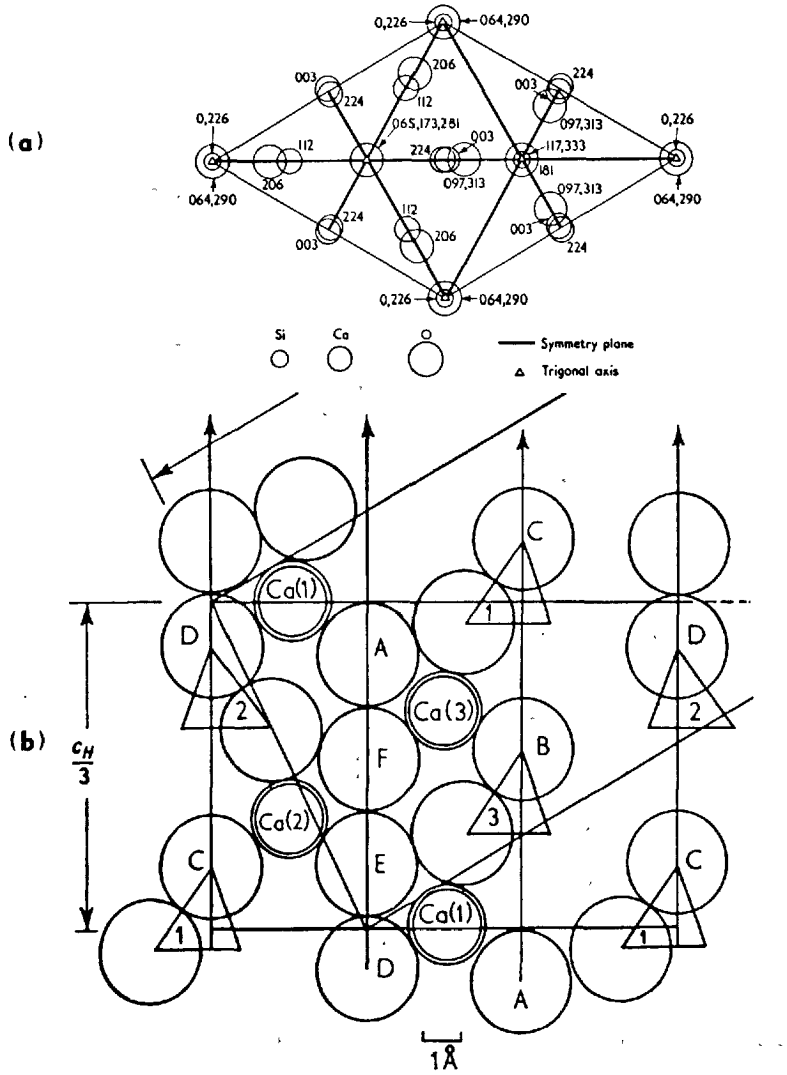

Figure 2

Tricalcium silicate: Jeffery's structure.

a) basal plane

b) vertical section through the long diagonal of the hexagonal cell. The relationship of the monoclinic axes to the hexagonal cell is shown. (Taylor: Chemistry of Cements, pp. 149-150).

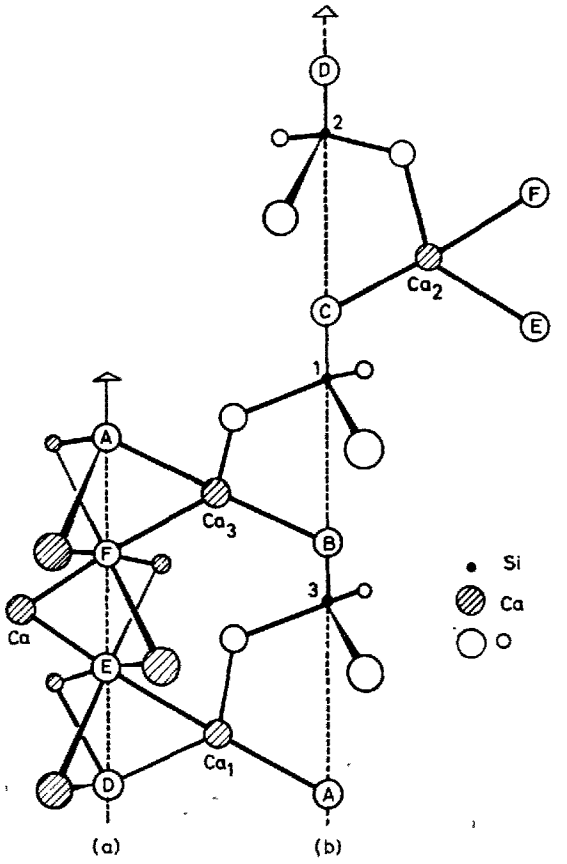

Figure 3

Tricalcium silicate: Jeffery's structure.

Two adjacent columns of tetrahedra and single O atoms, surrounded by Ca atoms. A complete column is obtained if (b) is placed on top of (a) and the labelling of the various atoms corresponds to that of Figure 2b). (Taylor: Chemistry of Cements, p. 148).

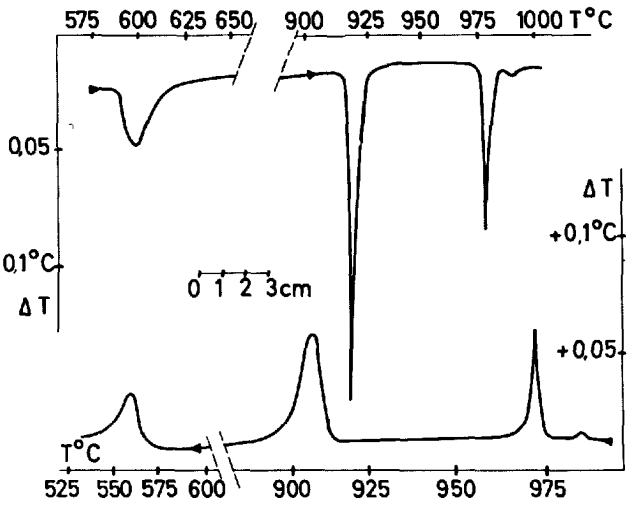

Figure 4

Tricalcium silicate. DTA diagram, heating rate 13°C/min. (Mazières).

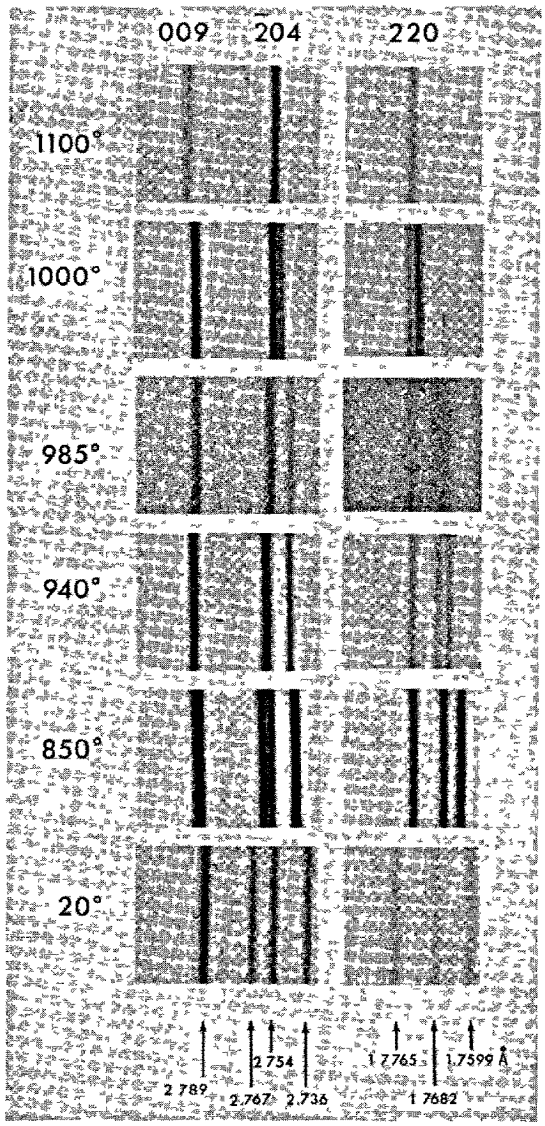

Figure 5

Tricalcium silicate. Evolution of the hexagonal reflexions 009, $\bar{2}04$, 220 from 1100° to ambient temperature. The powder patterns are obtained with a high temperature Guinier camera. At 1000° the components of the 220 doublet are separated by 3×10^{-3} Å, 220 ⟶ 1·786, 1·783 Å, and $\bar{2}04$ ⟶ 2·780, 2·776 Å (Regourd).

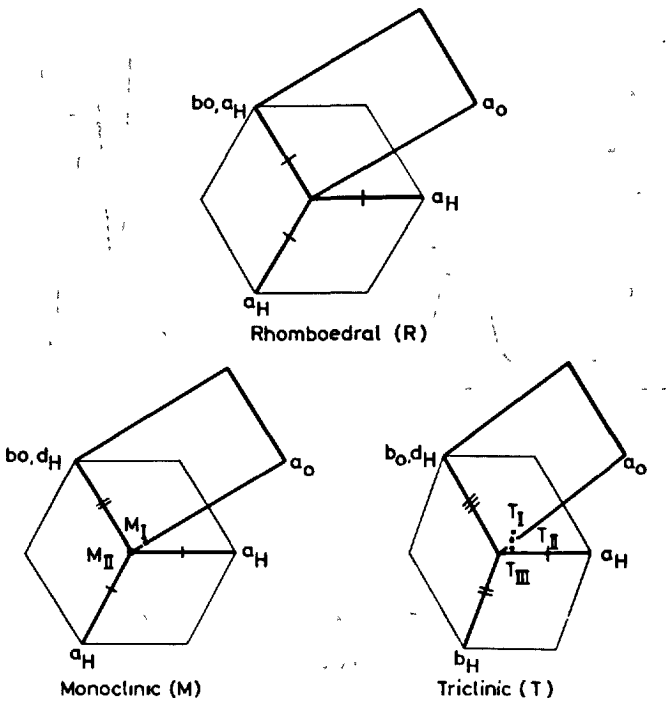

Figure 6

Tricalcium silicate: deformation of basal plane of the hexagonal cell. H = (pseudo-) hexagonal, O = (pseudo-) orthohexagonal. Dots indicate the projections of vectors [001] on the (001) plane. (Regourd).

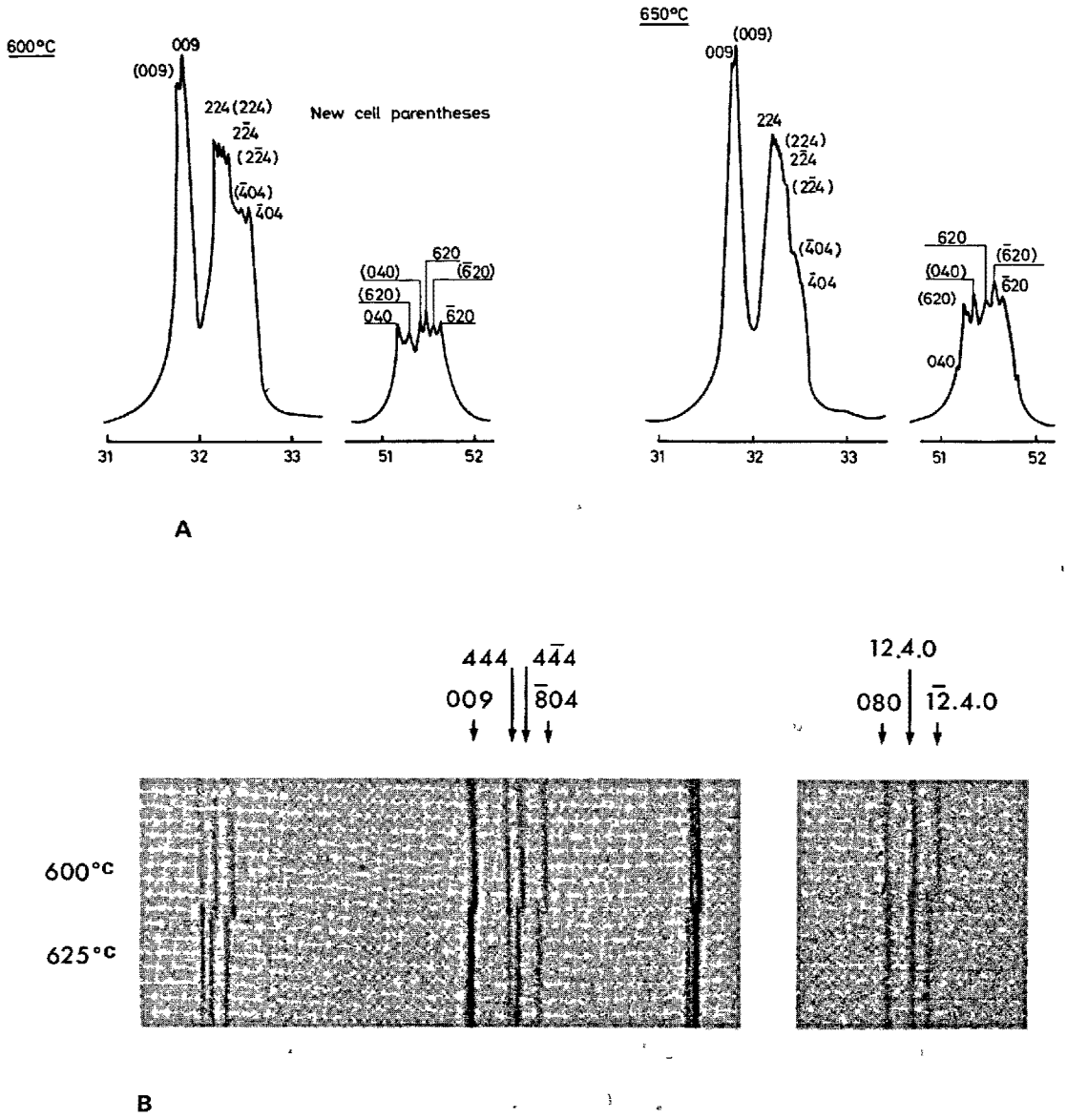

Figure 7

Tricalcium silicate. Comparison between: A) diffractometer traces by Miyabe and Roy taken at 680° and 650°C, showing a mixture of α and β phases; B) a pair of high temperature Guinier photographs showing T_I at 600° and T_{II} at 625°C. (Yannaquis, Regourd, Mazieres, Guinier).

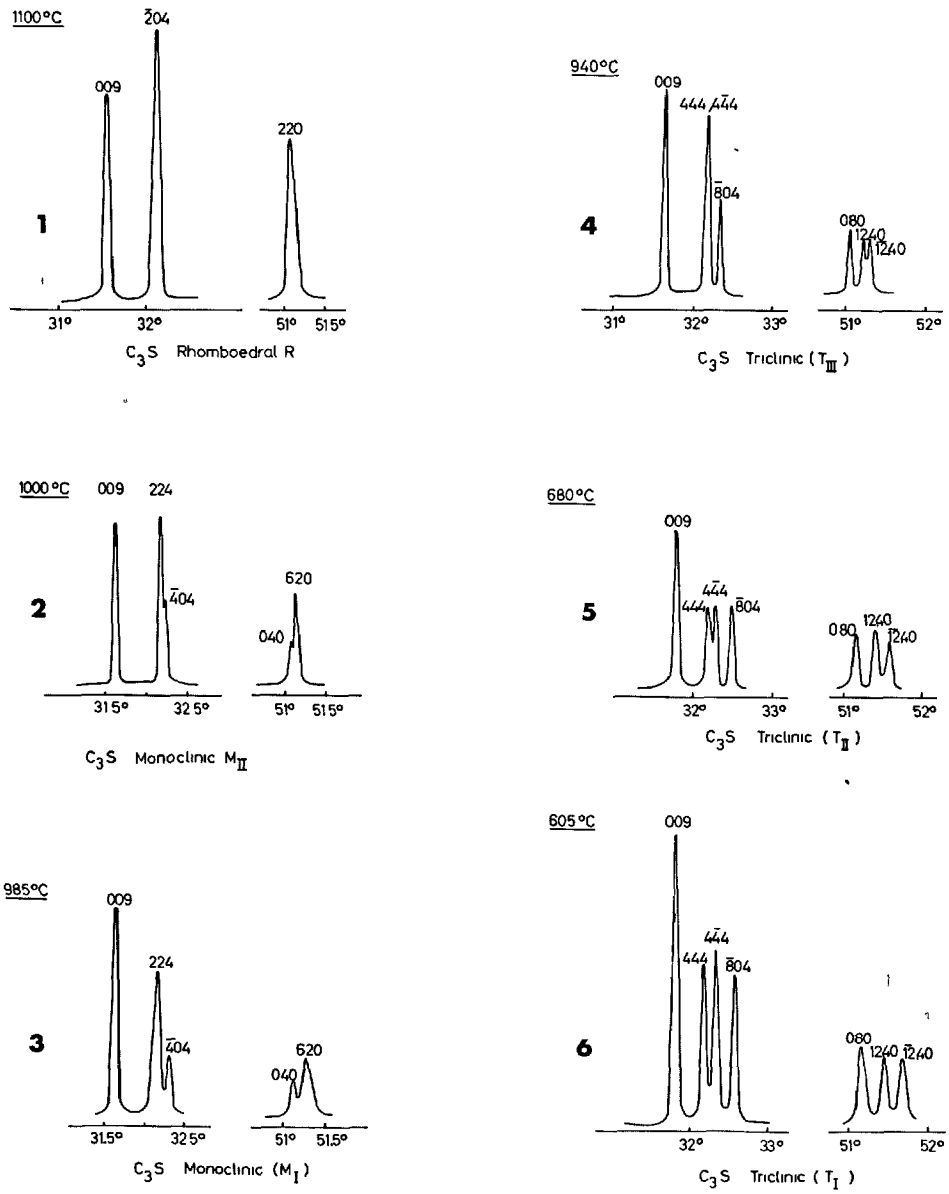

Figure 8

Tricalcium silicate. Characteristic reflexion groups in the powder patterns of the various modifications.

A) microdensitometer tracings of high-temperature focussing film patterns (Regourd);

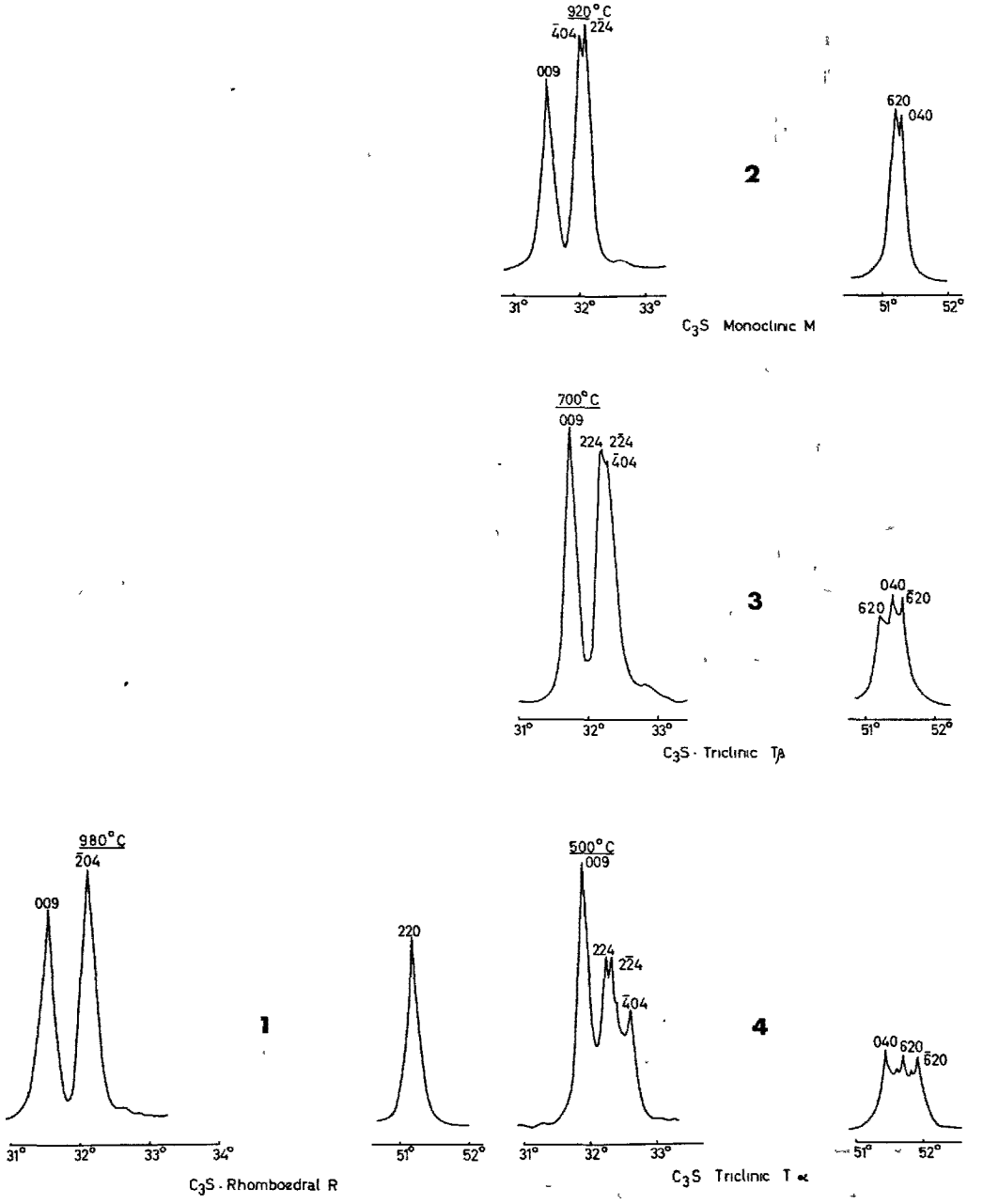

B) high-temperature diffractometer tracings (Miyabe and Roy).

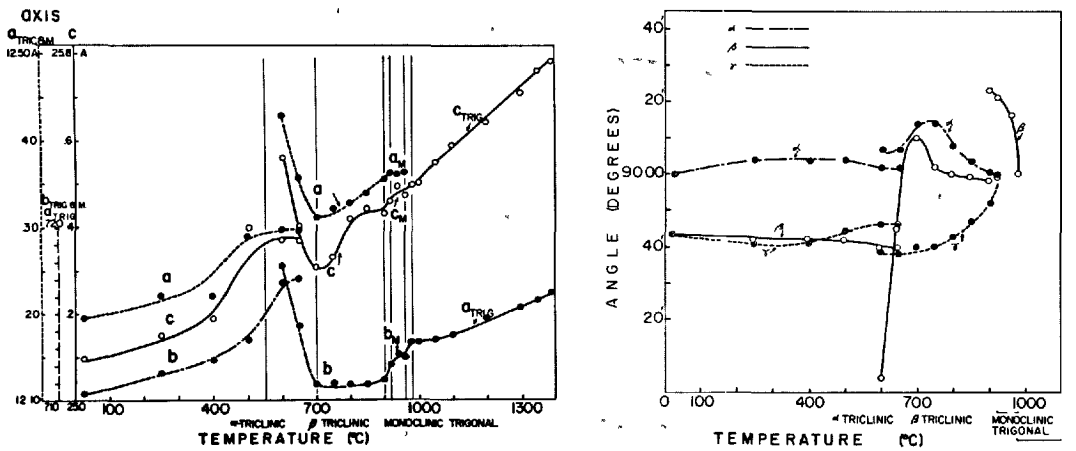

Figure 9

Tricalcium silicate: variation of pseudo-orthohexagonal lattice constants with temperature (Miyabe and Roy).

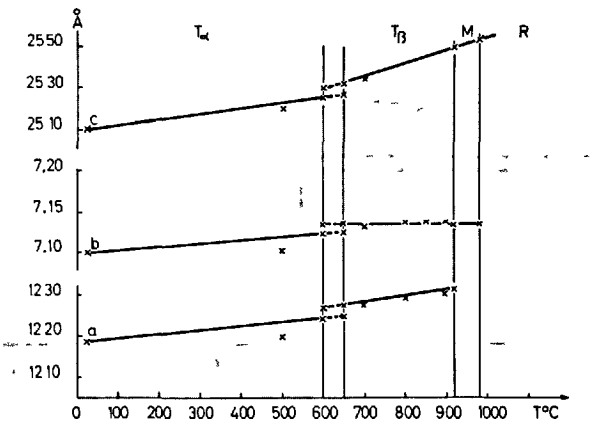

Figure 10

Tricalcium silicate. Variation of pseudo-orthohexagonal lattice constants with temperature, re-calculated from data of Miyabe and Roy.

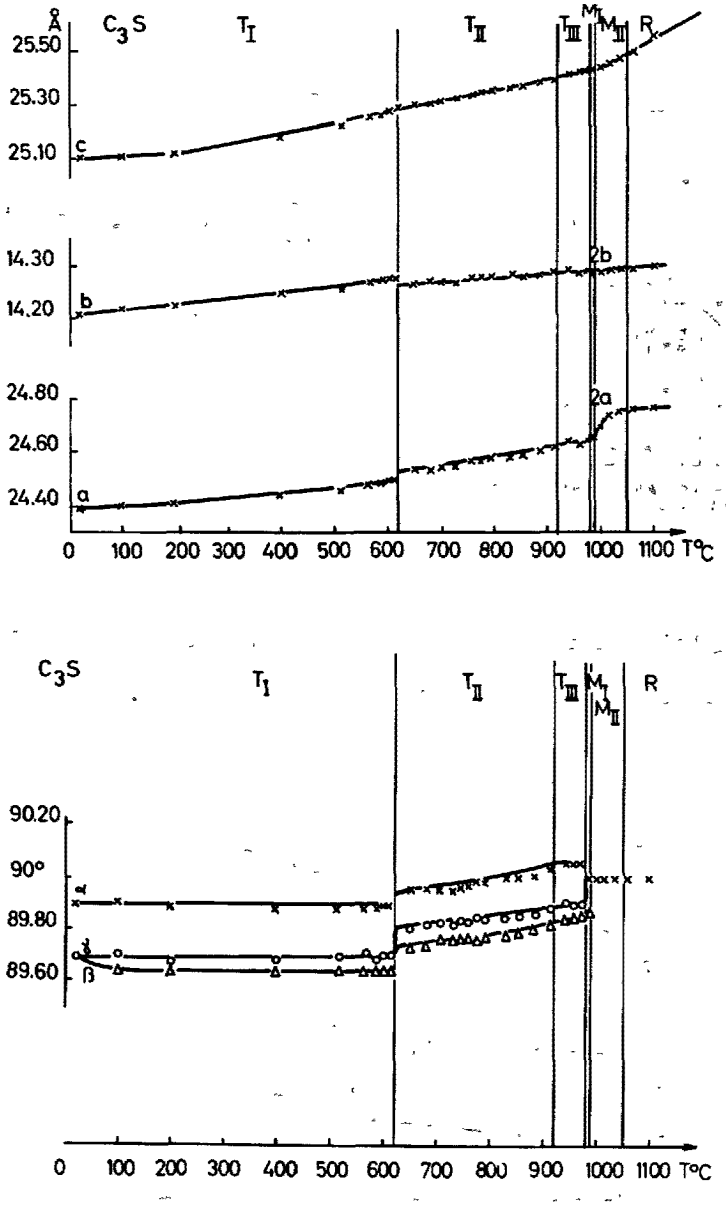

Figure 11

Tricalcium silicate. Variation of pseudo-orthohexagonal lattice constants with temperature. (Regourd).

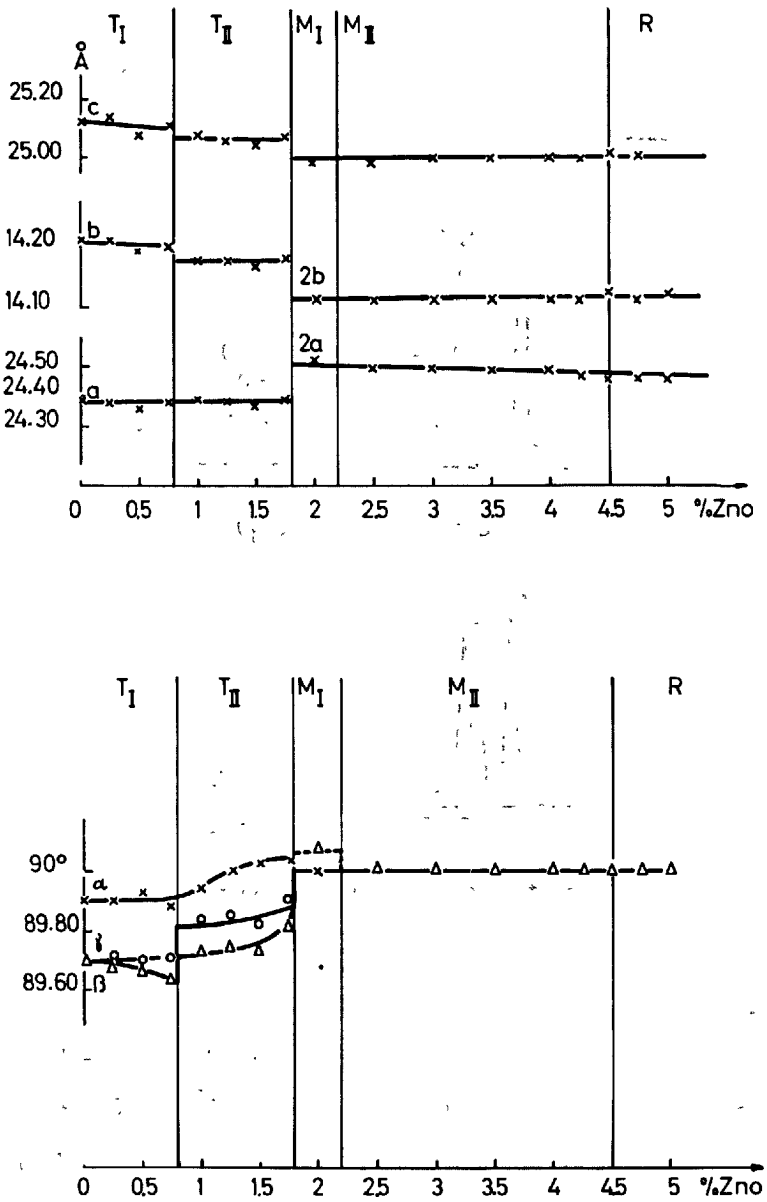

Figure 12

Ca_3SiO_5-ZnO solid solutions. Variation of pseudo-orthohexagonal lattice constants with composition at room temperature in the Ca_3SiO_5 -ZnO solid solution series. (Woermann, Hahn and Eysel).

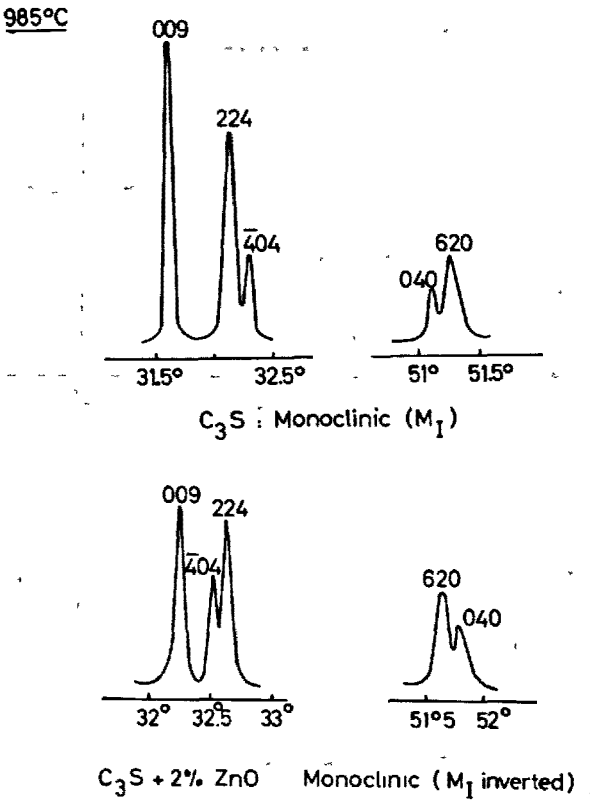

Figure 13

Comparison of densitometer records showing characteristic reflexions of monoclinic forms of pure C_3S at 985° and C_3S + 2% ZnO at ambient temperature. In the solid solution (C_3S + 2% ZnO) the 224, $\bar{4}04$ and 620, 040 reflexions are inverted.

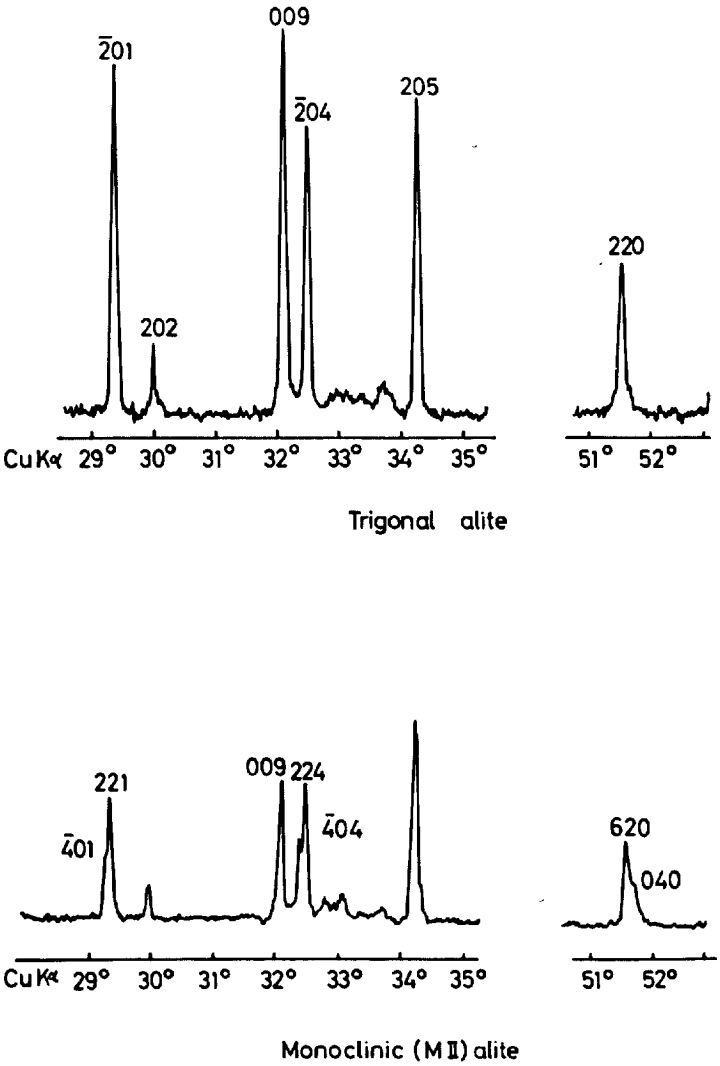

Figure 14

Densitometer records of powder patterns (Guinier camera) of two clinkers, in which the alite is respectively trigonal and inverse monoclinic.

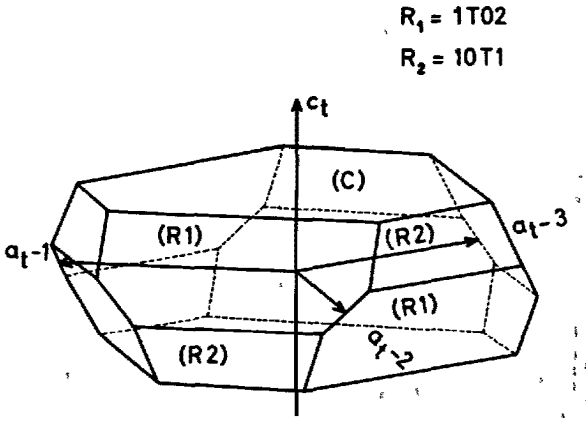

Figure 15

Relation between the trigonal axes $a_t - 1$, $a_t - 2$, $a_t - 3$, c_t and the crystal habit of a clinker alite. (Yamaguchi and Ono).

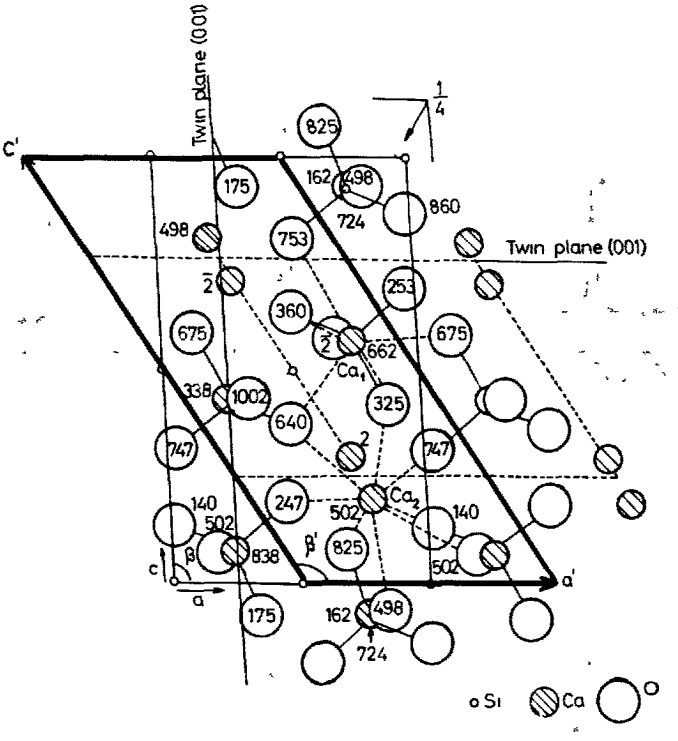

Figure 16

Dicalcium silicate. The projection of β C_2S structure on a plane perpendicular to the b-axis (Midgley). The pseudo-hexagonal cell, axes a' and b', is shown (Yamaguchi, Ono, Kawamura and Soda).

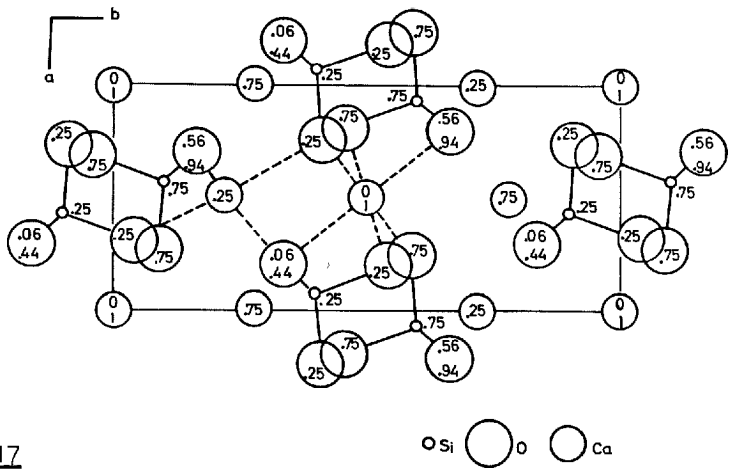

Figure 17

Dicalcium silicate. The projection of γC_2S structure on a plane perpendicular to the c-axis (Smith, Majumdar and Ordway).

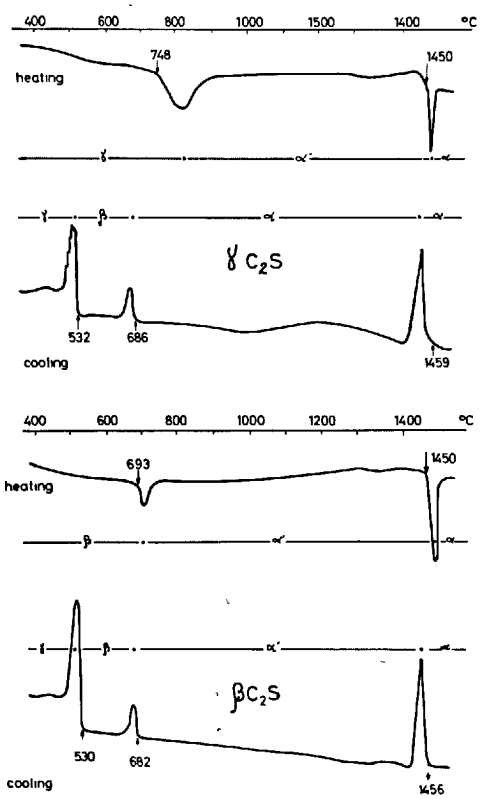

Figure 18

Dicalcium silicate. DTA diagram of γC_2S and βC_2S (Courtault) The temperatures of transformations seem higher than usual.

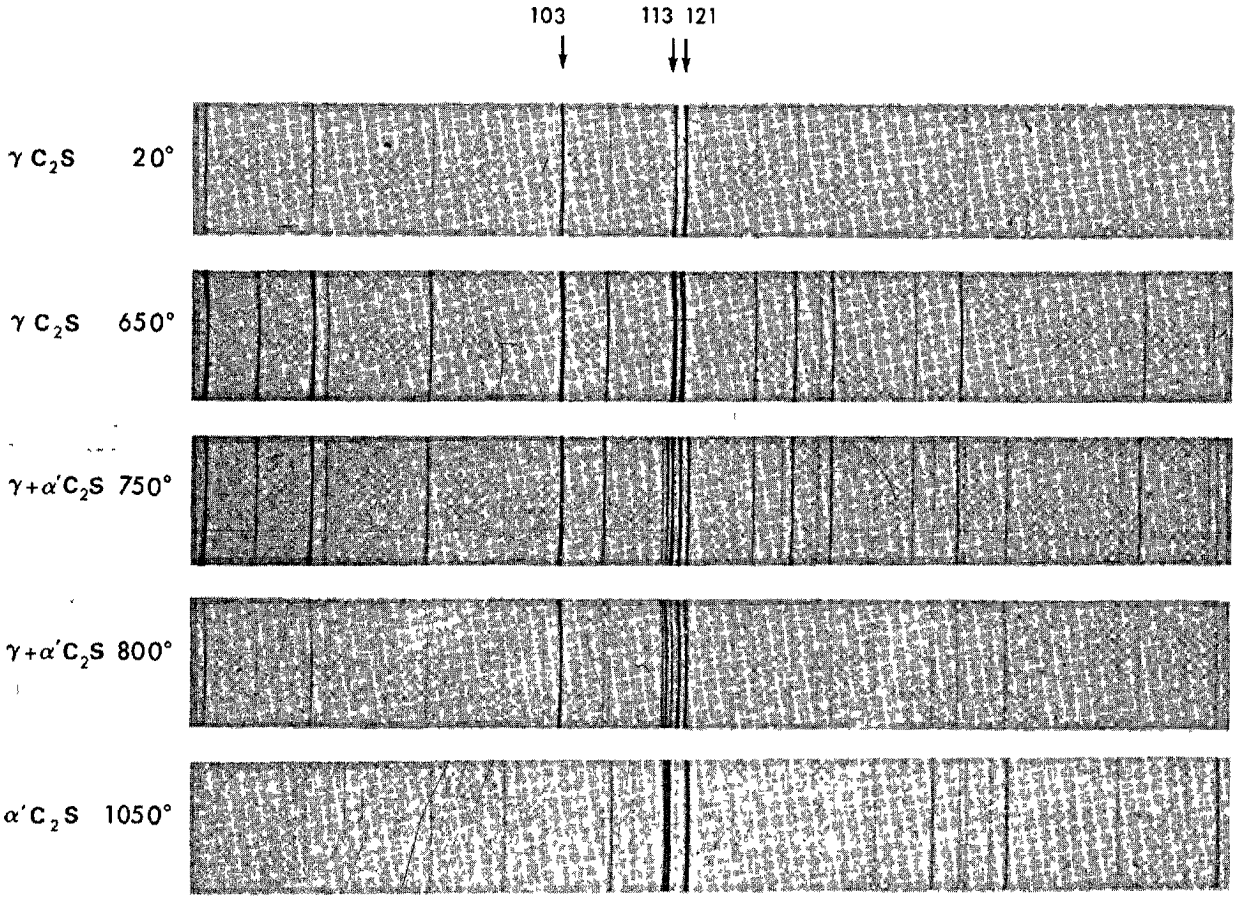

Figure 19

Dicalcium silicate. $\gamma \longrightarrow \alpha'_H$ transformation investigated by high-temperature X-ray powder patterns. At 750° and 850°C, the γ and α'_L forms coexist.

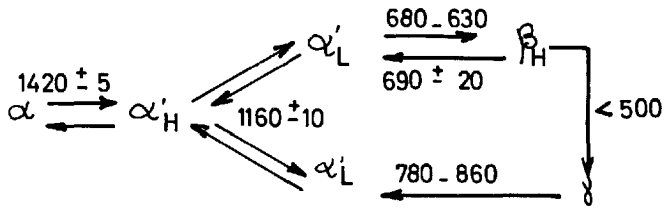

Figure 20

Dicalcium silicate. Schematic diagram of C_2S transformations. (Niesel and Thormann).

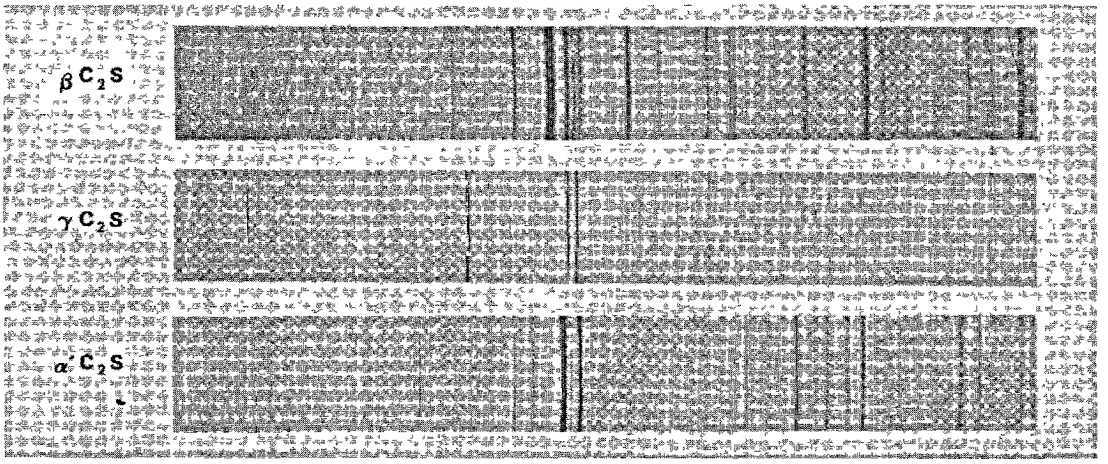

Figure 21

Dicalcium silicate. X-ray powder patterns of high-temperature Guinier camera with a stationary sample. The lines of γ C_2S are spotty while, under the same conditions, those of β C_2S are continuous.

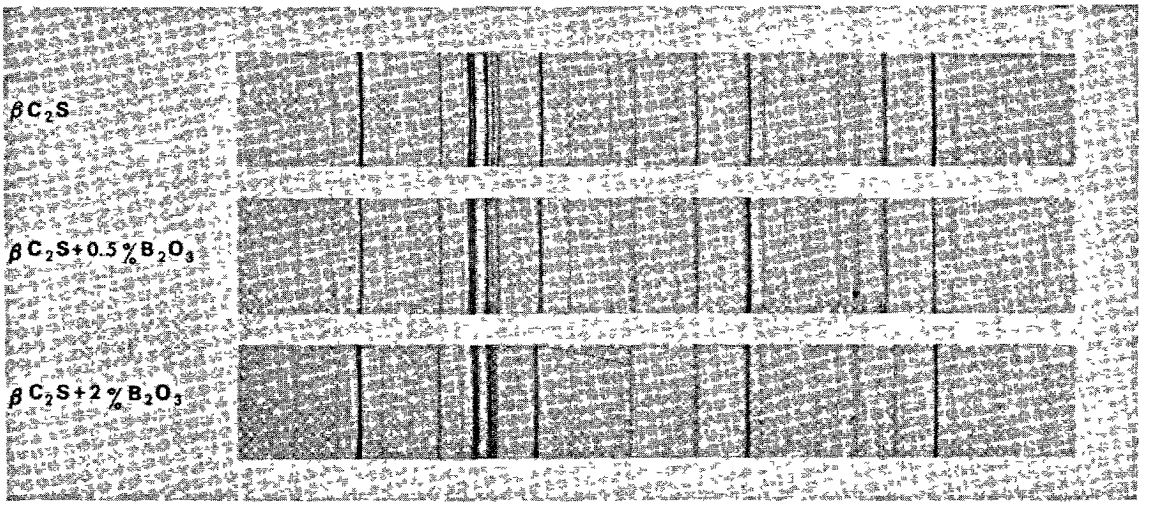

Figure 22

Dicalcium silicate and its solid solutions with B_2O_3. The lattice of β C_2S + 0·5% B_2O_3 is not significantly altered.

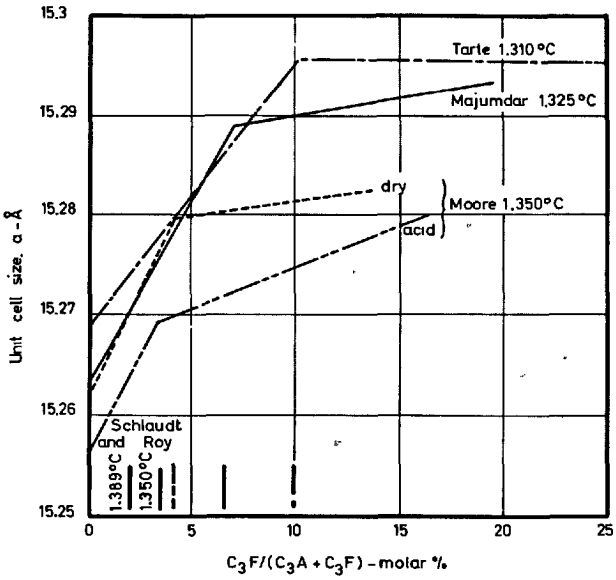

Figure 23

Tricalcium aluminate. Change in lattice parameter of C_3A with replacement of Al^{3+} by Fe^{3+}. (Moore).

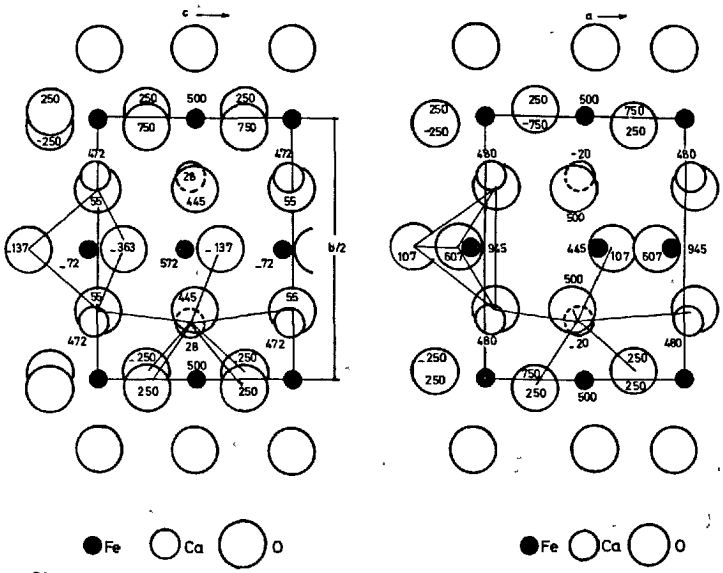

Figure 24

Dicalcium ferrite. Structure of C_2F. The projections along a and c axes are very similar. (Bertaut, Blum and Sagnières).

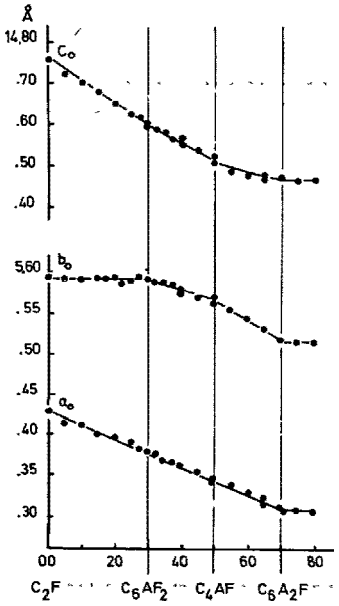

Figure 25

C_2F solid solutions: variation of C_2F lattice constants a_o, b_o, c_o with composition in the C_2F - "C_2A" solid solutions series. (Woermann, Hahn and Eysel).

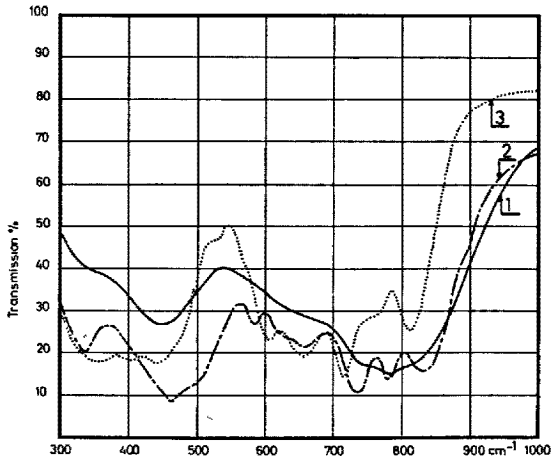

Figure 26

C_2F solid solutions. Infra-red absorption spectra (Tarte):

(1) of the vitreous phase formed from a composition $C_2(A_{0.80}F_{0.20})$;

(2) of the crystalline phases formed from the same composition as (1);

(3) of C_4AF.

Table 1

Characteristic properties of D.T.A. peaks of pure C_3S

Temperature of transformation (beginning of the signal during heating, °C)	Shape of the peaks - hysteresis	Estimated thermal effect related to the transformation (cal/g)	
		D.T.A.*	direct calorimetry**
585 ± 5	Broad peak up to 30° width depending on heating rate and strong hysteresis (20-40°C) upon cooling		0·6
917 ± 3	Sharp, strong peak, weak hysteresis (10°C)	1	1·3
975 ± 3	Sharp, strong peak without appreciable hysteresis	0·5	0·6
990 ± 2	Sharp, very small peak without appreciable hysteresis	0·05	

* From area of the peaks and comparison with the area of the peak obtained in high-low quartz transition. For this last thermal effect 1·4 cal/g was admitted as given by R. ROY(9).

** In this set of experiments(13) the thermal effect of the quartz transition was found to be 2 cal/g.

TABLE 2

Lattice constants of the modifications of pure C_3S (Average errors : a, b, c: $\pm$ 2 x 10^{-3} Å; α, β, γ : $\pm$3 x 10^{-2} degree)

Pseudo-hexagonal lattice constants

Temperature °C	Allotropic form	a (A)	b (A)	c (A)	α (°)	β (°)	γ (°)
1100	Rhomboedral R	7.150	7.150	25.560	90	90	120
1000	Monoclinic M_{II}	7.130	7.130	25.434	90	90	119.88
985	Monoclinic M_I	7.125	7.125	25.420	90.13	89.88	119.84
940	Triclinic T_{III}	14.229	14.249	25.412	90.10	89.85	119.76
			Possibly doubling of a and b				
680	Triclinic T_{II}	14.169	14.209	25.298	90.22	89.80	119.62
			Possibly doubling of a and b				
20	Triclinic T_I	14.080	14.147	25.103	90.30	89.77	119.53

Table 3

Characteristic properties of the transitions in pure $Ca_3Si_2O_5$

Transition temperatures (°C)	Characteristic effects		Type of transition *	Allotropic form	Space group
	X-Ray	D.T.A.			
1050	Change of symmetry, continuous deformation of the cell	No peak	Type a continuous	Rhombohedral (R)	R3m
				Monoclinic II (M_{II})	C1m1
990	No change of symmetry, change of cell volume	Very small reversible peak	Type a discontinuous	Monoclinic I (M_I)	C1m1
980	Change of symmetry, change of cell volume; superstructure : doubling of a and b to 14 Å	Strong reversible peak	Type a + b discontinuous	Triclinic III (T_{III})	C1
920	No change of symmetry, no change of subcell volume; (possibly second superstructure)	Strong reversible peak	Type b discontinuous	Triclinic II (T_{II})	C1
600	No change of symmetry, small deformation of the cell; possibly second superstructure	Broad reversible peak	Type a discontinuous	Triclinic I (T_I)	C1

* Type a : with decreasing temperature the degrees of freedom of the thermal vibrations are reduced thus leading to discontinuous or continuous changes in cell volume. The structural groups are slightly deformed but their periodicity is unaffected.

Type b : upon cooling, in the arrangement of the groups, regular stacking faults perpendicular to the c axis are produced, leading to the formation of superstructures but not affecting appreciably the volume of the subcell.

Table 4

Stabilisation of high-temperature allotropic forms by various oxides

Oxide	Composition ranges of allotropic forms quenched to room temperature, weight % added oxide					Limit of solid solution at 1550°C, weight % added oxide
	T_I	T_{II}	M_I	M_{II}	R	
Cr_2O_3	0-1·4	-	-	-	-	1·4
Fe_2O_3	0-0·9	0·9-1·1	-	-	-	1·1
Ga_2O_3	0-0.9	0·9-1·9	-	-	-	1·9
Al_2O_3	0-0·45	0·45-1·0	-	-	-	1·0
MgO	0-0·55	0·55-1·45	1·45-2·0	-	-	2·0
ZnO	0-0·8	0·8-1·8	1·8-2·2	2·2-4·5	4·5-5·0	5·0 (1400°)

Proceedings of
The Fifth International Symposium
on the
Chemistry of Cement
Tokyo, 1968

PART II
HYDRATION OF CEMENTS
(Volume II)

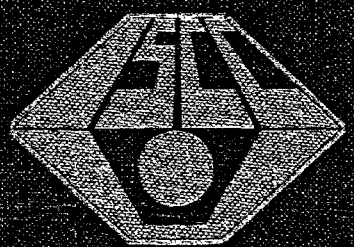

The Organizing Committee
for the Fifth International Symposium
on the Chemistry of Cement

The Cement Association of Japan

Verein Deutscher Zementwerke e. V.
Düsseldorf, Tannenstr. 2

Proceedings of
The Fifth International Symposium
on the
Chemistry of Cement
Tokyo, 1968

PART II
HYDRATION OF CEMENTS
(Volume II)

Symposium held October 7–11, 1968 at the
Tokyo Metoropolitan Festival Hall, Tokyo

Proceedings published in 4 volumes December 31, 1969

Explanatory Notes

Abbreviations.

The following symbols, which have been universally recognized by cement chemists for formulating more complex compounds, are used interchangeably with the respective oxide formulas throughout this book:

$C = CaO$, $S = SiO_2$, $A = Al_2O_3$, $F = Fe_2O_3$, $M = MgO$, $N = Na_2O$, $K = K_2O$, $H = H_2O$,

Less common abbreviations of this type are defined as they occur.

Commonly used abbreviations of more general nature are as follows:

DTA = differential thermal analysis
EPMA = electron probe micro analysis
IR = infrared
NMR = nuclear magnetic resonace
psi (or p.s.i.) = pounds per square inch
rh (or RH) = relative humidity
w/c (or W/C) = water – cement ratio
XRD = X-ray diffraction

Identification Number of Supplementary Papers

Example: Supplementary Paper III—50, III is session III and 50 is the arrival number of contribution. This number coincides with the number used in the preprint of papers distributed in advance of the symposium.

Contents

Volume II

Part II. Hydration of Cements

Session II-1 Crystal Structures and Properties of Cement Hydration Products (Calcium Silicate Hydrates)

Session II-2 Crystal Structures and Properties of Cement Hydration Products (Hydrated Calcium Aluminates and Ferrites)

Session II-5 Hydration of Portland Cement

SESSION II-1 CRYSTAL STRUCTURES AND PROPERTIES OF CEMENT HYDRATION PRODUCTS (CALCIUM SILICATE HYDRATES)

Principal Paper The Calcium Silicate Hydrates

H. F. W. Taylor*

Synopsis

This paper reviews progress on structural and phase equilibrium aspects of the calcium silicate hydrates and some related substances, under the following headings:

Introduction
New experimental techniques
Crystal structures: general points
Crystalline calcium silicate hydrates: new data
Crystalline calcium silicate hydrates: equilibria and conditions of formation
Crystalline calcium silicate hydrates with additional ions
Poorly crystalline calcium silicate hydrates
Paste hydration of C_3S and β–C_2S
Isomorphous substitution

The paper deals only with progress made since the Washington Symposium, and familiarity with the state of knowledge as summarized in the proceedings of the latter is assumed.

It is suggested that the evidence relating the hydration products formed in calcium silicate or cement pastes to tobermorite is weak and that the term "tobermorite gel" should not be used.

Introduction

In this paper, we shall review work on the structures, properties, and phase equilibria relating to the calcium silicate hydrates and some related compounds since the time of the Washington Symposium. It will be assumed that the reader is familiar with the state of knowledge at that time, as summarized in the proceedings (1). We shall deal only incidentally, if at all, with the kinetics, energetics and mechanisms of reactions yielding calcium silicate hydrates, and with the microstructures of calcium silicate or cement pastes and their relation to physical and mechanical properties.

Table 1 gives the names and compositions (in some cases, approximate) of the better established crystalline calcium silicate hydrates, and of some other related, crystalline phases that will be mentioned in this review. Not included in Table 1 is an indefinite range of semicrystalline and near-amorphous calcium silicate hydrates, which are nevertheless of great importance to cement chemistry. Their C/S ratios probably range from 0.5 to 3.0, and their H/S ratios from zero to about 2.0.

Table 1. *Crystalline calcium silicate hydrates, with some structurally related compounds*

Calcium silicate hydrates		*Other compounds**	
Structures related to wollastonite			
Nekoite	$C_3S_6H_8$	Wollastonite	β-CS
Okenite	$C_3S_6H_6$	Scawtite	$C_7S_6H_3\bar{C}$
Xonotlite	C_6S_6H	Jennite	$Nc_6S_5H_{11}$
Foshagite	C_4S_3H	Pectolite	NC_4S_6H
Hillebrandite	C_2SH	Miserite	$KC_8S_{10}H_3$

*Department of Chemistry, University of Aberdeen, Old Aberdeen, United Kingdom.

Table 1 (continued)

Calcium silicate hydrates		*Other compounds**	
Tobermorite group			
14 Å Tobermorite	$C_5S_6H_9$	9.7 Å Tobermorite	C_5S_6
11 Å Tobermorite	$C_5S_6H_5$		
9.3 Å Tobermorite	C_5S_6H		
12.6 Å Tobermorite	(?)		
10 Å Tobermorite	(?)		
Gyrolite group			
Z-phase	CS_3H_2	Reyerite	$KC_{28}S_{48}H_{15}$
Truscottite	$C_6S_{10}H_3$		
Gyrolite	$C_8S_{12}H_9$		
Structures related to γ-C_2S			
Calciochondrodite	C_5S_2H	γ-Dicalcium silicate	γ-C_2S
		Kilchoanite	C_3S_2
		—	C_8S_5
		Fluor-calciochondrodite	$Ca_5(SiO_4)_2F_2$

Calcium silicate hydrates		*Other compounds**	
Other structures			
Tacharanite	CSH	Cuspidine	$Ca_4(Si_2O_7)F_2$
Suolunite	CSH	Tilleyite	$C_5S_2\bar{C}_2$
Rosenhahnite	C_3S_3H		
Afwillite	$C_3S_2H_3$		
α-Dicalcium silicate hydrate	C_2SH		
Rustumite	C_4S_3H		
Dellaite	C_6S_3H		
Tricalcium silicate hydrate	$C_6S_2H_3$		

*$\bar{C} = CO_2$

New Experimental Techniques

The Electron Microprobe

Since the time of the Washington Symposium, the electron microprobe has become a tool of major importance in the study of anhydrous systems. Its applications in the field of hydrated compounds are probably more limited, but it has been used to establish the compositions of some newly discovered calcium silicate hydrate minerals (2), and also in synthetic investigations (3).

X-ray Spectroscopy

The wavelengths of the characteristic X-rays emitted by an atom are influenced by the configuration of its valence electrons and its surroundings, and can therefore provide information on such matters as oxidation state, coordination number, bond lengths, and order-disorder effects. Unlike X-ray diffraction, the method is not affected by the degree of long-range order, and can therefore be used for amorphous as well as crystalline substances. X-ray spectra of silicates are conveniently studied either by fluorescence techniques, or by electron-excited emission using the electron microprobe.

The first applications of X-ray spectroscopy to silicate structures were concerned with aluminium coordination, White, McKinstry and Bates (4), Brindley and McKinstry (5) and Day (6) showing that four and six coordination could be distinguished in this way. Applications to Al-substituted calcium silicate hydrates are mentioned later in this review. Another application of X-ray spectroscopy, also mentioned later, concerns the environment of sulphate groups substituted in a silicate structure. Lastly, White and Gibbs (7) have shown that the method can be used to provide information on mean Si–O bond lengths and thereby on the degree of condensation of silicate anions. This has not yet been applied to calcium silicate hydrates, but should afford a valuable check on the chemical methods discussed below.

Chemical Methods for Studying Degrees of Anion Condensation in Silicates

Murata (8) showed that the behaviour of silicate minerals with acids was related to the degree of condensation of the anion. If the anion was of low molecular weight, as with ortho- and pyrosilicates and framework structures containing much tetrahedral aluminium, gelatinuous silica was formed; silicates with highly condensed anions, in contrast, yielded silica pseudomorphs. Subsequently, various attempts have been made to identify the anions in silicates more precisely by attacking the solids with acids under conditions that would break the bonds between metal cations and oxygen, while leaving the silicon-oxygen bonds intact, followed by identification of the resulting silicic acids. Such conditions are difficult to achieve with certainty, and the problem is further complicated by the fact that the silicic acids tend to condense to form larger units. Three methods have been developed recently in attempts to overcome these difficulties, and each has been applied to calcium silicate hydrates.

(i) Lentz (9, 10, 10a) decomposed the silicate in a solution containing HCl, hexamethyldisiloxane ($Me_3SiOSiMe_3$), isopropyl alcohol, and water. The hexamethyldisiloxane decomposed to give Me_3SiOH and Me_3SiCl, which in turn reacted with the silicic acids to yield esters. These were identified by gas chromatography; it was assumed that esterification occurred rapidly enough to forestall changes in the silicic acids, and that the esters were themselves stable. In practice, condensation of the silicic acids was not entirely avoided, orthosilicates such as olivine or C_3S yielding appreciable proportions of the pyrosilicate ester as well as that of the orthosilicate. On the other hand, it is possibly more widely applicable than either of the other methods.

(ii) Funk and Frydrych (11) and Funk (12) decomposed the silicate in methanolic HCl. This reagent was preferred to aqueous HCl because the silicic acids were more soluble and had a much lower condensing rate. The solution was then mixed with an aqueous molybdic acid solution and the rate of formation of the molybdosilicic acid followed by a volumetric methods. Previous investigators had shown that the molybdic acid reacts only with orthosilicic acid; the rate-determining step if condensed silicic acids are present is their hydrolysis to orthosilicic acid. The method was shown to give satisfactory results for a number of silicates containing alkali or alkali earth cations, including Ca^{2+}, but to be less satisfactory in the presence of Mg^{2+} or Al^{3+}.

(iii) Thilo, Wieker and Stade (13) and Wieker and Stade (14) added the finely powdered silicate directly to an acidified, aqueous solution of ammonium molybdate and followed the rate of formation of the molybdosilicic acid spectrophotometrically. The method can be applied only if dissolution of the silicate is sufficiently rapid. It was shown to give satisfactory results for a number of alkali and alkali earth silicates.

It would be premature to attempt to assess further the relative merits of these three methods, applications of which to calcium silicate hydrates are metnioned later in this review.

Crystal Structures: General Points

The main principles governing calcium silicate structures were established by the time of the Washington Symposium, and will only be briefly summarized here. The metal cations play an essential part in controlling the manner in which SiO_4 tetrahedra condense; anions similar to those found in the pyroxenes, amphiboles, and micas do not occur in calcium silicates, because they do not fit onto the bands or sheets of linked CaO_6 octahedra. In contrast, anions of the types found in wollastonite or xonotlite occur, because they fit onto these bands or sheets.

Belov (15) has since emphasized the important role in many calcium silicate structures of the pyrosilicate group, which is of the correct size to bridge two corners of a CaO_6 octahedron. The essential feature of such structures is therefore the occurrence of lines of Si_2O_7 groups (Fig. 1a), and the linkage of these in some cases into wollastonite-type chains by the interpolation of additional tetrahedra (Fig. 1b) is almost incidental. Below drew attention to the frequent occurrence of structures based on lines of Si_2O_7 groups condensed with puckered sheet or three-dimensional nets of linked CaO_6 octahedra, as in tilleyite ($Ca_5(Si_2O_7)(CO_3)_2$) and cuspidine ($Ca_4(Si_2O_7)F_2$).

These structures are interesting, not only because they illustrate structural principles that apply to other crystalline calcium silicates, but also because they suggest a possible way in which deterioration of crystallinity and variation in composition could occur. It would appear possible for some of the silicon atoms in a wollastonite chain (up to one in three in extreme

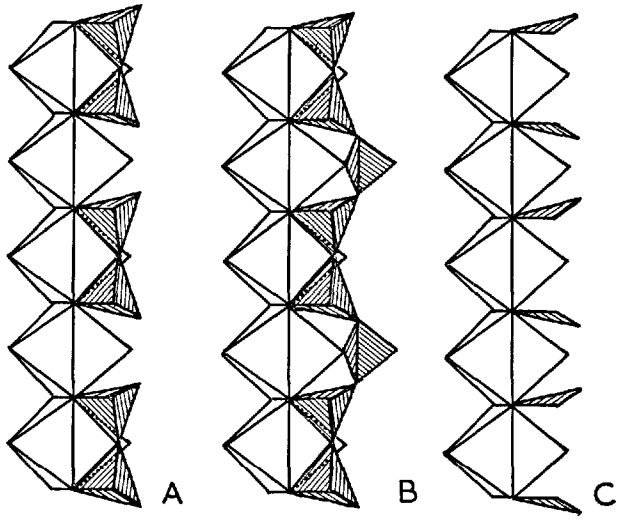

Fig. 1. *Ribbons of linked* MO_6 *octahedra with attached silicate or borate anions (after Belov).*
A, *Pyrosilicate groups.* B, *Wollastonite chain.* C, *Orthoborate groups (shown slightly tilted in alternate directions to emphasize the relation to* A *and* B).

cases) to be omitted, thus decreasing the chain length and increasing the C/S ratio, without basically destroying the structure. This accords with the hypothesis advanced by Taylor and Howison (16) and developed in a modified form by Brunauer and Greenberg (17) to explain the variable C/S ratio in the poorly crystalline calcium silicate hydrates. As is discussed later in this review, even relatively highly crystalline tobermorites, of both synthetic and natural origin, appear frequently to be deficient in silicon, and the same explanation may well apply.

Mamedov and Belov (18) have noted that close similarities exist between certain borate and silicate structures; thus warwickite ($Mg_3Ti(BO_3)_2O_2$) is structurally very similar to cuspidine. Two BO_3^{3-} groups in warwickite occupy a position analogous to that of an $Si_2O_7^{6-}$ group in cuspidine (Fig. 1a and c). Mamedov (19) has pointed out that the similarity extends to some carbonates, such as malachite ($Cu_2(CO_3)(OH)_2$). These relationships are interesting because they suggest a way in which small amounts of CO_3^{2-} or BO_3^{3-} could enter the structures of silicates containing chains of the wollastonite or similar types. Such substitution appears to occur in several cases, such as xonotlite, scawtite and tobermorite. If it occurs in the way suggested here, it would be at the expense of silicon and would thus cause a break in the silicon-oxygen chain.

It is inherent in the ideas developed above that the anions in many long-chain calcium silicate hydrates are in reality probably often far from infinite in length, as the idealized crystal structures would indicate. A distribution of chain lengths presumably exists. The new experimental techniques mentioned in the previous section should permit this hypothesis to be tested.

The essential role of metal cations in controlling the condensation of SiO_4 tetrahedra leads to a prediction as to the mechanism whereby calcium silicate hydrates precipitate from solution. It is surely not correct to regard the condensation of the SiO_4 tetrahedra as the primary process, with the metal cations only becoming involved later, for if this was so, anions entirely inappropriate to the structure might well be formed. It is much more likely, either that condensation of SiO_4 tetrahedra and of metal cation—oxygen polyhedra occur simultaneously, each process influencing the other, or alternatively, that the metal hydroxide sheets are formed first and act as a matrix for subsequent condensation of the SiO_4 tetrahedra. This latter view has been argued in the analogous case of the clay minerals (20). If the language of polymer chemistry is adopted, it is misleading to regard the formation of a complex silicate primarily as a case of condensation polymerization of the silicate anions. It is at least as important, perhaps more important, to regard the process as one of coordination polymerization in which the metal cations play an essential part.

Crystalline Calcium Silicate Hydrates: New Data

Nekoite, Okenite, Xonotlite, Foshagite and Hillebrandite

These compounds, in common with wollastonite, the crystalline tobermorites, and some calcium silicate hydrates containing additional ions, have 7.3 Å repeat distances in one direction and are known or believed to have structures containing wollastonite-type chains. Little new information of significance has emerged about any of them since the Washington Symposium, and foshagite (21) and xonotlite are still the only two of which the crystal structures have been determined. A new analysis of nekoite (22) shows the composition to be $C_3S_6H_8$ and not $C_3S_6H_6$ as previously reported. Nekoite and okenite remain unsynthesized. Polytypism (occurence of stacking modifications of the same, basic structure) in xonotlite and foshagite has been studied using selected area electron diffraction, and a system of nomenclature devised to designate the polytypes in these and similar cases (23, 24). The formula of xonotlite is still generally written as C_6S_6H, although, as was pointed out at Washington (25), published analyses and weight-loss curves of both natural and synthetic specimens suggest a slightly higher water content. The formula is perhaps better written as C_5S_5H, or $Ca_6Si_6O_{17}(OH)_2 \cdot O \cdot 2H_2O$. Thilo, Wieker and Stade (13) and Wieker and Stade (14) have applied the chemical method previously mentioned to determine the degree of anion condensation in hillebrandite. They concluded (14) that single metasilicate chains were present; this does not support the structure postulated on unit-cell evidence by Mamedov and Belov (26).

Crystalline Tobermorites

14 Å tobermorite, previously known to occur in

nature only as a constituent of intergrowths with other minerals, has now been found pure at Crestmore, California (27). An X-ray, infrared, and thermal decomposition study of this specimen has been reported (28). The composition approximates to $C_5S_6H_9$, with small amounts of B_2O_3 and CO_2; the borate probably occurs as planar BO_3^{3-} ions, which, along with the CO_3^{2-}, probably replace parts of the metasilicate chains as suggested earlier in this review. At 55 ± 5°C there is a sharp loss of water, and an 11.3 Å tobermorite, of approximate composition $C_5S_6H_5$, is formed. This gradually loses water at 55–220°C; the X-ray pattern remains sharp up to about 120°C, but thereafter becomes progressively more weak and diffuse, and at 200–220°C both 11.3 and 9.35 Å tobermorites are present. The 11.3 Å tobermorite can probably lose part of its water before collapse to the 9.35 Å form occurs, and this is reflected by slight changes in X-ray pattern and infrared absorption spectrum. The weight-loss curve shows a step corresponding to the approximate composition C_5S_6H at 250–450°C and it was concluded that the 9.35 Å tobermorite has this definite composition; the higher water contents indicated by some earlier studies appear to be in error, at least for the product obtained from the Crestmore mineral. At 450–650°C, the remaining water and the CO_2 are lost, and the basal spacing gradually *increases* again, to 9.7 Å. This can perhaps be attributed to the condensation of SiOH groups in chains of adjacent layers to form new SiOSi links, which might be expected to cause some change in packing. The 9.7 Å phase thus has the approximate composition C_5S_6. At 730–770°C, it changes topotactically (*i.e.*, with partial preservation of crystalline order) to an imperfectly crystalline wollastonite. Crystallization of wollastonite is completed at 850–900°C.

The C/S ratio of 11.3 Å tobermorite can range from the idealized value of 5:6 to about 1.0 (29) or possibly somewhat higher. It is suggested that C/S ratios above 5:6 arise through omission of Si rather than incorporation of extra Ca. If this is so, one would expect increase in C/S ratio to be accompanied by decrease in chain length and probably also by decrease in layer thickness. Funk (12) reported some results that suggest that increase in C/S ratio is in fact accompanied by decrease in chain length. He made three autoclaved preparations at 150°C with C/S ratios of 0.81, 1.01 and 1.1, all of which he showed to consist of 11 Å tobermorite mixed with xonotlite, and determined the proportion of the total silica extracted by methanolic HCl in each case. The proportions increased from zero for the 0.81 C/S preparation, to 6% for the 1.1 C/S preparation. He obtained similar but more detailed results for preparations of C–S–H (I), which can probably be considered a structurally degenerate tobermorite; these are described later. The layer thicknesses of natural and synthetic tobermorites range from about 11.0 to about 11.5 Å, but it is difficult to distinguish the contributions to this variation from variations in C/S ratio, H/S ratio, and Al substitution; research into this would be of value. With C–S–H (I), the layer thickness seems definitely to decrease with increasing C/S ratio (30).

Lentz (10a) used his extraction method to study a mixed 14 Å–11.3 Å tobermrite from Crestmore. He found that about one-half of the total SiO_2 occurred in anions containing a mean of 28 terahedra, and that, of the rest, most was insoluble in acid and thus presumably more highly condensed.

No new information of significance seems to have been reported for the crystalline 10 Å and 12.6 Å tobermorites that occur in nature in intergrowths at Crestmore (31, 32). The 10 Å form occurs intergrown with 14 Å tobermorite, and on heating yields 9.3 Å tobermorite (32); it is therefore most unlikely to be identical with the anhydrous 9.7 Å form mentioned previously. It is possibly a lime-rich variety with substantial deficiency of silicon. The anomalous characteristics of certain 11.3 Å tobermorites, such as that from Loch Eynort, Scotland, also remain unexplained.

Tacharanite

A new mineral, named tacharanite, was reported as a natural mineral from Skye, Scotland, by Sweet (33) and may belong to the tobermorite group. It is particular interest because its composition and X-ray powder pattern are nearer to those to C–S–H (I) than are those of any other *crystalline* calcium silicate hydrate (the natural mineral, plombierite, which is semi-crystalline, is virtually identical with C–S–H (I) (34)). Tacharanite was found only in milligram amounts, in amygdules in dolerite in association with tobermorite, gyrolite, saponite, calcite and various zeolites. Chemical analysis indicated the approximate composition $0.86CaO \cdot SiO_2 \cdot 1.21H_2O$ with some Al_2O_3 and MgO. The mineral was cryptocrystalline and had a mean refractive index of 1.537 and a density of about 2.36 g cm^{-3}. X-ray powder data and a weight loss curve were also given; the water was lost gradually over the range 100–1000°C though the curve showed slight arrests at 350° and 650°C. Sweet reported that, on exposure to air, the mineral changed

to give tobermorite and gyrolite, and suggested that it might be the parent mineral from which these had been formed.

A few mg of the mineral were kindly made available to the author for study. Part of this sample was heated successively at 50° (6 hr.), 110° (15 hr.), 160° (15 hr.), 260° (5 hr.), 400° (5 hr.), 580° (4 hr.), 700° (15 hr.), 800° (2 hr.) and 1000°C (2 hr.); after each period of heating, the material was cooled to room temperature and an X-ray powder pattern obtained. The X-ray pattern of the original mineral agreed well with that reported by Sweet. No significant changes were observed up to 700°C. The 800°C sample gave a modified pattern, still recognizably similar to that of the original mineral; the 1000°C sample gave a pattern of wollastonite.

These results are not easily reconciled with Sweet's observation that the mineral changes spontaneously in air to gyrolite and tobermorite; the total time occupied by the series of heating periods and X-ray exposures was about one week. Further study of tacharanite would be of much interest but is restricted by the extreme scarcity of material. Attempts by the writer and others to find more material at the original locality have been unsuccessful.

Suolunite

This name was given to a new hydrated calcium silicate mineral which was reported from Inner Mongolia by Huang (35). As the original note describing the mineral is in Chinese, and the composition of the latter is in a range of great importance to cement chemistry, the main observations will be reported here in some detail. The mineral was found as a narrow vein cutting into a diabase vein in the centre of an ultrabasic rock body; the name was derived from the locality. Chemical analysis gave SiO_2 43.38, CaO 42.95, H_2O^+ 13.17 (total 99.50), corresponding to the formula $CaO \cdot SiO_2 \cdot H_2O$. The X-ray powder pattern was not given in full, but was reported to have strong peaks at 4.03, 3.11 and 2.80 Å. The mineral was reported to form transparent, colourless, rod-like or granular crystals, with no definite cleavage; optical properties were $\alpha = 1.610$, $\beta = 1.620$, $\gamma = 1.623$, $-2V = 30$–$50°$ (a later paper gives 30–35° (36)). DTA curves showed a strong endotherm at 440°C. The unit cell was orthorhombic, with a 11.15, b 19.67, c 6.08 Å, space group F dd2; specific gravity 2.683, $Z = 16$. The subsequent paper (in English) by Tseng, Hsüeh and Peng (36) reports a crystal structure determination. The structure contains Ca^{2+} and $(Si_2O_7)^{6-}$ ions and oxygen atoms not directly bonded to silicon; it was suggested that the ionic constitution might be $Ca_2H_2(Si_2O_7) \cdot H_2O$ or $Ca_2H_4(Si_2O_7)O$. The calcium ions are 8-coordinated, and the axes of the Si_2O_7 groups lie in two directions in the ab—plane.

These results indicate that suolunite is quite different from any other calcium silicate hydrate, natural or synthetic; it does not even appear to be closely related to any of the other compounds. The occurrence of a new phase of this composition and the fact that it does not appear to have been obtained in any of the numerous synthetic studies are of the greatest interest. The results are also of considerable crystal chemical interest, in that they appear to demand the presence of pyrosilicate ions containing Si–OH groups ($Si_2O_5(OH)_2^{4-}$ or, less probably, $Si_2O_3(OH)_4^{2-}$), which have not hitherto been reported. Further information, including especially the complete X-ray powder pattern, would be of great interest.

Rosenhahnite

This phase was originally reported as a synthetic product by Pistorius (37) and has subsequently been found to occur in California as a natural mineral by Pabst, Gross and Alfors (38). It has the composition $3CaO \cdot 3SiO_2 \cdot H_2O$ and forms only at high pressures. Pistorius obtained it at pressures of about 25–50 kilobars and temperatures around 400°C; at lower pressures, it was prelaced by xonotlite and at higher temperatures by wollastonite. Pabst, Gross and Alfors (38) determined the unit cell and the optical properties, and also studied the morphology and behaviour on heating. They found that it was slowly converted to wollastonite at 400–500°C in air, the latter being formed in an unusually perfect topotactic relation.

The unit cell does not indicate any close relation to other calcium silicate hydrates. The phase is thus of considerable general crystal chemical interest, although it does not appear to be of direct importance to cement chemistry.

Gyrolite and Related Phases

Suggestions have been made that the formula of gyrolite is $C_3S_4H_3$ (39) or CS_2H_2 (40), but a careful synthetic study, together with an appraisal of the analyses of natural specimens, led Harker (41) to conclude that the generally accepted formula $C_2S_3H_2$ agrees better with the evidence. More recently, Cann (42) concluded from a study of a newly discovered natural specimen from Scotland that the idealized

formula is $Ca_{16}Si_{24}O_{60}(OH)_8 \cdot 14H_2O$, or $C_8S_{12}H_9$. This is perhaps the most satisfactory formula yet proposed. Harker (41) found that molecular water lost on static heating at 215°C was resorbed on treatment with boiling water. The ready loss and regain of molecular water, which recalls the behaviour of zeolites, may explain the difficulty in assigning an exact H/S ratio to this phase.

Gyrolite has been shown to exhibit polytypism, two- (39), three- (42) and six- (43) layer modifications all having been reported. Stacking mistakes are frequent (40, 41, 43). These effects may be expected to cause slight variability in the X-ray powder pattern.

There has been some uncertainty over the use of the names reyerite and truscottite. Strunz and Micheelsen (39) and Meyer and Jaunarajs (40) concluded that the natural minerals originally described by these names were identical, and if this is accepted, the name reyerite has priority. However, subsequent work by Chalmers, Farmer, Harker, Kelly and Taylor (44) showed that small but distinct differences exist in the layer thickness, which is about 19.0 Å for reyerite and 18.7 Å for truscottite, and in infrared spectrum. The minerals from Greenland (44) and from Scotland (42, 44) were shown on these criteria to be reyerite, while those from Sumatra and from Japan were shown to be truscottite. Chemical analysis of the Greenland mineral indicated the idealized formula $KCa_{14}Si_{24}O_{60}(OH)_5 \cdot 5H_2O$ and it was concluded that potassium was probably an essential constituent of reyerite, as opposed to truscottite. Cann (42) concluded from a chemical analysis of the Scottish mineral that the latter had a similar composition, but with considerable isomorphous replacement, including some Na^+ for K^+, $4OH^-$ for SiO_4^{4-} and possibly $(Al^{3+} + OH^-)$ for $(Si^{4+} + O^{2-})$.

Truscottite appears to contain no essential components other than CaO, SiO_2 and H_2O; synthetic preparations containing only these components have been shown to resemble truscottite rather than reyerite (44). The exact composition of truscottite has been a matter of some controversy. Analyses of the Sumatra mineral are difficult to interpret, mainly because the mineral is closely admixed with quartz. They have been held to support formulas ranging from C_2S_4H (45, 46) to C_3S_4H (39). Meyer and Jaunarajs (40) concluded from work on synthetic preparations that the composition was C_2S_4H, but their evidence appears to show only that the Ca:Si ratio is between 0.5 and 0.67. There appears to be no evidence for a Ca:Si ratio above 0.67. Funk (47) also concluded from work on synthetic preparations, which included determinations of unreacted silica by a chemical extraction method, that the composition was C_2S_4H. In contrast, Harker (41, 48) found that, in equilibrium preparations of bulk Ca:Si ratio 0.5, truscottite was always accompanied by significant amounts of silica; he obtained it pure, in sealed systems, only at bulk Ca:Si ratios of 0.57–0.60. He also reported thermal weight-loss curves, and concluded that the idealized formula was $C_6S_{10}H_3$.

Neither of these formulas is easily reconciled with crystallographic data. By analogy with gyrolite and reyerite, the presence of the $Si_{24}O_{60}$ grouping in the unit cell might be assumed. To yield this, Harker's formula must be written $Ca_{14.4}(Si_{24}O_{60})(OH)_{4.8}(H_2O)_{4.8}$. It is tempting to approximate this to $Ca_{14}(Si_{24}O_{60})(OH)_5(H_2O)_5$, which would be in accordance with the very close resemblance to reyerite; however, this gives an X-ray density of 2.57 g cm^{-3}, which is well above the range (2.36–2.48) of observed values. The formula C_2S_4H, on the other hand, appears to indicate the cell contents and constitution $Ca_{12}(Si_{24}O_{60}) \cdot 6H_2O$. This gives a more satisfactory X-ray density of 2.41 g cm^{-3} (the value of 2.47 g cm^{-3} given by Heller and Taylor (31) is wrongly calculated), but the implied absence of hydroxyl water does not agree with the infrared (44) or thermal weight-loss (41, 46) evidence. The position is further complicated by the possibility of appreciable substitution of 4H for Si, as was postulated for the Scottish reyerite (42). The idealized formula must therefore still be regarded as uncertain, though it would appear definitely to lie within the range C_2S_4H–$C_6S_{10}H_3$. A variable composition does not seem to be ruled out.

Harker (41) reported the formation of mixed-layer crystals of gyrolite and truscottite in some of his preparations. Gyrolite, truscottite, and reyerite all yield pseudowollastonite on heating at 800°C; (44, 47) an earlier observation (46) that truscottite behaves differently is incorrect.

Assarsson (49) described a product of approximate composition CS_2H_2 (or CS_2H_3) which he called Z-phase, this appears (25) to be essentially similar to one which Funk and Thilo (50) considered to be $CaH_4Si_2O_7(CS_2H_2)$. This product, which is especially characterized by an X-ray powder spacing of about 15 Å, has been further studied by Funk (47), Harker (41) and Wieker (51). Harker concluded that the composition was uncertain but that the phase was richer than gyrolite in both SiO_2 and H_2O. Funk (47) recorded new X-ray powder data, electron micrographs, and DTA curves, and concluded that material dried over silica gel had the composition $C_2S_4H_3$. Some loosely held, molecular water may well have been lost

by this drying technique. Electron micrographs showed crumpled foils resembling those of C–S–H (I), but the powder pattern was distinct from that of the latter and it appears likely to the present author that the phase belongs structurally to the gyrolite group. Wieker (51) concluded from application of the chemical method mentioned earlier (13, 14) that layer silicate anions were present; this supports the above conclusion.

Kilchoanite and Related Phases

A phase substantially identical with the "Phase Z" of Roy (52, 53) has been found to occur as a natural mineral and named kilchoanite (54). This phase is entirely different from the Z-phase mentioned previously and, to avoid confusion, the mineral name is to be preferred. The crystal data reported at the Washington Symposium for the synthetic material (25) have since been reported more fully (55, 56) and closely similar data have been given for the natural mineral (54). The preparations originally described by Roy had the composition C_9S_6H (53), but the natural mineral, as well as synthetic preparations made at about 700°C (55), are anhydrous. The anhydrous phase thus appears able to accommodate a little water in its structure. Some further data bearing on this problem have been published (56), but the explanation of the effect must await determination of the crystal structure.

At the Washington Symposium it was suggested that the material generally known as γ-dicalcium silicate hydrate of $C_2SH(C)$ was probably a mixture of calciochondrodite with a lime-rich, hydrous variety of kilchoanite (25). Further work (56, 57) has confirmed that the material is a mixture having calciochondrodite as one major constituent. The other major constituent is a previously unrecognized phase which has the idealized composition C_8S_5; in addition, xonotlite seems usually also to be present as a minor constituent.

C_8S_5 has not yet been obtained pure, but can be obtained mixed with other phases by hydrothermal treatment of γ-C_2S-quartz mixtures over a wide range of conditions (56, 57). In its ordered form, it appears to have a crystal structure consisting of alternate slabs of γ-C_2S and kilchoanite; this gives the composition C_8S_5. When it is formed in "γ-dicalcium silicate hydrate" (e.g. by treatment of γ-C_2S with water under saturated steam pressures at 180°C), the layer sequence appears to be somewhat disturbed, the proportion of γ-C_2S layers being increased. This raises the Ca:Si ratio from 8:5 in the direction of a limiting value of 2:1.

Thilo, Wieker and Stade (13) and Wieker and Stade (14) showed by a chemical extraction method that the products which Funk (58) named C_2SH (CI) and C_2SH (CII) both contained a mixture of ortho- and pyrosilicate ions. C_2SH (CI) has been shown to be identical with "γ-dicalcium silicate hydrate", i.e. to be essentially calciochondrodite and C_8S_5, while C_2SH(CII) is a mixture of calciochondrodite and kilchoanite (56). The chemical extraction results are thus readily explained, since calciochondrodite and γ-C_2S are orthosilicates, while the formula of kilchoanite suggests that it is almost certainly a pyrosilicate.

No new data of significance have been reported for calciochondrodite, but the fluoride analogue, $Ca_5(SiO_4)_2F_2$, has been prepared (59).

Other Calcium Silicate Hydrates

Since the Washington Symposium, the compound described by Roy as "Phase Y" (52, 53) has been found as a natural mineral and named dellaite (2). New X-ray and other data have been reported for this phase, for which the composition C_6S_3H originally proposed by Roy is confirmed (60).

A new calcium silicate hydrate phase has been reported as a natural mineral and named rustumite (2). Electron-probe analysis indicated the composition C_4S_2H; X-ray powder data, optical properties, density and the unit cell and space group (obtained from single-crystal X-ray study) were also given. The ionic constitution is possibly $Ca_4(Si_2O_7)(OH)_2$. This is analogous to cuspidine ($Ca_4(Si_2O_7)F_2$), but the unit cell parameters are somewhat more akin to those of tilleyite. As explained earlier, the tilleyite and cuspidine structures are quite closely related, and rustumite most probably belongs structurally to this group of minerals. It does not appear to be identical with any of the synthetic products described in the literature.

Thilo, Wieker and Stade (13), Wieker and Stade (14) and Lentz (10) confirmed by their respective chemical extraction methods the presence of orthosilicate anions in α-dicalcium silicate hydrate (13, 14) and afwillite (10). Mamedov and Belov (18) have modified an earlier suggestion (61) as to the crystal structure of tricalcium silicate hydrate, but there is still no crystallographic evidence other than unit cell parameters (62) whereby either of their suggested structures can be tested.

Crystalline Calcium Silicate Hydrates: Equilibria and Conditions of Formation

The Sub-System $CaSiO_3$–SiO_2–H_2O

The difficulty of reaching equilibrium in the CaO–SiO_2–H_2O system is well known. Harker (41) has recently discussed some of the problems, which are especially acute for siliceous compositions below about 150°C. At least four crystalline phases—nekoite, okenite, suolunite, and techaranite—that have been reported as natural minerals, and that might reasonably be expected to have stability fields in this part of the system, have never been synthesized, and one further phase in this category (14 Å tobermorite) has only once (63) been reported as a synthetic preparation. On the other hand semi-crystalline phases such as C–S–H (I), and poorly defined crystalline ones such as Z-phase, are readily formed. C–S–H (I) in particular is formed reproducibly from a variety of starting materials and is even known to occur as a natural mineral, plombierite. It may nevertheless be doubted whether any of these phases has a true field of stability.

A further complication arises where silica is present as a solid phase. In calcium-containing hydrothermal systems below about 450°C, this is usually formed in a hydrous, amorphous variety or as cristobalite, although quartz is the stable polymorph under these conditions. Coombs, Ellis, Fyfe and Taylor (64) have suggested that this effect may be caused by the formation on cristobalite particles of protective films of calcium silicate hydrates. The same authors have shown that this variation in the polymorphic form of the silica is likely to influence the equilibria profoundly. This has two practical consequences. First, it may help to explain the differences which are known to exist between the behaviour of quartz and that of other forms of silica, such as diatomite, in industrial processes. Second, hydrous silica is not a precisely defined phase; this may be epxected to contribute to the difficulty of obtaining reproducible equilibria, even of a metastable nature.

Equilibria in the $CaSiO_3$–SiO_2–H_2O subsystem have recently been comprehensively studied and reviewed by Harker (41) and by Roy and Johnson (3). Harker's main results are shown in Fig. 2. He assumed the solid phases in the subsystem at low temperatures to be C–S–H (I) and silica (Field 1), although he recognized that C–S–H(I) was probably metastable relative to other and more crystalline phases; he regarded the reactions occurring at progressively higher temperatures as a series of dehydration processes. Above about 110°C for saturated steam pressures, gyrolite and 11 Å tobermorite appear (Field 2). Two aspects only of Harker's results will be discussed: the stability fields of gyrolite and truscottite, and the conditions under which 11 Å tobermorite gives place to xonotlite.

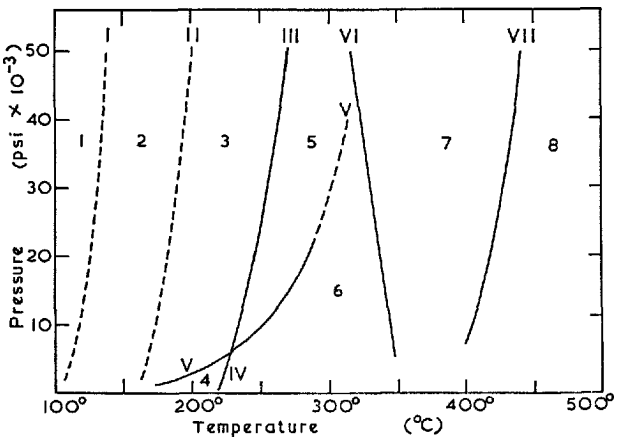

Fig. 2. *Equilibria in the sub-system* $CaSiO_3$–SiO_2–H_2O, *according to Harker* (41).

Curves		*Fields (solid phases only)*	
I	$S + C = Gy + H_2O$	1	S + C
II	$Q + Gy = Tr + H_2O$	2	Q + Gy + To
III	$Gy = Tr + To + H_2O$	3	Q + Tr + Gy + To
IV	$Gy = Tr + Xo + H_2O$	4	Q + Tr + Gy + Xo
V	$To = Xo + H_2O$	5	Q + Tr + To
VI	$Tr = Q + Xo + H_2O$	6	Q + Tr + Xo
VIII	$Xo = Wo + H_2O$	7	Q + Xo
		8	Q + Wo

Abbreviations

Q = Quartz	Gy = Gyrolite
S = Silica	To = 11 Å Tobermorite
C = C–S–H(I)	Xo = Xonotlite
Tr = Truscottite	Wo = Wollastonite

Curves I–IV and curve VI (Fig. 2) define the stability fields of gyrolite and truscottite. They imply that for saturated steam pressures and appropriate bulk compositions, gyrolite is stable at about 110–220°C and truscottite at 160–350°C. For high pressures (around 30,000 p.s.i.) these temperature ranges are about 140–230°C and 180–320°C respectively. These lower limits for the formation of truscottite are difficult to determine. In the presence of a mineralizer (2% of NaF) truscottite can be formed above about 160°C under saturated steam pressures, but in its absence, gyrolite-truscottite intergrowth are formed around 160–220°C and pure truscottite crystals only appear to be obtainable above about 220°C (47, 65).

Harker concluded from his own results and those of earlier workers that the C/S ratio of crystalline, 11 Å tobermorite could vary between 0.8 and 1.0. He regarded the replacement of 11 Å tobermorite by xonotlite as a dehydration reaction in which no other solid phase was involved. If this is accepted, 11 Å tobermorite and xonotlite can coexist stably only along a univarient P-T curve (Fig. 2, curve V). He concluded that the dehydration temperature at saturated steam pressures was 170 ± 20°C, and, in accordance with the earlier results of Buckner, Roy and Roy (66), that it rose sharply with pressure to about 300°C at 25,000 p.s.i. This marked dependence on pressure is unusual in this system; Harker suggested that it might be explained by assuming that slightly different forms of 11 Å tobermorite were involved at different points on the curve. The occurrence of such different forms was discussed at the Washington Symposium (25), and earlier in the present review.

Roy and Johnson (3) considered that the C/S ratio of 11 Å tobermorite in its most stable form could vary only slightly from the ideal value of 5-6, and represented the decomposition of this phase under high pressures as yielding xonotlite, truscottite and water. If this is accepted, 11 Å tobermorite and xonotlite can coexist over a field of pressure and temperature and not merely at points on a P-T curve. Roy and Johnson concluded that, for pressures of 30,000–45,000 p.s.i., the two phases coexisted stably from 285°C down to at least as low as 175°C, which was the lowest temperature studied.

There appear to be good experimental grounds for accepting Roy and Johnson's view, at least for high pressure conditions (15,000–45,000 p.s.i.). In this case, the upper part of Harker's curve V (Fig. 2) must be taken to represent the decomposition of 11 Å tobermorite to give xonotlite, truscottite, and water, and xonotlite must be added to the phase assemblages existing at temperatures below this curve. A need for further experimental work to establish the temperatures below which xonotlite becomes unstable is indicated.

The significance of these considerations for equilibria at saturated steam pressures may now be discussed. If 11 Å tobermorite is assumed to have a fixed C/S ratio of 5:6, it could coexist with xonotlite at temperatures below the value of 170°C proposed by Harker (41). It is suggested that the available data could be largely explained if the stable calcium silicate hydrate phases in the $CaSiO_3$–SiO_2–H_2O pseudo-system at saturated steam pressures are as follows (all temperatures are ±10 deg. C):

100–130°C: Gyrolite, 11 Å tobermorite, afwillite
130–160°C: Gyrolite, 11 Å tobermorite, xonotlite
160–170°C: Truscottite, gyrolite, 11 Å tobermorite, xonotlite.
170–220°C: Truscottite, gyrolite, xonotlite
>220°C: Truscottite, xonotlite

The lower limit of 130°C for the stability of xonotlite is supported by recent observations of Funk (12). The situation is complicated by the strong tendency for tobermorite of high C/S ratio (around 1.0) to persist metastably in place of xonotlite. Two conclusions of possible practical importance emerge. Firstly, at bulk C/S 5:6, 11 Å tobermorite may be stable relative to xonotlite up to 170°C; this may explain why it is formed in preference to xonotlite in many commercial products. Secondly, if formation of xonotlite is desired, there might be a possibility of achieving this in practicable times at temperatures as low as 130° if a way could be found to de-stabilize the 11 Å tobermorite of 1:1 Ca:Si ratio.

Equilibria in the $CaSiO_3$–H_2O system at very high pressures (5–53 k bars) were studied by Pistorius (37). His results define the stability fields of xonotlite, wollastonite and rosenhahnite in this region. His P-T curve for the dehydration of xonotlite to give wollastonite connectes smoothly with those obtained by Buckner, Roy and Roy (66) and by Harker (41) (Fig. 2, curve VII) at lower pressures.

The Sub-System $CaSiO_3$–CaO–H_2O at High Pressures

Roy and Johnson (3) reported the results of a study dealing with equilibria at high pressures (20,000–45,000 p.s.i.). Their results largely confirm and partly modify those presented at the Washington Symposium by Roy and Harker (65). The conclusions resulting from these two investigations, as regards the stable anhydrous or hydrated calcium silicate phases in this pressure region, where as follows (TSH = tricalcium silicate hydrate):

160–235°C Xonotlite—afwillite—hillebrandite—TSH
250–290°C Xonotlite—hillebrandite—calciochondrodite—TSH
290–355°C Xonotlite—foshagite—hillebrandite—calciochondrodite—TSH
355–430°C Xonotlite—foshagite—dellaite—calciochondrodite—TSH
430–520°C Wollastonite—foshagite—dellaite—calciochondrodite—TSH

520–650°C Wollastonite—foshagite—dellaite—calciochondrodite
650–810°C Wollastonite—dellaite—calciochondrodite

In the range 810–840°C, dellaite is replaced by α'–C_2S and rankinite appears. Subsequent work on the high temperature part of the system was reported by Harker, Roy and Tuttle (67), who showed that metling begins in the ternary system $Ca(OH)_2$–Ca_2SiO_4–CaO at 820°C. At 15,000 p.s.i., calciochondrodite melts incongruently at 955°C, giving Ca_2SiO_4 and liquid.

The role of kilchoanite in the system has presented much difficulty. Roy and Johnson (3) noted that this phase forms readily at about 15,000 p.s.i. over the approximate range 250–820°C and did not wholly exclude the possibility that it might form stably in part of this range. On balance, however, they considered that, at least at high pressures, it was probably metastable at all temperatures up to that of the foshagite decomposition (~650°C); above this temperature it possibly had a stable existence. In general agreement with this view, Agrell (2) considered that at 5000 p.s.i. foshagite was a stable phase below about 550°C, above which temperature it was replaced by kilchoanite.

Several values have been reported for the kilchoanite-rankinite inversion temperature, which because of the smallness of the volume change must be almost independent of pressure. Roy (53) placed it at 800–850°C, Agrell (2), quoting unpublished work by McConnell, at 700°C, and Speakman, Taylor, Bennett and Gard (56) at about 625°C. The latter investigators obtained evidence consistent with the view that, at high pressures, kilchoanite had a narrow temperature range of stability around 600°C. They considered that at lower temperatures, it was possibly replaced by wollastonite plus dellaite at 500–550°C, and by foshagite plus dellatie below 500°C.

The considerations of the last two paragraphs suggest that the stable phases at 430–810°C at high pressures are possibly:

430–500°C Wollastonite—foshagite—dellaite—calciochondrodite—TSH
500–520°C Wollastonite—dellaite—calciochondrodite—TSH
520–550°C Wollastonite—dellaite—calcio calciochondrodite
550–625°C Wollastonite—kilchoanite—dellaite—calciochondrodite
625–810°C Wollastonite—rankinite—dellaite—calciochondrodite

The Sub-System $CaSiO_3$–CaO–H_2O at Saturated Steam Pressures

The semicrystalline or near-amorphous calcium silicate hydrates that are formed at room temperature on hydration of portland cement or in other ways appear to be indefinitely persistent, but they are probably metastable relative to afwillite and $Ca(OH)_2$ (68). This probably accounts for the formation of afwillite when C_3S is ball-milled with water at room temperature (69).

The stability relations of kilchoanite relative to xonotlite, foshagite and hillebrandite at saturated steam pressures present some difficulty. Kilchoanite, or related phases or mixtures such as "γ-dicalcium silicate hydrate", are readily formed from mixtures of β- or γ–C_2S with silica at temperatures around 200°C and saturated steam pressure, and appear under these conditions to persist indefinitely. Lime-silica mixtures under similar conditions sometimes yield kilchoanite or related phases (70), but more often give xonotlite, foshagite, hillebrandite, or combinations of these phases, and these latter three phases then appear to be indefinitely persistent. Roy and Johnson (3) suggested that kilchoanite might have a stability field at low pressures, and Speakman, Taylor, Bennett and Gard (56) observed that this would be compatible with their results obtained in runs using γ-C_2S as the principal starting material. In contrast, workers who used other starting materials, such as Peppler (71) and Assarsson (49), concluded that xonotlite and hillebrandite coexist stably at temperatures around 180°C.

The problem probably cannot be resolved by runs using simple starting materials, and Ahmed and Taylor (72) therefore adopted a different approach, which is illustrated by the following example. A mixture of γ-C_2S and quartz of bulk Ca/Si ratio 1.5 was autoclaved at 180°C and gave a product consisting largely of kilchoanite. A mixture of lime and quartz was similarly treated and gave a product consisting mainly of xonotlite, hillebrandite, and foshagite. The two products were then mixed to yield a mixture which will be called (I). Portions of (I) were re-autoclaved at 180°C for various times to yield a series of products. The X-ray patterns of these products were compared with that of the mixture (I) in order to see which phases were increasing, and which decreasing in relative amount. The results indicated clearly that xonotlite and hillebrandite were stable relative to kilchoanite and foshagite. A similar group of experiments showed that at 250°C the stable phases at bulk Ca/Si ratio 1.5 were foshagite and hillebran-

dite. There were indications that calciochondrodite was unstable at both 180° and 260°C, but the results in this respect were not conclusive.

Evidence regarding the stability fields of other phases in the $CaSiO_3$–CaO–H_2O subsystem at saturated steam pressures was largely summarized at the Washington Symposium (25, 65). From this and the newer results presented here the stable calcium silicate hydrate phases in this subsystem at saturated steam pressure appear to be as follows:

<100°C	14 Å tobermorite—afwillite
100–130°C	11 Å tobermorrite—afwillite
130–140°C	Xonotlite—afwillite
140–150°C	Xonotlite—afwillite—hillebrandite
150–180°C	Xonotlite—hillebrandite
180–250°C	Xonotlite—hillebrandite—TSH
250–320°C	Xonotlite—foshagite—hillebrandite—calciochondrodite—TSH
>320°C	Xonotlite—foshagite—dellaite—calciochondrodite—TSH

Further work is needed to clarify a number of points, including the following:

(i) Does a crystalline phase related structurally to either C–S–H (II) or jennite (both of which are discussed later) have a stability field in the system?

(ii) Does rustumite have a stability field, and under what conditions can it be synthesized?

(iii) What are the lower temperature limits of stability of calciochondrodite and of tricalcium silicate hydrate? The values given above rest on slender evidence.

(iv) Does α-dicalcium silicate hydrate have any true stability field? This phase is formed very readily from a variety of starting materials at 100–180°C. It appears always to be metastable relative to hillebrandite or to afwillite plus $Ca(OH)_2$, but this cannot be considered certain.

(v) Under what conditions are kilchoanite or structurally related phases formed from lime-quartz mixtures? Kalousek, Logiudice and Dodson (70) obtained some results bearing on this question, but further work is needed.

(vi) What is the nature of the material that Aitken and Taylor (73) called "Phase F", ($C_5S_3H_2$ approx.)? This, or a similar material, has again been obtained from lime-quartz mixtures (72), but its nature is still obscure.

Crystalline Calcium Silicate Hydrates with Additional Ions

Of the various compounds in this category, we shall consider only those that appear especially important for cement hydration chemistry and for which significant work has been reported since the Washington Symposium. Substitution of additional ions in structures already described (e.g. of Al^{3+} in 11 Å tobermorite) is considered later.

Scawtite

This is identical with the phase which has been called CSH (A). Harker (74) has discussed the conditions of formation and stability of this phase, for which he assumes the general formula $Ca_{14}(OH)_4(Si_{16-x-y}C_xH_{4y})O_{44}$. He noted that scawtite has frequently been observed to form in runs in the CaO–SiO_2–H_2O system in which slight CO_2 contamination had occurred, and found that it could be synthesized at low partial pressures of CO_2 in the presence of excess water; its stability range appeared to extend from 140° to 300°C and to be independent of water pressure from saturated steam pressures up to at least 50,000 p.s.i. Harker obtained scawtite pure by using as starting material a mixture of $Ca(OH)_2$ and silicic acid, together with excess water containing the calculated amount of dissolved CO_2, so as to give the molar ratios Ca:Si:C = 14:12:1 or 14:12:2. Below 140°C, scawtite was unstable relative to 11 Å tobermorite and calcite, while above 300°C it was unstable relative to xonotlite and calcite; it was thus formed largely at the expense of xonotlite in the CaO–SiO_2–H_2O system. At 21°C, it was decomposed by stirring with CO_2-saturated water at 1 atmosphere for 16 hours.

Jennite

Jennite is a sodium calcium silicate hydrate of approximate composition $Na_2Ca_8Si_5O_{30}H_{22}$.* As will be shown later in this review, it is possibly more nearly related in structure to the predominant calcium silicate hydrate of cement pastes than is any other crystalline phase, including tobermorite. The available information about it will therefore be considered in some detail.

Jennite has so far been found as a crystalline phase only as a natural mineral. The formula given above is

*Subsequent analytical work (107) does not confirm the presence of appreciable sodium into in this mineral.

based on the analysis of the first specimen to be discovered which was found at Crestmore, California, and studied by Carpenter, Chalmers, Gard, Speakman and Taylor (75). A second specimen has since been discovered in Israel and shown by Heller (76) to give X-ray single crystal patterns identical with those of the Crestmore mineral, but no chemical analysis or other data for this second specimen have yet been reported.

Jennite forms small, blade-shaped crystals or fibrous aggregates. The unit cell was determined and indexed X-ray powder data obtained, together with infra-red, thermal decomposition, density, and electron microscope and diffraction data. There is a repeat distance of 7.25 Å parallel to the *b* or needle axis, with very marked pseudohalving; reflections corresponding to the 7.25 (as opposed to 3.625) Å repeat were invisible on X-ray rotation photographs, and only a few extremely weak ones were detectable on oscillation photographs. The triclinic cell has a thickness (d_{001}) of 10.42 Å in the direction perpendicular to the cleavage. The cell parameters (*a* 10.56, *b* 7.25, *c* 10.81 Å, α 99°42′, β 97°40′, γ 110°04′) somewhat resemble those of cuspidine, but the cell contents are distinctly different ($Na_2Ca_8Si_5O_{30}H_{22}$ for jennite, $Ca_{16}Si_8O_{28}F_8$ for cuspidine). From infrared and thermal decomposition evidence, it was suggested that the ionic constitution was possibly $Na_2Ca_8(SiO_3)_3$-$(Si_2O_7)(OH)_6 \cdot 8H_2O$, wollastonite-like chains and pyrosilicate groups thus both being present.

If jennite is heated in air at 70–90°C, four molecules of water are lost from the above formula unit, and the unit cell shrinks in the *c*-direction to give a layer thickness of 8.66 Å. The product thus formed is called metajennite. It closely resembles jennite as regards the *ab*-face of the unit cell, the general distribution of intensity in reciprocal space, as shown in single-crystal X-ray patterns, and the infrared absorption spectrum. Metajennite is therefore presumably derived from jennite by loss of water molecules from between layers which themselves undergo little or no change.

Meta-jennite loses water gradually at 90–750°C; with increasing temperature within this range the product becomes progressively less crystalline. By 450°C, X-ray diffraction shows only diffuse powder rings with spacings of about 3.0, 2.8, 2.0, and 1.8 Å. At 900–1060°C, wollastonite forms, and at 1100°C the main product is β-C_2S.

Subsequent to the publication of the above results, the present author has derived a tentative crystal structure from X-ray fibre rotation data; more certain results will be difficult to obtain because the crystals are poor. Fig. 3 shows the essential features. The structure is based on corrugated Ca–O sheets lying parallel to the (001) plane. On both faces of these, some of the oxygen atoms are shared with Si–O chains, which run parallel to the *b*-direction. These chains are probably highly disordered and contain frequent gaps: they are not of uniform length, and probably have a minimum chain length of two, and a mean chain length of five tetrahedra. In configuration they resemble portions of wollastonite chains. Of the oxygen atoms of the Ca–O sheets that are not linked to silicon, some must occur in water molecules, and others in hydroxyl groups. The structure is completed by the addition of interlayer sodium ions and water molecules. The sodium ions may not be essential; calcium might possibly replace them, especially in poorly crystallized material, if some appropriate balancing replacement also occurred.

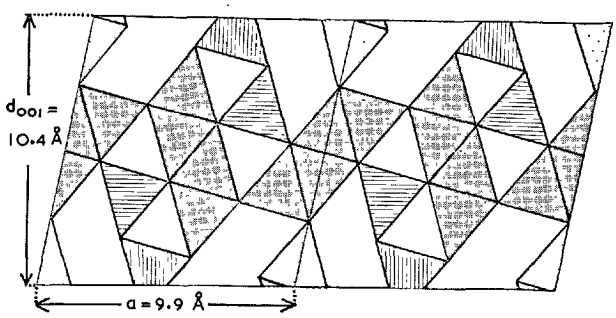

Fig. 3. *Suggested crystal structure for jennite (idealized and tentative), viewed along the* b*-direction. Axes relate to the monoclinic pseudocell with* a *9.9,* b *3.6,* c *10.6* Å, β *102°. Diamonds with dense point-shading represent* Ca(O, OH, $H_2O)_6$ *octahedra, which are linked to form a corrugated sheet that is seen edge-on and runs horizontally across the figure. Diamonds with light point-shading represent interlayer* $Na(H_2O)_6$ *octahedra, Triangles with horizontal line-shading represent* Si_2O_7 *groups, seen end-on. Triangles with vertical line—shading represent oxygen tetrahedra of which about one-half, statistically distributed, contain silicon atoms, which link the* Si_2O_7 *groups into short chains of various lengths. For clarity, tetrahedra of this type belonging to the two adjacent layers are omitted. The chains are seen end-on.*

The suggested structure, of which the tentative nature is emphasized, has features in common with those of tilleyite, cuspidine, and one of the structures suggested for tricalcium silicate hydrate (18). It has some broad similarities to that of tobermorite (77), but also some important differences. The most important of these are the very different configurations of the Ca–O sheets, which lower the repeat distance in the tobermorite a-direction from 11.2 Å in tobermorite to 9.9 Å in jennite, and the presence in jennite of hydroxyl ions and water molecules within these sheets. The two structures are compared schematically below:

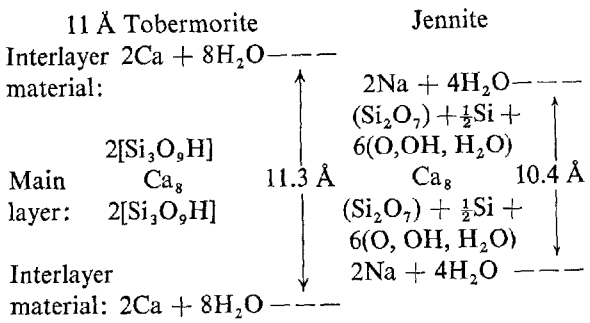

they considered to have the constitution $NaCaHSiO_4$, by hydrothermal treatment of Na_2CaSiO_4 in saturated steam (not liquid water) at 180°C.

Sazhin and co-workers (82, 83) reported studies on the N–C–A–S–H system at 240–280°C. They obtained in additions to $Ca(OH)_2$ and a hydrogarnet phase, two compounds which they considered to be $NC_2S_2H_n$ and $N_4C_2A_3S_6H_3$. In a similar study at 280°C, Ni and co-workers (84–86) reported the formation of $NC_2S_2N_n$ and $N_{1.25}C_{0.5}AS_2H$. Similarities of crystal morphology and refractive indices suggest that these phases may have been identical with the corresponding ones of Sazhin and co-workers. The X-ray powder data and refractive indices reported by the latter for $NC_2S_2H_n$ are, in turn, near to those of pectolite, but the formulae differ and the resemblances could be accidental. The relation between the $NC_2S_2H_n$ phases reported in these investigations and the $NaCaHSiO_4$ of Thilo, Funk and Wichmann (81) requires investigation. None of the synthetic products mentioned above appears to resemble jennite. Further work is needed to correlate the results of the various investigators.

Several other studies on the C–S–H system in the presence of alkalis have been reported recently (87–91) but most are mainly concerned with the influence of alkalis on the reactivity of anhydrous calcium silicates, and none with the formation of hydrated phases containing alkalis as essential constituents. A number of other calcium silicate hydrates with essential sodium or potassium are known as natural minerals, but apart from reyerite, which has already been mentioned, the only one whose composition appears to be in a range of apparent significance for cement hydration chemistry is miserite ($KCa_4Si_5O_{13}(OH)_3$) (92).

Synthetic Studies on Alkali-Containing Systems

Several studies have recently been reported on aspects of the N–C–A–S–H system relevant to cement chemistry. This system is of interest for several reasons. Firstly, as already mentioned in the case of jennite, some of the sodium-containing compounds may be structurally related to pure calcium silicate hydrates. secondly, raw materials containing alkalis and Al_2O_3, such as felspars, are used in some autoclave processes. Thirdly, in probably all processes of cement hydration the alkali present in the cement, though small in absolute amount, appears to go into solution rapidly, so that in the early stages of hydration the effective ratios of alkali oxides to other constituents may be quite high.

The early work of Clark and Bunn (78) and Thilo and Funk (79) showed that pectolite ($NaCa_2HSi_3O_9$) can readily be synthesized from a variety of starting materials of appropriate composition by hydrothermal treatment at 180–200°C under saturated steam pressures. This phase is structurally closely related to wollastonite (80). Thilo, Funk and Wichmann (81) described also the synthesis of a compound which

Poorly Crystalline Calcium Silicate Hydrates

This term will be used to denote all calcium silicate hydrates giving X-ray powder patterns significantly poorer than those of typical crystalline phases. It is convenient to divide them arbitrarily into semi-crystalline and near-amorphous phases. We shall use the term "near-amorphous" for phases or materials giving not more than three X-ray powder lines, which in general will usually be more or less broadened. The calcium silicate hydrate present in normally cured cement pastes (so-called "tobermorite gel") is typical of this group. In such materials only short-range order would seem to occur. The term "semi-crystalline" will be used for phases or materials whose X-ray powder patterns contain more than three lines, but give clear indication of absence of full three-dimensional order either because too few lines are present, or because of marked broadening or some other reason. The phase known as "C–S–H (I)" is typical of this group. It is, of course, assumed that fewness of lines is not due solely to use of an inadequate X-ray technique or to the fact that the phase is present as a minor constituent of a mixture. In the author's experience X-ray goniometers designed for single-crystal work are considerably more satisfactory for studies on poorly crystallized calcium silicate hydrates than are diffractometers, Guinier cameras,

or conventional Debye-Scherrer powder cameras.

Many workers in this field, including the present writer, have regarded all poorly-crystalline calcium silicate hydrates as structurally degenerate varieties of tobermorite and have called them tobermorites or tobermorite-like phases. While in some cases this view is probably correct, in others the evidence is weak, and in yet others there are positive grounds for postulating a closer relation to crystalline phases other than tobermorite. We shall use the term C–S–H to denote any poorly-crystalline calcium silicate hydrate, whether semicrystalline or near-amorphous. The letters C–S–H stand for "calcium silicate hydrate", and hyphens are inserted to show that no particular composition is implied.**

The classification of C–S–H varieties is rendered difficult by the indefinite nature of these materials, which probably comprise, not a finite number of phases each of definite composition and structure, but a largely continuous range with a number of variable parameters which are only partly correlated. It will be convenient to consider them in sequence of increasing C/S ratio.

Materials of Low C/S Ratio

In 1955, Funk and Thilo (50) described a virtually amorphous preparation which they obtained by mixing $Na(H_3SiO_4)$ and $CaCl_2$ solutions at 0°C. After drying over silica gel, it had the composition CS_2H_3 and they considered it to have the constitution $Ca(H_3SiO_4)_2$. On being autoclaved at 180°C, it yielded a product described as $CaH_4Si_2O_7$, and which appears to have been identical with Assarsson's "Z-phase" (25, 49). Funk (47) later repeated the preparations of CS_2H_3 and Z-phase, and described additional poorly crystalline products obtained by autoclaving CS_2H_3 at 120°C, for which he gave X-ray powder, DTA, TGA and electron microscope data. He considered that these products might be mixtures. The X-ray data do not agree with those of C–S–H (I) or other known phases. The nature of these products is still not clear, but it is at least possible that they are structurally related to gyrolite rather than to tobermorite. There appears to be little evidence for the ionic constitution $Ca(H_3SiO_4)_2$ assigned by Funk and Thilo (50); indeed, Wieker (93) showed by the chemical method described earlier (13, 14) that layer silicate anions were present. This is consistent with the hypothesis of a gyrolite-like structure.

The occurrence of a poorly-crystalline calcium silicate hydrate of low C/S ratio as an initial product in hydrothermal reactions employing lime and silica glass or gel is suggested by the results of Buckner, Roy and Roy (66), Assarsson (49) and Kondo (94). Such a product, if formed, could possibly be similar in structure to the poorly-crystalline materials discussed above.

C–S–H (I)

This term will be used to denote the product which has a C/S mole ratio of 0.8–1.5, appears as crumpled foils under the electron microscope, and gives an X-ray powder pattern consisting mainly of reflections corresponding to a two-dimensional, centred, orthogonal lattice with *a* 5.6, *b* 3.6 Å approx. There may or may not also be a strong basal reflection with a spacing of 9–14 Å, this value depending on the H/S and C/S ratios. C–S–H (I) is formed from a wide range of starting materials, most characteristically in aqueous suspensions at room temperature, but also hydrothermally as an intermediate reaction product. Natural plombierite of low C/S ratio (34) is substantially identical with C–S–H (I).

The X-ray powder pattern of C–S–H(I), and the changes in basal spacing that occur on dehydration (32), suggest strongly that the phase is a structurally degenerate form of tobermorite. This implies some degree of condensation in the silicate anions. Chemical studies of this problem have led to divergent conclusions. Brunauer and Greenberg (17), reporting unpublished work by Greenberg and Pressler, concluded that increasing depolymerization occurred with increasing C/S ratio. They gave no quantitative conclusions, but for a preparation with C/S 0.8 made at 85°C, the rates of dissolution in 0.5 M aqueous HCl and of reaction of the extract with an aqueous molybdic acid reagent suggested a substantial degree of condensation. Greenberg and Chang (95), reporting further unpublished results of Greenberg, Pressler and Chang, however concluded that "products of the reaction of calcium oxide, silica and water mixtures begin to dissolve completely in HCl at a CaO/SiO_2 mole ratio of 1. Therefore, in the $CaO–SiO_2–H_2O$ system, silica is completely depolymerized at this mole ratio." From this and other evidence, they concluded that preparations having C/S $\geqslant$ 1 contained a substance of formula CaH_2SiO_4.

The formula CaH_2SiO_4 was earlier assigned by

**Several prominent workers in the field, e.g. Assarsson (49), appear never to have accepted the hypothesis that all poorly-crystalline calcium silicate hydrates are tobermorite-like in structure. The writer thanks Professor H. Funk, for pointing out to him the weakness of this hypothesis, and Miss A. E. Moore, M. Sc., for suggesting the term C-S-H.

Thilo, Funk and Wichmann (81) to a product that was almost certainly C–S–H (I); these authors, too, considered that orthosilicate ions were present. However, Wieker (93) concluded from his chemical method that this product in fact contained chain-type silicate anions.

Funk (12) studied the degrees of condensation in C–S–H (I) preparations by his method based on dissolution in methanolic HCl and subsequent reaction with a molybdic acid solution. He concluded that, in all preparations studied, a distribution of anion sizes occurred. He considered that reliable information could be obtained regarding trends, but that absolute degrees of condensation could only be roughly estimated. The degree of condensation decreased with increasing C/S ratio over the range 0.81–1.1, and increased on raising the temperature of preparation from room temperature to 110°C. Funk made the following estimates for the anion size distributions of two preparations (apparently made at room temperature):

	Approx. percentages of SiO_2 present as anions of:			
C/S ratio	3–4 tetrahedra	4–6 tetrahedra	6–10 tetrahedra	>10 tetrahedra
1.01	—	10	80	10
1.1	20	40	40	—

He reported parallel results for preparations autoclaved at 130–170°C. These were shown by X-rays to contain tobermorite or xonotlite or both; the extent of condensation was found to increase further with increased temperature of preparation or decrease in C/S ratio. Funk's and Wieker's conclusions, unlike those reported by Greenberg and Chang, can readily be reconciled with the X-ray evidence.

New studies on the equilibria involving C–S–H (I) have been reported by Greenberg and his colleagues. Greenberg, Chang and Anderson (96) prepared solids at 85°C that appear to have been essentially C–S–H (I). They equilibrated these with aqueous solutions at 25°C, and from determinations of pH and Ca^{++} and silicic acid concentrations in solution derived values for two solubility products which were formulated as

$$K_{SP_1} = {}^{a}Ca^{++} \times {}^{a}H_2SiO_4^{2-}$$

and

$$K_{SP_2} = {}^{a}Ca^{++} \times {}^{a^2}H_3SiO_4^{-}.$$

They found $pK_{SP_1} = 7.0 \pm 0.1$ and $pK_{SP_2} = 8.5 \pm 0.1$. K_{SP_1} was assigned to an equilibrium between CaH_2SiO_4 and solution, and K_{SP_2} to an equilibrium involving $Ca(H_3SiO_4)_2$.

Greenberg and Chang (95) later reported a study of the pH values and Ca^{++} and silicic acid concentrations in solutions coexisting with solids of a range of C/S ratios. Their results were similar to those reported by numerous earlier workers. They concluded that at C/S 0.14–1 the solid consisted of CaH_2SiO_4 plus silica; the evidence for $Ca(H_3SiO_4)_2$ was not conclusive. At C/S 1–1.75, the solid was regarded as a solid solution of composition $CaH_2SiO_4 \cdot nCa(OH)_2$, and a distribution coefficient was derived relating the activity of the $Ca(OH)_2$ dissolved in this solid to its value in solution. The lack of positive evidence for $Ca(H_3SiO_4)_2$ in these results does not necessarily conflict with the observations of Funk and Thilo (50) metnioned earlier, as these workers used different preparative conditions.

Lawrence (97) has studied the dehydration of C–S–H (I) preparations of varying C/S ratios. Preparations with C/S 0.5–0.9 showed only minor changes in X-ray pattern up to 700°C; the 12.5 and 5.5 Å reflections disappeared and the remaining spacings were slightly shortened. At 770°C, there was a sharp transition to wollastonite. He showed that formation of β–C_2S, reported earlier by Gard, Howison and Taylor (98) occurred only if contamination by CO_2 had occurred. He considered that (uncarbonated) C–S–H (I) with C/S 0.5–0.9 could lose most or all of its water without serious disruption of the structure; the rapid increase in velocity of transformation to β–CS at 770°C suggested that some form of nucleation process controlled the reaction. Preparations with C/S 1.0–1.5 behaved differently, a near-amorphous intermediate material being formed at 550–770°C. At C/S 1.0–1.2 this yielded β–CS at 770°C; at C/S 1.2–1.5 it gave β–CS and β–C_2S. Wollastonite was also formed at 550–770°C if heating was prolonged. These results can perhaps be correlated with the DTA results of Kalousek (99), who showed that the sharp exotherm at about 800°C was depressed to lower temperatures with increase in C/S ratio. The cocurrence of this exotherm with C–S–H (I), which contrasts with its absence for crystalline Al-free tobermorite (63), suggests that the mechanism of wollastonite formation differs in the two cases.

The similarity of the X-ray powder patterns and compositions of C–S–H (I) and tacharanite has already been mentioned; it may, however, be fortuitous.

Grudemo (100) has published new electron micrographs and diffraction patterns for C–S–H (I) and other calcium silicate hydrates; these substantially confirm and augment those reported earlier (30, 101).

The balance of the existing evidence regarding C–S–H (I) seems clearly to support the view that material with C/S ~ 0.8 is a structurally degenerate tobermorite. There is little evidence that C/S can fall below 0.8 without silica occurring as a separate phase. Increase in C/S above 0.8 seems definitely to be associated with lower average degrees of condensation (12, 17) and with decrease in layer thickness (30). The only explanations that appear consistent with both these facts are ones in which the structure is modified by omission of tetrahedra from the chains, as suggested originally by Taylor and Howison (16), and supported in modified form by Brunauer and Greenberg (17). At the higher C/S ratios, omission of entire chains and their replacement by hydroxyl groups possibly also occurs; this could happen in a variety of ways, such as the incorporation of regions of jennite-like structure, or the replacement of the whole of one side of a layer as suggested by Gard, Howison and Taylor (98) and Grudemo (101). This matter has been further discussed elsewhere (102). The variable characteristics and generally indefinite nature of C–S–H (I) of high C/S ratio suggest strongly that several different causes of variable C/S ratio may operate.

C–S–H (II)

This term will be used to denote any semi-crystalline calcium silicate hydrate with a C/S ratio of 1.5 or above. Such products are more varied in character, and almost always less crystalline, than C–S–H (I), and the term may therefore cover a number of phases of different structural affiliations.

The most crystalline variety of C–S–H (II) that has been described is probably that which forms under certain conditions from C_3S (103) or β–C_2S (17) in aqueous solutions at room temperature, appears as characteristic fibre bundles in the electron microscope (17, 100, 101, 104), and gives an X-ray powder pattern somewhat similar to that of C–S–H (I) and having a longest spacing of 9.8 Å (31). In recent studies, Grudemo (100) and Gard (104) were unable to obtain selected area electron diffraction patterns from this material, but Copeland and Schultz (105) found that it gave a distorted hexagonal pattern with reflections having d-spacings of 3.07, 2.80 and 1.83 Å; this would appear to indicate a tobermorite-like structure. Some support for this hypothesis is provided by the X-ray powder pattern (31), which is relatively close to that of 10 Å tobermorite (31), especially if the effect of the slightly differing basal spacings is allowed for. If the C–S–H (II) preparations discussed above are structurally related to tobermorite, their high C/S ratios must presumably be explained in one or more of the ways already mentioned in relation to C–S–H (I).

Glasser and Taylor (107) studied the thermal decomposition of C–S–H (II) preparation D-69 of Brunauer and Greenberg (17), which is of the variety discussed above. On being heated at 10 deg C min^{-1}, this shows no significant change in X-ray pattern up to 250°C. Above about 300°C the 9.8 Å reflection disappears and some other minor changes occur, and at somewhat higher temperatures the material becomes almost amorphous. Neither these results, nor the DTA curve or the infrared absorption spectrum which were also obtained, provide any definite indications as to the structure.

Kurczyk and Schwiete (106) described hydration products of C_3S and β–C_2S that were possibly identical with the fibrous C–S–H (II) preparations discussed above. Like the preparation studied by Copeland and Schulz (105), these appear to have given tobermorite-like electron diffraction patterns.

Funk and Fahlke (108) found that two different hydration mechanisms operate with β–C_2S. If the solution was supersaturated with $Ca(OH)_2$, reaction proceeded by dissolution and represipitation, and yielded a product having C/S 1.86, showing as foils in the electron microscope, and giving broad X-ray powder spacings of 1.83, 3.05 and 11–14 Å. If the $Ca(OH)_2$ concentration was kept below saturation, the reaction appeared to proceed by a conversion of the crystals *in situ*. The intensities of the β–C_2S powder reflections changed relative to each other, and eventually needle-shaped crystals of a hydration product with C/S 1.54 were formed. These were possibly identical with the relatively crystalline form of C–S–H (II) discussed above. Funk and Fahlke (108) concluded that the second of these mechanisms was topotactic. In-situ conversion of dicalcium silicate to C–S–H has also been reported to occur in nature (68).

The other poorly crystallized calcium silicate hydrates with C/S $\geqslant$ 1.5 that have been described are of so low a degree of crystallinity that they might be considered to show only short range order and some are discussed later in connection with calcium silicate pastes. Several new electron microscope and diffraction studies have been made (100, 105, 109), but otherwise there has been little progress since the Washington Symposium. The electron microscope studies confirm that a range of morphologies occurs. Some forms, like that described previously, appear to give tobermorite-like electron diffraction patterns, but others give only a single, broad powder ring of

spacing 2.8–3.1 Å, together sometimes with either a second powder ring or a pair of relatively sharp reflections corresponding to a fibre repeat distance of about 1.8 Å. Such patterns could be taken as indicating a structural resemblance to any one of a number of crystalline phases. The application of new experimental methods, such as those mentioned earlier in this review, is probably essentiall if significant further progress is to be made in elucidating the structures of these materials.

Paste Hydration of C_3S and β-C_2S

It is well known that the products of hydration of C_3S or β-C_2S in pastes at room temperature are $Ca(OH)_2$ and a near-amorphous C–S–H. The latter is frequently called "tobermorite gel", but this name may be criticized on two grounds. First, the evidence relating it structurally to the crystalline tobermorites is weak; it amounts largely to a correspondance of the two or three broad X-ray powder reflections of the C–S–H constituent of the gel with strong *hko* reflections of the tobermorites, together with indirect support from what is known or suspected concerning the structures of the semi-crystalline products, C–S–H (I) and C–S–H (II). As will be shown, the hydration products formed in pastes probably comprise a range of phases of differing compositions, depending on such factors as time, temperature, and water: cement ratio. Some of them may be structurally related to tobermorite, but others probably are not; electron diffraction evidence suggests that some, at least, of the fibrous particles that have been observed may be more nearly related to jennite. The second objection to "tobermorite gel" is that a gel is, by definition, a heterogeneous material of a particular type, and to apply the name to a single phase in such a material is incorrect and may well lead to confusion of thought. We shall therefore refer to the calcium silicate hydrate formed in these pastes as C–S–H, particularizing further when necessary, on the basis of composition, morphology, or other characteristics.

Chemical Composition and Specific Surface

Since the Washington Symposium, Brunauer and his colleagues have extended the studies which they reported there (17) on the chemical composition and specific surface area of the C–S–H in calcium silicate pastes (110, 111, 112). Their results for C/S ratios are based on the use of extraction methods (112, 113), which enabled a distinction to be made between Ca^{2+} present in the C–S–H and that present as crystalline or amorphous $Ca(OH)_2$. The C/S ratio appears to depend on the degree of hydration, temperature, and water: cement ratio, but not on the fineness of grinding, assuming that pastes with the same degree of hydration are compared.

In 1962, Kantro, Brunauer and Weise (110, 111) reported results for C_3S and β-C_2S pastes at water: cement ratio 0.7. Their results were summarized by Brunauer (114) and Brunauer and Kantro (115). Specific surface areas and C/S and H/S ratios for the C–S–H were plotted against percentages of the anhydrous compound reacted, which in turn were plotted against time, for temperatures of 5°, 25° and 50°C. The main results were as follows:

(i) With both C_3S and β-C_2S, the C/S ratios are high initially possibly equalling those of the anhydrous phases themselves, and the specific surfaces are relatively low. With β-C_2S, the C/S ratio passes through a minimum at the same degree of hydration as the specific surface passes through a maximum; this stage is reached in about 12 hr at 25°C. With C_3S, the C/S ratio does not show a minimum, but the specfic surface does show a maximum, which is reached in 6 hr at 25°C. The lowest C/S ratios observed (for β-C_2S pastes at 5°C) are around 1.1, and the final C/S ratios are 1.4–1.7.

(ii) Temperature affects the percentages of hydration corresponding to maximum specific surface, and (for β-C_2S pastes) minimum C/S ratio, in a complex way. For β-C_2S pastes the final C/S ratios rise slightly with temperature, but for C_3S pastes there is no clear trend.

(iii) For the end products of the reaction, the H/S ratios are related to the C/S ratios; for materials dried over ice at −78°C, the compositions can be written approximately as $C_{(0.5+n)}SH_r$.

Kantro, Brunauer and Weise (111) interpreted these results to indicate the occurrence of three stages in the reaction. Firstly, a product of high C/S ratio and low specific surface was formed. They considered this to be a skin adhering to the particles of the anhydrous compounds and calculated that it grew to some tens of molecular layers in thickness. The second stage was the splitting-off of particles of a low C/S, high surface area intermediate, which were calculated to be either one or two layers thick, together with $Ca(OH)_2$. The final stage was the growth of these particles to a thickness of three layers. It was suggested

that the two- and three-layer products had C/S ratios of 1.39 and 1.73 respectively. The observed kinetics could be explained by assuming that the rate-determining step was, in the early stages, the reaction between the anhydrous silicate and water, and later the diffusion of ions through the gel layer. The second and third stages were distinct with β–C_2S, but not with C_3S.

In 1966, Kantro, Weise and Brunauer (112) extended their observations by studying the effects of varying the fineness and the water: cement ratio. The fineness was found to have no effect other than on the rate; i.e., if C/S ratio or other parameters were plotted against degree of hydration, fineness had no effect. The water: cement ratio, in contrast, had an important effect; values of 0.45–0.70 were studied. The general trends found in the earlier work were confirmed for all the water: cement ratios studied. The most important effect of water: cement ratio was that the C/S ratios of the final products increased as the water: cement ratios decreased; thus for C_3S at 25°C, the final C/S ratio was 1.42 for W/C = 0.7 and 1.61 for W/C = 0.45. Corresponding values for β–C_2S were 1.66 for W/C = 0.7 and 1.80 for W/C = 0.45. This effect was explained by assuming that the smaller amount of space available at low water: cement ratios favoured the formation of the denser three-layer product which, as already seen, was considered to be of higher C/S ratio.

Locher (116) has reported results for C_3S pastes at 20°C which agree in many respects with those of Brunauer and his colleagues. He worked with pastes of water: cement ratios 0.25–2 (those above 0.8 did not harden); $Ca(OH)_2$ was determined by a chemical extraction method and by TGA. Water contents were determined after drying over ice at −79°C. No results were reported for degrees of hydration below about 28%. For water: cement ratios $\geqslant$0.6 Locher found little variation in C/S with the percentage of hydration over the range studied; the chemical extraction method gave 1.4–1.6, and TGA 1.6–1.9. At lower water: cement ratios (especially at 0.25–0.35), the C/S ratios were higher, and rose not only with decreasing water: cement ratio, but also with increasing time. For W/C = 0.45, the final value was about 1.75 (by chemical extraction) or 2.05 (by TGA). Corresponding values for W/C = 0.25 (about 80% hydration) were around 2.15 and 2.37 respectively. Water contents were found to be correlated with C/S ratios, the general formula of the C–S–H being given as $C_{(0.34+n)}SH_n$. Locher concluded that the phase had a tobermorite-like structure in which the high C/S ratio was caused by the presence of attached $Ca(OH)_2$ layers, together possibly with replacement of silicate by hydroxyl ions on one side of the tobermorite sheet as suggested previously (98, 101).

Stein and Stevels (117) and de Jong, Stein and Stevels (117a) reported some studies on the kinetics and mechanism of the C_3S—water reaction in suspensions which led them to conclude that three successive reaction products are formed. They considered that the initial product had a rather high C/S ratio and that it adhered strongly to the C_3S from which it was formed; it was replaced by a product which had a lower C/S ratio and adhered less strongly. Electron microscopic studies (discussed later) gave some indications that this second product might initially be C–S–H (I), which later gave place to fibrous C–S–H (II). These conclusions seem to agree well with those of Kantro, Brunauer and Weise (111). Greenberg and Chang (118) concluded from a somewhat similar study that reaction proceeded by the reaction of Ca^{2+} and $H_2SiO_4^{2-}$ ions in solution to give a hydration product that crystallized initially on the C_3S surface; Stein and Stevels (119) considered that these results could be reinterpreted in a manner compatible with their own hypothesis.

Degree of Anion Condensation

Lentz (10) has studied the changes in the degree of condensation of the silicate anions in C_3S and portland cement pastes by his method based on formation of trimethylsilyl derivatives. The C_3S paste was 2.7 years old and had a W/C ratio of 0.7, and the C_3S had presumably largely or completely reacted. Lentz reported the following distribution of anion types expressed as percentages of the total acid-soluble silica present in each form):

SiO_4^{4-}	$Si_2O_7^{6-}$	$Si_3O_{10}^{8-}$	$Si_4O_{12}^{8-}$	Highly condensed
9.5	22.4	3.8	1.9	50.8

The $Si_4O_{12}^{8-}$ was considered to be a cyclic anion. A 14.7 year old portland cement paste gave closely similar results but showed a higher proportion (17.0 %) of silica present as SiO_4^{4-}. A study of cement pastes of differing ages showed a progressive trend to higher degrees of condensation with increase in curing time (Fig. 4). It was not established to what extent the orthosilicate contents could be attributed to unreacted C_3S and β–C_2S.

Lentz obtained evidence that the highly condensed material contained a variety of anion sizes. A later study (10a) indicated a mean anion size of 15.8 tetrahedra in a 15-year old paste. The rapid develop-

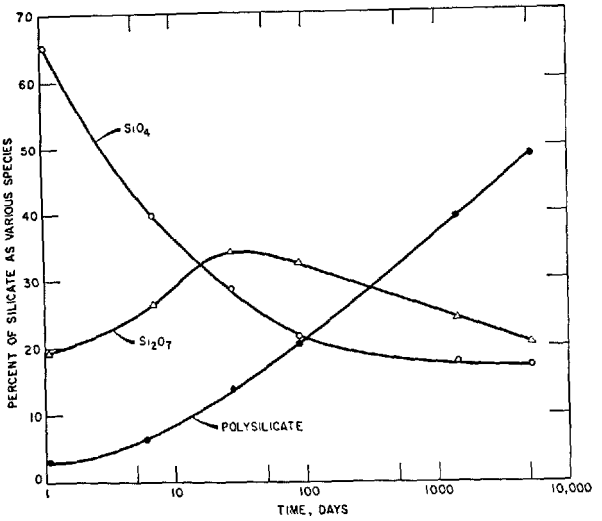

Fig. 4. *Variation with time in the distribution of anion sizes in a portland cement paste (W/C = 0.7; Lentz* (101)).

ment of $Si_2O_7^{6-}$ anions (19.8% of the soluble silica at 1 day, rising to a maximum of 34.3% at 28 days) is especially noteworthy. It would be of great interest to make a similar study on C_3S pastes of different ages and to carry out X-ray determinations of the unreacted C_3S at each stage so that the contributions of this constituent to the SiO_4^{4-} content could be assessed. Lentz's results suggest that (i) an orthosilicate may or may not be formed as the immediate product of reaction, (ii) if it is, it is quickly replaced by a pyrosilicate, which is relatively persistent, and (iii) the subsequent condensation of the silicate anions into larger units continues to advance for at least 15 years.

Electron Microscopy and Diffraction

Electron optical studies on C_3S, β–C_2S and alite pastes have been reported since the Washington Symposium by Copeland and Schulz (105), Copeland, Bodor, Chang and Weise (120), Grudemo (100), Stein and Stevels (117) and others. Grudemo (100, 101) reported that fully hydrated C_3S pastes with water: cement ratio 0.7 contained two types of C–S–H particles, in comparable amounts. One type appeares as small, thin particles, which showed at most in electron diffraction patterns a single, very diffuse ring at 2.8–3.1 Å. The other appeared as needles or rods, which seemed to be made of bundles of fibres or rolled sheets. The same two forms were observed in β–C_2S pastes.

The acicular particles have also been described by Copeland and Schulz (105) and Copeland, Bodor, Chang and Weise (120). They give a characteristic

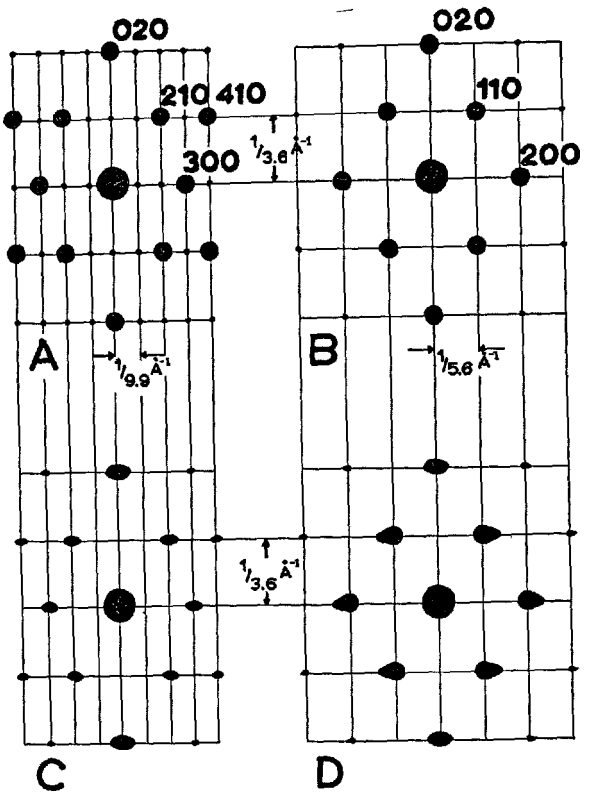

Fig. 5. *Idealized representations of some real or hypothetical electron-diffraction patterns.*
A. *Jennite or metajennite; crystal lying on*(001) *face.* B. *Tobermorite (any variety); crystal lying on* (001) *face.* C. *Fibre from alite paste* (120). D. *Tobermorite; thin foil with* (001) *surface rolled about an axis parallel to the 3.6* Å *repeat. In all cases, systematically weak groups of reflections corresponding to ordering of the Si-O parts of the structures are omitted.*

electron diffraction pattern (100, 101, 120) which was recorded particularly clearly by Copeland, Bodor, Chang and Weise, and is shown diagramatically in Fig. 5c. It differs markedly from the tobermorite-type of pattern (Fig. 5b) which is given by certain C–S–H (II) preparations mentioned earlier. The difference cannot be attributed to rolling of a thin tobermorite sheet, which would be expected to elongate the 110 and 200 reflections as shown in Fig. 5d; a tobermorite-like structure thus seems to be ruled out. The pattern in Fig, 5c does, however, show some similarity to the weighted reciprocal lattices of jennite and metajennite, which have groups of especially strong reflections with 30° and 21° indices, as well as a strong 020 reflection (Fig. 5a). Rolling of a thin crystal of jennite-like structure might be expected to change the pattern to something resembling that shown in Fig. 5c. The acicular particles in C_3S and β–C_2S pastes may therefore have a structure related to that of jennite.

Stein and Stevels (117) recorded some electron micrographs for C_3S pastes with water:cement ratio 1.0. For ages up to 2 hours, crinkly foils were observed, but after 4 hours these seemed to split into needle-like fragments, some of which appeared to be combined into cigar-shaped agglomerates. Copeland and Schulz (105) observed similar changes in the early hydration of cement pastes.

No systematic attempts seem to have been made to see whether the intensities of the C–S–H peaks or bands in the X-ray powder patterns of C_3S or β–C_2S pastes are always the same relative to each other, or not. It would be of interest to see whether any such variation occurs, and if so, whether it can be correlated with such factors as degree of hydration, temperature, or water: cement ratio, or with the relative proportions of acicular and flaky or foil-like particles revealed by electron microscopy. One might expect acicular particles to be associated with increased intensity of the 1.82 Å reflection, and flaky particles with increased intensity of the band or bands in the 2.8–3.1 Å region.

Calcium Silicate Pastes: Discussion

Lentz's (10) observation that the mean anion size rises continuously with time of hydration is readily correlated with the initial fall in C/S ratio postulated by Kantro, Brunauer and Weise (110) and by Stein and Stevels (117), as increased condensation must, in the absence of other changes, be associated with expulsion of Ca^{2+} from the structure. The subsequent rise in C/S ratio found by Kantro, Brunauer and Weise (110) can be attributed to incorporation of the elements of $Ca(OH)_2$ into the structure in amounts sufficient to outweigh the effect of increased condensation. The hypothesis that particles of jennite-like structure occur in fully hydrated pastes agrees with this explanation.

It is tentatively suggested that the following forms of C–S–H and sequence of changes occur in C_3S and β–C_2S pastes. Initially, a high C/S product is formed as a surface coating. It is probably composed initially of Ca^{2+}, $H_2SiO_4^{2-}$ and OH^- ions and H_2O molecules, and has a C/S ratio close to that of the starting material. Nothing is known of its structure; it may be amorphous. Anion condensation to, or perhaps beyond, the pyrosilicate stage may occur in this material. The second product is formed from the first by dissolution and reprecipitation. It probably has a C/S ratio of 1.0–1.5 and forms foils or platelets some 10–20 Å thick; it may be a very poorly crystallized C–S–H (I), with a tobermorite-like structure. How this low-lime phase coexists with free $Ca(OH)_2$ does not seem to have been explained; perhaps a high concentration gradient exists. Further anion condensation may occur within this material, either by *in situ* transformation or by repeated dissolution and reprecipitation. The third product has, in its most developed form, a fibrous morphology and a jennite-like structure, with a C/S ratio of 1.5–2.0. The distinctions between the second and third products, and calcium hydroxide particles, are probably not sharp; the small, thin particles which Grudemo (101) observed in fully hydrated C_3S pastes could have structures based on more-or-less continuous Ca–O layers, both surfaces of which are coated with a highly disordered mixture of hydroxyl ions and silicate anions of various sizes. Within any one such layer, the structure might in some places approximate to that of tobermorite or C–S–H (I), in others to that of jennite, and in yet others to that of $Ca(OH)_2$; this would explain the very poor electron diffraction pattern. Still greater disorder probably occurs in the presence of other ions, such as aluminate or sulphate; this is discussed in the next section.

Isomorphous Substitution

Substitution in Crystalline Tobermorite

In 1957, Kalousek (121) showed that Al^{3+} could enter the structure of 11 Å tobermorite. His results have recently been confirmed and extended by Diamond, White, and Dolch (122) who studied the synthesis of this phase in the presence of Al^{3+}, Mg^{2+}, and Fe^{3+}. Al^{3+} was added as kaolinite or as $Al(OH)_3$. In approximate agreement with Kalousek's results, it was shown that Al^{3+} could be present in amounts corresponding to replacement of about 15% of the Si^{4+} in the structure before a hydrogarnet appeared as an additional phase, and that this replacement caused the basal spacing to increase. Diamond, white and Dolch reported that the 002 spacing increased from 11.18 Å in the Al-free compound to 11.45 Å for maximum substitution. X-ray spectroscopy indicated that the Al^{3+} was in fourfold coordination, thus supporting the view that it replaced Si^{4+} in the structure.

Diamond, White and Dolch (122) found that entry of Al^{3+} into the structure caused only minor changes in the infrared spectrum, peaks at 1207 and 745 cm^{-1} being shifted to 1175 and 700 cm^{-1} respectively. Electron microscopy also showed no marked changes in morphology with Al-substitution, all the specimens examined consisting of platey crystals with sometimes a slight tendency to elongation. Specific surface areas (78 m^2/g for the Al-free preparation) showed no systematic trend with substitution. D.T.A. curves gave results broadly similar to those reported by Kalousek; the unsubstituted preparation showed a broad endotherm at about 275°C and a weak exotherm at 815°C, and the main effect of maximum Al-replacement was greatly to increase the size of the exotherm and to shift it to 835°C. X-ray results showed that both unsubstituted and substituted specimens had changed to the 9 Å hydrate by 350°C. Al-rich specimens appeared partly fused when cooled from 775°C or over. It was suggested that both this and the increased size of the exotherm might be caused by the formation of some quasi-amorphous phase, such as an Al–Si spinel.

As Diamond, White and Dolch pointed out, Farmer (123) has suggested that the infrared peak at about 1200 cm^{-1} in preparations such as those under discussion could be attributed to xonotlite. The conditions of preparation used by Diamond, White and Dolch (19 hour treatment of a lime-quartz slurry at 175°C under saturated steam pressure) might have caused partial conversion to xonotlite. The presence of a little xonotlite in the preparations would not invalidate the main conclusions reached by these authors.

Diamond, White and Dolch also studied the preparation of 11 Å tobermorite in the presence of Fe^{3+}, added as hematite or as goethite, and in the presence of Mg^{2+}, added as MgO. The hematite did not react. The results obtained using goethite and MgO suggested that both Fe^{3+} and Mg^{2+} could enter the structure, but reproducible results were not obtained and no detailed conslusions were reached.

Roy and Johnson (3) reported equilibrium studies on the hydrothermal treatment of mixes of compositions C_5S_6A and $C_{10}S_{12}A$ at 20,000–45,000 p.s.i. They expressed their results in terms of compatibility volumes within the C–A–S–H tetrahedron, which were shown projected on the C–S–H face for four temperature ranges. At 175–255°C, an Al-rich tobermorite coexisted with a hydrogarnet of approximate composition C_3ASH_4; at 260–275°C, a range of substituted tobermorites coexisted with xonotlite, and a particular one with xonotlite and a hydrogarnet. At 280–330°C the only stable tobermorite was an Al-substituted one, which above 330°C became unstable relative to a hydrogarnet and xonotlite. Roy (124) considered that the presence of Al^{3+} accelerated the crystallization of tobermorite, that it raised the upper temperature limit of its stability and that there was little evidence that it accelerated the change from tobermorite to xonotlite.

Substitution in C–S–H Preparations

It has long been recognized that ill-crystallized forms of C–S–H such as those produced in cement pastes may well contain ions other than those of the pure $CaO–SiO_2–H_2O$ system. At the London Symposium in 1952, Kalousek (99) suggested that all of the Al^{3+}, Fe^{3+} and SO_4^{2-} ions present in the cement tend eventually to enter the C–S–H. Although subsequent work has not supported this extreme view, at any rate for normally cured cement pastes, it still appears likely that these ions are partly present in the C–S–H. In the case of the sulphate ion, Kalousek (125) has recently placed this suspicion on a firmer basis by determining the amounts of crystalline SO_4–containing phases, which he showed to be inadequate to account for all the SO_4^{2-} ion present.

Copeland, Bodor, Chang and Weise (120) have studied the preparation of lime-rich C–S–H in the presence of Al^{3+}, Fe^{3+} and SO_4^{2-}, and the reactions with these ions of C–S–H gel preparations already made. Two types of evidence showed that Al^{3+} can enter the structure of the lime-rich C–S–H formed in C_3S and β–C_2S pastes. Firstly, experiments were carried out in which a hardened C_3S paste was ground and then treated with water and a reactant such as C_4AH_{13}. The only phases detected in the product were $Ca(OH)_2$ and a C–S–H gel phase. Essentially the same products were obtained on paste hydration of alite, or by ball-milling of mixtures of C_3S and C_3A. Secondly, it was shown that the morphology of the C–S–H gel particles changed if sufficient Al^{3+} was present. Thus a C_3S paste that had been ground and then shaken with water for 3 months was shown by electron microscopy to contain rolled sheets or fibres. If the experiment was repeated with C_4AH_{13} present during the shaking, the particles observed were ribbed sheets or laths similar to those formed during the early stages of hydration of cement. Evidence was obtained that the maximum amount of Al^{3+} that could be incorporated in the C–S–H was around 1 atom of Al per 6 atoms of Si. The variations in C/S and H/S ratios with Al-substitution were studied. They suggested that Al^{3+} could enter the structure in two ways: in the first,

$Al^{3+} + H^+$ replaced Si^{4+}, and in the second, $2Al^{3+}$ replaced $3Ca^{2+}$. In support of this conclusion, X-ray spectroscopy suggested that both octahedral and tetrahedral Al^{3+} were present.

These results may be compared with those of Diamond, White and Dolch (122) for crystalline tobermorite. The upper limits of Al/Si ratio in the structure are comparable in the two cases, but in the crystalline tobermorite, Al^{3+} seems to replace only Si^{4+} and not also Ca^{2+}.

Copeland, Bodor, Chang and Weise (120) prepared iron-substituted C–S–H gels by milling hardened pastes of C_3S with different proportions of C_2F. From studies of C/S and H/S ratios, they concluded that $2Fe^{3+}$ replaced $Ca^{2+} + Si^{4+}$. The upper limit of substitution was one atom of Fe^{3+} to six atoms of silicon.

Sulphate substitution was studied in several ways. In one, mixtures of C_3S and gypsum were hydrated in the ball-mill. X-ray and electron optical studies showed no phases in the product except C–S–H and $Ca(OH)_2$. The compositions of the products suggested that S^{6+} replaced $Si^{4+} + 2H^+$. X-ray spectra showed the sulphur K_α peak to be nearer that found with $K_2S_2O_7$ than that found with gypsum. It was concluded that sulphur replaced silicon in a chain anion. The upper limit of sulphur substitution was one atom of S per six atoms of Si.

Some additional experiments were carried out to show that C–S–H in hardened pastes reacts with sulphate solutions even when the pastes are not first ground and re-dispersed: replica studies with the electron microscope showed that changes in morphology occur on treatment with a SO_4^{2-} solution.

The results described above suggest clearly that Al^{3+} Fe^{3+} and SO_4^{2-} ions can all enter the structure of C–S–H formed in calcium silicate pastes. Their presence is likely to render the C–S–H formed as the final product in paste hydration of cement even less definite in structure than that given by the calcium silicates.

References

1. Chemistry of Cement: Proceedings of the 4th International Symposium, 1960 (2 vols.), 1962.
2. S. O. Agrell, "Polythermal metamorphism of limestones at kilchoan, Ardnamurchan" Mineral. Mag., **34**, 1–15 (1965).
3. D. M. Roy and A. M. Johnson, "Investigations of stabilities of calcium silicate hydrates at elevated temperatures and pressures", Proc. Symp. Autoclaved Clacium Silicate Building Products, 1966, 114–120 (1967).
4. E. W. White, H. A. McKinstry and T. F. Bates, "Crystal chemical studies by X-ray fluorescence", Proc. 7th Conf. Indust. Appl. of X-ray Anal., 239–245 (1959).
5. G. W. Brindley and H. A. McKinstry, "Kaolinite–mullite reaction series: IV, the coordination of aluminum", J. Amer. Ceram. Soc., **44**, 506–507 (1961).
6. D. E. Day, "Determining the coordination number of aluminium by X-ray emission spectroscopy", Nature, **200**, 649–657 (1963).
7. E. W. White and G. V. Gibbs, "Structural and chemical effects on the SiK_β X-ray line for silicates", Amer. Mineral., **52**, 985–993 (1967).
8. K. J. Murata, "Significance of internal structure in gelatinizing silicate minerals", U. S. Geol. Survey Bull., No. 950, 25–34. (1946).
9. C. W. Lentz, "Silicate minerals as sources of trimetyhlsilyl silicates and silicate structure analysis of sodium silicate solutions", Inorg. Chem., **3**, 574–579 (1964).
10. C. W. Lentz, "The silicate structure analysis of hydrated portland cement paste", Proc. Symp. Structure of Portland Cement Paste and Concrete, 1965, 269–283 (1966).

10a. C. W. Lentz, "Analysis of tobermorite by the silicate derivative technique", Mag. Concr. Res., **18**, 231–236 (1966).

11. H. Funk and R. Frydrych, "The degrees of anion condensation in silicic acids and silicates", Proc. Symp. Structure of Portland Cement Paste and Concrete, 1965, 284–290 (1966).
12. H. Funk, "Chemical alteration of poorly crystallized calcium silicate hydrates by hydrothermal treatment", Proc. Symp. Autoclaved Calcium Silicate Building Products, 1966, 122–124 (1967).
13. E. Thilo, W. Wieker and H. Stade, "On the relations between the degree of polymerization of silicate anions and their rates of reaction with molybdic acid" (in German), Zeit. Anorg. Allg. Chem., **340**, 261–276 (1965).
14. W. Wieker and H. Stade, "The degree of condensation of the silicate anions in the dicalcium silicate hydrates A, B and C", Proc. Symp. Autoclaved Calcium Silicate Building Products, 1966, 125–129 (1967).
15. N. V. Belov, "Crystal chemistry of large-cation silicates" (translation from Russian), Consultants Bureau, New York (1963).
16. H. F. W. Taylor and J. W. Howison, "Relationships between calcium silicates and clay minerals", Clay Minerals Bull., **3**, 98–111 (1956).
17. S. Brunauer and S. A. Greenberg, "The hydration of tricalcium silicate and β-dicalcium silicate at room temperature", Reference (1), 135–165 (1962).
18. Kh. S. Mamedov and N. V. Belov, "On the structural

analogy (isostructurism) between diorthosilicates and orthoborates" (in Russian), Geokhimiya, No. 11, 1087–1096 (1964).
19. Kh. S. Mamedov, private communication.
20. S. Hénin and S. Caillère, "Synthesis of minerals at low temperature: Attempt at a survey" (in French), Clay minerals Bull. **5**, 265–271 (1963).
21. J. A. Gard and H. F. W. Taylor, "The crystal structure of foshagite", Acta Crystallogr., **13**, 785–793 (1960).
22. R. A. Chalmers, A. W. Nicol and H. F. W. Taylor, "The composition of nekoite", Mineral. Mag., **33**, 70–71 (1962).
23. J. A. Gard, "Interpretation of weak reflections in electron diffraction patterns", Proc. Eur. Reg. Conf. on Electron Miscroscopy, 1960, **1**, 203–206 (1961).
24. J. A. Gard, "A system of nomenclature for the fibrous calcium silicates, and a study of the xonotlite polytypes", Nature, **211**, 1078–1079 (1966).
25. H. F. W. Taylor, "Hydrothermal reactions in the system $CaO–SiO_2–H_2O$ and the steam curing of cement and cement-silica products", Ref. (1), 167–190 (1962).
26. Kh. S. Mamedov and N. V. Belov, "On the crystal structure of hillebrandite" (in Russian), Dokl. Akad. Nauk SSSR, **123**, 741–743 (1958).
27. J. Murdoch, "Crestomre, past and present", Amer. Mineral., **46**, 245–257 (1961).
28. V. C. Farmer, J. Jeevaratnam, K. Speakman and H. F. W. Taylor, "Thermal decomposition of 14 Å tobermorite from Crestmore", Proc. Symp. Structure of Portland Cement Paste and Concrete, 1965, 291–299 (1966).
29. G. L. Kalousek and A. F. Prebus, "Crystal chemistry of hydrous calcium silicates: III morphology and other properties of tobermorite and related phases", J. Amer. Ceram. Soc., **41**, 124–132 (1958).
30. Å. Grudemo, "An electronographic study of the morphology and crystallization properties of calcium silicate hydrates", Swedish Cement and Concrete Research Inst. Proc. No. 26 (1955).
31. L. Heller and H. F. W. Taylor, "Crystallographic data for the calcium silicates", H. M. Stationary Office, London (1956).
32. H. F. W. Taylor, "Hydrated calcium silicates. Part V. The water content of calcium silicate hydrate (I)", J. Chem. Soc., 1953, 163–171.
33. J. M. Sweet, "Tacharanite and other hydrated calcium silicates from Portree, Isle of Skye", Mineral. Mag., **32**, 745–753 (1961).
34. J. D. C. McConnell, "The hydration of larnite (β–Ca_2SiO_4) and bredigite (α'–Ca_2SiO_4) and the properties of the resulting gelationous mineral, plombierite", Mineral. Mag., **30**, 672–680 (1955).
35. Huang Yang-hwei, "Suolunite–a new mineral" (in Chinese), Geological Review (Pekin), **23**, 7 (1965).
36. Tseng Jo-ku, Hsuech Chi-yueh and Peng Chin-chung, "The crystal structure of suolunite", Kexue Tongbao, **17**, 45–48 (1966).
37. C. W. F. T. Pistorius, "Thermal decomposition of portalndite and xonotlite to high pressures and temperatures", Amer. J. Sci., **261**, 79–87 (1963).
38. A. Pabst, E. B. Gross and J. T. Alfors, "Rosenhanite, a new hydrous calcium silicate from Mendocino County, California", Amer. Mineral., **52**, 336–351 (1967).
39. H. Strunz and H. Micheelsen, "Calcium phyllosilicates" (ih German), Naturwiss., **45**, 515 (1958).
40. J. W. Meyer and L. K. Januarajs, "Synthesis and crystal chemistry of gyrolite and reyerite", Amer. Mineral., **46**, 913–933 (1961).
41. R. I. Harker, "Dehydration series in the system $CaSiO_3–SiO_2–H_2O$", J. Amer. Ceram. Soc., **47**, 521–529 (1964).
42. J. R. Cann, "Gyrolite and reyerite from S Airde Beinn, Northern mull", Mineral. Mag., 35, 1–4 (1965).
43. Al L. Mackay and H. F. W. Taylor, "Gyrolite", Mineral. Mag., **30**, 80–91 (1953).
44. R. A. Chalmers, V. C. Farmer, R. I. Harker, S. Kelly and H. F. W. Taylor, "Reyerite", Mineral. Mag., **33**, 821–840 (1964).
45. P. Hövig, "Gold ores of the Lebong District (Benkoelen)" (in Dutch), Jaarbock Mijnwezen Ned. Oost.–Ind. (Batavia) **41**, 202 (1914).
46. A. L. Mackay and H. F. W. Taylor, "Truscottite", Mineral. Mag., **30**, 450–457 (1954).
47. H. Funk, "Chemical investigations of silicates: XXVI, On calcium silicate hydrates with composition $CaO·2SiO_2·0·5–2H_2O$ and synthesis of reyerite (truscottite) ($CaO·2SiO_2·0.5H_2O$)" (in German), Z. Anorg. Allg. Chem., **313**, 1–13 (1961).
48. R. I. Harker, "Dehydration series in the system $CaSiO_3–SiO_2–H_2O$", Bull. Geol. Soc. Am., **71**, 1881 (1960).
49. G. O. Assarsson, Contribution to Discussion, Ref. (1), 190–194 (1962).
50. H. Funk and E. Thilo, "Acid silicates: IV, calcium trihydrogen monosilicate $Ca[OSi(OH)_3]_2$ and its conversion into calcium tetrahydrogen disilicate $Ca[Si_2O_3(OH)_4]$" (in German), Z. Anorg. Allg. Chem, **278**, 237–248 (1955).
51. W. Wieker, Contribution to Discussion, Proc. Symp. Autoclaved Calcium Silicate Building Products, 1966, 205 (1967).
52. D. M. Roy, "Studies in the system $CaO–Al_2O_3–SiO_2–H_2O$: III, new data on the polymorphism of Ca_2SiO_4 and its stability in the system $CaO–SiO_2–H_2O$", J. Amer. Ceram. Soc., **41**, 293–299 (1958).
53. D. M. Roy, "Studies in the system $CaO–Al_2O_3–SiO_2–H_2O$. IV, phase equilibria in the high-lime portion of the system $CaO–SiO_2–H_2O$", Amer. Mineral., **43**, 1009–1028 (1958).
54. S. O. Agreel and P. Gay, "Kilchoanite, a polymorph of rankinite", Nature, **189**, 743 (1961).
55. D. M. Roy, J. A. Gard, A. W. Nicol, and H. F. W. Taylor, "New data for the calcium silicate, 'Phase Z' ", Nature, **188**, 1187–1188 (1960).
56. K. Speakman, H. F. W. Taylor, J. M. Bennett and J. A. Gard, "Hydrothermal reactions of γ-dicalcium silicate", J. Chem. Soc., *A* 1967, 1051–1060.
57. J. M. Bennett, J. A. Gard, K. Speakman and H. F. W. Taylor, "$Ca_8Si_5O_{18}$ and the nature of 'γ-dicalcium silicate hydrate'", Nature, **209**, 1127 (1966).
58. H. Funk, "On the products of the action of water on

the different forms of Ca_2SiO_4 at 120° to 350°C and their conditions of formation" (in German), Zeit. Anorg. Allg. Chem., **297**, 103–114 (1958).
59. K. W. Andres, "Research on the constitution of steelworks refractories", Refractories J., **37**, 66–77 (1961).
60. L. S. Dent Glasser, H. Funk, W. Hilmer and H. F. W. Taylor, "The identity of some dicalcium silicate hydrates", J. Appl. Chem., **11**, 186–190 (1961).
61. Kh. S. Mamedov, R. F. Klevtsova and N. V. Belov, "On the crystal structure of tricalcium silicate hydrate", Dokl. Akad. Nauk SSSR, **126**, 151–154 (1959).
62. E. R. Buckle, J. A. Gard and H. F. W. Taylor, "Tricalcium silicate hydrate", J. Chem. Soc., 1958, 1351–1355.
63. G. L. Kalousek and R. Roy, "Crystal chemistry of hydrous calcium silicates: II, characterization of interlayer water", J. Amer. Ceram. Soc., **40**, 236–239 (1967).
64. D. S. Coombs, A. J. Ellis, W. S. Eyfe and A. M. Taylor, "Zeolite facies; with comments on interpretation of hydrothermal syntheses", Geochim. Cosmochim. Acta, **17**, 53–107 (1959).
65. D. M. Roy and R. I. Harker, Contribution to Discussion, Ref. (1), 196–201 (1962).
66. D. A. Buckner, D. M. Roy and R. Roy, "Studies in the system $CaO–Al_2O_3–SiO_2–H_2O$: II, the system $CaSiO_3–H_2O$", Amer. J. Sci., **258**, 132–147 (1960).
67. R. I. Harker, D. M. Roy and O. F. Tuttle, "Melting phenomena in the system $CaO–SiO_2–H_2O$: I, the join $Ca_2SiO_4–Ca(OH)_2$", J. Amer. Ceram. Soc., **45**, 471–473 (1962).
68. J. V. P. Long and J. D. C. McConnell, "A mineralogical application of X-ray absorption microspectroscopy: the hydration of larnite", Mineral. Mag., **32**, 117–127 (1959).
69. D. L. Kantro, S. Brunauer and C. H. Weise, "The ball-mill hydration of tricalicum silicate at room temperature", J. Colled Sci., **14**, 363–376 (1959).
70. G. L. Kalousek, J. S. Logiudice and V. H. Dodson, "Studies on the lime-rich crystalline solid phases in the system lime-silica-water", J. Amer. Ceram. Soc., **37**, 7–13 (1954).
71. R. B. Peppler, "System of $CaO–SiO_2–H_2O$ at 180°C", J. Res. Nat. Bur. Stand., **54**, 205–211 (1955).
72. A. H. W. Ahmed and F. H. W. Taylor, new data.
73. A. Aitken and H. F. W. Taylor, "Hydrothermal reactions in lime-quartz pastes", J. Appl. Chem., **10**, 7–15 (1960).
74. R. I. Harker, "Scawtite and its synthesis", Mineral. Mag., **34**, 232–236 (1965).
75. A. B. Carpenter, R. A. Chalmers, J. A. Gard, K. Speakman and H. F. W. Taylor, "Jennite, a new mineral", Amer. Mineral., **51**, 56–74 (1966).
76. L. Heller, private communication.
77. H. D. Megaw and C. H. Kelsey, "Crystal structure of tobermorite", Nature, **177**, 390–391 (1956).
78. L. M. Clark and C. W. Bunn, "The scaling of boilers. Part IV: identification of phases in calcium silicate scales", J. Soc. Chem. Ind., **59**, 155–158 (1940).
79. E. Thilo and H. Funk, "On some chemical properties of pectolite, $Ca_2Na[HSi_3O_9]$, and its synthesis" (in German), Z. Anorg. Allg. Chem., **262**, 185–191, (1950).
80. M. J. Buerger, "The determination of the crystal structure of pectolite, $Ca_2NaHSi_3O_9$", Z. Kristallogr., **108**, 248–262 (1956).
81. E. Thilo, H. Funk and E. M. Wichmann, "Chemical investigations of silicates. XIV. The normal and acid salts of low-molecular silicic acids and their condensation products" (in German), Abhandl. Deut. Akad. Wiss. Berlin, Klasse Math. u. Allgem. Naturw., 1950, No. 4 (1951).
82. V. S. Sazhin, O. I. Shor, O. I. Arakelyan, A. I. Volkovskaya and I. A. Koletsnikova, "On the solid phases formed in the system $Na_2O–Al_2O_3–SiO_2–CaO–H_2O$" (in Russian) Ukr. Khim. Zh., **29**, 1123–1128 (1963).
83. V. S. Sazhin, O. I. Shor, O. I. Arakelyan, A. I. Volkovskaya and L. G. Shebeko, "Investigations on the solid phases in the system $Na_2O–CaO–Al_2O_3–SiO_2–H_2O$" (in Russian), Ukr. Khim. Zhur. **32**, 293–400 (1966).
84. L. P. Ni and L. V. Bunckuk, "Interactions in the system $Na_2O–Al_2O_3–SiO_2–CaO–H_2O$ under the conditions of hydrochemical processes and at varying ratios of CaO: SiO_2" (in Russian), Tr. Inst. Met. i Obogashch., Akad. Nauk Kaz. SSR, **9**, 56–62 (1964).
85. L. P. Ni, B. E. Medredkov and V. D. Ponomarev, "Reactions in the $Na_2O–CaO–SiO_2–H_2O$ system at 280°C" (in Russian), Tr. Inst. Met. i Obogashch., Akad. Nauk Kaz. SSR, **9**, 69–75 (1964).
86. L. P. Ni, L. V. Bunchuk, O. B. Khlyapina and V. D. Ponomarev, "Reactions in the system $Na_2O–Al_2O_3–CaO–SiO_2–H_2O$ at 280°C" (in Russian), Zh. Prikl. Khim., **38**, 288–295 (1965).
87. I. Yu. Uvarova and O. I. Luk'yanova, "Nature of the induction period of setting in the interaction of Na and Ca silicates in concentrate suspensions" (in Russian), Fiz.-Khim. Mekhan. Dispersnykh. Struktur, Akad. Nauk. SSSR, Sb. Statei, 1966, 253–259.
88. A. V. Lagoida, Yu. M. Butt and V. M. Kolbasov, "Hydration of $3CaO \cdot SiO_2$ in the presence of potsah at different temperatures" (in Russian), Tr. Mosk. Khim.—Tekhnol. Inst., No. 50, 123–127 (1966).
89. V. F. Chernykh, I. F. Ponomarev and R. D. Azelitskaya, "Study of the process of hydration of calcium silicates and the effect of potsssium oxide on it" (in Russian), Tr. Novocherk. Politekhn. Inst., **1963**, 15–25.
90. M. F. Malyshev "Reaction of β–$CaO \cdot SiO_2$ with sodium hydroxide solutions", (in Russian), Tsvetn. Metal., **38**, 57–59 (1965).
91. G. D. Uryvaeva, "The cementing properties of γ-dicalcium silicate" (in Russian), Izv. Sibirsk. Otd. Akad. Nauk SSSR, Ser. Khim. Nauk 1965, No. 2, 113–118.
92. W. T. Schaller, "Miserite from Arkansas; a renaming of natroxonotlite", Amer. Mineral., **35**, 911–921 (1950).
93. W. Wieker, Contribution to Discussion, Proc. Symp. Autoclaved Calcium Silicate Building Products, 1964, 205 (1966).

94. R. Kondo, "Kinetic study on hydrothermal reaction between lime and silica", Proc. Symp. Autoclaved Calcium Silicate Building Products, 1965, 92–97 (1966).
95. S. A. Grenberg and T. N. Chang, "Investigation of colloidal hydrated calcium silicates, II. Solubility relationship in the calcium oxide-silica-water system at 25°C", J. Phys. Chem., **69**, 182–188 (1965).
96. S. A. Greenberg, T. N. Chang and E. Anderson, "Investigation of colloidal hydrated calcium silicates. I. Solubility products", J. Phys. Chem., **64**, 1151–1156 (1960).
97. D. Lawrence, "The dehydration of calcium silicate hydrate C–S–H (I)", Proc. 7th. Conf. Silicate Ind., 1963. 259–263 (1965).
98. J. A. Gard, J. W. Howison and H. F. W. Taylor, "Synthetic compounds related to tobermorite: an electron-microscope, X-ray, and dehydration study", Mag. Concrete Res., **11**, 151–158 (1959).
99. G. L. Kalousek, "Application of differential thermal analysis in a study of the system lime-silica-water", Proc. 3rd. Int. Symp. Chem. of Cement, 1952, 296–311 (1954).
100. Å. Grudemo, "The microstructures of cement gel phases", Trans. Royal Inst. of Technology, Stockholm, No. 242 (1965).
101. Å. Grudemo, "The microstructure of hardened cement paste", Ref. (1), 615–655 (1962).
102. H. F. W. Taylor, "The calcium silicate hydrates", Chapter 5 of "The chemistry of cements", Vol. 1, H. F. W. Taylor, Editor, Academic Press, London and New York, (1964).
103. H. F. W. Taylor, "Hydrated calcium silicates. Part I. Compound formation at ordinary temperatures", J. Chem. Soc., 1905, 3682–3690.
104. J. A. Gard, "Electron microscopy and diffration", Chapter 21 of "The chemistry of cements", Vol. 2, H. F. W. Taylor, Editor, Academic Press, London and New York, (1964).
105. L. E. Copeland and E. G. Schultz, "Electron optical investigation of the hydration products of calcium silicates and portland cement", J. P. C. A. Res. and Dev. Labs., **4**, 2–12 (1962).
106. H. G. Kurczyk and H. E. Schwiete, "Concerning the hydration products of C_3S and β-C_2S", Ref. (1), 349–358 (1962).
107. F. P. Glasser and H. F. W. Taylor, new data.
108. H. Funk and B. Fahlke, "Chemical investigations of silicates, XXX. On the two different hydration mechanisms of dicalcium silicate (Ca_2SiO_4) by which calcium silicate hydrates (tobermorite-like phases) are formed" (in German), Z. Anorg. Allg. Chem., **334**, 99–108 (1964).
109. Z. Sauman, "System CaO–SiO_2–H_2O under hydrothermal conditions" (in Czech), Silikaty, **6**, 149–161 (1962).
110. D. L. Kantro, S. Brunauer and C. H. Weise, "Development of surface in the hydration of calcium silicates" Advances in Chemistry Series, **33**, 119–219 (1962).
111. D. L. Kantro, S. Brunauer and C. H. Weise, "Development of surface in the hydration of calcium silicates. II. Extension of investigations to earlier and later stages of hydration", J. Phys. Chem., **66**, 1804–1809 (1962).
112. D. L. Kantro, C. H. Weise and S. Brunauer, "Paste hydration of beta-dicalcium silicate, tricalcium silicate, and alite", Proc. Symp. Structure of Portland Cement Paste and Concrete, 1965, 309–327 (1966).
113. E. E. Pressler, S. Brunauer, D. L. Kantro and C. H. Weise, "Determination of the free calcium hydroxide contents of hydrated portland cements and calcium silicates", Anal. Chem., **33**, 877–882 (1961).
114. S. Brunauer, "Tobermorite gel—the heart of concrete", Amer. Scientist, **50**, 210–229 (1962).
115. S. Brunauer and D. L. Kantro, "The hydration of tricalcium silicate and β-dicalcium silicate from 5°C to 50°C", Chapter 7 of "The chemistry of cements" Vol. 1, H. F. W. Taylor, Editor, Academic Press, London and New York (1964).
116. F. W. Locher, "Stoichiometry of tricalcium silicate hydration", Proc. Symp. Structure of Portland Cement Paste and Concrete, 1965, 300–308 (1966).
117. H. N. Stein and J. M. Stevels, "Influence of silica on the hydration of $3CaO \cdot SiO_2$", J. Appl. Chem., **41**, 338–346 (1964).
117a. J. G. M. de Jong, H. M. Stein and J. M. Stevels, "Hydration of tricalcium silicate", J. Appl. Chem., **17**, 246–250 (1967).
118. S. A. Greenberg and T. N. Chang, "The hydration of tricalcium silicate", J. Phys. Chem., **69**, 553–561 (1965).
119. H. N. Stein and J. M. Stevels, "Remarks on the hydration of tricalcium silicate, J. Phys. Chem., **69**, 2489–2490 (1965).
120. L. E. Copeland, E. Bodor, T. N. Chang and C. H. Weise, "Reactions of tobermorite gel with aluminates, ferrites, and sulphates", J. P. C. A. Res. and Dev. Labs., **9**, 61–74 (1967).
121. G. L. Kalousek, "Crystal chemistry of hydrous calcium silicates: I, substitution of aluminum in lattice of tobermorite", J. Amer. Ceram. Soc., **40**, 74–80 (1957).
122. S. Diamond, J. L. White and W. L. Dolch, "Effects of isomorphous substitution in hydrothermally-synthesized tobermorite", Amer. Mineral., **51**, 388–401 (1966).
123. V. C. Farmer, "Infra-red spectroscopy of silicates", Chapter 23 of "The chemistry of cements", Vo.l 2, H. F. W. Taylor, Editor, Academic Press, London and New York (1964).
124. D. M. Roy, Reply to Discussion, Proc. Symp. Autoclaved Calcium Silicate Building Products, 1966, 121 (1967).
125. G. L. Kalousek, "Analyzing SO_3-bearing phases in hydrating cements", Materials Research and Standards, **5**, 292–304 (1965).

Written Discussion

Jerzy R. Dyczek

Introduction

The information contained in your report about the influence of the concentration of $Ca(OH)_2$ on the reaction of the hydration of calcium silicates are in a good agreement with the results of my latest work concerning the dependence of the texture of the products of hydration of cement on the type and amount of calcium sulphate added to the cement.

It is known, that the presence of more or less soluble calcium sulphate ($CaSO_4 \cdot 2H_2O$ or $CaSO_4 \cdot \frac{1}{2}H_2O$) has an important influence on the solubility of $Ca(OH)_2$.

Procedure

The cements used in the following tests were prepared in the following way: two industrial clinkers of the chemical compositions given in Table 1 were ground and then mixed in a laboratory ball mill with the addition of ground calcium sulphate. Calcium sulphate was added in such quantities as always to ensure 2% content of SO_4^{2-} in the cements. Thus six cements were obtained of which two had no calcium sulphate addition and were pure ground A and B clinkers, the two next were A and B clinkers with 2% addition of SO_4^{2-} introduced in the form of $CaSO_4 \cdot 2H_2O$ and designated in abbrevation as A_2 and B_2, and finally the two cements with 2% addition of SO_4^{2-} introduced in the form of $CaSO_4 \cdot 0.5H_2O$ and designated as $A_{0.5}$ and $B_{0.5}$.

The compression, bending strengths and the setting time were determined and the degree of grinding was checked for the cements tested by screen analysis and by determining their specific surfaces by the Blaine method (results given in Table 2).

To make possible a comparison of the specific surfaces of the hardened cement pastes (determined by the BET method) prepared from the above mentioned cements, a knowledge of the degree of hydration was indispensable. Therefore for corresponding hardening times the evaporable water was determined by the method described by Copeland, the results being given in Table 3.

The cement pastes intended for determination of the specific surfaces were prepared with such a quantity of water as to obtain a water-cement ratio of 0.4.

The paste samples were stored in a thermostatic bath (20°C ± 2°) in hermetically sealed glass test tubes.

After the elapse of 3, 7, 14, 21 and 28 days the test tubes with corresponding pastes were broken, the paste crushed and, after the evaporable water in it was determined, approximately 2 g of the hardened paste was transferred to the BET apparatus in order to determine the specific surface. Nitrogen was used as the absorbed gas.

The results of determination of the specific surfaces are presented in Fig. 1.

Considerable differences observed in the specific surfaces for the same hardening times of the cements tested and differing only in the form of calcium sul-

Table 1.

	A(%)	B(%)
L. of ign.	0.17	0.88
Ins.	0.18	0.20
SiO_2	20.24	21.86
Al_2O_3	7.62	4.54
Fe_2O_3	3.58	4.62
CaO	66.33	66.00
MgO	1.51	1.40
SO_3	0.44	0.42

Table 2.

		A	A_2	$A_{0.5}$	B	B_2	$B_{0.5}$
Com. st. after:							
(kg/cm^2) Days	3	88	176	160	68	152	136
	7	134	204	164	164	212	192
	28	200	268	228	208	328	287
Bend. st. after:							
(kg/cm^2) Days	3	25.8	57.0	47.0	22.2	44.5	44.5
	7	44.6	61.5	52.0	42.5	55.5	54.5
	28	37.5	80.5	71.5	61.0	87.0	73.5
Initial set. (min)		—	80	120	—	148	118
Fin. set. (min)		—	165	180	—	362	418
Specific surf. (acc. to Blaine) (cm^2/g)		3700	3620	3690	3260	3090	3080

Table 3.

	Evaporable water (%)			
Days:	3	7	14	28
A	13.26	9.77	9.22	8.05
B	16.21	12.96	12.54	11.25
A_2	12.74	9.82	8.42	7.96
B_2	15.76	13.96	12.07	10.31
$A_{0.5}$	12.44	8.64	8.32	8.24
$B_{0.5}$	13.12	11.95	11.02	10.41

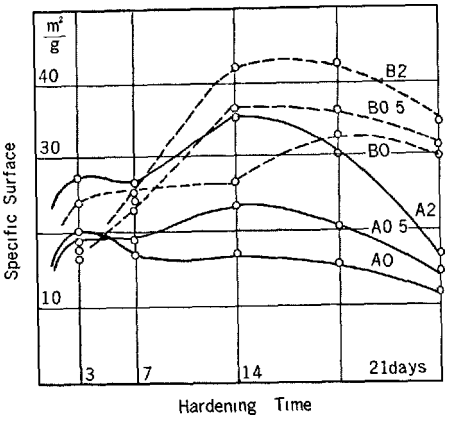

Fig. 1.

phate added were the reason for taking a series of photographs by means of an electron microscope.

The microscope preparations were made by the extraction replica technique, spraying the carbon and platinum at a 30° angle onto a triofal foil taking a fresh fracture of a hardened cement paste.

The Results and Their Discussion

From a comparison of the results of the determinations of the evaporable water in the pastes from cements produced from A and B clinkers respectively it appears that slightly more uncombined water was removed from the cements containing calcium sulphate dihydrate than from those of cement with calcium sulphate semihydrate. The greatest quantity of evaporable water (identified with that chemically uncombined) was removed from the hardened pastes made from the clinkers without a calcium sulphate addition (Table 3). The pastes that had undergone the reaction with water to a smallar degree did not always displayed a small specific surface. After three days hardening the pastes made from clinkers without a calcium sulphate addition had rather big specific surfaces (Fig. 1), while after longer hardening times (7, 14, 21 and 28 day respectively) the specific surfaces were smallest.

The greatest specific surfaces were measured in the pastes made from cements with calcium sulphate dihydrate and these cements had also the highest mechanical properties after hardening. A maximum may be observed occurring after about 14 days on the curves illustrating the specific surfaces depending on the hardening time. The later reduction of the surface may be explained by the recrystallization of the hydration and hydrolysis products with a simultaneous hindering of the reaction of that part of the cement grains which have not undergone reaction with water caused by the products of these reactions surrounding them (coatings hindering the access of water to the cement grains). A similar decrease in the specific surface of the reaction products of the alite and belite with water was observed by Copeland who explained this by the formation of a two and then of a three layer tobermorite. The differences in the specific surfaces of the investigated hardened pastes which clearly depended on the presence of calcium sulphate dihydrate and calcium sulphate semihydrate may be explained as follows: during the first moment after mixing the cement with water the better soluble $CaSO_4 \cdot 0.5H_2O$ passing into the solution reduces considerably the solubility of $Ca(OH)_2$ causing its precipitation in a spherical shape. The low concentration of $Ca(OH)_2$ may favour the formation of the lime poor habits of tobermorite (CSH I).

After mixing the cement with water in the presence of the less soluble $CaSO_4 \cdot 2H_2O$ more $Ca(OH)_2$ will be able to pass into the solution and the crystallization of the tobermorite-similar phase will occur in conditions favouring the formation of the lime rich fibrous CHS II variety. The differences in the crystal habit of these two varieties of tobermorite-like phase (CSH I—lamellae; CSH II—fibres of tubular structure) may be explained by the differences in the observed specific surfaces of the pastes tested.

In spite of the fact that after several minutes after mixing with water the calcium sulphate semihydrate initially present in the cement will become hydrate, the further course of crystallization will follow the already existing model.

Microscopic examinations support the interpretation of the results given above:

A total of about 150 photographs were taken. Only chosen examples are presented here. The single crystals designated on the photographs were identified by the electron diffraction method. Photographs No. 1–4 illustrate the cement pastes from A series with calcium sulphate dihydrate, No 5–8 with calcium sulphate semihydrate, No. 9–10 from pure clinker without calcium sulphate addition.

A better crystallization of the fibrous habits of CSH II and the presence of elongated aggregates of this variety (Photo 1–4) which are longer than those in the cement pastes with $CaSO_4 \cdot 0.5H_2O$ may explain the better strength properties after hardening of the cement pastes with calcium sulphate dihydrate and the tubular structure of the CSH II the large specific surface of these pastes.

In the pastes produced from the cements with calcium sulphate semihydrate the lamellar shapes of

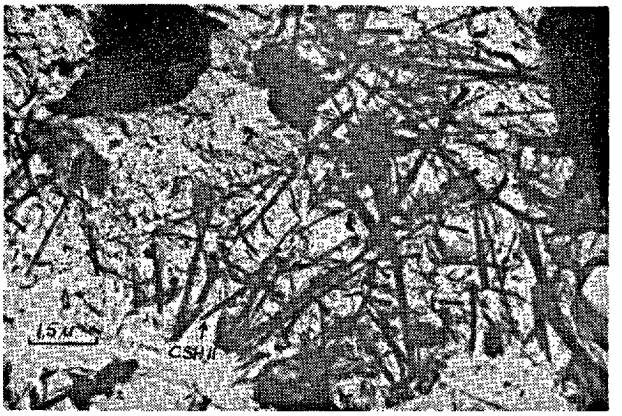

Photo 1.

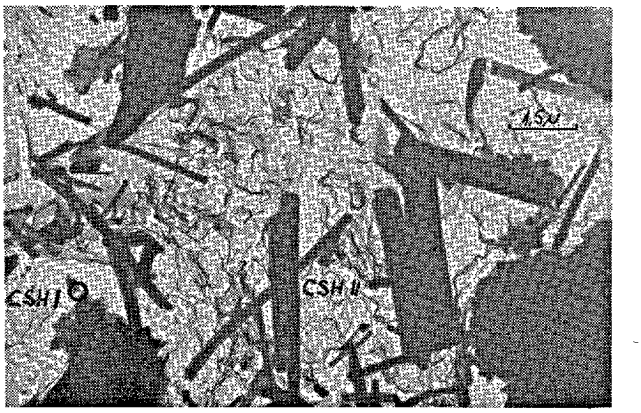

Photo 2.

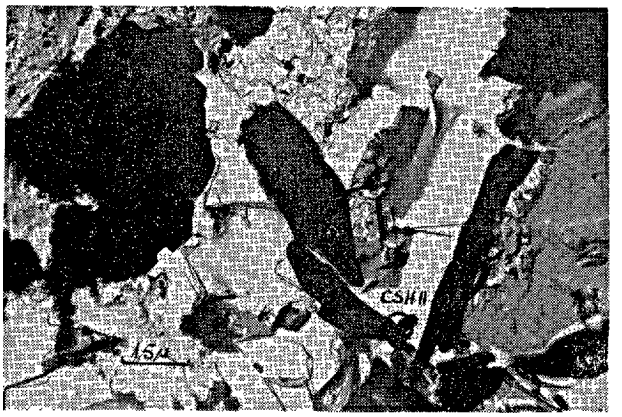

Photo 3.

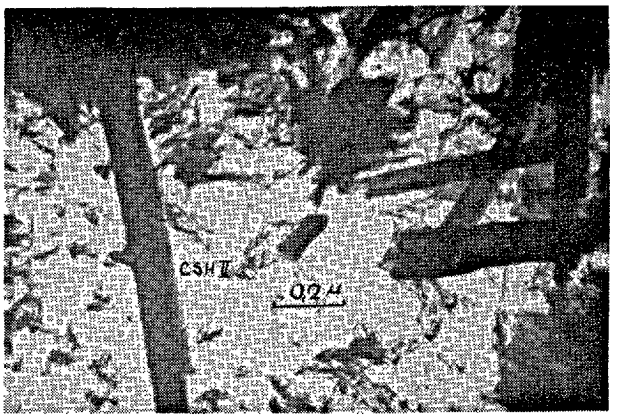

Photo 4.

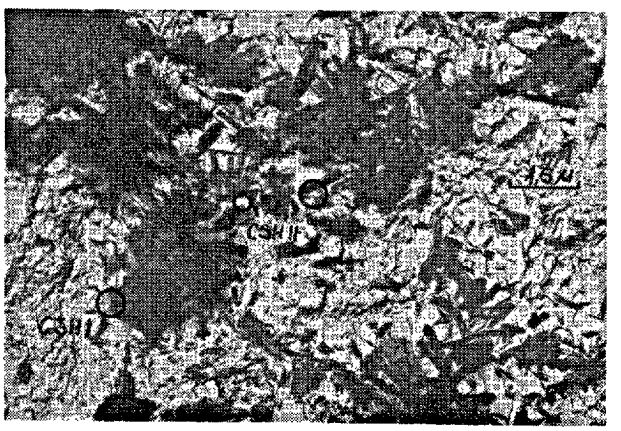

Photo 5.

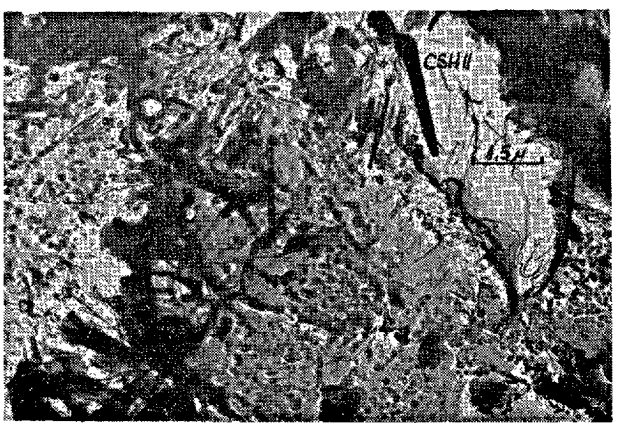

Photo 6.

the CSH I may be observed more often as irregular aggregates.

In all the preparations both varieties of the calcium hydroxide were observed. However, the portlandite occurred most often in the preparations taken from pastes made of cements with calcium sulphate dihy-

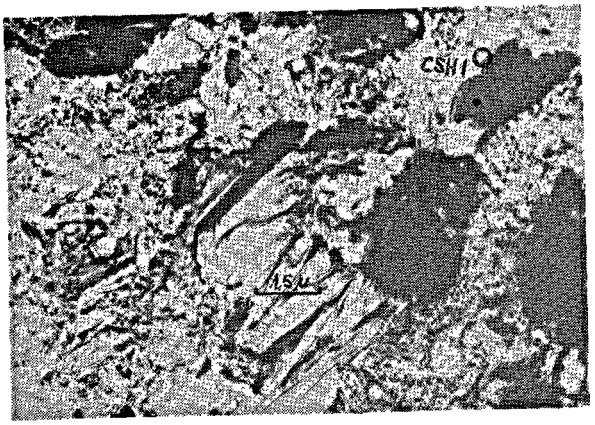

Photo 7.

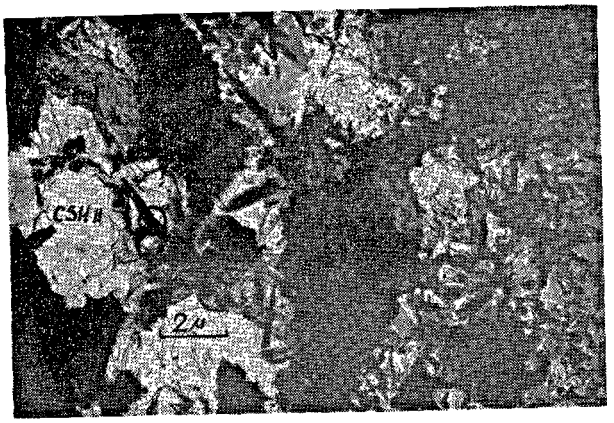

Photo 8.

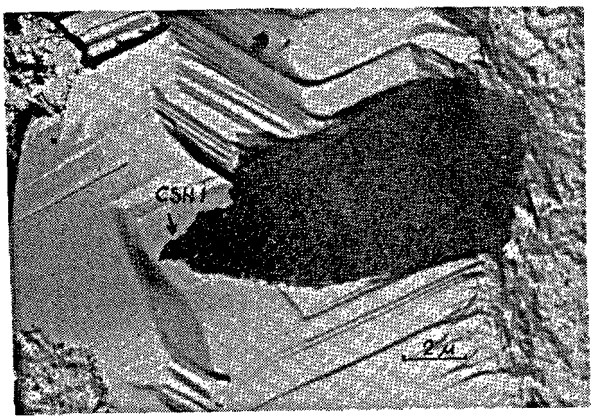

Photo 9.

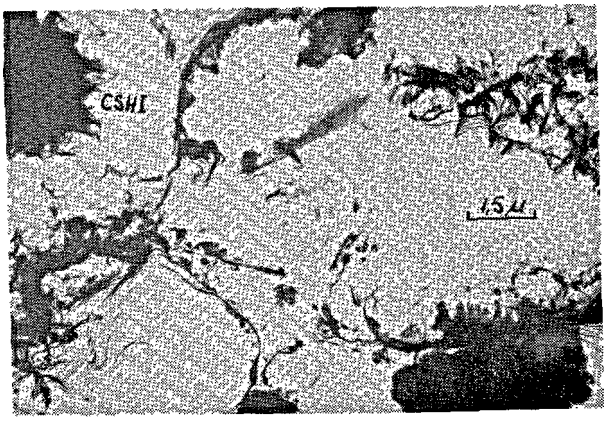

Photo 10.

drate.

Conclusions

From the results presented above it may be concluded that the disadvantageous effects of false setting (decrease in mechanical strength, surface hardness, etc) are caused by the changes in the texture of the products of the reaction of the cement with water, and in particular of the tobermorite-similar phase. When the cement contains $CaSO_4 \cdot 0.5H_2O$ less fibrous habits of CSH II form in the paste made of it than in the paste with the calcium sulphate dihydrate where CSH II will form moreover elongated and better crystallized habits.

Additional Note

I think, that the results of my work given above may contribute to the better understanding of the phenomena of false setting and its influence on some properties of cement in use.

Written Discussion

Paul Longuet

The works which have been done for some years upon the paste hydration of pure tricalcium silicate seem to be able to bring some complements to the calorimetric studies mentioned in the principal paper. Specially the use of the isothermal calorimeter on the first stage of hydration allowed new observations. We reproduce here the communication of B. Courtault (1) on this subject.

"D. L. Kantro, S. Brunauer and C. H. Weise (2, 3), A. Van Bemst (4) and H. N. Stein and J. M. Stevels (5) deduce from their works, the formation of several hydrated phases during the hydration in paste of the tricalcium silicate. Those authors found as a rule their speculations on the analytic results of the hydrated products and their characterizations by means of electronmicroscopy.

Calorimetry and more specially the often used isothermal calorimetry (5, 6, 7, 8) seems to be the ideal mean to show the real evolution of the different hydrated forms but in practice this prospect has not yet been confirmed. Two reasons seem responsible for this seeming failure: the usual conditions in the technical employment which lead to the mixing of solid-liquid outside the calorimeter and the lack of exact definitions of the heterogeneous system studied.

For the first point, we suggested a calorimetric device allowing the recording of the thermal phenomena at the initial stage of hydration (8). For the second one, we studied the influence of the tricalcium silicate grading, of the experiment temperature, of the hydrated state of the solid phase, of the composition of the liquid phase in touch with the solid, of initial additions to the solid or liquid phase.

Grading conditions affect the saturation rate of the liquid phase and the formation rate of the hydrated phase. The conclusions are summarized on the Fig. 1. A large and fairly coarse grading gives a simple thermogram of the type usually mentioned in literature (5, 6) while a granulometric portion, fine and well definite allows to specify the different phases of the thermal reaction.

The rate of the different reactions is conditioned by the temperature (Fig. 2). The slowing down due to the temperature drop permits to make a peak obvious in the first stage, on the thermograms at 6°C and 15°C.

The relations between the thermal effects and the equilibrium state of the system have been established point by point upon the solution in touch, after pressing out and upon the solid after hardening and elimination of free water by cryosublimation (this process used at the CERILH since 1955 consists in freezing suddenly the sample and to sublimate the produced ice under high vacuum).

The extracted solution allows to determinate the lime content of the solution at a definite time. The thermogravimetric measurements of the cryosublimated solid give the amount of $Ca(OH)_2$ released during the hydration and the amount of water bound to the hydrated portion.

The whole determinations made upon the same sample are shown on the Fig. 3. Their examination

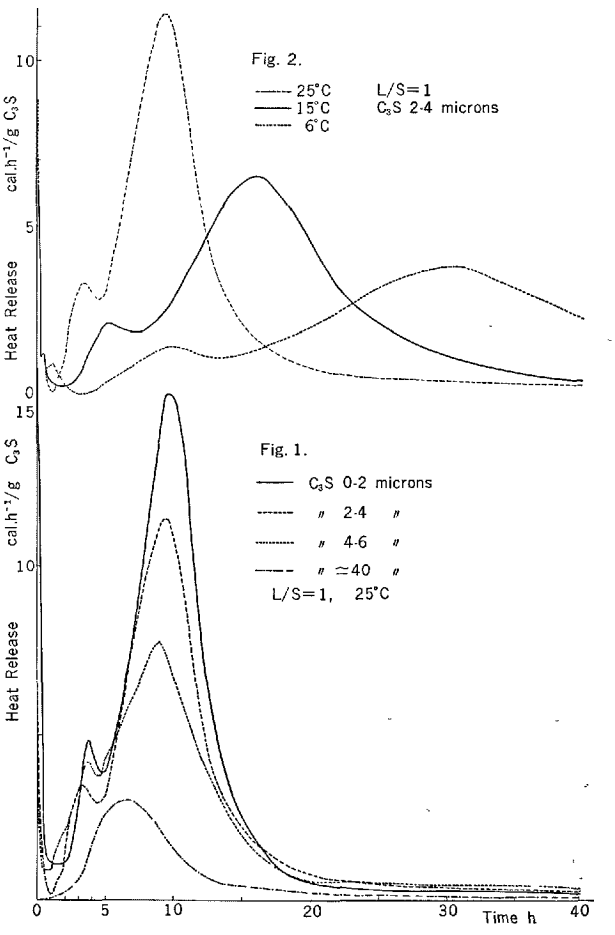

Fig. 1. *Grading influence*
Fig. 2. *Temperature influence*

brings the following remarks:

—The biginning of the endothermic effect is bound to a definite concentration of lime in solution.

—The development of the endothermic effect corresponds to a temporary increase of the lime concentration in the solution in touch.

Those two effects characterize a hydrolysis reaction (transition for a definite concentration of the solution, to a less saturated salt with release of base).

—The formation rate of $Ca(OH)_2$ released by hydration, increases before the endothermic effect while the formation rate of the hydrated phase grows only after the end of this effect.

To sustain the supposition of the hydrolysis reaction, the effects due to changes of lime concentration in solution in touch must be verified (Fig. 4). The addition of amorphous silica, already studied by Stein and Stevels (5) accelerates the hydration, inducing a decrease of the lime concentration in the liquid phase.

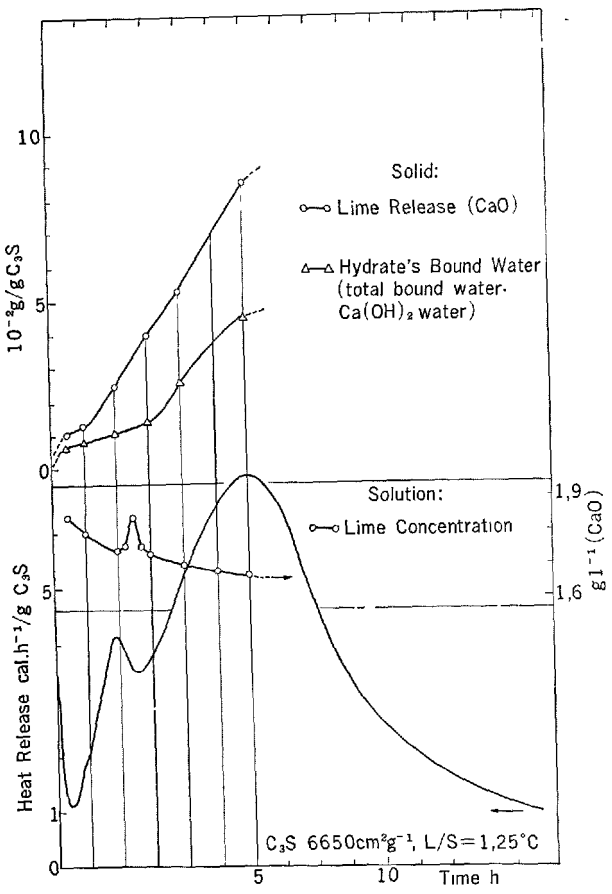

Fig. 3. *Solid, solution and heat release modifications*

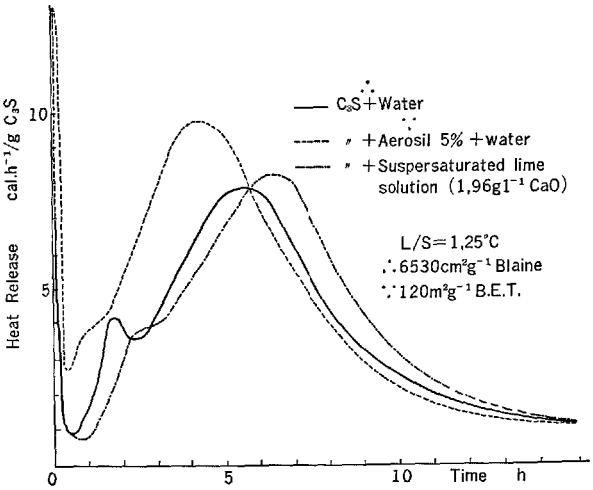

Fig. 4. *Hydration's medium influence*

On the other hand, when the initial water is substituted by a super-saturated lime solution, prepared according to Longuet and Zelwer (9), the hydrolysis equilibrium is displaced and the hydration is delayed. The study of the anomaly in the thermograms obtained by isothermal calorimetric measurements, gives an experimental confirmation of the supposed transformation of an hydrate with high C/S ratio, formed in the first stage of the reaction between water and C_3S (Kantro, first hydrate of Stein) in a hydrate with lower C/S ratio of CSH I type (second hydrate of Stein).

References

1. B. Courtault, "Contribution de la calorimétrie isotherme à l'étude de l'hydratation en pâte du C_3S", Communication intérieure, CERILH, France, (Juin 1968).
2. D. L. Kantro, S. Brunauer and C. H. Weise, PCA, Bull. **140**, (1961).
3. D. L. Kantro, S. Brunauer and C. H. Weise, J. Phys. Chem. **66**, 1804 (1962).
4. A. Van Bemst, Bull, Soc. Chim. Belg. **64**, 333 (1955).
5. H. N. Stein and J. M. Stevels, J. Appl. Chem. London, **14**, 338 (1964).
6. N. Kawada and A. Nemoto, Zement-Kalk-Gips, dtsch. **2**, 65 (1967).
7. G. E. Monfore, Ost Borje, J. of PCA **8** 13 (1966).
8. B. Courtault and P. Longuet, XXVIe Congrès de Chimie Industrielle, Bruxelles (1966).
9. P. Longuet and A. Zelwer, 37e Congrès de Chimie Industrielle, Madrid (1967).

Written Discussion

O. P. Mchedlov-Petrosyan, I. P. Vyrodov and L. P. Papkova.

D. I. Mendelejev (1) a prior noted that interaction between lime and aggregate is inevitable in durable mortars, while V. N. Young (2) has found by the use of chromatic reactions the presence of calcium hydrosilicates in the mortars of ancient buildings. Some reliable investigators denied the possibility of active interaction between binder and aggregate (3) and considered the formation of calcium carbonate to be

the only cause of the durability of ancient lime mortars (4).

Even the present time literature still uses the term "inert aggregates".

Our numerous attempts to explain experimentally the processes of prolonged hardening of lime mortars aged up to 2000 years (5–9) were conducted with the use of a complex of various physico-chemical and biochemical methods and allow us to picture a certain supposed course and nature of interaction between the components of durable mortars.

However we consider the results of X-ray examination of ancient lime-mortars as a decisive factor in solving the problem.

We used the method of X-ray ionization recording. This method is used widely in the investigation of mortars.

The apparatus used are: USR-50-IM and USR-50-I.

Some of the specimens of ancient mortars were examined by means of Deby's method (powder-method) with X-ray apparatus URS-55-A.

To determine reliable data of the phase-contents of ancient mortars we conducted X-ray investigation on specimens aged from 200 to 2000 years by means of three different apparatus in three different laboratories because we could not find the data of X-ray examination of ancient mortars in the modern Russian and foreign literature (12 and others).

The Table 1 displays the results of X-ray examination of these mortars; their study show that after centuries hardening the following products are observed:

1. The main component is calcite, increasing with the age of mortars;
2. The content of calcium hydrosilicate is much lower than of calcite; though all the specimens contain the hydrosilicates of following types: C_2SH(A, B, C); CSH(B); C_2S_2H; $C_3S_2H_3$; tobermorite etc. These calcium hydrosilicate are hydration products of portland-cement in which they are however presented in great quantity (10);
3. The investigation of the majority of examined specimens (11 of 12) has shown the presence of hillebrandite (C_2SH(B)), which is known as a product of hydro-thermal treatment of portland-cement paste; most of specimens contain, besides it, the hydrosilicates of the tobermorite group;
4. Several specimens showed the presence of amorphous silica; the hollow galls (eroded gall) in X-ray data indicate it's presence.
5. The content of hydrosilicates of calcium as well as that of calcite increases with the age of lime mortars.

The X-ray investigation has shown in all specimens of ancient mortars similar phase content according to nomenclature of products of hardening in the specimens of various climate zones.

The results of X-ray examination of all ancient mortars agree with the data obtained through other experimental methods, thermo-analysis, chemical-petrographical, luminescentical analysis and electron-microscopical analysis etc. and confirm the presence of calcium hydroscilicates (6–9). The content of calcium hydrosilicates confirms the presence of the hydrosilicate-type of hardening in ancient lime mortars similar to the hardening of portland-cement.

The presence of hillebrandite (C_2SH(B)), afwillite ($C_3S_2H_3$), gyrolite ($C_2S_3H_3$), riversidite (C_2S_2H) and others in ancient lime-mortars, which are formed under hydrothermal conditions in portland-cement, allows to assume, that the replacement of thermal treatment by long-time hardening (and vice versa) may give qualitatively the same results (11).

Table 1. *Results of X-ray analysis of ancient mortars.*

Number ordinal	Specimen number	Century of building	Phase composition
1	2	3	4
1	53[x)]	I	calcite; C_2SH(C); C_2SH(A); tobermorite; C_2SH(B); CSH(B)
2	72	IV	calcite; C_2SH(C); C_2SH(A); C_2SH(B); tobermorite; CSH(B).
3	59[x)]	XII	calcite; C_2SH(C); tobermorite; C_2SH(A); CSH(B).
4	80	XII	calcite; C_2SH(B); C_2SH(A); tobermorite; C_2SH(C); CSH(B).
5	85	XIII	calcite; C_2SH(C); C_2SH(A); C_2SH(B); tobermorite.
6	25	XV	calcite; C_2SH(B); C_2SH(A); tobermorite; C_2SH(C); CSH(B).
7	33	XVII	calcite; C_2SH(B); C_2SH(A); tobermorite; C_2SH(C); CSH(B).
8	54	I	calcite; C_3SH_2; hillebrandite.
9	87	VII	calcite; hillebrandite.
10	1	XI	calcite; hyrolite; hillebrandite. calcite; C_2S_2H-macro-crystallic.[xx)]
11	24	XIV	calcite; hyrolite; afwillite.
12	46	XVIII	calcite; hillebrandite; C_3SH_2; C_2SH.

Notes: Specimens 1-7 were analysed by means of the X-ray apparatus URS-50-IM; specimens 8-12—by means of the apparatus URS-50-I; specimen 10[xx)]—by means of the apparatus URS-55-3I (Deby-method). In specimens I and 3 there were observed "hollow galls" proving the presence of amorphous silica.

In spite of the essential differencies in phase-content of hardened lime and portalnd-cement stones they contain qualitatively the same products of hardening. This fact apparently allows, to a certain extent, to suppose the considerable durability of artificial stone made of portland-cement under unaggressive conditions of service. The age of portland-cement stone is only about 150 years, while the age of lime mortars is several thousands of years.

References

1. D. I. Mendelejev—Principles of chemistry. p. 665, 1906.
2. V. N. Young—On ancient Russian mortars. Scientific works on cementing materials. Gostechisdat, Moskow, 1948.
3. Ed. Donath—Die Chemie des Ziegelmauerwerkes. Sammlung, chemische und chemisch-technische Vorträge. Band 30, heft 5,6. Stuttgart, 1928.
4. G. F. Hüttig and E. Rosenkranz—Zur Kenntnis des ternären System CaO-CO_2-SiO_2. Zeitschrift Elektrochemische und angewandte physikalische Chemie, N 6, Band 35, S. 308–314, 1929.
5. J. G. Belik and L. P. Parkova—Some investigations of building materials of the Kiev Golden Gates. Isvestia Akad. Nauk SSSR, Ser. Geologie N 5, pp. 124–131, 1953.
6. V. F. Solotuchin, J. G. Belik and L. P. Parkova—On durable plasterings of ancient buildings. Works Lenin politechnical institute of Kharkov, vol. IV. Series of the chemical technology. Issue 2, pp. 223–239, 1954.
7. L. P. Parkova, J. G. Belik, A. P. Kononenko and O. P, Mchedlov-Petrossian—Experimental investigation of some mortars of old Baku buildings. Sovetskaja archeologia, N 1, pp. 292–296, 1966.
8. L. P. Parkova, Kh. O. Gevorkian and O. P, Mchedlov-Petrossian—On cementing materials of some ancient buildings in Armenia. Isvestia Academii Nauk Armyanskoj SSR, vol. XVII, N 2, pp. 61–66, 1964.
9. O. P. Mchedlov-Petrossian and L. P. Parkowa—Kristallisations-Strukturbildung in der Kontaktzone zwischen Bindemittel und Zuschlagstoff bei langdauernder Erhärtung. Silikattechnik, No. 10, S. 319–321, 1967.
10. L. E. Kopeland, D. L. Kantro and G. Verbeck—Chemistry of hydration of portland-cement, Procedings of the Fourth International Symposium on the Chemistry of Cement, 1960, Washington. Translation into Russian, Strojisdat, Moscow, pp. 305–352, 1964.
11. I. I. Ryvlin and L. P. Parkova—Formation of buildings materials from gypsum without thermal treatment. Works of Lenin politechnical institute of Kharkov, vol. VIII; issue 3, series of the chemical technology, pp. 219–233, 1956.
12. I. L. Znachko-yaworski—Essays on the history of cementing materials from ancient times to the middle of XIX century. Isd. AN SSSR, Moscow, 1963.

Oral Discussion

Udo Ludwig and Hans E. Schwiete

1. During hydration of glasses of the chemical composition of melilites in lime saturated water we found out together with Würth and Grieshammer that the glasses rich in MgO are leading to a formation of a foil-like C_2MS_2 aq.

The 12.6 Å interference was absent when we added anhydrite to the starting mixtures (Fig. 3). The formation of gehlenite-hydrate, ettringite and monosulphate-hydrate and hydrogarnet should be in this case out of discussion.

2. Together with Seiler we found out, that the C/S-ratio of the calcium silicate hydrates was in the range of 2.25 and 2.70 when the starting material was as follows:

The last results show a maximum C/S ratio of 3. When starting with a industrial retarder we found

Table 1. *Reaction of retarders with lime saturated solutions*

Research Nr.	Starting mixture retarder	[ml]	CaO [g]	Reaction time [h]	CaO (filtrate) [g/l]	C/S-ratio of CSH-phase	Weight of the solid [g]	Spec. surface [m²/g]	pH (filtrate)
1	$MgSiF_6$ 5%	10.5	3.4	0.5	0.575	2.25	5.3782	109.0	13.00
2		10.5	4.1	0.5	1.040	2.70	5.6476	100.7	
3		10.5	3.4	24	0.580	2.25	5.3538	116.0	13.00
4		10.5	4.1	24	1.051	2.70	5.6700	102.6	
5	"R"	10.0	4.1	0.5	0.564	2.70	6.6782	60.5	12.77
6	"R"	10.0	4.5	0.5	0.805	2.97	7.0104	83.9	
7	"R"	10.0	4.1	24	0.673	2.49	6.5272	61.3	12.81
8	"R"	10.0	4.5	24	0.834	2.90	6.8325	81.6	
9	"N"	6.0	3.79	0.5	1.280		3.3433	10.7	13.03
10	"N"	6.0	4.00	0.5	1.349		3.5506	11.2	
11	"N"	6.0	3.79	24	1.364		3.2323	11.5	13.03
12	"N"	6.0	4.00	24	1.321		3.5697	11.6	
13	"P"	15.0	3.90	0.5	1.180		4.3464	32.1	13.01
14	"P"	15.0	4.00	0.5	1.194		4.3948	33.4	
15	"P"	15.0	3.90	24	1.126		4.4216	33.2	13.00
16	"P"	15.0	4.00	24	1.133		4.5830	35.3	

"R" industrial retarder (main compound: $MgSiF_6$)
"N" industrial relarder (main compound: Hexite)
"P" industrial relarder (main compound: Polyhydroxy carbonic acids)

a range of 2.49 to 2.97. The X-ray diagram and the morphology are shown in the Fig. 4.

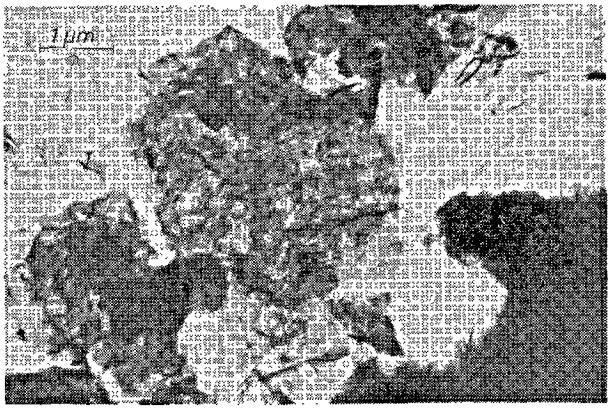

Fig. 1. *Foil-like* $C_2MS_2 \cdot aq$

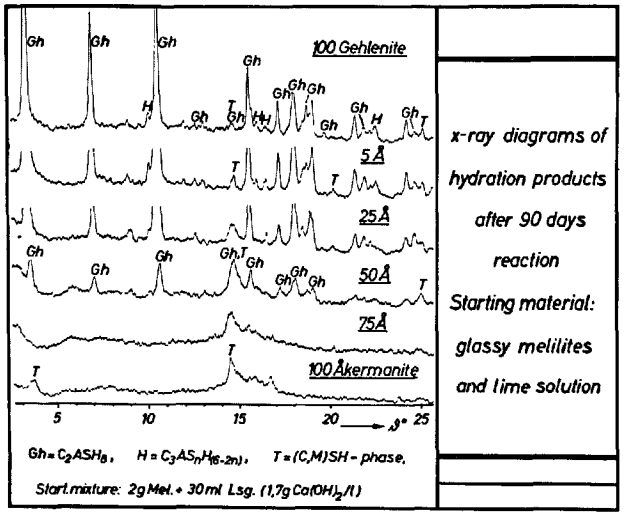

Fig. 2.

The electron micrographs were conducted by Dr. Buss.

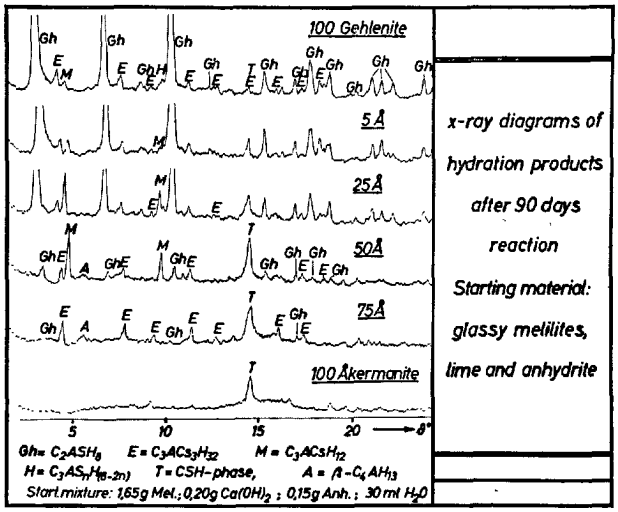

Fig. 3.

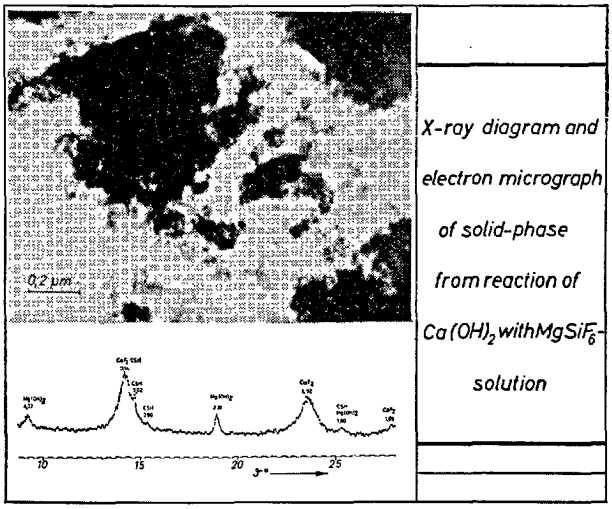

Fig. 4.

References

1. H. E. Schwiete, U. Ludwig, K. E. Würth and G. Grieshammer "Hydration products of the hydration of blast-furnace slags" (in German)—Vortrag von H. E. Schwiete am Min. Institut der Universität Leipzig im Nov. 1965.

2. K. Seiler: "The influence of retarders with special view on silico-fluoride containing retarders" Thesis, Institut für Gesteinshüttenkunde der RWTH Aachen 1958.

Oral Discussion

Della M. Roy

Professor Taylor has emphasized the importance of establishing equilibrium conditions when defining reactions taking place under hydrothermal conditions or at saturated steam pressures. Recently it has been suggested that C–S–H phases having a Ca: Si ratio of 3:2 are metastable with respect to afwillite. Another instance where metastable reaction products are

apparently produced is the case where high-SiO_2 phases such as gyrolite or truscottite are formed by reacting mixtures which contain a high surface area source of SiO_2. Presumably the stable equilibrium product under the given pressure-temperature-composition conditions would contain tobermorite. Does the author know of any work related to this problem? Particularly, is there any evidence that such metastable products eventually yield to the stable equilibrium phases?

SESSION II-2 CRYSTAL STRUCTURES AND PROPERTIES OF CEMENT HYDRATION PRODUCTS (HYDRATED CALCIUM ALUMINATES AND FERRITES)

Principal Paper Crystal Structures and Properties of Cement Hydration Products (Hydrated Calcium Aluminates and Ferrites)

Hans E. Schwiete and Udo Ludwig*

Introduction

In the following communication a review is given of the structures and properties of hydrated calcium aluminates and hydrated calcium ferrite aluminates together with those of the hydrates and double salts derived from them.

Following upon the knowledge that was available at previous symposia a report is presented of new results:

1. Previous data have been confirmed by new work.
2. Progress has been made particularly in investigating dehydration and in distinguishing the various hydrated tetra- and carboaluminates.
3. Numerous crystallographic data have been worked out for the double salts of general composition $3\,CaO \cdot Al_2O_3 \cdot Ca(X, Y_2) \cdot nH_2O$.
4. Two other double salts were synthesized and are described.
5. The only fully-clear structure is still that of C_3AH_6 which is derived from grossularite (C_3AS_3).

Crystal Structure and Properties of the Hydrated Calcium Aluminates and Ferrites

Amongst the calcium-rich hexagonal or pseudo-hexagonal hydrated calcium aluminate or calcium aluminate ferrites one must distinguish between those that contain three molecules of a calcium-bearing compound ($CaSO_4$, $Ca(OH)_2$, $CaCl_2$, $CaSiO_3$ and $CaCO_3$) and those which contain only one molecule of these compounds per unit of formula. Based on a suggestion of Smolczyk (1) it seems appropriate to designate the hexagonal hydration products which crystallize with three molecules of a calcium salt per unit of formula and whose prototype is ettringite ($C_3ACs_2H_{32}$) as "AFt phases". This is an abbreviation of (tricalcium)-aluminate *f*errite·*t*ri (sulphate, -hydroxide, etc.)·(hydrate)-*phase*. Consequently it is reasonable to name the corresponding phases whose prototype is C_4AH_{19} as "AFm"-phases (*m* = mono).

The distinction into these two groups is useful since the structures and properties of the AFt and AFm phases are fundamentally different.

The AFt phases are morphologically recognizable as hexagonal columns or needles in which the water of crystallization is contained in channels parallel to the *c*-axis. The AFm phases on the other hand are hexagonal or pseudo-hexagonal sheets in which the water of crystallization is bound in layers normal to the *c*-axis. These differences have an effect on the properties of dehydration.

*Institut für Gesteinshüttenkunde, Technische Hochschule Aachen, Aachen, West Germany.

One can further distinguish a group of hexagonal or pseudo-hexagonal hydrated calcium aluminates or calcium aluminate ferrites with a low calcium content which occur in high alumina cement or in slag-rich blast-furnace cements. A final group comprises the isometric hydrated calcium aluminate ferrites in which two molecules of water can be replaced by one molecule of SiO_2.

AFt Phases

In the following sections are described in more detail a phase of the composition $C_3A \cdot 3CaCl_2 \cdot 30H_2O$ and the AFt phases in which calcium hydroxide is wholly or partially replaced by calcium sulphate. For the corresponding calcium silicate and calcium carbonate phases reference is made to the original literature (2, 3).

$C_3AC_3H_{32}$

The hydrated tricalcium-aluminate-trisulphate is called ettringite after the natural mineral of the same composition. The mineral ettringite (named after Ettringen in the Eifel Mountains, Germany) was first discovered and investigated by Lehmann (4) in 1874. Michaelis (6) was probably the first to synthesize it in 1892. Bannister, Hey and Bernal (7) carried out a structural determination in 1936 and found for the lattice constants $a_0 = 11.24$ Å and $c_0 = 21.45$ Å. The space group was found to be $P6_3/mmc$. The density is 1.75 – 1.79 g/cm³. The lattice constants and the space group were confirmed by Feitknecht and Busser (12), as well as by Swanson, Gilfrich, Cook, Stindfield and Parks (13). In our own investigations (14) we found experimentally a density of 1.72, and one of 1.75 g/cm³ from X-ray data (Table 1).

In a recent publication Bezjak and Jelenic (15) determined by a Patterson synthesis the distances between the single atoms and the atomic groups and they are listed in Table 1. A final report on these investigations has not yet been published.

Bereczky (16) determined the pH value of ettringite as 10.52. From our own measurements (14) the value lies between 10.2 and 10.3. By boiling with the ester of acetic acid for one hour 4.74% CaO was dissolved from ettringite.

$C_3(A, F)C_3 \cdot H_{32}$

All the work so far carried out on ettringite in which

Table 1. *Investigations on ettringite*

Hydrates	Basal interfer. [Å]	Meth. of preparation r.h./temperature [%] [°C]	Properties	Authors (date)
—	—	—/—	Mineral from Ettringen(Eifel)	Lehmann(1874)
$C_3A \cdot Cs_{2.5} \cdot H_{59}$	—	—/room temp.	from CA-and Cs-solution	Candlot(1890)
$C_3A \cdot Cs_3 \cdot H_{30}$	—	above H_2SO_4/room temp.	from $Al_2(SO_4)_3$-and CaO-sol.	Michaelis(1892)
$C_3A \cdot Cs_3 \cdot H_x$	—	—/room temp.	x varied; depends on drying conditions	Deval(1902); Poirson(1911); Klein, Phillips(1915); Kühl and Albert(1923); Lafuma(1925); Mc Intire and Shaw(1925)
$Ca_{12}Al_4(OH)_{24}$ $(SO_4)_6 \cdot 52H_2O$	—	—/—	natural mineral $a_0 = 11.24$Å; $c_0 = 21.45$Å $n_\omega = 1,4661$; $n_\varepsilon = 1.4612$ $d = 1.75$–1.79g/cm³ (Laue-diagrams) group $P6_3/mmc$; $Z = 2$	Bannister, Hey and Bernal (1936)
$C_3A \cdot Cs_3 \cdot H_{31}$	9.62	—/—	$a_0 = 11.2$Å $c_0 = 21.4$Å	Feitknecht and Busser(1949)
$C_3A \cdot Cs_3H_{32}$	9.73	—/room temp.	$a_0 = 11.23$Å; $c_0 = 21.44$Å $d = 1.754$g/cm³(röntg.)$P6_3/mmc$	Swanson, Gilfrich, Cook, Stindfield and Parks (1956)
$C_3A \cdot Cs_3H_{32.5}$	9.72	alcohol/22	$d = 1.72$(exp.), 1.75g/cm³(röntg.) $a_0 = 11.25$Å $c_0 = 21.49$Å	Schwiete, Ludwig and Jäger (1967)
$[Al_2Ca_6(OH)_{12}24H_2O]$ $(SO_3)_3 \cdot 2H_2O$	—	—/—	Structure determination by Patterson-Synth, bond length: H–H_2O H–SO_4^{2-}2.70–2.74Å Ca–OH CA–$OH_2$2.38–2.44Å Al–OH Al–$OH_2$1.90–1.94Å	Bezjak and Jelenic(1966)

the Al^{3+} ions are replaced by Fe^{3+} ions is shown in Table 2. It can be seen that McIntire and Shaw (11) in 1925 were the first to prepare an iron-ettringite. Aruja and Rosaman (17) were the first to establish the a_0 value as 11.23 Å and the c_0 value as 22.14 Å. Smolczyk (1) found the a_0 value to be 11.25 Å and that of c_0, 22.02 Å.

According to our own investigations (14) the values are $a_0 = 11.25$ Å and $c_0 = 21.49$ Å, i.e. the values found by us are closer to those of the normal aluminium-ettringite. On the other hand the investigations of Malquori and Cirilli (19) and those of Cirilli (19) have shown that the solid solution series,—i.e. the replacement of aluminium by iron is incomplete. They found a maximum F/A ratio of 3:1.

We have carried out several thermo-chemical investigations (20, 14) on ettringite and also on a reaction mixture of iron-ettringite and monosulphate hydrate (Fig. 1). Both kinds of ettringite continuously give off water above 40°C and the maximum of the endothermal peak is reached at 130°C. Normal ettringite shows a second endothermal peak at 270°C which has not been found for iron-ettringite. Instead the latter has the additional characteristic peaks of monosulphate hydrate and calcium hydroxide.

$C_3A \cdot 3CaCl_2 \cdot H_{30}$

A chlorine-bearing hydrate which corresponds in composition to ettringite i.e. which contains $3CaCl_2$ instead of $3CaSO_4$, was described by Serb-Serbina (21) in 1956. He established that this hydrate is formed at low temperatures and he examined its thermal properties by means of DTA.

We have investigated (22) the formation of $3CaO \cdot Al_2O_3 \cdot 3CaCl_2 \cdot 30H_2O$ at temperatures between +20° and −10°C in the presence of various concentrations of calcium chloride. The starting materials were C_3A and $CaCl_2 \cdot H_2O$ (analyticgrade) and doubly distilled water.

Our infra-red spectroscopic investigations of ettringite ($3CaO \cdot Al_2O_3 \cdot 3CaSO_4 \cdot 32H_2O$) which was produced by hydration of C_3A in the presence of gypsum, and of $3CaO \cdot Al_2O_3 \cdot 3CaCl_2 \cdot 30H_2O$ (Fig. 2) show a structural similarity between these two hydrate phases. In both hydrates the water is present in two different forms. The absorption band at a wave length of 2.8 μm indicates the presence of hydroxyl groups whilst that at 6.2 μm represents molecular water. The bands at 7 μm suggest the formation of carbonate during the infra-red investigation; the reso-

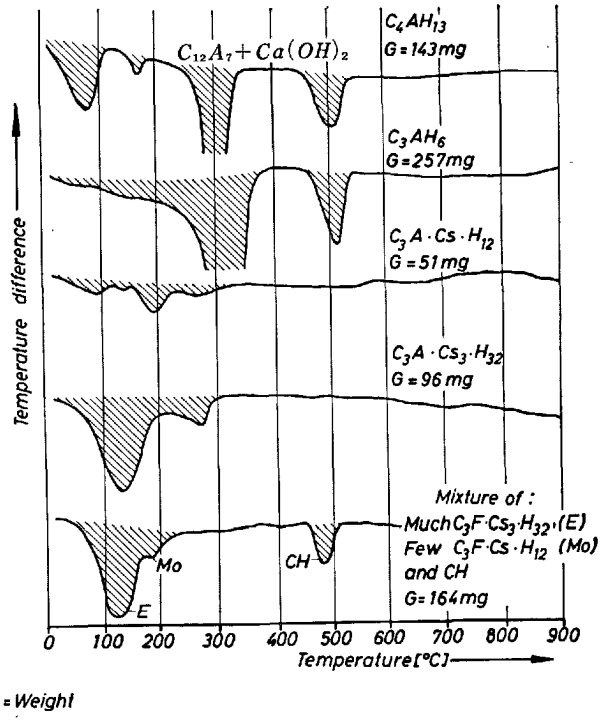

Fig. 1. *DDK—Investigation on calcium aluminate hydrates and calcium ferrite hydrates (Schwiete, Ludwig, Jäger 1967)*

Table 2. *Investigations on "ferrous" ettringite*

Hydrates	Basal interfer. [Å]	r.h./temperature [%] [°C]	Properties	Authors (date)
$C_3FCs_3H_{32}$	— — —	—/25	$n_\omega = 1.486$ $n_\varepsilon = 1.492$ hexagonal needles	Mc Intire, Shaw(1925) Bogue, Lerch and Ashton(1929) Jones(1945)
$C_3FCs_3H_{31-33}$	9.78	—/—	$a_0 = 11.23$Å, $c_0 = 22.14$Å hexagonal unit cell	Aruja, Rosaman and Midgley, Rosaman (1959)
$C_3F_xA_{1-x}Cs_3H_{32}$	—	—/—	imperfect formation of mixed crystals with $C_3ACs_3H_{32}$ on to F/A = 3/1	Malquori, Cirilli(1940) Cirilli (1943)
$C_3FCs_3H_{32}$	—	from ferrous-sulphate + $CaSO_4$-solution		Budnikov, Gorshkov (1959)
$C_3FCs_3H_{32}$	9.77 9.77	above H_2SO_4/22°	hex. a = b = 11.23Å c = 22.02Å from C_3F, gypsum resp. anhydrite, CaO and H_2O at 22°C	Smolczyk(1961) Schwiete, Ludwig, Jäger (1967)

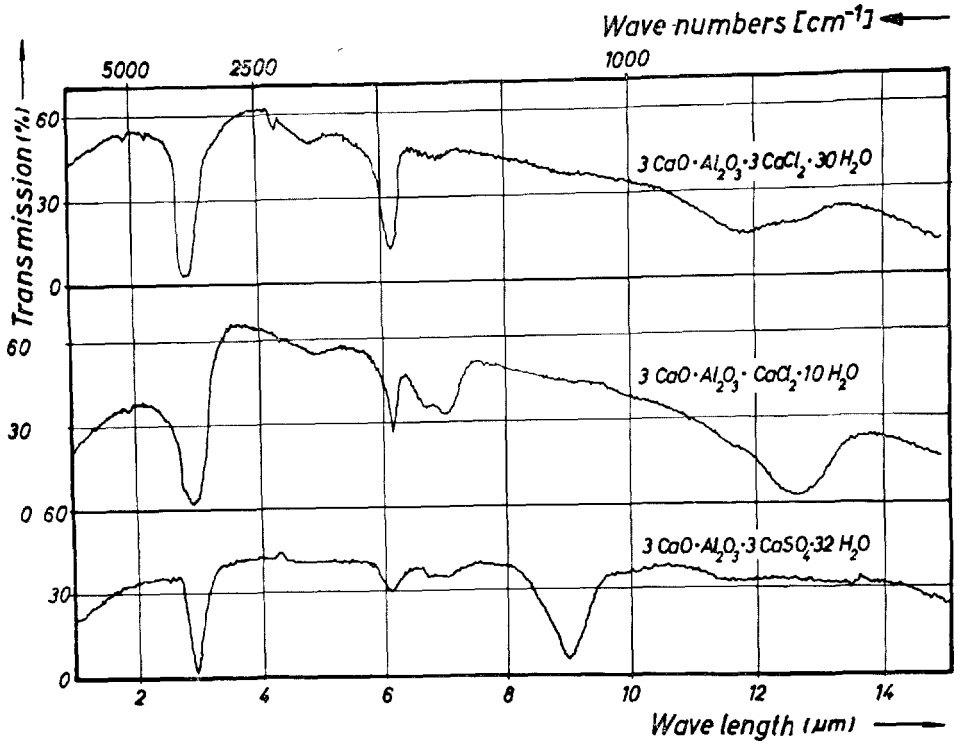

Fig. 2. *Infrared-spectroscopic investigations on calcium aluminate hydrates (Schwiete, Ludwig, Albeck 1967)*

nances at 9 μm and 15 μm of the ettringite are characteristic for the S-O-bonds of the SO_4^{2-} groups whilst in the range 11–13 μm the vibrations for the Al-O-bonding of the compound $3CaO \cdot Al_2O_3 \cdot 3CaCl_2 \cdot 30H_2O$ appear. The shapes of the DDK curves for ettringite and the corresponding calcium chloride-bearing compound (Fig. 3) also show good agreement. For ettringite the main endothermal peak begins at 70°C and has its maximum at 140°C. Release of water from the chlorine analogue begins at 50°C and reaches a maximum at 160°C.

Because of the structural relationship of $3CaO \cdot Al_2O_3 \cdot 3CaCl_2 \cdot 30H_2O$ with ettringite the equations for the hexagonal system were used for determining the (hkil)-values. In this way all the interference lines on the powder photograph could be given an (hkil)-value. Single crystal photographs were not possible because of the minute dimensions of the crystals. In Table 3 the calculated lattice constants and the density

Table 3. *Crystallographic data of hydrates with the composition* $3CaO \cdot Al_2O_3 \cdot 3Ca(X, Y_2) \cdot nH_2O$

Phase	a_0 (Å)	c_0 (Å)	Density (g/cm³)	Reference
$C_3AC_3H_{32}$	11.23	21.44	—	Swanson and co-worker
	11.18	21.48	1.72	Schwiete and co-worker
$C_3A \cdot 3(CaCl_2)H_{30}$	11.738	20.71	1.686	Schwiete and co-worker

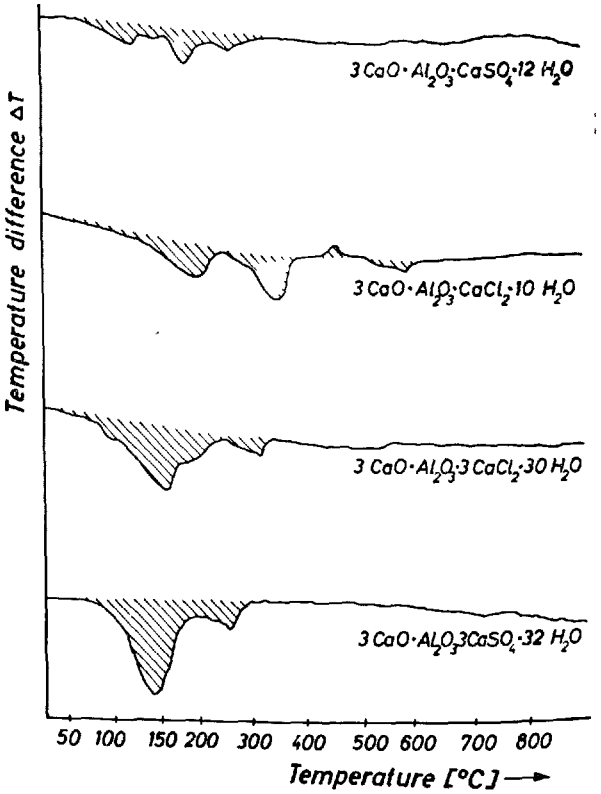

Fig. 3. *DDK—Investigation on calcium aluminate sulphate-and-chloride hydrates (Schwiete, Ludwig, Albeck 1967)*

of ettringite and those of the calcium-bearing analogue are compared.

Investigations with the scanning electron microscope show that the crystallographic habit of the chlorine-bearing compound is the same as that of ettringite, however whilst the length of the ettringite needles may reach 10 μm those of the latter are not longer than 1.5 μm.

Current attempts to prepare hydrate with the composition $3CaO \cdot Fe_2O_3 \cdot 3CaCl_2 \cdot 30H_2O$, starting from C_2F, CaO and calcium chloride, at $-10°C$ prove that a corresponding iron-bearing compound exists.

C_3A (CaS, $CaSO_4$)Hx

Furthermore we (22) succeeded in preparing an AFt-phase with CaS instead of $CaSO_4$ which shows the ettringite-like X-ray interferences and in normal and scanning electron microscope hexagonal prisms.

We are going on to find out more data of this compound that is from importance in accordance to the question of slag containing cements.

AFm Phases

The structure of the prototype of the AFm phase, C_4AH_x, has not yet been explained, although Brandenberger (23), Tilley, Megaw and Hey (24), Buttler, Dent Glasser and Taylor (25) and Grudemo (26) have attempted a clarification. They assume a layer structure and that the total oxygen is bonded as hydroxyl groups within the structural element $Ca_2Al(OH)_7$ of the compound C_4AH_7, a compound which is free of water of crystallization. There is difference of opinion about the sequence and composition of the various layers. According to Buttler, Dent Glasser and Taylor the pseudo-cell contains only one layer of octahedra which is similar in construction to portlandite. One can imagine that in a portlandite layer one of three Ca^{2+} positions is replaced by Al^{3+} (Fig. 4). To balance the charges the seventh (OH)-ion of the structural element $(Ca_2Al(OH)_6)OH$ is situated above the aluminium positions in the gaps between the (OH) belonging to the octahedra. The true cell is not known, however this hypothesis permits an explanation of the one-dimensional swelling parallel to the *c*-axis.

Assuming that the pseudo-cell of C_4AH_x is correct, Kuzel (27) derived the pseudo-cell for the analogue C_3ACsH_{12} as being three layers of the composition $1/2(Ca_4Al_2SO_4(OH)_{12} \cdot 6H_2O)$. The lattice constant, a_0, differs only slightly from that of C_4AH_{13} although two (OH) groups are replaced by one SO_4^{2-}. The thickness of the layers, however, is increased from 7.92 Å to 8.93 Å.

We see in the diagrams a relationship between the hydrates which we shall find again for the other chlorine- and sulphate-bearing compounds.

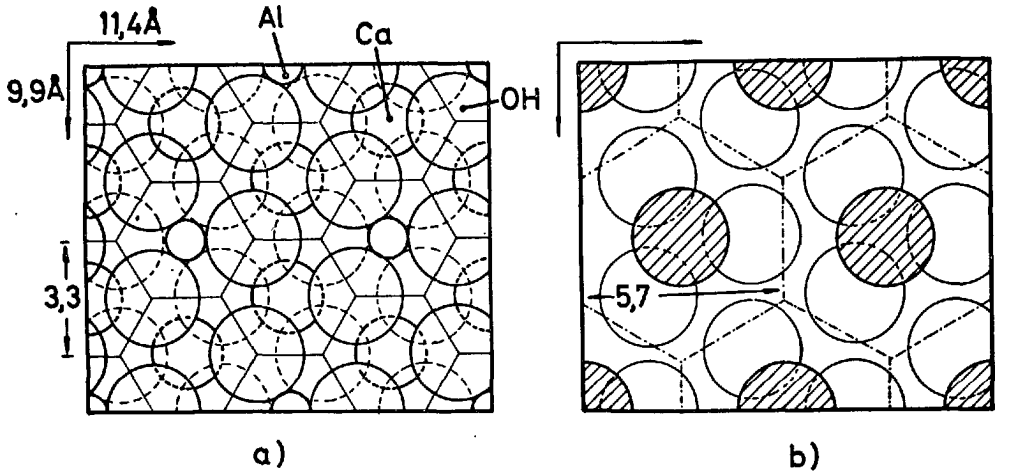

Fig. 4. *Structural element of* C_4AH_{19} *calculated by Buttler, Dent-Glaser and Taylor (in Dosch 1967)*
a) octahedra layer, b) "outer OH" (hatched) orded or statistically distributed on both sides of the octahedra layer

C_4AH_{19}

In 1957 Roberts (28) prepared and investigated C_4AH_{19}. In Table 4 the work that has so far been published on this compound is listed. It can be seen that one can distinguish between an α_1- and α_2-form of C_4AH_{19}. In his first experiments Roberts could only prove the existence of one form for which he assumed the existence of a solid solution series with C_2AH_8. Later Roberts and Jones (29) found that two tetracalcium aluminate hydrate phases exist. In 1960–1 Aruja (30) proved that the α_1 phase is trigonal and the α_2, hexagonal. In all investigations the basal interference of C_4AH_{19} was between 10.6 and 10.77 Å. Furthermore these papers have shown that the most hydrous forms of tetracalcium aluminate hydrate are stable only at a relative humidity of more than 88% at 25°C.

The unstable α_1 phase has a greater volume and a density of 1.79 g/cm³ in contrast to the stable α_2 phase with a density of 1.81 g/cm³.

In addition Aruja's work showed that a solid solution series with α_2–C_2AH_8 does not exist. This Roberts had previously assumed on the grounds of similar cell dimensions.

Analogous hydration products with 19 molecules of water, in which the aluminium oxide is wholly or partly replaced by iron oxide, have not yet been reported in the literature. It should be pointed out, however, that as early as 1883 Le Chatelier (31) found a tetracalcium aluminate hydrate with 21 molecules of water existing under humid conditions, which inverted to a 12-hydrate form at temperatures above 40°C. It is not impossible that this is the same hydrate phase which 75 years later was re-discovered.

Dehydration Products of C_4AH_{19}

Far more numerous are the authors (34-38) who, willingly or unwillingly, have found the dehydration products of C_4AH_{19} on their hands, as Table 5 shows. Here again we can recognize the existence of an α and a β phase, as in the case of C_4AH_{19}. But for C_4AH_{13} they can be distinguished on the grounds of their basal interference. Buttler, Dent Glasser and Taylor (25) proved in 1959 that the pseudo-cell of the β-modification contains only a single layer of octahedra with the composition $(Ca_2Al(OH)_6)OH$. Further structural determinations on the dehydration products of tetracalcium aluminate hydrate have not so far been published i.e. the arrangement of the structural elements in the true cell is not yet known.

At relative humidities between 84% and 12% only mixtures of α-and β–C_4AH_{13} were obtained. Dosch and zur Strassen (33) were able to show that at relative humidities of less than 80% only α–C_4AH_{13} is stable; at 22% humidity this reverts to β–C_4AH_{12}, at 11% to C_4AH_{11}, and at 8×10^{-5}% or by drying at 120°C, to C_4AH_7. Furthermore in 1962 Alégre (39) showed that the conversion to β–C_4AH_{13} is reversible. According to the latter investigations the α–C_4AH_{13} with a basal interference of 8.18 Å reverts in the presence of lithium chloride to β–C_4AH_{12} with a basal interference of 7.82 Å. With a saturated solution of calcium sulphate he managed to prepare α–C_4AH_{13} again. Thus Alégre's work showed for the first time, that β-tetracalcium aluminate hydrate contains one molecule of water less than its α-counterpart.

Table 4. *Investigations on* C_4AH_{19}

Hydrates	Basal interfer. [Å]	Preparation r.h./temperature [%] [°C]	Properties	Authors (date)
C_4AH_{21}	—	kept humid	> 40°C loss of $9H_2O \rightarrow$ 12-Hydrate	Le Chatelier(1883)
C_4AH_{19}	10.6	>88 / 25	d* = 1.79; solid solution C_2AH_8–C_4AH_{19}	Roberts(1957)
α_1-C_4AH_{19}	10.6	>88 / 25	—	Jones, Roberts(1962)
α_2-C_4AH_{19}	10.6	>88 / 25	d* = 1.81	Jones, Roberts(1962)
α_1-C_4AH_{19}	10.68	>88 / 25	d* = 1.79; trigonal a = 5.77 ± 0.01Å; c = 64.08 ± 0.1Å Z = 3; V = 18.46Å³	Aruja(1960/61)
α_2-C_4AH_{19}	10.68	>88 / 25	d = 1.81, hexagonal a = 5.77 ± 0.01Å; c = 21.37 ± 0.03Å Z = 1; V = 616.1Å³	
C_4AH_{19}	10.77	—/—	dehydration radiographically observed	Seligmann and Greening(1962)
	10.60	>88 / 25		zur Strassen and Dosch(1965)

*d in g/cm³

No difference between the α- and β-phases has so far been found on structural grounds. Various authors (33, 39) have shown that the β-phase has a lower water content of only 12 molecules of H_2O. Thus it appears that the phases contain different amounts of water.

Whereas the density of the α_1-phase of C_4AH_{19} is 1.79 g/cm³ and that of the α_2-phase is 1.81 g/cm³, the density for α- and β-C_4AH_{13} was determined as 2.02 g/cm³. As the water content falls to 11 and 7 molecules of water the density rises to 2.08 and 2.28 g/cm³ respectively. For comparison, the density of hydrocalumite, the naturally-occurring tetracalcium aluminate hydrate with 1.8% CO_2 and 11.6–11.8 molecules of water, is 2.12 g/cm³. Fig. 5 shows the mole ratio of H_2O to Al_2O_3 in C_4AH_{13} plotted against temperature. There figures were produced by Buttler, Dent Glasser and Taylor (25) using a thermal balance or by weighing after cooling. The results agree well with the data on the dehydration products of C_4AH_{19} shown in Table 5. In addition the authors showed that at temperatures above 600°C free CaO is split off $C_4A \cdot aq$ and that between 150° and 250°C a compound of the composition $C_4A_3H_3$ is formed.

Lavanant and Barret (40, 41) investigated the stability ranges of various tetracalcium aluminate hydrates and their P-T-diagram is seen in Fig. 6. It is obvious from this diagram that C_4AH_{12} has only a very narrow stability field which is the reason for the common occurrence of mixtures of hydrate phases with various water contents.

The adsorption of organic molecules by inorganic layer-lattice minerals has long been known, particularly for the clays, and has been described by numerous authors. Recently, in Germany, Weiss (43, 44), in particular, has investigated what can be taken up by these lattices and, in this connection, has examined more than 1000 organic compounds.

Nothing was previously known about the adsorption of organic compounds within the structures of the hydration products of cement, in spite of the fact

Table 5. *Tetracalcium aluminate hydrates of lower humidity*

Hydrates	Basal interfer. [Å]	Meth. of preparation r.h./temperature [%] [°C]	Properties	Authors (date)
C_4AH_{13}	—	—/—	$n_\omega = 1.532$; $n_\varepsilon = 1.505$; plates, spherulitic	Le Chatelier(1904), Lafuma(1925); L. S. Wells(1928)
$C_4AH_{13.5}$	—	—/—	$n_\omega = 1.538$; $n_\varepsilon = 1.510$; 2V = 14°, opt. negative	Assarson(1931)
C_4AH_x x = 13 x = 12	7.9	—/— above P_2O_5/~25	6 different methods of obtaining	Myllus(1933), Feitknecht(1942)
C_4AH_x x = 11.6 x = 11.8	—	—/<90–95	hydrocalumite; nat. mineral with 1.8%CO_2; hardness 3, density 2.15, monoclinic, pseudohexag, pseudocell: a = 9.6; b = 5.7; c·sin β = 7.86Å; space group C_{2h}^3–P2; or C_{2h}^3–$P2_1/m$	Tilley, Megaw and Hey(1934)
α- and β-C_4AH_{13}	8.2 and 7.92	1) 84-12/25 2) washing of C_4AH_{19} by alcohol or acetone	d = 2.02*; hexagonal a_0 = 5.74Å, c_0 = 8.2Å, a_0 = 5.74Å, c_0 = 7.92Å	Roberts(1957), Jones, Roberts(1962), Buttler, Dent Glasser and Taylor(1959)
α-C_4AH_{13}	8.2	<81/25		zur Strassen, Dosch(1965)
α- and β-C_4AH_{13}	(d = 8.18Å)α-C_4AH_{13} $\xrightarrow[\text{sat. } CaSO_4\text{-sol.}]{\text{above LiCl}}$ β-C_4AH_{12} (d = 7.82Å)			Alègre(1962)
$C_4AH_{13,12,11}$	—	between 1.75–15.8 torr and 13–50°C		Lavanant, Barret (1962)
α-C_4AH_{13} β-C_4AH_{13} C_4AH_{11}	8.28 8.01 7.40	by dehydration of C_4AH_{19}(d = 10.77Å)		Seligmann, Greening(1962)
β-C_4AH_{13}	7.763	—65/25	a_0 = 5.761Å, c_0 = 7.763Å	Schwiete and Iwai(1962)
	7.88	washed with alcohol/22°C dried above H_2SO_4		Schwiete, Ludwing and Jäger(1967)
C_4AH_{12}	7.8	22/25		zur Strassen and Dosch (1965)
C_4AH_{11}	7.4	11/25	d = 2.08*	Roberts(1957), zur Strassen, Dosch(1965)
C_4AH_7	7.4 7.7	8.10^{-5}/25° above P_2O_5 (or 120°C)	d = 2.28*	Roberts(1957) zur Strassen, Dosch(1965)

*[g/cms]

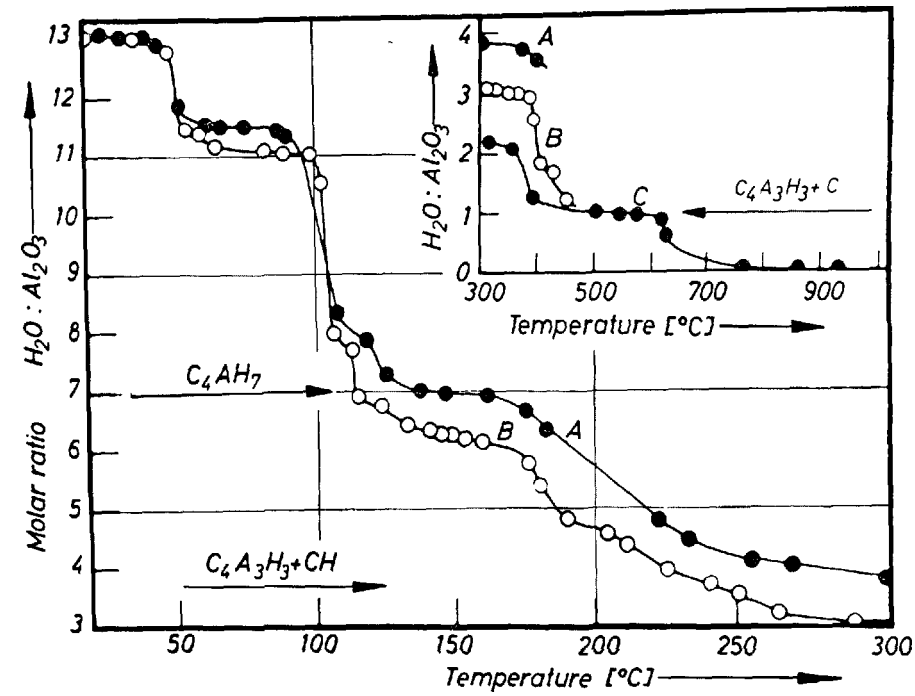

Curves A = direct determination by thermo-balance
Curves B and C = weighing after cooling

Fig. 5. *Dehydration of* C_4AH_{13} *(Buttler, Dent-Glasser and Taylor 1959)*

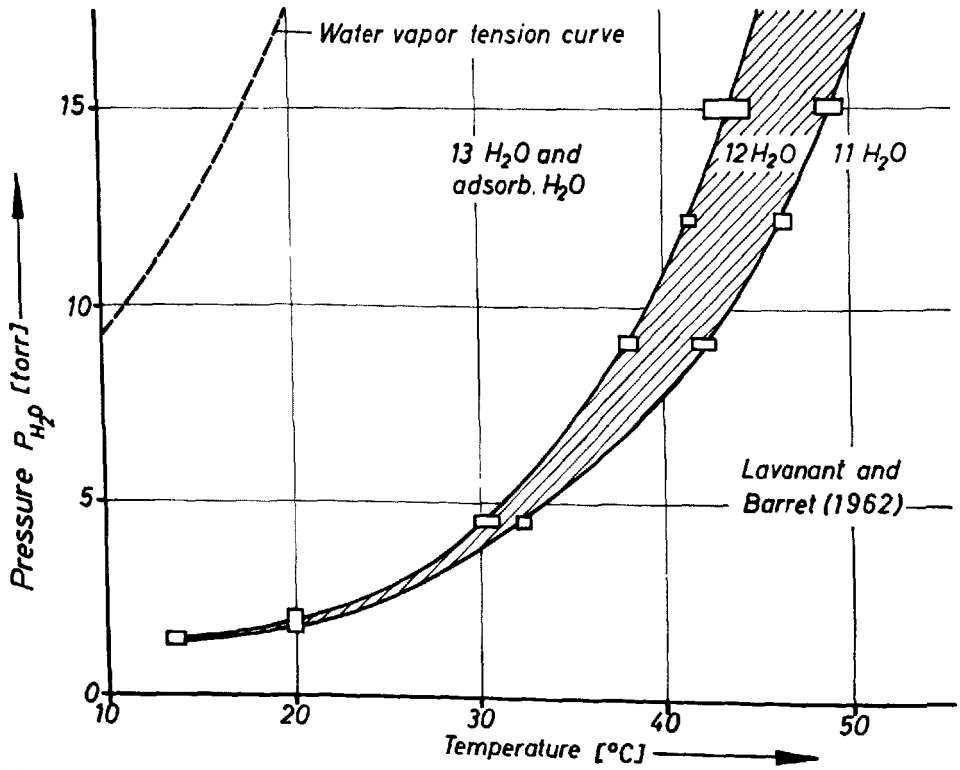

Fig. 6. *Content of hydrate water of tetracalcium aluminate hydrate in* p-T *diagram (Lavanant, Barret 1962)*

that numerous organic materials are added to cements in order to influence their properties. Recently Dosch (42) has reported the inclusion of organic molecules within tetracalcium aluminate hydrate, and more than 500 adsorption complexes have been prepared by this author.

In contrast to the clays, which are formed of layers of macro-ions held together by exchangeable ions of a different charge, tetracalcium aluminate hydrate is composed of neutral layers. The organic molecules are, in general, attracted by van der Waals forces or held by hydrogen bonds. In some cases they form covalent bonds with the inorganic host lattice.

Dosch has prepared and X-rayed complexes with the following organic compounds:

monovalent alcohols
multivalent alcohols, sugars and oxy-acids
mercaptane
amines
aldehydes
carbonic acids

He also succeeded in alkylising tetracalcium aluminate hydrate.

Primary alcohols have well-developed basal reflections which shift to smaller angles as the number of the carbon atoms increases (Fig. 7). As one ascends the alcohol series the speed of the adsorption reaction decreases. This is also true for the branched-chain alcohols. It is apparent form the X-ray data that the chains of alcohol in C_4AH_x are arranged perpendicular to the layers of the host mineral, whereas in montmorillonite an arrangement parallel to them is favoured by the energy requirements.

Multivalent alcohols, sugars, oxy-acids, mercaptane and amines are included in a similar fashion; both the perpendicular and the parallel type of arrangement is found. Aldehydes and carbonic acids react with C_4AH_x showing strong thermal effects. The underlying chemical reaction is not yet completely clear in the case of aldehydes. The carbonic acids presumably react to form esters with the basic (OH)-groups of the C_4AH_x lattice.

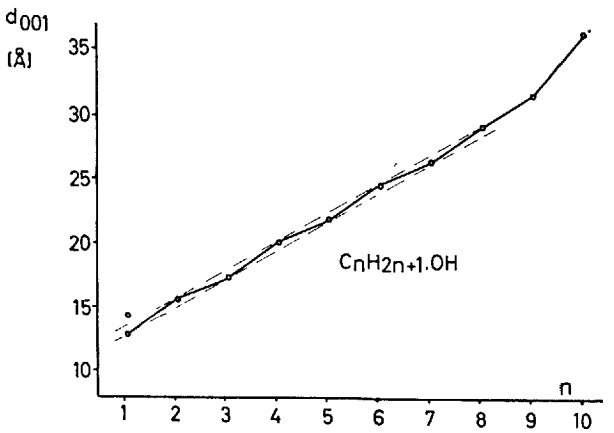

Fig. 7. C_4AH_x *adsorption complexes of* n*—alcohols (Dosch 1967)*

By means of dynamic differential calorimetry the amount of water in the hydrates and how strongly it is bonded can be determined (20, 42). Our own investigations (14) in connection with tetracalcium aluminate hydrates show four pronounced endothermal reactions (Fig. 1). The first minimum occurs at 75°C, the second at 170°C, the third at 300°C and the fourth at 500°C. The first two minima are caused by the splitting-off of water; the third is due to the release of lime and the formation of $C_{12}A_7$. The fourth minimum occurs when the liberated calcium hydroxide is finally dehydrated (14).

Our investigation shows that at about 300°C a splitting-off of $Ca(OH)_2$ with the formation of $C_{12}A_7$.* The dehydration curves of Taylor also do not show to the same extent the dehydration of calcium hydroxide at about 500°C. In Taylor's investigations there is a strong thermal effect above 600°C which does not appear in our diagram.

Bereczky (16) measured the pH value of a suspension of $C_4A \cdot aq$ in water as 12.36. The values of our own measurements (14) lie between 12.7 and 12.8. With the ester of acetic acid we dissolved 26.1 % of CaO from C_4AH_{13}. This is 65 % of the total lime content. An amount of lime remains which is roughly that stoichiometrically necessary for the formation of $C_4A_3H_3$ (14). Fig. 8 shows, amongst other things, the I-R diagram for C_4AH_{13}. Besides the characteristic vibrations for this compound at 7 μm, there is one for CO_3^{--}. This is due to the preparation of the sample with KBr and does not occur if paraffin oil is used.

$C_4F \cdot aq$ and $C_4(A, F) \cdot aq$

The corresponding tetracalcium ferrite hydrate was prepared for the first time in 1851 by Pelouze (46) in the form of white hexagonal plates and later on this was repeated by Le Chatelier (31), Hoffmann (47) and Malquori and Cirilli (Table 6). Malquori and Cirilli established, as Feitknecht (38) and Schwiete and Iwai (45) have also done, that a solid solution $C_4F_xA_{1-x}H_{13}$ $(0 \leq x \leq 1)$ exists. In 1966 Carlson (48) confirmed the earlier results of Schwiete and Iwai that at less than 16°C hexagonal tetracalcium alumi-

*takes place while Buttler, Dent-Glasser and Taylor (25) in 1959 found a formation of $C_4A_3H_3$ in this range of temperature.

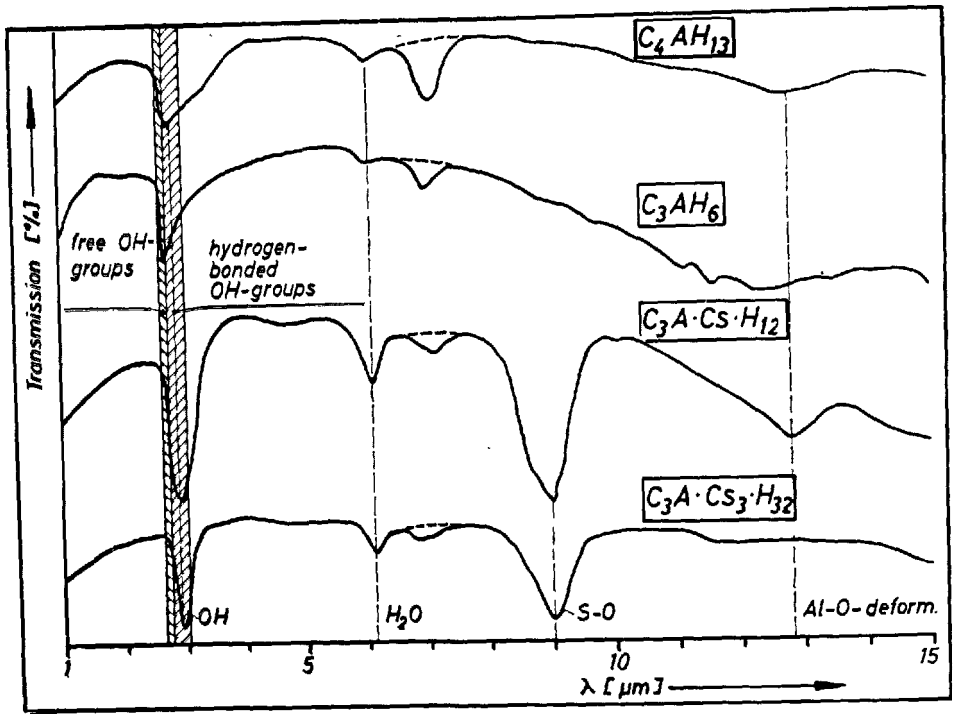

Fig. 8. *Infrared-spectroscopic investigations on calcium aluminate hydrates (Schwiete, Ludwig, Jäger 1967)*

Table 6. *Investigations on tetracalcium aluminate ferrite hydrates*

Hydrates	Basal interfer. [Å]	Meth. of preparation r.h./temperature [%] [°C]	Properties	Authors(date)
C_4FH_x	—	—/room temp.	white hexagonal plates prep. from $Fe(OH)_3 + Ca(OH)_2 + H_2O$	Pélouze(1851) Le Chatelier(1884)
C_4FH_{14}	—	—/20	prep. from $C_2F + CH + H_2O$	Hoffmann(1935)
C_4FH_7	—	—/50	obtained from $C_2F + CH + H_2O$	Hoffmann(1935)
		—/60	from dehydration	Malquori, Cirilli(1943)
C_4AH_{13}	7.9	above $CaCl_2$ /room temp. in vacuum/ //	solid solution observed $a_0 = 3.36$Å; $c_0 = 7.9$Å	Feitknecht(1942)
C_4FH_{14}	8.0		$a_0 = 3.42$Å; $c_0 = 8.0$Å	Feitknecht(1942)
$C_4A_xF_{1-x}H_{14}$	—	—/0	form. of solid solution(hexag.)	Malquori, Cirilli(1943 and 1952)
$C_3A_xF_{1-x}H_6$	—	—/25	form. of solid solution(cubic)	Malquori, Cirilli(1943 and 1952)
β-C_4AH_{13}	7.763	—65/25	$a_0 = 5.761$; $c_0 = 7.768$Å	Schwiete, Iwai(1962)
$C_4(A, F)H_{13}$	7.831		$a_0 = 5.829$; $c_0 = 7.881$Å	
C_4FH_{13}	7.902		$a_0 = 5.897$; $c_0 = 7.702$Å complete solution confirmed	
β-C_4AH_{13}	8.00	—79(above NH_4Cl-sol.)/15–35		Carlson(1966)
$C_4(A, F)H_{13}$	8.05–7.81			
C_4FH_{13}	7.80			

nate ferrite hydrate is formed and that above 35°C cubic tricalcium aluminate ferrite hydrate occurs, whilst between 15° and 25°C a mixture of the two hydrates can be observed. According to Feitknecht (38) and Schwiete and Iwai (45) the basal interference of the iron-bearing hydrate is higher than that of the aluminium phase, although Carlson (48) finds it to be lower.

Schwiete and Iwai (45) produced C_4AH_{13}, the mixed crystal $C_4A_{0.5}F_{0.5}H_{13}$ and C_4AH_{13} by precipitation from calcium hydroxide and iron- or aluminium chloride solutions. They calculated the lattice constants from the interferences of the lattice planes (002), (110) and (112). These values are listed in Fig. 9 and it is

apparent that the a_0 value rises from 5.76 Å for C_4AH_{13} to 5.90 Å for C_4FH_{13}, whilst the c_0 values go from 7.76 to 7.90 Å. The pH value of a suspension of C_4Faq was determined by Bereczky (16) as 12.16 to 12.36.

$C_3A(CaCO_3, Ca(OH)_2)aq$

In the older literature a series of tricalcium aluminate hydrates are described which today are identified as carboaluminate hydrates. Because of this it is necessary to deal with the carboaluminate hydrates in detail. Table 7 shows the present state of knowledge. It is apparent that one can distinguish between the so-called "quarter-carbonate" the semi-carbonate and the mono-carbonate. In addition a compound is known which corresponds to ettringite but which contains $3CaCO_3$ instead of $3CaSO_4$. The latter compound was first found by Flint and Wells (49) in 1941 and later its existence was confirmed by Carlson and Berman (50) in 1960. It crystallizes in needles, as ettringite does. The carboaluminate hydrate with 1/4–1 molecules of $CaCO_3$, however, forms hexagonal plates.

By comparing the basal interferences of the tetracalcium aluminate hydrates with those of the carboaluminate hydrates one finds that it is possible to distinguish the members of the two groups by the position of the basal interference of their dehydration products, as zur Strassen and Dosch (33) have illustrated (Fig. 10). With respect to the stability of the semi-carbonate it should be pointed out that the hydrate first described by Seligmann and Greening (32) has not been confirmed by zur Strassen and Dosch (33). As dehydration product a compound with 9 molecules of

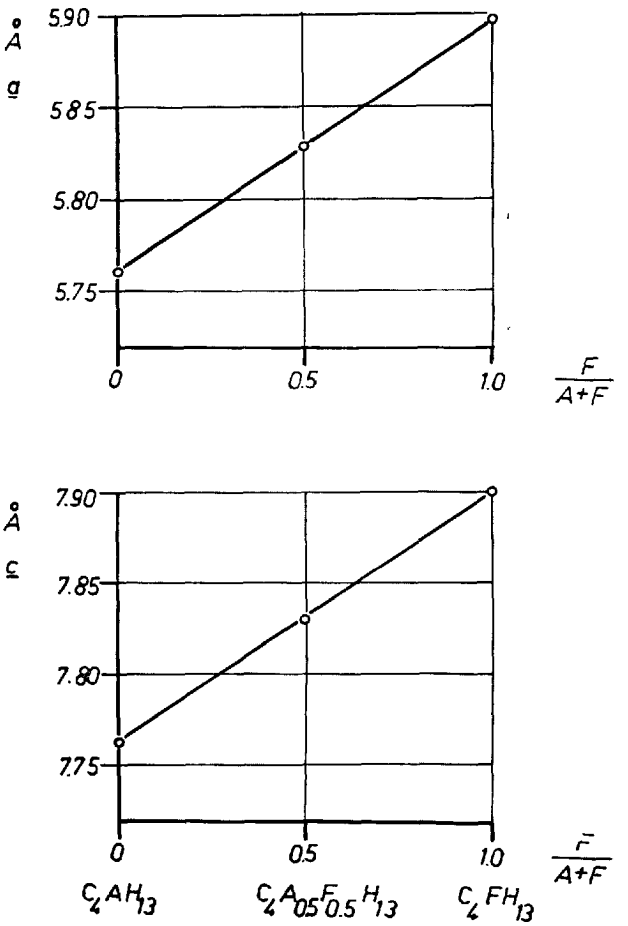

Fig. 9. *Lattice constances of hexagonal hydrates in the system* C_4AH_{13}–C_4FH_{13} *(Schwiete, Iwai 1964)*

Table 7. *Investigations on carboaluminate hydrates*

Hydrates	Basal interfer. [Å]	Preparation r.h./temp. [%] [°C]	Properties	Authors (date)
"Quarter carbonate" $C_3A \cdot 3/4CaO \cdot 1/4CaCO_3 \cdot H_{11-12}$	8.2	81/25	differs from α-C_4AH_{13}(d = 8.2Å by dehydration prod.	zur Strassen and Dosch(1965)
$C_3A \cdot 3/4CaO \cdot 1/4CaCO_3 \cdot H_9$	7.7	11/25	dehydr. prod. with $9H_2O$	
"Half carbonate" $C_3A \cdot 1/2CaO \cdot 1/2CaCO_3 \cdot H_x$	8.11–8.42	>11/25	by zur Strassen and Dosch(1965) not confirmed	Seligmann and Greening(1965)
"Monocarbonate" $C_3A \cdot CaCO_3 \cdot H_{10-11}$	7.6 7.56 7.62	33/—20 $8 \cdot 10^{-5}$/—	hexagonal plates $n_\omega = 1.552$, $n_\varepsilon = 1.532$	Turriziani and Schippa(1956) Carlson and Berman(1960) Bessey(1938) Seligmann and Greening (1962) and (1964) zur Strassen and Dosch(1965)
$C_3A \cdot CaCO_3 \cdot H_6$	6.3 7.15	—/150 —/120	dehydr. prod. with $6H_2O$	Turriziani and Schippa(1956) zur Strassen and Dosch(1965)
$C_3A \cdot 3CaCO_3 \cdot H_{32}$	9.41	79/—20	needles; dried above $Mg(ClO_4)_2$ loss of $3H_2O$	Flint and Wells(1941) Carlson and Berman(1960)

water was observed in the case of the quarter-carbonate and one with 6 molecules of water in the case of the mono-carbonate. In the former instance the basal interference decreased from 8.2 to 7.7 Å; in the latter case, the drying temperature is 150°C according to the work of Turriziani and Schippa (51) and 120°C according to zur Strassen and Dosch (33).

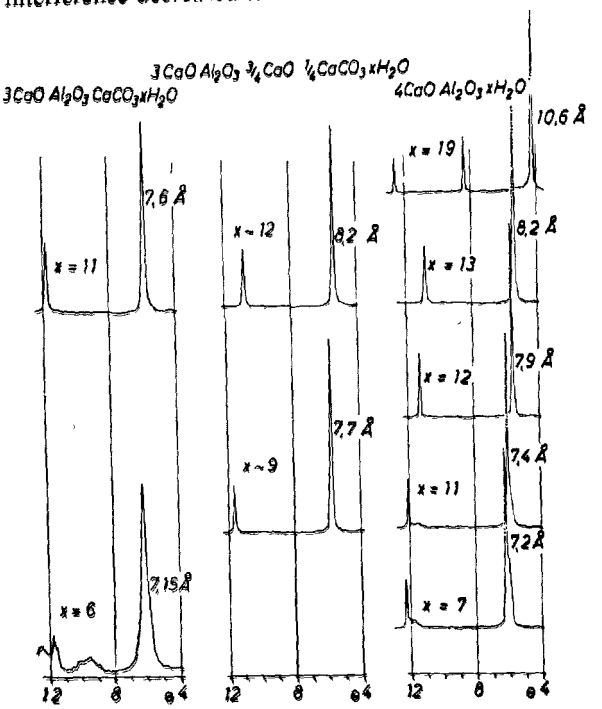

Fig. 10. *Dehydration products of calcium aluminate hydrates with and without* $CaCO_3$ (*Dosch, zur Strassen 1965*)

Spohn and Lieber found out, that test specimens of C_3A or C_4AF or portland cement with $CaCO_3$ attain higher strengths than specimens without carbonate admixture. They detected the formation of $C_3A \cdot CaCO_3 \cdot H_{10}$ formed in aqueous suspensions or in pastes.

$C_3ACs \cdot aq$

Table 8 lists the work on the calcium aluminate monosulphate hydrates. According to Turriziani and Schippa (53) the compound richest in water crystallizes with 16 molecules H_2O and is only stable at a relative humidity of more than 90 % at 20°C.

The latest structural determination on monosulphate hydrate was carried out by Kuzel (27) in 1965 and yielded the lattice constants $c_0 = 26.79$ Å and $a_0 = 5.76$ Å; the symmetry is probably trigonal. He determined the density as 1.90 g/cm³. The dehydration products have mostly been investigated by Turriziani and Schippa (53) who found a least hydrous compound with 7 molecules of water which was obtained at 110°C A number of workers have observed the formation of a solid solution between monosulphate hydrate and C_4AH_{13}. This was first recorded by Kalousek (55)

Table 8. *Investigations on monosulfate hydrates*

Hydrates	Basal interfer. [Å]	Preparat. r.h./temp. [%] [°C]	Properties	Authors (date)
$C_3A \cdot Cs \cdot H_{18}$	9.59	>90/20		Turriziani and Schippa(1955)
$C_3A \cdot Cs \cdot H_{12}$	—	washed with alcohol/20	$n_{\omega} = 1.504$, $n_{\varepsilon} = 1.488$ $d = 1.95 g/cm^3$	Lerch, Ashton, Bogue (1929) Mylius(1933)
$C_3A \cdot Cs \cdot H_X$ $x = 12$ $x = 8$ $x = 7$ $x = 6$ $x = 3$	—	—/< 185 —/< 200 —/< 225 —/< 325 —/ab 325	dehydration products	Malquori and Cirilli(1940)
$C_3A \cdot Cs \cdot H_{12}$	8.99	>35/20	c = 9.01Å a = 8.85Å a = 5.75Å	Turriziani, Schippa, Fratini(1955) Roberts(1960)
$C_3A \cdot Cs \cdot H_y$	10.39	>94/1		
$C_3A \cdot Cs \cdot H_y$ and $\cdot H_{12}$	8.99 u. 10.3	—/12–17		
$C_3A \cdot Cs \cdot H_{10}$	8.26	0.2torr/20	dehydration products	Turriziani and Schippa(1955) Schippa(1958)
$C_3A \cdot Cs \cdot H_8$	8.05	above P_2O_5/—		
$C_3A \cdot Cs \cdot H_7$	—	—/110		
$C_3A \cdot Cs \cdot H_{10-12}$	8.93	30–50/—25	$c_0 = 26.79 \pm 0.03$Å; $a_0 = 5.76 \pm 0.02$Å $d = 1.99 g/cm^3$; $V = 7.69$Å³	Kuzel(1965)
$C_3A \cdot Cs_X \cdot CH_{1-X} \cdot H_{12}$	7.92–8.93	—/—	mixed crystals with C_4AH_{13}	Kalousek(1941), Kuzel(1965)
	—	—/20	$(0 \leq X \leq 1)$, optically determined	D'Ans and Eick(1953)
	7.9; 8.2–8.9	alcohol/22	$(-0.4 \leq X \leq 1)$, radiogr. determined	Schwiete, Ludwig, Jäger(1963 and 67)
by $x = 1$ and 14–15 H_2O	8.75–9.02	—/—	$(0.6 \leq X \leq 1)$, radiogr. determined	Seligmann and Greening(1964)

in 1941 and according to D'Ans and Eick (56) the solid solution is complete. Our investigations (14), which agree with those of Seligmann and Greening (57), show a miscibility gap at the sulphate-poor end of the series. Fig. 1 shows the differential calorimetric investigations on pure C_3ACsH_{12}. Several endothermal reactions are recognizable in the range 50°–300°C. The strongest of these occurs at about 200°C.

We determined the pH value of C_3ACsH_{12} to be 12–12.1 (14). No CaO was dissolved out after boiling for one hour in ester of acetic acid.

Dosch and zur Strassen (57a) found a hitherto unknown hexagonal or pseudo-hexagonal sodium-bearing hydrate whose approximate composition is $4CaO \cdot 0.9Al_2O_3 \cdot 1.1SO_3 \cdot 0.5Na_2O 16H_2O$; the alkali content in particular is variable. Table 9 lists the basal interference and the water content in relation to relative humidity.

Fig. 11 shows a completely indexed X-ray photograph. Whereas the *c*-axis shrinks on drying, the *a*-axis remains constant at 5.75 Å which permits this hydrate to be grouped in the same family to which monosulphate hydrate and tetracalcium aluminate hydrate also belong. The authors presume that the new hydrate can be derived from monosulphate hydrate by the loss of Al^{3+} from the basal layer, which thus acquires a negative charge. The intermediate layer contains water of crystallization, sodium sulphate and Na^+ ions to balance the charges.

Table 9. *Range of Hydration of the* $4CaO \cdot 0.9Al_2O_3 \cdot 1.1SO_3 \cdot 0.5Na_2O \cdot 16H_2O$ *(Dosch and zur Strassen)*

rel. humidity	$H_2O/4CaO$	d_{001} (Å)
95	16	10.0
50	16	10.0
10	12	9.3
10–1	12	9.3
10–2	8	8.1
10–4	8	8.1

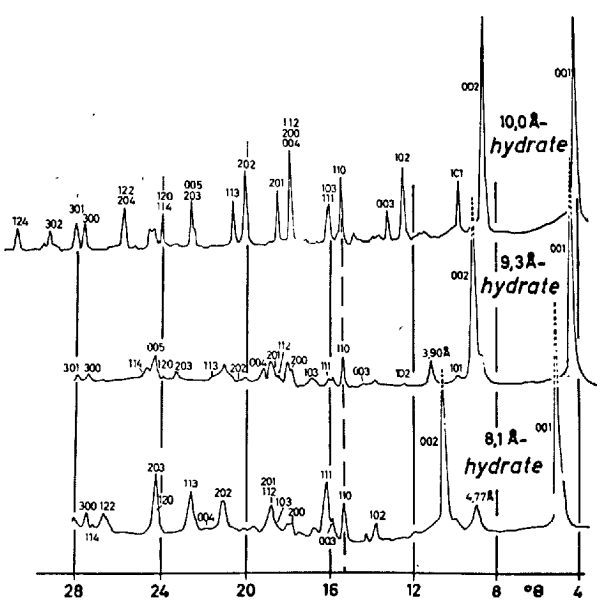

Fig. 11. *Hydrates of phase "U_s" (Dosch, zur Strassen 1967)*

The new hydrate was prepared both from monosulphate hydrate and trisulphate hydrate in the presence of an equilibrium solution of alkali aluminate, alkali sulphate and caustic soda. The content of caustic soda, aluminate and sulphate ions in the solution must be sufficiently high.

$C_3(A, F)Cs$ aq

In the monosulphate hydrates the aluminium can be completely replaced by iron. Malquori and Caruso (18) in 1938 were the first to observe C_3FCsH_x (Table 10). Together with Cirilli, Malquori (9) investigated the dehydration products of C_3FCsH_{10} and found hydrates with 10, 8, 6 and 4–5 molecules of water. Schippa (58) investigated the monosulphates and observed a water-rich iron monosulphate with 13–14 molecules of water and a basal interference of 10.45 Å. According to him the hydrate with 11–12 molecules of water has a basal interference of 8.98 Å. In addition he determined the lattice constants a_o and c_o and indicated the possibility of a solid solution between C_3FCsH_x and C_3ACsH_x.

Our experiments (14) also show a solid solution between iron and aluminium sulphate hydrates. Our starting materials were C_2F, C_4AF and C_6A_2F. Recently we have observed the formation of a solid solution in which not only is aluminium replaced by iron but also calcium sulphate by calcium hydroxide. In connection with C_2F we found only a pure monosulphate hydrate and no further solid solubility with tetracalcium ferrite hydrate. For C_4AF and C_6A_2F there are only solid solutions in the range of more than 0.4 mole calcium sulphate, i.e. as in the case of tricalcium monosulphate hydrate there is no solid solution with the corresponding tetracalcium aluminate ferrite hydrate in the calcium sulphate-poor region. A clear presentation of our values is given in Fig. 12.

$C_3(A, F)(CaSO_4, CaCl_2, Ca(OH_2))aq$

Since the description by Friedel (59) of a hydrate with composition $3CaO \cdot Al_2O_3 \cdot CaCl_2 \cdot 10H_2O$ (later known as Friedel Salts) and by Malquori and Caruso (18), Turriziani and Schippa (62), Mylius (37), Lafuma

Table 10. *Investigations on tricalcium ferrite monosulphate hydrate* ($C_3F \cdot Cs \cdot H_x$)

Hydrates	Basal interter. [Å]	Preparat. r.h./temp. [%] [°C]	Properties	Authors (date)
$C_3F\ Cs\ H_x$	—	—/—	—	Malquori, Caruso(1938), Hedin(1945)
$C_3F\ Cs\ H_{12}$	—	—/< 120	Dehydration products	Malquori, Cirilli(1940)
$C_3F\ Cs\ H_{10}$	—	—/< 160		
$C_3F\ Cs\ H_8$	—	—/< 195		
$C_3F\ Cs\ H_6$	—	—/< 325		
$C_3F\ Cs\ H_3$	—	—/< 325		
$C_3F\ Cs\ H_{13-14}$	10.45	> 94/18	$a_0 = 8.80 \pm 0.02$Å, $c_0 = 10.40 \pm 0.02$Å	Schippa(1958)
$C_3F\ Cs\ H_{11-12}$	8.98	55/—20	$a_0 = 8.80 \pm 0.02$Å, $c_0 = 8.98 \pm 0.02$Å; Mixed crystals with $C_3A \cdot Cs \cdot H_{12}$ possible	
$C_3F_xA_{1-x}CsH_{12}$	8.98 8.84 8.84	alcohol/22	Mixed crystals with $C_3A \cdot Cs \cdot H_{12}$: x = 1.0; from C_2F x = 0.5; from C_4AF x = 0.33; from C_6A_2F	Schwiete, Ludwig Jäger(1967)
$C_3F_xA_{1-x}$ $Cs_y(CH)_{1-y}H_{12}$	8.98 8.30 8.30–8.84		Mixed crystals with $C_4(A, F)H_{13}$ x = 1.0; from C_2F: y *only 1* x = 0.5 and 0.33 from $C_4AFa \cdot C_6A_2F$: y—0.5 x = 0.5 and 0.33 from $C_4AFa \cdot C_6A_2F$: $0.4 \leq y \leq 1$	

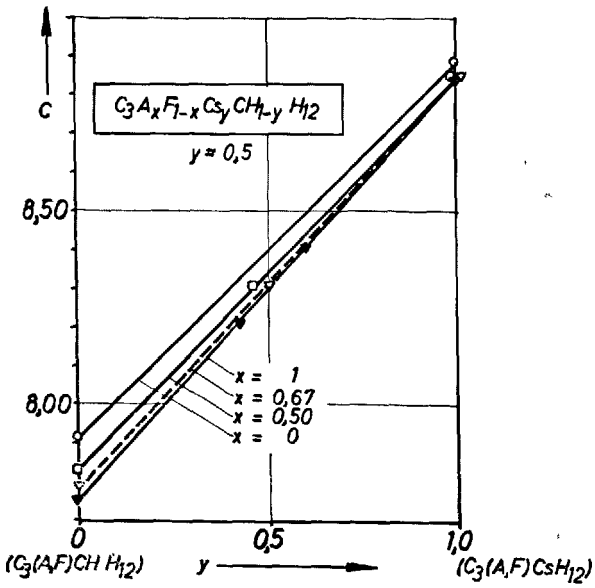

C = 1/3 of the lattice constants in c-axis direction

Fig. 12. *Formation of* $C_3(A, F)(Cs, CH)H_{12}$ *in hydration experiments with* C_3A, C_6A_2F, C_4AF *or* C_2F *(Schwiete, Ludwig, Jäger 1967)*

(34) and others of the corresponding compound $3CaO \cdot Fe_2O_3 \cdot CaCl_2 \cdot 10H_2O$, various authors have dealt with the effect of calcium chloride on the clinker minerals during the hydration of cement. The work of Wells (35), Lieber and Bleher (66), Roberts (67), Rosenberg (68) and the new investigations of Tenoutasse (69) are noteworthy (Table 11).

In recent hydrothermal experiments Kuzel (64) could prove that there were two polymorphs of $3CaO \cdot Al_2O_3 \cdot CaCl_2 \cdot 10H_2O$ whose inversion point was found by DTA to be $28° \pm 2°C$. By reactions at normal temperature we (65) only found out the β–$C_3A \cdot CaCl_2 \cdot H_{10}$.

Single crystal X-ray photographs of the monoclinic α-phase, stable at lower temperatures, indicate a monoclinic cell with $a_o = 9.98 \pm 0.04$ Å, $b_o = 5.74 \pm 0.02$ Å, $c_0 = 16.79 \pm 0.04$ Å and $\beta = 110.2°$. The space group is C2/c or Cc. The unit cell of α–$C_3A \cdot CaCl_2 \cdot H_{10}$ probably contains two identical layers of the composition $Ca_4Al_2(OH)_{12} \cdot Cl_2 \cdot 4H_2O$. The density determined with the pycnometer shows that that of the α-form is 2.03 g/cm³.

The trigonal modification has a unit cell in which $a_o = 5.74 \pm 0.02$ Å and $c_o = 46.88 \pm 0.08$ Å. Assuming the same density of 2.03 g/cm³ the unit cell contains 2.9 units of formula and is composed of six layers with the composition $Ca_2Al(OH)_6 \cdot Cl \cdot 2H_2O$.

Kuzel (64) could not find a solid solution between α- or β–$3CaO \cdot Al_2O_3 \cdot CaCl_2 \cdot 10H_2O$ and $3CaO \cdot Al_2O_3 \cdot CaSO_4 \cdot 12H_2O$. However he found a new compound of the composition $6CaO \cdot 2Al_2O_3 \cdot CaSO_4 \cdot CaCl_2 \cdot 24H_2O$ with a trigonal unit cell having the lattice constants $a_0 = 5.74 \pm 0.02$ Å, $c_0 = 100.6 \pm 0.2$ Å and a space group R3c or $R\bar{3}c$. The density of this hydrate is 2.2 g/cm³. Its pseudo-cell with c = 16.76 Å is about twice as large as those of C_3ACsH_{12} and $C_3A \cdot CaCl_2 \cdot H_2O$. Kuzel assumed double layers of the composition $Ca_4Al_2(OH)_{12} \cdot Cl \cdot 1/2\ SO_4 \cdot 6H_2O$ in which SO_4^{--} and Cl^- ions alternate in planes parallel

Table 11. *Investigation on Friedel—salt*

Hydrates	Basal interf. [Å]	Preparation	Properties	Authors(date)
$3CaO \cdot Al_2O_3 \cdot CaCl_2 \cdot 10H_2O$	—	hydrothermal at 400–500°C	$D_{14°C} = 1.8929$ g/cm³	Friedel(1897)
$3CaO \cdot Al_2O_3 \cdot CaCl_2 \cdot 18H_2O$	—	—	—	Lafuma(1925)
$3CaO \cdot Al_2O_3 \cdot CaCl_2 \cdot 10H_2O$	—	at 20°C dried by alcohol and ether above water free $CaCl_2$ pH > 10.9	$n_\omega = 1.550 \pm 0.003$ $n_\varepsilon = 1.533 \pm 0.003$	Wells(1928)
$3CaO \cdot Al_2O_3 \cdot CaCl_2 \cdot 10H_2O$	—	washed with H_2O and dried above water free $CaCl_2$	$n_\omega = 1.552 \pm 0.003$ $n_\varepsilon = 1535 \pm 0.003$	Mylius(1933) Forsén(1935)
$3CaO \cdot Al_2O_3 \cdot CaCl_2 \cdot 10H_2O$	7.90	—	—	Bunn, Clark(1938)
$C_3A \cdot CaCl_2 \cdot H_{10}$ $C_3F \cdot CaCl_2 \cdot H_{11}$	—	from solutions	dehydration and X-ray(Debey)	Malquori and Caruso(1938)
$3CaO \cdot Al_2O_3 \cdot CaCl_2 \cdot 10H_2O$	7.94	at 17–18°C dried above waterfree $CaCl_2$	formation of solid solution with $3CaO \cdot Al_2O_3 \cdot Ca(OH)_2 \cdot 12H_2O$	Turriziani, Schippa (1955/1956)
α-$3CaO \cdot Al_2O_3 \cdot CaCl_2 \cdot 10H_2O$	7.89	hydrothermal at 150°C, washed with methanol and dried at 35% r.h.	reversible conversion at 28°C ± 2°C in β-$3CaO \cdot Al_2O_3 \cdot CaCl_2 \cdot 10H_2O$ $a_0 = 5.74 \pm 0.02$Å $c_0 = 16.79 \pm 0.04$Å $\beta = 110.2°$ space group $C2_{/c}$ or C_c unit cell corresponding to pseudo-cell of hydrocalumite D = 2.03 g/cm³	Kuzel(1966)
β-$3CaO \cdot Al_2O_3 \cdot CaCl_2 \cdot 10H_2O$	7.81	at 35°C from α-$3CaO \cdot Al_2O_2 \cdot CaCl_2 \cdot 10H_2O$	$a_0 = 5.74 \pm 0.02$Å $c_0 = 46.88 \pm 0.08$Å No solid solution between α- or β-monocloride and $3CaO \cdot Al_2O_3 \cdot CaSO_4 \cdot 12H_2O$ observed. New compound $6CaO \cdot 2Al_2O_3 \cdot CaSO_4 \cdot CaCl_2 \cdot 24H_2O$	Kuzel(1966)
$3CaO \cdot Al_2O_3 \cdot 0.9CaCl_2 \cdot 10H_2O$	7.86	at 20°C 1 hour drying with isopropyl alcohol over H_2SO_4	only 1 modification observed	Schwiete, Ludwig, Albeck(1967)

to (0001).

The investigations of Turriziani and Schippa (62) in 1955 showed a complete miscibility between the compounds $3CaO \cdot Al_2O_3 \cdot Ca(OH)_2 \cdot 12H_2O$ and $3CaO \cdot Al_2O_3 \cdot CaCl_2 \cdot 10H_2O$.

Furthermore we (22) succeeded in preparing at ordinary temperatures as well as Kuzel at hydrothermal conditions an AFm-phase with CaS, which is of great importance in case of the slag bearing cements.

Hexagonal Hydrates with a Low $Ca(OH)_2$ Content

The following hydrates also have a layer structure but in contrast to the previous ones they occur only in high aluminate cements or occasionally in blast furnace cements rich in slag.

C_2Aaq

It can be seen from Table 12 that Allen and Roger (70) in the year 1900 were the first to prepare and investigate dicalcium aluminate hydrate. This compound crystallizes as hexagonal plates. Schwiete, Büssem and Salmoni (71) were able to isolate a series of dicalcium aluminate hydrates with variable water contents. The maximum water content was 13 molecules; at 300°C all the water was driven off. Roberts and Jones (29) distinguished an α_1, and α_2 and a β–C_2AH_8. The α_2-form is metastable relative to the α_1-form. Lavanant proved that the dehydration of C_2AH_8 to C_2AH_6 is a reversible reaction. The basal interference of α_2- and β–C_2AH_8 lies between 10.5 and 10.8 Å. By means of diboranhydrolysis he could distinguish how the water is bonded in the dicalcium aluminate hydrates. Whereas he found only hydroxyl groups in the hydrates with 5 molecules of water, in those richer in water he found, in addition, molecular and zeolitic water.

Lavanant (41) represented the water content of the dicalcium aluminate hydrates in a P-T-diagram (Fig. 13). One can see on the graph the equilibrium curves for C_2AH_5, C_2AH_6 and finally for C_2AH_9, which

Table 12. *Investigations on dicalcium aluminate hydrates*

Hydrates	Basal interfer. [Å]	Preparation r.h./temperature [%] [°C]	Properties	Authors(date)
C_2AH_7 and $C_2AH_{5.63}$	—	—/—	hexagonal plates	Allen and Rogers(1900)
$C_2AH_{8.6-9.1}$	—	—/—	spherulit hexagonal plates	Assarson(1931)
$C_2AH_{6.8-7.3}$	—	—/<50°	$n_\omega = 1.522$; $n_\varepsilon = 1.502$	Mylius(1933)
C_2AH_x, x = 13	—	—/—	confirmed by Henning(1966)	Schwiete, Büssem, Salmoni(1933)
x = 9	—	—/—	similar X-ray interferences, D = 1.959g/cm³	
x = 7	—	above $CaCl_2$/—20°		
x = 5	—	at 105°C, above P_4O_{10},	obtained in boiling water	
x = 3	—	—/<150°	give similar X-ray interferences	
x = 1	—	—/<400°		
x = 0	—	—/<400°		
C_2AH_x, x = 8.3	—	13.5 torr/17°	$n_\omega = 1.520$ $n\varepsilon = 1.505$	Lea and Bessey(1937)
x = 7.6	—	2.8 torr/17°	$n_\omega = 1.521$ $n\varepsilon = 1.512$	
C_2AH_x, x = 7.3, x = 8, x = 9	—	—/< 50°		Lafuma(1925), Lefol(1933)
x = 6.5, x = 5	—	—/<100°		Mylius(1933), Nacken(1936)
x = 4.9	—	—/<105°		Lea and Bessey (1937)
x = 5, x = 4	—	—/<150°		Lea and Jones (1938)
α_1-C_2AH_8	—	—/—	from C_4AH_{19} by substitution of 3H by $3AH_3$ hexag.; $a_0 = 9.65$, $b_0 = 11.6$, $c_0 = 24.1$Å $\beta = 64°$; V = 24.20Å³; Z = 8	Roberts(1957); Roberts, Jones(1962)
α_2-C_2AH_8 and β-C_2AH_8	10.5–10.7	100/—	instable relative to α_1-C_2AH_8	
C_2AH_6	8.8	—/—	C_2AH_8 can be stabilized by $CaHPO_4$ C_2AH_6 is formed in the presence of colloidal SiO_2	Carlson(1958), Crowley(1964)
—	—	<50k bar/200–800°	C_2AH_x is not formed	Pistorius(1962)
C_2AH_8	—	—/—	can be prepared with $C_{12}A_7$,CA,CA_2 and H_2O	Lehmann, Leers(1963)
C_2AH_x, x = 9, x = 8	10.5–10.7	4–21 torr/25°	$\Delta S_{298°} = 2 \times 35$ cal/°mole ± 10; determination of type boncing of H_2O and OH using Diborn-hydrolysis	Lavanant(1955)
x = 6, x = 5	8.5	<4 torr/25°		
C_2AH_x, x = 13	8.84	above $CaCl_2$/<5°	from C_2A^- and H_2O at 0–5°C	Henning(1966)
x = 9	—	above C_2H_5OH/20°	from CA and H_2O at 0°C	
—	—	—/—	8-7-and 3-hydrates not observed	
x = 5		from a) C_2AH_9 after 24h standing with C_2H_5OH b) 13 hydrate dried above P_2O_5 in vacuum		
x = 2	—	—/—250°	from 5 hydrate after 24h	
x = 1	—	—/—350°		
C_2AH_x	—	—/—	infrared absorption wave numbers	

practically coincide with the curve for water vapour.

There are numerous other hydrates which have been reported by Schwiete, Büssem and Salmoni (71) and more recently by Henning (80) but their significance in terms of energy has not yet been investigated. Chatterji and Majumdar (84) found by means of X-ray studies hexagonal hydrates with the composition C_2FH_y and a = 10.8 Å (as compared with 10.7 Å for C_2AH_8) together with the corresponding mixed crystals $C_2(A, F)H_8$. Their starting materials were C_2F, $C_2F_{0.7}A_{0.3}$ and $C_2F_{0.3}A_{0.7}$ with a ratio of water/solids of 0.6.

CA · aq

Monocalcium aluminate hydrate is principally responsible for the hydraulic hardening of cement. It crystallizes as needles with a density of 1.7 g/cm³ (Table 13).

It, too, forms hydrates with a varying water content. From the present knowledge it appears that the most hydrous member contains 10 molecules H_2O. Henning

Table 13. *Investigations on monocalcium aluminate hydrates*

Hydrates	Basal interference [Å]	Preparation r.h./temperature [%] [°C]	Properties	Authors (date)
$CAH_{9.4-10.8}$	7.68	—/<5° or 100/<22°	at 2.5g Al_2O_3/l available D = 1.70g/cm³; n = 1.43 crystallizes poorly, needles	Assarson(1931); Bessey(1938); not observed by Mylius(1933)
CAH_{10}	—	81/<20°	n = 1.470–1.48 a_0 = 9.45 c_0 = 14.60 D = 1.70g/cm³ hexag. prisms to 25 um length;	Brocard(1948) Lea and Desch(1956)
		—/—	from hydration of pastes also C_2AH_8	Carlson(1958)
	14.6 (7.3)	>45/15–20 <45/15–20	from CA-solution by freezing at 50°C	
$CAH_{7.3-5.5}$	—	or above P_2O_5	dehydration tests	Longuet(1952)
$CAH_{2.5}$	—	48h at 105°	>600°C: dehydrated	
CAH_7	13.6 14.2 (7.16)	—/— above $CaCl_2$	n_ω = 1.480; n_ε = 1.477 at 175°C destroyed	Lhopitallier(1960) Carlson(1957), Henning(1966)
CAH_x x = 10	—	data of the wave numbers of the infrared adsorption washed with acetone and ether at 0° (needles);		Henning(1966)
x = 8	10.50	〃 〃 〃 〃		
x = 7	—	〃 〃 〃 〃		
x = 6	10.14	dried above dehydrated $CuSO_4$, afterwards $CaCl_2$		
x = 4	8.71	dried in vacuum above P_4O_{10};		
x = 2	8.84	from CAH_8 by tempering 200–250°C		

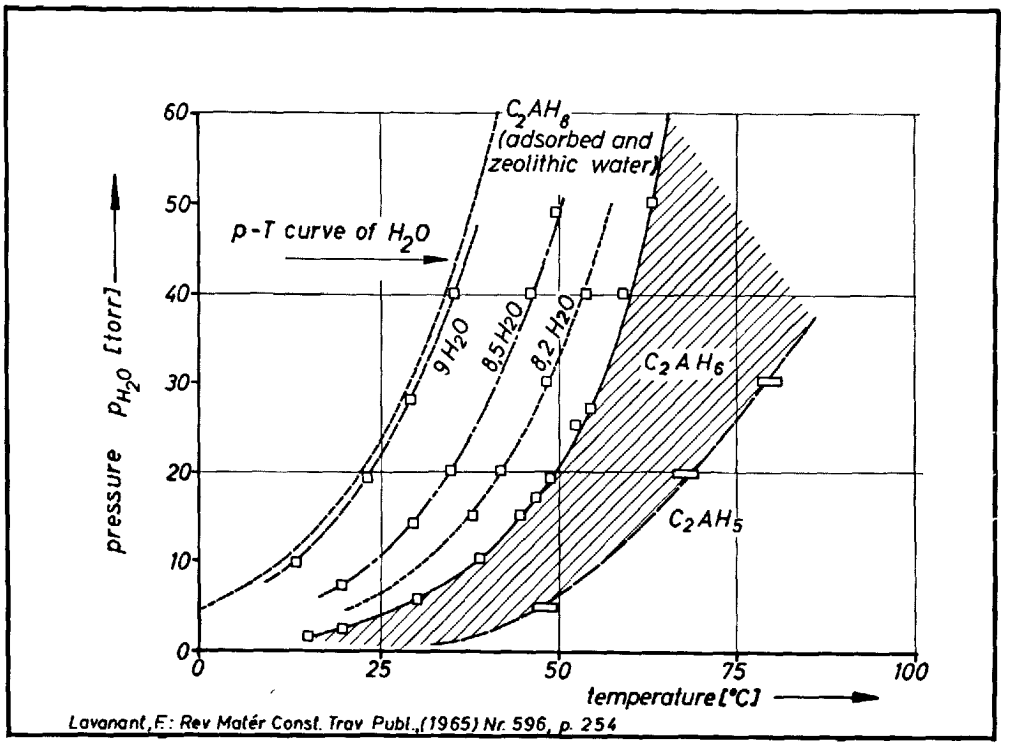

Fig. 13. *Dicalcium aluminate hydrates in the* p-T-*diagram* (*Lavanant 1965*)

(80) found hydrates with 10 to 2 molecules of water. The basal interference of the form with 10 molecules is 14.6 Å. At 200–250°C Henning obtained a hydrate with two molecules of water whose basal interference was 8.84 Å. According to Longuet (87) the last water is expelled at temperatures above 600°C.

No descriptions have appeared so far of a monocalcium aluminate hydrate in which the aluminium is partly or wholly replaced by iron although the existence of such a hydrate is to be expected.

C_2ASH_8

C_2ASH_8 is easily obtained by the reaction of at 600–800°C calcined kaolin or glass of the composition of gehlenite with a saturated solution of lime. It is probably by this reaction that Rebuffat (88) synthesized a hydrate of the composition C_2ASH_8 for the first time.

However, Strätling and zur Strassen (89) have shown later that by starting with calcined kaolin two hydrates are formed and thus Rebuffat was unable to separate the gehlenite hydrate by means of chemical methods. Contrary to the results of Fratini and Turriziani (90) who assumed hexagonal symmetry for C_2ASH_8, Schmitt (91) found it to have a monoclinic symmetry with an *a*-axis of 9.96 Å; he used the intensity distribution in a single-crystal electron diffraction photograph. In addition he found that 0.3 molecules of Al_2O_3 can be replaced by Fe_2O_3 causing a increase in the length of the *a*-axis from 9.96 Å to 10.07 Å and a decrease in the *c*-axis form 12.56 Å to 12.52 Å; the refractive index rises from 1.512 to 1.525. By exact measurement (92) of the impulse rate at intervals of $0.1° = 2\theta$ we established the monoclinic symmetry for gehlenite hydrate with $a_o = 9.9153$ and $c_o = 12.4458$. The starting materials were glasses of the composition of melilite and others with compositions in the solid solution series gehlenite (C_2AS)-akermanite (C_2MS_2). Measurement of the values for the interferences (003), (302) and (300) indicated how the lattice constants varied in the direction of the *c*- and *a*-axis. It can be seen from Fig. 14 that at amounts of up to 5% akermanite glass in melilite glass the lattice expands strongly in the a- and c-directions. A further increase in the akermanite fraction of the glass leads to an expansion along the *c*-axis only.

Using the ionic radii of Ahrens (1952) with the values $Mg^{++} = 0.64$ Å, $Al^{+++} = 0.50$ Å and $Ca^{++} = 1.02$ Å one can calculate a contraction of the lattice by 49% if Mg^{++} replaces Ca^{++}. The exchange by Al^{+++} produces a dilation of 28%. If magnesium is taken into the lattice, therefore, it probably replaces aluminium. The re-arrangement in the lattice necessary to maintain electrostatic neutrality can only be solved by a structural analysis.

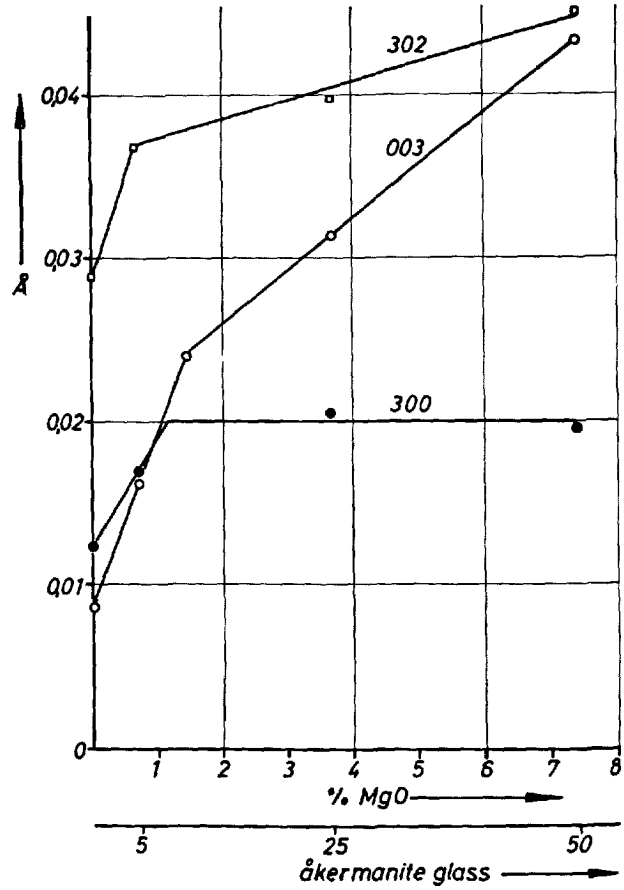

Fig. 14. *Lattice constants of gehlenite hydrate as a function of MgO content (Schwiete, ludwig, Würth, Grieshammer 1965)*

Interesting work was produced by Krönert, Schwiete and Wetzel (93) who allowed kaolin to react with an aqueous solution of calcium hydroxide at temperatures between 20° and 100°C for 8 weeks. The kaolin was either left unprepared or was treated mechanically by grinding. The untreated kaolin was not altered to gehlenite hydrate. In the case of the ground kaolin, however, at temperatures up to 60°C the formation of gehlenite hydrate was observed. Whereas at temperature of 40°C the amount of gehlenite hydrate remained constant for the 8 weeks, at 60°C it decreased rapidly and was replaced by hydro-garnet.

Cubic Hydration Products

C_3AH_6

Since the previous symposium in Washington it has been established that no pure tricalcium ferrite hydrate exists. Thus Allen and Roger (70) in 1900 were probably the first to deal with the cubic hydrate (Table 14). According to Wells, C_3AH_6 crystallizes in icositetrahedra or rhombic dodecahedra.

Table 14. *Investigations on tricalcium aluminate hydrate*

Hydrates	Basal interfer. [Å]	Preparation r.h./temp. [%] [°C]	Properties	Authors(date)
C_3AH_{12}	—	—	hexag. plates from C_3A and cold H_2O	Candlot(1889) and others
C_3AH_6	—	above $CaCl_2$	from Al and hot limewater	Allen and Rogers(1900), Mylius(1933)
	$a_0 = 12.56$	—	icositetrahedron a. rhombicdodecahedr.	L.S. Wells(1928), Flint, Mitarb.(1941)
	$a_0 = 12.576$	18.1/21 or above CaO at 21°C	cubic body centered space group Ia 3d $Z = 8$; $D = 2.522$ g/cm³ derive of the grossularite by substitution of $1SiO_4^{4-}$ by $4OH^-$, structure proven	Thorwaldson, Grace, Vigfusson(1929) Brandenberger(1933), Schwiete, Iwai(1962) Köberich(1934), Bogue, Lerch(1934)
	—	—/<275 resp. 330°C	from dehydration > 330°C loss of $4^1/_2$ moles H_2O	Schneider, Thorwaldson(1941) Kalousek, Davis, Schmertz(1949) Turriziani and Schippa(1954) Majumdar and Roy(1956)
$C_3AH_{1.5}$	—	—/<275	from dehydr. > 550°C form. of $C_{12}A_7$ + CaO >1050°C form. of C_3A	Majumdar and Roy(1956)
C_3AH_6, AH_3 $C_4A_3H_3$	—	≥ 800°C 5–20 k bar	formation of $C_4A_3H_3$($d_{basis} = 3.59$Å)	Majumdar and Roy(1956) and Pistorius(1962)
	—	≥ 350°C 5–50 k bar	form. of $C_4A_3H_3$ ($d_{basis} = 3.58$Å) form. of $C_4A_3H_3$ ($d_{basis} = 3.644$Å)	Majumdar and Roy(1956) Pistorius(1962)
C_3AH_6	—		reaction: $C_4AH_{13} \xrightarrow[\text{marked with } C^{45}]{\text{irreversible}} C_3AH_6 + CH + 6H$	Kelly(1960)
C_3AH_x	—		system C–A–H with variable P and T system C–A–H a) with analytic grade b) with spectroscopic grade starting points	Lavanant(1965) Crowley(1964)

Important investigations were carried out by Thorvaldson, Grace and Vigfusson (94) in 1929. They proved that the lattice of C_3AH_6 is cubic body-centred and that the space group is Ia3d. The unit cell contains 8 units of formula. The density is 2.52 g/cm³. The authors derived the structure of C_3AH_6 from that of grossularite, whereby one SiO^{4+} is replaced by $4(OH)^-$. According to Farmer (95) the Al^{3+} is in sixfold co-ordination. As a dehydration product, Majumdar and Roy (97) identified a hydrate with 1.5 molecules of water, stable at temperatures below 275°C. Above 550°C, $C_{12}A_7$ is formed together with free CaO, and at temperatures above 1050°C, C_3A. Later on the same authors observed the formation of $C_4A_3H_3$ with a basal interference of 3.58Å under conditions of increased temperature and pressures of between 5 and 20 kilobars; similar observations were made by Pistorius (82) at a pressure range reaching 50 kilobars. His product had a basal interference of 3.64 Å. Pistorius investigated C_3AH_6 under various conditions of temperature and pressure. He found equilibrium curves for C_3AH_6 and diaspore on the one hand, and $C_4A_3H_3$ on the other. His curves are for the range 5–50 kilobars and 200–370°C. At higher temperatures and lower pressures he investigated the stability of $C_4A_3H_3$ and of $C_{12}A_7$, CA_2 and H_2O. He could show that up to 800°C and 20 kilobars the hydrate of the composition $C_4A_3H_3$ occurs (Fig. 15).

There is interesting work by Kelly (102), who showed by means of radio-actively marked calcium, that $C_3AH_6 + Ca(OH)_2$ cannot be transformed into C_4AH_{13}. This confirmed the earlier observations according to which C_3AH_6 is the only stable pure calcium aluminate hydrate present, under normal conditions of temperature and pressure, in the system Al_2O_3–CaO–H_2O.

Fig. 1 shows our differential calorimetric investigations (14) of the endothermal reactions of C_3AH_6. One can see a distinct endothermal effect at about 300°C, as in the case of tetracalcium aluminate hydrate. It is due to the formation of $C_4A_3H_3$ with the release of free $Ca(OH)_2$. Once again the dehydration of calcium hydroxide occurs at about 500°C.

Bereczky found the pH value to be 12.1 (16). Our measurements give values of 12.1–12.2 which show a good agreement. No CaO was dissolved out of C_3AH_6 after one hour's boiling with the ester of acetic acid.

$C_3(A, F)S_n H_{(6-2n)}$

In the lattice of the cubic C_3AH_6, Al^{3+} can be replaced by Fe^{3+}, and two H_2O by one SiO_2 (Table 15). When one or more of these substitutions occur

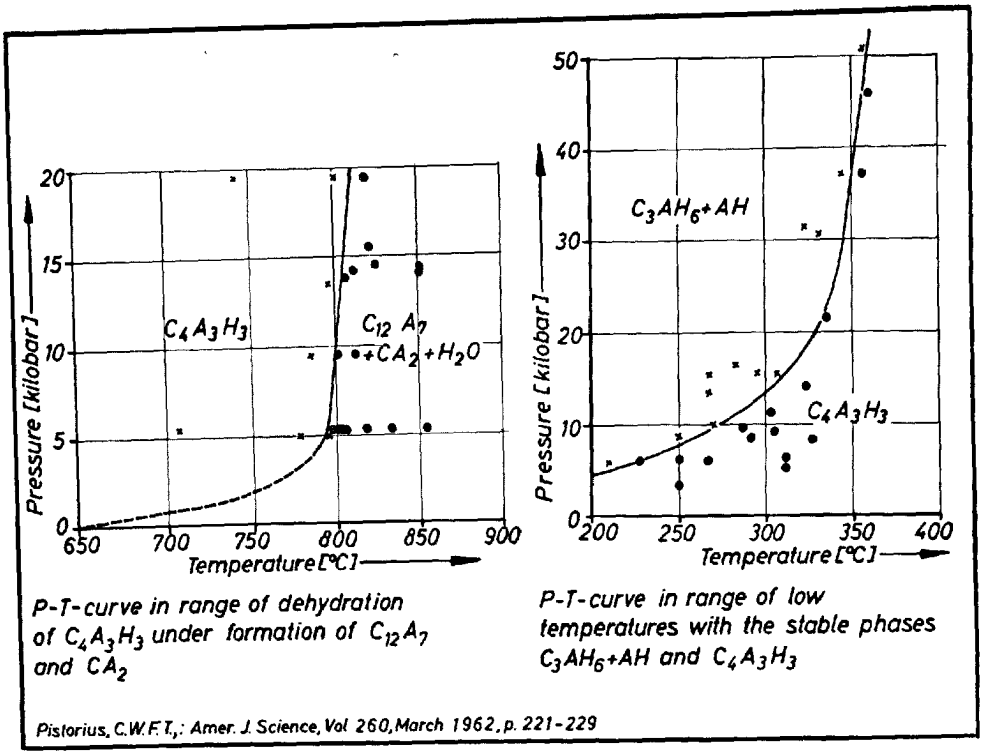

Fig. 15. p-T-*diagram of* C_3AH_6, AH *and* $C_4A_3H_3$ (*Pistorius 1962*)

Table 15. *Investigations on hydrogarnets* ($C_3A_xF_{1-x}S_yH_{6-2y}$)

Hydrates	Basal interfer. [Å]	r.h./temperature [%] [°C]	Properties	Authors(date)
C_3FH_6	$a_0 = 12.71$	—/<105	from $Fe(OH)_3 + Ca(OH)_2 + H_2O$ Drö = 2.790 g/cm³; <0.25CaO/l	Eiger(1937)
C_3FH_2	—	—/<300	formation of C_2FH_5 >600° loss of 2 moles H_2O	
C_3FH_6	a = 12.74	—		Flint, McMurdie and Wells(1941)
C_3FH_6	$a_0 = 12.56$	—/—	free of silica	Burdese and Gallo(1952)
C_3FH_2	$a_0 = 12.39$	—/<500		
"C_3F"	$a_0 = 15.36$	—/>500	>800°C formation of $C_2F + CaO$	
$C_3A_xF_{1-x}H_6$ $(0.163 \leq x \leq 1)$	$a_0 = 12.70$		C_3AH_6 to maximum $C_3A_{0.2}F_{0.8}H_6$	zur Strassen and Dörr(1958)
			" " " $C_3A_{0.188}F_{0.812}H_6$	Schwiete and Iwai(1962)
	$a_0 = 12.716$		" " " $C_3A_{0.163}F_{0.837}H_6$	Carlson(1956 and 1966)
$C_3A \cdot S_{0.3-4}H_{5.2-5.4}$	—	—/50	from burnt kaolin + lime water	Turriziani, Schippa(1954)
$C_3A \cdot S_{0.4-0.7}H_{4.6-5.2}$	a_0—12.30	—/—	from C–A–S-glass + lime water	zur Strassen, Dörr(1958, 1962)
$C_3(A, F)S_3$, general $R_3''R_2'''Si_3O_{12}$	—		natural garnets (isomorph. mixture) R'' = Ca,Mg,Fe,Mn; R''' = Al,Fe,Cr	Ford(1915)
$C_3(A, F)S_yH_{6-2y}$ $(0 \leq y \leq 3)$	$a_0 = 12.60$	hydrothermal	observed substitution of Al^{3+} by Fe^{3+} and SiO_4^{4-} by $4OH^-$ $C_3(A, F)H_6 + CS \cdot aq \rightarrow C_3(A, F)SH_4$, C_3AH_6 to $C_3AS_3H_2$(2000atm/360°C), Grossular(C_3AS_3)	Flint, McMurdie, Wells(1941) zur Strassen and Dörr(1958) D. M. Roy and R. Roy(1960)
$C_3A_{0.5}F_{0.5}SH_4$	$a_0 = 12.42$		from $C_4AF + CaO + C_3S$	Schwiete and Iwai(1962)
$C_3AS_{0.12}H_{5.74}$	$a_0 = 12.51$	40°C/20 torr	from kaolin and $Ca(OH)_2$ at temp. 20–100°C	Krönert, Schwiete, Wetzel(1967)

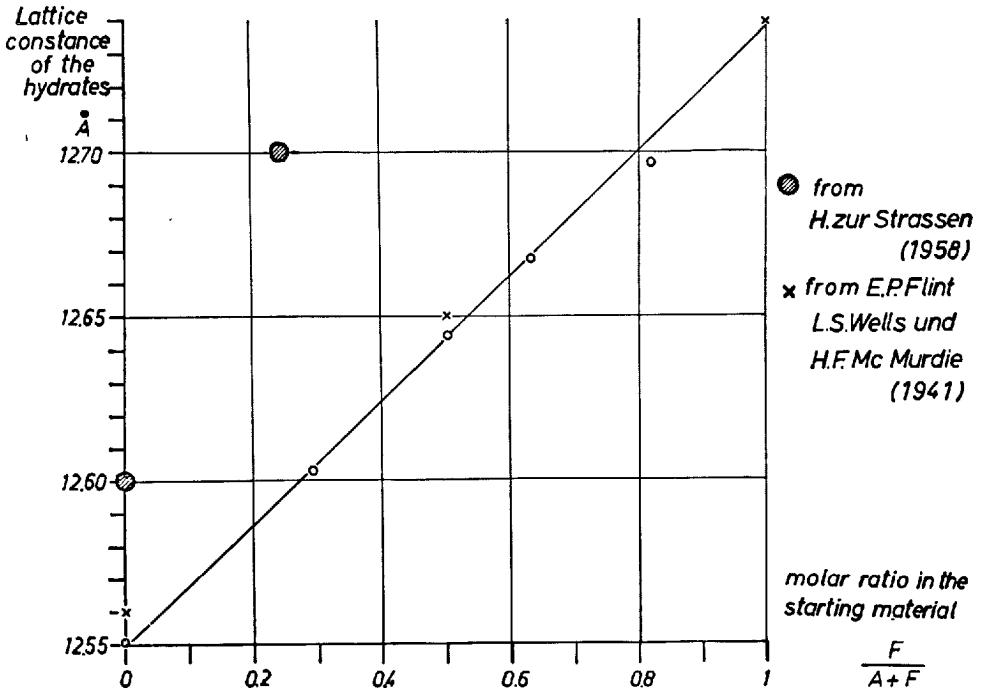

Fig. 16. *Lattice constants of hydrates in the system* C_3AH_6–C_3FH_6 *(Schwiete, Iwai 1964)*

the product is called hydrogarnet. A hydrogarnet in which the Al^{3+} is replaced by Fe^{3+} was first prepared by Eiger in 1937 (103). zur Strassen and Dörr (104, 105) are of the opinion that pure C_3FH_6 does not exist. According to them, and to Carlson (106) and Schwiete and Iwai (45) 0.163 molecules of Al^{3+} must be contained in hydrogarnet. Schwiete and Iwai calculated the lattice constants for the solid solution series C_3AH_6–C_3FH_6 using the Bragg equation for the cubic system with the strong reflections (321), (400), (420), (422), (431) and (521) and (532). They compared their values with those of Flint, Wells and McMurdie (96) and zur Strassen and Dörr (104, 105). The lattice constant rises from 12.55 Å for pure C_3AH_6 to 12.7 Å for $C_3A_{0.2}F_{0.8}H_6$ and there is a linear dependence. The value of Flint and co-workers for pure "C_3FH_6" lies on the extension of this line at 12.74 Å (Fig. 16).

Krönert, Schwiete and Wetzel (93) succeeded in preparing a silica-bearing hydrogarnet of the composition $C_3AS_{0.13}H_{5.74}$ at temperatures between 40° and 100°C and normal pressure, starting from uncalcined kaolin and calcium hydroxide. Further, silica-bearing garnets have been produced by Fratini and Turriziani (90) from calcined kaolin and lime water, and by zur Strassen (104) and Dörr (105) from calcium aluminate silicate glasses and lime water. Flint, McMurdie and Wells (96) allowed tricalcium aluminate ferrite hydrate and calcium silicate hydrate react under hydrothermal conditions and found a $C_3(A, F)SH_4$ with lattice constant of 12.42 Å.

Schwiete and Iwai (45) investigated reaction mixtures of C_4AF with CaO and increasing proportions of C_3S in aqueous solution under normal conditions of temperature and pressure. They observed a decrease in the lattice constant from 12.65 Å for the hydrogarnet prepared from C_4AF to 12.42 Å for the compound richest in silica, whose approximate composition is $C_3A_{0.5}F_{0.5}SH_4$. These results are in good agreement with those of Flint and Wells (49) as Fig. 17 shows. Thus in the hydrogarnets we observe an increase in the lattice constant with increasing iron content and a decrease in that with increasing silica.

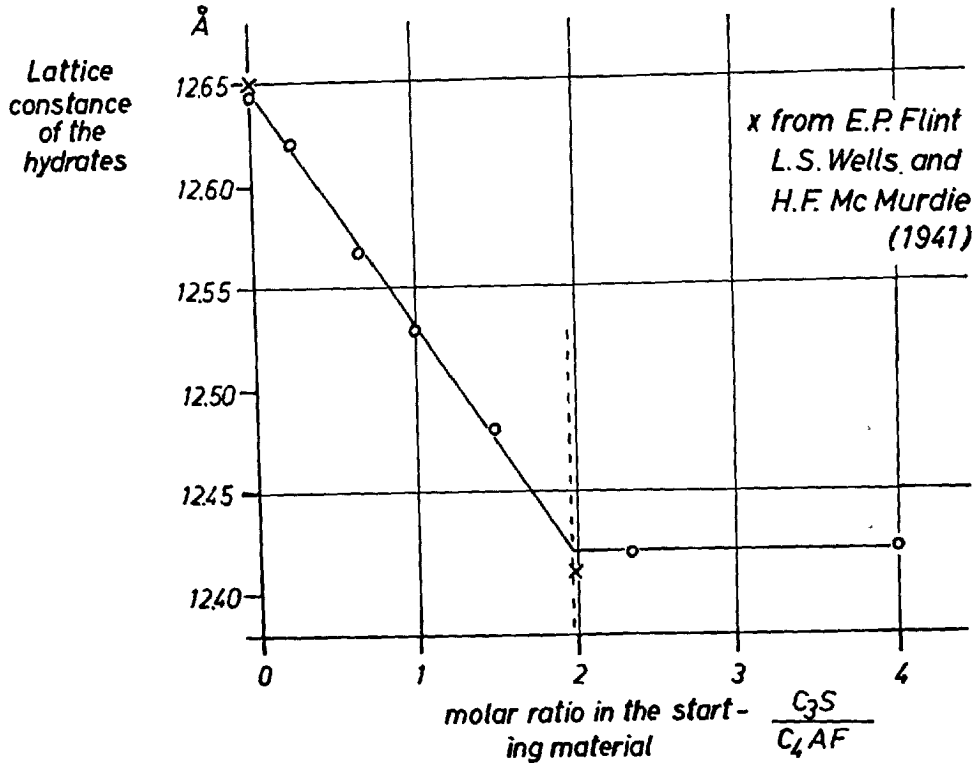

Fig. 17. *Lattice constants of Hydrogarnets in the system* C_4AF–C_3S–CaO–H_2O *(Schwiete, Iwai 1964)*

Investigations in the System CaO–Al_2O_3–H_2O at High Pressure with Varying Temperature

Crowley (81) examined the pseudo-binary system CaO–Al_2O_3–H_2O, at a pressure of 1055 kg/cm² and with increasing temperatures, firstly starting with spectrographically pure $CaCO_3$, and secondly with chemically pure $CaCO_3$.

Fig. 18 shows the diagram for spectrographically pure $CaCO_3$. In the calcium-rich region, at low temperatures, one can recognize the stability field of C_4AH_{19}, a field in which α–C_4AH_{19} co-exists with α–C_2AH_8, one with α–C_2AH_8 and CAH_{10}, and finally one in which CAH_{10} and AH_3 occur together. At temperatures above 25°C C_2AH_8 is transformed to C_3AH_6, whilst α–C_4AH_{19} and CAH_{10} remain stable. C_4AH_{19} and CAH_{10} are also altered to C_3AH_6 and gibbsite (AH_3) or C_3AH_6 and calcium hydroxide ($Ca(OH)_2$) respectively, depending on the starting material. Gibbsite inverts to diaspore above about 140°C. At temperatures of nearly 250°C C_3AH_6 is transformed into $C_4A_3H_3$ and $Ca(OH)_2$ or diaspore. It is interesting to note that, independent of the high pressures applied (1055 kg/cm²), the same reactions and phases are observed as can be found at normal temperatures e.g. by differential calorimetry or in experiments of isobaric decomposition.

In Fig. 19 a similar diagram is shown, which is obtained when chemically pure $CaCO_3$ is used as the starting material. It is interesting that here in the lime-rich region C_4AH_{13} is stable together with $Ca(OH)_2$ at temperatures up to 150°C. In the lime-poor region up to 250°C the C_2AH_6 is also partly stable, however the equilibrium temperature falls as the Al^{3+} content in the starting material increases. The use of less pure calcium carbonate thus leads to an important increase in the stability field of the tetra- and dicalcium aluminate hydrates, which according to previous work, are known to be unstable phases. Above 250°C $C_4A_3H_3$ is again observed with $Ca(OH)_2$ or aluminium hydroxide and it is remarkable that, in contrast to the experiments with spectrographically pure $CaCO_3$ the reactions of the low temperature phases are reversible if only chemically pure $CaCO_3$ is used.

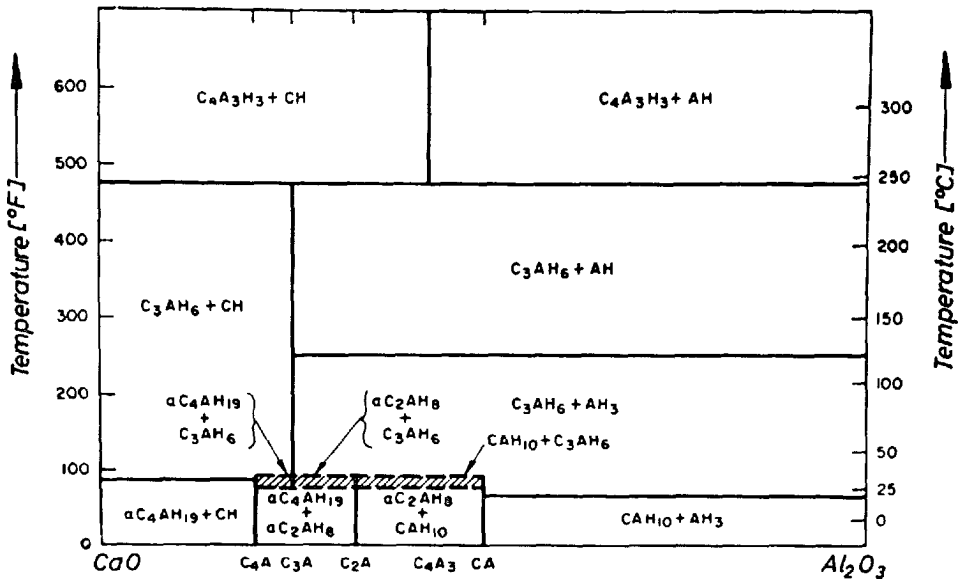

Crowley, 1964; with application of spectroscopic grade $CaCO_3$ (starting point)

Fig. 18. *Pseudobinary diagram of the system* $CaO–Al_2O_3–H_2O$ *at 1000 kg/cm²* (*Crowley 1964*)

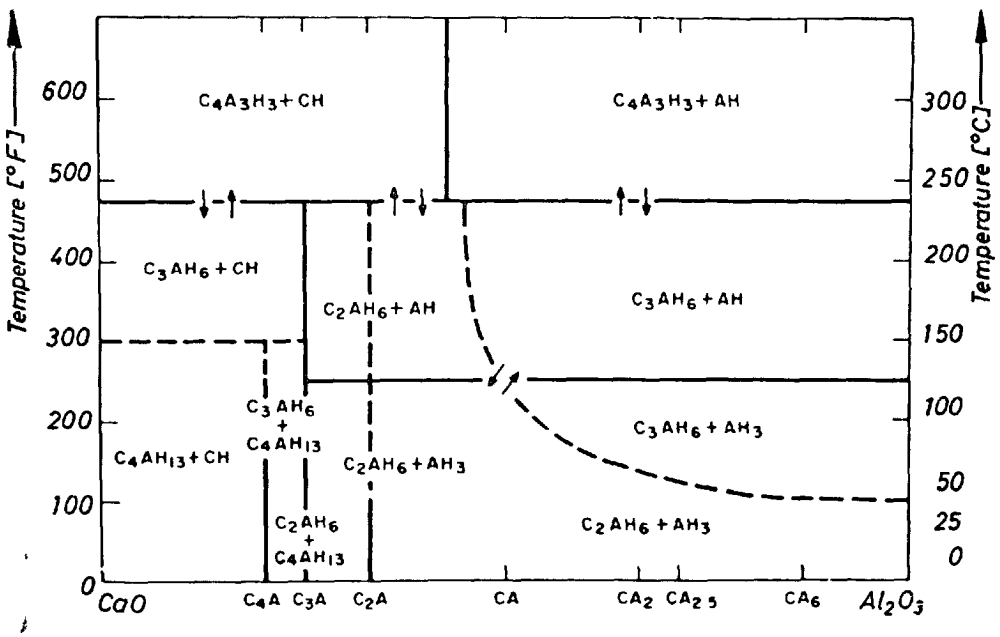

Crowley 1964; with application of analytical grade $CaCO_3$ (starting point)

Fig. 19. *Pseudobinary diagram of the system* $CaO–Al_2O_3–H_2O$ *at 1000 kg/cm²* (*Crowley 1964*)

Properties

The properties of calcium aluminate hydrates and calcium aluminate ferrite hydrates respectively are judged in different ways. In the following section, a distinction is to be made between the properties of the

hydration products during the formation of the cement stone and those of the hydration products in the cement stone itself.

Properties during the Formation of the Cement Stone

The calcium aluminate and aluminate ferrites respectively are characterized by their high reaction speeds in aqueous solution; the reaction speed increases as the ferrites contain a higher percentage of Al_2O_3. These reactions are accompanied by a high liberation of heat. The thermodynamic computations by V. J. Babuskin, G. M. Matveev and O. P. Mchedlov-Petrosyan (1965) have furnished us with a lot of data (Table 16). With the cements that contain much lime this quick reaction is delayed by the addition of calcium sulphates and by the resulting formation of an ettringite cover. $C_3(A, F)CsH_x$ and the mixed crystals of $C_3(A, F)CsH_x$ with $C_4(A, F)H_x$ respectively are formed only after the concentration of sulphate has fallen short of the minimum necessary for the formation of ettringite. The reaction by which ettringite is formed takes place, topochemically, at C_3A, $C_2(A, F)$ or at the granulated aluminate containing slag grain. If the percentage of sulphate is carefully harmonized with the composition and the fineness of the cement, the main formation of ettringite takes place at the early stage of setting and hardening so that it is only rarely possible to observe any expansion.

In contrast to the cements that contain much lime, the formation of ettringite in the supersulphated cements that contain less lime takes place through the phase of solution and contributes towards cementation. In the case of these cements, an expansion in the course of the formation of ettringite is observed only when this cement is produced with a too high percentage of clinker; by this circumstance, the pH-value is increased during the setting and the hardening.

In the case of the reaction of alumina and of iron from clinker and granulated blast furnace slags, when phases with very much lime are formed, one must in addition reckon with a lime combination by which, according to the law of the mass effect, the hydration of the calcium silicates must be accelerated.

Because of the quick reaction of the calcium aluminates and the calcium aluminate ferrites, one must furthermore reckon with the creation of additional surfaces on the calcium silicates so that the entire progress of the hydration will be favourably influenced by this circumstance, too.

Therefore this exposition demonstrates two facts; on the one hand, the calcium aluminates and the calcium aluminate ferrites respectively from the cements can bring about a decrease in strength at the beginning of the setting and the hardening by an eventual expansion; on the other hand, however, they can favourably influence the hydration and the hydrolysis of the cements in several ways by the high heat liberation, by their quick hydration and by the resulting creation of additional surfaces as well as by the lime combination.

In the case of the high alumina cements, the calcium aluminate hydrates CAH_{10} and C_2AH_8 are responsible for the hydraulic strength.

Table 16. *Thermodynamic data of aluminate hydrates*

Hydration product	ΔH_{298} kcal/mol	ΔG_{298}
C_4AH_{19}	−2409	−2092
C_4AH_{13}	−1983	−1749
C_3AH_6	−1317.6	−1187.6
C_2AH_8	−1291	−1142
C_3ACsH_{12}	−2082.8	−1843.6
$C_3ACs_3H_{31}$	−4110.9	−3556.4

By V. J. Babuskin, G. M. Matveev and O. P. Mchedlov-Petrosyan Thermodynamik der Silikate-VEB-Verl. Berlin 1965.

Properties in the Cement Stone

With the exception of the above-mentioned qualifications with regard to the formation of the cement stone and with the exception of the formation of ettringite which possibly has an expansion effect, the installation of the calcium aluminate ferrite hydrates in the cement stone may, to begin with, be expected to contribute in increasing its strength and its density. According to investigations by Spohn and Lieber (52) in 1965, an addition of $CaCO_3$ to C_3A or C_4AF results in an increase of the strength. This increase, however, results already from the strong increase in specific volume of solids which takes place when the anhydrous phases changes in the hydration products; the increase in specific volume is to be derived from the low densities of the calcium aluminate ferrite hydrates.

The contribution which the calcium aluminate hydrates make to strength becomes particularly obvious in the high alumina cements during the formation of the hexagonal or pseudo-hexagonal hydrates which contain little lime.

In this context, however, we must not consider without qualification the stability of these phases in dependence on temperature, pressure and relative humidity; from the above-mentioned thoughts we know that the hydrates rich in water, especially those

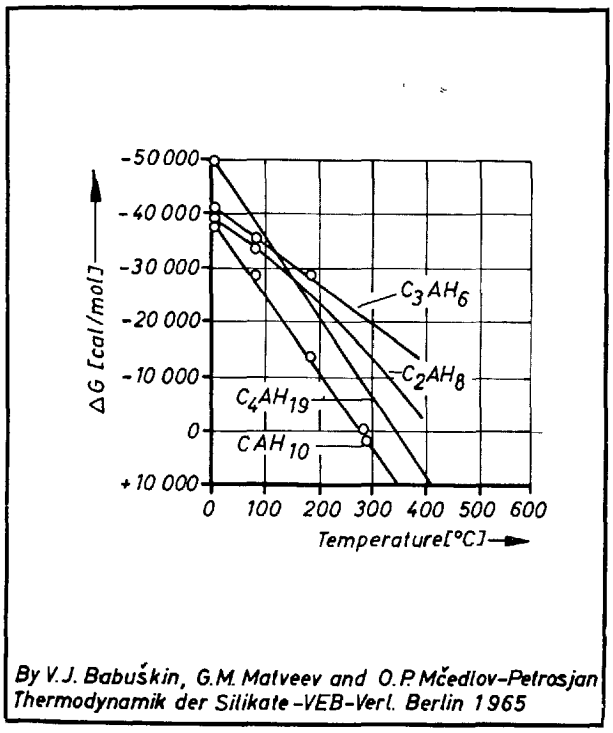

Fig. 20. $\Delta G_{react} = f(T)$ *in the system of* $3CaO \cdot Al_2O_3 - H_2O$

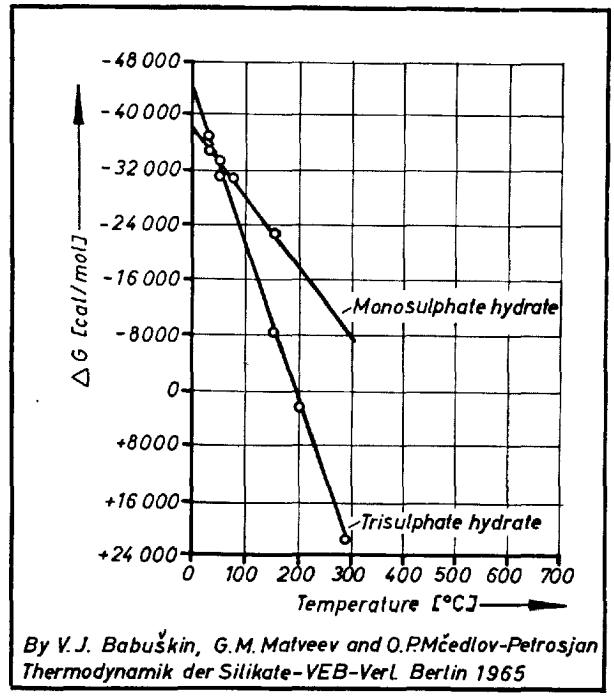

Fig. 21. *Stability of monosulphate and trisulphatehydrate*

of the AFm-phases, can only be preserved at high relative humidities. According to the present state of investigations, the AFt-phases and the hydrogarnets are more stable. The stability of some calcium aluminate hydrates, the ettringite and the monosulphate hydrate is shown in function of the temperature by Babuskin, Matveev and Mchedlov-Petrosyan in the following Figs. 20 and 21.

In the case of the high alumina cements, especially when the atmosphere is moist, temperatures >23°C have a negative accelerative effect on the conversion of the voluminous hexagonal or pseudo-hexagonal hydrates into denser cubic hydrogarnets; the reason is that the latter ones have a smaller volume where by the porosity of the cement stone is greatly increased and the strength are reduced. One tries to counteract that circumstance by making this set and harden at higher temperatures with a small water cement ratio whereby the stable phases form directly.

The stability of the AFm-Phases and the cubic tricalcium aluminate hydrates is additionally endangered by changes in concentration. When parts of cement stone contain these hydration products and can come into contact with solutions that contain sulphate, one has to reckon with the formation of ettringite which can lead to the destruction of the building. However, the intensity of the attack which must be expected depends on the density of the cement stone, on the strength of the sulphate concentration, on temperature and on the way in which the sulphate attacks, that is on the question whether the transport takes place by means of diffusion or capillarity.

When considering the stability of the phases in question one must not, however, forget to take into account that, according to investigations carried out by Copeland, Bodor, Chang and Weise (111) in 1967, a strong reaction of tobermorite geles on the aluminates, ferrites and sulphates takes place whereby these phases can most certainly be heavily reduced in dependence on time. These investigations fit in very well with our own frequent observations that often in old mortars and concretes no or only very low percentages of calcium aluminate and of aluminate ferrite hydrates are found. It is therefore probable that the entire complex of problems must be gone over and revised anew.

Summary

1. It has been possible to determine the inter-atomic distances in the compound $C_3ACs_3H_{32}$ by means

of a Patterson synthesis. Moreover, starting from C_2F, an ettringite has been repeatedly prepared in which Al^{3+} is completely replaced by Fe^{3+}.

2. The formation of $C_3A \cdot 3CaCl_2 \cdot H_{30}$ was not observed above 20°C, however, between 0° and −10°C (under conditions of increasing calcium chloride concentration, it was found in increasing quantities. From the d-spacing the (hkil)-values for the hexagonal system have been calculated. The existence of an iron-bearing analogue is to be expected. Moreover an AFt-phase of the composition $C_3A(CaS, CaSO_4)Hx$ was found.
3. Contrary to earlier results it has been shown that there is only one modification of C_4AH_{13} and that the previously assumed α- and β-phases only differ in having water contents of 13 and $12H_2O$ respectively.
4. Dehydration of C_4AH_{19} produced hydrates with 13, 12, 11 and 7 molecules H_2O. A complete solid between C_4AH_{13} and C_4FH_{13} has been reconfirmed.
5. For the carboaluminate hydrates the phases with the composition $C_3A \cdot 1/4CaO \cdot 1/4CaCO_3 \cdot H_{11-12}$, $C_3A \cdot 1/2CaO \cdot 1/2CaCO_3 \cdot H_x$ and $C_3A \cdot CaCO_3 \cdot H_{10-11}$ exist. They can be distinguished amongst themselves and from C_4AH_{13} on the grounds of their basal interference and those of their hydration products.
6. $C_4A_3H_3$ can be produced only from C_4AH_{13} and C_3AH_6 by splitting-off $Ca(OH)_2$. The solid solution between C_3AH_6 and C_3FH_6 has been confirmed. The most iron-rich member has the composition $C_3A_{0.163}F_{0.837}H_6$. The compound richest in silica has the composition $C_3A_{0.5}F_{0.5}SH_4$ under normal conditions of temperature and pressure.
7. Crystals of C_3ACsH_{12} were found to have a hexagonal pseudo-cell with $a_o = 5.76$ Å, and $c_o = 26.79$ Å; the space group is R3 or $R\bar{3}$. More recent investigations have proved a partial miscibility with C_4AH_{13}. This solid solution is also found when Al^{3+} is partly replaced by Fe^{3+} but not if pure C_2F is used as the starting material.
8. A hydrate of the composition $C_4A_{0.9} \cdot 1.1SO_3 \cdot 0.5Na_2O \cdot H_{16}$ was prepared from C_3ACsH_{12} and was examined by X-rays. It is one of three hydrates with 16, 12 and $8H_2O$ respectively.
9. According to investigations under normal and hydrothermal conditions no solid solubility exists between $C_3A \cdot CaCl_2 \cdot H_{10}$ and C_3ACsH_{12}, but there is another compound of the composition $C_6A_2 \cdot CaSO_4 \cdot CaCl_2 \cdot H_{24}$ with $a_o = 5.74$ Å and $c_o = 100.6$ Å; its space group is R3c or $R\bar{3}c$.
10. An α- and a β-form of $C_3A \cdot CaCl_2H_{10}$ can be distinguished, whose reversible inversion point is 28°C + 2°. The β-form stable above 28°C, has the lattice constants $a_o = 5.75$ Å and $c_o = 46.88$ Å, if a trigonal symmetry is assumed. According to rotation-, Weissenberg- and precession-photographs, α-$C_3A \cdot CaCl_2 \cdot H_{10}$ has a monoclinic pseudohexagonal unit cell with $a_o = 9.98$ Å, $b_o = 5.47$ Å and $c_o = 16.79$ Å; $\beta = 110.2°$.
11. A new AFm-phase with CaS is $C_3A \cdot CaS \cdot Hx$ whose formation was found as well at ordinary temperatures as at hydrothermal conditions.
12. For the di- and monocalcium aluminate hydrates the principal investigations in recent years have been on dehydration. Only partial agreement has been found with earlier results. X-ray investigations under controlled conditions of temperature and humidity are still lacking. Only substitution of Al^{3+} by Fe^{3+} was observed for C_2AH_8 and none in the case of CAH_{10}.
13. When small amounts of MgO are added to glasses of the composition melilite the lattice of C_2ASH_8 expands both in the a-and c-directions. With larger amounts an expansion along the c-axis only is observed. The dilation of the lattice is probably due to replacement of Al^{3+}.
14. The stability fields of the unstable hexagonal or pseudo-hexagonal phases are shifted towards higher temperatures if impure starting materials are used.
15. Complete data on density and pH values are given.

The writers express their appreciation to Dr. Ing. P. A. H. Otto for help with the manuscript. Our own work was supported by the Verein Deutscher Zementwerke (Düsseldorf), Arbeitsgemeinschaft Industrieller Forschungsvereinigungen (Köln) and the Deutsche Forschungsgemeinschaft (Bad Godesberg).

References

1. H. G. Smolczyk, "The ettringite phases in blast furnace cement" (in German).—Zement-Kalk-Gips **14**, 277–284 (1961).
2. E. P. Flint and L. S. Wells, "Analogy of hydrated calciumsilicoaluminates and hexagonal calciumalminates to hydrated calcium sulphoaluminates".—J. Research N. B. S. **33**, 471–478 (1944).
3. J. Mohri, "In regard to $C_3A \cdot 3CS \cdot H_{31}$" (in Japanese).—Semento Gijutsu Nenpo **12**, 9–11 (1958).
4. J. Lehmann, Neues Jahrbuch für Mineralogie 273 (1874).
5. F. Candlot, "Properties of cements and hydraulic binders" (in French).—Bull. Soc. d'encour. ind. nat. **89**, 682–685 (1890).
6. W. Michaelis, "The Zementbazillus" (in German).—Tonindustrie-Zeitung **16**, 105 (1892).
7. F. A. Bannister, M. H. Hey and I. D. Bernal, "Ettringite from Scawt Hill, County Atrim",—Min. Mag. **24**, 324–329 (1936).
8. L. Deval, "The effect of calcium sulfates on cements", (in German) —Tonindustrie-Zeitung **26**, 913–915 (1902).
9. Poirson (1911), Kühl and Albert (1923), Ref. in Proc. of the III. Int. Symp. on Chem. Cement, London, (1952).
10. A. A. Klein and A. J. Phillips, "The hydration of portland cement", Technolog. Papers, Bureau of Standards, Washington No. **43**, (1915).

11. W. H. Mc. Intire, and W. M. Shaw, Soil Sci. **19**, 125 (1925).
12. W. Feitknecht and H. Busser, Ref. in Mag. of Concrete Res. **9**, 17–24 (1957), ASTM Card 2-0059.
13. H. E. Swanson, Gilfrich, Cook, Stindfield and Parkes, "Standard X-ray diffraction powder patterns",—NBS Circular No. 539, 26th Sept. (1956), pp. 62, ASTM Card 6-0226.
14. H. E. Schwiete, U. Ludwig and P. Jäger, "Investigation on the hydration of C_3A, C_2F, C_4AF and C_6A_2F with calcium hydroxide and calcium sulphates".—Published by the Institut of Gesteinshüttenkunde (1967).
15. A. Bezjak and J. Jelenic, "The crystal structure investigation of calcium aluminium sulphate hydrate—ettringite",—Report on the VII, Int. Kongr. Kristallogr. Moskau, 1966.
16. A. Bereczky, "On the durability of concrete" (in German).—Baustoffindustrie **5**, 300 (1962).
17. E. Aruja and D. Rosaman, Proc. IV. Int. Symp. Chem. Cement 206 (1960).
17a. H. G. Midgley and D. Rosaman, "The composition of ettringite in set portland cement",—Proc. IV. Int. Symp. Chem. Cement, 259–262 (1960).
18. G. Malquori and E. Caruso, "The sulpho-, chlor- and nitro-ferrites of calcium" (in Italian), Atti del X. Congr. Intern. di Chim., Vol. ii., 713–718 (Rome 1938).
19. G. Malquori and V. Cirilli, "Hydrated calcium ferrites and compounds produced by the combination of tricalcium ferrite and various calcium salts" (in Italian), La Ricerca Scientifica Note 1, **18**, 316–321 (1940), Note 2, **18**, 434–442 (1940), Note 3, (by V. Cirilli) **14**, 27–30, Note 4, **21**, 78 (1943).
20. H. E. Schwiete and G. Ziegler, "Fundamentals of the application of the DDK" (in German).—Ber. Dtsch. Keram. Ges. **35**, 193–204 (1958).
21. N. N. Serb-Serbina, Yu. A. Savvina and U. S. Zhurina, "Formation of hydrated calcium chloroaluminates and their effect on the structure of hardened cement" (in Russian),—Doklady Akademii Nauk S. S. S. R. **3**, 659–662 (1956).
22. H. E. Schwiete, U. Ludwig and J. Albeck, "Investigations on $3CaO \cdot Al_2O_3 \cdot 3CaCl_2 \cdot 30H_2O$" (in German) Die Naturwissenschaften **55**, (1968) 179 and oral presentation of Principal Paper Tokyo 1968.
23. E. Brandenberger, "Investigations on the crystal structure of calcium aluminate hydrates" (in German).—Schweiz min. petrograph. Mitt. **13**, 569–570 (1933).
24. C. E. Tilley, H. D. Megaw and M. H. Hey, "Hydrocalumite ($4CaO \cdot Al_2O_3 \cdot 12H_2O$), a new mineral from Scawt Hill, Co. Antrim",—Miner. Mag., **23**, 607–615 (1943).
25. F. G. Buttler, H. S. Dent Glasser and H. F. W. Taylor, "Studies on $4CaO \cdot Al_2O_3 \cdot 13H_2O$ and the related natural mineral, hydrocalumite".—J. Amer. Ceram. Soc. **42**, 121–126 (1959).
26. A. Grudemo, "The microstructure of hardened cement paste".—Chem. of Cement, Proc. Fourth Intern. sym. Washington 1960, p. 615–647.
27. H. J. Kuzel, "Preparation and X-ray study on $3CaO \cdot Al_2O_3 \cdot CaSO_4 \cdot 12H_2O$" (in German).—N. Jb. für Mineralogie, **7**, 193–197 (July 1965) and S. P. "X-ray investigations of some complex calcium aluminate hydrates and related compounds," Tokyo 1968.
28. M. H. Roberts, "New calcium aluminate hydrates".—J. Appl. Chem. **7**, (1957) 543–546.
29. F. E. Jones, (M. H. Roberts), "Hydration of calcium aluminates and ferrites".—Proc. IV. Intern. Symp. Chem. Cement, Washington 205–246 VIII-3 (1960), J. Phys. Chem. **49**, 344–357 (1945).
30. E. Aruja, "Unit cell and space group determination of tetra-and dicalcium aluminate hydrates, the unit cell and space group of C_4AH_{19} polymorphs".—Acta cryst. **13**, (1960) 1018, **14**, (1961) 1213–1216.
31. H. Le Chatelier, Bull. Soc. Chim. **41**, 377 (1883), **42**, 88 (1884).
32. P. Seligmann and N. R. Greening, "New techniques for temperature and humidity control in X-ray diffractometry".—I. PCA Res. Developm. Labor. 4 (1962) 2–9, PCA Res. Dep., Bulletin 143, (1962).
33. W. Dosch and H. zur Strassen, "Investigation of tetracalcium aluminate hydrate, 1. the various hydrate stages and the effect of carbonic acid" (in German). —Zement-Kalk-Gips **18**, 233–237 (1965).
34. H. Lafuma, "Investigations on calcium aluminates and the combinations with calcium chloride and sulphate" (in French).—Thése, Paris 1925, Librairie Vuibert, p. 24.
35. L. S. Wells, "Reaction of water on calcium aluminates", —J. Res. Bur Standards Vol. 7–12, p. 951–1009 (1928).
36. G. Assarson, "Investigations on calcium aluminates I and II" (in German).—Zeitschr. für anorg. und allg. Chemie Bd. 200, 393 (1931), Bd. 205, 338 (1932).
37. C. R. W. Mylius, "On calcium aluminate hydrates and their double salts", (in German).—Acta Acad. Aboensis Math. et Phys. **7**, (5933) 151.
38. W. Feitknecht, "The formation of double hydroxides between bivalent and trivalent metals" (in German). —Helv. Chim. Acta **25**, 555–569 (1942).
39. R. Alégre, "Investigations on hexagonal C_4AH_x" (in French).—Rev. Mater. Constr. No. 566, Nov. 1962, Sonderdruck Publ. Techn. No. 135.
40. F. Lavanant and P. Barret, "Contribution to the study of the different hexagonal tetracalcium aluminate hydrates $4CaO \cdot Al_2O_3 \cdot 12H_2O$" (in French).—Comptes rendus de l'Academie des Siences 13. juillet, (1962).
41. F. Lavanant, "Contribution on the study of some calcium aluminate hydrates" (in French).—Revue des Materiaux de construction page 1–10, 76–87, 193–207, 251–261, 298–304 (1965).
42. W. Dosch, "Interlayer adsorption of water and organic compounds on C_4AH_x" (in German).—N. Jb. f. Mineralogie 200–239 (April 1967).
43. A. Weiß, "Organic derivates of micatype layer silicates", (in German).—Angew, Chem. **2**, 113–122 (1963).
44. A. Weiß, "Micatype layer silicates with alkylammonium ions".—Clays and Clay Miner. **10**, 191–234 (1963).
45. H. E. Schwiete and T. Iwai, "The ferrite phase of the

cament and its behaviour during hydration" (in German).—Forschungsber. des Landes NRW Nr. 1549 (1965)—Zement-Kalk-Gips **17**, 379–386 (1964).

46. J. Pelouze, "Observations on lime and two new combinations of this base with iron and chromium sesquioxides" (in French).—Ann. Chim. et Phys. **33**, 5–14 (1851).
47. H. Hoffmann, "Calcium ferrite hydrates" (in German). —Dissertation Berlin 1935, Zement **25**, 113–117, 130–132, 675–680, 693–698, 711–716 (1936).
48. E. T. Carlson, "Some properties of the calcium aluminate ferrite hydrates".—Building Science Series 6, M. S. Dep. of Commerce N. B. S. Washington 1966.
49. E. P. Flint and L. S. Wells, "Relationship of garnet-hydrogarnet series to sulfate resistance of portland cement".—J. Research Nat. Bur. Standards, **27**, 171–180 (1941).
50. E. T. Carlson and H. E. Berman, "Some observations on the calcium aluminate carbonate hydrates".—J. Research N. B. S. **64A**, 333–341 (1960).
51. R. Turriziani and G. Schippa, "Concerning the existence of a hydrated calcium monocarboaluminate" (in Italian).—Ricerca Scientifica **26**, 2792–2797 (1956).
52. E. Spohn and W. Lieber, "Reactions between calcium carbonate and portland cement, contribution to the systems C_3A–$CaCO_3$–H_2O and C_4AF–$CaCO_3$–H_2O" (in German).—Zement-Kalk-Gips **18**, 483–485 (1965).
53. R. Turriziani and G. Schippa, "Investigation of the quaternary solids CaO–Al_2O_3–$CaSO_4$–H_2O by X-ray and D. T. A. methods" (in Italian).—Teil 1: Ric. Sci. **24**, (11) 2356–2363 (1954), Teil 2: Ric. Sci, **25**, (10) 2894–2998 (1955).
54. W. Lerch, F. W. Ashton and R. H. Bogue, "The sulpho-aluminates of calcium".—I. Res. Nat. Bur. Stand. 2, 715–731 (1929).
55. G. L. Kalousek, "The sulpho-aluminates of calcium as stable and metastable phases and a study of a portion of the five-component system CaO–Al_2O_3–Na_2O–H_2O–SO_4".—Thesis, Univ. of Maryland, (1941).
56. I. D'Ans and H. Eick, "The system CaO–Al_2O_3–$CaSO_4$–H_2O at 20°C" (in German).—Zement-Kalk-Gips **6**, 302–311 (1953).
57. P. Seligmann and N. R. Greening, "Studies of early hydration reactions of portland cement by X-ray diffraction".—Highway Res. Record Nr. 62 80–105 (1964).

57a. W. Dosch and H. zur Strassen, "An alkali-containing calcium aluminate sulphate hydrate" (in German)—Zement-Kalk-Gips **20**, 392–401 (1967).

58. G. Schippa, "The sulphoferrite hydrates of calcium" (in Italian) Ric. Sci. **28**, 2334–2340 (1958).
59. A. Friedel, "A hydrated calcium chloro-aluminate hydrothermaly prepared" (in French).—Bull. Soc. Franc. Minéral **20**, 122–136 (1897).
60. L. Forsen, "On the chemistry of the portland cement" (in German) Zement **24**, 77–82 (1935).
61. C. W. Bunn and L. M. Clark, "The role of sodium aluminate in water softening, part IV reactions in lime-soda-sodium aluminate reaction vessels: a study of calcium aluminate hydrates". J. Soc. Chem. Ind. **57**, 399–405 (1938).
62. R. Turriziani and G. Schippa, "Contribution to the knowledge of hydrated calcium chloro-aluminates" (in Italian).—Ricerca Scient. **25**, 3102–3106 (1955).
63. G. Schippa and R. Turriziani, "The reaction of pozzolanas with calcium hydroxide in the presence of calcium chloride" (in Italian).—Ricerca Scient. **26**, 3715–3728 (1956).
64. H. J. Kuzel, "X-ray investigation in the system $3CaO \cdot Al_2O_3 \cdot CaSO_4 \cdot nH_2O$–$3CaO \cdot Al_2O_3 \cdot CaCl_2 \cdot nH_2O$–$H_2O$" (in German).—N. Jahrbuch f. Mineralogie **7**, (July 1966).
65. H. E. Schwiete, U. Ludwig and J. Albeck, "Investigation on the reaction between calcium chloride and clinker minerals" (in German) (unpublished).—Inst. f. Gesteinshüttenkunde der RWTH Aachen (1967).
66. W. Lieber and K. Bleher, "Is calcium chloride aggressive to steel?" (in German).—Beton **9**, 207–209 (1959).
67. M. H. Roberts, "Effect of calcium chloride on the durability of pre-tensioned wire in prestressed concrete".—Magazine of Coner. Res. **14**, 143–154 (1962).
68. A. M. Rosenberg, "Study of the mechanism through which calcium chloride accelerates the set of portland cement".—J. Amer. Concrete Inst. Proc., **61**, 1261–1269 (1964).
69. N. Tenoutasse, "Investigation on the kinetics of the hydration of tricalcium aluminate in the presence of calcium sulphate and calcium chloride" (in German).—Zement-Kalk-Gips **20**, 459–467 (1967).
70. E. T. Allen and H. F. Rogers, Ref. in Bessey, G. E.: "On calcium aluminate and silicate hydrates".—Symp. Chem. Cements, Stockholm 1938, Ingeniörsvetenskapsakademien, Stockholm 1939 p. 178–215 and Am. Chem. J. 1900 **24**, (4) 304–318.
71. H. E. Schwiete, E. Büssem and R. Salmoni, "Investigation on hydrated dicalcium aluminate".—Tonind.-Ztg. **58**, 168–169 (1934) and Zement **22**, 523–526 (1933).
72. H. E. Schwiete, U. Ludwig and P. P. Müller, "Investigations on hydrates of calcium aluminates" (in German).—Betonsteinzeitung **32**, 238–243 (1966).
73. G. E. Bessey, "The calcium aluminate and silicate hydrates".—Proc. Chem. Cem., Stockholm 1938, (1939) p. 178–230.
74. F. M. Lea und G. E. Bessey, J. Chem. Soc., 1612 (1937).
75. J. Lefol, Compt. rend., **17**, 919–921 (1933).
76. R. Nacken, "Behaviour of calcium silicates and aluminates in solutions of water. The problem of hardening of cement" (in German).—Zement **25**, 564–570 (1936), Zement **26**, 715–719 (1937).
77. F. M. Lea, The Chemistry of Cement and Concrete.—London 1956, 2. Edition (Edward Arnold Publishers, Ltd.)
78. P. Lhopitallier, "Calcium aluminates and high-alumina cements", Proc. IV. Intern. Symp, Chem. Cement, Washington (1960) VIII-4, p. 1007–1033.
79. E. T. Carlson, "Some observations on hydrated mono-

calcium aluminate and monostrontium aluminate". —J. Res. Nat. Bur. Standard **59**, 107 (1957).
79a. E. T. Carlson, "The system lime-alumina-water at 1°C".—J. Res. Nat. Bur. Standard **61**, 1–11 (1958).
80. O. Henning, "Formation, structure and hydration of the alkaline earthaluminates and high-alumina cements" (in German).—Habilitationsschrift Weimar 1966.
81. M. S. Crowley, "Effect of starting materials on phase relations in the system $CaO-Al_2O_3-H_2O$".—J. Amer. Ceram Soc. **47**, 144–148 (1964).
82. W. F. T. Pistorius, "Phase relations in the system $CaO-Al_2O_3-H_2O$ at high pressures and temperatures".—Amer. J. Science **260**, 221–229 (1962).
83. H. Lehmann and K. J. Leers, "Reactions during hardening of high-alumina cements" (in German).—Tonind.-Ztg. **87**, 29–41 (1963).
84. S. Chatterji and A. J. Majumdar, "Studies of the early stages of paste hydration of high-alumina cements".—The Indian Concrete Journal **40**, 51–55 (Febr. 1966), **40**, 152–155 (April 1966) and 40, (June 1966).
85. J. Brocard, "Hydration and hydrolysis of calcium silicates and aluminates as a function of temperature" (in French).—Ann. Inst. Techn. du Batiments Trav. Publ. Nr. 12 (1948).
86. F. M. Lea and C. H. Desch, "The chemistry of cement and concrete". London p. 56, 1956.
87. P. Longuet, "Note on a hydrated monocalcium aluminate".—Proc. III. Intern. Symp. Chem. Cement, London p. 328 (1952).
88. O. Rebuffat, Gazz. Chim. Ital. **30**, 182 (1900).
89. W. Strätling and H. zur Strassen, "The reaction between calcined kaolin and calcium hydroxide in water" (in German).—Z. für anorg. allgem. Chemie **245**, 267 (1940).
90. N. Fratini and R. Turriziani, "Contribution to knowledge of a hydrated calcium silico aluminate (Strätlings Compound)" (in Italian).—Ric. Sci. **24**, 1654–1657 (1954).
91. C. H. Schmitt, "Discussion", Chemistry of Cement, Proc. of the fourth Intern. Symp., Washington 1960, Vol. I, p. 244.
92. H. E. Schwiete, U. Ludwig, K. E. Würth and G. Grieshammer, "Hydration products of the hydration of blast-furnace slags" (in German).—Vortrag von H. E. Schwiete am Miner. Inst. der Universität Leipzig im Nov. 1965.
93. W. Krönert, H. E. Schwiete and K. Wetzel, "Reaction of alkaline earth oxides with clay minerals in water" (in German).—Die Naturwissenschaften **51**, 381–182 (1964). (complete publication is prepared).
94. T. Thorvaldson, N. S. Grace and V. A. Vigfusson, "The hydration of the aluminates of calcium, II. The hydration products of tricalcium aluminate".—Canad. I. Res. 1 201 (1929).
95. V. C. Farmer, "Infra-red spectroscopy of silicates and related compounds", in Taylor (1964) Bd. 2, p. 291.
96. E. P. Flint, L. S. Wells and H. F. McMurdie, "Hydrothermal and X-ray studies of the garnet-hydrogarnet series and the relationship of the series to hydration products of portland cement"—J. Research N. B. S. **26**, 13–33 (1941).
97. A. J. Majumdar and R. Roy, "The system $CaO-Al_2O_3-H_2O$".—J. Am. Ceram. Soc. **39**, 434–42 (1956).
98. F. Köberich, Diss. Berlin, 1934.
99. W. G. Schneider and T. Thorvaldson, "The hydration of aluminates of calcium".—Canad. J. Res. B. **19**, (1941) 123 and **21**, 34–42 (1943).
100. G. L. Kalousek, C. W. Davis and W. E. Schmertz, "An investigation of hydrating cements and related hydrous solids by differential thermal analysis".—J. Am. Concr. Inst. **45**, 673–712 (1949).
101. R. H. Bogue and W. Lerch, "Hydration of portland cement compounds". Industr. Ing. Chem. **26**, 837 (1934).
102. R. Kelly, "Solid-liquid-reactions. Part. II, Solid-liquid-reactions amongst the calcium aluminates and sulphoaluminates".—Can. J. Chem. Vol. **38**, p. 1218–26 (1960).
103. A. Eiger, "A new hydrated calcium ferrite" (in French).—Rev. Mat. Constr. **32**, 141 (1937).
104. H. zur Strassen, "The chemical reactions involved in the hardening of cement" (in German).—Zement-Kalk-Gips **11**, p. 137–43 (1958).
105. F. H. Dörr, "Studies in the system $CaO-Al_2O_3-SiO_2-H_2O$" (in German).—Dissertation, Mainz 1956.
106. E. T. Carlson, "Hydrogarnet formation in the system lime-alumina-water".—J. Research N. B. S. **56**, 327–35 (1956).
107. W. E. Ford, "A study of the relations existing between the chemical, optical and other physical properties of the members of the garnet group".—Am. Journ. Sci. 4th Series, Vol. XL, No. 235, Juli 1915.
108. D. M. Roy and R. Roy, "Crystalline solubility and zeolitic behaviour in garnet phases in the system $CaO-Al_2O_3-SiO_2-H_2O$".—Chem. Cem. 4th Intern. Symp. Washington 1960, N. B. S. Monograph 43, p. 307–14.
109. A. Burdese and S. Gallo, "Investigation of the dehydration products of tricalcium ferrite hexahydrate" (in Italian).—Ann. di Chim. **42**, 349–355 (1952).
110. O. P. Mchedlov-Petrosyan, V. J. Babuskin and G. M. Matveev: Thermodynamics of Silicates (in German) VEB-Verlag für Bauwesen, Berlin 1965.
111. L. E. Copeland, E. Bodor, T. N. Chang and C. H. Weise: Reactions of tobermorite gel with aluminates, ferrites and sulphates. J. P. C. A. Res. and Dev. Labs., **9**, 61–74 (1967).

Appendix *Infra-red absorption wave numbers of calcium aluminate hydrates*

C_4AH_{13}			C_3AH_62				$C_3A \cdot Cs \cdot H_{12}$		$C_3A \cdot Cs_3 \cdot H_{32}$					Type of oscillaiton
1	2	3	4	5		3	2	3	1	6	7	8	3	
		398		410	405	408	426				420	425	401	Ca–O
	427	462		500	423		526				555	540	590	S–Al–O
	542	522			535	578	592			606	610	608	606	ν_4–SO_4
	588												637	
704	660							732					676	
780	722	770			805	800	780	775			770	770		ν–Al–O
860	816					859			850	848	835	840		
880	878					895			875				860	
970	950				965									
1015							1075	1105	1110		1121	1130	1110	ν_3–SO_4
1075	1074	1106												
			1156				1163							
1330			1396			1425		1390	1450		1430	1432		internal CO_3–
											1490	1490		vibration
	1660		1555		1655		1630	1625	1620	1667	1646	1638	1635	S–H_2O
	1704													
							2000	2100						
			2273											
			2381			2910					3100	3100		ν–OH assoc.
3125	3150				3160				3230					
	3376	3490						3400		3340				
	3552	3590		3600	3540	3590	3590							
	3636		3799		3635	3640								
	3686		4000		3680		3710				3700	3700		ν–OH free
			4200											

1. Midgley (1960)
2. Henning (1966)
3. This investigation
4. Majumdar (1956)
5. Lehmann (1960)
6. Schwiete, Lipinski, Niel (1964)
7. Henning, Danowski (1964) Ettringite 1(cold precipitated)
8. like 7., Ettringite 2(precipitated by boiling temperature)

Appendix *X—ray data of AFm—phases (Kuzel)*

$3CaO \cdot Al_2O_3 \cdot CaSO_4 \cdot 12H_2O$			α-$3CaO \cdot Al_2O_3 \cdot CaCl_2 \cdot 10H_2O$			β-$3CaO \cdot Al_2O_3 \cdot CaCl_2 \cdot 10H_2O$			$6CaO \cdot 2Al_2O_3 \cdot CaSO_4 \cdot CaCl_2 \cdot 24H_2O$		
hkil	d (Å)	Int.	hkl	d (Å)	Int.	hkil	d (Å)	Int.	hkil	d (Å)	Int.
0003	8.90	100	002	7.89	100	00.6	7.81	100	00.6	36.5	5
0006	4.45	90	$\bar{1}11$	4.93	<5	10.2	4.85	<5	00.12	18.32	100
10.4	3.99	20	110	4.89	<5	00.12	3.90	80	00.18	5.56	10
10.5	3.64	<5	111	4.44	<5	10.8	3.79	30	10.4	4.87	<5
10.7	3.03	<5	$\bar{1}13$, 004	3.94	80	10.10	3.41	<5	10.8	4.63	<5
0009	2.97	<5	112	3.85	50	11.0	2.87	80	10.10	4.45	<5
11.0	2.88	10	204	3.72	10	11.3	2.82	<5	00.24	4.18	100
10.8	2.77	<5	202	3.51	<5	11.6	2.69	<5	10.14	3.91	<5
11.3	2.74	5	$\bar{1}14$	3.39	<5	00.18	2.60	10	10.16	3.90	5
20.1	2.48	<5	113	3.29	<5	10.16	2.52	10	10.20	3.53	5
20.2	2.45	10	$\bar{3}12$, 020	2.87	50	11.9	2.51	20	00.30	3.35	40
11.6	2.42	20	021, 313	2.82	<5	20.2	2.47	<5	11.0, 11.3	2.87	50
10.10	2.36	10	310	2.75	<5	20.4	2.43	10	11.6	2.83	<5
20.4	2.336	<5	022	2.69	<5	11.12	2.311	50	00.36	2.79	5
20.5	2.260	<5	006	2.63	20	20.8	2.288	20	11.9	2.78	<5
00012	2.233	30	204	2.60	<5	20.10	2.196	50	11.12	2.72	10
10.11	2.189	20	311	2.57	<5	10.20	2.120	10	10.32	2.66	<5
20.7	2.090	<5	023, $\bar{1}16$	2.52	10	11.15	2.113	10	11.15	2.64	<5
11.9	2.070	20	402, $\bar{2}21$	2.49	5	20.12	2.095	<5	11.18	2.55	<5
20.8	2.000	<5	$\bar{3}15$	2.48	5	20.14	1.994	<5	20.4	2.47	<5
10.13	1.906	10	220	2.44	5	10.22, 00.24	1.956	<5	11.21	2.46	5
21.2	1.867	<5	$\bar{4}04$	2.41	<5	11.18	1.928	<5	20.8	2.44	20
20.10	1.826	10	312	2.37	10	20.16	1.895	<5	00.42	2.39	30
00015, 10.14	1.786	10	221	2.349	<5	21.4	1.856	<5	11.24	2.37	30
11.12	1.765	<5	400	2.336	5	21.8	1.790	<5	10.38	2.335	<5
20.11	1.743	<5	024	2.319	10	21.10	1.744	<5	20.16	2.312	10
			$\bar{3}16$	2.277	10		.		11.27	2.271	<5
			$\bar{2}24$	2.272	10		.		10.40	2.244	20
			222	2.221	5				20.20	2.229	10
									20.22, 11.30	2.182	5
			116, $\bar{4}06$	2.157	30				00.48, 20.26	2.092	20
			025	2.121	<5				10.44	2.077	10
			$\bar{2}08$	2.098	20				20.28	2.043	<5
				.						.	
				.						.	

Appendix *X—ray data*

hkl	$3CaO \cdot Al_2O_3 \cdot 3CaSO_4 \cdot 32H_2O$ (Schwiete, Ludwig, Jäger) $a_0 = 11.18$ Å, $c_0 = 24.48$ Å		$3CaO \cdot Fe_2O_3 \cdot 3CaSO_4 \cdot 32H_2O$ (Schwiete, Ludwig, Jäger) $a_0 = 11.25$ Å, $c_0 = 21.49$ Å		$3CaO \cdot Fe_2O_3 \cdot 3CaSO_4 \cdot 31H_2O$ (Smolczyk) $a_0 = 11.23$ Å, $c_0 = 22.02$ Å		$3CaO \cdot Al_2O_3 \cdot 3CaCl_2 \cdot 30H_2O$ (Schwiete, Ludwig, Albeck) $a_0 = 11.738$ Å, $c_0 = 20.71$ Å	
	d (Å)	Int.	d (Å)	Int.	d (Å)	Int.	d (Å)	Int.
100	9.72	100	9.77	100	9.77	100	10.15	100
101	8.84	9	8.84	20				
110	5.60	73	5.58	81	5.63	70		
112	4.95	17			5.01	(10)		
200	4.84	4	4.87	46			5.06	14
104	4.70	36			4.796	10	4.69	11
314	4.35	2	4.435	18				
203	4.03	5	4.04	16	4.058	15		
114	3.87	53	3.914	66	3.934	45	3.94	3
210	3.67	4	3.67	3				
204	3.60	13	3.62	16	3.648	15	3.663	27
212	3.47	30	3.48	30	3.486	25		
213	3.27	5						
300	3.23	24	3.235	20	3.243	25	3.375	2
116	3.02	7	3.04	10	3.058	(<10)	3.11	5
220	2.80	5	2.80	51	2.805	(<20)	2.93	4
304	2.77	39	2.78				2.862	2
222	2.72	4						
310	2.71	14					2.82	4
008	2.68	5	2.686	3				
312	2.61	16	2.622	51				
216	2.565	50	2.59	32	2.600	(<15)		
313	2.52	2	2.53	30				
224	2.49	4			2.501	(10)		
400	2.43	2					2.57	18
118					2.468	(10)	2.48	2
306	2.41	10			2.420	(10)	2.42	2
208	2.35	5					2.366	2
320	2.22	8			2.230	35		
226	2.21	43					2.291	9
322	2.18	4						
316	2.15	19			2.173	15		
323	—							
410	2.12	6					2.225	1
412	2.08	3						
324	2.06	5					2.162	4
413	—		( ) = partly disturbed interferences				2.135	3
317	2.00	2						
325	1.98	5						
414	—						1.960	4
500	1.945	11						
407	1.90	5					1.920	4
503	1.87	2						
2.1.10	1.853	7						
332	1.845	6						
421	1.83	3						
504	—						1.907	3
422	1.81	3						
2.0.11	.							
0.0.12	.						1.822	3

Written Discussion

Melville H. Roberts

Synopsis

The present note is a contribution to the written discussion of a paper by H. E. Schwiete and U Ludwig entitled 'Crystal structures and properties of cement hydration products (Hydrated calcium aluminates and ferrites), to be presented at the Fifth International Symposium on the Chemistry of Cement, Tokyo, October 1968. Available evidence for the con-

clusion that cubic $3CaO \cdot Al_2O_3 \cdot 6H_2O$ is a metastable or unstable phase in solution at temperatures slightly below 20°C is discussed. Additional results are presented which appear to confirm this conclusion, since this cubic hydrate is partially transformed into the hexagonal-plate hydrates $2CaO \cdot Al_2O_3 \cdot 8H_2O$ and $4CaO \cdot Al_2O_3 \cdot 19H_2O$ in water and lime solutions at 1°C. Slight carbonation and the formation of quaternary carbonate hydrates also occurred, and to elucidate the influence of carbonate contamination the effects of carbon dioxide on $3CaO \cdot Al_2O_3 \cdot 6H_2O$ in aqueous suspensions at 25°C are briefly described.

Schwiete and Ludwig in their principal paper state that "C_3AH_6 is the only stable pure calcium aluminate hydrate present, under normal conditions of temperature and pressure, in the system Al_2O_3–CaO–H_2O". While this statement is also very probably true, even at high pressures, at temperatures up to about 225°C, there is some evidence pointing to the conclusion that cubic C_3AH_6 is a metastable or unstable phase with respect to the hexagonal-plate hydrates C_2AH_8 and C_4AH_{19} in solution at temperatures slightly below 20°C. In the following, the available data are discussed and some additional results are presented which appear to confirm this conclusion.

Buttler and Taylor (1) treated samples of C_3AH_6 with water and lime solutions at 5°C for various periods up to about 8 months, and they observed that the C_3AH_6 apparently dissolves congruently to give solution compositions near to the solubility curve for C_3AH_6 previously obtained at 20–21°C by other investigators (2, 3). On the other hand, in similar experiments at 1°C over periods from 9 to 16 months with intermittent shaking Carlson (4) found that partial transformation into C_2AH_8 or "C_4AH_{13}" occurred in some reaction mixtures, though not in all. some carbonation also took place in these tests, as shown by the presence of $C_3A \cdot CaCO_3 \cdot 11H_2O$ in all final solids, and this may possibly account for the erratic results. Nevertheless, Carlson concluded on the basis of these experiments that C_3AH_6 is less stable than C_2AH_8 or "C_4AH_{13}" at 1°C. While the difference in temperature might account for the different results at 1°C and 5°C, Jones (5) later inferred in his comprehensive review of the equilibria in the CaO–Al_2O_3–H_2O system that C_3AH_6 is still the only stable ternary phase at 1°–5°C. However, van Aardt and Visser (6) carried out further investigations in which C_3AH_6, with and without solid $Ca(OH)_2$, was treated with water for 7 days, and X-ray examination of moist solids showed the formation of C_4AH_{19} or C_2AH_8 at 5°C but not at 25°C. The X-ray powder patterns also indicated the presence of basal spacings at 8.2 Å and 7.6 Å, and though not recognized as such by these authors these spacings evidently arise from the quaternary carbonate hydrates $C_4A \cdot \frac{1}{2}CO_2 \cdot 12H_2O$ and $C_3A \cdot CaCO_3 \cdot 11H_2O$, respectively. In this case, contamination by atmospheric CO_2 may have mainly occurred during the X-ray diffractometer examination, whereas to account for previous work (1, 4) where little or no conversion of the C_3AH_6 apparently occurred after many months, it is conceivable that the results were also influenced by inadvertent carbonation in that the quaternary carbonate hydrates possibly formed a protective coating on the C_3AH_6 crystals in the aqueous suspensions.

Additional evidence for the instability of C_3AH_6 at 5°C is provided by the X-ray diffraction investigation of Seligmann and Greening (7). These authors studied the behaviour at different temperatures of a sample consisting initially of a mixture of C_4AH_{19}, $Ca(OH)_2$ and $C_4A \cdot \frac{1}{2}CO_2 \cdot 12H_2O$ and contained in a special X-ray diffractometer sample holder with an atmosphere of moist nitrogen. It was found that the C_4AH_{19} converted into C_3AH_6 and $Ca(OH)_2$ after 2 hours at 80°C, but subsequent storage over water for 17 hours at 5°C resulted in the disappearance of the X-ray pattern of C_3AH_6 and the restoration of that of C_4AH_{19}. A reversible transformation between C_3AH_6 and C_4AH_{19} has also been observed in later work by Carlson (8), who used a technique involving the microscopical observation of crystals in aqueous suspensions. By this means, it was shown that surface alteration of the C_3AH_6 crystals, evidently through the formation of C_4AH_{19}, occurred after 1 day at 10°C, and was removed after 2 days at 30°C. This surface alteration also took place at 15°C, but 14 days at 20°C produced no change in the C_3AH_6 crystals. Furthermore, a reversible transformation between the hexagonal and cubic phases was also observed to occur with various closely related calcium aluminoferrite hydrates over similar temperature ranges.

In contrast to these results, which indicate that C_3AH_6 is unstable in solution even at temperatures up to 15°C, Feldman and Ramachandran (9) studied the hydration of C_3A compacts at various tempera-

tures and concluded from DTA investigations that there is immediate formation of the hexagonal-plate hydrates at 2°, 12° and 23°C, followed subsequently after some time at these temperatures by conversion into cubic C_3AH_6. In view of the very different crystal structures of C_3AH_6 and the hexagonal-plate hydrates, together with the general observation that the conversion only takes place in the presence of water, it is probable that the transformation into C_3AH_6 occurs by a "through-solution mechanism" involving the crystallization of C_3AH_6 from solution and the dissolution of C_2AH_8 and/or C_4AH_{19} to maintain the solution composition. The DTA thermograms obtained by Feldman and Ramachandran, showing the presence of small amounts of C_3AH_6 in hydrated solids after 10 days at 2°C, after 6 hours at 12°C and after 30 minutes at 23°C, would thus seem to indicate that C_2AH_8 and C_4AH_{19} are unstable with respect to C_3AH_6 at these temperatures. While this conclusion is very probably true at 23°C, an alternative interpretation can be suggested for the results at 2° and 12°C. Thus, it should be noted that the hydrated samples were dried superficially, presumably at room temperature, before examination and that water will also be liberated by dehydration of the hexagonal-plate hydrates during the initial heating period in the DTA apparatus. It seems possible therefore that sufficient water may be present so that some C_3AH_6 could form during the course of the preparation and DTA examination of the hydrated samples, and all the C_3AH_6 may be formed in this way in the samples hydrated at 2°C, and possibly also at 12°C, and not actually be present in the samples at low temperature. A similar explanation may also account for the apparent formation of C_3AH_6 at 2° and 12°C in later work by Feldman and Ramachandran (10) with C_3A + $CaSO_4 \cdot 2H_2O$ compacts. There may therefore really be no conflict between the data of these authors for C_3A compacts and the view that C_3AH_6 is unstable with respect to C_2AH_8 and C_4AH_{19} at low temperature.

In order to examine further the stability of C_3AH_6 at low temperature, some additional tests have recently been made in which 1 g samples of C_3AH_6 were added to 100 ml water, or various lime solutions, at 1°C. After continuous shaking at 1°C for different periods, the reaction mixtures were filtered in the absence of atmospheric CO_2, the filtrates analysed for CaO and Al_2O_3, and an X-ray examination made on the solid phases while still moist with mother-liquor. The results are summarised in Table 1, and the final solution compositions are plotted in Fig. 1, superimposed upon the solubility curves at 1°C given by Jones (5) on the basis of a re-interpretation of the data of Carlson (4).

The C_3AH_6 remained essentially unchanged after shaking for 7 days in water (mixes 1 and 2), and the solution compositions were near to the CaO/Al_2O_3 = 3 composition line, indicating practically congruent solubility. However, at longer times of shaking up to 35 days (mixes 3 and 4) there was partial transformation of C_3AH_6 into C_2AH_8 (or possibly a "C_2AH_8–C_4AH_{19}" solid-solution composition) and the solution concentration changed to that of the solubility curve TY for the "hexagonal-plate" solid solution. Conversion of C_3AH_6 into C_2AH_8 or C_4AH_{19} also could not be detected at 7 days when C_3AH_6 was added to lime solutions of concentration up to about 1.2 g CaO per litre (mixes 5–8), but the formation of C_4AH_{19} was observed in saturated lime solution with excess crystalline $Ca(OH)_2$ at 7 days (mix 9), though

Table 1. *Composition of solid phases obtained by treatment of* C_3AH_6 *with water and lime solutions at 1°C (1 g* C_3AH_6 *in 100 ml solution)*

Mix No.	Initial CaO concentration (g/litre)	Time of shaking (days)	Molar ratio CaO/Al_2O_3 in final solid*	Compounds identified in final moist solids from X-ray patterns				
				C_3AH_6 (5.1Å)	C_2AH_8 (10.7Å)	C_4AH_{19} (10.7Å)	$C_3A \cdot CaCO_3 \cdot 11H_2O$ (7.6Å)	$C_4A \cdot \frac{1}{2}CO_2 \cdot 12H_2O$ (8.2Å)
1	0	7	3.02	much			trace	little
2**	0	7	2.98	much				
3**	0	28	2.87	much	some†			
4	0	35	2.84	much	much†		trace	little
5	0.245	7	3.03	much			trace	little
6	0.490	7	3.04	much			trace	little
7	0.735	7	3.05	much			trace	little
8	1.225	7	3.09	much			trace	little
9	saturated***	7	5.50	much		much††		little
10	saturated***	39	5.53	much		much††		little

*Calculated from total initial composition of reaction mixture and composition of filtrate.
**Freshly-prepared sample of C_3AH_6 used.
***Excess CaO added and $Ca(OH)_2$ present in final solid phase.
†Remains after drying at 81 per cent RH.
††Converted to C_4AH_{13}(7.9Å) after drying at 81 per cent RH.

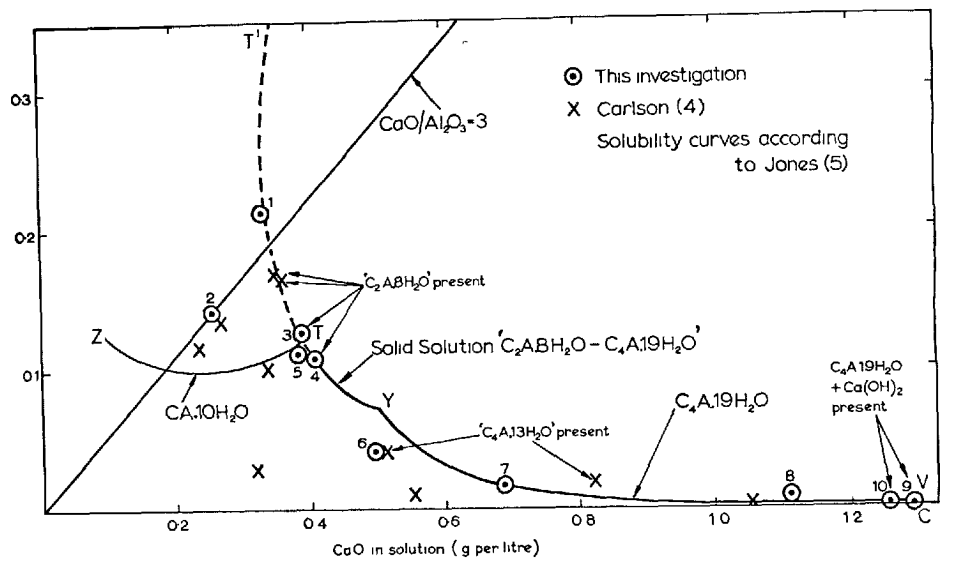

Fig. 1. *System* $CaO–Al_2O_3–H_2O$ *at 1°C. Treatment of* C_3AH_6 *with water and lime solutions*

some C_3AH_6 still remained after 39 days (mix 10). With these reaction mixtures of C_3AH_6 in lime solutions, all the final solution compositions were near to the solubility curves TY and YV, the latter being for C_4AH_{19}. Even at 7 days in mixes 5–8, it is possible therefore that the hexagonal-plate hydrates were present in small quantities, insufficient for detection by X-rays, and these may determine the solution compositions, though the quaternary carbonate hydrates present may also play some part. Small amounts of $C_4A\cdot\frac{1}{2}CO_2\cdot 12H_2O$, and usually traces of $C_3A\cdot CaCO_3\cdot 11H_2O$, were detected in all final solids, except for mixes 2 and 3 where a freshly prepared sample of C_3AH_6 was used. This carbonation may have mainly arisen from the use in most reaction mixtures of an old C_3AH_6 preparation, since the X-ray pattern of this preparation showed the presence of additional weak spacings at 7.9 Å and 7.6 Å, presumably from quaternary carbonate hydrates. In as much as similar results were obtained with mixes 2 and 3 in comparison with mixes 1 and 4, it does not appear that the carbonate contamination has affected the rate of conversion of C_3AH_6 in the continuously shaken suspensions. The transformation of C_3AH_6 into C_2AH_8 or C_4AH_{19} apparently does not occur very readily at 1°C, possibly because the latter hydrates precipitate as a protective coating on the C_3AH_6 crystals.

The above results are broadly similar to those obtained by Carlson (4) in his experiments on the solubility of C_3AH_6 in water and lime solutions at 1°C, and the solution compositions are included for comparison in Fig. 1. It is seen that some of these solution compositions are near to the plotted solubility curves, especially when the presence of "C_2AH_8" or "C_4AH_{13}" is indicated, but others differ markedly from these curves. In the latter cases, and perhaps aggravated by the intermittent shaking procedure, it is possible that the quaternary carbonate hydrates which are also present may be dominant, as a protective coating, in determing the solution compositions.

In connection with the effects of carbonate contamination, it has been observed in other experiments that C_3AH_6 is decomposed in the presence of CO_2 or $CaCO_3$ in aqueous suspensions at 25°C and marked changes in solution composition then occurred. On the basis of an X-ray examination of moist solid phases, it was indicated that treatment of C_3AH_6 suspensions in mother-liquor with increasing amounts of CO_2 at 25°C resulted initially in the formation of $C_4A\cdot\frac{1}{2}CO_2\cdot 12H_2O$, then increasing amounts of $C_3A\cdot CaCO_3\cdot 11H_2O$ and $C_4A\cdot\frac{1}{2}CO_2\cdot 12H_2O$ (or a similar solid-solution composition) were formed until the C_3AH_6 eventually disappeared, and subsequently hydrated alumina as well as calcite were precipitated. At the same time, the solution composition changed, and starting from a composition of about 0.56 g CaO per litre, 0.07 g Al_2O_3 per litre in the presence of a little $C_4A\cdot\frac{1}{2}CO_2\cdot 12H_2O$, the CaO concentration decreased slightly while the Al_2O_3 concentration increased appreciably, reaching values of 0.39 g CaO per litre and 0.32 g Al_2O_3 per litre. The solution compositions in the presence of $C_4A\cdot\frac{1}{2}CO_2\cdot 12H_2O$ (or a similar solid-solution composition) thus followed a path approximately parallel to the solubility curve TY for "C_2AH_8–C_4AH_{19}" solid solutions obtained at 25° by Jones and Roberts (11), and displaced to sligh-

tly lower CaO and Al_2O_3 concentrations. It may be noted that these solution compositions are very similar to those observed by Stein (12, 13) during the hydration of C_3A, with and without quartz, in aqueous suspensions at 25°C when increasing amounts of C_3AH_6 were being formed from the initially precipitated hexagonal-plate hydrates. It can therefore be suggested that, in spite of the precautions taken to obtain CO_2-free conditions, these results may have been influenced by inadvertent carbonation and the resulting formation of $C_4A \cdot \frac{1}{2}CO_2 \cdot 12H_2O$, rather than by a mechanism involving the alleged slower transformation of "C_4AH_n" then C_2AH_8 and the supposed precipitation of hydrous alumina, as indicated by Stein.

With the larger additions of CO_2 to C_3AH_6 suspensions, when hydrated alumina and calcite were present together with $C_3A \cdot CaCO_3 \cdot 11H_2O$ and $C_4A \cdot \frac{1}{2}CO_2 \cdot 12H_2O$, the solution concentration decreased to about 0.2 g CaO per litre, 0.08–0.10 g Al_2O_3 per litre. A similar solution composition was also obtained when $C_3A \cdot CaCO_3 \cdot 11H_2O$ was treated with water at 25°C, while in lime solutions of increasing concentration the Al_2O_3 concentration decreased rapidly to practically nil at about 0.3 g CaO per litre and remained barely detectable at higher lime concentrations up to saturation. The solubility curve of $C_3A \cdot CaCO_3 \cdot 11H_2O$ at 25°C appears to be very similar to that reported (11) for $C_3A \cdot 6H_2O$, but the latter hydrate should be more soluble than $C_3A \cdot CaCO_3 \cdot 11H_2O$.

Similar effects of carbonation on the solution composition to those described above at 25°C are to be expected at 1°C, and since small amounts of the quaternary carbonate hydrates were present in most of the reaction mixtures, some of the solution compositions reported may have been influenced by carbonation. However, although the results are not completely satisfactory in this respect, they support the conclusion that cubic C_3AH_6 is a metastable or unstable phase with respect to the hexagonal-plate hydrates C_2AH_8 and C_4AH_{19} at 1–5°C. The C_3AH_6 may also be unstable in solution at temperatures up to about 15°C, as observed by Carlson (8), but further work seems to be needed to check this observation.

References

1. F. G. Buttler and H. F. W. Taylor, 'The system $CaO–Al_2O_3–H_2O$ at 1°C, J. Chem. Soc., 2103–2110 (1958).
2. L. S. Wells, W. F. Clarke and H. F. McMurdie, "Study of the system $CaO–Al_2O_3–H_2O$ at temperatures of 21°C and 90°C", J. Res. Nat. Bur. Stand., **30**, 367–406 (1943).
3. J. D'Ans and H. Eick, "The system $CaO–Al_2O_3–H_2O$ at 20°C and the hardening of aluminous cement" (in German), Zement-Kalk-Gips, **6**, 197–210 (1953).
4. E. T. Carlson, "The system lime-alumina-water at 1°C", J. Res. Nat. Bur. Stand., **61**, 1–11 (1958).
5. F. E. Jones, "Hydration of calcium aluminates and ferrites", Proceedings Fourth International Symposium on the Chemistry of Cement, Washington 1960. U. S. Bureau of Standards Monograph 43, Vol. 1, 205–242 (1962).
6. J. H. P. van Aardt and S. Viesser, "Some reactions of tricalcium aluminate hexahydrate at medium temperatures", Cement and Lime Manufacture, **40**, 7–11 (1967).
7. P. Seligmann and N. R. Greening, "New techniques for temperature and humidity control in X-ray diffractometry", JPCA Res. and Devel. Labs., **4**, No. 2, 2–9 (1962).
8. E. T. Carlson, "Some properties of the calcium aluminoferrite hydrates", U. S. Dept. of Commerce, Nat. Bur. Stand., Building Science Series 6 (1966).
9. R. F. Feldman and V. S. Ramachandran, "Character of hydration of $3CaO \cdot Al_2O_3$", J. Am. Ceram. Soc., **49**, 268–273 (1966).
10. R. F. Feldman and V. S. Ramachandran, "The influence of $CaSO_4 \cdot 2H_2O$ upon the hydration character of $3CaO \cdot Al_2O_3$", Magazine of Concrete Research, **18**, No. 57, 185–196 (1966).
11. F. E. Jones and M. H. Roberts, "The system $CaO–Al_2O_3–H_2O$ at 25°C", Building Research Current Papers, Research Series 1 (1962).
12. H. N. Stein, "Influence of quartz on the hydration of $3CaO \cdot Al_2O_3$", Symposium on Structure of Portland Cement Paste and Concrete, Highway Research Board Special Report 90, 368–377 (1966).
13. The Science of Ceramics (Academic Press Inc., London and New York, 1967). Edited by G. H. Stewart. See paper by H. N. Stein entitled "The influence of quartz on the hydration of $3CaO \cdot Al_2O_3$", pages 109–128.

Written Discussion

W. Dosch, H. Keller and H. zur Strassen

Synopsis

A low-temperature phase of C_4AH_{19} was found below $-15°C$.

In solid solutions $Ca_2Al(OH)_6[(1-y)OH \cdot yX] \cdot aq$ the substitution rate y ranges in the complexes with carbonate from $y = 0.25$ to 0.5, with halides from 0.25 to 1 and with sulphate from 0.5 to 1, the basal distances being constant or nearly constant (CO_3, Cl, Br) or with a slight shift of ~ 0.2 Å (I. SO_4). In reaction mixtures low in iodide, a phase built up by regularly interstratified layers of C_4AH_{19} and the iodide-poorest solid solution was found, besides the separate phases. The halide complexes show a steeply increasing solubility of the halide ion in the solid solution range, among the carbonate complexes the quarter carbonate has an extremely low solubility.

The highest hydration stage of monosulphate (10.3 Å $16H_2O$) is formed only when the crystals are well ordered.

C_2AH_x is formed like quaternary complexes by replacing the exchangeable OH in $Ca_2Al(OH)_6OH \cdot aq$ by the anion $Al(OH)_4^-$.

The presence of the exchangeable OH is essential for the sorption capacity of C_4AH_x for organic molecules.

This contribution deals with a new modification of C_4AH_x and with various aspects of the solid solutions $Ca_2Al(OH)_6$ (OH, X)·aq, where X means a monovalent anion or an equivalent part of a polyvalent anion. Numerous anions, chosen after crystallochemical or geometrical features, were embedded into the C_4AH_x—lattice, only the main results will be reported here. Furthermore, new results on hydration stages of monosulphate, on C_2AH_8 and organo-complexes will be presented.

Low Temperature Modification of C_4AH_{19}

At room temperature, C_4AH_{19} exists in two polytypes, α_1– and α_2–C_4AH_{19} (1). Both modifications are built up by the same pseudocell, differing only in the stacking sequence of the elementary layers. By means of DTA and X-ray analysis, we found at low temperatures a modification of C_4AH_{19}, which has different dimensions of the pseudocell (2). The transformation

$$\alpha_2\text{–}C_4AH_{19} \xleftrightarrow{-15 \pm 2°C} \beta\text{–}C_4AH_{19}$$

is reversible at $-15 \pm 2°C$ and was observed only with exceptionally well crystallized C_4AH_{19}. The longest basal spacing of this "β–C_4AH_{19}" is 10.42 Å, the (110)—parameter enlarges from 2.88 Å (α_2–C_4AH_{19}) to 2.90 Å. Further work will be undertaken to get more complete X-ray data and to establish the symmetry of the new phase. With lower hydration stages of C_4AH_x there was no corresponding thermal transformation observed which originated in dimensional changes of the pseudocell.

Solid Solutions $Ca_2Al(OH)_6(OH, X) \cdot aq$

Preparation

Quaternary derivatives of C_4AH_x were prepared with reaction mixtures of CaO, $NaAlO_2$, H_2O and the calcium or alkali salt of the wanted anion. These mixtures were shaken at room temperature for at least one week. The same results are obtained by exchange of the outer OH's in preformed C_4AH_x against the wanted anions (added as salts) using aqueous or nonaqueous suspensions (exchange reactions). It is possible to produce the quaternary complexes also by neutralization: $Ca_2Al(OH)_6OH \cdot aq + HX \rightarrow Ca_2Al(OH)_6X \cdot aq + H_2O$, provided that the addition of the acid is extremely slow. This interlamellar sorption process preferably is done in C_4AH_x-benzene suspensions.

X-ray Characteristics

Regarding a certain hydration state, quaternary complexes derived from C_4AH_x are characterized by distinct basal spacings. Generally the same basal spacings are observed with members of the solid solution series $Ca_2Al(OH)_6(OH, X)\cdot aq$, however, some exceptions are noteworthy.

Constant Basal Distances

The CO_2-containing phases are of special interest with regard to cement hydration. Repeating an older work (3), we investigated once more the system C_4AH_x $-CO_2$, the CO_2-increments being this time more closer. We obtained the following results (Fig. 1):

The low carbonate phase (8.2 Å) is the only reaction product when the substitution rate y has reached values between 0.25 and 0.3. The basal distance keeps constant (8.2 Å) until $y = 0.5$. Exceeding amounts of CO_2 produce monocarbonate (7.6 Å) as a second phase and the 8.2 Å-phase disappears gradually until at $y = 1$ monocarbonate alone is present. Our investigations show, that the low carbonate phase (8.2 Å) has a varying composition: $Ca_2Al(OH)_6\left[(1-y)OH\cdot y\frac{CO_3}{2}\right]\cdot aq$ $(y = 0.25 - 0.5)$. Within this tolerance both statements of Dosch and zur Strassen (3) (1/4-carbonate) and Seligmann and Greening (4) (1/2-carbonate) are reconciled.

A continuous range of solid solution formation was also observed with halogenes and other anions. In the case of Cl- and Br- complexes, a single phase $Ca_2Al(OH)_6[(1-y)OH\cdot y\,Hal]\cdot aq$ was obtained, when y reached 0.25. The basal distance is almost the same as for the corresponding saturated complexes ($y = 1$) and does not shift significantly during further embedding of halogenes (Table 1).

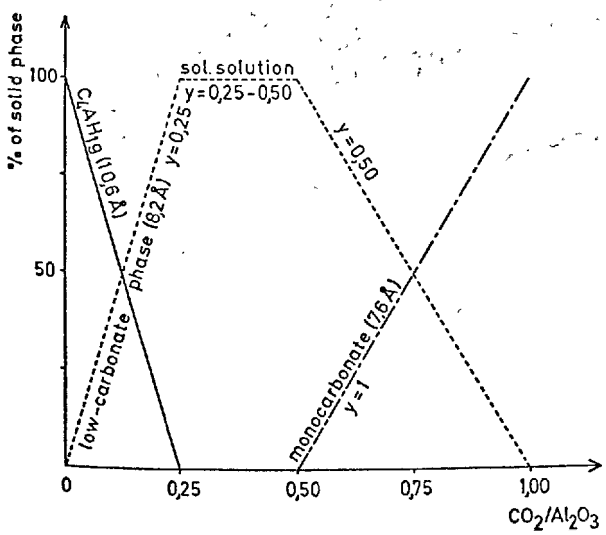

Fig. 1. *Sequence of carbonate complexes* $Ca_2Al(OH)_6\left[(1-y)OH\cdot y\frac{CO_3}{2}\right]\cdot aq$

Shift of Basal Distances

Examples for a distinct shift of the basal spacing with increasing replacement of OH by anions are the solid solution series with monoiodide (Table 1) or with monosulphate (Fig. 2).

When in the latter solid solution series the substitution rate y is below $0.5C_4AH_{19}$ and a sulphate bearing C_4AH_x ($c' = 8.78$ Å) coexist. Above 0.5, there are only mixed crystals. With increasing sulphate content the basal spacings get longer. The rate of increase is at first great, then becomes smaller. The end member, monosulphate-12-hydrate, is characterized by the longest basal distance of 8.94 Å, the total shift of the basal distances thus being about 0.2 Å.

The slope of the first part of the curve, where basal spacings of specimens with molar ratios SO_4^{2-}/Al_2O_3 below 0.5 are plotted, is reliable. But since the basal reflections of these specimens are weak and broad, they are measurable less accurately than those of compounds rich in sulphate. It is assumed that randomly interstratified layers of C_4AH_x and 1/2-monosulphate are formed when the molar ratios SO_4^{2-}/Al_2O_3 of the reaction mixtures are below 0.5. Since in these reaction products C_4AH_{19} is present as a second phase, the ratio of C_4AH_x to sulphate containing layers cannot be determined.

Table 1. *Solid solutions* $Ca_2Al(OH)_6[(1-y)OH\cdot yHal]\cdot aq$ *All reaction mixtures contain 10 mmoles* Al_2O_3 *(added as* $NaAlO_2$*), 40 mmoles* CaO *and 400 ml* H_2O. *The halides were added as sodium halides.*

Halide	Halide added mmoles	Halide in solution mmoles/l	Halide in solid phase y	X-ray reflections of moist solid c′ (Å)
Cl	1	0.6	0.04	10.6 ≫ 8.2† > 7.9
	2.5	1.5	0.10	10.6 > 8.2† ≧ 7.9
	5	1.8	0.22	7.92 ⫻ 10.6
	10	4.0	0.42	7.92
	15	10.2	0.54	7.92
	20	19.0	0.62	7.91
	30	37.5	0.75	7.87
	40	57.5	0.85	7.84
Br	1	0.3	0.04	10.6 ≫ 8.2
	2.5	0.5	0.12	10.6 > 8.2
	5	0.2	0.24	8.19 ≫ 10.6
	10	3.5	0.43	8.19
	15	11.0	0.53	8.19
	20	19.2	0.62	8.19
	30	40.2	0.70	8.18
	40	54.0	0.92	8.17
I	2.5	2.0	0.08	10.6 ≫ 19.18 > 8.4 b
	5	2.0	0.21	8.47 ≫ 19.18 ≧ 10.6
	7.5	3.0	0.32	8.55 ≫ 8.14† > 20
	10	6.2	0.38	8.58 ⫻ 8.22†
	15	12.5	0.50	8.62 ⫻ 8.22†

†traces of low-carbonate phases

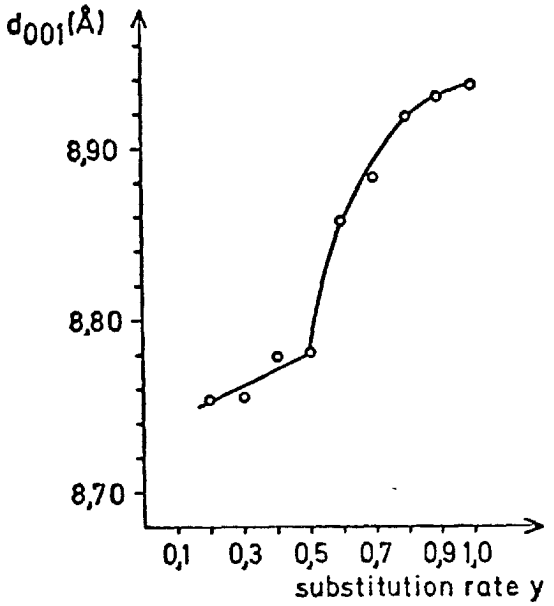

Fig. 2. *Basal distances of solid solutions* $Ca_2Al(OH)_6\left[(1-y)OH \cdot y\frac{SO_4}{2}\right] \cdot aq$

Regularly Interstratified Layers

Another type of solid solution formation was observed in mixed crystals $Ca_2Al(OH)_6[(1-y)OH \cdot yI] \cdot aq$ ($y = 0 - 0.25$). The reaction products, when still moist with mother liquor, showed among other basal reflections (Table 1) weak, but sharp integral 001—reflections, the longest basal spacing being 19.2 Å. This value originates from regularly interstratified sheets of C_4AH_{19} (10.6 Å) and sheets of monoiodide (8.62 Å): 10.6 + 8.6 = 19.2. This regularly stratified structure is destroyed on drying or when more iodide —ions are added to the starting reaction mixture. Exceeding the substitution rate y = 0.25, only mixed crystals are present, the basal spacing of which shifts from 8.5 to 8.6 Å, when half of the exchangeable OH is replaced by I.

Conclusions

We conclude, that in most cases of solid solution formation a certain low amount of embedded anions is sufficient to produce the basal spacing which is characteristic for a certain hydration stage of the corresponding saturated complex. Since under equal humidity and temperature conditions the basal distances of the quaternary compounds are in most cases widely separated from those of C_4AH_x and since there are always integral series of 001—reflections observed, it is concluded, that the solid solutions are not composed of randomly interstratified layers of $Ca_2Al(OH)_6OH \cdot aq$ and $Ca_2Al(OH)_6X \cdot aq$, or

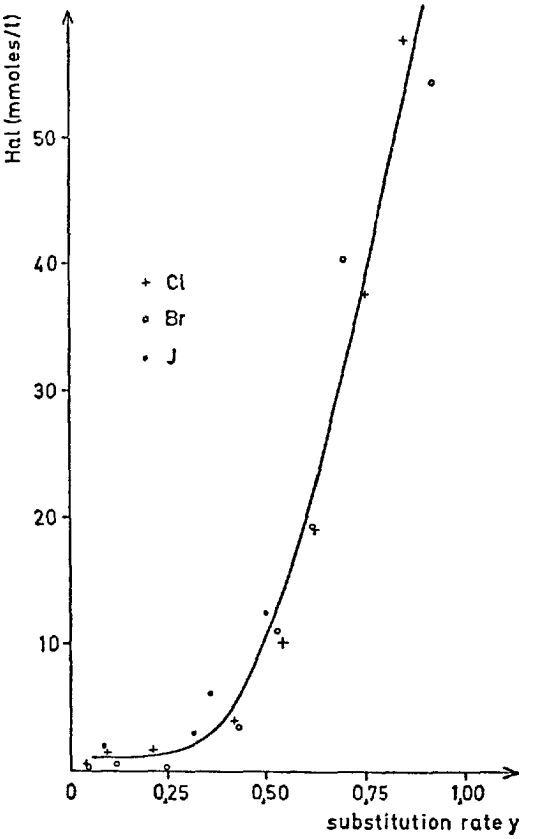

Fig. 3. *Solubility curves of solid solutions* $Ca_2Al(OH)_6[(1-y)OH \cdot yHal] \cdot aq$

intergrowths of larger stacks of ternary and quaternary compounds. The replacement of OH—ions by anions X takes place statistically on the surfaces of all $Ca_2Al(OH)_6$—principal layers. The resulting basal distance depends on the effective thickness of the anion X, but not on the total amount of exchanged anions. A minimum quantity, which is different for different anions, suffices to widen the elementary layers to the characteristic basal spacing of the quaternary complex. Further exchange of anions probably only has an influence on the crystal symmetry. But this picture is only a rough one, because it does not take into consideration the variation of the interlayer water during the sorption of anions by C_4AH_x.

The solid solution crystals are not very stable. Long storage or de- and rehydration cycles result in products giving rather complex X-ray patterns. Part of them indicate irregular interstratified layers, others show separation into ternary and quaternary phases.

Sorption Equilibria

The solubilities with regard to the sorbed anions

of the various complexes are very different. Extremely low solubilities have for instance the complexes with carbonate, sulphate, molybdate and uranate. C_4AH_x is, therefore, suitable for quantitative determinations of these anions or for the disintegration of salts and minerals, for example, calcite, coelestine and the like. Other quaternary complexes (for instance those of chromate, permanganate, chlorate, nitrate, halides) are strongly dissociated in aqueous solutions.

In Fig. 3. there is the halide content in solution plotted against the substitution rate. The solid consists (Table 1) of one single phase when y reaches 0.25. At lower contents of halide, there are two phases, C_4AH_{19} and the halide-poorest member ($y = 0.25$) of the solid solution series.

In agreement with this the first part in Fig. 3 indicates a very low and nearly constant solubility of the anion. The slope of the solubility curve begins at $y = 0.25$, when the solid consists of one phase. Very high solubilities have the saturated compounds ($y = 1$).

It was shown that an equimolecular mixture of calcite and tricalcium aluminate when shaken in aqueous suspension reacts by forming monocarbonate hydrate (5). The same decomposition of calcite is obtained when shaken with tetracalcium aluminate hydrate (Table 2, reaction 1). This shows that the solubility of calcite is higher than that of the carbonate complex. In the same way it can be demonstrated that the solubility with respect to the CO_3—anion is still lower in the low carbonate solid solution phase. Monocarbonate hydrate is decomposed by tetraclacium aluminate hydrate to semicarbonate (reaction 2), the later by additional CO_2—free phase to quarter carbonate (reaction 3). Monocarbonate and quarter carbonate react to semicarbonate (reaction 4). It is noteworthy that these transformations take place in spite of the extremely low solubility of the phases.

Table 2. *Reactions in aqueous suspension demonstrating the decreasing solubility of the carbonate complexes with decreasing carbonate content.*

1. $\frac{1}{2}CaCO_3 + Ca_2Al(OH)_6OH \cdot aq \longrightarrow Ca_2Al(OH)_6\left[\frac{CO_3}{2}\right] \cdot aq + \frac{1}{2}Ca(OH)_2$
   calcite — C_4AH_x — monocarbonate
2. $Ca_2Al(OH)_6\left[\frac{CO_3}{2}\right] \cdot aq + Ca_2Al(OH)_6OH \cdot aq \longrightarrow 2Ca_2Al(OH)_6\left[\frac{1}{2}OH \cdot \frac{1}{2}\frac{CO_3}{2}\right] \cdot aq$
   monocarbonate — C_4AH_x — semicarbonate
3. $Ca_2Al(OH)_6\left[\frac{1}{2}OH \cdot \frac{1}{2}\frac{CO_3}{2}\right] \cdot aq + Ca_2Al(OH)_6OH \cdot aq \longrightarrow 2Ca_2Al(OH)_6\left[\frac{3}{4}OH \cdot \frac{1}{4}\frac{CO_3}{2}\right] \cdot aq$
   semicarbonate — C_4AH_x — quarter carbonate
4. $Ca_2Al(OH)_6\left[\frac{CO_3}{2}\right] \cdot aq + 2Ca_2Al(OH)_6\left[\frac{3}{4}OH \cdot \frac{1}{4}\frac{CO_3}{2}\right] \cdot aq \longrightarrow 3Ca_2Al(OH)_6\left[\frac{1}{2}OH \cdot \frac{1}{2}\frac{CO_3}{2}\right] \cdot aq$
   monocarbonate — quarter carbonate — semicarbonate

Hydration Stages of Monosulphate Hydrate

Much uncertainty still seems to exist about the hydration stages of monosulphate. The following results (6) were obtained:

All de- and rehydration processes were followed stepwise by X-ray analysis, using a humidity and temperature controlled specimen cell. From reaction mixtures prepared above 10°C, 9.5 Å—monosulphate ($14H_2O$) is obtained. At room temperature and 95% r.h. this phase dehydrates to the 12—hydrate (8.9 Å), which exists within the range of 95% r.h. to 20% r.h.. Below 20% r.h. monosulphate-10-hydrate (8.15 Å) is formed. Over P_2O_5 and at temperatures between 30 and 50°C two more molecules of interlayer water are splitt off. This phase has a basal spacing of 7.95 Å. At room temperature it rehydrates rapidly at relative humidities below 1% to the 10—hydrate (8.15 Å). The latter phase rehydrates to the 8.9 Å—monosulphate at 30% r.h., 25°C. Further rehydration to the 9.5 Å—phase is possible in 100% r.h. at temperatures above 55°C. This phase converts to the 10.3 Å—phase, when the sample is cooled to below 8°C. Rising the temperature, 9.5 Å—monosulphate again is obtained. Not all preparations of monosulphate showed the re- and dehydration process forming the 9.5 Å and 10.3 Å—product. However, this conversion was always found with monosulphate which was prepared at temperatures around 0°C and which was X-rayed when still moist with mother liquor. Apparently only well ordered crystals—slowly grown at low temperatures—are able to de- and rehydrate at 8°C. We estimate the water content of the 10.3 Å—phase to be 16.

There is another example which indicates that some quaternary complexes of C_4AH_x must be of high crystalline orderliness to get their highest possible hydration stage: Foret (7) described the compound

$C_3A \cdot Ca(NO_3)_2 \cdot 16H_2O$, no X-ray data were given. Examining the solid solution series $Ca_2Al(OH)_6(OH, NO_3) \cdot aq$ we obtained the 16—hydrate ($c' = 10.39$ Å) only when the substitution rate y in the solid exceeded 0.75.

Since the H_2O dipoles are oriented not only to the octahedral OH's of the principal layer $Ca_2Al(OH)_6$ but also to the embedded anions, we conclude, that a high order of the anion arrangement is necessary to admit the formation of additional H_2O—layers, especially double layers of H_2O with or without participation of anionic oxygens. Lower hydration stages are far more tolerant of disordered crystals.

C_2AH_8, a Derivative of C_4AH_x

Among the numerous anions which are sorbed by C_4AH_x, there is also $Al(OH)_4^-$. This anion is of special interest since the interlamellar exchange of OH by $Al(OH)_4^-$ in C_4AH_x results in a compound which has the chemical composition of C_2AH_x:

$$Ca_2Al(OH)_6OH \cdot aq + Al(OH)_4^- \longrightarrow Ca_2Al(OH)_6Al(OH)_4 \cdot aq + OH^-$$

Indeed, our expectation to get C_2AH_x by this reaction was realized. According to that, C_2AH_x could be nominated "tetracalcium aluminate monoaluminate hydrate".

Our experiments were carried out using well crystalline C_4AH_x (average diameter 70μ) which was suspended in a concentrated alkaline $NaAl(OH)_4$ solution. Since in a strongly alkaline medium at room temperature the conversion of C_4AH_x to C_3AH_6 takes place readily, temperatures around 0°C had to be employed. The innercrystalline sorption of $Al(OH)_4^-$ is performed within 12 hours. One could argue that C_4AH_x disintegrates to form with $Al(OH)_4^-$ new crystals of C_2AH_x. But samples, which were examined at intermediate times during the sorption process did not exhibit any signs of decay. The C_2AH_8 ($c' = 10.7$ Å) formed this way is distinguishable from C_4AH_{19} ($c' = 10.7$ Å) by X-ray analysis only by its behaviour on dehydration.

Sorption of Organic Material by C_4AH_x

Until recently, we were not informed that Lavanant and Barret (8) were the first who found an organic sorption compound of C_4AH_x. However, the authors succeeded only to prepare a complex with methanol. Having no success with gaseous ethanol and benzene, they did not pursue such experiments.

Among cement hydration products, only C_4AH_x seems to possess the capability of innercrystalline swelling on the addition of organic substances, although the other hydration products partly form various hydration stages (9).

Esters, fatty acids and other acids are generally rapidly saponified by C_4AH_x. Recent IR-examinations have shown, that fatty acids are bonded as anions, there is no ester—like bond to the C_4AH_x—layers as was formerly supposed (10).

Free lime in cements is determined by the Franke method, using acetoacetic ester. At room temperature, this reagent violently disintegrates C_4AH_x, Ca-enolate and aluminium hydroxide being the reaction products. Therefore it is obvious that the Franke method is not applicable in the presence of C_4AH_x. Except calcium silicate hydrates, other products of cement do not react with acetoacetic ester.

Inorganic derivatives of C_4AH_x like monosulphate, Friedel's salt do not interlamellarly adsorb organic molecules. But solid solutions with C_4AH_x in which the exchangeable OH is only partially replaced by inorganic anions are capable to absorb organic molecules, though this process is rather complicated because partial decompositions into inorganic and organic derivatives of C_4AH_x take place. From this follows, that the sorption of organics is based on the existence of the exchangeable OH in $Ca_2Al(OH)_6 \cdot aq$ (9).

It must be pointed out, that there are two types of derivatives of C_4AH_x, which are capable to swell one-dimensionally with organic substances:

a) Inorganic derivatives of C_4AH_x containing anions which due to a certain electron configuration are able to fix organics. An example for this case is the quaternary complex $Ca_2Al(OH)_6Ni(CN)_4 \cdot aq$. Because of steric hindrances, only small molecules like methanol, formamide, acetone, pyridine are absorbed (2).

b) Alkali-monosulphate, though more widely differing from C_4AH_x, is the other compound showing sorption properties for organic molecules. In this compound, alkali cations which are situated between

negatively charged elementary layers are replaceable by alkylammonium cations, analogous to mica-like layer silicates (9).

References

1. F. E. Jones and M. H. Roberts, "The system CaO–Al_2O_3–H_2O at 25°C", Building Research Station, Research Series 1, 1959/1962.
2. H. Keller, Thesis, University of Mainz (in preparation).
3. W. Dosch and H. zur Strassen, "Untersuchung von Tetracalciumaluminathydraten. I. Die verschiedenen Hydratstufen und der Einfluss von Kohlensäure", Zement-Kalk-Gips **18**, 233–237 (1965).
4. P. Seligmann and N. R. Greening, "New techniques for temperature and humidity control in X-ray diffractometry", J. of P. C. A. Research and Development Labs. **4**, 2–9 (1962).
5. E. T. Carlson and H. A. Berman, "Some observations on the calcium aluminate carbonate hydrates", J. Research Nat. Bur. Standards **64A**, 333–341 (1960).
6. H. Keller, "Isotherme und isohygrische De- und Rehydratationen mit Tetracalciumaluminatmonosulfathydrat", Diplom-Arbeit, Mainz (1967).
7. J. Foret, "Sur le nitroaluminate de calcium", Comptes rendus **191**, 52–54 (1930).
8. F. Lavanant and P. Barret, "Contribution à l'étude des différents hydrates de l'aluminate tétracalcique hexagonal 4CaO, Al_2O_3, nH_2O", Comptes rendus **13**, 1122–1124 (1962). F. Lavanant, "Contribution à l'étude de quelques aluminates de calcium hydratés, Revue des Matériaux de Construction No. 592, 1–10; No. 593, 76–87; No. 595, 193–207; No. 596, 251–261; No. 597, 298–304 (1965).
9. W. Dosch, "Die eindimensionale innerkristalline Quellung natürlicher und synthetischer Schichtkristalle, insbesondere von Tetracalciumaluminathydrat", Habilitations-schrift, Mainz (1968).
10. W. Dosch, "Die innerkristalline Sorption von Wasser und organischen Substanzen an Tetracalciumaluminathydrat", N. Jb. Miner. Abh. **106**, 200–239 (1967).

Oral Discussion

Alice E. Moore and Harry F. W. Taylor

We have determined the crystal structure of ettringite by single-crystal X-ray methods, and our results do not support the structure of Bezjak and Jelenić

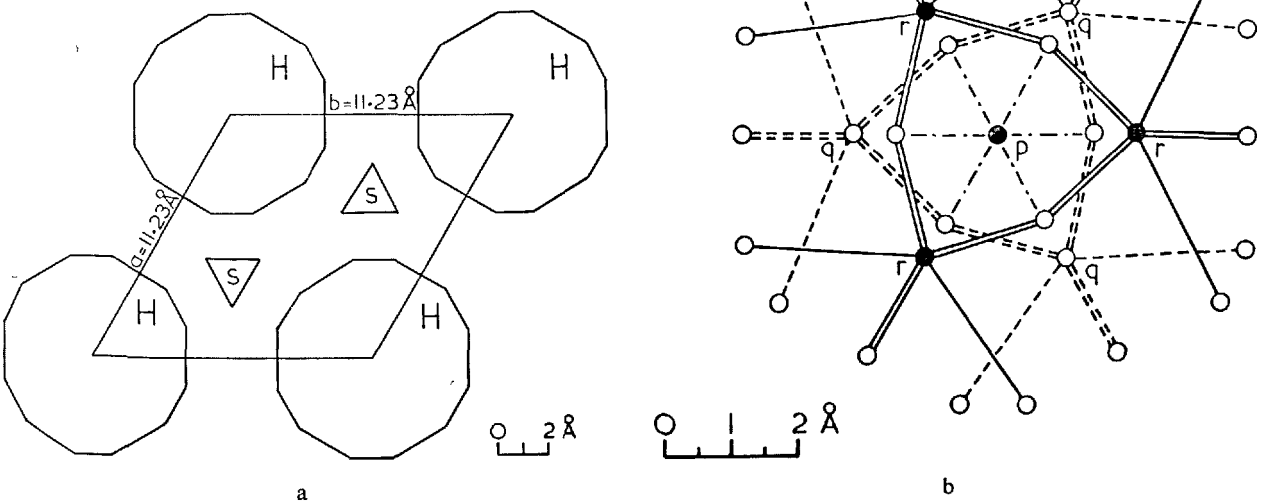

Fig. 1. *General features of the structure.* A, *Projection along* c, *showing the outlines of the columns* (*H*) *and of the sulphate groups* (*S*). B, *One of the columns in greater detail, also projected along* c. p, Al^{3+} *ions at* $z = 0$ *and* $\frac{1}{2}$ *(coincident in projection);* q *and* r, Ca^{2+} *ions at* $z = \frac{1}{4}$ and $\frac{3}{4}$, *respectively. Unlabelled circles represent either* OH^- *ions (co-ordinated to both* Al^{3+} and Ca^{2+}) *or* H_2O *molecules (co-ordinated only to* Ca^{2+} *within the columns).* Ca–O *bonds at* $z > \frac{1}{2}$ *are shown with full lines, and those at* $z < \frac{1}{2}$ *with broken lines. All the* z*-coordinates are given as fractions of the height of the pseudocell (10.72 Å). Reproduced, by permission of the editor and publishers, from ref. (2).*

(1) which is mentioned in the Principal Paper. We have reported preliminary results elsewhere (2), and have since refined the structure further using three-dimensional methods to give an R-factor of 0.11 for about 700 independent reflections.

The true space group is $\underline{P}31\underline{c}$ and the apparently hexagonal symmetry of some crystals must be attributed to disorder. The structure (Fig. 1a) is based on columns, of empirical composition $[Ca_3 \cdot Al(OH)_6 \cdot 12H_2O]^{3+}$, running parallel to the $\underline{c}$- or needle axis. In the channels between these columns occur the sulphate ions and remaining water molecules. Fig. 1b shows the structure of an individual column. Each Al^{3+} ion is octahedrally coordinated by hydroxyl ions, and each Ca^{2+} ion is 8-coordinated, by 4 hydroxyl ions and 4 water molecules. The Ca^{2+} and Al^{3+} polyhedra share edges. The surface of the column is formed by the H_2O molecules, and it is reasonable to suppose that the net positive charge of the column is distributed, more or less uniformly, among the hydrogen atoms of these water molecules.

Considering now the material in the channels, refinement of site-occupancies suggests that there are $1.5H_2O$ molecules per $3SO_4^{2-}$ ions, thus indicating the composition $Ca_6[Al(OH)_6]_2(SO_4)_3 \cdot 25\frac{1}{2}H_2O$, or $C_3A \cdot 3CaSO_4 \cdot 31\frac{1}{2}H_2O$, for ettringite. The contents of each channel follow the sequence SO_4–SO_4–SO_4–$1.5H_2O$, where the latter term represents a mean of $1.5H_2O$ molecules distributed statistically among 3 sites disposed symmetrically around the axis of the channel.

Further refinement is in progress and is beginning to show the positions of the hydrogen atoms.

References

1. A. Bezjak and I. Jelenić, Croat. Chim. Acta, **38**, 239 (1966).
2. A. Moore and H. F. W. Taylor, Nature, **218**, 1048 (1968).

Authors' Closure

Hans E. Schwiete and U. Ludwig

Roberts states in his paper that there is some evidence that C_3AH_6 is not the only stable pure calcium aluminate hydrate under normal conditions of temperature and pressure in the system Al_2O_3–CaO–H_2O at temperatures below 20°C.

We are in the opinion that it is very difficult in time to give a clear answer on this question. There is a lot of work stating the stability of C_3AH_6 at low temperatures and there are too experimental data from which we can derive instability and formation of C_2AH_8 and C_4AH_{19}. But when instability was found mostly there was found some impurity of CO_2 and in this case we have not the pure ternary system. From our own work we know, that it is not very easy to produce pure C_3AH_6 without any unhydrated C_3A, that could form afterwards C_4AH_{19} together with $Ca(OH)_2$. Together with Roberts we think that this is still a problem and further experimental work seems to be needed.

Dosch, Keller and zur Strassen gave in their paper some new data of the tetracalcium aluminate hydrate and the complex salts which can derived from it. We took care of this results already in our oral presentation of principal paper and appreciated the authors to their new data, specially the conversion of C_4AH_{19} at −15°C, and the explanation of the formation of complex salts by replacing exchangeable OH in $Ca_2Al(OH)_6OH \cdot aq$ and given boundary of the substitution rate of complex salts with CO_3, halides and SO_4.

A. E. Moore and H. F. W. Taylor gave a new space group for the crystal structure of the ettringite with $P31c$. This new space group is not only in contrast to the work of Bezjak and Jelenić but is also a correction of the former work of Bannister, Hey and Bernal.

The given composition of the ettringite with $Ca_6(Al(OH)_6)_2(SO_4)_3 \cdot 25\frac{1}{2}H_2O$ is in good agreement with our measurement of dehydration of ettringite that shows two endotherm peaks at about 60° to 200°C and 200° to 300°C with minima at 130° and 260°C.

The R-factor of 0.11 for about 700 reflections shows the accuracy of the given work. We are very much interested in the last details of the new structure of ettringite the authors announced.

(A) Papers regarding Structures

Supplementary Paper II-14 Quaternary Calcium Aluminate Hydrates: Crystal Structure of Calcium Aluminate Monobromide Hydrate

François Le Bel and Guy Grasland*

Synopsis

Quaternary calcium aluminate hydrates, belonging to one or other of two series of compounds with formulae:

$$Ca_2Al(OH)_6\,X\cdot nH_2O \text{ or } [Ca_2Al(OH)_6]_2Y\cdot nH_2O$$

(X and Y being respectively mono and divalent anions), are discussed. Synthesis methods used for monocrystal preparations are described.

The structural data concerning the calcium aluminate monobromide hydrate are given; the compound is trigonal (R3), the triple hexagonal cell includes three $Ca_2Al(OH)_6\,Br\cdot 2H_2O$ units, its parameters are:

$$a = b = 5.76\ \text{Å} \qquad c = 24.45\ \text{Å}$$

A structure determination obtained from 145 independent reflexions leads to a R index of 0.20. New intensity measurements associated with absorption corrections are being made to obtain a more precise determination of the structure.

The structure can be described as follows: Ca^{2+} and Al^{3+} ions, located in octahedral sites existing between two hydroxyl group layers are surrounded by six OH^-, polyhedrons of coordination having a common edge. Water molecules layers are found on both sides of the hydroxy-layers, the neighbouring of each Ca^{2+} ion is so completed with one water molecule. The Br^- ions are surrounded by six water molecules belonging to two successive layers.

A comparison is made with structure hypothesis formerly given.

Introduction

Present knowledge concerning the structure of hydrated calcium aluminates is very limited. This blank arises from the fact that it is very difficult to obtain single crystals of proper size, making possible direct analysis by X-ray diffraction.

At present, the only well-known structure is that of C_3AH_6. It was assessed by analogy with that of the glossularite C_3AS_3, by Flint, Wells and MacMurdie (1), and recently further specified by Weiss, Grandjean and Pavin (2).

The hydrocalumite, a natural mineral close to C_4AH_{13}, was the subject of a research on single crystals by Tilley, Megaw and Hey (3): however, the structure is still poorly understood.

Bezjac and Jelenic (4) recently presented a description of the structure of the ettringite, the work being carried out on powder photographies.

Studies on single crystals permitted Kuzel (5) to give crystal space groups and the unit cell of several calcium chloro and sulfoaluminates.

Lastly, many theories were proposed concerning the structure of the various hydrated calcium aluminates, in particular: Brandenberger (6); Tilley, Megaw and Hey (3); Bessey (7); Buttler, Dent Glasser and Taylor (8); Grudemo (9); Feitknecht and Buser (10).

The present work concerns the direct assessement of the structure of hydrated calcium monobromoaluminate, by X-ray analysis on single crystals.

*Ciments Lafarge, Paris, France.

Foreword

The hydrated calcium bromoaluminate $C_3A \cdot CaBr_2 \cdot 10H_2O$, belongs to the series of hydrated quaternary calcium aluminates. These compounds conform to the general formula $C_3A \cdot CaX_2 \cdot nH_2O$ or $C_3A \cdot CaY \cdot nH_2O$, X being a monovalent anion and Y a divalent anion. The series of these bodies was mainly studied by Buser (11). Chloroaluminates ($X = Cl^-$) sulfoaluminates ($Y = SO_4^{2-}$), carboaluminates ($Y = CO_3^{2-}$), compounds encountered in the hydration of cements, were particularly studied, as well as "hexagonal" aluminates to this series, with respective anions $Al(OH)_4^-$ and OH^-.

All these compounds present strong analogies, both by their crystallography (hexagonal facies of crystals, hexagonal parameter close to 5.7 Å..) and by their physical properties (easy cleavage parallel to 001, behaviour on dehydration, phyllitous nature . . .).

The choice of the calcium bromoaluminate within the series of these compounds was guided on one hand by the presence of the "heavy" bromine atom, on the other hand by the possibility of producing single crystals.

Preparation of Single Crystals

The hydrated calcium bromoaluminate $C_3A \cdot CaBr_2 \cdot 10H_2O$ can be produced as single crystals using the method described by H. W. Buser (11). This method uses the slow diffusion of a solution A, containing $Al(OH)_4^-$ and OH^- ions, and of a solution B, containing Br^- ions, into a third solution C, which may be either water, or a solution containing Br^- ions. According to the strengths of the three solutions A, B and C, the quality of crystals varies. The best conditions were obtained with:

Solution A(250 cm³)
$Al(OH)_4$: 0.05M; OH^- 0.1M; NaBr 0.6M
Solution B(250 cm³)
$CaBr_2$: 0.1M; NaBr 0.4M
Solution C(500 cm³)
NaBr: 0.6M

Crystals produced in this way appear as hexagonal plates 40 microns thick and 400 microns wide.

We also obtained single crystals by hydrothermal synthesis from lime, alumina and calcium bromide. A similar method was used by Friedel (12), who obtained crystals of calcium chloroaluminate; similarly, H. J. Kuzel (13) used this method to produce single crystals of chloro and sulfoaluminates. However synthesis remained smaller than that of diffusion crystals.

Structure of the Hydrated Calcium Bromoaluminate

This structural study was carried out in cooperation with Prof. Weiss's laboratory, of the Strasbourg University.

The X-ray diffraction study (powder diagram, rotating crystal, Weissenberg camera) indicates that the hydrated calcium bromoaluminate is rhombohedral. The parameters of the triple cell are $a = b = 5.76$ Å, $c = 24.45$ Å; it contains $1.5C_3A \cdot CaBr_2 \cdot 10H_2O$ units or, more precisely, three $Ca_2Al(OH)_3Br, 2H_2O$ units.

The only symmetry element is a ternary axis; the condition for the existence of reflections is $-h + k + l = 3n$.

Thus, possible space groups are R3 and $R\bar{3}$. The structure leads to the assumption of the R3 group.

The intensities of 145 independent reflections were recorded on Weissenberg camera, using CuKα-radiation. A first determination of the structure was made, leading to a quality factor R of about 0.20.

With such value, it is not possible to assert the accuracy of the structure; it can be explained by the high radiation absorption. At present, the intensities of about 500 independent reflections were measured with a Philips automatic diffractometer, using MoKα-radiation. Moreover, absorption corrections are now in progress, which will allow a greater accuracy.

In the present state of our knowledge, the structure can be described in the following way. (see Figs. 1, 2 and 3.)

Br, Ca, H_2O atoms are in special positions 00z of the R3 group, hydroxyl groups being in general xyz position. Ca^{2+} and Al^{3+} ions are located in octahedral cavities between two layers of hydroxyl groups. Each aluminium atom is thus surrounded by six hydroxyl groups, the same holding for each calcium

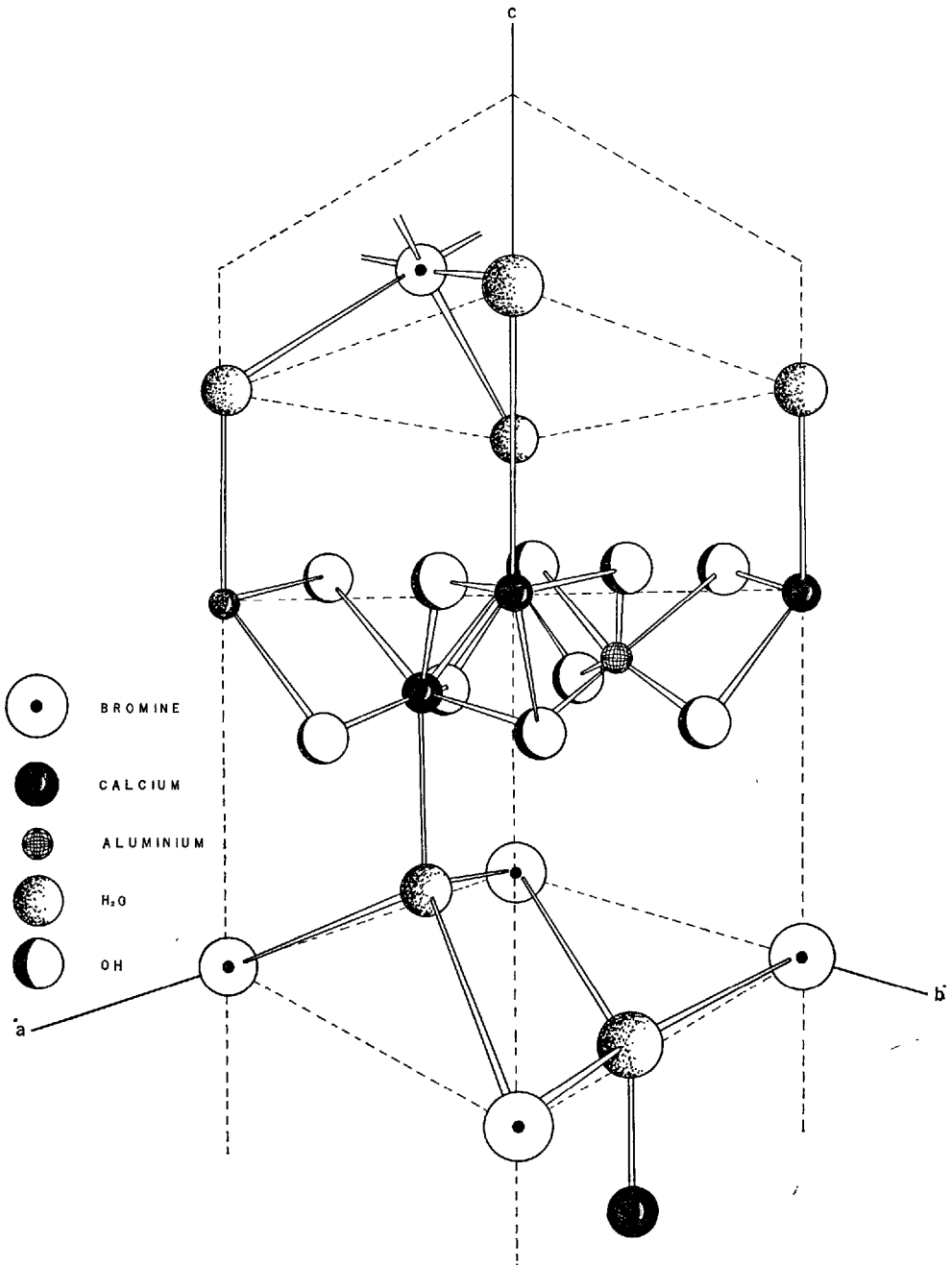

Fig. 1. $Ca_2Al(OH)_6Br \cdot 2H_2O$ *General view of the structure* ($\frac{1}{3}$ *of the cell*)

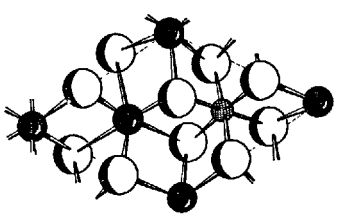

Fig. 2. $Ca_2Al(OH)_6$ *Layer: (001) projection*

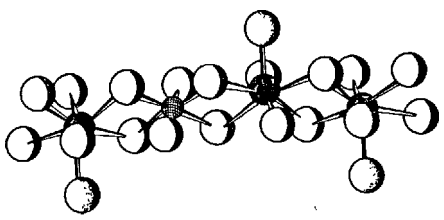

Fig. 3. $Ca_2Al(OH)_6$ *Layer: (110) projection*

atom. Coordinating polyhedrons have a common edge. Between hydroxyl layers there are two calcium atoms for one aluminium atom. Water molecules are located on both sides of these layers. The surrounding of each Ca^{2+} ion is thus completed by one water molecule.

Water molecules form layers parallel to hydroxyl layers. Bromine atoms are located between these layers, each Br^- being thus surrounded by six water molecules.

The structure is of the ionic type, and it can be easily shown to follow Pauling's rules.

Discussion of the Structure

Owing to the structure, we think it better to write the formula of the bromoaluminate as $Ca_2Al(OH)_6Br \cdot 2H_2O$. More generally, hydrated quaternary calcium aluminates should then be written:

$$Ca_2Al(OH)_6X \cdot nH_2O \text{ or } [Ca_2Al(OH)_6]_2Y \cdot nH_2O$$

Such writing is more representative of the properties of these compounds, as it lays stress on the hexacoordinance of aluminium and marks hydration water molecules.

The octahedral surrounding of aluminium is corroborated by the work of Fripiat (14) who showed an hexacoordinance of aluminium in $Ca_2Al(OH)_6 \cdot 3H_2O (C_4AH_{13})$ and in $[Ca_2Al(OH)_6]_2CO_3 \cdot 5H_2O$ $(C_3ACaCO_3H_{11})$ by measurements of X-ray emission wave length. Similarly, in C_2AH_8, half of the aluminium is hexacoordinated and the other half tetracoordinated, which is properly expressed by the formula: $Ca_2Al(OH)_6Al(OH)_4 3H_2O$.

The dehydration of the bromoaluminate conduces to the loss of two water molecules at approximately 180°C. This, in turn, produces a shortening of the *c*-axis which, according to Buser, changes from 8.1 to 7.15 Å.

The layer arrangement of water molecules and the relative weakness of the linking with the anion are in accordance with the easiness of cleavage parallel to 001.

The presence of the anion between layers explains the variations of the c-parameter in connection with the anion size (H. W. Buser) (11).

The works of Michel (15) and Buser (11), as well as our own experiences, indicated that it was very easy to carry out anion exchanges in quaternary aluminates; likely, this feature can be explained by the comparatively weak linking with the anion.

Previously Proposed Structures (Assumptions)

A review of previous theories about the structure can be found in Taylor's work (16).

We shall not go into the details of these assumptions, the only one close to that established by us for the calcium monobromoaluminate being that of Buttler, Dent Glasser and Taylor (8).

However, we can say that:

The structures proposed by Tilley (3) and Bessey (7) consider the substitution of H_2O to some Ca^{2+} ions in octahedral layers, and are inconsistent with a parameter remaining unchanged during dehydration.

The structure proposed by Grudemo (9) contradicts the hexacoordinance of aluminium.

The structure proposed by Buser (10–11) differs by the position of Al^{3+} ions, outside octahedral layers.

As to Buttler's assumption (8), recently modified by Dosh (17), it is very similar to that established for the bromoaluminate, owing to the existence of the octahedral layer $Ca_2Al(OH)_6$; the difference is mainly due to the fact that OH^- anion is assumed directly linked to the octahedral layer while, as we already saw, the Br^- anion is located between water molecule layers. Possibly, this difference may be explained by the size difference between Br^- and OH^- anions.

Conclusion

The production of single crystals permitted the direct assessment of the structure of the hydrated calcium monobromoaluminate $Ca_2Al(OH)_6B_2 \cdot 2H_2O$.

This structure is in accordance with several characteristics common to this compound and to the group of quaternary aluminates. It is essentially characterized by the existence of a double layer of hydroxyl

ions, containing calcium and aluminium atoms; anions are located between the layers of water molecules linked to the calcium.

Among previous theoreis, the structure proposed by Buttler, Dent Glasser and Taylor (8) is the nearest to our interpretation.

Addendum

It is only after completing the writting of this publication, that the work by Ahmed and Taylor (18), concerning the structure of a compound offering similitudes with $4CaO \cdot Al_2O_3 \cdot 13H_2O$, was known to us.

There is a very strong analogy between the structure of the said compound and that of bromoaluminate. Indeed, one may observe an octahedric layer $Ca_2Al(OH)_6$ and the presence of anions between two layers of water molecules. Calcium environment is actually completed to 7 by those water molecules.

A thorough comparison will be interesting when both of said structures will be definitely settled.

References

1. E. P. Flint, M. MacMurdie and L. S. Wells, "Hydrothermal and X-ray studies of the garnet-hydrogarnet series and the relationship of the series to hydration products of portland cement", J. Res. Nat. Bur. Stand., **26**, 13–33 (Jan. 1941).
2. R. Weiss, D. Grandjean and J. L. Pavin, "Structure de l'aluminate tricalcique hydraté, $3CaO \cdot Al_2O_3 \cdot 6H_2O$", Acta Cryst., **17**, No. 10, 1329–1330 (1964).
3. C. E. Tilley, H. D. Megaw and M. H. Hey, "New mineral found at Scawt Hill: Hydrocalumite ($4CaO \cdot Al_2O_3 \cdot 12H_2O$) "Mineral Mag. **17**, 607–615 (1932–1934).
4. A. Bezjak and I. Jelenic, "Crystal structure investigation of calcium aluminium sulphate hydrate—ettringite". Croat. Chem. Acta, **38**, No. 3, 239–242, (1966).
5. H. J. Kuzel, "Synthese und Röntgenuntersuchung des $3CaO \cdot Al_2O_3 \cdot CaSO_4 \cdot 12H_2O$", Neues Jahrb. Mineral, Monatsh., No. 7, 193–197, (1965).
6. E. Brandenberger, "Kristallstruktur und Zementchemie. Grundlagen einer Stereochemie der Kristallverbindungen in der Portland Zementen", Schweiz. Arch. Angew. Wiss. Tech., **2**, 45–58 (1936).
7. Proceedings of the Symposium on the Chemistry of Cements, Stockholm 1938, See discussion of W. Büssein, X-rays and Cement Chemistry" by G. E. Bessey 167–173, and G. E. Bessey, "The calcium aluminate and silicate hydrates", 177–215.
8. F. G. Buttler, J. S. Dent Glasser and H. F. W. Taylor, "Studies on $4CaO \cdot Al_2O_3 \cdot 13H_2O$ and the related natural mineral hydrocalumite", J. Am. Ceram. Soc., **12**, No. 3, 121–126. (1959).
9. A. Grudemo, "The microstructure of hardened paste", Preprint of Fourth International Symposium on Chemistry of Cement, Washington, p. 53 (1960).
10. W. Feitknecht and H. W. Buser, Helv. Chim. Acta, **32**, 2298 (1949).
11. H. W. Buser, "Beitrag zu Chemie und Konstitution der Calcium—Aluminium—Hydroxo-Doppelsalze und—Doppelhydroxyde" Inauguraldissertation zur Erlangung der Doctowürde—Hohen philisophischen Fakultat II der Universität Bern (1949) (Bern drückerei R + B Berthoud Bern 18, 1950).
12. G. Friedel, "Sur un chloroaluminate de clacium hydraté se maclant par compression", Bull. Soc. Franç. Minéral., **20**, 122–136, (1897).
13. H. J. Kuzel, "Röntgenuntersuchung im System $3CaO \cdot Al_2O_3 \cdot CaSO_4 \cdot nH_2O$–$3CaO \cdot Al_2O_3 \cdot CaCl_2\ nH_2O$", Neues Jahrb. Mineral, Monatsh., No. 7, 193–200 (1966).
14. J. Fripiat, private Communication.
15. Michel, Diss. Bern (1946).
16. H. F. W. Taylor, "The chemistry of cement" vol. 1 (Academic Press Inc. London, England and New York, U.S.A. 1964).
17. W. Dosch, "Die innerkristalline Sorption von Wasser und organischen Substanzen on Tetracalciumaluminat hydrate", Neues Jahrb. Mineral. Abhand., **106**, No. 2, 200–239, (1967).
18. S. J. Ahmed and H. F. W. Taylor, "Crystal structure of the lamellar aluminates hydrates", Nature, **215**, 622–623 (1967).

Supplementary Paper II-15 Contribution to the Study of Complex Aluminates: Hydrated Calcium and Magnesium Monocarboaluminates

Gérard Sadran and Bernard Cottin*

Synopsis

The authors have pointed out the existence of a series of calcium and magnesium aluminate monocarbonate hydrates derived from calcium aluminate monocarbonate hydrate by substitution from 0 to 95% of calcium by magnesium.

The analysis of these compounds conforms to the following formula:

$$[Mg_xCa_{2-x}Al(OH)_6]_2CO_3 \cdot 5H_2O$$

x varying from 0 (calcium aluminate monocarbonate hydrate) to 1.90.

These products have been prepared synthetically. Their X-ray patterns closely resemble the calcium aluminate monocarbonate pattern, except for high degrees of substitution in which case the principal lines only remain and are very much broadened.

The authors have ascertained that calcium and magnesium aluminate monocarbonate hydrates appear during the hydration of mixtures of aluminous cement and magnesium hydroxycarbonate. Their formation is effected from the hydrates usually precipitated during the set of aluminous cement: $CaO \cdot Al_2O_3 \cdot 10H_2O$ and $2CaO \cdot Al_2O_3 \cdot 8H_2O$. This formation is the result of a topochemical reaction, since no previous dissolution of the magnesium carbonate is observed. The reaction is easier using a carbonate with a large surface area.

The initial aim of this work was to state the particular conditions liable to promote the abundant crystallization of hydrated monocarboaluminate, both in the conditions of crystal synthesis and in pure pastes, mortars or concretes of aluminous cements. In fact, it is well known that, in usual conditions, this phase is very often present, but in limited amount, and that it is very difficult to increase its importance.

Further we were led to extend this research to the possibilities of isomorphic substitution between calcium and magnesium within the monocarboaluminate.

The existence of calcium and magnesium monocarboaluminate according to the formula $3CaO \cdot Al_2O_3 \cdot CaCO_3 \cdot 11H_2O$ was considered as likely by G. E. Bessey (1) as early as 1938. This body was further synthetically produced by R. Turriziani and G. Schippa (2) and its properties were studied by many authors using X-ray diagrams, differential and gravimetric thermal analysis crystal parameters, ...

The formation of hydrated calcium monocarboaluminate was observed during the air-carbonation of alumina and lime solutions (R. Turriziani and G. Schippa (2)—E. T. Carlson and H. A. Berman (3)) and of specimens of pure aluminous cement paste (G. Schippa (4)).

It was also observed during the hydration of anhydrous calcium aluminates and of portland or aluminous cement, in the presence of finely ground calcite: J. Farran (5)—T. Manabe, N. Kawada and M. Nishiyama (6)—Budnikov, Kolbasov and Panteleev (7).

These authors, as well as J. Farran (8) noted the coming out of an hydrate similar to the calcium monocarboaluminate by hydration of portland cement and of anhydrous calcium aluminates in the presence of dolomite or of magnesium carbonate.

In the presence of anhydrous carbonates such as $CaCO_3$ or $CaMg(CO_3)_2$, the formation of monocarboaluminates is a real fact, but this mineral appears only in small amounts and always accompanied by the other types of hydrated calcium aluminates: $CaO \cdot Al_2O_3 \cdot 10H_2O$–$2CaO \cdot Al_2O_3 \cdot 8H_2O$–$3CaO \cdot Al_2O_3 \cdot 6H_2O$—and $4CaO \cdot Al_2O_3 \cdot nH_2O$.

On the other hand, we observed that the reaction of anhydrous calcium aluminates or of their solutions, with hydromagnesite according to the formula $3MgCO_3 \cdot Mg(OH)_2 \cdot 3H_2O$ permitted the formation of very large amounts of monocarboaluminate, and even a complete reaction, the monocarboaluminate in such conditions becoming the only hydrated calcium aluminate present in the medium.

*Centre de Recherches de la Jonchère-Côte de la Jonchère, Ciments Lafarge, Paris, France.

Synthesis Conditions

We realized the production of hydrated monocarboaluminate by stirring a solution of lime and alumina, of molecular ratio $CaO/Al_2O_3 = 3$ in the presence of hydromagnesite. We selected this ratio because we hoped to obtain a monocarboaluminate by fixation of lime and alumina on the magnesium carbonate.

This solution (2.7 liters at 1130 mg/l of CaO and 690 mg/l of Al_2O_3) was obtained by adding 1.7 liter of a saturated lime solution to one liter of aluminous cement filtrate.

Stirring was carried out at room temperature, in 5-liter flasks, in the presence of increasing amounts of hydromagnesite, from 0.5 to 6 grams. In order to simplify, we shall denote by A_n the result of the stirring operation in the presence of n grams of hydromagnesite. $A_{1.5}$ corresponds to the amount of hydromagnesite just required for total combination with the lime and the alumina of the solution, resulting in an hydrated calcium and magnesium monocarboaluminate of assumed formula:

$$3CaO \cdot Al_2O_3 \cdot MgCO_3 \cdot xH_2O$$

After one week of stirring, the precipitate was filtered on sintered glass, dried by acetone washing followed by ether-washing, analysed and X-ray tested.

Simultaneously, we made a reference preparation of hydrated calcium monocarboaluminate, according to the method developed by R. Turriziani and G. Schippa (2). We shall denote by T. S. the result of this preparation.

Study of Resulting Products

X-ray Analysis

The study of obtained diffractograms indicates that for $A_{1.5}$ stirring, resulting spectra are that of pure hydrated calcium monocarboaluminate. The only impurity, unnoticeable by this method, appears by differential thermal analysis: a small amount of $Mg(OH)_2$ brought by the hydromagnesite.

For lower amounts of hydromagnesite, the monocarboaluminate is mixed with hydrated dicalcium aluminate, the A_0 stirring giving practically pure $2CaO \cdot Al_2O_3 \cdot 8H_2O$. $A_{0.5}$ stirring moreover indicates the presence of a body at 8.2 Å and 4.1 Å, corresponding to a solid solution of $3CaO \cdot Al_2O_3 \cdot Ca(OH)_2aq$ (or $4CaO \cdot Al_2O_3aq$) and of $3CaO \cdot Al_2O_3 \cdot CaCO_3aq$, according to W. Dosch and H. zur Strassen (9).

For higher hydromagnesite amounts, the monocarboaluminate is in the presence of $CaCO_3$, the proportion being the higher as the hydromagnesite at the onset is more important. However A_6 stirring, except for calcite lines, only gives highly broadened lines, corresponding to the strongest lines of the hydrated calcium monocarboaluminate.

Table 1 gives a summary of our results. Figures are proportional to the heights of the lines of the various bodies obtained, being understood that these heights are not rigorously proportional to concentrations, owing to preferring orientation. Nothing in the position of lines, or in their relative intensities, permits a discrimination between obtained calcium-magnesium products and purely calcium monocarboaluminate, the diagram of which was given by various authors.

Thermal Analysis

The dosing by ponderance thermal analysis of the various constituents was not possible because water, hydroxyl and CO_2 losses are not enough differentiated and take place continuously.

On the other hand, the differential thermal analysis, in an air atmosphere, enabled us to corroborate and complete X-ray tests, as shown in Table 2. According to the stirring type, one notes the presence of endothermic peaks characteristic of hydrated dicalcium aluminate, of hydrated magnesia $Mg(OH)_2$, of calcium carbonate and of hydrate monocarboaluminate. This latter presents the same endothermic peak at 200°C as the hydrated calcium monocarboaluminate and is

Table 1. *Synthesis of hydrated monocarboaluminates X-ray diffraction lines intensities*

	Monocarbo-aluminate	2 CaO Al_2O_3 8 H_2O	Compound	Calcite	Aragonite	$Mg(OH)_2$
	7.6 Å	10.8 Å	8.2 Å	3.035 Å	3.396 Å	2.365 Å
A_0		450				
$A_{0.5}$	110	370	115			
A_1	360	45				
$A_{1.5}$	450			ε		
A_2	360			35		
$A_{2.5}$	330			40	15	
A_3	400			60	55	
A_6	50 broadened			400		ε 30

mixed with $2CaO \cdot Al_2O_3 \cdot 8H_2O$ or $CaCO_3$ according to the amount of hydromagnesite at the onset.

The endothermic peak at 380°C, corresponding to the dehydration of $Mg(OH)_2$, is proportional to the weight of hydromagnesite used in the various stirring conditions. The magnesium hydroxide, present in the hydromagnesite at the onset did not react and is found unchanged in precipitates.

Chemical Analysis

The chemical analysis of precipitates, after acetone-ether washing, are reported in Table 3.

The knowledge of the phases present in these precipitates, determined by X-ray tests and by differential thermal analysis, permits the computation of the relative proportions of these phases and an approximate analysis of obtained hydrated monocarboaluminates, with the use of following assumptions:

—the molecular ratio CO_2/Al_2O_3 of these monocarboaluminates is 1.

—the basic portion $Mg(OH)_2$ of the hydromagnesite did not react, and is found unchanged in precipitates.

The results of these computations are presented in Table 4; they do not present any incompatibility with X-ray tests and differential thermal analysis. The various molecular ratios of monocarboaluminates are shown in Table 5. $(CaO + MgO)/Al_2O_3$ and MgO/Al_2O_3 are respectively about 4 and 11–12, except for $A_{0.5}$ stirring, for which we already indicated that X-rays showed the formation of an hydrate at 8.2 Å, for which we did not make allowance in our computations.

Conclusions

Our results permit us to say that a substitution is possible between MgO and CaO in the monocarboaluminate formula, and to assume, for all these products, a general formula

$$[Ca_{2-x}Mg_xAl(OH)_6]_2CO_3 \cdot 5\text{–}6H_2O$$

where x varies from 2 to 0, showing that this substitution can take place in any proportions.

Thus we have a continuous series of hydrated calcium and magnesium monocarboaluminates, one pole of which is the calcium monocarboaluminate (for which $x = 0$).

X-ray spectra of these hydrated calcium and magnesium monocarboaluminate are identical with that of hydrated calcium monocarboaluminate, at least up to 50% of substitution of MgO to CaO. For higher degrees of substitution, the product is not so well crystallized and shows only the highly broadened main lines of the monocarboaluminate.

The formation of calcite or aragonite, on stirring in the presence of more than 1.5 gram of hydroma-

Table 2. *Synthesis of hydrated monocarboaluminates heights of endotherms observed by differential thermal analysis*

	Monocarbo-aluminate	$2CaOAl_2O_38H_2O$			$Mg(OH)_2$	$CaCO_3$
	200°	100°	185°	310°	380°	around 800°
A_0	0	55	10	35	0	0
$A_{0.5}$	80	25	5	20	0	0
A_1	105	5		ε	15	0
$A_{1.5}$	85				20	0
A_2	75				30	10
$A_{2.5}$	70				30	15
A_3	45				45	25
A_6	very broad				105	90
T.S.	120				0	0

Table 3. *Synthesis of hydrated monocarboaluminates chemical analysis of precipitates*

	CaO	MgO	Al_2O_3	CO_2	H_2O
$A_{0.5}$	33.90	3.45	19.05	4.05	38.80
A_1	32.20	6.00	18.50	7.35	36.10
$A_{1.5}$	31.00	7.30	17.85	7.70	36.15
A_2	30.30	9.60	15.60	8.65	35.35
$A_{2.5}$	29.10	11.45	14.50	11.50	32.50
A_3	28.45	13.50	13.55	13.60	31.25
A_6	24.15	21.25	9.00	22.20	22.00
T.S.	38.60	0	17.60	7.65	35.45

Table 4. *Synthesis of hydrated monocarboaluminates computed composition of precipitates*

	$2CaO$ Al_2O_3 $8H_2O$	$CaCO_3$	$Mg(OH)_2$	Hydrated monocarboaluminate				
				CaO	MgO	Al_2O_3	CO_2	H_2O
$A_{0.5}$	33.95	0	1.60	23.25	2.35	9.40	4.05	24.65
A_1	5.25	0	2.90	30.55	4.00	17.00	7.35	33.10
$A_{1.5}$	0	0	3.40	31.00	5.00	17.85	7.70	35.05
A_2		4.30	4.10	27.90	6.80	15.60	6.75	34.05
$A_{2.5}$		11.95	4.90	22.40	8.05	14.50	6.25	31.00
A_3		17.60	5.50	18.60	9.70	13.55	5.85	29.55
A_6		41.45	9.70	1.00	14.55	9.00	3.90	19.00
T.S.		0.10	0	38.55	0	17.60	7.60	35.45

Table 5. *Synthesis of hydrated monocarboaluminates molecular ratios of hydrated calcium and magnesium monocarboaluminates*

	$\frac{CaO}{Al_2O_3}$	$\frac{MgO}{Al_2O_3}$	$\frac{CaO + MgO}{Al_2O_3}$	$\frac{H_2O}{Al_2O_3}$	$\frac{MgO}{CaO + MgO}$ *
$A_{0.5}$	4.5	0.6	5.1	14.7	7%
A_1	3.3	0.6	3.9	10.9	15%
$A_{1.5}$	3.2	0.7	3.9	11.0	18%
A_2	3.2	1.1	4.3	12.2	24%
$A_{2.5}$	2.8	1.4	4.2	12.0	33%
A_3	2.5	1.8	4.3	12.2	42%
A_6	0.2	4.1	4.3	11.8	96%
T.S.	4.0	0	4.0	11.1	0

*Substitution rate of CaO by MgO

gnesite, may be explained by the fact that the total molecular ratio CO_2/Al_2O_3 is higher than unity, which would corroborate the assumption used for the computations of formula. The excess of CO_2, precipitates as $CaCO_3$, less soluble than $MgCO_3$, and the corresponding lime is replaced by magnesia, in the lattice of the hydrated monocarboaluminate.

Other Conditions of Formation

In view of applications, various experimentations were carried out to check the possibility of an abundant formation of this phase in other conditions, and, in particular, in the conditions of "pastes" in the presence of limited water amounts.

Formation during the Hydration of Anhydrous Aluminates

These tests were carried out on aluminous cement pure pastes, mortars or concrete, with the addition of 10 and 20% of hydromagnesite, percentages corresponding either to the amount required to hydrate the $CaO \cdot Al_2O_3$ present in the cement as monocarboaluminate, either to an excess amount; i.e. in conditions similar to $A_{1.5}$ and A_3 stirring conditions of the above paragraph.

Results were studied by X-ray diffraction on pure paste, in the case of the 10% mixture, in order to study reaction kinetics. In the case of 20% additions, phenomena were similar, except for the additional coming out of calcium carbonate, according to the results obtained in the cases of synthesis.

Hydration in the Presence of Excess Water

The mixture aluminous cement*-hydromagnesite is stirred at room temperature in ten times its weight of water: ponderance ratio water/solid = 10. At predetermined times, a residue is obtained by filtration and tested by X-ray diffraction.

The Fig. 1 gives the peak intensities for the various bodies observed, in relation with time. After 4 hours of stirring, the hydrated monocalcium aluminate appears, increasing up to about 25 hours. At approximately 15 hours, an hydrate is formed, the main peak of which, at 9.4 Å, also reaches a maximum after about 25 hours, possibly the hydrated tricarboaluminate according to E. T. Carlson and H. A. Berman (3). These two hydrates gradually disappear and are replaced by the hydrated monocarboaluminate.

Note that we never observed magnesia in solution in obtained filtrates.

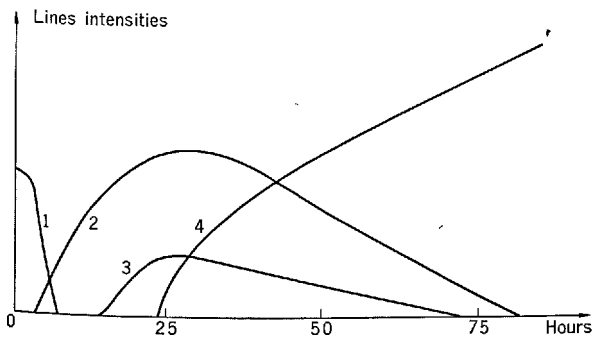

Fig. 1.

"Ciment Fondu" Stirred at 20°C + 10% hydromagnesite
W/S = 10

1. $CaO \cdot Al_2O_3$: 2.97 Å
2. $CaO \cdot Al_2O_3 \cdot 10H_2O$: 7.16 Å
3. Compound: 9.5 Å
4. Hydrated monocarboaluminate: 7.6 Å

Normal Paste Hydration

The mixture of aluminous cement* and hydromagnesite is mixed with a water/solid ratio of 0.5. The resulting paste hydrates in the sample holder of an X-ray diffractometer. The sample-holder is enclosed in a sealed chamber, the temperature of which is controlled. Figs. 2, 3 and 4 present the variation with time of the peak intensities of the various hydrates obtained at 20°C, 50°C and 70°C.

At 20°C, after a latency time of 20 hours or so, the anhydrous monocalcium aluminate hydrates, giving an hydrated monocalcium aluminate and a body with a broadened main line corresponding to a reticular distance of 8–8.5 Å. According to P. Seligmann and N. R. Greening (11) and to W. Dosch and H. zur Strassen (9), this line may correspond either to the hydrated hydroxyaluminate $4CaO \cdot Al_2O_3 \cdot 13H_2O$ or $3CaO \cdot Al_2O_3 \cdot Ca(OH)_2 \cdot 12H_2O$, either to a solid solution between the hydrated hydroxyaluminate and the hydrated monocarboaluminate $3CaO \cdot Al_2O_3 \cdot xCa(OH)_2 \cdot (1 - x)CaCO_3 \cdot yH_2O$. In our experience, the hydrated monocarboaluminate appears only after about 40 hours.

At 50°C, hydration reactions are much more rapid. The hydrated dicalcium aluminate appears after some

*Trade mark "Ciment Fondu"

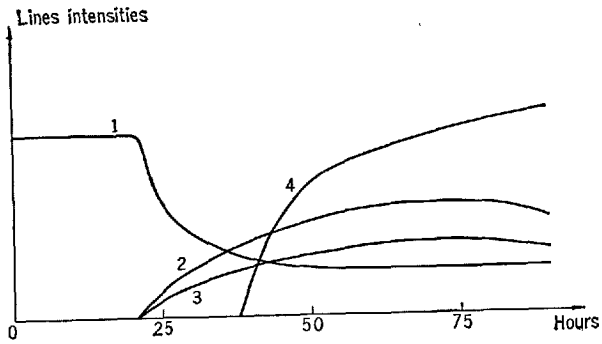

Fig. 2.

"Ciment Fondu" paste +10% hydromagnesite, Temp. = 20°C

1. $CaO \cdot Al_2O_3$: 2.97 Å
2. $CaO \cdot Al_2O_3 \cdot 10H_2O$: 7.16 Å
3. Compound: 8–8.5 Å
4. Hydrated monocarboaluminate: 7.6 Å

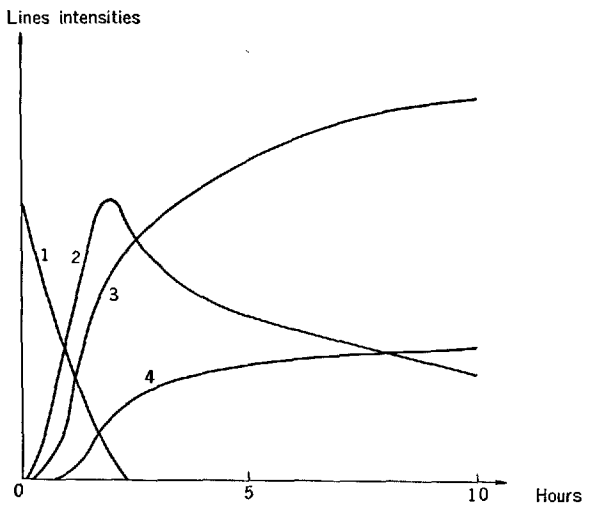

Fig. 3.

"Ciment Fondu" paste +10% hydromagnesite
W/S = 0.5, Temp. = 50°C

1. $CaO \cdot Al_2O_3$: 2.97 Å
2. $2CaO \cdot Al_2O_3 \cdot 8H_2O$: 10.6 Å
3. Hydrated monocarboaluminate: 7.6 Å
4. Gibbsite: 4.34 Å

minutes, and immediately after it, the hydrated monocarboaluminate and the gibbsite. $2CaO \cdot Al_2O_3 \cdot 8H_2O$ reaches its peak intensity after about 10 hours, then slowly decreases while the intensity of the monocarboaluminates still increases.

At 70°C, reactions are still more rapid. An hydrate, at 7.9 Å, forms immediately and disappears within one hour; this line corresponds to the hydrated hydroxyaluminate $4CaO \cdot Al_2O_3 \cdot 12H_2O$. The hydrated dicalcium aluminate reaches its peak intensity within one hour and completely disappears within three hours. The hydrated monocarboaluminate appears after one

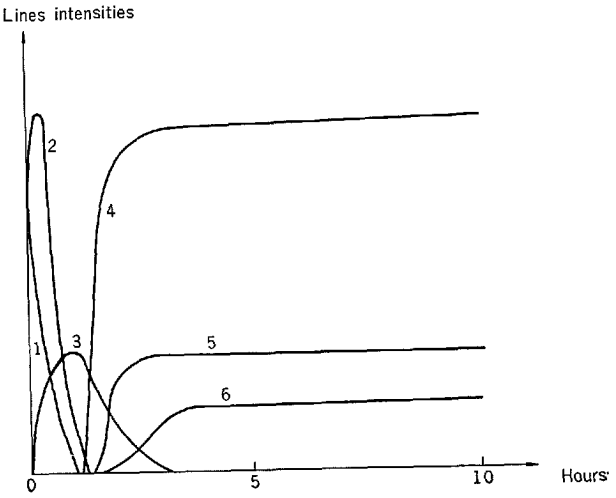

Fig. 4.

"Ciment Fondu" paste +10% hydromagnesite.
W/S = 0.5, Temp. = 70°C

1. $CaO \cdot Al_2O_3$: 2.97 Å
2. Compound: 7.9 Å
3. $2CaO \cdot Al_2O_3 \cdot 8H_2O$: 10.6 Å
4. Hydrated monocarboaluminate: 7.6 Å
5. Gibbsite: 4.34 Å
6. $3CaO \cdot Al_2O_3 \cdot 6H_2O$: 5.14 Å

hour, then rapidly increases. Lastly some gibbsite, then some hydrated cubic aluminate are formed after about one hour and half.

Whatever the hydration temperature of the aluminous cement* hydromagnesite mixture may be, hydrated calcium and magnesium monocarboaluminate is obtained. But this hydrate is not the first produced: it appears, according to the hydration temperature, after monocalcium, dicalcium or tetracalcium—more or less carbonated—hydrated aluminates, and to their detriment. Thus, we thought interesting to study the conditions of production of the monocarboaluminate from synthetic hydrated aluminates, in the presence of hydromagnesite.

Formation from Hydrated Calcium Aluminates

We mixed synthetic hydrated calcium aluminates $CaO \cdot Al_2O_3 \cdot 10H_2O$–$2CaO \cdot Al_2O_3 \cdot 8H_2O$–$3CaO \cdot Al_2O_3 \cdot 6H_2O$ and $4CaO \cdot Al_2O_3 \cdot 12H_2O$ with hydromagnesite and with the required water in order to get a fluid and well-homogenized paste. The proportions of hydromagnesite were computed in order to realize following theoretical reactions

$$3(CaO \cdot Al_2O_3 \cdot 10H_2O) + MgCO_3 = 3CaO \cdot Al_2O_3 \cdot MgCO_3 \cdot xH_2O + 2(Al_2O_3 \cdot 3H_2O)$$

*Trade mark "Ciment Fondu"

i.e. about 10% of hydromagnesite

$$\tfrac{3}{2}(2CaO \cdot Al_2O_3 \cdot 8H_2O) + MgCO_3 = 3CaO \cdot Al_2O_3 \cdot MgCO_3 \cdot xH_2O + \tfrac{1}{2}(Al_2O_3 \cdot 3H_2O)$$

i.e. about 17% of hydromagnesite

$$3CaO \cdot Al_2O_3 \cdot 6H_2O + MgCO_3 = 3CaO \cdot Al_2O_3 \cdot MgCO_3 \cdot xH_2O$$

i.e. about 23% of hydromagnesite

$$4CaO \cdot Al_2O_3 \cdot 12H_2O + MgCO_3 = 3CaO \cdot Al_2O_3 \cdot MgCO_3 \cdot xH_2O + CaO \cdot H_2O$$

i.e. about 17% of hydromagnesite.

These pastes, stored at room temperature in sealed bottles, were tested by X-ray diffraction after various times, after washing and drying with acetone-ether.

Figs. 5 to 8 show the variations of peak intensities with time. The identification of hydrates was made

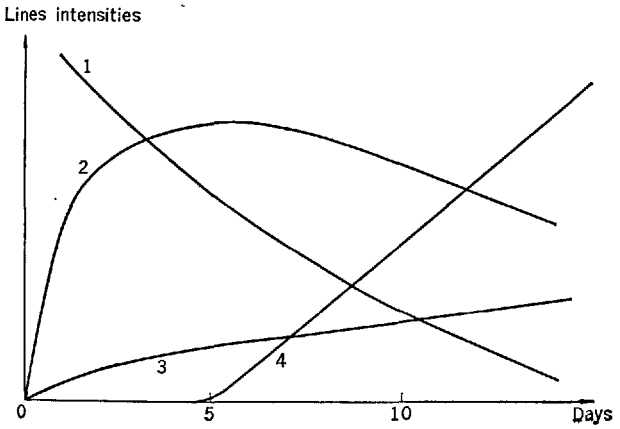

Fig. 5.

$CaO \cdot Al_2O_3 \cdot 10H_2O$ paste +10% hydromagnesite
Temp. = 20°C

1. $CaO \cdot Al_2O_3 \cdot 10H_2O$: 7.16 Å
2. Calcite: 3.04 Å
3. Gibbsite: 4.36 Å
4. Hydrated monocarboaluminate: 3.80 Å

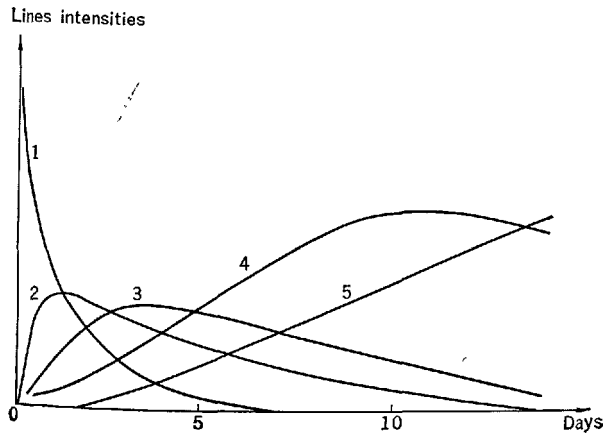

Fig. 6.

$2CaO \cdot Al_2O_3 \cdot 8H_2O$ paste +17% hydromagnesite
Temp. = 20°C

1. $2CaO \cdot Al_2O_3 \cdot 8H_2O$: 10.6 Å
2. Calcite: 3.04 Å
3. $4CaO \cdot Al_2O_3 \cdot 12H_2O$: 3.93 Å
4. $4CaO \cdot Al_2O_3 \cdot \frac{3}{4}CaO \cdot \frac{1}{4}CaCO_3 \cdot 9H_2O$: 3.82 Å
5. Hydrated monocarboaluminate: 3.80 Å

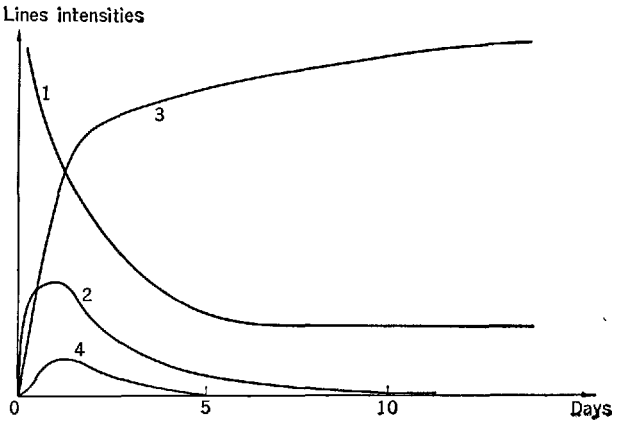

Fig. 7.

$3CaO \cdot Al_2O_3 \cdot 6H_2O$ paste +23% hydromagnesite
Temp. = 20°C

1. $3CaO \cdot Al_2O_3 \cdot 6H_2O$: 5.14 Å
2. Calcite: 3.04 Å
3. Hydrated monocarboaluminate: 3.80 Å
4. $4CaO \cdot Al_2O_3 \cdot 12H_2O$: 3.93 Å

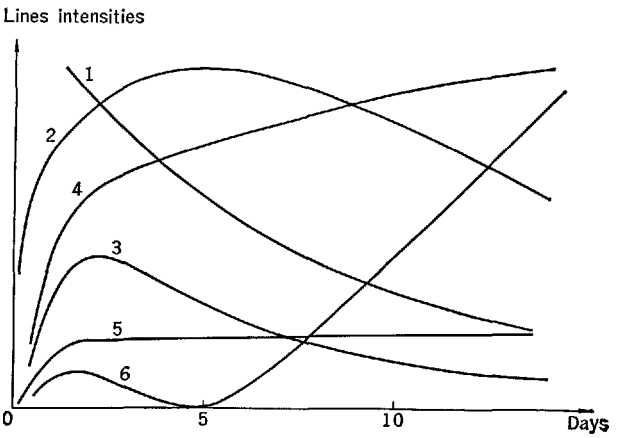

Fig. 8.

$4CaO \cdot Al_2O_3 \cdot 12H_2O$ paste +17% hydromagnesite
Temp. = 20°C

1. $4CaO \cdot Al_2O_3 \cdot 12H_2O$: 3.93 Å
2. $4CaO \cdot Al_2O_3 \cdot 13H_2O$: 4.09 Å
3. Calcite: 3.04 Å
4. Hydrated monocarboaluminate: 3.80 Å
5. $3CaO \cdot Al_2O_3 \cdot \frac{3}{4}CaO \cdot \frac{1}{4}CaCO_3 \cdot 9H_2O$: 3.82 Å
6. $4CaO \cdot Al_2O_3 \cdot 19H_2O$: 3.53 Å

according to the data of W. Dosch (10).

In every case, calcite is rapidly formed. The advent of the spectrum of the calcium and magnesium monocarboaluminate coincides with the decrease of the amount of calcite. In the presence of lime, which is dissolved, the magnesium is completely or partially transformed into less soluble calcium carbonate, then the calcium and magnesium monocarboaluminate seems to be formed, at least partially, from the calcite precipitated in this way.

Hydrated Monocalcium Aluminate

Its incongruent solubility promotes the precipitation of hydrated alumina. The hydrated monocarboaluminate appears only after more than 48 hours. After 50 days, $CaO \cdot Al_2O_3 \cdot 10H_2O$ has completely disappeared, but calcite still remains.

Hydrated Dicalcium Aluminate

The hydrated monocarboaluminate appears only between 24 and 48 hours. But there is intermediary formation of $4CaO \cdot Al_2O_3 \cdot 12H_2O$ and of a solid solution between $4CaO \cdot Al_2O_3 \cdot 12H_2O$ and the hydrated monocarboaluminate. After 50 days, $2CaO \cdot Al_2O_3 \cdot 8H_2O$ and $CaCO_3$ have disappeared, togeher with $4CaO \cdot Al_2O_3 \cdot 12H_2O$.

Hydrated Tricalcium Aluminate

The monocarboaluminate forms after only 5 hours. After 14 days, the reaction seems completed, but some cubic remains in the presence of the monocarboaluminate.

Hydrated Tetracalcium Aluminate

The advent of the monocarboaluminate is also very rapid. But reactions are more complex, owing to the more or less transient formation of $4CaO \cdot Al_2O_3 \cdot 19H_2O$, $4CaO \cdot Al_2O_3 \cdot 13H_3O$ and a solid solution between $4CaO \cdot Al_2O_3 \cdot xH_2O$ and the hydrated monocarboaluminate. The hydrated lime begins to crystallise after less than 7 days.

Note that, in our experimental conditions, the hydrated cubic aluminate, well-known for its stability, is, among hydrated calcium aluminates, the one most rapidly transformed into monocarboaluminate. The following assumption can be made.

The solubility of $3CaO \cdot Al_2O_3 \cdot 6H_2O$ is congruent. The molecular ratio CaO/Al_2O_3 of the solution is then favourable to the rapid formation of a complex aluminate, according to the formula $3CaO \cdot Al_2O_3 \cdot MgCO_3 \cdot 11H_2O$. The same is true of the solution in contact with $4CaO \cdot Al_2O_3 \cdot xH_2O$, the molecular ratio CaO/Al_2O_3 is still higher, the excess lime precipitating as hydrated lime. On the other hand, the solubility of $CaO \cdot Al_2O_3 \cdot 10H_2O$ is incongruent. The hydrated alumina slowly precipitates and the molecular ratio CaO/Al_2O_3 of the solution gradually increases and reaches a value of 3 which favours the precipitation of the hydrated monocarboaluminate. The case of $2CaO \cdot Al_2O_3 \cdot 8H_2O$ appears more complex, but the intermediary formation of an hydrated tetracalcium aluminate shows that the molecular ratio CaO/Al_2O_3 of the solution is high and permits the precipitation of the monocarboaluminate.

Conclusions

Experiences already described show that the hydrated monocarboaluminate in fact corresponds to a series of formula:

$$[Ca_{2-x}Mg_x \cdot Al(OH)_6]_2CO_3 \cdot 5\text{–}6H_2O$$

where the substitution of magnesium to calcium can take place in any proportions; the calcium monocarboaluminate, the best known at present, is only the calcium pole of this series. The magnesium pole $[Mg \cdot 2Al(OH)_6]_2CO_3 \cdot xH_2O$ was practically reached in our A_6 conditions of stirring.

These hydrates were not isolated, but their analysis can be deduced from chemical analysis, X-ray diffraction spectra and differential thermal analysis.

This series is remarkable for the steadiness of positions and intensity ratios of X-ray diffraction lines: even in the extreme magnesian case, there is no noticeable change of the position of strongly weakened lines.

In the presence of hydromagnesite, the formation of these monocarboaluminates may be very abundant, and may even lead to the crystallization of this only phase as hydrate.

The hydrated calcium and magnesium monocarboaluminate seems to form directly from CaO and Al_2O_3 solutions, but the study of other production conditions indicated that, in the presence of small amounts of water, its cristallization took place after the formation of conventional hydrated aluminates.

In particular, this is the case for the hydration of aluminous cement in the presence of hydromagnesite; the calcium and magnesium monocarboaluminate is formed after preliminary precipitation of hydrated

mono-, bi- or tetracalcium aluminates.

In the presence of hydromagnesite, the formation of monocarboaluminate is very easy, even from aluminates known as stables; the reaction is the simplest and the most rapid with the hydrated cubic aluminate. With hydrated mono- and dicalcium aluminates, it is preceded by the formation of other hydrates (gibbsite and tetracalcium aluminate), which seems to corroborate the possibility of direct precipitation from solutions with a molecular ratio $CaO/Al_2O_3 = 3$, and would in particular explain the rapidity of the reaction with the cubic aluminate, for which the congruent solubility permits to directly reach this value of the molecular ratio in the solution.

References

1. G. E. Bessey. "The calcium carbonate and silicate hydrates", Proceedings of the Symposium on the Chemistry of Cements, Stockholm, 1938, 178–215.
2. R. Turriziani and G. Schippa, "Sull'esistenza del monocarboalluminate di calcio idrato" Ric. Sci., **26**, No. 9, 2792–2797, (1956).
3. E. T. Carlson and H. A. Berman, "Some observations on the calcium aluminate carbonate hydrates". J. Res. Nat. Bur. St. A, **64**, No. 4, 333-341, (Jul. Aug. 1960).
4. G. Schippa, "Idratazione del cemento aluminoso" Ric. Sci, **28**, No. 10, 2120–2124, (1958).
5. J. Farran "Contribution minéralogique à l'étude de l'adhérence entre les constituants hydratés des ciments et les matériaux enrobés", Publication technique No. 78 (Centre d'Etudes et de Recherches de l'Industrie des Liants Hydrauliques, Paris, France 1956).
6. T. Manabe, N. Kawada and M. Nishiyama, "Studies on $3CaO \cdot Al_2O_3 \cdot CaCO_3 \cdot nH_2O$ (Calcium monocarboaluminate hydrate)" J. C. E. A. Rev. of 15th Gen. Meeting, p 48–55 (Japan Cement Engineering Association Tokyo, Japan, 1961).
7. P. P. Budnikov, V. M. Kolbasov and A. S. Panteleev, "The reaction of $3CaO \cdot Al_2O_3 \cdot Fe_2O_3$ with calcium and magnesium carbonates". Proc. Acad, Sci. USSR, Chem. Technol. Sec. (English Transl.), **129**, No. 5, 167–169. (1959).
8. J. Farran "Sur l'adhérence entre ciments et matériaux enrobés", Compt. Rend. **237**, 73–75, (6 Juillet 1953).
9. W. Dosch and H. zur Strassen, "Untersuchung von Tetracalciumaluminathydraten"—1—Die verschiedenen Hydratstufen und der Einfluss von Kohlensaüre", Zement Kalk Gips, **18**, 233–237 (1965).
10. W. Dosch, "Die Innerkristalline Sorption von Wasser und organischen Substanzen an Tetracalciumaluminathydrat" Neues Jahrb. Mineral, Abhandl., **106**, 2, 200–239 (1967).
11. P. Seligmann and Nathan R. Greening "Studies of early hydration reaction of portland cement by X-ray diffraction". PCA Res. Dept. Bull 185 (1964).

Supplementary Paper II-19 X-ray Investigations of Some Complex Calcium Aluminate Hydrates and Related Compounds

Hans J. Kuzel*

Synopsis

Single crystals of several calcium aluminate hydrates of the type $3CaO \cdot Al_2O_3 \cdot CaX \cdot nH_2O$ and $3CaO \cdot Al_2O_3 \cdot CaY_2 \cdot nH_2O$ with $Y = Cl^-$, Br^-, J^-, NO_3^-, BrO_3^- and $X = SO_4^{2-}$, CrO_4^{2-} were prepared by hydrothermal methods. Rotation, Weissenberg and precession photographs showed that the structures are usually completely ordered containing only one polytypic modification. The true unit cells have monoclinic, trigonal or rhombohedral symmetry. Ordered structures containing one, two, three or six layers have been observed. Space groups and unit cells of the compounds are given. Results of powder and single crystal investigations of $3CaO \cdot Ga_2O_3 \cdot CaBr_2 \cdot 10H_2O$, $3CaO \cdot Cr_2O_3 \cdot CaCl_2 \cdot 10H_2O$, $3CaO \cdot Cr_2O_3 \cdot CaSO_4 \cdot 12H_2O$, $3CaO \cdot Fe_2O_3 \cdot CaCl_2 \cdot 10H_2O$ and $3CaO \cdot Fe_2O_3 \cdot CaSO_4 \cdot 12H_2O$ are presented. A structure proposed by F. G. Buttler, L. S. Dent Glasser and H. F. W. Taylor (12) was confirmed by the determination of z-coordinates of the atoms in some compounds of this type.

Introduction

The composition of the complex calcium aluminate hydrates with layer structures may be represented by the general formula $3CaO \cdot Al_2O_3 \cdot CaY_2 \cdot nH_2O$ and $3CaO \cdot Al_2O_3 \cdot CaX \cdot nH_2O$ where Y is an univalent and X a divalent anion. At relative humidities of 35–45 percent the water content is $n = 10$–$12H_2O$. Many synthetic complex salts of this type were prepared and described by W. Lerch, F. W. Ashton and R. H. Bogue (1), J. Foret (2), W. Mylius (3), W. Feitknecht and M. Gerber (4), W. Feitknecht and H. Buser (5) and many other authors. Early work in this field was reviewed by F. E. Jones (6) and more recent contributions are mentioned by H. F. W. Taylor (7), R. Turriziani (8) and F. E. Jones (9).

The exact crystal structures of the complex calcium aluminate hydrates are not known. Since all compounds of this type crystallize in hexagonal or pseudohexagonal plates with perfect (0001) cleavage, E. Brandenberger (10) concluded that they have layer structures. C. E. Tilley, H. D. Megaw and M. H. Hey (11) proposed a crystal structure for hydrocalumite, a natural mineral which resembles the synthetic compound $3CaO \cdot Al_2O_3 \cdot Ca(OH)_2 \cdot 12H_2O$ in morphology and composition. The structure contained $Ca(OH)_2$ layers in which one Ca^{2+} out of three was replaced by H_2O alternating with layers of Al^{3+} ions, the remaining H_2O molecules and OH^- groups. This structure gave good agreement between observed and calculated 001 intensities.

A somewhat different crystal structure was suggested by F. G. Buttler, L. S. Dent Glasser and H. F. W. Taylor (12) based on packing considerations and single crystal X-ray examination of hydrocalumite and synthetic $3CaO \cdot Al_2O_3 \cdot Ca(OH)_2 \cdot 12H_2O$. The structure of these authors contains layers of the composition $[Ca_2Al(OH)_6]^+$ in which the octahedral sites are occupied by $2Ca^{2+}$ and one Al^{3+} in ordered positions. The seventh OH^- ion is placed between the layers where it is associated with the remaining water.

The OH group outside the octahedral layer may be completely replaced by other anions. The number of water molecules between the layers depends on relative humidity. F. G. Buttler, L. S. Dent Glasser and H. F. W. Taylor reported that even thin crystals of synthetic $3CaO \cdot Al_2O_3 \cdot Ca(OH)_2 \cdot 12H_2O$ contained two or more polytypes and perhaps stacking faults "so that the true structure only repeats after a large number of layers".

Of nearly all complex calcium aluminate hydrates with layer lattice only the pseudocells are known. The lattice constant a_0 appears to be about 5.7 Å. The thickness of the pseudocell depends on the size of the anions X and Y and the number of water molecules between the octahedral layers. More detailed data on the unit cells and space groups of the

*Institut für Kristallographie der Universität Frankfurt, Frankfurt, West Germany.

compounds $3CaO \cdot Al_2O_3 \cdot CaCl_2 \cdot 10H_2O$, $3CaO \cdot Al_2O_3 \cdot CaSO_4 \cdot 12H_2O$ and $3CaO \cdot Al_2O_3 \cdot 1/2CaSO_4 \cdot 1/2CaCl_2 \cdot 12H_2O$ based on single crystal X-ray investigations were reported by H.-J. Kuzel (13, 14). The structures of these complex salts were completely ordered. The true cells contained 2, 3 and 6 layers.

Other compounds are derived from these hydrated calcium aluminates by substitution of the larger cations Ga^{3+}, Cr^{3+} and Fe^{3+} for Al^{3+}. Several calcium ferrite hydrates of the type $3CaO \cdot Fe_2O_3 \cdot Ca(X, Y_2) \cdot nH_2O$ are already known. Preparations of the compounds $3CaO \cdot Fe_2O_3 \cdot Ca(OH)_2aq$, $3CaO \cdot Fe_2O_3 \cdot CaSO_4 \cdot 12H_2O$, $3CaO \cdot Fe_2O_3 \cdot CaCl_2 \cdot 10H_2O$ and $3CaO \cdot Fe_2O_3 \cdot Ca(NO_3)_2 \cdot 10H_2O$ were reported by G. Malquori and V. Cirilli (15). These authors summarized evidence for the close analogy between hydrated calcium ferrites and aluminates containing the same anion. The replacement of Al^{3+} by Fe^{3+} seems to be nearly isomorphous in that the essential features of the layer structures are not affected.

In the present work the unit cells, space groups and crystal structures of several compounds of the type $3CaO \cdot R_2O_3 \cdot Ca(X, Y_2) \cdot nH_2O$ have been investigated using X-ray single crystal and powder methods.

Experimental Procedure

Methods of Preparation

The determination of unit cells and space groups of compounds with large lattice constants is usually possible only with the aid of single crystal methods.

Since many complex calcium aluminate hydrates of the layer lattice type are stable at temperatures above 100°C under saturated steam hydrothermal methods have been used in preparing single crystals suitable for X-ray work. Crystals up to 0.1–0.2 mm across were made by heating calculated amounts of CaO and $Al(OH)_3$ (bayerite) with calcium salt solutions in simple Morey bombs at temperatures between 100°C and 200°C for several weeks.

Larger crystals could be often made by treating synthetic $3CaO \cdot Al_2O_3 \cdot 6H_2O$ with calcium salt solutions at 150°C. Hexagonal plates of $3CaO \cdot Al_2O_3 \cdot CaSO_4 \cdot 12H_2O$ and $3CaO \cdot Al_2O_3 \cdot CaCrO_4 \cdot 12H_2O$ up to 1 cm across were obtained by this method. Details of the experimental procedure were given in preceeding papers (13, 14).

Bulk preparations of all compounds were made by the usual method mixing solutions of calcium salts and lime water with a metastable calcium aluminate solution. The crystals from each method were hexagonal flakes with perfect (0001) cleavage. Faces of rhombohedrons were observed on crystals of $3CaO \cdot Al_2O_3 \cdot CaSO_4 \cdot 12H_2O$, $3CaO \cdot Al_2O_3 \cdot CaJ_2 \cdot 10H_2O$ and $3CaO \cdot Al_2O_3 \cdot Ca(NO_3)_2 \cdot 10H_2O$.

Except α–$3CaO \cdot Al_2O_3 \cdot CaCl_2 \cdot 10H_2O$ and α–$3CaO \cdot Ga_2O_3 \cdot CaCl_2 \cdot 10H_2O$ all compounds were uniaxial negative.

No single crystals of compounds $3CaO \cdot R_2O_3 \cdot CaY_2 \cdot nH_2O$ and $3CaO \cdot R_2O_3 \cdot CaX \cdot nH_2O$ where $R = Cr^{3+}$ and Fe^{3+} could be produced. Powders were made by mixing freshly precipitated Cr^{3+}-and Fe^{3+}-hydroxides with solutions of the desired calcium salt and lime water. The mixtures were shaken for several weeks at temperatures below 100°C. All products were filtered in a glove box under CO_2-free conditions and dried over saturated $CaCl_2$ at about 37 percent relative humidity.

The water contents of the various compounds were determined by heating the powder in a vacuum thermobalance and recording the loss of molecular water. At heating rates of 4°C/h the dehydration curves showed definite steps corresponding to the loss of the molecular water between the octahedral layers. At about 37 percent relative humidity the composition of the layers may be given by the general formulas $Ca_2Al(OH)_6 \cdot Y \cdot 2H_2O$ and $Ca_2Al(OH)_6 \cdot 1/2X \cdot 3H_2O$.

X-ray Investigations

In case single crystals were available lattice constants and space groups were determined using rotation, Weissenberg and precession cameras with filtered copper and iron radiation. The water contents of complex salts which contain tetrahedral anions are very sensitive towards alterations to relative humidity. These compounds were exposed to X-rays under controlled atmospheric conditions.

Powder diffraction patterns were taken with a Philips Norelco diffractometer using Si (Schuchardt 99.999%, $a_0 = 5.4308$ Å) as an internal standard. The powder patterns were indexed by aid of single crystal data. The lattice constants were refined by least squares methods.

Results

Unit Cells and Space Groups of Compounds $3CaO \cdot Al_2O_3 \cdot Ca(X, Y_2) \cdot nH_2O$

The results of X-ray examinations of some calcium aluminate hydrates containing other anions are listed in Table 1.

Crystals made under hydrothermal conditions were usually completely ordered if dried with caution and handled carefully. Compounds prepared by precipitation from metastable calcium aluminate solutions often showed considerable disorder.

On heating the monoclinic low temperature form α–$3CaO \cdot Al_2O_3 \cdot CaCl_2 \cdot 10H_2O$ changes to the rhombohedral β-phase, the transformation taking place readily and reversibly at 28 ± 2°C. The unit cell of α–$3CaO \cdot Al_2O_3 \cdot CaCl_2 \cdot 10H_2O$ contains two identical layers of the composition $Ca_4Al_2(OH)_{12} \cdot 2Cl \cdot 4H_2O$. The β-phase was investigated with the help of a little furnace attached to a precession camera. The observed reflections of β–$3CaO \cdot Al_2O_3 \cdot CaCl_2 \cdot 10H_2O$ agree with the space groups R3c and R$\bar{3}$c. Fig. 1 illustrates the relations between the unit cells of $Ca(OH)_2$, α–$3CaO \cdot Al_2O_3 \cdot CaCl_2 \cdot 10H_2O$ and β–$3CaO \cdot Al_2O_3 \cdot CaCl_2 \cdot 10H_2O$ in the ab plane. The structure of the β-phase is based on a 6R polytypic modification as well as that of $3CaO \cdot Al_2O_3 \cdot CaBr_2 \cdot 10H_2O$.

The unit cells of $3CaO \cdot Al_2O_3 \cdot CaJ_2 \cdot 10H_2O$, $3CaO \cdot Al_2O_3 \cdot CaSO_4 \cdot 12H_2O$ and $3CaO \cdot Al_2O_3 \cdot CaCrO_4 \cdot 12H_2O$ contain three layers in regular stacking sequences. Other polytypic modifications were not observed. Large crystals of the compounds with tetrahedral anions are considerably disordered when the freshly prepared specimens were dried quickly at 37 percent relative humidity, probably due to the loss of a part of the molecular water between the octahedral layers. The precession photographs showed diffuse streaks along the reciprocal lattice rows parallel c.

The only known complex calcium aluminate hydrate with a one-layer-structure appears to be $3CaO \cdot Al_2O_3 \cdot Ca(NO_3)_2 \cdot 10H_2O$. For the compounds $3CaO \cdot Al_2O_3 \cdot CaSO_4 \cdot 16H_2O$ and $3CaO \cdot Al_2O_3 \cdot Ca(BrO_3)_2 \cdot 10H_2O$ only powder diffraction data were available. The condition for hexagonal indexing of a rhombohedral lattice $-h + k + l = 3n$ ($n = 0, 1, 2, \ldots$) was clearly satisfied in both cases. Reflections h0hl with $h \neq 3n$ occur only with $l \neq 3n$, reflections hh$\bar{2}$hl were observed only for $l = 3n$. The space groups would therefore probably be R3, R$\bar{3}$, R32, R3m and R$\bar{3}$m. Which one of these is the correct space group cannot be decided from powder data and a further subdivision is impossible without knowledge of the Laue symmetries.

Single crystals of another compound similar to $3CaO \cdot Al_2O_3 \cdot 1/2CaSO_4 \cdot 1/2CaCl_2 \cdot 12H_2O$ with the composition $3CaO \cdot Al_2O_3 \cdot 1/2Ca(NO_3)_2 \cdot 1/2CaCl_2 \cdot 10H_2O$ were prepared with hydrothermal methods. The unit cell contains 6 double layers $Ca_4Al_2(OH)_{12} \cdot NO_3 \cdot Cl \cdot 4H_2O$. The Cl^- ions as well as NO_3^- probably occupy positions in alternating layers parallel (0001). Even the layers of these long period compounds were

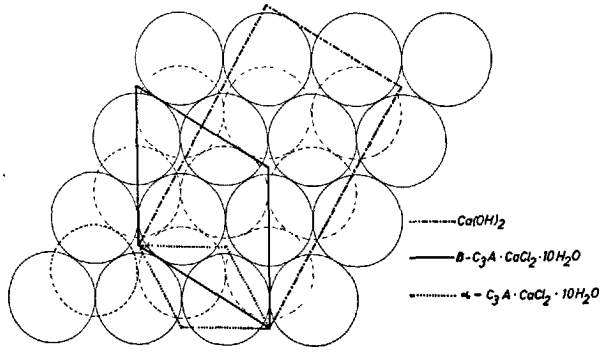

Fig. 1. *Relations between the unit cells of* $Ca(OH)_2$, α-$3CaO \cdot Al_2O_3 \cdot CaCl_2 \cdot 10H_2O$ and β-$3CaO \cdot Al_2O_3 \cdot CaCl_2 \cdot 10H_2O$

Table 1. *Unit cells and space groups of compounds* $3CaO \cdot Al_2O_3 \cdot Ca(X, Y_2) \cdot nH_2O$

Composition	Lattice constants in Å a_0	b_0	c_0	β	Pseudocell in Å c'	Space groups
α-$C_3A \cdot CaCl_2 \cdot 10H_2O$	9.962 ± 3	5.735 ± 1	16.836 ± 3	110.49 ± 2	—	C2/c, Cc
β-$C_3A \cdot CaCl_2 \cdot 10H_2O$	5.739 ± 1	—	46.87 ± 1	—	7.811	R3c, R$\bar{3}$c
$C_3A \cdot CaBr_2 \cdot 10H_2O$	5.761 ± 1	—	49.06 ± 1	—	8.177	R3c, R$\bar{3}$c
$C_3A \cdot CaJ_2 \cdot 10H_2O$	5.771 ± 1	—	26.572 ± 6	—	8.857	R3, R$\bar{3}$
$C_3A \cdot Ca(NO_3)_2 \cdot 10H_2O$	5.743 ± 1	—	8.623 ± 3	—	—	P3, P$\bar{3}$
$C_3A \cdot Ca(BrO_3)_2 \cdot 10H_2O$	5.7532 ± 4	—	29.425 ± 4	—	9.808	R3, R$\bar{3}$, R32, R3m, R$\bar{3}$m
$C_3A \cdot CaSO_4 \cdot 12H_2O$	5.756 ± 1	—	26,811 ± 4	—	8.937	R3, R$\bar{3}$
$C_3A \cdot CaSO_4 \cdot 16H_2O$	5.751 ± 1	—	28.672 ± 2	—	9.557	R3, R$\bar{3}$, R32, R3m, R$\bar{3}$m
$C_3A \cdot CaCrO_4 \cdot 12H_2O$	5.75 ± 2	—	26,91 ± 5	—	8.97	R3, R$\bar{3}$
$C_3A \cdot 1/2CaSO_4 \cdot 1/2CaCl_2 \cdot 12H_2O$	5.7502 ± 7	—	100.62 ± 2	—	16.770	R3c, R$\bar{3}$c
$C_3A \cdot 1/2Ca(NO_3)_2 \cdot 1/2CaCl_2 \cdot 10H_2O$	5.744 ± 8	—	98.28 ± 3	—	16.380	R3c, R$\bar{3}$c

Table 2. *Unit cells and space groups of compounds* $3CaO \cdot R_2O_3 \cdot Ca(X, Y_2) \cdot nH_2O$

Composition	Lattice constants in Å a_0	c_0	Pseudocell in Å c'	Space groups
$3CaO \cdot Al_2O_3 \cdot CaSO_4 \cdot 12H_2O$	5.756 ± 1	26.811 ± 4	8.937	R3, $R\bar{3}$
$3CaO \cdot Cr_2O_3 \cdot CaSO_4 \cdot 12H_2O$	5.831 ± 1	26.585 ± 2	8.862	R3, $R\bar{3}$, R32, R3m, $R\bar{3}m$
$3CaO \cdot Fe_2O_3 \cdot CaSO_4 \cdot 12H_2O$	5.888 ± 1	26.625 ± 9	8.875	R3, $R\bar{3}$, R32, R3m, $R\bar{3}m$
β-$3CaO \cdot Al_2O_3 \cdot CaCl_2 \cdot 10H_2O$	5.739 ± 1	46.87 ± 1	7.811	R3c, $R\bar{3}c$
$3CaO \cdot Cr_2O_3 \cdot CaCl_2 \cdot 10H_2O$	5.8164 ± 5	23.291 ± 4	7.764	R3, $R\bar{3}$, R32, R3m, $R\bar{3}m$
$3CaO \cdot Fe_2O_3 \cdot CaCl_2 \cdot 10H_2O$	5.858 ± 1	23.267 ± 5	7.756	R3, $R\bar{3}$, R32, R3m, $R\bar{3}m$
$3CaO \cdot Ga_2O_3 \cdot CaBr_2 \cdot 10H_2O$	5.8358 ± 3	24.386 ± 3	8.129	R3, $R\bar{3}$

completely ordered. Both compounds contained traces of other unknown polytypic modifications.

A c-axis rotation photograph of $3CaO \cdot Al_2O_3 \cdot 1/2CaSO_4 \cdot 1/2CaCl_2 \cdot 12H_2O$ is shown in Fig. 2.

Numerous experiments showed that intermediate compounds of this type should be expected in systems of complex calcium aluminate hydrates which contain anions of considerably different sizes.

Several other complex salts of this type with the anions S, NO_2, WO_4, and MoO_4 were prepared but not yet investigated.

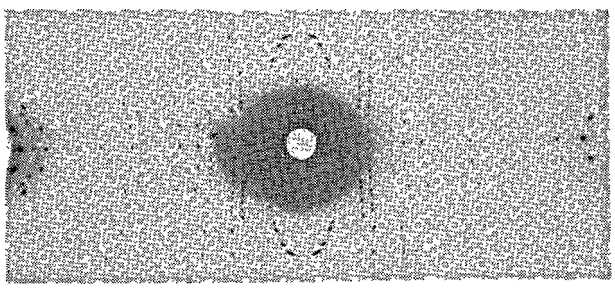

Fig. 2. A c-axis *rotation photograph of* $3CaO \cdot Al_2O_3 \cdot 1/2CaSO_4 \cdot 1/2CaCl_2 \cdot 12H_2O$ (CuK_α *radiation*)

Unit Cells and Space Groups of Compounds $3CaO \cdot R_2O_3Ca(X, Y_2) \cdot nH_2O$

Several complex hydrates $3CaO \cdot R_2O_3 \cdot Ca(X, Y_2) \cdot nH_2O$ with R = Fe^{3+}, Cr^{3+} and Ga^{3+} were prepared and investigated with X-ray methods. The results are listed in Table 2. The X-ray powder diagrams showed that the compounds containing Cr^{3+} and Fe^{3+} have ordered three-layer-structures independant of the method of preparation. The crystal structures are closely related to those of the complex aluminate hydrates.

The lattice constants a_0 increase with increasing radius of the cation R^{3+}. The basal spacings decrease in the same direction. This evidence agrees with the structural model proposed by F. G. Buttler, L. S. Dent Glasser and H. F. W. Taylor (12) the cations R^{3+} occupying octahedral sites. Increasing the radius of the cation R^{3+} causes probably higher OH–OH distances within the octahedral layer in directions perpendicular to c, the anions and water molecules between the layers being able to glide into the space between the OH-ions. The compound $3CaO \cdot Ga_2O_3 \cdot CaCl_2 \cdot 10H_2O$ seems to be closely related to the corresponding aluminate showing the same polymorphic transition at about 30°C.

Crystal Structures

The now available data from X-ray investigations on complex calcium aluminate hydrates of the type $3CaO \cdot R_2O_3 \cdot Ca(X, Y_2) \cdot nH_2O$ support the view of F. G. Buttler, L. S. Dent Glasser and H. F. W. Taylor (12) of the crystal structures of these compounds. To clear the question whether their structural model is correct or the one proposed by C. E. Tilley, H. D. Megaw and M. H. Hey (11) the z-coordinates of the atoms in some compounds which contain simple anions between the octahedral layers were determined from the intensities of 001 reflections.

The intensities of about 20 001 reflections of α–$3CaO \cdot Al_2O_3 \cdot CaCl_2 \cdot 10H_2O$, $3CaO \cdot Al_2O_3 \cdot CaBr_2 \cdot 10H_2O$, $3CaO \cdot Ga_2O_3 \cdot CaBr_2 \cdot 10H_2O$ and $3CaO \cdot Al_2O_3 \cdot CaJ_2 \cdot 10H_2O$ were measured with the aid of a single crystal counter diffractometer using MoK_α-radiation. The rhombohedral crystals were mounted along the a-axis, the monoclinic α–$3CaO \cdot Al_2O_3 \cdot CaCl_2 \cdot 10H_2O$ along b. From the intensity data relative structure factors were computed.

Since there existed a set of isomorphous crystals, the light and heavy atoms of which should be in the same positions, the replaceable atom method was applicable to determine the phases of high intensity reflections. A preliminary Fourier synthesis of $3CaO \cdot Al_2O_3 \cdot CaJ_2 \cdot 10H_2O$ calculated with 13 structure

Table 3. *Z-coordinates of the atoms of some complex calcium aluminate hydrates referred to the pseudocells*

$3CaO \cdot Al_2O_3 \cdot CaJ_2 \cdot 10H_2O$			$3CaO \cdot Al_2O_3 \cdot CaBr_2 \cdot 10H_2O$		
Atom	z(c′)	B	Atom	z(c′)	B
Al	0		Al	0	
2Ca	0.0647 ± 5	1.3	2Ca	0.077 ± 1	1.2
6OH	0.1127 ± 5		6OH	0.112 ± 1	
$2H_2O$	0.339 ± 2		$2H_2O$	0.369 ± 3	
J	1/2	2.1	Br	1/2	1.4
$3CaO \cdot Ga_2O_3 \cdot CaBr_2 \cdot 10H_2O$			α-$3CaO \cdot Al_2O_3 \cdot CaCl_2 \cdot 10H_2O$		
Ga	0		Al	0	
2Ca	0.0679 ± 5	1.4	2Ca	0.080 ± 1	0.7
6OH	0.1227 ± 1		6OH	0.126 ± 1	
$2H_2O$	0.379 ± 2	2.5	$2H_2O$	0.386 ± 3	2.1
Br	1/2		Cl	1/2	

factors indicated the z-coordinates (referred to the pseudocell with $c' = 8.857$ Å) to be about $z_{Al} = 0$, $z_{OH} = 0.11$, $z_{H_2O} = 0.35$, $z_J = 1/2$, the Ca^{2+} ions being displaced by about 0.5 Å out of their ideal position at $z = 0$. When these data and separate isotropic temperature factors for the octahedral layer and the layer containing the anion and the water molecules were refined by least squares methods on the basis of 22 001-intensities, the R-factor dropped to 3.2 percent.

With the data obtained for $3CaO \cdot Al_2O_3 \cdot CaJ_2 \cdot 10H_2O$ the z-coordinates of the other compounds were refined.

The results listed in Table 3 are compatible with the centrosymmetric space groups $R\bar{3}$ for $3CaO \cdot Al_2O_3 \cdot CaJ_2 \cdot 10H_2O$ and $3CaO \cdot Ga_2O_3 \cdot CaBr_2 \cdot 10H_2O$, $R\bar{3}c$ for $3CaO \cdot Al_2O_3 \cdot CaBr_2 \cdot 10H_2O$ and C2/c for α–$3CaO \cdot Al_2O_3 \cdot CaCl_2 \cdot 10H_2O$. Particularly the refinement of the z-parameters of the compound $3CaO \cdot Ga_2O_3 \cdot CaBr_2 \cdot 10H_2O$, the light cation Al^{3+} being replaced by the heavy Ga^{3+}, shows that the structural model proposed by F. G. Buttler, L. S. Dent Glasser and H. F. W. Taylor is correct.

Thus, in the case of the rhombohedral compounds, the x- and y-coordinates of all atoms, with the exception of the OH^- ions of the octahedral layers, are special coordinates. The octahedral layer contains both Ca^{2+} and the cation R^{3+} in ordered positions. These results are confirmed by the X-ray work of R. Allmann (personal communication) on the compound $3CaO \cdot Al_2O_3 \cdot CaSO_4 \cdot 12H_2O$. The resulting positive charge of the octahedral layers is balanced by the anion situated in $z = 1/2$ of the pseudocell. The constitution of these compounds at about 37 percent relative humidity may be given by the formulas

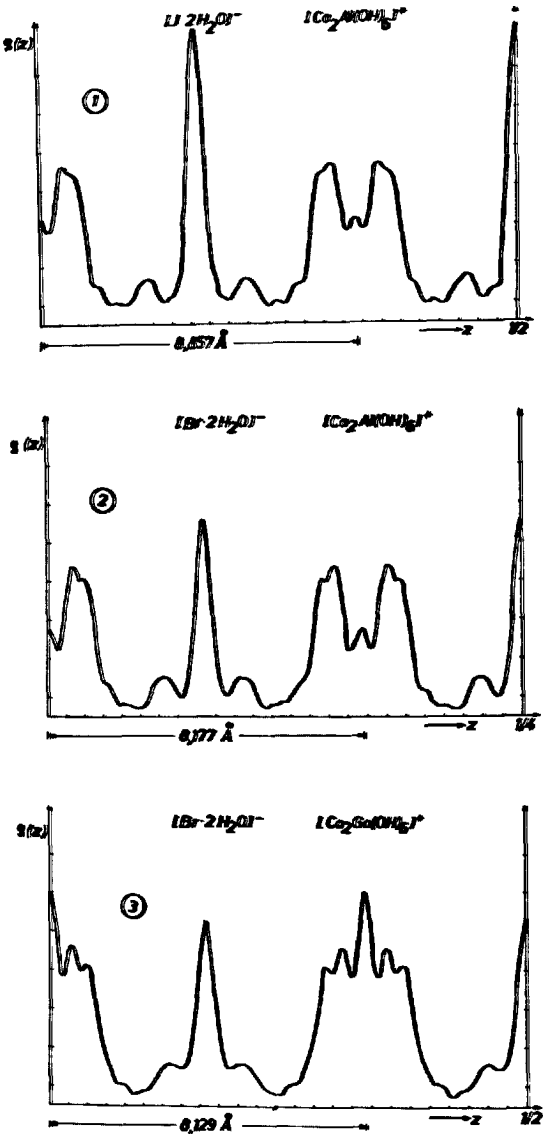

Fig. 3. *One dimensional Fourier projections $p(z)$ of* $3CaO \cdot Al_2O_3 \cdot CaJ_2 \cdot 10H_2O$ (1), $3CaO \cdot Al_2O_3 \cdot CaBr_2 \cdot 10H_2O$ (2) and $3CaO \cdot Ga_2O_3 \cdot CaBr_2 \cdot 10H_2O$ (3)

$$[Ca_2R(OH)_6]^+[Y \cdot 2H_2O]^-$$

and

$$[Ca_2Al(OH)_6]^+[1/2X \cdot 3H_2O]^-$$

In the case of the anions Cl^-, Br^- and J^- situated between the octahedral layers, there is not enough space left for the remaining water molecules at $z = 1/2$. These are, therefore, shifted off the position $z = 1/2$ along the c-axis. This is clearly indicated by the Fourier projections $p(z)$ shown in Fig. 3.

Table 4. *Observed and calculated structure factors*

$C_3A \cdot CaJ_2 \cdot 10H_2O$			$C_3A \cdot CaBr_2 \cdot 10H_2O$			$C_3Ga \cdot CaBr_2 \cdot 10H_2O$			α-$C_3A \cdot CaCl_2 \cdot 10H_2O$		
1	F_{obs}	F_{calc}	1	F_{obs}	F_{calc}	1	F_{obs}	F_{calc}	1	F_{obs}	F_{calc}
3	23.89	24.19	6	31.98	33.67	3	52.61	51.62	2	47.52	48.46
6	78.05	79.00	12	57.82	58.48	6	79.04	79.69	4	42.85	42.22
9	30.71	−30.21	18	31.03	−30.21	9	11.43	−10.72	6	20.66	−19.33
12	9.11	8.68	24	13.28	−13.60	12	4.91	4.71	8	25.99	−26.38
15	58.04	−57.65	30	42.03	−40.77	15	21.06	−21.29	10	24.46	−24.35
18	16.38	16.16	36	6.56	7.45	18	14.81	15.31	12	6.17	− 6.47
21	32.88	−31.51	42	22.31	−19.60	21	7.95	− 7.17	14	6.43	− 4.81
24	20.01	19.09	48	22.15	21.63	24	21.60	22.06	16	12.85	12.22
27	9.58	− 9.84	54	6.98	− 5.79	27	2.17	− 1.71	18	2.72	2.73
30	14.84	14.37	60	12.04	12.95	30	10.95	11.09	20	6.76	8.93
33	9.41	− 9.82	66	3.73	− 2.75	33	1.96	− 1.37	22	2.36	2.11
36	8.69	9.89	72	6.38	7.42	36	6.40	5.22	24	3.26	4.35
39	7.75	− 7.32	78	0.	− 0.67	39	2.64	2.57	26	2.92	4.21
42	7.08	7.77	84	8.58	9.42	42	7.75	7.88	28	6.44	5.89
45	1.17	0.85	90	1.75	1.30	45	5.41	5.76	30	4.38	5.04
48	7.96	8.51	96	4.36	6.76	48	7.53	7.28	32	3.56	3.74
51	3.22	3.16	102	0.	− 0.44	51	5.19	3.41	34	0.	0.07
54	6.03	6.15	108	0.	0.35	54	1.97	2.26			
57	1.40	0.30	114	2.94	− 2.85	57	0.	− 0.11			
60	0.	0.90	120	0.	0.62	60	0.	− 0.53			
63	0.	1.99				63	0.	− 0.70			
66	0.	0.42									
R = 3.2 percent			R = 6.1 percent			R = 3.7 percent			R = 5.5 percent		

Acknowledgements

The author wishes to thank Prof. H. O'Daniel, for high interest in and constant support of this work. Furthermore thanks are due to the "Deutsche Forschungsgemeinschaft" for support with equipment and computer time and to the "Verein Deutscher Zementwerke e. V." for financial help.

References

1. W. Lerch, F. W. Ashton and R. H. Bogue, "The sulforaluminates of calcium", J. Research NBS **2**, 715–731 (1929).
2. J. Foret, "Sur le chloro, le bromo et l'iodo-aluminate de chaux", Compt. rend. **191**, 711–713 (1930).
3. W. Mylius, "Über Calciumaluminathydrate und deren Doppelsalze", Acta Acad. Aboensis **7**, 3–145 (1933).
4. W. Feitknecht and M. Gerber, "Zur Kenntnis der Doppelhydroxyde und basischen Doppelsalze II. Über Mischfällungen aus Calcium-Aluminiumsalzlösungen", Helv. Chim. Acta **25**, 106–131 (1942).
5. W. Feitknecht and H. Buser, "Über den Bau der plättchenförmigen Calcium-Aluminiumhydroxysalze", Helv. Chim. Acta **34**, 128–142 (1951).
6. F. E. Jones, "The calcium aluminate complex salts", Proc. Symp. on Chemistry of Cements, 231–245 (Stockholm 1938).
7. H. F. W. Taylor, "The chemistry of cement hydration", Progress in Ceramic Science **1**, 89–145 (1961).
8. R. Turriziani, "The chemistry of cements", Vol. 1, p. 233–286, (Academic Press Inc., London, England, 1964).
9. F. E. Jones, "Hydration of calcium aluminates and ferrites", Proc. Fourth Int. Symp. on the Chemistry of Cement, 205–242 (Washington 1960).
10. E. Brandenberger, "Kristallstrukturelle Untersuchungen an Ca-Aluminathydraten", Schweiz. min. petrogr. Mitt. **13**, 569–570 (1933).
11. C. E. Tilley, M. D. Megaw and M. H. Hey, "Hydrocalumite ($4CaO \cdot Al_2O_3 \cdot 12H_2O$), a new mineral from Scawt Hill, Co. Antrim.", Miner. Mag. **23**, 607–615 (1934).
12. F. G. Buttler, L. S. Dent Glasser and H. F. W. Taylor, "Studies on $4CaO \cdot Al_2O_3 \cdot 13H_2O$ and the related mineral hydrocalumite", J. Amer. Ceram. Soc. **42**, 121–126 (1959).
13. H.-J. Kuzel, "Syntheses und Röntgenuntersuchung des $3CaO \cdot Al_2O_3 \cdot CaSO_4 \cdot 12H_2O$", N. Jb. Miner. Mh. 193–197 (1965).
14. H.-J. Kuzel, "Röntgenuntersuchung im System $3CaO \cdot Al_2O_3 \cdot CaSO_4 \cdot nH_2O$–$3CaO \cdot Al_2O_3 \cdot CaCl_2 \cdot nH_2O$–$H_2O$", N. Jb. Miner. Mh. 193–200 (1966).
15. G. Malquori and V. Cirilli, "The calcium ferrite complex salts", Proc. Third Int. Symp. on the Chemistry of Cement, 321–328 (London 1952).

Supplementary Paper II-27 Proton Magnetic Resonance Studies of C_3AH_6

Ryôiti Kiriyama, Hideko Kiriyama and Masanori Takagawa*

Synopsis

The proton magnetic resonance studies on crystal powders of synthetic $Ca_3Al(OH)_{12}$, abbreviated as C_3AH_6 in cement chemistry, were carried out over the temperature range between −186° and 110°C. The experimental values obtained for the second moment are 22.7 ± 0.3 and 19.6 ± 0.5 gauss^2 at liquid nitrogen and room temperatures, respectively. The samller value of the second moment found at room temperature is due to the increased amplitudes of the proton motions. The lattice constant is 12.536 Å at −170° and 12.566 Å at 24°C. Many structural models are tested by calculating the second moments for them and comparing the results with the experimental value. Thus, the positions of protons are located in a restricted region within the lattice of C_3AH_6: the representative parameters are given as $x_H = 0.093$, $y_H = 0.074$, and $z_H = 0.681$. This most probable sites of hydrogen atoms in the $Al(OH)_6$ group are not found on the production of the Al–O lines. There is no distinct tendency to form a H_4-cluster inside the oxygen tetrahedron which corresponds to the SiO_4 tetrahedron in the isomorphous silicate, grossular $Ca_3Al_2(SiO_4)_3$.

Introduction

Among many calcium aluminate hydrates, the isotropic structure of C_3AH_6, the abbreviation of the garnet type hydroxide $Ca_3Al_2(OH)_{12}$, presents a striking contrast to predominant layer structures of many others. The knowledge of chemical constitution of the hydroxyl groups in these compounds should be important to discuss the mechanism of hydration or dehydration process in cement chemistry. The determination of the hydrogen positions in the crystal lattice by X-ray diffraction technique is very difficult owing to the low scattering power of hydrogen atoms. The broad line proton magnetic resonance (PMR) is useful for the locating of the hydrogen positions and consequently it has been recommended as a supplementaty method for structure analysis. For this purpose, the knowledge about the atomic positions other than hydrogen's is required, which has been obtained by precise X-ray structure analysis. However, PMR gives an accurate information about the mutual interaction among the nearest protons as compared with the result obtained by any method of diffraction crystallography.

There has been another structural interest remaining in C_3AH_6. That is the possibility of a wide sense isomorphism between $Ca_3Al_2(SiO_4)_3$ and $Ca_3Al_2(OH)_{12}$ which implies the substitution of Si^{4+} by $4H^+$ for the charge balance requirement. The question whether a H_4-cluster is formed inside the oxygen tetrahedron or not is one of the important problems of the current crystal chemistry, and is a good problem for study by PMR.

Materials

Synthesis

C_3AH_6 was synthesized by adding aluminium powders slowly into a saturated aqueous solution of $Ca(OH)_2$ in the atmosphere free from carbon dioxide under a moderately warm condition. All reagents used were of extra-pure grade. The white precipitate was filtered quickly to avoid carbonate formation in air, and then was dried at 150°C. The samples were put into a glass tube and sealed off in vacuum. This glass sample tube was fitted in the PMR probe.

*The Institute of Scientific and Industrial Research, Osaka University, Osaka, Japan.

Identification

Chemical Analysis

Quantitative analyses of CaO and Al_2O_3 by ordinary wet gravimetric methods and the weight loss by ignition were as follows:

	obs.	calc.
CaO	45.27%	44.48%
Al_2O_3	27.45	26.95
H_2O	27.29	28.57
	100.01	100.00

The weight loss by ignition should be attributed to the water content for the chemical formula, $3CaO \cdot Al_2O_3 \cdot 6H_2O$. Thus the analysis agreed closely with the value calculated from the chemical formula. The slightly less value of the water content of the synthetic sample than that of the calculated one means that the dried powder contains no detectable water adsorbed.

X-ray Diffractometry.

All the diffraction patterns of the C_3AH_6 powder obtained by a X-ray diffractometer using filtered Cu K radiations were well indexed as the cubic, garnet type lattice and the line profiles were sharp. No diffraction lines other than those of the garnet type lattice were observed. Therefore, the synthetic C_3AH_6 was identified with pure, well-crystallized powder.

The lattice constants at 24°C and also at −170°C were determined by an inner-standard method using silicon powder.

a_o	12.566 Å	at 24°C
a_o	12.536 Å	at −170°C

The mean linear expansion coefficient between −170° and 24°C was calculated from these data: $\alpha = 1.25 \times 10^{-5}$ degree^{-1}.

Partial dehydration occurred between 270° and 350°C and amorphous diffraction patterns were observed in this temperature range. Above 370°C, the crystalline phase of $12CaO \cdot 7Al_2O_3$ appeared. The ignition product of C_3AH_6 at 900°C was well crystal lized $12CaO \cdot 7Al_2O_3$ powder.

Infra-red Absorption

In the O-H stretching vibration region a sharp absorption peak at 3600 cm^{-1} and a rather broad band with a shoulder at about 3500 cm^{-1} were observed, indicating the hydroxyl group to be free from any hydrogen bond. No peak was found in the neighbourhood of 1600 cm^{-1}, the H-O-H bending region. The lack of the absorption at 1600 cm^{-1} suggests that the sample contains no detectable adsorbed water.

Experimental Procedure

A PKW type broad line nuclear magnetic resonance spectrometer was used throughout the PMR measurements. The first derivative of the absorption line was recorded by keeping r.f. frequencies at 12 and 20 Mc/sec and sweeping the magnetic field. The amplitude of the magnetic field modulation was set less than 1/12 of the line width. Because the precise measurement of the second moment was required, the value of time varying applied field was continuously calibrated by a field tracking nuclear resonance gaussmeter. In our experiments on C_3AH_6, more than fifteen such curves were obtained at 25°C and −190°C. The experiments at low temperatures were performed to minimize line narrowing by thermal motion of the protons. Also it was found that spectra of better S/N ratios were obtained at liquid nitrogen temperatures.

The experimental value of the second moment was corrected for the modulation broadening according to the Andrew's formula (1).

$$\Delta H_2^2(\text{exp}) = \Delta H_2^2(\text{obs}) - \tfrac{1}{4}H_m^2 \qquad (1)$$

where H_m is the modulation amplitude in gauss.

The samples of about 3 g of C_3AH_6 powders sealed in a glass tube of 40 mm length and of 20 mm diameter were used in the PMR measurement.

Some of the experimental curves obtained at 12.000 Mc/sec are reproduced in Fig. 1.

The absorption was a broad, bell-shaped curve without resolved structure. The narrow component observed at room temperatures is due to the free water molecules, possibly included at the time of sealing off the glass sample tube. In the temperature range measured, the absorption lines showed only a slight motional narrowing. The line widths, taken as the separation in gauss of the maximum and minimum of the derivatives, were 15.1 and 14.1 gauss at −186°C and 25°C, respectively. A mean value of the second moment obtained from twenty low-temperature curves and that obtained from fifteen room-temperature curves were as follows:

ΔH_2^2(exp) at −186°C	22.7 ± 0.3 gauss^2
at 25°C	19.6 ± 0.5 〃

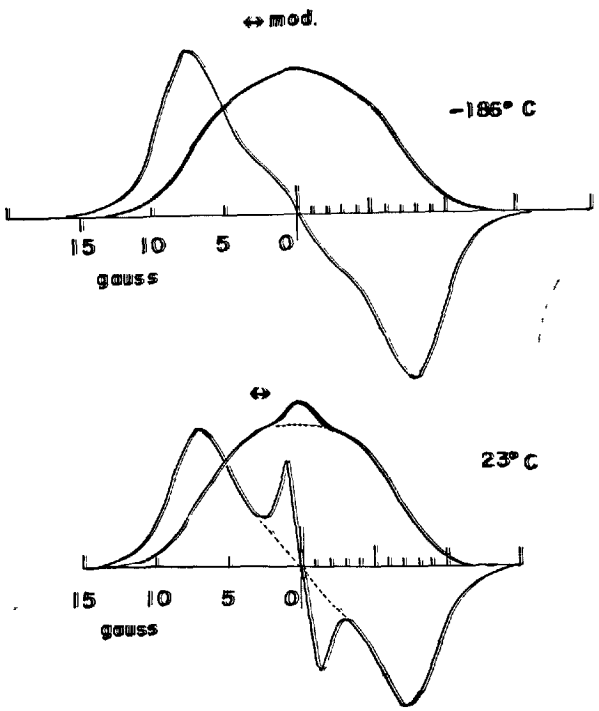

Fig. 1. *PMR absorption curves and those derivatives for C_3AH_6 powder.*

These values of the second moment of PMR are the main results obtained experimentally for the determination of the hydrogen positions.

Result

The crystal structure of C_3AH_6 was refined by Weiss (2) using X-ray diffraction. The space group is Ia3d and the lattice constant at a room temperature is 12.573 Å. The positions of heavy atoms are as follows:

16	Al	in	(a)	(0, 0, 0)
24	Ca	in	(c)	$(\frac{1}{8}, 0, \frac{1}{4})$
96	O	in	(h)	(x_0, y_0, z_0)

where x_0 is 0.030, y_0 is 0.052 and z_0 is 0.640.

From the symmetrical consideration, the hydrogen atoms must take the equivalent positions of 96(h), that is, the positional parameters are x_H, y_H and z_H. From the PMR experiment for C_3AH_6 powder, only one value of the second moment is available, so that the three structural parameters of the hydrogen positions in the crystal lattice can not be determined independently. However, some electrostatic and chemical considerations have often bring a useful and reasonable prediction of the arrangement of hydrogen atoms. Thus the possible structure would be considerably restricted.

In order to obtain the structural information from the PMR spectra, the theoretical second moment must be calculated by the method of Van Vleck (3) for various model structures.

Firstly, it is assumed that the hydrogen atom, or the proton in PMR phenomena, lies on the Al–O–H straight line and locates with an O-H distance changed between 0.96 and 1.12 Å.

In the case of C_3AH_6 the magnetic nuclei occupy structurally equivalent sites, so the second moment is expressed by the simple form

$$\Delta H_2^2(\text{calc}) = 358.1\sum_k r_{jk}^{-6} + 126.0\sum_m r_{jm}^{-6} \qquad (2)$$

where the first term is due to the magnetic dipole interaction between the protons and the second term is the interaction between the proton and aluminium nucleus. Because the second moment depends upon inverse sixth power of the inter-nuclear distance, the summation $\sum r_{jk}^{-6}$ in equation (2) converges rapidly as r_{jk} becomes large. Therefore, in calculating theoretical second moment for comparison with the experimental one, the terms in $\sum r^{-6}$ were obtained explicitly only for the neighbouring magnetic nuclei, hydrogen and aluminium, within a radius of 6 Å. The residual contributions by more distant nuclei were approximated by integration assuming the magnetic

moments of nuclei to be distributed uniformly. In this calculation, the cell dimension of 12.536 Å for −170°C was used and the coordinate parameter for oxygen was assumed to be the same as for room temperatures.

As shown in Fig. 2, the O–H distance fitted to the experimental second moment of 22.7 gauss² is given as 1.10 Å. This bond distance, however, seems to conflict with the result of the infrared absorption. On the other hand, O–O distance in the oxygen tetrahedron in C_3AH_6 lattice are 3.06 Å and 3.22 Å. It is, therefore, expected that the OH group in C_3AH_6 is free from any hydrogen bonding and the O–H distance of 0.98 Å is the most reasonable one. Moreover, in the above model, the nearest H–H separation is calculated to be 1.74 Å. This value is much shorter than the extreme value of 1.9 Å found in brucite, $Mg(OH)_2$, or an ordinary interhydrogen van der Waals separation of 2.0 ~ 2.4 Å. From such considerations, the model of the linear Al–O–H arrangement must be abandoned, and the hydrogen atom should be located deviating from the Al–O straight line having an apparent oxygen bond angle less than 180°.

Secondly, the location of the hydrogen nucleus was searched out by trial and error on assumptions: (i) the O–H distance is 0.98 Å and (ii) the hydrogen atom keeps the neighbouring calcium ions at a distance. If the O–H distance is fixed, unknown positional parameters should be diminished from three to two. Instead of three parameters, x_H, y_H and z_H, two new parameters α_H and β_H were taken. Angle α_H is defined as the azimuthal angle of the vector joined the origin of the unit cell to one selected hydrogen site $H_{68}(\frac{1}{2} + z_H, \bar{x}_H, y_H)$, which is measured from the X-axis in the XY-plane, and β_H is the polar angle of this vector. In the same manner, the oxygen parameters of $\alpha_O = -12°$ and $\beta_O = 20°$ were calculated for $O_{68}(\frac{1}{2} + z_O, \bar{x}_O, y_O)$ using the oxygen parameters found by Weiss. (2)

The value of β_H was fixed to some selected values of 20°, 18°, 16° and 14° and for each of β_H the parameter α_H was varied from −12° to −36° at 1° or 2° intervals. Fig. 3 shows the dependence of ΔH_2^2(calc) upon the parameters α_H and β_H. By comparing these results with the experiment, it was found that a locus for the points A, B and C in the Fig. 3 was the acceptable region for the actual location of the proton. The interatomic distances for each model are tabulated in Table 1.

Table 1. *Interatomic distances* (Å) *in* C_3AH_6

	oxygen polyhedron	model A	model B	model C	neutron diffraction
H–H	tetrahedron	1.96(4)	1.93(4)	2.06(4)	1.89(4)
	〃	2.56(2)	2.17(2)	1.84(2)	2.53(2)
H–H	dodecahedron	2.02	2.59	3.11	2.01
	〃	3.17	2.70	2.37	3.87
H–Al	octahedron	2.72	2.82	2.88	2.48
H–Ca	dodecahedron	2.61	2.65	2.70	2.86
	〃	3.04	2.78	2.48	3.11
angle	Al–O–H	138°	152°	168°	117°
angle	Ca–O–H	84°	86°	90°	103°
	〃	116°	98°	79°	123°

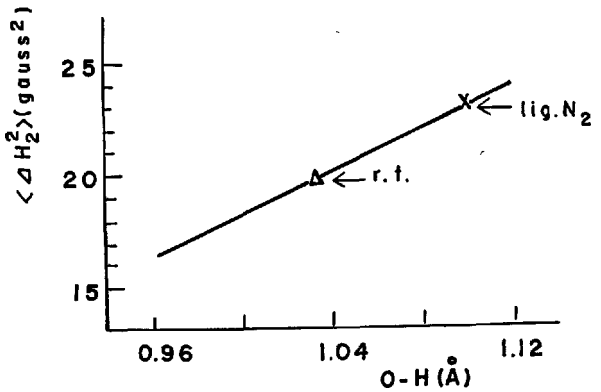

Fig. 2. *Dependance of the calculated second moment upon the O–H distance. The experimental values at −186°C and 23°C are also plotted.*

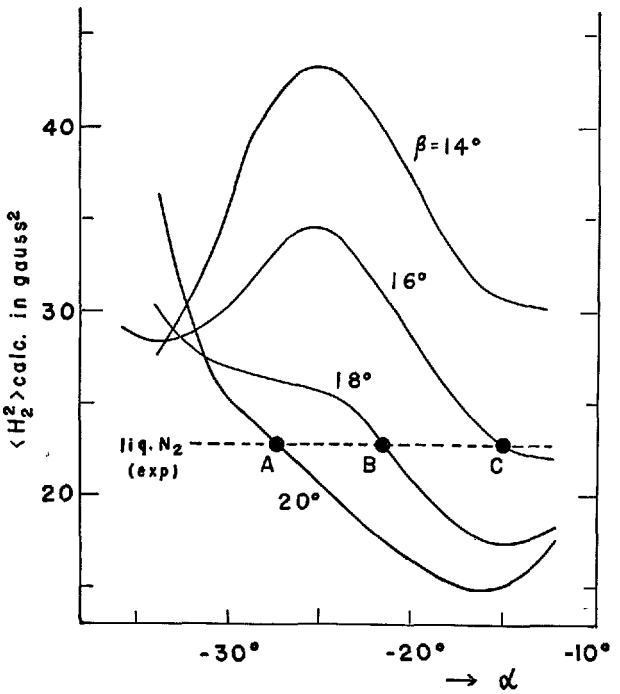

Fig. 3. *Dependence of the theoretical second moment upon the hydrogen position parameters α_H and β_H. The experimental value is indicated by a dashed line.*

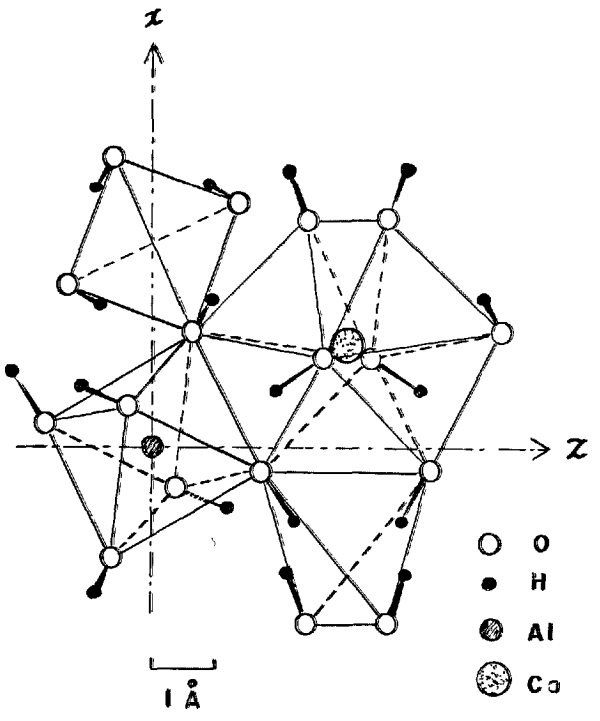

Fig. 4. *Projection of the crystal structure of* C_3AH_6 *on (010). Only the octahedron* $Al(OH)_6$ *at (000) and the neighbouring atoms around* H_{68} *are included.*

It seems that the location A of the hydrogen position is more preferable than the others in view of electrostatic energy. The atomic coordinates for the selected point A can be obtained from α_H, β_H and the assumed O–H distance of 0.98 Å:

$$x_H = 0.093,\ y_H = 0.074,\ z_H = 0.681.$$

The projection for the model A on (010) is shown in Fig. 4 with respect to H_{68} (hydrogen atom at $\frac{1}{2} + z_H, \bar{x}_H, y_H$) and its neighbours. It is noted that the hydrogen atoms occur outside of the oxygen tetrahedron (apart from the face less than about 0.2 Å) and consequently any discrete H_4-cluster is not formed. Thus, the H-H distances are 1.96 and 2.56 Å in the same $(OH)_4$ tetrahedron, while the shortest distance between adjacent tetrahedrons is 2.02 Å. In table 1 some results obtained by Cohen-Addad, Ducros, and Bertaut (6) are also included in comparison with ours.

Discussions

One of us, H. K., (4) reported a preliminary determination of the hydrogen position in C_3AH_6 by PMR experiments. In this earlier study the second moments measured were 17.6 gauss^2 at 105°C and 18.5 gauss^2 at −170°C. Cohen-Addad et al. (5) investigated independently the structure of C_3AH_6 by PMR and neutron diffraction and reported that the location of hydrogen position by neutron diffraction was confirmed by PMR. However, their measurement of the second moment was made at a room temperature only and effects of motional line narrowing were neglected. Their value of the second moment of 28 ± 3 gauss^2 was far larger than the value of 18 gauss^2 obtained by us. Such a disagreement led us to make a more precise measurement of the second moment at liquid nitrogen temperatures.

Recently, Cohen-Addad, Ducros and Bertaut (6) have refined the hydrogen coordinates by neutron diffraction at 4°K: $x_H = 0.101$, $y_H = 0.049$ and $z_H = 0.662$. From these values and the lattice constant found by us at −170°C, the theoretical second moment for the static model is estimated to be 26.9 gauss^2. This value is also appreciably larger than the experimental values of 22.7 gauss^2 at liquid nitrogen temperatures. The fact that the line narrowing between −186° and 25°C is relatively small indicates that the hydrogen atoms are bound to their structural sites by relatively strong forces. This, in turn, implies that thermal motion of the hydrogen is so reduced that a static model is applicable at the lower temperature. Therefore, in the present study the value of the experimental second moment at −186°C is used to locate the hydrogen positions in C_3AH_6.

One would not expect from the PMR data only to obtain accurate values of proton coordinates but an acceptable region for them. Nevertheless, the proton positions located by Cohen-Addad, Ducros and Bertaut (6) are not included in the allowed region. Thus, an ambiguity about the proton positions arises from the somewhat different results by different methods.

However, essential features of the hydroxyl radical in C_3AH_6 are similar as regards the fact that there is no discrete H_4-cluster inside the oxygen tetrahedron of the garnet lattice and also no definite hydroxyl bonds as like as proposed in $Al(OH)_3$. As may be seen in Table 1 and Fig. 4, some of the H-H distances between the neighbouring hydroxyl tetrahedra i.e. in the dodecahedron are close to twice the van der

Waals radius as occurred in the same tetrahedron.

Consequently, it is concluded from a viewpoint of crystal chemistry that the hydroxyl groups in C_3AH_6 are closely connected with the Al^{3+} ion forming a hydrogen-aluminate ion or hexahydroxoaluminate anion $[Al(OH)_6]^{3-}$, and these aluminate ions construct the ionic lattice of a garnet type with Ca^{2+} cations. If the anion $[Al(OH)_6]^{3-}$ is free, the Al-O-H bond should be linear owing to electrostatic interactions. Within the crystal lattice, however, the approach of the ions causes the O-H bond direction to have an appreciable deflection from the Al-O line. The position of the hydrogen deduced from the present PMR experiment will be favourable from these considerations. Namely, the hydrogen atom locates in 2.61 and 3.04 Å apart from two neighbouring Ca^{2+} ions and the separation of Al-H and the apparent bond angle of Al-O-H in its ion $[Al(OH)_6]^{3-}$ are 2.72 Å and 138°, respectively. The nearest inter-anionic hydrogen separation is 1.96 Å, suggesting a van der Waals contact with each other. In contrast to ours, the values found by neutron diffraction are 2.47 Å for Al-H distance and 117° for the bond angle of oxygen atom. The significance of their values may be difficult to assess at present.

References

1. E. R. Andrew, "Nuclear magnetic resonance modulation correction", Phys. Rev. **91**, 425 (1953).
2. R. Weiss and D. Grandjean, "Structure of tricalcium aluminate hydrate, $3CaO \cdot Al_2O_3 \cdot 6H_2O$ (in French), Acta Cryst. **17**, 1329–1330 (1964).
3. J. H. Van Vleck, "The dipolar broadening of magnetic resonance lines in crystals", Phys. Rev. **74**, 1168–1183 (1948).
4. H. Kiriyama, "Structure analyses of metal hydroxides by proton magnetic resonance" (in Japanese), Preliminary Abstracts of the 3rd Symposium on NMR at Osaka, Chemical Society of Japan, Tokyo, p. 152–155 (1963).
5. C. Cohen-Addad, P. Ducros, A. Durif, E. F. Bertaut and A. Delapalme, "Determination of the atomic position of hydrogens in hydrogarnet, $Al_2O_3 \cdot 3CaO \cdot 6H_2O$ by nuclear magnetic resonance and neutron diffraction" (in French), J. Phys. Fr. **25**, 478–483 (1964).
6. C. Cohen-Addad, P. Ducros, and E. F. Bertaut, "Studies on the substitution of SiO_4-group by $(OH)_4$ in the garnet type compounds, $Al_2Ca_3(OH)_{12}$ and $Al_2Ca_3(SiO_4)_{2.16}(OH)_{3.36}$" (in French), Acta Cryst. **23**, 220–230 (1967).

Supplementary Paper II-29 Calcium Aluminate Hydrates and Related Basic Salt Solid Solutions

Melville H. Roberts*

Synopsis

The composition and identity of different tetracalcium aluminate hydrates are studied in order to elucidate conflicting views in the literature. It is shown that two polytypes of $4CaO \cdot Al_2O_3 \cdot 19H_2O$ normally occur in contact with the liquid phase, and three lower hydrates with $13H_2O$, $11H_2O$ and $7H_2O$ are produced by dehydration under different drying conditions. Previous claims for the existence of $4CaO \cdot Al_2O_3 \cdot 13H_2O$ and $4CaO \cdot Al_2O_3 \cdot 12H_2O$ giving X-ray patterns with respective longest basal spacings of 8.2 Å and 7.9 Å are therefore not supported by the present study, and it is suggested instead that the 7.9 Å basal spacing originates from $4CaO \cdot Al_2O_3 \cdot 13H_2O$ and the 8.2 Å spacing from a related quaternary carbonate hydrate of composition $4CaO \cdot Al_2O_3 \cdot \frac{1}{2}CO_2 \cdot 12H_2O$.

The possibilities for the replacement of hydroxyl ions in the crystal lattice of calcium aluminate hydrates by other anions to give solid-solution series are examined. The previously reported replacement of sulphate ion by hydroxyl ion in $3CaO \cdot Al_2O_3 \cdot 3CaSO_4 \cdot 31H_2O$ is not confirmed, but solid solutions involving $4CaO \cdot Al_2O_3 \cdot 13H_2O$ are obtained under suitable conditions. Direct X-ray evidence is presented for the formation of a partial solid-solution series with compositions varying from $3CaO \cdot Al_2O_3 \cdot CaSO_4 \cdot 12H_2O$ to $3CaO \cdot Al_2O_3 \cdot \frac{1}{2}Ca(OH)_2 \cdot \frac{1}{2}CaSO_4 \cdot 12H_2O$ and a longest basal spacing decreasing within this range from 8.96 Å to 8.77 Å. A quaternary carbonate hydrate of composition $4CaO \cdot Al_2O_3 \cdot \frac{1}{2}CO_2 \cdot 12H_2O$ is readily formed by the action of CO_2 on $4CaO \cdot Al_2O_3 \cdot 19H_2O$ suspensions. The probable formation of a partial solid-solution series $4CaO \cdot Al_2O_3 \cdot \frac{1}{2}CO_2 \cdot 12H_2O$–$3CaO \cdot Al_2O_3 \cdot CaCO_3 \cdot 11H_2O$ giving basal spacings in the range 8.2–7.6 Å is also indicated. Preliminary results for chloride-containing solid solutions suggested the formation of similar partial solid-solution series with values for the basal spacings slightly higher than those for $4CaO \cdot Al_2O_3 \cdot 13H_2O$ and $3CaO \cdot Al_2O_3 \cdot CaCl_2 \cdot 10H_2O$. It is also indicated that related quinary solid solutions containing chloride and sulphate, or carbonate and sulphate may be formed in some circumstances.

Introduction

A comprehensive review of the then available knowledge of calcium aluminate hydrates in relation to the hydration of cement was made by Jones (1) at the Fourth International Symposium on the Chemistry of Cement. These hydrates have subsequently been the subject of many other studies (2–9), but some uncertainties still remain and conflicting views occur in the literature. In this connection, it may be noted that there are many difficulties in carrying out experimental work on calcium aluminate hydrates and related compounds, and two considerations are of particular importance. In the first place, many of the compounds exist in different hydration states, depending on the conditions of drying, and it is therefore necessary to maintain precise control over "H_2O" content and to prevent any interconversion between different hydrates, either by dehydration or rehydration, which may arise during subsequent treatment and examination of solid phases. Secondly, the hydrates are very susceptible to attack both by any carbonate in the reaction mixtures and by atmospheric CO_2, and all possible care must be taken to prevent such carbonation at every stage of preparation, treatment and examination, or if need be to make allowance for the effects of any carbonation that may occur unavoidably.

Carbonation is responsible for some erroneous interpretation in the past, as for example in the case of the so-called "C_3AH_{12}", which on the basis of many investigations (2, 10–13) is now accepted to be really the quaternary carbonate hydrate $C_3A \cdot CaCO_3 \cdot 11H_2O$. The opportunity for similar confusion and misinterpretation in identification still exists especially

*Building Research Station, Herts, United Kingdom.

with the tetracalcium aluminate hydrates, because of their close similarity to the related quaternary basic salt hydrates and particularly to the carbonate-containing hydrates which may occur with varying composition. The possibility of the formation of quaternary carbonate hydrates has therefore been given careful consideration in the first part of this study dealing with the tetracalcium aluminate hydrates. In addition, an attempt has been made to resolve the difficulties with regard to identification, and some experiments have been made to further investigate previous findings on these hydrates with the aim of elucidating the existing controversy on the composition and identity of different tetracalcium aluminate hydrates.

The existence of quaternary basic salt hydrates of the hexagonal-plate type, such as calcium monosulphoaluminate, monocarboaluminate, and monochloroaluminate, is well established (5). In view of the close structural relationship that evidently exists between these quaternary hydrates and C_4Aaq, there is therefore the possibility of the formation of "solid solutions" of varying degree of complexity involving the replacement of hydroxyl ions in the crystal lattice of calcium aluminate hydrates by any or all of such anions as sulphate, carbonate and chloride. The existence of these solid solutions has indeed been generally accepted, but little direct X-ray evidence of their formation appears to be available. The purpose of the remaining part of the present investigation is to examine the possibilities for the formation of such complex solid-solution series, particularly taking into account the more recent findings on calcium aluminate hydrates. An attempt has also been made to obtain data on the composition ranges and X-ray properties of the solid solutions, and some preliminary, though rather incomplete, results are given for basic salt solid solutions containing sulphate, carbonate or chloride.

Experimental

Materials and Procedures

The procedures for the preparation, filtration, analysis, and examination of different phases were very similar to those described by Jones and Roberts (13). In all cases, precautions were taken against contamination arising from carbonation by avoiding as much as possible any contact with atmospheric CO_2 at every stage of the preparation and subsequent treatment and examination, but attack by atmospheric CO_2 was not always completely prevented though the effects were probably minimised.

The basic ingredients of the reaction mixtures were a supersaturated monocalcium aluminate solution and freshly-ignited CaO, the former being prepared by treating a calcium aluminate cement ("Secar 250") with CO_2-free water and the latter by igniting "Analar" $CaCO_3$ at 1000°C. Quaternary compositions were obtained by adding to the calcium aluminate hydrate suspension either weighed quantities of the calcium salt ($CaCO_3$, $CaSO_4 \cdot 2H_2O$, or $CaCl_2 \cdot 2H_2O$), or, where appropriate, known volumes of the salt solution; all the salts were "Analar" chemicals. In the case of the quaternary carbonate compositions, incomplete reaction of the added $CaCO_3$ often occurred, and it was found to be preferable to introduce the carbonate by means of a method based on an adaptation of the barium hydroxide vacuum method for the determination of carbonate as described by Jones (14). This procedure involved the decomposition of a weighed amount of $CaCO_3$ with acid, and absorption at reduced pressure of the liberated CO_2 in a continuously stirred suspension of the calcium aluminate hydrate in mother-liquor contained in a conical filter flask.

The different reaction mixtures, contained in sealed "polythene" bottles, were shaken continuously at 25°C, for various periods, usually at least 7 days, before filtration either on a sintered-glass or a sintered stainless steel funnel in the absence of atmospheric CO_2. The solid phases obtained in the earlier stages of the investigation were dried to constant weight at room temperature and reduced pressure in a vacuum desiccator containing either a saturated salt solution to give the required relative humidity (usually 81% R. H.) or another drying agent, but since this procedure almost invariably resulted in some slight carbonation a different drying technique was later used. A sintered-glass funnel assembly fitted with ground glass joints and taps was used; the solid collected on the funnel after filtration being first washed with acetone, followed by ether, and evacuated for several minutes to remove the ether. The funnel was then disconnected from the filter flask, and, after closing at the top and bottom with ground glass joints fitted with small taps, was placed in an air thermostat at 25°C and connected to a supply of nitrogen which had previously been conditioned to

the required relative humidity by passing it through a saturated salt solution, or other drying agent as appropriate. The stream of nitrogen was continuously passed through the sintered-glass disc and the solid, and the funnel and contents weighed at 24 hour intervals until constant weight (± 1 mg) was obtained.

X-ray Examination

X-ray powder photographs were taken of a thin-layer specimen of solid using CuK_α radiation in a Guinier-type focusing camera with a diameter of 115 mm. To avoid both carbonation and possible changes in state of hydration, the specimens were prepared in a glove-box containing CO_2-free air at an appropriate relative humidity, and in general were exposed to X-rays in a sealed envelope formed by sealing each side of the power layer with self-adhesive "polythene" tape. Furthermore, to establish the hydrates actually present in contact with the liquid phase the X-ray examination was always, first of all, made on solid phases immediately after filtration and while still moist with mother-liquor. Subsequently, the solid phases were usually dried in a desiccator before X-ray examination, but difficulties often then arose from changes in the water content of the solid during preparation and from inadvertent carbonation of samples. To overcome these difficulties, some X-ray examinations were also made using a humidity-controlled specimen cell, as described by Aruja (15), whereby nitrogen at various relative humidities was passed over the X-ray powder specimen and the formation of different hydrates during drying or rehydrating cycles could be rapidly surveyed by X-ray examination with minimum risk of contamination by atmospheric CO_2 and of changes in state of hydration. Complete X-ray powder data for many of the hydrates considered have been published elsewhere (13, 16).

Results and Discussion

Tetracalcium Aluminate Hydrates

Results of the present investigation relating to the different states of hydration of hydrated tetracalcium aluminate are summarised in Table 1, which also includes results for some closely related quaternary carbonate hydrates. In the following discussion, the difficulties with regard to identification of different tetracalcium aluminate hydrates are examined, and the data of Table 1 are used to interpret and explain results previously obtained by other investigators.

Table 1. *Characteristics of tetracalcium aluminate hydrates and some related quaternary carbonate hydrates*

Composition	Drying conditions*	Basal spacings in X-ray powder patterns (Å)
C_4AH_{19}	moist with mother-liquor,	10.7
(α_1 and α_2)	or $>$ 88% R.H.	5.35
C_4AH_{13}	81–11% R.H.,	7.9
	or 25% R.H. at 40°C	3.95
C_4AH_{11}	anhydrous $CaCl_2$,	7.4
	or solid NaOH	3.70
CA_4H_7	P_2O_5	ca. 5.5†
$C_4A{\cdot}1/2CO_2{\cdot}12H_2O$	moist with mother-liquor,	8.2
	or 81–53% R.H.,	4.10
	or 25% R.H. at 40°C	
$C_4A{\cdot}1/2CO_2{\cdot}10H_2O$	11% R.H.,	7.7
	or anhydrous $CaCl_2$	3.85
$C_4A{\cdot}1/2CO_2{\cdot}8(?)H_2O$	P_2O_5	ca. 7.3
$C_4A{\cdot}CO_2{\cdot}11H_2O$	moist with mother-liquor,	7.6
(or $C_3A{\cdot}Ca{\cdot}CO_3{\cdot}11H_2O$)	or 81% R.H.,	3.80
	or anhydrous $CaCl_2$	

*At room temperature, unless stated otherwise.
†Poor X-ray pattern with weak and diffuse reflections.

C_4AH_{19}

In agreement with previous work by the present author (11, 13, 17), the tetracalcium aluminate hydrate in metastable equilibrium with mother-liquor at 25°C was found to be C_4AH_{19} (α_1 and α_2) with a longest basal spacing of 10.7 Å. This result has also been confirmed by many other investigators (3, 8, 9, 18–21), and on the basis of this work it is indicated that when hydrated tetracalcium aluminate is formed at temperatures in the range 1° to 50°C and at atmospheric pressure it is present as a $19H_2O$ hydrate in contact with the liquid phase. It has also been shown that this fully-hydrated C_4AH_{19} occurs in two polytypes, designated α_1 and α_2, which give X-ray patterns showing the same basal spacings and only differing slightly in the positions of non-basal reflections (13, 22).

Dehydration of C_4AH_{19} takes place very readily at room temperature at relative humidities below about 88%, and depending on the actual drying conditions, various lower hydrates not relevant to the aqueous system are formed. Consequently, in order to establish the presence of C_4AH_{19} in a hydrated product, it is generally advisable to undertake an X-ray examination of the moist solid in contact with mother-liquor with precautions to prevent loss of water from the specimen. This procedure may, however, result in some difficulty if C_2AH_8 is also present in the solid, because this hydrate gives basal spacings practically

identical to those of C_4AH_{19}. In this case, the often-used procedure of drying the moist solid phase in some way before X-ray examination may be helpful in distinguishing between the dicalcium and tetracalcium hydrates, but the utmost care most then be taken to prevent any carbonation both before and during the X-ray examination. If carbonation occurs, the X-ray examination of dried solids presents the opportunity of confusion of the X-ray patterns of quaternary carbonate hydrates with those of dehydrated C_4Aaq, as will be shown later. Furthermore, since these carbonate compounds may also be formed other than by carbonation of C_4Aaq, some uncertainty may then arise as to whether C_4AH_{19} was ever present in the original solid phase, as appears to be the case with some solid phases in many previous investigations (23–27).

C_4AH_{13}

As shown in Table 1, the present study has indicated the existence of a single C_4AH_{13} with a longest basal spacing of 7.9 Å. In contrast to this result, it was thought in earlier work by the present author (11, 13) that dehydration of C_4AH_{19} at 81% R.H. resulted in the formation of two polymorphs of C_4AH_{13}, designated α– and β–C_4AH_{13} and characterised in the X-ray patterns by longest basal spacings of 8.2 Å and 7.9 Å, respectively. However, Jones and Roberts (13) later suggested in an addendum to their paper that β–C_4AH_{13} was a true ternary hydrate, and that α–C_4AH_{13} contained carbonate in its structure. This conclusion was based on observations made on "C_4Aaq" preparations both with the deliberate introduction of CO_2 and with the rigid exclusion of atmospheric CO_2. Exposure of β–C_4AH_{13} to atmospheric CO_2 and treatment of suspensions of C_4AH_{19} in mother-liquor with $CaCO_3$, Na_2CO_3, or CO_2 resulted in the formation of "α–C_4AH_{13}" with a longest basal spacing of 8.2 Å. On the other hand, when X-ray examinations were made in a CO_2-free atmosphere using a humidity-controlled specimen cell (15), the passage of nitrogen at 81% R. H. over samples of α_1– and α_2–C_4AH_{19}, and C_4AH_{11} produced a single hydrate corresponding to β–C_4AH_{13} with a longest basal spacing of 7.9 Å. These observations have been confirmed by additional experiments on many other C_4Aaq preparations, and some typical results for a few preparations subjected to successive dehydration and rehydration cycles are given in Table 2. These results show that a basal spacing of 7.9 Å is obtained alone at relative humidities in the range 81 to 11%, provided that adequate precautions are taken

Table 2. *X-ray examination of* C_4Aaq *and* $C_4A\cdot\frac{1}{2}CO_2\cdot aq$ *during successive dehydration and rehydration cycles in X-ray specimen cell at room temperature.*

Relative humidity of nitrogen (%)	Longest basal spacing in X-ray powder pattern (Å)			
	$C_4Aaq(1)$	$C_4Aaq(2)$	$C_4Aaq(3)$	$C_4A\cdot1/2CO_2\cdot aq$
100	10.7(α_1)	10.7(α_1 + α_2)	10.7(α_1)	8.2
81	7.9	7.9	7.9†	8.2
33	7.9			8.2 +7.7(medium)
11	7.9			7.7 +8.2(medium)
ca. 1*	7.4	7.4	7.4	7.7
11	7.9 +8.2(very weak)			7.7
33	7.9 +8.2(weak)			8.1†† +7.7(medium)
81	7.9 +8.2(weak)	7.9	7.9	8.1†† +7.7(medium)
81**	7.9 +8.2(very weak)			8.2
81***		7.9 +8.2(medium)	7.9 +8.2(medium)	

*Nitrogen dried by anhydrous $CaCl_2$
**Nitrogen passed through solid on sintered glass funnel
***Solid dried in vacuo in desiccator
†Passage of air at 81% R.H. over separate sample gave spacings of 7.9+8.2 (medium)
††Slightly different from original X-ray pattern.

to exclude atmospheric CO_2. In some of the tests, particularly at the later stages of the cycling treatment, a basal spacing of 8.2 Å with a weak or very weak intensity was also present, but this spacing was observed with greater intensity in samples dried in desiccators or deliberately exposed to the atmosphere. This 8.2 Å spacing evidently arises by carbonation and the resulting formation of the so-called "α–C_4AH_{13}", or really $C_4A\cdot\frac{1}{2}CO_2\cdot12H_2O$ as established by other work involving deliberate carbonation (see later). With regard to the water content of the 7.9 Å hydrate, results from loss on ignition (1000°C) tests on several different C_4Aaq samples dried by N_2 at relative humidities in the range 81–33% at room temperature, or dried at 25% R. H. at 40°C, and only containing traces, if any, of the 8.2 Å hydrate, gave values in the range 41.2–42.5%, as compared with theoretical values of 41.8% H_2O for C_4AH_{13} and 39.9% H_2O for C_4AH_{12}. It is indicated, therefore, that the 7.9 Å hydrate (or "β–C_4AH_{13}") corresponds to a true ternary C_4AH_{13} hydrate, while the 8.2 Å hydrate (or "α–C_4AH_{13}") is actually a closely related quaternary carbonate hydrate.

In agreement with the above results Seligmann and Greening (3, 20) have also concluded that "α–C_4AH_{13}" was not a ternary phase, but really a "hemicarboaluminate" with a composition $C_3A\cdot\frac{1}{2}Ca(OH)_2\cdot\frac{1}{2}CaCO_3\cdot XH_2O$. However, in contrast with these views on "α– and β–C_4AH_{13}", Alègre (4) and Lavanant (7) have suggested instead that there existed a

C_4AH_{13} (8.2 Å) and a C_4AH_{12} (7.9 Å). This conclusion is not supported by the present study, particularly in that samples dried at room temperature over a range of relative humidities from 81% to about 22% showed a composition very near to C_4AH_{13} (7.9 Å) and this changed to C_4AH_{11} (7.4 Å) on further dehydration, together with the fact that the X-ray powder data given by Alègre and Lavanant for C_4AH_{13} (or "α–C_4AH_{13}") and C_4AH_{12} (or "β–C_4AH_{13}") are practically identical to those now obtained for $C_4A\cdot\frac{1}{2}CO_2\cdot 12H_2O$ and C_4AH_{13}, respectively.

It should also be noted that the question of contamination by atmospheric CO_2 was only considered by Alègre and Lavanant in so far as it might result in the formation of $C_3A\cdot CaCO_3\cdot aq$, since other quaternary carbonate hydrates were not recognised at that time. Although strict precautions were taken against contact with atmospheric CO_2, there is nevertheless still some doubt as to whether these precautions were completely successful in excluding CO_2 from the samples. This doubt arises from the use of techniques involving very small samples with consequent greater risks of carbonation effects, and in addition X-ray diffraction work on a Geiger-counter diffractometer which is vulnerable with regard to carbonation because the diffracting surface is only a very thin layer of the surface of the sample, particularly liable to be affected by any atmospheric CO_2 with magnified effects. It would appear to be very probable, therefore, that the results of these two previous studies were affected in some degree by carbonation and consequent formation of $C_4A\cdot\frac{1}{2}CO_2\cdot 12H_2O$ and $C_4A\cdot\frac{1}{2}CO_2\cdot 10H_2O$ (see Table 1) and indeed it is possible to interpret the results on this basis. For example, it could be suggested that the results obtained by Alègre for the alleged conversion of "C_4AH_{12}" (7.9 Å) into "C_4AH_{13}" (8.2 Å) at high relative humidity (Figs. 2 and 3 of original paper) are actually caused by carbonation during the course of X-ray examination with the resulting formation of $C_4A\cdot\frac{1}{2}CO_2\cdot 12H_2O$ (8.2 Å). Furthermore, this suggestion is then supported by the results at low relative humidity (Figs. 4 and 5, and Table 4 of original paper) which contrary to the opinion of Alègre do not appear to show conversion of "C_4AH_{13}" (8.2 Å) into "C_4AH_{12}" (7.9 Å), but rather that first of all $C_4A\cdot\frac{1}{2}CO_2\cdot 12H_2O$ (8.2 Å) dehydrates to the lower $10H_2O$ hydrate (7.7 Å), and at longer times the true C_4AH_{13} (7.9 Å) also dehydrates to C_4AH_{11} (7.4 Å). Alègre interpreted the final X-ray results at this low relative humidity (about 10% R. H.) as indicating the presence of C_4AH_{11} and C_4AH_7, but the formation of C_4AH_7 under this drying condition is extremely unlikely since the results given in Table 1 and 2 show that C_4AH_{11} is still stable at a lower relative humidity over anhydrous $CaCl_2$ or solid NaOH and that much more rigourous drying conditions are necessary to form C_4AH_7.

Similar alternative interpretations can also be suggested for the results on C_4Aaq obtained by Lavanant(7). In this investigation, it is noteworthy that the results for the immediate X-ray examination of compositions near to C_4AH_{13} at relative humidities of 80% and 50% do, in fact, indicate that a longest basal apacing of 7.9 Å is predominant. Lavanant preferred, however, to place greater reliance on results from samples "aged" in desiccators at these humidities, and it is not surprising that the longest basal spacing of 8.2 Å then predominated because it is very difficult, if not impossible, to prevent some carbonation of the samples under these conditions.

The question of the composition of "α– and β–C_4AH_{13}" together with the effect of carbonation on C_4Aaq have also recently been considered by Dosch and zur Strassen (8), and based on X-ray diffractometer studies it was concluded that the 7.9 Å basal spacing arose from a C_4AH_{12}, while the 8.2 Å spacing was derived both from a C_4AH_{13} and from a "quarter-carbonate" compound of composition $C_3A\cdot\frac{3}{4}CaO\cdot\frac{1}{4}CaCO_3\cdot 12H_2O$. Leaving aside the question of the composition of the quaternary carbonate hydrate, which is discussed again later, this work would appear to reconcile the two opposing points of view on "α– and β–C_4AH_{13}" which have already been considered above. However, the evidence presented by Dosch and zur Strassen for the existence of the two hydrates C_4AH_{13} (8.2 Å) and C_4AH_{12} (7.9 Å) is inconclusive and also inconsistent in some respects. In particular, very little data for the actual water content of preparations of the alleged "$13H_2O$" and "$12H_2O$" hydrates were given by these authors. A $12H_2O$ composition was said to be obtained after drying at 22% R. H. at 25°C, but the $13H_2O$ composition was only assumed on the basis of an incorrect interpretation of previous work. This single water content determination is not in agreement with the results for the water content of the 7.9 Å hydrate now obtained in the present investigation, which as shown above gave a composition nearer to C_4AH_{13} than to C_4AH_{12}.

Dosch and zur Strassen have also indicated that the "$12H_2O$" hydrate (7.9 Å) and the lower hydrates are converted into the "$13H_2O$" hydrate (8.2 Å) on storage at 81% R. H., but unfortunately detailed results for these transformations based on X-ray examination of pure C_4Aaq during dehydration and rehydration cycles were not given. The results of such an examina-

tion were only elaborated (Fig. 5 of original paper) in the case of a deliberately carbonated sample, consisting initially of a mixture of C_4AH_{19} (10.7 Å) and the related 8.2 Å carbonate hydrate, and consequently the position with regard to the possible existence of a C_4AH_{13} hydrate with a longest basal spacing of 8.2 Å was not clearly established. The authors interpreted these results as showing that C_4AH_{19} (10.7 Å) is dehydrated at 81% R. H. to a "$13H_2O$" hydrate with a longest basal spacing of 8.2 Å coincident with the 8.2 Å spacing of the quaternary carbonate hydrate, but against this interpretation no increase in intensity of the 8.2 Å spacing was shown in the diffractometer traces. It is, therefore, possible that difficulty may have occurred initially in resolving the 8.2 Å spacing of the carbonate hydrate from the 7.9 Å spacing which present results have indicated to be obtained from C_4AH_{13} under these conditions. Furthermore, these particular results given by Dosch and zur Strassen also appear to show the formation of a 7.9 Å spacing, together with a 8.2 Å spacing, when C_4AH_{11} (7.4 Å) and the dehydrated quaternary carbonate compound (7.7 Å) are rehydrated at 81% R. H., and this indication agrees with the present study but not with the conclusion of Dosch and zur Strassen that C_4AH_{13} with a longest basal spacing of 8.2 Å is formed at 81% R. H. It is also noteworthy that complete X-ray powder data for the quaternary carbonate hydrate and the alleged "C_4AH_{13}" with the same basal spacing of 8.2 Å were not given by Dosch and zur Strassen. Such data would appear to be necessary to confirm their separate existence, since some differences would be expected in other spacings in the X-ray patterns, but such differences have not so far been demonstrated. Finally, despite the elaborate precautions that were taken against atmospheric CO_2, it is likely, for reasons given above, that storage of solids in desiccators and X-ray examination by means of a diffractometer still offer the possibility of inadvertent carbonation having some effect on the results obtained by Dosch and zur Strassen.

C_4AH_{11}

Tables 1 and 2 show that the tetracalcium aluminate hydrate formed in samples dried over anhydrous $CaCl_2$ or solid NaOH is a $11H_2O$ hydrate with a longest basal spacing of 7.4 Å. This result is in agreement with similar previous results of many other investigators (3, 8, 11, 13, 28), though it has also been claimed by Alègre (4) and Lavanant (7) that C_4AH_{11} gave an X-ray pattern with characteristic spacings at 7.6 Å and 3.79 Å. However, pure C_4AH_{11} was not obtained in the latter two studies and, as already indicated above, some confusion and misinterpretation in identification of the mixture of hydrates appears to have arisen. Thus, it is likely that the spacings of 7.6 Å and 3.79 Å really originated from a dehydrated quaternary carbonate hydrate, while the other spacings of 7.4 Å and 3.70 Å were actually those of C_4AH_{11} and not C_4AH_7 as concluded by Alègre and Lavanant.

With regard to the range of drying conditions under which C_4AH_{11} is formed, some previous work (4, 7, 8) has indicated that this hydrate is obtained at 11% R. H. at 25°C (saturated LiCl solution), whereas the results in Tables 1 and 2 show the presence of C_4AH_{13} (7.9 Å) at this relative humidity. This minor point of difference may possibly be attributed to this drying condition giving a water vapour pressure near to the limiting value for the transition between the $13H_2O$ and $11H_2O$ hydrates, coupled with the fact that there may be some lack of precise control of the actual water vapour pressure obtained with saturated LiCl solution in different circumstances.

C_4AH_7

The results of the X-ray examination of C_4Aaq dried at room temperature over P_2O_5 were a little uncertain in that the preparations examined gave very poor X-ray patterns with a few weak and diffuse reflections. The water content obtained by loss on ignition (1000°C) tests on such samples was in the range $7–8H_2O$ indicating that only "hydroxyl" water is retained over P_2O_5, and it is possible that the almost complete removal of "inter-layer" water may have resulted in some deterioration of the crystallinity affecting the X-ray pattern. These patterns showed a weak basal spacing at about 5.5 Å, and this value is in approximate agreement with data for C_4AH_7 given by Feitknecht (29) and Buttler, Dent-Glasser, and Taylor (28).

In contrast to the above results, other investigators (4, 7, 8, 11) have claimed that C_4AH_7 gave an X-ray pattern with a longest basal spacing of about 7.4 Å. Such a spacing was obtained in earlier work by the present author (7), but this result was probably influenced by the effects of rehydration and/or carbonation under the conditions of examination used at that time. Alègre (4) and Lavanant (7) have also given a basal spacing of 7.4 Å for C_4AH_7, though as discussed above the X-ray patterns with sharp reflections which were attributed by these authors to C_4AH_7 actually correspond very closely to the X-ray pattern

of C_4AH_{11}. An X-ray pattern with sharp basal reflections, the longest being at 7.2 Å was obtained by Dosch and zur Strassen (8) when C_4Aaq was dried over P_2O_5 at 25°C. This finding is difficult to reconcile with present results, but two possible explanations may be suggested. In the first place, there is the possibility of rehydration of C_4AH_7 to C_4AH_{11}, which occurs very readily, causing some confusion in the X-ray patterns, and secondly inadvertent carbonation may have affected the results. Some support for the latter suggestion seems to be provided by the results now obtained for one quaternary carbonate preparation dried over P_2O_5, since as shown in Table 1 this preparation gave a reasonably sharp X-ray pattern with a longest basal spacing of about 7.3 Å very near to the value of 7.2 Å given by Dosch and zur Strassen for C_4AH_7.

Prossible Influence of Other Trace Impurities

The above discussion has clearly shown that control of water content of solid phases and prevention of carbonate contamination are two important factors in studies of hydrated calcium aluminates. Another possible complicating factor arises from the conclusion of Crowley (6) that trace impurities of foreign metal ions in the starting materials may have a pronounced influence on the phase relations in the system $CaO–Al_2O_3–H_2O$. Since stringent precautions as to the purity of the initial reactants were not taken in the present study, it appears to be necessary to examine the basis for this conclusion.

Crowley studied the phase relations at temperatures from 4° to about 300°C under high pressure, and reported that the phase diagram of the $CaO–Al_2O_3–H_2O$ system obtained from starting materials prepared from "reagent-grade" $CaCO_3$ was markedly different from that observed using an allegedly purer "luminescent-grade" $CaCO_3$. However, it is noteworthy that the phase diagram in the latter case (Fig. 1 of original paper) appears to agree reasonably well with other published work (13, 30–32) on the system $CaO–Al_2O_3–H_2O$, even though strict precautions as to the purity of the starting materials were not taken in these other investigations. Furthermore, when the initial reactants consisted of impure calcium aluminate cements or contained admixtures of different clays and various salts and bases the results were mainly in agreement with this diagram, suggesting that some factor other than the presence of trace impurities was operative in the case of different results obtained with "reagent-grade" $CaCO_3$.

The main differences in the diagram obtained using "reagent-grade" $CaCO_3$ (Fig. 5, of original paper) were that the compounds C_2AH_8 and CAH_{10} were not included, and instead a large field of stability, even up to about 240°C, for a "C_2AH_6" hydrate was obtained. This so-called "C_2AH_6" was not characterised clearly by Crowley, but it was implied that it was a dehydrated form of C_2AH_8, and presumably it was therefore identified in the X-ray powder patterns by a longest basal spacing in the region 8.7 Å to 8.8 Å on the basis of previous work (11, 13, 33). However, in these other investigations at atmospheric pressure, it was shown that the dehydrated from of C_2AH_8 was only obtained under fairly rigorous drying conditions and that rehydration to C_2AH_8 occurred very readily. In view of these results, together with the fact that Crowley also indicated the simultaneous presence of "C_2AH_6" and $Ca(OH)_2$ in some hydration products, it would appear that the true identity of the so-called "C_2AH_6" obtained by Crowley is far form clear. It may be conjectured that in some instances the preparation of the reaction mixtures was defective in that the initial reactants were contaminated with the nitrate ion involved in their preparation. If this were the case, the quaternary hydrate $C_3A \cdot Ca(NO_3)_2 \cdot aq$ would be formed, and since the X-ray pattern of this hydrate, as given by Van Aardt (34), shows a longest basal spacing of about 8.8 Å which is practically identical to that reported for the dehydrated form of C_2AH_8, it is possible that some confusion may have arisen.

In addition, the carbonate compounds "α–C_4AH_{13}" and $C_3A \cdot CaCO_3 \cdot 11H_2O$ were identified in many of the hydration products, and it is clear therefore that the effects of contamination by atmospheric CO_2 must also have played some part in the results reported by Crowley. The occurrence of such contamination is indeed to be expected when it is considered that little care was taken to exclude atmospheric CO_2 and that the techniques which were used involved the treatment of very small samples (20 mg of initial solid) and air-drying of the hydrated products before X-ray examination. The many inconsistencies in the detailed results reported, suggesting that some uncontrolled factor is operating, may therefore be attributed, at least partly, to the effects of variable carbonation of samples.

On the basis of the above remarks, it appears to the present author that Crowley's conclusion with regard to the marked influence of trace impurities of foreign metal ions in studies of hydrated calcium aluminates has not been substantiated, but rather that the effects of contamination by atmospheric CO_2 and lack of precise control of water content of solid phases are the principal factors to be guarded

against in such studies.

Quaternary Solid Solutions Containing Sulphate

Several possibilities exist for the replacement of OH^- in the crystal lattice of calcium aluminate hydrates by SO_4^{--}. The probable formation of five interconnected solid-solution series has been suggested by Kalousek (5, 35), but some of these can now be dismissed on the basis of more recent evidence. The supposed solid solution between C_3AH_{12} and $C_3A \cdot CaSO_4 \cdot 12H_2O$ can no longer be accepted, since it has been shown that the allged "C_3AH_{12}" is actually $C_3A \cdot CaCO_3 \cdot 11H_2O$ (2, 10–13). In addition, the suggested formation of the two solid-solution series $C_3A \cdot CaSO_4 \cdot 12H_2O$–$C_3A \cdot 3CaSO_4 \cdot 31H_2O$ and C_4AH_{13}–"$C_6A \cdot aq$" would appear to be ruled out by the different crystal lattice structures involved, and indeed the experimental evidence obtained by several investigators (36–38) has shown that the two aluminate sulphates do not form solid solutions.

The existence of the supposed solid solution between $C_3A \cdot 3CaSO_4 \cdot 31H_2O$ and "$C_6A \cdot aq$" is also rather doubtful, because no satisfactory evidence for the formation of "$C_6A \cdot aq$" has so far been obtained, despite many attempts by the writer and others (39, 40) to prepare this compound. Nevertheless, Midgley and Rosaman (40) still considered that limited replacement of SO_4^{--} by OH^- could occur in $C_3A \cdot 3CaSO_4 \cdot 31H_2O$, though the X-ray evidence obtained for this limited solid-solution formation was based solely on very slight apparent differences in the 100 reflection at about 9.7 Å, which is liable to appreciable error in measurement. In an attempt to obtain more conclusive evidence for this reported solid solution, some additional solid samples, prepared by the same methods as used by Midgley and Rosaman, were examined in the present study. It was found that the X-ray powder patterns of the various moist solids were practically identical to that shown by pure $C_3A \cdot 3CaSO_4 \cdot 31H_2O$, even in the case of the high angle reflections, and the alleged solid-solution formation was therefore not confirmed. Chemical analysis of the preparations gave values for the $CaSO_4/Al_2O_3$ molar ratio in the range 2.83–3.14, but difficulties occurred in the analytical determinations because of the presence of sugar, as may also well have been the case in the work of Midgley and Rosaman. It seems therefore that the evidence available at present for the replacement of SO_4^{--} by OH^- in $C_3A \cdot 3CaSO_4 \cdot 31H_2O$ is inconclusive, and further work is needed before its occurrence can be accepted.

The remaining possibility for solid-solution formation is that involving $C_4A \cdot aq$ and $C_3A \cdot CaSO_4 \cdot aq$, and several investigators (35–37) have indicated the existence of a solid-solution series between these two hydrates on the basis of variations in the refractive indices observed with dried solids of varying composition. However, in view of the difficulties arising in microscopical examination of finely divided solids, as well as possible changes produced during drying of the solids, this evidence cannot be regarded as completely satisfactory. Moreover, it has also been questioned (5, 38) whether such optical data provide evidence of the existence of a true solid solution, and it was suggested instead that the phenomenon might be caused by the formation of intergrowths of a particular kind. This situation arises from the investigation made by Turriziani and Schippa (38), in which it was observed that quaternary solids with $CaSO_4/Al_2O_3$ molar ratios of 0–1, dried over $CaCl_2$, gave X-ray patterns with reflections due to both "α–C_4AH_{13}" and $C_3A \cdot CaSO_4 \cdot 12H_2O$, whereas a single solid phase with varying refractive indices was obtained optically. The significance of these results is however not clear, since the formation of C_4AH_{11} (7.4 Å) and $C_3A \cdot CaSO_4 \cdot 10H_2O$ (8.2 Å) is to be expected on drying over $CaCl_2$ if $C_4A \cdot aq$ and $C_3A \cdot CaSO_4 \cdot aq$ were present, and complications due to changes produced by drying the moist solids, as well as by carbonation, may well have had some influence. Yet another possible complicating factor arises from the occurrence in the aqueous system of three different modifications of $C_3A \cdot CaSO_4 \cdot aq$, characterised in the X-ray powder patterns by respective longest basal spacings of 10.3 Å, 9.6 Å and 9.0 Å. While it is widely accepted that the 9.0 Å hydrate corresponds to $C_3A \cdot CaSO_4 \cdot 12H_2O$, the problem of the composition of the other two modifications has not yet been conclusively resolved, because their formation appears to depend both on the temperature and on the initial composition of the reaction mixture in relation to the final position in the quaternary CaO–Al_2O_3–$CaSO_4$–H_2O system. On the basis of some work by the present author, it has been indicated (41) that the 10.3 Å hydrate is a $15H_2O$ hydrate which is more stable at temperatures below 25°C, and that the 9.6 Å and 9.0 Å hydrates are polymorphs of a $12H_2O$ hydrate, the 9.6 Å hydrate being formed especially in solutions of low lime content. However, water contents of $16H_2O$ and $18H_2O$ for the 9.6 Å hydrate have also been reported (5, 42), and further work is needed to elucidate the problem of the composition and behaviour of the 9.6 Å and 10.3 Å hydrates.

In order to further investigate the possibility of the formation of a solid-solution series between $C_4A \cdot aq$ and $C_3A \cdot CaSO_4 \cdot aq$, some reaction mixtures in the $CaO–Al_2O_3–CaSO_4–H_2O$ were prepared, involving the treatment of a suspension of C_4AH_{19} in mother-liquor with increasing additions of $CaSO_4 \cdot 2H_2O$. The initial compositions of these mixtures were so arranged as to leave some $Ca(OH)_2$ in the final solid phases, so that the reflections due to $Ca(OH)_2$ in the X-ray powder patterns could be used as an internal standard to calibrate the measurements on other reflections. Furthermore, it was also found that in the presence of excess lime only one modification of $C_3A \cdot CaSO_4 \cdot 12H_2O$, the 9.0 Å hydrate, was formed, and complications due to the presence of the other two forms of this compound did not arise. X-ray powder photographs were taken of moist solid phases immediately after filtration, and the results from measurements on certain selected interplanar spacings from each of the various preparations are given in Figs. 1 and 2. The indexing of these particular reflections was based on the hexagonal pseudocell with $a = 5.76$ Å and $c = 26.79$ Å determined by Kuzel (43) for $C_3A \cdot CaSO_4 \cdot 12H_2O$, and the measurements for 006 were corrected against the $Ca(OH)_2$ reflection at 4.91 Å the 110 against the $Ca(OH)_2$ reflection at 3.110 Å, the 119 and 208 against the $Ca(OH)_2$ reflection at 1.927 Å, and the 300 against the $Ca(OH)_2$ reflection at 1.687 Å. Such internal calibration of the measurements was found to be necessary because small variations in the location of the specimen in the focusing camera caused the position of the reflections to change slightly from one photograph to the next.

The X-ray examination results (Figs. 1 and 2) showed that the 110 and 300 reflections remained practically constant for all solid phases, but the 006, 119 and 208 reflections only remained constant with the mixed solid phases giving $CaSO_4/Al_2O_3$ molar ratios of 0.09–0.50 and 1.0–1.25, and at intermediate values there was a gradual shift of these reflections. The same changes are apparent in Fig. 2, which gives mean values for $\frac{1}{3}c$ (corresponding to the longest basal spacing, 003) and mean values of a calculated from measurements on the particular reflections examined. These results indicated that solids of $CaSO_4/Al_2O_3$ molar ratio of 1 or higher consisted of mixtures of $C_3A \cdot 3CaSO_4 \cdot aq$ and a $C_3A \cdot CaSO_4 \cdot aq$ hydrate with $a = 5.75$ Å and $\frac{1}{3}c = 8.96$ Å, while a solid-solution series was formed with solids of $CaSO_4/Al_2O_3$ ratio varying from 1 to 0.50, the longest basal spacing decreasing gradually in this composition range from 8.96 Å to 8.77 Å but a remaining constant at 5.75 Å. Solids of $CaSO_4/Al_2O_3$ ratio below 0.50 consisted of mixtures of C_4AH_{19} and the limiting solid solution $C_4A \cdot \frac{1}{2}SO_3 \cdot aq$ with $a = 5.75$ Å and $\frac{1}{3}c = 8.77$ Å, the amount of C_4AH_{19} increasing with decreasing $CaSO_4/Al_2O_3$ ratio. In general agreement with these

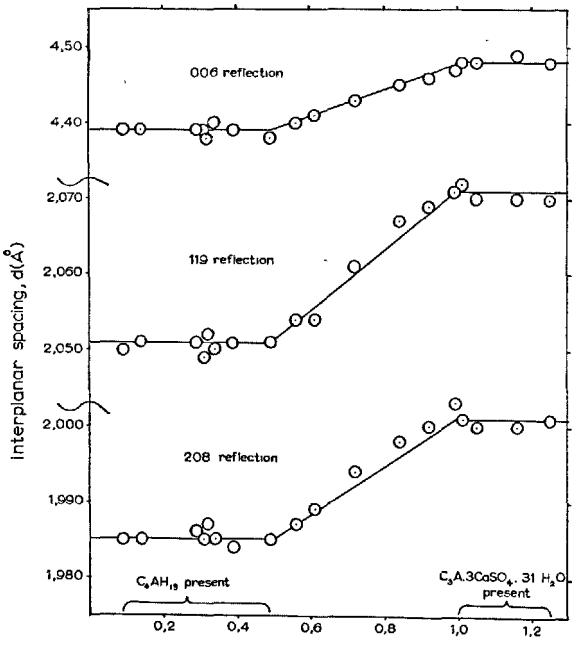

Fig. 1. *Selected interplanar spacings of* $C_4A \cdot aq–C_3A \cdot CaSO_4 \cdot aq$ *solid solutions in series of preparations in system* $CaO–Al_2O_3–CaSO_4–H_2O$

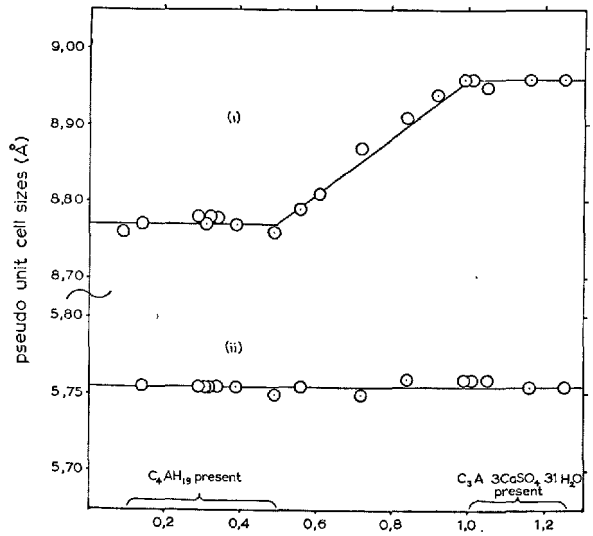

Fig. 2. *Pseudo unit cell sizes of* $C_4A \cdot aq–C_3A \cdot CaSO_4 \cdot aq$ *solid solutions in series of preparations in system* $CaO–Al_2O_3–CaSO_4–H_2O$

(i) mean values for $1/3c$ calculated from 006, 119, and 208 reflections

(ii) mean values for a calculated from 110 and 300 reflections

results, Seligmann and Greening (20) have given brief indications of the formation of similar solid-solutions in solid phases obtained from the hydration of C_3A with $Ca(OH)_2$ and $CaSO_4 \cdot 2H_2O$, but the limiting solid solution composition was reported as $C_4A \cdot \frac{3}{5}SO_3 \cdot aq$.

A few tests were made in the X-ray specimen cell to examine the stability of the solid solutions under different drying conditions. The X-ray pattern of the solid solution was found to remain unchanged after drying with N_2 at 81% R. H., but with N_2 dried by solid NaOH the X-ray pattern deteriorated markedly and a weak and diffuse basal spacing was observed at about 8 Å, which may be compared with the value of 8.2 Å for $C_3A \cdot CaSO_4 \cdot 10H_2O$ under the same drying conditions. The original X-ray pattern with a spacing at about 8.8 Å returned on rehydration at 81% R. H.. Only a few water-content determinations were made on the solid-solution compositions. Three preparations with $CaSO_4/Al_2O_3$ molar ratios of 0.56, 0.39 and 0.55 gave water contents corresponding to $12.6H_2O$, $12.3H_2O$ and $12.1H_2O$ after drying at 81% R. H. at room temperature. It is, therefore, indicated that this solid solution is formed between $C_3A \cdot CaSO_4 \cdot 12H_2O$ and C_4AH_{13}, and the replacement of OH^- by SO_4^{--} evidently results in the loss of "interlayer" water from C_4AH_{19}.

Very little information is available on the effect of slight carbonation on $C_3A \cdot CaSO_4 \cdot aq$ and the quaternary sulphate solid solutions, and on the possible formation of a complex solid solution containing sulphate and carbonate. This problem was encountered by Seligmann and Greening (20), but it was not resolved and it was only possible to indicate in the X-ray patterns that the basal spacing of the sulphate-containing hydrates fell within the limits of 9.6 Å for one form of $C_3A \cdot CaSO_4 \cdot aq$ to 7.6 Å for $C_3A \cdot CaCO_3 \cdot 11H_2O$. It has also been shown (12) that in contact with solution the presence of carbonate can result in some circumstances in the formation of $C_3A \cdot CaCO_3 \cdot 11H_2O$ and $C_4A \cdot \frac{1}{2}CO_2 \cdot 12H_2O$ coexisting with $C_3A \cdot CaSO_4 \cdot 12H_2O$ and $C_3A \cdot 3CaSO_4 \cdot 31H_2O$. However, a weak basal spacing in the region 8.3–8.5 Å was frequently observed in the X-ray patterns of some of the above solid-solution compositions after drying in desiccators at 81% R. H., and this spacing may possibly arise from carbonation with the consequent formation of a quinary solid solution containing carbonate and sulphate.

Table 3. *Composition of solid phases formed in system* $CaO–Al_2O_3–CaCO_3–H_2O$ *by action of* CO_2 *on* C_4AH_{19} *suspensions in mother-liquor.*

Molar composition solid dried at 81% R.H.				Compounds identified in moist solids from X-ray patterns				
CaO	Al_2O_3	CO_2	H_2O	C_4AH_{19} (10.7Å)	Solid solution* (8.2Å)	mono-carbonate** (7.6Å)	$Ca(OH)_2$	Calcite
4.02	1	0.13	13.8	much	some			
3.99	1	0.18	13.1	much	some			
4.04	1	0.35	12.9	little	much			
3.94	1	0.48	12.2†		much			
4.02	1	0.52	12.5††		much			
4.02	1	0.53	12.4		much			
3.96	1	0.67	11.9		much	little		
4.40	1	0.78	12.2		much	some	little	
4.06	1	0.95	11.6		trace	much		
4.29	1	0.98	11.6		trace	much	little	trace
4.15	1	1.12	11.2			much		little
6.82	1	1.62	14.1			much	much	some

*Composition indicated to be $C_4A \cdot 1/2CO_2 \cdot 12H_2O$
**$C_3A \cdot CaCO_3 \cdot 11H_2O$
†Solid dried by nitrogen at 56% R.H.
††Solid dried by nitrogen at 81% R.H.

Quaternary Solid Solutions Containing Carbonate

Similar considerations to those already discussed for quaternary sulphate solid solutions would seem to apply to the possibilities of solid-solution formation between calcium aluminate hydrates and the quaternary carbonate hydrates, and only the solid-solution series $C_4A \cdot aq–C_3A \cdot CaCO_3 \cdot aq$ was therefore studied. A series of reaction mixtures in the $CaO–Al_2O_3–CaCO_3–H_2O$ system were prepared by treating suspensions of C_4AH_{19} in mother-liquor, sometimes together with $Ca(OH)_2$ with increasing amounts of CO_2 and the compositions of the final solid phases are given in Table 3. These results showed that with small additions of CO_2 mixtures of C_4AH_{19} and a quaternary carbonate hydrate with a longest basal spacing of 8.2 Å were formed. This 8.2 Å hydrate increased in amount with increasing additions of CO_2 until at a CO_2/Al_2O_3 molar ratio near to 0.5 only this carbonate compound was obtained. With still larger additions of CO_2, $C_3A \cdot CaCO_3 \cdot 11H_2O$ was also formed and this monocarbonate increased in amount, while the 8.2 Å hydrate diminished, until the solid consisted mainly of $C_3A \cdot CaCO_3 \cdot 11H_2O$ at CO_2/Al_2O_3 ratios near to 1. At higher CO_2/Al_2O_3 ratios mixtures of $CaCO_3$ and $C_3A \cdot CaCO_3 \cdot 11H_2O$ were present.

Although the behaviour with CO_2 additions to C_4AH_{19} was similar in some respects to that already described for additions of $CaSO_4 \cdot 2H_2O$, an important difference was the formation of a mixture of the 8.2 Å carbonate-containing hydrate and $C_3A \cdot CaCO_3 \cdot 11H_2O$ at CO_2/Al_2O_3 ratios above 0.5. Furthermore, with all the preparations given in Table 3 it was not possible to detect any differences in the X-ray patterns

indicative of the formation of a solid-solution series. These results, therefore, appeared to suggest the formation of an unique quaternary carbonate hydrate of composition approximating to $C_4A \cdot \frac{1}{2}CO_2 \cdot 12H_2O$, and giving an X-ray pattern identical to that previously reported (13, 16) for "α-$C_4A \cdot H_{13}$". However, other results obtained with reaction mixtures of different compositions indicated the existence of other C_4AH_{13}–$C_3A \cdot CaCO_3 \cdot 11H_2O$ solid-solution compositions. When $C_4A \cdot \frac{1}{2}CO_2 \cdot 12H_2O$ was treated with lime solutions of varying concentrations, the X-ray patterns of the moist solids were unchanged with final lime concentrations in solution down to about 0.6 g CaO/litre, but at final concentrations of 0.52 g CaO/litre, 0.49 g CaO/litre, 0.42 g CaO/litre and 0.28 g CaO/litre the moist solid phases gave X-ray patterns with basal spacings of 8.15 Å, 8.10 Å, 8.05 Å, and 7.8 Å, respectively. At the same time, the Al_2O_3 concentration of the solution increased with decreasing lime concentration and the CO_2/Al_2O_3 molar ratio of the solid solution phase also gradually increased. Similar changes in the X-ray patterns, with a decrease in the basal spacings, were also frequently observed when samples containing the quaternary carbonate solid-solution were dried in a desiccator at 81% R. H., or subjected to lengthy cycling treatment in the X-ray specimen cell, and thus were vulnerable to further attack by atmospheric CO_2. Longest basal spacings in the range 8.2–7.6 Å may, therefore, be obtained for a solid-solution series with compositions probably varying from $C_4A \cdot \frac{1}{2}CO_2 \cdot 12H_2O$ to $C_3A \cdot CaCO_3 \cdot 11H_2O$.

The value of 8.2 Å for the longest basal spacing obtained from the carbonate-containing solid solution appears to be anomalous in that it is higher than the corresponding values for C_4AH_{13} (7.9 Å) and $C_3A \cdot CaCO_3 \cdot 11H_2O$ (7.6 Å). This situation may possibly arise from variations in the amount of H_2O displaced by the introduction of CO_3^{--} since full replacement of $2OH^-$ in C_4AH_{13} by CO_3^{--} to give $C_3A \cdot CaCO_3 \cdot 11H_2O$ also results in the loss of $1H_2O$. Unlike $C_3A \cdot CaCO_3 \cdot 11H_2O$, all the solid-solution compositions behaved in a similar manner to C_4AH_{13} and lost water when dried over anhydrous $CaCl_2$, and then gave X-ray patterns with basal spacings at about 7.7 Å. The results obtained with a sample of $C_4A \cdot \frac{1}{2}CO_2 \cdot 12H_2O$ subjected to successive dehydration and rehydration cycles are included in Table 2, and it is shown that dehydration occurred more readily than with C_4AH_{13} since it began at 33% R. H. and the longest basal spacing of 7.7 Å was obtained alone at 1–11% R. H.. As shown in Table 1, samples of $C_4A \cdot \frac{1}{2}CO_2 \cdot$ aq dried over anhydrous $CaCl_2$ gave a water content approximating to $10H_2O$, and the X-ray pattern of this hydrate showed low-angle spacings of medium or strong intensity at 7.7 Å, 4.57 Å, 3.85 Å, 3.78 Å and 2.87 Å. Further loss of water occurred on drying over P_2O_5 and the basal spacing decreased to about 7.3 Å.

Similar results to those given in Table 3 have also been obtained by Dosch and zur Strassen (8) for reaction mixtures consisting of CaO, $CaCO_3$ and sodium aluminate solution, but the 8.2 Å quaternary carbonate hydrate was given a composition $C_4A \cdot \frac{1}{4}CO_2 \cdot 12H_2O$ and the 7.7 Å hydrate obtained by dehydration at 11% R. H. had a composition $C_4A \cdot \frac{1}{4}CO_2 \cdot 9H_2O$. These compositions differ appreciably from those obtained in the present study, and it can only be suggested that this discrepancy may possibly arise from the results obtained by Dosch and zur Strassen being affected by additional carbonation from atmospheric CO_2 during the X-ray diffractometer examination of the various solids.

Quaternary Solid Solutions Containing Chloride

A limited number of experiments were made to study the solid solutions which have been reported (5) to be formed between C_4A·aq and $C_3A \cdot CaCl_2 \cdot 10H_2O$. Table 4 gives the results of the X-ray examination of moist solid phases prepared by treating C_4AH_{19} suspensions with increasing additions of $CaCl_2$, together with the molar compositions, the latter being obtained by calculation and thus perhaps subject to some error. Solids of calculated $CaCl_2/Al_2O_3$ molar ratios from 0.96 to 0.88 gave X-ray patterns with low-angle spacings at 7.8 Å (strong), 4.87 Å

Table 4. *Composition of solid phases formed in system* CaO–Al_2O_3–$CaCl_2$–H_2O *by action of* $CaCl_2$ *on* C_4AH_{19} *suspensions in mother-liquor.*

Molar composition solid*			Compounds identified in moist solids from X-ray pattern		
CaO	Al_2O_3	$CaCl_2$	C_4AH_{19} (10.7Å)	Solid solution (8.0–7.9Å)	$C_3A \cdot CaCl_2 \cdot H_{10}$ (7.8Å)
3.83	1	0.13	much	little	
3.78	1	0.17	much	some	
3.92	1	0.17	little	much	
3.60	1	0.40	trace?	much	
3.42	1	0.58		much	
3.37	1	0.67		much	
3.24	1	0.72		much	
3.21	1	0.88			much
3.25	1	0.94			much
3.21	1	0.96			much

*Calculated from total initial composition of reaction mixture and composition of filtrate.

(very weak), 3.91 Å (medium), 3.80 Å (medium), 3.41 Å (weak) and 2.87 Å (strong), and these patterns appeared to be identical to that of a pure preparation of $C_3A \cdot CaCl_2 \cdot 10H_2O$ (analysed composition 2.99 $CaO \cdot 1Al_2O_3 \cdot 0.97CaCl_2 \cdot 10.4H_2O$) obtained by reaction of a mixed $CaCl_2$–$AlCl_3$ solution with NaOH solution. These patterns also corresponded to that of β–$C_3A \cdot CaCl_2 \cdot 10H_2O$ as given by Kuzel (44). A quaternary chloride compound was also obtained alone with solids of $CaCl_2/Al_2O_3$ ratio in the range 0.72–0.58, but visual comparison of the X-ray patterns now showed slight differences from one preparation to the next and the basal spacings had also increased somewhat as compared with those of $C_3A/CaCl_2 \cdot 10H_2O$. With solids of still lower $CaCl_2 \cdot Al_2O_3$ ratio in the range 0.40–0.13, mixtures of C_4AH_{19} and apparently the same quaternary chloride hydrate with a basal spacing of about 8.0 Å were formed. This behaviour with $CaCl_2$ additions to C_4AH_{19} resembles that already described for the formation of quaternary sulphate solid solutions, and it is therefore indicated that C_4AH_{13} and $C_3A \cdot CaCl_2 \cdot 10H_2O$ form a limited solid-solution series over a restricted range of compositions. Further work is, however, needed to establish the changes in the X-ray patterns more precisely, and to correlate these changes with varying $CaCl_2/Al_2O_3$ ratio in the solids.

No information seems to be available on the effect of slight carbonation on the quaternary chloride hydrates, and on the possible formation of quinary solid solution containing chloride and carbonate, but some evidence was obtained for such a solid solution containing chloride and sulphate. Treatment of $C_3A \cdot CaCl_2 \cdot 10H_2O$ (1.00 g) with 150 ml $CaSO_4$ solution (0.66 g $CaSO_4$/litre), both without added $Ca(OH)_2$ and in the presence of excess $Ca(OH)_2$, was found to result in the complete removal of sulphate from solution and in the displacement of chloride from the original solid. X-ray examination of the moist solid phases showed the presence in each case of a single compound giving a longest basal spacing of 8.4 Å. The solid obtained in the absence of excess $Ca(OH)_2$ gave a composition $3.09CaO \cdot 1Al_2O_3 \cdot 0.39CaCl_2 \cdot 0.49CaSO_4 \cdot 12.3H_2O$ after drying at 81% R. H., and it is therefore indicated to be a quinary solid solution. This composition is very near to that of the compound $C_3A \cdot \frac{1}{2}CaCl_2 \cdot \frac{1}{2}CaSO_4 \cdot 12H_2O$ with a basal spacing of 8.3 Å which was prepared under hydrothermal conditions by Kuzel (44), but it is possible that a range of compositions exist for these quinary hydrates containing chloride and sulphate.

Conclusions

The results obtained in the present investigation, together with a critical examination of previous studies, give a substantial clarification of the existing uncertainties with regard to the composition and identity of different tetracalcium aluminate hydrates. The available data lead to the conclusion that there are five modifications of this compound, and these are characterised in the X-ray powder patterns by longest basal spacings of 10.7 Å (α_1– and α_2–C_4AH_{19}), 7.9 Å (C_4AH_{13}), 7.4 Å (C_4AH_{11}) and approximately 5.5 Å (C_4AH_7).

It is widely accepted that C_4AH_{19} is the only hydrate present in contact with the liquid phase at temperatures in the range 1° to 50°C and at atmospheric pressure, but some controversy exists with regard to the lower hydrates produced by dehydrating C_4AH_{19} under different drying conditions. It is suggested that some confusion and misinterpretation in identification of the various hydrates examined in previous studies has arisen from lack of precise control of water content of solid phases and especially from the effects of contamination by atmospheric CO_2. In this connection, it may be noted that X-ray diffraction work carried on a Geiger-counter diffractometer is particularly likely to be subjected to the influence of these two factors, because a very thin layer of the sample is the diffracting surface and this is where the effects of carbonation, dehydration or rehydration are very liable to occur unless extensive precautions are taken. Even when extreme care is exercised by the use of specially designed sample holders with a surrounding controlled atmosphere, it may be virtually impossible to completely exclude atmospheric CO_2 from the samples, and some caution must therefore be exercised in the interpretation of X-ray diffractometer data obtained with calcium aluminate hydrates, and related basic salt hydrates.

Inadvertent carbonation by atmospheric CO_2, and the resulting unrecognised presence of closely related quaternary carbonate hydrates are probably mainly responsible for the conflicting views in the literature on the lower hydrates of $C_4A \cdot aq$, especially with regard to the composition of the hydrates heretofore called α– and β–C_4AH_{13}, giving longest basal spacings of 8.2 Å and 7.9 Å, respectively. On present evidence, it is considered that the existence of a

C_4AH_{13} with a basal spacing of 8.2 Å and a C_4AH_{12} with a basal spacing of 7.9 Å has not been conclusively established, and it is concluded instead that a single 13 H_2O hydrate (corresponding to "β–C_4AH_{13}") with a basal spacing of 7.9 Å exists, while "α–C_4AH_{13}" with a basal spacing of 8.2 Å is actually a related quaternary carbonate hydrate of composition $C_4A \cdot \frac{1}{2}CO_2 \cdot 12H_2O$. The latter compound is dehydrated to a $10H_2O$ hydrate with a basal spacing of 7.7 Å and this spacing has occasionally in the past been incorrectly attributed to C_4AH_{11} which actually gives a basal spacing of 7.4 Å. In addition, provided that adequate precautions are taken to prevent both rehydration to C_4AH_{11} and carbonation, it is shown that the lowest hydrate C_4AH_7 gives a longest basal spacing of approximately 5.5 Å, and not 7.2–7.4 Å as indicated in some previous investigations.

With regard to the formation of solid-solution series between ternary calcium aluminate hydrates and related quaternary basic salts, the previously reported existence of solid solutions involving the hypothetical hexacalcium aluminate hydrate is not confirmed and only those involving tetracalcium aluminate hydrate are shown to be formed. Although the latter compound normally occurs only as the $19H_2O$ hydrate in contact with the liquid phase, it appears that replacement of hydroxyl ions in the crystal lattice by other anions results in the loss of "inter-layer" water so that effectively C_4AH_{13} is concerned in the solid-solution formation. Furthermore, complete solid-solution series are not formed but only partial series over restricted composition ranges, at any rate with basic salt solid solutions containing sulphate, or carbonate or chloride. With these anions, the behaviour when added to C_4AH_{19} suspensions is similar though not identical. The existence of a partial solid-solution series between C_4AH_{13} and $C_3A \cdot CaSO_4 \cdot 12H_2O$ is established over the range of compositions from $C_3A \cdot CaSO_4 \cdot 12H_2O$ to $C_3A \cdot \frac{1}{2}Ca(OH)_2 \cdot \frac{1}{2}CaSO_4 \cdot 12H_2O$, the longest basal spacing in the X-ray powder patterns decreasing within this range from 8.96 Å to 8.77 Å. The possible existence of solid solutions involving the 9.6 Å and 10.3 Å modifications of $C_3A \cdot CaSO_4 \cdot aq$ which also occur in the aqueous system still remains to be examined. A quaternary carbonate hydrate $C_4A \cdot \frac{1}{2}CO_2 \cdot 12H_2O$ is readily obtained, and, although variations in its composition and X-ray pattern are not observed in preparations obtained from C_4AH_{19} suspensions, it is probable that under other conditions a solid-solution series $C_4A \cdot \frac{1}{2}CO_2 \cdot 12H_2O$–$C_3A \cdot CaCO_3 \cdot 11H_2O$ is formed giving basal spacings in the range 8.2–7.6 Å. Some preliminary results obtained for the quaternary chloride solid solutions suggest that the behaviour is almost the same as with the sulphate-containing solid solutions, though the change in basal spacing with solid-solution formation to give higher values than those of C_4AH_{13}, and $C_3A \cdot CaCl_2 \cdot 10H_2O$ resembles that observed with the carbonate-containing solid solutions. It is suggested that the latter effect arises from variations in the amount of H_2O displaced by the incorporation of Cl^- or CO_3^{--} in the crystal lattice. Brief indications are also obtained that related quinary solid solutions containing chloride and sulphate, or carbonate and sulphate, may exist under suitable conditions. Further investigations are needed to establish more precisely the compositions and X-ray properties of these quinary solid solutions and the quaternary chloride-containing solid solutions, as also appear necessary to map out the various solid-solution fields in the equilibria of the relevant aqueous systems.

References

1. F. E. Jones, "Hydration of calcium aluminates and ferrites", Proceedings Fourth International Symposium on the Chemistry of Cement, Washington 1960. U. S. Bureau of Standards Monograph 43, Vol. 1, 205–242 (1962).
2. R. Rabot and M. T. Mounier, "Investigations on the existence of hexagonal tricalcium aluminate" (in French), Rev. Mat. Constr., No. 554, 449–464 (1961).
3. P. Seligmann and N. R. Greening, "New techniques for temperature and humidity control in X-ray diffractometry", J.P.C.A. Res. and Devel. Labs. 4, No. 2, 2–9 (1962).
4. R. Alègre, "Investigations on the hexagonal hydrated tetracalcium aluminate" (in French), Rev. Mat. Constr., No. 566, 301–314 (1962).
5. The Chemistry of Cements, Vol. 1 (Academic Press Inc., London and New York, 1964) Edited by H. F. W. Taylor. See chapter by R. Turriziani entitled "The calcium aluminate hydrates and related compounds".
6. M. S. Crowley, "Effect of starting materials on phase relations in the system CaO–Al_2O_3–H_2O", J. Am. Ceram. Soc. **47**, 144–148 (1964).
7. F. Lavanant, "Contribution to the study of some calcium aluminate hydrates" (in French), Rev. Mat. Constr., No. 592, 1–10; No. 593, 76–87; No. 595, 193–207; No. 596, 251–261; No 597, 298–304 (1965).
8. W. Dosch and H. zur Strassen, "Investigation of tetra-

calcium aluminate hydrate. I. The various hydrate stages and the effect of carbonic acid" (in German), Zement-Kalk-Gips **18**, 233–237 (1965).
9. J. H. P. van Aardt and S. Visser, "Some reactions of tricalcium aluminate hexahydrate at medium temperatures", Cement and Lime Manufacture **40**, 7–11 (1967).
10. G. Schippa and R. Turriziani, "Hydrated calcium aluminates" (in Italian), Ricerca Sci. **27**, 3654–3661 (1957).
11. M. H. Roberts, "New calcium aluminate hydrates", J. Appl. Chem. **7**, 543–546 (1957).
12. M. H. Roberts, Discussion of paper by P. Lhopitallier, Proceedings Fourth International Symposium on the Chemistry of Cement, Washington 1960. U. S. Bureau of Standards Monograph 43, Vol. 2, 1033–1034 (1962).
13. F. E. Jones and M. H. Roberts, "The system CaO–Al_2O_3–H_2O at 25°C", Building Research Current Papers, Research Series 1 (1962).
14. F. E. Jones, "A method for the determination of carbonate in small amounts of materials", J. Soc. Chem. Ind. **59**, 21–23 (1940).
15. E. Aruja, "A humidity and temperature controlled specimen holder for a focusing X-ray diffraction camera", J. Sci. Instrum. **39**, 393 (1962).
16. The Chemistry of Cements, Vol. 2 (Academic Press Inc., London and New York, 1964), Edited by H. F. W. Taylor. See Appendix 1.
17. M. H. Roberts, Discussion of paper by S. Chatterji and J. W. Jeffery, Magazine of Concrete Research **16**, No. 49, 236–238 (1964).
18. F. G. Buttler and H. F. W. Taylor, "The system CaO–Al_2O_3–H_2O at 1°C", J. Chem Soc. 2103–2110 (1958).
19. A. Percival and H. F. W. Taylor, "Monocalcium aluminate hydrate in the system CaO–Al_2O_3–H_2O at 21°C", J. Chem. Soc. 2629–2631 (1959).
20. P. Seligmann and N. R. Greening, "Studies of early hydration reactions of portland cement by X-ray diffraction", Highway Research Record, No. 62, 89-105 (1964).
21. E. T. Carlson, "Some properties of the calcium aluminoferrite hydrates", U. S. Bureau of Standards, Building Science Series 6 (1966).
22. E. Aruja, "The unit cell and space group of 4 CaO·Al_2O_3·19H_2O polymorphs", Acta Cryst. **14**, 1213–1216 (1961).
23. S. Chatterji and J. W. Jeffery, "Studies of the early stages of paste hydration of cement compounds, I", J. Am. Ceram. Soc. **45**, 536–543 (1962).
24. H. Lehmann and K. J. Leers, "Hardening reactions of alumina cements" (in German), Tonind. Ztg. **87**, 29–41 (1963).
25. S. Chatterji and J. W. Jeffery, "The effect of various heat treatments of the clinker on the early hydration of cement pastes", Magazine of Concrete Research **16**, No. 46, 3–10 (1964).
26. H. E. Schwiete, U. Ludwig and P. Muller, "Studies of calcium aluminate hydrates" (in German), Silikattechnik **16**, 103–109, 146–152 (1965).
27. H. N. Stein, "Influence of quartz on the hydration of 3CaO·Al_2O_3", Symposium on Structure of Portland Cement Paste and Concrete, Highway Research Board Special Report 90, 368–377 (1966).
28. F. G. Buttler, L. S. Dent Glasser and H. F. W. Taylor, "Studies on 4CaO·Al_2O_3·13H_2O and the related natural mineral hydrocalumite", J. Am. Ceram. Soc. **42**, 121–126 (1959).
29. W. Feitknecht, "The solid hydroxy salts of bivalent metals" (in German), Fortschr. Chem. Forschung. **2**, 670–757 (1953). See p. 736.
30. R. B. Peppler and L. S. Wells, "The system lime, alumina and water from 50°C to 250°C", J. Res. Nat. Bur. Stand. **52**, 75–92 (1954).
31. A. J. Majumdar and R. Roy, "The system CaO–Al_2O_3–H_2O", J. Am. Ceram. Soc. **39**, 434–442 (1956).
32. C. W. F. T. Pistorius, "Phase relations in the system CaO–Al_2O_3–H_2O to high pressures and temperatures", Am. J. Sci. **260**, 221–229 (1962).
33. E. T. Carlson, "The system lime—alumina—water at 1°C" J. Res. Nat. Bur. Stand. **61**, 1–11 (1958).
34. J. H. P. van Aardt, "Deterioration of cement products in aggressive media", Proceedings Fourth International Symposium on the Chemistry of Cement, Washington 1960. U.S Bureau of Standards Monograph 43, Vol. 2, 835–848 (1962). See page 844.
35. G. L. Kalousek, "Sulfoaluminates of calcium as stable and metastable phases and a study of a portion of the five-component system CaO–SO_3–Al_2O_3–Na_2O–H_2O at 25°C", Thesis, University of Maryland (1941).
36. F. E. Jones, "The quaternary system CaO–Al_2O_3–$CaSO_4$–H_2O at 25°C", J. Phys. Chem. **48**, 311–356 (1944).
37. J. D'Ans and H. Eick, "The system CaO–Al_2O_3–$CaSO_4$–H_2O at 20°C" (in German), Zement-Kalk-Gips **6**, 302–311 (1953).
38. R. Turriziani and G. Schippa, "Investigation of the quaternary solids CaO–Al_2O_3–$CaSO_4$–H_2O by X-ray and DTA methods" (in Italian), Ricerca Sci. **24**, 2356–2363 (1954).
39. E. T. Carlson and H. A. Berman, "Some observations on the calcium aluminate carbonate hydrate", J. Res. Nat. Bur. Stand. **64A**, 333–341 (1960).
40. H. G. Midgley and D. Rosaman, "The composition of ettringite in set portland cement", Proceedings Fourth International Symposium on the Chemistry of Cement, Washington 1960. U. S. Bureau of Standards Monograph 43, Vol. 1, 259–262 (1962).
41. Building Research 1965, Ministry of Technology. H. M. S. O., London. See page 72.
42. P. K. Mehta and A. Klein, "Investigations on the hydration products in the system 4CaO·3Al_2O_3·SO_3–$CaSO_4$–CaO–H_2O". Symposium on Structure of Portland Cement Paste and Concrete, Highway Research Board Special Report 90, 328–352 (1966).
43. H. J. Kuzel, "Synthesis and X-ray investigations of 3CaO·Al_2O_3·$CaSO_4$·12H_2O" (in German), Neues Jahrb. Mineral. Monatsh. No. 7, 193–197 (1965).
44. H. J. Kuzel, "X-ray investigations in the system 3CaO·Al_2O_3·$CaSO_4$·nH_2O–3CaO·Al_2O_3·$CaCl_2$·nH_2O–H_2O" (in German), Neues Jahrb. Mineral. Monatsh. No. 7, 193–200 (1966).

Supplementary Paper II-77 Crystal Structures and Reactions of C_4AH_{12} and Derived Basic Salts

S. J. Ahmed, L. S. Dent Glasser and Harry F. W. Taylor*

Synopsis

The crystal structure of a phase approximating in composition to C_4AH_{12}, with some structural CO_3^{2-}, has been determined. It is based on considerably distorted brucite-like layers of composition $[Ca_2Al(OH)_6]^+$, with interlayer H_2O, OH^- and CO_3^{2-}. Some of the interlayer water molecules occupy well-defined sites adjacent to Ca^{2+} ions, the coordination numbers of which are thereby raised to seven. The remaining H_2O molecules and OH^- and CO_3^{2-} ions occupy cavities and are only semi-ordered.

The thermal dehydration reactions of $Ca_2Al(OH)_6Cl\cdot 2H_2O$, $Ca_2Al(OH)_6Br\cdot 2H_2O$, and $Ca_2Al(OH)_6(NO_3)\cdot 1\frac{1}{2}H_2O$ have been studied by static and dynamic weight-loss curves, differential thermal analysis, and X-ray, infrared, and chemical examinations of heated material. In each case, the molecular water is lost below 100°C (static) or 200°C (dynamic). The dehydration products thus formed decompose at 200–500°C, with loss of part of the hydroxyl water, to give amorphous products. Dehydroxylation is only completed when CaO and $C_{12}A_7$ or related phases crystallize at 500–1000°C. The position is complicated by loss of chloride (or bromide) in the case of the halides, and by the successive decompositions to nitrite and eventually to oxide in that of the nitrate.

C_4AH_{12} and C_4AH_{19} readily undergo anion exchange reactions when placed in 2M solutions of $NaNO_3$, Na_2SO_4, or $NaO_2C\cdot CH_3$. This provides a possible method for growing crystals for X-ray structure determinations.

The crystal structures of the entire group of lamellar double hydroxides and basic salts related to C_4AH_{12} are almost certainly essentially similar to that of the latter phase, the only important differences lying in the composition of the interlayer material and the stacking sequences of the $[Ca_2Al(OH)_6]^+$ layers. Known or probable features of the structures of the hydroxide, halide, sulphate, carbonate and hydroxoaluminate (C_2AH_8) members of the group are discussed.

Introduction

Some of the lamellar calcium aluminate hydrates and related basic salts, such as C_4AH_{12} and $C_3A\cdot CaSO_4\cdot 12H_2O$ respectively, play important roles in the chemistry of cement hydration. We have recently determined the crystal structure of one of these phases (1). In the present paper, these results are summarized, some additional observations on thermal decomposition and anion exchange reactions described, and some conclusions reached as to the structures of these compounds in general.

Studies by Alègre (2) and Dosch and zur Strassen (3) have shown that the hydroxide phase having a layer thickness of 7.9 Å is C_4AH_{12} and not C_4AH_{13}, as has widely been supposed. This conclusion is compatible with the data for natural hydrocalumite, (4, 5) which has a layer thickness of 7.86 Å and a composition approximating to $Ca_{16}Al_8(OH)_{54}(CO_3)\cdot 20$–$21H_2O$. This composition, if the formula with 20 H_2O is assumed, is equivalent to C_4AH_{12} with minor replacement of $2OH^-$ by CO_3^{2-}.

*Department of Chemistry, University of Aberdeen, Old Aberdeen, United Kingdom.

Crystal Structure Determination

The crystals studied were selected from a preparation approximating in composition to C_4AH_{12-13} with some structural CO_3^{2-}. Because of the small amount available, exact chemical analysis was not possible, but the available chemical and optical evidence, toghther with the crystallographic results to be described, suggested that the probable composition was the same as that of hydrocalumite, of which the material was possibly a polytype.

X-ray single crystal studies showed the crystals to be trigonal, with space group $R\bar{3}c$. The unit cell, with $\underline{a} = 5.73$, $\underline{c} = 47.16$ Å (referred to trigonal axes), contains six formula units of mean composition $Ca_2Al(OH)_{6(3/4)}(CO_3)_{1/8} \cdot 2\frac{1}{2}H_2O$. The crystal structure was determined using three-dimensional data. Within the unit cell, there are six layers of composition $[Ca_2Al(OH)_6]^+$, which lie perpendicular to $\underline{c}$ and will be called "principal layers". They are 7.86 Å apart in the $\underline{c}$-direction. Between the principal layers lie regions of interlayer material. Each principal layer, with the interlayer material on one side of it, contains a single formula unit, each interlayer region thus having the mean composition $(OH^-)_{3/4}(CO_3^{2-})_{1/8} \cdot 2\frac{1}{2}H_2O$.

Fig. 1 shows the main features of the structure. The principal layers (Fig. 1 A and C) are completely ordered, and might be described either as distorted, brucite-like layers in which Ca^{2+} and Al^{3+} are regularly arranged, or as agglomerates of Ca^{2+} and $Al(OH)_6^{3-}$ ions. Comparison of Fig. 1 A and C indicates the stacking relation between adjacent layers.

The interlayer material (Fig. 1 B) is only partly ordered. Water molecules occur on the sites marked P and raise the Ca-coordination to seven; probably all of these P-sites are occupied. The remaining H_2O molecules and OH^- and CO_3^{2-} ions occur in cavities of the type centred on X, and must necessarily be statistically distributed. The composition may now be re-written as $[Ca_2Al(OH)_6 \cdot 2H_2O](OH)_{3/4}(CO_3)_{1/8}(H_2O)_{1/2}$, the contents of the cavities being represented by the material outside the square brackets.

The experimental data gave only an approximate indication of the arrangement of the material within the cavities, but were consistent with the following interpretation. One-half of the cavities contain a single OH^- group at X. One-eighth contain a CO_3^{2-} ion, with the carbon atom at or near X and the oxygen atoms at or near sites of the type marked Q. One-eighth contain two H_2O molecules, and the remainder (one-quarter) an OH^- ion and an H_2O molecule. In the two last-mentioned cases, the oxygen atoms occur at, or more probably near to two of the Q-sites. Space considerations make it unlikely that they actually occur on the Q-sites, or that more than two oxygen atoms can occur in the same cavity unless they form part of a CO_3^{2-} ion; this is discussed more fully later. The results gave no indication of any ordering among the various types of occupancy of the cavities, though the weak X-ray reflections by which this could have been detected might well have been unobserved with the small crystal used. They also did not show whether or not a continuous solid solution series exists between the hydrocalumite composition and C_4AH_{12}.

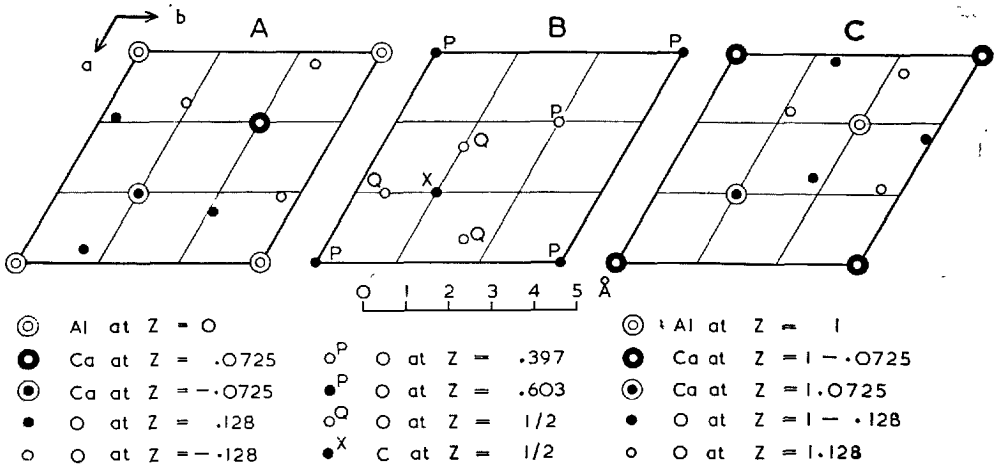

Fig. 1. *Diagram of parts of the structure, seen in projection along the $\underline{c}$-axis; $\underline{z}$-coordinates are given as fractions of the single layer thickness of 7.86 Å. A, principal layer with Al at $\underline{z} = 0$; B, interlayer region around $\underline{z} = \frac{1}{2}$; C, principal layer with Al at $\underline{z} = 1$. The full coordinates of one of the hydroxyl groups of the principal layers are (0.310, 0.057, 0.128).*

Tarte (6) concluded independently that these structures contain isolated AlO_6 (or $Al(OH)_6^{3-}$) octahedra on the basis of the infrared spectra. From an X-ray crystal structure determination, Allmann (7) independently found a closely similar structure for $C_3A \cdot CaSO_4 \cdot 12H_2O$; the two structures are virtually identical as regards the principal layers and the H_2O molecules in the P-sites. In the sulphate derivative, one-half the cavities contain an SO_4^{2-} ion, and the rest two H_2O molecules. The very close crystallographic similarities between all the members of this group of phases make it appear highly probable that the same principal layers occur in all of them. The H_2O molecules in the P-sites seem usually also to be present, except in dehydration products such as C_4AH_7-$(Ca_2Al(OH)_7)$. The phases differ essentially in the composition and structure of the interlayer material and in the stacking sequences of the principal layers.

Comparative single-crystal X-ray studies showed that natural hydrocalumite must have a structure differing only in minor respects from that of the synthetic material discussed above. The structure which Tilley, Megaw, and Hey (4) proposed for this phase is incorrect.

Thermal Decomposition Reactions

Previous workers have reported on the thermal decompositions of C_4AH_{13} and hydrocalumite (5), and of $C_3A \cdot CaCO_3 \cdot 11H_2O$ (8). We have now studied the decomposition of $C_3A \cdot CaCl_2 \cdot 10H_2O$, $C_3A \cdot CaBr_2 \cdot 10H_2O$ and $C_3A \cdot Ca(NO_3)_2 \cdot 9H_2O$ using static and dynamic weight-loss curves, differential thermal analysis, and X-ray, infrared and chemical examination of heated material.

Experimental

The starting materials were prepared as described by Mylius (9). Static weight-loss curves were obtained by heating a sample to constant weight in N_2 at successively higher temperatures. Dynamic weight-loss (TGA) curves were obtained in air, using a Stanton thermobalance, with a heating rate of 10 deg C min^{-1}. DTA curves were obtained on a Dupont instrument, in a N_2 atmosphere, also at 10 deg C min^{-1}. X-ray powder patterns were recorded using film techniques; for high-temperature work (up to 200°C) a nickel-foil heating element (10) was used. Infrared absorption spectra were recorded using a double-beam instrument and the KBr disk technique.

$C_3A \cdot CaCl_2 \cdot 10H_2O$

The specimen, which contained about 10% of C_4AH_{12} as impurity, gave an X-ray powder pattern and optical data agreeing with those reported by Kuzel (11) for β-$C_3A \cdot CaCl_2 \cdot 10\,H_2O$. The data were inadequate to show whether the C_4AH_{12} was present in solid solution or as a separate phase, but the apparent stabilization at room temperature of a stacking modification otherwise stable only above 28°C (10) possibly favours the former explanation. The infrared absorption spectrum was compatible with that found by Tarte (7), the main bands in the 650–4000 cm^{-1} region being at 785 cm^{-1} (Al–O–H bending), 1130 cm^{-1} (?), 1620 cm^{-1} (H–O–H bending), and 3450 and 3600 cm^{-1} (O–H stretching). In subsequent discussion, we shall consider the material as if it were pure $C_3A \cdot CaCl_2 \cdot 10H_2O$.

Interpretation of the weight-loss curves is rendered complicated by the loss of Cl^- at the higher temperatures. Chemical analyses showed that no loss of Cl^- occurs on static heating up to 640°C, but some loss occurs by 800°C, and a sample heated to constant weight at 1000°C retained only 15% of the Cl^- initially present. Loss of the Cl^- was slow, and was negligible on dynamic heating at 10 deg C min^{-1} up to 880°C, the highest temperature studied. Separate experiments showed that $CaCl_2$ begins to yield HCl at 850°C when heated in air of ordinary humidity.

Both static and dynamic weight-loss curves (Fig. 2) show distinct steps. The first occurs mainly at 40–100°C (static) or 90–170°C (dynamic) and is in either case complete by 200°C. The product at 200°C has the composition $C_3A \cdot CaCl_2 \cdot 6H_2O$, or $Ca_2Al(OH)_6Cl$. High-temperature X-ray photographs taken at 100–200°C broadly resembled that of the initial material, but indicated a layer thickness of 6.8 Å. X-ray patterns of samples cooled from these temperatures were closely similar to that of the initial material, but with some deterioration of crystallinity in the case of the 200°C sample; rehydration had occurred within a few hours on cooling. The infrared absorption spectra of samples cooled from 100–200°C resembled that of the initial material, but all bands were more diffuse, the 1620 cm^{-1} band was weakned, and the two O-H stretching bands were replaced by a single, broad band peaking at 3400 cm^{-1}. These results are

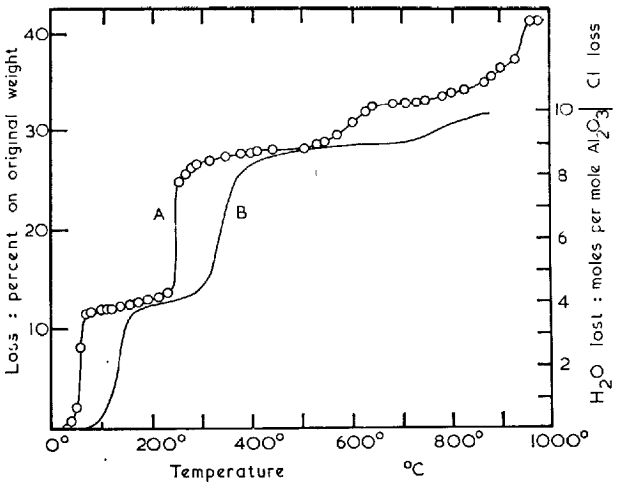

Fig. 2. *Weight-loss curves for* $Ca_2Al(OH)_6Cl \cdot 2H_2O$: *A, static; B, dynamic.*

compatible with loss of the molecular water, if it is assumed that partial rehydration occurred before the spectrum could be recorded.

The second step in the weight-loss curves occurs mainly at 240–270°C (static) or 290–380°C (dynamic) and is complete in either case by 500°C. The 500°C product has the approximate composition $C_3A \cdot CaCl_2 \cdot H_2O$, or $Ca_2Al(OH)O_{2(1/2)}Cl$. X-ray patterns of samples cooled from 300–500°C showed these to be almost amorphous, apart from some calcite which probably formed during the exposure. The infrared spectra of these samples somewhat resembled that of the 200°C product, but became progressively more diffuse with increase in temperature.

The third step in the weight-loss curve occurs mainly at 550–650°C (static) or 740–880°C (dynamic). It corresponds to loss of the remaining hydroxyl, so that the product has the bulk composition $C_3A \cdot CaCl_2$. X-ray powder photographs of samples cooled from these temperatures showed only amorphous material, but the infrared spectrum of a sample cooled from 650°C was consistent with formation of either $C_{12}A_7$ or $C_{11}A_7 \cdot CaCl_2$, and DTA evidence, described shortly, confirmed that crystallization of new phases from the amorphous material begins well before 750°C under dynamic heating conditions. The arrest in the loss of water around 500°C which separates the second and third steps in both static and dynamic curves may be explained by assuming that the amorphous dehydroxylation product tenaciously retains a proportion of the hydroxyl groups initially present, and that these are only lost when the temperature is high enough to bring about the crystallization of new phases. It is most unlikely to be associated with any structural feature of the initial material.

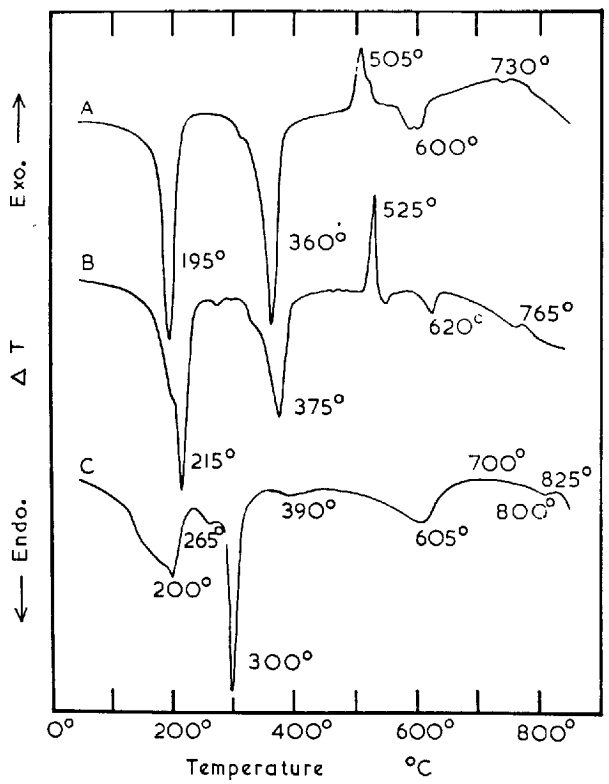

Fig. 3. *Differential thermal analysis curves for A,* $Ca_2Al(OH)_6Cl \cdot 2H_2O$; *B,* $Ca_2Al(OH)_6Br \cdot 2H_2O$; *C,* $Ca_2Al(OH)_6(NO)_3 \cdot 1\frac{1}{2}H_2O$.

The dynamic curve was not continued beyond 880°C, but the static curve showed a further weight loss at 650–1000°C. Comparison of the Cl^- contents of samples cooled from 640° and 1000°C showed that this loss could be attributed to the replacement of $2Cl^-$ by O^{2-}. The necessary oxygen for this reaction may have come from water or oxygen impurities in the nitrogen atmosphere. X-ray photographs and infrared spectra of samples cooled from 700–1000°C together showed that progressive crystallization of $C_{11}A_7 \cdot CaCl_2$ and CaO occurs over this range. The former product was shown to be $C_{11}A_7 \cdot CaCl_2$ rather that $C_{12}A_7$ or $C_{12}A_7H$ by its $\underline{a}$-axial length, which was found using an X-ray powder diffractometer to be 12.010 Å; a specimen of $C_{12}A_7$ for comparison, gave $\underline{a} = 11.991$ Å. Jeevaratnam, Glasser, and Dent Glasser (12) reported 12.004 Å for $C_{11}A_7 \cdot CaCl_2$, 11.983 Å for $C_{12}A_7H$, and 11.977 Å for $C_{12}A_7$. The amount of Cl^- remaining in the product at 1000°C agrees with that expected assuming stoichoimetric formation of $C_{11}A_7 \cdot CaCl_2$ and CaO.

The infrared spectrum of a sample cooled from 1200°C showed that C_3A had been formed.

On the DTA curve (Fig. 3A), the first two endo-

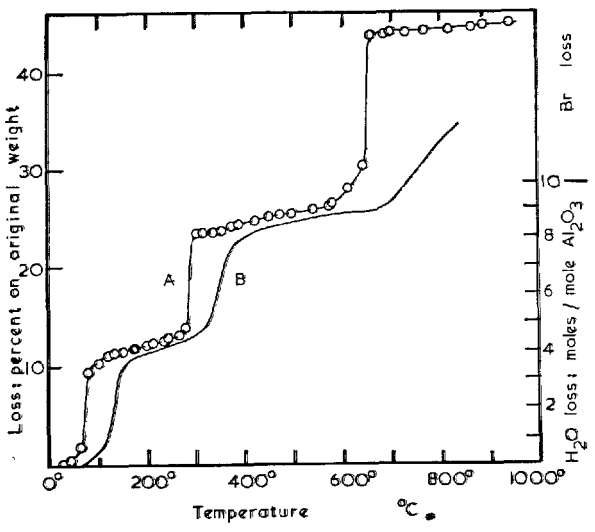

Fig. 4. *Weight-loss curves for* $Ca_2Al(OH)_6Br \cdot 2H_2O$: *A, static; B, dynamic.*

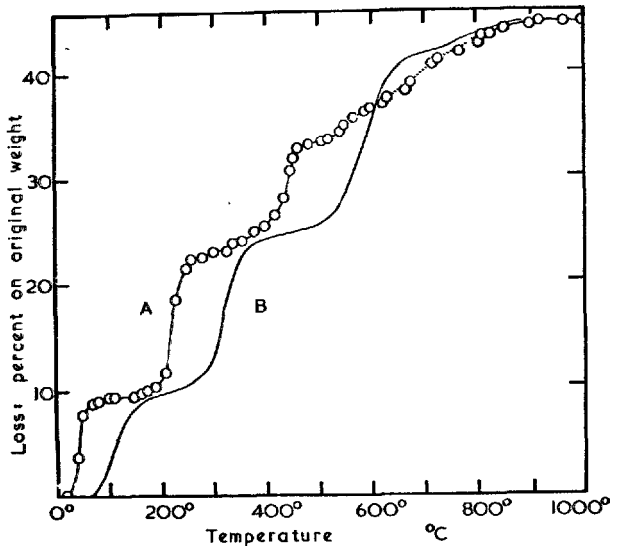

Fig. 5. *Weight-loss curves for* $Ca_2Al(OH)_6(NO_3) \cdot 1\frac{1}{2}H_2O$: *A, static; B. dynamic. The part of the static curve at 450–850°C is possibly in error due to absorption of water vapour or* CO_2 *during cooling.*

therms (195° and 360°C) correspond to the first and second steps respectively of the weight-loss curves. The exotherm at 505°C is attributed to the beginning of crystallization; evidently DTA is more sensitive than X-ray diffraction for detecting this process. The broad endotherm around 600°C is attributed to the final stage of dehydroxylation and the very broad, exothermic bulge around 730°C to continued development of crystallization.

$C_3A \cdot CaBr_2 \cdot 10H_2O$

This was studied by the same methods as the chloride derivative and gave closely similar results, which will therefore not be reported in detail. The X-ray pattern of the initial material indicated a layer thickness of 8.16 Å; this agrees with the value (8.1 Å) earlier reported by Feitknecht and Buser (13). The first two steps in the weight-loss curves (Fig. 4) correspond to formation of $Ca_2Al(OH)_6Br$ and $Ca_2Al(OH)O_{2(1/2)}Br$ respectively. The first of these products gave an X-ray pattern broadly similar to that of the initial material but indicating a layer thickness of 7.1 Å; it readily rehydrated in moist air. The second, like the corresponding product obtained from the chloride, was substantially amorphous. Loss of Br^- began at 600°C on static heating in N_2, and by 660°C much of the Br^- initially present had been lost. There was no arrest in the curve corresponding to that at about 700°C for the chloride. About 50% of the Br^- initially present was lost by 850°C on dynamic heating in air, and 85% by 950°C on static heating in N_2. X-ray and infrared studies indicated the progressive crystallization of CaO and either $C_{12}A_7$ or $C_{12}A_7H$ at 600–1000°C. In agreement with the findings of Jeevaratnam, Glasser and Dent Glasser (12), no evidence was obtained of the formation of a compound $C_{11}A_7 \cdot CaBr_2$ analogous to $C_{11}A_7 \cdot CaCl_2$, and the manner in which the residual Br^- is held at 1000°C was not established. The DTA curve (Fig. 3B) resembles that of the chloride and its features can be interpreted in the same way.

$C_3A \cdot Ca(NO_3)_2 \cdot 9H_2O$

Chemical analysis indicated this composition for a preparation dried over $CaCl_2$ at room temperature; Mylius (9) reported H_2O: Al_2O_3 ratios of 8.54–9.34 for similarly dried material. X-ray powder photographs indicated a layer thickness of 8.66 Å, which agrees with the value (8.6 Å) reported by Feitknecht and Buser (13). In agreement with Mylius's observation, the crystals were optically positive. The infrared absorption spectrum in the 650–2000 cm^{-1} region showed strong or moderate peaks at 785 cm^{-1} (Al–O–H bending), 1385 cm^{-1} (N–O stretching) and 1620 cm^{-1} (H–O–H bending).

Interpretation of the weight-loss data (Fig. 5) is complicated by the effects of the decompositions of NO_3^- to NO_2^- and of NO_2^- to O^{2-}. Chemical analyses

of cooled samples showed that the NO_3^- content is unaffected by static heating at 100°C. By 300°C, the NO_3^- has been completely converted to NO_2^-. Conversion of NO_2^- to O^{2-} is negligible at 300°C, but has reached 90% by 500°C and is virtually complete by 1000°C. No nitride (N^{3-}) was detected at any stage.

Both static and dynamic weight-loss curves show well-defined steps. The first, which occurs at 30–100°C (static) or 50–200°C (dynamic), yields $Ca_2Al(OH)_6(NO_3)$. High-temperature X-ray powder photographs of this product broadly resembled the pattern of the initial material but indicated a layer thickness of 7.9 Å. The material readily rehydrated on cooling. The infrared spectrum of the 100°C product confirmed that the molecular water had been lost and that the NO_3^- remained.

The second step occurs at 200–350°C (static) or 250–450°C (dynamic). As shown above, the NO_3^- is converted to NO_2^- in this range. Allowing for this, the composition of the product formed on completion of this step is thus found to be $Ca_2Al(OH)_3O_{1(1/2)}(NO_2)$. X-ray photographs of samples cooled from around 300°C showed these to be virtually amorphous, apart from some calcite which had probably formed during the exposure. Infrared spectra showed that some NO_3^- was still present at 300°C, but not at 400°C; this is compatible with the analytical results, if the higher sensitivity of the spectroscopic method is allowed for. The reason for the ending of the second step probably lies in the completion of the NO_3^- decomposition, rather than in any structural feature. Some OH^- ion remains, but is relatively firmly bound in the amorphous product at these temperatures (350–450°C).

The third step begins at 350°C (static) or 450°C (dynamic). The initial sharp rise in each case is caused largely by the decomposition of NO_2^- to O^{2-}, which is almost complete by 500°C under static heating conditions; the subsequent slower rise is due, partly to completion of the NO_2^- decomposition, but mainly to loss of residual hydroxyl. As with the halides, this process occurs mainly above 700°C, and was shown from X-ray photographs to be associated with the crystallization of CaO and $C_{12}A_7$ or $C_{12}A_7H$.

The DTA curve (Fig. 3C) shows an initial, broad endotherm peaking at 200°C, which can be attributed to loss of molecular water. The subsequent endotherms at 265°C (weak), 300°C (strong), and 390°C (weak) can be associated with the second step of the weight-loss curves, and thus with decomposition of the NO_3^- and partial dehydroxylation. The broad endotherm at 605°C is associated mainly with decomposition of the NO_2^-, and the exothermic bulge around 700°C with recrystallization. A sharp exotherm corresponding to the one near 500°C observed with the chloride and bromide is not seen, perhaps because it is swamped by the 605°C endotherm. The effects at 800 and 825°C possibly represent the completion of dehydroxylation and crystallization respectively.

Anion Exchange Reactions

Dosch (14) has shown that C_4AH_{13} reacts with solutions of many different organic substances, the molecules of which penetrate between the layers, causing major changes in layer thickness. These results suggested that exchange of interlayer anions could possibly be effected by placing crystals in appropriate aqueous salt solutions. Preliminary experiments have shown that this is indeed the case. Crystals of either C_4AH_{12} or C_4AH_{19} were placed in 2M-solutions of either Na_2SO_4, $NaNO_3$, or $NaO_2C\cdot CH_3$, the C_4AH_{19} being introduced as a concentrated suspension in its own mother-liquor. After a few hours, the crystals were removed and examined microscopically and by X-ray single-crystal methods. Some crystals had partly dissolved but all gave diffraction patterns. The layer thicknesses thus found showed that either partial or total replacement of the interlayer anion had occurred. These results are of interest because of their bearing on possible mechanisms of sulphate attack on concrete, and also because they provide a possible method of obtaining single crystals suitable for X-ray structure determination of phases for which these are otherwise difficult to prepare.

Discussion

Hydroxides

As a result of the work of Alègre (2) and Dosch and zur Strassen, (3) five C_4A hydrates now appear well-established; these are listed, with their layer thicknesses, below:

$C_4AH_{19} = [Ca_2Al(OH)_6 \cdot 2H_2O]OH \cdot 4H_2O$ (10.6 Å)
$C_4AH_{13} = [Ca_2Al(OH)_6 \cdot 2H_2O]OH \cdot H_2O$ (8.2 Å)
$C_4AH_{12} = [Ca_2Al(OH)_6 \cdot 2H_2O]OH \cdot \frac{1}{2}H_2O$ (7.9 Å)
$C_4AH_{11} = [Ca_2Al(OH)_6 \cdot 2H_2O]OH$ (7.4 Å)
$C_4AH_7 = [Ca_2Al(OH)_6]OH$ (5.8–7.4 Å)

The layer thickness of C_4AH_7 depends on how the phase is formed, values of 7.2–7.4 Å being recorded for preparations made by dehydrating the higher hydrates at room temperatures over powerful dehydrating agents (3, 15), while lower ones of 5.8–6.5 Å result from heating at 100–150°C (5).

The layer thickness of C_4AH_{11} could be explained by assuming the interlayer OH^- ion to lie on the X-site; this would place it about 3.3 Å away from both the water molecules and the OH^- ions of the $Al(OH)_6^{3-}$ groups, a distance which is comparable with the OH–OH separation in $Ca(OH)_2$. The retention of a 7.4 Å layer thickness in C_4AH_7 can be explained by supposing the water molecules to be lost without further change occuring. A reduction in layer thickness to a minimum of about 6 Å can be explained if it is assumed that the $Al(OH)_6^{3-}$ octahedra rotate about axes parallel to $\underline{c}$ and the Ca^{2+} ions undergo small displacements parallel to this axis; these changes are made possible by the loss of the H_2O molecules, and permit the OH^- ion to replace the latter in the coordination spheres of the Ca^{2+} ions. The final result of this process, though not the intermediate stages, could also be described in terms of migration of the OH^- ion to a new site of the type $(\frac{1}{3}, \frac{2}{3}, \underline{z})$ or $(0, 0, \underline{z})$, together with a change in stacking. The former mechanism is perhaps more probable, as it explains the apparently gradual nature of the decrease in layer thickness. The process presumably occurs when dehydration is effected by heating because this supplies some necessary energy which is not made available when dehydration occurs at room temperature.

In C_4AH_{13}, two oxygen atoms (one present as H_2O and one as OH^-) must be accommodated within the cavity centred on the X-site. As mentioned earlier, it seems most unlikely that these occur exactly on the Q-sites (Fig. 1B), although the X-ray evidence strongly suggests that they are not far away from them. Fig. 6 gives a possible interpretation of the results. Within each cavity, there are six possible sites; these occur in paris, and each is about 0.7 Å away from one of the Q-sites. For steric reasons, only two out of the six sites in a given cavity can be occupied, of which one must be of higher, and the other of lower z-coordinate than the X- and Q-sites. This arrangement gives each OH^- ion or H_2O molecule a tetrahedral environment, with 4(OH, H_2O) at 2.6–2.7 Å.

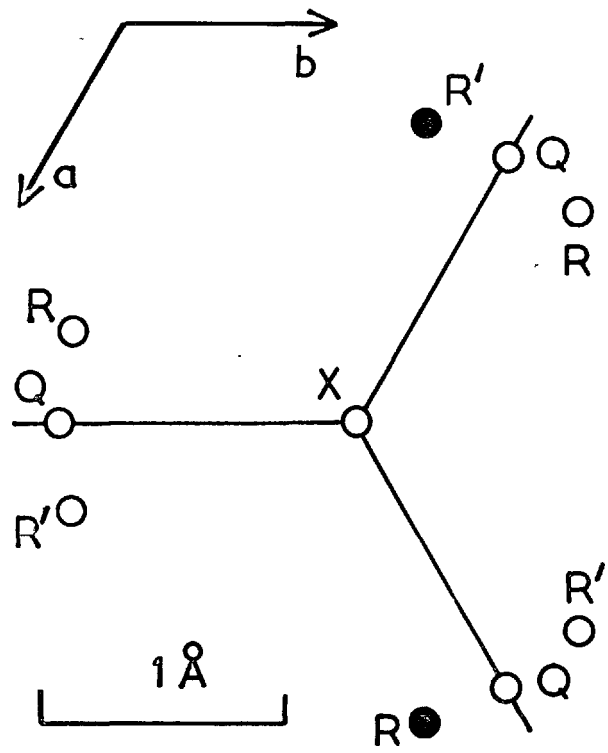

Fig. 6. C_4AH_{13}: *part of the interlayer region showing a possible arrangement of material in the cavities centred on the X-sites. Sites X and Q have the same significance as in Fig. 1B. Sites R and R' lie at* $\underline{z}$*-coordinates about 0.6Å respectively above and below that of the X- and Q- sites. In a given cavity, any one R- site, and the R'—site furthest away from it, can be occupied by* (H_2O, OH^-). *The full circles indicate one of the three ways in which this can occur.*

Dosch (14) suggested that C_4AH_{12} might be a randomly interstratified compound composed of layers of C_4AH_{11} and C_4AH_{13}. This is a possible explanation, and is consistent with the X-ray structure evidence described earlier in this paper. However, it does not appear to explain the apparently constant composition and layer thickness of this phase and more detailed study is required.

C_4AH_{19} can readily be explained as being derived from C_4AH_{13} by interpolation of an additional layer of water molecules between each $Ca_2Al(OH)_6$ layer and the next.

Nitrates

The positive optic sign and relatively great layer thickness (8.66 Å) of $C_3A \cdot Ca(NO_3)_2 \cdot 9H_2O(Ca_2Al(OH)_6 \cdot (NO_3) \cdot 1\frac{1}{2}H_2O)$ strongly suggest that the NO_3^- groups lie with their planes perpendicular to (0001). It may also be assumed that the NO_3^- groups occur in

the cavities centred on X. To satisfy the symmetry of the cavities, it is necessary to assume, either that the NO_3^- ions rotate freely about axes normal to (0001), or that they are statistically distributed as regards orientation. In the latter case at least three orientations are required, for which the planes of the NO_3^- ions are 120° apart. There does not appear to be sufficient room to permit free rotation of the ion, but several ways can be found of placing the ion in three or more equivalent orientations which would give reasonable distances between its oxygen atoms and the surrounding hydroxyl ions and water molecules. It does not appear profitable to discuss the matter further on the basis of the present evidence. No certain explanation can be offered for the apparent absence of H_2O molecules from some of the P-sites, though the ease with which the molecular water is lost (Fig. 5) suggests that the amount present may depend critically on the atmospheric temperature and humidity.

For the dehydration product, $Ca_2Al(OH)_6 \cdot (NO_3)$, the relatively high layer thickness (7.9 Å) suggests that the NO_3^- groups remain oriented perpendicular to the layers, but further investigation is needed before this can be considered certain.

Carbonates

The results obtained in the present investigation indicate that, in the material studied, the CO_3^{2-} ions lie with their planes parallel to (0001), with the carbon atom approximately at X and the oxygen atoms on Q-sites (Fig. 1B). The possibility of slight shifts from this situation, to bring the oxygen atoms onto sites similar to those proposed for C_4AH_{13} (Fig. 6) cannot be excluded. Packing considerations make it appear highly probable that the CO_3^{2-} ion occurs in this situation in all phases having a layer thickness under about 7.9 Å, such as $C_3A \cdot CaCO_3 \cdot 11H_2O$ (7.6 Å) and hydrocalumite. In the 8.2 Å phase, to which compositions $C_3A \cdot \frac{1}{2}CaCO_3 \cdot \frac{1}{2}Ca(OH)_2 \cdot \underline{x}H_2O$ (16) and $C_3A \cdot \frac{1}{4}CaCO_3 \cdot \frac{3}{4}CaO \cdot 12H_2O$ (3) have variously been assigned, the CO_3^{2-} groups may also occur in the same situation, but the possibility is not excluded that they are packed with their planes normal to (0001), similarly to the NO_3^- groups in $C_3A \cdot Ca(NO_3)_2 \cdot 9H_2O$.

Halides

It is tempting to assume that the halide ions, because of their spherical shape, lie in the centres of the cavities, on the X-sites. For $Ca_2Al(OH)_6I \cdot 2H_2O$, this assumption taken in conjunction with the observed cell parameters (19) gives I-OH_2 distances in reasonable agreement with the sum of the ionic radii, and is furthermore in accordance with evidence from the intensities of the 0001 X-ray reflections. (17) For $Ca_2Al(OH)_6Br \cdot 2H_2O$ ($C_3A \cdot CaBr_2 \cdot 10H_2O$), and especially for $Ca_2Al(OH)_6Cl \cdot 2H_2O$, in contrast, the halogen-water distances considerably exceed the sums of the ionic radii, and it is possible that the ions do not lie in the centres of the cavities.

The layer thicknesses of the dehydration products $Ca_2Al(OH)_6Cl$ and $Ca_2Al(OH)_6Br$ found in the present investigation can be satisfactorily explained if it is assumed that displacements within the principal layers or migration of the interlayer anions occurs, as was suggested for C_4AH_7.

Hydroxoaluminates

The compound C_2AH_8 and its various lower hydrates are closely related in structure to the group of phases under discussion. It is here suggested that they may be hydroxoaluminate members of the group; if this is so, the constitution of C_2AH_8 may be represented as $[Ca_2Al(OH)_6 \cdot 2H_2O]Al(OH)_4 \cdot 3H_2O$. The layer thickness is close to that of C_4AH_{19}; this is compatible with the above hypothesis.

Sulphates

As mentioned earlier, Allmann (7) has determined the crystal structure of $C_3A \cdot CaSO_4 \cdot 12H_2O$. The SO_4^{2-} groups, which occur in one-half of the cavities, are randomly distributed between two orientations. For both of these, the sulphur atoms lie at the X-sites, and one S–O bond is perpendicular to (0001), the other three oxygen atoms occupying sites similar to three of those shown in Fig. 6. The two orientations are related by inversion through a centre of symmetry at the X-sites, which occurs in this phase by virtue of the stacking sequence of the principal layers.

General

The ions discussed above are only a few of the many that can serve as interlayer anions in these phases (9, 13, 14); it is clear that anions of widely differing shapes and sizes can be accommodated, and also that the interlayer content frequently varies from point to point within a single crystal. In some respects, the interlayer regions resemble the channels in zeolites, but they differ in being extensible in one dimension and in that they are required to have a negative, and not a positive charge. Several especially important

and mutually related questions require clarification. First, the scale on which variation in composition occurs in individual cases is, in general, not known; there is a continuous range of possibilities extending from mixtures of physically separate crystals of different compositions, through intergrowths and randomly or regularly interstratified structures, to solid solutions or intermediate phases with random or regular variation in the composition within each individual layer. For a given bulk composition, more than one scale of mixing may be possible, depending on the conditions of formation. Secondly, many problems of the degree of order or disorder require to the studied. Lastly, the occurrence of continuously variable ranges of composition and, conversely, of miscibility gaps or of intermediate phases of apparently definite composition (e.g. C_4AH_{12}) need to be explained in the light of such considerations as those mentioned above.

Acknowledgments

We thank Dr. R. Allmann and Dr. P. Tarte for making available typescripts of papers in advance of publication, Dr. R. A. Chalmers for the nitrogen analyses, Mrs. L. Ingram M. Sc. and Miss W. Bissett for assistance with experimental work, and the editor, and publishers of "Nature" for permission to reproduce Fig. 1.

References

1. S. J. Ahmed and H. F. W. Taylor, "Crystal structures of the lamellar calcium aluminate hydrates", Nature, **215**, 622–623 (1967).
2. R. Alègre, "Recherches sur l'Aluminate Tétracalcique Hydraté Hexagonal", Rev. Mat. Constr., Publ. Tech. No. 134 (1962).
3. W. Dosch and H. zur Strassen, "Untersuchung von Tetracalciumaluminathydraten. I. Die verschiedenen Hydratstufen und der Einfluss von Kohlensäure", Zement-Kalk-Gips, **5**, 233–237 (1965).
4. C. E. Tilley, H. D. Megaw, and M. H. Hey, "Hydrocalumite ($4CaO \cdot Al_2O_3 \cdot 12H_2O$), a new mineral from scawt hill, country antrium", Mineral. Mag., **23**, 607–615 (1934).
5. F. G. Buttler, L. S. Dent Glasser, and H. F. W. Taylor, "Studies on $4CaO \cdot Al_2O_3 \cdot 13H_2O$ and the related natural mineral hydrocalumite", J. Amer. Ceram. Soc., **42**, 121–126 (1959).
6. P. Tarte, personal communication.
7. R. Allmann, "Die Doppelschichtstruktur der plättchenförmigen Calcium—Aluminium—Hydroxisalze am Beispiel des $3CaO \cdot Al_2O_3 \cdot CaSO_4 \cdot 12H_2O$", Neues Jahrb. Mineral., Monatshefte, in the press.
8. R. Turriziani and G. Schippa, "Sull' Esistenza del Monocarboalluminato di Calcio Idrato", Ricerca Sci., **26**, 2792–2797 (1956).
9. C. R. W. Mylius, "Über Calciumaluminathydrate und deren Doppelsalze", Acta Acad. Åboensis. Math. et Phys., **7**, No. 3 (1933).
10. A. Barcley and J. D. Donaldson, "Improved attachment for high-temperatures single-crystal X-ray work", J. Sci. Instrum., **38**, 286–287 (1961).
11. H.-J. Kuzel, "Röntgenuntersuchung im system $3CaO \cdot Al_2O_3 \cdot CaSO_4 \cdot nH_2O$–$3CaO \cdot Al_2O_3 \cdot CaCl_2 \cdot nH_2O$", Neues Jahrb. Mineral., Monatshefte, 193–200(1966).
12. J. Jeevaratnam, F. P. Glasser, and L. S. Dent Glasser, "Anion substitution and structure of $12CaO \cdot 7Al_2O_3$", J. Amer. Ceram. Soc., **47**, 105–106 (1964).
13. W. Feitknecht and H. W. Buser. "Über den Bau der plättchenförmigen Calcium—Aluminimhydroxysalze", Helv. Chim. Acta, **34**, 128–142 (1951).
14. W. Dosch, "Die innerkristalline Sorption von Wasser und organischen Substanzen an Tetracalciumaluminathydrat". Neus Jahrb. Miner., Abhandl., **106**, 200–239 (1967).
15. M. H. Roberts, "New calcium aluminate hydrates", J. Appl. Chem., **7**, 543–546 (1957).
16. P. Seligmann and N. R. Greening, "New techniques for temperature and humidity control in X-ray diffractometry", J. Portland Cement Assoc. Res. Develop. Lab., **4**, 2–9 (1962).
17. H.-J. Kuzel, unpublished work quoted in reference (7).

Oral Discussion

Shigeaki Koide

It is of much interest that all the compounds have ionized layers of composition $[Ca_2Al(OH)_6]^+$. Concerning the minute structure of the layer, however, we hope the authors to present their comment. It seems difficult to consider the layer to be of the above mentioned composition so long as Ca^{++} and Al^{3+} played the roles of octahedral and tetrahedral cations, respectively. Comparing the ionic radii of both cations, they might not be surrounded with the same number of hudroxyl ions.

What coordination numbers are considered for Ca^{++} and Al^{3+} in the layer, and whether the hydrates are analogous to clay minerals in their layer structure or not?

Authors' Closure

S. J. Armed, L. S. D. Glasser and H. F. W. Taylor

In reply to Dr. Koide, the Al^{3+} ions are octahedrally, and the Ca^{2+} ions seven-coordinated. The structures resemble certain clay minerals in their ability to accommodate varying amounts of interlayer water, with corresponding changes in layer thickness, and in some other ways. However, the layers are positively charged, whereas those of the clay minerals are negatively charged, and the structures of the layers themselves are only distantly related to those of the clay minerals.

Supplementary Paper II-137 The Alteration of Silicate Anions in Tobermorite Gels

Herbert Funk*

Synopsis

All tobermorite gels studied were found, by standing or drying condensation proceeds, to contain several silicate anions of different condensation degrees. The extent of condensation is influenced by the CaO/SiO_2 ratio.

Introduction

The calcium silicate hydrates which are formed in hardening portland cement are not uniform substances. Their composition and the form of their smallest particles differ. X-ray diffraction patterns of these substances are not always identical, yet have certain similarities with those of the mineral tobermorite, $5CaO \cdot 6SiO_2 \cdot 5H_2O$, and are therefore called "tobermorite like calcium silicate hydrates" or "tobermorite gels". The symbols C–S–H (I) or (II) are also commonly used for the hardening silicate. In the present paper these substances will be abbreviated as CSH.

About the Estimation of the Degrees of Condensation of Dissolved Silicic Acids. The Dissolving of Silicates and Formation of Corresponding Silicic Acids.

By an earlier described method (1) it can be determined, whether an acid-soluble silicate contains uniform silicate anions or different degrees of condensation. Changes in the degree of condensation by the reaction of the SiOH-groups of the anions to form SiOSi bonds can also be estimated. This method is not applicable to all silicates, but it can be used for tobermorite-like CSH.

For the determination of silicate anions of low degree of condensation, the CSH is dissolved in methanolic HCl. This yields primarily the free silicic acids, which corresponds to the silicate anions in the dissolved silicate. In order to get them into solution unchanged, certain rules of caution have to be obeyed (1, 2). The error that occurs during the dissolving of CSH due to condensation can be kept down to about 5%. To the silicic acid solution in methanol paramolybdate solution is added as soon as the weight sample has dissolved. By mixing the two solutions the complexing reaction proceeds under standardized conditions with a rate depending only on the degree of condensation of the dissolved silicic acid.

*Institut für Anorganische Chemie, Freie Universität Berlin, Berlin, West Germany.

The rates of molybdato silicic acid $H_4SiMo_{12}O_{40}$ formed after certain complexing times—calculated as % SiO_2 of the silicic acid in solution—are plotted against the complexing times on a logarithmic scale, thus producing the reaction or complexing curve (3, 4).

Fig. 1 represents the reaction curves of various silicic acids that are straight lines if there is only one type of silicic acid in solution. The complexing rates of uniform silicic acids, therefore, follow a first order reaction. In order to obtain only one type of silicic acid in solution crystallized test silicates of known structure, that had been finely powdered, were dissolved in methanolic HCl (10 mg SiO_2 in 10 ml methanol). Fig. 1 shows that the not highly condensed silicic acids are well to distinguish. The particular lines represents the complexing rates of

Curve 1: H_4SiO_4, monosilicic acid, from β–Ca_2SiO_4,
Curve 2: $H_6Si_2O_7$, disilicic acid, from $Na_6Si_2O_7$,
Curve 3: $H_6Si_3O_9$, tricyclosilicic acid, from α–$CaSiO_3$ (5) (Pseudowollastonite)
Curve 4: $H_8Si_4O_{12}$, tetracyclosilicic acid, from $K_4H_4Si_4O_{12}$ (6, 7),

Curve 5: $H_{12}Si_6O_{18}$, hexacyclosilicic acid, from $Cu_6Si_6O_{18} \cdot 6H_2O$ (8) (Dioptase)

If—e.g.— monosilicic acid solution is allowed to stand at normal temperature for 10 minutes, the reaction rates leave the straight line received for pure monocilicic acid and then proceeds with increasing curvature. After a standing time of one hour —e.g.— only less than 30% monosilicic acid remains and the curvature of the complexing curve increases.

Curve 6 (Fig. 1) shows the complexing curve of a two component solution, mixed of 4 moles mono— and 1 mole tetracyclosilicate. The first part of the curve has the slope of curve 1 (monosilicic acid), the remainder agrees with curve 4 (tetracyclosilicic acid). Extrapolation of the last part of the curve to the ordinate shows that both silicic acids are present with 50% (calculated as SiO_2). In this manner the type and amount of components of only simple mixtures can be determined. Curve 6 would not end as a straight line—as can be extrapolated—if further, higher silicic acids were present. Such complexing curves had, as already mentioned, not only been observed for dissolved silicic acids after standing, but for all dissolved CSH examined until now.

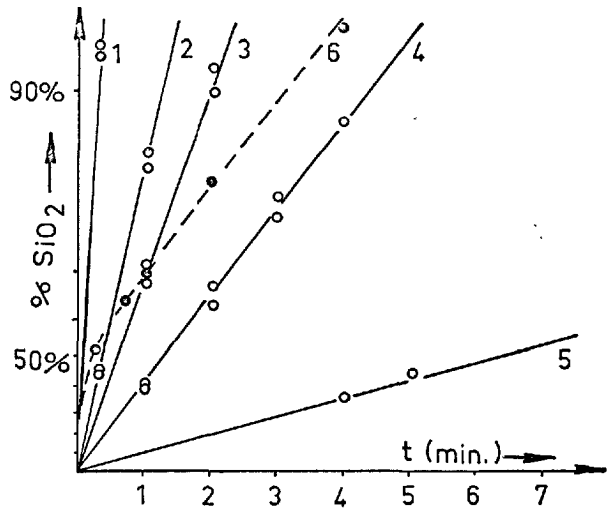

Fig. 1. *Complexing rates of uniform silicic acids in methanolic solutions:*

1.: Mono
2.: Di
3.: Tricyclo
4.: Tetracyclo
5.: Hexacyclo
6.: Mono + Tetra (50% + 50%SiO_2)

The Examination of Tobermorite Gels (CSH)

Different degrees of condensation are present in the anions of CSH formed by hydration of C_3S or β–C_2S: Fig. 2, Curve 1 represents the complexing rates of a C_3S hydration product (composition: $2CaO \cdot SiO_2 \cdot 2H_2O$). Curve 2 shows the complexing rates of a corresponding CSH (composition: 1.65 $CaO \cdot SiO_2 \cdot 1.9H_2O$) formed by hydration of β–C_2S at 25°C. In both cases the starting material is a monosilicate, yet both hydration products contain no noticeable monosilicate. Disilicate is present only to 20–30%, the greater part of CSH has higher condensed anions. Silicates with more than $6SiO_4$-tetrahedra are produced by C_3S (Curve 1) to less than 40%, by β–C_2S (Curve 2) about 50%.

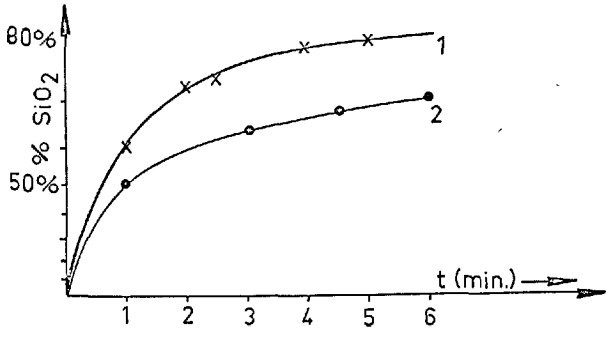

Fig. 2. *Complexing curves of* CSH *indicating condensation of silicate anions,*

1. C_3S hydration product
2. β-C_2S hydration product

The different condensation degrees in both hydration products of Fig. 2 are not characteristic to CSH produced from C_3S and β–C_2S, respectively. This is indicated by the differences of complexing rates in Fig. 3. Three CSH samples, that had been formed by hydration of C_3S, are represented by the Curves 1, 2 and 3 and differ to a greater extent than do the curves in Fig. 2.

Curve 1: C_3S, 90 days (25°C) with supersaturated $Ca(OH)_2$ solution (2:20 g):
$1.76CaO \cdot SiO_2 \cdot 2.5H_2O$.

Curve 2: C_3S, 90 days (25°C) with water (2:20 g):
$1.54CaO \cdot SiO_2 \cdot 2.0H_2O$.

Curve 3: C_3S, 5 years (paste):
$1.51CaO \cdot SiO_2 \cdot 1.09H_2O$.

Curve 1: The highest condensation degree in this CSH is a tetrasilicate, the sum of mono—, di—, tri—and tetrasilicate is therefore about 100%. In the CSH, used for Curve 2, not more than 50% di-, tri-

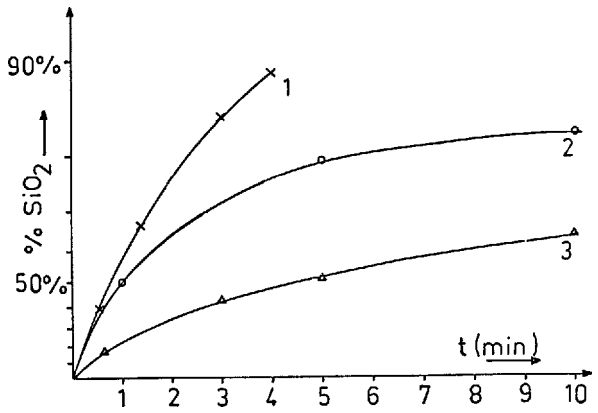

Fig. 3. C_3S *hydration under different conditions yielding different degrees of condensation*

and tetrasilicates are present, while more than 40% of the SiO_2 have a condensation degree of six or more. The differing degrees of condensation expressed by Curves 1 and 2 may be caused by the different CaO/SiO_2 ratios of the CSH products. The higher condensation in the CSH represented by Curve 3 is mainly due to a 5 years' standing as paste. The CaO/SiO_2 ratio does not change appreciable in this time, but the water content is lower, as can be expected for higher condensed silicates. The free $Ca(OH)_2$ that is always formed in considerable excess by the action of water on C_3S does not hinder the condensation of the primarily monomeric silicate anions.

The relationship between the degrees of condensation in CSH and its CaO/SiO_2 ratio was studied in further experiments.

CSH Gels of Different CaO/SiO_2 Ratio

Tobermorite gels having different CaO/SiO_2 ratios are easily obtained by precipitation from $Ca(ClO_4)_2$ solution with 0.1 molar $Na_2H_2SiO_4 \cdot 8H_2O$ in solution. An addition of NaOH to the silicate solution yields CSH higher in lime content. After rinsing the precipitated gels, voluminous water rich gels (95–97% H_2O) are obtained. Neither do the lines characteristic for $Ca(OH)_2$ appear on the X-ray diffraction pattern nor is more than 0.5% of the CaO soluble when the dried substance is extracted with a mixture of acetoacetic ester and isobutanol (9). This both facts indicate that all CaO contained in the CSH is bonded to the silicate. The X-ray patterns show merely some broad hko interferences which are typical of ill-crystallized CSH (10).

In the following descriptions about factors influencing the condensation of anions in CSH, the results are illustrated not only with the help of curves but also with tabulations. These tables contain complexing values obtained after 1, 5 and 10 minutes and make a general picture possible. From Table 1 and Fig. 1 it can be seen that all monosilicate and most of di- and trisilicate have been complexed after one minute.

The complexing curves of four precipitated CSH gels are presented in Fig. 4.

Table 1. *Complexed portions (approximate) of defined silicic acids (calculated as* $\%SiO_2$*) after*

	1	5	10	minutes
mono	100	100	100	$\%SiO_2$
di	85	100	100	
tri	65	100	100	
tetra	35	90	100	
hexa	10	40	65	

Curve 1A: CSH of $1.41 CaO/SiO_2$ and 95% H_2O, complexing rates taken 3 days after preparation;
Curve 1: same; 14 months after preparation;
Curve 2: CSH of $1.31 CaO/SiO_2$ and 97% H_2O (after 14 months);
Curve 3: CSH of $1.19 CaO/SiO_2$ and 96% H_2O (after 14 months);
Curve 4: CSH of $0.89 CaO/SiO_2$ and 96% H_2O (after 14 months).

From Fig. 4 it can be recognized that a decreased

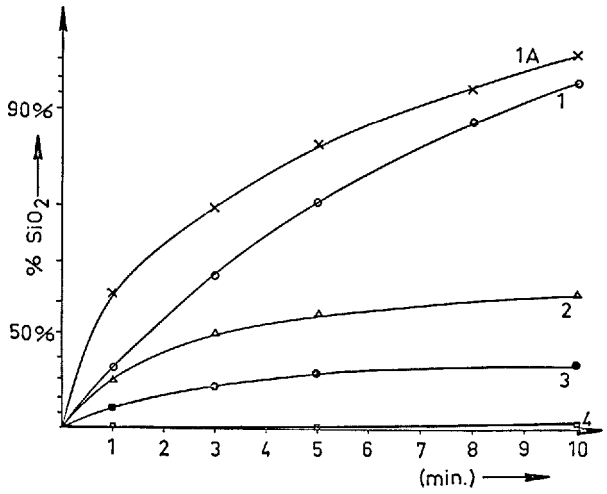

Fig. 4. *Condensation degrees in* CSH *gels depends on* CaO/SiO_2 *ratios*

1.: 1.41 CaO/SiO_2
2.: 1.31 "
3.: 1.19 "
4.: 0.89 "

1A: 1.41 CaO/SiO_2, 3 days after preparation
1—4: 14 months after preparation

Table 2. *Condensation of CSH by standing, indicated by decreased complexing rates.*

CSH precipitated: CaO/SiO_2		$\%H_2O$	Complexed $\%SiO_2$ after 1	5	10 minutes
1.18		88	44	65	71
	2 weeks later		41	62	70
1.34		92	61	83	91
	2 weeks later		46	77	85
	4 weeks later		46	76	82
1.41		95	63	87	94
	14 months later		34	79	91

Table 3. *Condensation in CSH gels by drying*

Tobermorite like CSH CaO/SiO_2	$H_2O\%$	Complexing time 1	5	10 minutes	
0.81	97%	6	14	22	$\%SiO_2$
	26%	4	11	19	complexed
0.86	95%	11	26	30	
	25%	7	15	21	
0.98	94%	23	40	52	
	26%	15	30	42	
	18%	14	28	32	
1.01	95%	26	50	63	
	24%	26	47	53	
	18%	24	42	52	
1.41	95%	65	90	95	
	25%	33	80	93	

Table 4. *Condensation degrees of silicate anions in CSH depending on CaO/SiO_2-ratios.*

Tobermorite like calc. sil. hydrates with CaO/SiO_2	$\%SiO_2$ were complexed after 1	5	10 minutes
0.81	6	15	24
0.81 (other preparation)	6	14	23
0.86	11	26	30
0.98	23	40	52
1.00	21	47	61
1.01	26	50	63
1.03	26	52	60
1.11	39	63	70
1.18	44	65	71
1.41	65	90	95

lime content produces a decreased complexing rate. The degrees of condensation of the silicate anions, therefore, are influenced by the CaO/SiO_2 ratio in CSH. This dependance is also clearly indicated by further examples shown in Table 4.

The difference in Fig. 4 between Curve 1 A and Curve 1 (3 days and 14 months after preparation) shows that by standing of the CSH, the condensation degree is increased. Further examples in Table 2. show that wet tobermorite gels have changed already after 14 days. In a freshly prepared CSH gel condensation also occurs by drying, as can be seen from the complexing values shown in Table 3.

These changes by drying are mainly observed for water containing CSH gels obtained by precipitation from aqueous silicate solutions. Drying causes condensation to a similar extent as does month-long storage at 25°C under wet conditions. Storage of a dried CSH does not cause any further condensation while standing of CSH with water showed noticeable condensation after 5 years (Fig. 3, Curve 3).

Discussion of the Results

The studied tobermorite-like CSH were found to contain always silicate anions of different degree of condensation. With regard to the anion mixtures obtained in the CSH, the way of preparation and—if the starting materials are identically—the details of reaction conditions for the CSH are of influence.

It can be assumed, that the tobermorite gels contain anions of SiOH-groups that are able to react one with another increasing the number of SiOSi-bonds. This reaction is analogous to the condensation of SiOH-groups of free silicic acids.

The extent of anion condensation depends—with in certain limits—upon the CaO/SiO_2 ratio in the respective CSH. This may be explained by the fact that the tendency to form higher condensed units increases with the number of SiOH-groups. Moreover, there is a relationship between calcium ions bonded to silicate and SiOH groups on the other hand, since calcium ions—leaving the silicate by hydrolysis to form $Ca(OH)_2$—yield simultaneously and necessarily SiOH groups.

Crystallized CSH have—in comparison with tobermorite gels—only one type of anion. The mixture of different silicate anions occurring in tobermorite gels may well be the reason for the always ill-crystallized state of the CSH. The crystal quality does not improve upon standing for months or even for years at room temperature. Only under hydrothermal conditions may condensation yield long-chain anions that are able to crystallize within certain limits of the CaO/SiO_2 ratio. This way the "actual" tobermorite is formed at about 160°C. This CSH is very similar in X-ray diagramm to one form of tobermorite found as mineral in Scotland. This tridimensional and crystalline ordered "actual" tobermorite has a definite composition and is a terminal member of a great number of possible tobermorite-like CSH. It is not to include into the group of tobermorite like CSH.

The nearly amorphous tobermorite gels are much more reactive than any form of crystallized CSH, which—e.g.—do not yield higher condensed silicates at ordinary temperature. Therefore, the behaviour of

the well crystallized tobermorite is much more similar to other crystallized CSH than to a tobermorite gel. Some important properties, characteristic of tobermorite gels—in comparision with crystallized CSH including "actual" tobermorite—are

1. ill-crystallized or nearly amorphous state in the CSH with typically hko-interferences,
2. several silicates of different condensation degrees are present in the CSH, probably causing the ill-crystallized state,
3. the higher reactivity of tobermorite gels
   a) of SiOH groups in silicate anions to form higher condensation degrees,
   b) of calcium ions toward hydrolysis.

References

1. H. Funk and R. Frydrych, "The degrees of anion condensation in silicic acids and silicates", Sympos. on Struct. of Portl. Cem. Paste and Concr., Special Report 90, Highway Research Boad, Washington, D. C. (1966).
2. E. Thilo, W. Wieker and H. Stade, "Über Beziehungen zwischen dem Polymerisationsgrad silicat. Anionen und ihrem Reaktionsvermögen mit Molybdänsäure", Zeitschr. anorg. allg. Chemie, Vol. 340, p. 261 (1965).
3. G. B. Alexander, "The reaction of low molecul. weight silicic acids with molybdic acids", Jour. Amer. Chem. Soc., Vol 75, p. 5655 (1953).
4. E. Weitz, H. Franck and M. Giller, "Untersuchungen an Kieselsäuren", Zeitschr. anorg. allgem. Chem., Vol. 331, p. 249 (1964).
5. W. Hilmer, "Zur Strukturbestimmung von $SrGeO_3$", Naturwissenschaften, Vol. 45, p. 249 (1964).
6. H. Funk and H. Stade, "Die Herstellung der Kaliumhydrogensilicate ($KHSiO_3$) u.a. aus Methanol", Zeitschr. anorg. allgem. Chem., Vol. 315, p. 79 (1962).
7. W. Hilmer, "Die Kristallstruktur des sauren Kaliummetasilicates $K_4(HSiO_3)_4$", Acta crystall., Vol. 17, p. 1063 (1964).
8. H. G. Heide, K. Boll-Dornberger, E. and E. M. Thilo, "Die Struktur des Dioptas $Cu_6(Si_6O_{18})\cdot 6H_2O$", Acta crystall., Vol. 8, p. 425 (1955).
9. B. Franke, "Bestimmung von CaO und $Ca(OH)_2$ neben Calciumsilicat", Zeitschr. anorg. allgem. Chem., Vol. 247, p. 180 (1941).
10. L. Heller and H. F. W. Taylor, "Crystallographic data for the calcium silicates", London, Her Majesty's Stationery Office, Dep. of Scientif. and Industr. Res., Building Res. Station (1956).

(B) Papers regarding Properties

Supplementary Paper II-6 Stability of Hydrogarnet Series Terms to Sulphate Attack

Bernardo Marchese and Riccardo Sersale*

Synopsis

Resistance to sulphate ions of terms belonging to "tricalcium aluminate-grossularite" (hydrogarnets) series, has been investigated.

Low silica hydrogarnets have been prepared by hydrothermal treatment of suitable glasses, and tested for crystallinity by thermogravimetric analysis and electron microscopy. Successively, they have been treated with saturated lime solutions containing different amounts of calcium sulphate. The ettringite produced has been identified by differential thermal analysis, X-ray diffraction, and electron microscopy.

Rate and degree of completeness of the reaction have been measured with good accuracy by means of differential calorimetry and X-ray diffraction. Minimum amount of silica required for hydrogarnet stability toward sulphate attack has been evaluated around 0.3 mols SiO_2 per mol of compound.

Resistance to sulphate ions of terms in the series "tricalcium aluminate hexahydrate-grossularite" (hydrogarnets), besides theoretical considerations, is of considerable importance on technical ground because the resistance of certain cement works, for instance steam-cured concrete (1), to sulphate containing solutions, can be ascribed to it.

Foundamental contributions to the study of hydrogarnet stability in presence of sulphate ions have been given by Flint and Wells, zur Strassen and, more recently, by Schwiete and Iwai, Richartz, Yang (2). It has been pointed out that tricalcium aluminate hexahydrate (extreme term in the already mentioned series) as well as tricalcium aluminate, are rapidly transformed into ettringite after contact with calcium sulphate solutions. The substitution of silica in place of water, as far as the cubic aluminate turns into grossularite, bears a lattice shrinkage (3) which corresponds to an increased sulphate resistance, as will be shown later.

The minimum amount of silica which gives resistance towards sulphate to hydrogarnets, seem thus to be of great importance. It has been evaluated by zur Strassen around 0.3 mols.

We have studied reactivity of hydrogarnets of suitable composition in contact with sulphate solutions, measuring rate and degree of completeness of reaction. This has led to the necessity of measuring with good accuracy the amount of ettringite formed in each run. The two different techniques used, which will be described later, have allowed also the evaluation of silica amount capable of transforming hydrogarnet series terms into virtually resisting compounds. In this note an account will be given of the experimental work done and of the corresponding conclusions.

Preparation of Specimens

Four intermediate terms in the hydrogarnet series have been prepared. Their composition resulted from chemical analysis were:

1) $C_3AS_{0.225}H_{5.56}$
2) $C_3AS_{0.28}H_{5.44}$
3) $C_3AS_{0.35}H_{5.30}$
4) $C_3AS_{0.43}H_{5.10}$

They have been prepared, according to literature

*Istituto di Chimica Industriale, Università di Napoli, Napoli, Italy.

(4), by long hydrothermal treatment (around 350 hrs), at 150°C, of glasses obtained by quenching melts of appropriate composition.

Soon after, the completeness of glass → crystal transformation has been tested. In fact, glasses with composition falling in the interval explored by us, are rapidly attacked by sulphate contact solution, with formation of ettringite. A small amount of residual glass in the hydrothermally crystallized product would thus invalidate the measurement of rate of fixation, especially at shorter times.

Control of "Crystallinity" by TGA and by EM

Weight losses of each specimen, before and after hydrothermal treatment, have been measured with methods of thermogravimetric analysis with a "Mass-flow thermobalance" of Stanton Instr. Inc. For example, curves relative to specimen No. 2 (0.28 mol SiO_2), before (a) and after (b) hydrothermal crystallization, have been reported in Fig. 1. The weight loss of the glass specimen is practically negligible (~1%), while that of the crystallized specimen amounts to 25.28% (stoichiometric value is 25.40%). Electron microscope observations are in good agreement with this result. The same specimen, observed after hydrothermal treatment, shows micrograph a) in Photo 1, only monometric crystals without glass particles. Crystals appear to be well formed even if edges are rounded by continuous shaking.

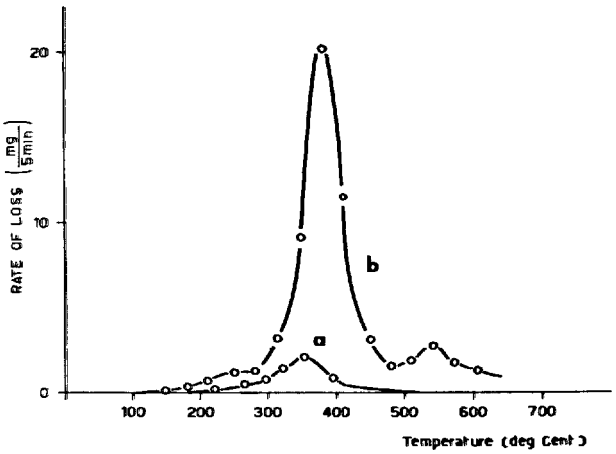

Fig. 1. TGA *of* $C_3AS_{0.28}H_{5.44}$:
a) *before hydrothermal crystallization*
b) *after* " "

Sulphate Fixation Rate Measurement

After evaluation of "crystallinity", for each specimen has been measured the rate of calcium sulphate fixation in continuous saturated lime solution. Experimental procedure has been described in a previous work (5). Rate curves, i.e. amount of sulphate fixed at room temperature against time of fixation, have been reported in Fig. 2.

Plots show a decrease in the amount of sulphate fixed in compounds with higher silica content. An abrupt decrease is shown passing from the 0.225 mols SiO_2 to the 0.28 mols term. It corresponds to the diminished reactivity toward attack solution already mentioned by zur Strassen (2).

X-ray Diffraction

Only diffraction data concerning the 0.28 mol terms have been reported.

Patterns in Fig. 3 (symbols as in Fig. 2) show, as time increases, transformation of reactant in contact with a constantly lime saturated and initially sulphate saturated solution, and point out progressive formation of ettrinigite (reflections at 9.73, 5.61, 3.88 Å). For reference purposes patterns of initial hydrogarnet of ettringite and of $Ca(OH)_2$ have been reported.

Unit-cell sizes of four hydrogarnet series terms with increasing SiO_2 content, have been measured. Values, reported in Fig. 4, show a cell shrinkage, which corresponds to an increase of lattice stability.

Differential Thermal Analysis

Differential thermal analysis curves in Fig. 5 are limited to products obtained from the 0.28 mol term

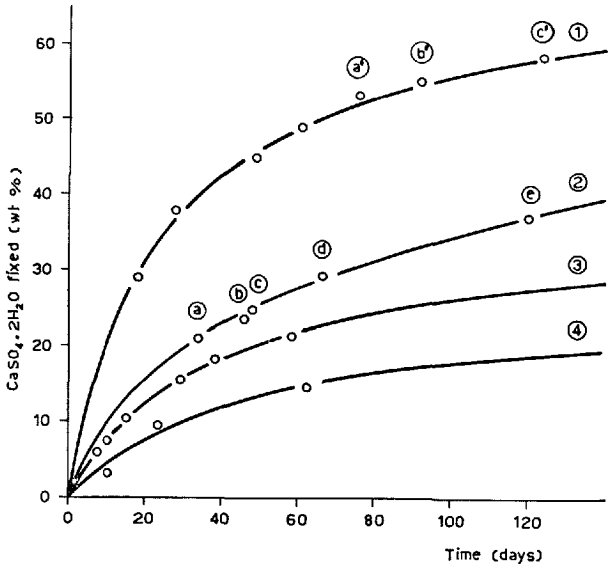

Fig. 2. *Fixation of* $CaSO_4 \cdot 2H_2O$ *by four hydrogarnet series terms*

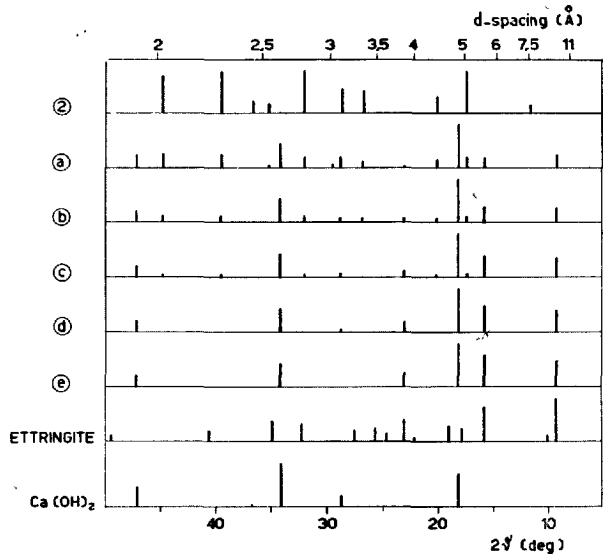

Fig. 3. *X-ray powder diffraction patterns of* $C_3AS_{0.28}H_{5.44}$, *in five successive stages of ettringite formation (symbols as in Fig. 2.)*

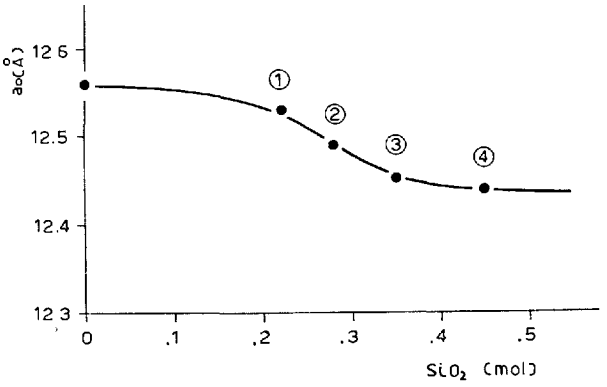

Fig. 4. *Decrease of hydrogarnet series terms unit-cell size, when* SiO_2 *content increases*

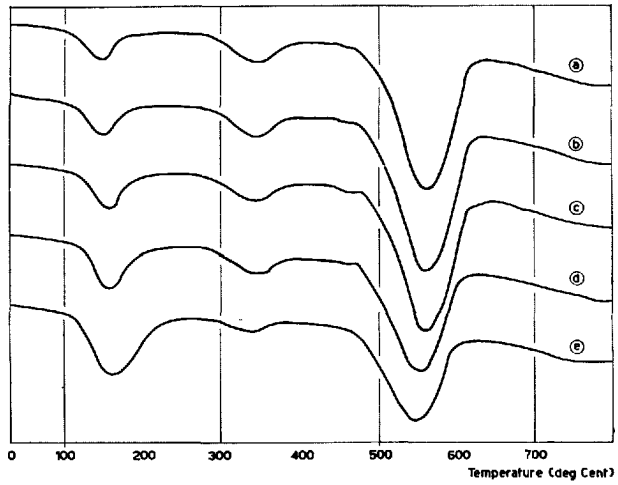

Fig. 5. DTA *of reaction products (symbols as in Fig. 2 and 3)*

only: all other terms show similar behaviour.

While the endothermic peak of hydrogarnet series term at 350°C decreases, the endothermic peak at 150°C corresponding to ettringite increases and the thermal effect with maximum at 550°C, corresponding to the dehydration of free calcium hydroxide, decreases.

Microscope Examination

Nucleation and successive growth of ettringite needles, during sulphate attack of hydrogarnet series terms studied, have been systematically followed with both optical (phase contrast) and electron (carbon replica method) microscopes.

Micrograph b) in Photo 1 corresponds to an intermediate stage of the attack: fragments of hexagonal plates on which sites of successive evolution into ettringite crystals can be recognized, are shown.

Micrograph c) in Photo 2 shows a more advanced stage in which the recently formed ettringite can be observed.

Micrograph d), corresponding to a standard specimen of ettringite prepared according to the literature (6), has been reported for comparison purposes.

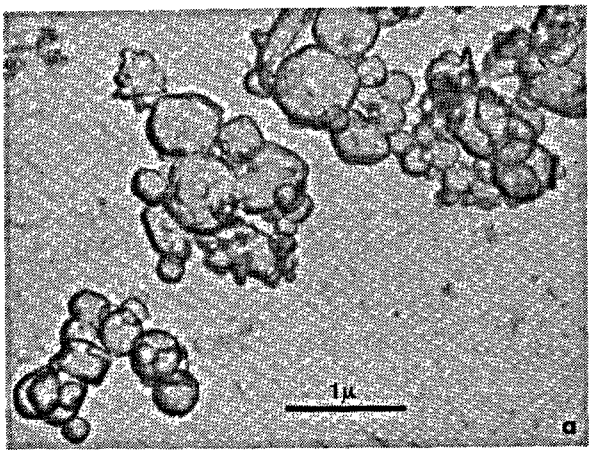

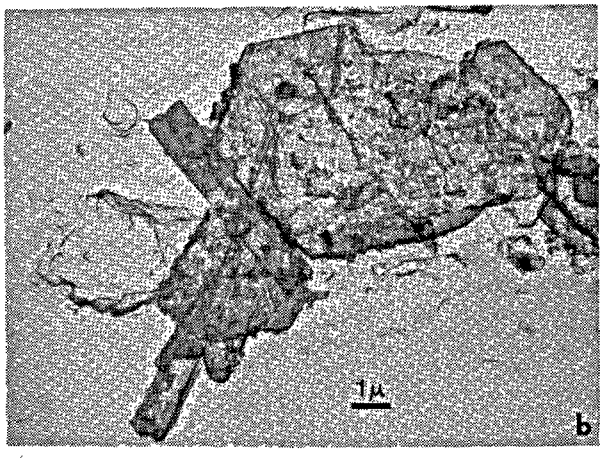

Photo 1.

a. *Monometric crystals of hydrogarnet after hydrothermal treatment*

b. *Initial and intermediate stages of ettringite formation*

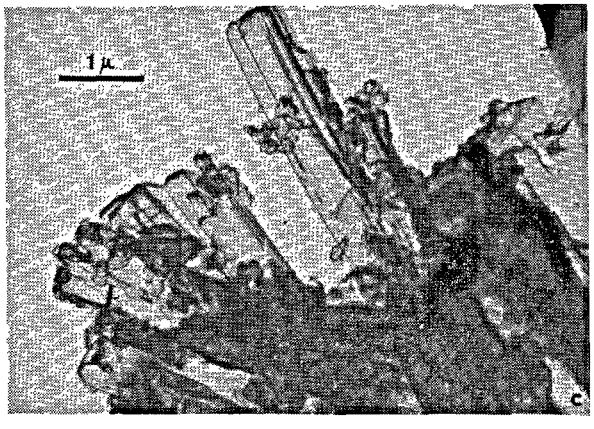

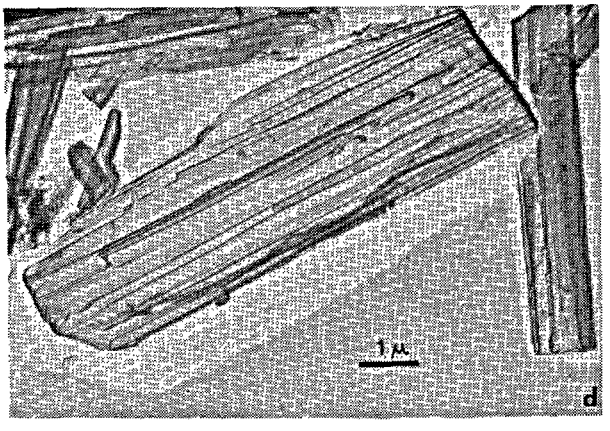

Photo 2.

c. *Advanced stage of ettringite formation*

d. *Specimen of standard ettringite*

Differential Calorimetry

A Perkin-Elmer DSC-1B apparatus has been used. Uniform drying of products has been necessary before examination. After passing a stream of cold dry air on them, powders have been kept for 24 hours on $CaCl_2$. Even if great care should be used during this treatment otherwise, a small amount of dehydration could lead to a defective determination of hydrogarnet and ettringite, the calorimetric determination resulted simple and rapid, thanks to the straightforward relation between mass and enthalpy. In the system being investigated, the degree of completeness of reaction has been evaluated measur-

Table 1. *Wt % of ettringite and hydrogarnet in different mixtures*

Sample	Chemical analysis ($CaSO_4 \cdot 2H_2O$ fixed)	DDC				X-ray
		Hydrogarnet		Ettringite		Ettringite
	wt %	ΔH $\frac{cal}{g\ mixt.}$	*wt %*	ΔH $\frac{cal}{g\ mixt.}$	*wt %*	*wt %*
2	—	155	100	0	0	0
a	21.5	29	18.7	27.5	12.7	11
b	23.1	25	16.1	40	18.5	17
d	28.6	22	14.2	51	23.6	23
e	36.3	11	7.1	90	41.7	41
a′	32.4	9	6	101	46.8	47
b′	54.5	7	5	111	51.4	51
c′	57.3	0	0	128	59.2	54
Ettringite	—	0	0	216	100	100

ing, on the same thermogram, both the decrease of reactant hydrogarnet and the increase of ettringite produced.

Calorimetric measurements on products corresponding to 0.225 and 0.28 mols terms have been reported in Table 1. Percentage of each chemical species has been evaluated on the basis of heats of transformation of pure products (hydrogarnet and ettringite) which also have been reported in Table 1. These percentages are in good agreement with those calculated on the basis of peak intensity of X-ray diffraction.

Conclusions

The whole of experimental results corroborates the statement according to which in the series tricalcium aluminate (cubic)-grossularite, substitution of H_2O with SiO_2 causes resistance to sulphate attack. Small amounts of silica are sufficient to induce resistance; the term with 0.28 mols SiO_2 is much more stable than term with 0.225 mol, so that a term with 0.30 mol SiO_2 can be considered practically sulphate resistant.

The product originated after reaction of initial hydrogarnet with sulphates, is a calcium sulphoaluminate (with high sulphate content) formed with a mechanism of dissolution and successive precipitation from calcium hydroxide and calcium sulphate solution.

Differential calorimetry has made possible precise and rapid determination of the degree of attack suffered by reactant hydrogarnet; the determination is comparable, as it concerns accuracy, with the results of X-ray diffraction analysis.

References

1. The Chemistry of Cements, Vol. I (Academic Press Inc. London, Ltd. 1964), Edited by H. F. W. Taylor. See chapter II by H. F. W. Taylor entitled "The steam curing of portland cement products".
2. E. P. Flint and L. S. Wells "Relationship of the garnet-hydrogarnet series to the sulphate resistance of portland cements", J. Res. Nat. Bur. Stand, **27**, 171 (1941)

—H. zur Strassen, "Die Chemischen Reaktionen bei der Zementhärtung", Zement-Kalk-Gips **4**, 137 (1958).

—J. C. Yang, "Hydrogarnet chemical resistance", Proc. 4th Int. Symp. Chem. Cement, Washington 1960, N. B. S. Monograph 43, vol. II (1962).

—H. E. Schwiete and T. Iwai, "Über das Verhalten der ferritischen Phase im Zement während der Hydratation", Zement-Kalk-Gips **9**, 379 (1964).

—W. Richartz, "Über die Bildung tonerdhaltiger Hydratphasen bei der Zementhärtung", Tonind. Ztg. **10**, 449 (1966).

3. H. Zeeh, "Versuche zur Aufklärung der Erhärtung von Zementen. Untersuchungen im eisenfreien System $CaO–Al_2O_3–SiO_2–CaSO_4–H_2O$", Dissertation, Main (1956).
4. E. P. Flint, H. F. McMurdie and L. S. Wells, "Hydrothermal and X-ray studies of the garnet-hydrogarnet series and the relationship of the series to hydration products of portland cement", J. Res. Nat. Bur. Stand., **26**, 13 (1941).
5. R. Sersale, V. Sabatelli, G. Frigione and R. Aiello, "Sul Comportamento di Vetri ad Alto Contenuto di SiO_2, Al_2O_3, CaO verso Soluzioni Sature di Idrossido e di Solfato di Calcio", Ric. Sci. **35** (II-A); 175 (1965).
6. F. M. Lea, The Chemistry of Cement and Concrete, page 199 (E. Arnold Publ., London, England, 1956).

Supplementary Paper II-40 Formation of Hydrated Gehlenite through the Reaction of Clay Minerals and Lime

Akira Ariizumi*

Synopsis

Hydrated gehlenite was firstly found by Strätling (1940) as the reaction product of metakaolin and lime. Later the properties of the hydrate were investigated by Turriziani (1954). It was observed by various authors, zur Strassen (1958), Locher (1960) and Goto (1962) that the hydrate can be formed also through the reaction of slag (or generally C-S-A glass) and lime. The crystal structure of the hydrate was discussed by zur Strassen.

The present author, on investigating the pozzolanic reaction of clay minerals, found out that allophane, hydrated halloysite or finely ground kaolinite results hydrated gehlenite as the product of lime reaction. Further an almost pure sample of the hydrate was obtained through the reaction of coprecipitated Al_2O_3–SiO_2 gel and lime, and some properties of the hydrate were examined.

It was demonstrated that the reactivity of the hydrate, which forms easily ettringite on the presence of gypsum, can be utilized for the soil stabilization in the Kanto-loam zone around Tokyo, of which dominant clay minerals are allophane and hydrated halloysite.

Introduction

Soils of volcanic origin are widely distributed in Japan. "Kanto loam" around Tokyo vicinity is the most typical of them. Dominant clay minerals contained in this loam are allophane and hydrated halloysite, which cause unfavorable soil mechanical properties. Investigation into soil stabilization is to be done for highway construction works in order to ensure a good trafficability. Conventional soil-cement method which needs a great quantity of cement to achieve a desired effect is not economical, and lime admixing method possesses such defect that development of strength is slow. It was found that admixing of lime and gypsum is effective and economical for soil stabilization.

The present author carried out a basic study on the mechanism of soil stabilization by means of the reaction of soil-lime and soil-lime-gypsum. It was confirmed that hydrated gehlenite (1) is formed in the mixture of allophane-lime at the room temperature and cement bacillus is formed by admixing lime and gypsum. It was further found that hydrated halloysite reacts easily with lime to result hydrated gehlenite. As these studies belong to an applied field of cement chemistry, here is reported the result of investigation which has been made in the Public Works Research Institute, Ministry of Construction, during the last ten years.

Materials Resulting from Reaction of Allophane-Lime and Allophane-Lime-Gypsum

Allophane was separated from various volcanic soils of Japan, and treated with lime solution or lime-gypsum solution under various reaction conditions. The resulting materials were examined through X-ray diffraction, DTA, infra-red absorption and chemical analysis. The following are the summary of the study.

The present author (2) (3) reported that lime can be absorbed by allophane when placed in lime solution, forming hydrated gehlenite C_2ASH_n. The nature of C_2ASH_n was examined. The reaction was found to be common for allophanes of various localities. The reactivity could be improved through heat treatment of allophane, eliminating the formation of C_4AH_{13}. The reaction mechanism was not disturbed with Truog's deferration processing or EDTA processing, but was disturbed with deferration processing of Tamm's reagent or alternative processing

*Kajima Construction Co., Ltd., Tokyo Japan.

of Na_2CO_3–HCl which removes free oxides. It was also confirmed that three layer clay minerals and their heat-treated materials do not result in C_2ASH_n.

The present author and Ohba (4) studied on the relationship of such reaction conditions to the resulting materials as lime concentration, lime-allophane ratio, temperature involved and reaction time. Thereby the decrease of lime during reaction process was examined. As the resultants, the following materials were identified as C_2ASH_n, C_3AH_6 (C_3ASH_4 after long reaction time), C_4AH_{13}, 7.6 Å hydrate (seems to be carboaluminate) and X-ray amorphous lime-absorbed allophane. C-S-H phase was not identified.

The reaction started with lime absorption, then C_4AH_{13} and 7.6 Å hydrate were formed, finally C_2ASH_n appeared and simultaneously 7.6～8.2 Å lines disappeared after lime concentration had dropped. Within 35 days of reaction time, C_2ASH_n was obtainable at the reaction temperature below 50°C, C_3AH_6 at 80°C. At 60°C, C_2ASH_n appeared with low lime concentration, C_3AH_6 with high lime concentration.

When lime concentration was too low, C_2ASH_n could not exist. Amount of lime absorbed should be more than 20% of allophane in order to bring about C_2ASH_n. Reaction of C_2ASH_n formation was observed to be slow when it was proceeded in a paste form.

Under an excess amount of lime, C_4AH_{13} was obtained instead of C_2ASH_n.

The present author and Wada (5) investigated the reaction between coprecipitated SiO_2–Al_2O_3 gel and lime solution. Various SiO_2–Al_2O_3 gels with mol ratio of 0.18～10.1 were prepared, among which the gels with mol ratio of 0.23～5.1 were found to have properties similar to those of natural allophane.

With a high mol ratio Al_2O_3/SiO_2, gibbsite, boehmite and bayerite were identified in the prepared materials.

1 g of gel and 1*l* of saturated lime solution brought out C_2ASH_n at 20°C when Al_2O_3/SiO_2 was 0.3～8.5, they resulted also C_3AH_6 when gel contained gibbsite or other minerals. When Al_2O_3/SiO_2 was very small, C-S-H phase was presumably formed.

X-ray diffraction pattern of C_2ASH_n was best-defined when Al_2O_3/SiO_2 was 1. At 80°C, C_3AH_6 was obtainable when a large amount of lime was absorbed. The reaction mechanism of C_2ASH_n formation was favored by heat treatment, intensifying the X-ray diffraction pattern of resultant. Heat treated gel with large Al_2O_3/SiO_2 ratio gave 11.1 Å and 5.5 Å lines which were not identified. Coprecipitated Fe_2O_3–SiO_2 gel($Fe_2O_3/SiO_2 = 0.4$) and lime brought out X-ray amorphous material at 20°C, but well-defined lines of C_3FH_6 at 80°C.

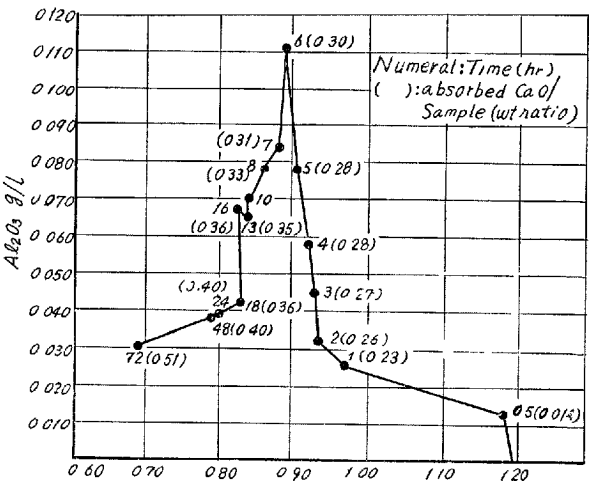

Fig. 1. *Composition of liquid phase during the reaction of coprecipitated* Al_2O_3–SiO_2 *gel with lime solution*

A further investigation into this reaction was made by the present author (6). Coprecipitated gel ($Al_2O_3/SiO_2 = 1$) was prepared as the starting material.

0.1 g of the gel was treated with 100 cc of saturated lime solution at 20°C. The resulting material was identified through X-ray diffraction, and the liquid phase examined by chemical analysis. The concentration of Al_2O_3 and CaO in the liquid phase is shown in Fig. 1.

According to the X-ray analysis, 7.6 Å line, 8.2 Å line and very weak lines of C_2ASH_n could be identified within 30 minutes of reaction time. The lines of C_2ASH_n became stronger after 1 hr, they were quite well-defined after 2 hrs. The main resultant, C_2ASH_n, became dominant, while the by-product with 7.6 Å line tended to disappear. It can be assumed that the natural allophane behaves similarly to the coprecipitated gel, although the reaction speed is slow. As was described by Strätling (1), the reaction of allophane with lime solution proceeds topochemically, and there is pseudo equilibrium between absorbed lime and liquid phase concentration, or between the resulting crystal material and liquid concentration. To investigate this mechanism, the next experiment was made. Coprecipitated Al_2O_3–SiO_2 gel ($Al_2O_3/SiO_2 = 1.00$) was heated at 600°C for 1 hr, added to lime solutions of various concentration, aged at 20°C for 35 days. As Fig. 2 shows, the amount of absorbed lime and the concentration of lime in liquid phase after the reaction were examined.

The relationship presented in Fig. 2 gives no straight line, but a line with three-steps gradient. This relationship was observed in air-dried allophane, but sometimes AC was straight line in the case of heat-treated

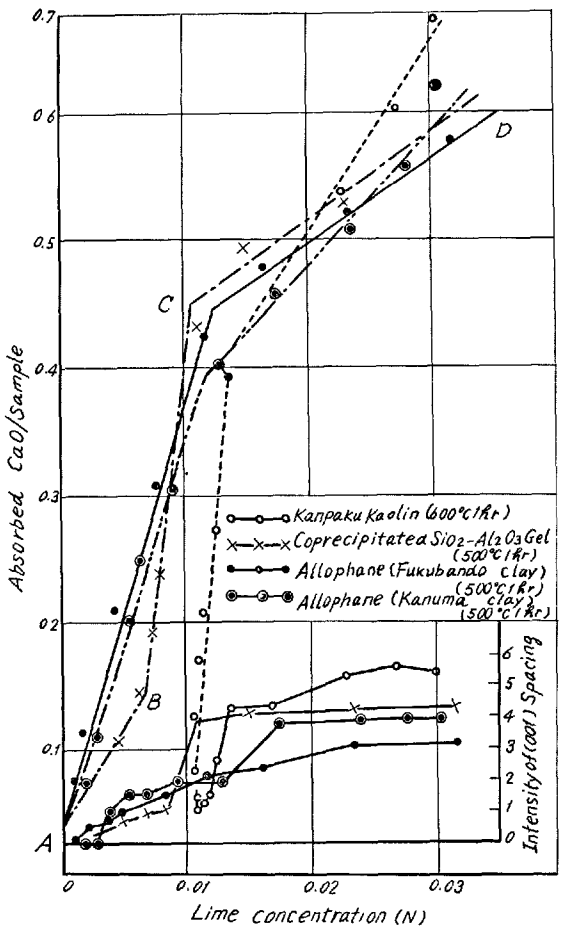

Fig. 2. *Relationship between lime absorbed and lime in liquid phase after reaction (Also intensity of basal reflexion of resulted material is plotted against lime concentration.)*

allophane. Between A and B no resulting crystal phase was identified, between B and C the intensity of the basal reflexion of C_2ASH_n was observed to increase gradually, and between C and D the intensity stayed unchanged. This characteristics was common with other experiments using allophanes from "Kanuma clay" and "Fukubando clay" or metakaolin from "Kanpaku kaolin". Points B and C correspond to 0.008 N and 0.013 N respectively.

Although the behavior of SiO_2 was not clarified with the above examination, the behavior of CaO could be summarized as the following. In the lime-poor region allophane exists together with lime-absorbed allophane, in the next region up to 0.013 N C_2ASH_n co-exists, in which the formation of C_2ASH_n from absorbed body proceeds. In the further lime-rich region, the reaction speed for the C_2ASH_n formation slows down, lime absorption continues gradually. In the region near to lime-saturation it is assumed that C_2ASH_n changes to C_4AH_{13}. The absorption reaction, C_2ASH_n formation through topochemical reaction or other possible reaction takes place simultaneously, and true equilibrium is not to be established.

The present author and Ohba (7) investigated the reaction of allophane with lime-gypsum solution.

0.15 g of allophane was treated with 100 cc of the solution of various components, varying the reaction time and temperature. With 5% gypsum added to allophane, low sulphate bacillus was obtained within a few hours. At 20°C C_4AH_{13} coexisted, the resulting bacillus re-dissolves as the lime in liquid phase was consumed by the absorbing reaction. At 60°C the resulting bacillus and C_4AH_{13} disappeared when original lime amount was more than 65% to allophane, C_3AH_6 appeared instead as a stable phase. With less than about 50% lime, C_3AH_6 could not be formed, and resulting bacillus tended to decrease while C_4AH_{13} increased.

With more than 15% gypsum added to allophane, high sulphate bacillus was formed as a stable phase at room temperature. Lime in liquid phase was consumed through both of bacillus formation and C_2ASH_n formation. During high sulphate bacillus redissolved as the results of lime consumption, it behaved approximately along the dissolving curve of bacillus to lime. The existence of gypsum disturbed the C_2ASH_n formation.

The present author and Maki (8) made laboratory experiment as well as field experiment on the soil stabilization, using "Kanto loam" treated with lime and gypsum. It was established that bacillus formation is attributable to the strength development in soil-lime-gypsum mixture, and the existence of gypsum gives the initial strength. When lime-gypsum was added to allophane clay with high sensibility as well as with high moisture content (more than liquid limit), it was observed that the strength and the bearing power were not sensitive to the moisture content, the resulting soil had enough strength to bear pedestrian's weight one hour after mixing, bringing out a sufficient initial trafficability.

Materials Resulting from Reaction of Hydrated Halloysite and Lime

As was described, allophane reacts with lime at room temperature to result in C_2ASH_n. Behavior of hydrated halloysite was not established. To clarify this point, the present author and Fujisaki (9) carried

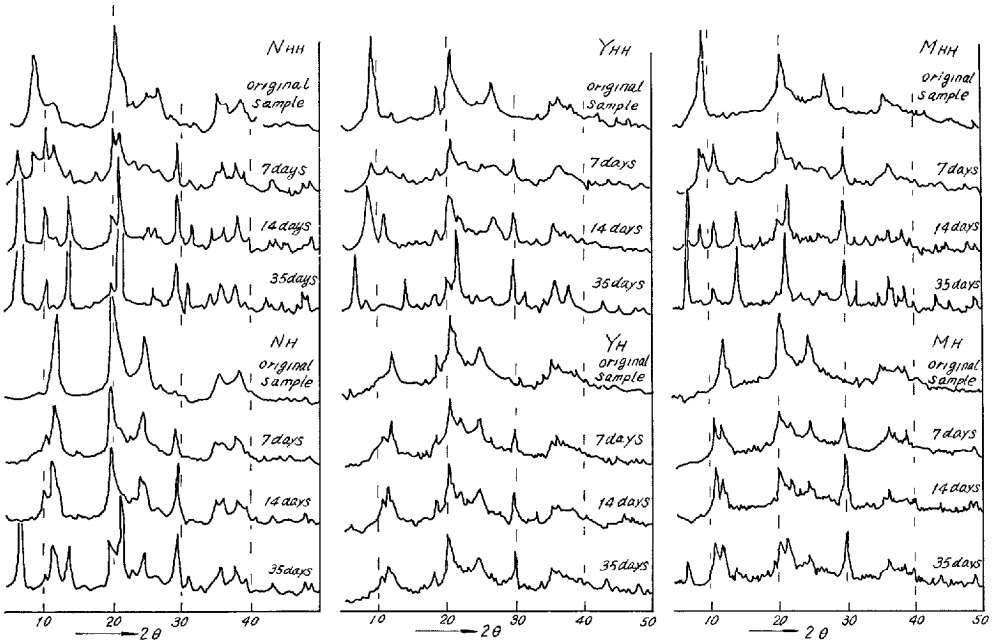

Fig. 3. *X-ray diffraction diagrams of reaction products 0.100 g sample to 100 cc lime saturated solution*

out an investigation similar to that in the case of allophane using three kinds of specimen of hydrated halloysite. It was confirmed that C_2ASH_n could be easily formed through the reaction and the reactivity decreased through dehydration of the starting material.

Specimens and Experimental Method

Naegihakudo clay, Yame clay and Musashino loam were treated with Kelley's method (10) to bring out Ca-clay specimen of less than 1μ. The specimens were kept in a desiccator with 60% moisture. Each specimen was named N_{HH}, Y_{HH} and M_{HH}. The specimens were heated at 150°C for 20 minutes to give N_H, Y_H and M_H. Besides N_{HH} was heated at 350°C for 2 hours to give 7.3 Å spacing. Hong Kong kaolin was named H_H. Also, well-crystallized Kanpaku kaolin was used for grinding experiment.

0.100 g of specimen was treated with 100 cc of lime saturated solution at room temperature for various reaction times (3, 7, 14, 21 and 35 days). Reaction vessel was of polyethylene, and care was taken to avoid CO_2 contamination. After the reaction was completed, lime concentration in liquid phase was measured and the amount of absorbed lime was determined. The reacted specimens were washed and kept in a desiccator with 60% moisture to give constant weight. X-ray diffraction, self-recording DTA and electron microscope were applied to examine the resultants. Care was taken to prevent dehydration of hydrated halloysite.

Experimental Results

Clay minerals were identified through X-ray diffraction and DTA, as shown in Figs. 3 and 4. All specimens could be identified as hydrated halloysite. Y_{HH} contained a small amount of gibbsite, M_{HH} a small amount of allophane. The order of structural perfectness was found to be $N_{HH} > M_{HH} > Y_{HH}$. On heating at 150°C, (001) spacing of all specimens shifted to 7.5 Å. The relationship between absorbed lime and reaction time is shown in Fig. 5.

The better crystallized specimens absorbed more lime. As is similar to the case of allophane, the C_2ASH_n formation started after the amount of absorbed lime had attained a limited value. The reactivity decreased through the dehydration of specimens when it was heat-treated.

According to X-ray diffraction, Y_{HH} gave 8.2 Å line and 7.6 Å line after 3 days. 8.2 Å line was intensified with age, then disappeared after 21 days. 7.6 Å line was not to be seen after 7 days. C_2ASH_n was not recognized before 21 days, but was recognized distinctly after 35 days. On the other hand, (001) spacing of hydrated halloysite became very weak after 3 days, and it disappeared almost completely after 35 days. (02) spacing, however, stayed unchanged. M_{HH} showed the same tendency as Y_{HH}, but C_2ASH_n formation started earlier, the existence of the new phase being recognized after 14 days. N_{HH} resulted C_2ASH_n further earlier.

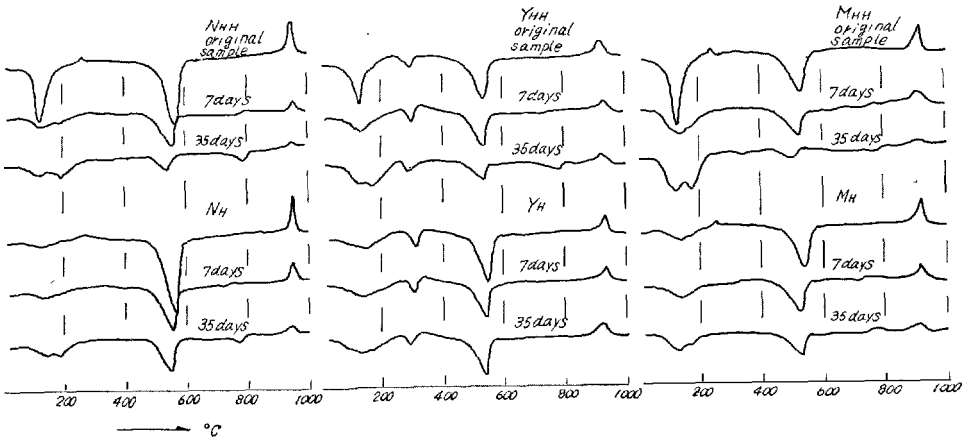

Fig. 4. *DTA diagrams of reaction products 0.100 g sample to 100 cc lime saturated solution, 20°C*

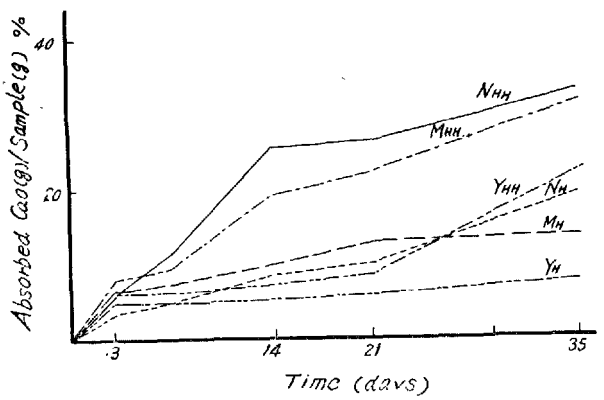

Fig. 5. *Lime absorption velocity at 20°C*

Y_H presented both of 8.2 Å line and 7.6 Å line for each reaction age, the pattern of X-ray diffraction remained almost unchanged, although the amount of absorbed lime was measurable. M_H showed greater reactivity than Y_H, (001) spacing became weak with age, a small amount of C_2ASH_n was observed after 35 days. N_H behaved similarly to M_H, but C_2ASH_n formation started earlier.

DTA curves of reacting specimens were found to have the following general tendency. The endothermic peak of 550°C shifted to lower temperature side, diffusing itself and becoming shallow. The exothermic peak of 970°C shifted to lower temperature side, the height of peak becoming lower and the profile rounded.

Gibbsite did not disappear, and loose endothermic peak of 750°C~800°C was observed. In correspondence to the structural perfectness of the specimens, the DTA curves were varied. The appearance of 200°C peak, which was based on C_2ASH_n, was in a good agreement with the results of X-ray analysis. The change of (001) spacing of hydrated halloysite, however, was in a poor agreement with the DTA analysis. The curves of N_H, M_H and Y_H presented a tendency similar to that of the hydrated specimens, although the profiles were not quite in evidence.

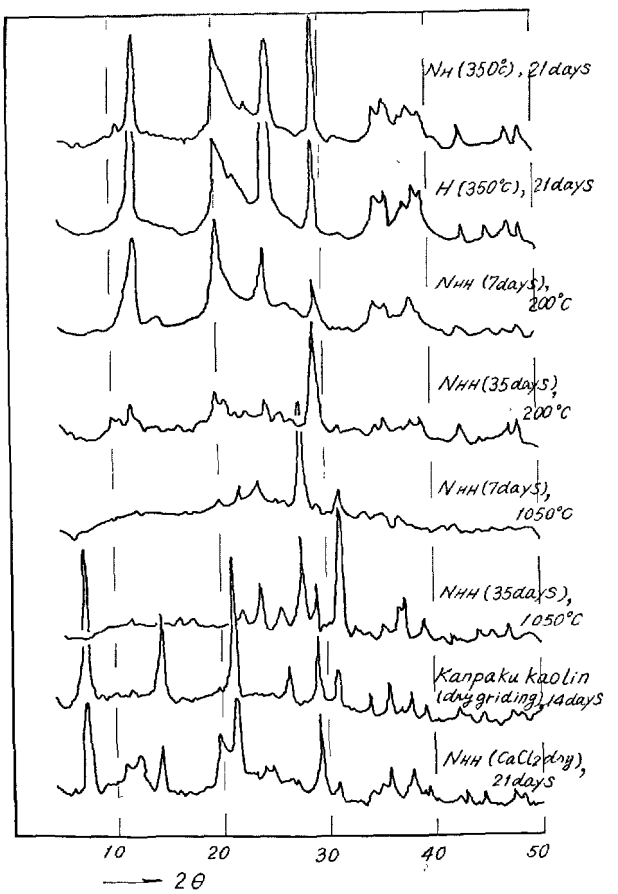

Fig. 6. *X-ray diffraction diagrams of reaction products with various treatment*

Fig. 6 shows X-ray diffraction patterns of resulted

material through the reaction between heated specimens and lime as well as of heat-treated resultants. Treatment conditions were the following.

a. N_{HH}, heated at 350°C for 2 hrs (7.35 Å), 21 days reaction
b. H_H, heated at 350°C for 2 hrs (7.25 Å), 21 days reaction
c. N_{HH}, 7 days reaction, then heat-treated at 200°C
d. N_{HH}, 35 days reaction, then heat-treated at 200°C
e. N_{HH}, 7 days reaction, then heat-treated at 1050°C
f. N_{HH}, 35 days reaction, then heat-treated at 1050°C
g. Kanpaku kaolin, ground, 14 days reaction
h. N_{HH}, kept in $CaCl_2$-desiccator for long time (7.5 Å), then 21-day reaction

As is observed in Fig. 6, the preheated specimens caused a decreased reactivity. When well-reacted specimen, which showed strong lines of C_2ASH_n and no (001) spacing of hydrated halloysite, was post-heated, then C_2ASH_n decomposed and halloysite appeared instead. On post-heating the reacted specimen at 1050°C, patterns of C_2AS and wollastonite were to be observed. Well-crystallized kaolinite, when dry-ground in agate mortar to give X-ray amorphous material, reacted easily with lime and resulted in C_2ASH_n. N_{HH} specimen, when dehydrated in $CaCl_2$ desiccator to give 7.5 Å line of halloysite, formed C_2ASH_n easily.

It was observed through electron microscope that clay specimen formed aggregate, then the aggregate changed into an edge-shaped form, crystal growth being started. This transformation is shown in Fig. 7.

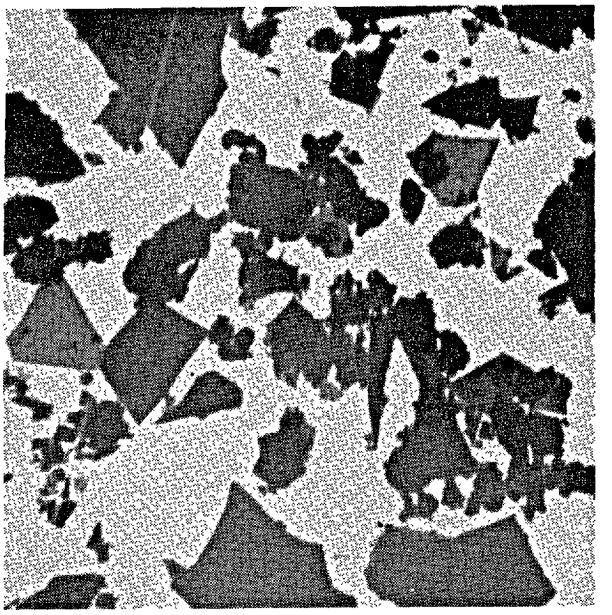

Fig. 7. *Electron micrograph of reaction product N_{HH}, 35 days, 20°C, Magnification ×5,000*

Discussion

Hydrated halloysite (N_{HH}, M_{HH}, Y_{HH}) absorbed lime when it was placed in lime solution, C_2ASH_n could be recognized by X-ray analysis after the amount of absorbed lime had attained a limited value. Even in the stage when the amount of absorbed lime was small and C_2ASH_n lines were not to be seen, (001) spacing of hydrated halloysite became weak, but the intensity of (02) spacing stayed unchanged. It can be assumed from this observation that the disorder along c-axis became greater with the reaction, lime being absorbed between layers. Further, the absorbed lime reacted with the adjacent layer, which resulted in forming C_2ASH_n. From the X-ray diffraction patterns of the heat-treated specimen causing decomposition of C_2ASH_n, it can be assumed that the clay remained retaining its crystallinity almost intact during the reaction process.

Eades and Grim (11) described about the mechanism of lime-clay reaction as such reaction with solution starting on the edge of crystals for three-layers minerals. According to the opinion of Diamond and Kinter (12), the reaction proceeds between absorbed lime and surface layers of clays. These observations are based on experiment with clay minerals of rather poor reactivity. From the present auther's experiment, in which such clay mineral of high reactivity and with interlayer water as hydrated halloysite was used, it is concluded that the reaction on surface layer could be more dominant than the one on layer's edge. It is also described that the resultant materials from clay minerals of poor reactivity are calcium aluminate hydrates and calcium silicates hydrate but not C_2ASH_n.

In the case of allophane, it was found that C_4AH_{13} and 7.6 Å hydrate appeared transiently and disappeared as C_2ASH_n began to be formed. This phenomenon, as was confirmed also by the case of hydrated halloysite, could be explained as that a part of Al_2O_3 dissolved into liquid phase when lime was absorbed. To satisfy the resulting condition of C_2ASH_n, the amount of absorbed lime should be more than 10% to the weight of air-dried hydrated halloysite. The value for allophane being about 20%, the deviation is caused by the difference of crystal structure of each clay mineral.

Generally speaking, the better-crystallized hydrated halloysite was found to possess the greater reactivity. This tendency was also confirmed with specimens, which were pre-heated at 150°C and showed 7.5 Å basal reflexion of halloysite. The pre-heat treatment, however, deteriorated the reactivity. It is assumed that high structural perfectness favored the invasion of lime between layers or the orientation of lime on layer surface. When specimens were heated at 350°C, interlayer water evaporate away and (001) reflexion shifted to about 7.3 Å, then the invasion of lime became difficult, the reactivity being decreased to a great extent.

Well-crystallized kaolinite, which is usually of poor reactivity, could be activated through dry-grinding to react easily with lime. The X-ray amorphous dry-ground kaolinite could recover its layer structure through the lime reaction, forming well-crystallized C_2ASH_n.

The final or metastable from materials resulting from the lime-clay reaction are, as is well known, dependent upon the reaction conditions such as paste form, slurry form or suspension form. Kudo, Tukiyama and Okabe (13) investigated the lime-clay (hydrated halloysite) reaction in paste form, in which C_4AH_{13} and C_2ASH_n were identified through X-ray analysis in early stage of reaction, tobermorite gel was identified through electron microscope in later stage, and the resulting crystal materials of early stage disappeared gradually as the reaction time elapsed. The reaction in paste form proceeds in the saturated lime solution, and the reaction speed is slow, thus giving different results compared with the present author's results.

Although no detailed examination was made to confirm the existence of calcium silicate hydrates, it is assumed that the endothermic peak of 750°C~800°C could be related to both of calcite and tobermorite gel. Davidson and Hilt (14) examined the 7.6 Å hydrate which was obtained by the lime-montmorillonite reaction, and concluded that a part of Al in C_4AH_{13} could be substituted isomorphously by Si, thus giving 7.6 Å line instead of 8.2 Å. This problem needs a further investigation.

Properties of Hydrated Gehlenite

On the properties of C_2ASH_n, which is obtainable by the lime-allophane reaction, some descriptions were already made (2) (3). The behavior of SiO_2 in allophane or of Fe_2O_3 as the contaminant is still unknown. The present author made detailed examinations on the properties of C_2ASH_n, which was prepared as purest as possible, comparing the newly obtained data with the published ones.

Specimens and Experimental Method

There was 20 g of coprecipitated gel(H_2O^- 17.5%, H_2O^+ 8.80%, Al_2O_3 46.45%, SiO_2 27.35%, Al_2O_3/SiO_2 = 1.00) was added to 20*l* of saturated lime solution, aged for 1 year at 20°C in a CO_2 free atmosphere. White crystal of C_2ASH_n was filtered out and kept in $CaCl_2$ desiccator. Chemical analysis, X-ray diffraction, DTA, TGA, infra-red analysis and electron microscope were applied to the obtained C_2ASH_n. Also the specific gravity and the heat of solution against 2N HNO_3 containing small amount of HF were measured.

Experimental Results

Chemical analysis (%) gave the following;

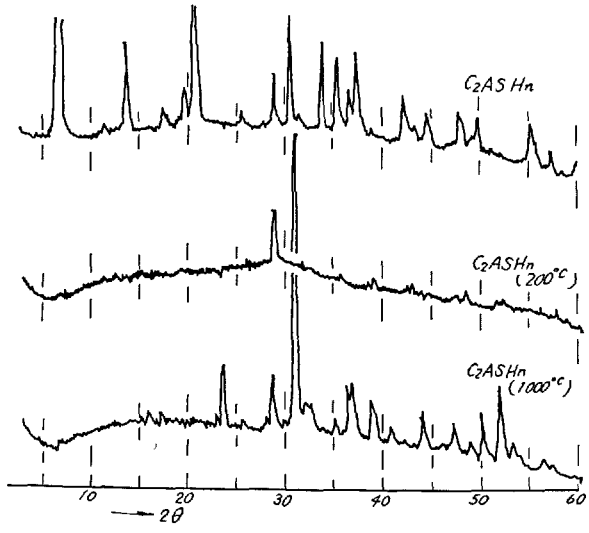

Fig. 8. *X-ray diffraction diagrams of* C_2ASH_8

H_2O^-: 7.60, H_2O^+: 25.25, CaO: 29.45,
SiO_2: 13.65, Al_2O_3: 21.40, CO_2: 1.69

Figs. 8, 9, 10 and 11 show respectively the results of X-ray diffraction, DTA and TGA, infra-red analysis and electron microscope. Heat of solution was found with unheated sample, with 500°C heated sample

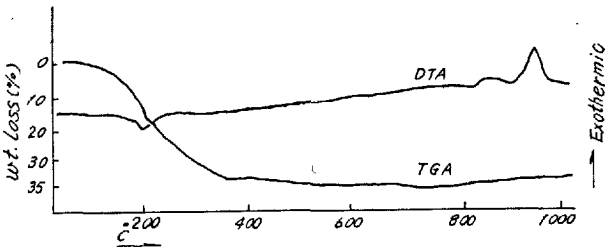

Fig. 9. *DTA diagrams of* C_2ASH_8

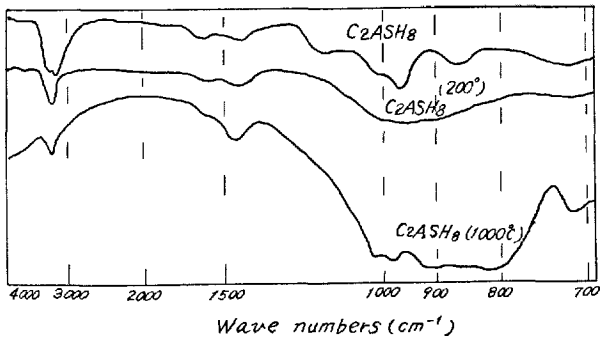

Fig. 10. *Infrared absorption spectrum of* C_2ASH_8

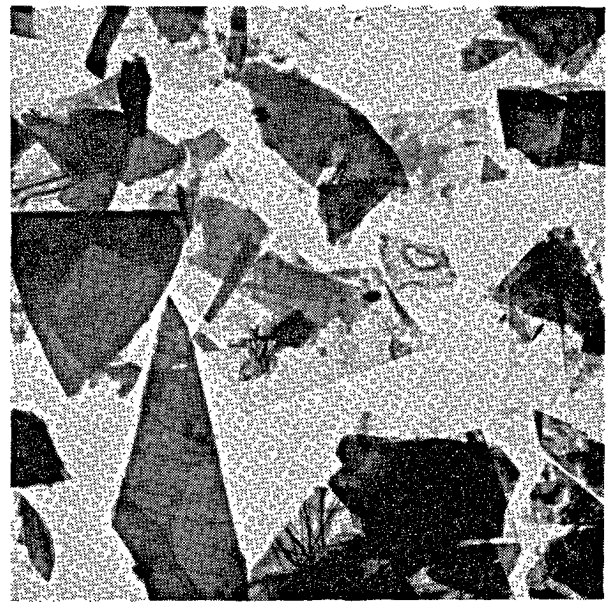

Fig. 11. *Electron micrograph of* C_2ASH_8 *Magnification* $\times 10{,}000$

(ig. loss 5.33%) and with 950°C heated sample respectively to be 336 cal/g, 577 cal/g, 672 cal/g. Specific gravity was measured to be 1.89.

Discussion

C_2ASH_n was firstly obtained by Strätling (1) who examined the resulting material of the reaction between meta-kaolin and lime solution. Turriziani and Schippa (15) confirmed this substance when they carried out the same experiment as the above, and investigated the nature of C_2ASH_n in detail. According to the study of Dörr, as is cited by Locher (16) and by zur Strassen (17), C_2ASH_n was formed through the reaction of C_2AS-glass and lime solution. C_2ASH_n could be obtainable from various starting materials through lime reaction such as quenched slag with high Al_2O_3 contents (18) (19) (20), dry ground amorphous kaolin (21) (9), allophane (2) (22), hydrated halloysite (9) (13), kaolinite (although reaction time elapsed very long) (23), coprecipitated SiO_2–Al_2O_3 gel (5) and metakaolin (1) (5) (24). C_2ASH_n was found also in the hydrates mixture of pozzolan cement of low alkali portland cement and burnt kaolin (25). Although the formation of C_2ASH_n has been reported by many authors, its properties are not yet clear because it is difficult to prepare C_2ASH_n in pure form.

Chemical composition can be calculated on the basis of the results of chemical analysis, being denoted by the formula $C_{2.33}AS_{1.08}H_{8.70}$. If CO_2 exists in the form of $CaCO_3$, and a small amount of lime is absorbed, the resulting material should be $C_2ASH_{8.45}$ together with a small amount of C_2SH to be assumed to exist. Thus the purity of the sample is about 90%. Dörr's sample, as was referred already, has the formula $C_{2.5}ASH_{9.3}$, which could be re-written as C_2ASH_8 when the existence of hydrogarnet is taken into consideration. Schmitt's sample (20), which was obtained through lime reaction of $C_2A_{(1-x)}F_xS$ glass, has the formula C_2ASH_8. The present author's sample, which was proved to be in relatively pure form through X-ray analysis as well as electron microscope, possesses the approximate composition of C_2ASH_8.

On the X-ray diffraction patterns, as shown in Fig. 8, calcite is found to be in existence, but no carboaluminate is to be seen. Calcium silicate hydrates were not recognized while weak lines of hydrogarnet are identified. Not regarding the lines, of which intensity is less than 10% to the intensity of (001) spacing, and eliminating the lines of above stated contaminants, C_2ASH_8 should possess the following spacing:

12.54(100)	6.24 (44)	4.92 (12)	4.17 (100)	2.868(60)
2.614(44)	2.495(27)	2.488(34)	2.405(20)	2.378(40)
2.118(16)	2.076(10)	2.014(12)	1.888(10)	1.824(16)
1.658(25)	1.645(14)	1.605(10)	1.542(10)	1.435(15)

Spacing values of C_2ASH_8 are already given by Strätling (1), Turriziani and Frantini (26), Schmitt

(20) and the present author (3). Now the above values are compared with the data of Schmitt. Lines of 4.28 Å and 3.52 Å, which are given by Schmitt, are not found by the present author. On the other hand, line of 2.01 Å is found here, lines of 2.50 Å and 2.38 Å showing doublet profile, and intensity of 2.87 Å line being greater than that of (002) spacing. When the above data are compared with the one already reported by the present author, all spacings possess a smaller value, and the intensity of lines is relatively strong as compared with the intensity of (001) spacing. From this observation it can be concluded that the sample is of high purity as well as of high degree of crystallinity, and isomorphous substitution by Fe is not assumable.

On DTA diagram a relatively sharp endothermic peak at 210°C and exothermic one at 940°C are to be seen. At 840°C calcite shows endothermic peak. Peaks based on gibbsite, hydrogarnet, tobermorite or hydrated lime are not recognized. Peak of 210°C results from the decomposition of hydrate water, 940°C peak results from the formation of C_2AS. According to the TGA diagram, dehydration starts at 50°C, it is intensified above 150°C. Up to 350°C, 90% of hydrate water decomposes. Weight loss above 750°C is attributable to calcite decomposition.

On infra-red absorption diagram, as shown in Fig. 10, absorption of calcite, Si–O, O–Al–OH, water and hydrogen bond are to be observed. Besides these, unidentified absorption bands are found as follows:

1500, 1380, 1160, 960, 865 (cm^{-1})

When heat treated at 200°C, 1160 band and 865 band disappeared, and a broad 800～1200 band, which allophane shows, comes out instead. These two bands are thought to be related to C_2ASH_8.

Electron microscope was applied to samples in which crystals of more than 5μ are removed through sedimentation method. As seen in Fig. 11, C_2ASH_8 possesses an irregular plate form, and hexagonal crystal is not observed. The edge of plates is not of straight line, but of curved line, and they tend to elongate. Degree of crystallinity is high. No gel substance is to be seen. Electron diffraction pattern which is taken along c-axis of crystal gives regular hexagonal figure. The results agree with the data of zur Strassen (17).

For this study, carried out in chemistry section of Public Works Research Institute, Ministry of Construction, the auther is much obliged to the co-workers, Mr. M. Ohba, Mr. T. Maki, Mr. K. Fujisaki and Mr. S. Wada as well as the assistant researchers, Mr. T. Kaibara and Mr. T. Nishijima.

References

1. S. Strätling, "Die Identifizierung der Reaktion Produkte von gebraunten Kaolin im Zussamenhang mit dem System Kalk-Kiesersäure-Tonerde-Wasser", Zement, **29**, 427–432, 441–445, 455–460, 475–477 (1940).
2. A. Ariizumi, "Pozzolanic reaction of allophane" (in Japanese), Semento Gijitsu Nenpō, **13**, 339–345 (1959).
3. A. Ariizumi, "On the stabilization of Kanto loam (allophanic clay) by means of lime-gypsum admixture: I, Formation of hydrated gehlenite through the reaction of allophane with lime" (in Japanese), Doboku Kenkyusho Hokoku, No. 110, p. 97–112 (1962).
4. A. Ariizumi and M. Ohba, ibid. "II, Factors affecting the formation of hydrated gehlenite" (in Japanese), No. 110, p. 113–126 (1962).
5. A. Ariizumi and S. Wada, ibid. "III, Formation of hydrated gehlenite through the reaction of coprecipitated SiO_2–Al_2O_3 gel with lime" (in Japanese), No. 111, p. 105–110 (1962).
6. A. Ariizumi, ibid. "IV, Discussion of the results" (in Japanese), No. 111, p. 105–110 (1962).
7. A. Ariizumi and M. Ohba, ibid. "V, Formation of cement bacillus through the reaction of allophane with lime-gypsum solution" (in Japanese), No. 119, p. 83–101 (1964).
8. A. Ariizumi and T. Maki, ibid. "VI, Mechanical Properties of clay-lime-gypsum mixture" (in Japanese), No. 122, p. 35–60 (1964).
9. A. Ariizumi and K. Fujisaki, "Formation of hydrated gehlenite through the reaction of hydrated halloysite with lime" (in Japanese), Semento Gijitsu Nenpō, **19**, 182–188 (1965).
10. W. P. Kelley, W. H. Dore, A. D. Woodford and S. M. Brown, "The colloidal constituents of California soils", Soil Sci., **48**, 201–255 (1939).
11. J. L. Eades and R. E. Grim, "The reaction of hydrated lime with pure clay minerals in soil stabilization", HRB Bull. No. 262, p. 51–63 (1960).
12. S. Diamond and E. B. Kinter, "Mechanism of soil-lime stabilization", Public Road, **33**, 260–273 (1966).
13. N. Kudo, K. Tukiyama and Y. Okabe, "Studies on hardening in Kanto loam-lime stabilization" (in Japanese), Gypsum & Lime, No. 84, p. 12–19 (1966).
14. G. H. Hilt and D. T. Davidson, "Isolation and investigation of a lime-montmorillonite crystalline reaction product", HRB Bull., No. 304, p. 51–64 (1961).
15. R. Turriziani and G. Schippa, "DTA of reaction products between dehydrated kaolin and hydrated lime" (in Italian), Ric. Sci., **24**, 366–374 (1954).
16. F. W. Locher, "Hydraulische Eigenschaften von

Kalkreichen Glässern des Systems $CaO–Al_2O_3–SiO_2$", Schriften der Zementindustrie, Düsseldorf. No. 25, p. 19 (1960)
17. H. zur Strassen, "Discussion of the paper: Hydration of calcium aluminates and ferrites" Proceedings of the Fourth International Symposium on the Chemistry of Cement, Washington, p. 244–245 (1960).
18. F. W. Locher, "Hydraulic properties and hydration of glasses of the system $CaO–Al_2O_3–SiO_2$", Proceedings of the Fourth International Symposium on the Chemistry of Cement, Washington, p. 267–276 (1960).
19. K. Goto, M. Hanada and H. Miyairi, "Studies on portland blast-furnace slag cements: mainly on the influence of chemical components of slag mixed in portland blast-furnace slag cements", Semento Gijitsu Nenpo, **16**, 162–168 (1962).
20. C. H. Schmitt, "Discussion of the paper: hydration of calcium aluminates and ferrites", Proceedings of the Fourth International Symposium on the Chemistry of Cement, Washington, p. 244 (1960).
21. W. Krönert, H. E. Schwiete and K. Wetzel, "Reaktionen von Erdalkalihydroxiden mit Tonmineralien in Wasseriger Suspension", Naturwissenschaften, **51**, 381 (1964).
22. S. Kaneko and T. Sudo, "Variations of mineralogical properties on the profile of Kanto loam" (in Japanese), Advances in Clay Sci. **3**, 125–135 (1959).
23. T. Kohashi, "Reaction of calcium hydroxide with allophane-kaolinite clay minerals", Clay Sci., **3**, 11–36 (1967).
24. J. Jambor, "Hydrationsprodukte der Kalk-Puzzolan Bindemittel", Zement-Kalk-Gips, **16**, 177–186 (1963).
25. E. J. Benton, "Cement-pozzolan reactions", HRB Bull., No. 239, 56–65 (1960).
26. N. Frantini and R. Turriziani, "Contributo alla conoscenza di un silico-alluminato idrato calcio (composito di Strätling)", Ric. Sci., **24**, 1654–1657 (1954).

Supplementary Paper II-67 Successful Prevention of Loss of Strength in Concrete Made with High-Alumina Cement

Povindar K. Mehta*

Synopsis

Utilization of High-Alumina cement for structural purposes is seriously limited due to the gradual loss of strength which High-Alumina cement concretes undergo especially under hot-wet environments. This phenomena is accompanied by conversion to C_3AH_6 of the hexagonal phase CAH_{10}, which is the initial product of hydration.

A calcium sulfoaluminate additive was added to a High-Alumina cement which was used for making 2″×4″ concrete cylinders at 40° to 50°F. The concrete was wet cured for 28 days at 40° to 50°F, and later exposed to warm water at 100°F. At regular intervals the cylinders were tested for strength up to a period of 168 days from the date of hydration. No loss of strength was observed. X-ray diffraction studies on the corresponding concrete samples showed that only an insignificant portion of CAH_{10} converted to C_3AH_6.

As compared with portland cements, High-Alumina cements (HA cements) are known to possess superior characteristics with regards to refractoriness, high early strength and resistance to chemical attack by acidic and sulfate-bearing waters. Development of high early strength is a valuable property for application of this cement both for emergency repair and construction jobs, and for production of prestressed concrete.

In spite of the advantages offered by HA cements, their use for structural purposes is handicapped due to partial loss of strength after long periods, particularly when the concretes are exposed to hot-wet environments. The loss of strength in certain cases is reported to have caused structural failures. Some countries have, therefore, forbidden the use of HA cement for structural applications.

Hypotheses on Loss of Strength

The main constituents in HA cements is generally the compound, CA. In his comprehensive review of aqueous cementitious systems containing lime and alumina, Steinour (1) states that, of the eight different hydrates reported by several investigators, only the following four are commonly present in the products of hydration of commercial calcium aluminate cements: C_4AH_{13}, CAH_{10}, C_2AH_8 and C_3AH_6. The former three hydrates are hexagonal and they crystallize as thin acicular needles which contribute to the binding strength of the hydrating cement. The hexagonal phases, however, are metastable and they transform eventually to the stable cubic C_3AH_6.

The data from the investigation of Lea (2), Neville (3) Lehmann and Leers (4), and several other investigators have proved beyond any doubt that the conversion of hexagonal calcium aluminate hydrates to the cubic phase is related to strength loss in HA cement concretes. Regarding the precise mechanism which is responsible for retrogression of strength, Lehmann and Leers (4) attributed this to the intrinsic properties of the hydrates involved. According to them, the cubic morphology of C_3AH_6 does not permit a high surface area to become necessary for development of strong binding forces. The data from the investigation of Gitzen and Hart (5), and Neville (3), however, shows that the loss strength may also be attributed to increased porosity in the concrete structure when CAH_{10} converted to C_3AH_6. Mehta (6) has made calculations to show that for every cubic centimetre of CAH_{10} which transform to C_3AH_6, the solids undergo a reduction in volume by about one—half of cubic centimetre. Such a reduction in the volume of solids after hardening of concrete would evidently lead to a porous structure, which not only is inherently weak with regards to load-bearing capacity, but is also more susceptible to corrosion by permeating acidic fluids, especially when calcium hydroxide is not present in the products of hydration of HA cements.

*The University of California, Berkeley, California, U.S.A.

Additives Already Investigated for Preventing Conversion

Robson (7) lists several chemical additives which have been tried by different investigators to prevent the conversion of CAH_{10} to C_3AH_6. The additives mentioned are preformed calcium aluminate hydrates, calcium sulfate, aluminum sulfate, ammonium chloride, sodium phosphate, polysaccharides and polyhydric alcohols, anionic, cationic and non-ionic surface active agents, etc. But, according to him, "No reliable and effective method has been discovered which will greatly retard or prevent the conversion process when the condition for the latter are especially favourable."

According to Young (8), presence of ligno-sulfonate yielded thermodynamically more stable hexagonal calcium aluminate hydrate phases, but the hydration reactions were considerably retarded. Obviously, therefore, such additives which do not interfere with the rate of hydration of CA (or rate of formation of CAH_{10}) but which counteract the conditions favouring conversion of CAH_{10} to C_3AH_6 seem to hold promise for solution of this problem.

Materials and Experimental Procedure

In carrying out this investigation a HA cement composed principally of mono-calcium aluminate was used. This cement was produced by heat treatment at 2600°F of stoichiometric quantities of reagent quality calcium carbonate and alumina hydrate. The chemical analysis of cement showed 35.5 percent CaO and 64.5 percent Al_2O_3. It was ground to 3130 cm^2/g Blaine. When this cement was hydrated at 40–70°F, the principal product of hydration, as determined by powder X-ray diffraction analysis, was CAH_{10}. For preventing conversion of CAH_{10} to C_3AH_6 under hot-wet conditions, a calcium sulfoaluminate additive was included in the HA cement. The additive consisted of a high-purity chemical compound having the molar composition $4CaO \cdot 3Al_2O_3 \cdot SO_3$. It was prepared by heat treatment at 2600°F of stoichiometric amounts of reagent quality calcium carbonate, calcium sulfate and alumina hydrate for a time sufficient to complete the reaction. It was also ground to 3130 cm^2/g Blaine. To chemical analysis of the additive showed 36.8 percent CaO, 50.1 percent Al_2O_3, and 13.1 percent SO_3. Using 0.6 water-cement ratio, graded Standard Ottawa sand (ASTM Standard No. C109) and 3/8″–1/2″ crushed quartz as coarse aggregate 2″ × 4″ cylinders were prepared from a six-sacks per cubic yard concrete, with and without the presence of the additive in the HA cement. Series A shown in Table 1 represents a concrete mix which had no additive in the cement, while series B represents the concrete mix which had 5 percent additive by weight of the total cementitious material.

In order to prevent the instantaneous formation of some C_3AH_6 due to high heat of hydration normally produced during the rapid hydration of High-Alumina cement at early ages, the concretes were made with cold water (40° to 50°F), cast in pre-chilled 2″ × 4″ C. I. molds, and the molds stored in a cold room maintained at 40° to 50°F. They were stripped after 24 hours, and finally cured in 40° to 50°F water for 27 days. This procedure of curing helped to hydrate most of the CA of the HA cement to CAH_{10} without producing any detectable C_3AH_6 in the specimens. On the 28th day three concrete cylinders from each series were tested, both for compressive strength and for changes in the compound composition of the cement. The other cylinders were moved to a water storage maintained at a constant temperature of 100°F. The purpose of curing in warm water was to test whether the presence of calcium sulfoaluminate additive helped to prevent conversion of CAH_{10} to C_3AH_6 and thereby checked the resultant loss in strength. At 35, 56, 84, 112, 140 and 168 days, tests were made to determine both the changes in compressive strength and the compound composition of cement. In addition, modulus of elasticity of both the concretes was also determined before exposure to hot-wet curing and after exposure to hot-wet curing for 140 days.

The cylinders were capped and tested for compressive strength in accordance with the Standard ASTM procedures (C192–62T and C39–64). Representative

Table 1. *Mix proportions of HA cement concretes both with and without the additive.*

Materials	Proportion by weight Series A	Series B
High-Alumina cement	564	536
Additive	nil	28
Water	338	338
Graded standard ottawa sand	1500	1500
3/8″–1/2″ crushed quartz	1648	1648

Table 2. *XRD peaks selected for semi-quantitative estimation of compounds*

Compound	Selected peak	
	d,Å	2θ CuKα
$CaO \cdot Al_2O_3$	2.996	30.1
$CaO \cdot Al_2O_3 10H_2O$	7.132	12.4
$3CaO \cdot Al_2O_3 \cdot 6H_2O$	5.121	17.3

samples of mortar were collected from the broken pieces of concrete. The mortar was crushed, sifted through a 100 mesh sieve in order to remove most of the sand, and tested by powder X-ray diffraction analysis for determining the compound composition of the cement paste. Phillips Norelco X-ray diffraction equipment with copper target, nickel filter and scintillation counter was used.

In Table 2 are shown the specific peaks of the X-ray diffraction (XRD) pattern which were selected for identification and for semi-quantitative evaluation of the respective compounds by comparison of their relative peak intensities (counts per second at 1/8 degrees 2θ scanning rate).

Results and Discussion

The results of these tests are shown in Table 3, and are also plotted in Fig. 1:

It is evident from the strength data that substitution of 5 percent $4CaO \cdot 3Al_2O_3 \cdot SO_3$ in HA cement did not alter the compressive strength characteristics of concrete specimens cured at 40° to 50°F for 28 days, the strength values (average of three specimens) being about 8.3 Ksi in both the additive-containing and the nonadditive-containing concretes. The X-ray diffraction analysis of the cement paste showed that in both cases the hydration product consisted mainly of the hexagonal phase, CAH_{10}. No cubic phase, C_3AH_6, was detected, while a substantial amount of anhydrous CA was still present in the samples. When the specimens were exposed to moist curing at 100°F, initially, the strengths rose to a value of about 11.0 Ksi in both cases (due to hydration of the remaining unhydrated CA as confirmed by X-ray diffraction data), but later on started to decline. It can be seen from the curves in Fig. 1 that while the strength of HA cement concrete having no additive declined from about 11.0 Ksi to about 2.1 Ksi during the hot-wet curing period of 56 days to 168 days, the strength loss under the same conditions during the corresponding period for HA cement concretes having 5 percent $4CaO \cdot 3Al_2O_3 \cdot SO_3$ as additive was insignificant (within the value of experimental error).

In fact, the average compressive strength of reference specimens of Concrete B stored continuously in cold water (40° to 50°F) for 168 days was found to be 10.47 Ksi as against 10.28 Ksi for the identical specimens of concrete which were initially cured with cold water (40° to 50°F for 28 days) and later exposed to a prolonged period of hot-wet conditions (stored continuously under water at 100°F until age 168 days). Furthermore, prolonged hot-wet curing (under water at 100°F from age 28–168 days) of cylinders of Concrete A showed a drop in the modulus of elasticity from 5.23×10^6 psi to 2.74×10^6 psi., whereas under the same conditions the values of modulus of elasticity for cylinders of Concrete B remained essentially unchanged (5.67×10^6 psi.,

Table 3. *Compressive strengths and XRD peak ratios of Concretes A and B at different ages*

Age	Concrete A (made with cement containing no additive)		Concrete B (made with cement containing additive)	
	Compressive strength Ksi.	XRD, ratio of peak intensities C_3AH_6/CAH_{10}	Compressive strength Ksi.	XRD, ratio of peak intensities C_3AH_6/CAH_{10}
28	8.24	0	8.29	0
35	10.69	0.145	11.38	0.06
56	11.55	0.25	10.85	0.08
84	7.98	0.39	10.98	0.14
112	5.50	2.50	10.10	0.14
140	2.48	9.70	10.03	0.19
168	2.17	11.00	10.28	0.19

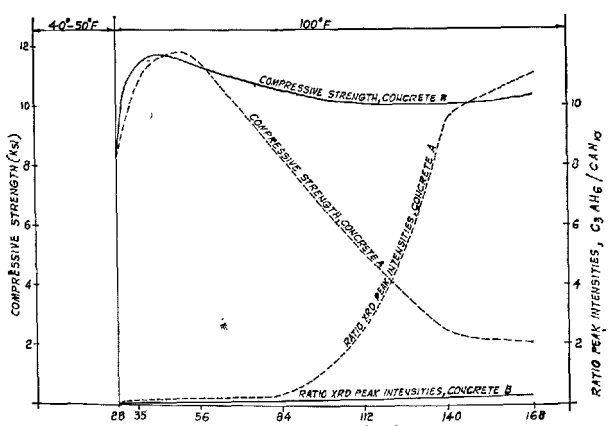

Fig. 1. *Compressive strength and XRD peak ratios of Concretes A and B at different ages of curing*

before exposure to hot-wet conditions, and 5.56×10^6 psi., after exposure to hot-wet conditions for 140 days).

The intensity ratios of diffraction peaks indicate that during the hot-wet curing period of 28 days to 168 days, the ratio of C_3AH_6 to CAH_{10} peaks increased from zero to about 11 for HA cement concrete having no additive, while it increased from zero to only 0.20 for HA cement concretes containing the calcium sulfoaluminate additive.

Conclusion

It can be concluded from the results of this investigation that, under the test conditions employed, the presence of $4CaO \cdot 3Al_2O_3 \cdot SO_3$ additive during hydration at high-alumina cement was capable of stabilizing the compound CAH_{10} under hot-wet conditions, thus ensuring that no loss in compressive strength of concretes resulted when such concretes were exposed to hot-wet conditions. It can also be concluded that the presence of this additive did not, in any derogatory way, interfere with the initial hydration rate of CA.

It is, however, realized that some further tests are necessary to show the details of behaviour under other conditions such as exposure to hot-wet conditions at different stages of hydration.

Acknowledgement

This research was sponsored by the University of California. The research work was conducted at the Laboratories of Structural Engineering and Structural Mechanics Division of the University of California at Berkeley.

References

1. H. H. Steinour, "Aqueous cementitious systems containing lime and alumina," Bulletin No. 34, (Portland Cement Association, U.S.A., 1951).
2. F. M. Lea, The Chemistry of Cement and Concrete pp. 441, 43, (St. Martins Press Inc., London, New York 1956).
3. A. M. Neville, "The effect of warm storage conditions on the strength of concrete made with high-alumina cement", Proc. Inst. Civil Eng. V. 10, pp. 185–92, 1958.
4. H. Lehmann and K. J. Leers, "Reactions during hardening of high-alumina cement", (in German), Tonindustrie Zeitung V. 87, No. 2 pp. 29–41, 1963.
5. W. H. Gitzen and L. D. Hart, "Explosive spalling of refractory castables bonded with calcium aluminate cement", Bull. Am. Cer. Soc, V. 40, No. 8, pp. 503–510, 1961.
6. P. K. Mehta, "Retrogression in the hydraulic strength of calcium aluminate cement structures", Minerals Processing, pp. 16–19, Nov. 1964.
7. T. D. Robson, "High alumina cement and concretes," First Edition (John Wiley and Sons, New York, 1962).
8. J. F. Young, "Hydration of tricalcium aluminate with lignosulfonate additions", Mag. Conc. Re. V. 14, No. 42, pp. 137–42, 1962.

Oral Discussion

Shunro Ueda and Renichi Kondo

Dr. Mehta emphasized that CAH_{10} could be stabilized by the addition of calcium sulfoaluminate. We formerly tested the effect of calcium sulfoaluminate on the conversion of the aluminous cement in water at 50°C, because the aluminous cement manufactured in Japan by the sinter process using rotary kiln and heavy oil usually contains a certain amount of calcium sulfoaluminate in the clinker. In our test, not only CAH_{10} but also C_2AH_8 transformed to C_3AH_6 and gibbsite and the strength of the test pieces decreased. But the rate of the conversion was generally little retarded by the presence of additives such as

calcium sulfoaluminate.

You did not discuss the reason of the stability of CAH_{10}. However we think the prevention of the conversion cannot be explained by the consideration that the phase equilibrium of $CaO–Al_2O_3–H_2O$ system changes with the addition of SO_3 ion. We would like to ask you about those points.

Oral Discussion

Keiko Okada

It is of much interest that $C_4A_3\bar{S}$ added in alumina cement on hydration prevents the hydrate CAH_{10} from converting into C_3AH_6 during long age without losing any strength of the cement.

To stabilize CAH_{10}, however, we have found it necessary to keep the hydrate specimen at relatively low temperature during such a long time as 28 days even if any additives were present.

Practically, however, it seems to be difficult to keep the large specimen under those conditions.

We should like to ask the author's opinions what properties were expected when the concrete having $C_4A_3\bar{S}$ were placed and cured at room temperature.

Author's Closure

Povindar K. Mehta

Reply to S. Ueda and R. Kondo

The author used 5% addition of a laboratory-made specimen of $C_4A_3\bar{S}$ for stabilizing strengths of concretes made with high-purity calcium aluminate cement. No conversion of CAH_{10} to C_3AH_6, and correspondingly no strength loss was observed when the concrete specimens, initially cured for 28 days at 40–50°F, were finally exposed to hot-wet conditions at 40°C for 140 days. The discussers used different types of high alumina cements, differently made from calcium sulfoaluminate additive with perhaps unknown ratio of additive to cement, and different curing conditions (50°C). Since their materials and the experimental conditions differed significantly from those of the author, it is possible that the discussers also obtained different results. The author already acknowledged that more work is needed using a wider range of materials and curing conditions before complete success in solving the problem of retrogression of high-alumina cement concretes is attained.

Regarding the mechanism of CAH_{10} stabilization, no work has yet been done in this direction, and author's thoughts on the subject are still of a speculative nature.

Reply to K. Okada

Results of research on properties of calcium aluminate cement concretes containing $C_4A_3\bar{S}$ additive, and placed-cured at room temperature, are not yet available. The author appreciates the concern of the discusser that the results may not be the same under more practical conditions of placement and curing. Research work is being planned in this direction at the Structural Engineering and Structural Mechanics Laboratory of the University of California.

In the mean time, the findings reported in this paper clearly establish that an initial long period of low temperature curing is not adequate by itself to prevent CAH_{10} conversion of concretes exposed to hot-wet conditions at later ages. The presence or absence of the $C_4A_3\bar{S}$ additive did make all the difference between final strengths and CAH_{10}-stabilization characteristics of Concretes A($C_4A_3\bar{S}$ absent) and B($C_4A_3\bar{S}$ present), considering that both the concretes were subject to identical conditions of placement and curing, i.e. cured at 40–50°F for the first 28 days and thereafter at 100°F in water.

Supplementary Paper II-68 Amorphous Phase in the $CaO-Al_2O_3-CaCl_2-H_2O$ System

Ferenc Tamás*

Synopsis

The reaction between supersaturated aqueous monocalcium aluminate solution and diluted calcium chloride solution in the presence of calcium hydroxide was studied formerly by Turriziani and Schippa. The precipitate being formed in this process was always a crystalline solid solution of Friedel's salt ($3CaO \cdot Al_2O_3 \cdot CaCl_2 \cdot 10H_2O$) and C_4AH_{13}. In this study the same reaction was re-examined, but extending the range to more saturated $CaCl_2$ solutions and the absence of calcium hydroxide as well. In the absence of calcium hydroxide, the precipitate is crystalline and completely amorphous if the $CaCl_2$ solution is diluted and concentrated, respectively. This change is not abrupt but gradual: $CaCl_2$ solutions of 0.5 molar or above cause amorphous, $CaCl_2$ solutions of 0.375 molar or less cause crystalline precipitates. The crystalline precipitates have an X-ray pattern very similar to that of Friedel's salt, but their chemical composition varies, aluminium content is always higher, calcium content always lower than indicated by the formula. The chloride contents are not volatilized by ignition: a common feature of crystalline and amorphous precipitates. Infrared spectra of the amorphous and crystalline phases differ quantitatively but are qualitatively similar. The two phases are entirely different under the electron microscope.

Introduction

The reaction between supersaturated aqueous monocalcium aluminate solution and aqueous calcium chloride solution yields precipitates. Composition and mineralogy of these solutions were cleared by the systematic study of Turriziani and Schippa (1): they consist of solid solutions of $C_3A \cdot CaCl_2 \cdot xH_2O$ and C_4AH_x. The $CaCl_2/Al_2O_3$ ratios of the products range from 0.1 to 1.0, this latter conforming to pure tricalcium aluminate-calcium chloride-dekahydrate (hereinafter called "Friedel's salt" for short).

However, the Italian authors have studied the reaction using rather diluted (56 g/l, i.e. roughly 0.5 mol/l as a maximum) calcium chloride solutions only; further this solutions were saturated in respect to $Ca(OH)_2$. It thus occurred promising to re-examine this reaction and extend the range towards more saturated $CaCl_2$ solutions, and without $Ca(OH)_2$-saturation too. As a further difference, pure monocalcium aluminate was used as a starting substance in this study as contrasted to the aluminous cement raw material of Turriziani and Schippa (1).

Experimental

Preparation of Samples

Supersaturated, metastable monocalcium aluminate solution was prepared by shaking synthetically produced, pure CA (containing no alkalies and free lime) for 30 mins with CO_2-free distilled water in polythene flasks. Shaking was done machinally at room temperature.

The clear, supernatant liquor was sucked down and added to an equal volume of $CaCl_2$-solution, of concentrations ranging from 0.125 M to 2.0 M. Precipitation occurred usually within a few seconds; the mixtures were allowed to stand for 1 hr, then filtered and washed with a little water.

All the mixing, shaking, filtering, and other operations were made in a controlled atmosphere cabinet (glove box) in pure nitrogen atmosphere. Distilled water was always used after a previous vigorous

*Central Research and Design Institute for Silicate Industry, Budapest, Hungary.

boiling for 10 mins; the hot water was cooled to room temperature in the glove box. These rigorous measures eliminated the danger of contamination of the products by airborne carbon dioxide against which they are extremely sensitive.

Sample preparation was made at laboratory temperature (about 22–25°C); some additional experiments were made at 0°C and 70°C too.

X-ray Investigation

Filtered precipitates were examined partly in moist state and partly after drying in a $NaOH + CaO$ filled desiccator. For the X-ray tests a Japanese diffractometer (Type Geigerflex, Rigaku-Denki) was used, with filtered Cukα radiation. The scanning speed was usually 1 deg/min; in some cases a lower speed was used to enable a better resolution.

Chemical Analysis

The precipitates were only partly soluble in nitric acid; thus they were analysed for CaO, Al_2O_3 and Cl^- after attacked with $KNaCO_3$. The melts were dissolved in diluted nitric acid and stock solutions made. CaO and Al_2O_3 were determined volumetrically by EDTA, Cl^- by adding an excess amount of 0.1N $AgNO_3$ and back-titrated with 0.1N NH_4SCN. All analytical results are given, on an anhydrous basis, in terms of mols taking the amount of Al_2O_3 as unit.

Results

The most striking result is that not all products are crystalline. The crystallinity of the product depends primarily on the concentration of the calcium chloride solution: dilute $CaCl_2$ solutions yield crystalline, concentrated ones amorphous precipitates. The limit is slightly below 0.5 M.

The crystalline products have a sharp pattern, diffraction peaks are intensive; positions and intensities are almost identical with those obtained by Turriziani and Schippa (1). Table 1 gives some characteristic crystalline patterns selected from more than 200 patterns of crystalline precipitates obtained during the last two years; additionally, two patterns published by the cited authors as well as that of standard Friedel's salt (card 2–0081 of the ASTM Powder Diffraction File). The similarity of the patterns is striking, though two peaks mentioned in the ASTM card are missing. But these two peaks have never been found in the präparat patterns neither during this study nor by the Italian authors, so they must be considered as incorrect data.

Table 1. *X-ray patterns of calcium aluminate chloride hydrates (d_{hkil} values in Å)*

1.	2.	3.	4.	5.	6.	7.
7.94 vs	8.10 vs	7.90 vs	7.76 vs	7.87 vs	7.96 s	7.86 vs
—	6.36 vw	—	4.77 w	4.79m?	—	5.13 w
4.36 w	4.45 w	4.35 w	4.35 w	4.35 m	—	4.42 w
3.94 s	4.01 s	3.94 s	3.92 s	3.95 s	3.96 m	3.93 s
3.83 w	3.88 w	3.80 w	3.83 m	3.89 w	3.83 vw	3.86 s
—	—	—	—	—	—	3.76 s*
3.46 w	—	—	3.42 vw	3.45 w	—	3.39 w
—	—	—	—	—	—	3.13 w*
2.88 m	2.89 w	2.87 m	2.88 m	2.88 m	2.88 w	2.86 s
2.79 vw	2.66 w	2.68 w	2.70 vw	2.71 w	—	2.79 w
—	—	—	2.61 m	2.63 w	—	2.68 m
2.63 w	2.59 w	2.54 w	2.54 vw	2.55 w	—	—
2.54 w	2.40 w	2.45 m	2.44 w	2.44 m	—	2.43 m
2.32 m	2.35 w	2.32 m	2.32 m	2.33 m	2.32 w	2.30 s (diff)
—	—	—	2.20 vw	—	—	2.19 w
2.13 m	2.18 m	2.14 m	2.13 m	2.14 m	2.14 vw	2.12 w
2.02 vw	2.00 m	—	—	—	2.02 vw	2.03 w
1.97 m	1.96 w	1.97 w	1.96 w	1.97 w	—	—
—	1.89 vw	—	—	—	—	—
1.71 m	1.74 vw	—	1.71 w	1.71 vw	—	1.70 w
1.63 vw	1.66 vw	—	1.66 w	1.66 vw	—	1.65 m

1. Preparate with $Al_2O_3/CaCl_2 = 1.0(1)$
2. Preparate with $Al_2O_3/CaCl_2 = 0.22(1)$
3. Preparate at lab. temperature with 0.25 m $CaCl_2$ soln. $Al_2O_3/CaCl_2 = 0.228$
4. Preparate at lab. temperature with 0.125 m $CaCl_2$ soln. $Al_2O_3/CaCl_2 = 0.205$
5. Preparate at 70°C temperature with 0.125m Ca Cl_2 soln. $Al_2O_3/CaCl_2$ n.d.
6. Preparate at lab. temperature with 0.450 m $CaCl_2$ soln. $Al_2O_3/CaCl_2 = 0.650$
7. Card No. 2-0081($3CaO \cdot Al_2O_3 \cdot CaCl_2 \cdot 10H_2O$) in ASTM Powder Diffraction File

*These two lines have never occurred in our samples.

The amorphous precipitates showed no peaks at all, not even the slightest trace of them; only one broad ring was visible extending over 20–25 degrees in more than 150 amorphous samples investigated.

The change in preparation temperature has had no marked effect upon the crystallinity of the precipitates.

To elucidate phenomena in more detail, additional experiments were made with $CaCl_2$ solutions in the concentration range between 0.250 and 0.500 M, in steps of 0.05 M; in the range of 0.450 and 0.500 M in steps of 0.005 M. For the examination of these samples a scanning speed of 1 deg/4 min. was chosen and only a narrow range, $\theta = 4$–8 deg. was scanned for the main (0001) peak of Friedel's salt and its solid solutions appear in this range. The relative intensities of this peak as read off from the diffractometer tracing against the background are given in Table 2.

As well seen from these data, the changeover from crystalline to amorphous is not abrupt but gradual.

Table 2. *Intensity of the (0001) peak in X-ray patterns of precipitates made with 0.250 M—0.500 M* $CaCl_2$ *solutions*

Molarity of $CaCl_2$ soln.	Intensity
0.250	100
.300	100
.350	100
.400	100
.450	78
.455	71
.460	68
.465	62
.470	38
.475	25
.480	5
.485	2
.490	0

In any case, the samples made with $CaCl_2$ solutions being more concentrated than 0.5 M are undoubtedly amorphous, and those with $CaCl_2$ solutions less concentrated than 0.400 M crystalline.

The chemical composition of the precipitates showed very great variability; at present this will not be discussed in detail. The ignition of samples at 1000°C for three hours causes no loss of Cl^-. The examination of thermal behavior of crystalline and amorphous substances has not been finished yet.

Infrared spectra of the crystalline and amorphous preparates are similar, though the crystalline samples give more distinct bands. OH stretching vibrations do not occur; the source of the double band in the range of 2800–3000 cm^{-1} is the Al–O stretching vibration. The 1480 cm^{-1} band is presumably due to water molecules coordinated to calcium.

Crystalline and amorphous preparates are entirely different under the electron microscope.

References

1. R. Turriziani and G. Schippa: "Contributo alla conoscenza degli allumino-chloruro complessi", Ricerca Scientifica **25**, 3102–3106 (1955).

Supplementary Paper II-81 Barium Aluminate and Barium Silicate and Their Hydraulic Properties

Hiroshi Uchikawa and Koichi Tsukiyama*

Synopsis

The crystal structure and hydraulic properties of principal hydraulic compounds of refractory barium aluminous cement ($BaAl_2O_4$) and rapid hardening barium silicate cement (Ba_2SiO_4) were investigated.

Crystal structure of $BaAl_2O_4$, Ba_2SiO_4 and their hydration products of $Ba(OH)_2 \cdot H_2O$, $BaAl_2O_4 \cdot 6.5H_2O$, $BaSiO_3 \cdot 6H_2O$ were precisely determined by electron diffraction of single crystal and powder X-ray diffraction using IBM 7040 and IBM 360 computer from the structure model and Patterson or Fourier synthesis.

Stoichiometry of the hydration of barium aluminate and barium orthosilicate was proposed by the identification of produced compounds based on the analysis of crystal structure, electronmicroscopic observation and liquid phase equilibrium.

Physical properties and structural change of barium aluminate and silicate hydrate under various atmosphere and at elevated temperature were discussed in relation to crystallographic consideration.

Introduction

It has been reported that there are two kinds of barium cement consisting mainly of barium aluminate ($BaAl_2O_4$) (1) and barium orthosilicate (Ba_2SiO_4) (2). The high refractoriness of barium aluminous cement and high early strength of barium silicate cement as well as the radioactive rays absorbing property have been interested in from the viewpoint of industrial utilization. But owing to the lack of the foundamental knowledge of the constituent compounds, produced hydrates and the mechanism of hydration, it has been very inconvenient for us to increase the production and utilization of these barium cements. In order to make clear these undissolved problems, the authors performed a series of crystal chemical studies on both of the hydrated and unhydrated barium aluminate and barium silicate as summerized later.

Method of the Precise Measurement of the Position and the Intensity of Diffracted X-ray Peak

X-ray diffraction was carried out using the powdered sample with X-ray diffractometer as it is too difficult to obtain the single crystal large enough to do single crystal X-ray diffractometry. Conditions of the X-ray diffraction are summerized in Table 1. The sample was finely ground to under five microns so as to avoid the preferred orientation of the crystal and the microabsorption effect of the X-ray. Silicon or magnesium oxide fine powder was used as an internal standard in order to determine the Bragg angle precisely and avoid the variation of the apparatus. Possible slow scanning speed and fine slit were selected to satisfy the relation of the time width. Five measurements were performed on each sample, and the error in this case was smaller than 0.01° in 2θ and 3% in intensity.

Table 1. *Conditions of X-ray diffraction*

X-ray	CuKα radiation (Ni filtered)
Distance from X-ray source to sample	180 mm
Distance from sample to receiving slit	180 mm
Width of receiving slit	0.2 mm
Horizontal divergence	1°
Vertical divergence	1°
Time constant	4 sec or 2sec
Scanning speed	1/4°/min
Ratemeter scale factor	8

*Central Research Laboratory, Onoda Cement Co., Ltd, Tokyo, Japan.

So we can conclude that the measurement has good reproducibility enough to use in the present work.

Method of the Determination of the Lattice Constants and the Atomic Coordinates

Reciprocal cell of a crystal is capable of being represented independently of its symmetry, as triclinic cell using six appropriate vectors. If we choose $E(\theta)$ as a function of systematic error, next equation is right in general case.

$$4\sin^2\theta = h^2a^{*2} + k^2b^{*2} + l^2c^{*2} + 2hka^*b^*\cos\gamma^* + 2hla^*c^*\cos\beta^* + 2klb^*c^*\cos\alpha^* + E(\theta)$$

Observed 2θ value and random sets of (hk$l$) are given to the computer as input in ascending order. The computer then solves the above-given equation by means of least square method as the observed 2θ values are numerous in comparison with variable reciprocal vectors. When calculated $1/d^2_{obs}$ is not fitted to observed $1/d^2_{cal}$, this set of (hk$l$) is eliminated as unsuitable. This procedure is repeated until all sets of (hk$l$) are satisfied by selected lattice parameter.

Atomic coordinates are first estimated roughly by means of Patterson synthesis and heavy atom method. Precise determination is performed by slight removal of the atoms considering the crystal symmetry and by the calculation of diffracted X-ray intensity to the corresponding positional parameter so as to minimize the

$$R(=\sum|(I_0)-(I_c)|/|I_0|) \text{ value.}$$

All calculation was carried out by the computers, types of which were IBM 7040 and IBM 360.

Barium Aluminate and Barium Orthosilicate

Crystal Structure of Barium Aluminate ($BaAl_2O_4$)

Precedent Works

In 1937, X-ray diffraction data on barium aluminate was first reported by S. Wallmark and A. Westgren (3). Structural survey for a series of K_2AlSiO_4, $BaAl_2O_4$, K_2LiSO_4 and Na_2AlSiO_4 has been performed by W. Nowachi (4) using the relationship to β-tridymite, but the precise determination of $BaAl_2O_4$ cell and atomic coordinates have not been clarified. Recently, precise determination of $BaAl_2O_4$ structure and certification of the formation of the iron-bearing solid solution were reported by the authors (5).

Precise Determination of the Lattice Constants and Atomic Coordinates.

$BaAl_2O_4$ was synthesized by heating the stoichiometric mixture of barium carbonate and α-Alumina in a electric furnace at 1500°C for four hours. The chemical compositions and specific gravity and powder X-ray diffraction patterns of synthesized $BaAl_2O_4$ are shown in Table 2 and Fig. 1. Indexing of the powder diffraction peaks was carried out by referring the S. Wallmark and A. Westgrens' crystal data (3)

Table 2. *Chemical composition, specific gravity and refractive index of* $BaAl_2O_4$.

Compound	Chemical composition				Free BaO	Specific gravity (g/cm³)	Refractive index (20°C)
	Ig. loss	Al_2O_3	BaO	Total			
$BaAl_2O_4$	0.28	39.54	60.07	99.89	0.01	4.004	1.682 ± 0.003

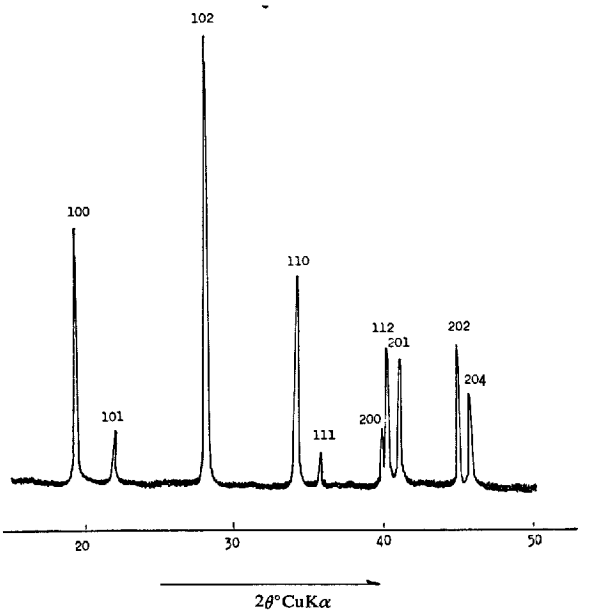

Fig. 1. *Powder X-ray diffraction pattern of* $BaAl_2O_4$

considering the close resemblance of the pattern. The unit cell dimensions determined by means of a least-squares treatment were $a = 5.224$ Å, $c = 8.777$ Å. Assuming that $Z = 2$, the density at room temperature was calculated as 4.087 g/cm³, which was good agreement with observed density (4.004 g/cm³).

(hk*l*) reflections are observed only when (00*l*) is even, which corresponds to the space group D_6^6–$P6_322$.

A two dimentional Fourier synthesis with reflection normal to *c*-axis and at intervals of 1/120 along *a*- and *c*-axis was computed by IBM 7040 computer using the atomic coordinates reported by W. Nowachi (4). From the calculated electron density distribution diagram of $BaAl_2O_4$, the interval of positional parameter of aluminum correspond to the same electron density along *z* direction was determined as ± 0.009 and oxygen along x direction as ± 0.08. Possible positional parameter of aluminum and six oxygen atom were selected from each of fifty values from -0.05 to 0.15 along *c*-axis and from 0.16 to 1.16 along *a*-axis, respectively. With these 2500 sets of positional parameters, structure of $BaAl_2O_4$ was refined by comparing the calculated intensities with observed one. When suitable atomic coordinates are selected, final *R* value for all observed reflections was 0.175, which is better than $R = 0.181$ obtained from our calculation to W. Nowachi's atomic coordinates. Final atomic coordinates of $BaAl_2O_4$ are given in Table 3. Observed diffracted X-ray intensities, calculated structure factors and intensities are shown in Table 4. The interatomic distances calculated from above-mentioned atomic coordinates are listed in Table 5.

Crystal Structure

The atomic arrangement projected along *c*- and *b*-axis is shown in Fig. 2. Two barium atoms in special position in the cell are situated at 1/4 and 3/4 level of *c*-axis and four AlO_4 in the unit cell form distorted tetrahedron with covalent bonding. Each of the oxygen situated at the apex of AlO_4 tetrahedra is shared with two inversed AlO_4 tetrahedra. Other three basal oxygens are situated at the same levels along *c*-axis. The average Al–O distance in AlO_4 tetrahedra is 1.79 Å, which shows good coincidence with 1.78 Å obtained by J. W. Smith (6). Another average value is reported in anorthite as 1.788 Å and 1.719 Å ac-

Table 3. *Atomic coordinates of* $BaAl_2O_4$

Atom	Atomic coordinate		
	x	y	z
Ba_1	0	0	0.250
Ba_2	0	0	0.750
Al_1	0.333	0.667	0.046
Al_2	0.667	0.333	0.954
Al_3	0.667	0.333	0.546
Al_4	0.333	0.667	0.454
O_1	0.333	0.667	0.250
O_2	0.667	0.333	0.750
O_3	0.647	0	0
O_4	0	0.647	0
O_5	0.353	0.353	0
O_6	0.647	0	0.500
O_7	0	0.647	0.500
O_8	0.647	0.647	0.500

Table 4. *Comparison of calculated structure factors and intensities of* $BaAl_2O_4$ *with observed intensities*

h k l	W. Nowachi		Authors		$I_{obs.}$
	$\|F_{cal.}\|$	$I_{cal.}$	$\|F_{cal.}\|$	$I_{cal.}$	
1 0 0	70.6	52.7	66.9	43.8	52.7
1 0 1	25.1	10.5	24.3	9.1	12.1
1 0 2	98.7	100.0	102.6	100.0	100.0
1 1 0	116.0	47.5	116.3	44.3	46.2
1 1 1	37.0	8.9	36.4	8.0	11.5
2 0 0	59.8	9.5	66.0	10.7	13.7
1 1 2	88.6	41.3	87.4	37.1	24.2
2 0 1	206.0	20.0	199.0	19.5	20.0
2 0 2	87.7	32.5	82.5	26.7	25.8
1 0 4	68.7	19.2	64.6	15.7	15.9
2 1 0	54.2	9.0	54.8	8.5	7.1
1 1 4	80.5	19.3	84.0	19.4	14.3
2 1 2	80.4	34.6	80.2	31.9	26.9
2 0 4	63.0	10.4	66.1	10.6	11.5
3 0 0	137.6	22.8	136.3	20.7	11.0
0 0 6	60.9	1.4	56.6	1.1	6.0
1 0 6	60.0	7.4	63.6	7.7	8.8
2 1 4	58.8	13.5	57.9	12.1	9.9
2 2 0	89.5	7.3	90.3	6.9	6.0
1 1 6	93.1	15.2	89.0	12.9	9.3

Table 5. *Interatomic distances of various ions in* $BaAl_2O_4$

a) Al–O bonds, in Å

Key number of tetrahedron	Atoms		Length
	Al	O	
1	Al_1	O_1	1.790
	Al_1	O_4	1.737
	Al_1	O_5	1.821
	Al_1	O_9	1.745
2	Al_2	O_2	1.791
	Al_2	O_3	1.730
	Al_2	O_5	1.699
	Al_2	O_{12}	1.772
3	Al_3	O_2	1.791
	Al_3	O_6	1.699
	Al_3	O_8	1.750
	Al_3	O_{11}	1.772
4	Al_4	O_1	1.791
	Al_4	O_7	1.740
	Al_4	O_8	1.735
	Al_4	O_{10}	1.817

Mean value of tetrahedral Al–O bonds is 1.761 Å

c) Ba–O bonds, in Å

Atoms	Length
Ba_1—O_5	2.841
Ba_1—O_7	2.865
Ba_2—O_7	2.867
Ba_2—O_6	2.842

b) O–O bonds in Å

Atoms	Length
O_1—O_4	2.770
O_1—O_5	2.823
O_1—O_9	2.774
O_5—O_4	3.000
O_6—O_8	2.868
O_4—O_9	2.932
O_5—O_9	2.774
O_6—O_{11}	2.927
O_1—O_8	2.768
O_8—O_{11}	3.000
O_1—O_{10}	2.820
O_7—O_8	2.931
O_2—O_{11}	2.793
O_7—O_{10}	3.000
O_8—O_{10}	3.000
O_2—O_3	2.765
O_2—O_5	2.747
O_2—O_{12}	2.791
O_3—O_5	2.849
O_3—O_{12}	2.983
O_5—O_{12}	2.927
O_2—O_6	2.747
O_2—O_8	2.779
O_1—O_7	2.770
Means	2.856

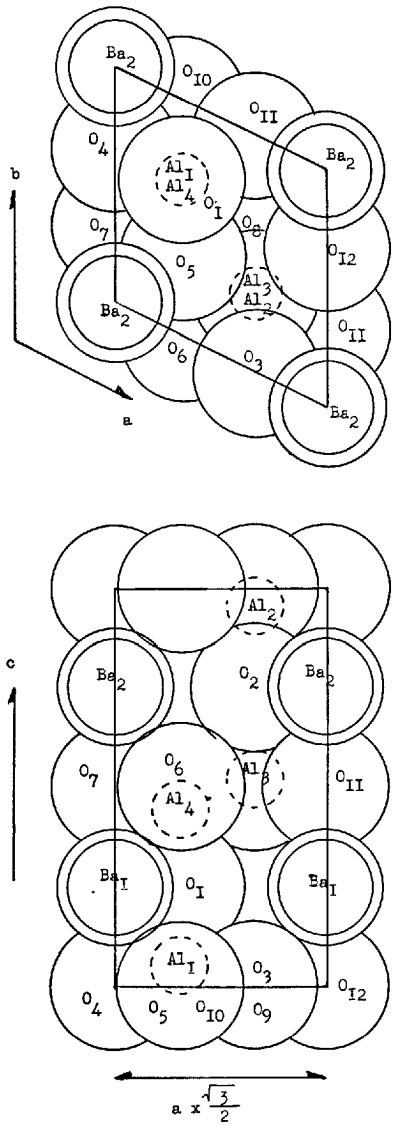

Fig. 2. *Packing diagram of* $BaAl_2O_4$

cording to its AlO_4 structure (7) and 1.77 Å in layer silicate minerals (8). Obtained Al–O distances in $BaAl_2O_4$ are considered to be reasonable compared with the generally accepted values with the character of covalent bonding. Average interatomic distance of O–O and Ba–O are 2.86 Å and from 2.84 to 2.87 Å, respectively, which indicate the ionic bonding.

Iron-Bearing Solid Solution

Powder X-ray diffraction pattern of the sample synthesized by the addition of ferric oxide showed the expansion of cell as shown in Table 6 and Table 7. The degree of lattice expansion was variable according to the content of Fe_2O_3 which indicates the formation of iron-bearing solid solution. To account for the

Table 6. *Interplaner spacing of iron bearing solid solutions*

Fe_2O_3 added (%)	Interplaner spacing d(Å)						
h k l	0	1.0	3.0	5.0	7.5	10.0	15.0
2 0 1	2.1975	2.1974	2.1976	2.2015	2.2001	2.2212	2.1959
2 0 2	2.0104	2.0111	2.0153	2.0162	2.0170	2.0128	2.0153
1 0 4	1.9769	1.9754	1.9786	1.9803	1.9794	1.9918	1.9770
2 1 0	1.7095	1.7095	1.7125	1.7153	1.7172	1.7166	1.7137
1 1 4	1.6814	1.6811	1.6828	1.6845	1.6857	1.6851	1.6828
2 1 2	1.5928	1.5923	1.5958	1.5988	1.5992	1.5994	1.5973
2 0 4	1.5759	1.5764	1.5778	1.5803	1.5788	1.5803	1.5778
3 0 0	1.5072	1.5074	1.5105	1.5122	1.5134	1.5136	1.5127
0 0 6	1.4642	1.4646	1.4654	1.4665	1.4668	1.4667	1.4658
1 0 6	1.3937	1.3933	1.3952	1.3959	1.3955	1.3937	1.3937
2 1 4	1.3492	1.3486	1.3479	1.3496	1.3496	1.3493	1.3486
1 1 6	1.2777	1.2775	1.2787	1.2799	1.2799	1.2769	1.2787

Table 7. *Change of lattice constants by the formation of solid solution with* Fe_2O_3.

Quantities of added Fe_2O_3(%)	Lattice constant (Å)	
	a	c
0	5.224	8.777
1.0	5.225	8.777
3.0	5.233	8.779
5.0	5.239	8.796
7.5	5.240	8.797
10.0	5.244	8.789
15.0	5.258	8.734

mechanism of the substitution and the situation of iron ions in $BaAl_2O_4$, the diffracted X-ray intensities of high (hk*l*) reflection were calculated in the following three cases on the assumption that the space group of $BaAl_2O_4$ is kept independent to the formation of solid solution and the X-ray scattering of oxygen atoms interfere with each other, consequently intensities of $BaAl_2O_4$ and iron-bearing $BaAl_2O_4$ are affected only by the atomic scattering factor of aluminum and iron ion.

1) Fe^{3+} substitutes at random for Al^{3+}
2) Fe^{3+} substitutes systematically for the two Al^{3+}(Al_3^{3+} and Al_4^{3+})
3) Fe^{3+} substitutes for one Al^{3+}(Al_4^{3+})

Fig. 3. shows the observed relationship between diffracted X-ray intensities and quantities of added Fe_2O_3, and Fig. 4. does the relation between calculated relative intensities and quantity of added Fe_2O_3 to the above-mentioned three cases. Iron bearing solid solution is considered to be formed by the systematic substitution of two Al^{3+}(Al_3^{3+}, Al_4^{3+}) or one Al^{3+}(Al_4^{3+}) when substituted quantities of Fe^{3+} is small, but over 10% random substitution of Al^{3+} occurs accom-

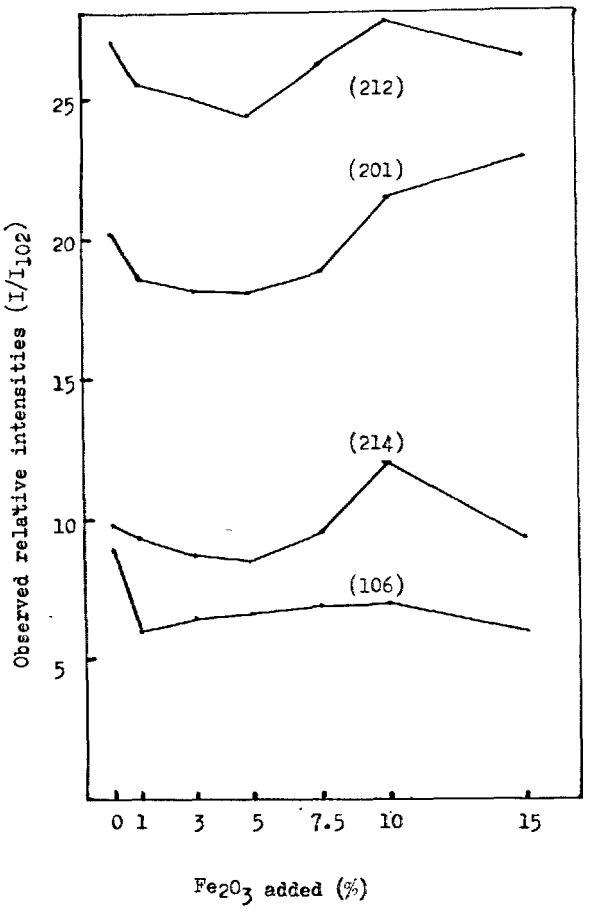

Fig. 3. *Relation between observed relative intensities and the quantity of added* Fe_2O_3

panying with the partial transformation of the coordination of Fe^{3+} from FeO_4 to FeO_6.

Crystal Structure of Barium Orthosilicate (Ba_2SiO_4)

Precedent Work

Crystal structure of Ba_2SiO_4 was proposed by H. O'Daniel and L. Tscheischwilli (9) that this compound belongs to orthorhombic system with $a = 5.77$ Å, $c = 7.56$ Å as a series of structural studies on the orthosilicates such as K_2BeF_4 and $SrSiO_4$. H. P. Rooksby (10) suggested that the structure of Ba_2SiO_4 has a close resemblance to β-K_2SO_4 and E. M. Levin and G. M. Ugrinic (11) measured the interplaner spacing and relative intensities of Ba_2SiO_4 by powder X-ray diffraction. The structure of Ba_2SiO_4 has been considered isostructural with β-K_2SO_4 from the close resemblance of both ionic radius of barium to potassium and silicon to sulfur as well as $(SiO_4)^{2-}$ to $(SO_4)^{2-}$.

Recently indexing of powder X-ray diffraction patterns and the precise determination of lattice constants and atomic coordinates of Ba_2SiO_4 using structure model of β-K_2SO_4 were reported by the authors (12).

Indexing of the Powder X-ray Diffraction Patterns and Precise Determination of Lattice Constants

Ba_2SiO_4 was synthesized stoichiometric mixture of guaranteed reagents of barium carbonate and silicic anhydride powder by heating in platinum crucible in electric furnace at 1500°C for seven hours. Chemical compositions, refractive indices and powder X-ray pattern are shown in Table 8 and Fig. 5.

Table 8. *Chemical compositions, specific gravity and refractive indices of synthesized* Ba_2SiO_4

Synthesized sample	Ig. loss	SiO_2	BaO	Total	Free BaO	Specific gravity (g/cm³)	Refractive index (20°C)
Ba_2SiO_4	0.29	17.25	82.19	99.73	0.05	5.427	n = 1.80 n = 1.80 n = 1.826

Powder X-ray diffraction peaks of barium orthosilicate were indexed by using the H. O'Daniel and L. Tscheischwilli's (9) approximate cell constants. Then precise cell constants were determined from previously obtained (hk*l*) and the precise peak position by the aid of least square method. The lattice constants obtained by these procedures were $a = 5.772$ Å, $b = 10.225$ Å, $c = 7.513$ Å. The extinctions of (0k*l*) with $k + l = 2n + l$, (hk0) with $h = 2n + l$ and (h00) (0k0) (00*l*) with h, k, $l = 2n + l$ lead to the determined space group D_{2h}^{16}–Pmcn.

Atomic Coordinate

From the above-mentioned space group, presumed structure was built up on the assumption that eight barium atoms were placed in position (4c), four silicon atoms and eight oxygen atoms in (4c) and the other eight oxygen atoms in (8d) to form the exact tetrahedron of SiO_4 keeping 1.61 Å of Si–O distance. Diffracted X-ray intensities were calculated for each of barium atom with systematically variable positional parameters of 81 cases for range of 6.37% of b value along b-axis and 6.06% of c value along c-axis. While x coordinate was fixed on the mirror plane. The atomic coordinates in the first approximation obtained in comparison with calculated and observed diffracted X-ray intensities are shown in

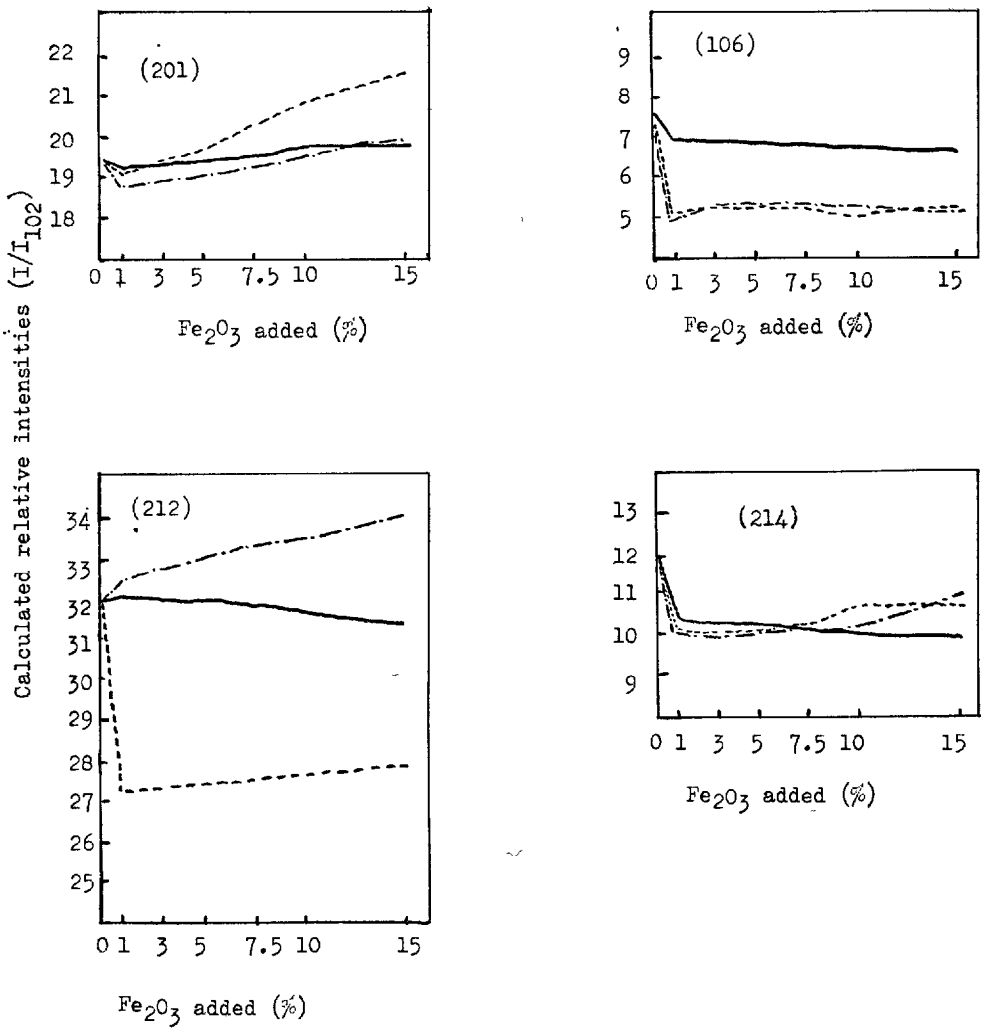

Fig. 4. *Relation between the calculated relative intensities and the quantity of added* Fe_2O_3

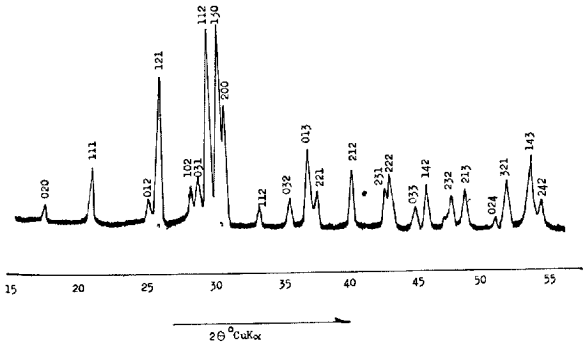

Fig. 5. *Powder X-ray diffraction pattern of synthesized* Ba_2SiO_4

Table 9. Obtained R value in this case was 0.249.

The same procedure was applied to the determination of silicon and oxygen atomic coordinates to attain

Table 9. *Atomic coordinates of* Ba_2SiO_4 *obtained by the first approximation*

	Atomic coordinate					
Parameter	Ba_1	Ba_2	Si	O_1	O_2	O_3
x	0.2500	0.2500	0.2500	0.2500	0.2500	0.0410
y	0.0761	0.7046	0.4155	0.4032	0.5579	0.3482
z	0.1768	−0.0123	0.2358	0.0315	0.2970	0.2997

the more accurate results. The range of variation of the positional parameter is ±2.90% of *b* value along *y* direction, ±2.66% of *c* value along *z* direction and *x* coordinate was fixed on mirror plane. For the oxygen atoms, range of the variation of positional parameter is the same as Si atom except for 1.64% of a value along *x* coordinate. From this, the final refined

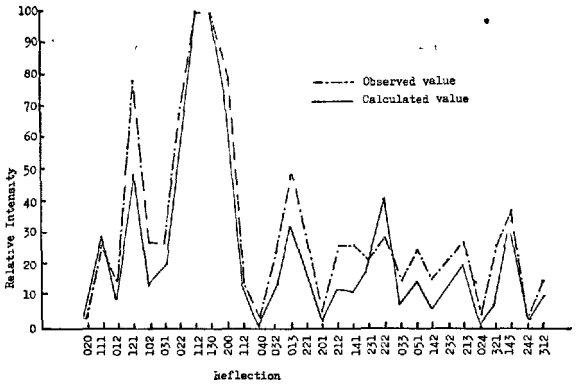

Fig. 6. *Comparison of the observed and the calculated intensities using the atomic coordinates shown in Table 10*

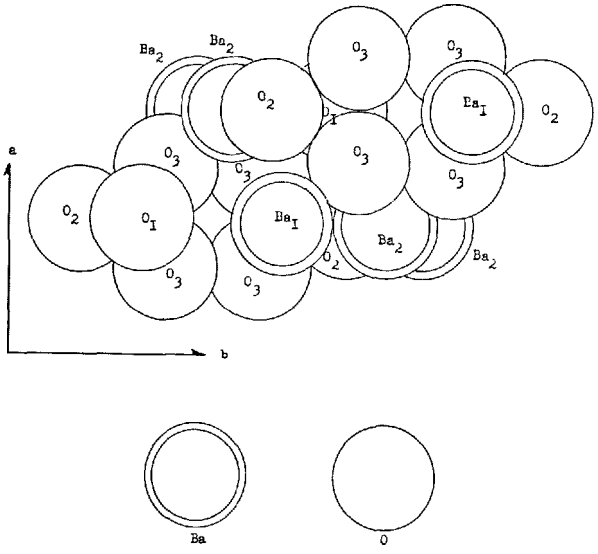

Fig. 7. *Packing of atoms in the* Ba_2SiO_4 *structure with their ionic sizes*

atomic coordinates for Ba_2SiO_4 are obtained as shown in Table 10. Calculated F value and the comparison with observed diffracted X-ray intensities are shown in Fig. 6.

Reliability calculated from thirty peaks was 0.171, which is better than the *R* value of 0.249 in first approximation. Interatomic distances in Ba_2SiO_4 structure are listed in Table 11.

Crystal Structure

Packing diagram of Ba_2SiO_4 illustrated by the sphere with their ionic radius is given in Fig. 7. In Fig. 8. are shown ab, bc projection of Ba_2SiO_4 structure about barium atom and SiO_4 group. Ba_1, Ba_2, Si, O_1 and O_2 atom are situated on the mirror plane perpendicular to *a*-axis and SiO_4 forms distorted tetrahedron having 1.60 Å, 1.67 Å and 1.61 Å intera-

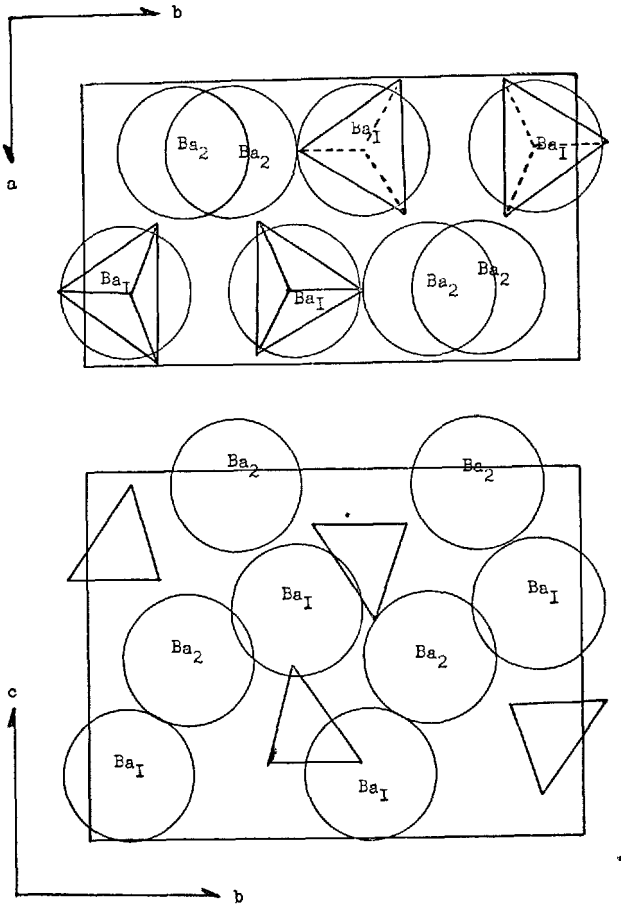

Fig. 8. ab, bc-*projection of the* Ba_2SiO_4 *structure*

Table 10. *Determined atomic coordinates of* Ba_2SiO_4

Atomic coordinate	Ba_1	Ba_2	Si	O_1	O_2	O_3
x	0.2500	0.2500	0.2500	0.2500	0.2500	0.0324
y	0.0761	0.7046	0.4445	0.4322	0.6019	0.3715
z	0.1768	−0.0123	0.2624	0.0488	0.3236	0.3523

Table 11. *Interatomic distances*

Atom	Distance (Å)
Ba_1—O_1	2.79
Ba_1—O_2	3.22
Ba_1—O_3	2.79
Ba_2—O_1	2.82
Ba_2—O_2	2.74
Ba_2—O_3	2.76
Si—O_1	1.61
Si—O_2	1.69
Si—O_3	1.60
O_1—O_2	2.70
O_1—O_3	2.67
O_2—O_3	2.68

tomic distances of Si–O_1, Si–O_2 and Si–O_3. As O_2 atom is influenced by the neighbouring Ba_2, Si–O_2 distance is somewhat larger than in the exact SiO_4 tetrahedron. Resonanced structure of double and single bond of Si–O is suggested from the value 1.77 Å observed in the single covalent bond. Average interatomic distance of Ba and O was 2.87 Å which indicate the ionic bonding of Ba–O in Ba_2SiO_4.

Hydration of Barium Aluminate and Barium Orthosilicate

Stoichiometry of the Hydration of Barium Aluminate and Barium Orthosilicate

Precedent Work

Al. Braniski (1) reported the equation on the hydration of $BaAl_2O_4$ and Ba_2SiO_4 but no detailed explanation for the derivation of the equation has yet been attempted.

Stoichiometry of the Hydration

One of the produced barium aluminate hydrate and barium orthosilicate are $BaAl_2O_4 \cdot 6.5H_2O$ and $BaSiO_3 \cdot 6H_2O$ mentioned later. In the hydration of $BaAl_2O_4$ initially liberated $Ba(OH)_2 \cdot H_2O$ was consumed in the process of hydration as shown in Fig. 9. On the contrary, $Ba(OH)_2 \cdot H_2O$ was recognized in the later stage of hydration in Ba_2SiO_4 by powder X-ray diffraction of hydrated specimen. Electronmicroscopic observation of the sample obtained from the early stage of hydration of $BaAl_2O_4$ indicates the gel hydrate of $Al(OH)_3$. In the early stage of hydration of Ba_2SiO_4, thin plate of $BaSiO_3 \cdot 6H_2O$ and spindle shaped $Ba_2SiO_4 \cdot nH_2O$ were observed, but the latter disappeared with the passage of time (Fig. 11, Photo 4 and 5). From these experimental results we supposed the stoichiometry of the hydration of $BaAl_2O_4$ and Ba_2SiO_4 as follows:

$BaAl_2O_4$

$$2BaAl_2O_4 + 11.5H_2O = BaAl_2O_4 \cdot 6.5H_2O + Ba(OH)_2 \cdot H_2O + 2Al(OH)_3 \quad \text{(initial reaction)}$$

$$BaAl_2O_4 + Ba(OH)_2 \cdot H_2O + 7H_2O = Ba_2Al_2O_5 \cdot 9H_2O \quad \text{(successive reaction)}$$

$$3BaAl_2O_4 + 18.5H_2O = BaAl_2O_4 \cdot 6.5H_2O + Ba_2Al_2O_5 \cdot 9H_2O + 2Al(OH)_3 \quad \text{(reaction as a whole)}$$

Ba_2SiO_4

$$Ba_2SiO_4 + nH_2O = Ba_2SiO_4 \cdot nH_2O \quad \text{(reaction at early stage)}$$

$$Ba_2SiO_4 \cdot nH_2O + (8-n)H_2O = BaSiO_3 \cdot 6H_2O + Ba(OH)_2 \cdot H_2O \quad \text{(reaction at later stage)}$$

$$2Ba_2SiO_4 + 8H_2O = BaSiO_3 \cdot 6H_2O + Ba(OH)_2 \cdot H_2O \quad \text{(reaction as a whole)}$$

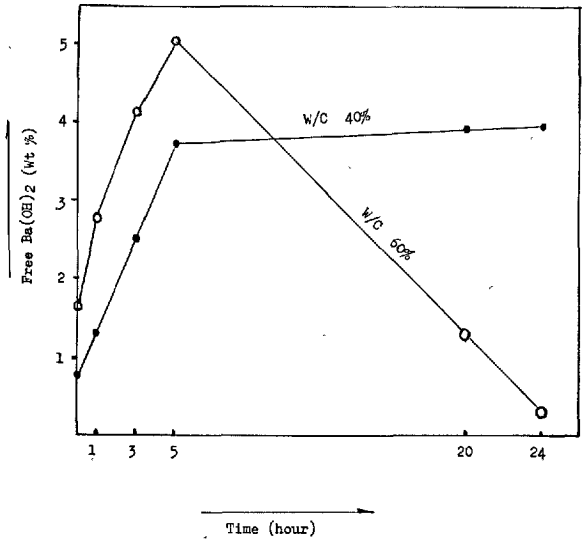

Fig. 9. *Change of produced barium hydroxide in the hydration of* $BaAl_2O_4$

Equilibrium Relationships of Liquid Phase in the Initial Stage of Hydration

The process of the dissolution of unhydrated compounds was followed by the chemical analysis of liquid phase separated from hydrated specimen. Relation between molar concentration of each ion in aqueous solution and time of hydration are summarized in Fig. 10 (13).

Composition of Liquid Phase in the Hydration of $BaAl_2O_4$

Stepwise change in the composition was recognized as in Fig. 10. Increase in concentration in the first step corresponds to initial hydration which contains the absorption of water to the surface of unhydrated particles, the diffusion of water into unhydrated particles, the formation of thin rectangular and gel-like hydrate.

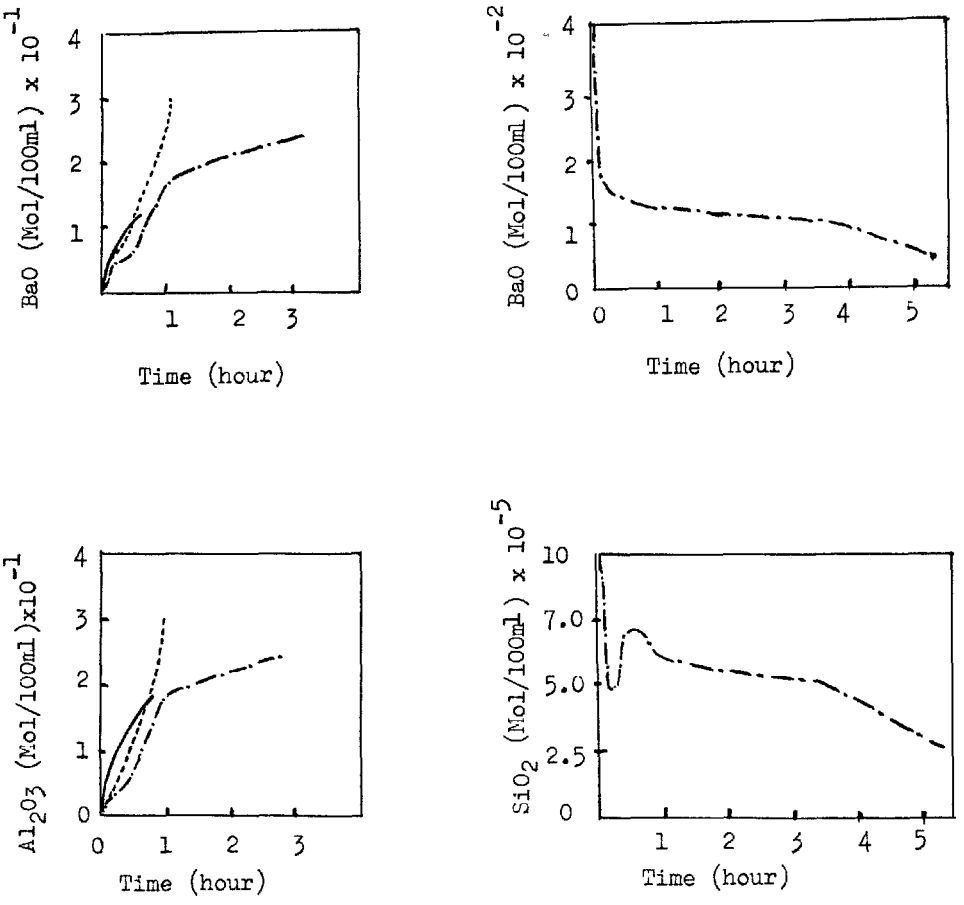

Fig. 10. *The compositions of liquid phase in the early stage of hydration of* $BaAl_2O_4$ *and* Ba_2SiO_4

In this period the vivid dissolution of unhydrate is predominant over the crystallization of hydrate, so the concentration of barium and aluminum ion increases until equilibrium is completed. The second step has to do with the successive reaction mentioned before. High ion concentration in low content of water is considered to be caused by the high super satulation concentration in equilibrium state. As little liberated $Ba(OH)_2 \cdot H_2O$ is recognized, when monoclinic hydrate is produced, from the equimolecular relation between BaO and Al_2O_3 in liquid phase, it comes to a conclusion that the rectangular barium aluminate hydrate is equimolecular compound.

Composition of Liquid Phase in the Hydration of Ba_2SiO_4

As the hardening of Ba_2SiO_4 is quick, the separation of liquid phase was very difficult without addition of large quantity of water. Barium ion concentration showed monotonous decreasing while silicon ion showed maximum value at thirty minutes after mixing with water, but its absolute value was very small in comparison with barium ion.

Hydraulic Properties of $BaAl_2O_4$

Electronmicroscopic Observation

Electronmicrographs of hydrated barium aluminate in W/C = 0.6 at room temperature are shown in Fig. 11 (14). At thirty minutes after mixing, thin plate like crystal of $BaAl_2O_4 \cdot 6.5H_2O$ and groups of minute granular substance of $Al(OH)_3$ were produced among the unhydrated particles. Besides these substances, spherical hydrates of $Ba(OH)_2 \cdot H_2O$ were recognized (Fig. 11, Photo 1). At one hour after mixing, plate like hydrates gradually widened into rectangular plate and spheric hydrate disappeared (Fig. 11, Photo 2). After five hours of hydration rectangular crystal increased the thickness and irregular polyhedral hydrate which was considered to be $Ba_2Al_2O_5 \cdot 9H_2O$ from the hexagonal pattern of electron diffraction was appeared (Fig. 11, Photo 3a, b).

Degree of Hydration

Degree of hydration of $BaAl_2O_4$ calculated from the ignition loss, free $Ba(OH)_2$ and unhydrated $BaAl_2O_4$ measured by quantitative X-ray diffraction analysis are shown in Fig. 12 (14). The larger the water content, the higher was the rate of hydration of $BaAl_2O_4$. One of the reason for this is supposed to be the higher

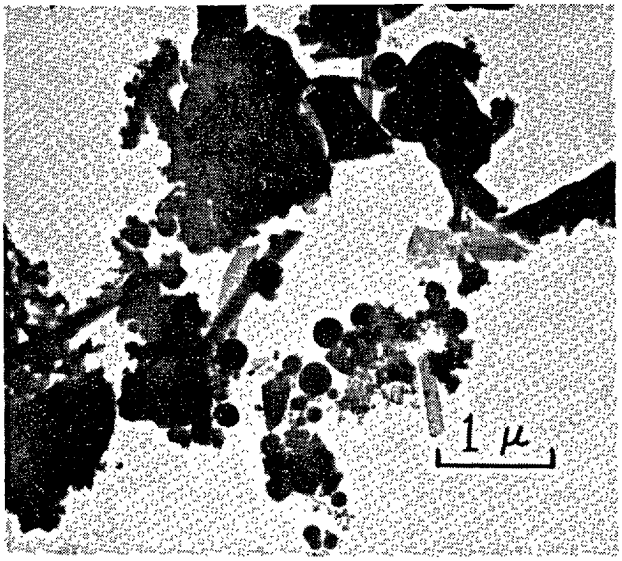

Photo 1. *W/C = 0.6, 30 minutes after mixing* ($BaAl_2O_4$)

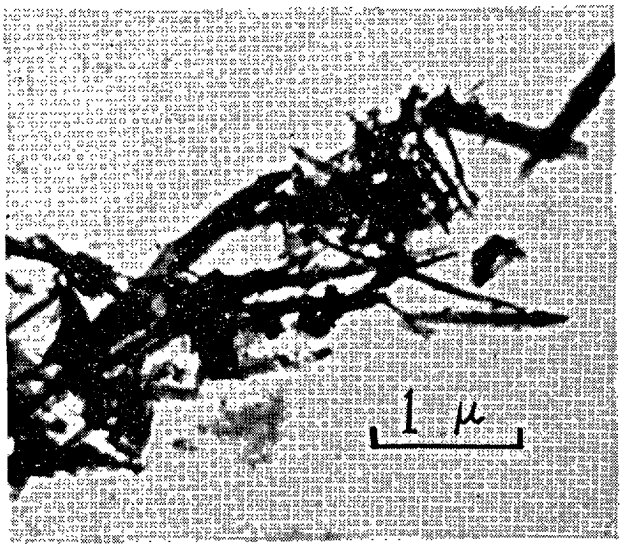

Photo 2. *W/C = 0.6, 1 hour after mixing* ($BaAl_2O_4$)

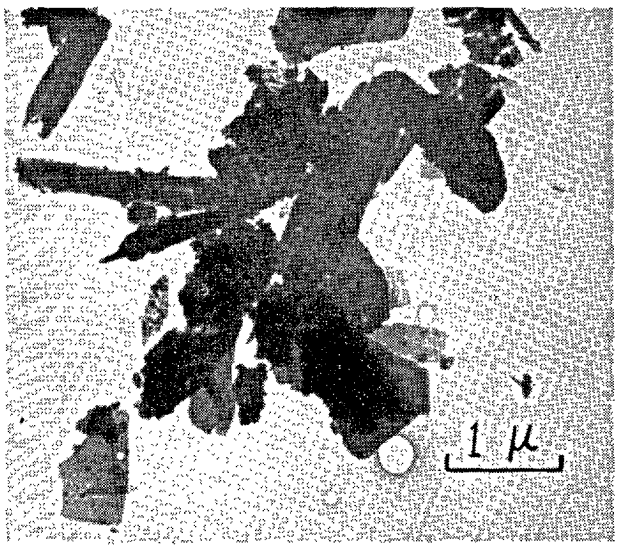

Photo 3a. *W/C = 0.6, 5 hours after mixing* ($BaAl_2O_4$)

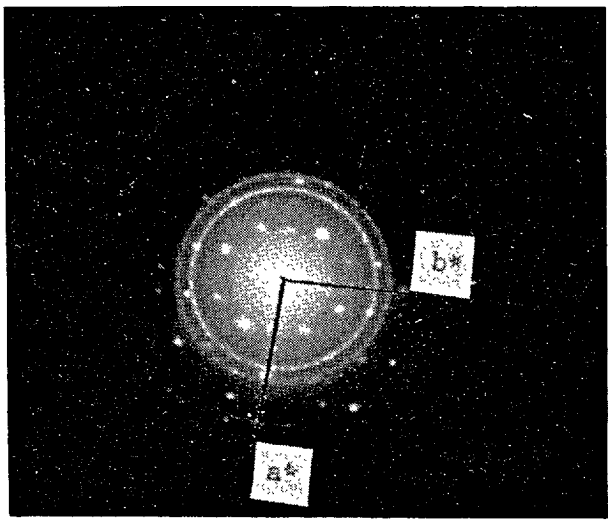

Photo 3b. *W/C = 0.6, 5 hours after mixing; Electron diffraction pattern* ($BaAl_2O_4$)

(Fig. 11.)

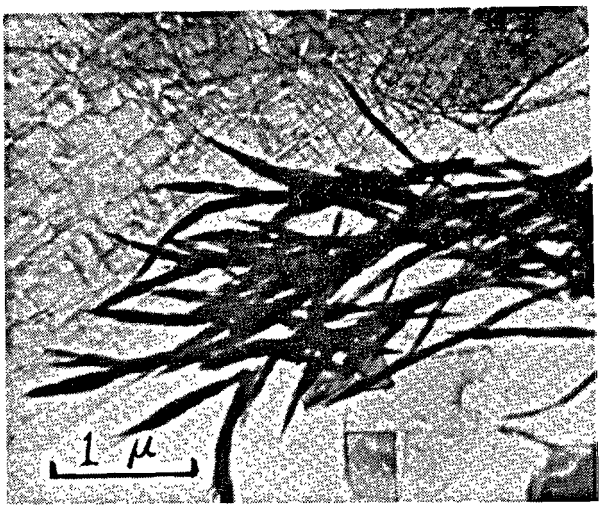

Photo 4. *W/C = 2.0, 15 minutes after mixing* (Ba_2SiO_4)

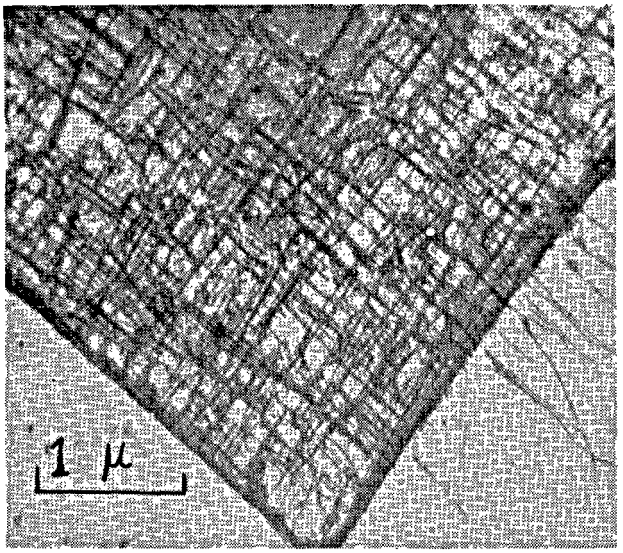

Photo 5. *W/C = 2.0, 1 hour after mixing* (Ba_2SiO_4)

Fig. 11. *Electronmicrographs of hydrated* $BaAl_2O_4$ *and* Ba_2SiO_4

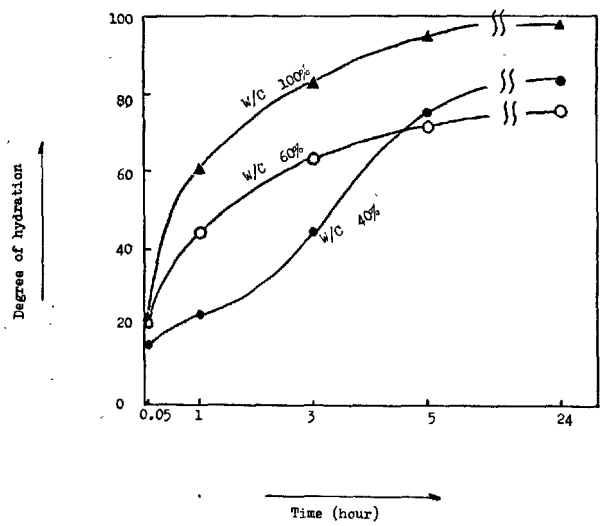

Fig. 12. *Degree of hydration of* $BaAl_2O_4$ *measured by means of X-ray diffraction*

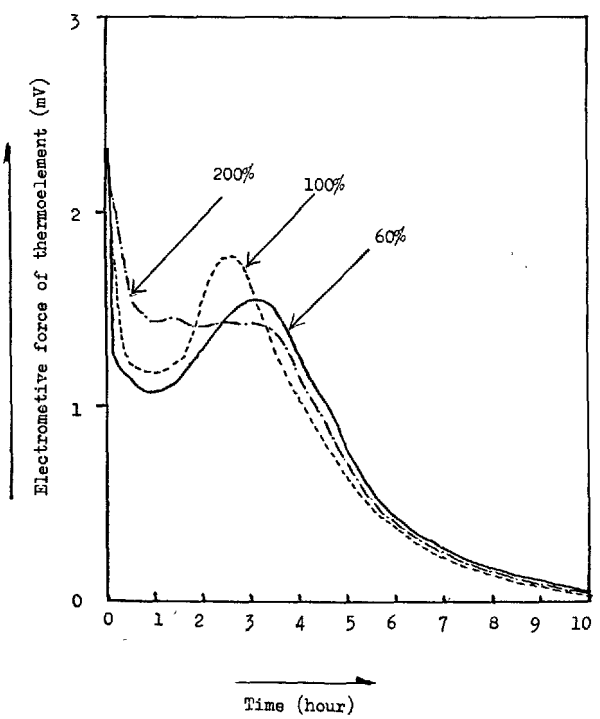

Fig. 13. *Liberated heat in the hydration of* $BaAl_2O_4$ *measured by conduction calorimeter*

rate of dissolution of $BaAl_2O_4$ caused by the large gradient of concentration between the liquid and the margin of $BaAl_2O_4$. The other is low rate of deposition of hydrate on account of the smaller degree of liquid saturation, which helps the development of crystal and deposition of hydrates apart from unhydrated $BaAl_2O_4$. The third is the formation of skeleton structure even if the hydrate deposits around the unhydrated particles. The period of the appearance of these hydrates is variable owing to the difference of the activity of synthesized $BaAl_2O_4$ and of other conditions such as fineness, water content, temperature.

Rate of Liberation of Heat in the Early Stage of Hydration

The rate of heat liberation in the early stage of hy-

dration of $BaAl_2O_4$ was measured by conduction calorimeter. Heat distribution curves consist of three divisions as shown in Fig. 13 (15). The first peak immediately after mixing with water is considered to be caused by the rapid hydration of directly contacted active $BaAl_2O_4$. The formation of porous film of hydrates on the surface of $BaAl_2O_4$ particles is responsible to the successive flat division appeared two hours after mixing, but this is different essentially from the dormant period recognized in the hydration of portland cement owing to higher electromotive force of some ten times than in the case of portland cement. The final peak at later than three hours is supposed to occur from the partial destruction of hydrates film caused by the formation of different hydrate such as $Ba_2Al_2O_5 \cdot 9H_2O$ by the consumption of $Ba(OH)_2 \cdot H_2O$. The sum of the liberated heat within one day was about 80–90% of the heat of hydration measured by the specimen cured for six months.

Table 12. *Heat of hydration calculated from heat of solution*

Water (%)	Heat of hydration (cal/g)			
	1 day	3 days	7 days	6 months
40	69.2	72.8	75.8	80.4
60	72.3	76.3	78.6	

Heat of Hydration

Heat of hydration of $BaAl_2O_4$ in various curing period calculated from the heat of solution to mixed strong acid of 4N–HNO_3 and hydrofluoric acid is listed in Table 12.

From Table 12 heat of complete hydration is considered to be about 80 cal/g. In some case of larger water content than 60%, reduction of the heat of hydration observed in longer period of curing. This may probably suggest the transformation to another stable phase.

Crystal Structure of Barium Hydroxide, Barium Aluminate Hydrate and Barium Silicate Hydrate

Crystal Structure of Barium Hydroxide Monohydrate ($Ba(OH)_2 \cdot H_2O$)

Precedent Work

The coordination polyhedra of hydrated barium compounds such as $Ba(OH)_2 \cdot 8H_2O$ and $Ba(ClO_4) \cdot 3H_2O$ were reported that barium atom is coordinated by eight water oxygens in the former, while in the latter coordinated by twelve oxygen (16). No investigation, however, was intended to analyse the crystal structure of barium hydroxide monohydrate.

Determination of Lattice Constants and Other Crystallographic Data

Sample to be analysed was obtained from the hydrated Ba_2SiO_4 specimen for six months which contained about 50% of $Ba(OH)_2 \cdot H_2O$. Considering the strong resemblance of powder X-ray diffraction pattern and the ionic radius of metallic ion to $Sr(OH)_2 \cdot H_2O$ and $Eu(OH)_2 \cdot H_2O$ (17), isostructure was presumed on the $Ba(OH)_2 \cdot H_2O$. Approximate lattice constants of a and b were obtained from (hk0) reflection taken by the electron diffraction of $Ba(OH)_2 \cdot H_2O$ single crystal. Precise lattice constants were determined as $a = 6.99$ Å, $b = 6.33$ Å and $c = 3.92$ Å from the dissolution of the least square equation using the (hk$l$) indexed on the $Sr(OH)_2 \cdot H_2O$. The systematic extinction in (h0l) and (h00) reflection with h odd indicates the same space group of $Sr(OH)_2 \cdot H_2O$ as C_{2v}^2–$P2_1am$. The number of molecule in the unit cell is four and the calculated density is 4.589 g/cm³.

Atomic Coordinates

The unit cell of $Ba(OH)_2 \cdot H_2O$ contains two barium atom, two water and four hydroxyl oxygen. All of them situated in special position from the space group symmetry. In the calculation of diffracted X-ray intensities positional parameter of barium atom was fixed in the same position of strontium as in $Sr(OH)_2 \cdot H_2O$, but the positional parameter of oxygen atoms was fixed only z direction and variable ± 0.349 Å (correspond to $\pm 5\%$ for x coordinate) for O_2 and O_3 along x direction and 0.317 Å (correspond to $\pm 5\%$ for y coordinate) for O_1 and O_3 along y direction. Suitable atomic coordinates were decided to the best R value obtained from abovementioned combinations of positional parameter as shown in Table 13. Calculated intensities in this case are shown

Table 13. *Determined atomic coordinates of* $Ba(OH)_2 \cdot H_2O$

	x	y	z
Ba	0.250	0.372	0
O_1	0.376	0.842	0
O_2	0.191	0.063	0.500
O_3	−0.011	0.563	0.500

in Table 14 and interatomic distance are listed in Table 15.

Crystal Structure

The packing diagram of $Ba(OH)_2 \cdot H_2O$ structure projected on a plane perpendicular to *c*- and *b*-axis is shown in Fig. 14. The barium and oxygen atoms exist in the layer at zero level and hydroxyl oxygens are situated at about 1/2 level along *c*-axis. Barium atoms between hydroxyl oxygen layers are coordinated by six hydroxyl oxygens and form a distorted octahedron as shown in Ba–O distance from 2.61 Å to 2.94 Å. It is interesting to compare the barium atoms in barium hydroxide octahydrate coordinated by water oxygen molecules.

Table 14. *Comparison of the observed and the calculated diffracted X-ray intensities of* $Ba(OH)_2 \cdot H_2O$

h k l	I_{obs}	I_{cal}	I_{cal} (Using $Sr(OH)_2 \cdot H_2O$) (atomic coordinate)
0 1 0	54	74	98
1 1 0	100	100	100
0 0 1	52	49	53
2 0 0	48	47	56
0 1 1	37	36	41
1 1 1	64	49	54
1 2 0	66	67	60
2 0 1	59	51	50
0 2 1	13	2	4
2 1 1	50	58	66
1 2 1	83	91	98
3 1 0	21	18	23
0 3 0	13	7	6
1 3 0	13	12	16
0 0 2	19	17	19
3 1 1	21	23	22
0 1 2	20	6	8
2 3 0	18	9	12
4 0 0	11	7	9
2 0 2	12	12	13
2 1 2	14	7	7
2 3 1	11	15	13
4 0 1	5	6	6
4 1 1	10	9	12
3 3 1	20	7	4
2 1 2		12	10
		R = 0.157	R = 0.210

Table 15. *Interatomic distances in* $Ba(OH)_2 \cdot H_2O$

Atom	Distance (Å)
Ba_1—O_2	2.80
Ba_1—$O_{3'}$	2.61
Ba_1—O_3	2.94
Ba_2—O_3	2.61
Ba_2—$O_{2'}$	2.80
Ba_2—$O_{3'}$	2.94
Ba_1—O_1	3.10
Ba_2—O_1	2.94
O_1—$O_{2'}$	3.01
$O_{1'}$—$O_{2'}$	2.74
O_1—O_2	2.74
$O_{1'}$—O_2	3.01

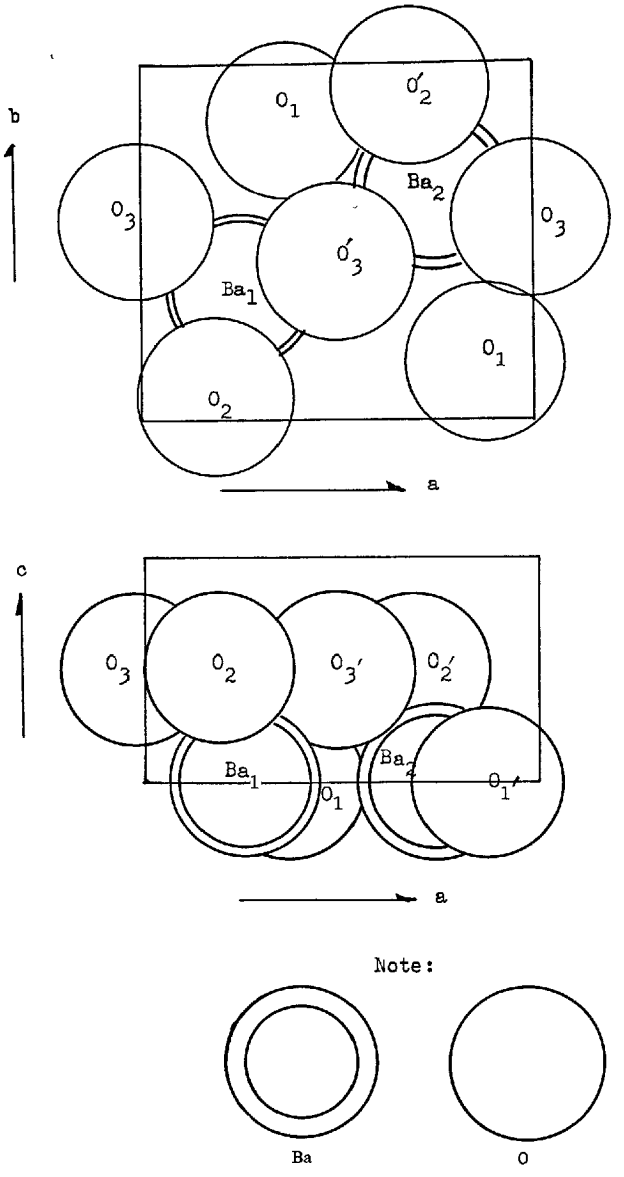

Fig. 14. *The packing diagram of* $Ba(OH)_2 \cdot H_2O$ *structure*

Crystal Structure of Barium Aluminate Hydrate ($BaAl_2O_4 \cdot 6.5H_2O$)

Precedent Work

Some kinds of barium aluminate precipitated from barium and aluminum hydroxide aqueous solution were first identified by E. T. Carlson and L. S. Wells (18) with X-ray and chemical analysis. Since then many studies have been reported on the optical, physical properties, X-ray diffraction data, but crystal structure of barium aluminate hydrates has not been determined.

Determination of Lattice Constants and Other Crystallographic Data

Sample was prepared by the hydration of $BaAl_2O_4$ at W/C = 0.6 at room temperature. The barium aluminate hydrates produced at the early stage of hydration of $BaAl_2O_4$ were a mixture of two kinds of hydrates and aluminum hydroxide, but latter hydration they changes into a kind of hydrate in the laterstage of hydration which has the composition of $BaO \cdot Al_2O_3 \cdot 6.5H_2O$ as shown in Table 16.

From the electron diffraction pattern of a single crystal of $BaO \cdot Al_2O_3 \cdot 6.5H_2O$, symmetry elements were deduced to be twofold or twofold screw axis parallel to *c*-axis and a mirror plane on the *a-b* face. Approximate lattice constants were $a = 8.5$ Å $b = 7.0$ Å and $\gamma = 92°55'$. Unit cell dimension along *c*-axis was determined as about 16.7 Å from the powder X-ray diffraction data and observed density (2.519 g/cm³). Space group of this hydrate is assumed to be C_{2h}^2–$P2_1/m$ since the (00*l*) reflections are systematically absent with *l* odd. More precise lattice constants were obtained from a least squares fit of 23 lines of powder X-ray diffraction. That is $a = 8.523$ Å $b = 6.939$ Å, $c = 16.667$ Å and $\gamma = 92°55'$. Numbers of the molecules contained in unit cell were determined as four from the lattice constants and observed density.

Atomic Coordinate

A detailed study of the crystal structure was difficult because of small numbers of reflections, so we calculate the electron density by means of one dimensional Patterson function along *c*-axis using (00*l*) reflection intensities. From this we assumed the approximate positional parameters of barium and oxygen along *z* direction. One dimensional Patterson synthesis was also performed in consideration of the coordinate of all atoms in this structure. As shown in Fig. 15, the electron density distribution represents a centrosymmetric structure and two barium atoms are situated at each levels of 0 and 0.5, five oxygen atoms at 0.125, 0.250, 0.375, 0.625, 0.750 and 0.875, respectively. Aluminum atoms are situated two by two at the neighbouring oxygen positions and are coordinated by oxygen atoms. The other oxygen atoms must be distributed according to space group C_{2h}^2–$P2_1/m$. The calculated (00*l*) reflection intensities using above-mentioned positional parameters showed comparatively good coincidence with observed one, so that above-mentioned parameters are able to be adopted as approximate atomic coordinates along *z* direction. The atomic arrangement along *b*-axis was introduced from comparative resemblance of *a*-direction in $Ba(OH)_2 \cdot H_2O$ and the packing of three oxygen atoms was thought to be positioned along *a*-axis.

Table 16. *Chemical compositions and specific gravity of hydrated barium aluminate*

Ig. loss	Insol.	Al_2O_3	BaO	Total	Specific gravity (g/cm³)
30.39	2.90	26.33	39.83	99.45	2.519

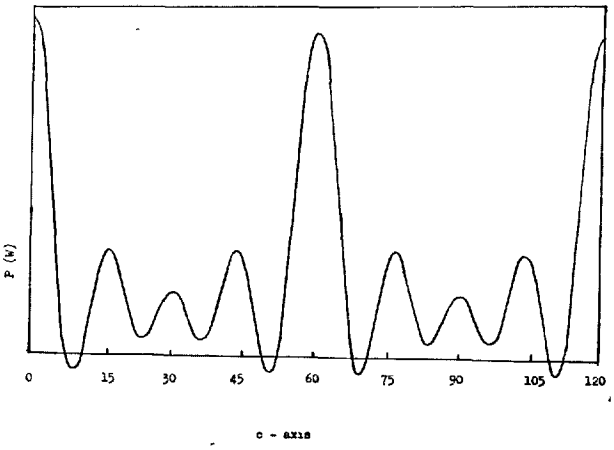

Fig. 15. *Electron density distribution curve of* $BaAl_2O_4 \cdot 6.5H_2O$ *along c-axis calculated from Patterson function*

Possible atomic positions derived from Fourier synthesis along *z* direction and previous mentioned structure on ab-plane was then refined by trial and error method considering much contribution of heavy barium atom on the diffracted X-ray intensities. In this calculation barium atom positional parameters are variable in the range of ± 0.04 considering the framework of $Ba(OH)_2 \cdot H_2O$ in the structure. The most suitable atomic coordinates in many calculation and interatomic distances are given in Table 17 and Table 18. *R* value obtained in this case was 0.147 as shown in Table 19.

Table 17. *Determined atomic coordinates of* $BaAl_2O_4 \cdot 6.5H_2O$

Atom	Coordinate		
	x	y	z
Ba	0.598	0.259	0.0
Al_1	0.176	0.692	0.221
Al_2	0.516	0.490	0.221
O_1	0.176	0.692	0.125
O_2	0.551	0.490	0.125
O_3	0.821	0.202	0.125
O_4	0.458	0.0	0.125
O_5	0.176	0.922	0.250
O_6	0.340	0.576	0.250
O_7	0.669	0.591	0.250
O_8	0.516	0.245	0.250
O_9	0.012	0.576	0.250
O_{10}	0.246	0.389	0.0
O_{11}	0.141	0.101	0.125
O_{12}	0.880	0.836	0.125
O_{13}	0.0	0.476	0.087

Table 18. *Interatomic distances of* $BaAl_2O_4 \cdot 6.5H_2O$

Atom	Distance (Å)
$Ba_I—O_2$	2.70
$Ba_I—O_3$	2.84
$Ba_I—O_4$	3.00
$Ba_2—O_1$	2.99
$Ba_2—O_2$	2.85
$Ba_2—O_4$	2.79
$Ba_I—O_{10}$	2.78
$Ba_2—O_{10}$	2.78
$Al_I—O_1$	1.60
$Al_I—O_5$	1.72
$Al_I—O_6$	1.73
$Al_I—O_9$	1.76
$Al_2—O_2$	1.63
$Al_2—O_8$	1.74
$Al_2—O_7$	1.75
$Al_2—O_8$	1.78

Table 19. *Comparison of the calculated intensities of diffracted X-ray with the observed one of* $BaAl_2O_4 \cdot 6.5H_2O$

h k l	I_{obs}	I_{cal}
0 0 2	100	100
0 1 2	6	5
1 1 1	3	6
1 0 3	8	7
1 1 2	3	3
0 0 4	51	58
1 1 3	6	4
$\bar{1}$ 1 3		3
$\bar{2}$ 1 0	18	19
$\bar{2}$ 1 1	13	15
$\bar{1}$ 2 0	17	15
2 1 3	6	5
2 0 4	4	2
0 0 6	11	7
3 1 0	11	10
2 2 2	9	5
1 1 6	7	9
$\bar{2}$ 2 3	3	2
$\bar{2}$ 2 4	20	25
$\bar{1}$ 3 0	8	11
2 1 6	15	17
0 3 3	5	3
4 0 2	12	14
$\bar{4}$ 1 2	5	5
		R = 0.147

Crystal Structure

Fig. 16 shows the projection of the assymmetric unit on (00*l*). Each barium atom is coordinated by six oxygen atoms which form a framework of barium hydroxide monohydrate, so average Ba–O distance of 2.84 Å is almost equal to the value in $Ba(OH)_2 \cdot H_2O$. Other two oxygen atoms neighbouring the barium atom on the zero level along *c*-axis may belong to water molecules because they exist apart from other six oxygen atoms. The apex oxygen atom of AlO_4 tetrahedron in special position is bounded to both of two AlO_4 tetrahedra like as in $BaAl_2O_4$. The basal three oxygens of these tetrahedra link to oxygen atom surrounding the barium atoms keeping the interatomic distance from 1.72 Å to 1.78 Å. Three kinds of another oxygen atom in general position are not contact with barium or aluminum

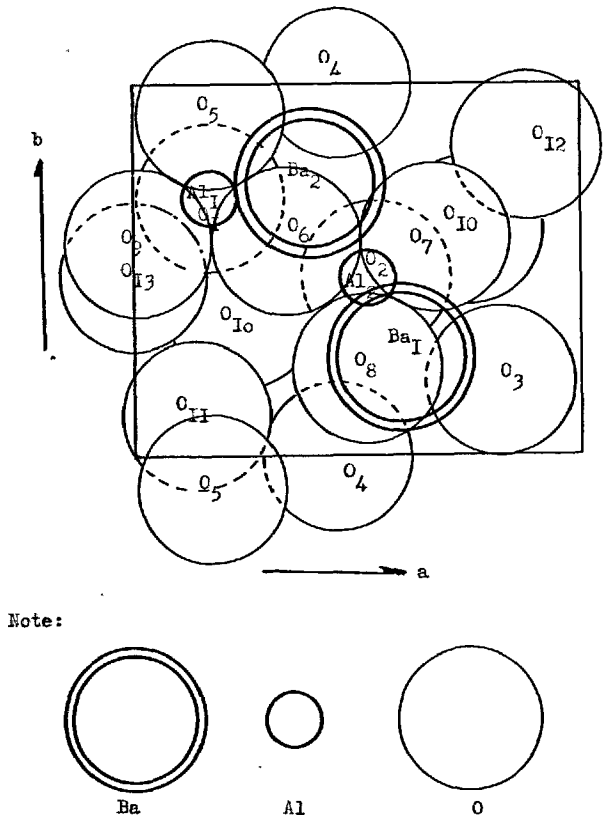

Fig. 16. *Packing diagram of* $BaAl_2O_4 \cdot 6.5H_2O$

atom but it occupies a possible situation in the vacancy of oxygen packing. $BaAl_2O_4 \cdot 6.5H_2O$ is built up from the framework of $Ba(OH)_2 \cdot H_2O$ and the linkage of two AlO_4 tetrahedra extending along *c*-axis. The existence of a set of AlO_4 tetrahedra sharing the apex oxygen atom is observed in unhydrated $BaAl_2O_4$ which is considered to be one of the reasons why $BaAl_2O_4$ paste has high refractoriness.

Crystal Structure of Barium Silicate Hydrate ($BaSiO_3 \cdot 6H_2O$)

Precedent Work

$BaSiO_3 \cdot 6H_2O$ was recently studied by E. Höhen and K. Dornbergen-Schift (19) who determined the crystal structure by means of two and three dimensional Patterson function synthesis. Barium silicate hydrate in the hydrated sample of Ba_2SiO_4, however, have not been identified clearly and their crystal structure have not been determined.

Determination of Lattice Constants and Other Crystallographic Data

Sample was prepared by the complete hydration of

Ba_2SiO_4 in 200% water suspension for a month at room temperature. The hydration products of Ba_2SiO_4 in later stage of hydration are $BaSiO_3 \cdot 6H_2O$ and $Ba(OH)_2 \cdot H_2O$ as mentioned before, so we can easily distinguish barium silicate hydrate from barium hydroxide monohydrate. The electron diffraction pattern of barium silicate hydrate single crystal showed the structural accordance with $BaSiO_3 \cdot 6H_2O$ reported by E. Höhen and K. Dornbergen-Schift (19), and approximate lattice constants were determined to be $a = 8.4$ Å and $b = 13.0$ Å. As the powder X-ray diffraction patterns is characterized by systematic decreasing in diffracted X-ray intensities keeping the constant intervals of the diffraction peaks toward high angle, these peaks are considered to correspond to (00l) reflection of the crystal. Cell dimension of c-axis was therefore decided to be about 15 Å. Using these approximate lattice constants, observed X-ray diffraction peaks were first indexed for all possible set of (hk$l$) as the lattice constants were large and less precise. Precise lattice constants were next determined by the least squares fit of twenty-six lines as $a = 8.44$ Å, $b = 13.00$ Å and $c = 15.06$ Å, space group was C_{2v}^9–$P2_1cn$ and the extinction was for (hk0) with $h + k = 2n$, for (hk0) with $h + k = 2h$ for (h0l) with $l = 2n$, for (h00), (0k0) and (00l) with $h = 2n$, $k = 2n$, $l = 2n$, respectively. The numbers of molecules in unit cell were eight and calculated density was 2.603 g/cm³.

Atomic Coordinate

The diffracted X-ray intensities were calculated for the range that the changes of the positional parameters of barium atom were ±0.337 Å (correspond to ±0.04 for x coordinate) along x direction and ±0.518 Å (correspond to ±0.05 for y coordinate) along y direction under the condition that barium atom is bound to oxygen atom by ionic bonds. In this calculation the positional parameters of SiO_4 tetrahedra were fixed in the Höhen and Dornbergen-Schifts (19) structure because of less contribution to the structure factor compared with barium atoms. From the condition that (002) reflection must be the strongest intenstiy, the positional parameters of Ba_1 and three Ba_2 to be variable were stricted to the combination of 0.250 and 0.210 along x direction and 0.109 and 0.049 along y direction. So that the selected combinations became $2 \times 2 \times 3 \times 3$. The strongest intensity was calculated in (022), (131), (113) and (021) reflection in combinations of another parameters, so that these were eliminated. From these calculation, it was concluded that suitable atomic coordinates of Ba_1 and Ba_2 along x direction must be in the range from 0.210 to 0.250 and from 0.710 to 0.790, respectively from the restriction for Ba–O ionic distances. After the calculation on eighty-one combinations of barium positional parameters on all the possible 101 reflections, atomic coordinates of all atoms in unit cell were determined as given in Table 20. Calculated intensities in this case showed good coincidence with observed one as represented by $R = 0.124 \sim 0.159$ in Table 21. Ba–O distances calculated from deter-

Table 20. *Atomic coordinates of* $BaSiO_3 \cdot 6H_2O$

Atom		Coordinate x	y	z
Ba_1	case A	0.250	0.109	0.241
	case B	0.210	0.109	0.241
	case C	0.210	0.109	0.241
Ba_2	case A	0.250	0.234	0.248
	case B	0.790	0.234	0.248
	case C	0.710	0.234	0.248
Si_1		0.160	0.434	0.065
Si_2		0.340	0.434	0.456
O_1		0.340	0.435	0.051
O_2		0.100	0.398	0.154
O_3		0.170	0.166	0.482
O_4		0.650	0.043	0.487
O_5		0.160	0.430	0.440
O_6		0.420	0.426	0.364
O_7		0.340	0.160	0.041
O_8		0.850	0.044	0.018
O_L		0.730	0.436	0.143
O_K		0.770	0.422	0.354
O_G		0.590	0.298	0.216
O_H		0.080	0.298	0.287
O_A		0.580	0.043	0.207
O_B		0.920	0.033	0.271
O_C		0.0	0.180	0.121
O_D		0.500	0.179	0.369
O_E		0.670	0.185	0.062
O_F		0.830	0.193	0.433

Table 21. *Comparison of the calculated intensities of diffracted X-ray in several cases with the observed one.*

h k l	I_{obs}	$I_{cal.}$ (case A)	$I_{cal.}$ (case B)	$I_{cal.}$ (case C)
0 0 2	100	100	100	100
1 0 2	5	2	3	3
1 1 2	32	27	41	27
0 2 2	44	40	40	40
2 0 0	50	69	55	74
1 1 3	61	53	54	52
2 1 1	12	11	10	10
0 0 4	42	47	47	47
2 1 2	5	3	3	4
2 2 1	21	30	22	26
0 2 4	5	6	6	6
1 2 4	6	2	2	2
2 3 2	6	2	3	2
1 4 2		2	2	2
0 2 5	14	15	13	15
3 1 1	24	22	25	22
1 1 6	5	2	4	2
1 4 4		2	2	2
1 2 6	4	2	2	2
0 6 0	5	7	7	7
4 0 0	4	4	0	6
1 5 4	14	14	13	13
4 2 0	13	5	8	3
0 2 7		6	6	6
2 6 0	10	11	9	10
0 0 8	9	5	5	4
		R = 0.159	R = 0.124	R = 0.157

Table 22. *Interatomic distances of* Ba–O *in the coordination of eight and ten oxygens*

Atom		Distance (Å)		
		Case A	Case B	Case C
Ba_1—O_A		2.94	3.25	3.25
Ba_1—O_B		3.06	2.78	2.78
Ba_1—O_C		2.92	2.71	2.71
Ba_1—O_D		2.99	3.25	3.25
Ba_1—O_G		2.86	3.04	3.04
Ba_1—O_H		2.93	2.77	2.77
Ba_1—O_K		2.82	2.86	2.86
Ba_1—O_L		2.84	2.84	2.84
	Ave.	2.92	2.94	2.94
Ba_2—O_A		2.88	3.05	2.74
Ba_2—O_B		2.99	2.85	3.17
Ba_2—O_C		2.93	2.71	3.18
Ba_2—O_D		2.87	3.12	2.65
Ba_2—O_E		2.94	3.03	2.88
Ba_2—O_F		2.91	2.84	3.00
Ba_2—O_G		2.94	3.26	2.65
Ba_2—O_H		2.96	2.65	3.27
Ba_2—O_K		2.91	2.91	2.95
Ba_2—O_L		3.06	3.09	3.05
	Ave.	2.94	2.95	2.95

mined atomic coordinate were listed in Table 22.

Crystal Structure

Projections of the structure of $BaSiO_3 \cdot 6H_2O$ to (010) is shown in Fig. 17. Barium atoms in general position make two types of polyhedra coordinated by eight and ten oxygen atoms. SiO_4 tetrahedra lie independently in general position contacting with the oxygen atoms which form barium octa—and deca—hydrates. Two water molecules in $Ba(H_2O)_{10}$ coordinate polyhedra are not shared two barium atom, that is, exist in free water. It is very interesting to note that $BaSiO_3 \cdot 6H_2O$ consists of positionally unstable barium atoms which can remove in the limited range without influence on the diffracted X-ray intensities. The differences in barium atomic coordinates and

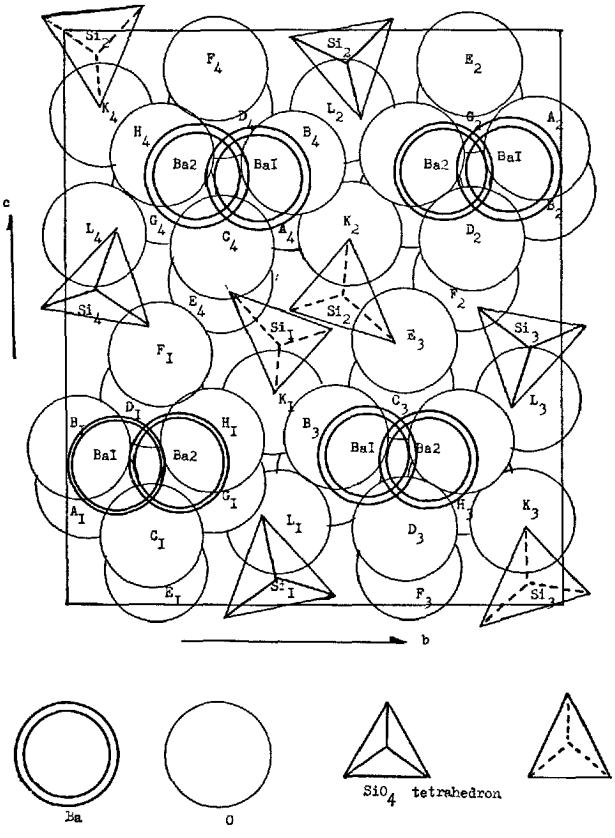

Fig. 17. *Packing diagram of* $BaSiO_3 \cdot 6H_2O$

interatomic distances in the authors and previous research (19) have probably been caused by the difference of the source of sample and consequently by the difference of condition and process of crystalization. The mean Ba–O distance in both of polyhedron coordinated by eight and ten oxygens, however, are 2.94 Å and 2.95 Å, which is good coincidence with precedent work (19).

Physical and Crystal Chemical Properties of the Produced Hydrates

Physical Properties of Barium Aluminate Hydrate

Specific Surface Area of Hydrated Barium Aluminate

The specific surface area of $BaAl_2O_4 \cdot 6.5H_2O$ and $BaAl_2O_4 \cdot 4H_2O$ produced in lower water sample ratio were measured with BET method by N_2 gas adsorption. Period of hydration of samples are both three months. Obtained values were 2 m^2/g for $BaAl_2O_4 \cdot 6.5H_2O$ and 6.0 m^2/g for $BaAl_2O_4 \cdot 4H_2O$ (14) which indicate the existence of these hydrates in complete crystalline state.

Mechanical Strength of Hydrated Barium Aluminate

The compressive and bending strength of hydrated barium aluminate by using the mortar specimen is shown in Fig. 18 (17). When the amount of hydration water is small, the mechanical strength of $BaAl_2O_4$ mortar is high. Therefore, it seems that the theory of the water cement ratio for portland cement may also be applied in this case, but the mechanism of the development of strength is quite different from the

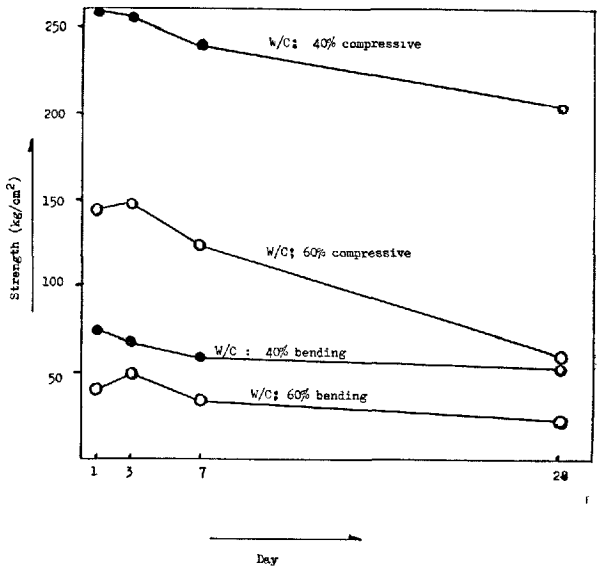

Fig. 18. *Compressive and bending strength of barium aluminate mortar* ($BaAl_2O_4$: Sand = 1 : 2)

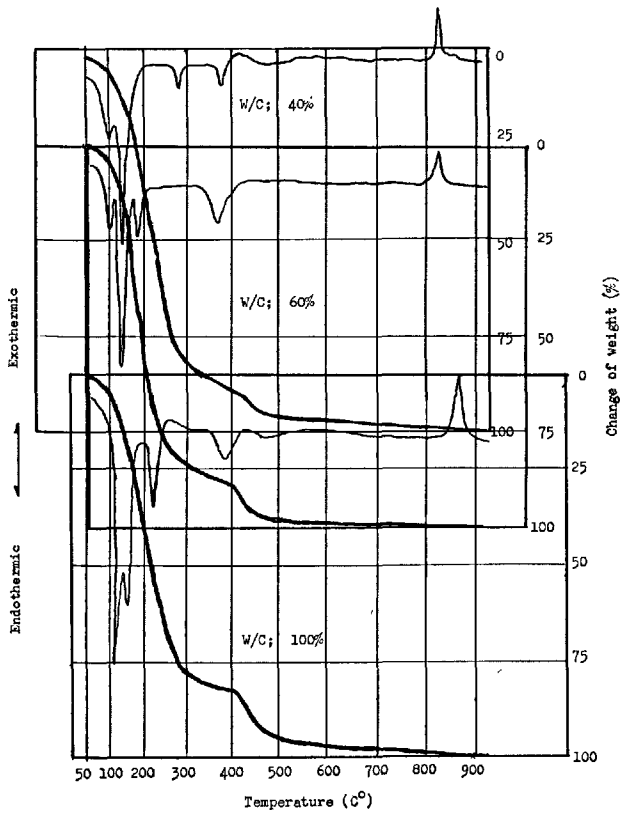

Fig. 19. *Differential thermal analysis and thermogravimetry curves of hydrated* $BaAl_2O_4$

case of portland cement. Orthorhomic double salt ($lBaCO_3 \cdot mBa(OH)_2 \cdot nH_2O$) was recognized in the

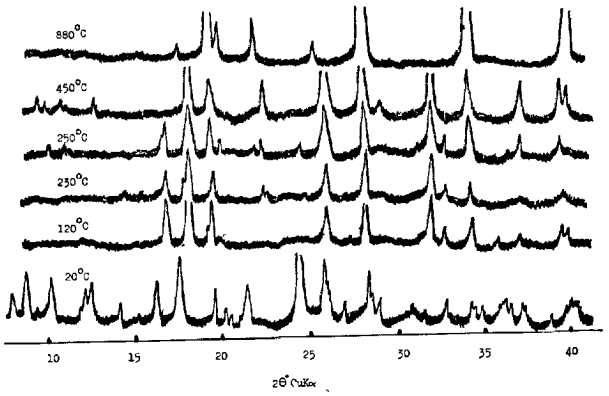

Fig. 20a. *Powder X-ray diffraction patterns of hydrated* $BaAl_2O_4$ *at high temperature. W/C; 40%*

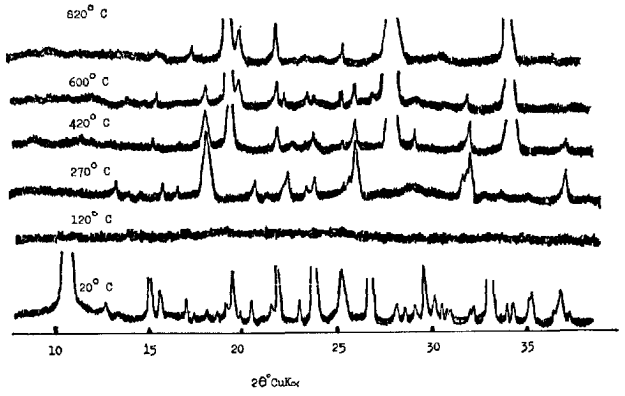

Fig. 20b. *Powder X-ray diffraction patterns of hydrated* $BaAl_2O_4$ *at high temperature. W/C; 60%*

mortar specimen cured in wet air for four weeks by the powder X-ray diffraction which may probably be one of the reason for the decrease in strength with age.

Properties of Hydrated Barium Aluminate at Elevated Temperature

Structural Change of Hydrate in Heating

Differential thermal analysis, thermogravimetry and powder X-ray diffraction at high temperature was done to pursue the dehydration and structural change of hydrate in heating (15). Results are represented in Fig. 19 and Fig. 20. A greater part of the combined water dehydrated under 350°C leaving one molecule of water, but the remarkable difference in dehydration process was observed between the sample hydrated with 40% of water and others. This was probably due to the difference of originally existed hydrate. Amorphous and illcrystalized phase was clearly observed at 100 to 300°C in the specimen

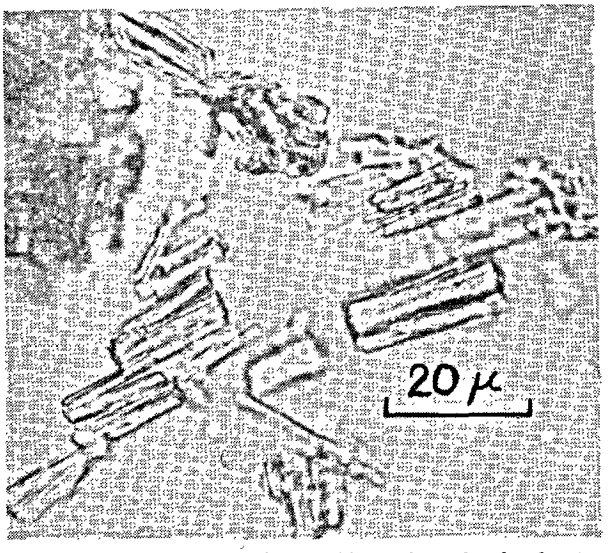

Fig. 21. *Opticalmicrograph of* $BaAl_2O_4 \cdot 6.5H_2O$ *after heating at 300°C*

hydrated over 60% of water which indicate the destruction of original crystal structure and the rearrangement of atoms. As the crystal correspond to the amorphous state keeps the external form of original hydrate as shown in Fig. 21, it is reconfirmed that the set of two AlO_4 tetrahedra shared the apex oxygen remained as they are through all period of heating. This may be one of the reason why limited decrease in the mechanical strength at elevated temperature.

Phase Relation in Heating

Phase relation of hydrated barium aluminate in heating is summerized in Fig. 22. Converted phase appeared above 200°C was agreed with the cubic hydrate of $BaAl_2O_4 \cdot H_2O$ reported by E. T. Carlson, T. J. Chaconas and L. S. Wells (18).

Mechanical Strength

Mechanical strength of mortar specimen at various elevated temperature is shown in Fig. 23. When the water cement ratio is low such as 0.4, unstable hydrate (probably be $BaAl_2O_4 \cdot 4H_2O$) is tend to be formed, which shows the favorable influence on the development of the mechanical strength. Compressive strength is first increase by the drying of the specimen and then decreased according to the temperature. The degree of decrease in strength, however, is fairly small compared with calcium aluminous cement as well as portland cement. Remarkable increase above about 700°C is caused by the formation of $BaAl_2O_4$, which contributes the favorable effects on the utilization of

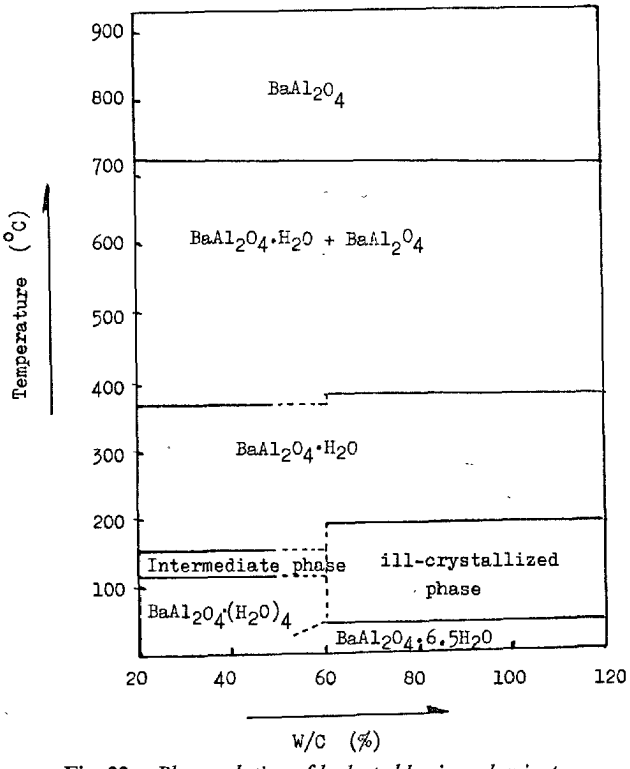

Fig. 22. *Phase relation of hydrated barium aluminate*

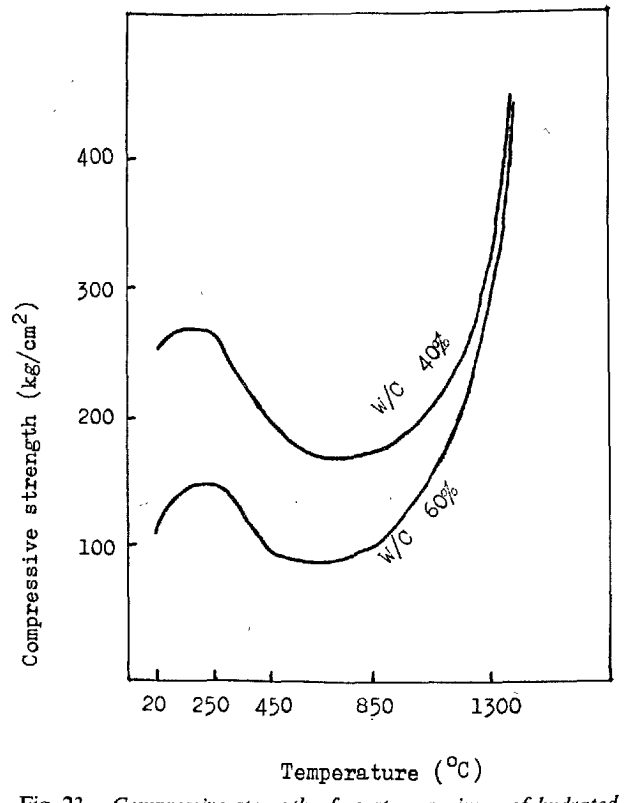

Fig. 23. *Compressive strength of mortar specimen of hydrated barium aluminate at various elevated temperature* ($BaAl_2O_4$: Sand = 1:2)

barium aluminous cement.

Effect of the Atomosphere on the Structure of Hydrates (20)

Method of Experiment

Completely hydrated sample prepared by the bottle hydration for twenty-eight days at room temperature with 500% of water is dried under 1 mmHg and then mounted on the sample holder of X-ray diffractometer which is specially designed for the control of humidity and atmosphere. The optical system of the diffractometer including the sample mount was filled with desired gas with selected humidity which was attained by the passage of the gas through aqueous solution of suitable salts. The powder X-ray diffraction patterns of samples under various conditions were recorded by this method.

Effect of Humidity

Fig. 24 shows the change of X-ray diffraction patterns of hydrated barium aluminate exposed in dry and wet nitrogen gas after being dried under 1 mmHg. The third chart of X-ray diffraction are that of the sample redried by the exposure of dried nitrogen gas. The interplaner spacing of the barium aluminate hydrate ($BaAl_2O_4 \cdot 6.5H_2O$) represented by the diffraction profiles in 2θ CuK$\alpha = 11 \sim 12°$ shows the reversible change in accordance with the variation of humidity. These experimental facts lead us to the conclusion that the structure of $BaAl_2O_4 \cdot 6.5H_2O$ contains barium hydroxide monohydrate layer and water molecules stacked along *c*-axis which is able to remove without destruction of crystal structure.

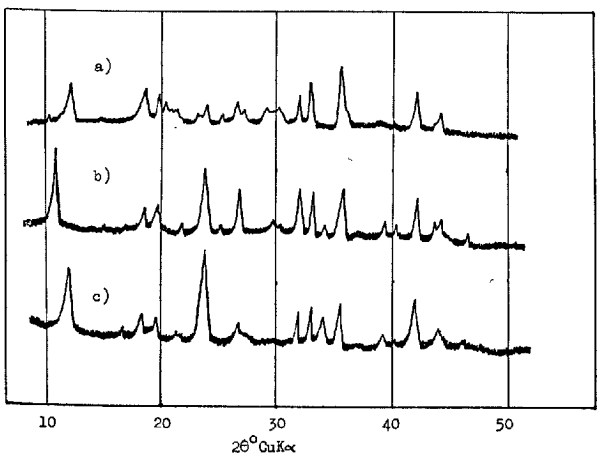

Note: a) Saturated with dry nitrogen gas
b) Saturated with wet nitrogen gas (R.H = 100%)
c) Resaturated with dry nitrogen gas

Fig. 24. *X-ray diffraction patterns of hydrated barium aluminate exposed in various humidity after dried under 1 mm Hg.*

Results on the hydrated barium silicate obtained under same experimental conditions are illustrated in Fig. 25. Crystal structure of $BaSiO_3 \cdot 6H_2O$ and $Ba(OH)_2 \cdot H_2O$ showed no essential change by the mere repetition of dry and wet cycle. This is easily deduced from the crystal structure of $BaSiO_3 \cdot 6H_2O$ that SiO_4 (probably $Si(OH)_4$) tetrahedra arranged along *a*-axis contacted fairly tight to water molecule neighbouring barium atom. But unfortunately small amount of carbon dioxide mixed into the sample space, carbonation of $Ba(OH)_2 \cdot H_2O$ occurred as shown in Fig. 25 (a) and (b).

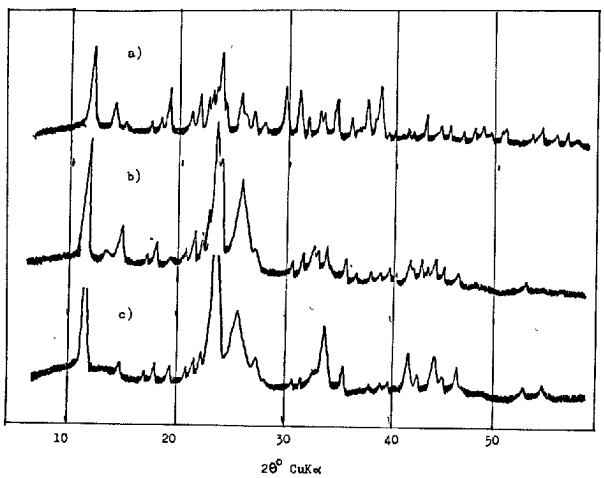

Note: a) Saturated with dry nitrogen gas
b) Saturated with wet nitrogen gas (R.H. = 100%)
c) Resaturated with dry nitrogen gas

Fig. 25. *X-ray diffraction patterns of hydrated barium silicate exposed in various humidity after dried under 1 mm Hg.*

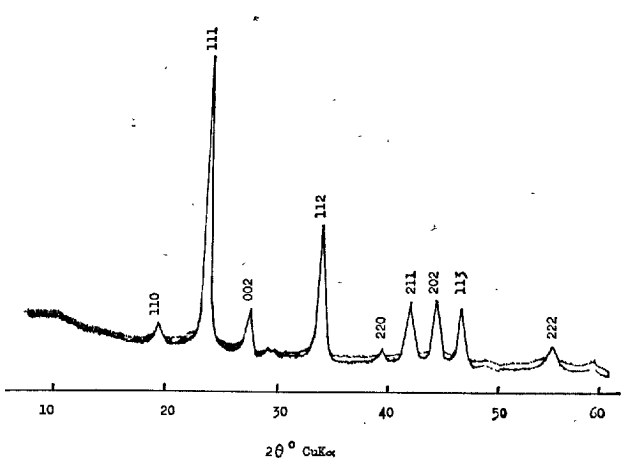

Fig. 26. *X-ray diffraction pattern of hydrated barium silicate exposed in wet carbon dioxide after dried under 1 mm Hg.*

Effect of Carbon Dioxide

Diffraction profiles of $d = 2.56$ Å, 2.62 Å and 3.72 Å gradually appeared when hydrated barium aluminate expose for long time to wet carbon dioxide gas. The above-mentioned diffraction peaks are considered to be carbonated barium hydroxide hydrate ($l BaCO_3 \cdot mBa(OH)_2 \cdot nH_2O$). The formation of this compound is slow and small.

Hydrated barium silicate was irreversibly changed immediately by the exposure of wet carbon dioxide gas into the carbonated barium hydroxide hydrate. X-ray diffraction pattern of the hydrate is resemble to that of witherite ($BaCO_3$) as shown in Fig. 26. As SiO_4 tetrahedra exist separately without formation of both chain and network, main structure of $BaSiO_3 \cdot H_2O$ resemble to barium octahydrate. This may be one of the reasons why hydrated barium silicate is easily carbonated under high humidity.

Summary and Conclusions

Crystal structure of barium aluminate, barium silicate and their hydrated products were determined as follows:

$BaAl_2O_4$:
D_6^6–$P6_322$, hexagonal, $z = 2$, $\rho_{obs} = 4.004$ g/cm³, $a = 5.224$ Å, $b = 8.777$ Å, atomic coordinate, see Table 3.

Ba_2SiO_4:
D_{2h}^6–Pmcn, orthorhombic, $z = 4$, $\rho_{obs} = 5.427$ g/cm³, $a = 5.772$ Å, $b = 10.225$ Å, $c = 7.513$ Å, atomic coordinate, see Table 10.

$Ba(OH)_2 \cdot H_2O$:
C_{2v}^2–$P2_1am$, orthorhombic, $z = 2$, $\rho_{cal} = 4.589$ g/cm³, $a = 6.99$ Å, $b = 6.33$ Å, $c = 3.92$ Å, atomic coordinate, see Table 13.

$BaAl_2O_4 \cdot 6.5H_2O$:
C_{2h}^2–$P2_1/m$, monoclinic, $z = 4$, $\rho_{obs} = 2.519$ g/cm³, $a = 8.523$ Å, $b = 6.939$ Å, $c = 16.667$ Å, $\gamma = 92°55'$, atomic coordinate, see Table 17.

$BaSiO_3 \cdot 6H_2O$:
C_{2v}^9–$P2_1cn$, orthorhombic, $z = 8$, $\rho_{cal} = 2.603$ g/cm³, $a = 8.44$ Å, $b = 13.00$ Å, $c = 15.06$ Å, atomic coordinate, see Table 20.

Stoichiometry of the hydration of barium aluminate and barium orthosilicate with enough water was proposed as follows:

$BaAl_2O_4$:

$$2BaAl_2O_4 + 11.5H_2O = BaAl_2O_4 \cdot 6.5H_2O + Ba(OH)_2 \cdot H_2O + 2Al(OH)_3 \quad \text{(initial reaction)}$$

$$BaAl_2O_4 + Ba(OH)_2 \cdot H_2O + 7H_2O = Ba_2Al_2O_5 \cdot 9H_2O \quad \text{(successive reaction)}$$

$$3BaAl_2O_4 + 18.5H_2O = BaAl_2O_4 \cdot 6.5H_2O + Ba_2Al_2O_5 \cdot 9H_2O + 2Al(OH)_3 \quad \text{(reaction as a whole)}$$

Ba_2SiO_4:

$$Ba_2SiO_4 + nH_2O = Ba_2SiO_4 \cdot nH_2O \quad \text{(reaction at early stage)}$$

$$Ba_2SiO_4 \cdot nH_2O + (8 - n)H_2O = BaSiO_3 \cdot 6H_2O + Ba(OH)_2 \cdot H_2O \quad \text{(reaction at later stage)}$$

$$2Ba_2SiO_4 + 8H_2O = BaSiO_3 \cdot 6H_2O + Ba(OH)_2 \cdot H_2O \quad \text{(reaction as a whole)}$$

Barium aluminate hydrate changes into $BaAl_2O_4$ at a considerable low temperature through intermediate phase (probably be $BaAl_2O_4 \cdot H_2O$) without destruction of external crystal form. Completely hydrated barium aluminate shows the reversible change of interplaner spacing along c-axis in accordance with the variation of humidity. These experimental facts are able to be explained by the arrangement of AlO_4 tetrahedra and the stacking of water molecules in the structure of $BaAl_2O_4 \cdot 6.5H_2O$.

Rapid hardening and high strength development of hydrated barium silicate in wet atmosphere are considered due to the network structure of hydrogen bonding among SiO_4 (probably be $Si(OH)_4$), $Ba(H_2O)_8$ and $Ba(H_2O)_{10}$ judging from the fairly long interatomic distance of Ba–O. The property of the hydrate being easily carbonated can also be illustrated from its crystal structure.

References

1. Al. Braniski, "Refractory barium-aluminous cement and concrete", Proc. 4th Intern. Symposium Chem. Cement, Washington, D.C. P. 1075–1091, NBS Monograph 43, U.S. Department of Commerce, 1962.

2. H. Lehmann and K. H. Müller, "Der Einflüss des Mineralaufbaus von Bariumzementen auf ihre Hydraulichen Eigenschaften", TIZ-Zbl, **86**, 578–584 (1962).
3. S. Wallmark and A. Westgren, "X-ray analysis of barium aluminates", Arkiv. Kemi. Mineral. Geol. **12B** No. 35, 4–11 (1937)
4. W. Nowachi, "Relations among $K[AlSiO_4]$ (kaliophilite), $Ba[Al_2O_4]$, $K[LiSO_4]$, $Na[AlSiO_4]$ (nepheline) and $[Si_2O_4]$ (β-tridymite)", Naturwissenschaften, **30**, 4712–4720 (1942).
5. H. Uchikawa and K. Tsukiyama, "Precise determination of $BaAl_2O_4$ cell and certification of the formation of iron bearing solid solution", J. Ceram. Assoc. Japan, **74**, 15–20 (1966).
6. J. V. Smith, "A review of the Al–O and Si–O distances", Acta Cryst. **7**, 479–481 (1954).
7. H. D. Megaw, C. J. E. Kempster and E. W. Radoslovichi, "The structure of anorthite, $CaAl_2Si_2O_8$. I. Structure Analysis", Acta Cryst. **15**, 1005–1017 (1962).
8. J. V. Smith and S. W. Bailey, "Second review of Al–O and Si–O tetrahedral distances", Acta Cryst. **16**, 801–811 (1963).
9. H. O'Daniel and L. Tscheischwilli, "The structure of γ-Ca_2SiO_4 and Na_2BeF_4", Z. Krist, **104**, 124–141 (1942).
10. H. P. Rooksby, "Identification by X-rays of interface compounds on "oxide" cathodes", Nature, **159**, 609–610 (1947).
11. E. M. Levin and G. M. Ugrinic, "The system barium oxide—basic oxide-silica", J. Res. NBS, **51**, 37–56 (1953).
12. H. Uchikawa and K. Tsukiyama, "Indexing of the X-ray difiraction patterns and precise determination of the crystal structure of Ba_2SiO_4", J. Ceram. Assoc. Japan, **73**, 106–110 (1965).
13. H. Uchikawa, K. Tsukiyama and M. Mochizuki, "The equilibrium relationships of liquid phase in the hydration of Ba_2SiO_4 and $BaAl_2O_4$", J. Japan Cement Eng. Assoc. **20**, 75–79 (1966).
14. H. Uchikawa, K. Tsukiyama and M, Mochizuki, "On the hydration of $BaAl_2O_4$" J. Japan Cement Eng. Assoc. **19**, 81–87 (1965).
15. H. Uchikawa and K. Tsukiyama, "Structural change and mechanical strength of hydrated barium aluminate at elevated temperature", J. Chem. Soc. Japan, Industrial Chemistry Section, **69**, 1710–1715 (1966).
16. H. Manohar and S. Ramaseshan, "The crystal structure of barium hydroxide octahydrate", Z. Krist. **119**, 357–374 (1964).
17. H. Bärnighausen und J. Weidlein, "Die Kristallstruktur von Strontium-hydroxid-Monohydrat", Acta Cryst. **22**, 252–258 (1967).
18. E. T. Carlson, T. J. Chaconas and L. S. Wells, "Study of the system barium oxide-aluminum oxide-water at 30°C", J. Res. NBS, **45**, 381–398 (1950).
19. E. Höhen and K. Dornberger-Schift, "Die Kristallstruktur des Wasserhaltigen Bariumsilikats $BaO \cdot SiO_2 \cdot 6H_2O$", Acta Cryst. 1298 (1961).
20. H. Uchikawa and K. Tsukiyama, "Structural change of completely hydrated barium aluminate and barium orthosilicate under various humidity" J. Japan Cement Eng. Assoc. **18**, 51–57 (1964).

SESSION II-3 PHASE EQUILIBRIA OF CEMENT-WATER

Principal Paper Phase Equilibria of Cement-Water

Paul Seligmann and Nathan R. Greening*

Synopsis

The solid phases at complete hydration in the cement-water system are identified as a calcium silicate hydrate gel containing appreciable quantities of alumina, sulfate, and alkalies, the low sulfate form of calcium sulfoaluminoferrite hydrate, the lowest sulfate form of calcium sulfohydroxyaluminate hydrate, an alumina-silica hydrogarnet, and calcium hydroxide. Ettringite or its iron analogue is also present in cements low in C_3A, but more often forms as a result of carbonation.

Questions still remain on the thermodynamic stability of some of the phases at ultimate hydration. Evidence is presented that indicates that afwillite and calcium sulfohydroxyaluminate hydrate may be stable at ordinary temperatures of cement hydration.

The early hydration reactions can be considered to be an essentially continuous sequence of phase equilibrium situations. The contact between cement and water immediately produces a set of reactions determined by local solution concentrations at the cement-water interfaces to produce materials such as calcium sulfoaluminate hydrates and a hydrogarnet. These local reactions are followed by a period of slow hydration in which the solution composition is relatively constant as ettringite precipitates and lime supersaturation persists. When the calcium hydroxide nucleates, a calcium silicate hydrate gel containing sulfate and a little alumina forms. Ettringite continues to form until the gypsum is depleted; the solution sulfate concentration drops. Rapid solution of the ettringite and the remaining aluminate and ferrite phases causes formation of a gel, richer in alumina, the calcium sulfoaluminoferrite hydrate, and the low sulfate form of calcium sulfoaluminate hydrate. The formation of further aluminasilica hydrogarnet at this stage may be due to local depletions of sulfate in the liquid phase. After the ettringite is depleted, the lowest sulfate form of calcium sulfohydroxyaluminate is ultimately produced.

Introduction

The techniques of portland cement manufacture and of the production of strong, durable concrete were originally developed largely empirically, as has usually been the case in processes involving naturally occurring complex raw materials and equally complex products. These developments were accompanied by research that originated with observed correlations between variations in the processes and the performance of the products and ultimately produced a sophisticated applied science and technology. As the science of the cement and concrete field has developed, progress has been reflected in specifications, codifications, and quality control procedures. As a consequence, control of the properties of concrete and prevention of concrete deterioration has been facilitated. In addition, considerable fundamental understanding of the nature and mechanisms of cement hydration and concrete deterioration has been achieved.

By contrast, more fundamental scientific research on the chemistry of cement, or any other complex material or process, must necessarily begin with studies of vastly oversimplified situations. The real situation is approached as progress is made. Complications can then be added to the study. In fundamental

*Portland Cement Association, Research and Development Laboratories, Skokie, Illinois, U. S. A.

research on the chemistry of cement hydration, studies of phase equilibria of aqueous systems involving particular components found in cement have been a focal point for many years. The relationship between these studies and actual cement hydration have frequently been somewhat tenuous, because of the complexity of the cement-water system.

The purpose of the present paper is to apply current knowledge of the phase equilibria of pure cement constituents and water to improve understanding of the chemistry of the cement hydration process. This procedure implies certain limitations that must be set forth at the outset. Cement hydration in field concrete, on the one hand, can be influenced by various factors such as carbonation, aggregate reactivity, etc., that are not strictly part of the cement-water system. On the other hand, portland cement contains trace quantities of oxides for which systematic phase equilibrium studies are not available. Furthermore, the cement hydration process is known to be affected qualitatively by additional factors such as the amount of SO_3 in the cement and perhaps the water content of the hydrating system.

The process to be considered here is therefore the hydration of a cement at or near the optimum gypsum content (1) and showing a depletion of the solid calcium sulfate phase at 18–24 hours of hydration (2). This cement is assumed to be in a paste with a water-cement ratio in or slightly above the range normally found in concrete. The data available limit the presentation to the behavior of the major oxides in the cement and largely to a consideration of the nature of just the solid phases, since analyses of the liquid phase in the cement-water system are available only at early ages. The value and potential utility of a study with these limitations must be judged by its adequacy. It is shown that many features of the chemistry of cement hydration, from the time of first contact with water, can be qualitatively interpreted in terms of phase equilibria. The analysis made here naturally provides, often merely by implication, possible directions of future research in resolving those uncertainties, difficulties, and discrepancies that still remain.

The presentation in the present paper begins with evaluation of some aspects of the experimental identification of solid phases in the cement-water system. A discussion of the final products of cement hydration is followed by consideration of the thermodynamic stability of these products. Finally, the relation of the early hydration reactions to phase equilibria is presented.

Details of the phase equilibria involving pure compounds will be developed only where needed. Excellent reviews of these equilibria have been published quite recently (3) and will be referred to where appropriate. Other reference to work in this field will be largely confined to papers published since the appearance of these reviews.

Some of the conclusions drawn result from previously unpublished original work. For completeness, details of this work are given where appropriate. The emphasis of the study is perhaps slightly selective, since the authors have not had experience with all of the various aspects of the cement-water system.

The present paper is based largely on information on cement hydration developed since the Fourth Symposium. The expansion of knowledge during this period has been made possible by extensive use of relatively new instruments, especially the X-ray diffractometer. Results of considerable interest have also been obtained with the Mössbauer spectrometer, a very new instrument.

Studies of a condensed heterogeneous system must commence with the identification of the phases present and the determination of their composition. The following section deals with certain problems and techniques of identification that are important in studies of the cement-water system.

Identification of Solid Phases

An examination of recent literature reveals that present knowledge of the equilibrium state of the cement-water system has come a long way since that time, only twenty years ago (4), when it appeared that the only solid phases present at ultimate hydration were crystalline calcium hydroxide and an essentially undifferentiated, poorly crystallized solid consisting primarily of a calcium silicate hydrate. The progress that has been made has resulted largely from the improvement of techniques for identifying solid phases in hydrated portland cement.

It has been shown, for example, that the calcium silicate hydrate has an X-ray diffraction pattern that has at least a rudimentary crystallinity (5). Additional diffraction lines have been observed that can be associated with crystalline phases containing aluminum and iron, by comparison of the patterns with those of the corresponding pure compounds (6). Great pro-

gress has also been made in recent years in the preparation and characterization of both simple and complex calcium aluminates such as might occur in hardened cement paste (7).

The X-ray diffractometer has a great advantage over many other techniques for identifying solid phases in the cement-water system in that the state of the material under study can be rigorously controlled (8). The same can be said for the optical microscope and also for the Mössbauer spectrometer, to be discussed later. Many other techniques, such as differential thermal analysis, thermogravimetric analysis, and electron microscopy, require that the sample be subjected to treatments, such as preheating in a laboratory atmosphere or evacuation, that can demonstrably change its character prior to observation. Since the optical microscope is limited by its resolving power, results from X-ray diffraction studies are considered the primary source of data for identification of phases for present purposes. Results from other techniques are used as confirmatory evidence or for consideration of ambiguities not yet resolved or inherently not resolvable by X-ray diffraction studies.

The above paragraph is not meant to imply that all existing X-ray diffraction studies provide a complete and consistent picture. This is certainly not the case. Many uncertainties and even contradictions appear in the published literature. It is believed, however, that presently available information provides a basis for resolving many of the problems that have been encountered and for identifying most or even all of the solid phases that exist during the hydration of portland cement.

No attempt will be made here to analyze all of the various uncertainties that have appeared in the literature. The following sections deal primarily with those aspects of instrumentation that are essential for the present argument and that can aid in resolving many problems that have been encountered.

Effect of Carbonation

Published examinations of hydrated cement pastes or of calcium aluminate and ferrite hydrates have generally shown the presence of one or more carbonated phases. It has proved to be extremely difficult to prepare materials of this type that are truly free of carbon dioxide (9). In most instances where exclusion of carbon dioxide has been claimed, the claim has not been substantiated by a chemical determination of CO_2. It is of course recognized that the presence of a small proportion of a carbonated phase has little effect on the gross composition or properties of a bulk phase; even slight carbonation, however, can cause gross misinterpretation of diffraction patterns of materials because the bulk of the carbonation may occur precisely at the surface where the diffraction is taking place. As a result, a slight degree of carbonation, while only a small proportion of the bulk phase, can result in a diffraction pattern that has little relation to the material being studied. For example, Wells, Clarke, and McMurdie (10) gave a basal spacing of 8.2 Å as characteristic of their preparation of the tetracalcium aluminate hydrate. Even though this spacing is now known to belong to a carbonated phase (8), this fact does not in itself imply that the bulk material was unduly carbonated nor prove the rest of that phase equilibrium study invalid. In terms of the small quantities of materials used in the powder cameras of that time, carbonation could have occurred very early during handling of the sample, so that the material in the camera was simply no longer representative of the bulk of material under study. This illustration does, however, point up the need both for care in interpreting diffraction patterns and for recognition of the effects of carbonation on the phases present.

The above conclusion applies directly to the significance of an identification of the high sulfate form of calcium sulfoaluminate (hereinafter called *ettringite*) in hydrated cement pastes. It has been found that carbon dioxide reacts with the low sulfate form of calcium sulfoaluminate hydrate (hereinafter generally referred to as *monosulfate*) to produce the calcium hemicarboaluminate hydrate and ettringite:

$$3[Ca_3A \cdot CaSO_4 \cdot 12H_2O] + CO_2 + 20H_2O \rightarrow 2[C_3A \cdot \tfrac{1}{2}Ca(OH)_2 \cdot \tfrac{1}{2}CaCO_3 \cdot 12H_2O] + C_3A \cdot 3CaSO_4 \cdot 32H_2O$$

Further carbonation then converts the hemicarboaluminate to the carboaluminate and ultimately to some form of calcium carbonate. Fig. 1 illustrates the effect. Here carbonation was deliberately induced by blending calcium carbonate with Long-Time Study cement 18 in pastes at a water-cement ratio of 0.5. The cement composition is shown in Table 1. The top pattern shows the diffraction pattern of the carbonate-free

Table 1. *Compositions(48) of cements used in study of ettringite as an ultimate hydration product*

Cement	LTS 18	LTS 41
C_3S	44.5%	20.0%
C_2S	28.0	51.0
C_3A*	12.2	3.4
C_4AF	6.8	15.2
SO_3	1.83	1.98
Alkalies as Na_2O	0.22	0.84

*Corrected for minor oxides (49).

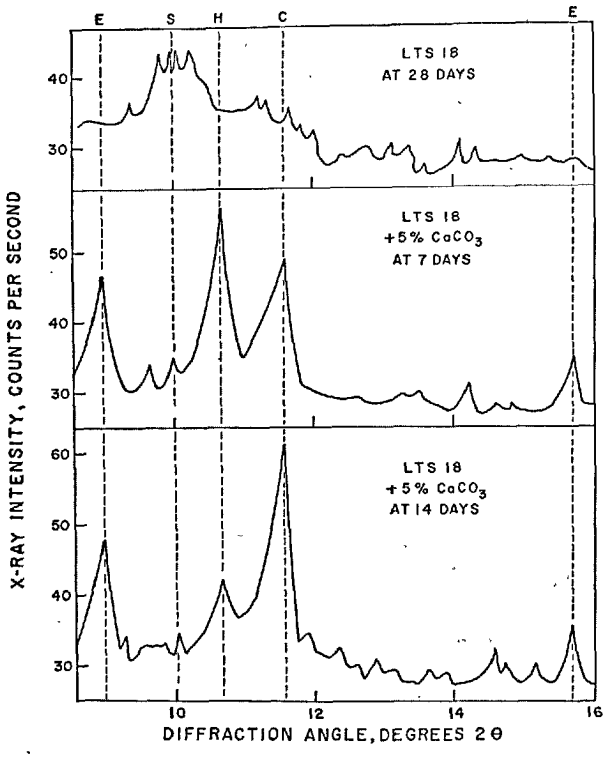

Fig. 1. *Carbonation of cement produces secondary ettringite. Legend: E = ettringite; S = calcium sulfohydroxyaluminate hydrate; H = calcium hemicarboaluminate hydrate; C = calcium carboaluminate hydrate.*

paste after 28 days of moist curing. The ettringite peaks are absent. In the presence of the carbonate, as shown in the other two patterns at 7 and 14 days, respectively, the peaks for ettringite and the carbonated phases are very prominent, whereas the monosulfate-hydroxide solid solution (11) (hereinafter referred to as *calcium sulfohydroxyaluminate hydrate*) pattern that is prominent in the top pattern is essentially absent in the others.

Thus, the presence of ettringite in a well hydrated paste or similar system containing lime, alumina, sulfate, and water does not in itself indicate this compound to be a primary equilibrium product, but may merely indicate that this material was formed as a secondary product from incidental carbonation. It is believed that this reaction explains many of the reported inconsistencies regarding the presence of ettringite in well-hydrated pastes. Since diffraction studies on hydration of simulated cement pastes (11) have shown that the sulfate ultimately forms monosulfate and the sulfohydroxyaluminate, it appears that the ultimate hydration products of the cement-water system in the absence of carbon dioxide may not always include ettringite.

In an extension of this study, samples of pastes made from longtime study cements 18 and 41, whose compositions may be found in Table 1, were examined after 14 years of continuous moist curing. The samples were sawed out of the centers of 2 × 6 inch paste cylinders made up at a water-cement ratio of 0.5. The diffraction pattern for cement 18 gave no indication of carbonation and also no indication of ettringite. That for cement 41, on the other hand, contained the ettringite peaks and yet displayed no evidence of carbonation. Occurrence of ettringite as an ultimate hydration product of the cement-water system, as discussed later, depends upon the cement composition.

Although the existence of the calcium hemicarboaluminate hydrate was reported some years ago (8), the evidence for its existence and composition was not published at that time. Since the reported composition has been viewed with considerable skepticism (12, 13), and since recognition of this material is of great importance in diffraction studies of the cement-water system, it is essential that the details of this identification be presented here. The following discussion also covers the preparation and the properties of the material and gives some indication of the reasons for the existing confusion.

In the present work, a suspicion that the material was not a form of C_4AH_{13} as had been generally supposed, arose when it was found that it could not be converted to a higher hydrate. Thus, when a solid exhibiting the diffraction pattern of this material and C_4AH_{13} was repeatedly wetted and dried, the C_4AH_{13} would transform reversibly to C_4AH_{19}, whereas the 8.2 Å line would remain unchanged. The material responsible for this line therefore had to be either some form of C_4AH_{13} that was metastable toward absorption of water or some other compound. Although no C_4AH_{13} preparation could be made that was free of this line, routine CO_2 determinations revealed that the intensity of the 8.2 Å line varied with the CO_2 content of the preparation.

A series of preparations was then made using slurries containing tricalcium aluminate, calcium carbonate, and calcium hydroxide, in which the mole ratio $CaCO_3/C_3A$ was varied from 0.1 to 1 in steps of 0.1, and the mole ratio $Ca(OH)_2/C_3A$ was held constant at 1. These slurries were agitated at 40°F, to avoid formation of the cubic C_3AH_6, for 70 days. After filtration of the slurries, diffraction patterns were made of the wet solids. The material with a mole ratio $CaCO_3/C_3A$ of 0.5 had a major diffraction intensity for a basal spacing at 8.2 Å whereas the preparation with lower $CaCO_3/C_3A$ ratios showed increasing intensities of the 10.7 Å spacing of C_4AH_{19},

and those with higher $CaCO_3/C_3A$ ratios showed increasing intensities of the 7.6 Å spacing of $C_3A \cdot CaCO_3 \cdot 12H_2O$. The intensity of the 8.2 Å peak varied with the carbonate-to-alumina ratio and attained its maximum at $CaCO_3/C_3A = 0.5$.

Subsequently, preparations of the hemicarboaluminate have been made to study its properties. For these preparations, 1 mole of C_3A, 0.45 mole of $CaCO_3$, and 0.55 mole of $Ca(OH)_2$ are mixed in a slurry and agitated until the C_3A is hydrated. It has been found that the preparation can be made at room temperature since the hemicarboaluminate, unlike C_4AH_{13}, is stable with respect to the cubic phase, C_3AH_6; in fact, the complex also forms, although slowly, from similar mixtures in which the C_3A is replaced by C_3AH_6. The slight deficiency in carbonate is deliberately introduced, since the mix absorbs enough atmospheric CO_2 during filtration and subsequent handling to produce the desired composition. Chemical analyses of these preparations are within 0.25 per cent of the composition demanded by the assigned formula. Successive drying over $CaCl_2 \cdot 2H_2O$ and then $CaCl_2$, followed by equilibration at 50 per cent relative humidity over dilute sulfuric acid, yields the desired compound with the 8.2 Å basal reflection and close to 12 moles of water per formula weight. A very weak pattern for C_3AH_6 also appears in the diffraction charts of these preparations.

Microscopic examination shows the material to crystallize in poorly defined hexagonal plates that are uniaxial negative with refractive indices: $N_O = 1.537 \pm 0.002$, $N_E = 1.510 \pm 0.002$.

The X-ray diffraction pattern obtained agrees essentially with that already published and indexed as "C_4AH_{13}" by Wells, Clarke, and McMurdie (10) on the basis of a hexagonal cell with $a = 8.89$ Å, $c = 8.20$ Å. The spacings and indices obtained by Wells et al are reproduced in Table 2 for reference.

Dehydration of the material produces successive structures with successive reduction of the longest spacing from 8.20 Å to 7.74 Å, 7.30 Å, 6.80 Å, and 6.09 Å. The last value was obtained by prolonged drying over phosphorus pentoxide and corresponded to a measured water content of 6.78 moles of water per mole of Al_2O_3. The first stage of dehydration was observed by Dosch and zur Strassen (12), who reported a spacing of 7.7 Å and a water content of $9H_2O$ per Al_2O_3.

Table 2. *Interplanar spacings and miller indices for calcium hemicarboaluminate hydrate(10)*

d(Å)	hkl	d(Å)	hkl
8.2	001	2.06	004
4.1	002	2.000	104
3.9	111	1.951	222
2.9	210	1.766	320
2.73	211	1.670	410
2.64	103	1.637	411
2.55	300	1.554	403
2.45	301	1.500	501
2.37	212	1.475	323
2.31	113	1.440	420
2.24	203		

The indexing given in Table 2 is confirmed by the observation that dehydration causes systematic shifts in all low-order lines except the one at 2.88 Å, which is the only low-order spacing of the form (hk0). Thus, the dehydration can be explained on the basis of changes in the c spacing only. This material is then quite different from the other materials of the type $C_3A \cdot CaX_2 \cdot yH_2O$, to which a spacing of the order of 5.7 Å has been attributed (14).

The major source of confusion in the identification of calcium hemicarboaluminate hydrate as a form of C_4AH_{13} arises from the fact that a very small degree of surface carbonation of a sample in an X-ray diffractometer can produce a high intensity 8.2 Å line. The existence of the dehydration states of the hemicarboaluminate helps further to explain the confusion regarding the number of calcium aluminate hydrates. When the phase changes in these materials occur on dehydration, the shifts in the X-ray diffraction pattern are accompanied by line broadening. As a result, the 7.9 Å line of the C_4AH_{13} overlaps the 7.7 Å peak of the first dehydration state of the carbonated phase, and the 7.4 Å line of the C_4AH_{11} overlaps the peak for the second dehydrated carbonate state at 7.3 Å. Thus, the hemicarboaluminate and the C_4AH_{13} have appeared to produce identical dehydration states.

Calcium Hemicarboferrite Hydrate

The results described above naturally lead to the question of whether the behavior of the calcium ferrite and aluminoferrite hydrates on carbonation is analogous to that of the calcium aluminate hydrates. Two sets of experiments have demonstrated that this analogous behavior actually does occur.

In one study, samples of tetracalcium aluminoferrite were hydrated at 40°F in the presence of systematically varied quantities of calcium carbonate, just as already described for tricalcium aluminate. Each slurry contained four moles of calcium hydroxide per mole of C_4AF to bring the $CaO/(Al_2O_3 + Fe_2O_3)$ mole ratio to 4. The original slurries were dark colored, but became white upon completion of the hydration. The diffraction patterns of the products were completely parallel to those of the C_3A series. The peak for the

highest spacing of the $C_4(A, F)H_{19}$ decreased with increasing carbonate contents and disappeared when the $CO_2/(Al_2O_3 + Fe_2O_3)$ mole ratio reached 0.5. At this point, the peak for the 8.2 Å spacing reached its maximum intensity, decreasing at higher CO_2 contents as the peak for the 7.6 Å spacing for the calcium monocarboaluminoferrite hydrate became stronger. The alumina-ferric oxide combination apparently forms a series of carbonated calcium salts completely analogous to those of the alumina alone.

The evidence for the formation of a hemicarboferrite comes from a test in which very finely ground C_2F was hydrated in a slurry at 40°F with two moles of $Ca(OH)_2$. After 8 days of agitation considerable reaction had occurred. X-ray diffraction showed major spacings of 10.7 Å and 8.20 Å, indicating that atmospheric CO_2 had produced the calcium hemicarboferrite hydrate in the absence of alumina. The *c* spacings for these carbonated phases containing alumina or ferric oxide appear to be identical.

Alumina Versus Ferric Oxide

Cement hydration is usually discussed in terms of the alumina in the cement despite the fact that ferric oxide forms a set of high limed hydrates completely analogous to the calcium aluminate hydrates and their complexes (15). Since those compounds based on ferric oxide are essentially indistinguishable from their alumina counterparts by X-ray diffraction, attempts to study the role of the ferric oxide in the cement-water system have encountered formidable experimental problems. Recently, a new instrument, the Mössbauer spectrometer, has become available for studies of the state of the iron. The presence of aluminum does not complicate such studies. The instrument has yielded results that provide considerable insight regarding the separate roles of the alumina and the ferric oxide in cement hydration.

The space available here does not permit a discussion of the principle and the operation of this instrument, other than to say that an X-ray spectrographic technique is used that is somewhat analogous to one used recently to determine the coordination number of aluminum in various compounds (16). The Mössbauer technique, however, measures total resonance absorption, by the sample, of radiation from a very different type of radiation source and is much more sensitive than the usual type of X-ray spectrograph. The interested reader can find a good and inexpensive elementary English language text readily available (17).

Reference patterns for the use of this instrument have been obtained from tests run for these laboratories by Dr. R. L. Collins of Austin Science Associates, Inc. Two fully hydrated mixtures prepared by long time agitation of slurries of tetracalcium aluminoferrite, gypsum and calcium hydroxide were submitted for examination. A light colored material made from a slurry having a $SO_3/(Al_2O_3 + Fe_2O_3)$ mole ratio equal to one and containing sufficient calcium hydroxide to produce a $CaO/(Fe_2O_3 + Al_2O_3)$ mole ratio of 4 gave an X-ray diffraction pattern characteristic of the monosulfate and a characteristic Mössbauer pattern shown in Fig. 2.

In this figure, the ordinate, reading downward, represents the absorption, in percent, of the incident beam by the sample. No calibration was made for this exploratory test, so that the energy units on the abscissa simply represent channel numbers of the memory in the recording analyzer. Under proper calibration, as shown later in the present paper, these channel numbers represent numerical values for velocities that are proportional to differences in beam energy from that represented by the mid-line that intersects the horizontal scale. Two parameters are used to characterize these spectra. One is the displacement of the center of gravity of the spectrum from the zero of the figure. This parameter is known as the *isomer shift*. The other parameter, known as the *quadrupole splitting* is the difference in energy (expressed as velocity) between the two absorption peaks that frequently appear for a single solid phase, particularly for crystals of low symmetry.

A much darker material prepared from a similar mixture, but with only half the quantity of gypsum per unit C_4AF, gave a diffraction pattern identical with that of the light colored material, so far as could be determined with copper Kα radiation without special monochromators. Special care might perhaps have detected a broad peak, but it is certain that no other well-crystallized phase was present. The dark material produced the Mössbauer pattern shown in Fig. 3. This figure can be interpreted as indicating the presence of at least two phases, one of which is probably the one responsible for the pattern shown in Fig. 2. It thus becomes quite clear that the instrument is responsive to changes in the state of the iron in the presence of lime, alumina, sulfate and water. The result indicates further that the color of the product provides an index to the purity of the phase. Since it had been found that mixtures of intermediate composition produced dark products, it could be conclude that the light colored single phase with the highest sulfate content was the low sulfate from of calcium sulfoaluminoferrite hydrate, $C_6AF \cdot 2CaSO_4 \cdot xH_2O$.

A further confirmation of the sensitivity of the instrument was obtained from a Mössbauer pattern of the aluminoferrite analog of ettringite as prepared from a slurry of aluminum and ferric sulfates and calcium hydroxide in the appropriate stoichiometric ratios. Again a pattern for a single compound was found. This pattern was, moreover, distinctly different from that of the monosulfate.

The above considerations have now paved the way for a discussion of the existing evidence regarding the nature of the ultimate hydration products of portland cement.

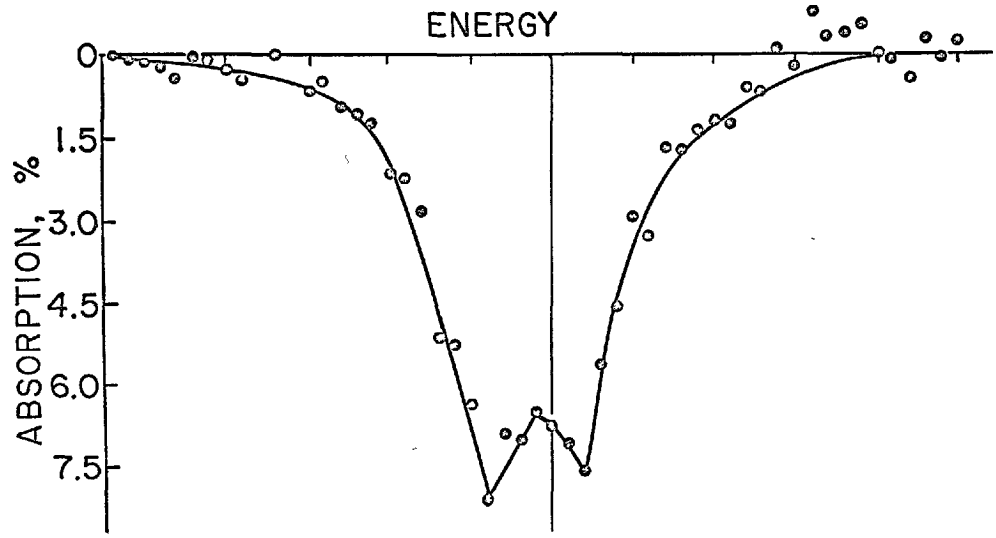

Fig. 2. *Mössbauer spectrum of the low sulfate form of calcium sulfoaluminoferrite hydrate.*

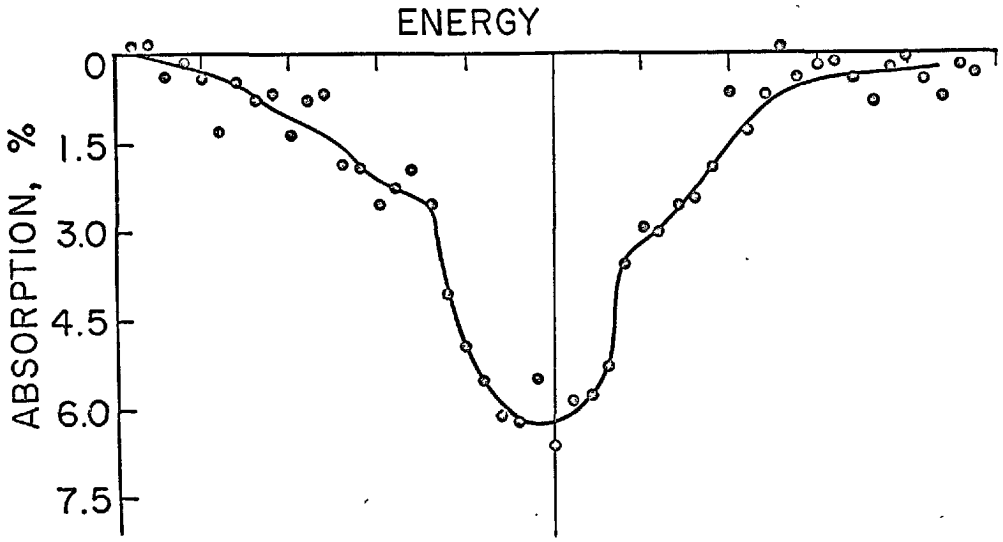

Fig. 3. *Mössbauer spectrum of a fully hydrated material with the molar composition:* $C_4AF + 3CaO + CaSO_4 \cdot 2H_2O$.

The Ultimate Hydration Products

The most comprehensive survey by X-ray diffraction of the phase composition of the ultimate hydration products in portland cement is the study of well aged pastes by Kantro, Copeland and Anderson (6).

After exclusion of the carbonated phases as not properly belonging in the cement-water system, and of ettringite in the presence of CO_2 as frequently secondary, the patterns obtained consistently show the presence of a calcium silicate hydrate gel, sulfated calcium aluminate and ferrite hydrates, a hydrogarnet phase, and calcium hydroxide.

Since no work has been reported on the composition of the liquid phase in equilibrium with all of these ultimate hydration products, present knowledge of the final state of the cement-water phase equilibrium is necessarily limited to the nature, composition, and thermodynamic stability of these materials. The calcium hydroxide is very well defined and crystallized, and is always present, in the normal range of cement compositions, in sufficient quantity to saturate the liquid phase in the cement-water system. The interest here therefore centers on the nature and composition of the remaining solid phases. The matter of thermodynamic stability is considered later.

The Calcium Silicate Hydrate Phase

The calcium silicate hydrate gel found in portland cement pastes is the primary cementitious material. It is a very poorly crystallized material, whose presence and general characteristics have been recognized for many years. It is only relatively recently, however, that X-ray diffraction techniques have demonstrated a fragmentary pattern of three lines (5), and electron microscopy has demonstrated a characteristic morphology for dried samples (18). Crystallographically, the material is a distorted version of the structure known as CSH (I) that is usually formed in room temperature equilibrium studies in the CaO–SiO_2–H_2O system (19). The most significant structural difference between the cement product and CSH (I) is the absence, in the former, of any lines involving a c spacing. The spacings that are observed in both materials are also found in the naturally occurring crystalline mineral tobermorite (19).

Paste hydration of tricalcium silicate or beta-dicalcium silicate at room temperature yields a gel with the same X-ray pattern as the cement hydration product. It thus appears that the structure of the product is little affected by the presence of the other constituents of portland cement. This conclusion is strengthened by the close agreement that has been found between the heats of hydration of the anhydrous silicates and the values for the corresponding phases in portland cement as calculated by least squares from the heats of hydration of cements of various compositions (20). The electron microscope, however, does show a difference in morphology (18).

It is not surprising that a material as poorly defined as this major cement hydration product should show minor variations in composition. Various studies have shown that small quantities of alumina, ferric oxide, sulfate, or alkalies can be incorporated in the material without causing a change in X-ray pattern. It thus appears that changes in composition of this phase could accompany changes in the equilibrium liquid phase. Such changes are of interest in relation to the early hydration reactions and are discussed in that context after consideration of the effects of other solid hydration products on the liquid phase composition. It is, however, pertinent to consider here the ranges of composition that have been found for individual substituents and combinations of them.

The work of Copeland, Bodor, Chang, and Weise (21) indicates that alumina, ferric oxide, or sulfate ion can be incorporated into the gel by substitution of the aluminum, iron, or sulfur atoms, respectively, for calcium or silicon atoms up to a maximum of one atom of substituent per six atoms of silicon in the hydrate. These preparations were made by wet ball milling of the anhydrous C_3S or alite with an appropriate anhydrous or hydrated calcium compound containing the constituent and appear to be good approaches to equilibrium. It was also found that exposure of an alumina substituted gel to a sulfate solution produced ettringite. This result provides a direct demonstration of the effect of the liquid phase on the gel composition, even though no quantitative analyses of the liquid phases were made.

It will be shown later that the calcium silicate hydrate phase finally formed in hydrated cement paste contains considerable alumina and little ferric oxide or sulfate ion.

Effect of Alkalies

The classical study of Kalousek (22) on the Na_2O–CaO–SiO_2–H_2O system determined equilibrium points for gels prepared by reaction of calcium hydroxide with sodium silicate solutions. Equilibrium as measured by constancy of solution composition, was attained in a few weeks. It was pointed out, however, that the equilibria depended strongly on the nature of the solid phase and that slow changes in crystallinity of that phase over a long period of time could produce very different equilibrium points. Little has been reported since the time of that study in relation to the effect of alkalies on calcium silicate hydrate gels.

Powers and Steinour (23), in their study of alkali-aggregate reaction, have reported alkali contents of

solutions and solid phases resulting from two year contact of water with five hydrating cements beginning with pastes one day old. It was found that the alkali contents of the gels were much lower than would be expected from the results obtained by Kalousek,

Recent studies at these laboratories have indicated the reason for the discrepancy and have provided a limited amount of additional information regarding the role of the alkalies in the gel of the cement-water system. In these studies, various cements, anhydrous calcium silicates, and synthetic calcium silicate hydrates with a range of lime-to-silica ratios up to 1.45 were treated as slurries with alkali solutions from 0.125 molar up to 2 molar in sodium or potassium hydroxide for a period of six months. X-ray diffraction patterns were made of the wet solid phases obtained by filtration of these slurries. In many cases, the filtrates were weighed and analyzed to determine the distribution of alkalies in the system. Inconsistencies in the analytical results indicated that equilibrium had probably not been attained in six months, particularly at the higher alkali contents. The present discussion of these results is limited to those essentially qualitative aspects believed significant in the cement-water system.

The alkali contents of the solid phases were in all instances of the magnitude found by Powers and Steinour and considerably less than those found by Kalousek. The tests of the effect of potash were limited to the synthetic calcium silicate hydrate gels; for these preparations, with a range of lime-to-silica ratios of 0.9 to 1.45, the potash and soda behaved very similarly.

After six months of exposure to alkali, all solid phases, including those of the cements, developed some degree of crystallinity, as revealed by the presence of a peak for the (002) spacing of tobermorite in the diffraction patterns. Some variation of the position of this peak was noted at low alkali contents for the tests on C_3S and β–C_2S, where spacings as low as 9.6 Å were observed. At the higher alkali contents the peak became sharper and in all cases attained a spacing of 12.3–12.4 Å, the constant spacing observed for the highest limed calcium silicate hydrate at all alkali contents. The results clearly confirm Kalousek's surmises regarding the dependence of the equilibria on the state of the gel and the presence of slow crystallization processes.

An additional feature of interest in the tests on the highest limed calcium silicate hydrate was the presence of the peaks for the (001) and (101) spacings for calcium hydroxide. These lines appeared at soda or potash concentrations above 0.25 molar and increased in intensity with increasing alkali contents.

A comparison of these results with Kalousek's data indicates that the limiting alkali concentration for appearance of solid calcium hydroxide was much lower for his gels. The equilibrium state for the present gel is characterized by a higher lime content as well as a lower alkali content.

It might be speculated that the increasing crystallinity of the gel with time of exposure might be accompanied by a decreased tolerance for alkalies in the structure. An indication of this effect was observed in another series of tests in which the soda content of the gel formed from the highest limed calcium silicate hydrate decreased during the time from 20 to 98 days of exposure. Unfortunately, this series of tests included sodium chloride in solution as an additional source of alkali, so that secondary effects may have occurred even though no appreciable change of the chloride ion concentration in solution was observed.

Since diffraction patterns of hydrated cements do not normally exhibit the d_{002} spacing found in the above study, it must be assumed that the significant quantities of alumina present in cement gel affect the structure. Evidence for this has been found in the electron microscope (21). A more complete study of the role of the alkalies in the cement-water system would therefore require the addition of alumina to the calcium silicate hydrates. The evidence already presented, however, indicates that the difference in capacity for alkali between a high limed calcium silicate hydrate gel and the gel in hydrated cement must be small. The primary conclusion to be drawn from the studies just described is that the alkali content of the gel in cement paste must be quite low and of the order of magnitude found by Powers and Steinour.

The Sulfated Aluminate and Ferrite Hydrates

A large number of studies have produced evidence for the existence of calcium sulfoaluminates at the various stages of cement hydration. The best evidence available for the ultimate hydration state is probably that of the X-ray diffraction study already cited (6). As already mentioned, caution must be used in the evaluation of such studies with respect to the presence of ettringite as a final hydration product in the cement-water system in the presence of carbonated phases.

The most interesting recent development in this area has been the use of the Mössbauer spectrometer in studies of cement paste. Wittmann, Pobell, and Wiedemann (24) have used the instrument to study the hydration of a single cement with a potential

compound composition of 33 percent C_3S, 38 percent C_2S, 14 percent C_3A, and 9 percent C_4AF, and with an SO_3 content of 3.1 percent (25). The spectrometer was used to monitor the state of the iron during the hydration of the cement in pastes at water-cement ratios of 0.4 and 1.0. Hydration was complete after two years.

The results are shown in Fig. 4. The spectrum of the original cement is shown at the top of the figure. The work of Pobell and Wittmann (26) on the ferrite solid solution series has shown this pattern to be characteristic of C_4AF. This pattern was also obtained from the pastes for the first two days after mixing. Thus, it appears that no hydration had taken place during this period. The middle spectrum was obtained for the paste with a water-cement ratio of 1.0 at 27 days. Here the C_4AF peaks have decreased in intensity and two peaks for a hydrated phase have appeared. Finally, at 200 days, the bottom spectrum was obtained. Here, only the pattern for the hydrate appears; it can be assumed that the material was completely hydrated. The phase appearing at ultimate hydration was the only hydrated phase that was found throughout the hydration process. This phase was not identified.

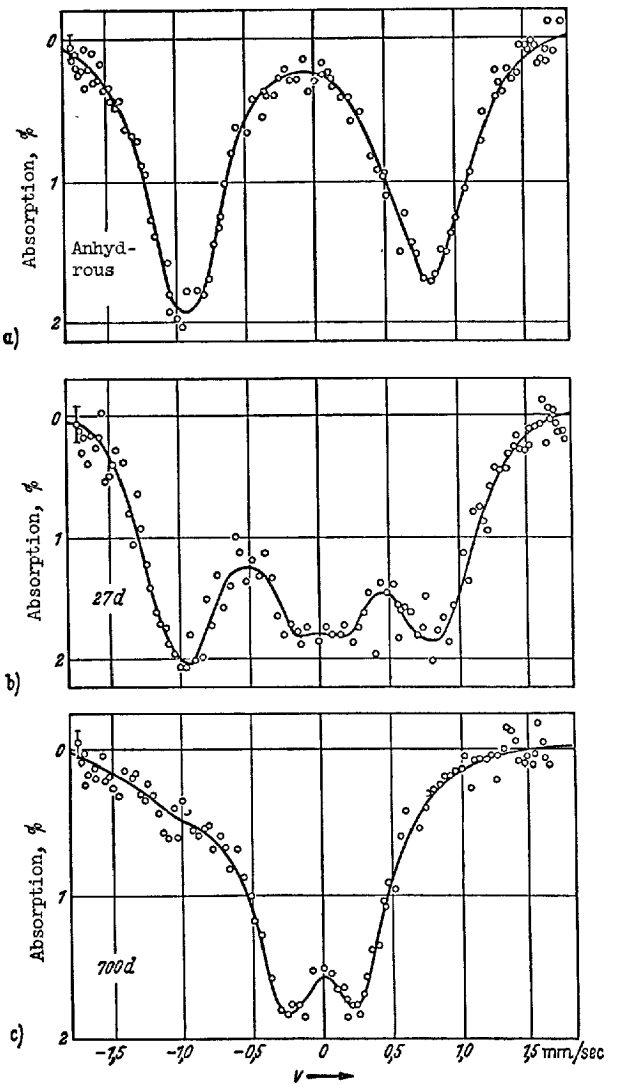

Fig. 4. *Mössbauer spectra of a cement at successive stages of hydration (from Reference 23).*

Comparison with the results obtained by Collins reveals that the final spectrum of Fig. 4 is identical with that shown in Fig. 2. This matching identifies the hydrated ferrite as the low sulfate form of calcium sulfoaluminoferrite hydrate. It must be recognized that this identification cannot be regarded as complete until Mössbauer patterns of all other possible alternatives are available; it is believed, however, that general experience with the sensitivity of the instrument indicates that other materials containing ferric oxide, such as the sulfate-free C_4FH_x or $C_4(A, F)H_x$, would give distinctly different patterns. This identification is also made with the qualification that the Mössbauer spectrometer is known to be insensitive to highly dispersed states of iron (26), i.e., a small quantity of ferrite hydrate dispersed in the gel would probably not be detectable by this means.

From the result obtained, definite conclusions can be drawn regarding the final distribution of the alumina and the ferric oxide in the cement tested by Wittmann. The mole ratio of Fe_2O_3 to SO_3 in this cement is 0.477. Thus, the Mössbauer results indicate that for each mole of sulfate present, $2 \times 0.477 = 0.954$ mole is ultimately transformed to a calcium sulfoaluminoferrite hydrate and 0.477 mole of alumina is consumed. The mole ratio of Al_2O_3 to SO_3 is 1.814. From the X-ray evidence, it is reasonable to assume that the lowest sulfate form of calcium sulfohydroxyaluminate hydrate is present. The experimental evidence, as shown later in the present paper and also in reference 11, indicates that this compound contains about 0.6 mole of SO_3 per mole of alumina. The 0.046 mole of sulfate not accounted for in the ferrite complex can thus combine with $0.046/0.6 = 0.077$ mole of alumina. This supposition still leaves $1.814 - 0.477 - 0.077 = 1.260$ mole of alumina per mole of sulfate unaccounted for. If this 69 percent of the alumina in the cement were to combine with the free calcium hydroxide that must be present in the hydration products, a tetracalcium aluminate hydrate would form and could be identified by diffraction. Since this hydrate has not been found in well hydrated pastes, it must be concluded that the remaining alumina is

ultimately distributed between the calcium silicate gel and the calcium aluminosilicate hydrogarnet phase discussed later. Without X-ray diffraction patterns of saturated, well-aged, uncarbonated pastes of the cement studied by Wittmann, however, it is not feasible to verify this analysis.

A Mössbauer spectrometer study of the pastes described in reference 6 is now underway in cooperation with the National Bureau of Standards. To at least a first approximation, all pastes tested have produced spectra similar to Fig. 2 for the hydrated ferrites. It thus appears that the above analysis should be quite generally applicable.

The above calculation of the distribution of cement components into the ultimate hydration products can always be performed provided that the mole ratio Al_2O_3/Fe_2O_3 is at least unity and the mole ratio SO_3/Fe_2O_3 is at least two. The first of these requirements is met by all portland cements except certain special cements designed to have a zero C_3A content. The second requirement is met by most present-day normal cements, such as ASTM Type I, especially with the continuing rise in specification limits for SO_3 content (27), but not by low heat or sulfate resistant cements or even by many older cements with relatively low SO_3 contents. In well hydrated pastes made from cements not meeting the second requirement, preliminary results from the present cooperative study reveal that only unhydrated C_4AF can be found as an additional iron-containing phase, even in pastes cured continuously moist for 10 years. Thus, it appears that hydration of the ferrite phase in cement essentially ceases when sulfate is no longer available for formation of the sulfoaluminoferrite complex. These cements with the unhydrated C_4AF residue are the very ones whose X-ray diffraction patterns indicate the presence of ettringite as an ultimate hydration product. It is therefore apparent that the hydration in these pastes is of a character more usually associated with the early hydration reactions and will be discussed further when these reactions are considered.

With respect to the phase equilibria in the cement-water system a problem remains in that some cements produce pastes containing an unhydrated residue at later ages that is certainly not an equilibrium phase, and yet one that hydrates so slowly that no hydration products are identifiable in a reasonable time.

Effect of Alkalies

With regard to the possible effect of alkalies on the sulfated aluminates and ferrites, it is necessary to consider the recent work of Dosch and zur Strassen (28) dealing with a solid calcium sulfoaluminate hydrate phase containing soda. After a great deal of effort, these workers were unable to establish either the precise composition of the phase or the boundaries of its region of stability. Both of these problems proved to be very complex. It was concluded that this phase, with the approximate composition:

$$4CaO \cdot 0.9Al_2O_3 \cdot 1.1SO_3 \cdot 0.5Na_2O \cdot 18H_2O,$$

was unlikely to occur in cement paste, except possibly in dried pastes at very early ages.

The results of a series of studies by the present authors on the effect of sodium hydroxide solutions on the concentrations of sulfate that are in equilibrium with calcium sulfoaluminate and sulfoferrite hydrates add a little more to the story. Examination by X-ray diffraction of the solid phases obtained in this study revealed the presence of calcium hydroxide and the solid phase with the 10.0 Å and 5.0 Å spacings studied by Dosch and zur Strassen. Those workers found it necessary to use relatively low lime and high alumina levels in order to determine the composition of the solid phase. The present work, on the other hand, with solid $Ca(OH)_2$ present and with very low Al_2O_3 in solution, represents a range of liquid phase compositions that is much closer to those occurring in cement pastes.

In one series of tests, mixtures of ettringite with a series of solutions of sodium hydroxide with concentrations from 0.4 to 8.6 percent NaOH were agitated in polyethylene bottles for 4 weeks. The new phase was detected in many of the tests. In only one case, however, did the reaction proceed to the point that ettringite was no longer detectable by diffraction. In this test, 5 grams of ettringite were treated with 40 ml of 2.55 N sodium hydroxide. On the assumption of the Dosch and zur Strassen composition for the alkali-containing solid, it was to be expected that the final solution would contain 6.69 percent Na_2O and 1.25 percent SO_3. The actual values found were 7.59 percent Na_2O and 1.30 percent SO_3. The result indicates that the new phase can form in highly alkaline media in the presence of excess lime and in the absence of excess alumina. There is, further, an indication here that the phase has a different composition under these conditions.

An analogous set of experiments with the high sulfate form of calcium sulfoferrite hydrate yielded similar results, with considerably greater sulfate solubility at low alkali concentrations and with similar reduction in Na_2O in the liquid phase. Here the basal spacing of the new phase was 10.3 Å, which is the same as that for the low sulfate form of calcium

sulfoferrite hydrate. It appears that, in principle, either the aluminate or the ferrite can form this type of solid phase.

A similar set of tests with the calcium sulfohydroxyaluminate hydrate showed slight but definite increases in SO_3 and decreases in Na_2O solution concentrations. However, excessive carbonation prevented careful diffraction studies of the solid phases.

In the course of the previously discussed tests on the effect of alkalies on the gel in hydrated cement, the 10.0 Å and 5.0 Å spacings were observed in the diffraction patterns of the solids from various reaction mixtures. It was found that when slurries made from one part of cement and as much as 8 parts of 8 percent sodium hydroxide solution were hydrated, these peaks represented the only identifiable sulfate-containing phase in the solid. It thus appears that the compound can form in cement in the presence of excess alkali, although it has not been detected under oridinary conditions of cement hydration.

The Hydrogarnet Phase

Kantro, Copeland and Anderson (6), in their X-ray studies, reported the presence of a set of diffraction peaks attributable to a cubic hydrogarnet phase. This pattern appeared quite early in the hydration process and did not increase appreciably in intensity during aging of pastes. The unit cell edge, 12.40 Å, was definitely different from the 12.58 Å of the tricalcium aluminate hydrate, C_3AH_6. Since substitutions, both of alumina by ferric oxide and of water by silica, are possible, the observed cell size could not be used for identification of the composition. The formation of this phase has been confirmed by electron microscope studies (29).

The persistence of the hydrogarnet phase during the remainder of the hydration process indicates a high degree of stability. On the other hand, the inability of the phase to nucleate C_3AH_6 is of considerable interest. Apparently the cell sizes and compositions are too different for this process to occur. Another alternative is that C_3AH_6 is not a stable phase in the $CaO–Al_2O_3–SO_3–H_2O$ system in the presence of excess lime, a possibility that is considered later.

The Mössbauer results provide a clue regarding the composition of the material. Cubic phases are known to give spectra different from those of hexagonal phases. All of the pastes that have been studied by this technique have produced spectra with appreciable intensities only for the patterns of unhydrated C_4AF and the calcium sulfoaluminoferrite hydrate. Strong evidence thus exists for the absence of ferric oxide in the hydrogarnet phase. Comparison of the observed cell edge of 12.4 Å with those found by Flint, McMurdie, and Wells (30) indicates that the hydrogarnet formed should have a composition on the order of $C_3AS_{0.5}H_5$.

Summary

The present knowledge of the cement-water system indicates that five hydrated solid phases are ultimately formed. These phases are a calcium silicate hydrate gel containing significant quantities of alumina, sulfate, and alkalies, the low sulfate form of calcium sulfoaluminoferrite hydrate, the lowest sulfate form of calcium sulfohydroxyaluminate hydrate, and aluminasilica hydrogarnet, and calcium hydroxide. In cements with relatively low C_3A contents, such as ASTM Type IV or Type V, ettringite and unhydrated C_4AF may also be present.

Thermodynamic Stability of the Ultimate Hydration Products

Although true thermodynamic equilibrium in a condensed heterogeneous system implies the presence of stable solid phases, the continued presence of a solid phase in a reaction mixture does not rule out a metastable situation. In fact, previous studies and reviews on the cement-water system and related phase equilibria have indicated considerable doubt regarding the stability of some of the solid phases that have been found.

The purpose of the present section is to review the available information insofar as it bears on the cement-water system. In particular, recent original studies have produced results of considerable interest.

The Calcium Silicate Hydrate Gel

Work on the lime-silica-water phase equilibrium has generally shown that, at ordinary temperatures and high lime contents, the silica in the system occurs as a calcium silicate hydrate gel (19). The lime concentration in solution varies with the lime to silica ratio of the gel. As already indicated, the gel phase in hydrated cement appears to be a high limed, poorly organized, and partially substituted version of the

calcium silicate hydrate gel found in the phase studies.

A variety of crystalline calcium silicate hydrates have been prepared by hydrothermal means and have usually been considered as stable only at elevated temperatures. A single exception is the room temperature preparation of afwillite, by $C_3S_2H_3$, Brunauer, Copeland, and Bragg (31), which was accomplished by ball milling of slurries of tricalcium silicate in water. In this exceptional instance, it could, however, be argued that the milling process introduced sufficient energy to produce a metastable phase.

Further work has confirmed the possibility that afwillite may well be the stable room temperature calcium silicate hydrate in the lime-silica-water system, but yet may not be the stable phase in the cement-water system. These studies centered around the discovery that the presence of small quantities of afwillite during hydration of tricalcium silicate in pastes caused formation of crystalline afwillite rather than the usual gel. The results obtained and the properties of the material formed are believed of sufficient interest for inclusion here.

Table 3 shows properties of a set of 1/2-inch cubes prepared from C_3S at the water-to-solids ratios shown. Nucleation was accomplished with 2 percent, by weight of the C_3S, of an afwillite formed spontaneously in hydration of a C_3S slurry and purified by leaching with water until no calcium hydroxide was detectable by X-ray diffraction. The cubes were stored in the molds for one day and then in water until the time of test. X-ray diffraction of the specimens indicated a more rapid hydration and the formation of afwillite rather than gel in the seeded cubes. The increase in hydration rate is reflected in the increase in non-evaporable water at 7 days, as measured by the method of Copeland and Hayes (32), and also in the relatively high compressive strengths at that age.

Table 3. *Effect of nucleation by afwillite on the properties of tricalcium silicate pastes*

One half inch cubes stored in the mold for one day and then cured under water until time of test.

Sample No.	Admixture	Water-to-solids ratio	Non-evaporable water		Compressive strength	
			7d.	28d.	7d.	28d.
1	none	0.25	0.109	0.142	10,300	14,800
2	2% afwillite	0.25	0.175	0.177	12,550	14,000
3	none	0.40	0.097	0.151	1,800	5,600
4	2% afwillite	0.40	0.179	0.201	4,900	6,600

Fig. 5 shows conduction calorimeter curves for

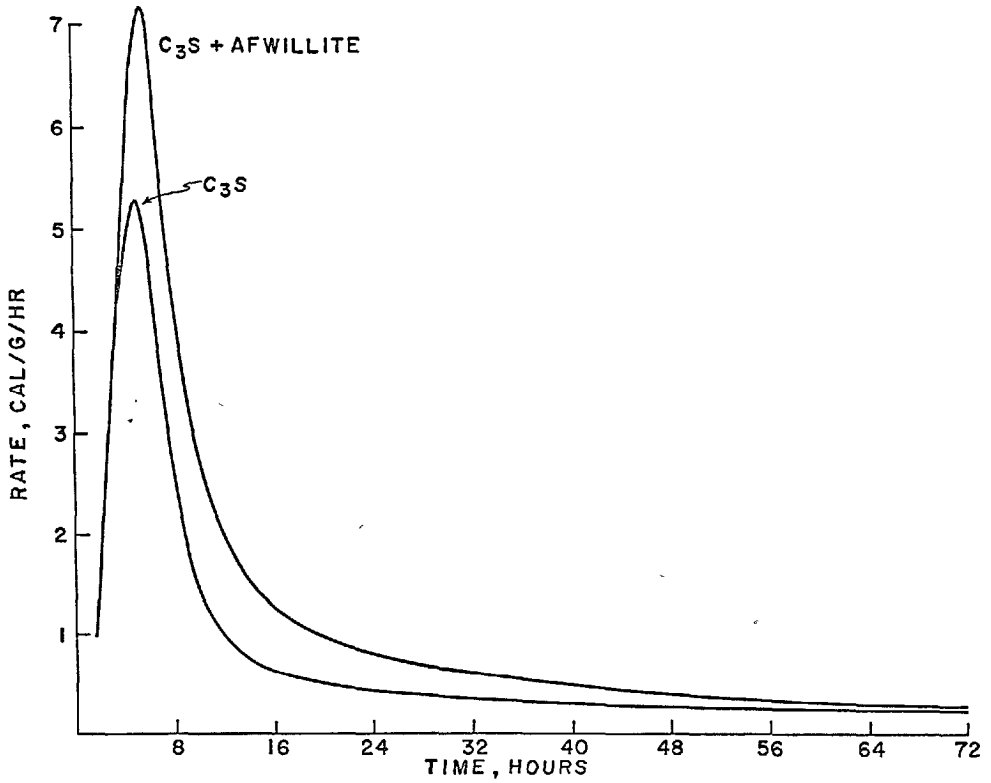

Fig. 5. *Nucleation by afwillite increases the rate of heat liberation during the hydration of tricalcium silicate.*

both seeded and unseeded C_3S pastes made from a sample ground to a specific surface of 4400 cm^2/g (Blaine). The results, from pastes at a water-to-solids ratio of 0.40, reveal a great difference in heat evolution at times as early as 8 hours. After 24 hours the total heat evolved for the nucleated sample was 57.4 cal/g as opposed to 38.6 cal/g for the paste without the afwillite.

The crystalline material also showed the expected reduction in shrinkage as compared with the behavior of an ordinary paste. Fig. 6 shows shrinkage as a function of water content for seeded and unseeded material for 1/4 × 1/4 × 6 inch bars with a gauge length of 5 inches cast from pastes with a water-to-solids ratio of 0.40. After a 28 day cure in water, the bars were stored successively in CO_2-free atmospheres at 85, 65, 55, 45, 25, 7 and 0 percent relative humidity for 24 days at each exposure. It can be seen that, below 85 percent, the shrinkage of the paste containing the crystalline silicate was consistently less than one-third of that of the paste containing the poorly crystalline material.

Further studies included attempts to induce afwillite crystallization in pastes of materials closer in composition to cement and in cement itself. Crystallization could, indeed, be induced in pastes of an alite that has a composition corresponding to the Jeffery formula $C_{54}S_{16}AM$ (33), and also in pastes of alites having alumina and magnesia contents 1/3 to 2/3 of those required by the Jeffery formula. However, crystallization could not be induced in pastes of beta-dicalcium silicate, a mixture of 90 percent C_3S and 10 percent C_3A, or cement.

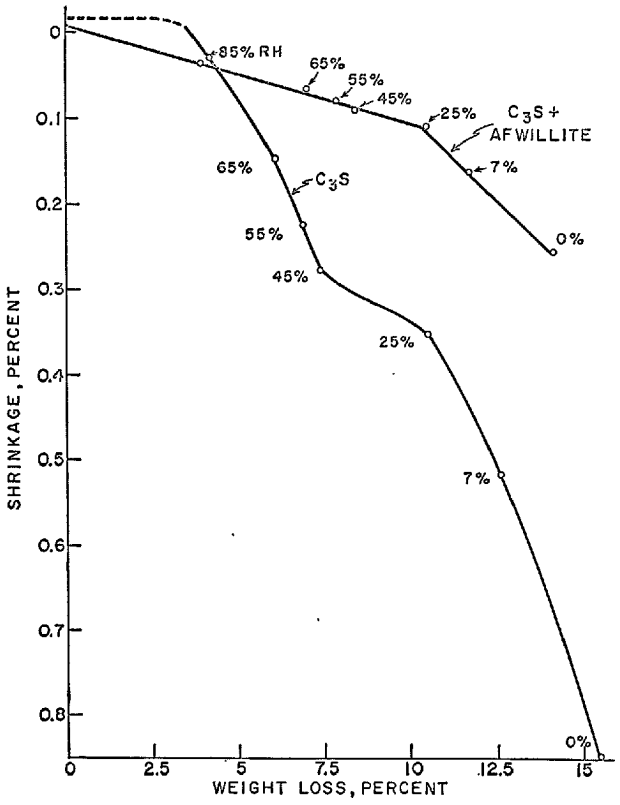

Fig. 6. *Nucleation by afwillite reduces the drying shrinkage of hardened tricalcium silicate pastes*

From the results obtained, it appears that the nature of the stable equilibrium state of the substituted calcium silicate hydrate in cement is still open to question. The difference in free energy between afwillite and the pure calcium silicate hydrate gel may be quite small. It is also possible that the introduction of appreciable quantities of sulfate or alumina into the gel to produce the material found in cement may reverse this free energy difference. Such an explanation would account for all results except the failure to nucleate crystalline afwillite from the dicalcium silicate paste. The presence of the stabilizer in that compound, however, may also have affected the free energy difference.

The Calcium Aluminate Hydrate Phase

Although the alumina and the ferric oxide can potentially form analogous hydrates in cement hydration, only the alumina is of interest in the present context; the cubic tricalcium aluminate hexahydrate, C_3AH_6, has long been recognized as a stable phase in the $CaO–Al_2O_3–H_2O$ system at room temperature, even though it is found to be unstable at temperatures just above the freezing point of water in the presence of excess lime (8). The ferrite analog, C_3FH_6, on the other hand, appears to be structurally unstable (7).

The stability of C_3AH_6 in the presence of sulfate and excess alumina has been clearly established. However, in the presence of sulfate and excess lime, the area of interest in cement chemistry, the picture is much less clear. Considerable controversy over this matter has appeared in the literature and has been summarized by Steinour (34). In relation to the cement-water system it must be noted that the presence of C_3AH_6 in hydrated cement pastes has not been observed by X-ray diffraction, even though a closely related cubic phase, the hydrogarnet, has been found, even at early ages. The latter phase may indeed be only metastable, since it is present only in small quantity throughout the hydration. This phase also appears incapable of nucleating the closely related C_3AH_6. Tests conducted at these laboratories indicate that sulfate inhibits the formation of C_3AH_6

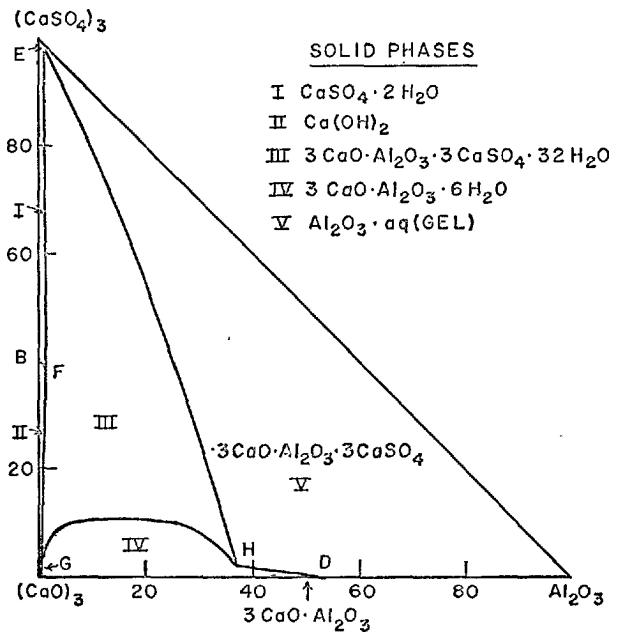

Fig. 7. *System* $CaO–Al_2O_3–CaSO_4–H_2O$ *(with alumina gel) at 25°C (Jones(46)). The diagram is distorted slightly at the left side to show the fields there more distinctly (from Reference 33)*

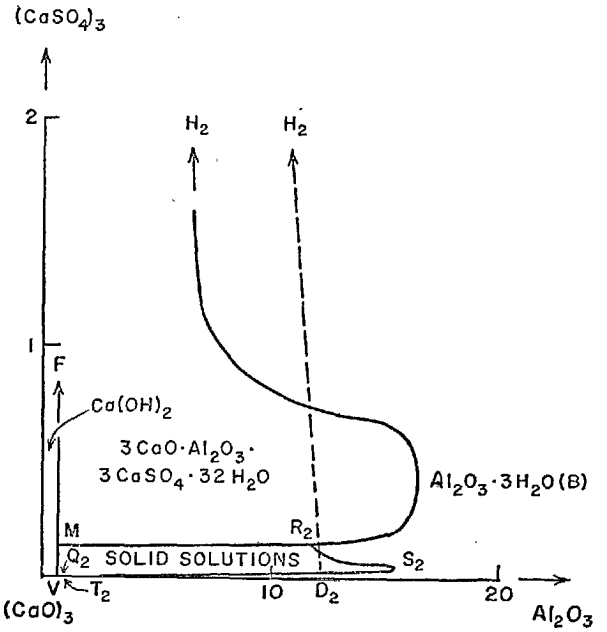

Fig. 8. *Portion of the system* $CaO–Al_2O_3–CaSO_4–H_2O$ *at 25°C showing the region of calcium sulfohydroxyaluminate hydrate (according to Jones(47), from Reference 33).*

in the cement-water system (11). In more recent studies of clinkers having high C_3A contents, C_3AH_6 was observed by diffraction to form in pastes, early and quite readily, in the absence of sulfate.

A previously unpublished study of the calcium sulfohydroxyaluminate hydrates is believed to throw additional light on the stability relations in the $CaO–Al_2O_3–SO_3–H_2O$ system. As background for the discussion of this study and for later reference, it is necessary at this point to review the principal features of that portion of the system where calcium hydroxide exists as a solid phase.

Figs. 7 and 8, from Steinour (34), show the features of interest. These figures are so-called Janecke projections and are particular representations of the four component system. An excellent discussion of this type of representation has been given by Purdon and Slater (35). In Fig. 7, the origin represents pure CaO. For convenience in considering the stoichiometry, the composition of an aqueous mixture, containing calcium, sulfate, and aluminate ions, is expressed in terms of moles of $(CaO)_3$, $(CaSO_4)_3$ and Al_2O_3. On this basis, the mole fraction of Al_2O_3 in the mixture is plotted along the abscissa and the mole fraction of $(CaSO_4)_3$ along the ordinate. Moles of water per mole of total solid can be visualized as being plotted along a third axis perpendicular to the paper. Solution compositions are then represented as surfaces in space. The lines in the figure are vertical projections of the boundaries of the fields of the various phases. The figure shows the liquid phase compositions for the "stable" equilibria at 25°C under the condition that free Al_2O_3, when present, occurs as a gel. The present paper is concerned only with the high lime portion of the system (along CaO–G–F–E in the figure), thus the form of the alumina is irrelevant.

Fig. 8 shows the situation of "metastable" equilibria at 20°C. Here the point G has been replaced by the segment MV. The point M represents the liquid phase composition in equilibrium with three solids: calcium hydroxide, ettringite, and monosulfate.

Studies of the effect of small percentages of alkalies on this system have revealed (34) that the boundaries of the fields shift only quantitatively in the high-lime region and that no new phases appear. Figs. 7 and 8 will therefore also be referred to in relation to appropriate systems containing alkalies.

In a major investigation of the calcium sulfohydroxyaluminate hydrates, three sets of slurries were made in which C_3A and $Ca(OH)_2$ in equimolar proportions were mixed in an excess of water with various quantities of gypsum necessary to introduce 0.1 to 1.1 mole of SO_3 per mole of alumina. These mixtures were agitated in polyethylene bottles for periods up to one year at temperatures of storage of 40°F, 73°F, and 100°F. Periodic examinations of the solid phases at

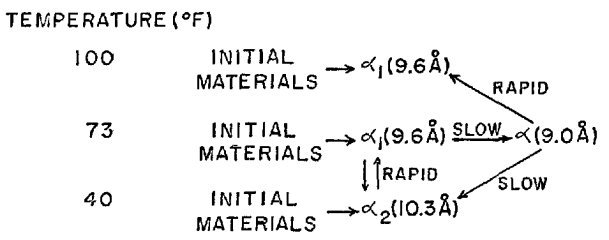

Fig. 9. *Stabilities and conversion rates of the crystalline forms of the low sulfate form of calcium sulfoaluminate hydrate.*

the storage temperatures were made by X-ray diffraction. After the final filtration, the wet solids were subjected to temperature changes while in the diffractometer.

The results shown in Fig. 9, for a mole ratio of $SO_3/C_3A = 1$, indicate that the structure of the monosulfate is highly dependent on temperature. The results shown duplicate in part those of Turriziani (36), whose notation is used here. The α_1 form is stable at 100°F; the α form, at 73°F; and the α_2 form, at 40°F. At 73°F, the α_1 form is produced first, either from the raw materials or by warming of the α_2 form. The α phase, once formed, is relatively stable toward cooling, but converts quite rapidly to the α_1 phase on heating.

The range of calcium sulfohydroxyaluminate hydrates found at SO_3/Al_2O_3 ratios from 0.7 to 1.0 indicated that the solid solutions are stable at 73° and 100° but not at 40°F, where they decompose into the α_2 form of the monosulfate and C_4AH_{19}. The range of d spacings for these calcium sulfohydroxyaluminate hydrates is 8.80–9.01 Å, with the higher spacings corresponding to higher sulfate contents. They are formed at both 73°F and 100°F, after initial formation of the α_1 form of the monosulfate. The rate of formation from the α_1 form was found to decrease rapidly with increase in sulfate content of the system, requiring years at sulfate contents near unity.

It is believed significant that in those mixtures with the very low SO_3 contents stored at 100°F, both C_3AH_6 and the lowest sulfate form of the calcium sulfohydroxyaluminate hydrate were formed, with no trace, in the diffraction patterns, of the ettringite that would be formed from decomposition of the solid solution into the phases usually considered stable. This result would tend to indicate stability for the solid solution at that temperature, and would establish the existence of a boundary in Fig. 8 between the fields of the hexagonal solid solution and the cubic calcium aluminate hydrate. At both 40°F and 73°F, the excess alumina in these low sulfate mixes appeared as C_4AH_{19}. It is to be expected that the C_4AH_{19} would eventually convert to C_3AH_6 and $Ca(OH)_2$ at 73°F.

It is therefore proposed that another invariant point occurs between M and V in Fig. 8 that represents the liquid phase composition in equilibrium with $Ca(OH)_2$, C_3AH_6, and the lowest sulfate form of calcium sulfohydroxyaluminate hydrate as the solid phases. The segment from that point to V would then be the boundary between a C_3AH_6 field and the $Ca(OH)_2$ field. The complete phase diagram would then include a new boundary extending from the low limit of the solid solution field on MV to some point on MR_2, to the left of the field of Al_2O_3.

An exploratory test, completed while the present paper was being written, provides somewhat more direct evidence for the stability of the lowest sulfate form of calcium sulfohydroxyaluminate hydrate. The test was based on various previous studies that indicated a high degree of stability of the α_1 form of the monosulfate in the presence of excess lime over the temperature range 100–190°F. In the present test a slurry containing this form of the monosulfate together with C_3AH_6 and excess lime was stored at 100°F. After 3 weeks, weak diffraction peaks appeared for the lowest sulfate form of the calcium sulfohydroxyaluminate hydrate. The estimated 3–4 percent of the reaction product are believed to constitute direct evidence for its thermodynamic stability at 100°F.

In another study, the details of which are beyond the scope of the present paper, it was found that slurries of appropriate proportions of C_3AH_6, $Ca(OH)_2$, and calcium carbonate formed the calcium hemicarboaluminate hydrate on prolonged agitation at room temperature. It was thus demonstrated that C_3AH_6 is not stable with respect to formation of the $C_3A \cdot \frac{1}{2}CaCO_3 \cdot \frac{1}{2}Ca(OH)_2 \cdot 12H_2O$ in the $CaO–Al_2O_3–CO_2–H_2O$ system.

Phase Equilibria and the Early Hydration Reactions

Although the early stages of portland cement hydration cannot represent equilibrium states, the studies that have been made of the equilibria among the phases involved have provided considerable insight into the nature of the reactions that are occurring. The reactions that occur in this heterogeneous system are relatively slow in comparison with those occurring, for example, among inorganic ions in aqueous

solution. The processes limiting the rates of reaction appear to be those of solution and of crystallization that occur at interfaces between solid and liquid phases. The nature of these processes will naturally depend upon the composition of the liquid phase at these interfaces. For very rapid reactions, this composition will be only locally uniform; for the slower reactions in pastes, on the other hand, the composition of the entire liquid phase can be considered uniform. Thus, in the absence of high activation energies, the reactions at these interfaces can be considered as heterogeneous equilibrium situations that involve shifts in composition as the hydration reactions continue. The existing evidence indicates that this description furnishes adequate mechanisms for many features of the early hydration reactions. It is in this sense that the stages of early hydration can be related to phase equilibria in the cement-water system.

The earlier writers on phase equilibria of those aqueous systems that include components of cement made predictions only reluctantly with regard to the course of the early hydration reactions. This reluctance had several based, namely, that slow reaction rates could prevent attainment of a predicted equilibrium situation, that the presence of other cement constituents would cause radical changes in the limited systems that they were studying, that there was no clear-cut experimental evidence to support their conclusions, and, finally, that there was considerable uncertainty regarding the nature and stability of the solid phases present in cement pastes, or even in some of the more limited systems studied. A major cause of the uncertainties was probably the presence of products from rapid local reactions and from carbonation. Present knowledge largely confirms the premise that many aspects of the early hydration are entirely predictable from the phase equilibrium studies.

The background for the present interpretation comes from the published studies on phase equilibria, from the more recent studies of the early hydration reactions and, finally, from the excellent recent studies of the composition of the liquid phase (37, 38, 39). The approach used here is to interpret the hydration process from the time of the first contact of the cement with water to the time of formation of the ultimate hydration products already described. Because of the nature of this approach, little attention will be given to the components of the original cement. It will generally be assumed that the various components diffuse into the solution until the sources of the components are exhausted. A major exception is the ferrite phase, for which the results from Mössbauer spectroscopy, as well as evidence from X-ray diffraction (40) indicate a considerable delay in initiation of hydration. It is therefore assumed that ferrite is initially "absent".

Of the various recent studies of the liquid phase at early ages, that of Lawrence (37) appears to be the most complete and to give the most detail. The results of this study are used in the following sections wherever references to a uniform liquid phase composition are appropriate.

Fig. 10 is a reproduction of one of Lawrence's plots of liquid phase composition, up to about 16 hours, for a cement paste having a water-cement ratio of 1.0. This figure displays most of the features relevant to the present discussion. After the initial contact with the cement, the liquid phase has high lime and sulfate concentrations. The alkalies of the cement are released gradually. The lime concentration passes through a maximum, which is accompanied by a drop in sulfate concentration. This sequence is accompanied by an increase in the alkalinity (basicity). The composition then remains relatively constant with slow increase in alkalies until rapid decreases in lime and sulfate concentration occur, accompanied by a rise in alkalinity. The cement composition was not given, but the plot indicates that the material is undersulfated, by the present criterion, since sulfate depletion occurs before 18 hours. Most of the features of the plot are included in the interpretation given below.

First Contact Between Cement and Water

The period of first contact between cement and water is a time of highly energetic reaction, as evi-

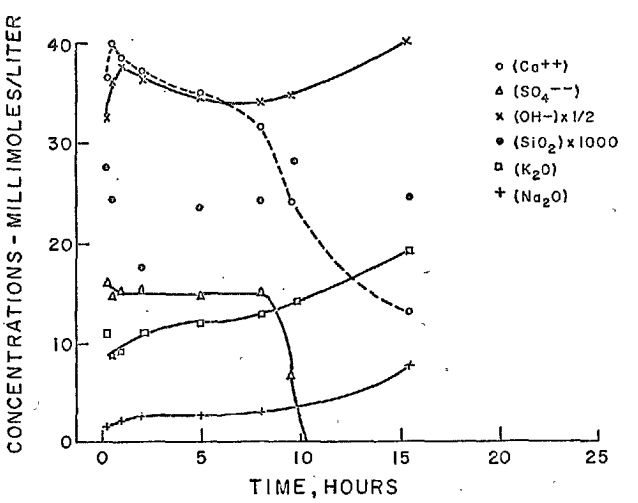

Fig. 10. *Composition of the liquid phase during early hydration reactions of a cement at 25°C (from Reference 37).*

denced by the rate of heat evolution. It is to be expected that solution compositions and temperatures vary widely over the entire body of liquid during this brief period and that the highest concentrations and temperatures occur in the liquid layer closest to the cement particles. It is therefore not surprising that considerable uncertainty has existed regarding the first alumina-containing phase to be precipitated.

Under an assumption of localized approaches to equilibrium, it is perfectly possible for a variety of immediate hydration products to form. The solid product would merely depend upon the local temperature and the local concentrations of lime, sulfate, silica, alumina, and alkali existing at the surface of the hydrating cement particle. This expected variety has in fact actually been observed in an electron microscope study of the products of brief periods of hydration (29). By means of a replica technique, various products formed after as brief a hydration period as 30 seconds have been observed. Rods of ettringite, plates of calcium aluminate hydrates probably containing various amounts of sulfate, and cubic crystals of hydrogarnet were observed against a background of gel, as might be expected from local variations in alumina and sulfate ion concentrations.

Dormant Phase

After the immediate reactions the liquid phase is supersaturated with calcium hydroxide and saturated with calcium sulfate. Alkalies are also present. Unfortunately, values for the alumina content of the liquid phase during that period are not available but are known to be very low. Relative to the components shown in Fig. 7, or its analogue at low alkali concentrations (41), the solution composition could be represented along a metastable extension of the boundary EF toward G. This point could not lie on the boundary FG, since this position would imply the presence of calcium hydroxide as a solid phase. Along the boundary EF, the solid phases are calcium sulfate and ettringite, as in the present case. During the period before the crystallization of calcium hydroxide, when the rate of heat evolution is very low, the alumina, which is already dissolving from the tricalcium aluminate, reacts with the calcium sulfate in solution to produce the solid ettringite. Thus, as shown for the first six hours in Fig. 10, the solution composition remains relatively constant except for changes in calcium hydroxide supersaturation as represented along the prolongation of the boundary EF in Fig. 7. The increase in supersaturation tends to decrease the sulfate concentration because of the common ion effect, as shown in Fig. 10 for the initial hour. The alkalinity remains quite constant during the period because the alkali released from the cement reacts with the calcium sulfate to form calcium hydroxide (42):

$$2KOH + CaSO_4 \rightarrow Ca(OH)_2 + K_2SO_4 \qquad (1)$$

Since the alumina concentration at F is very small, and is probably decreased by the increase in lime, the metastable extension of EF must be almost parallel to the $(CaO)_3$–$(CaSO_3)_3$ axis and probably turns slightly toward that axis. The effect of the release of alkalies on alumina concentration has not been measured directly, but can be estimated from the phase equilibrium studies, which indicate that the alumina concentration at point F in Fig. 7 is decreased in the presence of alkalies.

So far nothing has been said about the silicates. It has been indicated, however, that the liquid phase rapidly becomes supersaturated in lime. This calcium hydroxide must result primarily from the reaction of water with the alite phase. The crystallization of $Ca(OH)_2$ from this solution usually initiates the setting process.

Reactions at the Time of Set

The formation of crystalline calcium hydroxide is accompanied by a great increase in the rate of cement hydration. The alite phase hydrates rapidly with considerable heat evolution and deposition of calcium silicate hydrate gel. In view of the high sulfate and low alumina concentrations in solution at this time, it is to be expected that the gel formed contains appreciable sulfate. This composition has been verified for C_3S hydration by Celani and coworkers (38), who used their results to verify that the gel was the location of "missing" sulfate, as postulated by Kalousek (43) in a very careful study of the early hydration reactions by differential thermal analysis.

The phase equilibrium diagram of Fig. 7 indicates that the precipitation of the $Ca(OH)_2$ should produce a decrease in calcium ion concentration and a corresponding increase in sulfate ion in solution. Fig. 10 does not show this effect because the gypsum becomes depleted during this period. Other data of Lawrence do, however, show the anticipated result. The system moves from the metastable state to point F and remains there as long as the three solid phases, ettringite, calcium hydroxide, and gypsum are present in the system.

A discussion of the variation of the lime to silica ratio in the gel during early hydration can be found in

another paper in the present symposium (44).

Hydration of the Aluminate and Ferrite Phases

For a cement of the type being considered, the solid gypsum in the cement-water system becomes depleted between 18 and 24 hours after initial contact of the cement with water. This period is marked by a final rise in the rate of heat evolution. The reactions that occur at this time have again proved to correspond to expectations arising from phase equilibrium studies.

When the solid gypsum is no longer present, the requirements for point F in Fig. 7 are no longer satisfied. The sulfate ion concentration in solution drops as this ion continues to react with the tricalcium aluminate, which is still slowly dissolving to produce a further crystallization of ettringite. The loss of sulfate from solution is accompanied by the reverse reaction of Eq. (1) and a consequent rise in alkalinity, as shown in Fig. 10 for the period after 6 hours. The solution composition moves from point F toward point M in Fig. 8, the invariant point at which the three solids calcium hydroxide, ettringite, and the monosulfate can coexist. When the sulfate concentration at point M is reached, the monosulfate begins to precipitate.

X-ray diffraction and Mössbauer studies have produced evidence that the rapid hydration of C_3A is accompanied by rapid hydration of the ferrite phase at this point. Although the delay of the ferrite hydration in the cement studied by Wittmann appears lengthy, the result is understandable because the composition indicates that the cement may be "oversulfated". As already indicated, the reaction product of the ferrite appears to be the low sulfate form of calcium sulfoaluminoferrite hydrate. During this period, therefore, the ettringite reacts with C_3A and C_4AF to produce monosulfate and the complex ferrite hydrate. Lawrence (37) has observed that the sulfate concentration at this transition point is higher when there is a higher alkali concentration.

Although the precise mechanism for the high rate of reaction at point M in Fig. 8 is unknown, it appears possible that the decreased sulfate concentration causes a rapid solution of ettringite and a high reactivity of the C_4AF and the remaining C_3A phases. This explanation provides a mechanism that is completely analogous to the observed increase in rate of alite hydration as the lime supersaturation decreases at the time of setting. It is assumed here that the process involves a dissolution of the ettringite, and of the anhydrous aluminate and ferrite phases followed by a reaction in the liquid phase to produce the solid low-sulfated products. The rapid increase in reactivity of the anhydrous phases can be attributed to dissolution of an ettringite coating on the tricalcium aluminate. No explanation has yet been found for the absence of any very early hydration product for the ferrite phase of the cement studied by Wittmann.

The Wittmann results thus indicate that the sulfate is preferentially taken up by the aluminoferrite rather than by the aluminate. The absence of any iron-containing phase other than the sulfoaluminoferrite indicates that the equilibrium concentration of sulfate from this phase must be less than that for the corresponding aluminate phase at point M in Fig. 8. The rate of ferrite hydration must be controlled by some factor other than solution concentration, since the hydration is much slower than the rate of solution of the ettringite.

Electron microscope evidence indicates that some hydrogarnet phase forms during this period (45). No good explanation exists for this phenomenon, other than that widely varying local solution concentrations during the rapid reaction may be the cause.

Finally, after the ettringite is depleted, the sulfate ion concentration again decreases. The remaining C_3A and C_4AF react with the monosulfate to give the lowest sulfate form of calcium sulfohydroxyaluminate hydrate and the calcium sulfoaluminoferrite hydrate; part of the alumina also goes into the gel. The system moves along the line MV in Fig. 8 to the invariant point involving the lowest sulfate solid solution. This stage of the hydration is not attained by the cements with low C_3A contents. Thus, the final products from hydration of the C_3A and C_4AF phases in these cements are the calcium monosulfoaluminoferrite hydrate, the monosulfate, and ettringite; a portion of the C_4AF apparently remains unhydrated indefinitely.

The continued hydration of the remaining calcium silicates and the C_4AF result in the ultimate hydration products discussed earlier.

Gel Composition

Few direct measurements are available on the extent of substitution by other cement constituents in the calcium silicate hydrate gel formed during cement hydration at ordinary temperatures and at the water-cement ratios found in concrete. The type and degree of substitution must depend both on the composition of the liquid phase and on the rate of the process.

At equilibrium, a given gel composition must be in contact with a liquid phase of definite composition. From the known variations in the liquid phase and

from the information available regarding the stoichiometry of the hydration process during the early hydration reactions, as already described, it is possible to survey the type of variations in gel composition that can occur.

With respect to the alkalies, the results of Powers and Steinour (23) and the original work already described indicate the orders of magnitude to be expected. The liquid phase compositions obtained by Lawrence (37) indicate the variations in the alkali concentrations that occur during the hydration process. The actual alkali content of the gel depends primarily on the rate of substitution, which appears to be slow.

The available Mössbauer spectrometer results indicate the degree of iron substitution to be very small.

For a discussion of the degree of substitution by alumina and sulfate ion, it is convenient to consider the variations in solution composition shown in Figs. 7 and 8. These variations have been plotted schematically in Fig. 11. For the cement-water phase equilibria, the values obtained for the $CaO–Al_2O_3–SO_3–H_2O$ system must be modified by the presence of alkalies, ferric oxide, and silica. The numbers in Fig. 11 therefore represent only orders of magnitude and are based on exploratory tests below the level of saturation of calcium silicate hydrate gel by the substituents (45).

For each point on the curve of Fig. 11, there must correspond an equilibrium gel of definite composition in the presence of calcium hydroxide as an additional solid phase.

The points of interest are labeled to conform with the corresponding points in Figs. 7 and 8, which represent the corresponding silica-free system. Thus point B represents the concentration of SO_3 in the liquid phase in contact with calcium sulfate, calcium hydroxide, and gel saturated with SO_3, similar to that described in reference 21. Point F represents the alumina concentration necessary to initiate precipitation of ettringite. Point M represents an invariant point where the solid phases are $Ca(OH)_2$, the monosulfoaluminoferrite, ettringite, and the gel. This point has been approximated in original experiments with the iron-free system in which C_3S was hydrated in the presence of about 40 percent of its weight of calcium monosulfoaluminate hydrate. Ettringite was formed during the hydration; its proportion increased with the degree of C_3S hydration. Evidently, the gel

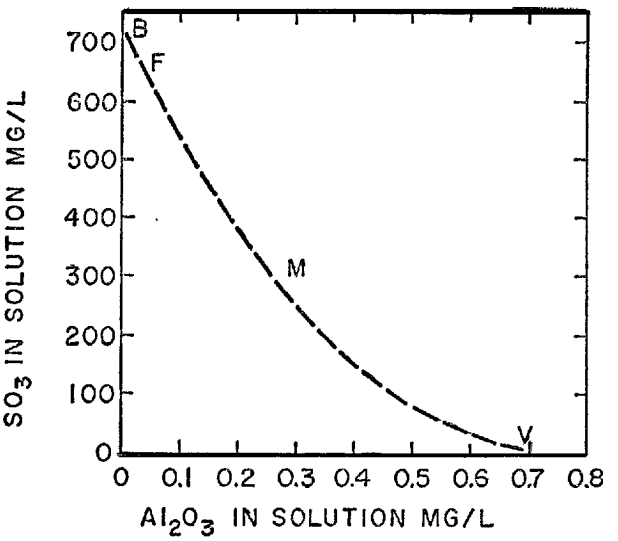

Fig. 11. *Schematic phase diagram of the variation in liquid phase composition during cement hydration.*

at this equilibrium point contains more Al_2O_3 than SO_3 on a molar basis. The portion of the curve to the right of M then represents those compositions higher in alumina where the solid phases are, successively, the monosulfate, the solid solution sulfohydroxyaluminate, and finally, C_4AH_{19}. Point V would then represent a sulfate-free system in which the solid phases are $Ca(OH)_2$, C_4AH_{19} or C_3AH_6, and an alumina-saturated gel similar to that described in reference 21.

Good experimental evidence exists to indicate that shifts in gel composition during cement hydration are sufficiently rapid to attain or at least closely approach equilibrium. The high sulfate content of the gel at point F has been observed (38, 43). No crystalline alumina-containing phase free of sulfate, such as C_3AH_6 or C_4AH_{19} has been observed as the hydration proceeds from F through M toward V. This fact, together with the high alumina content of the gel at ultimate hydration indicates that the alumina must be absorbed by the gel rapidly during the hydration of the C_3A and C_4AF remaining at point M after the gypsum has become depleted. Presumably, there is a simultaneous release of SO_3 from the gel during this period to participate in the formation of the calcium sulfoaluminoferrite hydrate.

Conclusion

No attempt will be made here to summarize the various equilibria that have been described. It is of

interest, however, that the major features of cement-water phase equilibria can be condensed into a diagram of the type shown in Fig. 11. A series of curves for various alkali contents on such a plot would represent the appropriate small portion of the seven-component system $CaO–SiO_2–Al_2O_3–Na_2O–K_2O–SO_3–H_2O$. The calcium silicate hydrate gel and calcium hydroxide are always present as solid phases. There must be definite equilibrium values for the lime and silica in solution at each point of the curves for alkali content. The gel composition should vary in accordance with the equilibrium liquid phase. Other solid phases are associated with the various ranges of solution composition. By the use of a third dimension, the effect of Fe_2O_3 content could be represented as well.

References

1. W. Lerch, "The influence of gypsum on the hydration and properties of portland cement pastes," Am. Soc. Testing Mater., Proc. **46**, 1251–1292 (1946). Reprinted as Portland Cement Assoc. Res. Dept. Bull. 12.
2. "The optimum gypsum content of portland cement" reported by Committee C-1 on Cement through its Working Committee on SO_3 Content, Am. Soc. Testing Mater. Bull. No. 169, 39–45 (Oct. 1950).
3. The Chemistry of Cements, Vol. 1 (Academic Press, London and New York, U. S. A., 1964), edited by H. F. W. Taylor. See Part II entitled "Chemistry of hydrated cement compounds".
4. T. C. Powers and T. L. Brownyard, "Studies of the physical properties of hardened portland cement paste, Part 1. a review of methods that have been used for studying the physical properties of hardened portland cement," Proc. Am. Concrete Inst. **43** 105–132 (1947). See pp. 109–110. Reprinted in Portland Cement Association Research Department Bulletin 22.
5. L. E. Copeland and D. L. Kantro, "Chemistry of hydration of portland cement at ordinary temperature," Chapter 8 of Reference 2. See p. 336.
6. D. L. Kantro, L. E. Copeland and E. R. Anderson, "An X-ray investigation of hydrated portland cement pastes," Am. Soc. Testing Mater., Proc. **60**, 1020–1035 (1960). Reprinted as Portland Cement Assoc. Res. Dept. Bull. 128.
7. R. Turriziani, "The calcium aluminate hydrates and related compounds," Chapter 6 of Reference 2. See pp. 234–243.
8. P. Seligmann and N. R. Greening, "New techniques for temperature and humidity control in X-ray diffractometry," J. Portland Cement Assoc. Res. Develop, Lab. **4**, No. 2, 2–9 (May 1962). Reprinted as Portland Cement Assoc. Res. Dept. Bull. 143.
9. H. A. Berman, "Preparation of a carbonate-free complex calcium aluminate," J. Res. Nat. Bur. Std. **69A** 45–51 (1965).
10. L. S. Wells, W. F. Clarke, and H. F. McMurdie, "Study of the system $CaO–Al_2O_3–H_2O$ at temperatures of 21° and 90°C," J. Res. Nat. Bur. Std. **30** 367–409 (1943).
11. P. Seligmann and N. R. Greening, "Studies of early hydration reactions of portland cement by X-ray diffraction," Highway Res. Record, No. 62, 80–105 (1964). Reprinted as Portland Cement Assoc. Res. Dept. Bull. 185.
12. W. Dosch and H. zur Strassen, "Investigation of tetracalcium aluminate hydrate. I. The various hydrate stages and the effect of carbonic acid," Zement-Kalk-Gips **18**, 233–237 (1965).
13. F. Lavanant, "Contribution to the study of some hydrated calcium aluminates," Rev. Mater. Construct. Trav. Publ. No. 592 1–10; No. 593, 76–87; No. 595, 193–207; No. 596, 251–261; No. 597, 298–304 (1965). See p. 207.
14. H. F. W. Taylor, "Tabulated crystallographic data," Appendix in Volume 2 of Reference 2. See pp. 395–396, 399.
15. See pp. 277–280 of Reference 7.
16. D. E. Day, "Determining the coordination number of aluminium ions by X-ray emission spectroscopy," Nature **200** 649–651 (1963).
17. G. A. Wertheim, Mössbauer Effect: Principles and Applications, (Academic Press, London, England and New York, U. S. A. 1964).
18. L. E. Copeland and E. G. Schulz, "Electron optical investigation of the hydration products of calcium silicates and portland cement," J. Portland Cement Assoc. Res. Devel. Lab. **4**, No. 1, 2–12 (Jan. 1962). Reprinted as Portland Cement Assoc. Res. Dept. Bull. 135.
19. H. F. W. Taylor, "The calcium silicate hydrates," Chapter 5 of Reference 2. See pp. 192–196.
20. G. Verbeck, "Chemistry of hydration of portland cement. III. Energetics of the hydration of portland cement," Proc. Intern. Symp. Chem. Cement, 4th, 1960, pp. 453–463 (Pub. 1962). Reprinted in Portland Cement Assoc. Res. Dept. Bull. 153.
21. L. E. Copeland, E. Bodor, T. N. Chang, and C. H. Weise, "Reactions of tobermorite gel with aluminates, ferrites, and sulfates," J. Portland Cement Assoc. Res. Devel. Lab. **9**, No. 1, 61–74 (Jan. 1967). Reprinted as Portland Cement Assoc. Res. Dept. Bull. 211.
22. G. L. Kalousek, "Studies of portions of the quaternary system soda-lime-silica-water at 25°C," J. Res. Nat. Bur. Std. **32**, 285–302 (1944).
23. T. C. Powers and H. H. Steinour, "An interpretation of published researches on the alkali-aggregate reaction. Part 1—the chemical reactions and mechanisms of expansion," Proc. Am. Concrete Inst. **51** 497–516 (1955). Reprinted in Portland Cement Assoc. Res. Dept. Bull. 55. See pp. 514–516.

24. F. Wittmann, F. Pobell, and W. Wiedemann, "Examination of the hydration of iron-containing clinker components with the help of the Mössbauer effect," Z. Angew. Phys. **19**, 281–4 (1965).
25. Personal communication from F. Wittmann.
26. F. Pobell and F. Wittmann, "Mössbauer effect of 14.4 kev-γ-line of Fe 57 in the superparamagnetic ferrites of portland cement," Z. Angew. Phys, **20**, 488–492 (1966).
27. T. B. Kennedy, "Significance of test for calcium sulfate in hydrated portland-cement mortar," Am. Soc. Testing Mater. Proc. **61** 1035–1038 (1961).
28. W. Dosch and H. zur Strassen, "An alkali-containing calcium aluminate sulfate hydrate," Zement-Kalk-Gips **20** 392–401 (1967).
29. H. E. Schwiete, U. Ludwig, and E. Niel, "Studies on the beginning of hydration of clinker and cement," Proc. 7th Conf. Silicate Industry, Akadémiai Kiadó, Budapest, pp. 221–273 (1963).
30. E. P. Flint, H. F. McMurdie, and L. S. Wells, "Hydrothermal and X-ray studies of the garnet-hydrogarnet series and the relationship of the series to hydration products of portland cement," J. Res. Nat. Bur. Std. **26** 13–33 (1941).
31. S. Brunauer, L. E. Copeland, and R. H. Bragg, "The stoichiometry of the hydration of tricalcium silicate at room temperature: I—Hydration in a ball mill," J. Phys. Chem. **60** 112–116 (1956). Reprinted in Portland Cement Assoc. Res. Dept. Bull. 65.
32. L. E. Copeland and J. C. Hayes, "The determination of non-evaporable water in hardened portland cement paste," ASTM Bull., No. 194, 70–74 (Dec. 1953) Reprinted as Portland Cement Assoc. Res. Dept. Bull. 47.
33. H. G. Midgley, "The formation and phase composition of portland cement clinker," Chapter 3 of Reference 2. See pp. 90–91.
34. H. H. Steinour, "Aqueous cementitious systems containing lime and alumina," Portland Cement Assoc. Res. Dept. Bull. 43 (1951). See pp. 68–70.
35. F. F. Purdon and V. W. Slater, Aqeous Solution and the Phase Diagram, pp. 93–130 (Edward Arnold and Co., London, England, 1946).
36. R. Turriziani, "The process of hydration of portland cement," Ind. Ital. Cemento **29** 185–189, 219–223, 244–246, 276–280, 282 (1959).
38. C. D. Lawrence, "Changes in composition of the aqueous phase during hydration of cement pastes and suspensions," Highway Res. Board, Special Report 90, pp. 378–391 (1966).
38. A. Celani, M. Collepardi, and A. Rio, "The influence of gypsum and calcium chloride on the hydration of tricalcium silicate," Ind. Ital. Cemento **36** 669–678 (1966).
39. A. Rio, A. Celani, and M. Collepardi, "A contribution to the study of the hydration of portland cement during early ages," Ind. Ital. Cemento **35** 275–286 (1965).
40. L.E. Copeland and D. L. Kantro, "Chemistry of hydration of portland cement. II. Kinetics of the hydration of portland cement," Proc. Intern. Symp. Chem. Cement, 4th, 1960, pp. 443–453 (Pub. 1962). Reprinted in Portland Cement Assoc. Res. Dept. Bull. 153.
41. Reference 33. See pp. 63–64.
42. W. C. Hansen and E. E. Pressler, "Solubility of $Ca(OH)_2$ and $CaSO_4 \cdot 2H_2O$ in dilute alkali solution," Ind. Eng. Chem. **39** 1280–1282 (1947).
43. G. L. Kalousek, "Analyzing SO_3-bearing phases in hydrating cements," Mater. Res. Std. **5** 292–304 (1965).
44. L. E. Copeland and D. L. Kantro, "Hydration of portland cement," This Symposium, Paper II-5.
45. Personal communication from L. E. Copeland.
46. F. E. Jones, "The quaternary system CaO–Al_2O_3–$CaSO_4$–H_2O at 25°C," Trans. Faraday Soc. **35** 1484–1510 (1939).
47. F. E. Jones, "The quaternary system CaO–Al_2O_3–$CaSO_4$–H_2O at 25°C equilibria with crystalline $Al_2O_3 \cdot 3H_2O$, alumina gel, and solid solution," J. Phys. Chem. **48** 311–356 (1944).
48. W. Lerch and C. L. Ford, "Long-time study of cement performance in concrete. Chapter 3. Chemical and physical tests of the cement," Proc. Am. Concrete Inst. **44** 743–795 (1948). Reprinted in Portland Cement Assoc. Res. Dept. Bull. 26. See p. 761.
49. "Twenty-year report on the long-time study of cement performance in concrete," by the Advisory Committee, Long-Time Study of Cement Performance in Concrete, Portland Cement Assoc. Res. Dept. Bull. 175. See p. 14.

Oral Discussion

Shunro Ueda and Renichi Kondo

The effect of the addition of the seed crystals on the rate and mechanism of cement hydration was mentioned in your paper and also briefly in our principal paper. In your case, the reaction may be promoted and the physical properties of the paste are remarkably changed. It seems that not only the formation of the outer product but also that of the inner product are affected considerably. Especially when the composition of the seed crystal is similar to that of the hydrate, the transformation of the ordinary hydrate into the stable hydrate may occur easily because the migration of atoms is not needed during the transformation.

Whether the additive acts as a seed or as a catalizer may be determined by the identification of the product.

Oral Discussion

Heinrich zur Strassen

The authors as well as Dr. Roberts (1) confirm their former results that the low-carbonate phase with a basal spacing of 8.2 Å is only a semicarbonate. Some years ago, we were of the opinion that the low-carbonate phase would be a quarter carbonate (2), but now we have found, as explained in our Written Discussion (3) to the Principal Paper No. II-2 that there exists a solid-solution range between semicarbonate and quarter carbonate.

The solid solution is not easily to be detected because all compositions have the same basal distance of 8.2 Å. The most convincing experiment is reaction 4 in Table 2 of the Written Discussion: Quarter carbonate free from rests of tetracalcium aluminate hydrate is prepared and controlled by X-rays (Fig. 1).

This substance is shaken together with monocarbonate in the molar ratio 2 to 1 in aqueous suspension. After one week, the monocarbonate has disappeared completely whereas the remaining reflections which now must belong to the semicarbonate phase have not changed their position.

The disappearance of monocarbonate would be impossible if there would exist only a single phase of lower CO_2 content than the monocarbonate phase, either a quarter carbonate as we thought before, or a semicarbonate as the other authors believe.

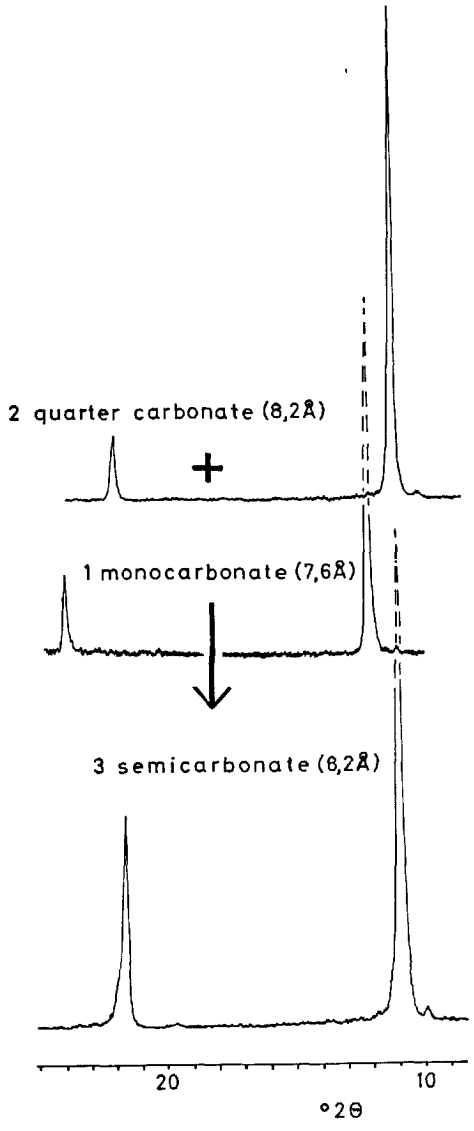

Fig. 1. *Reaction between quarter-carbonate and monocarbonate.*

References

1. M. H. Roberts, "Calcium aluminate hydrates and related basic salt solutions". This Symposium, Supplementary Paper No. 11–29.
2. W. Dosch and H. zur Strassen, "Untersuchung von Tetracalciumaluminathydraten. I. Die verschiedenen Hydratstufen und der Einfluss von Kohlensäure". Zement-Kalk-Gips **18**, 233–237 (1965).
3. W, Dosch, H. Keller and H. zur Strassen, "Additional remarks on tetracalcium aluminate hydrate and its quaternary complex salts". This Symposium, Written Discussion No. 11–21.

Authors' Closure

Paul Seligamann and Nathan R. Greening

Dr. zur Strassen has not indicated the temperature at which his tests were made. It will be recalled that our tests were made at 40°F to avoid formation of the cubic phase, C_3AH_6. At room temperature, the cubic phase does indeed form, but its presence is manifested by only a very weak X-ray diffraction pattern in comparison with that of the calcium hemicarbonate hydrate. This pattern is very easily overlooked. The tetracalcium aluminate hydrate, on the other hand,

has a pattern with an intensity comparable with that of the carbonated phase.

We have made tests of the type described by Dr. zur Strassen both at room temperature (73°F) and at 40°F. The results confirm our original conclusion. Room temperature mixes with a molar CO_2/Al_2O_3 ratio between 0.25 and 0.5 show little beside the hemicarbonate pattern; cooling to 40°F, however, reveals the true situation as the cubic hydrate converts to the hexagonal and the intense lines of the latter phase appear. We have no reason to expect that the formation of the C_4AH_{19} pattern is accompanied by any shift in the binding of the carbonate in the mix, since there is no change in the intensity of the hemicarbonate pattern.

In response to the discussion by Mr. Ueda and Dr. Kondo, the paper perhaps did not make sufficiently clear that the pastes whose properties were reported in Figs. 5 and 6 and Table 3 were examined by diffraction and found to contain crystalline afwillite rather than the gel obtained without nucleation. The properties are thus attributable to the change in paste structure rather than to the changed reaction rate, which itself appears characteristic of the transformation to the afwillite rather than the gel.

SESSION II-4 KINETICS OF HYDRATION OF CEMENTS

Principal Paper Kinetics and Mechanisms of the Hydration of Cements

Renichi Kondo* and Shunro Ueda**

Synopsis

This paper deals with the results obtained by the authors as well as by reviewing related literatures which appeared mainly during 1960 to 1967 in order to provide the present, advanced knowledge on the kinetics and the mechanisms of hydration of cements.

The accuracy of conduction calorimetry and quantitative X-ray diffractometry among methods for the estimation of the degree of hydration have been greatly improved and they are being widely used. While the measurements on the surface electron diffraction and the pore size distribution are still under development, they are already providing useful information. Interesting results can also be expected by the application of electron microscope either with electron microprobe analyzer attached or of the scanning type.

Such chemical properties as hydraulic, latent hydraulic and pozzolanic of cement components as well as the reaction with additives are compared and discussed. An attempt was made to explain the concepts of the so-called topo-chemical and through solution. Important factors which are dealt with are the fineness of cement, the water cement ratio and the curing temperature.

Since the rate of hydration is closely related with the properties of the hydrates, it is necessary to study the concentration and constitution of the liquid phase, nucleation and crystal growth, the composition and morphology of hydrates, the pore structure, and permeability and diffusion.

As the rate and mechanism of hydration vary, in general, with the progress of reaction, it is divided into 5 stages and each of these are discussed in detail with reference to the hydration of tricalcium silicate as an example. Some comments are made on the rate equations of the solid state reaction which appeared previously and an equation which explains the rate of the whole hydration process is derived in consideration of the above mentioned complexity in the process.

Introduction

As most inorganic cements harden by the hydration reaction, investigations concerning the rate and mechanism of their reaction not only have scientific interest but also practical importance. In this paper chiefly the hydration of pure substances will be dealt with to elucidate fundamentally the rate and mechanism of their reactions. Problems such as the hydration of actual cement or the rate and mechanism of the development of strength are not described in this paper. These problems will be explained by the other authors in this Symposium.

Most researches up to 1960 have been presented at the Washington Symposium. Particularly the stoichiometry, kinetics and energetics of the hydration of portland cement have been described by Copeland, Kantro and Verbeck (1). Accordingly fundamental researches concerning subjects reported from 1960 to 1967 will be reviewed in this paper, together with some results obtained by authors. The contents of this paper are under the following headings:

* Research Laboratory of Engineering Materials, Tokyo Institute of Technology, Tokyo, Japan.

**Research Laboratory, Nihon Cement Co. Ltd., Tokyo, Japan.

Determination of the degree of hydration
Reactivities of cement components and types of reaction
Several factors concerned with the rate of hydration
Properties of hydrates concerned with the rate of hydration
Relation between the rates and mechanisms of hydration

Determination of the Degree of Hydration

The degree of the hydration of cement components is measured by various methods. The degree of hydration is usually shown by the amount of residual reactant as the compositions and the crystallinities of hydrates change widely with the progress of the reaction. We can measure the amount by X-ray diffractometry and optical observation but there are still problems concerned with the accuracy. The former is more hopeful than the latter.

The determinations of the amount of non-evaporable water and free $Ca(OH)_2$, and also the measurements of the electric conductivity, the heat of hydration and the strength conveniently give the relative values for the degree of hydration with rather good reproducibility.

Differential thermal analysis, thermo-gravimetric analysis, differential thermo-gravimetry, infra-red absorption, electron microscopic observation, and selected-area electron diffraction are frequently used for studying the hydration mechanism.

Besides the phase-contrast microscope, the recently-developed electron microprobe analyzer and scanning electron microscope will find use in the near future. Ueda, Hashimoto and Kondo (2) applied the method of surface electron diffraction to the study on the hydration process.

The characteristics and the problems involved in the methods commonly used with respect to the rate and the mechanism of hydration are discussed.

X-ray Diffractometry

The measurement of quantities of unhydrated reactants using X-ray diffractometry have been attempted as a useful method for determining the degree of hydration since the development of X-ray diffractometer. The reliability of this analysis has been remarkably improved recently. The large error by this analysis is due to the difference in the distortion and the fineness of powder. When the unhydrated particle is enveloped by the hydrates, the reproducibility is especially reduced. The accuracy is improved by analysis with the digital computer.

The following two methods are generally used in quantitative X-ray analysis. Seligmann and Greening modified X-ray sample holder to provide control of the temperature of the sample and the humidity and composition of the ambient atmosphere surrounding the sample, and studied the reaction occurring in a mixture of tricalcium aluminate, calcium hydroxide, gypsum and water (3), and the dehydration reactions of calcium aluminate hydrates (4). Angstadt and Hurley observed that the hydration rate of the alite in portland cement paste reaches the maximum after 7 hours in the case of the internal standard method, whereas it is reached slightly faster in the hydration of neat paste on X-ray goniometer (5)(6). Tsumura and Kawachi (7) and Tsumura (8) determined the hydration rate of each clinker mineral in paste form by a similar method. The operation of this direct method is very easy but it has some defects such as the preferential deposition of hydrates on the surface of the film, the appearance of a large halo by film and hydrated layer, and the amount of unhydrated reactant is apt to be estimated lower than the real amount.

The most common quantitative X-ray diffraction analysis is the internal standard method. In this method, the effect of mass absorption coefficient can be neglected theoretically, however Smolczyk (9) pointed out that the correct application of mass absorption coefficient must be considered in actual experiments. The calibration curves of alite, $Ca(OH)_2$ and ettringite were obtained by Smolczyk (10) after the theoretical correction for loss on ignition of hydrates has been made since the presence of H_2O and CO_2 decreases the diffraction intensity. The curves of alite and $Ca(OH)_2$ are in accordance with the theory, but a large error still exists in that of ettringite. The results of the progress of hydration determined by X-ray diffractometry are shown in Fig. 1.

In the estimation of the degree of hydration using X-ray diffractometry, it is necessary to calibrate the presence of poor-crystalline hydrates particularly at the early stage and the formation of products on the surface of unhydrated grain in order to obtain better accuracy. The diffraction lines $2\theta = 41°$ and $43°$ CuKα were selected for C_3S (tricalcium silicate) and MgO as the internal standard respectively in the estimation of the degree of hydration of C_3S by the

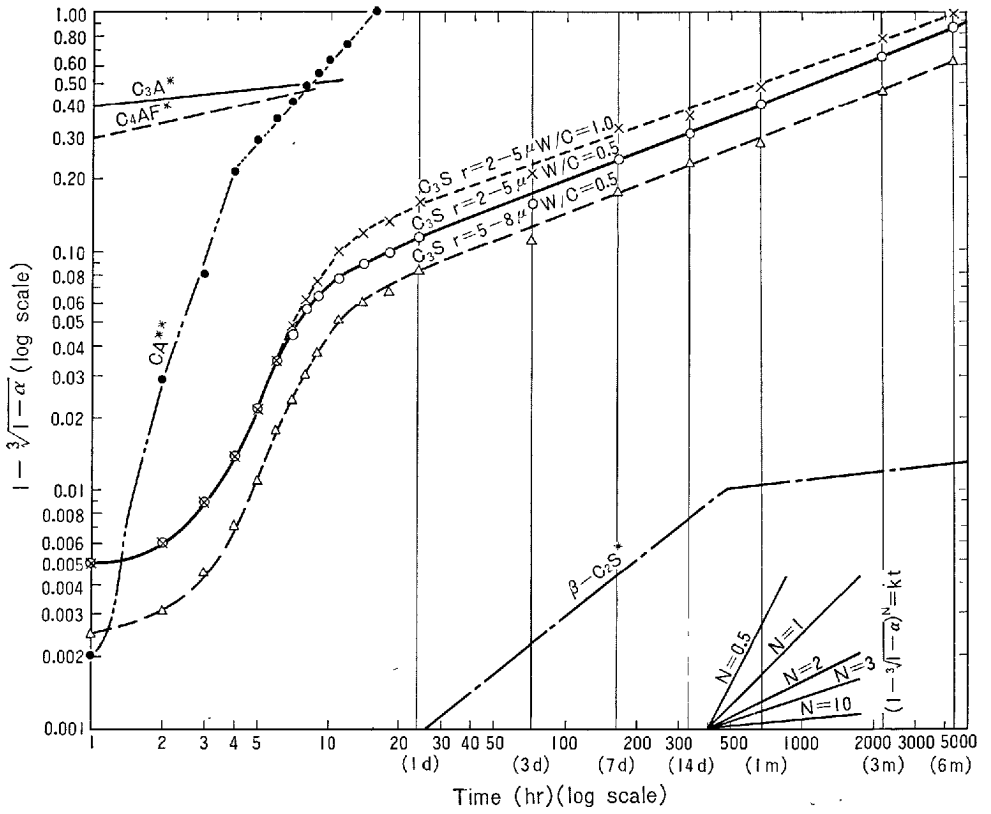

Fig. 1. *Rate of hydration of cement composing minerals by quantitative X-ray analysis.*
C_3S *is hydrated at 25°C.*
**β*-C_2S, C_3A *and* C_4AF *are measured by direct method. After Tsumura and Kawachi (7) and Tsumura (8).*
***Bottle hydration of aluminous cement with W/C=4.0. After Sakurai, Ueda, Hashimoto and Fukunaga (120).*

authors. It is necessary to repeat measurements 12 times in order to obtain a mean value with an accuracy as high as $2\sigma = 4\%$.

Calorimetry

The heat-of-solution, the adiabatic and the conduction calorimeters are used for the measurement of the heat of hydration. In the measurement by the heat-of-solution continuous result of hydration heat cannot be obtained, but it is possible to accurately measure the heat of hydration of the sample curing for a long time. Continuous curve of temperature change can be obtained with the adiabatic calorimeter but it is not suitable for obtaining the heat change for long time and it has the defect of change in curing temperature due to heat liberation. The conduction calorimeter which was adopted by Lerch (11) is most suitable as heat can be obtained continuously at almost constant cured temperature and in addition, it is self-recording. This type of calorimeter has been made smaller by Danielson (12), Stein (13), and Monfore and Ost (14), and also it has made possible the measurement of several grams of synthesized sample.

The conduction calorimeter expresses differentially the relation between the heat liberation and the curing time.

$$q = \sigma \Delta T + H_{\text{eff}} \frac{d(\Delta T)}{dt}$$

where q is the heat flows into the container per unit time dt, σ is the coefficient of heat transfer, ΔT is the temperature difference between the container and an isothermal body with a large heat capacity, and H_{eff} is the effective heat capacity of the sample, container and heat conductor. The temperature change of the isothermal body shifts the base line, however,

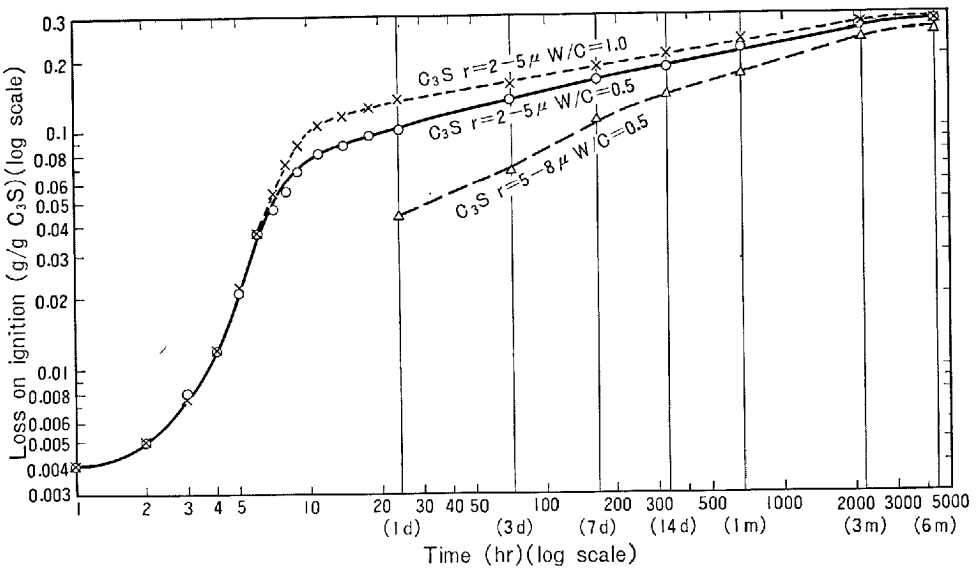

Fig. 2. *Change in content of non-evaporable water per original C_3S with progress of hydration*

the isothermal body and container are coupled by relatively good heat conductor in a conduction calorimeter. In order to remove this defect the twin-type conduction calorimeter has been developed and widely used, in which two of the same kind of calorimeter are differentially connected to offset the various heat changes. The hydration rate and mechanism by the results of heat liberation will be discussed later in detail.

The same reaction is not carried out from the early stage to the later stage in the hydration of cement, and particularly at the early stage unstable products are formed to liberate low heat of hydration compared with the degree of hydration. Accordingly, the absolute value of the degree of hydration reaction cannot be determined by the heat evolution as in the case of the amount of free $Ca(OH)_2$ and the thermo-gravimetric result. However, the results of calorimetry indicate a parallel tendency with the degree of hydration reaction obtained by X-ray diffractometry. It is convenient to study the effect of the factors on the rate of hydration as the relative value of the degree of hydration can be obtained with high sensitivity especially at early stage.

Chemical Analysis

The quantity of the non-evaporable water of hydrated sample depends on the drying conditions. Copeland and Hayes (15) revised the evacuated drying method at the temperature of dry ice (−79°C). They asserted that the time to reach an end point is usually shorter, and that the partial pressure of water vapor can be maintained constant in 0.5×10^{-3} mmHg with great ease, and that the obtained value is more nearly equal to the chemically combined water. However it must be considered that most of the combined water in some aluminate hydrates, ettringite and gypsum is lost under this condition.

The amount of the non-evaporable water in cement paste, as is shown in Fig. 2, increases with the curing time to give a similar result as the curve of the reduction of reactant. But the former result does not coincide exactly with the latter, as the stoichiometry of products is indefinite at the early stage of hydration. Kondo, Ueda and Kodama (16) showed that the molar H_2O/SiO_2 and CaO/SiO_2 ratios of calcium silicate hydrate changed very irregularly within 24 hours.

The amount of free $Ca(OH)_2$ is determined by the Lerch-Bogue method (17), Franke method (18), X-ray diffractometry and thermal measurement method. Yamaguchi, Takemoto, Uchikawa and Takagi (19) pointed out that in Lerch-Bogue method a small part of the lime was removed from the hydrate due to heating of the sample for a long time, whereas a single extraction by the Franke method did not come even close to removing all the free $Ca(OH)_2$. Brunauer and Greenberg (20) described that the free $Ca(OH)_2$ could be accurately determined by modified Franke method characterized by multiple extraction. In our

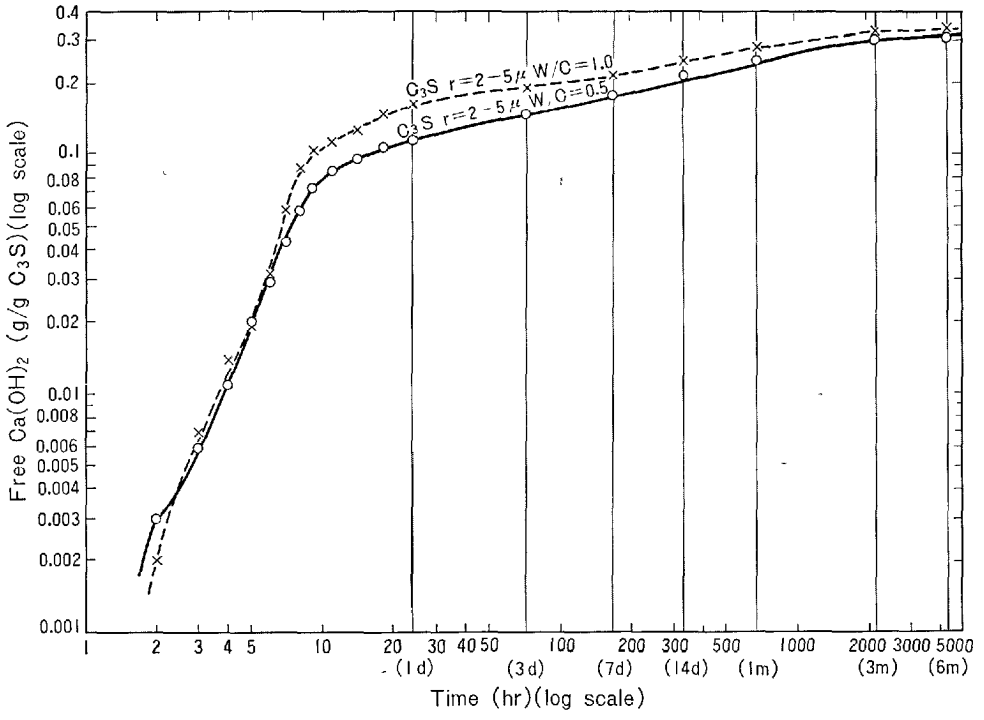

Fig. 3. *Change in content of free* $Ca(OH)_2$ *per original* C_3S *with progress of hydration*

laboratory we adopted the modified multiple extraction method and obtained the results of Fig. 3. One of the reasons for the different compositions of calcium silicate hydrate given by the different investigators may be attributed to the difference in the experimental condition.

Chemical analysis and the measurement of electric conductivity of the liquid phase with the progress of reaction are frequently carried out. The concentration and constitution of liquid phase has indispensable effect on the nucleation and crystal growth of the hydration product.

Surface Area and Pore Size Distribution

The multiple adsorption theory has been applied to the measurement of surface area as the BET method (21). Not only the surface area, but also the pore size distribution and the shape of the open pore of hardened cement paste can be determined by the measurement of adsorption and desorption isotherms. A greater part of the surface area of hardened sample is due to the poor crystalline C–S–H gel. There have been many discussions on the adsorbate used and the surface area of calcium silicate hydrate in water vapor is from 2 to 3 times that in nitrogen gas. Regarding this matter, Kalousek (22) pointed out that the smaller size of water molecule enabled it to penetrate into pore spaces which were inaccessible to the large nitrogen molecules. However the pore size distribution calculated from nitrogen adsorption by Eipeltauer, Schilcher and Czernin (23) indicates that there are no pores of less than $d = 16$ Å. This value is larger than the size of nitrogen molecule, so they proposed that nitrogen adsorption showed the true surface area, as persorption phenomena is caused by water vapor adsorption such as is seen in zeolite. On the other hand Brunauer, Kantro and Weise (24) pointed out that nitrogen adsorption did not measure the true surface area because of leading to negative surface energy value in C–S–H gel.

The differences of surface area due to the difference in water cement ratio, according to Hunt (25), are small at 1 day but become very large as hydration proceeds. Besides, Mikhail and Selim (26) showed that water vapor always gave larger areas than the other gases of larger molecule, and gases of moderate molecules, such as nitrogen and methanol, resulted in different values of surface area depending on the difference in water cement ratio as shown in Fig. 4.

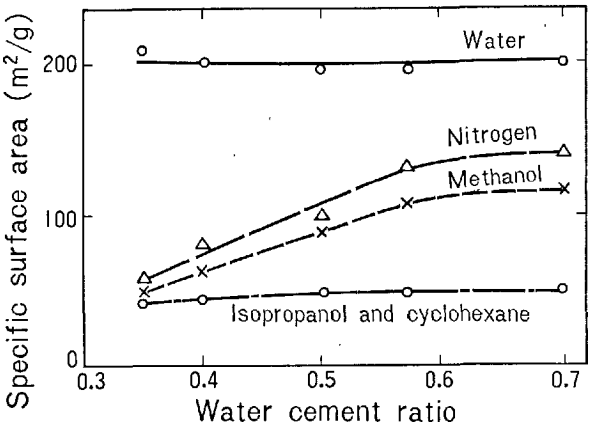

Fig. 4. *Variation with water cement ratio of surface area available to the different adsorbates. After Mikhail and Selim(26)*

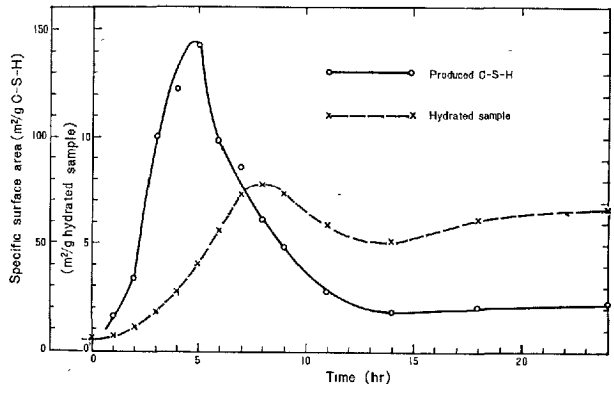

Fig. 5. *Change in specific surface area of hydrated* C_3S *($r = 2 \sim 5\mu$) with progress of hydration. ($W/C = 1.0$, at 25°C)*

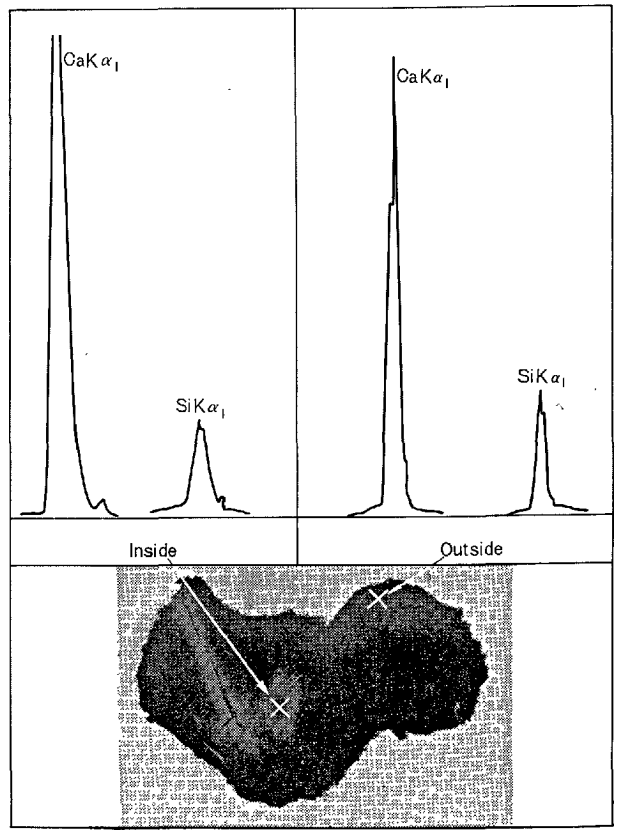

Fig. 6. *An example of chemical analysis by electron microprobe analyzer attached to an electron microscope*

The quantity of nitrogen adsorption, according to Kondo, Ueda and Kodama (16), has a maximum value at first and then reaches a minimum value at the early stage and thereafter increases gradually, as is shown in Fig. 5. That is, it is possible to discuss the crystallinities and the changes of the related properties of hydrated products from the result of adsorption. However, the degree of hydration is not so closely related with the surface area.

The pore size distribution of porous material such as hardened cement paste is measured by adsorption, mercury penetration, fluid permeation, back diffusion, electron microscope, selective adsorption and so on.

In the mercury penetration method the pore size distribution is calculated, on the assumption that the shape of the pore is cylindrical. However the pore radius measured by this method is smaller than the true value as the size of the neck of the capillary is measured. Particularly this error appears in case of sample in large lump form.

In the mercury pressure method all the pores in the gel cannot be measured owing to the difficulty of the high pressure technique and the minimum radius to be determined is 15 Å. On the contrary in the adsorption method the pores between several hundred Å and 10 Å in diameter can be measured. In calculation of the pore size distribution from adsorption data, the Cranston-Inkley method (27), which assumes the pore as a cylindrical capillary is widely used for instance, by Eipelatuer, Schilcher and Czernin (23). The Innes method (28) used by Hunt (25) assumes that the pores are in parallel plates.

Electron Microscope

A high resolution electron microscope is effective for the study of hydrate because of its low crystallinities. The morphologies of hydrates have been clarified considerably by Grudemo (29) (30) who published many results obtained with the electron microscope. As the electron beam has a much larger

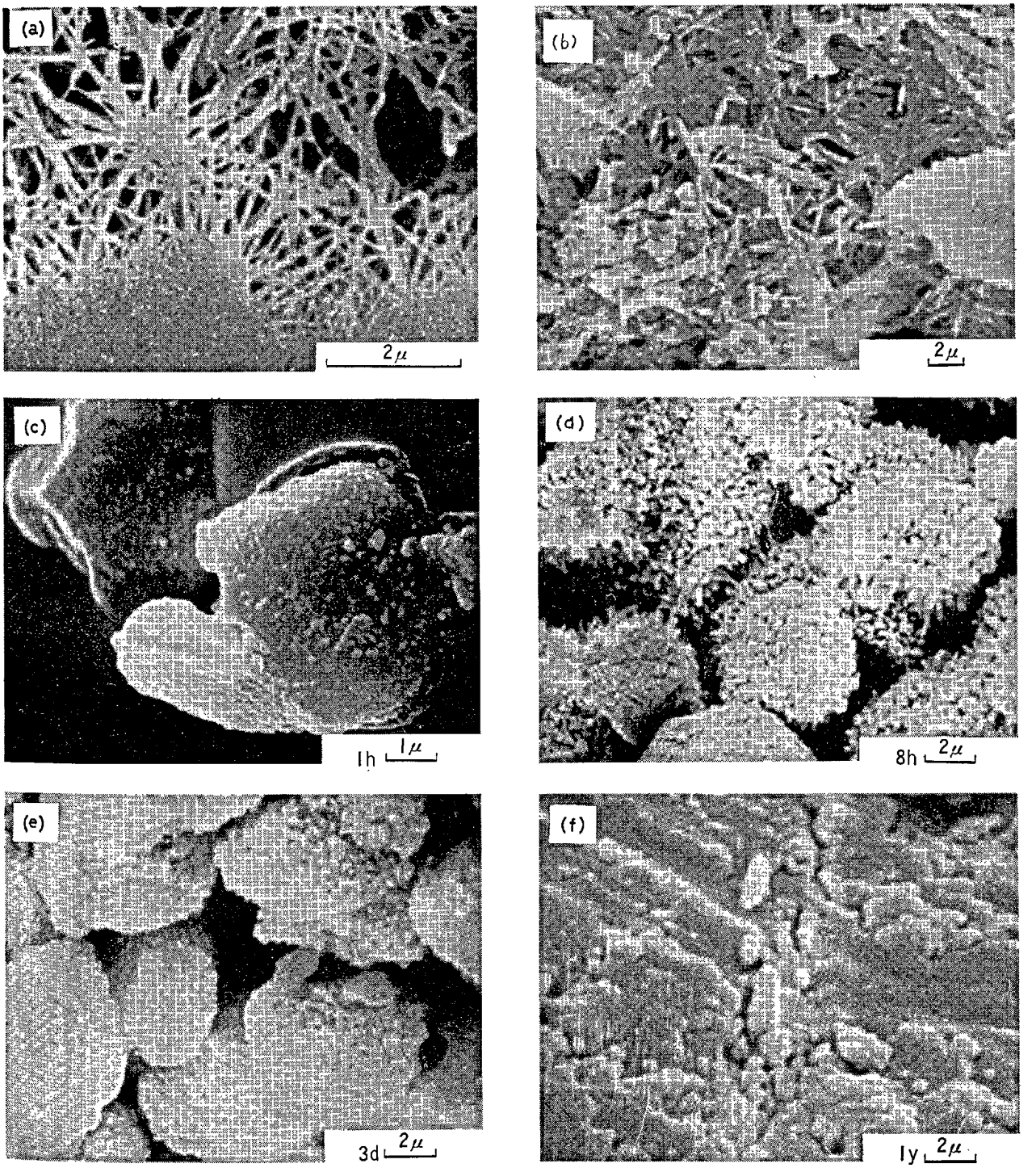

Fig. 7. *Textures at broken surface examined by a scanning electron microscope.* (a), (b): *sand-lime brick by G. Sudoh,* (c)~(f): *surface state of* C_3S *powder in hydration with* $W/C = 0.5$ *by Kondo, Daimon and Ueda(55)*

sectional area of adsorption and scattering amplitude than X-ray and neutron beams, it provides sufficiently strong diffraction pattern so that measurement even in thin crystal is possible while it can pass about 1000 Å of the thickness of crystal without disappearance of coherency.

Direct observation and diffraction of fine crystal are obtained by the suspension method but the observation of the surface of hydrated particle is also important for the study of the hydration of cement. However, there are many problems when observing the particle boundary and distinguishing the figure by two step replica method. The character of the evaporation film of carbon has been applied in the one step replica method and this is being studied (31). It is considered that this method is suitable for study to distinguish the reactivities of various crystal surfaces in hydration.

The microtome technique is useful instead of the single crystal experiment as it is difficult to obtain in hydration. The preparation of ruby or diamond knife and the embedding method are being studied (32). Application of high voltage electron microscope is also interesting.

The method of using surface electron diffraction was used by Ueda, Hashimoto and Kondo (2) for the study of the state of the cement particle at the induction period which was only assumed in the past.

The recently developed electron microscope with electron microprobe analyzer may also assist the study of hydration. It becomes possible by this to identify the chemical composition, with the exception of observation of the figure and the diffraction pattern. As an example, the result obtained on hydrated C_3S particle is shown in Fig. 6.

On the other hand the scanning electron microscope which was recently developed in England and Japan has a deep focal length and this is useful for direct observation of the surface of sample. The broken plane of the sand lime brick treated in an autoclave as well as the surface state of the C_3S particle in hydration are shown in Fig. 7.

Reactivites of Cement Components and Types of Reaction

The hydration reaction is first of all affected by the natures of the reactants which possess hydraulic, latent hydraulic or pozzolanic reactivities. So-called clinker minerals have unstable crystal structure and low bond energy. The conditions of heat treatment and cooling, and the presence of minor components affect their crystal structure and lattice defect. Admixtures such as retarder and accelerator control the hydration rate and the properties of hardened pastes owing to the changes in species, morphology and volume of the hydrated product. There are many discussions on the mechanism of hydration whether it progresses by through solution or topochemically.

Reactivities of Hydraulic Components

Calcium silicates, calcium aluminates, calcium alumino-ferrites and calcium sulfates are well known as components which react with water to harden. There are components in which strontium or barium replaces calcium, or germanium replaces silicon. Some kind of phosphates, for instance $Al(H_2PO_4)_2$ and $Zn(PO_4)_2$, have also hydraulic properties.

The free energy in a certain system must be decreased in order to carry out the hydration reaction. The values of ΔG_{298} per mole of CaO or MgO for the hydration of CaO, calcium silicates, calcium aluminates, calcium sulfates and lime-silica mixtures are given in Table 1. As can be seen in Table 1, the energy gains for the Ca–O bond for these reactions are near the values of ΔH_{298}. The low values of bond energy of the cement components are considered to be attributed to low coordination number of Ca^{++} and Al^{+++} ions by Brandenberger (33) and to the coordination with low symmetry by Bredig (34). According to Jeffery (35) Ca^{++} ion in C_3S is surrounded by six oxygens, and five of them are in one hemisphere, and only one is in the other hemisphere whereby a large hole. C_3S is therefore reactive. Kondo (36) studied the structure of $Ca_8Al_{12}O_{24}(SO_4)_2$ and found that Al^{+++} ion was in a fourfold coordination, and that Ca^{++} ion was surrounded asymmetrically by oxygen, and also found the presence of free SO_4^{--} ion. Accordingly this compound is reactive with water. Burdick and Day (37) mentioned that most of the aluminium ions in tricalcium aluminate were in fourfold coordination.

When the cement composing minerals are brought into contact with water, a decrease of bond energies is promoted and is dissolved by thermodynamic instability. According to Mchedlov-Petrosyan and Babushkin (38), calcium ion dissolves together with oxygen, whereas Si^{4+} ion hydrates in water and polymerizes in order to neutralize its charge and finally forms nuclei. The supersaturated solution permits crystal growth of the hydrated compound

Table 1. *Heat of formation and free energy change of various hydration reactions. After Mchedlov-Petrosyan and Babushkin (38) modified by Kondo.*

Hydration reactions	ΔH_{298} (kcal/mole CaO)	ΔG_{298} (kcal/mole CaO)
$CaO + H_2O \rightarrow Ca(OH)_2$	−15.60	−13.21
$MgO + H_2O \rightarrow Mg(OH)_2$	− 8.84	− 6.45
$3CaO \cdot SiO_2 + 2.17H_2O \rightarrow 2CaO \cdot SiO_2 \cdot 1.17H_2O + Ca(OH)_2$	− 8.17	− 6.23
β-$2CaO \cdot SiO_2 + 1.17H_2O \rightarrow 2CaO \cdot SiO_2 \cdot 1.17H_2O$	− 3.40	− 0.86
γ-$2CaO \cdot SiO_2 + 1.17H_2O \rightarrow 2CaO \cdot SiO_2 \cdot 1.17H_2O$	− 2.90	− 0.36
β-$CaO \cdot SiO_2 + 0.585H_2O \rightarrow 1/2(2CaO \cdot SiO_2 \cdot 1.17H_2O) + 1/2SiO_2$	+ 3.47	+ 4.89
$5Ca(OH)_2 + 6SiO_2$(quartz) $+ 0.5H_2O \rightarrow 5CaO \cdot 6SiO_2 \cdot 5.5H_2O$	− 7.32	− 4.67
$5Ca(OH)_2 + 6SiO_2$(silica glass) $+ 0.5H_2O \rightarrow 5CaO \cdot 6SiO_2 \cdot 5.5H_2O$	−10.80	− 8.47
$3CaO \cdot Al_2O_3 + 6H_2O \rightarrow 3CaO \cdot Al_2O_3 \cdot 6H_2O$	−23.03	−18.67
$12CaO \cdot 7Al_2O_3 + 48H_2O \rightarrow 3(4CaO \cdot Al_2O_3 \cdot 12H_2O) + 8Al(OH)_3$	−19.07	−16.60
$CaO \cdot Al_2O_3 + 4H_2O \rightarrow 1/2(2CaO \cdot Al_2O_3 \cdot 5H_2O) + Al(OH)_3$	−17.77	
$CaSO_4 \cdot 1/2H_2O + 1.5H_2O \rightarrow CaSO_4 \cdot 2H_2O$	− 4.61	− 1.32
$CaSO_4 + 2H_2O \rightarrow CaSO_4 \cdot 2H_2O$	− 4.00	− 0.25

with higher Ca–O bond energy and low solubility.

Compared with many cement composing minerals, the reactivity of the reactant with high lime content is generally high because of the decrease in free energy or the increase in bond energy gain. The hydration rate of such a reactant is accelerated due to difference in concentration between the reactant interface and the surrounding liquid becoming larger. Compared with silicates, aluminates are generally high in reactivity and have rapid hydration rate due to high solubilities of both the unhydrate and hydrate, and also to the increase in the difference of concentration. However, when hydrates are formed on the surface of the particles of reactant to control the overall reaction by ion diffusion in pores, the hydration rate is significantly affected by the physico-chemical properties of hydrates. A comparison of the hydration rates of the principal compounds of cement is shown in Fig. 1.

Next we will consider the reactivities of hydraulic components with approximately the same chemical composition. It is well known that minor components and conditions of heat treatment and cooling produce several polymorphisms of C_3S and C_2S. Yamaguchi, Shirasuka and Ota (39) found that monoclinic alite hydrated slightly faster, but early strength of the triclinic one seemed to be a little higher, in comparison with polymorphisms of alite with the same composition. Lehmann, Traustel and Jacob (40) measured the heat of hydration of alites, which were prepared by various rates of cooling, and found that alite subjected to slow cooling had lower heat of hydration and strength than that subjected to rapid cooling. Ono and Soda (41) reported that crystal structure with high energy level caused acceleration of the hydration rate.

According to Kondo (42), the hydration rate of C_3S is accelerated if it contains SO_3 and the reactivity of C_3S with water is decreased if it contains P_2O_5. Kondo and Yoshida (43) confirmed that the alite which is defined as a solid solution containing Al_2O_3 and MgO has a higher hydration rate than pure C_3S, and when alite or C_3S contains TiO_2 the reaction within 1 day is retarded, but the subsequent reaction is remarkably accelerated. It is regarded that the reactivity is increased because of the substitution of Al and Ti for Si in the structure of C_3S but the retardation of the induction period in the C_3S and alite containing Ti may be attributed to the difficulty of the growth of nuclei of more stable hydrate formed in the impermeable coating.

When $KC_{23}S_{12}$ and NC_8A_3 are compared with β–C_2S and C_3A, according to Kryzhanovskaya, Mirak'yan, Shokotova and Horodnui (44) a significantly different hydration rate is not indicated.

Imperfections, such as lattice defects and dislocations, play important roles in the chemical reactivities of solids and a surface may be considered to be a giant lattice defect. When particles and water are brought into contact, ionic species dissolve apart from particles. Dislocation density contributes to the rate of the dissolution. The formation of dislocation etch pits is generally attributed to enhanced chemical reactivity resulting from the lattice strain in the vicinity of edge or screw dislocations. But Gatos (45) indicated that dislocations could also be revealed at low angle boundaries where they possessed no additional lattice energy, and that the lattice strain associated with dislocations was not of primary importance in determining their increased chemical reactivity. In certain instances surfaces with dislocation can become entirely inactive in the presence of adsorbed molecules in solution. If the surface reaction is the slow step the dissolution of the surface becomes activation-controlled, and differences in reactivity among surfaces with various indices (hkl) may be observed. However, differences in reactivity shall not be observed when the mass-transport is the slow

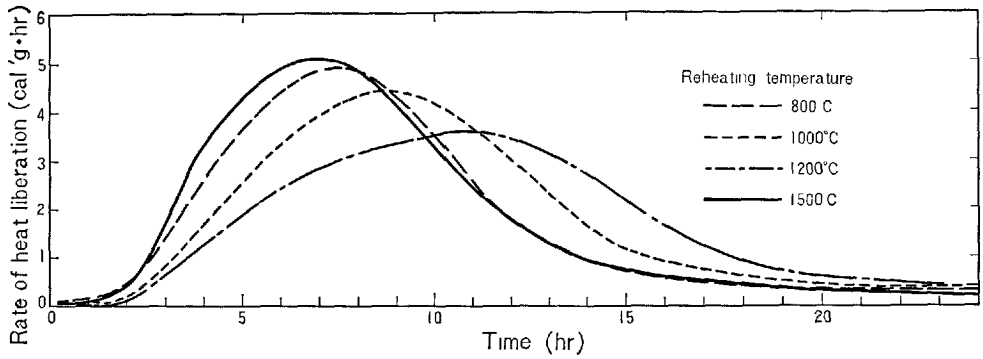

Fig. 8. *Variation with reheating temperature of heat liberation of* C_3S. *(W/C = 0.5, at 25°C)*

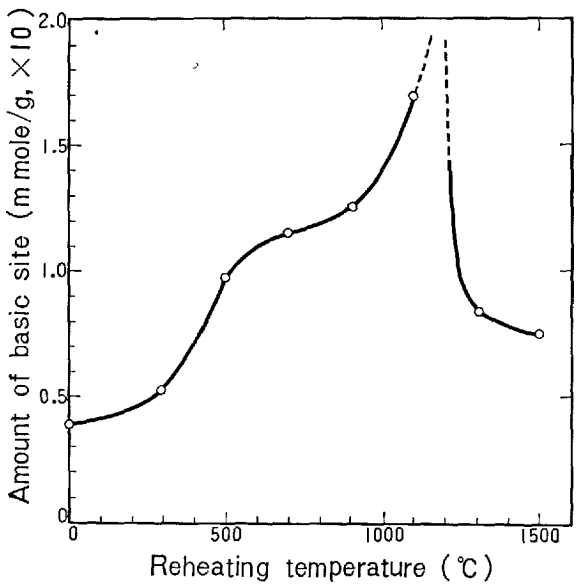

Fig. 9. *Amount of basic site of reheated* C_3S.

step.

Kondo, Daimon and Akiba (46) investigated the relationship between the amount of basic site and the hydration rate of C_3S. The change in the amount of basic site in reheated C_3S corresponds to that of the hydration rate as is seen in Figs. 8 and 9. With the increase in annealing temperature, C_3S powder loses adsorbed water at about 400°C and dissociates into CaO and C_2S at the surface and the amount of basic site increases rapidly at about 1100°C. If it is reheated above 1300°C, however, C_3S is stabilized at its surface and the amount of basic site decreases. The surface which easily accepts proton or donates the electron pair seems to lower the hydration rate.

Through Solution and Topochemical Reactions

There are two theories about the mechanism of cement hydration, particularly with respect to the location forming hydrates. It has long been discussed whether it takes place by through solution or topochemically.

Through Rolution Seaction

The through solution theory at present is close to the crystallization theory of LeChatelier (47). According to him, the dissolution of the cement composing mineral takes place at first and then the dissolved species are hydrated in the solution. During this period as the hydration compounds produced has lower solubility than the reactants, crystallization is commenced in solution.

Brunauer and Greenberg (20) proposed the following process, if the hydration reaction is advanced with the through solution mechanism.

1. the hydrated ions form at the surface.
2. they diffuse away from the surface.
3. they react with each other to form C–S–H molecules.
4. the molecules form nuclei.
5. the nuclei grow.
6. colloidal particles precipitate and flocculate.

They practically observed that $Ca(OH)_2$ separated out of the solution as relatively large particles and was overlaid by C–S–H gel or grew around and occluded C–S–H gel, and the gel appeared to form at considerable distances from the grains. According to Richartz and Locher (48), calcium silicate hydrates grow from the surface of the alite and belite particles into the surrounding water as large as the pore space allows.

Table 2. *Hydration mechanism of* C_3S.
(t_r = intermediate phase t_i = inner product t_o = outer product P_1 = first portlandite P_2 = second portlandite).
After Terrier and Moreau (54) partly modified by Kondo, Daimon and Ueda (55).

Stage	0	I	II	III	IV		V		
	Water	Solution		Solution	Solution	P_1	Solution	P_1	
						t_o		P_2	t_o
↑ Original particle boundary	C_3S	t_r $CaO/SiO_2 = 3$	$t_r \rightarrow (t_i)$	$t_r \rightarrow t_i$	t_i $CaO/SiO_2 = 1.6$		t_i outside $CaO/SiO_2 = 1.6$ t_i inside $CaO/SiO_2 = 2$		
		C_3S		t_i C_3S	C_3S		C_3S		

Topochemical Reaction

A type of hydration other than through solution is so called topochemical reaction. According to Michaelis (49), when the Ca-rich silicious clinker mineral is brought into contact with water, Ca^{++} ion is liberated into the solution and the Ca-poor skeleton of crystal remains. This skeleton is swollen by the action of the prepared lime solution to form gel. He assumed that inner suction took place towards the interior of the cement particles.

Hansen (50) concluded that the hydrolysis of C_3S to form hydrated silicate and $Ca(OH)_2$ took place topochemically, as he could not detect a significant amount of SiO_2 and Al_2O_3 in the filtrate. Funk (51) showed by X-ray diagrams and optical observations that β–C_2S crystals took up H_2O at 100°C and 100% relative humidity to form the intermediate products with low refractive indices, however it alters into the C–S–H phase with increasing water content.

Feldman, Ramachandran and Sereda (52) believed that the hydration of C_3A in the vapor phase at 50% relative humidity took place and the reaction would proceed by a direct mechanism, because only one or two molecular layers of adsorbed water are present on the surface under these conditions and a through solution mechanism does not have any meaning. Trojer (53), who observed the formation of the intermediate products of decreased refractive indices inside the original cement particle, considered that ionic species transported by lattice diffusion, i.e. Ca^{++} ion, migrated toward the outside and H^+ ion penetrated from the liquid in order to maintain the electrical neutrality of the lattice. Terrier and Moreau (54) affirmed by optical observations that the hydration of a silicate proceeded topochemically and calcium moved from the reactant interface which shifted inwards gradually, through the inner product layer to the outside of the grain as is seen in Table 2, which is partly modified by Kondo, Daimon and Ueda (55).

Hydration of plaster of Paris is generally regarded to take place with through solution mechanism, but Eipeltauer (56) observed the formation of inner product.

From the consideration of the specific volume and the pore space of hydrated gel, Taplin (57) and Powers (58) considered that the hydration reaction proceeded towards the interior of the cement particle to form the inner product, but simultaneously 1.2 times the volume of the reacted part was required by the outer product. Accordingly the formation of inner and outer products in the respective stages of the process must be examined with consideration given to counter diffusion through the product layer.

Kondo, Ueda and Kodama (16) examined the hydration of C_3S by calorimetry, quantitative X-ray analysis, chemical analysis of liquid phase and microscopic observation. In the extension of this study Kondo, Daimon and Ueda (55) pointed out that SiO_2 content of the suspension of only the outer products exceeded SiO_2 concentration of the extracted liquid phase and thus confirmed the existence of C–S–H gel other than $Ca(OH)_2$ as the outer products formed in solution.

However before the end of the induction period CaO concentration of the liquid rises rapidly to commence precipitation of $Ca(OH)_2$ crystal. The difference in CaO concentration between the C_3S interface and liquid increases due to the beginning of the precipitation of $Ca(OH)_2$ and liberation of Ca^{++} ion becomes easier. On the other hand SiO_2 concentration in the C_3S interface of the exceedingly high CaO concentration decreases and the liquid phase remains in the saturated state. Therefore it will become difficult for Si^{4+} ion to migrate due to the small SiO_2 concentration difference.

Kondo, Ueda and Kodama (16) have studied the hydration process of single particle of C_3S under the

microscope. After 8 hours the surface alters slightly, as can be seen in Fig. 10. The inner product which has a double refraction of almost zero extends toward the interior of the particle with the progress of hydration. The unhydrated part has been eliminated by 8 days in the case of fine particles. As shown in Fig. 10, the hydration seems to proceed without any remarkable changes in shape and size of the original C_3S grain. The outer products which are formed outsides the C_3S particle consist of $Ca(OH)_2$ crystals which are growing large and calcium silicate hydrate gel appears on the slide glass and the cover glass. With the exception of the early stage, the reaction proceeds topochemically, while liberating Ca^{++} ion and also keeping the original shape. Similar microscopic observation in the hydration of $C_4A_3\bar{S}$ were separately reported by Okushima, Kondo, Muguruma and Ono (59). $C_4A_3\bar{S}$ reacts with water to form inner products, while the particle expands by topochemical reaction when $C\bar{S}H_2$ and CH are existing.

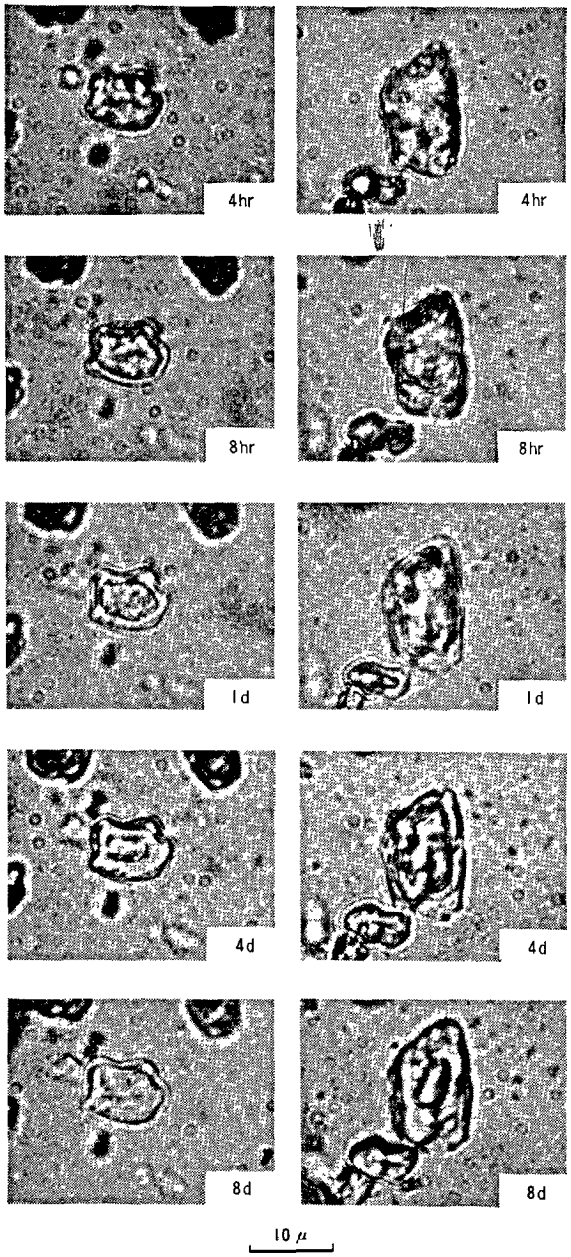

Fig. 10. *Hydration process of single particle of* $C_3S(r = 2 \sim 5\mu)$ *under microscope. After Kondo, Ueda and Kodama(16)*

It was also pointed out by Kondo, Ueda and Kodama (16) that the crystallization of the inner product was by no means chaotic, but proceeded epitaxially, from the observation of the Becke line around the particle whose reaction was considerably advanced. McConnell (60) has found similarly by a single-crystal X-ray technique that the *b*-direction of the hydrated phase is oriented parallel to the *c*-direction of the parent bredigite (natural α'–C_2S). Such epitaxial crystal growth as mentioned above may have taken place due to the similarity between the arrangements of SiO_4 tetrahedra in C_3S and that in tobermorite as pointed out by Kawada and Nemoto (61).

As mentioned above, C_3S is hydrated to form C–S–H with a definite direction without much change in the Si site of the original C_3S. The oxygen site is generally not changed in the so-called topotactic reaction. On the other hand, the SiO_4 tetrahedra migrates slightly to drop the energy level in the hydration of C_3S because the original SiO_4 tetrahedra is independent while that of the product is in chain.

A reactant which participates in mutual reaction and moreover has a large dissolution rate, for instance, gypsum in portland cement, reacts by the through solution mechanism. Cement components generally form the outer products by the through solution mechanism while they form the inner product topochemically. Topochemical reaction is characterized by taking place near the interface of reactant and includes not only a topotactic reaction but also a local through solution mechanism.

Latent Hydraulic and Pozzolanic Materials

Besides the hydraulic components, calcium aluminosilicate glass such as granulated blast-furnace slag produces hydrates and hardens in the presence of activators, and also reactive silica or silicates hydrates and hardens by the reaction with lime.

Latent Hydraulic Materials

There are calcium alumino-silicate glass and $CaSO_4$

Table 3. *pH of suspension with calcium alumino-silicate glass powders. After Kondo (62).*

	Latent hydraulic					Intermediate			Hydraulic					
CaO	48.2	44.5	52.9	40.8	41.0	41.2	38.1	48.0	55.8	58.1	48.6	51.0	49.5	58.3
Al_2O_3	—	18.6	18.6	37.2	18.6	—	50.9	37.3	20.3	26.4	51.4	30.8	43.7	33.0
SiO_2	51.8	36.9	28.5	22.0	33.0	44.0	11.0	14.7	23.9	15.5	—	18.2	6.8	8.7
MgO	—	—	—	—	7.4	14.8	—	—	—	—	—	—	—	—
Mineral composition	CS	CS 50 C_2AS 50	C_2S 50 C_2AS 50	C_2AS	C_2AS 50 C_2MS_2 50	C_2MS_2	C_2AS 50 CA 50	C_2AS etc.	C_2AS etc.	C_2S 44 $C_{12}A_7$ 39 C_3A 17	$C_{12}A_7$	C_2AS etc.	$C_{12}A_7$ 64 C_2S 19 CA 17	C_3A 44 C_2A_7 31 $C_{12}S$ 25
pH 3 min.	10.0	8.4	10.2	8.5	8.4	10.1	10.5	10.2	10.8	11.9	12.0	10.9	11.7	11.5
pH 3 hr.	10.3	8.8	10.7	8.8	8.6	11.1	11.8	11.9	12.1	11.9	11.7	11.9	11.9	11.8
pH 2 d.	10.6	8.9	10.3	8.5	9.2	11.5	11.9	11.8	12.1	12.2	12.0	12.0	12.0	11.8

as materials which react with water to form hydrated products and to which an activator is added in order to accelerate their very slow reaction rate. Ortho silico-ethyl ester $Si(OC_2H_5)_4$ is hydrolized and hardened at a present of exciter such as acid or organic base.

Kondo (62) studied the hydration of calcium alumino-silicate glass powders in excess water and obtained the pH values of liquid shown in Table 3. Glasses with composition of above 50% CaO and below 20% SiO_2 content have hydraulic properties and the pH values become more than 11～12. Glasses which indicate pH values lower than this due to their CaO contents have latent hydraulic properties.

Granulated blast-furnace slag is a glass whose main potential constituents are C_2AS–C_2MS_2 solid solution, CS and C_2S. Kondo (62) studied the mechanism of the hydration of latent hydraulic materials using C_2AS glass to simplify the complicated composition of slag. Compared with C_2MS_2 or CS, C_2AS is difficult to dissolve in water. Particularly the amount of SiO_2 and Al_2O_3 liberated is very low when compared with that of CaO (Fig. 11). The dissolution rate of these compound is in general slightly larger in the glassy state than in the crystalline state.

In the suspension hydration of C_2AS glass powders, a low permeable coating which is approximately ASH_6 in composition and 0.2μ in thickness is formed on their surfaces. D'Ans and Eick (63) similarly reported that the surface of the slag was covered with acid gel by reaction with water. Fig. 12 shows that the suspension hydration of C_2AS glass is accelerated by the addition of $Ca(OH)_2$ to form the hydrate with approximately C_3ASH_5 composition because SiO_2 and particularly Al_2O_3 are apt to be liberated and the solubility of hydrate also decreases under this condition. Nevertheless if C_2AS is in a crystalline state, the amount of dissolution does not increase even in the presence of $Ca(OH)_2$.

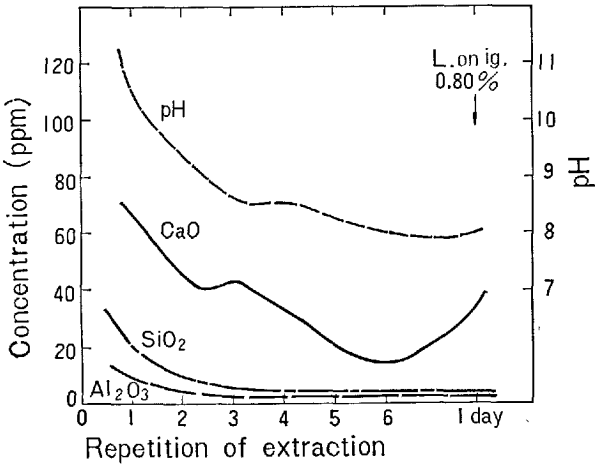

Fig. 11. *Repeated extraction of C_2AS glass. (5 grams of C_2AS per 100 c.c. of water) After Kondo(62)*

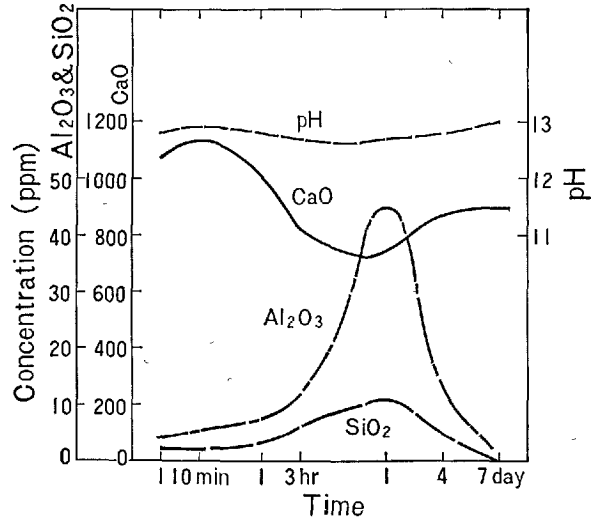

Fig. 12. *Solubility of C_2AS glass with 2 moles of $Ca(OH)_2$. (1 gram of solid per 100 c.c. of water) After Kondo(62)*

$CaSO_4$ is not an exciter in super-sulfate slag cement but an important reactant on account of its hydration. The reaction between both reactants, however, is not proceeded in the absence of an alkaline exciter.

While there is no example of investigation on the degree of hydration of slag in the portland blast-furnace cement and super-sulfate slag cement. The reason for this is that a suitable method for estimation of residual slag in hydrated cement paste has not been found. Kondo and Ohsawa (64) developed a method and determined the rate of hydration of slag in various slag cements.

Pozzolanic Materials.

The pozzolanic cement is a kind of blended cement and historically the oldest cement.

In the pozzolanic cement the reactive silicas and silicates, which are called pozzolanic materials, combine with lime at ordinary temperature in the presence of water to form hydrates similar to those found in the hydration of portland cement. There are natural and artificial pozzolanic materials and their mineral constituents and properties have been reviewed by Malquori (65). Colloidal silica, opal, diatomite, alumino-silicate glass, zeolites, allophane, halloysite and metakaolin have been found to be reactive components. The hydration of pozzolanic materials containing a reactive alumina is especially accelerated by the addition of gypsum, besides lime. Quartz which has low reactivity at ordinary temperature reacts with lime rapidly at a high curing temperature.

Halstead and Lawrence (66) and also Greenberg (67) examined the rate of reaction between colloidal silica and lime solution. It is shown that the surface of silica is covered with acidic silanol groups, SiOH, which react immediately with $Ca(OH)_2$ in an acid-base reaction. Concentration of C–S–H is expressed in the solubility products as $[Ca(OH)_2]^x [SiO_2] = k$, in which $x = 1.9$ and $k = 3.4$ (66) (68).

The pozzolanic reactivities of silica glass and quartz are compared at various temperatures and the results are mentioned later (69).

Mutual Reactions and the Effect of Admixtures

The addition of additives in cement or mixing water changes the rate of hydration. As additives sometimes a large amount of materials such as blast-furnace slag or pozzolan is added to the portland cement and occasionally a nearly inert powder of quartz or limestone is added. On the contrary, materials such as gypsum, calcium chloride and surfactants affect hydration reaction considerably even when a small amount is added. To avoid quick-setting of C_3A, which is contained to some extent in portland cement, gypsum is always added.

Interaction of Silicates

The concentration of the liquid phase in paste is varied by the addition of admixtures. Kondo, Daimon and Ueda (55) examined the hydration of C_3S with liquids supersaturated with respect to both $Ca(OH)_2$ and C–S–H. The fresh C_3S was hydrated with this liquid and then it was found that its hydration is extremely retarded as seen in Fig. 13 (70). Steinour (71) and de Jong, Stein and Stevels (72) reported similar results. When the surrounding liquid is in supersaturation, the dissolution of C_3S is retarded to extend the induction period.

According to Kawada and Nemoto (61), the hydration of C_3S is accelerated when gypsum is added as the supersolubility with respect to $Ca(OH)_2$ rises in the presence of gypsum. According to Kurczyk and Schwiete (73), a small amount of $CaCl_2$ accelerates the hydration of C_3S and the pH value of liquid

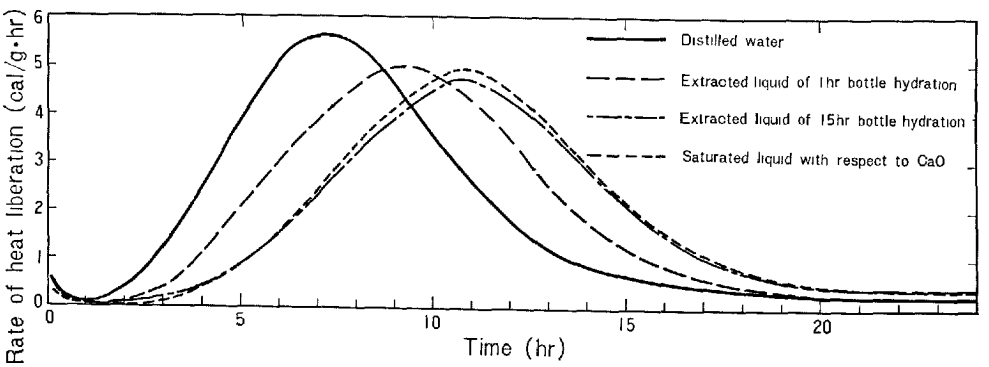

Fig. 13. *Variation with mixing liquid of heat liberation of* C_3S. *($r = 2 \sim 5\mu$, $W/C = 0.5$, at 25°C)*

decreases with the amount of addition. But when $CaCl_2$ above 2% is added the pH value drops to below 12 to hinder the formation of a C–S–H gel. Stein and Stevels (74) reported that the hydration of C_3S was accelerated by an autocatalytic type of reaction, as the addition of aerosol changed in calcium ion and silicate concentrations, and pH value.

Admixtures also change the composition, morphology and amount of hydrated products which are closely related to the rate of mass-transfer. According to Kurczyk and Schwiete (73), the addition of gypsum impedes the hydration of β–C_2S due to the low degree of crystallization of acicular product.

The rate of reaction of β–C_2S is retarded at the early stage in the presence of C_3S but it is accelerated after liquid is supersaturated by the dissolution of C_3S (75). The hydration of β–C_2S is retarded considerably in the presence of $C_{12}A_7$ (76).

Interaction of Aluminates

There are many studies on the mutual reactions of aluminates with admixtures such as gypsum because these reactions are concerned with retardation of the setting of portland cement and with the expansion of expansive cement.

According to Kondo (62), when C_3A powder is hydrated in excess water, it dissolves stoichiometrically and the concentration of liquid indicates high supersolubility with respect to hydrates, which precipitate rapidly as shown in Fig. 14. The surface of C_3A particle is covered with an ettringite coating from the beginning if gypsum is added to decrease the dissolution rate and the Al_2O_3 concentration of the liquid until gypsum is consumed as shown in Fig. 15. Similarly Fig. 16 shows that the hydration rate is kept low in the presence of $Ca(OH)_2$. Particularly when gypsum and lime are added simultaneously to the hydration of C_3A, the solubility of ettringite decreases further to form very small crystals and causes an increase in the compactness of coating. Therefore the hydration rate of C_3A is retarded ex-

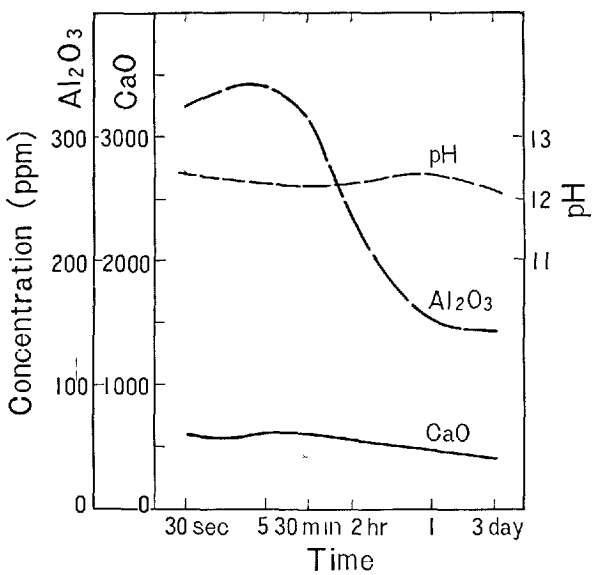

Fig. 14. *Solubility of* C_3A. *(2 grams of* C_3A *per 100 c.c. of water) After Kondo*(62)

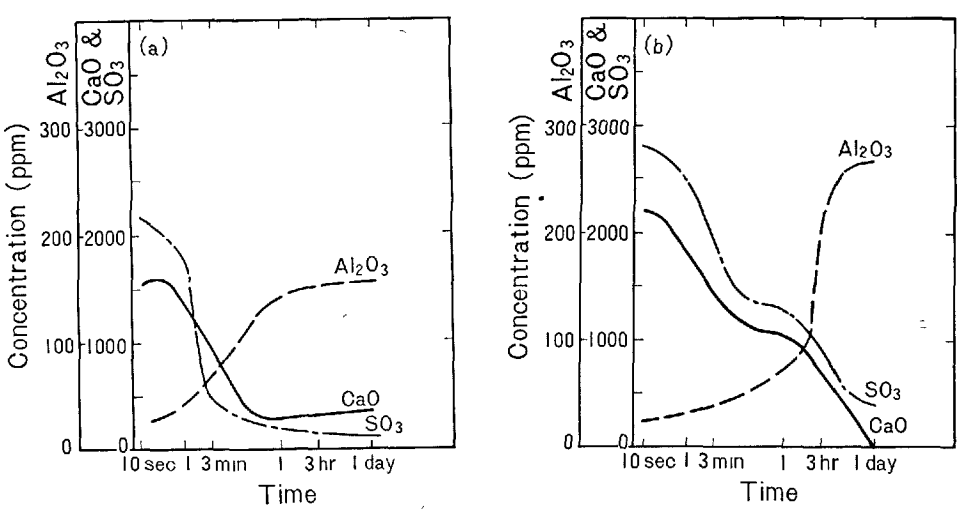

Fig. 15. *Effect of* $CaSO_4 \cdot \frac{1}{2}H_2O$ *on solubility of* C_3A.
(a) C_3A + 1 mole of $CaSO_4 \cdot \frac{1}{2}H_2O$
(b) C_3A + 2.5 mole of $CaSO_4 \cdot \frac{1}{2}H_2O$
After Kondo(62).

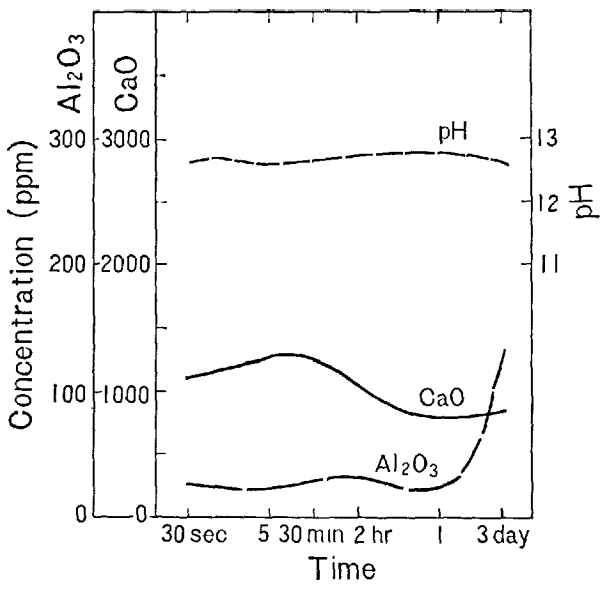

Fig. 16. *Effect of* $Ca(OH)_2$ *on solubility of* C_3A. (*Addition of 1 mole of* $Ca(OH)_2$) *After Kondo(62)*

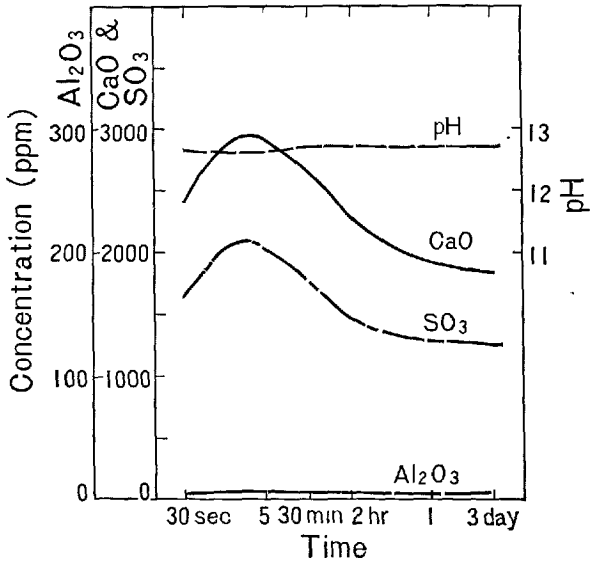

Fig. 17. *Effect of* $CaSO_4 \cdot \frac{1}{2}H_2O$ *plus* $Ca(OH)_2$ *on solubility of* C_3A. (*Addition of 1 mole of* $CaSO_4 \cdot \frac{1}{2}H_2O$ *and 1 mole of* $Ca(OH)_2$) *After Kondo(62)*

tremely, and the Al_2O_3 concentration of liquid is kept very low as shown in Fig. 17.

The hydration rate of C_3A, according to Stein (77), is attributed to the degree of crystallization of calcium sulfoaluminate hydrate corresponding to the amount of additives. The formation of acicular crystal seems generally to have a tendency to accelerate hydration, however, less soluble products such as

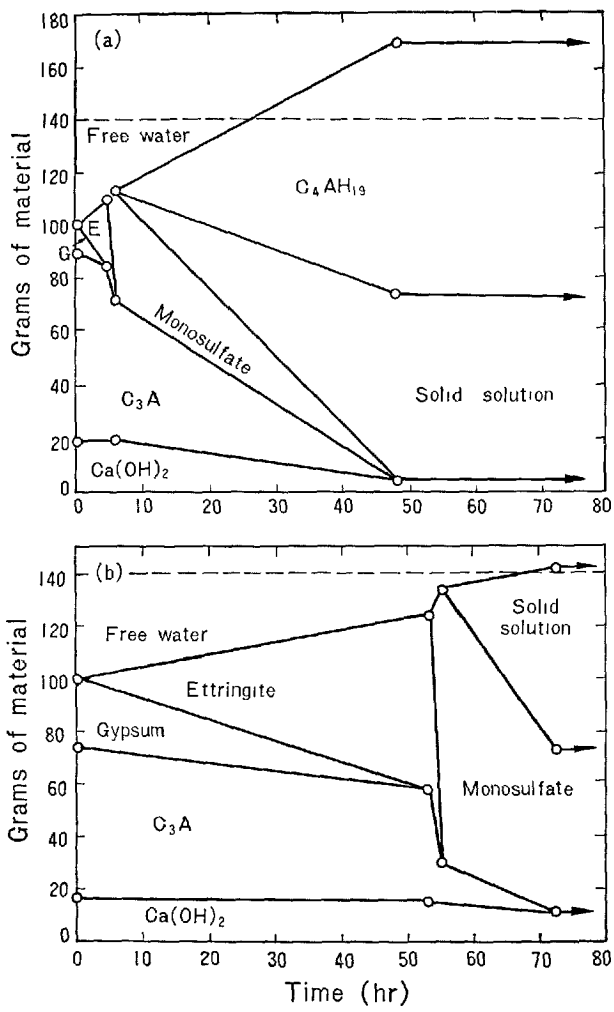

Fig. 18. *Effect of gypsum on aluminate hydration reaction with* $W/S = 0.4$. *Molar proportion of reactants* C_3A, $Ca(OH)_2$ *and* $CaSO_4 \cdot 2H_2O$; (a) $1:1:\frac{1}{4}$, (b) $1:1:\frac{3}{4}$. E = *Ettringite*, G = *Gypsum. After Verbeck(79)*

ettringite retards the reaction due to its lower permeability.

Schwiete, Ludwig and Jäger (78) found that a layer of ettringite was topochemically formed around the C_3A particles immediately after the addition of water, enveloping them in "hedge hog" fashion and owing to the formation of this layer the following reaction between C_3A and sulfate ions was considerably retarded. These ions are thought to diffuse to form additional ettringite at the C_3A interface. As long as the sulfate ion concentration is sufficient for an ettringite formation, the ettringite skin is sound or healed by new formation when it breaks in consequence of crystallization pressure. After the concentration of sulfate ion is lowered by the consumption of gypsum a rapid reaction of the remaining C_3A occurs.

According to Verbeck (79), after the consumption of gypsum the conversion of ettringite to monosulfate hydrate commences as seen in Fig. 18. Henning and Danowsky (80) discussed the mechanism of hydration with the measurement of high frequency conductivity. According to them, Ca^{++} ion and $[Al(OH)_6]^{---}$ group liberate from C_3A, and SO_4^{--} ion and Ca^{++} ion from gypsum. SO_4^{--} ion reacts with the C_3A surface to form monosulfate film on it and $[Al(OH)_6]^{---}$ ion with the gypsum surface to form acicular trisulfate on it.

Tenoutasse (81) observed that the time required for consumption of gypsum was in square proportion to the amount of added gypsum and was reduced with increasing temperature. The hydration of C_3A with gypsum is accelerated, if $CaCl_2$ is added, and after the consumption of gypsum the reaction between C_3A and the Cl^- ions commences. He applied the kinetic equations conventionally but the model of reaction was not given.

According to Okushima, Kondo, Muguruma and Ono (59), hydration of C_3A or $C_4A_3\bar{S}$ forms monosulfate at the interface of reactant locally even in such a case to form ettringite as an inner product. On the other hand it is difficult to form products at the surface of gypsum which has a large solubility and rate of dissolution. They also discussed the mechanism of hydration of expansive cement accompanying with an expansion which occurred in the consumption of mechanical energy.

Feldman and Ramachandran (82) proposed that the formation of ettringite did not have any direct role in the retardation and rather the presence of $CaSO_4$ in solution decreased the reaction rate of C_3A by sorption of SO_4^{--} which affected the operation of surface source of dislocation. Feldman and Ramachandran (82) also found a two step reaction in which C_3A and gypsum first formed the hexagonal hydro-aluminates immediately on contact with water, and then the gypsum reacted partly with the hexagonal hydro-aluminates to form the trisulfate hydrate.

The surfactants in general lower the water requirement and retard the setting, however, Young (83) reported that C_3A formed needle-like crystals at a presence of more than 3% of lignosulfonate. According to Kawada and Nishiyama (84), C_3A does not physically adsorb calcium lignosulfonate but reacts chemically to form a new hydration product. However, when the concentration of anionic calcium lignosulfonate is low, C_3S or C_2S adsorbs physically to satisfy the Langmuir's equation. Thus the hydration is retarded. The retardation mechanism was explained by Kasai (85) from the standpoint of the complex chemistry whereby the structure of hydrate had been explained by Forsén (86).

Stein (87) found that the hydration of C_3A became faster as more C_3AH_6 was added, so that the second peak in the hydration of C_3A is dependent upon the formation of C_3AH_6 from the intermediates. He also stated in a later report (88) that the precipitation of amorphous hydrous alumina inactivated the nuclei of C_3AH_6 to stop the reaction and this effect was lowered in the presence of quartz because the precipitation occurs partially on the quartz surface. According to Feldman, Ramachandran and Sereda (52), the effect of the addition of $CaCO_3$ does not seem to be significant. Stein (13) reported that the addition of sodium carbonate accelerated the hydration of C_3S, whereas it retarded the hydration of C_3A as the result of the formation of $3CaO \cdot Al_2O_3 \cdot CaCO_3 \cdot 11H_2O$.

Several Factors Concerned with the Rate of Hydration

Pulverizing of cement not only makes the surface area of sample large but also changes the energy state of its surface. These variances affect the reactivity with water. The water cement ratio and curing temperature are the most effective factors on the hydration reaction. Furthermore hydration may be affected by vibration and ultrasonic treatment in the casting of paste, and by the relative humidity and the existence of CO_2 gas during atmospheric curing.

Fineness of Cements

The particle size or the surface area of powder contributes to the rate of hydration and in general of solid state reaction and is inclusive in the kinetic constant. The hydration rate of the classified C_3S is accelerated further, the finer the C_3S grain, as shown in Fig. 1. From these data the thickness of the hydration layer can be calculated under an assumption in which the thickness of the hydration layer in C_3S particle increases in correlation with time, without any relation with particle size. It is presumed that the time required for the reaction to be completed is about 1 year in particles with 8μ radii and is about 10 years in particles with 20μ radii.

Sylvan (89) pointed out that the specific surface

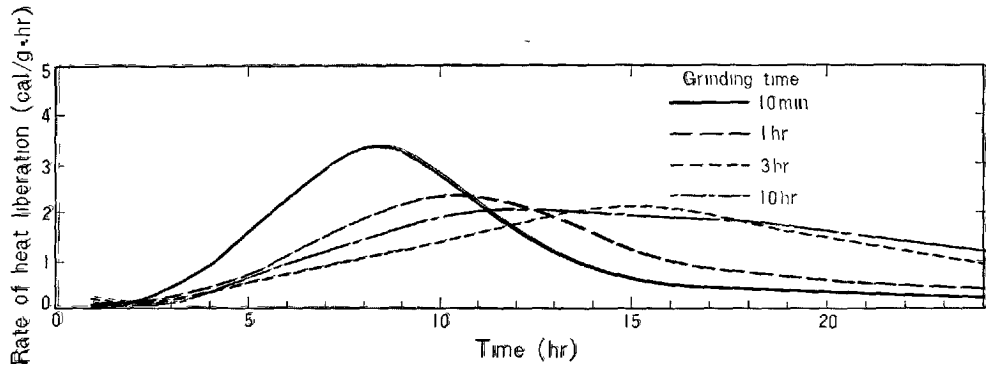

Fig. 19. *Variation with grinding time of heat liberation of* C_3S. *($r = 2 \sim 15\mu$, $W/C = 0.5$, at 25°C)*

was to a large extent dependent upon the measure of dispersion of the grading, whereas the hydrated quantity was not. The strength of the hardened cement paste is more closely bound up with the average value of the particle size and with the degree of hydration than with the specific surface.

From the measurement of the amount of non-evaporable water, Gronau (90) proposed an equation to determine the degree of hydration. It was derived from the assumptions that the thickness of reaction layer did not depend on the particle size and the particle size of cement was in a logarithmic regular distribution.

$$\alpha = \frac{1}{\sqrt{2\pi}}\int_{-\infty}^{1/\sigma \ln h/r_0} e^{-t^2/2}dt + \frac{3h}{r_0}e^{\sigma^2/2}\int_{t_1}^{\infty}\frac{1}{\sqrt{2\pi}}e^{-u^2/2}du - \frac{3h^2}{r_0^2}e^{2\sigma^2}\int_{t_2}^{\infty}\frac{1}{\sqrt{2\pi}}e^{-v^2/2}dv + \frac{h^3}{r_0^3}e^{9/2\cdot\sigma^2}\int_{t_3}^{\infty}\frac{1}{2}e^{-w^2/2}dw$$

where $t = 1/\sigma \cdot \ln \cdot r/r_0$, $u = 1/\sigma \cdot \ln \cdot r/r_{01}$, $v = 1/\sigma \cdot \ln \cdot r/r_{02}$, $w = 1/\sigma \cdot \ln \cdot r/r_{03}$, $h = f(t)$, r_0 is the median of volume distribution, σ is the variance and α is the degree of hydration. This equation can be solved by the help of the table of Gauss' error function as all the right side terms are this type of function. The relation between α and g H_2O/g cement is experimentally obtained.

Otherwise the surface energy of the particle changes with the degree of grinding. Beke and Opoczky (91) obtained a very fine powder by grinding of clinker minerals by addition of tri-ethanolamine as a grinding aid to avoid adhesion and aggregation. It was observed by X-ray diffraction that the intensity of the fine powder decreased with grinding time and the width of peak became broad and also that split peaks became a single peak. They explained that the fine grinding of clinker mineral assisted the formation of lattice distortion and lattice defect, and then the rearrangement of atom in the crystal structure. Ueda, Hashimoto and Kondo (2) studied the hydration rate on classified C_3S with different grinding time with results illustrated in Fig. 19. The surface structure was also investigated by surface electron diffraction and its results are shown in Fig. 20. X-ray diffraction intensity of a sample ground for 10 hours decreases but there are no changes in the peak width and the background. The surface electron diffraction pattern shows that the surface is to some extent amorphous and the thickness of this amorphous layer increases with the grinding time. The hydration rate is retarded with the grinding time and the volume of heat evolution immediately after the addition of water is not in linear correlation with the grinding time. Accordingly, it is clear that the lattice defect does not always promote the reactivity of C_3S particle at least in the early stage of reaction.

In order to accelerate the hydration such a study on the pulverizing method to obtain the reactant powder with limited particle size distribution must be important, however, we must simultaneously consider the rheological properties of cement paste.

Water Cement Ratio

The water cement ratio of the paste determines the space of the capillary void where the reaction progresses, and particularly controls the state of the outer products. The relationship between the water cement ratio and the concentration of the liquid extracted from the paste is shown in Fig. 21. This figure indicates that the degree of supersaturation becomes higher with decrease in the water cement ratio. The degree of supersaturation contributes significantly to the rate of nucleation. The reaction rate is accelerated with increase in the water cement ratio when the slow

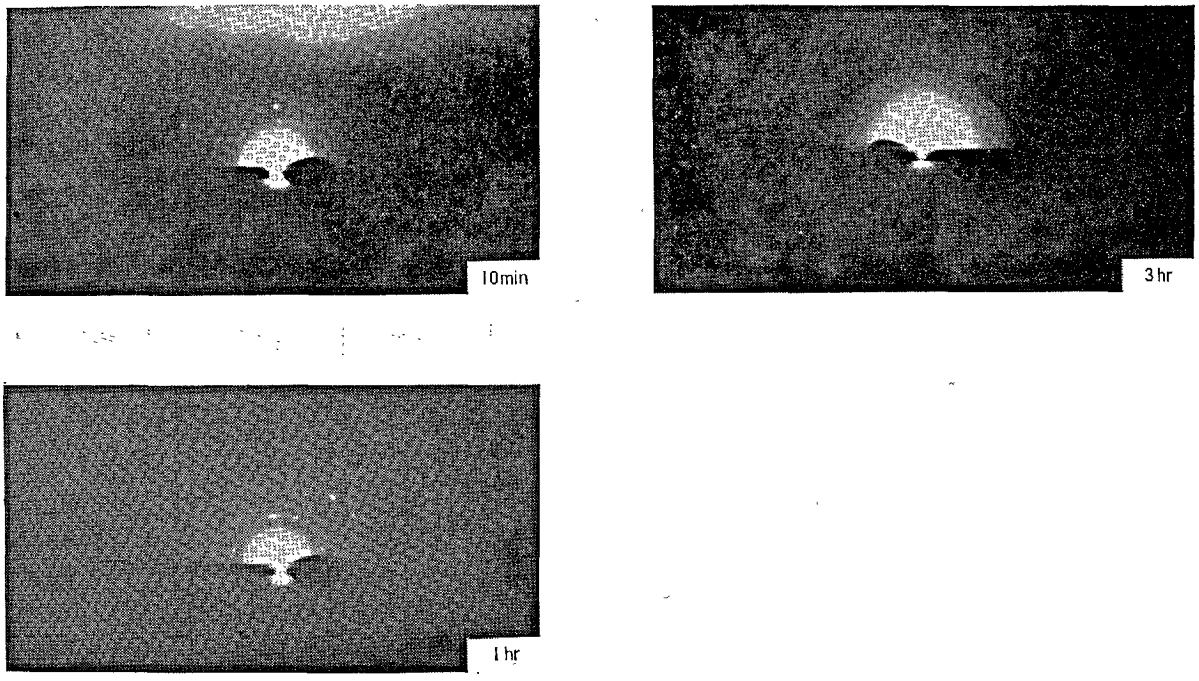

Fig. 20. *Surface electron diffraction patterns of* C_3S *with different grinding time*

step is dissolution but with decrease in the water cement ratio when the rate of hydration is controlled by nucleation.

Different results have been reported by numerous investigators on the dependence of the water cement ratio upon the rate of hydration. Sudoh and Mori (92), and Kantro, Weise and Brunauer (93) noted that at an early age the degree of hydration of C_3S and β–C_2S was nearly the same for W/C = 0.3 to 0.7, whereas at a later age it gave a higher value with increase in the water cement ratio. According to Kondo, Ueda and Kodama (16), the hydration rate of C_3S within 6 hours does not seem to depend upon the difference between W/C = 0.5 and 1.0, however, the following reaction is distinctly accelerated to a great extent in a large W/C ratio. As is shown in Fig. 1, the degree of hydration in W/C = 1.0 is about 2 times that in W/C = 0.5 within a short time but the difference between them decreases in case of a long time. This indicates that the hydration reaction is determined neither by solution control nor by nucleation control.

The amount of combined water of the product increases with increase in the water cement ratio at the early stage, while it is kept constant regardless of different water cement ratios at the later stage as is shown in Fig. 22.

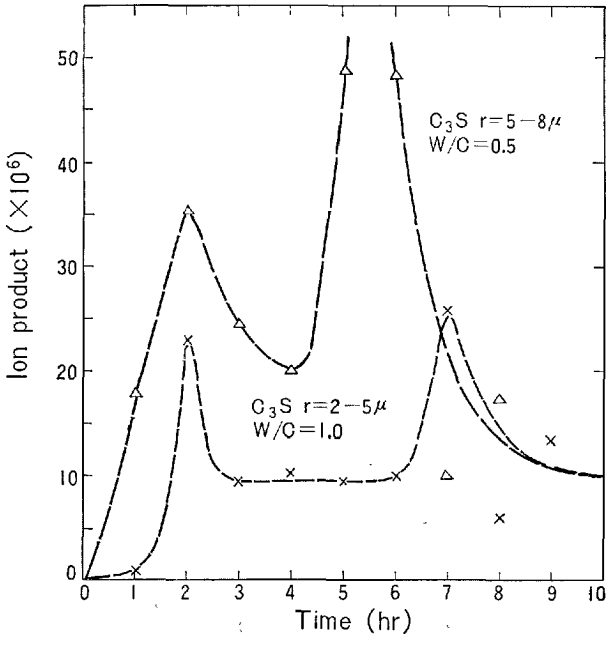

Fig. 21. *Concentration of extracted liquid from* C_3S *paste*

In contrast with the above results, Locher (94) recently reported that with increase in the amount of mixing water the degree of hydration decreases until the age of 7 days and reaches the minimum

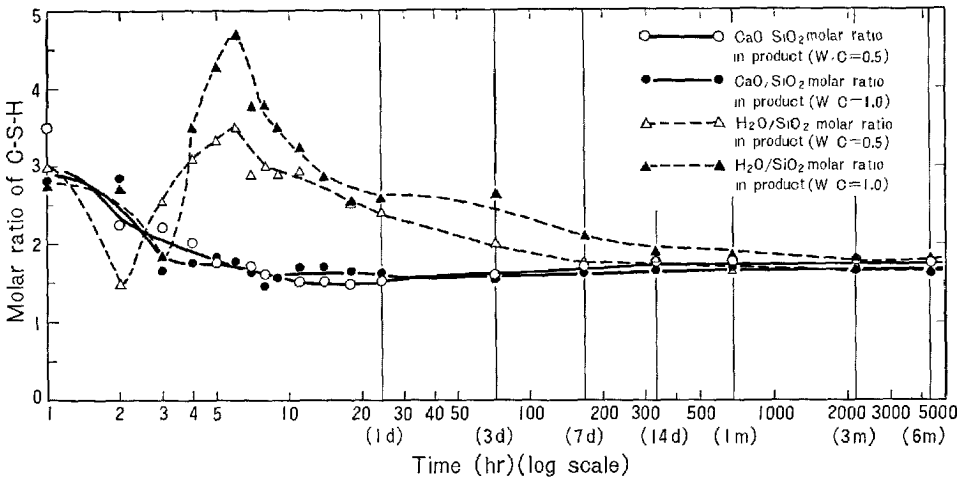

Fig. 22. *Change in molar ratio of produced calcium silicate hydrate in hydration of* C_3S. ($r = 2 \sim 5\mu$, *at 25°C*)

with W/C = 0.8. However he did not discuss the significance of this. According to Locher (94), C–S–H occurs with approximately equal CaO/SiO_2 ratio in the C_3S paste at above W/C = 0.6, but in samples with low water content CaO-rich C–S–H whose CaO/SiO_2 ratio rises with decreasing W/C value are formed.

Kantro, Brunauer and Weise (95) studied the hydration of C_3S in a steel ball mill at room temperature and found that $Ca(OH)_2$ and hydrate III were formed at the early stage but the latter was unstable and was converted gradually to well-crystallized afwillite.

According to Tsumura and Kawachi (7), the hydration rate of C_3A is accelerated with increase in the water cement ratio, while the early stage of C_4AF is accelerated by the decrease in the ratio. Seligmann and Greening (3) found that at the very early stage the hydration in C_3A-gypsum-water system was accelerated by the presence of excess water.

Curing Temperature

Curing temperature has a large effect on the hydration of cement and introduces the changes in the products and the reaction rate. The reaction is generally accelerated with rise in temperature. On the contrary, for instance, the hydration product of CA is transformed at about 20°C and consequently the rate of hydration is not accelerated with the curing temperature. When C_3S or C_2S is hydrated at temperatures higher than 70 to 80°C, hydrates are produced in high lime and low surface area and then the strength of the hardened paste decreases.

The rate of the hydration reaction of lime-quartz mixture is very slow at room temperature but is accelerated with rise in temperature. Accordingly such binding materials are subjected to curing at about 180°C in industry using an autoclave. For convenience's sake the effect of curing temperature is explained by separating it into that of lower than 100°C and that of higher than 100°C. However, the practical problems on temperature treatment will be described in detail at part III of this Symposium.

Reaction Occurs under Atmospheric Condition

Kantro, Brunauer and Weise (96) found that in the comparison of hydration of C_3S at 5°, 25° and 50°C, the reaction rate at the early stage was accelerated with the temperature. However, the temperature dependence after 1 day becomes ambiguous. Kondo and Daimon (70) studied the effect of curing temperature on the early hydration of C_3S. The difference in heat evolution is shown in Fig. 23, and the results will be discussed in the later section.

Mchedlov-Petrosyan and Chernyavskii (97) studied the effect of low temperature, even below the freezing point and reported that the reaction rate was retarded by increase in the specific volume of silicate gel.

According to Carlson (98) who studied the hydration of aluminates, the hexagonal hydrates are more stable than C_3AH_6 at low temperature. Compared with the hydration at ordinary temperature, the hydration mechanism itself is different at low temperature.

Hydrothermal Reaction

The reaction between lime and pozzolan proceeds

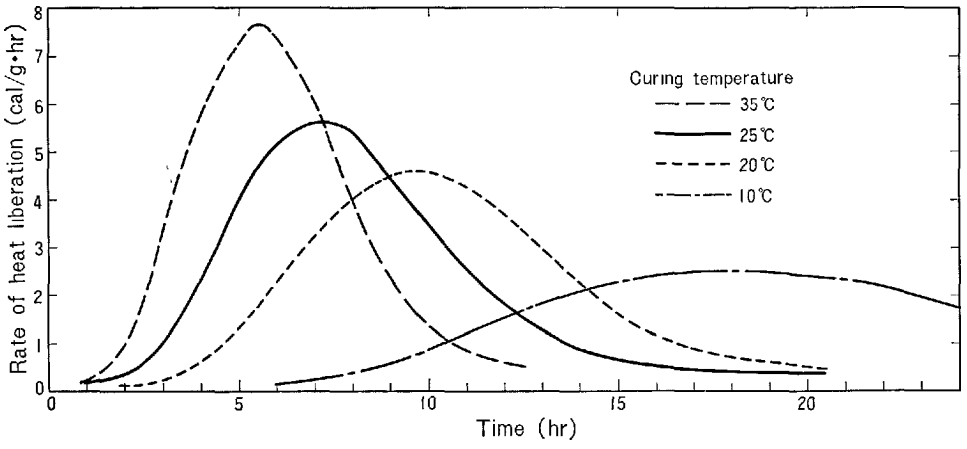

Fig. 23. *Variation with curing temperature of heat liberation of* C_3S. ($r = 2 \sim 5\mu$, $W/C = 0.5$)

considerably even at ordinary temperature but the reaction of lime-quartz mixture cannot appreciably take place, although this is accelerated by heat treatment. The autoclave is used for heat treatment at a temperature higher than 100°C in order to avoid loss of the liquid phase.

Mchedlov-Petrosyan and Babushkin (38) reported on the free energy change of the hydrothermal reaction in a CaO-quartz-H_2O system. The result of the free energy change when compared with that in CaO–SiO_2–H_2O system in which quartz is replaced by silica glass is shown in Fig. 24. The hydrothermal reaction in the CaO–SiO_2–H_2O system was summarized by Taylor (99), and the reaction rate was discussed by several authors.

Moorehead and McCartney (100) suspended a crystal quartz in saturated lime solution and treated it in an autoclave. It was shown that tobermorite was formed at 235°C and xonotlite at 335°C on the surface of crystal quartz. They proposed that the reaction was a diffusion-controlled process limited by the diffusion of $H_2SiO_4^{--}$ species through the product layer formed on the outside. The higher temperature of this experiment makes probably the silica concentration in the solution very high and the calcium concentration very low. It is therefore possible that the diffusing species and the precipitation sites of products may differ in the reaction at temperatures of 150° to 200°C which are used in industry.

Krzheminskii, Rashkovich, Sudina and Vorlamov (101) developed a method for quantitative X-ray diffraction analysis while carrying out autoclave treatment. They carried out treatment at 150°C and found that at the early stage the reaction rate was determined by the nucleation process and at the later

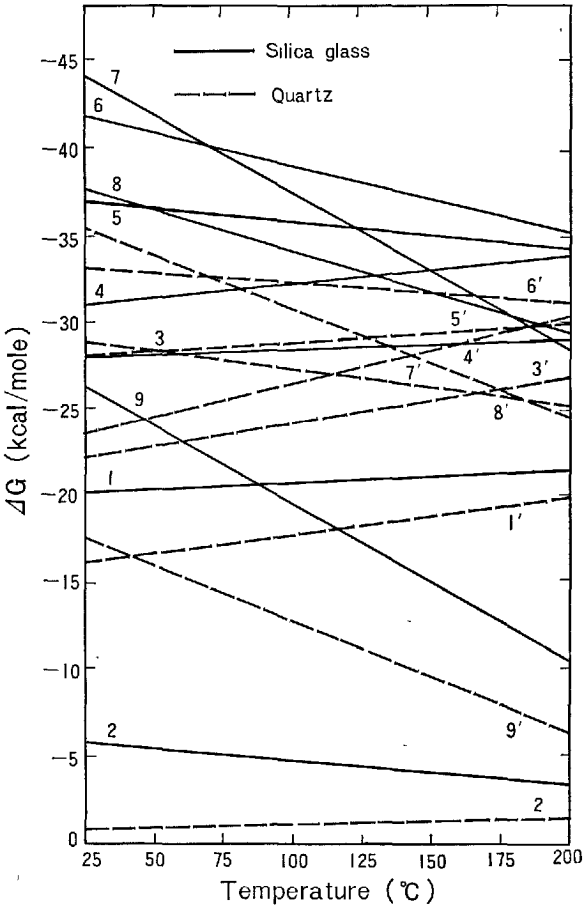

Fig. 24. *Free energy changes in hydrothermal reaction. (1. hillebrandite 2. afwillite 3. foshagite 4. xonotlite 5. 9Å tobermorite 6. 11Å tobermorite 7. 14Å tobermorite 8. gyrolite 9. okenite) After Mchedlov-Petrosyan and Babushkin(38), partly modified by Kondo(69)*

stage by the diffusion which is proportional to the root of the absolute temperature.

Sauman (102) studied the hydration of β-C_2S at 175°C and found that α-C_2S hydrate began to form after 4 hours and it was converted into β-C_2S hydrate after 7 days. He also described that the addition of quartz stopped the hydration of β-C_2S due to the formation of silica gel but the addition of a small amount of $Ca(OH)_2$ or C_3S accelerated the formation of CSH (I) and tobermorite.

Kondo (69) studied the kinetics of hydrothermal reaction between lime and silica. As representatives of the silica reactants, silica glass and quartz were chosen, the former being a species of pure silica, which possessed pozzolanic properties and the latter being the most stable form of silica, widely used for manufacturing autoclaved products. The particles of silica reactants between 5 and 10μ in radius were mixed with calcium oxide in a molar ratio of 1:1. The specimens were processed in an autoclave at various temperatures between 80 and 216°C, for various periods between 0.5 and 24 hours.

In the case of quartz, the reaction proceeds regularly without falling into any slump in a wide range of conditions, as shown in Fig. 25. The reaction of silica glass, on the other hand, is retarded excessively with the progress of reaction except when it is below 100°C or in the initial stage at higher temperature. As the reaction progresses, the lime-silica ratio of the product is converted from high to low in the case of quartz but a reverse trend is observed in case of a product obtained from silica glass as shown in Fig. 26. The rate of reaction seems to have a close relationship with the compactness of the product which varies with the process of formation. Such differences in composition or compactness of the product may be closely associated with the magnitude of solubilities of quartz and silica glass in the liquid phase.

It was found furthermore by Kondo, Ohsawa, Matsumaru, Kitamura and Kato (103) that the reaction rate was remarkably lowered by replacement of a part of the quartz with silicates, such as clay minerals, feldspar and fly ash, all of which contained alumina. Accelerating effect of alkali, on the contrary, is probably due to the increase in solubility of quartz. The results are shown in Fig. 27.

In connection with the composition of hydrous calcium silicate, they noticed that it was difficult for SO_3 to enter into the tobermorite lattice, in which, however, certain amounts of Na_2O, K_2O, Al_2O_3 and P_2O_5 seemed to be dissolved. Considerable amount of alumina was also found dissolved into α-dicalcium silicate hydrate as a sub-component.

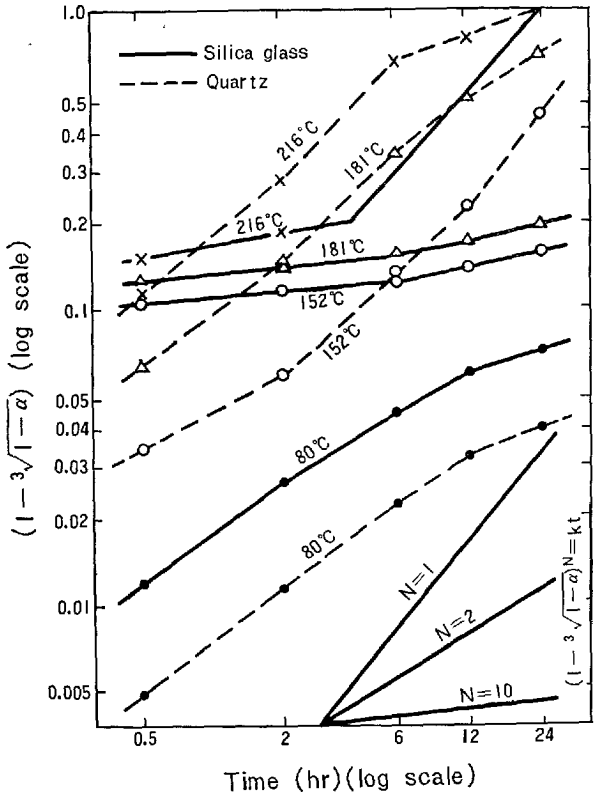

Fig. 25. *Rate of hydrothermal reaction between lime and quartz or silica glass. After Kondo(69)*

Next, they dealt similarly with the reactivity of diatomite. It tends to react easily with lime even at below 100°C to form a hydrate in bulky gel state, with considerable combined water and indefinite lime silica ratio which changes from low to high with the progress of reaction.

Temperature Dependence on the Rate of Hydration

Temperature dependence on the processes such as dissolution or hydration is frequently expressed perfunctorily as an activation energy. The activation energy is sometimes estimated as more than 10 kcal/mole even when the hydration of cement is controlled by diffusion. This seems to depend on the effect of the increase in pore size and pore volume due to the crystal growth of product with increase in curing temperature, however the chemical restriction may partly be concerned.

The temperature coefficients on the hydration rate of C_3S and C_2S are positive, according to Knoblauch (104), but on the other hand, van Bemst (105) shows negative values. According to Kantro, Brunauer and Weise (96), it is positive for hydration of C_2S and C_3S up to 70 and 30 percent degree of hydration,

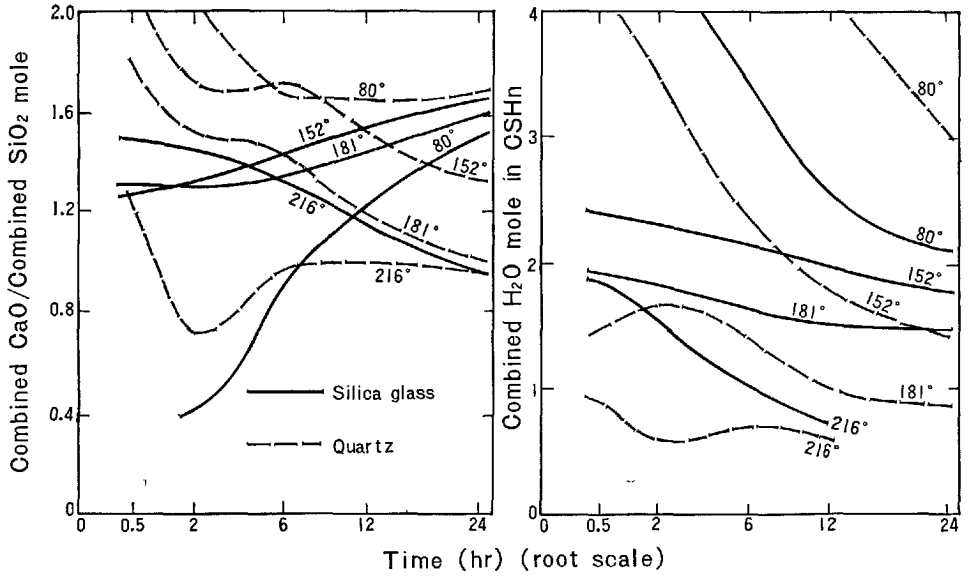

Fig. 26. *Changes in combined* CaO/SiO_2 *ratio (left) and combined* H_2O/SiO_2 *ratio (right) with processing time. After Kondo(69)*

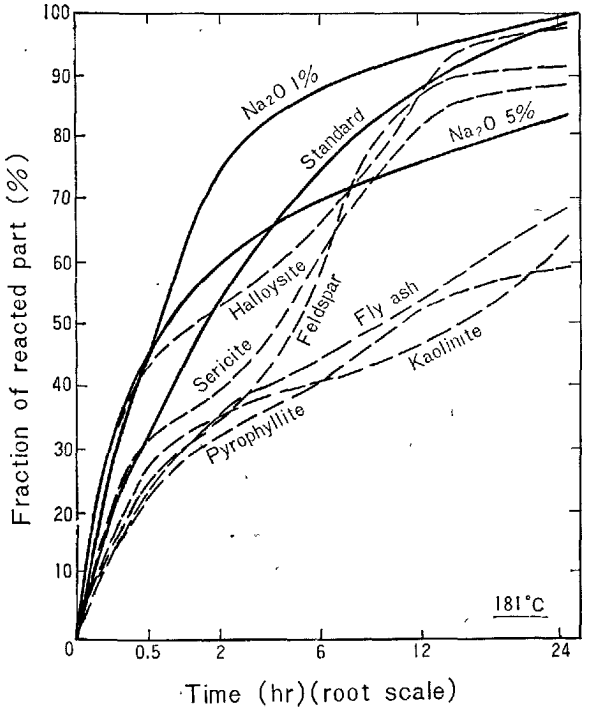

Fig. 27. *Effect on reaction rate of solubility alumina for 10% of silica by replacing part of quartz by other silicates, and of added alkali. After Kondo, Ohsawa, Matsumaru, Kitamura and Kato (103)*

respectively. Copeland and Kantro (106) examined the kinetics of overall reactions of portland cement from the heat of hydration, and found that the apparent activation energy was not a constant, but decreased from 8 to 2.3 kcal/mole with the degree of hydration.

The dissolution process of colloidal silica powder into lime solution is a reaction with an average activation energy of 16.7 kcal/mole by Halstead and Lawrence (66) and 9.4 to 18.4 kcal/mole by Greenberg (67). In the hydrothermal reaction between quartz and lime Kondo (69) indicated that an activation energy is 14.3 kcal/mole in the early reaction and 12.5 kcal/mole in the later. According to Moorehead and McCartney (107), the activation energy to produce xonotlite hydrothermally is 52.1 kcal/mole but this unusually high value probably depends on the change in pore volume.

The activation energy in the reaction of gypsum in a C_3A-gypsum system, according to Tenoutasse (81), is 12 kcal/mole. Tanaka, Murakami and Sato (108) reported that the activation energy in the early reaction of C_4AF to form hexagonal hydrates such as C_4AH_{13} and C_4FH_{13}, was 9.1 kcal/mole and that the subsequent reaction was retarded by the transformation of hexagonal hydrates to cubic ones. Layden and Brindley (109) obtained an activation energy of 16.1 kcal/mole in the hydration of magnesium oxide.

There are few data on the diffusion coefficients in hydration product of cement at various temperatures. For reference, the temperature dependence on the diffusion coefficient of the cation exchange in clay and

zeolite is given. According to Low (110) the activation energy for exchangeable ion movement in bentonite changed parallel with the specific volume of the adsorbed water, and the electrical interaction between ion and clay have little effect on the activation energy; that is, the activation energies for the migration of Li^+, Na^+ and K^+ ion in pure solution are 4.0, 3.9 and 3.4 kcal/mole respectively, and those in clay are only about 0.5 kcal/mole higher than in the former. The self-diffusion coefficients of Na^+ and SO_4^{--} ion in water and in bentonite are given by Lai and Mortland (111) as shown in Table 4. According to Rao and Rees (112), the diffusion coefficient in mordenite crystal at 60°C is expected as low as 1.0×10^{-12} in Na and 0.47×10^{-12} cm²/sec in K. The diffusion of Na which is controlled in the Na form by 2.8 Å windows has an activation energy of 8.74 kcal/g.ion.

Table 4. *Diffusion coefficients of* Na^+ *and* SO_4^{--} *ions in Na-bentonite plug and film. After Lai and Mortland(111).*

Ion	$D(cm^2sec^{-1}) \times 10^5$ in clay plug at 25°C	$D(cm^2sec^{-1}) \times 10^5$ in film at 25°C	$D(cm^2sec^{-1}) \times 10^5$ in water at 25°C
Na^+	0.467–0.535	0.00074	1.35
SO_4^{--}	1.15–1.27		1.08

Properties of Hydrates Concerned with the Rate of Hydration

The rate and mechanism of hydration are affected by the reactivity of the reactant and the various factors mentioned previously. However it is controlled more directly by the concentration and the constitution of the liquid phase at various sites, nucleation and crystal growth in the liquid or in hydrates, the composition and morphology of hydrates, the pore structure and the easiness of the mass transfer in the product.

Concentration and Constitution of Liquid Phase

The concentration of the liquid phase in cement paste and in suspension is equal to the solubilities of the hydrates when the reaction is completed. On the other hand, during the progress of hydration it is in the supersaturated state with respect to the outer hydration product. The liquid phase coexists with the outer product and is in the lower concentration with respect to the inner hydration product.

According to Mchedlov-Petrosyan and Babushkin (38), Ca^{++} ion dissolves accompanying with oxygen from reactant suface and Si^{4+} ion joins with existing OH^- group or forms double bonds with oxygen. $HSiO_3^-$ ion is stable at the range $pH = 8 \sim 13$. Whereas at $pH > 13$ SiO_3^{--} ion is the principal constitution unit. In the presence of Ca^{++} ion the latter polymerizes to form chains $(Si_6O_{17})^{10-}$, layers $(Si_{12}O_{31})^{14-}$ and networks $(Si_6O_{15})^{6-}$. Greenberg (67) reported that the silicate ion in the solution was monosilicic.

In the bottle hydration of C_3S with $W/C = 20$, according to Kondo, Daimon and Ueda (55) the concentration of the liquid after 1 hour is not saturated with respect to $Ca(OH)_2$, but is supersaturated with respect to C–S–H. After 3 hours it rises slightly with respect to $Ca(OH)_2$ and falls with respect to C–S–H than at 1 hour but both are in the supersaturated state. Thereafter the concentration of the liquid remains almost constant. Greenberg and Chang (113) also found similar results in the bottle hydration of C_3S.

The results of the chemical analysis of the liquids extracted from the C_3S paste were reported by Malinin, Lopathikova, Guseva and Klishanis (114), and Kawada and Nemoto (61) (75).

In addition, two maxima in the concentration are observed by Kondo, Ueda and Kodama (16) at the beginning and at the end of the acceleratory period as shown in Fig. 21. The coating layer produced or C_3S dissolves very slowly until the liquid reaches supersaturation with respect to $Ca(OH)_2$ during the induction period. After the supersaturation the outer products which consist mainly of $Ca(OH)_2$ are precipitated. The liquid concentration remains almost constant as the crystallization rate is larger than the rate of Ca^{++} ion supply from unhydrated C_3S. The crystal of $Ca(OH)_2$ grows rapidly but the rate of the growth decreases slightly after $7 \sim 9$ hours and thereby the liquid concentration becomes the second peak. At the same time C_3S particles begin to be enveloped by the growing crystals of $Ca(OH)_2$. Therefore the liquid concentration drops again because hydration reaction becomes retarded. It is difficult to estimate the very low SiO_2 concentration in the presence of CaO.

Greenberg and Chang (113) examined a C_3S paste with $W/C = 0.7$ and found that the saturation with respect to C–S–H was obtained within 2.75 min.

The liquid concentration in the suspension hydration of calcium aluminates or aluminous cement is independent of the composition difference of reactants as reported by Wells and Carlson (115).

Electric conductivity or resistance is sometimes

measured besides chemical analysis. It was reported by Greenberg and Chang (113) that the electric resistance in suspension hydration of C_3S showed a sudden drop within several minutes and a plateau appeared between 10 and 20 min. This fact seems to indicate very rapid dissolution of C_3S and the existence of time lag for nucleation.

The measurement of pH value is not difficult in excess water. Mchedlov-Petrosyan and Salop (116) developed tungsten and molybdenum electrodes which could act stably even in the hardening process.

In the above-mentioned studies only the liquid concentration outside the particle was measured. The method for measurement of the concentration and the constitution of the liquid in the interface of unreacted reactant has not been established, however it is very important to elucidate hydration reaction.

Nucleation and Crystal Growth

The free energy difference ΔG between the solute molecule and the solute crystallite in solution goes through a maximum when the radius of the crystallite increases to a certain value. The crystallite, which is larger in size than the critical nuclei of radius, commences to grow as a stable nucleus. When the liquid concentration becomes larger than supersolubility, the liquid becomes unstable to form a solute crystallite.

For nucleation from condensed phases Melia (117) proposed the rate equation

$$\log_{10} J = \log_{10} A - \frac{16\pi\sigma^3 V^2 N^3}{3(2.303\ RT)^3(\log_{10} S)^2}$$

where J is the nucleation rate, A is the kinetic constant, σ is the interfacial free energy per unit area between the forming phase and the metastable phase, V is the volume of a single molecule of the forming phase, R is the gas constant, and N is Avogadro's number. The nucleation rate, accordingly, is determined by the supersaturation ratio S, which is the ratio of the activities of the solute in the supersaturated solution and in the saturated solution.

Greenberg and Chang (113) measured the rates of formation of products from solutions of monosilicic acid and calcium ions by light-scattering measurements. They found that the rate of change of scattering increased with calcium concentration and pH in solution. They also observed that the dissymmetry values $Z = i_{45}/i_{135}$ decreased with reaction time, and proposed that the dissymmetry had to be attributed partially to the changes in size of the growing particles, to the anisotropy of hydrated calcium silicate particles, and to flocculation.

The precipitation of $Ca(OH)_2$ crystal commences at the end of the induction period. Kondo, Ueda and Kodama (16) observed C_3S hydration under a polarizing microscope and found that the outer product consisted of a few but yet well-crystallized $Ca(OH)_2$ and the C–S–H gel. The presence of the latter was confirmed by electron microscope, appearing very thin on the slide glass and the cover glass. The crystal growth rate of $Ca(OH)_2$ in the C_3S paste at W/C = 0.5 is shown in Fig. 28 (55). In view of this, they considered the formation of the metastable phase of the nuclei of $Ca(OH)_2$ and C–S–H gel based on Takiyama's consideration (118) with the relationship between supersolubility and solubility as shown in Fig. 29.

Ueda, Hashimoto and Kondo (2) reported from the result of surface electron diffraction that the depth of the intermediate product layer was 200–300 Å. According to Uhara (119) the size of the critical nuclei at which free energy becomes the maximum is in the order of 10^{-6} cm in case of solid nuclei. The C–S–H produced after 1 day grows to the extent a surface electron diffraction pattern is indicated (2).

Composition and Morphology

The rate of species migration through the hydrated product layer seems to be influenced mainly by the pore size distribution and morphology of the inner products. The particle size and morphology of the hydrate are closely related with its chemical composition. Furthermore the rate of hydration of C_3S in the later stage is related with the crystal size of $Ca(OH)_2$ produced.

The composition of hydration products illustrated in Fig. 22 shows that the reaction takes place with the same stoichiometry at the later stage. However, the hydration reaction of calcium silicate is not carried out with the same stoichiometry at least until the formation of stable hydrated product and becomes diffusion-controlled reaction. The compositions of hydrated products have been calculated from the results of several experiments. Particularly the different compositions at the very early stage have been reported by several investigators. Ueda, Hashimoto and Kondo (2) attempted to determine the composition and performed an experiment in which the hydrated particle was gradually dissolved with weak acid solution from its surface.

The difference in the morphology of C–S–H gel depending upon the difference of its composition has been discussed in detail by Richartz and Locher

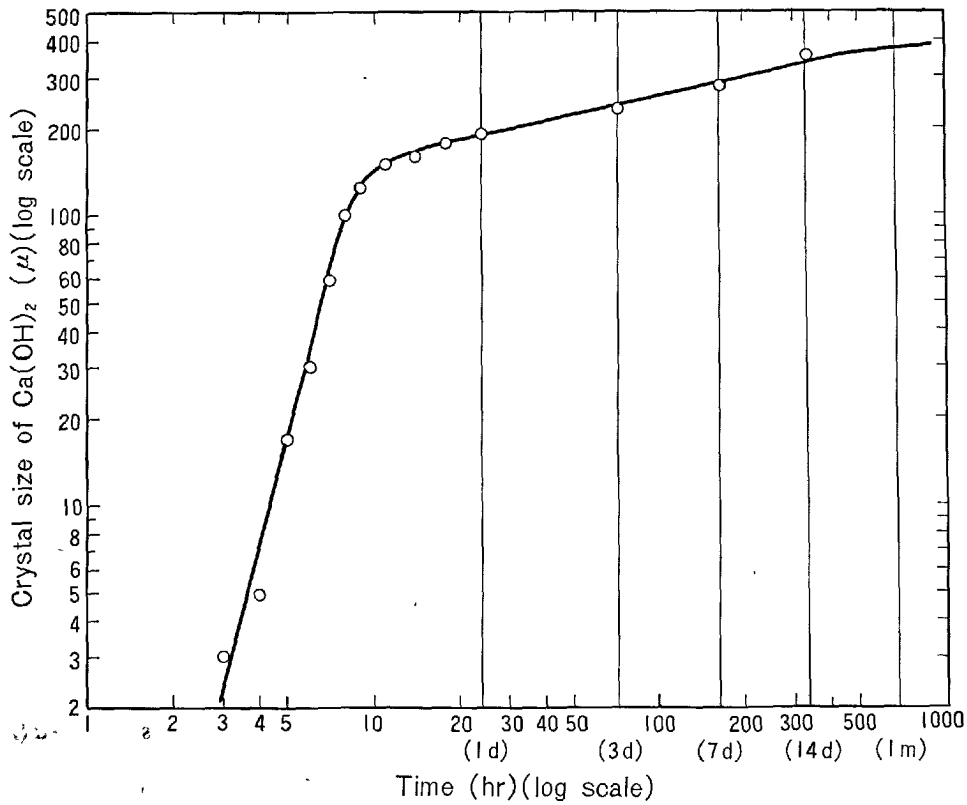

Fig. 28. *Crystal growth of* $Ca(OH)_2$ *in paste hydration of* C_3S. *($r = 2 \sim 5\mu$, $W/C = 0.5$, at 25°C)*

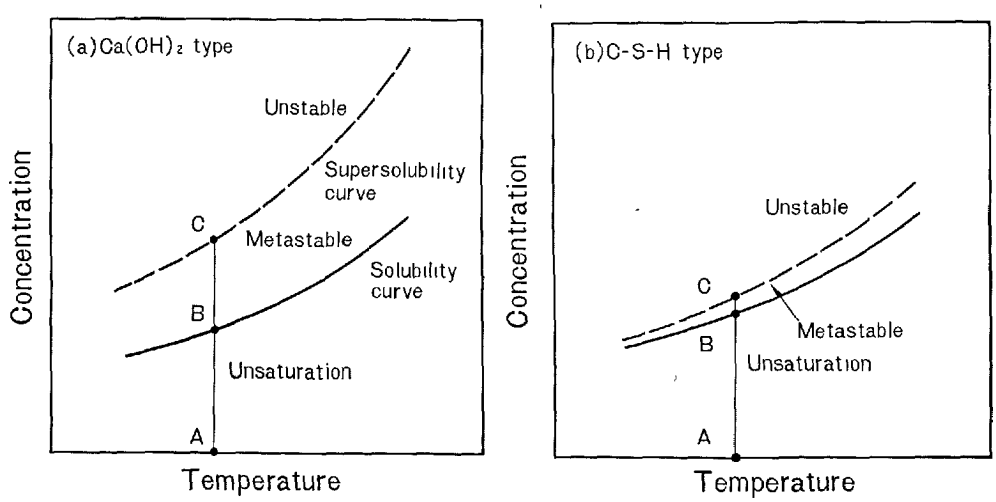

Fig. 29. *Relation between solubility and supersolubility.*

(48). Calcium silicate hydrates with a molar CaO/SiO_2 ratio of 1.0 crystallize in pseudorhombic foil and those of 1.3 in partly rolled-up foil, whereas those with a ratio above 1.4 form fibrous crystal. The electron diffraction of this fibre shows a diffuse pattern perpendicular to the fibrous direction. Thus, they confirmed that this fibre was of the rolled-up form. According to Sakurai, Ueda, Hashimoto and Fukunaga (120), CAH_{10} may also be of the rolled-up form.

Stein and Stevels (74) observed that the hydrate

habit converted from the crinkly foil (CSH(B)) to needle-like cigar-shaped agglomerates (C_2SH_2) before and after the induction period. But they thought that the acceleration of the hydration rate of C_3S depends upon the conversion of crinkly foil from closely fitting hydrate. The conversion begins in the induction period and then accelerates the main reaction. The kinetic equations were given by them as described later. Kondo, Daimon and Ueda (55) have further proved the changes of the surface state of C_3S powder in hydration by a scanning electron microscope as shown in Fig. 7. In 1 hour hydration, the particle surface is covered with scale-like products and the hydration itself does not make any progress, but 8 hours later the hydrate becomes active and the particle surface is highly progressed as can be seen in this figure. It can also be realized that in 3 days and 1 year the product gradually develops and as a result retarding the hydration.

Funk, Schreppel and Thilo (121) studied the hydration of β–C_2S and found that on the surface of crystal there was a zone of low refractive index and the thickness of this zone increased with increasing binding water to grow into the tobermorite-like phase. They called this product with low refractive index the intermediate product. McConnell (60) found the formation of gel pseudomorphs with relict lamellae twinning after natural β–C_2S (larnite). Such investigators, Trojer (53), Terrier and Moreau (54), Kondo, Ueda and Kodama (16), who studied the process of C_3S hydration with an optical microscope found that an intermediate product with low birefringence has formed surrounding the C_3S particle. According to Kondo, Ueda and Kodama (16), the inner product is formed epitaxially with a preferred orientation to the direction of the parent C_3S.

Until recently the calcium hydroxide in cement paste has not received much attention. According to Terrier and Moreau (54) (122), the $Ca(OH)_2$ crystal appears in the interstices of cement particles and crystallizes preferentially in larger pore to grow in 7 to 90 days to the extent the space permits. They also observed the second portlandite in the matrix between above cited first-crystallized portlandite and clinker particles. According to Kondo, Ueda and Kodama (16), a particle of $Ca(OH)_2$ grows not only in the pore space but also envelops the C_3S grains. This fact has a significant meaning as the acceleratory period of C_3S approximately coincides with the period of the largest crystal growth rate of $Ca(OH)_2$.

Aluminium substitutes silicon in hydrates and changes the properties of the products. Copeland, Boden, Chang and Weise (123) discussed in detail the relations among the molar CaO/SiO_2, H_2O/SiO_2 and Al_2O_3/SiO_2 ratios in a series of C–S–H gels containing different amounts of alumina. They also found that the aluminium substituted gel looked very much like the gel formed in the early stages of hydration of cement. Diamond (124) found also by X-ray fluorescence spectroscopy that Al^{+++} ion could substitute 15% of Si^{4+} ion in tobermorite produced by hydrothermal synthesis.

Pore Structure

The rate of hydration is occasionally discussed with the results of loss on ignition and free $Ca(OH)_2$ as the degree of hydration and even with strength. The pore volume is also closely related with the degree of hydration and strength, independently of the composition of cement. The pore structure of product in the radial direction to the reactant particle is most desirable to be elucidated in connection with the rate of hydration.

The pore system is divided into capillary pore and gel pore by Powers (125). Edel'man, Sominskii and Kopchikova (126) reported as a result of measurement with a mercury pressure porosimeter that the large capillary pores were the matrix between unhydrated clinker particles and new products, and the small pores correspond to the pore in the texture among the growing produced crystals. Mikhail, Copeland and Brunauer (127) reported that the nuclei of hydration products could not grow into crystals in small pores. Whereas Richartz and Locher (48) pointed out that there was a continuous size distribution for the entire pore space as the diameters of the calcium silicate hydrate tubes varied over a wide range. There may be no distinct difference between the small and large pore systems. The result of Kondo, Ueda and Kodama (16) indicates a continuous pore size distribution.

The relationship between pore size distribution and curing time is shown in Fig. 30. This figure shows that both the total pore volume and the size of pore decrease with the progress of hydration.

The fact that the pore shape in hardened cement paste is not always cylindrical was found by Schwiete and Ludwig (128) in observation of electron microscope. The shape of the pore can be determined to some extent by the hysteresis loop of adsorption and desorption isotherms. Mikhail, Copeland and Brunauer (127) pointed out that the shapes of hysteresis loops in hardened portland cement pastes came closest to those classified as type D loops by de Boer (129). Such type of capillaries is consisted of wide

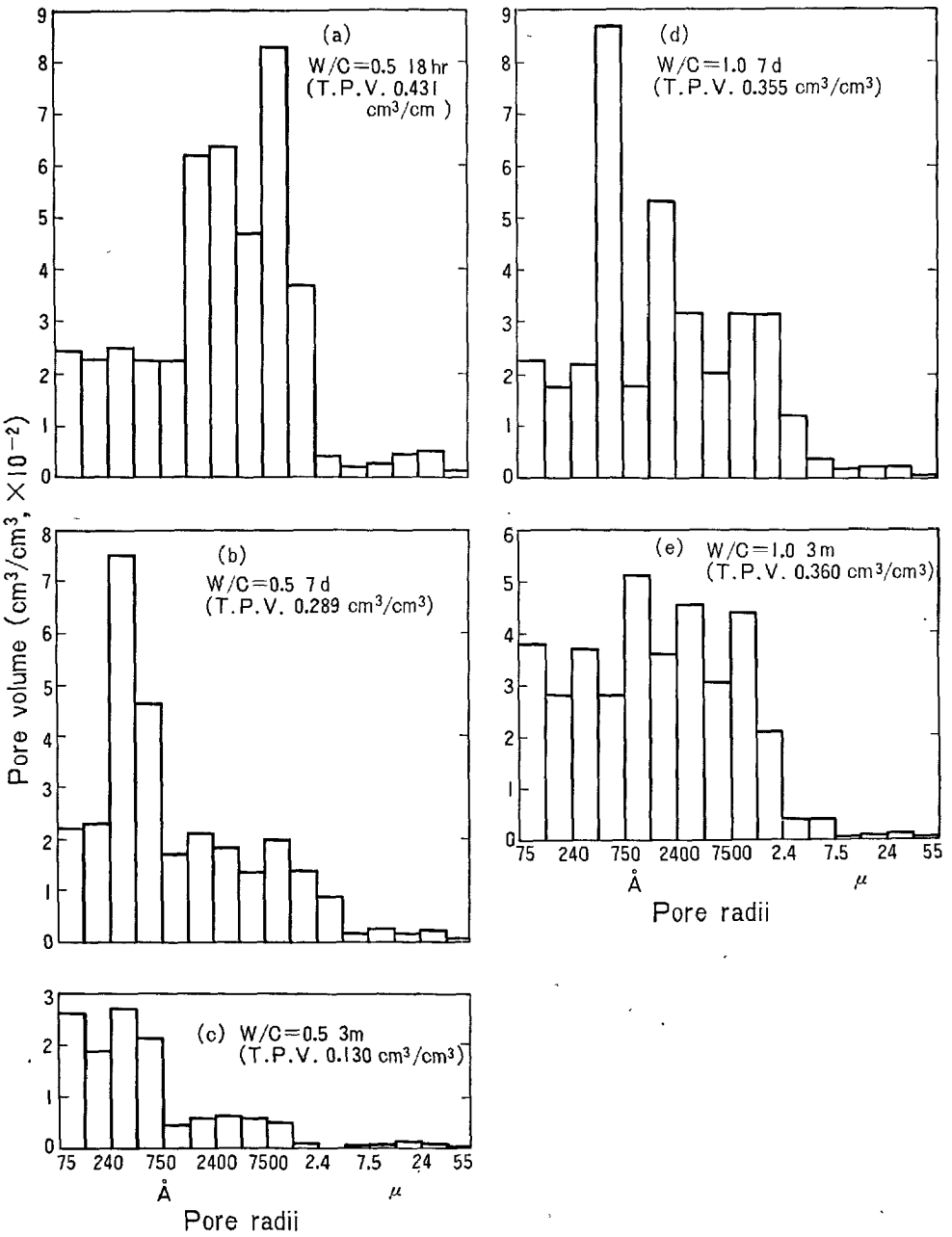

Fig. 30. *Pore size distribution of* C_3S *paste hydrated at 25°C. T.P.V. indicates total pore volume.*

bodies having a varying range of narrow short necks.

Besides open pore and sack-like pore, Powers, Copeland and Mann (130) pointed out the creation of capillary cavity. The necessary curing time for the creation of capillary cavity are affected by water cement ratio and temperature. For standard laboratory conditions, they were as follows: W/C = 0.7, 1 year; 0.6, 6 months; 0.5, 14 days; 0.45, 7 days; 0.40, 3 days. The fact suggests an increase in the hydration rate with water cement ratio. It has been confirmed that the surface area and the pore size distribution change due to the difference in water cement ratio by Hunt (25) and also by Kondo, Ueda and Kodama (16).

As a special experiments on the pore size distribution change with curing time, Feldman and Ramachandran (131) and Feldman and Sereda (132) studied on the hydration of C_3A compact. The effects of sand

cement ratio and CO_2 curing are studied by Kroone and Crook (133) (134). The effects of autoclaving are examined by Moorehead and McCartney (100) and also by Kondo, Ohsawa, Matsumaru, Kitamura and Kato (103).

Permeability and Diffusion

As hydration progresses, the interstices among cement particles are filled with the outer products to decrease the pore volume and particularly the pore size. As a result the permeability or the diffusivity in the hardened cement paste is lowered. This effect relates also with such as water permeation, rate of hydration, carbonation of hardened paste, sulfate attack and so on.

The rate of permeation and diffusion is expressed by the following equation,

$$Q = \frac{v}{t} = PA\frac{h}{\xi} = DA\frac{C}{\xi}$$

where v is the volume of permeation (cm^3), t is time (sec), P is the coefficient of permeability $P = \xi \cdot v/A \cdot h \cdot t$ (cm/sec) and A is sectional area (cm^2), h is the pressure difference (cm), ξ is the thickness (cm), D is the diffusion coefficient $D = \xi \cdot v/A \cdot C \cdot t$ (cm^2/sec) and C is the concentration difference (vol/vol).

The rate of permeation through a pore Q is expressed by the Poiseuille's equation as follows:

$$Q = \frac{\pi r^4}{8\eta} \cdot \frac{h}{l}$$

where r and l are the radius and length of single pore and η is the viscosity of the fluid.

In the case of gas, D decreases proportionally with r if r is less than about 1000 Å.

$$D = \frac{4r}{3}\sqrt{\frac{2RT}{\pi m}}$$

where m is the molecular weight of gas.

The molecules and ions in solution usually are hydrated with water molecules. The strongly hydrated species move less easily through the pore, whereas water molecule is most permeable because of its small size.

The membrane permeability coefficient P is equal to the value obtained by multiplying the diffusion coefficient in pore D by the pore volume ratio Ae/A and the tortuosity. D gives a lower value when compared with the diffusion coefficient in solution D because of the interaction of the adsorption sites along the pore. When the hydrated layer is electrically charged, the effect of the Coulomb's force appears. If it is negatively charged, it will be difficult for anion to migrate in the pore and it is the opposite in case of cation. Colloidal particles diffuse by Brownian motion and its diffusion coefficient D' is expressed as

$$D' = \frac{RT}{N} \cdot \frac{1}{3\pi\eta d}$$

where N is the Avogadro's number and d is the diameter of the particle.

In the hydration of cement, the outer reactants such as gypsum dissolve and diffuse inwards with water through the product layer around another reactant particle so that the latter reacts at the interface and a part of hydrate deposits to form inner products while the remainder diffuses outwards to form outer products. The pore size in the cement paste is exceedingly small and has a peak of pore volume at radii of 10 to 20 Å, and therefore interaction with diffusing ions cannot be neglected. Colloid particles formed as inner product hardly migrate outward. On the other hand, according to Moorehead and McCartney (100), the product treated in an autoclave at a very high temperature has big pores with radii of 2700 to 10800 Å. Thus, it appears that the migration is not affected by the interaction along the pore. They also determined the diffusion coefficient of Na^+ or Ca^{++} ion in these specimen (100).

In the hydration of hydraulic compound it is difficult to measure the concentration of the interface, and also it is almost impossible to study the diffusion coefficients of the produced layer after this layer is removed from the unhydrated particles.

Ionic diffusion in pores is comparatively well known in clay paste, zeolites and high-polymer film and some of these have already been mentioned. But it has not yet been examined the relationship between diffusion coefficient and the pore structure of hydrated cement.

Ratinov, Kurcheryaeva and Melentéva (135) measured the dissolution rate of pellets of C_3S, β–C_2S and hydrothermally synthesized C_3SH_2 and $C_2SH(A)$. The solubility of C_3S is 0.256, 0.338 and 0.387 g/l at 2°, 10° and 20°C, respectively. They also obtained the diffusion coefficients, which were 0.26×10^{-5} at 2°C, 0.30×10^{-5} at 10°C and 3.4×10^{-5} cm^2/sec at 20°C.

Spinks, Baldwin and Thorvaldson (136) determined the diffusion coefficient of hardened cement paste with a radioactive tracer. The diffusion coefficient D of 1:2 mortar in 4 weeks is 2.8×10^{-10} cm^2/sec for Ca^{++} and that of neat paste is smaller. They also found that anion generally indicated a diffusion coefficient higher than that of cation.

As the diffusion coefficient changes with the pore

structure, precise experiments to elucidate the relationship between the pore structure and the diffusion coefficient or the rate of hydration must be systematically carried out in the future.

The diffusion-controlled exchange between calcium in calcium silicate hydrate crystal and its surrounding solution was measured by Forrester and Lawrence (137). The self-diffusion coefficient for calcium in the hydrate crystal is very low, however it increases from 1.08×10^{-23} to 60.7×10^{-23} cm^2/sec as the molar CaO/SiO_2 ratio of hydrates change from 0.36 to 1.39. They considered that the low mobilities of calcium ion accounted for the slowness with which calcium silicate hydrate came to equilibrium with its aqueous solution and for the high durability of portland cement products.

Relation between the Rates and the Mechanisms of Hydration

The hydration mechanism of cement components changes with the progress of reaction even in the case of a certain single component. Therefore an equation which explains a single step cannot represent the actual rate which changes complexly. The kinetics of hydration should correspond to the mechanism but a strict model for the later stage especially is difficult to be given and an accurate measurement of the degree of reaction is also difficult particularly in the very early stage.

Variation in the Hydration Mechanisms with the Progress of Reaction

Periodical changes in the rate and the mechanism are generally observed in the hydration of plaster of Paris, portland cement, aluminous cement and so on. The variation with progress of hydration will be described in the case of C_3S as an example for it can represent the behavior of portland cement.

The result of measurement of heat evolution of C_3S with a conduction calorimeter gives the characteristic curve as shown in Fig. 31. Kondo, Ueda and Kodama (16) classified this characteristic curve into five stages to discuss the hydration process.

- S_I: The stage in which a short but rapid reaction takes place immediately on contact with water.
- S_{II}: The stage which corresponds to the so-called dormant period and the reaction rate is very low.
- S_{III}: The stage in which the reaction takes place very actively and is accelerated with time.
- S_{IV}: The stage in which the reaction rate is decreased after the most active reaction is over.
- S_V: The stage in which deceleration is more remarkable.

The whole process can also be differently divided into 3 periods. S_I and S_{II} correspond to the induction period, S_{III} is the acceleratory period and S_{IV} and S_V belong to the decay period. The variations in the properties of the liquid phase and the solid phase are summarized in Table 5.

The Induction Period

It had been considered that the exothermic reaction which took place immediately on contact of portland cement with water was due to the rapid hydration of C_3A, as already described but it was confirmed that

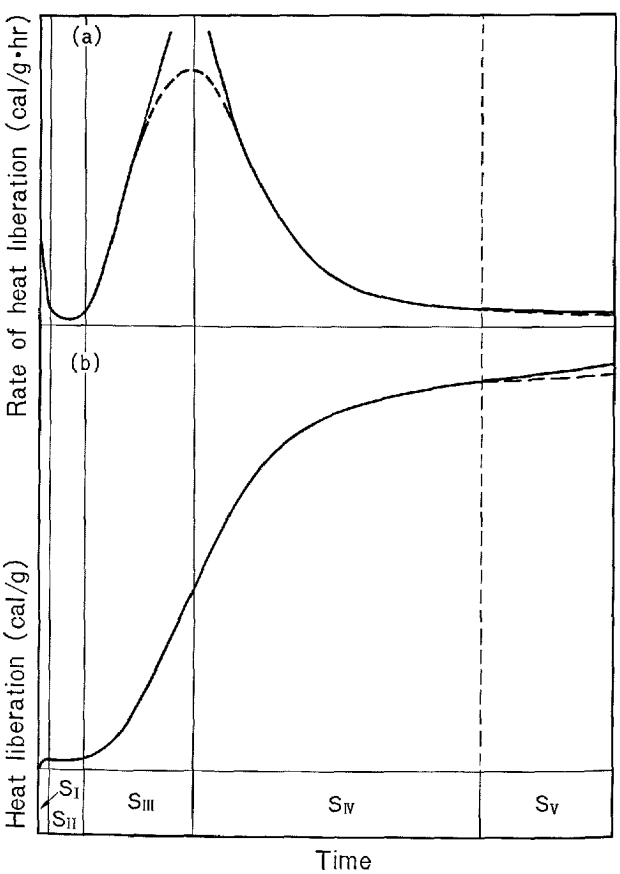

Fig. 31. *Classification of hydration stages of* C_3S

Table 5. *Characters of respective stages.*

	Stage	Induction period I	Induction period II (Dormant p.)	III (Acceleratory period) Start to reaction	III (Acceleratory period) Most active	Decay period IV	Decay period V
Liquid	CaO concentrn.	negligible	promptly up	down	a little up	down	
	(OH) concentrn.	negligible	promptly up	down	suddenly up	down	
	Ion product	negligible	promptly up	down	suddenly up	down	
Solid	Degree of hydrn. or combined H_2O	a little	dormant	start again	most actively up	gradually up	slowly up
	Amount of $Ca(OH)_2$	negligible		up	most actively up	gradually up	slowly up
	Amount of C–S–H	negligible		up	actively up	gradually up	slowly up
	C/S of C–S–H	about 3		suddenly down	constant	constant 1.6	1.6 → 1.7
	H/S of C–S–H	about 3		highest	down	down	2.5 → 1.7
	Surface area of total solid	small		up	highest	down	gradually up
	Surface area of C–S–H	small		highest	down	gradually down	

it appeared in the paste of C_3S.

According to Greenberg and Chang (113) the supersaturation with respect to C–S–H is reached within only 2.75 min. in a C_3S paste with W/C = 0.7. As the amount of C–S–H is large but of poor crystallinity, its metastable region is narrow as shown in Fig. 29 and it precipitates soon after the supersaturation. It may be formed on the surface of the C_3S particle, as Richartz and Locher (48) and Greenberg and Chang (113) pointed out.

The composition of the product which is formed immediately after C_3S is brought into contact with water, differes with investigators but it is believed to coincide with C_3S to which water has combined as shown in Table 5. This can be understood from the fact that the CaO concentration of the liquid is very low. Kondo, Ueda and Kodama (16) pointed out that the product layer is only less than 200 Å in thickness at 1 hour after the addition of water. The critical nucleus has the maximum difference of interfacial free energy at a product layer of the order of 10^2 Å by Uhara (119).

Kondo and Daimon (70) discussed the causes of formation of such a thin and compact layer in accordance with the following three hypotheses: (1) The formation of a protective layer of very low diffusion coefficient by the addition of water to the reactant. (2) The conversion of the amorphous layer around the reactant surface formed by grinding. (3) Minimizing the free energy by the strain energy of the surface product. In the third hypothesis the chemical free energy decreases with increase in the thickness of the layer but the total free energy reaches the minimum at a certain thickness due to the surface free energy of the thin layer. It reaches the maximum due to the compressive strain with increase in thickness. The strain energy which is stored at the surface of C_3S is

$$\Delta G_{\text{strain}} = \int_0^{k\sqrt{\delta}} \frac{4}{k^4}(k\sqrt{\delta} - y)^2 dy = \left[\frac{4}{3k^4}(k\sqrt{\delta} - y)^3\right]_0^{k\sqrt{\delta}} = c\delta^{3/2}$$

where δ is the thickness of the compressed layer, $k\sqrt{\delta}$ is the thickness of the stretched layer, y is a distance from the interface of C_3S and c is a constant. The ratio of the dependence of hypotheses (1)~(3) to the mechanism of actual hydration is not clear.

After the formation of metastable nuclei at the product layer, the inner products, which consist mainly of C–S–H with high CaO content, are topochemically formed and liberated excess Ca^{++} ion dissolves into the liquid. The outer product which is formed in solution may consist of much $Ca(OH)_2$ and lesser amount of C–S–H as the concentration of silica is lowered by increase in lime concentration of the liquid.

When a reaction does not begin immediately but has a time lag, this time is called the induction or incubation period. The term dormant period used in the hydration of cement is equivalent to this period.

Powers (138) assumed in the hydration of portland cement that during the dormant period the exposed surface of C_3A became coated by small amounts of their own products, and the physical characteristics of cement paste are not altered appreciably. But various kinds of chemical changes may take place during this period. The most characteristics in this period is the change in liquid concentration as shown in Table 5. The composition and the surface area of reaction product seems to be altering gradually. Namely the induction period is the stage in which the dissolution of Ca^{++} ion mainly takes place through the protective coating layer. This gradual dissolution continues until the liquid reaches to the unstable degree of supersaturation. According to Ueda, Hashimoto and Kondo (2), a 1 hour hydrated sample does not indicate a

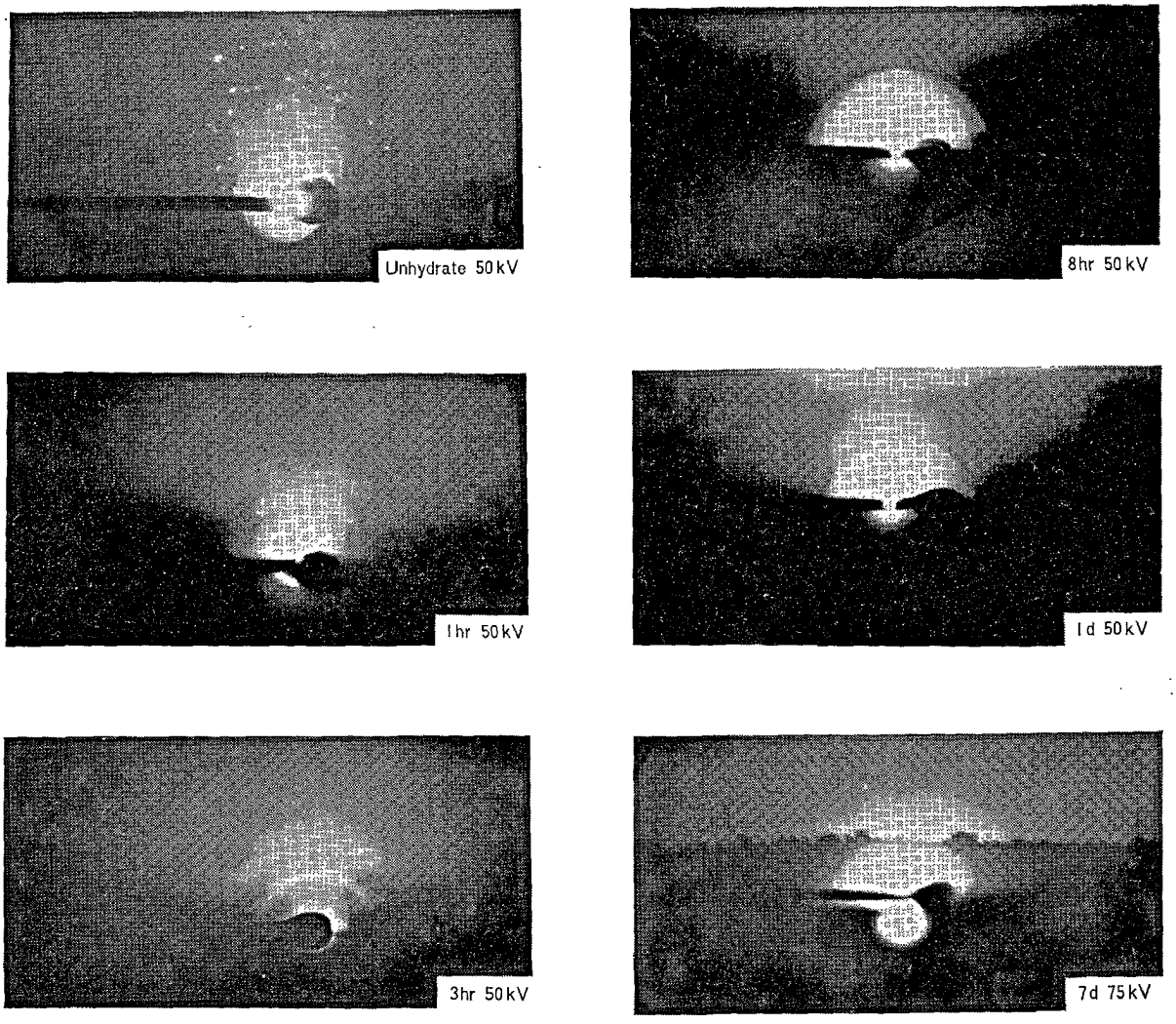

Fig. 32. *Surface electron diffraction patterns of hydrated* C_3S *particles.*

surface electron diffraction pattern but a 3 hour hydrated sample, which has already passed through the induction period, indicates a weak pattern. These results are shown in Fig. 32. It seems that the product layer liberates Ca^{++} ion during this period to give low mass absorption coefficient.

As is shown in Fig. 13, the hydration of C_3S with the saturated solution is to some extent retarded when compared with the case of pure water. According to Kondo and Daimon (70), the dissolution of Ca^{++} ion is decreased due to the small concentration difference by which the formation of topochemically produced nuclei is retarded.

Experiments on hydration by addition of seed crystal have been attempted. Funk (51) found that β-C_2S was practically transformed into dicalcium silicate α-hydrate at 100° to 200°C through the solution, if seed crystals of this compound were added. Stein (87) also found that the hydration of C_3A was accelerated by an addition of C_3AH_6. Kondo and Daimon (70) examined the hydration of C_3S paste by the addition of seed which was prepared by grinding 6 months hydrated paste, and found that the hydration became more retarded as more seed crystal was added as seen in Fig. 33. This suggests that the seed crystal plays the role of only increasing the liquid concentration due to the dissolution of $Ca(OH)_2$ in the seed. Accordingly the seed crystal seems to give only the same effect as the hydration with the saturated solution as has already been shown in Fig. 13. While de Jong, Stein and Stevels (72) found that the addition of CaO or $Ca(OH)_2$ to C_3S paste resulted in

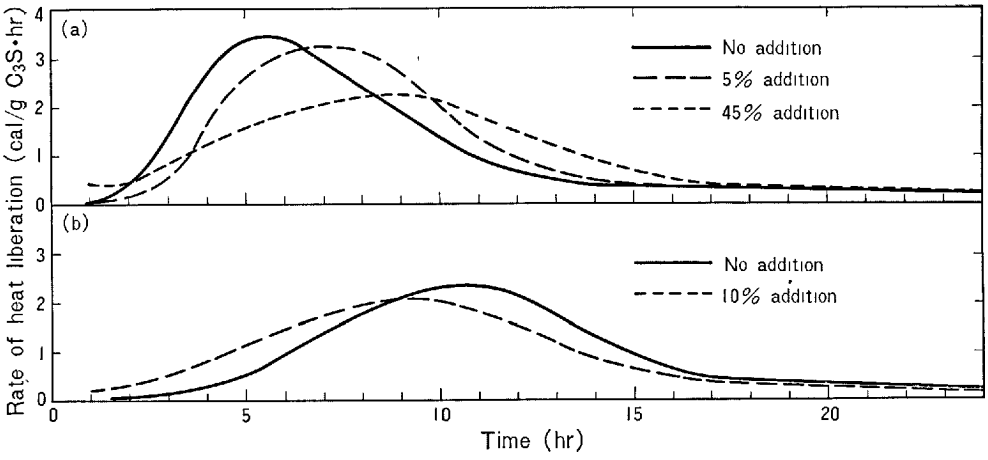

Fig. 33. *Effect of added seed on heat liberation of* C_3S. ($r = 2 \sim 5\mu$, $W/S = 0.5$, *at* 25°C) (*a*) *by pure water.* (*b*) *by saturated solution with respect to* $Ca(OH)_2$ *and* C–S–H

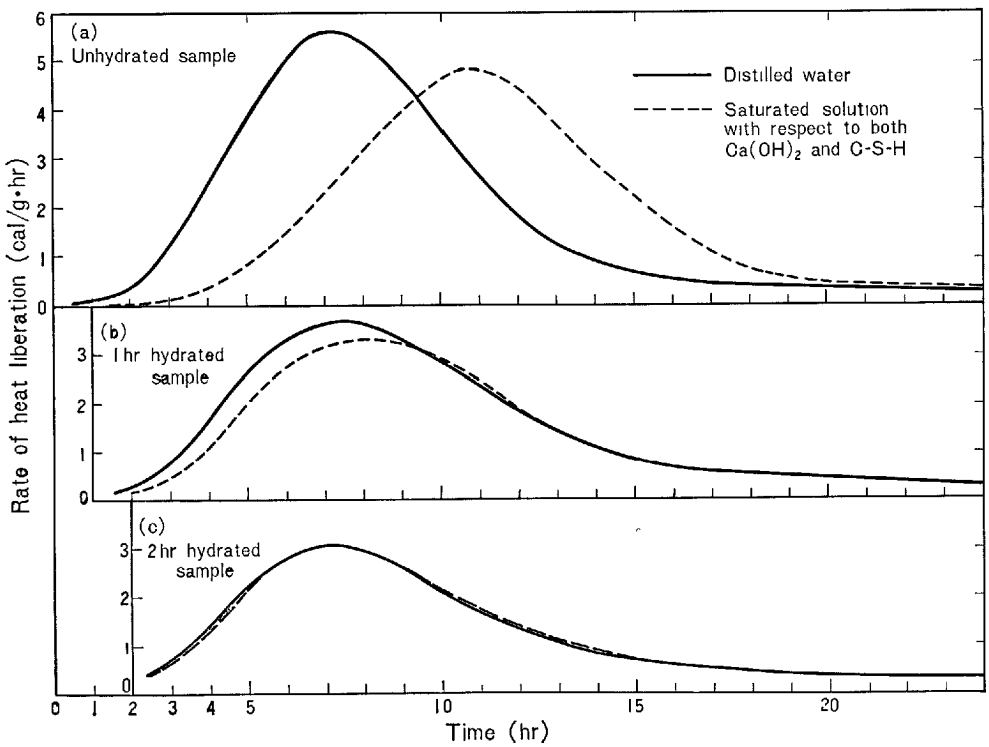

Fig. 34. *Heat liberation rate of rehydration of* C_3S.

the retardation, which was supposed to be due to suppressing the nucleation of meta-stable hydrate from unstable coating. On the other hand, Kondo and Daimon (70) pointed out that the hydration of C_3S with the saturated liquid with respect to both $Ca(OH)_2$ and C–S–H is accelerated if seed crystals are added as shown in Fig. 33. It seems desirable to testify the effect of seeds of various hydrates previously removed $Ca(OH)_2$ to avoid the complexity. The effect of seed consisting of C–S–H is considered to be the acceleration of the deposition of the outer product by increasing the growing sites and also to be the improvement of the crystallinity of the inner product which controls the rate of hydration.

On the other hand, despite of the cessation of hydration by drying the paste at a certain time of the induction period the hydration proceeds successively as usual as shown in Fig. 34 when dried sample is re-

wetted. This suggests that the metastable nuclei produced promotes the following reaction.

S_{II} is after all the stage in which the nuclei of C–S–H is being formed in the coating layer accompanying with increasing the liquid concentration. Thereafter not only the inner product but also the outer product are formed in S_{III} stage due to increase of the permeation of the protective layer.

The Acceleratory Period

There are various theories for the reason why a reaction begins to be accelerated after a certain period. Powers (138) considered that at the inside of a gel coating on a particle of cement osmotic pressure developed to split off pieces of the gel covering and the crystal surface was immediately accessible to water and thus permitted rapid reaction. Brunauer and Kantro (139) also considered that a protective skin on the unhydrated substrate had the same CaO/SiO_2 ratio as the substrate and such a high-lime gel coating might be unstable and decomposed with the liberation of calcium hydroxide, accompanied by the splitting off of thin layer of the second intermediate. Stein and Stevels (74) thought that the hydration of C_3S was accelerated by the conversion from a closely fitting hydrate to a crinkly foil hydrate with the change in liquid concentration. Kawada and Nemoto (75) considered that the seed crystal precipitated and at the same time the thickness of the intermediate product layer on the substrate decreased to make the diffusion of water easy and accelerated the hydration of C_3S. However, the theories mentioned above cannot explain satisfactorily the changes in the stoichiometry and morphology of hydrates and also the fact that the induction period is never appeared in the reaction of refreshed reactant surface.

Kondo, Ueda and Kodama (16) considered that the properties of the early produced protective layer with low permeability might be changed. Kondo, Daimon and Ueda (55) proposed further that the protective layer became porous. That is, when the nuclei of metastable C–S–H in the protective layer are grown to an extent of the thickness of the layer, the hydration of reactant begins again as the result of increase in permeability of the layer due to the liberation of lime. The rate of hydration reaction of C_3S in this period must be controlled by the degree of the sectional area of permeable part in the protective layer. The inner product composes of metastable C–S–H which has not become thick enough to control the rate of reaction in S_{III} stage.

When t_i is the time required for the induction period to be over, and k' is the slope of the differential for rate d^2q/dt^2, k' becomes smaller as t_i becomes longer as seen in Fig. 35. According to Kondo and Ueda (140), it was confirmed that d^2q/dt^2 was always positive, independent of the slope k', and the reaction proceeded with positive acceleration. When k' is positive, there is almost no resistance to retard the reaction effects and so the acceleration of hydration reaction increases with time. As is shown in Fig. 36, however, when the thickness of the inner product layer increases the material transfer is limited and k' becomes negative. As is shown in Fig. 36, when the degree of hydration is large and consequently the inner product is thick and $Ca(OH)_2$ crystals are large, the time required for k' to become negative shortens.

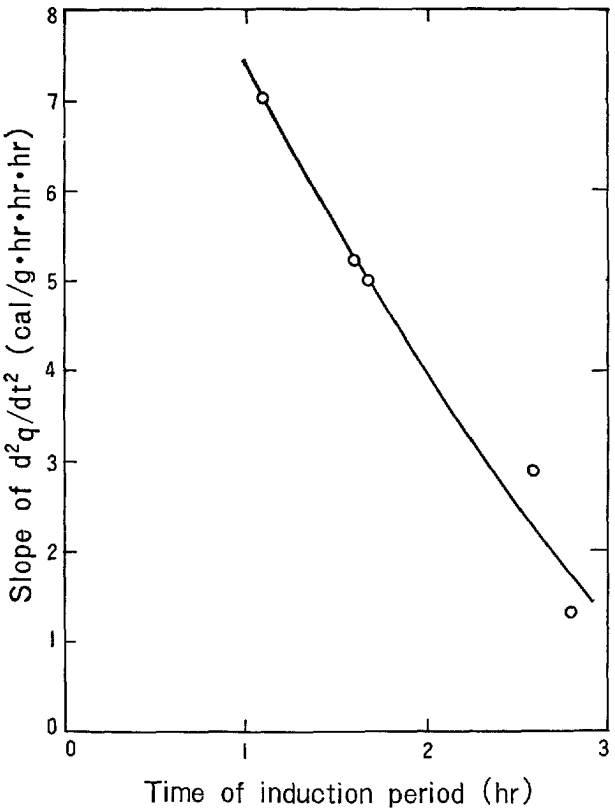

Fig. 35. *Change in velocity of acceleration of* C_3S *hydration with time of induction period*

The Decay Period

When the reaction proceeds further, it indicates negative $d^2\alpha/dt^2$ and the rate begins to decrease. At the beginning of this period the thickness of the inner product exceeds 2000 Å and the surface of the original C_3S particle seems to be changed as is seen in Fig. 10. The reaction in this period depends upon the rate $N = 2$ as seen in Fig. 1, and is controlled by the outer diffusion through the inner product layer. $Ca(OH)_2$

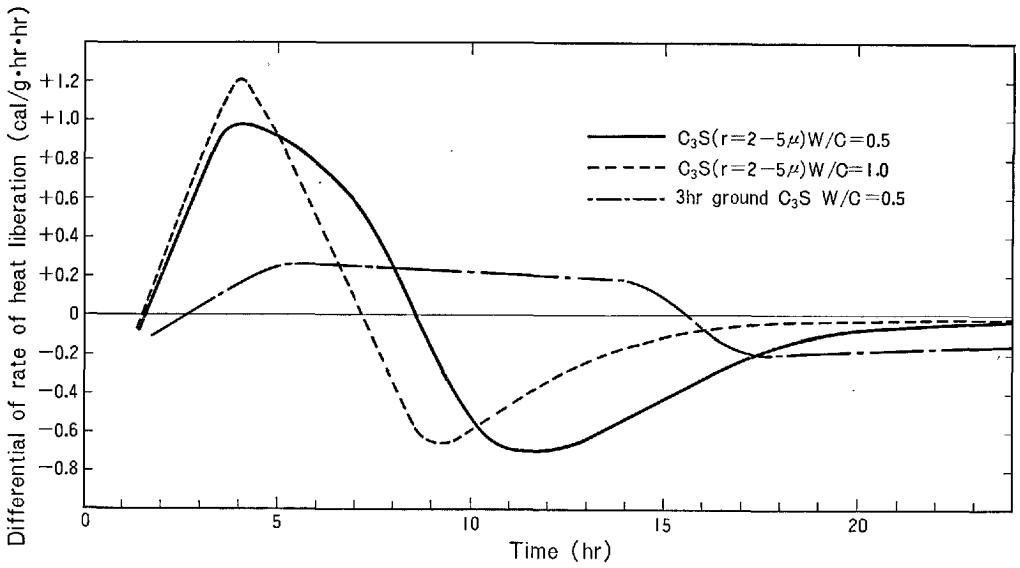

Fig. 36. *Curve of differential of heat liberation rate*

formed in the outer hydration space becomes larger than 100 μ and envelops many C_3S particles.

It is apparent from Fig. 32 that the S_{IV} stage shifts to S_V stage gradually. The inner product increases in compactness and is enveloped by $Ca(OH)_2$, and the reaction is controlled by a diffusion such as $N > 2$, namely the diffusion coefficient decreases with increase in time.

At the beginning of the S_V stage the size of the $Ca(OH)_2$ crystal reaches already 200 μ. Thereafter it grows gradually and envelops most of C_3S particles as is shown in Fig. 37. According to Kondo, Daimon and Ueda (55), it has been confirmed that the inner product consists of two zones in a perfectly hydrated sample. Compared with the outside part, the inside part indicates greater refractive index. Terrier and Moreau (54) observed two kinds of inner products and reported that the inside part had the higher CaO/SiO_2 ratio. The C_3S enveloped by $Ca(OH)_2$ cannot react with the outer water, but reacts with the gel water held in the product previously formed. Therefore the inside part may consist of a product of higher CaO/SiO_2 ratio and lower H_2O/SiO_2 ratio than the outside part which is formed before. The second portlandite is formed surrounding the C_3S particle as mentioned by Terrier and Moreau (54). According to Ueda, Hashimoto and Kondo (2), the inner product at 1 day grows to indicate the surface electron diffraction pattern, as shown in Fig. 32.

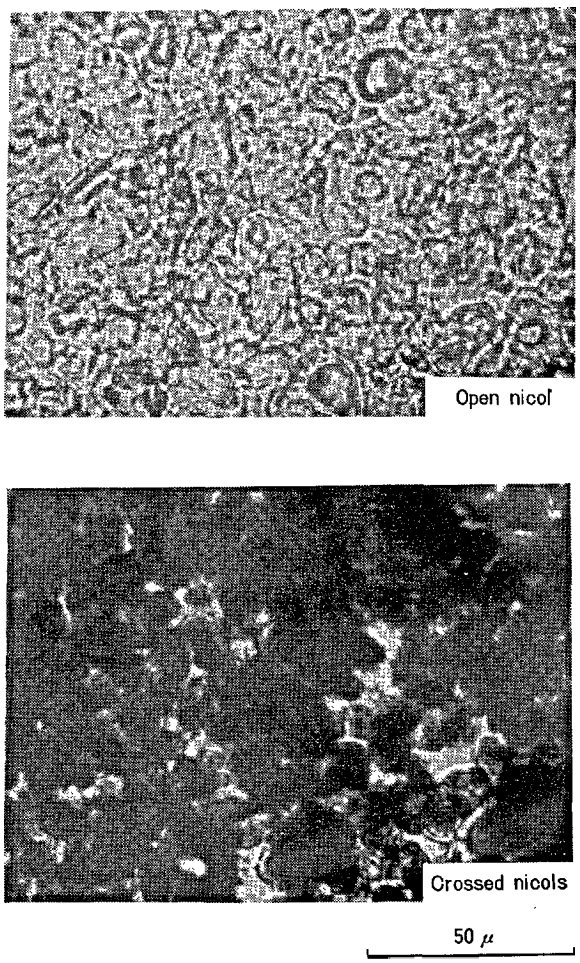

Fig. 37. *Inside and outside products in inner product*

Rate Equation of Hydration

The rate of hydration of cement components is

generally determined by the mass transfer through the product layer formed around the reactant particles, except at the early stage of paste hydration and ball-mill hydration. The rate equation for whole hydration process is shown, although the rate determining step changes with progress of reaction. As the rate has already been discussed for the case in which the particle size of the reactant is distributed, it will be discussed here by assuming a sphere of a single size.

Non-Diffusion Controlled Reaction

First, the rate equations other than the diffusion controlled step, for instance the boundary reaction being a slow step, will be reviewed. Furthermore, several reports have applied conventionally the rate equations for homogeneous reaction to discuss the order of reaction and empirical equations which do not correspond to an actual model.

As cited previously, Halstead and Lawrence (66) and also O'Connor and Greenberg (68) discussed the rate of reaction between colloid silica and lime solution and expressed the results by the following equation.

$$1 - x^{1/3} = kt$$

where x is the fraction of silica remaining in solid form after time t. In this reaction the dissolution of silica is the slow step and the rate is proportional to the surface area of reactant. The rate of solution is independent of the hydroxyl-ion concentration in the range of 15–40 milli-equivalents/ liter.

Greenberg and Chang (113) determined the rate of hydration of C_3S from the measurement of concentration and electric resistance of the solution, as C_3S dissolved congruently about 0.25 g per liter of water. The rate equation is as follows

$$-\frac{d(C_3S)}{dt} = k_1 S - k_2(C_3S)_a S$$

where (C_3S) is the concentration of unreacted C_3S, $(C_3S)_a$ is the concentration of dissolved C_3S, S is the surface area of unreacted C_3S, and k_1 and k_2 are the rate constants of dissolution and precipitation on the surface of particles, respectively. However, this does not always correspond to the experimental results.

According to Brunauer and Kantro (139), the reaction of C_3S in ball-mill hydration is always accelerated as the gel coating is removed. If it is assumed that the reducing rate of C_3S is equal to the disappearing rate of the gel coating, this can be expressed by the following equation.

$$-\frac{d(C_3S)}{dt} = k(C_3S)^{2/3} \qquad (1)$$

The rate is proportional to the surface area of C_3S. k is $0.095\,h^{-1}$ and then C_3S reacts completely at 31.5 h.

In the case of the hydration of calcum sulfate hemihydrate, a maximum in the rate was found by Taplin (141) near the mid-point of the reaction. The precipitation of gypsum controls the rate until the maximum, and thereafter the control passes to the dissolution of hemihydrate, which may be related with diffusion. An equation mentioned below is given

$$\frac{1}{\frac{d\alpha}{dt}} = \frac{1}{g} \cdot \alpha^{2/3} + \frac{1}{h} \cdot (1 - \alpha)^{2/3}$$

where g and h are the empirical rate constants for the precipitation and for the dissolution respectively. In practice the exponents become more than 2/3. The accelerators usually increase the rate of precipitation.

Knoblauch (104) examined the rate of hydration of C_3S and C_2S at several temperatures and reported that the former was the reaction of the third order and the latter was 1.5. Brunauer and Greenberg (20) suggested that these reactions were rather the diffusion controlled reaction. zur Strassen (142) interpreted from the result of Knoblauch (104) that the hydration of C_2S was obeyed by the surface controlled reaction from several days up to 120 days and it was controlled by diffusion thereafter, and that the hydration of C_3S was diffusion controlled until 30 days.

The rate of dissolution can be apparently expressed by an equation for the first order reaction which was derived by Nernst. As an example of such reaction there is the hydration of magnesia studied by Coleman and Ford (143). When the sample is exposed to an atmosphere saturated with water vapor, the hydration rate can be expressed by such type of equation as follows,

$$\ln(1 - \alpha) = -kt$$

The relationship between the rate and the mechanism is not clear, but they concluded that this hydration was the result of capillary condensation of water-vapor in the micro-pores of MgO and its rate was dependent, not on specific surface, but on the difference in the starting materials and calcination temperatures. On the other hand Layden and Brindley (109) found an incubation period in the hydration of magnesia and interpreted that an interface reaction controlled the progress of the overall reaction. The rate of hydration of magnesia in the vapor-phase can be expressed by similar equation as like (1).

Rate Equations of the Solid State Reaction

Rate equations of the solid state reaction controlled by diffusion are given by many investigators. Particularly the equation derived by Jander (144) is frequently used. The equation is as follows:

$$[1-(1-\alpha)^{1/3}]^2 = kt$$

where α is the reaction ratio and t is time. This equation was derived by assuming the sectional area of diffusion being the original surface but the area should be the geometric mean between the former and the interface of the reactant which reduced with progress of reaction. However it was reported by Kondo and Choi (145) that this equation conformed to another kind of the solid state reaction which took place in the presence of melt, for an example $C + C_2S \rightarrow C_3S$ in the portland cement formation.

Ginstling and Brounshtein (146) obtained a more accurate equation. Their equation can be modified to express by the function of the thickness of reaction layer in convenience of later discussion and to elucidate the meaning of the rate constant.

$$[1-(1-\alpha)^{1/3}]^2 - \frac{2}{3}[1-(1-\alpha)^{1/3}]^3 = 2DCt \cdot \frac{1}{ar_0^2} \quad (2)$$

where α is the reaction ratio, D is the diffusion coefficient, C is the concentration difference expressed as g reactant/1000 $cm^3 \cdot \rho$, where ρ is the density (g/cm^3) of the solid reactant and "a" is a constant described later and r_0 is the radius of the original reactant particle. As shown in the above equation, the first term of the left side dominates the reaction in the early stage to coincide with Jander's equation and on the other hand, the second term dominates the reaction in the later stage to complete faster.

The above two rate equations are given under a very simple assumption that the mass transfer depends only upon inward diffusion and the volume of the reacted reactant is equal to that of the formed product. Thereafter Carter (147) proposed an equation in which the volume ratio of the reacted part to the formed product was considered. But all of these equations are not natural because of the assumption that the product is formed only at the interface of reactant. If it is true each particle must be expanded and the rate constant cannot remain unchanged owing to the destruction of the texture of the formerly formed product.

Regarding this matter Taplin (57) considered that the outer product and inner product were formed simultaneously by counter diffusion in the hydration of C_2S and gave the equation (148) in which two diffusion coefficients on both products were taken into account. The following equation is a modification of Taplin's equation to make easy to compare with the equations mentioned above.

$$\frac{1}{D_i}\left[1-(1-\alpha)^{2/3}-\frac{2}{3}\alpha\right] + \frac{1}{D_o}(z-1)\left\{1+\frac{2}{3}(z-1)\alpha-[1+(z-1)\alpha]^{2/3}\right\} = \frac{2Ct}{ar_o^2}$$

where D_i and D_o are the diffusion coefficients on the inner and outer products, respectively, and z is the volume ratio of the product to reactant.

The above equation is reduced to Carter's equation if $D_i = D_o$, and coincides with the equation of Ginstling and Brounshtein if $z = 1$. The meaning of rate constant is here clarified, however it is not described by Ginstling and Brounshtein (146) and Carter (147). A factor "a" in the right side term must not be neglected, nevertheless it is not considered by Taplin (148) as all of the reacted reactant does not diffuse outward but only a part "a" of this diffuses. In addition, "a" is to be $(z-1)/z$ when the densities of inner and outer products are the same. It is obvious from the above equation that particularly the rate at the later stage decreases when the diffusion through the outer product is the slow step.

Mass Transfer Controlled by Diffusion

The rate equations mentioned above is applicable to the case of hydration if the diffusion is a slow step. Furthermore some rate equations mainly concerned with the hydration reaction will be reviewed.

Greenberg and Chang (113) considered that the rate of the hydration of C_3S was controlled by the rate of diffusion of the ions into the surrounding solution through the product layer and applied an equation given by Brunner and Tolloczko.

$$-\frac{d(C_3S)}{dt} = kS[(C_3S)_s - (C_3S)_d]$$

where k is a function of diffusion, S is the surface area of C_3S particle, (C_3S), $(C_3S)_s$ and $(C_3S)_d$ are the concentrations of unhydrated C_3S, dissolved C_3S on the interface of unhydrated C_3S and dissolved C_3S in the solution far from the unhydrated particle surface respectively. This equation, however, does not coincide with the experimental results. It seems that it is necessary to take into consideration the thickness of the product layer.

On the other hand, Ratinov and Lavut (149) discussed the early stage of suspension hydration of C_3S.

with the rate of solution. The solution rate of a disk is as follows.

$$\frac{dl}{dt} = \frac{D}{\rho\delta}(C - C')$$

where, l is the size of particles, D is diffusion coefficient, ρ is density, δ is the effective thickness of the diffusion layer and estimated from the study of Levich as $\delta = kD^{1/3}$ in which convection and diffusion are taken into consideration, C is saturated concentration and C′ is the concentration of the liquid. The dissolution rates of the pressed pellets of C_3S, C_2S or hydrothermally synthesized product such as C_3SH_2 or $C_2SH(A)$ are obtained (135). Both results were substituted in the above equation, by which the following equation was derived.

$$\frac{1}{k_1}(m_1^{\frac{1}{3}} - m_{1.0}^{\frac{1}{3}}) - \frac{1}{k_2}(m_2^{\frac{1}{3}} - m_{2.0}^{\frac{1}{3}}) = -D^{\frac{2}{3}}(C_1 - C_2)t$$

where, m_1 and m_2 are the weight of reactant and product, respectively, at time t, $m_{1.0}$ and $m_{2.0}$ are those at $t = 0$. As l_1 and l_2 are in the order of $10 \sim 50\ \mu$ and $100 \sim 500$Å respectively, $C_1' - C \gg C - C_2'$, and $k_1 D^{2/3}(C_1 - C_2)$ can be approximated as a constant, so that

$$m_1^{\frac{1}{3}} - m_{1.0}^{\frac{1}{3}} \simeq -kD^{\frac{2}{3}}(C_1 - C_2)t$$

In the case of cement, C_2 can be ignored as $C_1 \gg C_2$. The determined value of $-k \cdot 10^4$ is $1.0 \sim 1.1$ at $20° \sim 65°$C. The value $m_1^{1/3} - m_{1.0}^{1/3}$ is kept nearly zero for $2 \sim 3$ hr, thereafter it increases proportionally with lapse of time. The slope of the line obtained from this equation becomes steeper, which implies that the reaction is accelerated by the addition of a salt such as $NaNO_2$, KCl and K_2SO_4. This rate equation is dealt with carefully but this cannot be utilized for paste hydration in which the diffusion through the product layer becomes the slow step.

Stein (150) discussed the retardation of the reaction of C_3A by the formation of ettringite in the presence of gypsum and lime. If the amount of the ettringite produced is P, f is the fraction of ettringite formed around the interface of reactant to cause retardation, the following equation was obtained from Fick's first law of diffusion.

$$-\frac{d\ln f}{dt} + 2\frac{d\ln \mathrm{A}}{dt} = \frac{1}{\mathrm{P}} \cdot \frac{d\mathrm{P}}{dt} + \frac{\dfrac{d^2\mathrm{P}}{dt^2}}{\dfrac{d\mathrm{P}}{dt}}$$

The relation of P vs t is a straight line when the beginning of the second peak of the rate of heat liberation is taken as t. He substituted Blaine's surface of C_3A for A which is the area of the relevant surface concerned with diffusion as he intended only to apply to the early stage of reaction.

Rate Determining Steps in Hydration

In the case of the reaction of spherical particle the relation between the thickness of the reacted layer ξ and time t is expressed as $\xi = kt$ when the rate determining step is boundary reaction. On the other hand when the reaction is controlled by diffusion, the relation $\xi^2 - \frac{2}{3}\xi^3 = kt$ is given as shown by equation (2) but this equation becomes approximately $\xi^2 = kt$ in the very early stage.

It is hold for many reactions an empirical equation in which the N power of the function of the thickness of reaction layer $1 - (1 - \alpha)^{1/3}$ is regarded as being equal to kt. The value of N is 1 if the slow step is boundary reaction and approximately 2 if it is diffusion. This value sometimes becomes less than 1 or more than 2, however almost no discussion has been made on hydration reaction in the past.

When N is less than 1, an autocatalytic reaction is expected and the rate is accelerated with progress of reaction. This type of reaction occurs at the acceleratory period.

It can be considered that an impermeable product layer formed at the S_I stage decreases in thickness gradually to become permeable at the S_{III} stage. However, the consideration of the change of rate with time and of mechanism leads us to a conclusion that the formation and growth of nuclei start by the transformation from unstable to metastable phase during S_{II} stage already. When the size of transformed spots reaches the thickness of protective layer, this layer becomes permeable to change to S_{III} stage and further growth of these spots seems to increase the sectional area of permeable part. This process leads to a proportional increase in the rate of hydration.

Kondo and Daimon (70) proposed a following rate equation for transformation in the product layer. They considered that the reaction was boundary controlled, and that the transformed part grew linearly at a constant rate k.

$$\alpha_j = \frac{\pi}{2}k^2(t - t_g)^2$$

where α_j is the transformed volume and t_g is the time when the center of transformation is formed. If the rate of increase of the center is k', the following equation is obtained.

$$\alpha - \alpha_i = \sum_{t_g=t_i}^{t} k'\alpha_j = \frac{\pi}{2}k^2k' \int_{t_i}^{t} (t - t_g)^2 dt_g$$

$$\alpha - \alpha_i = \frac{\pi}{6}k^2k'(t - t_i)^3$$

The rate of increase in α_j is practically decreased by

the collision of the growing fronts and the roughness of the particle surface. k' is also saturated by the end of S_{III}.

If we next assume diffusion as being the slow step,

$$d\alpha = \frac{3DC\epsilon}{\xi r}dt = k\epsilon\, dt$$

where ϵ is the volume fraction of the permeable part. In case of the transformed part grows in length and width with time,

$$\epsilon(t) = k'(t - t_i)^2$$
$$d\alpha = kk'(t - t_i)^2\, dt$$
$$\alpha - \alpha_i = \frac{1}{2}kk'(t - t_i)^3$$

where ϵ is a fraction of the total transformed metastable phase ϵ'. Accordingly, ϵ' increases in the S_{II} stage but ϵ remains zero.

On the other hand, from the heat liberation data during the S_{III} stage, the following equation is given.

$$\frac{d^2q}{dt^2} = k(t - t_i)$$

where, k(cal/g·hr^3) indicates the rate of increase in the permeable area, and t_i is the time of the induction period. Since the temperature dependance of k is as large as 37 kcal/mole, the hydration of C_3S at the S_{III} stage is regarded as being controlled by the chemical reaction in which the protective layer is transformed into the metastable phase.

When N is a value larger than 2, the diffusion may be the slow step, however the diffusion coefficient decreases gradually. The reaction at the S_V stage mentioned above is an example of this type. The diffusion coefficient through the hydration product is generally smaller than in bulk liquid so that the ratio of sectional area of the total through pores to the relevant surface is smaller than 1, the tortuosity is higher than 1 and chemisorption of capillary is also effective. When the pore structure becomes more dense, it can be expressed by $\xi^N = kt$ where $N > 2$. In general $\xi^2 = vt$, where v is a variance, which is expressed as $v = k'/\xi^{N-2}$. Accordingly the diffusion coefficient D decreases in this case at a rate of $1/\xi^{N-2}$ with progress of reaction.

In the hydration of C_3S, the S_{IV} stage whose reaction is controlled by diffusion through only inner product is very short. In the S_V stage most particles are enveloped by the growing $Ca(OH)_2$ crystal and thereafter the subsequent hydration is very limited as the gel water in the inner product formed before is only available for hydration. Then the value of N of the overall reaction after 1 day becomes 2.5 to 2.8.

Kinetics of the Whole Hydration Process Having Various Stages.

The complicated change occurring in the hydration of cement with progress of reaction has already been explained. Kondo and Kodama (151) tried to formulate these complicated changes without over simplification. Here the whole hydration process containing the five stages from S_I to S_V will be described. The equations obtained are also applicable to somekind of solid state reactions having induction and acceleratory periods.

A dense protective layer seems to be formed on the reactant suface during the early part of the reaction and this follows the parabolic law as a kind of an erosion reaction.

$$\frac{d\xi}{dt} = \frac{k}{\xi} \qquad \text{or} \qquad \xi^2 = kt + k'$$

where, k' refers to the very early chemical reaction term which is not affected by diffusion. In this period, it can be considered that ξ will be proportional to α, so

$$\alpha^2 = k_\alpha t + k'_\alpha$$

The change of $d\alpha/dt$ or α with time is shown in Fig. 38, (a) and (b), respectively.

Next, the geometry of a single sphere of reactant whose original radius and the radius of the partly reacted reactant are r_o and r, respectively, is shown in Fig. 39. Among the overall transport processes of the chemical species, the slowest one is assumed to govern the rate of reaction.

Now, let us consider the situation where the reaction $d\alpha$ advances in the duration dt at time t. The flux of the material or ion in relation to the rate determining transport process F, is formed in proportion to $d\alpha$, so that the flux in a single spherical particle can be expressed by the following equation.

$$F = \frac{4}{3}\pi r_o^3\, a\frac{d\alpha}{dt}$$

where, "a" is the proportionality constant when the chemical species concerning the rate controlling diffusion are formed in proportion to the quantity of the hydrated reactant.

Hence, it is possible to derive the following equations.

$$C_1 - C_2 = \frac{4}{3}\pi r_o^3\, a\frac{d\alpha}{dt}\cdot\frac{\Delta r_a}{D_a\cdot S_a} \tag{3}$$

$$C_2 - C_3 = \frac{4}{3}\pi r_o^3\, a\frac{d\alpha}{dt}\cdot\frac{\Delta r_b}{D_b\cdot S_b} \tag{4}$$

$$C_3 - C_4 = \frac{4}{3}\pi r_o^3\, a\frac{d\alpha}{dt}\cdot\frac{1}{D_c\cdot S_c} \tag{5}$$

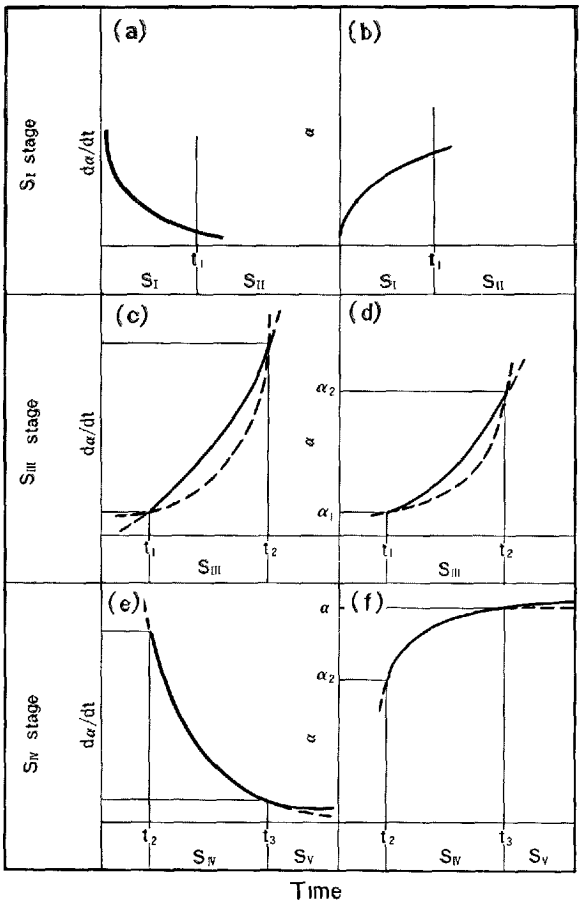

Fig. 38. *Relation between hydration rate or degree of hydration and time at each stage*

where, C_1, C_2, C_3 and C_4 are the concentrations of the rate determining chemical species in each position, D_a, D_b and D_c are the mass transfer coefficients of the rate determining chemical species in each position, and S_a or S_b is the geometric mean surface between S and S_o', or between S_o' and S_o, respectively. By combining (3), (4) and (5), we obtain,

$$\frac{4}{3}\pi r_o^3 a\frac{d\alpha}{dt} = \frac{C_1 - C_4}{\dfrac{\Delta r_a}{D_a \cdot S_a} + \dfrac{\Delta r_b}{D_b \cdot S_b} + \dfrac{1}{D_c \cdot S_o}} = \frac{C}{\sum_{i=1}^{3} R_i} \tag{6}$$

where, C is the overall concentration difference, and R refers to the resistance to the flux of the rate determining process, and is expressed by,

$$R_1 = \frac{\Delta r_a}{D_a \cdot S_a},\quad R_2 = \frac{\Delta r_b}{D_b \cdot S_b},\quad R_3 = \frac{1}{D_c \cdot S_o}$$

Now, the flux of the rate determining process is given from equation (6).

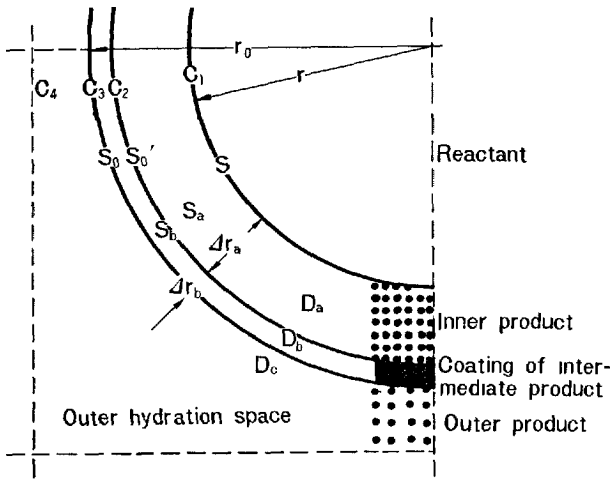

Fig. 39. *Schematic diagram of hydrated spherical particle*

$$\frac{4}{3}\pi r_o^3 a\frac{d\alpha}{dt} = \frac{S_o \cdot C}{\dfrac{\Delta r_a \cdot S_o}{D_a \cdot S_a} + \dfrac{\Delta r_b \cdot S_o}{D_b \cdot S_b} + \dfrac{1}{D_c}} \tag{7}$$

where S_o, S_a and S_b are

$$S_o = 4\pi r_o^2$$

$$S_a = (S_o' \cdot S)^{\frac{1}{2}} \fallingdotseq [4\pi r_o^2 \cdot 4\pi r_o^2(1-\alpha)^{\frac{2}{3}}]^{\frac{1}{2}} = 4\pi r_o^2(1-\alpha)^{\frac{1}{3}}$$

$$S_b = (S_o' \cdot S_o)^{\frac{1}{2}} \fallingdotseq 4\pi r_o^2$$

The protective layer is first simply assumed to become gradually thiner linearly with time by the dissolution process. Thence,

$$\Delta r_a = r_o[1 - (1-\alpha)^{\frac{1}{3}}] \tag{8}$$

$$\Delta r_b = \xi_o - k_s(t - t_1) \tag{9}$$

where, ξ_o is the layer thickness at time t_1.

Hence, from equations (7), (8) and (9), we obtain the following differential equation which should be solved.

$$\left\{\frac{r_o}{D_a}\cdot\frac{1-(1-\alpha)^{\frac{1}{3}}}{(1-\alpha)^{\frac{1}{3}}} + \frac{1}{D_b}[\xi_0 - k_s(t-t_1)] + \frac{1}{D_c}\right\}\frac{d\alpha}{dt} = \frac{3C}{ar_0} \tag{10}$$

If we assume that in the S_{III} stage the process which governs the overall rate is the mass transfer through the protective layer, $R_2 \gg R_1 + R_3$. When the R_1 term is ignored and the equation (10) is integrated from α_1 to α and from t_1 to t,

$$\int_{\alpha_1}^{\alpha} d\alpha = \frac{3C}{r_0 a}\int_{t_1}^{t}\frac{1}{\left(\dfrac{\xi_0}{D_b} + \dfrac{1}{D_c}\right) - \dfrac{k_s}{D_b}(t-t_1)}dt$$

The solution which gives the relationship between α and t in the S_{III} stage is

$$\alpha - \alpha_1 = A_3 \ln \frac{1}{1-(t-t_1)/B_3}$$

where,

$$A_3 = \frac{6.9C}{ar_0} \cdot \frac{D_b}{k_s} \quad \text{and} \quad B_3 = \frac{D_b}{k_s}\left(\frac{\xi_0}{D_b} + \frac{1}{D_c}\right)$$

The solid curves shown in Fig. 38 as (c) and (d) represent the relationship between t and $d\alpha/dt$ or α, respectively.

It was assumed after equation (9) that the coating layer became thin linearly but the rate of reaction for the acceleratory period increased in the proportion of nearly second power of time. This leads to the hypothetical mechanism that the area of permeable part in the coating layer increases in two dimensions with time.

Thus, the term, $1/D_b[\xi_0 - k_s(t-t_1)]$, in equation (10) must be changed to $\xi_0/k(t-t_1)^n$. The following equation is similarly obtained by ignoring the R_1 and R_3 terms,

$$\alpha - \alpha_1 = \frac{3kC}{(n+1)ar_0\xi_0}(t^{n+1} - t_1^{n+1}) = k'(t^{n+1} - t_1^{n+1})$$

The dotted curves (c) and (d) in Fig. 38 are from calculated value.

As for the S_{IV} stage, we assume that the process which governs the overall rate is the mass transfer through the inner products, so that $R_1 \gg R_2 + R_3$, by which equation (10) reduces to

$$\frac{r_0}{D_a} \cdot \frac{1-(1-\alpha)^{\frac{1}{3}}}{(1-\alpha)^{\frac{1}{3}}} d\alpha = \frac{3C}{ar_0} dt$$

When integrated from t_2 to t and from α_2 to α,

$$\frac{r_0}{D_a}\int_{\alpha_2}^{\alpha}[(1-\alpha)^{\frac{1}{3}} - 1]d\alpha = \frac{3C}{ar_0}\int_{t_2}^{t} dt$$

The solution which gives the relationship between α and t in the S_{IV} stage is

$$t = A_4[B_4 - \frac{3}{2}(1-\alpha)^{\frac{2}{3}} - \alpha] \qquad (11)$$

where $A_4 = \frac{ar_o^2}{3D_aC}$

and $B_4 = \frac{3}{2}(1-\alpha_2)^{\frac{2}{3}} + \alpha_2 + \frac{3D_aC}{ar_o^2}t_2$

Equation (11) corresponds to that derived by Ginstling and Brounshtein (146) if t_2 and α_2 are zero because the reaction has no induction and acceleratory periods. If we assume the value C is in the order of g/l, and "a" is about 0.5, although they have not been experimentally confirmed in cement hydration, the order of D may be evaluated from the data of the hydration rate as $10^{-11\sim12}$. In Fig. 38, (e) and (f) show the relationship between t and $d\alpha/dt$ or α in the S_{IV} stage.

Further, in the later period of hydration in which the unsteady diffusion process through the inner and outer products is the rate determining step, the diffusion equation is generally given by Fick's second law rewritten in spherical coordinates as follows.

$$\frac{\partial C(r,t)}{\partial t} = \frac{1}{r^2}\frac{\partial}{\partial r}\left(Dr^2\frac{\partial C}{\partial r}\right)$$

where $D(r, C, t)$ is not a constant. This equation represents the S_V stage and expresses a trend for retarding qualitatively more than the rate of reaction in the S_{IV} stage. We do not have sufficient information on the structures and concentrations of the system at this stage but the rate of the overall reaction can be expressed by an empirical equation, $[1-(1-\alpha)^{1/3}]^N = kt$, in which $N > 2$ generally and $N = 2.5\sim2.8$ in the case of paste hydration of C_3S, as previously described.

Finally, the whole hydration process consisting of various stages can be expressed as shown in Fig. 31, in which the solid curves are the sum of the results shown in Fig. 38 for every stage and the dotted curves are for the actual reaction course.

References

1. L. E. Copeland, D. L. Kantro and G. Verbeck, "Chemistry of hydration of portland cement", Proceedings of the Fourth International Symposium on the Chemistry of Cement, Washington, 1960, NBS Monograph 43, 429–465 (1962).
2. S. Ueda, M. Hashimoto and R. Kondo, "Study on the hydration of cement by surface electron diffraction" (in Japanese), Semento Gijutsu Nenpo **22**, 67–72 (1968).
3. P. Seligmann and N. R. Greening, "Studies of early hydration reactions of portland cement by X-ray diffraction", Highway Research Record No. 62, 80–105 (1964). Research Lab. Portland Cement Association, Bull. **185**, 80–105 (1964).
4. P. Seligmann and N. R. Greening, "New techniques for temperature and humidity control in X-ray diffractometry", J. of the PCA Res. and Dev. Lab. (Portland Cement Association) **4**, No. 2, 2–9 (1962).
5. R. L. Angstadt and F. R. Hurley, "Hydration of the alite phase in portland cement", Nature, London, **197**, 688 (1963).
6. F. R. Hurley and R. L. Angstadt, "The early hydration of tricalcium silicate and β-dicalcium silicate in neat portland cement pastes", J. appl. Chem. **16**, 162–165 (1966).
7. S. Tsumura and H. Kawachi, "Hydration of C_3A

and C_4AF" (in Japanese), Semento Gijutsu Nenpo **18**, 45–50 (1964).
8. S. Tsumura, "On the hydration mechanism of clinker minerals" (in Japanese), Semento Gijutsu Nenpo **19**, 88–92 (1965).
9. H. G. Smolczyk, "The X-ray determination of the crystalline phases of portland cement clinker" (in German), Zement-Kalk-Gips **14**, 558–566 (1961).
10. H. G. Smolczyk, "An optimum treatment for the quantitative X-ray analysis of hydrated cement" (in German), Tonindustrie-Zeitung **86**, 261–267 (1962).
11. W. Lerch, "The influence of gypsum on the hydration and properties of portland cement pastes", Proceedings, American Society for Testing Materials **46**, 1252–1292 (1946).
12. U. Danielson, "Heat of hydration of cement as affected by water-cement ratio", Proceedings of the Fourth International Symposium on the Chemistry of Cement, Washington, 1960, NBS Monograph **43**, 519–526 (1962).
13. H. N. Stein, "Influence of some additives on the hydration reactions of portland cement. I. Non-ionic organic additives", J. appl. Chem. **11**, 474–482 (1961).
14. G. E. Monfore and Borje Ost, "An isothermal conduction calorimeter for study of the early hydration reactions of portland cements", J. of the PCA Res. and Dev. Lab. (Portland Cement Association) **8**, No. 2, 13–20 (1966).
15. L. E. Copeland and J. C. Hayes, "Determination of non-evaporable water in hardened portland-cement paste", ASTM Bull. No. 194, 70–74 (Dec. 1953).
16. R. Kondo, S. Ueda and M. Kodama, "Reaction process of the hydration of $3CaO \cdot SiO_2$" (in Japanese), Semento Gijutsu Nenpo **21**, 83–90 (1967).
17. W. Lerch and R. H. Bogue, "Determination of uncombined lime in portland cement", Ind. Eng. Chem. **18**, 739–743 (1926).
18. B. Franke, "A new method for determining calcium oxide and calcium hydroxide in the presence of hydrous and anhydrous calcium silicate" (in German), Z. anorg. u. allgem. Chem. **247**, 180–184 (1941).
19. G. Yamaguchi, K. Takemoto, H. Uchikawa and S. Takagi, "Researches on the quantitative analytical methods for calcium hydroxide in hydrated portland cement" (in Japanese), Semento Gijutsu Nenpo **14**, 47–57 (1960).
20. S. Brunauer and S. A. Greenberg, "The hydration of tricalcium silicate and β-dicalcium silicate at room temperature", Proceedings of the Fourth International Symposium on the Chemistry of Cement, Washington, 1960, NBS Monograph 43, 135–165 (1962).
21. S. Brunauer, P. H. Emmett and E, Teller, "Adsorption of gases in multimolecular layers", J. Am. Chem. Soc. **60**, 309–319 (1938).
22. G. L. Kalousek, "Fundamental factors in the drying shrinkage of concrete block" Proceedings of the Am. Concrete Inst. **51**, 233–248 (1954–1955).
23. E. Eipelatuer, W. Schilcher and W. Czernin, "The problem of pore distribution in cement hydration products" (in German), Zement-Kalk-Gips **17**, 543–546 (1964).
24. S. Brunauer, D. L. Kantro and C. H. Weise, "The surface energy of tobermorite", Can. J. Chem. **37**, 714–724 (1959).
25. C. M. Hunt, "Nitrogen sorption measurements and surface areas of hardened cement pastes", Symposium on Structure of Portland Cement Paste and Concrete, Highway Research Board, 112–122 (1966).
26. R. Sh. Mikhail and Suzy A. Selim, "Adsorption of organic vapors in relation to the pore structure of hardened portland cement pastes", Symposium on Structure of Portland Cement Paste and Concrete, Highway Resdarch Board, 123–134 (1966).
27. R. W. Cranston and F. A. Inkley, "The determination of pore structures from nitrogen adsorption isotherms", Adv. in Catalysis **9**, 143–154 (1957).
28. W. B. Innes, "Use of a parallel plate model in calculation of pore size distribution", Analytical Chemistry **29**, 1069–1073 (1957).
29. Åke Grudemo, "The microstructures of cement gel phases", (Swedish Cement and Concrete Research Institute at the Royal Institute of Technology, Stockholm, 1965).
30. Åke Grudemo, "The microstructure of hardened cement paste", Proceedings of the Fourth International Symposium on the Chemistry of Cement, Washington, 1960, NBS Monograph 43, 615–648 (1962).
31. R. Kondo and S. Ueda, new data.
32. R. Kondo and S. Ueda, new data.
33. E. Brandenberger, "Intercrystalline structure and the chemistry of cement. Basis of a stereochemistry of the crystalline compounds present in portland cement" (in German), Schweizer Archiv. **2**, 45–58 (1936).
34. M. Bredig, discussion of paper by R. W. Nurse, "The dicalcium silicate phase", Proceedings of the Third International Symposium on the Chemistry of Cement, London, 1952, Cement and Concrete Association, 82–84 (1954).
35. J. W. Jeffery, "The tricalcium silicate phase", Proceedings of the Third International Symposium on the Chemistry of Cement, London, 1952, Cement and Concrete Association, 30–48 (1954).
36. R. Kondo, "The synthesis and crystallography of a group of new compounds belonging to the hauyne type structure" (in Japanese), Yogyo Kyokaishi **73**, 1–8 (1965).
37. V. L. Burdick and D. E. Day, "Coordination of aluminum ions in tricalcium aluminate", J. Am. Ceram. Soc. **50**, 97–101 (1967).
38. O. P. Mchedlov-Petrosyan and W. I. Babushkin, "Thermodynamics of the hardening processes of cement", Proceedings of the Fourth International Symposium on the Chemistry of Cement, Washington, 1960, NBS Monograph 43, 533–544 (1962).
39. G. Yamaguchi, K. Shirasuka and T. Ota, "Comparison of hydration properties between monoclinic and inverted triclinic alite", Symposium on Structure of Portland Cement Paste and Concrete, High-

way Research Board, 263–268 (1966).
40. H. Lehmann, S. Traustel and P. J. Jacob, "Investigation for the determination of disorder of alite" (in German), Tonindustrie-Zeitung **86**, 316–321, 339–344 (1962).
41. Y. Ono and Y. Soda, "Effect of the crystallographic properties of alite and belite on the strength of cement" (in Japanese), Semento Gijutsu Nenpo **19**, 93–103 (1965).
42. R. Kondo, "Effects of special components on the mineral composition of portland cement clinker" (in Japanese), Semento Gijutsu Nenpo **17**, 42–49 (1963).
43. R. Kondo and K. Yoshida, "Miscibilities of special elements in tricalcium silicate and alite and the hydration properties of resulted solid solutions", paper is presented in this Symposium.
44. I. A. Kryzhanovskaya, V. M. Mirak'yan, V. M. Shokotova and B. G. Horodnui, "Hydration of alkali minerals in clinker" (in Russian), Tsement 1965, No. 5, 10–11 (1965).
45. H. C. Gatos, "Crystalline structure and surface reactivity", Science **137**, No. 3527, 311–322 (3 Aug. 1962).
46. R. Kondo, M. Daimon and T. Akiba, "Study on the hydration of cement by calorimetry" (in Japanese), Semento Gijutsu Nenpo **22**, 73–78 (1968).
47. H. Le Chatelier, "Experimental researches on the constitution of hydraulic mortars" (translated by J. L. Mack) (McGraw Publ. Co., N. Y., 1905).
48. W. Richartz and F. W. Locher, "A contribution to the morphology and combination with water of calcium silicate hydrates and to the structure of the hardened cement paste" (in German), Zement-Kalk-Gips **18**, 449–459 (1965).
49. W. Michaelis, "The hardening process of calcium bearing hydraulic materials" (in German), Kollid Z. **5**, 9–22 (1909).
50. W. C. Hansen, discussion of paper by H. H. Steinour, "The reactions and thermochemistry of cement hydration at ordinary temperature", Proceedings of the Third International Symposium on the Chemistry of Cement, London, 1952, Cement and Concrete Association, 318–321 (1954).
51. H. Funk, "Two different ways of hydration in the reaction of β-Ca_2SiO_4 with water at 25 to 120°C", Proceedings of the Fourth International Symposium on the Chemistry of Cement, Washington, 1960, NBS Monograph 43, 291–295 (1962).
52. R. F. Feldman, V. S. Ramachandran and P. J. Sereda, "Influence of $CaCO_3$ on the hydration of $3CaO \cdot Al_2O_3$", J. Am. Ceram. Soc. **48**, 25–30 (1965).
53. F. Trojer, "A contribution to the information of intermediate phase by the hydration of cement clinker mineral" (in German), Zement und Beton **29**, 1–5 (1964).
54. P. Terrier and M, Moreau, "Study on the mechanism of pozzolanic reaction of fly ash with cement" (in French), Rev. Matér, Constr. Trav. Publics No. 613, 379–396 (1966) and No. 614, 440–451 (1966).
55. R. Kondo, M. Daimon and S. Ueda, new data.
56. E. Eipeltauer, "Manufacture of expansive-free prefabricated units from anhydrite in an extrusion press" (in German), Zement-Kalk-Gips **17**, 60–66 (1964).
57. J. H. Taplin, "A method for following the hydration reaction in portland cement paste", Australian J. Appl. Sci. **10**, 329–345 (1959).
58. The Chemistry of Cements, Vol. I (Academic Press, London and New York, 1964), Edited by H. F. W. Taylor. See chapter 10 by T. C. Powers entitled "The physical structure of portland cement paste".
59. M. Okushima, R. Kondo, H. Muguruma and Y. Ono, "Development of expansive cement with calcium sulfoaluminous cement clinker", paper is presented in this Symposium.
60. J. D. C. McConnell, "The hydration of larnite (β-Ca_2SiO_4) and bredigite (α'-Ca_2SiO_4) and the properties of the resulting gelatinous mineral plombierite", Min. Mag. **30**, 672–680 (1955).
61. N. Kawada and A. Nemoto, "Calcium silicates in the early stage of hydration" (in German), Zement-Kalk-Gips **20**, 65–71 (1967).
62. R. Kondo, "Fundamental study on the manufacture of slag cement", Dr. Thesis in Tokyo Institute of Technology (1958).
63. J. D'Ans and H. Eick, "Investigations on the setting process of hydraulic blast furnace slag" (in German), Zement-Kalk-Gips **7**, 449–459 (1954).
64. R. Kondo and S. Ohsawa, "Studies on a method to determine the amount of granulated blastfurnace slag and the rate of hydration of slag in cements", paper is presented in this Symposium.
65. G. Malquori, "Portland-pozzolan cement", Proceedings of the Fourth International Symposium on the Chemistry of Cement, Washington, 1960, NBS Monograph 43, 983–1006 (1962).
66. P. E. Halstead and C. D. Lawrence, "Kinetics of reaction in the system CaO–SiO_2–H_2O", Proceedings of the Fourth International Symposium on the Chemistry of Cement, Washington, 1960, NBS Monograph 43, 321–324 (1962).
67. S. A. Greenberg, "Reaction between silica and calcium hydroxide solutions. I. Kinetics in the temperature range 30 to 85°", J. Phys. Chem. **65**, 12–16 (1961).
68. T. L. O'Connor and S. A. Greenberg, "The kinetics for the solution of silica in aqueous solutions", J. Phys. Chem. **62**, 1195–1198 (1958).
69. R. Kondo, "Kinetic study on hydrothermal reaction between lime and silica", International Symposium on Autoclaved Calcium Silicate Building Products, London, 1965, Soc. of Chem. Ind. 92–97 (1967).
70. R. Kondo and M. Daimon, "A solid reaction with induction and acceleration periods: Early hydration of tricalcium silicate", J. Am. Ceram. Soc. **52**, (1969).
71. H. H. Steinour, "Aqueous cementitious systems containing lime and alumina", Research Lab. Portland Cement Association Bull. **34**, (1951).
72. J. G. M. de Jong, H. N. Stein and J. M. Stevels, "Hydration of tricalcium silicate", J. appl. Chem. **17**, 246–250 (1967).
73. H. G. Kurczyk and H. E. Schwiete, "Electron microscopic and thermochemical investigation on the hydration of calcium silicate $3CaO \cdot SiO_2$ and β-$2CaO \cdot SiO_2$ and the effect of calcium chloride and gypsum on the hydration process" (in German),

Tonindustrie-Zeitung **84**, 585–598 (1960).
74. H. N. Stein and J. M. Stevels, "Influence of silica on the hydration of $3CaO \cdot SiO_2$" J. appl. Chem. **14**, 338–346 (1964).
75. N. Kawada and A. Nemoto, "Hydration process of calcium silicates during first 24 hrs." (in Japanese), Semento Gijutsu Nenpo **20**, 68–74 (1966).
76. R. Nagano and H. Wada, "On the hydration of C_2S" (in Japanese), Semento Gijutsu Nenpo **15**, 42–46 (1961).
77. H. N. Stein, "Influence of some additives on the hydration reactions of portland cement. II. Electrolytes", J. appl. Chem. **11**, 482–492 (1961).
78. H. E. Schwiete, U. Ludwig and P. Jäger, "Investigations on the system $3CaO \cdot Al_2O_3$–$CaSO_4$–CaO–H_2O" (in German), Zement-Kalk-Gips **17**, 229–236 (1964).
79. G. Verbeck, "Cement hydration reactions at early ages", J. of the PCA Res. and Dev. Lab. (Portland Cement Association) **7**, No. 3, 57–63 (1965).
80. O. Henning and W. Danowsky, "Studies of the hydration of calcium (3:1) aluminate in the presence of gypsum. Part 1: High-frequency conductivity measurements" (in German), Silikattechnik **16**, 284–286 (1965).
81. N. Tenoutasse, "Investigation into the kinetics of the hydration of tricalcium aluminate in the presence of calcium sulphate and calcium chloride" (in German), Zement-Kalk-Gips **20**, 459–467 (1967).
82. R. F. Feldman and V. S. Ramachandran, "The influence of $CaSO_4 \cdot 2H_2O$ upon the hydration character of $3CaO \cdot Al_2O_3$", Mag. of Concrete Research **18**, No. 57, 185–196 (1966).
83. J. F. Young, "Hydration of tricalcium aluminate with lignosulphonate additives", Mag. of Concrete Research **14**, No. 42, 137–142 (1962).
84. N. Kawada and M. Nishiyama, "Actions of calcium lignosulfate upon portland cement clinker compounds" (in Japanese), Semento Gijutsu Nenpo **14**, 41–47 (1960).
85. J. Kasai, "Hydration of cements from the view point of complex chemistry", Yogyo Kyokaishi **71**, C55–59 (1963).
86. L. Forsen, "The chemistry of portland cement as complex chemistry" (in German), Zement **22**, 73–77 (1933).
87. H. N. Stein, "Mechanism of the hydration of $3CaO \cdot Al_2O_3$", J. appl. Chem. **13**, 228–232 (1963).
88. H. N. Stein, "Influence of quartz on the hydration of $3CaO \cdot Al_2O_3$", Symposium on Structure of Portland Cement Paste and Concrete, Highway Research Board, 368–377 (1966).
89. P. Sylvan, "The granulometric composition of cement" (in German), Zement-Kalk-Gips **17**, 299–301 (1964).
90. J. Gronau, "A new method for determining the degree of hydration of portland cement brick" (in German), Silikattechnik **18**, 143–146 (1967).
91. B. Beke and L. Opoczky, "Structural deformation by pulverizing of clinker in extreme fine grade" (in German), Dechema-Monographien Nr. 993–1026 Band 57 Zerkleinen 495–508 (1967).
92. G. Sudoh and H. Mori, "The influence of the different amounts of mixing water and alkali on the hydration of C_3S" (in Japanese), Semento Gijutsu Nenpo **15**, 46–54 (1961).
93. D. L. Kantro, C. H. Weise and S. Brunauer, "Paste hydration of beta-dicalcium silicate, tricalcium silicate and alite", Symposium on Structure of Portland Cement Paste and Concrete, Highway Research Board, 309–327 (1966).
94. F. W. Locher, "Stoichiometry of tricalcium silicate hydration", Symposium on Structure of Portland Cement Paste and Concrete, Highway Research Board, 300–308 (1966).
95. D. L. Kantro, S. Brunauer and C. H. Weise, "The ball-mill hydration of tricalcium silicate at room temperature", J. Colloid Sci. **14**, 363–376 (1959).
96. D. L. Kantro, S. Brunauer and C. H. Weise, "Development of surface in the hydration of calcium silicate. II. Extension of investigations to earlier and later stages of hydration", J. Phys. Chem. **66**, 1804–1809 (1962).
97. O. P. Mchedlov-Petrosyan and V. L. Chernyavskii, "Influence of low temperatures on the process of hydration of portland cement" (in German), Silikattechnik **18**, 72–76 (1967).
98. E. T. Carlson, "The system lime-alumina-water at 1°C" J. Research NBS **61**, 1–11 (1958).
99. H. F. W. Taylor, "A review of autoclaved calcium silicates", International Symposium on Autoclaved Calcium Silicate Building Products, London, 1965, Soc. of Chem. Ind. 195–205 (1967).
100. D. R. Moorehead and E. R. McCartney, "The mechanism of the quartz-lime solution reaction at temperatures up to 500°C", International Symposium on Autoclaved Calcium Silicate Building Products, London, 1965, Soc. of Chem. Ind. 86–91 (1967).
101. S. A. Krzheminskii, L. N. Rashkovich, N. K. Sudina and V. P. Vormalov, "Influence of the composition of the mixture and the temperature of hydrothermal treatment on the kinetics of interaction of lime and quartz", International Symposium on Autoclaved Calcium Silicate Building Products, London, 1965, Soc. of Chem. Ind. 110–113 (1967).
102. Z. Šauman, "Hydration rate of dicalcium silicate in mixes with quartz under hydrothermal conditions", International Symposium on Autoclaved Calcium Silicate Building Products, London, 1965, Soc. of Chem. Ind. 101–109 (1967).
103. R. Kondo, S. Ohsawa, H. Matsumaru, M. Kitamura and T. Kato, "The hydrothermal reactions between lime and siliceous materials" (in Japanese), Semento Gijutsu Nenpo **21**, 91–100 (1967).
104. H. Knoblauch, "Hydration velocity of the cement clinker minerals tricalcium silicate and dicalcium silicate" (in German), Tonindustrie-Zeitung **82**, 36 (1958).
105. A. van Bemst, "Hydration of calcium silicate: Determination of the chemical composition of hydrosilicate formed" (in French), Industrie Chim. belge. **20**, 67–70 (1955).
106. The Chemistry of Cements, Vol. I (Academic Press, London and New York, 1964), Edited by H. F. W.

Taylor. See chapter 8 by L. E. Copeland and D. L. Kantro entitled "Chemistry of hydration of portland cement at ordinary temperature".
107. D. R. Moorehead and E. R. McCartney, "Hydrothermal formation of calcium silicate hydrates", J. Am. Ceram. Soc. **48**, 565–569 (1965).
108. H. Tanaka, K. Murakami and M. Sato, "Studies on the hydration of calcium aluminoferrite phase and its glass in portland cement clinker" (in Japanese), Yogyo Kyokaishi **74**, 20–27 (1966).
109. G. K. Layden and G. W. Brindley, "Kinetics of vapor-phase hydration of magnesium oxide", J. Am. Ceram. Soc. **46**, 518–522 (1963).
110. P. F. Low, "Influence of adsorbed water on exchangeable ion movement", Clays and Clay Minerals Vol. 9 (Pergamon Press, Oxford, London, New York, Paris, 1962). 219–228.
111. T. M. Lai and M. M. Mortland, "Self-diffusion of exchangeable cations in bentonite", Clays and Clay Minerals Vol. 9 (Pergamon Press, Oxford, London, New York, Paris, 1962). 229–247.
112. A. Rao and L. V. C. Rees, "Kinetics of ion exchange in mordenite" Trans. Faraday Soc. **62**, 2505–2512 (1966).
113. S. A. Greenberg and T. N. Chang, "The hydration of tricalcium silicate", J. Phys. Chem. **69**, 553–561 (1965).
114. Yu. S. Malinin, L. Ya. Lopathikova, V. I. Guseva and N. D. Klishanis, "On hydration and hardening of portland cement", paper is presented at the International Conference on the Problems of Accelerated Hardening of Concrete in Manufacturing Precast Reinforced Concrete Units, RILEM, Moscow July 1964, 34 pp.
115. L. S. Wells and E. T. Carlson, "Hydration of aluminous cements and its relation to the phase equilibria in the system lime-alumina-water", J. Research NBS **57**, 335–348 (1956).
116. O. P. Mchedlov-Petrosyan and G. A. Salop, "Study of the setting process by measurement of the pH value" (in German), Silikattechnik **17**, 205–209 (1966).
117. T. P. Melia, "Crystal nucleation from aqueous solution", J. appl. Chem. **15**, 345–357 (1965).
118. K. Takiyama, "Precipitation from homogeneous solution (V)" (In Japanese), Hyomen **3**, 854–860 (1965).
119. I. Uhara, "Crystal nucleus" (in Japanese), Hyomen **5**, 611–619 (1967).
120. T. Sakurai, S. Ueda, M. Hashimoto and M. Fukunaga, "Early hydration of aluminous cement" (in Japanese), Semento Gijutsu Nenpo **20**, 86–91 (1966).
121. H. Funk, B. Schreppel and E. Thilo, "On the primary intermediate product by the hydration of β-Ca_2SiO_4 and on the formation mechanism of lime-rich tobermorite-like calcium silicate hydrate" (in German), Z. anorg. u. allgem. Chem. **304**, 12–24 (1960).
122. P. Terrier and M. Moreau, "Microscopic examination of portland cement paste" (in French), Rev. Matér. Constr. Trav. Publics No. 584, 129–137 (1964).
123. L. E. Copeland, E. Boden, T. N. Chang and C. H. Weise, "Reactions of tobermorite gel with aluminates, ferrites and sulfates", J. of the PCA Res. and Dev. Lab. (Portland Cement Association) **9**, No. 1, 61–74 (1967).
124. S. Diamond, "Coordination of substituted aluminum in tobermorite", J. Am. Ceram. Soc. **47**, 593–594 (1964).
125. T. C. Powers, "Physical properties of cement paste", Proceedings of the Fourth International Symposium on the Chemistry of Cement, Washington, 1960, NBS Monograph 43, 577–609 (1962).
126. L. I. Edel'man, D. S. Sominskii and N. V. Kopchikova, "Pore size distribution in cement rock" (in Russian), Kolloid Zhur. **23**, 228–233 (1961).
127. R. Sh. Mikhail, L. E. Copeland and S, Brunauer, "Pore structures and surface area of hardened portland cement pastes by nitrogen adsorption", Can. J. Chem. **42**, 426–438 (1964).
128. H. E. Schwiete and U. Ludwig, "On the determination of open pores in cement stone" (in German), Tonindustrie-Zeitung **90**, 562–574 (1966).
129. The Structure and Properties of Porous Materials (Butterworths Scientific Publications, London, 1958), Edited by D. H. Everett and F. S. Stone. See paper by J. H. de Boer entitled "The shapes of capillaries", 68–94.
130. T. C. Powers, L. E. Copeland and H. M. Mann, "Capillary continuity or discontinuity in cement pastes", J. of the PCA Res. and Dev. Lab. (Portland Cement Association) **1**, No. 2, 38–48 (1959).
131. R. F. Feldman and V. S. Ramachandran, "Character of hydration of $3CaO \cdot Al_2O_3$", J. Am. Ceram. Soc. **49**, 268–273 (1966).
132. R. F. Feldman and P. J. Sereda, "Sorption of water of compacts of bottle-hydrated cement. I. The sorption and length-change isotherms. II. Thermodynamic considerations and theory of volume change", J. appl. Chem. **14**, 87–93, 93–104 (1964).
133. B. Kroone and D. N. Crook, "Studies of pore size distribution in mortars", Mag. of Concrete Research **13**, No. 39, 127–132 (1961).
134. B. Kroone and D. N. Crook, "Further studies of pore size distribution in mortars", Mag. of Concerte Research **14**, No. 40, 43–46 (1962).
135. V. B. Ratinov, G. D. Kurcheryaeva and G. G. Melentéva, "Thermodynamic and diffusion characteristics of the silicate components in portland cement in their dissolution process in water" (in Russian), Dokl. Akad. Nauk SSSR. **136**, 875–878 (1961).
136. J. W. T. Spinks, H. W. Baldwin and T. Thorvaldson, "Trace studies of diffusion in set portland cement", Can. J. Techn. **30**, 20–28 (1952).
137. J. A. Forrester and C. D. Lawrence, "Self-diffusion of calcium ions in the equilibrium system calcium silicate hydrate-lime solution", J. appl. Chem. **11**, 413–420 (1961).
138. T. C. Powers, "Some physical aspects of the hydration of portland cement" (in German), Zement-Kalk-Gips **14**, 81–87 (1961). Research Lab. Portland Cement Association Bull. **125**, 47–56 (1961).

139. The Chemistry of Cements, Vol. I (Academic Press, London and New York, 1964), Edited by H. F. W. Taylor. See chapter 7 by S. Brunauer and D. L. Kantro entitled "The hydration of tricalcium silicate and β-dicalcium silicate from 5°C to 50°C".
140. R. Kondo and S. Ueda, new data.
141. J. H. Taplin, "Hydration kinetics of calcium sulphate hemihydrate", Nature, London, **205**, 864–866 (1965).
142. H. zur Strassen, "The problem on the non-selective hydration of cement minerals" (in German), Zement u. Beton No. 16, 32–34 (1959).
143. D. S. Coleman and W. F. Ford, "The effect of crystallite size and micro porosity on the hydration of magnesia", Trans. Brit. Ceram. Soc. **63**, 365–373 (1964).
144. W. Jander, "Solid state reactions at high temperature" (in German), Z. anorg. u. allgem. Chem. **163**, 1–30 (1927).
145. R. Kondo and S. Choi, "Mechanisms and kinetics of portland cement clinker formation for an example of the solid state reaction in the presence of a liquid phase", paper is presented in this Symposium.
146. A. M. Ginstling and B. I. Brounshtein, "Concerning the diffusion kinetics of reactions in spherical particles", J. Appl. Chem. (USSR) **23**, 1327–1338 (1950).
147. R. E. Carter, "Kinetic model for solid-state reactions", J. Chem. Phys. **34**, 2010–2015 (1961).
148. J. H. Taplin "The temperature coefficient of the rate of hydration of β-dicalcium silicate", Proceedings of the Fourth International Symposium on the Chemistry of Cement, Washington, 1960, NBS Monograph 43, 263–266 (1962).
149. V. B. Ratinov and A. L. Lavut, "Study of hydration kinetics of portland cement clinker minerals" (in Russian), Dokl. Akad. Nauk SSSR. **146**, 148–151 (1962).
150. H. N. Stein, "Some characteristics of the hydration of $3CaO \cdot Al_2O_3$ in the presence of $CaSO_4 \cdot 2H_2O$", Rec. trav. chim. pays-bas **81**, 881–889 (1962).
151. R. Kondo and M. Kodama "On the hydration kinetics of cement" (in Japanese), Semento Gijutsu Nenpo **21**, 77–82 (1967).

Written Discussion

Hans N. Stein

Dr. Kondo and Mr. Ueda are to be congratulated for having derived mathematical expressions that can be applied to the mechanism proposed for the hydration of C_3S by Kantro, Brunauer and Weise (1) and by Stein and Stevels (2) (3) (4).

These authors adduced experimental arguments indicating that during the accelerated phase of C_3S hydration, the reaction rate is determined by the transition of a closely fitting, strongly retarding first hydrate (=F. H., probably C_3SH_n) into a second one, less retarding one (=S. H., probably CSH-I). This transition was found to be determined by the amount of S. H. nuclei present. It appears from Kondo and Ueda's paper that this mechanism is corroborated by recent measurements of theirs.

The equations of Kondo and Ueda are, in principle at least, capable of dealing with this mechanism. However, in their derivation one very important factor, viz. the rate of formation of S. H. nuclei, has not yet been fully worked out. In Kondo and Ueda's paper, the rate of S. H. nucleus formation is thought to be independent of time, i.e. independent of the concentrations in the aqueous phase. This, however, is improbable and at variance with the experimental results that led to the mechanism mentioned (viz. the influence of amorphous silica on the suspension hydration of C_3S). The introduction of parameters (t_1 and n in Kondo and Ueda's final equation) may make the equation fit experimental data, but this procedure may conceal rather than solve the fundamental difficulties. It is clear that the theory must be supplemented on this point before it can be applied with confidence.

References

1. D. L. Kantro, S. Brunauer and C. H. Weise, J. Phys. Chem. **66**, 1804 (1962).
2. H. N. Stein and J. M. Stevels, J. Appl. Chem. **14**, 338–346 (1964); Silicates Industriels **32**, (10), 337–343 (1967).
3. H. N. Stein and J. M. Stevels, J. Phys. Chem. **69**. 2489 (1965).
4. J. G. M. de Jong, H. N. stein and J. M. Stevels, J. Appl. Chem. **17**, 246–250 (1967).

Written Discussion

John H. Taplin

Kondo and Ueda state that a kinetic equation of mine (1) defines two diffusion constants but omits a factor which is the fraction of material which eventually diffuses outwards. The equation was originally given as:

$$i[1 - (1 - F)^{2/3} - 2F/3] + (o/v)[1 + 2vF/3 - (1 + vF)^{2/3} = 2Ct/R^2 \quad (1)$$

The quantities i and o were stated to be specific resistances. If C is the concentration difference and if D_i is the diffusion coefficient of outward moving material, in the inner products, then a/D_i can be written for i. However "a" is not the fraction of material which diffuses out, it is the concentration in the cement mineral, of the material involved in the rate controlling diffusion.

In a Supplementary paper to this Symposium (2) it has been argued that equation (1) is more likely to apply to the inward diffusion of water than to the outward diffusion of soluble products. However equation (1) could still apply to outward diffusion if the cement mineral, or some thin impermeable coating or its surface, is able to come to equilibrium with the aqueous solution so as to maintain the constant concentration difference, C, which was assumed in deriving equation (1).

However, equation (1) applies to a particle of radius R. In order to take account of the particle size distribution possessed by most powders, it is convenient to approximate equation (1). It is more accurate (3) to use equation (2) rather than Jander's eqaution.

$$dF/d(t^z) = k_z(1 - F)^N/R \quad (2)$$

where $z = 2$ for parabolic kinetics and where N is always well below the 2/3 value given by Jander's approximation. For example:

N = 0.43 for quadratic kinetics (all diffusion resistance in the inner products)

N = 0.30 for $i = 0$, as in Valensi's equation (4), and $v = 1$

Of course, the exact effect of particle size distribution on the reaction kinetics of a powder depends on the nature of the particle size distribution. However, the effect can be illustrated for linear kinetics, as follows. Let $(f)_R$ be the frequency function on a weight basis so that the proportion of the powder consisting of particles with a radius greater than R is $\int_R^\infty (f)_R\, dR$. If the particles keep their shape as they react then:

$$(1 - F)_R = (1 - p/R)^3 \quad (3)$$

where p is the distance the reaction has penetrated a particle of size R. For simplicity, assume linear kinetics so that p is independent of R, $p = kt$. For the whole powder

$$\int_p^\infty (1 - F)_R\, (f)_R\, dR \quad (4)$$

By differentiating equation (4) four times with respect to p it follows that:

$$(1 - F) = 6\,(f)_p/p^3$$

or

$$(f)_p = p^3(1 - F)^{IV}/6 \quad (5)$$

Integrating equation (5) by parts, we obtain:

$$\int_0^P (f)_R\, dR = F - \sum_1^3 (-p)^n\, (1 - F)^n/n! \quad (6)$$

An important difference between a mono-sized powder and one with a range of sizes is that the surface area of the mono-sized powder decreases more slowly as it reacts. This fact suggests a modification of equation (2) where allowance is made for a range of sizes by increasing the value of N. Assume

$$dF/dt = Akp(1 - F)^M \quad (7)$$

for a powder reacting by linear kinetics where A is the specific surface area, ρ the density and $M > 2/3$. By using $p = kt$, making the necessary differentiations, and substituting in equation (6), the appropriate cumulative particle size distribution is found. For example for $M > 1$.

$$\int_0^x (f)_x\, dx = 1 - q^L[1 + x/q + Mx^2/2q^2 + M(2M - 1)x^3/6q^3] \quad (8)$$

where $L = 1/(1 - M)$ and $q = 1 - (1 - M)x$

Fig. 1 is a log probability plot of three distributions of size which, for linear kinetics, will obey equation (7) with M = 1, 1.5 and 2.0. It will be seen that at the lower values of M the distributions are approximately lognormal.

This effect of particle size distribution, means that plots of $\ln[1 - (1 - F)^{1/3}]$ versus $\ln(t)$, as used by Kondo and Ueda in their Fig. 1, are difficult to interpret except for closely sized materials such as their C_3S samples. Consider particle size distributions such as are found for commercial portland cements. The

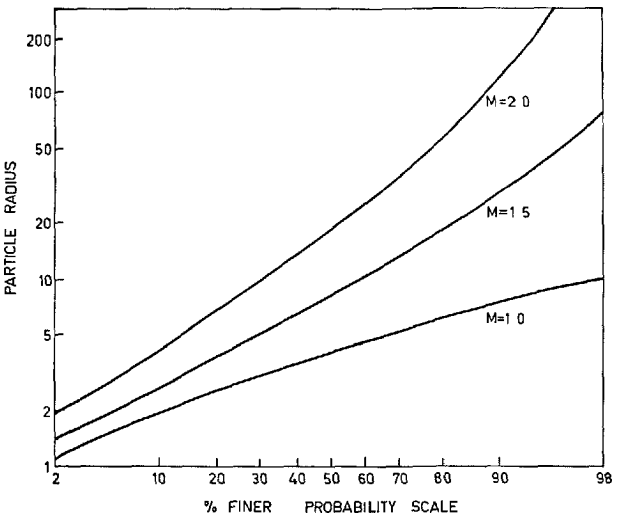

Fig. 1. *Log probability plots of particle size distributions of powders which, for linear kinetics, meet the following requirements: (i) the reaction rate is proportional to* $(1 - F)^M$ *(ii) the particles retain their shape as they react*

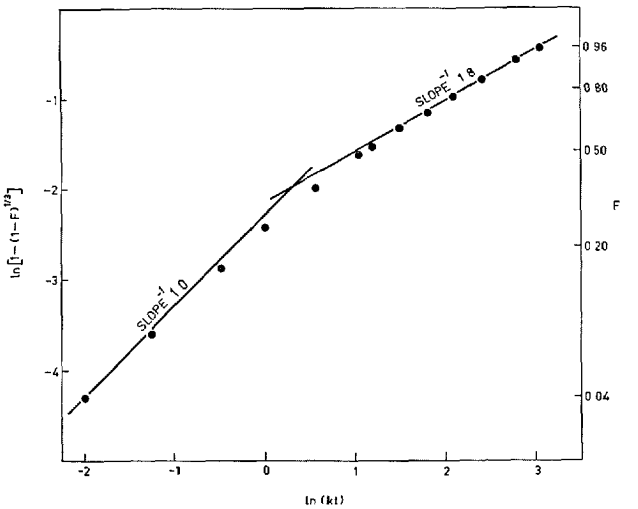

Fig. 2. *The failure of the relation,* $[1 - (1 - F)^{1/3}] \propto t$, *for the linear reaction of a hypothetical powder of spherical particles with a Furnas distribution of sizes approximating that found in commercial portland cements*

Furnas distribution usually fits cement data closely from a radius of 1.7 to about 25 microns (5), i.e. from about 8 to 90% passing. For $C \neq 0$, the Furnas distribution is

$$\int_0^x (f)_R \, dR = (R^C - R_0^C)/(R_1^C - R_0^C)$$

The linear and quadratic kinetics were computed for a size distribution typical of a cement, $C = 1/2$, $R_0 = 0.84$ microns and $R_1 = 31.5$ microns. Fig. 2 is a plot of $\ln [1 - (1 - F)^{1/3}]$ versus $\ln (kt)$ for linear kinetics. If interpreted as the kinetics of a mono-sized powder it would suggest a transition to diffusion kinetics at about a third of the way through the reaction. Fig. 3 is a similar plot for quadratic kinetics. Again the initial slope is that expected for a mono-sized powder and again it falls as the reaction proceeds. These plots would show even greater curvature if allowance was made for the usual deviation of cement from the Furnas distribution. There is usually 5–10% of material which is coarser than the fitted R_1.

Nucleation, crystal growth, dissolution and diffusion are some of the possible rate controlling processes in the hydration of cement. In trying to distinguish between them, the effect of particle size distribution can hardly be ignored. In the later stages

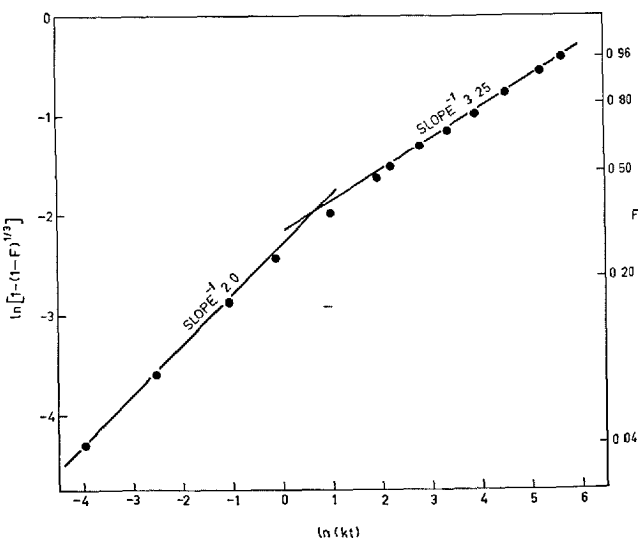

Fig. 3. *The failure of the relation,* $[1 - (1 - F)^{1/3}]^2 \propto t$, *for the parabolic reaction (diffusion resistance in inner products) of a hypothetical powder of spherical particles with a Furnas distribution of sizes approximating that found in commercial portland cements*

of the reaction, this size distribution effect is generally about as great in comparison with a mono-sized powder as is a change from a linear to a parabolic reaction mechanism.

References

1. J. H. Taplin, Proceedings of the Fourth International Symposium on the Chemistry of Cement, Washington, D. C. 1960, N. B. S. Monograph 43, 263–266 (1962).
2. J. H. Taplin, "On the hydration kinetics of hydraulic cements", paper II-70 this Symposium.

3. J. H. Taplin, "A steady state kinetic model for solid-fluid reactions" to be presented to the American Ceramic Society in October, 1968.
4. M. G. Valensi, Comptes Rendus **202**, 309 (1936).
5. J. H. Taplin, unpublished.

Written Discussion

Rolf F. Feldman

In this very comprehensive review the authors have discussed the various parameters that control the rate of hydration of a solid. These can be categorized as follows:

(a) Reactivity of the solid,
(b) Nucleation and crystal growth,
(c) Mass transfer through the solid product.

The authors have also outlined how these parameters may be affected by the addition of foreign molecules or ions. It is the purpose here to discuss the effect of sulphate ions on the hydration of C_3A.

On the assumption that the rate-controlling process is the rate of decomposition of the solid, sorption of ions on surface sources of dislocation may decrease the reaction rate, effectively decreasing the reactivity of the solid. Foreign molecules can also affect the number of nuclei available for crystallization and modify the rate of growth and morphology of crystals. They may even alter the product of hydration more drastically: for example, the presence of sulphate ion prevents, for a time, the conversion of hexagonal hydro-aluminates to the cubic hexahydrate (1) in the hydration of C_3A. It is this conversion that accelerates the normal hydration of C_3A (2).

The additive might affect the rate of hydration through the third category by changing the nature of the solid product (as stated previously) that might accumulate around the reactant. This has been the most common explanation for the retardation of C_3A hydration in the presence of additions of gypsum. It has been concluded that ettringite forms a dense impermeable layer around unhydrated C_3A grains, thereby retarding the reaction.

The main purpose of this discussion is to show that the above conclusion may be premature. If it is accepted that the rate of diffusion through the solid product is the rate-controlling process, then one is faced with two possibilities:

(1) The product modified by the additive has a greater density and impermeability than the product formed without the additive. In the case of the hydration of C_3A in the presence of gypsum, it is generally concluded that ettringite, which forms around the unhydrated C_3A, has these properties of high density and impermeability relative to the properties of the hexagonal hydroaluminate. The latter product forms around the C_3A during its earlier periods of hydration in the absence of gypsum.

(2) The effect of the sulphate ion in small pores with its high electric-field intensity may significantly reduce the rate of mass transport through the solid product.

This mechanism for retardation will then remove the necessity of giving special properties to the ettringite layer.

The importance attached to the nature of the solid product requires an understanding of the formation of the structure of a body when the solid product forms during hydration. The nature of the stresses and strains produced during hydration should provide some information on whether the layer around the unhydrated grains will be dense and impermeable.

The final structure of an agglomeration of particles of a solid which may undergo a reaction with water depends upon many factors. The morphology of the product and the place where it is deposited must be considered as part of the over-all reaction mechanism; reaction conditions may affect all of these. The state of the structure and the volume change of the body reflect the morphology of the product and its place of deposition. Volume or length change may be large or small; a large length change does not necessarily lead to a weak and soft body. When the expansion leads to a weak and soft structure, it is considered disruptive.

Compaction of the solid reactant tends to emphasize some of the properties of the reaction by bringing particles in contact and, although compaction may alter the relative periods at the different stages of the reaction, it must be kept in mind that a body of low porosity is also the final product of normal paste hydration. Studies of length change of compacts of several materials during hydration have been made to aid in understanding the nature of the stresses and strains involved during formation of the solid product. It was assumed that the forces that cause expansion of the body would also operate in the formation of a layer around a grain of unhydrated material; results have led us to believe that this is so.

The fact that hydration reactions involve an increase in the volume of solid product over solid reactants

does not account for the various types of length change and structuring during reaction. At the beginning of hydration, expansion of the compact is caused by the thrust of the product at or close to the points of contact of the grains of the reactants. In some cases, this expansion is slight and a fairly dense impermeable product is built around each grain and penetrates into the pore spaces. The structure of the body would then consist of a dense impermeable product and should be and is of good strength and low porosity. The hydrate product is probably continuous but the unhydrate material is embedded in it, and the reaction is terminated or almost so by the lack of space or water. Examples of this type of reaction with the solid in compact form are C_3S and β-C_2S both with linear expansion of 0.10 to 0.15 per cent (3) and portland cement with 0.3 per cent (4).

The hydration of $CaSO_4 \cdot 1/2H_2O$ compacts (5) is accompanied by somewhat larger linear expansions (from 1 to 4 per cent,) depending upon the hydration conditions, but also produces a strong fairly dense body. The expansion in this case is not disruptive. Slurries of calcium sulphate hemi-hydrate may produce linear expansions of 0.5 per cent. CaO hydrates with a disruptive expansion in the presence of water vapour (6); there is a weakening of the structure during hydration, little or no reduction in reaction rate, and a complete disintegration of the body, leaving only a powder. Under these conditions, one cannot visualize the formation of a dense impermeable product around the CaO particles because this would mean that the unhydrated material was joined together and surrounded by the dense product (thereby forming a strong body) and that the reaction rate had been drastically reduced.

The reaction of CO_2 with compacts of $Ca(OH)_2$ in the presence of water vapour (7) is an example of another type of structuring. Although the reaction produces an increase in solid volume, densification of the body is accompanied by shrinkage up to 0.3 per cent linear measurement.

These examples show something of the complex nature and relationship of length change to structuring and reaction mechanism.

The expansive behaviour observed for the compacts of mixtures of C_3A with 10 and 20 per cent gypsum was disruptive; the body was in fact a "much". It is difficult to see how, in the light of the above discussion, this can be the result of a special dense and impermeable product of ettringite. The retardation of C_3A hydration by gypsum when the reaction is controlled by diffusion is thus considered to be due to the effect of the electric field intensity of sulphate ions upon mass transport through small pores.

In contrast to this, hydration of C_3A at 52°C (8) produced a firm strong product, and the expansion of the compact was only 0.7 per cent after 4 days, most of this taking place in less than one hour. The degree of hydration was only 17 per cent although plenty of pore space was available for hydrate product. It appeared clear that, under these conditions of hydration, there was a dense impermeable product of $C_3A \cdot H_6$ around the C_3A grains.

References

1. R. F. Feldman and V. S. Ramachandran, "The influence of $CaSO_4 \cdot 2H_2O$ upon the hydration character of $3CaO \cdot Al_2O_3$", Mag. of Concrete Research **18**, No. 57, 185–196 (1966).
2. H. N. Stein, "Mechanism of the hydration of $3CaO \cdot Al_2O_3$," J. Appl. Chem. **13**, 228–232 (1963).
3. R. F. Feldman, unpublished information.
4. R. F. Feldman, P. J. Sereda and V. S. Ramachandran, "A study of length changes of compacts of portland cement on exposure to H_2O," Highway Research Board, No. 62, 106–118 (1964).
5. P. J. Sereda, R. F. Feldman and V. S. Ramachandran, "Hydration of gypsum plaster by the compact technique," Amer. Cer. Soc. Bull. **44**, 151–155 (1965).
6. V. S. Ramachandran, P. J. Sereda and R. F. Feldman, "Mechanism of hydration of CaO," Letter to Nature **201**, 288–289 (1964).
7. E. G. Swenson and P. J. Sereda, "A mechanism for carbonation shrinkage of lime and hydrated cement," J. Appl. Chem. **18**, 111–117 (1968).
8. R. F. Feldman and V. S. Ramachandran, "Character of hydration of $3CaO \cdot Al_2O_3$", J. Amer. Ceramic Soc. **49**, 268–273 (1966).

Oral Discussion

J. Albeck, Udo Ludwig and Hans E. Schwiete

Our investigations (1, 2) of the hydration of aluminate-ferrite phase (W/S = 1.0–1.2) of portland clinker and of technical clinkers (W/S = 0.5) together with $CaSO_4$ (as anhydrite or dihydrate) and increasing amounts of $CaCl_2$ in lime saturated pastes can be summarized as follows:

1. In accordance with Schwiete, Ludwig and Jäger (3) we found a decrease of reaction velocity of the following clinker minerals with dihydrate and anhydrite in lime saturated pastes:

$$C_3A \longrightarrow C_6A_2F \longrightarrow C_4AF \longrightarrow C_2F$$

Correspondingly the sulphate combination velocity of clinkers decreases with decreasing C_3A content of the clinker.

2. With anhydrite the sulphate fixation of the aluminate-ferrite phases and the clinkers itself is more rapid than with dihydrate. This is due to the lower dissolving velocity and the therefore minor tendency for initial formation of ettringite coatings.

3. The addition of $CaCl_2$ accelerates the sulphate fixation. Increasing amounts of $CaCl_2$ are effecting increasing accelerations. This effect is due to the reduction respectively prevention of the ettringite layer on the aluminate-ferrite phases of the clinker grains.

4. With 20% of Cl^- addition we found in the first minutes of hydration (up to 30 minutes) the simultaneous formation of $C_3(A, F)\cdot 3CaCl_2\cdot H_{30}$, $C_3(A, F)\cdot 3CaSO_4\cdot H_{32}$ and $C_3(A, F)\cdot CaCl_2\cdot H_{10}$, afterwards the formation of the two latter salts only. That means in disagreement with Tenoutasse (4)—that $CaCl_2$— and $CaSO_4$-fixation runs at higher $CaCl_2$-content simultaneous.

5. The reaction of $CaCl_2$ to Friedel salt stabilizes the initial formed ettringite for there are minor aluminate ions for the formation of $C_3(A, F)\cdot CaSO_4\cdot H_{12}$ or the solid solution series $C_3(A, F)\cdot(Ca(OH)_2, CaSO_4)H_{12}$.

6. On slurries (W/S = 10) with C_3A an increasing $CaCl_2$-content leads to an increasing Al_2O_3 and a decreasing SO_3 content and pH value in the filtered solution. By this we establish the minor formation of ettringite coatings.

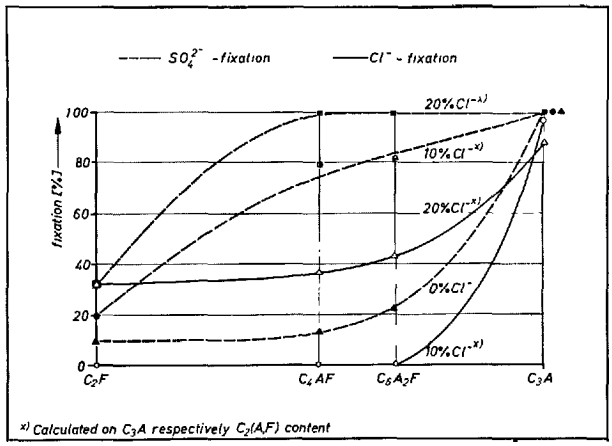

Fig. 1. *One day's* $CaCl_2$*-and* $CaSO_4$ *fixation of aluminatic ferritic clinker phases* ($W/S = 1.0 - 1.2$)

Table 1. Al_2O_3 *-and* SO_3*-concentration and pH-value after 30 minutes hydration in lime saturated solution*

1) 10,0 g C_3A + 6,0 g $CaSO_4\cdot 2H_2O$ + 1,82 g $Ca(OH)_2$
2) 10,0 g C_3A + 6,0 g $CaSO_4\cdot 2H_2O$ + 1,82 g $Ca(OH)_2$ + 1,82 g $CaCl_2\cdot H_2O$
3) 10,0 g C_3A + 6,0 g $CaSO_4\cdot 2H_2O$ + 1,82 g $Ca(OH)_2$ + 3,64 g $CaCl_2\cdot H_2O$
x) Calculated on C_3A-content
W/S = 10 t = 30 min

		Al_2O_3 (mg in solution)	SO_3 (mg in solution)	pH
1	0% Cl^-	0,14	149,40	12,85
2	10% $Cl^{-x)}$	0,17	110,00	12,63
3	20% $Cl^{-x)}$	0,26	106,25	12,50

References

1. H. E. Schwiete, U. Ludwig, and J. Albeck: "Investigations of $3CaO\cdot Al_2O_3\cdot 3CaCl_2\cdot 30H_2O$"(in German), Die Naturwissenschaften 55 (1968) 179.
2. H. E. Schwiete, U. Ludwig, and J. Albeck: "Fixation of $CaCl_2$ and $CaSO_4$ during hydration of aluminate-ferrite clinker minerals" (in German)—Zement-Kalk-Gips (report is prepared).
3. H. E. Schwiete, U. Ludwig and P. Jäger: "Investigations on the hydration of C_3A, C_2F, C_4AF and C_6A_2F with calcium hydroxide and calcium sulphates," Published by the Institut für Gesteinshüttenkunde der RWTH Aachen (1967).
4. W. L. De Keyser and N. Tenoutasse: "Physico-chemical principles of the action of the admixtures with various cements and concretes," International Symposium on Admixtures and Concrete, Brussels, August 30th—September 1st 1967.

Authors' Closure

Renichi Kondo and Shunro Ueda

Three written discussions were given to our paper. First of all, Dr. Stein pointed out the similarity of ideas on the explanation of acceleratory period between our's and of other investigators. But the reason why the reaction in the acceleratory period takes place can hardly be explained logically simply by insisting that the propective layer splits off as viewed by Messers Kantro, Brunauer and Weise. Their theory cannot explain satisfactorily the mechanism that the reaction of this period is accelerated as the splitting off makes expose the new unreacted surface. According to us, the sudden reaction in the acceleratory period can be explained mathematically by considering that the protective layer partially becomes porous. We made reference to this point in our principal paper.

Dr. Stein also pointed out that the kinetic equation of the nucleation as conceived by us didn't take the concentration of liquid into our consideration. To this comment we have described that the nucleation rate is functioned with the liquid concentration, in the section of "Nucleation and Crystal Growth". On the other hand, our own data shows that the liquid concentration remains for a while in comparatively same level during the course of the acceleratory period. By taking advantage of this phenomenon, we obtained the equation as shown in the section "Rate determining step in hydration" by going so far as setting the liquid concentration at constant.

In his discussion, an empirical equation which appeared in principal paper's last page was criticized as having escaped the difficulty in the fundamental solution. In response to this comment, we wish to point out that there is a fear of perfunctory handling even if a theoretical equation is forcively induced, as there are many doubtful points in later stages of the reaction. As a first-hand step to cope with the difficulties, we are going ahead with a plan to seek the diffusion coefficient by using the radioactive isotope and observing the hydrate's structure by the electron microscope either scanning type or using the microtome.

The equation in which N was referred to as parameter is an empirical one. However, we explained already the relationship between N and diffusion coefficient or the compactness of the product layer in the section mentioned above so far as the concentration difference is constant. This is the very reason why we gave a temporary conclusion by utilizing this equation.

Next, Mr. Taplin raised an objection to our opinion in his written discussion that the factor "a" in the rate constant must be regarded as a concentration in the cement mineral of the material involved in the rate controlling diffusion, instead of a fraction of material which diffuses out. Our view on the terms, C, "a" and D in the rate constant will be here described in detail, since the examination of the rate constant is important in order to evaluate the magnitude of diffusion coefficient, although it is not incorrect to combine the terms such as "a" and D in the so called resistance as treated by Mr. Taplin.

As described in our principal paper, Mr. Taplin's equation can be reduced to the Ginstling's equation when the diffusion in the inner product layer determines the rate of reaction, and Ginstling's equation was improved by Kondo as follows:

$$[1-(1-\alpha)^{1/3}]^2-\frac{2}{3}[1-(1-\alpha)^{1/3}]^3=2DCt\frac{1}{ar_0^2}$$

where C is the concentration difference of the species involved in the rate controlling diffusion between outside and inside interfaces of the inner product. C is expressed as follows in consideration of the material balance:

$$\frac{\text{wt. difference of dissolved reactant (g)}}{\text{unit volume (cm}^3\text{)}}\times\frac{1}{\text{density of reactant (g/cm}^3\text{)}}$$

And the factor "a" is taken as the weight fraction of the material diffused out to the reacted reactant.

An example will be shown to clarify the characters of C and "a", and also to examine the order of D in a hydration reaction.

At first let us assume that the amounts and compositions of inner and outer products are the same in the hydration of C_3S, and the difference of concentrations in the liquid phase is 1.63 gC_3S/l. When the concentration is expressed on the liquid phase, it must be multiplied by a ratio of pore volume to total volume of the inner product, and this ratio estimated is approximately 0.2. And the density of C_3S is 3.2 g/cm³. Then

$$a=\frac{1}{1+1}=0.5,\quad C=\frac{1}{3.2}\times 0.2\times\frac{1.63}{1000}=0.0001$$

If we use C_3S powder with $r_0=3.5\,\mu$, the thickness of the reacted layer reaches $1-(1-\alpha)^{1/3}=0.06$ in 5 hrs (18000 sec.) from 5th to 10th hr. in early hydration, and $1-(1-\alpha)^{1/3}=0.285$ in 27 days (2330000 sec.) from 1st to 28th day in later hydration.

Then the magnitude of D can be estimated as follows. In the case of early hydration,

$$0.06^2-\frac{2}{3}\cdot 0.06^3$$

$$= 2 \times D \times 0.0001 \times 18000 \times \frac{1}{0.5 \times 0.00035^2}$$

$$D = 5.8 \times 10^{-11} \text{ cm}^2/\text{sec}$$

In the case of later hydration,

$$0.285^2 - \frac{2}{3} \cdot 0.285^3$$

$$= 2 \times D \times 0.0001 \times 2330000 \times \frac{1}{0.5 \times 0.00035^2}$$

$$D = 8.5 \times 10^{-12} \text{ cm}^2/\text{sec}$$

Next we shall assume that 1 mole C_3S reacts topochemically with water to form $C_{1.5}SH_n$ as the inner product and 1.5 mole CaO diffuses outerward to form $1.5Ca(OH)_2$ as the outer product, and the concentration difference is 1.2 gCaO/l. Then

$$a = \frac{1.5 \times \text{m.w. of CaO}}{\text{m.w. of } C_3S} = 0.37$$

This value may be called as the concentration in C_3S, of the material involved in the rate controlling diffusion as Mr. Taplin stated.

$$C = \frac{1}{3.2} \times \frac{\text{m.w. of } C_3S}{3 \times \text{m.w. of CaO}} \times 0.2 \times \frac{1.2}{1000}$$
$$= 0.0001$$

The value D can similarly be evaluated as follows: In the case of early hydration,

$$D = 4.3 \times 10^{-11} \text{ cm}^2/\text{sec}$$

In the case of later hydration,

$$D = 6.2 \times 10^{-12} \text{ cm}^2/\text{sec}$$

The evaluated value of D in hydration, thus obtained is a little lower than in paste or mortar. This is expectable, as only radial through pores around the reactant particles are available for material transfer in hydration reaction. On the other hand the diffusion in bulk specimen of paste or mortar must be mainly taken place in the pores of outer product. Regardless of the considerable amount of pore volume, the order of diffusion coefficient in hydration product, even in the bulk specimen, is as low as that in zeolites with very fine pores of several Å. Chemical interaction between the surface of pores and the diffusing species seems to be responsible for lowering the diffusion coefficient and worth systematical study in future.

In addition, we have recently received a private communication from Mr. Taplin, whose opinion is not fully agreed with us, but he described that we had the density of the reactant as a factor C whereas he had it as a factor of "a". He granted us an "a" which was the fraction of material which diffused out if we wrote for the right hand side of the equation $2DCt/apr_0^2$, where ρ is the density of reactant.

On the other hand, Mr. Taplin in his written discussion emphasizes the importance of the particle size distribution on the rate of hydration and gives the equation, which are believed very useful. However we do not think that we have ignored the effect of particle size distribution, so that we have used elutriated samples and discussed about it not only in the paper but also especially in the paper refered as number (69) in the former.

Finally it is generally considered that the retardation mechanism of C_3A hydration by added gypsum is attributable to the formation of a dense ettringite coating. But Mr. Feldman and his colleague have put forward an idea to the effect that the sorption of SO_4^{--} ions over the dislocations of the particle surface is related thereto. This idea was already referred to in our principal paper.

Mr. Feldman supplemented afresh with a view that where diffusion is rate controlling, the transport rate of mass such as water molecules can be reduced by the high electric field of SO_4^{--} ion within the small pore.

In connection with the hydration rate of cement, we attach importance to the necessity of clarifying the hydrate's conditions on the surface of cement compounds, and are actually going ahead with researches by utilizing either the surface electron diffraction or scanning electron microscope. As a matter of fact, we already have obtained considerably clear results which cover silicate hydration just as we mentioned in our principal paper. We further expect to be able to solve the problem of aluminate hydration by the similar method.

While on the other hand, we cited an example in Table 4 of our principal paper with respect to the mobility of various ions in the porous body. However, it is difficult to recognize such special trend as SO_4^{--} ion serving to lower down the diffusion coefficient more than other ions. Thus it is desirable to verify by further experiments Mr. Feldman's idea that the electric field has an effect on the rate of hydration.

In any case, we believe that his idea will serve as useful working hypothesis in pushing forward more detailed fundamental researches in days to follow.

(A) Papers regarding Mechanism

Supplementary Paper II-26 The Influence of Sugars on the Hydration of Tricalcium Aluminate

James F. Young*

Synopsis

The influence of monosaccharides and polysaccharides on the paste hydration of tricalcium aluminate (C_3A) was studied for periods up to 90 days using X-ray diffraction, thermal analysis and electron microscopy. Each of the sugars used was found to retard the hydration of C_3A. Sucrose and raffinose were strongly retarding at all ages, and trehalose, xylose and ribose were the least retarding. The other sugars studied gave intermediate results, although lactose, xylose and fructose were strongly retarding at very early ages. It was shown that the presence of sugars prevents the rapid formation of C_3AH_6 which is observed in pastes without additives. The principal hydration product was C_4AH_{13} while C_2AH_8 was often present; the morphology of these hydrates was considerably modified.

Sugars also influenced the formation of sulphoaluminates in pastes of C_3A and gypsum. Apart from some early acceleration by xylose, fructose and glucose, all sugars retarded the rate of formation of ettringite and its subsequent conversion to the low-sulphate sulphoaluminate hydrate. An increase in the rate of formation of ettringite was apparent after 14 days in pastes containing lactose, raffinose and sucrose. The morphology of ettringite was also modified by sugars.

The experimental results are discussed with reference to the different mechanisms of retardation that have been postulated. It is suggested that the complexing of organic compounds with metals, such as calcium or aluminium, could be the main factor underlying their behaviour as retarders.

Introduction

Interest in the use of organic compounds as potential set-retarding additives for cement has prompted several recent investigations (1–4) on their effects on the setting characteristics and hydration of cement pastes. However, apart from lignosulphonates and related materials, and with the exception of work by Suzuki and Nishi (2), no detailed study of the physical and chemical effects of organic additives on the hydration of cements and cement compounds has been reported.

This paper presents results of preliminary studies on the influence of organic compounds on the chemistry of the hydration of cement compounds. The saccharides were chosen for this initial study because earlier reports indicated that these compounds generally behave as strong retarders. Interest in sugars was stimulated by previous work with lignosulphonates (5) which themselves contained appreciable amounts of sugars and other carbohydrates as impurities. It has been shown (6) that the performance of lignosulphonate additives is not impaired by a high carbohydrate content and that sucrose behaves satisfactorily (6, 7) as an additive to concrete at low dosages (0.05% by wt. of cement) giving some decrease in water requirements and slight gains in strength at 7 and 28 days. Nevertheless, it appears that sugars are still viewed with concern by the concrete industry.

With the exception of trehalose (4) it has generally been found that all saccharides strongly retard the set of cement even when used at moderately low dosages. An earlier report (1) that fructose and raffinose are not strong retarders has not been substantiated (2, 4). Although sucrose may be the strongest retarding sugar, all sugars show complete inhibition of set after several days at high concentrations (> 0.25%) (1, 2). Suzuki and Nishi (2) found that large additions of sugar (1% by wt.) tend to promote flash set when the water: cement ratio is low.

*Chemistry Division, Department of Scientific and Industrial Research, Wellington, New Zealand.

Experimental

Materials

C_3A was prepared by repeatedly firing at 1300°C and grinding pellets made from the appropriate mixture of the constituent oxides. The C_3A had a specific surface area of 3430 cm^2/g. (air-permeability method), an initial free lime content of 2.1% and an iron content of 0.5% (from ball-mill contamination). No other phase was detected by X-ray diffraction, but a differential thermal analysis showed that the free lime was partially hydrated or carbonated and that trace amounts of C_3A were hydrated.

C_3A-gypsum mixtures were prepared by blending 2 parts by weight of C_3A to 1 part of AR gypsum in a Pascall end-runner mill.

The sugars were of laboratory reagent grades and were used without further purification. The following were used in this study: ribose, xylose, glucose, mannose, fructose (monosaccharides); sucrose, lactose, $\alpha\alpha$-trehalose (disaccharides); and the trisaccharide raffinose.

Preparation of Pastes

The sugars were dissolved in CO_2-free distilled water and the solutions cooled to 0°C before being mixed with solid. The concentration of the solutions was such that 1% sugar by wt. of C_3A was added at a water: solid ratio of 0.6. This dosage gives a sugar: C_3A ratio similar to that when 0.05–0.10% sugar is added to a typical cement, and it is sufficiently high to ensure that any change occurring is readily detectable.

The pastes were mixed by hand for 1–2 minutes in the glass vials in which they were stored. The tightly stoppered vials were then stored at 21°C over CO_2-free distilled water in a desiccator containing soda-lime. This procedure ensures protection against CO_2 during the hydration period and the maintenance of 100% R. H. within the vials.

At the end of each hydration period a vial was opened, the contents crushed where necessary and washed with acetone to remove excess water and stop hydration. A sample was set aside for immediate X-ray diffraction analysis and the remainder dried to constant weight over $MgCl_2 \cdot 6H_2O$ at 21°C (33% R. H.) in the absence of air. As the pastes were not protected from CO_2 during crushing and washing, the carbonation later observed would have occurred at this stage. The reactivity of different pastes with CO_2 from the air during this brief exposure was found to vary. The dried pastes were subsequently subjected to thermal analysis and, in some cases, to quantitative X-ray diffraction analysis.

Apparatus

Differential thermal analysis (DTA) was carried out on a "Deltatherm" instrument (Technical Equipment Corp.) using chromel-alumel thermocouples in contact with the samples and a heating rate of 10°C/min. Thermogravimetric analyses (TGA) were run on a Chevenard thermobalance at 5°C/min. A specially designed "cylinder and piston" sample, similar to that described by Garn and Kessler (8), was used so that the samples decomposed in self-generated atmospheres.

A Phillips Norelco X-ray diffractometer was used for diffraction (XRD) work using CuKα radiation with nickel filters. The scanning speed was 1° 2θ/min., the scale factor 4 and the time constant 4. Commercial titanium dioxide (Rutiox CR, British Titan Products), having an average particle size of 0.25 μ, was used without further treatment as an internal standard in quantitative work.

Electron micrographs were taken on a Phillips EM200 microscope at 80 kV. Samples were prepared by dispersing a small portion of the paste in alcohol and evaporating a drop of the suspension on a copper grid backed with a carbon film supported on collodion. No shadowing was used.

Results

C_3A Pastes

All pastes, except those containing trehalose, were quite fluid on mixing. Using a fixed water: solids ratio, pastes containing trehalose remained as a thick slurry after the initial mixing; but there was no evidence of premature set. All the other sugars showed slight water-reducing properties in pastes as evidence by bleeding which was not observed in the control pastes without sugars.

Table 1. *Hydration products in C_3A pastes hydrated with sugars*

Time of hydration	3 hours			24 hours			5 days			14 days			90 days		
Hydration products*	C_4	C_2	C_3	C_4	C_2	C_3	C_4	C_2	C_3	C_4	C_2	C_3	C_4	C_2	C_3
Additives															
None	mw†	—	mw	mw	—	s				mw	—	s	mw	—	vs
Ribose	mw	—	—	m	w	—	m	mw	w	m	mw	mw			
Xylose	tr	—	—	mw	w	w	m	w	mw	m	w	m	ms	—	m
Mannose	w	—	—	mw	tr	tr	m	—	vw	m	—	mw	m	—	m
Glucose	w	—	—	mw	vw	w	mw	w	vw	mw	w	mw	m	w	m
Fructose	vw	—	—	mw	vw	w	mw	w	tr	m	w	w	m	vw	m
Sucrose	vw	—	—	w	—	tr	mw	—	tr	mw	—	vw	mw	—	vw
Lactose	—	—	—	tr	—	—	mw	tr	—	m	tr	w	ms	—	w
Trehalose	mw	—	—	m	w	tr	m	mw	w	m	mw	w	ms	m	w
Raffinose	tr	—	—	w	—	—	mw	—	—	mw	—	—	mw	—	—

*C_4 = C_4AH_{13} and carbonated products; C_2 = C_2AH_8; C_3 = C_3AH_6
†tr = trace, vw = very weak, w = weak, m = medium, s = strong.

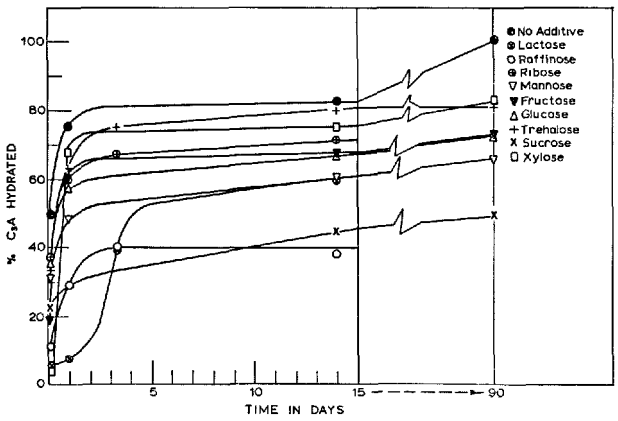

Fig. 1. *The rate of hydration of C_3A pastes*

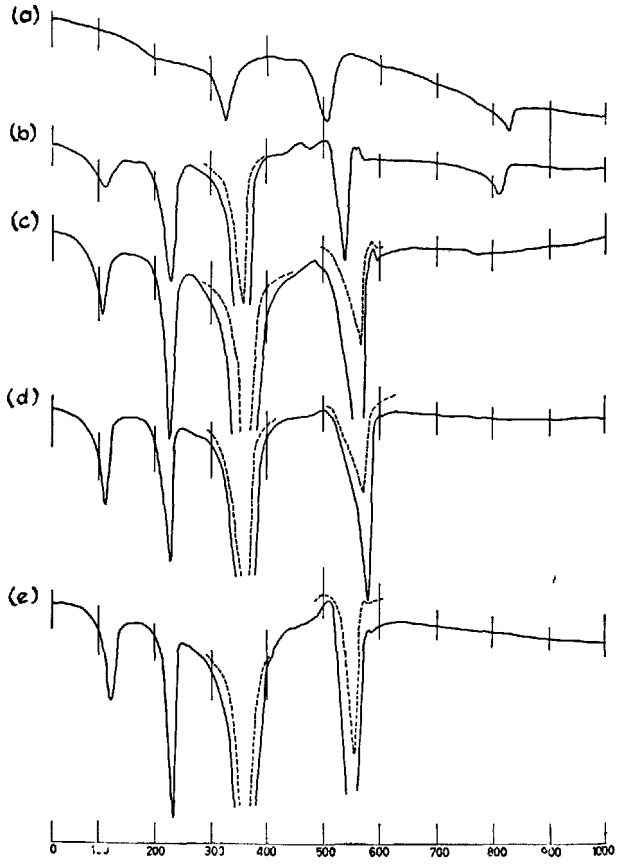

Fig. 2. *DTA thermograms of C_3A hydrated without additives. (a) No hydration (b) 3 hours hydration (c) 24 hours (d) 14 days (e) 90 days. Dashed curves were recorded at half sensitivity*

Amount of Hydration

Fig. 1 shows the rate of hydration of C_3A in pastes as determined by quantitative XRD analysis. Very little hydration occurs within 3 hours in pastes containing xylose and lactose. This is confirmed by thermal analyses and by the lack of any strength development in these pastes. In the case of lactose this abnormal behaviour continues during the first 24 hours and appreciable hydration occurs only later. On the other hand pastes with xylose hydrate very rapidly between 3 and 24 hours, and from this point hydration is but weakly retarded as compared with that observed in pastes without additives. Pastes with fructose show a behaviour similar to that of xylose, but to a lesser degree. Both sucrose and raffinose are strongly retarding at all ages. The weakest retarders are trehalose, xylose and ribose.

Hydration Products

Table 1 lists the hydration products detected in C_3A pastes by DTA and XRD. In DTA thermograms, of which typical examples are given in Figs. 2–4 the hexagonal phases C_4AH_{13}* and C_2AH_8 are recognized by

*Throughout the text the formula C_4AH_{13} is taken to include the carbonation products of this hydrate. XRD shows the predominant phase to be generally α-C_4AH_{13} (10) but sometimes $C_3A \cdot CaCO_3 \cdot 12H_2O$ is present in appreciable quantities.

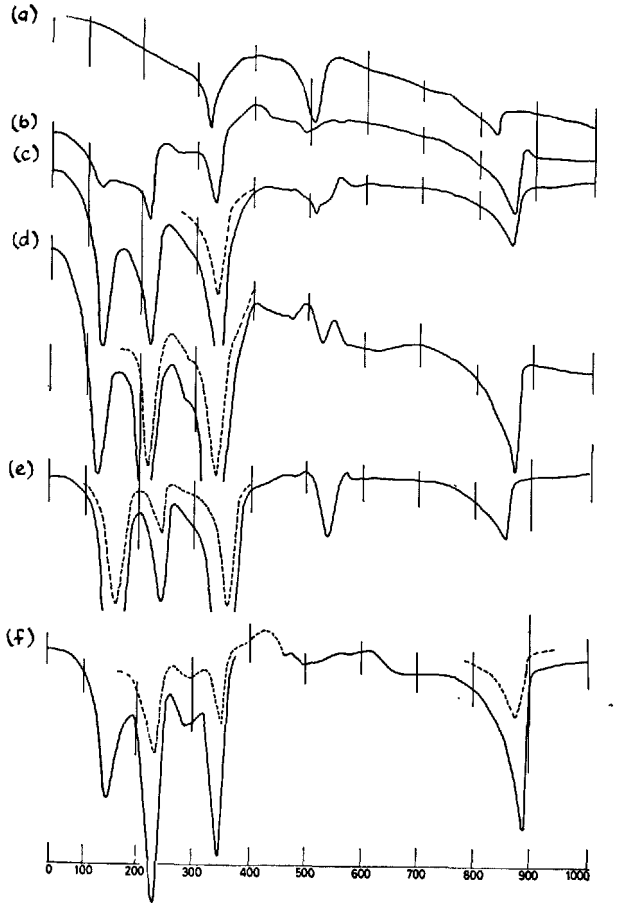

Fig. 3. *DTA thermograms of* C_3A *hydrated with 1% sucrose. (a) No hydration (b) 3 hours hydration (c) 24 hours (d) 5 days (e) 14 days (f) 90 days. Dashed curves were recorded at half sensitivity*

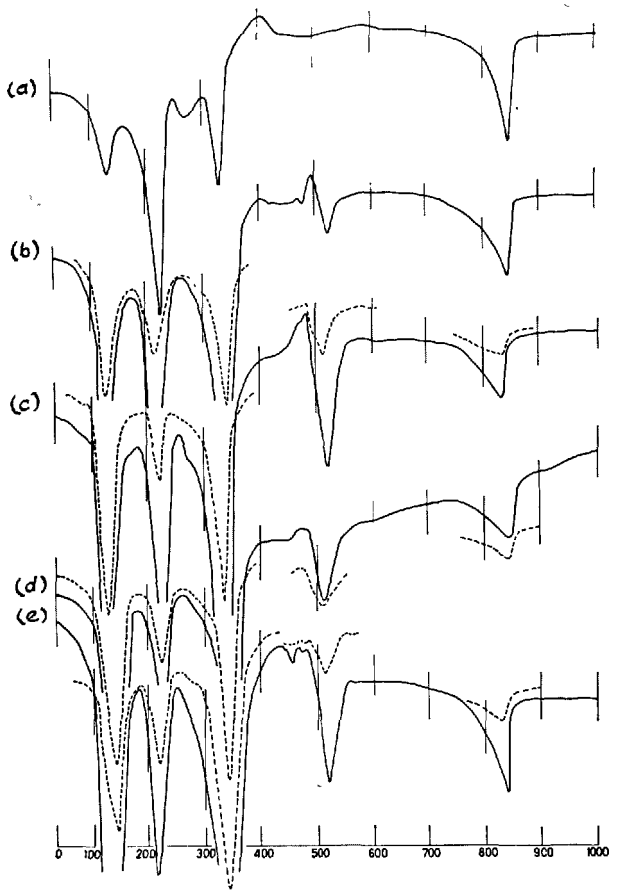

Fig. 4. *DTA thermograms of* C_3A *hydrated with 1% trehalose. (a) 3 hours hydration (b) 24 hours (c) 5 days (d) 14 days (e) 90 days. Dashed curves were recorded at half sensitivity*

three endotherms peaking just above 100°, 200° and 300°C respectively. C_3AH_6 is characterized by a strong endotherm at 300–350°C, superimposed on an endotherm due to the hexagonal phases, and another at about 550°C which originates from the dehydration of calcium hydroxide formed in the first dehydration step (9). An exothermic hump at about 400°C (Figs. 3 and 4), usually only readily seen at early ages, is attributed to the combusiton of organic matter. These results agree with earlier observations (5). It is not easy to distinguish between C_4AH_{13} and C_2AH_8 by DTA because their thermograms are so similar, but in samples where C_2AH_8 is detected by XRD the initial 100°C endotherm is more intense than that at 200°C (Fig. 2) whereas these two endotherms are of comparable intensity (Figs. 3 and 4) when C_2AH_8 is absent. The endothermic effects of DTA correspond to successive weight-loss steps in the TGA curves with a correlation between the intensities of the endotherms and the magnitude of the weight losses. As expected, TGA shows that there is appreciable overlap of the first three dehydration steps under the experimental conditions used.

The hexagonal hydrates were estimated from the XRD patterns by the relative intensities of their basal reflections and C_3AH_6 from its reflections at 4.43 Å and 3.14 Å, which are free of interference from C_3A. Small quantities of C_3AH_6 were preferably estimated by DTA using the intensity of the endotherm at about 550°C. Several samples did not show this endotherm, although their XRD patterns apparently indicated that small amounts of C_3AH_6 were present. It is our experience that DTA is more sensitive in detecting trace amounts of hydrates. The 3-hour pastes with xylose and fructose, and the 23-hour paste with lactose showed very small quantities of the hexagonal hydrates to be present, although these were not detected by XRD.

The relative amounts of the hydrates listed in Table 1 have only been estimated qualitatively, and hence

the details must be treated with caution. However, the main trends are clear, and two main points should be noted: (1) the large amount of C_3AH_6 found in pastes without additives compared with the much smaller quantities found in all other pastes even after 90 days, and (2) the formation of C_2AH_8 in appreciable amounts in the majority of pastes hydrated with sugars. The pastes in which no C_2AH_8 (or only trace amounts) was detected, contain those sugars (mannose, lactose, sucrose and raffinose) which are the strongest retarders. C_2AH_8 was not detected in pastes without additives, although it has been reported by others (11, 12) and was detected in low temperature hydration (5).

TGA Data as a Measure of Hydration

It was not possible to obtain reliable quantitative data on the amounts of the different hydrates present in the pastes. Although attempts were made to calculate these quantities from TGA curves using empirical methods, consistent results could not be obtained. The main difficulty arises from the variability in the relative magnitudes of the weight loss steps of the curves. It should be possible to obtain reliable figures from TGA data by paying closer attention to the control of experimental conditions. Making TGA measurements in steam atmospheres may achieve a separation of the overlapping dehydration steps.

The quantitative XRD estimation of the hydrates is not considered to be practicable at present because of (a) the uncertainty of detecting small amounts of C_3AH_6, as discussed previously, and (b) the strong tendency to preferred orientation of the hexagonal hydrates and the difficulty in preparing suitable samples for calibration.

Nevertheless, a remarkably good linear relationship was found between the ignition loss at 1100°C, as measured by TGA, and the amount of C_3A hydrated as measured by XRD (Fig. 5). This is due to the fact that most of the pastes form mainly the hexagonal hydrates which have very similar percentage weight losses for total dehydration. The ignition losses for the pastes without additives lie on a separate straight line as a result of their high C_3AH_6 contents. The lower slope of this line indicates that the C_3AH_6: C_4AH_{13} ratio is always much higher than in other pastes.

Crystal Development and Morphology

The behaviour of the pastes hydrated without additives is distinctive in that large amounts of C_3AH_6 are formed at all ages. The TGA data in Table 2 indicates that after the first 24 hours the C_4AH_{13} content

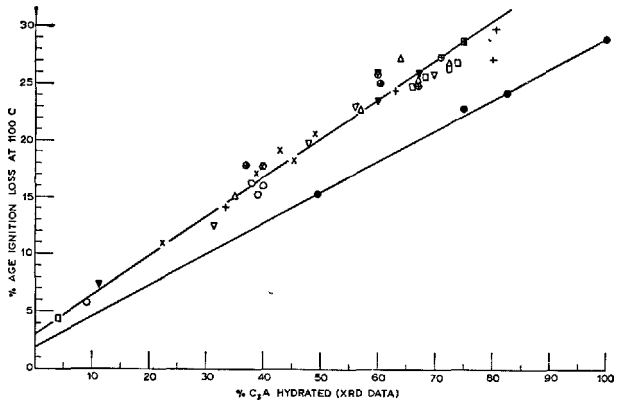

Fig. 5. *The relationship between ignition loss and the amount of* C_3A *hydrated. (Key as in Fig. 1)*

Table 2. *Percentage weight losses for* C_3A *pastes hydrated without additives*

	Time of hydration			
Temp. interval	3 hrs	24 hrs	14 days	90 days
Up to 200°C	3.2	3.4	3.4	3.4
200—400°C	7 5	14.0	15.4	18.1

remains constant throughout the hydration period and only the C_3AH_6 content increases. The weight loss up to 200°C represents only C_4AH_{13} and the loss from 200–400°C represents both C_4AH_{13} and C_3AH_6. It is generally assumed that C_3AH_6 forms from the conversion of the metastable hexagonal hydrates which are the first products of reaction. Therefore it would seem that after the initial period of hydration a steady state is set up as the rate of conversion to C_3AH_6 equals the rate of formation of the intermediate hydrates. The question then arises as to why the hexagonal hydrates readily convert to C_3AH_6 in pastes which do not contain additives, but are stable in the presence of sugars. It is possible that, as a result of the initial rapid heat evolution that occurs when sugars are not present, the temperature in the control pastes may rise sufficiently high for the conversion to become quite rapid. However, the experimental procedures were designed to prevent this.

An examination of the hydration products by electron microscopy (Fig. 6) show changes in crystal morphology which may be the main cause of this difference in reactivity. Fig. 6a shows the well-developed hexagons of C_4AH_{13} normally found in C_3A pastes. These are up to 2 microns in diameter, but are very thin since the electron beam can penetrate through the stacks of crystals which are generally found. Nevertheless, the crystals are quite stable in the beam.

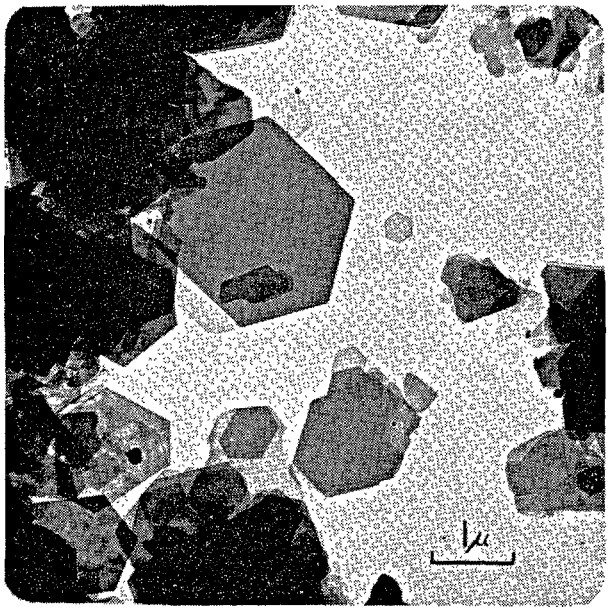

(a)

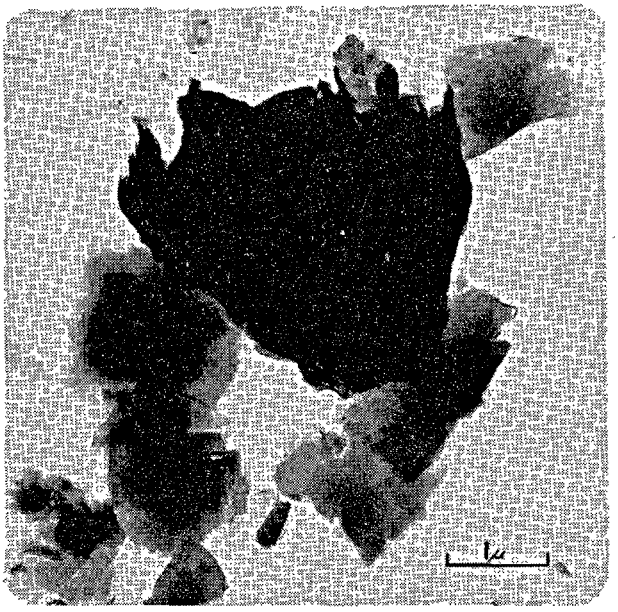

(b)

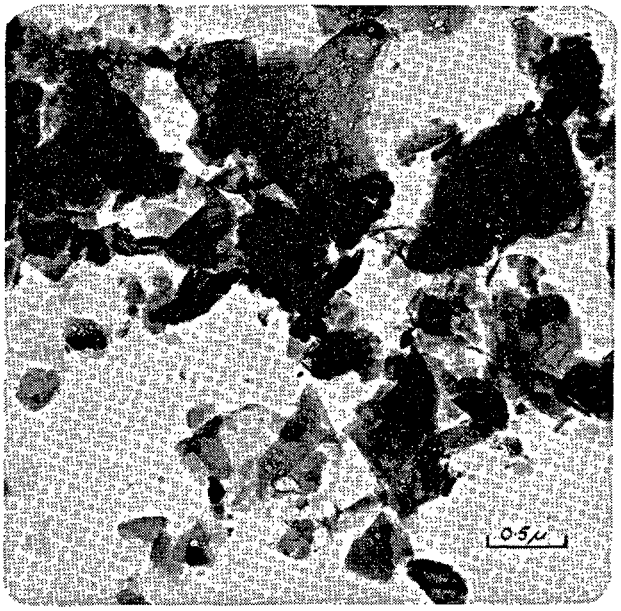

(c)

Fig. 6. *Electron micrographs of* C_3A *pastes after 24 hours.* (*a*) *No additive* (×*19,750*) (*b*) *with 1% mannose* (×*24,650*) (*c*) *with 1% trehalose* (×*37,500*).

The stippled material superimposed on some hexagons is most probably dehydrated aluminium hydroxide which must be formed with C_4AH_{13}. Figs. 6b and 6c show the typical material formed when sugars are present. There is no sign of hexagonal crystals, but instead there are extremely thin laminae which have no regular shape. They are usually piled up on each other in a large number of layers to give large aggregates of hydrated material 1–2 microns in diameter (Fig. 6b), but when the laminae are smaller, e.g. < 1 micron across, the material tends to be more scattered as in Fig. 6c. This latter micrograph clearly shows

the extreme thinness of the laminae and indicates that they are much less stable under the electron beam than the well-formed hexagonal crystals. The "bubbly" appearance probably results from free water released from the structure after having been trapped between laminae, and it occurs at relatively low beam intensities. Electron diffraction experiments show multicrystal patterns revealing hexagonal symmetry, and thus confirm the nature of the material. These patterns were much weaker than those of the hexagonal crystals and, although they were more distinct in the case of material hydrated for 3 or 4 days, hexagonal crystals were not seen.

XRD and DTA of pastes indicate that in pastes with sugars C_4AH_{13} is much more susceptible to attack by CO_2 than in pastes without additives, the latter showing very little carbonation. The extent of carbonation precludes any estimate of line broadening in XRD reflections which would result from poor crystallinity. Nevertheless, it is clear that the crystallinity of the hexagonal hydrates is less well developed in the presence of sugars. Lignosulphonate additives have also been found (5) to alter crystal morphologies and stabilize the hexagonal hydrates with respect to C_3AH_6. It is not yet certain how the changes in crystallinity affect the formation of C_3AH_6, but the observed decrease in the rate of this reaction could have an influence on the rate of hydration of C_3A. Stein (11) has suggested that the acceleration of C_3A hydration by the addition of C_3AH_6 is due to the C_3AH_6 particles acting as nuclei and thereby hastening its formation from the hexagonal hydrates.

C_3A-Gypsum Mixtures

C_3A pastes containing gypsum had a C_3A: gypsum ratio of 2 which is similar to that found in many cements. Sufficient C_3A is present to allow ettringite, which forms initially, to convert completely to the low-sulphate sulphoaluminate, but this change does not occur until later ages and was not studied in detail. Nevertheless, several interesting observations were made.

Hydration Products

In all pastes ettringite was the only product of hydration in the first 14 days. Qualitative estimations of ettringite by XRD generally give the same trends as calculated values (see Figs. 7 and 8), but in some cases preferred orientation gave misleading results. Although ettringite gives sharp reflections, it could not be detected at concentrations less than about 8%. Typical DTA thermograms are shown in Figs. 7 and 8.

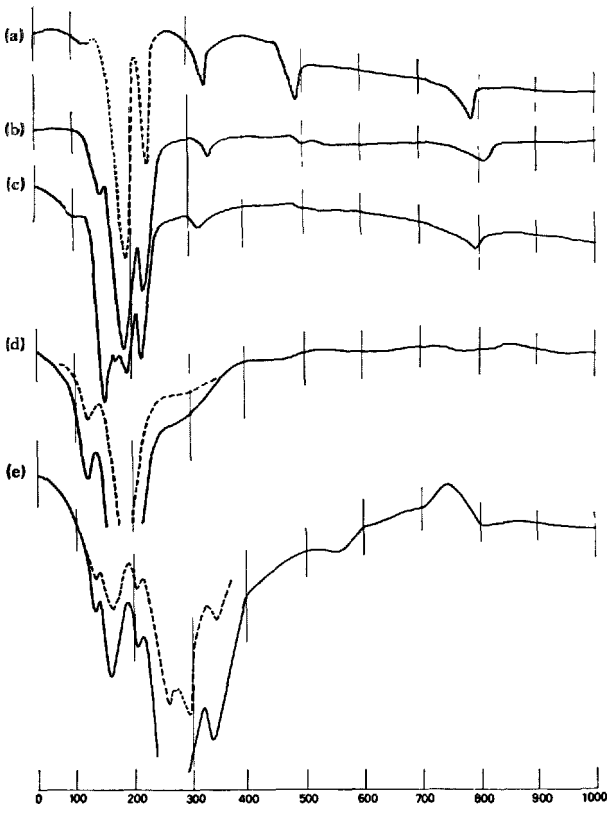

Fig. 7. *DTA thermograms of C_3A-gypsum pastes hydrates without additives. (a) No hydration (b) 3 hours hydration (c) 24 hours (d) 14 days (e) 90 days. Dashed curves were recorded at half sensitivity*

In the early stages of hydration four overlapping endotherms lie between 150°C and 250°C. The lowest endotherm is due to ettringite, and later it grows so intense that it obscures the whole region. The two highest endotherms are attributed to gypsum even though their relative intensities are different from that which is usually observed. The gypsum peaks are obscured eventually by the growing ettringite endotherm. The fourth endotherm at 150–200°C has not been positively identified, but is tentatively assigned to water adsorbed on the gypsum. Adsorbed water has been detected earlier in this laboratory (13a) as an endothermic shoulder on the lower gypsum peak. In pastes without additives a small endothermic shoulder appears on the low temperature side of the strong ettringite peak (Fig. 7d). This effect has been shown (13b) to be due to water adsorbed on ettringite. The peak was not observed with pastes containing sugars.

A broad exothermic effect at about 400°C (Fig. 8) is again attributed to the organic matter, but

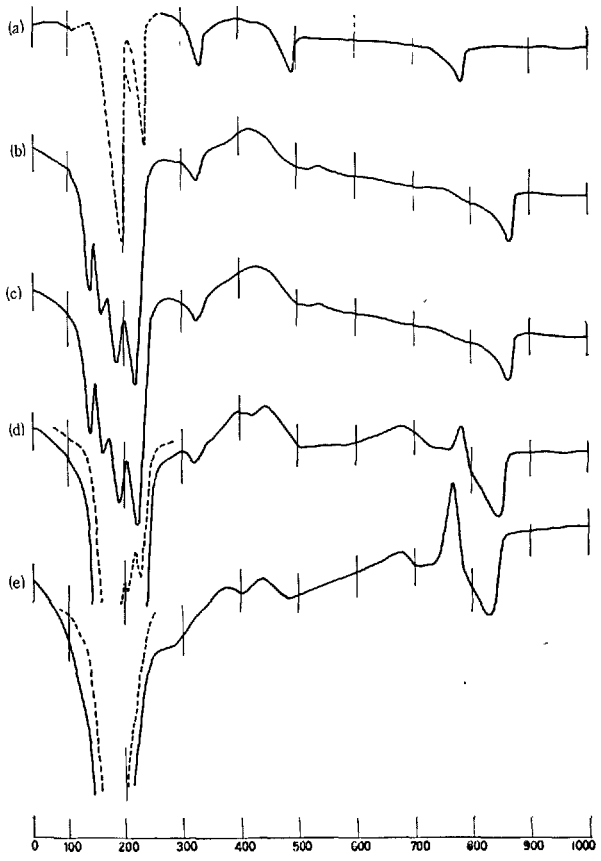

Fig. 8. *DTA thermograms of C_3A-gypsum pastes hydrated with 1% sucrose. (a) No hydration (b) 3 hours hydration (c) 24 hours (d) 14 days (e) 90 days. Dashed curves were recorded at half sensitivity*

probably also arises from the formation of insoluble anhydrite after the gypsum has dehydrated. A broad exotherm at about 650°C and the sharper one at about 750°C (Fig. 8) are dependent on the amount of ettringite that was initially in the pastes, but are not found either in the thermograms of pastes hydrated without additives (Fig. 7) or in the thermograms of synthetic ettringite. These effects have previously been observed (5) in C_3A-gypsum pastes, but their origin is still not clear.

The presence of the low-sulphate sulphoaluminate is readily detected by XRD and DTA. In DTA thermograms the endothermic region is shifted to 200–300°C (Fig. 7e) and the broad exotherm at 750°C has been shown (14) to be characteristic of the low-sulphate sulphoaluminate. Low-sulphate sulphoaluminate has only been detected at 28 days in pastes without additives and by 90 days in pastes containing lactose, trehalsoe and raffinose (Table 3). It can be seen (Table 3) that C_4AH_{13} appears before the conversion of the sulphoaluminates is complete.

Table 3. *The conversion of ettringite to low-sulphate sulphoaluminate in C_3A-gypsum pastes*

Additive	Time of hydration			
	14 days	28 days	60 days	90 days
None	Ett*, vs†	Ett, m LS, vs C_4, tr	Ett, tr LS, vs C_4, w	Ett, tr? LS, vs C_4, mw
Lactose	Ett, ms	Ett, s	Ett, vs	Ett, m LS, vs C_4, mw
Trehalose	Ett, vs	Ett, vs	—	Ett, ms LS, ms
Raffinose	Ett, ms	—	—	Ett, vs LS, vw

*Ett = ettringite; LS = low-sulphate sulphoaluminate; $C_4 = C_4AH_{13}$
†vs = very strong, s = strong, m = medium, w = weak, tr = trace

Table 4. *Percentage ettringite formed in C_3A-gypsum pastes*

Additive	Time of hydration					
	3 hours	24 hours	14 days	28 days	60 days	90 days
None	10.3*	1.59	52.3	LS†	LS	LS
Xylose	11.8	22.6	42 2	—	—	48.6
Glucose	8.2	16.5	37.7	—	—	50.0
Fructose	11 2	15.0	33.8	—	—	46.9
Sucrose	8.7	10.5	24.8	—	—	50.0
Lactose	10.3	9.6	32.0	38.2	42.0	LS
Trehalose	6.0	15.6	48.9	55.5	—	LS
Raffinose	7.5	8.8	33.9	—	—	LS

*Complete reaction of gypsum gives a maximum of 62.0% by weight of ettringite.
†Low-sulphate sulphoaluminate was present and the amount of ettringite could not be calculated.

Rate of Hydration

The amounts of ettringite formed in pastes, calculated, as described below, from TGA data, are presented in Table 4. The weight losses up to 400°C for gypsum and ettringite were determined on pure samples. If it is assumed that no reaction has occurred, then the theoretical weight loss due to gypsum is known and the extra loss observed in any sample is attributed solely to ettringite. Using the reaction

$$C_3A + 3CaSO_4 \cdot 2H_2O + 26H_2O \longrightarrow C_3A \cdot 3CaSO_4 \cdot 32H_2O$$

the amount of gypsum reacted to form ettringite can be calculated, and this leads to a new value for the amount of ettringite formed. By successive approximations the concentrations of gypsum and ettringite are eventually determined. The assumption that adsorbed water does not contribute to the TGA weight losses is probably not justified in view of DTA interpretations (see previous section). However, accurate corrections would be difficult to make, because adsorbed water was not distinguished in TGA data, and consequently they have been neglected. Although the calculated values of ettringite may consequently be too high (and this would explain the apparent insen-

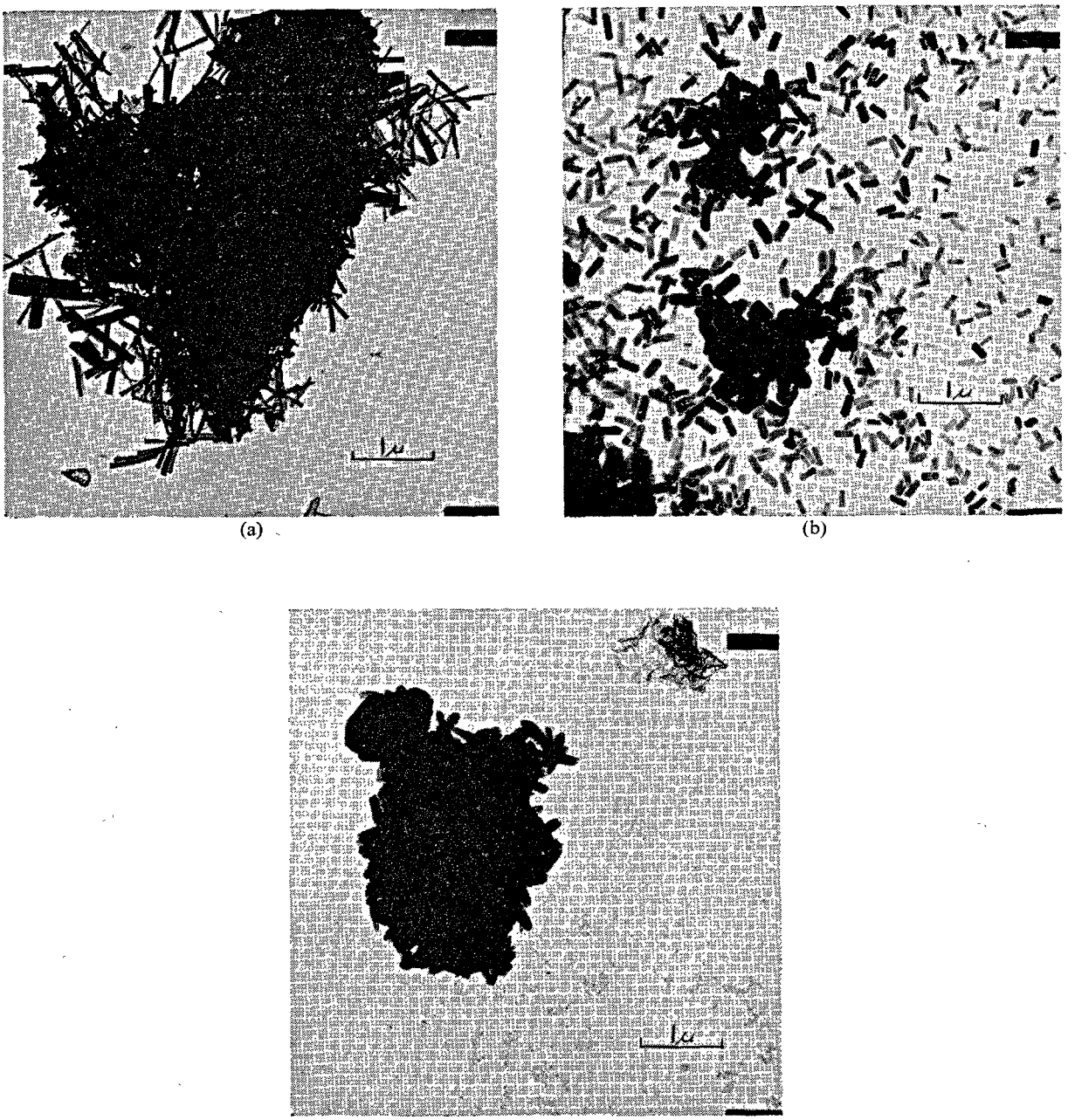

(a) (b)

(c)

Fig. 9. *Electron micrographs of* C_3A*-gypsum pastes after 24 hours* (×*24,650*). (*a*) *No additive* (*b*) *with 1% xylose* (*c*) *with 1% glucose*

sitivity of XRD), the general trends will not be affected.

The formation of ettringite is retarded by the addition of sugars. However, there is a small, initial acceleration in pastes with xylose, fructose and glucose, although the rate of formation of ettringite appears to be less at later ages in these pastes. On the other hand pastes with raffinose, trehalose and lactose are initially strongly retarding and the appearance of low-sulphate sulphoaluminate by 90 days is the consequence of an increase in the rate of formation of ettringite at later ages. Sucrose also shows this later

acceleration in rate, but to a smaller extent.

This action of the sugars is rather different from their effects in C_3A pastes. Thus xylose and fructose accclerate hydration at early ages, but retard strongly later. Raffinose and lactose are initially strongly retarding, but only moderately retarding later; while sucrose is again strongly retarding at all ages. Trehalose, apart from an initial strong retardation, delays hydration less than the other sugars.

Crystal Morphology

A brief electron microscopic examination of C_3A-gypsum pastes show that sugars also modify the morphology of ettringite. The familiar needles of ettringite are well formed in pastes without additives by 24 hours (Fig. 9a), although good electron diffraction patterns could not be obtained. These needles are also present in pastes hydrated with trehalose, but are not generally as well developed. Usually they have been modified to small rectangular crystals (Fig. 9b) or to thick chunky crystals (Fig. 9c). The needles were not observed with other sugars and only the modified forms were present. However, no appreciable strength was developed in C_3A-gypsum pastes until the low-sulphate sulphoaluminate was formed, so that ettringite does not contribute to the strength of pastes whether modified or not.

Discussion

The Behaviour of Sugars in Pastes

Structures

At the beginning of this study it was hoped to be able to relate the effects of the different sugars to their structural differences; but no definite pattern has emerged. From this point of view the saccharides are not good compounds to study because they are complex structurally. Sugars are capable of existence in an open chain form and as 5-membered (furanose) or 6-membered (pyranose) ring forms and these are all rapidly interconvertible. Most saccharides exist predominantly in the pyranose form in neutral aqueous solutions, but fructose is mainly in its furanose form, and ribose has abnormally high amounts of the open-chain form. Thus the equilibria between the different structural forms may vary widely under the experimental conditions.

Reactivities

Sugars are also very labile in strongly alkaline solutions (15) such as occur in cement pastes. Initially isomerizations to other saccharides takes place and the hydrolysis of polysaccharides may also occur. Using gas chromatography it has been shown (16) that these reactions occur quite rapidly in saturated calcium hydroxide or in C_3A solutions (Table 5). Slower reactions also occur (15) which involve the formation of saccharinic acids and the breakdown of sugars into fragments which can then re-combine. These reactions cause the yellowing of alkaline sugar solutions and account for the yellow tints observed in the dried C_3A pastes from 24 hours onwards. The disappearance of the original sugars in alkaline solutions, as estimated from gas chromatography, cannot be wholly accounted for in the formation of other sugars, and the appreciable discrepancies are attributed to the formation of other undetected products. However, ribose and trehalose show no appreciable isomerization, hydrolysis or degradation and these sugars are moderately weak retarders. Therefore, it is possible that the degradation products may be more effective retarding compounds than the sugars themselves. Bruere (4) has earlier remarked on the stability of trehalose towards alkali.

Table 5. *The isomerization of sugars in saturated calcium hydroxide solution*

Initial sugar	New products detected by gas chromatography
Ribose	None
Xylose	Arabinose, Lyxose?
Mannose	No other hexoses, unidentified pentoses
Glucose	Galactose, mannose, fructose, xylose, arabinose
Fructose	Glucose, mannose
Sucrose	Glucose, fructose, traces of pentoses
Lactose	Galactose, glucose (only traces of both)
Trehalose	None
Raffinose	Galactose, glucose, fructose, traces of pentoses

Mechanisms of Retarding

Complexing

Taplin (3) has suggested that the HO–C–C=O grouping is an essential feature of any organic compound which is an effective retarder. This chemical grouping is one which can readily complex with metals by chelation. Taplin has pointed out that the two oxygen atoms must also be able to approach each other and this is also a necessary condition for chelation. The 5-membered chelate ring such as would be formed is the ring size of optimum stability. Those com-

pounds which are classed by Taplin as weak or negligible retarders are, in fact, generally poor complexing agents. However, the weak retarding action of some recognized strong complexing agents (e.g. acetylacetone, 8-hydroxyquinoline, salicylaldehyde, EDTA) suggests that the position of equilibria between complexed and uncomplexed forms may be important.

Although sugars are formally polyhydroxy aldehydes with the HO–C–C=O grouping, they exist predominantly in ring forms (as discussed above) in which the aldehyde group has become an ether linkage. Nevertheless, sugars complex with salts and hydroxides of the alkali metals (17), alkaline earth metals (17) and other metals (18), although the structures of these complexes are not definitely established. Sugars also complex with hydroxy complexes of metals (19, 20) such as borates, germanates, stannates, arsenites, and aluminates (21, 22). In these complexes it is considered (19, 20) that the sugar molecule chelates to the central metal atom by substituting for two metal hydroxyls to form two C–O–M bonds through adjacent hydroxy groups.

We consider, therefore, that complexing of metals, especially calcium, aluminium and iron, may be an important factor in the retarding action of organic compounds. The concentration of the metal in solution will increase on complexing, and this should influence the hydration reactions. Suzuki and Nishi (2) have observed increases in the total concentrations of aluminium, iron and silica in cement pastes containing sugars. It is anticipated that specific ion electrodes will be useful tools in the investigation of complexing in cement chemistry.

Adsorption

Hansen (23) has suggested that retarders adsorb on cement surfaces thereby preventing attack by water, and Taplin (3) has pointed out that adsorption on hydrate surfaces would also lead to retardation. Adsorption may be regarded as a special case of complexing in that the metal ions involved are located on solid surfaces and not in solution. Sugars have been found to have water-reducing properties, and this is usually explained by the repulsion of solid particles through adsorption.

The behaviour of trehalose is puzzling in that the particles appear to be attracted rather than repelled. Trehalose is a non-reducing sugar not readily attacked by alkali so that it will exist as two pyranose rings even in cement pastes. This contrasts with the isomerization or hydrolysis observed for other saccharides which indicates that the open-chain forms are readily formed under these conditions. Therefore, it is plausible to suggest that the structure of trehalose allows it to adsorb on solid surfaces in such a way that it can adsorb to a second surface simultaneously, as has been suggested (24) for additives which increase the flocculation of cement pastes.

Solubility

Suzuki and Nishi (2) have suggested that additives act through the precipitation of insoluble complexes which are assumed to prevent further reaction by coating the cement grains. They have suggested that a relationship exists between the solubilities of the calcium salts of carboxylic acids and their retarding properties. However, contrary to their statement, complexes of sucrose and other sugars with calcium hydroxide are very soluble in aqueous solutions (17). The solubility product of metal complexes on salts will play a part since this also affects the concentration of the metal in solution.

Concluding Remarks

At the present time it is not possible to do more than generalize about the theories of retarders, but it is likely that the three approaches discussed above are merely different aspects of the one phenomenon and can all be involved in influencing the hydration of cement. However, until more data is available to the cement chemist the details of mechanisms cannot be clarified, and more work is therefore required on the chemical aspects of retardation such as the rate of formation of hydration products and changes in their reactivity, the rate of release of components into the liquid phase, the extent and nature of adsorption and the chemical behaviour of additives in the alkaline environment of a cement paste. Our results have, therefore, been presented at this stage, although several points require further investigation. This work is being developed further with special attention being given to the possibilities of complexing.

Acknowledgements

I wish to thank the Director of Physics and Engineering Laboratory, D. S. I. R. for the use of the

Phillips Electron Microscope, and Mr. N. B. Milestone and Mr. G. T. Mentzer for assistance with the experimental work. I am indebted to Mr. R. A. Kennerley for his critical reading of the manuscript and his continued interest in this work. This paper is published with the permission of the Director of Chemistry Division.

References

1. W. Sandermann and M. Brendel, "The 'Cement-poisoning' effect of wood components and their dependance on chemical constitution" (in German), Holz als Roh-und Werkstoff, **14**, 307 (1956).
2. S. Suzuki and S. Nishi, "The effects of saccharides and other organic compounds on the hydration of cement" (in Japanese), Semento Gijustu Nenpo, **13**, 160 (1959).
3. J. H. Taplin, Discussion on Paper by H. E. Vivian, (Ref. 23), Proc. 4th. Int. Symp. Chem. Cement, Natl. Bur. Standards, Monogr. 43, Vol. II, 927 (1960).
4. G. M. Bruere, "Set-retarding effects of sugar in portland cement pastes", Nature, **212**, 502 (1966).
5. J. F. Young, "Hydration of tricalcium aluminate with lignosulphonate additives", Mag. Concr., Res., **14**, No. 42, 137 (1962).
6. L. H. Tuthill, R. F. Adams and J. M. Hemme, "Observations in testing and use of water-reducing retarders", Amer. Soc. Test. Mater., Spec. Tech. Publ., No. 266, **97**, (1960).
7. R. Ashworth, "Some investigations into the use of sugars as an admixture to concrete", Proc. Inst. Civil Engrs., **31**, 129 (1965).
8. P. D. Garn and J. E. Kessler, "Thermogravimetry in self-generated atmospheres", Anal. Chem., **32**, 1563 (1960).
9. W. G. Schneider and T. Thorvaldson, "The dehydration of tricalcium aluminate hexahydrate", Canad. J. Res., **B19**, 123 (1941).
10. P. Seligmann and N. R. Greening, "New techniques for temperature and humidity control in X-ray diffractometry", J. Portland Cement Assocn. Res. Dev. Labs., **4**, No. 2, 2 (1962).
11. H. N. Stein, "Mechanisms of the hydration of $3CaO \cdot Al_2O_3$", J. Appl. Chem., **13**, 228 (1963).
12. R. F. Feldman and V. S. Ramachandran, "Character of hydration of $3CaO \cdot Al_2O_3$", J. Amer. Ceram. Soc., **49**, 268 (1966).
13(a) D. A. St. John, personal communication.
13(b) R. A. Kennerlay, unpublished results.
14. J. F. Young, unpublished results.
15. The Carbohydrates (Academic Press Inc., London, England and New York, U.S.A., 1957). Edited by W. Pigman. See article by M. G. Blair on "Sugars in solution in the presence of alkalis", p. 60.
16. N. B. Milestone and J. F. Young, to be published.
17. J. A. Rendleman, "Complexes of alkali metals and alkaline-earth metals with carbohydrates", in Advances in Carbohydrate Chemistry, **21**, 209 (1966) (Academic Press Inc., London, England and New York, U.S.A., 1966). Edited by M. L. Wolform.
18. E. J. Bourne, R. Nery and H. Weigel, "Metal chelates of polyhydroxy compounds", Chem. & Ind., 998 (1959).
19. G. L. Roy, A. L. Laferriere and J. O. Edwards, "Comparative study of polyol complexes of arsenite, borate and tellurate ions", J. Inorg. Nucl. Chem., **4**, 106 (1957).
20. H. Weigel, "Paper electrophoresis of carbohydrates" in Advances in Carbohydrate Chemistry, **18**, 61 (1963). (Academic Press Inc., London, England and New York, U.S.A., 1963). Edited by M. L. Wolfrom.
21. E. Calvet, H. Thebon and R. Ugo, "Reactions between sodium aluminate and calcium saccharate solutions" (in French), Bull. Soc. Chim. France, 1346 (1965).
22. B. K. Davison, "Hydroxy-oxo-aluminium polyol complexes", U. S. Patent 3, 198, 332 (Chem. Abstr., **63**, 16446c (1965)).
23. W. C. Hansen, "Actions of calcium sulphate and admixtures in portland cement pastes", Amer. Soc. Test. Mater., Spec. Tech. Publ. No. 266, 3 (1960).
24. H. E. Vivian, "Some chemical additions and admixtures in cement pastes and concrete", Proc. 4th Int. Symp. Chem. Cement, Natl. Bur. Standards Monogr. 43, Vol. II, p. 909 (1960).

Sapplementary Paper II-41 Some Principles in Cement Hydration

Albert Joisel*

Synopsis

During the hydration of cements their constituents, C, S, A, F, N, K, M, etc., regain a certain individuality.

1) *Calcium silicates* have an incongruent dissolution: lime passes into solution much faster than silica, the richer the silicate is in lime and the higher the concentration of strong anions in the interstitial water; it alone can result in a crystallization of portlandite.

Hydrated calcium silicates are not stoichiometrically defined.

2) *Calcium aluminates* pass into solution in their stoichiometric ratio faster, the richer they are in lime, the poorer in iron oxide, the higher the concentration of strong cations and the lower the concentration of strong anions in the interstitial water.

The crystallization of hydrated aluminates starts with a coacervation: the network of hydrates includes all the constituents present in the interstitial liquid: hydroxides, sulphates, chlorides, carbonates, etc. The most stable hydrated aluminate is C_3AH_6.

3) *Anions or cations in the interstitial solution* can precipitate on the calcic cement grains in an anhydrous form: they coat their surface and thus retard their hydration. Above the concentration corresponding to a monomolecular layer on the surface of the grains, they precipitate into the solution and contribute to the gelation of the aqueous interstices.

Anions in the interstitial solution can also precipitate with the calcium ion of the solution in a hydrated form and contribute to gelation without coating the cement grains.

4) *Calcium sulphate*, which is relatively soluble, is amphoteric. It behaves as a strong anion for silicates and highly calcic aluminates and as a strong cation for aluminates low in calcium.

It can also contribute to the gelation of aqueous interstices when partially dehydrated.

Introduction

The study of cement hydration which originated at the end of the last century, has only made strides in the course of the last scores of years. It has considerably developed during the last twenty years. A mere careful scrutiny of the book-reviews of the last symposiums on the chemistry of cements, mainly those of 1952 and of 1960 suffices to convince one of this development.

The science of hydration has still to improve a great deal and above all let's say that the existing data are often lacking in accuracy. It is due to the fact that the hydrated cement constitutes an *artificial rock*, and one knows there exists and infinite variety of rocks in nature . . .

Hence one can understand why hydrated cement is highly heterogeneous. One must not expect to find in it only perfectly defined bodies, from the stoichiometric point of view, and, a fortiori, from the crystallographic point of veiw, except in some particular cases affecting special cements only.

Yet, hydration is of the highest interest as it exerts an influence of primary importance on all the various properties of concretes: rapidity of setting; mechanical strength; stability of volume; impermeability; resistance to agressive agents, to freezing, to flames; protection of the reinforcement; and so on.

Conversely all that can be known concerning these different properties should be fully taken to account in the study of hydration, and provide indispensable precisions, complement to the mineralogical studies of hydrated products (chemical composition, water fixation, crystallography, etc.).

Two general methods may be envisaged for this study: the first one consists in examining separately the evolution of certain compounds, in presence of water, under certain conditions, as best as possibly can be defined, as for instance the evolution of calcium silicates, that of calcium aluminates, the influence exerted by minor components and by admix-

*Centre d'Etudes et de Recherches de l'Industrie des Liants Hydrauliques, Paris, France.

tures (i.e. by sulphates, chlorides, carboxolates, etc.), the influence of temperature, the consequence of the water/cement ratio, etc. The second method consists in taking advantage of the total results accumulated during the laboratory researches, and also in the practical experience of the utilization of cements. The first method is mainly *deductive*, it bears on the scale from the simple to the complex. The second method is more *inductive*, it tends to extract certain simple principles out of a complex entity. Most of the works published for the last scores of years, dealing with hydration, have generally adopted the first method. But one must not neglect the possibilities of intellectual induction, working from scientific observations, either technical or practical, on the greatest possible variety of cements (portlands, slags, pozzolanas) used under the most varied conditions (fineness, dilution, temperature, admixtures, etc.). On all cases it is imperative that *the basic principles of the science of hydration should be verified by all checked inferences, without any exception.*

The principles we wish to set out concern the studies which are carried out at the CERILH in France, after a very important confrontation of the works having been published in different countries in the world. We will mostly refer to data universally known and admitted by experts such as for instance the acceleration of the hydration of portland clinker by means of calcium chloride, or the retardment provoked by sodium fluoride. We will therefore not indicate the origins.

General Points

As from its initial mixing, concrete is heterogeneous, since it is a three-phased element: it has a solid phase (the aggregate grains and the cement grains), a liquid phase (water, or rather interstitial solution) and a gaseous phase, intended or not (the voids, and the air or hydrogen bubbles). The aggregates and the gases remain almost inert, at least at ambient temperatures, during a certain time. Hydration therefore occurs essentially in the paste constituted by the cement grains and the water.

The hydraulic components of the cement grains enter into solution in water, where they precipitate in a hydrated form, but this dissolution is accompanied by a *hydrolysis*, that is to say, that the acids (particularly silica and alumina) and the bases (mainly lime), which constitute the cement, regain *a certain individuality* at the time of dissolution.

This is particularly characteristic with silicates: for instance the lime of the clinker alite may escape alone from the cement grains in order to crystallize in the aqueous interstices in hydroxide form (which has been termed portlandite that may be easily observed under the microscope and with a microprobe on polished sections, and on thin plates) or even to form stalactites out of the rims of certain cracked reservoirs. This is true, too, for aluminates, though alumina passes into solution more easily than silica; the effects are the polystoichiometry of hydrated aluminates, the proportion of "fixed" water, the rising of the pH to a rate of about: from 11 to 13, etc . . . Cements are always basic, for lime is a strong base, whereas cement acids (silica, alumina) are weak, not much soluble, and not very much dissociated. Moreover, the dissolution of alkaline components present on occasion, is easy and rapid. So it may be noted that the main *stable* cement hydrates may be written as follows:

$$s\mathrm{SiO_2},\ a\mathrm{Al(OH)_3},\ f\mathrm{Fe(OH)_3},\ c\mathrm{Ca(OH)_2},\ n\mathrm{H_2O}$$

(This formulae is a generalization of that which had been formerly proposed by Brandenberger).

s, a, f, c, n are whole numbers. The OH have not the infrared absorption bands of water, and do not obey its laws of evaporation. For example, the curves of thermogravimetric analysis always present a level corresponding either to a $\mathrm{C_cS_sH_c}$ or to a $\mathrm{C_cA_aH_{3a+c}}$ formulae as $\mathrm{C_3S_2H_3}$, $\mathrm{C_3AH_6}$, $\mathrm{C_3FH_6}$ etc. Conversely, the $n\mathrm{H_2O}$ are *more or less "free"*, and they evaporate therefore more or less easily, and especially in keeping with the conditions of temperature and of steam pressure, and *their elimination is more or less reversible* in normal temperature.

The formulae shows that aluminates fix more water than silicates.

Hydration of Silicates

One may be tempted to argue in the following way: we know, according to the original theory of Le Chatelier, that the anhydrous silicates dissolve and crystallize in an hydrated form (that may be appre-

ciated by X-rays); then, whatever the initial fineness of the cement may be, the hydrated paste obtained in course of time depends only on the initial (water/cement) ratio. This would be proved by the fact that the mechanical strength is effectively almost the same in course of time, whatever the initial fineness. But it is to be noticed that the water taken out of the solution, at the start of mixing, contains lime, but contains almost no silica. Besides, the permeability of the hydrated paste varies in relation to the initial fineness and the hydraulic drying shrinkage is almost in proportion to the initial Blaine fineness, for usual portland cements, whatever the duration of hydration before they are exposed to the air. In other words the cement does not so soon forget its specific surface, and consequently it keeps intact the surface of its grains.

Hence, one is to think that hydration occurs as is described, in schematizing, on Fig. 1, for instance for tricalcium silicate and this is not annuled by microscopic observations and by microanalysis with the Castaing probe. *The initial surface of the cement grains remains a solution of continuity in the hydrated paste during the hydration. The topochemical "gel" formed inside a silicate grain and the gel created in the interstices initially filled with water, are quite distinct gels.*

Since the silicate grains keep the same surface during the hydration and thus keep their contact points between one another and with the aggregates, one understands why in wet medium and in constant temperature the apparent volume of the cement paste, and a fortiori, that of concrete are not modified: *there is no mould shrinkage for the portland cements which are rich in silicates.*

The interestices between the grains have, in fact, a lime concentration independent from the fineness of the cement, provided that the (water/cement) ratio remains the same; and one can think that the mechanical strength depends mainly on this concentration. But the network of interestices has ramifications depending on the fineness of cement, and one knows, too, that permeability, capillarity, hydraulic shrinkage depend on this texture: the permeability-meters used for the measuring of the fineness of cement originate in these principles, and the clay pastes shrinkage is consonant to them.

During the hydration the bonds which are formed in the interstices of the grains are in increasing number: they are represented on Fig. 1, in schematizing, by the $\boxed{CH}$.

The penetration of a fluid into a porous solid almost occurs in conformity to the usual law:

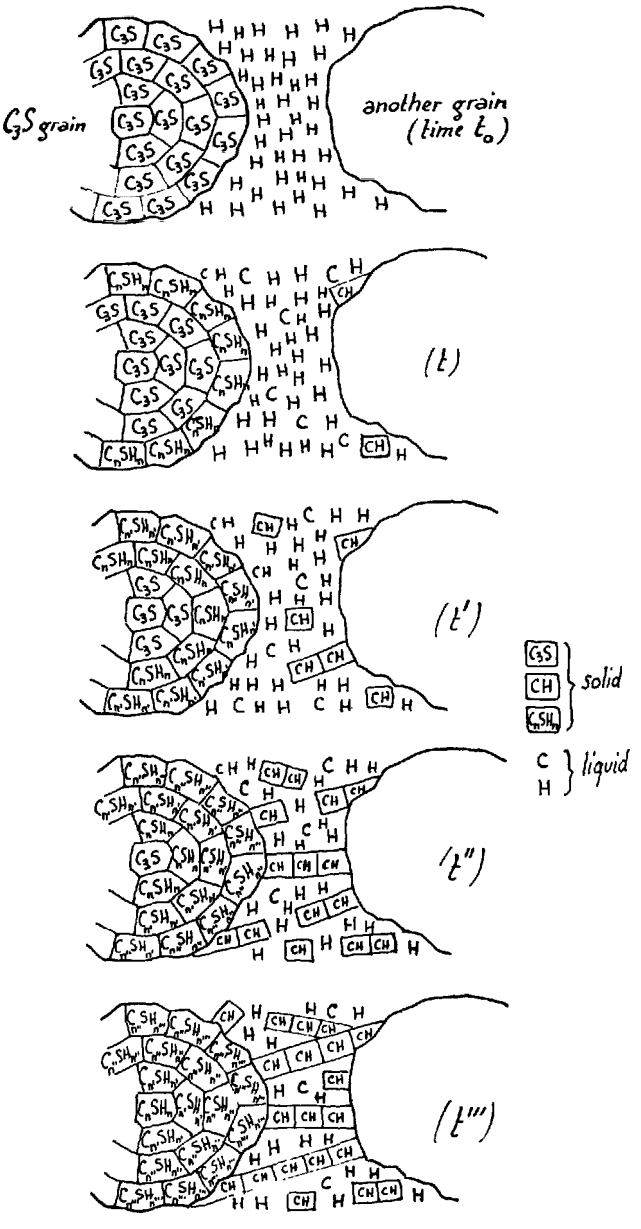

Fig. 1.

$$\text{depth } \boxed{x = k_s\sqrt{\text{time } t}}$$

For the silicate grains which are hydrolyzed by water, the expression of the penetration is, no doubt, a little more complex; but anyway this penetration of water into the grains occurs more and more slowly since the thickness of silicate that water must get through is increasing during the hydration: *one conceives that the setting of highly silicated portland cements is slow and that their mechanical strength is progressively and regularly increasing.*

A part of the lime in the calcic silicate passes into the interstitial water, leaving a free space for the penetration of water, for the molecules of water are smaller than those of lime. Besides, those among the molecules of lime which become hydrated, while staying at the same place in silicate grains, may undergo some changes in position. But if two lime molecules of a silicate are taken out, instead of one, the penetration of water is not two times more rapid. To understand the preceding statement it is enough to remember that the flow of a liquid in a pipe is in proportion to the square of its section. One then deduces that *tricalcium silicate hydrates more rapidly than dicalcium silicate*; and monocalcium silicate is not easily hydrated.

For one given (water/cement) ratio of the paste, the amount of portlandite in of the interstices is all the higher, the stronger the lime content of the silicates is, that is to say the alite content is higher.

During the hydration of an alite grain, the core of the grain may have remained anhydrous and one conceives that the hydrated part of the grain which is very near this core remains relatively rich in lime. But silica has little affinity with lime (one knows, for instance, that calcium silicates are relatively seldom found in nature, and that the burning of cement needs considerable energy). So, when recovering a certain individuality, during the hydration, *the lime has a propensity to make its concentration roughly uniform in the whole paste* containing the initial grains and the aqueous interstitial phase. As, in concrete, cement takes up a volume which is about 1/3 to 1/2 of the volume of the paste (cement + water), the hydrated silicate, which has a propensity to replace alite C_3S in wet medium, has a total composition roughly situated between CSH and $C_{1.5}SH_{1.5}$, but *there is no stoichiometrically defined hydrated calcium silicate*, and as a consequence, during the hydration, intermediate compositions may exist locally, compositions which can reach C_2SH_2, or even CH (as we saw previously).

As it is diffused in all the interstitial solution, the lime originating in the silicate grains, reinforces all the bonds. A vibration being effected on concrete, after the first precipitations are made, and even after the first bonds are established, i.e. a little moment after the initial set, no an ill effect on the final strength.

The penetration of water into the grains, and the concomitant migration of their lime into the interstices, depends on the viscosity of this water which lowers when temperature increases. It results that *the speed of hydration of the silicates increases with temperature*. One knows that the solubility of the lime diminishes when temperature increases; but it is the speed of dissolution which must be taken into account much more than solubility.

Silica is much less mobile than lime, during the hydration, but it is not strictly insoluble, in a water the pH of which is high. So, around the grains, *in course of time*, there are, undoubtedly, some movements of molecules or of siliceous anions in the silicates (alite or belite), in presence of lime in solution, and above all in presence of alkalies (see par. Accelerators and Retarders).

Hydration of Aluminates

It is to be noticed that *the water which is extracted from the paste of calcium aluminate, at the initial mixing, contains alumina and lime in the same C/A ratio, as the anhydrous aluminate: the hydrolysis of calcium aluminates is therefore quite different from that of the silicates*. Their hydration occurs as is indicated (in schematizing) in Fig. 2 for instance for the tricalcium aluminate.

The surface of the grains in contact with the solution is progressively dissolved by water. It disappears in so far as it is a discontinuity of the hydrated paste. It, therefore, establishes no solid bond with the aggregate grains (or the other cement grains) which are around it. A surface that is dissolving even prevents the bonds from being strongly established in the area in which it is found. It is only when the dissolution is complete in an area that strong bonds may be established. It results that the hardening occurs immediately after the moment in which the first bonds are established, that is, after the initial set. *Thus this hardening is always rapid:* after one day the average compressive strength of normal mortar ISO is of 600 kg/cm² for an aluminous cement, whereas it is ten times weaker for a portland cement having the same setting time.

It results also that a mixing or a vibration of concrete after the moment when the first bonds are established, i.e., after the initial set, breakes these bonds and considerably reduces the final strength. It is what happens with the aluminous cement, as with plaster, for the same reasons.

One could assert, in schematizing, that the bonds between silicate grains are produced one beside the other, in parallel; they are more and more numerous,

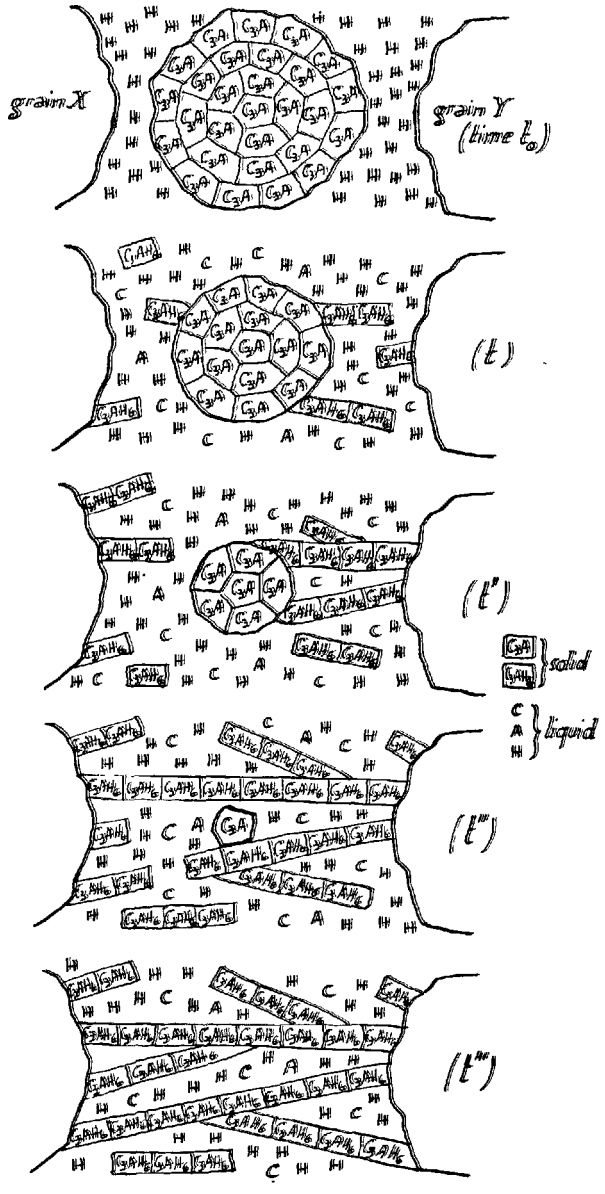

Fig. 2.

stronger and stronger, *they give one another more strength*, whereas the bonds between aluminate grains are produced, at least partly, one at the end of the other, in series. Every re-mixing breaks the bonds and if the latter afterwards go on extending, they are weakened once for all. This weakening, moreover, may be stressed by the fact that aluminates absorb more water than silicates, and the workability is more affected by the initial hydration.

The hydration of aluminates occuring with a shrinkage of the whole (solid + water), *the cement concrete rich in aluminate shows a mould shrinkage*, conversely to what happens with the cements which are rich in silicates. It is all the same, a fortiori, with neat cement paste, and specially with aluminous cement.

Whatever the initial fineness of the aluminate grains may be, the hydrated paste has about the same texture if the (water/cement) ratio is the same. It results that *the drying shrinkage does not much depend on the initial fineness of the aluminate*. Actually it is known that it is so, for the aluminous cement: the increase of the cement shrinkage due to the increase of fineness is small. It originates, to a great extent, in the small proportion of silicate that it contains. One conceives, too, that the permeability, the capillarity, and the freezing strength of concretes of aluminous cement little depend on the fineness of cement, contrary to what happens with the portland cements.

As the surface of the grains dissolves when it comes into contact with the interstitial water, the penetration of this water into the grains keeps more or less the $\boxed{x = k_a \cdot t}$ law, whereas for silicates we saw that it was rather $x = k_s\sqrt{t}$. It is one of the reasons why *the hydration of aluminates is more rapid than that of the silicates* for the same molar proportions of lime in relation either to the alumina or to the silica.

During the hydration of calcium aluminate, the alumina and the lime pass into solution, but alumina is much less soluble and much less mobile than lime. *Hydration therefore is the more rapid, the richer in lime the alminate is*: aluminate which is highly calcic grants the quick-setting cement a quick set. The same holds true in respect of the tricalcium aluminate of the portland, provided it is not retarded by the gypsum (see par. Accelerators and Retarders). Conversely, the aluminate of the aluminous cement, which is not very calcic, and the composition of which corresponds more or less to CA, is a slow-setting one.

Ferric oxide is still less soluble and less mobile than alumina, at least for the simple reason that the iron atom is more voluminous than the aluminium atom. Thus *the smaller their A/F ratio is, the less rapidly the aluminoferrites hydrate*.

Crystallization of hydrated aluminates in the interstitial solution has some common points with a coacervation: the aluminates which have passed into solution and have precipitated, behave like colloids in certain respects, and *they enclose in their networks the components contained in the interstitial liquid, i.e. hydroxides, sulphates, chlorides, carbonates, etc.* It results in a formation either of aluminates enriched with lime or of complex aluminates: sulphoaluminates, chloroaluminates, carboaluminates, etc. It is not the same thing with silicates.

Since the alumina of the aluminate passes into

solution at the same time as the lime, the changes in structure of the hydrated aluminate may possibly occur, and this explained why *the more stable hydrated aluminate eventually tends to be effected.* It is known that usually, it is C_3AH_6, above all if temperature rises above 30°C.

Accelerators and Retarders

The products which accelerate or retard the dissolution of the hydraulic components of cement, especially, lime, silica, and alumina, are accelerators or retarders. These admixtures, thus, must be *soluble* in the mixing water. If they are hydrolized, they behave like a mixture of the ionized acid and base which constitute them. In order to understand their activity one must consider that *the medium has always a high pH.*

1) The *accelerators* are essentially:

—the "*acid*" *anions* which accelerate the dissolution of the lime: hydrochloric, nitric, and sulphuric anions. These are *the acids of which the calcium salts are comparatively soluble*, and particularly the chloride whose anion is the smallest one, and thus the most mobile one.

—the "*basic*" *cations* which accelerate the dissolution of alumina and of silica: alkaline cations (sodium, potassium, ammonium, etc.) for all the aluminates and silicates; calcic cation for the aluminates which are poor in lime.

These are the bases of which the silicic or aluminic salts are comparatively soluble.

But *the alkaline cations remain "dissolvent" and hence weakening* for the final strengths, mainly if the cements are very much calcic (portlands).

The portland cement acts upon the aluminous cement as if it were a basic accelerator. The two cements, therefore, are incompatible.

One deduces from the above that the best accelerator salt of the portland cements is the *calcium chloride;* nitrate is more expensive than chloride, and moreover it is more dangerous for the reinforcement. For less calcic cements, containing high proportions of blast-furnace slag or of natural pozzolana or of artificial pozzolana (fly ash), an alkaline chloride may be preferred.

Alkaline hydroxides are accelerators for all the cements made of calcium silicates and aluminates. The alkaline salts of weak acids behave like the corresponding bases: silicates, aluminates, carbonates, etc. They are therefore accelerators. In strong dose, besides, they are "gelificators", too (see par. Setting and False-Setting).

The accelerating action varies regularly and more or less *in proportion to the concentration* of the accelerating admixture in the mixing water. But one understands that the slower the crystallization of the hydrated bonds is the more easily it is effected. The best final strengths, thus, are usually all the higher the more slowly the setting is.

2) *Retarders* can behave in two different ways. They are:

a) "*Reducers of solubility*": their presence in solution in the mixing water lowers the rate of solubility of the anhydrous cement components. For instance, calcium hydroxide retards the portland since it hinders the dissolution of the lime of the silicates; calcium chloride retards the "slag cement with lime" made mainly of slag (vitreous silico-aluminate of a potential composition which is very near $C_6S_3A_6$) and of $Ca(OH)_2$, since the Cl^- anion, like all the anions, retards the dissolution of silica and of alumina, and the Ca^{++} cation is already existing in the lime.

The activity of these reducers of solubility regularly varies with their concentration.

b) "*Coaters*": They form with a cement constituent, *on the surface of its grains in contact with the mixing water, an anhydrous compound almost insoluble*, and thus impermeable. It is the case of alkaline tetraborates, fluorides, phosphates and carboxilates, and of certain organic substances, such as the sugars, which form, with the calcium, compounds which are much less soluble than lime and which, therefore, fix the calcic cement ions and inhibit the dissolution of the silicates and aluminates. The latter are retarders for all cements (schema in Fig. 3).

It is the same case, too, for the cations which correspond to almost insoluble bases. These bases precipitate, by means of an exchange with $Ca(OH)_2$, on the surface of the cement grains, that is to say, where the OH^- anions are more concentrated (schema in Fig. 4). These hydroxides contain OH hydroxiles, but they are anhydrous, like all coaters.

These cations can originate in oxides insoluble in pure water and brought into solution in presence of cement alkalies. This is why, for instance, zinc oxide, which has no effect on cements without soluble alkalies (since it is insoluble), is a retarder for usual portlands which contain small amount of alkalies.

The coaters are retarders for a low proportion, since it is enough for them to form *a monomolecular layer* on the surface of the grain to be effective. Beyond

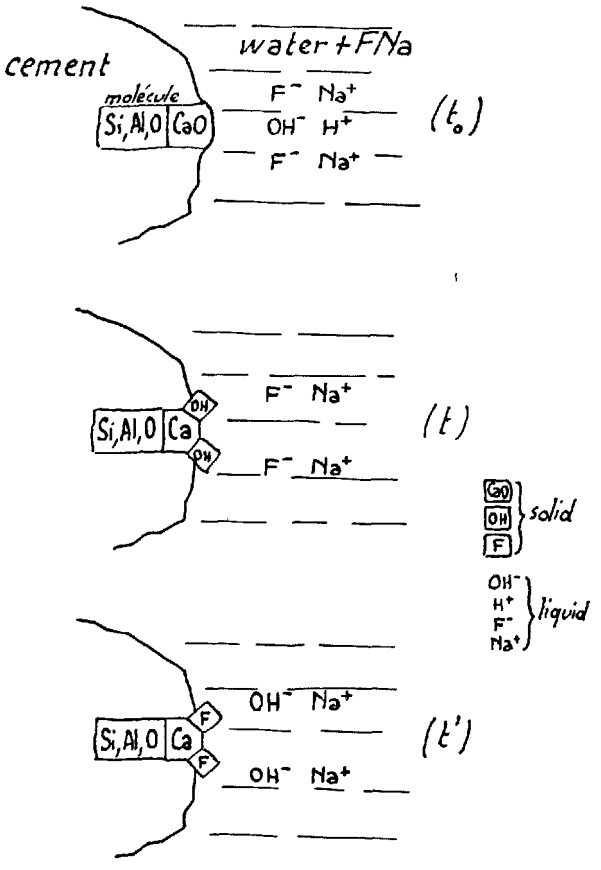

Fig. 3.

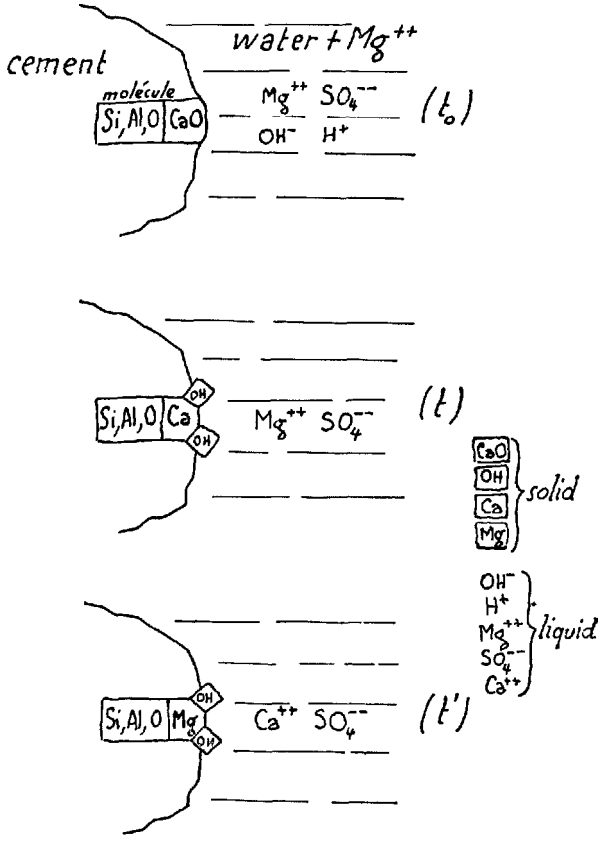

Fig. 4.

this proportion the retard does not become more marked in proportion to the addition. The coating coat is not rigorously impermeable. Hydration is just retarded and the final resistances may be excellent.

3) Certain compounds are *amphoterous*: They are either accelerators or retarders according to their effect on one or the other of the cement components. Or else these compounds include two ions the effects of which may act against each other. Generally speaking, to understand their effects, one must study the cement components the dissolution of which is absolutely necessary:

—To accelerate a silicate, one has better act upon its lime,

—To accelerate an aluminate, one must act upon its alumina,

—To retard something, one has better act upon the lime.

So, *calcium sulphate* is:

—By the *sulphate anion*, comparatively strong,

—An accelerator for calcium silicates (in which it accelerates the dissolution of the lime),

—A retarder for highly calcic aluminates, in which it retards the dissolution of the alumina (it is a "reducer of solubility").

It is, therefore, a regulator of setting and of hardening for the portlands. Its best proportion is all the stronger, the more rapid the initial hydration of the clinker is, and thus:

—the finer,
—the richer in alkalies (see below: 4)
—the richer in C_3A

} the clinker is.

—By the *calcium cation*, relatively strong, the sulphate is an accelerator for the aluminates and for the alumino-silicates, little calcic, and particularly for slags and pozzolanas.

If the action of the calcium sulphate must be extended so that it should not be wholly fixed from the initial hydration by hydrated aluminates, it must be little soluble. This is why the supersulphated cement (mainly composed of slag and of calcium sulphate) is made of anhydrite burnt in some special conditions. But if the supersulphated cement concrete, conceived to give good strengths in ordinary conditions of tem-

perature, is steam cured, the sulphate passes too rapidly into solution and the final strengths chance to be mediocre, as though gypsum instead of anhydrite had been used in normal conditions of temperature.

Amphoterous admixtures tend sometimes to behave differently according to the ambient temperature.

When two ions of a salt have opposing effects, *it is generally the retarding ion that prevails.* For example, calcium chloride is a retarder for aluminous cement although Ca^{++} tends to accelerate the dissolution of the alumina, because the Cl^- ion is a retarder for the same dissolution.

In particular, when an ion of the admixture is a coater, it is always its action which prevails.

Certain anionic tensio-active admixtures are:
—accelerators for the aluminates by means of the Na^+ cation,
—retarders for the silicates by means of R^- anion.

4) *Certain cement components*, which rapidly pass into solution in the mixing water, can, in certain respects, be considered as admixtures. This is the case of calcium sulphates added to most cements, of a part of the portland cement clinker alkalies, and even of the calcium hydroxide produced by the silicates of the clinkers, particularly by the alite (see par. Setting and False-Setting).

Setting and False-Setting

We have seen (par. General Points) that hydration of cements is produced by the dissolution of certain components of the grains in the interstitial water and crystallization in these interstices in a hydrated form. This dissolution takes place progressively as regards the aluminates (par. Hydration of Aluminates) and principally as regards the silicates (cf. par. Hydration of Silicates) since the penetration of water into the grains is itself progressive.

The concentration (in the initial aqueous phase) of hydrated solid products, therefore, progresses regularly, and this results in a higher shearing strength, which was initially null: by definition a fluid has no shearing strength. The Vicat needle measures, in fact, a shearing strength of the paste and allows one to appreciate what is termed the "*initial*" *and* "*the final setting time*".

The addition of a retarder-coater admixture such as sodium fluoride delays the "setting". For this a dose corresponding to a monomolecular coating of calcium fluoride on the cement grains suffices. That is:
—surface of grains × thickness of the coating × volumic mass of fluoride,
for instance, for one gram of cement of the specific surface of 3,000 cm^2/g:

$$3{,}000\ cm^2 \times 3.5 \cdot 10^{-8}\ cm \times 3.2\ g/cm^3 = 0.00034\ g$$

It follows that the dose of sodium fluoride of *0.4 per 1000* (in respect to the weight of the cement) sufficies to retard considerably the setting. For the coating admixtures having more important molecules than those of sodium fluoride, more important doses would be necessary. This is the case of for example, certain sodium lignosulfites which are retarders-coaters when they are used at high doses.

Yet the sodium fluoride is used as an "accelerator" for certain uses but at a rather high does. In fact, it is true that the fluoride is a *retarder for the cement hydration*, but if it is added in sufficient quantity to the mixing water saturated with lime by the initial hydration of the cement, it precipitates also with the Ca^{++} ions, *within the aqueous interstices*. So it is a "*gelificator*" or "*thickener*" for these interstices; it is rather a "pseudo-accelerator".

Water saturated with lime contains about 1 gram of calcium per litre. One can calculate that its precipitation under the CaF_2 form, requires about 2.1 gram of NaF per litre, that is to say about *one thousandth* of the cement for usual concretes. One obtains so, to get the gelification, a minimum dose of calcium fluoride of $0.4 + 1 = 1.4$ per 1.000. But the Ca^{++} ions which are precipitated by F^- ions are renewed by Ca^{++} ions originating in the cement and the stronger the dose of fluoride is, the more marked is the gelification. In fact doses of about 1 % or even more are used.

Thanks to this example one can distinguish "setting" from "false-setting":
—*The setting originates in the hydration of cement grains* which pass into solution and crystallize in the aqueous interstices.
—*The false-setting originates in the precipitation of admixtures* initially soluble, in the aqueous interstices.

One must take as admixtures, in this respect (as we saw it in par, Accelerators and Retarders), not admixtures specially added to the cement, but also the hydration products which pass into solution *during the mixing*: alkalies, lime originating in portland cement clinkers, calcium sulphate.

The setting and the false-setting have, of course, common points, in particular, both of them need the presence of the cement components which precipitate in the aqeuous interstices. But they show noteworthy differences which are deduced from the principles we have enacted:

—1) The false-setting is always quick (a few minutes, at most);

—2) It is almost not retarded by cold;

—3) *It does concern but a trifling proportion of the cement components* (a few per cent, and even sometimes less than 1 %);

—4) It only results in trifling strengths (a few kg/cm² at most);

—5) It only occurs with a trifling liberation of heat;

—6) It is "broken" by a re-mixing.

Even though the fringe between the setting and the false-setting is not quite defined, it is absolutely necessary to characterize clearly their respective process. The understanding of the latter may allow one to avoid them, to obviate their inconveniences or to use them rationally. We will give some examples of what is above:

1) We saw previously that the alkaline fluorides are either strong retarders or pseudo-accelerators (it means accelerators of setting, but retarders of hardening). They can so be used in order to get a false-setting, for instance, in the case of *projected concrete* or of rapid withdrawing from the mould. It is all the same with other admixtures which precipitate in presence of Ca^{++}: tetraborates, phosphates, carboxilates. This is why tensio-active admixtures (air entraining agents, plasticizers, fluidifiers) sometimes increase the viscosity of concrete, at a high dose, whereas they are retarders at a weak dose.

2) One can create a false-setting by means of the admixtures which precipitate in basic medium as, for instance, the ferric sulphate which involves the gelification of the aqueous interstices by the precipitation of $Fe(OH)_3$ and eventually of the hydrated calcium sulphate.

3) The *chlorideless accelerators* may be alkaline bases; but on one hand they are caustic for the workers, and, on the other hand they weaken the final strengths. They are generally replaced by salts of weak acids: silicates, aluminates, carbonates which behave like the corresponding alkaline ions (for the same molarity), and of which the anions participate in the gelification of the aqueous interstices by means of the precipitation with the lime originating in the portland cement, under the hydrated forms of calcium silicates, aluminates and carbonates. The final strengths can this way be not too much lowered.

4) This gelification is used too for the *waterproofing agents*, but in order to avoid a disturbing false-setting one must sometimes reduce the proportion of the lime of the cement which passes into solution, and must add for this effects a small dose of coater (a phosphate for instance).

5) A part of the *alkalies of portland cement* rapidly passes into solution in the course of the mixing. It can be said that the clinker alkalies are auto-accelerators. Their action is somewhat moderate for the reason that their dissolution is progressive; and so, a portland cement containing, for instance, 1 % of K_2O is not so rapid as when the corresponding proportion of caustic potash is added to a similar cement without alkalies. But it does happen that the aeration of certain cements relatively rich of soluble alkalies confers them a false-setting, although the aeration generally retards the setting. The *carbonation of the alkalies* entails at the time of mixing, in the aqueous interstices, the precipitation of the alkaline carbonates, in presence of the lime in solution, in the form of calcium carbonate.

6) The common false-setting is that of *dehydrated gypsum at the time of grinding* when the temperature of the cement is above 100°C. The setting of the plaster thus formed provokes the false-setting of the cement. This is really a false-setting in the proper sense that must be given to this term.

7) A sulphate false-setting is also provoked by the addition of barium chloride to cements which contain gypsum.

8) The acceleration of aluminous cement by means of lime or of portland (which rapidly liberates lime) proceeds partly from what we have termed a false-setting: in the aqueous interstices this lime passed into solution is precipitated in presence of calcium aluminate coming out of the aluminous cement.

Mechanical Strengths and Homogeneity

It results from the principles of hydration which we have exposed, that the strengths of the hydraulic binders are obtained with the normal fineness and at the normal temperature:

—*During the first minutes*, thanks to the very calcic aluminates (quick-setting cement, aluminous cement mixed with lime);
—*During the first hours*, to the little calcic aluminates (aluminous cement) or to the very calcic aluminates retarded by gypsum (portlands rich in C_3A);
—*On the first days*, to the very calcic silicates (portlands);
—*At a longer period*, to silicates and to silico-aluminates little calcic (slag cements, pozzolanic cements, portland cements relatively poor in lime and alkalies).

The obtainment of these strengths can be accelerated by favouring the dissolution of hydratable compounds:

—higher grade of fineness,
—addition of accelerating admixtures,
—heating,

Heating is more favourable to silicates than to aluminates: the portland cements rich in C_3A (from 12% to 15% of C_3A) have lower strengths when warm than when cold. Aluminous cements also.

The cement paste which confers strength to concrete has a *high heterogeneity* for different reasons:

1) Immediately after the mixing and the working stage the relatively soluble components which diffuse from the grains in the liquid, particularly alkalies, calcium sulphate, lime, are uniformly distributed to the aqueous interstices as they have only a few dozens of microns to travel for that purpose *in a liquid;* but as crystallization of the hydrates goes on, this phase acquires a shearing strength and the concrete acquires *ipso facto* a mechanical strength. The diffusion of the different components is progressively slowed down, so much their ions and molecules are bigger and less mobile, that is to say, less soluble. Thus the lower the (water/cement) ratio is, the less rapid the hydration.

The electrons themselves become less mobile from one atom to the other in the course of hydration and the *electrical conductibility* diminishes at the "end of the setting".

2) The cement grains have various dimensions: the grains inferior to a micron (the number of which is of the same importance as that of the grains superior to a micron) are rapidly hydrated (often in less than 24 hours) whereas the hydration of bigger grains sometimes lasts several years.

3) Cement grains are heterogeneous: they contain different silicates, aluminates, ferrites, sulphates, etc.. They can contain clinker, slag, pozzolana, gypsum. The diffusion of their components and their hydrations can be more or less rapid. The interior surfaces of the aqueous interstices have their origin from cement grains or from aggregates or from reinforcement, or from moulds.

4) Concrete is not always homogeneous for multiple reasons (mixing, segregation etc.).

5) The medium of conservation of concrete can create heterogeneities: evaporation of water, carbonation by the atmosphere, percolation of aggressive waters (either pure, acid, or sulphated).

One must, therefore, not be surprised at the diversity of hydrates occasioned during hydration.

Conclusion

The problem of hydration of cements is not simple; but one can already grasp at least qualitatively most of the phenomenons which are inherent: setting, hardening, hydraulic shrinkage, etc. No method should be neglected in order to progress in this respect, and further knowledge cannot be considered as acquired, unless all observations and all possible measures are corroborated. It is conspicuous to realize for instance that the first values of the dimension of the minute interstices which subsist between the solid hydrated surfaces were determined, thirty years ago, by measuring hydraulic shrinkage, and their order of importance has never been canceled since.

One can hope that ulterior researches will allow one to precise the present knowledge concerning hydration, particularly on the point of view of the quantitative data. One cannot, however, dissimulate that the way will be long, since cement hydrates are evidently more complex than water, and many particularities of this simple substance are not yet enlightened.

Supplementary Paper II-43 Contribution of Analysis by Means of an Electron Microprobe to the Cement Chemistry

Pierre Terrier*

Synopsis

The study of minerals and anhydrous glasses in cement and their change during hydration is carried out in CERILH using analysis with an electron microprobe. This enables the qualitative and quantitative analysis to be made by X-ray emission of the elements present in a volume of some cubic microns under the polished surface of the sample examined with a microscope.

Anhydrous silicates and aluminates in portland cement contain precipitated inclusions and impurities in solution. Microanalysis characterizes them in industrial clinkers.

The chemical composition of fly ashes used in cements is relatively constant; however, in the same ash some heterogeneity can occur between the grains as a consequence of the rapid passage of unburnt coal through the flame. The glass produced belongs to the silica-mullite-anorthite system and contains different proportions of iron, alkalies and magnesia.

In cement pastes, the hydration of aluminates with fixation of the sulphate ion leads to the formation of acicular crystals grouped in separate positions in the intergranular interstices. The hydration of tricalcium silicate is effected by the penetration of water which converts the anhydrous silicate into hydrated silicate in place while part of the lime diffuses outside the grain and crystallized in the form of hydroxide.

The reaction of ash grains in cement or lime pastes is effected by a superficial change of the vitreous grains with the formation of an hydrated envelope with a mainly low silica content which diffuses into the interstices and combines with lime.

Introduction

In 1949, A. Guinier and R. Castaing proposed a physical method of elements microanalysis at the congress in Delft. In 1951, R. Castaing described in his thesis the electron microprobe (1). Since then, the equipment has been perfected and the analysis has as much developed in metallurgy as in mineralogy and in biology.

We give, here, some examples of the use of this method in regard to cement chemistry. They deal with the composition of the minerals of cement clinker, the composition of fly ashes, the hydration of portland cement and the "pozzolanicity" of the ashes.

Electron Microprobe Analysis

A solid target bombarded under vacuum, with an electron beam, emits an X-ray radiation. The latter contains a continuous background, and lines representative of the constituent elements of the target, and there exists a relationship between the intensity of a line and the concentration of the element emitting it. The different lines are analysed, that is to say, separated by means of spectrometers.

A variable self-bias triode-type gun produces an electron beam which is focussed on the section to be studied, by means of two electro-magnetic lenses. An adjustment of electronic intensity eliminates the influence of possible variations in the emission of the electron gun.

The specimen contains a diamond-polished section; its surface is made conductive by a film of nickel deposited under vacuum. The observation of the impact of the electrons on the target is obtained by means of a microscope having a mirror objective which permits the coaxial focus of the electron and light beams. Two chambers, placed on each side of the

*Centre d'Etudes et de Recherches de l'Industrie des Liants Hydrauliques, Paris, France.

column, contain the curved crystals spectrometers and the gas-flow proportional counters, which are combined to them. These spectrometers allow the revelation of the radiations of the elements classified by Mendeleev, except for the first four elements.

The displacement of the analyzing crystal and of the detector on a focussing circle crossing the point of impact permits the qualitative analysis of the target. The quantitative analysis is achieved by clamping the spectrometer in an appropriate position, and by comparing the intensities of the radiation when emitted by the sample under consideration, and by a standard.

One may also possibly shape the image of the distribution of an element, by means of an oscilloscope: a small area of the specimen is scanned by the electron beam, in synchronism with the spot of the oscilloscope, the latter being modulated in intensity by the signal of the counter.

By modulating the intensity of the oscilloscope beam by a signal proportional to the number of electrons absorbed by the specimen, one forms the electron image, i.e. a data comparable to an optic view, but in which the fluctuation of the average atomic number from one phase to another comes into account for the differentiation.

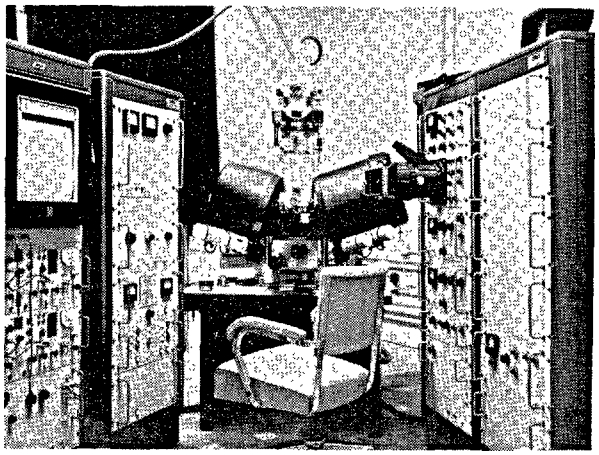

Fig. 1. *Electron microprobe. General layout*
Center: Electron and light optics. Spectrometers
Left: Two pens recorders; two channels. EHT supply and adjustment; vacuum meters and control.
Right: Nanoamperemeter; X-ray and electron display; condenser supply, objective supply; astigmatism control and illuminator supply. Sweep chassis

The Clinker Minerals

The study of the influence of the various elements on the formation and the stability of the minerals depends on the solution of the problem of the composition of the minerals contained in industrial clinkers.

Images of the distribution of the elements in the crystals have been obtained by means of the microprobe by Philibert and Weinryb for an aluminous clinker (2). Taylor (3), later Moore (4), and more recently Terrier, Hornain and Socroun (8) have expounded those relative to portland clinkers.

Wright (3) has determined the calcium in alite and belite. Determinations in alite have been effected by Moore for MgO, by Terrier and Capitant (5) for Al_2O_3 and Fe_2O_3 and by Peterson (7) for MgO, Al_2O_3 and Fe_2O_3. In belite, Moore has determined MgO and Peterson K_2O. These authors have also effected determination in the interstitial phase.

The CERILH has undertaken the complete analysis of the clinker minerals. The values shown in Table 1 have been extracted from the "Revue des Matériaux" (8) in which our first results have been published.

It appears that the alite contains about 3% of minor oxides, the contents of which change from one clinker to another. Belite contains as far as 5% minor oxides; it is richer than alite in Al_2O_3, Fe_2O_3 and alkaline oxides.

Table 1. *Compositions of the crystals of alite and belite expressed in percentages*

Alite				Belite		
Clinker 1	Clinker 2	Clinker 3		Clinker 1	Clinker 2	Clinker 3
71.0	70.9	73.1	CaO	63.2	63.6	63.7
24.9	24.9	25.3	SiO_2	31.5	31.5	33.7
1.1	1.3	0.7	Al_2O_3	1.8	1.8	1.3
0.6	0.6	0.8	Fe_2O_3	0.9	0.8	1.1
0.9	0.3	0.4	MgO	0.5	0.3	0.3
0.2	0.2	—	K_2O	0.8	0.7	0.4
0.1	0.1	0.1	Na_2O	0.2	0.2	0.4
0.2	0.4	0.2	TiO_2	0.3	0.1	0.3
trace	0.1	0.1	P_2O_5	0.3	0.3	0.1
99.0	98.8	100.7	Total	99.5	99.3	101.3

The determinations relative to the C_3A and C_4AF aluminates are delicate if one takes into consideration the fact that the modern kilns deliver quenched products in which the components of the interstitial phase are often closely entangled. From the measures we have gathered, one can infer that the C_3A phase contains about 3% SiO_2, 5% Fe_2O_3, 0.6% MgO, 0.9%

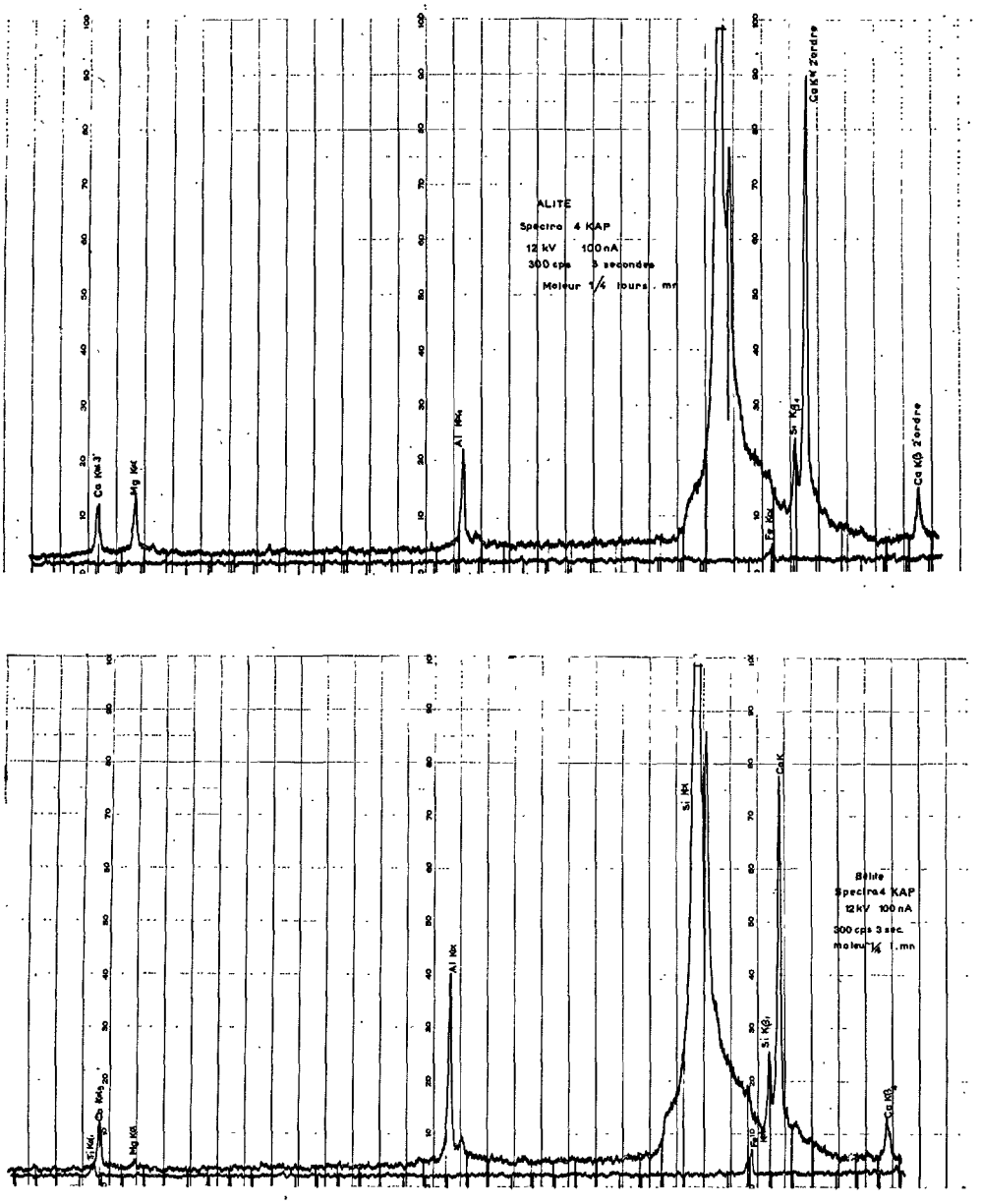

Fig. 2. *Qualitative composition of Alite and Belite crystals in clinker; lines records*

K_2O, 0.4% Na_2O and 0.3% TiO_2; whilst the percentages in the C_4AF phase are of about 2% SiO_2, 2% MgO and 1.8% TiO_2.

These determinations are still carried on at the CERILH, in collaboration with the crystallographic research team, by the study of the correlations which exist between the composition and the allotropic form in which the silicates occur in the clinkers.

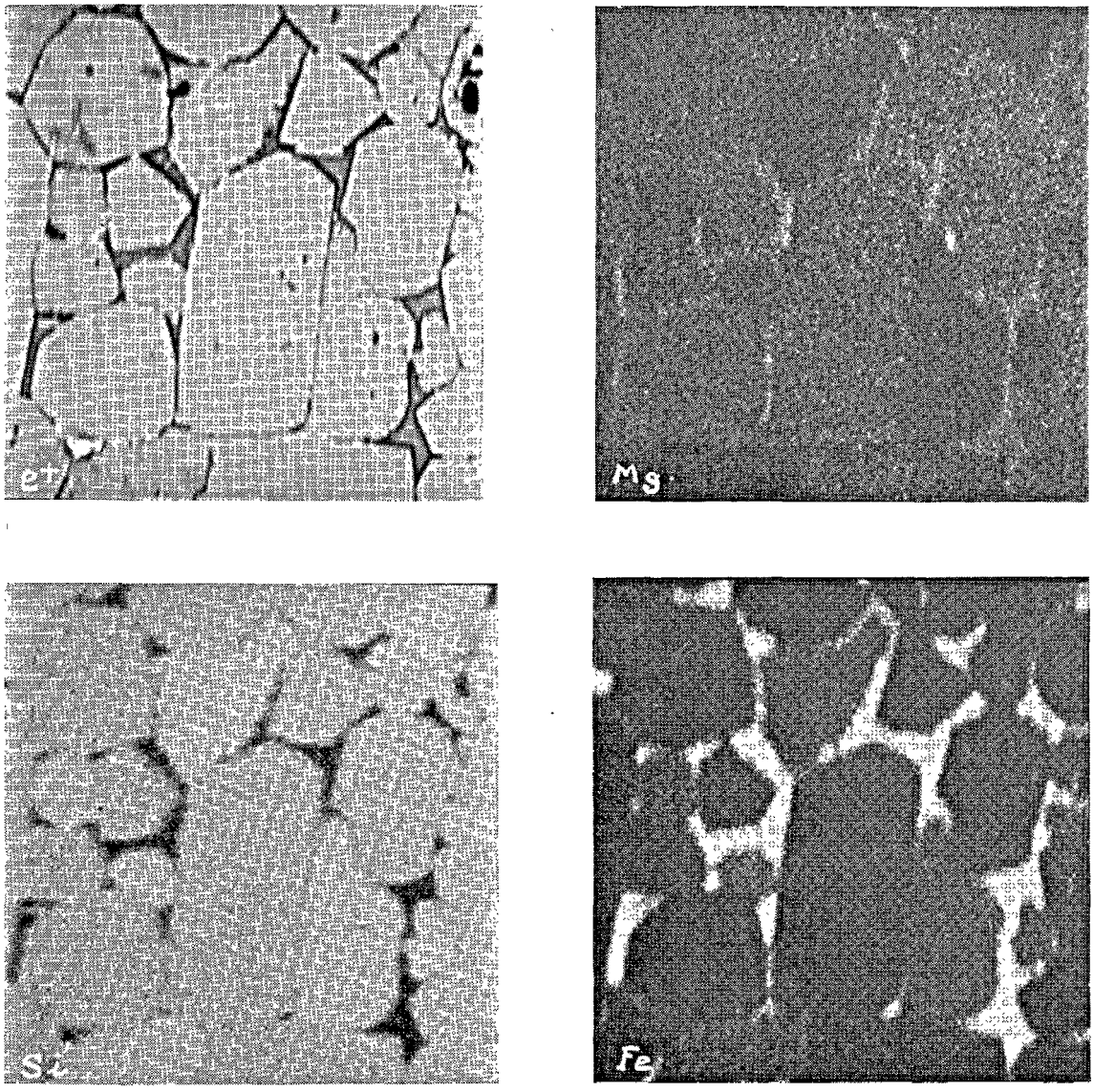

Fig. 3. *Electron image* (e^+) *and X-ray images for* Mg, Si, Fe.
Polished section of clinker; 100 microns side

Fly-Ashes

The fly-ashes issued by the flame of the generating plant result from the melting of coal leavings: clay, quartz, pyrites, calcite, gypsum, dolomite, etc.

Among the uses of ashes which profit of the spheric form of the grains, their lightness, their composition, or their pozzolanicity, the incorporation into cement particularly engage our attention, in France, an attention which is based at the same time on a long industrial experience and on laboratory studies in which the CERILH was very early involved.

The ashes are constituted by vitreous spheres, either solid or hollow, by spongy fragments, by mineral grains, and by unburnt fragments. The fineness of the ashes is related to that of the coal and to the type of the collector; the unburnt substance is related to the nature of the coal and the type of generating plant. The proportion of vitreous phase is due to the nature of the leavings, to the fineness of grinding, and to

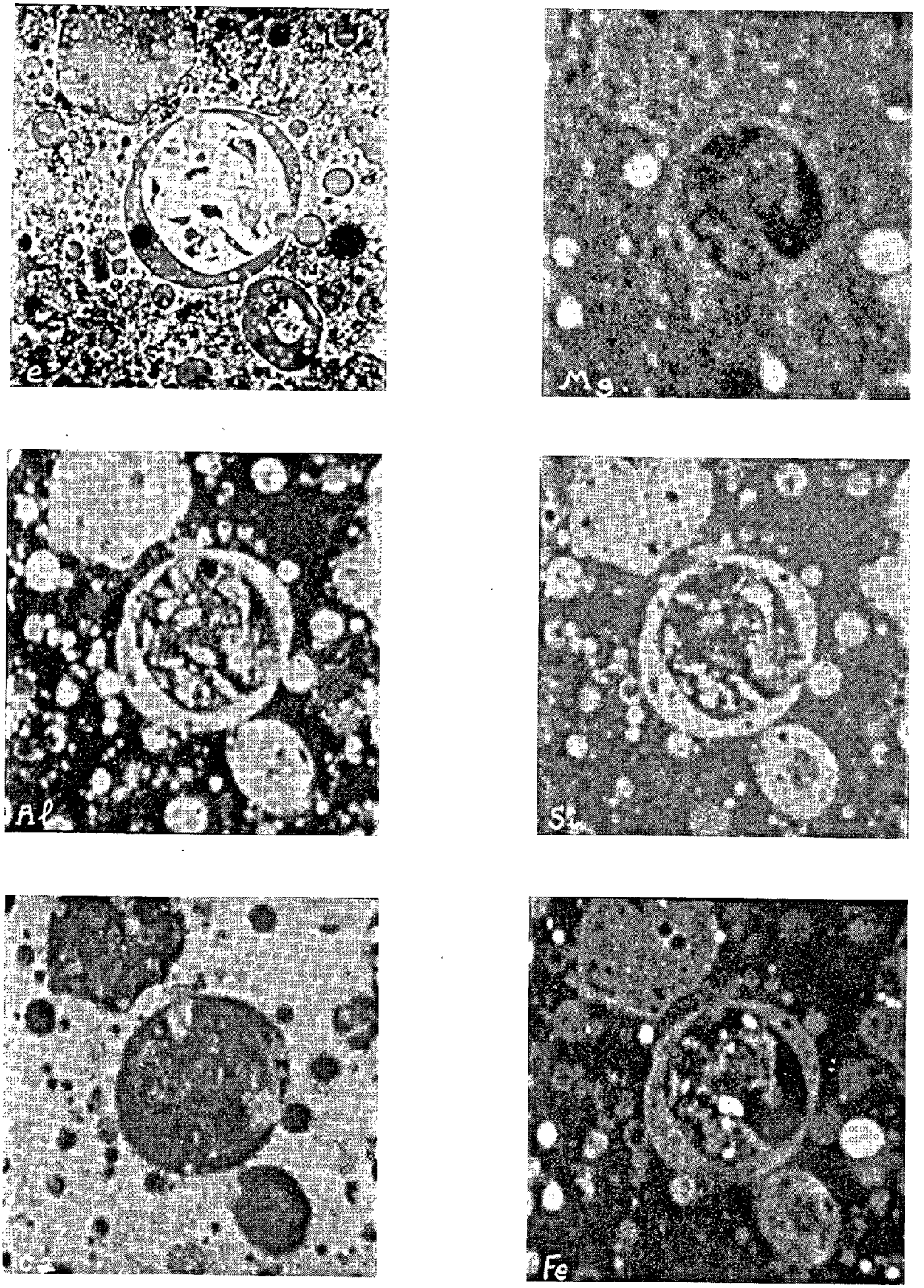

Fig. 4. *Electron image* (e^+) *and X-ray images for* Mg, Al, Si, Ca *and* Fe. *Polished section of lime and fly ash mixture; 100 microns side.*

Table 2.

	Composition of the ashes	
	2A Mean of the ashes of French coal	2B The studied ash*
SiO_2	50	51.4
Al_2O_3	30	27.7
Fe_2O_3	7	9.0
CaO	2	3.1
MgO	2	2.0
SO_3	0.5	0.1
Na_2O	1	0.8
K_2O	4	4.2
TiO_2	1	1.6

*Special granulometric fraction 7 to 80μ

the thermal treatment.

The study of the representative samples taken in the generating plant shows a constant variation of all the properties of the ashes from the furnace to the end of the dust collector. The first precipitated fragments are the most important in size. They are porous and heterogeneous, whilst the finest ones, recovered at the end, are compact.

Table 3. *Elementary compositions obtained by probe for grains of a same ash*

SiO_2	Al_2O_3	Fe_2O_3	CaO
58	36.1	3.0	2
53.1	33.1	6.3	—
51.1	42.9	5.1	—
43.5	24.2	9.6	18.4
42.5	30.2	12.9	7
42.1	29.3	17.9	4.6
42.1	24.2	26.8	—
42	29.5	20.8	—

To the constancy of the macroscopic composition of coal ashes (Table 2) is opposed a microscopic heterogeneity, the consequence of the rapid passage of the coal leavings through the flame which does not allow a diffusion of the bodies in presence and a complete reaction.

Eight characteristic analyses of vitreous grains of the same ash are shown on Table 3. The glasses potentially contain mullite, quartz, anorthite and ferrites. They contain, moreover, 0 to 7% K_2O and variable contents of MgO. The unmelted quartz and the mullite of devitrification are associated to them.

Hydration of Portland Cement

The study of the hydration of portland cement has been undertaken on pastes of particular granulometric graduation (7 to 80μ) and pastes of complete granulometric gradation.

The hydration of aluminates takes place with fixation of the sulphate ion, and produces acicular crystals which are grouped in discrete sites in the intergranular interstices. Three determinations of this phase shown on Table 4 demonstrate that it has an intermediary composition between an aluminate and a sulphoaluminate of calcium.

Table 4. *Composition of the acicular crystal groups in portland pastes**

After	2 years	2 years	3 years
CaO	44.5	45.1	41.2
Al_2O_3	21.9	23.2	24.0
SO_3	9.8	9.0	9.2

*of 7–80μ granulometry.

The hydration of tricalcium silicate is obtained by a penetration of water which transforms anhydrous silicate into hydrated silicate whilst a part of the lime diffuses outside the grain and crystallizes in the hydroxide form: portlandite. The measurements obtained by the electron microprobe have shown that the hydrated silicate had a mean molecular ratio CaO/SiO_2 of 1.65 for a duration up to 90 days for the 7 — 80μ fraction tested (6). This ratio varies from one crystal to another. We have discussed the mechanism of the hydration of alite which probably begins by a topochemical reaction.

In the portland paste, the portlandite contains in course of time, small quantities of SiO_2, Al_2O_3 and K_2O. At the end of three years, the portlandite crystals have the following composition: CaO = 74.2, SiO_2 = 2.5, Al_2O_3 = 1.7, K_2O = 0.7.

Pozzolanicity of the Ashes

The reaction of the ash grains in cement or lime pastes takes place with a superficial transformation of the vitreous grains with formation of a "corroded" envelope, poor principally in silica.

Twenty compositions of active grains are shown in Table 5. It does seem that the vitreous phase is reac-

Table 5. *Compositions of active grains of the same ash*

SiO_2	Al_2O_3	CaO	Fe_2O_3
57.8	33.8	0.4	2.6
57.4	39.5	0.6	2.5
55.9	35.2	2.7	5.4
55.5	38.5	0.5	3.0
55.4	33.8	0.3	3.7
53.9	37.0	4.5	3.0
53.2	31.2	7.7	2.3
52.9	35	0.3	3.1
52.1	30.2	6.3	5.1
49.9	38.9	0.8	3.9
49.9	32.5	0.7	11.2
49.2	35.9	0.4	7.0
49.1	29.7	5.3	3.7
47.6	23.6	1.5	18.0
47.4	32.8	4.1	11.6
46.2	30.4	7.6	6.4
44.0	27.6	2.0	17.9
43.7	27.4	2.4	22.8
41.9	25.7	1.5	21.5
39.6	29.7	0.3	25.6

tive in a large area of composition.

The study of the diffusion of the elements of the ash in the interstices of the pastes is undertaken for pastes of fly-ash cement and for lime-ashes mixtures. In the latter the progression of the diffusion of the silica and of the alumina terminates in concentrations of 14% SiO_2 and 2% Al_2O_3 in the interstices which also contain after 600 days of conservation at 60°C small quantities of MgO and K_2O.

The preparation of synthetic glasses having analogy of compositions with the fly-ashes was effected by means of the Verneuil blowpipe and allows one to carry on the study of the mechanism of the pozzolanic activity by the study of systems having a more limited number of variables.

Conclusion

It is often difficult to make the best of the microscopic observations that can be effected on anhydrous or hydrated products, because of the heterogeneity of the substance. The electron probe, which permits to analyze, point by point, what can be seen with a microscope, is thus a precious tool for the interpretation of the observations. Its high resolution ability is adapted to a great number of problems which concern the grains of the hydraulic binders as they are for the greater part visible with the microscope.

The method is applied whenever localized variations of the composition which cannot be appreciated by the global methods of analysis, impose the necessity of a punctual technique and direct investigation.

The electron probe is a basic research instrument which is unique for the punctual analysis by comparison with standards placed in the same geometry and detected by the same radiation.

Although corrections are necessary, they can be greatly reduced by the choice of standards neighbouring the phases to be analyzed.

Up to the present, the electron probe microanalysis only shows the quantitative distribution of the elements but not their bonding.

These studies which are developed at the CERILH thanks to the intensification of technical research in the French cement profession are effected with the participation of the Centre d'Etudes et de Recherches des Charbonnages de France and the financial help of the Communauté Européenne du Charbon et de l'Acier.

References

1. R. Castaing, "Application de Sondes Electroniques à une Méthode d'Analyse Ponctuelle, Chimique et Cristallographique", ONERA Publication No. 55 (1952).
2. J. Philibert and E. Weinryb, "Quelques Applications du Balayage Automatique sur la Microsonde de Castaing", Journal de Microscopie, **1**, No. 1, 13–22 (1962).
3. H. F. W. Taylor, "The chemistry of cements", Academic Press, London and New York. vol. 1, 119–120 and P. W. Wright (mentioned by Taylor,) (1964).
4. A. E. Moore, "Examen d'un Clinker de Ciment Portland par Microanalyse à la Sonde Electronique" Silicates Industriels Belgique **30**, No. 8, 445–50 (1965).
5. P. Terrier and M. Capitant "Etude de l'Hydration du Ciment Portland par Microanalyse (émission X)", 4° Congrès International Optique des Rayons X et Microanalyse. Orsay. Hermann Edition Paris (1965).
6. P. Terrier and M. Moreau, "Recherche sur le Mécanisme de l'Action Pouzzolanique des Cendres Volantes dans le Ciment", Revue Matériaux Construction France. No. 613–614. Publication Technique CERILH No. 176 (1966).
7. O. Peterson, "Untersuchung von Portland-Klinker mit der Mikrosonde", Zement-Kalk-Gips No. 2, 61–4 (1967).
8. P. Terrier, H. Hornain and G. Socroun, "Quelques Applications de l'Analyse par Microsonde Electronique à l'Etude des Minéraux du Clinker", Revue Matériaux Construction (1968). No. 3.

Oral Discussion

Renichi Kondo and Shunro Ueda

As the thickness of the hydration layer of C_3S particle is very thin, Dr. Roy and Mr. Grutzeck could not recognize the reaction rim by X-ray microanalyzer. Kondo and Ohsawa pointed out that the thickness of the hydration layer of slag was thinner. Accordingly the spot analysis of the hydrate by using X-ray microanalyzer with usual technique seems to be difficult. Therefore we used an electron microscope attached with X-ray microanalyzer and studied semiquantitatively the difference of the compositions between the inside part and the outside part of hydrated C_3S particle as was shown in Fig. 6 of the principal paper II-4.

It must be useful for us if Mr. Terrier shows his experimental conditions as his experiment seems to have good accuracy. Furthermore, if he has some experimental results on various hydrates of cements and additives which are not shown in his supplementary paper, it might be very interesting to show these results.

Oral Discussion

Della M. Roy

Dr. Terrier reports analyses of C_3S hydration products indicating that the phase has a 1.65 $CaO:SiO_2$ ratio. Was this observation made only after relatively long periods of hydration, or was it found to be true also of shorter reaction periods? Indication was also given that analyses varied from grain to grain. What were the limits of variation observed?

Author's Closure

Pierre Terrier

First ages observation of cement hydration products, by means of the EPMA, is difficult. The first condition for the analysis is the following one: the phase to be analysed must be optically defined, which is, generally, not the case. On the other way, the electron probe enters into the target and risks to get through the phase to be analysed. In the way to avoid it, we use an accelerating voltage of the 12 KV, limiting the penetration (while the current limitation limits the heating). The choice of a particular grading (7–80 microns) enables, in some way, to dilate the timescale, and to obtain the optically defined hydrates for which, between 28 and 90 days, the paste strength becomes 950 kg/cm² from 500 kg/cm². Our tests are related to this period and beyond it.

The knowing of the CaO/SiO_2 ratio, which is between 1.35 and 2.00, with a mean value of 1.65, for 28 to 90 days, is a first approach. We must table in account the alumina, the magnesia and the SO_3, and this has been yet well studied by EPMA, for anhydrous products only.

It is showed by Kondo and Ohsawa (1) that the thickness of the reacted layer on C_3S in C_3S-slag mixture is about 0.5 μ at 28 days and the thickness of the reacted layer on the slag particles is about 0.4 μ at the same time.

About C_3S we (2) observed that the thickness is higher on alite in cement, about 3 μ at 28 days, (and not the same from one to another crystal). This agrees with the fact that in the investigation you made (1) more than 70% of C_3S react in portland cement at 28 days and only 30% of C_3S in C_3S-slag mixture.

It is possible to observe the reacted layer on alite by EPMA after 28 days and to examine the ratio Ca/Si with V = 12 kV and I = 30 mA for example. Quantitative measurements are made point by point with a stationary beam on the specimen and on the standard (wollastonite). This conditions and those of Roy and Grutzek (4) are similar but these authors studied synthetic compounds.

Relating to cement aluminates hydration, your experiments (3) show that the simultaneous presence of $Ca(OH)_2$ and of semihydrated calcium sulfate makes the alumina practically insoluble, which undergoes little replacement. The hydrated aluminates are forming from the anhydrous aluminates and are developing in the interspace with fixation of the sulfate-ion, which is evidenced by the joint figures obtained with the microprobe for the cement granulometry of 7–80 μ, after three years curing.

On the other hand, the hydration mechanism with internal hydrates and external hydrates formation applies not only to portland cement, but also to high furnace slag. A 5–80 μ slag hydrated with 10% soda, with a W/C ratio = 0.46, has a compressive strength of nearly 500 kg/cm².

That was studied with the microprobe. The evolution is recapitulated in Table 1 for molar ratios and

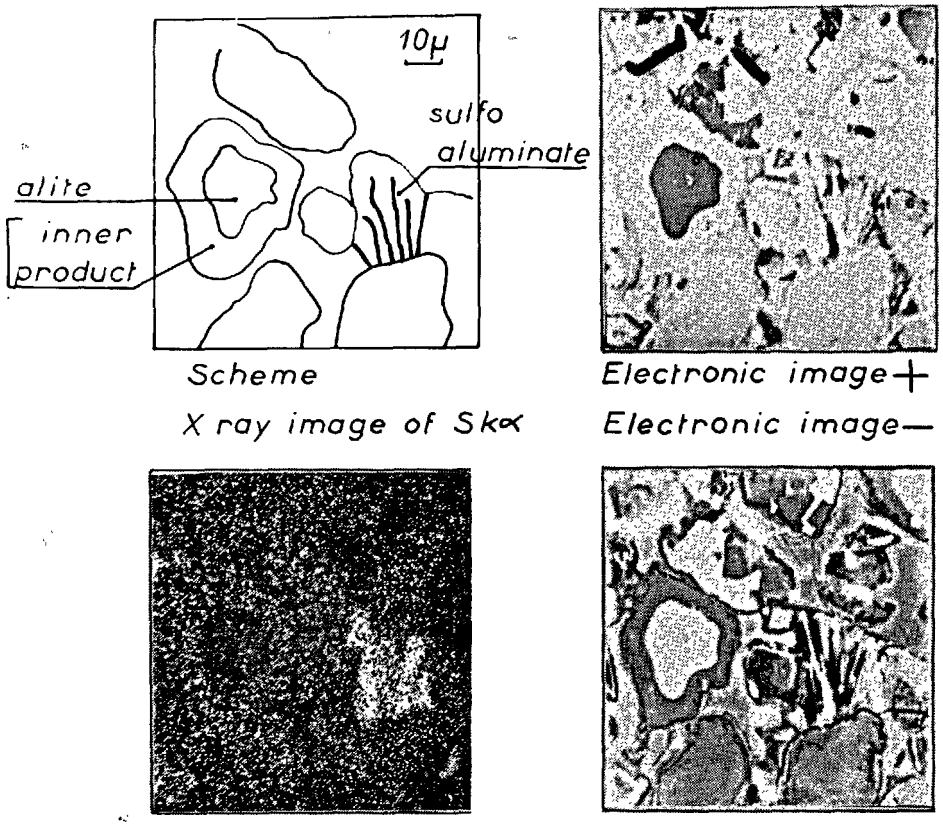

Fig. 1. *Electronic images and scanning of S cement 7–80 μ. Pure paste after 3 years.* $\frac{e}{c} = 0.28$

Table 1.

	Slag	Inner product	Outer product
$\frac{CaO}{SiO_2}$	1.46	1.07	1.75
$\frac{SiO_2}{Al_2O_3}$	3.46	4.65	2.16

by the diagram, Fig. 2.

You indicate (3), in good place, that the hydration rate of alite is modified by the minor elements. In some way, cement contains an impressive amount of additives whose action and ending are not already known. EPMA is useful to study this and we have done recently a new approach of the composition of alite (5).

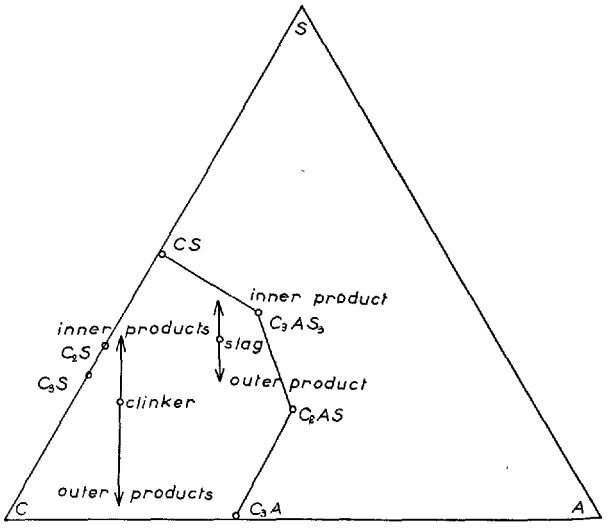

Fig. 2.

References

1. R. Kondo and S. Ohsawa, Studies on a method to determine the amount of granulated blastfurnace

slag and the rate of hydration of slag in cements. Part IV. Session 3. V. ISCC.
2. P. Terrier and M. Moreau, 1966.
3. R. Kondo and S. Ueda, Kinetics and mechanisms of the hydration of cements. Part II. Session 4. V. ISCC.
4. D. M. Roy and M. W. Grutzeck, Electron microprobe studies of cement phases. Part II. Session 4a. V. ISCC.
5. P. Terrier, H. Hornain and G. Socroun, Sur la composition des alites. Rev. Mater. Constr. 1968. to be published.

Supplementary Paper II-62 The Behavior of Aluminate-Ferrite Phase during Hydration

Paul Jäger, Udo Ludwig and Hans E. Schwiete*

Introduction

In continuation of our earlier work (1, 2) the mechanism which occurs when the aluminate-ferrite clinker minerals C_3A, C_6A_2F, C_4AF and C_2F react with calcium hydroxide and gypsum or anhydrite in aqueous solution have been investigated by chemical means, by infra-red spectroscopy, by X-ray diffraction and with the aid of the electron microscope. The chosen fractions of C_3A or calcium aluminate ferrite and calcium sulphate correspond approximately to commercial portland cement. The amount of calcium hydroxide added was sufficient to form ettringite and convert the remaining C_3A and calcium aluminate ferrite into tetracalcium aluminate ferrite and into tetracalcium aluminate ferrite hydrate respectively in the presence of a saturated lime solution.

As an indicator for the rate of hydration the absorption of water and free sulphate were measured.

Reactions in the System C_3A–$CaSO_4$–CaO–H_2O

The investigation of C_3A was carried out with 0, 30, 60 and 90% gypsum relative to the C_3A content.

In the pure C_3A system the principal product in the first hours was hydrogarnet (C_3AH_6) and later tetracalcium aluminate hydrate (C_4AH_{19}). The proportion of tetracalcium aluminate hydrate remained the same during a three-year observation period, and this means that for a long while no appreciable recrystallization of the unstable C_4AH_{19} to the stable C_3AH_6 took place.

With 30% gypsum ettringite was first formed but disappeared again after 8 hours. In its place the sulphate-bearing phases monosulphate hydrate or the mixed crystals of this with tetracalcium aluminate hydrate were observed. The occurence of C_3AH_6 as well as C_4AH_{19} was clearly recognizable.

With 60% gypsum ettringite was stable over a greater range. Monosulphate hydrate and its mixed crystals with tetracalcium aluminate hydrate only appeared after a full day's hydration.

After 60 days ettringite reappeared and was still present after 300-day hydration together with monosulphate hydrate, the mixed crystals with tetracalcium aluminate hydrate and pure tetracalcium aluminate hydrate.

With 90% gypsum it was only after 2 days that a marked decrease in the content of the initially-formed ettringite was observed. Simultaneously monosulphate hydrate appeared in the reaction mixture. However, in contrast to the other mixtures, no solid solution between monosulphate hydrate and tetracalcium aluminate hydrate was observed.

The results of these experiments can be summarised in the following table:

These results show that with rising content of gypsum the amount and stability of ettringite increases in the period before monosulphate hydrate or the mixed crystals with tetracalcium aluminate hydrate are formed. The formation of monosulphate hydrate and tetracalcium aluminate hydrate or the mixed crystals of the two begins only when all the sulphate ions have been used to form ettringite or when the concentration of sulphate ions is no longer sufficient to allow this mineral to crystallize. Concomitant with the formation of monosulphate hydrate the initially-formed ettringite is decomposed and the remaining C_3A is hydrated. The amount of gypsum added determines the speed of hydration of C_3A.

Table 1. *Formation of* $C_3A \cdot Cs_3 \cdot H_{32}$ *and* $C_3A(Cs, CH) \cdot H_{12}$ *in the system* C_3A–$CaSO_4$–CaO–H_2O

Amount of $CaSO_4 \cdot 2H_2O$ added %	Occurrence of $C_3A \cdot Cs_3 \cdot H_{32}$	Occurrence of $C_3A \cdot Cs \cdot H_{12}$ $C_3A(Cs, CH) \cdot H_{12}$
30	at once†	12 h
60	at once	24 h
90	at once	48 h

†observed under the electron microscope after 30 sec.

*Institut für Gesteinshüttenkunde, Technische Hochschule Aachen, Aachen, West Germany.

Reactions in the System (C_2F–C_6A_2F)–$CaSO_4$–CaO–H_2O

In the experiments with the calcium aluminate ferrites C_2F, C_4AF and C_6A_2F a constant amount of sulphate containing 27.9% SO_3 was added; this corresponds to 60% dihydrate or 47.4% anhydrite. The amount of calcium hydroxide added was such that, allowing for the formation of the most lime-rich phases, a saturated solution of lime was still present.

Bonding of Sulphate

The combination of sulphate with calcium aluminate ferrite was determined, making allowance for the free sulphate in the solution and as a residue. Fig. 1 shows the amount of sulphate combining with C_6A_2F in the presence of lime in aqueous solution. It can be seen that the reaction is much faster in the case of anhydrite than if dihydrate is used. After only 6 hours 70% of the anhydrite has reacted but only 43% of the dihydrate. After 12 days both compounds are completely fixed.

C_4AF, also, is hydrated much faster in the presence of anhydrite than with dihydrate, as is obvious from Fig. 2. The combination of sulphate is only complete after 90 days in the case of anhydrite and in the case of the dihydrate it is almost complete after 180 days.

As may be expected, the slowest reaction is shown by C_2F, although for this compound also the reaction proceeds much faster in the presence of anhydrite than with dihydrate (Fig. 3). In this case the combination of sulphate is only complete after 180 — 270 days.

The reaction of calcium aluminate ferrite with gypsum or anhydrite shows the influence of the different sulphates on the concentration of sulphate ions in the solution. It was observed that the sulphate concentration increases with increasing ferrite con-

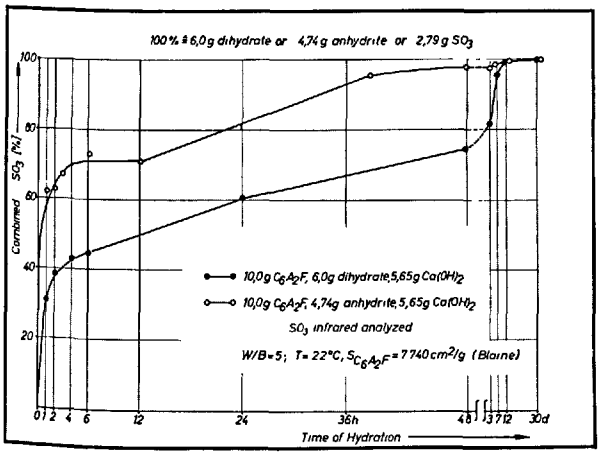

Fig. 1. *Sulphate-bonding in system* C_6A_2F–$CaSO_4$–CaO–H_2O

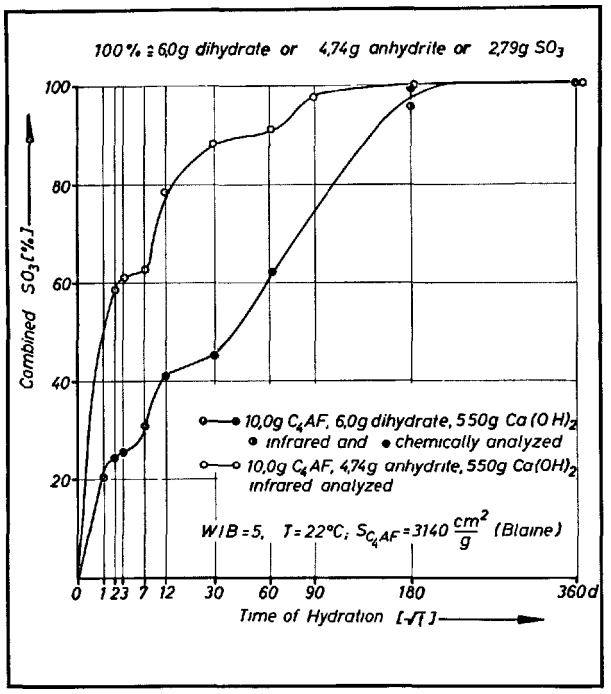

Fig. 2. *Sulphate-bonding in system* C_4AF–$CaSO_4$–CaO–H_2O

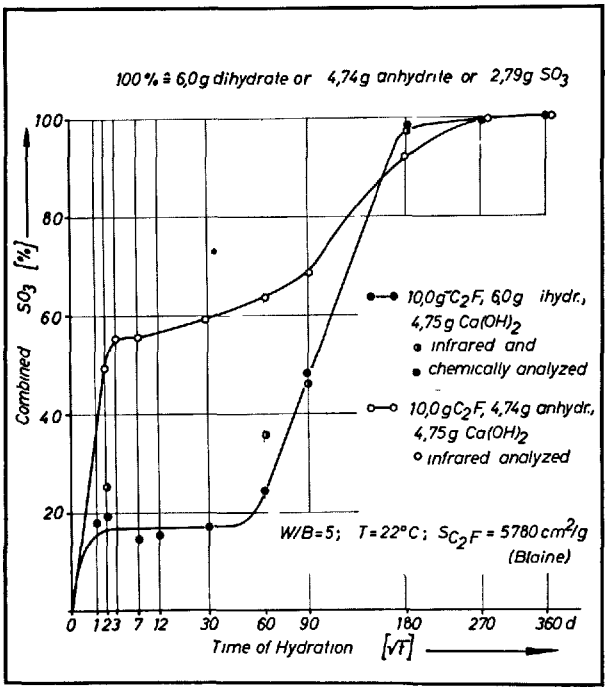

Fig. 3. *Sulphate-bonding in system* C_2F–$CaSO_4$–CaO–H_2O

Table 2. *Sulphate bearing hydration products after 2 years in the system* $C_2(A, F)$–$CaSO_4$–CaO–H_2O

	$C_3(A, F)Cs \cdot H_{12}$	$C_3(A,F) \cdot (Cs, CH) \cdot H_{12}$	$C_3(A, F) \cdot Cs_3 \cdot H_{32}$
C_6A_2F	+	+	weak
C_4AF	+	+	"
C_2F	+	–	"

tent of the calcium aluminate ferrite, but decreases with rising aluminate content.

These reactions show in particular that C_6A_2F reacts so fast that at no time is the solution saturated with respect to anhydrite, or even with the dihydrate, under normal conditions of temperature and grain size of the reagents.

Formation of the Hydrates

The formation of hydrates in the residue was determined by X-rays over a period of 2 years. To begin with ettringite, phases ($C_3(A,F)\ Cs_3H_{32}$) with varying ratios of Al^{3+} to Fe^{3+} were formed almost exclusively. With increasing aluminate content of the calcium aluminate ferrites, the trisulphate hydrates are altered faster into the monosulphate hydrates and the mixed crystals of this with tetracalcium aluminate hydrate by using up the remaining ferrite. The solid solutions do not occur with C_2F. For the remaining ferrites C_4AF and C_6A_2F these mixed crystals prove increasingly unstable with time, i.e., their amount decreases, the longer the hydration continues, with the formation of monosulphate hydrate. As in the case of C_3A the appearance of the mixed crystals is less likely as the amount of sulphate is increased. In the case of the calcium aluminate ferrites, the formation of the mixed crystals decreases with increasing iron content of the ferrite, and is less pronounced in the presence of anhydrite than in the presence of dihydrate.

Hydrogarnets were observed in all the reaction mixtures. Their amount increases with a rising aluminate content of the ferrites.

The following table show the sulphate bearing hydration products formed by the reaction of calcium aluminate ferrite with anhydrite and lime in aqueous solution after a hydration period of two years.

Discussion and Summary

On the basis of previous and present work on the hydration of the aluminate ferrite phases in aqueous solutions of calcium hydroxide and calcium sulphate, we have been able to confirm our opinion that, directly after the addition of water, the calcium aluminates and calcium aluminate ferrites become protected from further rapid hydration by a layer of ettringite-like phases.

In the presence of solutions rich in sulphate and lime ettringite forms as soon as water is added, together with negligible amounts of monosulphate hydrate and its mixed crystals with tetracalcium aluminate hydrate. Only when the sulphate ion concentration is too low to allow ettringite to crystallize are monosulphate hydrate and the corresponding mixed crystals formed to any extent. The ettringite initially precipitated is then altered to monosulphate hydrate or the mixed crystals with tetracalcium aluminate hydrate by reaction with the remaining C_3A. The point at which all the remaining C_3A is used up and the ettringite decomposes is dependent upon the amount of sulphate present and the grain size of the C_3A. Similar results were found for the calcium aluminate ferrites.

Determination of the amounts of water and sulphate combined, and examination by X-rays and in the electron microscope have shown that the rate of hydration of the calcium aluminate ferrites increases with increasing alumina content in the system $C_2(A, F)$–$CaSO_4$–CaO–H_2O. This is seen in Fig. 4. If one refers the amounts of calcium aluminate ferrite to a common specific surface area, the increase in weight of the residue shows that, after one day the quantity of C_2F that has reacted is only 50% of the amount in the case of C_4AF, 30% in the case of C_6A_2F and 15% in the case of C_3A.

The schematic presentation in Fig. 5, which includes ideas of Manabe (3), shows that, during hydration in the presence of solutions rich in sulphate and lime, the principal hydration products of the aluminate ferrite phases in portland cement clinkers are trisulphate hydrate together with small amounts of monosulphate hydrate and its mixed crystals with tetracalcium aluminate hydrate. This occurs directly after the addition of water. Only when the sulphate ion concentration is insufficient to form ettringite do monosulphate hydrate and the mixed crystals begin to appear in increasing amounts. The trisulphate first formed is more or less completely altered to monosulphate hydrate after a few hours depending upon the amount of sulphate present.

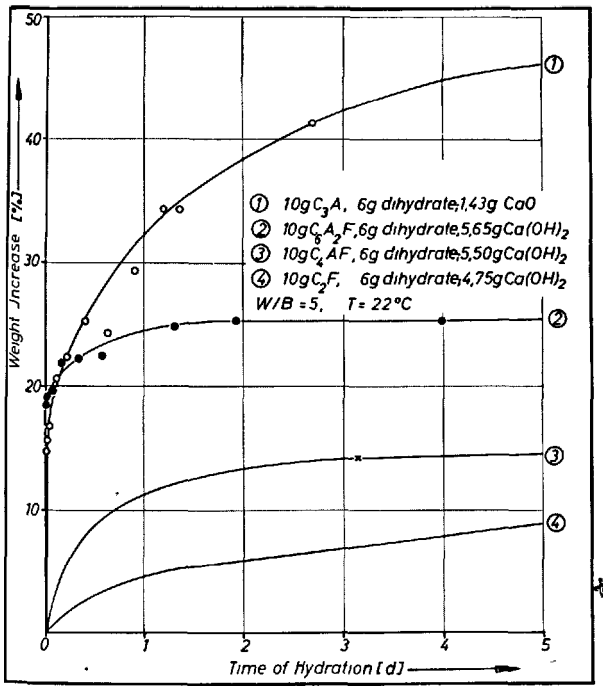

Fig. 4. *Weight increase of the precipitation during hydration of aluminate—ferrite phase based on the specific surphace of 1000 cm²/g (Blaine)*

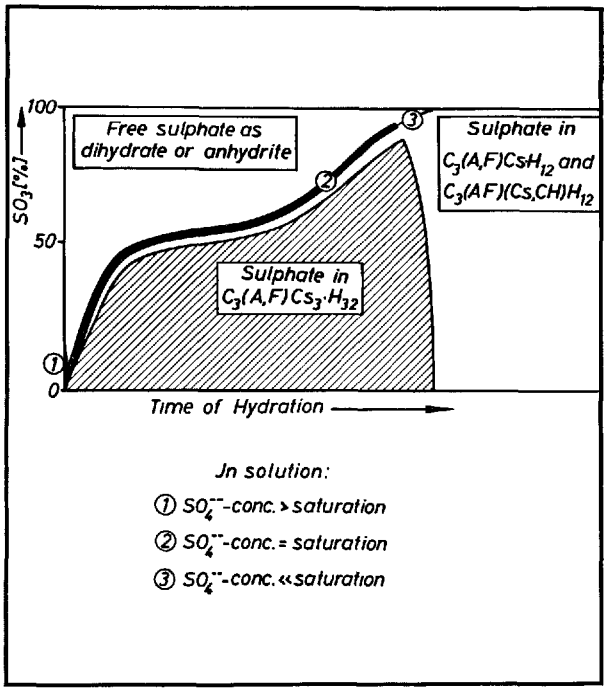

Fig. 5. *Reaction of sulphate during hydration of* C_3A *and* $C_2(A,F)$

The experimental results show that the amount and kind of the calcium sulphate added is of prime importance for the rate of hydration of the C_3A and the calcium aluminate ferrites.

Furthermore the formation of tri- and monosulphate hydrate from the calcium aluminate ferrites is only possible by combining 1 molecule of calcium hydroxide. This contrasts with the reaction for C_3A. When the formation of tri- and monosulphate hydrate is complete, hydration of the aluminate or aluminate ferrites to tetracalcium aluminate ferrite hydrate occurs by combination with calcium hydroxide which is split off the calcium silicates. Thus the hydrolysis and hydration of the calcium silicates is influenced and controlled by the course and speed of the hydration of the tricalcium aluminate and calcium aluminate ferrites and their combination with lime.

Also important is the fact that more or less rapid hydration of C_3A and the calcium aluminate ferrites has an effect on the area of reactive surface of the calcium silicates in the clinker.

It follows from the above results that the amount and kind of the calcium sulphate added has a complex influence on the rate of the initial hydration of the aluminate-ferrite phases of the clinker:

1. by retarding and controlling the hydration of C_3A and the calcium aluminate ferrites,
2. by fixing the free calcium hydroxide released by hydrolysis of the calcium silicates in the clinker, which is then combined with the crystallizing trisulphate hydrate, monosulphate hydrate and tetracalcium aluminate ferrite hydrate. This causes an acceleration in the hydrolysis of the calcium silicates and
3. by creating a greater reactive surface area in the calcium silicates of the clinker.

In practice the accelerative effect of anhydrite as compared to the dihydrate is of great importance, in particular in the production of portland cements low in, or free of C_3A.

We are grateful to the Association of German Cement Producers, Düsseldorf, for their financial support.

References

1. H. E. Schwiete, U. Ludwig and P. Jäger: "Investigations on the system $3CaO\cdot Al_2O_3$–$CaSO_4$–CaO–

H_2O" Zement-Kalk-Gips **17**, 229–236 (1964).
2. H. E. Schwiete, U. Ludwig and P. Jäger: "Investigations on the system $3CaO \cdot Al_2O_3$–$CaSO_4$–CaO–H_2O" Special Report 90, Symp, on Structure of Portland Cement Paste and Concrete Highway Research Board Washington 1966 p. 353–367.
3. T. Manabe: "Discussion to the work of A. Hansen" Chem. Cem. Proc. 4. Intern. Symp. Washington, D.C. 1960, p. 404.

Supplementary Paper II-96 Synthesis of the Analogues of Portland Cement and Other Binding Materials on the Basis of Acidic-Basic Reactions

Nikolai F. Fedorov*

Synopsis

The analysis shows that the hardening of portland cement and other most widely distributed binding materials of normal and autoclave hardening (lime, phosphate and oxychloride cements) is the result of chemical reactions in which acid radicals and metal cations take part together with the protons and hydroxyl groups and which, therefore, are the reactions of acid-base interaction.

The results of investigation of binding properties of a great number of combinations are considered in the paper, the components of which were selected so that the process of acid-base interaction would take place.

Four groups of materials have been investigated on the basis of the following type systems:

1. Mineral-water systems, where minerals are the analogoues of calcium silicates or aluminates, viz. plumbates, stannates, titanates and zirconates of alkali earths.
2. Metal oxide-acid systems, where acids are HCl, H_3PO_4, H_2SO_4, $H_2C_2O_4$, etc.
3. (The binding materials of autoclave hardening). MeO–MeO_2–H_2O systems, where MeO are the oxides of alkali earths and MeO_2 are TiO_2, SnO_2, PbO_2 and ZrO_2.
4. Metal oxide-polyatomic alcohol systems (glycernie, glycol).

In each group, for a great number of investigated combinations the formation of stone-like materials has been established, physico-mechanical properties of the latter having been investigated and for separate, most typical ones, the phase composition of new formation has been investigated by means of X-ray, infrared and chemical analysis.

Introduction

At present it is difficult to find such an industry where artificial stone would not be used. Artificial stone is used both in the most ancient industries such as construction and the most modern ones, such as radioelectronics (1).

Among the methods of technical stone synthesis, the methods and ways of silicate technology are the most popular ones, including several varieties. Their common feature is the transition from the solid powder material of natural or artificial origin to the monolith—an artificial stone having a certain complex of properties. Schematically, separate varieties of silicate technology may be represented in the following way:

1. Ceramic technology:
   powder→moulding→burning→artificial stone
2. Technology of glass-crystalline materials:
   powder→melting→moulding→heat treatment →artificial stone.
3. Technology of cements:
   powder→mixing with fluid→artificial stone.
4. Technology of autoclave materials:
   powder→moulding→hydrothermal treatment →artificial stone.

The comparison of separate methods shows that, from the technological point of view, the most convenient one is the method of producing artificial stone by the technology of binding materials. However, in spite of this rather important fact, the technology of ceramics and glass have achieved the greatest progress in their development lately. So, during only one or two decades man has learned to produce and organized the industrial production of materials having unique electrical and magnetic characteristics, the ones having good mechanical properties in conditions under the influence of high temperatures, etc. by the ceramic technology, i.e. by the technology which was once developed for producing red brick, porcelain, and pottery.

The transition from traditional ceramic materials and glass to the new ones was stipulated in most cases not by any special changes in the technology of their production, but mainly by the expansion of the

*Chemical Technology of Cement, Leningrad Lensoviet Institut of Technology, Leningrad, U.S.S.R.

"geography" of the chemical elements used, by the substitution of the widely used in nature and readily available elements such as O, Si, Al, Fe, Ca, Na, K, Mg, H, etc. by less distributed and even rare ones, such as Ti, Sn, Pb, Zr, Nb, W, Mo, Sr, Ba, Ni, Co, F, etc.

The range of materials produced by the technology of binding materials may also be widened, and, if one takes into account the simplicity of the production and the fact that the development of technology is often hindered by the lack of suitable materials giving possibility, for instance, to cement together metals, ceramics, glass, plastics, particularly under ordinary conditions, the range of such materials has to be enlarged.

According to the experience of ceramic technology, when developing the new kinds of binding materials, it seems necessary to reject the idea of using only inexpensive, readily available raw materials. The search should be carried out very widely, enveloping possibly greater number of elements, including even the rare ones. In order that the search of the new kinds of binding materials would be more specific and economical it is necessary to proceed, first of all, from the ideas developed by V.F. Zhuravlev (2) and from his main conclusion in particular: "Binding properties are not something permanent and inherent only to a limited number of mineral compounds. The display of binding properties is a common link of the chain of phenomena subject to definite regularities; there are numerous other combination and chemical reactions, the binding properties of which should be expressed stronger or weaker than the known ones".

From numerous family of chemical reactions it is necessary first to consider the ones that are the main reactions for the preparation and application of the widely distributed binding materials.

The analysis shows that the hardening of portland cement, alumina cement and other most widely distributed binding materials (gypsum, lime, phosphate, and oxy-chloride cements) is the result of the crystallization of the products resulting from the chemical reactions in which acid radicals and cations of metals along with protons and hydroxyl groups interact. Chemical reactions of such kind are called acid—base reactions. So, one of the directions when searching for new binding materials which are the analogues of the traditional binding materials, should be the detailed consideration of all possible acid-base reactions; the range of the objects to be investigated should be limited by the reactions in the solid-liquid systems and solid-H_2O (vapour) ones, although acid-base reactions may be realized:

a) through a solution, b) in the saturated water vapour medium, c) through the melt, d) in the solid phase, and e) in the gaseous phase.

As it was stated above, in the present paper the range of the objects studied was limited by considering only such systems and such chemical reactions as have long been used for preparing binding materials, viz. 1) mineral (salt)—water, 2) oxide (hydroxide) —acid (salt), 3) base oxide-acid oxide (in the saturated vapour medium), 4) oxide (hydroxide)—organic compounds having acidic properties.

Binding Materials on the Basis of Mineral-Water System

The principal chemical reaction resulting in the hardening of the binding materials of this type is the exchange reaction with water when the hardly soluble compounds are formed. This reaction takes place when portland and alumina cements harden, to be more exact, when calcium silicates and aluminates react with water. It has long been noticed that calcium silicates and aluminates are not the only representatives of chemical compounds which are capable of being hydrolyzed. Zhuravlev and the collaborators of the Chair of Chemical Technology of Cement, Leningrad Lensoviet Technological Institute showed experimentally that there exist the analogues of calcium silicates, aluminates and ferrites, strontium and barium silicates and aluminates, in particular, as well as titanates, manganates, chromates and stannates of calcium, strontium and barium (2–6).

According to the periodic system of D.I. Mendeleev, one should expect the plumbates of the alkali earths to be hydraulically active ones. So, the comparative investigation of the binding properties of plumbates and other silicate analogues—stannates, titanates and zirconates of the alkali earths has been done in the given section, the latter having been investigated from the point of view of hardening in the hydrothermal conditions, since it has not been done before.

All the minerals in $MeO–MeO_2$ systems about which there is certain information have been synthesized. Due to the fact, that a number of systems formed by the dioxides of group IV and by the alkali earth oxides have not been investigated, the compositions corresponding to the investigated systems have been

chosen for the synthesis. The oxides of Mg, Cd, Zn, Ba, as well as the calcium and strontium carbonates and the Ti, Sn, Pb, Zr dioxides have been taken as the original materials. The synthesis has been done in the following way: the original materials were weighed in the amount corresponding to the stoichiometry of the mineral to be synthesized and then ground in the laboratory ball mill. The duration of the grinding was such that all the ground powder would pass through the sieve No. 0063. From the raw mixture prepared in this way the samples have been made, the tiles, having dimensions of 5 × 5 × 4 cm under the pressure of 500 kgs. per sq. cm., which have been burned. The burning has been done either in the muffle furnace or in the laboratory furnace with carborundum heaters. The temperature of burning was chosen according to the melting temperature of the minerals, and it amounted to 0.8–0.9 of the melting temperature. The readiness of the synthesised minerals was checked by chemical determination of the content of unreacted base oxide (excluding zinc and cadmium minerals) as well as by the X-ray or infrared analysis. The data of the condition of sample synthesis are given in Table 1. The samples which are not monomineral ones are marked with the sign "*".

All the products obtained were ground till they passed through the sieve 0063 mesh, and were mixed with water until the paste of ordinary consistense was prepared. The samples to be tested for mechanical strength were made of the paste in the shape of cubes having the edge of 1.41 cm long.

The results of investigating the strength properties of the materials obtained are given in Table 2. It should be noted that the hardening of all samples took place both in the normal and hydrothermal conditions of hardening, the autoclaving being done under the pressure of 8 and 16 atmospheres during 4 or 8 hrs. respectively, at a maximum pressure.

Consideration of the data given in Table 2 allows one to draw the following conclusions: When reacting with water minerals—calcium silicate analogues show pronounced binding properties, in contrast to minerals —silicates the binding properties of calcium plumbates and stannates, strontium and barium distinguishing themselves when the basicity of the mineral is

Table 1. *Conditions of synthesis of the minerals studied*

Preparation	Number of burnings	Total keeping at maximum temperature	Temperature °C	Amount of free MeO in % by weight
	Minerals—plumbates			
*$CaO \cdot 2PbO_2$	1	8	960	—
*$CaO \cdot PbO_2$	4	24	960	0.56
$2CaO \cdot PbO_2$	4	27	900	0.21
*$SrO \cdot 2PbO_2$	1	8	900	—
*$SrO \cdot PbO_2$	3	18	920	3.2
$2SrO \cdot PbO_2$	1	8	940	—
*$BaO \cdot 2PbO_2$	1	8	910	—
*$BaO \cdot PbO_2$	3	20	930	0.25
$2BaO \cdot PbO_2$	5	36	900	3.15
$MgO \cdot PbO_2$	1	8	900	not checked
	Minerals—titanates			
$CaO \cdot TiO_2$	1	8	1380	0.20
$3CaO \cdot 2TiO_2$	2	16	1380	0.73
$2CaO \cdot TiO_2$	2	16	1380	16.00
$SrO \cdot TiO_2$	1	8	1380	—
$3SrO \cdot TiO_2$	1	8	1380	—
$2SrO \cdot TiO_2$	1	8	1380	—
$BaO \cdot TiO_2$	1	8	1300	—
$3BaO \cdot 2TiO_2$	1	8	1280	—
$2BaO \cdot TiO_2$	1	8	1380	—
$MgO \cdot TiO_2$	1	8	1380	—
$CdO \cdot TiO_2$	1	8	1380	—
$ZnO \cdot TiO_2$	1	8	1380	—
	Minerals—stannates			
$MgO \cdot SnO_2$	2	12	1380	—
$2MgO \cdot SnO_2$	3	18	1380	—
$CaO \cdot SnO_2$	1	6	1350	—
$2CaO \cdot SnO_2$	3	18	1380	—
*$3CaO \cdot 2SnO_2$	1	6	1350	—
$SrO \cdot SnO_2$	2	12	1350	—
$2SrO \cdot SnO_2$	2	12	1350	—
$BaO \cdot SnO_2$	2	12	1350	—
*$2BaO \cdot SnO_2$	4	24	1380	45.5
	Minerals—zirconates			
$CaO \cdot ZrO_2$	1	6	1350	—
$SrO \cdot ZrO_2$	1	6	1350	—
*$2SrO \cdot ZrO_2$	2	12	1350–1400	12.0
$BaO \cdot ZrO_2$	1	6	1350	—
$ZnO \cdot ZrO_2$	1	6	1400	not determined
$2ZnO \cdot ZrO_2$	1	6	1400	〃
$CdO \cdot ZrO_2$	1	6	1350	〃
$2CdO \cdot ZrO_2$	1	6	1350	〃

Table 2. *Compressive strength (kg/cm²) of the minerals—calcium silicate analogues*

Mineral	Compression limit (kg/cm²)				
	Under ordinary conditions of hardening			Under hydrothermal conditions of hardening	
	3 days	7 days	28 days	8 atm	16 atm
$CaO \cdot 2PbO_2$	0	0	0	70	165
$CaO \cdot PbO_2$	10	80	100	170	435
$2CaO \cdot PbO_2$	525	600	625	560	810
$SrO \cdot 2PbO_2$	0	0	0	95	150
$SrO \cdot PbO_2$	5	10	110	390	560
$2SrO \cdot PbO_2$	45	75	140	495	560
$BaO \cdot 2PbO_2$	10	15	120	180	230
$BaO \cdot PbO_2$	35	75	145	280	350
$MgO \cdot PbO_2$	0	0	0	0	0
$MgO \cdot SnO_2$	0	0	0	0	0
$2MgO \cdot SnO_2$	0	0	0	15	30
$CaO \cdot SnO_2$	0	10	15	70	75
$2CaO \cdot SnO_2$	100	150	150	415	500
$3CrO \cdot 2SnO_2$	75	100	100	340	365
$SrO \cdot SnO_2$	15	30	30	70	115
$2SrO \cdot SnO_2$	225	300	300	70	115
$BaO \cdot SnO_2$	0	15	15	10	25
$2BaO \cdot SnO_2$	does not harden				
$BaO \cdot TiO_2$	0	0	0	130	200
$3CaO \cdot 2TiO_2$	5	10	15	165	210
$2CaO \cdot TiO_2$	30	15	10	195	255
$SrO \cdot TiO_2$	0	0	0	75	100
$3SrO \cdot 2TiO_2$	15	15	45	85	125
$2SrO \cdot TiO_2$	45	70	95	125	230
$BaO \cdot TiO_2$	0	0	0	65	95
$2BaO \cdot TiO_2$	185	195	360	170	195
$2ZnO \cdot TiO_2$				30	
$2CdO \cdot ZrO_2$				620	
$3CdO \cdot ZrO_2$				230	
$SrO \cdot ZrO_2$				0	
$CaO \cdot ZrO_2$				0	
$BaO \cdot ZrO_2$				45	

equal to 1. Autoclaving intensifies the process of hardening of the greater majority of the minerals investigated and it results in displaying the hydraulic activity for a number of them, e.g., monobasic calcium titanates, strontium and barium, which shows that monobasic strontium, calcium, and barium titanates are not hydraulically inert compounds as it was thought before. Since, as it was found in the laboratory of the chair, the same refers to the low basic silicates of the alkali earths. Therefore, speaking about some substance exhibiting binding properties or not doing so it is necessary to state the conditions under which it does so.

The fact that cadmium zirconates display binding properties contradicts to the point of view of V. F. Zhuravlev and a number of other investigators, according to whom minerals—silicates of zinc, cadmium and magnesium and their analogues are not able to display binding properties. The hydraulic activity of cadmium zirconates which is rather pronounced requires further attentive investigation. To find out the character of the hydration process of the minerals —calcium silicate analogues, the investigation of the hardening products formed during their reaction with water has been carried out when calcium stannates were hardening in particular.

For investigation the methods of thermography, X-ray and infrared analysis have been used. The comparison of thermograms, X-ray patterns, and the spectra of the original minerals and the hardening products showed their substantial differences. The respective curves for calcium ortho and metastannates also differ from each other. There are no effects on the thermograms of the original stannates while on the thermograms of the hardening products of dicalcium stannate are four endothermic effects at the temperature of 140–160°, 310–350°, 470–520° and 770–800°C and an exothermic one at the temperature of 700–730°C. The thermogram of the hardening products of calcium metastannate differs from that of the orthostannate by the absence of endothermal effect at the temperature of 470–520°C and by less intensive other effects. According to the available information in literature (5), the endoeffects at the temperature of 310–350° and 770–780°C appear to be due to the dehydratation of the calcium hydrostannate, and the one at the temperature of 470–520° is due to the decomposition of calcium hydroxide. As to the exothermal effect at the temperature of 700–730°, it is likely to be connected with the recrystallization of the amorphous calcium metastannate. Therfore, it may be suggested from the thermographic data that during the hardening process calcium orthostannate is hydrolyzed giving off calcium hydroxide and forming hydrostannate, while metastannate is hydrated.

The results of X-ray and infrared analysis confirm the fact that the original materials are converted into new hydrated compunds which is demonstrated by the appearance of new diffraction maxima in the X-ray patterns and new lines of absorption in the spectra. When calcium orthostannate hardens hydrolysis also takes place since on the X-ray patterns of the hardening products of calcium orthostannate along with the new diffraction maxima $d/n = 4.66$; 4.04; 2.32; 2.14; 2.08; 1.64; 1.38; 1.34 which are likely to be inherent to the calcium hydrostannates, the strongest lines of calcium hydroxide being distinguished when $d/n = 4.83$; 2.62; 2.40; 1.80. The latter are completely absent in the X-ray patterns of the hardening products of calcium metastannates.

The information given above allows to draw the conclusion that minerals—stannates and possibly, minerals analogues of calcium silicates, in general, when mixed with water are either hydrated or hydrolyzed forming hydrated compounds which are difficult to dissolve and the crystallization of which leads to the formation of cement stone. Exchange reactions with water are known to envelop an extensive class of chemical compounds—salts. So, the minerals considered in the given paper are a small part of chemical compounds which may be employed to obtain new binding materials. Thus, there are prospects for new materials search especially if one takes into account that hydrolysis should be looked upon as a particular case of solvolysis, i.e., an exchange reaction of a solute and a solvent in general. The facts that have been considered in the present paper in combination with the information received by other authors are a sound foundation for obtaining a great number of binding materials of the following type: $MeO–MeO_2–Me_2O_3$, where MeO_2 and Me_2O_3 may be represented both by separate compunds such as PbO_2 and Al_2O_3 and by numerous combinations of the oxides of the same type with each other.

Binding Materials on the Basis of Metal Oxide—Acid (Salt) Systems

Among various binding materials which have been widely used along with cement, gypsum and lime there are two more groups of binding materials—magnesium oxychloride and phosphate or dental cements. The

former are obtained by mixing powder magnesium oxide and its chloride solutions, the latter by mixing certain oxides or the compositions prepared on their basis and phosphoric acid. Until now those groups of binding materials have been considered separately, but the chemical basis of their hardening is nevertheless the same: acid-base reaction. The kinds of cements mentioned above seem to be particular representatives of a large family of binding materials prepared on the basis of solid—liquid systems, when solutions of acids and salts are taken as liquids and the solids are represented by the oxides and compositions formed on their basis.

The given section of the paper has been devoted to checking up the possibility of synthesis of artificial stone on the basis of oxides of different groups of D.I. Mendeleev's Periodic Table and a number of acids: HNO_3, diluted H_2SO_4, HCl, HI and $H_2C_2O_4$ as well as the solutions of sodium acid phosphates which may be used for obtaining the binders (7).

To determine the availability of binding properties the original oxides were ground in the agate mortar and the powder made was mixed with such amount of an acid or salt which was necessary to prepare the paste of normal consistency. Balls or pellets were formed from the paste which were kept under normal conditions during 1–3 days after which they were crushed. The availability of binding properties has been determined, as it was stated above, in the systems MeO–HNO_3, where MeO–ZnO, Bi_2O_3, CdO, ZnO, ZrO_2. If sulphuric acid was used, the hardening compositions were prepared on the basis of the following oxides: Fe_2O_3, Bi_2O_3, PbO, CdO, MgO. When mixing the compounds with HCl solution, the compositions hardened on the following basis: CaO, I_2O_3, La_2O_3 and other rare earths, ZrO_2, TiO_2, Nb_2O_5, Sn_2O, NiO, and all the alkali earth oxides and, when HI was used, the ones on the basis of V_2O_5, BaO, Co_2O_3, ZrO_2. In case the oxides were mixed with oxalic acid, the following oxides gave the cement stone: Sb_2O_5, Co_2O_3, MgO, ZrO, TiO_2 and others.

In the experiments where the oxides were mixed with solutions of acid phosphates of sodium the compositions containing P_2O_5 in the amount of 35% by weight were used. The binding properties were found in the following oxides: Co_2O_3, Fe_2O_3, FeO, CuO, CdO, HgO, PbO_2, SnO_2 when mixed with monosubstituted sodium phosphate in normal conditions of solidification, and in SiO_2, TiO_2, Cr_2O_3, V_2O_5 when heated at 200—300°C. The use of disubstituted sodium phosphate as a mixing agent allows one to obtain the binding properties on the basis of SiO_2, TiO_2, Al_2O_3, ZrO_2, MgO, CaO, SrO, Co_2O_3, Fe_2O_3, FeO, SnO_2, ZnO, CdO. The strength characteristics of some binding materials obtained were determined. The samples from the paste 1:0 having the shape of cubes the size of which was 1 × 1 × 1 cm were tested for compressive strength. The samples were stored in air during 3, 7 and 28 days. The results obtained are given in Table 3. For comparison, the results of testing the samples of portland cement are also given, the latter having been prepared and stored in a similar way.

The data obtained confirm the fact that on the basis of metal oxide—acid systems a whole number of cements may be synthesized, the strength characteristics of the latter being similar to those of portland cement and sometimes even much greater.

More detailed investigation of the binding substances of this kind will result in such new binding materials which will surpass the already well—known magnesia, oxychloride and dental cements. The investigation of the binding substances in the MeO—HCl systems, in particular, showed that the cements obtained by mixing CuO with solutions of cupric chloride or hydrochloric acid in contrast to magnesia cement appear to be not air but hydraulic binding materials since they can harden not only in air but also under water.

As to the cements formed on the basis of metal oxide—phosphoric acid systems, they are used, at present, not only in the dental technique. There are numerous kinds of phosphate cements which are used as heat resistant binders, vacuum lutes for cementing various materials. In the near future the scope of employing such binding materials is likely to become still wider as there are all necessary requisites for this:

Table 3. *Compressive strength (kg/cm²) of cements on the basis of metal oxide—acid (salt) systems*

No	System	Strength (kg/cm²) in 3 days	7 days	28 days
1	Sb_2O_5–$H_2C_2O_4$	37	95	110
2	MgO–$H_2C_2O_4$	69	80	94
3	ZrO_2–HNO_3	20	25	40
4	MgO–HI	30	90	150
5	CdO–H_2SO_4	400	540	700
6	Cement of trade mark 500	58	90	105
7	V_2O_5–Na_2HPO_4	180	—	—
8	MgO–Na_2HPO_4	240	—	—
9	CdO–NaH_2PO_4			
10	CuO—$CuCl_2$			
	a/ 10% sol $CuCl_2$	58	60	63
	20% " "	66	66	68
	30% " "	79	80	84
	40% " "	165	115	120
	50% " "	155	100	180
	60% " "	225	235	240
11	CuO–HCl			
	a/ 15% sol. HCl	60	65	68
	b/ 25% " "	150	150	160
	c/ 30% " "	165	165	180

first, both the composition of the powder constituent and the mixing fluids for such cements may be varied greatly, second, the reacting capacity of the powder and the chemical activity of a mixing fluid may be changed, i.e. one may influence the processes of chemical interaction of solid and liquid components of the binder and the processes of structural formation of artificial stone and, as a result of this, to direct the synthesis of the artificial stone with predetermined properties.

Binding Materials of Autoclave Hardening on the Basis of $MeO-MeO_2-H_2O$ Systems

At present there is no such a definition as binding materials of autoclave hardening in spite of the fact that such materials have long been used in construction. The author suggests an idea of calling by this name solid powder materials of different chemical and mineralogical composition which change into strong stone-like body after moulding and hydrothermal treatment. The typical representatives of this group of materials known from the time of Michaelis are the silicate articles made of finely divided silica and lime, i.e., the articles that result from the reaction of acid and base oxides in the medium of saturated water vapour.

The author considers it probable to expect the existence of numerous analogues of such lime silicate materials.

The investigations carried out by D.I. Tchemodanov and his collaborators (8) as well as by the investigators from the Chair of Chemical Technology of Cement, Leningrad Lensoviet Institute of Technology, confirm the existence of such analogues. The results given below demonstrate this statement.

The following systems have been considered as the objects to be investigated: $MeO-H_3BO_3$, where MeO are the oxides of Mg, Ca, Sr, Ba, Zn and Cd; MeO_2 were taken as acid oxides, i.e. TiO_2, ZnO_2, PbO_2 and SnO_2.

The original samples were prepared from the raw mixture of variable composition from base and acid oxides or an acid. The raw mixture composition varied from 0 to 100% of each component every other 10% by weight. The raw mixtures were ground by means of wet grinding in a ball mill until the fineness of 0063 mesh. The samples were pressed from the mixture, under the pressure of 100 kgs. per sq. cm., their dimensions being $1.41 \times 1.41 \times 1.41$ cm. They were placed into an autoclave. The autoclaving was carried under the pressure of 8 and 16 atm. according to the scheme of raising the pressure—keeping at the same pressure—lowering the pressure during 2–8–2 hrs and 2–4–2 hrs respectively. On the day following the autoclaving the testing of the samples has been made. The testing results are given in Table 4.

The analysis of the data obtained from the quantitative point of view appears to be difficult since the materials of different granulometric composition were used in various combinations in the experiments and the conditions of the hydrothermal treatment were not strictly identical. Nevertheless, it is quite evident that the original statement about the possibility of the artificial stone synthesis by the technology of autoclave materials on the basis of the mixtures of the oxides of groups II and IV of the D.I. Mendeleev's Periodic Table or for the mixtures of H_3BO_3 and MeO is fully justified. The strength of the samples depends upon the nature of acid and base oxides, upon their concentration and as the special experiments proved, both upon the parameters of the hydrothermal treatment and upon the pressure of pressing the samples. One should note that all the systems of $MgO-MeO_2$ investigated are a good foundation for producing the artificial stone the strength of which

Table 4. *Compressive strength (kg/cm^2) of binding materials of hydrothermal hardening on the basis of* $MeO-MeO_2-H_2O$ *systems. $P = 8$ atm*

Base oxide		Acid oxide content in % by weight 20	40	50	60	80
MgO	1	75	300	110	110	240
	2	215	400	495	550	305
	3	95	180	235	195	110
	4	—	—	—	—	—
	5	100	100	60	30	0
CaO	1	15	25	35	75	50
	2	255	475	610	600	325
	3	130	260	335	280	140
	4	100	60	80	60	70
	5	170	40	30	50	40
SrO	1	0	0	0	0	0
	2	170	345	445	410	220
	3	60	110	140	130	75
	4	30	0	0	0	0
	5	70	94	0	0	0
BaO	1	0	0	0	0	0
	2	0	0	0	0	0
	3	45	80	105	95	35
	4	0	0	0	0	0
	5	0	60	130	0	0
CdO	1	—	—	—	—	—
	2	—	—	—	—	—
	3	0	0	0	0	0
	4	450	190	—	70	60
	5	—	—	—	—	60

1. $MeO-SnO_2$ system
2. $MeO-PbO_2$ system
3. $MeO-TiO_2$ system
4. $MeO-ZrO_2$ system
5. $MeO-H_3BO_3$ system

does not yield to that of the samples obtained with other alkali earths. The formation of magnesia compounds of calcium hydrosilicate type is likely to occur much easier from the oxides than in case the anhydrous magnesium titanates, stannates, plumbates and other analogues are used since the artificial stone does not form the latter even in the hydrothermal conditions as it is stated in the first section of the paper.

An interesting phenomenon also takes place in the systems containing zink and cadmium oxides. The combination of those oxides and zirconium dioxide allows one to synthesize the stone having rather high strength.

If the results of mechanical testing of the stone produced on the basis of the same systems of $MeO–MeO_2–H_2O$ by the technology of binding materials and using autoclaving as a hardening intensifier, i.e. with the preliminary synthesis of the anhydrous minerals—calcium silicate analogues were compared with the ones for the stone obtained by the technology of autoclave materials, the preference should be given to the latter ones since, in this case, the expensive operation of burning specially prepared raw material to obtain anhydrous materials has been eliminated.

In conclusion, it may be stated that the hydrothermal treatment of the samples, the components of which were chosen so that the acid—base reaction would take place among them, is an effective means of artificial stone synthesis.

Binding Materials on the Basis of Metal Oxide–Polyatomic Alcohol Systems

A whole number of organic compounds are known to display acid properties when reacting with metals and their oxides. Polyatomic alcohols refer to such kind of compounds in particular, the interaction of a representative of polyatomic alcohol—glycerine and lead oxide being used to obtain a special lute.

In the light of ideas developed by the author, this kind of binding materials may be expected to have analogues, too.

The interaction of the oxides of the elements of groups II, III, IV of the Periodic Table and glycerine or glycol have been investigated from the point of view of obtaining binding materials. The method of making an experiment was the same as the one in the second section of the paper. The results of testing are given in Table 5. They indicate the fact that calcium, strontium, barium, lead and minimum oxides when mixed with glycerine or glycol form quick hardening, high-strength binding materials, the strength of which (e.g., strontium oxide—glycerine system) amounts to 1000 kg. per sq. cm. exceeding that of cement having trade mark 500 and tested under similar conditions approximately fivefold. It should be noted that a number of combinations on the basis of the mixture of the oxides investigated and glycerine produce high—strength binding materials differing from other kind of cement in greater adhesion in relation to glass and metals.

Table 5. *Compressive strength (kg/cm²) of binding materials on the basis of* MeO*—polyatomic alcohol systems (air—kept)*

Oxide	Glycerine			Glycol		
	1 day	3 days	7 days	1 day	3 days	7 days
PbO	185	315	390	150	175	240
CaO	125	600	570	35	640	550
SrO	400	970	1050	—	—	—
70% PbO + 30% CaO	920	850	870	500	340	380
70% PbO + 30% SrO	200	780	—	—	—	—

As it was stated above, among organic compounds there are ones having both acid and basic properties. On account of this fact the author believes that the combination of a solid inorganic powder component and organic liquids will give possibility to synthesize a lot of new binding materials and, possibly, a new separte chapter of the chemistry of binding materials will develop on this basis.

Conclusion

While fulfilling the present investigation, the author set the task to investigate the possibility of synthesis of the new kinds of binding materials having taken the main thesis of V.F. Zhuravlev about binding properties of substances being chemical properties as a foundation. The author assumes that, when developing new binding substances, one should be guided by those chemical reactions which are the main ones in obtaining already well-known, widely distributed binding materials. Large experimental

material gathered indicate the correctness of the above idea, and shows the rich possibilities of the chemistry of binding materials in the synthesis of artificial stone the strength properties of which surpass those of portland cement and which has or, at least, may have specific properties that are the distinctive features of a solid powder component. The ideas of Prof. V.N. Young (9) who considered cement stone to be "microconcrete" containing unreacted grains of original minerals and compounds may be taken for the basis of such a conclusion. If one takes into account the statement mentioned above and the results of the experiments, it is theortically possible to obtain binding materials with most varied properties, such as electrophysical and others as well as binding materials having greater adhesion to metals, glass and ceramics than the cements known to-day.

References

1. U. D. Kingery "Introduction to ceramics" 2nd edition, (translated from English into Russian) St. Publ. of. for Constr. Lit., Moscow. USSR. (1967).
2. V. F. Zhuravlev, "Chemistry of binding materials" (in Russian) Goskhimizdat. Leningrad. Moscow. (1951).
3. S. D. Okorokov and S. L. Golinko-Volfson, U. V. Nikiforov, "Binding properties of manganates of group II periodic system of D. I. Mendeleev" in the Bulletin "Chemistry and practical application of silicates" (in Russian) CBTI Lensovnarkhoz (1960).
4. S. D. Okorokov, S. L. Golinko-Volfson and U. Ya. Starodubtsev "Binding properties of manganates of group II periodic system of D. I. Mendeleev" (in Russian) Proc. Lensoviet LTI VI edition. Leningrad (1960).
5. A. Braniski "Stabiliziertes Tristrontiumsilikat". Zement-Kalk-Gips (in German), No 10, p. 398 (1957).
6. A. Braniski "Strontium Hüttenzemente". Silikattechnik (in German) No. 10, p. 450 (1957).
7. E. Wainer USA Patent No. 2372236. 27. III (1945).
8. D. I. Tschemodanov, I. N. Astafiev, N. S. Tschikovani, L. K. Polozova, E. T. Shmikova, A. T. Sartakova and L. A. Denisova "About binding properties of $CaO-_xO_y-H_2O$ systems in the conditions of autoclaving" in "News of High Inst." No. 3, p. 70 (in Russian) Novosibirsk (1965).
9. V. N. Young. "The foundation of technology of binding materials". Promstroiizdat (in Russian) Moscow, p. 511 (1951).

Supplementary Paper II-122 Electron Microprobe Studies of Cement Phases

Della M. Roy and Michael W. Grutzeck*

Synopsis

The electron microprobe has been applied to the study of cement phases and their hydration products. The instrument used was an ARL-EMX modified microprobe equipped with three spectrometers. Visual cathode-ray tube displays of characteristic Ca–K_α, Al–K_α and Si–K_α emission, and electron back scatter (EBS) displays have been used to follow the progress of hydration of cement phases. In addition, counting techniques were employed to obtain quantitative analytical data. The C_3A hydration process was studied in detail as a function of time as it proceeds from C_3A through the early stage hydration products to C_3AH_6. The C_3S hydration was studied similarly, and finally mixtures of a simplified cement containing C_3A, C_3S and C_2S were examined. It is believed that techniques have been demonstrated which will apply more generally to the study of cement hydration problems.

Introduction

Portland cement offers the researcher a complex multicomponent system, replete with temperature and composition sensitive hydration reactions, poorly crystalline hydrates and extremely small grain size. In order to solve the complex problems involved in the hydration of portland cement researchers have been continually searching for new insights and new methods. An analytical tool which does not depend on crystallinity and which is well suited for non-destructive, in situ analysis of small grains is the electron microprobe. This investigation was begun with the intention of exploring the feasibility of applying the microprobe to various unsolved problems involving portland cement hydration.

While the microprobe was initially applied to the study of metals and sections of large single crystals, White (1, 2) in our laboratories has adapted the microprobe technique to the analysis of crystalline powders. More recently, Moore (3) and Yamaguchi (4) have conducted exploratory work with the microprobe on the identification and distribution of material in cement clinker phases. The microprobe has been recognized as an extremely powerful tool; however, it has not as yet been used to investigate portland cement hydration products. The specific purpose of this research was to adapt electron microprobe methods for examination of hydration products of cement compounds individually and in mixtures, to collect sufficient data to evaluate the method, to compare the results with data obtained by other means and, if possible to establish techniques that could be applied generally.

Experimental Method

General

Standard anhydrous compounds** and hydrates were prepared, identified and examined for purity by optical and X-ray diffraction methods. These were mounted in plastic and were used as microprobe standard samples. Repeated counts were made on different grains of the same material and the resulting data were treated statistically. Several of these materials were also used for preparation of hydrated pastes. Wherever possible, the results of microprobe analyses were compared with X-ray diffraction and optical data. In some cases these data were supplemented by thermogravimetric analysis data.

*Materials Research Laboratory and Department of Geochemistry and Mineralogy, The Pennsylvania State University, Pennsylvania, U.S.A.

** Throughout the paper standard cement nomenclature abbreviations are used as follows:
$C = CaO$, $A = Al_2O_3$, $S = SiO_2$, $H = H_2O$, $F = Fe_2O_3$

Equipment

Electron Microprobe

The electron microprobe used in this investigation was an ARL-EMX electron microprobe* modified with an automatic print out of three spectrometers, a preset time mode of collecting data and a step scanner which moved the sample one micron under the beam between each counting period.

Two types of data were collected: the first entailed the use of a rastering electron beam operating in unison with an oscilloscope. The output, in the form of electron back scatter (EBS) and elemental displays was photographed from the cathode ray tube. The second type of data involved the use of a stationary beam to perform quantitative analyses, registering the counts of characteristic X-rays emitted from the sample. The microprobe was operated at 30 kev with a one-to-two micron diameter spot size. For the rastering beam analysis the current used was 0.03 microamperes on the 3×10^{-8} A scale, while the current used for stationary beam analysis was 0.01 microamperes on the 10×10^{-9} A scale.

Microscopes

A standard Zeiss petrographic microscope and a Leitz reflecting light microscope were used to identify the materials and to follow the course of hydration in pastes.

X-ray Diffractometer

A GEXRD-5 wide range diffractometer equipped with a copper tube was used throughout the study. In addition to standard powder techniques, the diffractometer was used for some constant monitor experiments. In the latter case, the hydrating sample was placed in a square shallow depression in a glass or plexiglass slide and was covered with a 0.001 inch thick Mylar sheet. Repeated scans were then taken until the desired stage of hydration had been reached.

Sample Preparation

Preparation of Standards

Analyzed reagent-grade chemicals used as starting materials have as their highest levels of impurity, $CaCO_3$ (0.08% Na); Al_2O_3 (0.005% Cl); SiO_2 (0.005% heavy metals). The anhydrous compounds CA, C_3A, CA_2, pseudowollastonite (α-CS), β-C_2S and C_3S were prepared by reaction in the dry state at 1400°C. Calcium aluminoferrites were eliminated for simplicity because of the difficulty in analysis of Fe-containing compounds. 1% Al_2O_3 was added to the C_3S before firing to promote crystal growth, and β-C_2S contained 1% B_2O_3 as stabilizer. C_5S_2H (calciochodrodite) was prepared hydrothermally at 650° and 4000 psi (5, 6). For electron microprobe standards it was necessary to select crystals distinguished by their optical properties and X-ray diffraction pattern. It was found that sieved grains in the 44 to 74 μ size range made the best standards and starting materials for hydration studies. These sieved grains entirely contained the electron beam, and at the same time assured us that the observed hydration rims were due only to the outward growth of individual grains. Analysis of such materials and their use as standards of reference made it possible to correct for many of the sources of error in microprobe analysis.

Hydration of Sample for Microprobe Studies

Hydrated pastes of compounds and "synthetic cements" were prepared by mixing the above-mentioned size fraction with water, having a 0.5 water: solids ratio for C_3A, and 0.4 water: solids ratio for C_3S and the synthetic cement. The paste was mixed in a mortar, compacted into a 5 mm. I.D. glass tube, transferred to a rubber-stoppered shell vial and sealed with wax. The temperature of reaction ranged from 28 to 30°C. After the allocated reaction time the sample was immersed in liquid nitrogen (7) and the glass tube was broken away. In the usual case the hydration product was crushed gently in a mortar to enable examination of individual grains with their rims. The samples were then washed in very cold absolute alcohol and vacuum desiccated for five hours.

Sample Preparation for Microprobe

Initial experiments using a "cold-setting" resin, Quickmount revealed an undesirable temperature rise. The final material selected was a mixture of Selectron RS-5003 polyester (98.5 wt.%)**, Nuodex Cobalt Naphthenate (1.0 wt.%)*** here acting as a retarder and the catalyst t-butyl hydroperoxide (0.5 wt.%)****. A dough-like paste was made by adding a few drops of this material to about 250 mg of sample. This paste was placed in the center of a greased microscope

*Built by Applied Research Laboratories, Inc., 3713 Park Place, Glendale, Calif., and modified by Dr. E. W. White, Materials Research Laboratory, The Pennsylvania State University.

** Selectron RS-5003, manufactured by Pittsburgh Plate Glass Co., Pittsburgh, Pa.

*** Nuodex, from Nuodex Products Division, Heyden Newport Chemical Co., Elizabeth, N.J.

**** From Lucidol Division, Walace and Tiernan, Inc., Buffalo, N.Y.

slide, surrounded by a greased section of 3/4" I.D. combustion tubing which was filled with additional plastic material, and covered with a greased 7/8" thinness zero cover glass square. Approximately four days was required for the set. A preliminary polish with 6, 3 and 1 μ Geonite diamond paste* and Metadi oil** was followed by buffing on pads of optical quality SnO_2. Absolute alcohol was used to clean the surfaces between each step. The final sample surface was coated with a few hundred Å layer of carbon and then mounted in brass sample holders.

Experimental Results

EBS Photographs and Elemental Displays

An electron back scatter (EBS) photograph conveys information as to the mean atomic weight of the material under the beam, and is very useful in detecting rims of hydrate formed around a crystal or grain. Such displays, as well as the cathode ray tube displays of the characteristic radiation for the major elements, CaK_α, AlK_α, and SiK_α were obtained for the various samples. Fig. 1 gives an example of EBS, Ca and Al displays for anhydrous C_3A and a sample of C_3A hydrated for one day. While the crystal boundaries are shown to be sharp, and the element distribution homogeneous in the anhydrous compound (1a), the hydrated sample (1b) reveals a distinct grain boundary observable between the hydrate and central core C_3A. Such rims were not clearly observable with C_3S samples, presumably because of the slower rate of hydration. However, occasional $Ca(OH)_2$ crystals were observed in C_3S hydrates as confirmed by the elemental displays.

Quantitative Analysis

Calibration-Standardization

In order to eliminate the effect of many non-random sources of error in obtaining quantitative analyses (such as described by McKinley (8); Birks (9) and Keil (10)) empirical correction was made by use of calibration standards. Calibration curves were constructed for calcium aluminates and silicates derived from measurement of Ca, Al and Si intensities for the compounds C_3A, CA, CA_2, C_3S, β-C_2S, α-CS and C_5S_2H. Measurements were made on five to ten grains of each compound. Values for grains showing high variation were discarded, and the remaining values used. The usual coefficient of variation ranged from 0.80 to 1.75%. The data are summarized in Fig. 2 and 3, which include the experimentally determined data, as well as interpolated and extrapolated values for calcium aluminates and calcium silicates, respectively. These curves were employed to analyze the data obtained for hydration products at various stages.

Effect of Dehydration

In order to correct for the effect of dehydration in the electron beam two lines of experiment were performed. In the first, the weight loss of a hydrate was determined as a function of temperature under a vacuum comparable to microprobe conditions. A thermobalance curve of C_3AH_6 run at a 10^{-5} torr vacuum is shown in Fig. 4a. It is seen that the weight loss is insignificant below 200°C.

To examine the effect of actual operating conditions in the microprobe, grains of C_3AH_6 having a 20 micron diameter were prepared in the usual manner and exposed to a 0.01 microampere sample current at 30 kev accelerating voltage with a one micron spot for ten minutes during which Ca and Al intensities were recorded simultaneously. Under these conditions Ca and Al intensities should have changed proportionately to the amount of water lost.

Fig. 4b shows the change in intensity of characteristic radiation as function of time, also plotted as a percent of the total water lost. It is seen that, within the relatively short time for quantitative analysis (10 seconds on a spot) the water loss would be negligible. When working with hydrates whose thermal properties are unknown, however, it is best to take precautions against dehydration by keeping the beam power as low as possible, selecting a short counting period, and spreading the beam spot over as wide an area as possible.

Problems of Sample Geometry

In addition to the calibration curves obtained above, it was occasionally necessary to correct for the effect of crossing a grain boundary. This was particularly necessary in examining the course of hydration when pursuing a traverse from the center of an unhydrated crystal through a hydration rim to the grain-plastic

* Geonite diamond paste from Geoscience, Inc., New York, N.Y. (concentration S was used).

** Metadi oil, trade name for thin polishing oil, Buehler, Ltd., Evanston, Ill.

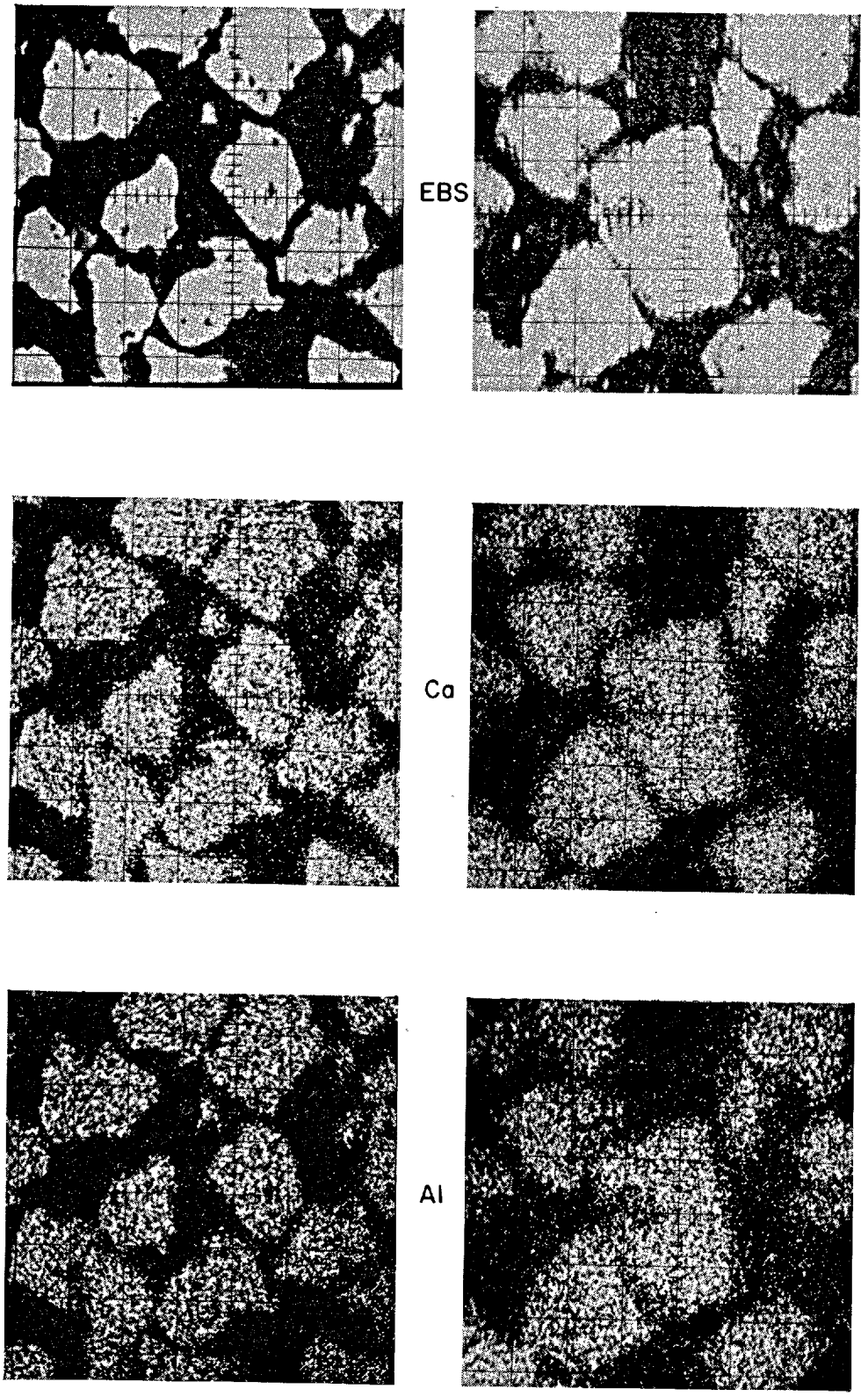

Fig. 1. *EBS and elemental displays for* C_3A *samples. (a) anhydrous; (b) hydrated for one day: note hydration rim. Small grid division is* 5μ

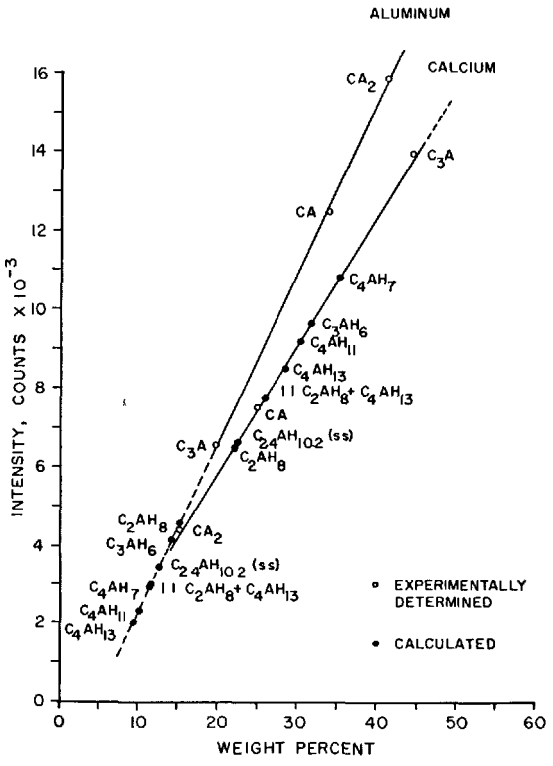

Fig. 2. *Calcium aluminate calibration curves: aluminum and calcium X-ray intensities as a function of weight percent of element*

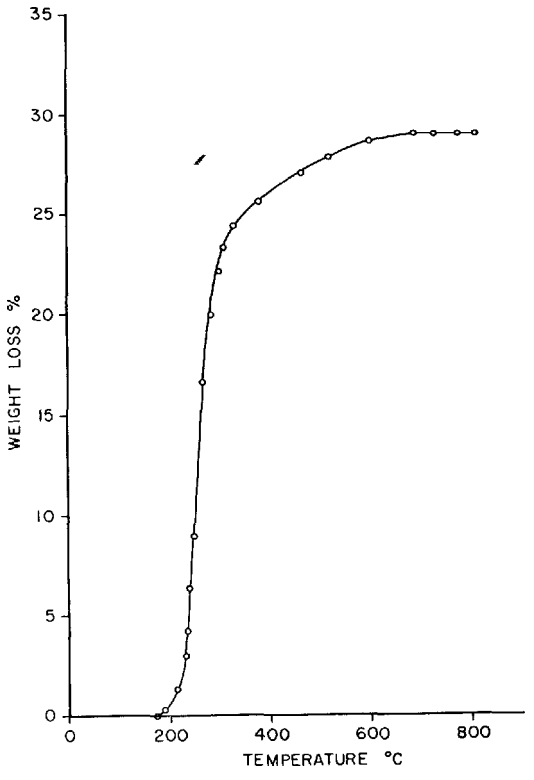

Fig. 4(a). *Thermobalance curve showing dehydration of* C_3AH_6 *at a vacuum of* 10^{-5} *torr. Rate of heating was 2°C/minute*

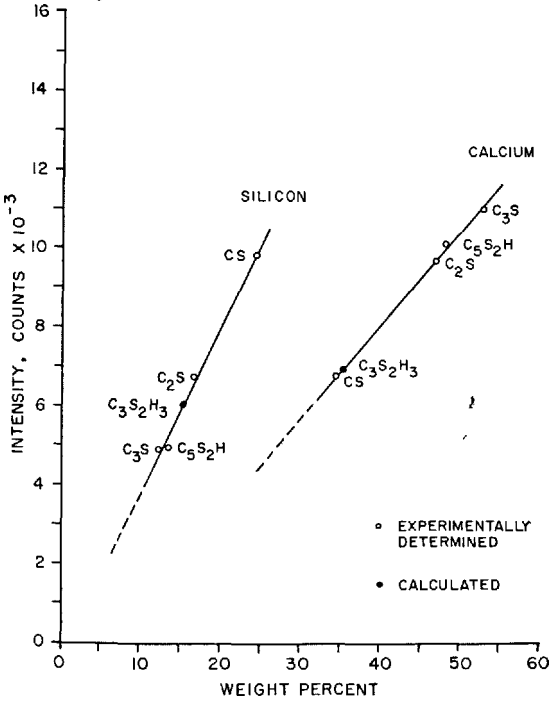

Fig. 3. *Calcium silicate calibration curves*

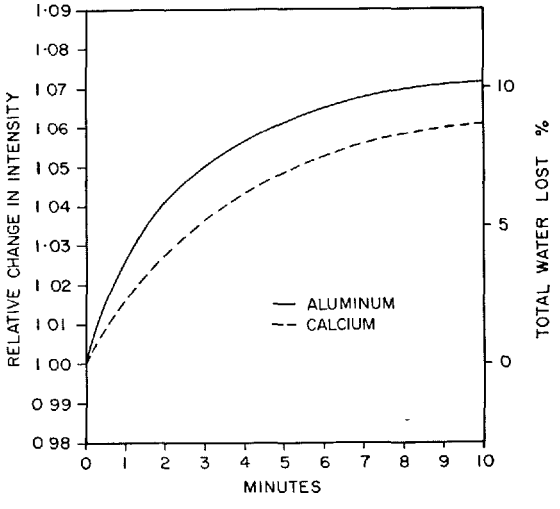

Fig. 4(b). *Loss of water in* C_3AH_6 *as a function of time under the electron beam in the microprobe, calculated from change in measured X-ray intensities*

boundary. X-ray intensity measurements made on a crystal surrounded by different widths of hydration rim are shown schematically in Fig. 5a. If the hydra-

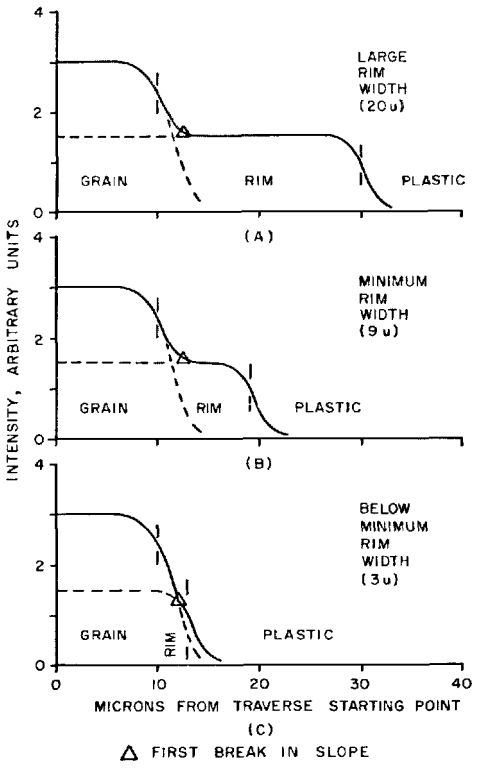

Fig. 5(a). *The effect of width of hydration rim on the measured position of the first break in slope in the X-ray intensity curve (schematic)*

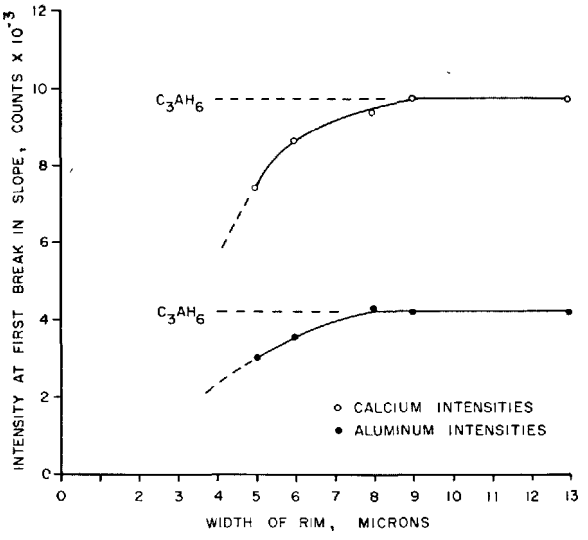

Fig. 5(b). *Measured variation in position of first break in slope as a function of width of hydration rim for calcium aluminates*

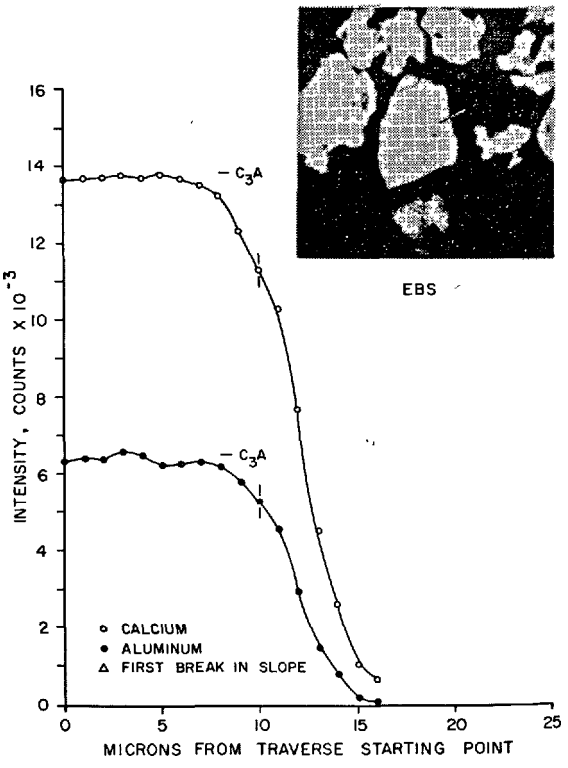

Fig. 6. *X-ray intensities measured in traverse across an anhydrous C_3A grain/plastic boundary. Vertical line shows position of boundary. Small grid division in EBS photo is 5μ*

tion rim is sufficiently large, a shoulder levels off and enables accurate measurement of the X-ray intensity. If not, the only measurement possible is the position of the first break in slope of the curve. Under the experimental conditions employed, it was necessary to have a minimum rim width of approximately 9 μ in order to record directly accurate X-ray intensities of the material in the hydration rim. Fig. 5b gives actual intensities of Ca and Al emission measured as a function of thickness of the rim. Using this latter fig. it was possible to calculate a correction factor when the rim width was below 9 μ.

Analytical Data Obtained from C_3A-Hydrate Traverses

X-ray intensities were measured with the microprobe for anhydrous C_3A and C_3A which had been hydrated for one, seven and twnety-one days, respectively. In each Case EBS displays were also recorded. Examples of the actual data obtained are shown in Figs. 6, 7, and 8 which give the measured X-ray intensities at 1 micron intervals, along with the EBS photograph showing the position of the traverse. The results for a typical unhydrated sample (Fig. 6) are unambiguous, and the interpretation of Fig. 7 is based on the information contained in Fig. 5 and 6 where it is seen that the point of first break in slope is significant and measurable. For the one-day hydration product this point represents a $CaO:Al_2O_3$ ratio of approxi-

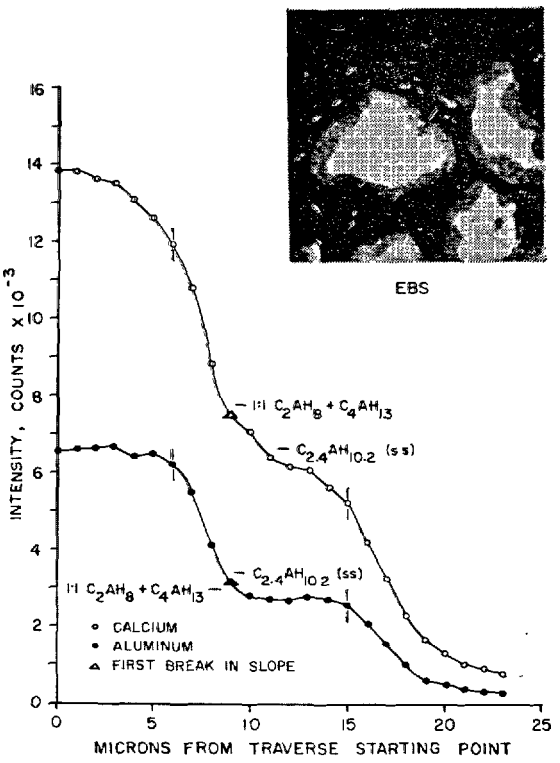

Fig. 7. *Measured X-ray intensities in traverse across a grain of* C_3A *hydrated for one day. Vertical lines show position of central core/hydrate and hydrate/plastic boundaries. Small grid division in EBS photo is 5μ*

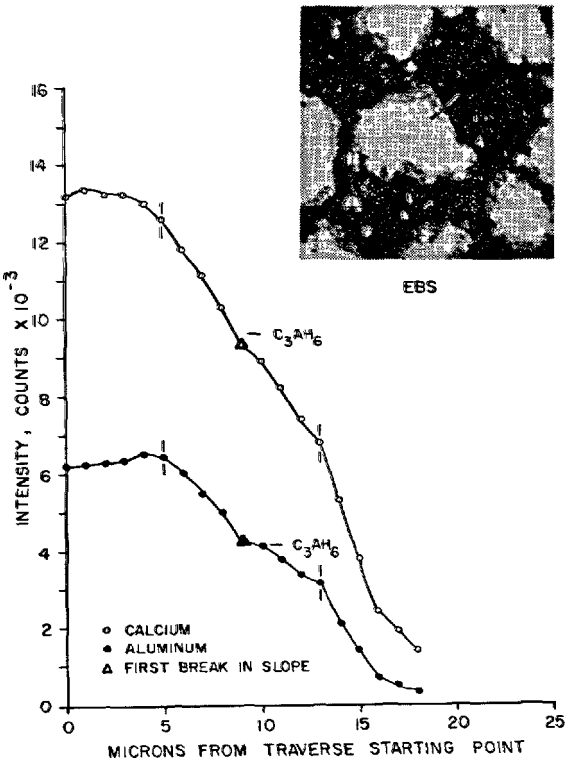

Fig. 8. *Traverse for* C_3A *hydrated seven days. Small grid division in EBS photo is 5μ*

mately 2.8. The hydration product at one day had been tentatively identified by X-ray diffraction as C_4AH_{13}. However, it is probable, in view of the microprobe analysis data, that the hydrate is either a crystalline solution of C_4AH_{13} with C_2AH_8 in its lattice, or a 1:1 mixture of crystalline C_4AH_{13} and amorphous C_2AH_8, which would provide the measured stoichiometry. Refractive indices of the plate-like crystals were different ($\omega = 1.552$, $\epsilon = 1.539$) from the reported values for C_4AH_{13} ($\omega = 1.534$–1.539, $\varepsilon = 1.514$–1.524), (II) suggesting probable crystalline solution. In any event, a total $CaO : Al_2O_3$ ratio of approximately 3:1 seems reasonable in view of conservation of matter from the original C_3A.

Data obtained after seven days of hydration (Fig. 8) show an initial break in slope on the Ca and Al intensity curves at a $CaO: Al_2O_3$ ratio of approximately 3.0. This agreed with the observed X-ray diffraction and optical data which indicated that the hydrate present was C_3AH_6.

After twenty-one days of hydration, the first break in slope was also observed at a $CaO: Al_2O_3$ ratio near 3.0; however, it was usually more difficult to determine this position precisely because of grain

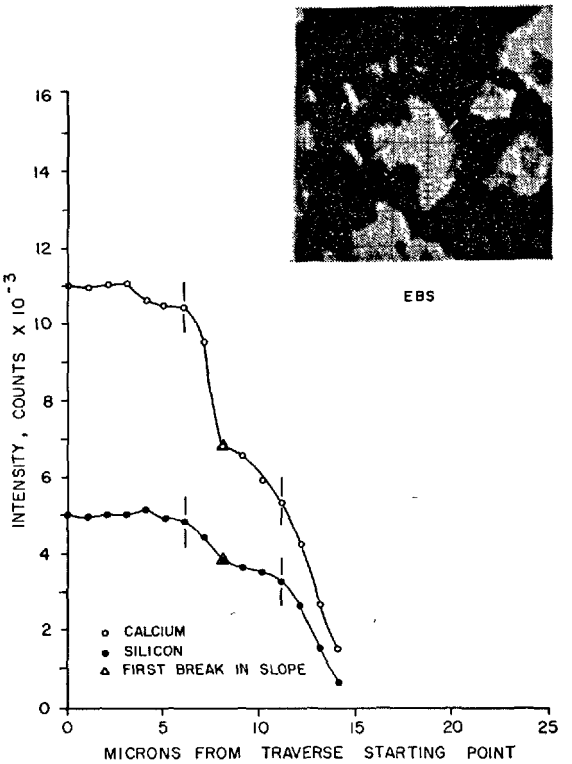

Fig. 9. *Traverse for* C_3S *hydrated twenty-one days. Small grid division in EBS photo is 5μ*

deterioration. The results are in general agreement with X-ray diffraction and optical data, which showed the presence of C_3AH_6.

Analytical Data Obtained from C_3S Traverses

X-ray intensity data were collected on anhydrous C_3S, and C_3S hydrated for three, twenty-one and forty-two days. No substantial rim build-ups were observed even after forty-two days had elapsed.

Data from a typical traverse after twenty-one days, hydration are given in Fig. 9, where an initial break in slope occurs at a $CaO: SiO_2$ ratio of about 2.4. The position of the traverse is shown in the EBS photograph. The first break in slope suggests the presence of a hydrate having a composition of the type $C_5S_2H_x$. Insufficient data were available to provide a valid correction factor due to small rim size, and hence no further inferences have been made. A somewhat lower $CaO: SiO_2$ ratio in the hydrate is reasonable in view of the existence of $Ca(OH)_2$ as identified both in the X-ray diffraction pattern and in the microprobe display. It appears that the relatively slow rate of hydration of C_3S prevents sufficient build-up of the hydration rim for accurate analysis to be possible at this stage.

Data on a Synthetic "Cement"

Preliminary studies were made on a synthetic "cement" composed of a mixture of the C_3A and C_3S

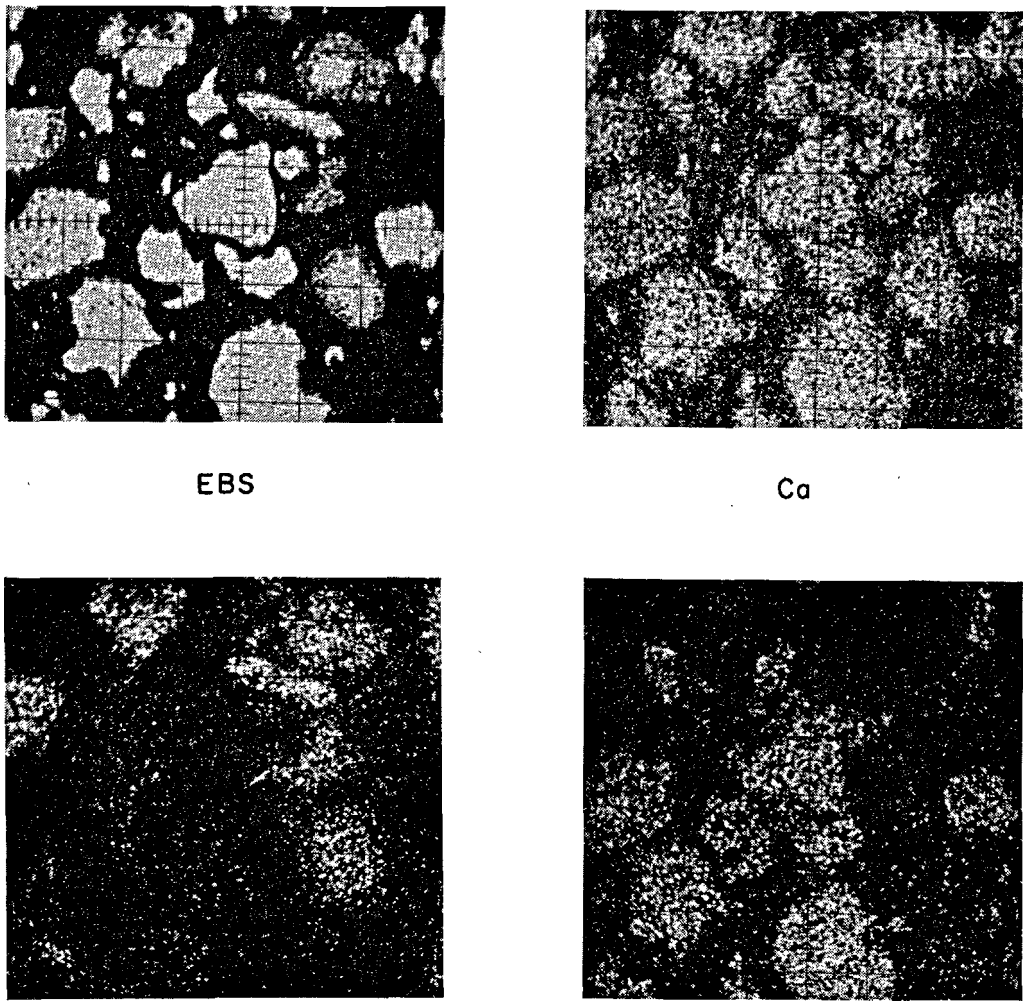

Fig. 10. *EBS and elemental displays for* C_3S–C_2S–C_3A *"cement" hydrated seven days. Small grid division is* 5μ

used in earlier experiments, along with β-C_2S*. Data were obtained on samples hydrated for seven and twnety-one days. Visual displays of the Ca, Al and Si emission, as well as the EBS for a typical sample hydrated for seven days are shown in Fig. 10. The EBS shows that some grains have substantial hydration rims while others do not. Elemental data indicate that the rimmed grains are C_3A, while the others are silicates, consistent with the data on the individual compounds. Insufficient time was available to carry these studies as far as desirable. However, the results showed comparatively little inter-reaction between the silicate and aluminate phases in this relatively early stage of reaction. It would appear that the aluminate hydrates early, and only after an extended period makes water available for silicate hydration.

Summary and Conclusions

Existing electron microprobe techniques have been successfully modified to cope with the specialized problems inherent in portland cement hydration studies. Limits of error in quantitative measurements have been established by applying standardization techniques and studying geometrical factors and effects of dehydration.

Two principal techniques have been employed: the use of electron back scatter (EBS) and elemental display data; and the analysis with a stationary beam at successive one micron intervals across a hydration rim. The first offered a physical description of the grain-hydrate relationships during the progress of the hydration and the possibility of observing the relative rate of hydration of aluminate and silicate phases both individually and combined in a synthetic cement. The second, the elemental analysis data taken along traverses, made it possible to follow the progress of the hydration in a quantitative manner Agreement between published and observed data and similar data gathered with the microprobe was good, and discrepancies could be explained.

The advantages of the method are: the direct analysis available on a micron scale; the visual nature of display data clearly showing inter-relationships; and rapid identification of individual grains. The disadvantages are concerned with the difficulty in sample preparation for quantitative analysis and the time consumed in obtaining significant quantitative data. It is believed that the advantages outweigh the disadvantages, and that the use of the microprobe should be extended to help solve many of the problems relating to portland cement and its hydration.

Acknowledgment

The authors are indebted to Dr. Eugene White and his staff for cooperation and helpful suggestions with the electron microprobe, and to Dr. Joseph Greig for help with experimental microscopic techniques and sample preparation. Financial assistance through NSF grants GP-2291 and GK-1154 made this study possible.

References

1. E. W. White, "Microprobe technique for analysis of multiphase microcrystalline powders," Am. Min. **49** 196–7 (1964).
2. E. W. White, P. J. Denny and S. M. Irving, "Quantitative microprobe analysis of microcyrstalline powders," *the electron microprobe*, T. D. McKinley, *et al.* eds., John Wiley and Sons, Inc., New York, 1966.
3. A. Moore, "Examination of a portland cement clinker by electron probe micro-analysis," Silicates Industriels **30**, 445–50 (1965).
4. G. Yamaguchi, private communication.
5. D. M. Roy, "Studies in the system CaO–Al_2O_3–SiO_2–H_2O: *IV* Phase equilibrium in the high-lime portion of the system CaO–SiO_2–H_2O" Am. Min., **43**, 1009–28 (1958).
6. E. R. Buckle and H. F. W. Taylor, "A Calcium analogue of chondrodite," Am. Min. **43**, 818–23 (1958).
7. R. F. Feldman and V. S. Ramachandran, "Character of hydration of $3CaO \cdot Al_2O_3$," J. Am. Ceram. Soc. **49**, 268–73 (1966).
8. T. D. McKinley, K. F. J. Heinrich and D. B. Wittry, eds., *The electron microprobe*, John Wiley and Sons,

*The synthetic "cement" consisted of 25 wt.%C_3A, 45 wt.% C_3S and 30 wt.% β-C_2S. These proportions were chosen to match type I portland cement except for the absence of a ferrite phase.

Inc., New York, 1966.
9. L. S. Berks, *Electron probe microanalysis*, Interscience Publishers, New York, 1963.
10. K. Keil, "The electron microprobe X-ray analyzer and its application in mineralogy," Fortschritte der Mineralogie **44**, 4–66 (1967).
11. M. H. Toberts, "New calcium aluminate hydrates." J. Appl. Chem. 7, 543–46 (1957).

Oral Discussion

Giichi Sudoh

In the C_3S paste, it is difficult to observe the hydration rim even after 42 days' curing.
Dr. Roy and Mr. Grutzeck assume that this is because of the slow rate of hydration of C_3S, we also assume that there may be some other reasons causing difficulty in observing the C_3S hydration rim.

Among the above are as follows: and we should like to ask Dr. Roy on these points.

(1). The effect of the polishing conditions on the hydration rim of C_3S may be more sensitive than on that of the C_3A hydrates.
(2). The dehydration phenomena during observation may disturb the electron back scattering display.

Furthermore, in Dr. Roy's and Mr. Grutzeck's paper, it is reported that their C_3S hydrate has high molecular ratio of lime to silica, about 2.4.
This high ratio is considered to come from the dehydration of C_3S hydrates, isn't it?

Authors' Closure

Della M. Roy and M. Grutzeck

It is true that the rims observed on C_3S were smaller than those observed for C_3A. We do not believe that C_3S hydration rims were broken off during polishing. Great care was taken during mounting and polishing to prevent this happening. In addition, optical examination under high power indicated that the final polished surfaces are flat for both the C_3A and C_3S sample plaques.

Some dehydration undoubtedly does take place under the electron beam. While we investigated this for CA hydrates, we were not able to establish quantitatively the limits for "CSH gel", since it is difficult to produce a standard material for analysis. The absolute measured intensities of Ca and Si increase with loss of H_2O, but the Ca: Si ratio changes much less. Recent data obtained on C_3S samples hydrated for longer periods of time yield data which speak to both questions. Larger hydration rims were visible on these samples, and the size appears to be a function of time. In addition we obtained lower Ca: Si ratios in the latter analyses, close to those predicted by many for C-S-H gel. The dehydration effect does not appear in these instances to cause a substantial increase in Ca: Si ratio.

These supplementary data are reported elsewhere.

(B) Papers regarding Kinetics

Supplementary Paper II-35 Mutual Interaction of C_3A and C_3S during Hydration

J. G. M. de Jong, Hans N. Stein and J. M. Stevels*

Synopsis

The following mechanism can be proposed for the mutual interaction of C_3A and C_3S during hydration: the compounds start to react individually, C_3A forming hexagonal aluminate hydrates, C_3S forming "first hydrate" (F.H.). Soon, however, the presence of silicate ions in the water phase influences C_3A hydration and the presence of calcium and aluminate ions in the water phase influences C_3S hydration.

A. The former can be understood by two opposing effects:
   1. an acceleration of the formation of C_3AH_6 nuclei
      a. by silicate ions incorporated into the C_3AH_6 nuclei
      b. because C_3S can be used in this case as precipitation place for amorphous $Al(OH)_3$ by which the C_3A hydration can carry through.
   2. a retardation of C_3AH_6 nucleus formation by a lowering of aluminate ion concentration in the water phase. The aluminate ions are taken away from the water phase and incorporated into the calcium hydrosilicates formed.
   If a small amount of C_3S is present, the former influence (A1) predominates, in the presence of larger amounts of C_3S the latter (A2) predominates.

B. C_3A retards the appearance of the C_3S heat evolution peak, since
   1. aluminate ions can be incorporated into F.H. This is more stable with respect to recrystallisation than aluminium-free calcium silicate hydrate.
   2. the calcium- and hydroxyl concentration in the water phase originating from the hydration of C_3A, retard the transition F.H. → S.H. too.

Introduction

Until now only limited research has been devoted to the mutual interaction of C_3A and C_3S during hydration.

Earlier work includes that by Chatterji and Jeffery (1) investigating mixtures of alite, C_3A, C_4AF and water by electron microscopy, electron diffraction and X-ray diffraction. As hydration products hexagonal crystals of $Ca(OH)_2$, $C_3A \cdot CaCO_3 \cdot H_{12}$ and C_4AH_x were found. After longer hydration times the hexagonal C_4AH_x changed into the cubic C_3AH_6 (hydrogarnet). Calcium silicate hydrates were observed too.

Strätling and zur Strassen (2, 3) investigated $C_3S - C_3A$ mixtures (molar ratio 2:1) in dilute suspensions, following CaO and Al_2O_3 concentrations in the water phase. They concluded that the "Al_2O_3" was probably incorporated into the calcium hydrosilicate, forming a quaternary compound.

Iwai (4) ground mixtures of C_3A and C_3S for 1 week in a ball mill (w/s = 5/1), left the resulting systems for 1 week, dried the mixture and investigated the hydration products by X-ray diffractometer. If only C_3A was present, the cubic C_3AH_6 was formed exclusively. The intensities of the X-ray peaks of this hydrate were smaller with increasing C_3S/C_3A ratio. In contrast with experiments with mixtures of C_4AF and C_3S, no silicate ions were build into the lattice of the cubic crystal. By hydration of C_3S afwillite ($C_3S_2H_3$) came into existence.

Richartz (5) found in mixtures of C_3S and C_3A, which were shaken in water (w/s = 5/1) for 28 days, that the quantity of hydrogarnet increased at small quantities of C_3S. At larger concentrations of C_3S the quantity of hydrogarnet decreased whereas more C_4AH_{13} was present which was ascribed to the influence of $Ca(OH)_2$ liberated. Because SiO_2 had been

*Laboratory of Inorganic Chemistry, Technological University, Eindhoven, Netherlands.

built into the lattice, the hydrogarnet had the composition $C_3AH_{5.6}S_{0.2}$.

According to Copeland et al. (6) aluminate ions can be incorporated in tobermorite gel which comes into existence by the hydration of C_3S. On account of the introduction of aluminium ions the morphology of tobermorite gel changes. Afwillite is the product formed by the hydration of pure C_3S in the ball mill (7) but simultaneous hydration of C_3S and C_3A (C_3S/C_3A ratio = 10/1) gives $Ca(OH)_2$ and tobermorite gel only. A hydrogarnet was detected when the proportion of C_3A was increased by 10 percent.

Bobrov et al (8) found by shrinkage measurements that the hydration of a mixture of C_3A and C_3S was more sluggish than would be expected from a summation of the hydration reactions of the separate compounds.

In this study the mutual interaction of C_3A and C_3S during hydration has been investigated both in pastes and in suspensions.

In pastes heat evolution rate was measured, supplemented by X-ray and DTA analyses of hydration products after predetermined hydration times.

In suspensions the electrical conductivity and the pH have been determined, and the calcium, aluminate and silicate ion concentrations were determined analytically. The solid phases were characterized by their X-ray diffraction patterns.

Experimental

Materials

C_3S

Calcium carbonate (reagent grade "Merck") and quartz (reagent grade "Merck"), ground separately in an agate ball mill, were ground together in an excess of benzene. There was a very slight excess of quartz over the stoichiometric amount in order to minimize contamination by free calcium oxide. The mixture was heated overnight in a vacuum oven (40°C) in order to remove the benzene and then heated for 40 hours at 1600°C. Every 8 hours the product was taken out of the furnace and ground in dry first, and then with water; after the last firing, the product was ground in dry only.

X-ray analysis showed that the product contained a very slight quantity of free CaO only, but that it was also contaminated with a small amount of γC_2S. From examination by microscope it was concluded that no other C_2S modification was present. The amount of γC_2S was estimated to be 3 to 4%. The percentage of free CaO was determined according to the method of Pressler et al. (9) and was found to be less than 0.3% by weight. The specific surface of this C_3S preparation was found by air permeability (10) to be 1.76×10^3 cm^2g^{-1}.

C_3A

This compound was prepared by heating a stoichiometric mixture of $CaCO_3$ (reagent grade "Merck") and Al_2O_3 (reagent grade "U.C.B."; loss on ignition 4.5%), ground previously in an agate ball mill, during four hours at 1375°C. Thereafter the mixture was heated two times for four hours at 1500°C. Between all firings, the product was ground in dry first, then with water. After the last firing, the product was only ground in dry in agate ball mills. The X-ray diffractogram of the product agrees completely with the data, mentioned by Taylor (11).

The percentage of free CaO, determined according to the method of Pressler et al. (9), was less than 0.8% by weight.

The specific surface, determined by air permeability (10) was 1.0×10^3 cm^2g^{-1}.

Water

The water used was twice distilled. All water had been boiled and cooled shortly before use so as to minimize contamination of the pastes or suspensions by CO_2.

Nitrogen

The nitrogen, used in the suspension measurements, was purified by passage successively through an adsorption tube filled with 13 — 20 mesh carbosorb, a washing bottle filled with 20% NaOH solution and a washing bottle filled with water.

Method

Paste Experiments

Preparation of the Pastes

The water/solid ratio in the pastes was 1 : 1 (2.00 g of solid with varying C_3A/C_3S ratio and 2.00 ml of water). The C_3A and C_3S mixed in dry; the mixture was transferred to a porcelain dish, after which the water was added. This paste was ground for 1 min.

with a porcelain pestle and transferred into the isothermal calorimeter.

At predetermined times, samples were taken and dispersed by being ground in a porcelain dish for 1½ to 2 min. in an excess of absolute ethanol (10 ml.). The ethanol was added in order not only to arrest the hydration reaction at a fixed moment but also to provide protection against CO_2 (12). It is generally held that the ethanol affects neither the nature of the hydrated phase nor that of the unhydrated phase (13; 14). The sample was dried in a vacuum oven (25 – 35°C) overnight.

Isothermal Calorimeter

The isothermal calorimeter which has been described earlier (15; 16) was placed in a thermostat (25 ± 0.1°C), situated in a constant temperature room (25 ± 0.25°C).

X-ray Analysis

Qualitative X-ray analysis was carried out with a Philips diffractometer (PW 1051) using CuK α_1 rays with a Ni filter.

Differential Thermal Analysis

As a reference Al_2O_3 (reagent grade "Merck"), heated previously to 1200°C was used. The equipment used (Licence CNRS; model M1) required only a few mg of sample. The rate of temperature increase was about 10°C per min.

Suspension experiments

Preparation of the Suspensions

Water (60 ml), brought previously to temperature, was pipetted into a glass beaker provided with a thermostating jacket. Stirring was started and the solid phase was added through a small hole in the cover that was closed immediately afterward by a rubber stopper. During the hydration the suspension was magnetically stirred and purified nitrogen was passed over the suspension. The nitrogen exit tube was protected against back flow of air by a carbosorb-filled tube. The speed of the magnetic stirrer was kept constant during any series of experiments. Care was taken that the magnetic stirrer swept the whole bottom of the thermostatic beaker (with the exception of a rim of about 1 mm. width) so as to avoid "dead spots" in stirring and to prevent settling of the suspended solids.

Determination of the Electrical Conductivity

Electrical conductivity in the suspensions during hydration was followed by means of a Philips PR 9501 direct reading conductometer in combination with a Philips PR 9510 immersion conductivity cell and a Philips PR 4069 M/00 recorder.

Determination of pH

Determination of pH was performed using conventional high alkali glass and calomel electrodes. The glass electrode was placed directly in the suspension, the calomel electrode in a 1 N KCl solution. The boundary between suspension and 1 N KCl solution was formed through a capillary as described by MacInnes and Belcher (17) and renewed once every 5 minutes in the earliest reaction stages, after one hour once every 10 min. After 7 hours' hydration, boundary renewal was omitted and only started again after 22 hours' hydration. Precipitation of hydrates near the boundary tended, if these precautions were not taken, to influence the pH measurements.

The pH was recorded by an Electrofact Laboratorium pH meter type 53 A and a Philips type PR 4069 M/00 recorder.

Chemical Analysis of the Water Phase

Separation of Liquid and Solid Phases

The suspension was filtrated with suction directly from the thermostatic beaker by way of a siphon through a Schott 1 G 4 sintered glass funnel. During filtration, purified nitrogen was passed still over the suspension by which the suspension was protected against contact with air. The filtration time varied from some seconds to sometimes fifteen minutes. Samples of the filtrate were pipetted for chemical analysis immediately after filtration; the solid phases were washed with absolute ethanol and dried in a vacuum oven overnight.

Determination of the Calcium Concentration

Calcium was titrated with EDTA after acidification, addition of 5 ml of a triethanolamine-water mixture, dilution to about 200 ml and addition of 10 ml 4 N KOH solution with murexide as indicator.

Determination of the Aluminate Concentration

Aluminium was determined gravimetrically with 8-hydroxyquinoline (18).

Determination of the Silicate Concentration

The silicate concentration was determined spectrophotometrically by the Mullin and Riley method (19) as modified by van Lier (20).

Experimental Results

The Results of the Paste Experiments

The results of the measurements in the isothermal calorimeter have been reproduced in Fig. 1, in which the heat evolution rate has been expressed as a function of the time. Some experiments have been stopped after predetermined times and the hydration products have been investigated by X-ray analysis. These results, forming the basis for the interpretation of the calorimetric data have been reproduced in Table 1.

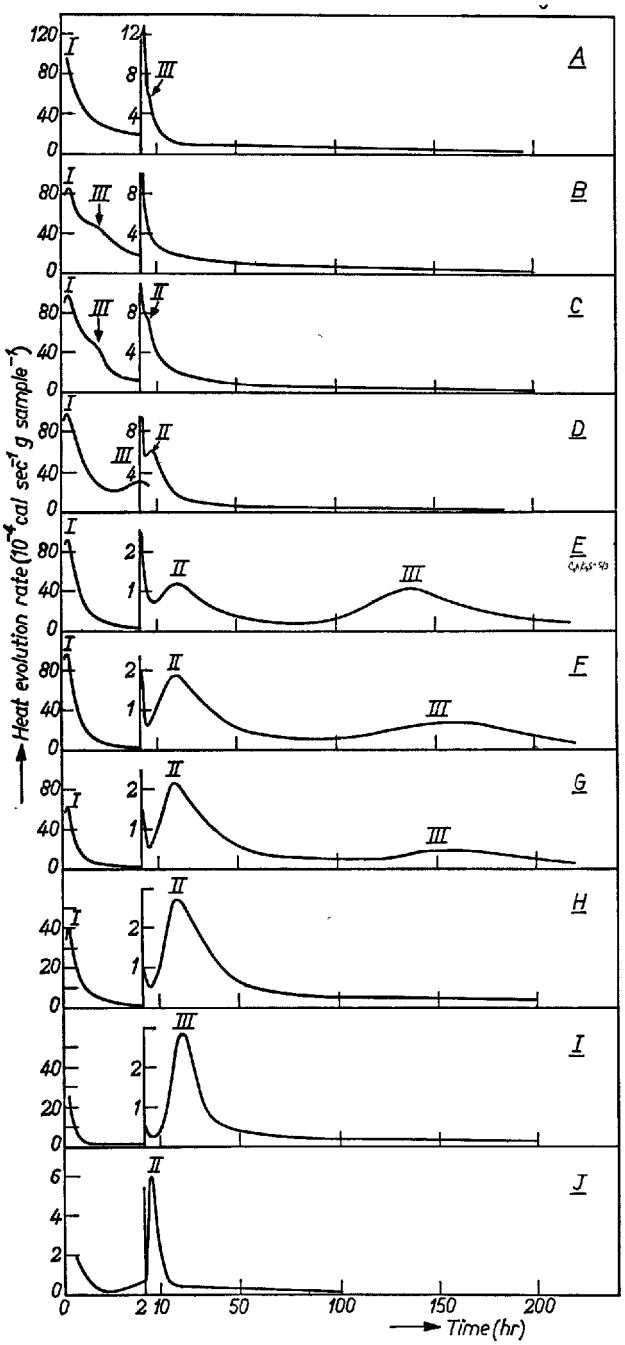

Fig. 1. *Heat liberation curves for pastes, containing* C_3A, C_3S *and water. Letters indicate the reactions as in Table 1*

The heat evolution per unit of time during the hydration of C_3S increased after an induction period, during which practically no reaction took place as described earlier (21, 22). It shows with the C_3S used a maximum after 5 hours and then decreases gradually (Fig. 1. J). By the addition of a small quantity of C_3A this C_3S heat peak (peak II) shifts from 5 to 20 h, it becomes lower but more spread out (Fig.

Table 1. *The date of the X-ray diffraction patterns of the reaction:* xg C_3A + yg C_3S + 2 ml H_2O

		C_3A	C_3S	C_4AH_n*	C_3AH_6	$Ca(OH)_2$
A.	2.00 g C_3A + 2.00 ml H_2O					
	after 20 h	m	—	—	vs	—
	7 months	—	—	—	vs	—
B.	1.90 g C_3A + 0.10 g C_3S + 2.00 ml H_2O					
	after 2 h	vs	vw	—	s	—
	20 h	m	—	—	vs	w
	200 h	vw	—	—	vs	w
C.	1.75 g C_3A + 0.25 g C_3S + 2.00 ml H_2O					
	after 1h.30 min.	vs	m	—	s	—
	20 h	m	vw	—	vs	m
	200 h	vw	—	—	vs	m
D.	1.50 g C_3A + 0.50 g C_3S + 2.00 ml H_2O					
	after 1 h	vs	s	w	w	—
	4 h	m	s	w	vs	—
	20 h	w	vw	—	vs	s
E.	1.25 g C_3A + 0.75 g C_3S + 2.00 ml H_2O					
	after 5 h	vs	vs	bb	—	—
	70 h	vs	w	w	—	vs
	200 h	vw	vw	vw	vs	vs
F.	1.00 g C_3A + 1.00 g C_3S + 2.00 ml H_2O					
	after 5 h	vs	vs	bb	—	—
	70 h	vs	m	w	—	vs
	200 h	w	w	—	vs	vs
G.	0.75 g C_3A + 1.25 g C_3S + 2.00 ml H_2O					
	after 5 h	s	vs	bb	—	—
	70 h	s	m	—	—	vs
	200 h	w	w	—	vs	vs
H.	0.50 g C_3A + 1.50 g C_3S + 2.00 ml H_2O					
	after 5 h	m	vs	—	—	—
	70 h	m	m	vw	—	vs
	200 h	w	m	—	s	vs
I.	0.10 g C_3A + 1.90 g C_3S + 2.00 ml H_2O					
	after 5 h	—	vs	—	—	—
	70 h	—	m	—	—	vs
	200 h	—	m	—	—	vs
J.	2.00 g C_3S + 2.00 ml H_2O					
	after 20 months	—	m	—	—	vs

vs = very strong; s = strong; m = medium; w = weak; vw = very weak; bb = broad band; tr = traces

*Includes also the compound with small amounts of CO_3^{2-}; C_2AH_n was not found.

1.I). At still smaller C_3S/C_3A ratios this peak becomes lower always but more spread out too. This peak II shifts again to about $5\frac{1}{2}$ hours if peak III comes into existence after smaller hydration times (Fig. 1.C and 1.D).

In pastes of C_3A two heat evolution peaks are found (23; 24): the first one directly after the beginning of the hydration (peak I), the second one, for the sample used in the present investigation a very small effect (peak III) after about $6\frac{1}{2}$ hours (Fig. 1.A.). This peak III has been connected with the conversion of intermediate hexagonal hydrates into the cubic C_3AH_6 (24). By the addition of a small quantity of C_3S to C_3A this peak shifts to earlier reaction times and is more intensified (Fig. 1.B, 1.C, 1.D). If the C_3S/C_3A ratio $\geqslant 3/5$ the C_3A hydration and the C_3AH_6 formation is retarded strongly (Fig. 1.E, 1.F etc.).

This interpretation of the heat evolution peaks based on X-ray data (Table 1) is confirmed by DTA measurements (Fig. 2.): After 5 hours' reaction in pastes 1 g C_3A + 1 g C_3S + 2 ml H_2O (F) exclusively endothermal peaks of the hexagonal aluminate hydrates can be observed; after 70 hours the strong peak of $Ca(OH)_2$ at 475°C has appeared. After 200 hours the peaks of the hexagonal hydrates have disappeared almost but the strong peak of C_3AH_6 at about 330°C has appeared. The second, more weak peak of C_3AH_6 can not be distinguished from the peak of $Ca(OH)_2$.

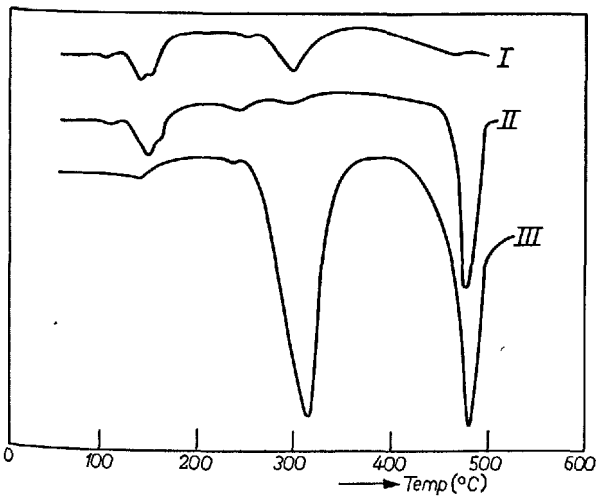

Fig. 2. *D.T.A. of the paste reaction:*
1.00 g C_3A + 1.00 g C_3S + 2.00 ml *water*
The reaction has been stopped after:
I 5 h
II 70 h
III 200 h

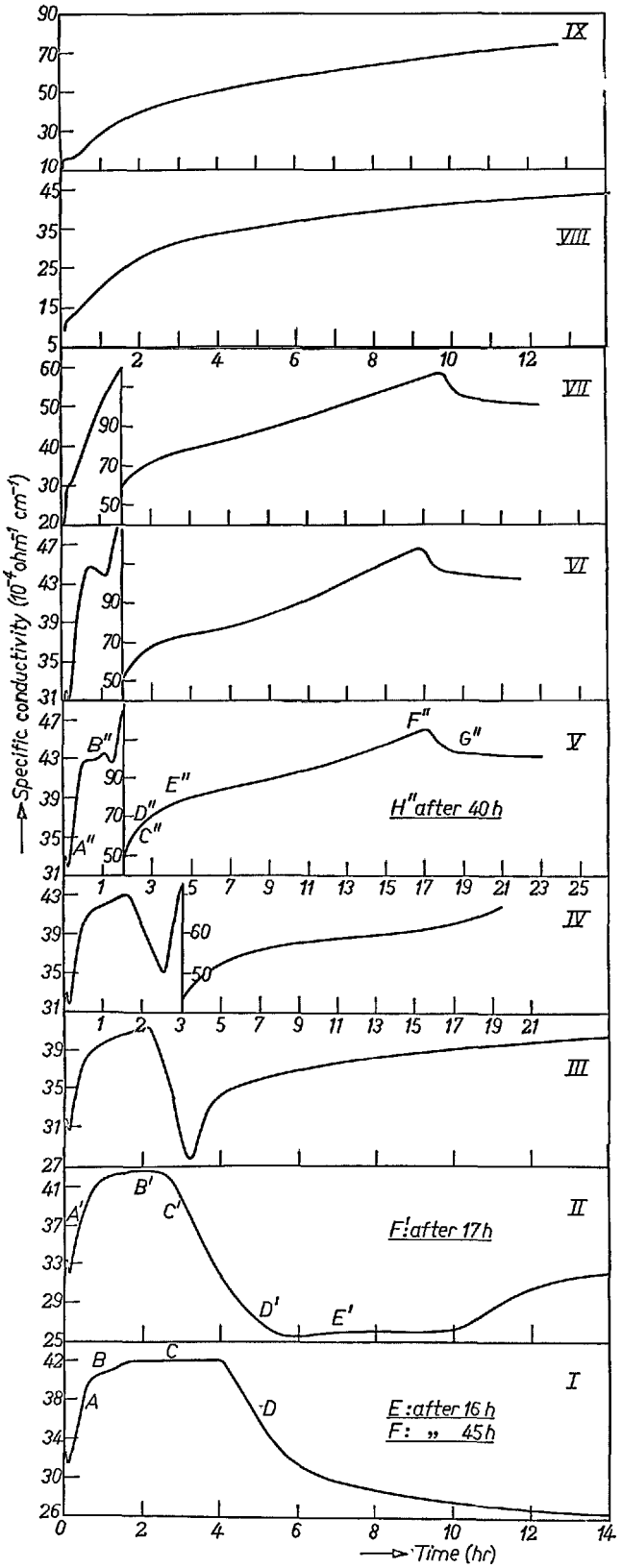

Fig. 3. *Electrical conductivity vs. time for suspensions, containing* C_3A, C_3S *and water. Numbers indicate the reactions as in Table 3*

The Results of the Suspension Experiments

The specific conductivity for suspensions with different C_3S/C_3A ratios has been reproduced as a function of the time in Fig. 3., the pH in Fig. 4. This pH has, in general, a similar course as the specific conductivity. The decrease of the conductivity which is found after 4 hours in the absence of C_3S, took place after earlier hydration times when a small quantity of C_3S had been added to the C_3A. The crystallisation of C_3AH_6 which causes this decrease in the specific conductivity (32), took place therefore earlier as is also evident from Table 2 where the X-ray diffractograms of the solid phases have been reproduced for some reactions. The conductivity increase, caused by the C_3S hydration (see later), shifts to earlier reaction times with increasing C_3S content of the paste and converges ultimately with the first part of the curve, caused by the C_3A hydration. The C_3S quantity decreases very gradually. After 16 hours hydration time (during experiment V) practically no C_3A is present but still a distinct amount of C_3S.

The X-ray patterns of the products of all these reactions after 24 hours hydration time have been reproduced in Table 3. It is seen that the sudden decrease of the specific conductivity in some experiments (V, VI, VII) after about 17 hours hydration time is caused by crystallisation of $Ca(OH)_2$. Usually no quaternary compound was formed, but in some cases traces of gehlenite hydrate were found.

By the addition of a small quantity of C_3A to C_3S the specific conductivity is distinctly lowered (Fig. 3. VIII).

The results of the analyses for calcium and aluminate ion concentrations in the water phase during the reactions I, II and V have been reproduced with the Jones and Roberts phase diagram for the ternary system, $CaO–Al_2O_3–H_2O$ (26) as a background (Fig. 5). The results of the ion concentrations during the reactions V and IX have been reproduced in Table 4, respectively Table 5. The results of Strätling and zur Strassen (2, 3) are in accordance with these results.

The addition of C_3S to C_3A does not change the concentration course in the beginning up to the time of establishment of a solution saturated towards both C_4AH_{19} and C_2AH_8. In the presence of small quantities of C_3S the crystallisation of C_3AH_6 takes place more

Table 2. *The data of the X-ray diffraction patterns of the reactions:* 0.60 g C_3A + xg C_3S *in* 60 ml H_2O *in the course of its hydration.*

I. 0.60 g C_3A in 60 ml H_2O	after 50 min.	3 h 30 min.	7 h	24 h			
C_3A	vs	—	—	—			
αC_2AH_8	vs	vs	m	w			
C_4AH_n	m	vs	?	w			
C_3AH_6	—	w	vs	vs			
II. 0.60 g C_3A + 0.05 g C_3S in 60 ml H_2O	**after 20 min.**	**2 h**	**3 h**	**5 h**	**7 h**	**17 h**	
C_3A	vs	s	w	—	—	—	
αC_2AH_8	m	m	w	—	—	—	
$C_3A \cdot CaCO_3 \cdot H_{12}$	m	s	m	vw	—	—	
C_3AH_6	s	vs	quantity increases →				
C_4AH_n	m	s	m	vw	—	—	
V. 0.60 g C_3A + 0.60 g C_3S in 60 ml H_2O	**after 7 min.**	**35 min.**	**2 h**	**3 h 30 min.**	**16 h 30 min.**	**19 h**	**40 h**
C_3S	vs	vs	vs	vs	s	m	tr
C_3A	vs	quantity decreases →			tr	tr	—
C_3AH_6	—	m	quantity increases →		vvs	vvs	vvs
$Ca(OH)_2$	—	—	—	—	w	m	vvs
C_2ASH_8	—	—	—	tr	tr	tr	—
$C_3A \cdot CaCO_3 \cdot H_{12}$	—	—	—	—	—	w	—

Table 3. *The X-ray data after 24 hours' hydration time of the reactions:* xg C_3A + yg C_3S *in* 60 ml H_2O.

	C_3S	C_3A	C_2ASH_8	$Ca(OH)_2$	C_2AH_8	C_4AH_n	C_3AH_6
I. 0.60 g C_3A in 60 ml H_2O	—	—	—	—	w	w	vs
II. 0.60 g C_3A + 0.05 g C_3S in 60 ml H_2O	—	—	—	—	—	—	vs
III. 0.60 g C_3A + 0.15 g C_3S in 60 ml H_2O	vw	—	—	—	—	—	vs
IV. 0.60 g C_3A + 0.30 g C_3S in 60 ml H_2O	w	—	—	vw	—	—	vs
V. 0.60 g C_3A + 0.60 g C_3S in 60 ml H_2O	m	—	tr	m	—	tr	vs
VI. 0.30 g C_3A + 0.60 g C_3S in 60 ml H_2O	m	—	tr	vs	—	—	s
VII. 0.15 g C_3A + 0.60 g C_3S in 60 ml H_2O	m	—	w	vs	—	tr	—
VIII. 0.05 g C_3A + 0.60 g C_3S in 60 ml H_2O	vs	—	w	—	—	—	—
IX. 0.60 g C_3S in 60 ml H_2O	vs	—	—	—	—	—	—

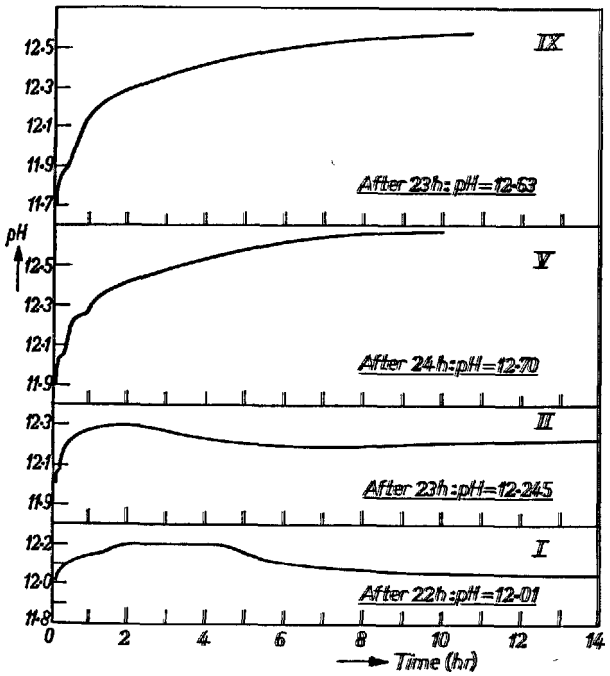

Fig. 4. *pH vs time for suspensions, containing* C_3A, C_3S *and water. Numbers indicate the reactions as in Table 3*

Table 4. *The results of the analyses for calcium, aluminate and silicate ion concentrations in the water phase during the reaction* 0.60 g C_3A + 0.60 g C_3S *in* 60 ml *water* (V)

	hydr. time	Ca conc. (mg CaO/l)	Al conc. (mg Al_2O_3/l)	Si conc. (mg SiO_2/l)
A″	7 min	491	211	0.05
		520	190	0.15
		539	198.5	0.0
B″	40 min	654	103	0.1
		650	97.5	0.2
		622	106	0.8
C″	1 h 45 min	712	94	2.8
D″	2 h	917	37.5	2.5
E″	3 h 30 min	1132	71	1.95
		1260	65	1.35
F″	16 h 30 min	1738.5	20	0.55
		1750	47	0.90
G″	19 h	1656	0.5	0.75
		1687	18	0.0
H″	40 h	1413	1	—

quickly; the concentration course in that stage resembles that found in pastes C_3A + amorphous

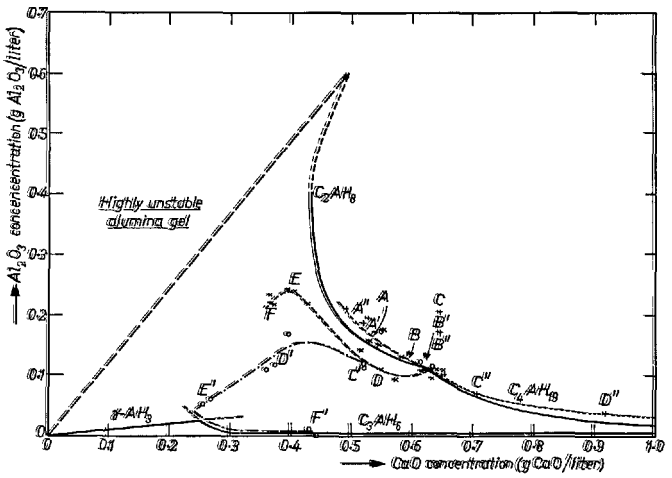

Fig. 5. *Concentration relations in the water phase of suspensions of:*
x——x 0.60 g C_3A in 60 ml water
o——o 0.60 g C_3A + 0.05 g C_3S in 60 ml water
+—+ 0.60 g C_3A + 0.60 g C_3S in 60 ml water

Table 5. *The results of the analyses for calcium and silicate-concentrations in the water phase during the reaction* 0.60 g C_3S *in* 60 ml *water*

hydr. time	Ca-conc. (mg CaO/l)	Si-conc. (mg SiO_2/l)
10 min	223.5	—
	232	50
	226.5	54
1 h	393.5	18
	393.5	12
17 h	1404.5	0
	1348	0

SiO_2 + H_2O (33) but equilibrium conditions (concentrations corresponding to solutions saturated towards C_3AH_6) are reached more quickly. In the presence of larger quantities of C_3S the concentration line leaves the point of metastable coexistence of solution with C_4AH_{19} and C_2AH_8 no longer in the same way as in suspensions of pure C_3A but along the C_4AH_{19} saturation line. It follows that the rising part of the conductivity curve is caused by the C_3S hydration; this is evident from the silicate determinations, too.

Discussion of the Experimental Results

C_3S Hydration

The following mechanism, proposed by Stein and Stevels (22; 26) based partly on results of Kantro et al. (27; 28), agrees with all data available concerning the hydration of C_3S:

$3CaO \cdot SiO_2 + H_2O$

$\downarrow$

$3CaO \cdot SiO_2 \cdot mH_2O$(F. H. = first hydrate)

$\downarrow$

$Ca(OH)_2 + (0.8 - 1.5)CaO \cdot SiO_2 \cdot nH_2O$
(C–S–H(I); S. H. = second hydrate)

$\downarrow$

$(1.5–2)CaO \cdot SiO_2 \cdot pH_2O$(C–S–H(II) or tobermorite gel; T. H. = third hydrate).

The influence of small quantities of C_3A added to C_3S is understood if it is supposed that the transition F. H. $\rightarrow$ S. H. is retarded. This is evident both in suspensions (see Fig. 3) and in pastes (see Fig. 1). There may be two reasons for this as for as the authors can see:

1. Aluminium ions are incorporated into the calcium silicate hydrate formed. This aluminium-containing calcium hydrosilicate is thought to be more stable with respect to recrystallisation than aluminium-free calcium hydrosilicate, in analogy to Kalousek's results on Al-containing tobermorite (29). This is the reason why addition of bayerite, or still more clearly, the addition of amorphous $Al(OH)_3$ retards the hydration of C_3S (28).

2. The calcium and hydroxyl ions in the water phase, resulting from the hydration of C_3A, retard the transition F. H. $\rightarrow$ S. H. too. It is already known that CaO or $Ca(OH)_2$, added to C_3S, retards the C_3S hydration (30).

Of these two possible mechanisms, the first-mentioned appears to be much more probable than the last-mentioned, though the latter may not be excluded. Although in C_3S + water systems $[Ca^{2+}]$ and $[OH^-]$ are generally higher than in C_3A + water systems, during the very first stages rapid reaction of C_3A may provide still higher $[Ca^{2+}]$ and $[OH^-]$ in mixed $C_3A + C_3S$ + water systems than are found in C_3S + water systems. It is known from the work of Stein and Stevels (22) that the calcium and hydroxyl ion concentrations during the first hydration stages have a far-reaching effect on C_3S hydration.

Larger quantities of C_3A are found not to exert this strong retarding action on C_3S hydration. The transition between both mechanisms lies at a C_3S/C_3A ratio less than 3/5 in pastes. The reasons for this changed mechanism are at present far from clear; it should be remembered, however, that in suspensions a rather striking difference in concentration course is found between suspensions with low C_3S/C_3A ratio and suspensions with high C_3S/C_3A ratio: the point of metastable coexistence of C_4AH_{19}, C_2AH_8 and solution is left in the former case more or less along the C_2AH_8 saturation line, in the latter case along the C_4AH_{19} saturation line (see Fig. 5). This suggests the following explanation: In the presence of large amounts of C_3A, C_3AH_6 precipitation occurs in such a way as to lower the aluminate ion concentration to a value represented by the C_3AH_6 saturation line in the $CaO–Al_2O_3–H_2O$ phase diagram. In this case only a slight amount of aluminium ions is incorporated into the calcium silicate hydrates:

C_3S hydration is not noticeably retarded. On the other hand, in the presence of small amounts of C_3A, C_3AH_6 precipitation is suppressed. The aluminate ion concentration in the water phase remains high (corresponding to a value represented by the C_4AH_{19} metastable saturation line in the $CaO–Al_2O_3–H_2O$ phase diagram), more aluminium ions are incorporated into the calcium silicate hydrates: C_3S hydration is considerably retarded. From the suspension measurements one would expect that this mechanism can be operative at later hydration times only; but it should be remembered that the suspension measurements are not to be taken too strictly as indications for the time scale of the paste mechanism; especially for the formation of C_3AH_6 nuclei an acceleration with decreasing water solids ratio has been reported (32).

The explanation offered is consistent with data by Copeland et al. (6) who report that a minimum amount of 20% C_3A should be present in order to make possible C_3AH_6 formation. It is confirmed by the calorimetric and X-ray data on paste experiment I (Table 1) obtained in the present investigation. If a small quantity of C_3A is added to C_3S the specific conductivity is lower. This is in accordance with the hypothesis that aluminate ions are incorporated into the calcium hydrosilicate formed by which the hydration of C_3S is retarded. For this reason less calcium and hydroxyl ions, which determine the conductivity, come into the solution.

C_3A Hydration

The following mechanism can explain the hydration of C_3A (32): in the first reaction stage, hexagonal metastable hydrates are present on the C_3A surface. After conversion of this layer, C_3AH_6 and hydrous alumina are precipitated, the latter also on the C_3A surface so that the C_3A hydration is retarded again. It has been found earlier that the addition of an inert material, like quartz, on which the amorphous $Al(OH)_3$, can precipitate, accelerates the reaction (32). If amorphous silica is added to C_3A, peak III in the heat evolution rate curve, connected with the conversion of intermediate hexagonal hydrates into the cubic one, shifts to earlier reaction times and is

intensified more clearly (33).

De Jong et al. (33) have demonstrated quantitatively, Richartz (5) and Chernykh et al. (34) qualitatively that at comparable times the quantity of hydrogarnets in the presence of amorphous silica is larger. Especially, the formation of C_3AH_6 nuclei appears to be accelerated by the presence of silicate ions. If a small quantity of C_3S is added to C_3A, the effect of this C_3S is analogous to that of amorphous silica, viz, and acceleration of the formation of C_3AH_6 nuclei by silicate ions. Peak III shifts, therefore, to earlier hydration times and is intensified. In accordance with this explanation Richartz (5) found, in the presence of small quantities of C_3S, a larger quantity of hydrogarnets. Since in this case no aluminium ions are incorporated into the F. H., the C_3S hydration is not perceptibly retarded.

For C_3S/C_3A ratio $\geqslant 3/5$ the retardation of the formation of C_3AH_6 nuclei by a lowering of aluminate ion concentration plays the most important part. The aluminium ions are incorporated in an early reaction stage into the F. H., in a later reaction stage into the tobermorite gel. By the absence of large quantities of aluminate ions, the formation of C_3AH_6 nuclei is retarded and therefore the C_3A hydration, too, because the hexagonal aluminate hydrates remain as a protecting layer around the C_3A grains. It is typical of the extreme case of high C_3S/C_3A ratio that in suspensions the invariant point of coexistence of solution with C_4AH_{19} and C_2AH_8 is left following the C_4AH_{19} saturation line (Fig. 5.), and that C_3AH_6 is observed late if at all by X-rays both in suspension and in pastes.

Acknowledgment

The authors express their gratitude to Miss Y. Leeuwenburgh for chemical analysis and for assistance in the X-ray diffraction work.

References

1. S. Chatterji and J. W. Jeffery, J. Amer. Ceram. Soc. **46**, 187 (1963).
2. W. Strätling, Zement **29**, 427; 441; 455; 475 (1940).
3. W. Strätling and H. zur Strassen, Zeitschrift für Anorg. und Allg. Chemie **245**, 257 (1940).
4. T. Iwai, Ph. D., Thesis T. H. Aachen, 1963, p. 61.
5. W. Richartz, Tonind. Ztg. **90**, 449 (1966).
6. L. E. Copeland, E. Bodor, T. N. Chang and C. H. Weise, J. PCA Res. and Dev. Labs., 1967, p. 61.
7. S. Brunauer, L. E. Copeland and R. H. Bragg, J. Phys. Chem. **60**, 112 (1956); PCA Research Department Bulletin 65.
8. B. S. Bobrov, M. B. Epel'baum and N. M. Pogorelov, Tsement **33**, 8 (1967).
9. E. E. Pressler, S. Brunauer and D. L. Kantro, Analyt. Chem. **28**, 896 (1956).
10. F. M. Lea and C. H. Desch, "Chemistry of cement and concrete", Revised Edn. p. 327 (1956) (London: Edward Arnold).
11. H. F. W. Taylor, In: "The chemistry of cements" Vol. 2., (H. F. W. Taylor, ed.), (Academic Press, London and New York) p. 347 (1964).
12. A. Grudemo, Proc. 4th. Int. Symp. Chem. Cement, p. 135 (1960).
13. R. F. Feldman and V. S. Ramachandran, J. Am. Ceram. Soc. **49**, 268 (1966).
14. S. Chatterji and A. J. Majumdar, Indian Concr. J. **40**, 51 (1966).
15. H. N. Stein, J. Appl. Chem., **11**, 474 (1961).
16. J. de Jong and L. Marquenie, Instrum Pract, **16**, 45 (1962).
17. D. A. MacInnes and D. Belcher, Ind. Eng. Chem. Anal. Ed. **5**, 199 (1931).
18. R. Frenseius and G. Jander, Handbuch der analytischen Chemie III. Teil. Band 3, p. 258, Berlin (1942).
19. J. B. Mullin and J. P. Riley, Anal. Chim. Acta **12**, 162 (1955).
20. J. A. van Lier, Ph. D. Thesis, Utrecht, p. 8 (1959).
21. L. R. Forbrich, J. Am. Concr. Inst. **37**, 161 (1940).
22. H. N. Stein and J. M. Stevels, J. Appl. Chem. **14**, 338 (1964).
23. E. Calvet and P. Longuet, Comptes Rendus du 27 me Congrés Int. de Chimie Industrielle, Bruxelles, **3**, 31 (1954); Chem. Abstr. **50**, 9131a (1954).
24. H. N. Stein, J. Appl. Chem. **13**, 228 (1963).
25. F. E. Jones and M. H. Roberts, Building Research Current Papers, Research Series 1, June (1962).
26. a. H. N. Stein and J. M. Stevels, J. Phys. Chem. **69**, 2489 (1965).
    b. H. N. Stein and J. M. Stevels Silic. Ind. **32**, 337 (1967).
    c. H. N. Stein, J. M. Stevels and J. G. M. de Jong, Zement-Kalk-Gips **20**, 347 (1967).
27. D. L. Kantro, S. Brunauer and C. H. Weise, J. Phys. Chem. **66**, 1804 (1962).
28. H. F. W. Taylor, see ref. 9, vol 1, p. 287.
29. G. L. Kalousek, C. T. Davis and W. E. Schmertz, J. Amer. Concr. Inst. **20**, 693 (1949).

30. J. G. M. de Jong, H. N. Stein and J. M. Stevels, to be published.
31. J. G. M. de Jong H. N. Stein and J. M. Stevels, J. Appl. Chem. **17**, 246 (1967).
32. a. H. N. Stein, Highway Research Board, Washington, Special Report 90, 368 (1966).
    b. H. N. Stein, Chemisch Weekblad **62**, 279 (1966).
    c. H. N. Stein, Science of Ceramics (G. H. Stewart Ed) Academic Press, London and New York, 109 (1967).
33. J. G. M. de Jong, H. N. Stein and J. M. Stevels, to be published.
34. V. F. Chernykh, R. D. Azelitskaya and J. F. Ponomarev, Ivestiya Visshikh Uchebnykh Zavedenii SSSR, "Khimiya i khimicheskaya technologiya", 967 (1964), Chem. Abstr. **63**, 2730c.

Supplementary Paper II-44 The Mathematical Simulation of Chemical, Physical and Mechanical Changes Accompanying the Hydration of Cement

Geoffrey J. C. Frohnsdorff, William G. Fryer and Paul D. Johnson*

Synopsis

In order to aid the understanding of the factors affecting cement performance, a quite general mathematical model has been developed to show the interrelationships between several important experimentally measurable variables.

The central and most complex part of the model is the representation of the kinetics of hydration. Once the kinetics are satisfactorily represented, many important properties of the system at any given point in time can be calculated from the quantity and composition of the liquid phase, the quantities and particle size distributions of the solid phases and the known properties of the phases.

The model is described and its use is illustrated by calculations depicting the chemical changes, heat liberation, volume changes, and changes in flow and mechanical properties accompanying the hydration of tricalcium silicate.

Introduction

When an inorganic cement is mixed with water, chemical and physical changes begin to take place which, in some cases, can continue for many years. These changes are, in large part, responsible for the engineering performance of the cement. While some qualitative relationships between the physics and chemistry of cement hydration and specific aspects of cement performance have been recognized, there is a need for improved insight into the physical and chemical factors affecting performance. A method for contributing to the insight which has recently become practicable is mathematical simulation using electronic computers. This paper illustrates the method and discusses its advantages and limitations.

Simulation has already been applied successfully to complex problems in many scientific, engineering and business applications and it appears to be equally applicable to the problem of cement hydration. In this case, the most general simulation could be described as a physical-chemical-mechanical model since it would have to relate physical, chemical and mechanical effects.

The desirability of being able to relate the engineering performance of cements to chemical and physical changes was apparent to Le Chatelier (1) in the late 19th century, and this recognition appears to have stimulated his important contributions to the field. In subsequent years, many persons have tried to relate specific aspects of cement performance to recognizable chemical and physical characteristics, and they have generally contributed in an important way to understanding. Examples of contributions of this sort for the case of portland cement have been those of Powers (2), Helmuth (3) and Volkov (4) and their collaborators, while the work of Ridge (5) and Schiller (6) has been concerned with gypsum plaster, and the work of Koishi (7) with dicalcium plumbate. The contributions of Volkov, Ridge, Schiller, and Koishi are particularly relevant to the present work since each developed mathematical expressions for the kinetics of the hydration reactions in which they were interested and, in some cases, attempted to relate experimentally determined performance characteristics (e.g. heat liberation, setting, etc.) to chemical changes. The present work illustrates how more comprehensive and more generally useful mathematical models for use with computers can be developed.

The application of computers to complex problems in chemical kinetics has recently been demonstrated by DeTar (8) and others (9, 10). Though their work has been oriented towards reactions in homogeneous systems, similar methods can be applied to reactions in heterogeneous systems, such as cement paste, in which reactions at the solid-liquid interface have to

*American Cement Corporation, Riverside, California, U.S.A.

be taken into account. In the physical-chemical-mechanical model to be described below, a quite general approach has been taken which may be applied to any solid-liquid system in which solution, nucleation and precipitation are taking place. Because of the complexity of the cement hydration process, it is not to be expected that the model as described will be entirely realistic but it does have features which can account for a number of aspects of cement behavior and it may be modified to deal with its shortcomings as they become apparent.

Outline of the Incremental Solution-Precipitation Model

The model which is to be described can be used with a computer of moderate capacity such as the IBM 360, Model 30. It is an incremental model which proceeds in steps covering more or less short time intervals. Starting from an input defining the state of the cement-water system at the start of mixing, calculations are made which allow the prediction of physical, chemical and mechanical changes which take place in successive time intervals. The predicted values are the output of the program. In this section, the input to and the output from the calculations and the calculations themselves will be outlined prior to the fuller discussion to be given in Section 3. The way in which the input, the output, and the calculations are related is indicated in the flow chart of Fig. 1.

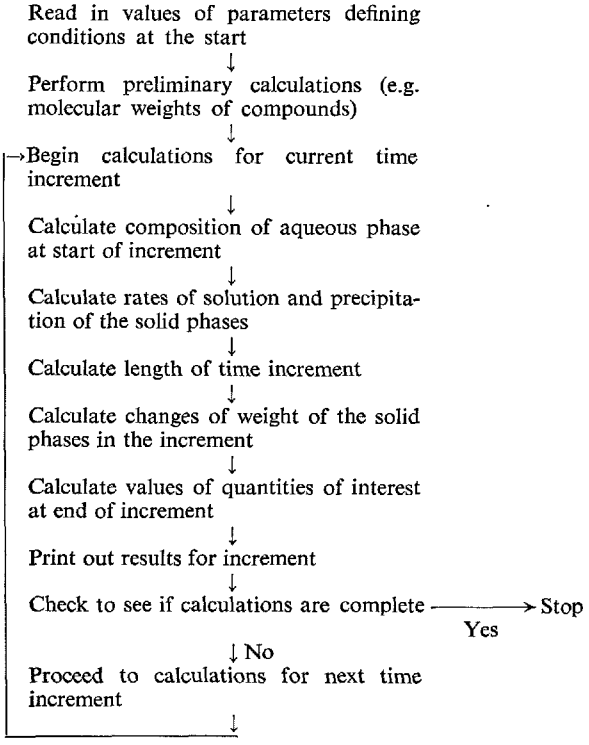

Fig. 1. *Flow chart depicting major subdivisions of the model calculations*

Input—The State of the System at the Start of Mixing

The characteristics used to describe the system at the start of mixing and which form the input to the calculations are (i) the quantities, compositions, and particle size distributions of the solid phases present in the cement, and (ii) the quantity and composition of the mixing water. In addition, it is necessary to know or assume the compositions of the possible reaction products and the values of the relevant chemical and physical properties of both products, and reactants. These properties include solubilities rate constants for solution, nucleation and precipitation, heat contents, and specific gravities together with other constants needed for calculation of mechanical properties.

Output—The Calculated Characteristics of the System at Various Points in Time

The output of the calculations consists of the quantities and particle size distributions of the solid phases present, the quantity and composition of the aqueous phase, the heat liberated, the volume, density, porosity, viscosity, and modulus of elasticity of the system. It must be emphasized that the quality of the output depends upon the quality of the input and upon the correctness of the many assumptions incorporated in the model.

Calculations

For simplicity, calculations are based on the assumption that each solid phase in the system consists of spherical particles which, depending on the composition of the aqueous phase, will either dissolve or precipitate when in contact with the aqueous solution. The rate of solution or precipitation of a compound at any point in time is governed by the degree of saturation of the solution with respect to that compound. Calculations of the rates of solution of dissolving phases and of the rates of nucleation and

growth of particles of precipitating phases make possible the further calculations of the changes which take place in the system over a suitably short time interval. Then, proceeding in steps over successive time intervals, the incremental calculations can be extended to cover the whole course of the reactions. In addition to the state of the system in terms of the quantities and particle size distributions of the phases present at a point in time, the calculations are extended to cover the porosity of the system, the rate of heat liberation, viscosity, and modulus of elasticity.

Details of the Model as Applied to Cement Hydration

The calculations associated with the chemical and physical changes taking place in the system are of three main types. These are calculations of the composition of the aqueous phase, calculations of rates of solution of dissolving phases, and calculations of rates of nucleation and growth of precipitating phases. The other major calculations are those of mechanical properties. These aspects of the calculations will now be discussed individually.

Calculation of Rates of Solution of Dissolving Phases

In the simplest case, the rate of solution (R_s) of a dissolving phase can be expressed in terms of the surface area (S) of the phase and the degree of unsaturation of the aqueous phase with respect to the dissolving compound (11). This is expressed by the equation:

$$R_s = k_s \cdot S \cdot (I_{sat} - I) \qquad (1)$$

where k_s is a constant, I is related to the ionic product for the compound in solution at a given point in time, and I_{sat} is the value of I for a saturated solution of the compound. For the compound $A_1B_mC_n \ldots$, I is given by:

$$I = \left[[A]^1 \cdot [B]^m \cdot [C]^n \cdot \ldots\right]^{\frac{1}{1+m+n\cdots}} \qquad (2)$$

where [A], [B], [C], ... are the concentrations of the ions in solution.

Calculation of the Rates of Nucleation and Growth of Precipitating Phases

Just as the rate of solution of a compound can be expressed by equation (1), so can the rate of growth of existing particles of the compound. However, calculations of precipitation are more complex than those of solution since the possibility of the nucleation of new particles must be taken into account (11). The rate of nucleation (R_n) may be expressed by the equation:

$$R_n = k_n \cdot (I - I_{sat})^p \qquad (3)$$

where p is an exponent characteristic of the particular compound and k_n is a constant. The value of p usually lies between about 4 and 20. In the calculations, it is assumed that all nuclei of a given compound are of the same size.

Calculation of the Composition of the Aqueous Phase

The most difficult part of the calculations for any given point in time involves the determination of the composition of the aqueous phase. In the terms used by DeTar, the aqueous phase is "a steady state intermediate" whose composition changes at a rate which is very low compared with the rates of change of the quantities of the solid phases in the system. This makes it difficult to use a material balance based on solution and precipitation calculations to calculate the composition of the aqueous phase. A more satisfactory method is to calculate the composition of the solution from the knowledge that its rate of change with time is close to zero. In this procedure, the rates of solution and precipitation of the solid phases at the point in time are calculated as functions of solution composition using the previously calculated surface area values, and then selecting the solution composition which minimizes the sum of squares of the relative rates of change of the concentrations of the ions in solution. Although the concept is straightforward, the calculations required are lengthy and account for the greater part of the computations.

Calculation of Physical and Mechanical Properties

Examples of the physical and mechanical properties which the model may be used to interpret are heat liberation, porosity, viscosity, and modulus of elasticity.

The calculation of the heat liberation as a function of time requires a knowledge of the molar heat contents of the individual phases in the system. Then the total heat content of the system at a point in time is given by the equation:

$$H = \sum_{1}^{n} N_i \cdot \tilde{H}_i \qquad (4)$$

where N_i is the number of moles of phase i in the system and $\tilde{H}_i$ is its molar heat content. The rate of heat liberation is calculated as the rate of change of the heat content of the system with time.

The viscosity n at moderate rates of shear can be related to the volume concentration of solids in the system using one of the well-known equations for the viscosity of concentrated suspensions. The volume concentration ϕ is calculated from the previously calculated weights of solid and water in the system at the particular point in time. While it is not yet known which viscosity equation is best suited to the case of cement paste, the one used in the present form of the model is the Mooney equation (12):

$$\eta = \eta_0 \exp\left(\frac{2.5\phi}{1 - k\phi}\right) \qquad (5)$$

In this equation, η_0 is the viscosity of the liquid phase and k is a constant.

Whereas the volume concentration of solid in the liquid governs the viscosity and other flow properties, the porosity of the system plays a major part in governing mechanical properties such as elastic moduli and compressive strength. The proosity is the fraction of the volume within the outer bounds of the mass which is not occupied by solid. Thus, the pores may be filled with water or air. Since the overall volume of a cement paste seldom changes more than a small fraction of 1 percent during hydration, the proosity ε at a point in time may be calculated from the expression:

$$\varepsilon = \frac{\text{volume of solid in system at the given time}}{\text{initial volume of system (solid + liquid)}} \qquad (6)$$

The porosity calculated in this way is used to calculate changes in the modulus of elasticity E using the equation:

$$E = E_0 \cdot (1 - \varepsilon)^3 \qquad (7)$$

where E_0 is a constant which may be interpreted as the modulus for zero porosity (3).

Application of the Model to the Case of C_3S Hydration

Calculations using the model have been made for a few hypothetical cases in which the hydration of C_3S* was considered to be represented by the equation:

$$2Ca_3SiO_5 + 5H_2O \longrightarrow Ca_3Si_2O_7 \cdot 2H_2O + 3Ca(OH)_2 \qquad (8)$$

The calculations differed in the values chosen for parameters such as the rate constants for solution, nucleation and growth, and I_{sat} for the solid phases. This approach, which was dictated by the lack of information about the actual values of the parameters, gave an insight into the sensitivity of the calculations to the choice of values.

An example of the results obtained is illustrated in Figs. 2 and 3. Only one set of calculations is represented since the work has not progressed sufficiently far for any critical evaluation to have been made. The values of the parameters used are given in Table 1. The axes of the curves in Figs. 2 and 3 have linear scales, but they are not marked in absolute units since, in view of the arbitrary choice of parameters for the calculations, these would not be meaningful. However, the curves do share a common time scale and may be compared with each other.

Table 1. *Values of parameters used in the illustrative calculations*

	C_3S	$C_3S_2H_2$	$Ca(OH)_2$
k_s	0.01	0.1	1.0
k_n	10^{18}	10^{21}	10^{18}
Diameter of nucleus	10^{-7}	10^{-7}	10^{-7}
p	3	3	3
I_{sat}	10^{-5}	10^{-8}	10^{-5}
Particle diameter at start	6×10^{-4}	0	0
Weight at start	1.0	0	0

*The cement industry nomenclature used in this paper employs the symbols C = CaO, S = SiO_2 and H = H_2O.

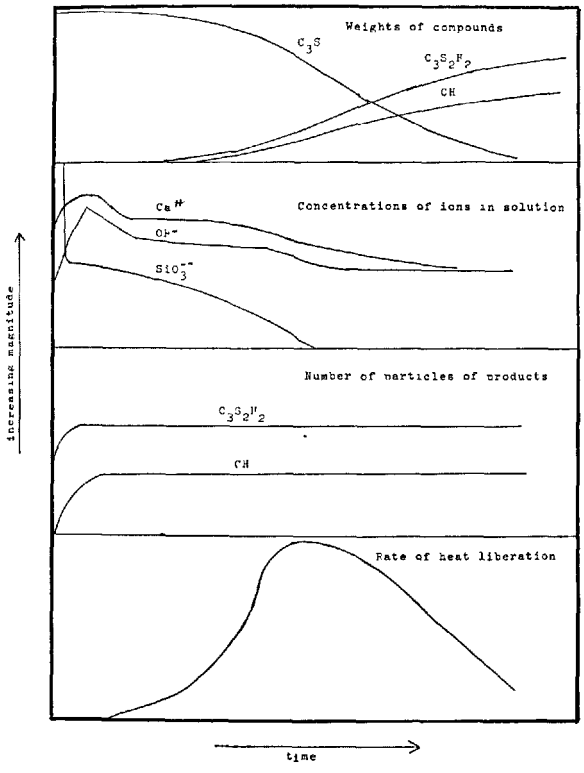

Fig. 2. *Results of an illustrative set of model calculations*

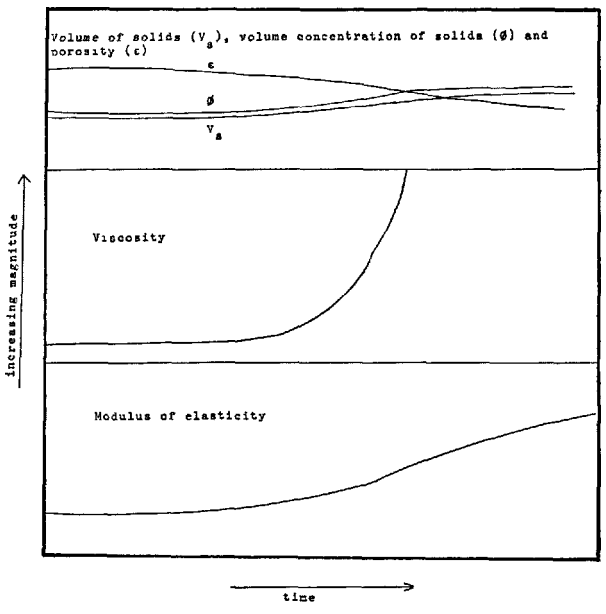

Fig. 3. *Results of an illustrative set of model calculations*

Discussion

Because the calculations represented in Figs. 2 and 3 merely represents an early attempts to simulate the hydration of a cementing material using a computer, the forms of the curves shown should not be considered to have great significance. What is significant is that the curves illustrate how physical, chemical and mechanical changes taking place in an hydrating cement can be interrelated. The capability of being able to relate so many different aspects gives hope of obtaining improved insights into the interrelationships between them.

Referring to Fig. 2, the changes in the weights of the solid phases with time shows several expected features such as an initial "dormant" period followed by a period of increasing rate of reaction. A wide range of control over the length of the dormant period and over the steepness of slope of the curve can be exercised through modification of the input parameters. However, in its present form, the model does not appear to have the capability of accounting for experimental data for the hydration of C_3S such as that obtained by de Jong, Stein and Stevels (13). de Jong's data showed the induction or dormant period to be followed by a period of fast reaction and a still later period of prolonged slow reaction. These findings were interpreted in terms of a sequence of reactions in which hydrated calcium silicates with different C/S ratios were formed and de Jong *et al* postulated that these products have different retarding effects on the hydration of C_3S. While the present model does not take into account effects such as those postulated by de Jong, such effects could easily be included in future versions of the model.

The relationships between the changes in weights of the solid phases and other variables such as the number of particles of the products, heat liberation and the porosity and volume concentration of solids in the system is apparent from Figs. 2 and 3, but the curves showing concentrations of ions in solution have a shape which is unexpected in the light of Lawrence's experimental data (14) for hydrating cements. However, the forms of these curves are particularly sensitive to the values of the input parameters and should not be considered as necessarily being representative.

The calculated values lead to an initially high rate of nucleation of the product compounds which is followed by a continuing period of growth without significant nucleation.

It is clear that no precipitation of reaction products can take place without the formation of particles of the compounds by nucleation, and this is consistent with results shown in the third frame of Fig. 2.

The first set of curves in Fig. 3 are closely related to the changes in weights of the compounds, and show no unexpected features. The curves for the volume of solids and the volume concentration of solids are closely similar, but they would diverge more if the calculations had been for a lower water/cement ratio than 0.6. From the calculated volume concentration of solids and the porosity, the calculations of viscosity and modulus of elasticity shown in the lower portions of the figure were made. The results indicate that the viscosity of the system increases markedly with time as a result of the volume concentration of solids increasing. This effect would be related, at least in part, to the setting of cement systems. Little can be said about the calculated curve of the modulus of elasticity except that the calculations are only likely to be useful for rigid systems. Thus, calculations of the modulus for early ages are unlikely to be of value, just as calculations of viscosity at late ages when the system is rigid are also of little value. The modulus increases with time because of the decreasing porosity. The changes in the modulus would be much more marked if the calculations had been made for a lower water-cement ratio. This draws attention to the fact that one of the uses of this and similar models is to attempt to predict the effects of changes of water/cement ratio, compound composition, particle size distribution and other variables on the performance of cement-containing systems and it will also be useful in aiding the design of experiments to test the predictions. In addition, the predictions will raise questions about the chemistry and physics of cement hydration which may stimulate research to answer them. An example of such a question concerns the nature of nuclei and the role of nucleation in affecting cement performance.

In conclusion, the advantages which a mathematical model offers to the individual researcher or cement technologist are

(a) A self-consistent, easily modified, representation of the state of knowledge concerning cement performance.
(b) An ability to test the implications of new concepts concerning cement performance.
(c) An aid to the planning and interpretation of research work.
(d) An educational tool for the teaching of concepts relevant to the understanding of cement behavior.

While it must be emphasized that the success which any general model will have in the prediction of cement performance from fundamental physical and chemical properties may be limited, there can be no doubt that such a model is an important aid to understanding. This is particularly true when the model is used as an evolving representation of the state of knowledge and is improved whenever its shortcomings are identified.

Summary

In this paper, we have shown how a general mathematical model for the hydration of cement and other materials can be developed. The model has been outlined and its use illustrated by calculations depicting the hydration of C_3S. The calculations were based on a single set of somewhat arbitrarily chosen parameters and are not expected to approximate closely to the real system. While the application of the model to the interpretation of real data has not been attempted, the results of the calculations have been discussed with reference to data in the literature and to known features of cement performance.

Acknowledgment

The authors wish to express their thanks to Mr. James P. Giles, President of American Cement Corporation, for granting permission to publish this paper.

References

1. H. Le Chaterlier, Constitution of Hydraulic Mortars, trans. by J. L. Mack, McGraw-Hill, New York

(1905).
2. T. C. Powers, Proceedings of the Fourth International Symposium on the Chemistry of Cement, Washington, D. C., Vol. 2, p. 577 (1962).
3. R. A. Helmuth and D. H. Turk, Special Report 90, Highway Research Board, Washington, D. C., p. 135 (1966).
4. O. S. Volkov, L. G. Karlova, A. F. Polak and V. B. Ratinov, Kolliod. Th., **29**.
5. M. J. Ridge, Nature, **204**, 70 (1964).
6. K. Schiller, J. Appl. Chem., **13**, 572 (1963); **14**, 209 (1964); **15**, 581 (1965).
7. J. Koishi, Bull. Chem. Soc. Japan, **39**, 2406 (1966).
8. F. D. DeTar and C. E. DeTar, J. Phys. Chem., **70**, 3842 (1966).
9. C. Giese, Simulation, p. 141, March, 1967.
10. R. A. Nesbitt and R. D. Engel, Simulation, p. 133, March 1967.
11. A. Van Hook, Crystallization: Theory and Practice, Reinhold, New York (1961).
12. M. Mooney, J. Colloid Sci., **6**, 162 (1951).
13. J. G. M. de Jong, H. N. Stein and J. M. Stevels, J. Appl. Chem., **17**, 246 (1967).
14. C. D. Lawrence, Special Report 90, Highway Research Board, Washington, D. C., p. 378 (1966).

Supplementary Paper II-53 Study on Hydration of Alumina Cement by Ultrasonic Method

Shigeaki Koide and Keiko Okada*

Synopsis

Change in the mechanical property of alumina cement during hydration process was searched continuously by tracing the velocity of ultrasonic wave propagated through neat paste of the cement.

For the hydration of the cement paste a paraffine-made vessel was prepared which was a long parallelepiped and had a couple of transducers made of $BaTiO_3$ facing each other on both ends of the vessel. They were electrically connected with an electric oscillator as well as an amplifier followed by an oscilloscope. Generated power from the oscillator vibrated the specimen to propagate sonic wave between both the transducers, and finally a sinusoidal mode appeared on a screen of the oscilloscope. When the oscillator was directly connected with the oscilloscope, however, a similar mode was obtained having a phase different from the former. From the phase difference relating to the time necessary for the propagation of sound, sound velocity (v) could be obtained as follows:

$$v = l/(n\mathrm{T}_0 + \Delta\mathrm{T}),$$

where l is distance between both transducers, n is number of waves standing within both ends of the specimen, T_0 is period of vibration, and ΔT is phase difference, respectively.

At first the velocity in the paste was mostly constant for several hours, the value being near to that in water. After gradual increase in the next period, the velocity increased steeply and reached the constant value, both the period length and the final velocity depending on hydration temperature.

Mechanical strength was predicted on the basis of Young's modulus calculated from sound velocity of the hardened specimen. Between the above obtained result and that of crushing test carried out on corresponding specimen, a fairly good agreement was found out. Thus the progressive change in sound velocity in hydrating cement shows the hardening process. A time when the sound velocity has reached a saturated value, i.e., the hardening time, is more important to estimate the strength development of alumina cement than so-called setting time.

Introduction

There have been many studies dealing with hydration of alumina cement, and some proper phenomena appearing in early stage, e.g., remarkable heat evolution, sudden decrease of electric conductivity, etc., have often been discussed in comparison with rapid hardening of the cement (1). A number of studies on various crystalline and amorphous hydration products have made clear their structures as well as their crystallization processes depending on conditions, e.g. temperature, water-to-cement ratio, that were much influential on early strength development (2). Recently the early developed strength was discussed in quite a few studies, referring not only to hydrates produced in early stage of hydration, but also to their conversion in each other (3). Although the early strength was considered to be due to chemical reaction accompanied with heat evolution, very few has been reported on correlation between mechanical and chemical properties at the very early stage of hydration of the cement (4). In the present investigation a set of direct measurements of mechanical properties changing in the hydration process were carried out by means of ultrasonic method. The change in mechanical properties was continuously searched by tracing the velocity of ultrasonic wave propagated through the neat paste of the cement.

Although ultrasonic wave has well been used in many studies on cement and concrete (5), e.g., non-

*College of Technology, Seikei University, Tokyo, Japan.

destructive test on strength, non of the results reported hitherto has concerned such a slurry or muddy state that had been found in very early stage of hydration. The reason is considered to come from the fact that it was difficult to measure sound velocity in a muddy substance continuously which change entirely into solid. In the present work it was the most important subject to establish a method to transduce the sonic wave into the specimen and to pick it up out of the specimen as well as to keep off any trouble preventing a stable propagation during the hydration.

The sound velocity in the neat paste of the cement increased to the saturated values depending on conditions of hydration, the elastic modulus derived from the velocity showing the correspondence to mechanical strength of the hardened cement paste. And this happened coincidentally with the characteristic heat evolution as well as the sharp drop of electric conductivity.

Specimen, Apparatus and Procedures

Specimen

Through the whole experiment one of the commercial alumina cements produced by electro-fusion was used as specimen, the chemical composition being illustrated in Table 1. In preliminary experiment, however, some pure calcium aluminates prepared from chemical reagents, $CaCO_3$ and Al_2O_3, were also used in addition to the cement above mentioned. The specimen was confirmed to consist of $CaAl_2O_4$ in great majority and of $12CaO7Al_2O_3$ and $4CaOAl_2O_3Fe_2O_3$ as minor portions, although glassy or amorphous parts could not be inspected since the mineralogical inspection was carried out only by X-ray diffraction on the cement powder.

Physical properties of the specimen were shown in Table 2 and 3 which were obtained by the test based upon JIS-R-5201. Hydraulic strength and setting time of neat paste specimen were measured at several levels of curing temperatures and water-to-cement ratios to compare them with data on mechanical properties which would be obtained in later.

Table 1. *Chemical composition of specimen*

SiO_2	2.90	MgO	0.32
Al_2O_3	40.34	Na_2O	tr.
Fe_2O_3	13.28	K_2O	0.20
FeO	3.98	Ig. loss	−0.10
Fe	0.01	Total	100.40
TiO_2	2.25		
CaO	37.15	Insol.	0.65

Table 2. *Characteristics of specimen*

Particle size distribution		Specific surface area (cm^2/g) 3000			
size-group (microns)	weight (%)		Setting time		
			20°C	30°C	35°C
88<	0.4				
88~40	32.51				
40~30	9.90	Initial	3^h–45^m	4^h–48^m	2^h–06^m
30~20	10.36	Final	4^h–20^m	8^h–44^m	3^h–11^m
20~15	14.99	Water content (%)	28.7	29.1	30.0
15>	32.24				

Apparatus and Procedures

Behavior of sound propagation in a substance is generally different depending either on its physical state, or on mechanical properties. There was obtained on the other hand, a set of close relations between mechanical strengths and elastic moduli of hardened alumina cement (6). Since the experiment searching early strength development was desired to be carried out by means of continuous and non-destructive measurement, the velocity of sound propagation through neat paste of the cement was being traced throughout the hydration process.

A couple of tansducing elements made of $BaTiO_3$ crystal were used both to propagate sonic wave into the specimen and to pick it up out of the specimen. Both the elements had high directional characteristics that was necessary for efficient transducing and good prevention of sonic wave from dispersion in the specimen.

For the hydration of the cement paste a parallelepiped vessel was prepared which was 15 cm × 2 cm × 2 cm on the inside and had a couple of $BaTiO_3$ elements facing each other on both ends of the vessel.

Table 3. *Physical properties of specimen*

Hydration time	Flexural strength (kg/cm^2)	Compressive strength (kg/cm^2)
4 hours	2.4	10
5 〃	20.6	89
6 〃	38.2	241
24 〃	49.7	409
2 days	57.0	461
3 〃	58.8	479
7 〃	66.8	577
28 〃	75.4	671

Flow value 210 (mm) w/c (%) 60

The vessel was made of paraffine in which the sound velocity was lower than that in the cement paste. Thermally molten paraffine was poured into a steel mold and cooled to make the vessel into the long parallelepiped. Ratio of length to cross section of the vessel was so large that sonic wave was propagated through the specimen in longitudinal mode.

The transducers were electrically connected with an electric oscillator and an amplifier followed by an oscilloscope respectively. The arrangement was shown in Fig. 1. Thus, generated electric power from the oscillator vibrated the specimen with frequency ranging from 30 to 40 kc to propagate the sonic wave between both the transducers, and finally a sinusoidal mode appeared on a screen of the oscilloscope. Electric signal generated in a pick-up (one of $BaTiO_3$ elements) had the mode somewhat different from the perfect sine-wave because of unavoidable dispersion and reflection of sound in the specimen. So, such an amplifying circuit as a cathod-follower type was used to amplify the signal with high S-to-N ratio. The main amplifying circuit was shown in Fig. 2.

When the oscillator was directly connected with the oscilloscope, however, a similar mode was obtained having a phase different from the former. The phase

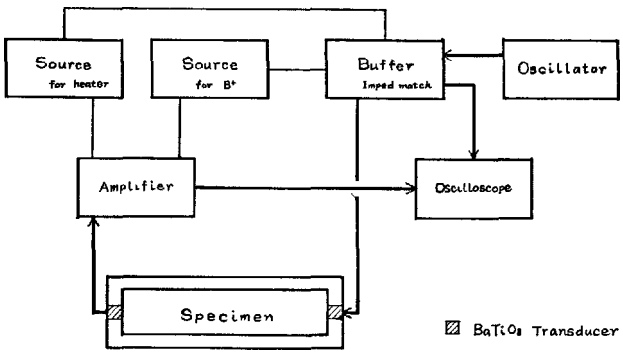

Fig. 1. *Arrangement of circuits on measurement of sonic wave*

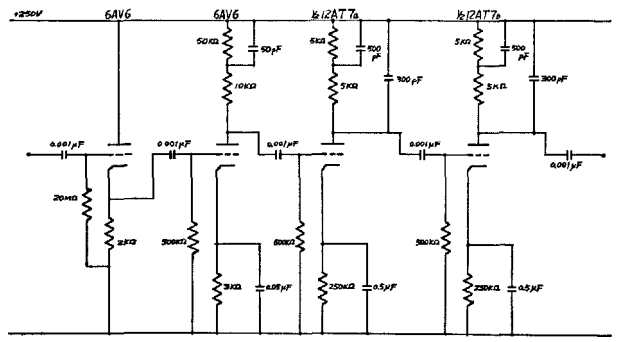

Fig. 2. *Amplifying circuit*

difference (ΔT) was obviously to correspond to the time necessary for the propagation of sound through the specimen. So, the sound velocity (v) in the cement paste could be obtained as follows:

$$v = l/(nT_0 + \Delta T),$$

where l is distance between both transducers,
T_0 is period of vibration, and
n is number of waves standing within both ends of the specimen.

The relation among v, l, T_0 and ΔT was shown in Fig. 3 schematically. ΔT was exactly measured on the oscilloscope and n was determined in preliminary experiment in which the relations of n to l had been obtained at the various distances.

After the transducers were molded in both ends of the vessel, it was put into a case in which temperature was controlled within 20 ~ 35°C with an accuracy of $\pm$0.05°C and relative humidity was kept over 85%. The control was carried out by means of both the electric heater and the coolant set in water stored at the bottom of the case. Alumina cement powder and water previously stored in a thermostat at the same temperature as that in the case were mixed with each other by a series of water-to-cement ratios ranging from 0.24 to 0.30. The mixture was kneaded for about 3 min., and poured into the vessel with a slight tapping. The progressive change in phase of mode of ultrasonic wave propagated through the specimen was recorded in photographs that were taken at regular intervals until the specimen hardened completely. The whole apparatus was shown in Fig. 4.

A couple of electrodes, on the other hand, made of copper plate with area of 2 cm × 3 cm was inserted in the specimen along the side walls of the vessel so as to face each other in parallel to the path of sonic wave as shown in Fig. 5. Applying alternative current between both the electrodes, electric conductivity of the specimen was continuously kept in an electronic recorder. The progressive change of the conductivity

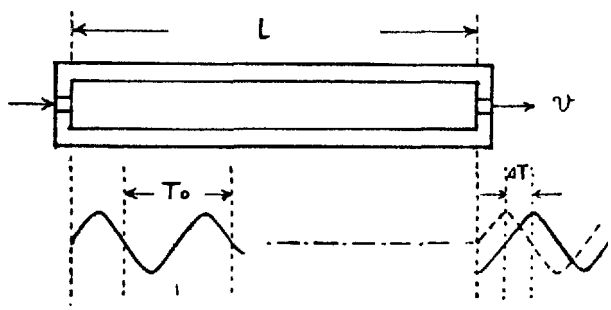

Fig. 3. *Phase difference of sonic wave induced by propagation through specimen*

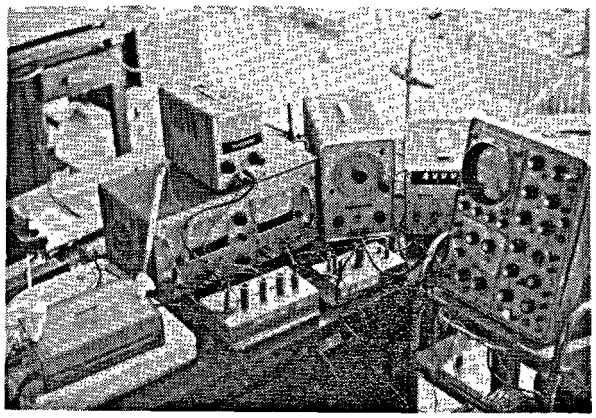

Fig. 4. *Bird's-eye-view of apparatus*

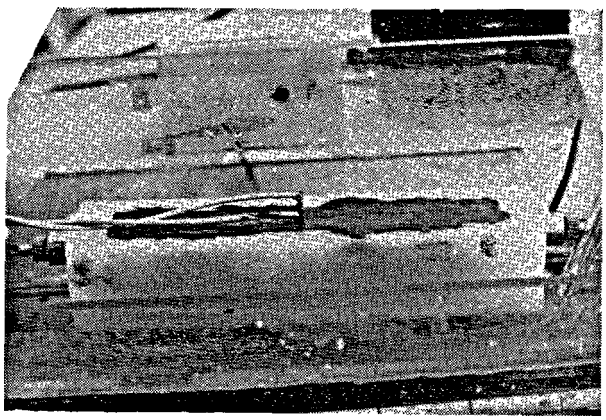

Fig. 5. *Electrodes inserted in vessel*

was measured simultaneously with that of sound velocity during hydration. Since it was avoided in the experiment to electrolyse the specimen, data were not obtained on D. C.—conductivity, but on admittance accompanied with capacitance. Keeping track of characteristic change in electric impedance of the specimen was of good use in this work even if the capacitance could not be measured separately. Therefore, voltage drop generated by alternative current flowing through the specimen was traced during hydration.

Results and Discussion

Sound Velocity

Characteristic patterns of progressive changes in sound velocities propagated through the specimens were obtained throughout the hydration. Fig. 6 showed both the modes of propagated (lower) and standard (upper) sonic waves on a dual beamed screen. The phase difference scarcely changed during the first 2 hours. Through a gradual increase the difference became rapidly greater. The velocity was mostly constant for the first period, the length of which was different depending on hydration temperature and water-to-cement ratio; the value of the velocity was near to that in water, about 1,400 m/sec. After a gradual increase in the second period, the velocity rose up suddenly, then reached again a constant value. Both the length of the second period and the final velocity were also dependent on hydration conditions, the values of them falling into $2 \sim 10$ hours and $2{,}400 \sim 4{,}600$ m/sec respectively.

Effect of Water-to-Cement Ratio

When specimen were prepared with water-to-cement ratio lower than 0.28, it was difficult to obtain sharp modes of sonic wave on the oscilloscope because the specimens were not sufficiently plastic to be molded homogeneously enough for stable propagation of sound. As for the specimens with water-to-cement ratios ranging from 0.28 to 0.30, measurements of the velocities were easily carried out and their progressive changes similarly appeared with a little differences depending on the ratio. The dependence of the pattern of progressive change in sound velocity on water-to-cement ratio was not so remarkable compared with that on hydration temperature. Therefore, the further experiments were carried out on the specimens with constant viscosity (or workability) irrespective of water-to-cement ratio.

Temperature Dependence of Progressive Change in Sound Velocity

Change in sound velocity during hydration was so much influenced by temperature as were periods of heat evolution and of setting as well as of strength development. The temperature dependence was obviously much more remarkable than that on water-to-cement ratio. In Fig. 7 each pattern of progressive change in sound velocity was shown as a function of hydration time with hydration temperature as a parameter. The characteristic increase of the velocity retarded with the increase of hydration temperature up to 30°C, at which the retardation reached the maximum. Over this temperature, on the other hand, the period of velocity-increase became earlier again. At

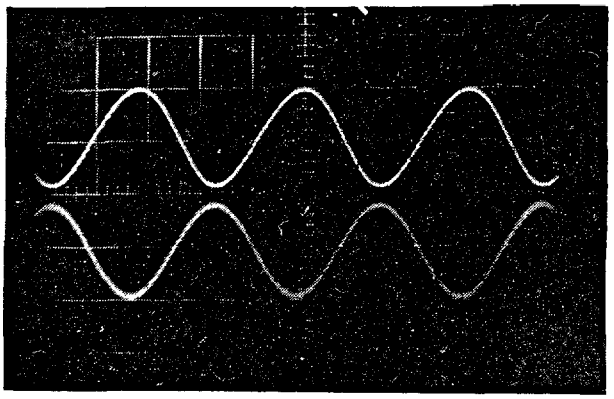

(1) 2 hrs

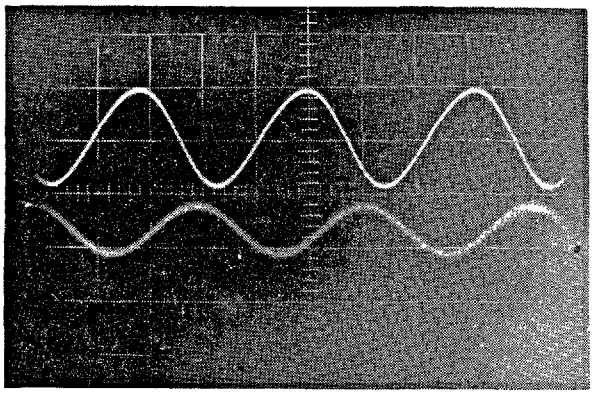

(2) 2.5 hrs

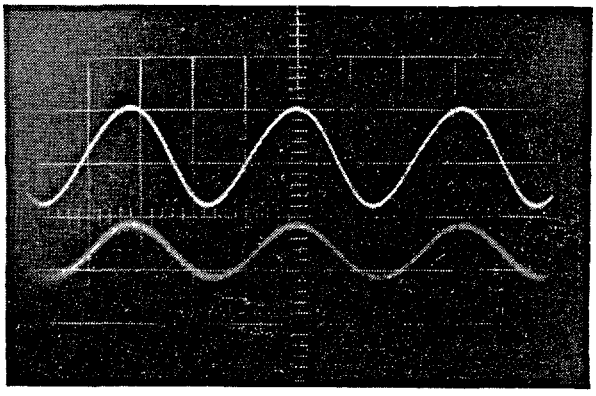

(3) 3.5 hrs

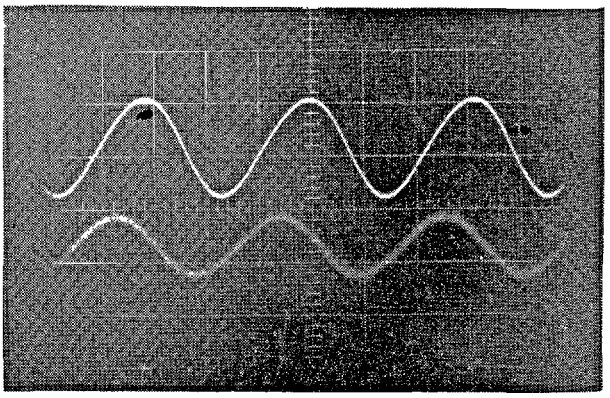

(4) 4.2 hrs

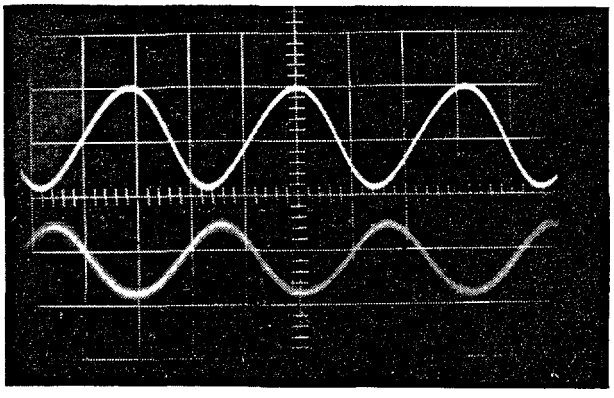

(5) 5 hrs

Fig. 6. *Progressive change in phase of sonic wave propagated through specimen (40 kc, 20°C)*

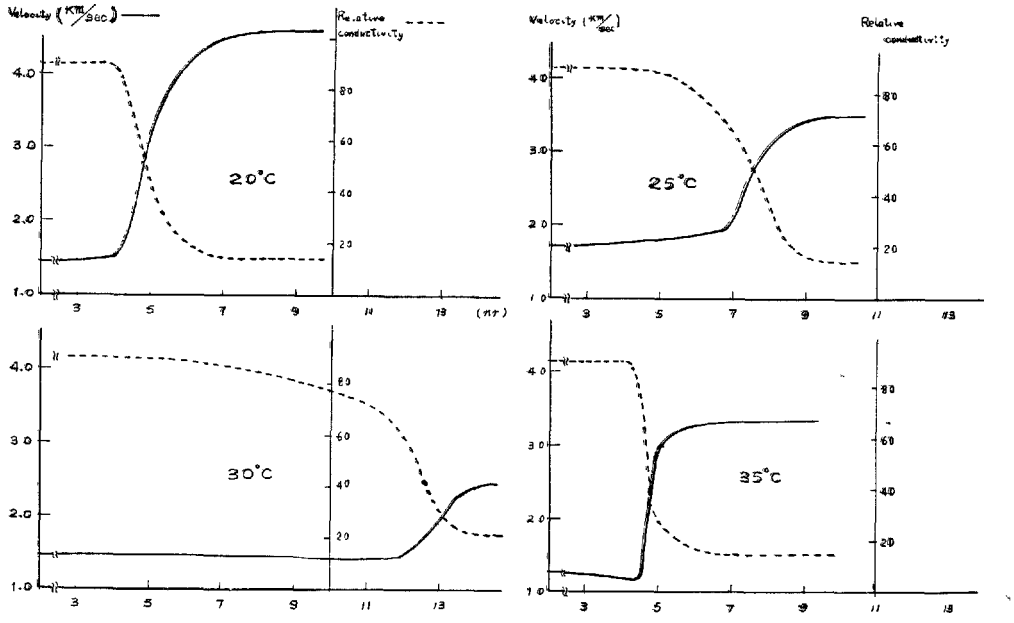

Fig. 7. *Sound velocity and electric conductivity in specimen as functions of time*

30°C, the slope of the velocity-increase became the smallest. Comparing these results with those previously reported (8), it was found out that correlation between the progressive change in sound velocity and hydration temperature closely resembled that between heat evolution and the temperature.

Electric Conductivity

During hydration of the specimen, electric conductivity decreased in characteristic manner depending on hydration temperature. The patterns of change in the conductivity were exactly same as those obtained previously (1). At 20°C, like the sound velocity, electric conductivity decreased scarcely for the first several hours, then sudden drop appeared after which the conductivity reached very low constant value. It is of interest that the time when the sudden drop appeared was exactly coincident with the sudden increase in the sound velocity.

When hydration proceeded at temperatures merely below 30°C., electric conductivity began to decrease gradually after the first period in which no change in the conductivity was found. Decrease in the conductivity continued thereafter with the slope becoming progressively steep, and finally the low constant value was reached. At 30°C, change in the conductivity was the most gradual without such a sharp drop as found at 20°C, although the steepest slope was recognized at a time about 12.5 hours after the beginning of hydration.

Since the electric conductivity was measured using alternative current, obtained data showed somewhat lower value of impedance than pure resistance against D. C.—current. The latter was usually 2~7 times as large as the former. It should be noted that the hardened specimen showed capacitance ranging from 100 pF to 0.01 μF, which was remarkably large compared with those reported on ordinary concrete (7).

At every hydration temperature, the coincidence of characteristic drop in electric conductivity with proper rising in the sound velocity was preserved as shown in Fig. 7. This fact suggests that characteristic change in mechanical properties of alumina cement during hydration exactly corresponds to chemical change.

Young's Modulus and Mechanical Strength

In the present work, sonic wave propagated through the specimen could be considered to be longitudinal wave, since the vessel used for measurement was a long parallelepiped. Therefore, the elastic constant regarded as the function of the obtained sound velocity is "volume modulus" until the specimen hardens, and is "Young's modulus" after hardening. For the sake of simplicity, we used Young's modulus to discuss the mechanical properties of the cement paste through-

Table 4. *Sound velocity and Young's modulus in neat paste of alumina cement during hydration*

Temperature (C°)	Time (hr)	3	4	5	6	7	8	9	10	11	12	13	14
20	V(km/sec)	1.48	1.50	3.16	4.16	4.50	4.60	4.61	4.61				
	E(10^5 kg/cm^2)	0.467	0.487	2.13	3.71	4 34	4.52	4.55	4.55				
25	V(km/sec)	1.71	1.78	1.81	1.86	1.96	3.13	3.45	3.48				
	E(10^5kg/cm^2)	0.624	0.676	0.700	0.739	0.821	2.10	2.54	2.59				
30	V(km/sec)								1.43	1.43	1.47	1.90	2.43
	E(10^5 kg/cm^2)								0.436	0.436	0.461	0.77	1.18
35	V(km/sec)	1.25	1.18	3.00	3.27	3.31	3.32	3.34					
	E(10^5 kg/cm^2)	0.334	0.298	1.93	2.28	2.345	2.36	2.385					

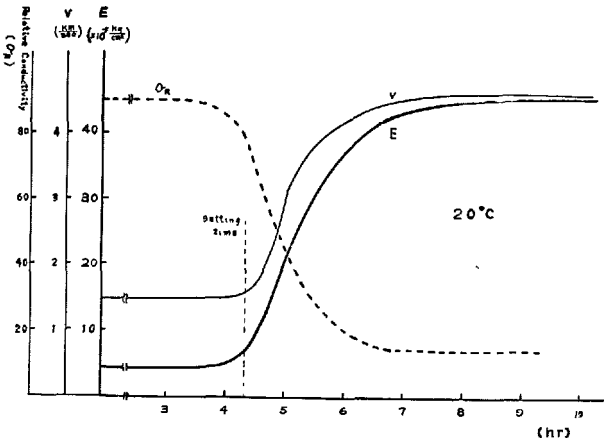

Fig. 8. *Correlation between Young's modulus and hydration time*

out the hydration process, since the latter could approximately take the place of volume modulus. Young's modulus of the specimen was derived from

$$E = \rho v^2,$$

where E is Young's modulus,
ρ is bulk density of specimen, and
v is velocity of longitudinal sonic wave in specimen.

Using the bulk density of specimen known to be 2.0 g/cm^3 at the beginning of hydration and finally to become 2.1 g/cm^3, Young's modulus of the cement paste was calculated at the various hydration temperatures as shown in Table 4. Young's modulus calculated from sound velocity and electric conductivity were shown in Fig. 8 as functions of time during hydration at 20°C. The modulus reached the final value of ca. 4.28×10^5 kg/cm^2 corresponding to the final velocity of sound. The coincidence of the characteristic period of change in Young's modulus with that in electric conductivity was, of course, preserved.

In our previous study (6), it has been found out that there were fairly good correlations between crushing

Table 5. *Correlation between predicted and measured strength*

Hydration temperature (°C)	Predicted strength (kg/cm^2)	Measured strength (kg/cm^2)	Hardening time (h-m)
20	800≦	675	7–20
25	450～500	420	9–15
30	150～200	141	13–40
35	390～440	378	6–40

strengths of hydrated alumina cement and their Young's moduli irrespective of hydration conditions. On the basis of the results mechanical strengths of the specimens were predicted from their Young's moduli. After the experiments, on the other hand, the hardened specimen were subjected to crushing test. Both the predicted and the measured strengths of the specimens hydrated at various temperatures were shown in Table 5. There were a fairly good agreement between them so that the estimation of the strength by ultrasonic method seemed to be possible even in early stage of hydration of alumina cement. Thus, it is clear that sound velocity propagated through the neat paste of alumina cement corresponds to its mechanical strength that is being developed during hydration, and that the progressive change in the velocity shows the hardening process of the cement.

The setting time was also different with hydration temperatures as shown in Table 2, the temperature dependence being similar to that of the saturation time of sound velocity. Comparing the final setting time with the saturating time of the velocity at each temperature in Fig. 7, however, it was difficult to find out quantitative relations between both the times. Therefore, a time when the sound velocity has reached a saturated value is considered to be more essential to the strength development of alumina cement than the setting time.

It was shown that alumina cement hardened within a short period accompanied by rapid increase in sound velocity as well as sharp drop of electric con-

ductivity which had been reported to coincide with a remarkable heat evolving time in the hydration process of the cement (8). This leads to the fact that all the characteristic properties change coincidentally with each other during hydration. On the basis of the experimental results, we propose that the hardening time be defined as a time when sound velocity in the cement paste has reached a saturated value. The hardening time is considered to be of more useful as a measure of strength development in alumina cement than the setting time.

Conclusion

To investigate the process of early strength development in alumina cement, a set of experiments were carried out measuring sound velocity in neat paste of the cement during hydration. For the measurement a method was established to transduce the sonic wave into and out of the muddy specimen that changed into solidus state during hydration, as well as to keep a stable propagation.

The progressive change in the sound velocity was obtained at each hydration temperature of 20°, 25°, 30° and 35°C. The velocity changed scarcely at first, gradually in the next period and then suddenly rose up to the saturated value, the manner of change and the final value depending on hydration temperature. The change proceeded more slowly with rising hydration temperature below 30°C, above that the change became faster again. The pattern of change in the velocity closely resembled that of electric conductivity and the final period in both patterns were exactly coincident.

Mechanical strength was predicted on the basis of Young's modulus calculated from sound velocity of the hardened specimen. The results was compared with that of crushing test carried out for corresponding specimen, and a fairly good agreement was found between them. Thus, the progressive change in sound velocity in hydrating cement is considered to show the hardening process. A time when the sound velocity has reached a saturated value, i.e., the hardening time, is more important to discuss the early strength development of alumina cement than the setting time.

References

1. J. Cellaja, J. Amer, Concr. Inst., **50**, 349–60, 1953. "Determination of setting and hardening time of high-alumina cements by electrical resistance techniques". A. Majumdar, and R. Roy, J. Amer. Ceram. Soc., **39**, 434–38, 1956 "The system $CaO–Al_2O_3–H_2O$". S. Koide, M. Kawano and K. Kaiden, Asahi Glass Co. Res. Lab. Rep., **7(1)**, 44–53, 1957. "Hydration process of alumina cement affected by temperature in early stage". Ch. Eyrand, M. Murat and P. Barriac, Bull. Soc. Chim. France, **10**, 3730–32, 1967. "Etude la déshydration d'un solide par mesure de conductivité électrique. Application a la déshydration du gypse".
2. J. D'Ans and H. Eick, Zement-Kalk-Gips, **6**, 197–210, 1953. "Das System $CaO–Al_2O_3–H_2O$ bei 20°C und das Erhärten des Tonerdezements". L. S. Wells and E. T. Carson, J. Res. Nat. Bur. Stand., **57**, 335–53, 1956. "Hydration of aluminous cements and its relation to the phase equilibria in the system lime-alumina-water". E. T. Carlson, ibid., **61**, 1–11, 1958. "The system lime-alumina-water at 1°C". H. zur Strassen, Zement-Kalk-Gips, **11**, 137–43, 1958. "Die chemischen Reaktionen bei der Zementerhärtung". F. W. Jones and M. H. Roberts, Proc. IV intern, Symp. Chem. Cement, Washington, 205–42, 1960. "Hydration of calcium aluminates and ferrites"
3. J. S. Schneider, J. Amer. Ceram. Soc., **42**, 184–93, 1959. "Effect of heat-treatment on the constitution and mechanical properties of some hydrated aluminous cement". S. Koide, J. Ceram. Assoc. Japan, **69**, C43–51, 1961. "Hydration of alumina cement". W. C. Hansen, Mat. Res. Stand., **2**, 490–93, 1962. "Solid-liquid reactions in portland cement paste". F. W. Locher, Zement-Kalk-Gips, **17**, 175–82, 1964. "Die chemischen Reaktionen der Zementerhärtung".
4. H. G. Midgley, Trans, Brit. Ceram. Soc., **66(4)**, 161–87, 1967. "The mineralogy of set high-alumina cement".
5. P. Klieger, J. Amer. Concr. Inst., 481, 1957. "Long-time study of cement performance in concrete, Chapter 10—Progress report on strength and elastic properties of concrete".
6. S. Koide, K. Kaiden and M. Kawano, Asahi Glass Co. Res. Lab. Rep., **8(2)**, 83–95, 1958. "Relation between mechanical strength and sonic properties of alumina cement".
7. T. D. Robson, High Alumina Cements and Concretes, pp. 82–83, 1962.
8. S. Koide, M. Kawano and M. Kaiden, Asahi Glass Co. Res. Lab. Rep., **7(1)**, 44–53, 1957. "Hydration process of alumina cement affected by temperature in early stage".

Oral Discussion

Renichi Kondo

We are much interested in the use of ultrasonics in cement chemistry, which seems to give some influences on the rate and mechanism of hydration and to be of much interest for practical purposes. The authors showed the relation between the sound velocity and the electric conductivity of each specimens at each curing temperature in Fig. 7. It is considered that the sound velocity is concerned with the structure of hydrated specimens, while electric conductivity show the liquid phase concentration. I would like to know how to understand the relation between these physical and chemical properties and hydration mechanism of alumina cement. Especially, the relative conductivity in early stages is almost constant in many cases. How do you think about the hydration mechanism in relation to this fact?

Authors' Closure

Shigeaki Koide and Keiko Okada

Sound velocity and electric conductivity of alumina cement paste progressively change showing the characteristic pattern as a function of hydration time. On the basis of the pattern the mechanism of hardening process of the cement is considered to be as follows:

When the cement powders contact with water, CA immediately decomposes into calcium- and aluminum-ions on its surface, and some amount of the ions migrate out of the powder with the steep concentration gradient at a vicinity of the surface of the cement powder. While the rest of ions precipitate mostly on the surface of the powder turning into nuclei of CAH_{10} the new ions are produced by the reaction of CA with water diffusing through the surface layer.

The migrating ions seem to be kept in almost constant amount, so that the electric conductivity is also constant in this period, although it is not the case in which water to cement ratio becomes higher or some additives are present in the water. The length of the period (so-called induction period) falls into several hours depending on hydration temperature, water to cement ratio, amount of additives, etc. At the end of the period acicular CAH_{10} crystals are produced which bridge the aggregate with anhydrous cement powders. Then, the paste hardens into the solid with rigid texture, and the remained free water vaporizes due to the heat liberated coincidentally. So, the increase of elastic modulus and drop of electric conductivity occur simultaneously at a time which may be called the hardening time. The time is considered to be more effective aim of strength development of the cement than the setting time.

Supplementary Paper II-70 On the hydration Kinetics of Hydraulic Cements

John H. Taplin*

Synopsis

The hydration kinetics of seven hydraulic cements are explored. They are magnesia in 1.5–0.05 molar magnesium chloride or sulphate solution, anhydrite in potassium alum solution, one β–C_2S preparation without boric oxide and one with it, two preparations of monoclinic C_3S with excess alumina and a triclinic C_3S without excess alumina. From the particle size distributions of six of these cements, hypothetical linear and quadratic kinetics are calculated and used as a guide as to whether the rate of hydration depends on the reacting surface area or on the rate of diffusion of material to or from the surface.

The cements were stirred in some experiments and hardened in others. In all stirred experiments the kinetics are either approximately linear or approximately quadratic. Hardening specimens of magnesia, anhydrite and in final stages C_3S show a rate decay which is even more rapid than quadratic kinetics and which is taken to be controlled by resistance to diffusion through merging and perhaps thickening outer products.

Some aspects of the possible basis for a linear-diffusion kinetics model are treated. For a single discrete particle, for example, it is shown that a diffusion process is unlikely to control the rate either at the very beginning or at the very end of the reaction.

A possible mechanism by which the outward diffusion of a substance could control the rate is postulated and found to lead to joint linear-diffusion control. No direct evidence could be found in the stirred experiments for such a joint kinetics although the possibility exists when the rate is controlled by merging outer products.

Linear rate constants and apparent activation energies are quoted for several of these hydraulic cement systems. The ageing of C_3S preparations was found to slow the diffusion process and refiring to speed it up.

Introduction

The hydration of a hydraulic cement involves the reaction of discrete particles of the cement with an aqueous solution, and the formation of a coherent network of solid hydration products. It has been argued previously (1) that at least the outer products must be formed from material which has been transported by diffusion. Here we will consider the simple alternatives of a rate (i) proportioned to the surface area of cores of unreacted cement and (ii) invesely proportional to the resistance to diffusion provided by a coherent coating of reaction products.

The kinetics of (i) above will be referred to as "linear." The term "diffusion kinetics" will be used for a reaction rate controlled by any diffusion process, "parabolic kinetics" for control by diffusion through one or more layers of products each assumed to have a constant specific permeability and, "quadratic kinetics" for parabolic kinetics with the resistance of the outer products negligible compared to that of the inner products. Linear and quadratic kinetics have been discussed previously in relation to the hydration of β–C_2S (2).

The hydraulic cements to be described here are: magnesia in magnesium chloride and sulphate solution at concentrations below those needed for basic salt formation, anhydrite in potassium alum solution, two preparations of β–C_2S and three of C_3S. To test for linear or diffusion kinetics, the experimental hydration data are compared with hypothetical linear and quadratic curves computed from the measured particle size distribution (p.s.d.) assuming spherical shape and uniform reactivity. Quadratic kinetics was chosen as a test for diffusion kinetics because the inner products might be expected to provide most of the diffusion resistance for isolated particles with coherent coatings. It is also a useful choice in that the effect of a more complex parabolic reaction or other diffusion modifications such as for example a decreasing product porosity can be expected to show up as

*Commonwealth Scientific & Industrial Research Organization, Department of Civil Engineering, Sydney University, Sydney, Australia.

a deviation from quadratic kinetics in the direction of an even more rapidly falling rate, i.e., in the direction away from linear kinetics. Such deviations are to be expected under conditions of high strength since both phenomena are due to the outer products filling most of the space between the original cement particles.

Experimental

The hydration of the calcium silicates was followed by the method of Taplin (1), i.e., the reaction was stopped by vacuum drying, the specimens further dried at 125°C in an atmosphere of steam and the "chemically combined" water determined as the loss on heating to 540°C. For magnesia the procedure was modified by omitting the steam atmosphere in the oven and, for stirred magnesia, by first washing out most of the chloride or sulphate before vacuum drying. The weight loss between vacuum dry and 540°C was the hydration measure for anhydrite. The hydration values assumed for complete reaction are: 0.45 for magnesia, 0.26 for anhydrite, 0.21 for C_2S and 0.25 for C_3S.

Two types of specimen were made. The "stirred" specimens consisted of an aqueous suspension of cement in a glass bottle or tube sealed with a rubber gasket or stopper and attached to a wooden frame rotating about four times a minute. The curing temperature was 21°C and the suspension had a water cement ratio of 5, 8 or 10 depending on the tendency of the cement to stiffen.

The "hardening" specimens were paste specimens unless referred to as mortars. The water-cement ratio (W/C) is quoted by weight. The early specimens were $\frac{1}{2} \times \frac{1}{2} \times 4$ inch bars tested in compression as modified cubes. The anhydrite specimens were $\frac{1}{2}$ inch cubes and the 1967 C_3S specimens were cylinders, $\frac{1}{2}$ inch diameter, $1\frac{1}{4}$ inches high. Only the β-C_2S (5106) specimens at W/C = 0.35 were produced by mechanical compaction in a tamping machine. A vibrating table was used to help remove air bubbles from the more fluid mixes. The earlier specimens were kept saturated by the addition from time to time of a few drops of water to the tube in which they were cured. The cylinders were cured under water. Only the hydration results of these specimens will be discussed here.

The experimental p.s.d. of the cements are plotted on logarithmic probability paper in Fig. 1. For the purpose of computing linear and quadratic kinetics, these data were approximated by double composite lognormal distributions obtained by fitting two lines which meet at the median size and pass through the upper and lower parts of the distribution respectively. This p.s.d. was then treated as a histogram with each step containing one per cent of the powder at a size which was the median in the range. At various hypothetical reaction times, the fraction reacted was computed for each step of the histograms, by interpolating in tables of F versus t/R and F versus t/R^2 construc-

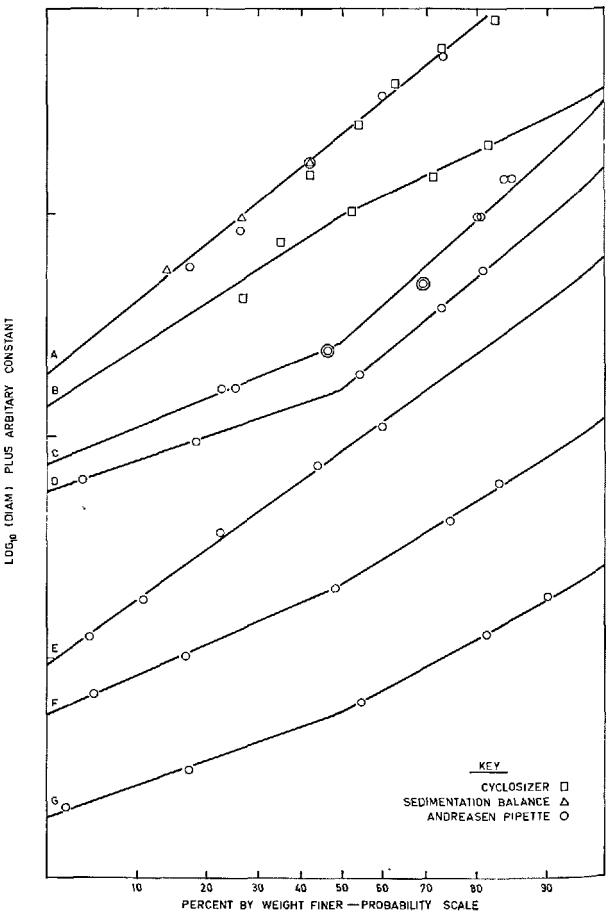

Fig. 1. *Particle size distributions of the hydraulic cements on log probability paper. The suspending medium for the cyclosizer was water and for the sedimentation balance and Andreasen pipette it was ethanol with 0.01% calcium chloride. The mineral identifications are:*

A Fused magnesium oxide,
B Sintered anhydrite,
C β-C_2S(5106),
D β-C_2S(5108),
E Alite(608),
F C_3S(620),
G C_3S(620) re-fired.

ted from equations (1) and (2) for linear and quadratic kinetics respectively.

$$1 - (1 - F)^{1/3} = k_1 t/R \qquad (1)$$

$$1 - (1 - F)^{2/3} - 2F/3 = k_2 t/R^2 \qquad (2)$$

where k_1 and k_2 were put equal to unity for the computation and then adjusted in attempts to fit the experimental hydration data. The distributions used in the computations can be described by the diameters in microns at the 15, 50 and 84% levels, they are: "fused" MgO 3.45/13.2/51, sintered anhydrite 7/20/44, β-C_2S (5106) 2.8/5.2/24, β-C_2S (5108) 4.8/8.6/34, alite (608) 7.1/23/77, C_3S (620) 5/10.3/29, C_3S (620) re-fired 5/9/22.

Magnesium Oxide

This material is a commercial "fused" magnesia with a chemical analysis of MgO 96%, SiO_2 3.0% and Fe_2O_3 0.4%. It had been ground in a ball mill. One sample of this material was separated into closely sized fractions by use of a cyclosizer (3).

Another sample "B", was analysed for size distribution by use of the cyclosizer, and the Andreasen pipette, the result in Fig. 1 (a) show good agreement.

Powdered magnesia mixed with concentrated solutions of magnesium chloride or magnesium sulphate forms basic magnesium salts which are the basis of sorel cement. However, at concentrations below about 2 molar, the X-ray diffraction patterns of the basic salts disappear and are replaced by that of a colloidal brucite. Although giving less strength than with the basic salts, the system still acts as a hydraulic cement.

The stirred experiments with the various size fractions in 1.25 molar magnesium sulphate show approximately linear kinetics as shown in Fig. 2 which is a plot of curing period versus $1 - (1 - F)^{1/3}$ where F, the fraction reacted, is the ratio of hydration value to 0.44. A logarithmic plot of the slopes of the lines in Fig. 2 versus the mean particle size in Fig. 3 has a slope approaching unity and tends to confirm the linear kinetics. Note that the non-spherical shape of the particles tends to compensate for the non-uniform particle size. Examination of reacted particles from this experiment showed a coherent coating of brucite about the unreacted cores. See Photo 1.

As the concentration is reduced the brucite becomes

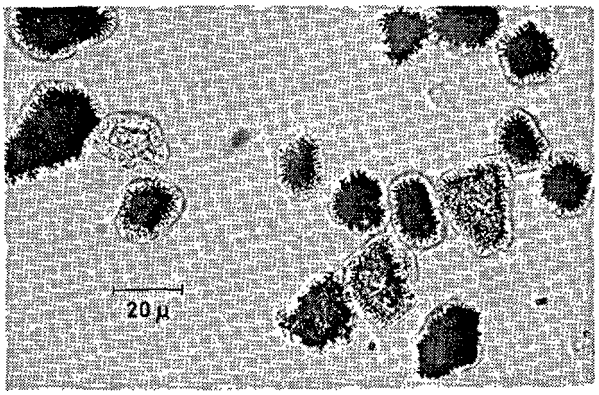

Photo 1. *Magnesia particles with brucite coatings. The 15–24μ fraction, hydrated 430 hours in stirred 1.25MgSO₄ solution, dried and later photographed by transmitted light ×640*

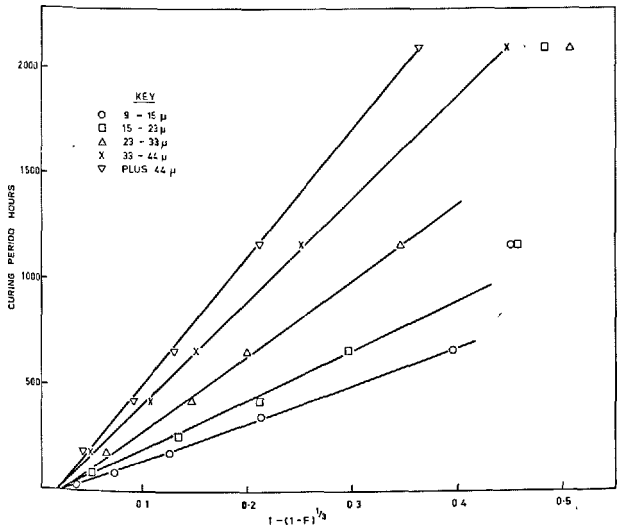

Fig. 2. *The hydration of sized magnesia fractions stirred in a slurry of 1.25 molar magnesium sulphate solution. The data fit linear kinetics for the first 80% of the reaction*

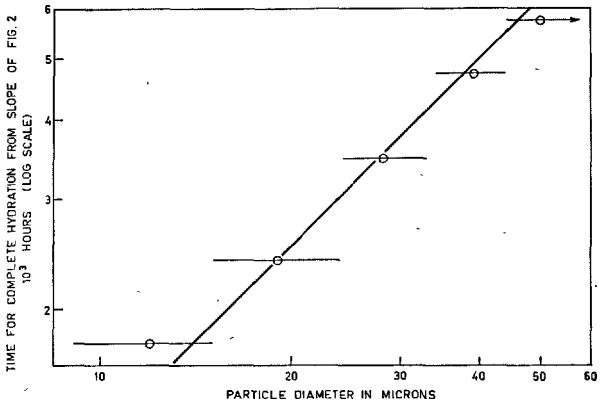

Fig. 3. *A logarithmic plot of the slopes of the lines in Fig. 2 versus the mean size of the particles in each fraction. The range of particle sizes in each fraction is indicated. A slope of unity indicates that the linear rate constant is independent of particle size*

more crystalline and at concentrations below about 0.05 molar the rate decays more rapidly than it does for linear kinetics. This phenomena is illustrated by Fig. 4 for both chloride and sulphate. In the region where linear kinetics apply the rate constants are 5.3×10^{-3} and 9.5×10^{-3} microns per hour for sulphate and chloride respectively.

The rate also decays more rapidly than for linear kinetics in hardened specimens. Data for a W/C ratio of 0.40 and 1.25 molar magnesium sulphate are plotted in Fig. 5. The continuous lines are drawn for the purpose of estimating an activation energy of 18 kcal in Fig. 8. They show a rate decay greater than that for quadratic kinetics. The broken line indicates the course of the reaction at a W/C ratio of 0.17 and 42°C. This rapid decay of the rate at low W/C ratios is not due to the specimens drying out because they were kept saturated by the addition from time to time of a drop of water to the tubes in which they were cured.

The way in which the reaction is choked off at low W/C ratios suggests the same explanation that was given for the similar behaviour of portland cement (1), i.e., the reaction rate becomes limited by the rate of diffusion of material to, and of nucleation of products in, water filled voids of above a certain critical size.

The difficulty with this explanation is to provide a mechanism, by which the lack of space in which to precipitate products, can slow down the decomposition of unstable oxide minerals to their thermodynamically more stable hydrated products. This difficulty will be taken up later.

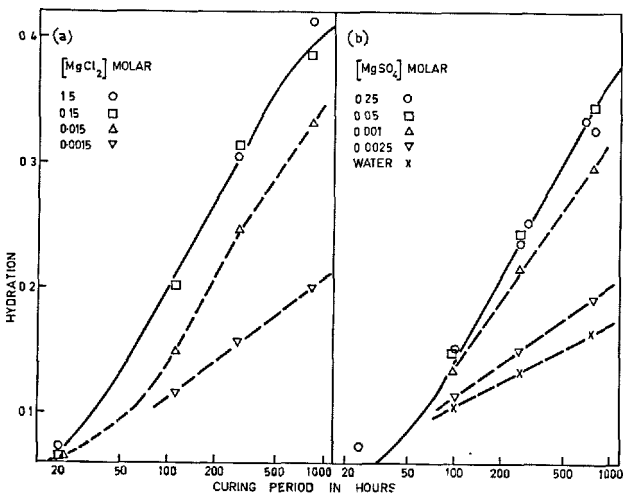

Fig. 4. *The hydration of a magnesia powder in a stirred slurry. The continuous lines represent linear kinetics as calculated for the p.s.d. in Fig. 1(A). The broken lines indicate the more rapidly falling rate at lower concentrations of (a) magnesium chloride, (b) magnesium sulphate*

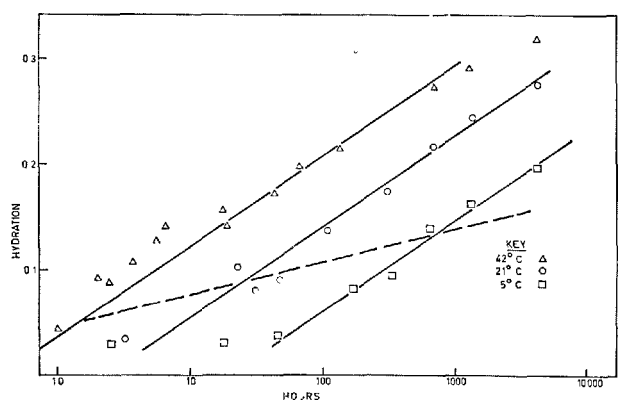

Fig. 5. *Hydration rate of hardening specimens of magnesia with 1.25 molar magnesium sulphate at a W/C ratio of 0.40. The broken line indicates the course of the reaction at a W/C ratio of 0.17 and at 42°C*

Anhydrite

Prepared from A. R. gypsum by adding one per cent of sodium chloride, kneading with water and sintering at 860°C. The chemical analysis is CaO, 40.61; SO_3, 58.60; NaCl, 1.59; SiO_2, 0.08; Al_2O_3, 0.04; MgO, 0.03; Fe_2O_3, 0.02. The material was ground with pestle and mortar and a particle-size analysis was carried out with the cyclosizer. The p.s.d. shown in Fig. 1(b) is probably in error in appearing too disperse at the fine end due to dissolution in the cyclosizer.

A 3% solution of potassium alum was the electro-

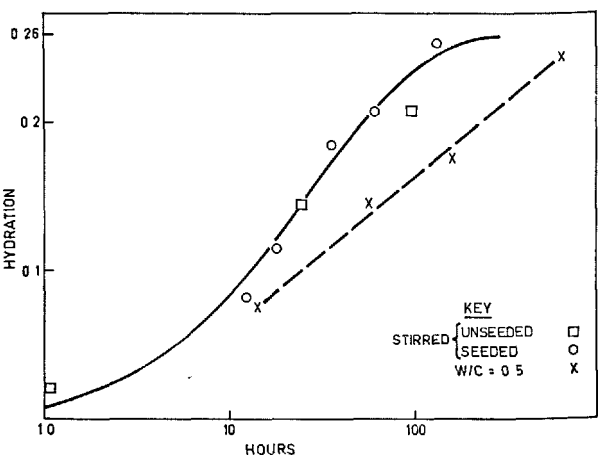

Fig. 6. *Hydration of anhydrite in 3% potassium alum solution. By assuming an induction period of ten and forty hours for seeded and unseeded experiments, stirred hydration approximates to linear kinetics represented here by the continuous line*

lyte used to promote hydraulic activity. The result of two stirred runs are shown in Fig. 6. In the run marked "seeded" 0.25 grams of A. R. calcium chloride were rapidly stirred into 80 mls of 3% alum solution and the resulting suspension of small gypsum crystals used as electrolyte. In order to approximate to the linear kinetics as calculated from the p.s.d. an induction period of ten and forty hours was assumed for the seeded and unseeded experiments respectively. The estimated linear rate constant is 8.5×10^{-2} microns per hour. An error in the fine end of the p.s.d. will not explain away more than an hour or so of the apparent induction period of the stirred experiment. However, it could be due to non-spherical shape and to different rates of dissolution along different axes of the anhydrite crystals.

For hardening specimens the rate decays more rapidly as is shown by the (1:1:0.5 sand, anhydrite, water) mortar specimens in Fig. 6 or by the specimens with a W/C ratio of 0.30 in Fig. 7. The approximation of these 0.3 W/C ratio runs to quadratic kinetics is probably no more than an indication of a diffusion process controlling the rate. Certainly the coarse network of gypsum crystals appears very different from the coherent coating of inner-products which are assumed in calculating quadratic kinetics.

Beta C_2S (5106)

This material was prepared from precipitated silica and A. R. calcium carbonate by a repeated procedure of grinding with pestle and mortar, mixing to a stiff paste with ethanol or water, pressing into small pellets and firing to 950°C. After five cycles the material contained no free lime by White's reagent. The crystal size is very small, but it was estimated that at least 80% of the material had a refractive index above 1.695. The X-ray diffraction pattern is that of β-C_2S. The p.s.d. obtained from the Andreasen pipette is shown in Fig. 1(c).

The kinetics of stirred specimens is considered with aid of Fig. 9. It will be seen that the rate appears to decay too slowly for linear kinetics and this suggests the remedy previously invoked for anhydrite, of

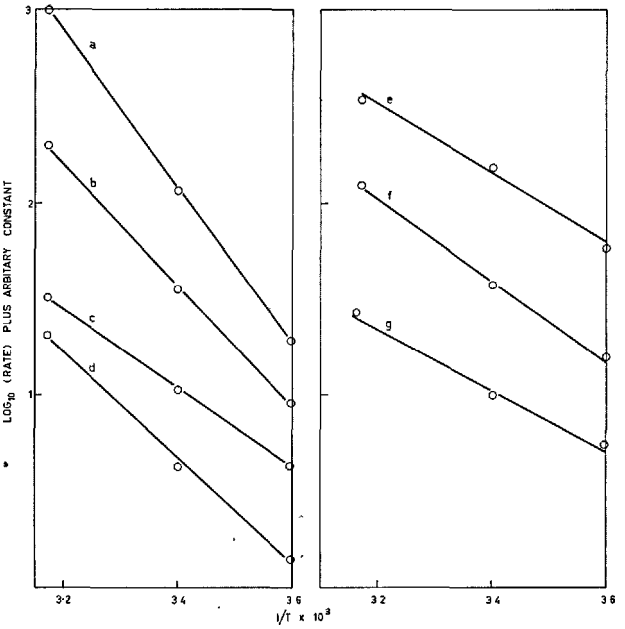

Fig. 8. *Logarithm of empirical rate constant versus reciprocal of absolute temperature. The identification are:*
(a) MgO from Fig. 5.
(b) β-C_2S, $1/T_0$ from Fig. 11.
(c) β-C_2S, $1/T_R$ from Fig. 11.
(d) β-C_2S (5108) linear rate constant from Fig. 13.
(e) Alite (608) linear rate constants Fig. 18(a).
(f) Alite (608) linear rate constants Fig. 18(c).
(g) C_3S (620) quadratic rate from Fig. 20(b).

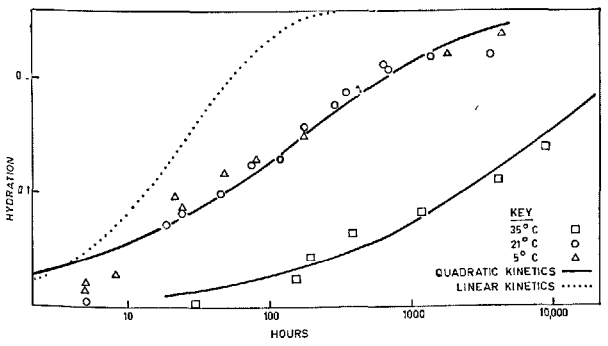

Fig. 7. *At a W/C ratio of 0.3 the hydration of anhydrite in 3% potassium alum approximates to quadratic kinetics (the continuous lines)*

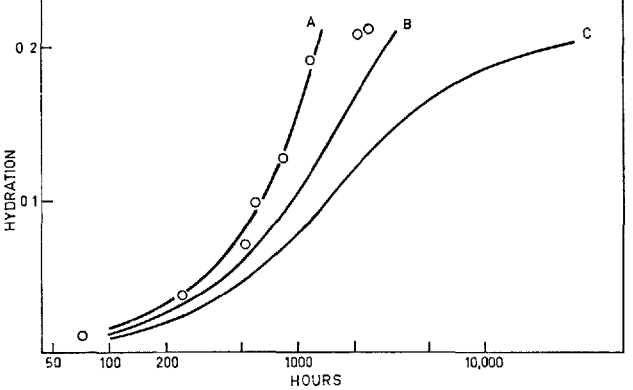

Fig. 9. *Hydration of β-C_2S (5106) in a stirred slurry compared to: (a) constant rate, (b) linear kinetics, (c) quadratic kinetics*

supposing an induction period. However when this is done, the data still give a better fit to constant rate kinetics as in Fig. 10.

The hydration rates of hardening specimens also approximate to constant rate kinetics as is shown in Fig. 11. Without taking this induction period plus constant rate model more seriously than is warranted by the data, it is of interest to note that, by treating the induction period as the completion time of a rate process, we obtain an apparent activation energy of 15 kcal from Fig. 8(b) compared to 9.6 kcal from Fig. 8(c) for the constant rates themselves.

Beta C_2S (5108)

This material was prepared from the same materials as (5106) but with the addition of 0.5% boric oxide which was assumed to replace silica. It was fired four times to 1400°C until White's reagent showed negligible free lime. It was much better crystallized than 5106, but had a very similar X-ray diffraction pattern. The p.s.d. obtained by Andreasen pipette is indicated in Fig. 1(d).

Fig. 12 suggests that linear kinetics fit the hydration of stirred specimens better than either constant rate or quadratic kinetics.

At a W/C ratio of 0.525 and curing temperatures of 42, 21 and 5°C the kinetics are again approximately linear as shown in Fig. 13. The linear rate constants are 41×10^{-4}, 8.5×10^{-4} and 2.8×10^{-4} microns per hour with an apparent activation energy of 13 kcal compared to our previous (2) estimates of 6×10^{-4} microns per hour at 25°C and 16 kcal for a previous β-C_2S which was also stabilized by boric oxide. If allowance is made for the discrepancy for irregular particles between Stoke's law and Feret diameters and for the difference in curing temperatures, the earlier preparation is seen to be reacting at only a third the rate of 5108.

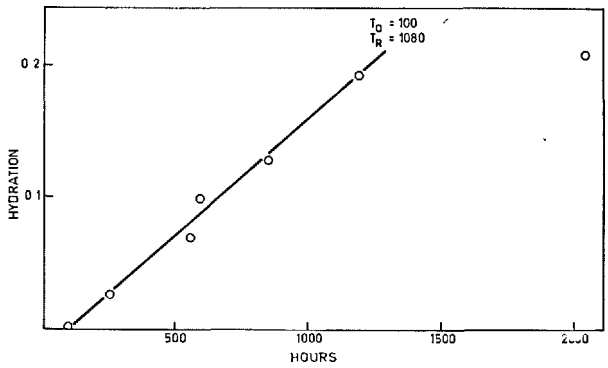

Fig. 10. *Stirred hydration of β-C_2S (5106) replotted from Fig. 9 to show the induction period T_0 and reaction time, T_R, of the constant rate kinetics*

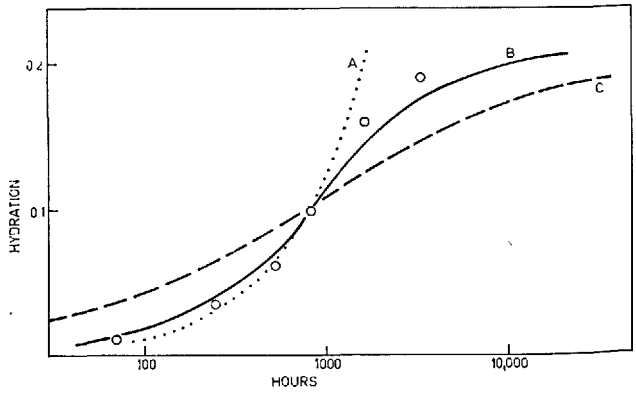

Fig. 12. *Hydration of β-C_2S (5108) in a stirred suspension compared with the following kinetics: (a) constant rate, (b) linear, (c) quadratic*

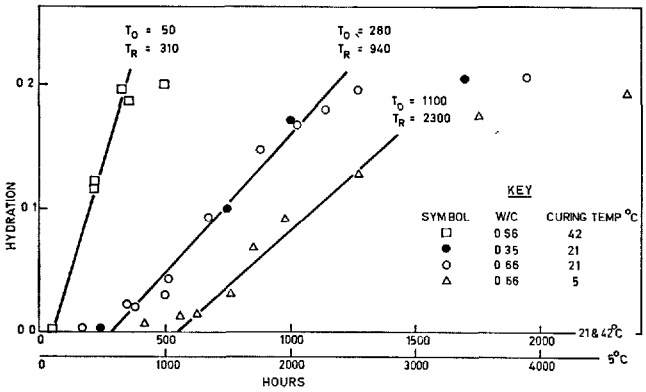

Fig. 11. *Constant rate plots for hardening specimens of β-C_2S (5106)*

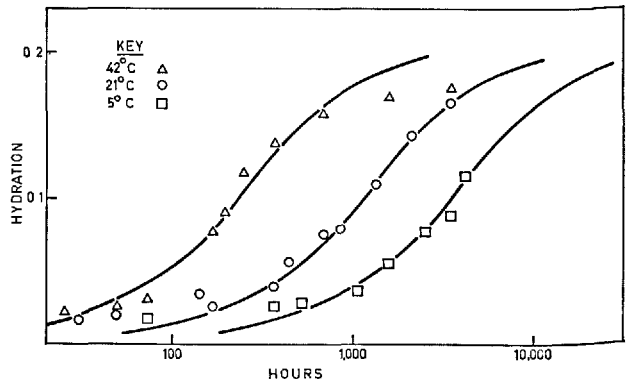

Fig. 13. *Hardening specimens of β-C_2S (5108) at a W/C ratio of 0.525. The lines represent linear kinetics as calculated from the p.s.d.*

Alite 286

This material was prepared in 1956 from a 99% pure calcium carbonate and 96% pure silica sand. Extra alumina and magnesia were added in an attempt to approach $C_{54}S_{16}AM$. The materials were interground overnight in a ball-mill and fired to 910°C. The powder was pressed into 2 inch diameter pellets, fired to 1500°C, cooled and reground. After three cycles of this treatment there was little free lime. Many particles had small inclusions which are thought to be C_2S. A chemical analysis gave the overall composition $C_{53}S_{16}A_{1.06}M_{0.53}F_{0.05}$. Both the X-ray diffraction pattern and a single endotherm at 835°C in the first D.T.A. heating cycle indicate (4), (5) a monoclinic crystal structure.

Two hydration experiments at a W/C of 0.525 were made with this material. The runs of 1956–7 are shown in Fig. 14. Simplifying the figure by means of the reference lines does not hide the complicated movement of the temperature coefficient of the rate which is first positive, then negative and finally approaches zero. The experiments of 1959 were undertaken to see if ageing slowed the reaction and if reheating would restore the rate. Fig. 15 shows that, although reheating to 540°C increased the rate by about a quarter, both experiments have similar kinetics. It seems that only at very early ages and low temperatures can the reaction be linear. For the test of the reaction the rate falls rapidly suggesting a diffusion or precipitation controlled reaction. Lack of a measured p.s.d. precludes a more detailed analysis of these experiments.

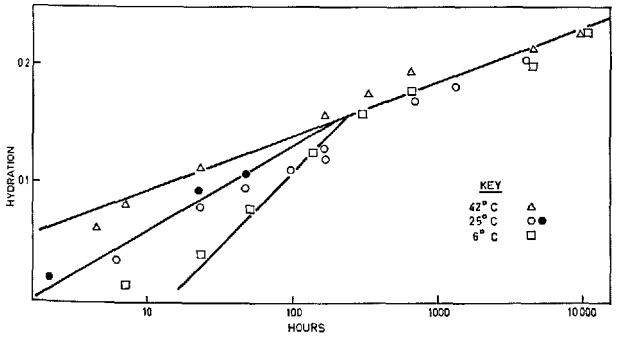

Fig. 14. *Hydration of alite (286) at a W/C ratio of 0.525. Specimens made Nov. 1956 and Feb. 1957 are given shaded and open symbols respectively. The lines are for comparison with Fig. 15.*

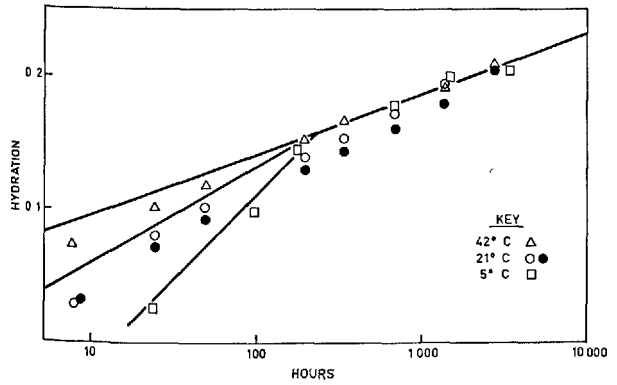

Fig. 15. *The 1959 hydration of alite (286) at a W/C ratio of 0.525. The shaded circles represent untreated material, the open symbols represent material re-heated to 540°C. The reference lines are for comparison with Fig. 14*

Alite 608

Prepared in 1959 by methods similar to those described for Alite 286 from precipitated silica and A. R. calcium carbonate, alumina and magnesia. The chemical analysis of this material can be written $C_{54}S_{16}A_{1.0}M_{0.8}F_{0\ 02}$. D.T.A. runs were made in 1960 and on untreated material in 1967 with the same result. Endotherms at 770 and 840°C were found in the first heating cycle but only the second endotherm occurred in later cycles. The first endotherm and a weight loss of 5% above 540°C are ascribed to carbonation of the aged material. The X-ray diffraction pattern indicated a monoclinic structure. A small region of this pattern is shown in Fig. 16. The p.s.d. is shown in Fig. 1.

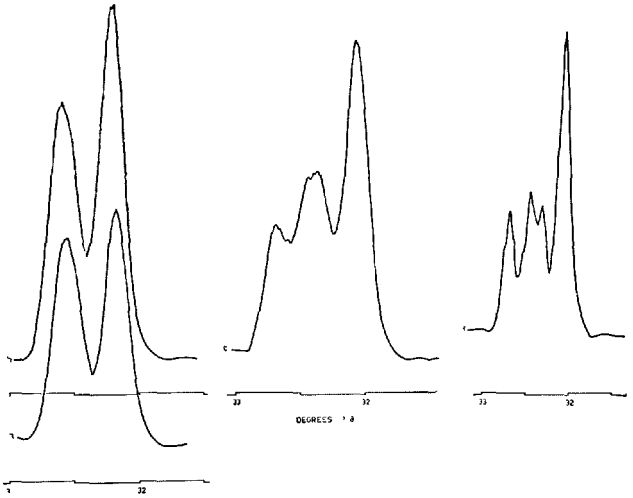

Fig. 16. *A small but characteristic portion of the X-ray diffraction pattern of the tricalcium silicate phase*
(a) alite (608) untreated, 1967; (b) alite (608) refired 1400°C, 1967; (c) C_3S (620) untreated, 1967; (d) C_3S (620) refired 1400°C, 1967

There are three sets of experiments: (a) those of 1960, (b) those with untreated material in 1967, (c) those with material re-fired to 1500°C in 1967. No change in X-ray diffraction pattern was detected except that re-firing had reduced the intensity of the very weak calcite pattern. Patterns (b) and (c) were prepared much more carefully than was pattern (a). There was insufficient of (c) for a full particle size analysis but it is probably very similar to (b) since the percentages passing a 30 micron sieve are 52 and 50 respectively.

From Fig. 17 it will be seen that the kinetics of (a) and (c) are linear but those of (b) are quadratic. The linear rate constant of (a) is 1.25×10^{-2} microns per hour.

Fig. 18 shows that hardening specimens react as they did when stirred except that now, as the water voids fill with outer products, a diffusion or precipitation process controls the rate for the last 30 or 40% of reaction. The apparent activation energies of the linear portions of (a) and (c) are found from the plots of Fig. 8(e) and (f) to be 8.5 and 9.7 kcal respectively.

C_3S (620)

This material was prepared from precipitated silica and A. R. calcium carbonate by repeated pressing to pellets, firing to 1500°C and grinding with pestle and mortar. The chemical analysis can be written $C_{3.06}SA_{0.005}M_{0.003}F_{0.0006}$. A D.T.A. run in 1960 gave sharp endotherms at about 920 and 970°C on heating and exotherms about 30° lower on cooling. Another run on untreated material in 1967 gave the same behaviour plus an additional endotherm at 780°C for the first heating cycle only. A Tα pattern was obtained by X-ray diffraction in 1960 and for untreated material in 1967.

The experiments fall into the same three groups as did those of alite (608): (a) 1960, original material; (b) 1967, untreated material; (c) 1967, material re-fired to 1400°C. The original and re-fired material have similar p.s.d. as can be seen from Fig. 1(f) and (g). However, re-firing has produced a Tβ X-ray diffraction pattern. Fig. 16 compares alite and C_3S patterns at 32° 2θ for CuKα.

The stirred hydrations all approximate to quadratic kinetics as shown by Fig. 19. The rate constants of (b) and (c) are only 27 and 36% of (a) and this represents a substantial change in rate without a change in kinetics.

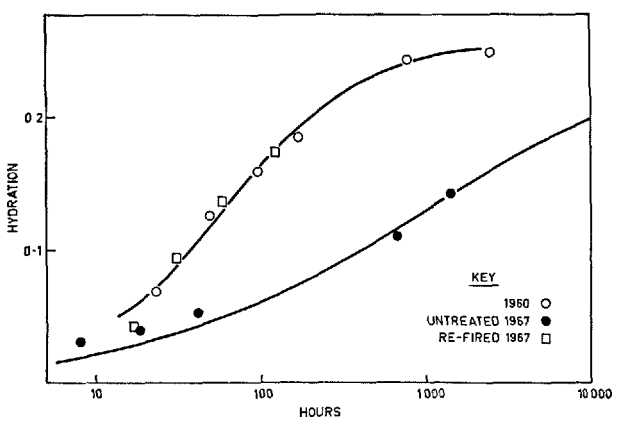

Fig. 17. *Stirred hydration of alite (608). The lines (A) and (B) are linear and quadratic kinetics respectively, they are calculated from the p.s.d. of the untreated material*

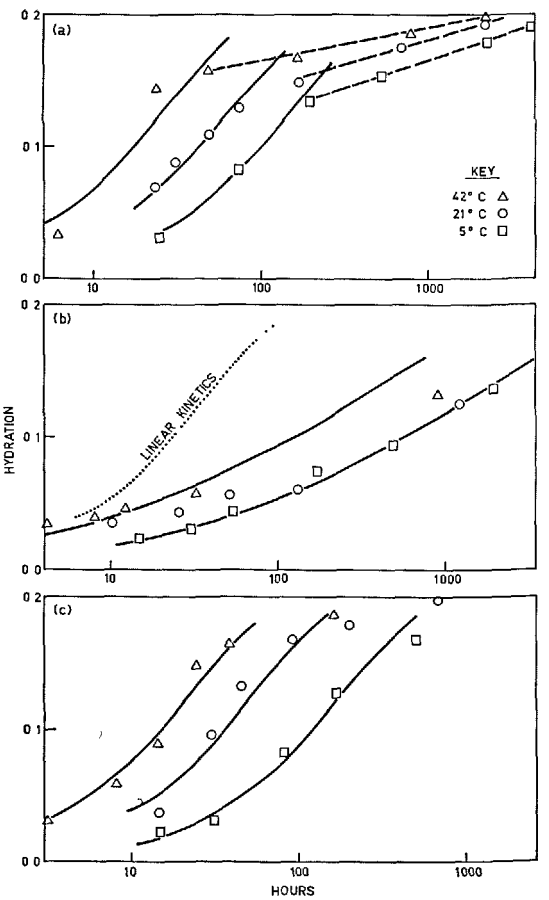

Fig. 18. *Hardening specimens of alite (608)*

(a) the 1960 runs at W/C ratio of 0.35. The continuous lines represent linear kinetics for this p.s.d.

(b) the 1967 runs for untreated material at W/C ratio of 0.436. The lines are for the quadratic kinetics of this p.s.d.

(c) the 1967 runs with re-fired material at W/C of 0.367. The lines are for linear kinetics of the p.s.d. of the untreated material.

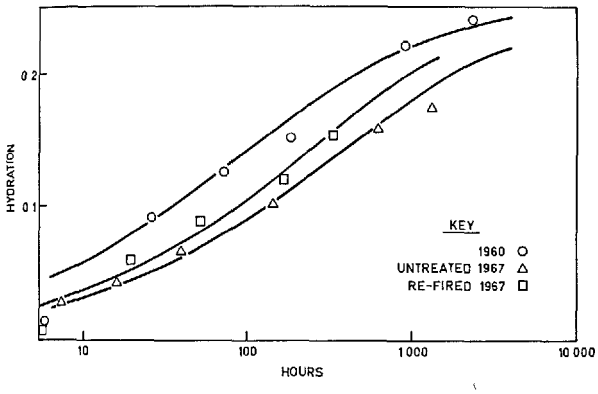

Fig. 19. *Stirred hydration of* C_3S *(620) compared with quadratic kinetics as calculated from the relevant p.s.d.*

Fig. 20 shows that the hydration kinetics of hardening specimens is again approximately quadratic, with the rate falling even more rapidly as the reaction approaches completion. The kinetics of (a) and (c) are similar to those of alite (286) in that the curves are initially separated but merge later. There is also the same suggestion of linear reaction at early ages and lower temperatures. The kinetics of (b) are different because there is no suggestion of an early linear reaction and yet the temperature coefficient remains fairly large. The apparent activation energy from Fig. 8(g) is 7.4 kcal. This aged material like that of alite (608) has a weight loss of 5% above 540°C which is ascribed to carbonation, although the calcite pattern is barely detectable.

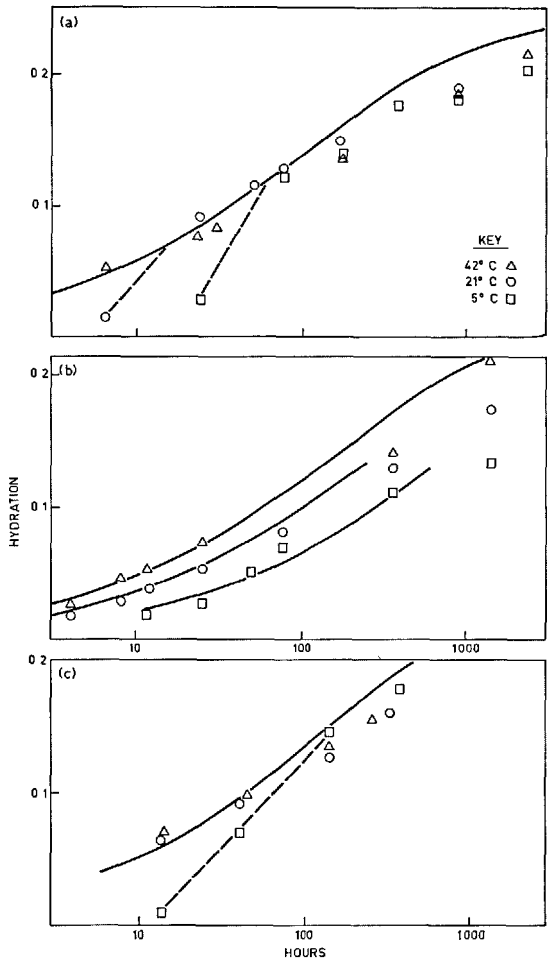

Fig. 20. *Hardening specimens of* C_3S *(620). The continuous lines represent quadratic kinetics as calculated from the relevant p.s.d. The different experiments are shown as follows:*
(a) 1960, W/C = 0.40.
(b) 1967 untreated material, W/C = 0.50.
(c) 1967 material re-fired to 1400°C, W/C = 0.50.

Discussion

For stirred experiments where the particles can be considered as reacting without interference from their neighbours, the data are consistent with either linear or quadratic kinetics except for β–C_2S (5106) where the rate decays too slowly for even linear kinetics. The lack of an effect for W/C ratio suggests that the constant rate process is not a homogeneous reaction in solution. However the presence of an induction period for this material indicates a process which accelerated the rate. If such an effect were to continue throughout the reaction, it would tend to counteract the effect of the decreasing reaction surface and produce an approximately constant rate from what might be essentially linear kinetics.

When the cements are allowed to harden, the rate tends to decay more rapidly than for the same material stirred. This effect depends on the W/C ratio and at the values used here is most pronounced for magnesia and anhydrite, it affects the C_3S phases only at later ages and has little effect on β–C_2S.

Generally, then, the data is not inconsistent with the attractively simple model of a reaction which starts linear but which may become diffusion controlled if the resistance of the diffusion process exceeds that of the surface decomposition. Where diffusion kinetics hold for isolated particles, the rate approximates to

quadratic kinetics. However, when the reaction becomes diffusion controlled due to merging outer products, then the kinetics vary with W/C ratio and possibly depend on the relative specific permeabilities of inner and outer products.

Even a good fit to a kinetic equation does not establish it as a mechanism, but merely fails to eliminate it. The present data is not precise and it is plotted against the integrated form of the rate equation which is a notoriously insensitive test (6) for a kinetic model. Consequently, the possible basis for this simple linear diffusion kinetics will be treated next.

The Linear-Diffusion Kinetic Model

Consider the general model, put forward by this author (1) in 1959, to account for the phenomenon of hydraulic hardening. It is suggested that at least the outer-products must form a coherent network; and, to minimize the generation of disruptive stress, that these products must be precipitated from material which has diffused away from the cement grains. For portland cement, the limited growth of the crystals of hydration product and their supposed inability to nucleate in pores below a critical size, are phenomena invoked to further limit the generation of stress and to explain the very great reduction in hydration rate which occurs at low W/C ratios as the outer-products fill the space available to them. Under these conditions it is probable that diffusion or precipitation control the rate. However, neither in this (1) account of the argument nor in the later versions of Powers (7), Verbeck (8) or Brunauer and Greenberg (9) is any mechanism offered to explain the difficulty to which we alluded in describing the limited hydration of magnesia at low W/C ratios.

The difficulty is this. In order to prevent the accumulation of products at the cement mineral surface and the consequent generation of disruptive stress, the outward diffusion process must always keep pace with the rate of mineral decomposition. If we suppose that the hydration rate is controlled by the inward diffusion of water, then this implies that the outward diffusion of hydrated material occurs more readily. This is difficult to accept in view of the higher concentration and greater mobility of water compared to say divalent cations in aqueous solution. On the other hand, if we suppose that outward diffusion or precipitation controls the rate, then we need a mechanism to prevent the cement decomposition from exceeding this rate.

Such a mechanism is not hard to find when the free energy change and hence solubility difference between cement mineral and hydration product is small. Anhydrite is an instance of this and at low W/C ratios when the precipitation of gypsum is hindered the concentration rises towards the solubility of anhydrite, slowing the rate of its dissolution. However, for more thermodynamically unstable materials such as C_3S, such a mechanism is not possible.

A possible mechanism for such unstable materials is that a stable surface is produced by the adsorption of an outward diffusing chemical species which in this way poisons the reaction if its concentration rises. From such a mechanism we have derived (10) the following rate equation:

$$r^2 k\eta_A + rKX_i\eta_W + rk([A]_o + K) = X_i[W]_o K \quad (3)$$

where r is the reaction rate, k is the resistance to a linear reaction, η_A and η_W are the respective resistances of the intermediate product A and water to diffusion across the product coating, (1/K) is the Langmuir adsorption coefficient for A on the cement, X_i is the surface area of the unreacted cement cores and $[A]_o$ and $[W]_o$ are the concentration of A and water at the outer surface of the reaction coating.

If the third term of the left hand side dominates, we get linear kinetics. For example, equation (1) is obtained by expressing X_i in terms of the fraction reacted of a sphere.

If the second term of the L. H. S. dominates we get parabolic kinetics for the inward flow of water. Substituting an expression for the resistance due to the inner products of a spherical particle gives the equation (2) for quadratic kinetics. Introducing the resistance of the outer products of an isolated sphere gives equation (4) of reference (2).

If the first term dominates, we get joint control by the surface decomposition and by the outward diffusion of the poisoning species. For a plane surface $F^{3/2} = a + bt$, compared to $F = bt'$ for linear and $F^2 = a + bt$ for parabolic kinetics. For joint kinetics the empirical rate constant b is compound (11) and the activation energy is half the sum of the enthalpy charge for adsorption and the activation energies for diffusion and linear reaction. The rate equation for the joint kinetics of a sphere is complicated.

The condition for joint kinetics is

$$\eta_A k[W]_o K\eta_W \gg X_i\eta_A \gg k([A]_o + K)^2/k[W]_o \quad (4)$$

If $X_i\eta_A$ lies below these limits the reaction is linear, if above, it is parabolic. Notice that $X_i\eta_A$ tends to zero at both the beignning and at the end of the reaction so that it must start and finish linear. If inequality (4) does not hold, the reaction is either completely linear; or starts linear, becomes parabolic and then ends linear. The necessity for a linear finish is not

explicit in earlier treatments (2), (12), (13). Such an effect is unlikely to be of experimental importance as the particles will generally reach this final stage at different times depending on their size and the proximity of their neighbours.

Alternatively, we could provide a mechanism for outward diffusion to control the rate by postulating a direct coupling between this process and the inflow of water.

Evidence from the Experiments

These experiments produce no direct evidence for joint kinetics. Hydration curves on log time for the joint kinetics of isolated particles will have slopes which lie between those of our calculated linear and quadratic kinetics. Examination of the figures for stirred hydration show no such evidence. We must conclude that, if joint kinetics exists in our experiments, it can be only in those regions where the kinetics are affected by merging outer products. Unfortunately it is just here that the geometry of the diminishing water spaces makes calculation of the kinetics most difficult.

Two of these cements, β–C_2S (5106) and anhydrite show a definite induction period. That of β–C_2S has an apparent activation energy of 15 kcal, whereas that of anhydrite appears only in stirred experiments and is greatly reduced if the solution is already seeded with gypsum.

It should be mentioned that, if the magnesia is fired to 910°C and then stirred in 1.25 molar magnesium sulphate, as in Fig. 4, then it gives the usual linear kinetics after an induction period of 170 hours. There is no evidence in these experiments from which one can draw conclusions about factors which might affect the linear reaction constants of these cements.

There is evidence in Figs. 17–20 to show that the diffusion process for C_3S is affected by the ageing or re-firing of the cement. This result is somewhat surprising and requires further investigation. It seems to imply a difference in either the structure of the gel of hydration products or in the concentration difference driving the process or both. It may be due to the presence of carbonate.

Conclusions

For the seven hydraulic cements described here and with only a few additional hypotheses it is possible to describe the hydration kinetics at least approximately by an attractively simple model in which the rate after allowance for particle shape, particle size distribution and the merging of outer products, is controlled by either linear or parabolic kinetics. The additional hypotheses are the induction period for β–C_2S (5106) and anhydrite, and an extra accelerating process for β–C_2S (5106) which counteracts the effect on the rate of the diminishing reaction surface on linear kinetics.

Consideration of the possible basis of such a model leads to the dilemma that it is difficult to see how the rate of diffusion of water in through a coherent coating of products should be slower than the outward diffusion of products, yet, if the outward diffusion is slowest, then a mechanism must be provided to prevent the rate of cement decomposition exceeding the rate of outward diffusion. A solution to this dilemma is to suppose that an outward diffusing substance can adsorb on, and poison, the cement surface. This hypothesis raises the possibility of joint linear-diffusion control. It is shown that, regardless of the nature of the linear-diffusion transistion, the rate must obey linear kinetics at the very end of the reaction of a discrete particle. No evidence is found in these experiments for joint kinetics, but it is not possible to rule out this possibility in the region where the merging of outer products controls the rate.

Evidence for the effect of ageing and re-firing of C_3S suggests that these effects are due to a change in the rate of a diffusion process.

Acknowledgments

Miss B. Terrell for chemical analyses.

Mr. J. Weymouth for Photo 1.

References

1. J. H. Taplin, "A method for following the hydration reaction in portland cement paste", Aust. J. Appl. Sci. **10**, 329–345 (1959).

2. J. H. Taplin, "The temperature coefficient of the rate of hydration of β-dicalcium silicate", Proc. of Fourth Internat. Symposium on the Chem. of Cement, **1**,

263–266 (1960).
3. D. F. Kelsall and J. C. H. McAdam, "Design and operating characteristics of a hydraulic cyclone elutriator", Trans. Instn. Chem. Engrs., **41**, 84–95 (1963).
4. G. Yamaguchi, K. Shirasuka and T. Ota, "Comparison between monoclinic and inverted triclinic alite", Symposium on Structure of Portland Cement Paste and Concrete, Highway Research Board special report 90, 263–286 (1965).
5. Y. Ono, T. Uno and Y. Kanai, "Synthesis of five polymorphic modifications of C_3S", Review of Nineteenth General Meeting—Technical Session, The Cement Association of Japan, 35–41 (1965).
6. J. H. Taplin, "Hydration kinetics of calcium sulphate hemihydrate", Nature, **205**, No. 4874, 864–866 (1965).
7. R. C. Powers, "Physical properties of cement paste". Fourth Internat. Symposium on the Chem. of Cement, Washington D.C., 1960, Proc., **2**, 577–613 see p. 591–594.
8. L. E. Copeland, D. L. Kantro and G. Verbeck, "Chemistry of hydration of portland cement". Fourth Internat. Symposium on the Chem. of Cement, Washington D.C., 1960. Proc., **1**, 429–465 see p. 456.
9. S. Brunauer and S. A. Greenberg, "The hydration of tricalcium silicate and β-dicalcium silicate at room temperature", Fourth Internat. Symposium on the Chem. of Cement, Washington D.C., 1960. Proc., **1**, 135–163, see p. 162.
10. J. H. Taplin—to be submitted for publication. Presented to Amer. Ceramic Soc. 24 Oct. 1968.
11. J. H. Taplin, "Significance of experimental rate constants", Nature **194**, No. 4827, 471–472 (1962).
12. G. Valensi, "Cinetique de l'oxydation de spherules et de poudres metalliques", Comptes vendus, **202**, 309–312 (1936).
13. R. E. Carter, "Kinetic model for solid state reactions", J. Chem. Phys. **34**, 2010–2015 (1961).

Supplementary Paper II-73 Effect of the Temperature on the Early Hydration of the System $3CaO \cdot Al_2O_3$–$CaSO_4 \cdot 2H_2O$–$Ca(OH)_2$–H_2O

Hitoaki Mori and Keiichi Minegishi*

Synopsis

The hydration course of $3CaO \cdot Al_2O_3$ with $CaSO_4 \cdot 2H_2O$ and $Ca(OH)_2$ at 5°C to 70°C has been investigated mainly by using twin-type conduction calorimeters. The hydration reaction of the present system can be classified into four stages: 1) the first rapid reaction (the first heat evolution peak), 2) the dormant period after the first peak, 3) the rapid reaction of the remaining $3CaO \cdot Al_2O_3$ (the second heat evolution peak), and 4) the suppressed reaction after the second peak. These stages appear successively.

The reaction rate in the first stage is not greatly affected by the hydration temperature. In the second stage, however, a considerable increase in the rate of hydration is observed when the temperature is raised, because the physical properties of the ettringite coating vary with temperature. The reaction of forming a coating on the surface of the $3CaO \cdot Al_2O_3$ grains proceeds below 40°C, while the reaction proceeds on the surface of $3CaO \cdot Al_2O_3$ at 70°C without forming a protective layer. The change in the properties of the ettringite coating has a greater effect on the reaction rate. The presence of sufficient $Ca(OH)_2$ restrains the dissolution of $3CaO \cdot Al_2O_3$ and ettringite, and makes the ettringite layer more dense. The addition of $Ca(OH)_2$ has a similar effect to the lowering of the temperature.

The reaction in the third stage appears when the $CaSO_4$ content in the solution becomes insufficient to form ettringite, and calcium monosulfate precipitates from the liquid phase near the $3CaO \cdot Al_2O_3$ grains and simultaneously the ettringite coating is removed by being dissolved. The reaction of $3CaO \cdot Al_2O_3$ with ettringite is fairly rapid and is accelerated by raising temperature.

In the fourth stage, the hydrates which are produced in the second rapid reaction enclose the unhydrated $3CaO \cdot Al_2O_3$ grains and suppress the subsequent hydration.

Introduction

The early hydration of $3CaO \cdot Al_2O_3$ has been known to be retarded by the presence of $CaSO_4 \cdot 2H_2O$. Recently the kinetics and the mechanisms of the reaction of $3CaO \cdot Al_2O_3$ (C_3A) with $CaSO_4 \cdot 2H_2O$ have been discussed in many papers (1–7). In general, it has been found that $CaSO_4 \cdot 2H_2O$ can retard the hydration of C_3A by the forming of the ettringite ($C_3A \cdot 3CaSO_4 \cdot 32H_2O$) coating on the surface of the C_3A grain, and that the reaction proceeds with the diffusion of sulfate ions through the coating in the earlier stage and with the occurrence of cracking in the coating in consequence of the formation of more ettringite in the later hydration (2, 3). On the other hand, there are papers in which the formation of monosulfate on the C_3A grains in the very early hydration (5) and the retardation of calcium aluminate hydrates on the hydration of C_3A, not of ettringite (6) have been reported. It follows that there is some doubt about the hydration course of the present system.

Calorimetric methods are often used successfully to trace continuously the hydration process, and calorimeters which were constructed in laboratories have been used to study the hydration of C_3A (1, 2). The heat of hydration in the present system at a temperature ranging from 5°C to 40°C was studied in the previous paper (7). This experiment is concerned with the early hydration of the system at 5°C to 70°C. The hydration course of C_3A with $CaSO_4 \cdot 2H_2O$ and $Ca(OH)_2$ has been studied by analyzing quantitatively the effects of the hydration temperature and the reactant composition on the heat evolution rate, and by determining the hydration product and the degree of hydration by X-ray diffraction analysis.

*Chichibu Cement Co., Ltd., Tokyo, Japan.

Materials and Methods

Materials

C_3A was prepared from reagent grade $CaCO_3$ and Al_2O_3. These reagents were weighed in the fixed molar ratio and, after mixing, they were heated three times in an electric furnace at 1450°C. Free CaO determined by the alcohol-glycerol method was 0.2%, and loss on ignition was 0.2%. SiO_2 and Fe_2O_3 determined by the chemical analysis as other impurities were 0.1 and 0.1% respectively. The synthetic product had a CaO/Al_2O_3 molar ratio of 2.96 and was free of other calcium aluminates. The product was pulverized in a porcelain potmill to 2980 cm^2/g of Blaine value in this experiment. Reagent grade $CaSO_4 \cdot 2H_2O$ was dried at 40°C after washing sufficiently with pure water. $Ca(OH)_2$ was prepared by mixing CaO with CO_2-free water and by desiccating the hydrate. CaO was made by heating reagent grade $CaCO_3$ at 900°C. Prepared $CaSO_4 \cdot 2H_2O$ and $Ca(OH)_2$ contained few impurities.

These preparations were mixed with each other so as to get mixtures containing the molar ratio as shown in Table 1. All of the samples were dry-mixed throughly until they became homogeneous. The effects of the $CaSO_4 \cdot 2H_2O$ content and the hydration temperature on the early hydration of C_3A were determined from the results of calorimetric measurements on samples No. 1 to 6, and the effect of the CaO concentration was determined by measuring the heat evolution of samples No. 7 to 11 at 20°C.

Ettringite, which was used to examine its reactivity with C_3A, was prepared by suspending 1 mole of C_3A and 3 moles of $CaSO_4 \cdot 2H_2O$ in excess pure water in a tightly closed 300-ml Erlenmeyer flask. The flask was shaken sufficiently for six months at 20°C. The result of the X-ray powder diffraction in Table 2 showed that no reactant was present and most of the lines were found to be due to ettringite. The differential thermal analysis curve of the product was also identical with the ettringite one. Loss on ignition of the synthetic ettringite was 44.6% of its weight.

Table 1. *Molar ratio of the starting samples*

Sample No.	$3CaO \cdot Al_2O_3$ (mole)	$CaSO_4 \cdot 2H_2O$ (moles)	$Ca(OH)_2$ (moles)
1	1.0	0	0
2	1.0	0	0.5
3	1.0	0.25	0.5
4	1.0	0.5	0.5
5	1.0	1.0	0.5
6	1.0	3.0	0.5
7	1.0	0.25	0
8	1.0	0.25	(S)
9	1.0	0.25	0.1
10	1.0	0.25	1.0
11	1.0	0.25	2.0

(S): Saturated solution of $Ca(OH)_2$

Methods

The measurements of heat evolution, which was observed in the hydration of the mixed samples at a temperature ranging from 5°C to 70°C, were performed at an interval of 5°C or 10°C. This temperature range was decided on because the hydration reaction at 5°C is similar to the reaction which occurs in concrete casted in winter, and because the conditions at 70°C are near to those in the steam curing of concrete. The reaction processes of samples were traced by using twin-type conduction calorimeters which were designed by Amaya (8). Block diagrams of the two conduction calorimeters improved to be installed with temperature controlled baths are shown in Fig. 1. The one for lower temperature was used at a temperature from 5°C to 40°C, and the calorimeter for higher temperature was used at 50°C to 70°C. The temperature in the baths was controlled by the thermister temperature regulator and the temperature of the reaction vessel was kept within ± 0.1°C and ± 0.03°C of the desired temperature for the former and for the latter respectively. For measurement at higher temperature, the reaction vessel was kept as tight as possible so as to prevent the water-solid ratio from varying during the hydration of the paste.

Table 2. *X-ray powder data for ettringite preparation*

Preparation		NBS		Preparation		NBS	
d Å	intensity	*d* Å	intensity	*d* Å	intensity	*d* Å	intensity
10.74	8			2.701	10	2.714	6
9.72	100	9.73	100	2.682	12	2.697	12
8.86	9	8.86	12			2.680	7
7.21	3			2.617	20	2.616	21
5.72	12			2.565	52	2.564	45
5.61	80	5.61	81	2.523	3	2.524	4
4.98	24	4.98	24	2.489	4	2.487	3
4.86	8	4.86	6	2.442	2	2.434	2
4.70	44	4.69	36	2.423	4	2.422	2
		4.41	3	2.402	10	2.401	10
4.03	10	4.02	10	2.350	6	2.347	4
3.88	61	3.88	51	2.230	10	2.230	20
3.68	6	3.67	7	2.209	42	2.209	43
3.60	14	3.60	14	2.184	8	2.185	8
3.48	34	3.48	31	2.154	25	2.154	23
3.26	12	3.27	4	2.128	5	2.130	2
3.24	22	3.24	19	2.123	6	2.124	5
3.02	9	3.02	6	2.080	3	2.081	4
2.81	8	2.81	6	2.062	5	2.062	5
2.77	45	2.77	38				

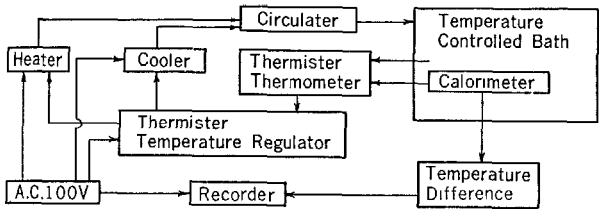

(1) Calorimeter for lower temperature

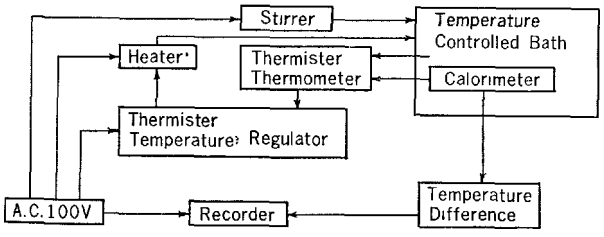

(2) Calorimeter for higher temperature

Fig. 1. *Block diagram of twin-type conduction calorimeter*

These calorimeters have installations for stirring and are suitable for continuous measuring of heat evolution after the addition of water when the hydration was made with the mixed sample in paste form. Sensitivity of the heat conductor used is 6.5 mv/°C at 20°C.

Pastes for calorimetric investigation were prepared by mixing 4 g of sample with 2 ml of distilled pure water for 5 minutes at a speed of 60 r.p.m. In these experiments the hydration reaction up to a period of 3 days was traced and discussed.

Heat of hydration of the sample was calculated from the ratio of the area within the curve of heat evolution rate of the sample to the area within the curve of heat evolution rate of a manganin coil (100 cal/hr) over a fixed time. And the rate of heat evolution was determined by the ratio of thermo-electromotive force measured during the hydration of the sample at a fixed time to that of the standard coil.

The increase in temperature of the paste during hydration was about 4°C at its maximum when either gypsum and $Ca(OH)_2$ were absent or the hydration temperature was raised. To determine the reproducibility of a measurement, the heat evolution of CaO and C_3A, which are known to be very active for water, were measured three times at 20°C. These results showed that the heat of hydration of CaO after 1 hour was 252 ± 3.5 cal/g and the heat of 1 hour hydration of C_3A was 103 ± 1.8 cal/g, and that heat evolution rates of C_3A at the first peak after the addition of water agreed within $\pm 3.6\%$. When measurements were taken with an amount of C_3A ranging from 3 g to 5 g, results obtained were within the same range as above. The reproducibility of measurements was satisfactory enough.

The hydration products were identified by X-ray diffraction analysis and differential thermal analysis. The hydration degree of C_3A against time was determined by means of the calorimeter when the reaction rate was greater, considering it to be proportional to the heat of hydration, and by the X-ray internal standard method when the reaction became steady. The hydration was stopped by suspending the product in acetone, and the product was dried over soda lime and/or $CaCl_2$ in a desiccator at room temperature.

Results and Discussion

Effect of the Hydration Temperature and Gypsum Content on the Heat Evolution

Table 3 and Figs. 2 to 5 show the heat of hydration which were liberated during the hydration of samples No. 1 to 6 containing different amounts of gypsum at 5°, 20°, 40° and 70°C. From Fig. 2 it is evident that the immediate hydration of samples No. 1 and 2 with no gypsum occurs at a slower rate at 5°C than at a higher temperature, and that the heat of hydration after 1 hour is found to be less. The heat evolution rate after that, however, decreases so slowly in both cases that considerable increases in the heat of hydration after 1 day are observed in Table 3. C_2AH_8 and C_4AH_{13} were detected during the hydration of sample No. 1, and C_4AH_{13} was the only product in the hydration of No. 2. These products seem to have had no great retarding effect on the hydration of C_3A.

The presence of gypsum decreased the rate of heat evolution when the C_3A grains came in contact with water and also the rate after the first peak. Accordingly, heat of hydration of only 16.7 to 22.3 cal/g. C_3A were measured after 1 day. The difference in the gypsum contents hardly affected the hydration reaction for 3 days. The second peak of heat evolution, which was accompanied by the conversion of ettringite to monosulfate, did not appear in this time. It is apparent that by the formation of an impermeable

Table 3. *Heat of hydration and hydration products of the system* C_3A–$CaSO_4 \cdot 2H_2O$–$Ca(OH)_2$–H_2O

Sample No.	Temperature (°C)	Heat of hydration (cal/g C_3A)		Hydration product	
		1 hr.	1 day	1 hr.	1 day
1	5	58.2	161	C_2AH_8, C_4AH_{13}	C_2AH_8, C_4AH_{13}
	20	103	184	C_3AH_6, C_4AH_{13}	C_3AH_6
	40	104	143	C_3AH_6	C_3AH_6
	70	88	127	C_3AH_6	C_3AH_6
2	5	80	186	C_4AH_{13}	C_4AH_{13}
	20	137	241	C_3AH_6, C_4AH_{13}	C_3AH_6, C_4AH_{13}
	40	155	227	C_3AH_6	C_3AH_6
	70	91	192	C_3AH_6	C_3AH_6
3	5	8.1 (2.5)*	16.7 (6.9)*	Ett	Ett
	20	13.6 (3.6)	182 (48.4)	Ett	Ett, Mono, S.S.
	40	24.6 (7.1)	214 (61.5)	Ett	Mono, C_3AH_6, S.S.
	70	54.7(24.3)	163 (72.1)	Mono	Mono, C_3AH_6
4	5	8.9 (3.2)	24 6 (7.5)	Ett	Ett
	20	16.5 (3.9)	59.4(13.9)	Ett	Ett
	40	23.2 (5.8)	249 (62.2)	Ett	Mono, C_3AH_6, S.S
	70	110 (47.5)	166 (71.4)	Mono, Ett	Mono, C_3AH_6
5	5	9.3 (2.6)	21.1 (6.2)	Ett	Ett
	20	15.4 (3.8)	49.5(13.3)	Ett	Ett
	40	24.4 (5.0)	233 (48.0)	Ett	Mono, Ett
	70	77.1(17.5)	315 (71.4)	Ett	Mono
6	5	9.5 (2.8)	22.3 (6.6)	Ett	Ett
	20	17.8 (4.6)	62.2(13.5)	Ett	Ett
	40	20.0 (5.2)	206 (49.8)	Ett	Ett
	70	73.1(11.6)	266 (63.0)	Ett	Ett

1) *; degree of hydration (%)
2) Ett; $C_3A \cdot 3CaSO_4 \cdot 32H_2O$, Mono; $C_3A \cdot CaSO_4$ $12H_2O$, S.S; solid solution of C_3A $CaSO_4 \cdot 12H_2O$ and C_4AH_{13}

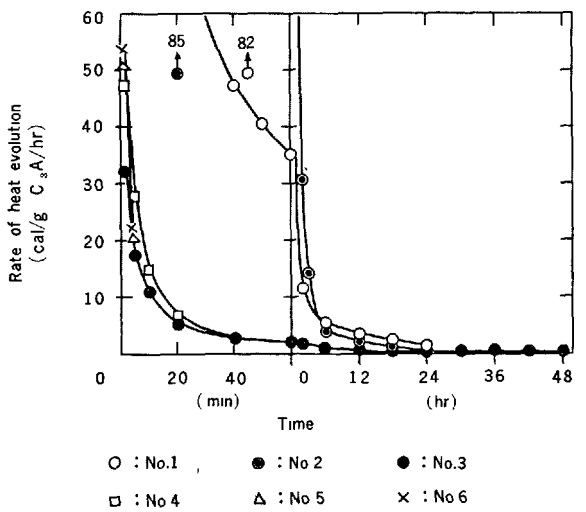

Fig. 2. *Effect of* $CaSO_4 \cdot 2H_2O$ *content on the early hydration of* C_3A *at 5°C*

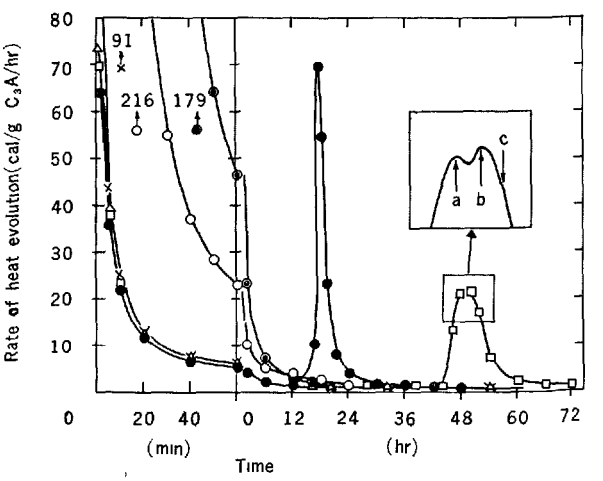

Fig. 3. *Effect of* $CaSO_4 \cdot 2H_2O$ *content on the early hydration of* C_3A *at 20°C (symbols as in Fig. 2)*

and dense coating around the C_3A grains ettringite retards the hydration of C_3A more effectively at 5°C.

At 20°C the rates of hydration at the first peak of samples No. 1 and 2 were two times as great as that at 5°C, subsequent rates, however, tended to decrease markedly. The products fromed during 1 hour's hydration were some C_3AH_6 and a little C_4AH_{13}. It is found that C_3AH_6 is able to form a more impermeable coating than C_2AH_8 and C_4AH_{13}. A small peak of heat evolution, which can not be shown in Fig. 3, appeared after about 2 hours during the hydration course of No. 2. This peak was observed at 15°C, but was not recognized for 3 days either at a temperature below 10°C or above 25°C. The small peak corresponds to a heat effect which is due to crystallization of C_3AH_6 from the intermediate C_4AH_{13}, as

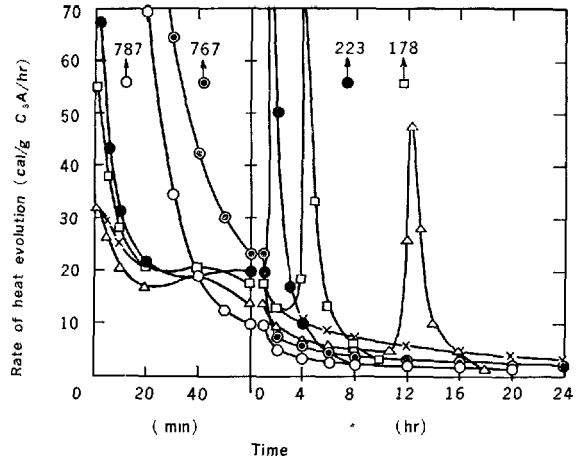

Fig. 4. *Effect of* $CaSO_4 \cdot 2H_2O$ *content on the early hydration of* C_3A *at 40°C (symbols as in Fig. 2)*

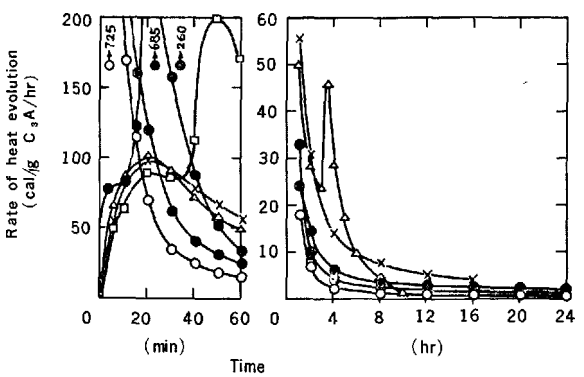

Fig. 5. *Effect of* $CaSO_4 \cdot 2H_2O$ *content on the early hydration of* C_3A *at 70°C (symbols as in Fig. 2)*

observed previously by Stein (9), because an apparent increase in the amount of C_3AH_6 was observed after this peak.

During the hydration courses of samples No. 3 to 6 which contained gypsum, gypsum effectively retarded the hydration of C_3A at 20°C. As shown in Fig. 3, the second peak of heat evolution occurred after 12 and 44 hours for samples No. 3 and 4, respectively. The second peak of No. 4 was divided in two parts. This phenomenon will be discussed later. The second peak took place when most of the added gypsum had reacted with the C_3A. It is assumed that ettringite forms a coating on the surfaces of the C_3A grains and the retarding effect of the coating on the hydration of C_3A increases as the reaction proceeds.

After 3 days only ettringite was detected in the products of samples No. 5 and 6 in which the molar ratios of $CaSO_4 \cdot 2H_2O/C_3A$ were 1.0 and 3.0, respectively. The second peak was not observed during 3 days hydration.

At 40°C No. 1 and 2 formed C_3AH_6 just after the addition of water, and then the immediate hydration was promoted more markedly than at 20°C. After 1 hour, however, the reaction rate decreased sharply as stated by Tanaka, Murakami and Sato (10). The heat of 1 day's hydration of No. 1 at 40°C was 41 cal/g C_3A less than at 20°C.

In the cases of samples No. 3 to 6, the heat evolution rates of the first peak were lower at 40°C than at 20°C. But the decrease in the rates was gradual afterwards, and the reaction was so markedly accelerated that the heat evolution rate at the onset of the second peak was fourteen or fifteen times that at 20°C. And the reaction of the second peak was also accelerated and, therefore, the heat of 1 day's hydration increased. It might be said that at 40°C gypsum acted as an accelerator for the hydration of C_3A. In Fig. 4 small heat effects are recognized after about 40 minutes in No. 3 to 6. These effects were already observed at 35°C. After the peak no change could be recognized in the hydration product except a noticeable increase in the amount of ettringite.

At 70°C gypsum hardly retarded the hydration of C_3A. Fig. 5 shows that in the hydration of lower gypsum content the second peaks occur after 10 and 35 minutes for No. 3 and 4 respectively without an apparent decrease in the rate following the broad first peak. The onset of the second peak of No. 5 with higher gypsum content was 6 hours earlier than at 40°C, though a considerable decrease in the rate is observed after the first peak. After the second peak, however, the heat evolution rate declined rapidly. Since sample No. 6 had stoichiometric amounts of C_3A and gypsum for ettringite, it formed only ettringite even at 70°C and the ettringite did not convert to monosulfate. For 1 day's hydration of No. 6, 6.6% of C_3A hydrated at 5°C, 13.5% at 20°C, 49.8% at 40°C, and 63.0% at 70°C. These results show that the retarding effect of gypsum decreases with increasing temperature.

The same tendency was shown by the calorimetric measurements at other temperatures which were not included in Table 3 and Figs. 2 to 5. In Fig. 6, it is evident that the hydration of C_3A is continuously promoted by temperature increase. At a lower temperature, a fast heat evolution after the addition of water is followed after about 2 hours by a slow increase in the heat of hydration. In this dormant period added gypsum reacts with C_3A and retards the hydration of C_3A by forming ettringite. Marked differences among the inclines of heat evolution against time are observed

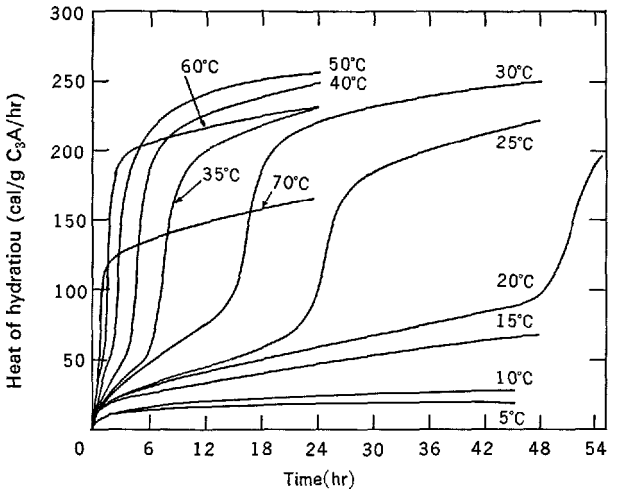

Fig. 6. *Heat of hydration of sample No. 4 at various temperatures*

Table 4. *Volume shrinkage of pastes during the hydration of* C_3A *with* $CaSO_4 \cdot 2H_2O$

Sample No.	Volume shrinkage (ml/100g solid)			
	calculation[a]	20°C	40°C	70°C
3	1.27	1.2	1.3	—
4	2.26	2.3	1.8	1.8
5	3.73	—	5.6	3.9

a: Data were calculated from the following equation.

$$C_3A + 3CaSO_4 \cdot 2H_2O + 26H_2O \rightarrow C_3A \cdot 3CaSO_4 \cdot 32H_2O \quad \ldots\ldots(-53.9\ cm^3)$$

in the dormant period, showing that the retarding effect of gypsum became apparently smaller above 35°C.

The relations between the heat of hydration before the start of the second peak and the hydration temperature, and between the onset of the second peak and the temperature are illustrated in Fig. 7. Linear decreases in the heat of hydration by raising temperature are observed. Using the heat of formation of ettringite, 347 cal/g C_3A, the heats of hydration before the second peak were calculated to be 29.4, 58.8, and 117 cal/g C_3A for No. 3, 4 and 5 respectively from added gypsum contents. On comparing the calculated values with the measured values, the latter were greater than the former at a lower temperature, but at a higher temperature were inversely smaller. The same trend is recognized in Table 4, where the volume shrinkages of pastes from 30 minutes after the addition of water are shown. These shrinkages are responsible for the formation of ettringite. The formation of such a product as C_3AH_6, for which both the heat of formation and the volume shrinkage accompanied by the formation are smaller than for ettringite, might be expected. But its presence in the products was not observed by X-ray

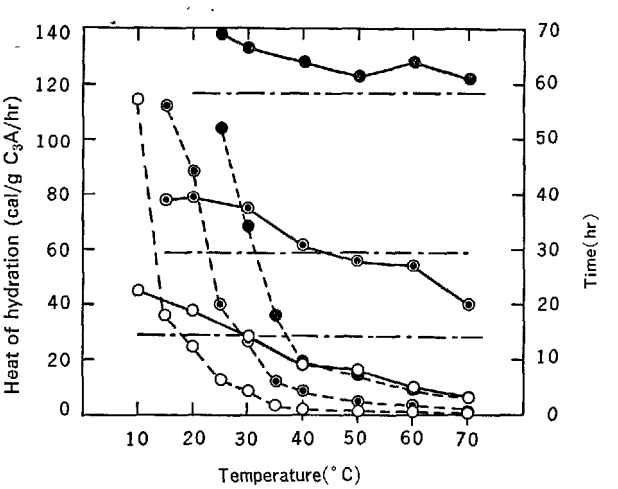

—— heat of hydration before the second peak
- - - - onset of the second peak
—·—· calculated value of heat of hydration
○: No. 3 ⊙: No. 4 ●: No. 5

Fig. 7. *Effect of temperature on the heat of hydration before the second peak and the onset of the second peak*

analysis and differential thermal analysis (DTA). The amount of unhydrated C_3A determined by X-ray quantitative analysis at the onset of the second peak undoubtedly decreased when the temperature was raised. As stated by Lieber (11), the reaction between C_3A and $CaSO_4 \cdot 2H_2O$ is not quantitative especially with a lower gypsum content and at a higher temperature.

The onset of the second peak is shortened with temperature rise as shown in Fig. 7. Though this trend is affected to some extent by temperature and the gypsum content, it may be said that below 40°C the time for the complete reaction of gypsum with C_3A decreases to one fourth or one third when the temperature is raised by 10°C, and above 50°C decreases to about one half when the temperature is raised by 10°C. The effect of gypsum on the reaction time is recognized more distinctly below 30°C, and the time measured for the hydration of No. 4 is three times that for No. 3 and that for No. 5 is about three times that for No. 4. Added gypsum retards the hydration of C_3A more strikingly as the amount of it is increased at a temperature below 30°C. As already mentioned, it is thought to be caused by a structural change of the ettringite coating, e.g., an increase of its thickness or a decrease in the void space.

It may be concluded from the calorimetric measurements that gypsum retards the early hydration of C_3A and its action becomes more effective by increasing the amount, but the effect of gypsum is weakened above 35°C.

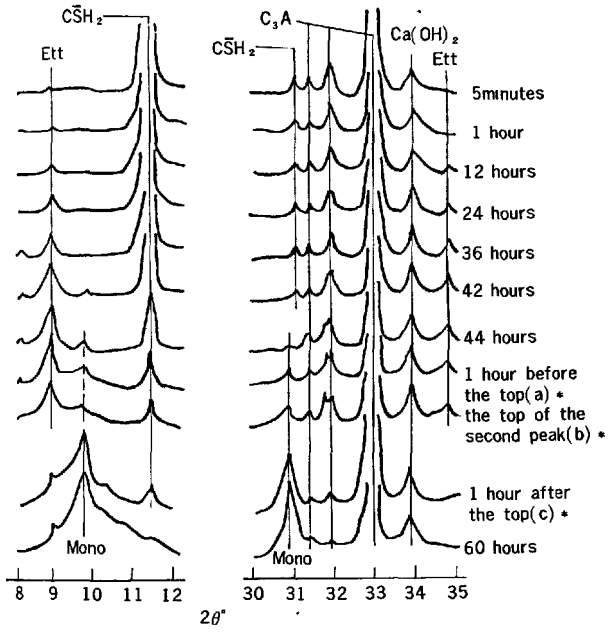

Ett: ettringite $C\bar{S}H_2$: $CaSO_4 \cdot 2H_2O$
Mono: calcium monosulfate

Fig. 8. *X-ray diffraction patterns of product during the hydration of sample No.4 at 20°C (*: symbols as in Fig. 3)*

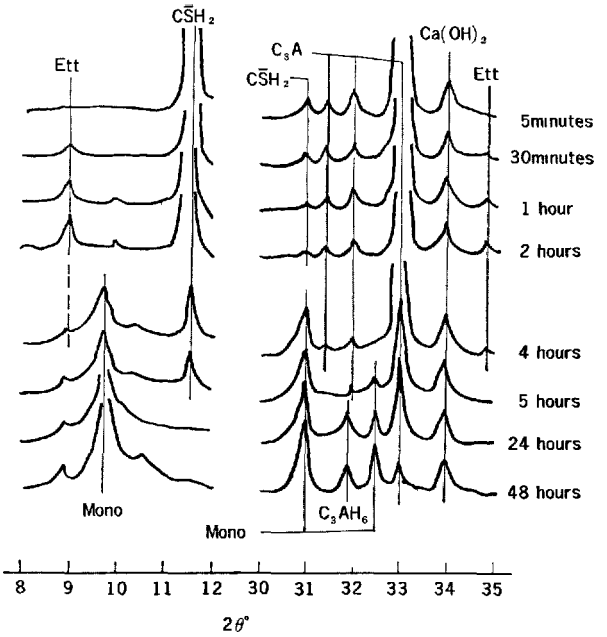

Fig. 9. *X-ray diffraction patterns of product during the hydration of sample No. 4 at 40°C (abbreviations as in Fig. 8)*

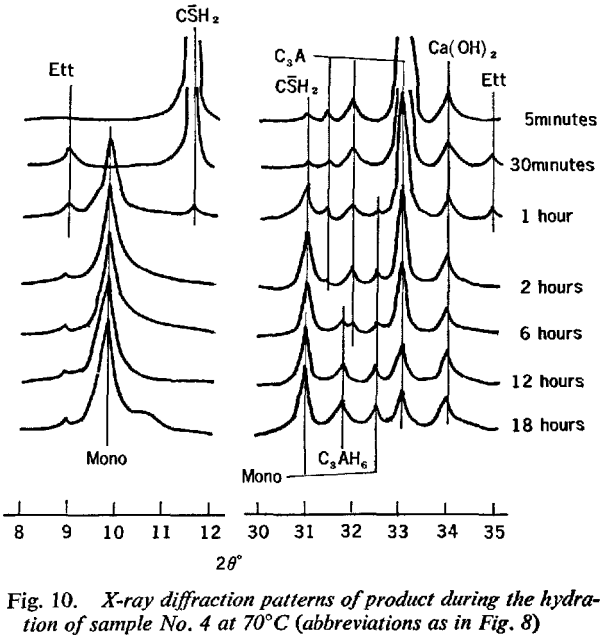

Fig. 10. *X-ray diffraction patterns of product during the hydration of sample No. 4 at 70°C (abbreviations as in Fig. 8)*

Hydration Products and Reaction Sequence

So as to compare the changes in the hydration products with results by the calorimeters, X-ray analysis and DTA were carried out on the products which were prepared under the same procedure as employed for the calorimetric measurement. The hydration products which were detected after 1 hour and 1 day are listed in Table 3. Figs. 8 to 10 show the X-ray diffraction patterns of the products during the hydration of sample No. 4. In Fig. 8 the pattern after 5 minutes indicates the presence of a slight peak of ettringite at 9°. In addition, a small endotherm at 155°C, which was responsible for ettringite, was observed in the DTA curve of the same product. However, both analyses showed the formation of no other product, such as monosulfate, C_4AH_{13}, or C_3AH_6. Up to the onset of the second heat evolution peak, continuous decreases in the amounts of unhydrated C_3A and gypsum and a continuing increase of ettringite are observed. No change was observed in the amount of $Ca(OH)_2$ which was determined by the loss in weight between 500°C and 600°C on the thermogravimetric curve. Therefore, no significant reaction between $Ca(OH)_2$ and C_3A occurred. Immediately after the second peak starts, a peak at 31° appears indicating the formation of monosulfate and, on the other hand, the interference of gypsum is noticeable. As the hydration proceeds the interferences of C_3A, gypsum, and ettringite decrease. The interference of ettringite can not be recognized any

longer after 1 hour from the top of the second peak, and that of gypsum disappears entirely at the end of the peak. At the same time a considerable increase in the intensities of monosulfate interferences at 9.8° and 31.0° appears. A line of monosulfate was observed at 9.2° in the wet specimen, but it shifted to 9.8° when washed with acetone and further to 10.4° upon drying over $CaCl_2$. Accordingly, after the onset of the second peak the samples were preserved on soda lime in a desiccator. After 1 hour from the top of the heat evolution peak, $Ca(OH)_2$ decreases considerably and an interference of monosulfate at 9.8° is found to be extending to about 11°. These observations show that a solid solution of monosulfate with C_4AH_{13} had already formed. It can be seen from Fig. 8 that monosulfate is formed at first, followed by the formation of the solid solution, and that the doubled peak of sample No. 4, as already shown in Fig. 3, are explained in the following way; the first half shows the formation of monosulfate and the second the solid solution.

The reactions at 40°C and 70°C produced the same products as at 20°C. But a great increase in peak intensity at 9.8° was observed, and little solid solution was formed. At 40°C after 1 day C_3AH_6 was present in the product instead of the solid solution. At 70°C the formation of C_3AH_6 was so accelerated as to be recognized after 6 hours. In the hydration of No. 3 with lower gypsum content, C_3AH_6 was formed in greater quantities above 30°C. In No. 5 with higher gypsum content, however, after the second peak the formation of monosulfate was only observed over the entire temperature range.

On comparison of the thermal processes to the change in the hydration products with time, it is found that the first peak of heat evolution and following slow evolution are responsible for the heat of formation of ettringite. The second intense reaction occurs with the conversion of ettringite to monosulfate, and with the formation of monosulfate and the solid solution of monosulfate and C_4AH_{13}, or with the formation of monosulfate and C_3AH_6.

Stein (12) pointed out that from the fact that the presence of unhydrated C_3A and ettringite can be demonstrated when the second peak must have been passed, this second peak corresponds to the scaling-off of a protective layer of ettringite and its replacement by a layer of C_4AH_{19}, monosulfate or a mixed phase of these two compounds. The results of present investigation indicate the presence of ettringite even after the onset of the second peak, but the amount of ettringite decreases considerably because it reacts with the remaining C_3A forming monosulfate or the solid solution.

To determine the reactivity of C_3A with ettringite, the hydration reactions of the mixtures, which had the same compositions that samples No. 3, 4, and 5 had at the beginning of the second peak, were traced by the conduction calorimeters, X-ray diffraction analysis, DTA and thermogravimetic analysis (TGA). Fig. 11 shows the development of heat of hydration, and changes in the amounts of the reactants and the products of the mixture, $11C_3A + C_3A \cdot 3CaSO_4 \cdot 32H_2O$ (ettringite) $+ 6Ca(OH)_2$, which corresponds to the composition of No. 3 after a complete consumption of the gypsum. The amounts of unhydrated C_3A, and both ettringite and $Ca(OH)_2$ were determined by X-ray internal standard method and by TGA respectively. DTA endotherms between 200° and 300°C are thought to contribute to the dehydration of monosulfate and/or the solid solution of that with C_4AH_{13}. In Fig. 11 an immediate hydration with great velocity is followed by a rapid decrease in the reaction rate. Free C_3A, ettringite, and $Ca(OH)_2$ decrease rapidly at first, but after 10 minutes decrease slowly. After 6 hours the presence of ettringite is not observed at all. No calcium aluminate hydrate other than monosulfate and its solid solution with C_4AH_{13} can not be observed in the X-ray diffraction patterns. It can be concluded from the results in Fig. 11 that the reactivity of ettringite with C_3A in water is very high. And it is thought that the second peak takes place when ettringite begins to react with the remaining C_3A, and that a great increase in the heat of hydration is responsible for the reaction of C_3A with ettringite, and further reaction of the system C_3A–$Ca(OH)_2$–H_2O.

Kinetics of the Hydration Reaction

From the results by the conduction calorimeters, it seems that the ettringite coating, which was fomred

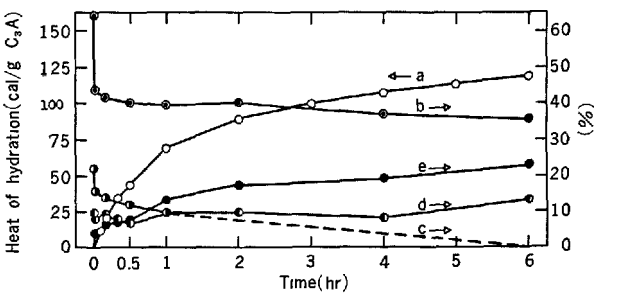

a: heat of hydration b: hydration degree of C_3A
c: ettringite d: $Ca(OH)_2$
e: loss in weight during 200° to 300°C endotherm

Fig. 11. *Heat of hydration and hydration degree of the system* C_3A–$C_3A \cdot 3CaSO_4 \cdot 32H_2O$–$Ca(OH)_2$–$H_2O$

on the C_3A grains in the hydration of C_3A with gypsum and $Ca(OH)_2$, acts as a diffusion layer. However, the rate of heat evolution varied noticeably with varying temperature and the dependence of the rate upon the temperature was considerable.

In general, the hydration reaction of the present system can be classified into four stages; 1) the rapid reaction after the addition of water (the first peak of the heat evolution), 2) the dormant period after the first peak, 3) the second rapid reaction (the second peak of the heat evolution) and 4) the suppressed reaction after the second peak. The equation of the reaction rate which was introduced by Kondo (13), $(1-\sqrt[3]{1-\alpha})^N = kt$, was applied to interpret these processes; where α is the degree of hydration, k is the rate constant, t is the hydration time and N is the value which is variable according to the reaction type. The logarithms of $(1-\sqrt[3]{1-\alpha})$, which were calculated from the degree of hydration as a function of time, were plotted against the logarithms of the hydration durations. In Fig. 12 there are linear relationships between them over the whole temperature range, and except at 5°C three straight lines are observed. The values of N in the equation were determined from the slopes of the first lines in the second stage when the reaction became steady. The estimations are listed in Table 5. The reaction of C_3A is retarded at a temperature below 40°C because the ettringite, which is formed in the very early hydration, forms a coating on the C_3A grains and the solution probably containing Ca^{2+} and SO_4^{2-} ions have to diffuse through the coating. At 70°C, however, the type of the reaction differs considerably from that at a lower temperature.

The reaction processes for sample No. 4 as shown in Fig. 12 are discussed in detail as follows: At 5°C the slope becomes fairly gradual after the first 20 minutes of the reaction. Then N is about 4. This means that ettringite has formed dense coating around the C_3A grains, and that the coating has become more compact in structure and simultaneously the resistance of the coating to the diffusion increases as the reaction proceeds. Accordingly the reaction is retarded markedly after the first peak of heat evolution and is followed by a decrease in rate. Namely at 5°C, the saturated concentration of CaO in the liquid phase is higher, and the solubility of ettringite is lower, so the dissolution of C_3A into the solution is suppressed and the oversaturation of ettringite is attained more easily, and then a large number of nuclei will be formed. It is assumed that fairly fine crystals of ettringite, which are formed near the surface of the C_3A grains, form an impermeable layer by filling up capillary pores in the layer with more ettringite.

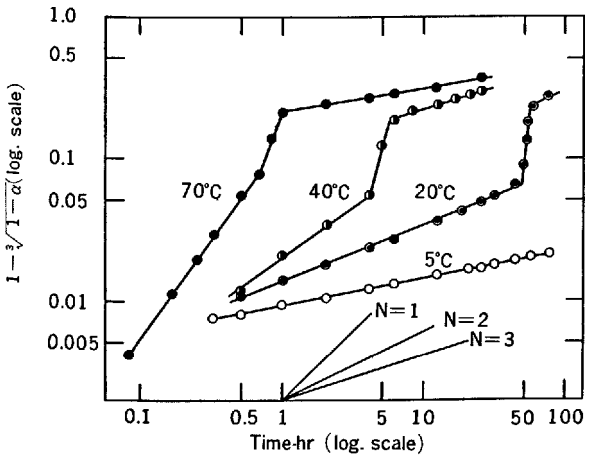

Fig. 12. *Determination of the value of N in the equation,* $(1-\sqrt[3]{1-\alpha})^N = kt$, *on the hydration of sample No. 4*

At 20°C, the value of N was about 3 at a duration from 30 minutes to 44 hours. The value of N shows the formation of a fairly compact coating. But the concentration of CaO becomes lower and the solubility of ettringite is greater than at 5°C; therefore, the ettringite crystals must grow larger. It is evident from the above that the reaction has been promoted by a decrease in the resistance of the ettringite coating to the diffusion of the solution.

At 40°C this trend is encouraged more and more. The value of N is about 2 from 30 minutes to 4 hours, and the equation is near to Jander's equation. It is assumed from the value of N that an increase in the amount of ettringite during the progress of the reaction increases the thickness of the coating, but brings no change in the structure. Furthermore, the diffusion constant increases with rising temperature. These cause apparent increases in the reaction rates so that considerable differences in the heat evolution rates are observed in Figs. 2 to 7.

The reaction at 70°C is not divided into four stages because of overlapping of the first stage with the second one. The first linear relationship is observed after only 5 minutes in Fig. 12. The slope of this line

Table 5. *Determination of the value of N on the hydration of* C_3A *with* $CaSO_4 \cdot 2H_2O$

Sample No.	Temperature (°C)			
	5	20	40	70
3	3.5	2.5	1.5	1
4	4	3	2	1
5	3.5	2.5	1.5	1(1.5)
6	3.5	2.5	1.5	1(1.5)

is about 1 unitl 40 minutes' hydration. This value of 1 shows that ettringite does not interfere with the progress of the reaction of C_3A, and the reaction proceeds on the surface of the C_3A grains. However, for samples No. 5 and 6, higher in gypsum content, the first lines were broken into two parts on their way to the third stage. Namely, for No. 5 N was about 1 for the next 25 minutes, but about 1.5 for the following 2.5 hours, and for No. 6 the value of N was about 1 for the next 45 minutes and after that N was approximately 1.5. In the hydration at 70°C ettringite crystals grew large enough to be visible under the optical microscope, and did not form what is called a protective layer. An increase in the quantity of ettringite, which was formed near the C_3A grains, would decrease the reaction rate after some duration in the hydration of the sample high in gypsum content.

The nitrogen adsorption measurement of the surface area (BET method) was carried out on the hydration products of sample No. 6, at 5°, 20°, 40°, and 70°C, after sufficient washing with acetone. An outgassing of the products, which were dried over soda lime and $CaCl_2$, was performed at −20°C and under 10^{-5} mmHg for 2 hours to prevent the ettringite from decomposing. Under these conditions no decomposition of ettringite was apparent according to X-ray diffraction analysis and DTA. Table 6 shows increase of the surface area after 1 day. As above described sample No. 6 had always formed only ettringite. A loss on ignition in Table 6 is caused only by ettringite, and the quantity of ettringite can be calculated from the ignition loss. An increase in the surface area of the product means the difference between the surface area of the product and that of the reactant. It has been corrected by the decreases in the areas of C_3A and gypsum which are calculated from the degree of hydration. Hence, the increase is approximately equivalent to the surface area of ettringite, because most of the ettringite is separated from the C_3A grains by suspension in acetone with enough mixing to break up the product. In Table 6 the increase in the area markedly varies with the hydration temperature as the degree of hydration increases with rising temperature. The surface area per gram of ettringite is at a maximum at 5°C and decreases with temperature increase. It is evident from these results that the manner in which ettringite is formed is variable according to the hydration temperature. In this discussion a growth of ettringite crystal as the result of recrystallization can be neglected because of the low watersolid ratio of 0.5.

Table 6. *Increase in surface area of hydrated product of sample No. 6 after 1 day by nitrogen adsorption method*

Temperature (°C)	Increase in loss on ignition (%)	Ettringite formed[a] (g/g product)	Increase in surface area[b] (m^2/g)	b/a (m^2/g ettringite)
5	2.30	0.062	3.30	53.2
20	5.11	0.137	5.62	41.0
40	14.17	0.380	12.44	32.7
70	20.94	0.561	12.71	22.7

It can be concluded from the above results that, the type of the reaction differs with the temperature because, at a temperature below 20°C, the fine crystals of ettringite form a dense coating around the C_3A grains and, at a higher temperature, the crystals grow larger and cannot form such a compact layer and finally ettringite forms no protective layer at 70°C. In these experiments, the gypsum content did not affect the N value distinctly. But the effect of temperature on the hydration rate of the sample higher in gypsum content tended to decrease at a temperature above 40°C.

The heat evolution of samples No. 7 to 11, in Table 1, were measured at 20°C by the conduction calorimeter to examine the dependence of the retarding effect of gypsum upon the physical properties of the ettringite layer. In Fig. 13 the reaction rate of C_3A with gypsum is significantly influenced by the presence of $Ca(OH)_2$, especially, in the early stage. The extent of the effect of $Ca(OH)_2$ reaches a maximum

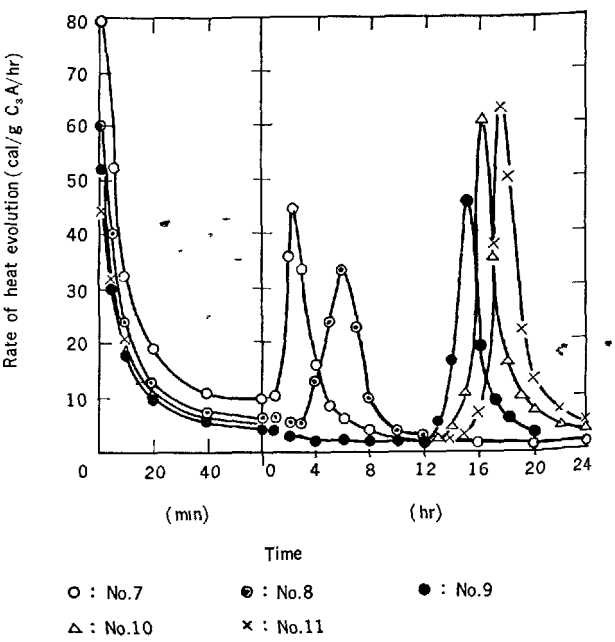

Fig. 13. *Effect of* $Ca(OH)_2$ *concentration on the hydration of* C_3A *with* $CaSO_4 \cdot 2H_2O$

at a higher $Ca(OH)_2/C_3A$ molar ratio than 0.1. The addition of $Ca(OH)_2$ is similar to the lowering of the temperature and the reaction rate of sample No. 7 without $Ca(OH)_2$ at 20°C is equivalent to that of No. 3 with 0.5 $Ca(OH)_2/C_3A$ molar ratio at about 35°C. During the continuous observations of the hydration reaction at water-solid ratio of 5.0 by the optical microscope, needle-like crystals were observed after only 10 minutes, if $Ca(OH)_2$ was not present, and grew to a few score μm in length after several hours. Then the crystals covered the C_3A grains radial like. The increase of $Ca(OH)_2$ concentration shortened the crystal and, in the case of saturated solution, the ettringite crystals became invisible under the microscope. Thus, $Ca(OH)_2$ suppresses the dissolution of C_3A and ettringite, and disturbs the growth of the ettringite crystals. In the calorimetric measurements at low water-solid ratio of 0.5, the relation between them may be expected to differ from that described above. But even at low water-solid ratio $Ca(OH)_2$ may retard the hydration of C_3A with gypsum in the same manner as at water-solid ratio of 5.0, because the surface area of the product increased after raising the $Ca(OH)_2$ content.

It seems from the above results that the effect of the $Ca(OH)_2$ concentration on the hydration rate of C_3A with gypsum can be explained in terms of the size of the ettringite crystal and the manner in which the crystal covers the C_3A grains.

The values of N, as shown in Table 5, were substituted for N in the equation, $(1-\sqrt[3]{1-\alpha})^N = kt$. The mean value of k was determined from the calculations at various hydration times during the reaction in the second stage, using the equation of $\ln k = N \times \ln(1-\sqrt[3]{1-\alpha}) - \ln t$. For the hydration of sample No. 4 at 5°, 20°, 40° and 70°C, mean value of k was calculated to be 5.7×10^{-8}, 3.9×10^{-6}, 9.1×10^{-4}, and 2.5×10^{-1} (hr^{-1}) respectively. Similar values to these were given for other samples. The considerable differences in the values of the rate constant, k, is thought to be caused chiefly by the changes in the physical properties of the ettringite coating, because the dependence of the diffusion constant upon temperature must be too small to account for the variation of k. The reaction rate is determined by the changes in the properties of the ettringite coating.

The discussion of the sequence of the second rapid reaction, as already described, leads to the investigation of the possible cause of the reaction. In Fig. 12, the value of N is always smaller than 1 for the rapid reaction, and it shows that the reaction proceeds with increasing velocity. Fig. 14 shows free CaO and free

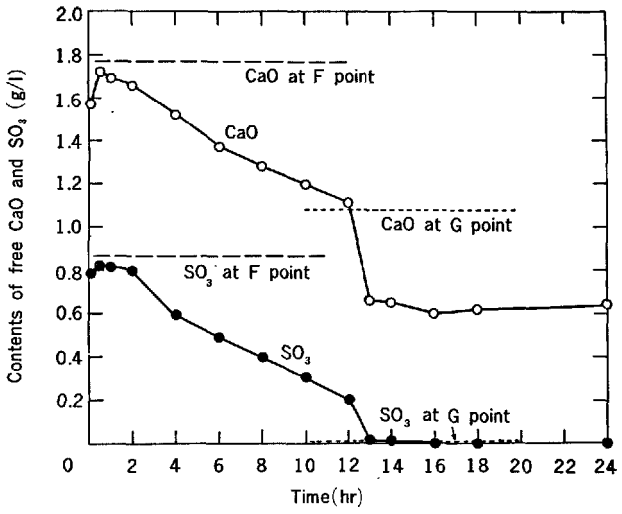

Fig. 14. *Free CaO and SO_3 contents in the liquid phase during suspension hydration of sample No. 3 at 20°C*

SO_3 contents in the solution during the suspension hydration of sample No. 3 in 20 water-solid ratio at 20°C. Free CaO was determined by the EDTA titration method and free SO_3 was by gravimetric analysis. Since no important change was observed in the characteristic pattern of heat evolution by increasing water-solid ratio to 20, it was chosen so as to get the conditions as similar as possible to those at the onset of the second peak when little gypsum was present in the solid phase. In Fig. 14 free CaO and free SO_3 concentrations exist in the region near to Jones' F point (14) for 2 hours after the addition of water and decrease gradually to the composition at G point. After 12 hours considerable decreases in their concentrations, during which the contents of free CaO and SO_3 dropped below those at G point, were observed. These rapid decreases correspond to the start of the second peak in the heat evolution curve.

From these results, it may be concluded that monosulfate crystallizes thereby withdrawing free CaO and free SO_3 from the liquid phase when CaO and SO_3 contents in the solution become insufficient to form ettringite, and that simultaneously the ettringite coating is removed by being partially dissolved. Then the second rapid reaction, that is, the third stage occurs with increasing velocity because more ettringite must be removed in proportion to time.

After the second peak the hydrates around the C_3A grains formed a new barrier and the value of N in the equation of the reaction rate was greater than 2. Thus the reaction rate decreased again, so that a slow decrease in the amount of unhydrated C_3A was observed.

Conclusion

The following conclusions may be drawn from this investigation:

1. For the sake of the convenience the reaction can be classified into four stages; 1) the rapid reaction after the addition of water (the first peak of the heat evolution), 2) the dormant period after the first peak, 3) the second rapid reaction (the second peak of the heat evolution), and 4) the suppressed period after the second peak.

2. The reaction in the first stage is not greatly influenced by the temperature and reveals its maximum rate at a temperature ranging from 15°C to 25°C. But the rate is markedly decreased by the presence of both gypsum and $Ca(OH)_2$.

3. On the other hand, the hydration in the second stage is considerably affected by the hydration temperature and the $Ca(OH)_2$ concentration. The degree of these effects is closely related to the properties of the ettringite layer. At a temperature below 40°C, and further by the presence of sufficient $Ca(OH)_2$, the reaction of forming a coating on the surface of the C_3A grains proceeds with decreasing velocity in proportion to the lowering of the temperature. This is because, the lower the hydration temperature, the finer the crystals of ettringite which are formed and the more compact the ettringite coating. At 70°C, even if sufficient $Ca(OH)_2$ is present, the ettringite crystals grow larger and do not form a protective layer. Then the reaction takes place with little decrease in rate. From considerable increases in the rate constant with rising temperature, it is considered that the changes in the properties of the ettringite layer rather than the diffusion through the layer or the occurrence of the cracking in the layer determine the reaction rate at a temperature between 5° to 70°C.

4. The second rapid reaction in the third stage occurs when the gypsum content in the solution is insufficient to form ettringite. This reaction also accelerated by a rise in temperature. Great increases in the heat of hydration during the second peak are responsible for the reaction of the remaining C_3A with dissolved ettringite and, when more C_3A is present, are responsible for the further hydration of the system C_3A–$Ca(OH)_2$–H_2O.

5. In the last stage, the reaction seems to proceed with the diffusion of the solution through the clusters of the hydrates which have formed around the C_3A grains.

Acknowledgment

The authors wish to express their gratitude to Ass. Prof. Dr. R. Kondo of Tokyo Institute of Technology and Mr. S. Akaiwa, Head of Research Department of Chichibu Cement Co., Ltd., for invaluable advices and useful suggestions. The authors also extend their thanks to Mr. T. Ohtomo, President, and Mr. M. Horiguchi, Vice-president of Chichibu Cement Co., Ltd., for granting permissions to publish the paper.

References

1. H. Tanaka, K. Murakami, I. Monna and T. Karaki, "Studies on the hydration of $3CaO \cdot Al_2O_3$ by calorimetry" (in Japanese), J. Ceram. Assoc. Japan **70**, No. 11, 302–312 (1962).
2. H. N. Stein, "Some characteristics of the hydration of $3CaO \cdot Al_2O_3$ in the presence $CaSO_4 \cdot 2H_2O$", Silicates Industrials 141–145 (1963).
3. H. E. Schwiete, U. Ludwig and P. Jäger, "Investigations in the system $3CaO \cdot Al_2O_3$–$CaSO_4$–CaO–H_2O", Symposium on Structure of Portland Cement Paste and Concrete, Highway Research Board, Special Report 90, Washington D.C., p. 353–367 (1966).
4. C. D. Lawrence, "Changes in composition of the aqueous phase during hydration of cement pastes and suspensions", Symposium on Structure of Portland Cement Paste and Concrete, Highway Research Board, Special Report 90, Washington D.C., p. 378–391 (1966).
5. O. Henning and W. Danowski, "Investigations of the hydration of tri-calcium aluminate in the presence of gypsum" (in German), Silikat Technik **16**, No. 9, 284–286 (1965).
6. R. F. Feldman and V. S. Ramachandran, "The influence of $CaSO_4 \cdot 2H_2O$ upon the hydration character of $3CaO \cdot Al_2O_3$", Magazine of Concrete Research **18**, 185–196 (1966).
7. H. Mori and K. Minegishi, "Influence of gypsum content and hydration temperature on the hydration characteristics of $3CaO \cdot Al_2O_3$" (in Japanese), Semento Gijutsu Nenpo **21**, 71–76 (1967).
8. K. Amaya, "Microcalorimetry" (in Japanese), Bussei

4, No. 10, 588–595 (1963).
9. H. N. Stein, "Mechanism of the hydration of $3CaO \cdot Al_2O_3$", J. appl. Chem. **13**, 228–232 (1963).
10. H. Tanaka, K. Murakami and M. Sato, "Studies on the hydration of calcium aluminoferrite phase and its glass in portland cement clinker" (in Japanese), J. Ceram. Assoc. Japan **74**, No. 1, 20–27 (1966).
11. W. Lieber, "Ettringite formation at elevated temperature" (in German), Zement-Kalk-Gips **16**, No. 9, 364–365 (1963).
12. H. N. Stein, "Influence of some additives on the hydration reaction of portland cement. I. non-ionic organic additives", J. appl. Chem. **11**, 474–482 (1961).
13. R. Kondo, "The chemistry of cement and new-type cement" (in Japanese), Kagaku Kogyo **17**, No. 5, 1–7 (1966).
14. F. E. Jones, "The quaternary system CaO–Al_2O_3–$CaSO_4$–H_2O at 25°C", J. Phys. Chem. **48**, 311–356 (1944).

Supplementary Paper II-93 Hydration of Tricalcium Silicate in a Very Early Stage

Kinjiro Fujii and Wakichi Kondo*

Synopsis

Hydration of tricalcium silicate which occurred immediately after mixing with water (C_3S/water 1:0.7) was studied by following the evolution of heat, the increase in combined water, and the dissolution of calcium and silicate ions. The heat evolution was followed by using a twin type conduction calorimeter and the combined water was measured by micro-electrometric titration using Karl—Fischer's reagent with the hydrate sample as wetted with petroleum ether, which was obtained first by mixing the sample of paste with alcohol to interrupt the progress of hydration, and then by replacing the alcohol with petroleum ether centrifugally. To determine the concentrations of calcium and silicate ions in the aqueous phase, the solutions were squeezed out of the paste by hand loading through a plunger and absorbed into the filter papers, which were then subjected to chemical analysis.

As a result, there were obtained curves of combined water versus period of hydration, in which a rapid increase of combined water was observed during the first five minutes, followed by a dormant period which continued for half an hour at 20°C. At this immediate stage combined water amounted to 0.05 wt. % of tricalcium silicate used, irrespective of the temperature for hydration, while the concentration of Ca^{++} ions in the aqueous phase was 9 millimoles/l and tricalcium silicate was found to dissolve instantaneously as it was mixed with water in a ratio of $CaO/SiO_2 = 3$, that is, congruently, it being suggested that the dissolution of one mole layer of C_3S on the surface of the grain would result in adsorption of 3 or 4 mole layers water on it.

Once the immediate hydration has ceased, it begins the sluggish stage durable for about three hours, in which the heat evolution and the increase in combined water are mild and sluggish. During this stage are observed the supersaturation of Ca^{++} ion in the aqueous phase, the maximum concentration being about twice as high as the solubility of $Ca(OH)_2$ in water, and the exceedingly large mean heat of hydration per mole combined water. From these data available together with electron micrographs, it was considered that until the end of the sluggish stage, about four mole layers of C_3S (equivalent to a depth of 20 Å) on the surface of original grains should be hydrated, and the outmost of the four mole layers does emigrate elsewhere through a solution-precipitation process (in the immediate stage), however the remaining three mole layers will be hydrolyzed in situ under the participation of the adsorbed water to form an intermediate substance prior to tobermorite—formation (in the sluggish stage).

Introduction

When tricalcium silicate ($3CaO \cdot SiO_2$ or C_3S for brevity) comes into contact with water, a rapid hydration reaction occurs with evolution of some detectable heat. This early hydration has been followed by several means containing electron microscope (1) (2), calorimetry (3), measurement of specific surface area (4), and analysis of solution (5). Much elaborate work has been reported, nevertheless the detailed mechanism of the hydration of C_3S in a very early stage is likely to remain ambiguously. The present study, therefore, was undertaken with the hope of obtaining some information necessary for a quantitative approach.

*The Government Chemical Industrial Research Institute, Tokyo, Japan.

Experimental

Materials

Tricalcium silicate

Tricalcium silicates used in this study had such characteristics as are shown in Table 1. And the preparative method for them was as follows:

A slight excess of tetraethyl silicate over the stoichiometric amount was added into an aqueous suspension of $Ca(OH)_2$ at room temperature and the whole mixture was shaken for a while to cause ethyl silicate to hydrolyze into the formation of calcium hydrosilicate gel. After drying, the mixture was so ground as to pass through 80 mesh sieve, subjected to chemical analysis and then corrected by adding a necessary amount of $CaCO_3$ for the stoichiometric ratio of CaO to SiO_2 3:1. The calcium carbonate used was a reagent suitable for flame photometry. The mixture was then moistened with ethyl alcohol, hand-pressed to form cylindrical shapes, prefired at 1400°C for two hours, ground, shaped again by hand-pressing, fired for two hours at 1500°C, then ground, shaped repeatedly under a pressure of 1250 kg/cm², fired for five hours at 1550°C and so ground as to pass through 200 mesh sieve (for sample No. 1). For sample No. 2, the second heating and a relating process was omitted. It is indispensable for the reproducibility of kinetic data on the hydration in an early stage to use an almost completely moisture-free tricalcium silicate, so that before used, it was reheated at 1300°–1350°C, followed by distintegration of lumps in a porcelain mortar while hot (300°–400°C) and preservation in a P_2O_5 desiccator.

Isothermal Calorimetry

The isothermal calorimetry was performed in a constant temperature room (20°C ± 0.3°C) by use of the twin type conduction calorimeter which has been described earlier (6). Ten grams of tricalcium silicate was fallen down into the reaction vessel and mixed with ten milliliters of decarbonated water, resulting in liberation of heat, which was detected by a recorder through the circuit of wire connecting two thermoelement in twin form and having a sensitivity of 3 millivolt/1°C.

The curves to be traced in a chart are the ones representing the rates of heat evolution, and from these data the integral curves can be made to show an overall amounts of the heat evolved during any predetermined reaction time, if account is taken of the heat conserved in the reaction vessel at the end of that time. This conserved heat will be measured from the area under the attenuation curve which for any heat evolution rate would be traced from the moment at which the evolution of heat will be suddenly stopped. In practice, the relations between the areas under the attenuation curves and the heat evolution rates were made previously by use of a standard heater having a known resistivity, and were utilized as calibration curves.

Analysis of Aqueous Solution in the Paste

To determine the concentrations of calcium and silicate ions in the aqueous phases, the solutions were squeezed out of the paste by hand loading through a plunger and absorbed into the filter papers as shown in Fig. 1.

That is, 5 g of C_3S was mixed with decarbonated water in a cylindrical vessel (stainless steel, inner diameter 45 mm, depth 15 mm), the ratio of water to C_3S being 0.7, and the mixture was enclosed therein tightly with a lid, submerged in a thermostat. At predetermined time it was taken, and then closely upon the mixture were placed five sheets of 100% nylon cloths, on which further ten sheets of filter papers No. 7 supplied by Toyo Roshi Kaisha, Ltd. were successively placed. The nylon clothes, which were nonchemically treated as woven and had a fine texture suitable for the purpose of making umbrella, were used after precoating with a thin slurry of low soda alumina

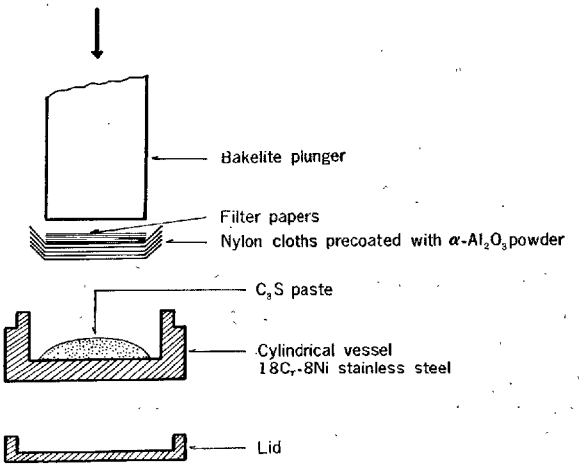

Fig. 1. *Assembly for sequeezing the aqueous solution from the paste*

(α–Al_2O_3, mean grain size of 3μ) and then drying, to secure the liquid absorbed in filter papers from the contamination with C_3S particles. Care should be paid here not to substitute filter papers for nylon clothes, because the filter papers commercially available do adsorb substantial amount of Ca^{++} ion from the basic aqueous solution to be analyzed. After hand-loading through a plunger, the whole filter papers were separated from, weighed, mixed with 30 ml of 0.03 N HCl, filtered and washed. The solutes in the filtrate thus obtained were analyzed as follows: After adding about 2 ml of 0.1 mol Mg-EDTA solution to the half filtrate, the content of calcium ion was determined by titration with 0.001 mol EDTA under the indicator of BT (7). To determine the SiO_2 content in the other half filtrate, molybdenum blue photometric method (8) was carried out, a Hitachi Spectro-photometer Model EPU-2 being utilized for the purpose.

Combined Water

After hand pressing, the residue left under the nylon sheets was taken and the combined water therein was measured as follows: The residue (about 5 g in dry basis) was diluted with about 70 ml of absolute iso-propyl alcohol to interrupt the progressive hydration of C_3S and was centrifugalized. The sediment was mixed with another 70 ml of absolute alcohol and re-centrifugalized, this treatment being repeated successively four times, followed by replacements with each 70 ml of petroleum ether three times. The sediment thus obtained was then placed, as wetted with petroleum ether, on a combustion boat made of silica glass and the combined water therein was released by heating in a tube furnace, absorbed in a methanol—glycol solution and titrated with Karl Fischer's reagent (3 mg H_2O /ml) as described in the recent paper (9). To obtain a correct value, it was necessary to run through blank test with almost the same amount of α-alumina —petroleum ether paste and to make a corresponding reduction (i.e. equivalent to 0.2–0.3 ml of the reagent) from the result of analysis. Thus, the combined water described in this paper should be defined as the one combined to the solid phase tightly enough not to be released by the dissolving effect of absolute iso-propyl alcohol.

Electron Micrograph

The electron micrographs were made by means of a Nippon Denshi K. K., Model JEM-7A. Samples treated with organic solvent at predetermined times were air-dried and sprinkled over a collodion film supported by a grid in the usual manner.

Results

Immediate Heat Liberation of C_3S as Mixed with Water

In Fig. 2 the heat evolution rate during the hydration of C_3S is plotted versus time. A peak of heat evolution rate appears immediately after mixing C_3S with water, but soon declines to a minimum, the minimum being at around 30 min.—in this paper the period until the minimum appears is refered to as immediate stage,— and then the heat evolution rate increases gradually but almost linearly with time (sluggish stage), followed by an abrupt raising (hardening stage).

From the peak area in Fig. 2, the heat liberated in the immediate stage was calculated to be 0.096 cal/g C_3S or 0.25 cal/m² C_3S for the sample C_3S (I) and 0.14 cal/g C_3S or 0.33 cal/m² C_3S for the sample C_3S (II). The discrepancy between both calorimetric values would be in a close relation to the difference in the specific gravity, as shown in Table 1. It is further noticeable that these calorimetric values were so small in comparison with those of portland cements, the values being around 4 cal/g cement in general (6). Passing through a minimum heat evolution rate, there came the sluggish stage, which was durable for about

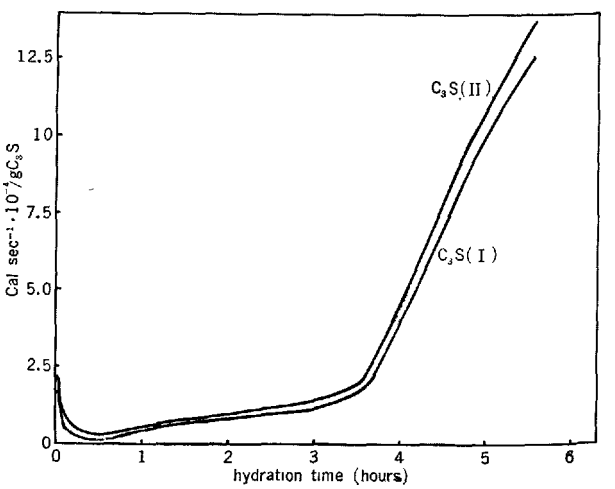

Fig. 2. *Heat evolution rates versus hydration time at 20°C* (C_3S: *water* = *1* : *1*)

Table 1. *Characteristics of* $3CaO \cdot SiO_2$ *used*

Sample	Ignition loss†	Mole ratio CaO/SiO_2	F-CaO	Density	Surface area m^2/g*	Spectrochemical analysis Cu**	Mg	Fe
C_3S (I)	0.10	2.98	0.05%	3.14	0.38	W	Tr	Tr
C_3S (II)	0.15	2.99	0.05%	3.12	0.43	F	Tr	Tr

* by B.E.T. method
**probable contamination from the abrasion of sieve wire
† before use, the moisture was removed by heating at 1300–1350°C.

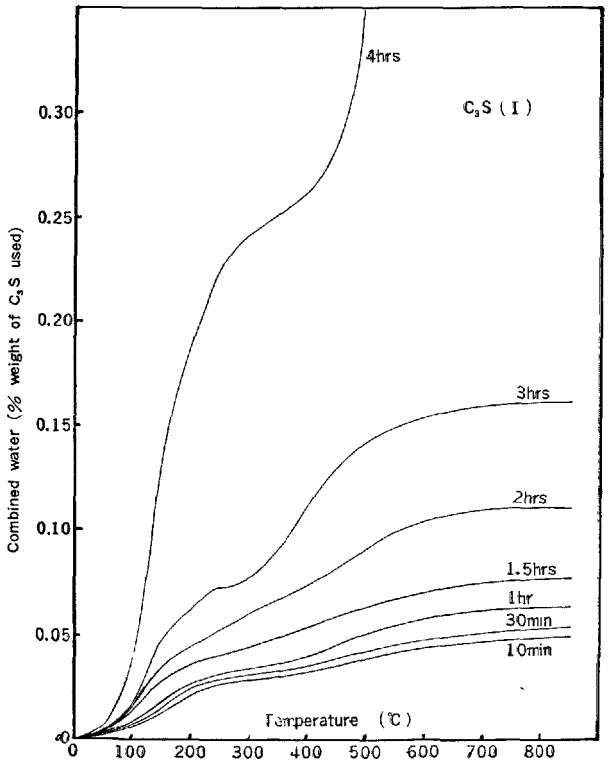

Fig. 3a. *Dehydration curves of* C_3S(I) *hydrated for various periods at 20°C, heating rate 5°C/min*

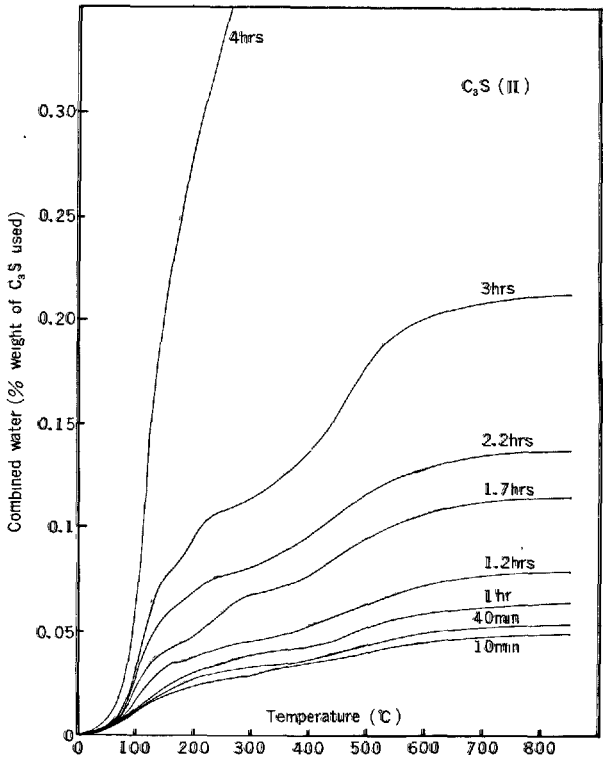

Fig. 3b. *Dehydration curves of* C_3S(II) *as in Fig. 3a*

three hours and showed a mean heat evolution rate of one cal. sec^{-1}. 10^{-4}/g C_3S.

Increase in Combined Water

Based upon the application of the devised analytical method mentioned above, it was made possible to follow clearly the increase in combined water during the early stage of hydration.

From the titers of Karl Fischer's reagent, the percentage of water by weight released from the solid samples were plotted against temperaturs as shown in Fig. 3 a. b., where the continuous dehydration curves were seen over the temperature range up to 700°C, but slight sharp slopes were observed at around 100°C and between 400°C–500°C. Such dehydration curves were obtained for the series of samples which had been hydrated at various temperatures of 10°C, 20°C and 40°C, and the total amounts of water released by heating up to 850°C were determined and refered to as a combined water in the hydrated sample, the results being shown in Fig. 4.

The curves in Fig. 4 indicate that after mixing C_3S with water a combined water is formed almost instantaneously and the amount thereof soon reaches to a constant value of about 0.05 ± 0.005 wt.% irrespective of the temperatures for hydration. This constant value holds for a while (i. e. for a dormant period) but the durations thereof are considered as depending upon the temperatures for hydration. Passing through

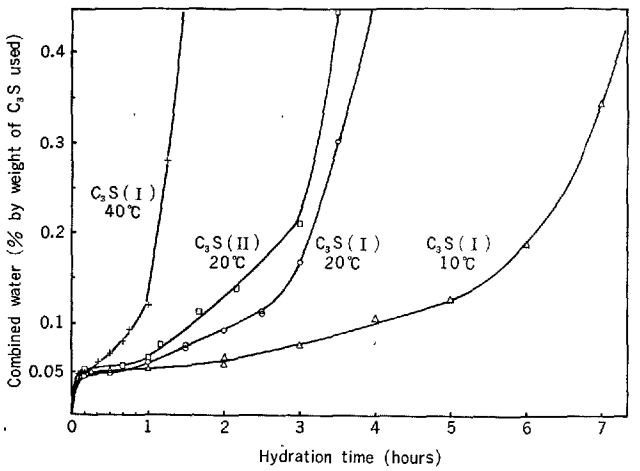

Fig. 4. *The amounts of combined water (wt.% by weight of C_3S used) versus hydration time*

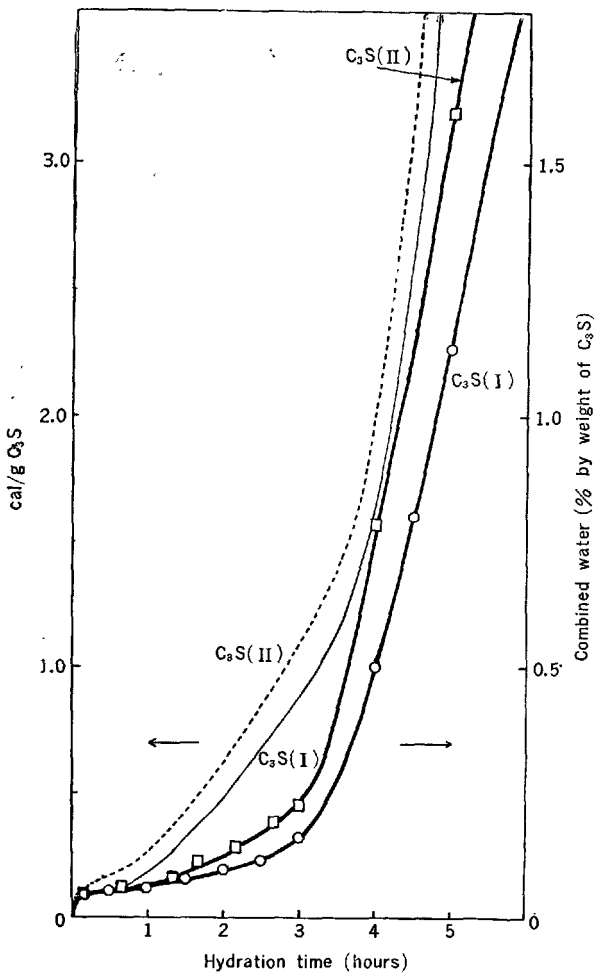

Fig. 5. *Cumulative curves of the amounts of heat evolved and combined water versus hydration time, at 20°C*

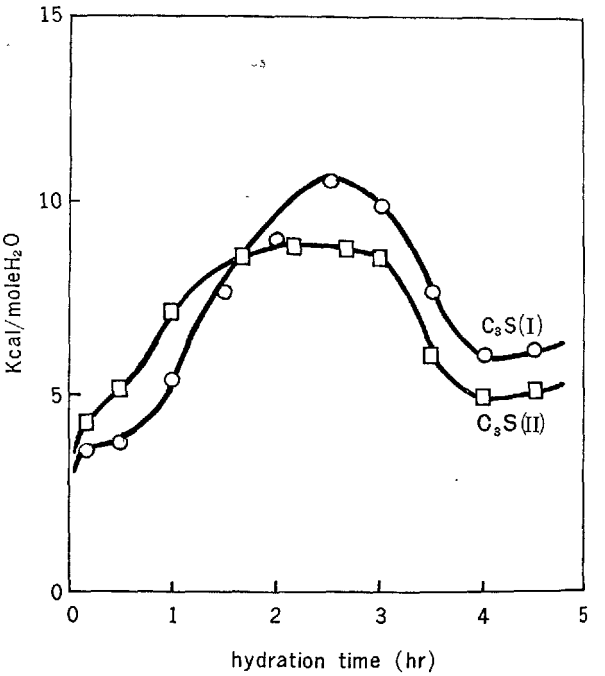

Fig. 6. *Mean heat of hydration per mole of combined water versus hydration time, at 20°C*

the dormant period, the curves are rising with a nearly linear slope up to the point indicating about 0.12 wt.% of combined water, this period being corresponding to the sluggish stage in Fig. 2.

To make clear the relationship between the liberation of heat and the formation of combined water, it is necessary to transform the curves shown as heat evolution rate versus time in Fig. 2 into the one in the form of integral amount of heat evolved versus time. The results obtained are shown in Fig. 5, wherin are seen the cumulative curves of the amounts of heat evolved (in this case however, the heat of solution or crystallization of Ca $(OH)_2$ is excluded) and combined water versus time during hydration (at 20°C), indicating that a remarkable difference in the slopes of curves occurs at the time range from 1 hour to 3.5 hours. When the mean heat of hydration per one mole of combined water may be presented as (cumulative amount of heat evolved)/(cumulative amount [moles] of water combined), so the values can readily be calculated as shown in Fig. 6.

From Fig. 6, it was revealed that at the immediate stage the mean heat of hydration was as small as about 3.5 Kcal/mole H_2O, but gradually became larger until a maximum of 10 Kcal/mole H_2O was reached in a later sluggish stage, followed by a sudden decrease at the beginning of the hardening stage.

Analytical Results of Aqueous Phases

The aqueous phase in a paste with a 0.7:1 water—tricalcium silicate ratio by weight was squeezed out in the immediate stage and subjected to chemical analysis.

As shown in Fig. 7 a, b, c, the dissolutions of both calcium ion and silicic acid did occur immediately as tricalcium silicate was mixed with water and the amount of silicic acid was recorded to be about one millimole/l soln. at a reaction time of 0.5 min. The concentration of silicic acid, however, reduced rapidly in contrast with gradual increase in that of calcium ion along with time. Such trends were observed not only for C_3S(I) at 20°C but also for the same at 10°C and for C_3S(II) at 20°C, and when these data were represented so as to illustrate the variation in CaO/SiO_2 ratio with time, then were obtained the curves shown in Fig. 8.

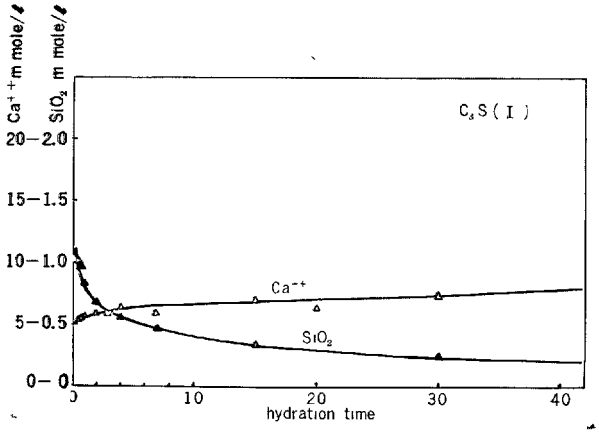

Fig. 7a. *Dissolutions of calcium ion and silicic acid from* C_3S(I), *at 20°C*

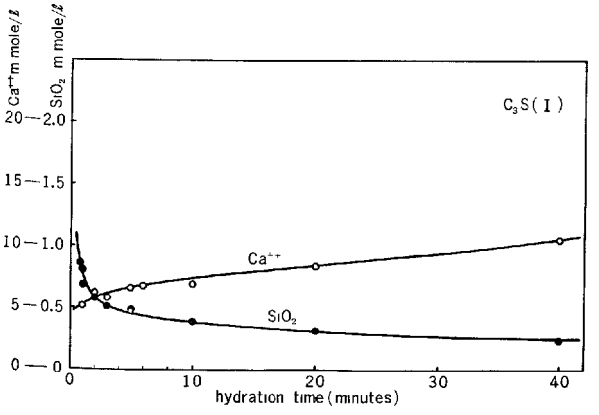

Fig. 7b. *Dissolutions of calcium ion and silicic acid from* C_3S(I), *at 10°C*

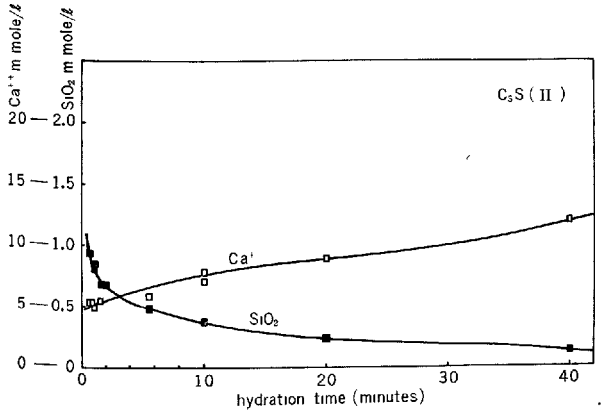

Fig. 7c. *Disolutions of calcium ion and silicic acid from* C_3S(II), *at 20°C*

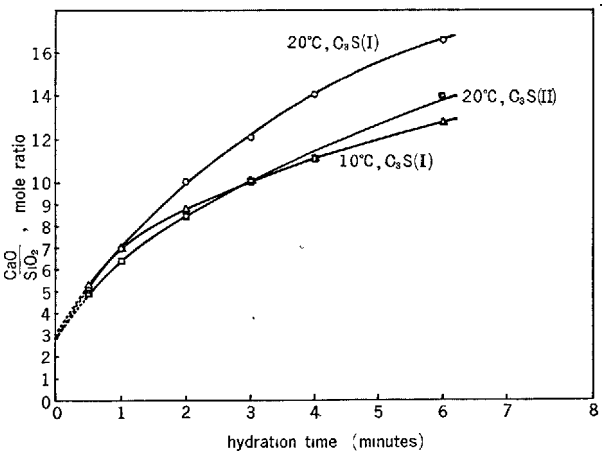

Fig. 8. *Variations in* CaO/SiO_2 *mole ratio in the aqueous phases of pastes with hydration time*

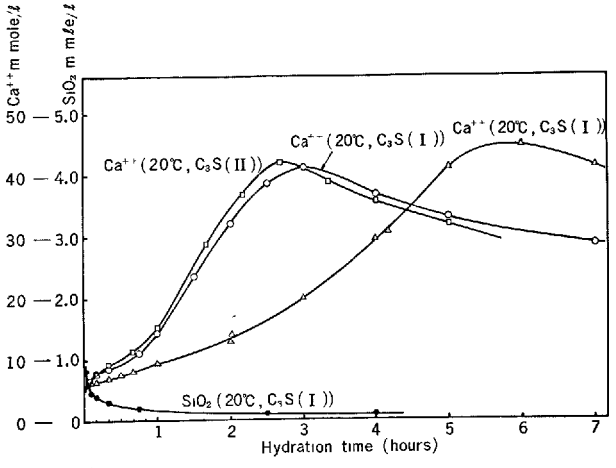

Fig. 9. *Concentrations of Calcium ion and silicic acid in aqueous phase versus hydration time (view over the long period)*

Extrapolating the curves to a reaction time of zero in Fig. 8, so the CaO/SiO_2 ratio of 3 was probably attained, it being suggested that at the moment of their mixing with water, some surface layers of tricalcium silicate were likely to dissolve instantaneously in water at a stoichiometric ratio or congruently, and that the silicic acid once dissolved would soon precipitate from aqueous solution presumably as a calcium hydrosilicate.

The concentration of calcium ion in the aqueous phase varied with reaction time, and the feature could be viewed until after seven hours as shown in Fig. 9.

In the immediate stage, the concentration of calcium ion as CaO was far below the level of saturation, and remained unsaturated until a hydration time of 1.3 hours (at 20°C) and 3.2 hours (at 10°C) has elapsed. After reaching the saturation, however, a further increase in concentration took place continuously up to the maximum concentration which was about twice as high as the solubility of calcium hydroxide. It is worthwhile to note that the time at which the maximum concentration was attained was in a later sluggish stage, that is, a start on the crystallization of $Ca(OH)_2$ from the supersaturated solution would likely be in a close relation to the beginning of the hardening stage.

Discussion

Based on the data described above, some interpretations may be put on the hydration processes of tricalcium silicate in an early stage.

An Immediate Stage

On mixture with water, tricalcium silicate was found to dissolve instantaneously in a ratio of $CaO/SiO_2 = 3$, that is congruently (See Fig. 8). If such dissolution should occur from the surface of the grain, the amount of dissolution of one mole layer on the outer shell of C_3S can be calculated to be (specific surface area of C_3S)/(mean area occupied by one molecule of C_3S) × (Avogaro's number), where the mean area occupied by one molecule of C_3S may be 25.2 Å², the value being obtained as

$$(\text{abc. sin } \beta . \sin\gamma/Z)^{2/3}$$

unit cell constants (10): $a = 12.915$ Å $\quad \alpha = 90° \quad Z = 18$; $b = 7.104$ Å $\quad \beta = 89.8°$; $c = 25.096$ Å $\quad \gamma = 89.8°$

Therefore, the amount of dissolution of one mole layer on the outer shell of C_3S can be expected to be 2.54×10^{-3} millimoles/g C_3S(I) or 2.86×10^{-3} millimoles/g C_3S(II), namely the concentration of C_3S dissolved in the aqueous phase of the paste ($C_3S : H_2O = 1:0.7$ in weight ratio) will amount to 2.54/0.7 millimoles/1 = 3.63 millimoles/1 for C_3S(I) or 2.86/0.7 millimoles/1 = 4.08 millimoles/1 for C_3S(II). These values are fairly comparable with the concentrations of calcium ion in the aqueous phases 8.5 millimoles/1 for C_3S(I) and 9.0 millimoles/1 for C_3S(II), measured at a hydration time of twenty minutes, the time being at a later immediate stage, (see Fig. 7 a, b, and Fig. 2), because the hydrolysis of one mole of tricalcium silicate dissolved should split off more than one mole of $Ca(OH)_2$ in accordance with the following formula.

$$3CaO \cdot SiO_2 + (3 + m - n)H_2O = nCaO \cdot SiO_2 \cdot mH_2O + (3-n)Ca(OH)_2 \quad (1)$$

for calcium silicate hydrate (I), $n = 1$–1.5

Providing n to be 1, so the calculated concentrations of calcium ion in the aqueous phases would become $2 \times 3.63 = 7.26$ millimoles/1 for C_3S(I) and $2 \times 4.08 = 8.16$ millimoles/1 for C_3S (II).

The amount of the combined water formed at the end of the immediate stage was found to be about 0.05% by weight of C_3S used, as seen in Fig. 4a, and the nature of this combined water will be mentioned in the following.

The combined water described in this work will be hydrated water to form calcium hydroxide and calcium hydrosilicate, the remainder presumably being an adsorbed water. An approximate estimation of each combined water would be possible, provided that the calcium hydrosilicate crystallized out of the solution during the immediate stage has a mole ratio H_2O/SiO_2 of 2.0 in based on the value given by Taylor (11), that was obtained for calcium silicate hydrate (I) dried with alcohol and ether, in the present work also the same drying procedure with organic solvent being employed. If m in the equation (1) is thus supposed to be 2, so the equation (1) becomes as follows:

$$3CaO \cdot SiO_2 + (5 - n)H_2O = nCaO \cdot SiO_2 \cdot 2H_2O + (3 - n)Ca(OH)_2 \quad (2)$$

The amount of one mole layer of C_3S on the outmost surface dissolved into aqueous phase could be estimated to be 2.54×10^{-3} millimoles/g C_3S (I) or 2.86×10^{-3} millimoles/g C_3S (II) as mentioned

above, and should the C_3S thus dissolved hydrolyze to precipitate nCaO·SiO_2·2H_2O with remaining $Ca(OH)_2$ formed in an aqueous phase, the amount of three species of combined water could be calculated and the result is shown in Table 2.

From Table 2, an adsorbed water can be considered as a principal constituent of the combined water. It will be reasonable to suppose that the adsorbed water should be formed on the surface of C_3S grains as compensation for the dissolution of one mole layer of C_3S situated on the outmost surface. Then, the number of layers of water molecules adsorbed on the C_3S grains can be calculated using the cross sectional area of 11.4 Å^2 for one water molecule (12) and the

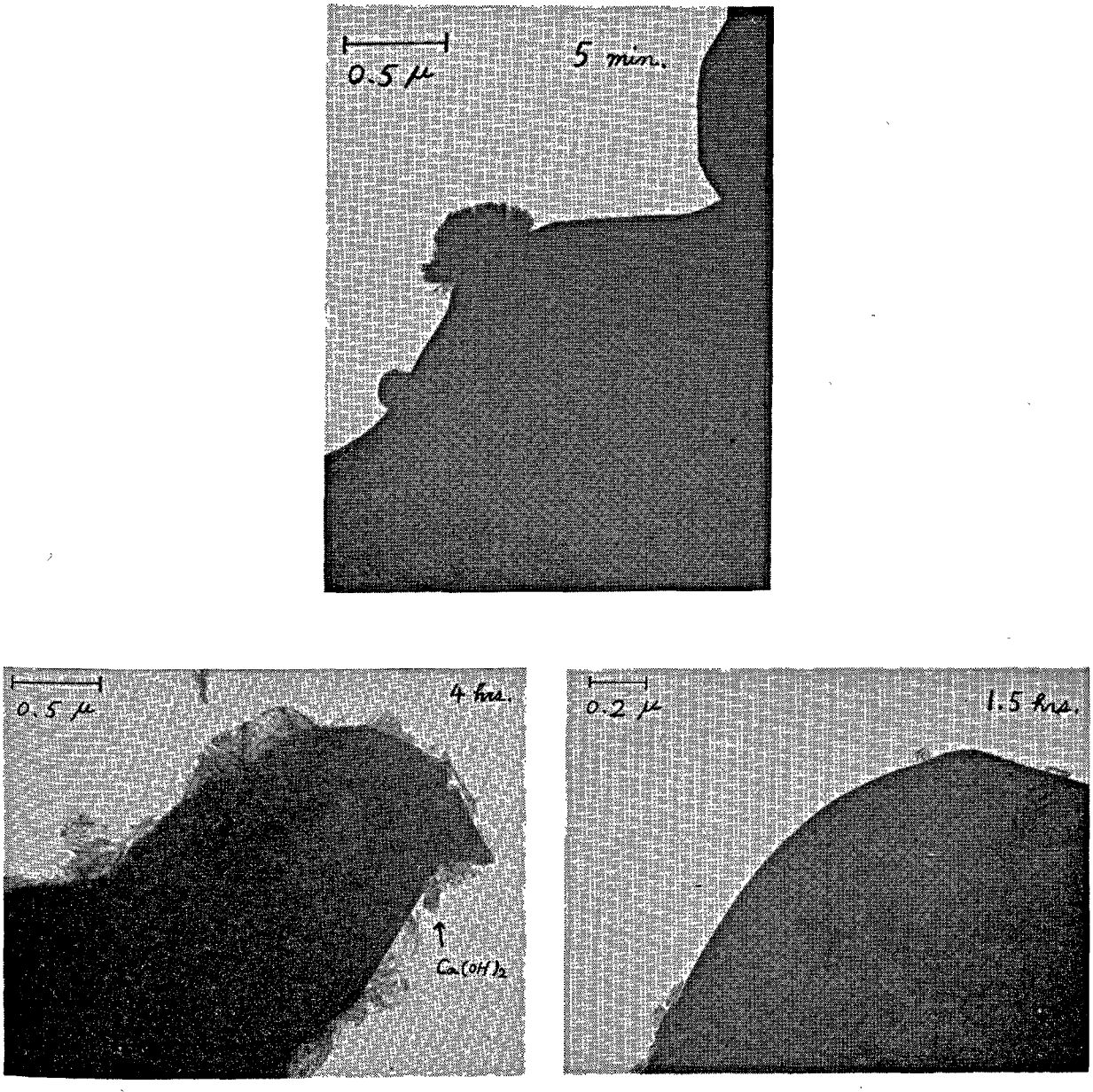

Fig. 10. *Electron micrographs of* C_3S *hydrated for various periods at 20°C*

Table 2. *Adsorbed water (wt%) on C_3S grains during the immediate stage (Calculated by use of eq. 2)*

Species of H_2O	n = 1.0		n = 1.5	
	C_3S(I)	C_3S(II)	C_3S(I)	C_3S(II)
$nCaO \cdot SiO_2 \cdot 2H_2O$	0.009	0.010	0.009	0.010
$Ca(OH)_2$*	0.005	0.006	0.004	0.005
Adsorbed water	0.036	0.034	0.037	0.035
Total comb. water	0.050	0.050	0.050	0.050
Number of layers of H_2O molecules adsorbed on the C_3S grain	3.6	3.4	3.3	3.1

*About 40% by weight of total amount of solution in the paste tested was squeezed out for analysis of the solution. Therefore, the amount of the combined water for $Ca(OH)_2$ in the solution must be $0.6 \times 0.009 = 0.005$ for $n = 1.0$, C_3S(I) and so on.

results are also shown in Table 2. The mean values are seen to be 3.5 for $n = 1$ and 3.2 for $n = 1.5$, but, the most probable number of layers of adsorbed water molecules will be 4, because that the alcohol added to the paste to interrupt the progressive hydration of C_3S does dissolve a very few but, influential amount of $Ca(OH)_2$ and if account is taken of the low concentration of Ca^{++} ions in the aqueous phase at the immediate stage, the value of n will probably be 1.2–1.3.

The Sluggish Stage

Once the immediate reaction of C_3S with water has ceased, it begins the durable sluggish stage in which the heat evolution is mild and the increase in the amount of combined water is sluggish. Of the data obtained in this work, the followings seem to be important for understanding the characteristic reaction that has occured in the sluggish stage.

1. The concentration of calcium ion reached to about 40 millimoles/l soln. in a later sluggish stage, this maximum concentration being about twice as high as the solubility of $Ca(OH)_2$ in water (Fig. 9).

2. From Fig. 6, the mean heat of hydration per one mole of combined water in the sluggish stage is found to be exceedingly large in comparison with those in the immediate stage and the hardening stage.

3. From the electron microscope data (Fig. 10), no distinct changes could be observed in the sluggish stage and the fibrous or crinkly foil-type hydrate lying stragglingly on the C_3S grains will most likely be a precipitate of calcium hydrosilicate from the solution during the immediate stage.

Based on these facts, it will be possible to put some interpretations on the characteristic reactions at the sluggish stage. In the first place, it may reasonably be deduced that at the later sluggish stage, about four mole layers of C_3S (equivalent to a depth of about 20 Å) on the surface of original grains should be hydrated with splitting off Ca ion into solution in accordance with the formula 1, because that the concentration of $Ca(OH)_2$ thus splitted off into the solution at the later sluggish stage (40 millimoles/l) is four times as high as that at the end of the immediate stage, the latter being approximately equivalent to one mole layer of C_3S as mentioned above. The outmost of the four mole layers does emigrate elsewhere through a solution—precipitation process. However the remaining three mole layers will be hydrolyzed in situ to form an intermediate substance as was anticipated from the concentration of silicic acid shown in Fig. 7 and 9, the intermediate compound being presumably a non-crystalline hydrate prior to tobermorite—formation.

In the second place, about four mole layers of the adsorbed water which have been made presumably loosely on the surface of grains during the immediate stage, must rearrange themselves to form hydrates and contribute to heat evolution during the sluggish stage. This effect will be one of the causes for the exceedingly high mean heat of hydration observed during the sluggish stage (Fig. 6).

Lastly, it will be interesting to note the fact that the beginning of crystallizing calcium hydroxide out of the solution with a maximum supersaturation did timely correspond with the entrance into the hardening stage. However, further investigation will be necessary to solve the problem as to whether both are in a causal relation or not.

References

1. J. G. M. de Jong, H. N. Stein and J. M. Stevels, "Hydration of tricalcium silicate," J. appl. Chem. London **17**, 246–250 (1967).
2. G. Sudoh and H. Mori, "Influence of alkali and amount of water on the hydration of tricalcium silicate," Semento Gijutsu Nempo **15**, 46–54 (1961).
3. H. N. Stein and J. M. Stevels, "Influence of silica on the hydration of $3CaO \cdot SiO_2$", J. appl. Chem. London, **14**, 338 (1964).
4. D. L. Kantro, S. Brunauer, and C. H. Weise, "Development of surface in the hydration of calcium silicates (II) Extention of investigation to earlier and later stages of hydration," J. Phys. Chem. **66**, 1804 (1962).
5. S. A. Greenberg and T. N. Chang, "The hydration of tricalcium silicate," J. phys. Chem. **69**, 553–561

(1965).
6. K. Fujii, T. Watanabe, and S. Hagiwara, "Immediate heat liberation of portland cement as mixed with water," Semento Gijutsu Nempo **18**, 120–24 (1964).
7. W. Biedermann and G. Schwarzenbach, Chimia (Switz.) **2**, 56 (1958). cf. K. Ueno, "Kireito Tekitei Ho" (The method of Chelate Titration) published by Nanko Do, Tokyo, 1962, P230.
8. I. Iwasaki and T. Tarutani "Silica in water, V. Salt effect on the colorimetric determination of silica in concentrated salt solution," Bull, Chem. Soc. Japan, **32**, 32 (1959).
9. K. Fujii, W. Kondo and N. Mashimo "Presence of syngenite in commercial portland cement," J. ceram. Assoc. Japan (Yogyo-Kyokai-Shi) **76** (1968) (in English).
10. "The chemistry of cements" edited by H. F. W. Taylor, vol 2, P367, (1964) Academic Press.
11. ibi, vol. 1, P195.
12. S. Brunauer and S. A. Greenberg, "The hydration of tricalcium silicate and β-dicalcium silicate at room temperature," Chemistry of Cement, Proceeding IV international Symposium (Washington D.C.) vol. 1, P149.

Oral Discussion

Shunro Ueda

You stated that the combined water was only 0.05% of C_3S immediately after the mixing with water. Our tests have shown that powered C_3S usually contains about 0.1% moisture and combines with 0.3 to 0.4% water immediately after the mixing. You considered that the thickness of the reaction layer was about 20 Å at the end of the sluggish stage. Terrier and Moreau presumed the thickness to be several Å while we presumed it to be 200 to 300 Å in agreement with the thickness of a nucleus, based on our tests by surface electron diffraction.

I would like to ask your opinion on these points.

Arthor's Closure

Kinjiro Fujii

It would be due to the hydration condition of C_3S varying with each other that our results remarkably differ from those obtained by Mr. Ueda and Dr. Kondo, that is, in our test C_3S was hydrated at a water/C_3S ratio of 0.7, while Mr. Ueda and Dr. Kondo studied on the hydration of C_3S in a suspension state, the water/C_3S ratio being 20. Our determination of calcium ions concentration in the solution one hour after mixing with water showed that the amount of Ca^{++} dissolved was only 0.01 m. mole/g. C_3S at a water/C_3S ratio of 0.7, while in case of water/C_3S ratio of 200, under which Greenberg and Chang (1) studied on the kinetics of the hydration of C_3S, it was about 1.7 m. moles/g.C_3S, that is 170 times of the former. From this, different conclusions may be conducted on the hydration layer thickness.

With regard to the determination of combined water content of C_3S hydrated in a short period, a satisfactory result may be obtained by the analytical procedure written in the present paper within a error of $\pm$0.005 wt/% of C_3S used. From our blank test by Kirl-Fischer's method, it was estimated that the absorbed moisture content of original sample which was heated in advance and allowed to cool in desiccator was 0.01 wt% or less. D-dry method stated by Copeland and Hayes is said to require two days in drying, and so there remains some different questions in its application for the study on hydration process of C_3S in a very early stage.

References

1. S. A. Greenberg and T. N. Chang, The hydration of tricalcium silicate, J. phy. chem. **69**, (2) 553 (1965).
2. L. E. Copeland, J. C. Hayes, Determination of non-evaporable water in hardened portland-cement paste, ASTM Bull. T. P. 214, (12) 70 (1953).

Supplementary Paper II-118 The Hydration Mechanism of C_3A and C_3S in the Presence of Calcium Chloride and Calcium Sulphate

Nemat Tenoutasse*

Synopsis

We have studied the paste hydration of C_3A and C_3S in the presence of gypsum and/or $CaCl_2$.

The methods of investigation used in this work are: isothermal microcalorimetry, X-rays, chemical analysis, measurements of specific surface area (B.E.T. method), etc.

During this investigation we have developed a simple method for determining free $CaCl_2$ in the system C_3A–$CaCl_2$–H_2O; this method is based on the high solubility of $CaCl_2$ in ethyl alcohol.

The influence of the temperature on the hydration of $C_3A + CaCl_2$ and $C_3A + CaSO_4 \cdot 2H_2O$ is determined by microcalorimetry.

The activation energy for hydration is also determined.

The hydration of the system C_3A–$CaCl_2$–$CaSO_4 \cdot 2H_2O$ has shown that $CaCl_2$ accelerates the reaction between C_3A and gypsum.

In the hydration of C_3A in the presence of SO_4^{--} and Cl^-, the SO_4^{--} ions react first, and the C_3A reacts with the Cl^- ions only after the gypsum has been used up.

The trisulphoaluminate remains stable as long as the aqueous phase contains calcium chloride.

Our results on the system C_3S–$CaCl_2$–H_2O show that the $CaCl_2$ which can be extracted by alcohol decreases during hydration.

Using all of our results as a basis, we discuss the mechanism by which $CaCl_2$ and $CaSO_4 \cdot 2H_2O$ influence the hydration of tricalcium aluminate and silicate.

Introduction

Calcium sulphate and chloride are two substances frequently used to control the setting and hardening of portland cement.

The action of gypsum ($CaSO_4 \cdot 2H_2O$) on the hydration of cement and its constituents has been the subject of numerous investigations.

Jones (1) has carried out a detailed investigation of the system CaO–Al_2O_3–$CaSO_4$–H_2O. The chemical nature and the stability domains of the various hydrates have been determined. D'Ans and Eick (2) have also studied the calcium sulphoaluminates.

Schwiete, Ludwig and Jäger (3) have recently studied the system C_3A–$CaSO_4$–$Ca(OH)_2$–H_2O; amongst the various hydrates of the system CaO–Al_2O_3–$CaSO_4 \cdot H_2O$, there are two of particular interest in cement chemistry:

1. Calcium trisulphoaluminate, $C_3A \cdot 3CaSO_4 \cdot 32H_2O$ (Candlot's salt); this is found in nature as ettringite.

2. Calcium monosulphoaluminate or $C_3A \cdot CaSO_4 \cdot 12H_2O$; this hydrate is isomorphous with C_4AH_{13}; calcium monosulphoaluminate crystallises as thin hexagonal platelets.

As far as research on the role of $CaCl_2$ in the setting and hardening of cements is concerned, a literature review by Vollmer (4) should be mentioned. The latter summarizes almost 200 publications on the role of $CaCl_2$ in the hydration of cements.

Most of the research on the behaviour of cement in the presence of $CaCl_2$ is concerned with the technological aspect and with mechanical characteristics; the exact mechanism by which $CaCl_2$ exerts its effect is not well understood.

Calcium chloride modifies the hydration kinetics of all the constituents of cement; it accelerates the hydration of silicates and slows down that of aluminates and aluminoferrites.

Certain investigators believe that the acceleration of the hydration of silicates by $CaCl_2$ is due to a lowering of the pH of the aqueous phase by the calcium chloride.

*Centre National de Recherches Scientifiques et Techniques pour l'Industrie Cimentière, Bruxelles, Belgium.

Amongst the chlorine-containing hydrates of interest in cement chemistry, the following ones should be mentioned:

monochloroaluminate: $C_3A \cdot CaCl_2 \cdot 10H_2O$ (Friedel's salt)

trichloroaluminate: $C_3A \cdot 3CaCl_2 \cdot 32H_2O$

calcium oxychloride: $3CaO \cdot CaCl_2 \cdot 15H_2O$.

Calcium monochloroaluminate is the only hydrate formed in the usual conditions of cement use.

It is known that aluminates and aluminoferrites containing $CaCl_2$ do not influence positively the mechanical performance of cements. The favorable results obtained by the addition of $CaCl_2$ are due essentially to its role in the hydration of C_3S.

We shall discuss briefly below our work on the hydration of C_3A and C_3S in the presence of $CaSO_4 \cdot 2H_2O$ and/or $CaCl_2$.

Materials and Methods

C_3S and C_3A are prepared by heat treatment from stoichiometric mixtures of the oxides.

The purity of the final products is checked by X-rays and by a determination of free lime using a method developed by the author (5).

The products thus obtained are crushed until they pass through an A.S.T.M. 325 sieve.

In order to obtain fractions of definite grain sizes, we fractionated C_3A and C_3S using a BAHCO elutor-centrifuge.

The gypsum and $CaCl_2$ used are Merck "pro analisi" reagents.

The determination of gypsum and $CaCl_2$ was carried out as described previously (6 and 7).

The thermal phenomena accompanying the hydration of our samples are followed using an isothermal microcalorimeter.

The technical characteristics of this apparatus have been described by Stein (8) and the author (9).

In order to determine the structure of the hydrates we used X-rays. The apparatus employed is the Philips P. W. 1010 diffractometer, fitted with a P. W. 1050/30 wide-angle goniometer.

Results and Discussion

$C_3A + CaSO_4 \cdot 2H_2O$

Literature data on the hydration of C_3A in the presence of gypsum indicates that ettringite (the trisulphoaluminate) is formed at the beginning of hydration: it persists until the SO_4^{--} ions are used up; afterwards it is converted into monosulphoaluminate which, in turn, forms mixed crystals with C_4AH_{13}.

It is well-known that gypsum influences the hydration kinetics of C_3A; isothermal microcalorimetry is a useful method for confirming the role of $CaSO_4 \cdot 2H_2O$ in the hydration rate of tricalcium aluminate.

The thermograms in Fig. 1 show the influence of various gypsum concentrations on the thermal phenomena accompanying hydration.

An examination of the curves shows that a variation in the percentage of $CaSO_4 \cdot 2H_2O$ greatly modifies the profile of the thermograms; in fact, the gypsum concentration of the samples influences not only the time necessary for the appearance of thermal phenomena, but the amplitude of the peaks (hydration rate) is also changed.

An analysis of the sample by X-rays, and also by chemical analysis, shows that at the top of the second thermal phenomenon, the gypsum has been entirely used up. It is, therefore, possible to measure the time necessary for the consumption of a definite quantity of gypsum by microcalorimetry; in fact, it is sufficient to measure the time which has passed in order to

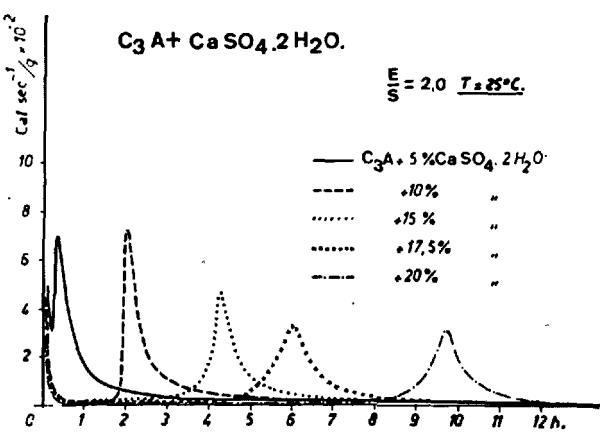

Fig. 1.

obtain the maximum of the second thermal phenomenon.

This time has been calculated from the thermograms of Fig. 1 for several gypsum concentrations. It is seen that the gypsum consumption time varies linearly with the square of the gypsum percentage (Fig. 2). In other words the delay caused by gypsum in the appearance of the second thermal phenomenon is proportional to the square of the $CaSO_4 \cdot 2H_2O$ concentration.

The fact that the gypsum consumption time depend linearly on the square of its concentration suggests that the gypsum reacts by a diffusion mechanism.

The effect of temperature on the hydration kinetics is demonstrated by microcalorimetric tests at various temperatures.

If rate constants are calculated from peak heights, the Arrhenius equation is shown to be valid.

Using the thermograms carried out at different temperatures, we have determined the activation energy for hydration for the system $C_3A + CaSO_4 \cdot 2H_2O + H_2O$. This energy is of the order of 12 $Kcal \cdot mole^{-1}$.

$C_3A + CaCl_2$

The hydration kinetics of C_3A in the presence of $CaCl_2$ has been studied under the same conditions as $C_3A + CaSO_4 \cdot 2H_2O$. The role of $CaCl_2$ in influencing the thermal phenomena is analogous to that of $CaSO_4 \cdot 2H_2O$. Fig. 3 shows the thermograms obtained for the hydration of C_3A in the presence of various quantities of $CaCl_2$; the ratio E/S = 1.2; calcium chloride is dissolved in the water before tempering.

It can be seen from Fig. 3 that an increase in the concentration of $CaCl_2$ in the aqueous phase retards the appearance of the second thermal phenomenon.

We have followed the $CaCl_2$ consumption during hydration. We shall denote by α the degree of transformation (percentage of $CaCl_2$ which has reacted).

By studying the function $F(\alpha) = A(t)$ where t is the hydration time, it is observed that the hydration kinetics is controlled by diffusion processes.

Amongst the different relations proposed by various investigators, the equation for diffusion in a sphere is in best agreement with our experimental results:

$$[1 - (1 - \alpha)^{1/3}]^2 = Kt$$

The straight lines in Fig. 4 show satisfactory agreement between this expression and the experimental data.

$C_3A + CaSO_4 \cdot 2H_2O + CaCl_2$

The paste hydration of C_3A in the presence of Cl^- and SO_4^{--} ions is of an obvious practical interest; when $CaCl_2$ is added to portland cement, the tricalcium aluminate of the cement is hydrated under the simultaneous influence of calcium chloride and calcium sulphate. Roberts (10) has investigated this problem, but his experimental methods do not enable a determination of the chloride which has reacted to be carried out. Our method, on the other hand, ena-

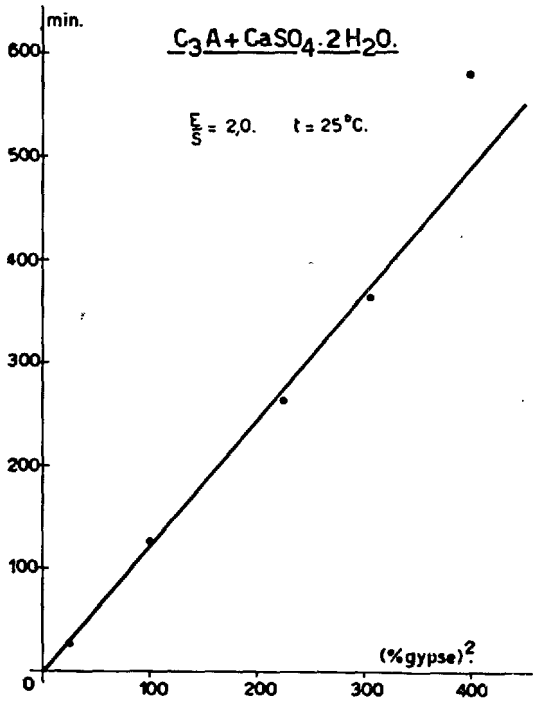

Fig. 2.

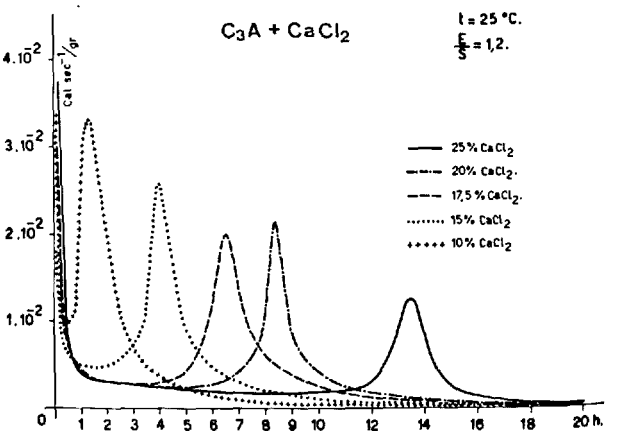

Fig. 3.

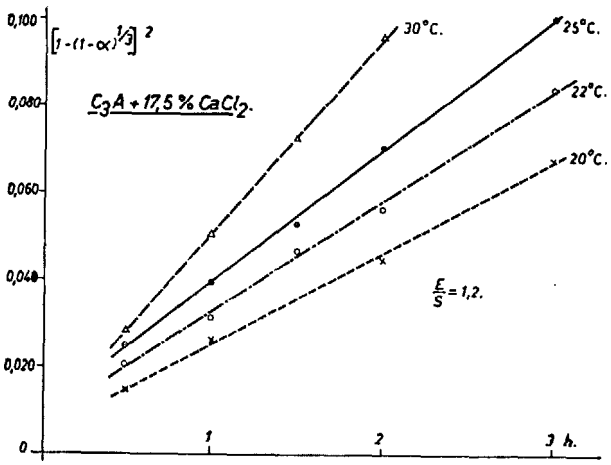

Fig. 4.

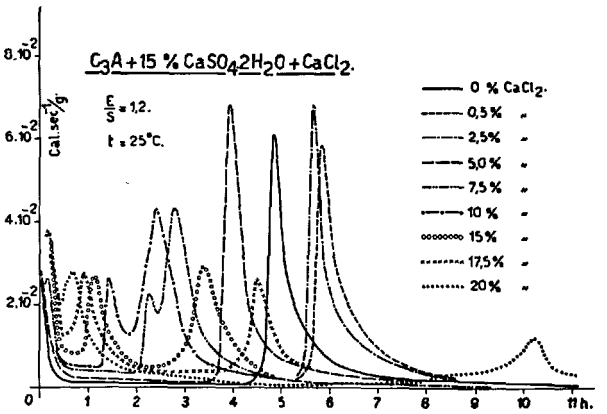

Fig. 5.

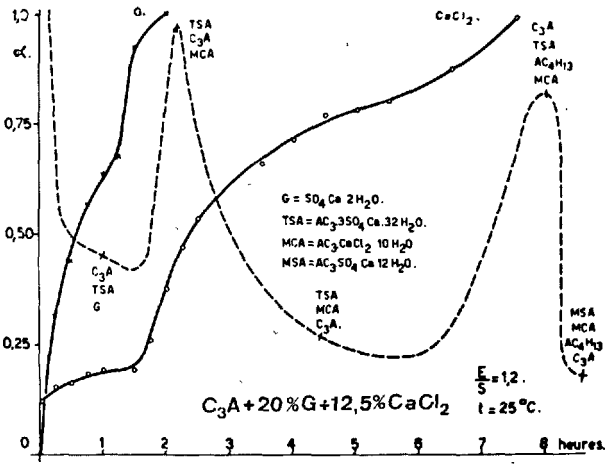

Fig. 6.

bles one to determine precisely how much $CaCl_2$ has been consumed at a given time; the presence of $CaSO_4 \cdot 2H_2O$ has no effect on the estimation of $CaCl_2$.

Microcalorimetry has provided us with valuable information on the action of $CaCl_2$ in the hydration of $C_3A + CaSO_4 \cdot 2H_2O$.

The curves in Fig. 5 show the influence of various percentages of $CaCl_2$ on the hydration of a mixture of $C_3A + 15\%\ CaSO_4 \cdot 2H_2O$.

An examination of these thermograms shows that percentages of $CaCl_2$ greater than 5% accelerate the appearance of the thermal phenomena; above 7.5% $CaCl_2$ the main thermal phenomenon is doubled; $CaCl_2$ concentrations less than 5% slow down the appearance of the thermal phenomena; it seems that the addition of small amounts of $CaCl_2$ (less than 5%) increases the effect of gypsum.

To arrive at a better understanding of the hydration process, we shall consider in particular the hydration of a sample having the following composition:

$$C_3A + 20\%CaSO_4 \cdot 2H_2O + 12.5\%CaCl_2$$

The choice of the composition of this sample is based on microcalorimetric data, since with these percentages of sulphate and chloride, the thermal phenomena are considerably separated and one can easily stop the hydration between two microcalorimetric peaks.

The hydration of this sample is followed by the methods listed below:

1. The thermal phenomena are recorded using an isothermal microcalorimeter.

2. The $CaCl_2$ consumption is followed by estimation of the $CaCl_2$ which has not reacted (free chloride).

3. The reaction between C_3A and $CaSO_4 \cdot 2H_2O$ is studied by determining the gypsum percentage by radiocrystallography.

4. The hydration products are identified throughout hydration by X-rays.

Our results are shown schematically in Fig. 6.

At the beginning of hydration, a small amount of $CaCl_2$ reacts to give chloroaluminate; but it is observed in particular that SO_4^{--} ions react at first to give calcium trisulphoaluminate.

Consumption of Cl^- ions begins only after the SO_4^{--} ions have been completely used up; the complete consumption of $CaCl_2$ coincides with the maximum of the third peak.

In the light of these results, one can represent the hydration process of C_3A in the presence of Cl^- and SO_4^{--} by the following reaction steps;

A. first microcalorimetric peak "liquid-solid contact"

$$C_3A + 3CaSO_4 + 32H_2O \rightarrow C_3A \cdot 3CaSO_4 \cdot 32H_2O$$
$$C_3A + CaCl_2 + 10H_2O \rightarrow C_3A \cdot CaCl_2 \cdot 10H_2O$$

B. between the first and second peaks

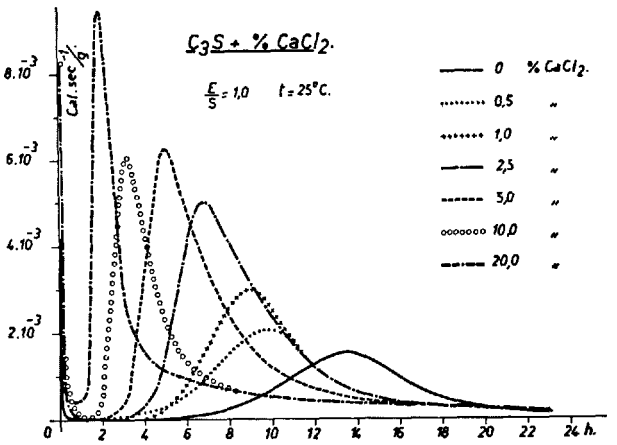

Fig. 7.

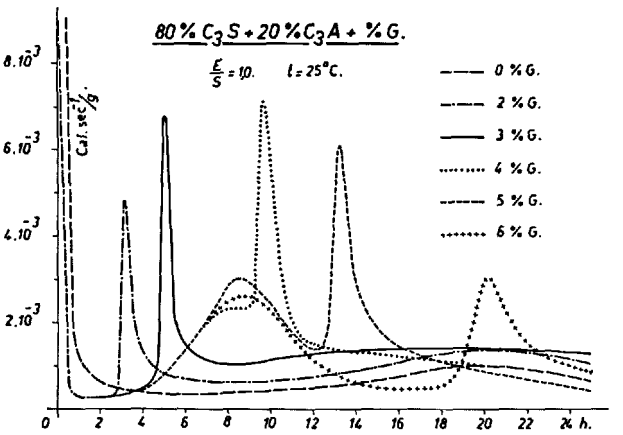

Fig. 8.

$$C_3A + 3CaSO_4 + 3H_2O \rightarrow C_3A \cdot 3CaSO_4 \cdot 32H_2O$$

This reaction proceeds until the gypsum has been completely used up; during this period the $CaCl_2$ does not react.

C. between the second and third thermal phenomena

$$CaCl_2 + C_3A + 10H_2O \rightarrow C_3A \cdot CaCl_2 \cdot 10H_2O$$

D. after the third thermal phenomenon

The remaining C_3A is hydrated to give $C_3A \cdot Ca(OH)_2 \cdot 12H_2O$; this hydrate converts the trisulphoaluminate into monosulphoaluminate (after the Cl^- ions have been used up):

$$C_3A \cdot 3CaSO_4 \cdot 32H_2O + 2C_3A \cdot Ca(OH)_2 \cdot 12H_2O \rightarrow 3C_3A \cdot CaSO_4 \cdot 12H_2O + 20H_2O + 2CH_2$$

After conversion of the ettringite (the trisulphoaluminate) the hydrates having a hexagonal structure; $C_3A \cdot Ca(OH)_2 \cdot 12H_2O$, $C_3A \cdot CaCl_2 \cdot 10H_2O$ and $C_3A \cdot CaSO_4 \cdot 12H_2O$ form solid solutions.

The Hydration of C_3S

The hydration of C_3S has been studied in particular by isothermal microcalorimetry.

Fig. 7 shows the effect of $CaCl_2$ on the hydration kinetics of C_3S. It can be seen that $CaCl_2$ accelerates the appearance of the second thermal phenomenon.

It should also be noted that an increase in the concentration of $CaCl_2$ in the aqueous phase causes the height of the peak to increase.

X-ray examination of samples of C_3S hydrated in the presence of $CaCl_2$ did not enable us to detect any compound containing $CaCl_2$, except in the sample containing 20% $CaCl_2$; in fact, X-rays show that this sample contains calcium oxychloride ($3CaO \cdot CaCl_2 \cdot 15H_2O$).

We have also studied the hydration of mixtures of C_3S and C_3A; our first results show that the presence of C_3A considerably modifies the thermal phenomena accompanying the hydration of C_3S. Tricalcium aluminate slows down the hydration of C_3S.

In Fig. 8 are shown thermograms for a mixture of C_3S and C_3A, containing increasing percentages of gypsum.

An examination of the curves in Fig. 8 shows that; when the microcalorimetric peak due to the complete consumption of the gypsum lies before the peak due to the hydration of C_3S, the latter peak is greatly retarded.

On the other hand, when the thermal phenomenon attributed to the hydration of $C_3A + CaSO_4 \cdot 2H_2O$ lies after the thermal phenomena due to the hydration of C_3S, the latter peak is practically unchanged.

General Conclusions

In the present investigation, we have studied the hydration of C_3S and C_3A in the presence of $CaCl_2$ and/or $CaSO_4 \cdot 2H_2O$.

Great importance is attached to the kinetic aspect of hydration.

In order to study the hydration kinetics, adequate methods of investigation are above all necessary to follow the transformation.

By using simple methods, we have followed with precision the concentration of Cl^- and SO_4^{--} in the liquid phase.

In this way we have been able to show the determining role of diffusion processes in the hydration of C_3A in the presence of calcium chloride or calcium sulphate.

We have proposed equations to describe the hydration kinetics.

Our microcalorimetric investigations have led us to devise a simple method for determining the activation energy for hydration.

The values obtained by microcalorimetry for the activation energy are in agreement with those measured by chemical methods.

As regards the nature of the hydration products, it should be remembered that the hydration of pure C_3A gives unstable hydrates with a hexagonal structure (C_4AH_{13}, C_2AH_8) which are converted into the cubic hydrate C_3AH_6, which is the only stable hydrated calcium aluminate in the system CaO–Al_2O_3–H_2O; but according to our X-ray crystallographic data, the hydration of C_3A in the presence of $CaSO_4 \cdot 2H_2O$ and $CaCl_2$ gives rise to sulpho- and chloroaluminates which have the hexagonal structure. These complex hydrates containing Cl^- and SO_4^{--} form solid solutions with C_4AH_{13}. The formation of a solid solution stabilises C_4AH_{13} and greatly slows down its conversion into C_3AH_6.

A study of the nature of the hydrates in the hydration of the system C_3A–$CaSO_4 \cdot 2H_2O$–$CaCl_2$ enables us to define certain aspects of the hydration of C_3A in the presence of Cl^- and SO_4^{--}:

I. $CaCl_2$ accelerates the reaction between gypsum and C_3A.

II. When C_3A is hydrated in the presence of $CaCl_2$ and $CaSO_4 \cdot 2H_2O$, the SO_4^{--} ions react first to give the trisulphoaluminate; formation of monochloroaluminate begins only after the SO_4^{--} ions have been used up.

III. The trisulphoaluminate formed in the presence of $CaCl_2$ is converted into monosulphoaluminate only after all the $CaCl_2$ has been used up.

IV. $CaCl_2$ accelerates the reaction between C_3A and $CaSO_4 \cdot 2H_2O$.

V. Calcium hydroxide does not alter the hydration mechanism of C_3A in the presence of Cl^- and SO_4^{--} ions.

Our work on the kinetic aspect of the hydration of $C_3A + CaCl_2$ and/or $CaSO_4 \cdot 2H_2O$ has shown that for a complex kinetic study, it is useful to use several methods of investigation such as; isothermal microcalorimetry, X-ray crystallography, chemical analysis, etc.

As regards the hydration of the binary system $C_3S + C_3A$ in the presence of $CaCl_2$ and $CaSO_4 \cdot 2H_2O$, our first results are encouraging, but further research is necessary to understand the hydration mechanism of $C_3S + C_3A$.

Abbreviations

The following symbols are used:

$$C = CaO$$
$$S = SiO_2$$
$$A = Al_2O_3$$
$$F = Fe_2O_3$$
$$H = H_2O$$
$$\frac{E}{S} = \frac{\text{water}}{\text{solid}}$$

This work is part of the research sponsered by the Centre National de Recherches Scientifiques et Techniques pour l'Industrie Cimentière (C.R.I.C.). We thank Mr. A. De Donder for his technical assistance.

Our thanks are also due to the Institut pour l'Encouragement de la Recherche Scientifique dans l'Industrie et l'Agriculture (I.R.S.I.A.) for financial assistance.

University of Brussels Laboratory for Chemistry of Solids Director: Prof. W.L. De Keyser

References

1. F. E. Jones, "The quaternary system CaO–Al_2O_3–$CaSO_4$–H_2O at 25°C. Equilibria with crystalline $Al_2O_3 \cdot 3H_2O$, alumina gel and solid solution", J. Phys. Chem. **48**, 311 (1944).
2. J. D'Ans and H. Eick, "Das System CaO–Al_2O_3–$CaSO_4$–H_2O bei 20°C", Zement-Kalk-Gips **6**,

No. 9, 302–311. (Sept. 1953).
3. H. E. Schwiete, U. Ludwig and P. Jäger, "Untersuchungen in system $3CaO \cdot Al_2O_3$–$CaSO_4$–CaO–H_2O" Zement-Kalk-Gips, **17**, No. 6, 229–236 (June 1964).
4. H. C. Vollmer, "Annotated bibliography on calcium chloride in concrete", Highway Res. Board, Bibliography **13**, (1952).
5. N. Tenoutasse, Unpublished work.
6. N. Tenoutasse, "Influence du gypse sur l'hydratation de la phase ferrite des ciments Portland" Rev. Mater. Construct. Trav. Publ. No. 604, 18–26 (Jan. 1966).
7. N. Tenoustasse, "Une méthode simple pour la détermination du chlorure de calcium au cours de l'hydratation des ciments", RILEM-ABEM. Intern. Symp. on admixtures for mortar and concrete, Brussels, Aug. 30th–Sept. 1st 1967. V/15 ABEM, Brussels, p. 251–269 (1967).
8. H. N. Stein, "Influence of some additives on the hydration reactions of portland cement. I. Nonionic organic additives", J. Appl. Chem., **11**, 474–482 (1961).
9. N. Tenoutasse, "L'action du gypse sur l'hydration de la phase ferrite Aspect cinétique (II)", Rev. Matér. Construct. Trav. Publ. No. 614, 452–458 (Nov. 1966).
10. M. H. Roberts, "Effect of calcium chloride on the durability of pre-tensioned wire in prestressed concrete", Mag. Concrete Res. **14**, No. 42, 143–154 (Nov. 1962).

Supplementary Paper II-120 The Hydration of the Ferrite Phase of Cements

Walter L. De Keyser and Nemat Tenoutasse*

Synopsis

It is generally accepted that the ferrite phase of cements is a solid solution having the formula $C_6A_xF_y$.

During the investigation of the hydration of cements, we have studied some aspects of the solid solution of the ferrite phase under different conditions for pastes having a low water to solid ratio.

The action of iron during hydration was established by chemical analysis of the hydrated phase separated from the mixture by heavy liquids.

We have also studied the hydration of alumino-ferrites in the presence of gypsum and the latter was found to influence strongly the kinetics of hydration. The nature and stability of different hydrates was determined by X-ray studies and by electron microscopy.

The part dealing with the kinetics is entirely devoted to studies of the effect of the following parameters, which influence the rate of reaction:

I. time of contact of the specimens with gypsum,
II. water to solid ratio,
III. specific surface area,
IV. temperature, and
V. chemical composition of the specimens.

Introduction

The system Al_2O_3–CaO–H_2O has been studied in many investigations, and we now have a good understanding of it; this is neither the case for the system Fe_2O_3–CaO–H_2O, nor that of the system Al_2O_3–Fe_2O_3–CaO–H_2O, obtained by hydration of the ferrite phase, symbolically represented by $C_6A_xF_y$, where $x + y = 3$.

It should be remembered that a study of the system Fe_2O_3–CaO–H_2O presents difficulties owing to the instability of hydrates containing iron: for example FC_3H_6 is a hydrate which is difficult to synthesize in the pure state, while the synthesis of AC_3H_6 presents no difficulty.

In this investigation we have looked into the hydration of certain components of the solid solution of the ferrite phase in a pure paste or in the presence of $Ca(OH)_2$. The hydration of the ferrite phase is also studied in the presence of certain setting regulators such as $CaSO_4 \cdot 2H_2O$ and $CaCl_2$.

The hydration of tricalcium aluminate in the presence of gypsum and/or $CaCl_2$ is the subject of a paper presented at this symposium (1).

This paper is a condensed summary of work carried out over the last few years.

Materials and Methods

Nine components of the solid solution of $C_6A_xF_y$ were synthesized from "pro analisi" reagents. Mixtures of $CaCO_3$, Fe_2O_3 and $Al(OH)_3$ having a definite stoichiometry (lying between C_2F and C_6A_2F) are subjected to three heat treatments at 1340°C.

After the heat treatments the product is crushed until it passes through an ASTM 325 sieve (16,900 mesh/cm²).

In order to obtain fractions of definite granulometries, we carried out a fractionation of the products after sieving, using a BAHCO elutriator-centrifuge.

The gypsum used is U.C.B. "pro analisi" $CaSO_4 \cdot 2H_2O$ (No. 1234); it is passed through an ASTM 325

*Centre National de Recherches Scientifiques et Techniques pour l'Industrie Cimentière, Bruxelles, Belgium.

sieve (limiting mesh diameter 44 microns).

The gypsum is also elutriated to obtain fractions with different specific surface areas. In all the experiments we used Merck "pro analisi" $CaCl_2 \cdot 2H_2O$ (2832). The $CaCl_2$ content is always expressed as a percentage of anhydrous $CaCl_2$ respect to anhydrous aluminoferrite.

The calcium chloride is always dissolved in the water before tempering.

In order to follow the $CaCl_2$ concentration during hydration, we extracted the $CaCl_2$ which had not reacted by means of ethyl alcohol. After the alcohol extraction the chloride is determined by the silver nitrate method in a non-aqueous medium.

The thermal phenomena accompanying the hydration of our samples are followed using an isothermal microcalorimeter, described previously (2).

In order to determine the nature of the hydrates, we employed thermogravimetric analysis: the differential thermobalance was developed in 1953 by W. L. De Keyser (3).

Since then this method has been used frequently in studying the hydration of cement and its constituents.

The applications of differential thermogravimetry to cement chemistry are dealt with in a publication by De Keyser, Derie and Van Bemst (4).

In order to identify the structure of the hydrates, we used X-ray diffraction and electron microscopy.

We should like to point out that we have studied only the paste hydration of aluminoferrites.

The synthesized products were mixed with freshly boiled distilled water to obtain a plastic paste; the amount of water necessary to obtain such a paste varies from 25 to 40% depending on the nature of the aluminoferrite.

The hydration of the aluminoferrites was carried out at 25°C; the samples were stored in an atmosphere saturated with water and free from CO_2.

Results and Discussion

The Hydration of the Ferrite Phase in the Pure State and in the Presence of $Ca(OH)_2$

The rate of hydration of C_2F is very small. At the beginning of hydration the X-ray diagram of the sample of $C_2F + H_2O$ resembles that of the anhydrous substance.

As the iron is progressively replaced by aluminium in C_2F, the rate of hydration increases. For instance, C_6AF_2 is hydrated more rapidly than C_2F.

As regards the nature of the hydrates obtained by the hydration of C_6AF_2, it should be remembered that these hydrates are similar to those obtained by hydration of C_4AF and C_6A_2F.

The hydration of C_4AF is more rapid than that of C_2F and C_6AF_2. After five minute hydration, electron microscopy enables one to identify hydrates of hexagonal structure (Fig. 1).

24 hours later, the platelets are thicker, but the hexagonal platelets disappear gradually and hydrates of the cubic system are observed to appear. Fig. 2 shows an electron micrograph of a C_4AF sample hydrated for 4 months.

Fig. 3 shows differential thermogravimetric analysis

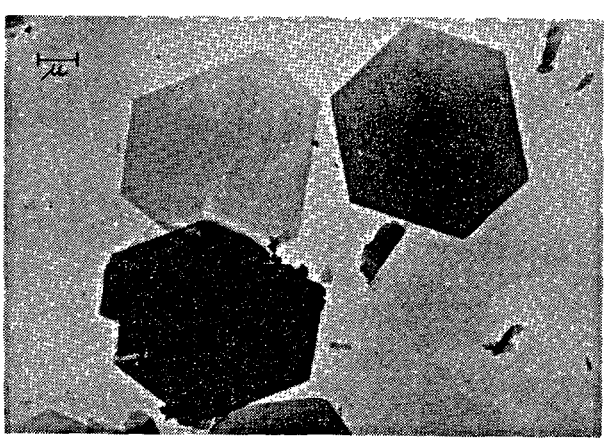

Fig. 1.

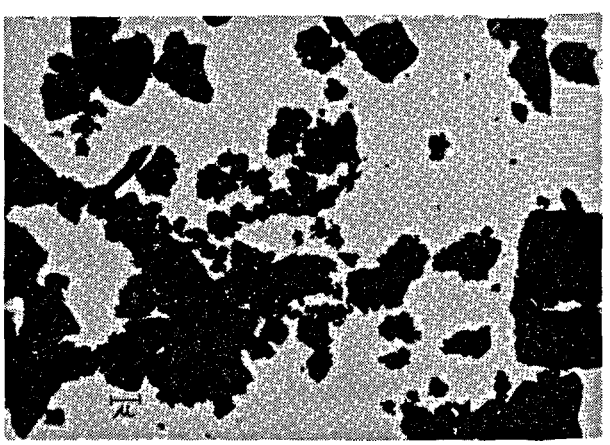

Fig. 2.

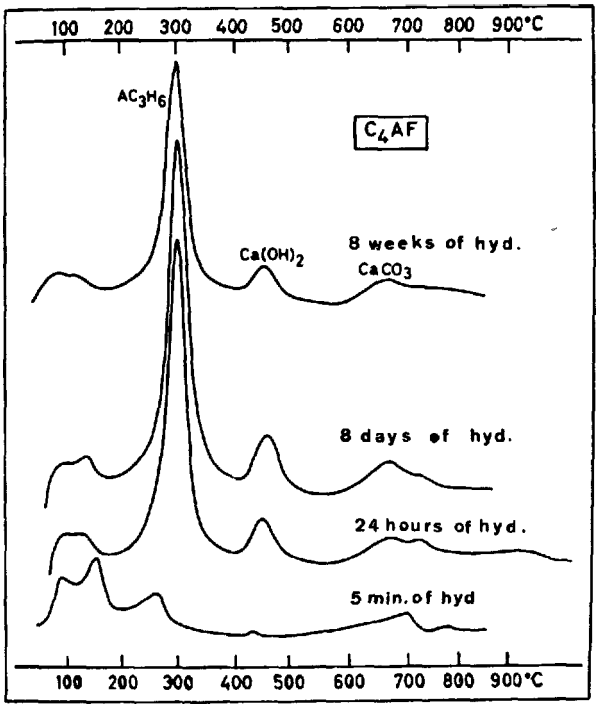

Fig. 3.

curves obtained after various hydration times. An examination of the curves in Fig. 3 shows clearly that after 5 minute hydration there are various peaks situated in the region lying between 100°C and 250°C, the peak at 150°C being characteristic of the hexagonal compounds.

But after 24 hour hydration it is seen that these peaks disappear gradually and an important peak appears at 300°C corresponding to the dehydration of the cubic compounds (A, F)C_3H_6. The appearance of this peak at 300°C is accompanied by that of another peak at 450°C, which corresponds to the dehydration of the $Ca(OH)_2$ liberated by the dehydration of the cubic hydrate.

It can, therefore, be seen that during this hydration hexagonal compounds are formed at first; these then turn into cubic compounds.

The process by which C_6A_2F is hydrated is very similar to that of C_4AF; however, the hydration of C_6A_2F is even faster than that of C_4AF.

When aluminoferrites are hydrated in the presence of $Ca(OH)_2$, the hydration process changes considerably.

This investigation was undertaken on account of its practical importance. This is due to the fact that portland cements liberate $Ca(OH)_2$ during hydration.

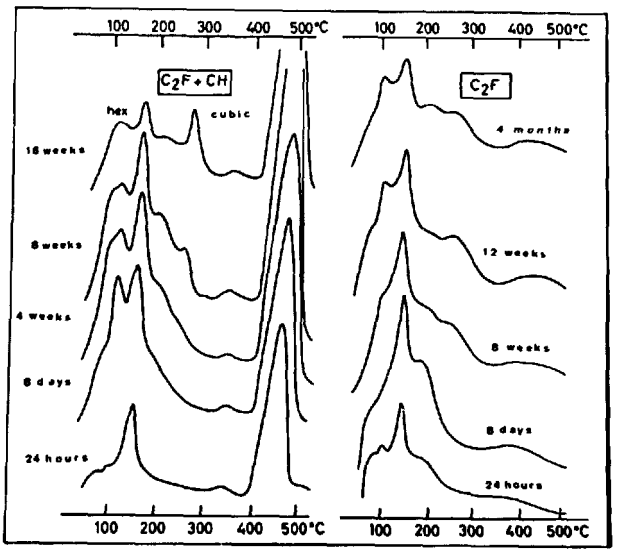

Fig. 4.

The role of $Ca(OH)_2$ in the hydration of C_2F is illustrated in Fig. 4; this figure shows the differential thermogravimetric analysis curves for C_2F hydrated in the presence and in the absence of lime.

It can be seen that in the system $C_2F + Ca(OH)_2$, hexagonal compounds are formed at first; but after 16 weeks hydration a peak characteristic of cubic compounds appears.

It seems that in this case the hydration process is greatly accelerated by lime and that hexagons are first formed, followed by cubes, which are not observed in the case of C_2F free from lime, even after 4 months hydration.

When C_4AF is hydrated in the presence of $Ca(OH)_2$, the formation of hexagonal hydrates can be demonstrated using an electron microscope.

An examination carried out after 8 weeks shows the persistence of hexagonal platelets, while for C_4AF free from lime these platelets had then completely disappeared.

It follows that $Ca(OH)_2$ considerably slows down the conversion of hydrates having the hexagonal structure.

The evolution of the hydration of C_6A_2F in the presence of $Ca(OH)_2$ is similar to that of C_4AF. Here too, lime slows down the conversion of hexagonal hydrates.

The slower conversion of hexagonal crystals into cubic ones enables one to obtain cubic crystals having better shapes, which is moreover explained by the general rules of crystallochemistry.

The Hydration of the Ferrite Phase in the Presence of Gypsum and/or $CaCl_2$

The Hydration of $C_6A_xF_y$ in the Presence of $CaSO_4 \cdot 2H_2O$

We shall describe here our results on the hydration of C_4AF in the presence of $CaSO_4 \cdot 2H_2O$. Fig. 5 shows the effect of various gypsum concentrations on the thermal phenomena accompanying hydration.

To arrive at a better understanding of the hydration mechanism, we shall consider the hydration of the mixture $C_4AF + 10\%$ $CaSO_4 \cdot 2H_2O$ (Fig. 6). The hydration of this sample is stopped at the points M, N, O and P marked on the curve. After each interruption of hydration, the hydrated phase is identified by X-rays. Fig. 6 summarizes clearly the hydration process of $C_4AF + CaSO_4 \cdot 2H_2O$.

Using the microcalorimetric method we have studied the influence of several parameters on the hydration kinetics. The thermograms in Fig. 7 illustrate the influence of the specific surface area of C_4AF on the appearance time of the thermal phenomena. It can be seen that an increase in the specific surface area reduces the time required for the appearance of the second thermal phenomenon.

The thermograms in Fig. 8 show the influence of the water/solid ratio on the hydration kinetics.

The Hydration of the Ferrite Phase in the Presence of $CaCl_2$ and $CaSO_4 \cdot 2H_2O$

Our work on the hydration of C_3A in the presence of $CaCl_2$ shows that $CaCl_2$ considerably retards the hydration of tricalcium aluminate; the thermal phenomena accompanying the hydration of $C_3A + CaCl_2$ can easily be recorded using the isothermal microcalorimeter (1).

Microcalorimetric experiments show that $CaCl_2$ reacts so fast with aluminoferrites that it is very difficult to analyse the effect of $CaCl_2$ on the hydration kinetics of C_4AF by this method. It should be remembered here that it is the second thermal phenomenon which reveals the retarding effect of $CaCl_2$ or $CaSO_4 \cdot$

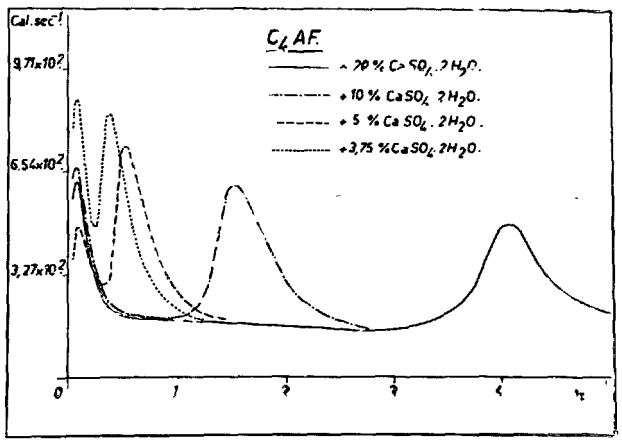

Fig. 5.

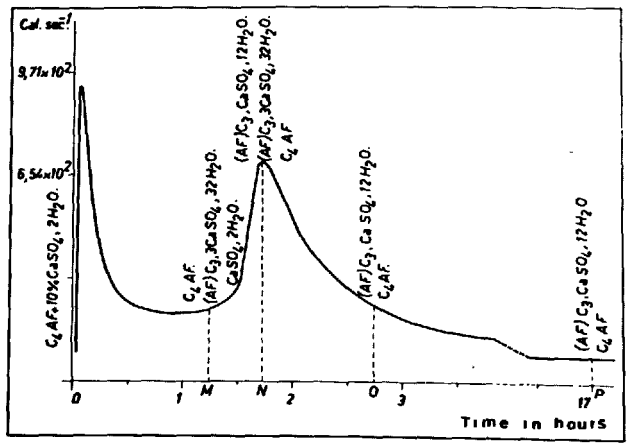

Fig. 6.

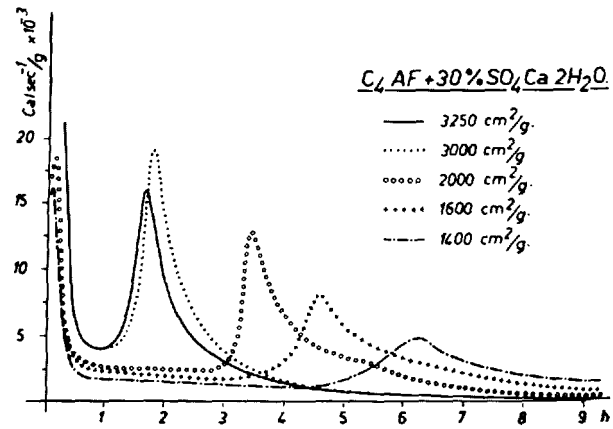

Fig. 7.

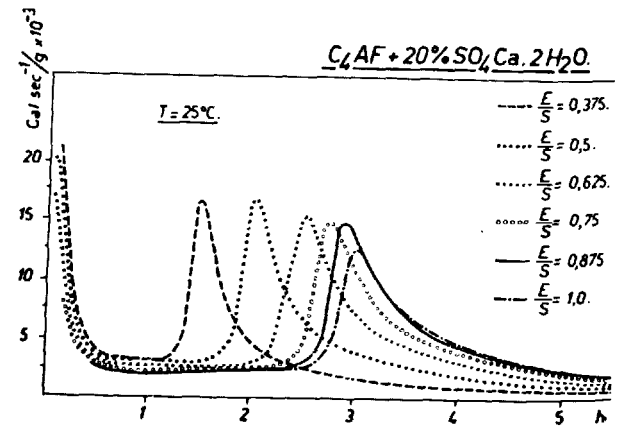

Fig. 8.

$2H_2O$. In the system $C_4AF + CaCl_2$, the $CaCl_2$ consumption is so rapid that practically only one thermal phenomenon is recorded.

A study of the system $C_4AF + CaCl_2$ has shown us that under certain conditions, the hydrate $C_3(AF) \cdot 3CaCl_2 \cdot 30H_2O$, rich in chlorine, is formed. But the trichloroaluminoferrite is easily converted into monochloroaluminoferrite. Fig. 9 shows a micrograph of $C_4AF + 20\%$ $CaCl_2$ after five minute hydration. Fig. 10 shows a micrograph of the same sample after one hour hydration.

In Fig. 9, needles of $C_3(AF) \cdot 3CaCl_2 \cdot 30H_2O$ are easily distinguished; $C_3(AF) \cdot 3CaCl_2 \cdot 30H_2O$ closely resembles ettringite, $C_3A \cdot 3CaSO_4 \cdot 32H_2O$. When the variation of $CaCl_2$ concentration is followed during the hydration of $C_4AF + 30\%$ $CaCl_2$, a rapid consumption of $CaCl_2$ with formation of trichloroaluminoferrites is observed (Fig. 11); afterwards the $CaCl_2$ consumption decreases.

This phenomenon is observed better when the hydration is carried out with D_2O; in fact, the replacement of H_2O by D_2O greatly reduces the rate of hydration and a plateau can easily be distinguished on the $CaCl_2$ consumption curve (Fig. 11).

When $CaCl_2$ is added to portland cement, the hydration of the ferrite phase of the cement is influenced by the simultaneous presence of calcium sulphate and calcium chloride; this is why the paste hydration of the ferrite phase in the presence of Cl^- and SO_4^{--} ions presents an obvious practical interest.

The thermograms in Fig. 12 illustrate the effect of various percentages of $CaCl_2$ on the hydration of a mixture of $C_4AF + 25\%$ $CaSO_4 \cdot 2H_2O$. It can be seen that $CaCl_2$ accelerates the appearance of the thermal phenomenon. When the $CaCl_2$ concentration reaches 5%, the second thermal phenomenon is doubled.

We have studied the progress of the hydration of the mixture $C_4AF + 25\%$ $CaSO_4 \cdot 2H_2O + 7.5\%$ $CaCl_2$ by stopping the hydration after the various times indicated on the thermogram of the sample. After

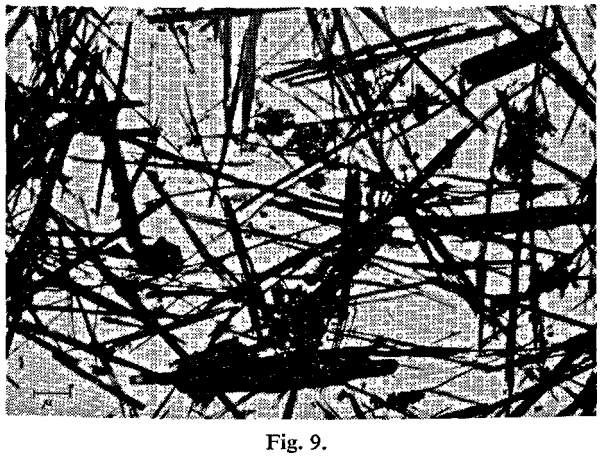

Fig. 9.

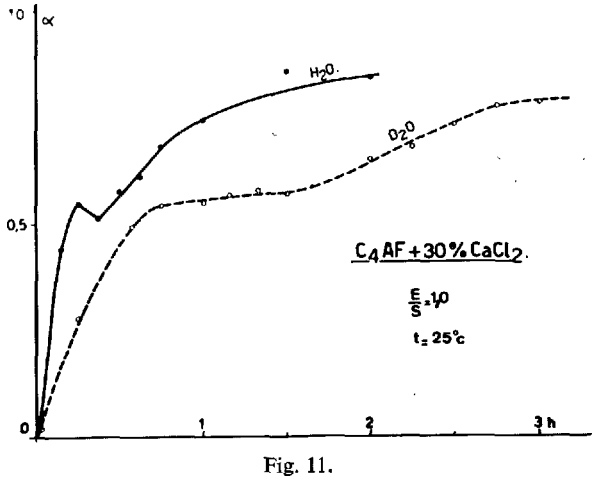

Fig. 11.

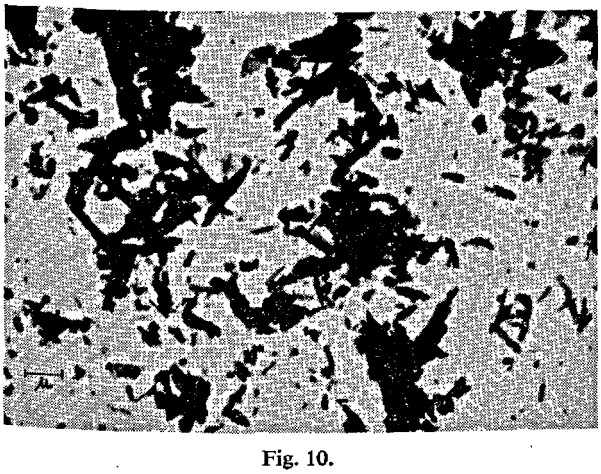

Fig. 10.

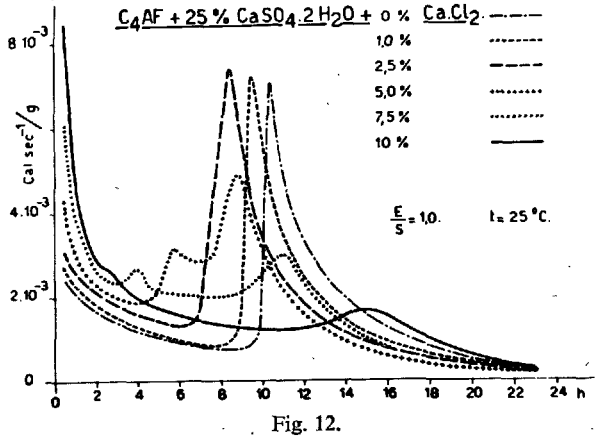

Fig. 12.

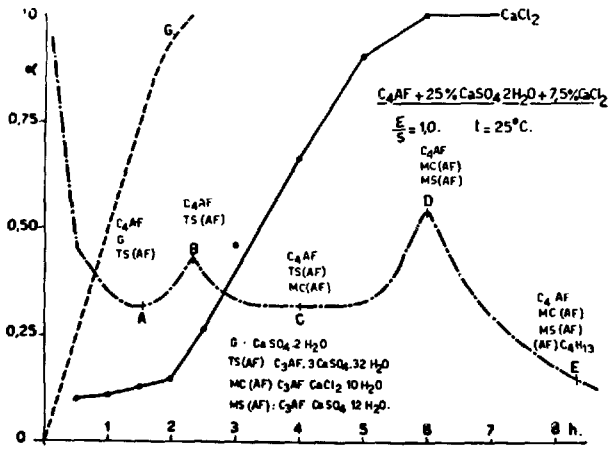

Fig. 13.

the hydration has been stopped, the sample undergoes chemical analysis and X-ray crystallography.

Fig. 13 shows all of our results. Using the results illustrated schematically in Fig. 13 as a basis, we can summarize the hydration process of C_4AF in the presence of Cl^- and SO_4^{--} ions as follows:

A. Between the first and second peaks: the gypsum reacts to give calcium trisulphoaluminoferrite. On the X-ray diagram of the sample at point A, the principal line of $C_3(AF)\cdot 3CaSO_4\cdot 32H_2O$ can be detected at 9.75 Å: the presence of $CaSO_4\cdot 2H_2O$ and anhydrous C_4AF is also confirmed by X-ray crystallography.

B. The gypsum consumption continues up to point B: the X-ray diagram of the sample at point B shows that all the gypsum has been consumed; between points A and B, there is an increase in intensity of the trisulphoaluminoferrite line which we shall designate by TS(AF). At the top of the second thermal phenomenon (point B), the gypsum has been completely used up. After the complete consumption of $CaSO_4\cdot 2H_2O$, the Cl^- ions begin to react to form calcium monochloroaluminoferrite.

C. In the system $C_3A + CaSO_4\cdot 2H_2O$ and $C_4AF + CaSO_4\cdot 2H_2O$, at the top of the second calorimetric peak (point B), when the gypsum has been used up, the hydrates rich in sulphate are converted into hydrates poor in sulphate; in other words, the trisulphated phases are converted into monosulphated phases. In the presence of Cl^- ions this transformation does not occur.

X-ray crystallography shows that at point C (between the second and third thermal phenomena) TS(AF) and MC(AF) are present. This observation supports our conclusions on the system $C_3A + CaCl_2 + CaSO_4\cdot 2H_2O + H_2O$ (1).

D. Between the second and third thermal phenomena (points B and D), $CaCl_2$ reacts to give monochloroaluminoferrite. At point D all the $CaCl_2$ has reacted and the TS(AF) begins to be converted into monosulphoaluminoferrite MS(AF).

E. When the $CaCl_2$ has reacted completely (point D), the hydration continues on account of the presence of anhydrous C_4AF; after point D the hydration of C_4AF gives hexagonal hydrates $(AF)C_4H_{13}$. This hydrate forms solid solutions with $C_3(AF)\cdot CaCl_2\cdot 10H_2O$ and $C_3(AF)CaSO_4\cdot 12H_2O$.

General Conclusions

Literature data tell us that aluminoferrites behave in a similar manner to calcium aluminates.

According to the work of Malquori and Caruso (5), there is a great similarity between $FC_3\cdot CaSO_4\cdot 12H_2O$ and $C_3A\cdot CaSO_4\cdot 12H_2O$.

In our work we have dealt with the hydration kinetics, using various means of investigation.

Our results on the hydration of the ferrite phase in the pure state show that the hydration rate increases from C_2F up to C_6A_2F.

As regards the nature of the hydrates, it is observed that, in the initial period of hydration, the hydrates are of hexagonal structure, but that under our experimental conditions the hexagonal hydrates (AC_2H_8, AC_4H_3) are unstable; they are converted into cubic hydrates (AC_3H_6); calcium hydroxide considerably slows down this transformation.

In the presence of $CaSO_4\cdot 2H_2O$, calcium trisulphoaluminoferrite $C_3(AF)\cdot 3CaSO_4\cdot 32H_2O$ is formed at the beginning of the hydration. After the gypsum has been used up, the trisulphate phase is converted into calcium monosulphoaluminoferrite $C_3(AF)\cdot CaSO_4\cdot 12H_2O$.

An inspection of our results on the hydration of the system $C_6A_xF_y + CaSO_4\cdot 2H_2O$ shows that there is a great similarity between the effect of gypsum on the ferrite phase and its role in the hydration of C_3A.

Our conclusions on the hydration of the ferrite phase are in agreement with the results of Chatterji and Jeffery (6, 7).

A study of the hydration mechanism of the system $C_4AF + CaSO_4\cdot 2H_2O + CaCl_2$ shows that the hydration process of this system is similar to that of C_3A in the presence of Cl^- and SO_4^{--} ions (1).

$CaCl_2$ accelerates the reaction between gypsum and C_4AF.

When C_4AF is hydrated in the presence of $CaCl_2$ and $CaSO_4 . 2H_2O$, the SO_4^{--} ions react first to give trisulphoaluminoferrite; during the consumption of SO_4^{--} ions the Cl^- ions do not react. The formation of monochloroaluminoferrite begins only after the complete consumption of SO_4^{--} ions.

The trisulphate phase (calcium trisulphoaluminoferrite) formed in the system $C_4AF + CaSO_4 \cdot 2H_2O + H_2O$ is converted into a monosulphate phase after the complete consumption of $CaSO_4 \cdot 2H_2O$. In the presence of $CaCl_2$ the trisulphate phase persists after the complete consumption of the gypsum, in other words the presence of $CaCl_2$ prevents the conversion of TS(AF) into MS(AF).

This phenomenon can be explained by the fact that it is above all the hydrated calcium aluminoferrites, $(AF)C_4H_{13}$ and $(AF)C_2H_8$, which react with the trisulphate phase to convert it into the monosulphate phase. When the aqueous phase contains Cl^- ions, the calcium aluminoferrites react with $CaCl_2$ to give hydrated chloroaluminoferrites, and as long as there are Cl^- ions in the liquid phase, the trisulphoaluminoferrite is not converted into monosulphoaluminoferrite.

In this work we have separated off the hydrated phase by using heavy liquids: the A/F ratio of the hydrates is different from the A/F ratio of the anhydrous aluminoferrite.

In the hydration of C_4AF, the phases hydrated under different conditions have an A/F ratio greater than 1. It, therefore, seems that only part of the iron is to be found in the hydrates; the rest may be in the form of ferric hydroxide.

We have investigated the influence of certain parameters on the hydration kinetics. Differential microcalorimetry has proved to be a useful method for determining the influence of various factors such as the E/S ratio, the grain size, etc, on the hydration of the ferrite phase.

We have seen above that C_4AF forms hexagonal hydrates after five minutes hydration.

Recently we have shown directly that these hexagonal platelets contain iron.

It is by means of an electron microprobe that one can demonstrate the presence of iron in the hexagonal platelets (8).

As a sample mount for the microprobe examination we used a single crystal of MgO.

It should be remembered that a study of the role of iron in the hydration of cements is of an obvious practical interest; indeed it is well known that cements rich in Fe_2O_3 are very resistant to agressive media (sea-water, water containing sulphates, etc.).

References

1. N. Tenoutasse, "The hydration of mechanism of C_3A and C_3S in the presence of calcium chloride and calcium sulphate", In: Vth Intern. Symp. Chemistry of Cement, Tokyo, 6–12 Oct. 1968.
2. N. Tenoutasse, "L'action du gypse sur l'hydration de la phase ferrite. Aspect cinétique", Rev. Mater. Construc. Trav. Publ. No. 614, 452–458, (nov. 1966).
3. W. L. De Keyser, "Differential thermobalance: a new research tool" Nature (London) **172**, 364 (1953).
4. W. L. De Keyser, R. Derie and A. Van Bemst "Application of differential thermogravimetry to the study of the hydration of cements", In: Highway Res. Board. Symp. on structure of Portland cement paste and concrete. Highway Res. Board, Special report 90, publ. 1389, 398–405 (1966).
5. J. Malquori and E. Caruso, Atti Congr. Intern. Chim. 10. Rome, **2**, (713) 1938.
6. S. Chatterji and J. W. Jeffery, "Studies of early stages of paste hydration of cement compounds I", J. Am. Ceram. Soc. **45**, No. 11, 536–543 (nov. 1962).
7. S. Chatterji and J. W. Jeffery, "Studies of early stages of paste hydration of cement compounds II", J. Am. Ceram. Soc. **46**, No. 4, 187–191 (apr. 1963).
8. N. Tenoutasse. Unpublished work.

Abbreviations

The following symbols are used:

$C = CaO$
$A = Al_2O_3$
$F = Fe_2O_3$
$S = SiO_2$

$\frac{E}{S} = \frac{\text{water}}{\text{solid}}$

$MCA = C_3A \cdot CaCl_2 \cdot 10H_2O$
$MC(AF) = C_3(AF) \cdot CaCl_2 \cdot 10H_2O$
$MS(AF) = C_3(AF) \cdot CaSO_4 \cdot 12H_2O$

$TS(AF) = C_3(AF) \cdot 3CaSO_4 \cdot 32H_2O$

$TC(AF) = C_3(AF) \cdot 3CaCl_2 \cdot 32H_2O$

This work is part of the research sponsered by the Centre National de Recherches Scientifiques et Techniques pour l'Industrie Cimentière (C. R. I. C.).

We thank M. A. De Donder and M. R. Smitz for their technical assistance.

Our thanks are also due to the Institut pour l'En couragement de la Recherche Scientifique dans l'Industrie et l'Agriculture (I.R.S.I.A.) for financial assistance.

SESSION II-5 HYDRATION OF PORTLAND CEMENT

Principal Paper Hydration of Porltand Cement

L. E. Copeland and D. L. Kantro*

Synopsis

Various factors influence the reactions of alite and belite in cement; temperature, water-cement ratio and composition are among these. Their effects on cement are comparable with their effects on the corresponding "pure" compounds.

The temperature data lead to activation energy results consistent with early age solution reaction processes and later age diffusion processes. The hydration factors are of two types, one involving the composition of the alite or belite phase itself and the nature of the polymorphic form and the other concerning the presence of other substances, i.e., C_3A, $CaSO_4 \cdot 2H_2O$ and $CaCl_2$.

These various factors also influence the composition of the hydration products of the "pure" phases. For example, the C/S ratio of C–S–H gel has been found to increase significantly with decreasing w_0/c ratio.

The presence of other substances such as sulfate ion in the hydrating system leads to the formation of substituted C–S–H gels.

The hydration of C_3A starts immediately upon contact with water. The products that form depend upon the composition of the solution phase. If sulfate ion and $Ca(OH)_2$ are present the first product is hexacalcium aluminate trisulfate. When the sulfate ion is depleted further hydration of C_3A produces tetracalcium aluminate sulfate. Thereafter the solid solution of monosulfate and tetracalcium aluminate is formed. The presence of the ferrite solid solution phases leads to substitution of F for A in all hydration products.

Sufficient sulfate ion is present in properly retarded cements to assure that the conversion of hexacalcium aluminate trisulfate to tetracalcium aluminate sulfate does not occur until after the paste has hardened.

Introduction

The hydration of portland cement consists of sets of simultaneous and consecutive chemical reactions that are practically impossible to investigate in detail if study is limited to the cement-water system. However much progress has been made by studying this complex cement-water system. One method of study has been to make the tacit assumption that cement is one component of a two component system and use an estimate of the "chemically bound" water (such as the non-evaporable water) or the heat of hydration as a measure of the amount of cement that has hydrated. Many characteristics of hardened neat cement pastes are closely related to the extent of hydration of the cement so deduced. It is also possible to identify most of the hydration products of cement without any knowledge of the hydration characteristics of the individual compounds that comprise cement, and most of the hydration products that normally occur had been so identified at the time of the Fourth International Symposium on the Chemistry of Cement.

The attempt to obtain more detailed information on hydration characteristics of the individual cement compounds was started long ago with studies of the hydration of each of the pure compounds individually. More recently the hydration of pure compounds under conditions like those that exist in the cement-water system have proven to be fruitful. The primary

*Portland Cement Association, Research and Development Laboratories, Skokie, Illinois, U.S.A.

purpose of this paper is to review pertinent information on the hydration of "pure" cement compounds, individually and in mixtures; to compare this information with information obtained from hydration of portland cement; and finally to describe a sequence of events in the early hydration reactions of cement that seems to be consistent with the experimental results and the interpretations of most researchers.

The Hydration of Silicate Phases of Portland Cement

The Consumption of Alite and Belite

Dependence on w_0/c

The disappearance of alite and belite in cement is conveniently observed by means of X-rays. Examples of the type of results obtained are given in the 1960 Symposium (1, 2). Since that time, other investigators (3, 4) have also employed the X-ray method.

Some of these authors (1, 4) have indicated the difficulty in obtaining good precision in the belite results because of the small amount of material in the cement. The difficulty is compounded if the belite line at 2.88 Å is used, as was pointed out by von Euw (5) a decade ago.

The X-ray analysis procedure for the silicate phases in cements and clinkers reported a few years ago (6) may be used with only minor modifications (7) for alite and more reliable belite analyses than is obtained from use of the 2.88 Å line of partly hydrated cement pastes.

Alite and belite data have recently been obtained for cement pastes hydrated under various conditions (7). The curves in Fig. 1 represent data obtained from an ordinary (ASTM Type I) cement hydrated at two different water-cement ratios. The curves show that the percentages of alite that had hydrated by 1 day are about the same at both water-cement ratios. The curves diverge from 1 day on, more alite hydrating at the higher water-cement ratio in a given time.

As can be seen from the data points on the figure, somewhat greater scatter occurs in the case of the belite. Nevertheless, the belite results have characteristics somewhat similar to those of alite. At 1 day the amount of belite hydrated is almost independent of water-cement ratio. The curves diverge thereafter, although, in contrast to the alite curves, they reconverge to some extent at later ages.

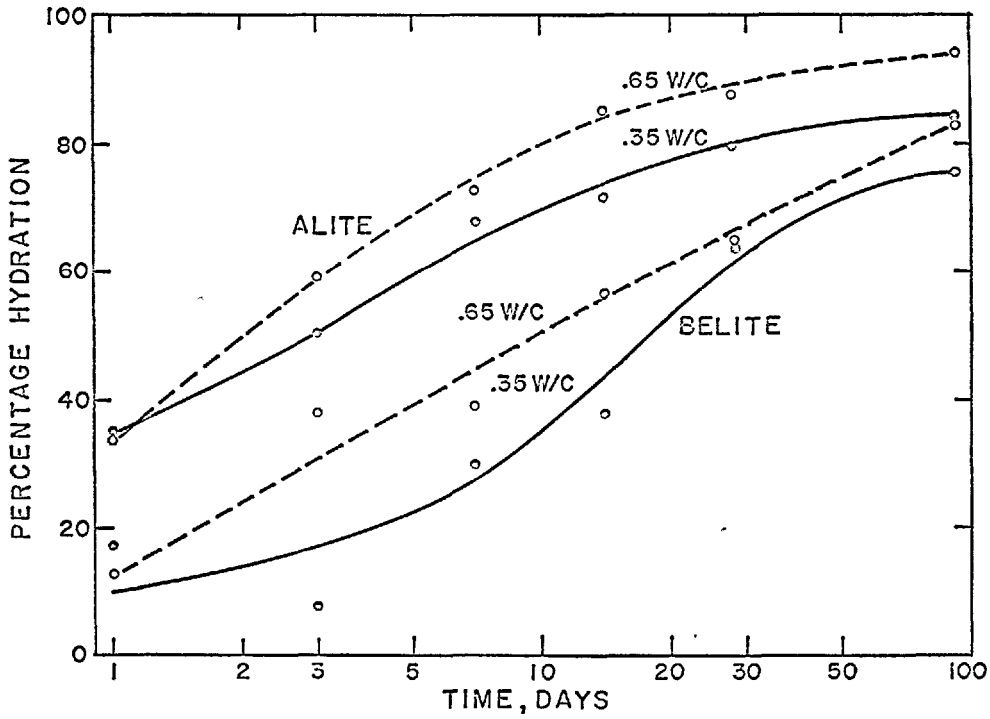

Fig. 1. *Alite and Belite hydration in an ordinary portland cement. (Initial alite, 57.8 percent; initial belite, 19.6 percent).*

The X-ray results in Fig. 1 indicate the same type of effect of water-cement ratio on cement hydration as do the fixed water data given previously (8).

The investigation of the hydration of C_3S and C_2S as a function of w_0/c-ratio has led to similar results (9, 10, 11). Thus, in general, it is found that more C_3S and C_2S hydrate in a given time, the higher the w_0/c ratio. However for ages up to 7 days, Locher finds that the degree of hydration of C_3S decreases with increasing w_0/c, above a value of .35 w_0/c, reaching a minimum at .80 w_0/c. We have found this same type of effect at shorter times but only in a lower w_0/c range, .20 to .35. Various factors, such as mixing conditions, fineness of C_3S, and sample size and shape may influence these earlier age results.

Alite and belite data were obtained for another oridinary portland cement hydrated at 3 different temperatures, 5, 25 and 50°C (7). The alite results are shown in Fig. 2. A very significant temperature influence can be seen, especially during the early stages of hydration, since the widest divergence in results occurs at the earliest age investigated, 12 hours. Nevertheless, the curves begin to converge significantly only after about 1 day. The rate of alite hydration at 50°C becomes very low after about 14 days of hydration.

These alite results may be compared with the results obtained for the hydration of pure C_3S at the same 3 temperatures (12). As can be seen in Fig. 3, the 5° results at early ages are lower than the results at 25 and 50°C; these latter two do not differ significantly. Furthermore, the percentage hydration from about 1 day on is independent of temperature over the entire range examined, the data for all pastes falling on the same curve within experimental error. Hence the rate of hydration is independent of temperature. Earlier results, by others, have indicated small regular temperature dependence (13) and small inverse temperature dependence (14).

The small or zero temperature dependence indicates a diffusion controlled hydration process (15). As is well known, diffusion controlled processes have low temperature coefficients of rate (16), and hence low activation energies.

Rates of hydration of alites in cement at different temperatures have been obtained from the data in Fig. 2. The apparent activation energies at 60 and 70 percent hydration were calculated from the ln R vs. 1/T plots shown in Fig. 4.

The value obtained at 60 percent hydration, 9.8

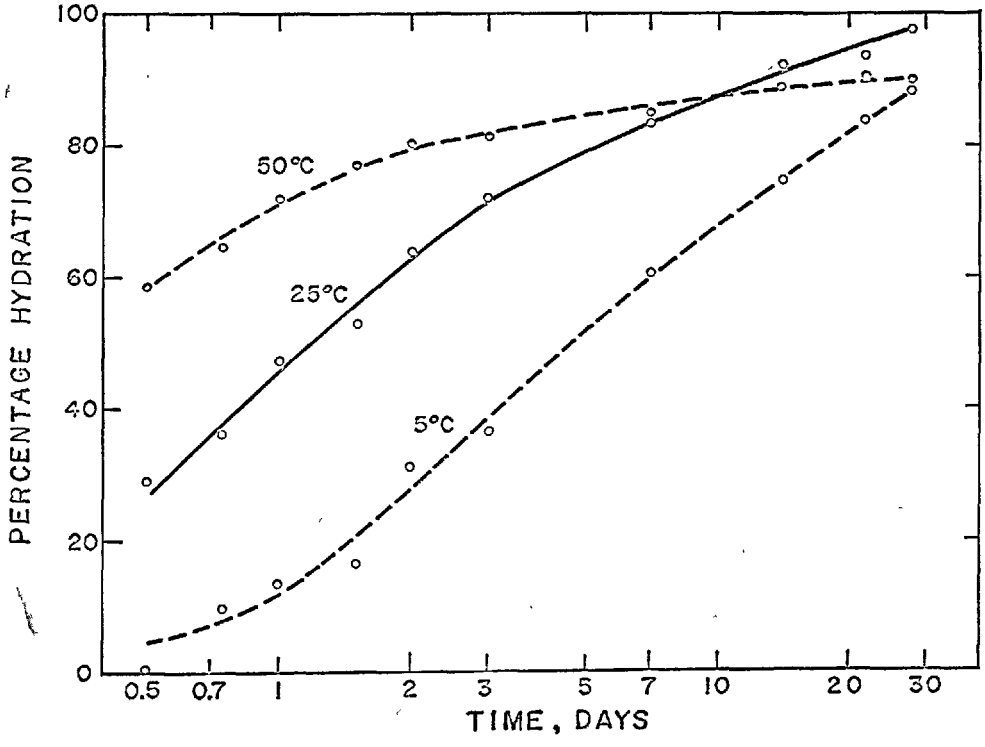

Fig. 2. *Alite hydration in an ordinary portland cement at different temperatures. (Initial alite, 50.0 percent, initial belite, 31.1 percent; $w_0/c = 0.57$.)*

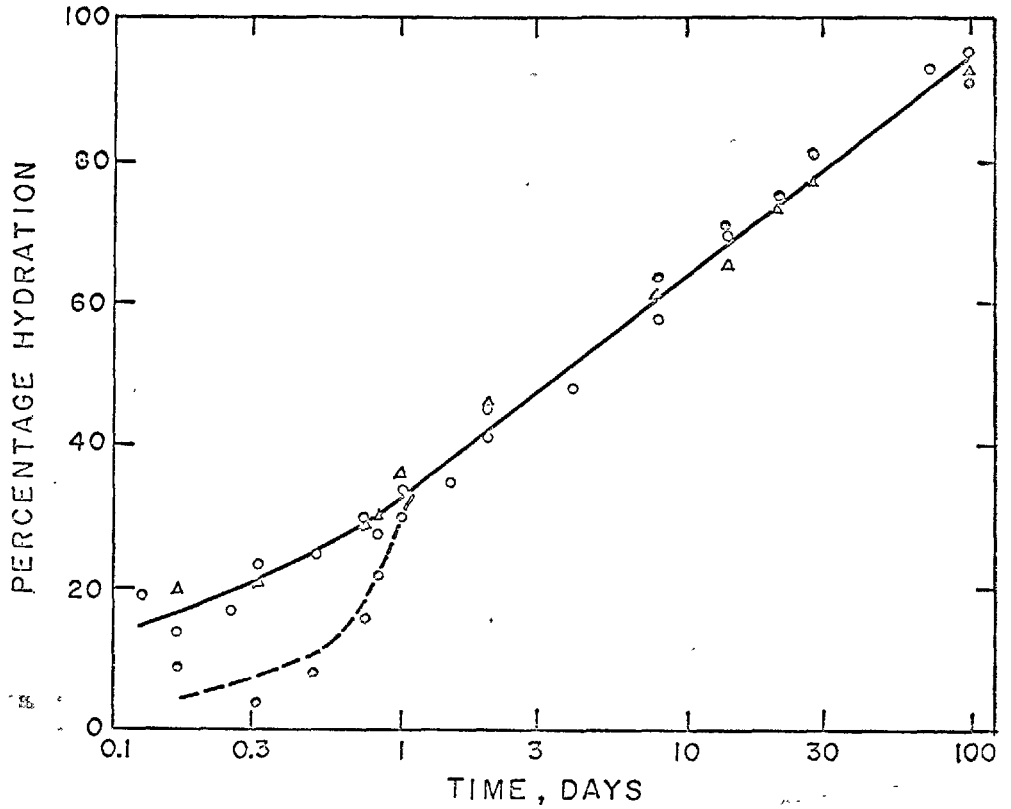

Fig. 3. *Hydration of* C_3S *at different temperatures* ($w_0/c = 0.70$; ●5°C; ○25°C; △50°C)

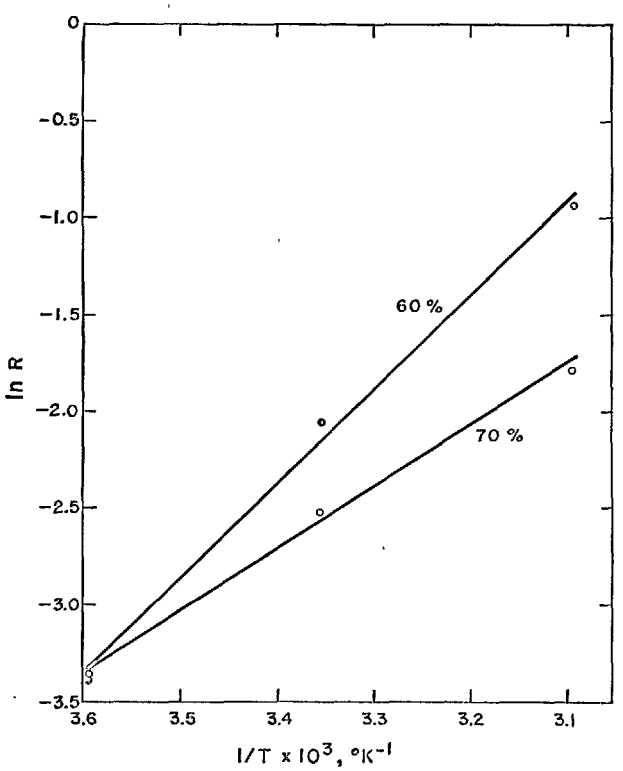

Fig. 4. *ln R vs 1/T plots, cement alite at 60 and 70 percent hydration.*

kcal/mol, is considerably higher than values attributed to diffusion processes (17), but is in the range of values given by Iler (18) for the acid and base catalyzed polymerization of silicic acid. The hydration of alite and belite to a calcium silicate hydrate gel also include silicate polymerization steps. As has been recently shown by Lentz (19) and by Funk and Frydrych (20) C_3S and C_2S both consist of orthosilicate ions; these same authors have shown that the calcium silicate hydrate consists of condensed silicate chains of various lengths, in agreement with Taylor's hypothesis (21).

The apparent activation energy of the cement alite at 70 percent hydration is 6.30 kcal/mol. The significant decrease in the apparent activation energy from 60 to 70 percent hydration indicates that the hydration process is becoming more and more diffusion-controlled.

Taplin (22) reports a value of 10 kcal/mol for portland cement paste. An apparent activation energy of about 9.3 kcal/mol was obtained for C_3S during its early stages of hydration from conduction calorimeter data (10). Taplin reports a value of 10 kcal/mol for one C_3S preparation.

A comparison of the C_3S results (Fig. 3) with those of alite (Fig. 2) suggests that the hydration of C_3S is probably diffusion-controlled by the time 25 percent hydration has occurred; while for alite, even at 60 percent hydration, the reaction may still be controlled primarily by the rate of polymerization of orthosilicate ions and diffusion has not yet become the rate determining step.

The belite results corresponding to the alite data of Fig. 2 are shown in Fig. 5. These results may be compared with similar data obtained for β–C_2S (B_2O_3-stabilized) (12), shown in Fig. 6. The two sets of curves do show some similarities, as contrasted to the alite and C_3S results. However a greater fraction of the belite in cement hydrates in a given time than of β–C_2S by itself, possibly simply because of the smaller amount of belite in cement, as compared to the relatively pure material. The cement belite hydration has a greater temperature dependence than the β–C_2S hydration. The apparent activation energies calculated at 40 percent hydration are 13.5 and 7.4 kcal/mol respectively for belite and β–C_2S. These values indicate that diffusion control occurs at lower extents of hydration in C_2S as compared to the belite in cement, just as it does in the case of C_3S as compared with cement alite.

Apparent activation energy values for different β–C_2S preparations examined by Taplin (22) were stated to be 18 kcal/mol and greater than 10 kcal/mol. These values were based on moisture loss data.

Dependence of Alite Hydration on Composition

The reactions of C_3S and alite are also influenced by the composition of the hydrating mixture. Three different types of composition variation may be considered: the presence of small amounts of other constituents in C_3S, making it an alite, the presence of other cement compounds, and the presence of other substances, such as gypsum or calcium chloride. Although the behavior of alite in cement is the principal concern of this section, C_3S is considered in some detail, because it serves as a convenient reference material with which to compare cement alite.

Tricalcium silicate has a number of polymorphic forms, stable in various temperature ranges (23). The presence of small amounts of foreign ions in the C_3S structure will stabilize one or another of these polymorphic forms at room temperature, as has been done by Woermann, Hahn and Eysel (24). Different polymorphic forms of alite in different portland cements were observed by Midgley, Fletcher and

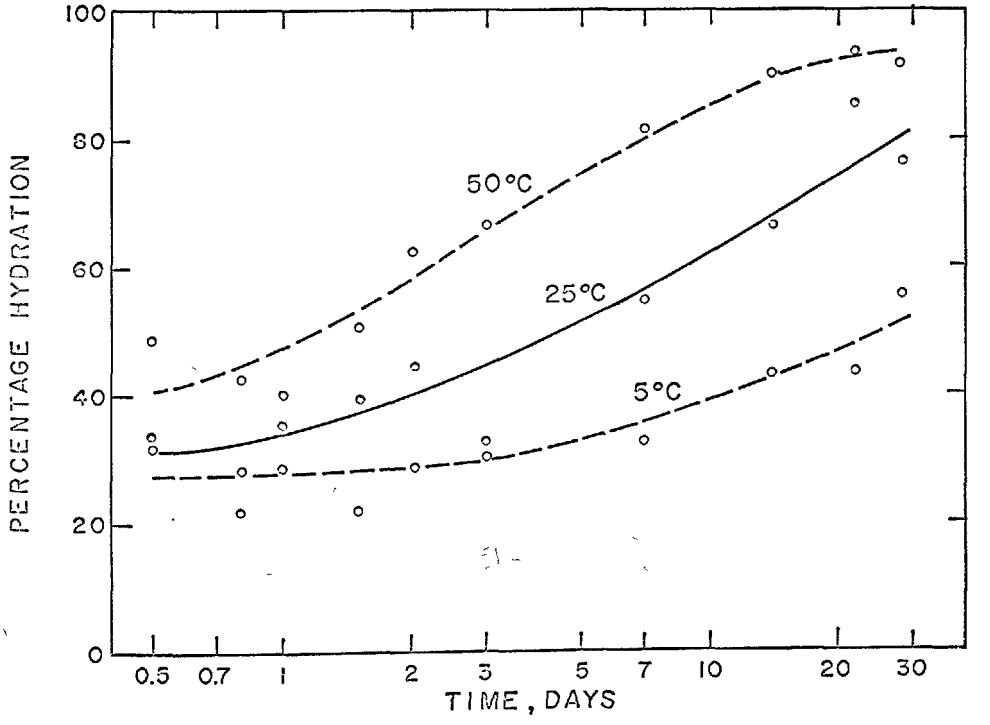

Fig. 5. *Belite hydration in an ordinary portland cement at different temperatures. (Initial alite, 50.0 percent; initial belite 31.1 percent; $w_0/c = 0.57$)*

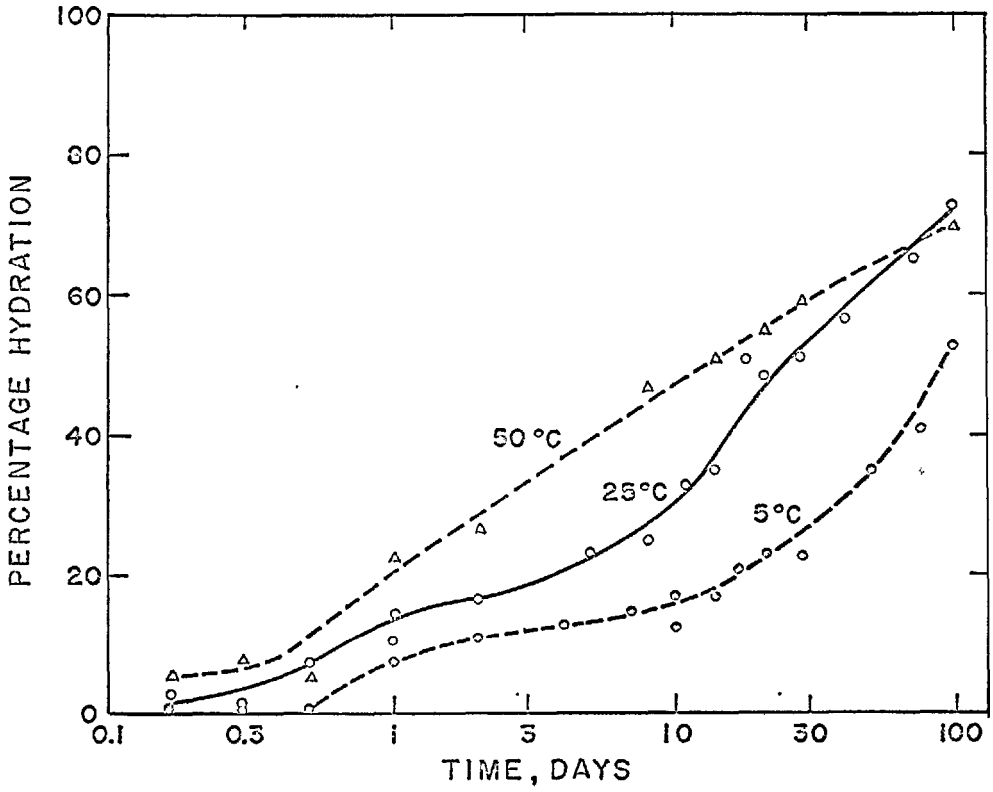

Fig. 6. *Hydration of β-C_2S at different temperatures.* ($w_0/c = 0.70$; ●5°C; ○25°C; △50°C)

Cooper (25) and by Ono, Uno and Kanai (26). With the knowledge that different alites can occur in different cements, the question immediately arises as to how the hydration characteristics of these alites differ. Differences can occur because of differences in crystal structure, differences in composition, or both. Yamaguchi, Shirasuka and Ota (27) have succeeded in obtaining alite of one composition, $C_{29.5}M_6S_{99}A$, in two polymorphic forms, triclinic and monoclinic. Pastes of each of these alite modifications were hydrated, and the alite residues at various ages were determined by X-rays. The results are given in Fig. 7. The results show that the monoclinic form hydrates slightly more rapidly between 5 hours and one day; thereafter, the two curves run approximately parallel. Nurse, Midgley, Gutt and Fletcher (28) used compressive strength as a measure of reactivity in an investigation of the various polymorphic forms of C_3S. These forms were obtained by inclusion of MgO, F, MnO, and a combination of MnO + F in various amounts in the alite. The results for preparations including only magnesia are in general agreement with those of Yamaguchi and his coworkers, showing a slight increase in strength from the lowest symmetry form

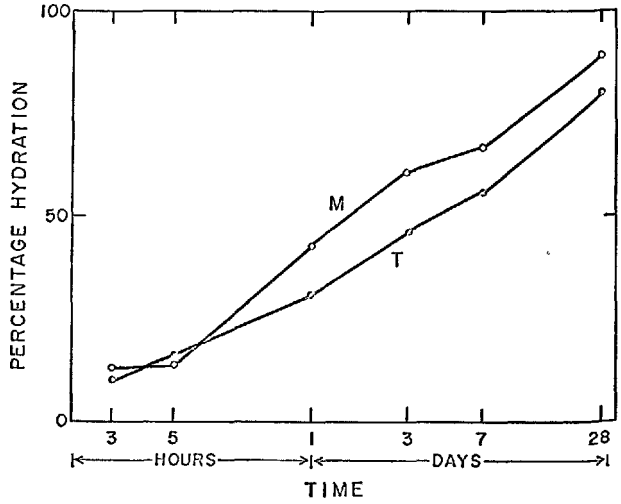

Fig. 7. *Hydration of different alite polymorphs.* (*M = Monoclinic, T = Triclinic*) (*ref. 27*)

(triclinic) to the highest (monoclinic). The alites containing fluorine did not show any clear-cut relationship.

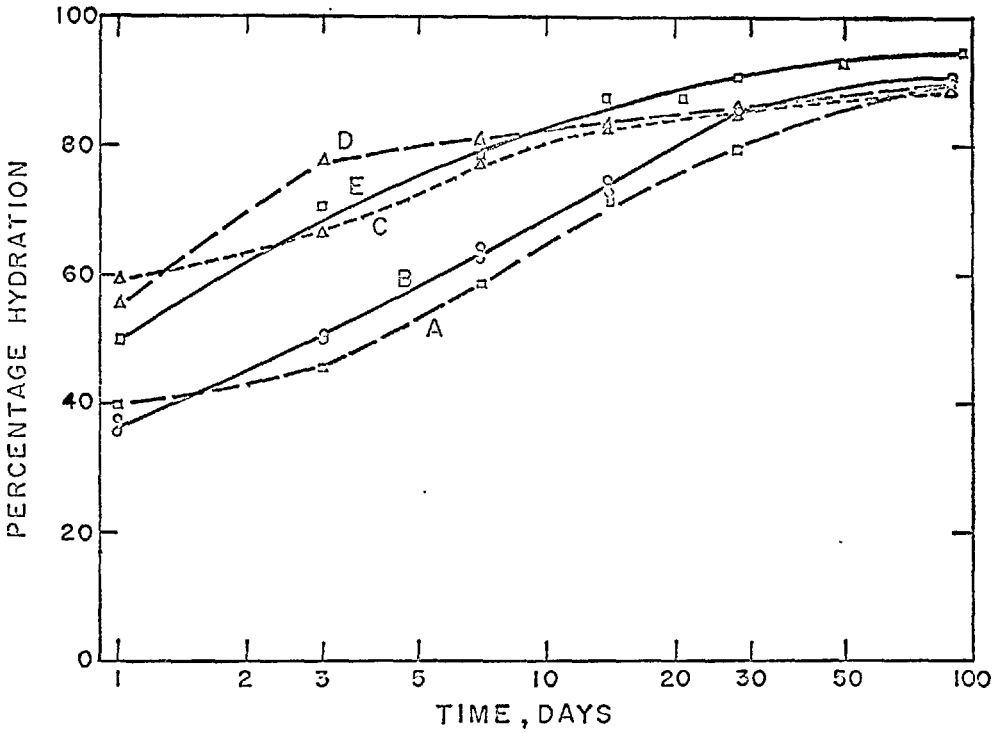

Fig. 8. *Hydration of alite and* C_3S. ($w_0/c = 0.45$; *high-speed blender mixing;* A ■ C_3S; B, ○ *triclinic alite and* ● *monoclinic alite;* C, △ *alite* +*2.3 percent* C_3A; D, ▲ *alite* +*4.5 percent* C_3A; E, □ *cement LTS-11 [57.1 percent alite and 8.3 percent* C_3A])

The presence of other compounds along with alite in pastes can have a significant effect on the hydration characteristics. Alites containing small amounts of free C_3A have been hydrated and the alite residues at various times determined by X-rays (29). The results are shown in Fig. 8. Also included in this figure are results for C_3S, a triclinic alite (9), a monoclinic alite, all of which are C_3A-free, and a normal portland cement. The triclinic alite contains 1 percent Al_2O_3 and 0.3 percent MgO; the monoclinic alite contains 1 percent Al_2O_3 and 1 percent MgO.

The curves A and B in Fig. 8 indicate the same kind of differences Nurse, Midgley, Gutt and Fletcher found.

Curve A represents the case of a pure C_3S, which is triclinic, T_I in the nomenclature of Woermann, Hahn and Eysel (24). Curve B is the composite of data from a triclinic alite, T_{II}, and a monoclinic alite which was prepared from the triclinic alite by reburning with additional MgO. These two alites behave alike. Effects that may have been caused by differences in their structures must therefore be compensated for by effects due to differences in their composition. It seems probable that the difference between curves A and B is caused by the difference in alumina of the corresponding materials, 0.1 percent in C_3S and 0.9 percent in each of the alites. The higher reactivity of the monoclinic alite reported by Yamaguchi, Shirasuka and Ota (27) may be attributed to the fact that the companion triclinic form was the stable phase at the hydration temperature.

The two alites represented by curves C and D both contain 1 percent Al_2O_3. One (curve C) contains 0.7 percent MgO and the other (curve D) 1 percent MgO. This latter alite is almost identical in composition to the monoclinic alite of curve B. The alite in cement LTS-11 is also monoclinic. In all cases in which free C_3A is present, as can be seen from the curves, a significant increase in the rate of hydration occurs during the first day of hydration, the rate then remaining higher even beyond the second day for the two highest C_3A cases (curves D and E).

The accelerating action of gypsum on alite hydration has been deduced from heat liberation data (8) and from DTA data such as has been reported by Raccanelli (30). The latter finds alite hydration in

cement is accelerated by either gypsum or alkali sulfate, but the acceleration is independent of sulfate concentration. He does find, however, that the duration of the acceleration is proportional to the alkali sulfate concentration.

A normal portland cement clinker hydrated with various gypsum additions was subjected to X-ray analysis (7). Some of the results are shown in Fig. 9. There is an indication from these data that there is an "optimum" gypsum level for maximum rate of hydration of alite in cement. This effect is particularly noticeable in the 1 and 3 day hydration curves. By 7 days the "optimum" value, if one exists, is below 1 percent SO_3. It appears from these results that the "optimum" value decreases with time of hydration. The accelerating effect of the gypsum is rather small however, and in fact, with larger gypsum additions, a significant retarding action occurs.

A number of investigators have examined the influence of gypsum on C_3S hydration. Kurczyk and Schwiete (31) conclude on the basis of free lime results that gypsum admixtures up to 4 percent by weight have no effect on the hydration kinetics of C_3S. Celani, Collepardi and Rio (32) conclude, also from free lime data, that gypsum does accelerate C_3S hydration, but only during the first day.

Pastes of C_3S with different amounts of admixed gypsum were analyzed by X-rays for unhydrated C_3S residues after various hydration times (10). A significant acceleration occurred even with the lowest amount of gypsum added, 0.7 percent as SO_3, as can be seen in Fig. 10. There was some evidence for an "optimum" effect, but the variation was rather small over the entire range of amounts added, 0.7 to 3.0 percent as SO_3. The C_3S with added SO_3 hydrates at about the same rate as the alite in a properly retarded cement.

The accelerating action of $CaCl_2$ on cement hydration is well known. Kurczyk and Schwiete (31) found, by an X-ray method, that at a time when 68 percent of C_3S in a paste had hydrated, 96 percent had hydrated in a paste also containing 2 percent $CaCl_2$. Results of a similar nature were obtained by Celani, Collepardi and Rio (32).

Alite analyses have been made on hydrated pastes of 3 widely differing cements, one a normal cement, one a white cement, and one a nominal zero-C_3A cement (33). The results are shown in Fig. 11. The curves for the alites of these cements all follow approximately the same paths. However, the shape of curve

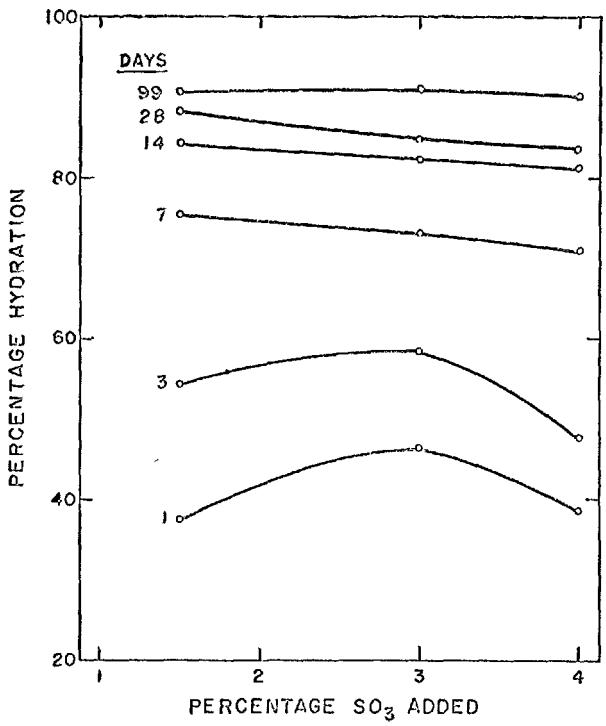

Fig. 9. *Hydration of cement alite in the presence of gypsum.* ($w_0/c = 0.45$; *low frequency vibration mixing*)

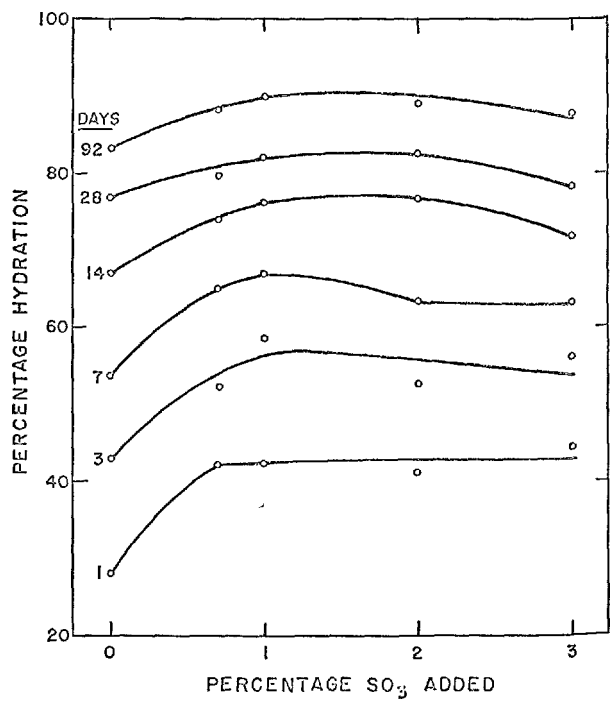

Fig. 10. *Hydration of* C_3S *in the presence of gypsum.* ($w_0/c = 0.45$; *low frequency vibration mixing*)

C, for the zero C_3A-cement is slightly different from those of A and B.

Dependence of Belite Hydration on Composition

Dicalcium silicate is a polymorphic material; four different forms are known (34, 35). Of these four forms, α, α', β and γ the first and last are considered to be nonhydraulic (36, 37) although Yamaguchi, Ono, Kawamura and Soda (38) have reported strength development of mortars made with α–C_2S.

The normal belite phase in portland cement consists of the β–modification. The α'–modification has been reported to occur also, but this could be the alkali silicate $KC_{23}S_{12}$. Both Nurse and Midgley indicate that $KC_{23}S_{12}$ is a potassium stabilized α'–C_2S.

It has not been possible to compare hydration characteristics of different polymorphs of C_2S having the same composition. However, some investigations of the effect of belite composition including more than one polymorph have been carried out (38, 39).

Yamaguchi, Ono, Kawamura and Soda (38) investigating mortars made with the α, α' and β-forms, observed that there was little difference in strengths between mortars of α' and β forms, but found that mortars of the α-form gave much more strength. Strength results, however, do not give a good indication of the hydration characteristics of the anhydrous materials because of the influence of other factors, such as the composition and morphology of the hydration product.

Kryzhanovskaya, Mirak'yan, Shokotova and Kholodnyi (39) investigating the bound water content as a function of time for pastes of $KC_{23}S_{12}$ and β–C_2S found little difference in the hydration characteristics of these two materials.

The results reported with regard to similarity in hydration characteristics of $KC_{23}S_{12}$ and β–C_2S are rather surprising in view of the significant influence that the composition of β–C_2S has on its hydration properties (28, 34). Results of X-ray analyses have been obtained for paste series of β–C_2S preparations stabilized in different ways (29). Among these preparations were a β–C_2S stabilized with 0.8 percent SO_3, added as $CaSO_4$, as described by Funk (40), a β–C_2S stabilized with 1.9 percent Al_2O_3 and 0.9 percent MgO (41), and two stabilized in the conventional way with B_2O_3, one containing 0.5 percent and the other 0.8 percent. The results of the X-ray analyses are shown in Fig. 12. These results show that all the C_2S

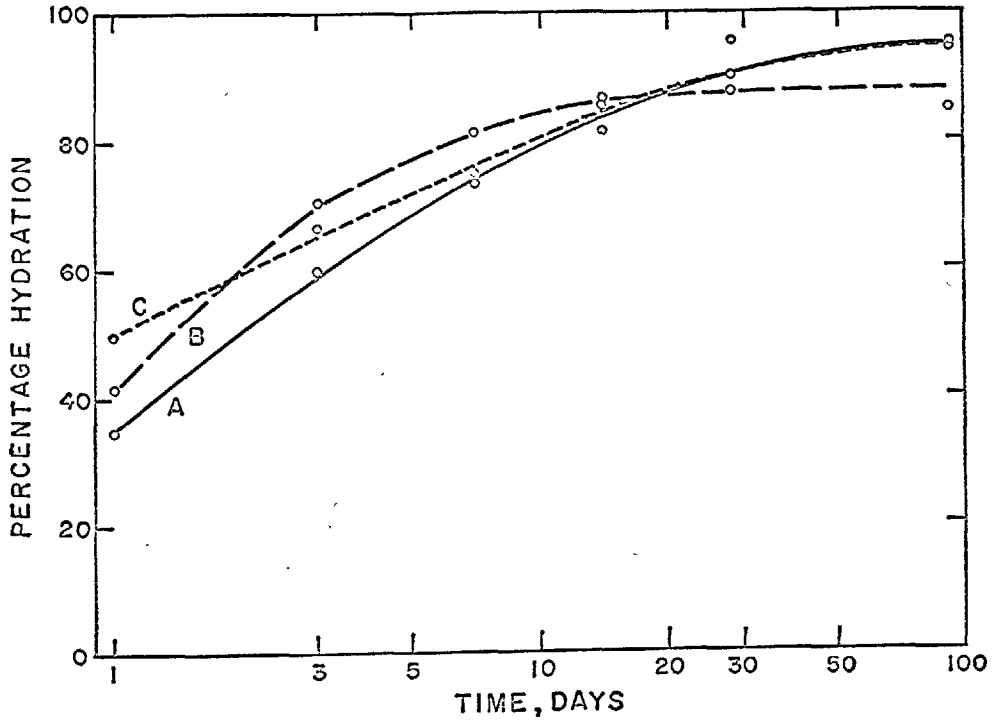

Fig. 11. *Hydration of alites in different cements.* ($w_0/c = 0.65$; A, *normal cement, 57.8 percent alite;* B, *white cement, 50.8 percent alite;* C, *zero-C_3A cement, 67.2 percent alite*)

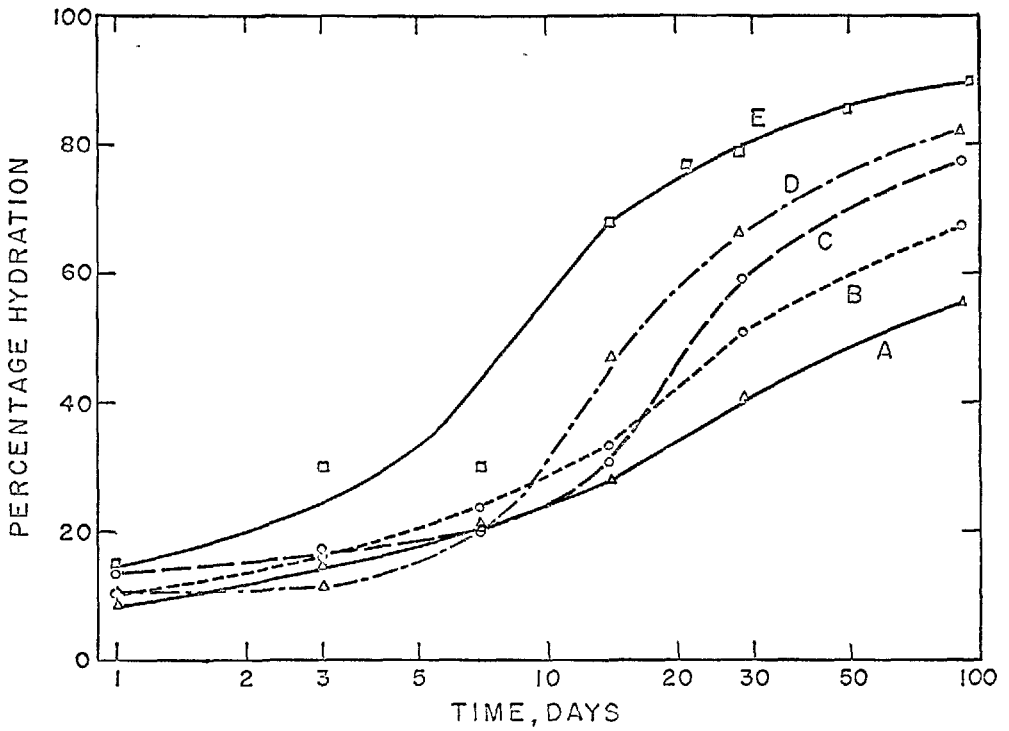

Fig. 12. *Hydration of different* β-C_2S *preparations and of cement belite.* ($w_0/c = 0.45$; A, △ *0.8 percent* B_2O_3; B, ● *0.5 percent* B_2O_3; C, ○ *1.9 percent* Al_2O_3 + *0.9 percent* MgO; D, ▲ *0.8 percent* SO_3; E, □ *cement belite, LTS-11*)

preparations hydrate to about the same extent during the first week of hydration. Thereafter, the influence of the stabilizer becomes apparent. The B_2O_3–stabilized preparations (curves A and B) hydrate to a lesser extent at later ages, the highest B_2O_3 content material (curve A) hydrating the least. The Al_2O_3–MgO and SO_3–containing materials (curves C and D) react to a greater extent than do the B_2O_3–containing materials, but still do not demonstrate the reactivity of belite in an ordinary portland cement (curve E). Although the Al_2O_3–MgO stabilized C_2S was made in an attempt to reproduce a cement belite, it is likely that either there is still some difference in the compositions of these two, or the cement belite is influenced by the presence of some other substance, such as sulfate of C_3A. As an example of a composition variation, the cement belite may have a somewhat higher Al_2O_3 content, and possibly some iron as well (34).

Belite results in cement were obtained which are analogous to the alite results in Fig. 9 (7). A slight "optimum" effect was observed at all ages for the paste series with 1.5 percent SO_3 added. The curves for 3 and 4 percent SO_3 additions were almost alike and higher additions resulted in a marked decrease in belite hydration.

Belite hydration is also accelerated by $CaCl_2$. Kurczyk and Schwiete report 48 percent hydration of β–C_2S as compared with 82 percent hydration when 2 percent $CaCl_2$ was present. Funk (42) had previously reported complete hydration of β–C_2S in 30–40 days in the presence of 15 percent $CaCl_2$. This result may be compared with hydration times for pure β–C_2S greater than 1 year, even in an excess of water (43).

Belite results analogous to the alite results in Fig. 11 have also been obtained (33) and are shown in Fig. 13. The belite in the white cement appears to be less reactive than the belites in the other two cements. Because of the absence of iron in the white cement, the composition of the belite may be slightly different from its compositions in the other two cements. It is also possible that the amount of belite present has some relationship to the behavior. Not enough data is available at the present time to allow any definite conclusions to be made.

The Alite and Belite Hydration Products

The Calcium Silicate Hydrate Phase

The hydration products of portland cement consist

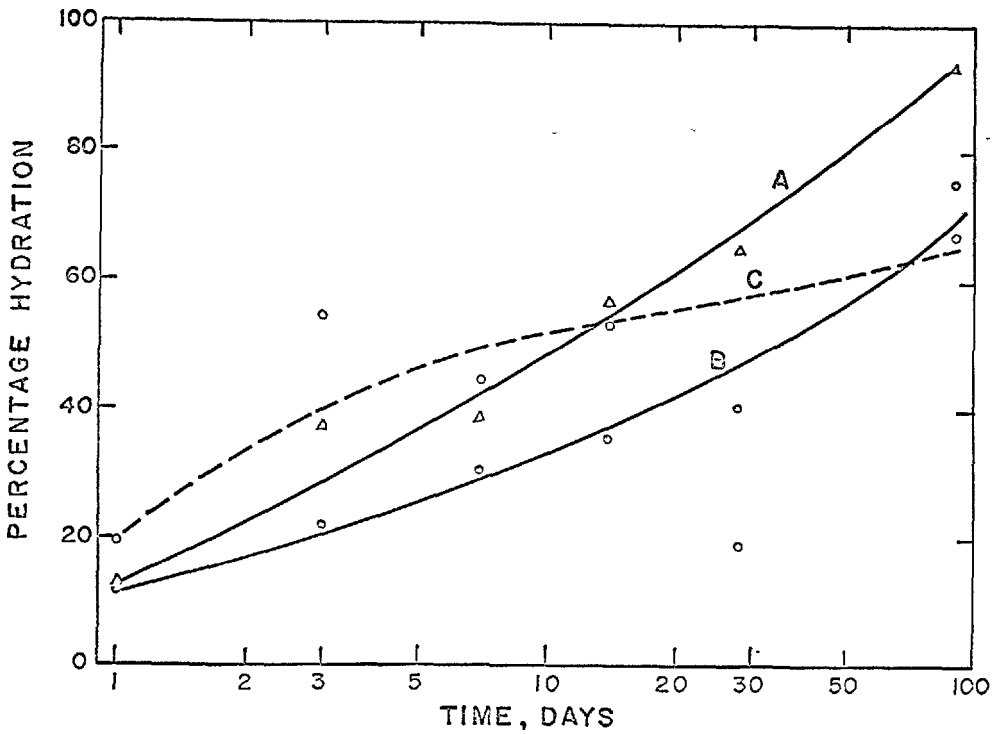

Fig. 13. *Hydration of Belites in different cements.* ($w_0/c = 0.65$; A, △ *normal cement, 19.5 percent belite;* B, ● *white cement 40.0 percent belite,* C, ○ *zero-*C_3A *cement, 13.7 percent belite*)

of two types of materials—substances that are relatively well-crystallized, such as calcium hydroxide and ettringite, and a substance that is poorly crystallized, namely a calcium silicate hydrate gel. For some years, this calcium silicate hydrate has been called variously tobermorite, tobermorite (G) and tobermorite gel. The tobermorite designation was applied because of some similarity of this material to the well-crystallized natural mineral of the same name. The primary similarity is in the X-ray diffraction diagram. Three broad peaks are obtained for the calcium silicate hydration product, these peaks corresponding approximately in d-spacing to three strong natural mineral tobermorite X-ray peaks. In this respect the calcium silicate hydrate resembles tobermorite more than it does any other calcium silicate hydrate.

On the other hand, the composition of the calcium silicate hydrate gel is quite different from that of natural mineral tobermorite, or even of hydrothermally prepared tobermorite (21). In order to distinguish between the product of paste hydration of tricalcium, dicalcium silicate, alite, or belite on the one hand, and any other calcium silicate hydrate on the other, the poorly crystallized calcium silicate hydrate gel which is the product of the paste hydration is here designated C–S–H gel.

Of primary importance in the present discussion is the composition of the C–S–H gel that is produced by the hydration of portland cement. Unfortunately, because of the complexities of the system little is known about this composition, except by analogy with the products of hydration of C_3S and β–C_2S.

The Determination of the Composition of C–S–H Gel

Various investigations have been carried out in recent years on the composition of C–S–H gel. Even in the case of the hydration of the "pure" calcium silicates, the determination of the composition of the calcium silicate hydrate gel presents certain difficulties. No method has yet been devised that will permit direct determination of the C/S and H/S ratios of this gel. It is therefore necessary to determine all of the other constituents in the system, and obtain the composition and amount of the calcium silicate hydrate gel by difference (44). To obtain the difference requires determination of the unhydrated residue and the calcium hydroxide content of the material. Several methods have been used to determine the calcium hydroxide content (15, 43). Three such methods may be considered. These are chemical extraction using ethyl

acetoacetate, X-ray analysis, and thermogravimetric analysis. The chemical extraction method gives higher results than the other two, both of which give about the same result (43).

Two different points of view have been expressed in explanation of this phenomenon (15, 21, 43, 45). One is that the lime not detected by X-rays is lime which is chemically extracted from lime-rich regions of the C–S–H gel. The other is that some amorphous lime is present, which cannot be detected by X-rays and which consequently would not give a sharp step in the thermal weight loss curves. One explanation for the formation of amorphous lime was given by Grudemo (46). More recently Locher (11) reported results obtained on free lime contents of hydrated C_3S pastes by both chemical and thermogravimetric methods. His observed difference in $Ca(OH)_2$ values, in terms of moles $Ca(OH)_2$ per mole SiO_2, appeared to be nearly independent of the C/S ratio of the C–S–H gel. If both the firmly bound lime and the labile lime were associated with the silica in a given C–S–H gel, one might expect from spatial considerations that if an increase in firmly bound lime occurred, a corresponding decrease in labile lime could occur. If, however, the lime were amorphous and not associated with the gel, no relationship would need to exist between its amount and the C/S ratio of the gel.

In further discussion of gel compositions, values based on chemical lime determination will be considered.

Influence of Time, Temperature and w_0/c on Composition of the C–S–H Gel

Investigations in recent years have shown that various paste hydration conditions, such as time, temperature, water-solids ratio and presence of other substances can affect the composition of the C–S–H gel hydration product.

The effect of time on the hydration of C_3S and C_2S has been examined for pastes hydrated at .70 w_0/c at three different temperatures (12, 44) for periods from 1/2 hour to 400 days. The results indicated that both C_3S and β–C_2S formed initial hydration products with C/S-ratios near those of the original anhydrous compounds. These C/S-ratios decreased during the early stages of hydration. In the case of C_3S, the initial decrease was rapid, and was followed by a slow decrease during the remainder of the hydration reaction. In the case of C_2S, the early age decrease was also rapid; however it was followed by a slower rise during the remainder of the hydration (9).

The influence of temperature on the C/S-ratio of the C–S–H gel formed by hydration of C_3S appears to be negligible over the temperature range examined. The lowest C/S-ratios were obtained for pastes hydrated at 25°C; pastes hydrated at either 5 or 50°C gave slightly higher values.

In the case of C_2S pastes, there appeared to be a correlation of C/S-ratio with hydration temperature, the value of the C/S-ratio increasing with increasing temperature, as had been observed previously (40) (43).

The influence of w_0/c on the composition of the hydration product is significant. Investigations by Locher (11, 45), Sudoh and Mori (47) and by the present authors and their coworkers (9, 10) have yielded results in quite good agreement. It is found that as the w_0/c-ratio is decreased the C/S-ratio increases. Over the entire range of w_0/c-ratios covered by these various investigators, 2.00 to 0.20, the C/S-ratio was found to vary from about 1.3 to 2.3. It was also found that C_3S pastes below a certain w_0/c value, about 0.45, showed a slight increase in C/S-ratio with time at later ages. One set of results is shown in the upper curve in Fig. 14 (10). The data points represent average values obtained from pastes hydrated 6 months or more. All of these pastes were hydrated more than 60 percent, a time beyond which any further increase in C/S at a given w_0/c is negligible.

The H/S values associated with the C–S–H gel are

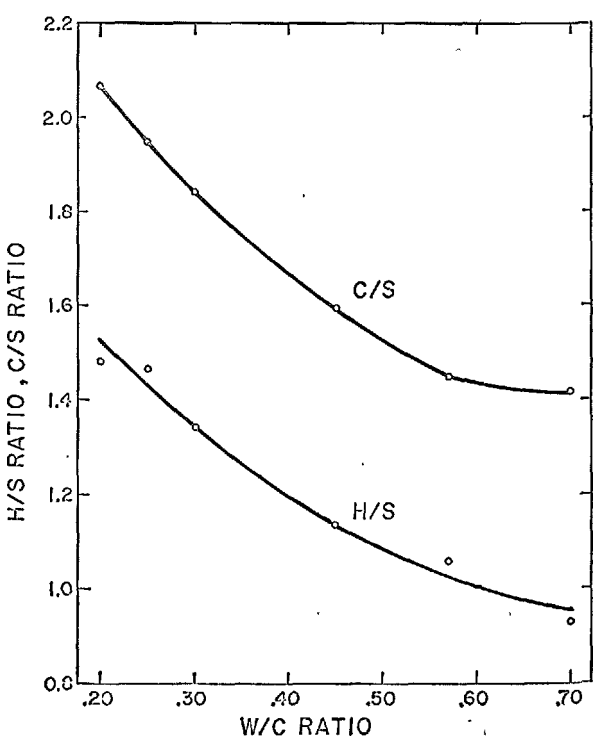

Fig. 14. *Influence of* w_0/c *on* C–S–H *gel composition*

first of all related to the extent to which moisture has been removed from the paste at the end of the hydration period. Various methods of drying have been used. In the investigation of C_3S and C_2S pastes, one method has been to remove water with the aid of organic agents such as cyclohexanol followed by drying in CO_2-free air (11). Another has been vacuum drying, the so-called "D-drying" (9, 15). These two methods lead to results not too different from one another, as is indicated by the fact that the amounts of water retained, after drying, by fully hydrated C_3S pastes were found to be about the same by both methods.

The H/S ratios calculated for a given paste are obtained from loss on ignition data (1000–1050°C) corrected for the water in the free $Ca(OH)_2$ and for the CO_2 present. For well-hydrated systems, it has been found that the H/S ratio is about 0.5 mole/mole SiO_2 less than the C/S ratio, as is shown in Fig. 14. This indicates that the composition of C–S–H gel varies as calcium hydroxide enters or leaves it. The general composition of C–S–H gel in well-hydrated systems may, as a first approximation, be represented by the expression.

$$C_xSH_{x-0.5}$$

where x is the C/S ratio. However, another type of H/S variation has also been observed, which depends on time. The above expression may therefore be modified to

$$C_xSH_{x-0.5+y}$$

where y is the difference in H/S-ratio between the experimental value and that estimated from the C/S-ratio. Results on the hydration of C_3S (11, 44) and C_2S (44) have shown that values of y are negative during the early stages of hydration. In the case of C_2S at 5°C, the value of y at the earliest stages of hydration was almost $-(x - 0.5)$, that is, the net H/S ratio was nearly zero. A similar observation was reported by Kawada and Nemoto (48). As hydration progresses, the value of y increases, finally becoming slightly positive, of the order of 0.1 moles H_2O/mole SiO_2. Upon reaching this value, y remains approximately constant.

Substituted C–S–H Gels

The above discussion has dealt with "pure" C_3S and C_2S. Some analogy may be drawn to the behavior of alite and belite in cement. Turriziani, Rio and Collepardi (49) found some similarities regarding free-lime formation in clinker and C_3S. It is well-known that a C–S–H gel also forms by hydration of cement, this gel having properties similar in many respects to those of the gel formed by C_3S or C_2S hydration. The gel formation in cement is probably controlled to a significant extent by the same factors operating in C_3S and C_2S pastes. However, other variables exist in the cement system, these being related to the presence of other substances—gypsum, other cement compounds, alkali. Furthermore, the alite and belite phases contain small amounts of other substances—Al_2O_3, Fe_2O_3, MgO, K_2O, in solid solution, which may have an important bearing on their behavior.

The composition and properties of the hydration products are more important in the following discussions than are the influences of these various "impurities" upon the hydration characteristics of C_3S and C_2S. In the past few years, work by a number of investigators has shown that substances such as alumina or calcium sulfate could enter the calcium silicate hydrate structure chemically without destroying the identity of the gel. Kalousek (50) prepared samples of tobermorite hydrothermally containing as much as 6.5 percent Al_2O_3. His results indicated that the alumina substituted for silica in the structure. In addition Kalousek suggested that this type of substitution is possible in the products of hydration of cement at ordinary temperatures. A similar hydrothermal investigation was also carried out by Diamond, White and Dolch (51), in which such products containing iron or magnesium were also prepared. Kurczyk and Schwiete (31) and Celani, Collepardi and Rio (32) found that when C_3S was hydrated with added gypsum, a morphologically altered hydration product resulted. The latter investigators also observed that the sulfate in the paste present as gypsum was less after a period of hydration than the amount added initially. They concluded that some of the sulfate had entered the C–S–H gel lattice.

Recently a study was made of the reaction products of hydrated C_3S pastes with C_3A, C_2F and $CaSO_4 \cdot 2H_2O$ (52). Substituted C–S–H gels were produced in all cases, as was indicated from X-ray analysis and electron microscopic examination.

The substitution of other species for silica or for lime in the C–S–H gel lattice is not, strictly speaking, an isomorphous substitution, inasmuch as slight structural changes must occur because of valence differences between the substituent species and the normally present species. Furthermore, these reactions may easily be considered as addition reactions, since, for example, silica is not released in the reaction between C–S–H gel and calcium sulfate; the entry of the sulfate into the lattice is essentially a structural

Fig. 15. C_3S *paste after agitation in water 3 months.*

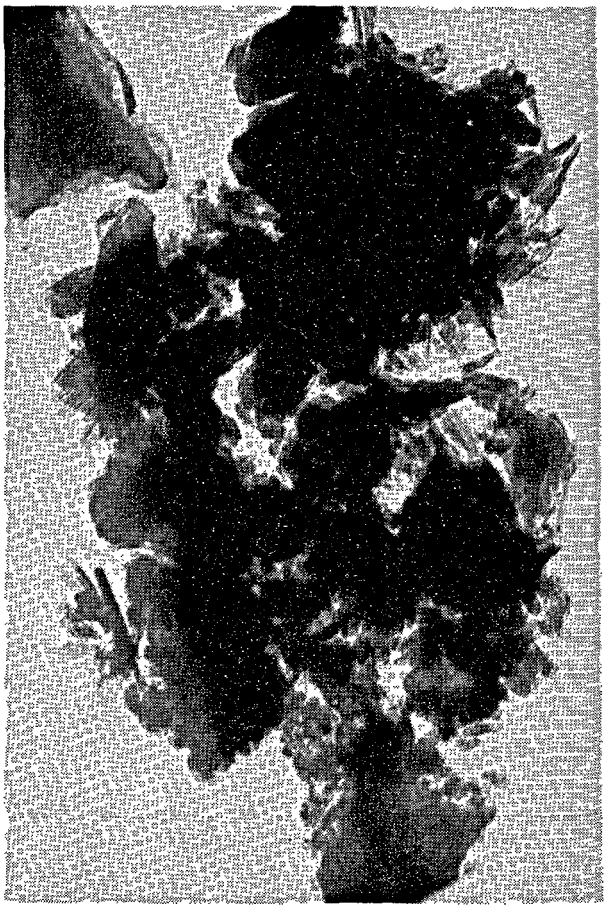

Fig. 16. C_3S *paste containing added* C_4AH_{13} *after agitation in water 3 months*

extension in which more gel is produced.

The maximum ratio of substituent ion to silica was found to be 1/6, for sulfate, aluminum, or iron. The substitution reaction occurs either during formation of the gel or between the gel and the substituting species. Substitution for both calcium and silica by the same species can occur. Thus it was found that, at maximum substitution of alumina, 74 percent of the total alumina had replaced silica; the remainder substituted for calcium. In the case of iron, 50 percent substitutes for silica, and all sulfate substitutes for silica. Electron microscopic examinations indicate that significant morphological changes occur along with the substitution reactions. Examples of the changes observed are shown in Figs. 15–17. Fig. 15 shows a field of a hardened C_3S paste after agitation in water for 3 months; Fig. 16 shows a field of this same material with added C_4AH_{13} after agitation in water for 3 months; Fig. 17 shows a field of the C_3S paste with 20 percent added gypsum after agitation in water for 3 months. The rolled sheet type of structure evident in Fig. 15 and characteristic of C_3S pastes is absent in Figs. 16 and 17. In Fig. 16, the gel more nearly resembles that formed during the early stages of cement hydration, and in Fig. 17, a less fibrous product (than in Fig. 15) occurs with an indication of numerous small platelets.

The examination of the substitution reactions has been extended to the hydrating paste system (10). Pastes of C_3S have been hydrated in the presence of various quantities of gypsum up to 3 percent as SO_3 on the C_3S basis. The net effect of the sulfate in the case of reaction in a hydrating system was much the same as in the case of reaction with a previously formed C–S–H gel. The results obtained by the two methods are shown in Fig. 18, in which the linear relationships between C/S-ratio of the gel, and the extent of sulfate substitution in the gel, expressed as the molar SO_3/SiO_2 ratio, are illustrated. The lower line was obtained by the reaction in an agitated slurry, and the upper curve by the direct reaction in a hydrating paste. The intercepts of the lines represent the

Fig. 17. C_3S *paste containing added gypsum after agitation in water 3 months*

C/S ratios of unsubstituted gels obtained with the respective reaction conditions, and the slopes represent the uptake of lime accompanying the SO_3 substitution. If the only lime to enter with the sulfate were that required to extend the structure, the slope would be equal to the intercept, that is, the C/SO_3 ratio would equal the initial C/S ratio. However, the slopes of both lines exceed the intercept values by 1.5 moles of lime per mole of SO_3. One mole of this amount may be considered to enter the structure so as to maintain charge balance.

The H/S results are consistent with the C/S results. The value of the slope of the H/S line is 0.5 moles/mole SiO_2 less than the value of the slope of the C/S line, maintaining the difference in the initial H/S and C/S ratios. The difference between the slope and the intercept of the H/S line is 1.5 moles/mole SiO_2, indicating that the additional lime, over that required for structure extension and charge balance, entering in with the SO_3, enters in as $Ca(OH)_2$.

The morphological changes which accompany entry of sulfate into the structure are similar regardless of when during the history of the C–S–H gel this entry occurs. This is illustrated by the stereo pairs of electron micrographs of surface replicas shown in Fig. 19. Pair (a) represents a field obtained from a C_3S paste hydrated for 5 years at 0.7 w_0/c; pair (b) represents a field of this same paste after immersion in 0.15 M K_2SO_4 for 30 days. The sulfate-treated paste shows only vague suggestions of the structure that appeared in the untreated paste. The rosettes of cone-shaped particles have completely disappeared.

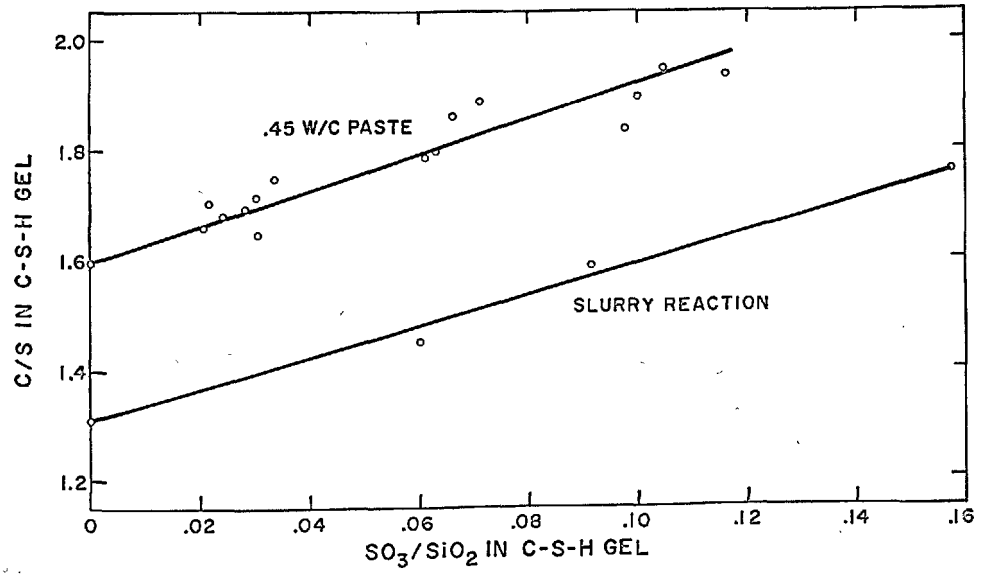

Fig. 18. *Effect of sulfate substitution in* C–S–H *gel*

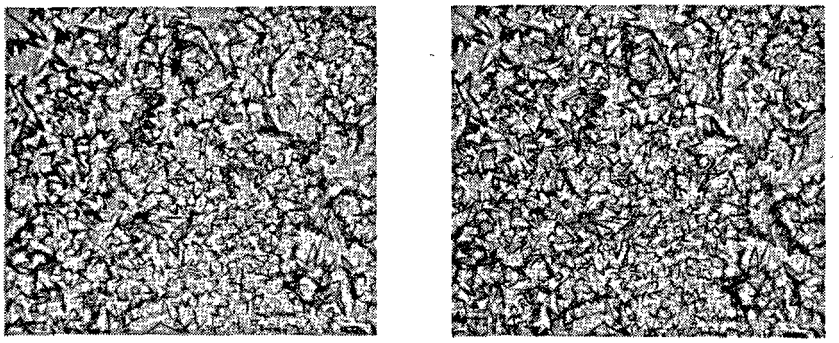

(a) *Untreated* C_3S *paste, initial* $w_0/c = 0.7$ *cured 5 years.*

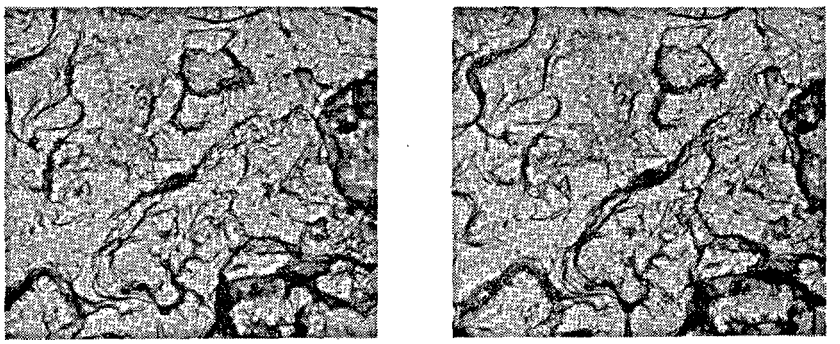

(b) *Same paste after 30 day immersion in 0.15* M K_2SO_4.

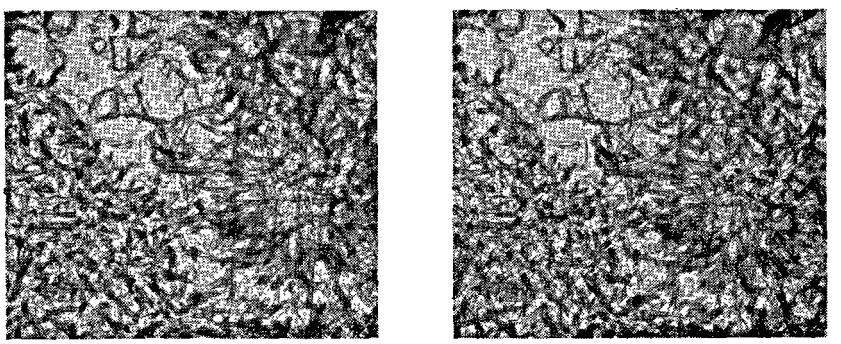

(c) *Pure* C_3S *paste, initial* w/C_3S, *cured 28 days.*

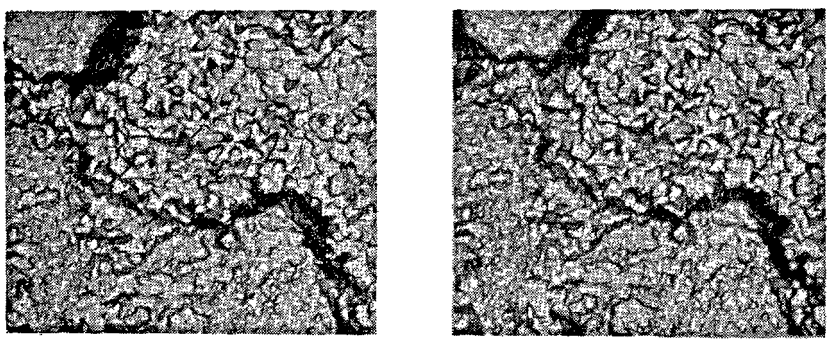

(d) *Paste of* C_3S *plus 3 percents* $\overline{S}$ *as gypsum, initial* $w_0/c = 0.45$, *cured 28 days.*

Fig. 19. *Surface replicas of hardened* C_3S *pastes (Mag.* $\times 5000$)

Fig. 20. *Alite paste after agitation in water 3 months*

Pairs (c) and (d) represent fields of C_3S paste hydrated at .45 w_0/c in the absence and in the presence of 3 percent SO_3 as gypsum. The pastes are 28 days old. Pair (c) shows particles similar to those in pair (a), except that they are much more elongated. They, too, seem to grow out of the substrate in clusters, or rosettes. Pair (d) shows broader, thicker and much shorter cones. The change in morphology from (c) to (d) is not at all as severe as in the case of (a) and (b). Pairs (a) and (b) represent the case of attack on an already existing C–S–H gel, while (c) and (d) represent formation without or with gypsum present.

The investigation of the composition of the hydration products of alite pastes brings one a step closer to the cement-water system. In past years, one alite, containing approximately 0.9 percent Al_2O_3 has been investigated (9, 12, 44). Recently, the hydrations of two other alite preparations containing excess alumina, as C_3A, have been examined (29). Alumina was found to enter the C–S–H gel as a substituent. An electron micrograph of an alite paste is shown in Fig. 20. Fewer rolled sheets of the type shown in Fig. 15 are found in alite pastes; there is a similarity in the appearance of the field in Fig. 20 to that of a C_4AH_{13} treated C_3S paste shown in Fig. 16.

The C/S ratios obtained for pastes with various alumina contents, hydrated at .45 w_0/c for 28 days or more are shown in Fig. 21, along with the results obtained from the slurry reaction products of hydrated C_3S paste and C_4AH_{13}. Linear relationships were obtained for the two series, the lines having about the same slope, corresponding to an uptake of 1 mole

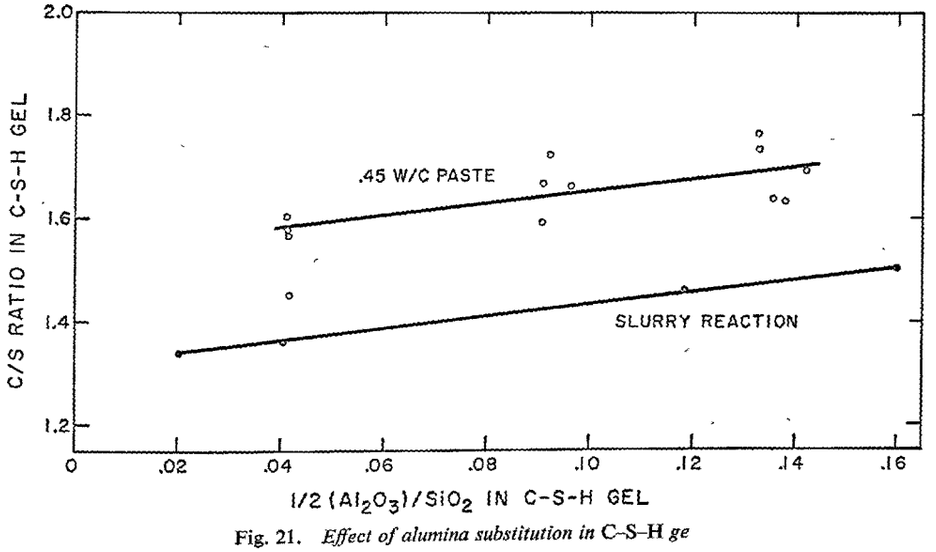

Fig. 21. *Effect of alumina substitution in* C–S–H *ge*

CaO per equivalent of Al_2O_3.

Two investigations have been carried out that suggest that substitution in C–S–H gel occurs during hydration of cement. In one of these Kalousek (53) found, using a quantitative DTA technique, that not all the sulfate in cement paste was accounted for by the amounts of gypsum and sulfoaluminate phases present. Some sulfate was "missing"; Kalousek suggests that this "missing" SO_3 is a "lattice substituent" in the gel. As much as 2.83 percent SO_3 of this type was determined. If all the SiO_2 in the cement used was in the silicate phases, this would correspond to a SO_3/SiO_2 ratio of 0.10, which is below the maximum ratio of 1/6, given above. Since the pastes used by Kalousek were not completely hydrated, the ratio 0.1 should be somewhat higher, probably by about 25 percent. In the other Smolczyk (54) observed that the calcium aluminate hydrates could not account for all the alumina present in blast furnace slag cement paste. He pointed out that the concentration of Ca^{2+} and OH^- was too high to permit the presence of amorphous alumina and concluded that the C–S–H phase retained the "missing" alumina.

It has been demonstrated that a significant morphological change in C–S–H gel produced by cement hydration occurs when sulfate enters the gel (55). This is demonstrated by electron micrograph stereo pairs of replicas of the gel produced by hydration of a clinker and by hydration of the cement (containing 4 percent SO_3 as gypsum) shown in Figs. 22a and 22b, respectively.

Some consideration has been given to the simultaneous substitution of both alumina and sulfate in C–S–H gel. Kalousek suggests that the amounts of these materials that can enter the gel are interdependent to the extent that less of each can enter when both are present.

More recently, it was found that ettringite reacted

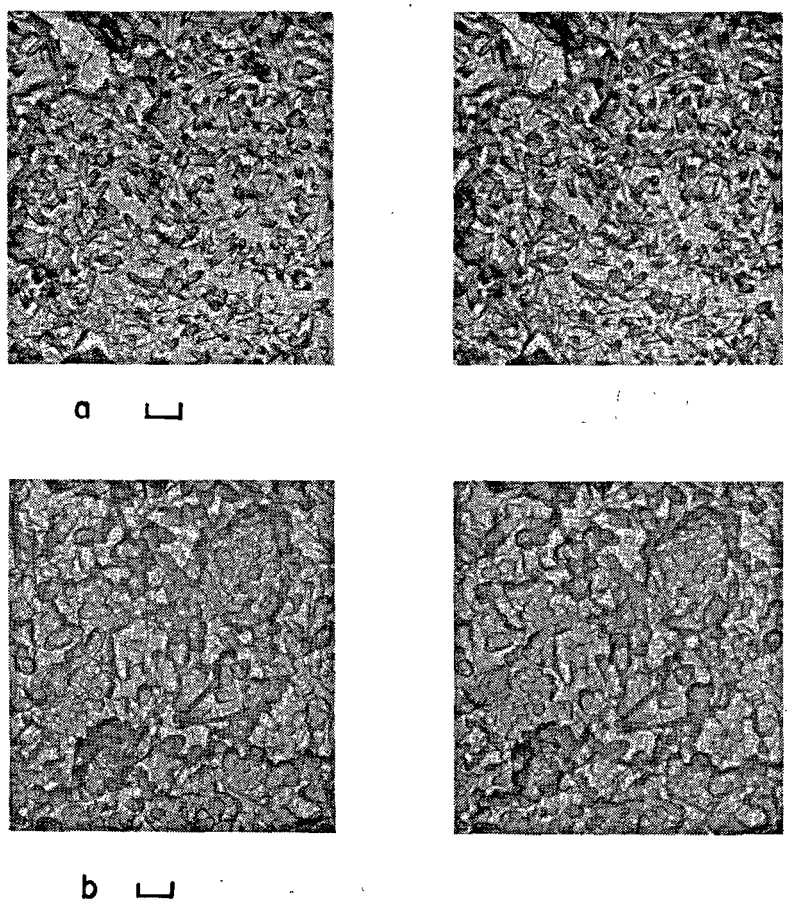

Fig. 22. *Stereo pairs of electron micrographs of hardened cement pastes.* a, *clinker paste made with* $w_0/c = 0.45$, *cured 14 days.* b, *paste of same clinker plus 4 percent* SO_3 *as gypsum,* $w_0/c = 0.45$, *cured 14 days. Mark represents 1* μ.

only slightly with C_3S paste, but that the sulfoferrite analog reacted more extensively (52). Furthermore, it was observed that ettringite was a product of the reaction of calcium sulfate with the alumina-substituted gel formed by hydration of alite, and also a product of the reactions of C_3A and tetracalcium aluminate hydrate with sulfate substituted C–S–H gel. However, the conversions to ettringite were apparently not complete; the evidence indicated that some alumina and sulfate could coexist as substituents in C–S–H gel.

The structural changes occurring because of substitution result in changes in other physical characteristics besides particle morphology. Of great significance with regard to cement technology is the influence of these various reactions on the strength properties of the paste. The compressive strengths of C_3S pastes (.45 w_0/c) as a function of extent of sulfate substitution are shown in Fig. 23. The strength drops significantly with increasing sulfate content. The strength at the highest sulfate content (3 percent on the C_3S basis) is 56 percent of that of the corresponding sulfate free paste, for both percentage hydrations illustrated, 75 and 90 percent. Possibly the lack of resistance of many cements to sulfate attack is at least in part related to these changes caused by replacement of Si^{4+} by S^{6+} in the gel.

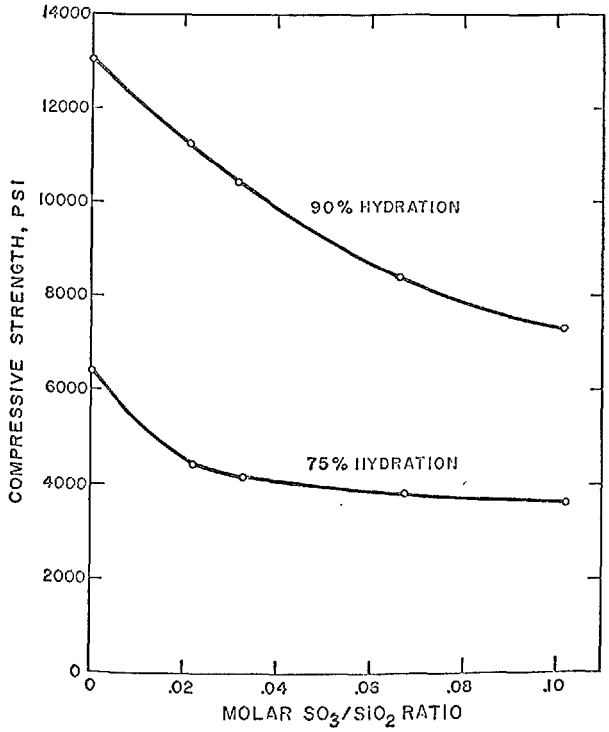

Fig. 23. *Variation of compressive strength with extent of sulfate substitution at constant amount of* C_3S *hydration*

The data obtained regarding the influence of alumina substitution on compressive strength indicate that a slight improvement may result.

Early Hydration Reaction of C_3S

The results of most researches on the hydration of C_3S are generally compatible; the minor differences in interpretation that do exist are probably caused by the fact that most groups of workers do not have the time or facilities to make a complete study. Nevertheless by comparing the work of all it is possible to propose a sequence of reactions during the first few hours that is fairly consistent with all results.

Kawada and Nemoto (48) studied most of the aspects of the early stages of C_3S hydration. They showed that when C_3S was mixed with water there was an immediate liberation of heat for a few minutes, after which the rate of heat liberation fell to a low level. Later the rate of heat liberation increased, passed through a maximum and decreased to a low level again in about eighteen hours. The essential features of this heat liberation curve have been duplicated in our own laboratories. They, Turriziani, Rio and Collepardi (49), as well as Celani, Collepardi and Rio (32) measured the increase in lime content in solution as well as in the solid phases during the early reactions. The solution phase becomes saturated with lime in less than an hour after mixing; concentration of lime continues to increase until maximum supersaturation is reached at 2–6 hours. At about 6 hours crystalline calcium hydroxide can be detected by X-ray diffraction. Turriziani, Rio and Collepardi report free lime in the solid phases is found at about 4 hours by chemical extraction but not by X-ray diffraction. They consider this lime to be amorphous, as have Brunauer, Kantro and Copeland (56). The lime concentration in solution remains high until crystalline $Ca(OH)_2$ begins to be formed; after that it drops slowly to the saturation value.

Greenberg and Chang (57) report that in suspensions of C_3S in water the concentration of silicate ion in solution decreased rapidly as the concentration of $Ca(OH)_2$ in solution increased, and that the silicate ion in the solution phase of C_3S pastes reached a concentration of 6.7×10^{-5} moles per liter within 2 minutes after first contact with water. The Ca^{2+} concentration was .032 moles with a pH = 12.8; comparison of these values with values they obtained (58) by analysis of the solution formed by prolonged stirring of aqueous suspensions of well hydrated C_3S

pastes (wherein the silica concentration was less than 10^{-5} molar in solutions containing .0193 M Ca^{2+} at a pH = 12.46) shows that within 2 minutes the solution became supersaturated with respect to calcium hydroxide and also with respect to the C–S–H gel in C_3S paste.

The results of determining C/S ratio in the hydration (or hydrolysis) product that have been obtained by different research teams differ to some extent. Kawada and Nemoto (48) find the C/S ratio is about 1.5 initially; it rises to 2.5 at about 6 hours, after which it falls and remains essentially constant at 1.5. On the other hand Kantro, Brunauer and Weise (12), and Locher (11) find that the first product formed has a C/S ratio nearly 3. This high ratio decreases rapidly to an approximately constant value, depending upon the water/C_3S ratio of the paste. In pastes, mixed with w_0/C_3S equal to 0.7 and 0.57, the reaction product at 30 minutes had a C/S ratio of 2.9; after 4 hours (14% hydration) the C/S ratio had fallen to about 1.7; it then decreased slowly to about 1.5 at complete hydration in 1 year. Kawada and Nemoto report that the calcium silicate formed initially has practically no bound water. Kantro, Brunauer and Weise as well as Locher also have reported that the water content of the hydration products of C_3S pastes at early ages is essentially the water bound in calcium hydroxide.

These results indicate that the first reaction upon contact of C_3S with water is hydrolysis of C_3S. The solid product of the hydrolysis is a reaction intermediate left as a coating remaining on C_3S surfaces, which retards the reaction. The intermediate product has a C/S ratio somewhat below 3 (but perhaps not far below 3) and has little, if any, bound water. The hydrolysis proceeds to form a solution that is supersaturated with respect to calcium hydroxide and also with respect to the C–S–H gel finally formed. The increase in rate of heat liberation at about 2 hours indicates that cleaning of surfaces by dissolution of the intermediate product to form C–S–H gel has started. Maximum lime concentration in solution is reached at about this time. The increase in rate of hydration is accompanied by a decrease in C/S ratios of the reaction product and the first appearance of extractable lime (between 2 and 4 hours). At 4 hours the C/S ratio of the C–S–H gel has fallen to about 1.6. The lime concentration has decreased somewhat. Crystalline $Ca(OH)_2$ is nucleated in the period between 4 and 6 hours at which time the rate of hydration reaches its maximum. The rate of hydration then decreases as surfaces become covered and space becomes filled with C–S–H gel.

As hydration proceeds, more and more available space becomes filled with hydration products. Calcium hydroxide precipitates with increasing difficulty and the hydration products leave the anhydrous silicate only with greater difficulty. The net result is an increase in the C/S-ratio of the gel with formation of proportionately less free lime, and an increase in the distance which ions must diffuse through hydration product in order to arrive at the solution boundary. The effect of limited available volume becomes more significant, the lower the w_0/c-ratio, and accounts for the marked increase in the C/S ratio of the C–S–H gel that occurs as the w_0/c-ratio of the paste is decreased.

The Hydration of Alumina-Bearing Phases

Tricalcium Aluminate Phase

Hydration in Pure Water

The study of the hydration of pure C_3A in water has been shown to have little similarity to the hydration of C_3A in cement because in cement or clinker pastes the solution formed quickly attains relatively high concentrations of $Ca(OH)_2$, alkalies, and sulfates. These solutes influence the rate and also the products that are formed in the hydration of C_3A. Nevertheless, a brief review of the simple system will serve to illustrate the sensitivity of this component of cement to the conditions of hydration.

Steinour (59) reports that Candlot and LeChatelier believed that C_3A hydrated to form C_3AH_{12}. Klein and Phillips (60) later reported that hexagonal plates, needles, and spherulites, all with the same optical properties were formed by hydration of C_3A at room temperature. The chemical analysis showed the hydrate to have a C/A ratio of 3. In 1929 Thorvaldson and Grace (61) prepared pure cubic crystals of C_3AH_6 by hydration of C_3A at 150°C and also at room temperature. Nacken and Mosebach (62), among others, showed that hydration of C_3A does not always produce a hydrate with a C/A ratio of 3. They found that the solution formed in the first few days was not congruent, and became so only when the "hexagonal" phase transformed to the cubic C_3AH_6. Wells, Clarke, and McMurdie (63) were able to show that the "hexagonal" hydrates formed by hydration of C_3A

in water consisted of two compounds: $C_2A \cdot Aq$ and $C_4A \cdot Aq$.

Recently H. N. Stein (64, 65) examined the hydration reaction of C_3A using calorimetric, conductometric, and X-ray diffraction techniques. Two heat evolution maxima were found in pastes of C_3A, $w_0/C_3A = 1.0$. The first started immediately upon mixing the paste with water, the second, appearing 2 to 3 hours later, was connected with the conversion of the intermediate hexagonal hydrates, C_2AH_8 and C_4AH_{19}, into C_3AH_6 and hydrous alumina. Addition of C_3AH_6 to the C_3A-water paste shifted the second peak to earlier time without affecting its intensity appreciably. Addition of finely ground quartz to the C_3A-water pastes had little effect upon the time of appearance of the second maximum, but did increase its intensity, Fig. 24. Decreasing the water to C_3A ratio shifted the second peak to shorter times. These results are consistent with a mechanism in which the hexagonal hydrates begin to form immediately upon contact of the C_3A with water, and later convert to the more stable C_3AH_6. The results show that C_2AH_8 disappears more rapidly than does C_4AH_{19}. The decreased rate of conversion was attributed to deposition of hydrous alumina upon the C_3AH_6 crystal faces. The action of added C_3AH_6 was to provide seed so that the conversion of hexagonal to cubic phase could start sooner. Addition of quartz to the pastes apparently did not provide nucleation sites for C_3AH_6, but did provide surfaces for precipitation of hydrous alumina, and thus gave some protection to the surface of the C_3AH_6 crystals.

This mechanism seems consistent with the results of Feldman and Ramachandran (66) who studied the

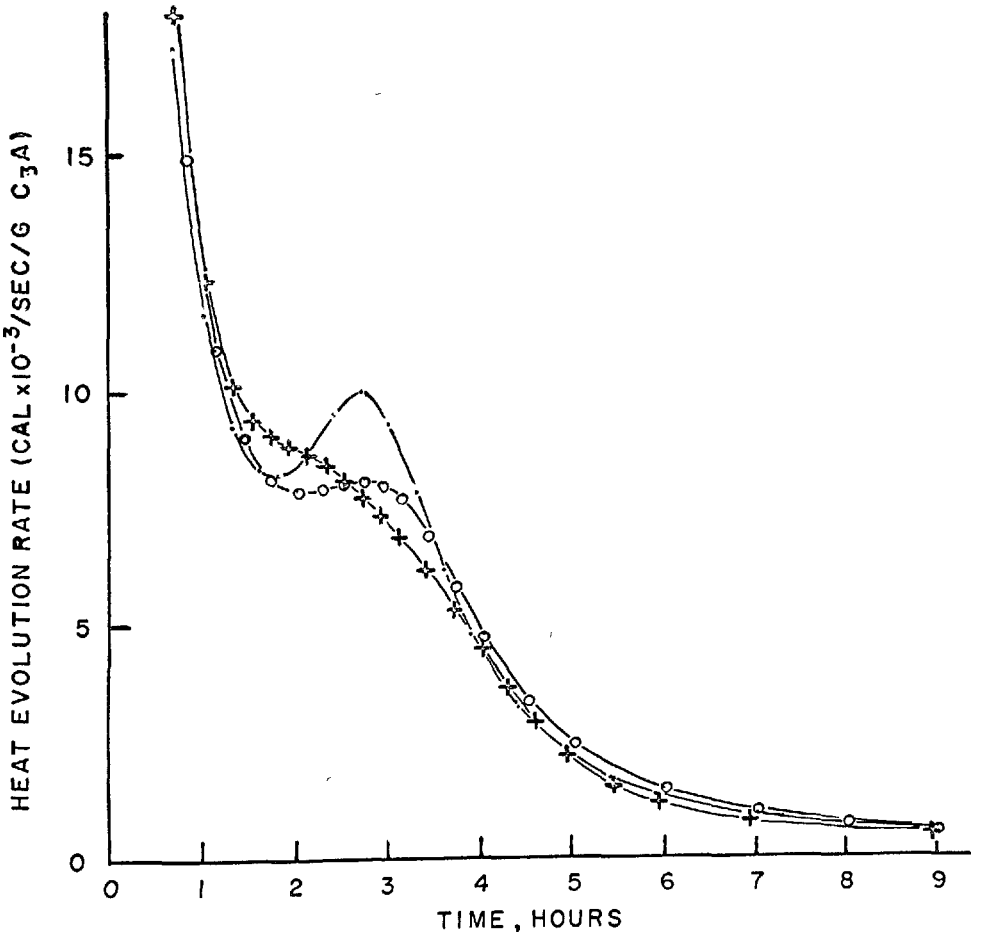

Fig. 24. *Influence of quartz on heat evolution characteristics of* C_3A + *water pastes.* C_3A: *batch B, surface area 16.3* × $10^2/g$
+ —*0.9991 g* C_3A + *1000 g water.*
○—*1.0004 g* C_3A + *0.1228 g quartz* + *1000 g water.*
·—*0.9985 g* C_3A + *0.3747 g quartz* + *1000 g water*

hydration of compacts of C_3A in water at different temperatures and examined the products by DTA and expansion measurements. They found that hexagonal phases formed first at all temperatures, although only small amounts were formed above 50°C. At temperatures above 52°C conversion to C_3AH_6 occurred rapidly and hydration of C_3A virtually ceased at that time. These authors suggest that at the higher temperatures the C_3AH_6 formed directly on the C_3A surfaces and blocked the entrance of water. At room temperature, and below, the hexagonal phases formed on the surface of the C_3A grains; their conversion to C_3AH_6 cleaned the surface and accelerated hydration for a time.

Effect of Gypsum

Feldman and Ramachandran also studied the influence of gypsum upon the hydration of C_3A (67) using identical techniques. C_3A contained 2 percent free lime; this amount is not sufficient to supply all the lime needed to prevent the hydrolysis of C_3A. The amount of gypsum, which was mixed with the C_3A before making the compact, was varied from 0.25 percent to 20 percent. Consequently even the highest gypsum content contained a smaller proportion of gypsum relative to C_3A than would normally be found in portland cement even if its C_3A content were high. Nevertheless they did find that the rate of hydration was retarded even at the lowest gypsum level (0.25 percent) although they could not identify hexacalcium aluminate trisulfate hydrate (ettringite) as a product of hydration. They reported that at all other gypsum levels except the highest (20 percent) the hydration products comprised a mixture of C_2AH_8 C_4AH_{13}, and $C_6A\bar{S}_3H_{32}$. Conversion of the hexagonal hydrates to C_3AH_6 was delayed but not prevented by the presence of SO_4^{2-}. With 20 percent gypsum at 52°C the rate of expansion of the compact was very much higher than observed in the corresponding compact without gypsum. Apparently the hexacalcium aluminate trisulfate formed with gypsum present retards the hydration of C_3A less than does the C_3AH_6 that forms at high temperatures in the absence of gypsum. Feldman and Ramachandran concluded that although the formation of the mixed hexagonal aluminates on the surface of the C_3A retarded the reaction to some extent, the adsorption of SO_4^{2-} ion on the surface of C_3A was still the major factor. Other workers seem not to agree with this conclusion.

Effect of Gypsum Plus Calcium Hydroxide

Seligmann and Greening (68) monitored, by X-ray diffraction examinations of wet pastes, the hydration reaction of C_3A in pastes containing gypsum and equimolar quantities of C_3A and $Ca(OH)_2$. The water: solids ratio was 0.4. Fig. 25 shows a series of X-ray patterns obtained from a paste containing 1/4 mole SO_3 per mole of alumina, which is a lower gypsum content than corresponds to most portland cements.

The results are semiquantitative and show that the sequence of hydration reactions can be divided into three stages: In the first stage the hydration reaction produces hexacalcium aluminate trisulfate hydrate $C_6A\bar{S}_3H_{32}$. The second stage starts when the SO_4^{2-} is depleted; the hexacalcium aluminate trisulfate $C_6A\bar{S}_3H_{32}$ reacts with C_3A to produce tetracalcium aluminate monosulfate hydrate, $C_4A\bar{S}H_{14}$. In the third stage the hydration of tricalcium aluminate produces the tetracalcium aluminate hydrate—tetracalcium aluminate monosulfate hydrate solid solution, and tetracalcium aluminate hydrate.

In Fig. 25 the pattern at 15 minutes shows peaks of gypsum (G) and tricalcium aluminate (A); weak lines for hexacalcium aluminate trisulfate hydrate (E) are present. By 2 hours the gypsum peaks are considerably reduced and the peaks for hexacalcium aluminate trisulfate hydrate are stronger. The first stage of hydration ends by 5 hours when the gypsum has completely reacted. By six hours the second stage of hydration is completed; the hexacalcium aluminate trisulfate hydrate has converted completely to tetracalcium aluminate monosulfate hydrate. This reaction produces the heat evolution peak marking rapid reaction of C_3A shown by Lerch (69). The final stage is completed at 48 hours when the C_3A has completely reacted. In this stage the monosulfate peak at 9.2° (2θ) increases in intensity and shifts to higher angles as the monosulfate reacts with tricalcium aluminate and calcium hydroxide to form a solid solution. The monosulfate peak at 31.0° (2θ) eventually disappears. By 12 hours the peak of tetracalcium aluminate hydrate at 8.3° (2θ) appears and continues to increase in intensity with continued hydration of C_3A. The fact that tetracalcium aluminate hydrate coexists with the solid solution suggests that there is an upper limit to the amount of $Ca(OH)_2$ that can be taken up in formation of the solid solution phase. Hydration of pastes with higher gypsum contents showed essentially the same effects except that when enough gypsum was present the monosulfate persisted as the final calcium aluminate hydrate phase.

Stein (70) showed the sequence of the reactions involving hydration of tricalcium aluminate in the presence of gypsum and enough calcium hydroxide to insure formation of tetracalcium aluminate hydrate by use of calorimetric measurements and X-ray dif-

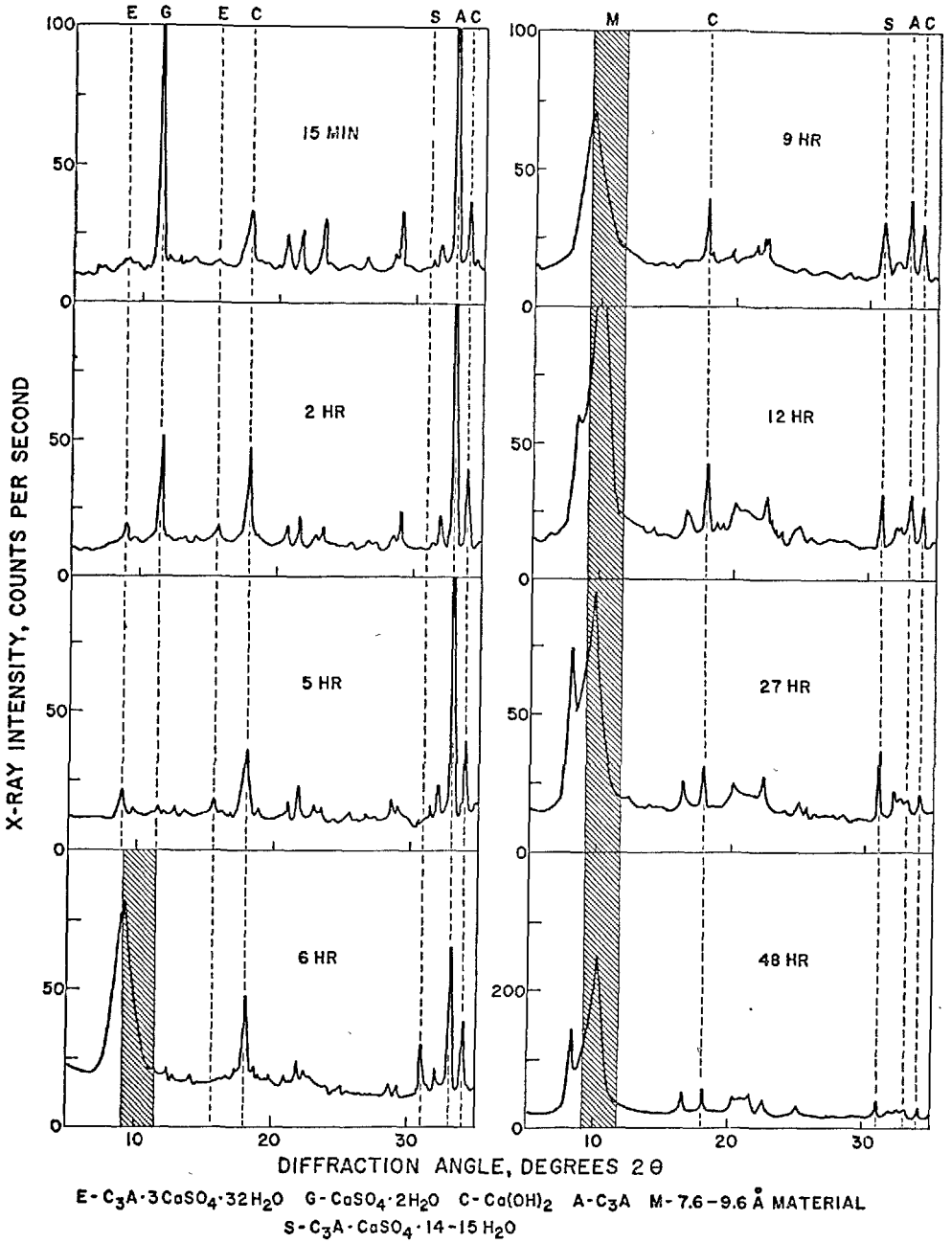

Fig. 25. *Diffraction patterns of base mixture with 3/4 mole* SO_3 *per mole alumina*

fraction examinations. His heat curve is shown in Fig. 26. As with cement there is at first a large heat liberation peak followed by a "dormant" period, in which the rate of heat liberation is low until the gypsum has completely reacted. Immediately following there is a second large peak during which the hexacalcium aluminate trisulfate hydrate formed in the "dormant" period reacts with tricalcium aluminate to form tetracalcium aluminate monosulfate hydrate. Stein concluded: (1) that the trisulfate is formed first on the surfaces of the tricalcium aluminate grains, and (2) that the layer of trisulfate must eventually peel off because the volume of the trisulfate is so much larger than the volume of the tricalcium aluminate from which it was formed. Schwiete, Ludwig and Jäger (71) concur with Stein's proposed mechanism on the basis of their

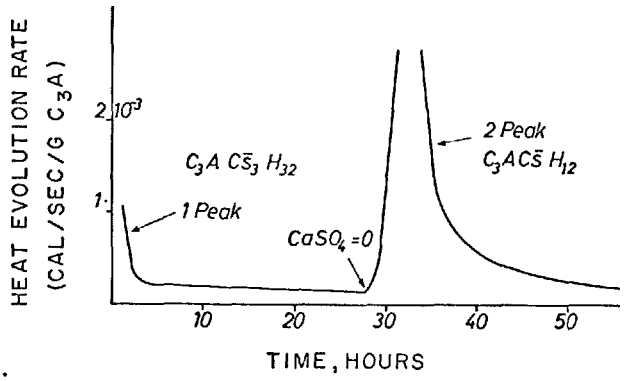

Fig. 26. *Isothermal heat liberation of* C_3A–$CaSO_4 \cdot 2H_2O$–$Ca(OH)_2$–H_2O; *mixture—3 g.* C_3A, *0.4 g.* $CaSO_4 \cdot 2H_2O$ *2 cc 0.0196 m* $Ca(OH)_2$ *solution. (Ref. 71)*

own experimental results. They followed the rate of disappearance of SO_3 and CaO from solution in slurries of tricalcium aluminate, CaO, and gypsum in distilled water. X-ray examination of the reaction products showed the same sequence of reactions reported by Stein, and Seligmann and Greening. Their conception of Stein's proposed mechanism is illustrated by their diagram reproduced in Fig. 27. Schwiete and his coworkers were able to show by electron microscopy, Fig. 28, that hexacalcium aluminate trisulfate hydrate formed upon the surface of C_3A grains within thirty second after the introduction of water.

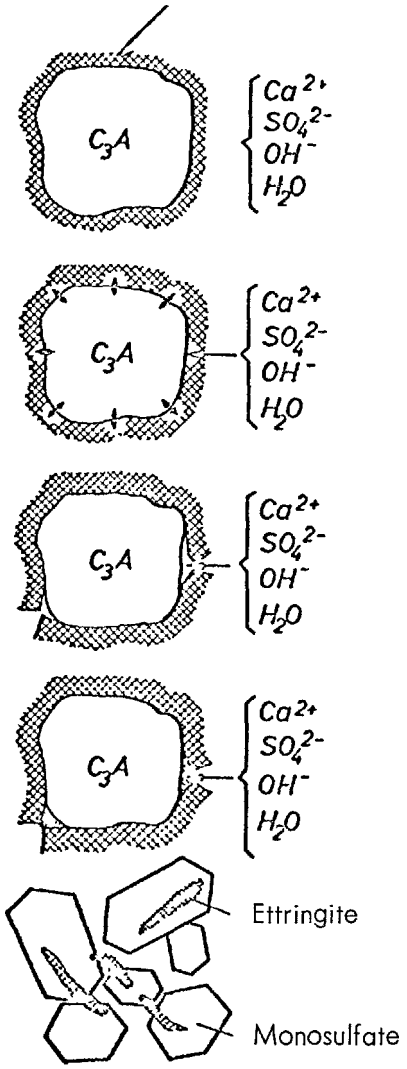

First stage: Formation of a thin cover of $C_6A\bar{S}_3H_{32}$ on the C_3A surface.

Second stage: A thicker layer of $C_6A\bar{S}_3H_{32}$ formed on the C_3A surface produces crystallization pressure.

Third stage: Bursting of $C_6A\bar{S}_3H_{32}$ layer caused by pressure of crystallization.

Fourth stage: Burst section sealed by newly formed $C_6A\bar{S}_3H_{32}$.

Fifth stage: Insufficient $\bar{S}$ for formation of $C_6A\bar{S}_3H_{32}$; complete hydration of C_6A with consumption of $C_6A\bar{S}_3H_{32}$ to form $C_4A\bar{S}H_{12}$ and $C_4A(\bar{S}, OH)H_{12}$.

Fig. 27. *Schematic description of retarded setting caused by sulfates (after Stein, as modified by Schweite). (Ref. 71)*

Hydration of the Calcium Aluminate Ferrites

The reactions of the calcium aluminate ferrite solid solution phases are more complicated than those of tricalcium aluminate although there are many similarities between the two sets of reactions. In the discussion of these solid solutions we shall for brevity use the symbol, F_{ss}, in place of the name "calcium aluminate ferrite" solid solution. Whenever it is necessary to designate a particular composition of the solid solution the symbol will be written $F_{ss}(p)$, where p is the mole ratio, $A/(A + F)$; thus tetracalcium aluminate ferrite will be written either $F_{ss}(1/2)$ or $F_{ss}(0.5)$. The range of p is thus $0 \leq p \leq 2/3$; the solid solution phase found in portland cement usually lies in the range $1/3 \leq p \leq 2/3$.

F_{ss} Reaction with Pure Water

Carlson (72) investigated the action of pure water on six different F_{ss} phases in leaching experiments, and found it possible to remove all of the alumina and most of the lime from the solid solutions and leave most of the iron as oxide with a little lime adsorbed upon it. If F_{ss} is shaken with water the solution becomes sufficiently concentrated to precipitate C_2AH_8 at room temperature. At 70°C the precipitate that forms is hydrogarnet with about ten percent of A replaced by F. The rate of the reaction increases with temperature and decreases with increasing iron content in the F_{ss}. The presence of $Ca(OH)_2$ in solution will retard the dissolution reaction but will not prevent it even at lime saturation.

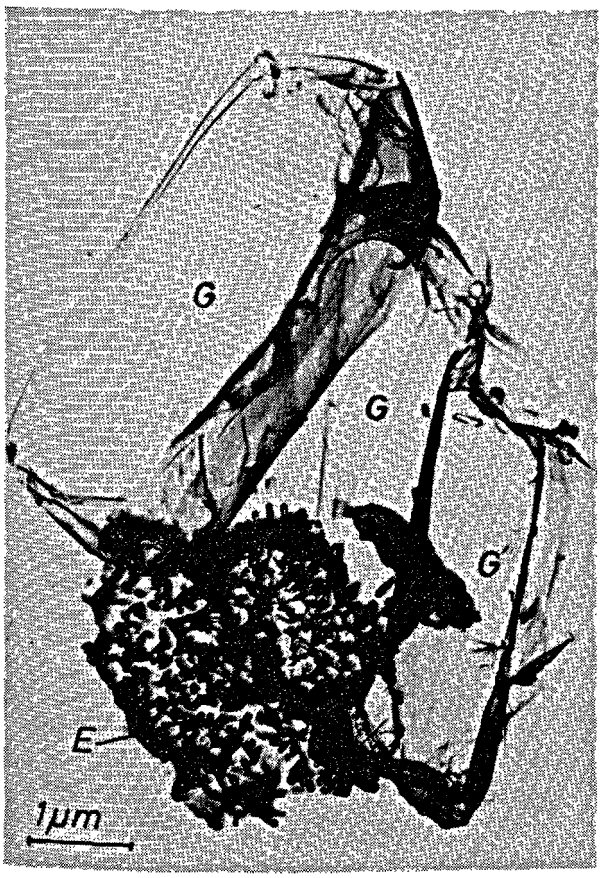

Fig. 28. *Electron micrograph of replica of field in* C_3A–$C\bar{S}$–C–H *system.* $E = C_6A\bar{S}H_{32}$, $C_2 = C\bar{S}H_2$

The reactions in pastes with water are similar in most respects. The composition of the hydrogarnet varied with the composition of the F_{ss}, but the iron to alumina ratio of the hydrogarnet was always lower than that of the F_{ss} phase. When p of the F_{ss} phase is small (high iron content) the hydration product is $C_4(A, F)H_x$, especially at low temperature. If p is high and the temperature is low, C_2AH_8 is formed. The reactivity of F_{ss} decreases with increasing iron content. Chatterji and Jeffery (73) reported that pastes of $F_{ss}(1/2)$ with water/solids ratio of 0.6 were a deep brick red and remained soft up to three months. Hexagonal plates forming early in the hydration (4 min.) were identified as C_2AH_x. Calcium carboaluminate and a small quantity of C_4AH_x were also found. The predominant hydrate was hydrogarnet. No calcium hydroxide, iron oxide, nor any other iron compound was identified by either electron or X-ray diffraction. The lack of iron compounds and calcium hydroxide along with the occurrence of some shift in the magnitude of a_H for the hexagonal phases lead to the suggestion that iron may substitute for aluminium in the hydration products. Carlson's work shows that such substitution does occur; substitution also occurs in C_4AH_x, trisulfate, and monosulfate phases but the diffraction patterns are almost identical to the unsubstituted hydrates (74) so it is generally difficult to detect substitution from the diffraction pattern alone.

Pastes of F_{ss} + $Ca(OH)_2$

Chatterji and Jeffery (73) found that pastes of F_{ss} (1/2) mixed with a suspension of lime-water did not harden in three months. The color of the paste changed from a brick red to a light yellow during this time. Hexagonal hydrates began to form within 4 minutes after mixing. At 24 hours small cubic crystals were also seen. The diffraction patterns showed presence of $C_4(A, F)H_x$, carboaluminate, $C_3(A, F)H_6$, $Ca(OH)_2$ and C_4AF. During the 3 month period, the $Ca(OH)_2$ disappeared while the proportions of $C_4(A, F)H_x$ and $C_3(A, F)H_6$ increased. The fading of the red color of the paste to yellow indicated that the proportion of iron in the hydration products increased during the

hydration period. At 3 months the unit cell of the cubic phase was 0.5 percent larger than that of the cubic phase formed in the C_4AF-water pastes at the same age. During the same period the a parameter of the hexagonal phase in the pure water increased from 5.7 to 5.8 Å. (Chatterji and Jeffery report a for the pure iron compound to be 5.8 Å) They concluded that the iron remained in the hexagonal phase and did not substitute for aluminium in the cubic phase unless excess lime was present.

Schwiete and Iwai (75) studied the hydration of C_4AF mixed with the stoichiometric quantity of CaO needed to form the hexagonal hydrate. The mixture was ground with water, water/solid ~ 5, in an agate mill for 24 hours, then one portion was stored at 5°C, and a second portion was stored at 25°C for a month. At 5°C the C_4AF hydrated to $C_4(A, F)H_{13}$ and $C_3(A, F)H_6$. At 25°C the cubic hydrate was formed with only a meager quantity of the hexagonal hydrate. They also hydrated F_{ss} phases with various iron contents with the stoichiometric quantity of CaO necessary to produce the corresponding cubic hydrate. For F_{ss} phases with iron contents below $p \sim 0.2$ the diffraction lines of the cubic hydrates were sharp and shifted to lower angles with increasing iron content. At higher iron contents the diffraction peaks were not clearly defined because of the low reactivity of the iron-rich F_{ss} phases. The lattice constant a for the cubic hydrates varied with p of the F_{ss} phases in good agreement with the values found by Flint, McMurdie, and Wells (76) for the hydrogarnets.

Work of Carlson (77) has corroborated the findings of Schwiete and Iwai to a large extent. Carlson hydrated a series of F_{ss} solid solutions with the necessary quantity of lime to produce either the hexagonal phase or the cubic phase. He was able to achieve colorless, or light yellow hydrates with p of the hydrate the same as for the F_{ss} phase. He was not successful in preparing C_3FH_6, and found that hydration became more sluggish as the iron content of the F_{ss} phase was increased.

Pastes of F_{ss} + Gypsum

In their study of pastes of C_4AF and gypsum Chatterji and Jeffery (73) found that the first hydration product formed as needles on C_4AF surfaces. The needles did not give an electron diffraction pattern, but had the morphology of ettringite, and their X-ray diffraction patterns showed them to be that. At 14 days the hydration product was a mixture of two types of hexagonal plates. One type had $a = 6.14$ Å; the other had a pseudo cell with $a = 5.66$ Å but also showed joint intermediate spots indicating a doubled a axis. The hexagonal phase with $a = 6.14$ Å was not identified. The other is tetracalcium aluminate monosulfate or its solid solution phase. Some C_4AH_x was also present. Gypsum and ettringite had disappeared. At 3 months the sample was a mixture of the cubic phase, C_4AH_x and the monosulfate. The paste was brick red in color so only a part, if any, of the iron was in the hydration products. Tenoutasse (78) studied the behavior of C_2F, C_6AF_2, C_4AF, and C_6A_2F with gypsum in pastes. C_2F hydrated slowly to give hexagonal plates identified as $C_4F\bar{S}H_x$. With C_6AF_2 the trisulfate was the first hydration product. Hexagonal plates, identified as $C_4(A, F)\bar{S}H_{12}$ and $C_4(A, F)H_{13}$, appeared in a week, and at the end of a month the trisulfate phase had practically disappeared. No cubic phases appeared. The hydration reactions of C_4AF and C_6A_2F were examined in more detail and proved to be similar to each other. Calorimetric measurements showed that when water was added to the F_{ss} phase and gypsum there was an immediate heat evolution which subsided after a short time. Some time later there was a second peak in the heat curve. The time of appearance of the second peak depended upon the quantity of gypsum that had been added. The trisulfate hydrate was formed immediately on adding water. After the gypsum had completely reacted, the second heat peak developed with the further reaction of F_{ss} and trisulfate to produce the monosulfate phase. The A/F ratios of the hydration products were found to be higher than those of the F_{ss} phases from which they were formed. This reaction sequence is like that of C_3A + gypsum.

Pastes of F_{ss} + $Ca(OH)_2$ + Gypsum

Chatterji and Jeffery (73) found that the trisulfate phase was formed immediately when a paste containing C_4AF: $Ca(OH)_2$: gypsum = 10:1:1, was mixed, but that the rate of formation was very low in comparison to the rate of formation in the absence of lime. The X-ray diffraction peaks of the trisulfate were somewhat diffuse so it could not be determined whether or not there was substitution of F for A in the trisulfate phase. After 3 months the paste contained mostly the monosulfate phase with some $C_3(A, F)H_6$ and $C_4(A, F)H_x$. The color of the paste changed from grey at the time of mixing to light red at 3 months. The color indicates that amorphous ferric oxide was liberated slowly; some substitution of F for A must have taken place. These results agree with those of Seligmann and Greening (68) who examined the F_{ss} solutions with $p = 0$, 1/3, 1/2 and 2/3. In all instances the rates of hydration were low, even at low SO_3 levels; C_2F gave no hydration products

even after 13 days. They did find that the hydration sequence of the other F_{ss} phases was like that of C_3A; that is three stages occur: the trisulfate phase formed first in Stage I, Stage II started when SO_3 was depleted and further hydration produced the monosulfate phase, but Stage III differed in that absorption of $Ca(OH)_2$ was not accompanied by the changes in the X-ray pattern in the 7.6–9.6 Å range. Their pastes were also red and they were unable to determine the extent of substitution of F for A. Seligmann and Greening also found that not only were the rates of hydration of the ferrite phases low, but also that C_3A hydrated slowly in pastes containing $C_3A:C_4AF = 2:1$ with lime and gypsum at a constant ratio of SO_3/total Al_2O_3, i.e., the presence of C_4AF under these conditions retarded the hydration of C_3A.

Effect of Tricalcium Silicate Phase on Hydration of $C_3A + F_{ss}$

Aside from the comparative reactivity of tricalcium aluminate and the F_{ss} phases their hydration characteristics are similar, and their hydration products are so similar that it is difficult to differentiate between them under the most favorable conditions. The presence of calcium hydroxide has a pronounced effect upon both the rate and the products formed in the hydration reactions. Since the silicates are sources of calcium hydroxide in cement it is important to know how the hydrations of the aluminates and ferrites in the presence of gypsum are affected when the calcium hydroxide in the system must be obtained by the hydrolysis of the silicate phases. Some work has been reported on hydration of simple (relative to cement) mixtures of gypsum, C_3S, or alite, with C_3A and/or F_{ss}.

Pastes of C_3S, C_3A with Gypsum

Seligmann and Greening (68) found that the Stage I hydration of C_3A was accelerated when the $Ca(OH)_2$ in their mixture was replaced by 3 moles of C_3S. This effect is probably caused by the initial absence of calcium hydroxide in solution. The later hydration though was markedly retarded, and the hydration products were poorly crystallized relative to those obtained in the mixture containing calcium hydroxide. Finally, no C_4AH_{19} was formed.

The retardation of Stage II and III reactions probably results from the decreased rate of imbibition of water caused by hardening of the paste. The effects of C_3S are shown in Fig. 29 where diffraction patterns of pastes with increasing C_3S contents are compared

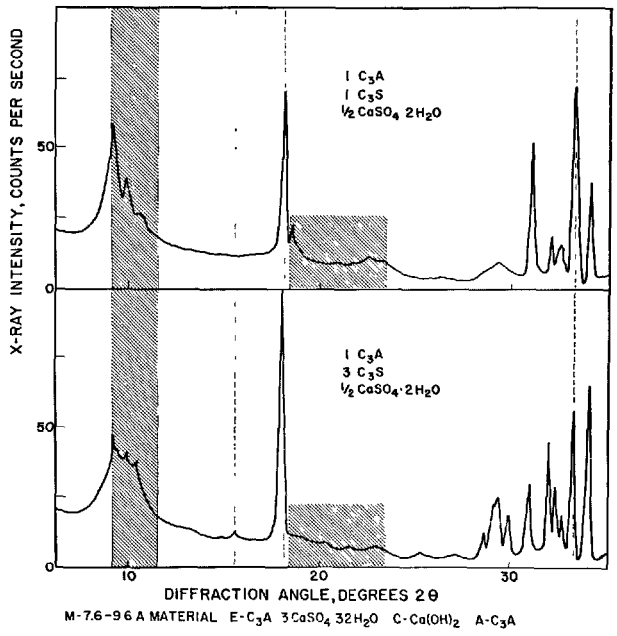

Fig. 29. C_3S *retards hydration of base mixture and causes formation of poorly crystallized products*

after 24 hours of hydration. One must consider, of course, that the C_3A content of the pastes is reduced as the C_3S content increases. In the paste containing 3 moles of C_3S per mole of C_3A a faint line for ettringite is still visible indicating that Stage II hydration has not been completed, yet the tetracalcium aluminate sulfate is already converting to the mixed hydrate M shown by the broad peaks in the 7.6–9.6 Å region. The peaks in the 4 Å region are hardly discernible. Pastes containing 1 mole of C_3S per mole of C_3A show no tetracalcium aluminate trisulfate, but do show the 9.6 Å monosulfate peak. Nevertheless, except for the monosulfate peak, the peaks in the 4 Å region are not resolved. The results suggest that Stages II and III are not clearly separated in the presence of C_3S.

The fact that no C_4AH_{19} is found in the hydration products of pastes containing C_3S may be related to the ability of the calcium silicate gel to absorb alumina, which is discussed in the section "Substituted C–S–H Gels".

Pastes of C_4AF, C_3S and Lime

Schwiete and Iwai (75) prepared hydrogarnets by hydration of C_4AF with different preparations of C_3S chosen to achieve different degrees of substitution of silica for water. They found a linear decrease in the value of the lattice constant of the hydrogarnet with increasing mole ratio of C_3S/C_4AF of the starting

material up to a ratio of 2. Above 2 the lattice parameter was constant. The values of the unit cell parameters agree very well with the values reported by Flint, McMurdie and Wells (76) if it is assumed that the cubic phase produced by C_4AF in excess lime was $C_3(A_{0.5}F_{0.5})H_6$ and S substituted for 2H until the composition became $C_3(A_{0.5}F_{0.5})SH_4$, i.e., below the mole ratio of 2 the iron, alumina, and silica were present in the hydrogarnet in the same proportion as in the starting materials. The final value of the unit cell parameter was 12.419 Å; a value that agrees closely with value usually found in cement pastes (8).

Paste Hydration of Mixtures of Alite, C_3S and C_4AF, with and without Gypsum

The hydration of mixtures of alite, C_3A and C_4AF should be as good a model for cement hydration as it is possible to get by mixing pure phases. It is encouraging that a study of this model by Chatterji and Jeffery (79) produced results that are consistent with the results on simpler systems. In the absence of gypsum thin foils and small hexagonal plates formed on particles in the mixture. Neither gave electron diffraction patterns. After 3 hours the hexagonal plates gave hexagonal electron diffraction patterns with $a_H =$ 5.7 Å showing that they were calcium aluminate hydrates. At 24 hours the paste had set. The foils appeared to have transformed to splines that look very much like the splines of C–S–H gel observed in hydrated cement at 4–6 hours (80) and observed in C–S–H gel after exposure to C_4AH_{13} in a slurry, see Fig. 16. It may be that substitution of alumina for silica in C–S–H gel causes the change in morphology.

Weak X-ray lines at 8.1 Å and 7.6 Å showed the presence of calcium carboaluminate hydrate and α–C_4AH_{13}, which contains essential CO_2 (81). At 14 days the cubic aluminate phase had formed; the X-ray pattern showed a smaller unit cell size, which indicates that silica had replaced some water in the crystallites. At 3 months the alite had reacted completely, but C_3A and C_4AF were still present. There was essentially no change in the hydration product. In another set of experiments 0.1 N NaOH was used to mix the pastes. The only difference noted was a slight delay in the formation of hexagonal phases.

Pastes made with gypsum were more fluid when mixed and setting occurred during the first day. Ettringite and foils of C–S–H gel were present after 4 minutes. Splines of C–S–H gel appeared at 3 hours. At 14 days the monosulfate and tetracalcium aluminate hydrate with a little ettringite were present as well as another unidentified hexagonal phase with $a_H =$ 6.3 Å. At 3 months the ettringite had disappeared; only a trace of alite was present along with C_3A and C_4AF. The presence of 0.1 N NaOH had little effect on the hydration characteristics except that the splines of C–S–H gel appeared within 4 minutes.

Early Reactions in Portland Cement Pastes

Reaction Sequence

In a normally regulated cement the SO_4^{2-} ion will be depleted in about 24 hours; this then is the length of the Stage I period for hydration of the aluminates, and the early cement reactions are completed during this time. The hydration characteristics of pure C_3S, C_3A, and F_{ss} phases provide a basis for understanding the early hydration reactions of cement. These reactions start immediately upon contact of the cement and water. Schwiete, Ludwig and Niel (82, 83) showed that hydration products formed on the surface of cement particles within 30 seconds after contact of the cement with water. Bar-shaped crystals, hexagonal plates, and gel could be delineated in electron micrographs. After 20 minutes ettringite was identified; larger hexagonal plates and hydrogarnets were also observed. The hexagonal plates could be either the monosulfate phase or the dispropor tionation products of C_3A, i.e., C_2AH_8 and C_4AH_{19}. The fact that hydrogarnet was also found implies that the SO_4^{2-} concentration was low and that consequently the hexagonal plates were the disproportionation products. It is possible that some of the gel first observed was amorphous Fe_2O_3 from hydrolysis of F_{ss}. Chatterji and Jeffery (84) identified ettringite as a product of hydration of cement after 4 minutes. They followed the hydration reactions through 3 months time, and found trisulfate, monosulfate, and carboaluminate in all samples after 24 hours. Carbonation at concentrations as low as is provided by calcite will react with the monosulfate phase to form the trisulfate phase and the hemicarboaluminate (α–C_4AH_{13}), or carboaluminate, depending upon the amount of available monosulfate phase (85).

The free lime in the clinker and the hydrolysis of alite furnish the lime to retard the hydrolysis of the calcium aluminate and F_{ss} phases. Because the hydration of the calcium silicates in cement also starts immediately upon contact with water (82, 84) so

shortly after the introduction of water both calcium hydroxide and sulfate ion are available to retard the hydration of the alumina-bearing phases and to accelerate the hydration of alite if the proper amount of SO_4^{2-} is present. Several investigators (see for example (32, 48, 49, 86, 87)) have shown that the solution phase in contact with clinker, portland cement, or C_3S quickly becomes supersaturated with respect to $Ca(OH)_2$. Among these workers, Lawrence found that the silica concentration in the solution phase quickly exceeded the saturation value with respect to the system C–S–$\bar{S}$–A, then remained practically constant during the early hydration period. Kawada and Nemoto found that the solution in contact with C_3S and gypsum never became supersaturated with gypsum, but remained saturated for about nine hours. Rio, Celani and Collepardi observed that the first crystalline calcium hydroxide began to precipitate at about 4 hours; this is about the same time as the rate of heat liberation from the hydration of alite begins to increase. The Ca^{2+} ion concentration of the solution phase continued to increase after the first appearance of crystalline $Ca(OH)_2$, and passed through a maximum during the time interval in which rapid hydration of alite is normally observed.

These observations and the interpretations offered by the various research teams suggest a mechanism for setting of cement pastes. In a freshly mixed paste hydrolysis of all phases starts immediately. Before the SO_4^{2-} concentration can be built up the alumina bearing phases should produce C_2AH_8, C_4AH_{19}, hydrous Fe_2O_3, and sometimes hydrogarnet. The hydrolysis of alite soon supersaturates the liquid phase with respect to calcium hydroxide and produces a high concentration of silicate ions, simultaneously leaving the surfaces of alite coated with a metastable product, probably with high C/S and low H/S ratios (12, 48).

The gypsum dissolves rapidly to produce a saturated solution (in some instances the solution must become supersaturated with respect to gypsum, depending upon the form of $CaSO_4$ in the cement). The high concentrations of $Ca(OH)_2$ and $CaSO_4$ soon transform the aluminate hydrates to $C_6(A, F)\bar{S}_3H_{32}$. Evidence from X-ray diffraction, DTA, and electron microscopy indicates that all this happens within 30 seconds to 4 minutes. The hydration of the alumina bearing phases to produce the trisulfate proceeds slowly simultaneously with the hydrolysis of alite which increases the concentration of $Ca(OH)_2$ in solution and produces a thicker layer of the metastable product. Eventually nuclei for crystallization of $Ca(OH)_2$ appear throughout the system, and crystalline $Ca(OH)_2$ appears. At about the same time nucleation of the stable C–S–H gel starts. When this nucleation occurs the unstable gel that coats alite surfaces dissolves to precipitate on nuclei, some of which may appear within the coating itself; as the alite surface becomes cleaner the hydration of alite accelerates and the supersaturation of Ca^{2+} increases. As the alite surfaces again become coated (with the stable gel this time) the rate of hydration increases less rapidly and passes through a maximum. The concentration of Ca^{2+} ion also passes through a maximum at about the same time. During the period of rapid hydration of alite the stable C–S–H gel forms in laths protruding from the clinker grains and starts to precipitate upon calcium hydroxide surfaces as well. The gel soon forms a continuous network throughout the paste and setting occurs.

The intergrowth of gel and $Ca(OH)_2$ has been observed microscopically using time-lapse photography by Erlin and Greening (88). Evidence of it is sometimes found in surface replicas of hardened pastes. One method of preparing these is to slice the paste with a fine-grit diamond saw using water as a lubricant (52). Calcium hydroxide crystals in the cut surface are dissolved away during this process. The voids remaining frequently show that C–S–H gel had intergrown with the $Ca(OH)_2$ in a preferred orientation, see Fig. 30. H. F. W. Taylor (89, 90) has pointed out that the octahedral arrangement of OH^- around each Ca^{2+} in the $Ca(OH)_2$ crystal has a spacing such that an SiO_4^{4-} tetrahedron can share an edge of the octahedron with only a little distortion. This ability of the tetrahedra to share edges of octahedra could well lead to epitaxial growth of gel on crystal surfaces. It also suggests that the nuclei for formation of crystalline $Ca(OH)_2$ may be similar to those that form stable C–S–H gel; that the two kinds of nuclei form under similar conditions.

Stages II and III of the aluminate reactions may be prolonged in hardened portland cement pastes. An example of the transformation of the trisulfate phase to the monosulfate phase in a portland cement paste is shown in Fig. 31. The portland cement had a potential C_3A content of 14.3 percent with 3 percent SO_3 added as gypsum. The paste, $w_0/c = 0.45$, had been stored continuously moist for 14 days. Rods of the trisulfate phase and hexagonal plates of the monosulfate phase are both present. Some of the rods seem to pierce the plates of the monosulfate phase.

Optimum Gypsum

Lerch's work (69) on the influence of gypsum upon

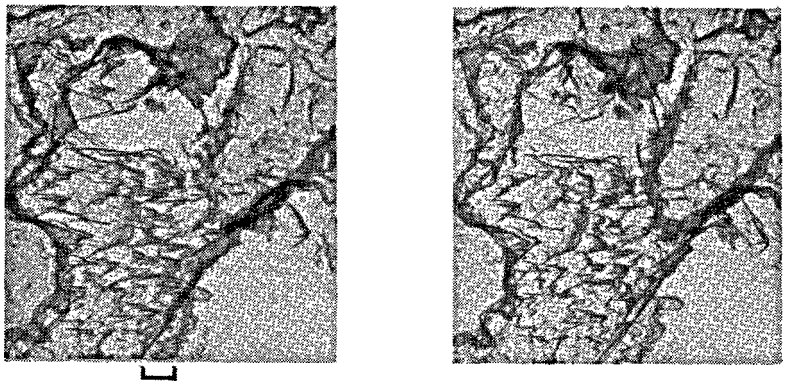

Fig. 30. *Stereo pair of electron micrographs of surface replicas of hardened portland cement paste,* $w_0/c = 0.7$. *Depressions in surface resulted from dissolution of* $Ca(OH)_2$ *crystals during preparation of the slice of paste. The dentate growths of gel in the "saddle" between the depressions probably resulted from intergrowth of gel and calcium hydroxide during hydration. Mark represents 1μ.*

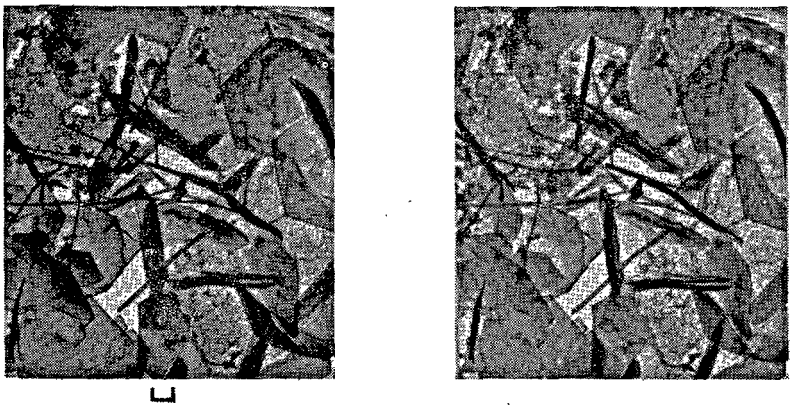

Fig. 31. *Stage II of hydration of* C_3A *in portland cement paste. This stereo pair of electron micrographs shows hexagonal plates of* $C_4(A, F)\bar{S}H_{14}$ *and rods of* $C_6(A, F)\bar{S}_3H_{32}$ *present after 14 days of hydration. Some of the rods appear to pierce the hexagonal plates. Mark represents 1μ.*

hydration of cement was undertaken to examine the basis for specifications on SO_3 content of cements. As a result of the work he found that there was a quantity of gypsum for each cement that would produce a maximum strength and a minimum drying shrinkage in mortars. In only a few instances did cements with optimum gypsum show larger expansions than were found with the maximum permissible SO_3 content (ASTM Specifications). This quantity of gypsum he called the optimum gypsum content. Its magnitude depends upon the composition and fineness of the cement. In addition to the properties of the cement, the conditions of use of the cement must be also considered, for example, the optimum gypsum content for cement used for making concrete at 4°C is lower than for cement ground from the same clinker and used for making concrete at 20°C. Lerch found that the optimum gypsum content was that quantity that would be completely reacted in 18 to 24 hours. From the preceding discussion it is clear that optimum physical properties of hardened pastes and concretes will be attained when Stage I of the hydration of the alumina containing phases is extended through the period of setting and into the period of hardening of the paste.

The sequence of early hydration reactions provides some insight into why an optimum gypsum content exists. Too much gypsum extends the Stage I hydration for too long a time; SO_4^{2-} ion will be present to produce the trisulfate phase long after setting, causing

a continuous expansion of the paste structure that inhibits the development of strength. If too little gypsum is used Stage I hydration ends before the hardening of the paste is well enough advanced; the reaction transforming the trisulfate to the monosulfate proceeds very rapidly; and this reaction is followed by the formation of the solid solution between the monosulfate and $C_4(A, F)H_{19}$, which reduces the high concentration of $Ca(OH)_2$. The decreased $Ca(OH)_2$ concentration permits further hydrolysis of C_3S to the metastable product, delays the nucleation of the stable gel, and consequently retards the development of the C–S–H gel structure, as described in the previous section.

References

1. L. E. Copeland, D. L. Kantro and George Verbeck, "Chemistry of hydration of portland cement," Proc. Fourth International Symp. Chemistry of Cement, Natl. Bur. Stds. Monograph No. 43, Washington, D. C. Vol. I, pp. 429–465 (1960) PCA Res. Dept. Bull. 153.
2. G. Yamaguchi, K. Takemoto, H. Uchikawa and S. Takagi, "Rate of hydration of cement compounds and portland cement estimated by X-ray diffraction analysis," Proc. Fourth International Symp. Chemistry of Cement, Natl. Bur. Stds. Monographs No. 43, Washington, D. C. Vol. I, pp. 495–499 (1960).
3. R. L. Angstadt and F. R. Hurley, "Hydration of the alite phase in portland cement," Nature **197**, 688 (1963).
4. Yu. S. Malinin, M. M. Mayants and V. R. Ryazin, "Determination of the degree of hydration of minerals of portland cement clinker by quantitative X-ray diffraction analysis" (in Russian), Nauchn. Soobshch. Gos. Vses. Nauchn.-Issled. Inst. Tsementn. Prom. **16**, 46–50 (1963).
5. M. Von Euw, "Quantitative analysis of portland cement clinker by X-rays" (in French), Silicates Ind. **23**, 643–9 (1958).
6. D. L. Kantro, L. E. Copeland, C. H. Weise and Stephen Brunauer, "Quantitative determination of the major phases in portland cement by X-ray diffraction methods," J. Res. Develop. Lab., Portland Cement Assoc. **6**(1) 20–40 (Jan. 1964). PCA Res. Dept. Bull. 166.
7. D. L. Kantro, L. E. Copeland and C. H. Weise, unpublished results.
8. The Chemistry of Cement, Vol. I (Academic Press, London, 1964), Edited by H. F. W. Taylor. See chapter by L. E. Copeland and D. L. Kantro entitled "Hydration of cement".
9. D. L. Kantro, C. H. Weise and Stephen Brunauer, "Paste hydration of beta-dicalcium silicate, tricalcium silicate and alite," Symposium on Structure of Portland Cement Paste and Concrete, Special Report 90, Highway Research Board, Washington, pp. 309–327 (1966) PCA Res. Dept. Bull. 209.
10. D. L. Kantro, C. H. Weise and L. E, Copeland, "Influence of the sulfate content and water-solids ratio on the paste hydration of tricalcium silicate," to be published.
11. F. W. Locher, "Stoichiometry of tricalcium silicate hydration," Symposium on Structure of Portland Cement Paste and Concrete, Special Report 90, Highway Research Board, Washington, pp. 300–308 (1966).
12. D. L. Kantro, Stephen Brunauer and C. H. Weise, "Development of surface in the hydration of calcium silicates. II. Extension of investigations to earlier and later stages of hydration," J. Phys. Chem. **66**, 1804–9 (1962). PCA Res. Dept. Bull. 151.
13. A. van Bemst, "The hydrates of calcium silicate," (in French) Bull. Soc. Chim. Belges. **64**, 333–351 (1955).
14. H. F. Schwiete and H. Knoblauch, "The hydration of beta-dicalcium silicate and tricalcium silicate," (in German) Forschungsgerichte des Landes Nordrhein-Westfalen, No. 748 (1959).
15. The Chemistry of Cement, Vol. I (Academic Press, London, 1964), Edited by H. F. W. Taylor. See chapter by Stephen Brunauer and D. L. Kantro entitled "Hydration of Calcium Silicates".
16. S. Glasstone, K. J. Laidler and H. Eyring, The Theory of Rate Processes, p. 370 (McGraw-Hill Book Co., New York, 1941).
17. S. Glasstone, K. J. Laidler and H. Eyring, op. cit., pp. 522 ff.
18. R. K. Iler, The Colloid Chemistry of Silica and the Silicates, pp. 48 ff (Cornell Univ. Press, Ithaca, N. Y., 1955).
19. C. W. Lentz, "The silicate structure analysis of hydrated portland cement paste," Symposium on the Structure of Porltnad Cement Paste and Concrete, Special Report 90, Highway Research Board, Washington, ff. 269–283 (1966).
20. H. Funk and R. Frydrych, "The degrees of anion condensation in silicic acid and silicates," Symposium on the Structure of Portland Cement Paste and Concrete, Special Report 90, Highway Research Board, Washington, pp. 284–290 (1966).
21. The Chemistry of Cement, Vol. I (Academic Press, London, 1964), Edited by H. F. W. Taylor. See chapter by H. F. W. Taylor entitled "The calcium silicate hydrates".
22. J. H. Taplin, "The temperature coefficient of the rate of hydration of β-dicalcium silicate," Proc. Fourth International Symp. Chemistry of Cement, Natl. Bur. Stds. Monograph No. 43, Washington, D. C. Vol. I, pp. 263–266 (1960).
23. M. Regourd, "The polymorphic transformations of tricalcium silicate" (in French) Rev. Mater. Construct. Trav. Publ. **620**, 167–176 (May, 1967).
24. E. Woermann, T. Hahn and W. Eysel "Chemical and structural investigations on the solid solutions of tricalcium silicate" (in German), Zement-Kalk-

Gips **16**, 370–375 (1963).
25. H. G. Midgley, K. E. Fletcher and A. G. Cooper, "The identification and determination of alite in portland cement clinker," The Analysis of Calcareous Materials, S. C. I. Monograph 18, Society of Chemical Industry, London, pp. 362–370 (1964).
26. Y. Ono, T. Uno and Y. Kanai, "Synthesis of five polymorphic modifications of C_3S," Semento Gijutsu Nempo, English Synopses **19**, 37–41 (1965).
27. G. Yamaguchi, K. Shirasuka and T. Ota, "Comparison of hydration properties between monoclinic and inverted triclinic alite," Symposium on the Structure of Portland Cement Paste and Concrete," Special Report 90, Highway Research Board, Washington, pp. 263–268 (1966).
28. R. W. Nurse, H. G. Midgley, W. Gutt and K. E. Fletcher, "Effect of polymorphism of tricalcium silicate on its reactivity," Symposium on the Structure of Portland Cement Paste and Concrete, Special Report 90, Highway Research Board, Washington, pp. 258–262 (1966).
29. D. L. Kantro and C. H. Weise, unpublished results.
30. A. Raccanelli, "Effects of additions of alkali sulfates and calcium sulfate on the early reactions of portland cement hydration" (in Italian), Ind. Ital. Cemento **34** (1), 3–14 (Jan. 1964).
31. H. G. Kurczyk and H. E. Schwiete, "Electron microscope and thermochemical studies of the hydration of calcium silicates $3CaO \cdot SiO_2$ and β–$2CaO \cdot SiO_2$, and the effect of calcium chloride and gypsum on the hydration process" (in German), Tonind.-Z. **84**, 585–598 (1960).
32. A. Celani, M. Collepardi and A. Rio, "The influence of gypsum and calcium chloride on the hydration of tricalcium silicate" (in Italian), Ind. Ital. Cemento **36** (7), 669–678 (July, 1966).
33. D. L. Kantro, unpublished results.
34. R. W. Nurse, "The dicalcium silicate phase," Proc. Third International Symp. Chemistry of Cement, Cement and Concrete Assoc., London, pp. 30–48 (1952).
35. F. Ordway, "Crystal structures of clinker constituents," Proc. Fourth International Symp. Chemistry of Cement Natl. Bur. Stds., Monograph No. 43, Washington, Vol. I, pp. 39–58 (1960).
36. R. W. Nurse, "Phase equilibria and constitution of portland cement clinker," Proc. Fourth International Symp. Chemistry of Cement, Natl. Bur. Stds. Monograph No. 43, Washington, D. C. Vol. I, pp. 9–21 (1960).
37. The Chemistry of Cement, Vol. I (Academic Press, London, 1964) Edited by H. F. W. Taylor. See chapter by H. G. Midgley entitled "The formation and phase composition of portland cement clinker".
38. G. Yamaguchi, Y. Ono, S. Kawamura, and Y. Soda, "Strength of mortars made from the modifications of Ca_2SiO_4", Semento Gijutsu Nempo **17**, 64–66 (1963), J. Res, Onoda Cement Co. (Tokyo) **15** (58), 195–205 (Dec. 1963).
39. I. A. Kryzhanovskaya, V. M. Mirak'yan, B. G. Shokotova and A. G. Kholodnyi, "Hydration of alkali minerals in clinker," Tsement (5) 10–11 (1965) Cement and Lime Manufacture **34** (3) 45–48 (May, 1966).
40. H. Funk, "The products obtained from the action of water on β–Ca_2SiO_4 up to 120°" (in German), Z. Anorg. Allgem. Chem. **291**, 276–293 (1957).
41. L. E. Copeland, Stephen Brunauer, D. L. Kantro, Edith G. Schulz and C. H. Weise, "Quantitative determination of the four major phases of portland cement by combined X-ray and chemical analysis," Anal. Chem. **31**, 1521–1530 (1959). PCA Res. Bull. 108.
42. H. Funk, "Two different ways of hydration in the reaction of β–Ca_2SiO_4 with water at 25 to 120°C," Proc. Fourth International Symp. Chemistry of Cement, Natl. Bur. Stds. Monograph No. 43, Washington, D. C. Vol. I, pp. 291–295 (1960).
43. Stephen Brunauer and S. A. Greenberg, "The hydration of tricalcium silicate and β-dicalcium silicate at room temperature," Proc. Fourth International Symp. Chemistry of Cement, Natl. Bur. Stds. Monograph No. 43, Washington, D. C. Vol. I, pp. 135–165 (1960).
44. D. L. Kantro, Stephen Brunauer and C. H. Weise, "Development of surface in the hydration of calcium silicates," Advances in Chemistry Series No. 33, American Chemical Society, Washington, 1962, pp. 199–219 PCA Res. Bull. 140.
45. F. W. Locher, "The chemical reactions of the hardening of cement" (in German), Zement-Kalk-Gips **17**, 175–187 (1964).
46. The Chemistry of Cement, Vol. I (Academic Press, London, 1964), edited by H. F. W. Taylor, see chapter by A. Grudemo entitled "Electron microscopy of portland cement pastes".
47. G. Sudoh and H. Mori, "The influence of difference amounts of mixing water and alkali on the hydration of C_3S," Semento Gijutsu Nempo, English Synopses **19**, 43–48 (1961).
48. N. Kawada and A. Nemoto "Calcium silicates in the earlier stages of hydration" (in German), Zement-Kalk-Gips **56**, 65–71 (1967).
49. R. Turriziani, A. Rio and M. Collepardi, "Observations on the mechanism of hydration of tricalcium silicate" (in Italian), Ind. Ital. Cemento **35**, 635–644 (1965).
50. G. L. Kalousek, "Crystal chemistry of hydrous calcium silicates: I, substitution of alumina in lattice of tobermorite," J. Am. Ceram. Soc. **40**, 74–80 (1957).
51. S. Diamond, J. L. White and W. L. Dolch, "Effects of isomorphous substitution in hydrothermally synthesized tobermorite", Am. Mineralogist **51**, 388–401 (1966).
52. L. E. Copeland, E. Bodor, T. N. Chang and C. H. Weise, "Reactions of tobermorite gel with aluminates, ferrites, and sulfates," J. Res. Dev. Lab., Portland Cement Assoc. **9** (1), 61–74 (Jan. 1967), PCA Res. Bull. 211.
53. G. L. Kalousek, "Analyzing SO_3-bearing phases in hydrating cements," Mater. Res. Std. **5**, 292–304 (1965).
54. H. G. Smolczyk, "Hydration products of cements with high contents of blast furnace slag" (in

German), Zement-Kalk-Gips **5**, 238–246 (1965).
55. L. E. Coepland, unpublished results.
56. Stephen Brunauer, D. L. Kantro and L. E. Copeland, "The stoichiometry of the hydration of beta-dicalcium silicate and tricalcium silicate at room temperature," J. Am. Chem. Soc. **80**, 761–767 (1958) PCA Res. Bull. 86.
57. S. A. Greenberg and T. N. Chang, "Hydration of tricalcium silicate", J. Phys. Chem. **69**, 553–561 (1965).
58. S. A. Greenberg and T. N. Chang, "Investigation of colloidal hydrated calcium silicate. II. Solubility relationships in the calcium oxide-silica-water system at 25°", J. Phys. Chem. **69**, 182–188 (1965). PCA Res. Bull. 180.
59. H. H. Steinour, Aqueous Cementitious Systems Containing Lime and Alumina, Portland Cement Assoc. Res. Develop. Lab. Res. Dept. Bull. **34**, Stokie, Illinois, USA (1951).
60. A. A. Klein and A. J. Phillips, "The hydration of portland cement," Natl. Bur. Standards (U.S.) Technol. Paper No. 43, 71 pp. (1914).
61. T. Thorvaldson and N. S. Grace, "The hydration of the aluminates of calcium. I. A new crystalline form of tricalcium aluminate," Can. J. Research **1**, 36–47 (1929).
62. R. Nacken and R. Mosebach, "Investigation of the system CaO–SiO_2–H_2O" (in German), Z. Anorg. Allgem. Chem. **227**, 328–36 (1936).
63. L. S. Wells, W. F. Clarke and H. F. McMurdie, "Study of the system CaO–Al_2O_3–H_2O at temperatures of 21° and 90°C," J. Res. Nat. Bur. Std. **30**, 367–409 (1943).
64. H. N. Stein, "Mechanism of the hydration of $3CaO \cdot Al_2O_3$" J. Appl. Chem. (London) **13**, 228 (1963).
65. H. N. Stein, "Influence of quartz on the hydration of $3CaO \cdot Al_2O_3$," Symposium on the Structure of Portland Cement Paste and Concrete, Special Report 90, Highway Research Board, Washington, pp. 368–377 (1966).
66. R. F. Feldman and V. S. Ramachandran, "Character of the hydration of $3CaO \cdot Al_2O_3$," J. Am. Ceram. Soc. **49**, 268–273 (1966).
67. R. F. Feldman and V. S. Ramachandran, "The influence of $CaSO_4 \cdot 2H_2O$ upon the hydration character of $3CaO \cdot Al_2O_3$," Mag. Concrete Res. **18**, 185–196 (1966).
68. P. Seligmann and N. R. Greening, "Studies of early hydration reactions of portland cement by X-ray diffraction," Highway Research Record **62**, 80–105 (1964), PCA Res. Bull. 185.
69. W. Lerch, "The influence of gypsum on the hydration and properties of portland cement pastes," Am. Soc. Testing Mater., Proc. **46**, 1252–1292 (1946), PCA Res. Bull. 12.
70. H. N. Stein, "Some characteristics of the hydration of $3CaO \cdot Al_2O_3$ in the presence of $CaSO_4 \cdot 2H_2O$," Silicates Ind. **28** (3), 141–5 (1963).
71. H. E. Schwiete, V. Ludwig and P. Jäger, "Investigations in the system $3CaO \cdot Al_2O_3$–$CaSO_4$–CaO–H_2O," Symposium on the Structure of Portland Cement Paste and Concrete, Special Report 90, Highway Research Board, Washington, pp. 353–367 (1966).
72. E. T. Carlson, "Action of water on calcium aluminoferrites," J. Res. Nat. Bur. Std. **68A**, 453–463 (1964).
73. S. Chatterji and J. W. Jeffery, "Studies of early stages of paste hydration of cement compounds. I.," J. Am. Ceram. Soc. **45**, 536–543 (1962).
74. R. Turriziani, "The process of hydration of portland cement" (in Italian), Ind. Ital. Cemento **29**, 185–189, 219–233, 244–246, 276–280, 282 (1959).
75. H. E. Schwiete and I. Iwai, "The behavior of the ferrite phase in cement during hydration" (in German), Zement-Kalk-Gips **53**, 379–386 (1964).
76. E. P. Flint, H. F. McMurdie and L. S. Wells, "Hydrothermal and X-ray studies of the garnet-hydrogarnet series and the relationship of the series of hydration products of portland cement", J. Res. Nat. Bur. Std. **26**, 13–33 (1941).
77. E. T. Carlson, "Some properties of the calcium aluminoferrite hydrates," Building Science Series 6, Building Research Division, Institute for Applied Technology National Bureau of Standards, Washintgon (1966).
78. N. Tenoutasse, "Influence of gypsum on the hydration of the ferrite phase of portland cement" (in French), Rev. Mater. Construct. **104**, 18–26 (Jan. 1966).
79. S. Chatterji and J. W. Jeffery, "Studies of early stages of hydration of cement compounds. II.", J. Am. Ceram. Soc. **46**, 187–191 (1963).
80. L. E. Copeland and E. G. Schulz, discussion of paper by A. Grudemo, "The Microstructure of hardened cement paste," Proc. Fourth International Symp. Chemistry of Cement, Natl. Bur. Standards Monograph No. 43, Washington, Vol. II, pp. 648–655 (1960).
81. P. Seligmann and N. R. Greening, "New techniques for temperature and humidity control in X-ray diffractometry," J. Res. Develop. Lab., Portland Cement Assoc. **4** (2), 2–9 (May, 1962), PCA Res. Bull. 143.
82. H. E. Schwiete, U. Ludwig and E. Niel, "Studies on the beginnings of hydration of clinker and cement," Proc. Seventh Conf. on the Silicate Industry, Akademiai Kiado, Budapest, pp. 221–233 (1965).
83. H. E. Schwiete and E. M. G. Niel, "Formation of ettringite immediately after gaging of a portland cement," J. Am. Ceram. Soc. **48**, 12–14 (1965).
84. S. Chatterji and J. W. Jeffery, "Studies of early stages of paste hydration of different types of portland cement," J. Am. Ceram. Soc. **46**, 268–273 (1963).
85. P. Seligmann and N. R. Greening, "Phase equilibria of cement-water," Fifth International Symp. on the Chemistry of Cement.
86. C. D. Lawrence, "Changes in composition of the aqueous phase during hydration of cement pastes and suspensions," Symposium on Structure of Portland Cement Paste and Concrete, Special Report 90, Highway Research Board, Washington, pp. 378–391 (1966).
87. A. Rio, A. Celani and M. Collepardi, "A contribution to the study of the hydration of portland cement during early ages" (in Italian), Ind. Ital. Cemento **35**, 275–286 (1965).

88. B. Erlin and N. R. Greening, "Hydration studies by time lapse photomicrography," J. Res. Develop. Lab., Portland Cement Assoc. **10** (2), 58–59 (May, 1968).
89. H. F. W. Taylor, private communication.
90. H. F. W. Taylor, "The chemistry of cement hydration," Proc. Seventh Conf. Silicate Industry, Akademai Kiado, Budapest, pp. 199–220 (1965).

Written Discussion

J. G. M. de Jong, Hans N. Stein and J. M. Stevels

In the survey on the early hydration of C_3S, given by Dr. Copeland and Dr. Kantro, one point is only shortly mentioned that may be of some other than trivial nature: the accelerated, "autocatalytic" character of the hydration of C_3S during the first day.

The phenomenon has been known from calorimetric measurements as early as 1940 (1). It has been confirmed by later calorimetric experiments (2, 3), and its interpretation of indicating accelerated conversion of C_3S has been corroborated by X-ray measurements (4, 5).

The accelerated character of the hydration of C_3S has been ascribed (2, 6, 7) to the conversion of a first, strongly retarding hydrate (F. H.) into a second, less retarding one (S. H.) under the action of nuclei of the second hydrate. F. H. was assumed, following Kantro, Brunauer and Weise (8), to have the composition C_3SH_n; S. H. resembles C–S–H–I samples as regards electron microscope habit, and may therefore be supposed to have a much lower CaO/SiO_2 molar ratio.

The following facts are consistent with this mechanism:

a. The hydration of C_3S can be accelerated by artificially lowering the Ca^{2+} and OH^- concentrations during the first minutes by the addition of amorphous silica. Indeed, the formation rate of S. H. nuclei from F. H. is expected to be accelerated by the lowering of calcium and hydroxyl ion concentrations.
b. The hydration of C_3S can be retarded by the addition of CaO or $Ca(OH)_2$ (9). This equally can be explained by the mechanism mentioned: the formation of S. H. nuclei from F. H. is expected to be retarded by an initial excess of calcium and hydroxyl ions in the water phase.
c. The hydration of C_3S is retarded by the addition of aluminate ions, either as $Al(OH)_3$ (10) or as C_3A (11), when the aluminate ion concentration surpasses a certain limit. This is explianed through incorporation of aluminium ions into F. H., retarding its conversion, as found by Kalousek (12) for the case of the conversion of tobermorite into xonotlite.

Some results reported by Copeland and Kantro (Fig. 8 of their paper) appear to indicate an increase rather than a decrease of the hydration rate of C_3S by the presence of aluminium ions. However, their first data were obtained after 1 day's hydration. Indeed we found calorimetrically that the *total* heat evolved during the C_3S hydration peak is increased by aluminate ions; by means of quantitative X-ray analysis, it was found that after 96 hours more C_3S had been converted in the presence of $Al(OH)_3$ than in its absence (10).

As regards C_3A hydration in the presence of $CaSO_4 \cdot 2H_2O$, Copeland and Kantro remark that the ettringite layer first formed on the C_3A surface is supposed to be removed by a "scaling off" mechanism. This indeed was the view supported in 1962 by one of the present authors (13). However, later (14) some results were obtained indicating a chemical rather than a mechanical destruction of this layer. This interpretation had been, as appears now, anticipated by Seligmann and Greening (15), and has been confirmed recently by Mori and Minegishi (16). There rests the difficulty of explaining the persistent coexistence of ettringite and monosulfate or C_4AH_{19} crystals in hardening cement pastes, as mentioned by Copeland and Kantro (Fig. 31). Most probably a rapid conversion of ettringite demands high values of calcium and aluminate ion concentrations as are found in a hardening cement paste locally only, in the direct vicinity of a C_3A surface.

References

1. L. R. Forbrich. J. Amer. Concrete Inst. Proc., **37**, 161 (1940).
2. H. N. Stein and J. M. Stevels, J. Appl. Chem. (London) **14** (8), 338–346 (1964).

3. N. Kawada and A. Nemoto, Zement-Kalk-Gips **56**, 65–71 (1967).
4. R. L. Angstadt and F. R. Hurby, Nature (London) **197**, 688 (1963).
5. F. R. Hurley and R. L. Angstadt, J. Appl. Chem. (London) **16**, 162 (1966).
6. H. N. Stein and J. M. Stevels, J. Phys. Chem. **69**, 2489 (1965).
7. H. N. Stein, J. M. Stevels and J. G. M. de Jong, Zement-Kalk-Gips **56** (8) 347 (1967).
8. D. L. Kantro, S. Brunauer and C. H. Weise, J. Phys. Chem. **66**, 1804–9 (1962).
9. J. G. M. de Jong, H. N. Stein and J. M. Stevels, J. Appl. Chem,. (London) **17**, 246–250 (1967).
10. J. G. M. de Jong, H. N. Stein and J. M. Stevels, J. Appl. Chem. (London) **18**, 9–17 (1968).
11. J. G. M. de Jong, H. N. Stein and J. M. Stevels, Supplementary Paper submitted for the 5th. Intern. Symp. on the Chemistry of Cement. See also N. Tenoutasse, ib.
12. G. L. Kalousek, J. Am. Ceram. Soc **40**, 74 (1957).
13. H. N. Stein, Rec, trav. chim. Pays Bas **81**, 881 (1962).
14. H. N. Stein, J. Appl. Chem. (London) **15** 314–325 (1965).
15. P. Seligmann and N. R. Greening, Highway Research Record **62**, 80–105 (1964).
16. H. Mori and K. Minegishi, as ref. (11).

Oral Discussion

John H. Taplin

In a Written Discussion of paper II-4 by Kondo and Ueda I have made a plea that where researchers do not have closely sized materials, they should measure the particle size distribution.

This request is perhaps even more relevant here. Copeland and Kantro have quoted a great deal of kinetic data but much of the kinetic significance has been lost because of a lack of particle size information about the anhydrous cement materials.

Authors' Closure

L. E. Copeland and D. L. Kantro

Mr. Taplin is correct in the sense that little of the data presented in our paper gives information about the effects of particle size upon the kinetics of hydration. Nevertheless, something has been learned about the effects of factors other than fineness (or particle size), and there is much more to be learned. The effects of temperature, water/cement ratio, and chemical composition can be studied individually by working with cements ground by the same procedures to a constant fineness. The conclusions reached in this type of study may have to be modified if there is a strong interaction between fineness and one or more of the other factors.

The results of hydration studies by independent teams of workers are fairly consistent with each other and suggests that interactions between fineness and other factors are probably not strong over the range of finenesses usually encountered in cements.

Supplementary Paper II-2 Contribution of Calcium Thiosulphate to the Acceleration of the Hydration of Portland Cement and Comparison with Other Soluble Inorganic Salts

Keiichi Murakami and Hirobumi Tanaka*

Synopsis

In this paper, the accelerating ability of calcium thiosulphate which was newly discovered by the authors is investigated by means of various methods, in comparison with other soluble inorganic salts, such as calcium chloride, calcium nitrate etc.

The accelerating action of calcium thiosulphate on the setting of portland cement is approximately similar to that of calcium chloride. The early development of strength of portland cement gradually increases as the quantity of calcium thiosulphate in portland cement increases. Especially, the early strength of mortar of portland blast furnace slag cements (consisting of granulated blast furnace slag 65 and portland cement 35), when calcium thiosulphate is used at concentration of 3% to the cement, is developed near that of ordinary portland cement.

The result of corrosion test showed that the test pieces of mild steel buried in mortar containing respectively 3% and 6% calcium thiosulphate weres carcely corroded after the mortar was exposed under the atmosphere for 6 months. Under the same condition, the test piece of mild steel buried in the mortar containing 2% calcium chloride was markedly corroded after only one month.

The acceleration of hydration of portland cement by inorganic salts results from the acceleration of hydration of alite phase. The order of effectiveness of anions and cations as the accelerators of hydration of portland cement is $Cl^- > S_2O_3^{--} > SO_4^{--} > NO_3^-$, $Cl^- > Br^- > I^-$ and $Ca^{--} > Mg^{--} > Na^-$. The anion in salt is closely related to the tangent of the ascending portion in the heat liberation curve of the hydration of alite. The cation is closely related to the beginning time of the second peak in the heat liberation curves of the hydration of portland cement.

The hydration products of C_3S at later stage of hydration are generally CSH(II) when calcium chloride was used, are CSH(I) when no additives was used and can not be evidently detected when calcium thiosulphate is present.

At early stage of the hydration without gypsum, the hydration products of C_3A which are obtained in the presence of calcium chloride and calcium thiosulphate are gel-like substance, however, when calcium nitrate is present, the hydration products are polygonal crystalline particles and hexagonal plate-like crystals.

Introduction

Calcium chloride is now well known as an excellent accelerator of the hydration of portland cement. However, the chloride attack to the steel in reinforced concrete is hardly ignored from the viewpoint of the maintenance of concrete constructions. Furthermore, a troublesome problem connected with the chloride attack is being brought about by the use of beach-sand that resulted from the lack of fine aggregates in making concrete in large cities in Japan. Therefore, it is very favorable if the chloride ion remaining in concrete can be turned into the very difficult soluble compound and so be inactivated. But it may be now very difficult.

In the present study, the accelerating action of calcium thiosulphate discovered by the authors is investigated and is compared with other soluble inorganic salts, such as calcium chloride, calcium nitrate, calcium sulphate etc. Because, it is suggested that calcium thiosulphate does not probably give any corrosion to the steel in concrete.

A number of studies have been undertaken to clarify the accelerating actions of various salts and, especially, the effect is brought about by the addition of calcium chloride to portland cement.

*Faculty of Engineering, Tohoku University, Sendai, Japan.

Shinohara and Naritomi (1), Nagai (2), Narahashi, Amamiya and Nakajima (3) examined the influences of various salts on the setting and hardening of portland cement. Their results showed that calcium chloride and barium chloride have a most effective accelerating action among various salts used. The heat liberation process of the hydration of portland cement containing the accelerators was studied by Bogue (4), Stein (5), Edwards and Angstadt (6), Angstadt and Hurley (7), Zimonyi and Balazs (8), etc. by the use of conduction calorimeter. They obtained an identical conclusion, in which the accelerators do not promote the hydration of C_3A, but predominantly accelerate the hydration of C_3S phase of portland cement. Edwards and Angstadt (6) reported that both cations and anions are ranked according to their general effectiveness as accelerators of the hydration of the C_3S phase: $Ca^{++} > Mg^{++} > Li^{+} > Na^{+} > H_2O > Zn^{++}$ and $OH^{-} > Cl^{-} > Br^{-} > NO_3^{-} > SO_4^{--} > H_2O > CH_3COO^{-}$. It was reported by Bogue (9) and Jones (10) that, although calcium chloride does not accelerate the hydration of C_3A, such complex salts as $C_3A \cdot CaCl_2 \cdot 10H_2O$ and $C_3A \cdot 3CaCl_2 \cdot 30H_2O$ are produced by the reaction between calcium chloride and C_3A. The reaction with C_3A and $CaSO_4 \cdot 2H_2O$ was found by Rosenberg (11) to occur rapidly than the reaction with C_3A and $CaCl_2$, when C_3A was added to the aq.solution containing $CaCl_2$ and $CaSO_4 \cdot 2H_2O$. Calcium chloraluminate complex salts are produced after gypsum was depleted. Andreeva and Segalova (12) reported that the concentration of Cl^- in the liquid phase of C_3S paste containing $CaCl_2$ does not vary with time. Therefore, it was suggested that the accelerating action of calcium chloride on the hydration of C_3S may be catalytic. Moreover, Johnston (13) confirmed that the concentration of Ca^{++} in the liquid phase of portland cement paste is increased by the addition of calcium chloride. It was shown by Libermann and Kireev (14) that some calcium salts, as $CaCl_2$, $MgCl_2$, etc., however, may so reduce the OH^- concentration of aq. solution, even though saturated with lime. Recently, Kawada and Nemoto (15) have reported that the addition of calcium chloride at a optimum concentration on the acceleration brings about an increase of the quantity of lime and silicate which are saturated in liquid phase and therefore, that the early strength development of portland cement is given by the great precipitation of resultant hydration products. Another study suggested that the coagulation of CSH may be strengthened by the ionic strength which was increased by the addition of calcium chloride. The morphologie of CSH produced in the presence of calcium chloride were studied by Richartz and Locher (16) by electron microscopic observation. They stated that the high strength obtained by the addition of calcium chloride may resulted from the cross-linking of the long fibrous crystals of CSH.

Experimental

Materials

In this study, each of commercial portland cement, commercial portland blast furnace slag cement and commercial early strength portland cement was employed. Tricalcium aluminate, tricalcium silicate and alite as clinker mineral of portland cement were synthesized and were also employed.

Crystals of calcium thiosulphate can be prepared (17) by making a 3/4 saturated solution of $CaCl_2 \cdot 6H_2O$, adjusting the pH of 8–9 with CaO, and adding pure $Na_2S_2O_3 \cdot 5H_2O$ excluding air and CO_2 with a stream of N_2. After 4 hours, at 40°C, the solution is freed of precipitated salt by filtration, and two corps of calcium thiosulphate are obtained, one at 0°C and a second at −20°C. In order that the crystals are completely freed from Cl^-, subsequently, a series of such operations as dissolution, crystallization and washing with water is twice repeated. The resultant crystals were very pure.

Calcium thiosulphate has a molecular equation as $CaS_2O_3 \cdot 6H_2O$ and a large solubility in water. Since the vapor tension of crystal water is very high, some portions of crystal water are easily lost and simultaneously sulphur and calcium sulphite is produced as decomposed compounds, when the crystal is kept standing in dry atmosphere. Therefore, calcium thiosulphate must be stored in a vessel with saturated humidity, however, it is stable for long period in the aqueous solution.

Fig. 1 shows the DTA curve of calcium thiosulphate crystal and its thermal balance curve. The curves indicate the loss of crystal water (50°C), the dehydration of the calcium sulphite crystal (100°C), the combustion of the sulphur (300°C) and the oxidation of the calcium sulphite (600°C).

Procedures

In order to investigate the accelerating action of

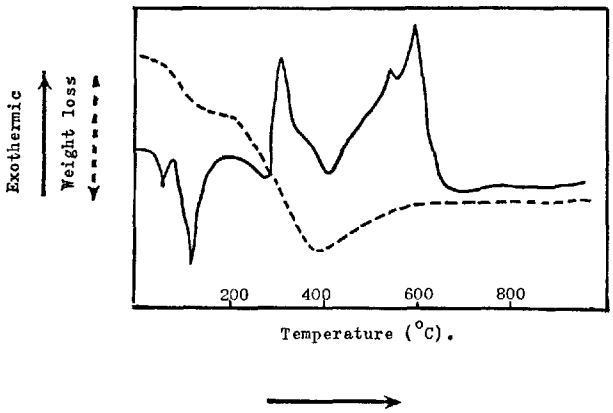

Fig. 1. *DTA of calcium thiosulphate crystal. Heating rate: 5°C/min., Standard substance: α-Al_2O_3., Sample holder: Pt, Thermocouple: Pt-PtRh 13%. Solid curve: DTA, Broken curve: Thermal balance.*

calcium thiosulphate and other soluble inorganic salts, various methods are used, namely, setting and strength development test, measurement of the heat liberation on the hydration of portland cement, quantitative and qualitative X-ray analysis, differential thermal analysis, thermal balance, electron microscopic observation, measurement of free lime, corrosion test and measurement of specific surface area.

Results and Discussion

The time of set of paste made from portland cement containing $CaCl_2$, CaS_2O_3 and $Ca(NO_3)_2$ is shown in Table 1. When 1% of calcium chloride was added to the portland cement, the setting time is reduced to half that of portland cement with only gypsum. Calcium nitrate accelerates the set at concentration of 0.5% to the cement, but it acts as a retarder beyond its concentration. Calcium thiosulphate is very effective as an accelerator to the setting of ordinary portland cement, portland blast furnace slag cement and early strength portland cement. The results are shown in Tables 2 and 3. The strength development of mortar made from portland cement containing $CaCl_2$, CaS_2O_3 and $Ca(NO_3)_2$ is shown in Table 4. The accelerating effect of calcium chloride on the strength development at early stage of the hydration of portland cement is largest among them. However, there is a tendency that the strength development of the 28 day of portland cement with calcium chloride is relatively less than that of portland cement without calcium chloride. From this result, it is suggested that an optimum amount of calcium chloride for the acceleration of portland cement hydration may be 2%. Calcium nitrate does not reveal the accelerating action on the strength development of portland cement mortar.

Table 1. *Effects of calcium chloride, calcium nitrate and calcium thiosulphate on the setting time of portland cement*

	$CaCl_2$				
	$CaCl_2$/portland cement (%)				
	0	0.5	1.0	3.0	6.0
Initial set (hr.-min.)	2—50	1—58	1—18	0—45	0—05
Final set (hr.-min.)	4—20	3—15	2—02	1—20	0—11
	$Ca(NO_3)_2$				
	$Ca(NO_3)_2$/portland cement (%)				
	0	0.5	1.0	3.0	6.0
Initial set (hr.-min.)	2—28	1—52	1—35	1—40	3—05
Final set (hr.-min.)	4—10	2—12	2—40	3—30	5—55
	CaS_2O_3				
	CaS_2O_3/portland cement (%)				
	0	1.2	1.8	2.9	
Initial set (hr.-min.)	2—44	1—21	1—04	0—23	
Final set (hr.-min.)	3—56	1—54	1—39	0—40	

Table 2. *Effect of calcium thiosulphate on the setting time of portland blastfurnace cement*

	CaS_2O_3/portland blastfurnace cement (%)			
	0	1.0	2.0	3.0
Initial set (hr.-min.)	4—14	1—48	1—16	0—32
Final set (hr.-min.)	6—24	2—30	2—01	0—57

Composition of portland blastfurnace slag cement: Granulated blast furnace slag (65) + portland cement (35).

Table 3. *Effect of calcium thiosulphate on the setting time of early strength portland cement*

	CaS_2O_3/early strength portland cement (%)	
	0	1.0
Initial set (hr.-min.)	2—13	1—16
Final set (hr.-min.)	3—25	1—41

Table 4. *Effects of calcium chloride, calcium nitrate and calcium thiosulphate on the strength development of portland cement mortar*

		1 day		3 days		7 days		28 days	
	%	B	C	B	C	B	C	B	C
	0	15.8	39.0	34.3	120	52.8	221	79.0	379
$CaCl_2$	1.0	20.8	69.5	40.0	150	54.9	291	76.1	381
	2.0	24.2	82.5	46.9	172	51.5	243	77.1	352
	3.0	26.7	85.3	45.5	177	55.5	265	74.9	364
$Ca(NO_3)_2$	2.0	7	18.7	34.2	113	47.3	193	74.6	316
	5.0	15.1	42.3	41.0	173	63.1	261	77.3	351
CaS_2O_3	1.0	17.1	44.7	34.6	117	51.9	210	73.6	341
	2.0	18.1	46.7	35.6	127	53.2	203	76.2	328
	3.0	18.8	55.8	37.8	130	53.1	237	75.2	366
	5.0	20.1	59.3	40.6	150	55.7	205	66.1	310
	6.5	21.1	69.3	37.6	143	50.9	207	63.4	268

B: Bending strength, C: Compressive strength, unit of strength: kg/cm².

The accelerating action of calcium thiosulphate, which is relatively less than that of calcium chloride, however, is gradually strengthened in proportion to the amount of calcium thiosulphate added to the cement. Consequently, a high strength is obtained at the one and three days, but the strength development at the 28 days is less, as in the case of calcium chloride, than that of portland cement with only gypsum.

An interesting example in the acceleration of strength development by the addition of calcium thiosulphate is shown in Table 5. The early strength development of portland blast furnace slag cement containing a large quantity of granulated blast furnace slag is generally poor, according to the delayed hydration of blast furnace slag, on the other hand, the strength development at later stage of the hydration is very high. When calcium thiosulphate was added at concentration of 3% to the blast furnace slag cement, not only the early strength development can be approached to the value near that of ordinary portland cement, but also a higher value can be kept at later stage without such adverse reduction that is frequently observed when the accelerators were used, because the quantity of portland cement clinker is only 35% of the blast furnace slag cement, in which the influence of portland cement on the strength development of the blast furnace slag cement will be small at later stage. Therefore, it can be suggested that the hydration mechanism of granulated blast furnace slag is markedly different from that of portland cement and the accelerating action of calcium thiosulphate is scarcely related to the hydration of slag.

It is evident that calcium thiosulphate is effective as an accelerator on the 15 hour strength development of early strength portland cement, however, it

Table 5. *Effect of calcium thiosulphate on the strength development of portland blast furnace slag cement*

		1 day		3 days		7 days		28 days	
	%	B	C	B	C	B	C	B	C
	0	8.4	17.9	25.4	65.8	46.8	161	63.9	318
	1.0	11.6	26.8	30.0	81.8	54.4	173	73.7	335
CaS_2O_3	2.0	13.6	28.8	33.7	93.1	61.2	175	75.5	339
	3.0	13.2	33.0	43.2	122	70.4	179	82.0	350

Composition of portland blast furnace slag cement: Granulated blastfurnace slag (65) + portland cement (35). Unit of strength: kg/cm².

Table 6. *Effect of calcium thiosulphate on the strength development of early strength portland cement*

	1 day		3 days			15 hrs	
%	B	C	B	C	%	B	C
0	26.7	78.8	67.5	273	0	14.2	43.2
3.0	26.8	81.6	71.7	263	6.5	21.7	74.5

Unit of strength: kg/cm².

Table 7. *Effect of calcium thiosulphate and hot curing on the strength development of portland cement*

CaS_2O_3 (%)	Curing method	B	C	(kg/cm²)
6.5	5 hrs at 20°C	1.2	7.1	
6.5	8 hrs at 20°C	3.1	12.1	
6.5	5 hrs at 20°C + 4 hrs at 60°C	27.3	78.8	
6.5	5 hrs at 20°C + 8 hrs at 60°C	35.1	126	

Hot curing was undertaken in hot water.

has not an available action on the one and three day strength development (Table 6). On the manufacture of ready-made concrete products, if the high early strength can be developed by the addition of calcium thiosulphate, consequently, the rate of production will be accelerated and the economical production will be accomplished. As an example of this attempt, Table 7 shows the strength development of portland cement mortar containing calcium thiosulphate after 5 and 8 hour curing in air at 20°C and, in addition, subsequently after 6 hour hot curing in hot water. From this result, it may be suggested that the removing of concrete products from frame can be accelerated by the use of calcium thiosulphate.

Corrosion Test

In order to compare with the corrosive character of $CaCl_2$, CaS_2O_3 and $Ca(NO_3)_2$, the test pieces made of mild steel were buried in portland cement mortar containing a definite quantity of each salt. Then, the mortars was kept standing for a definite period in outdoors. The occurrence of corrosion was observed on the surface of all the test pieces buried in the mor-

tar with 2% and 5% additions of $CaCl_2$ after only one month. On the contrary, the corrosion on the surface of test pieces buried in the mortar containing calcium thiosulphate and calcium nitrate was scarcely observed after 6 months, even when both salts were respectively used at concentration of 5%. Consequently, calcium thiosulphate has been confirmed to be an accelerator without the corrosive action.

Effect of Accelerators on the Heat Liberation Process of the Hydration of Portland Cement and Clinker Minerals

An adiabatic calorimeter, of which the detailed operating procedure and construction were described in the previous paper (18), was used. The compositions of cement samples charged in the calorimeter are shown in each figure. From Fig. 2 to 9, the heat liberation caused by the hydration of sample in the calorimeter is plotted as "Temperature rising" (Thermal electromotive force μV by thermocouple) versus hydration time. This device uses such paste that contains a large water- content and is not entirely

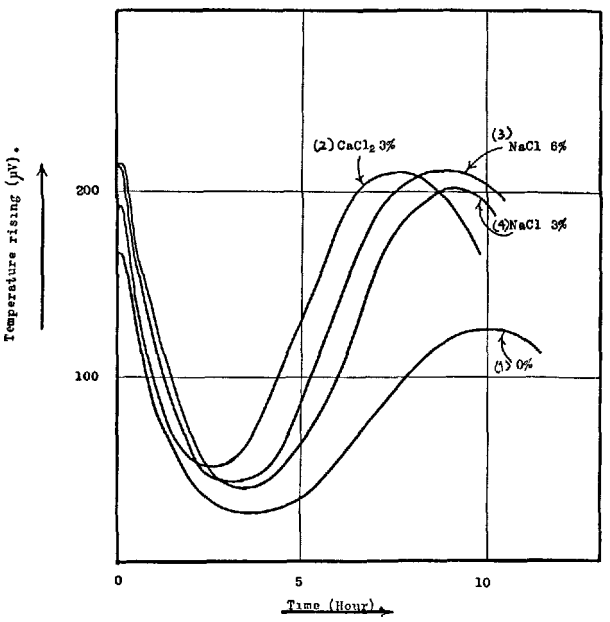

Fig. 2. *Heat liberation curves of the hydration of portland cement pastes containing* $CaCl_2$ *and* NaCl
Compositions of pastes:
(1) Portland cement(8g) + α-Al_2O_3(16g) + H_2O(13ml).
(2) Portland cement(8g) + α-Al_2O_3(16g) + 2%$CaCl_2$ aq. solution(13ml).
(3) Portland cement(8g) + α-Al_2O_3(16g) + 4%NaCl aq. solution(13ml).
(4) Portland cement(8g) + α-Al_2O_3(16g) + 2%NaCl aq. solution(13ml).
Hydration temperature: 25°C.

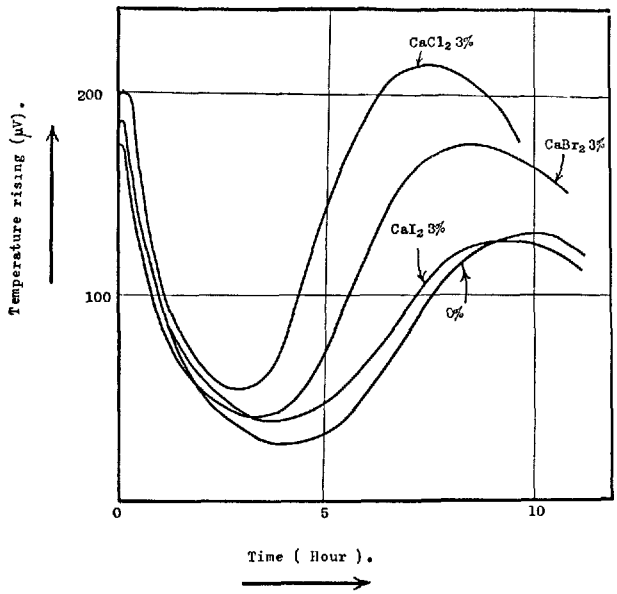

Fig. 3. *Heat liberation curves on the hydration of portland cement pastes containing* $CaCl_2$, $CaBr_2$ *and* CaI_2
Compositions of pastes:
Portland cement(8g) + α-Al_2O_3(16g) + 2%$CaCl_2$ aq. solution(13ml).
Portland cement(8g) + α-Al_2O_3(16g) + 2%$CaBr_2$ aq. solution(13ml).
Portland cement(8g) + α-Al_2O_3(16g) + 2%CaI_2 aq. solution(13ml).
Hydration temperature: 25°C.

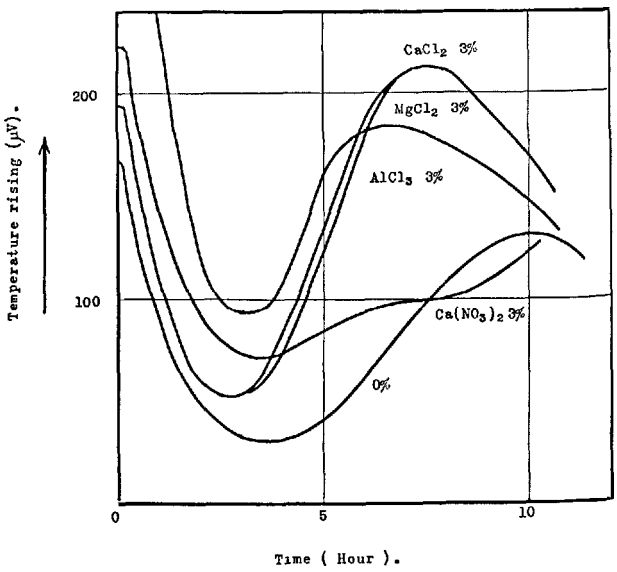

Fig. 4. *Heat liberation curves on the hydration of portland cement pastes containing* $CaCl_2$, $MgCl_2$, $AlCl_3$ *and* $Ca(NO_3)_2$
Compositions of pastes:
Portland cement(8g) + α-Al_2O_3(16g) + 4%$MgCl_2$ aq. solution(13ml).
Portland cement(8g) + α-Al_2O_3(16g) + 4%$AlCl_3$ aq. solution(13ml).
Portland cement(8g) + α-Al_2O_3(16g) + 4%$Ca(NO_3)_2$ aq. solution(13ml).
Hydration temperature: 25°C.

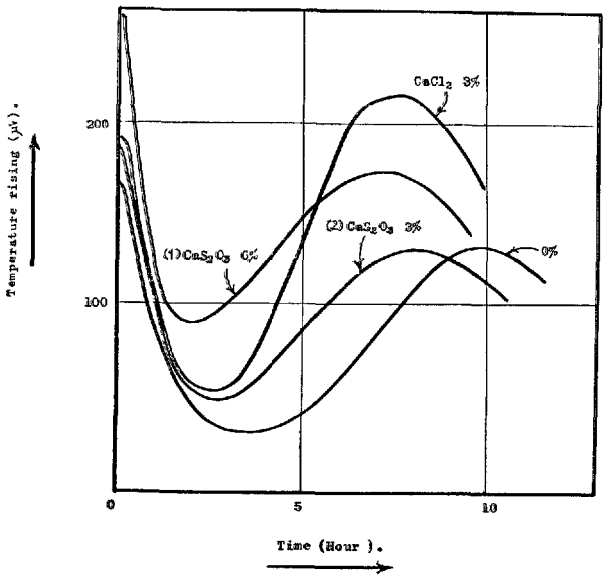

Fig. 5. *Heat liberation curves on the hydration of portland cement pastes containing* $CaCl_2$ *and* CaS_2O_3

Compositions of pastes:
(1) Portland cement(8g) + α-Al_2O_3(16g) + 4%CaS_2O_3 aq. solution(13ml).
(2) Portland cement(8g) + α-Al_2O_3(16g) + 2%CaS_2O_3 aq. solution(13ml).
Hydration temperature: 25°C

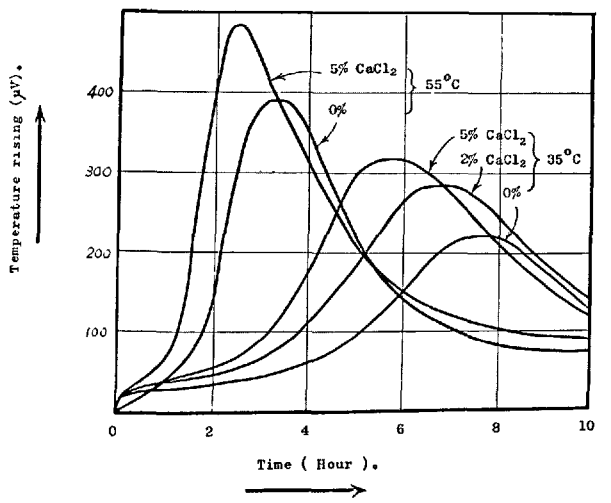

Fig. 6. *Effect of calcium chloride on the heat liberation of the hydration of alite*

Compositions of pastes:
Alite(3g) + Gypsum(0.5g) + α-Al_2O_3(20.5g) + H_2O(13ml).
Alite(3g) + Gypsum(0.5g) + α-Al_2O_3(20.5g) + 0.46% $CaCl_2$ aq. solution(13ml).
Alite(3g) + Gypsum(0.5g) + α-Al_2O_3(20.5g) + 1.15% $CaCl_2$ aq. solution(13ml).
Hydration temperature: 35°C and 55°C.

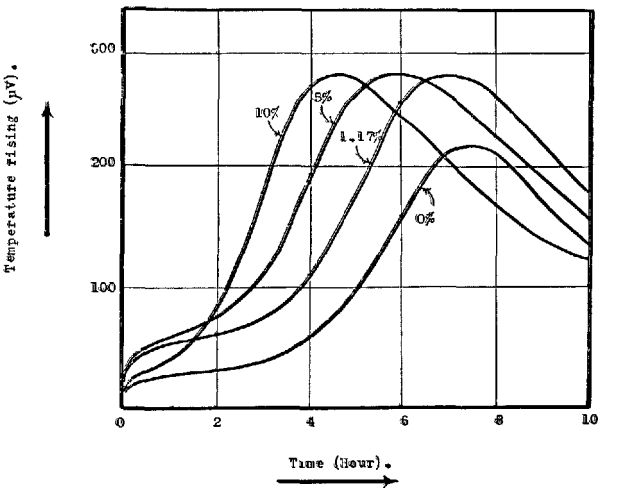

Fig. 7. *Effect of calcium thiosulphate on the heat liberation of the hydration of alite*

Compositions of pastes:
Alite(3g) + Gypsum(0.5g) + α-Al_2O_3(20.5g) + 0.45% CaS_2O_3 aq. solution(13ml).
Alite(3g) + Gypsum(0.5g) + α-Al_2O_3(20.5g) + 1.15% CaS_2O_3 aq. solution(13ml).
Alite(3g) + Gypsum(0.5g) − α-Al_2O_3(20.5g) + 2.30% CaS_2O_3 aq. solution(13ml).
Hydration temperature: 35°C.

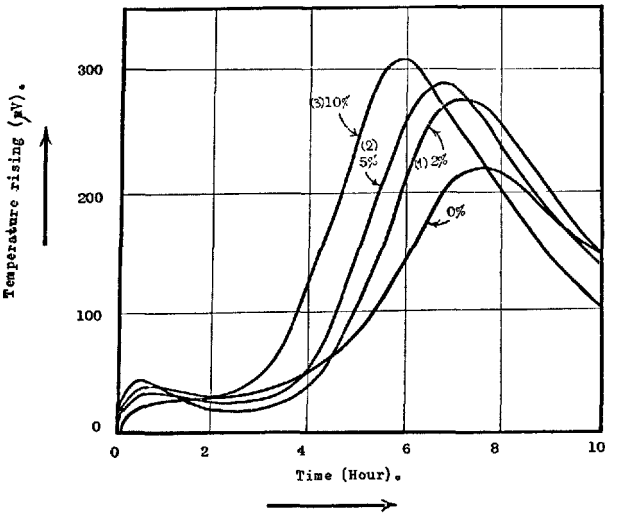

Fig. 8. *Effect of calcium nitrate on the heat liberation of the hydration of alite*

Compositions of pastes:
(1) Alite(3g) + Gypsum(0.5g) + α-Al_2O_3(20.5g) + 0.45%$Ca(NO_3)_2$ aq. solution(13ml).
(2) Alite(3g) + Gypsum(0.5g) + α-Al_2O_3(20.5g) + 1.15%$Ca(NO_3)_2$ aq. solution(13ml).
(3) Alite(3g) + Gypsum(0.5g) + α-Al_2O_3(20.5g) + 2.30%$Ca(NO_3)_2$ aq. solution(13ml).
Hydration temperature: 35°C.

agitated. The heat liberation of hydration immediately after portland cement contacted into with water can be measured by this device, on the other hand, it is impossible with the conventional conduction calorimeter. Furthermore, when the heat liberation of hydra-

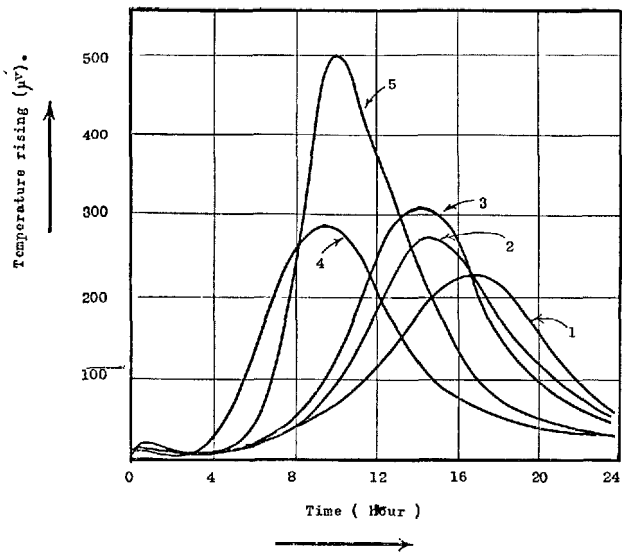

Fig. 9. *Effects of* $CaCl_2$, CaS_2O_3, $Ca(NO_3)_2$ *and* $CaSO_42H_2O$ *on the heat liberation of the hydration of* C_3S

Compositions of pastes:

(1) $C_3S(8g) + \alpha\text{-}Al_2O_3(16g) + H_2O(13ml)$.
(2) $C_3S(8g) + \alpha\text{-}Al_2O_3(16g) + 2\%Ca(NO_3)_2$ aq. solution (13ml).
(3) $C_3S(8g) + \alpha\text{-}Al_2O_3(16g) + CaSO_4 \cdot 2H_2O(0.27g) + H_2O(13ml)$.
(4) $C_3S(8g) + \alpha\text{-}Al_2O_3(16g) + 2\%CaS_2O_3$ aq. solution (13ml).
(5) $C_3S(8g) + \alpha\text{-}Al_2O_3(16g) + 2\%CaCl_2$ aq. solution (13ml).

tion of portland cement containing accelerators is measured by conduction calorimeter, generally, there is a tendency that the analysis of accelerating action becomes very difficult by overlapping of both the first and second cycle in the heat liberation curve, because the hydration of alite phase corresponding to the second cycle is considerably accelerated by the agitation. The separation between the both cycles is approximately possible in the heat liberation curve given by the use of this device.

Fig. 2 shows the accelerating actions of acidic salt $CaCl_2$ and neutral salt NaCl. They accelerate the set and hardening of portland cement by accelerating the hydration of alite phase, namely, by accelerating the occurrence of the second cycle. Besides, it is suggested that the anion of salts is closely related to the tangent of ascending portion of the second cycle, and that the cation, to the beginning time of second cycle. When the both salts are used at the same concentration, the beginning time is more shortened by calcium chloride than by sodium chloride. When sodium chloride is used at a concentration of 6%, the beginning time is slightly shortened than that in the case of 3% sodium chloride, however, it is still longer than that in the case of 3% calcium chloride.

The effects of some salts consisted of a common cation Ca^{++} and different anions of halogens Cl^-, Br^- and I^- on the hydration of portland cement are shown in Fig. 3. From this result, it is found that the stronger the non-metallic character of anions, the larger the tangent of ascending portion of the second peak. The addition of salt containing anion with a strong metallic character causes the second peak to be less intense.

Fig. 4 shows the accelerating action of some chlorides with different cation and calcium nitrate on the hydration of portland cement. $CaCl_2$ and $MgCl_2$ have a similar accelerating effect on the hydration of alite. On the other hand, the heat liberation curves of the hydration of portland cement with $AlCl_3$ 3% and $Ca(NO_3)_2$ 3% are anomalous. In the case of the former, especially, there is a considerable increase, which can be caused by the flash set of alumina-gel which is most likely produced by the reaction with an acidic salt $AlCl_3$ and lime in liquid phase or aluminate phase, in the initial heat evolution. The produced gel will coat the cement grains and will hinder the hydration of cement, therefore, the second peak may not be consequently developed in spite of the presence of chloride ion. Calcium nitrate shows an abnormal curve as if it not only indicates the absence of accelerating action, but also may obstructs the hydration of alite phase. From this fact, it will be considered that the hydration behaviors of calcium aluminate in the presence of accelerators must be also studied for understanding the acceleration of hydration of portland cement.

The second peak of the hydration of portland cement accelerated by 3% $CaCl_2$ has an intensity which is twice larger than that accelerated by calcium thiosulphate at the same concentration as shown in Fig. 5. Namely, the tangent of ascending portion of the second peak with 3% $CaCl_2$ is also twice that of the case of 3% CaS_2O_3. When the concentration of CaS_2O_3 was increased from 3% to 6%, the second peak in the heat liberation curve is slightly accelerated and also is leveled up with the original profile. Although calcium thiosulphate accelerates the occurrence of the second peak in the heat liberation of portland cement hydration, it does not relate to the increase in tangent of ascending portion of the second peak. A considerable increase in the initial heat evolution, in the case of 6% CaS_2O_3, is supposed apparently to be caused by the interaction between CaS_2O_3 and C_3A or calcium aluminoferrites.

In order to confirm the accelerating action on the hydration of only alite, the effect of calcium chloride

on the hydration of synthetic alite was studied at both temperatures of 35°C and 55°C. The result is shown in Fig. 6. The accelerating action of calcium chloride is apparent by the facts that the beginning time of heat liberation is gradually shortened and the intensity of heat liberation is rapidly strengthened in proportion to the increasing amount of calcium chloride. However, the effect of temperature is so great that the hydration at 55°C corresponds to that with the addition of 10% $CaCl_2$.

Fig. 7 shows the accelerating action of calcium thiosulphate on the hydration of synthetic alite. The principal effect is a shifting of the peak of maximum heat liberation to an earlier age. Of course, an increase in the heat liberation during the first ten hours is larger than that of the case without calcium thiosulphate, however, the liberated heat is not increased as the addition of calcium thiosulphate increases. It seems a tendency in the accelerating action of calcium thiosulphate.

Although the accelerating action of calcium nitrate has not been observed in Fig. 4 and Tables 1 and 4, the hydration of alite is slightly accelerated as shown in Fig. 8. But, a shifting of the peak is less than that with $CaCl_2$ or CaS_2O_3, in spite of the increasing additions. Fig. 9 shows the effect of representative accelerators used in this experiment on the hydration of synthetic tricalcium silicate. The general order of effectiveness as accelerator is $Cl^- > S_2O_3^{--} > SO_4^{--} > NO_3^-$. But, only the order of the last two obtained in this experiment is contrary to that shown by Edwards and Angstadt (6).

pH of Liquid Phase of Paste Containing Accelerators

Libermann and Kireev (14) already stated that pH of liquid phase of portland cement is lowered when the accelerator was added. Table 8 shows the pH in liquid phase of portland cement paste immediately after the paste was prepared. Although the lowering of pH by the addition of possible accelerators is evidently observed, it is not always true that all the salts which lower the pH of liquid phase are accelerators.

Hydration Products of C_3S Paste Containing $CaCl_2$ CaS_2O_3 and $Ca(NO_3)_2$

Various phenomena in the hydration process are affected not only by the addition of accelerators, but also by the different morphologie and different physicochemical properties of the hydration products which were formed in the hydration process. Fig. 10 shows the DTA curves of the 7 hour hydration products of C_3S pastes containing such $CaCl_2$, $CaSO_4 \cdot 2H_2O$, CaS_2O_3 and $Ca(NO_3)_2$. The intensity of endothermic peaks near 100°C and 500°C shows approximately the rate of hydration. A shoulder of peak at 500°C indicates the presence of amorphous calcium hydroxide. The two endothermic peaks at temperature of over 900°C show the two inversions of C_3S, namely, triclinic $\xrightarrow{923°C}$ monoclinic $\xrightarrow{980°C}$ trigonal. The defference between $CaCl_2$ and CaS_2O_3 is apparently demonstrated by the continued two exothermic peaks occurred at a temperature range from 600°C to 700°C. The DTA and thermal balance curves of the 24 hour hydration products, which are shown in Fig. 11, indicate evidently the differences mentioned above. In the case of $CaCl_2$, since the exothermic peak at 650°C does not brings about any changes in weight,

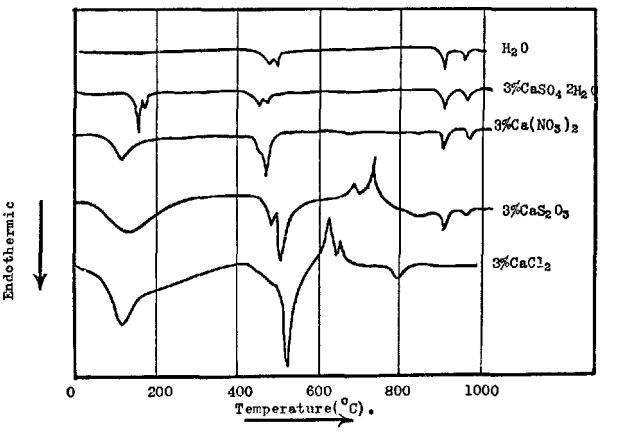

Fig. 10. *DTA curves of the hydration products (After 7 hour hydration) of C_3S in the presence of various salts.*
Water-C_3S ratio: 40%, Hydration temperature: 20°C, The quantity of each salt added to C_3S is 3%. Heating rate: 5°C/min. Thermocouple: Pt–PtRh 13%.

Table 8. *pH of liquid phase in portland cement paste containing various salts*

Salt	$AlCl_3$	$CaBr_2$	Na_2SO_4	$CaCl_2$	$Ca(NO_3)_2$	NaCl	CaS_2O_3	MgS_2O_3	$MgCl_2$	Nil
pH	6.78	11.90	12.74	11.63	11.87	12.18	12.27	11.81	11.11	12.88

Composition of paste:
Portland cement(100g) + 6% Each salt aq. solution(50g).
Agitation of paste: 1 min., Filtration was undertaken immediately after 1 minute agitation of paste. Time of filtration is 1~5 minutes.
Hydration temperature: 20–23°C.

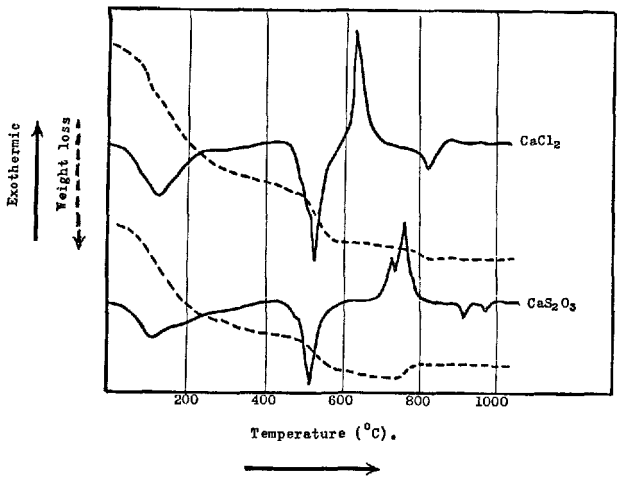

Fig. 11. *DTA and TB curves of the 24 hour hydration products of* C_3S *in the presence of* $CaCl_2$ and CaS_2O_3. *Preparation of paste and operating condition of DTA and TB are similar to the cases of Fig. 10*
Solid curves: DTA, Broken curves: Thermal balance.

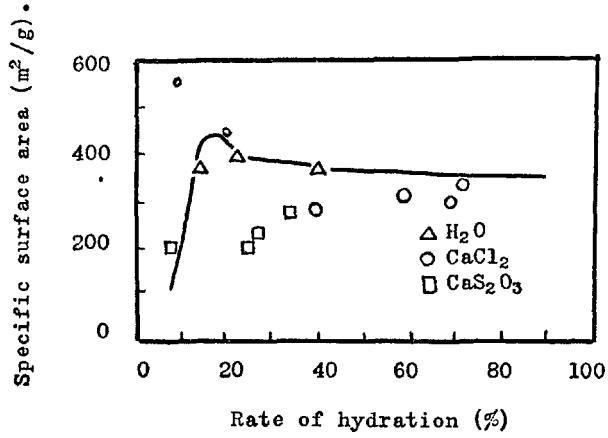

Fig. 12-1. *Specific surface area of the 100 day hydration products of* C_3S *in the presence of various salts*
Hydration temperature: 20°C, Adsorbent: Water-vapor, Solid curve: Kantro's results. Hydration temperature: 25°C.

it is seen as the heat evolution due to the crystallization of CSH. In the case of CaS_2O_3, the first heat evolution without the change in weight and the second heat evolution with some increments in weight are observed. Therefore, it is suggested that the second heat evolution shows the oxidation reaction of calcium sulphite as the decomposed compound of calcium thiosulphate. Assuming that the first heat evolution is due to the combustion of sulphur as the decomposed product of calcium thiosulphate, the weight loss in thermal balance curve should be observed naturally. But, it is not observed in Fig. 11. This reason is not yet clarified.

In general, it has been well known that the hydration products of C_3S or portland cement at room temperature are mainly CSH(I) and CSH(II), of which the occurrence is controlled by the lime concentrations of liquid phase. These CSH are poor in crystallinity at early stage of the hydration of C_3S or portland cement, therefore, it can be scarcely detected by X-ray diffraction. The X-ray diffraction patterns of the 100 day hydration products of C_3S paste showed CSH(II) when calcium chloride was added, did not evidently indicate either CSH(I) or (II) when calcium thiosulphate was added and showed CSH(I) when any additives were not added.

According to the fact that CSH(II) is converted by heating, the production of CSH(II) in the hydration of C_3S in the presence of calcium chloride has been confirmed by the formation of β–C_2S in the 24 hour hydration products by heating at 650°C. Kalousek (19) reported, using DTA, that synthetic CSH(II) is converted into β–C_2S by heating at temperature of over 900°C. The principal cause may be that, in the hydration products of C_3S, the large amounts of fine grain calcium hydroxide which are present near CSH(II) will promote the inversion to β–C_2S, however, in the case of synthetic CSH(II), any calcium hydroxide is not present near it.

One of the main characteristics of CSH is a large specific surface area. It has been suggested that the measurement of specific surface area of CSH will be an available method for detecting the effect of accelerators on the properties of CSH. Therefore, the specific surface area of CSH in the hydration products of C_3S produced in the presence of $CaCl_2$, CaS_2O_3 and $Ca(NO_3)_2$ were measured by following various methods; the measurement of specific surface area of the hydration products of C_3S by BET with water-vapor, the X-ray quantitative analysis of the remaining unhydrated C_3S in hydration products and the quantitative analysis of the produced calcium hydroxide by new Franke method (20).

Fig. 12–1 shows the change of specific surface area of CSH in the hydration products of C_3S. The CSH in the hydration products of C_3S hydrated in the presence of $CaCl_2$ has a considerable large surface area at earlier age, however, this high value of surface area reduces gradually in proportion to curing age and, consequently, it approaches to the value of CSH in the hydration products without any accelerators at later age. In the case of the addition of calcium thiosulphate, on the contrary, the surface area of CSH is small, but it increases with curing age as if it approaches to the value of CSH in the hydration products without any accelerators.

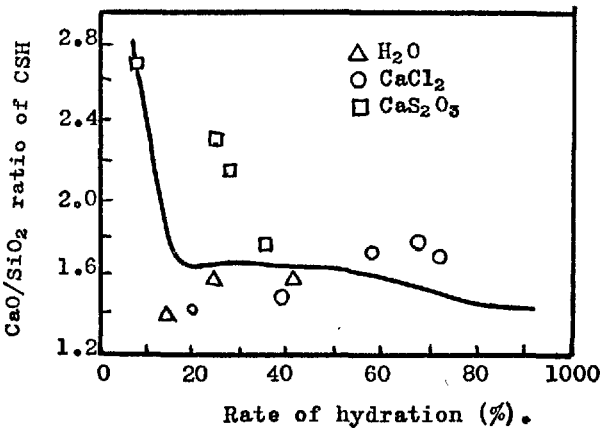

Fig. 12-2. CaO/SiO_2 *molar ratio of* CSH *in the 100 day hydration products of* C_3S *in the presence of various salts* Hydration temperature: 20°C, Solid curve: Kantro's result.

Fig. 12–2 shows CaO/SiO_2 ratio of CSH in the hydration products. Comparing with Kantro and others results (21), the CaO/SiO_2 ratio of CSH in low rate period of hydration is near 1.60 when any accelerators are not used, is 1.70 when calcium chloride is used and is 2.72 at 8% hydration when calcium thiosulphate is used. These values gradually approach to that of the case without any accelerators as the degree of hydration increases. The principal cause of the irregularity of CaO/SiO_2 ratio of CSH at early stage of the hydration may be explained by the hypothesis that CSH is produced from aq. solution in the state of non-equilibrium, in which the formation of CSH is initiated before the aq.solution is saturated with lime and silicate ions.

In another experiment, the CSH with CaO/SiO_2 ratio 0.8 was prepared, using CaO and SiO_2 gel, at 50°C for 7 hours in the presence of such various salts as calcium chloride, calcium thiosulphate and calcium nitrate. These specific surface areas showed an identical value; 328 m^2/g when any accelerators were not used, 339 m^2/g when calcium chloride was added and 323 m^2/g when calcium thiosulphate was added. From this result, it can be considered that the presence of accelerators in the hydration process of C_3S markedly affects the hydration process and the physicochemical properties of produced CSH, however, that the presence in the synthetic process of CSH is not closely related to the properties of resulted CSH.

Electron Microscopic Observation of the Hydration Products of C_3S

CSH, having a large specific surface area, is generally regarded as a gel-like substance, therefore, it can not be confirmed evidently by X-ray diffraction. The application of electron microscope is very significant to observe the morphologie of CSH.

Photo 1 shows the hydration products of C_3S pastes with H_2O/C_3S 0.5 at 35°C. In the C_3S–$CaSO_4 \cdot 2H_2O$ system, the fibrous hydration products are produced, but it does not markedly grow. In the C_3S–$CaCl_2$ system, the hydration products, regarding as calcium hydroxide from Grudemo's study (22), grow as if it likely forms the cross-linked net work. When gypsum was added to the system, the net work structure is progressively developed and, simultaneously, the cigarette type CSH which has been known as CSH(II) is produced.

The presence of CSH(II) in the hydration products of C_3S paste with calcium chloride not only was already confirmed by X-ray diffraction, but also is found by electron microscope. The considerable development of strength of portland cement by the

C_3S–H_2O
After 5 hour hydration.

C_3S–$CaSO_4 \cdot 2H_2O$–H_2O
After 10 hour hydration.

(Photo 1.)

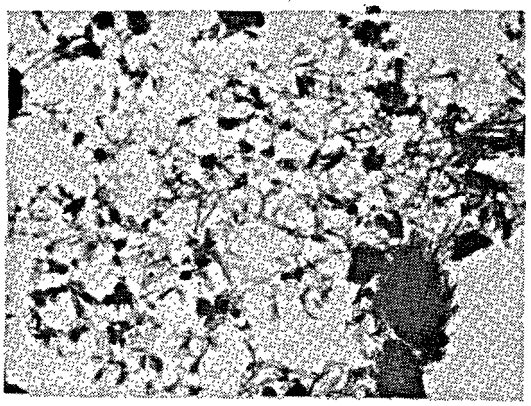

C_3S–$CaCl_2$–H_2O
After 8 hour hydration.

C_3S–$CaSO_4 \cdot 2H_2O$–$CaCl_2$–H_2O
After 8 hour hydration

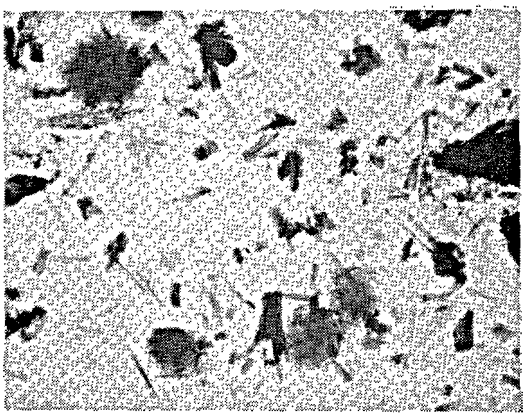

C_3S–$Ca(NO_3)_2$–H_2O
After 3 hour hydration.

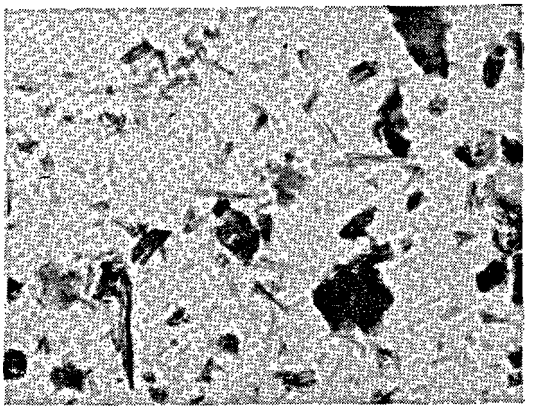

C_3S–$CaSO_4 \cdot 2H_2O$–$Ca(NO_3)_2$–H_2O
After 3 hour hydration.

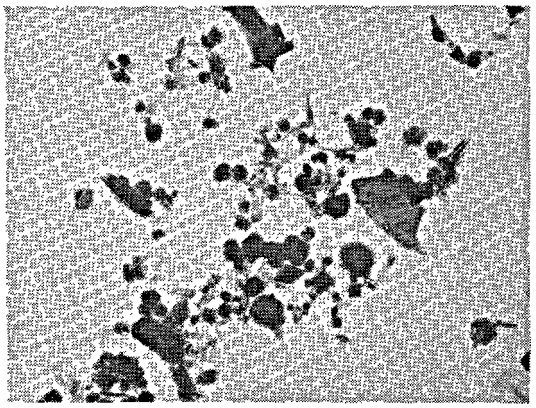

C_3S–CaS_2O_3–H_2O
After 8 hour hydration.

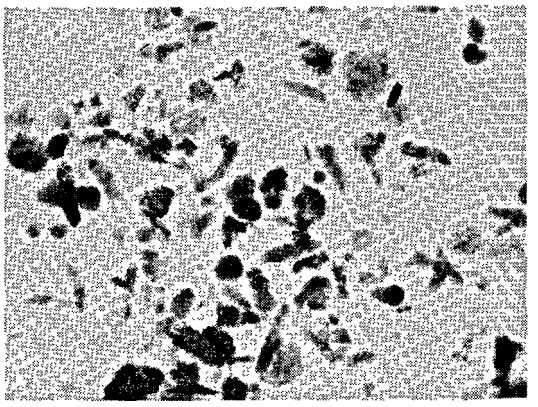

C_3S–$CaSO_4 \cdot 2H_2O$–CaS_2O_3–H_2O
After 8 hour hydration.

Photo 1. *Electron micrographs of hydration products of* C_3S *in the presence of each salt*
Hydration temperature: 35°C, Water- C_3S ratio of paste: 50%, Magnification: ×25,000.

addition of calcium chloride may be caused by the co-operative effect of both the progress of hydration and the three dimensional development of net-work structure mentioned above. When calcium nitrate was added, the thin plate-like products are predominantly produced after 3 hours hydration. When calcium thiosulphate was used, the large amounts of the fibrous and hexagonal-plate like products are produced. Especially, only the latter is identified with calcium hydroxide. The relationship between the morphologie of these products and the strength development is not yet sufficiently studied.

Effect of Accelerators on the Hydration of C_3A

Figs. 13 and 14 show the X-ray diffraction patterns and the DTA curves of the hydration products of C_3A which hydrated in the presence of $CaCl_2$, CaS_2O_3 and $Ca(NO_3)_2$ Photo 2. is the electron micrographs of the hydration products. These results, which were obtained from the C_3A-Accelerator-H_2O system without gypsum, may not be appropriate for understanding the effects of accelerators on the hydration of portland cement. However, it will be useful as one of possible feature in the hydration of portland cement in the presence of accelerators.

A large and broad diffraction pattern in the range of from 5° of 2θ to 10°, when calcium chloride and calcium thiosulphate were added, is observed in the hydration products after 10 minutes hydration. This diffraction pattern probably demonstrates that many kinds of hydration products, which are small in quan-

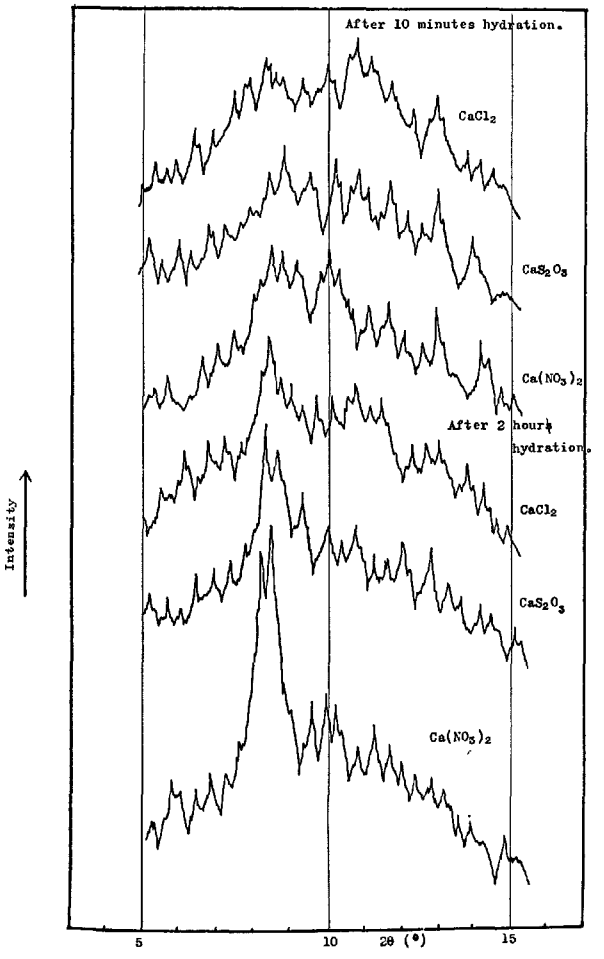

Fig. 13. *X-ray diffraction patterns of the hydration products of* C_3A *in the presence of* $CaCl_2$, CaS_2O_3 *and* $Ca(NO_3)_2$
Temperature of hydration: 20°C, H_2O/C_3A: 50%. The quantity of each salt is 3% to C_3A. Cu-Kα 30KV, 15mA.

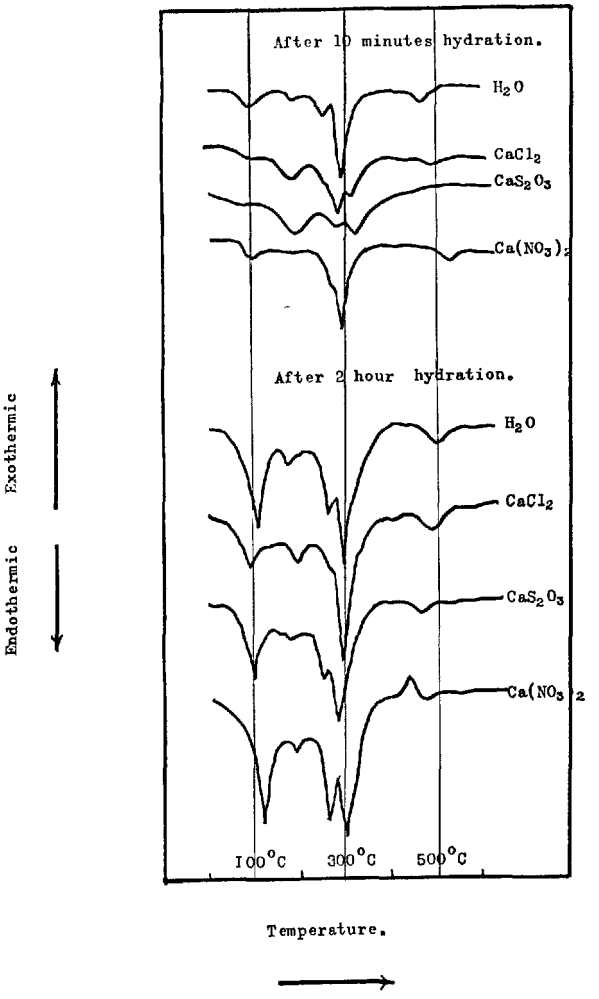

Fig. 14. *DTA of the hydration products of* C_3A *in the presence of* $CaCl_2$, CaS_2O_3 *and* $Ca(NO_3)_2$
Temperature of hydration: 20°C., H_2O/C_3A: 50%., The quantity of each salt is 3% to C_3A., Rate of heating: 5°C/min., Thermocouple; Pt–PtRh 13%., Standard substance: α-Al_2O_3.

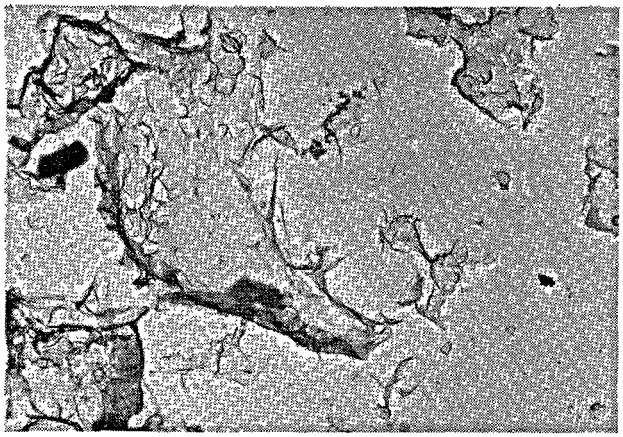

C_3A–$CaCl_2$
After 10 minute hydration.

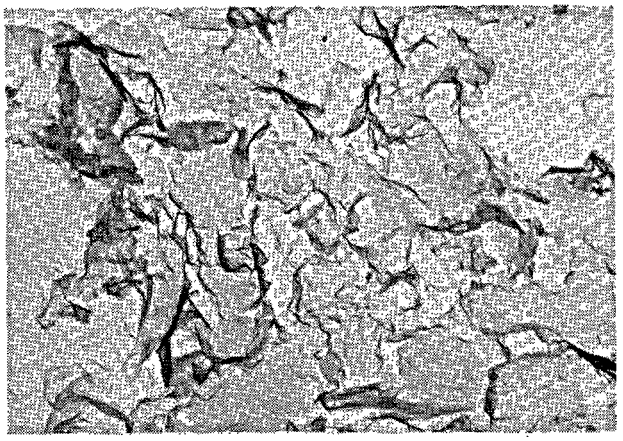

C_3A–$CaCl_2$
After 2 hour hydration.

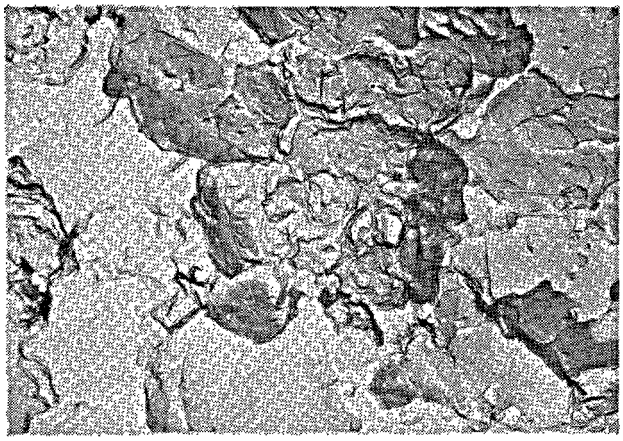

C_3A–CaS_2O_3
After 10 minute hydration.

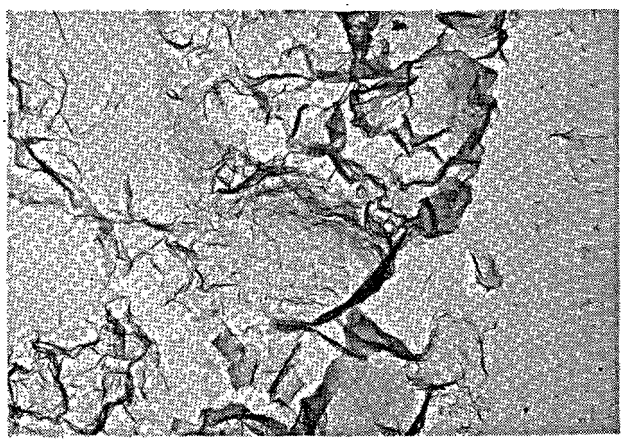

C_3A–CaS_2O_3
After 2 hour hydration.

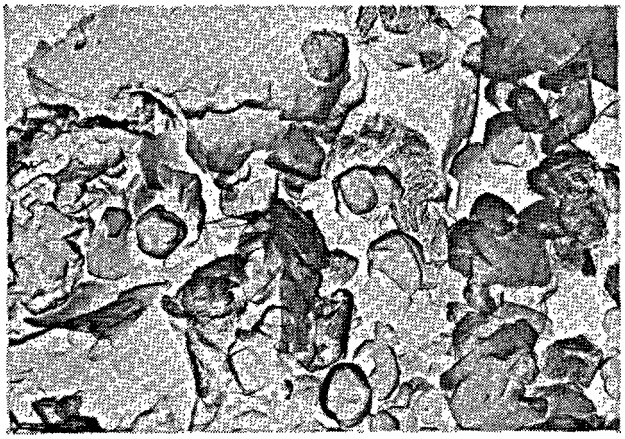

C_3A–$Ca(NO_3)_2$
After 10 minute hydration.

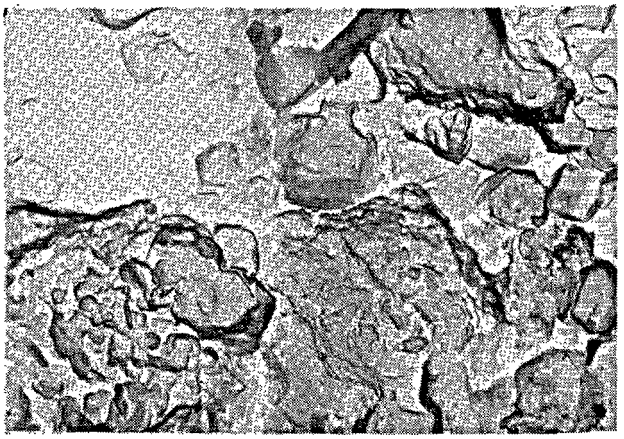

C_3A—$Ca(NO_3)_2$
After 2 hour hydration.

Photo 2. *Electron micrographs of the hydration products of* C_3A *in the presence of* $CaCl_2$, CaS_2O_3 *and* $Ca(NO_3)_2$
Temperature of hydration: 20°C, H_2O/C_3A: 50%. The quantity of each salt is 3% to C_3A. ×6,000.

tity and poor in crystallinity, with the lattice constants corresponding to the above diffracted range are produced. On the other hand, when calcium nitrate was added, the two relatively sharp diffractions at 8°–9° and 10° of 2θ are observed. Such diffractions are not observed evidently in the hydration products with calcium chloride and calcium thiosulphate. In the DTA curves, a few of endothermic peak are observed near 100°C, 200°C and 300°C. Above all, the endothermic peak at 300°C is most sharp when calcium nitrate was added. Furthermore, Photo 2 shows that the gel-like hydrates are product in plenty when calcium chloride and calcium thiosulphate were added, on the contrary, that the polygonal small particles and plate-like hydrates are markedly produced when calcium nitrate was added.

All the X-ray diffraction lines of the hydration products after 2 hour hydration are considerably developed. Both the diffraction lines with calcium nitrate at 8°–9° and 10° of 2θ are most sharply strengthened. Also, all the endothermic peaks in DTA curves are remarkably developed. The two endothermic peaks near 100°C and 200°C which likely belongs to an identical hydration product are more strengthened together in the hydration products after 2 hour hydration than that after 10 minute hydration.

The electron micrographs of the hydration products show an unchangeable feature also at 2 hour hydration as well as at 10 minute hydration, when calcium chloride and calcium thiosulphate were added. Only in the case of calcium nitrate, the different products from the two formers are observed.

It has been already reported, by Heller and Ben—Yair (23), that a synthetic $C_3A \cdot CaCl_2 \cdot XH_2O$ as the complex salt between C_3A and $CaCl_2$ shows the basal spacing at 7.9 Å of d and has a sharp endothermic peak at 215°C and four kinds of weak endothermic peaks at 110°C, 256°C, 330°C and 550°C. The X-ray diffraction patterns of the hydration products at the two curing ages show the diffraction lines indicating that the product corresponded to calcium chloroaluminate by Heller and Ben-Yair(23). Simultaneously, the formation of $C_3A \cdot Ca(OH)_2 \cdot 18H_2O$ and $C_2A \cdot 8H_2O$ is also observed, therefore, it is suggested that the formation of solid solution between $C_3A \cdot CaCl_2 \cdot XH_2O$ and $C_3A \cdot Ca(OH)_2 \cdot XH_2O$ are likely possible. In the cases of calcium thiosulphate and calcium nitrate, although the detailed information about the complex salts containing $S_2O_3^{--}$ and NO_3^- has not been reported, the products substituting these anions for some portions of OH^- in the structure of $C_3A \cdot Ca(OH)_2 \cdot XH_2O$ may be produced.

In the cases of calcium chloride and calcium thiosulphate, it is thought that the endothermic peaks at 100°C and 280°C in DTA curves show the dehydration of $C_2A \cdot 8H_2O$ and that the endothermic peaks at 200°C and 300°C show the dehydration either of $C_3A \cdot Ca(OH)_2 \cdot XH_2O$ or of products substituting Cl^- or $S_2O_3^{--}$ for OH^- in the structure. The formation of $C_3A \cdot 6H_2O$ is not detected by X-ray diffraction. The polygonal small particles in the hydration products of C_3A which hydrated in the presence of calcium nitrate are confirmed as $C_3A \cdot 6H_2O$ by X-ray diffraction, therefore, the endothermic peak at 300°C in DTA curve shows the dehydration of $C_3A \cdot 6H_2O$.

When the weak accelerating action of calcium nitrate is connected with the fact that the hydration reaction of C_3A with calcium nitrate is very different from that with calcium chloride or calcium thiosulphate, it should be naturally considered that, for understanding the accelerating action on the hydration of portland cement, the effect of accelerators on the hydration of C_3A must be studied together with that on the hydration of C_3S.

Conclusion

Although calcium chloride is being used as an excellent accelerator on the hydration of portland cement, the corrosive action of Cl^-, remaining in concrete, to steel is considerable and can be scarcely avoided. It will be most favorable if an appropriate accelerator without corrosive character is found and used.

The accelerating action of calcium thiosulphate studied in the present paper is slightly lower than that of calcium chloride. However, it seems that calcium thiosulphate is available as an accelerator without the corrosive character to the steel in reinforced concrete.

The accelerating action of calcium thiosulphate increases in proportion to the amount of addition to cement. However, the effect on the strength development of mortar is not available beyond the three day age. The use of a large amount of accelerator will cost one dear.

When calcium thiosulphate is added to portland blast furnace slag cement which consists of, for example, the granulated blast furnace slag 65 % and portland cement 35 %, the accelerating action is predominantly given for the hydration of portland cement. Therefore, if the same quantity of calcium thiosulphate is

respectively added to the two cements, the hydration of portland cement in the blast furnace slag cement will be doubly affected by the calcium thiosulphate. The initial strength development, comparing with that of the blast furnace slag cement without calcium thiosulphate, is considerably promoted.

Besides, since the slag hydrates independently of whether the accelerators are present or not, namely, the hydration mechanism of the slag greatly differs from that of portland cement, the high strength development at later stage can be kept, without any fall in the strength development, by the hydration of slag.

References

1. K. Shinohara and S. Naritomi, "Availability of some chemical reagents as the accelerator of set and strength development of portland cement", Semento Gijutsu Nenpo **IV** 309–313, (1949).
2. S. Nagai, "Semento Gairon", 5th ed., 310–316, (1947), Maruzen Shuppan Co., (Tokyo).
3. K. Narahashi, T. Amamiya and K, Nakajima, "Influences of various salts on the false set of portland cement", Semento Gijutsu Nenpo, **XI**, 66–74, (1956).
4. R. H. Bogue, "The chemistry of portland cement", 2nd ed., p. 661, 664, (1955), Reinhold Publishing Corp., N. Y.
5. H. N. Stein, "Influence of some additives on the hydration reactions of portland cement, I. Non-ionic organic additives, II. Electrolytes," J. apple. Chem., **11**, 474–481, 482–492, (1961).
6. G. C. Edwards and R. L. Angstadt, "The effect of some soluble inorganic admixtures on the early hydration of portland cement", J. apple. Chem., **16**, 166–168, (1966).
7. R. L. Angstadt and F. R. Hurley, "Hydration of the alite phase in portland cement", Nature **197**, 688, (1963).
8. Gy. Zimonyi and Gy. Balazs, "Physikalische Prüfung des Wirkungs Mechanismus von Kalziumchlorid", Silikattechnik, **17**, 14–16, (1966).
9. R. H. Bogue, "The chemistry of portland cement", 2nd ed., p. 571–579, (1955), Reinhold Publishing Corp., N. Y.
10. F. E. Jones, "Hydration of calcium aluminates and ferrites", Chemistry of Cement, Proceedings of the Fourth International Symposium Washington, 1960, US Department of Commerce National Bureau of Standards Monograph 43—Vol.-1.
11. A. M. Rosenberg, "Study of the mechanism through which calcium chlorides accelerates the set of portland cement", Journal of the American Concrete Institute, 1261–1269, Oct., (1964).
12. E. P. Andreeva and E. E. Segalova, "Kinetics of structure formation in suspensions of tricalcium and β-dicalcium silicates in presence of calcium chloride", Translated from Kolloidnyl Zhurnal, **22**, 503–505, (1960).
13. J. Johnston and C. Grove, "The solubility of calcium hydroxide in aqueous solutions", J. Am. Chem. Soc. **53**, 3967, (1931).
14. G. V. Libermann and V. A. Kireev, "Reaction of tricalcium aluminate with water in the presence of the chlorides of calcium, sodium and potassium at elevated temperature", Translated from Zurnal Prikladnoi Khimii, Vol. 37, 194–196, (1964).
15. N. Kawada and A. Nemoto, "Hydration process of calcium silicate phase at early stage", Semento Gijutsu Nenpo, XX, 68–75, (1966).
16. W. Richartz and F. W. Locher, "Ein Beitrag zur Morphologie und Wasserbindung von Calciumsilicat Hydraten und zum Gefüge des Zementsteins", Zement-Kalk-Gips, **18**, 449–459, (1965).
17. H. Ballczo and O. Kaufmamn," Preparation of calcium thiosulfate", Monatsh, **80**, 220–231, (1949), Chem. Ab, 865, (1950).
18. H. Tanaka, K. Murakami, I. Monna and T. Karaki," "Studies on the hydration of $3CaOAl_2O_3$ by calorimeter, influence of chemicals on the setting of cement, I" J. Ceram. Assoc. Japan, **70**, 116–126, (1962).
19. G. L. Kalousek, "Chemistry of Cement", Proceedings of the Third International Symposium, London 1952, Cement and Concrete Association, London.
20. E. E. Pressler, S. Brunauer, D. L. Kantro and C. H. Weise, "Determination of the free calcium hydroxide contents of hydrated portland cements and calcium silicates" Analytical Chemistry, **33**, 877–882, (1961).
21. D. L. Kantro, S. Brunauer and C. H. Weise, "Development of surface in the hydration of calcium silicates, II. Extension of investigations to earlier and later stages of hydration." J. Physi. Chem., **66**, 1804–1809, (1962).
22. A. Grudemo, "The microstructure of cement gel phases", Translated from Kungl. Tekniska Högskolans Handlinger (Transactions of the Royal Institure of Technology Stockholm Sweden No. 242, 1965,
23. L. Heller and M. Ben-Yair, "Effect of chloride solutions on portland cement", J. apple. Chem., **16**, 223–226, (1966).

Supplementary Paper II-4 Significance of Total and Water Soluble Alkali Contents of Cement

Walter J. McCoy and Ottomar L. Eshenour*

Synopsis

The portion of the alkalis in the clinker that are water soluble depends on the form the alkalis are in, which in turn depends on the chemical composition of the raw mix and the conditions during the burning operation. It was found that the amount of the alkalis that are water soluble can vary from less than 10% to over 60% of the total alkali content. In some cases a better correlation was obtained between the soluble alkali content and the amount of alkali-aggregate expansion than between the total alkali content and the amount of expansion. Soluble alkalis were found to have a significant effect on the rate of hydration but not on the pH of the aqueous extract from cement pastes. Even after hydration at room temperature for 1 year a considerable portion of the alkalis in cement may not be water soluble.

Introduction

The subject of alkalis, namely, sodium oxide (Na_2O) and potassium oxide (K_2O) in cement and the various aspects of the alkali-aggregate reaction has been the subject of numerous papers and symposia during the past 25 years. The interest in alkalis and the concern with the alkali-aggregate problem has steadily increased since 1940 when P. H. Bates, Chief, Clay & Silicate Production, National Bureau of Standards (and Chairman ASTM Committee C-1 on Cement), invited cement company representatives to attend a conference at the Bureau where they were advised of the findings of T. E. Stanton (1**) that excessive expansion of concrete could be caused by chemical actions between cements of relatively high alkali content and certain aggregates. Since that time most of the investigations concerning alkalis in cement have been in connection with the alkali-aggregate reaction. Practically all of these studies refer to the total alkali content, and this is especially true of the many investigations of the relationship between alkali content and the amount of expansion. Alkali specifications for cement are based on total alkali content calculated as Na_2O equivalent. Test data have been obtained which indicate that in some cases there is a better correlation between the soluble alkali content and the amount of expansion than between the total alkali content and the amount of expansion. To complicate the situation, tests on a large number of various cements have shown that the amount of alkalis that are water soluble within the first hour of hydration can vary from 10 to 60% of the total alkali content.

Since the findings of our study includes other important aspects of the alkali content of cement besides that associated with the alkaliaggregate reaction, it seems appropriate to review some background information regarding the alkali component of cement.

Background

Alkalis, namely, Na_2O and K_2O occur in varying amounts in cement raw materials, and coal ash with the natural silicate or clay mineral components of the raw mix usually being the principal sources. In the burning of the clinker a portion of the alkali is volatilized when the natural alkali containing silicates react with the lime in or near the clinkering zone in the kiln. The amount of the alkalis volatilized can depend on a number of factors such as:

(a) Whether alkalis are present principally as potassium or sodium compounds since a survey of 73 cement plants showed that on the average

*Lehigh Portland Cement Co., Allentown, Pennsylvania, U.S.A.

**The numbers in brackets refer to list of references appended to this paper.

no Na_2O is volatilized until about 30% of the K_2O is volatilized, and above the 30% mark the additional volatilization of the K_2O will be 50% greater than the amount of Na_2O that is volatilized (2).

(b) Temperature of burning zone in the kiln which in turn is somewhat limited by the composition of the raw mix.

(c) The amount of sulfur compounds in the raw mix or fuel since sulfate in the clinker and SO_3 in the combustion gases tend to retain the alkalis.

(d) With other conditions being similar, higher alkali volatilization is obtained with gas and with oil than with coal as a fuel (3).

(e) Chloride, if added to the kiln feed, is effective in volatilizing K_2O.

If we had to pick a figure for the average amount of alkali volatilized during the burning operation, it would be of the order of 40–50% of that present in the kiln feed. If stack dust is collected and returned to the kiln, the amount volatilized could be significantly less.

Alkali Compounds in Portland Cement Clinker

The alkalis in portland cement clinker occur in many different forms depending upon the composition of the kiln feed, conditions of burning and rate of cooling (4). In most cases the alkalis combine with the available SO_3 during the burning operation to form an alkali phase that contains both K_2O and Na_2O with the K_2O predominating. The amount of sulfate present is usually sufficient to combine with only part of the alkalis and the remaining portion is combined with the aluminates and silicates with Na_2O principally in the aluminates and the K_2O in the silicates. According to Kryzhanovskaya and Mirakyan (5), the principal compounds formed in this case are NC_8A_3 which is a solid solution of Na_2O in C_3A and $KC_{23}S_{12}$ which represents a solid solution of K_2O in C_2S. $KC_{23}S_{12}$ which is formed by this reaction of K_2O and C_2S is a stable compound, and is not converted to C_3S during the burning operation even in the presence of excessive free lime. It is possible for a clinker with less than 1% K_2O to have all the potential C_2S in the form of $KC_{23}S_{12}$. If there is more than enough K_2O to convert all the C_2S to $KC_{23}S_{12}$, then some of the C_3S in the clinker may be decomposed by the K_2O to form additional amounts of $KC_{23}S_{12}$ and free lime. Burnability test data in a paper by Yu M. Butt, V. V. Myshlyaeva and T. A. Osokina (6) clearly show that the presence of alkalis in the raw mix slows down the clinkering reactions.

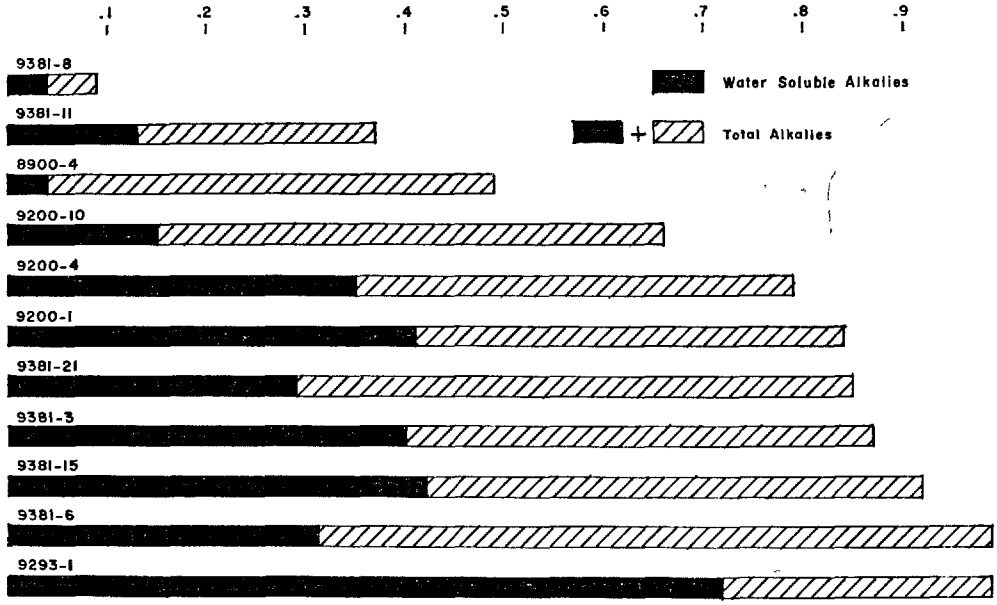

Fig. 1. *% total alkalies vs. % water soluble alkalies—Type I cements*

When cement is mixed with water, the alkali sulfates dissolve immediately, and the concentration of K_2O in solution is usually greater than Na_2O at very early ages. The Na_2O phases tend to dissolve more rapidly than the other K_2O phases since the aluminates hydrate more rapidly than the silicates. In view of the foregoing, the portion of the alkalis that are water soluble after any given period of hydration can vary considerably depending on the clinker. This variation in the portion of the alkalis that are water soluble is illustrated by Figs. 1, 2 and 3 which show both the total and water soluble alkali contents for a number of Type I, II and III cements respectively. The total and water soluble alkalis were determined by

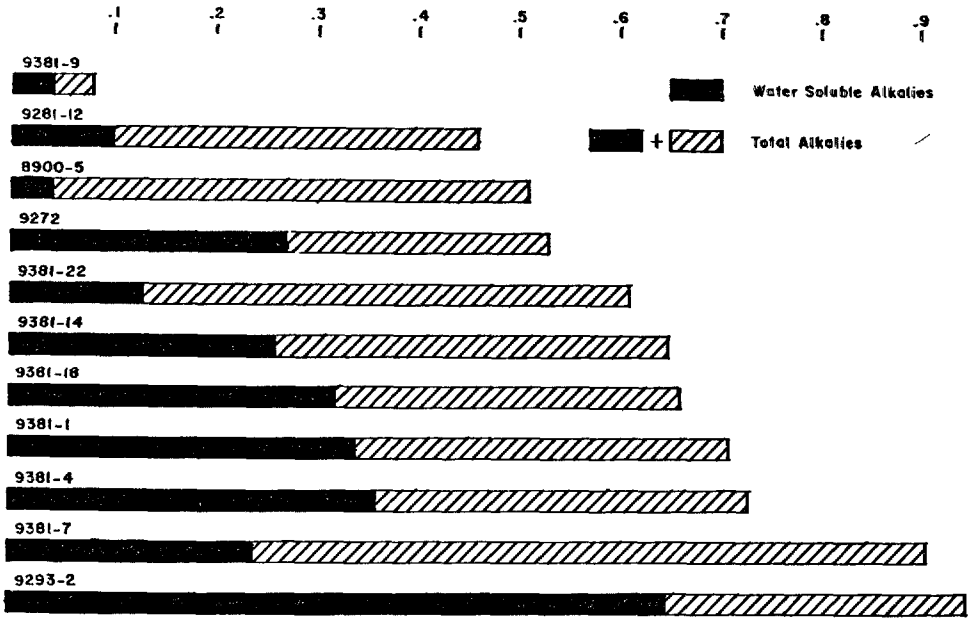

Fig. 2. *% total alkalies vs. % water soluble alkalies— Type II cements*

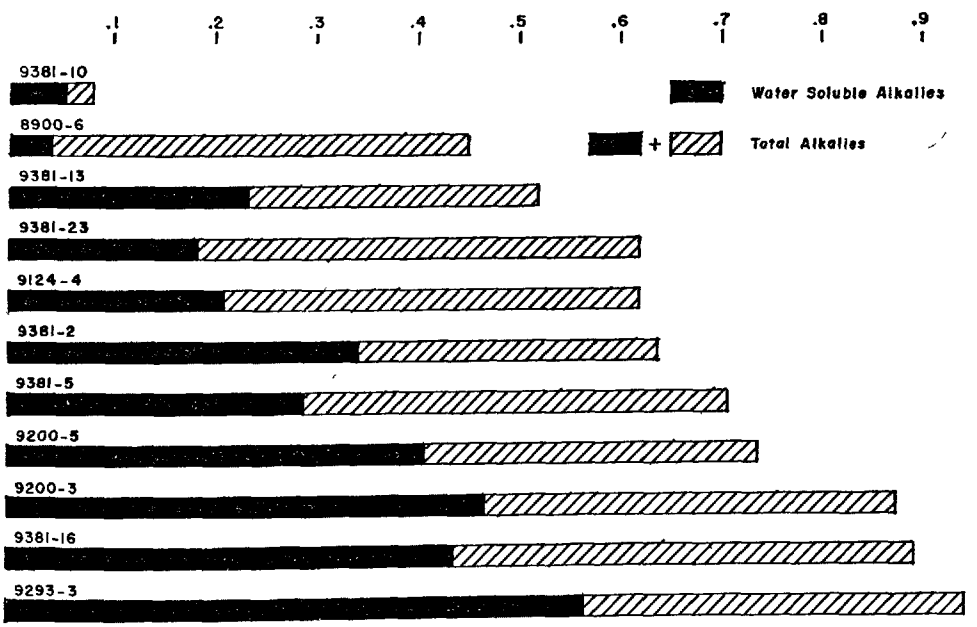

Fig. 3. *% total alkalies vs. water soluble alkalies— Type III cements*

ASTM Method C 114–65. Figs. 1–3 illustrate that the amount of alkali in a cement that is water soluble varies from less than 10% to over 60% of the total alkali present.

A high water soluble K_2O content as determined by ASTM Method C 114–65 will frequently indicate that the cement clinker contained appreciable quantities of K_2SO_4 in which case it would not be unusual for the cement to have satisfactory or high strengths at 1 and 3 days but a relatively poor strength gain between 3 and 28 days. This is illustrated by the ASTM Method C 109 mortar cube strengths given in Table 1 which were obtained for the cement with the highest and lowest soluble K_2O as illustrated in Fig. 1. These two Type I cements had similar potential C_3S, C_3A and fineness characteristics.

Alkalis in cement are usually thought of as serving no useful purpose, and the lower the amount of alkali the better. To obtain information on this subject, we prepared some portland cement clinker in the laboratory that contained no alkalis, and compared the strength characteristic of portland cement from that clinker with a cement prepared from similar clinker except for a nominal amount of alkalis. These two clinkers were prepared from a lot of commercially burned Type I clinker which was divided into two portions. One lot was reburned in a laboratory kiln with no additions, and had an alkali content of .57% Na_2O equivalent most of which was potassium. The other portion was similarly reburned except for a quantity of ammonium chloride (NH_4Cl) which was added to effect a volatilization of the alkali during the reburning, and this reburned clinker had no alkali. NH_4Cl was used to remove the alkali since all this material would be volatilized, along with the alkali, so that the only change in the chemical composition of the clinker was the loss of the alkali.

Both clinkers were ground with gypsum to the same fineness and ASTM C 109 mortar cubes were fabricated from each of the two cements, and the compressive strength determined at 1, 3, 7 and 28 days. A similar set of mortar cubes was also made with the zero alkali cement to which potassium hydroxide (KOH) was added equivalent to .4% Na_2O on the basis of the cement content. These data as given in Table 2 indicate that the alkali component has an appreciable beneficial effect on the early strength development. Further tests showed that small additional quantities of alkali in excess of the .4% had no significant effect on early strength development unless they were added in another form such as carbonate, sulfate or chloride which is an entirely different situation because of the effect of the anion.

A series of tests was made to determine what effect the quantity of alkali in a cement would have on the pH of an aqueous extract from a cement paste after 1/2 hr. hydration with water-cement ratios of 0.5 and 2.0 and after 24 hr. with a water-cement ratio of 2.0. In the 24 hr. test series the samples were continuously agitated. The data obtained are given in Table 3, and show that the quantity of alkali has very little effect on the pH of the aqueous phase. The extracts of the cements which had alkali contents ranging from .03% to 1.19% Na_2O equivalent all had a pH in the range of 12.3 to 12.7 even after the 24 hr. extraction period.

Studies of the significance of total and water soluble alkali with regard to the amount of expansion obtained with reactive aggregates in ASTM C 227 mortar bar tests have not shown a uniform relationship. In some cases such as with Bishop and Saticoy sands from

Table 1. *Compressive strength of mortar cubes containing cements with high and low soluble K_2O contents*

	Cement No. 9381–8 soluble K_2O = .03%	Cement No. 9293–1 soluble K_2O = .61%
1 day	1220	1420
3 day	2550	2660
7 day	4020	3540
28 day	6540	4700

Table 2. *Compressive strength, psi; Effect of the absence of alkali*

Cement sample	1 day	3 day	7 day	28 day
Type I (alkali = .57%)	660	1750	2670	4250
Type I (no alkali)	160	300	2150	3650
Type I (no alkali + KOH)	540	1410	2410	3830

Table 3. *Effect of alkali content on pH of aqueous extracts from neat pastes*

Cement	Na_2O equiv.	Water soluble alkalis W/C = 2; 24 hrs.		pH W/C = 0.5	pH W/C = 2	pH W/C = 2
		K_2O g/liter	Na_2O g/liter	1/2 hr.	1/2 hr.	24 hr.
7305–4	.03	.03	.06	12.3	12.3	12.3
8517	.29	.64	.31	12.2	12.3	12.3
8661–8	.42	.87	.35	12.4	12.4	12.4
8046–7	1.19	3.6	1.4	12.6	12.5	12.7

California, the amount of expansion correlated better with the total alkali content than with the amount of soluble alkali. However, this was not true in the tests with reactive dolomite obtained by H. H. Newlon and W. C. Sherwood (7) who have pointed out that certain types of carbonate rock are alkali reactive, and that the reaction differs from the well known alkali-silica type. Mortar bar tests with a reactive sand from Watertown, South Dakota described in U. S. Army Engineer Waterways Experiment Station Paper No. 6-530 (8) shows better correlation between the amount of expansion and the soluble alkali content than with the total alkali content. Both the reactive dolomite and the Watertown sand were tested for expansion characteristics by ASTM C 227 mortar bar procedure with three portland cements which had the same total alkali content and soluble alkali contents of .48%, .32% and .14% respectively. The expansion data are given in Table 4.

Some additional C 227 expansion tests were made with the reactive dolomite and three portland cements which had the same approximate soluble alkali content but different total alkali contents. A similar series of tests were made on a sample of Republican River aggregate. The results obtained on this series of tests which are given in Table 5 also show a better correlation between the amount of expansion and the soluble alkali content than with the total alkali content.

J. L. Gilliland and T. R. Bartley (9) have pointed out that "water-soluble alkali" in portland cement is a relative quantity, which depends upon the length of time that the cement has hydrated as well as the testing technique. He reported that for cements hydrating at 100°F substantially all of the alkalis are rendered water-soluble within 90 days, sodium becoming soluble somewhat faster than potassium does. Apparently Gilliland used a high water cement ratio in making up the specimens used in his tests since he explains the procedure as follows: "Ten grams of cement are placed in a small vial. The vial is filled with distilled water and the mixture thoroughly stirred. The vial is then sealed and stored in an over at 100°F."

Tests were made on a series of neat cement bars similar to those used in ASTM Method C 151 to determine what effect hydration of cement with a "normal consistency" water-cement ratio at 23°C (73.4°F) would have on increasing the relative amount of alkalis in a cement that are water soluble. The specimens were stored in a moist closet with a relative humidity in excess of 90 percent. After storage, the hydrated bars were crushed, dried and ground to the same approximate fineness as the cement was originally. The soluble alkalis were determined on the finely ground hydrated samples with appropriate corrections being made for the water of hydration. The results are given in Table 6 and clearly show that, even after hydration for one year under the condition described, a considerable portion of the alkalis are still insoluble in water.

Table 4. *Expansion of ASTM C 227 mortar bars; Water soluble Vs. total alkali*

Cement	% Na_2O equiv.		% Expansion			
	total	water-sol.	1 mo.	3 mo.	6 mo.	1 yr.
Reactive dolomite (Virginia)						
8658–1	.83	.48	.026	.040	.054	.068
8660–3	.83	.32	.024	.037	.049	.062
8664–8	.84	.14	.018	.028	.034	.048
Watertown sand (So. Dakota)						
8658–1	.83	.48	.013	.022	.028	.036
8660–3	.83	.32	.008	.014	.015	.022
8664–8	.84	.14	.002	.005	.005	.010

Table 5. *Expansion of ASTM C 227 mortar bars; water soluble Vs. total alkali*

Cement	% Na_2O equiv.		% Expansion			
	total	water-sol.	1 mo.	3 mo.	6 mo.	1 yr.
Reactive dolomite (Virginia)						
8664–8	.84	.14	.018	.028	.034	.048
8658–5	.62	.19	.024	.042	.052	.064
8670–10	.45	.19	.020	.034	.042	.056
Republican river (Nebraska)						
8664–8	.84	.14	.060	.156	.212	.306
8658–5	.62	.19	.031	.138	.186	.204
8670–10	.45	.19	.012	.102	.175	.234

Table 6. *Effect of hydration on the relative solubility of alkalis*

Cement	8658–1	8664–3	9293–1
Unhydrated			
Total K_2O, %	1.1	.56	.74
Total Na_2O, %	.13	.26	.25
Total alkali, %	1.23	.82	.99
Water-soluble K_2O, %	.68	.10	.57
Water-soluble Na_2O, %	.03	.02	.11
Water-soluble alkali, %	.71	.12	.68
% of alkali, water soluble	58	15	68
Hydrated 1 year			
Water soluble K_2O, %	.71	.22	.45
Water soluble Na_2O, %	.08	.16	.15
Water soluble alkali, %	.79	.38	.60
% of alkali, water soluble	64	46	60

Conclusions

1. The presence of alkalis in the raw mix can slow down the clinkering reactions.

2. The amount of alkali in a cement that is water soluble can vary from less than 10% to over 60% of the total alkali present.

3. A relatively high water soluble K_2O content frequently indicates the cement clinker contained appreciable quantities of K_2SO_4 in which case a relatively poor strength gain is sometimes obtained between 3 and 28 days.

4. If a cement has no alkali the early strength can be abnormally low.

5. The amount of total or water soluble alkali in a cement has very little effect on the pH of the aqueous extract from cement pastes.

6. With some reactive aggregates a better correlation was obtained between the amount of expansion and the soluble alkali content than with the total alkali content.

7. Even after hydration at room temperature for 1 year, a considerable portion of the alkalis in cement may not be water soluble.

References

1. T. E. Stanton, "Expansion of concrete through reaction between cement and aggregate", Proceedings, ASCE Vol 66, p. 1781 (1940).
2. J. P. Draper, "Alkali removal in the cement burning process", Manufacturing Research Report No. **69**, PCA, (1954).
3. R. A. Loveland, Portland Cement Association, Personal Communication (1948).
4. T. F. Newkirk, "The alkali phases in portland cement clinker", PCA Assoc. Fellowship Paper No. **63**, (1952).
5. I. A. Kryzhanovskoya and V. M. Mirakyan, "Hydration of alkali minerals in clinker", Cement and Lime Manufacture, pp. 45–48 (May 1966).
6. Yu M. Butt, V. V. Myshlyaeva, and T. A. Osokina, "The effect of alkalies on the process of clinker formation and on the strength of cement", Tsement, Vol. 23, No. 5, p. 9–14 (1957).
7. H. H. Newlon, Jr. and W. C. Sherwood, "An occurrence of alkali-reactive carbonate rock in Virginia", Highway Research Board Bulletin No. **355**, (1962).
8. "Alkali-silica and alkali-carbonate reactivity of a South Dakota sand", Miscellaneous Paper No. **6–530**, U. S. Army Engineer Waterways Experiment Station, (September 1962).
9. J. L. Gilliland and T. R. Bartley, "Water solubility of alkalis in portland cement", Proceedings, ACI Vol 47, p. 153, (1950).

Oral Discussion

Arthur W. Brown

I would comment that with respect to soluble alkali sulphates, the results in Table 6 would plot well on Fig. 3 of our paper on "The distribution of alkalis in portland cement clinker". However our work shows that the idea of the soda not as sulphate migrating to C_3A and the potash not as sulphate going preferentially to C_2S is an oversimplification. It also suggests that the restriction of combination by the stabilisation of belite with potash is not generally as serious a risk as the paper appears to suggest, although that it does occur as a real problem is illustrated by photo 5 from our paper which shows alkali stabilized belite coexisting in contact with free lime and demonstrating this restriction of combination. Finally I would like to take this opportunity of congratulating the authors, more especially for illustrating the importance of the nature of the alkalis as distinct from their quantity in the context of alkali-aggregate reactions.

Oral Discussion

Heinz G. Smolczyk

Concerning the very interesting paper II-4 of W. J. McCoy and O. L. Eshenour, I want to make a contribution to a widely interesting problem:

The authors found that in most of the cases not the amount of total alkali but the amount of water

soluble alkali shows the better relation to the expansion through alkali-aggregate reaction. This better relation is confirmed even more clearly if not only portland cements but also other types of cement e.g. pozzolanic cements and blastfurnace slag cements are included in this kind of studies. These cements often have a higher content of total alkali but only a very small amount of water soluble alkali.

This is one reason for the wellknown favourable effect of blastfurnace slag or pozzolanas on the elimination of alkali reaction which is also mentioned once again by O. Valenta in his Principal Paper III-2 "*Durability of Concrete*". And this is a very serious point for all countries with a greater amount of mixed cements because the wellknown American recommendation of 0.6% total alkali is based on tests with portland cements only.

As we have been asked about this problem, sometimes even in Germany, we were forced to develop an approximate but safe formula which takes into consideration the amount of granulated slag. On the basis of leaching experiments with well-hydrated and afterwards finely ground cement mortars we got the following safe alkali limit for slag cements:

$$\text{Alkali } \% \cong 0.60 + 0.075 \text{ slag } \%$$

Soon after we had found this (April 1967) we received the results of the very precise studies of P. Klieger and A. W. Isberner (PCA) on this same problem. A graphical comparison of their expansion-test values with our approximate formula proved a nearly complete accordance (*see Fig. 1*).

On account of all the wellknown experiences and the new facts I think it would be a good idea to extend the American recommendation of 0.6% total alkali to a more characteristic limit, which should take into consideration the far more characteristic amount of water soluble alkali or the special composition of the cement, and which then would possibly be valid for all the other types of cements, too.

We are working hard on this problem and we will be grateful for any help or advice of the colleagues with special experience in this difficult field.

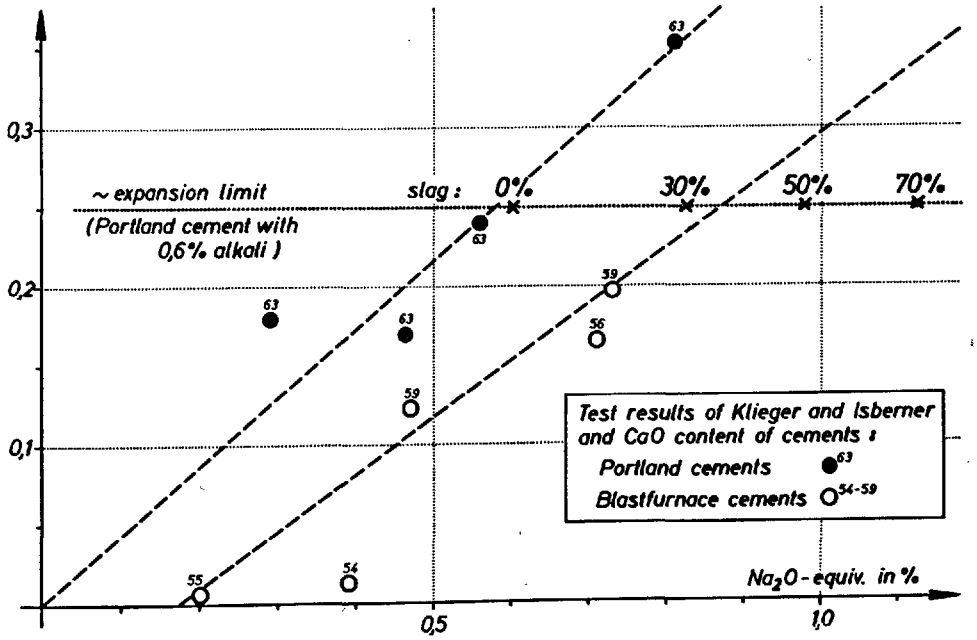

Fig. 1. *1 years' results of Klieger, Isberner and formula: Alk. $\% \cong 0.60 + 0.0075 \cdot$ Slag %*

Reference

P. Klieger and A. W. Isberner: "Laboratory studies of blended cements—Portland blastfurance slag cements" PCA-Research Department Bulletin No. 218 (Sept. 1967).

Supplementary Paper II-22 The Influence of Lead and Zinc Compounds on the Hydration of Portland Cement

Werner Lieber*

Synopsis

Small amounts of lead oxide PbO and zinc oxide ZnO of less than 0.1 % cause a retardation of the setting time of portland cement. Equivalent other simple lead and zinc compounds show the same influence. The retardation effect of definite amounts of the retarding agents depends on the specific surface area and on the C_3S content of a cement. PbO and ZnO have an influence on the C_3S only, which will be retarded. The strengths of cements will be increased after 28 days by these admixtures.

X-ray diffraction studies revealed that the portland cements do not hydrate and that no $Ca(OH)_2$ is formed during the retardation period, while the initial reaction of the aluminate and ferrite phases with the gypsum takes place as usual.

During the retardation period another zinc compound, calcium-trihydroxo-aquozincate, $Ca[Zn(OH)_3H_2O]_2$, is formed.

Adding the complex zincate instead of simple zinc compounds to a cement, the retardation period will be very short, but even the early strengths after one day will be increased up to 20% and more. The formation of the silicate hydrates tends into the range of fibrous phases.

Introduction

Thirty years ago L. Forsén (1) reported on the effect of admixtures on ground portland cement clinker. A certain group of admixtures was defined by him as "cement destroying", as they may considerably reduce the strength of the cement clinker and even prevent its hardening.

To this group belong, for instance, lead and zinc compounds. Even small quantities of less than 0.1% of lead oxide or zinc oxide retard the setting time by many hours. Other authors (2, 3), too, reported on the retarding effect of lead and zinc compounds.

This paper describes the influence of lead and zinc compounds on the setting and hardening of portland cement.

The Effect of Lead Compounds

Among the oxides PbO, PbO_2, Pb_3O_4 and the hydroxide $Pb(OH)_2$, the PbO_2 is practically inert, while the Pb_3O_4 has a rather insignificant retarding effect. The lead (II)oxide and the lead hydroxide retard the setting and hardening of portland cements very much. Equivalent quantities show approximately the same effect. Water soluble lead salts, for instance, lead nitrate, have practically the same strong retarding effect, because in the cement paste the formation of lead hydroxide takes place immediately.

The experiments described here, therefore, deal exclusively with the action of PbO.

Setting Time

The determination of the setting time, according to Vicat, leads to less exact results particularly when the setting is very much retarded. A more exact method is the measurement of the temperature evolution of cement pastes in relation to time. For that purpose resistance thermometers are imbedded into pastes of 500 grams of cement and 175 grams of water. The temperature is registered continuously. The initial

*Portland-Zementwerke Heidelberg A. G., Heidelberg, West Germany.

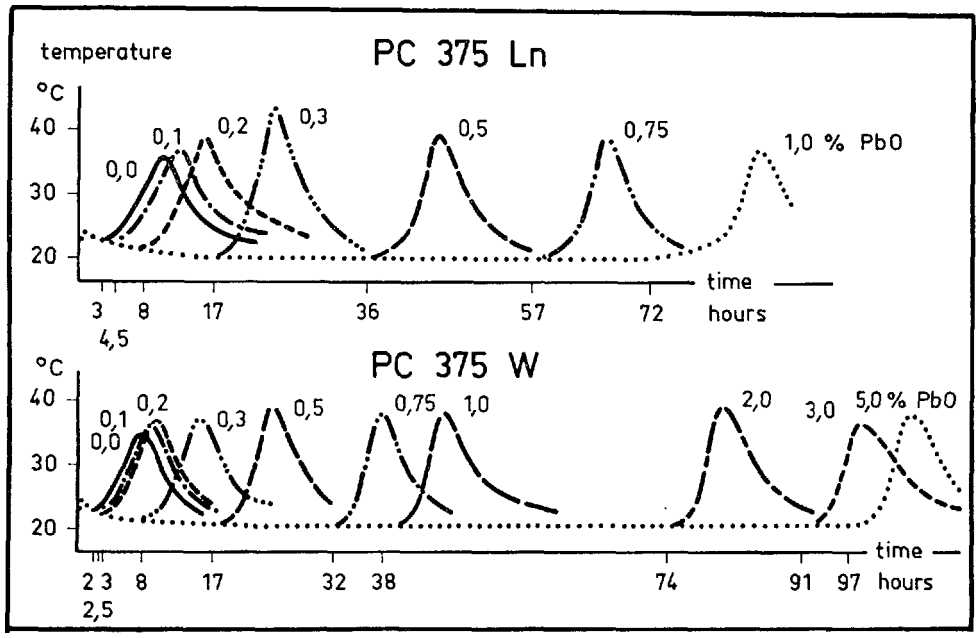

Fig. 1. *Set-retarding effect of lead oxide, represented by the temperature evolution of pure cement pastes (w/c = 0.35)*

set starts at approximately the same time as the marked rise in temperature.

Fig. 1 shows the time-temperature curves of cement pastes with lead oxide. It can be seen that equal quantities of PbO cause, in different cements, different retardations. It can also be observed, however, that the retarded cements–even after an interval of 100 hours–continue to show completely normal reactions as soon as the retardation period has been finished. There was no loss of quality. In many cases it can even be observed that the maximum temperature rises with PbO, which indicates a more intensive reaction as compared with the blank test. Fig. 2 shows the initial setting time as a function of the lead oxide content.

When cements of different degrees of fineness are ground from the same kind of clinker and the action of lead oxide on them is studied, it results that the retardation period is inversely proportional to the specific surface area of the cements (Fig. 3).

Strength

The path of the time-temperature curves permitted the conclusion that the cements are in no way damaged by means of lead oxide, but when the retardation period has been finished, they harden as well as cements not containing lead oxide and attain even better final strengths.

Specific Influence

W. Koenne (3) has reported that gypsum slag cement is not retarded by PbO. As a result of experiments carried out in our laboratories, it has been found that all types of portland cement and all slag containing cements are retarded by PbO, and that, however, the specific surface is not the exclusive criterion for the intensity of the retardation. From systematic research with pure phases of clinker prepared in the laboratory it resulted that the PbO has exclusively an influence on C_3S. The other phases of clinker, C_2S, C_3A and C_4AF are not retarded.

By means of X-ray diffraction studies with pastes consisting of C_3S with and without PbO, it could be demonstrated that no formation of calcium hydroxide takes place during the retardation period which may last for many hours or even several days, depending on the quantity of PbO. Thermogravimetric studies

Table 1. *Compressive strength of portland cements (DIN 1164) without and with lead oxide*

Days	% PbO			% PbO		% PbO	
	0	0.1	0.3	0	0.2	0	0.4
1	95	104	72	132	118	77	60
3	242	249	259	258	292	228	260
7	340	337	353	350	386	348	377
28	457	466	498	431	491	425	507

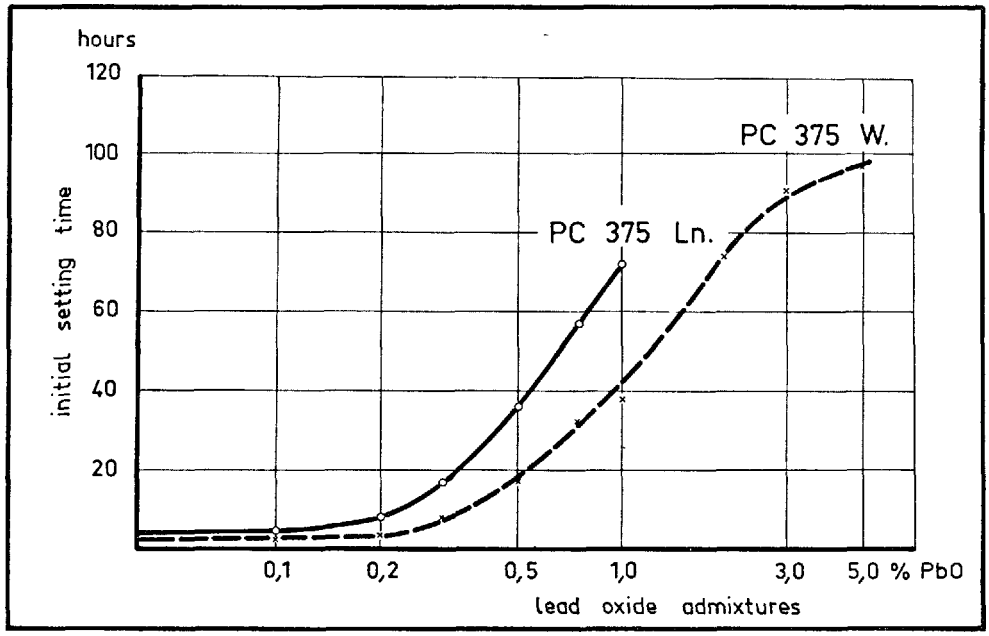

Fig. 2. *Initial setting time of pure cement pastes with lead oxide (w/c = 0.35)*

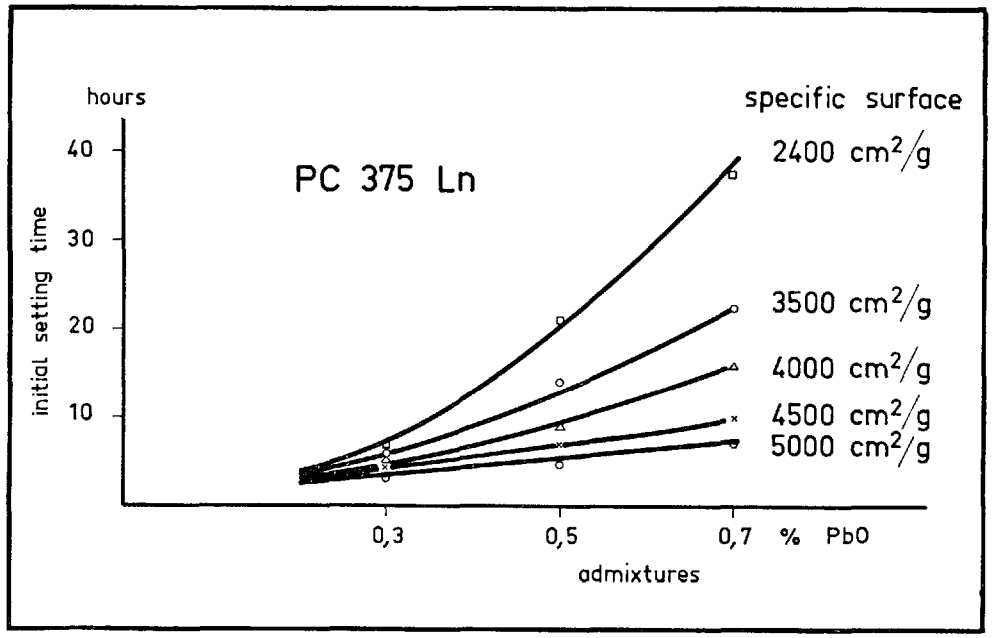

Fig. 3. *Relation between initial setting time, lead oxide admixture and specific surface*

showed that practically no water is bound. Immediately after the termination of the retardation period, however, a very rapid hydration and hydrolysis of C_3S takes place.

It seems that a cement retarded by lead oxide shows no reaction at all during the retardation period. It is true, however, that the typical reaction between gypsum and aluminates and ferrites in the first minutes after mixing a cement with water is not delayed.

The amount of water-soluble sulfate, still unbound

and consequently extractible, which is present in an unretarded cement normally decreases, within the first hour, from approximately 3% to about 1.5%. The sulfate is then bound rather slowly and decreases continuously and, after a period of 24 hours, water-soluble sulfate is no longer detectable. The first period of rapid sulfate binding to form the ettringite is not delayed by lead oxide, respective retardation concerns exclusively the subsequent binding process. As soon as the retardation period has been finished, the concentration of the water-soluble sulfate decreases rapidly (Fig. 13).

At present no satisfactory explanation of the surprising effect of PbO exists. There will be no doubt as to a blocking up of the surface of C_3S. The relation between retardation time end specific surface area is rather apparent. It is still unclear, however, which factor causes the hydration to start. The initial period of the hydration is accompanied by a simultaneous marked decrease in intensity of the X-ray interferences of the PbO which finally disappear completely. On the other hand, no new peaks from any lead compound can be detected.

The Effect of Zinc Compounds

Several authors, including H. Kühl (2, 4), W. Koenne (3), F. Keil (5) and F. Spalovsky (6) reported on the retarding effect of simple zinc compounds, particularly of zinc oxide. Some of these authors stated that zinc compounds would "destroy" the cement.

Several experiments have shown (7) that the effects of zinc oxide are practically the same as those of lead oxide. Equivalent quantities of other simple zinc compounds as, for instance, $Zn(OH)_2$, $Zn(NO_3)_2$, $ZnSO_4$ etc. have the same effect as ZnO itself.

The Effect of ZnO

It can be seen from Fig. 4 that small quantities of ZnO have a marked retarding effect on the setting process, without causing any damage to the cement. Equal quantities of ZnO cause retardation periods of different duration in different cements (Fig. 5).

Experiments carried out with pure clinker phases which have been prepared in the laboratory showed that ZnO has a specific retarding influence only on the C_3S. The retarding action of a defined quantity of ZnO is inversely proportional to the fineness and the C_3S content of the cements. The early strengths of the cements are, of course, in many cases, reduced by the retarding action of the ZnO; however, equal strengths can be observed after seven days, and after 28 days great strengths are principally attained as compared with cements which do not contain ZnO.

Reactions during the Retarding Period

Numerous experiments with pure C_3S and different portland cements show that practically no hydration and hydrolysis of the C_3S takes place during the retarding period. The characteristic reaction of the sulfate with the aluminates and ferrites which takes place during the first minutes after mixing the cement with water is, however, not delayed by zinc oxide which acts only on the subsequent binding of the sulfate (Fig. 13).

X-ray diffraction studies have shown that during the retardation period practically no formation of calcium hydroxide takes place. The intensity of the ZnO reflexes decreased continuously, whereas the characteristic lines (Fig. 7) of a calcium-hydroxo-zincate appeared which will be described later. The ZnO was completely transformed into the complex zincate, and then a very rapid hydrolysis of the C_3S and the formation of $Ca(OH)_2$ could be observed. Simultaneously the zincate also disappeared.

Formation of Calcium-Hydroxo-Zincate

It is known that, due to their amphoteric character, zinc oxide and zinc hydroxide have the tendency to form alkali zincates. Also a calcium-hydroxo-zincate has long since been known (8, 9, 10), but it became known as such only some 30 years ago. Its formula is $Ca[Zn(OH)_3H_2O]_2$. The zincate contains 18.1% CaO, 52.7% ZnO and 29.2% H_2O.

Notwithstanding its low solubility, the formation of this compound takes place within a few hours, for instance, by precipitation of zinc salts with a solution of calcium hydroxide or by a reaction of an alkali zincate solution with calcium hydroxide. Fig. 6 shows some crystals of calcium zincate. Fig. 7 shows the X-ray diffraction diagram of the compound.

By means of X-ray diffraction studies it has been possible to demonstrate that the synthetically pro-

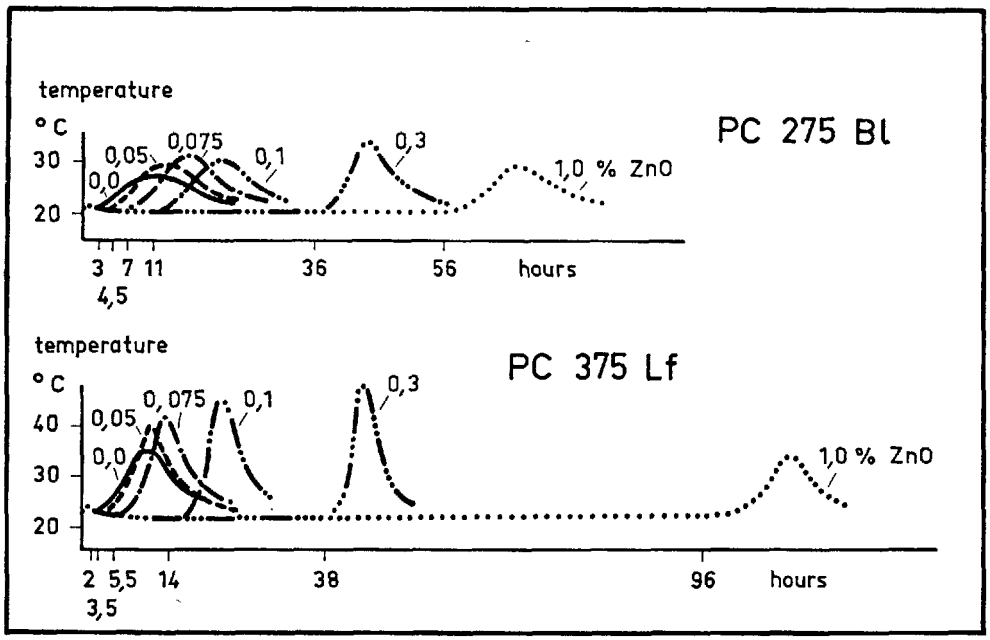

Fig. 4. *Set-retarding effect of zinc oxide, represented by the temperature evolution of pure cement pastes*

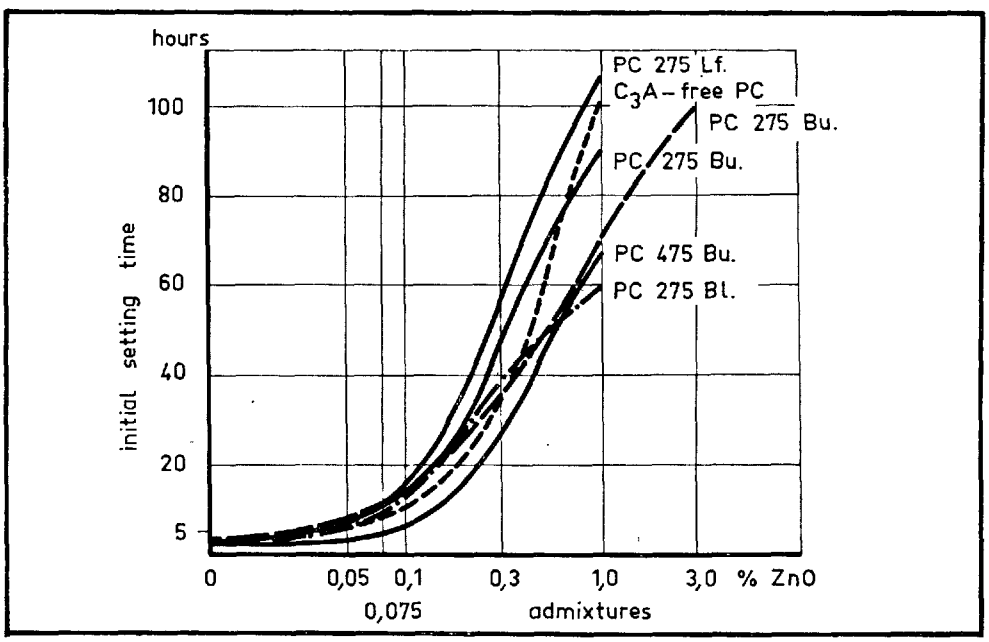

Fig. 5. *Initial setting time of pure cement pastes with zinc oxide* ($w/c = 0.35$)

duced calcium-hydroxo-zincate is identical with the zincate which is formed in pastes of C_3S or portland cement with ZnO. Consequently, the formation takes place without difficulty according to the equation:

$$2ZnO + Ca(OH)_2 + 4H_2O \rightarrow Ca[Zn(OH)_3H_2O]_2$$

Reactions of C_3S Pastes Containing Calcium Zincate

Tests carried out with zinc oxide showed that the formation of calcium-hydroxo-zincate takes place

during the very long retardation period, and that the hydration starts at about the same time when the zincate begins to disappear. Due to this fact, experiments were made in order to study the reactions taking place when calcium zincate instead of ZnO is mixed to the C_3S. For that purpose pastes were prepared of pure C_3S with and without 2% calcium zincate and tightly closed up in glass tubes. The heat of hydration, the loss on ignition and the formation of $Ca(OH)_2$ has been determined at different time intervals.

Figs. 8 and 9 show that 2% zincate (which are equivalent to 1% ZnO) cause only a very slight retardation of the hydration and the hydrolysis of the C_3S.

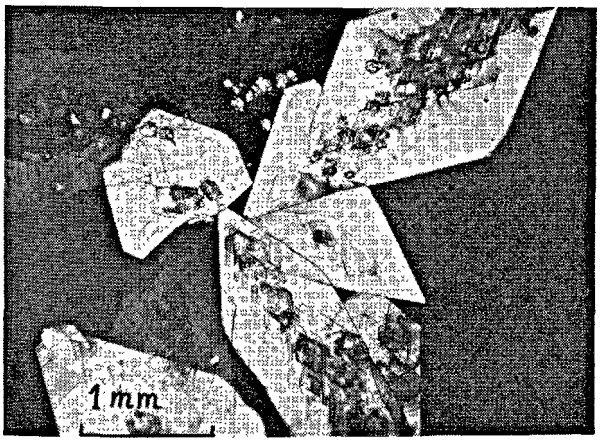

Fig. 6. *Calciumtrihydroxo-aquo-zincate crystals. Crossed nicols*

X-ray diffraction studies in several test series with different contents of zincate showed that during the short retardation period the intensity of the calcium zincate is reduced by leaps and bounds. Only then the hydrolysis of C_3S and the formation of $Ca(OH)_2$ begins. The zincate is no longer detectable by X-ray diffraction.

When C_3S reacts in an aqueous suspension with a small quantity of calcium zincate, intensive corrosion (see Fig. 10) can be observed as soon as 24 hours later on the originally sharp developed zincate crystals. Most of the small crystals disappeared after 3 days, while the big crystals showed corrosion phenomena particularly on sharp-developed corners and edges. In spite of its remarkable low solubility, the zincate does react. It is supposed that during this process an even more stable compound is formed. But, as there is no new zinc compound detectable, the zinc must have been entered the crystal lattice of the calcium silicate hydrates.

Influence of Calcium Zincate on Portland Cement

According to the described results, it was to be supposed that also mortars made from portland cements will be only slightly retarded by calcium zincate, and that, however, the strength could be in-

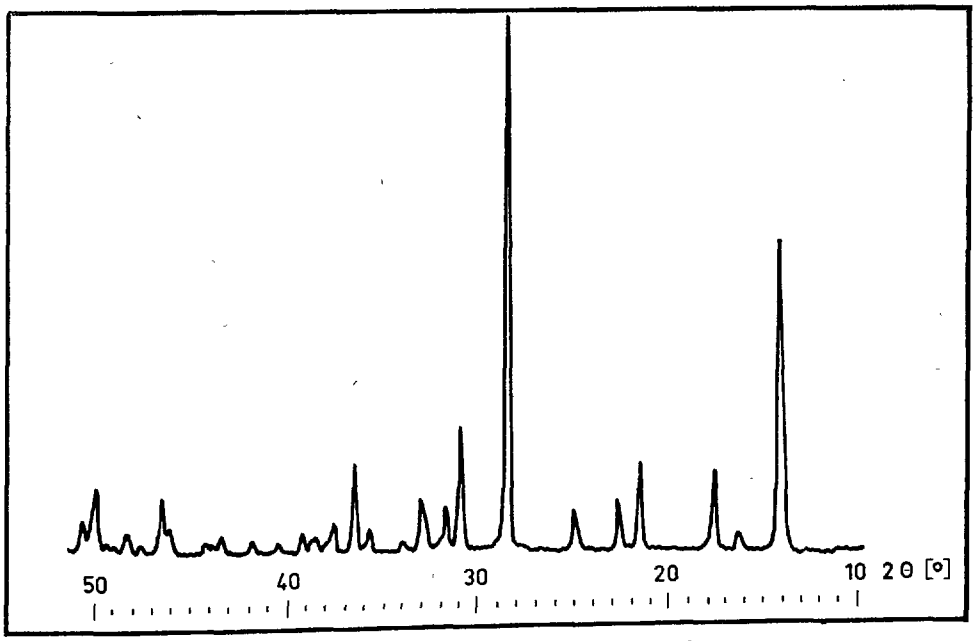

Fig. 7. *X-ray diffraction pattern of calciumtrihydroxo-aquo-zincate* Cu k_α

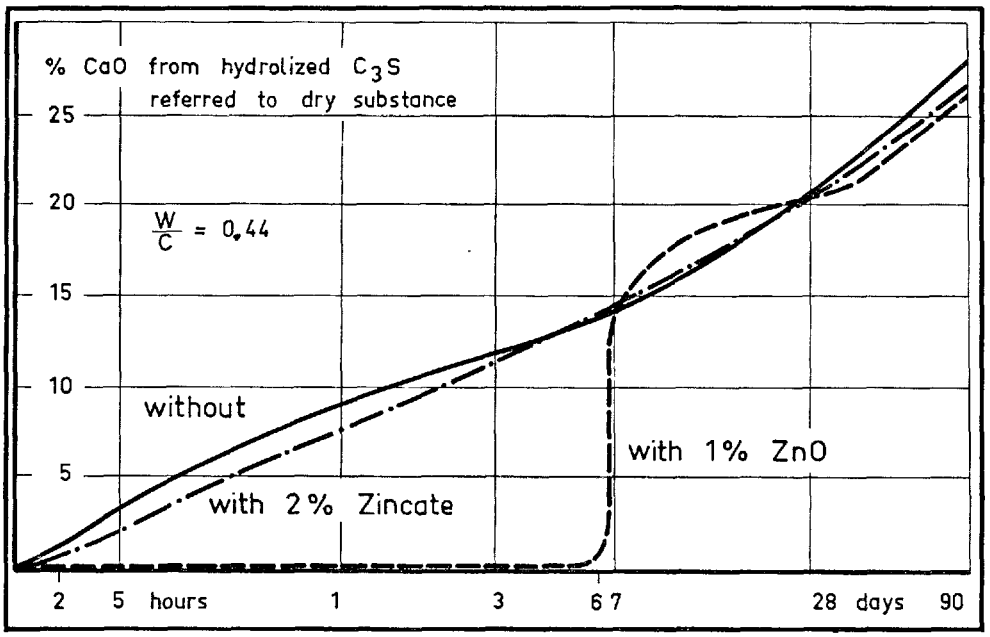

Fig. 8. *Hydrolysis of* C_3S, *containing zinc compounds*

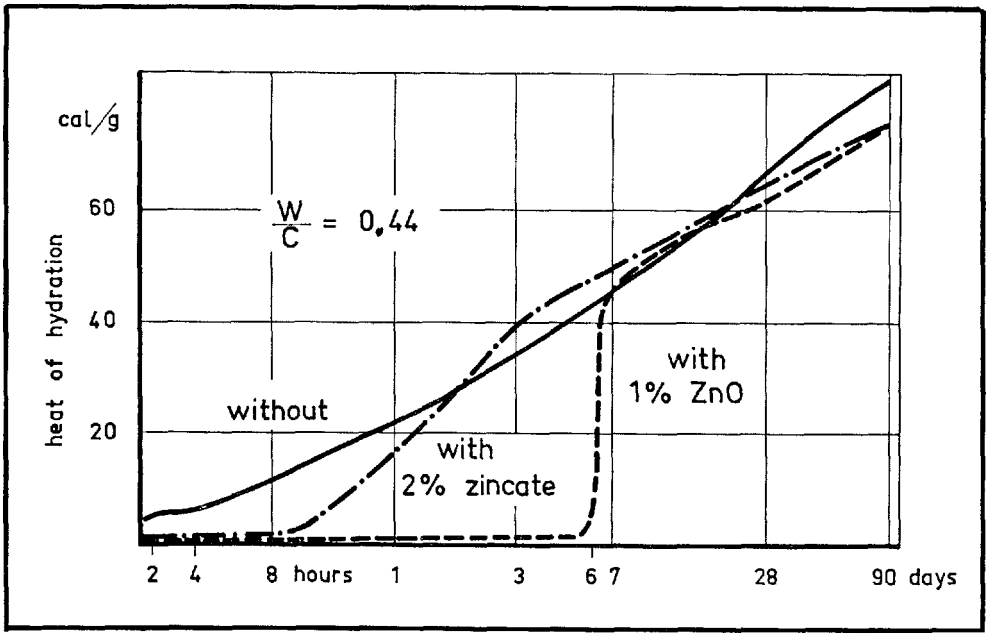

Fig. 9. *Heat of hydration of* C_3S, *containing zinc compounds*

creased. Fig. 11 shows some time-temperature curves of hydrating pure cement pastes with and without calcium zincate.

It results that the retardation period in the presence of calcium zincate is extremely shorter than with an equivalent quantity of ZnO.

Fig. 12 shows that for any cement a definite optimal quantity of calcium zincate admixture can be determined. This optimal quantity depends substantially on the specific surface area and the C_3S content. For obtaining optimal strengths a very fine cement containing much C_3S can be mixed with a larger quantity

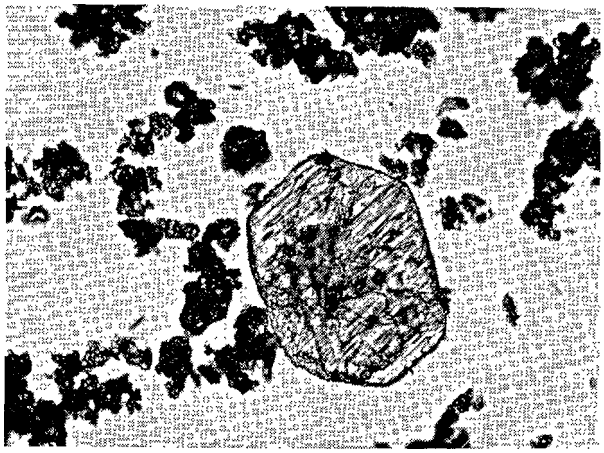

Fig. 10. *Corroded calcium zincate crystal in a* C_3S*-suspension*

of zincate than a coarse cement with a low C_3S content. Even larger quantities added cause no harm.

The chemical reaction between sulphate (of the gypsum contained in the cement) and the aluminates and ferrites is represented in Fig. 13. The cement containing no admixture shows the well-known decrease of the water-soluble SO_3. With 1 % of $CaCl_2$ somewhat less sulphate is bound during the first hour. After a period of 8 hours the quantity of sulphate bound in the cement which contains no admixtures is somewhat larger than the quantity of sulphate bound in the cement containing calcium zincate. The total quantity of sulphate is bound after a period of 24 to 48 hours. Lead and zinc oxide, however, cause marked retardations so that all of the sulphate is bound after 4 days only.

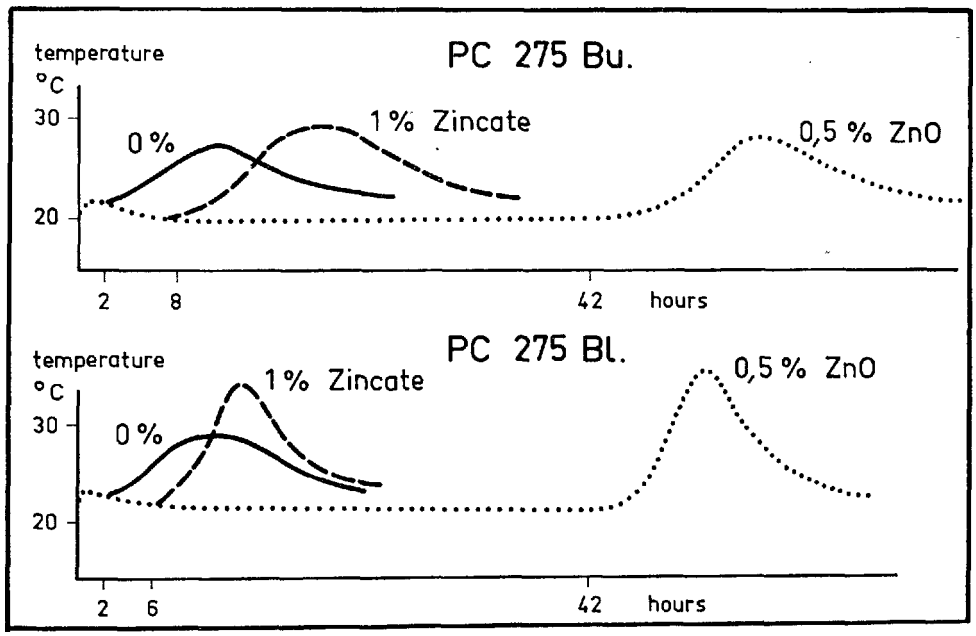

Fig. 11. *Influence of calcium zincate on the setting time of pure cement pastes* ($w/c = 0.35$)

Table 2. *Compressive strength (DIN 1164) of cements with calcium zincate admixtures*

Probe % zincate	PC 375 Bl 0	PC 375 Bl 0.7	PZ 475 Bl 0	PZ 475 Bl 1.0	PC 375 Bu 0	PC 375 Bu 0.8	PZ 375 Lf 0	PZ 375 Lf 0.8	PZ 375 W 0	PZ 375 W 0.8
setting time										
inital	4:20	9:25	2:25	5:15	1:45	4:15	3:00	6:10	2:10	4:50
final	5:30	10:45	4:00	7:35	4:00	7:35	4:00	7:30	2:55	5:45
compressive strength kg/cm²										
1 day	77	100	160	237	140	170	120	142	128	148
3 days	265	342	332	435	300	360	310	375	290	315
7	395	472	470	580	415	475	437	508	400	440
28	520	602	575	623	578	645	535	600	525	575
56	545	620	630	692	650	720	560	620	555	605
90	580	650	632	705	700	755	570	635	560	620
180	600	690	630	705	725	780	570	635	580	630
360	617	700	660	715	737	783	570	635	580	630

Although the setting time of the cements is slightly retarded by the admixture of calcium zincates, a remarkable increase in the strengths was demonstrated after only 24 hours, as is shown in Tables 2 and 3. This increase was observed over the entire hardening period. In many cases it was even higher.

It was also of particular interest to know whether the zinc which did evidently enter the crystal lattice of the calcium silicate hydrates, influences their chemistry and their morphology as compared with the silicate hydrates containing no admixtures. In some experiments hydrates have been found exhibiting a

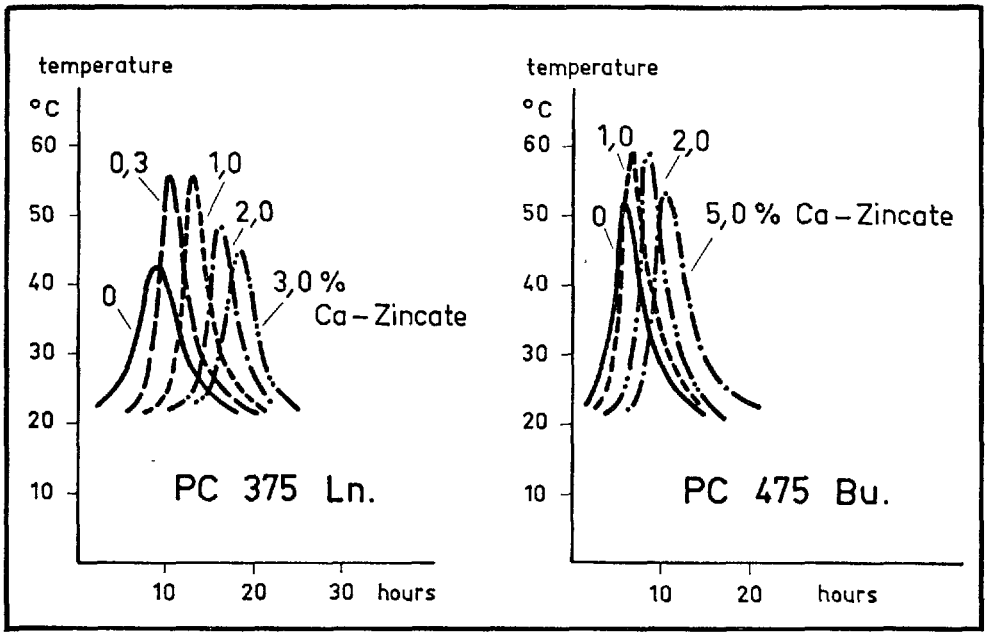

Fig. 12. *Effect of various zincate admixtures*

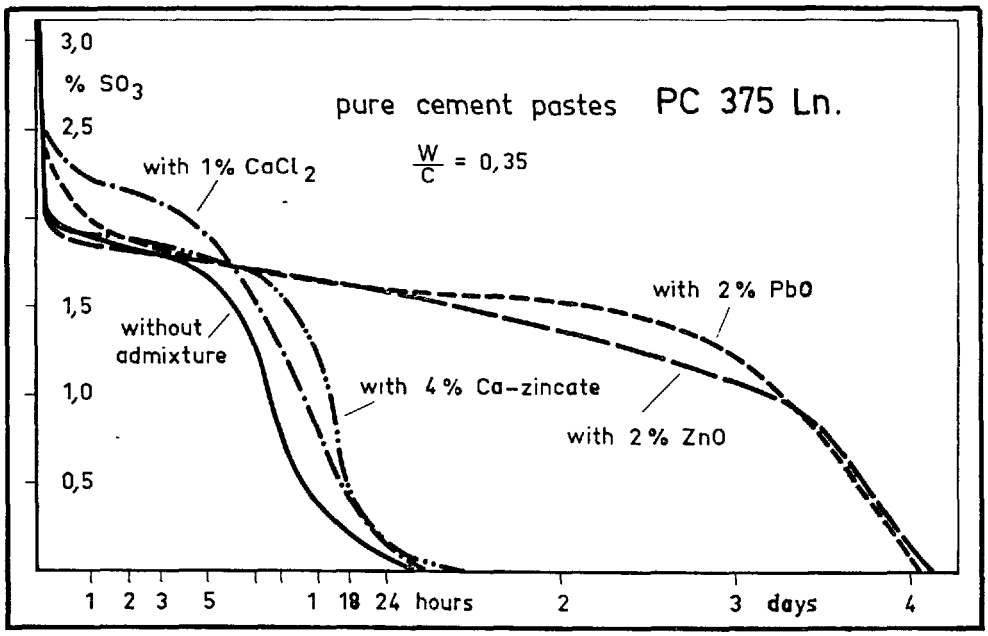

Fig. 13. *Reaction of the sulfate with clinker in the presence of lead and zinc compounds*

Table 3. *Compressive strength (DIN 1164) of cements with calcium zincate admixtures*

Probe	White PC		Swedish PC–Li		Swedish PC–He		Japanese PC–N	
% zincate	0	1.0	0	0.75	0	0.75	0	0.9
compressive strength kg/cm²								
1 day	82	75	108	109	106	137	151	172
3 days	221	309	288	300	239	308	387	465
7	296	421	350	432	338	378	524	631
28	503	576	465	525	428	488	645	750
56			525	595	458	501	673	770
90							679	774

ratio $CaO:SiO_2$ of approximately 2.0, whereas this ratio was approximately 1.5 without calcium zincate.

Electron micrographs carried out by W. Richartz (11) showed that the C_3S with 2% calcium zincate and 1% ZnO (Figs. 8 and 9) preferably forms long-fibered silicate hydrates, while the other one containing no admixture preferably exhibits foil-shaped hydrates. Fig. 14 shows hydrated C_3S with 2% calcium zincate after seven days of hydration. It can be seen that long fibres cover the pore.

Calcium hydroxozincate is an admixture which, in spite of its slight retarding effect, influences the hydrating process in a very favorable way by forming long-fibered silicate hydrates, thus increasing remarkably even the strengths in early stages and the long time strengths, too.

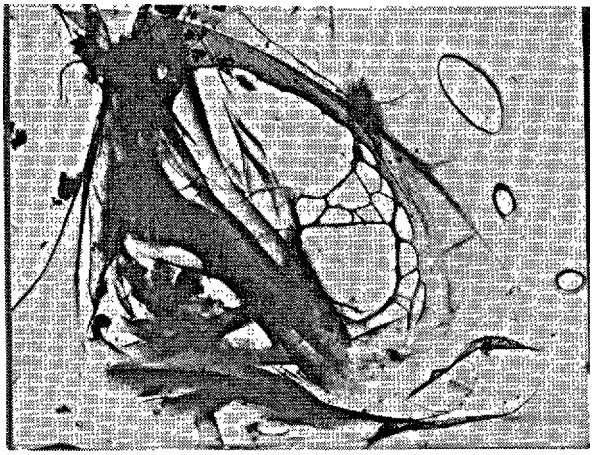

Fig. 14. *Electron micrograph of* $C_3S(w/c = 0.44)$ *after seven days*

References

1. L. Forsén, "The chemistry of retarders and accelerators", Proceedings of the second Internat. Symposium on the Chemistry of Cement, Stockholm 1938, pages 289–333 (1938).
2. H. Kühl, "Die Chemie der hochwertigen Zemente" (in German), Zement **17**, 686 (1928).
3. W. Koenne, "Set retardation by metal oxides" (in German), Zement-Kalk-Gips **14**, 158 (1961).
4. H. Kühl, "Zementchemie", Band III, S. 303, VEB-Verlag Technik Berlin, 3. Aufl. 1961.
5. F. Keil, "Studies on concrete admixtures" (in German), Tagungsberichte der Zementindustrie, Heft 7, 213 (1952).
6. F. Spalovsky, Austrian Patent 176 498, October 1953. Applicant: Perlmooser Zementwerke AG, Wien: "Method to retard the setting of cements" (in German).
7. W. Lieber, "Influence of zinc oxide on the setting and hardening of portland cements" (in German) Zement-Kalk-Gips **20**, 91–95 (1967).
8. M. G. Bertrand, "Studies on earth-alkali zincates (in French) Compt. rend. **115**, 939, 1028 (1892).
9. G.W. Heise and E.A. Schumacher, "An air-depolarized primary cell with caustic alkali electrolyte", Trans. electrochem. Soc., **62**, 383–391 (1932).
10. R. Scholder and H. Breuning, Diplomarbeit, Karlsruhe 1955, not published
11. W. Richartz, "Structure and strength of hardened cement pastes" (in German), presented on the Herbsttagung of Verein Deutscher Zementwerke, 13th October 1966 at Munich.

Oral Discussion

Giichi Sudoh

I have listened with profound interest to Dr. Lieber's presentation of his research findings, and I want to ask a few questions.

He has stated that the remarkable retardation effect of ZnO on the setting time is due to a blocking-up of the surface of C_3S particles, and may I consider here that the blocking-up compound is zincate? If this compound be zincate, what is the reason the sharp hydrolysis of C_3S starts at the same time that all of the ZnO has been transformed into the zincate?

Also he has stated that Zn is dissolved into calcium

silicate hydrate, and interesting is the phenomenon of the C/S mol ratio of calcium silicate hydrate rising as a result of the dissolution. In this case, what is the form of dissolution? Also what is approximately the maximum amount of dissolution?

Oral Discussion

John H. Taplin

Dr. Lieber is to be congratulated on his research. He may like to comment on the following idea which has occured to me since I discussed the action of retarders in the 1960 Symposium. In the early stages alite reacts slowly due to the formation of an impermeable coating of products or because of the presence of a stable surface. With the nucleation of a stable C–S–H phase the reaction accelerates. Because many organic and inorganic retarders have such similar effects, I suggest that all retarders may act by delaying the nucleation of a stable C–S–H phase and thereby extending the normal dormant period. Retarding action may therefore be independent of any adsorption on anhydrous minerals.

Author's Closure

Werner Lieber

The retardation effect of both PbO and ZnO as well is due to a blocking-up of the surface of C_3S. The ZnO is transformed into the calcium zincate, while a related lead compound could not be detected yet. In the case of retardation by zinc oxide, the rapid hydrolysis of C_3S starts at about the same time, at which all of the ZnO has been transformed into the zincate. Although a similar transformation of lead oxide into a plumbate is not to be observed, the retardation with PbO is about as long as that with ZnO. So I don't think that the rapid hydrolysis of C_3S is the result of a rapid dissolution of the zincate.

It can be seen from the Figs. 8 and 13 that the zincate has only a small influence on the speed of the hydration, the more it has an influence on the morphology of the CSH-phase (Fig. 14). With help of electron microscopy we were able to show that only a very small amount of C_3S reacts with water and forms extremely long-fibered hydrates. This process goes on during the dormant period. I agree with Mr. Taplin that many retarders act by delaying the nucleation of the CSH-phase. The hydration and hydrolysis of the C_3S is significant for the setting and hardening of the portland cements, at least those of usual composition. The aluminate and ferrite phases do not play such an important role as usually mentioned in the literature.

Mr. Sudoh's question is an interesting one. We have examined many samples of hydrates C_3S-pastes by electron microprobe and found that about 3% zinc oxide enter the CSH-phase, when we hydrated mixtures of 90% C_3S and 10% calcium zincate. But, 3% seem not to be the maximum amount. The amount of entering zinc is variable and depends on the quantity of calcium zincate mixed to the C_3S before starting the hydration. I suppose the zinc will enter the lattice of the CSH-phases as $Zn(OH)_2$ interlayer material.

Supplementary Paper II-47 Some Observations upon the Determination of Heat of Hydration of Slag and Portland Cements by the Method of Differential Heat of Solution

Georges A. Toubeau*

Synopsis

The determination of heat of hydration of cements by the method of differential heat of solution is at present studied in many countries in order to establish a classification according to this very important property. So, the C.E.T.I.C. Chemical Commission and a Cembureau Sub-Committee have for many years been working upon this problem. On the other hand, the R.I.L.E.M. has recently proposed a classification of cements based on the value of heat of hydration after conservation during three days at +5°C.

With a view to promotion of concerting in winter, a complete study of the Belgian cements was done in collaboration by several laboratories. This study involved specially the measure of heat of hydration by the solution method.

The base procedure was this one proposed by Santarelli and Goggi, inspired from the old A.S.T.M. method. However, several modifications were made at this original procedure: standard dimensions for the tubes for the conservation of the hydrated cement pastes, conservation in a thermostatic water-bath, mechanical grinding of the hydrated cement under alcohol in a special mill, introduction of the loss on ignition's value in the calculations for the slag and supersulphated cements.

From the numerous determinations that were carried out, it appears clearly that it is absolutely necessary to normalise the following conditions in order to obtain good, comparable and reproducible results: preparation of hydrated cement samples (temperature, tubes), conservation, grinding of the hydrated cement (time, fineness, liquid), drying of the ground sample (time, temperature), determination of heat capacity (preparation, quality and quantity of the ZnO), loss on ignition determination. Of these conditions the drying process seems to be the most important.

Numerous examples give an idea of the errors that can be made in case of variation of the above-mentioned conditions.

Introduction

The determination of the heat of hydration of cements has long formed the subject of many researches. As it is not possible to mention them all, we shall quote here three types of methods put forward, that is adiabatic (1), (2), (3), thermometric or semi-adiabatic (4), (5), (6), (7), (8), and solution (9), (10), (11), (12), (13), (14).

Notwithstanding the existence of these three methods, however, the choice of such and such a cement was based more on the chemical composition than on the direct determination of the heat of hydration and its development speed in terms of time, and mortar and concrete preservation conditions. The standards issued by the different countries did not, as a matter of fact, make any express provision as regards this cement property.

Now, an evolution of the tendencies in this field has been observed in the last few years. Some research work in order to promote cold weather concreting depends on the determination of the heat of hydration; making rapid progress, the R.I.L.E.M. proposed, besides, to classify cements in terms of their heat of hydration at 3 days and ±5°C determined by the solution method.

Some countries intend, moreover, to introduce in their standards characteristics other than mechanical strengths and, more particularly, the value of the heat of hydration. This is, for example, the case with the new German standards issued in 1967 (15).

Such an evolution obviously calls forth an important problem of methodology. It must be added that many international organizations are anxious to co-

*S. A. Ciments d'Obourg, Obourg, Belgium.

ordinate their efforts and investigations in order to attain a method valid both from a national and an international point of view. In this regard we will, more particularly, quote the work achieved by the Chemical Commission of the C.E.T.I.C. (8), (16), (17) and by the Cembureau Sub-committee "Testing of cement and concreté".

Within the limits of this problem of methodology we think it advisable to inform you about the results and observations achieved by our laboratory during a lot of series of tests made by the solution method. In order to promote winter concreting in Belgium an extensive programme of research work is being carried on. This programme consists, more particularly, of an attempt to classify all Belgian cement types in terms of the above mentioned R.I.L.E.M. criterion.

A first attempt of classification using the *original A.S.T.M. method* failed; this was due to possible cement class overlappings (see Table 1, 1st column). The problem was then studied on new bases using the *modified solution method* by Santarelli and Goggi (13), (18) with, however, a few adjustments.

The results achieved by various laboratories showed an excellent concordance (see Table 1, 2nd column) and allowed a classification of Belgian cements into 6 classes spaced from 5 to 10 calories (see Table 1, third column).

During a second series of tests intended for the selection of 6 cements for concrete testing, however, important differences, some of them amounting to 15 and even 20 calories per gram appeared between these laboratories. This led to a revision of the initial cement classification and, what is more, of the validity of the solution method as a calculation method.

Now, a checking of these differences showed that some laboratories had modified the mode of procedure initially put forward. This ascertainment led the laboratory of the S. A. Ciments d'Obourg to start a series of additional researches in order to determine the possible causes of error and to emphasize the problems set with a view to subsequent standardization.

Table 1bis. *Influence of the value of the heat capacity determined with different quantities of* ZnO *on the value of the heat of hydration*

Basic data $\begin{cases} \theta_c \text{ for anhydrous cement: } 4.2383 \\ \theta_c \text{ for hydrated cement: } 4.104 \\ R = \dfrac{100 - PFi}{100 - PFa} = 0.8865 \end{cases}$

Quantity of ZnO used for the stamping	Heat capacity M	Dispersion constant K	Heat of solution of the anhydrous cement in cal/g	Heat of solution of the hydrated cement in cal/g	Heat of hydration in cal/g
14	814.08*	0.02165	575.05	538.39	36.66
12.5	815.97*	0.0238	576.38	539.64	36.74

*Each of these values is the mean of a minimum of six simple determinations.

Table 1. *Comparison between the values of heat of hydration of various cements, measured according to the prescriptions of the original A.S.T.M. method and the modified A.S.T.M. method.*

Cement type	Heat of hydration measured according to the original A.S.T.M. method in cal/g	Heat of hydration Q measured according to the modified A.S.T.M. method in cal/g	Proposed classification after the value of Q measured after conservation 3 days at +5°C in cal/g
PN	35.48–35.05–38.45	33.05–32.52–33.74–36.84–36.50–36.3	35 ± 5
PHR	41.52–35.52–32.73	42.89–39.89–41.65–35.72–47.30	45 ± 5
PDR	63.54–57.61	49.85–59.12–64.39–64.55–52.07–56.6	55 ± 5
HFN	23.45–33.93–37.82	25.89–23.60–21.80	25 ± 5
HFHR	20.14–17.70–27.87–30.76	30.20–32.40–28.00	30 ± 5
HFDR	49.38–44.46	52.54–46.10–48.30	50 ± 5
PMN	21.08	19.63	—
SHR	29.72	17.00	—

PN = normal portland PHR = high strength portland PDR = rapid hardening portland
HFN = normal slag cement HFHR = high strength slag cement HFDR = rapid hardening slag cement
PMN = "permetallurgique" slag cement SHR = high strength supersulphated cement.

Description of the Equipment Used

—The calorimeter used here is described in the publication by Santarelli, Piselli and Covarelli (13), (16)

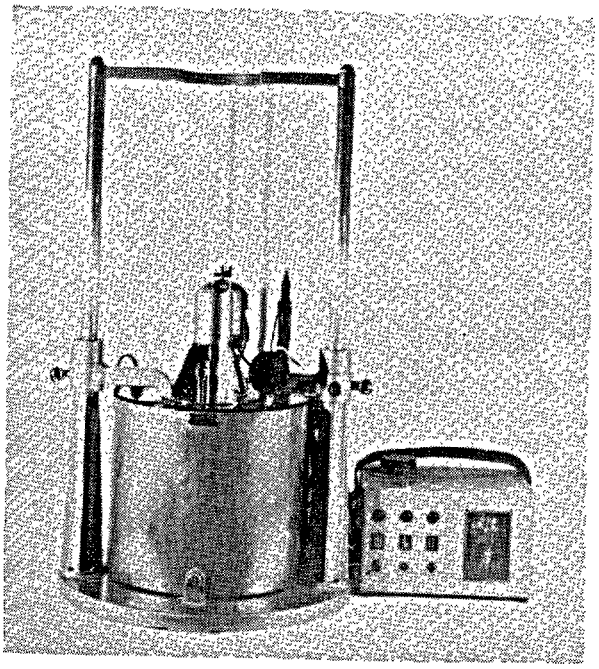

Photo 1. *Calorimeter*

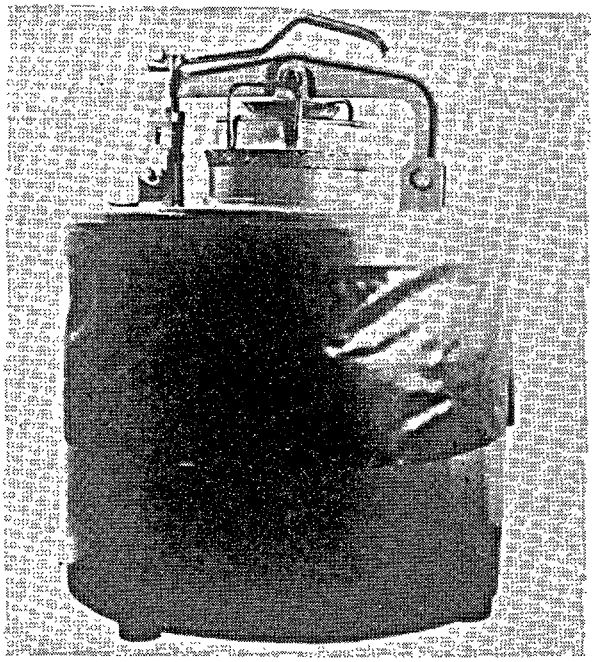

Photo 3. *Laboratory swinging disk grinder*

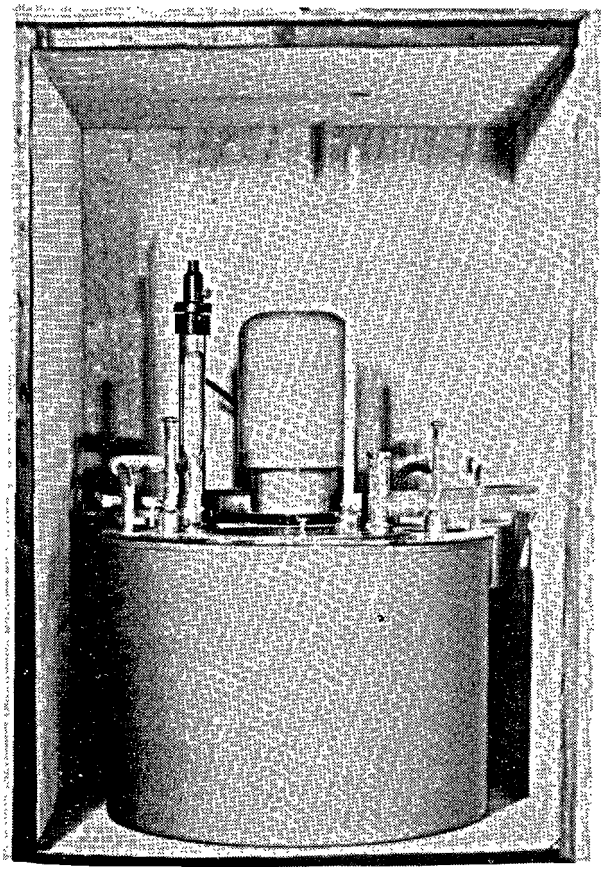

Photo 2. *Ultrathermostat*

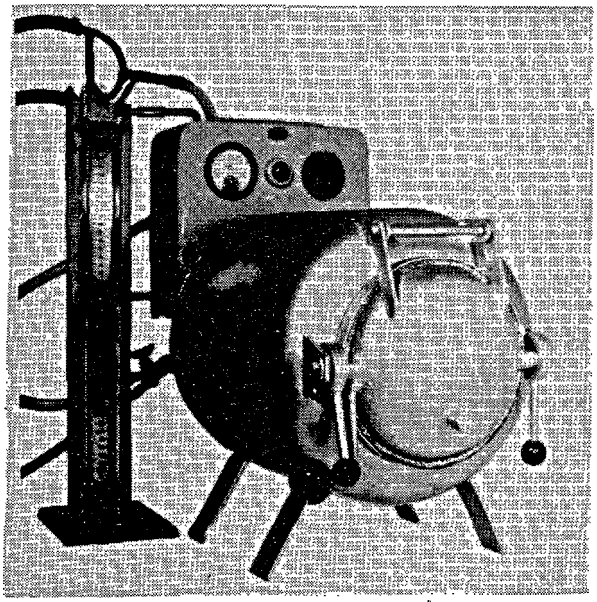

Photo 4. *Nitrogen forced circulation laboratory kiln*

(19) (see photo 1.)

Although other calorimeters of the same design can yield excellent results, we recommend the use of a funnel for introducing samples into the acid bath. The use of this funnel, as a matter of fact, allows an uniform and rapid introduction. Besides, any risk of carbonation of the sample is avoided and the temperature of the substance to be solved

can be risen to the same temperature as the acid solution before starting the measurements. The use of this funnel also make it possible to work in a room with a steady and regular temperature.

—An ultrathermostat allowing the preservation of the cement pastes with an accuracy of $\pm 0.01°C$ (photo 2).

—Small laboratory swinging disk grinder to grind hydrated cement samples (photo 3),

—Nitrogen forced circulation laboratory kiln for measuring the loss on ignition in a nitrogen atmosphere of metallurgic cements (photo 4).

—Vacuum pump.

Method for the Determination of the Heat of Hydration

The method used here has been described in a lot of publications issued by Dr. Goggi (16), (19). Nevertheless, three important modifications were introduced:

Sample Preservation

The preservation in the air of cement pastes could not be guaranteed with accuracy for a temperature of $5°C \pm 0.1°C$. We chosed, therefore, a preservation in water, the temperature of the bath being kept at $\pm 0.01°C$ by means of an ultrathermostat.

The cement pastes are preserved in polyethylene tubes of standardized dimensions (height 68 mm, diameter 26 mm). They are sealed with paraffin and horizontally set in the body of the ultrathermostat to avoid any segregation in the hydrated cement paste.

No matter how high the preservation temperature may be, we propose that the sample preservation in water be generalized.

Grinding of Hydrated Cement Samples

When cement pastes are preserved for three days at $+5°C$, the hardened pastes to be ground are still relatively humid. A dry grinding as prescribed by the original A.S.T.M. method is thus impossible. Besides, it is important to avoid any further reaction of the water still free with the particles of anhydrous cement.

The grinding by hand in alcohol and a nitrogenic atmosphere, which is long, difficult and not free from carbonation hazard, has been replaced by a grinding in alcohol in a swinging disk grinder. This allows a reduction of the grinding time which is now comprised between 1 and 4 minutes, a more even fineness of grinding and the cancellation of any contamination hazard by air CO_2, the cap of the grinder being hermetically closed.

Determination of the Heat of Solution of Hydrated Cement

The formula put forward for the determination of the heat of solution for metallurgic cements read as follows (16):

$$Q_x = \frac{\theta_c \times M}{P \times \frac{CaOi}{CaOa}} + 0.4(T_{30} - T_0) + 0.3(T_{30} - 20°) \quad (1)$$

It thus appeals to the CaO content value of anhydrous and hydrated cement samples. Now, a quick determination of CaO by complexometry is accurate at $\pm 0.5\%$ only. This corresponds to a possible error of 7 cal/g on the heat of solution of hydrated cement and, consequently, on the heat of hydration.

A CaO quantity determination could be devised using wet chemical analysis. In the case of metallurgic cements, however, the quantity of MnO and Mn_2O_3 which are always to be found in slags should be determined, too, and the necessary corrections be made as regards the CaO value. This, consequently, would seriously lengthen and complicate the solution method.

That is the reason why we replaced the quantity determination of CaO by the determination of the loss on ignition in nitrogen with an accuracy of $\pm 0.1\%$. In this case the heat of solution of hydrated cement is determined, as for portlands, by means of the following formula:

$$Q_x = \frac{\theta_c \times M}{P \times \frac{100 - PFi}{100 - PFa}} + 0.4(T_{30} - T_0) + 0.3(T_{30} - T_{20}) \quad (2)$$

After having described the equipment and the method of determination used here, we can now examine such parameters as may influence the measures studied in the course of our additional tests.

Description and Results of Additional Tests

Calibration of the Calorimeter with ZnO

In the course of collective tests it is important that the zinc oxide used for the calibration of the calorimeter should have an even quality. To avoid gross impurities, we recommend the use of ZnO p.a.

In addition, the ZnO preparation has to be standardized as regards the *calcination temperature* and the *fineness of grinding*.

Our experience led us to put forward the following preparation: ± 100 g. ZnO p.a. are calcined for an hour in a ALO_2 alloy dish at a temperature of 950°C. It is then slowly cooled down in a dessicator at 100–110°C, then ground in a china mortar till the whole mass can pass a 295 micron sieve. *A finer grinding should be avoided.* Some laboratories stipulate a fineness lower than 160 μ and even 148 μ. In this case, the ZnO powder tends to form clots by the imperfect dissolution, which in the acid mixture can make the calibration erroneous. The ground ZnO is carefully preserved in a hermetically closed flask.

As regards the quantity of ZnO to be used for calibration, it should be such that the thermal jump be of the same range as the one attained when proceeding with either 6 g. anhydrous cement or 7 g. hydrated cement. The ideal quantity of ZnO is thus 14 grams.

As a rule the ratio acid/ZnO is thus equal to 60. Should a greater ratio be adopted, for ex. 68, viz. a calibration with 12.5 g. ZnO, one can see from Table 1 bis that in spite of the variation of the calorific capacity M, the values of the heat of hydration remain unchanged.

However, to avoid greater errors, we think that the quantity of ZnO should not show a difference greater than 14 grams.

When it is not possible to perform a calibration with help of an electric method, it is then of great interest to accurately standardize the calibration by a thermochemical proceeding in order to attain, at least, anhydrous cement measures which can be compared between different laboratories.

Acid Mixture Composition

Our experiments compared with those of other laboratories showed that the composition of the acid mixture does not practically influence the heat of solution either of ZnO or of anhydrous or hydrated cements.

In order, however, to avoid the introduction of a cause of additional error, a standard mixture consisting of HNO_3 $2N \pm 0.05N$ and of HF 38 to 40% shall be used, preferably, in such a proportion that one has 10 ml HF per 425 grams acid mixture.

Mixing Conditions for Tests on Hydrated Cement

When measuring the heat of hydration after a 7 days preservation at $+20$°C, it should be noted that a mixing of the paste at the laboratory ambient temperature does not lead to any error.

On the contrary, when the mixing is followed by a preservation at $+5$°C, the question may be whether it may not be necessary or not that water and mixing temperature should amount to $+5$°C too.

To answer this question, we performed tests on two very different types of cement. The results are shown on Table 2.

This table shows that the mixing conditions do not influence—or very slightly influence—the results attained for metallurgic cements. In the case of rapid-hardening portland cements (i.e. the most unfavourable case), on the contrary, differences amounting to 2 calories per gram are possible.

With a view to attain an increased accuracy, it is

Table 2. *Influence of the mixing conditions of the cement paste on the heat of hydration after conservation during 3 days at +5°C*

Cement type	Heat of solution and of hydration after mixing of the cement paste at +20°C			Heat of solution and of hydration after mixing of the cement paste at +5°C		
	Heat of solution of the anhydrous cement	Heat of solution of the hydrated cement	Heat of hydration in cal/g	Heat of solution of the anhydrous cement	Heat of solution of the hydrated cement	Heat of hydration in cal/g
PDR (Rapid hardening portland cement)	596.0 595.7 } 595.9	527.7 527.6 528.1 } 527.8	68.1	595.9	529.8 529.6 } 529.7	66.2
HFHR (Slag cement)	582.9 582.7 } 582.8	549.0 549.0 } 549.0	33.7	582.8	548.9 549.5 } 549.2	33.5

therefore recommended to rise the temperature of mixing water to that of the subsequent paste preservation.

Influence of the Determination of the Loss on Ignition for Metallurgic Cements

As said above, the determination of the heat of hydration of metallurgic cements should be made by substituting the loss on ignition in nitrogen to the CaO calibration. This, however, supposes the determination of this loss on ignition at $\pm 0.1\%$ under accurately settled operating conditions.

We undertook some experiments with a view to attain accurate values for these. The results thereof are shown on Tables 3 to 5. These tables show every test series corresponding to 5 measures made from 5 crucibles introduced simultaneously in the nitrogen laboratory kiln and thus submitted to similar operating conditions. Owing to the large dimensions of the laboratory kiln, however, there are slight differences between the temperature recorded by the sheathed pyrometer and that of each sample. With a view to discussing our results we shall, therefore, consider the means attained, not taking extreme values into account.

The loss on ignition of the cement used for the tests amounts to 5.37% under the optimal testing conditions defined hereafter. Quoting this value, an examination of Tables 3 to 5 allows the following conclusions:

1. *the calcination temperature* of the sample should amount to at least 1,000°C. At lower temperatures an incomplete decarbonation leads to errors on the low side comprised between 0.5 and 2.5% (see Table 4).
2. *the calcination time* will be of *60 minutes*. Less time will yield errors on the low side of $\pm 0.3\%$ and more time does not give any important variation provided on proceeds with at least 1,000°C (see Table 5).
3. the samples should not be taken out of the nitrogen laboratory kiln at a temperature higher than 300°C. This is particularly important in calcinating the hydrated cements (see Table 3).

When these three conditions are fulfilled, our experiments show that an excellent accuracy and a very good reproducibility can be attained.

In order to better emphasize the importance of an accurate determination of the loss on ignition in nitrogen, Table 6 shows two examples with measures

Table 3. *Loss on ignition unter nitrogen—Influence of the exit temperature of the sample from the laboratory kiln*
Trial conditions: samples ignited 1/2 h. at 1,000°C

Exit temperature of the sample from the laboratory kiln	Loss on ignition in %					Mean value	Mean without extreme values
	1	2	3	4	5		
	a) Anhydrous slag cement						
140	5.19	5.26	5.30	5.43	5.59	5.39	5.33
300	5.32	5.34	5.41	5.54	5.55	5.43	5.43
400	5.26	5.39	5.43	5.56	5.59	5.44	5.46
500	5.20	5.23	5.30	5.38	5.46	5.31	5.30
	b) Hydrated slag cement						
140	9.84	9.91	9.94	9.98	10.00	9.93	9.94
200	9.89	9.97	10.01	10.05	10.06	9.99	10.01
300	9.85	9.88	9.90	9.92	9.89	9.89	9.90
400	9.73	9.85	9.88	9.93	9.97	9.87	9.89
500	9.68	9.70	9.83	9.85	9.87	9.78	9.79
600	9.58	9.59	9.60	9.68	9.73	9.63	9.62

Table 4. *Loss on ignition unter nitrogen—Influence of the maximum temperature of ignition*
Trial conditions:—sample maintained 1/2 h at the choosen temperature
—exit temperature of the sample: 140°C

Maximum ignition temperature in °C	Loss on ignition in %					Mean value	Mean without extreme values
	1	2	3	4	5		
800	2.58	2.81	2.86	2.94	2.98	2.83	2.87*
850	2.99	3.44	3.53	3.60	3.65	3.44	3.56
900	3.94	4.00	4.08	4.19	4.71	4.18	4.09
950	4.19	4.43	4.74	4.95	4.97	4.65	4.71
1,000	5.02	5.24	5.26	5.27	5.44	5.24	5.26

*The determination of the CO_2 content of the anhydrous cement has given 2.85%. The difference between the losses of ignition at 800°C and 1,000°C corresponds practically to some quantity of CO_2 not released.

Table 5. *Loss on ignition unter nitrogen—Influence of the ignition time at 1,000°C*

Ignition time in minutes	Loss on ignition in %					Mean value	Mean without extreme values
	1	2	3	4	5		
30	5.19	5.26	5.30	5.43	5.59	5.39	5.33
60	5.32	5.42	5.56	5.58	5.63	5.50	5.32

Table 6. *Influence of the value of the loss on ignition for a slag cement on the calculated head of solution of the same cement hydrated during 3 days at +5°C*

	Corrected θ_c in cal/g	Head capacity in cal/g	Loss on ignition of the anhydrous cement in %	Loss on ignition of the hydrated cement in %	Heat of solution of the hydrated cement in cal/g
Example 1: Slag cement HFHR					
Laboratory A	3.6425	813.06	4.47	21.78	516.71
Laboratory B	—	—	2.17	19.82	516.27
Example 2: Slag cement HFN					
Laboratory A	4.020	813.06	5.33	14.88	519.30
Laboratory B	—	—	1.57	9.97	510.50

performed in two different laboratories. These examples show that differences in the values of the loss on ignition used for the determination can lead either to differences which can bc overlooked (example 1) or to differences amounting to *10 calories per gram* for the heats of solution of hydrated cements (example 2).

An accurate standardization of the operating procedure is therefore quite justified.

Conditions for the Preparation of Hydrated Cement Samples

Mixing and drying hydrated cement samples are, in our opinion, the two delicates operations of the solution method. Owing to the numerous fests made in Belgium it appeared absolutely necessary to lay down with accuracy the conditions under which both operations should be carried out.

Samples are being preserved for a very short time (3 days at +5°C). Besides, it is important to take care to avoid any action of the atmosphere CO_2 which might alter subsequent measures. The grinding of hydrated cement is thus carried out in a liquid in order to avoid any contamination and prevent from hydration. As far as grinding is concerned, different finenesses of grinding can be attained.

Then the last traces of the liquid used must be removed by means of an ether rinsing and a more or less prolonged drying.

Carrying out all these operations showed some differences between Belgian laboratories, some of them amounting to 15 cal/g for the heat of hydration of the same cement type.

This prompted us to carry out a serie of tests to study the influence of the following parameters on the value measured for the heat of hydration:

1. *Nature of the liquid used for grinding.* Two types of liquid—which are the most commonly used—were used here; they are: ethyl alcohol and acetone.

2. *Fineness of grinding of hydrated cements.* Two finenesses of grinding were adopted: less than 147 microns and less than 297 microns.

3. *Drying time and drying temperature of the ground sample.* Four types of drying were considered:

—a vacuum drying for 45 minutes under ambient temperature conditions as initially put forward by Dr. Goggi (16). Conventionally, we will agree to consider the respective heats of hydration as *values of reference.*

—a vacuum drying for 1 hour at 35°C.

—a vacuum drying for 40 minutes at 30°C.

—a vacuum drying for $1\frac{1}{2}$ hour at 30°C.

Two cement types were used for these tests: a rapid hardening portland cement (PDR) and a rapid hardening blast-furnace cement (HFDR).

After mixing the cement pastes were preserved for three days at +5°C under above-defined conditions. At the time of settlment for testing the hydrated cements were ground and dried under various conditions. Then we measured their heat of solution. The heats

Table 7. *Determination of heat of hydration of PDR hydrated cement samples, crushed and dried in various conditions*
Basic data:—heat capacity M: 836.17 cal/g—heat of solution of the anhydrous cement PDR: 591.59 cal/g—loss on ignition of the anhydrous cement: 1.58%—grinding fineness: $< 147\,\mu$

Sample No.	Treatment of the hydrated cement after conservation 3 days at +5°C	θ_c measured	Heat of solution of the hydrated cement in cal/g	Heat of hydration in cal/g	Loss on ignition of the hydrated cement in %
13	crushed with ethyl alcohol, washed with ether and dried under vacuum at room temperature for 45 min.	3.570 3.571	533.66 533.79	57.88	20.80 20.77
14	crushed with ethyl alcohol, washed with ether and dried under vacuum at 35°C for 1 hour.	3.768 3.768	542.66 542.64	48.95	17.85 17.70
15	crushed with ethyl alcohol, dried under vacuum at 30°C for 40 min.	3.617 3.613	533.85 533.16	58.09	19.80 19.70
16	crushed with ethyl alcohol, dried under vacuum at 30°C for 1 1/2 h.	3.730 3.730	540.45 540.34	51.21	18.20 18.30
17	crushed with acetone, then dried under vaccum at room temp. for 45 min.	3.733 3.739	537.99 538.79	53.21	17.85 17.78
18	crushed with acetone and dried under vacuum at 35°C for 1 hour.	3.762 3.771	541.07 542.36	49.89	17.71 17.60
19	crushed with acetone, then dried under vacuum at 30°C for 40 min.	3.595 3.584	536.01 534.02	56.44	20.61 20.55
20	crushed with acetone, then dried under vacuum at 30°C for 1 1/2 h.	3.623 3.632	535.28 536.57	55.67	19.80 19.90

of hydration were determined after some additional measures of the heat of solution of anhydrous cement and of the losses on ignition of anhydrous and hydrated cements had been made.

Table 7 is a summary of the results attained for a PDR cement and Table 8 shows those attained for a HFDR cement, both to them being ground with a fineness lower than 147 microns, while Table 9 shows the results attained for cement pastes with a fineness lower than 297 microns.

In order to further investigate an eventual drying action of the grinding liquid and of the drying process on the mineralogic structure of hydrated cement, a certain number of ground and dried samples underwent some physical examination: X-ray diffraction, thermogravimetry and differential thermal analysis

Table 8. *Determination of heat of hydration of HFDR hydrated cement samples, crushed and dried in various conditions*
Basic data:—heat capacity M: 836.17 cal/g—heat of solution of the anhydrous cement HFDR: 573.66 cal/g—loss on ignition, unter nitrogen, of the anhydrous cement: 5.62%—grinding fineness $< 147\,\mu$

Sample No.	Treatment of the hydrated cement after conservation 3 days at +5°C	θ_c measured	Heat of solution of the hydrated cement in cal/g	Heat of hydration in cal/g	Loss on ignition of the hydrated cement in %(unter nitrogen)
1	crushed with ethyl alcohol, washed with ether and dried under vacuum at room temperature for 45 min.	3.469 3.477	517.98	55.68	23.83
2	crushed with ethyl alcohol with ether and dried under vacuum at 35°C for 1 hour.	3.780 3.769	534.18	39.48	16.1
3	crushed with ethyl alcohol, dried under vacuum at 30°C for 40 min.	3.473 3.482	514.74	58.92	23.22
4	crushed with ethyl alcohol, dried under vacuum at 30°C for 1 1/2 h.	3.868 3.869	539.07	34.59	18.41
5	crushed with acetone, then dried under vacuum at room temp. for 45 min.	3.814 3.822	535.04	38.62	18.89
6	crushed with acetone and dried under vacuum at 35°C four 1 hour.	3.853 3.855	535.11	38.55	18.11
7	crushed with acetone, then dried under vacuum at 30°C for 40 min.	3.833 3.832	534.02	39.64	18.40
8	crushed with acetone, then dried under vacuum at 30°C for 1 1/2 h.	3.851 3.852	531.70	41.96	17.61

Table 9. *Determination of heat of hydration of PDR and HFDR hydrated cement samples, crushed and dried in various conditions*
Basic data:—heat capacity M: 836.17 cal/g—heat of solution of the anhydrous PDR: 591.59 cal/g—heat of solution of the anhydrous HFDR: 573.66 cal/g—loss on ignition of the anhydrous PDR: 1.58%—loss on ignition, unter nitrogen, of the anhydrous HFDR; 5.62%—grinding fineness: $< 297\,\mu$

Cement type	Sample No.	Treatment of the hydrated cement after conservation 3 days at +5°C	θ_c measured in cal/g	Heat of solution of the hydrated cement in cal/g	Heat of hydration in cal/g	Loss on ignition in %
HFDR (Rapid hardening slag cement)	9	crushed with ethyl alcohol, dried under vacuum at room temperature for 45 min.	3.614 3.629	521.31	52.35	21.03
	10	crushed with ethyl alcohol, dried under vacuum at 35°C for 1 hour.	3.889 3.891	538.26	35.40	17.86
	11	crushed with ethyl alcohol, dried under vacuum at 30°C for 40 minutes	3.677 3.676	523.77	49.89	20.22
	12	crushed with ethyl alcohol, dried under vacuum at 30°C for 1 1/2 h	3.946 3.953	541.62	32.04	17.12
PDR (Rapid hardening portland cement)	21	crushed with ethyl alcohol, dried under vacuum at room temperature for 45 min.	3.464 3.471	525.09 527.03	65.09	22.10 22.05
	22	crushed with ethyl alcohol, dried under vacuum at 35°C for 1 hour.	3.627 3.632	534.58 535.34	56.64	19.70 19.60
	23	crushed with ethyl alcohol, dried under vacuum at 30°C for 40 minutes	3.510 3.516	533.30 534.26	57.82	22.02 22.09
	24	crushed with ethyl alcohol, dried under vacuum at 30°C for 1 1/2 h.	3.622 3.622	535.65 535.63	55.97	19.90 19.95

The essential features of the results of this examination are shown on Tables 10 and 11. The thermograms and diagrams obtained by DTA are also shown on Figs. 1 to 7.

Table 10. *Investigation on differently treated PDR and HFDR cement by X-ray diffraction and differential thermal analysis*

Cement type	Sample No.	X-ray diffraction		Differential thermal analysis	
		$Ca(OH)_2$ X-ray	Ettringite X-ray	Peak height in mm	
		reflex in mm	reflex in mm	between 80° and 150°C	between 400° and 600°C
HFDR (slag cement)	1	19	67	212	49
	2	17	53	176	62
	3	20	51	—	—
	4	13	49	—	—
	5	19	58	—	—
	7	20	85	—	—
	8	17	50	—	—
	9	18	62	—	—
PDR (Rapid hardening portland cement	13	42	55	226	168
	14	36	64	208	200
	15	32	50	—	—
	16	50	49	—	—
	21	40	40	—	—

A careful examination of above-mentioned documents leads to the following conclusions:

PDR Cement (Samples 13 to 24)

Influence of the Fineness of Grinding

We must compare measure series 13 to 16 and 21

Table 11. *Percentage weight loss from TGA in temperature ranges 80°–150°C and 400°–500°C*

Cement type	Sample No.	Weight loss in % between 80 & 150°C	Weight loss in % between 400 & 500°C
HFDR (slag cement)	1	7.30	0.80
	2	6.20	1.12
	3	7.50	0.76
	4	6.16	0.80
	5	6.64	1.00
	7	6.96	1.00
	8	6.30	0.88
	9	5.70	0.70
PDR (Rapid hardening portland cement	13	6.90	2.20
	14	6.70	2.35
	15	6.80	2.16
	16	7.20	2.40
	21	6.80	2.30

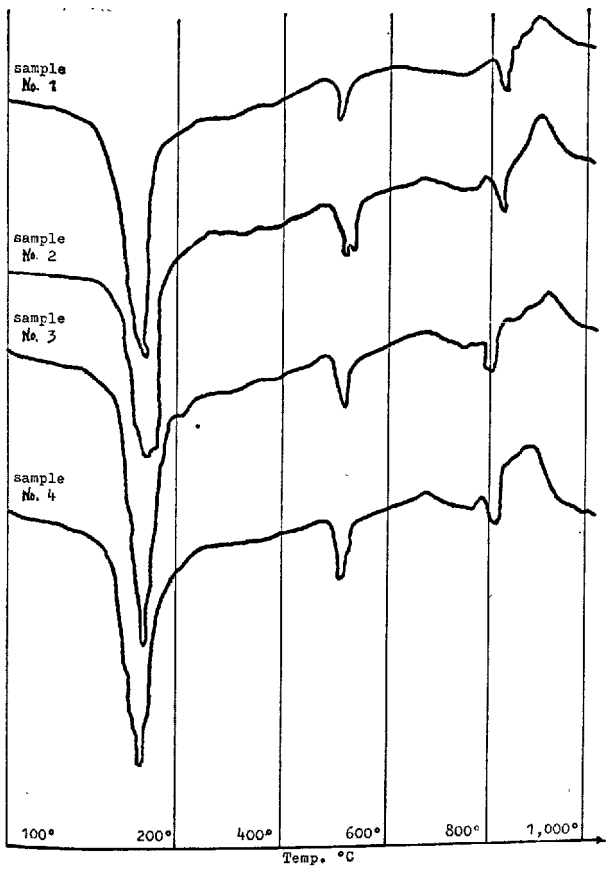

Fig. 1. *DTA graphs of hydrated cement samples*

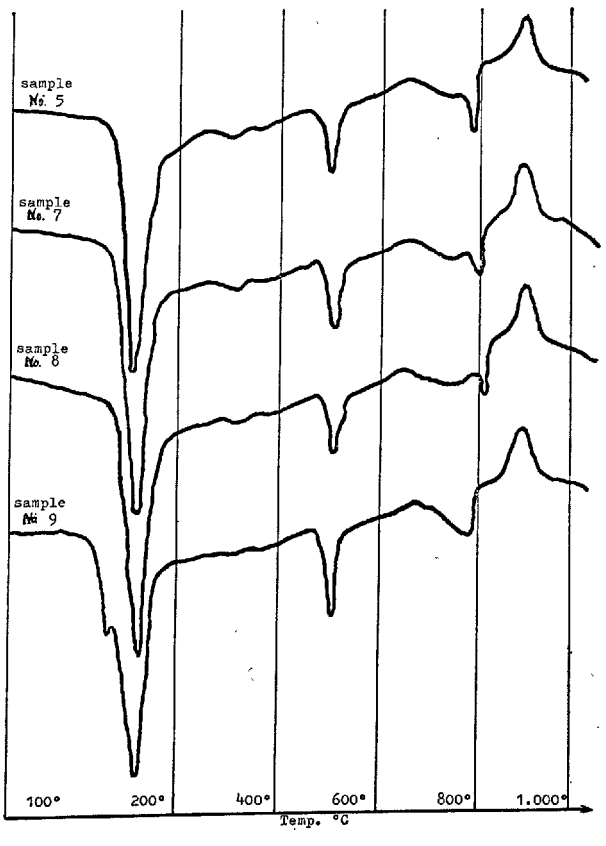

Fig. 2. *DTA graphs of hydrated cement samples*

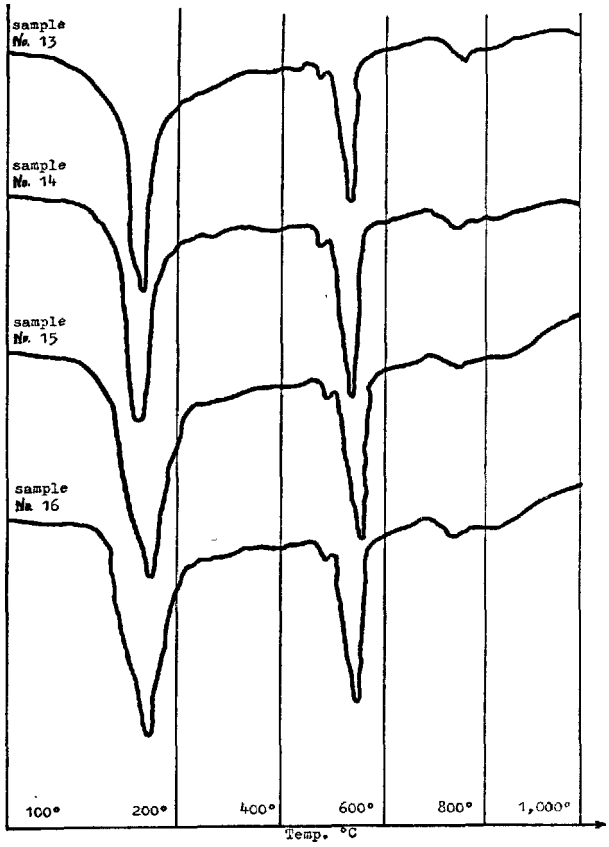

Fig. 3. *DTA graphs of hydrated cement samples*

to 24. Logically, a coarser sample grinding should eliminate alcohol-ether more easily. Now it is just the opposite with a PDR cement, as in this case, the losses on ignition of samples ground more coarsely are always higher by 1 to 2%. This is a systematic fact which is always recorded, *whatever the drying process adopted after grinding may be.*

The occurrence of some residual ethyl alcohol cannot, in our opinion, explain the recorded differences, some of which amount to 8 or 9 calories (see Tables 7 and 9). As it is not possible to find a logical explanation, we think that this parameter should be studied once again using portland cements of a lower fineness.

Influence of the Liquid used for Grinding

For a given drying process, the differences between the values of series 13 to 16 and 17 to 20 are comprised between 1 and 4 cal/g. Compared with ethyl alcohol, the differences attained when using acetone are sometimes on the higher, sometimes on the lower side.

It seems that the type of liquid does not play a fundamental part as far as portland cements are concerned. The differences recorded seem to be explainable through the occurrence of a certain quantity of residual alcohol or acetone.

Influence of the Drying Temperature and of the Drying Time

After treating samples 13 to 16 with *ethyl alcohol,* the following statements can be made:

—for a limited drying period, the values attained for the heat of hydration are almost identical, whether the drying be carried out at the ambient temperature or at 30°C.

—should the drying time be prolonged or the temperature risen to 35°C, important differences should be recorded, more particularly, when drying is being carried out for 1 hour at 35°C.

A reading on the thermograms does not allow to state that there is a loss of combination labile water of the hydration constituents.

The difference recorded in comparison with the value of reference 13, however, cannot be explained through a more complete alcohol elimination. And the 3% loss on ignition shows that a hydration water loss is probable.

It should thus be remembered that when using ethyl alcohol one should have a maximum temperature of 30°C and a drying time not exceeding 40 minutes.

The differences, when these two conditions are not complied with, are more important when proceeding with a high fineness of grinding.

When using acetone, it should be noted that:

—the effects of a drying period exceeding 1 hour are less important when using ethyl alcohol.

—the combination of a prolonged drying with a temperature of 35°C leads once more to a very important drop of the heat of hydration.

Conclusions

Owing to this series of tests, it can be stated that the values attained for the heat of hydration are comprised between 51 and 58 cal/g., i.e. a dispersion of 7 cal/g. This dispersion can sometimes be explained by an incomplete elimination of the grinding liquid, and also by a reduced elimination of combination labile water when the period of drying exceeds 40 minutes. This conclusion is valid whatever the liquid used and the adopted fineness of grinding may be.

On the contrary, it is clear that a drying at 35°C automatically leads to a more or less important destruction of the hydrated structure with a loss of labile water which is not to be overlooked. The dif-

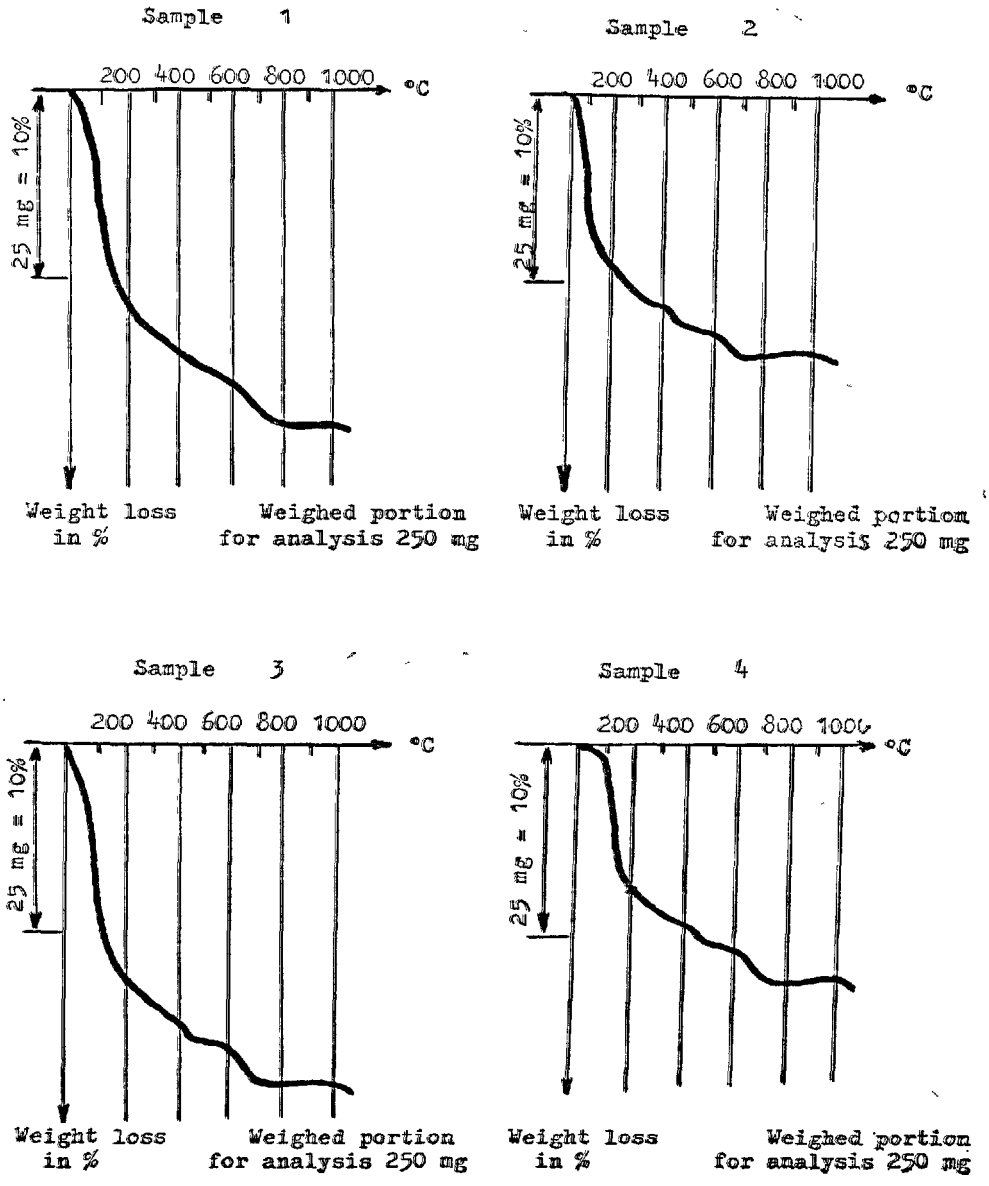

Fig. 4. *TGA graphs of hydrated cement samples*

ferences versus the value of reference may then amount to at least 8 and 9 cal/g.

HFDR Cement (samples 1 to 12)

Influence of the Fineness of Grinding

Lets us now compare measure series 1 to 4 and 9 to 12. It is found that samples ground more coarsely give less important values for the heat of hydration. As their loss on ignition is much lower, it appears that the ethyl alcohol elimination was more complete than for finely ground pastes. It is evident that in this case we are isolating the fineness parameter and that only two samples which underwent the same drying process can be compared with one another.

Influence of the Liquid used for Grinding

When comparing two by two the values of series 1 to 4 and 5 to 8, it clearly appears that the values 5 to 8 are very well grouped together within a mean

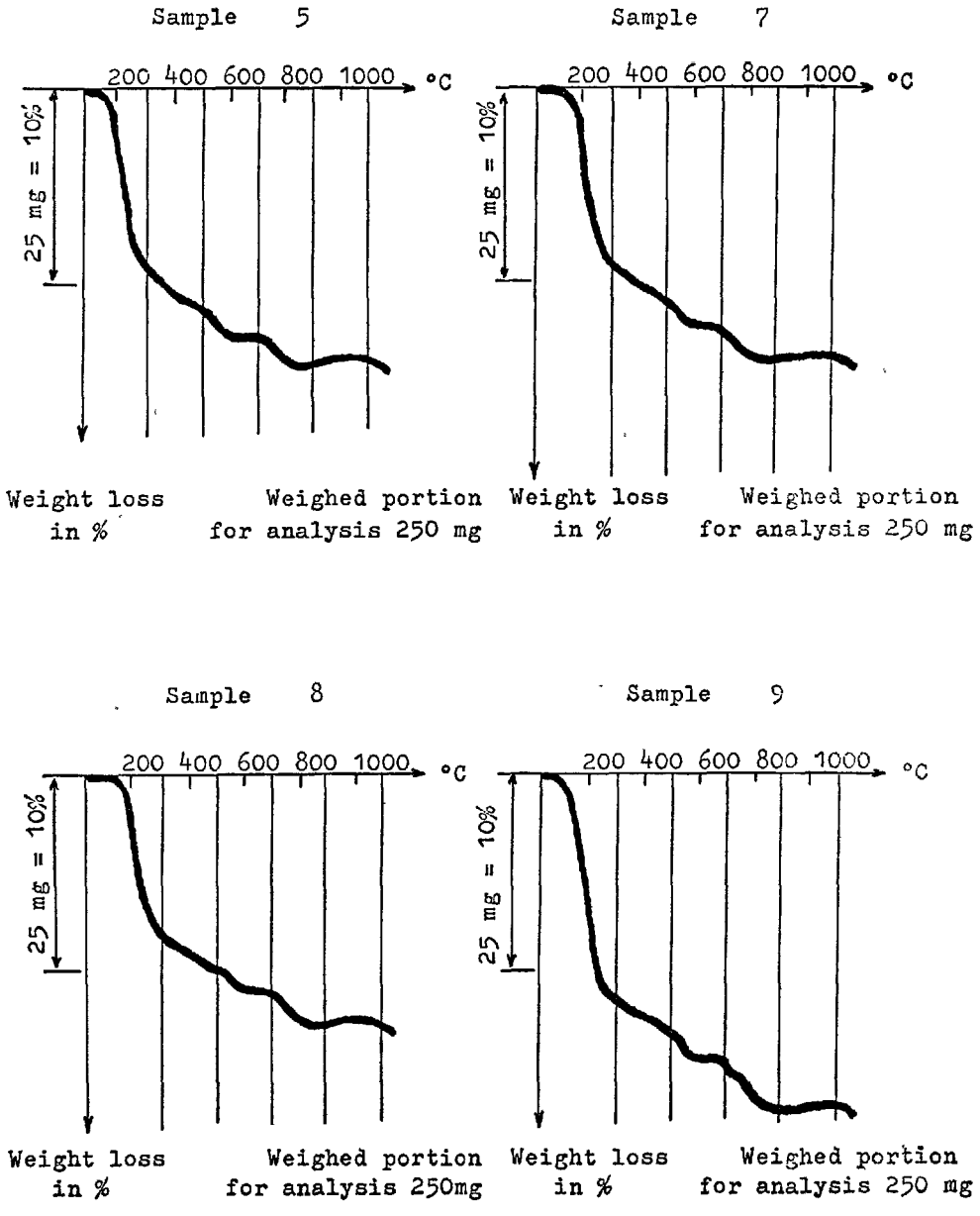

Fig. 5. *TGA graphs of hydrated cement samples*

range of 39 cal/g. Drying conditions seem, therefore, to have very little influence in the value of the heat of hydration when using *acetone*.

This clearly shows that the use of acetone under drying conditions similar to those used with ethyl alcohol leads to an exaggerated desiccation of the ground paste with an important labile water loss of the hydrated constituents. This loss is more particularly characterized by the thermogram features and the differences recorded as regards weight losses between 80°C and 150°C.

Influence of the Drying Temperature and of the Drying Time

For samples 1 to 4 which underwent an *ethyl alcohol treatment*, it appears that a non-prolonged drying period (with a maximum of 40 minutes) at a lower temperature than or equal to 30°C leaves very similar values for the heats of hydration measured.

Too long a drying or a temperature of 35°C only

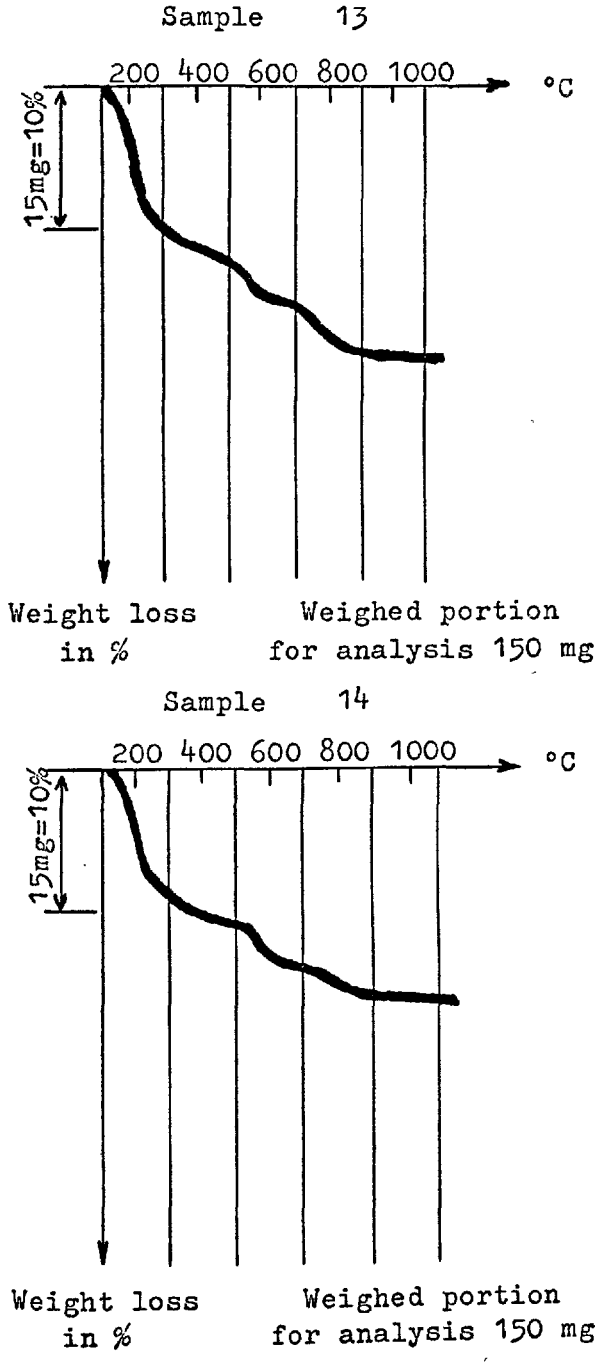

Fig. 6. *TGA graphs of hydrated cement samples*

leads to an indisputable degradation of the hydrated constituents of the paste.

When acetone is used there is always a degradation of the hydrated structure whatever the drying conditions may be.

Conclusions

When ethyl alcohol is used a coarser grinding allows a more complete elimination of this liquid. For a given fineness the value dispersion is of 2 to 3 cal/g. provided that moderate drying conditions be adopted.

When drying takes place under drastic conditions, however, there is an important degradation of the hydrated constituents of the paste and the values measured mean nothing any more.

The same thing occurs when using acetone whatever the adopted method of drying may be. The use of this liquid should thus be prohibited.

Conclusions

Above-mentioned tests dealt with two cement types only. The conclusions drawn, therefore, should not be considered as definitive ones, but rather as indications allowing a limitation of the problems set and an orientation with a view to subsequent researches. They may be summarized as follows:

a. The fineness of grinding of hydrated cement pastes should not be too high and a fineness lower than 300 microns should represent an adequate minimum. The elimination of the grinding liquid and of the rinsing ether will consequently be more complete. This conclusion, however, should be confirmed by subsequent testing on anhydrous cements of a lower fineness.

b. The use of acetone as a grinding liquid leads to the destruction of the structure of the cement paste whatever the subsequent drying conditions may be. Used of this liquid should thus be strictly prohibited.

c. When using ethyl alcohol drastic drying conditions should be avoided as these cause a more or less important loss of the combination labile water of hydrated components. The effect of an exaggerate drying is particularly bad in the case of blast-furnace cements.

In the present state of our research work we recommend a high vacuum drying for a maximum of 40 minutes, at a temperature not exceeding 30°C.

Subsequent research work should allow an increased accuracy of the limits thus determined.

It may also be questioned whether the combined action of alcohol and rinsing ether does not cause a substantial etching of residual hydrated and anhydrous constituents of the cement paste, this etching being characterized by the flowing of a certain quantity of soluble matter into the filtrate.

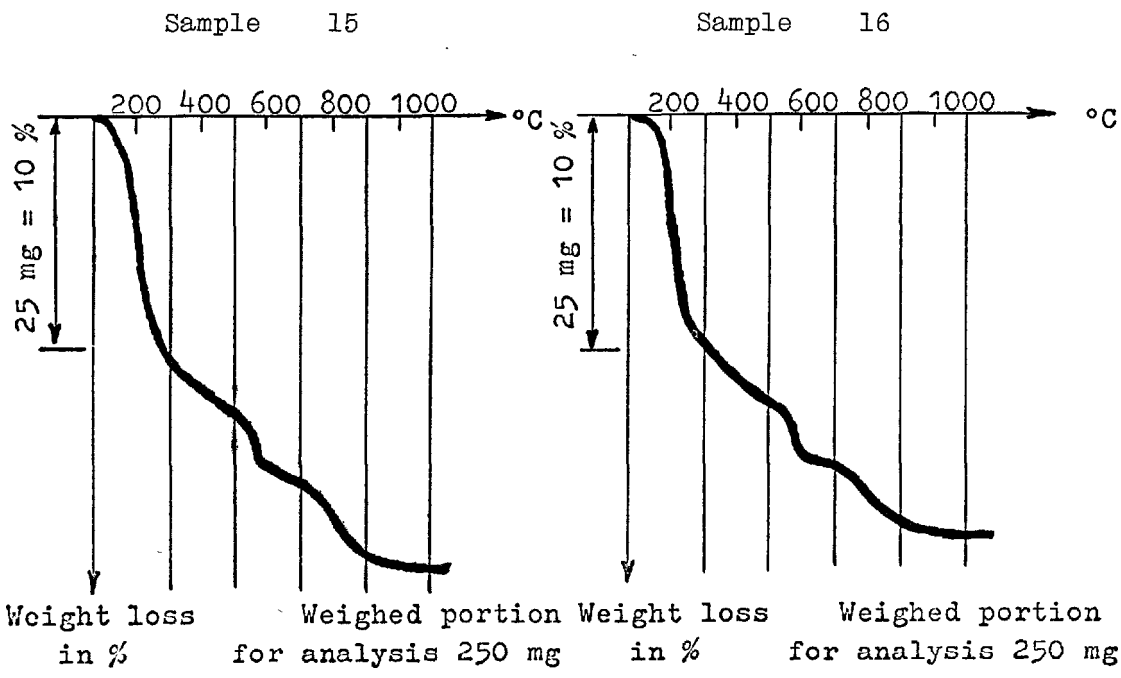

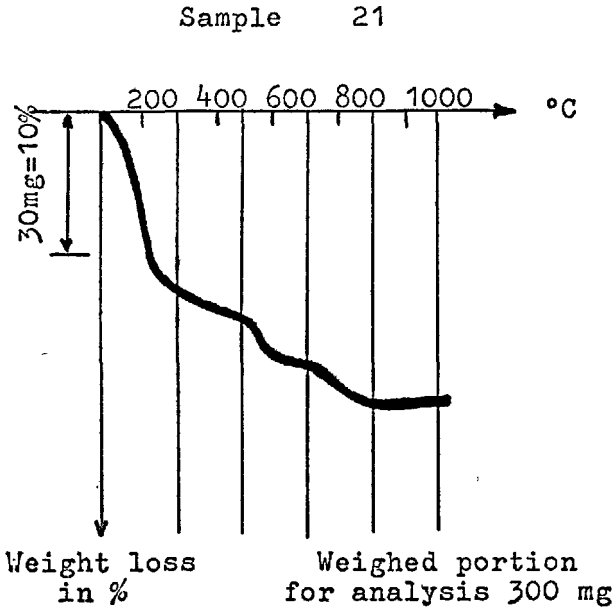

Fig. 7. *TGA graphs of hydrated cement samples*

To answer this question two types to tests were performed:

a) Chemical analysis of filtrates derived from the washing of hydrated cement samples with alcohol-ether.

The following results expressed in % of the quantity

of dry cement initially mixed were attained:

	Sample 1	Sample 2
SiO_2	% 0.0016	% 0.0009
R_2O_3	0.0022	0.0005
CaO	0.0008	0.0006
$Ca(OH)_2$ solved	0.0008	0.0009

b) Compared analysis of anhydrous, hydrated but not washed with alcohol-ether, hydrated then washed with alcohol-ether cement.

The following table shows analysis results determined with a null loss on ignition.

	PDR anhydrous cement	PDR hydrated cement, unwashed			PDR hydrated cement then washed with alcohol-ether
		1st test	2nd test	Mean	
	%	%	%	%	%
SiO_2	20.60	20.79	20.22	20.50	20.45
Al_2O_3	7.34	6.83	6.73	6.78	6.98
Fe_2O_3	3.27	3.26	3.26	3.26	3.26
CaO	65.96	65.33	65.05	65.19	65.14
MgO	0.82	—	0.74	0.74	0.74

The above-mentioned results clearly show that an usual grinding in ethyl alcohol followed by an ether rinsing will not modify in the least the chemical composition of the hydrated cement by matter flowing into the filtrate. The cause of the differences recorded should thus be searched elsewhere.

Conclusions

Very important differences, some of them amounting to 15 calories per gram were recorded between different laboratories when measuring the heat of hydration of the same cement type using the solution method.

A certain number of factors capable of explaining these differences have been studied in this record.

The calibration of the calorimeter will be carried out with 14 grams zinc oxide with an even but not too high fineness of grinding. The heat capacity M will be the mean of at least 6 determinations. If all these conditions are complied with, any cause of error due to a faulty calibration is eliminated.

Though it does not seem to have any influence on the values of the heats of solution measured, the composition of the acid mixture will be standardized, too.

The mixing of the cement will be carried out, if possible, with water having the subsequent paste preserving temperature. Errors of ± 2 calories per gram are possible when water is at the laboratory temperature whereas heating is being carried on at a low temperature.

The loss on ignition of anhydrous and hydrated cements interferes in the determination of the heat of solution of hydrated cement and has, consequently, an influence on the value of the heat of hydration. These losses on ignition will be determined by calcinating samples for an hour at $1{,}050°C \pm 50°C$. For blast-furnace cements this determination will be carried out in a laboratory kiln with a neutral atmosphere (nitrogen, argon). The procedure should be accurately described and strictly complied with. Should this not be done, differences of 10 calories per gram could be recorded between some laboratories.

It should be noted, however, that the standardization of above-mentioned operations allows the cancellation of practically any cause of systematic error. Such ideal operating conditions are, in our opinion, very well settled now and an agreement between laboratories on these various points is susceptible of being reached within a short time.

The delicate point of the solution method remains, therefore, the determination of the conditions for the preparation of hydrated cement samples. The tests which were carried out in our laboratories dealt with a limited number of cements and it is not possible, as a matter of fact, to draw now definite conclusions in this regard. In our opinion, however, these tests allowed a recording of some interesting facts which could be the base of new tests dealing with a greater number of cements having a different fineness and a different nature.

The following points should eseentially be recorded:

1. When heating of cement pastes occurs at a low temperature and for a very short time, it is absolutely necessary to use a liquid for grinding hydrated cement. Otherwise the carrying on of hydration and carbonation would cause errors which could only be estimated with much difficulty.
   Nevertheless for heatings of a longer period at a temperature of $+20°C$, the question remains whether it is advisable to use a liquid of which the subsequent elimination cannot be easily performed.
2. The liquid used should not modify the composition of the hydrated cement sample by matter flowing into solution. With ethyl alcohol this possibility does not practically exist.
3. The liquid used should be totally eliminated; if

not, the values of the losses on ignition and that of the heat of hydration determined could be altered. The fineness of grinding of hydrated cement should not be too high. We propose to limit it to a size non-remaining on a 297–micron sieve.

Besides, the elimination of this liquid by ether rinsing and vacuum drying should be performed under such conditions that the structure of some hydrated constituents should not be modified. More particularly, a loss of combination labile water of some hydrates should be avoided at all costs.

Owing to our experiments, we think that, provided a high vacuum drying (till 1 Torr) be performed, a drying period of a maximum 40 minutes at a temperature not exceeding 30°C is quite enough to eliminate totally a liquid like ethyl alcohol. On the contrary, the adoption of the same drying conditions in acetone leads most of the time to a high degradation of the hydrated paste structure. The use of such a liquid should, therefore, be prohibited.

Besides, we would like to emphasize that the above-recommended drying conditions were determined after a testing on rapid-hardening cements of which the Blaine specific surface is of about 5,000 sq. cm/g. It is thus quite clear that these conditions may be slightly modified for cements with a lower fineness, and that the period of drying may be further shortened. The temperature, however, should in no case exceed 30°C and it is, in our opinion, even preferable to proceed at the ambient laboratory temperature that is about 20°C.

It appears therefore absolutely necessary to carry out for the shortest possible time numerous tests enabling us to make a definite determination of the conditions for the preparation of hydrated cement samples allowing thus the accuracy and reproducibility of the measures performed.

As long as these optimal conditions remain indeterminate any attempt of a cement classification in which the differences between classes would not exceed 5 calories per gram appears to us as illusory and premature.

An important work of methodology remains to be done, as far as the solution method is concerned. Besides, it will be extremely interesting to compare the results attained with those concerned with other methods such as the predetermined dispersion method (6) and the isothermal calorimeter method (22).

We wish the work described here could contribute to some progress of this problem of methodology.

References

1. R. W. Carlson and L. R. Forbrich, "Correlation of methods for measuring heat of hydration of cement", Ind. and Eng. Ch., **16**, No. 7, 382–387, (1938).
2. R. Alègre, "La calorimétrie des ciments au C.E.R.I. L.H.", Rev. des Mat. de Constr., **544**, 1–12, (1961).
3. M. Minerbe, "Calorimètre adiabatique", Publication Technique du C.E.R.I.L.H., **98**, (1959).
4. J. Cléret de Langavant, Publication Technique du C.E.R.I.L.H., **7**, (1948).
5. J. Cléret de Langavant, Publication Technique du C.E.R.I.L.H., **67**, (1954).
6. L. Santarelli and F. Fonda, "La mesure de la chaleur d'hydratation des ciments avec la méthode thermométrique à dispersion prédéterminée", Rev. des Mat. de Constr., **544**, 13–19, (1961).
7. R. Alègre, "La calorimétrie des ciments au C.E.R.I. L.H.", Rev. des Mat. de Constr., **547**, 218–229 (1961); **548**, 247–262, (1961) et **549**, 300–314, (1961).
8. V. Vandenbosch, "Measure de la chaleur d'hydratation des ciments", Commission Chimique du C.E.T.I.C. 16ème séance (juin 1964).
9. W. Lerch, "A simple apparatus for determining heat of hydration of portland cement", Port. Cem., Ass., (1934–1936).
10. E. S. Newman, "A study of the determination of the heat of hydration of portland cement", J. of Res. of the Nat. Bur. of Stand, 45, 411, (1950).
11. T. W. Parker and R. W. Nurse, "Specification tests for heat of hydration of cement", Cem. and Lime Man., **26**, 1 (1953).
12. E. S. Newman and L. Shartsis, "A study of the heat of solution procedure for determining the heat of hydration of portland cement", A.S.T.M. Proc., vol. **43**, 905, (1943).
13. L. Santarelli, F. Piselli and C. Covarelli, "La mesure de la chaleur d'hydratation des ciments portland et pouzzolaniques", Rev. des Mat. de Constr., **533**, 31–42, (1960).
14. H. Schwiete, U. Ludwig and K. Rakel, Tonindustrie Zeitung, **89** (7/8), 166–169 (1965).
15. "Bestimmung der Hydratationswärme von Zement mit dem Lösungskalorimeter", Zem.-Kalk-Gips, **4**, 191–194, (1966).
16. G. Goggi, "Contribution a l'évaluation de la chaleur d'hydratation des ciments d'après la méthode par dissolution", XVIIème Réunion de la Commission Chimique du C.E.T.I.C., Bruxelles, 2 et 3 juin, (1965).
17. J. Daube, "Observations récentes sur la méthode de

mesure de la chaleur d'hydratation des ciments par dissolution", Commission Chimique du C.E.T.I.C., 19ème séance, (avril 1967).
18. A. Rio and Von Baldass, "La Determinazione del Calore d'Idratzione dei Cementi Pozzolanici con il Metodo del Calore di Soluzione", L'Ind. Ital. del Cem., 59 et 95, (1955).
19. G. Goggi, "Contributo alla calorimetria dei cementi con il metodo a soluzione", L'Industria Italiana del Cemento, Anno XXXV, 7, 447–458, (1965).
20. C. Brisi, "Determinazione del Calore di Idratazione dei Cementi per Soluzione in Acido Cloridirco", L'Ind. Ital. del Cem., (1956).
21. F. Piselli, "Il calorimetro a soluzione nella misura del calore di idratazione del cemento, Studio statistico", l'Industria Italiana del Cemento, (1957).
22. G. E. Monfore and B. Ost. "An isothermal conduction calorimeter for study of the early hydration reactions of portland cements", Journ. of the P.C.A., 13–20, (1966).

Supplementary Paper II-117 The Influence of Alkali-Carbonate on the Hydration of Cement

Egide M. M. G. Niël*

Synopsis

The setting and the strength-development of mortars of portland cements and blast furnace slag cements is affected by the presence of alkali-carbonate.

It has been noticed for all these cements that the setting time is retarded at first in proportion to the alkali-carbonate content (at about 0.2% K_2CO_3), and gets gradually shorter so that at about 2% K_2CO_3 a flash setting occurs.

At a further increase of the alkali-carbonate content this flash setting effect continues to occur, until at about 15% K_2CO_3 setting times of about 20 minutes show up again.

Also the strength-development of prisms of mortar shows clearly that alkali-carbonates exert an influence.

By following the hydration closely, an insight is gained in the reactions, to which the above mentioned phenomenons can be related.

For this examination chiefly use has been made of chemical analyses and semi-quantitative measurements with the help of X-ray diffraction and infrared measurements.

Introduction

Literature (1, 2, 3) chiefly mentions two cases in which the hydration process is influenced by alkali-carbonate, viz. when alkali-carbonate is added to cement in mortars, and in case of false set which occurs after long-stored cements are used.

The addition of alkali-carbonate in cement mortars either serves to accelerate set at a normal temperature or enables to use mortar at temperatures below 0°C.

However, the presence of alkali-carbonate in mortar causes several properties of this mortar to change during the stiffening an hardening process. This hardened mortar reacts differently from the usual mortar.

The investigations and tests have established that by addition of alkali-carbonate the following irregularities occur by the use of portland cement and blast furnace cement:

1) deviations in setting and workability
2) increase compressive strength and flexural strength
3) rise of the temperature of mortar

When moist air can penetrate the storage yard where cement is kept, hydration-reactions will occur on the cement particles. In these reactions the alkalies bound in the clinker can be liberated which react with carbon-dioxide from the air to form alkali-carbonate.

By some authors (1) this alkali-carbonate is held responsible for above mentioned irregularities.

In this contribution we have tried to find an explanation for these irregularities by investigating the hydration process as well as we could with the means available and by applying the results of this investigation to the above mentioned deviations.

Physical Tests

Paste Tests

The respective rheological behaviour and the hardening characteristics of the mortar to which alkali-carbonate has been added, result from the hydration-reactions in the cement paste.

To get an insight about the effect of the different alkali-carbonate proportions, tests have been carried out with cement pastes. After it appeared from orientation tests that sodium-carbonate had a similar activ-

*Eerste Nederlandse Cement Industrie, Maastricht, Netherlands.

ity as K_2CO_3, only potassium-carbonate was used for the rest of the series to be tested.

To start with a series of determinations of the setting time was carried out at five portland- and blast furnace slag cements with addition of K_2CO_3. They were carried out, according to the German specification DIN 1164, presuming that the temperature at preparing and preserving amounted to 4°C for one series and 20°C for the other series.

Potassium-carbonate was dissolved in the gauging water. The proportioning of this salt was calculated in the percentage of weight of the cement. The results of these series have been reproduced by means of examples on the Figs. 1 and 2.

The curve representing the relation between initial, final setting and the percentage of potassium-carbonate at a fixed temperature is practically the same for all cements, which means:

—at very small proportionings (0.2%) a considerable delay of the setting (especially at low temperatures)

—at proportionings of 2 to 10% a considerable shortening of the setting time, so that the cement paste can hardly be worked

—at large proportionings over 10% potassium-carbonate a less considerable shortening of the setting time.

Although sufficient data about the reduction of the setting time can be found in literature (3), the indications about the retarding effect are lacking. This effect however is such that it is worth while to pay attention. At 20°C the retardation amounts to 1 hour and 25 minutes; at 4°C to 22 hours (slag-cement).

The tests have been carried out with the laboratory portland cement "M".

With this, cement pastes have been made with gauging water containing potassium-carbonate. The above-mentioned characteristics changes in the setting time at 23°C proved to be most striking for the following K_2CO_3-proportionings: 0, 0.25, 2.5 and 20% (see Fig. 3).

In all the following tests and in the hydration examination, these mixing ratios were used.

The second part of the paste-tests aimed at obta-

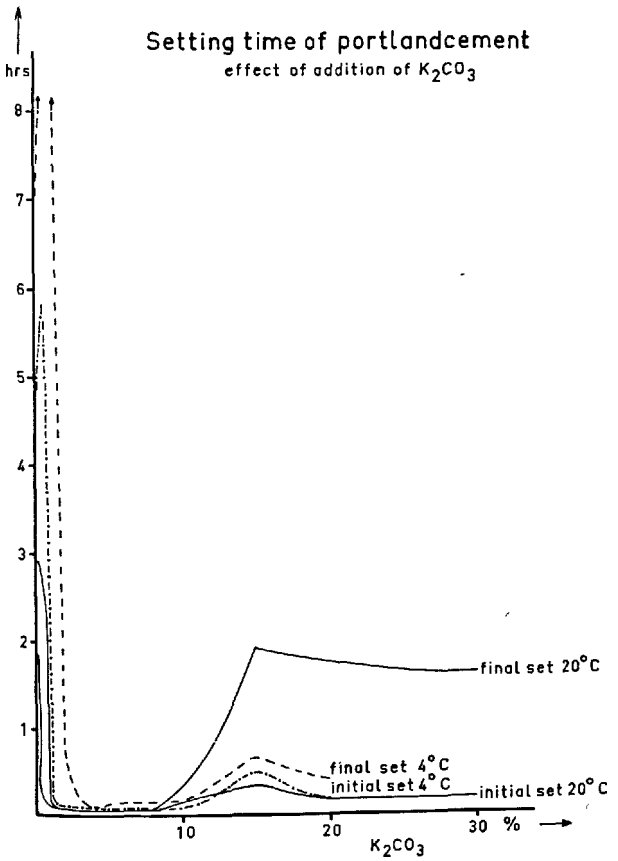

Fig. 1. *The initial and final setting time of portland cement at various additions of* K_2CO_3

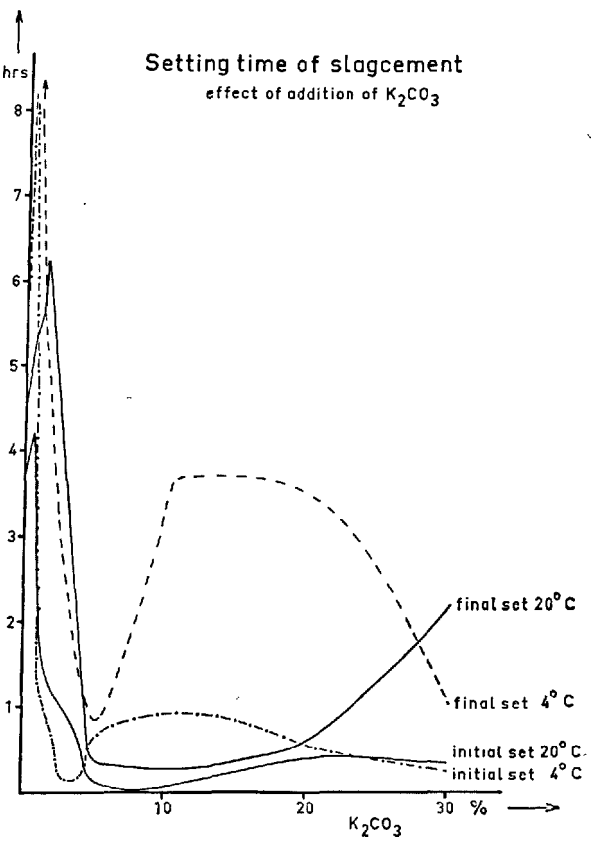

Fig. 2. *The initial and final setting time of slag cement at various additions of* K_2CO_3

ining more data about the behaviour of the pastes after the mixture was completed.

To that end determinations were carried out with the penetrometer according to Francardi (4, 5), with which the setting of the pastes can be watched continuously. Simultaneously, temperature measurements in the pastes were carried out. With the penetrometer, according to Francardi, a so-called consistency curve may be drawn up, which reproduces the course of setting.

In Fig. 4a the consistency curves of the 4 pastes have been reproduced. From these it can be read how the setting is accelerated when potassium-carbonate is present.

Moreover, it is clearly to be seen that, at a proportioning of 0.25% K_2CO_3, in the initial setting after slightly more than half an hour, K_2CO_3 changes into a retarder. This initial setting may be regarded as a flash setting. The degree of flash set is larger in proportion as more K_2CO_3 is added. The temperature measurements were carried out by inserting a thermocouple in the paste, with which a paste-container of the penetrometer had been filled.

The results of these measurements are shown in Fig. 4b. They were carried out simultaneously with the consistency-measurements with the penetrometer, and they show the change of temperature at the inside of the paste.

The retarding in the setting at 0.25% K_2CO_3 is accompanied by a retarded start of the temperature rise whereas the increase in temperature is less than in the reference sample. In the initial period after preparing the paste containing 0.25% K_2CO_3, a temperature rise occurs which however decreases after about half an hour. Linked with this is the early setting, which after this half an hour does not continue in a setting-course.

In the larger amounts, the steep change in consistency is in accordance with the violent increase of temperature shortly after preparation. About 2 hours after preparation the temperature rises to a second maximum.

Mortar Tests

The examination made of setting phenomena showed that when potassium-carbonate is added flash setting may occur. This may influence the workability of fresh concrete. Workability was measured by the slump method. With fresh concrete containing aggregates, graduated according to the Fuller-curve, and with 350 kg/m³ normal portland cement, at a water/cement ratio of 0.5 a slump of 10 cm was obtained. In Table 1 the changes caused by the addition of potassium-carbonate (calculated on cement) are shown. At small percentages the workability is lessened; in proportionings of over 5% the slump is again increased.

To get an idea of the influence of the potassium-carbonate on the strength development of mortars (according to Cembureau specifications) compres-

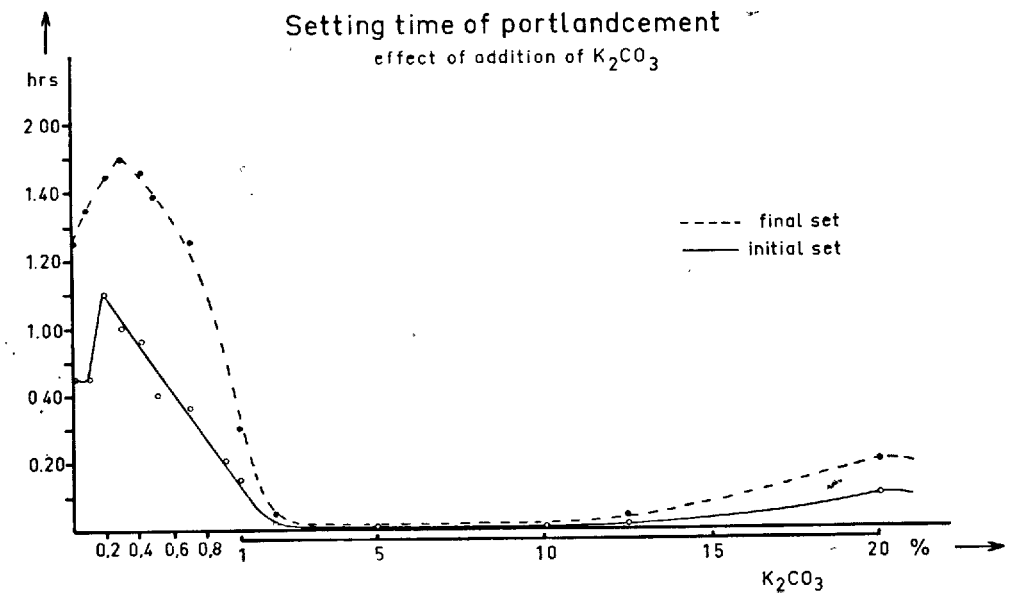

Fig. 3. *The initial and final setting time of portland cement "M" at various additions of* K_2CO_3 (20°C)

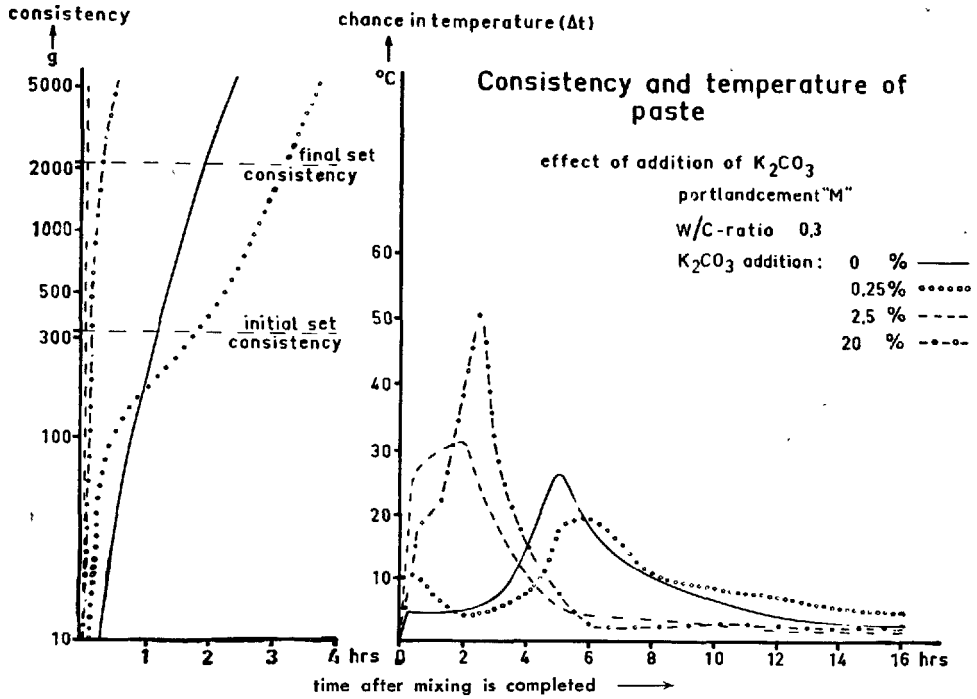

Fig. 4a. *Change in consistency of a portland cement paste in the course of hydration*

4b. *Development of temperature in the portland cement paste*

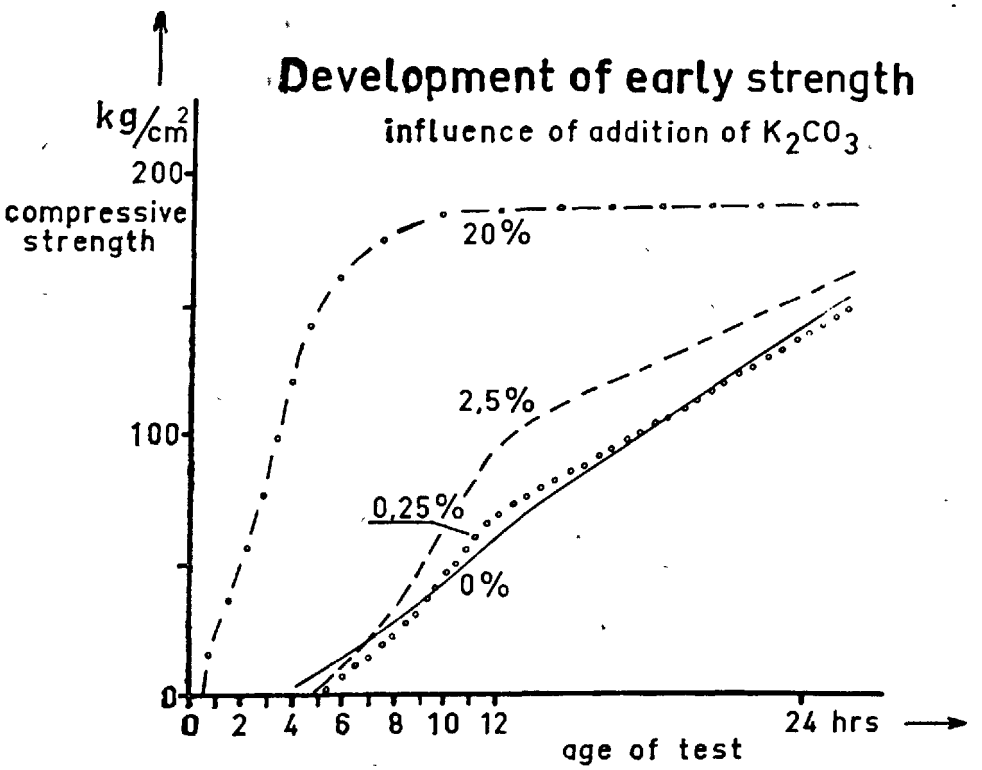

Fig. 5. *The development of early strength on mortar prisms of portland cement*

sive and bending/tensile strengths have been determined about hardened mortars, which originally were composed of sand, cement "M" and gauging water, in which 0–2.5 and 20% potassium-carbonate was dissolved. The results of these tests after 12 hours, 1–3–7 and 28 days of hardening, are shown in Table 2.

It may be concluded that at 12 hours after prepara tion, with a high proportioning of K_2CO_3 (20%) the strengths are already considerable. The increase of strength after these 12 hours is however relatively slight.

The lower proportionings showed this in a lesser degree, whereas 0.25% K_2CO_3 caused a decrease of the strengths after 12 hours in comparison with the reference sample.

In view of the considerable differences in strength after 12 hours of the various mortars a series of mortar prisms was prepared. Every hour after preparation prisms were tested; until the moment of testing they were left in the mould. In this way the development of strength in the initial period of the hydration could be observed.

Unfortunately, we had to use a clinker of a slightly different quality, owing to which the curves in Fig. 4 cannot be simply compared with the results in Table 2.

However, the same tendency may be observed, viz., the pastes with 20–2.5–0 and 0.25% start the hardening in this sequence and also reach in this sequence the highest strengths in the initial 12 hours.

Table 1. *The workability of concrete mortar. The influence of the addition of potassium-carbonate to cement "M".*

K_2CO_3 [%]	slump-test [cm]	temperature [°C]
0	10	23
0.25	2	21
2.5	0.5	23
5	10	22
20	23	29.5

Table 2. *The strength of portland cement "M". Influence of the potassium-carbonate on the development of strength*

	days	K_2CO_3				
		0%	0.25%	1.5%	2.5%	20%
compressive strength in kg/cm²	0.5	92	74	106	142	259
	1	214	211	212	266	271
	2	327	346	323	304	295
	3	426	426	372	298	316
	7	546	542	412	316	370
	28	620	627	501	451	446
bending/tensile strength in kg/cm²	0.5	20	16	18	30	57
	1	38	34	33	n.d.	58
	2	54	50	49	n.d.	53
	3	60	62	51	n.d.	55
	7	67	66	54	49	45
	28	75	71	66	61	50

Hydration-Reactions of Portland Cement with K_2CO_3

As pointed out in the foregoing 4th Symposium on Chemistry of Cement, the reactions which occur in the hydration of a portland cement are known for the greater part. The progress of the hydration of each of the clinker components has been examined by analysing pastes and suspensions of C_3S, C_2S, C_3A and the "ferrite phase".

In the last few years this examination has been extended to the more complex course of hydration in cement pastes (6, 7).

In this study the hydration-reactions which occur when K_2CO_3 is added to portland cement "M", have been observed.

Procedure

To get an idea of the reactions, which occur during the hydration process, the following procedure was adopted:

A paste is made from cement "M" with water (W/C 0.3), in which potassium-carbonate in the required percentages has been dissolved; this paste is put into a plastic bottle and stored in a water-bath of 23°C (±1°).

At definite times a small sample of paste was taken and the hydration was stopped immediately with isopropyl-alcohol. For the hardened paste it was necessary to pulverize the small sample prior to vibrating ultrasonic with excess of water-free isopropyl-alcohol. After that the samples were ground in an agate grinder to achieve a constant fineness. This constant fineness is necessary to achieve comparable measurements. This technique to put a stop to the hydration-reactions has been applied successfully in earlier studies (8, 9).

By suspending in excess of water-free isopropyl-alcohol the components, are precipitated practically completely and the so-called free water is eliminated from the particles, which has been confirmed ab origine by the infrared spectra. Practically no increase in the water peak at wave number 1650 cm^{-1} is perceptible.

Finally the alcoholic suspensions were filtered off by millipore filters (ϕ max. $= 0.45\ \mu$) and then the remaining residues of alcohol were removed in a drying-oven at 40°C and 60 mm Hg.

Then the small samples were examined, viz.:

a) by determining the loss on ignition
b) by X-ray diffraction
c) by infrared spectrography

Before discussing the results of the determinations, an elucidation to the methods of the examination is given.

a) loss on ignition

The loss on ignition was determined by heating at 1060°C for 10 minutes of the water-free sample.

b) X-ray diffraction

The X-ray diffraction recordings were carried out with the Philips diffractometer 1010/1050/1051/4082/. The further details are:

X-ray tube:	Cu-anode + Ni-filter (96 KV + 26 mA)
divergence slit:	1°
receiving slit:	0.2 mm
scatter slit:	1°
counter:	proportional counter (1700 V)
goniometer-speed:	1°/min.
paper-speed:	800 mm/h

Amplitude 25.5 V; channel width 20 V; discriminator: attenuation 4.

The sample was rotated during the measurement.

The following interferences were measured from the various components:

component	value
$C_3S + C_2S$	2.18 Å
C_3S	1.765 Å
C_3A	2.69 Å
"C_4AF"	2.64 Å
$Ca(OH)_2$ or CH	4.92 Å
$C_3A \cdot Ca(OH)_2 \cdot 12H_2O$ or C_4AH_{13}	8.2 Å
$C_3A \cdot CaCO_3 \cdot 11H_2O$ or $C_4A\bar{C}H_{11}$	7.56 Å
$C_3A \cdot 3CaSO_4 \cdot 31H_2O$ or $C_6A\bar{S}_3H_{31}$	9.7 Å
$C_3A \cdot CaSO_4 \cdot 12H_2O$ or $C_4A\bar{S}H_{12}$	8.9 Å
$3K_2CO_3 \cdot 2CaCO_3 \cdot 6H_2O$	2.07 Å
$CaCO_3$	2.49 Å
$CaSO_4 \cdot 2H_2O$	7.56 Å
K_2SO_4	4.17 Å

c) infrared spectrography

For the infrared measurements the Perkin-Elmer infrared spectrophotometer 337, speed 94 cm/min.-slit 3 was used. Sample: KBr-tablet.

Quantitative measurements were carried out. The contents could not be given in percentages, because not all the calibration lines are available; therefore, extinction values have been mentioned in the graphs.

The following components were measured quantitatively at the specific wave numbers mentioned behind:

$Ca(OH)_2$	at	3650 cm^{-1}
K_2SO_4	at	623 cm^{-1}
$CaSO_4 \cdot 2H_2O$	at	670 cm^{-1}
$K_2SO_4 \cdot CaSO_4 \cdot H_2O$	at	660 cm^{-1}
OH (total)	at	3400–3600 cm^{-1}

Data about Cement "M"

The cement was obtained by grinding 95 parts by weight of clinker with 5 parts of gypsum in a laboratory ball mill.

During this process of grinding gypsum did not decompose into semihydrate. The specific surface amounts to 5600 cm^2/g, according to Blaine. Under the microscope the mineralogical composition has been studied. The clinker minerals proved to be practically completely crystallized, with the exception of the ferrite phase, which is mainly glassy. The potential mineral composition of clinker calculated according to Bogue and the complementary data have been collected in Table 3.

Table 3. *Chemical composition and potential mineral composition of portland cement "M" according to Bogue*

Chemical composition of the cement		
loss on ignition	1.48%	
SO_3	2.34%	
K_2O	0.30%	
insoluble	0.35%	
Potential mineral composition according to Bogue		
C_3S —65.2%	lime saturation formula	94.1
C_2S —15.5%		
C_3A — 8.6%	free lime	0.64
C_4AF— 7.6%		

For the tests distilled water was used.
The added potassium-carbonate was a mixture of equal parts K_2CO_3 and $K_2CO_3 \cdot 1\frac{1}{2}H_2O$.

Interpretation of Measurements

Before proceeding to the discussion of the hydration-reactions, it may be observed that these measurements cannot give a complete picture of the hydration-reactions. The X-ray diffraction only allows to detect sufficiently crystallized compounds, which give sufficiently strong intensities, and the peaks of which do not coincide with those of other components. For these reasons it was not possible to measure C_2S at a separate peak but only as total $C_2S + C_3S$, and the fer-

rite phase was only partly perceptible. The important hydration products of the tobermorite phase were not or hardly measurable, whereas it is only possible to measure sufficiently clearly the monosulphate ($C_4A\bar{S}H_{12}$) after longer periods (>1 month) of hydration.

Also K_2CO_3 in hydrated cement is also hard to measure. With infrared the carbonates have strongly developed peaks, but from these the K_2CO_3-peak could be selected with difficulty. Due to such effects it may be possible that, when certain reaction products appear, they can only be observed at a somewhat later time. For the measurements for infrared as well as for X-ray diffraction, care has been taken so that they are carried out 3 times at least. The averages can be found back in the graph 6 as measuring-points.

In all the following graphs these measuring-points have been omitted to make the presentation more clearly.

The measurements are shown as intensities or as extinctions (infrared), because the X-ray diffraction and, to some extent, also the infrared measuring technique are not yet apt to carry out quantitative mineralogical analysis in weight percentages.

Since the measuring circumstances do not vary from measuring-point to measuring-point and each sample undergoes a similar particle-preparation, the variables which hamper a quantitative interpretation of measuring results are minimized. Since the measurements of the decrease of the intensities of the clinker minerals are least affected by crystal effect, they are reproduced separately in the graphs. Due to the hydration-reactions the weight of "solid material" increases. The values of the clinker minerals are only corrected with the losses on ignition. Some of these measurements have been repeated with an internal standard. After addition of 10% CdS to the probe, the mixture is homogenized by gently milling a suspension in cryclohexane. The clinker interference was measured at 2.18 Å ($C_3S + C_2S$). Also the degree of hydration of the calcium silicates was esti-

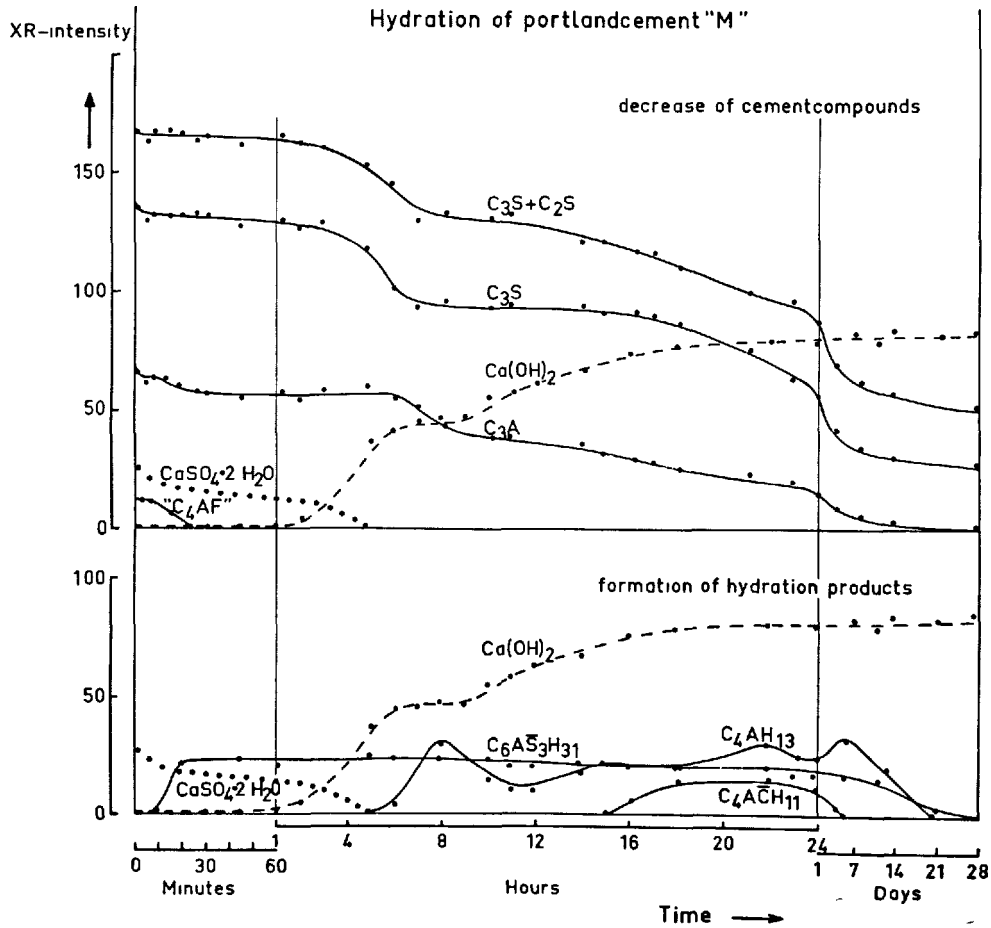

Fig. 6. *Hydration of portland cement "M"; W/C-ratio 0.3 X-ray measurements; indication of the average measuring-points*

mated at 60 minutes, and 7 days, being 3.5% and 63%. These results are in accordance with the degree of hydration which can be derived from the data in graph 6 by comparing the XR-intensities at these times with those of the unhydrated portland cement "M".

Discussion of the Results

The results of the measurements are shown in the graphs 6–13. Because a relation should be established between the reactions in the paste on the one hand, and the workability of the paste, the development of strength initially and after longer periods on the other hand, a classification in 3 periods with 3 different time scales has been made, viz., 1 hour, 1 day and 28 days. The first graph shows the averages of the measurements, the divergence and the times of the measurements.

In Table 4 the data regarding the measurements after 2 and 3 months have been recorded.

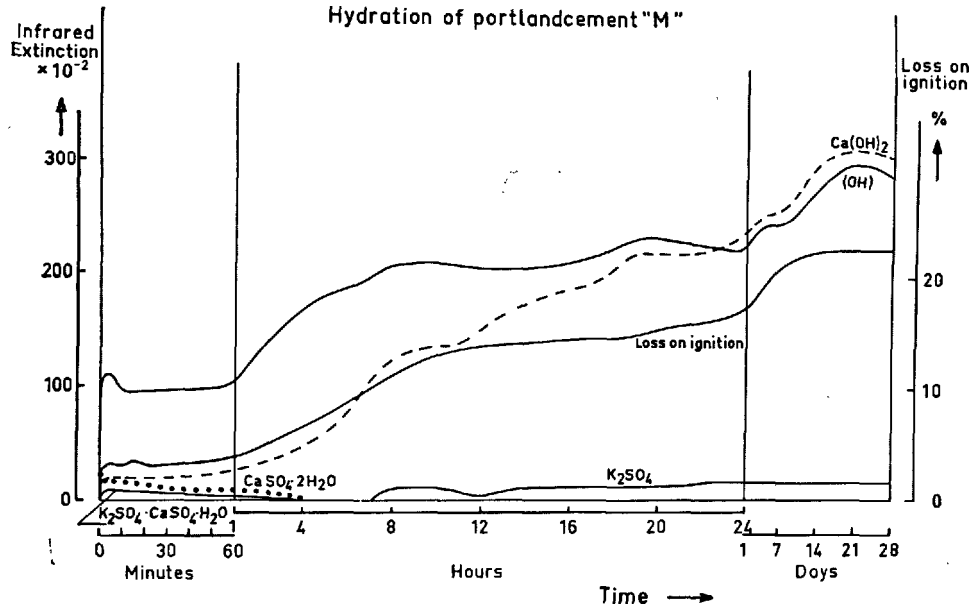

Fig. 7. *Hydration of portland cement "M"; W/C-ratio 0.3*
Infrared extinctions at different times

Table 4. *X-ray intensity and infrared extinction measurements on cement paste (W/C-ratio 0.3)*
Measuring values after a longer period of hydration

Component	Portland cement "M"				Portland cement "M" +0.25% K_2CO_3				Portland cement "M" +2.5% K_2CO_3				Portland cement "M" +20% K_2CO_3			
	1 day	1 month	2 months	3 months	1 day	1 month	2 months	3 months	1 day	1 month	2 months	3 months	1 day	1 month	2 months	3 months
measured by: X-ray diffr.																
$C_3S + C_2S$	88	52	36	7	96	42	32	9	91	62	40	9	93	70	46	14
C_3S	57	27	16	4	70	28	20	7	68	47	32	8	68	50	24	9
C_3A	16	—	—	—	26	4	—	—	15	14	8	—	10	—	—	—
C_4AH_{13}	25	—	—	—	22	8	—	—	—	—	—	—	—	—	—	—
$C_4A\bar{C}H_{11}$	10	—	—	—	—	—	—	—	39	38	32	34	71	69	46	92
$C_6A\bar{S}_3H_{31}$	19	—	—	—	26	10	—	—	—	—	—	—	—	—	—	—
$C_4A\bar{S}H_{12}$	—	—	52	24	—	—	26	18	—	—	—	—	—	—	—	—
$3K_2CO_3 \cdot 2CaCO_3 \cdot 6H_2O$	—	—	—	—	—	—	—	—	—	—	—	—	*	—	14	10
measured by: Infrared																
$Ca(OH)_2$	240	310	300	350	200	260	268	310	200	232	280	240	82	190	215	230
K_2SO_4	15	15	17	14	14	2	14	8	40	30	30	15	48	43	42	47
(OH)	206	290	280	315	320	240	290	300	190	250	250	271	n.d.	n.d.	n.d.	n.d.

*In the period preceeding to this measurement the component has been present.

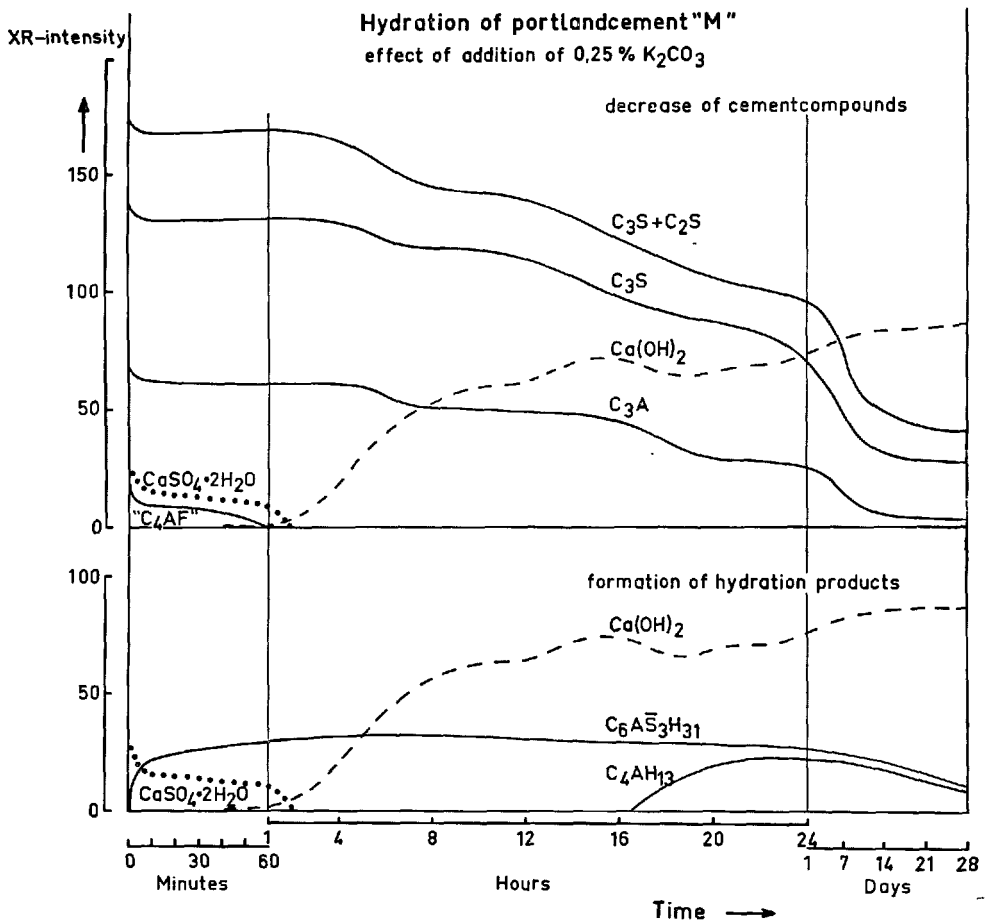

Fig. 8. *Hydration of portland cement "M" with 0.25% K_2CO_3*
X-ray measurements at different times

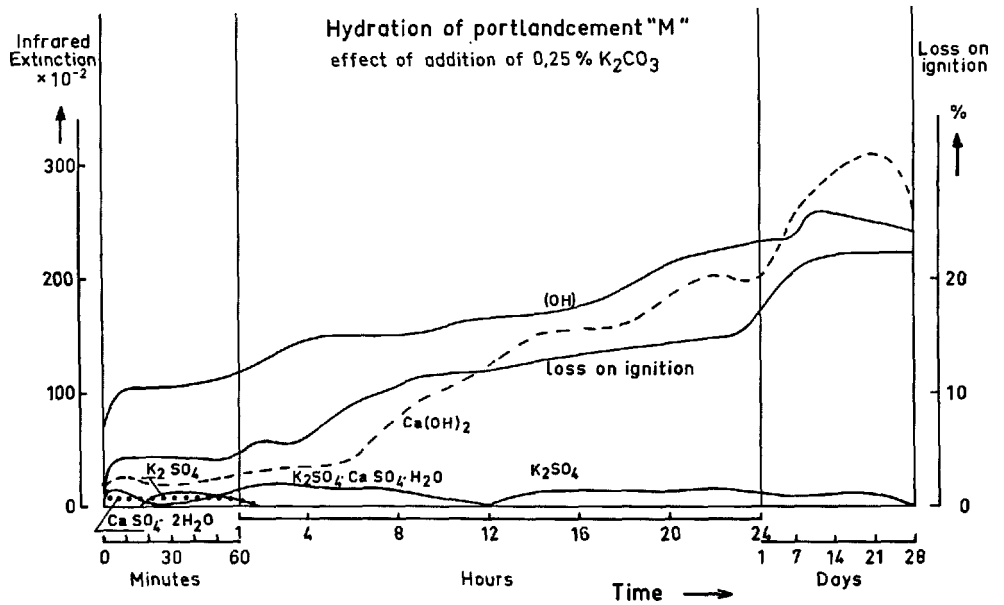

Fig. 9. *Hydration of portland cement "M" with 0.25% K_2CO_3*
Infrared extinctions at different times

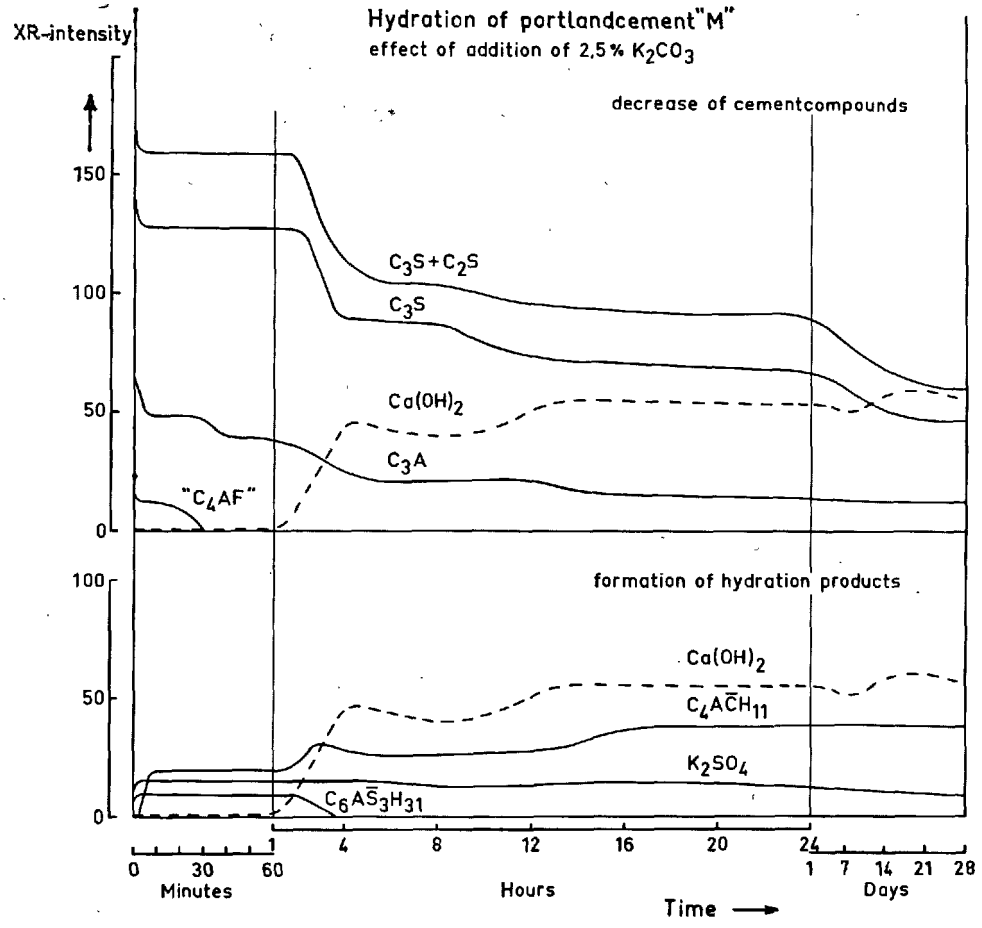

Fig. 10. *Hydration of portland cement "M" with 2.5%K_2CO_3 X-ray measurements at different times*

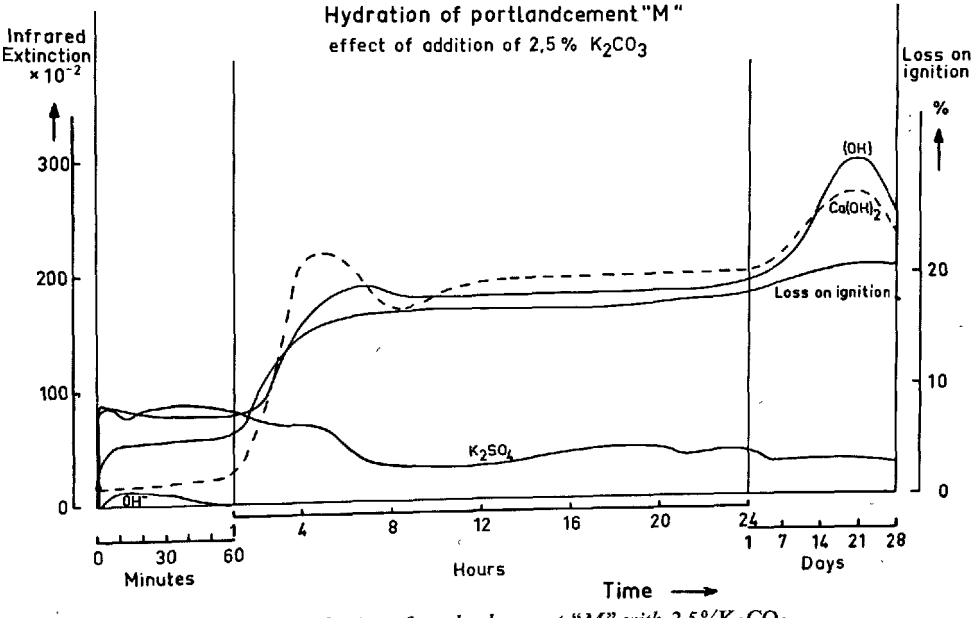

Fig. 11. *Hydration of portland cement "M" with 2.5%K_2CO_3 Infrared extinctions at different times*

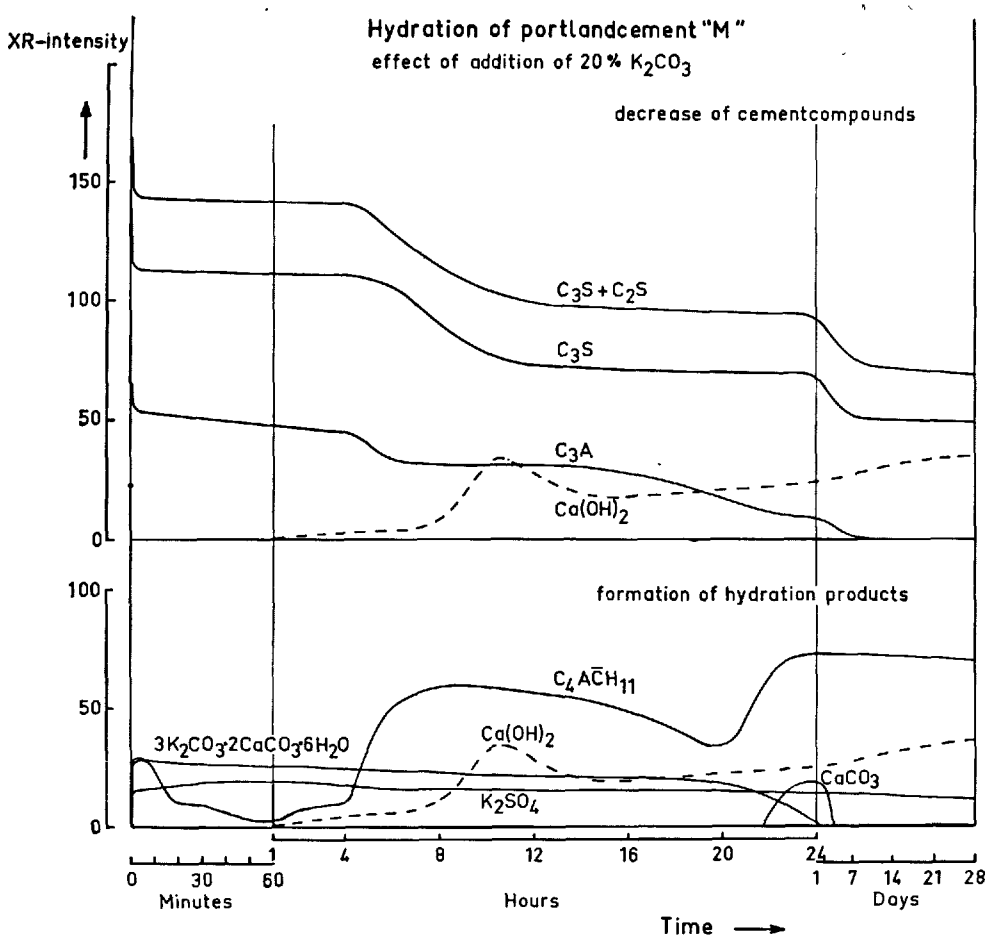

Fig. 12. *Hydration of portland cement "M" with 20%K_2CO_3*
X-ray measurements at different times

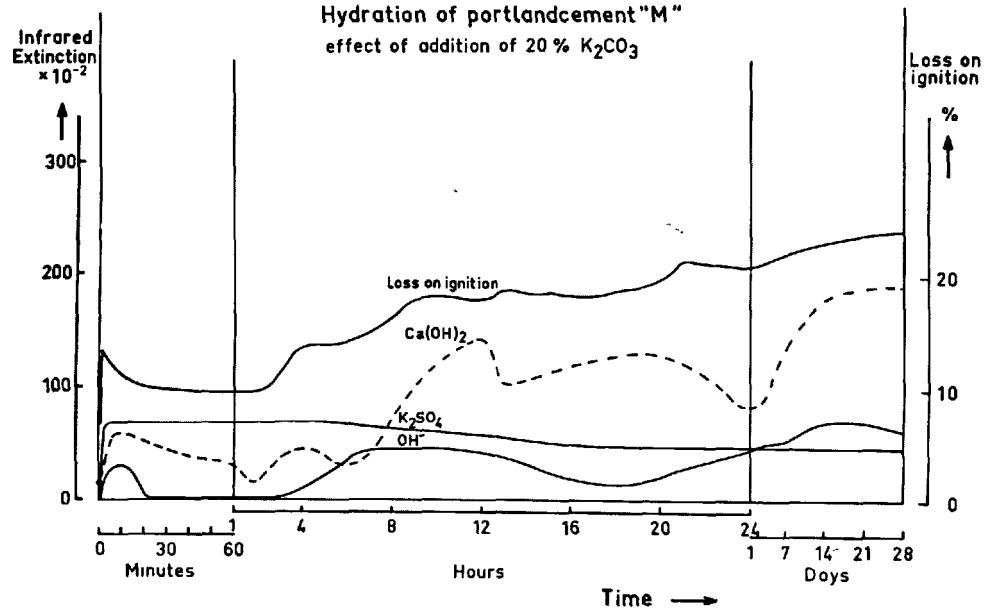

Fig. 13. *Hydration of portland cement "M" with 20%K_2CO_3*
Infrared extinctions at different times

Reactions in the Initial Period and Setting

The reactions of the portland cement "M" (see Figs. 6 and 7) correspond with the observations in the literature (10). G. Yamaguchi, K. Takemoto, H. Uchikawa and S. Takagi (7) ascertained that in the first 3 minutes slight hydration-reactions of the calcium-silicates and violent reactions of the aluminate-containing phases are to be expected. H. Schwiete and E. Niël (8) could follow by infrared measurements the reactions in which the sulphates are involved in the first minutes of the hydration. They came to the conclusion that in particular C_3A reacts in the first minutes, and that the reactions of the ferrite phase are of some importance only after about 15 minutes.

The calcium-hydroxide which is liberated during hydration can be measured by both analysing methods. Contrary to the X-ray measurements the hydrate could be established already in the first hour with infrared. The greater part of this calcium-hydroxide, however, was already present in the portland cement as free lime. Generally the amount of free calcium-hydroxide during hydration can be measured in a more sensible way with infrared. The little amount of syngenite, which has been formed in the first minutes of hydration reacts together with gypsum and the aluminate-containing phases. In Fig. 7 the measuring of the infrared absorption at 3400–3600 cm^{-1} is shown. In this absorption-band, many hydration products are represented. As there are uncertainties in the interpretations their diagram will not be further discussed.

Although not all the reaction products among which the important tobermorite phase could be measured, it is evident that the hydration-reactions of portland cement "M" are influenced by the presence of K_2CO_3. The larger is the amount of K_2CO_3. the larger is the share of the clinker phases and of gypsum in the reactions in the initial minutes. These reactions are promoted by the conversion of K_2CO_3 and gypsum, owing to which the regulating influence of the gypsum on the hydration-reactions decreases. This explains the effect of flash setting in the cement paste (high temperatures and early stiffening).

As a result of these conversions, the following salts appear at the various amounts of addition:

0.25% K_2CO_3—syngenite ($CaSO_4 \cdot K_2SO_4 \cdot H_2O$), little K_2SO_4 and $CaCO_3$

2.5% K_2CO_3—K_2SO_4 and $CaCO_3$

20% K_2SO_4–K_2SO_4 + $3K_2CO_3 \cdot 2CaCO_3 \cdot 6H_2O$ (in addition to non-converted K_2CO_3)

The aluminate phase and the ferrite phase react within a few minutes with the above-mentioned calcium salts. This is shown by the detection by means of X-ray diffraction of ettringite after 3 minutes (at 0% K_2CO_3), of ettringite immediately after gauging (at 0.25% K_2CO_3), of ettringite followed immediately by carbo-aluminate (at 2.5% K_2CO_3) and of only carbo-aluminate (at 20% K_2CO_3).

The formation of carbo-aluminate confirms the observations of K. T. Greene (10), who found peaks in the D. T. A.-curve of alkali carbonate-containing cement after 24 hours of hydration (W/C ratio 0.35) at room-temperature. These peaks bore a marked resemblance to the curve for the mono-carbo-aluminate given by Turriziani and Schippa. R. F. Feldmann, V. S. Ramachandran and P. J. Sereda (11) found that the hydration-reaction of C_3A is suppressed by $CaCO_3$-additions.

This is due primarily to the formation of the low form of calcium carbo-aluminate on the surface of the C_3A. The important addition of 20% K_2CO_3 does raise the temperature of the cement paste. Å. Grudemo (12) mentioned that the carboaluminate is not stable at a higher temperature. This is also visible in the course of the $C_4A\overline{C}H_{11}$-curve given in Fig. 12. The initial formed carboaluminate is not stable after a few minutes of hydration. Mono-sulphate and other aluminate-hydrates could not be proved on account of difficulties at the measurements.

In the initial period reactions causing the stiffening occur in the cement paste. In the cements containing potassium-carbonate, this stiffening is a direct result of the hydration-reactions, not controlled enough by Ca^{++}-ions. Obviously the stiffening starts by reactions of the aluminate-containing phases, as is established at the cement "M". At an addition of 0.25% K_2CO_3 the stiffening starts, under the influence of reactions of the ferrite phase. The stiffening will no doubt be supported by the formation of poor soluble calcium salts such as $CaCO_3$, $3K_2CO_3 \cdot 2CaCO_3 \cdot 6H_2O$ and $CaSO_4 \cdot K_2SO_4 \cdot H_2O$ (1).

After the rather important conversions in the initial minutes, C_3S and C_2S hardly react in the first hour of the hydration process. In this period the loss on ignition also hardly changes. Although rather important reactions occur, in which the aluminate-containing compounds are involved, the amount of fixed water hardly increases during the first hour. This may be an indication that the hydration products react mutually with the aluminate, ferrite phase or with one of the salts.

Period of Strength Development

In the first hours of this period the reactions, which

initiate the increase in the strength, start. The development of strength, such as measured at the mortar prisms, follows for portland cement practically a straight line, from the moment of the strength of 10 kg/cm² was measured till the strength at 24 hours of hydration. Also for portland cement "M" with an addition of 0.25 % K_2CO_3, the development of strength follows practically a straight line. The consumption of clinker components during the reactions in this period is in accordance with this representation. In the period that the hardening is initiated, rather important reactions take place, which are accompanied with the decrease of the amount of clinker components and a considerable increase of water, fixed during the hydration, as may be concluded from the determinations of the loss on ignition.

As far as the increase of the hydration products at portland cement "M" can be observed, C_3A reacts first with gypsum or with $CaSO_4$ from syngenite, probably to form mono-sulphate to react then with $Ca(OH)_2$, which is released at the hydration of lime and calcium silicates, under the formation of C_4AH_{13}. Although this product disappears partly within 2 hours of hydration, from 10 to 24 hours of hydration, a steady decrease of C_3A and an increase of calcium aluminate may be observed. This is accompanied with a slight decrease in ettringite. The K_2SO_4 which shows up after 8 hours of hydration may be formed as a result.

During the hydration of portland cement "M" with 0.25 % K_2CO_3 approximately the same pattern is shown. Again an increase of the loss on ignition, which is stronger till 9 hours of hydration than afterwards. C_3A reacts at about 6 hours of hydration less strongly than in the cement free from carbonate. After 16 hours C_3A reacts, however, while forming C_4AH_{13}. For the cements containing alkali-carbonate (2.5 and 20 %) the course of hardening differs from the portland cement "M". After obtaining measurable mortar strength this increase is at about 11 respectively 6 hours proportional, to change then into a less steep increase of strength. With 2.5 % K_2CO_3 the reactions develop most intensely in the first hours after hydration. The steep decrease of calcium silicates and C_3A is in accordance with the great development of heat. H. N. Stein (13) already mentioned that the heat development in this period of hydration is increased by the addition of alkali-carbonate to the portland cement. This heat development increases the paste temperature (see Fig. 4b). This will be the reason for the rather strange behaviour of the $Ca(OH)_2$-curve in the first hours of hydration.

In this period ettringite is fully disintegrated, the amount of carbo-aluminate increases, as well as the amount of free lime, of this increase something is retracted by reactions, in which besides $Ca(OH)_2$, also K_2SO_4 is involved (probably formation of mono-sulphate). The increase of the loss on ignition and free lime after 12 hours of hydration is very slight. Also the decrease of the clinker components is slight; only a temporary, weak revival of C_3A at about 14 hours simultaneously with an increase of carbo-aluminate may be ascertained. At an addition of 20 % K_2CO_3 the initial strength can be measured already after well over half an hour. In this period the temperature in the paste has also highly increased. The very strong development of strength, which follows hereupon, stops at about 5 hours. The basis for this course is already formed by the reactions during gauging. For any paste the decrease of the aluminate-containing phases and of calcium silicates is very important. The lime which is formed by the hydration-reactions of C_3S and C_2S in the environment rich in potassium-carbonate, is absorbed by the aluminate-containing phases in the form of carbo-aluminate. Lime is still formed, but for a few minutes no longer absorbed by C_3A. The decrease of C_3A, which is measured, shows that it still takes part in the hydration-reactions after the initial period. This is weak till 4 hours of hydration, but it is strong between 4 and 6 hours. The first hour after the initial reactions, the carbo-aluminate decreases, because it is not resistant to the high temperature, which has developed in the meantime, as well as the $Ca(OH)_2$ and increases then strongly between 4 and 6 hours in content, also again in the same order as in the initial phases. At the end of the first day, after 16 hours of hydration, C_3A is again remarkable active. The double-salt $3K_2CO_3 \cdot 2CaCO_3 \cdot 6H_2O$ is then disinte grated, $CaCO_3$ is formed, which partly combines with C_3A to carbo-aluminate.

Conclusion

The hydration of portland cement "M" was clearly influenced by the presence of potassium-carbonate. After correction on the loss on ignition, the consumption of clinker components during the hydration of portland cement "M" could be followed clearly by X-ray measurements.

These reactions are in accordance with the observations at the tests on stiffening and strength develop-

ment of the same cement. Less complete is the representation of the hydration products. Partly they are not apparent in this mixture of components or only measurable after they are either present in larger amounts or crystallized sufficiently. A particular case is the $Ca(OH)_2$-measurement with infrared spectrography or with X-ray diffraction. Although the large changes are observed with both methods, the infrared measurement is somewhat more sensitive, especially in the first hour and the last phase of the hydration. The following reactions and phenomena have been observed more in detail.

Setting

The gypsum present in cement, is converted during the period of gauging fully or partly by the potassium-carbonate into K_2SO_4, $CaCO_3$ or in the double-salts $3K_2CO_3 \cdot 2CaCO_3 \cdot 6H_2O$ and $K_2SO_4 \cdot CaSO_4 \cdot H_2O$. Owing to this gypsum and even a part of the calcium-ions ($Ca^{++} \rightarrow CaCO_3$) can no longer act as setting regulators. In this environment in which the concentration of the K^+-ions has been increased, the aluminate-containing phases react violently.

Dependent on the added amount of K_2CO_3 other reactions occur. Although not all the hydration products can be detected, the impression exists that, when 0.25% K_2CO_3 is added, the initial reactions are activated. Since sufficient gypsum is available for the formation of ettringite, the aluminate phase reacts faster and to a larger extent, while forming more ettringite than in samples without addition from alkali-carbonate. Owing to this, a better retarding envelopment is formed on the clinker particles, resulting in the absence of reactions of C_3A for a relatively long period. At the consistency measurements in the paste, this is reflected in a retardation period in the stiffening process. At a higher K_2CO_3-percentage (2.5%) all the gypsum starts reactions already during the gauging period. An amount of gypsum equivalent to the K_2CO_3-content converts into K_2SO_4 and $CaCO_3$, whereas the rest of gypsum and a part of the calcium-carbonate reacts spontaneously with C_3A.

Since the heat development starts initially and the stiffening in the cement-paste still goes on for a while, it may be concluded that the protective activity of the combination of carbo-aluminate and ettringite is inferior. Due to this C_3A continues to react still very strongly in the first hour, and incites the C_3S and C_2S to a rather violent activity.

When gauging the mixture consisting of cement with 20% K_2CO_3, the C_3A as well as "C_4AF" react violently. These violent reactions are controlled for a few minutes by the initially formed carbo-aluminate. This is, however, at the temporary high temperature of the paste not stable enough so that under breakdown of this hydrate, the stiffening process may go on.

The consequence of the temporary retardation of the hydration is that the setting times of cement with 20% K_2CO_3 are somewhat longer (about 10 minutes) than at the lower percentages (about 3 minutes).

Also the calcium-silicates in the clinker reacts differently due to the presence of potash. However, the initial reactions in portland cement "M" are small, the amount of C_3S which reacts in the cement-pastes rich in K_2CO_3 is considerable. Especially the splitting off of calcium-hydroxide, which is due to this reaction, will be sufficient for formation of $CaCO_3$. The crystallization of poor soluble calcium salts like $CaCO_3$, $3K_2CO_3 \cdot 3CaCO_3 \cdot 6H_2O$ and $CaSO_4 \cdot K_2SO_4 \cdot H_2O$ will support the early stiffening of the alkali-carbonate-containing cement-pastes.

Strength

After 5 hours of hydration an initial strength in mortars has been measured, this strength increases gradually till 24 hours. Mortars containing much potassium-carbonate do not react in the same way. The increase of strength till 12 hours after gauging is greater than from 12 to 24 hours. The hydration mechanism will be responsible for this. In the paste containing hardly any alkali-carbonate the course of hydration-reactions during the first day is such that a continuous decrease of the clinker phases can be recorded. At higher percentages of alkali-carbonate these reactions are rather important during the first few hours, after which at 8–11 hours a period of relative rest sets in, which goes on till the end of the first day. This decrease in strength development is explicable with the reactions of the fresh C_3A to carbo-aluminate, owing to which the clinker particles are well enclosed again.

The writer wishes to express his appreciation to the co-workers of the ENCI-Research Department for their assistance in the preparation of this paper. He is indebted to Mr. S. Brouns for his assistance in carrying out the X-ray measurements and to Mr. V. Vaessens for the infrared measurements.

References

1. H. H. Steinour, The setting of portland cement, (Portland Cement Association, Chicago, U.S.A.,

1958).
2. W. C. Hansen, False set in portland cement, p. 387-403 and 424–438, (Proceedings of the Fourth International Symposium on the Chemistry of Cement Washington D. C. 1960).
3. W. Schulze and J. Lange, "Kaliumcarbonat als Frostschutzstoff für Fugenmörtel", Baustoffindustrie **2**, 38–42 (1965).
4. M. T. Francardi, Détermination de la consistance et du temps de prise des pâtes de ciment par un type spécial de pénétromètre, Compte rendu de XXXI Congrès International de Chimie Industrielle, Liège, September 1958.
5. L. Santarelli, Discussion to Paper IV-2, 414–415, (Proceedings of the Fourth International Symposium on the Chemistry of Cement, Washington D. C. 1960).
6. L. E. Copeland, D. L. Kantro and G. Verbeck, Chemistry of hydration of portland cement, (Proceedings of the Fourth International Symposium on the Chemistry of Cement, Washington D. C. 1960).
7. G. Yamaguchi, K. Takemoto, H. Uchikawa and S. Takagi, Rate of hydration of cement compounds and portland cement estimated by X-ray diffraction analysis, 495–499, (Proceedings of the Fourth International Symposium on the Chemistry of Cement, Washington D. C. 1960).
8. H. E. Schwiete and E.M.M.G. Niël, "The determination of the various sulphates in cements during setting" (in German), Zement-Kalk-Gips **18**, No. 4, 157–163 (1965).
9. H. E. Schwiete and E.M.M.G. Niël, "Investigation of the formation of new compounds at the commencement of the hydration of clinker and cement" (in German), Zement-Kalk-Gips **19**, No. 9, 402–411 (1966).
10. K. T. Greene, Early hydration reactions of portland cement, 359–373, (Proceedings of the Fourth International Symposium on the Chemistry of Cement, Washington D.C. 1960).
11. R. F. Feldmann, V. S. Ramachandran and P. J. Sereda, "Influence of $CaCO_3$ on the hydration of $3CaO \cdot Al_2O_3$", J. Am. Ceram. Soc. **48**, 25–30 (1965).
12. Å. Grudemo, The condition of Cement Research, p. 11, Cembureau, Technical Notes, No. 3, 1965.
13. H. N. Stein, "Influence of some additives on the hydration reactions of portland cement", J. Appl. Chem., **11**. December 485 (1961).

Supplementary Paper II-129 Aqueous Phase in Portland Cement Pastes Containing Soluble Chloride Ion

Kenneth T. Greene and Kenneth E. Palmer*

Synopsis

Data which can be used as a basis for determining whether the aqeuous phase in a cement paste at any particular early age is undersaturated, saturated, or supersaturated with respect to gypsum and calcium hydroxide are useful in studies of cement hydration, and are pertinent to various theories which have been proposed to explain early stiffening phenomena. This paper presents such data for pastes containing calcium chloride in concentrations equivalent to those commonly used in concrete.

Concentrations of Ca^{++}, OH^-, and SO_4^{--} are reported for solutions in equilibrium with both $CaSO_4 \cdot 2H_2O$ and $Ca(OH)_2$ at 25°C, and which contain potassium from 0 to 0.20 mole per liter expressed as $(K^+)_2$ and chloride from 0 to 0.27 mole per liter expressed as $(Cl^-)_2$.

Extracts from actual cement pastes containing calcium chloride were analyzed and concentrations of the various ions compared with the determined equilibrium values. The data indicated that marked supersaturation with either $Ca(OH)_2$ or $CaSO_4 \cdot 2H_2O$ or both may exist in such pastes during the first few minutes after mixing.

Introduction

Freshly mixed portland cement pastes or slurries are not in equilibrium with respect to the ions in solution, and a knowledge of conditions of unsaturation, saturation, or supersaturation is useful in studies of early hydration reactions and early stiffening phenomena. The aqueous phase in a paste without admixture is predominantly a solution of the following ions: Na^+ and K^+, Ca^{++}, OH^- and SO_4^{--}. Some CO_3^{--} ions are invariably present as a result of carbonates in the cement or from atmospheric carbonation of the solution after mixing. CO_3^{--} ions often can be neglected, but an estimation of CO_3^{--} concentration is desirable to insure that carbonation has not been excessive.

Silica, alumina, iron and minor elements are also present in some form in the solution, but their concentrations are very much lower than those of the ions mentioned above. They may affect the properties of fresh cement pastes to a greater extent than now realized, but they can scarcely have any major effect on the solubility relationships of gypsum and calcium hydroxide, which many cement chemists regard as highly pertinent to early stiffening problems.

Hansen and Pressler (1) determined the composition of solutions containing varying concentrations of alkalies which were saturated with both gypsum and calcium hydroxide at 25°C and 30°C. Their data demonstrated that at a given temperature, the equilibrium or saturation concentrations of Ca^{++}, SO_4^{--} and OH^- ions, as determined by analysis, are fixed by the total concentrations of Na^+ and K^+. They provided a basis for determining whether the aqueous phase in a cement paste at any particular early age is unsaturated, saturated, or supersaturated with gypsum and calcium hydroxide.

Calcium chloride, a common admixture, is added to concrete to accelerate setting and hardening, particularly in cold weather. The presence of chloride ions in the aqueous phase of the cement paste alters the equilibrium concentrations of Ca^{++}, SO_4^{--} and OH^- ions in contact with gypsum and calcium hydroxide so that the Hansen and Pressler data cannot be used. The work reported in this paper was done to provide information similar to that of Hansen and Pressler for the aqueous phase of concrete containing chloride ion, since such data could not be found in the literature.

Hansen and Pressler showed that the effects of sodium and potassium were essentially equivalent and that mixtures of the alkalies gave very nearly the same

*Ideal Cement Co., Colorado, U.S.A.

results as the individual elements when converted to a molar basis. For this reason, potassium was used in the present study, except for two experiments using sodium. The following table shows the results obtained with two solutions of NaCl compared to two solutions of KCl of equal molarity.

	(Moles per liter)			
Alkalies	Ca^{++}	SO_4^{--}	$(OH^-)_2$	CO_3^{--}
$0.100(NaCl)_2$	0.0454	0.0208	0.0226	0.0013
$.100(KCl)_2$	.0462	.0216	.215	.0018
$.200(NaCl)_2$	.0501	.0263	.236	.0016
$.200(KCl)_2$	.0536	.0292	.0248	—

We report here the concentrations of Ca^{++}, SO_4^{--} and OH^- in equilibrium with gypsum and calcium hydroxide at 25°C for solutions containing potassium from 0 to 0.20 mole per liter expressed as $(K^+)_2$ and chloride from 0 to 0.27 mole per liter expressed as $(Cl^-)_2$. This latter level of chloride is approximately equivalent to the initial concentration in the aqueous phase of concrete of W/C = 0.50 to which 2 percent of $CaCl_2 \cdot 2H_2O$ by weight of cement has been added. This is usually the recommended upper limit of calcium chloride addition.

In the absence of chloride, the aqueous phase is a four-component system (considering mixed alkalies as one component) with three compositional degrees of freedom. If we stipulate that the two solid phases, gypsum and calcium hydroxide, must both be present in excess, we reduce the compositional degrees of freedom to one. If in addition we fix the level of alkali concentration and perform the experiment at a constant temperature and at one atmosphere pressure, the system becomes invariant, which means that the concentrations of Ca^{++}, SO_4^{--} and OH^- are also fixed. With chloride present, the compositional degrees of freedom increase by one and we must fix the chloride concentration as well as the alkali concentration in order to have an invariant system.

From the above relationship it follows that, if we know the total concentrations of alkalies and of chloride in any given cement extract, we can then determine the concentrations of Ca^{++}, SO_4^{--} and OH^- which represent the saturation conditions for $CaSO_4 \cdot 2H_2O$ and $Ca(OH)_2$ in that particular extract at the temperature in question.

When the solution is saturated with $CaSO_4 \cdot 2H_2O$, the ion product $(Ca^{++})(SO_4^{--})$ will be equal to a fixed value determined by the concentrations of alkalies and chloride. Likewise, at saturation with $Ca(OH)_2$ the ion product $(Ca^{++})(OH^-)^2$ will be fixed. These equilibrium or saturation products can be estimated from the data reported in this paper. By calculating the ion products in actual analyzed cement extracts and comparing them with the equilibrium or saturation products, we can determine whether the solutions are saturated, undersaturated, or supersaturated with respect to these phases and the approximate degree of supersaturation or undersaturation. An analytically determined product greater than the equilibrium product indicates supersaturation, while an analytical product smaller than the equilibrium product indicates undersaturation.

Materials and Methods

The solutions were made up from analytical reagent chemicals and distilled water which had been freshly boiled and cooled to room temperature to remove dissolved carbon dioxide. Starting solutions whose K:Cl molar ratio was less than 1 were prepared with mixtures of KCl and a standard solution of $CaCl_2$. Solutions with a K:Cl ratio greater than 1 were made with mixtures of KCl and K_2SO_4. One hundred ml. of each solution was prepared in a volumetric flask, then transferred to a 250-ml. conical flask. Sufficient solid $CaSO_4 \cdot 2H_2O$ and $Ca(OH)_2$ were added to saturate the solutions and leave a definite excess. The flasks were stoppered, and stored (with occasional shaking) for several days at approximately 25°C. Preliminary tests indicated that equilibrium was reached rather rapidly and that one week was more than sufficient.

Before filtering, the flasks were placed in a water bath at 25° ± 1°C for several hours. The solutions were filtered rapidly and aliquots taken for analysis.

We analyzed for Ca^{++}, SO_4^{--} and Cl^- by standard gravimetric or volumetric procedures. Hydroxide was determined by titration with dilute HCl or HNO_3. Carbonate was estimated in several of the solutions by titration to a pH of 8.5 to indicate the OH^- plus approximately one-half of the CO_3^{--}, followed by further titration to a pH of 3.9, which gave the OH^- plus essentially all the CO_3^{--}.

Concentrations were calculated with the aid of the following formulas:

For hydroxide: 2P − M
For carbonate: 2(M − P)
Where P = volume of standard acid to reach pH 8.5
M = volume of standard acid to reach pH 3.9

Potassium (K^+) concentrations were not determined analytically in the equilibrium experiments, but were taken to be those of the original solutions. We disregarded the very small change in K^+ and Cl^- concentrations caused by the solution of the $CaSO_4 \cdot 2H_2O$ and $Ca(OH)_2$. In experiments to be described later, in which actual cement extracts were analyzed, alkalies were determined by the flame photometer method.

Results

Solubility Studies

The compositions of the various solutions in equilibrium with solid $CaSO_4 \cdot 2H_2O$ and $Ca(OH)_2$ at 25°C are presented in Table 1. Since concentrations are expressed as moles per liter of $(K^+)_2$, $(Cl^-)_2$, Ca^{++}, SO_4^{--}, $(OH^-)_2$ and CO_3^{--}, all ions are on an equivalent basis and can be compared to one another without regard to valence. Four groups of data from Hansen and Pressler (1) for chloride-free mixes are included in the table.

It will be noted that about half of the $(Cl^-)_2$ values were determined by analysis, whereas the others were calculated by difference, i.e. the difference between the sum of the cations and the sum of the other anions. This is justified by the principle of electrical neutrality and the absence of appreciable quantities of other ions. In all cases where all the ions were determined analytically, the sums of the cations were in satisfactory agreement with the sums of the anions.

The data in Table 1 are shown graphically in Figs. 1, 2 and 3, in which the concentrations of Ca^{++}, SO_4^{--} and $(OH^-)_2$ are plotted against $(Cl^-)_2$ content at five levels of $(K^+)_2$ concentration.

Cement Extracts

To illustrate the application of the data, we studied several commercial cements by analyzing solutions extracted a few minutes after mixing. The water-cement ratio was 0.50 by weight in all cases, and calcium chloride was added to the mix water at the rate of either 1% or 2% $CaCl_2 \cdot 2H_2O$ by weight of cement. The data are presented in Table 2.

Table 1. *Compositions of solutions saturated with* $CaSO_4 \cdot 2H_2O$ *and* $Ca(OH)_2$ *at 25°C*

Mix No.	(Moles per liter)						Remarks
	$(K^+)_2$	$(Cl^-)_2$	Ca^{++}	SO_4^{--}	$(OH^-)_2$	CO_3^{--}	
22	none	0.0007	0.0322	0.0119	0.0190	0.0007	
10a	none	.1363*	.1603	.0084	.0156	N.D.**	
8a	none	.2723*	.2952	.0086	.0143	N.D.	
21	0.0250	.0251	.0369	.0153	.0214	N.D.	
	.0501	—	.0197	.0358	.0344	—	Interpolated from H. & P.(1)
23	.0500	.0160	.0252	.0291	.0258	.0010	
17b	.0500	.0505	.0382	.0171	.0201	.0007	
11a	.0500	.1325*	.1093	.0111	.0157	N.D.	
6a	.0500	.2735*	.2469	.0090	.0144	N.D.	
	.1002	—	.0161	.0722	.0444	—	From H. & P.(1)
24	.1000	.0338	.0200	.0536	.0319	.0010	
18	.1000	.1001	.0462	.0216	.0215	.0018	
12a	.1000	.1367*	.0695	.0156	.0172	N.D.	
5a	.1000	.2716*	.1969	.0105	.0148	N.D.	
	.1503	—	.0163	.1142	.0510	—	Interpolated from H. & P.(1)
15a	.1500	.0506	.0185	.0770	.0368	.0008	
13	.1500	.1343*	.0397	.0302	.0252	N.D.	
19	.1500	.1497	.0498	.0258	.0223	.0012	
7a	.1500	.2720*	.1502	.0137	.0145	N.D.	
	.2005	—	.0165	.1562	.0582	—	From H. & P.(1)
16	.2000	.0499*	.0185	.1210	.0476	N.D.	
25	.2000	.0673	.0186	.1110	.0397	.0012	
14	.2000	.1339*	.0262	.0594	.0329	N.D.	
20	.2000	.1977	.0536	.0292	.0248	N.D.	
9a	.2000	.2716*	.1043	.0163	.0164	N.D.	

*Calculated by difference.
**Not determined.

Table 2. *Compositions of solutions extracted from cement pastes containing calcium chloride*

Extract No.	Cement alkalies (%)		W/C	$CaCl_2 \cdot 2H_2O$ added	Approximate time after H_2O contact	Solution composition (moles per liter)						
	K_2O	Na_2O				$(K^+)_2$	$(Na^+)_2$	$(Cl^-)_2$	Ca^{++}	SO_4^{--}	$(OH^-)_2$	CO_3^{--}
1	0.91	0.25	0.50	2%	7–10 Min.	0.129	0.011	0.285	0.184	0.013	0.023	0.003
2	.22	.11	.50	1%	7–10 Min.	.009	.002	.137	.166	.012	.022	.003
3a	.52	.07	.50	1%	7–15 Min.	.049	.005	.126	.115	.014	.019	.005
3b	.52	.07	.50	2%	7–15 Min.	.049	.005	.265	.241	.012	.017	.005
4a	.03	.52	.50	1%	7–15 Min.	.001	.016	.126	.145	.012	.020	.002
4b	.03	.52	.50	2%	7–15 Min.	.001	.016	.265	.275	.011	.020	.003

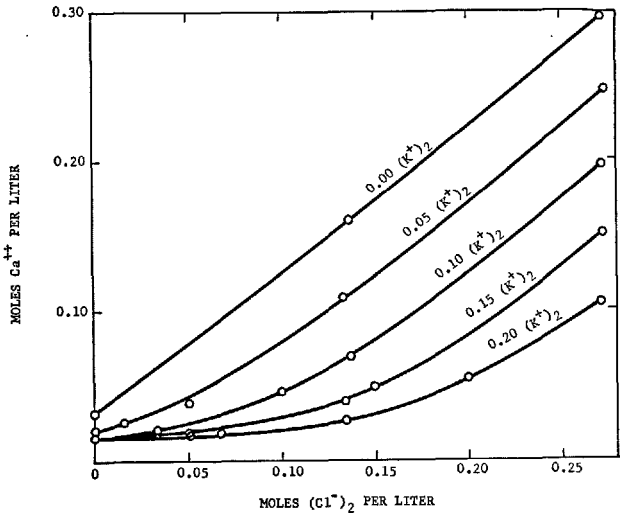

Fig. 1. *Concentration of* Ca^{++} *in solutions saturated with* $CaSO_4 \cdot 2H_2O$ *and* $Ca(OH)_2$ *at 25°C*

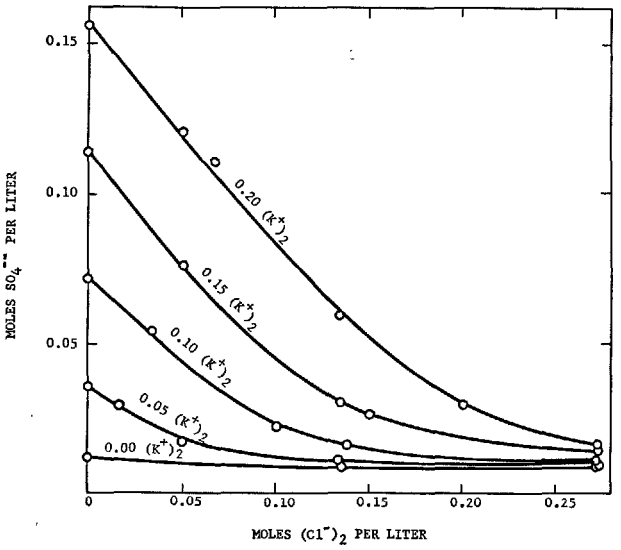

Fig. 2. *Concentration of* SO_4^{--} *in solutions saturated with* $CaSO_4 \cdot 2H_2O$ *and* $Ca(OH)_2$ *at 25°C*

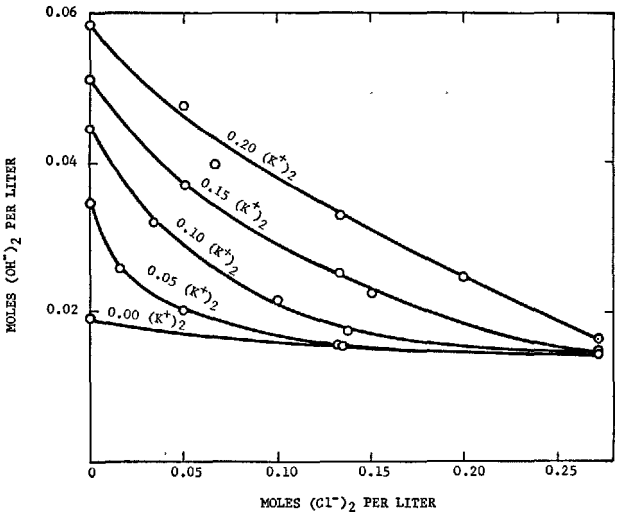

Fig. 3. *Concentration of* $(OH^-)_2$ *in solutions saturated with* $CaSO_4 \cdot 2H_2O$ *and* $Ca(OH)_2$ *at 25°C*

The equilibrium concentrations of Ca^{++}, SO_4^{--} and $(OH^-)_2$ in the cement extracts at the determined total alkali and chloride concentrations were estimated by interpolation from Figs. 1, 2 and 3. We then calculated the equilibrium ion products and compared them to the products calculated from the analytically determined concentrations of the ions so that saturation conditions could be determined. Table 3 shows these comparisons and the conclusions which were drawn.

Discussion

The data in Table 3 suggests that in cement pastes containing calcium chloride, some supersaturation with gypsum commonly exists up to approximately 15 minutes after mixing. Supersaturation with calcium hydroxide also appears to be common during this period and may sometimes be quite strong, giving ion products over twice the equilibrium value. The study of extracts as it applies to the hydration reactions and physical behavior of fresh cement pastes containing calcium chloride admixture would appear to be a fruitful area of research.

Table 3. *Comparison of equilibrium and analytical ion products in cement extracts*

Extract No.	Total $(K^+)_2 + (Na^+)_2$ moles/liter	$(Cl^-)_2$ moles/liter	Estimated equilibrium concentrations moles/liter			$(Ca^{++})(SO_4^{--})$ Equilibrium	$(Ca^{++})(SO_4^{--})$ Analytical	$(Ca^{++})(OH^-)^2$ Equilibrium	$(Ca^{++})(OH^-)^2$ Analytical	Conclusions
			Ca^{++}	SO_4^{--}	$(OH^-)_2$					
1	0.140	0.285	0.180	0.013	0.014	234×10^{-5}	239×10^{-5}	141×10^{-6}	389×10^{-6}	Approximately saturated with $CaSO_4 \cdot 2H_2O$. Highly supersaturated with $Ca(OH)_2$.
2	.011	.137	.152	.009	.016	137×10^{-5}	199×10^{-5}	156×10^{-6}	321×10^{-6}	Moderately supersaturated with $CaSO_4 \cdot 2H_2O$. Highly supersaturated with $Ca(OH)_2$.
3a	.054	.126	.096	.012	.016	115×10^{-5}	161×10^{-5}	98×10^{-6}	166×10^{-6}	Somewhat supersaturated with $CaSO_4 \cdot 2H_2O$. Moderately supersaturated with $Ca(OH)_2$.
3b	.054	.265	.236	.009	.014	212×10^{-5}	289×10^{-5}	185×10^{-6}	279×10^{-6}	Somewhat supersaturated with $CaSO_4 \cdot 2H_2O$. Moderately supersaturated with $Ca(OH)_2$.
4a	.017	.126	.132	.009	.016	119×10^{-5}	174×10^{-5}	135×10^{-6}	232×10^{-6}	Moderately supersaturated with $CaSO_4 \cdot 2H_2O$. Moderately supersaturated with $Ca(OH)_2$.
4b	.017	.265	.272	.009	.014	245×10^{-5}	303×10^{-5}	213×10^{-6}	440×10^{-6}	Somewhat supersaturated with $CaSO_4 \cdot 2H_2O$. Highly supersaturated with $Ca(OH)_2$.

Acknowledgments

The authors are grateful to the Ideal Cement Company for permission to publish this paper, and for the assistance of R. H. Patrick and K. L. Hillsten, who performed the analyses.

References

1. W. C. Hansen and E. E. Pressler, "Solubility of $Ca(OH)_2$ and $CaSO_4 \cdot 2H_2O$ in dilute alkali solutions," Ind. Eng. Chem. **39**, 1280–1282 (1947).

Supplementary Paper II-134 The Effect of Tricalcium Aluminate on the Hydration of Tricalcium Silicate and Portland Cement

Adriano Celani, Pietro A. Moggi and Arturo Rio*

Synopsis

The effect of tricalcium aluminate, present in portland cement in variable percentages, on the hydration kinetics of tricalcium silicate and development of mechanical strengths at early and later ages has been investigated.

To this aim, by means of physical-chemical measurements, the hydration of cements containing various percentages of tricalcium aluminate, with or without gypsum and with or without calcium chloride additions has been followed in the time.

The experimental results altoghther show the positive effect of tricalcium aluminate contents increasing up to an optimum value on the hydraulic properties of portland cement, and permit us to formulate some interesting hypothesis on the nature of hydration processes.

Introduction

In recent years several investigators have devoted themselves to study the reactions of hydration of cement and its compounds, with or without additions. These researches not only aimed at explaining the complex chemical-physical processes occurring by cement hydration, but tended often to state the best conditions to be realized for controlling setting and hardening processes in order to meet the latest requirements of the modern building technology. The problem of the first rank is how to obtain a sharp increase of mechanical strengths, especially at the early ages. Gypsum and calcium chloride have resulted to be the most affective additions in this regard, acting the former principally as a regulator of the setting phenomena and the latter by accelerating the hydration process of the most hydraulic compounds of cement (1, 2, 3).

Whilst it was studied hard for the hydration of the single cement compounds, C_3S, beta-C_2S, aluminates and ferrite phase, as well for the effects of addition compounds, such as gypsum and calcium chloride, little or nothing was done, on the other hand, to know how the compounds themselves influence each other, during hydration, when that structure develops which all they contribute to form.

In the group of cement compounds, C_3A is often regarded as useless, or deleterious because of the troubles it brings about by its rapid setting; its hydraulic properties are questioned and its action seems to be limited to make possible the clinker burning at no very high temperature (4). Actually, when pure tricalcium aluminate undergoes hydration the product obtained after quick set, under an intensive heat evolution, shows very low strengths, which scarcely increase with the time.

Nevertheless, some decades ago, many investigators (5, 6) noted, from their sometimes also contradictory results, that mixtures prepared by adding even appreciable C_3A amounts (19 and 15 per cent) to the other more sharply hydraulic compounds of cement, like C_3S and beta-C_2S, show strengths higher than those expected from additivity, or even higher than the strengths of pure C_3S, beta-C_2S or their mixtures at the same ages. The phenomenon occurs, sometimes emphasized, also when gypsum is added to the mixture.

It is evident that the significance of such results must have been undervaluated; indeed, since then on, the literature does not report any research thereon.

This feeling of a possitive effect of C_3A on the strength development may be indirectly confirmed by some data, deducible from W. Lerch's work (7), which refer to the influence of gypsum on portland cement hydration. Comparison between the mechanical strengths of cements containing different C_3A and equal alkalies shows that such strengths generally increase with the C_3A content, this effect being more remarkable at the early ages.

We have often noted this phenomenon by con-

*Soc. Calci e Cementi di Segni, Laboratorio Centrale, Rome, Italy.

trolling the strength development of cements, with different C_3A amounts, produced in several factories.

A systematic research was, therefore, undertaken to investigate the influence of the tricalcium aluminate present in various proportions in portland cement on the hydration of cement compounds, specifically C_3S, as well on the strength development at the early and later ages.

The hitherto obtained results and the possible deductions are the subject of the present paper.

Experimental

According to the considerations and purposes previously spoken of, a series of preliminary tests was carried out for determining the influence of C_3A on the hydration and strengths of portland cement. The tests were done on mixtures of C_3S and C_3A, prepared with pure compounds. The percentage of C_3S was kept constant, whereas that of the C_3A was variable. The mixture was completed with $CaCO_3$. Each mixture was added with 5 per cent of gypsum and the compressive strength at 1, 7 and 28 days was determined on 4 cm cubes of I.S.O. mortar 1:3, *w/c* ratio 0.50. The results are given in Table 1.

These results indicated that the highest strength is found with C_3A content ranging from 2 to 5 per cent, and that there was a very remarkable difference of behaviour between the addition of C_3A and that of the only carbonate of equal fineness.

Other preliminary tests for compressive strengths at 1, 3, 7 and 28 days were performed on specimens similar to the above, but made up with clinkers of different industrial source. These were corrected with an addition of pure compounds for obtaining an equal percentage of C_3S, thereafter they were reburnt and ground with 5 per cent of gypsum to the same fineness.

Table 1. *Compressive strengths of mixtures of pure compounds*

Compounds %	C_3S	80	80	80	80
	C_3A	—	2	5	10
	$CaCO_3$	15	13	10	5
	$CaSO_4 \cdot 2H_2O$	5	5	5	5
Compressive strengths kg/cm²	1 day	70	90	82	60
	7 days	144	208	184	178
	28 days	250	345	325	288

The results are given in Table 2 wherein all strength values are the average of two determinations.

Table 2. *Compressive strengths of industrial cements with the same C_3S percent*

Mineralogical composition %	C_3S	58.14	61.02	58.79
	C_2S	22.24	15.65	20.22
	C_3A	3.41	5.10	8.77
	C_4AF	12.29	13.81	9.12
Compressive strengths kg/cm²	1 day	138	194	142
	3 days	330	452	374
	7 days	391	502	459
	28 days	560	680	618

The positive effect of C_3A on the strengths appears clearly also from this series of measurements which besides confirms the presence of an optimum amount of C_3A ranging, in this series, from 5 to 8 per cent.

At this point, four clinkers were prepared by burning mixtures of pure $CaCO_3$, SiO_2, Al_2O_3 and Fe_2O_3 for 4 hours at 1450°C in order to prosecute the tests on materials of homogeneous chemical and physical properties. The mixtures were so proportioned to give burned products with constant C_3S and C_2S content (nearly 50 and 25 per cent respectively) and variable C_3A content (nearly 3, 5, 10, 15 per cent), the remaining being the ferrite phase.

After burning, the clinkers were cooled in air, ground in porcelain mills, analyzed by chemical analysis and submitted to successive burnings with the same procedure as before, till the complete disappearance of free lime. The final analysis of the four clinkers and the mineralogical compositions, calculated according to Bogue, are reported in Table 3.

The mineralogical composition of the four clinkers was also examined experimentally by reflected light microscope. The micrographs obtained are given in Fig. 1. The examination resulted to be in good aggreement with the mineralogical compositions calculated as above.

The clinkers were ground to an equal fineness corresponding to a residue of 15 per cent on the 40 micron sieve and to a Blaine specific surface of 3500 cm²/g. They were then utilized partly so as they were, partly with gypsum added.

The gypsum addition had been calculated in order

Table 3. *Chemical analysis and mineralogical composition of clinkers*

Clinker No.	1	2	3	4
CaO	65.47	62.11	66.70	67.58
SiO_2	22.95	22.40	22.14	21.65
Al_2O_3	4.96	5.65	6.62	7.60
Fe_2O_3	6.04	5.55	4.20	2.74
free CaO	0.30	0.20	0.30	0.40
C_3S	49.00	52.10	51.50	53.97
C_2S	29.12	25.22	24.92	21.65
C_3A	2.93	5.59	10.44	15.51
C_4AF	18.38	16.89	12.78	8.44

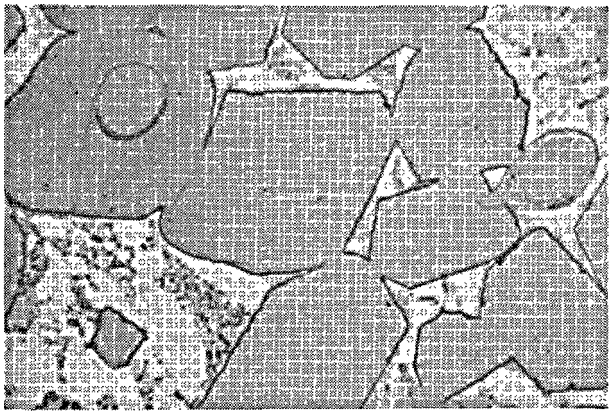

Clinker I

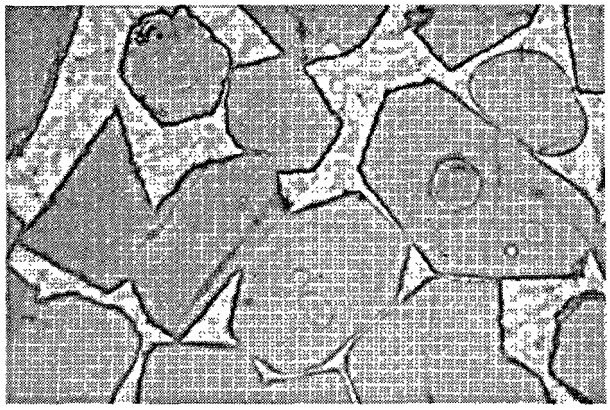

Clinker II

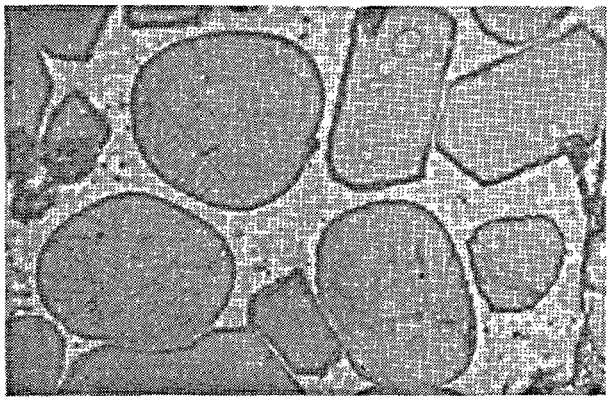

Clinker III

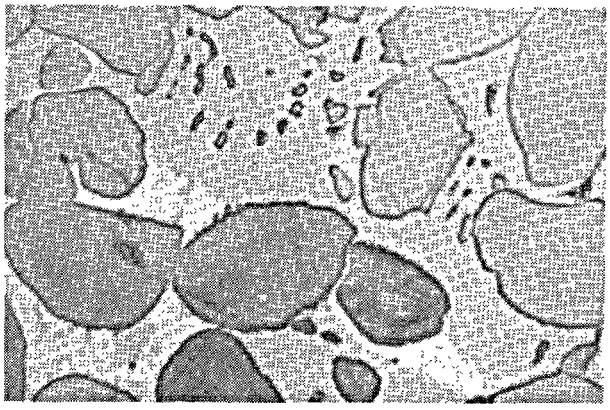

Clinker IV

Fig. 1. *Micrographs of the four clinkers* (×*1200—Etched with alcoholic* HCl)

to obtain a constant $C_3A/CaSO_4$ ratio for all four cements. It was roughly corresponding to the optimum gypsum content, as derived from W. Lerch's data (7) and a control was once more made on it by the chemical method of extraction with water and determination of SO_3 soluble, as proposed by the same author (A.S.T.M. C265–58T).

By this way it was tried that each cement had the best SO_3 concentration for developing strengths and an equal ratio during hydration between the C_3A combined as sulphoaluminate and the C_3A available, in order that the effect of the latter may be better isolated. The mineralogical compositions of the cements after addition of gypsum are reported in Table 4.

In connection with previous studies (3) of the influence of gypsum on the hydration process, tests were carried out by adding a constant amount of $CaCl_2$, corresponding to 2 per cent by weight of cement, dissolved in the mixing water.

With the cements prepared as described, a number of researches was made for studying the influence of different amounts of C_3A on the course of hydration of the tested cements using the following parameters:

—Mechanical strengths
—Hydration rate and extent of hydrolysis
—Development of the specific surface of hydrated pastes.

Table 4. *Mineralogical composition of cements with gypsum added*

Cement N.	1	2	3	4
C_3S	48.02	50.01	47.90	48.57
C_2S	28.54	24.21	23.18	19.49
C_3A	2.87	5.37	9.71	13.64
C_4AF	18.01	16.21	11.89	7.60
$CaSO_4$	1.58	3.16	5.53	7.90
$C_3A/CaSO_4$	1.82	1.70	1.76	1.73
Loss on ignition	0.67	1.11	1.61	2.31

Mechanical Strengths

The various cements were used to prepare 4 cm cubes of I. S. O. mortar 1 : 3, mixed with a constant water amount, corresponding to a *w/c* ratio of 0.5, although the consistency, measured according to the A.S.T.M. C 230–61 method, resulted clearly tending to increase with higher C_3A contents.

The compressive strengths were determined at 1, 3, 7, 28 days. The obtained values are given in Table 5.

The development of the strengths in the time may be seen on the graphs in Fig. 2.

From the results, the following considerations can be made:

—The compressive strengths at various ages show a maximum in correspondance of one of the four cements, or better, of a determined percentage of C_3A.

—For the same cement, the strengths are sharply higher for addition of gypsum and moreover of calcium chloride. The overall course is yet the same in the three series, therefore the addition of gypsum and calcium chloride does not alterate the effect of the different proportion of C_3A.

—The position of the maximum strength shifts from high C_3A contents at the early ages to low C_3A contents at the subsequent ages. Indeed, while at 3 days the maximum of strengths is found between cement III and IV, it has passed at 28 days between cement I and II.

To have also a quantitative indication on the development of the phenomenon, the strengths at a given age have been assumed as varying with the C_3A content according to a function of parabolic type and the maximum of such a function was calculated thereafter analytically. The obtained values for the C_3A content in correspondance to the maxima are gathered in Table 6.

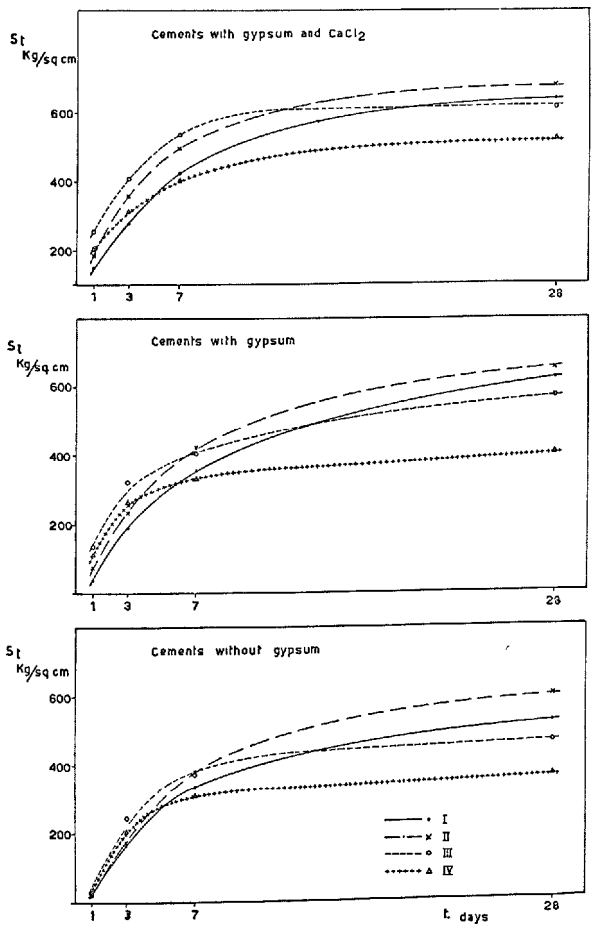

Fig. 2. *Compressive strengths vs. time*

Rate of Hydration and Extent of Hydrolysis

As we have done in earlier studies of hydration processes (1, 2, 3), we based our investigation on determination of hydrolysis lime and on analysis of the contact solution with cement paste.

Furthermore, for studying the rate of hydration of cements, we used the determination of the non-evaporable water content. Finally we have carried out

Table 5. *Compressive strengths of 4 cm cubes in ISO mortar 1: 3*

	Compressive strengths Kg/cm²			
	1 day	3 days	7 days	28 days
Cement without gypsum:				
N. 1	16	168	337	521
N. 2	18	175	381	599
N. 3	21	246	375	462
N. 4	25	212	312	364
Cement with gypsum:				
N. 1	37	187	356	628
N. 2	78	237	428	653
N. 3	137	325	409	572
N. 4	112	265	334	403
Cement with gypsum and $CaCl_2$:				
N. 1	150	278	424	653
N. 2	187	359	497	681
N. 3	253	406	537	618
N. 4	203	312	403	525

Table 6. *Optimum C_3A percent for compressive strengths at different ages*

	1 day	3 days	7 days	28 days
Cement without gypsum	—	10.8	8.1	6.5
Cement with gypsum	11.1	10.5	7.6	5.9
Cement with gypsum and $CaCl_2$	10 4	9.3	8.8	6.2

measurements of the specific surface to investigate the variations of this parameter with time, relating it to the course of hydration and to the development of strengths.

The determination of the free lime content in cement pastes was also used by other investigators (8) as an indirect method for studying the rate of hydration of the C_3S and C_2S in cement.

Furthermore, we found it useful to take into account also the measurement of the lime supersaturation of the contact solution. Indeed, it is known that the contact solution with portland cement pastes presents supersaturation phenomena at the early ages since the rate of passing into solution of the hydrolysis lime is greater than that of precipitation of the lime itself from the solution, according to the equilibrium

$$Ca(OH)_2 \text{ Solution} \rightleftarrows Ca(OH)_2 \text{ Solid}$$

This brings about a progressive accumulating of lime in the contact solution beyond the supersaturation value, which continues till the rate of precipitation of the lime becomes higher than the rate of its going into solution. At this moment, a maximum of the supersaturation is reached, and subsequently this decreases more or less rapidly.

Since the rate of hydrolysis of C_2S is negligible, the supersaturation of the contact solution may be considered as resulting from an equilibrium between the rate of hydration of the C_3S alone and the rate of precipitation of the lime, whereas the variation with the time of the free lime content of the solid phase will be influenced also by the hydrolysis of C_2S.

The content of non-evaporable water at the various ages, determined under equal conditions for all samples was assumed by a number of investigators (9) as index of the fixed water amount in the hydration products and therefore as a criterion for the measurement of the extent and rate of the cement hydration.

Finally, in many studies (10) the development of the specific surface of hydrated pastes in the time has been related to the extent and the rate of hydration of cement and its components. Furthermore, it is evident that there is a correlation between specific surface and mechanical strengths of a cement during hydration.

In the first series of test for studying the rate of hydration of C_3S at the early ages, all samples were hydrated with a w/c ratio $= 5$, in order to have a sufficient quantity of solution to analyze, and kept in a thermostat at 40°C till ages of 1, 2, 4, 8, 16, 24, 28, 72, 120 hours. At the end of the curing, the suspension was filtered rapidly in a CO_2 free atmosphere, while the solid phase was ground in a mortar with alcohol to interrupt the hydration, filtered again in the same a CO_2 free conditions, washed with ether and oven-dried for 2 hours at 105°C, in stream of CO_2 free air.

On the dried solid the free lime was determined, according to the T. V. M. method (11), by extraction in boiling by the solvent mixture isobutyl alcohol (87%)—acetoacetic ester (13%) and subsequent titration of the extract with isobutylic perchloric acid, thymol blue as indicator.

On the dried solid the ignition loss at 950°C was also determined. The alkalinity of the filtered solution was determined by titration with HCl, using methyl orange as indicator, and the CaO concentration was determined by complessometric titration with EDTA, using calconcarbonic acid as indicator.

The SO_3 concentration of the contact solutions with the cement samples with gypsum was determined by nephelometry. Finally, for the series to which also calcium chloride was added, the Cl^- ion concentration was determined by titration with $AgNO_3$ according to the method of Fayans, with fluorescein as indicator.

For cements without gypsum addition, the CaO concentrations at the equilibrium were calculated by means of the lime-alkali isotherm at 40°C (12). In the case of cements with gypsum addition it was necessary to examinate the more complex equilibrium CaO–SO_3-alkali (13, 1). Finally, for the series with calcium chloride also the CaO amount corresponding to the Cl^- ion concentration was considered.

The extent of the lime supersaturation of each solution is derived from the difference between the value of the CaO concentration found and the CaO concentration at the equilibrium.

The course of the CaO supersaturation of the three series of samples is reported as function of the time on the graphs in Figs. 3–4–5. On the side of each figure appears, enlarged, the evolution of free lime at the early stages of hydration.

The following observations can be done:

—The rate of hydrolysis of the C_3S increases with the C_3A content without a maximum being evident, at least in the field of the compositions examined. On the other side, it may be noted that the differences between the maximum supersaturations are not proportional to the differences between the C_3A contents, therefore a maximum should be nevertheless present for the rate of hydration of C_3S at the early ages, in correspondence to a given C_3A content.

—The accelerating effect of gypsum and calcium

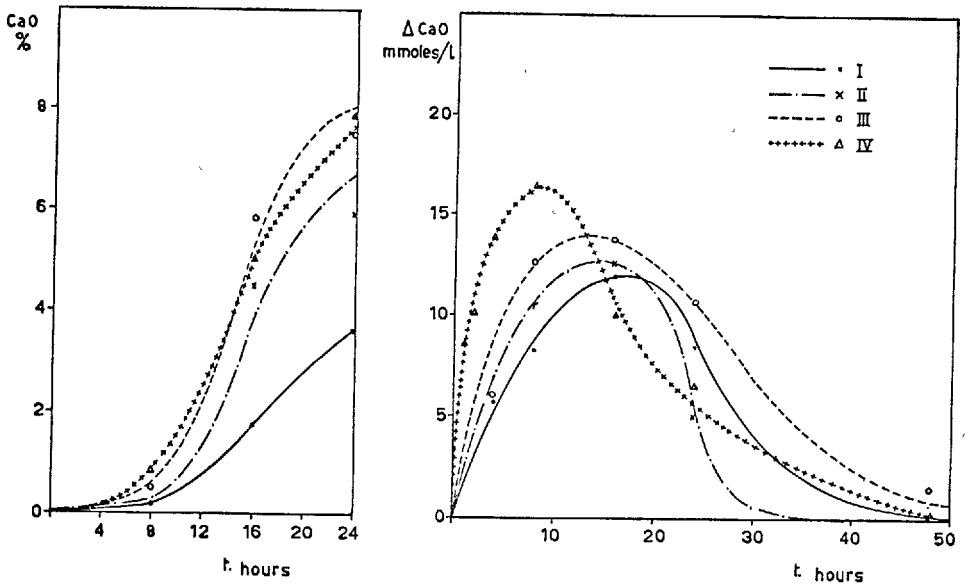

Fig. 3. *Development of* CaO *of hydrolysis at early ages and supersaturation of contact solution with cement pastes.*
A) Cements without gypsum

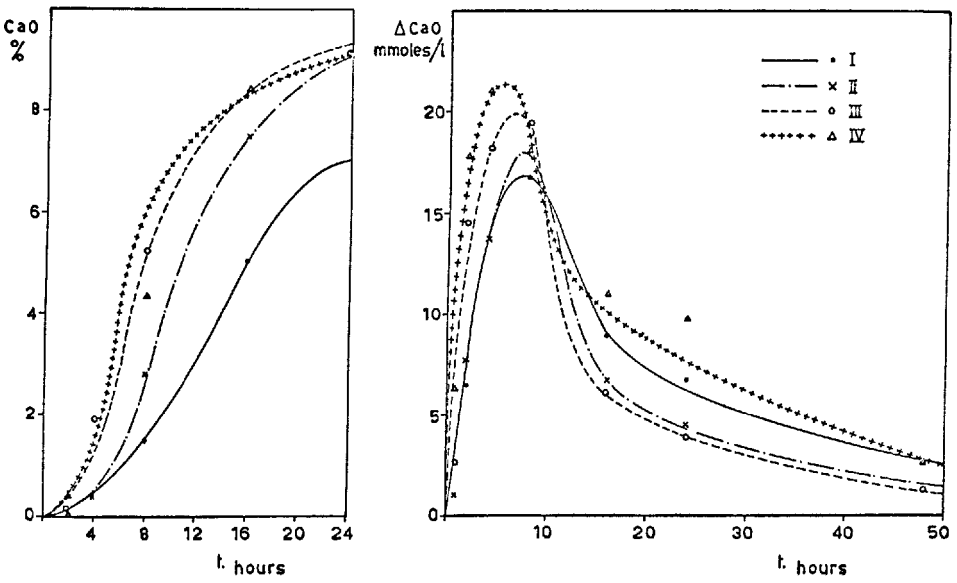

Fig. 4. *Development of* CaO *of hydrolysis at early ages and supersaturation of contact solution with cement pastes*
B) *Cements with gypsum*

chloride on the hydration is also evident; indeed the maxima of supersaturation of the three series are about in a ratio of 1 : 1, 4 : 3.

In the series with calcium chloride the maxima of supersaturation are very close to each other because the marked accelerating action of this salt conceals the differences due to the different C_3A content.

Within the earliest hours the free lime amount increases with increasing C_3A, without maxima being present, but already within the twelfth and the sixteenth hour a maximum free lime amount appears in correspondence of cement III. This observation agrees both with the results from the supersaturation and with the progressive shifting of the maximum of

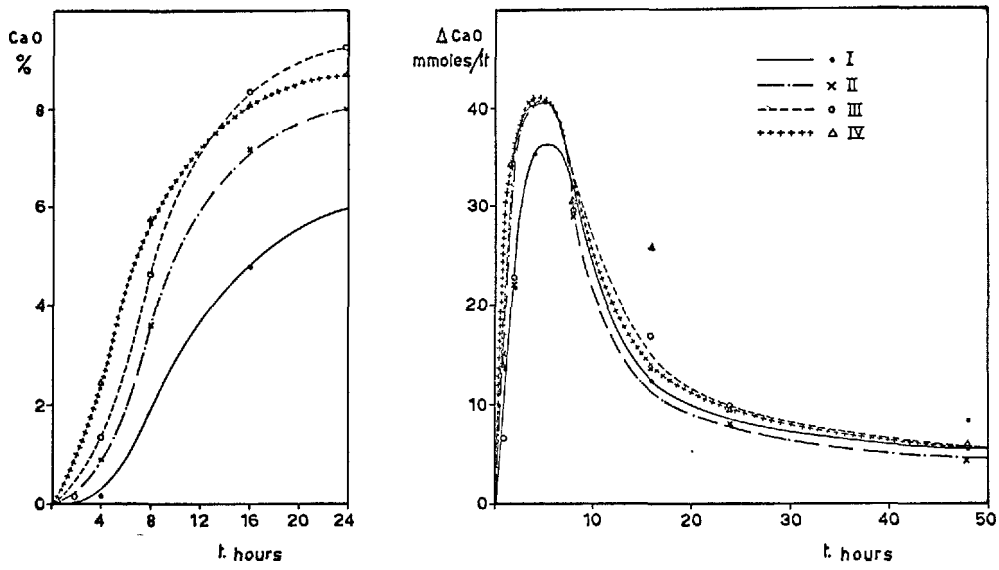

Fig. 5. *Development of* CaO *of hydrolysis at early ages and supersaturation of contact solution with cement pastes*
C) *Cements with gypsum and* $CaCl_2$

strengths towards lower C_3A contents which was observed during the course of hydration.

It is important to remark that the free lime amount in the solid phase, after the earliest hours, is clearly free from contributions due to the C_3A hydration which, by means of a mechanism "through solution" (14), could affect the supersaturation degree of contact solution. Therefore, from the differences found for the free lime amounts, the influence of C_3A on the rate of hydration of silicates appears evident.

In a second series of tests, all samples have been submitted to hydration as a paste with *w/c* ratio = 0.5. The pastes were kept in thermostat at 25°C till fixed ages of 1, 3, 5, 7, 14, 28, 60, 90 days. At the end of the curing the hydrated paste was treated with the same procedures as used for determinating the supersaturation. On the dried solid the free lime content and the loss on ignition at 950°C were determined.

From the free lime amount, the extent of hydrolysis was calculated, defined as the ratio between the amount of lime developed by hydrolysis at a given age and the amount of lime developed at the end of the hydration. To calculate the latter value, it was assumed that the stoichiometry of the hydration of the C_3S and beta-C_2S in the paste form be represented by the equations [1] and [2] (15).

$$2C_3S + 6H_2O = C_3S_2 \cdot 3H_2O + 3Ca(OH)_2 \quad [1]$$

$$2C_2S + 4H_2O = C_3S_2 \cdot 3H_2O + Ca(OH)_2 \quad [2]$$

From the loss on ignition at 950°C the content of the non-evaporable water was derived.

The results obtained for free lime and hydrolysis extent of the three series of samples; cement without gypsum, cements with gypsum, cements with gypsum and calcium chloride, are reported in Table 7. All values are referred to as percentage of the original anhydrous material.

—The course in the time of the hydrolysis extent of silicates (Fig. 6) agrees essentially with the development of the strengths. The presence of a maximum shifting for all series with the time, from high to low C_3A contents, appears clearly at each age.

To confirm the results from the strength tests, the proportions of C_3S corresponding to the maximum extent of hydrolysis of silicates at the ages of 1, 3, 7, 28 days were calculated, also in this case, analytically. The results are given in Table 8.

As may be seen, the accordance is very satisfactory.

—On comparing the results of the three series of tests with each other, the favourable effect of gypsum and also of calcium chloride on the rate of hydration of silicates is as yet remarkable.

It may be controlled that for the same cement, at the early ages, the addition of gypsum brings about an increment of nearly 150 per cent, and a further addition of calcium chloride brings about an increment of nearly 250 per cent for the extent of hydrolysis. Nevertheless, the action of these additions ends at the early ages. In fact the hydration rate becomes almost identical for all samples already after 5 days, and the initial difference of the extent of hydrolysis tend to disappear.

Table 7. *Hydrolysis extent of cement pastes*

		1 day	3 days	5 days	7 days	14 days	28 days	60 days	90 days	complete hydration
Cements without gypsum:										
N. 1	free CaO %	1.33	8.21	12.22	13.77	15.07	16.64	17.46	18.96	22.78
	hydrolysis %	5.80	36.00	53.70	60.50	66.20	73.10	76.70	83.30	—
N. 2	free CaO %	3.65	11.38	14.02	14.20	16.60	16.97	19.59	21.51	23.28
	hydrolysis %	15.70	48.90	60.30	61.00	71.30	72.90	84.60	92.50	—
N. 3	free CaO %	4.70	13.23	15.92	15.97	16.40	17.09	17.40	20.48	23.01
	hydrolysis %	20.40	57.50	69.20	69.40	71.30	74.30	75.60	89.00	—
N. 4	free CaO %	4.52	13.71	14.75	14.85	16.31	16.53	17.31	19.97	23.39
	hydrolysis %	19.30	58.60	63.10	63.90	69.80	70.70	74.70	85.40	—
Cements with gypsum:										
N. 1	free CaO %	4.89	9.35	12.20	13.86	14.92	16.45	17.59	18.21	22.32
	hydrolysis %	21.90	41.90	54.70	62.10	67.80	73.70	78.80	81.60	—
N. 2	free CaO %	5.68	9.61	10.80	13.87	14.38	15.37	17.82	18.61	22.35
	hydrolysis %	25.40	42.90	48.20	62.00	64.30	68.70	79.60	82.30	—
N. 3	free CaO %	6.26	10.47	12.31	14.03	14.21	15.67	17.20	17.61	21.41
	hydrolysis %	29.20	48.90	57.50	65.50	66.40	73.10	80.30	82.30	—
N. 4	free CaO %	6.51	9.80	10.35	13.03	13.96	14.69	15.19	15.57	21.05
	hydrolysis %	30.90	46.50	49.20	61.90	66.40	69.80	72.10	74.00	—
Cements with gypsum and $CaCl_2$:										
N. 1	free CaO %	9.78	11.75	12.29	12.94	14.02	14.36	14.63	15.63	22.32
	hydrolysis %	43.80	52.70	55.00	58.00	62.80	64.40	65.50	70.10	—
N. 2	free CaO %	10.42	13.69	14.10	14.35	14.93	15.30	15.61	16.58	22.35
	hydrolysis %	46.60	61.20	63.10	64.20	66.80	68.40	69.90	74.30	—
N. 3	free CaO %	10.73	13.91	14.06	14.12	15.05	15.67	15.73	16.35	21.41
	hydrolysis %	50.10	65.00	65.70	66.00	70.30	73.10	73.40	76.30	—
N. 4	free CaO %	8.98	12.66	12.84	13.09	13.29	14.93	15.05	15.70	21.05
	hydrolysis %	42.70	60.20	61.00	62.10	63.10	71.00	71.70	74.70	—

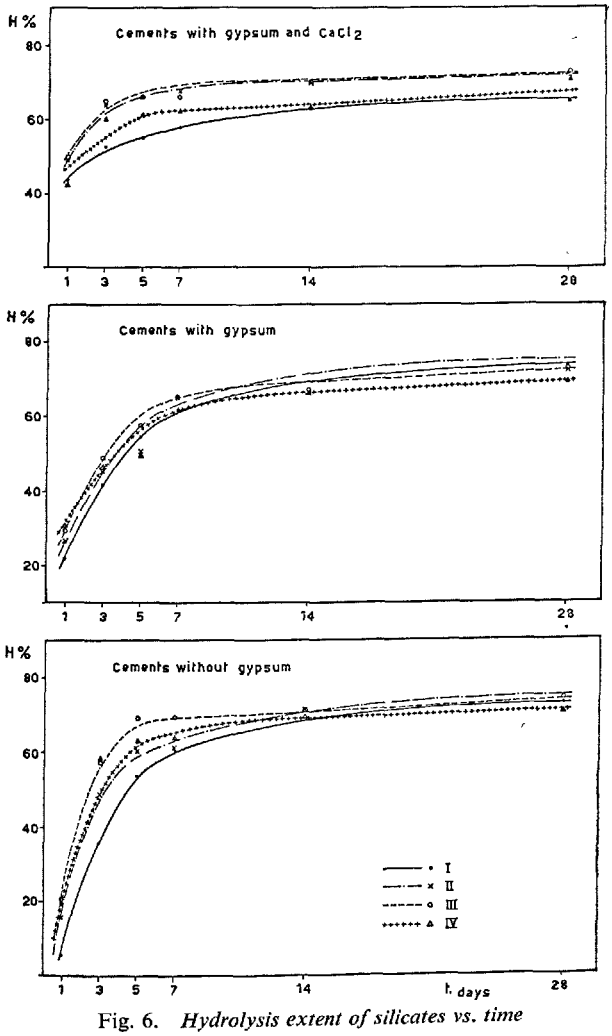

Fig. 6. *Hydrolysis extent of silicates vs. time*

Table 8. *Optimum C_3A percent for hydrolysis extent of silicates at different ages*

	1 day	3 days	7 days	28 days
Cements without gypsum	10.9	10.3	9.6	7.2
Cements with gypsum	—	10.2	9.2	5.8
Cements with gypsum and $CaCl_2$	9.7	8.5	8.2	6.2

In Table 9 there are reported the content of non-evaporable water of the hydrated pastes at various ages and the amount of the fixed water in the hydration products. This is calculated by subtracting the amount of the combined water in $Ca(OH)_2$ from the amount of the non-evaporable water.

The course of the non-evaporable water is affected both by the rate of hydrolysis of the silicates according to the above considered course and by the variable amount of the aluminates present. Generally it is noted that the amount of combined water increases within the same series with the tricalcium aluminate content. On passing from a series to another, the reactions of hydration to take into consideration become too much complex for an easy comparison.

Development of the Specific Surface of the Hydrated Pastes

The hydrated pastes of the cements with gypsum added, at ages of 1, 7, 28 days were tested for specific surface. The measurement was carried out by adsor-

Table 9. *Non-evaporable and fixed water of htdration of cement pastes*

		1 day	3 days	5 days	7 days	14 days	28 days	60 days	90 days
Cements without gypsum:									
N. 1	non-evaporable water %	3.46	9.19	12.28	14.94	17.44	19.56	20.10	22.30
	fixed water %	3.03	6.55	8.35	10.51	12.59	14.21	14.49	16.20
N. 2	non-evaporable water %	5.22	10.63	15.00	17.14	17.95	20.02	20.18	22.37
	fixed water %	4.05	6.97	10.49	12.57	12.62	14.56	13.85	15.45
N. 3	non-evaporable water %	6.25	11.66	16.32	18.30	19.82	20.84	21.40	22.85
	fixed water %	4.74	7.41	11.20	13.16	14.55	15.35	15.81	16.26
N. 4	non-evaporable water %	5.79	12.88	17.58	20.19	21.95	22.42	23.49	23.87
	fixed water %	4.34	8.47	12.84	15.38	16.70	17.10	17.92	17.45
Cements with gypsum:									
N. 1	non-evaporable water %	5.39	10.69	12.24	12.88	16.16	17.64	20.60	20.92
	fixed water %	3.83	7.68	8.42	8.42	11.36	12.36	14.95	15.06
N. 2	non-evaporable water %	7.40	11.65	14.44	15.01	17.57	19.63	21.10	21.22
	fixed water %	5.57	8.56	11.10	10.55	12.95	14.69	15.37	15.24
N. 3	non-evaporable water %	7.96	14.44	15.22	16.84	19.08	19.13	21.26	22.44
	fixed water %	5.94	11.08	11.26	12.32	14.51	14.09	15.73	16.78
N. 4	non-evaporable water %	8.37	12.30	15.71	18.11	20.77	20.97	21.75	24.62
	fixed water %	6.28	9.14	12.38	13.92	16.28	16.25	16.87	19.61
Cements with gypsum and $CaCl_2$:									
N. 1	non-evaporable water %	11.75	15.29	16.28	17.27	19.47	20.95	21.30	21.78
	fixed water %	8.61	11.51	12.33	13.11	14.96	16.34	16.62	16.78
N. 2	non-evaporable water %	13.00	15.49	17.81	18.32	21.33	21.46	21.82	22.02
	fixed water %	9.65	11.09	13.28	13.71	16.53	16.54	16.82	16.70
N. 3	non-evaporable water %	11.05	14.28	16.24	17.32	19.47	20.71	21.23	21.94
	fixed water %	7.60	9.81	11.72	12.78	14.64	15.68	16.19	16.71
N. 4	non-evaporable water %	10.98	12.20	14.55	15.26	20.21	20.44	21.12	21.82
	fixed water %	8.09	8.13	10.53	11.06	15.94	15.64	16.30	16.79

Table 10. *Specific surfaces of hydrated pastes of cements with gypsum added*

	Specific surface m^2/g			
	1 day	3 days	7 days	28 days
Cement N. 1	13.61	34.82	41.05	71.39
" N. 2	17.12	38.51	49.47	101.48
" N. 3	23.56	45.05	48.28	51.43
" N. 4	31.05	42.31	48.16	48.76

Table 11. *Optimum C_3A percent for specific surface of hydrated pastes of cements with gypsum added at different ages*

1 day	3 days	7 days	28 days
—	10.7	7.4	5.8

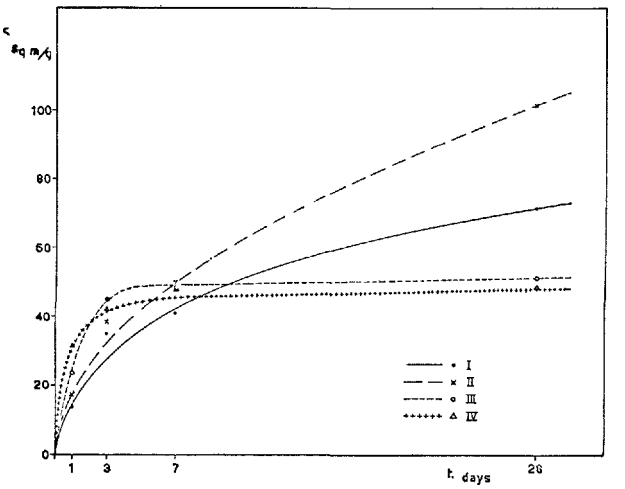

Fig. 7. *Specific surface vs. time. Cements with gypsum added.*

ption of nitrogen from mixtures nitrogen-helium after the B.E.T. method (16) by means of a Perkin-Elmer Sorpmeter mod. 212-D. Before being tested, the sample were degased for two hours at 150°C in helium stream.

The results are reported in Table 10, whereas the development of specific surface of the various samples is plotted in Fig. 7 as a function of the time.

On comparing this development with those of strengths and hydrolysis extent obtained for the same series (Figs. 2b and 6b), a good agreement is observed. This is also confirmed by the values, given in Table 11, which refer to the calculation of the percentage of C_3A corresponding to the maximum specific surface at the various ages (see Tables 7 and 9).

Discussion of the Results

The experimental results may be summarized, on the whole, as follows:

The presence of increasing C_3A contents in a portland cement has a sharply positive action on the devel-

opment of the strengths, particularly at the early ages. Such influence tends to become less appreciable, or even deleterious, if C_3A is present in too high amounts, at the most advanced ages. This is at least the results at the conditions of at our test.

The presence of increasing C_3A contents affects catalytically the hydration of C_3S; the rate of the lime supersaturation of the contact solution with the cement pastes increases and earlier appear appreciable amounts of free lime in the solid phase.

The hydrolysis extent of silicates rises with the C_3A content, especially at the early ages. Afterwards, the influence of C_3A becomes less appreciable, or even if high amounts of C_3A are present, its effect is negative for the progressing of the hydration.

In the first stage of hydration, the specific surface of the hydrated pastes rises sharply with the C_3A content. At the subsequent hydration stages the cements of high C_3A present a very slow development of their specific surface.

The results from the measurements of compressive strengths, hydrolysis extent of silicates, and specific surface of the hydrated pastes are concordant in indicating the presence of an optimum C_3A amount for these quantities, which ranges from 10–11 per cent at the early ages to 6–7 per cent at more advanced ages.

We intend to extend our investigation to other cement series by varying the C_3S content for the various series, but keeping it constant, as we have already done, for each series.

Furthermore, gypsum and calcium chloride produce an accelerating effect on the cement hydration, acting particularly on the C_3S. However they do not appreciably alterate the influence of the C_3A and the optimum values of this constituent at the different ages.

Most of our experimental results seem to agree with the theories of W. Foster (14) and P. Rehbinder (17), as well with the recent views of A. Joisel (18) on the hydration mechanism of tricalcium aluminate in portland cement.

In the presence of water, tricalcium aluminate goes into solution and dissociates into its constituents to give, among other things, calcium ions. Lime and alumina in solution then recombine as tricalcium aluminate hydrate, or, if gypsum is present too, as calcium sulpho-aluminate. These compounds precipitate from the supersaturated interstitial solution in the colloidal form at first giving hydrophil products of high specific surface which adsorb other ions and large amounts of water. The contribution of such compounds to strengths is negligible. Later the colloidal hydrates crystallize as local agglomerates which assemble and grow to give greater crystals of well defined structure and chemical composition.

It seems to us that the interpretation of the influence of the aluminates on the calcium silicates during hydration, as given by Bogue and Lerch (6), be inacceptable. According to these authors, the increase of strengths at early ages would be due to a lowering of water amount available to silicates, that is, a kind of local reduction of the *w/c* ratio caused by the rapid hydration of aluminates.

It is known that cement pastes, after a rapid surface reaction, prosecute to hydrate very slowly because of the difficulty met by the water in penetrating into the internal structure.

Therefore, the effect of C_3A could be that of promoting, with the rapid hydration and the originary formation of highly hydrophil colloidal products the penetration of water to the interior, so that greater amounts of this become available for the hydration of silicates which is anticipated and its rate is increased.

For this reason, higher C_3A contents at the early ages would not only give products of high specific surface, but also produce an accelerating effect on the hydration of silicates and consequently on the passing into solution of hydrolysis lime as well on the strength development.

Successively, however, the aluminate crystallize with formation of crystalline products which by themselves give a negligible contribution to the specific surface of hydrated pastes and to the strengths. Moreover, they would hinder the progress of hydration of silicates with their occupying the intergranular space, and would bring about a solution of continuity in the gels of hydrated silicates. In the presence of high C_3A amounts that would negatively effect the development of specific surface, hydrolysis lime and strengths at later ages. It would, thereafter, establish a balance between a sharply positive initial action of the increasing C_3A content and a subsequent negligible or even deleterious one. That would result in the appearance of an optimum amount of this compound ranging from high contents, at the early ages, to lower values, at the more advanced ages.

The value of such an optimum per cent of C_3A will be, of course, dependent on the amount of the more sharply hydraulic products, such as C_3S, in the cement. A systematic study of the C_3A action in cement also at other levels of C_3S amounts shall be therefore interesting.

Gypsum and calcium chloride accelerate the hydrating of C_3S appreciably (3). Their effect on the hydration of tricalcium aluminate has not yet been investi-

gated thoroughly (18, 19). It seems us, however, it is lower than that on C_3S and the mechanism of hydration is not essentially modified by it. Indeed, the phenomena due to different C_3A contents keep their particular course in the presence of gypsum and calcium as well. The accelerating effect of these salts on the C_3S hydration has the only result of making the hydration of C_3A less noticeable at the early ages, which gives account for the slightly lower optimum values of C_3A for the extent of hydrolysis of silicates and for the mechanical strengths at different ages.

Conclusions

The results of our investigation demonstrate that tricalcium aluminate influences positively the rate of hydration of the other constituents of cement, particularly the tricalcium silicate, and the development of mechanical strengths, principally at the early ages.

This is of great practical importance for the production of rapid hardening cements without having to resort to the addition of substances, which, as calcium chloride, may bave secondary negative effects under certain conditions.

The significance of the obtained results shows clearly the need of prosecuting a thoroughly study on the mutual influence of the cement compounds during hydration.

References

1. A. Rio, A. Celani and M. Collepardi, "A contribution to the study of portland cement hydration at the earlier ages" (in Italian), Ind. Ital. Cemento **35**, 275–286 (1965).
2. R. Turriziani, A. Rio and M. Collepardi, "Some observations on the hydration mechanism of tricalcium silicate" (in Italian), Ind. Ital. Cemento 35, 635–644 (1965).
3. A. Celani, M. Collepardi and A. Rio, "The influence of gypsum and calcium chloride on the hydration of tricalcium silicate" (in Italian), Ind. Ital. Cemento **36**, 669–678 (1966).
4. F. M. Lea and C. H. Desch, The Chemistry of Cement and Concrete, 2nd Ed., p. 82—Arnold Publ., London, England (1956).
5. P. H. Bates and A. A. Klein, "Properties of the calcium silicates and calcium aluminates occurring in portland cement" J. Frank. Inst. **182**, 398–401 (1916).
6. R. H. Bogue and W. Lerch, "Hydration of portland cement compounds", Ind. Eng. Chemistry **26**, 837–847 (1934).
7. W. Lerch, "The influence of gypsum on the hydration and properties of portland cement pastes", Proc. Am. Soc. Testing Materials **46**, 1252–1293 (1946).
8. S. Brunauer and S. A. Greenberg, "Hydration of tricalcium silicate and betadicalcium silicate at room temperature", Proc. of the 4th Int. Symp, on the Chem. of Cement, Washington 1960, Natl. Bur. Std. Monograph **43**, 135–165 (1962).
9. L. E. Copeland and D. L. Kantro, "Kinetics of the hydration of portland cement", Proc. of the 4th Int. Symp. on the Chem. of Cement, Washington 1960, Natl. Bur. Std. Monograph **43**, 443–453 (1962).
10. D. L. Kantro, S. Brunauer and C. H. Weise, "Development of surface in the hydration of calcium silicates", Advances in Chemistry Series **33**, 199–219 (1961). J. Phys. Chem. **66**, 1804–1809 (1962).
11. E. E. Pressler, S. Brunauer, D. L. Kantro and C. H. Weise, "Determination of the free calcium hydroxide contents of hydrated portland cements and calcium silicates", Anal. Chem. **33**, 877–882 (1961).
12. N. Fratini "Research on the CaO of hydrolysis in cement pastes" (in Italian), Ann. Chim. (Rome) **40**, 461–469 (1960).
13. W. C. Hansen and E. E. Pressler, "Solubility of $Ca(OH)_2$ and $CaSO_4 \cdot 2H_2O$ in dilute alkali solutions", Ind. Eng. Chem. **39**, 1280–1282 (1947).
14. W. D. Foster, "Hydration of C_3A" Cement and Cement Manuf, **6**, 97–104 (1933).
15. S. Brunauer, L. E. Copeland and R. H. Bragg, "The stoichiometry of the hydration of tricalcium silicate at room temperature. II. Hydration in paste form", J. Phys. Che . **60**, 116–120 (1956).
16. S. Brunauer, P. H. Emmett and E. Teller, "Adsorption of gases in multimolecular layers", J. Am. Chem. Soc. **60**, 309–319 (1938).
17. P. A. Rehbinder, "Physico-chemical concepts on the setting and hardening of mineral binders" (in Russian), Reports of Symposium on the Chemistry of Cements, State Publication of Literature on Structural Materials, Moscow, 1956, pp. 125–137.
18. A. Joisel, "Chemical action of admixtures: accelerators and retarders" (in French), Reports of International Symposium on Admixtures for Mortar and Concrete, Brussels, 1967, pp. 41–55.
19. N. Tenoutasse, "Hydration mechanism of C_3A in presence of $CaCl_2$" (in French), Rev. Mat. Constr. Trav. Publ. **622–623**, 265–272 (1967).

Oral Discussion

Shigeru Yamane

I will make a brief discussion of the interesting paper of Dr. Celani and coworkers.

1. The authors stated that C_3A acts catalytically on C_3S. What is the mechanism of this catalytic action?

2. In order to clarify the effect of C_3A, I think it is necessary and important that not only the alkalinity and C_2O, SO_3, Cl^- but also Al_2O_3 and SiO_2 in the liquid phase have to be investigated. What is your opinion on this point?

3. The addition of calcium chloride certainly promotes the hydration of C_3A and C_3S. According to my experimental results, the addition of $CaCl_2$ increases rapidly the amounts of Al_2O_3 and SiO_2 in the liquid phase in early stage of hydration of cement. With much Al_2O_3 in the liquid phase, the concentration of SO_3 decreases rapidly due to the formation of ettringite type hydration product. Namely, there is the interrelation between the concentrations of SO_3 and Al_2O_3 in the liquid phase. These facts can be useful keys for the clarification of the above problem.

Oral Discussion

Hans N. Stein

There is an apparent contrast between the results obtained by Celani, Moggi and Rio (especially as regards data on CaO of hydrolysis at very early ages) and those reported by de Jong, Stein and Stevels (see Supplementary Paper II-35): whereas Celani c.s. report an acceleration of C_3S hydration by small amounts of C_3A, de Jong c.s. find a retardation.

However, it should be kept in mind that Celani c.s. investigated systems at 40°C, at which temperature the recrystallization of hexagonal hydrates to C_3AH_6 is quite different from that at 25°C. A second complicating factor may be that Celani c.s. investigated systems of a much more complex character than de Jong c.s.

Authors' Closure

Adriano Celani, Pietro A. Moggi and Arturo Rio

Reply to S. Yamane

1) The positive influence of C_3A on the hydration of C_3S at early stages and of alite in portland cement has been shown by the authors, according to L. E. Copeland and D. L. Kantro, Principal Paper "Hydration of Portland Cement" Part II—Session 5.

About the reaction's mechanism, the authors tried to give in their paper a reasonable explanation. The subject is still a matter of investigation and the authors will give to Mr. Yamane all the eventual information.

2) In order to explain 1) the authors emphasize the opportunity to determine the Al_2O_3 and SiO_2 in the liquid phase.

3) Authors think there is no correlation between the accelerating action of $CaCl_2$ on C_3S and on alite in portalnd cement and the possible increase of the interaction between Al_2O_3 and SO_3 as reported by Mr. Yamane.

Reply to H. N. Stein

1) The positive influence of C_3A on the hydration of C_3S at early stages and of alite in portland cement has been shown by the authors, according to L. E. Copeland and D. L. Kantro, Principal Paper "Hydration of Portland Cement" Part II—Session 5.

About the reaction's mechanism, the authors tried to give in their paper a reasonable explanation. The subject is still a matter of investigation and the authors will give to Mr. Stein all the eventual information.

2) Authors agree that the investigated systems have a much more complex character than de Jong c.s. They, however, think the recrystallization of hexagonal hydrates to C_3AH_6 cannot explain the apparent contrast between the results.

Author Index

For Volume II

Subject Index

For Volume II

D

E

F

T

U

V

W

X

Y

Z

Proceedings of
The Fifth International Symposium
on the
Chemistry of Cement
Tokyo, 1968

PART II
PROPERTIES OF CEMENT PASTE AND CONCRETE
(Volume III)

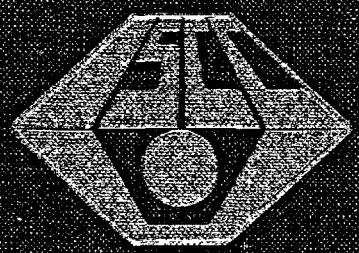

The Organizing Committee
for the Fifth International Symposium
on the Chemistry of Cement
The Cement Association of Japan

Proceedings of
The Fifth International Symposium
on the
Chemistry of Cement
Tokyo, 1968

PART III
PROPERTIES OF CEMENT PASTE AND CONCRETE
(Volume III)

Symposium held October 7–11, 1968 at the
Tokyo Metoropolitan Festival Hall, Tokyo

Proceedings published in 4 volumes December 31, 1969

Explanatory Notes

Abbreviations.

The following symbols, which have been universally recognized by cement chemists for formulating more complex compounds, are used interchangeably with the respective oxide formulas throughout this book:

$C = CaO$, $S = SiO_2$, $A = Al_2O_3$, $F = Fe_2O_3$,
$M = MgO$, $N = Na_2O$, $K = K_2O$, $H = H_2O$,

Less common abbreviations of this type are defined as they occur.

Commonly used abbreviations of more general nature are as follows:

DTA = differential thermal analysis
EPMA = electron probe micro analysis
IR = infrared
NMR = nuclear magnetic resonace
psi (or p.s.i.) = pounds per square inch
rh (or RH) = relative humidity
w/c (or W/C) = water — cement ratio
XRD = X-ray diffraction

Identification Number of Supplementary Papers

Example: Supplementary Paper III—50, III is session III and 50 is the arrival number of contribution. This number coincides with the number used in the preprint of papers distributed in advance of the symposium.

Contents

Volume III

Part III. Properties of Cement Paste and Concrete

Session III-1 Structures and Physical Properties of Cement Pastes

Session III-2 Durability of Concrete

Session III-3 Carbonation of Concrete

Session III-4a Hydration of Portland Cement Paste at High-Temperature under Atmospheric Pressure

Session III-4b High-Temperature Curing of Concrete under Atmospheric Pressure

Session III-5 High-Temperature Curing of Concrete under High Pressure

SESSION III-1 STRUCTURES AND PHYSICAL PROPERTIES OF CEMENT PASTE

Principal Paper Structures and Physical Properties of Cement Paste

George J. Verbeck and Richard H. Helmuth*

Synopsis

Pseudomorphs of the original cement grains in hardened pastes result from differences in hydration products deposited within and between the original grain boundaries. Structures of the various hydration products, as seen in the electron microscope are described. Pore size distributions for cement pastes obtained by a variety of methods are consistent. Surface area values measured by nitrogen adsorption decrease with the water-cement ratio. The distinctions between capillary, gel, and non-evaporable water are reviewed. The gel water resembles interlayer water in clays.

Strength depends primarily on the capillary porosity. The uniformity of distribution of the hydration products explains the effects of gypsum content and temperature.

Initial drying shrinkage is relatively independent of clinker composition at "optimum" gypsum content. The dependence of this shrinkage on water loss suggests independent effects from different classes of water in the paste. The dependence of this shrinkage on water-cement ratio and duration both of curing and of subsequent drying is discussed. Carbonation shrinkage varies with the ambient relative humidity. Releases of equal amounts of water by carbonation or drying result in equal shrinkages. Cycles of wetting and drying reveal that volume changes have reversible and irreversible components.

Thermal expansivity depends on moisture content, rate of temperature change, and the nature of the solid phases. Thermal conductivity changes little with water-cement ratio or temperature.

The elastic properties are primarily related to capillary porosity. Inelastic properties are discussed. The relationship between permeability and capillary porosity applies even to bleeding fresh pastes. Available data on moisture diffusion are sufficiently consistent to permit determination of the activation energy. The importance of osmotic and electrokinetic effects in studies of liquid flow is discussed.

Introduction

This paper is a selected review of the state of knowledge of the structure and physical properties of cement pastes. We have not attempted to repeat detailed review of each of the topics treated in the corresponding paper of the Fourth Symposium (1). Apart from space limitations this is because little information can be added to some of the topics treated in the 1960 review. On the other hand, we have included much new material, particularly on strength and shrinkage, and have included some properties not previously included.

In addition, some differences from previous points of view are presented. We have tended more to include primary data concerning the actual behavior of the pastes under different conditions, and less theoretical interpretation. We have, however, presented new interpretations of physical properties in terms of features of the structure wherever desirable.

*Portland Cement Association, Research and Development Laboratories, Illinois, U.S.A.

A second difference in point of view concerns the state of the water in hardened pastes. This has developed because it has become increasingly clear that much of the evaporable water is in a more highly organized state than previously supposed. Although it is not yet possible to make quantitative classifications different from those based on the concepts of gel water and capillary water, there is considerable evidence that some of the evaporable water in hardened pastes exists in distinct states similar either to the interlayer water in swelling clays or water of crystallization. Such water is therefore a component of the structure of the paste. Changes in water content therefore have important effects on the physical properties and dimensional stability of the structure.

The morphology of the hydration products as revealed by electron microscopy was covered in detail in the Fourth Symposium (2). We have therefore given only a brief summary of such work, and combined such results with newer methods of investigation of the paste structure, as given in the next section.

Structures of Hardened Pastes

In regard to the structure of hardened paste we will first consider the morphology or microstructure of the solid components of the hardened paste, then the microstructure of the pore system of the paste, and finally discuss the nature of the state of the water component of paste.

Microstructure of Hardened Paste

The microstructure of hardened paste has been studied by direct optical methods and by the electron microscope observing both the fragmented dispersed hydrated particles and replicas of sawed or fractured surfaces.

Optical Studies

Although optical examination of portland cement paste reveals little about its detailed structure, by such examination it can be directly observed that the space between clinker grains, initially water filled, soon becomes filled with hydration products formed by dissolution of portions of the clinker grains. Portions of the larger clinker grains hydrate and form hydration products in the space within the original grain boundary created by the prior solution process. These hydration products have optical properties which are somewhat different from those of the products precipitated in the water-filled space (3, 4) and thus remain visible as pseudomorphs of the original clinker particles. Under such conditions the original clinker structure appears to be preserved in the pseudomorph; outlines of the silicate phases are preserved. Portions of the larger clinker grains may remain unhydrated within the paste depending upon clinker grain size, the original water-cement ratio (w/c), of the paste, and the duration of exposure to water.

Crystals of calcium hydroxide can be seen to form in the waterfilled space between clinker grains about 4 hours after mixing. These crystals grow around any impediment, e.g., there is a continuous intergrowth of calcium hydroxide and gel; in mortars, grains of sand frequently appear to be engulfed in calcium hydroxide.

The hydration products other than calcium hydroxide are so finely divided that they cannot be resolved with an optical microscope, but the electron microscope has revealed information about the morphology of the hydration products as well as structure of the hardened paste. Information about morphology of hydration products is obtained by direct study of powdered and dispersed pastes; information about paste structure is obtained by electron microscopic examination of surface replicas of hardened pastes.

Electron Microscopic Studies

Direct electron microscopic examination of the individual products of hydration of cement pastes requires dispersion of the paste particles. Studies in which dispersion has been used have followed the course of hydration of cement, and also of the pure silicates, from the time of mixing of the paste through several days of hydration after which time the paste can no longer be properly dispersed. These studies have shown that hydration starts immediately upon contact of the cement with water. Ettringite is one of the first products that can be identified in cement pastes. It forms primarily as stubby hexagonal prisms on C_3A faces, but can also form as long hexagonal prisms away from cement particles in water-filled space. After about 2 hours thin acicular particles of calcium silicate hydrate are observed protruding from the surfaces of unhydrated grains of cement. These particles grow longer and broader to form thin laths which are striated along their length. At the time of final set they appear to be long enough and numerous enough to form an interlooking network through-

out the paste. By 24 hours the paste is somewhat difficult to disperse, but thin, striated sheets of calcium silicate hydrate are observed. The edges of the undispersed masses also show sufficient detail to confirm that these masses are aggregations of the thin sheets which sometimes occlude crystallites of calcium hydroxide (5, 6, 7).

The calcium silicate "gel" formed by hydration of pure calcium silicate is poorly crystalline. However a significant fraction of the gel comprises particles, which appear to be rolled sheets, that are sufficiently well crystallized to give single-crystal electron diffraction patterns. Occasionally the X-ray diffraction patterns of a wet, hardened paste of C_3S will show a layer spacing (8).

In comparison with the gel formed by hydration of pure calcium silicates the gel formed by hydration of cement is not nearly so well crystallized. Indeed, single-crystal electron diffraction patterns of gel particles have not been obtained. Since isomorphous substitution of aluminum and sulfur for silicon is possible in the calcium silicate hydrate "gel" (9), and since these substitutions are accompanied by changes in the morphology of the gel, it is likely that such substitution is the cause of the more nearly amorphous character of the gel formed from cement as compared to that formed from pure calcium silicate. Cement pastes stored under water for up to 10 years do not show any marked increase in crystallinity of its hydration products.

Electron microscopic examination of carbon replicas gives information about the arrangement of hydration products within hardened paste. Different techniques of preparing surfaces for replication emphasize different aspects of the structure of pastes. Two types of surfaces have been examined: (1) surfaces prepared by cutting a slice of paste with a diamond saw on a sectioning machine, using water as the saw lubricant, and (2) surfaces prepared by fracturing pastes.

Flushing the paste surface with water during the cutting dissolves calcium hydroxide crystallites in the surface region but reveals aggregations of calcium silicate hydrate "gel" and the crystallites of the hydration products of the alumina bearing phases. Details of the techniques used and several examples of replicas prepared from *sawed* surfaces can be seen in paper II-5 (Figs. 19, 22, 30, and 31) of this symposium. Comparison of the form of the calcium silicate hydrate seen in these replicas with that found by direct electron microscopic examination suggests that the particles seen in replicas are indeed aggregations of thin sheets. Pores both within and between these aggregations are too small to be revolved by the replica.

The aggregations of calcium silicate hydrate "gel" are not so prominent in replicas of *fractured* surfaces. Apparently the fracture passes through the aggregations instead of along boundaries between them. However cavities that may be several microns across are frequently seen; these contain acicular particles which implies that they grew in initially water-filled free space. Most frequently the particles in the cavities appear to be fibrous—these are calcium silicate hydrate—but sometimes crystallites of ettringite can be recognized protruding from the walls.

Fig. 1 is an example of a fractured surface of moist-cured hardened portland cement paste. The lower part of the field shows fractures approximately perpendicular to the cleavage plane of calcium hydroxide. It is likely that the striations in the crystal result from the manner in which gel and calcium hydroxide grow together which is illustrated at left in the field. In the upper part of the field, to the right of center, there is a cavity, approximately 6μ long, partially filled with a network of gel laths and a few prisms of ettringite (10).

Pore Size Distributions

General Considerations

The water-filled spaces between the cement particles in the fresh cement paste may be regarded as an interconnected capillary system. As hydration pro-

Fig. 1. *Photomicrograph of a carbon replica of a fractured hardened cement paste surface*

ceeds these spaces become partly filled with gel and microcrystalline hydrate particles. However, the manner of filling of the original water-filled spaces with hydration products depends upon the particle size distribution of the cement, upon the water-cement ratio, and upon the availability of water during hydration. If partial drying occurs during hydration, large pores empty and precipitation from solution cannot then occur in such spaces. We may thus expect differences in the pore size distributions depending upon whether the paste was kept saturated, kept sealed and hence allowed to self-desiccate, or allowed dry by direct loss of water.

Pore size distributions can be calculated from either of two different kinds of experimental results: 1, porosimetry, in which the volume of mercury that is forced into a porous system is measured as a function of the applied pressure, and 2, capillary condensation of vapors from either the adsorption or desorption isotherm of the porous system. In both techniques the Kelvin equation is used with an assumption that must be made about the shapes of pores. The assumption of a pore shape influences the calculated pore size distribution because the pressure at which a pore fills depends upon the curvature of a meniscus and therefore upon the shape of a pore. Most commonly the pores sizes are calculated as if they were either a system of cylindrical capillaries, or a system of parallel plates. Recently a method of calculating the pore size distribution without a model for the shapes of the pores has been proposed and it utilizes the "hydraulic radius" (pore volume/pore wall area), as a measure of pore size (11).

Mercury Porosimetry

Fig. 2 shows results of pore size distributions

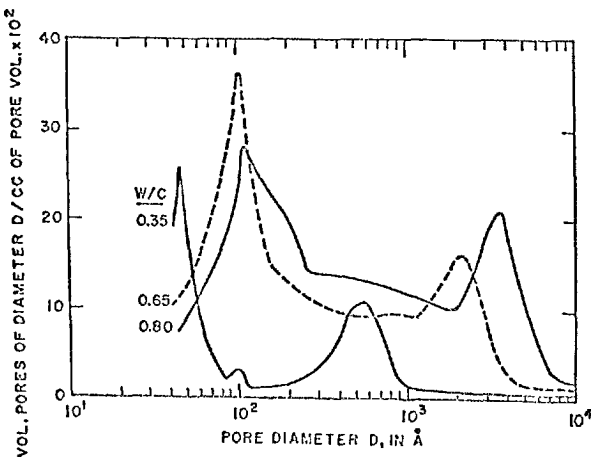

Fig. 2. *Pore size distributions of cement pastes, moist cured for 11 years, obtained with a high pressure mercury porosimeter.*

obtained with a high pressure (50,000 psi) mercury porosimeter (12). Results for 11 year moist-cured cement pastes at three water-cement ratios, 0.35, 0.65 and 0.80, are shown. The results span more than three orders of magnitude, from about 9×10^4 to about 40 Å. A logarithmic abscissa is used. The curves has been normalized. Each curve shows two clearly defined maxima. For the 0.35 paste maxima occur at pore diameters of 45 and 550 Å; for the 0.65 paste maxima occur at 105 and 2100 Å; for the 0.80 paste maxima occur at 110 and 3500 Å.

The large diameter maxima are in substantial agreement with those of another study (13) showing that they represented a class of pores that depended upon water-cement ratio, cement fineness, and curing. These are usually denoted by the term "capillary" pore (14). The small diameter maxima occurred at somewhat larger diameters than in Fig. 2, possibly because of differences in curing times. In addition to these maxima each distribution includes measureable pore volumes of intermediate sizes as well as very large pores with diameters exceeding 10^4 Å.

The main features of these pore size distributions are supported by two other kinds of experimental evidence: 1, as discussed above, large cavities or pores, are observed by electron microscopic examination of surface replicas of hardened pastes, and 2, the studies of ice propagation in freezing experiments (15) gave evidence of a bimodal distribution of pores that are completely compatible with the mercury porosimeter results. This agreement is of special importance because the freezing experiments were performed with pastes that had never been dried and the porosimetry and adsorption measurements are made on dried pastes. Since drying is known to product irreversible changes of structure it is possible that the indicated pore structures would be different. These results, however, do not indicate any great changes in the pore structure during drying.

The sizes of pores given by both the mercury porosimetry and the freezing propagation studies are not necessarily the sizes of the pores filled, but only the sizes of the entry ways.

Pore Structure from Adsorption Isotherms

Pore size distributions have been calculated from measurements of nitrogen adsorptions, Fig. 3 (16), and cyclohexane adsorption, Fig. 4, on a series of hardened pastes made with water-cement ratios in the range from 0.35 to 0.70 (17). The distribution curves calculated from the cyclohexane isotherms are not strictly comparable to those calculated from nitrogen

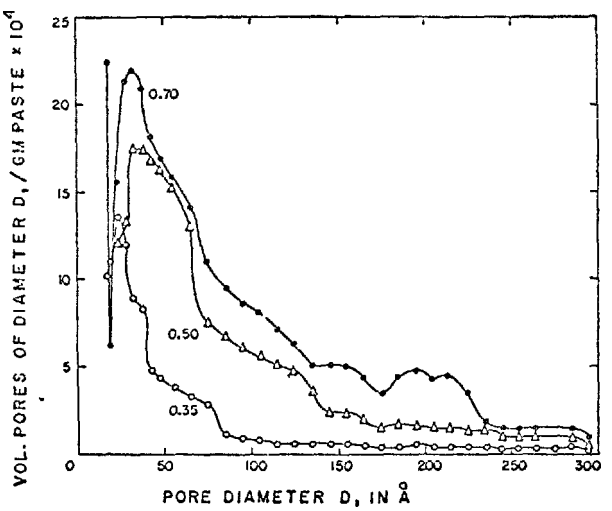

Fig. 3. *Pore size distributions of mature cement pastes obtained from nitrogen absorption*

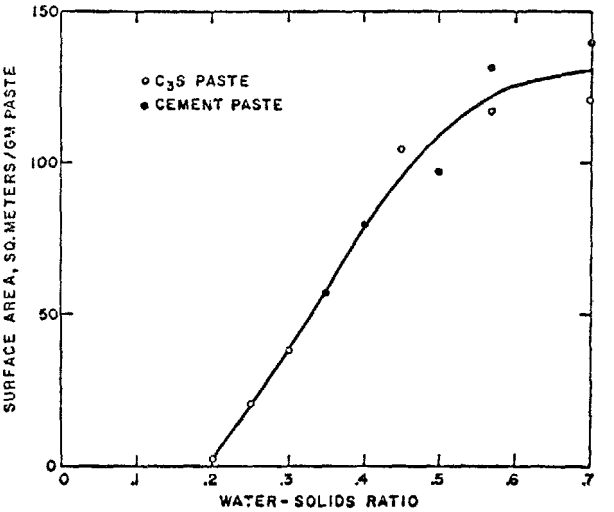

Fig. 5. *Nitrogen adsorption on cement pastes decreases with water-cement ratio*

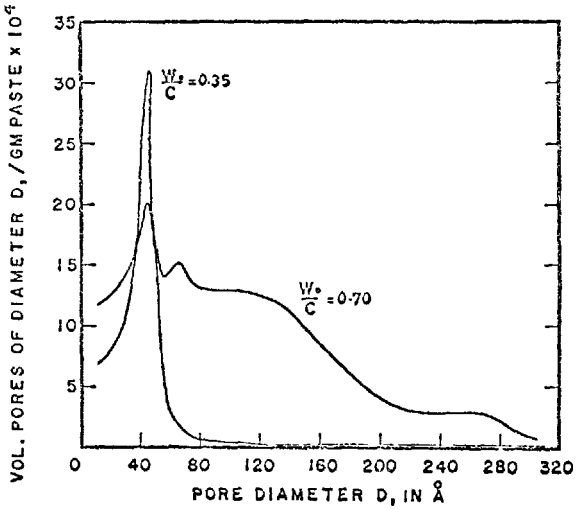

Fig. 4. *Pore size distributions of mature cement paste obtained from cyclohexane adsorption*

isotherms because the desorption branch was used for cyclohexane while the adsorption branch was used for nitrogen. All these distributions have a well defined mode; with cyclohexane the mode is at 45 Å for two pastes, one with $w_0/c = 0.35$, the other with $w_0/c = 0.70$; with nitrogen, the modes for these same two pastes were at 22 Å and 32 Å respectively. One cannot be certain whether the smaller diameters obtained from nitrogen resulted from its smaller molecular size or from using the adsorption branch of the isotherm. The effect of difference in size of the molecules is shown by the fact that the surface area and total pore volume calculated from cyclohexane isotherms were smaller than those calculated from nitrogen isotherms.

The largest pore diameters that can be calculated from sorption isotherm is limited to about 300 Å, consequently none of the these distributions reached a pore size large enough for the second mode shown in the porosimeter distribution curve.

The two methods agree in one respect; neither account for all the space occupied by evaporable water in hardened paste. About 70 percent of the pore volume is accounted for by the porosimeter and nitrogen in the more porous paste, cyclohexane fills less than 50 per cent of the space. A part of the effect is the result of molecular sizes. The inability of the porosimeter to fill all the space may be caused by the limited pressure than can be attained, but may also be caused by the inability of the non-polar molecule to enter some spaces that water can occupy.

It is well known that the "specific surface", (surface area per gram of cement gel), calculated from water-sorption data is a constant, approximately 200 square meters per gram, that is independent of w/c of the paste and its degree of hydration. Such is not the case for the specific surface as determined by nitrogen. The "nitrogen surface" is always smaller than the "water surface" and decreases with decreasing water/cement ratio of pastes (18). Recently a study of nitrogen surface areas of hardened pastes of tricalcium silicate with water-cement ratios as low as 0.2 was made (19). The results of this investigation agreed very well with results of other investigations using portland cement pastes. The lowest nitrogen area attained was 3.5 square meters per gram of gel on pastes with $w_0/C_3S = 0.2$ cured 14 months. The trend of the results, shown in Fig. 5, suggests that the

nitrogen area will become zero at a water-cement ratio slightly below 0.2.

The State of the Water in Hardened Paste

The state of the water in the pore system is important because any difference between the state of the water in the pores from that of liquid water implies the existence of forces on the water and reaction forces on the solid. This has important implications with respect to volume change and structural change phenomena.

Water in cement pastes may be arbitrarily classified into "evaporable water" and "non-evaporable water" (water not removed under a standard drying condition). The best defined drying condition for this purpose is drying in vacuum over ice at the dry-ice (solid CO_2) temperature, −79°C, sometimes called "D-drying" (20). The non-evaporable water determination is intended to remove nearly all of the "physically adsorbed" water and leave only "chemically bound" water. It is believed that this is accomplished, but there is uncertainty concerning the degree to which loss of the evaporable water represents loss of water of hydration.

The evaporable water in cement pastes may also be arbitrarily classified into "gel" water and "capillary" water (14). This is based upon the conception that the cement gel has a certain minimum porosity, which may be arbitrarily defined from measurements of water contents of saturated, well hydrated, low water-cement ratio pastes. In such pastes it is found that cement hydration virtually ceases before all the cement is hydrated. Such pastes are assumed to contain only gel water. Capillary water is defined as the difference between the total evaporable water of a paste and its gel water content.

The distinction between "capillary" water and "gel" water is useful in the discussion of the porosity of the paste for the following reason. By variation of water-cement ratio and curing time the capillary water content can be varied from zero to nearly the entire volume of the hydrated part of the paste. Hence it was possible to shown (21) by standard thermodynamic methods that the partial specific volume of the capillary water was constant at about 1.0. That is, capillary water in saturated pastes has near normal density. The gel water content, however, cannot be arbitrarily varied. Hence the partial specific volume of the gel water cannot be similarly determined, and various attempts have been made to estimate its volume by other methods (1).

The main problem then centers on the state of the gel water. This has two aspects: how much of the gel water is hydrate water, and what is the nature of that part of gel and capillary water not combined as hydrate water.

Evidence concerning the state of the water in pastes has been obtained from NMR (nuclear magnetic resonance) studies of some calcium silicate hydrates. The results have been summarized and compared with results obtained with ettringite, silica gel, and montmorillonite clays of different water contents (22). In NMR techniques one of the parameters measured is the transverse or spin-spin relaxation time, T_2. This quantity is a measure of the magnitude of local fields surrounding the protons. In strong local fields T_2 is very short because the resonating protons react quickly (spins flip over) to the local forces. In weak local fields T_2 is long. T_2 is thus a measure of how "tightly" the proton is bound. More correctly, T_2 is a measure of mobility of the magnetic moment of the proton rather than a thermodynamic property, such as bond energy. In liquid water T_2 is about 2.5 sec. In ice it is only 7 microseconds, indicating that the water molecules in ice have a strongly fixed "orientation".

Results of pulsed NMR measurements on some calcium silicate hydrates and other materials are given in Table 1. In an alite paste at 16 per cent RH values of T_2 ranged from 300–500 microseconds, in agreement with values for montmorillonite clay, 250 microseconds, and various other calcium silicate hydrate preparations at relative humidities ranging from 3×10^{-3} to 70 per cent. These results indicate that the water molecules in these systems were under the influence of local forces which caused relatively rapid reorientation after the pulsed radiation was cut off. A further indication of the strength of the local fields was given by the absence of spin echoes. Spin echoes are detected when the protons are in liquid water and water adsorbed on silica gel, but not in the calcium silicate hydrates, except at high water con-

Table 1. *Results of pulsed NMR measurements*

Sample number	Composition	Equilibrium relative humidity, %	Total water content, %	Echoes	T_2 microseconds
1	$C_{1.45}SH_{2.41}$	70	23.15	absent	300–500
2	$C_{1.28}SH_{2.08}$	50	21.96	absent	300–500
3	Alite	16	21.31	absent	300–500
4	C_3S	3×10^{-3}	16.62	absent	ca. 200
5	$C_3S + C_3A$	3×10^{-3}	17.70	absent	ca. 200
6	Ettringite	ca. 50	46	absent	300–500
7	Ettringite	< 1	13	absent	300–500
8	Silica gel	36	21	present	ca. 2300
9	Montmorillonite	20	18.02	absent	ca. 250
10	Montmorillonite	80	24.00	absent	ca. 320

tents.

The first five samples shown in Table 1 are samples in which no capillary water was present. The first two were synthesized from calcium hydroxide and silica gel; neither had capillary pores. The third was an alite paste that had been dried sufficiently to empty the capillaries. The fourth and fifth samples had only non-evaporable water. The T_2 values obtained for these materials are of the same order of magnitude as those calculated from wide-line NMR measurements on hardened cement pastes (23). Thus the evaporable water present in the first three samples can be assumed to be in the same state as gel water in hardened cement pastes; the results show that gel water is probably interlayer water and suggest that NMR may provide a good measure of capillary porosity in saturated samples.

Similarity of the calcium silicate hydrates to swelling clays is not limited to the spin-spin relaxation times. In addition, we may note that: 1) The montmorillonites and zeolites lose water continuously as do cement pastes even though the lattice spacing changes in discreet (1, 2, etc.) monomolecular layer steps. 2) The swelling of pastes is limited, as in the zeolites, rather than unlimited, as in the montmorillonites. 3) The irreversible loss of water and shrinkage during D-drying is very like the irreversible collapse of structure of the swelling clays observed during strong drying. 4) Much of the evaporable water in cement pastes seems to be part of the solid structure because of the decrease of the elastic moduli caused by drying.

Physical Properties of Hardened Pastes

Strength

The strength of hydrated portland cement paste, as with other porous materials, depends primarily upon its capillary porosity or its degree of space filling. In addition, the strength of hydrated paste depends upon the uniformity of distribution of the hydration product within the microstructure of the paste.

The "classical" concept of the relationship between the strength of hydrated cement paste and "gel-space ratio" is shown in Fig. 6. This concept has proven most useful in connection with many interpretations regarding the strength properties of hydrated cement paste but perhaps has been somewhat misleading regarding the strength producting qualities of "tobermorite gel" per se. In addition, it has not been satisfactory in providing an understanding of certain other factors that can significantly affect the strength of cement paste, such as the SO_3 content of the cement or the hydration temperature. The information present in Fig. 6 regarding the relationship between the compressive strength and gel-space ratio (24, 14) can be used to provide the corresponding relationship between the strength and the "capillary porosity" of these pastes. Such information is shown in Fig. 7. Here we see that within the limits of the concept of "capillary porosity" or "calillary water", as previously discussed, there is a close relationship between the amount of this relatively less strongly bound water and strength. In this particular comparison the relationship appears almost linear but must be curvilinear because there is obviously no strength at "100 per cent capillary porosity".

Fig. 7 contains three datum points that are specifically identified and which represent the compressive strengths and capillary porosities measured of fully autoclaved cement pastes made at the indicated water-cement ratios. These pastes contained essentially no "gel" as measured by the normal water vapor adsorption techniques. It can be seen that when the strengths of these autoclaved pastes containing no gel are compared with those of pastes containing

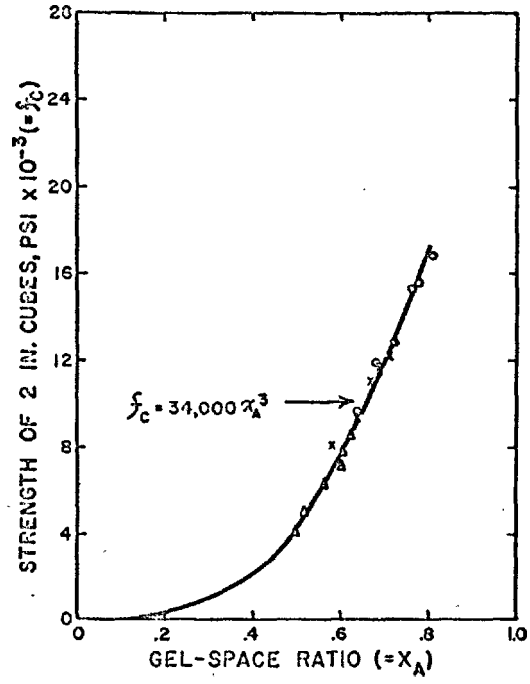

Fig. 6. *Cement paste strength depends on "gel-space ratio"*

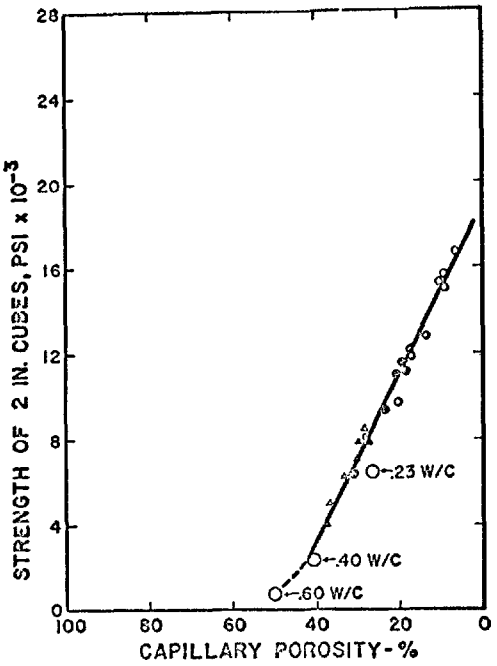

Fig. 7. *Cement paste strength depends on capillary porosity*

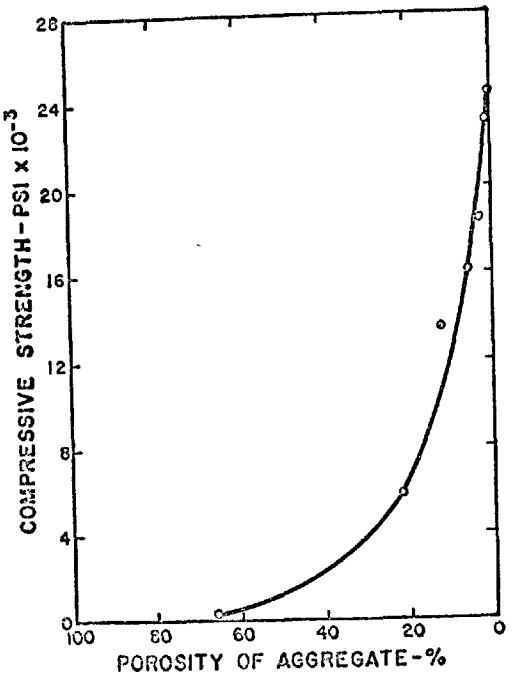

Fig. 8. *Aggregates strength depends on capillary porosity*

"gel" they demonstrated essentially the strength that would be anticipated on a capillary porosity basis. The point intended to be made here is that the low strength shown by autoclaved pastes (without added silica), which is quite low at water-cement ratios substantially above those of "normal consistency", is simply a result of the relatively low volume contributions of the hydration product produced under autoclaving conditions. Under normal curing conditions a product is obtained that has a volume approximately 2-fold that of the volume of the original cement. This is in large part due to the fact that the volume of this product is increased because the amount of water that it contained (interlayer water such as in a clay, zeolitic water, or water of crystallization) increases the volume of the hydration product and hence decreases the capillary porosity of the system. In essence it is more a matter of the degree of filling of the space rather than what the space is filled with.

Similar information can be obtained for other types of materials.

Fig. 8 shows the general relationship between the average compressive strengths and the average porosities of approximately 100 aggregates (25), the individual points representing the averages of groups of aggregates, ground on the basis of porosity range. It can be noted that the same general type of relationship is obtained.

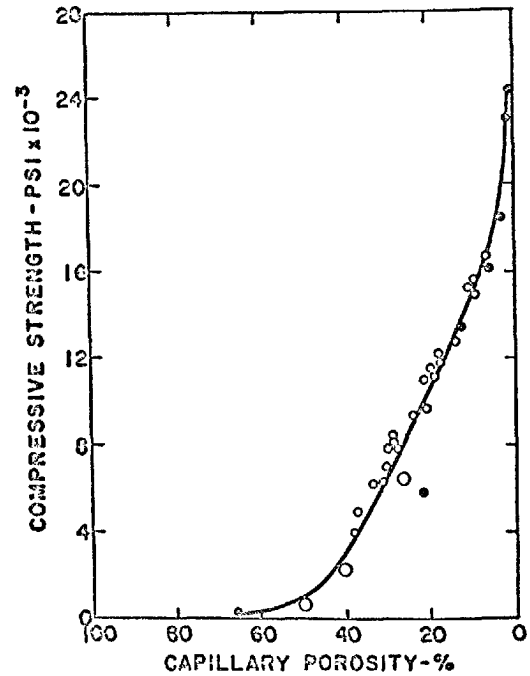

Fig. 9. *General relationship between capillary porosity and average strength of the various materials*

Fig. 9 compares all the data contained in Figs. 7 and 8. This represents data for normally cured paste containing "tobermorite gel" of normal curing, for

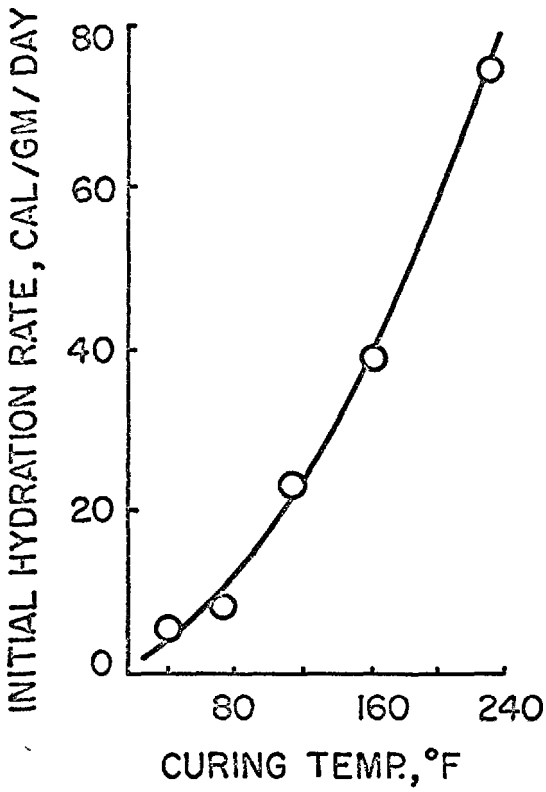

Fig. 10. *The initial rate of cement hydration increases with temperature*

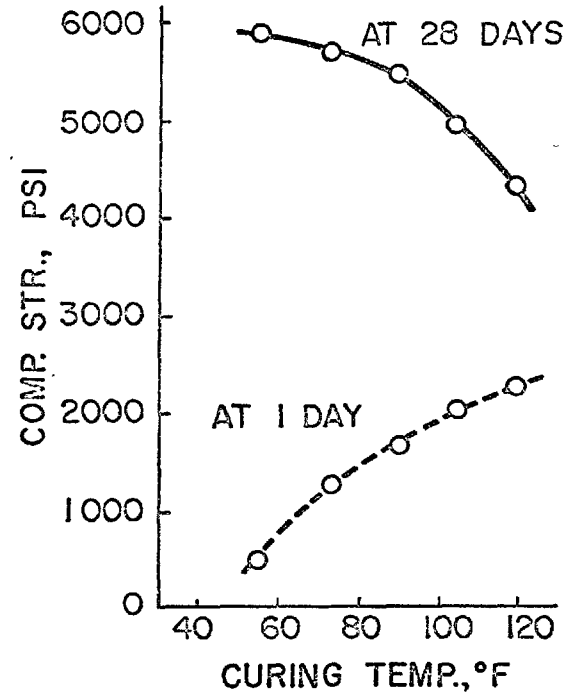

Fig. 11. *One day strength increases with increasing curing temperature but 28 day strength decreases with increasing curing temperature*

the crystalline non-gel-like material obtained by autoclaving, and for a wide variety of aggregates. This figure is taken to indicate that there is nothing greatly unusual about the strength properties of hydrated cement paste or of "tobermorite gel", but rather that in the case of any of these materials the primary factor influencing strength is the degree of space filling or, conversely, the capillary porosity of the system.

However, almost needless to say, it is well recognized that there are other factors that influence the strength of the various materials. There was considerable variation among the strengths of the aggregates within each group that were averaged to produce the relationship shown in Fig. 8. This variation certainly involves factors such as the size and distribution of the individual mineral constituents, the orientation of the bedding place during test and the elasticity of the material. Likewise, for normally hydrated cement paste, it is known that the strength that is developed by a hydrated paste is influenced by many factors other than its capillary porosity; these factors include the effect of "optimum" gypsum content and an apparently somewhat anomalous effect of hydration temperature, both effects will be shown below to be interpretable in terms of the early rate of cement hydration. However, it is also known that the SO_3 in a hydrating portland cement participates in the formation of the calcium silicate hydration product and thus may to some degree affect the inherent physical strength properties of the silicates.

The reaction between cement and water is like other chemical reactions in that the rate at which the reaction occurs increase with increasing temperature. Fig. 10 shows the relationship between the initial rate of hydration of cement, as measured by the rate at which heat is evolved by the chemical hydration reactions, and the temperature of the hydrating cement paste. The data cover the range from 40 to 230°F. The rapid increase of the initial rate of hydration of cement with hydration temperature would lead one to expect that at a given early age the strength of the concrete also would be higher, at a higher hydration temperature. That this expectation is true is shown in the lower curve of Fig. 11 which compares the compressive strengths of concretes after one day of moist curing at temperatures within the range 55 to 120°F. Thus, at 1 day, in the temperature range shown, the higher the curing temperature, the higher the compressive strength. One might expect that the same effect

would be true at later ages. However, the temperature variation of the strengths of these same concrete for a curing period of 28 days at these same temperatures is exactly opposite to that of the 1 day curve, as is shown in the upper curve of Fig. 11.

In the search for an explanation for these apparently anomalous results, the inherent nature of the hydration products obtained at different temperatures has been studied to see if it significantly changes with hydration temperature. The *chemical* nature of the hydration product can be evaluated to some degree from the relationship between the amount of water chemically combined and the heat evolved during the process of hydration. Fig. 12 shows immediately that the *chemical* nature of the hydration product, as measured by the ratio of the non-evaporable water to the heat evolved, does not vary with cement hydration temperature in the range from 40 to 230°F.

The *Physical* nature of the hydration product—that is, the degree to which the product is "colloidal"—can be evaluated from the amount of water vapor adsorbed by the product—its "surface area"—in relation to the amount of product formed, as measured by the heat evolved during hydration. Fig. 13 which contains such information, shows a measure of "surface area" per unit of hydration product (percent water vapor adsorbed at 36 per cent relative humidity per calorie of heat evolved) in relation to hydration temperature. Obviously the *physical* nature of the product of hydration is independent of the temperatures of hydration. Therefore the explanation of the variation of strength with temperature at later ages cannot involve either chemical or physical differences in the nature of the hydration product.

The explanation of the beneficial effect of high hydration temperatures on early strength and their detrimental effect on later age strength is believed, primarily, to involve two opposing factors. One factor is that an increased hydration temperature increases the initial rate of hydration and hence is beneficial to early hydration and to early strength. The opposing factor is that this same initial reaction, because of its rapidity, is detrimental to ultimate strength because it both retards subsequent hydration, as is indicated below, and because it produces a non-uniform distribution of hydration product within the paste microstructure. The non-uniformity of distribution within the microstructure of hydrated paste cannot be easily revealed by the classical methods for characterizing the hydration product, such as adsorption techniques.

One line of evidence for such an argument comes from the early hydration reactions of cement, as revealed by the conduction calorimeter. The heat evolution peak that occurs at about 6 to 8 hours at normal temperatures appears to have particular significance. During this period the cement is undergoing very rapid reaction at normal temperatures; perhaps 20 per cent of the cement hydrates a period of 2 or 3 hours. At elevated curing temperatures, these reactions are accelerated; at 105°F as much as 30 to 40 per cent of the cement may hydrate in a 2-hour period. At steam curing temperatures, perhaps 50 per cent or more of the cement hydrates in an hour or less. The rate in any instance depends upon cement composition and fineness, hydration and temperature. These very high rates of reaction can have a significant physical effect. The low solubility and low diffusibility of the cement hydration products make it appear doubtful that these products could diffuse to any significant distance from the surface of the hydrating cement grains within the time of the observed rapid hydration. In other words, when the cement hydrates at a low temperature, and therefore hydrates slowly, there is ample time for the hydration product to dif-

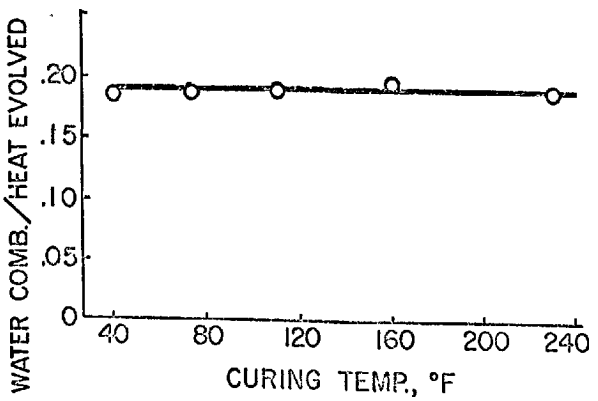

Fig. 12. *Evidence for temperature independence of the* chemical *nature of cement hydration products*

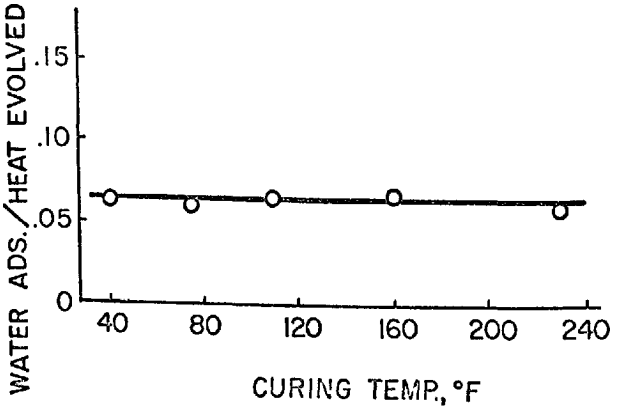

Fig. 13. *Thermal evidence for temperature independence of the* physical *nature of cement hydration products*

fuse and precipitate relatively uniformly throughout the interstitial space among the cement grains. However if the hydration is accelerated, as by increased curing temperature, the high rate of reaction does not allow time for such diffusion and therefore a high concentration of hydration product must be built up in the zone immediately surrounding the hydrating cement grain. If, in fact, this highly concentrated, dense and encapsulating layer does develop as postulated, then its presence should influence at least two properties of the paste. First, this relatively impermeable rim around the cement grain should retard subsequent hydration. That the rate of hydration of cement is significantly affected by the gel-space ratio of the paste has been demonstrated from such heat of hydration studies (26) as shown in Fig. 14. In addition, entirely independent studies have shown that the ultimate degree of hydration of C_3S (and also C_2S), as measured by X-ray diffraction techniques, is actually retarded by increased temperature during the early stages of hydration (27). This is demonstrated in Fig. 15 for C_3S pastes. This figure shows the degrees of hydration of C_3S at ages varying from 1 day to 5 years for C_3S pastes hydrated at different initial temperatures. It is seen that at 1 day the degree of hydration increases with the hydration temperature, as would be expected. However, at later ages a reversal is observed. It is believed that the dense zone of hydration product around the hydrating grain created by the rapid early hydration significantly reduces the ultimate degree of hydration of these silicate phases, even after 5 years of moist curing. Therefore, a high initial hydration temperature is detrimental to later age strength development because it, per se, reduces the degree of hydration of the cement at later ages.

The formation of the densified layer encapsulating the hydrating cement grain should cause a reduction in strength even if the same overall degree of cement hydration were attained. In Fig. 16 is shown the usually observed relationship between strength of mortars cured at "normal" temperature (solid line) and the concentration of the hydration product (measured as the "gel-space" ratio). As already discussed, this concentration is a function of original water-cement ratio and degree of cement hydration. The more concentrated the hydration product, the greater the observed strength. A paste having an overall gel-space ratio of, for example, 0.7 and a uniformly distributed hydration product would attain then a strength of about 12,000 psi as shown. However, at this same average gel-space ratio a non-uniform distribution of the hydration product could significantly influence the observed strength. For example, if one assumes a high concentration of 0.8 around the cement grain residues and 0.6 in the interstitial space, then a minimum strength of less than 8,000 psi would be antici-

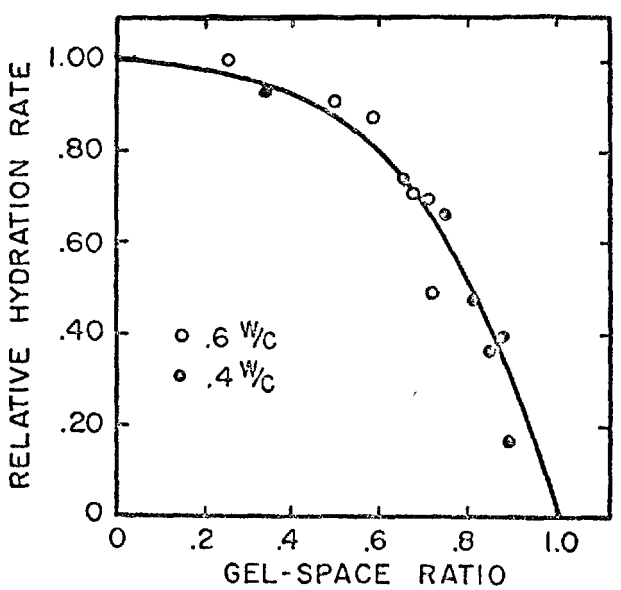

Fig. 14. *The denser the coating of hydration product the lower the rate of cement hydration*

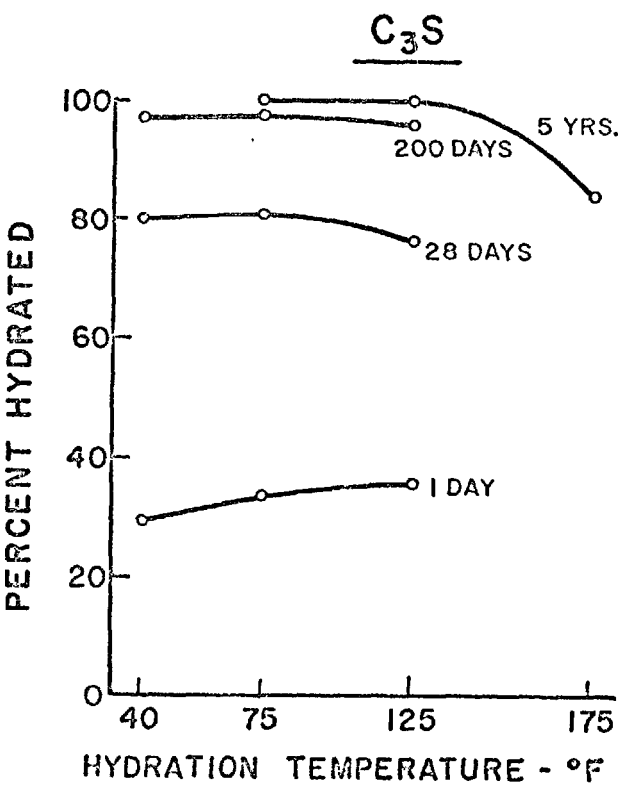

Fig. 15. *At later ages, degree of C_3S hydration was less for pastes initially cured at higher temperature*

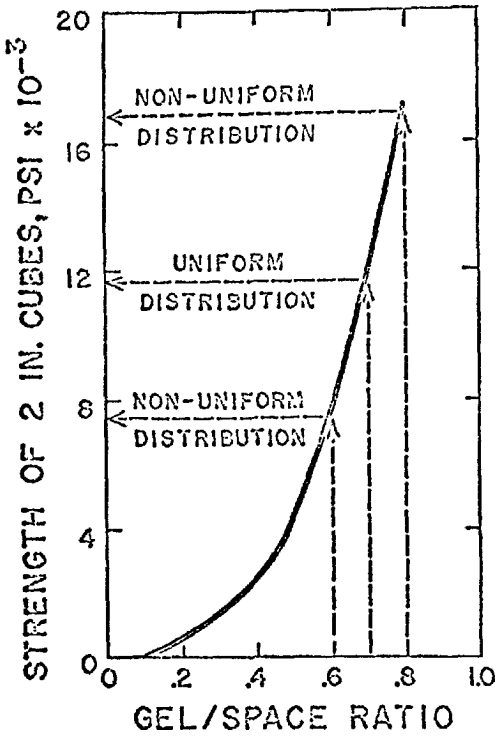

Fig. 16. *Uniform distribution of gel provides optimum strength. For the same average gel-space ratio but with non-uniform distribution the strength is reduced to that corresponding to the lower gel-space ratio*

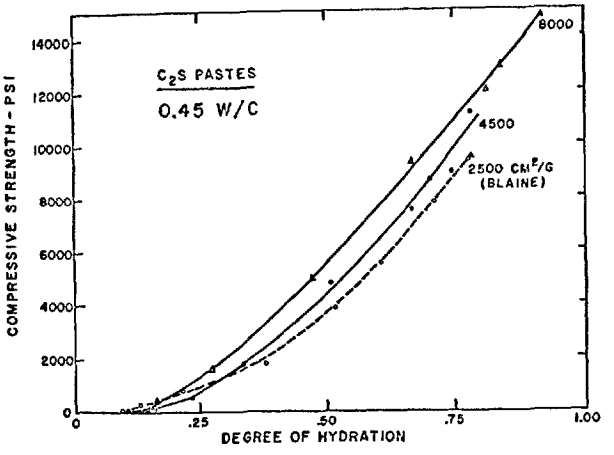

Fig. 17. *Finer grinding of C_3S produces increased strength at same degree of hydration because of greater uniformity of distribution of hydration product*

pated since the weaker portion of the paste must limit the strength attained (dashed lines). Both the retarded subsequent hydration and primarily the nonuniform distribution of the hydration product are presently considered to be the major causes of the detrimental effect of elevated curing temperatures. The role of gypsum at "optimum" gypsum content could be largely due to an optimization of the rate of early reactions in the sense of minimizing the development of such an encapsulating, retarding layer, thus permitting formation of a hydration product of more uniform density distribution and hence of higher inherent strength. This concept is also borne out by recent studies concerning of strength development (28) in pastes made with C_2S of different finenesses at various degrees of hydration, as is shown in Fig. 17. Here it may be noted that at comparable degrees of hydration, higher strengths were attained as the fineness of the C_2S increased. It can reasonably be expected that a more uniform, less disproportionated, hydration product should be obtained for a cement of higher fineness and hence that a greater strength therefore should be attained. Chemical studies of the hydration product obtained in these latter studies show the products at any particular degree of hydration to be essentially identical, since the CaO/SiO_2 ratio was observed to be independent of the fineness of the C_2S. It is anticipated that, using recently developed techniques, future studies of the pore size distribution in pastes of different SO_3 contents, cured at various temperatures, will be of considerable value in further elucidating the role of these factors in strength development.

Drying and Carbonation Shrinkage

The shrinkage of hydrated cement paste is influenced by many factors. These include the composition and fineness of the cement, the water-cement ratio, the degree of hydration, the degree of drying, and the conditions and degree of carbonation. The shrinkage of paste on first drying may or may not be reversible during subsequent rewetting and redrying cycles, depending upon details of the process of drying. We will consider first those factors that affect the shrinkage of paste on initial drying, a process that causes the largest shrinkage, except for effects associated with continued hydration or carbonation.

Cement

In regard to the effects of cement characteristics on shrinkage some previous investigators have concluded that the tricalcium aluminate and alkali contents of cement and its fineness, have large effects on shrinkage. At the time such observations were made they appeared correct from the data then available, but actually they have been found to be somewhat misleading. Most of these investigations were conducted

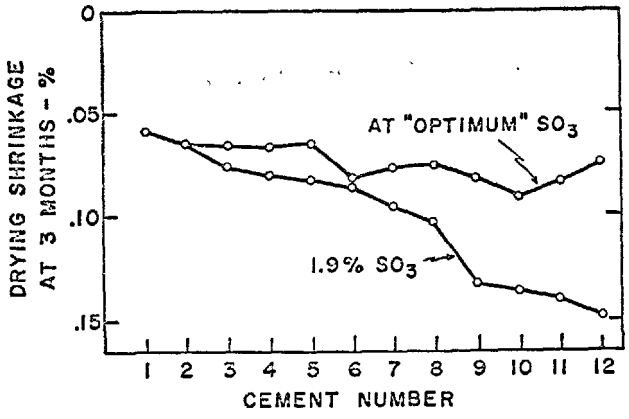

Fig. 18. *Drying shrinkage of mortars is relatively independent of clinker composition at "optimum" gypsum content*

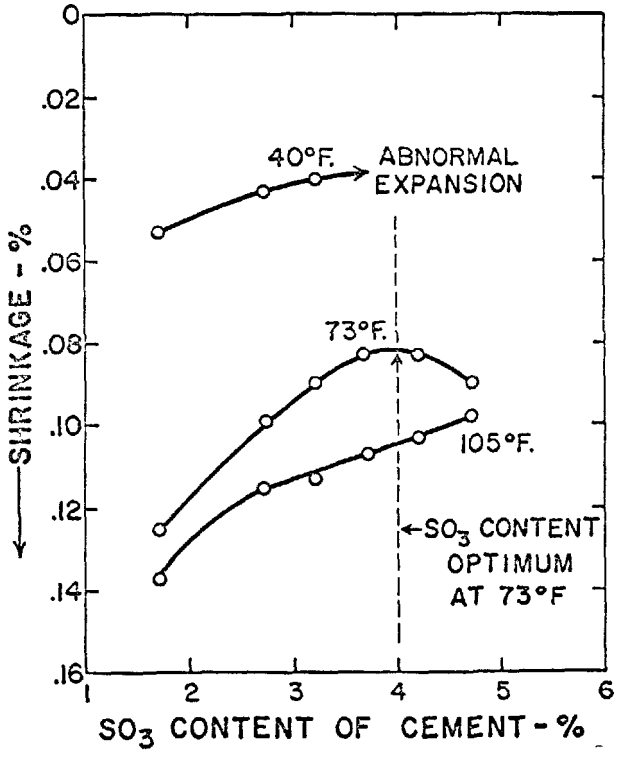

Fig. 19. *The "optimum" gypsum for minimum drying shrinkage changes with temperature of early hydration*

years ago during the period when it was thought that the primary effect of gypsum addition was to control the setting time of cement. The general practice throughout the cement industry was to use a relatively small and uniform amount of gypsum with little regard for the chemical composition of the clinker or the fineness of grinding. Subsequently it has been learned that if the gypsum content of cement is properly adjusted to an "optimum" level dependent upon the cement, the presumed detrimental effects of C_3A, alkalies, and fineness can be largely avoided and the differences among cements significantly reduced (29). This is demonstrated in Fig. 18 which compared the drying shrinkages of comparable mortars made with a group of cements varying in C_3A content from 2.4 to 14.3 per cent and in alkali content, expressed as Na_2O equivalent, ranging from 0.17 to 1.48 per cent. As shown in the lower curve, the cements have been arranged in order of increasing shrinkage as observed when a constant SO_3 content of 1.9 per cent was used with each clinker composition. From the least to the greatest shrinkage, there is approximately a 2-1/2 fold difference. From the upper curve it can be seen that the range of drying shrinkages of these mortars is considerably reduced when the SO_3 contents of the various cements were adjusted to "optimum". An increase in the C_3A content or the alkali content of a clinker increases the "optimum" SO_3 content requirements of the cement. Similar effects are found when the fineness of the cement is increased; with increasing fineness the amount of SO_3 required to minimize shrinkage and to maximize strength, under normal conditions of test, is also increased.

The "optimum" SO_3 content of a cement is not clearly definable even when tested under standard laboratory conditions. This "optimum" depends upon whether maximum strength or minimum shrinkage is required, and upon the age such qualities are required. In addition, it depends significantly upon the early hydration temperature of the cement. This effect is shown in Fig. 19. The effect of temperature on strength previously discussed, indicates that the SO_3 content that is optimum for minimum shrinkage increases as the early hydration temperature of the cement is increased. From Fig. 19, an SO_3 content of 4.0 per cent, which appears optimum for shrinkage when tested at 73°F, is almost 1 per cent low for minimum shrinkage if the early hydration reactions are at 105°F, and 1 per cent too high to prevent abnormal expansion during early moist curing at 40°F.

In addition to these influences on shrinkage, it has been shown that some chemical admixtures can increase the shrinkage characteristics of cement, perhaps by altering the SO_3 content required for "optimum" which had already been adjusted during manufacture of the cement. It is also possible that the size of the concrete section in which the cement is used (a temperature effect), and the duration of concrete mixing or agitation, might have important effects on the "optimum" SO_3 content of cement.

Water Content

At present the relationship between the water loss of a cement paste to its shrinkage can be expressed only in semi-quantitative terms. Certainly, in most of the investigations of this matter during the past several decades, pertinent details regarding either the nature of the materials used, or the environment to which the specimens were actually exposed, have been omitted from the published reports. Therefore, the present authors will draw largely upon their own studies that are believed to have taken into consideration at least most of the important factors. Of course, data from other sources will be incorporated where appropriate.

Realization of the complexity of this matter has increased in recent decades. Whereas the purpose of early investigators was to find means to reduce the shrinkage of field-placed concrete, current interest has broadened so that a major purpose of more recent investigators has been to develop an understanding of the phenomena of shrinkage itself, with the ultimate hope of minimizing or eliminating volume change property of the paste component itself.

As indicated in the discussion relative to the role of cement properties, there are many traditional concepts that may not have adequate technical support. The information to be presented here is believed to satisfactorily reveal at least the semi-quantitative influence of the various factors involved in the shrinkage of neat cement paste.

The over-all relationship between loss of water of a neat cement paste and the resulting change in length or volume, in an atmosphere free of even the low concentration of CO_2 present in normal air, is shown in Fig. 20. The data in this figure, as in the case of all data shown in Fig. 20 through Fig. 28, represent the shrinkages obtained during the first drying of individual neat cement paste or mortar specimens, each to a single "equilibrium" humidity (as contrasted to progressive step-by-step drying to "equilibrium" of single specimens, which produces irreversible structural effects within the pastes). The paste specimens now to be discussed were 1/4 × 1/4-inch in cross section, and the mortar specimens were 1/4 × 1/2-inch in cross section.

The data in Fig. 20 shows the relationship between shrinkage and water loss on "drying", in a CO_2-free atmosphere, from 100 per cent relative humidity RH, to 0 per cent RH (defined as "D-drying") and then with further dehydration accomplished by progressive heating to temperatures as high as 525°C.

There are several features of Fig. 20 that are of considerable significance. Six separate specimens are

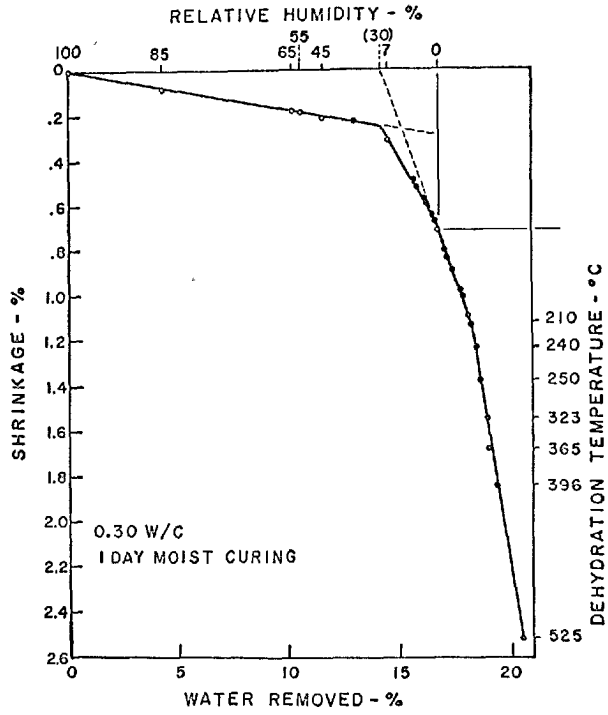

Fig. 20. *The variation of the first shrinkage of moist cured cement paste with water removed by drying in air and dehydration at elevated temperatures*

represented, each of which was dried to apparent length and weight "equilibrium" at a single relative humidity. The open circles represent these specimens equilibrated at the relative humidities shown. The closed dots represent non-equilibrium transient measurements made during drying of the specimen being equilibrated at 0 per cent RH. It can be noted that these non-equilibrium measurements fall consistently on the straight line segment representing data for equilibria from 100 to approximately 30 per cent RH, and similarly on the straight line segment extending from about 30 to about 1 per cent RH. A further change in relationship begins at about 1 per cent RH and extends to 0 per cent RH and beyond. In this experiment further increments of water were removed by heating the specimen to progressively higher temperatures; after each heating, the specimen was cooled to 23°C and its length and weight determined. It may be noted that this third segment extends to water removals attained by heating to about 210°C. The fourth segment extends from 210°C to approximately 525°C, a temperature at which the specimen showed physical disruption. In other experiments that involved various water-cement ratios and various degrees of hydration there has frequently been observed an initial horizontal segment representing satura-

ted pastes from which substantial water losses, perhaps approaching 10 per cent, could be sustained before there was any evidence of shrinkage.

The observed linearity of the segments and the abruptness of change between them suggests that the transitions mark stages of drying where the water is being removed from the different types of hydrated compounds or from sites within the calcium silicate hydrate and other hydrated phases. A belief that shrinkage is not due to loss of "adsorbed" water of the type found on a finely divided material such as silica gel is fully supported by recent studies using nuclear magnetic resonance techniques (22). These studies clearly show that all the water held below 80 per cent RH by paste or by hydrated calcium silicates is not "adsorbed" in that sense but rather in a state similar to that of interlayer water (such as in clays), zeolitic water, or hydrate water of crystallization (such as in ettringite, $C_3A \cdot 3CaSO_4 \cdot 32H_2O$).

Quantitative data on the shrinkage-weight loss relationships of the different linear segments, shown in Table 2, provides several interesting features. The 1:1 concordance between over-all loss of volume of the paste and loss of volume of water in the high temperature range, segment 4, would appear most unusual. This effect would appear to have considerable significance regarding the structure of the paste and the distribution of the residual water in the paste, and will be the subject of further study.

The relations among the $\Delta V_p/\Delta V_w$ of segments 1, 2 and 3 are particularly interesting and suggestive of the nature of the mechanism of shrinkage. These three segments can be interpreted to represent the loss of only two types of water, that represented by the relationship of segment 1 and that of segment 3. Indeed, as can be seen in Fig. 20 an extrapolation of segment 3 intercepts the axis of zero shrinkgae at almost exactly the weight loss and relative humidity at which the junction between segments 1 and 2 occurred. In addition, the $\Delta V_p/\Delta V_w$ factor of segment 2 is almost exactly the average of those for segments 1 and 3. This strongly suggests that segment 2 is simply a combined relation of simultaneous loss of water by the phenomena represented by segments 1 and 3. Upon drying of a saturated specimen, the segment 1 mechanism is joined by the segment 3 mechanism to produce segment 2, with the segment 1 mechanism participating from 100 per cent RH to about 1–3 per cent RH and the segment 3 mechanism participating from about 30 per cent RH to an extended drying condition represented by heating to approximately 210°C. The observation that the $\Delta V_p/\Delta V_w$ for segment 2 is the mean of those for segments 1 and 3 may be coincidental, or may indicate that in the range of 30 to 1–3 per cent RH equal numbers of water molecules are simultaneously released by both the segment 1 and 3 mechanisms, and hence the observed $\Delta V_p/\Delta V_w$ has the mean value of segments 1 and 3, or that in this range the loss of a water molecule results in two different shrinkage mechanisms. Special tests using a SO_3-free cement show a similarly abrupt change in relationship at about 30 per cent RH, thus establishing that the segment 2 or 3 mechanisms do not involve dehydration of the highly hydrated calcium sulfoaluminates.

Table 2. *Ratio of volume change of paste, ΔV_p, to volume of water removed, ΔV_w, during drying in air*

Segement	Range	$\Delta V_p/\Delta V_w$ (cc/cc)
1	100% RH—30% RH	0.025
2	30% RH—1% RH	0.22
3	1% RH—200°C	0.40
4	200°C—525°C	1.00

Subsequent discussion of shrinkage and dehydration phenomena will be limited to those that occur in the more usual range of 100 to 0 per cent RH.

Water-Cement Ratio and Duration of Curing

The relationships obtained between shrinkage and water loss for pastes of 0.3, 0.5 and 0.7 water-cement ratio, when dried in a CO_2-free atmosphere after periods of prior moist curing of 1, 7, 28, 90 and 365 days, are shown in Fig. 21. The points shown are "equilibrium" data obtained with duplicate paste specimens after drying to 85, 65, 55, 45, 7, or 0 percent RH. First it should be noted that the segmented type of shrinkage-water loss relationship previously shown in Fig. 20 is invariably obtained in this type of experimental procedure. The minor deviations from strict consistency of the data are attributable to small differences in the initial weights of the individual specimens. For the segment 1 portion of the relationships, from 10 to approximately 30 per cent RH, the shrinkage to water loss becomes greater the greater the duration of prior curing. It should also be noted that the water loss corresponding to the junction of the segment 1 and the segment 2 relationships decreases with duration of prior curing as might be expected. In general the slopes of the segment 2 relationship, at least for that data representing a single water-cement ratio, appears relatively independent of duration of hydration. For each of these general observations it may be noted that the greatest shift occurs between those specimens cured 1 day and those cured

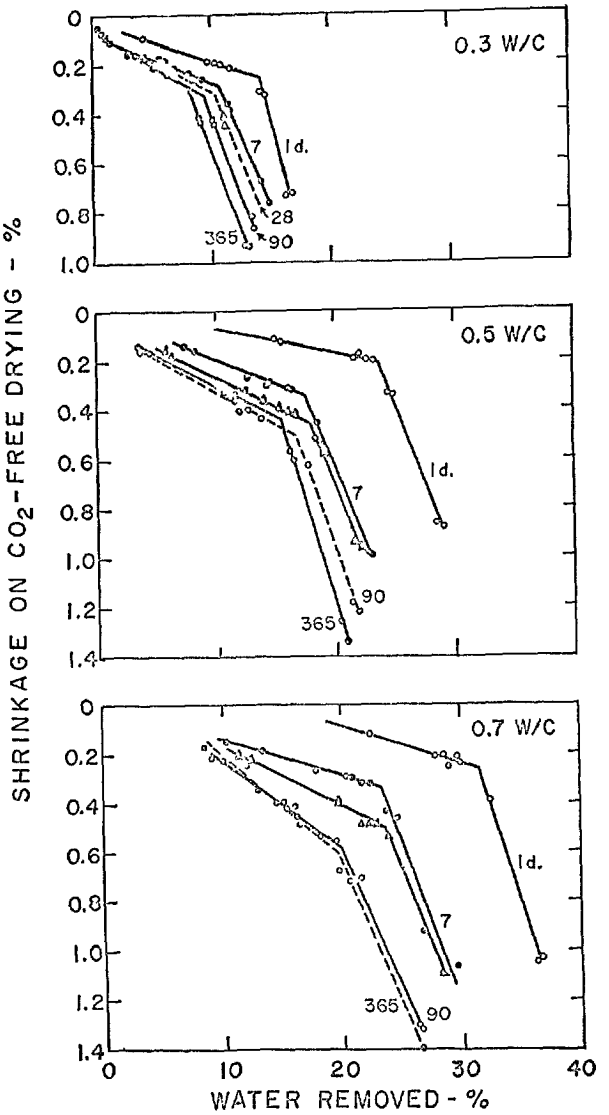

Fig. 21. *Drying shrinkage of cement pastes at various ages and water-cement ratios*

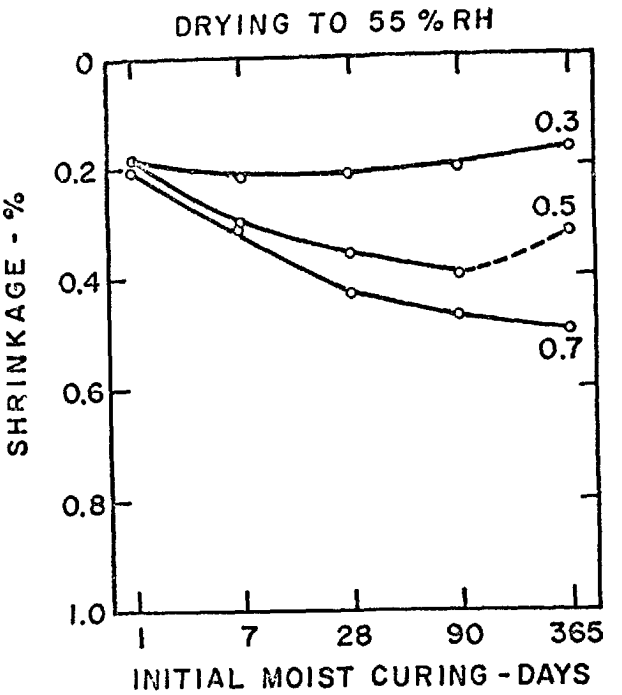

Fig. 22. *Dependence of first drying shrinkage on duration of moist curing and water-cement ratio*

for 7 days, as also might be expected since this period probably reflectes the greatest change in degree of hydration of the cement. A clearer understanding of the effect of duration of initial moist curing (degree of hydration of the paste) prior to CO_2-free drying is shown in Fig. 22. These data are again equilibrium data attained on exposure of the specimens, after the indicated periods of moist curing, to drying at 55 percent RH. As will be discussed later, some differences occurred in the total drying time of these individual specimens before "equilibrium" was attained, but it may be noted that at 0.30 water-cement ratio the shrinkage observed on drying to 55 per cent RH was little affected by curing for periods ranging from 1 to 365 days, and, if anything, the shrinkage at 365 days was slightly less than that at 1 or 7 days. However, at 0.7 water-cement ratio the longer the period of moist curing before drying the greater the subsequent shrinkage due to drying. This would be the normal expectation from "theoretical" considerations: the longer the period of hydration the greater the amount of the "shrinking gel" produced and the less the amount of "restraining" unhydrated clinker particles. The relationships obtained, particularly that at 0.5 water-cement ratio, suggest that for any initial water-cement ratio there may be a duration of initial moist curing that produces within the paste a concentration of hydration product that has maximum shrinkage potential. It should be noted that the shrinkages of the paste of 0.3, 0.5 and 0.7 water-cement ratio were essentially identical when the pastes were initially moist cured only 1 day.

Effect of Duration of Drying

In the previous discussion of shrinkage, the shrinkage values that have been reported were considered to be "equilibrium" values. However it has been observed in the conduct of these various tests that, whereas "equilibrium" was established relatively rapidly at intermediate humidities, decreases in length and weight of the specimens occurred very slowly at

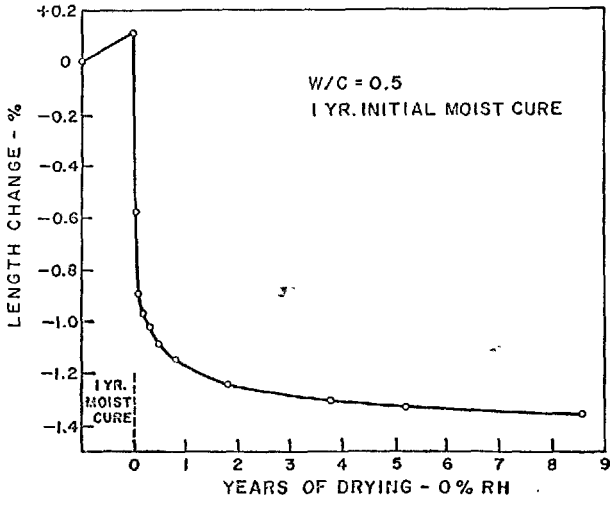

Fig. 23. *Drying shrinkage at 0 percent RH of a cement paste cured moist for 1 year*

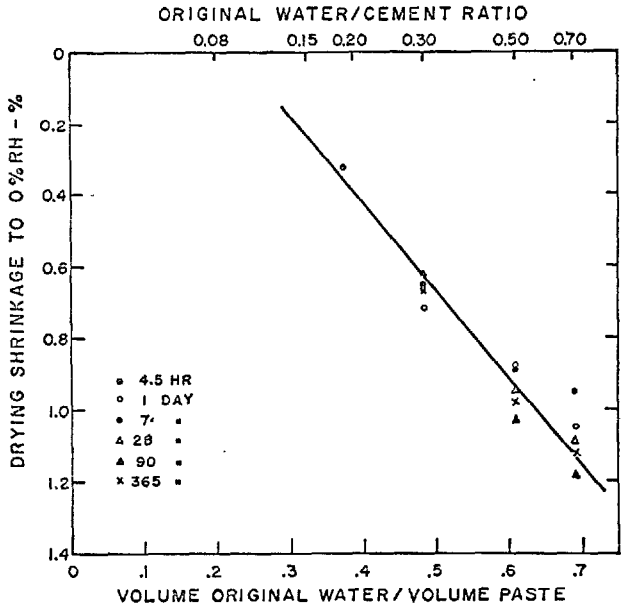

Fig. 24. *Drying shrinkages of cement pastes at 0 percent RH is a function of porosity of the original pastes. Pastes dried approximately 2 months*

very low humidities. Data for a neat cement paste of 0.5 water-cement ratio and initially cured 365 days prior to drying is shown in Fig. 23. Here it may be noted that an expansion of approximately 0.1 per cent occurred during the first 365 days of initial curing. Subsequent exposure of this specimen to "D-drying" condition (0.5μ water vapor pressure in a vacuum, CO_2-free, atmosphere) gave rise to a progressive shrinkage of the specimen during a period of 8–1/2 years of drying in this condition. This prolonged period for approach to equilibrium is not caused by drift of the measuring instrument because these changes in length were accompanied throughout this whole period by a corresponding, and constant, shrinkage-weight loss relationship. Furthermore, the times of drying are far too great to permit interpretation in terms of water release without corresponding changes in the solid phases. Thus, these data indicate that, under certain drying conditions at least, structural changes can occur within the cement paste over very extended periods of time.

This observation is of particular importance in connection with the interpretation of Fig. 21. In the tests shown in Fig. 21, it was found that those specimens receiving a preliminary curing of 90 or 365 days before drying at 0 per cent humidity required or were allowed significantly longer times to reach "equilibrium" than those cured 1, 7, or 28 days. It is of interest to examine the "terminal" shrinkages of the specimens at 0 per cent RH at a time that all of the specimens had been subjected to essentially equal durations of drying. Such information is shown in Fig. 24. Fig. 24 compares the average shrinkages to 0 per cent RH of those specimens initially cured 1, 7, 28, 90 or 365 days and having an original water-cement ratio of 0.3. 0.5 and 0.7. In Fig. 24 the data are presented both on an original water-cement ratio basis and an initial volume of water per volume of paste basis. In addition to the aforementioned data there is also shown a point representing the shrinkage of a similar paste of 0.18 water-cement ratio cured only 4.5 hours (set time). It may be seen that there is no consistent effect of duration of moist curing among the data and that the over-all shrinkage of a paste from 100 per cent to 0 per cent RH is essentially a linear function of original water porosity of the paste rather than its degree of hydration.

The observation that the total shrinkage of paste between 100 and 0 per cent RH is essentially independent of degree of hydration, at least for the type of specimen and drying used in this study, is paralleled by similar observations of the heat of adsorption of hydrated pastes (26). Fig. 25 shows that the total heat of adsorption from 0 per cent RH to saturation is essentially identical for two pastes hydrated to different degrees as reflected by their different non-evaporable water contents (0.156 and 0.204 g/g ign. wt.). The heat of adsorption-water content relationships are observed to consist of two essentially linear segments similar to the previously observed shrinkage-water content relationships. However, it is difficult to believe that the observed segments theore-

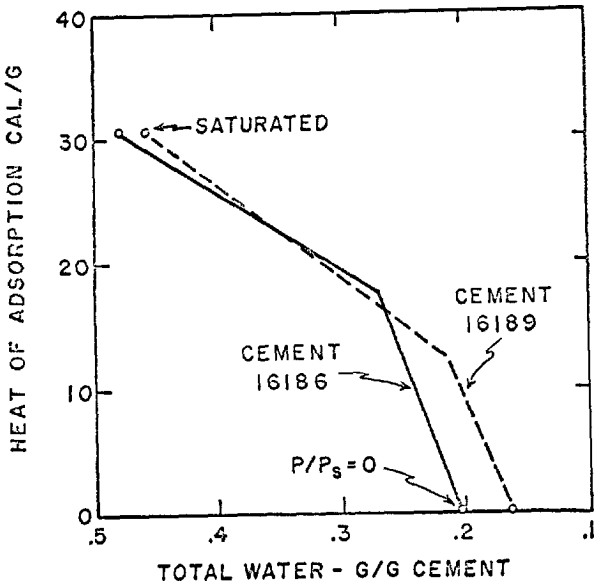

Fig. 25. *Variation of heat of water adsorption of paste follows a pattern similar to that of drying shrinkage with water content*

tically can be absolutely linear and that each increment of water between 100 per cent and 30 per cent RH has an equal energy of binding because the adsorption isotherm is continuous and not a step function. It would therefore appear that the energy increments that result in the different amounts of water that are adsorbed over this range in relative humidity are relatively small.

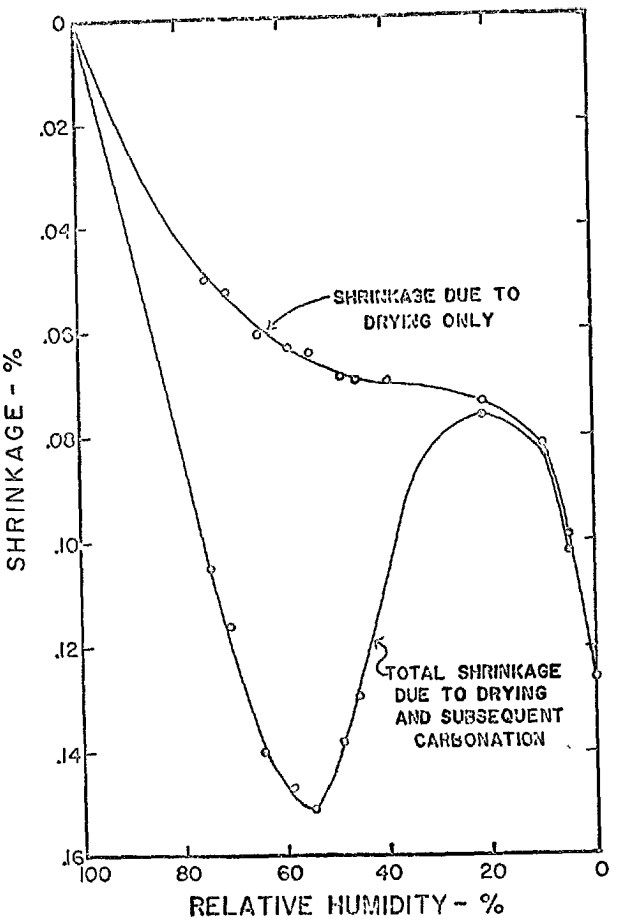

Fig. 26. *Contributions of drying and carbonation to total mortar shrinkages at various relative humidities*

Carbonation Shrinkage

It has been long established that cement paste, mortar, or concrete is also susceptible to that shrinkage caused by reaction with the CO_2, even at the low concentration present in normal air. That this reaction is very dependent upon the relative humidity of the environment in which the exposure to carbon dioxide occurs, is shown in Fig. 26. This figure shows the shrinkages of mortar bars exposed first to CO_2-free drying at relative humidities varying from 100 to 0 per cent and subsequently to atmospheres maintained at these same relative humidities but containing carbon dioxide. The shrinkage due to carbon dioxide is seen to be strongly dependent on humidity; although some carbonation did occur at 100 per cent RH, no shrinkage was found and at humidities below about 25 per cent no reaction or shrinkage resulted from exposure to CO_2. A maximum shrinkage due to chemical reaction with CO_2 was observed at approximately 55 per cent RH. It can be observed that the shrinkage at 55 per cent RH due to carbonation was greater than that due to drying alone at this same humidity. Carbonation in cement paste, mortar, or concrete extends to a much greater depth than is ordinarily assumed on the basis of the phenolphthalein indicator color test, which essentially indicates the depth to which the degree of carbonation is almost complete. It has been shown that the carbon dioxide can carbonate not only the calcium hydroxide liberated by the hydration reactions of the cement but can react with 85 per cent or perhaps more of all the solid components within the cement paste—the calcium hydroxide, the hydrated calcium silicates, the hydrated calcium aluminates, and the magnesium hydroxide. There has been some conjecture as to the mechanism of carbonation shrinkage, and it is believed that this matter can be now somewhat clarified.

In Fig. 27 is shown another typical drying shrinkage versus water loss relationship. The points represented are all "equilibrium" values. After reaching equilibrium in air at the indicated relative humidities

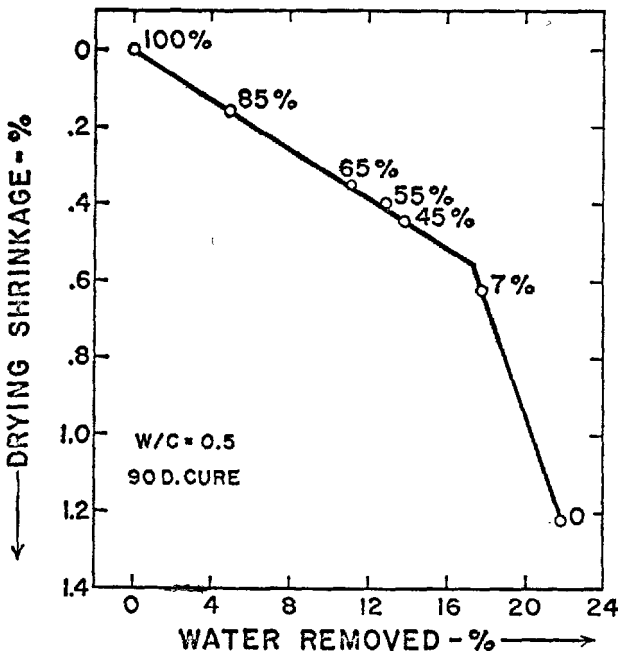

Fig. 27. *Drying shrinkages vs water removed relationship for paste specimens*

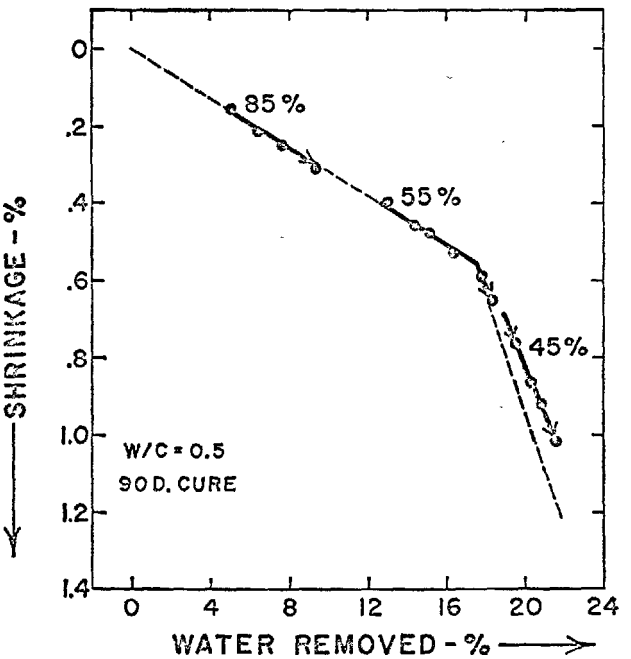

Fig. 28. *Effect of subsequent carbonation on the specimens used for the data in Fig. 27 on shrinkage as water removed relationship*

the specimens then were exposed to air, at the same indicated humidity, but containing relatively low concentrations of CO_2. Under these conditions, one mole of H_2O is released for each mole of CO_2 that reacts and from the gain in weight of a specimen, the loss in water that the specimen has sustained can be calculated. A typical shrinkage water loss due to carbonation relationship sustained by the same specimens of Fig. 27 is shown in Fig. 28 along with a dashed line representing the relationship for water loss due to drying alone, previously shown in Fig. 27. In Fig. 28 it may be noted that the specimen maintained at 85 per cent RH lost water due to reaction with CO_2 but that its shrinkage water loss relationship was identical with the relationship that had been previously established in Fig. 27 where the water loss resulted from the reduction in relative humidity alone. Similar concordance was observed for the specimen maintained at 55 per cent RH which lost water due to carbonation and it can be seen in Fig. 28 that the specimen underwent the transition from segment 1 to segment 2 in a manner strikingly similar to that which would have been expected had the specimen been subjected to reductions in relative humidity in the absence of CO_2. A portion of the relationship attained at 45 per cent RH is also indicated. The data shown in Fig. 28 are typical of those obtained during the carbonation of other specimens of this group at different water-cement ratios and subjected to different prior curing periods. This information can only indicate that the shrinkage-water loss relationship of a cement paste is similar whether the water loss results from evaporation due to a reduction in relative humidity of the specimen or from displacement during reaction with CO_2. It must be admitted at this state of our knowledge that the exact structural significance of these observations is not clearly interpretable. It is intended that these matters will be dealt with in much more quantitative detail in a subsequent paper dealing specifically with this subject.

As had been previously noted the discussion to this point has been limited essentially to the shrinkage properties of cement paste on first drying. The reaction of the cement paste on rewetting and the degree to which the length changes of the paste are reversible will now be considered.

Irreversibility and Stabilization by Drying

The experimental information presented in the following discussion of shrinkage of paste was obtained using thin paste slabs approximately 15 by 80 millimeters and varying in thickness from 0.5 to 3.0 millimeters in thickness (30). As previously discussed the shrinkage of a moist-cured cement paste during its first drying is always greater than the swelling that occurs upon rewetting. However, if the ce-

ment is completely hydrated and protected from carbonation during drying at a relative humidity not below 11 per cent then the swelling and shrinkage cycles that occur on subsequent rewetting and drying are reversible. Typical results are shown in Fig. 29. This particular paste specimen that had received 8 months of initial moist curing was subjected to 3 cycles of drying and rewetting at relative humidities between 11 and 100 per cent. The specimen was held at each of the humidity exposures for periods of about 5 to 8 weeks during which time the thin specimens closely approached equilibrium. The 3 cycles of rewetting and redrying following the first drying of the specimen differed somewhat in detail, as can be ascertained from the data points, which are numbered in chronological order. After the first drying to 11 per cent RH the data show good reproducibility within the range of 11 to 100 per cent RH and it is considered that the paste was essentially stabilized by the first drying. The difference between the length of a saturated specimen prior to first drying and the length attained at 100% RH on subsequent cycles of drying and wetting is the irreversible shrinkage component, and is accompanied by a corresponding irreversible loss of water content.

The first drying shrinkage of a cement paste to equilibrium at intermediate humidity has been shown in Fig. 21 to depend upon the water-cement ratio of the paste and the degree of hydration of the cement. Not all investigators have observed the linear and segmented relationships such as are shown in Fig. 21. The data in Fig. 21 was obtained in this instance by subjecting companion initially-saturated specimens directly to drying at the final humidity desired. In other studies a single specimen has been equilibrated at progressively lower relative humidities and it is believed that the irreversible changes that develop in a paste at each of the equilibrium levels could be the cause for the non-linearity of the relationships obtained. In other words, as the paste was moved progressively from "equilibrium" at a higher humidity to a lower humidity the inherent nature of the paste had been altered by its prior drying and hence the individual data points do not represent equivalent paste structures.

For paste dried to intermediate relative humidities, it has been observed that the irreversible component is strongly dependent upon the porosity of the paste whereas the reversible swelling-shrinking component that arises on subsequent cycling is independent of porosity. As an example, the results for portland cement paste moist-cured for approximately 6 to 7 months prior to drying at 46 per cent RH are shown in Fig. 30 (30). The lower line shows the first shrinkage of these pastes, which had initial water-cement ratios between 0.40 and 0.60. It may be seen that this first shrinkage varied linearly with the "total porosity" of the paste. The swelling of the paste upon rewetting to 100 per cent RH is practically independent of porosity, as indicated by the fact that the irreversible shrinkage line is essentially parallel to that for the first shrinkage. Drying to humidities lower than 47 per cent increases both the reversible shrinkage component and the irreversible shrinkage component of the paste. The first shrinkage of a saturated paste to 47 per cent

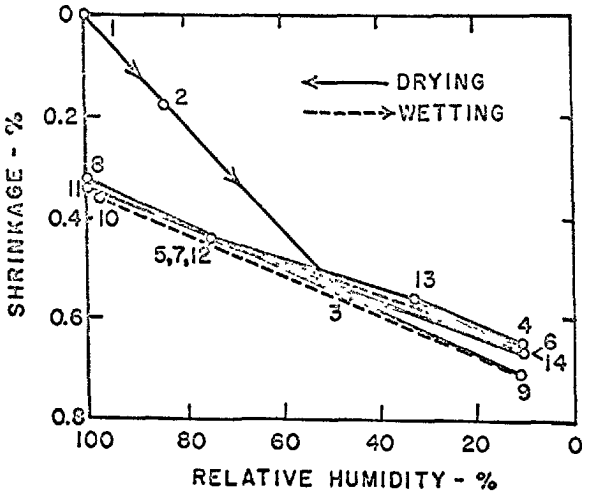

Fig. 29. *Reversibility of volume changes of pastes with relative humidity after first drying*

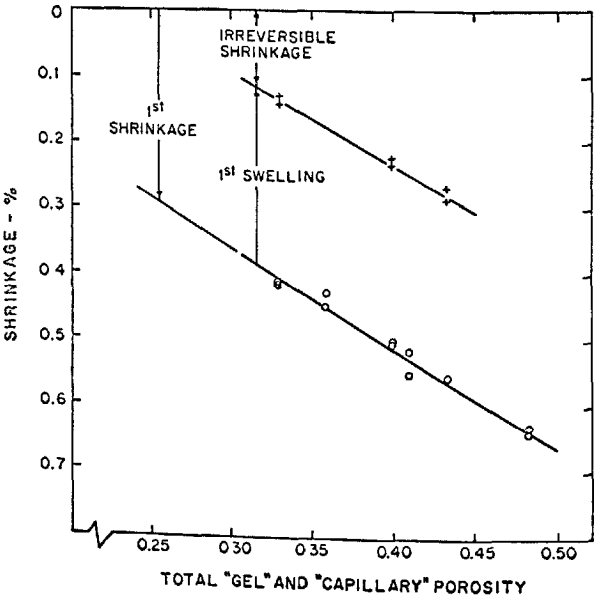

Fig. 30. *Dependence of reversible and irreversible components of drying shrinkage on paste porosity*

RH is found to depend somewhat upon the length of time that the specimen was held at the intermediate relative humidities. If the thin slabs were dried at 84 per cent RH for 5 weeks before drying at 47 per cent RH the effect was slight. However, if the pastes were dried in smaller steps at 92, 84, 75, 67 and 58 per cent RH, during a total of 31 weeks, before drying at 47 per cent RH, the first shrinkage was reduced by about 20 per cent below that by drying directly to 47 per cent RH.

The preceding results show that there can be a pronounced difference between the first drying shrinkage and the subsequent swelling and shrinkage behavior of a hydrated paste. The shrinkage-water content relationship during first drying and redrying appeared to depend significantly upon the length of time the specimen was held in the "dried" condition. Such information is shown in Fig. 31. These particular paste specimens were cured for 19 months, hence were essentially completely hydrated. Each of the 4 specimens was held at 47 per cent RH for different periods of time during first drying as indicated in Fig. 31. Very little irreversible shrinkage or irreversible water loss resulted from drying for only 0.1 days; the redrying curve agreed well with the first drying curve. Paste dried for 1 day or more showed considerable irreversible shrinkage and water loss. Although the loss of water during each redrying cycle is nearly as great as that during the first drying cycle, the swelling and redrying shrinkages are progressively reduced.

Progressive Changes and "Equilibrium" Values

In studies of the mechanism of shrinkage of paste it has often been presumed that the system itself does not undergo changes in structural properties between one "equilibrium" state and another. However, the above results clearly show that hardened cement pastes are subject to progressive irreversible changes during drying.

From the foregoing it seems obvious that there are numerous factors influencing and obscuring any direct quantitative or thermodynamic analysis of shrinkage phenomena. However, it is believed that studies of the nature herein described, supplemented by studies of a much more exploratory nature, may develop concepts and techniques capable either of the reduction in the inherent shrinkage potential of cement paste, or an understanding of those factors that create irreversibility during the first drying shrinkage of paste, so that a stabilizing mechanism can be brought about during the normal hydration process of cement paste.

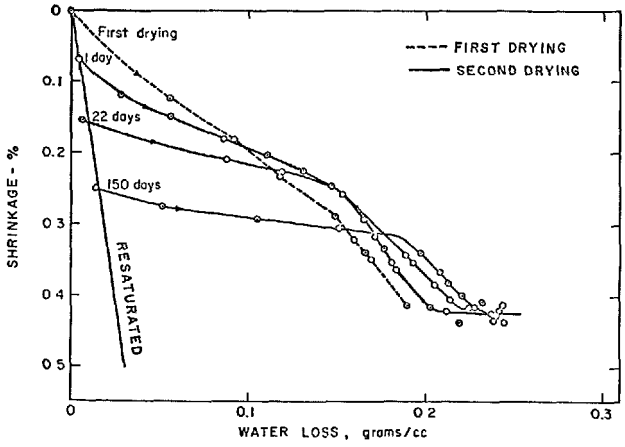

Fig. 31. *Effect of drying at 47 percent RH for periods indicated on length recovery on resaturation and on shrinkage vs water loss relationship of second drying*

Thermal Properties

The thermal properties of hardened cement paste have considerable practical importance. Since concrete structures are subjected to temperature changes and gradients a knowledge of their potential behavior under such conditions may be needed.

It is necessary to consider the relationship of each of these properties to cement paste porosity (initial water-cement ratio and degree of hydration), to moisture content, and to temperature.

Temperature: Effect on Paste Volume

Of the various thermal properties to be discussed here, the dimensional changes accompanying variations in temperature are the most complex.

Wet pastes. For an understanding of the effects of temperature on cement pastes hydrated under normal conditions and containing evaporable water, it is necessary to consider the effect of temperature on degree of saturation. The capacity of a paste for water, at a given vapor pressure, increases as the paste is cooled. This means that a paste not having access to water is effectively "dried" during cooling, and therefore should shrink simply because of this desiccation.

In addition to such a change in overall degree of saturation, distribution of moisture within the paste may occur. This effect, found with nearly saturated pastes (31), is illustrated in Fig. 32. It can be seen here that during rapid cooling (under conditions where there is a negligible temperature lag) the initial contraction coefficient is quite large, 29×10^{-6}/degree C. When cooling was stopped, the specimen began expanding (called "thermal swelling"). The expansion

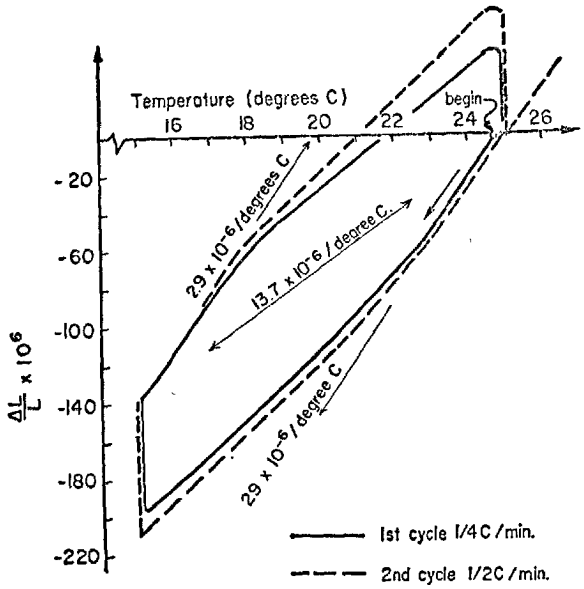

Fig. 32. *Effect of redistribution of moisture on paste volume after rapid temperature changes*

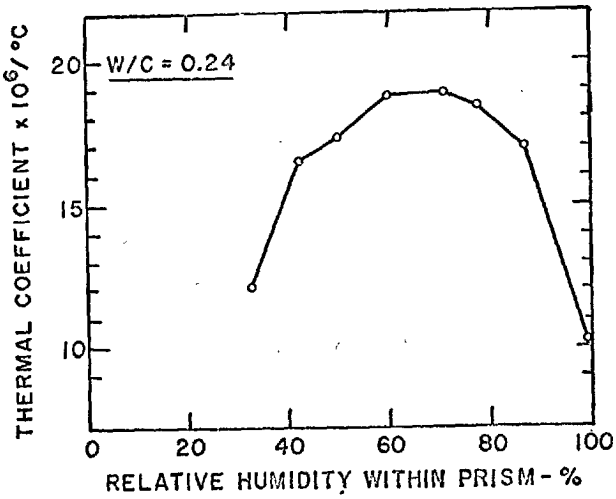

Fig. 33. *The thermal coefficient of expansion varies with the relative humidity within the paste*

followed an exponential decay curve until finally attaininig constant length. Warming caused the process to be reversed, and faster rates of cooling or warming caused greater lags of the length changes. Obviously a contraction (or an expansion) thus depends upon rate of temperature variation, being much lower at slower rates or when calculated from the end points obtained at "equilibrium". Note in Fig. 32 that the "equilibrium" thermal coefficient for this paste was 13.7×10^{-6}/degree C. If the specimen is immersed in water during the experiment, the moisture movement should be affected, and indeed additional swelling can occur after cooling (that is, less overall contraction results).

Dry pastes. Hardened cement pastes that have been completely dried show no time-dependent cooling or heating effects (32). The volume changes that do accompany temperature variations are reversible, except, in certain instances, for the first heating. Thermal coefficients ranging from $10.5–12.4 \times 10^{-6}$/degree C have been obtained (32, 33). The higher value represents a more highly hydrated paste; i.e., less restraining unhydrated cement particles.

Autoclaved pastes. The thermal behavior of an autoclaved paste appears independent of moisture content and the thermal expansion coefficient is about that of a dry paste (34).

Temperature: Discussion of "Coefficient of Thermal Expansion"

"Coefficient of thermal expansion" cannot be uniquely defined for a cement paste. The coefficient depends upon the moisture content of the paste and upon the rate of change of temperature. Three types of thermal coefficient have been usefully employed.

One coefficient, α_i, can be termed the "instantaneous" coefficient. It is used to measure a process too rapid to permit an appreciable redistribution of moisture within the specimen.

A different coefficient, α_w, measures a process that is slow enough for continuous redistribution of moisture to occur but without change in total moisture content.

For a process in which equilibrium is maintained in a paste that is saturated and has access to water, a coefficient, α_{sat}, is used. Several measurements of this coefficient are shown in Table 3. The last item in Table 3 may represent data for the only fully hydrated paste that has been studied.

Since a value of 6.1×10^{-6}/°C has been obtained (36) for a specimen that can be assumed to be clinker alone, the coefficient for the hydrated product appears to be about double that for unhydrated material.

Values of α_w depend greatly upon humidity. They are much highest at intermediate relative humidities than at either water-saturation or at extreme dryness (32, 33, 34, 35). Typical results are shown in Fig. 33. Similar results were obtained with pastes of higher water-cement ratio, but these experiments showed that as hydration proceeds the maximum coefficient decreases while at the same time the values at the extremes remain unchanged (34, 35).

Partial drying of hardened cement pastes can cause the recovery effect (that is, the swelling and contrac-

Table 3. *Thermal expansion coefficients, water-saturated hardened cement pastes*

w/c	Moist cure period	Temperature range (°C)	$\alpha_{sat} \times 10^6$ $(°C)^{-1}$	Reference
0.22–0.40	14–17 years	21 to 49	9.6 ± 0.3[a]	(34)
0.25–0.35	7–13 days	−9 to 21	10.9 ± 1.8[b]	(33)
0.26	197 days	20 to 60	10.0 ± 1	(35)
0.55	27 mos.	0 to 25	11.6 ± 0.6	(31)

[a]average of values for pastes made from 4 different portland cements.
[b]average of values for pastes made from 12 different portland cements.

Table 4. *Specific heat of cement paste calories per gram per degree C*

Temperature °C	Water-cement ratio	
	0.25	0.60
21	0.265	0.380
34	0.277	0.408
43	0.303	0.455
54	0.340	0.505
65	0.400	0.580

tions at constant temperature) to disappear completely. This results in a large increase in α_w, a value as high as 25×10^{-6}/°C has been obtained (31). This is nearly as high as the initial rates for rapid cooling shown in Fig. 32, and considerably higher than those of Fig. 33. Approximately similar results have been reported elsewhere (35).

Thermal Conductivity

Measurements under carefully controlled conditions (37) suggest that paste porosity and temperature have little effect on the thermal conductivity of saturated pastes. The values obtained, 7.3–9.3 BTU/(hr) (sq ft) (°F/in), are, however, about twice that calculated for oven-dried pastes.

Specific Heat

The specific heat of hardened cement paste has apparently not been measured under conditions where all the variables were known or controlled. For example, data (38) published for a single cement at two water-cement ratios and at a number of temperatures, although the pastes were described as well hydrated, no information was given on the degree of saturation The values, shown in Table 4, indicate strong dependence upon porosity and temperature.

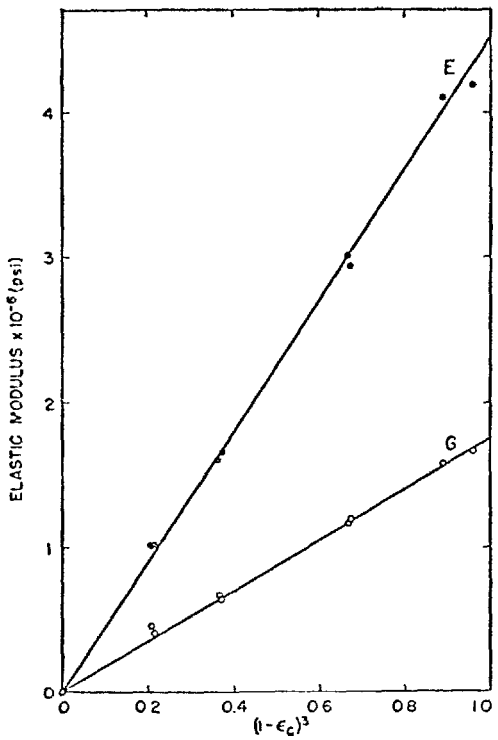

Fig. 34. *Dependence of elastic moduli of paste on "capillary" porosity*

Elastic Properties of Hardened Paste

We will now consider the elastic properties of hardened paste: Young's modulus, shear modulus, and Poisson's ratio, and the effects of porosity, temperature and drying on these properties.

Effect of Porosity

Elastic moduli have been determined for nearly fully hydrated portland cement pastes and tricalcium silicate pastes of various porosities (39). The Young's modulus, E, was found to depend upon the capillary porosity, ε_c, according to:

$$E = E_g(1 - \varepsilon_c)^3 \qquad (1)$$

where E_g is Young's modulus of the gel at "zero capillary porosity". A similar equation was found to hold for the shear modulus, G. Data for water-saturated portland cement pastes are shown in Fig. 34. It was also found that good conformance to Eq. (1) is obtained if the "total porosity" ("gel" and "capillary" porosity) is used as shown in Fig. 35 for the same set of results. The value of E when the "total porosity"

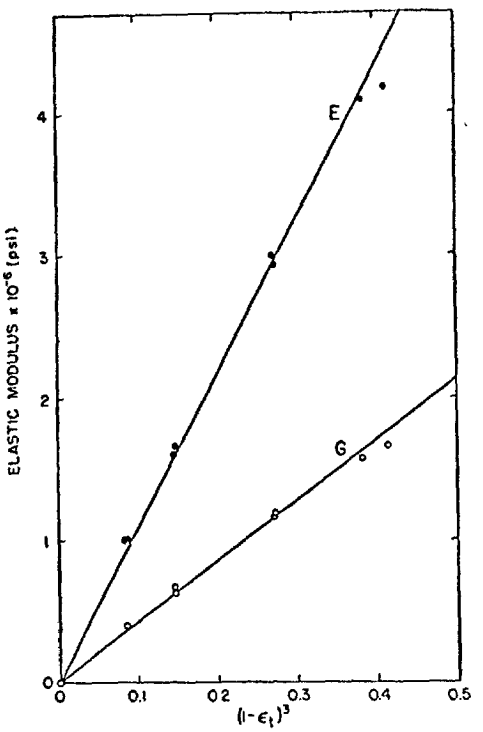

Fig. 35. *Dependence of elastic moduli of paste on "total" porosity*

Table 5. *Elastic moduli for hardened pastes of zero porosity (by extrapolation)*

	Gel phases				Solid phases			
Material	E_g × 10⁻⁶ (psi)	G_g × 10⁻⁶ (psi)	K_g × 10⁻⁶ (psi)	ν_g	E_s × 10⁻⁶ (psi)	G_s × 10⁻⁶ (psi)	K_s × 10⁻⁶ (psi)	ν_s
Tricalcium silicate	6.8	2.7	4.4	0.25	13.8	5.6	8.8	0.23
Portland cement	4.5	1.75	3.4	0.28	10.8	4.3	7.9	0.27

is zero, E_g, represents the average Young's modulus of the solid phases within the gel and the unhydrated cement particles. The bulk modulus, K, and Poisson's ratio, ν, were also calculated from the Young's and shear moduli. The limiting values on both the zero "capillary" and "total porosity" basis of all of these quantities are given in Table 5 for pastes made from pure tricalcium silicate and a portland cement, cured, saturated, and measured at 25°C. The data for E_g, G_g, etc. are of greater accuracy than the corresponding values for E_s, G_s, etc. because of the minimal extrapolation involved.

Effect of Curing

During curing, the originally water-filled spaces in the fresh paste fill with hydration products and the cement grains are progressively transformed into hydrated pseudomorphs. The moduli of all fresh pastes are zero, but during curing increase to values corresponding to the straight lines shown in Figs. 34 and 35 for mature pastes. Pastes at an early age or incompletely hydrated pastes may be regarded as a two phase system consisting of unhydrated cement particles embedded in a matrix of hydration products; the moduli in these instances may be approximated from equations for the elastic moduli of heterogenesis systems (40).

Effect of Temperature

The elastic moduli of concrete decrease with increasing temperature (41) but the information available is not sufficient for quantitative detailed analysis. With mortars of 0.35 water-cement ratio, with a 50 per cent volume of cement paste, that were cured 2 months in water at 20°C, it was found the dynamic Young's moduli varied according to (42):

$$E(10^6 \text{ psi}) = 5.11 - 0.016\ T°C \qquad (2)$$

The effect of temperature on the Young's moduli of neat pastes (0.35 water-cement ratio, cured at 97°C) has been determined over the range 0–100°C (43). For one such paste the temperature coefficient was only 0.0045×10^6 psi/°C, about one-fourth that for the room temperature cured mortar specimens of Eq. (2). Perhaps the difference is related to the effect of curing temperature on the nature of the hydration products, such as the degree of hydration and uniformity of hydration product as previously discussed in connection with the effect of temperature on strength.

Effect of Drying

Fig. 36 shows the effect of drying on the bulk moduli calculated from the resonance frequencies of thin slabs of hardened cement pastes. The wet (water-saturated) pastes have higher moduli than those dried to 47 to 7 per cent relative humidity. Also, rewetting causes a partial, but not complete, recovery. This result is taken to indicate that an irreversible change occurs in the structure of the paste during drying, in agreement with shrinkage and surface area measurements (30, 44).

Fig. 36 shows one other difference between water-saturated pastes and dried pastes. The data for the dried pastes fall on a straight line through the origin, just as found for the Young's and shear moduli data. The line for the rewet specimens and the line for the

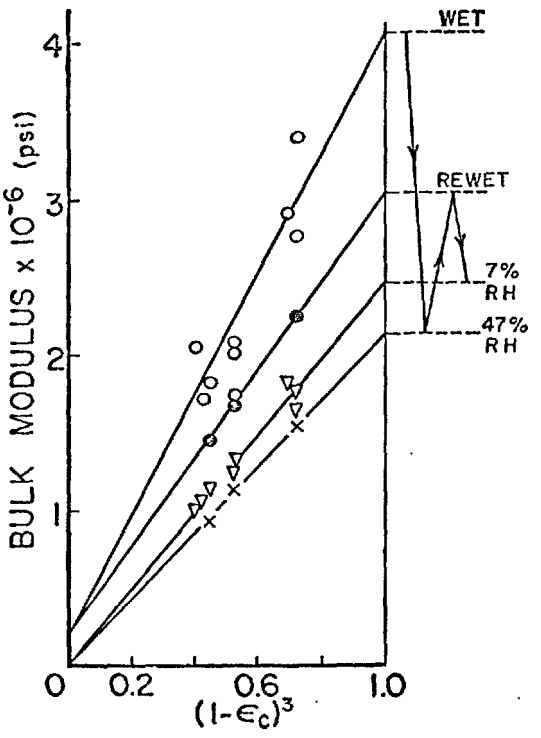

Fig. 36. *Dependence of the bulk modulus of paste on capillary porosity at different moisture conditions*

Table 6. *Changes of poisson's ratio with drying and rewetting*

Moisture condition	Poisson's ratio
Saturated	0.31
Dried to 47% RH	0.18
Rewetted	0.26
Dried to 7% RH	0.18

saturated pastes, however, show a finite intercept of about 0.2×10^6 psi, in approximate agreement with the bulk modulus of water, 0.3×10^6 psi.

Poisson's Ratio

Drying of nearly fully hydrated paste decreases Poisson's ratio (39) and the magnitude of the changes in the ratio appears to be independent of porosity of the paste within the precision of these measurements. Table 6 compares the average Poisson's ratio of saturated pastes, and the effects of drying to 47 per cent RH, rewetting (vacuum saturation), and redrying to 7 per cent RH. The pastes ranged in capillary porosity from about 0.1 to 0.3. The results are similar to those for the bulk moduli in indicating that irreversible changes are caused by drying.

Compressibility of the Hydrates

The compressibilities of an unhydrated portland cement and of "D-dried" solids in hydrated cement pastes have been measured at pressures up to 10,000 atmospheres (45). The compressibility of the unhydrated cement was found to vary with pressure range, being (0.21 ± 0.01) and $(0.12 \pm 0.01) \times 10^{-6}$/psi in pressure ranges of 0 to 4000 and 4000 to 10,000 atmospheres respectively. Compressibilities of the dried solids in hardened pastes cured for periods ranging from 1 to 32 weeks varied considerably but no correlation with curing time or initial water-cement ratio (0.3 to 0.7) could be developed. The mean value for ten such pastes was $(0.22 \pm 0.03) \times 10^{-6}$/psi. The mean value for compressibilities of the hydrates in these pastes (the paste compressibility corrected for the compression of the volume fraction of unhydrated cement) is calculated as $(0.24 \pm 0.08) \times 10^{-6}$/psi. Since the compressibility of dried calcium hydroxide (46), $(0.25 \times 10^{-6}$/psi) is very close to the value for dried pastes, the compressibilities of calcium hydroxide and "tobermorite" gel in the hardened paste cannot be very different.

The compressibilities of dried hydrates that were determined by application of hydraulic pressure (a light petroleum distillate) to the sample are about twice as great as the compressibilities determined by direct physical compression, or conversely, the bulk modulus of elasticity obtained by direct compression is only about half as great as that obtained by the hydraulic pressure technique. This discrepancy may indicate that the petroleum distillate did not penetrate all of the "gel" pores in the hardened paste even at 10,000 atmospheres pressure. Use of the $(1 - \varepsilon_c)^3$ relationship of Eq. (1) indicates that the lower bulk modulus corresponds to a porosity of about 24 per cent for the dried hydrates which agrees closely with the 26 per cent porosity generally assigned to the "gel" substance itself, Hence the discrepancies in compressibilities and bulk moduli can be explained if very little if any of the "gel" porosity was penetrated by the fluid during the compression measurements.

Inelastic Properties of Hardened Paste

Somewhat analogous to our knowledge concerning the shrinkage of pastes, the information available on the inelastic properties of pastes, mortars or concretes appears insufficient for quantitative description. The large number of papers on creep of concrete are somewhat conflicting and in many instances either the necessary details as to the exact nature of the material studied or an adequate description of the methods employed and precautions taken are lacking. However,

the discussion to follow is believed to represent, at least semi-quantitatively, some of the factors involved.

Creep

When hardened cement pastes are subjected to externally applied loads both instantaneous and time-dependent deformations occur. The instantaneous portion may include both a truly elastic deformation and a "permanent set". The time-dependent portions resulting from the applied stress is called "creep". The creep of cement, mortar, and concrete is generally regarded to result mainly from the creep of the cement paste fraction. At moderate stress level (below 30 to 40 per cent of the ultimate strength of the material) the creep deformation is proportional to the applied stress at equal times after loading (47, 48). The total creep deformation may be divided into two parts, one of which is reversible, and the other irreversible (49). Creep which occurs under constant humidity has been called "basic creep" (50). During drying while under load the total deformation is larger than can be accounted for by the drying shrinkage. The increase in the deformation may be called the "drying creep" (47).

A typical creep curve is shown in Fig. 37 (51). This curve shows compressive strain per unit stress (at 3500 psi) of a cement paste cylinder of 0.30 water-cement ratio. The specimen, a thin-walled (2.5 mm) hollow cylinder, was tested in water to insure water-saturation throughout the test. Three separate creep zones were identified as shown in the figure. The test was continued for 1300 hours, and although constant length had not yet been reached, the total strain was more than twice the instantaneous strain.

Flexural deflections of small, sealed, hardened cement paste beams of 0.32 water-cement ratio have been found to continue for about 500 days, attaining apparently constant values about four times as great as the instantaneous deflections (48).

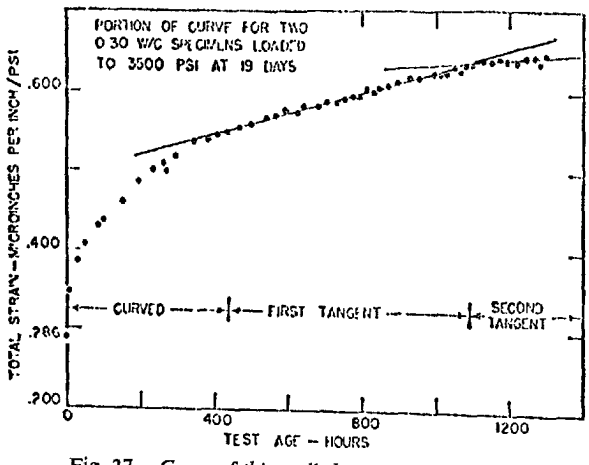

Fig. 37. *Creep of thin-walled cement paste cylinder*

Effect of Water-Cement Ratio and Curing on Creep

Although the creep of mortar and concrete can be approximately calculated from the volume fractions of cement gel and unhydrated cement in the cement paste fraction (41) (47) few detailed studies of this kind have been reported for cement pastes. The creep is known to increase with water-cement ratio and to decrease with curing time before loading. The effect of water-cement ratio on the creep is shown in Table 7 for water-saturated portland cement pastes cured for 29 days before loading (51).

Effect of Drying on Creep

If concrete or mortar is loaded at the same time that it is dried for the first time the total deformation can be several times as great as the sum of the shrinkage and the creep measured separately (52) (53). The effect is observed in shear as well as in compression and flexure (54). The effect was not observed during subsequent drying after rewetting (55). This fact indicates that the effect may be associated with an irreversible change of structure of the paste during first drying. To what extent this effect may depend upon reaction with atmospheric carbon dioxide is not known. However, as already discussed, it is known that irreversible changes of the shrinkage behavior occur during the first drying in the absence of carbon dioxide (30). It therefore seems likely that the irreversibility seen in the creep during first drying is not totally dependent upon carbonation. The phenomenological similarities and certain theoretical considerations indicate that drying shrinkage and creep may have a common origin (56).

Creep is practically eliminated if the paste is oven dried at 110°C before loading and kept dry while under load. Upon rewetting the paste may again creep under stress, but at a lower rate than before drying (51).

Table 7. *Effect of water-cement ratio on creep of water-saturated pastes*

w/c	Load* (psi)	Duration of load (hours)	Specific instantaneous strain	Specific creep strain
0.45	3370	800	0.47 × 10⁻⁶/psi	0.68 × 10⁻⁶/psi
0.40	4300	875	0.41 × 10⁻⁶/psi	0.56 × 10⁻⁶/psi
0.33	5825	875	0.30 × 10⁻⁶/psi	0.45 × 10⁻⁶/psi
0.30	6000	800	0.26 × 10⁻⁶/psi	0.35 × 10⁻⁶/psi

*Approximately 33 to 40 percent of compressive strength of specimens.

Effect of Temperature on Creep

Creep of moist mortars and concretes increases with temperature above 10°C, but shows irregular variations with temperature near 0°C. Results (55) reported for measurements on sealed, moist cured mortars of 59 per cent cement paste, 0.35 water-cement ratio, cured 6 months at 35°C before loading in flexure are given in Fig. 38. Also shown are results obtained by in similar tests (57) of for moist concretes moist cured 41 days before loading to compression. The relative creep, the ratio of the creep at each temperature to that at 20°C is given as a function of the temperature. The creep values were those determined after 24 days under load at about 30 per cent of the ultimate load. The agreement between the two sets of data is excellent. The relative creep for sealed, but not water-saturated, specimens of hardened portland cement paste beams of 0.32 water-cement ratio did not increase with temperature as much as indicated by the data of Fig. 38 (58). The higher creep at temperatures near 0°C is considered to be an artifact attributable to cyclic freeze-thaw action associated with the temperature control. Much larger deflections are observed when the specimen is subjected to temperature variations while loaded than when loaded at any constant temperature within the range (57, 42).

Internal Friction

The mechanical processes of creep under static loads have relatively long relaxation times. In addition, there are mechanical relaxation processes of much shorter duration which produce internal friction and damping when cement pastes are dynamically loaded. The "vibration damping" at very low frequencies may be a result of some of the same relaxation processes that control creep. Measurements of the logarithmic decrement, δ, at low frequencies show a marked increase in internal friction at frequencies below 2.5 cycles per sec., Hz (59). Portland cement pastes of 0.33 water-cement ratio, cured at 95 per cent RH for at least 2 weeks and dried in air until 2 months old showed a value of δ of 0.026 above 2.5 Hz, but δ increased to 0.036 at 0.5 Hz, the lowest frequency employed. The results suggest even greater damping at lower frequencies.

At higher frequencies it is sometimes more convenient to measure "tan δ" by measuring the width of a resonance peak, rather than the logarithmic decrement directly.

In a preliminary study of the temperature dependence of tan δ of cement pastes results were reported (43) for values of tan δ ranging from 0.005 for a partially dried cement paste cured at 27°C to peak values as high as 0.04 for water-saturated pastes that had been cured at 97°C (0.35 water-cement ratio). Five internal friction peaks were identified in the water-saturated pastes in the frequency range 500 to 3000 Hz between −30 and 100°C. The temperature dependence pattern indicated one peak to be a relaxation process associated with the flow of water of nearly normal viscosity. In the one partly dried paste no internal friction peaks were observed, but the value of tan δ was high enough to indicate the existence of relaxation processes differing widely in their relaxation times.

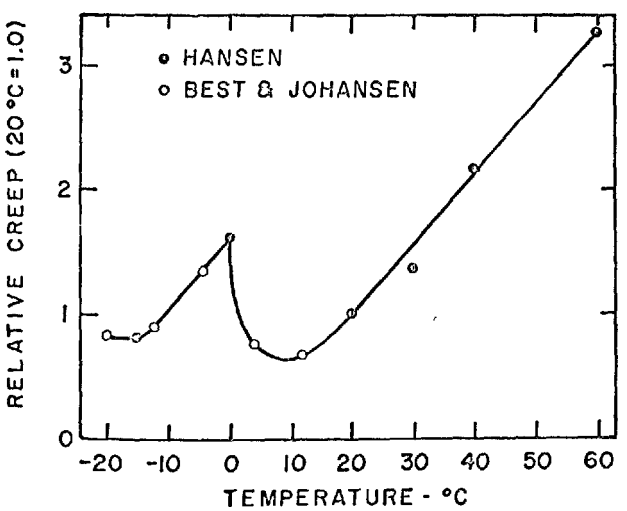

Fig. 38. *Variation of creep of sealed mortars with temperature*

Permeability to Water

Saturated Flow

The rate of flow of water through hardened cement pastes under the action of a hydraulic gradient, as given by D'Arcy's law, depends upon the paste structure and the viscosity of the fluid. The viscosity of the liquid phase may depend upon dissolved impurities, such as the alkalies present in most portland cements. Gradients in the concentration of dissolved alkalies may also cause "osmotic pressure" effects that cause apparent deviations from D'Arcy's law. When such "osmotic" effects occur a plot of the observed flow rate versus the applied hydraulic pressure is linear, but an intercept on the pressure axis is observed. The intercept on the pressure axis may be taken as the "osmotic" pressure, and the slope of the relationship used to calculate the permeability coefficient (60).

The relationships between permeability and other properties, such as porosity and "specific surface

area" are not simple. In a freshly mixed cement paste "bleeding" or "settlement" is observed. From bleeding measurements the permeability coefficient of fresh pastes can be calculated (1, 61). The total water content of the paste can be considered to be "capillary" space. Even after the paste has set, in the early stages of hydration, the originally water-filled spaces between the cement grains form a continuous system of capillaries; thus, the resistance afforded by the cement particles and hydration product is not great and the permeability remains high. As hydration proceeds these capillaries are partially filled by the hydration products, the permeability decreases, and, for well hydrated paste of intermediate water-cement ratio, becomes very low.

For sufficiently hydrated pastes the relationship between permeability and "total" porosity (gel and capillary porosity) was found to satisfy the following equation (62):

$$K_1 = \frac{1.36 \times 10^{-10}}{\eta(T)} \frac{\varepsilon^2}{1-\varepsilon} \exp\left[-\left(\frac{1242}{T} + 0.7\right)\frac{1-\varepsilon}{\varepsilon}\right] \quad (3)$$

in which K_1 is the permeability coefficient, $\eta(T)$ is the viscosity of water in poises at temperature T(°K), and ε is the "total porosity".

This equation has been previously applied to flow through both the "gel" and "capillary" pores, or the "total porosity", of the paste. However, in keeping with the prior discussions, if the "gel" water is considered to be part of the "solid" phase of the hydrated paste, and if the "total" porosity, ε, is replaced by only the "capillary" porosity, ε_c, then the equation applies over the whole range, from fresh, bleeding and plastic pastes, to mature pastes as is shown in Fig. 39.

This figure obtained for pastes of C_3S show acceptable conformance with Eq. (3) for fresh, bleeding pastes (61) and for hardened pastes after 4 to 242 days of hydration without any suggestion of major change in the permeated system, i.e., such as "continuous" versus "discontinuous" capillaries. It has been noted that pastes made of cements of normal fineness but at high water-cement ratio, 0.70 by wt., do not quantitatively conform to Eq. (3) until relatively well hydrated. Specimens prepared without special precautions at such water-cement ratios may contain "bleeding channels" that can produce misleadingly high experimental results.

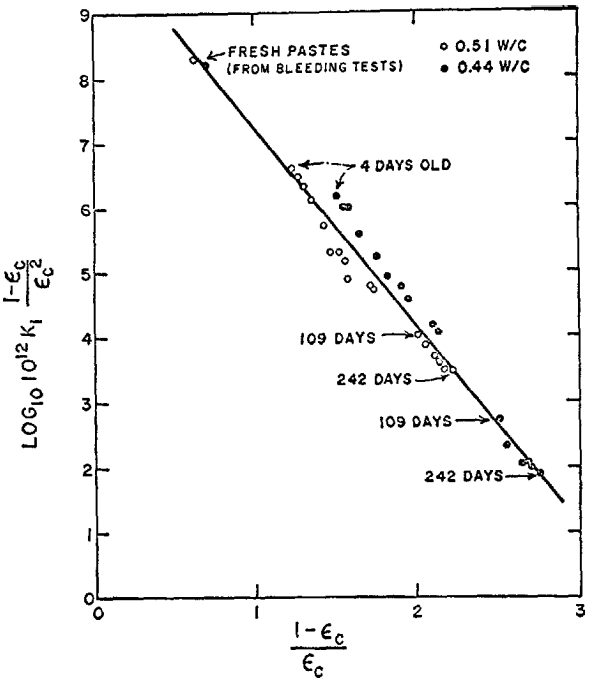

Fig. 39. *The functional relationship between permeability and capillary porosity is linear over the porosity range from fresh pastes (bleeding) to essentially fully hydrated pastes (242 days moist cured)*

Diffusion of Moisture in Unsaturated Pastes

Moisture may diffuse through an unsaturated paste because of concentration of dissolved material, humidity and temperature gradients. A general treatment for capillary porous systems, including both mass and heat transport, has been given (63). For isothermal, uniaxial flow, mass transport is proportional to the concentration gradient. In hardened cement pastes the diffusion coefficient is found to increase with paste porosity, moisture content and temperature, and to decrease with curing time (64, 65, 66, 67).

Most determinations of the water diffusion coefficients are based on transient measurements of water contents during drying rather than steady state conditions. In many instances, the drying rate then is not controlled by diffusion through the material, because of retardation by slow drying at the surface of the specimen. Unless a particular effort is taken to maintain humidity and temperature control at the specimen's surface the initial rate of drying will not be the diffusion controlled rate. When, in later stages of drying the rate becomes diffusion controlled, there is a marked change in the rate. Values of the "diffusion coefficient" may then be calculated from the drying curves.

Data on diffusion coefficients shown in Fig. 40 pertain to determinations on moist cured hardened cement pastes (67).

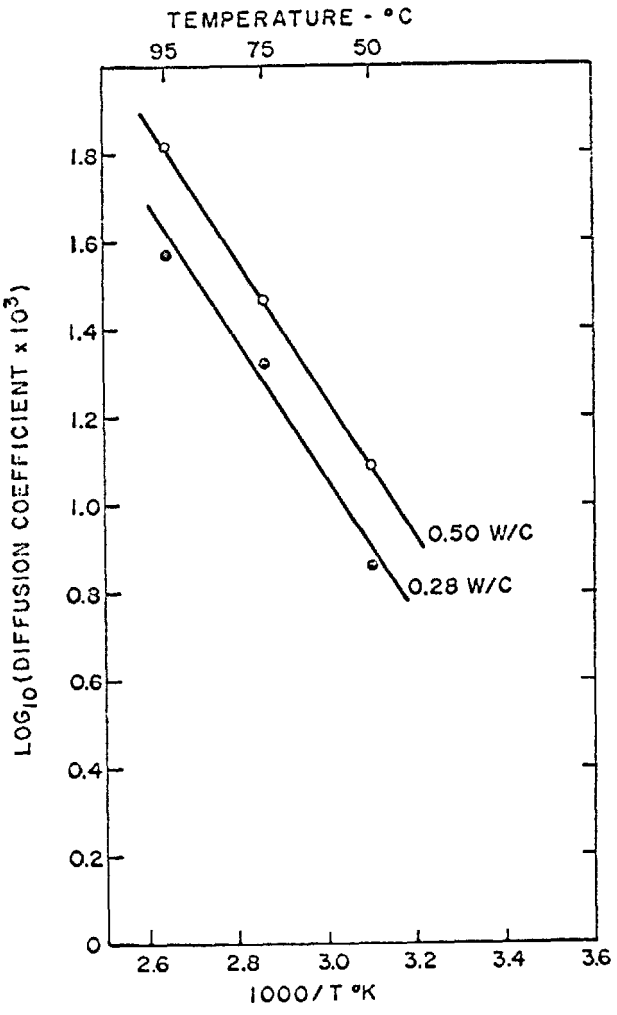

Fig. 40. *Moisture diffusion in paste varies with temperature*

The results agree with values obtained by other investigations (66) at the higher temperatures.

The temperature dependence of the diffusion coefficients may be used to calculate the activation energy for moisture diffusion through the paste; 6.5 ± 3 kcal/mole for 0.5 *w/c* and 7.5 ± 3 kcal/mole for 0.28 *w/c*. These values were derived from pastes from which more than half the evaporable water had been removed. Lower values would be expected at higher water contents.

Ionic Mobility and Electrokinetic Effects

The effects of "ionic mobility" and of "electrokinetic phenomena" in cement paste, although discussed only briefly in this paper, are believed to be of considerable importance in connection with various aspects of paste, mortar, and concrete properties. Because of their complexity these matters will be dealt with in necessary detail in a subsequent paper.

Ionic Mobility

The inherent mobility of the particular ionic species influences the relative ease with which they can be leached from paste and hence also presumably the relative ease with which they can penetrate the paste. For example, the hydrated lithium ion because of its relatively low ionic mobility (conductance) is leached less rapidly than the hydrated sodium ion which has an intermediate ionic mobility. The hydrated potassium ion, which has a mobility higher than sodium ion, is leached more rapidly.

There is also evidence that the relative ionic mobilities influence not only the distribution among ionic species during simultaneous leaching but also the overall rate of leaching of all ions. The addition of a lithium salt to cement containing soda and potash reduces the rate of leaching of all alkalies. Apparently the ion of lowest mobility present has a significant effect on the total leaching rate of all alkalies.

In addition to their influence on movement of ions within the paste, the mobilities of the ions can have considerable effect upon certain chemical reactions. For example, it has been shown (68) that at essentially equal thermodynamic activities, the rate of attack of the alkali hydroxides on siliceous aggregates is directly related to ionic mobility, i.e., lithium hydroxide is least aggressive, sodium hydroxide is moderately aggressive, and potassium hydroxide is the most aggressive. In other tests it has been shown that tetramethyl ammonium hydroxide is less aggressive than lithium hydroxide and that the tetramethyl ammonium ion has a correspondingly lower mobility than lithium ion.

We have found that consideration of ionic mobilities also successfully explains the effects of various chemical inhibitors of the alkali aggregate reaction (69).

Electrokinetic Effects

Cement paste behaves as a reasonably efficient semi-permeable membrane as indicated by observations of osmotic flow when differences exist in the thermodynamic activities of the water component of contact aqueous solutions.

In addition, cement paste appears to be a permselective, electronegative membrane and show phenomena associated with this type of membrane. Streaming potentials or electroosmosis results when

an electrolyte is forced through the paste or an electrical potential gradient applied. Also, since the paste membrane shows greater transference for cations, "anamalous osmosis" develops if gradients in activity of cations exist. A suitable description of the phenomena and the experimental results obtained are beyond the scope of this paper.

References

1. T. C. Powers, "Physical properties of cement paste," Proc. Fourth International Symp. Chemistry of Cement, Natl. Bur. Stds. Monograph No. 43, Washington, Vol. II, pp. 577–609 (1960) PCA Res. Dept. Bull. 154.
2. Chemistry of Cement: Proceedings of the Fourth International Symposium, Natl. Bur. Stds. Monograph No. 43, 2 Vols., Washington, USA (1960).
3. L. S. Brown, Discussion of "Microstructure of hardened cement paste," by Å. Grudemo, Proc. Fourth International Symp. Chemistry of Cement, U. S. Dept. of Commerce, Washington, pp. 655–656 (1962).
4. P. Terrier and M. Moreau, "Recherche sur le mechanisme le l'action pouzzolanique des cendres volantes dans le ciment" Revue de Materiaux de Construction "Ciments et Betons" No. 613–614, October et November (1966).
5. L. E. Copeland and E. G. Schulz, "Electron optical investigations of hydration products of calcium silicates and portland cement," J. Res. Develop. Lab., Portland Cement Assoc. **4**, (1) 2–12 (Jan. 1962) PCA Res. Dept. Bull. 135.
6. Å. Grudemo, "The microstructures of cement gel phases," Swedish Cement and Concrete Research Institute at the Royal Institute of Technology, Stockholm (1965), Reprint 30.
7. H. E. Schwiete, U. Ludwig and E. Niël, "Studies of the beginning of hydration of clinker and cement," Proc. of the Seventh Conference of the Silicate Industry, pp. 221–233, Akademai Kiado, Budapest (1965).
8. S. Brunauer, L. E. Copeland and R. H. Bragg, "The stoichiometry of the hydration of tricalcium silicate at room temperature," J. Phys. Chem. **60**, 112–120 (1956) PCA Res. Dept. Bull. 65.
9. L. E. Copeland, E. Bodor, T. N. Chang and C. H. Weise, "Reactions of tobermorite gel with aluminate ferrites, and sulfates," J. Res. Develop, Lab., Portland Cement Assoc. **9**, (1) 61–74 (Jan. 1967) PCA Res. Dept. Bull. 211.
10. L. E. Copeland, private communication (1968).
11. S. Brunauer, R. Sh. Mikhail and E. E. Bodor, "Pore structure analysis without a pore shape model," J. Colloid and Interface Sci., **24**, 451–463.
12. R. Brown, "Pore studies of carbonate aggregate by an evaporation technique," Ph. D. Thesis, Purdue University (1968).
13. L. I. Edel'man, D. S. Sominskii and N. V. Kopchikova, "Pore-dimension distribution in cement stone," (in Russian) Kolloid, Zhur, **23**, 228–233 (1961).
14. T. C. Powers and T. L. Brownyard, "Studies of the physical properties of hardened portland cement paste," Proc. Am. Concrete Inst., **41**, 101–132, 249–336, 469–504, 549–602, 669–712, 815–880, 933–992 (1946–1947) PCA Res. Dept. Bull. 22.
15. R. A. Helmuth, "Capillary size restrictions on ice formation in hardened portland cement pastes," Proc. Fourth International Symp. Chemistry of Cement, Natl. Bur. Stds. Monograph No. 43, Washington, Vol. II, pp. 855–869 (1960) PCA Res. Dept. Bull. 156.
16. R. Sh. Mikhail, L. E. Copeland and S. Brunauer, "Pore structure and surface areas of hardened portland cement pastes by nitrogen adsorption," Canadian Journ. Chem., **42**, 426–438 (1964) PCA Res. Dept. Bull. 167.
17. R. Sh. Mikhail and S. A. Selim, "Adsorption of organic vapors in relation to the pore structure of hardened portland cement pastes," "Symposium on structure of portland cement paste and concrete", Special Report 90, Highway Research Board, Washington, pp. 123–134 (1966).
18. C. M. Hunt, "Nitrogen sorption measurements and surface areas of hardened cement pastes," "Symposium on structure of portland cement paste and concrete", Special Report 90, Highway Research Board, Washington pp. 112–122 (1966).
19. D. L. Kantro, private communication (1968).
20. L. E. Copeland and J. C. Hayes, "The determination of non-evaporable water in hardened portland cement pastes," ASTM Bull. 194, 70–74 (1953).
21. L. E. Copeland, "Specific volume of evaporable water in hardened portland cement pastes," Jour. Am. Concrete Inst., Proc. **52**, 863–874 (1956).
22. P. Seligmann, "Nuclear magnetic resonance studies of the water in hardened cement paste," J. Res. Develop. Lab., Portland Cement Assoc. **10**, (1) 52–65 (Jan. 1968).
23. R. L. Blaine, "Proton magnetic resonance in hydrated portland cements," Proc. Fourth International Symp. Chemistry of Cement, Natl. Bur. Stds. Wash., Monograph No. 43, Vol. I, pp. 501–511 (1960).
24. T. C. Powers, "The physical structure and engineering properties of concrete," Lecture at Institute of Civil Engineers, Iondon, March 1956, PCA Res. Dept. Bull. 90.
25. J. A. Griffith, "Physical properties of typical American rocks," Iowa. Iowa State College, Engineering Experiment Station, Bull. No. 131, 56 pages (1937).

26. L. E. Copeland, D. L. Kantro and G. Verbeck, "Chemistry of hydration of portland cement," Proc. Fourth International Symp. Chemistry of Cement, Natl. Bur. Stds. Washington, Monograph No. 43, Vol. I, pp. 429–465 (1960) PCA Res. Dept. Bull. 153.

27a. S. Brunauer and S. A. Greenberg, "The hydration of tricalcium silicate and β-dicalcium silicate at room temperature," Proc. Fourth International Symp. Chemistry of Cement, Natl. Bur. Stds. Monograph No. 43, Washington, Vol. I, pp. 135–168 (1960) PCA Res. Dept. Bull. 152.

27b. D. L. Kantro, S. Brunauer and C. H. Weise, "Development of surface in the hydration of calcium silicates. II Extension of investigations to earlier and later stages of hydration," J. Phys. Chem. **66**, 1804–1809 (1962) PCA Res. Dept. Bull. 151.

28. D. L. Kantro, private communication (1968).

29. W. Lerch, "The influence of gypsum on the hydration and properties of portland cement pastes," Proc. Am. Society for Testing Matls., **46**, 1251–1292 (1946) PCA Res. Dept. Bull. 12.

30. R. A. Helmuth and D. H. Turk, "The reversible and irreversible drying shrinkage of hardened portland cement and tricalcium silicate pastes," J. Res. Develop. Lab., Portland Cement Assoc. **9**, (2) 8–21 (May 1967) PCA Res. Dept. Bull. 215.

31. R. A. Helmuth, "Dimensional changes of hardened portland cement pastes caused by temperature changes," Proc. Highway Research Board, **40**, 315–336 (1961) PCA Res. Dept. Bull. 129.

32. H. Dettling, "The thermal expansion of hardened cement paste, aggregates, and concretes," (in German) Deutscher Ausschuss für Stahlbeton, Heft 164, Part 2, 1–64 (1964).

33. L. J. Mitchell, "Thermal expansion tests on aggregates, neat cements, and concretes," Proc. Am. Society for Testing Matls., **53**, 963–977 (1953).

34. S. L. Meyers, "Thermal expansion characteristics of hardened cement paste and of concrete," Proc. Highway Research Board, **30**, 193–203 (1950).

35. L. Virronnaud and N. V. Thanh, "Dilatometer with an optical tripod, Part 2 tests and results of experiments," (in French) Annales de l'Inst. Tech. Batin et Trav. Publ. 7-78 531–540 (June 1954) Sec. Essais et Mesures (30) France, Centre D'Etudes et de Recherches de L'Industrie des Liants Hydrauliques, Publ. Tech. No. 65.

36. S. L. Meyers, "Thermal coefficient of expansion of portland cement," Ind. Eng. Chem., **32**, 1107–1112 (1940).

37. A. E. Lentz and G. E. Monfore, "Thermal conductivities of portland cement paste, aggregate, and concrete down to very low temperatures," J. Res. Develop. Lab., **8**, (3) 27–33 (Sept. 1966). PCA Res. Dept. Bull. 182.

38. R. W. Carlson and L. R. Forbrich, "Correlation of methods for measuring heat of hydration of cement," Ind. Eng. Chem., Analytical Edition **10**, 382–386 (1938).

39. R. A. Helmuth and D. H. Turk, "Elastic moduli of hardened portland cement and tricalcium silicate pastes: effect of porosity," "Symposium on structure of portland cement paste and concrete", Special Report 90, Highway Research Board, Washington, pp. 135–144 (1966) PCA Res. Dept. Bull. 210.

40. T. C. Hansen, "Influence of aggregate and voids in modulus of elasticity of concrete, cement mortar, and cement paste," Jour. Am Concrete Inst., Proc. **62**, 193–216 (1965).

41. T. C. Hansen, "On rheology of hardened concrete," (in English) Syenska Forskningsinstitut för Cement och Betong. Handlinger Nr. 37, 39 pages (1968).

42. T. C. Hansen and L. Eriksson, "Temperature change effect on behavior of cement paste, and concrete under load," Jour. Am. Concrete Inst., Proc. **63**, 489–504 (1966).

43. C. W. Richards and F. Radjy, "A new application of internal friction to concrete research," Materials Research and Standards, ASTM, **6**, 386–392 (1966).

44. C. M. Hunt, L. A. Tomes and R. L. Blaine, "Some effects of aging on the surface area of portland cement paste," J. Res. Natl. Bur. Stds., **64A**, No. 2, 163–169 (Mar-Apr 1960).

45. C. E. Weir, C. M. Hunt and R. L. Blaine, "Behavior of cements and related materials under hydrostatic pressures up to 10,000 atmospheres," J. Res. Natl. Bur. Stds., **56**, 39–50 (1956).

46. C. E. Weir, "The system lime-water at 21°C and high pressures," J. Res. Natl. Bur. Stds., **54**, 37–40 (1955).

47. I. Ali and C. E. Kesler, "Mechanisms of creep in concrete," Amer. Concrete Inst. Spec. Publ. 9, "Symp. on the creep of concrete" 35–57 (1964).

48. J. Glucklich, "Rheological behavior of hardened cement paste under low stresses," Proc. Am. Concrete Inst., **56**, 327–337 (1959).

49. O. Ishai, "Elastic and inelastic behavior of hardened mortar in torsion," Amer. Concrete Inst. Spec. Publ. 9, "Symp. on the Creep of Concrete" 65–94 (1964).

50. T. C. Hansen, "Creep of concrete—a discussion of some fundamental problems," (in English) Svenska Forskningsinstitut för Cement och Betong VII Meddelanden Nr. 33, 48 pages (1958).

51. W. G. Mullen and W. L. Dolch, "Creep of portland cement paste," Proc. Am. Society for Testing Matls., **64**, 1146–1170 (1964).

52. R. E. Davis and H. E. Davis, "Flow of concrete under sustained compressive stress," Proc. Am. Society for Testing Matls., **30**, 707–730 (1930).

53. R. E. Davis, H. E. Davis and J. S. Hamilton, "Plastic flow of concrete under sustained stress," Proc. Amer. Society for Testing Matls., **34**, Pt. II, 354–386 (1934).

54. C. M. Duke and H. E. Davis, "Some properties of concrete under sustained combined stresses," proc. Amer. Society for Testing Matls., **44**, 888–896 (1944).

55. T. C. Hansen, "Creep of concrete—the influence of variations in the humidity of the ambient atmosphere," Svenska Forskningsinstitut för Cement och Betong, Sartryck 8 (1960). Reprint from 6th Congr. Intl. Assn. for Bridge and Struct. Eng. Pre. Pub. 57–65 (1960).

56. T. C. Powers, "Some observations on the interpreat-

tion of creep data," RILEM Bull. 33, 381–391 (1966).
57. C. H. Best and R. Johansen, "Creep of concrete at varying temperature," (in Norwegian) Betongtekniske Publikasjoner **1**, 23–29 (1963).
58. J. Glucklich and O. Ishai, "The effect of temperature on the deformation of hardened cement paste," RILEM Symp. on Concrete and Reinforced Concrete in Hot Countries, Pt. I, Materials, 14 pages, Haifa (1960).
59. D. G. Cole and D. C. Spooner, "The damping capacity of hardened cement paste and mortar in specimens vibrating at very low frequencies," Proc. Amer. Society for Testing Matls., **65**, 661–667 (1965).
60. T. C. Powers, L. E. Copeland, J. C. Hayes and H. M. Mann, "Permeability of portland cement paste," Jour. Am. Concrete Inst., Proc. **51**, 285–298 (1954). PCA Res. Dept. Bull. 53.
61. H. H. Steinour, "Further studies of the bleeding of portland cement paste," PCA Res. Dept. Bull. 4 (1945).
62. T. C. Powers, H. M. Mann and L. E. Copeland, "The flow of water in hardened portland cement paste," Special Report 40, Highway Research Board, Washington, pp. 308–323 (1958) PCA Res. Dept. Bull. 106.
63. A. V. Luikov, "Heat and moisture transfer in capillary porous media," (in English) RILEM Bull. 29, 99–106 (Dec. 1965).
64. R. W. Carlson, "Drying shrinkage of large concrete members," Proc. Amer. Concrete Inst., **33**, 327–336 (1937).
65. S. E. Pihlajavarra, "On the main features and methods of investigation of drying and related phenomena in concrete," (in English) Finland. Valtion Teknillinen Tutkimuslaitos. Julkaisu 100, 142 pages (1965).
66. B. P. Hughes, I. R. G. Lowe and J. Walker, "The diffusion of water in concrete at temperatures between 50 and 95°C," Brit. J. Appl. Phys., **17**, 1545–1552 (1966).
67. N. L. Hancox, "A note on the form of the rate of drying curve for cement paste and its use in analyzing the drying behavior of this material," RILEM Bull. 36, 197–201 (Sept. 1967).
68. G. Berbeck and C. Gramlich, "Osmotic studies and hypothesis concerning alkali-aggregate reaction," Proc. Amer. Society for Testing Matls., **55**, 1110–1128 (1955).
69. W. J. McCoy and A. G. Caldwell, "New approach to inhibiting alkali reaction," Proc. Amer. Concrete Inst., **47**, 693–706 (1951).

Written Discussion

Sidney Diamond

Synopsis

New data on mercury intrusion into portland cement pastes are presented, and are interpreted as indicating a continuous distribution of pore sizes from an upper limit of the order of 0.1 to 1 microns, depending on water-cement ratio and maturity. Attention is drawn to the potential utility of the scanning electron microscope in elucidating the details of portland cement paste microstructure.

The microstructure of so complex a material as portland cement paste is far from perfectly understood, despite the very extensive assemblage of evidence of various kinds presented by Verbeck and Helmuth. The present discussion is aimed at adding several additional items of evidence in the specific areas of pore size distribution and of electron optical observation of microstructure.

Mercury Porosimetry of Cement Pastes

The pore size distributions of a number of cement pastes of various water-cement ratios and degrees of maturity have been examined by D. N. Winslow in the writer's laboratory, using slightly-modified commercial mercury intrusion equipment capable of intruding cylindrical pores down to an effective

diameter of slightly greater than 100 Å. These pastes were mixed under vacuum and hydrated in sealed containers for 24 hours, stripped and hydrated under lime-water for their remaining hydration period, then oven-dried. Representative pore size distribution curves are shown in Fig. 1 for young (3-day) and mature (320-day) pastes of 0.4 and 0.6 initial water-cement ratios. A wetting angle of 130° has been assumed.

In contrast to the curves discussed by Verbeck and Helmuth, these results are presented as cumulative distribution curves rather than as differential distribution curves. In point of fact the mercury intrusion data are obtained in precisely this fashion, that is, in terms of cumulative intrusion following stepwise increments of increasing pressure. For many interpretive purposes, especially those involving estimation of relative volumes of pore space existing between arbitrary size bounds, this form of presentation was found to be much more satisfactory than the differential functions.

Examination of the data suggests the following:

1. Cement pastes prepared in this manner show only a negligible content of "large" pores that is, those larger than one micron in diameter.
2. In each of the curves there is a pronounced inflection point at a pressure corresponding to that required to intrude pores of a size range somewhere between 1 micron and 0.1 micron, depending on water-cement ratio and degree of maturity.
3. For pressures higher than that corresponding to the inflection point, an increase in pressure always brings about a significant increase in mercury intrusion; i.e. from this point down the cumulative pore size distribution curve shows a continuous distribution of sizes down to pores (or interstices) corresponding to the limit of pressuring capacity of the instrument. There are no gaps corresponding to size regions where pores capable of being penetrated by mercury are lacking.

The curves obtained generally resemble those of Edelman, Sominskii and Kopchikova (1), for comparable water cement ratios and ages, but differ from them in that the latter show significant contents of pores larger than 1 micron. The difference is apparently due to the mode of hydration, the samples of Edelman et al. being hydrated at atmospheric humidity rather than under water. Presumably water was lost from some large capillary spaces early in the hydration process and these pores remained incompletely filled with hydration product even after prolonged periods.

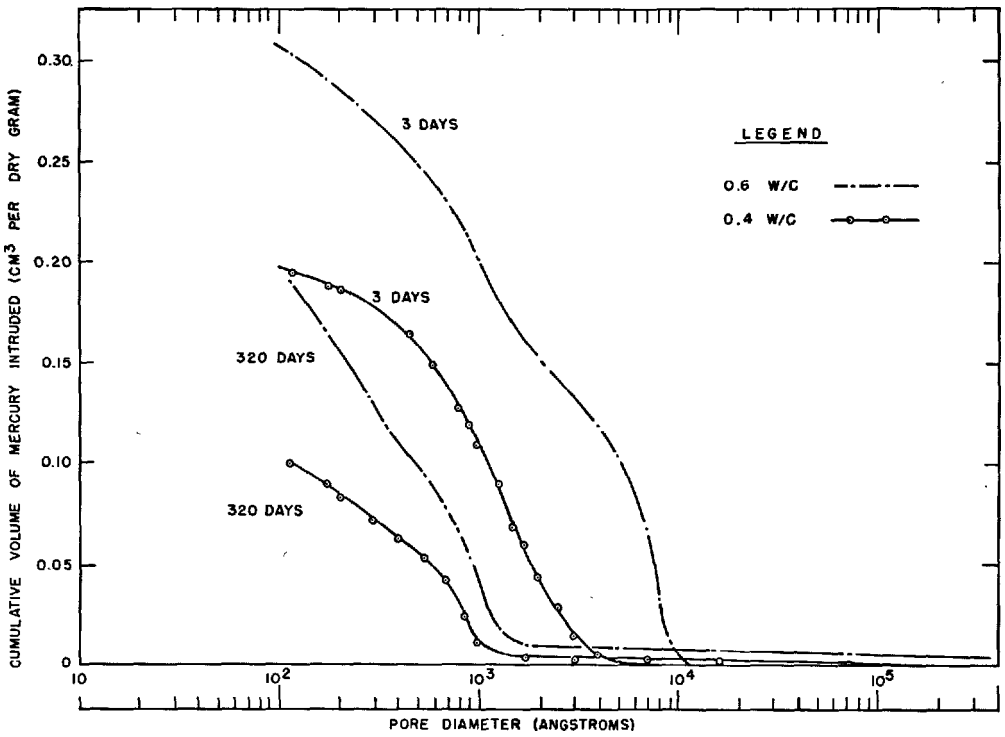

Fig. 1. *Pore size distribution curves for cement pastes*

It is entirely possible to plot such data in differential form and draw inferences about the number and extent of "modes" of pore sizes that seem to be present. It seems more to the point to the writer to emphasize the fact for sizes below the order of a significant fraction of a micron and above about 100 Å. a continuous distribution of pore sizes is indicated by mercury intrusion.

In all cases the volume of "space" potentially available in the paste (in terms of volume formerly occupied by water lost on drying) is substantially greater than the volume of mercury intruded. Thus the evidence cited here does not preclude the possibility of a significant gap in the pore size distribution between the roughly 100 Å lower limit explored and some hypothetical upper limit of a special category of "gel" pores, with the remaining volume of porosity concentrated in some narrow "gel" size range. However, the evidence of the nitrogen pore size distribution curves cited by Verbeck and Helmuth suggest that this is not the case; rather, that the continuous distribution of pore sizes also seems to exist between 100 Å (or more) and the lower limit of pore sizes. The significance of the apparent continuity in the cumulative pore size distribution curve is debatable. The writer, however, is led to the supposition that the distinction between "gel" pores and ordinary pores in cement paste may be largely conventional.

Application of Scanning Electron Microscopy

Another aspect of the microstructure of cement paste that is of current concern in a number of laboratories involves the application of the scanning electron microscope to the problem of delineating the significant details of the morphology and topographic arrangement of the particles and of the pore spaces between them. This instrument has several significant advantages over transmission electron microscopy for this purpose. In particular, one can examine a fracture surface directly, without the necessity of preparing replicas. Not only is the possibility of replication artifacts or imperfect reproduction of the surface avoided, but the entire surface of a relatively large sample may be scanned systematically and quickly; hence, much greater assurance is forthcoming that the small areas photographed are representative of the entire sample. The depth of field is extremely great, and the curved path taken by the secondary electrons which form the image permit visualization of details of microstructure within cavities and interstices between particles.

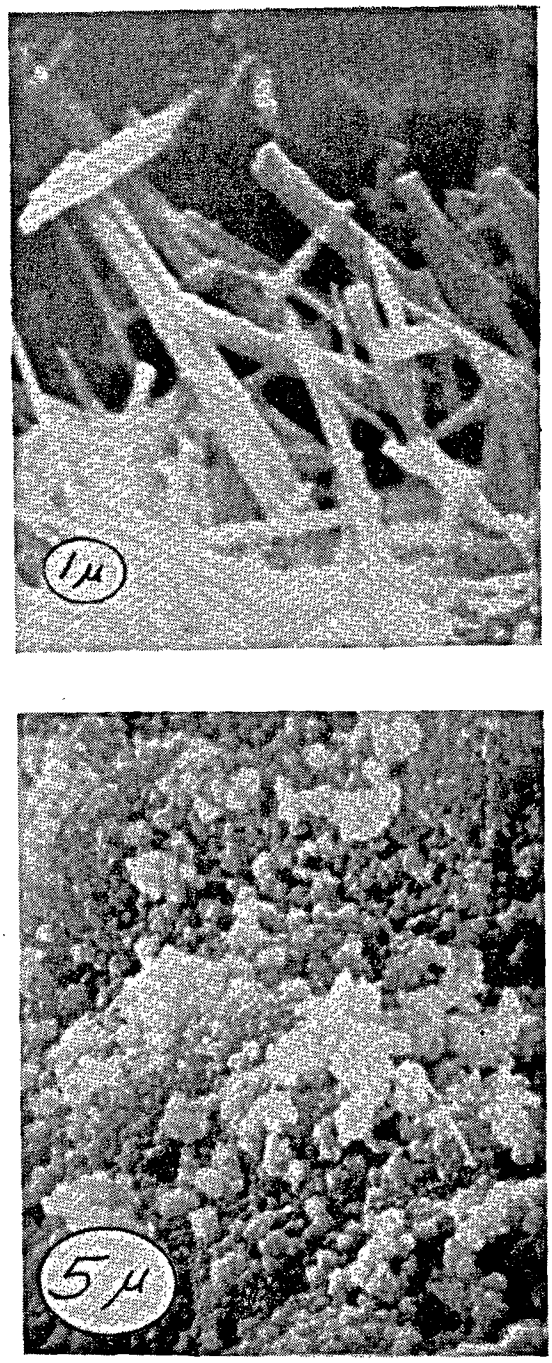

Fig. 2. *Scanning electron micrographs of cement pastes showing extremes of variation in locally-dominant particle morphology*

Details of the theory and practical aspects of image formation and interpretation have been authoritatively reviewed (2) and the proceedings of a recent conference (3) illustrated the wide range of applications possible. A direct comparison of the utility of scanning electron microscopy relative to that of examination of replicas of fracture surfaces

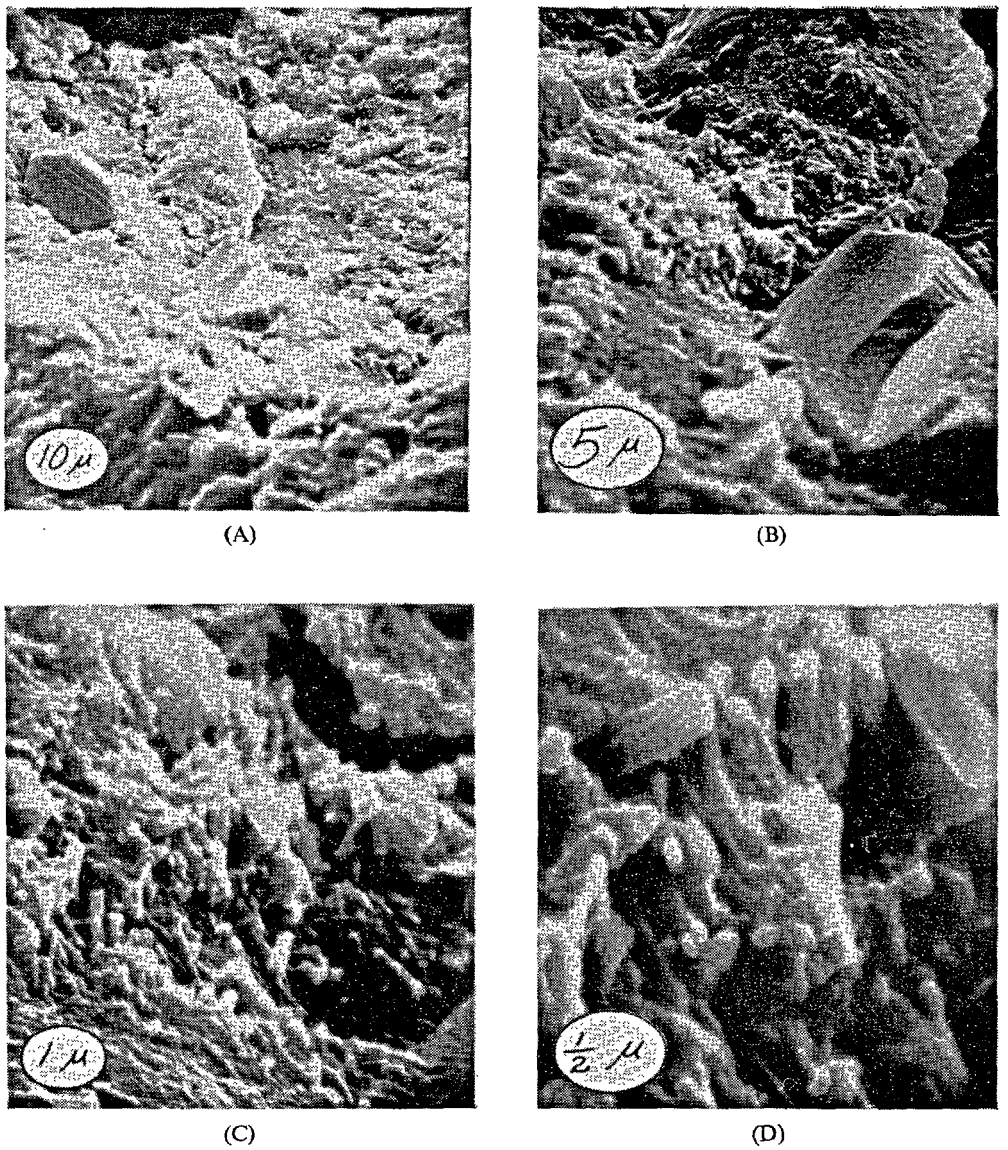

Fig. 3. *Scanning electron micrographs of a portion of the fracture surface of dried cement paste taken at progressively increasing magnification*

by transmission electron microscopy has recently been carried out (4) and examinations of the surface topography of ceramics and other materials related to cement paste have been published (5,6).

A preliminary examination of the three-dimensional arrangement of hydration products in set cement paste was reported by Chatterji and Jeffery (7) and in a subsequent paper (8) the same authors proposed a hypothesis of strength development based in part on their scanning electron microscope observations. In interpreting their observations of portland cement paste, these authors place major emphasis on their observation that the large elongated particles of ettringite and in particular the smaller needle-shaped particles of calcium silicate hydrate form an entangled mass in three dimensions.

Some very preliminary observations by the present writer illustrate that the cement paste morphology problem is much more intricate than this. In addition to areas where only entangled elongated particles are visible (Fig. 2A) we have observed areas comprising only more or less equant "gel bodies" (Fig.

2B) and areas where both particle morphologies occur in locally uniform mixtures.

Some indication of the potential of this instrument in delineating topographic relationships in cement pastes may be seen in Fig. 3 which represents several steps in a series of plates taken at the same spot on a fracture surface of a dried cement paste at progressively increasing magnifications. The sizes indicated are approximate; the ellipse indicates that the magnification indicated for the vertical direction is less than that indicated for the "horizontal" direction because of the tilt of the sample holder. The relation of Fig. 3B to Fig. 3A is obvious. Fig. 3C may be related to Fig. 3B by reference to the curved crack in the upper left hand portion which in Fig. 3B is found near the center of the figure. The advantage of the very large depth of field of the scanning microscope is apparent. Further, the complexity of the topographical features would seem to make successful replication of areas like this exceedingly difficult. Fig. 3D resolves individual particles sticking out of the ground mass. This figure illustrates one of the difficulties of scanning microscopy for viewing very small particles emerging from a base elevation; the excessive brightness observed in such cases is one of the characteristics of secondary emission and tends to obscure fine details of structure. This feature, and the limited present resolution of the scanning electron microscope (150-200 Å) makes it somewhat less satisfactory than the transmission microscope for viewing details of the finest ultimate particles of cement pastes, but its potential utility in elucidating details of microstructure on higher levels of organization appears to be very promising.

Acknowledgements

The courtesy of the Engis Equipment Company in making available their "Stereoscan" scanning electron microscope and that of Mr. Frank Rossi, who operated the instrument, are acknowledged with thanks. The data for Fig. 1 were obtained in connection with a research project sponsored jointly by the Indiana State Highway Commission and the Bureau of Public Roads, U.S. Department of Transportation. The opinions expressed, however, are entirely those of the writer.

References

1. L. I. Edelman, D. S. Sominskii and N. V. Kopchikova "Pore size distribution in cement rocks" (in Russian) Kolloid. Zhurnal **23**, 228–233 (1961).
2. C. W. Oatley, W. C. Nixon and R. F. W. Pease "Scanning electron microscopy", Advances in Electron Physics (L. Marton, ed.) **21**, 181–247 (1965).
3. Scanning Electron Microscopy, 1968 (O. Johari, ed.) Proceedings of the Symposium on the Scanning Electron Microscope, III Research Institute Chicago Illinois 60616, USA.
4. Om Johari "Comparison of transmission electron microscopy and scanning electron microscopy of fracture surfaces", Journal of Metals, 26–32 (June 1968).
5. R. F. M, Thornley and L. Cartz "Direct examination of cermaic surfaces with the scanning electron microscope" J. Amer. Ceram. Soc. **45**, 425–428 (1962).
6. L. H. Pruden, E. J. Korda and J. P. Williams "Characterization of surface topography with the scanning electron microscope", Ceramic Bull. 750–754 (1967).
7. S. Chatterji and J. W. Jeffery "Three-dimensional arrangement of hydration products in set cement pastes", Nature **209**, 1233–1234 (1966).
8. S. Chatterji and J. W. Jeffery "Strength development in calcareous cements" Nature **214**, 559–561 (1967).

Written Discussion

Rolf F. Feldman and Peter J. Sereda

It is appreciated that the authors faced a formidable task in writing on the broad subject of the structure and physical properties of cement pastes, and in this regard they are to be complimented. It must be noted, however, that the authors omitted an appreciable body of published information (1, 6, 8, 9, 10, 11, 16) and, having accepted a new concept for the "state" of the water in cement gel, did not attempt to reas-

sess the significance of this on much of the previously published information.

It is readily accepted and the authors adequately support the idea that in hydrated cement paste the physical and mechanical properties are intimately dependent and profoundly affected by the "adsorbed" water. This being the case, it has long been recognized that one of the key questions in the understanding of this system was the "state" of the water. In this regard two schools of thought have existed: one proposing that the "gel" water was physically adsorbed, and the other that at least part of this water was interlayer. The existence of these two divergent ideas in this field of science has not been documented by the authors.

The importance of these concepts pertaining to the state of the water cannot be overemphasized because they served as the basis for a model to explain the physical and mechanical properties. Most of the literature deals with these properties of hydrated cement on the basis that the "gel" water was physically adsorbed. The proposal that part of the "gel" water was interlayer water was first made by Kalousek and substantiated by extensive research at the Division of Building Research of the National Research Council of Canada.

It is gratifying to note that the authors of the principal paper under discussion are now supporting the idea that much of the "gel" water is interlayer based on the results from nuclear magnetic resonance (N. M. R.) measurements by Seligmann. The authors, however, have not discussed the profound implication of this fact on the understanding of the whole nature of hydrated portland cement and its properties. A reassessment of much previous work is certainly necessary. The work at the Division of Building Research of the National Research Council of Canada, dating from 1963, makes available a body of information and discussion on this vital question, culminating in a proposal of a new model for hydrated portland cement. The publications containing the results of these studies have not been cited as references by the authors of this principal paper, although we realize that they may not have had access to our most recent papers (12, 14, 17). This discussion, therefore, attempts to summarize the information that has been omitted from the paper under review.

We fully recognized the complex nature of cement paste and the simplified model proposed is merely another step in the development of the understanding of this system. Much has yet to be done to provide full understanding.

The development of the present model of hydrated portland cement has been largely based on surface chemical considerations; this involved the establishment of criteria to distinguish between chemically-combined and physically adsorbed water. The determination of the stoichiometry of the tobermorite gel, its water surface area, and its porosity were based on the above criteria.

Water adsorption experiments have been used to measure the porosity and surface area of hydrated portland cement; results of the latter have yielded values in excess of 200 m^2/g. This value was of great importance and was used to estimate the number of layers in the tobermorite gel "crystallites"; it also provided the basis for calculating other physical parameters.

Kalousek (1) observed that the surface area using N_2 as adsorbate yielded very low values compared with those of water; the N_2 value was shown by Mikhail et al (2) to decrease with the water-to-cement ratio to values below 30 m^2/g, and, as reported by the authors, by Kantro to values below 1 m^2/g. Similar results were obtained when organic vapours such as $CH_3 \cdot OH$ were used as adsorbates (3).

The determination of surface area by adsorption of N_2, together with a calculation based on the B. E. T. equation, has become a standard method in the realm of surface chemistry. Carbons with very high surface areas and very small pores have yielded nitrogen surface areas that approach 1000 m^2/g. Yet in the case of hydrated portland cement, the "water area" has been the one generally held "true and valid." It was considered that the N_2 molecule could not enter small pores and be adsorbed on the whole surface because of its large size (2). The diameters of the water, nitrogen, and methanol molecules are approximately 3.25, 4.05 and 4.4 Å respectively; it seems difficult to accept the situation where over 90 per cent of the area is excluded to N_2 because of the small difference in diameters. If the holes were part of the cyrstal structure as in certain "molecular sieves" that are cage-like molecules with small entrances, it would be realistic, but hydrated cement is not of this nature.

Several years ago, in the laboratories of the Division of Building Research of the National Research Council of Canada, it was decided to undertake a careful study of the water-hydrated portland cement sorption system. This study included measurement of both length change and weight change with changing relative humidity. The measurements were done simultaneously in carefully controlled conditions and in a high-vacuum apparatus. We believe, therefore, that we are correct in stating that the Division of Building Research of the NRC of Canada was the first laboratory to carry out this type of study on hydrated

portland cement.

In light of this, it is indeed surprising that the authors of this principal paper state, "... in most of the investigations of this matter during the past several decades, pertinent details regarding either the nature of the materials used, or the environment to which the specimens were actually exposed, have been omitted from the published reports, Therefore, the present authors will draw largely upon their own studies that are believed to have taken into consideration at least most of the important factors." This would seem to confine unduly the scope of the discussion presented in this principal paper.

Before these experiments could be started, it was necessary to understand the adsorption and length-change process. The project began, therefore, with studies of the adsorption of water on materials less complicated than hydrated portland cement, but related to it in some way. These materials included an alumino-silicate (molecular sieves), calcium sulphate hemihydrate, precipitated calcium carbonate, finely divided silica, porous glass and calcium hydroxide. A series of papers were published on this work (4 to 8).

The results of the early experiments on bottle-hydrated cement showed that it was possible to detect characteristic differences in the type of water that was being removed on drying (9). These characteristics provided the base for a hypothesis on the expansion and contraction of hydrated portland cement on sorption and desorption of water (10, 11). It must be emphasized that this hypothesis did not relate to the phenomena that operate during first drying. The hypothesis emphasized the role of the Gibbs and Bangham equations in the intermediate pressure regions and it was concluded that the expansion on sorption was initiated by the decrease in surface energy of the solid. It was not necessary to introduce the concept that individual crystallites could move back and forth with respect to each other. As will be shown later, other evidence also disproves this concept.

From the length change and weight change characteristics and the sorption isotherm (10, 11) it was recognized that the exit and entry of the interlayer water between the sheets of the tobermorite gel played an important role in expansion and contraction. At this stage no real quantitative estimate could be made as we have now been able to do.

The effect of interlayer water rehydration on water sorption properties may be easily illustrated. First, however, a brief discussion of some cases of sorption hysteresis will clarify the point.

Fig. 1 illustrates three forms of hysteresis that have been observed on various materials. A loop of type I is formed over a limited range of pressures and is generally considered to be associated with the formation of a meniscus. Scanning of the loop may be performed by desorbing after reaching X on the ascending boundary curve; thus, one reaches Y on the descending curve and may return to X by readsorption. Type II hysteresis, where the loop extends over the whole pressure range, has been observed for water on cellulose or protein fibres and also for polar adsorbates on montmorillonite. In type III, which combines the characteristics of the other types, the ascending and descending branches only join at very low or zero pressure. The dotted lines show the pattern followed if adsorption recommences at X. Type III loops are found with some graphites, clay minerals and, as has

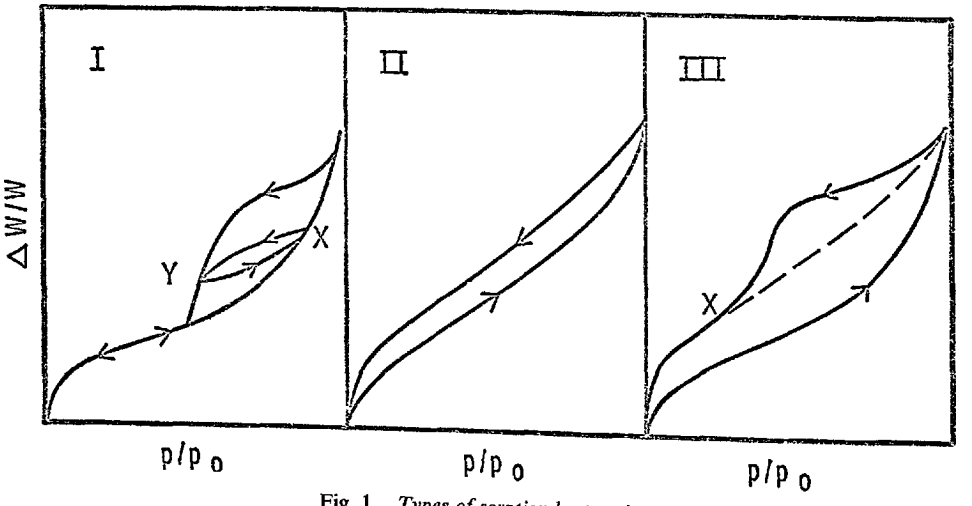

Fig. 1. *Types of sorption hysteresis*

been shown (10), with hydrated portland cement.

This low-pressure hysteresis phenomenon is usually attributed to irreversible intercalation of adsorbate within the structure of the solid. Quite often the solids have a layer structure and a change in the spacing of these layers has been observed. Unfortunately, because of the nature of the tobermorite gel with regard to the *c* axis, it has not been possible to confirm the interlamellar penetration by X-ray methods. It is clear, however, that somewhere along the ascending branch of the isotherm water is sorbed irreversibly. This would affect the over-all mechanism for the sorption-expansion phenomena, and the use of the ascending curve for B. E. T. calculations if interlayer water re-enters in the 0 to 35 per cent relative humidity range.

The importance of these results was realized at an early stage in our laboratories. Both the classification and role of the various forms of water became a prime objective of our activities; it was suspected that the entry of interlayer water might affect many mechanical properties. The effect of physically-adsorbed water on the bond between crystallites (and the nature of this bond) was also considered to be of critical importance. As a result, further work in our laboratories was planned to re-examine some areas in greater detail and to extend it in other areas.

Experiments at DBR/NRC can be divided into two categories:

i) measurement of the variation of adsorbed water, length, Young's modulus, flexural strength, and microhardness with relative humidity;

ii) measurement of the variation of Young's modulus, flexural strength, microhardness at constant conditions of relative humidity as a function of porosity, and method of fabrication.

The methods of fabrication involved were as follows:

(a) compaction of hydrated portland cement powder at different pressures to form rigid bodies of different porosity;
(b) cast samples at different water-cement ratios;
(c) recompacted cast samples to lower effective porosites than (b) above.

All these samples were made with small dimensions (= 30 mm diameter and 1 mm thick) to avoid stresses due to moisture gradients and to facilitate equilibrium.

These experiments were also performed on porous glass and some other materials of which more is known with regard to their properties and behaviour. The results from these were used to aid interpretation.

A discussion follows of the results of the various experiments.

Length and Sorption Isotherms and Scanning Loops

Some of this work has been presented in paper No. III-23 (12) of this Symposium and only those conclusions that contribute to this discussion will be restated. We would like to draw attention to Fig. 1 to 4 of the above paper. It was concluded that interlayer water was entering simultaneously as adsorption occurs up the isotherm.

From the scanning loops and from some assumptions that later provided to be justified, we were able to separate quantitatively the interlayer and physically adsorbed water and construct isotherms for both [Fig. 5 and 6 of paper No. III-23 (12)]. From these calculations we were able to make the following conclusions that completely supported this approach.

1. Surface areas from N_2 and H_2O adsorption are very similar.

2. The total interlayer water found by calculation from the scanning isotherms was equal to the difference between the total water sorbed and the total nitrogen or methanol sorbed for many samples. This had previously been ascribed to small pores that prevented nitrogen but not water from entering.

3. A plot of length change versus weight change for the reversible isotherms produced a linear plot up to a relative humidity of about 45 per cent. This type of linear plot has been observed for water adsorption on many relatively inert materials.

4. A plot of length change versus the surface-free energy change was constructed, using the Gibbs and Bangham equations:

$$\Delta L/L \propto \Delta F = RT/\sigma \int_0^p ndp/p$$

where $\Delta L/L$ is the length change, ΔF is the surface-free energy change, σ is the surface area (cm^2/g), n is the number of moles adsorbed per unit weight of material. This plot produced a straight line through zero, and thus the equations were obeyed (see Fig. 5, paper No. III-23).

5. From these calculations, Young's modulus for the solid material was calculated to be 4.35×10^6 lb/in^2. Helmuth and Turk (13) extrapolated from porosity E plots to get E of "gel phase" as 4.5 and of the "solid phase" as 10.8 lb/in^2. This latter value was similar to the extrapolation of Soroka and Sereda (14) (paper No. III-34 of this Symposium). Both these values suffer from including as porosity the interlayer water removed during "*d*-drying". Considering the assumptions, the value found for the modulus of the solid phases is very good and is considered as further evidence of the validity of this approach.

6. Further calculations from the scanning isotherms showed that less than 20 per cent of the total expansion along the isotherm was due to physically adsorbed water. On the desorption branch of the curve at 29 per cent R. H. only 15 per cent of the evaporable water is physically adsorbed.

This is consistent qualitatively with recent N. M. R. work (15) which suggests that no physically adsorbed water is present at 70 per cent R. H. and that the water is similar to the interlayer water in montmorillonite. It is difficult to agree with the authors' statement however, that no physically adsorbed water is present since nitrogen adsorption measurements do show a fairly significant surface area even at a water-to-cement ratio of 0.25.

Sorption and the Variation of Young's Modulus

In measuring Young's modulus as a function of relative humidity two types of responses have been observed for surface active materials:

(a) no change for rigid porous bodies (this has been observed with porous glass);

(b) a continuous decrease (this has been observed largely with cellulosic materials (see Fig. 2).

Hydrated portland cement gave results which partly conformed with the first type but in addition presented certain features which at first we could not explain. These results were published in 1966 (16) and at that time were explained generally by interlayer dehydration and rehydration. Fig. 3 is a representative sketch of some of the results.

As is shown, there was very little change in Young's modulus from 100 per cent R. H. to low humidites on drying and then on "*d*-drying" a large decrease in E. On sorption an increase in E took place just above 50 per cent R. H.

In the irreversible isotherms presented as Fig. 6 of paper No. III-23, for $\Delta L/L$ and $\Delta W/W$ versus relative humidity, it will be noted that there is a similarity between them and the E versus relative humidity plot. The hysteresis and effects beyond 50 per cent R. H. are the same, and the $\Delta L/L$ versus $\Delta W/W$ plot shows a sharp break just above 50 per cent R. H.

We were able to incorporate these results in a simple model which can explain most of the properties described. This model has already been described (17) and is referred to briefly in paper No. III-23.

The main points are that interlayer water re-enters between the layers from the outer edges, causing expansion by some opening of the layers (see Fig. 7 in paper No. III-23); the water acts as webs or cross-links; there will be no real increase in E until the middle starts to fill, similar to sandwich-type construction; when this filling takes place, E goes up markedly. The length-to-weight change results indicate a rapid increase of interlayer water with a not so great length change beyond 50 per cent R. H. The model shows that most of the expansion has already taken place from the edges. Emptying now starts from the edges but only at low pressures; this explains the hysteresis shown in these plots. "E" does not decrease until the water has left the middle of the layers, and this occurs only at

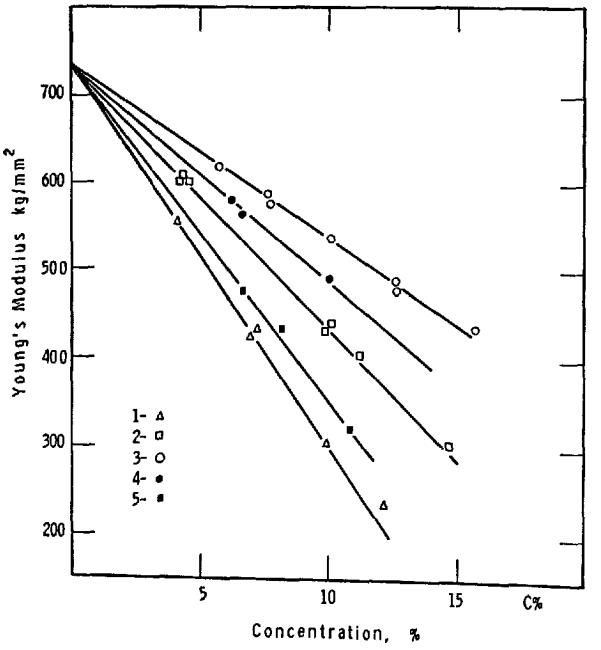

Fig. 2. *Effect of various gases on Young's modulus of acetate silk; 1-methyl alcohol, 2-ethyl alcohol, 3-butyl alcohol, 4-acetone, 5-water*

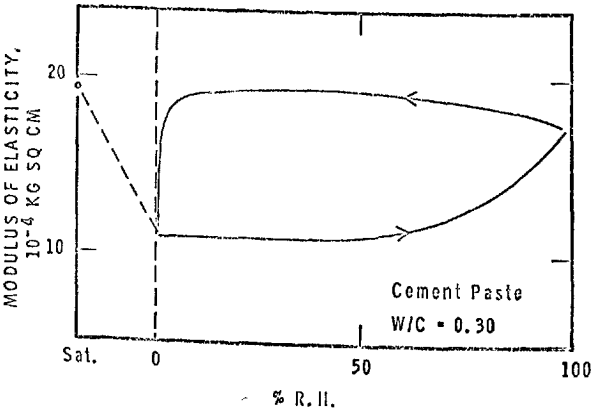

Fig. 3. *Modulus of elasticity as a function of relative humidity*

very low vapour pressures. In addition, since desorption starts from the edges when the middle is still full, the $\Delta L/L$ versus $\Delta W/W$ characteristics will be changed and a hysteresis must be expected in this plot also.

We must emphasize that this model is simplified and much work remains to be done to confirm it. The role of the hydrate water from the aluminates and sulphoaluminates will have to be taken into account.

Flexural Strength and Microhardness as a Function of Relative Humidity

On Fig. 4 is shown, relative to 0 relative humidity, the variation of strength or microhardness of porous silica glass, hydrated portland cement paste, and fused quartz. It will be noted that there is a great similarity. The results for hydrated portland cement were published in 1966 (16). In contrast, results for cellulosic products show a linear decrease with the amount sorbed, similar to Fig. 2 which shows results for the variation of E with amount sorbed.

These results are important; the decrease in flexural strength of cellulosic materials has been shown (8) to be due to the attenuation of hydrogen bonds between fibres by adsorbed water. These hydrogen bonds hold individual fibres together. A previous model for swelling of hydrated portland cement which visualizes a separation of individual crystallite units (18) is similar to the model for cellulosic materials and would require similar "E" and flexural strength variations with change in R. H. As this is not borne out, because of this and other evidence the old model for swelling and shrinking must be discarded.

The similarity in behaviour of hydrated cement and glass can be fully explained (8). Strained $-\overset{|}{\underset{|}{Si}}-O-\overset{|}{\underset{|}{Si}}-$ bonds at the apex of cracks yield at lower stresses in the presence of water vapour; this results in the formation of (–OH) groups. This process is regarded as a form of stress corrosion. Thus the change in flexural strength is due to the change in environment rather than a change in structure of the material.

The experiments under category ii) variation of mechanical properties as a function of porosity and method of fabrication, will now be discussed.

Interrelation of Hardness, Modulus of Elasticity and Porosity in Various Gypsum Systems

Generally, for otherwise identical conditions, mechanical properties such as strength and modulus of elasticity are related to porosity. The relation usually takes the form of an exponential expression

$$S = S_0 e^{-b_1 p} \qquad \text{or} \qquad E = E_0 e^{-b_2 p}$$

where S and E are the strength and modulus of elasticity of the specimen respectively, S_0 and E_0 are these parameters at zero porosity; and p is the porosity (8). This type of equation was found to hold for various gypsum systems (19).

Study of the gypsum systems which are distinctly crystalline and in which intergrowth of crystals during hydration is a possibility was considered useful for comparison with the cement systems.

Results may be summarized by Figs. 5 and 6 where "E" and hardness versus porosity are plotted for the several systems.

1. Hardness and modulus of elasticity are related to porosity. This relation can be described by the

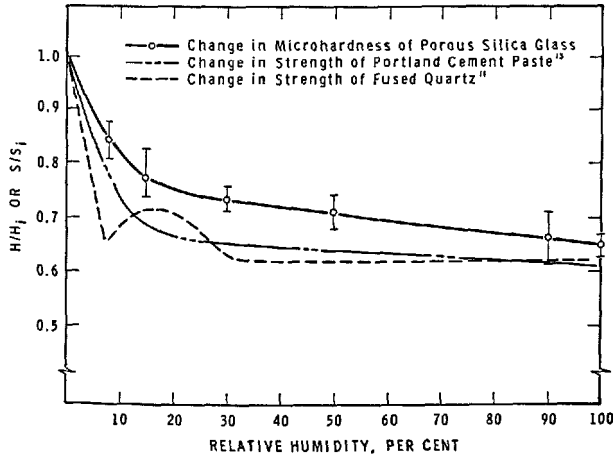

Fig. 4. *Effect of humidity on microhardness and strength*

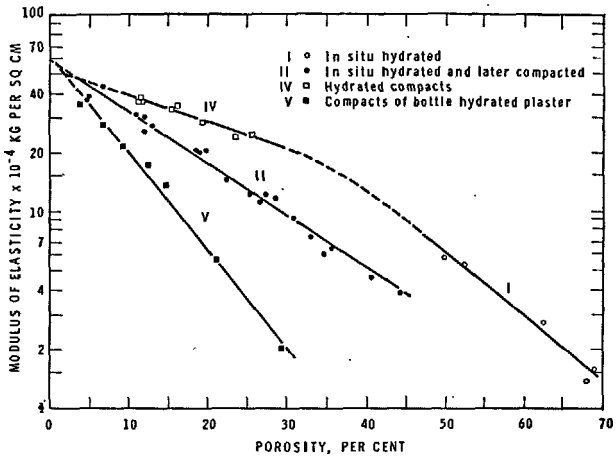

Fig. 5. *Modulus of elasticity vs porosity for the gypsum systems*

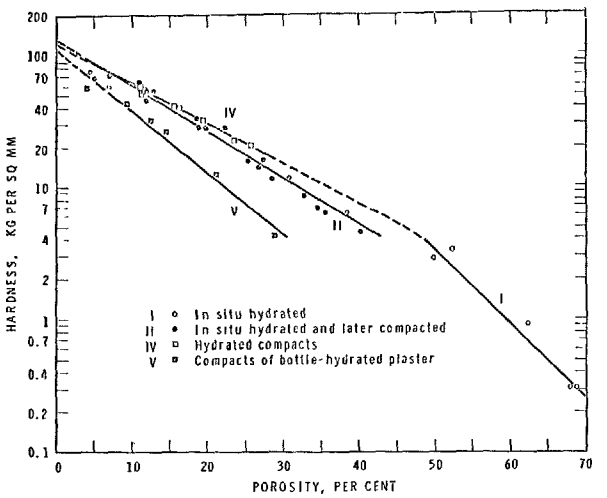

Fig. 6. *Hardness vs porosity for the gypsum systems*

exponential expression already discussed.

2. Intergrowth and interlocking of crystals formed during hydration significantly affect mechanical properties. Depending on the porosity, hardness values were as much as four times higher and modulus of elasticity up to ten times higher than corresponding values in otherwise identical systems in which crystal intergrowth is not very likely to occur. These latter systems were type V (Figs. 5 and 6), which had been prepared by compaction of bottle-hydrated plaster, and type II, which was in situ hydrated and recompacted.

Variation of Microhardness, Strength and Modulus of Elasticity of Hydrated Portland Cement

A detailed study of the above is presented to this Symposium (paper No. III-34); this study was instigated, however, by results obtained some time ago and published in 1966 (16). These results showed the then surprising fact that bottle-hydrated cement compacts showed almost identical porosity vs flexural strength and porosity vs E characteristics.

The results presented in paper No. III-34 to this Symposium have expanded this work and the following conclusions could be made:

1. The results for both hardness and modulus of elasticity could be plotted according to the following equations:

$$E = E_0 e^{-b_2 p}$$

$$H = H_0 e^{-b_3 p}$$

2. The values for the modulus of the compacts of bottle-hydrated cement fit very closely to those of the paste and compacted paste when plotted against porosity (Fig. 2, paper No. III-34).

3. The results of micro-hardness versus porosity lead to the same conclusions as the result for modulus (Fig. 3, paper No. III-34).

These results enabled the conclusion to be made that pressure produced either by compaction or hydration would yield the same type of solid-solid bonds between crystallites. This is, of course, in sharp contrast to the effect observed from the gypsum systems studied. In the gypsum system, the intergrowth of crystals seems to occur during hydration and forms "chemical" bonds which produce greater strength than do the bonds formed during compaction. Similarly, some recent work involving compacts of $Ca(OH)_2$ during ageing (20) and during carbonation (21) shows how these interparticle bonds can be increased because of recrystallization of the material or because of new products formed as the result of the reaction.

The further contrasting results between the gypsum systems and the hydrated cement system produces convincing evidence for the nature of the interparticle bond in hydrated cement. The experiments where hydrated cement paste was compacted to lower porosities involving a reduction of porosity varying from as little as 5 per cent to as much as 45 per cent showed that in all cases the modulus values fitted the same relation as for the hydrated paste samples. If a "chemical" bond were to be formed during hydration, such a bond would be broken during subsequent compaction and would not be remade, resulting in a lower modulus for compacted paste. This was not the case, which is evidence of the absence of "chemical" bonds and leads to the conclusion (mentioned previously) that the interparticle bonds are solid-to-solid which are responsible for the stable structure of cement paste after first drying. These bonds appear to be of such a nature that they can be broken and remade without suffering permanent decrease in modulus.

Before discussing some of the features of the interparticle bonds in hydrated cement, perhaps a more general discussion of interparticle bonds may be made by way of definition.

It is recognized that the terms "chemical" or "primary" and "secondary" bonds have been used in describing the structure of hydrated cement systems without a strict definition of their meaning. This has led to considerable midunderstanding. It is believed that what was meant by the "chemical" bond between the particles was a solid-to-solid contact similar to that of a grain boundary in a polycrystalline material where some atoms approach the spacing and arrange-

ment in the crystal. Such "chemical" bonds could be formed during a crystallization process accompanying a chemical reaction where the mobility of atoms allows for a regular arrangement resulting in an intergrowth of crystals. It follows that these bonds would be stong and when broken would not be remade in normal circumstances.

It is believed that the term "secondary" bonds as applied to the hydrated cement system arose from the assumption that physically adsorbed water was a constituent part of the interparticle bond; thus, the general term of van der Waals forces was considered appropriate. It is suggested, therefore, that a different interparticle bond be postulated which would involve a solid-to-solid contact resulting from the bringing together of surfaces (by pressure externally or internally generated by the hydration reaction) forming a particle boundary having little or no regular atomic arrangement or spacing. Atoms at such a boundary would engage a varying proportion of the long-range and short-range forces depending on the degree of disorder and the average spacing. It can be visualized that this interparticle bond can be broken and subsequently remade under appropriate loading conditions. This type of bond differs from the "chemical" bond just defined, which has a more regular atomic arrangement and the spacing of more of the atoms may approach that of the lattice spacing in the crystal. If water is involved in such a bond (it will be either chemisorbed, hydrated or interlayer), it is considered a constituent part of the crystal.

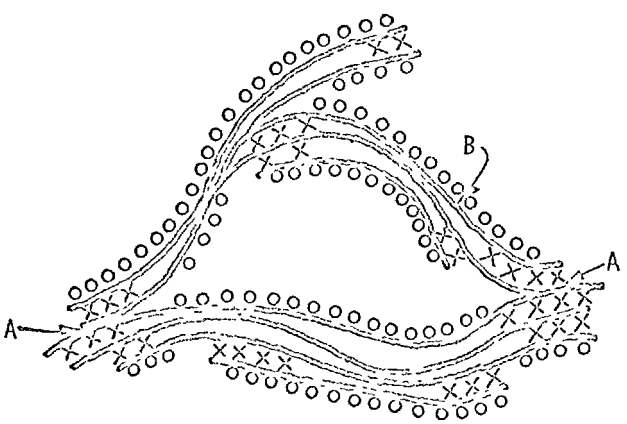

Fig. 7. *Simplified model for hydrated portland cement*

Of all the various experiments leading to the understanding of hydrated portland cement, and the bonding system involved in the structure, perhaps the most conclusive in support of the idea that interparticle bonds do not have adsorbed water at the boundary comes from the measurements of elastic modulus and strength at different conditions of relative humidity (16). If the adsorbed water were entering the interparticle bond area, the net result should be a decrease in modulus or strength as occurs in the case of cellulosic materials (8).

A very simplified and tentative model for the structure of hydrated portland cement is presented as Fig. 7 which shows the layerd structure of hydrated portland cement. The role of the types of water and possible bonding between sheets is shown. *The irreversible shrinkage* during first drying might involve formation of more solid-to-solid bonds or further aggregation of layers. First drying would involve great energy changes, and the structure may be subject to forces which demand new positions of stability.

Creep Phenomena

The establishment of a new model for hydrated cement enables a fresh approach in understanding some of its properties. A discussion of some possibilities with regard to creep follows:

1. The importance of interlayer water in hydrated portland cement is now recognized, and this interlayer water may be removed at low relative humidities. Under higher stress levels creep may be associated with a slow decomposition of the interlayer hydrates. This effect is influenced by relative humidity and may result in both reversible and irreversible creep.
2. The nature of the interparticle bonds which show the capacity for breaking and remaking may be involved in irreversible creep.
3. A large part of creep, when measured before first drying, might be related to the irreversible shrinkage phenomena.

Concluding Statement

It is hoped that the interpretation of experimental work described in this discussion, and the model evolved, may lead to further understanding and subsequently a more advanced model for hydrated portland cement.

References

1. G. L. Kalousek, "Fundamental factors in the drying shrinkage of cement block," J. Am Concrete Instt., 26, 233–248 (1954).
2. R. Sh. Mikhail, L. E. Copeland and S. Brunauer, "Pore structures and surface areas of hardened portland cement pastes by nitrogen adsorption," Can. J. Chem., 42, 426–438 (1964).
3. R. Sh. Mikhail and S. A. Selim, "Adsorption of organic vapours in relation to the hardened portland cement pastes," Highway Research Board Special Report 90, p. 123–134 (1966).
4. P. J. Sereda and R. F. Feldman, "Compacts of powdered materials as porous bodies for use in sorption studies," J. Appl. Chem., 13, 150–158 (1964).
5. R. F. Feldman and P. J. Sereda, "The use of compacts to study the sorption characteristics of powdered plaster of paris," J. Appl. Chem., 13, 158–167 (1963).
6. V. S. Ramachandran and R. F. Feldman, "Length change characteristics of $Ca(OH)_2$ compacts on exposure to water vapour," J. Appl. Chem., 17, 328–332 (1967).
7. R. F. Feldman and P. J. Sereda, "Moisture content, its significance and interaction in a porous body," Proc., Internat. Symposium on Humidity Measurements, Washington, C. D., 4, Ch. 28, 233–243 (1963).
8. P. J. Sereda and R. F. Feldman, "Mechanical properties and the solid gas interface." *In* The Solid Gas Interface, Edited by E. A. Flood, Vol. 2, Ch. 24, 729–764, Marcel Dekker Inc., New York (1967).
9. R. F. Feldman and P. J. Sereda, "A datum point for estimating the adsorbed water in hydrated portland cement," J. Appl. Chem., 13, 375–382 (1963).
10. R. F. Feldman and P. J. Sereda, "Sorption of water on bottle-hydrated cement, I; The sorption and length-change isotherms," J. Appl. Che ., 14, 87–93 (1964).
11. R. F. Feldman and P. J. Sereda, "Sorption of water on compacts of bottle-hydrated cement, II; thermodynamic considerations and theory of volume change," J. Appl. Chem., 14, 93–104 (1964).
12. R. F. Feldman, "Sorption and length change scanning isotherms of methanol and water on hydrated portland cement," Submitted to the Fifth International Sympositum on the Chemistry of Cement, Tokyo, October 1968.
13. R. A. Helmuth and D. H. Turk, "Elastic moduli of hardened portland cement and tricalcium silicate pastes: effect of porosity," Highway Research Board, Special Report No. 90, 135–144 (1966).
14. I. Soroka and P. J. Sereda, "The structure of cement-stone and the use of compacts as structural models," Submitted to the Fifth International Symposium on the Chemistry of Cement, Tokyo, October, 1968.
15. P. Seligmann, "Nuclear magnetic resonance studies of the water in hardened cement paste," J. Res. Develop. Lab., Portland Cement Assoc., 10, (1), 52–65 (1968).
16. P. J. Sereda, R. F. Feldman and E. G. Swenson, "Effect of sorbed water on some mechanical properties of hydrated cement pastes and compacts," Highway Research Board, Special Report No. 90, 58–73 (1966).
17. R. F. Feldman and P. J. Sereda, "A model for hydrated portland cement paste as deduced from sorption length change and mechanical properties," Presented at the RILEM Colloquium: The physical and chemical cause of creep and shrinkage of concrete, Munich, April 1968.
18. T. C. Powers, "Mechanism of shrinkage and reversible creep of hardened paste," Proc. Int. Conf. on Structure of Concrete, London, 1965.
19. I. Soroka and P. J. Sereda, "Interrelation of hardness, modulus of elasticity and porosity in various gypsum systems," J. Am. Cer. Soc., 51, 337–340 (1968).
20. E. G. Swenson and P. J. Sereda, "Some ageing characteristics of lime," J. Appl. Chem., 17, 198–202 (1967).
21. E. G. Swenson and P. J. Sereda, "A mechanism for carbonation shrinkage of lime and hydrated cement," J. Appl. Chem., in press.

(A) Papers regarding Fundamental

Supplementary Paper III-8 Changing of the Specific Surface of Cement Stone in Different Conditions of Hardening

Otar. P. Mchedlov-Petrosyan and Dmitrijs A. Uginčius*

Synopsis

The work on the determination of specific surface of cement stone is a part of the investigation in the field of hydration and structure formation and it attracts attention of many researchers. We can cite works of Brunauer, Greenberg, Kantro, Weise (4, 7), Copeland, Hayes (5) Khodakov, Edel'man, Kornienko (9) Hunt, Tomes, Blaine (6, 24), Krasil'nikov (10, 11), Mikhail, Selim (16, 17), Powers, Brownyard (18, 19), Stupachenko (22) and many others.

Naturally, the list does not cover all works, because such a review is not the task of the authors.

Two main reasons may explain the interest to this problem. Firstly, a developed enough surface of hydrosilicate component of cement stone determines to a great extent its strength, deformative properties and durability. Secondly, the data on paste surface development kinetics may essentially supply available information on hydration and structure formation kinetics, and the value of specific surface of cement stone is connected with the rate of cement hydration.

Among the methods of investigation mentioned, particularly, in reviews of Reitlinger, Chekhovski (20) and in ours (15), the BET method is employed. It is based on wellknown works of Brunauer, Emmett and Teller (1, 3). The BET method calls for preliminary sample preparation and for a long time experiment. That is why we were looking for a suitable method to study the kinetics surface development.

The following points are examined in this paper as a continuation of our previously published work (25):

1. The development of cement stone specific surface at room temperature.
2. The change of silicate gel specific surface.
3. The influence of water-cement ratio on the value of specific surface.
4. The influence of high temperature on the specific surface.
5. The influence of low temperature on specific surface.
6. The effect of chemical additives on the development and value of specific surface of cement stone.

Method

The experimental investigations have been carried out by means of the thermographic method elaborated by Kazanski (8). While choosing the method, we considered the peculiarity of hardening cement stone as an object of the investigation. The rate and character of the reactions taking place in cement stone are defined to a great extent by hydrothermal conditions of the medium.

The method is based on regularity of water desorption from a thin (1–2 mm) layer of dispersive body at the constant medium temperature.

While experimenting the sample temperature changing in coordinates "time-temperature difference of the sample and medium" (the desorption thermogram) and the kinetic curve of sample weight changing were registered (Fig. 1).

The singular points are defined on the thermogram which correspond according to Kazanski (8), to the following forms of bond of water:

1. Free water on the surface of the cement stone granules and between them.
2. Capillary water of macropores $r > 10^{-5}$ cm.
3. Capillary water of micropores $r < 10^{-5}$ cm.

Such a classification of macro- and micropores, suggested by Rehbinder, is given in Lykov's book (12).

4. Water of polymolecular adsorption.
5. Water of monomolecular adsorption (Vm).

*Railway Engineering Institute, Kharkov, U.S.S.R.

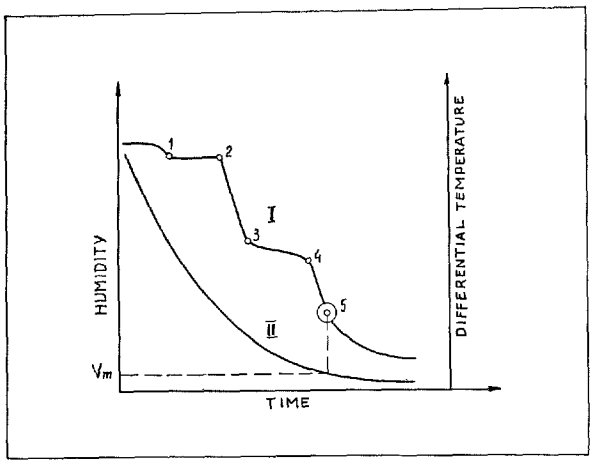

Fig. 1. *The desorption thermogram (I) and gravimetric curve (II). Monomolecular layer water amount determination by singular point 5*

We are now interested only in decoding of the value of singular point 5. By projecting point 5 on the gravimetric curve, we get the value Vm (Fig. 1). Counting begins from weight of the sample obtained by D-drying. In our point of view it is very important for maximum water content corresponding to point 5 to be defined under conditions close to normal (at temperatures less then 60°C and at air rarefaction up to residual pressure of 5 mm Hg.).

The sample soaked with water is placed into a vacuum thermostat in a cell suspended from the automatic photoelectric balance.

The sensitivity of weight recording is up to 0.4 mg for 1 mm of the scale of the self-recording potentiometer. The thermogram is recorded by a copper resistance thermometer.

The approximate temperature of the medium is maintained by thermistor relay and accurate control within ± 0.01°C is achieved with the help of proportional regulator.

The size of sample granules was made as 0.25–0.50 mm to prevent from appearing high temperature gradients in a single granule which makes thermogram recording difficult.

The value of specific surface of cement stone has been calculated by Vm in conformity with the BET theory (1), ωH_2O was assumed to be equal to 11.4 Å^2 according to Brunauer, Kantro and Copeland (2).

Object of Investigation

3 types of portland cement, with different phase composition and specific surfaces were investigated (Table 1).

The samples prepared of type 2 cement were kindly presented for the investigation during our joint work by Dr.-Eng. Werner Reichel from the Leipzig Building Institute.

Table 1.

Type	Specific surface, cm²/g	Phase composition, %				
		C_3S	C_2S	C_3A	$C_xA_yF_z$	$CaSO_4$
1	2870	51.2	26.9	6.6	10.5	1.6
2	3100	41.0	25.6	6.1	15.4	3.1
3	4912	67.6	8.7	7.6	12.5	2.5

Experimental

Normal Temperature

The samples were prepared of types 1 and 2 cement with water-cement ratio-0.24 in metal forms of $2 \times 2 \times 2$ cm and being vibrated with vibration frequency of 3000 ± 200 per minute and average amplitude of 0.35 mm for 30 seconds. Samples were kept at 20 ± 2°C and at 100% relative air humidity. The demoulding of the samples from the forms were made in a day after their preparation.

The type 1 cement stone underwent investigations each day for 28 days, the type 2 at 1, 3, 7, 14 and 28 days of hardening. About 2 g of cement stone were taken for one experiment. The results are given in Fig. 2.

The intensive increasing of specific surface is observed for both types of cements (and also for type 3, Fig. 5) up to 7–10 days, and then the perceptible stabilization takes place. Unfortunately, our method does not make it possible to investigate changing of the specific surface of cement paste at the beginning of hardening (for the first day) as the testing time becomes commeasurable with the sample age.

The data on absolute values of specific surface are in good conformity with the data of the authors listed by us in the synopsis. If we take into consideration

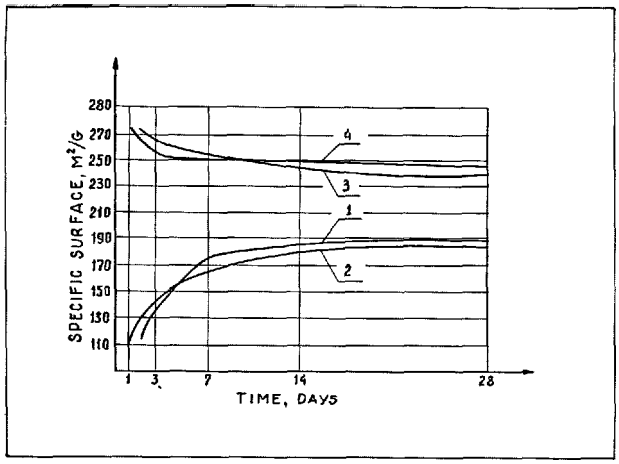

Fig. 2. *Hardening cement stone specific surface changing (1-type 1 cement, 2-type 2) and gel specific surface changing (3-type 1, 4-type 2)*

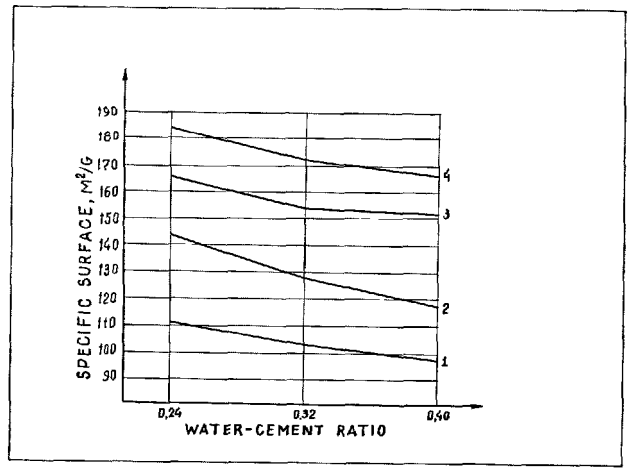

Fig. 3. *Specific surface of cement stone at the different water-cement ratios (type 2 cement) 1–1st, 2–3rd, 3–7th, 4–28th day of hardening*

that the main volume of hydrated cement, approximately 80% according to Brunauer and Greenberg's data (4), consists of tobermorite-like calcium hydrosilicates, then Fig. 2 will reflect the kinetics of silicate hardening.

Specific Surface of Gel

According to our data, the specific surface of gel of both types of cement are in the range of 275–240 m^2/g in different time of hardening, the gel having a clear tendency to "aging" due to recrystallization of hydrosilicates and formation of structure with more rough dispersity. Volzhenski (26) pays much attention to this phenomenon as the strength of cement stone along with the rate of hydration is determined by dispersity of gel particles.

The additional investigations made by us have shown that with increasing water cement ratio this gel tendency to "aging" increases to some extent.

Water-Cement Ratio

The samples of 2 type-cement were prepared for water-cement ratios of 0.24; 0.32; 0.40. To prevent from bleeding at large *w/c* for first two hours, the forms were turned over each 5 minutes.

The specific surface was determined at the 1, 3, 7, 28 days of hardening. The results of the experiments are given in Fig. 3.

The diminishing of the specific surface of cement stone with rising of *w/c* is observed during all investigated stages of hardening. This is explained, in general, by lower specific volume of silicate gel at larger *w/c* and, only to some extent, by more intensive "aging" of gel during later stages of hardening.

High Temperature

The samples prepared of type 1 cement with water-cement ratio of 0.24 in accordance with above-mentioned technique had been kept for 1 hour at $20 \pm 2°C$ and at 100% relative humidity, and then they were undergone steam curing with the following parameters:

the rate of rising temperature—40°C per hour;
the temperatures of isothermal heating—40, 60 and 90°C;
the time of isothermal heating—1–9 hours.

The samples were heated in closed forms. During steam curing after each hour of isothermal heating the samples were taken out of the chamber and placed into the exsiccators (desiccators) at $20 \pm 2°C$ and 100% relative air humidity, and they were kept there for 28 days and then investigated. In this way we tried to gain a certain comparison of the data obtained at normal and high temperatures of hardening.

The results obtained (Fig. 4) enable us to make the following conclusions:

The specific surface of the steam-cured cement stone is much less than the paste hardening under normal conditions.

The increasing of the temperature of isothermal heating leads to the decreasing of the specific surface.

It should be noted that the sample heated at 40°C

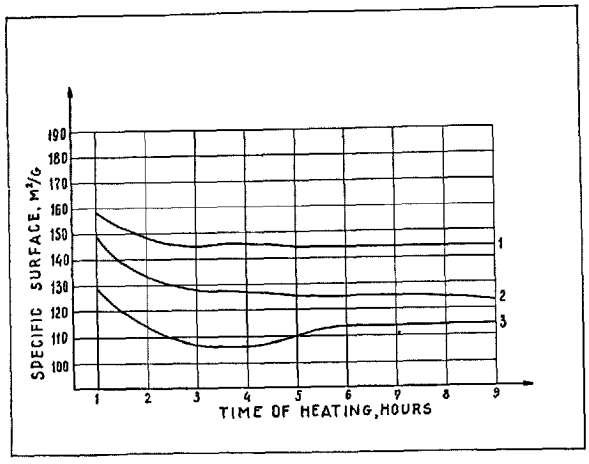

Fig. 4. *Specific surface of steam curing cement stone (on 28th day of hardening, type 1 cement) 1-at 40°C, 2-at 60°C, 3-at 90°C*

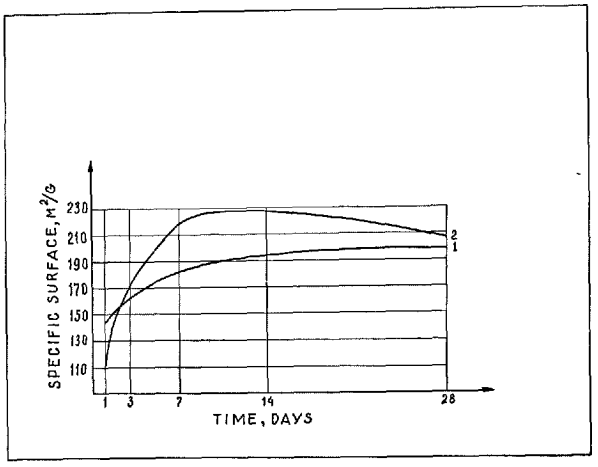

Fig. 5. *Changing of specific surface of control samples (1) and of cooled paste (2). Type 3 cement*

for more than 3 hours, at 60°C for more than 5 hours and at 90°C for more than 6 hours did not appear to cause any perceptible changes in the specific surface. In general, the specific surface decreases until this time.

The influence of temperature on cement hardening processes is connected with the regularities of proceeding the process in the diffusion area, described by Einstein. With temperature increase by 1°C, the hydration rate at the liquid/solid phases boundary is increased by 3–10 times.

Thus the rate ratio of heterogeneous processes is equal to 1, 2 and depends on the process duration as the thickness and density of diffusion layer changes from instant to instant.

However, in practice, the hydration processes at higher temperatures do not proceed quite satisfactorily Firstly, from the point of view of thermodynamics the heating contributes to proceeding the endothermal processes of hydrolysis and solution, but the hydration processes going with the decreasing of free energy proceed under unfavorable conditions.

Secondly, steam curing causes the formation of dense hydrate films on cement particles, thus retarding diffusion process of water and new formations.

All these results in formation of more rough dispersive structure of gel and in decrease of its specific volume in cement stone. Volzhenski (26) reports that the samples of cement paste with $w/c = 0.30$ after 8 hours of steam-curing at 90°C have specific surface of gel equal to 133 m^2/g, and at hardening at normal temperature on the 28th day-186 m^2/g. Thus, more rough gel dispersity was obtained. However, it is difficult to explain whether rough dispersity of gel or smaller rate of hydration cause the decrease of specific surface.

Low Temperature

The cement paste prepared from type 3 cement according to above-mentioned technique ($w/c = 0.29$) was immediately placed into a freezing chamber at -20 ± 1°C for one day. The further hardening took place up to the 28th day at +20°C and 100% relative humidity.

The specific surface was measured at 1, 3, 7, 14 and 28 days of hardening (Fig. 5).

The specific surface development of cement paste cooled in such a way proceeds more intensively than that of controlled samples.

This discrepancy decreases considerably with time, but it is still large enough at the 28th day.

From the thermodynamic and kinetic points of view, more favourable conditions for crystal structure formation are observed in this case. The temperature decreasing retards clinker mineral hydration, but the probability of high basic calcium hydrosilicate formation rises.

There is no doubt that at low temperatures the degree of solution of silicate clinker phase decreases and the probability of the appearing of a new phase reduces to a greater extent.

The decreasing of growth of hydrate crystal in comparison with the rate of initial phase solution causes the increasing of solution concentration (according to CaO). It creates favourable conditions for high basic tobermorite formation. The favourable conditions created at the primary cooling influence

greatly on further cement paste hardening at normal temperature.

Chemical Additives

Mchedlov-Petrosyan and Filatov (14) have suggested a compounded additive elaborated in conformity with so called "principle of compensated expansion". The additive consists of reaction accelerators (calcium chloride, aluminium sulphate), expander (aluminium powder) and retarder (sulphite-cellulose liquor).

The porous structure of such a cement stone was studied by Uginčius, Mchedlov-Petrosyan, Lutsyk and Kazanski (25). The combined introduction of these additives proved to provide higher density, strength of cement stone and to reduce its permeability.

The results of studying the influence of both the compounded additive and its components on the development of specific surface of cement stone (type 1 cement) are given in this paper; *w/c* was 0.24. The amount of components (in % to cement weight) was taken in accordance with the suggestion of the authors (14):

Aluminium powder (specific surface is 15000 cm^2/g)—0.01%
Aluminium sulphate (pure)—2%
Calcium chloride (pure)—2%
Sulphite-cellulose liquor (commercial)—0.15%

According to technological requirements aluminium sulphate solution and suspension of aluminium powder, calcum chloride and sulphite-cellulose liquor were poured together in the moment of paste mixing.

In the rest the technique of preparation, curing and testing of samples was the same.

Aluminium powder and aluminium sulphate did not greatly effect the value and changing of the specific surface.

The controlled samples and samples with compounded additive were tested at 1, 2, 3, 4, 5, 7, 9, 13, 14, 21 and 28 days of hardening, the samples with additives of calcium chloride and of sulphite-sellulose liquor at 1, 2, 3, 7, 14 and 28 days. The compounded additive appeared to increase greatly the specific surface, the process of its development taking place up to the 13th or the 14th day of hardening (control sample—up to the 7th or 8th day) (Fig. 6).

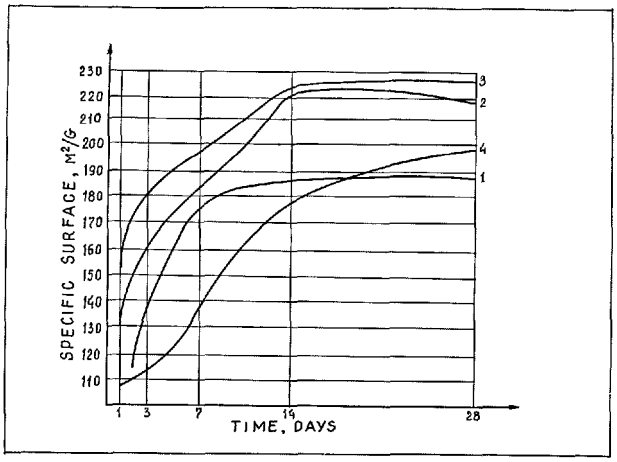

Fig. 6. *Influence of chemical additives on cement stone specific surface changing.; 1-control samples (type 1 cement),* 2-2% $CaCl_2 + 2\% Al_2(SO_4)_3 + 0.15\%$ *sulphite-cellulose liquor* +0.01% *aluminium powder,* 3-2% $CaCl_2$, 4-0.15% *sulphite-cellulose liquor*

We assumed that this compounded additive had a component causing a great effect on calcium silicate hydration processes. In fact, only silicate hardening products may affect the value of cement stone specific surface.

Calcium chloride proved to be such a component. It accelerates processes of silicate hardening and provides their plenitude for a long time (Fig. 6). The problem of mechanism that calcium chloride effect on silicate hardening processes is elaborated by Tamas (23). We think that results of great interest are obtained while investigating samples with sulphite-cellulose liquor known as plasticizer (21). The major component of this additive is calcium lignosulphonate, while adsorbing on cement particles retards silicate hardening processes.

However, the retarding of calcium hydrosilicate crystal growth under the influence of adsorption layers causes their dispergation (modification phenomenon). This phenomenon leads to some increasing of specific surface of cement stone.

Conclusion

The investigations have shown that various technological factors (water-cement ratio, temperature changing, chemical additives) influence on the value of specific surface of cement stone and on its changing.

It should be taken into account that the value of

specific surface is connected with such an important factor as strength of cement stone. Indeed, Powers and Brownyard (19) have found direct correlation between amount of water of monomolecular layer (Vm) and amount of "non-evaporable" water (Wn).

The value of Wn may serve as basis of new formation concentration calculation.

The strength of cement stone is in parabolic relationship to the concentration of new formations (18).

The increasing of cement stone specific surface is, first of all, the increasing of hydrosilicate gel specific volume which, in its term, increases material strength and density.

The creation of proper conditions for hardening, which change the value of gel specific volume, is one of the problems of so called "directed structure formation" (13).

The basis of this trend in cement materials technology should be kinetics control and intensification of silicate hardening processes.

References

1. S. Brunauer, "The adsorption of gases and vapors", V.1 (Princeton Univ. Press., USA, 1945).
2. S. Brunauer, D. L. Kantro and L. E. Copeland, "The stoichiometry of the hydration of beta-dicalcium silicate and tricalcium silicate at room temperature". J. Amer. Chem. Soc., **80**, 761–767 (1958).
3. S. Brunauer, P. H. Emmett and E. Teller, "Adsorption of gases in multimolecular layers". J. Amer. Chem. Soc., **60**, 309–319 (1938).
4. S. Brunauer and S. A. Greenberg, "The hydration of tricalcium silicate and beta-dicalcium silicate at room temperature". Chemistry of Cement. Proc. of the IV-th Int. Symp., Washington, USA, Vol. 1, 135–165 (1962).
5. L. S. Copeland and J. C. Hayes, "Porosity of hardened portland cement pastes". J. Amer. Concrete Inst., **27**, 6, 633–340 (1956).
6. C. M. Hunt, "Nitrogen sorption measurements and surface areas of hardened cement pastes". Symp. on Structure of Portland Cement Paste and Concrete. Highway Res. Board Spec. Rep. 90, Washington, USA, 112–122 (1966).
7. D. L. Kantro, C. H. Weise and S. Brunauer, "Paste hydration of beta-dicalcium silicate, tricalcium silicate and alite". Symp. on Structure of Portland Cement Paste and Concrete. Highway Res, Board, Spec. Rep. 90, Washington, USA, 309–327 (1966).
8. M. F. Kazanski, "An analysis of the form of moisture bonding in porous adsorbents by means of isothermal drying thermograms" (in Russian). Coll. J. 19, 6 622–667 (1957).
9. G. S. Khodakov, L. I. Edel'man and G. G. Kornienko, "Changes in the specific surface area of the solid phase in the hardening of mineral binders" (in Russian) Ibid., **24**, 3, 332–336 (1962).
10. K. G. Krasil'nikov, "Sorption of steam on calcium hydrosilicates" (in Russian). Rep. of Acad. Sci. of USSR, **143**, 4, 911–914 (1962).
11. K. G. Krasil'nikov, "The specific surface of tobermorite as calculated from its crystal lattice constants and adsorption data" (in Russian). Ibid., **149**, 4, 891–893 (1963).
12. A. V. Lykov, "The theory of drying", p. 46 (in Russian, State Publ. House on Energetics, Moskow, USSR, 1966).
13. O. P. Mchedlov-Petrosyan, "Modern views on processes of cement hardening" (in Russian, New in Cement Technology, State Publ. House on Building, Moskow, USSR, p. p. 144–152, 1963).
14. O. P. Mchedlov-Petrosyan and L. G. Filatov, "Expanding compositions on the basis of portland cement" (in Russian, State Publ. House on Building, Moskow, USSR, 1965).
15. O. P. Mchedlov-Petrosyan and D. A. Uginčius, "Methods of determining of porous structure of cement stone". (in Russian, Sci. Inform. of State Cement Ind. Inst., Moskow, USSR, 21, p. 34–42, 1966).
16. R. Ch. Mikhail, "Hydrated portland cemen-surtface area in relation to pore structure". Proc. of the VII-the Conf. on the Silicate Ind., Budapest, Hungary, 251–258. 1965.
17. R. Sh. Mikhail and S. A. Selim, "Adsorption of organic vapors in relation to the pore structure of hardened portland cement pastes". Symp. on Structure of Portland Cement Paste and concrete. Highway Res. Board. Spec. Rep. 90, Washington, USA, 123–134, 1966.
18. T. C. Powers, "Physical properties of cement paste" Chemistry of Cement. Proc. of the IV-th Int. Symp., Washington, USA, Vol. 2, 577–609 (1962).
19. T. C. Powers and T. L. Brownyard, "Studies of the physical properties of hardened portland cement paste." J. Am. Concrete Inst., **18**, 101–132, 249–336, 469–504, 549,–602, 669–712, 845–880, 933–992 (1947).
20. S. A. Reitlinger and Yu. Chekhovski, "Mechanism of transfer of gases and liquids through concrete and methods of investigation of porous structure of concretes". (in Russian, Publ. of Inst. of Pipe-Line Constr., Moskow, USSR, 1961).
21. V. I. Soroker, "Plasticized concretes" (in Russian, State Publ. House on Building, Moskow, USSR. 1963).
22. P. P. Stupachenko, "Structural porosity and its connection with properties of cement, silicate and gypsum materials" (in Russian, Trans. of Vladivostok Politechn. Inst., USSR, **63**, 3–62, 1964).
23. F. D. Tamas, "Acceleration and retardation of portland cement hydration by additives". Symp. on Structure of Portland Cement Paste and Concrete. High-

way Res. Board, Spec. Rep. 90. Washington, USA, 392–397 (1966).
24. L. A. Tomes, C. M. Hunt and R. L. Blaine, "Some factors affecting the surface area of hydrated portland cement as determined by water vapor and nitrogen adsorption", J. of Res. NBS, **59**, 357–364. (1957).
25. D. A. Uginčius, O. P. Mchedlov-Petrosyan, R. V. Lutsyk and M. F. Kazanski, "Kinetics of the formation of porous cement stone structures in the presence of compounded additives" Proc. of the VIIIth Conf. on the Silicate Ind., Budapest, Hungary, 307–318 (1966).
26. A. V. Volzhenski, Yu. S. Burov and V. S. Kolokol'nikov, "Mineral binding agents"., p.p. 225–226 (in Russian, State Publ. House on Building, Moskow, USSR, 1966).

Oral Discussion

Rolf F. Feldman

A great deal of research has been directed over a period of many years towards establishing criteria to distinguish quantitatively between adsorbed and hydrate water in hydrated cement paste.

These efforts were largely unsuccessful because of the slight differences in energy of attachment between the hydrate and adsorbed water.

In the field of surface chemistry it has been impossible, more often than not, to make a clear distinction between mono-molecular and multi-molecular adsorption even by accurate adiabatic calorimetry; clear distinctions between free water, capillary water in macropores, and capillary water in micropores, etc. as made by the authors (categories 1 to 4) are considered as unlikely occurrences. With these considerations in mind, it is difficult to explain the irregular curve obtained by the authors and surprising to see that the T.G.A. curve shows no change in slope at the positions corresponding to positions 1 to 5.

Another and perhaps more important area of discussion in this work is the fact that the authors have not included the decomposition of interlayer or other hydrates in their listing of the various types of water given off and it is suggested here that part of the water assessed as water of mono-molecular adsorption is hydrate water; surface areas calculated from water sorption and B.E.T. calculations are not valid for this reason, and it is unlikely that this thermal method is free of the above criticism.

Authors' Closure

O. P. Mchedlov-Petrosyan and D. A. Uginčius

Mr. Feldman in his paper and oral discussion of our paper spoke about a number of interesting problems concerning the sorption investigations of the structure of silicate materials; in this connection we take an advantage of giving our point of view as to this problem.

We think there is no reason to oppose water vapour and nitrogen adsorption methods while investigating the silicate structure.

We simply define different things: by nitrogen adsorption one can determine only external surface of hydrates because nitrogen molecules can not penetrate into the interlayer structure spaces, especially if we take into consideration that these spaces decrease as the result of dehydration up to 1 Å.

The water is adsorbed in interlayer spaces. This water is not a part of crystal lattice and its molecules have a mobility close to that of free water (7). Thus it is not necessary to take this "interlayer hydrate water" as a separate class.

This was clearly shown by K. G. Krasil'nikov while working with tobermorite (5, 6, 7,) It is he who in 1962 showed that characteristic vertical section caused by withdrawing water which is sorbed by swelling structure was seen on the adsorption isotherm of tobermorite when $P_0/P = 0.35$ (5).

That is why we may speak about a total surface S_{H_2O} and an external surface S_{N_2}.

The loss of some quantity of crystal water by high-basic hydrates can not greatly affect the results obtained. We can rather be afraid of compression effect of surface forces which was in particular pointed out by J. H. de Boer (1). Nevertheless, the results obtained by means of water vapour adsorption are in good accordance with samll angle X-rays method data (L. E. Copeland), which is precise enough and quite different.

We consider that at present there is no reason to reject the BET-method and to be satisfied with an approximate pattern of the cement stone porous structure.

The problem of fixing positions 1 to 5 on the desorption thermogram (given schematically in our paper)

was only mentioned at this Symposium. Therefore we should like only to refer to our previous paper (8) and particularly to a number of works by M. F. Kazansky (2, 3, 4) who suggested this method.

In conclusion we want to thank the V-ISCC Organizing Committee for giving us an opportunity to take part in this interesting discussion.

References

1. J. H. de Boer, "The dynamical character of adsorption", (Oxford at the Clarendon Press, 1953).
2. M. F. Kazanski, "An analysis of the forms of moisture bonding in porous adsorbents by means of isothermal drying thermograms" (in Russian), Coll. J., **19**, No. 6, 662–667 (1957).
3. M. F. Kazanski, "An investigations of the kinetics of drying natural high polymers" (in Russian), J. Phys. Eng. **1**, No. 6, 93–95 (1958).
4. M. F. Kazanski, "The use of kinetic drying curves in analysing the linkage forms and the state of the liquid adsorbed by a dispersed body" (in Russian), Rep. of Acad. Sci. of USSR, **130**, No. 5, 1059–1062 (1960).
5. K. G. Krasil'nikov, "Sorption of steam on calcium hydrosilicates" (in Russian), Ibid., **143**, No. 4, 911–914 (1962).
6. K. G. Krasil'nikov, "The specific surface of tobermorite as calculated from its crystal lattice constants and adsorption data" (in Russian), Ibid., **149**, No. 4, 891–893 (1963).
7. V. I. Kvlividze, K. G. Krasil'nikov, "The state of water adsorbed on calcium hydrosilicate, as investigated by means of nuclear magnetic resonance" (in Russian), Ibid., **145**, No. 6, 1305–1307 (1962).
8. D. A. Uginčius, O. P. Mchedlov-Petrosyan, R. V. Lutsyk and M. F. Kazanski, "Kinetics of the formation of porous cement stone structures in the presence of compounded additives", Proc. of the VIII-the Conf. on the Silicate Ind., Budapest, Hungary, 307–318 (1966).

Supplementary Paper III-23 Sorption and Length-Change Scanning Isotherms of Methanol and Water on Hydrated Portland Cement

Rolf F. Feldman*

Synopsis

The purpose of this work was to investigate the nature and the reversibility of the CH_3OH and H_2O isotherms, and to compare their length-change and sorption characteristics. These characteristics for water on hydrated portland cement have caused some controversy, due to several complicating features in the isotherm, with regard to the surface properties and stoichiometry of the compounds, and the length change and creep mechanisms.

Introduction

The development of the present model of hydrated portland cement has been largely based on surface chemical considerations; this involved establishing criteria for distinguishing between chemical and physio-sorbed water. The determination of the stoichiometry of the tobermorite gel, its water surface area, and its porosity was based on these criteria, and these parameters are among the most important factors related to the phenomena of expansion-contraction and creep, and the mechanical properties, strength and elasticity.

The most important experiments performed using the surface chemical approach have been the sorption and length change isotherms but, as no detailed investigation of the isotherms has been made, their validity and results obtained from them have been assumed to be correct. Results of surface area investigations, however, differ markedly from those obtained from nitrogen adsorption, and this has led to some suspicion of the results.

In a series of papers by the author and co-workers, (1, 2) a more detailed examination of the isotherms was started, involving both length change and weight change as function of the vapour-pressure of water; measurements of Young's modulus and relative breaking stress were also made as functions of vapour pressure. The results led the authors to conclude that the surface area of hydrated portland cement was considerably lower than the accepted value ($\simeq$200 m^2/gm), and that inter-layer hydrate water was playing a role in both the length change and sorption isotherms, and in the variation of Young's modulus with relative humidity.

The present work is a further stage in these investigations. Detailed cycling and scanning loops were obtained for samples dried at three different conditions during the determination of precise length change and weight change isotherms based on numerous data for water and methanol on bottle and paste-hydrated cement.

Results qualitatively confirmed the earlier work, although some assumptions made previously were proved to be not completely correct. The work enabled a revised model for portland cement paste to be made, however, and allowed further evolution of the theory of volume change and suggestions with regard to the creep phenomena.

*Division of Building Research, National Research Council of Canada, Ottawa, Canada

Experimental

Meterials

The cement used in this work was a type I; its composition was reported in a previous paper (1). The cement was hydrated in two ways; paste hydrated for 1 year at a water cement ratio (w/c) of 0.5 and bottle hydrated for a period of 4 months at a w/c ratio of 5.0. The degree of hydration and other properties are shown in Table 1. The bottle-hydrated cement was stored and conditioned in desiccators to 10 to 15 per cent relative humidity (R. H.) using a concentrated NaOH solution. The cast paste cylinders were sliced to 0.05 in. (1.27 mm) thickness and were approximately 1.25 in. in diameter and then stored as above. Compacts were formed at a load of 10,000 lb in a mould 1.25 in. (3.175 cm) diameter from the bottle-hydrated cement. The procedure for making the compacts and the samples has been described previously (2).

The methanol used in this work was purified by making a magnesium iodine Grignard complex by refluxing magnesium turnings and iodine in a large excess of 99 per cent pure methanol. After several distillations, the methanol was distilled directly into the high-vacuum apparatus.

Apparatus

The high-vacuum apparatus used for this work was designed to expose 12 samples simultaneously for long periods to the same vapour pressure conditions, with air excluded. Six of these samples were mounted in individual tubes on quartz spirals of the McBain-Bakr type and gave values of the weight changes to a sensitivity of 3.0×10^{-5} gm. The remaining six samples were mounted on modified Tuckerman optical extensometers and placed in individual cells equipped with optical windows (3). This determined the dimensional changes to a sensitivity of 4×10^{-6} in./in. A quartz Bourdon-type spiral gauge was used to measure the vapour pressure to a sensitivity of 1 micron and an absolute accuracy of 10 microns at low pressures.

A three-stage oil diffusion pump backed by a rotary vacuum pump was used to obtain pressures of 10^{-6} mm of mercury. The adsorbate was introduced into the system from a bulb immersed in a bath that could be controlled at temperatures down to −45°C within 0.05°C, although most of the pressure readings were taken with the Bourdon gauge. The samples were maintained at 21.3°C within 0.05°C by immersing the lower ends of the tubes and cells containing the samples to a depth of 12 in. in a controlled bath. Room temperature was controlled at 23°C ± 0.5.

Procedure

Two samples measuring 3 by 1 by 0.127 cm were cut from the discs and mounted, one section on the extensometer and the other on the quartz spiral. Samples were degassed by evacuating simultaneously through a manifold. The samples were heated during the evacuation. Three samples of bottle hydrated cement were used and one each was heated at: 80°C for 3 hours, 85°C for 3 hours, and 95°C for 3 hours plus 1 hour at 96°C. Two samples of hydrated paste were used and one each was heated at: 85°C for 3 hours, and 95°C for 3 hours plus 1 hour at 96°C. Preliminary work using a vacuum electro-balance and thermal balance techniques had established that vacuum degassing at 85°C for 3 hours with these samples produced the same result for the non-evaporable water as the conventional 'd-drying' procedure. For

Table 1. *Some sorption properties of the hydrated portland cement samples*

	Non-evaporable water		Nitrogen surface area, m^2/g, 85°C		Methanol area		Conventional water area					
	Wn	(Wn/25) × 100	Measured (a)	For complete hydration (b)	(a)	(b)	80°	(a) 85°	96°	80°	(b) 85°	96°
Bottle hydrated	21.5	86	30	35	37	43	130	142	150	151	165	174
Paste hydrated	23.0	92	47	51	—	—	—	152	147	—	165	160

(ΔL/L)/(ΔW/W) Values for bottle-hydrated cement degassed at 80°C.

	On adsorption		On desorption		Separation of adsorption-desorption curves at P/P_0 of 0.10
	Total	Reversible	Before datum point	After datum point	
Water	0.0770	0.0220	0.040	0.0860	0.0375
Methanol	0.0640	0.0525 (estimate)	—	—	0.0955

the methanol isotherm, 1 day was generally allowed for equilibrium between points; for the water isotherm from 1 day to as much as 33 days was allowed. Generally 1 to 3 days was found adequate. It took over 10 months to determine the whole isotherm. Adsorption was effected by allowing the manifold and samples to attain the desired vapour pressure by control of the temperature of the bath in which the adsorbate source was immersed, or by introducing or withdrawing adsorbate from the manifold and system and measuring the vapour pressure. It was found that equilibrium was attained more rapidly with the latter method.

Theory

Adsorption

The isotherm for a given solid gas system should be reversible if there is no irreversible change in the nature of the solid and/or gas, since there thus can be only one equilibrium state at a given vapour pressure. This is usually the case at low pressures but at high pressures the problem of primary hysteresis arises. This is usually related to the pore structure of the solid and a change in nature of the adsorbate.

The well-known B. E. T. equation, valid for the low pressure region, implicitly assumes reversibility and a constant surface area. There is an isotherm, however, referred to as Type C, which has the characteristic that the ascending and descending branches only join at very low or zero pressure(4). Type C loops are found with some graphites, clay minerals, and hydrated portland cement (1). This low-pressure hysteresis phenomenon is usually attributed to irreversible intercalation of adsorbate within the structure of the solid, which usually has a layer structure. Changes in the spacing of some of these layers has been observed (5) by X-ray methods, but unfortunately, due to the disordered nature of the layers of the hydrated silicates in hydrated portland cement, this has not been possible for this material.

Length Change due to Adsorption

The Gibbs' adsorption equation is extremely important in length-change adsorption theory (6), but it has been applied in different ways by various workers and sometimes not justifiably. The equation

$$\Delta F = -RT \int_0^P n \frac{dP}{P} \qquad (1)$$

represents the change in free energy of pure adsorbent from its initial state under its own vapour pressure to its combining state, provided that this integral represents a path of thermodynamic reversibility. n is the number of moles of adsorbate on a fixed mass of absorbent. If it is supposed that the constant solid surface area, σ m^2/g, has undergone a change in surface tension, $\Delta\gamma$, one can write

$$\Delta F = \sigma \Delta\gamma \qquad (2)$$

thus

$$\Delta\gamma = \frac{RT}{\sigma} \int_0^P n \frac{dP}{P} \qquad (3)$$

$\Delta\gamma$ in fact indicates changes in the state of stress of the solid brought about by the interaction of the adsorbed molecule with forces on the solid surface; these forces have placed the solid in a state of compressive stress.

The Bangham equation (7) provides a basis for testing Gibbs' equation on solids

$$\frac{\Delta L}{L} = k_1 \Delta\gamma \qquad (4)$$

where $\Delta L/L$ is the length change of an adsorbent during the reversible adsorption process. From another relation derived by Bangham and co-workers (7), the Young's modulus of the solid material may be calculated:

$$E = \rho \frac{\sigma}{k_1} \qquad (5)$$

where E is Young's modulus of the material, and, ρ, in g/cc, is the density. The equation is derived for plates, or infinitely long cylinders, where the only surface is that of the curved surface of the cylinder or the major surface of a thin plate. The latter model might approximate hydrated cement paste. As Gibb's equation requires thermodynamic reversibility it can only be used at low pressures where normal hysteresis does not occur. If low pressure hysteresis does occur, then this region of the isotherm may be also irreversible. As will be shown later, this is true for hydrated portland cement, but a way has been found to overcome it.

Some authors (8, 9, 10) have used an equation of the osmotic pressure type and applied it to the low pressure region:

$$\Delta P = \frac{RT}{\rho M} ln \frac{P_2}{P_1} \quad \text{or} \quad \frac{\Delta L}{L} = k_2 \frac{RT}{\rho M} ln \frac{P_2}{P_1} \qquad (6)$$

where ΔP is suggested as being the pressure of the adsorbed film. This equation can only be valid if the water-hydrated cement system is considered to be a dilute solution, i.e., a change in concentration of water with respect to the adsorbent is not taking place during adsorption or desorption, and if the adsorbed water is not adsorbed water but bulk water. Both of these assumptions are completely untenable in this region.

In the reversible high-pressure region of the isotherm where capillary condensation has occurred and menisci exist, one might assume that a change in concentration is not taking place, if one defines capillary water as being remote from the surface forces; thus the capillary water in this assumption will also be 'bulk'. The capillary water maintains equilibrium with different vapour pressures by changing the radius of its meniscus. The water within the range of surface forces, however, will still effect a change in surface free energy with a change in vapour pressure of the system even if one defines it as being constant at two molecular layers. This must be taken into account as in the equations for the capillary region:

$$\Delta\gamma = \frac{RT}{\sigma} \cdot n \int_{P_1}^{P_2} \frac{dP}{P} \quad \text{and} \quad \frac{\Delta L}{L} = \left(k_1 \frac{RT}{\sigma} \cdot n + k_2 \frac{RT}{\rho M}\right) ln \frac{P_2}{P_1} \tag{7}$$

Results and Discussion

Water Adsorption

The sorption and Length Change Isotherms

The sorption and length change isotherms for the bottle-hydrated cement degassed at 80°C and 96°C are shown in Figs. 1 and 2 respectively. Results for a degassing temperature of 85°C were also obtained, but are not presented here. They were of a similar nature, but gave a slightly different 'conventional water surface area, as is shown in Table 1. In addition, it was observed that the weight of water present (in per cent) on the descending boundary curves of the isotherm at P/P_0 of 0.14, for the three temperatures 96°, 85° and 80°C, was 8.51, 8.19 and 7.91 per cent respectively. These values were less than 0.5 per cent different from the weight lost on degassing. As the starting condition was only known approximately

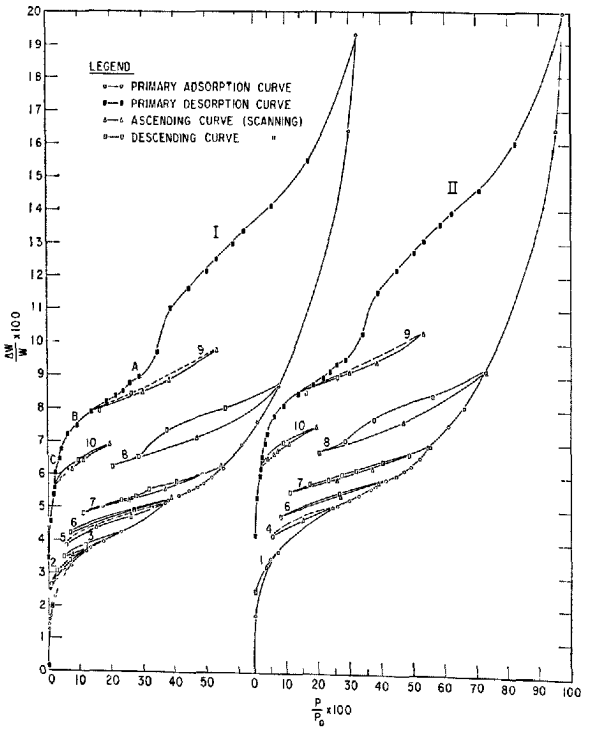

Fig. 1. *Weight change isotherms for bottle-hydrated portland cement compacts: I—degassed at 80°C; II—degassed at 96°C (scanning loops marked 1 to 10).*

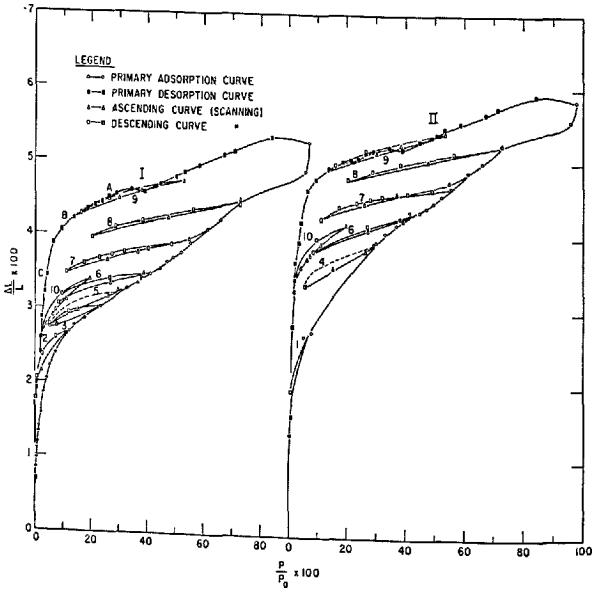

Fig. 2. *Length change isotherms for bottle-hydrated portland cement compacts: I—degassed at 80°C; II—degassed at 96°C (scanning loops marked 1 to 10).*

(P/P_0 of 0.10 to 0.15), it must be assumed that practically all the water lost on degassing was regained after the sample had been returned to the starting condition through the P/P_0 of 0.97. The degassing procedure, however, produced an irreversible shrinkage.

A general examination of both length and weight change in the two isotherms shows a large low pressure hysteresis formed by what will be called the adsorption (ascending) and desorption (descending) boundary or primary curves. Off the boundary curves are scanning loops, which contain descending and ascending portions. These loops are numbered on Figs. 1 and 2 from 1 to 10, and will be referred to as loop 1, 2, etc. It will be observed that the point where the scanning loop left the primary curve was always very close to, if not exactly at, the point where it rejoined the primary curve. This is considered as evidence for good equilibrium. The scanning loops determined for the two isotherms in Figs. 1 and 2 were not the same in all cases; detailed analysis of only the sample degassed at 80°C will be made here, however, and passing reference to the others included.

All the experimental points obtained for this sample are shown in Table 2, in the order in which they were obtained. The points with asterisks are those which have left the primary curves and are of scanning loops, both descending and ascending.

Length and sorption isotherms for one of the paste-hydrated samples, the one that was degassed at 85°C, are shown on Fig. 3. Again the similarity with the other samples is striking, although the extent of the low pressure hysteresis is not as great as for the paste samples. The general form of the primary curves for the paste- and bottle-hydrated samples agrees with that obtained from somewhat fewer data obtained by the authors and co-workers in a previous study (11), but the low-pressure hysteresis here is much larger than was obtained in an earlier investigation (1). It will be shown that this is due to the more severe drying used in the present study. No detailed analysis will be made here of the paste samples (Fig. 3), but it was again found that all the water lost on degassing was regained after the sample had been returned to the starting condition through the P/P_0 of 0.97; the surface areas for water and nitrogen are given in Table I. The areas, corrected for incomplete hydration, vary from 151 to 174 m^2/g for the water determination, and are only a bit lower than usually obtained, but,

Table 2. *Length change and weight change isotherms for the sample of bottle-hydrated cement degassed at 80°C*

P/P_0 × 100	ΔW/W × 100	ΔL/L × 100	T, days	P/P_0 × 100	ΔW/W × 100	ΔL/L × 100	T, days	P/P_0 × 100	ΔW/W × 100	ΔL/L × 100	T, days
Sorption				Sorption (Cont'd)				Desorption (Cont'd)			
0.27	1.27	.0844	6	8.21*	4.25	.3068	2	62.01	13.41	—	1
0.44	1.42	.0972	2	27.02*	4.94	.3352	2	58.51	13.02	.4940	1
0.59	1.58	.1108	3	38.72*	5.29	.3484	1.5	53.41	12.54	.4860	1
0.79	1.69	.1196	2	44.68	5.54	.3552	2	50.40	12.17	.4788	1
1.06	1.94	.1336	2	47.17	5.64	.3648	2	44.76	11.65	.4692	1
1.49	2.06	.1440	3	49.38	5.75	.3700	2	38.87	11.04	.4572	1
2.22	2.28	.1584	1	52.03	5.93	.3792	3	34.48	9.71	.4612	1
3.08	2.60	.1860	7	55.38	6.21	.3900	3	28.99	8.94	.4540	1
4.37	2.84	.2052	7	48.57*	6.04	.3884	2	26.14	8.77	.4500	1
5.44	3.08	.2220	7	40.46*	5.80	.3836	2	23.93	8.54	.4444	1
7.42	3.24	.2392	8	31.82*	5.58	.3772	1	21.38	8.35	.4396	1
12.31	3.70	.2688	8	27.53*	5.35	.3732	3	18.52	8.21	.4340	1
7.24*	3.44	.2608	11	23.10*	5.24	.3684	1.5	13.94	7.91	.4220	1
2.63*	3.07	.2384	8.5	17.48*	5.06	.3612	1	29.89*	8.51	.4472	1
0.84*	2.65	.2068	7.5	11.05*	4.85	.3484	2	38.35*	8.88	.4588	1
0.36*	2.36	.1780	13	25.91*	5.25	.3668	3	53.23*	9.78	.4740	1
2.42*	2.86	.2152	6	36.75*	5.59	.3780	2	26.37*	8.45	.4476	1
13.92	3.76	.2772	15	54.74*	6.32	.3956	2	16.32*	7.96	.4284	1
17.68	3.96	.2876	2	61.20	6.94	.4088	3	9.47	7.49	.4060	1
23.35	4.26	.3068	6.5	66.20	7.62	.4228	3	6.38	7.24	.3880	1
12.18*	3.85	.2952	6	72.70	8.75	.4452	3	4.43	6.75	.3448	1
5.14*	3.50	.2736	5	56.19*	8.05	.4340	2	3.58	6.49	.3228	1
7.90*	3.56	.2744	33	38.07*	7.35	.4180	2	2.32	6.05	.2880	1
31.00	—	.3240	1	28.66*	6.56	.4100	2	2.21	5.62	.2600	1
38.00	5.23	—	1	20.44*	6.26	.3972	2	4.17*	5.87	.2780	1
5.92*	3.87	.2760	3	47.29*	7.13	.4248	2	6.48*	6.09	.2896	1
15.30*	4.38	.2972	3.5	72.79	8.73	.4484	2	7.38*	6.14	.2952	1
26.38*	4.73	.3160	2	95.25	16.42	.4884	3	11.15*	6.41	.3116	1
29.95*	4.87	.3228	1	96.98	19.31	.5276	1	19.64*	6.92	.3392	1
32.80*	4.98	.3284	2	Desorption				9.66*	6.41	.3180	1
36.80*	5.18	.3356	2	84.01	—	.5340	2	1.89	5.36	.2396	1
38.00*	5.20	.3428	2	82.03	15.51	—	2	0.93	4.59	.1900	1
41.45	5.38	.3480	2	70.86	14.16	.5156	1	0.42	3.45	.0648	1
26.88*	4.95	.3404	2	67.33	—	.5096	1	0.005	0.07	−0.420	2

*Points on scanning curve

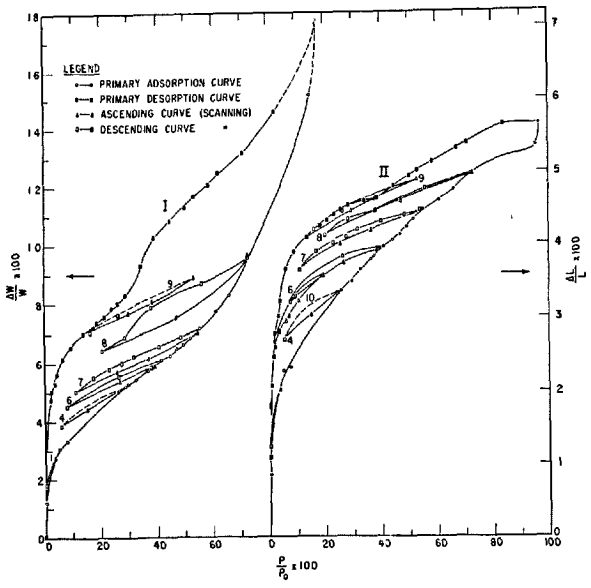

Fig. 3. *Weight change (I) and length change (II) isotherms of hydrated portland cement paste (water/cement ratio = 0.5). Scanning loops marked.*

as will be shown, a water area determination cannot be considered as a valid procedure. The nitrogen areas are, for these samples, 1/3 to 1/5 of the water areas, as has been observed by other workers (12).

Detailed examination of the isotherms, and especially the loops (Figs. 1 and 2), reveal the following:

(a) The isotherm is irreversible even at as low a P/P_0 value as 0.05 as is shown by loop 1; much of the irreversibly sorbed water, contributing to the low-pressure hysteresis, is sorbed below a P/P_0 of 0.35. (This irreversibly sorbed water, as will be shown, is interlayer hydrate water and will also be referred to as 'irreversible water.')

(b) All descending portions of loops 3 to 9 are essentially parallel and are much less steep than the primary curve. Thus means of course that a large part of the water sorbed on the primary adsorption curve is irreversible.

(c) In loops 7 and 8, where the descending curve has not gone below a P/P_0 of 0.11, the loops, although very close to, are not quite reversible.

(d) Both loops 7 and 8 exhibit a small primary hysteresis. This is to be expected since these loops leave the primary curve at P/P_0 values of 0.56 and 0.73 respectively. The desorption of the capillary water takes place between P/P_0 values of 0.38 and 0.29. This is lower than has been reported (8), but is confirmation of what was found previously (1).

(e) The primary desorption curve shows a large primary hysteresis. This primary hysteresis disappears between P/P_0 values of 0.39 and 0.29. The length change isotherm shows a small expansion in this region.

(f) The primary desorption curve below a P/P_0 of 0.29 shows that the low pressure hysteresis has increased markedly since the last loop, 8; the length change isotherm shows large changes between earlier loops, but does not show a further change in this region in the same relation to the irreverible water added.

(g) Fig. 3 shows the $\Delta L/L$ vs. $\Delta W/W$ plots for the sample degassed at 80°C; loops are numbered. Curve I contains most of the loops, curve II is a magnified version of I, and curve III shows only the primary ascending and descending curves. The $\Delta L/L$ vs. $\Delta W/W$ characteristics for the primary curve and the loops are completely different; the slope of the primary curve is much steeper and only if the loop goes below a P/P_0 value of 0.10 or thereabout does it become steep. This implies that the mean location of the water sorbed on the primary loop is different from that desorbed. The water sorbed on the primary curve is composed of a reversible and irreversible component and the $\Delta L/L$ vs. $\Delta W/W$ slope of this water is much greater in the low pressure range than the reversible component, most of which comes off separately if the loop is not carried to too low a pressure. It now seems clear that this 'irreversible water' is interlayer hydrate water. Sorption and length change theory (13) (see also earlier part of this paper) allows for length change due to physical adsorption by a decrease in surface energy of the solid. If a "crystal" is anisotropic, this may lead to the development of shear forces. In the case of hydrated cement, the hydrated silicate which has lost most of its intelayer hydrate water will accept physically adsorbed water (sometimes referred to as "reversible water") on its external surface, most of which is perpendicular to the *c*-axis. The resulting expansion on top of the layer should cause some warp at the edges, allowing some interlayer hydrate water to enter. This process will continue up the isotherm. (More will be said later about how this interlayer water enters and leaves and how it affects $\Delta L/L$ and Young's modulus.)

(h) The primary desorption curve below P/P_0 of 0.29, (Figs. 1 and 2) is surprisingly much steeper than all the desorption curves of the scanning loops. Loop 9 shows that 'irreversible water' was being desorbed in this region; the $\Delta L/L$ vs. $\Delta W/W$ slope (Fig. 4) for the primary desorption loop is much lower than in the primary adsorption region. Loop 9, however, is still steeper than loop 7, and it appears that some

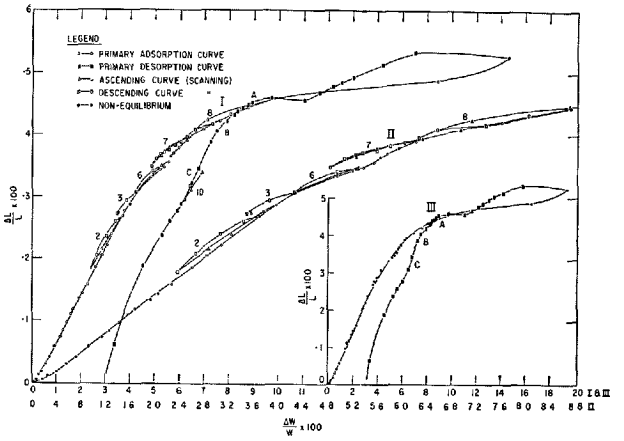

Fig. 4. ΔL/L vs. ΔW/W *plot for water sorbed on bottle-hydrated sample degassed at 80°C: I—containing all loops; II—enlarged portion of I; III—only showing primary sorption and desorption curves (scanning loops marked 1 to 10).*

interlayer hydration may be taking place along the adsorption curve of loop 9.

(i) ABC on Figs. 1, 2 and 4 mark the area where two regions of distinctly different slope of the ΔL/L vs. ΔW/W curve occurs on the primary desorption curve (2). As will be seen later, this probably represents a change in the response of length change due to unit weight loss of interlayer water. The assumption made previously (2) that this characteristic is constant now appears to be incorrect.

(j) The line BC marks the region where a considerable hysteresis in the ΔL/L vs. ΔW/W plot is formed (Fig. 4). (How this may illustrate the difference between entry and exit of interlayer water will be discussed later.) Below BC, the curve first gradually returns towards the zero point but then turns away, resulting in a large contraction below the zero point at zero ΔW/W.

(k) Loop 10 illustrates how a smaller low pressure hysteresis may be obtained in the isotherm when the sample has not been degassed as much as the initial degassing. Along the adsorption curve of the loop, a change in slope again occurs at about a P/P_0 of 0.10.

(l) Sorption and desorption measurements were taken at very low pressures (Table 2). On sorption the lowest P/P_0 value was 0.0027 and 0.0044 gave a ΔW/W × 100 value of 1.42. On desorption, the value was 3.45 at a P/P_0 value of 0.0042. This shows that there is large hysteresis in the sorption isotherm even at the lowest pressures. The length change isotherm shows a hysteresis in the other direction. At P/P_0 below 0.0093, a very large shrinkage occurs (0.420 per cent below the original zero). The pressure at zero was less than 1 micron of Hg (10^{-3} torr).

Construction of a Reversible Isotherm

The following conclusions can be derived from the previous discussion.

(a) The water isotherm for the several degrees of drying investigated is irreversible at all primary regions and, as such, cannot be used for B. E. T. calculations.

(b) As a large but unknown portion of the 'sorbed' water in the low pressure region is interlayer hydration, the surface area must be considerably lower than the original value calculated for water. The surface area obtained from N_2 will be considered here as the more reliable figure.

It still seems possible to separate, to some extent, the interlayer and physically adsorbed water from the isotherm. This can be done with the help of the scanning loops. If the desorption part of each loop up to the point where it overlaps with the inception of the previous loop (at a lower pressure)is regarded as reversible and involving only physically held water, one would be able to calculate for the pressure region over which the loop extended, the amounts of 'irreversible' and 'reversible' water sorbed along the primary adsorption curve. Since loops 7 and 8 exhibited primary hysteresis, the adsorption curve was used in these instances. For the estimate between P/P_0 of 0.727 and 0.97, it was assumed that no 'irreversible water' was desorbed between P/P_0 of 0.97 and 0.289; then the separation between this point on the primary desorption curve and loop 8, represented the water irreversibly sorbed between P/P_0 of 0.727 and 0.97. This procedure was also performed for the length change isotherm.

Fig. 5 shows the reversible length change and sorption isotherms. The desorption curve between P/P_0 of 0.97 and 0.289 was fitted on this curve. From the length change isotherm it is clear that too much contraction took place in this region to fit properly onto the adsorption curve. It is suspected that some 'irreversible water' was lost between at least P/P_0 of 0.345 and 0.289. Calculation of the reversible desorption between P/P_0 of 0.289 and 0.139 using loop 9 was not satisfactory since the validity of the assumption that the adsorption curve of the loop only involves physical water is suspect.

A plot of ΔL/L vs. ΔW/W (Fig. 5), shows a sharp deviation from the linear part of the curve at a P/P_0 of 0.10. This linear plot has been observed for the adsorption of water on porous glass, finely divided silica, precipitated calcium carbonate, calcium sulphate hemihydrate and $Ca(OH)_2$ and goes through

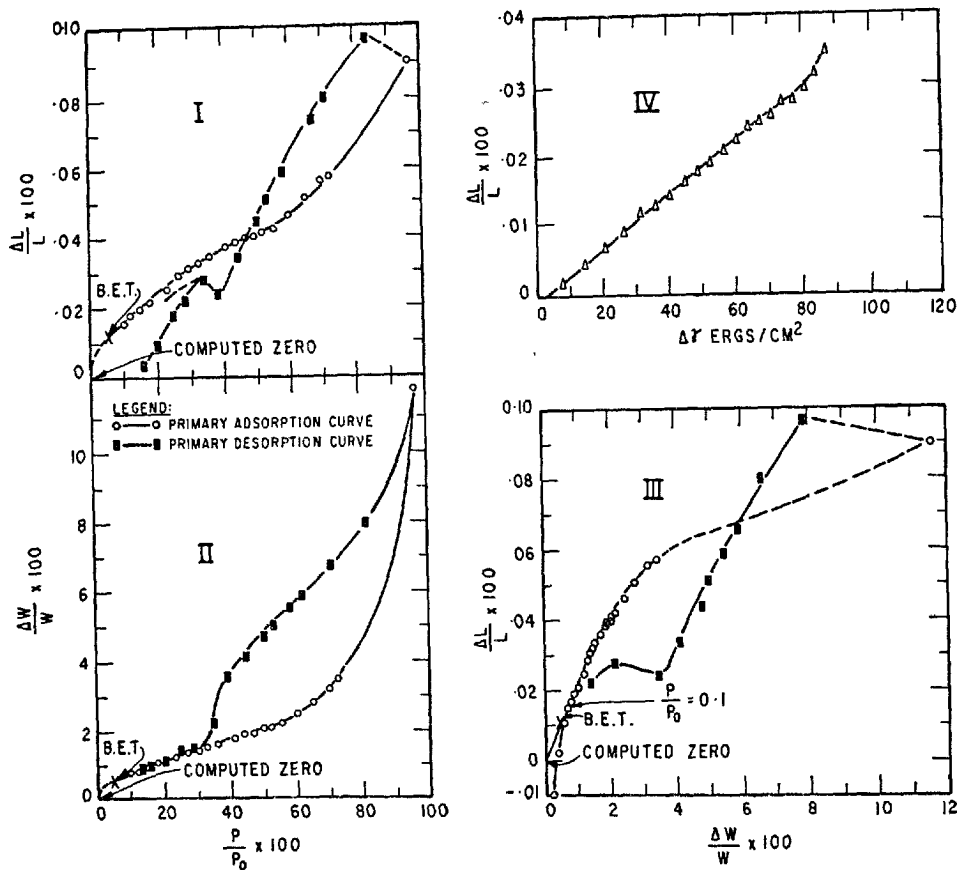

Fig. 5. *Constructed reversible water isotherm and computations: I*—$\Delta L/L \times 100$ vs. $P/P_0 \times 100$; *II*—$\Delta W/W \times 100$ vs. $P/P_0 \times 100$; *III*—$\Delta L/L \times 100$ vs. $\Delta W/W \times 100$; *IV*—$\Delta L/L$ vs. $\Delta\gamma$.

zero (14–17). Thus it is concluded that a larger amount of 'irreversible water' is removed below P/P_0 of 0.10, and so the physically held water cannot be estimated in this region using loops 1 or 2. An alternative procedure was used to achieve this. The N_2 surface area of 30 m^2/g (Table 1) was assumed to be approximately correct. Then, using the B.E.T. equation and adding different amounts of reversible water to represent that adsorbed below a P/P_0 of 0.10, calculations were made allowing the assumed surface area to vary slightly, until the monolayer capacity fell on a P/P_0 of 0.15 to 0.20. Using the area of the water molecule as 10.8 m^2/g, the water area obtained was 40.8 m^2/g; 0.70 per cent for $\Delta W/W \times 100$ was used for the 'reversible water' between P/P_0 of 0 to 0.10. From the B. E. T., a $\Delta W/W$ value for P/P_0 of 0.05 was obtained, and all other points below this were made by extrapolation of the curve. No significance was attributed to values below P/P_0 of 0.05 for 'reversible water.' Similar values for $\Delta L/L$ could be obtained by extrapolation of the $\Delta L/L$ vs. $\Delta W/W$ plot to the zero obtained for $\Delta W/W$.

All these results are included in Table 3 together with the results for the 'irreversible water,' which will be discussed together in more detail later.

Application of Gibbs' Equation and the Estimation of Young's Modulus from the Reversible Isotherm

An integration over the adsorption branch of the reversible isotherm was made between P/P_0 values of 0.05 (to avoid the extrapolated area and errors in integration as the pressure approaches zero) and 0.60, according to Gibbs' equation (Eqs. (1) and (3)). The change in state of stress of the solid $\Delta\gamma$, is plotted against $\Delta L/L$ according to Eq. (4). As shown on Fig. 5, this plot yields a very good straight line, and it appears that the whole procedure in constructing the reversible isotherm is justified. The slope of this line, k_1, from Eq. (4) is 3.90×10^{-6} cm/dyne.

Table 3. *Computed values for the reversible and irreversible isotherms*

P/P_0 range	Sorbed		Reversibly desorbed				Irreversibly Sorbed				% Irr.* of Total sorbed		% Rev.** of Total sorbed	
	ΔW/W × 100	ΔL/L × 100	ΔW/W × 100	Total	ΔL/L × 100	Total	ΔW/W × 100	Total	ΔL/L × 100	Total	ΔW/W	ΔL/L	ΔW/W	ΔL/L
0 → 0.003	1.27	0.084	—	—	—	—	—	—	—	—	—	—	—	—
0.003 → 0.03	1.25	0.098	0.71	—	0.063	—	0.54	—	0.035	—	—	—	—	—
0.03 → 0.052	0.56	0.040	0.20	—	0.012	—	0.36	—	0.028	—	—	—	—	—
0.052 → 0.08	0.26	0.022	0.19	—	0.009	—	0.07	—	0.013	—	—	—	—	—
0.08 → 0.10	0.18	0.013	0.11	—	0.004	—	0.07	—	0.009	—	—	—	—	—
0 → 0.10	3.52	0.257	0.70	0.70	0.016	0.016	2.82	2.82	0.241	0.241	80.1	93.8	19.9	6.2
0.10 → 0.123	0.16	0.011	0.10	0.80	0.002	0.018	0.06	2.88	0.009	0.250	78.3	93.3	21.7	6.7
0.123 → 0.15	0.16	0.010	0.11	0.91	0.002	0.020	0.05	2.93	0.008	0.258	76.4	92.8	23.6	7.2
0.15 → 0.18	0.15	0.009	0.11	1.02	0.002	0.022	0.04	2.97	0.007	0.265	74.4	92.3	25.6	7.7
0.18 → 0.234	0.28	0.017	0.18	1.20	0.004	0.026	0.10	3.07	0.013	0.278	71.9	91.4	28.1	8.6
0.234 → 0.27	0.22	0.009	0.10	1.30	0.004	0.030	0.12	3.19	0.005	0.283	71.0	90.4	29.0	9.6
0.27 → 0.30	0.18	0.008	0.09	1.39	0.002	0.032	0.09	3.28	0.006	0.289	70.2	90.0	29.8	10.0
0.30 → 0.33	0.20	0.009	0.08	1.47	0.001	0.033	0.12	3.40	0.008	0.297	69.5	90.0	30.5	10.0
0.33 → 0.36	0.20	0.007	0.09	1.56	0.002	0.035	0.11	3.51	0.005	0.302	69.2	89.6	30.8	10.4
0.36 → 0.414	0.30	0.013	0.16	1.72	0.002	0.037	0.14	3.65	0.011	0.313	68.0	89.4	32.0	10.6
0.414 → 0.44	0.13	0.006	0.12	1.84	0.002	0.039	0.02	3.67	0.004	0.317	66.6	89.1	33.4	10.9
0.44 → 0.47	0.15	0.010	0.05	1.89	0.001	0.040	0.10	3.77	0.009	0.326	66.6	89.1	33.4	10.9
0.47 → 0.50	0.17	0.008	0.12	2.01	0.001	0.041	0.05	3.82	0.007	0.333	65.5	89.1	34.5	10.9
0.50 → 0.52	0.14	0.005	0.05	2.06	0.001	0.042	0.09	3.91	0.004	0.337	65.5	88.9	34.5	11.1
0.52 → 0.55	0.28	0.013	0.12	2.18	0.001	0.043	0.16	4.07	0.012	0.349	65.1	89.1	34.9	10.9
0.55 → 0.60	0.52	0.014	0.26	2.44	0.004	0.047	0.26	4.33	0.010	0.359	64.0	88.4	36.0	11.6
0.60 → 0.65	0.65	0.015	0.32	2.72	0.005	0.052	0.33	4.66	0.010	0.369	63.2	87.7	36.8	12.3
0.65 → 0.70	0.82	0.017	0.41	3.13	0.005	0.057	0.41	5.07	0.012	0.381	61.8	87.0	38.2	13.0
0.70 → 0.727	0.53	0.009	0.29	3.42	0.001	0.058	0.24	5.31	0.008	0.389	60.8	87.0	39.2	13.0
0.727 → 0.97	10.58	0.082	8.32	11.74	0.035	0.093	2.26	7.57	0.047	0.436	39.2	82.4	60.8	17.6

P/P_0 range	Desorbed		Reversibly sorbed				Irreversibly desorbed				Comments
0.97 → 0.29	10.37	0.073	10.37	1.37	0.073	0.020	—	7.57	—	0.436	Assumed no interlayer water lost
0.29 → 0.25	0.27	0.006	0.15	1.22	0.005	0.015	0.12	7.45	0.001	0.435	—
0.25 → 0.20	0.39	0.011	0.19	1.03	0.008	0.007	0.20	7.25	0.003	0.432	—
0.20 → 0.16	0.24	0.009	0.15	0.88	0.007	0.000	0.09	7.16	0.002	0.430	—
0.16 → 0.14	0.13	0.006	0.07	0.81	0.003	—	0.06	7.10	0.003	0.427	—
0.14 → 0.05	0.96	0.060	0.35	0.46	0.007	—	0.61	6.49	0.053	0.374	Calculated from B. E. T.
0.05 → 0.044	0.20	0.017	0.03	0.43	0.001	—	0.17	6.32	0.017	0.357	Estimated values of reversible water
0.044 → 0.036	0.26	0.022	0.05	0.38	0.001	—	0.21	6.11	0.021	0.336	〃
0.036 → 0.023	0.44	0.035	0.07	0.31	0.002	—	0.37	5.74	0.033	0.303	〃
0.023 → 0.022	0.43	0.028	—	—	—	—	0.43	5.31	0.028	0.275	〃
0.022 → 0.0093	1.03	0.070	0.10	0.21	—	—	0.93	4.38	0.070	0.205	〃
0.0093 → 0.0042	1.14	0.125	0.21	0.00	—	—	0.93	3.45	0.125	0.085	〃
0.0042 → 0	3.38	0.485	—	—	—	—	3.38	0.07	0.485	−0.400	Actual value is −0.4200

* Total irreversible sorbed
**Total reversibly desorbed

Using a value of 2.86 g/cc for $Ca_3Si_2O_7 \cdot 2H_2O$ (18) since at a P/P_0 of 0.30 only about 40 per cent of the irreversible water has re-entered and since most of the adsorption is taking place on this "crystal" which constitutes most of the area, and using 40.8 m^2/g for the surface area, the value of 'E' from Eq. (5) is 2.99×10^{11} dyne/cm^2 or 4.35×10^6 lb/in.^{2}. This value is about 8 times as large as that measured for the equivalent compact (19), or of the equivalent water to cement ratio paste (20). This calculated value, however, represents 'E' for the solid material, not the porous body. Helmuth and Turk (20) extrapolated from porosity-E plots to get 'E' of 'gel phase' as 4.5, and of 'solid phase' 10.8 (lb/in.^{2}). This latter value was similar to the extrapolation of Soroka and Sereda (19). Both these values suffer from the difficulty of measuring the correct porosity; however, since a large part of the water removed during 'd-drying' is interlayer water which returns on sorption. Thus, the water porosity (determined by water) would be much lower than anticipated, making the extrapolated value much too high. Considering these assumptions, the value found for the modulus of the solid phases is very good and is considered as further evidence of the validity of this approach.

The Irreversible Isotherm

The method outlined in the previous section (construction of a reversible isotherm) also enables one to obtain the irreversible isotherm (Fig. 6 and Table 3). The large hysteresis in both length and weight change isotherms is evident. As already described, this hysteresis exists even to vapour pressures of only a few microns. The 'irreversible water' is sorbed at all pressures along the primary adsorption isotherm, and this explains why the time to attain equilibrium was always longer on this curve. Values below P/P_0

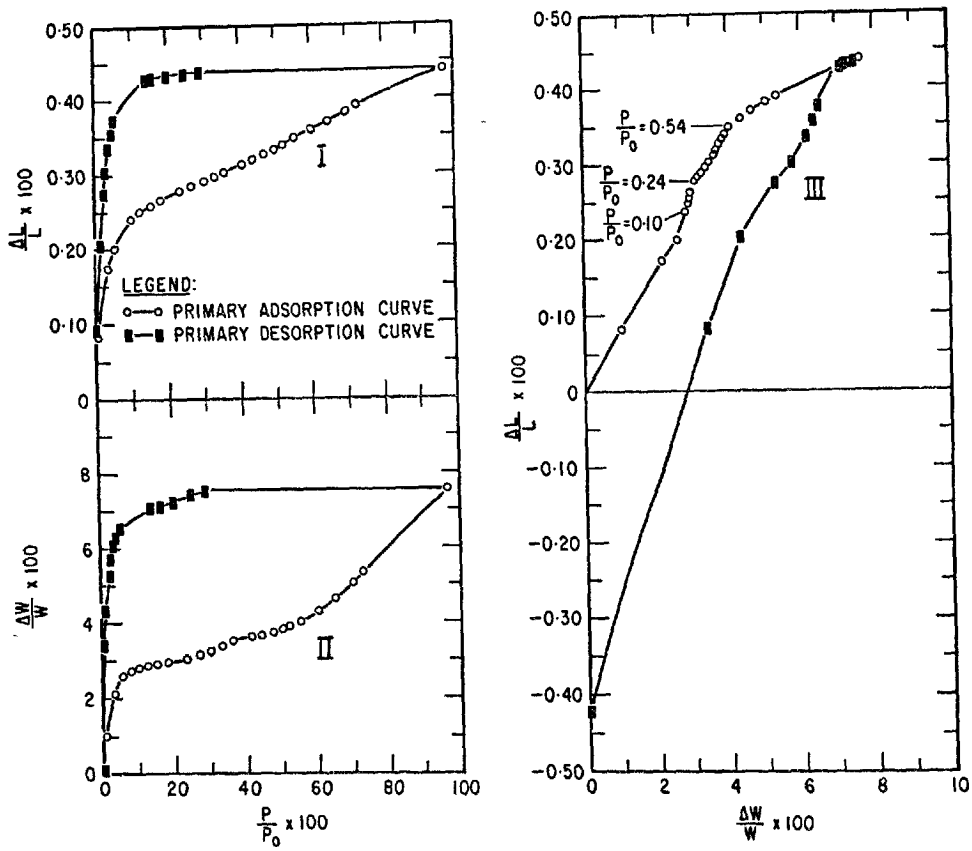

Fig. 6. *Constructed irreversible water isotherm: I*—$\Delta L/L \times 100$ vs. $P/P_0 \times 100$; *II*—$\Delta W/W \times 100$ vs. $P/P_0 \times 100$; *III*—$\Delta L/L \times 100$ vs. $\Delta W/W \times 100$.

of 0.05 were extrapolated for 'reversible water', but since this became small compared with the 'irreversible water', any error would be negligible.

The plot of the $\Delta L/L$ vs. $\Delta W/W$ shows the important change in slope on the sorption curve at P/P_0 of 0.54. This is precisely the point where the value of the modulus of elasticity (11) starts to increase, when measured as a function of relative pressure. In addition, the hysteresis of this curve shows that the withdrawal of interlayer water follows a completely different path from its entry. Again this might be implied from the results of the modulus measurements (11). As the desorption continued, it appeared as if the loop might gradually close, but below P/P_0 of 0.009 it diverged yielding a large irreversible shrinkage below the original zero by 0.420 per cent, although the zero for $\Delta W/W$ was the same.

This irreversible effect also occurred on the first degassing, but did not occur when degassing took place after a methanol cycle. Thus it must be associated with the effect of water. Solution effects of water on calcium hydroxide (14) are ruled out because the effect is considered too large; the explanation favoured is that when the final interlayer water is expelled, a reorientation of the layers occurs, resulting in an irreversible contraction. More work is needed in this area. Nevertheless, a plausible model can be suggested to explain most of the general behaviour of the entrance and exit of interlayer water and the variation of $\Delta L/L$ and modulus of elasticity with P/P_0.

Fig. 7 illustrates in model form the process of exit and entry of interlayer water: initially drying will take place from the edges with little contraction ((a) to (b)); drying to state (c) will provide some collapse and large contraction; drying at the edges probably occurs below P/P_0 of 0.30 and stronger drying (state (c)), below P/P_0 of 0.07; the final removal of the water in the middle will not take place above P/P_0 of 0.009. It is considered that this water in the centre provides the main bracing for a higher rigidity and, when it is removed, the modulus decreases as experiments show. This state of drying (d) also involves possible reorientation of the plates to produce an irreversible contraction. Resorption now occurs

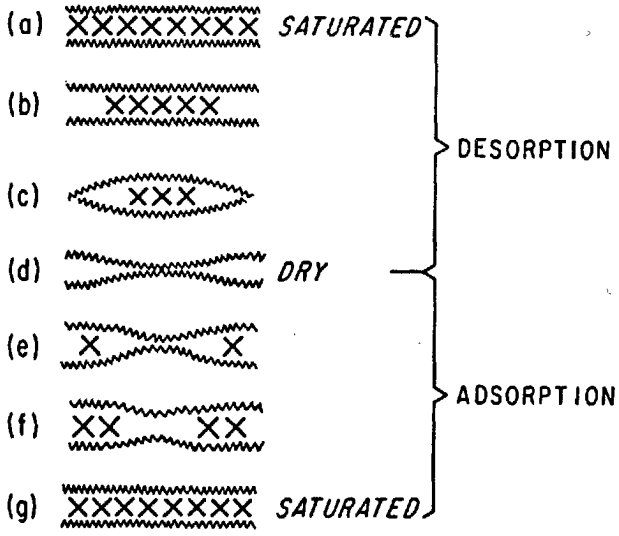

Fig. 7. *Simplified model for exit and entry of water between layers of tobermorite gel*

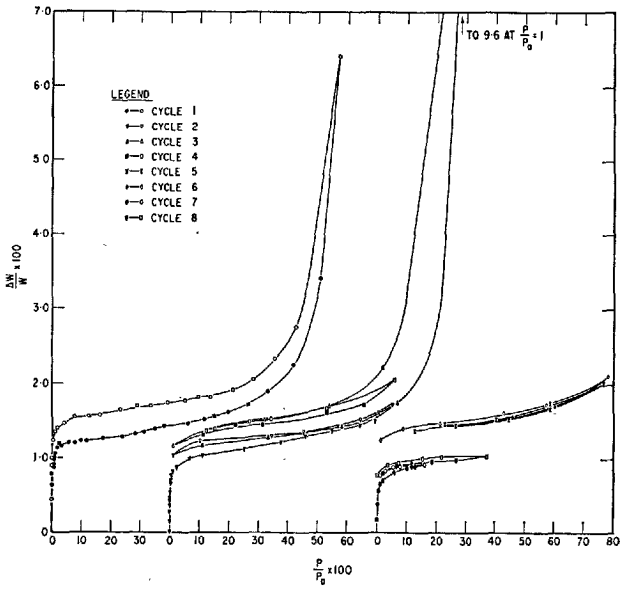

Fig. 9. *Length change isotherms of methanol on bottle-hydrated portland cement compacts degassed at 80°C.*

at the edges (states (e) and (f)), being initiated by physical adsorption and resultant surface free energy change on the external surfaces. Here, the pressure vs. $\Delta L/L$ or $\Delta W/W$ hysteresis is apparent, since interlayer water cannot enter until some external movement occurs. Further sorption will continue inward from the edges, causing large expansions. As the layers are filled towards the middle (states (f) to (g)), it is apparent that the modulus will start to increase due to "bracing" of the layers by the water molecules; the resultant $\Delta L/L$ will not be as large because most of the expansion occurred from the edges.

Further implications of the interlayer water can be observed from Table 3:

(a) Total interlayer water for this sample is 7.54 per cent, although it may be somewhat higher, as discussed above. This means that the difference between pore volumes obtained by water, on the one hand, and nitrogen and methanol, on the other, would be in the order of 0.08 ml/g. This explains the discrepancies in pore volume obtained by Mikhail and Selim (21) for pastes with a *w/c* of 0.35 to 0.57. It is postulated here that, since the interlayer penetration by nitrogen is very small, this gas would give the best pore volume for mechanical property extrapolations.

(b) Less than 20 per cent of the total expansion along the isotherm is due to physically adsorbed water. The percentages of physical and 'irreversible' water, and their concomitant length changes for the different pressure ranges are shown in Table 3.

The only remaining evidence to support the previous model of hydrated portland cement is the density measurements of Brunauer, Kantro, and Copeland (18). It is clear, however, that when the density is measured with a water solution, the interlayer water has already re-entered. The slow decrease in density obtained by these authors for some less severely dried samples is probably associated with some slow recovery of the irreversible shrinkage observed by Helmuth and Turk (22), or as observed here below P/P_0 of 0.009. Density measurements should be perhaps obtained with nitrogen.

Methanol Adsorption

Methanol sorption was measured on the same compacted sample degassed at 80°C.

The sorption results (Fig. 8) are very similar to those obtained by Mikhail (21) inasmuch as a surface area of similar magnitude was obtained (area of molecule taken as 18.1 Å², see Table 1), and the low pressure hysteresis is of the same magnitude (intermediate between water and nitrogen). Several cycles were performed, however, and length change measurements, (Fig. 9) were made during these cycles. Significant features of these results are the following:

(a) After significant sorption at very low pressures, the isotherm is very flat; for cycle 2 to P/P_0 of 0.75 the desorption is even flatter. This may be explained by the concept of autophobicity of alcohol adsorption (23), where the isotherms exhibit strong monolayer

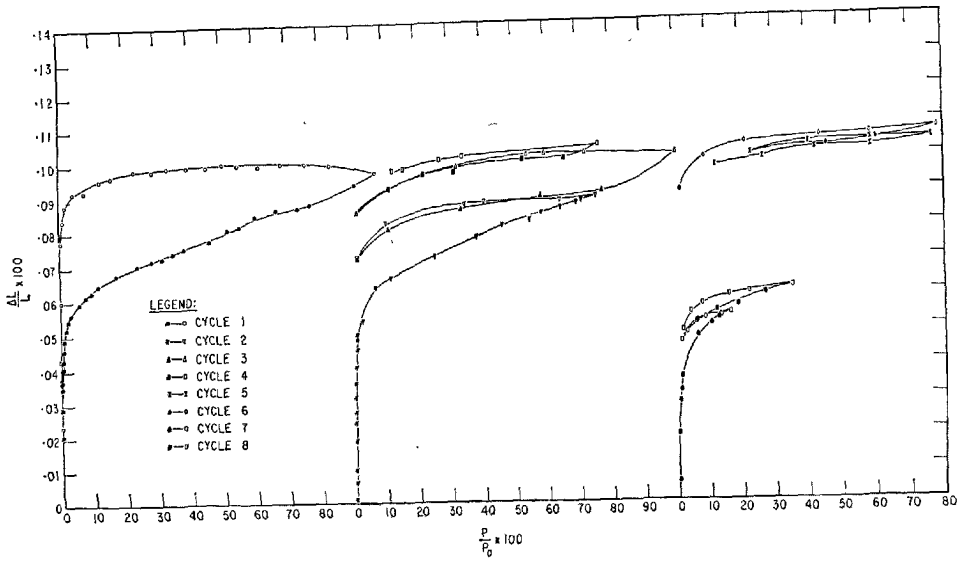

Fig. 8. *Sorption isotherms of methanol on bottle-hydrated portland cement compacts degassed at 80°C.*

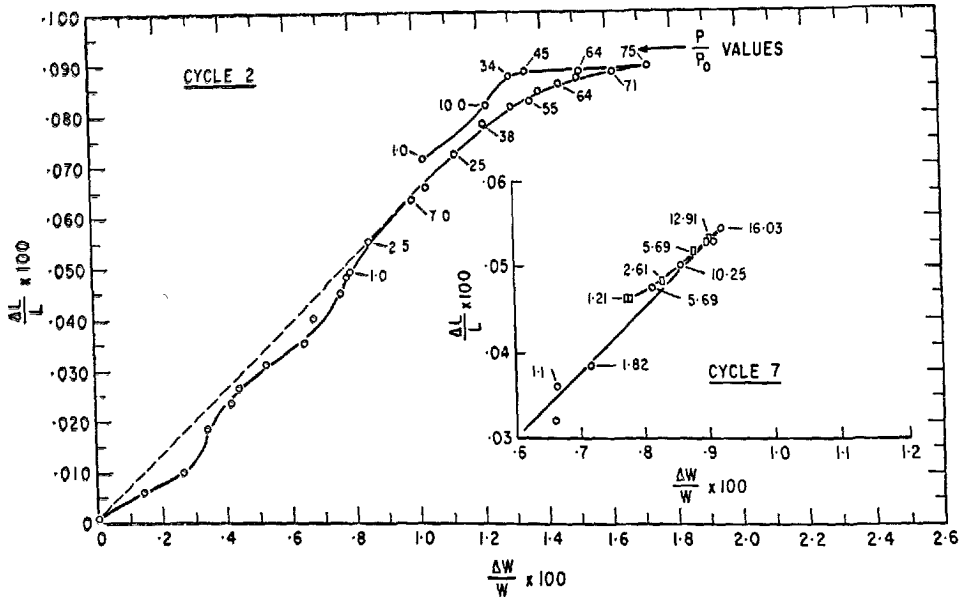

Fig. 10. ΔL/L vs. ΔW/W *plots for methanol sorbed on bottle-hydrated portland cement compact degassed at 80°C* (P/P_0 *values are* × *100*)

binding with little tendency toward multilayer formation; multilayer formation occurred almost asymptotically at high vapour pressures. The autophobicity is due to strongly oriented adsorption in the first adsorbate layer which would permit multilayer formation at a distance remote from the initial interface so that its influence is lost. The result would approximate to a Langmuir isotherm, but for methanol, whose hydrocarbon chain is not so long, this approximation is not completely attained.

(b) Cycles 2, 7 and 8 show that the hysteresis, like that for water, is cumulative, significant low pressure hysteresis occurring even after sorption to only P/P_0 of 0.17. Cycle 3 rejoins precisely where cycle 2 stopped on the adsorption curve, but for cycles 7 and 8, the rejoining is not so exact. Cycle 4 shows that some of the irreversibly sorbed methanol may be withdrawn at about P/P_0 of 0.01; cycle 5 shows that the isotherm

is close to reversible between P/P_0 of 0.12 and 0.77 on the descending branch, and cycle 6, that some irreversible sorbed methanol is added when this cycle goes to a higher pressure than did cycles 4 and 5.

(c) The length results show the same result as far as irreversibility is concerned. The ascending 'sorption' curves, however, cycles 1, 2, 3, show a significant length change at the beginning and all the way up the isotherm, contrary to the assumption of Mikhail and Selim (21). Despite the large desorption, there is very little contraction on the desorption curve. This length change plot looks very similar to the constructed irreversible plot for water. The explanation is clear: along the sorption curve, both physical adsorption (of a strong nature at low P/P_0), and interlayer penetration are taking place. The penetration is less than that of water because of the respective sizes of the molecules; on the desorption curve only weakly held methanol is coming off. At P/P_0 of 0.10, the slope $(\Delta L/L)/(\Delta W/W)$ for the hysteresis is taken to represent that for interlayer methanol (see Table 1); the value 0.0955 is more than that for water (0.0860) which is reasonable since the methanol molecule is bigger than water. Curve I in Fig. 10 shows the $\Delta L/L$ vs. $\Delta W/W$ plot. The points below P/P_0 of 0.01 show signs of specific interaction, but the adsorbed methanol cannot be separated from the interlayer methanol. If the average slope is taken and the surface area is assumed to be 30 m^2/g (nitrogen value), the physically adsorbed methanol will have a $(\Delta L/L)/(\Delta W/W)$ of 0.0525, over twice that for water. This is consistent with Gibbs' equation if, as assumed, a larger proportion of the methanol is adsorbed at low pressures. There would be reason to expect that the specific adsorption for methanol would be different from the one for water if the surface contains many hydroxyl groups (13). Details of this will not be included here, but it is apparent that the methanol isotherm is more complicated than previous interpretations (21), and that it is consistent in every way with the results obtained from water sorption.

Conclusions

1. Exposure of dried (below approximately 10 per cent R. H.) hydrated portland cement paste to water vapour at any pressure results in the entry of interlayer hydrate water simultaneously with physically adsorbed water.

2. Surface areas are much lower than was believed, the nitrogen area probably being the most reliable figure.

3. Less than 18 per cent of the expansion along the isotherm is due to physically adsorbed water.

4. Porosity values obtained from water sorption are too high. Nitrogen would give more reliable figures.

5. Gibbs' equation is obeyed for the constructed reversible isotherm, and a calculation of the modulus of elasticity of the solid material gives a reasonable value.

6. A model for the entry and exit of interlayer water is given which explains the effect of vapour pressure on the modulus of elasticity. This model suggests that the entry and exit of interlayer hydrate water plays an important part in creep phenomena.

7. Results from methanol sorption, which also involves interlayer penetration, are consistent with those of water.

Acknowledgements

The author is grateful to H. F. Slade and S. E. Dods for setting up the apparatus and collecting the data. This paper is a contribution from the Division of Building Research, National Research Council of Canada and is published with the approval of the Director of the Division.

References

1. R. F. Feldman and P. J. Sereda, "Sorption of water on bottle-hydrated cement I," J. Appl. Chem., **14**, 87–93 (1964).

2. R. F. Feldman and P. J. Sereda, "A Datum point for estimating the adsorbed water in hydrated portland cement," J. Appl. Chem., **13**, 375–382 (1963).

3. R. F. Feldman and P. J. Sereda, "Characteristics of sorption and expansion isotherms of reactive limestone aggregate," Proc., J. Amer. Concr. Inst., **58**, 203–214 (1961).
4. R. F. Feldman and P. J. Sereda, "A model of hydrated portland cement paste as deduced from sorption—Length change and mechanical properties." To be published.
5. H. Van Olphen, "Thermodynamics of interlayer adsorption of water in clays," J. Colloid Sci., **20**, 822–837 (1965).
6. R. F. Feldman and P. J. Sereda, "Sorption of water on compacts of bottle-hydrated cement, II. thermodynamic considerations and theory of volume change," J. Appl. Chem., **14**, 93–104 (1964).
7. D. Bangham and F. A. P. Maggs. "The strength and elastic constants of coals in relation to their ultrafine structure," In Proc., Conf. Ultra-fine Structure of Coals and Cokes, Brit, Coal Util. Res. Ass., 118–130, June 1943.
8. T. C. Powers and T. L. Brownyard, "Studies of the physical properties of hardened portland cement paste," PCA Bulletin No. 22, 304 p. (1948).
9. T. C. Powers, "Mechanism of shrinkage and reversible creep of hardened paste," Proc. Intern. Conf. Structure of Concrete, London (1965).
10. R. M. Mills, "Effects of sorbed water on dimensions, compressive strength and swelling pressure of hardened cement paste," Highway Research Board, Special Report No. 90, 84–111 (1966).
11. P. J. Sereda, R. F. Feldman and E. G. Swenson, "Effect of sorbed water on some mechanical properties of hydrated cement pastes and compacts," Highway Research Board, Special Report No. 90, 58–73 (1966).
12. R. Sh. Mikhail, L. E. Copeland and S. Brunauer, "Pore structures and surface areas of hardened portland cement pastes by nitrogen adsorption," Can. Jour. Chem., **42**, 426–438 (1964).
13. P. J. Sereda and R. F. Feldman, "Mechanical properties and the solid gas interface," *In* The Solid Gas Interface, Edited by E. A. Flood, Vol. 2, Ch. 24, 729–764, Marcel Dekker Inc., New York (1967).
14. V. S. Ramachandran and R. F. Feldman, "Length change characteristics of $Ca(OH)_2$ compacts on exposure to water vapour," To be published.
15. R. F. Feldman and P. J. Sereda, "The use of compacts to study the sorption characteristics of powdered plaster of paris," J. Appl. Chem., **13**, 158–167 (1963).
16. P. J. Sereda and R. F. Feldman, "Compacts of powdered materials as porous bodies for use in sorption studies," J. Appl. Chem., **13**, 150–158 (1963).
17. C. H. Amberg and R. MacIntosh, "A study of hysteresis by means of length changes of a rod of porous glass," Can. J. Chem., **30**, 1012–1032 (1952).
18. S. Brunauer, D. L. Kantro and L. E. Copeland, "The stoichiometry of the hydration of β-dicalcium silicate and tricalcium silicate at room temperature," Jour. of Phys. Chem., **80**, 761–767 (1958).
19. I. Soroka and P. J. Sereda, "The structure of cement—stone and the use of compacts as structural models," Submitted to 5th International Symp. on Cement Chemistry, Tokyo, 1968.
20. R. A. Helmuth and D. H. Turk, "Elastic moduli of hardened portland cement and tricalcium silicate pastes: effect of porosity," Highway Research Board, Special Report No. 90, 135–144 (1966).
21. R. Sh. Mikhail and S. A. Selim, "Adsorption of organic vapors in relation to the pore structure of hardened portland cement pastes," Highway Research Board, Special Report No. 90, 123–134 (1966).
22. R. A. Helmuth and D. H. Turk, "The reversible and irreversible drying shrinkage of hardened portland cement and tricalcium silicate pastes," J. Portland Cement Association, Research and Development Laboratories, **9**, 8–21 (1967).
23. J. Barto, J. L. Durham, V. F. Baston and W. H. Wade, "The gas phase autophobicity of alcohols adsorbed on alumina," J. Colloid and Interface Science, **22**, 491–501 (1966).

Supplementary Paper III-34 The Structure of Cement-Stone and the Use of Compacts as Structural Models

I. Soroka* and Peter J. Sereda**

Synopsis

The relation between hardness, modulus of elasticity and porosity was investigated in three different systems prepared from normal Type I portland cement. This study was undertaken to obtain some data on the structure of cement-stone, particularly with regard to the nature of the interparticle bonds and their effect on mechanical properties. The study also enabled the evaluation of the possible use of compacts in cement research.

The three cement systems, designated as I, II, and III, cement pastes (I) in which porosity varied from 40% to 70% and the degree of hydration from 73% to 98% (w/c ratio 0.40 to 1.20), compacted cement pastes (II) in which porosity varied within the range of 25% to 60%, and compacts of bottle hydrated cement (III) in which the porosity varied from 20% to 55% and the degree of hydration from 0% to 90% (i.e., unhydrated cement compacts were included).

Test results generally supported the concept that the strength of the cement-stone is mainly derived from a particular type of interparticle bond. It is concluded that this bond is a solid to solid contact resulting from the bringing together of surfaces, and that it is essentially the same in compacts as in cement paste.

The close agreement between values for mechanical properties of compacts as compared to paste suggests that compacts, used as a model of the cement-stone, are a promising and a reliable tool in cement research.

Introduction

It is generally accepted that the structure of cement-stone*** is rather complex, and there are still quite a few aspects concerning its nature awaiting clarification. Although extensive data exist to indicate that the hydration products are essentially comprised of colloidal-sized particles having a great variety of microstructure, as shown by Grudemo (1), little is known about the nature of the bonds between these colloidal particles to account for the strength of the cement-stone. Philleo in his review (2) discussed the various types of bonds and pointed out that limited swelling of the cement-stone in water has been considered as evidence for the existence of some chemical (primary) bonds between the gel particles but that the secondary bonds accounted for most of the strength of the cement paste. This conclusion was made on the grounds that adsorbed water was a constituent part of the bond, in order to account for some of the unusual physical and mechanical behaviour. Recent work at DBR (3–6), however, contradicts the above hypothesis.

It is recognized that the terms "chemical" and "secondary" bonds have been used in describing the structure of hydrated cement system without a strict definition of their meaning. This has led to considerable misunderstanding. It is believed that what was meant by the "chemical" bond between the particles was a solid to solid contact similar to that of a grain boundary in a polycrystalline material where some atoms approach the spacing and arrangement in the crystal. Such "chemical" bonds could be formed during a crystallization process accompanying a chemical reaction where the mobility of atoms allows for a regular arrangement resulting in an intergrowth of crystals. It follows that these bonds would be strong and, when broken, would not be remade in normal circumstances.

It is believed that the term "secondary" bonds as applied to the hydrated cement system arose out of the assumption that adsorbed water was a constitu-

* Building Research Station—Technion—Israel Institute of Technology Haifa, Israel.

**Division of Building Research, National Research Council, Ottawa, Canada.

***Cement-stone refers to the system of cement gel and the associated capillary space, and is an alternate name for the hardened cement paste.

ent part of the interparticle bond; hence the general term of van der Waals forces was considered appropriate.

Previous work in this laboratory has indicated that neither of these definitions would fit adequately the interparticle bonds in the hydrated cement system. It is suggested, therefore, that a different interparticle bond be postulated which would involve a solid to solid contact resulting from the bringing together of surfaces (by pressure or accommodation) forming a particle boundary having no regular atomic arrangement or spacing. Atoms at such a boundary would engage a varying proportion of the long range and the short range forces depending on the degree of disorder and the average spacing. It can be visualized that this interparticle bond can be broken and subsequently remade under appropriate loading conditions. This type of bond differs from the "chemical" bond defined above, which has a more regular atomic arrangement, and in which the spacing of the atoms may approach that of the lattice spacing in the crystal.

The vital question of the structural model for hydrated cement, therefore, has yet to be resolved, especially in regard to the nature of the particular interparticle bonds for which there is considerable evidence from the work at DBR involving compacts of hydrated cement. The present work was designed to shed some further light on the above questions of the structure of portland cement-stone.

In the first stage of the study, some mechanical properties of compacts and pastes were compared in a gypsum system, which is distinctly crystalline and where intergrowing of crystals is a distinct possibility. The results of this stage of the work were reported elsewhere (7), but the essential part is reproduced here to enable direct comparison of the gypsum system with the cement system.

In the second series of experiments reported here, essentially the same tests were carried out with Type I normal portland cement instead of gypsum. It was hoped that the comparison of results for the two systems (distinctly different in the degree of crystallinity) would reveal information about the nature of the bonds.

Experimental

In the tests described, the hardness and modulus of elasticity of portland cement pastes and of compacts with a wide range of porosities were compared. All specimens involved were flat, round plates 1.25 in. (approximately 32 mm) in diameter and 0.050 in. (approximately 1.25 mm) thick. Specimens of three different systems were prepared, all from the same brand of Type I normal portland cement.

Preparation of Specimens

System I—Cement Paste

The cement was mixed in vacuum with boiled distilled water to give cylinders measuring 1.25 in. in diameter and approximately 5 in. high. (For the chemical composition of the cement see reference (3), and for further details of mixing procedure see reference (8)). The water/cement ratio in the specimens varied from 0.40 to 1.20 resulting in pastes of seven different porosities ranging from approximately 40% to 70% (Table 1).

Specimens were demoulded after 48 hours and, to avoid carbonation, were wet-cured in tightly closed rubber bags. At the age of approximately 3 months the cylinders were taken out and sliced to give specimens having the required thickness of 0.050 in. Conditioning of specimens involved two stages; they were first allowed to dry at 30% R. H. and 22°C (saturated solution of $CaCl_2$), and then placed over a NaOH solution to reach equilibrium at 50% R. H. and 22°C both in a CO_2-free atmosphere.

The porosity of the samples was calculated from the weight, volume, and degree of hydration, taking the density of the unhydrated cement to be 3.15 g/cc and that of the hydration products to be 2.60 g/cc.

System II—Compacted Cement Paste

Some of the cement paste specimens (system I),

Table 1. *Summary of test data*
System I—*Portland cement pastes and compacts*

Designation	w/c ratio	Porosity, %	Hardness, kg per sq mm	Modulus of elasticity × 10 4, kg per sq cm	Degree of hydration, %
15	0.40	39.6	32.0	14.71	73.3
16	0.50	45.6	20.6	10.86	80.9
19	0.60	51.8	10.7	7.92	80.2
23	0.70	55.6	8.2	6.95	86.8
25	0.80	59.3	5.9	5.63	88.6
31	1.00	65.5	3.3	3.80	91.7
37	1.20	69.9	—	2.57	98.5

after being cured and sliced, were subjected to a compacting pressure in a closely fitting mould (0.003 in. nominal clearance). In each case the thickness of the sliced specimens was adjusted to yield the nominal thickness of 0.050 in. after compaction. Porosity was controlled by the amount of the applied pressure and ranged from approximately 25% to 60% (Table 2). When the initial porosity was known, porosity after compaction was determined simply from the change in the dimension of the specimens involved.

Compaction was affected when the paste specimens reached equilibrium at 30% R. H.; however, testing was carried out after they were conditioned at 50% R. H.

System III—Compacts of Bottle Hydrated Portland Cement

The hydrated cement was prepared by mixing 1:5 mixtures of cement and water in tightly closed bottles which were mounted on a rotating disc. The mixing period varied between 24 hours and 28 months, resulting in products of different degrees of hydration within the range of approximately 35% to 90% (Table 3).

When mixing was completed, the hydrated cement was filtered, dried at 30% R. H. over $CaCl_2$, and then screened through a 100-mesh sieve. The remaining fraction (mostly $Ca(OH)_2$ crystals) was ground and recombined with the sieved material. At this stage the powdered hydrated cement was used to produce the compacts by the method described elsewhere (3–5). Altogether, compacts of 5 different degrees of hydration were prepared within the porosity range of approximately 20% to 55% (Table 3). To complete the picture and to provide data for "zero" degree of hydration, compacts of unhydrated cement were also prepared in the porosity range of 18% to 31% (system IIIa-Table 4). As in system I (cement pastes) porosity was determined from the weight, volume and degree of hydration and using the density values mentioned previously. To conform with the

Table 2. *Summary of test data*
System II—*Compacted portland cement pastes and compacts*

Designation	Compacting pressure, kg per sq cm	Porosity, %	Hardness, kg per sq mm	Modulus of elasticity × 10^{-4}, kg per sq cm
15	1,430	39.1	41.6	4.90
	2,860	36.6	51.2	14.76
	5,730	30.0	69.9	22.41
	11,460	24.9	85.6	26.84
16	1.140	45.1	25.4	9.28
	2,290	40.4	41.4	12.36
	4.580	33.3	—	19.78
	5,730	30.3	63.2	22.10
	11,460	24.8	87.1	26.90
19	1,140	49.4	23.9	7.89
	2,290	41.5	38.7	14.79
	4,300	34.0	—	20.57
	5,730	31.1	64.9	23.36
	11,460	25.8	80.4	24.34
23	1,140	50.2	—	8.92
	1,430	47.3	26.0	10.82
	1,720	46.8	—	11.24
	2,290	40.4	—	14.20
	2,860	37.3	46.0	15.98
	5,730	29.1	67.6	23.49
	11,460	24.6	85.8	27.94
25	860	53.5	15.3	7.67
	1,140	51.0	—	7.42
	1,430	49.0	—	9.72
	1,720	47.7	—	10.40
	2,000	44.5	30.3	12.08
	2,290	43.3	—	13.59
	4,300	33.5	56.6	20.08
	5,730	29.8	—	23.83
	6,870	28.2	69.3	25.90
	11,460	25.7	83.7	27.31
31	860	56.7	10.8	5.20
	1,140	53.3	—	6.99
	1,720	49.0	—	9.56
	2,290	44.1	32.1	11.75
	2,860	39.8	—	16.29
	5,730	30.8	62.0	17.66
	11,460	25.6	79.5	25.92
37	570	59.4	—	4.72
	740	57.6	10.4	5.08
	860	54.7	—	6.67
	1,140	51.0	—	8.11
	1,430	48.9	20.8	9.20
	1,720	46.7	—	9.92
	3,440	37.9	45.9	16.35
	4,300	33.9	—	20.58
	5,730	31.0	66.9	27.24
	10,020	25.9	—	27.03
	11,460	25.2	77.9	26.99

Table 3. *Summary of test data*
System III—*Compacts of bottle hydrated portland cement*

Designation	Mixing time	Degree of hydration, %	Compacting pressure, kg per sq cm	Porosity, %	Hardness, kg per sq mm	Modulus of elasticity × 10^{-4}, kg per sq cm
B1	1 day	34.1	860	45.7	10.4	5.80
			2,860	34.0	37.2	15.16
			5,730	26.7	62.6	22.38
			11,460	19.9	92.8	29.46
B3	3 days	49.8	860	48.9	13.0	6.14
			2,860	36.8	38.9	15.20
			5,730	28.3	69.1	23.17
			11,460	21.3	99.0	30.84
B7	7 days	63.8	860	47.9	16.0	6.73
			2,860	35.5	40.4	16.31
			5,730	30.6	50.1	20.50
			11,460	28.7	51.4	21.15
B28	28 days	75.5	860	49.7	16.0	7.84
			2,860	37.3	35.5	16.95
			5,730	34.5	43.8	19.06
			11,460	33.9	—	—
BM	28 months	90.7	860	54.8	9.1	4.08
			2,860	41.0	30.8	11.57
			5,730	31.5	52.4	19.22
			8,020	26.6	70.5	25.75
			11,460	23.2	81.7	27.16

Table 4.
System IIIa—*Compacts of unhydrated portland cement*

Compacting pressure, kg per sq cm	Porosity, %	Hardness, kg per sq mm
1,430	31.1	19.6
2,860	26.8	28.3
5,730	22.4	50.8
11,460	18.1	81.6

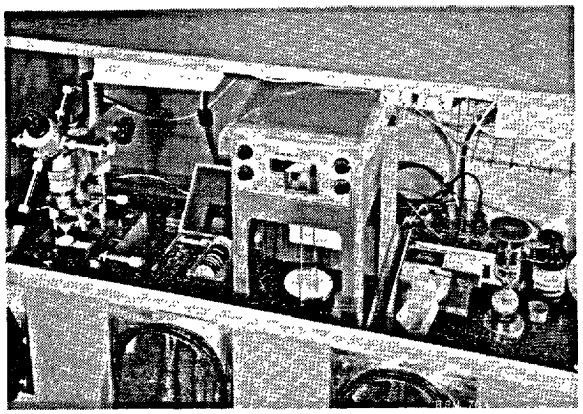

Fig. 1. *General view of testing layout*

other systems, testing was carried out after specimens reached equilibrium at 50% R. H. and 22°C.

Testing Methods

All tests were carried out in a gloved box which was conditioned at 50% by means of a NaOH solution (Fig. 1). The following tests were conducted.

Hardness

Vickers hardness was determined with a Leitz Miniload hardness tester; the load was adjusted in each case to give indentation to a depth of 35 to 50μ. For each specimen tested, the hardness was taken as the average of 10 tests carried out along an arbitrary diameter at 0.1-in. spacing.

Young's modulus of elasticity was determined with an apparatus described elsewhere (5). Essentially the procedure involves the measuring of the deflection of a specimen when it is loaded at its centre and supported at three points located at the circumference of a circle 1 in. in diameter. Under such conditions, Young's modulus is related to centre-deflection as follows (9):

$$\text{Def} = \beta \frac{\text{P}a^2}{\text{E}h^3}$$

where P = the applied load
a = radius of circle of support
E = Young's modulus of elasticity
h = specimen thickness
β = parameter related to Poisson's ratio (μ), number of supports (m) and the ratio (t) between the radius of circle of supports (a) and radius of specimen (c).

To determine the value of β in the above formula, it was assumed that the modulus of elasticity in compression is equal to the value determined from the deflection test. In turn, the modulus of elasticity in compression was determined on cylinders 1.25 in. $\times$ 2 in. which were, in fact, the companion specimens of the cylinders used for preparing systems I and II.

The average of five tests was considered as Young's modulus for any given set of conditions.

Degree of hydration was determined by means of a thermo-balance test (TGA). The weight of the sample in a "dry state" was taken as the value recorded when no weight loss was observed (readings to the nearest milligram) with the oven temperature kept constant at 120°C. The amount of water required for complete hydration was considered to be 25.4% of the unhydrated cement weight. For each set of conditions, the degree of hydration was taken as the average of three or four such tests.

It is realized that the accuracy and reproducibility of the results of the above procedure are questionable to some extent. This, in fact, is somewhat indicated in the results reported in Tables 1 and 3. It can be seen that, contrary to what could have been expected, the degree of hydration in the paste with a w/c ratio of 1.20 was found to be higher than that observed in the cement which was bottle-hydrated for 28 months. It should be kept in mind, however, that for the purpose in hand, where the degree of hydration is used to calculate porosity, the use of a better established value is less critical than it perhaps would be under different conditions. Using, for instance, the formula suggested by Powers (10) it can be shown that a difference of 10% in the degree of hydration is associated only with approximately 3% variation in the porosity of denser pastes (w/c = 0.40) and 1% variation in high-porosity pastes (w/c = 1.20). It is, therefore, considered that possible errors of such order are not liable to affect materially the results and the use of the above procedure in no way limits the following conclusions.

Results and Discussion

In Figs. 2 and 3 respectively, hardness and modulus of elasticity are plotted against porosity, together

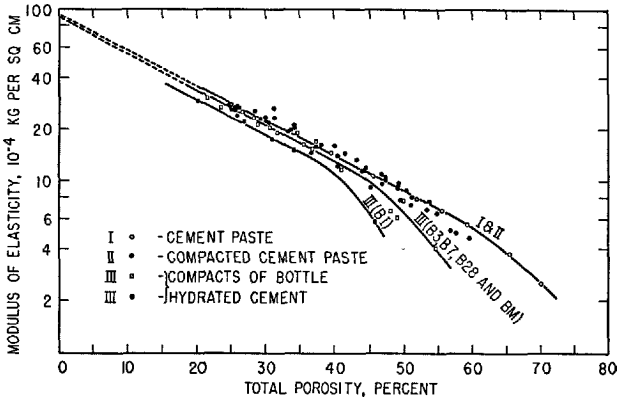

Fig. 2. *Modulus of elasticity vs. porosity for the cement systems*

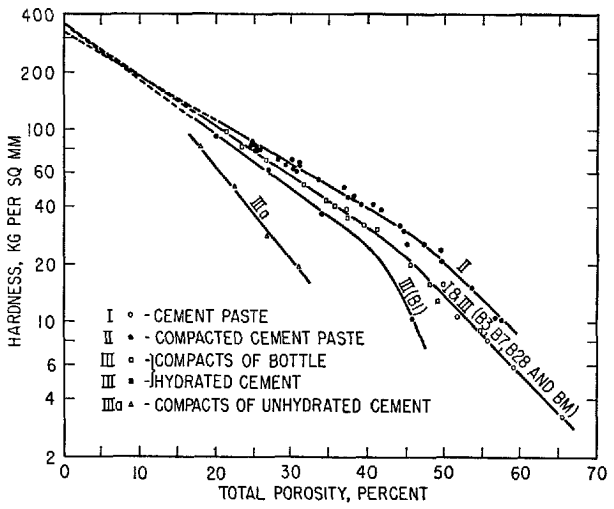

Fig. 3. *Hardness vs. porosity for the cement systems*

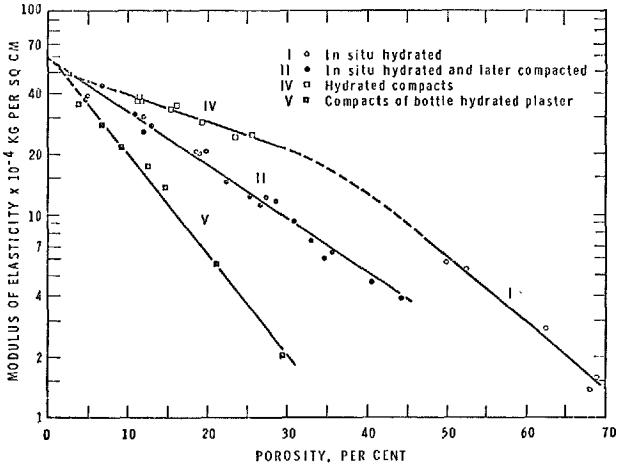

Fig. 4. *Modulus of elasticity vs. porosity for the gypsum systems*

with the corresponding regression line. These lines were calculated to fit test data employing the least squares method and assuming a semi-logarithmic relation between the factors involved. It can be seen that for each of the systems prepared, (excluding the higher end of the porosity range), such an assumption resulted in fairly good agreement with the experimental data. It should be realized, however, that the exponential expression used here, although suggested and used by others (11, 12), is purely empirical and therefore does not necessarily represent the "true" relation between the factors involved. Moreover, it is possible to devise other expressions to fit the very same data. In the present study, however, where the main object is the comparative evaluation of the different cement systems, this aspect becomes of secondary importance. In fact, for the present purpose, any other expression which can be shown to represent the experimental data may be used with more or less the same degree of success.

The most significant result, as shown in Fig. 2, is that the modulus versus porosity relation was the same for the compacted cement paste as for the cement paste despite the fact that paste samples, having an original porosity in the range of 40 to 70% were compacted to porosities in the range of 25 to 60%. This is strong evidence for the absence of "chemical" bonds because it is unlikely that these would not be broken (if they were present) when the pore volume is reduced by one half during compaction. The fact that the values for the modulus of the compacts of bottle hydrated cement fit so closely to that of the paste and compacted paste lends further support to the idea that this system has none or very few "chemical" bonds.

The above results are in striking contrast with the results for the gypsum systems presented in Fig. 4 (reproduced from reference (7)) where "chemical" bonds can be identified. In this case the modulus for the in-situ hydrated gypsum was an order of magnitude greater than for the compacts at the same porosity.

The results of microhardness versus porosity presented in Fig. 3 lead to the same conclusions as the results for modulus; the "chemical" bonds, if present in the paste, play an insignificant role because paste and compacts give the same relation with porosity. It is surprising, however, that the compacted paste samples give higher values for hardness. This may be related to a surface effect in the case of these samples.

It is also evident from the data in Figs. 2 and 3 that the degree of hydration is a significant factor only when its value is below 50% as represented by system III (B1). All series of cement compacts (system III) made from material in which the degree of hydration exceeded 50% (B3, B7, B28 and BM-Table 3) are

represented by a single line. This point is further demonstrated from the data related to systems I and II (Fig. 2). Here, although the degree of hydration varied in the various series (Tables 1 and 2), in all cases it exceeded 50% and the results from both systems are represented by a single line. A similar result was obtained by Sereda et al. (5) for cement pastes in which the degree of hydration exceeded 58%.

The above result suggests that, when cement is hydrated in excess of 50%, it is possible to obtain bonds between the hydrated and the unhydrated particles in the paste and in the compacts that are as strong as between hydrated particles themselves.

A case has been made for the absence in cement paste of "chemical" bonds which would fit the strict definition given and which seem to be present in other crystalline hydrates such as gypsum. This conclusion directs attention to the type of interparticle bonds in all the systems of hydrated cement prepared for this study. The nature of these bonds can now be deduced.

Any analysis of experimental results to be used in the deduction of the nature of the interparticle bond in cement must take into account the high total porosity of the system and, correspondingly, the fact that the bond area is small relative to the apparent cross-sectional area. This means that the bond area must always experience high stress concentrations relative to what the particle itself experiences. It is reasonable to postulate, therefore, that some of these bonds can be broken and remade for any loading condition because the system of particles is poorly organized and non-isotropic.

The interparticle bonds are undoubtedly solid to solid contacts which are responsible for the limited swelling. These bonds are obviously made by bringing the surfaces together with the appropriate pressure resulting from the chemical reaction or from the externally applied load. This being the case, increasing the pressure as in compaction increased strength or modulus in proportion to the reduction of the void volume. The increased modulus reflects either an increased area of contact or increased bond strength due to closer and more regular spacing of the atoms, but is probably due to both.

This concept of the nature of the interparticle bonds in cement paste allows for the possibility of one particle breaking its bond with one neighbouring particle and remaking a similar bond with another neighbour. The result would be permanent deformation but no net loss of strength, when the system is subjected to sustained load. These concepts of the structural model are further discussed by Feldman and Sereda (13).

These bonds may approach the character of the "chemical" bonds when the porosity approaches zero. In fact, the extrapolated regression lines for modulus of gypsum systems in Fig. 4 virtually intersect at zero porosity. This result from the study with the gypsum systems suggests that the extrapolated values of modulus for the cement systems have a definite meaning. It follows, therefore, that the modulus of elasticity of the systems at zero porosity is actually the modulus of elasticity of the solid phase of the cement gel. Under test conditions this extrapolated value was found to be 88×10^4 and 92×10^4 kg per sq cm, for systems I and II, and system III, respectively. It is of interest to note that the above values agree surprisingly well with the data reported by Helmuth and Turk (14). Although quite a different method was employed (resonance frequency), the reported values for the two cements tested were 76×10^4 and 81×10^4 kg per sq cm.

The above conclusions, regarding the bonds in the structure of hydrated portland cement paste, are applicable to the interparticle connections and not necessarily to the bond system operating within the postulated layered structure of the tobermorite gel particle. A suitable model for the particle itself, proposed by Feldman and Sereda (13) to explain its physical and mechanical behaviour, has been based on detailed analyses of sorption isotherms. In the proposed model for the gel particle, water molecules do act as structural components, but this water has not the characteristics of adsorbed water, in contrast to what was suggested by Powers (15).

It is hoped that the proposed structural model for hydrated cement paste will assist in resolving the physical and mechanical behaviour of this material.

The implication that compacts of bottle hydrated cement can serve as models of the cement-stone has been demonstrated by the present data, by data reported elsewhere (3–5), and by the experience gained at DBR. It is believed, therefore, that the compact is a reliable tool in cement research.

References

1. Å. Grudemo, "The microstructures of cement gel phases", Trans. Roy. Inst. Technol. Nr 242, Stockholm, Sweden, (1965).
2. R. E. Philleo, "The origin of strength of concrete",

Highway Res. Bd., Spec. Rpt. 90, 175–185, (1966).
3. R. F. Feldman and P. J. Sereda, "Sorption of water on compacts of bottle hydrated cement, I, the sorption and length isotherms", J. Appl. Chem. **14**, 87–93 (Feb. 1964).
4. R. F. Feldman and P. J. Sereda, "Sorption of water on compacts of bottle hydrated cement, II, thermodynamic considerations and theory of volume change", J. Appl. Chem. **14**, 93–104 (Feb. 1964).
5. P. J. Sereda, R. F. Feldman and E. G. Swenson, "Effect of sorbed water on some mechanical properties of hydrated portland cement and compacts" in Symposium on Structure of Portland Cement Paste and Concrete, Highway Res. Bd., Spec. Rpt. 90, 58–73 (1966).
6. R. F. Feldman, "Sorption and length change scanning isotherms of methanol and water on hydrated portland cement", submitted to 5th Intern. Sympsoium on Chemistry of Cement, Tokyo, 1968.
7. I. Soroka and P. J. Sereda, "The relation between hardness, modulus of elasticity and porosity in various systems of gypsum", submitted to J. Am. Ceram. Soc.
8. P. J. Sereda and E. G. Swenson, "Apparatus for preparing portland cement paste of high water-cement ratio", Mat. Res. Standards, 7, No. 4, 152–154 (April 1967).
9. A. F. Kirstien, W. H. Dell, R. M. Wooley and L. J. Davis, "Deflection of centrally loaded thin circular elastic plates on equally spaced point supports", J. Res. Natl. Bureau Standards, **70C**, No. 4, 227–234 (Oct.-Dec. 1966).
10. T. C. Powers, "The nonevaporable water content of hardened portland cement paste—its significance for concrete research and its method of determination", ASTM Bull. No. 158, 68–76 (May 1949).
11. W. O. Kingery and R. L. Coble, "A review of the effect of microstructure on mechanical behaviour of polycrystalline ceramics" in "Mechanical behaviour of crystalline solids". Natl. Bureau Standards, Monograph 59, 103–113 (March 1963).
12. R. J. Stokes, "Correlation of mechanical properties with microstructure", Natl. Bureau Standards Misc. Publ. No. 257, 41–72, (April 1964).
13. R. F. Feldman and P. J. Sereda, "A model for hydrated portland cement as deduced from measurements of sorption-length change and mechanical properties", submitted to RILEM Colloquium on Physical and Chemical Causes of Creep and Shrink-Age of Concrete, Munich, April 1–3, 1968.
14. R. A. Helmuth and D. H. Turk, "Elastic moduli of hardened portland cement and tricalcium silicate pastes: effect of porosity" in Symposium on Structure of Portland Cement Paste and Concrete, Highway Res. Bd. Spec. Rpt. No. 90, 135–144 (1966).
15. T. C. Powers, "Some observations on the interpolation of creep data", RILEM Bull, No. 33, 381–391 (December 1966).

Supplementary Paper III-46 Molecular Sieve Effect in Concrete

Ronald H. Mills*

Synopsis

Certain polar and non-polar fluids and gases including nitrogen are incapable of penetrating the finest pores in hydrated cement. Water is capable of greater, though incomplete penetration. The difference between the volumes of water and large-molecular fluid which can be accommodated in hydrated cement paste is a measure of cohesive forces which give concrete its strength and also of the extent to which such forces and dimensions of the gross structure may be modified by swelling or disjoining pressure.

Taking the volume of pore space occupied by water = V_w and that occupied by a fluid with large molecules = V_f, then the ratio: $k = (V_w - V_f)/V_w$ is shown to be a function of the rate and extent of hydration and of the $CaO:SiO_2$ ratio C/S. For a particular value of this ratio, strength σ is a linear function of k and the slope $d\sigma/dk$ increases with increase in C/S. On the other hand the relationship between strength σ and the volume concentration of hydrate C does not appear subject to variations in C/S.

Volume changes due to creep and shrinkage appeared to increase with increase in k but values of kV_w after shrinkage and creep had taken place were less than at the start of the test. This suggested a *collapse of structure* in the cement hydrate. The volume kV_w was found to represent between 1 and 3 monolayers capacity of water and corresponded to the water held at relative humidities of between 0 and 28 per cent. Shrinkage varied linearly with weight of water gained or lost within this range of relative humidities.

Introduction

Since publication of the classic studies of Powers and Brownyard in which it was apparent that gases such as nitrogen, hydrogen and helium and fluids with large molecules such as acetone, carbon tetrachloride and toluene (1) were excluded from sites accessible to water, other evidence (e.g. 2, 3, 4, 5) supported the view that cement hydrate acted as a molecular sieve.

More recently Copeland, Mikhail et al were able to make deductions regarding the pore structure of cement paste through study of sorption characteristics of various organic fluids. Of particular significance was their conclusion that large-molecular fluids such as cyclohexane could be accommodated only in capillary pores (6, 7).

Comparatively little attention seems to have been paid to the correlation of these phenomena with engineering properties such as strength and dimensional stability until Hrennikoff noted the almost total absence of swelling which accompanied saturation with kerosene, methyl alcohol and mineral oil (8). A year later Mills discussed the "wedging" action of water in relation to diminution of strength accompanying adsorption and postulated that absence of this effect when concrete was saturated with kerosene and carbon tetrachloride could be attributed to lack of penetration of these fluids into the gel structure (9).

A geometrical model based simply on exclusion of large molecules from narrow spaces admittedly neglects factors such as hydrogen-bonding and packing of molecules (10); but it is probably accurate enough for the present purpose. Contemporary models of the structure and behaviour of hardened cement paste assign great importance to the interaction of water and solid in zones of restricted adsorption (11, 12) and the molecular sieve effect provides a ready means of establishing the volume proportion of this class of pore water.

*Department of Civil Engineering, The University of Calgary, Alberta, Canada.

The Model

When cement reacts with water the products of hydration grow outward from the unhydrated nucleus into space originally occupied by the mixing water. This is illustrated in the electron micrographs of Figs. 1 and 2 which show calcium silicate hydrate *flowers* growing on a cement grain. The absolute volume of the hydrate is greater than that of the original cement but less than the sum of the volumes of the reacting components. In order to maintain saturation of pores an increment of water has to be supplied from an external source. This increment of water, Δw, is proportional to the non-evaporable water which has become part of the solid. For reasons discussed elsewhere (13) the characteristic ratio of w_n:Δw must be determined in a separate experiment by hydrating cement with water:cement ratio w_0 of 6 or more in a pycnometer bottle. Equations for the volume proportions of solid and water in cement paste may be set forth as follows:

volume concentration of unhydrated cement

$$V_{uhc} = \frac{1 - \alpha}{gw_0 + 1} \qquad (1);$$

volume concentration of hydrated cement,

$$V_{hc} = \frac{\alpha\left\{1 + gw_n^0\left(1 - \frac{\Delta w}{w_n^0}\right)\right\}}{gw_0 + 1} \qquad (2);$$

volume concentration of evaporable water,

$$V_w = \frac{w_0 g - \alpha g w_n^0\left(1 - \frac{\Delta w}{w_n^0}\right)}{gw_0 + 1} \qquad (3);$$

the volume concentration of hydrate in space available to accommodate it,

$$C = \frac{V_{hc}}{1 - V_{uhc}} \qquad (4);$$

where $1/g$ = the specific volume of the unhydrated cement cc/gm; w_0 = the original water: cement ratio; w_n^0 = the non evaporable water gm/gm of fully hydrated cement; Δw is the reduction in specific volume resulting from the complete reaction of w_n^0 and 1 gram of cement and α is the degree of hydration.

If the concrete is dried to equilibrium weight at 110°C and then vacuum saturated with a fluid having large molecules, the ratio:

$$k = \frac{V_w - V_f}{V_w} \qquad (5);$$

represents the fraction of water which has access to space which excludes the fluid. To a first approximation, kV_w is a measure of pore water strongly adsorbed in the micro-cellular structure of the cement hydrate.

The kV_w fraction is, in terms of the model, that portion of the pore water which is active in the sense

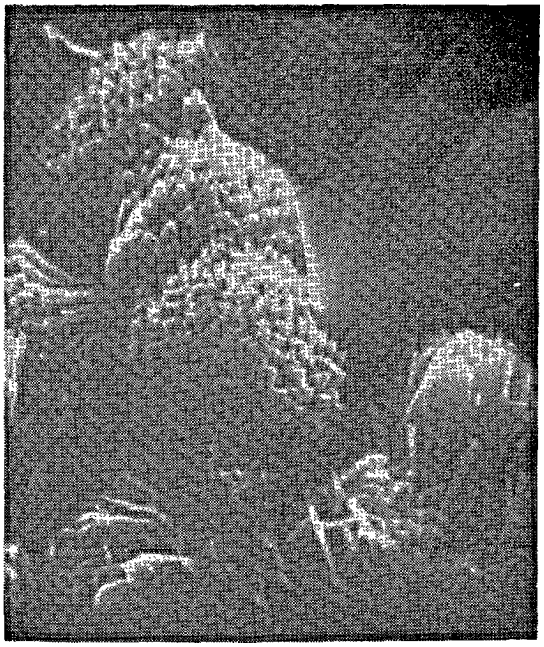

Fig. 1. *Growth of calcium silicate hydrate from the surface of a cement grain* (×6,500)

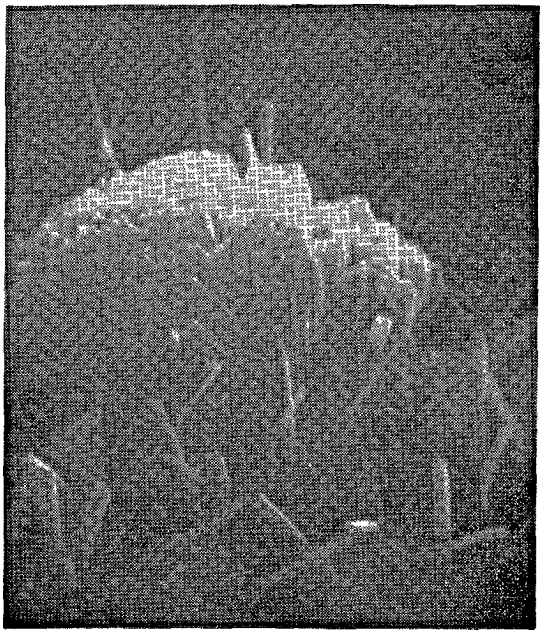

Fig. 2. *Cluster of calcium silicate hydrate fibres* (×13,500)

of applying swelling or disjoining pressure tending to separate primary particles of cement hydrate. It is under pressure at the time hydration products are laid down and this pressure is equilibrated in part by surface forces which tend to draw primary particles of solid together. As concrete drys, and meniscus forces become active, pressure is reduced and partial closure of spaces between primary particles results. At the same time, meniscus forces react on assemblies of primary particles (such as *petals*) and produce volume contraction of the gross structure. Both these effects would result in isotropic contraction of the paste.

The spaces separating primary particles are unlikely to have parallel sides and judging from Figs. 1 and 2 may be described as *wedge-shaped* with the sharp end of the *wedge* pointing in random directions. In terms of this model water is excluded from the apex of the *wedge* where inter-particle cohesion is provided by primary bonds. In drying concrete, increase in the magnitude of meniscus forces, or decrease in relative humidity in the pores would result in migration of water towards the wide part of the *wedge*. Retreat of water from sites on the surface would result in increase of surface energy residing in the solid surface and, in addition, closure of the gap between surfaces. As before this would give rise to isotropic strain in an unloaded specimen. In a specimen subjected to uniaxial load this effect would be supplemented by migration of water molecules out of spaces tending to be closed by the load and into spaces tending to be opened by the load. Thus creep may be viewed as one component of adjustment following variation of other components contributing to equilibrium of kV_w water whether or not drying occurs at the same time.

If the model is realistic, both creep and shrinkage should be accompanied by permanent exclusion of water from zones near the apex of the *wedge* in a process analogous to *sintering*. At first sight it is not easy to judge whether this would result in increase or decrease of the k factor: increase in k would imply that the walls of wedges had rotated about a point near the sharp end; and reduction of k would imply rotation in the opposite sense. In reality the platey structures of primary particles would probably buckle in a rather complicated fashion. In general the variation of k would not be the same for both loaded and unloaded specimens since both rotations and buckling would be of opposite sense parallel to and transverse to the load while drying shrinkage would have the same effect in all directions. This model is consistent with results appearing in recent reports (14, 15, 16) and the characteristics of models recently proposed by Powers (11, 12) and Ishai (17). Perhaps the only significant difference lies in the present emphasis on initial stress in pore water and the possibility of internal *seepage* even in saturated pastes.

Experimental

The data described herein was obtained during the course of other investigations in which the observation of k factors was not the primary objective. Although a considerable quantity of data has been accumulated over the past 10 years or so it is only recently that there has been sufficient incentive to process the observations. The data presented herein is typical but incomplete, particularly insofar as creep tests are concerned. More work is being prepared for publication.

Five series of experiments are described:

Series I

Two groups of mixes containing cement having $C/S = 2.82$ and 1.70 respectively were made with water: cement ratios of approximately 0.25, 0.50 and 0.80. Specimens were exposed to drying atmospheres after water curing for 7, 28 and 56 days. Linear shrinkage and moisture loss were determined for various values of the relative humidity p/p_s on both desorption and asorption cycles. Specimens were ovendried then vacuum saturated with methyl alcohol, ethyl alcohol, propyl alcohol, benzol and kerosene and then re-saturated with water. Values of k, mean V_w and V_f were observed.

Series II

Four mixes having C/S ratio 2.82 and water: cement ratios 0.25, 0.45, 0.65 and 0.85 were ovendried at 28 days; shrinkage, ε_s, moisture loss, V_w and k were observed as outlined in Series II above. Fluids used were methyl alcohol, ethyl alcohol, propyl alcohol, benzol, carbon tetrachloride and cyclo-hexane.

Series III

Various combinations of normal, and rapid hardening portland cement and blastfurnace slag were used to give variation of the C/S ratio in 12 mixes having $w_0 = 0.50$. Cubes were tested at various ages up to 112 days and observations of cube strength σ, w_n, Δw, and k from kerosene absorption were made at each age.

Series IV

k values using kerosene were observed before and after creep and shrinkage were recorded for mixes having $w_0 = 0.6$ and aggregate: cement ratio = 6, the period of testing being approximately 1200 days. A preliminary report of these tests appeared in 1958 (18) and the final report is due to be published in the same journal.

Series V

Concrete and mortar prisms were oven-dried and re-saturated in water and kerosene, methyl alcohol and benzol. The mean coefficient of expansion over the temperature range 10 to 45°C and the static and dynamic moduli determined at room temperature.

In all these tests it was found necessary to isolate specimens and fluids from contamination by atmospheric moisture. The specimens were, except for very brief periods, isolated in evacuated drums. The end-point of weighings was taken as that corresponding to disappearance of the surface sheen on saturated specimens. Irregularly shaped specimens were avoided as far as possible in k tests by using unbroken cubes. In Series IV, however, all the specimens subjected to k tests were end *pyramids* chosen from the debris of equivalent cube tests.

Chemical compositions of cements are recorded in Table 1 and constants obtained from bottle-hydrated cements in Table 2. Other details of mixes are given in Table 3.

Table 1. *Chemical analysis of cements*

Series	Mix	SiO_2	Fe_2O_3	Al_2O_3	CaO	MgO	SO_3	C/S ratio
I	1, 2&3	22.6	2.6	5.2	63.9	2.5	1.8	2.82
	4,5&6	27.8	1.6	10.7	47.2	11.3	0.9	1.70
II	1, 2, 3&4	22.6	2.6	5.2	63.9	2.5	1.8	2.82
III	1	22.6	2.6	5.2	63.9	2.5	1.8	2.82
	2	26.5	2.0	9.5	51.0	7.8	1.9	1.92
	3	27.7	1.6	10.8	48.2	10.7	0.8	1.74
	4	27.8	1.6	10.7	47.2	11.3	0.9	1.70
	5	22.1	2.8	4.9	64.1	1.7	1.8	2.90
	6	30.4	1.2	13.4	39.0	15.6	0.4	1.28
	7	30.2	1.2	13.3	39.1	15.4	0.5	1.29
	8	25.1	2.1	7.9	55.6	6.9	1.4	2.22
	9	29.1	1.4	12.0	43.0	13.4	0.7	1.48
	10	28.9	1.5	11.9	43.2	13.1	0.7	1.49
	11	26.5	1.9	9.3	51.4	9.1	1.1	1.94
	12	26.2	2.0	9.3	51.6	8.6	1.1	1.97

C/S ratio weight of CaO/weight of SiO_2

Table 2. *Constants obtained by ball-milling cements in pycnometer bottles*

Series	Mixes	g	w_n^0	$w_n^0/\Delta w$
I	1,2,3	3.22	1.253	3.87
II	1,2,3,4			
III	1,5			
III	8	3.16	0.255	3.42
	11,12	3.13	0.258	3.27
	2,3,4	3.09	0.261	3.10
	9,10	3.06	0.263	2.90
	6,7	3.03	0.264	2.70

g = specific gravity of cement gm/cc
w_n^0 = non-evaporable water per unit weight of cement gm/gm
Δw = water taken up from external source to compensate reduction in specific volume accompanying hydration process—gm/gm hydrated cement.
Note: Mixes I, 4,5,6 and III, 2,3,4 used the same cement.

Table 3. *Mix proportions of pastes, mortars and concrete*

Series	Mix	Water: cement ratio w_0	Agreegate: cement ratio A/C
I	1,4	0.25	0
	2,5	0.50	1.0
	3.6	0.80	2.2
II	1	0.25	0
	2	0.45	1.09
	3	0.65	2.13
	4	0.85	3.09
III	1 to 12	0.50	1.91
IV	1 to 7	0.60	6.0
V	1	0.45	4.5
	2	0.60	6.0
	3	0.35	1.0

Results and Discussion

Volume occupied by Various Fluids

The results of these tests are recorded in Tables 4 and 5. Typical curves are shown in Fig. 4 together with results taken from Mikhail and Selim (7). Although the ratio of molecular weight to density represents only a first approximation to molecular volume, the curves show a progressive reduction in V_f/V_w with increase in M/ρ except for saturation with cyclohexane. Discussion of packing density of molecules

Table 4. *Ratio of void space occupied by fluid to that occupied by water V_f/V_w*

Age days	Fluid		M/ρ cc/mole	Series I mix number 1	2	3	4	5	6
7	Methyl alcohol	CH_3OH	40.25	.59	.82	.90	.55	.68	.77
	Ethyl alcohol	C_2H_5OH	58.37	.58	.78	.87	.46	.63	.74
	Propyl alcohol	C_3H_7OH	74.70	.57	.76	.83	.44	.59	.69
	Benzol	C_6H_6	88.86	.46	.65	.72	.37	.53	.62
	Kerosene	—	—	.66	.79	.86	.51	.67	.76
28	Methyl alcohol	CH_3OH	40.25	.64	.76	.86	.51	.66	.77
	Ethyl alcohol	C_2H_5OH	58.37	.60	.74	.84	.45	.63	.73
	Propyl alcohol	C_3H_7OH	74.70	.60	.70	.81	.45	.58	.71
	Benzol	C_6H_6	88.86	.51	.60	.65	.36	.52	.61
	Kerosene	—	—	.64	.71	.84	.52	.66	.75
56	Kerosene	—	—	.63	.78	.82	.51	.64	.74

M = molar wieght ρ = density gm/cc M/ρ = nominal volume cc/mole.

Table 5. *Ratio of void space occupied by fluid to that occupied by water for mixes of Series II at 28 days*

Fluid		M/ρ cc/mole	Mix 1	2	3	4
Methyl alcohol	CH_3OH	40.25	.63	.81	.98	.99
Ethyl alcohol	C_2H_5OH	58.37	.61	.79	.97	.98
Propyl alcohol	C_3H_7OH	74.70	.55	.76	.90	.95
Benzol	C_6H_6	88.86	.51	.73	.88	.93
Carbon-tetrachloride	CCl_4	96.45	.53	.73	.85	.90
Cyclo-hexane	C_6H_{12}	108.04	.58	.77	.92	.97

M = molar weight ρ = density gm/cc M/ρ = nominal volume cc/mole

and the possible effects of hydrogen bonding is beyond the scope of this paper. It is sufficient for the present to note that substantial and apparently systematic differences exist between the volume occupied by water and other fluids. It may be noted from Table 4 that the shape of gel spaces varies with C/S. As C/S is reduced, the taper of the wedge apparently becomes more acute. Further, the acutance of the *angle* would seem to depend upon the water: cement ratio. This is, to some extent, verified by comparison of the size of *flowers* shown in Fig. 3 taken from a specimen having $w_0 = 0.4$ and Figs. 1 and 2 in which the water: cement ratio was effectively 1.0 (19).

Relationship between k Obtained by Kerosene Absorption and Various Parameters

Table 6 records the relationship between hydration factor α, volume of unhydrated cement V_{uhc}, volume of hydrated cement V_{hc}, V_w the volume of free water, C the volume concentration of hydrate in space avail-

Fig. 3. *Calcium silicate hydrate cluster in cement paste having water: cement ratio = 0.4 (×104,000)*

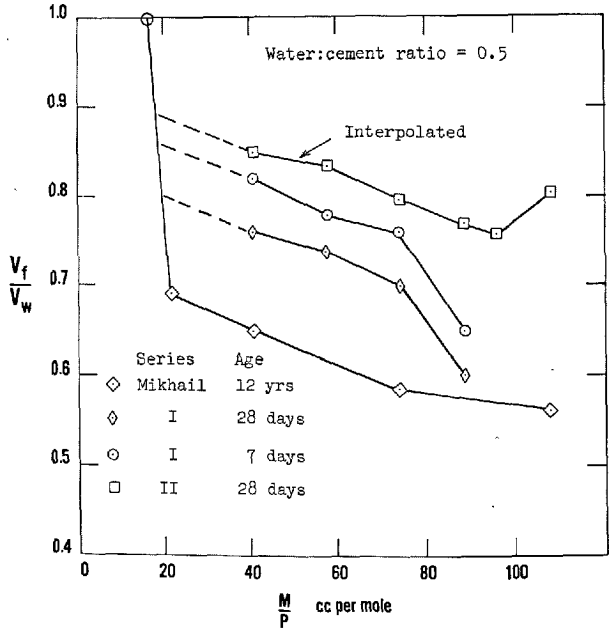

Fig. 4. *Volume occupied by various fluids*

able to accommodate it and kV_w the volume of water in zones of restricted adsorption. It is seen that increase in kV_w is associated with decrease in V_{uhc} and V_w and increase in α, strength σ, V_{hc} and C. In other words kV_w increases with increase in the volume of new solids produced by hydration. Not shown but reported elsewhere (20) is the systematic increase of V_w with α implicit in equations 2, 3 and 4.

Fig. 5 shows that the relationship between strength σ and C in this series is substantially independent of C/S. Fig. 6 on the other hand shows that the

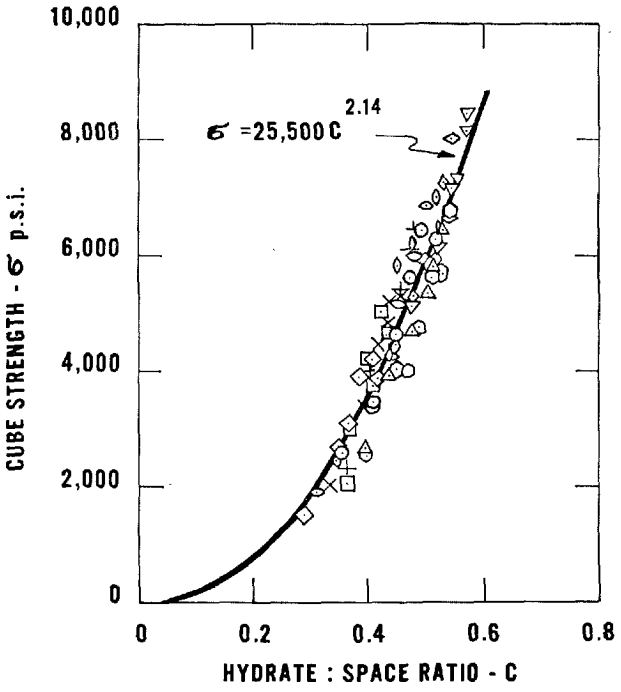

Fig. 5. *Cube strength vs volume concentration of cement hydrate C for mixes of Series III. For key to symbols see Table 4*

Table 6. *Hydration factor* (α), *volume proportions of unhydrated cement* (V_{uhc}) *hydrated cement* (V_{hc}) *and free water* (V_w) *in paste. Volume concentration of hydrate in space available to accommodate it* (C), *volume of water in space inaccessible to kerosene* kV_w *ratio* kV_w/V_{hc} *and cube strength* δ*—p.s.i. at various ages in days*

Mix	Parameter	Age—days 3	7	14	28	56	112
1	α	.587	.676	.743	.826	.852	.883
	V_{uhc}	.147	.115	.091	.062	.053	.042
	V_{hc}	.335	.386	.424	.472	.486	.504
△	V_w	.518	.499	.484	.466	.461	.454
	C	.393	.436	.466	.503	.513	.526
	kV_w	.0363	.0464	.0503	.0526	.0742	.0754
	kV_w/V_{hc}	.108	.120	.119	.112	.153	.1495
	σ	2670	3930	4730	5380	5800	6430
2	α	.508	.628	.705	.749	.799	.852
	V_{uhc}	.180	.136	.108	.092	.073	.054
	V_{hc}	.287	.355	.398	.423	.451	.481
○	V_w	.534	.510	.495	.486	.476	.465
	C	.350	.411	.446	.466	.486	.508
	kV_w	.0662	.0842	.0861	.0953	.119	.124
	kV_w/V_{hc}	.231	.237	.216	.255	.265	.258
	σ	2630	3470	4630	5750	6500	6290
3	α	.490	.676	.701	.741	.770	.801
	V_{uhc}	.186	.118	.109	.095	.084	.073
	V_{hc}	.277	.382	.396	.419	.435	.453
0	V_w	.537	.500	.496	.488	.482	.476
	C	.340	.433	.444	.463	.526	.513
	kV_w	.072	.097	.123	.124	.157	.146
	kV_w/V_{hc}	.259	.254	.311	.296	.360	.321
	σ	2590	4300	5890	6320	6600	7050
4	α	.443	.609	.690	.696	.753	.816
	V_{uhc}	.203	.143	.113	.111	.090	.067
	V_{hc}	.250	.344	.390	.393	.425	.461
○	V_w	.547	.514	.498	.497	.485	.473
	C	.314	.401	.440	.442	.467	.494
	kV_w	.058	.081	.095	.102	.138	.139
	kV_w/V_{hc}	.232	.236	.244	.259	.324	.301
	σ	1880	3450	4350	5400	6000	6940
5	α	.680	.767	.806	.830	.881	.881
	V_{uhc}	.123	.089	.074	.065	.046	.046
	V_{hc}	.418	.472	.496	.510	.542	.542
▽	V_w	.459	.439	.430	.425	.413	.413
	C	.477	.518	.536	.545	.568	.568
	kV_w	.053	.061	.070	.071	.072	.076
	kV_w/V_{hc}	.127	.129	.141	.139	.134	.141
	σ	5170	6300	7200	7590	8560	8200
6	α	.364	.451	.481	.506	.588	.566
	V_{uhc}	.253	.219	.207	.197	.164	.173
	V_{hc}	.218	.270	.287	.302	.352	.338
◇	V_w	.529	.511	.506	.501	.484	.489
	C	.292	.346	.362	.376	.421	.409
	kV_w	.069	.104	.117	.131	.135	.153
	kV_w/V_{hc}	.318	.385	.409	.434	.383	.451
	σ	1580	2740	3140	3960	3950	4280
7	α	.494	.502	.566	.532	.606	.585
	V_{uhc}	.201	.198	.173	.186	.157	.165
	V_{hc}	.295	.300	.338	.318	.362	.350
□	V_w	.503	.502	.489	.496	.481	.485
	C	.369	.374	.409	.391	.429	.419
	kV_w	.085	.124	.137	.157	.158	.178
	kV_w/V_{hc}	.286	.415	.406	.494	.437	.507
	σ	2010	3160	3810	4250	4680	5050
8	α	.533	.645	.714	.747	.816	.816
	V_{uhc}	.182	.138	.111	.098	.071	.071
	V_{hc}	.325	.393	.435	.455	.497	.497
⬡	V_w	.494	.469	.454	.477	.432	.432
	C	.397	.456	.489	.504	.535	.535
	kV_w	.040	.068	.066	.075	.072	.078
	kV_w/V_{hc}	.123	.173	.151	.164	.145	.157
	σ	2770	4140	4770	5600	5720	6810
9	α	.433	.535	.581	.614	.651	.666
	V_{uhc}	.224	.184	.166	.152	.138	.132
	V_{hc}	.262	.323	.351	.371	.393	.402
×	V_w	.515	.493	.484	.477	.470	.466
	C	.337	.396	.421	.438	.456	.463
	kV_w	.057	.092	.120	.127	.124	.144
	kV_w/V_{hc}	.218	.284	.343	.343	.315	.358
	σ	2010	3530	4570	4880	5180	5510
10	α	.473	.568	.618	.660	.692	.706
	V_{uhc}	.208	.171	.151	.134	.122	.116
	V_{hc}	.286	.343	.373	.399	.418	.426
+	V_w	.506	.487	.476	.468	.461	.458
	C	.361	.414	.439	.461	.476	.482
	kV_w	.068	.107	.135	.153	.149	.159
	kV_w/V_{hc}	.239	.312	.361	.384	.356	.373
	σ	2320	4070	5030	5400	6270	6620
11	α	—	.621	.703	.766	.787	.805
	V_{uhc}		.148	.116	.091	.083	.076
	V_{hc}		.378	.427	.466	.478	.489
◇	V_w		.485	.457	.443	.438	.435
	C		.444	.483	.512	.521	.529
	kV_w		.069	.085	.093	.086	.096
	kV_w/V_{hc}		.182	.200	.200	.180	.195
	σ		4470	5350	5790	5970	7250
12	α	—	—	.736	.818	.796	.835
	V_{uhc}			.103	.071	.080	.064
	V_{hc}			.447	.497	.484	.508
◇	V_w			.450	.432	.436	.428
	C			.498	.535	.526	.543
	kV_w			.088	.093	.097	.100
	kV_w/V_{hc}			.198	.187	.201	.197
	σ			5910	6590	7160	8170

Symbols used in Figs. 5 and 6 are shown below number of each mix.

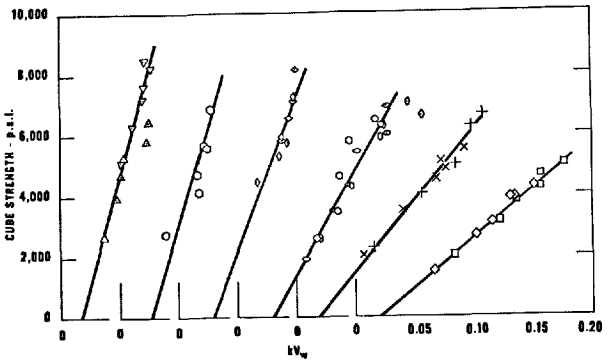

Fig. 6. *Cube strength versus volume of water in zones of restricted adsorption for mixes of Series III. For key to symbols see Table 6.*

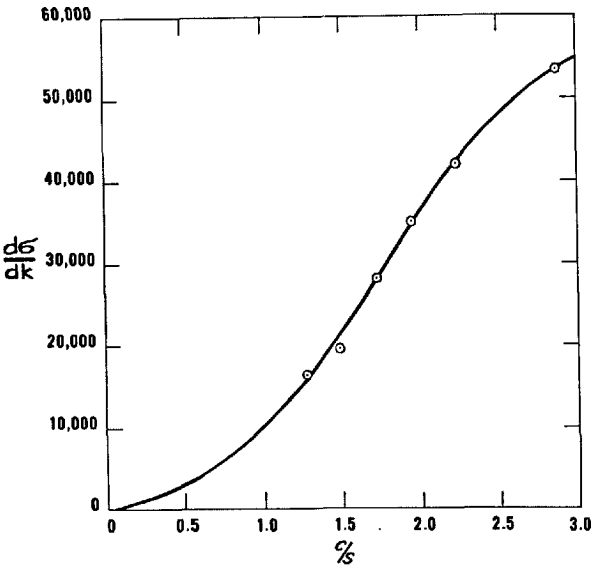

Fig. 7. *Slope of strength vs k factor as a function of the weight ratio of* CaO *to* SiO_2

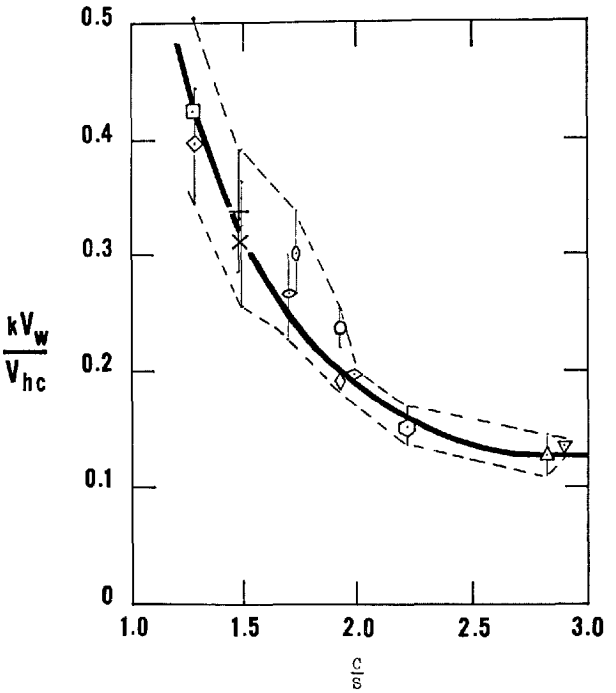

Fig. 8. *Variation of fraction of adsorbed water per unit volume of hydrated cement with the* CaO: SiO_2 *ratio. Broken line indicates one standard deviation. For key to symbols see Table 6*

Table 7.

Age days	Liquid		Ratio of volume of water in zones of restricted adsorption to monolayer capacity for mixes $\frac{V_w - V_l}{V_{ml}}$ 1	2	3	4	5	6
7	Methyl alcohol	CH_3OH	1.54	1.22	1.49	1.73	2.55	3.15
	Ethyl alcohol	C_2H_5OH	1.54	1.50	1.94	2.07	2.95	3.56
	Propyl alcohol	C_3H_7OH	1.62	1.63	2.54	2.15	3.27	4.25
	Benzol	C_6H_6	2.03	2.38	4.19	2.41	3.75	5.20
	Kerosene		1.65	1.43	2.09	1.88	2.64	3.29
28	Methyl alcohol	CH_3OH	1.20	1.54	1.95	1.75	1.72	2.85
	Ethyl alcohol	C_2H_5OH	1.33	1.67	2.22	1.96	1.87	3.34
	Propyl alcohol	C_3H_7OH	1.33	1.92	2.64	1.96	2.13	3.56
	Benzol	C_6H_6	1.62	2.56	4.86	2.29	2.44	4.81
	Kerosene		1.20	1.86	2.23	1.71	1.72	3.10
56	Kerosene		1.03	1.31	2.32	1.27	2.14	2.92

Table 8. *Values of relative humidity* p/p_s *corresponding to the adsorption of a quantity of water* $=(1 - k)V_w$ *for specimens of Series I cured for 56 days.* P/Ps *was determined by an isopiestic method with* H_2SO_4 *solutions and* k *was determined from kerosene absorption*

Mix	kV_w	p/p_s%
1	0.103	21.0
2	0.299	21.5
3	0.540	20.0
4	0.083	23.0
5	0.246	26.0
6	0.495	28.0

relationship between kV_w and σ varies according to the C/S ratio. The slope of these curves $d\sigma/dk$ appears to vary systematically with C/S as shown in Fig. 7. The ratio kV_w/V_{hc}, the volume of water in zones of restricted adsorption to the absolute volume of hydrate is seen from results plotted in Fig. 8 to increase with decrease in C/S.

It has been shown (21) that decrease in C/S favours the formation of 2 rather than 3 layer tobermorite. Thus, although the variation of strength with volume proportion of solids may indeed be independent of C/S, the surface area and morphology of hydration products are, on the other hand, profoundly influen-

ced by this ratio. This deduction is in agreement with observed behaviour of portland-blastfurnace cement pastes which are know to creep and shrink more than comparable portland cement pastes (13, 16).

Relationship between k and Monolayer Capacity

The ratio of kV_w to monolayer capacity, V_{ml}, as determined from kerosene absorption and B. E. T. surface area determinations are recorded in Table 7. It is seen that kV_w/V_{ml} increases with w_0 and C/S. This is interpreted as meaning that products of hydration form in a different way according to the space available to accommodate cement hydrate. Low C/S and high values of w_0 produce long narrow *petals* and hence long narrow *wedges*.

kV_w in Relation to Water Adsorbed at Various Relative Humidities

Table 8 shows the relation between kV_w expressed as a quantity of water taken up from *bare surface* condition and the corresponding value of p/p_s as determined by an isopiestic method (15).

kV_w is seen to correspond with the quantity of water held at values of p/p_s lying between 20% and 28%, p/p_s increasing both with w_0 and C/S.

Shrinkage and the Value of k

As discussed in previous paragraphs kV_w as measure by kerosene absorption corresponds to the volume of water held by cement pastes at low relative humidities. Figs. 9 and 10 show the location of kV_w on curves of swelling of dried pastes and mortars of Series I versus gain in moisture and variation of p/p_s. Evidently sorption of water from the surface dry condition to kV_w results in expansion varying linearly with weight gain in moisture. Reverse curvature of the expansion-moisture gain plots probably results from the effect of surface tension following formation of menisci in about this region. This is to be expected from corresponding values of kV_w/V_{ml} and p/p_s which mark a transition zone between molecular adsorption in gel pores and condensation of liquid water in capil-

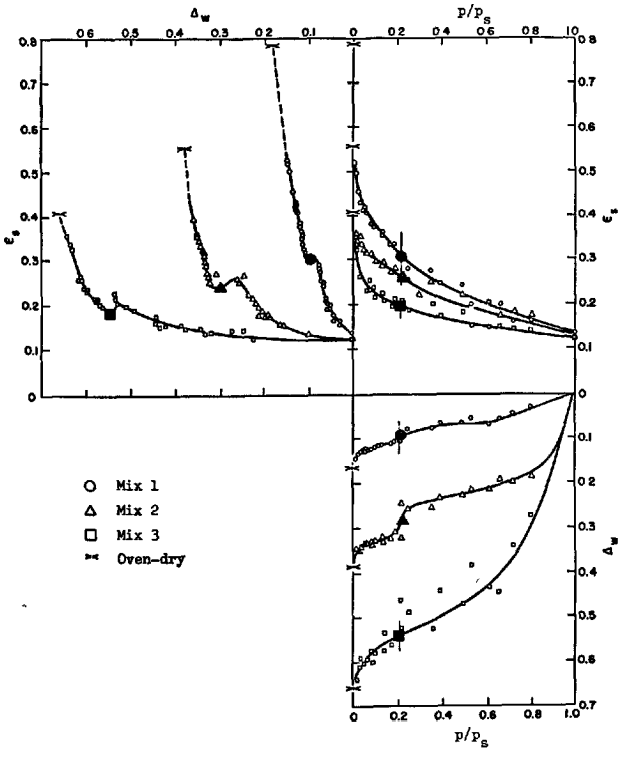

Fig. 9. *Relationship between* kV_w, Δw, p/p_s *and* ε_s *for Series I. Large black symbols represent pore volume which can accommodate water but which excludes kerosene*

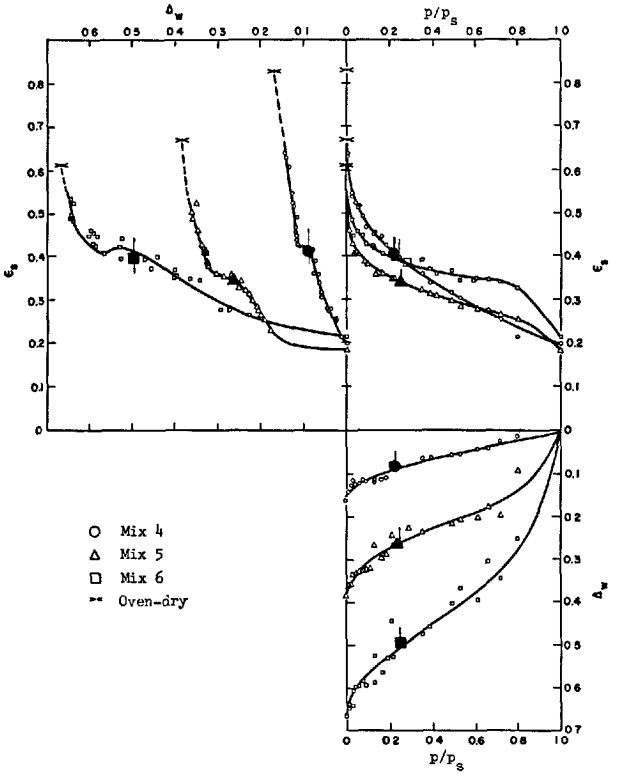

Fig. 10. *Relationship between* kV_w, Δw, p/p_s *and* ε_s *for Series I. Large black symbols represent pore volume which can accommodate water but which excludes kerosene*

laries.

Since kV_w increases with the hydration factor α and, consequently the surface area, it is to be expected that shrinkage would increase with kV_w or decrease with V_f/V_w. This was found to be the case with oven-dried shrinkages of Series II as shown in Fig. 11.

Collapse of Structure in Creep Experiments

In the case of creep and shrinkage experiments of Series IV as reported elsewhere (16), kV_w values obtained at the start of the tests and after 1200 days sustained loading were observed, with the results shown in Fig. 12. It appeared that kV_w reduced with both kinds of volumetric strain but that changes in kV_w over the test period were not the same for shrinkage and creep specimens. Generally, strains associated with change in kV_w were greater for creep and shrinkage than for shrinkage alone.

This would be consistent with opening of *wedge* shaped spaces having their axes parallel, and closure of those transverse, to the load.

Load-Bearing Water

The results of static elastic modulus, measured in uniaxial compression, and dynamic modulus as measured in Series V are recorded in Table 9. In many static modulus tests performed by the author there has been no convincing evidence of change in elastic modulus with moisture content. This was probably because drying was never taken far enough to remove water from areas of restricted adsorption. In the present tests the concrete was first oven-dried and then allowed to take up moisture and various liquids. It is clear from these tests that water capable of penetrating to sites of restricted adsorption in the gel is capable of bearing load and contributing to stiffness of the concrete. Other fluids which do not penetrate these areas do not make this contribution. It would be reasonable to assume therefore that strongly adsorbed water is capable of resisting shear stress while that

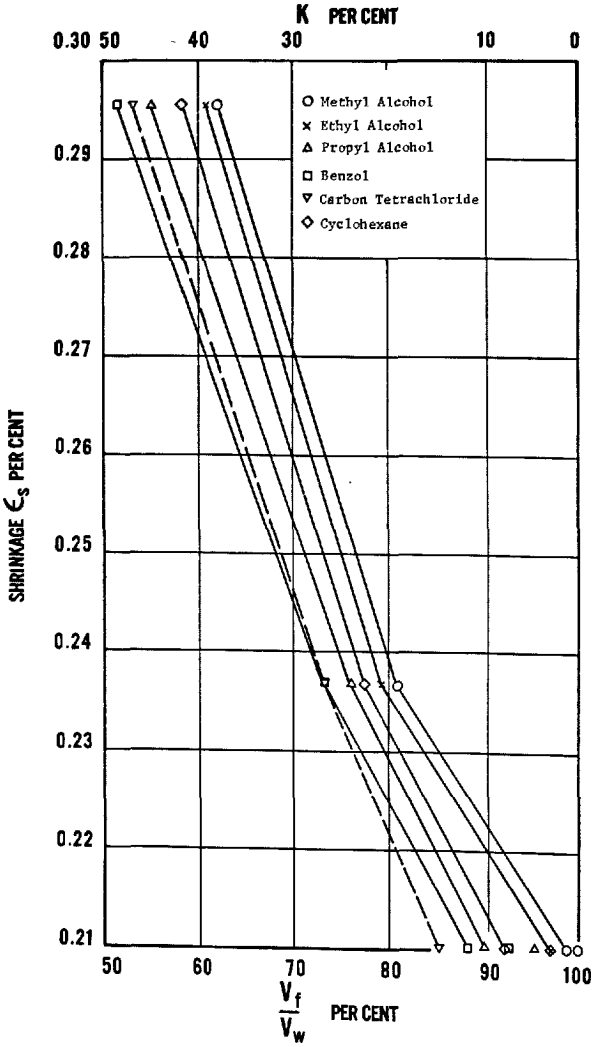

Fig. 11. *Variation of oven-dry shrinkage with fraction of pore volume filled by large-molecular fluids*

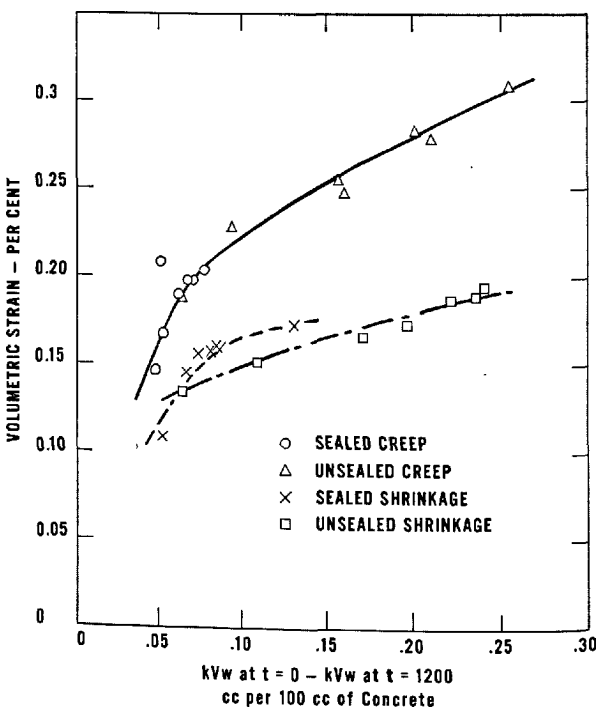

Fig. 12. *Relationship between plastic strain and reduction in volume of water in zones of restricted adsorption*

condensed in comparatively coarse capillaries is incapable of making this contribution.

Table 9. *Elastic moduli of concrete and mortar saturated with various fluids*

Series V Mix	Static and dynamic elastic moduli 10^6 p.s.i. when saturated with			
	Water	Kerosene	Methyl alcohol	Benzol
	Static modulus			
1	5.35	4.25	3.45	3.75
2	4.93	3.45	3.25	3.60
3	4.90	4.10	4.10	4.25
	Dynamic modulus			
1	4.66	3.96	4.21	3.62
2	4.30	3.65	3.58	3.52
3	4.15	3.47	3.52	3.36

Temperature Coefficient of Expansion

The temperature coefficients of expansion recorded in Table 10 clearly indicate that concrete containing even small quantities of water is subject to greater volume changes than dry concrete or concrete saturated in large molecular fluids which do not penetrate the gel structure. It would appear, though, that even large molecular fluids may contribute to the overall volume changes accompanying rise or fall of temperature. The lowest coefficients of expansion were recorded for concrete in the oven-dry condition.

By far the predominating influence, however, appeared to be due to thermal agitation of small quantities of water in areas of restricted adsorption.

Table 10. *Thermal coefficient of expansion of concrete and mortar containing various quantities of water and saturated with various liquids*

Liquid in pores	Thermal coefficient 10^{-6} per °C Series V mix number		
	1	2	3
H_2O saturated	11.20	11.45	11.95
1% by weight	15.60	15.40	15.75
2% by weight	15.50	15.79	15.55
4% by weight	13.50	13.21	13.98
Kerosene	9.61	9.78	10.01
Methyl alcohol	12.70	11.50	11.00
Benzol	10.00	11.49	11.90
Oven-dry	9.40	9.60	9.90

Conclusions

1. The detection of differences in the volumes of water and large molecular fluids taken up by dry concrete affords a convenient method of estimating the volume of pore water held in zones of restricted adsorption. Ordinary kerosene is a convenient fluid to use for comparison with water. The parameter $k = (V_w - V_l)/V_w$ is related to degree of hydration, surface area and strength. Further research may show close dependance of creep and shrinkage characteristics on this parameter.

2. Strongly adsorped water is capable of supporting mechanical load in short term tests. Any agency such as depression of external relative humidity or mechanical loading which disturbs the equilibrium state of water in areas of restricted adsorption will result in the time-dependant volume changes known as creep and shrinkage.

3. The shape of spaces separating the surfaces of colloidal particles in cement gel varies with water: cement ratio and the weight ratio $CaO:SiO_2$. This property may well depend upon the distance between nucleation sites from which calcium silicate hydrate *flowers* grow. The distance of separation would increase with increase in water: cement ratio and with decrease in $CaO:SiO_2$ ratio: this would tend to form attenuated *petals* and longer, narrower gel spaces.

Acknowledgements

The work described herein was performed in the laboratories of the University of the Witwatersrand. The help of Messrs. C. W. Wolhuter and G. Miqkela is acknowledged with thanks. Material assistance of Messrs. Slagment Ltd. and the financial support of the National Research Council of Canada is gratefully acknowledged.

References

1. T. C. Powers and T. L. Brownyard, "Studies of the physical properties of hardened portland cement paste", Portland Cement Assoc. Res. Bull. No. 22 (Mar 1948) See pp. 669–712. Reprinted from Proc. Am. Concrete Inst., **43** (Oct 1946—April 1947).
2. R. L. Blaine and H. J. Valis, "Surface available to nitrogen in hydrated portland cements", Jour. Res. Nat. Bur. Standards, **42**, 257–267 (1949), Research Paper RP 1967.
3. C. M. Hunt, L. A. Tomes and R. L. Blaine, "Some effects of aging on the surface area of portland cement paste", Jour. Res. Nat. Bur. Standards, **64A**, 163–169 (1960).
4. P. A. Rehbinder, L. A. Schreiner and K. F. Zhigach, "Hardness reducers in drilling". Academy of Science, U.S.S.R., Moscow 1944. Translated by C.S.I.R.O. Melbourne 1948.
5. C. E. Weir, C. M. Hunt and R. L. Blane, "Behaviour of cements and related materials under hydrostatic pressures up to 10,000 atmospheres", Jour. of Res. Nat. Bur. Standards, **56**, No. 1, 39–50 (1956).
6. R. Sh. Mikhail, L. E. Copeland and S. Brunauer, "Pore structures and surface areas of hardened portland cement pastes by nitrogen adsorption", Can. Jour. Chem., **42**, No. 2, 426–438 (Feb. 1964).
7. R. Sh. Mikhail and S. A. Selim, "Adsorption of organic vapors in relation to the pore structure of hardened portland cement pastes", Symp. on Structure of Portland Cement Paste and Concrete, H.R. B. S. R. 90, 123–134 (1966).
8. A. Hrennikoff, "Shrinkage, swelling and creep in cement", Proc. A.S.C.E., **85**, No. EM3, 111–135 (July 1959).
9. R. H. Mills, "Strength-maturity relationship for concrete which is allowed to dry", R.I.L.E.M. Int. Symp. on Concrete and Reinforced Concrete in Hot Countries, Haifa, Israel, (1960).
10. A. Bondi, "Molecular crystals, liquids and glasses", pp. 214–255 (J. Wiley and Sons Inc. New York, U.S.A., 1968).
11. T. C. Powers, "Mechanism of shrinkage and reversible creep of hardened cement paste", Int. Conf. on the Structure of Concrete, London, England, Paper G.1 (Sept. 1965).
12. T. C. Powers, "Some observations on the interpretation of creep data", R.I.L.E.M. Bull. No. 33, 381–391 (Dec 1966).
13. R. H. Mills, "Factors influencing cessation of hydration in water cured cement pastes", Symp. on Structure of Portland Cement Paste and Concrete, H.E.B. S. R. 90, 406–424 (1966).
14. F. Wittman and G. Englert, "Bestimmung der Mikroporen Verteilung im Zementstein", Mater. Sci. Eng. 2, 14–20 (1967).
15. R. H. Mills, "Shrinkage of concrete containing blast-furnace slag", R.I.L.E.M. Colloq. on Shrinkage of Hydraulic Concretes, Madrid, Spain (1968).
16. R. H. Mills, "Creep and shrinkage of concrete containing mixtures of portland cement and high-magnesia blast-furnace slag", Publication Under Review, Trans. South African Inst. of C.E.
17. O. Ishai, "Drying shrinkage mechanism in hardened cement paste and mortar", Appl. Mater. Res., **5**, No. 3, 154–161 (July 1966).
18. R. H. Mills, "A preliminary Investigation of the engineering properties of concrete incorporating high-magnesia slag", Trans. South African Inst. of C.E., **8** No. 9, 250–257, (Sept 1958).
19. R. H. Mills, "Influence of water in areas of restricted adsorption on properties of concrete", R.I.L.E.M. Colloq. Munich, Germany (1968).
20. R. H. Mills, "The relation between the reduction in specific volume of the products of hydration and strength of pastes, mortars and concretes made with portland cement, portland blast-furnace cement and mixtures of portland cement and blastfurnace slag," Trans. South African Inst. of C.E., 4, No. 7, 125–132 (July 1962).
21. S. Brunauer, "Tobermorite gel–the heart of concrete", Am. Scientist, **50**, No. 1, 210–229, (Mar 1962).

Oral Discussion

Rolf F. Feldman

It has been known for some time that hydrated portland cement that has been "d-dried" can "sorb" a greater volume of water than nitrogen, methanol, cyclo-hexane and several other sorbates (1, 2); it was clear that with large molecules such as cyclohexane, isopropanol, etc, some pores might exist that are too small to allow their entrance. For nitrogen, helium and methanol, however, this reasoning is not as clear; the determination of surface area by adsorption of N_2, together with a calculation based on the B.E.T. equation, has become a standard method in surface chemistry. Carbons with very high surface areas and very small pores have yielded nitrogen surface areas that approach 1000 m^2/gm. Yet, in the case of hydrated portland cement, the "water area" has been the one generally held "true and valid", and it was considered that the N_2 molecule could not enter pores and adsorb on the whole surface. The diameters of the water, nitrogen and methanol molecules are such as 3.25,

4.05 and 4.4 Å respectively; it seems difficult to allow for the situation where in some cases more than 99 per cent of the area is excluded to N_2.

Results have now shown clearly that the differences between surface areas, porosities and densities obtained by water on the one hand and nitrogen on the other, can be quantitatively accounted for when it is recognized that d-dried hydrated cement rehydrates as it is exposed to increasing humidities.

The importance of the hydrate of interlayer water must be emphasized; it is part of the crystal structure contributing to the mechanical properties of the solid. The removal of the water which may have specific sites for bonding, results in a collapse of the layers and causes a reduction in the modulus of elasticity of the material. It is clear that the role of interlayer water and the spaces between the layers are quite different from adsorbed water and pores, and the entrance or exit of interlayer water involves different forces and energy terms which should be included in accounting for total free energy changes during sorption.

A relation between the parameter $V_W - V_F$ of the author and the cohesive forces of hydrated cement is difficult to conceive; certainly the more hydrated silicate present in the porous body, the stronger the body will become because there will be a decrease in the porosity of this body and with this, a greater area of contact between crystallites; likewise, as the quantity of hydrated silicate increases, the amount of interlayer water will increase, i.e., $V_W - V_F$. This same reasoning also applies to the expansion observed on sorption of water; more than 80 per cent of the expansion observed on exposing "d-dried" hydrated cement to 100 per cent R.H. is due to interlayer rehydration. Thus, as the degree of hydration increases, more interlayer hydration sites exist and the expansion on rehydration will be greater.

Supplementary Paper III-50 A Statistical Study of the Effects of Trace Elements on the Properties of Portland Cement

Raymond L. Blaine*

Synopsis

A digital computer was used to find and evaluate significant relationships between the properties of a large number of portland cements and various independent variables which included chemical compounds, minor constituents, and trace elements. This article presents a review of the probable effects of minor constituents and trace elements on various properties including heat hydration, sulfate expansion, compressive strength with different curing conditions, shrinkage, and durability. On the basis of the statistical study, Na_2O or K_2O were associated with most of the properties measured but not always to the same degree. Very few of the individual trace elements had a highly significant relationship to the various properties measured, but when used in equations in addition to other commonly determined variables, there was usually a highly significant reduction in variance. The coefficients for Ba, Cu, SrO, P and Li were significant at the 0.01 probability level in some tests and at the 0.05 probability level in other tests. The coefficients for Cr, Ni, Rb, Ti, V, and Zr were significant at the 0.05 probability level in equations for some of the tests. The effects of the alkalies and trace elements were generally small compared to the effects of major constituents and other independent variables.

Introduction

During the past 50 years there have been four,—now five, international symposia on the chemistry of cement. Information on the many aspects of the nature of hydraulic cements and the hydration products which are formed have been published in the proceedings of these symposia. We have, as a result, a much better understanding of these complex materials, and the major compounds and reactions which are involved. There still appear to be some unsolved questions with respect to possible or probable modifications of the properties of cements by minor constituents and trace elements. Exploratory work was conducted at the National Bureau of Standards to determine the quantities of trace elements that occur in commercial portland cements, as well as their probable effects on properties of neat cements, mortars, and concretes. Most of this information has been published or is in process of analysis and publication (1, 2, 3, 4). These publications have dealt with the effects on various properties of both the major and minor constituents. The present article will summarize and review some of the results of these studies of the contributions of minor constituents and trace elements in non-air-entraining cements to the various properties that were determined.

Materials

The tests were made on 199 commercial portland cements, most of which were obtained from different manufacturing plants within the U.S.A., but a few were obtained from other countries. Of these cements, 185 were, according to our tests, non-air-entraining cements. These included 82 type I, 68 type II, 20 type III, 3 type IV, and 12 type V cements as classified on the basis of chemical and physical properties. There was, in most instances, a fairly broad but normal distribution of values for the chemical and physical properties.

*National Bureau of Standards, Washington, D.C., U.S.A.

Tests

The tests made on the cements included fineness, and the usual chemical analyses, plus flame photometric determinations of Na_2O, K_2O and SrO. Semiquantitative spectrochemical determinations were made on most of the cements for all the other trace elements which could be detected.

Other tests included heat of hydration at 7 days, 28 days, and 1 year, autoclave expansion, potential sulfate expansion, compressive strength of 1:2.75 (cement to sand) mortars at 1, 3, 7, 28 days, 1, 5 and 10 years, as well as compressive strength of mortars cured with steam at atmospheric pressure, and at 10 atmospheres steam pressure. Nonrestrained and restrained shrinkage tests were made on neat cements which had been cured in moist air for 24 hours.

Two series of concretes were made with each cement,—the one with a water/cement ratio of 0.635, and the other with the water adjusted to give a concrete with a 5 ± 1 inch slump. The cement content was 5 1/2 bags per cubic yard or about 300 kg/m³. Tests made on the concretes included shrinkage in air after 14 days moist curing and subsequent expansion when air-dried specimens were placed in water for 28 days. The weight loss and weight gain was determined as well as the dynamic Young's modulus of elasticity after the various curing conditions. Freeze-thaw durability tests were made on air-dried specimens; studies were made of the regain of strength of specimens after the freeze-thaw tests.

The details of the test methods and the results of the tests have previously been reported and, except for the range of values for the minor constituents and trace elements, will not be repeated in this article.

The semiquantitative spectrochemical values for the trace elements ranged from zero up to 1.0 per cent for Ti and Mn, to 0.5 per cent for P and Zr, to 0.2 per cent for Ba and Zn, to 0.1 per cent for V, to 0.05 per cent for Cu, Mo, and Pb, to 0.02 per cent for Cr, Li and Ni, and to 0.01 per cent for Co and Rb. The flame photometric values for Na_2O ranged from zero up to 0.75 per cent, for K_2O to 1.1 per cent, and for SrO to 0.4 per cent.

Statistical Treatment of Data

A digital computer was used to find and evaluate significant relationships between the results of tests (the dependent variables) and various independent variables which included chemical composition, minor constituents, and trace elements. Multivariable regression equations were calculated by a least-squares method using only commonly determined variables (including Na_2O and K_2O) and these variables together with trace elements. Numerous trial equations were required to determine which of the independent variables were significantly related to the dependent variable, and the combination of variables which resulted in the lowest estimated standard deviation for the equation.

Up to 13 independent variables could be accommodated in an equation with the computer program used. The output of the computer included the estimated coefficient of each of the independent variables used in the multivariable equation, as well as the estimates of the standard deviation of each of the coefficients. An independent variable was retained in an equation if the ratio of the estimated coefficient to its estimated standard deviation (coef./s.d.) was greater than 1.0. Although this represents a very low probability of significance, such independent variables were retained in an equation primarily because these studies were exploratory. Values between 1.0 and 2.0 for the coef./s.d., ratio may also be considered of doubtful significance, and further studies of the effects of such independent variables would be desirable. Values of 2.0 or greater for the coef./s.d. ratio would occur by chance with a probability of 0.05, and therefore independent variables having values of the coef./s.d. ratio between 2 and 3 will be referred to as probably having a significant relationship to the dependent variable. A coef./s.d. ratio of 3 or greater would occur by chance with a probability of less than 0.01, and therefore it can be assumed that the independent variable has a significant effect on the dependent variable. The probable significance of contributions of Na_2O and K_2O (when used in multivariable equations) to the independent variables were evaluated solely on the basis of the coef./s.d. ratios.

Various techniques were used to determine which of the trace elements were associated with the dependent variables when used in equations with commonly determined variables having coef./s.d. ratios greater than 1. The magnitude of the coef./s.d. ratio was also used in evaluating the significance of the individual trace elements. With the additional use of the trace

elements in an equation with commonly determined variables, there was usually a further reduction of variance,—that is, the mean square of differences between the observed values and the values computed from the equation. This offered another statistical means for evaluating the significance of contributions of the trace elements as critical values for significance at the 0.01 and 0.05 probability levels of Fisher's ratio of variances for different degrees of freedom are given in most mathematical textbooks.

Results of the Statistical Evaluation

The Effects of Na_2O and K_2O

When used as independent variables in multivariable equations, the coefficients for Na_2O and K_2O were, in some tests, highly significant and in other tests, variations in one or both of the alkalies had no apparent effect on the property measured. A summary of some of the results is presented in Table 1. In this table the sign of the coefficient (+ or −) is presented together with an index of significance in parentheses. The coef./s.d. ratio is here labeled "index of significance" for convenience, but this is not standard statistical terminology. A (0) indicates that when tried in an equation, the coef./s.d. ratio was less than 1.0; a (1) indicates that the coef./s.d. ratio was between 1.0 and 2.0; a (2) indicates the ratio was between 2.0 and 3.0; a (3) that the coef./s.d. ratio was 3.0 or greater. The first three lines of the table may be interpreted as follows:—an increase in the K_2O content was significantly associated (0.01 probability level) with an increase in the heat of hydration at 7 days but not at 28 days or 1 year. Also, an increase in the Na_2O content was probably associated (0.05 probability level) with a decrease in the heat of hydration at 1 year but not at 7 or 28 days. It may be noted also, that at 28 days, variations in the quantities of neither of the alkalies had a significant effect on the heat of hydration values.

As indicated in Table 1, higher K_2O contents were associated, or probably associated with higher 7 day heat of hydration, with higher sulfate expansion, with higher compressive strength of mortars at early ages, and with higher compressive strength of low-pressure-steam-cured mortars. Higher K_2O contents were also associated with higher shrinkage of neat cement pastes, with higher dynamic modulus of elasticity of concretes moist cured for 14 days, but with lower weight loss and gain of concretes in drying and wetting tests, with lower freeze-thaw durability. Higher Na_2O contents were associated, or probably associated, with lower heat of hydration at one year, with lower compressive strengths of mortars at 1 to 10 years, with higher shrinkage of neat cements at 7 days to 7 months and with higher dynamic modulus of elasticity of concrete at 14 days. Higher Na_2O contents were also associated with lower compressive

Table 1. *Sign and index of significance of coefficients for* Na_2O *and* K_2O *when used in multivariable equations together with other independent variables, as calculated for a number of properties of portland cements.*

Test	Sign and index of significance (see text)*		Reference**
	Na_2O	K_2O	
Heat of hydration			
at 7 days	(0)	+(3)	Eq 6 Table 5-2
at 28 days	(0)	(0)	Eq 6 Table 5-6
at 1 year	−(2)	(0)	Eq 6 Table 5-10
Sulfate expansion			
0–9% C_3A cements			
at 14 days	(0)	+(3)	Eq 12 Table 4-4
at 28 days	(0)	+(2)	Eq 25 Table 4-6
at 84 days	(0)	+(2)	Eq 19 Table 4-8
Autoclave expansion			
neat cements	+(2)	+(2)	Eq 3 Table 6-3
Compressive strength			
1 : 2.75 mortar cubes, water stored.			
at 1 day	(0)	+(3)	Eq 2 Table 7-3
at 3 days	(0)	+(2)	Eq 2 Table 7-7
at 7 days	(0)	+(2)	Eq 3 Table 7-11
at 28 days	(0)	(0)	Eq 4 Table 7-15
at 1 year	−(3)	(0)	Eq 4 Table 7-19
at 5 years	−(3)	(0)	Eq 3 Table 7-31
at 10 years	−(3)	(0)	Eq 5 Table 7-35
Compressive strength mortar cubes			
Low-pressure-steam cured.			
Cure start at 5 hours, tested dry	(0)	+(2)	Eq 2 Table 8-14
Cure start at 24 hours, tested wet	(0)	+(3)	Eq 2 Table 8-18
High pressure steam cured.			
Cure start at 5 hours, tested dry	−(3)	(0)	Eq 2 Table 8-22
Cure start at 24 hours, tested dry	−(3)	−(3)	Eq 3 Table 8-26
Dynamic modulus of elasticity concrete with constant water-cement ratio			
at 14 days, moist	+(3)	+(3)	unpublished data
after 8 weeks in lab air	(0)	+(1)	"
after 4 weeks resoaking	(0)	(0)	"
Shrinkage neat cement paste			
at 24 hours	+(1)	+(3)	Eq 3 Table 9-3
at 7 days	+(2)	+(3)	Eq 4 Table 9-7
at 28 days	+(3)	+(3)	Eq 3 Table 9-11
at 6 months	+(3)	+(3)	Eq 2 Table 9-15
Shrinkage constant w/c concrete 8 weeks in lab air	−(3)	(0)	Eq 3 Table 10-5
Expansion after resoaking 4 weeks	+(3)	(0)	Eq 4 Table 10-9
Weight loss of concrete in air drying 8 weeks	−(3)	−(3)	unpublished
Weight gain of concrete after reasoaking 4 weeks	−(3)	−(3)	"
Freeze-thaw durability	−(1)	−(3)	"

* See section on Results of the Statistical Evaluation.
**References are to individual equations in "Interrelations between Cement and Concrete Properties" as published or as proposed for publication.

strength of high-pressure-steam-cured mortars, with lower shrinkage of air-dried concretes, lower weight gain on rewetting, but with higher expansion when the air-dried specimens were resoaked.

Although there were many instances in these equations where the coefficients for Na_2O and K_2O were significant at the 0.01 probability level, the probable effects on the various properties were generally small compared with the effect of some of the major constituents or some of the other variables. Reference should be made to the complete equations in the published articles (1).

The Effect of Other Trace Elements

In Table 2 are presented the trace elements (and SrO) which were found to have coef./s.d. ratios greater than one when used in multivariable regression equations containing the commonly determined independent variables. The sign of each coefficient (+ or −) is presented as well as the coef./s.d. ratio. The significance of the numbers in parentheses are the same as for Na_2O and K_2O of the previous table. Also presented is the level of significance of the reduction in variance as a result of including the added independent variables,—the trace elements.

It may be noted that although the coefficients of most of the individual trace elements were not highly significant, the use in an equation of all having a coef./s.d. ratio greater than one resulted in a reduction of variance, significant at the 0.01 probability level in the equations for most of the properties measured. The reduction in variance was significant at the 0.05 probability level in a few equations and was less than that in equations for two of the properties.

SrO and the elements Ba, Cu, Rb and Zr appeared most often in Table 2. Zn, V, P and Cr were next in frequency, and Co, Ni, Mn, Li, Pb and Ti, appeared

Table 2. *Trace elements, their signs, and index of significance as well as the probability level of the reduction of variance when the trace elements were used in multivariable equations together with commonly determined independent variables*

Test	Trace elements sign and index of significance (see text)*	Level of significance of reduction of variance	References**
Heat of hydration			
at 7 days	+Cr(2), −Cu(2), −P(2), +Zr(2)	0.01	Eq 6 Table 5-2
at 28 days	−Co(1), −Cu(3), −P(2), −SrO(2), +Zr(1)	0.01	Eq 6 Table 5-6
at 1 year	−Ba(2), −Cu(3), −P(2), +V(2)	0.01	Eq 6 Table 5-10
Sulfate expansion			
0–9% C_3A cements			
at 14 days	−Cu(2), +SrO(1), +V(2), +Zn(1)	0.01	Eq 12 Table 4-4
at 28 days	−Cu(1), +Ni(2), +SrO(1)	0.05	Eq 25 Table 4-6
at 84 days	−Cu(1), +Ni(2), +SrO(1)	0.01	Eq 19 Table 4-8
Autoclave expansion	−Cr(1), +SrO(3), +V(3)	0.01	Eq 3 Table 6-3
Compressive strength			
1:2.75 mortar cubes			
at 1 day	+Ni(1), −P(2), −SrO(2)	0 01	Eq 2 Table 7-3
at 3 days	+ Cr(1), −Mn(2), −SrO(2), +V(1)	0.01	Eq 2 Table 7-7
at 7 days	−SrO(1)	not at 0.05 level	Eq 3 Table 7-11
at 28 days	−Co(2), −Cr(2), −SrO(1), +Zr(1)	0.01	Eq 4 Table 7-15
at 1 year	−Co(1), −Mn(1), −Rb(2), +Zr(2)	0.01	Eq 4 Table 7-19
at 5 years	+Ni(1), −Rb(2), +Zn(1), +Zr(1)	0.05	Eq 3 Table 7-31
at 10 years	+Cr(1), −SrO(1), +Zn(1), +Zr(2)	0.01	Eq 5 Table 7-35
Compressive strength,			
Low-pressure steam cured.			
Cure started at 5 hours, tested dry	−Ba(3), −Cu(1), −P(3)	0.01	Eq 2 Table 8-14
Cure started at 24 hours, tested wet	−Ba(2), −Cu(2), +Li(2)	0.01	Eq 2 Table 8-18
Compressive strength,			
High pressure steam cured.			
Cure started at 5 hours, tested dry	−Ba(2), +Cr(2), −Cu(3), +Li(3), −V(1)	0.01	Eq 2 Table 8-22
Cure started at 24 hours, tested dry	−Ba(1), −Rb(2), −SrO(2), −V(1)	0.01	Eq 3 Table 8-26
Dynamic modulus of elasticity concrete with constant water-cement ratio			
at 14 days, moist	−Mn(1), +Rb(1), +Zr(1)	unpublished	unpublished
after 8 weeks in lab air	−V(1)	〃	〃
after 4 weeks resoaking	−Ba(2), −Cu(2), +Zr(2)	〃	〃
Shrinkage neat cement paste			
at 24 hours	+Ba(1), +Cr(2), +P(1), −Zn(1)	0.01	Eq 3 Table 9-33
at 7 days	+Ba(2), +P(1), +Rb(2)	0.01	Eq 4 Table 9-7
at 28 days	+ Ba(3), +P(2), +Rb(2), −Zn(1)	0.01	Eq 2 Table 9-15
at 6 months	+Ba(3), +Ni(2), +Rb(2)	0.01	Eq 2 Table 9-15
Shrinkage constant w/c concrete,			
14 days moist, 8 weeks in lab air	+SrO(2), −Zn(2), +Zr(1)	0.01	Eq 3 Table 10-5
Expansion after resoaking 4 weeks	+P(1), −Pb(1), +Rb(2), −SrO(1), −Zn(1)	0.01	Eq 4 Table 10-9
Weight loss in air-drying 8 weeks	+Ba(1), −Rb(1), −Zr(1)	unpublished	unpublished
Weight gain after resoaking 4 weeks	+Ba(1), +Cu(1), −Rb(1), −Zr(1)	〃	〃
Freeze-thaw durability	−Ba(1), −Cu(2), −Pb(1), −Rb(1), −Ti(2)	〃	〃

* See section on Results of the Statistical Evaluation.
**References are to individual equations in "Interrelations between Cement and Concrete Properties" as published, or as proposed for publication.

least frequently. Mo, one of the trace elements detected in a few cements did not appear in any of the equations.

Of the four trace elements that appeared most frequently in the equations, higher Ba contents were probably associated with lower heat of hydration at one year, with lower compressive strength of both low- and high-pressure steam cured mortars, lower dynamic modulus of concrete, and higher shrinkage of neat cements,—especially at the later ages. Higher Cu contents were probably associated with lower heat of hydration, lower sulfate expansion, lower compressive strengths of steam cured and autoclaved mortars, and lower dynamic modulus of concrete after rewetting. Higher Rb contents were probably associated with lower compressive strength of mortars at 1 and 5 years, and lower compressive strength of high-pressure-steam-cured mortars when steam curing was started at 24 hours, and also with higher shrinkage of neat cements, and higher expansion of concretes when rewetted. Higher Zr contents were probably associated with higher heat of hydration at 7 days, higher compressive strengths at 1 and 10 years, and with higher dynamic modulus of elasticity of concretes after rewetting.

Of the other trace elements only Li, P and SrO had coefficients significant at the 0.01 probability level in any of the equations for the various properties. Increased SrO was associated with increased autoclave expansion, and probably with lower heat of hydration at 28 days, lower compressive strength of mortars at 1 and 3 days, lower compressive strength of mortars autoclaved at 24 hours. Higher SrO contents were probably associated with higher sulfate expansion and higher shrinkage of concrete when air dried. Increased Li was associated with higher compressive strength of autocalved mortars when curing was started at 5 hours.

As was found with the alkalies, Na_2O and K_2O, the probable effects of the other trace elements were generally small compared with the effects of some of the major constituents or some of the other variables. The combined effect was in most instances highly significant.

Discussion

In any statistical studies of this nature, the empirical equations derived are dependent on the adequacy of sampling of all possible portland cements. Somewhat different coefficients would be obtained with a different group of cements, with different methods of making the physical tests, and with different treatment of the data.

These tests were made with commercial portland cements and no information was available of the temperature at which the clinker was burned nor the rate of cooling. These factors may have contributed to an increased variance of the equations. Another contributing factor, especially with some tests, is the normal variation of the testing procedures and test-results. Relatively small quantities of cement are used in concrete, and the effect of the cement may be masked because of variations of the aggregates. The trace elements other than Na_2O, K_2O and SrO were reported to the closest value of a series such as 1, 2, 5, 10, 20 etc. More accurate means of analyses and values for the trace elements would be desirable.

Cements with a trace element value less than the minimum reported value, were assigned a value of zero for the element. All of these factors may have masked not only the actual effect of the trace elements which were indicated as probably having a significant relationship but may possibly have eliminated other elements as not having a significant relationship. The results of these statistical studies explain in part, however, some of the reasons why different cements may have somewhat different properties. Further work is necessary to determine the role that the trace elements may have in the hydration and hydration products of portland cements.

Summary and Conclusions

On the basis of the statistical evaluation, Na_2O and K_2O were associated with most of the properties of portland cement pastes, mortars, and concretes. The two alkalies sometimes have the same effect in some tests, but with other tests one may have a significant effect and the other not. Of the other trace elements, very few had a highly significant relationship to the various properties measured. However, by use of the trace elements in equations in addition to commonly determined variables, there was usually

a highly significant reduction in variance. Ba, Cu, Rb, SrO and Zr appeared most often in the equations for the various properties.

The probable effects of variations of Na_2O, K_2O as well as those of the other trace elements on the properties measured were small compared with the effects of variations of some of the major constitutents or some of the other independent variables. However, the contributions of the minor constituents and trace elements, although small, were in many instances, significant, and help to explain some of the differences in properties of portland cements.

References

1. "Interrelations between cement and concrete properties", Part 1, Building Science Series 2, National Bureau of Standards, Aug. 1965.
   R. L. Blaine, H. T. Arni and B. E. Foster, Section 1. "Materials and Techniques."
   R. L. Blaine, H. T. Arni and R. A. Clevenger, Section 2. "Water requirements of portland cement."
   R. L. Blaine, Leonard Bean and Elizabeth K. Hubbard, Section 3, "Occurrence of minor and trace elements in portland cement."
2. "Interrelations between cement and concrete properties", Part 2, Building Science Series 5, National Bureau of Standards, July 1966.
   R. L. Blaine, H. T. Arni and D. N. Evans, Section 4, "Variables associated with expansion in the potential sulfate expansion test."
   R. L. Blaine and H. T. Arni, Section 5, "Heat of hydration of portland cement."
   R. L. Blaine and H. T. Arni, Section 6, "Variables associated with small autocalve expansion value of portland cements."
3. "Interrelations between cement and concrete properties", Part 3, Building Science Series 8, National Bureau of Standards (to be published).
   R. L. Blaine, H. T. Arni and M. R. DeFore, Section 7, "Compressive strength of test mortars."
   R. L. Blane, H. T. Arni and M. R. DeFore, Section 8, "Compressive strength of steam-cured portland cement mortars."
4. "Interrelations between cement and concrete properties", Part 4, Building Science Series Natonal Bureau of Standards, (to be published).
   R. L. Blaine, D. N. Evans and H. T. Arni, Section 9, "Shrinkage of hardened portland cement pastes."
   R. L. Blaine and H. T. Arni, Section 10, "Shrinkage and expansion of concrete."

Supplementary Paper III-71 Cement Paste Shrinkage-Relationships to Hydration, Young's Modulus and Concrete Shrinkage

Harold Roper*

Synopsis

The paper presents paste shrinkage, hydration and Young's modulus data for sixteen cements with various chemical compositions. These cements fall into two categories, based on high or low shrinkage characteristics. Of the eight cements in the high shrinkage group, three showed definite evidence of the diagnostic triple peak heat of hydration phenomenon described by Lerch. The effects of chemical composition and fineness of the unhydrated cement are considered, and the paper stresses the relationships between shrinkage characteristics and other physical properties of the paste; namely the degree of hydration and the Young's modulus.

For individual cements, data over a wide range of water: cement ratios fit an equation of the form:

$$\frac{1}{\Delta L} = a - b(W_n)$$

where ΔL is the paste shrinkage, W_n is the non-evaporable water and a and b are constants.

When shrinkage data for the various cements are compared, the effect of the paste modulus and its interaction with the hydration must be considered. For all the data, highly significant correlations are observed between the shrinkage and hydration and Young's modulus. It is concluded that different pastes, with the same hydration and Young's modulus values, will undergo equal shrinkage irrespective of the chemical composition or fineness of the cement.

The paper compares briefly the paste shrinkage with concrete shrinkage at an equivalent water:cement ratio. Concrete shrinkage up to drying periods of at least one year can be satisfactorily predicted using paste shrinkage data. The importance of early shrinkage rates of the various concretes is noted.

Introduction

The stringent demands made by engineers who aim to decrease or eliminate cracking associated with the restraint of forces induced by concrete shrinkage, have stimulated research into the factors which influence paste shrinkage. The work of Lerch (1) and Pickett (2) demonstrated the role of C_3A and proved the importance of optimum gypsum contents in reducing shrinkage. More recent developments have been the presentation, by Fulton (3) and Hansen and Nielsen (4), of formulae which relate the shrinkage of concrete to the volume changes and elastic constants of paste and aggregate. Such formulae are fully applicable only if it is assumed that tests on neat paste reflect shrinkages in larger concrete specimens; this assumption has been criticized by Swayze (5, 6), but defended by Tremper (7).

The work described in this paper is a study of the relative magnitude of shrinkages of pastes under controlled conditions, and the comparison of these values with those of concrete shrinkages. Factors which influence the paste shrinkage and the conditions under which paste shrinkage becomes particularly important are considered.

*C.S.I.R.O., Department of Civil Engineering, Sydney University, Sydney, Australia.

Materials and Techniques

The investigation was limited to sixteen cements, which represented a random sample of Type A ordinary portland cements (in accord with the relevant Australian Standard (8)) produced in thirteen different plants during November 1965. Compositional and fineness data are given in Table 1 for these cements, which are arranged in increasing C_3A content.

Cement specimens $3 \times \frac{1}{4} \times \frac{1}{4}$ inch were cast at water: cement ratios ranging from 0.2 to 0.6, stripped at 24 hours and cured at 21°C under water for various periods of time. The cured length was taken as datum and the specimens were dried in desiccators at 20° ± 2°C and 50% relative humidity over a saturated salt solution and at a pressure of 460 mm of mercury. After 7 days drying the length was recorded to 0.0001 inch and the shrinkage calculated as a percentage decrease. This period of time allowed the cement pastes to closely approach equilibrium conditions. After completion of the shrinkage measurements the paste specimens were crushed and their non-evaporable water was determined by the method of Copeland and Hayes (9).

For Young's modulus determinations 2 inch diameter by 4 inch cylinders were case at different water: cement ratios, stripped at 24 hours and cured under water for 28 days. The specimens were brought to equilibrium in a 50% RH atmosphere before being loaded to their ultimate compressive strength. Strain measurements were recorded using resistance wire strain gauges attached on opposite sides of the specimens. The chord modulus was measured between the values of 1,500 and 3,500 lb/sq.in.; this value closely approximated the tangent modulus of the paste.

Table 1. *Composition and fineness of cements*

Cement	C_3S	C_2S	C_3A	C_4AF	SO_3	Free CaO	Na_2O	K_2O	Fineness Sq cm/gm Blaine
A	54.2	24.0	1.8	13.2	1.95	1.04	0.19	0.53	2930
B	47.7	28.0	3.5	12.3	2.35	0.83	0.65	0.06	2820
C	49.0	29.1	3.7	11.3	2.25	1.14	0.13	0.40	2830
D	36.7	39.5	3.8	10.2	3.10	1.58	0.14	0.41	2890
E	60.0	12.4	4.6	15.3	2.60	0.40	0.36	0.37	3340
F	49.5	24.1	4.6	10.5	2.40	2.86	0.21	0.21	4020
G	43.8	29.0	6.2	11.7	2.50	1.58	0.42	0.34	3450
H	48.3	27.8	6.5	10.6	1.70	0.53	0.09	0.74	2820
I	54.9	19.3	7.0	10.8	1.80	1.37	0.60	0.61	3090
J	50.4	26.0	8.4	9.0	1.60	0.44	0.48	0.32	3510
K	39.5	33.5	9.8	10.5	0.90	2.14	0.43	0.51	3290
L	50.0	21.4	10.3	9.4	2.00	1.94	0.06	0.86	3650
M	52.2	18.9	10.6	10.5	1.90	1.55	0.07	0.60	2620
N	34.1	38.4	10.9	9.3	1.90	0.69	0.06	0.87	3600
O	50.4	21.1	11.3	9.3	2.25	1.82	0.07	0.77	3400
P	56.0	16.4	11.8	10.0	1.70	0.88	0.06	0.30	3100

The coarse aggregate generally used in the concrete investigations was a river gravel. This aggregate yields concretes of relatively low shrinkage. In comparing concretes made with aggregates which affect the shrinkage characteristics, this river gravel was contrasted with a basic igneous rock known to produce higher shrinkage in concrete. The same quartz sand was used in both series of mixes.

Concrete shrinkages were measured to 0.0001 inch on $8 \times 3 \times 3$ inch specimens having anvils set vertically to provide a 6 inch gause length. Specimens were demoulded at the age of 24 hours during which period they were cured at 100% relative humidity. For the subsequent 6 days they were cured under water at 23° ± 2°C, after which time the zero reading was recorded. Drying occurred in laboratory air at 23° ± 2°C and a relative humidity of 50 ± 4%.

Cement Paste Shrinkage

Paste Shrinkage Data

Data for two typical cements using the paste shrinkage test procedure described, and a range of curing periods from 3 to 90 days are shown in Figs. 1 and 2. For the longer curing periods the shrinkages for the high water: cement ratio pastes in Fig. 1 are approximately twice those of pastes in Fig. 2; however, at low water: cement ratios and short curing periods differences betweeen the cements are small.

Similar data were obtained for the same curing periods for the sixteen cements having compositions as given in Table 1. However, since cracking was suspected to occur during the drying of some specimens having short curing periods, all paste data presented in this paper will henceforth refer to underwater curing for 28 days. Paste shrinkage data for this curing period, using the 16 cements, are given in Table 2.

Table 2. *Shrinkage, L(%); Non-evaporable water , W_n (gm/gm ignited cement) and Young's modulus, E (10^{-6} lb/sq in) Data for cement pastes*

Cement	Water: Cement ratio																							
	.250			.275			.300		.325			.350		.400			.450		.500			.600		
	ΔL	W_n	E	ΔL	W_n	E	ΔL	W_n	ΔL	W_n	E	ΔL	W_n	ΔL	W_n	E	ΔL	W_n	ΔL	W_n	E	ΔL	W_n
A	.174	.144	4.58	.176	.148	3.78	.198	.156	.204	.159	2.61	.214	.160	.218	.158	2.17	.216	.158	.220	.158	1.70	.220	.158
B	.188	.175	4.20	.196	.182	3.65	.228	.186	.236	.189	2.92	.241	.189	.252	.191	2.17	.266	.191	.264	.195	1.76	.270	.197
C	.170	.159	4.57	.186	.164	4.41	.210	.170	.212	.173	3.44	.210	.175	.214	.176	2.70	.224	.173	.228	.176	1.42	.228	.175
D	.220	.134	4.03	.230	.144	3.82	.238	.153	.238	.154	3.19	.244	.162	.250	.161	2.24	.252	.164	.256	.161	1.86	.260	.165
E	.208	.152	4.44	.220	.164	3.96	.244	.171	.248	.179	3.36	.278	.183	.270	.185	2.59	.276	.187	.286	.187	1.71	.282	.190
F	.210	.177	3.83	.220	.179	3.90	.240	.182	.240	.196	2.78	.252	.197	.274	.205	2.15	.278	.206	.288	.209	1.42	.292	.212
G	.192	.162	4.50	.206	.175	4.07	.216	.183	.226	.195	3.09	.246	.197	.258	.205	2.59	.260	.208	.282	.209	2.08	.292	.229
H	.188	.158	4.08	.204	.165	4.01	.212	.174	.234	.180	2.63	.232	.183	.260	.185	2.48	.256	.182	.252	.188	1.57	.258	.188
I	.196	.164	4.14	.228	.180	3.52	.266	.186	.282	.196	3.22	.358	.213	.432	.221	2.32	.446	.222	.460	.226	1.88	.440	.229
J	.186	.188	4.69	.222	.205	4.06	.252	.205	.316	.223	3.64	.338	.228	.452	.243	2.51	.572	.252	.660	.254	2.13	.768	.250
K	.222	.171	4.03	.258	.186	3.39	.294	.193	.348	.205	2.39	.396	.206	.486	.215	2.40	.560	.213	.658	.222	1.73	.848	.217
L	.172	.161	4.15	.234	.182	3.98	.258	.193	.300	.202	3.28	.326	.200	.384	.218	2.56	.474	.226	.534	.229	1.92	.624	.232
M	.162	.155	4.53	.198	.171	4.12	.236	.181	.272	.190	3.04	.302	.197	.370	.206	2.53	.434	.211	.496	.214	1.90	.520	.211
N	.232	.167	3.75	.261	.174	3.55	.294	.181	.332	.199	3.15	.380	.200	.468	.210	2.31	.608	.213	.716	.222	1.40	.800	.227
O	.182	.172	4.20	.200	.184	4.07	.234	.191	284	.205	3.60	.298	.212	.380	.220	2.41	.440	.226	.460	.215	1.87	.540	.225
P	.168	.179	4.12	.194	.188	4.09	.224	.201	.272	.215	3.55	.302	.220	.376	.237	2.39	.412	.242	.462	.245	1.69	.498	.251

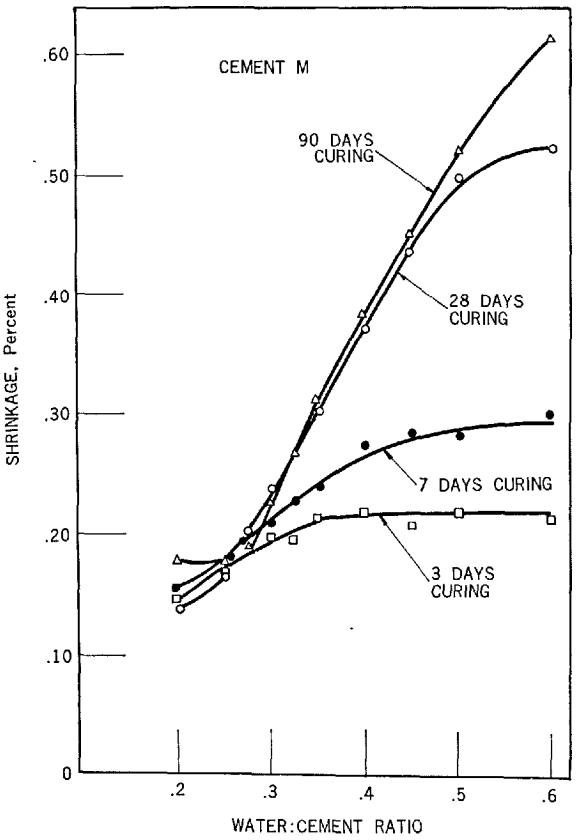

Fig. 1. *Paste shrinkage as a function of water: cement ratio and curing period for a cement exhibiting high shrinkage characteristics.*

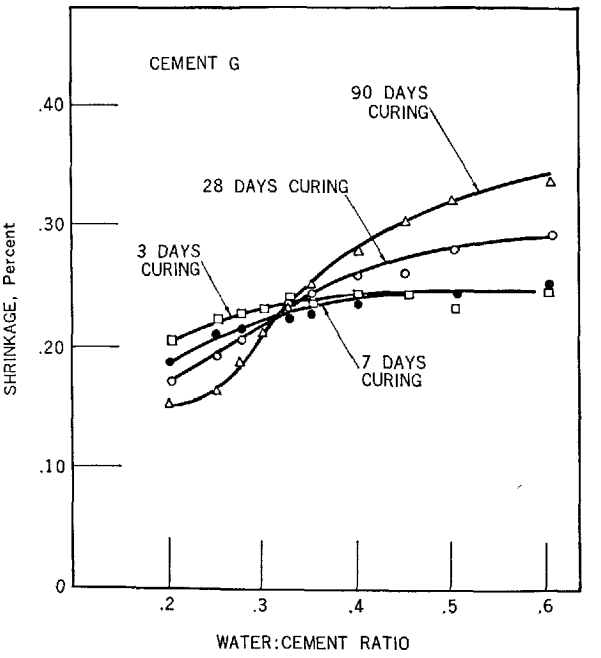

Fig. 2. *Paste shrinkage as a function of water: cement ratio and curing period for a cement exhibiting low shrinkage characteristics.*

Concrete Shrinkage

Relationships between Cement Composition and Paste Shrinkage

Linear regression analyses using various forms of equations relating paste shrinkage at constant water: cement ratio to cement composition, were calculated from the relevant data in Tables 1 and 2. Using an equation of the form:

$$\Delta L = a(C_3S) + b(C_2S) + c(C_3A) + d(C_4AF) + e(SO_3),$$

the only regression coefficient which was consistently significant was that of C_3A.

Comparisons of results of various equations indicated that the most significant one for the prediction of shrinkage is of the form:

$$\frac{1}{\Delta L} = f - g(C_3A).$$

The statistical data obtained using this equation for various water: cement ratios are given in Table 3. The constant term remains the same for all water: cement ratios, whereas the coefficient g changes systematically. All the correlation coefficients in the table are significant at the 0.1% significance level for 14 degrees of freedom; up to 80% of the variance of the paste shrinkage is explicable by the variation in C_3A. The addition of terms relating to the other components of the cement and to the fineness improved the fit insignificantly.

It was concluded from the results of all these analyses that the role of C_3A was dominant in explaining the variance in shrinkage of the cements, provided that the water: cement ratios equalled or exceeded 0.325. Increases in shrinkage which relate to C_3A may be affected in three ways, *viz.* greater shrinkage of the C_3A hydration products *per se*; depletion of SO_3, resulting in modified hydration rates and products; and increase in the hydration rates of the silicates by the presence of C_3A in solid solution or as discrete inclusions within the silicate clinker grains. It is probable that all three factors play a part in the outcome.

A noteworthy fact is that the cements used in this investigation show a negative linear association, significant at the 5% level, between C_3A and SO_3. This relationship is the opposite to what would be expected, however, the practical problems associated with establishing and maintaining an optimum gypsum content are complex and certain clinkers produced throughout the world have gypsum demands which exceed the SO_3 limits in cement specifications. The relatively high alkali contents of the tested cements tend to increase their gypsum demands. A further complicating factor is that some SO_3 derived from kiln fuels may be present in the clinker; up to 0.75% has been detected in the clinker of cement E. Such SO_3 in clinker minerals is not necessarily available for reaction in the same way as that derived from added gypsum, yet it is not considered as a different entity when SO_3 limits are imposed. High sulfate contents which satisfy the optimum requirements may lead to false set, thus solving one problem but creating another.

Table 3. *Statistical data for least squares fit for C_3A and shrinkage*

Water: Cement ratio	Constant (f)	Standard error	Coefficient of C_3A (g)	Standard error	Correlation coefficient (r*)
0.325	4.928	0.222	−0.149	0.028	0.816
0.350	4.782	0.284	−0.166	0.036	0.775
0.400	4.905	0.291	−0.234	0.037	0.861
0.450	5.001	0.319	−0.276	0.041	0.878
0.500	5.019	0.330	−0.299	0.042	0.888
0.600	5.082	0.335	−0.325	0.043	0.901

r = Correlation coefficient for 14 degree of freedom. An r value greater than 0.742 indicates a significant relationship at the 0.001 level.

An unpublished investigation undertaken by the author and J. H. Taplin indicated that three of the cements *viz.* K, L and O showed the typical diagnostic triple peak heat of hydration phenomena described by Lerch (1), indicating gypsum deficiency. Cement M showed a slight plateau on its second peak, but it was not sufficiently pronounced to demonstrate conclusively that the gypsum content was less than optimum. For the other cements no indications of more than two peaks were observed.

Despite the heat of hydration data it is noted that the shrinkage characteristics of cements A to H differ significantly from those of cements I to P providing the water: cement ratio exceeds 0.325. Those of the first group give shrinkage curves of the same type as those in Fig. 2, where Fig. 1 is typical of the higher shrinkage cements. In order to confirm the fact that a cement may have no sulphate deficiency by its hydration curve yet give relatively high shrinkage, cement P was selected for further study.

Clinker was ground to the fineness of the comparable cement, and gypsum, again of comparable fineness, was added to give a range from 0 to 5% SO_3. Paste bars with a water: cement ratio of 0.5 were cast from these blends and tested in the usual manner. The curve for paste shrinkage versus SO_3 % is given in Fig. 3. Two commercial cements, from the same plant but with different SO_3 levels were tested for shrinkage, and the data were plotted on the figure. It appears that, for the shrinkage measured by this technique, even at 5% SO_3, optimum gypsum content had not been reached. The results of gypsum addition in the laboratory closely approximate those obtained for the commercially ground products.

As further confirmation that the sulphate levels were low for certain of the cements, the effects of replacing small amounts of cement by a 1:1 mixture by weight of ground limestone and anhydrite were studied. Pastes having water: cement ratios of 0.45

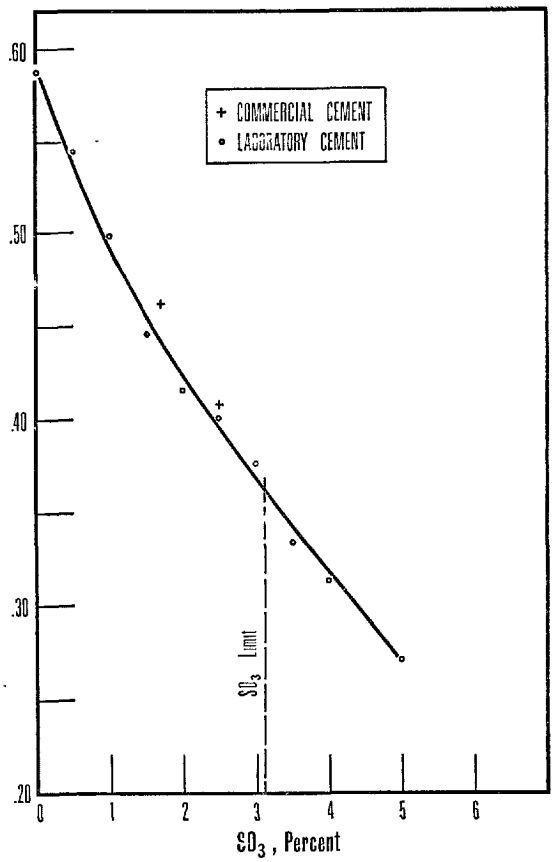

Fig. 3. *Paste shrinkage as a function of* SO_3 *content.*

were cast, using cements as received. Similar pastes were cast with 2, 3, 4 and 5% replacement by weight of the ground limestone and anhydrite. The specimens were cured, measured and dried in the usual manner. It was found that, although there was virtually no observable effect in the case of the low shrinkage cements, all the cements of the higher shrinkage group showed decreases in shrinkage of up to 35%. As expected, only some of these cements displayed an optimum SO_3 content within the replacement range. Although the use of such additions in concrete could overcome the rigid sulphate limits imposed by the cement specifications, the long term effects could be as detrimental to the concrete as the presence of SO_3 in the usual form.

Relationships between Non-Evaporable Water, Young's Modulus and Shrinkage of Cement Paste

It was considered that the effects of differences in hydration rates of the various cements were influencing the shrinkage results significantly and the non-evaporable water contents of the various pastes were measured as described. As was expected, the cements with high C_3A contents generally gave higher non-evaporable water contents at equal ages and at water: cement ratios within the range considered important for this investigation. The hydration rate of some of the high C_3A cements was very rapid, and for these very little change was noted between values measured at-28 days and 3 months. Such cements gave excellent 28 day concrete strengths. However, they cannot be considered ideal materials when design criteria depend on continued strength gain long after the first month of the life of a structure and when shrinkage cracking may be promoted by both the hygric dimensional change of the concrete and thermal dimensional changes accentuated by high heats of hydration at early ages.

In order to study relationships between paste shrinkage and hydration an empirical approach to the problem was adopted. Using the data given in Table 2 for the paste shrinkage and non-evaporable water, the following equation was found to apply for each individual cement:

$$\frac{1}{\Delta L} = a - b(W_n)$$

where ΔL is the paste shrinkage expressed as a percentage, W_n is the non-evaporable water and a and b are constants.

The interpretation of "a" in physical terms is that it represents the reciprocal of the percentage shrinkage which an unhydrated cement compact would undergo from a saturated state to the experimental drying conditions, always provided that the lines may be extrapolated. From the values of "a" it appears that such a compact could exhibit between 0.05 and 0.14% shrinkage under these conditions.

Plots of this equation for results on cements M and G for 28 days curing are given in Fig. 4. The conclusion, always allowing for the fact that direct causal relation may be through a third factor, is that, for a particular cement cured for the same period of time, the reciprocal of the paste shrinkage is a linear function of the hydration at the time of test.

When the 144 results of the cements are treated as a series of independent values, the following equation results:

$$\frac{1}{\Delta L} = 10.844 - 37.035W_n$$

with a correlation coefficient of 0.835 for 142 degrees of freedom and with standard errors of 0.397 and

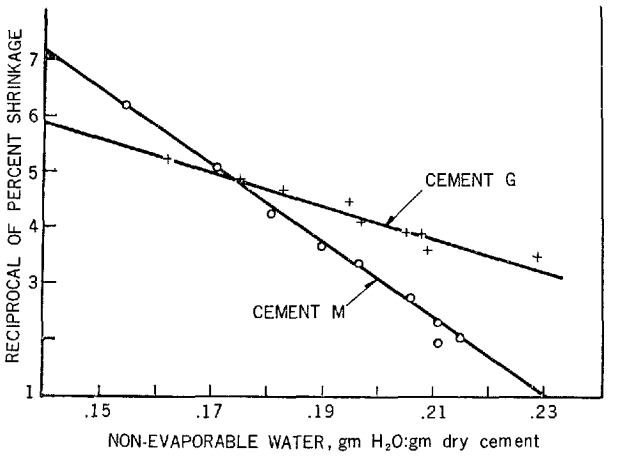

Fig. 4. *Relationship between the reciprocal of paste shrinkage and non-evaporable water.*

2.048 for the constant term and the coefficient of the variable respectively. Using this equation 70% of the variance in shrinkage of all cements is explicable by the nonevaporable water contents of the hydrated pastes.

In order to improve the fit of the equation, the inclusion of a term representing the compressibility of the paste was desirable. The Young's modulus of the material was selected rather than the compressibility since the measurement of the Poisson's ratio is tedious and relatively inaccurate. The technique of the modulus measurement has been described, and the results for the various cements are given in Table 2. Only eighty observations were available for computation. The resulting equation was:

$$\frac{1}{\Delta L} = 7.620 - 27.301W_n + 0.485E$$

with a multiple correlation coefficient of 0.890 for 77 degrees of freedom and with standard errors of 0.689, 2.808 and 0.076 for the three terms in that order. Statistical tests indicate that the inclusion of the Young's modulus term is advantageous and now 80% of the variance is explicable by these two variables. The only other attempt to improve the fit of the equation was to substitute the relative hydration, i.e., the ratio of non-evaporable water content to the non-evaporable water content at complete hydration, for the W_n term. This led to no improvement in the results.

It appears from the above results that different pastes with the same non-evaporable water content and equal Young's modulus values will undergo similar shrinkages, irrespective of the chemical composition or fineness of the cement. In practice, however, compositions which increase early strength generally lead to higher measured paste shrinkage due to the higher rate of hydration. Similarly, finer cements of identical chemical composition show an increase in shrinkage when tested after equal periods of curing simply due to the hydration effect.

In contrast, some low heat cements tend to give high shrinkage values when tested by the procedure used for the present series of cements. Since the hydration of these cements is relatively low at 28 days, a possible conclusion is that the effect of increased compressibility becomes dominant. Such a conclusion should be made with care since it is based on an empirical rather than a physical model.

Relationships between Cement Paste Shrinkage and Concrete Shrinkage

The study of this relationship has a two fold purepose, firstly, for the empirical prediction of concrete shrinkage from paste shrinkage data, and secondly, for the assessment of the accuracy of theoretical formulae which relate vairous physical properties of aggregate and paste to concrete shrinkage.

In order to establish whether a significant relationship exists between paste and concrete shrinkages, regression analyses were conducted on data from 15 of the Australian type A cements referred to in Tables 1 and 2. Paste shrinkage data for 28 days curing and a water: cement ratio of 0.50 were used. The comparative shrinkage data for concretes having maximum 3/8 inch aggregate and mix proportions of 3.0:2.4:1.0:0.5, gravel aggregate: quartz sand: cement: water, were provided by 8 × 3 × 3 inch specimens which were cured, measured and dried as previously described. The results are summarized in Table 4.

The concrete shrinkages after 7, 28, 90 and 365 days drying are recorded together with the correlation coefficient from linear regression analyses which relate paste shrinkage after 7 days drying to the concrete shrinkage at the various ages. It is concluded that highly significant correlation exists between the paste and concrete shrinkages even for drying periods up to 1 year.

Following the method used by Ross (10), final shrinkage values were calculated for each concrete from the test data by assuming that the shrinkage-time curves can be represented by a hyperbolic equation of the form:

$$\Delta L = \frac{\Delta L\infty \cdot t}{N + t}$$

where ΔL is the concrete shrinkage at time t,

Table 4. *Paste and concrete shrinkage data*
Water: Cement ratio = 0.5

Cement	Paste shrinkage per cent	Concrete shrinkage per cent					Prriod to reach half final shrinkage day
		7 day drying	28 day dyring	90 day dyring	1 year drying	Calculated final shrinkage	
A	.220	.012	.032	.048	.067	.075	37.3
C	.228	.015	.035	.052	.068	.075	29.5
H	.252	.018	.042	.063	.080	.090	29.1
B	.264	.015	.037	.055	.072	.079	30.8
E	.280	.017	.038	.057	.075	.082	29.1
G	.282	.015	.035	.050	.068	.075	29.6
F	.288	.017	.037	.052	.068	.074	24.8
I	.460	.023	.053	.070	.085	.091	19.5
O	.460	.022	.048	.062	.075	.080	17.7
P	.462	.025	.053	.068	.085	.091	19.4
M	.496	.025	.052	.065	.078	.083	16.8
L	.534	.022	.050	.063	.075	.083	18.1
K	.658	.028	.058	.070	.083	.088	15.1
J	.660	.028	.062	.077	.090	.095	15.2
N	.716	.032	.065	.080	.093	.099	14.9
	r*	.962	.966	.886	.841	.755	

r* = Correlation coefficient for 13 degrees of freedom. An r* value greater than 0.760 indicates a significant relationship at the 0.001 level.

$\Delta L\infty$ is the final shrinkage and
N is a constant equal to the time at which the shrinkage strain becomes half the final value.

By calculating $t/\Delta L$ as a linear function of t and fitting straight lines by least squares, $\Delta L\infty$ and N are easily obtained. Fig. 5 illustrates the type of data obtained from the concrete shrinkage measurements, and the linear form of this data for cement O. It should be noted that the relationship between the paste shrinkages and calculated final shrinkages no longer holds at the 0.1% significance level but does so at the 1% level.

Dependence of Concrete Shrinkage Rates on Cement

A result considered to be of more practical importance than the determination of the final shrinkage value, is that the shrinkage rates, particularly early in the shrinkage period, are significantly different for concretes cast with different cements.

In Table 4, values of N, the period in days required to reach half the ultimate shrinkage, are given for the concretes. Although the final concrete shrinkages differ at maximum by only 30% of the mean value, the period required to attain half of this final shrinkage varies by about 100% of the mean. At this laboratory, crack tendency tests, using embedded reinforcing rods to produce restraint to concrete shrinkage, have indicated that early shrinkage rates have a major influence on crack development. The longer the

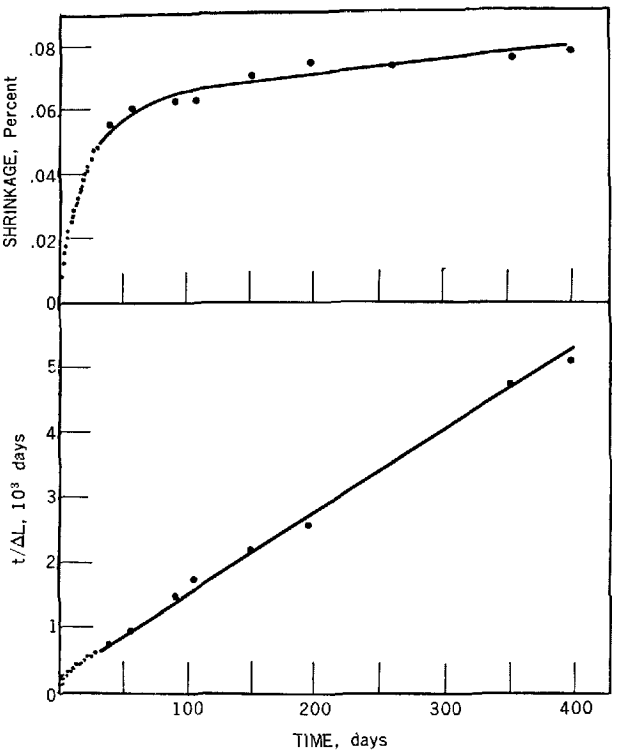

Fig. 5. *Observed and linearized relationships between shrinkage.*

elapsed period of drying without the formation of a crack, the less the possibility that cracking will occur. This fact is due to creep, which reduces the rate of tensile stress increment, and to the continued increase in tensile strength.

Three important warnings should be noted. Firstly, the size effect and drying conditions of concretes in the field will naturally modify the laboratory findings, but so far the crack tendency tests appear to correlate well with field observations. Secondaly, this rate effect is most important only when unsightly cracking occurs; indeed, from some other viewpoints, the more rapidly shrinkage reaches an asymptotic value, the better. Thirdly, under normal concreting conditions all the cements so far studied may give equally satisfactory results; however, in adverse circumstances, either in combination with other materials or due to extreme drying conditions, the likelihood of cracking is increased by cements with high early shrinkage rates.

Interaction Effects between Cement and Aggregate Shrinkages

The use of high shrinkage cements is of greatest

consequence when combined with aggregates which themselves exhibit dimensional changes due to adsorption and desorption of water. The interaction effects of various factors on the relative shrinkage value have been described (11); however, the effects on rate of shrinkage are again considered to be of prime importance in crack development.

Fig. 6 shows the shrinkage-drying time curves for three commercial concrete mixes which were designed to give equivalent strengths at 28 days using constant water contents. The difference in shrinkage behaviour using cement O and the two different aggregates is large, and the early shrinkage rates should be compared. When cement H was used with the dimensionally unstable aggregate, both the amount of shrinkage after 90 days drying and the rate of shrinkage was reduced relative to the companion specimen using cement O. For the first 18 days drying, a critical period for the development of strength and crack propagation, shrinkage rates of the concretes made with cements O and H and with the two aggregate materials were quite similar. This result suggests that when aggregates of doubtful quality must be used due to economic necessity, particuar attention should be paid to the cement-aggregate interactions and effects on both rates and absolute values of shrinkage.

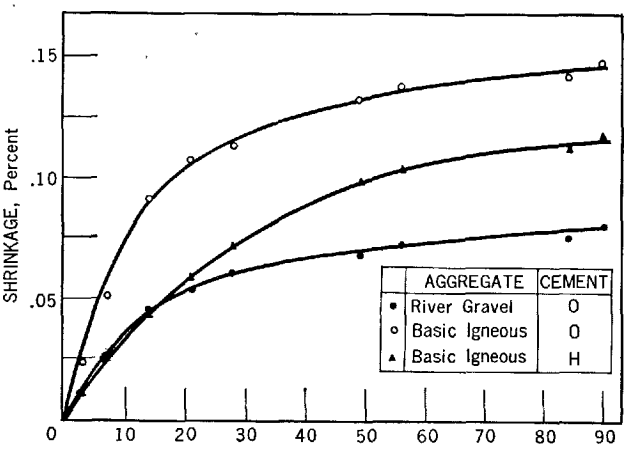

Fig. 6. *Shrinkage as a function of time for different cement and aggregate combinations.*

Conclusion

From the results presented in this paper it is concluded that, when satisfactory procedures are adopted, shrinkage tests on neat paste can be related to concrete shrinkage and chemical properties of the cement. Shrinkage should be considered as a rate process rather than in absolute terms when its effect on concrete cracking is studied. Future research should be oriented towards combinations of materials which effect early shrinkage rates, thereby influencing cracking tendency.

References

1. W. Lerch, "Influence of gypsum on hydration and properties of portland cement pastes", Am. Soc. Testing Materials Proc. **46**, 1252–1297 (1946).
2. G. Pickett, "Effect of gypsum content and other factors on shrinkage of concrete prisms", Proc. Am. Concrete Inst. **44**, 149–175 (1947).
3. F. S. Fulton, "A co-ordinated approach to the shrinkage testing of concretes and mortars", Mag. of Concrete Research **13**, No. 39, 133–140 (1961).
4. T. C. Hansen and K. E. C. Nielsen, "Influence of aggregate properties on concrete shrinkage", J. Am. Concrete Inst. **62**, 781–794 (1965).
5. M. A. Swayze, "Discussion on 'Volume changes in concrete,' by R. L'Hermite", Proc. Fourth International Symposium on the Chemistry of Cement **2**, 700–702 (1960).
6. M. A. Swayze, "Volume changes in concrete", Materials, Research and Standards **1**, 700–704 (1961).
7. B. Tremper, "Discussion on 'Volume changes in concrete', by M. A. Swayze", Materials, Research and Standards **1**, 704–708 (1961).
8. "Australian Standard A2–1963 Portland Cement", Standards Association of Australia, Sydney (1963).
9. L. E. Copeland and J. C. Hayes, "Determination of non-evaporable water in hardened portland cement paste", Am. Soc. Testing Materials Bul. **194**, 70–78 (1953).
10. A. D. Ross, "Concrete creep data", The Structural Engineer **15**, No. 8, 314–320 (London 1937).
11. B. Tremper and D. L. Spellman, "Shrinkage of concrete—comparison of laboratory and field performance", Highway Research Record **3**, 30–73 (1963).

Supplementary Paper III-115 On Some Main Aspects of Theory of Solidification and Strength Formation of Cement Stone and Concrete

Ivan Petrowitsch Vyrodov*

Synopsis

The present work deals mainly with a few aspects of the theory of hardening of mineral binding materials. It includes, for example such problems as the applicability of the main principles of molecular physics and thermodynamics to the study of the character and trends of conversion (Chapter 1). In this Chapter the most important principles were determined, that is, the connection between thermodynamic parameters and kinetic parameters of the system: between energy and thermodynamic potential of the process of activation.

In Chapter 2 some works are analyzed, which support the view that the process of hardening of binding materials takes place in a kinetic range. As a result of the analysis of some theoretical and experimental works it is considered that the hardening of binders is a complex process and it takes place (macroscopically) in the diffusional range. Further, it is confirmed that it is impossible to judge from the form of the principal kinetic equation whether the main process takes place in the diffusional, or in the kinetic range. The hardening process is much more complicated, than it could be imagined, judging by these two mutually eliminating conceptions.

In Chapter 3 the existing conceptions on the main aspects of the structure formation theory are critically analysed, and equations for strength of cement stone and concrete are introduced. They are more versatile in comparison with the ones in common use. The conception of ripeness of concrete is specified in connection with changes in strength properties of cement stone and concrete.

Concluding, the present work deals with the prospects of development of general problems of structure formation, that is, with the coagulation processes and with coalescence-cohesion processes. The author works out a cohesion-coalescence mechanism of structure formation resulting in a quantitative theory of hardening of mineral binding substances.

Introduction

The hardening of mineral binders is a very complex process. It takes place in a heterogeneous interaction of original substances and products of interaction. So in working out the quantitative theory of hardening of mineral binders, the use of laws formulated for homogeneous systems results in inadequate quantitative ratios.

Owing to limited space in this work, only a few principles of molecular physics and thermodynamics the most often used by scientists in their studies of heterogeneous systems are pointed out.

There is one peculiarity more, which we should like to point out and to which much attention is paid in this work because of its importance.

As distinct from the theory of coagulation structure formation, the mechanism of which is qualitatively investigated by P. A. Rehbinder and E. E. Segalova, a cohesion-coalescence mechanism of structure formation is presented in this work.

The main motivation for elaboration of this mechanism was as follows:

First, during the crystallisation of the resulting products from the oversaturated solution two processes are quite inevitable: the "distillation" process (coalescence), and the process of direct fluctuative formation of particles of the final product on the bases and inside the volume of solution.

Second, during the crystallising growth of the particles, the cohesive linkage of crystals is also inevitable. In highly oversaturated solutions cohesion results in a formation of so called true contacts, the strength of which, if we do not consider the marginal effects resulting in defective contacts, is similar to the strength of crystals in general.

Third, in highly oversaturated solutions the coagulation as a process of agglutination of particles in

*Krasnodar Polytechnical Institute, Krasnodar, U.S.S.R.

dispersion systems, taking place under the effect of molecular (van-der-Waals) forces, is quite out of question. The coagulation process may occur in systems which allow a very low solubility, where the process of coalescence, of "distillation" of the substrate through the solution does not take place. In the here investigated systems, characterized by a cohesive-coalescent mechanism of hardening, the coagulation as an ante-crystallisation period, is not necessary. It may be supposed that after the disappearance of the coalescent mechanism of crystallisation the coagulation of non-agglutinative crystals will begin to take place. Such supposition is hardly probable as in the formed cage the mobility of these crystals is hardly sufficient for the coagulation mechanism of increase of these particles to take place. But if these effects were present in the final step of the process, their role would be quite negligible in comparison with the principal process of crystallisation, with coalescence.

Taking into consideration the cohesive-coalescent mechanism of hardening of mineral binders, the author elaborates the quantitative theory of appearance of tixotropically irreversible properties of hardening cement pastes, which, unfortunately, is not reflected in the present work.

The present work deals with the actual problems of the theory of hardening and strength formation of cement stone (brick) and concrete, and the groundlessness of some conceptions is proved, which deny the limiting role of diffusion processes in hardening of mineral binders. It is proved, that to elaborate a valuable theory of strength of cement stone and concrete, it is necessary to operate with asymptotic functions of distribution of particles according to their size.

The modern theory of hardening of mineral binders according to the physical-chemical standpoint of P. A. Rehbinder and his co-workers is briefly reviewed and critically analysed in the present work.

Presenting of new formulas of strength of cement stone and concrete, the introduction of the conception of concrete ripeness qualitatively, and of a cohesive-coalescent scheme of hardening of mineral binders, all the above mentioned is to contribute to the development of the modern quantitative physical-chemical theory of hardening of mineral binders.

Chapter 1
On the Possibility of Applying the Main Principles of Molecular Physics and Thermodynamics to the Study of Character of Changes of Mineral Binders

Limitations for Applying the Common Phenomenological Thermodynamics to the Theory of Hardening of Mineral Binders

As it is known, in the fifties of the last century Berthelau formulated the principle, in accordance to which only exothermic reactions take place spontaneously, that is, the reactions which are followed with a decrease of the enthalpy value (thermal content) of the system H. In general case this principle is not adequete. For example some reactions are known where a negative thermal effect takes place (dissolving of salts, etc.). Later it was stated that the thermodynamic potential may be measure of chemical affinity, more exactly, it change. As the thermodynamic (isobaric-isothermic) potential is connected with the enthalpy and entropy S by a known equation (having P and T constant).

$$\Delta Z = \Delta H - T\Delta S, \qquad (1.1)$$

at low temperatures and low values of ΔS it follows from $\Delta Z \approx \Delta H$ and the Berthelau principle takes place. At high temperatures and high values of ΔS this approximated equation is not adequate.

Mathematical calculations of changes of the thermodynamic potential of the system for different types of reactions very often result in negative values of ΔZ. From the standpoint of chemical thermodynamics all these reactions are possible and it appears to some degree that it is possible to consider the reactions having a more negative value ΔZ to be more preferable. However, from the point of view of common thermodynamics it is impossible to predict in this case what variant will be realised. Intuitive assumptions on preferability of reactions with a more pronounced negative value of ΔZ, as it is shown later on, have the same basis as the Berthelau's principle.

The change of the thermodynamic potential for a standard state looks as follows:

$$\Delta Z^{\circ} = -RT \ln K_p, \qquad (1.2)$$

where $K_p = k_1/k_2$, k_i are constants of velocities of chemical (direct and inverse) reactions, $k_i - A_i \exp [-E_i/RT]$ we have:

$$E_1 = E_2 + RT \ln (A_1/A_2), \qquad (1.3)$$

where E_1 and E_2 are energies of activation of endothemic processes respectively. In the works of Polyani, Evans and Semenov it is shown that for many exothermic reactions (radical ones) the following expression is true: $E_2 = A - BQ$, where A and B are some constants, and Q is a thermal effect of the chemical reaction. Generally the values are: $B \approx 0.25$ $A = 11.5$. Substituting for E_2 in the above mentioned equation for E_1 and neglecting the entropic item $RT \ln(A_1/A_2)$, we will have $E_1 \sim C + \Delta Z^\circ$, where C is some new constant which changes within negligible limits. In these cases it is quite true, the reaction with a more negative value of ΔZ° is more preferable. In other words, preferable reactions take place more rapidly in comparison with other reactions.

Let us make one very short, but strict and consistent conclusion, which links the thermodynamic potential of activation with the change of the thermodynamic potential of the system. For this purpose we shall put down in accordance with the theory of transient state, the interaction between the constant of the chemical equilibrium K_p and the constant of equilibrium of the complex K_k:

$$K_p = K_k \frac{(2\pi m_k kT)^{1/2}}{h} \qquad (1.4)$$

Then, taking into consideration, that the constants of the equilibrium of the complex are valid for this equation, we shall put down the similar equation for the constant of the chemical equilibrium:

$$\Delta Z_A = -RT\left[\ln K_k - \ln \frac{\prod\limits_{(i)} a_{ik}}{\prod\limits_{(j)} a_{jk}}\right], \qquad (1.5)$$

and we shall get following formula, which links the thermodynamic potential of the activation system ΔZ_A with the change of the thermodynamic potential of the system ΔZ:

$$\Delta Z_A = \Delta Z - RT\left[\ln \frac{\prod\limits_{(i)} a_i}{\prod\limits_{(j)} a_j} - \ln \frac{\prod\limits_{(i)} a_{ik}}{\prod\limits_{(j)} a_{jk}}\right] + RT \ln \left[\frac{(2\pi m_k kT)^{1/2}}{h}\right] \qquad (1.6)$$

From the equation (1.6) for the standard change of the thermodynamic potential of the activation system we shall obtain the following equation:

$$\Delta Z_A^0 = \Delta Z^0 + RT \ln \left[\frac{(2\pi m_k kT)^{1/2}}{h}\right] \qquad (1.7)$$

The thermodynamic potential of the activation system represents a kinetic character of the system: the more is ΔZ_A^0 the less intensively does the reaction take place, as the constant of the velocity of the chemical reaction is determined by a known equation:

$$K = x \frac{kT}{h} e^{-\Delta Z_A/RT}, \qquad (1.8)$$

which follows from the theory of the transient state. It follows from the equation (1.7) that ΔZ_A^0 is fully determined by the change of the standard value of the thermodynamic potential of the system if the second, or, if the first item is much more than the second item. In this case we consider much more preferable those reactions which have the change of the thermodynamic potential the most negative from possible values of ΔZ^0. Thus the range of application of the principle of preferability of reactions is settled.

To illustrate the formula (1.7) we shall give below some calculations with ΔZ_A^0 for some hydration reactions and the total data are given in a table:

Original compound	ΔZ_1^0 298 ccal/M	Final compound	ΔZ_2^0 298 ccal/M	ΔZ_A^0 298 ccal/M
CaO	144.40	$Ca(OH)_2$	214.33	14.86
MgO	136.13	$Mg(OH)_2$	199.27	21.84
$CaSO_4 0.5H_2O$	342.78	$CaSO_4 \cdot 2H_2O$	429.19	27.12
H_2O	56.69	—	56.69	—
C_2S		$C_2SH_{1.17}$		25.86
C_2S		$C_2SH_{1.17}$		9.60
C_3A		$\frac{1}{2}(C_4AH_{19}) + \frac{1}{2}(AH_3)$		20.04

The given data are confirmed experimentally. It must be noted that the formation of C_4AH_{19} takes place without the energy of activation. In this case we do not take into consideration some peculiarities connected with the presence of the chemical potential gradient, which are favourable for the topochemical process. We must mention among these peculiarities, for example, the surface of the chemical reaction, which leads to the reduction of the surface tention according to the formula

$$\Delta\sigma = M\Delta\mu \qquad (1.9)$$

where $\Delta\sigma$ is a change of the surface tention, $\Delta\mu$ is the change of the chemical potential and M is the value of the surface transfer of the component.

Thus, the symbol ΔZ shows the possibility for the process to take place, and the numerical value of it gives the possibility to state the preferability of reactions (3).

On Applying the Basic Laws of Thermodynamics of Non-Equilibrium Processes To the Theory of Hardening of Mineral Binders.

From the above written it follows that the character of the change of the thermodynamic potential cannot serve as satisfying measure of chemical affinity. For a full description of the process we had a consideration of parameters determining the kinetics of the process. Such parameter which determines the chemical activity of the given transformation is the energy of activation, or, more exactly, the thermodynamic potential of activation: ΔZ_A. The calculation of these values in quantum mechanics is followed with considerable mathematical difficulties and the obtained data are not of high accuracy. Generally, the error of determination of energy of activation is about 20–25%. Consequently, it is quite natural from the part of the scientists in physics and in physical chemistry to try to obtain the correlaton between the energy of activation and the thermodynamic parameters, which reflect the change of state of the systems, what is calculated with much more accuracy than is indicated above.

Before pointing out this correlation it would be necessary to note the time scantiness of methods of phenomenological non-equilibrium thermodynamics, which follows from its linear phenomenological laws.

Its main disadvantage is that it describes the processes only in the neighborhood of their equilibrium state. However, despite of this very strict limitation in some cases we can obtain very valuable information on the process rate "in toto". These are the cases when linear approximations appear to be true with slight errors during the whole process of transformation, that is, when the law of acting masses is taken into consideration.

It may be supposed that the elaboration of methods of non-linear thermodynamics of irreversible processes will considerably enlarge the possibilities of thermodynamics in solving the most important problems of the chemical kinetics. First of all we must verbalize the conditions necessary to solve our problem and then we shall analyze the obtained results.

Let us consider the most simple case of the chemical transformation $I \rightarrow II$, which takes place in a diffusional region and draw a relation for the activation energy process E_A (an experimental value), and also for the thermodynamic potential of the activation process ΔZ_A. As further on for transfer processes we shall use linear phenomenological laws of thermodynamics of irreversible processes, so for the difference of thermodynamic potentials of different states of the system ΔZ in the given case we have an inequality: $\Delta Z \ll RT$, so we shall use the equality $\Delta Z \approx 0$. For sake of simplicity we shall consider only such systems which have the difference of the standard values of thermodynamic potentials of the original and final products $\Delta Z^0 \gg RT$, and the flow of substance ζ_n is stationary in relation to some internal coordinate of the system y.

Taking into consideration all the above mentioned we may take as an example the case of transformation of highly dispersed substance, which leads for E_A to the relation, similar to the known rule of Polyani-Semenov.

Let us present the chemical potential for a mass unit of the system $\mu(y)$ as follows:

$$\mu(y) = \frac{kT}{m} \ln \lambda(y) + \mu^\circ, \tag{1.10}$$

where m is the mass of the particle, y is some internal parmeter of the system, $\lambda(y)$ is the activity of the substance, μ^0 is a standard (true or hypothetic) value of the chemical potential of the substance. The true value of the chemical potential μ^0 is necessary to take for substances which allow a non-limited solubility, and hypothetic values of μ must be taken for such substances which allow only a limited solubility in some ambience where the chemical reaction occurs (transformation).

For the chemical reaction rate $j(y)$ which is proportional to the value of the flow $j_n(y)$ we shall write a phenomenological equation

$$j(y) = -L\frac{\partial \mu(y)}{\partial y} \tag{1.11}$$

Then we shall get from (1.10)and (1.11):

$$j(y) = -\frac{LkT}{m\lambda(y)} \frac{\partial \lambda(y)}{\partial y} \tag{1.12}$$

Introducing the "mobility" $u = L/\lambda$ and the "diffusion" coefficient $D = kTu/m$ according to some internal coordinate y we shall obtain:

$$j(y) = -D\frac{\partial \lambda(y)}{y} \tag{1.13}$$

writing it beforehand (3) in the following form:

$$j(y) = -\frac{LD}{u} \frac{\partial}{\partial y}[e^{\ln \lambda(y)}]\, 1^{-\ln \lambda(y)} \tag{1.14}$$

and multiplying the result by $u/LD \cdot 1^{\ln \lambda(y)}$, after integration by y, we shall get:

$$j = \alpha[1 - e^{-(A-A^0)/RT}] \tag{1.15}$$

where chemical affinities A and A^0 are equal to a difference of thermodynamic potentials: $A = Z_1 - Z_2 = -\Delta Z$, $A^0 = Z_1^0 - Z_2^0 = -\Delta Z^0$

and $$\alpha = \frac{e^{(Z_1 - Z_1^0)/RT}}{\int_1^2 D^{-1}(y)dy}$$

Now we shall draw out the relation for the chemical reaction rate. This reaction occurs in the diffusional region, judging by kinetic considerations.

Let us consider the interaction of the spherical part of the radius S_i, having the mass $m_i = \frac{4}{3}\pi S_i^3 d_0$ where d_0 is the density of the substance of the particle, with a gas·ous or liquid medium. The quantity of the substance dm_i which diffused into solusion during the time dt is so formulated after the first law of Fick:
From that

$$\frac{d\rho_i}{dt} = \frac{D}{d_0}\frac{\partial C}{\partial r}\bigg|_{r=\rho_i} \qquad (1.17)$$

The concentration change rate in the near-to-surface layer is

$$\frac{dC}{dt} = \varphi(K_i, C_\Pi) + D\frac{\partial^2 C}{\partial r^2}\bigg|_{r=\rho_i} \qquad (1.18)$$

After some time the concentration C reached some ultimate value C_Π in the near-to-surface layer. Let the process occur at $C(r = \rho_i) = C_\Pi$. Then from (1.18) we get:

$$D\frac{\partial^2 C}{\partial r^2}\bigg|_{r=\rho_i} = -\varphi(K_i, C_\Pi) \qquad (1.19)$$

From this by integration we get:

$$D\frac{\partial C}{\partial \rho_i} = \varphi(K_i, C_\Pi)\rho_i, \qquad (1.20)$$

as at $\rho_i = 0$ also $\frac{\partial C}{\partial \rho_i} = 0$
Substituting (1.20) into (1.17) we shall obtain:

$$\frac{d\rho_i}{dt} = -\frac{\varphi(K_i, C_\Pi)}{d_0}\rho_i \qquad (1.21)$$

From the evident equation

$$\frac{dm_i}{m_i} = 3\frac{d}{\rho_i} = -3\frac{\varphi(K_i, C_\Pi)}{d_0}dt \qquad (1.22)$$

we shall get:

$$\frac{dm_i}{dt} = -km \qquad (1.23)$$

Introducing some approximated value of the reaction rate constant

$$k = \frac{\sum k_i m_i}{m}, \text{ we shall get:} \qquad (1.24)$$

$$\frac{dm}{dt} = -km,$$

where m is the mass of the substance for a unit of the volume of the system.

Thus the reactions controlled by the diffusion are the reactions of the first order. According to this scheme the oxychloride gypsum and other mineral binders are hardening.

For these systems the time necessary to reach the critical concentration on the surface of hard bodies is about a few seconds.

To describe the character of the system it is necessary to choose the inner coordinate of the system. For this we must choose such a parameter which will reflect rather fully the state of the system and will lead to a single value of the chemical potential $\mu(y)$. If the surface of the particle was determined by a single value of the mass of the reacting substance, we could choose as an inner coordinate a value proportional to the mass of the reagent m or to the surfaces of its particles S_Π. However, it is necessary to take into consideration that during the process of chemical interaction as a result of an invasion of the adsorption active medium into the micropores of the particles, the process of chemical dispersion of the substance occurs too. As a result of two parallel processes we cannot indicate a single value correspondance between m and S_Π. Moreover, opening of new surfaces of the reaction leads to an occurence of an excessive free surface energy, which contributes in addition to the chemical (or thermodynamic) potential of the system. Further, when we have a known m we can determine the quantity of the substance in the solution. Thus, the parameters m and S_Π rather fully describe the state of the system but on the other hand they somewhat synonymously determine the chemical potential of the system. Considering the measure of y, $y = S_\Pi/\Delta m$ should be taken. This choice of the inner coordinate, as it will be shown below, does not contrdaict the conditions in which the laws of linear phenomenological thermodynamics of irreversible processes are valid.

Let us choose some mean value of D and thus suppose that D = const(y). Then

$$j = D\Delta m l^{(Z_1 - Z_1^0)/RT}\left[\frac{1 - e^{-(A - A^0)/RT}}{S}\right] \qquad (1.25)$$

In accordance with (1.24) we get:

$$k = \frac{j}{m} = -\frac{D}{\Delta S_\Pi}e^{(Z_1 - Z_1^0)/RT}(1 - e^{(\Delta Z - \Delta Z^0)/RT}) \qquad (1.26)$$

In accordance with data of the theory of transient state we write the constant of the reaction rate in the following form:

$$K = x\frac{kT}{h}e^{-Z_{\Delta\Pi}/RT} = x\frac{kTe}{h}e^{\Delta S_A/R}e^{-E_A/RT} = Be^{-E_A/RT}, \quad (1.27)$$

where x is the transmission coefficient, $x = 1$. K is the Boltsman's constant, S is the entropy of activation. Considering (1.27) we get the following:

$$-\frac{ekT\Delta S_\Pi}{Dh}e^{-(E_A+Z_1-Z_1^0-TS_A)/RT} = 1 - e^{(\Delta Z-\Delta Z^0)/RT} \quad (1.28)$$

or, as $Z_A = E_A - T\Delta S_A$:

$$e^{(\Delta Z-AZ^0)/RT}\left[1 - \frac{ekT\Delta S_\Pi}{Dh}e^{-(\Delta Z_A-\Delta Z-\Delta Z^0-Z_1-Z_1^0)/RT}\right] = 1 \quad (1.29)$$

Introducing the identifications:

$$Z_2^0 - Z_2 = \Delta Z_2 \qquad Z_1^0 - Z_1 = \Delta Z_1, \quad (1.30)$$

$$\Delta Z - \Delta Z^0 = \Delta Z_{12}, \quad (1.31)$$

instead of (1.29) we obtain:

$$e^{\Delta Z_{12}/RT}\left(1 - \frac{ekT\Delta S_\Pi}{Dh}e^{-(\Delta Z_A-\Delta Z_2)/RT}\right) = 1. \quad (1.32)$$

For a state near to a balanced Z the last equation must be re-written as

$$\Delta Z_A = RT\ln\left[-\frac{ekT\Delta S_\Pi}{Dh}\cdot\frac{e^{\Delta Z_2/RT}}{1 - e^{-\Delta Z_0/RT}}\right] \quad (1.33)$$

Taking into consideration the second equation formulated by us $|\Delta Z^0| \gg RT$, we get the following:

$$E_A = \Delta Z^0 + RT\ln\left[\frac{B\Delta S_\Pi}{Dh}e^{\Delta Z_2/RT}\right] \quad (1.34)$$

Taking for the reactions of the same type the expression $\Delta Z_2 + T\Delta S_A = \alpha\Delta Z^\circ$, where α is some factor, a constant item for the reactions of the same type, and supposing that $\gamma = 1 + \alpha$ we may write the following:

$$E_A = \gamma\Delta Z^0 + RT\ln\frac{-2\Delta D_i nekT}{DhD_i^{-3}}, \quad (1.35)$$

which is valid for the end of the process, when $\Delta Z_2 \approx 0$. In the above equation $S_\Pi = nd^2$, n is the number of reacting particles, d is their mean size, and $D_i = 1/d$ is the dispersion of the substance. This equation links the energy of the activation of the process with the heat of the phase conversion, and with the change of the standard values of thermodynamic potentials. This may be easily seen from the following example. The conditions for the reacting substance are: $|\ln \Delta S_\Pi T/D| \ll |\ln ek/h|$ and the reaction proceeds at temperature of T = 300°K. Then from (1.35) we get:

$$E_A = \gamma\Delta Z^0 + 13.8 \quad (1.36)$$

In the case of limited solubility of at least one of substances of the system instead of the Z^0 it is necessary to take $Z = Z^0 + G$ where G is some constant. Then $\Delta Z_2 + T\Delta S_A = \Delta Z_2^0 - Z_2 + T\Delta S_A = \alpha\Delta Z^0 - G$ and from the equation (1.34) we again get (1. 35 and 1. 36). Lastly it is necessary to note that for systems in which proceed the chemical reactions, linear phenomenological interrelations are carried out near to balanced states. or in conditions where the molecules of reacting substances during the reaction do not alter the Maxwell's distribution by velocities*. (* = It is evident, that as in the theory of transient state, this condition is not necessary). Thus, the obtained values of ΔZ_A characterize the rate of the system approximation to the final equilibrium state or to a state, characterised by an induction period.

On a Directed Change of Properties of Hardening Mineral Binders under the Effect of Surfactants

The directed change of properties of hardening mineral binders with the help of surfactants is one of the main and most difficult tasks of the chemical technology of building materials and concretes. Theoretical investigations here are far behind the actual requirements and successes of the practical branch of this science. Some attempts for creating the prerequisites explaining (but not predicting) the mode of action of surfactants were made by Academician P.A. Rehbinder (see, for example, the last work 4). As in the above mentioned work (4), in the preceding works the central item of the theory is the use of e-theorem of Boltzman for surfactants distributed by volume of liquid and on the surface of the solid.

But, as it was shown in the work (5), the utilization of Boltzman's e-theorem is rather limited. Particularly, it is not applied to heterogenous systems. Aside from the mathematical proof of its inapplicability to these systems which may be found in the thesis, it should be noted that the said inapplicability follows from the physical sense of Boltzman's e-theorem, obtained for gaseous states. The following conditions are necessary. First of all, the equation of state of ideal *gas* is utilised in deduction of the theorem. Uniformity and stability of temperature for the system are supposed, and uniformity of vector field in which the particles of the ideal system are. If at least one of these conditions is not present we do not obtain e-theorem. Thus it may be seen how complex is the problem for real heterogenous systems where vector fields act being

different in the whole volume of the system and not being a single value function of space coordinates.

Even in the most simple case, in the system "solid-liquid" the vector field on the surface of the solid differs from the vector field inside the liquid. Particularly this phenomenon is one of the main objections to the utilisation of e-theorem.

Under the effect of the internal field of isolated liquid and of the external field of gravity the Boltzman's distribution of particles by height really takes place. However, as the solution comes into contact with the adsorption-active medium this distribution is changed as a result of non-equilibrium process leading to the adsorption of the substance from the solution containing a surfactant. Similarly, as the trasformation of mineral binders takes place, the continued alteration of sequence of settling (but not settled) distributions not only inside the volume of the solution but near the surface of the transformated sbustance takes place. The character of the distribution of surfactants determines the rate of substance conversion. On the other hand the surfactants influence the rate of increase of particles of the new phase. The correlation between the dispersion of particles D_i and the rate of change of surface tension σ_i and of particle size l_i is established in the work (5):

$$\frac{\partial \sigma_i}{\partial t} : \frac{\partial l_i}{\partial t} = -\sigma_i D_i \qquad (1.37)$$

A very important conclusion thus follows. The surfactant action itself is not single-valued. When evaluating the action of surfactant it is necessary to consider kinetic particularities of converting substances and the temperature of the system too.

The study of influence of surfactants on dispersibility of forming particles leads to very interesting conclusions.

The relative concentration of additive surfactant C_g to achieve extreme dispercibility value D_i in the field of small D_{i3}, depends upon chemical potential of the additive surfactant:

$$C_g \text{ relative} = \frac{\gamma_0}{\mu_g}, \qquad (1.38)$$

where $\gamma_0 = \text{constant}$. It follows that the greater is the chemical potential of the substance of the additive, the less is portion necessary to obtain the same effect.

In the field of high values D_{i3} we have:

$$C_g = \frac{\gamma_{j0}}{k_j^1}, \qquad (1.39)$$

where

$$\gamma_{j0} = \sum \frac{1_q C_{qj}}{\gamma_j} \frac{\partial \tau_q}{\partial 1_q}; \quad k_j^1 = \rho(T) \qquad (1.40)$$

Thus, in the field of high values of D_{i3} the role of individual properties of surfactants is limited to a character of change of edge tensions determining the effectiveness of surfactant action and it is not dependant on the chemical potential of the additive. Here is the limit of utilisation of main thermodynamic parameters in high-dispersibility phases. The same is for Gibbs-Curie-Wolf principle stating the dependance of the process of crystals growth upon the surface tension of edges. By these parameters, that is, by rates of changes of edge tension and by particle bond energy the extreme strength of hardened binders is determined.

Chapter 2
Role of Diffusion Kinetics of Reactions in the Process of Hardening of Mineral Binders

Some Critique on Studies Denying the Diffusion Mechanism in the Process of Hardening of Mineral Binders

Some works based on the study (6), state that the diffusion kinetics does not limit the process of hardening of the mineral binders.

The conclusions of Shiller (6) are based on comparing two approximately evaluated items: the length of diffusion D path, and the coefficient of diffusion *l*. They are values of one order of smallness. The approximations are made with the exactitude of smallness order equal to 1. Consequently, the comparison of values of the same order of smallness, which are estimated with the same exactitude—one order of smallness—is absolutely senseless.

Moreover, it should be noted that K. Shiller uses the equation which reflects the effect of free diffusion, that is, the self-diffusion of Brown particles, as in reality in this system we see just another diffusion, of another origin, which takes place in the presence of concentration gradient. K. Shiller does not notice this, he substitutes diffusion by the selfdiffusion.

It should also be noted that Einstein's formula is

valid only for some mean value $l - \bar{l}$ (that would be sufficient for non-applicability of the said formula in solving the present problem) and for rather great values of time t. Having these conditions let us consider $t = \Delta t$ and $l = \Delta x$. Then the relation $\Delta t = \Delta x^2/2D$ is a criterion (a condition) of stability in solving the equation of diffusion in final-differential approximation. In this case particularly the Einstein's equation gets a definite interpretation with a diffusion conditioned by a presence of concentration gradients.

The above mentioned is sufficient to prove the K. Shiller's conclusions to be highly unconvincing.

Let us consider another study, which has something common with the conclusion of K. Shiller. This is the work of A. F. Polak (7), where the evaluation of character of the process is based on the Bertrand's formula (2. 75):

$$\xi = \frac{k_1 D}{k_1 \delta + D}(C_\infty - C), \qquad (2.1)$$

which is valid in "mixed" kinetics and is obtained by excluding the concentration of the substance C_x near the surface of the binder from two relations. One of them describes the kinetic field, the other the diffusion field of "dissolving".

Then, this relation is used for recording the Peckle's value:

$$Pe = \frac{k_1}{D/\delta} = \frac{\xi\delta}{D(C_\infty - C) - \xi\delta}, \qquad (2.2)$$

from which supposedly follows that with $Pe \gg 1$ the process is a diffusion one, and with $Pe \ll 1$ the process takes place in the kinetic field. Presenting the evaluation data for this formula A. F. Polak comes to the conclusion that at small oversaturations the process proceeds according to the "mixed" kinetics, and at high oversaturations it goes in the kinetic field. We consider these conclusions to be highly doubtful for following reasons.

Polak's intention to use Peckle's value to solve the above mentioned problem is reasonable. However, in the formula (2.2) the value of rate of loss of the molecule of the binder into the boundary layer:

$$\xi_k = k_1(C_\infty - C_x) \qquad (2.3)$$

and the value of rate of diffusion transport of particles from the boundary layer into the volume of solution:

$$\xi_D = \frac{D}{\delta}(C_x - C). \qquad (2.4)$$

should be used.

Then the Peckle's value would have the form:

$$Pe = \frac{\xi k}{\xi D} = \frac{k_1}{D/\delta}\frac{(C_\infty - C_x)}{(C_x - C)} \qquad (2.5)$$

Particularly this correct formula should be used for estimations rather than the formula (2.2). Using the formula (2.2) the author essentially can not overstep the limits of mixed kinetics as there is one condition in it: $\xi_D = \xi_K$.

On the other hand, excluding the $(C_\infty - C_x)/(C_x - C)$ (2.5) see formula (2.2), Polak records the wrong value for Peckle's number from the very beginning. By force of this second reason it is possible to get very controversing conclusion from the formula (2.2), what is actually characteristic for the work (7).

It is rather important to note the difference between the work (6) and (7). In considering the whole process the work (6) deals only with the stage of crystallisation of new formations, while the work (7) deals with the meachanism of "dissolving" of the binder. It is evident that these one-sided investigations can not be used as criteria in considering what is the scheme of the process.

Substantiation of Diffusion Mechanism of Solidification of Mineral Binders

A rather full substantiation of the diffusion mechanism of solidification of binders is the subject of the works of Ratinov V. B. and his co-workers. Diffusion coefficients and diffusion flows were experimentally obtained in these works. The comparison of diffusion flows with rates of solidification of binders is the first proof for a diffusion mechanism of solidification of binders. My thesis was confirmed with the works of V. B. Ratinov using experiments establishing the dependance of rates of solidification on intensity of blending cement dough and by solving corresponding equations of diffusion as well.

It should be specially noted that the works on diffusion from a mobile boundary gave as a result of using the computers URALS-1 the functions of change of size of particles depending on time. The obtained functions are near to linear. These results are very valuable as they show the limit of utilization of a highly utilized formula:

$$S = (Dt)^{1/2} \qquad (2.6)$$

to determine the coordinate ρ of the moving boundary of the phase conversion limited by diffusion. In our solved marginal problem the exponent at t is near to 1.

On Criterium of Applicability of Molecular Diffusion Equations to Solve More Complicated Problems of Turbulent Diffusion

Let the molecular diffusion coefficient be $D_m \sim v_m l_m$, where v_m is the diffusing particle velocity, l_m is the length of free path of molecule. A similar relation may be written for turbulent diffusion coefficient $D_T \sim v_T l_T$ having in mind that proportional coefficients D_m and D_T are taken into consideration between diffusion flows j and gradients of concentration of substances. v_T is here the mean value of turbulent fluctuation of velocity, being the measur of intensity of turbulence, l_T is the turbulence scale, a value similar to the length of free path, or after Prantle—the path of blending. Molecules moving along the distances $l \leq l_T$ are statistically bound with each other. If the turbulence scale l_T is very small in comparison with the region inside which the diffusion takes place, this turbulent diffusion is called a small scale diffusion, or a gradient diffusion, and its description is similar to that of the molecular diffusion, as in this case it is possible to carry out the condition of proportionality between the flows and concentration gradients of substances, and the processes of diffusion are described apparantly similar differential equations. When there is no continued blending of solidifying cement dough, a molecular diffusion proceeds, in the presence of distributed temperature gradients a turbulent small scale diffusion proceeds too.

But also in the case large scale turbulent diffusion, that is, in the presence of large turbulences the form of differential equations will not change. Only the interpretation of desired functions a parameter of equations will change in this case.

On the Main Kinetic Equation of Solidification of Mineral Binders

As it was already noted, there are two tendencies in our and foreign literature representing the basements for a quantitative theory of solidification of mineral binders.

The first tendency establishes the diffusion mechanism of solidification of mineral binders. According to the second tendency the process of solidification of binders proceeds in the kinetic region. Although the principle difference between the said tendencies is quite evident, it is quite stated in the work (8) that both tendencies are just and valid, as "... the process rate undergoes the general laws of chemical reactions kinetics ...". Naturally, if the process of solidification of binders proceeded in the diffusion region, the consideration of kinetics of chemical reactions from the general positions of physical chemistry would necessarily lead to the differential equation of diffusion. In this sense only it is possible to consider any process whether it proceeds in kinetic or in diffusion region, from general positions of chemical reactions. However, the experimental basements of any mechanism make easy drawing the conclusion of the main kinetic equation of the process of solidification of binders.

Some works may be found sometimes which confirm the second tendency basing on a check of "apriori" kinetic equation of the first order. But it is not difficult to demonstrate that the processes occuring in diffusion region are also described by equations of the first order. Thus and because of this the good confirmation between the theoretical formula and the experiment can not serve as a confirmation of any scheme of solidification of binders.

It is also necessary to note that the works (7) are characterised by numerous constants of the process. It should be borne in mind that the more constants we have the more arbitrariness in the choice of kinetic law, and the more incorrect is the conclusion about the mechanism of solidification of binders.

The process of solidification of binders is a very complicated one. Although in general the process of solidification of binders proceeds in diffusion region (5), some local processes are possible. They proceed in kinetic region. In these cases in some limits the local processes can be descirbed by the law of acting masses.

Before establishing the main kinetic equation according to this law we will consider the change of different forms of water which is present in solidifying binders.

According to our point of view all waters in solidifying concrete may by divided into three categories.

To the first category belongs the chemically bound water, B_{xc}. This is the water of the product of reaction. It includes zeolitic, structural and non-structural water.

The second category includes the sorption-bound water. This is the water adsorbed by the surface of the aggregate B_3 (physical sorption), by the surface of

cement grains $B_{u\partial}$ (chemisorbed water corresponding to pre-reactional period), and also water contained in the capillaries and micropores of product of hardening and of aggregate $B_{K\Pi}$.

The third category includes the free water into which come the dissociation products of new formations: B_c.

Such distribution is based on the principle of consideration of binding forces of water with solids contained in concrete mixtures, as the rate of activity of water to trasformations occuring in concrete depends on these bonds.

To put down the relation for the chemical reaction rate it is necessary to consider that in accordance with the law of acting masses the rate of change of the reaction product depends on the quantity of collisions of active molecules having the possibility to interact. Such molecules are the molecules of water $B_ц$ and the cement grain molecules on the surface of the grains, that is the active moecules of cement $Ц_a$. It may be seen that the reaction rate will not depend on B_c, even though how large this value would have been changed. Although B_c is not included into the law of acting masses it should be borne in mind that during the transport of reäction products inside the free water the rate of transport will depend on volume of this water. If the process is purely topochemical and the reaction products are left on the surface of the grains the water B_c does not affect the transformation rate. The principal mistake of the author of the work (8) is that while establishing the main kinetic equation is included in the active water.

Thus in accordance with the law of acting masses we have:

$$v = \frac{\partial m}{\partial t} = k B_ц^m Ц_A^n \qquad (2.7)$$

where m is the mass of reaction product.

$$m = B_x + \alpha B_x = (1 + \alpha) B_x \qquad (2.8)$$

Here α is stechiometric coefficient equal to the relation of mass of waterless part of reaction product to the mass of in it contained chemically bound water.

From equations (2.7) and (2.8) we have:

$$\frac{\partial B_x}{\partial t} = \frac{k}{1 + \alpha} B_ц^m Ц_A^n \qquad (2.9)$$

This equation essentially differs from that obtained in the work(8), representing the main equation in the theory of heat emission of concrete.

The values $B_ц$ and $Ц_A$ are proportional to the specific surface of the binder S, so we have:

$$B_ц^m Ц_A^n = \beta S^{m+n} \qquad (2.10)$$

Carrying out the integration in (2.9) with a consideration of (2.10) we get:

$$B_x = \frac{\beta}{1 + \alpha} \int_\partial^t k(t) S^{m+n}(t) dt \qquad (2.11)$$

It is possible to make the final integration of (2.11) only if we know the position in time of "constant" of chemical reaction rate $k(t)$ and $S(t)$. The introduction of system model is necessary at this stage.

In the work (5) is shown, that if the process is limited by diffusion, then having a rather large quantity of particles in a unit of volume their size will decrease linearly with the time. In this case

$$S = \sum S_i = \sum 4\pi R_i^2 = 4\pi(\bar{R}_0 - \gamma_1 t)^2 \qquad (2.12)$$

When the quantity of particles in the unit of volume is not high:

$$S = 4\pi(R_0 - \gamma_2 t) \qquad (2.13)$$

For a general case we may write:

$$S = S_0(1 - \gamma t)^\mu \qquad (2.14)$$

where μ may be any number.

Substituting (2.14) into (2.11) and taking into consideration that the process is almost isothermic we will get:

$$B_x = \frac{B k S_0}{1 + \alpha} \int_0^t (1 - \gamma t)^{\mu(m+n)} dt = \frac{C}{r}[1 - (1 - \gamma t)^r], \qquad (2.15)$$

where

$$C = \frac{B k S_0}{\gamma(1 + \gamma)}, \qquad (2.16)$$

$$r = \mu(m + n) + 1 \qquad (2.17)$$

As at the end of the process

$$B_{xk} = B - B_3 - B_{k\Pi} = \frac{C}{r}, \qquad (2.18)$$

instead of (2.15) we get

$$B_x = B_{xk}[1 - (1 - \gamma t)^r] \qquad (2.19)$$

As $B_x \sim m$, this equation represent not only the equation of hydration but also the main kinetic equation reflecting the transformation rate in general.

If we took, that the process took place not in the diffusion region, we would get another equation for specific surface of substance, and, consequently, another kinetic equation.

Let us suppose now, that in the process of transformation of original substance some part of its surface is permanently screened by products of reaction. If the constant of screening is not changed with time the kinetic equation will not change either. If the constant of screening changes with time the kinetic equation will change too.

It is necessary to note, that the form of kinetic equation is influenced not only by time dependance of specific surface of original binder, but also by time dependance of "constant" of reaction rate. In case of limiting role of diffusion this constant includes directly the diffusion coefficient and the degree of influence of volume of solving water B_c. As in case of diffusion mechanism the consideration of screening is quite necessary in the kinetic region. In both cases the consideration of sc eening does not influence the character of transformation, that is, the process being in diffusion region does transfer into kinetic region with the change of screening constant. On the other hand, the introduction of different constants(8) representing the physical sense of the character of the process does not give the possibility to reveal the nature of any of the processes. (This must be more detailed. The formation of solid surface films surely prevents the transportation and later on the chemical interaction of reagents. From this point of view the process macroscopically must be transferred from kinetic into the diffusion region. So, if the films representing the products of new formations are semi-permeable, the process can take place macroscopically in diffusion region or in the region of mixed kinetics. The character of interaction of original substances "in pure state" /"in nascent state"/is not changed.)

We may finish here the evaluation of the main kinetic equation. Finally, the most natural is the supposition that the "acting" surface (that is, not screened part of the surface) is proportional to whole surface. Thus it should be considered that the form of the principal kinetic equation (2.19) is not changed even if considering the screening effect. (We mean the case of practically impermeable films).

Let us now consider the case when the solidification of concrete is limited within the kinetic region. In this case $S = l(B_x)$. In fact:

$$\frac{4}{3}\pi(R_{0i}^3 - R_i^3) = kB_x \tag{2.20}$$

It is not difficult to obtain the following equation from the above equation for sherical particles:

$$S_i = S_{0i}\left(1 - \frac{B_{xi}}{B_{kxi}}\right)^{\frac{2}{3}} \tag{2.21}$$

For a poly-disperse substance and for a particle of random shape we get:

$$S = S_0\left(1 - \frac{B_x}{B_{kx}}\right)^{\nu}, \tag{2.22}$$

where ν is so far an uncertain number.

Considering (2.9) (2.10) we get:

$$\frac{\partial B_x}{\partial t} = \frac{K_\beta S_0}{1+\alpha}\left(1 - \frac{B_x}{B_{kx}}\right)^{N}, \tag{2.23}$$

where $N = (1 + n)\nu$. After integration of this equation with a constant K we get:

$$\left(1 - \frac{B_x}{B_{kx}}\right)^{-N+1} = 1 + \frac{K_\beta S_0}{1+\alpha}(N-1)B_{kx}t \tag{2.24}$$

or

$$B_x = B_{kx}[1 - (1 + \gamma_3 t)^{1/(N-1)}] \tag{2.25}$$

Using the denominations $B_{kx}(N-1)\gamma_2 = \gamma_3$ and $N - 1 = q$ we get the principal kinetic equation in the following form:

$$B_x = B_{kx}[1 - (1 + \gamma_3 t)^{-q^{-1}}] \tag{2.26}$$

The form of this equation is similar to the one of (2.19). Moreover at $N < 1$ and $r > 0$ these equations are analogous in the sense of their application to the description of the given process. We got this at first glance paradox conclusion because at the diffusion and "kinetic" mechanism of solidification of concrete the hydration rate is directly proportional to the specific surface S^N of the binding substance. In the first case the diffusion meehanism influences the character of dependance $S(t)$, and the value of N. Just the same we have in the case of the process occuring in the kinetic region.

The equations (2.19) and (2.26) can be used to study heat emission regularities. Taking into consideration that heat emission of concrete is ruled by the hydration process (not bearing in mind other transformations) we get:

$$Q = \alpha_0 B_x, \tag{2.27}$$

where α_0 is a coefficient.

The equations (2.19) and (2.26) can be used to determine the hydration degree K_r after the formula

$$K_r = \frac{B_x}{B_{kx}}. \tag{2.28}$$

The constants (parameters) of equations (2.19) and (2.26) are determined after the kinetic curves.

Chapter 3
On Some Principal Aspects of the Theory of Solidification and Strength Formation of Cement Stone And Concrete

Establishing of the Formula of Strength of Solidifying Pastes

In accordance with the data obtained in (21), the strength of the solidifying paste may be expressed in the following way:

$$R = \frac{9}{4d^2}\sum n_{ik}f_{ik} \tag{3.1}$$

where f_{ik} are forces of bonds between i-and k-ions of two different particles, n_{ik} is the density of saturating valence bonds determined by the structure of the substance, d is the mean size of the particles. With a rather good accuracy we may write:

$$\sum n_{ik}f_{ik} = f_{цц}(n_{цц} + \alpha_{цц}), \tag{3.2}$$

where $f_{цц}$ are forces generated by atoms of cement and $f_{\sigma ц}$ are forces of bonds appearing as the result of interaction of molecules of water with the atoms of cement.

As $n_{цц}$ and $n_{\sigma ц}$ are proportional to the mass of reacted substance m:

$$m = m_k(1 - e^{-kt}) \tag{3.3}$$

where k is the constant of rate of transformation, m_k is the mass of solidified product. Then the quantity of contacts and the quantity of bonds are proportional to the following item:

$$n_{цц} \sim m Ц^2; \qquad n_{\sigma ц} \sim m B Ц. \tag{3.4}$$

where B and Ц correspond to the total quantities of masses of water and cement respectively. Taking also into consideration the interval of concentrations, for which $d \sim B$, we get:

$$R \sim \frac{9}{4R^2}m_k(1 - e^{-kt})(Ц^2 + \alpha B Ц), \tag{3.5}$$

$$R = A(1 - e^{-kt})\left(\frac{Ц}{B}\right)\left(\alpha + \frac{Ц}{B}\right) \tag{3.6}$$

Thus we got a very important formula, which connects the strength of solidifying cement paste with the water-cement ratio, constant of transformation rate and the time of solidification. In the limit of a rather large time (for examble, after the Standard, for 28 days) the exponential member appears to be very small and we obtain the formula 31 in the work (21).

The obtained formula gives some perspectives to consider the dependance of strength of solidifying pastes on reduction effects, (shrinkage effects).

On Some Factors Influencing the Strength of Cement Stone and Concrete

On the preceding pages we considered the dependance of strength of solidifying cement stone and concrete R on time and water-cement ratio. This dependance is obtained by us in the form (3.6) where

$$A = R_k\left\{\left(\frac{Ц}{B}\right)_k\left[\alpha + \left(\frac{Ц}{B}\right)_k\right]\right\}^{-1} \tag{3.7}$$

Here the item "k" at B and Ц/B corresponds to the final values.

If in the process of concrete solidification (or cement) the ratio Ц/B is constant, that is, if $Ц/B = (Ц/B)_k$, the strength of concrete is expressed by a simple equation:

$$R = R_k(1 - e^{-kt}) \tag{3.8}$$

From here for difference $R_k - R = \Delta R$ we get:

$$\Delta R = R_k e^{-kt} \tag{3.9}$$

In accordance with existing standards $R_k = R_{28}$ If in the process of solidification the warer-cement ratio changes, then for ΔR a simple exponential dependance of type (3.9) will not be obtained.

In fact, if we denominate $Ц/B = x$, we shall get utilising (3.6) and (3.7) the following equation:

$$R = R_k\frac{x(\alpha + x)}{x_k(\alpha + x_k)}(1 - e^{-kt}) \tag{3.10}$$

From here

$$\Delta R = R_k\left[1 - \frac{x(\alpha + x)}{X_k(\alpha + x_k)}(1 - e^{-kt})\right] \tag{3.11}$$

From this relation we can establish the connection between x_0 and t_0 corresponding to relative extremes: on the strength curve $R(t)$. The knowledge of this connection is very important as with its help we can determine beforehand the moment in time during which it is necessary to introduce the corresponding intensification of the process (vibration, ultrasonic processing of concrete mixtures and so on) to eliminate the time loss of strength of concrete. We shall analyse the presence of the said connection only for a simpliest case.

Let us take the variation $\delta R = 0$ for variables x and t. Utilising (3.10) we get:

$$(\alpha + 2x_0)(1 - e^{-kt})\delta x + kx_0(\alpha + x_0)e^{-kt}\delta t = 0 \qquad (3.12)$$

From here

$$\frac{\delta x}{\delta t} = \frac{kx_0(\alpha + x_0)}{\alpha + 2x_0}\left(\frac{1}{1 - e^{kt_0}}\right) \qquad (3.13)$$

As by time the surface of the binder for a range of concrete mixtures increases linearly, so supposing we get:

$$\mu = \frac{kx_0(\alpha + x_0)}{\alpha + 2x_0}\left(\frac{1}{1 - e^{kt_0}}\right) \qquad (3.14)$$

From here

$$t_0 = \frac{1}{k}\ln\left[1 - \frac{kx_0(\alpha + x_0)}{\mu(\alpha + 2x_0)}\right] \qquad (3.15)$$

Considering that $\mu = \frac{x}{t} = \frac{x_0}{t_0} = \frac{x_k}{t_k}$ we re-write this expression in the form:

$$t_0 = \frac{1}{k}\ln\left[1 - \frac{kt_k\left[\alpha\frac{t_0}{t_k} + xk\left(\frac{t_0}{t_k}\right)^2\right]}{\alpha + 2x_k\frac{t_0}{t_k}}\right] \qquad (3.16)$$

Thus we have got a transcendent equation to determine t_0. If the curve of increase of strength is monotonous, that is, does not include relative extremes, then $t_0 = t_k$ and the expression (3.16) can be utilised to determine the constant α:

$$\alpha = x_k\left[1 + \frac{e^{kt_k} - 1}{e^{kt_k} - 1 + tk_k}\right] \qquad (3.17)$$

At $t_k \to \infty$ from (3.16) we obtain the following expression to determine t_0:

$$kt_0 = \ln(1 - kt_0) \qquad (3.18)$$

The solution of this equation (besides the above given) is the only one: $t_0 = 0$. From here follows, that at a linear change x the curve $R(t)$ increases monotonously. The change on monotonous character is thus determined by a change of x from linear interrelation $x = \mu t$, or from the interrelation $x = x_k$.

To find t_0 in a case of more complicated dependance $x(t)$ it is necessary to analyse the original products in the process of solidification of concrete.

This analysis can be done with the help of X-ray study of the solidifying dough.

The Concrete Age

With the help of the formula (3.8) it is possible to introduce the necessary notion of concrete age in the theory and practice of binders technology. In accordance with (30, 31) the concrete age is determined by a number equal to product of age by the temperature of solidification. If we consider the concrete age from the point of view of its approaching to a certain utmost state, then the most convenient property to determine the concrete age is the value ΔR. Let ΔR_{tn} and ΔR_t correspond some standard deviation and current deviation of strength. Generally $\Delta R \to 0$ at $t \to \infty$. However the state of $\Delta R = 0$ as a result of inevitable errors of measuring and smallness of ΔR will appear far more early. So we can consider the end of the process as some moment of time t_n, and the value corresponding to ΔR_{tn} we may consider as a standard value for the given type of binder and concrete. Then taking the concrete age in the form:

$$\mathscr{Z} = \frac{\Delta R_{tn}}{\Delta R_t} = e^{k(t_n - t)} \qquad (3.19)$$

we see, that the age of concrete is evaluated in parts of 1 and can not exceed it: $0 \leq \mathscr{Z} \leq 1$. From the last expression it is possible to calculate beforehand the time left to concrete to reach the full ripeness, if we have beforehand the admissible value of age $\mathscr{Z}_g$:

$$\Delta t_g = -\frac{1}{k}\ln \mathscr{Z}_g. \qquad (3.20)$$

In case if the solidification of concrete occurs at different temperature conditions the value k will be variable and to determine the concrete age (ripeness) it is necessary to use statistical methods.

Let $\bar{k}$ be the mean value of the "constant" of the process of solidification of concrete. Then the age may be introduced for each period of time within the limits of which k_i is constant according to the formula:

$$\mathscr{Z}_i = \frac{\Delta R_{tn}}{\Delta R_{ti}} = e^{-kt_n + (kt)_i} \qquad (3.21)$$

From here we may get the age of concrete as an arithmetic mean from the values of ripeness for each period:

$$\mathscr{Z} \approx \bar{\mathscr{Z}} = \frac{1}{n}\sum_{i=1}^{n}\mathscr{Z}_i = \frac{e^{-kt_n}}{n}\sum_{i=1}^{n}l^{(kt)_i} \qquad (3.22)$$

Using this expression it is possible to obtain the expression for some mean value of time left to reach the total ripeness at some mean value of ripeness given beforehand:

$$\bar{\mathscr{Z}}_g \approx \mathscr{Z}_g;\ \Delta\bar{t}_g = -\frac{1}{k}\ln \bar{\mathscr{Z}}_g$$

In comparison with in (30, 31) introduced term of age (ripeness), the term age, given by us, is somewhat absolute (28) and includes a certain physical sense. Using (3.2) it is possible to write the following generalised expression for concrete age:

$$\bar{\mathscr{Z}} = l^{-kt_n} \sum_{i=1}^{n} \frac{1}{1 - \frac{x_i(\alpha + x_i)}{x_n(\alpha + x_n)}(1 - e^{-(\bar{k}t)_i})} \quad (3.23)$$

where $x_i(t)$ is known function for the given type of concrete. Finally, it should be said that we have calculated the approximated value of $\alpha \approx 2x_k$ in the given work, and have noted the uncertainties for the expression (3.9), and also the reasons for temporary loss of strength of concrete. We have proposed universal expressions for determination of concrete age.

Diffusion Mechanism to Determine the Functions of Distribution of Particles by Size and the Solution of the Main Problem of the Theory of Strength.

As it is known the statistical theories of strength of Veibull, Kontorova and Frenkel give the possibility to explain the difference between the theoretical strengths of crystal grids of substances and their technical strengths.

However these theories have some important disadvantages, namely that they use some original formulae without serious physical basements.

Thus, in accordance with the most strictly phyisical-based physically theory of Kontorova and Frenkel (32) the mean value of strength F_{xp} is calculated from the expression:

$$\frac{\partial P(F_{xp})}{\partial F_{xp}} = \frac{\bar{n}V[P(F_{xp})]^2}{\int_{F_{xp}}^{\infty} P(F)dF}, \quad (7)$$

where $\bar{n}$ is the mean number of defects in the unit of the volume of the sample, V is the acting volume of the sample, P(F) is the function of distribution of defects by their danger in the sense of strength. In their works Kontorova and Frenkel used the normal law of distribution for the function of danger. This leads to some false conclusions from the theory in general. Chechulin (33) used the function of distribution of Pearson of the third type as the function of danger, although there is no physical basement for such utilization either. It is evident that the function of distribution of the defects by their danger for strength must correlate with the function of pores distribution or of cracks by sizes. In fact if some samples are made which have certain definite sizes of pores (or cracks), it is quite evident that the sample having more defects will be less strong.

The utilization of asymptotic functions of distribution of particles (or pores) by size, formed as a result of a continued diffusion breakdown of oversaturated solutions gives the possibility to base the choice of function of danger. Besides, the utilisation of asymptotic distributions of particles by sizes gives the possibility to elaborate a theory of strength having a sufficient basing its main positions.

The problem of considering the functions of distribution of particles by size must be a central item of scientific technology of cements and concretes.

There are only a few works on this subject so far, as the finding of functions of distribution is connected with considerable mathematical difficulties (34).

It was proposed in the work (35) to establish the functions of distribution of particles by size with the help of data of X-ray small angle method. This is more detailed in work (2).

Conclusions

The analysis of modern physical and chemical views on the theory of solidification of mineral binders, showed that the attempts to ignore the main physical and chemical properties of binders and the attempts to elaborate a modern theory of solidification of mineral binders only on the basement of qualitative non-single interpretations of some experimental curves having a very limited information lead to false impression about the modernisation of actual views in the theory of solidification of mineral binders, and in the theory of obtaining the strength of cement concrete.

Directed changes of the processes of solidification of concretes unfortunately have not so far scientifically basement. However, they can be explained (not solely, or hypothetically) only after some experimental statements.

It would be unreasonable to wish more on a present state of knowledge of these very complex phenomena. However, according to modern state of sciences, of physics, chemistry, mathematics and engineering

there are some possibilities to elaborate such theory. After all, there is a possibility to review the information contained in text books on some monomineral binders, for example, as manganese binders, the solidification processes of which are studied rather thoroughly (36).

It is also necessary that specialists of different branches of science collaborate for sake of establishment of this theory.

The critical analysis of main positions of modern physical and chemical theory of solidification of mineral binders of P. A. Rehbinder and his co-workers was necessary not because we consider their view not correct and new scientific and more adequate views must be confronted with theirs, but also because of following considerations.

Although the author published some critical remarks on main positions of the said modern physical and chemical theory of solidification of mineral binders, some foreign authors (37–39) consider these main positions to be theoretical basements of the "Russian scientific school", disregarding the fact that they are supported mainly by P. A. Rehbinder and his co-workers, (see work 38 at page 289). Proceeding with the critical analysis of the main experimental works of P. A. Rehbinder and his co-workers which are the basements of their theoretical views the said foreign authors (9, 38) give as examples contradictory experimental results, not those given and obtained by P. A. Rehbinder and his co-workers. For example, such is the position with experimental data on the change of the specific surface of the original mineral binder in the process of its solidification, and so on.

Thus the second task with which the author is confronted is to clear up the situation, which characterises the false views abroad concerning the achievements of the Soviet science and which lower the Russian scientific thought to the views of P. A. Rehbinder and his co-workers.

Some foreign and Soviet scientists share the false impression that P. A. Rehbinder and his co-workers continue the main hypothesis of Baikov (37) in their theory of solidification of mineral binders. It is a false impression and it could be easily clarified only with a single sentence from the second column of the main theoretical work of E. E. Segalova and P. A. Rehbinder (10), directed against the topochemical scheme of A. A. Baikov. This could be understood, as theoretical positions of P. A. Rehbinder and his co-workers are based on the "through-solution" mechanism of solidification of mineral binders.

In accordance with the through-solution mechanism of Le Chatellier the crystallisation of new formations occurs only from the solution.

A. A. Baikov divided the process into three periods:

1. Dissolving of the original mineral binder with the formation of an oversaturated solution as a result of that.

2. Colloidation, that is the formation by the chemical reaction on the surface of the binder of smallest particles of the final product sponsoring the formation of high oversaturations;

3. Crystallisation of amorphous gels.

These conceptions are seemed to be established in Soviet and foreign scientists. Very often the arguments for any of the conceptions are purely qualitative, while the main positions of the theory of solidification of mineral binders after A. A. Baikov (39), which are not very well known among foreign scientists, are falsely interpretated. Evidently, this happened because of publications where the Baikov's theory was denominated as a result of synthesis based on main positions of Le Chatellier and Michaelis. Such denomination is not correct, because the most valuable in the theory of A. A. Baikov is that view, in which it differs from the views of Le Chatellier and Michaelis on the scheme of solidification of mineral binders. The Baikov's theory continues the idea of Baikov about the permanent topochemical process occuring in solidification of mineral binders. This point differs it from the point of view of Le Chatellier and Michaelis.

The supporters of Le Chatellier's conception include D. Bernal (40) and other foreign scientists. In the work (40) it is stated that "the mechanism of solidification of silicates . . . confirms with the present knowledge on gypsum solutions . ." which are obtained ". . by dissolving a highly more soluble semi-hydrate $CaSO_4 \cdot 0.5H_2O$ . .". If this really occurs in this way, the author would like to see the experimental and theoretical basements of these conceptions made by D. Bernal and his colleagues.

We consider that the reference to the mechanism of solidification of gypsum is not valid, as the works of the author showed (17) that the crystals of dihydrate gypsum are formed in the system in the period before the maximum of oversaturation of the solution. In such cases, when the original substance chemically interacts with the liquid medium it is quite senseless to speak about the solubility of the substance.

Brunauer and Grinberg (9) point out that the mechanism of dissolving of the original mineral binder is not the single possible, but the topochemical process is possible too. As it was shown in the works (9, 41), the reactions on the surface are possible in the absence of the liquid phase, they occur as a result of interaction of the binder with the vapour of this phase.

Describing the "through-solution" mechanism, the authors (9) use some rather primitive standpoints. For example, at page 153 of the Russian translation of the works of the 4th International Congress on the chemistry of cement they write that the invaded into the liquid medium ions form the molecules, "the molecules form embryos, which grow up to colloidal sizes, the colloidal particles are sedimented from the solution and coagulate".

Here are the main objections to the above mentioned.

1. All the authors do not worry about the proofs of the mechanism of dissolving of original binder from the positions of thermodynamics and kinetics.

2. In the presence of oversaturated solutions do not all embryos grow. Part of them breaks down as a result of the mechanism of coalescence (after-critical particles "eat out" the pre-critical particles) during the permanently changing critical size of the particles. Thus the selection of regions of the fast formation of embryos and of crystals growth is rather artificial. The growth of crystals from dispersions occurs in the whole interval of concentrations over that one of saturation. Establishing the quantitative theory of the processes of solidification of cements without this character of the mechanism of solidification is quite impossible.

3. The coagulation process of particles is not typical at crystallisation from oversaturated solutions. Crystallisation at the presence of coalescence process leads to cohesion. This cohesive process of formation of the network of solidifying dough is well pronounced, and the more it is pronounced when the oversaturation of the solution and the time of oversaturation state of the system are larger. The mechanism of coagulation structure formation is possible only in the cases when the substances are low soluble and do not create visible oversaturations. In that case the rate of growth of crystals is very little and the diffusion collision of colloidal particles may lead to a formation of coagulation-van-der-Waals' bonds.

An illustration of the effect of van der Waals' bonds were the experiments of Chernin (43), who proved that the mixture of 100 g of well ground quartz sand (up to the specific surface 2 sq. meters) and of 20 g of water can withstand a load (when formed) up to 10 kg. This case is typical for low soluble substances.

If in slightly oversaturated solutions van der Waals' bonds are formed, then later, due to introduction of ions into the near-contact region in the oversaturated solution, there happens a lack of contacts originally possessing the van der Waals' bonds. Our electron-microscopic studies (44) proved that the character of this lack of contacts is determined by properties of the surfactant additives intoduced into the system. The more intensive this process of lack of contacts is, the more is the oversaturated solution. The typical binder for these conditions is the semi-hydrate gypsum.

The described mechanism of occurence of cohesion (chemical) bonds shows the methods for considering van der Waals and cohesion bonds from the quantitative point of view. These considerations are rather important. They admit the possibility of counter opposition of two different conceptions on the nature of bonds and about their role in the process of solidification of the binder at different steps of solidification of binders.

From the standpoint of cohesion-coalescence scheme of which the present author is a supporter, the effects of tixotropy are explained by a small quantity of cohesion bonds in the systems admitting the high solubility of reaction products and semi-products.

There is one consideration more in the work (38). "It is possible that the earliest reactions occur by means of dissolving and sedimentation, while the later hydration is controlled by diffusion and is near to the processes of solid phase type" (p. 290).

This statement contradicts the elegant experiments conducted in the work (45). They show that the products of the topochemical reaction on the grain surface of elyte cement were formed in the first minutes of interaction of the binder with water ($t = 5$ min).

As topochemical processes are thermodynamically more profitable in comparison with the processes of dissolving (as from the data of the work 46), we may consider that the local processes of dissolving in the systems may occur only in the presence of activating effect of heat emitted at topochemical reactions. This effect is the main process, the acting force of the mechanism of interaction of the binder with the liquid medium. Particularly by these by-effects and by dissolving of the products and semi-products it is possible to explain the crystallisation of new formed products beyond the limits of particles of the original binder. The alternative solution of the problem—what is the mechanism of solidification of binders—is possible only from the positions of adequate quantitative theory.

In accordance with our views based on experimental and theoretical data of the scheme of A. A. Baikov, the main, principal item is correct and it represents the motivating force of the process—that is the presence of topochemical reactions. And concerning the content of the stages, the periods of solidification, they are radically reviewed in our scheme.

Taking into consideration the material presented in

the D. Ch.'s Thesis (5) and in the paragraph I of the chapter III of the present communication it is possible to divide the mechanism of solidification of binders into three main processes:

1. Dissolving of hydrates of the products and semi-products of chemical interaction of binder with the liquid active medium.

2. Formation of crystalline products and semi-products on the surface of the binder in the period after settling of the concentration of the system, and of the utmost level of saturation, corresponding to the mean sizes of particles of new formations.

3. Process of crystallisation of new formations.

All the three above mentioned process may occur at the same periods of time.

We must detail the 3rd item of our scheme. It should be borne in mind that the process of crystallisation occurs at the expence of coalescence (distillation). The crystallisation occurs at the expence of direct intergrowth of formed crystals of new formations on the surface of original binder and the inner volume of solution. These both processes are interconnected. Mainly, at the crystallisation there happens the *selection* (thermodynamically) of more resistant, stable in the given conditions crystals of the final product as a result of dissolving of less stable particles of semi-products. As a result of this some surfaces are freed and serve as suppliers of new particles capable to intergrow to a distillation depending on defect degree and on the size. Crystallisation occurs due to a fluctuation formation of new particles on the surface of old particles containing the centers of embryo-formation. The rate of appearance of these particles is determined by the oversaturation rate of the solution and surface state of embryo-forming centers.

A. A. Baikov considered that the third period occuring in the solid phase represents the re-crystallisation of the amorphous jelly. Our X-rays graphic studies of the products of solidification of Cl-and sulphate-manganese cement, gypsum and other binders showed that the crystalline products are formed from the very beginning of interaction of the binder with the liquid medium. We stated also that at certain conditions which are not common to the processes of solidification in the products of solidification of some binders some amorphous phases can appear.

In accordance with the above presented scheme of solidification of mineral binders the main points of theory are determined. They include the compiling and solving of the equations which describe the kinetics of interaction between the liquid medium and the binder, and of equations which describe the presented mechanisms of crystallisation: coalescence, cohesion and fluctuation. The detailed study of the coalescence process makes possible to establish the distribution of particles of new formations by size at the moment of loss of flowing capacity of the mass, that is, by the moment of appearance of tixotrophically irreversible structures. While deducing the functions of distribution it is necessary to introduce corresponding corrections for fluctuation and cohesion mechanisms of particles growth. It is quite clear, that from the practical point of view very important moment of loss of tixotrophic reversible properties will be determined as by means of the total quantity of particles, as by the form of function of distribution of particles by sizes. The more shifted the maximum of this function is towards the smaller particles, the more uniformly will the particles be distributed for cohesion interaction and consequently, the more percentage of cohesion bonds will form in the unit of the volume of mass at the given moment of time.

The process of interaction of mineral binders leads to the formation of lyophilic dispersoidal systems, where the coagulation properties are pronouncedly weak, and we cannot use the rule of Schultz-Hardy in connection with them. Having such a low specific weight, we see that coagulation is governed by processes which correspond to the third item of our scheme of solidification of mineral binders. The study of these problems will contribute to the possibility of controlling the processes of solidification of mineral binders to obtain the desired properties of the products of their solidification. To these questions, to the main points of the theory of solidification of mineral binders predicting some prospective discoveries in the future is dedicated the D. Ch.'s thesis of the author (5).

In the present paper some details are considered. They include the cohesion-coalescence mechanism of solidification of mineral binders proposed by the author (5). Thus we see that our approach to the development of the theory of strength of concrete, being substantially semi-phenomenological, leads us to theoretical basement of well known empirical equations, which connect the strength of concrete with the water-cement ratio. As a result of our theoretical studies it became possible to clear up the physical sense of the parameters, which are part of these equations, and to establish the limits of utilization of the said equations. We consider that the establishment of the theory of solidification and of strength is an infinite process. But we show the way and we consider it right as it conforms to the experiment and has no controversies in itself.

References

1. S. de Groot and P. Mazur, Non-equilibrium thermodynamics. MIR Edition, 1964.
2. A. A. Zuchovitsky, V. A. Grigoryan and E. Michalik, Surface effect of the chemical process. DAN SSSR, 1964, 155, 392–394.
3. I. P. Vyrodov, Establishing of the direction of the process on the surface of binder by means of thermodynamic calculations. KAI Proceedings, Krasnodar, II, 39, 15–24, 1963.
4. P. A. Rehbinder, Surface and volume properties of solutions of surfactants. ZVHO Mendeleyev, XI, 4, 362–368, 1966.
5. I. P. Vyrodov, On some aspects of physics and chemistry of heterogenous systems with application to mineral binders. Abstract of the thesis of Docotor dissertation of Chemistry, Kharkov, 1964.
6. K. Schiller, Mechanism of re-crystallisation in calcium sulphate semihydrate plasters. J. Appl. Chem., 12, 135, 1962.
7. A. F. Polak, Solidification of monomineral binders. Strojezdat, Moscow, 1966.
8. I. P. Vyrodov, Some main problems of diffusion kinetics and their solution by means of integral formulations (unpublished); 1965.
9. S. Brunauer and S. A. Grinberg, Hydration of 3-Ca and β–Ca silicate at room temperature. 4th International Symposium on the Chemistry of Cement. Strojizdat, Moscow. 123–158, 1964.
10. E. E. Segalova and P. A. Rehbinder, Modern physical and chemical views on the processes of solidification of mineral binders. Stroitelniye Materialy, 21–25, 1960.
11. I. P. Vyrodov, Establishing of functions of distribution of particles by size and solution of the main problem of the theory of strength. Supplementary paper on the V Int. Symposium on the Chemistry of Cement.
12. E. D. Shtchukin and P. A. Rehbinder, Formation of new surfaces in deformation and breakdown of a solid in a surface active medium. Colloid. J. Journ. 5, 645–654, 1958.
13. V. I. Lichtmann, E. D. Shtchukin and P. A. Rehbinder, Physical and chemical mechanics of metals. Izd. AN SSSR, Moscow, 1962.
14. I. P. Vyrodov, On condition of a spontaneous dispersion of solids. Journ. Appl. Chem. 35, 191–192, 1962.
15. I. P. Vyrodov, On conditions of a spontaneous dispersion of solids. KAI Proceedings, Krasnodar, II, 39, 11–14, 1963.
16. I. P. Vyrodov, On some problems of the theory of solidification of mineral binders. Journ. Appl. Chem., 35, 2341–2343, 1962.
17. I. P. Vyrodov, X-ray graphic study of kinetics of solidification of chloromanganese cement and gypsum. Proceedings of the Kuban Agricultural Institute (KAI), Krasnodar, 11, 39, 50–55, 1963.
18. V. B. Ratinov, A. P. Lavut, S. M. Pimenova and I. A Smirnova, A study of kinetics of hydration of minerals of portland cement clinker. "News in chemistry and technology of cement." Gosstrojizdat, 286–294, 1962.
19. O. M. Todes, Kindtics of coagulation and increase size of particles in solcs. "Problems of kinetics and catalysis", Izd. AN SSSR, 7, 137–173, 1949.
20. A. I. Markov, N. V. Michailov and P. A. Rehbinder, On the approximated calculation of strength of cement concretes depending on degree of hydration of cement, on the water-cement ratio and on the volume of air involved. DAN SSSR, 167, 1342–1345, 1966.
21. I. P. Vyrodov, Elements of theory of strength of cement stone. KAI Proceedings, Krasnodar, II, 39, 40–49, 1963.
22. I. P. Vyrodov and O. P. Mchedlov-Petrosyan, Zur Ableitung der Formel fur die Zementstein und Betonfestigkeit. Silikattechnik, 15, 257–258, 1964.
23. I. P. Vyrodov and O. P. Mchedlov-Petrosyan, Zur Theorie der Festigkeit. Silikattechnik, 16, 109–110, 1965.
24. A. I. Markin and N. V. Michailov, On contraction and formation of contraction pores in processes of hydration solidification of cements. DAN SSSR, 168, 161–164, 1966.
25. L. A. Siltchenko, N. V. Michailov and P. A. Rehbinder, Kinetics of hydration of cement in concrete at high temperatures. DAN SSSR, 154, 391–394, 1966.
26. P. A. Rehbinder, E. D. Shtchukin and L. Y. Margolis, On mechanical strength of porous dispersoidal bodies. DAN SSSR, 154, 695–698, 1964.
27. A. F. Polak and V.V. Babkov, On the theory of strength of porous bodies. Physical and chemical mechanics of dispersoidal structure. Isd. Nauka, 28, 1966.
28. I. P. Vyrodov and O. P. Mchedlov-Petrosyan. On the theory of strength of cement brick and concrete (in German), Silikattechnik, 16, 312–313, 1965.
29. B. G. Skramtayev and Y. M. Bazenov, Clearing out the formula to determine the strength of concrete. "Concrete and armoured concrete". 11, 4, 25–27, 1965.
30. A. G. Saul, Mag. of Concrete Research, 6, 1951.
31. L. E. Copeland, D. L. Cantro and G. Verbeck, Chemistry of hydration of portland cement. 4th ISCC, Strojizdat, Moscow, 305–352, 1964.
32. T. A. Kontorova and Y. I. Frenkel, Statistical theory of strength of real crystals. Journ. Techn. Physics, XI, 3, 173, 1941.
33. B. B. Chechulin, On the statistical theory of brittle strength. Journ. Techn. Physics, 24, 2, 292–298, 1954.
34. I. P. Vyrodov, Diffusion kinetics of reaction. Int. Chem. Eng., 5, 512–517, 1965.
35. I. P. Vyrodov, On calculation of functions of distribution of particles by size by date of X-ray small angle method. Crystallography, 10, 6, 779–787, 1965.
36. I. P. Vyrodov, On structure forming of manganese cements, Journ. Appl. Chemistry, XXXIII, 2399–2404, 1960; On the problem of solidification of chloromanganese cements. Journ. Appl. Chemistry, XXXIV, 2099–2102, 1961.
37. A. Grudemo, Micro-structure of solidifying cement

paste. IVth INT. SCC, Strojizdat, Moscow, 439–469, 1964.
38. K. T. Grin, Reactions of hydration of portland cement on early stages. 4th ISCC, Strojizdat, Moscow, 275–304, 1964.
39. H. F. Taylor, The chemistry of cement hydration. Proc. of 7th Conference on the silikate industry. Academiai Kiado, Budapest, (Silikont, 1963, 199–220, 1965).
40. D. D. Bernal, Structures of cements hydration products. 3rd ISCC, Gosstrojisdat, Moscow, 137–176, 1958.
41. H. Funk, Z. anorg. u. allgem. Chemie. Chemische Untersuchungen von Silikaten, 296, 46–62, 1958.
42. N. Kawada and A. Nemoto, Calcium silicates in the early stage of hydration. Zement-Kalk-Gips, 20, 65–71, 1967.
43. W. Gzeznin, Zement und Beton, 16, 1959.
44. I. P. Vyrodov and B. N. Didenko, Electron Microscopic study of the influence of surfactants on the microstructure chloromanganese cement. Problems of progressive technology of building materials. Krasnoyarsk, 280–285, 1965.
45. V. Tchernin, Some unsolved problems of cement hydration. 4th ISCC, Strojizdat, Moscow, 50, 7–510, 1964.
46. I. P. Vyrodov and O. P. Mchedlov-Petrosyan, Über Feststellung der Richtung chemischer Reactionen und die Beziehung zwischen den kinetischen und thermodynamischen Parametern des Systems. Silikattechnik, 18, 252–253, 1967.

Supplementary Paper III-125 Electron Microscopic Investigations about the Relations between Structure and Strength of Hardened Cement

Wermer Richartz*

Synopsis

Electron microscopic investigations show that the hardening of cement may be classified in three stages.

Calcium hydroxide and ettringite are formed a short time after the addition of water. The first stage of hydration is finished after nearly one hour, as to that moment it is firstly possible to indicate that the calcium silicate hydrates are decisive to the development of strength.

The second stage of hydration takes about 24 hours. During this time the calcium silicate hydrates and the ettringite formed to relative long fibres or needles, may grow into the big pores of the labile basic structure. In the second stage of hydration it is established a structure which is decisive to the further development of the strength.

In the third stage of hydration the pores, still existing, will be filled up by the arising products of hydration and the structure will be consequently more compact. If the cement hardens at low temperature or under the influence of a retarder, in the second stage of hydration the calcium silicate hydrates may grow to longer fibres. Consequently the final strength can increase for 20%.

If the hydration is accelerated, less long fibrous calcium silicate hydrates are formed. In this case the final strength is lower than at normal hardening.

Calcium silicate hydrates have a small characteristic strength because of their high structural disorder. But still, they are the principal strength forming phases of the hardened cement. Foreign fibres of inorganic or organic materials may only increase the strength of the hardened cement, if the adherence to the hydration products is ensured.

Introduction

The structure of the hardened cement formed by hydration consists mainly of 4 crystalline phases. The calcium silicate hydrates are the most important constituents. They are formed by hydration of alite and β–C_2S and mainly consist of fibrous crystals which have a very small degree of structural order. The length of the fibrous crystals is about 1 μm, the diameter of the fibre varies between 50 Å and 1000 Å (0.005 and 0.1 μm).

The ettringite crystallizes in long acicular crystals as a product of the reaction of C_3A and C_4AF with gypsum. Ettringite and calcium hydroxide are the first hydration products which are formed immediately after the addition of the mixing water. Later on the ettringite can convert into monosulfate and calcium sulfate during the advanced hardening process. It is doubtful whether this phase with its low stability can give a significant contribution to a stable structure of the hardened cement.

Calcium hydroxide and calcium aluminate hydrate both crystallize in hexagonal-tabular form. Their contribution to the total strength of the hardened cement is quite small; therefore, they are no longer discussed.

The pores are also a quite important fact in the structure of hardened cement. The structural composition and the process of hardening can also be understood as an alteration of the pore space. The strength mainly depends on how the pores are bridged; according to this the investigations about the structure of the hardened cement has to be concentrated on the pores.

For the electron microscopic investigation the cement paste was filled into a glass- or plastic-tube. The water cement ratio was in the range between 0.40 and 0.45. The tube then was hermetically sealed. After a hydration time of at least 1 day, the tube was broken. From the very plain boudary surface of the hardened cement, carbon replicas were taken

*Forschungsinstitut der Zementindustrie, Düsseldorf, West Germany.

which reproduce fine details of the structure in the pores. Here the hydration took place undisturbed, and hence the walls of the pores reproduce the real structure of the hardened paste.

Most of the investigations were made with pastes of C_3S to facilitate the identification of the constituents of the structure.

Structure Development of Hardened Paste

Fig. 1 shows a pore of hydrated C_3S-paste, into which fibrous crystals of calcium silicate hydrate grow from all directions. Several parts of the pore are already bridged by long firbous calcium silicate hydrates. Inside the pore most of the calcium silicate hydrates can grow unhindered, because there is still enough space. The upper and the lower edge of the pore are connected by a few calcium silicate hydrate fibres only. That means, inside the pore the development of the structure is in an early stage. But in the lower part of the figure the structure consists of closely packed calcium silicate hydrates and has already reached the final stage of hydration.

Fig. 2 shows an originally larger pore in a 3-days-hydrated C_3S-paste. The pore is filled with interlocking fibrous crystals of calcium silicate hydrate. Several long fibres bridge the whole pore space, in the remaining very small pores grow short crystals only. Hence it follows that hydration starts with the crystallization of long fibres, which bridge the big pores originally filled out by mixing water. Consequently the big pores become subdivided into several smaller pores and the total pore volume has decreased. The smaller the pores, the shorter the calcium silicate hydrate fibres crystallizing during the further steps of hydration. This results in a condensing of the paste structure.

Fig. 3 shows the stage of C_3S-hydration after 90 days. It reveals a highly condensed structure, which consists of fine pores and short-fibrous calcium silicate hydrates only. The long fibres were covered during the hardening by the fine granular hydration products, and thus they cannot be detected.

The electron micrographs (Figs. 1–3) show the

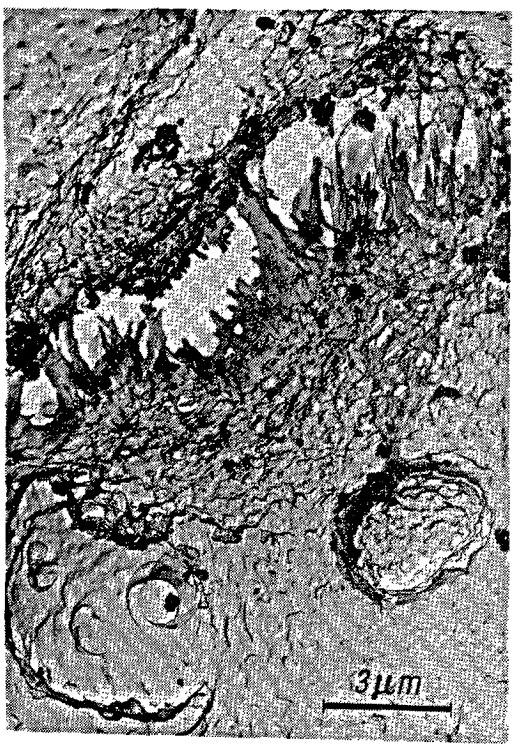

Fig. 1. *Electron micrograph of a* C_3S*-paste hardened 3 days* w/c = *0.44 (carbon replica)*

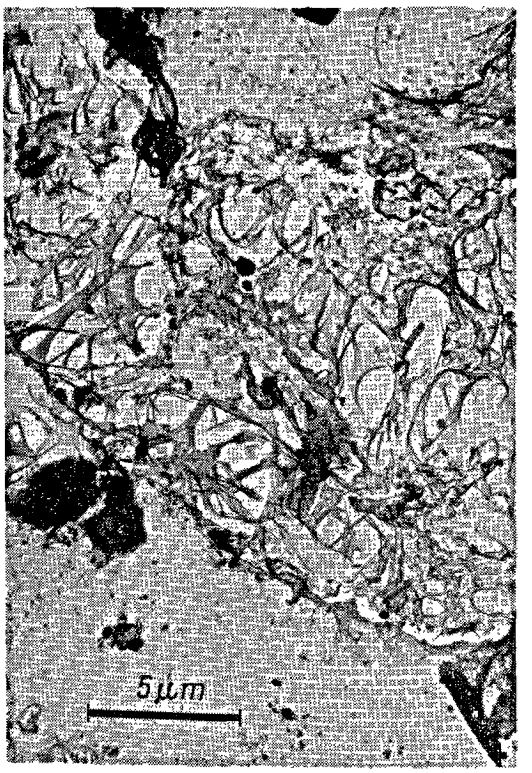

Fig. 2. *Electron micrograph of a* C_3S*-paste hardened 3 days* w/c = *0.44 (carbon replica)*

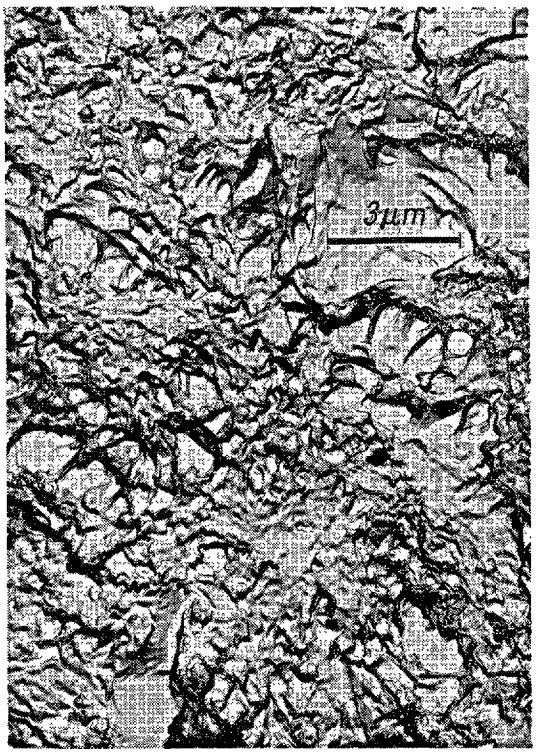

Fig. 3. *Electron micrograph of a* C_3S*-paste hardened 90 days* w/c = *0.44 (carbon replica)*

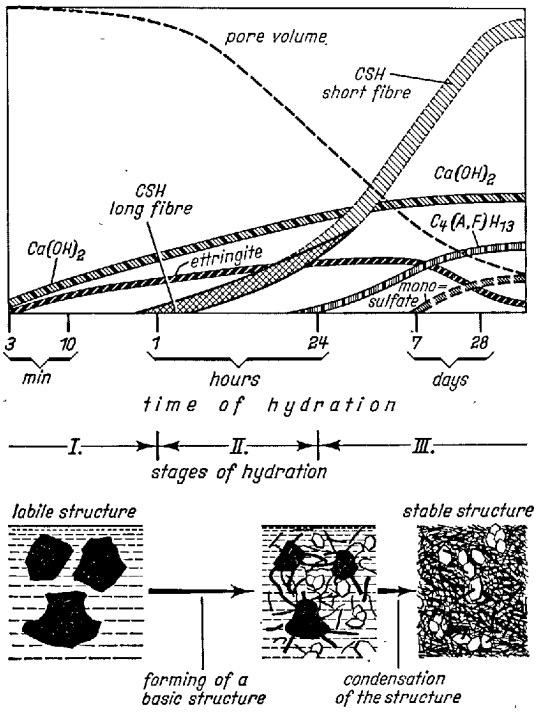

Fig. 4. *Formation of the hydrate phases and constitution of the structure during the hardening of the cement*

relations between the development of structure and strength of hardened cement. Simplifying this, they reveal the structural composition of a paste which consists of calcium silicate hydrates only. During hydration of cement, however, other hydration products,i.e., ettringite, monosulfate and tetracalcium aluminate hydrate are formed, not simultaneously but successively. Consequently, the whole process of hydration can be classified in 3 stages (Fig. 4). The first stage of hydration is designated by the formation of $Ca(OH)_2$ and ettringite, which can already be detected by electron microscope after 3 to 5 minutes. Ettringite grows on the surface of the cement grains, and calcium hydroxide crystallizes from the solution as thin plates. The second stage of hydration starts after about 1 hour. At this time the first formation of calcium silicate hydrates in at first very fine crystals can be identified. By this moment the volumes of the cement particles have not distinctly decreased, because only a thin surface layer has reacted. The interspace between the cement grains has still nearly the same size as at the beginning of the hydration. Consequently the calcium silicate hydrates grow to be long interlocking fibres. After the complete hydration such long fibres will act as a microreinforcement of the structure of hardened cement and will increase the ultimate strength. At the end of the second stage of hydration after about 24 hours, the formation of ettringite is finished as all gypsum has reacted. At this moment the structure mainly consists of long interlocked fibrous calcium silicate hydrates which bridge a condiderable part of the originally water filled space.

During the third stage of hydration from about 24 hours up to the end of the reaction the still remaining pores are filled out by new hydration products as described above. During this stage of hydration tetracalcium aluminate ferrite hydrate $C_4(A, F)H_{13}$ is formed instead of ettringite, and the ettringite can be converted into monosulfate. Therefore, its contribution to the total strength is doubtful but, in any case, it influences the setting of cement and the early strength.

Influences on the Structure of Hardened Paste

Retarded Hardening

K. Walz and J. Bonzel (1) report that the process of hardening is distinctly retarded at low temperatures of hydration, and that nearly always a higher ulitmate strength is reached. This can be explained in the following way:

Because of the reduced rate of reaction the different stages of hydration, especially, the second stage are extended. Consequently, in the second stage of hydration, more long-fibrous calcium silicate hydrates are formed. This influence of the temperature on the morphology of the calcium silicate hydrates was already reported in an earlier publication (2).

The hydration being retarded by chemical additions the structual constitution is influenced in the same way as afore mentioned. Fig. 5 shows an electron micrograph of C_3S-paste, which hardened 7 days efficaciously retarded. Fibres of calcium silicate hydrate are formed 10 μm long, several fibres have lengths up to 30 μm.

According to this distinctly changed structual constitution which is developed by the influence of a retarder, the final strengths were up to 20% higher than those of normally hardened cement paste. These investigations confirm and explain the results of measurements of K. Walz and H. Mathieu (3) who found that by addition of retarders always significantly higher final strengths result although the early strength is decreased.

The reaction inhibiting effect of retarders remains still today incompletely settled. A logical assumption is that the surface of the cement grains are blocked up by the retarding additions and so the cement reacts slower.

Accelerated Hardening

An accelerating of the reaction can be caused either by a higher fineness, higher temperature or addition of an accelerator. If an accelerator is added, the surface of the cement grains obviously is activated, so that the solution in the pores is always supersaturated. Hence the conditions for spontaneous nucleus formation and increased crystal growth are given. So

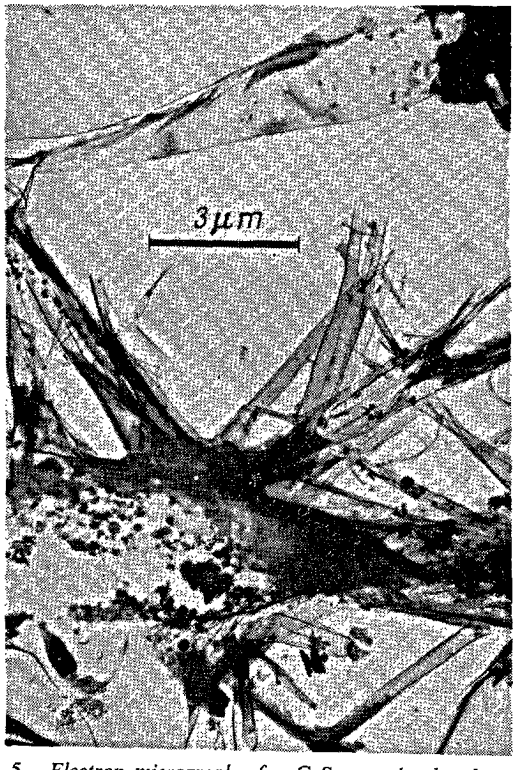

Fig. 5. *Electron micrograph of a C_3S-paste hardened 7 days with addition of a retarder* w/c = *0.44 (carbon replica)*

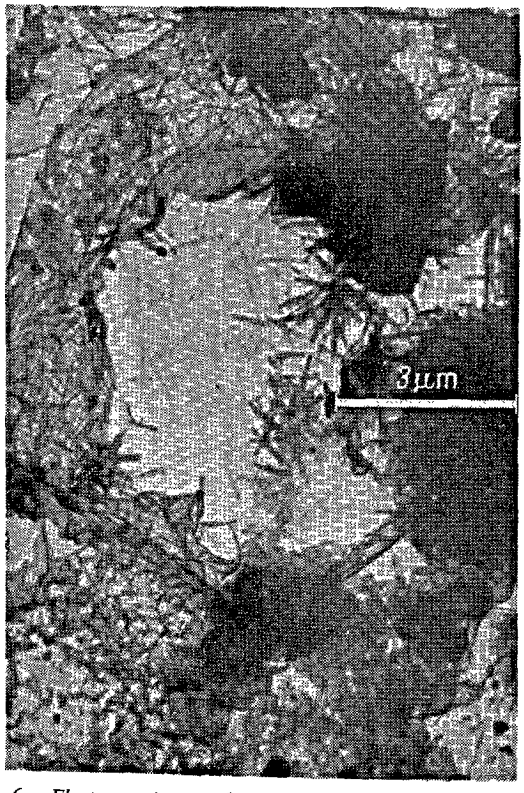

Fig. 6. *Electron micrograph of a C_3S-paste hardened 7 days with addition of an accelerator* w/c = *0.44 (carbon replica)*

only a few crystals can grow to be long fibres also in the second stage of hydration, although at this time there were space enough for the formation of long fibrous crystals. So, by the influence of an accelerator a structure with more short fibrous crystals is formed than by hydration under normal or retarding conditions as shown in Fig. 6.

The strength of the hardened paste after one day is distinctly higher as compared with a paste without accelerator because a higher degree of hydration is reached. Also, after a 7-days-hardening only a few calcium silicate hydrate crystals with a fibre length of more than 1 μm are formed.

The strength development of a cement without addition, with an accelerator and with a retarder is given in Fig. 7. The accelerated cement yields the highest initial strength because of the higher degree of hydration. After about 28 days the final strength is reached. The normally hardened cement shows a significant lower initial strength, but after 28 days it reaches approximately the strength of the accelerated cement and exceeds it during the further hardening.

The retarded cement gets a low initial strength. But after 28 days it reaches and after 90 days it exceeds the strengths of normal and accelerated cements.

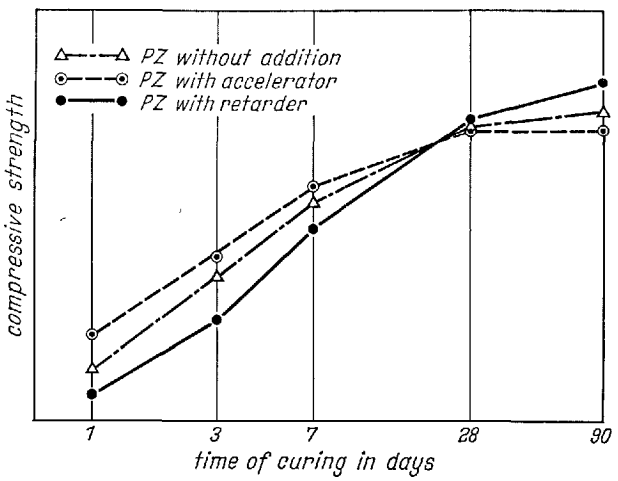

Fig. 7. *Development of strength of a normal, a retarded and an accelerated hardening*

These results show that a strict relationship exists between the development of the structure and of the strength. High initial strength is caused by a high degree of reaction, high final strength by a close packing and a significant part of fairly long calcium silicate hydrate fibres.

High Initial and Final Strength

If it is possible to get quickly a larger quantity of long fibrous crystals in the early stages of hydration, even a cement with a usual fineness can reach as well high initial as final strengths. A mixture of 75% C_3S and 25% tricalcium germanate (C_3G) is a model cement according to this condition. After one day the C_3G portion has nearly completely reacted. This is characteristic for an accelerated hardening. In spite of the high rate of reaction, the hydration products are long-fibrous interlocking crystals of calcium germanate hydrate (2). So, the conditions for a high final strength are satisfied. The subsequent hydration of C_3S supplies the mass of short-fibrous calcium silicate hydrates which fills out the space between the calcium germanate hydrate crystals forming the basic structure. Fig. 8 concerning a micrograph of the hardened paste of this germanate cement shows the long-fibrous crystals after one day of hydration.

The strength development of this mixture and of pure C_3S is given in Fig. 9. Special attention is called to the fact that strength of the mixture C_3S–C_3G after 1 day of hardening is about the same as the strength of pure C_3S after 28 days. After 28 days the strength of the mixture is still 20% higher than the corresponding strength of pure C_3S.

The example shows that the formation of long fibrous crystals during the second stage of hydration significantly raises the final strength, and that a high hydration activity increases the initial strength.

Fig. 8. *Electron micrograph of a* C_3S–C_3G*-paste hardened 1 day* w/c = *0.50 (carbon replica)* C_3G = *tricalcium germanate* = $3CaO \cdot GeO_2$

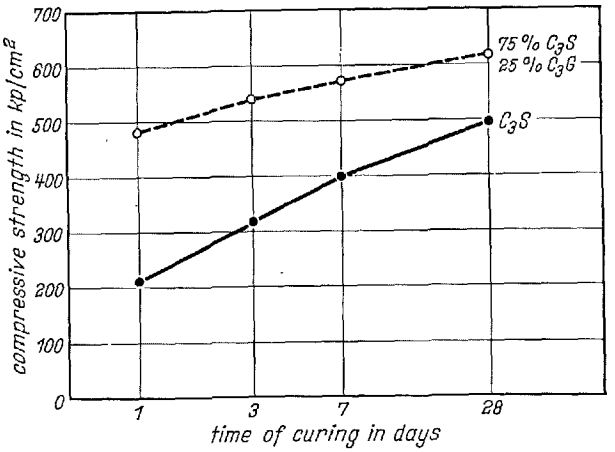

Fig. 9. *Development of strength of* C_3S *and of a mixture of* C_3S–C_3G, C_3G = *tricalcium germanate* = $3CaO \cdot GeO_2$

Reinforcing of Paste by Fibres

The favorable effect of long fibres on the strength suggests to examine the effect of fibres added to the cement as a micro reinforcement. Nylon threads with a diameter of 0.25 mm and 0.6 mm and a length between 5 and 10 mm were used as fibres. They were mixed with a portland cement in a quantity of 1% 3% and 5% by weight. The measured strengths are given in Fig. 10. It reveals that additions from 1 to 3% results in a higher strength at all ages. Additions of 5% on the other hand diminish the strength probably because of the difficulty to get a homogenous mixture with higher contents of fibres. The increase of the strength by addition of 1 and 3% of nylon threads was fairly small and did not fulfil the expectations.

The small effect of reinforcement of the paste by nylon threads is attributed to the poor adherence to the paste. But also with alkali resistant borosilicate glass fibres no better adherence was obtained.

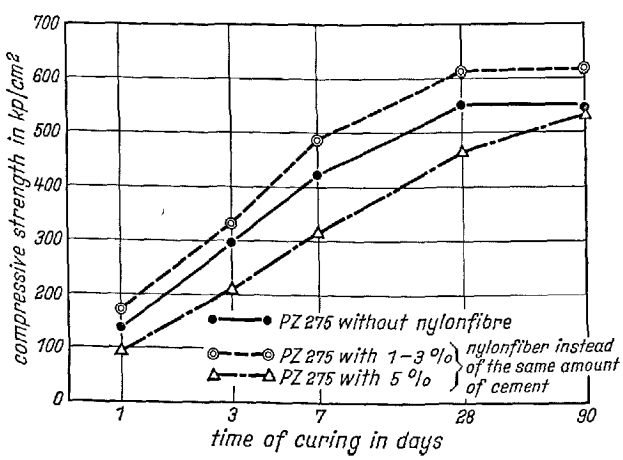

Fig. 10. *Compressive strength of cement mortar with various additions of nylon threads*

Adherence of Hydration Products in the Hardened Paste

Calcium silicate hydrates formed by cement hydration have a high degree of structural disorder. So, a single calcium silicate hydrate crystal has a comparatively low characteristic strength. On the other hand, the adherence of the calcium silicate hydrates with each other and with other hydrate phases is very strong. This is demonstrated by the electron micrographs of Fig. 11–13. They show replicas of C_3S and cement pastes, prepared with retarders and hardened 7 or 28 days. Fig. 11 shows a network-like arrangement of calcium silicate hydrates. All the fibres bridging the pore are connected with each other. The shadow of all fibres in the background indicates that the represented object is not a defect of the foil. Similarly the micrographs of Fig. 12 and 13 show the bridging effect and the adherence of the calcium silicate hydrate fibres. The fibres are strongly branched and form new cross connections between the bigger fibres and the walls of the pores. Besides it is probable that the joint between the fibres is improved by bristly calcium silicate hydrate crystals which are grown in similar orientation on the surfaces of the bigger crystals.

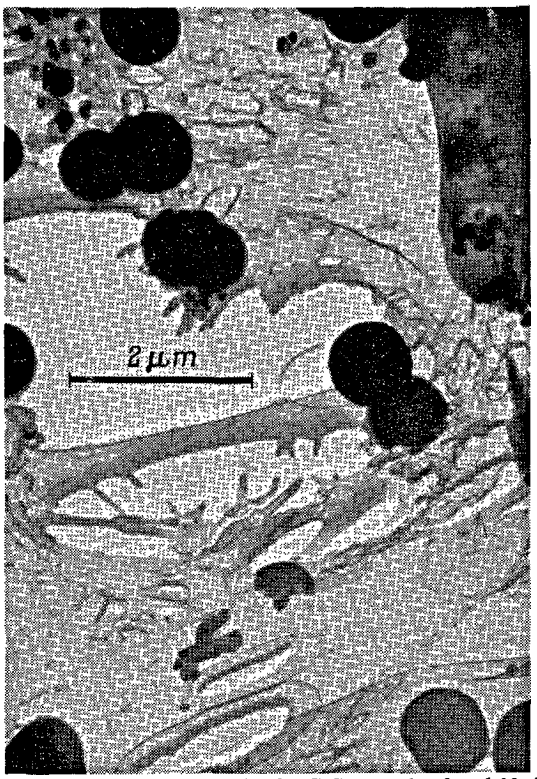

Fig. 12. *Electron micrograph of a* C_3S*-paste hardened 28 days with addition of a retarder* w/c = *0.44 (carbon replica)*

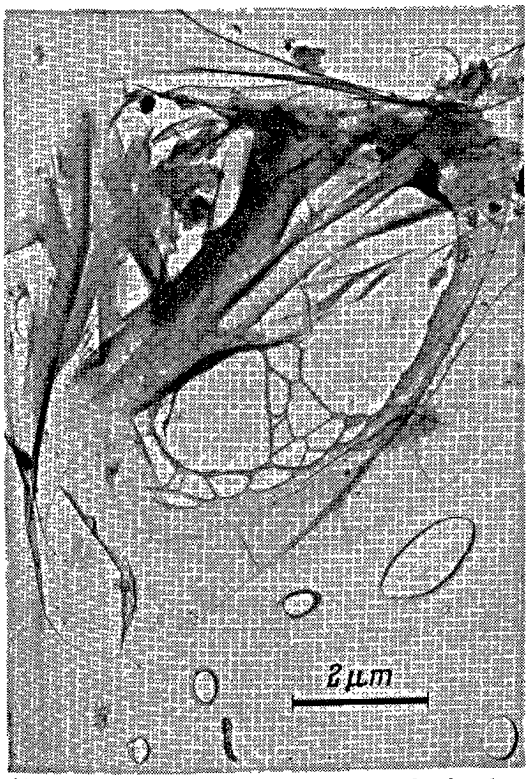

Fig. 11. *Electron micrograph of a* C_3S*-paste hardened 7 days with addition of a retarder* w/c = *0.44 (carbon replica)*

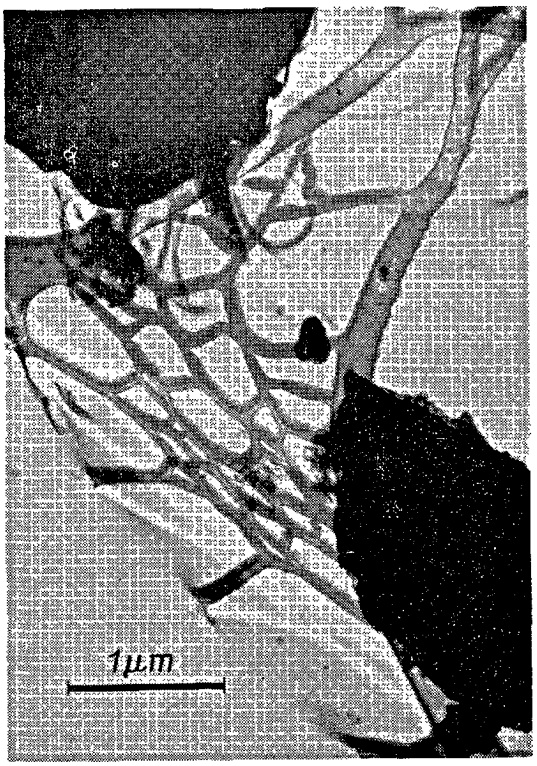

Fig. 13. *Electron micrograph of a blastfurnace slag cement paste hardened 28 days* w/c = *0.45 (carbon replica)*

Flexibility of Calcium Silicate Hydrate Fibres

Calcium silicate hydrates do not crystallize in form of rigid needles, they rather show the character of threads and a high flexibility. Fig. 14 shows calcium silicate hydrates formed by hydration of C_3S in presence of excessive water. The fibres are highly flexible. But during the microscopic investigation the calcium silicate hydrate fibres are exposed in this case to the alternating effect of the electron beam in contrast to the investigation mentioned before. For that reason it is not sure whether a more or less destruction of the structure has effected a deformation of the calcium silicate hydrates and simulates a flexibility. But the electron micrographs taken with the replica method indicate the same flexibility (Figs. 15–17).

When the hardened paste is broken, the calcium silicate hydrate fibres tear up. In the zone near the fracture the fibres orient themselves into the direction of the breaking stress owing to their flexibility. This is shown by the Figs. 18 and 19 which represent micrographs of the fracture surfaces of hardened cement paste. It is to be recognized that the ends of the torn calcium silicate hydrate fibres protrude out of the surface of the paste and have about the same orientation.

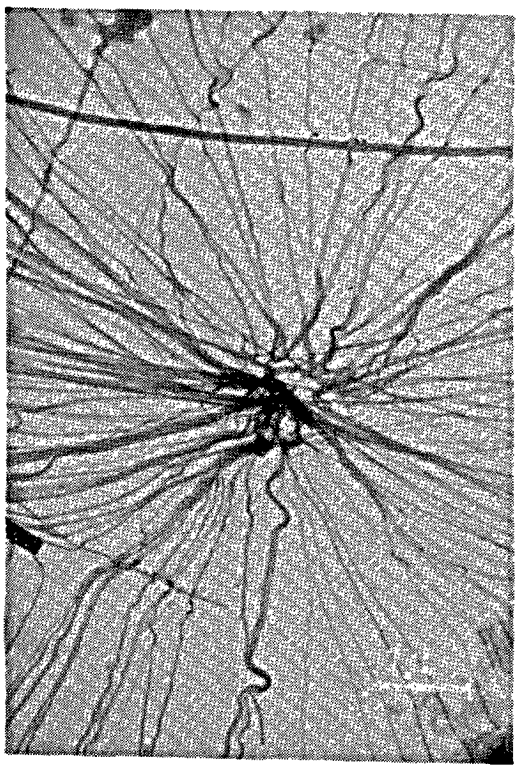

Fig. 14. *Electron micrograph of calcium silicate hydrates, originated by complete hydration of* C_3S *in water of 5°C*

Fig. 15. *Electron micrograph of a blastfurnace slag cement paste hardened 28 days* w/c = *0.45 (carbon replica)*

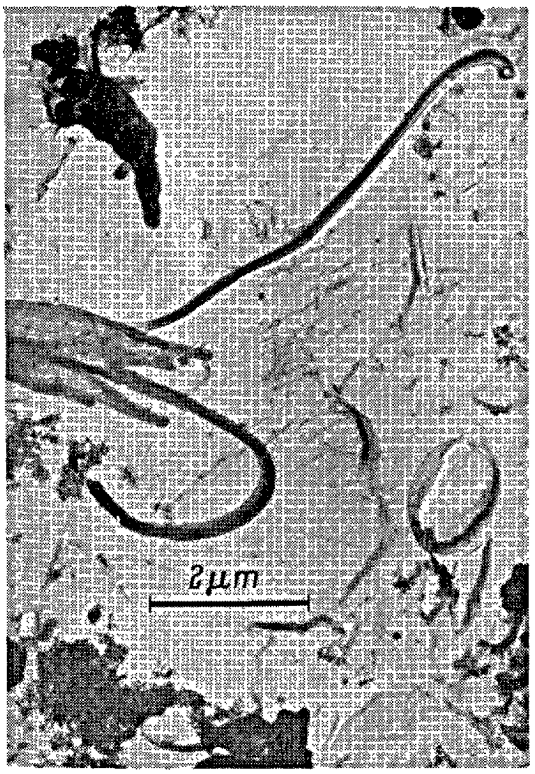

Fig. 16. *Electron micrograph of a blastfurnace slag cement paste hardened 28 days* w/c = *0.45 (carbon replica)*

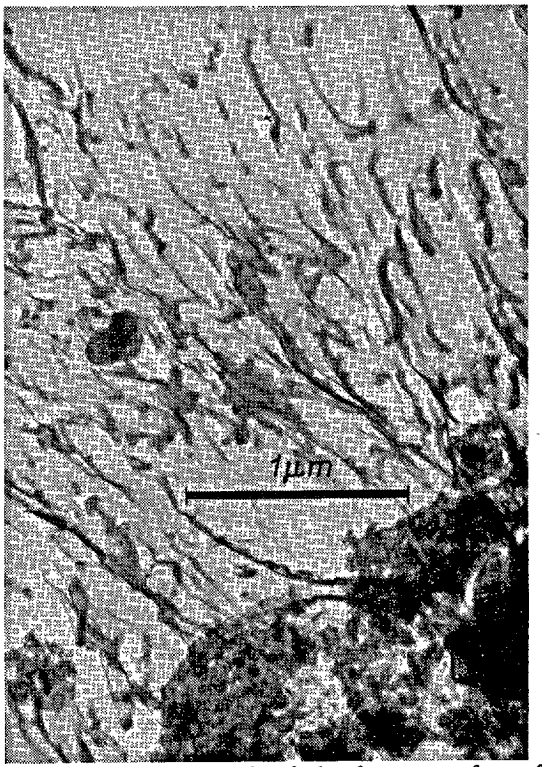

Fig. 18. *Electron micrograph of the fracture surface of a portland cement mortar hardened 28 days* w/c = *0.40 (carbon replica)*

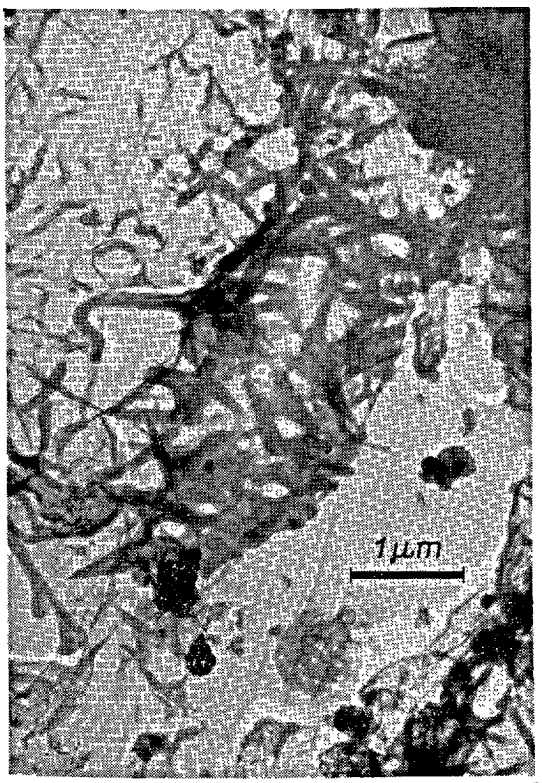

Fig. 17. *Electron micrograph of a* C_3S*-paste hardened 7 days* w/c = *0.44 (carbon replica)*

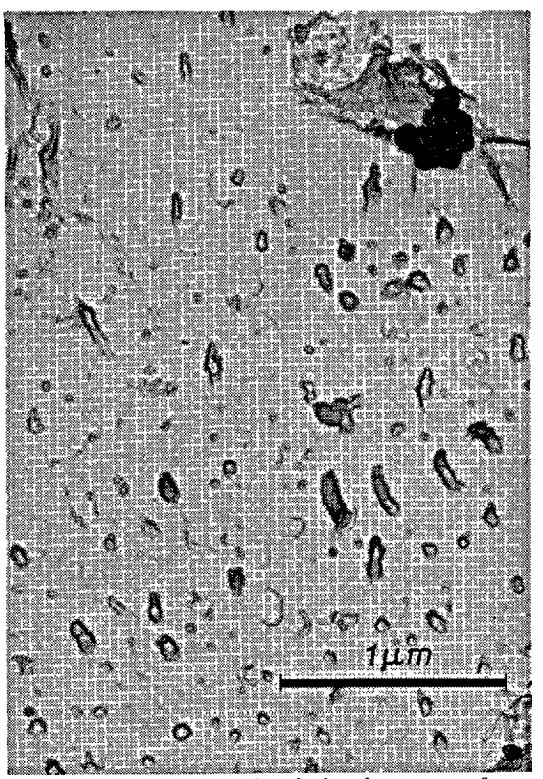

Fig. 19. *Electron micrograph of the fracture surface of a portland cement mortar hardened 4 months* w/c = *0.35 (carbon replica)*

References

1. K. Walz and J. Bonzel, "Development of strength of various cements at low temperature" (in German), Beton **11**, 35–48 (1961).
2. W. Richartz and F. W. Locher, "A contribution to the morphology and combination with water of calcium silicate hydrates and to the structure of hardened cement pastes" (in German), Zement-Kalk-Gips **18**, 449–459 (1965).
3. K. Walz and H. Mathieu, "Influence of the quantity of plastizising additions on the development of the strength of mortar" (in German), Beton **11**, 619–625 (1961).

(B) Papers regarding Application

Supplementary Paper III-1 Comparison of Various Measurements Concerning the Kinetics of Hydration of Portland Cements

Sandor Popovics*

Synopsis

The use of a simple cement model for the description of the kinetics of hydration of portland cement is the subject of this paper.

Following the general description of the proposed model, its application for the strength development is shown. Then, the kinetics of the developments of non-evaporable water content and vapor sorption of the hardening portland cement paste are investigated by using the cement model again. Calculated values are compared to pertinent experimental data. The similarities and dissimilarities of the kinetics of various hydration characteristics are also discussed. Finally, the model is applied to demonstrate the effect of temperature on the strength development of portland cement concretes.

Introduction

A simple model was recommended recently for the descritption of the hardening of portland cement paste, mortar, or concrete in terms of the compound composition of the cement and the age of the strength specimen (1). Strength values provided by that model were shown to be in a reasonable agreement with experimental data. In this paper, an attempt is made to develop similar models for two other characteristics of the hydration process, namely, the vapor sorption and non-evaporable water content of the hardened cement pastes. These models can be used conveniently for the comparison of strength, sorption, and other measurements connected with the kinetics of hydration of portland cements. It will also be shown that the model is suitable for the description of the effect of temperature on the hardening process.

A pertinent speculation of Philleo will conclude this introduction. He says, it can be shown from purely geometric considerations that for a given degree of hydration the standard deviation of hydration rate at various points is approximately proportional to the hydration rate (2).

General Description of the Model

The mathematical form of the model developed for strength is [1]:

$$f_{rel} = 100\frac{1 - pe^{-a_1 t} - (1-p)e^{-a_2 t}}{1 - pe^{-28a_1} - (1-p)e^{-28a_2}} \qquad [1]$$

where

f_{rel} = relative strength of portland cement paste, mortar or concrete, that is, the ratio of the strength at a certain t age and the 28-day strength, percent,

t = age of the strength specimen, day,

p = computed C_3S content of the portland cement, percent/100, and

a_1 and a_2 = parameters which are independent of the strength and age, but may be a function of the fineness and composition of the cement, curing and testing methods, etc.

This cement model satisfies the following conditions:

1. It consists of only two hardening components. The first component is the C_3S, the second component is a mixture of the other cement ingredients.

*Department of Civil Engineering, Auburn University, Alabama, U.S.A.

2. These two components hydrate simultaneously with differing rates but without any interaction. Thus, their resulting strengths can be superimposed.

3. The final strength of C_3S is the same as the final strength of the second component.

4. The decelerations of the hardening of both the C_3S and the second component are proportional at a given age to the remaining strength development at that time, but the two proportionality factors are different.

5. The proportionality factors may be functions of the C_3A content.

Thus, it is apparent that this model is a simplification of an actual portland cement; that is, in accordance with the technical meaning of the term "model" (3), it resembles a portland cement in several but not in all respects. The a parameters in Equation [1] represent the specific rates of hardening, that is, (rate of hardening)/(remaining strength at a given age). The squares of these parameters represent the specific decelerations of hardening. The a_1 parameter characterizes the early strength development, while the a_2 parameter characterizes the strength development at later ages. More specifically, the greater the value of a_1, the higher the early strengths will be as compared to the 28-day strength; and the smaller is the value of a_2 up to a certain limit, the longer and larger will be the relative strength increase after 28 days. Thus, these parameters can be used for the description of the kinetics of hardening of various portland cements.

Equation [1] is not the first attempt to establish a quantitative relationship between compound composition of cement and strength development. The previous attempts are based on the assumption that each cement compound contributes strength at a given age in proportion to the percentage of that compound present [(4) through (9)]. The mathematical form of this assumption for the four main compounds is as follows:

$$\text{Strength} = a(C_3S) + b(C_2S) + c(C_3A) + d(C_4AF) \quad [2]$$

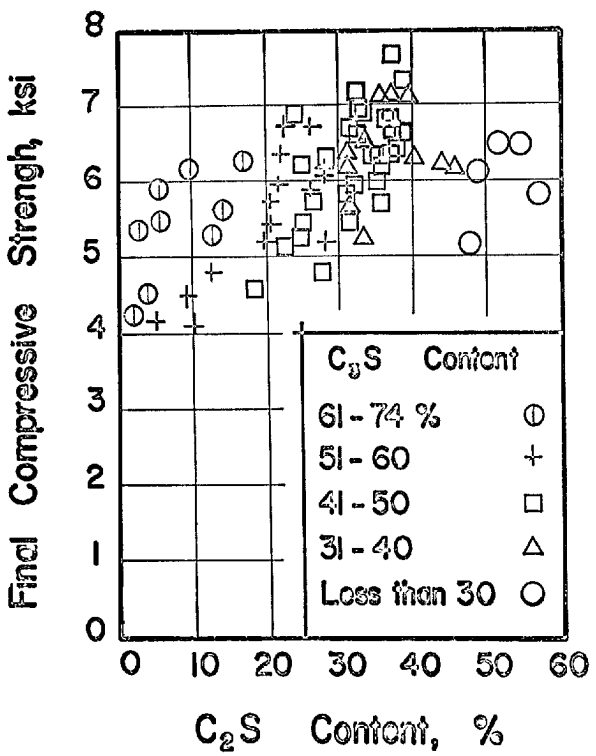

Fig. 1. *Final compressive strengths of 1: 2.75 mortars made with various portland cements as a function of the compound composition. The values are based on data published by Gonnerman (9). I*

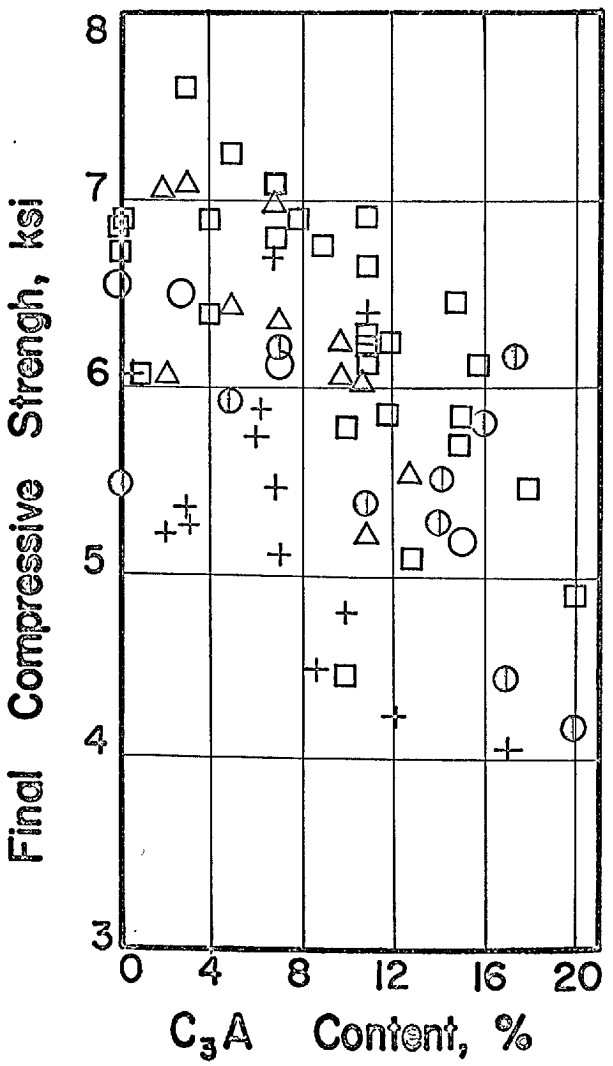

Fig. 2. *Final compressive strengths of 1: 2.75 mortars made with various portland cements as a function of the compound composition. The values are based on data published by Gonnerman (9). II. The symbols are the same as in Fig. 1*

where the symbols in parentheses represent the percentage by weight of the compound, and a, b, c, and d are empirical parameters representing the contribution of one percent of the corresponding compound to the strength of the hardened mixture at a given age.

Experimental data obtained by Gonnerman with Ottawa-sand mortars (9) showed reasonably satisfactory agreement with Equation [2]. Nevertheless, the linear model is objectionable for several reasons. First, the number of the empirical parameters is high, four for each age group. Another reason is that variations in burning and cooling condition, as well as differences in the mineralogical composition of the raw materials used in cement making, may affect the hardening process of cement (10). Therefore, without the consideration of these factors, one cannot expect a good correlation between the compound composition and strength of cement (Figs. 1 and 2). Finally, experimental evidence indicates that the hydration process of various clinker minerals, especially the calcium silicates and aluminum silicate, may interact with each other (8, 11, 12, 13). Thus, the simple superposition of the compound strengths is objectionable in principle. The cement model represented by Equation [1] eliminates some of these objections.

Application of the Model for the Strength Development

It has been demonstrated (1) that experimental results obtained by various investigators support fairly well the applicability of Equation [1]. By computing an average deviation between the calculated and experimental values (14), it was found to be less than 10 per cent.

It has also been shown that the values of a_1 and a_2 may be functions of the potential C_3A content of the portland cement (1). For instance, Table 1 presents a_1 and a_2 values for various cases that were obtained from pertinent experimental results (15) by the method of least squares. Fig. 3 illustrates how the model reproduces the effect of the C_3A content on the rela-

Table 1. *Specific rates of hardening for mortars and concretes tested by Klieger*

Type of test	w/c by weight (approx.)	a_1, 1/day	a_2, 1/day
Tensile strength of mortar (ASTM C 190-49)		0.80	$0.02C_3A$
Compressive strength of mortar (ASTM C 109-49)		0.20	$0.005C_3A$
Flexural strength of mortar		0.45	$0.01C_3A$
Compressive strength of concrete, 6 bags/cu yd	0.43	0.40	$0.002C_3A + 0.02$
Flexural strength of concrete, 6 bags/cu yd	0.43	0.55	$0.001C_3A + 0.02$
Compressive strength of concrete, 4½ bags/cu yd	0.54	0.30	$0.005C_3A$
Flexural strength of concrete, 4½ bags/cu yd	0.54	0.5	$0.005C_3A$
Compressive strength of concrete, 3 bags/cu yd	0.80	0.15	$0.003C_3A$
Flexural strength of concrete, 3 bags/cu yd	0.80	0.25	$0.004C_3A$

Note: C_3A designates the percent of the potential tricalcium silicate content of the portland cement computed according to the Bogue method. (16)

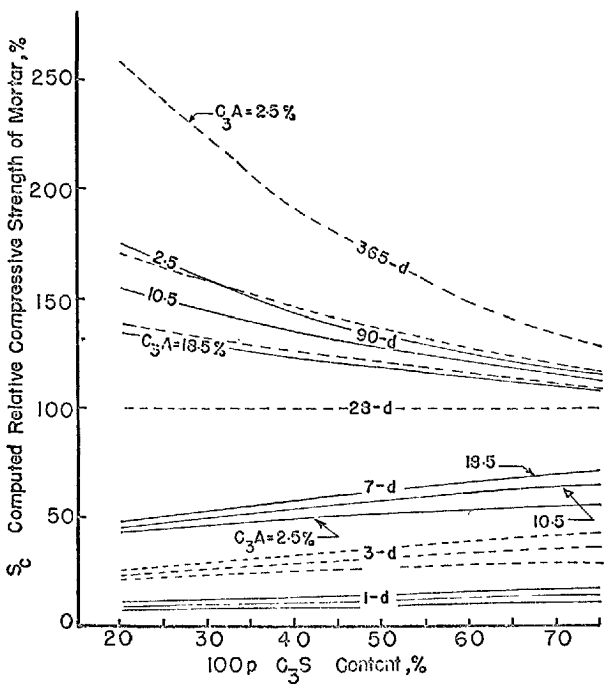

Fig. 3. *Effect of the* C_3A *content on the relative compressive strength of 1: 2.75 mortars at various ages. (1)*

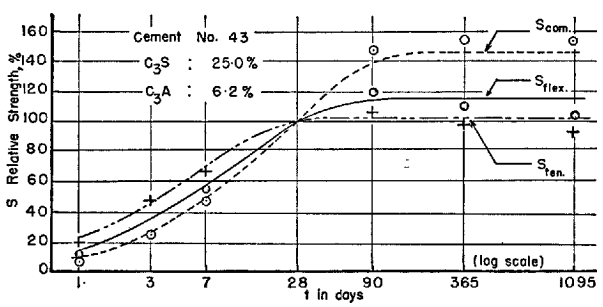

Fig. 4. *Comparison of experimental and computed values to illustrate the effect of test method on the kinetics of the hardening of portland cement in mortars. Experimental values are represented by points, computed values by lines. (1)*

tive compressive strength of 1:2.75 mortars tested by Gonnerman (9) at various ages.

A group of calculated values and experimental results is presented in Fig. 4. Here the relative values of tensile strength, compressive strength, and flexural strength of mortars made with the same cement are plotted as a function of age. Points represent the experimental values, and lines designate the values calculated by Equation [1] with the appropriate values of a_1 and a_2 of Table 1 (1). It can be seen that the rate of increase in the relative tensile strength of a portland cement is much higher than the rate of increase in the relative compressive strength, but the deceleration of the development of tensile strength is also stronger.

A comparison of the a values for concretes of two different cement contents reveals that the development of relative strength is quicker and the deceleration is stronger for higher cement contents and for lower water-cement ratios, other factors being equal.

Application of the Model for Non-Evaporable Water Content and Vapor Sorption

The applicability of this model concept to other characteristics of the hydration of portland cement may be questioned. Two such characteristics will be discussed here (as indicated in the title above). Investigations concerning a third characteristic, the heat of hydration, are in progress.

To answer the question raised above, experimental results of such portland cements should be analyzed where the compound composition is the sole variable; that is, where the fineness and gypsum content of the cements, curing and testing methods, etc. are practically identical. Such a test series was performed by Verbeck and Foster where the non-evaporable water contents and vapor sorptions of various Types I, II, IV, and V portland cements were measured up to the age of $6\frac{1}{2}$ years (17). Their results obtained with Type III cements are not applicable here because of the differing fineness of these cements.

Several attempts revealed that a better goodness of fit can be obtained for the experimental values of non-evaporable water content when the third condition of the model is modified. It seems suitable to apply the modification that the C_3S is capable of withholding three times as much non-evaporable water as the second component. The mathematical form of this modified cement model is the following:

$$w^0_{rel} = 100\frac{1 + 2p - 3pe^{-a_1 t} - (1-p)e^{-a_2 t}}{1 + 2p - 3pe^{-28a_1} - (1-p)e^{-28a_2}} \quad [3]$$

where

w^0_{rel} = relative non-evaporable water content of portland cement paste, percent of the 28-day non-evaporable water content.

The other symbols of Equation [3] are the same as the symbols of Equation [1].

A stepwise approximation provides the following a values for Equation (3) and the experimental values by Verbeck and Foster (17):

$$a_1 = 0.01C_3A + 0.25, \text{ 1/day} \quad [4]$$

$$a_2 = 0.0005C_3A + 0.010, \text{ 1/day} \quad [5]$$

where C_3A is again the percent of the potential tricalcium aluminate content of the portland cement computed according to the Bogue method (16).

The thus calculated and measured values are summarized in Table 2. The first digit of the cement numbers used indicates the standard type of the cement. For instance, cement No. 14 is a Type I portland cement. It can be seen that the calculated values of the non-evaporable water contents for Type I and Type II portland cements generally approximate the experimental values quite well within the time limits of 7 days and $6\frac{1}{2}$ years. The approximation for Types IV and V is not as good.

The reasonable goodness of fit shown in Table 2 appears to indicate that the kinetics of the increase of non-evaporable water content differs from the kinetics of hardening. The main difference is that the C_3S, at least in the model, binds more non-evaporable water for a given strength than the second component. Kantro and Copeland have presented a similar tendency (18). That is, in the case of an identical amount of non-evaporable water, a portland cement with a low C_3S content is expected to provide a greater f_{rel} relative strength at early ages than a comparable cement with a high C_3S content. It should be realized, however, that regardless of the validity of this mechanism of hydration, the model represented by Equation [3] seems applicable for the estimation of the amount of non-evaporable water at various ages for a large group of portland cements.

It may be mentioned that Powers and Brownyard (19), and later Kantro and Copeland (18) have published a linear empirical formula for the non-evaporable water content versus compound composition relationship in the form of Equation [2]. Essentially the same criticism is valid for this linear model that

was previously presented concerning the linear strength model of Gonnerman.

Less successful is the attempt to apply the presented model concept to the kinetics of vapor sorption, that is, to the kinetics of the development of specific surface of hardening cement pastes. The following a

Table 2. *Experimental and calculated relative non-evaporable water contents*
The "exp" experimental values were obtained from Verbeck and Foster's experiments. (17)
The "cal" calculated values were obtained by Eq. 3) with the following parameters:
$a_1 = 0.01C_3A + 0.25$, 1/day, and $a_2 = 0.0005C_3A + 0.010$, 1/day.
"T" designates cements that are comparable to present-day air-entraining cements.

Cement No.	C_3S %	C_3A %	Relative non-evaporable water content at 70°F, percent: 7-*d*		28-*d*	3-*m*		1-*y*		$6\frac{1}{2}$-*y*	
			exp	cal		exp	cal	exp	cal	exp	cal
11	50.0	12.1	87.1	85.7	100	109.2	112.0	116.7	118.9	126.0	119.0
11T	51.0	12.2	85.0	86.0	100	104.1	115.5	108.2	118.2	119.6	118.3
12	45.0	12.6	84.4	84.6	100	108.3	114.3	113.6	112.4	125.0	122.5
12T	46.0	12.5	75.4	84.8	100	107.9	113.8	113.0	121.6	122.2	121.7
13	50.0	10.1	77.6	85.0	100	116.9	111.9	125.3	119.5	136.2	119.6
14	42.5	8.2	83.5	82.3	100	103.3	115.4	113.0	126.3	125.2	126.5
15	64.5	12.1	86.1	88.6	100	107.5	106.9	108.5	110.9	120.0	111.0
16	53.5	7.5	86.1	84.6	100	109.1	110.4	113.8	117.9	123.6	118.1
16T	52.5	7.9	89.8	84.6	100	109.7	110.8	118.1	118.4	121.3	118.6
17	52.0	10.4	79.0	85.6	100	107.6	111.1	109.7	118.1	118.2	118.2
18	44.5	13.2	84.4	84.6	100	108.9	114.5	113.0	122.5	116.7	122.6
18T	44.0	13.2	84.2	84.4	100	104.0	114.8	107.5	122.9	111.0	123.0
21	40.0	6.4	79.3	80.8	100	116.7	116.7	123.2	129.6	133.3	129.9
21T	38.0	6.6	79.5	80.3	100	116.0	118.0	123.9	131.7	135.0	132.1
22	41.5	6.6	78.6	81.4	100	113.4	115.9	123.1	127.9	130.5	128.3
23	51.0	3.7	71.5	81.8	100		111.0	123.5	120.7	126.6	121.1
24	41.0	5.4	82.6	80.6	100		116.0	124.0	129.0	133.2	129.4
41	20.0	4.5	84.0	70.9	100		136.3	136.2	167.2	145.5	168.2
42	27.0	3.5	71.5	74.7	100	138.6	126.8	158.0	150.8	166.4	151.8
43	25.0	6.2	87.0	74.6	100	116.5	129.5	133.1	152.4	141.0	153.0
43A	29.0	5.3	77.6	76.4	100	127.1	125.1	147.1	145.4	156.9	146.1
51	41.0	3.7	80.8	79.6	100	122.9	115.8	144.0	129.8	152.2	130.4

Table 3. *Experimental and calculated relative vapor sorptions*
The "exp" experimental values were obtained from Verbeck and Foster's experiments. (17)
The "cal" calculated values were obtained by Eq. 1) with the following parameters:
$a_1 = 0.7$, 1/day, and $a_2 = 0.033$, 1/day.
"T" designates cements that are comparable to present-day air-entraining cements.

Cement No.	C_3S %	C_3A %	Relative sorption at 0.36 r.v.p. and 70°F, percent cement: 7-*d*		28-*d*	3-*m*		1-*y*		$6\frac{1}{2}$-*y*	
			exp	cal		exp	cal	exp	cal	exp	cal
11	50.0	12.1	83.4	74.8	100	115.0	121.6	118.2	124.8	130.0	124.8
11T	51.0	12.2	92.2	75.4	100	109.5	121.0	112.4	124.1	120.3	124.1
12	45.0	12.6	73.1	71.7	100	110.4	124.3	112.0	127.9	120.9	127.9
12T	46.0	12.5	93.8	72.3	100	104.6	123.8	115.3	127.3	121.5	127.3
13	50.0	10.1	78.5	74.8	100	113.7	121.6	133.1	124.8	151.0	124.8
14	42.5	8.2	94.4	70.0	100	118.5	125.8	129.8	129.6	133.1	129.6
15	64.5	12.1	66.7	83.0	100	106.0	114.3	113.6	116.4	119.7	116.4
16	53.5	7.5	68.4	76.9	100	110.6	119.7	116.0	122.6	126.3	122.6
16T	52.5	7.9	63.6	76.3	100	109.0	120.2	138.1	123.2	131.0	123.2
17	52.0	10.4	68.3	76.0	100	112.8	120.5	111.1	123.5	122.2	123.5
18	44.5	13.2	73.8	71.3	100	117.0	124.6	113.9	128.3	117.0	128.3
18T	44.0	13.2	69.1	71.0	100	113.1	124.9	113.1	128.6	116.1	128.6
21	40.0	6.4	65.5	68.4	100	114.5	127.2	125.2	131.3	114.5	131.3
21T	38.0	6.6	66.1	67.0	100	116.1	128.4	128.5	132.6	135.8	132.6
22	41.5	6.6	57.6	69.4	100	111.9	126.3	106.8	130.2	125.2	130.2
23	51.0	3.7	65.5	75.4	100		121.0	109.1	124.1	123.7	124.1
24	41.0	5.4	79.3	69.0	100		126.6	107.5	130.6	124.5	130.6
25	34.0	4.7	75.0	64.2	100		130.9	109.5	135.5	111.5	135.5
31	56.0	10.8	87.6		100			94.0		107.8	
33	60.0	10.4	87.5		100			95.3		106.1	
33T	57.0	10.5	90.5		100			100.0		109.5	
34	64.0	5.7	82.7		100			92.2		103.0	
41	20.0	4.5	72.5	53.3	100		140.5	111.9	146.5	127.2	146.5
42	27.0	3.5	68.8	58.9	100		135.5	129.1	140.8	146.0	140.8
43	25.0	6.2	80.5	57.4	100	132.6	136.9	128.1	142.4	150.0	142.4
43A	29.0	5.3	69.5	60.5	100	139.0	134.2	134.9	139.2	148.0	139.2
51	41.0	3.7	75.9	69.0	100	128.0	126.6	126.0	130.6	142.0	130.6

values appeared to be relatively the best with Equation [1]:

$$a_1 = 0.7 \text{ 1/day}, \quad \text{and} \quad a_2 = 0.033 \text{ 1/day} \qquad [6]$$

The values calculated with these parameters along with the corresponding values measured by Verbeck and Foster (17) are summarized in Table 3. The cements tested were the same as those presented in Table 2. It can be seen that the goodness of fit between the calculated and measured values is fairly poor. It should be pointed out, however, that at least a part of the discrepancies result from the uncertainty of the sorption measurements. For instance, cement No. 14 shows an unaccountably high vapor sorption at the age of 7 days as compared to cement No. 15, considering that both the C_3S and C_3A contents of the latter are much higher.

Despite this uncertainty, the difference between Equation [3] and Equation [1] appears to show that perhaps there is no single linear relationship between the non-evaporable water content and the corresponding vapor sorption (or strength) which is generally valid for every portland cement and every age. Certain experimental results also support this view (18, 20). Therefore, when one talks about the kinetics of hydration of portland cement, the characteristic of the hydration used (compressive strength, non-evaporable water content, etc.) should always be specified.

It should be reemphasized here that the influence of the water-cement ratio on the kinetics of hydration may be significant. This is demonstrated for strength in Table 1, and in (21). Pertinent data can also be found in the technical literautre concerning the non-evaporable water content (22), and the specific surface of the hardening cement paste (20).

It is also important that Equations [1] and [3] indicate the effect of C_3A on the kinetids of hydration in the model. Namely, they reveal that the specific rate of the hydration process is, in numerous cases, a linear function, and consequently, the specific deceleration is a quadratic function of the C_3A content with a reasonable degree of approximation. This relation is not restricted to the C_3A. It seems also applicable to many other factors that influence the hydration of portland cement, such as the fineness of cement, the curing temperature, etc. If a change in any of these factors increases the early strength by increasing the specific rate of hydration, then, simultaneously the same factor increases the deceleration of the hydration to a higher degree; thus the final strength, or at least the final relative strength, will be less. This principle is further illustrated in the next paragraph by the effect of temperature on strength.

Effect of Temperature on the Hardening

It will be shown now that the presented model concept is suitable for the demonstration of the effect of temperature on the hydration. A natural point of departure is the so-called Arrhenius equation:

$$a = A_0 e^{-Q/RT_a} \qquad [7]$$

where

a = specific rate of reaction,
Q = activation energy,
R = gas constant,
T_a = temperature, °K, and
A_0 = empirical constant.

One can obtain the following simplified form by expanding Equation [7] into a series:

$$a = A\left[B - \frac{Q}{R(273 + T)}\right] \qquad [8]$$

where

T = temperature of the mixture, °C, and
A and B = empirical constants.

The other symbols are identical with the symbols of Equation [7].

It may be assumed for this demonstration that the value of Q is independent of the temperature and is about 16,000 cal/g mol. If the usual assumption (that the hydration of portland cement ceases when the temperature is −10°C or lower) is also used, then the value of 30.4 can be computed for the B constant. The value of A is dependent on numerous factors, such as the measured characteristic of hydration, the hydrating cement component, the composition and fineness of the cement, the water-cement ratio, etc. As is shown in Table 1, the cements tested by Klieger (15), with 0.43 water-cement ratio and 23°C curing temperature, provided $a_1 = 0.40$ 1/day, and $a_2 = 0.002C_3A + 0.02$ 1/day values for the compressive strength of concrete. Thus, for this case

$$A_1 = \frac{0.40}{30.4 - 8000/296} = 0.12 \qquad [9]$$

Similarly,

$$A_2 = 0.0006C_3A + 0.006 \qquad [10]$$

Therefore, the a parameters of Equation [1] can be expressed as a function of temperature for this case

and for 10 percent C_3A content as follows:

$$a_1 = 0.12\left(30.4 - \frac{8000}{273 + T}\right) \quad [11]$$

and

$$a_2 = 0.012\left(30.4 - \frac{8000}{273 + T}\right) \quad [12]$$

A convenient way to check the extent of support given these speculations by experimental results is to apply the "maturity rule" to the formulas above. As is well known, the maturity rule states that within certain limits the effects of curing temperature and age on the strength of concrete can be expressed in terms of a single parameter given by the product of age and temperature where the temperature is reckoned from −10 °C (23, 24, 25). That is,

$$M = (T + 10)t \quad [13]$$

where

M = maturity, °C × day,
T = curing temperature of concrete, °C, and
t = age of the specimen at testing, days.

If one expresses the a_1t and a_2t parameters defined by Equations [11] and [12] in terms of maturity, the following is the result:

$$a_1t = \frac{3.6}{273 + T}M \quad [14]$$

and

$$a_2t = \frac{0.36}{273 + T}M \quad [15]$$

It can be seen that the strengths calculated by the presented cement model are dependent not only on the maturity but also on the curing temperature. However, within certain limits (e.g., 0 and 25°C), the temperature has little effect on Equations [14] and [15]. To help illustrate the temperature sensitivity of these equations, one can use the following expression for the strength development from Equation [1]:

$$f = f_0[1 - pe^{-a_1t} - (1 - p)e^{-a_2t}] \quad [16]$$

where

f_0 = compressive strength of concrete after infinitely long wet curing, and
f = compressive strength of the same concrete at the age of t.

The other symbols are identical with the symbols of Equation [1].

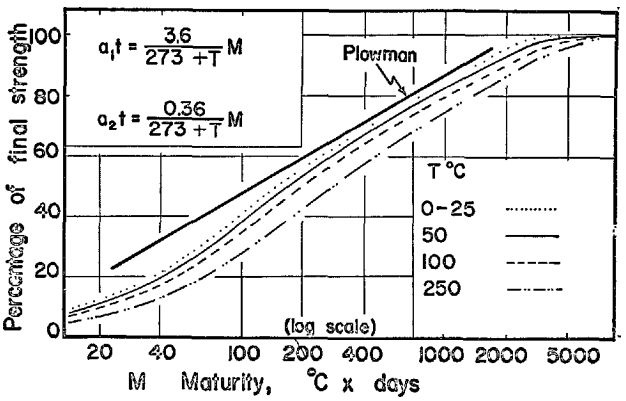

Fig. 5. *Compressive strength of concretes cured at differing temperatures as a function of maturity.*

By substituting Equations [14] and [15] into Equation [16], and introducing the $f^0_{rel} = 100f/f_0$ relative strength, the following relationship is obtained between the f^0_{rel} compressive strength of the concrete discussed and the M maturity:

$$f^0_{rel} = 100[1 - pe^{-3.6M/(273+T)} - (1 - p)e^{-0.36M/(273+T)}] \quad [17]$$

where the symbols are identical with the symbols of Equations [1] and [13].

Values of strength calculated by Equation [17] and with 50 percent C_3S content are shown in Fig. 5 for various temperatures. It can be seen that strengths related to a given maturity are lower when the curing temperature is higher. Experimental results by various authors show similar tendency (26, 27). The presented discussion of the temperature sensitivity of strength is also in accordance with a conclusion of Klieger (27), namely, that the relationship between strength and maturity is affected by the type of the cement and the composition of the concrete as well.

Fig. 5 also shows, with thick line, an empirical relationship for the effect of maturity on the relative compressive strength of concrete. This relationship was estimated from experimental data published by Plowman (28). This line also appears to support the applicability of the presented cement model for the estimation of the effect of temperature on the strength development of concrete.

Topics for Further Research

1. The approximation of the model for the hydration of Type IV and Type V portland cements at later ages is not entirely satisfactory. It is conceivable that a modification of the model would improve the ap-

proximation. For instance, the assumption of a composition for the C_3S different from the one used by Bogue, might be such a modification. Thus, further research in this direction is desirable.

2. A fundamental topic is the derivation of the form of the *a* parameters as a function of C_3A content from theoretical considerations.

3. An experimental topic is to determine the effects of fineness, temperature, mix proportion, admixtures, etc. on the numerical values of the *a* parameters.

4. An investigation is desirable concerning the cause of the differences between the kinetics of the various hydration characteristics.

5. It would be interesting to check the applicability of the model for high alumina cements.

Conclusions

1. The presented simple model concept seems applicable for the kinetics of various characteristics of hydration for a large group of portland cements.

2. The kinetics of the various hydration characteristics of a paste, (or mortar or concrete) may differ considerably. For instance, the rate and the deceleration of the development of tensile strength are much more intensive than those of the compressive strength of the same mixture. The kinetics of the non-evaporable water content, or that of the specific surface of a hardening cement paste seem also different.

3. Therefore, it is not expected that there exists a single linear relationship between any two of the discussed hydration characteristics which is valid for every age and every portland cement.

4. The presented cement model seems also suitable for the demonstration of the effect of temperature on the hydration process.

5. The goodness of fit between experimental data and values calculated by the model is reasonable enough to encourage further research for the refinement and further application of the presented model concept.

References

1. S. Popovics, "A model for the kinetics of hardening of portland cement", Highway Research Record No. 192. Highway Research Board, Washington, D. C. 1967. pp. 14–35.
2. R. E. Philleo, "The strength of concrete—a statistical view", Stanton Walker Lecture Series on the Materials Sciences No. 5. Presented at University of Maryland, Nov. 16, 1967.
3. G. Murphy, Similitude in Engineering, The Ronald Press. New York. 1950. pp. 57–61.
4. P. H. Bates and A. A. Klein, "Properties of the calcium silicates and calcium aluminate occuring in normal portland cement", Technologic Paper No. 78, National Bureau of Standards, June 9, 1917.
5. H. Woods, H. H. Steinour and H. R. Starke, "Effect of composition of portland cement on heat evolved during hardening", Industrial and Engineering Chemistry, Vol. 24, 1932. pp. 1207–14.
6. H. Woods, H. R. Starke and H. H. Steinour, "Effect of cement composition on mortar strength", Engineering News Record, Vol. 109, No. 15. 1932. pp. 435–437.
7. R. E. Davis, R. W. Carlson, G. E. Troxell and J. W. Kelley, "Cement investigation for the Hoover Dam" ACI Journal, Proc., Vol. 29. June, 1933, pp. 413–431.
8. R. H. Bogue and W. Lerch, "The hydration of portland cement compounds", Industrial and Engineering Chemistry, Vol. 26. August, 1934. pp. 837–847.
9. H. F. Gonnerman, "Study of cement composition in relation to strength, length changes, resistance to sulfate waters and to freezing and thawing, of mortars and concrete", Proceedings, ASTM, Vol. 34, Part II. 1934. pp. 244–295.
10. W. Czernin, Cement Chemistry and Physics for Civil Enginneers, Crosby Lockwood & Son Ltd. London, 1962. Part 3.
11. F. M. Lea and C. H. Desch, The Chemistry of Cement and Concrete, 2nd Edition. (Revised by F. M. Lea), Edward Arnold (Publishers) Ltd. London, 1956. p. 81.
12. M. Venuat, "Compte rendu d'un voyage d'etudes aux Etats-Unis et au Canada (Mai 1965)" (Report of a Study Tour in the United States and Canada, May, 1965). Revue des Materiaux de Construction "Ciments & Betons", October et December 1965, Nos. 601 et 603.
13. G. Verbeck, "Cement hydration reactions at early ages", Journal of the PCA Research and Development Laboratories, Vol. 7, No. 3, Sept. 1965. pp. 57–63.
14. S. Popovics, "A method for evaluating how well observed data fit the line Y = X", Materials Research and Standards, Vol. 7, No. 5. May, 1967. pp. 195–202.
15. P. Klieger, "Long-time study of cement performance in concrete". Chapter 10. Progress report on strength

and elastic properties of concrete", ACI Journal, Proc. Vol. 54, December, 1957. pp. 481–504.
16. R. H. Bogue, "Calculation of compounds in portland cement", Industrial and Engineering Chemistry (Analytical Edition), Vol. 1, October 15, 1929. p. 192.
17. G. J. Verbeck and C. W., Foster, "Long-time study of cement performance in concrete with special reference to heats of hydration" Chapter 6. Proceedings, ASTM, Vol. 50. 1950.
18. L. E. Copeland, D. L. Kantro and G. Verbeck, "Chemistry of hydration of portland cement", Chemistry of Cement. Proc. of the Fourth International Symposium. Monograph 43, Vol. I. Session IV. Washington, D. C., 1960.
19. T. C. Powers and T. L. Brownyard, "Studies of the physical properties of hardened portland cement paste—Part 9. General summary of findings on the properties of hardened portland cement paste", ACI Journal, Proc. Vol. 43, April. 1947. pp. 971–992.
20. C. M. Hunt, "Nitrogen sorption measurements and surface areas of hardened cement pastes", Symposium on Structure of Portland Cement Paste and Concrete, Highway Research Board, Special Report 90. Washington, D. C., 1966. pp. 112–122.
21. S. Popovics, "Factors affecting the relationship between strength and water-cement ratio", Materials, Research and Standards, Vol. 7, No. 12. December, 1967. pp. 527–534.
22. J. H. Taplin, "A method for following the hydration reaction in portland cement paste", Australian Journal of Applied Science, Vol. 10, No. 3. Sept., 1959. pp. 329–345.
23. R. W. Nurse, "Steam curing of concrete", Magazine of Concrete Research, Vol. 1, No. 2. London, June, 1949. pp. 79–88.
24. A. G. A. Saul, "Principles underlying the steam curing of concrete at atmospheric pressure", Magazine of Concrete Research, No. 6. March, 1951.
25. S. G. Bergstrom, "Curing temperature, age and strength of concrete", Magazine of Concrete Research, No. 14. Dec., 1953.
26. K. M. Alexander and J. H. Taplin, "Concrete strength, paste strength, cement hydration, and the maturity rule", Australian Journal of Applied Science, Vol. 13, No. 4. Dec., 1962. pp. 227–284.
27. P. Klieger, "Effect of mixing and curing temperature on concrete strength", ACI Journal, Proc. Vol. 54. June, 1958. pp. 1063–1081.
28. J. M. Plowman, "Maturity and the strength of concrete", Magazine of Concrete Research, Vol. 8, No. 22. March, 1956. pp. 13–22.

Supplementary Bibliography

F. S. Fulton, "The rate of hydration of portland cement", Laboratory Report, SF-4, Portland Cement Institute. August, 1962. Johannesburg, South-Aftica.

RILEM Symposium, Winter Concreting Theory and Practice, The Danish National Institute of Building Research, Special Report. Copenhagen, 1956.

T. C. Powers and T. L. Brownyard, "Studies of the physical properties of hardened portland cement paste—part 3. Theoretical interpretation of adsorption data", ACI Journal, Prov. Vol. 43. December, 1946. pp. 469–504.

D. L. Kantro, C. H. Weise and S. Brunauer, "Paste hydration of beta-dicalcium silicate, tricalcium silicate, and alite", Symposium on Structure of Portland Cement Paste and Concrete, Highway Research Board, Special Report 90. Washington, D.C 1966. pp. 309–327.

L. E. Copeland and D. L. Kantro, "Chemistry of hydration pf portland cement at ordinary temperature", The Chemistry of Cements, Edited by H. F. W. Taylor, Vol. I, Chapter 8, Academic Press, London & New York, 1964. pp. 313–370.

S. Brunauer and D. L. Kantro, "The hydration of tricalcium silicate and beta-dicalcium silicate from 5°C to 50°C", The Chemistry of Cements, Edited by H. F. W. Taylor, Vol. I, Chapter 7, Academic Press, London & New York, 1964. pp. 297–312.

U. Danielsson, "Conduction calorimeter studies of the heat of hydration of a portland cement", Handlingar, NR 38. Svenska Forskningsinstitutet for Cement och Betong vid Kungl. Tekniska Hogskolan I Stockholm.

B. Mather, "Cement performance in concrete", Technical Report No. 6–787, USAE Waterways Experiment Station, Vicksburg. September, 1967.

A. Nykanen and S. Philajavaara, "The hardening of concrete under winter concreteing conditions", The State Institute for Technical Research, Finland, Publication 35, Helsinki, 1958.

J. H. Taplin, "The temperature dependence of the hydration rate of portland cement paste", Australian Journal of Applied Science, Vol. 13. No. 2, June, 1962. pp. 164–171.

Supplementary Paper III-3 Mechanical Properties of Precompressed Cement-Mortar Specimens

Ori Ishai*

Synopsis

Mortar specimens, cured by different procedures, were subjected to creep and shrinkage tests, and their instantaneous mechanical properties were determined.

Experimental results indicate the superiority of specimens precompressed during the setting period (2–4 hours after mixing), to their counterparts subjected to ordinary moisture curing. Precompressed specimens were characterized by higher compressive strength, rigidity and density, lower creep, shrinkage and smaller thermal expansion. Oven-dried specimens showed negligible compressive creep.

The above characteristics are attributable to the reduction in both the voids ratio and the evaporable-water content, obtainable by the precompression and drying processes.

Introduction

Cement paste, mortar and concrete are highly-porous materials whose mechanical properties are strongly influenced by their porosity characteristics.

The porous phase covers a wide range of pore sizes, from 20–30 Å for gel pores to 10,000 Å for capillaries.

At the initial stage of hardening, almost the entire pore volume is filled with absorbed and adsorbed evaporable water. The role of the pores and the pore water on the mechanical properties of cementitious products was investigated and discussed extensively. It was found that while the voids ratio mainly influences time-independent properties such as elastic modulus and strength (1, 2, 3), content and distribution of the evaporable water within the microstructure are the predominant factors in the time-dependent behavior manifested by shrinkage (1, 4, 5, 6) and creep (7, 8, 9, 10).

It was concluded that while a higher voids ratio results in low strength and rigidity, a high evaporable-water content favors high time-deformation.

The object of the present work was:

a) An appropriate method of reducing both the voids ratio and the water content.

b) A study of the mechanical behaviour of the more compact and dry cementitious product obtained by such methods.

Experimental Prodecure

According to the main object, two extreme methods of treatment were chosen:

1) Almost total drying of hardened ordinary moist-cured mortar specimens, in order to expel the evaporable water.
2) Compaction of the fresh mortar mix, in order to reduce the voids ratio before hardening.

Compacted dry tubular (Fig. 1) (o.d. 7.5, i.d. 4, height 15 cm), compared to orinary moist-cured ones. Four mechanical parameters were studied: strength, rigidity, shrinkage and creep.

*Technion, Israel Institute of Technology, Haifa, Israel.

Preparation of Specimens

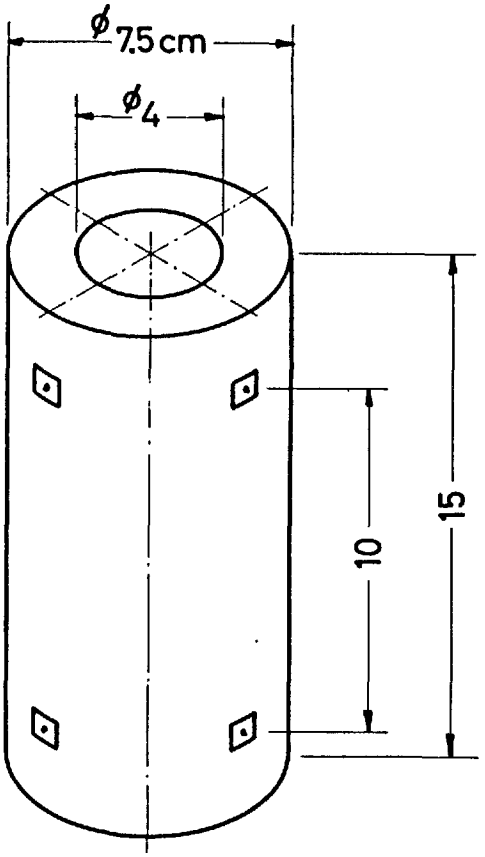

Fig. 1. *Mortar specimens used for testing the compressive deformational behavior*

Mix proportions were 1.1: 1 Leighton-Buzzard sand to portland cement by weight; initial water/cement ratio — w/c = 0.33.

Two main groups of specimens were prepared according to mode of curing and treatment as follows:

Group A: Ordinary Moist-Cured Specimens

Specimens were stored at 90% R.H. and water-cured for 6 more days after demolding.

Group B: Precompressed Specimens

The fresh mix was precompressed in the mold by a central axial force*, exerting an axial pressure of about 160 kg/cm² on the material. This pressure, transmitted by a prestressing device and counterbalanced laterally by the mold walls, was maintained for 3 days in a moist environment.

At 3 days, after release of the axial compression and demolding, the hardened specimens were moist-cured for 4 more days.

Procedure

Four series of test were conducted as follows:

Series I: Compressive Strength

The influence of precompression time (1, 2, 3 and 4 hours) on strength at 7 days, measured on a standard testing apparatus.

Series II: Young's Modulus in Compression

Longitudinal deformations under axial load applied at 7 days, measured by means of Steiger-type extensometers along the generatrices (Accuracy — 10^{-5} micro strains).

Series III: Shrinkage

Dry-wetting cycles applied at 7 days:
11 days at 90% R. H., 22°C
11 days at 50% R. H., 22°C
4 days oven-drying, 105°C
150 days at 90% R. H., 22°C
30 days under water, 22°C

Axial deformation measurements were taken daily (hourly during the oven-drying period).

Series IV: Creep

Wet specimens of both groups, moist-cured for 35 days, and insulated** specimens of group A oven-dried at 105°C to almost constant weight were kept under axial load in a climate room at 50% R. H. and 22°C.

Axial deformations were measured daily up to 130 days after loading.

*This compaction process resulted in immediate squeezing-out of water and an average volume contraction of about 10%.

**Dried specimens were immersed several times in liquid epoxy resin, which hardened and provided good insulation for at least 10 weeks.

Results and Discussion

The influence of precompression was evident in all cases. The resulting disruption of the setting process seemed to have no adverse effect on strength and other properties of the hardened mortar—rather to improve them. Expulsion of the evaporable water from the hardened mortar reduced appreciably all time-dependent deformations and almost eliminated creep.

Series I

Precompression 1 hour after mixing does not affect compressive strength, but when applied 3–4 hours after mixing a strength increase up to 100% is obtained.

Series II

Precompressed specimens showed modulus values higher by about 10%. The same trend is reflected in the higher density and lower coefficient of thermal expansion characterizing the specimens of group B.

Series III

Both groups exhibit the same general trend: increase of shrinkage during exposure to dry environment (higher rate at 50% R. H. compared to 90% R. H.), and a steeper increase, terminated by stabilization, during the oven-drying period. Shrinkage recovery during wetting follows the usual course of swelling, which becomes pronounced under immersion.

In all stages, precompressed specimens exhibit lower shrinkage and swelling characteristics and seem to tend to long-term total recovery (Fig. 3).

Series IV

Creep strain vs. time curves show, as expected, a high time-rate of deformation after loading, and a decreasing rate later on (Fig. 4). Precompressed

Table 1. *Effect of precompression on mechanical properties*

Group	Density gr/cm³	Young's modulus in compression kg/cm²	Compressive strength at 7 days kg/cm²	Coefficient of thermal expansion	Shrinkage (10 days) at 50% R.H.	Creep at 10 weeks under 160 kg/cm²
A Ordinary moist-cured	2.28	4.0×10^5	280	11.5×10^{-6}	43×10^{-5}	55×10^{-5}
B Precompressed 2 hours after mixing	2.42	4.5×10^5	420	10.8×10^{-6}	26×10^{-5}	30×10^{-5}

(average of at least two specimens, 4 deformation measurements on each).

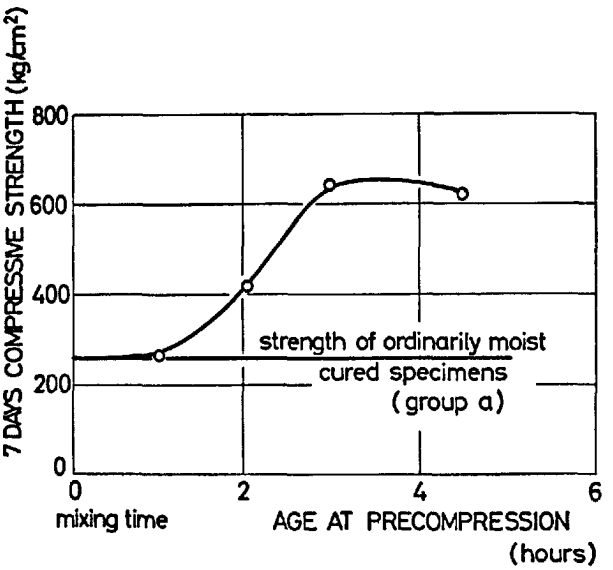

Fig. 2. *Influence of time at precompression on compressive strength of specimens*

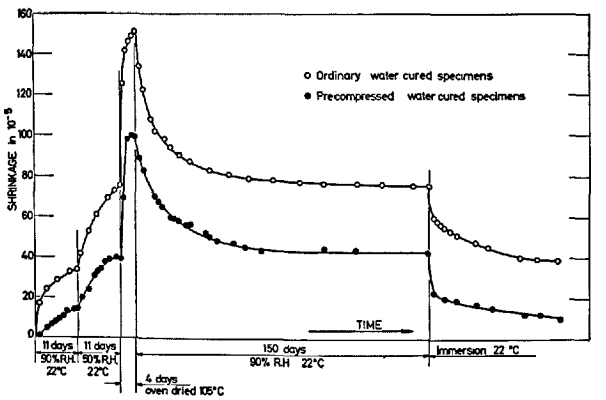

Fig. 3. *Shrinkage and swelling characteristics of wet specimens exposed to drying-wetting cycle*

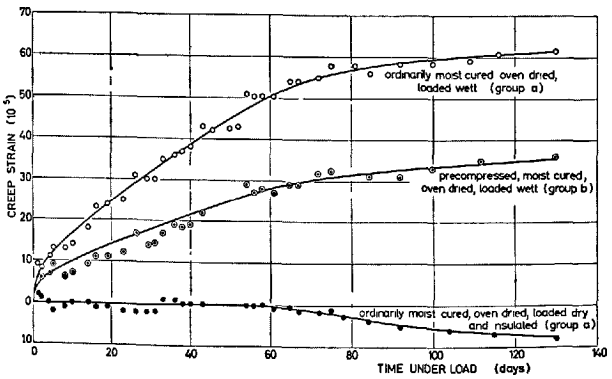

Fig. 4. *Compresive creep of specimens with different curing and treatment histories*

specimens show appreciably lower creep (up to almost 50%), but long-term slopes seem to be identical for both curves.

Dried specimens of group A showed no noticeable deformational change during the first 10 weeks after loading. Later a slight swelling was recorded (attributable to water diffusion through the insulating coating) followed by recovery.

In view of their higher voids ratio compared with group B, it is concluded that the evaporable-water content is the main factor governing the above creep behaviour.

Conclusions

1) Precompression of the mix during setting influenced appreciably the mechanical properties of the hardened product.

2) Precompression 3–4 hours after mixing seems to yield optimal results with regard to compressive strength.

3) Precompressed specimens are characterized by higher compressive strength and rigidity, higher density and lower coefficient of thermal expansion compared with their ordinary counterparts.

4) Precompressed specimens exhibit markedly lower shrinkage and creep characteristics compared with their ordinary counterparts.

5) Insulated oven-dried specimens show negligible creep under compressive load.

6) The superior quality of the precompressed and dried specimens is attributable to their low porosity and low evaporable-water content, believed to be the main factors determining the mechanical behavior of the hardened cement paste.

Acknowledgments

The project was sponsored in part by the Fohs Foundation. The author is indebted to J. Jerushalmi for assistance in conducting the experiments, and to P. Schechter for the drawings.

References

1. T. C. Powers, "Physical properties of cement paste", Proc. 4th Intern. Symp. on Chemistry of Cement, Washington 1960.
2. T. C. Hansen, J. A. C. I. **62**, 193 (1965).
3. O. Ishai, J. A. C. I., **58**, 611 (1961).
4. T. C. Powers, Fundamental Aspects of the Shinkage of Concrete, 3rd Int. Congr. of the Precast Concrete Industry, Stockholm, June 1960.
5. R. F. Feldman and P. J. Sereda, J. Appl. Chem. 14, 87 (1965).
6. O. Ishai, J. Appl. Materials Research, p. 154, July 1966.
7. J. Glucklich and O. Ishai, J. A.C.I., **59**, 923 (1962).
8. R. G. L'Hermite, "Volume changes of concrete" 4th Inster. Symp. on Chemistry of Cement, Washington 1961.
9. O. Ishai, "The time-dependent deformational behavior of cement paste mortar and concrete", Inter. Conf. on the Structure of Concrete, Sept. 1965, London.

Supplementary Paper III-33 Determination of Plain Concrete

Floyd O. Slate* and Bernard L. Meyers**

Synopsis

This paper describes and explains, in general terms, various aspects of deformations of the concrete system. The subject is introduced by a description of the composite material, followed by a breakdown into components, including aggregate, aggregate-paste interface, crystals, crystallites, gel, holes of various sizes, water, and air. The various individual components that are deformed (called Deformees), are discussed one-by-one, as related to deformation of the over-all system. Then the stimuli causing deformation (called Deformers) are listed and discussed. This is followed by a general discussion of the interactions between the Deformees and the Deformers, that result in significant engineering deformations. Finally, the paper attempts to show that local, internal deformations and their cumulative effects limit the usefulness of concrete, and are directly related to short-term deflection, long-term deflection, cracking, and failure.

The paper breaks down the various components of the system, and the various stimuli and actions, into individual variables, discusses them item-by-item, then combines them into the composite system concrete. Thus, the first portion of the paper is written from the point of view of structure of matter and materials science; as the paper proceeds, the emphasis is shifted toward the point of view of engineering applications.

Local, internal deformations, and their cumulative effects, are considered to be of overwhelming importance in determining the stiffness, deflections, and strength of concrete. These local deformations initiate cracking and creep; the progress of cracking and creep follows the progressive development of local deformations; and fracture or excessive deformation is the cumulative effect of local deformations. The proper isolation and study of the variables associated with local deformations should be fruitful in leading to a better understanding of the performance of concrete, and to its improvement.

Introduction

The purpose of this paper is to describe and explain, in general terms, various aspects of the deformation of concrete system. Several types of deformation as well as how and why they occur, are discussed. The paper is not intended to be a review of the literature, but rather to be the authors' analysis of concrete deformations, based on general principles, on existing knowledge, and on research carried out by the authors over a period of years. Consideration is limited to deformations caused by such things as loading and unloading, hydration, and changes in moisture content; deformations associated with such things as thermal changes and freeze-thaw action are not considered.

The general subject is introduced by a description of the concrete system, including aggregate, aggregate-paste interface, crystals, gel, holes of various sizes, water, and air. Deformations, prior to, during, and after the time under load, are explained and discussed in terms of the reaction of the concrete system and its elements to such stimuli as: load, moisture migration, hydration, and recrystallization. The general approach is based on consideration of a heterogeneous internal structure, and on the internal forces that hold matter together and govern its differential displacement and recovery. The first part of the paper is written from the point of view of materials science; as the paper proceeds, the emphasis is shifted toward the point of view of engineering application.

Many papers (only a few of which are referenced

*Cornell University, New York.
**The University of Iowa, Iowa, U.S.A.

here) have been written on the internal structure of concrete (1, 2, 3)*, on the general elastic and inelastic behavior of concrete under the action of loads of short duration (4, 5), on the shrinkage behavior of concrete (6), and on the time-dependent deformation of concrete caused by sustained load (7, 8, 9, 10, 11, 12). But very few authors (13) have tried to present a coordinated overall picture of the deformation of concrete.

Internal Structure of Concrete

A brief statement will be made here of those aspects of internal structure which have major effects on deformations. A later section of the paper, "Deformees—Things that are Deformed," will discuss one-by-one some of the individual components of the structure.

Concrete is a multiphase heterogeneous material. Its individual components and their interfaces act differently from each other, resulting in a very complex variation in local deformations throughout the material, including both differing magnitudes of deformations and differing time-deformation responses, in different parts of the same concrete specimen. In the opinion of the authors, local deformation is the item that is directly related to failure (or to local separation, fracture, or flow), and stress is thus only indirectly related to failure. For a proper understanding and explanation of failure of concrete, it is likely that approaches based on stress, or based on the assumption that "strain" is constant throughout the specimen, are doomed to limited sucess at best, and that an approach based on varying local deformations is both correct and necessary.

Interactions at the aggregate-past interface play an important role in the overall behavior and deformation of concrete (7, 14, 15). A considerable portion of the total deformation of concrete is probably usually concentrated at these interfaces.

The paste itself is also a multiphase material. It can be assumed that paste is made up of crystals, and of needles, plates, filaments, and crumpled sheets (2) of very small size (crystallites) arranged mostly at random in a three-dimensional system to form a gel (a colloidal, spongy structure). These crystallites that form the gel have surfaces that are multipolar, attract each other by secondary electrostatic forces, and are strongly hydrophillic. Thus, water is strongly attracted to the surfaces of the gel and into spaces between closely-spaced gel particles, tending to separate them. The thickness of these layers of adsorbed water varies from about one to ten molecules. There are also water-filled holes (pores, capillaries, and voids) of widely varying size in the concrete system. In addition, many of the larger holes (voids) hold only air.

Deformees—Things That are Deformed

An attempt will be made to list, as separate variables, the various parts of the concrete system that are deformed—that is, generally changed in position or shape. The basic consideration is any *relative* movement in space of atoms, ions, or molecules; the movement must be relative to other matter in the same concrete system.

Concrete as a Whole

It is customary to measure gross deformation in concrete, by use of deformators, compressometers, and strain gages. Then, on the assumption that the deformations are distributed equally throughout the specimen (or the gage length), "strains" are calculated to represent the concrete as a whole. Actually, the gross deformation measured is the sum total of, or the result of, very many small, varying, discreet deformations occurring in the various constituents and parts of the concrete. Thus highly localized deformations or "strains" may be greatly different from the average for the concrete as a whole. For example, the "strain" across an aggregate-paste interface where a crack opens up will probably be an order of magnitude greater than for the average of the specimen as a whole.

*Numbers in parenthesis refer to entries in the References at the end of this paper.

Aggregate

The mineral aggregates used in concrete are brittle under short-time loading. That is, deformations are small up to brittle fracture, and are largely elastic. Under long-time loading, inelastic deformation may take place; although it may be appreciable, especially for some aggregates such as some limestones, it is generally very small as compared to deformations of other parts of the concrete system. Formation of cracks in the aggregate is usually small until the moment of catastrophic failure of the concrete; for higher water-cement ratios, for younger ages, and with rounded aggregate, the total amount of ultimate cracking in the aggregate is usually very small-it generally increases with lower water-cement ratios, with greater ages, and with more angular aggregate. The mineral composition and lithologic structure influence all deformation and fracture properties. Since the deformations of aggregate are small as compared to those of paste, their primary significance is that of *differential* deformation at the interfaces, often leading to a greater *net* deformation across the interface.

Aggregate-Paste Interface

Ideally, the interface might be considered to be an infinitely thin surface, not subject to deformation across its surface. However, in this paper the interface will be considered to be the region extending slihtly into both aggregate and paste, and will still be called an aggregate-paste interface (cracked) even after a crack has been formed, consisting of a void of air or water, and in reality creating two new interfaces, aggregate-air (or water) and paste-air (or water).

The aggregate-paste interface (or aggregate-mortar interface, as it is sometimes called), has been shown to be the site of a very large amount of cracking, and thus of deformation, under many different conditions of loading, hydration, and drying (7, 14, 15, 16). The separation may be "clean," between aggregate and paste, or may occur partly within one or the other material. For example, soft, porous limestones may fail partially within the limestone, leaving some thin layers of limestone still adhering to the paste on the paste side of the separation. More often, the other case, of some failure through paste very close to the aggregate surface, is noted. The latter case seems to occur more often when the aggregate surface is rough, even on a microscopic scale, thus providing a greater area of bonding and sometimes forcing "brittle shear" to occur through one of the materials.

The interfacial bond should be primarily brittle in nature, and primarily elastic in action until actual separation. The separation can be more or less perpendicular to the interface, forming an opened crack-in this case a brittle tensile failure seems to be the predominating action. The local displacement can also occur as sliding along a compression-shear-loaded interface (presumably after an initial brittle failure of the bond), in which case friction could resist further sliding deformation (17). An interfacial crack may partially close upon removal of load, giving an effect of partial "elastic action."

In many cases, a crack-like "semi-void," or apparently a thin layer of paste of high water-cement ratio, can be seen adjacent to the interface. This weak region is presumably caused at the time of placement by gravity segregation (particularly at interfaces at the bottom surfaces of aggregate particles), and on all surfaces by vibration of aggregate particles, thus displacing all material away from the surfaces, followed by faster and greater return to the depleted region by water as compared to cement.

The deformations occurring at the interfaces have been shown to be directly related to, and to be a major influence controlling, the shape of the stress-strain curve (14) and to involve a portion of the average strain in long-time deformation (7). It is probable that a majority of the total short-time, uniaxial compressive deformation in concrete, from about 50% to 70% of ultimate load, (and almost all the inelastic deformation below 50% of ultimate), is contributed by the cumulative effect of interfacial deformations, particularly interfacial cracking. Of course, the paste phase, which is the continuous phase, must be deformed to allow deformation of the concrete as a whole, but in many or most concretes its local deformation is probably appreciably controlled and "forced" by deformations at interfaces, at least up to about 70 percent of the short-time ultimate strength.

Paste

An attempt will be made to divide paste into its basic material components, and to discuss each (crystals, crystallites, air, free water, capillary water, adsorbed water, water of hydration, and miscellaneous structures and effects such as holes, solution, deffusion, reprecipitation, and crystal-to-crystal contact) as a separate variable. It must be recognized that one

component may have a profound effect on another, and that the actual behavior is caused by interrelated properties of the system, rather than by additive effects of each part in turn. However, it will be fruitful to examine each part, as it exists within the system.

Crystals

This section refers primarily to those crystals large enough to be seen with the optical microscope. They are brittle in nature, both in short-time loading and long-time loading-long-time as understood for concrete (a few years). Their deformations, short of fracture, are small and primarily elastic. Rod, needle, plate, and sheet crystals should be able to withstand, without fracturing, much more deformation in certain directions than in others (such as bending of a beam as compared to direct compression). Deformations associated with fracture are non-recoverable. The sum total of deformations contributed by these "large" crystals is probably very small, at least until the moment of catastrophic fracture of the specimen, and perhaps even then. Thus, these deformations are relatively unimportant in concrete.

Crystallites

This refers to crystals (often highly imperfect) beyond the resolution of the optical microscope. Another useful definition (allowing a larger size) would be to place them within the colloidal range, with at least one dimension less than one-tenth micron. These tiny crystals (often needles, plates, filaments, and crumpled sheets), arranged more or less at random, separated more or less by thin layers of water, and containing various-sized spaces filled with water and air, constitute cement paste, and compose what is often called cement "gel," particularly when the larger spaces or holes are not considered. The crystallites can be expected to act much as do the larger crystals, but their total mass is so much greater that their cumulative deformation must be much greater. Their less-perfect crystal structures might allow more plastic crystal deformation, but the amount should still be small as compared to other deformations in concrete.

Air

Air is very easily deformed and easily compressed. Its solubility in water and aqueous solutions is appreciably increased by pressure, leading to reduced volume. It will readily flow from regions of high to lower pressure. Its flow may be inhibited by water saturation of all spaces that otherwise could afford routes of flow.

Free Water

This refers generally to water at distances greater than about 1 mm. from crystal or crystallite surfaces. It is present in the larger spaces, holes, and voids. Its compressibility is so small that it can be ignored. It is very easily deformed, and will tend to flow easily and quickly from regions of high to low pressure, if unrestricted. Its flow may be restricted by the smallness of the holes through which it must flow, leading to significant time effects. Free water is relatively easily removed from the system by evaporation.

Capillary Water

This refers generally to water at distances between about 1 mm. and 30 Å from crystal or crystallite surfaces. It is attracted with appreciable, but not great, force to those surfaces, which are highly hydrophillic. The attraction to the surfaces (primarily polar, secondary forces) will oppose and delay, but not prevent, movement of the water away from the surfaces. Thus an additional time effect is present for deformation (or movement) of this water; it will be removed from a surface, or evaporated, slower and with more difficulty than free water. Otherwise, its characteristics are the same as those listed above for free water, with one vitally important exception: upon removal of a load (or effect causing evaporation) which has removed capillary water from an attractive surface, the water will tend to return. Since removal of the water caused crystal surfaces to move closer together (or vice versa), return of the water will cause the crystal surfaces to move apart. Thus deformations from load or drying, and involving capillary water, can be recovered with time. For example, water between two crystals could be squeezed out into a relatively large air void; upon removal of the load, the water would tend to return and spread the space between the two crystals to its original distance.

Adsorbed Water

This refers generally to water at distances between 0 and about 30 Å from crystal and crystallite surfaces, and represents a layer of water from one to ten molecules thick. The attraction of the surface varies greatly across this distance, and there is no sharp dividing line between adsorbed water and capillary water. The adsorbed water is held very tightly by the strongly hydrophillic surfaces of the crystals

and crystallites. It can be moved by load or evaporation, but only with great difficulty (large pressure) and only slowly. It generally acts very much in the manner described above for capillary water, except it moves from a surface with more difficulty and more slowly. Its removal from a region will result in deformation, and it will *strongly* tend to return in time after load (or other driving force) is removed, causing a delayed recovery of deformation. The first three molecular layers of water are probably not much affected through most of the concrete system, even at catastrophic failure of the system (although they may be, at isolated points of great pressure), and the innermost molecular layer is probably deformed or removed little if at all.

Water of Hydration

This term is often used somewhat loosely. It should refer to water of crystallization held directly in a crystal lattice, in a definite combining ratio with the other building blocks of the crystal. It often refers to water held tightly in variable hydrates, and sometimes apparently even to very tightly bound surface water on a crystal. Thus the binding forces vary from primary chemical bonds to secondary chemical bonds (such as hydrogen bonds) and even to very strong secondary physico-chemical bonds in adsorbed layers. In all cases, the water is held very tightly, and most tightly of all water in the system. Some of this water can be moved by elevated temperatures, still within expected experience for some concrete, by very low external relative humidities, and by high local pressures caused by external load. This latter point may be of appreciable importance, although deformations involving water of hydration should be expected (except possibly in cases of extreme temperature leading to disintegration) to be relatively small as compared to those involving other forms of water.

Holes

Holes are not properly component materials of the paste, but perhaps a brief consideration of them may be helpful. In general, by holes is meant any space not occupied by a solid. Thus holes may be filled with air, with water (solutions), or with some of each. They vary in size from "huge" spaces in honeycombed concrete to tiny spaces between crystallites in the gel system, measured in a few angstrom units. In general, whenever the fluid (air or water) is removed from the hole by some force, the hole becomes smaller, and the solid surfaces bounding the hole come closer together—both local and gross deformations can then be observed. The effect is greater for smaller holes. Upon removal of the force which caused removal of the fluid, the system will attempt to reach a new equilibrium. If the hole is small enough that its attraction for water is appreciably large, and if water is available to move into the hole, water will flow back into the hole, the hole will become larger, and both local and gross deformations (of recovery) can be observed. Such recovery will be time dependent.

There will be a tendency for all similar solid surfaces to be covered by an equal thickness of water film, at true equilibrium. This condition will not exist for concrete at any time, including before loading. As loading re-distributes the water films, the new position of some of the water will be expected to be nearer true equilibrium conditions, even for non-loaded concrete. Thus some of the water will never return to its original position after unloading of the concrete, and some of the deformation will be non-recoverable.

Crystal-to-Crystal Contact

There may be points of crystal-to-crystal contact, without any intervening layers of water, although this point is not at all certain. Such contact should vary from an intimate relationship in which one crystal is part of the system of the other (as in twinning) where primary chemical bonds (electrovalent for these mineral systems) are involved, down to a touching of neighboring adjacent, but independent, crystals, which would attract each other by multipolar, secondary chemical forces. In either case, the bond should be brittle, and should be relatively strong, even for the weaker case of independent crystals with multipolar forces of attraction. If these bonds from crystal-to-crystal contact exist, they may be one of the last points of failure or deformation to occur just before or at the moment of catastrophic failure of the concrete specimen, and may appreciably influence the ultimate strength of concrete, in both short- and long-time loading.

Solution, Diffusion, and Reprecipitation

The solubility of crystals and crystallites increases under pressure. The load through concrete must be transmitted unevenly through the mass, at least on a micro scale. Therefore, at concentrated load-bearing points, some material dissolves, diffuses to a region of lower pressure (or where a newly-precipitated crystal would be under less pressure),

and precipitates out (as in a void). This represents a permanent deformation, is a time-dependent process, and is non-recoverable creep. The effect under short-time load should be much smaller than under long-time load, but might still result in a small amount of non-recoverable deformation even for the short-time load. This process *must* occur, qualitatively. It probably is of considerable importance in autogenous healing of concrete under load.

Deformers—Things That Cause Deformation

We have seen that each part of the concrete system, from the largest piece of aggregate to the smallest gel crystallite and on to individual water molecules, contributes to the overall deformation. Deformation is induced in each of the components by various influences. The most important of these influences are those which alter pressure in, and hygral equilibrium of, the system; other influences are such things as hydration and carbonation.

Hydration and Carbonation

An autogenous shrinkage of the paste is caused by hydration of cement (in the absence of available external free water) because the products of hydration occupy a smaller volume than do the reactants. If external free water is available and allowed to enter the system, a net expansion of the paste occurs, as expansion from ingress of water to adhere to and spread newly-formed hydrophillic hydrate surfaces, more than overcomes shrinkage from hydration. Carbonation (an acid-base reaction involving carbonic acid and the basic paste components) apparently involves solution of basic crystals such as calcium hydroxide, perhaps under pressure from drying shrinkage, and precipitation of resulting carbonates in open void spaces.

Change of Average Load or Pressure

The application and the removal of load affects the overall pressure causing deformation in various parts of the system. Change of load also induces localized pressure peaks and troughs because of the heterogenity of the system. Change of load, in addition, affects hygral equilibrium because of load-induced moisture migration.

Change of Local Pressure

The pressure at various local internal places can be expected to change greatly as the external load is changed; as the volume changes from wetting, drying, hydration, and carbonation; and as internal redistribution of individual portions of the structure forces changes of load-bearing points and areas. These localized regions of pressure differential must strongly influence diffusion of water, solution of solids, diffusion of dissloved material, and positions of crystal reprecipitation.

Wetting and Drying

These actions increase or decrease the thickness of water films separating the hydrophillic hydrate surfaces, forcing them apart upon wetting, or forcing them together upon drying as internal pressure falls below that of the external environment. These effects occur for both adsorbed water and capillary water. There is little effect from change in "free" water content in the larger voids and honeycomb spaces.

Physical Processes Caused by the Deformers

There is generally an intermediate step between application of a Deformer and the physical occurrance of deformation. This intermediate step consists of physical processes that are caused by the Deformers, and which in turn cause, control, or result in deformations. These physical processes that are caused by the Deformers include such things as the following: Direct deformation and breakage of crystals and crystallites, Separation of interfaces, Flow, Diffusion, Solution, and Reprecipitation. Any process involving diffusion can be expected to be strongly time-dependent; therefore, all deformations—either primary or of recovery—involving diffusion should be strongly time-dependent, and all such deformations from load and from drying should be partly recoverable and partly non-recoverable, depending on the relative stability or energy levels before and after diffusion, and the possibility of irreversible processes following diffusion.

Deformation Behavior

In this section the deformation of concrete as an engineering material is discussed in detail. The discussion is divided into the following sections: Deformation without Load, Deformation due to Short-Time Load, and Deformation due to Long-Time Load. This rather arbitrary separation is not intended to imply that the various types of deformation are independent. It is recognized that all components of deformation can occur ar the same time and are highly dependent on each other.

Deformation without Load

Volume changes caused by the hydration process and by carbonation are time-dependent and may be considered small compared to the deformations caused by load.

The deformation caused by the migration of water into and out of a specimen is of sufficient magnitude to affect the structural performance. In most practical cases, the relative humidity of a concrete specimen is higher than that of its surroundings. Thus, the matrix will lose water in an effort to establish hygral equilibrium with its environment. Moisture is evaporated first from the larger pores and capillaries, introducing small volume changes, and later from the smaller capillary spaces and from the layers of water adsorbed to the gel surfaces, introducing relatively large volume changes. The resulting deformation is defined as drying shrinkage (normal range = 0.0001 to 0.001 in/in). If water is returned to the matrix a corresponding swelling will take place.

Since drying shrinkage and swelling take place in the paste, tensile stresses are introduced at the interface between the paste and the relatively rigid aggregate particles (15). When the tensile strength of the interface is exceeded, microcracks are developed, resulting in non-recoverable deformation. Microcracks are also developed, to a lesser degree, by the volume changes caused by the hydration process and by carbonation.

Deformation Due to Short-Time Load

When loads of short duration (10 to 10^3psi/sec) are applied to a concrete specimen, elastic and inelastic deformations take place. The stress-strain curve of concrete can be divided into three ranges. From 0 to about 30% of the ultimate strength, the deformation is elastic and linear. Between 30 and 70% of the ultimate strength, both elastic and inelastic deformations take place, the majority being inelastic. Above 70% of the ultimate strength, most of the deformation is inelastic. The inelastic and elastic deformation caused by loads of short duration are not affected by strain rate and, therefore, are not time-dependent.

The general behavior of concrete subjected to short-time loads, described above, will now be analyzed in detail by discussing the deformation of each component of the matrix.

Aggregate

The deformation of the aggregate particles is small compared to the total deformation and may be assumed to be linear and elastic.

Paste

The deformation of the paste is also, for the most part, linear and elastic. As load is applied, atoms (ions) and molecules move. For each crystal and crystallite, if this local motion is less than 1/2 of the ionic or molecular diameter, the resulting deformation is completely recoverable and linear. The gel crystals bend, deform, and return to their original configurations upon removal of the load. If the load is of sufficient magnitude, some of the weaker cyrstals will break, introducing non-recoverable deformation.

Aggregate-Paste Interface

Most of the inelastic, nonrecoverable strain exhibited by the short-time stress-strain curve of concrete is a result of cracking at the aggregate-paste interface and through the paste (14). As the load is applied, existing cracks do not propagate and new ones do not form until the load reaches about 30% of the ultimate strength. Above this load, bond cracks start to increase in width, length and number. As the load is further increased, some cracked interfaces continue to carry, by friction, about the same load that caused the initial failure. All additional load is carried by the uncracked interfaces and the surrounding paste. Local cracks begin to form in the paste, at the tip of existing bond cracks, allowing the aggregate particles to slide relative to the paste, causing the initial inelasticity of the short-time stress-strain curve. As the load is increased above about 70% of the ultimate strength, the local cracks start to bridge between adjacent aggregate particles causing additional inelasticity and internal disruption that ultimately

leads to failure of the specimen (17).

Water

The water in the system will also move under the influence of short-time load introducing a relatively small amount of deformation. In contrast, the time-dependent migration of moisture within and to the surface of the system has a much more pronounced effect on the creep of concrete, and will be discussed more fully later in the paper.

Deformation Due to Long-Time Load

If a load is applied, and maintained at a constant stress level, or applied at a rate slower than about 1 psi/sec, a concrete specimen continues to deform without any increase in applied stress. This time-dependent deformation is usually 1 to 4 times greater than the initial strain from the applied load, for specimens on which a load within the working stress range is maintained for more than about a month. Upon release of the sustained load, part of the total strain is immediately recovered, part is slowly recovered, and part is never recovered.

Stress is developed throughout the matrix when it is subjected to a sustained load: in the aggregate, in the hydrated cement gel, at the aggregate-paste interface, and in the various types of water. The long-time, load-induced deformation of concrete consists of the response of all of the above to stress: progressive internal microcracking at the aggregate-paste interface, elastic and inelastic deformation of the aggregate and of the paste, migration of load-bearing water within and to the surface of the specimen, solution and recrystallization of gel particles, and other stress-induced changes in the gel structure.

Moisture Movement

When load is applied, the pressure and the hygral equilibrium within the specimen are altered. In order to re-establish equilibrium the water contained in the larger holes (pores, capillaries and voids) is forced out of its original position, through capillaries and between gel surfaces to air voids and to the surface. The resulting volume change, which takes place rather quickly (probably in a few weeks or less), may be considered increased or accelerated shrinkage caused by the sustained load. It is non-recoverable, unless water is returned to the specimen after the sustained load is removed (3).

The water strongly adsorbed to the gel surface diffuses from its original position very slowly. As this water diffuses from between the gel surfaces to larger holes, and eventually to the surface of the specimen, the gel particles are forced closer together by the load. The resulting deformation (creep) takes place very slowly and probably never completely reduces the thickness of the adsorbed water layers to zero (9).

If there is no change in the internal structure of the gel and the amount of water in the specimen remains constant, creep should be completey recoverable. When load is removed, the hydrophillic gel attracts water which deffuses from the larger holes back to the closely spaced gel surfaces, tending to force them apart. The resulting deformation is creep recovery.

The magnitude of the deformation caused by internal moisture migration (creep and creep recovery) depends on the properties (such as surface area) of the cement gel, on the water content, and on the storage conditions at the time of load application and during the time under load.

Effect of Adsorbed Water

In most practical mixes the hydration of the cement continues for six months or more. During this time the surface area of the gel increases and available water is attracted to the surfaces between the new gel particles, increasing the number of and the total thickness of the adsorbed water layers. At some stage of hydration the adsorbed layers may begin to decrease in average thickness, as the area of the gel increases and the amount of available free water is decreased through combination with cement and by evaporation. Therefore, a specimen sealed prior to and during the time under load will exhibit more creep than a companion specimen that is allowed to dry prior to and during the time under load. The total deformation of the unsealed specimen, including increased shrinkage, may or may not be greater than that of the sealed specimen, depending on the age and drying at the time of loading (9).

Effect of Recrystallization and Changes in Internal Structure

The solubility of the gel (of all the solids) is increased by load. Gel and crystals dissolve, in water, at regions of high load intensity, diffuse to new locations, and reprecipitate as new crystals or on existing crystals in areas of lower load intensity. As a result of this diffusion, undissolved particles will move closer together as material is dissolved away from between them. The magnitude of this deformation depends on the maturity and stability of the gel at the time of load application. If the specimen is loaded early in the hydration process, a large amount of recrystalli-

zation will be introduced by the load. On the other hand, if the specimen is loaded when hydration is near completion, the gel will be more stable and additional deformation due to recrystallization will be small. Since the deformation described above is a result of a permanent change in the structure of the gel, it is non-recoverable (9).

Non-recoverable deformation is also introduced if the sustained load is of sufficient magnitude to break some of the gel crystallites and crystals.

Since the deformation resulting from internal changes in gel structure is non-recoverable, creep cannot, in fact, be completely recoverable. If the load is applied and maintained on a young specimen for a long period of time, recovery will be small compared to creep. On the other hand, if an older specimen is loaded for a shorter period of time, recovery will be large compared to creep (9).

Microcracking

Sustained load causes the propagation of more microcracking than an equal short-time load. If the sustained load is below about 70% of the ultimate strength, the same amount of bond cracking is introduced by time-dependent strain as would be by a short-time strain of equal magnitude. However, there is no increase in mortar (paste) cracking. For loads above 70% of the ultimate strength, mortar cracks are introduced by creep strain, and the specimen will probably fail after some time under a constant load. Deformation due to time-dependent microcracking is non-recoverable (7).

Relationships between Deformations and Failure or Deflection (19, 20, 21)

Local, internal deformations and their cumulative effects limit the usefulness of concrete, and are directly related to short-term deflection, long-term deflection, cracking, and failure. The distance between individual building blocks of matter, such as atoms, ions, and molecules, governs the attraction and repulsion between them, and thus controls the resistance to initial or further deformation, strain, or separation at any given load or stress. Attraction or repulsion is a geometric function of distance.

There should be a limiting deformation at each point (really two adjacent points) within concrete, that will result in brittle separation, excessive flow, or excessive deformation or deflection. It must be emphasized that the limiting deformation will vary greatly among the various Deformees in the system, and that it will be changed by conditions (such as rate of deformation) for any given Deformee. Therefore, *failure should be a deformation-dependent phenomenon*, with the critical deformation a function of various things, such as composition, rate of deformation, and environment.

There should be a limiting over-all deformation for a concrete specimen, that will result in failure. The amount of this limiting deformation should be about the same for all specimens of a given concrete, under a given set of conditions. However, a different concrete, or a different rate of deformation (for example), should cause a change in the limiting deformation. It seems reasonable that many or most concretes, under a variety of general conditions, but with a few critical conditions stated or controlled, should exhibit limiting deformations within a usable reproducible range. The range or general level of limiting deformations might then change with such things as age, moisture content, and rate of deformation, and even with the testing set-up for laboratory specimens.

Attempts to relate a maximum strain with failure, for complex heterogenous systems such as concrete, have generally not been successful, because only gross or over-all strain or deformation has been considered; consideration must also be given to local deformations or to control of those variables influencing local deformations and thus ultimately influencing gross deformations. If it is true that local deformations ultimately control deflection and failure of concrete, then it follows that the weaknesses and deficiencies of concrete related to deflection and load limit, can perhaps profitably be isolated, investigated, and alleviated by study of local deformations and their interactions.

For example, a concrete showing a large gross deformation or strain under a short-time uniaxial compressive load will probably contain more internal microcracks than a concrete showing a smaller gross deformation; in this case, any change (such as increase of aggregate-paste interfacial strength) that reduces the amount of microcracking at a given load will reduce the gross strain and deflection of the concrete at that load. Such sorting and isolation of variables moves studies for understanding and improvement of materials away from empiricism.

Acknowledgement

This paper is connected with work done at Cornell University and sponsored by the National Science Foundation.

References

Only a few selected references are listed; no attempt has been made to present an extensive list from the large number of publications related to this general subject. An excellent bibliography was prepared by l'Hermite (reference 13 below).

1. T. C. Powers and T. L. Brownyard, "Studies of the physical properties of hardened portland cement paste", J. Am. Conc. Inst., Proc. **41**, 101–132, 249–336, 469–504, 549–602, 669–712, 845–880, 933–992 (Oct. 1946–Apr. 1947). Reprinted as Research Lab. Portland Cement Assoc. Bull. 22 (1948).
2. A. Grudemo, "The microstructure of hardened cement paste", Proc. Fourth Internat. Symp. on the Chemistry of Cement, Washington D. C., Vol. 2, 615–658 (1960). U. S. Natl. Bur. Stds. Monograph 43.
3. T. C. Powers, "Physical properties of cement paste", Proc. Fourth Internat. Symp. on the Chemistry of Cement, Washington D. C., Vol. 2, 577–613 (1960). U. S. Natl. Bur. Stds. Monograph 43.
4. T. J. Hirch, "Modulus of elasticity of concrete affected by the elastic moduli of cement paste matrix and aggregate", J. Am. Conc. Inst., Proc. **59**, 427–451 (Mar. 1962).
5. T. C. Hansen, "Theories of multi-phase materials applied to concrete, cement mortar and cement paste", Internat. Conf. on The Structure of Concrete, Imperial College, London (1965).
6. T. C. Powers, "Mechanisms of shrinkage and reversible creep of hardened cement paste," Internat. Conf. on The Structure of Concrete, Imperial College, London (1965).
7. B. L. Meyers, F. O. Slate and G. Winter, "Relationship between time-dependent deformation and micro-cracking of plain concrete", sumbitted for publication to the Am. Conc. Inst. in Aug. 1967.
8. B. L. Meyers and F. O. Slate, "Creep and creep recovery of plain concrete as influenced by moisture conditions and associated variables", submitted for publication to the Am. Conc. Inst. in Aug. 1967.
9. B. L. Meyers and F. O. Slate, "A general hypothesis for the creep of concrete", submitted for publication to the Am. Conc. Inst. in Aug. 1967.
10. O. Ishai, "Time-dependent deformational behavior of cement paste, mortar and concrete", Internat. Conf. on The Structure of Concrete, Imperial College, London (1965).
11. W. Ruetz, "A hypothesis for the creep of hardened cement paste and the influence of simultaneous shrinkage", Internat. Conf. on The Structure of Concrete, Imperial College, London (1965).
12. C. E. Kesler and I. Ali, "Mechanism of creep", Am. Conc. Inst. Special Publn. 9, Symp. on Creep of Concrete (1964).
13. R. G. l'Hermite, "Volume changes of concrete", Proc. Fourth Internat. Symp. on the Chemistry of Cement, Washington D. C., Vol. 2 659–702 (1960). U. S. Natl. Bur. Stds. Monograph 43.
14. T. T. C. Hsu, F. O. Slate, G. M. Sturman and G. Winter "Microcracking of plain concrete and the shape of the stress-strain curve", J. Am. Conc. Inst., Proc. **60**, 209–224 (Feb. 1963).
15. T. T. C. Hsu, "Mathematical analysis of shrinkage stresses in a model of hardened concrete", J. Am. Conc. Inst., Proc. **60**, 371–390 (Mar. 1963).
16. F. O. Slate and R. E. Matheus, "Volume changes on setting and curing of cement paste and concrete from zero to seven days", J. Am. Conc. Inst., Proc. **64**, 34–39 (Jan. 1967).
17. S. P. Shah and G. Winter, "Inelastic behavior and fracture of concrete", J. Am Conc. Inst., Proc. **63**, 925–930 (Sept. 1966).
18. K. Newman, Complex and Heterophase Materials, (Elsevier Publishing Co., London, 1965). See chapter on "Concrete systems".
19. O. Ya Berg. "The problem of the strength and plasticity of concrete", Dokladi Akademii Nauk USSR **70**, No. 4, 617–620 (1950).
20. R. Jones, "Testing of concrete by ultrasonic-pulse technique", Highway Research Board, Proc. **32**, 258–275 (1953).
21. M. F. Kaplan, "Strains and stresses of concrete at initiation of cracking and near failure", J. Am. Conc. Inst., Proc. **60**, 853–880 (July 1963).

Supplementary Paper III-72 Correlation of Strength and Hydration with Composition of Portland Cement

Kenneth M. Alexander, John H. Taplin and John Wardlaw*

Synopsis

The paper presents the results obtained by multiple regression analysis of strength and hydration data from recent surveys of normal portland cement in Australia. Differences between the cements are largely attributed to C_3A. The effect is thought to be mainly an acceleration of the hydration of the cement as a whole. C_3A dominates at water/cement ratios from 0.35 to 0.80, curing temperatures from 5 to 75°C, and throughout most of the period from 1 day to 6 months. Strength is most sensitive to C_3A content under conditions which are frequently encountered in laboratory test work, namely, water/cement ratio 0.5, age 28 days, curing temperature 21°C.

With the present cements there is a smaller, but significant effect, for median particle size, whereas the effect of quite appreciable differences in C_3S content is of minor importance. The influence of other cement characteristics such as minor oxide compositions, surface areas, etc., is either non-significent, or can be accounted for as another aspect of the C_3A and size effects. Possible exceptions are the positive correlations of strength with Mn_2O_3 at early ages, and the negative correlations of strength with free lime at high water/cement ratio and later ages.

Introduction

As a result of recent investigations in these laboratories, a considerable volume of data on cement strength and hydration has been accumulated, both as a byproduct and as the main objective of several in dependent lines of enquiry. Spanning the full range of normal portland cements in Australia, these studies cover performance at early and later ages, from near freezing to steam curing conditions, and from the upper to the lower limits of water/cement ratio encountered in practice. In this paper, six thousand measurements from these studies are assembled and analysed for relationships between performance and mineral composition, fineness, minor element content, and other characteristics of cement.

Previous studies, for example, by Gonnerman and Lerch (1), support the widely held belief that the rate of hardening depends on the fineness and the C_3S content of cement. Gonnerman (2) found the contribution of C_3A to strength was important until 28 days, but with further curing it declined, to become zero or negative after a year or more. The accelerating effect of C_3A has been supported by authors such as Powers (3) and Budnikov and Erschler (4).

Experimental

The various series of experiments which are assembled in this paper fall naturally into two groups that will be analysed separately. The results in Experimental I are by Alexander and Wardlaw, those in Experimental II are by Taplin, and the analyses are by Alexander and Taplin respectively. Only the one statement of conclusions is presented, and this is based on the findings of both analyses.

Experimental I

The 15 cements used in this section of the investigation were commercial products from 15 different plants. All materials complied with the Australian Standard Specification A2 for Type A Ordinary

*C.S.I.R.O., Department of Civil Engineering, Sydney University, Sydney, Australia.

Table 1. *Oxide compositions, surface areas and median particle sizes for cements 1 to 15*

Cement No.	Surface area in cm^2/g	Median particle diameter in microns	Ign. loss (%)	Oxide compositions (per cent)											
				SiO_2	Al_2O_3	Fe_2O_3	CaO	MgO	SO_3	Na_2O	K_2O	Mn_2O_3	P_2O_5	TiO_2	Free lime
1	3410	20.0	1.54	20.75	5.05	3.55	64.30	1.35	2.50	0.60	0.68	0.05	0.06	0.19	1.18
2	3890	13.8	0.99	20.90	5.15	3.10	65.60	1.65	1.20	0.04	0.67	0.09	0.05	0.22	1.02
3	3160	19.0	1.14	20.45	6.30	3.35	66.10	0.40	1.90	0.03	0.28	0.07	0.05	0.40	0.26
4	3410	19.0	1.27	21.70	4.65	2.50	63.95	1.55	2.70	0.70	0.06	0.05	0.09	0.42	1.49
5	3130	24.0	0.91	22.85	3.55	4.20	64.80	0.75	2.20	0.19	0.55	0.01	0.08	0.21	1.17
6	3440	19.8	1.52	20.20	6.15	3.00	65.50	0.80	2.40	0.06	0.86	0.11	0.06	0.27	2.44
7	3430	19.8	2.49	21.00	4.45	4.00	62.95	1.50	2.50	0.53	0.56	0.07	0.08	0.31	2.04
8	3540	16.2	0.72	20.20	4.65	5.20	64.50	1.30	2.50	0.36	0.39	0.28	0.12	0.30	0.63
9	4380	15.0	1.84	20.65	4.05	4.90	64.25	1.40	2.25	0.24	0.22	0.03	0.10	0.33	3.47
10	3680	19.0	1.41	19.40	6.40	3.45	64.80	1.60	2.05	0.08	0.57	0.11	0.11	0.34	2.01
11	3190	23.0	0.90	23.35	3.60	3.50	64.20	0.85	2.50	0.10	0.38	0.10	0.07	0.22	0.87
12	3500	18.9	1.62	20.00	6.20	3.20	64.30	1.65	2.00	0.03	0.88	0.11	0.06	0.26	2.55
13	3720	20.6	2.14	21.20	3.55	4.90	63.15	2.00	1.90	0.30	0.32	0.02	0.10	0.33	2.40
14	3460	17.5	1.24	21.25	5.30	3.20	64.75	1.50	1.60	0.36	0.34	0.16	0.08	0.37	1.63
15	3260	22.0	0.95	21.90	4.50	3.55	64.25	1.55	2.30	0.07	0.62	0.13	0.07	0.31	0.62

Portland Cement. The chemical and physical characteristics of these cements are given in Table 1, and their potential mineral compositions, calculated by the method of ASTM Standard C150–64, and corrected for free lime, are in Table 2. Surface areas were determined by air permeability, in accordance with ASTM Standard C204–55.

In the main series of tests, compressive strengths were determined on $\frac{1}{2}$-inch cubes of machine mixed paste which had been cured continuously under water at 21°C. Strength measurements were made at 1, 3, 7, 28, 56, 90 and 180 days on pastes with water/cement ratios 0.35, 0.50 and 0.80 by weight. The pastes with water/cement ratios of 0.80 were stabilized with 3%, by weight, of pre-gelled bentonite. A subsidiary group of tests was run at water/cement ratio 0.45, ages 16 to 56 days, and under water curing at 5, 21 and 43°C.

The results for the main series (Table 3) are means of at least 10 replications per point. Data for this table originated in the Organization's laboratories in Sydney and Melbourne. Co-ordination between the two laboratories was checked in a series of 600 tests at 1 to 180 days, using half the present range of cements. A coefficient of correlation of 0.993 was obtained.

Data for the subsidiary tests are in Table 8.

The compound compositions of cements 1 to 15 range from 44.5 to 61.7% for C_3S, 11.1 to 33.2% for C_2S, 1.1 to 11.2% for C_3A, and 7.6 to 15.8% for C_4AF. Surface areas are from 3130 to 4380 cm^2/g. At highest water/ cement ratios and earliest ages the highest paste strengths are about 3 times the lowest, whilst at the opposite extreme of late age and low water/cement ratio, this strength ratio is about 1.5 to 1.

Attention is drawn to the point that in the accompanying discussion, significance at the 5, 1 and 0.1% levels of probability will be termed significant, highly significant, and very highly significant respectively.

Table 2. *Potential mineral compositions for cements 1 to 15*

Cement No.	Potential mineral composition (per cent)			
	C_3S	C_2S	C_3A	C_4AF
1	53.8	18.8	7.4	10.8
2	60.3	14.3	8.5	9.4
3	60.8	12.7	11.0	10.2
4	47.3	26.3	8.1	7.6
5	50.1	27.5	2.3	12.8
6	51.4	19.0	11.2	9.1
7	46.4	25.0	5.0	12.2
8	61.7	11.1	3.6	15.8
9	50.9	20.5	2.4	14.9
10	55.3	13.6	11.1	10.5
11	44.5	33.2	3.7	10.6
12	48.1	20.9	11.0	9.7
13	51.0	22.1	1.1	14.9
14	51.3	22.0	8.7	9.7
15	51.4	23.9	5.9	10.8

Experimental II

The fifteen cements, numbers 16 to 30, used in these experiments came from the same cement works as those quoted in the previous section but were, with one exception, completely different samples. The potential mineral composition was calculated by the method of ASTM C150 after correcting for free lime. Table 10 lists the relevant data on chemical composition and median particle size. The minor oxides TiO_2, P_2O_5 and Mn_2O_3 were also included in some statistical analyses their mean % values are 0.26, 0.07 and 0.09 respectively.

The cements, and those quoted in the previous section were sized by the method of Andreasen using

Table 3. *Paste compressive strengths for cements 1 to 15 at water/cement ratios 0.35 to 0.80 and ages 1 to 180 days*

Compressive strength in p.s.i. Mean of 10 determinations

Cement No.	Age in days																	
	1	3	7	28	56	90	1	3	7	28	56	90	180	1	3	7	28	56	90
	Water/Cement ratio 0.35						Water/Cement ratio 0.50							Water/Cement ratio 0.80					
1	3400	6850	10200	15960	16460	17940	562	2160	4550	9420	11240	11720	12970	280	771	1330	2520	2860	2820
2	3910	8050	12960	19190	20090	20610	970	2790	5480	10920	11700	12330	13260	274	948	1720	3080	3360	3180
3	2890	5670	10730	17740	20770	19960	956	2300	4140	9010	10870	9400	12600	275	795	1290	2790	2970	2910
4	2450	5660	11140	15740	17380	18880	970	2300	4210	7930	9930	11500	11540	292	737	1080	2350	2900	3060
5	2880	5790	9310	14010	15290	16560	900	2490	3530	5430	8040	9920	10550	184	564	836	1880	2510	2700
6	2990	7300	12810	16570	18660	17950	1260	3470	5420	9290	10440	12460	10790	387	910	1520	2520	2770	2640
7	2640	5160	7360	11720	14230	16450	880	2070	3110	5330	7280	9200	9680	200	668	1040	2070	2440	2680
8	4990	9340	11140	15690	17880	18280	1180	2570	3790	7370	8620	9790	10670	563	1120	1420	2370	2700	2840
9	3460	7170	9620	14940	16690	17340	1010	2380	3650	5850	7380	9220	9820	248	761	1010	1960	2320	2540
10	3830	6960	11260	16030	17080	17390	716	2460	4310	8640	11040	10560	11620	245	736	1220	2570	2380	2500
11	2020	3980	7830	14250	16220	16130	694	1500	2640	5830	8270	10260	10720	240	759	983	2090	2660	2990
12	3080	7130	12510	18900	19030	20330	687	2940	4790	10770	11700	12610	12450	357	984	1700	2820	2550	2400
13	2080	5000	7290	12500	13140	13620	331	1400	2410	5420	6690	7620	8950	208	648	960	2000	2300	2520
14	3100	5090	11010	17250	20420	20760	868	2360	4290	9240	11060	11680	12090	264	845	1240	2870	2950	3120
15	2650	5090	9030	14620	17790	18460	546	2280	3480	6670	8800	10460	11890	375	792	1020	2300	2770	3100

Table 10. *Oxide composition, potential mineral composition and median size of cements*

P.C.[1]	Oxide composition × 10⁴										Potential minerals × 10³				μ
	SiO_2	Al_2O_3	Fe_2O_3	CaO	MgO	SO_3	Na_2O	K_2O	I.L.[2]	F.L.[3]	C_3S	C_2S	C_3A	C_4AF	Dm
16	2250	410	350	6425	80	260	8	46	104	100	471	288	50	106	23.0
17	2220	445	350	6435	145	200	6	76	78	54	510	250	59	106	23.0
18	2000	395	495	6405	130	245	22	23	187	335	553	154	22	151	14.9
19	2155	350	515	6320	165	200	24	38	129	292	459	269	6	157	21.0
20	2185	500	330	6440	150	165	37	49	94	119	488	257	76	100	21.5
21	2060	440	350	6400	155	245	61	8	123	231	537	184	58	106	20.8
22	2165	455	375	6240	150	280	52	56	155	153	402	316	57	114	21.5
23	2225	345	440	6465	70	195	21	52	106	174	526	239	18	134	22.0
24	2060	590	330	6455	70	230	5	93	148	238	463	240	100	100	19.0
25	2015	485	515	6470	135	215	34	42	92	89	617	109	41	157	18.0
26	2055	590	305	6485	135	195	4	80	164	214	501	209	105	93	20.0
27	2035	595	340	6460	155	195	6	57	145	169	516	192	101	103	19.0
28	2145	495	360	6445	125	210	59	66	162	87	521	221	70	109	20.0
29	2125	520	295	6590	125	175	4	74	133	54	611	147	88	90	17.2
30	2065	620	335	6675	40	190	4	28	111	31	622	121	108	102	19.0

1 portland cement
2 ignition loss
3 free lime

ethanol with 0.01% calcium chloride. The measurements were made at 30, 20, 10, 5 and 3.4 μ and gave reasonably straight lines when plotted on log probability paper. The median size was obtained by interpolation. The cements were also sieved with uncalibrated 30 and 20 μ electro-formed sieves and this method indicated a median size 3 μ smaller than quoted. The correlation between the methods is 0.88.

Stirred Specimens

Tubes about two thirds filled by ten grams of cement and forty mls of water are attached to a slowly rotating frame so that they revolve end-over-end about four times a minute. At the appropriate time the specimen is filtered, dried under vacuum and the hydration determined by the method of Taplin (5). Hydration, in this paper, means the weight loss defined by this method. The curing periods are 5, 9, 16, 24, 30, 48, 96, 168, 240, 672, 2000 and 4000 hours.

Hardened Specimens

These specimens were $\frac{1}{2}$ inch diameter, 1.3 inches high, paste cylinders and were cured entirely under water. The ends were ground parallel, prior to testing in compression. These tests were made in duplicate and the remains of the cylinders were dried and used in hydration determinations. For those specimens which were cured entirely at 21°C the curing periods were 9, 16, 24, 72, 168, 240, 672, 2000, and 4000 hours. The specimens were made at W/C ratios of 0.35 and 0.60 by weight.

Complete sets of strength determinations at

W/C = 0.35 are available only to ten days. Additional specimens were given simulated steam curing after standing for 1, 4 and 7 hours at 21°C. The standard size glass jar containing the specimens under water was then placed in an oven at 75°C for twenty hours, the specimens were then cooled under running water for half an hour, and tested. The temperature of the specimens rose 30°C in the first hour in the oven. Only for one cement did the specimens show a significant increase in strength with the length of standing time at 21°C. The results were averaged over standing period giving nine replications to each measurement.

The pastes at W/C = 0.60 were stabilized against bleeding by the addition of one per cent, by weight of the cement, of bentonite. The bentonite was gelled by standing overnight in the mixing water. The 4000 hour results are not yet complete at the time of writing. The simulated steam curing procedure was also repeated at this W/C ratio but this time at 65°C, and an extra set of steamed specimens was given an additional 27 days curing at 21°C.

Discussion I

The Regression of Strength on Composition at Ages 7 to 180 Days

In this section, relationships between strength and potential mineral content for cements 1 to 15 (Tables 2 and 3) are studied by the techniques of multiple linear regression analysis. Attention is concentrated on curing periods from 7 to 180 days, and the discussion begins by considering the situation where all four major compounds, C_3S, C_2S, C_3A and C_4AF are included in the analysis.

Table 3 contains 13 sets of strengths for ages 7 to 180 days and water/cement ratios 0.35 to 0.80. All coefficients of multiple correlation for the regressions of these strengths on compound composition are found to be significant whereas, among the 13 sets of 4 regression coefficients, only 2 of the 52 individual values are significant. At this, the 5% level of significance, the observed proportion of significant regression coefficients could readily have occurred by chance.

The fact that the regressions as a whole are significant, whereas the influence of each individual variable is not, can be explained by the observation that the mineral contents of the cements do not vary independently. In this instance, the simple correlation coefficients for C_3S on C_2S and C_4AF on C_3A are both highly significant. A better description of observed strength is thus likely to be obtained by a regression in which the silicates and aluminates are each represented by only one independent variable. The analogous situation for heats of hydration has been analysed by Hald (6).

The point is illustrated by Fig. 1, where the coefficient of multiple correlation (R) is plotted for suc-

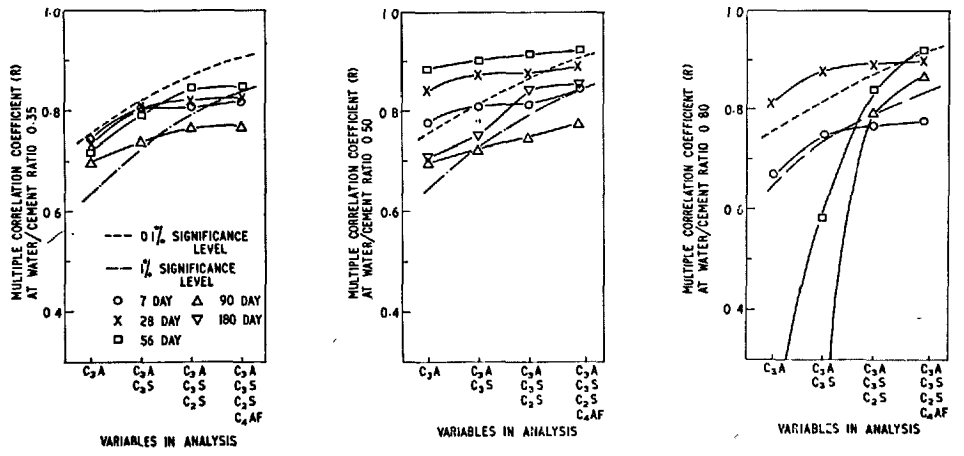

Fig. 1. *The regression of strength on potential mineral content: multiple correlation coefficients and significance levels for successive regression analyses, starting with a constant and one independent variable.*

cessive analyses in which the independent variables are added in the order C_3A, C_3S, C_2S, C_4AF, suggested by the simple correlations. It will be seen that at water/ cement ratios 0.35 and 0.50, the elimination of C_4AF and C_2S from the analysis has only a slight adverse effect on the significance of the association of strength with mineral composition. At water/cement ratio 0.80 these same conclusions apply up to 28 days, beyond which time the regression of strength on C_3A becomes non-significant, and the present order of analysis is no longer recommended.

Further details of the analysis show that the only occasion when the regression on C_3A, C_3S and C_2S is significantly better than on C_3A, C_3S, is at 180 days, where the data are, unfortunately, restricted to the single water/cement ratio 0.50. This limited evidence does however, serve as advance warning that C_2S should not be excluded at ages of 6 months and greater.

Within the range of cement compositions studied here, it is profitable to continue the process of elimination beyond the stage where silicates and aluminates are each represented by a single variable. It can be shown, by intermediate solution of the analyses, that with the exception of one borderline case at 7 days (water/cement ratio 0.80), C_3S itself can be omitted. In Fig. 1 the general effect of this omission is seen as a slight decrease in the coefficient of multiple correlation, coupled with an increase in the significance of the regression.

It is, therefore, concluded that for the present cements, the most significant association between strength and compound composition lies in the regression involving C_3A alone, and not in the more complex analyses involving two or more cement minerals. Over a wide range of water/cement ratios and ages, the significance of the regression on C_3A never falls below the 1% level and, in a high proportion of cases, exceeds the requirements for significance at the 0.01% level of probability.

In view of the key role indicated for C_3A, a further set of regressions on strength was calculated, using the proportion of C_3A determined by X-ray. The correlation between X-ray and potential C_3A was highly significant, but the correlation coefficients for the regressions of strength on the X-ray values averaged 15% lower than those for potential C_3A.

A more detailed examination will now be made of the regression of strength on C_3A. Consider, for example, the information in Table 4, where coefficients for the regression of strength on C_3A are given for curing periods from 7 to 90 days, and water/cement ratios 0.35 to 0.80. To facilitate comparisons within and between experiments the regression coefficients in this table are also given as proportions of the mean strength for the 15 cements tested under each combination of age and water/cement ratio. On first inspection it is perhaps tempting to identify patterns of behaviour among these transformed relationships. However, it can be shown by analysis of variance (Table 5) that the differences between the intercepts and between the slopes* of the regression lines are not significant (7). Thus, between the ages of 7 and 90 days, and for most water/cement ratios encountered in practice, the behaviour of these cements can be

Table 4. *The regression of paste compressive strength on* C_3A

W/C ratio	Age in days	Coefficients for the regression of compressive strength on % C_3A: In p.s.i. Const.	In p.s.i. Coeff. for C_3A	Relative to mean strength for normal portland cement: Const.	Relative to mean strength for normal portland cement: Coeff. for C_3A	Multiple correlation coefficient (R)	Number
0.35	7	7670	389	0.746	0.0378	0.746	1
	28	12720	439	0.812	0.0280	0.738	2
	56	14410	445	0.828	0.0256	0.720	3
	90	15490	381	0.858	0.0211	0.698	4
0.50	7	2670	196	0.670	0.0491	0.779	5
	28	4680	465	0.600	0.0595	0.841	6
	56	6620	434	0.694	0.0455	0.886	7
	90	8670	285	0.819	0.0269	0.703	8
0.80	7	880	52	0.718	0.0419	0.673	9
	28	1850	84	0.745	0.0350	0.814	10
	56	2440	38	0.906	0.0140	0.463	11
	90	2770	5	0.989	0.0016	0.064	12

Table 5. *Analysis of variance (2) for transformed regressions 1 to 10 from Table 4*

Variation	Degrees of freedom	Sums of squares	Mean square	Variance ratio: Observed	Variance ratio: 5% point
Ascribable to regression	1	2.435	2.435		
Ascribable to differences between regression coefficients	9	2.344×10^{-1}	2.604×10^{-2}	1.91	1.95
Ascribable to distances between regression lines	9	1.060×10^{-4}	1.178×10^{-5}	0.00	1.95
Unaccountable	130	1.769	1.361×10^{-2}		
Total	149	4.438			

*Although non-significant at the 5% level, the variance ratio testing the differences between coefficients is sufficiently high to warrant further investigation.

represented by a single regression:

$$Y = 0.75 + 0.037x \quad (1)$$

where

Y is the strength relative to the mean for all cements tested at that age and water/cement ratio,

and

x is the percentage of C_3A.

Since the sum of the silicates in the present cements is virtually constant (mean of 73%, standard deviation 2.6), one interpretation of the constant term in equation (1) is that, within the limits of the experiment, there is a specific strength for silicates.

Although equation (1) seems to imply that the strength of a particular cement is the sum of the strengths for silicates and C_3A, it is likely that some or most of the C_3A effect could be attributed to this component modifying the silicates, or accelerating their contribution to strength. One further point is that from 7 to 90 days, the relative importance of the silicate and C_3A effects is independent of age and water/cement ratio. Evidence presented later shows that this conclusion is unlikely to apply at early ages for, at 1 and 3 days, there is no significant relationship between strength and C_3A. The validity beyond 90 days too is doubtful, for, in this region, increasing age brings increasing departures from linearity in the relationships between strength and composition.

Although thus far, C_3S and C_2S have been treated collectively, under the heading of silicates, the present data can provide some indication of the relative contribution that each of these compounds makes to strength. With this object in mind, the analyses were repeated, but with the assumption that the regression should pass through the origin. Such a model has been used by Gonnerman (2), who retained all four major cement minerals in the analysis. However, for reasons analogous to those stated in developing the standard form of the analysis, a regression involving only C_3S, C_2S and C_3A is preferred here. Additional justification for omitting C_4AF comes from tests on cements containing constant amounts of C_3S, C_2S and C_3A, but variable amounts of C_4AF, which indicate that the latter compound has little or no effect on strength (2).

The results, given in Fig. 2, show a number of interesting features. For example, in accordance with the known properties of the pure compound, C_2S exhibits only a slow rate of strength development. At medium and high water/cement ratios (Figs. 1 (b) and (c)) it is about 90 days before the contribution made by each 1% of C_2S matches that of a corresponding amount of C_3S. Lowering the water/cement ratio to 0.35 (Fig. 2a) prevents the more slowly reacting constituent, C_2S, from attaining equality with C_3S, even at the latest age covered by these experiments.

Regarding C_3A ,the influence that this component exerts, relative to that of the silicates, rises to a maximum at water/cement ratio 0.50 and between the ages of 2 to 10 weeks (Fig. 2b). Under these conditions, each 1% increase in C_3A is accompanied by a 400 p.s.i. increase in compressive strength, thus equalling the maximum absolute contribution associated with this constituent in the stronger pastes at water/cement ratio 0.35. The influence of C_3A becomes negligible at late ages in the pastes of highest water/cement ratio (Fig. 2c). Finally, attention is drawn to the close agreement between the regression coefficients for C_3A in Fig. 2, and those calculated by the alternative form of analysis (Table 4).

Owing to a combination of uncertainties involved when the regression is forced through the origin (8), and when there are strong associations between the independent variables, the implications of the type of analysis in Fig. 2 should be viewed with considerable

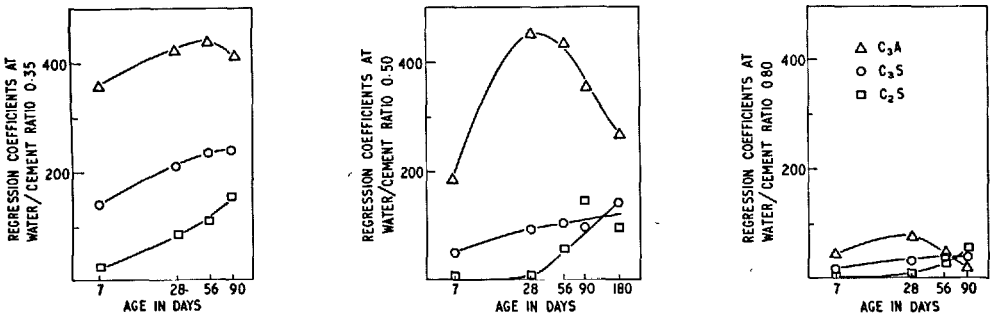

Fig. 2. *Regression coefficients (b_n), in p.s.i., for the regression:* $Y = b_1(\%C_3S) + b_2(\%C_2S) + b_3(\%C_3A)$

reservation. However, despite these limitations, it can be seen that there is an appreciable measure of agreement between the behaviour illustrated by this diagram, and some of the known properties of the cement minerals.

The Effect of Particle Size, Free Lime, Potassium, Phosphorous and other Factors, on the Strength of Cement

It has been shown that for the cements in Table 1, the addition of any major compound, or any combination of major compounds, almost invariably reduces the significance of the regression of strength on composition. However, the regression on C_3A never accounts for more than 80% of the total sum of squares. This raises the question of whether any of the other properties measured in this investigation could explain a useful proportion of the residual variation.

In order to check this possibility, the simple correlations between strength, and the following variables, were calculated for all ages and water/cement ratios: surface area, median particle size, MgO, SO_3, Na_2O, K_2O, Mn_2O_3, P_2O_5, TiO_2, free lime, ignition loss. The more promising leads were then followed by means of multiple regression analyses in which selected variables were added to C_3A singly, and in groups. Only particle size, free lime and potassium were significantly correlated with strength, although there were occasional borderline cases of significance for phosphorous.

In the case of phosphorous, the evidence suggests that the relationship with strength is not causal. There is significant positive correlation between the P_2O_5 and Fe_2O_3 levels in the oxide analyses of the cements and, in addition, the pattern of water/cement ratios at which significant negative correlations occur between strength and phosphorous, conforms to a stronger pattern of highly and very highly significant negative correlations between strength and iron.

With the alkalis, significant strength correlations are found only for potassium, and even then, only at the intermediate water/cement ratio of 0.50. These correlations are positive, and approach or attain significance at all ages from 7 to 90 days. Apart from one isolated exception there is no suggestion of significance at other water/cement ratios.

Turning finally to particle size and free lime, analysis shows that compared with phosphorous and potassium, the significance levels are higher and, in addition, the ages and water/cement ratios at which significance occurs, form a wider and more consistent pattern of behaviour. The influence of particle size and free lime is shown in Figs. 3 and 4, in which values of

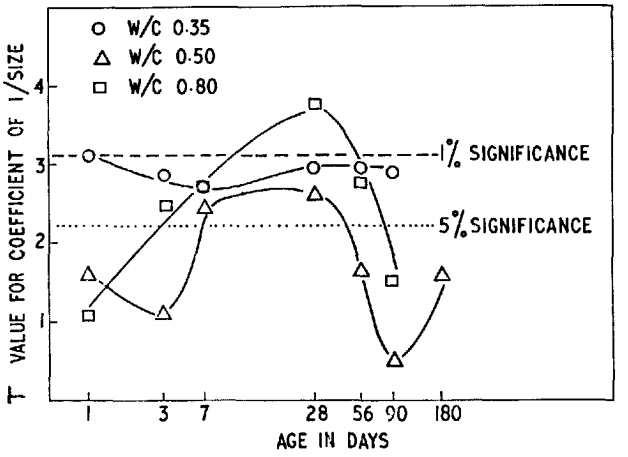

Fig. 3. *Significance of the coefficient (b_5) for particle size in the regression:*
$Y = b_0 + b_1(\%C_3A) + b_5((1/D_m) \times 10^3) + b_6(\%$ free lime$)$
where D_m is median particle diameter in microns

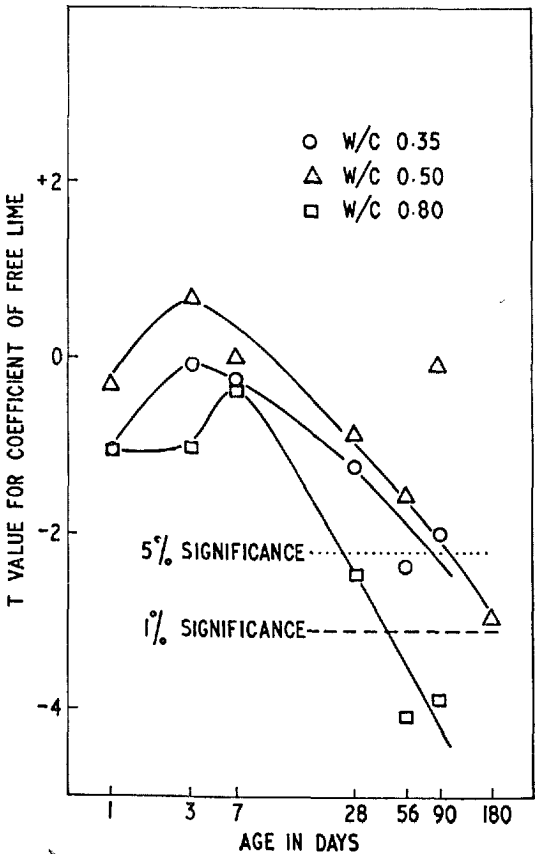

Fig. 4. *Significance of the coefficient (b_6) for free lime in the regression:*
$Y = b_0 + b_1(\%C_3A) + b_5((1/D_m) \times 10^3) + b_6(\%$ free lime$)$
where D_m *is median particle diameter in microns*

Student's T for the coefficients b_2 and b_3 in equation (2) are plotted against log time:

$$Y = b_0 + b_1x_1 + b_2x_2 + b_3x_3 \qquad (2)$$

where

Y = compressive strength of cement paste, in p.s.i.
$b_0 \ldots 3$ = regression coefficients
x_1 = percentage of C_3A
x_2 = reciprocal of median particle diameter in mm
x_3 = percentage of free lime

In these relationships, the reciprocal of particle diameter is preferred to the diameter itself, for reasons outlined later. Fig. 3 shows that at the water/cement ratios 0.35, 0.50 and 0.80, particle size is significant at 1 to 90 ,7 to 28, and 3 to 90 days respectively. Fig. 4 shows that the negative effect of free lime on strength begins to appear at about 7 days, reaching significance at about 90 days in pastes of low and medium water/cement ratio, and at 28 days in pastes of high water/cement ratio. At this latter water/cement ratio, free lime exerts a highly significant effect after about 6 weeks.

Coefficients for the regression of strength on C_3A and other significant factors are given in Table 6.

The Regression of Strength on Composition and other Variables at Ages less than 7 Days

The regression of strength on composition at 1 and 3 days differs markedly from that at 7 days onwards. Little will be said on this aspect, however, for there are too few results available at the earliest ages, the pattern of behaviour is more variable than at later ages, and significance is found in only a small proportion of cases.

Table 7 gives data for major components and other variables that are significantly correlated with strength at earliest ages. The best combination of two variables is also listed, whereas combinations of more than two are omitted since they are less significant.

The analysis is particularly unrewarding at water/cement ratio of 0.50 for, with the exception of C_3A at 3 days, neither major nor minor components, nor particle size, nor any combination of these variables gives a significant regression on strength.

At the extreme water/cement ratios C_2S is the major compound most significantly correlated with strength. The slight advantage over C_3S probably indicates that, at early ages, the proportion of this component, rather than the proportion of C_3S, is the more effective index of silicate quality. Particle size, as would be expected, is significantly correlated with strength on several occasions. However, greater interest lies in the very highly significant correlation between strength and the manganese content of cement at high water/cement ratio, and the analogous, though less striking, effect at low water/cement ratio.

Regression of Strength and Hydration on Compound Composition at Temperatures other than 21 Degrees

In a preliminary survey of the effect of temperature on the relationships between strength and composition, compressive strengths were measured for 0.45 water/cement ratio pastes which had been cured for 56, 28 and 16 days at 5, 21 and 43°C respectively. According to the empirical formula used by Saul (9), such pastes should be of equivalent maturity. The

Table 6. *Coefficients for the regression of strength on % C_3A, particle size, and % free lime*

W/C ratio	Age in days	Const.	C_3A	$\frac{1}{\text{Median Size in mm}}$	Free lime	Multiple correlation coefficient
0.35	7	2840	360	94	—	0.856***
	28	7280	407	106	—	0.847***
	56	9930	397	116	−862	0.874***
	90	11150	338	107	−683	0.858**
0.50	7	580	184	41	—	0.866***
	28	790	442	76	—	0.899***
	56	6620	434	—	—	0.886***
	90	8670	285	—	—	0.703**
	180	10630	244	—	−605	0.824**
0.80	7	101	47	15	—	0.816**
	28	1070	77	19	−113	0.931***
	56	2010	30	16	−215	0.850**
	90	3110	1	—	−201	0.706*

* = significant at 5% level
** = significant at 1% level
*** = significant at 0.1% level

Table 7. *Simple and multiple correlations for 1 and 3 day strength*

W/C	Age in days	Correlation coefficient					Multiple correlation coefficient
		C_3S	C_2S	C_3A	$\frac{1}{\text{Median Size}}$	Mn_2O_3	C_2S and Mn_2O_3
0.35	1	0.740**	−0.780***	0.158	0.657**	0.613*	0.843***
	3	0.652**	−0.755**	0.207	0.662*	0.447	0.769**
0.50	1	0.304	−0.307	0.232	0.443	0.344	0.389
	3	0.301	−0.446	0.607*	0.346	0.287	0.460
0.80	1	0.432	−0.465	0.181	0.250	0.827***	0.838***
	3	0.498	−0.565*	0.373	0.561*	0.799***	0.840***

* = significant at 5% level
** = significant at 1% level
*** = significant at 0.1% level

maturity was also assessed by measuring the degree of hydration.

Only the regressions on C_3A are examined here. The results (Table 8) indicate that of the two groups of regressions, strength on C_3A, and hydration on C_3A, the latter is the more highly significant at all curing temperatures. Both groups attain highest significance at 21°C. The relative coefficients in Table 8 show that the greatest effect of temperature occurs with strength, and between 21 and 43°C, where there is a considerable reduction in the influence of C_3A.

Regressions in Terms of Transformed Variables

During this examination of the regression of strength on composition a search was made for improvements which could be achieved by the transformation of variables. Dependent and independent variables alike were subjected to transformations. The following two types of transformations were employed:

(a) Transformations by grouping and processing the raw variables into forms which have straightforward chemical or physical significance in the present context. Examples are the formation of variables to represent the quality of the silicate and aluminate phases, and the calculation of regressions for strength in terms of oxide analyses rather than compound compositions.

(b) Mathematical transformations with no immediately obvious physical interpretation.

Neither type of transformation produced consistent improvement throughout the range of ages and water/cement ratios used here, although some marginal gains could be made for the regression of 180 day strength on composition by correcting for departures from linearity. On the question of conducting regression analyses for strength directly on the oxide values, the procedure showed no general advantage in so far as levels of significance were concerned. However, in view of the convenience of working with oxide results rather than potential mineral contents, a summary of results is given in Table 9.

Table 9 shows that the level of significance for the regression of strength on alumina is similar to that for the regression on C_3A, and that the same conclusion applies to the comparison between multiple regressions on the four major compounds, and those on the four major oxides. It is of interest to note that in building up the regressions from the 1 to 4 oxide level, the best order for introducing the variables is Al_2O_3, CaO, Fe_2O_3, SiO_2.

An example of analysis on one of the more useful combinations of transformed variables is shown in the last column of Table 9, where multiple correlation coefficients are given for regressions on the calcium/silica and alumina/iron ratios. This set of transformations gives improved significance at early ages at the expense of some marginal loss of significance at later age.

Table 8. *Coefficients for the regression of strength and hydration on C_3A at 5, 21 and 43°C*

W/C ratio	Age in days	Curing temp. °C	Property	Coefficients expressed as proportion of mean strength for all cements		Correlation coefficient
				Const.	C_3A	
0.45	56	5	Strength	0.803	0.0292	0.553*
	56	5	Hydration	0.839	0.0240	0.741**
	28	21	Strength	0.675	0.0484	0.865***
	28	21	Hydration	0.740	0.0387	0.912***
	16	43	Strength	0.915	0.0127	0.379
	16	43	Hydration	0.783	0.0324	0.858***

* = significant at 5% level
** = significant at 1% level
*** = significant at 0.1% level

Table 9. *Simple and multiple correlation coefficients for the regression of strength on composition in terms of potential minerals and oxides*

W/C ratio	Age in days	Correlation coefficient		Multiple correlation coefficient		
		C_3A	Al_2O_3	C_3A C_3S C_2S C_4AF	Al_2O_3 CaO Fe_2O_3 SiO_2	(CaO/SiO_2) (Al_2O_3/Fe_2O_3)
0.35	1	0.158	0.338	0.802*	0.773*	0.743**
	3	0.207	0.366	0.784*	0.845**	0.753**
	7	0.746**	0.741**	0.819*	0.890**	0.813**
	28	0.738**	0.713**	0.820*	0.854**	0.750**
	56	0.720**	0.700**	0.849**	0.862**	0.710*
	90	0.698**	0.649	0.771*	0.752	0.690*
0.50	1	0.232	0.274	0.348	0.546	0.337
	3	0.607*	0.630*	0.648	0.739	0.679*
	7	0.779***	0.737**	0.848**	0.930***	0.816**
	28	0.841***	0.802***	0.890**	0.887**	0.847***
	56	0.885***	0.812***	0.921***	0.907***	0.863***
	90	0.703**	0.546*	0.777*	0.805*	0.743**
	180	0.709**	0.603*	0.859**	0.782*	0.675*
0.80	1	0.181	0.293	0.486	0.444	0.398
	3	0.373	0.464	0.589	0.559	0.536
	7	0.672**	0.700**	0.773*	0.781*	0.748**
	28	0.814***	0.785***	0.894**	0.843**	0.802**
	56	0.463	0.317	0.916***	0.783*	0.557
	90	0.064	0.108	0.885**	0.670	0.542

* = significant at 5% level
** = significant at 1% level
*** = significant at 0.1% level

Discussion II

It is to be expected that the rate at which a cement hydrates and hardens will depend on its particle size distribution as well as on its composition. The initial rate may depend on the specific surface area but, since the coarsest half of a cement may contribute as little as ten per cent of the surface area and, since the after the first day or so, reaction is mainly of these coarser particles, it follows that the specific area may be a poor indicator of the reaction rate in the later stages. A similar objection for the opposite reason can be made to the use of a sieve residue involving only a few per cent of the cement. In this paper, as a simple compromise, the median diameter by weight (Dm) is used as a measure of cement fineness.

The rate of hydration and hardening of cements 16 to 30 is indicated in Figs. 6 and 7; the vertical lines at each curing period represent a range of one standard deviation (S. D.) about the mean. The actual range is greater, but not distributed symmetrically about the mean. The experimental design is described in "Experimental II."

The almost traditional method (2) (10) (11) of analysing effects in terms of potential mineral composition is to fit an equation of the form

$$y = b_1(C_3S) + b_2(C_2S) + b_3(C_3A) + b_4(C_4AF)$$

This equation seems to assume that the effect of each mineral is linear and independent of the cement composition. These assumptions may be difficult enough to justify near complete hydration but seem quite inappropriate at early ages. Fig. 7 shows the result of such an analysis of the present data. It will be seen that, in each experiment, and for both hydration and strength, the initial coefficients for both of the silicates are negative. Even in the more mature pastes where the silicate coefficients are positive, the analysis ascribes the effect disproportionately to the aluminates, especially to C_3A. Of course C_3A does react more rapidly and combines more water than do the silicates, but this alone can not account for an effect as large as shown in Fig. 7. In particular, the high

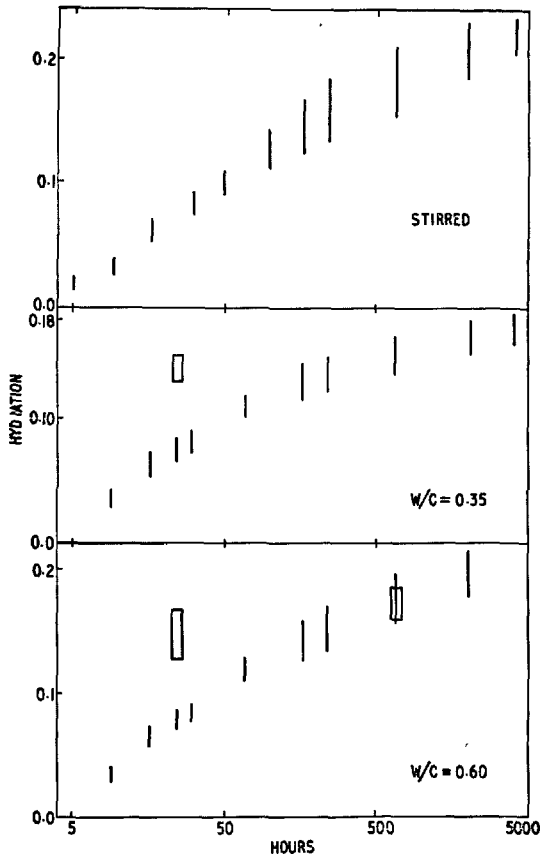

Fig. 5. *The hydration of cements 16 to 30. The range at each curing condition represented by a standard deviation about the mean. Vertical lines: specimens cured entirely at 21°C. Rectangles: specimens given a steam-curing treatment on the first day*

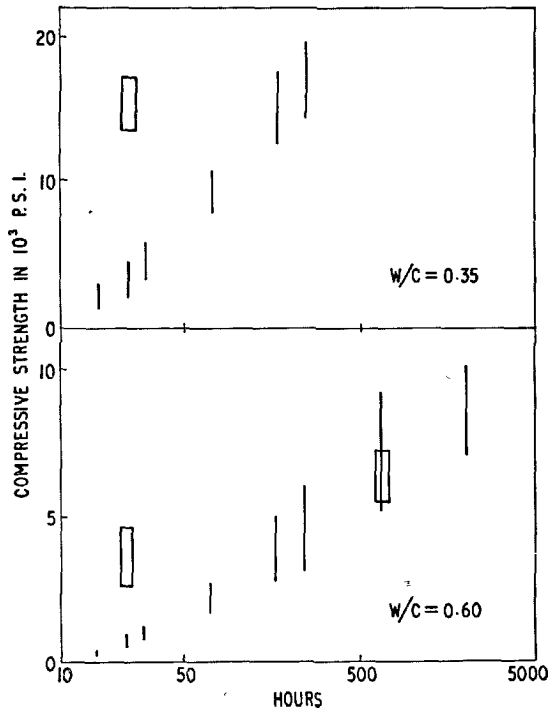

Fig. 6. *Compressive strength of cements 16 to 30. The range at each curing condition represented by a standard deviation about the mean. Vertical lines: specimens cured entirely at 21°C. Rectangles: specimens given a steam-curing treatment on the first day*

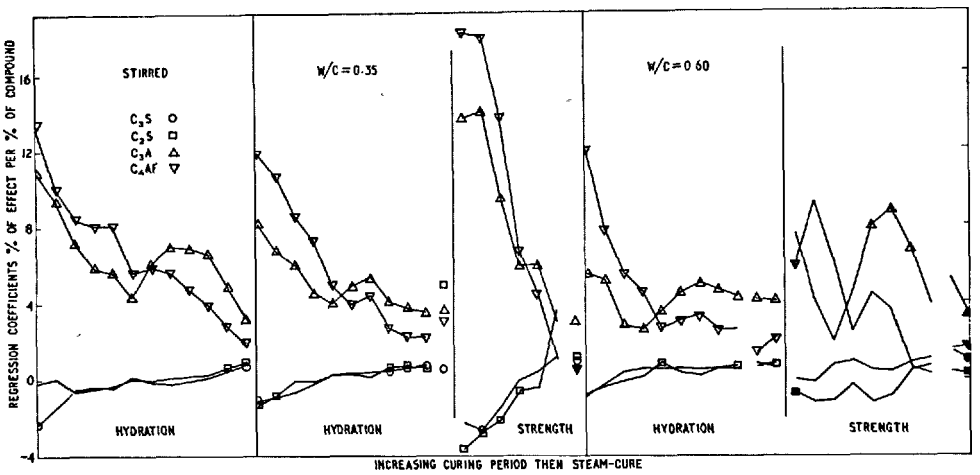

Fig. 7. *Regression coefficients for:*

$$y/\bar{y} = b_1(\%C_3S) + b_2(\%C_2S) + b_3(C_3A) + b_4(\%C_4AF)$$

where y is the hydration or strength at a particular curing period. The open symbols denote coefficients which are significantly above or below zero, the solid symbols identify the curves only

Table 11. *Correlations coefficients* ($\times 10^3$) *between potential mineral compositions and median particle size*

	C_2S	C_3A	C_4AF	Dm	$C_3S + C_2S$	$C_3A + C_4AF$	C_3S/C_2S	C_3A/C_4AF
C_3S	−939	153	069	−565	225	357	932	137
C_2S	1000	−222	−119	747	123	−540	−950	−192
C_3A		1000	−840	−122	−186	747	151	990
C_4AF			1000	−222	−139	−267	195	−872
Dm				1000	484	−489	−653	−111
$C_3S + C_2S$					1000	−500	−003	−148
$C_3A + C_4AF$						1000	508	691

Table 12. *Correlation coefficients* ($\times 10^3$) *between various items from the cement oxide compositions*

	SiO_2	Al_2O_3	Fe_2O_3	Dm	WL[1]	FL[2]	K_2O	C_3A	C_2S
CaO	−237	579	−386	−334	−213	−519	092	556	−696
SiO_2	1000	−502	−150	813	−491	−359	204	−291	726
Al_2O_3		1000	−627	−298	151	−330	374	949	−390
Fe_2O_3			1000	−222	−001	441	−460	−840	−119
Dm				1000	−558	−269	126	−122	747
W.L.[1]					1000	579	090	116	−036
F.L.[2]						1000	−234	−402	150
K_2O							1000	455	290

1. ignition loss
2. free lime

coefficient for C_3A in the strength regressions is surprising because of the suggestion of Powers and Brownyard (12) that C_3A, in excess of that which forms sulpho-aluminate, weakens cement paste.

The likely explanation of the results in Fig. 7 is that the silicate minerals are hydrating more rapidly in the cements with the higher aluminate contents. The same explanation accounts for inflated aluminate coefficients, especially of C_3A, in the equations of Gonnerman (2), Powers and Brownyard (10) and Verbeck (11). The acceleration of cements with higher aluminate contents could be due to (i) direct interaction between aluminate and silicate phases, (ii) changes in the aluminium and iron substitutions in the silicates, (iii) finer grinding of cements with higher aluminate content, or (iv) a higher C_3S content in cements with a higher aluminate content.

The Hydration of Stirred Specimens

Tables 11 and 12 show that the cements with a higher aluminate ($C_3A + C_4AF$) content tend to have both a smaller median size and a higher C_3S/C_2S ratio. However, before drawing any conclusions from this, we will look at correlation coefficients (r) between hydration and various cement characteristics and between these characteristics themselves. Fig. 8 shows *r* between hydration of stirred specimens and various quantities associated with the cements, plotted against

the curing periods for this experiment as listed in "Experimental II." The curve for ($C_3A + C_4AF$) shows an r which is significant for almost the whole period from 5 hours to 6 months. The r for Dm is less significant. Correlations for 1/Dm were also evaluated because one might expect the hydration rate to depend on some power of this reciprocal but the significance level is little changed by this transformation. The negative r for C_2S is less significant than that of Dm, although more significant than the generally positive r of C_3S (not shown). Because both Dm and C_3S are highly correlated with C_2S, it seems that the correlation between hydration and ($C_3A + C_4AF$) is not explained by particle size or C_3S content.

Referring again to Fig. 9, the correlation of ($C_3A + C_4AF$) with hydration can be compared with those of C_3A and Al_2O_3, and it will be seen that, although less significant at early ages, these two curves are more significant than that of C_3A beyond 10 and 7 days respectively. The r for C_4AF on the other hand becomes significantly negative for these later curing periods. It should be noted that total aluminate content has a positive correlation with both C_3A and alumina but a slightly negatively correlation with C_4AF. Arguing then from the strength of the correlations with hydration and from the inter-correlations of the various cement characteristics, it seems possible that the correlation between hydration and total aluminates is due mainly to an effect of C_3A or alumina, helped to some extent by the effects of median size and C_4AF. The C_3S/C_2S ratio is also in a position to help, but since the silicates are correlated with Dm but give a poor correlation with hydration, this possibility must be somewhat discounted. It is risky to argue from simple correlations alone, but extensive multiple linear regression analysis did not reveal any hidden interactions. The multiple regression of hydration on C_3A and Dm is significant from 16 hours onwards and is more significant over-all than the simple regression on total aluminates alone. The

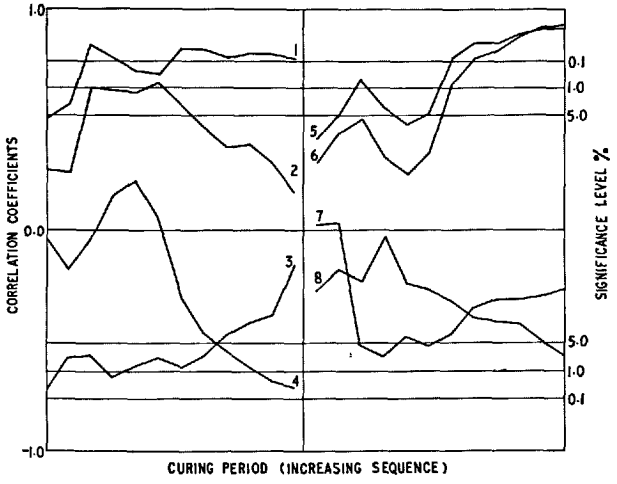

Fig. 8. *Simple correlations coefficients for stirred specimens, between hydration and* (1) $C_3A + C_4AF$ (2) *Minus* D_m (3) $C_3S + C_2S$ (4) C_4AF (5) Al_2O_3 (6) C_3A (7) C_2S (8) *Minus* K_2O

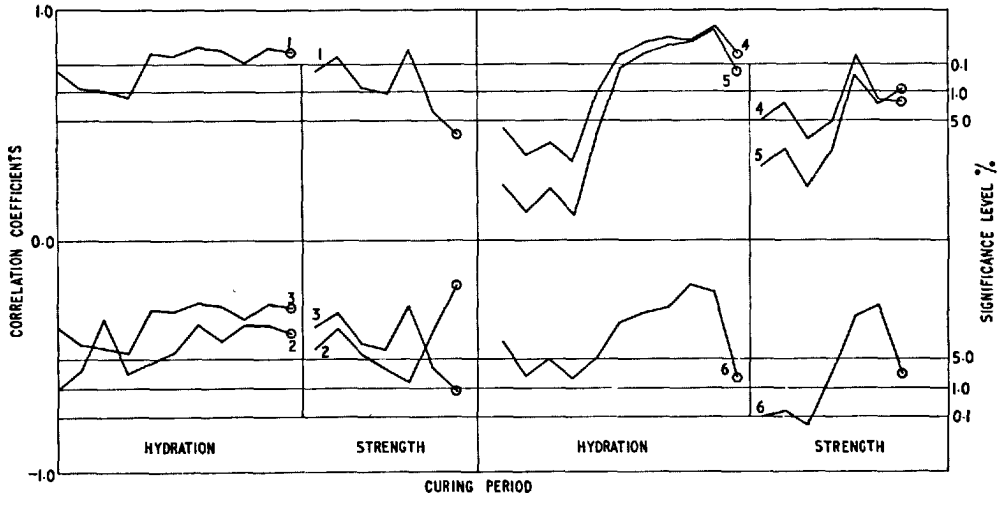

Fig. 9. *Correlations for the hydration and hardening of cement paste at* $W/C = 0.35$. *Coefficients for correlation between hydration or strength and* (1) $C_3A + C_4AF$ (2) D_m (3) $C_3S + C_2S$ (4) Al_2O_3 (5) C_3A (6) *Minus* Mn_2O_3. *Curing periods at 21°C in sequence, followed by 1-day steam-cured specimens shown by circles*

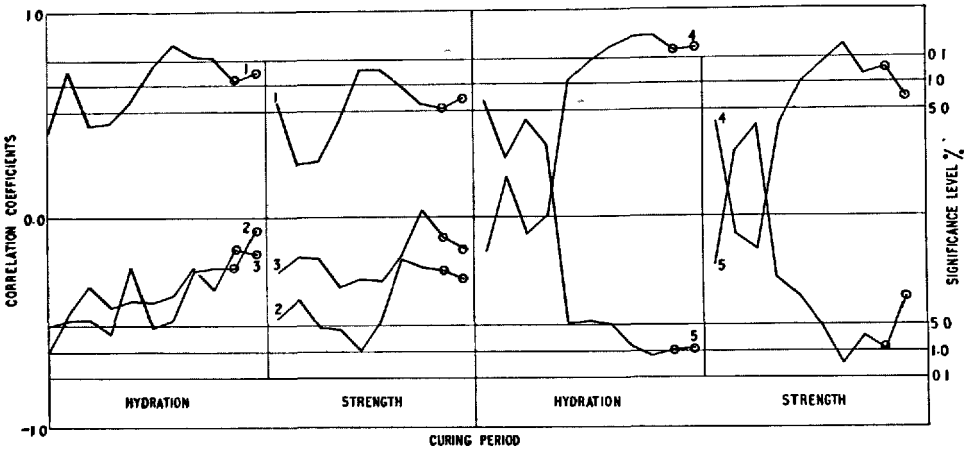

Fig. 10. *Correlations for the hydration and hardening of cement paste at W/C = 0.60. Coefficients for correlation between hydration or strength and* (1) $C_3A + C_4AF$ (2) D_m (3) $C_3S + C_2S$ (4) C_3A (5) C_4AF. *Curing periods at 21°C in sequence then steam-cured specimens shown by circles*

correlation curves in Fig. 8 for total silicates and for K_2O are at least partly explained by their dependence on Dm and C_3A respectively.

Hardened Specimens

The correlation coefficients between both hydration and strength and various cement characteristics are plotted for W/C = 0.35 in Fig. 9 and for W/C = 0.6 in Fig. 10. It will be seen that the curves of *r* versus curing period are of the same general shape as the corresponding curves of Fig. 9 but the correlation of C_3A with strength is not as significant as it is for hydration. Generally the steam cured specimens show the same behaviour as specimens cured entirely at 21°C to the same hydration value. Although the correlations are not shown, it must be stated that the correlation curve of C_2S is less significant than that of Dm but more significant than that of C_3S. A curve for the positive correlation of manganese is shown in Fig. 9. It reaches higher levels for strength than it does for hydration. It is less significant at the higher W/C ratio. The correlation between strength and both K_2O and Na_2O is shown in Fig. 11. It has already been suggested that the positive *r* for hydration on K_2O is partly a reflection of the C_3A effect but the possibility of a real alkali effect, as suggested by Fig. 11 can not be ruled out. However, such an effect is likely to be associated with the composition of the clinker minerals rather than the effect of alkali in solution because no difference was found by Alexander and Davis (13) who added both alkalies to the mix water.

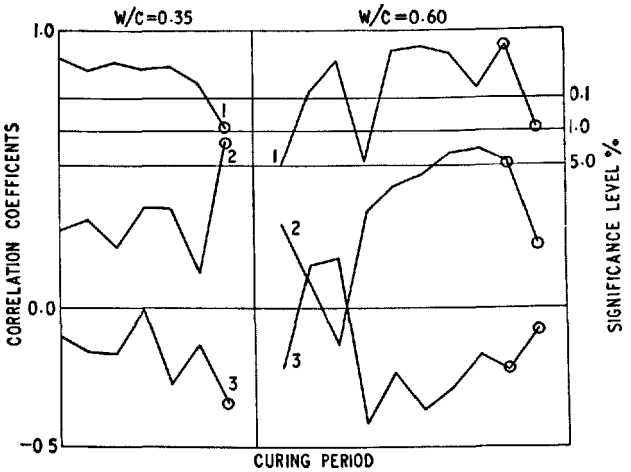

Fig. 11. *Coefficients for correlation between paste strength and* (1) *Hydration* (2) K_2O (3) Na_2O. *Curing periods at 21°C in sequence, then steam-cured specimens shown by circles*

The correlations of strength with hydration are also shown in Fig. 11. It will be seen that this correlation holds through all curing periods and is generally more significant than correlations shown here previously. Multiple regression analysis for strength on hydration and various cement characteristics gave no consistent pattern and an improvement in significance was found only occasionally for the addition of Dm, C_2S and TiO_2. In the multiple regression of strength on hydration and C_3A the coefficients for C_3A are not significantly different from zero. This means that, for these cements and at least

until six months, C_3A has little effect on the strength except that of accelerating the hydration reaction. The same conclusion can be stated in terms of Al_2O_3. From this study it is not possible to distinguish between the effect of C_3A itself and the effect of additional alumina on the properties of the other phases.

Conclusions

In this survey of commercial portland cements, differences between the strengths and between the hydrations are mainly attributed to differences in C_3A content. This factor dominates at water/cement ratios from 0.35 to 0.80, curing temperatures from 5 to 75°C, and throughout most of the 1-day to 6-month range of curing periods investigated. Strength is most sensitive to C_3A content under conditions which are frequently encountered in laboratory test work, namely, water/cement ratio 0.5, age 28 days, curing temperature 21°C.

With the present cements there is a smaller, but significant effect, for median particle size, whereas the effect of quite appreciable differences in C_3S content is of minor importance. Earlier work (1), which attributes differences in strength between older and more recent cements largely to differences in C_3S and in fineness, is not inconsistent with the present study, since the cements in the former investigation had a nearly constant level of C_3A.

The influence of other cement characteristics such as minor oxide composition, surface area, etc., is either non-significant, or can be accounted for as another aspect of the C_3A and size effects. Possible exceptions are the positive correlations of strength with Mn_2O_3 at early ages, and the negative correlations of strength with free lime at high water/cement ratio and later ages.

The C_3A effect is thought to be mainly an acceleration of the hydration of the cement as a whole. However, in assessing the influence of C_3A on the quality of cement, it should be borne in mind that the rate of strength gain is but one aspect. The possibility that, at late ages, C_3A may have a negative effect on strength must be considered (2), and allowance must also be made for any effects on drying shrinkage (2) (14), sulphate resistance, and heat of hydration.

Acknowledgments

The authors are indebted to Mr. C. H. Gray, of the Division of Computing Research, for Table 5, and to Dr. R. T. Leslie and Staff, of the Division of Mathematical Statistics, for helpful discussions. The oxide analyses of the cements are by Miss B. Terrell, and the X-ray determination of C_3A are by Mr. A. Wilson, both of the Division of Applied Mineralogy. Messrs. C. Larrewyn, B. Murphy and B. Press, of the same Division, participated in the conduct of the tests. The above are all members of the C.S.I.R.O., Australia.

References

1. H. F. Gonnerman and William Lerch, "Changes in characteristics of portland cement as exhibited by laboratory tests over the period 1904 to 1950", Am. Soc. Testing Materials, Special Publication No. 127, (1951); Research Labs., Portland Cement Assoc. Bull. No. 39, 1–56 (1952).
2. H. F. Gonnerman, "Study of cement composition in relation to strength, length changes, resistance to sulphate watersand to freezing and thawing, of mortars and concrete", Am. Soc. Testing Materials, Proc. (2), **34**, 244–295 (1934).
3. T. C. Powers and T. L. Brownyard, "Studies of the physical properties of hardened portland cement paste, 6. Relation of physical characteristics of the paste to compressive strength", Proc. Am. Concrete Inst. **43**, 845–857 (1947), p. 857.
4. P. P. Budnikov and E. Ya. Erschler, "Studies of the processes of cement hardening in the course of low-pressure steam curing of concrete", Symposium on the Structure of Portland Cement Paste and Concrete, Highway Research Board, Special Report 90, 425–466 (1960).
5. J. H. Taplin, "A Method for following the hydration reaction of portland cement paste", Australian J. Appl. Sci., **10**, 329–45, (1959).
6. A. Hald, Statistical Theory with Engineering Applica-

tions, Chapter 20 (John Wiley and Sons, Inc., U.S.A., 1952).
7. M. H. Quenoulle, Associated Measurements, p. 76–79 (Butterworth and Co., London, 1952).
8. E. J. Williams, Regression Analysis (John Wiley and Sons Inc., New York, U.S.A., 1959).
9. A. G. Saul, "Principles underlying the steam curing of concrete at atmospheric pressure", Mag. Concr. Research, **3**, 127–140 (1951).
10. T. C. Powers and T. L. Brownyard, *loc. cit.*, "9. General summary of findings on the properties of hardened portland cement paste", p. 975.
11. G. Verbeck, "Energetics of the hydration of portland cement", Fourth Internat. Symposium on the Chem. of Cement, Washington (1960), **1**, paper IV-3 (III), 453–465, p. 461–462.
12. T. C. Powers and T. L. Brownyard, *loc. cit.*, "6. Relation of physical characteristics of the paste to compressive strength," p. 853.
13. K. M. Alexander and C. E. S. Davis, "Effect of alkali on the strength of portland cement paste", Australian J. Appl. Sci., **11**, 146–156 (1960).
14. H. Roper, "Cement paste shrinkage—relationships to hydration, Young's modulus and concrete shrinkage", This Symposium.

Supplementary Paper III-88 Relation between the Hydration of Alumina Cement Mortars and Their Strength in the Early Stages

Kiyotaka Mishima*

Synopsis

Mineralogical changes involved in the early stages of the hydration of alumina cement mortar have been investigated under various conditions (w/c = 0.4 ~ 0.7, curing temperature 10 ~ 40°C) in comparison with changes in compressive strength. And setting time of neat alumina cement paste has also been measured in different temperatures.

When the mortar specimens were cured at temperatures lower than 30°C, CAH_{10} and C_2AH_8 were observed and their strengths were higher than those of specimens cured above 30°C. But above 30°C., the first hydration product was only C_2AH_8, which was converted to C_3AH_6 in later stages. In this temperature region CAH_{10} was not observed at any stage. The compressive strength had increased only for the first 1 to 3 days before lowering and their maximum strengths were lower than those cured below 30°C. At approximately 30°C, no hydrated product was observed until 12 hrs. of curing, then C_2AH_8 and CAH_{10} were produced and the strength developed very slowly. But no deterioration of strength was found until 7 days of curing. These results corresponded to the fact that setting time was extremely long at around 30°C.

There is no obvious relationship between the quantities of hydrates and the strength of mortars because the strength seems to be rather greatly influenced by their structure and behaviour of amorphous parts. However, distinct relationship is observed between the species of hydrates and strength of mortar specimens. That is, it may be said that the strengths of mortar specimens containing CAH_{10} is greater than those containing $C_2AH_8 + AH_3$ or $C_3AH_8 + AH_3$.

As to the reduction of hydration reaction at temperatures around 30°C, it is likely to be considered that two reactions take place at the same time, as follows:

$$CA + H \longrightarrow CAH_{10} \longrightarrow C_2AH_8 + AH_3$$
$$CA + H \longrightarrow C_2AH_8 + AH_3$$

Both hydrates, CAH_{10} and C_2AH_8, have their optimum temperatures for crystal growth below and above 30°C, respectively. Consequently, the rate of crystal growth seems to reach the minimum value about 30°C. which leads to the extremely long setting time.

Introduction

The main phases in anhydrous alumina cement are mostly CA, CA_2, $C_{12}A_7$, C_2AS, C_2S, C_2F and C_4AF. The rapid hardening qualities are attributed to the calcium aluminates, especially CA. The several hydrates are produced on the hydration of alumina cement and the most prominent hydrates are CAH_{10}, C_2AH_8, C_3AH_6 and AH_3 (gibbsite). It is said, however, that the only stable hydrates, at ordinary temperature, are gibbsite and cubic C_3AH_6. The metastable hexagonal calcium aluminate hydrates, CAH_{10} and C_2AH_8, are only formed at low temperatures.

It was thought that the main hydrate produced from alumina cement was C_2AH_8, but it is now believed that the most important phase of normal hydration is CAH_{10}. Recent work by Percival Buttler and Taylor (1) has shown that CAH_{10} is a persistent metastable phase at temperature lower than 21°C. However, Wells and Carlson have indicated that it was still main hydrate at 24°C., in paste hydration studies. Johns and Roberts (2) concluded that there was a transition temperature at 22°C above which C_2AH_8 was stable towards CAH_{10} in the aqueous phase.

It is thought that the metastable hexagonal CAH_{10} converts first to C_2AH_8 and then finally to stable

*Research Laboratory, Asahi Glass Co., Ltd., Yokohama, Japan.

C_3AH_6. And the rate of conversion is known to be very slow below about 25°C, but it increases with rising temperature. It has also been known that there is the loss in strength of alumina cement for a long time ageing or at high temperature curing. To explain the cause of strength reduction many investigations have been done. Wells and Carlson suggested that the loss in strength was due to crystallization of AH_3 from alumina gel. More recent work by Midgley (3) showed that the strength reduction was due to change of porosity associated with conversion and was affected by the rate of conversion. In the opinion of Robson (4) change of strength by conversion was mostly influenced by initial water cement ratio. But the exact causes have not been completely ascertained.

The effect of temperature on the setting time of alumina cement has been investigated by many workers. It is known that in the temperature range $1 \sim 30$°C the setting time becomes progressively longer as the temperature rises and over 30°C, the setting time rapidly becomes shorter again.

This phenomenon corresponds to the fact that the development of initial strength is retarded the most at 30°C, and the rate of hydration passes through a minimum value at around the same temperature.

The causes of the anomalies at around 30°C have not also been known exactly.

In this investigation mineralogical changes involved in the early stages of hydration of alumina cement mortar have been investigated under various curing temperature in comparison with changes in compressive strength.

On the basis of this experimental results, the relation between the mineralogical state of hydrates produced in mortar and compressive strength of mortar has been discussed. And some observation on the hydration reaction has also been carried out, then anomalies of hydration has been discussed at about 30°C.

Experimental Procedures

Preparation of Specimens

The specimens used in strength measurement and mineralogical analysis were made from 1:2 alumina cement: sand mortars to bring the test condition close to that of concrete. They were made in the form of prisms $4 \times 4 \times 16$ cm. The mixed materials for prisms were kneaded by hand and tamped into a steel mould. The specimens were usually cured in the mould up to 6 hrs., then were removed from the mould and cured in moist-air until they were subjected to test. All these operations were done in the curing room which was kept at testing temperature and at a relative humidity above 85%.

The neat alumina cement paste was employed in the measurement of setting time which were also carried out in that curing room.

The alumina cement used in this investigation was a commercial high alumina cement. The chemical analysis of the cement is given in Table 1. X-ray examination of the cement showed the following minerals to be present: CA, C_4AF and $C_{12}A_7$.

Table 1. *Chemical compositions of alumina cement*

	Weight (%)
Al_2O_3	40.34
CaO	37.15
SiO_2	2.90
FeO	3.95
Fe_2O_3	13.28
MgO	0.32

Condition of Hydration and Curing

For the strength measurements and the mineralogical analyses, the specimens were made from the mortars with four different water cement ratios: 40, 50, 60 and 70%. To find the effect of temperature of hydration and curing on the strength and the mineralogy, mortar specimens were examined in temperatures ranging from 10°C to 40°C with interval of 5°C. At each testing temperature the specimens were stored at a relative humidity above 85%.

Strength Measurements

The measurements of compressive strength were carried out for the specimens cured at various temperatures for the following periods: 6 hrs., 12hrs., 24hrs., 3days and 7 days.

Mineralogical Examinations

The mineralogical analyses were carried out by X-ray powder diffraction just after the strength measurements were done. The broken pieces of

specimens obtained in the test of compressive strength were used in the mineralogical analyses. The material from the specimens was roughly ground, then it was screened by 170-mesh sieve for separating the cement from the sand.

The specimens which did not perfectly harden were treated with absolute methanol in order to remove the water and separated from the sand by 170 mesh sieve in methanol.

The hydrated cements got by the such way were subjected to X-ray examination.

The quantitative determinations of unhydrated CA and hydrated crystals were tried by X-ray powder diffraction method. But the exact determination of minerals was not made, because the cement was not completely separated from sand, so the quantitative analysis by using the internal standard was not carried out. Therefore, the quantity of crystals was determined in comparison of the intensity of each peak of X-ray diffraction patterns.

As the method by means of integral intensities of each peak was generally better than by comparison of height in each peak, the measurements of area of each peak were carried out by fixed-time-method for some specimens. However, since the result showed a good agreement with that of height measurement, the determination by comparison of height in each peak was adopted in this investigation.

Measurement of Setting Time

The setting time of the neat alumina cement was determined at temperatures ranging from 5°C to 40°C with interval of 2°C by Vicat needle method. The water cement ratios of the specimens were determined by the normal consistency at each testing temperature.

Experimental Results

Compressive Strength

Table 2 shows the compressive strengths of mortar prisms which were made with different water cement ratios and cured at various temperatures and for various periods. For example, the strength of specimens made with a W/C = 40% and cured at various conditions is given in Fig. 1.

Table 2. *Compressive strength of mortar prisms cured at various temperatures for various periods*

Curing temp.	W/C	6 hrs.	12 hrs.	1 day	3 days	7 days
10	40	320	402	485	539	593
	50	232	425	573	605	676
	60	186	455	621	634	624
	70	166	473	543	523	628
15	40	229	376	438	503	571
	50	237	353	443	539	508
	60	156	356	446	491	556
	70	123	355	413	449	498
20	40	277	406	441	488	494
	50	284	384	405	481	531
	60	292	373	416	490	571
	70	170	328	364	433	518
25	40	164	342	423	441	507
	50	204	357	392	502	488
	60	175	332	394	454	468
	70	132	264	312	369	339
30	40	—	198	419	476	508
	50	—	257	342	369	335
	60	—	211	317	301	266
	70	—	164	253	249	219
35	40	317	387	459	452	465
	50	260	315	326	390	378
	60	241	289	288	281	277
	70	194	234	224	206	237
40	40	322	391	357	297	300
	50	273	274	243	201	217
	60	241	224	193	185	201
	70	186	191	150	152	172

The strength of specimens cured at a temperature below 30°C increased steadily with age until 7 days

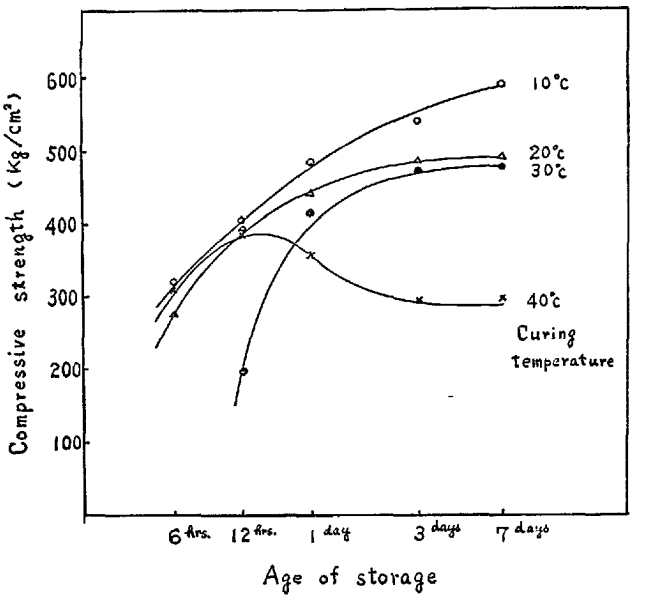

Fig. 1. *Strength of prisms made with alumina cement mortar of W/C = 0.4, cured at various temperatures*

and, the lower the curing temperature, the strength became the higher. At 30°C, the strength did not increase in the first 12 hrs., and then increased rapidly, the strength at 7days was lower than those found in specimens cured for the 7 days at below 30°C. Above 30°C, the strength increased during 1 to 3 days, then decreased gradually and the maximum strength was lower than those cured below 30°C.

As for the water cement ratio (Fig. 2, Fig. 3), at curing temperature up to 25°C, there was not clear correlation between the compressive strength and the water cement ratio, but above 25°C, the strength decreased with the ratio.

Mineralogical Examination

The results of semi-quantitative analyses by X-ray diffraction are given in Fig. 4. In this figure only CA of unhydrates is shown for simplification.

The hydrated crystals found in the mortar specimens were CAH_{10}, C_2AH_8, C_3AH_8, C_3AH_6 and gibbsite (AH_3). At low hydration temperatures the main phase produced on hydration was CAH_{10}, followed by C_2AH_8. At high temperatures, the primary hydration product was only C_2AH_8 which was converted to C_3AH_6 in later stages. The higher the temperature, the more rapidly this conversion proceeded.

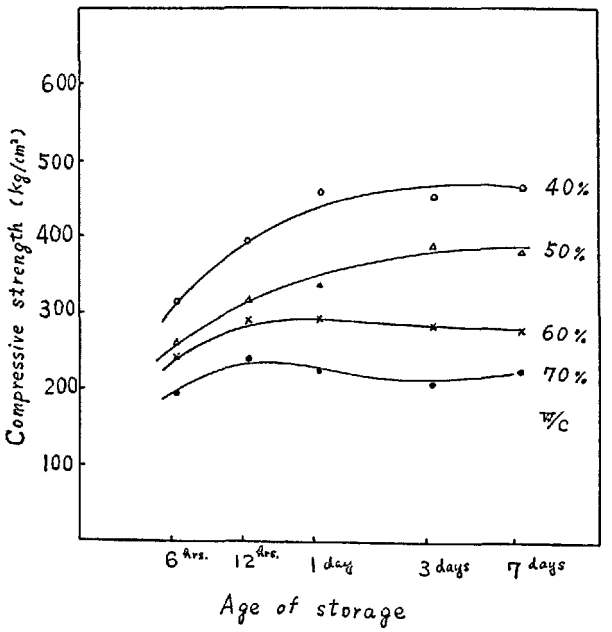

Fig. 3. *Strength of mortar prisms cured at 35°C for various periods*

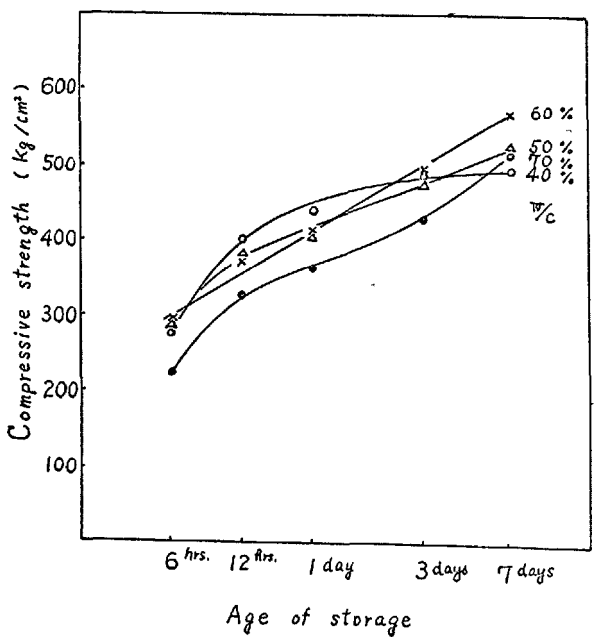

Fig. 2. *Strength of mortar prisms cured at 20°C for various periods*

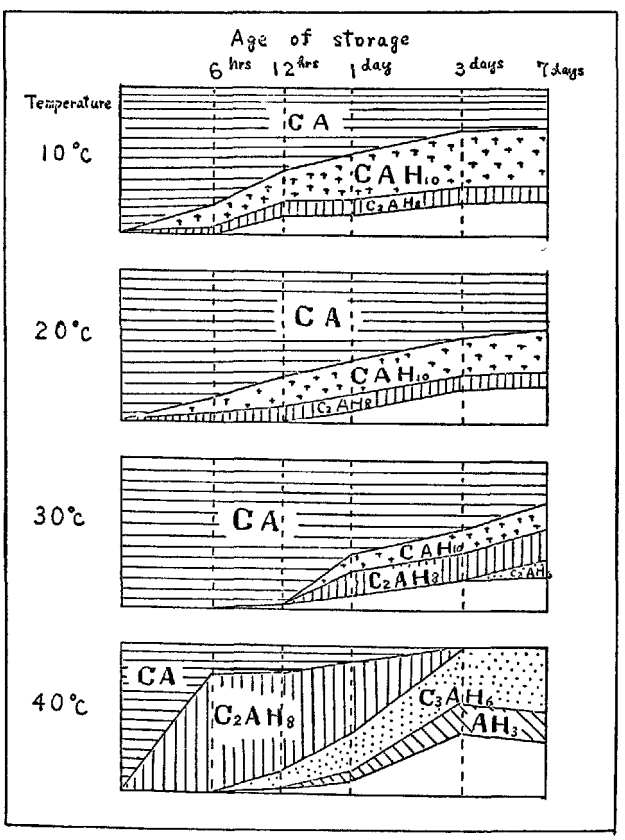

Fig. 4. *Results of X-ray examination. Quantity of crystals observed in specimens made with alumina cement mortar of W/C = 0.4, cured at various temperatures for various periods*

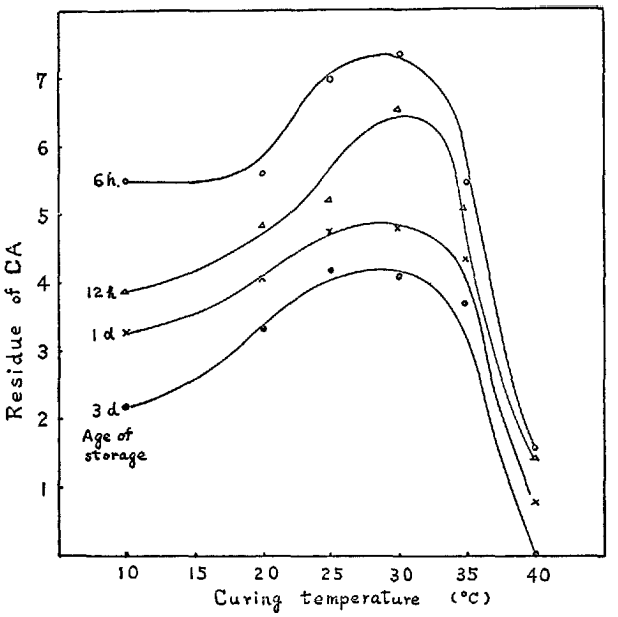

Fig. 5. *Residue of CA in the mortars cured at various temperatures for various periods*

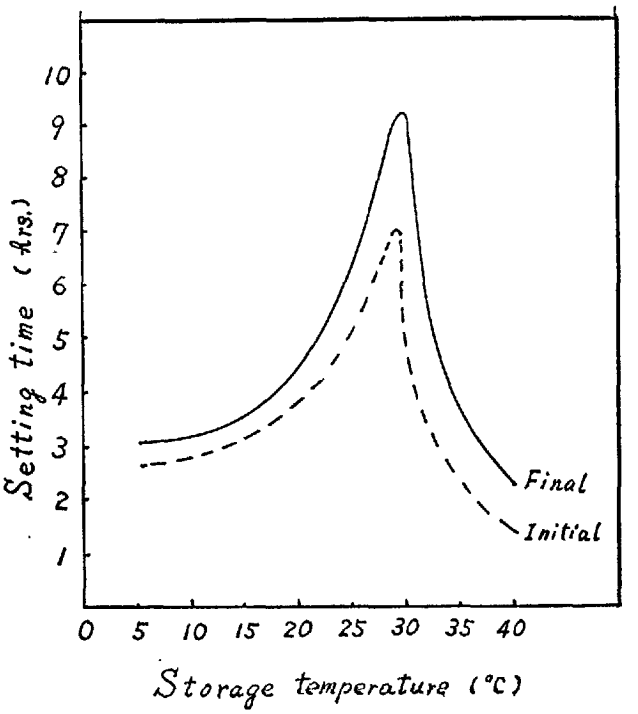

Fig. 6. *Setting time of neat cement pastes at various temperatures*

The changes of the amounts of CA are given in Fig. 5. The results showed that there was no obvious relationship between the reaction rate of CA and the temperature. There was an increase in remaining amounts of CA as the temperature was raised from 10°C to 30°C, but there was a decrease again at 40°C. Consequently, the quantities of hydrates produced in the reaction were very little at 30°C, in the early stage.

CAH_{10} was produced at temperatures below 30°C, above which it had never been observed. The amounts of CAH_{10} increased with the fall of temperature and the increase of the curing period.

C_2AH_8 observed always whenever the hydrated crystals were formed, and there was an increase in quantities as the temperature and curing age increased. However, when the hydration temperature was raised to 40°C, the amounts of C_2AH_8 increased up to 12 hrs. and then decreased and conversely the quantities of C_3AH_6 increased.

C_3AH_6 was not observed up to 7 days at temperatures below 25°C, but at higher temperature it was produced in the early stages. It was formed at the time more than 7 days at 30°C, and at 24 hrs. at 40°C respectively. The amounts of C_3AH_6 increased monotonically with curing periods.

Gibbsite was usually crystallized at the time of a little later than production of C_3AH_6.

As for the effect of water cement ratio on mineralogy, it was observed that the rate of hydration increased with a rise of water cement ratio.

Setting Time

The results of setting time measurements are given in Fig. 6. In the range from 5°C to 30°C the setting time of alumina cement paste became progressively longer as the temperature rose and above 30°C rapidly shortened again.

The results agree with the results of many workers.

Discussion

Relation between the Hydrates and the Strength

There is no obvious relationship between the quantities of crystalline hydrates produced in mortar specimen and the strength of mortar, because the strength seems to be rather greatly influenced by the structure of the whole body containing amorphous parts. However, supposing that the specimens made with

same water/cement ratio have the same structure, there are following relationships between the hydrates and the strength of the specimens with same water/cement ratio;

1. The strength increases with the amounts of CAH_{10}.
2. When the both crystals, CAH_{10} and C_2AH_8, are present simultaneously, the strength increases as the ratio of CAH_{10} to all produced hydrated crystals increases.
3. When the hexagonal C_2AH_8 and cubic C_3AH_6 exist together, that is, the conversion reaction proceeds, the strength decreases with the increase of C_3AH_6.
4. Whenever cubic C_3AH_6 is produced, the strength falls.

On the basis of these results, the following relation may be considered as existing among the three hydrates as to the strength

$$CAH_{10} > C_2AH_8 \gg C_3AH_6$$

This relation has not always shown that the binding strength of C_3AH_6 is less than that of CAH_{10} or C_2AH_8. Rather it has concerned the strength of whole body of mortar containing each hydrate, irrespectively of whether it is produced by conversion or not, that is, the strength of the mortar specimen containing CAH_{10} crystals is greater than that of the specimen containing C_2AH_8 or C_3AH_6.

The causes of strength reduction at higher temperature are thought as follows;

1. The binding strength of CAH_{10} is greater than C_3AH_6.
2. The change of structure by conversion of hexagonal hydrates to cubic hydrate.
3. The change of behavior of amorphous parts like a alumina gel by rising the temperature.

However, in this investigation, it could not be confirmed which reason is the most effective.

Setting Time and Hydrates

At temperatures around 30°C, the setting time is most delayed and final set is about 9 hrs., when no hydrated crystal is observed. CA decreases little until 12 hrs. of curing at this temperature. These results correspond to the fact that the strength develops very slowly. However, after 12 hrs. the reaction proceeded rapidly, so C_2AH_8 and CAH_{10} were produced and the strength increased rapidly, too.

There is a critical temperature at about 30°C above which crystal of CAH_{10} is not observed by X-ray diffraction. And at 30°C., sometimes C_2AH_8 is observed in earlier stage than formation of CAH_{10}.

Generally setting time agrees with the time when the hydrates begin to form the hydrate and crystals of hydrates grow enough to be found by X-ray diffraction in 2 or 3 hrs. after the final set.

Hydration Reaction at Each Curing Temperature

Generally the hydration reaction of CA is considered to proceed as follows;

$$CA + H \longrightarrow CAH_{10} \longrightarrow C_2AH_8 + AH_3 \longrightarrow C_3AH_6 + AH_3$$

At the first stage on hydration of CA metastable hexagonal compound CAH_{10} is produced, then it is subsequently converted to hexagonal C_2AH_8, and at ultimate stage C_2AH_8 is converted to stable cubic C_3AH_6. The rate of conversion of the metastable hydrates to the stable cubic hydrate is heavily dependent on the temperature. Therefore, at higher temperature, it seems apparently that the direct reaction from CA to C_2AH_8 will proceed and CAH_{10} is not observed.

But on the basis of these experimental results, it seems reasonable to consider that the following two reactions take place at the same time

$$CA + H \longrightarrow CAH_{10} \longrightarrow C_2AH_8 + AH_3 \longrightarrow C_3AH_6 + AH_3 \quad (1)$$

$$CA + H \longrightarrow C_2AH_8 + AH_3 \longrightarrow C_3AH_6 + AH_3 \quad (2)$$

that is, the reaction (1) is an ordinary way and the reaction (2) is direct reaction of CA to C_2AH_8.

Fig. 4 shows the quantities of CAH_{10} and C_2AH_8 produced at various temperature respectively. These figures show that the rate of hydration decreases gradually towards 30°C, at which it falls to its lowest, and then above 30°C, rapidly increases with the rise of temperature. To explain this fact it is favourable to consider that two reactions proceed simultaneously. And it is also explained smoothly that C_2AH_8 is produced at earlier stage than CAH_{10} at 30°C, and is observed always when the other hydrates are formed at any temperatures. However, at temperatures above 30°C, it may be considered that the reaction (1) does not occur practically.

To explain the reduction of hydration at 30°C, it is necessary to confirm the hydration mechanism of CA. Although the exact mechanism of the CA-water reaction is very difficult to prove conclusively, it seems reasonable for the explanation of above results to

consider as follows. When the CA grain gets in contact with water, at the first stage thin hydrated amorphous layer is formed on the surface of the grain (It may be considered that the layer is made from the saturated solution of the CA). This product probably retards the reaction by restraining the water supply to the CA (or by controlling the dissolution of the CA). As the layer becomes some thick to some extent, it appears that the reaction is not proceeding. At later stage in the reaction the crystallization of hexagonal hydrates occur in the layer and poorly crystalline hexagonal CAH_{10} and C_2AH_8 are formed. But in this stage they are not yet observed by X-ray diffraction. As the crystals of hexagonal hydrates become bigger, the water permeability of the layer may increase and the reaction progresses again. While from the Fig. 6, it may be considered that there is an optimum temperature of growth of hexagonal CAH_{10} crystal in lower temperatures, and C_2AH_8 crystal has an optimum temperature to grow in high temperature regions. These optimum temperatures are presumed to be below and above 30°C, respectively. Therefore in low temperature region crystals of CAH_{10} grow up in the early stage (C_2AH_8 grow little) and the layer becomes porous, the reaction proceeds rapidly. At high temperatures, too, the reaction accelerates by growth of C_2AH_8 crystals. But at approximately 30°C, the rate of hydration reaction decreases extremely because it is difficult for the crystal of two hexagonal hydrates to grow. Consequently, it is observed at temperatures around 30°C that the setting time is very delayed and the strength develops very slowly.

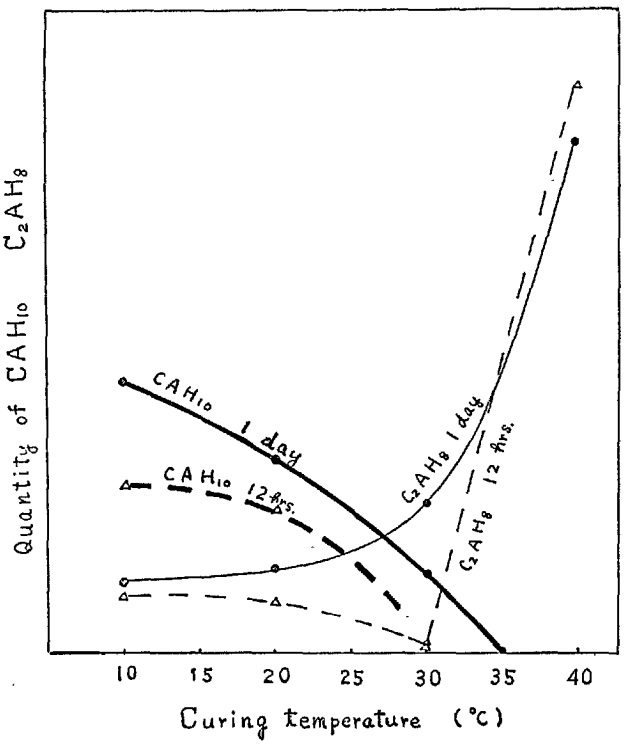

Fig. 7. *Quantity of* CAH_{10} *and* C_2AH_8 *produced at various temperatures for 6 hrs. and 1 day*

Summary

Mineralogical changes involved in the early stages of the hydration of alumina cement mortar have been investigated under various curing temperature (10 ~ 40°C) with different water cement ratios (40 ~ 70%), and associated changes in compressive strength have been determined. The setting time of neat alumina cement paste has also been measured in various temperatures (5 ~ 40°C).

On the basis of these experimental results the relation between the mineralogical state of produced hydrates and the compressive strength has been discussed. Some observation on the hydration reaction has also been carried out.

There was no obvious relationship between the quantities of hydrates produced on the hydration and the compressive strength of mortar because the strength seemed to be rather greatly influenced by its structure and behavior of amorphous parts produced in mortar specimens. However, distinct relationship was observed between species of hydrates produced in mortar specimens and mortar strength, as follows;

$$CAH_{10} > C_2AH_8 + AH \gg C_3AH_6 + AH_3$$

This relation shows that the strength of mortar containing CAH_{10} is greater than that containing $C_2AH_8 + AH_3$ or $C_3AH_6 + AH_3$.

To explain the reduction of hydration reaction at temperatures around 30°C, it seems reasonable to consider that two reactions take place at the same time, as follows;

$$CA + H \longrightarrow CAH_{10} \longrightarrow C_2AH_8 \longrightarrow C_3AH_6$$

$$CA + H \longrightarrow C_2AH_8 \longrightarrow C_3AH_6$$

At very early stage of hydration hydrated amorphous layer is formed around the CA grain. This product probably retards the reaction by restraining the water supply to the CA. At the next stage the hexagonal hydrates (CAH_{10}, C_2AH_8) crystallize in the

layer. As the crystals of hydrates grow, the water permeability of the layer increases and the reaction progresses again. There is an optimum temperature of growth of CAH_{10} crystal in lower temperature, on the other hand, C_2AH_8 crystal has an optimum temperature to grow in high temperature regions. Therefore, in low temperature regions crystals of CAH_{10} grow up at early stage and reaction proceeds rapidly. At high temperature the reaction also accelerates by growth of C_2AH_8 crystal. But at approximately 30°C the rate of hydration reaction decreases extremely because it is difficult for the crystals of two hexagonal hydrates to grow. Consequently, it is observed at temperatures about 30°C that the setting time is very delayed and the strength develops very slowly.

Acknowledgment

The author is grateful to Dr. S. Koide for helpful discussions and to Mr. K. Omata for collecting the data.

References

1. A. Percival, F. G. Buttler and H. F. W. Tayler, "The precipitation of $CaO \cdot Al_2O_3 \cdot 10H_2O$ from supersaturated calcium aluminate solution at 21°C", Chemistry of Cement Proc. 4th Int. Symp. Washington Vol. I 277–283 (1960).
2. F. E. Jones and M. H. Roberts. "Hydration of calcium aluminates and ferrites", Chemistry of Cement Proc. 4th Int. Symp. Washington Vol. I 205–242 (1960).
3. H. G. Midgley, "The mineralogy of set high-alumina cement", Trans. Brit. Ceram. Soc. **66(4)** 161–187 (1967).
4. T. D. Robson, "High-alumina cements and concretes" (1962), Contractors Record Ltd., London.

Supplementary Paper III-97 Effects of Hydration of Cement on Compressive Strength, Modulus of Elasticity and Creep of Concrete

Singo Seki, Kiyoshi Kasahara, Takeo Kuriyama and Makoto Kawasumi*

Synopsis

Relation between rate of hydration of cement and compressive strength, modulus of elasticity, and creep of concrete was examined from data of bound water of cement paste and wave velocity in it, and compressive strength and creep tests of concrete.

Introduction

It is natural to consider that the strength, modulus of elasticity, creep and many other properties of concrete are closely related to the hydration of cement.

We showed in the previous paper that the compressive strength of concrete is linearly related, regardless of its age to the weight ratio of hydrated cement to the mixing water, and derived an empirical formula to be used practically. In this paper, are summarized only important results of the above study. And descriptions are given on the result of some attempts to estimate modulus of elasticity of concrete at any age when the properties of aggregate are known. And the result on the relation between creep and progress of hydration of cement will also be stated.

The original mix proportion of the concrete of the specimens studied are shown in Table 1. And this is the one which was used to construct the Kurobe No. 4 Dam, one of the representative large dams in Japan. The concrete specimens, however, were made with the concrete wet screened through a sieve with 40 mm openings.

Table 1. *Mix proportion of full mix concrete*

Maximum size of aggregate (mm)	Cement (kg/m³)	Water (kg/m³)	Fine aggregate (kg/m³)	Coarse aggregate (kg/m³)	Water-cement ratio w/c (%)
180	180	85	434	1722	47.0

And the type of cement was moderate heat portland cement.

Measurement of the Amount of Bound Water in Cement Paste

In order to get the relation between the amount of bound water in cement paste and the strength of concrete, the amount of bound water in the cement paste with water-cement ratios (W/C) of 25, 35, 40 and 55%, at the ages of 7, 28, 91, 365 days were measured.

Type of Cement

The type of cement used in experiments was moderate heat portland cement and its mineral composition is shown in Table 2.

Table 2. *Mineral composition of cement*, (%)

C_3S	C_2S	C_3A	C_4AF	$CaSO_4$	Total
46.9	30.9	3.4	13.0	2.0	96.2

Manufacture of Specimens and Testing Procedures

Specimens for the measurement of the amount of bound water were prepared using the mold of 4 × 4 × 16 cm, cured in a constant temperature and

*Technical Laboratory, Central Research Institute of Electric Power Industry, Tokyo, Japan.

humidity chamber at 24°C and 80% RH for twenty hours after casting. Their respective water-cement ratios were 25, 35, 40 and 55%. After the mold was removed, they were cured in the waterpool with 21 ±1°C respectively for 7, 28, 91, 365 days.

Measurement of the weight of bound water was made with specimens cured in closed glass tubes, but as the purpose of the present experiments was to investigate the compressive strength of concrete cured in water, we particularly examined the amount of bound water found in cement cured in water. The method we used in testing was as follows:

After the specimens were ground in a steel mortar, they were passed through a sieve with 0.15 mm openings. About 5 grams of passed sample were dried in vacuum-type desiccator under a pressure of 5 mm mercury and stored in a silica gel dryer for three days to remove free water. Then after being put into a platinum melting pot, they were ignited in an electric furnace with the temperature of 900–950°C for about three hours. In the case of cement-paste with water-cement ratio 60–65%, the testing was given up as the materials were so badly segregated that the preparation of specimens became impossible.

The Result of the Measurement

The result of the measurement of the amount of bound water of cement-paste with different water-cement ratios is shown in Fig. 1.

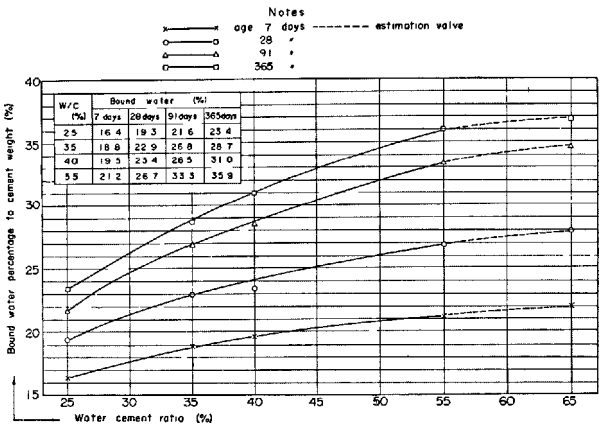

Fig. 1. *Bound water of moderate heat cement paste with different water cement ratios at each age (cured in water at 20°C)*

According to Kondo (1), the amount of bound water measured by weight when the cement is perfectly hydrated is said to account for 35–37%, of the weight of whole cement while Kinji Shinohara (2) regarded it as 32–37%. In consideration of these two experimental values, the amount of perfectly bound water will be estimated to be 37%. Or estimating from the results of experiments of concrete made by the authors, it is proper to consider its value as 37% in the case of moderate heat portland cement.

Rate of Hydration of Cement (R_H)

Experimental results on the relation between the amount of bound water and water-cement ratio with different ages are shown in Fig. 1, and according to it, the rate of hydration of cement increases with the water-cement ratio and the age. If the percentage of bound water to original cement by weight is 37% as described above, when the whole cement is hydrated in our experiment, the rate of hydration of moderate heat portland cement is calculated as shown in Table 3. When cement is cured in water for one year with its water-cement ratio of 55%, the rate of hydration is 35.9/37 = 0.97, that is, 97% of the cement is supposedly hydrated. The ratio of amount of bound water in hydrated cement at a specified age to that of bound water in its perfectly hydrated cement shows the rate of progress of hydration.

$$\text{Rate of hydration } (R_H) = \frac{\text{bound water at the specified age}}{\text{bound water in perfectly hydrated cement}} \quad (1)$$

This rate of hydration changes with the water-cement ratio and the age of cement paste. The relation between them is shown in Fig. 2. From this chart, the rate of hydration of cement at any water-cement ratio and age, can be obtained.

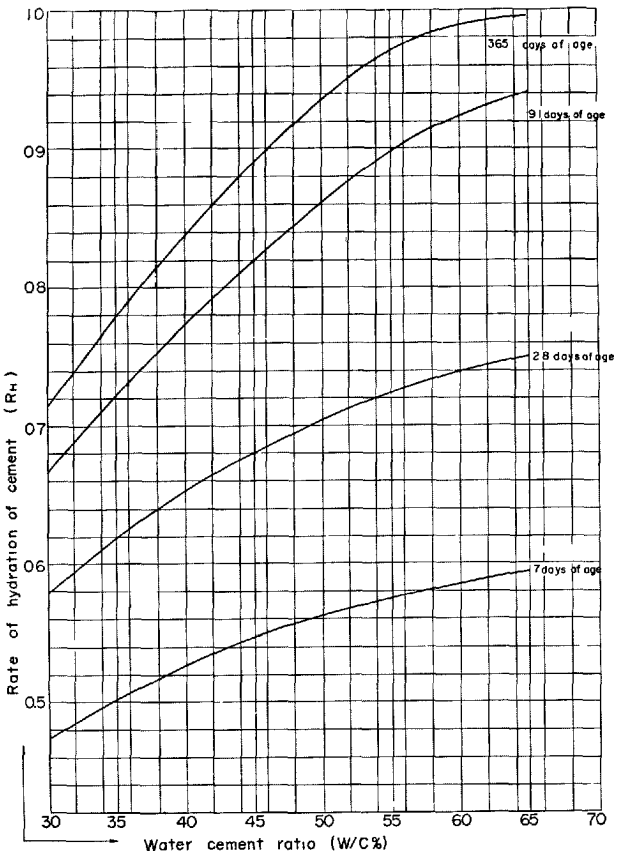

Fig. 2. *Relation between water-cement ratios and rates of hydration at early age (type of cement: moderate heat cement, 37% of perfect bound water)*

Table 3. *Rate of hydration* (R_H) *calculated from the amount of bound water*

W/C (%)	Amount of bound water (%)				Rate of hydration of cement (R_H) (%)				Remarks
	7 days	28 days	91 days	1 year	7 days	28 days	91 days	1 year	
25	16.4	19.3	21.6	23.4	44.3	52.2	58.4	63.2	○
30	17.5	21.4	24.6	26.4	47.3	57.8	66.5	71.4	□
35	18.6	22.8	26.8	28.8	50.3	61.6	72.4	77.8	○
40	19.5	24.2	28.5	31.0	52.7	65.4	77.0	83.8	○
45	20.2	25.4	30.3	33.0	54.6	68.6	81.9	89.2	□
50	20.8	26.2	31.9	34.6	56.2	70.8	86.2	93.5	□
55	21.2	26.7	33.3	35.9	57.3	72.2	90.0	97.0	○
60	21.6	27.2	34.2	36.6	58.4	73.5	92.4	98.9	□
65	22.0	27.8	34.8	36.8	59.5	75.1	94.1	99.5	□

Note: (1) The amount of perfectly bound water of cement is 37% of the total weight of the cement.
(2) Sign ○ expresses experimental values, and sign □ values read from figures.

Effective Cement-Water Ratio and the Compressive Strength of Concrete

Compressive strength of concrete is supposedly related to the effective cement-water ratio expressed in the following formula:
Effective water-cement ratio (C_H/W)

$$= \frac{\text{cement weight per 1 m}^3\text{ concrete (kg/m}^3) \times \text{rate of hydration of cement } (R_H)}{\text{weight of water per 1 m}^3\text{ concrete (W) (kg/m}^3)}$$

$$= \frac{\text{weight of original cement that has become hydrated per 1 m}^3 \times \text{concrete } (C_H)\text{ (kg/m}^3)}{\text{weight of water per 1 m}^3\text{ concrete (W) (kg/m}^3)} \quad (2)$$

It became clear that the relation between the effective cement-water ratio calculated from the rate of hydration of cement and the compressive strength of concrete are showed almost on the same line at any age. Fig. 3 shows especially the relation between compressive strength of concrete used for the Kurobe No. 4 Dam and its effective cement water ratio at each age.

The mineral composition of this cement is almost the same as the one used for the measurement of bound water. Fig. 4 shows the plot of 36 values obtained from experiments in our laboratory and 28 experimental values of other dams.

From the data shown in Fig. 4, the following linear regression line was derived by the method of least squares,

$$\sigma_c = -281.2 + 413.97\,(C_H/W)\ \text{kg/cm}^2 \quad (3)$$

where σ_c is the compressive strength of concrete. A95% confidence prediction interval for future observation about the compressive strength of con-

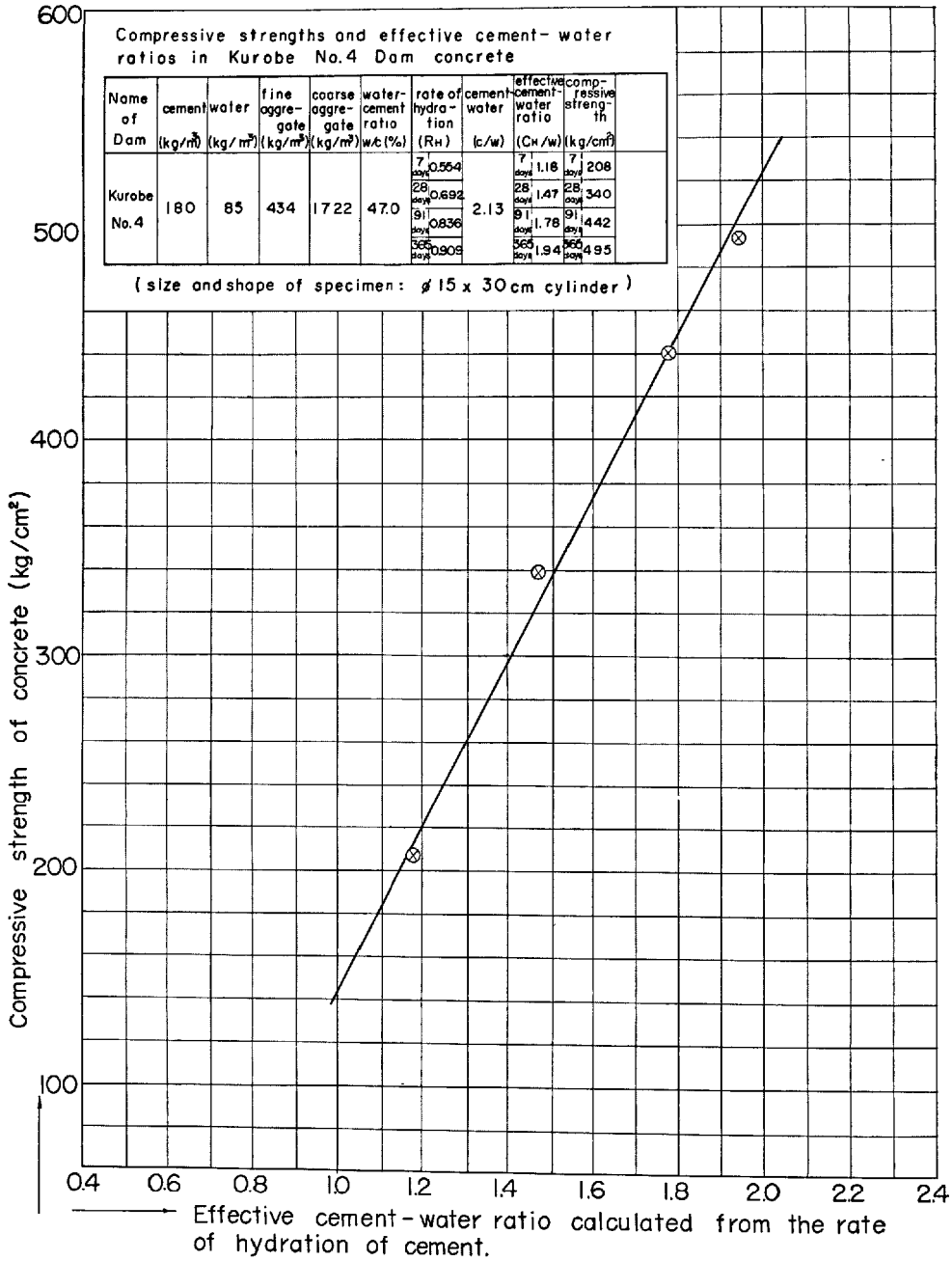

Fig. 3. *Relation between compressive strength of concrete and effective cement-water ratio calculated from the rate of hydration of cement in the Kurobe No. 4 Dam concrete. (type of cement: moderate heat cement, ages 7, 28, 91, 365 days)*

crete is also shown in Fig. 4.

We must recall that T. C. Powers and T. L. Brownyard stated in 1947 that the strength of cement-paste and mortar is expressed as a linear function of the ratio of the volume of hydrate of cement and void contained therein to the amount of water initially used (gel-space ratio) (3). Later developments are concisely summerized in Powers' report (4). Here, we derived a

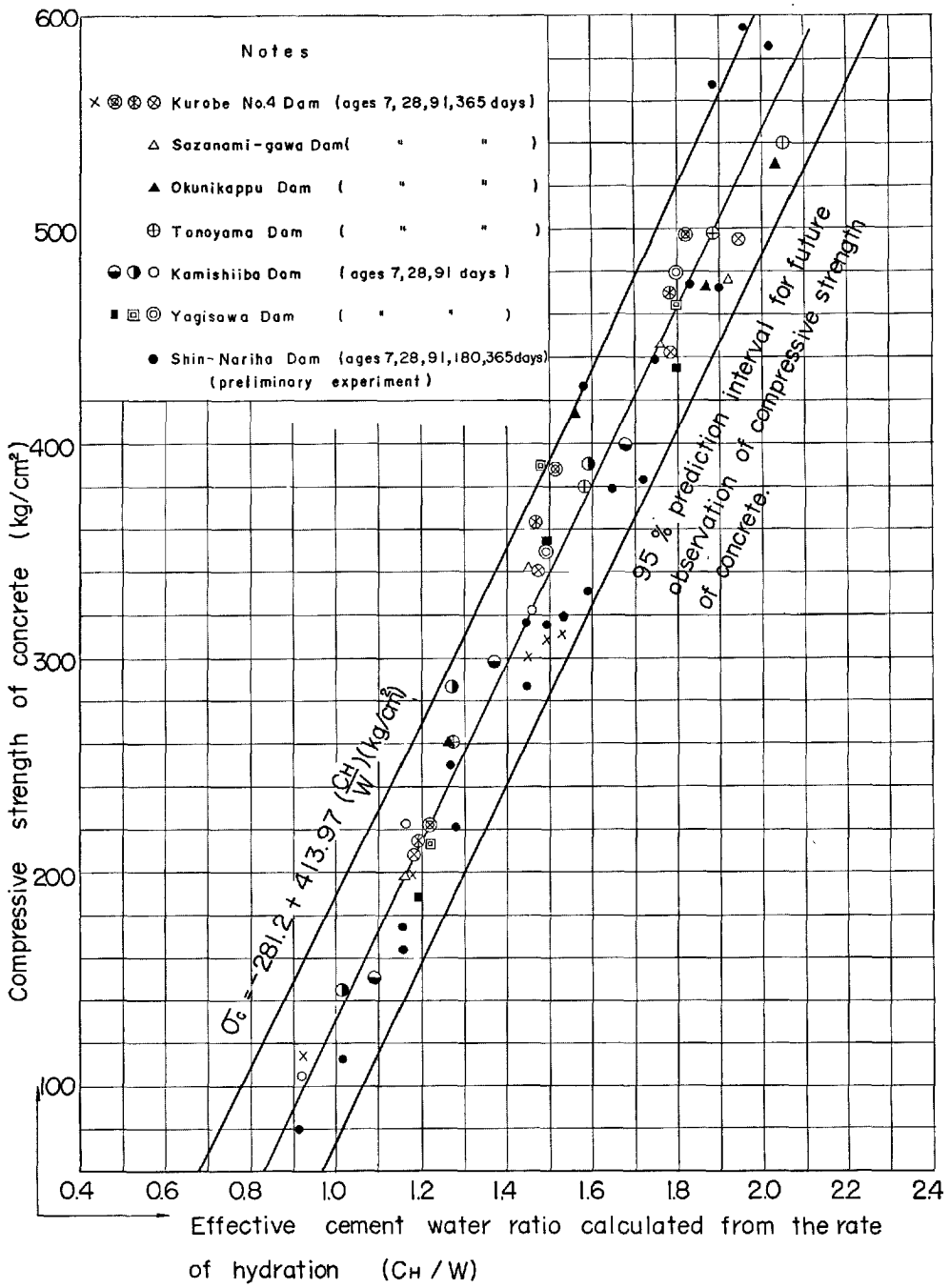

Fig. 4. *Relation between compressive strength of concrete and the effective cement-water ratio calculated from the rate of hydration (with perfect bound water ratio 37%)*

practical formula of broader application on the strength of concrete in terms of C_H/W.

The value C_H/W shows the hydrated cement-water ratio, and seems to be more suitable in the chemical terminology. But it shows the effective amount of cement-water ratio contributing to the enhancement of compressive strength of concrete, so this value was named effective cement-water ratio.

Measurement of Longitudinal Wave Velocity in Cement Paste

Longitudinal wave velocities in cement pastes with w/c, 26, 36, 44.5, 52% at the time of demoulding were measured at the ages of 7, 28, 91, 365 days, by ordinary direct pulse method using of an oscilloscope.

Size of specimens was $\phi 5 \times 10$ cm, and four specimens were used for each measurement. The results are shown in Table 4.

The densities of specimens at the times of measurement are shown, in Table 5.

Table 4. *Longitudinal wave velocities in cement pastes with different w/c and ages*

W/C (%)	Longitudinal wave velocity (m/sec)			
	Age (days)			
	7	28	91	365
26	4,040	4,320	4,420	4,610
36	3,660*	3,870	3,980*	4,240
44.5	3,170	3,700	3,750	3,890
52	3,030	3,410	3,450	3,850

*With two specimens.

Table 5. *Densities of cement pastes at each age (kg/cm³)*

W/C (%)	Age (days)			
	7	28	91	365
26	2.18	2.21	2.21	2.21
36	2.12	2.15	2.14	2.12
44.5	2.00	2.01	2.01	2.00
52	1.93	1.94	1.94	1.98

Longitudinal Wave Velocity and Volume of Unhydrated Water in Cement Paste

The problem of longitudinal wave in cement paste will be treated from the two stand points,—the one is that of the elastic wave propagating through granular media and the other that of the wave through porous media. And with the former, there are theories described Takahashi—Y. Sato (5), S. Nagumo (6) and T. Momoi (7) and with the latter, by Y. Sato (8) (9).

But here, we try to find the effect of progress of hydration of cement on wave velocity experimentally.

In Fig. 5, is shown relation between volume of unhydrated water in cement paste and longitudinal wave velocity in it.

The volume of unhydrated water in cement paste were caluculated by the following formula:

$$V_{W-WH} = V_W - \frac{0.37C_H}{\rho_W} = V_W - \frac{0.37R_HC}{\rho_W} \quad (4)$$

where V_{W-WH}: volume of unhydrated water in 1 m³ cement paste [m³/m³]

V_W: volume of water in cement paste at the beginning [m³/m³]

C: cement mass in 1 m³ cement paste [kg/m³]

C_H: hydrated cement mass in 1 m³ cement paste [kg/m³]

R_H: rate of hydration of cement

ρ_W: density of water = 1000 kg/m³

From this figure, it was shown as a first approximation that the velocity is linearly dependent on the volume of unhydrated water as shown by the least squares solution,

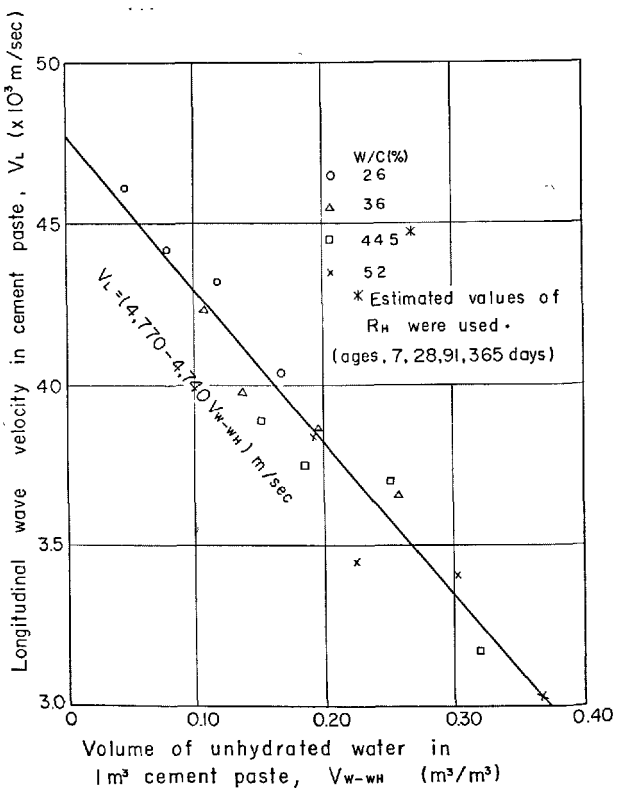

Fig. 5. *Relation between volume of unhydrated water in cement paste and longitudinal wave velocity*

$$V_L = 4{,}770 - 4{,}740 V_{W-WH} \quad \text{m/sec} \qquad (5)$$

where V_L: longitudinal wave velocity [m/sec]

In this calculation the data for those with w/c = 44.5% were excluded because only estimated values of R_H were available for those specimens.

Estimation of Young's Modulus of Cement Paste

The dynamic Young's modulus of cement paste by pulse method was calculated by the formula,

$$E_p = \rho \frac{(1+\sigma)(1-2\sigma)}{1-\sigma} V_L^2$$

$$= \rho \frac{(1+\sigma)(1-2\sigma)}{1-\sigma} (477{,}000 - 474{,}000\, V_{W-WH})^2$$

$$\text{dyne/cm}^2 \qquad (6)$$

where E_P: dynamic Young's modulus of elasticity of cement paste by pulse method

V_L: longitudinal wave velocity [cm/sec]

σ: Poisson's ratio of cement paste

ρ: density of cement paste [kg/cm³]

As the dynamic Poisson's ratio could not be measured, $\sigma = 0.2$ was assumed. Then the above formula with engineering units becomes,

$$E_P = 9.184 \rho_S (4{,}770 - 4{,}740\, V_{W-WH})^2 \times 10^{-3}$$

$$= 9.184 \rho_S \left\{ 4{,}770 - 4{,}740 \left(V_W - 0.37 \frac{R_H C}{\rho_W} \right) \right\}^2$$

$$\times 10^{-3} \text{ kg/cm}^2 \qquad (7)$$

where ρ_S: specific gravity of cement paste.

In Fig. 6, E_P/ρ_S vs. volume of unhydrated water in cement paste is shown.

To estimate static Young's modulus of cement paste from dynamic modulus, the relation we have obtained between static Young's modulus and dynamic modulus of dam concrete by resonance method was used, namely,

$$E_D = 1.369 E_S \qquad (8)$$

where E_D: dynamic Young's modulus by resonance method

E_S: static Young's modulus

And also $E_D = E_P$ was assumed. Experimental results between E_S and E_D are shown in Fig. 7.

These results are neither about cement paste nor by pulse method. But so far as the authors' other

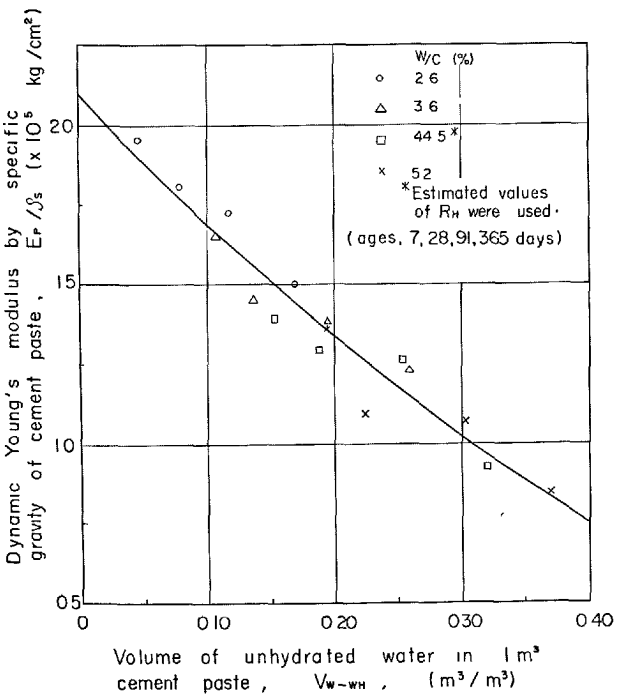

Fig. 6. *Relation between dynamic Young's modulus by specific gravity and volume of unhydrated water in cement paste*

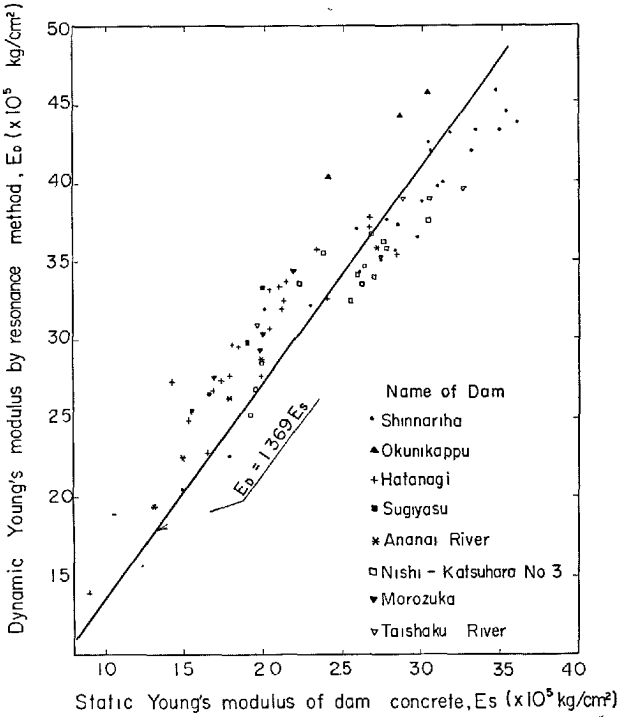

Fig. 7. *Relation between static Young's modulus and dynamic Young's modulus by resonance method in dam concrete* (ages, 4–365 days)

experiments are concerned, cement paste seems to obey the nearly equal rule. Though the ratio E_p/E_s may change with age, this effect was neglected.

The estimated dynamic and static moduli of cement paste with w/c = 47% by means of the above mentioned method are shown in Table 6.

Table 6. *Estimated dynamic and static elastic moduli of cement paste with w/c = 47%*

Age (days)	Dynamic Young's modulus (kg/cm²)	Static Young's modulus (kg/cm²)
7	177,200	129,400
28	213,400	155,900
91	254,900	186,200
365	277,600	202,800

Estimation of Modulus of Elasticity of Concrete

The elastic moduli of the Kurobe No. 4 Dam concrete cured in water were calculated at each age and compared with the experimental results shown in Table 7.

The aggregate used is granite, and its properties are shown in Table 8.

The static Young's modulus of the actual aggregate which was used for concrete specimens was not measured. But the values of the granite taken from the quarry were measured by H. Ishigai, K. Kasuya and K. Saito in wet condition by means of an Okhuizen compressometer (10).

The results are shown in Table 9.

Thus the mean value of static Young's moduli was as follows:

$$E_a = 284{,}000 \text{ kg/cm}^2 \tag{9}$$

This value will be used in the following calculations.

The present aspects of researches on the theory of elasticity of random media has been reviewed by Z. Hashin (11).

Here, several formulas which have been used by other authors for concrete research will be used to compute elastic modulus of concrete at each age.

From now on, the following symbols will be adopted,

E_c: static Young's modulus of concrete [kg/cm²]
E_a: static Young's modulus of aggregate [kg/cm²]
E_m: static Young's modulus of cement paste matrix [kg/cm²]
V_a: volume of aggregate in 1 m³ concrete [m³/m³]
V_m: volume of cement paste in 1 m³ concrete [m³/m³]

In case of wet screened the Kurobe Dam concrete,

$V_a = 0.7623$, $V_m = 0.2377$, and
$E_a = 284{,}000$ kg/cm²

Em at each age is taken from Table 6.

The formulas are,

$$E_c = V_a E_a + V_m E_m \tag{10}$$

$$\frac{1}{E_c} = \frac{V_a}{E_a} + \frac{V_m}{E_m} \tag{11}$$

by Dantu, Kaplan, and T. C. Hansen (12)

$$E_c = \left[\frac{(1 - V_a)E_m + (1 + V_a)E_a}{(1 + V_a)E_m + (1 - V_a)E_a}\right]E_m \tag{12}$$

Table 7. *Unit weight, modulus of elasticity, compressive strength of the Kurobe No. 4 Dam concrete*

Age (days)	Unit weight (kg/m³)	Static Young's modulus, Es (kg/cm²)	Compressive strength (kg/cm²)
7	2,335	174,000	208
28	2,331	224,000	340
91	2,352	258,000	442
366	2,356	303,000	495

Table 8. *Physical properties of aggregate*

Item	Fine aggregate	Coarse aggregate
Kind of aggregate	granite	granite
Specific gravity	2.59	2.64
Amount of water absorption (%)	0.6	0.7
Weight loss by soundness test* (%)	8.0	7.8

*Five times tests were repeated with sodium sulfate solution.

Table 9. *Properties of granite taken from the quarry for the Kurobe No. 4 Dam concrete*

Place	Specific gravity	Water absorption (%)	Compressive strength (kg/cm²)		Static Young's modulus in wet condition (kg/cm²)
			dry	wet	
Quarry A	2.61	0.45	2,290	2,360	264,000
Quarry A	2.69	0.47	2,800	1,970	335,000
Quarry B	2.63	0.66	2,230	1,520	254,000
Mean	2.64	0.53	2,440	1,950	284,000

which Hansen (12) simplified the results due to Hashin (13), assuming Poisson's ratio of both aggregate and cement paste is 0.2,

$$\text{and,}\quad \frac{1}{E_c} = \frac{1-\sqrt{V_a}}{E_m} + \frac{1}{\left(\frac{1-\sqrt{V_a}}{\sqrt{V_a}}\right)E_m + E_a} \qquad (13)$$

by Counto (14).

Relation between the calculated static Young's moduli of concrete by the above formulas and the estimated static Young's moduli of cement paste are shown in Fig. 8.

Experimental results are also illustrated in the same figure.

Judging from these results, the difference % between them reaches about 30% at the maximum, although the trend of the calculated values coincide with the experimental.

These errors are attributable to the inaccuracies of elastic moduli of cement paste and aggregates, and the lack of sufficient accuracy in the above formulas. But it is not clear whether factor is most predominant or not.

To solve this problem, further efforts will be needed. As an additional remark, it may be worthy of mention that the results by Hashin-Hansen and by Counto almost coincide with those and other results obtained by rather gross assumptions are not so far from the results by a theoretical formula.

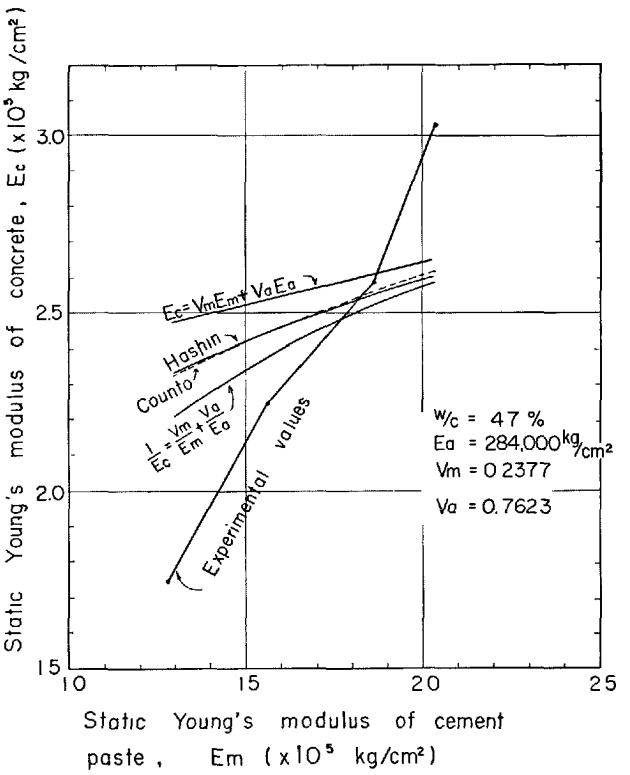

Fig. 8. *Static Young's modulus of cement paste vs. static Young's modulus of concrete*

Hydration of Cement and Creep of Concrete

The following fact has been well recognized that, in a creep test about a same kind of concrete, the later is the loading age, the smaller is the creep strain. This may be due to hardening of cement paste. But the definite relation between creep and hydration of cement has not been known to the authors.

As the first step of approaching this problem, relation between creep factor and volume of unhydrated water at the age of loading in our creep test is investigated and is shown in Fig. 9.

The term creep factor adopted here is defined in the following expression used for the analysis of creep curves per unit stress, and the factors are proportional to creep strains when the age is fixed.

$$\varepsilon_{(t)} = \frac{1}{E_i} + F(k)1_n(t+1) \qquad (14)$$

$\varepsilon_{(t)}$: elastic and creep strain per unit stress [1/kg/cm²]

E_i: instantaneous elastic modulus [kg/cm²]

k: age of loading [day]

$F(k)$: creep factor [1/kg/cm²]

t: days after loading [day]

This expression has been used by U.S. Bureau of Reclamation to analyse creep of dam concrete.

However, for analysis of the data obtained from 7 days loading, the fittness at the early ages was not good, so the following expression was introduced:

$$\varepsilon_{(t)} = \frac{1}{E_i(2)} + \left(\frac{1}{E(\infty)} - \frac{1}{E_i(2)}\right) \tanh\left\{\left(\frac{F^{(2)}_{(k)}}{\frac{1}{E(\infty)} - \frac{1}{E_i(2)}}\right)1_n(t+1)\right\}$$

$$= \varepsilon^{(2)}_{(0)} + (\varepsilon(\infty) - \varepsilon^{(2)}_{(0)})\left(1 - \frac{2}{1+(t+1)^{2\alpha}}\right) \qquad (15)$$

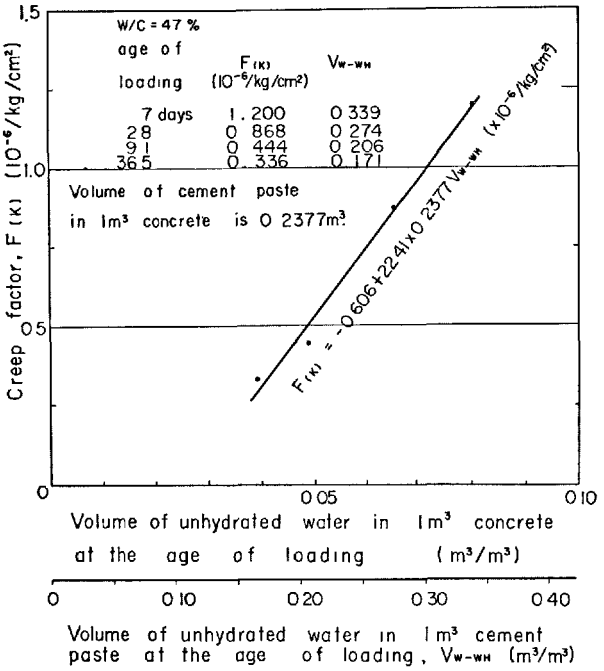

Fig. 9. *Relation between volume of unhydrated water in concrete or cement paste at the age of loading and creep factor*

where

$$\alpha = \frac{F^{(2)}_{(K)}}{\frac{1}{E(\infty)} - \frac{1}{E_i(2)}}$$

When $\ln(t+1)$ is sufficiently small the above expression tends to

$$\varepsilon^{(2)}_{(t)} \cong \varepsilon^{(2)}_{(0)} + F^{(2)}_{(K)} \ln(t+1) \qquad (16)$$

And when t is sufficiently large,

$$\varepsilon_{(t)} \to \frac{1}{E(\infty)} \qquad (17)$$

The creep curves obtained from a experiment is shown in Fig. 10.

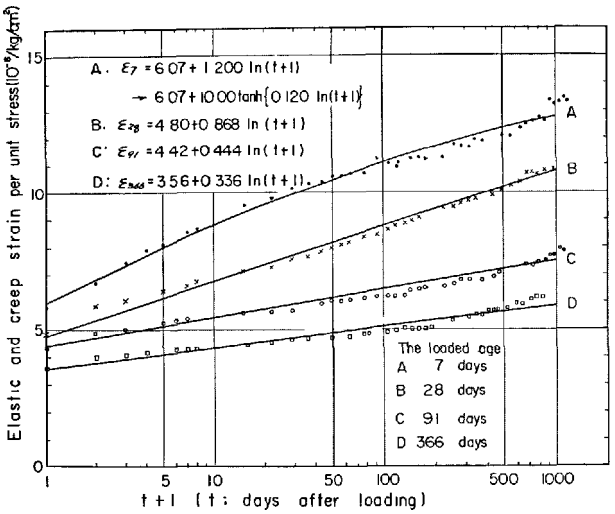

Fig. 10. *Creep curves of the Kurobe No. 4 Dam concrete*

The strains were measured by embedded Carlson type strain meters.

The mix of concrete was the same above, and the size of specimen was ϕ 15 × 60 cm. The specimens were sealed with rubber just after demoulding. The curing condition of these specimens therefore differs from water curing. The data on hydration of cement, however, were substituted by the value of hydration of the water cured cement paste obtained in the experiment previously referred to.

According to Fig. 9, creep factors are linearly related to the volumes of unhydrated water in the range for practical applications.

But the creep factor of 7 days loading was based on the data of strains observed at the relatively early ages. Then this linearlity including the result of 7 days loading, will hold true for limited ages.

This may be a natural consequence, because creep strain will be affected not only by the degree of hydration at the age of loading, but also by the progress of hydration thereafter.

Conclusion

A very close relation was observed between rate of hydration of cement and compressive strength of concrete. And a formula was presented expressing compressive strength of concrete at any age by a linear function of effective cement-water ratio.

This effective cement-water ratio introduced in our report means the ratio of hydrated cement weight to the weight of mixing water.

Linear relation between volume of unhydrated water in cement paste and velocity of longitudinal wave in it was observed. And a formula was derived to express dynamic modulus of elasticity of cement paste in terms of rate of hydration of cement and w/c.

Several formulas expressing elastic modulus of concrete in terms of the moduli of cement paste and aggregate and their relative volumes were examined.

A result showing the linear dependence of creep factor on the volume of unhydrated water at the age of loading was presented.

More advanced microscopic physico-chemical studies are recognized as necessary to make clear problems concerning compressive strength, elasticity, creep and other fundamental properties of concrete.

References

1. K. Asaoka, "Theoretical cement chemistry" (in Japanese), (Kunitachi Press Inc., Tokyo, Japan) 1946.
2. K. Shinohara, "Study on cement-paste" (in Japanese), Bulletin of Kyushu Univ. (1938, 1940).
3. T. C. Powers and T. L. Brownyard, "Studies of the physical properties of hardened portland cement paste, Part 6. Relation of physical characteristics of the paste to compressive strength", Journal of ACI, **18**, No. 7, 845–864 (Mar. 1947).
4. T. C. Powers, "Physical properties of cement paste", Chemistry of Cement, Proc. of the 4th International Symposium, Washington, Vol. 2. 577–613 (1960).
5. T. Takahashi and Y. Sato, "On the theory of elastic waves in granular substance 1", Bull. of Earth quake Research Institute, **27**, 11–16, (1949).
6. S. Nagumo, "Studies on the elastic wave velocity in clastic rock", Bull. of the Geological Survey of Japan, **8**, No. 9, 27–44, (1957).
7. T. Momoi, "On the longitudinal wave velocity in the moist granular media (I) (II)" (in Japanese), Journal of the Seismological Society of Japan, 2nd Series **14**, No. 3, 201–203, (Sept, 1961).
8. Y. Sato, "Velocity of elastic waves propagated in media with small holes", Bull. of Earthquake Research Institute, **30**, 179–190, (1952).
9. Y. Sato, "Velocity of elastic waves propagated in media with small obstacles", Bull. of Earthquake Research Institute, **31**, 1–18, (1953).
10. K. Ishigai, K. Kasuya and K. Saito, "Some considerations on basic properties of deformation of rock" (in Japanese), Technical Report of Central Research Institute of Electric Power Industry, Civil Engineering 59017, (1960).
11. Z. Hashin, "Theory of mechanical behavior of heterogeneous media", in Applied Mechanics Surveys, 263–275, (Spartan Book, Washington, D. C., U.S.A.) 1966.
12. T. C. Hansen, "Influence of aggregate and voids on modulus of elasticity of concrete, cement mortar, and cement paste", Journal of ACI, **62**, No. 2, 193–216, (Feb. 1965).
13. Z. Hashin, "The elastic moduli of heterogeneous materials", Trans. of ASME., Journal of Appl. Mech., **29** Ser. E., No. 1, 143–150. (Mar. 1962).
14. U. J. Counto, "The effect of the elastic modulus of the aggregate on the elastic modulus, creep and creep recovery of concrete", Mag. of Concrete Research, **16**, No. 48, 129–138, (Sept. 1964).

Supplementary Paper III-119 Some Recent Advances in the Study of Cement and Concrete

Harold E. Vivian*

Introduction

During the past 20 years a considerable amount of basic research has been carried out on the crystal lattice structures of clinker compounds and on their hydrated products. In addition many kinetic studies on cement in pastes and suspensions as well as in concrete have been made in order to describe the basic performance of hydrating cement. While all this work is necessary for an understanding of the nature and behaviour of the compounds that make up clinker and cement, it does not always allow the performance of clinker and cement to be predicted or controlled.

Much of the work done on cement performance in paste and concrete has also failed to demonstrate clearly and unequivocally how and for what reasons the observed physical phenomena occur. The immediate reasons for these failures arise from the complexity of clinker and the problems encountered in studying and understanding the hydration reactions and compound interactions in cement. However, behind all these difficulties lie some important and intractable problems. Commercially-produced clinker is not controlled sufficiently closely in any characteristic other than its gross chemical composition. Consequently cement used in experimental work is inadequately described especially in relation to certain physical characteristics that can exert a profound effect on paste and concrete performance. Thus it will be seen that arguments based on the performance of an inadequately described cement are liable to prove unsound and confusing if applied to the performance of cement paste and concrete in general. Additional difficulties associated with sampling and test methods have greatly confused the overall understanding of cement performance.

In recognition of these problems, studies are being made into the performance of clinker compounds in mixtures of identical chemical composition but different and closely-controlled physical characteristics. The purpose of this paper, therefore, is to indicate how some of the results of these studies may help in clarifying the performance of cement and concrete.

Clinker

It is well known that argillaceous limestones usually clinker readily even when coarsely ground. The fineness of grinding and the intimacy of mixing of the raw material components are major factors in controlling clinkering when mixtures of pure limestone and clay or shale are used. In large manufacturing plants chemical control testing is adequate but control of the particle size of the raw meal constituents may be so meagre that the desired levels of uniformity in burning and in the properties of clinker are not always maintained.

Coarse limestone and shale or silica particles, which do not undergo complete reaction during the time that they are resident in the buring zone in the kiln, modify the clinker composition both in their immediate vicinity and in more remote zones. Such particles, therefore, cause the clinker composition to be changed from that calculated, increasing the uncombined lime and residual silica. To minimize such defects a long burning time is required with consequent reduction in kiln output and a general deterioration in kiln performance. Clinker produced under these conditions is generally coarsely crystallized and inhomogeneous in composition. Fine grinding on the other hand produces finely-crystallized clinker with a high degree of uniformity and reduces the burning time required to give a low free lime content.

Two contrasting microphotographs shown in Fig. 1 illustrate the differences in crystal size and uniformity of clinker produced from raw meals of different particle size but identical chemical composition. These microphotographs show (1) a uniform, finely-crystallized clinker produced from raw meal particles that were all in the 12–24μ range and (2) a non-uniform, coarsely-crystallized clinker produced from

*C.S.I.R.O., Chemical Research Laboratories Melbourne, Australia.

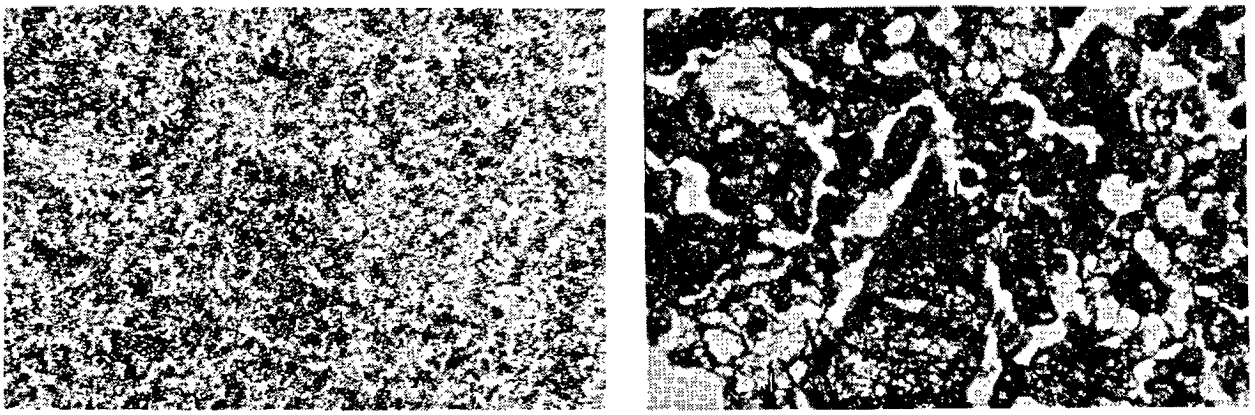

A. Produced from raw meal particles 12-24μ

B. Produced from raw meal particles $+36\mu$ and up to 150μ

Fig. 1. *Photomicrographs of sections of clinker having the same calculated chemical composition*—C_3S 71.0%, C_2S 12.0% C_3A 5.0%, C_4AF 12.0%, *and burnt at 1400°C for 15 minutes. Magnification* ×40. (*Microphotographs by J. H. Weymouth*)

raw meal of the same chemical composition and made up of particles that were $+36\mu$ and up to 150μ. Commercial clinker is generally intermediate between these two extremes but tends to approach the more variable, coarser crystalline type. In the finely-crystalline clinker the crystals are generally-12μ whereas in the coarsely-crystalline clinker C_2S and C_3S crystals may be up to 300μ. C_3A and C_4AF are present in much smaller amounts and occur in finer crystals than those of C_2S and C_3S. The subsequent performance of these clinkers, when ground, appears on present indications to be different in many respects.

Control over the size of raw meal particles in commercial plants requires (1) a large scale separator that is capable of achieving a clean separation of the particles below 70μ from the ground raw meal and further studies may indicate that it is desirable for the maximum particle size to be smaller and (2) rapid and accurate test procedures to ensure that the required separation is being obtained consistently.

Cement Grinding

Although the principles of ball milling appear to be relatively simple certain factors in mill operation can adversely affect the uniformity and performance of cement. Two of these factors will be discussed. It has long been known that the gypsum content of the -12μ fraction of cement is generally much greater than that of the coarser fractions. Gypsum and clinker when ground together in a mill break down into different particle size distributions. Surface area measurements used for mill control do not distinguish between these two distributions and variations between the relative grindability of clinker and gypsum cannot be detected. Any circumstances leading to a coarser gypsum particle size distribution can result in the cement behaving as though it contained inadequate sulphate. Conversely excessive proportions of gypsum in the -12μ fraction can give the impression that the gypsum content of the cement is adequate or even excessively large at least in the behaviour of cement at early ages while the later behaviour of the cement may indicate some deficiency in sulphate. This type of variation can only be detected and minimized by using a control procedure based on a combination of particle size separation and determination of the gypsum content of each fraction.

Closed circuit grinding in air-swept mills accentuates problems arising from contact of cement particles with large volumes of air containing moisture and carbon dioxide. Such systems promote the surface hydration and carbonation of active clinker components, especially C_3A. These surface reactions modify the changes that occur in paste during the mixing period and cause premature stiffening and early loss of workability. Methods of minimizing this problem include a reduction in the amount and temperature of the circulating air-stream, closed circuitry of the air system as far as possible and reducing the residence time of the fine cement particles in the circuit by

increasing separator efficiency.

Consistency and Workability

The water requirement for normal consistency of cement paste is a function partly of the particle size distribution and partly of the effects produced by the early chemical reactions which change the solid-water relationship and produce stiffening. Finely-ground cement, which has been over-heated during grinding, and especially if it has also been aerated in a humid atmosphere, rapidly develops stiffening tendencies which may be caused by a wide range of factors.

A different stiffening phenomenon can occur generally at a time longer than ten minutes after mixing ceases. There are indications that this stiffening is influenced by a reduction in the availability of dissolved sulphate due to the rapid occlusion of gypsum particles by films of reaction products. Clinker particles deprived of sulphate then tend to hydrate as though unretarded and the paste stiffens rapidly. Although this unstable system of occluded gypsum may persist for a long time under static wet conditions, the sulphoaluminate reaction proceeds very slowly in the hardened paste and may ultimately cause expansion and cracking. One way of avoiding stiffening, which results from sulphate occlusion, is to provide a greater quantity of gypsum in the fine particle size range than would normally be necessary.

The actual amount of clinker hydrated, when stiffening occurs, is usually quite small. Finely-ground clinker without added gypsum undergoes a hard set very rapidly and when it is less than 5 per cent hydrated. Free water, however, can be readily removed under pressure from such hardened paste.

Since clinker hydration and chemical interactions begin as soon as cement and water are mixed together, the stiffening of paste may develop rapidly and can be modified in some instances by vigorous mixing especially in pastes containing low water contents. The stiffening reactions affect the consequent properties such as strength development, shrinkage, cracking tendencies and durability of hardened paste and concrete. Paste consistency and concrete workability can be improved by various procedures which involve modifications in clinker composition, coarser grinding, reduced aeration and reduction in grinding temperature.

Dimensional Stability of Paste

Experiments have shown that gypsum can react with C_3A and then become occluded by the reaction products. When gypsum is occluded by reaction products in hydrating cement paste, a certain proportion of the undissolved gypsum is either prevented from going into solution or is able to dissolve at only a very slow rate. This arrested solution condition can persist under static wet conditions for very long periods of time, at least for several years. Under continuously dry conditions the paste will remain permanently in its contracted state without undergoing any further changes. When pastes are subject to dry-wet cycling conditions, and especially when given heat-cool cycles as well, a certain amount of gypsum is intermittently released into solution during each wet cycle and this gypsum, on reacting with C_3A, can cause local and progressive expansion and eventual disruption of the paste. This appears to be the cause of a type of surface crazing that is apparent in concrete exposed to wet-dry and heat-cool cycles. Some heating in conjunction with drying is necessary to induce the maximum amount of change in the layers of reaction product surrounding the gypsum particles in order to ensure that further amounts of undissolved gypsum become available for reaction with C_3A.

The presence of gypsum in cement paste tends to reduce the magnitude of drying shrinkage because it reacts with C_3A to produce calcium sulphoaluminate. This latter compound has two effects in paste. It retrains shrinkage movements and, as a result of its continued formation, it causes an expansion that counteracts some of the drying shrinkage movement.

The internal restraint reduced in paste by sulphatoaluminate is roughly comparable with the more macroscopic restraining action of aggregate particles in mortar and concrete. The restraint imposed by the aggregate particles reduces the overall measured shrinkage but induces very considerable numbers of internal cracks. The development of crack patterns

in paste, mortar and concrete constitutes an important phenomenon which is indicative of the condition of the material and the types of actions that are proceeding in it.

The particle size distribution of the cement and particularly that of the clinker fraction exerts a major influence on the magnitude of shrinkage. In addition the dependent variable, the water/cement ratio, tends to accentuate shrinkage as it increases. Both of these factors increase the interparticle spacings in the cement paste and these distances in turn determine the shrinkage potential of the paste. When the interparticle distances in the paste are large, the effect on shrinkage of the particle size distribution will exceed that of any other factor.

The physical condition of the hydrated compounds and the conditions of their development in paste largely determine their shrinkage tendencies. Hydrated compounds produced at atmospheric temperature have colloidal properties and, therefore, undergo a marked volume decrease that is approximately proportional to their water content and to the initial interparticle spacing in the paste. When pastes are made from (a)-12μ clinker particles and (b) 24 – 36μ clinker particles and at identical water/solid ratios, the drying shrinkages of the fine particle pastes are always larger than those of the coarse particle pastes. Shrinkages of these pastes are shown in Fig. 2.

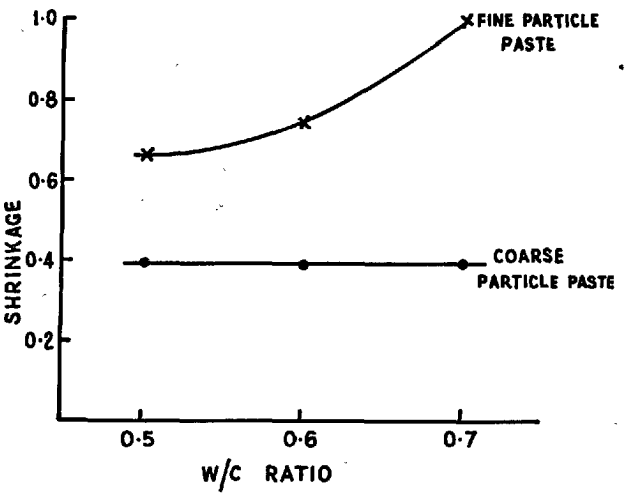

Fig. 2. *The drying shrinkages of clinker pastes made from* (a) -12μ *and* (b) *24–36*μ *particles at the same water/solid ratios*

The fine particle pastes contain more colloidal hydrated material and possess less internal restraint than the coarse particle pastes.

Strength

Movements of hydrated products from single particles and in paste have been observed to occur over finite distances. On mixing with water, hydration and interaction products deposit rapidly as a skin on the surface of the clinker particles. This surface layer then tends to retard but does not inhibit further hydration. As hydration and reaction proceed inwards, the internal pressure on the surface skin increases, the surface skin becomes distended and is eventually disrupted. This allows some of the internal hydrated product to escape and deposit in the freshly opened space in the surface skin or in the surrounding water-filled space. These hydrated products make contact with similar hydrated products derived from adjacent clinker particles or with aggregate particles.

These observations have indicated that fine and coarse clinker particles behave in somewhat different ways in pastes. The hydrated material derived from a fine particle is not present in sufficient quantity to move through such a large distance as that derived from a coarse particle of clinker. Moreover, as a result of particle contacts, pastes consisting only of coarse particles tend to expand as hydration occurs while pastes consisting only of fine particles never undergo serious expansion during hydration. This behaviour is consistent with the local disruptive forces being greater in large hydrating particles than in very small hydrating particles. In addition, in an equivalent volume of paste composed of fine particles, the ratio of hydrating material to available space is less than that in pastes composed of coarse particles. The hydrated product is, therefore, accommodated in the former without generating severe local stress concentrations. The water-filled space in fine particle pastes is approximately 30 per cent by volume while that in coarse particle pastes of approximately equivalent consistency is 15 –20 percent by volume.

In mixtures of fine and coarse particles, which produce pastes that are approximately equivalent to pastes produced from commercially-ground cements, the fine particles hydrate in contact with the coarse particles and contribute a large volume of hydrated product to form the skin on the surface of the coarse particles. The hydration of the coarse particles is thereby retarded to such an extent that they do not cause undue paste expansion.

The clinker compounds show marked difference in their rates of hydration. C_3A in water hydrates very rapidly and to such a great depth that even + 36μ particles are completely hydrated within a few days. C_3A particles, therefore, swell to a marked extent as they hydrate and, even though the hydrated develop some adherence and strength, the continued hydration and swelling of the particle disrupts and displaces the externally developed surface layers. In compacted pastes, the swelling particles produce large inter-particle forces that disrupt the mass. C_3S which is also a relatively rapid hydrating compound causes very minor expansion and disruption in pastes composed only of coarse particles. Pastes composed of fine C_3S particles are quite stable in volume. C_2S and C_4AF generally undergo slow or limited hydration reactions which do not proceed sufficiently deeply into the particles to cause paste expansion and disruption. Pastes made from these compounds appear to be stable and strong.

The presence of small amounts of gypsum and other compounds in the mixing water changes the physical condition of the hydration products that form the surface skin on the clinker particles and modifies the bonding characteristics of these products. Some admixtures form voluminous surface skins on clinker particles whereas others appear to suppress the hydration rate of clinker particles. Gypsum has been observed to promote the disruptive action in paste by reacting slowly with C_3A to form calcium sulphoaluminate. Thus, even though gypsum initially retards clinker hydration, the continued slow reaction of C_3A and gypsum increases the total amount of clinker hydrated over a long period of time. The continuing reaction of gypsum and clinker increases the rate of strength development and the ultimate strength attained by the paste.

Environmental Conditions and Durability

Environmental conditions affect the performance of hardened cement pastes and concrete. Observations have indicated that the drying shrinkage and re-wetting expansion of clinker pastes, as opposed to comparable movements of cement pastes, are quite dissimilar. Clinker pastes undergo a large initial drying shrinkage and on re-wetting expand to approximately 60 per cent of their initial length. Thereafter dry-wet cycling produces shrinkage and expansion movements that remain approximately constant. Cement pastes on the other hand differ from this type of behaviour in having an initial shrinkage that is only about 70 per cent of that given by a clinker paste and, on re-wetting, the cement paste expands almost to its initial dimensions. The initial dry-wet cycling movements of cement paste are therefore somewhat greater than those of clinker pastes. Subsequent cycles of drying and wetting can cause finely-ground cement pastes to undergo a positive expansion on each wetting cycle. Coarsely-ground cement pastes do not show a comparable tendency to undergo expansion when cycled. Clinker pastes composed of either fine or coarse particles do not undergo expansion when given cycles of drying and wetting. These differences are indicated in Fig. 3 which shows the length changes after each drying and wetting cycle of finely-ground clinker and cement pastes made up at the same water content. The slow expansion of the cement paste is caused by the reaction of C_3A and gypsum.

On account of its very many useful functions in paste, gypsum plays an important role in modifying behaviour and promoting desirable properties. How-

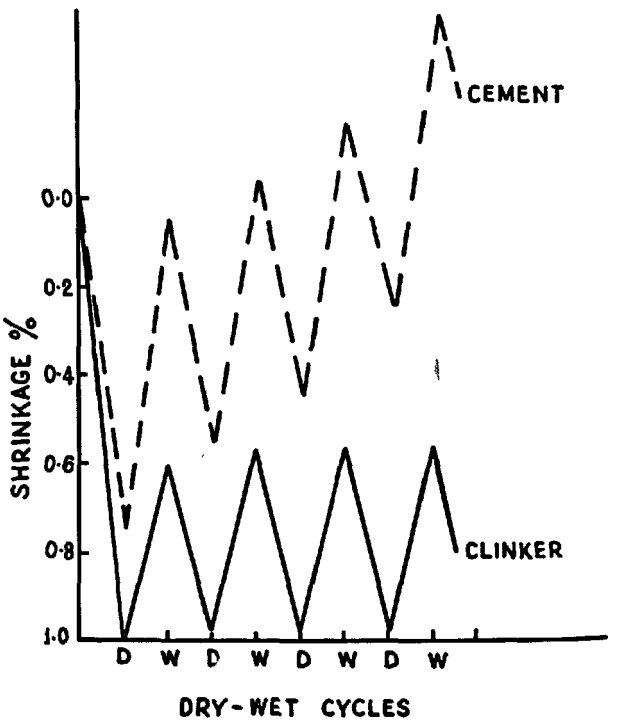

Fig. 3. *The dry-wet cycling movements of finely-ground (—12μ) clinker and cement pastes made at 0.7 water/solid ratio*

ever, since it can become occluded, undissolved gypsum and unreacted C_3A can co-exist in a paste under static wet conditions for long periods of time, at least several years. When the pastes are subjected to dry-wet cycling, and especially if given heat-cool cycles as well, some gypsum is intermittently released during each wetting cycle. When this soluble gypsum reacts with C_3A, expansion and disruption of the paste occurs. The expanding paste develops a closely-spaced crack pattern and undergoes a progressively increasing expansion.

These comments indicate the importance of C_3A and its interactions with gypsum on the durability of hardened cement paste and suggest that there is an increasing need to understand and control the mode of occurrence of C_3A in clinker. Deleterious changes in concrete usually occur slowly, and become obvious only after the concrete has been in service for a long time. At this late stage the basic causes of deterioration are often difficult to determine. To ensure durability of hardened paste ways should be found to minimize movements which are caused by cycling environmental conditions, and to reduce the undesirable expansive reactions that occur when gypsum continues to react slowly with C_3A.

Concluding Remarks

Some of the developments discussed briefly in this paper should be investigated further for possible future use in the cement manufacturing industry. The performance and uniformity of cement depend largely on the burning and grinding processes and grinding processes and improvements can be effected by a variety of modifications.

1. Increased control over clinkering and the uniformity of clinker can be achieved by a more stringent control over the particle size distribution of raw meal.

2. Control over the particle size distributions of both clinker and gypsum in cement is necessary to ensure satisfactory and uniform cement performance in paste and concrete. Reduction in grinding temperature, and in aeration and carbonation of cement will also assist in improving the performance of cement.

3. It would be advantageous to develop some new equipment including sampling devices and an effective large scale partial size separator.

4. Additional tests should be made to increase cement uniformity in performance and to indicate its potential behaviour in concrete. Determination of particle size distribution should become a normal test procedure in order to correct defects in grinding and determination of sulphate in the separated fraction would ensure the maintenance of a satisfactory gypsum grind.

5. Concrete performance tests under dry-wet and heat-cool cycling conditions would indicate the stability of hardened paste and its tendency to crack and undergo abnormal changes.

6. More attention should be given to studying the volume stability and durability of concrete especially as affected by the slow reaction of gypsum in hardened paste and concrete.

SESSION III-2 DURABILITY OF CONCRETE

Principal Paper Durability of Concrete

Oldřich Valenta*

Synopsis

Concrete durability is the most important factor of the durability and long time safety of concrete structures. Homogenity of concrete is more important for its durability than for its strength. Protection, systematic maintenance with timely repairs are other factors that significantly bear on concrete durability. The properties of the cement-aggregate joint are of utmost importance, too.

The various processes of concrete deterioration can be divided into three groups. Generally, concrete durability importantly depends on a number of physical and mechanical properties of the material: porosity, permeability, absorptivity, capillarity, tensile strength and bond of the components. The essential point is to express the extent and the properties of the pore system. Air entrained concrete is an example of a suitable system of pores.

Cement and hardened cement paste play a decisive role in the durability of concrete. The degree of hydration at the time concrete is attacked by aggressive agents is a very important factor in this respect. Many other factors—cement composition, fineness in grinding, etc.—have a lot to do with it too. Very important is the part played by admixtures, air entraining agents in particular. Formation and extent of cracks also significantly affect concrete durability as regards ingress of water and of other agents in concrete, and the tensile strength. Cracks have a number of causes: shrinkage, heat of hydration, load, pathologic phenomena, and aggressive agents.

Tests of concrete durability and their relation to actual concrete deterioration are of utmost importance for the control and design of concrete with specified durability, There are many requirements made on suitable tests while the existing ones have a number of shortcomings. Long-term observations and studies should be considered as an indispensable part of an appropriate system of durability tests leading to determination of the rate of concrete deterioration. Thence we should deduce the rate of deterioration and loss of safety of concrete structures. Cooperation in introducing suitable test methods is very important.

The fundamental requirements on further research work and the need of international cooperation are discussed in the conclusion.

General Observations on the Durability of Concrete Structures

Introduction

Considering the total volume and in particular, the diversity of applications ranging from light foam concrete of insulating walls to heavy concrete for shielding nuclear reactors, from pavement slabs to tall, slender masts, bridges and dams, cement concrete is without dispute the most important structural material the world over. The broad field of concrete uses indicative on the one hand of its outstanding possibilities, puts in on the other hand in greatly varying conditions of stress, mainly so far as it concerns the secondary effects of external media—no matter whether of natural (climatic phenomena and different waters) or industrial (mostly chemical) origin. The unfavourable action of those conditions, especially on the mechanical properties of concrete—a yardstick of its quality in most cases—has opened up

*Building Research Institute, Technical University, Prague, Czechoslovakia.

the question of the durability of concrete and concrete structures, the importance of which continues to grow proportional to the scope of applications and the volume of concrete used.

The durability of concrete cannot be separated from the durability of concrete structures—an important factor of their economy at present. The durability of concrete structures must be ensured on a complex basis—starting from the choice of the building site and suitable system of construction, and ending with the design proper and its task to take into consideration the nature of the surrounding medium, and the technology of concrete with its all important choice of suitable materials, composition, manufacture, placing and curing. As to the durability of concrete structures: it is imperative that proper care be accorded to finished structure, too; this can be done by the application of regular checks, timely maintenance or possibly repair.

Protection of concrete and concrete structures against excessive effects of aggressive media (underground waters, industrial effluents in particular) forms an inseparable part of measures designed to ensure durability. Such measures include: weakening or neutralization of aggressive substances before they come in contact with concrete, draining of such substances and reducing their contact with concrete to a minimum, immediate protection of concrete surface against direct contact with aggressive substances.

The significance of the durability and homogeneity of concrete becomes obvious once we start to consider the high demands that are imposed on the quality of any surface protection of concrete for the reason that it is the weakest spot that decides.

The durability of concrete structures is a very complex problem with two principal aspects: *physical* and *economical.*

The physical durability of concrete and concrete structures is expressed in terms of the loss of the decisive mechanical and physical properties of concrete to a value that ensures the minimum required safety of the structure no longer.

The economical durability of concrete and concrete structures follows from the minimum of total cost expended in its building and maintenance. This cost can be expressed by the relation

$$N = N_i + N_u + p_r S + N_1 \qquad (1)$$

where

N_i—the primary investment cost of the structure
N_u—the total maintenance cost for time T_r during which the structure is in use
p_r—the probability that the structure will collapse in time T_r
S—material damages caused by structure collapse
N_1—the cost of tearing down and removing the structure.

The economical durability of a structure is then given by the condition that is $\delta N/\delta T = 0$.

Considering that the last term of eq. 1 is virtually invariable, the main factors involved here are the ratios A, B of the investment cost, repair and maintenance costs, and the risk of failure of the structure (Fig. 1).

Savings in the investment cost usually lead to higher total cost of the structure during the time of its use.

Gradual deterioration of concrete texture caused by the most diverse external agents depends on the properties of concrete components and their relationships. Unlike under static action, it is the weakest spot of the structure (thin-wall members, concrete texture weakened by pores or cracks, aggregate grains-hardened cement paste joint) that are subjected to the most intensive attack of aggressive agents. This is the reason why such high demands are imposed by the durability on the quality of concrete and its ingredients with respect to homogeneity.

Professional literature all over the world has accorded considerable attention to the durability of concrete all along. The large amount of research studies published in the last 30 years notwithstanding, there are still not enough data or information avilable today to enable us to deal with the durability of concrete as we do with its strength. Yet an adequate understanding of the problem is just the thing that could help us in making concrete structures more economical by the application of refined methods of design.

As we have already pointed out, the relationships involved—be they ever of mechanical, physical or chemical character—are highly complicated and closely related to the nature of the components and the properties of concrete. Their elucidation is not

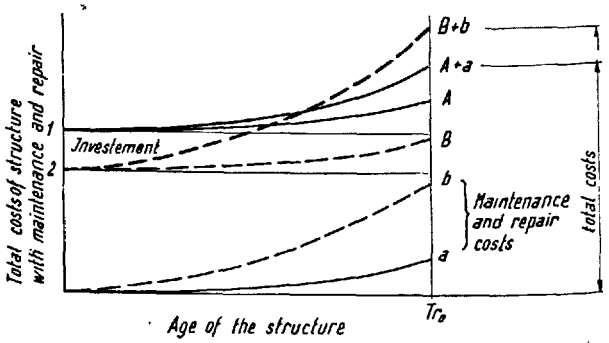

Fig. 1. *Effect of investment costs and maintenance on total costs of structure*

possible unless one resorts to the most modern techniques of research into the texture of concrete and its changes.

Even though it is necessary when ensuring the durability of concrete structures to consider those relations in all the stages of their realization (choice of building site, system of construction, materials and technology, protection) and their use (overloading, maintenance, repair), the crucial point of the whole problem lies in concrete technology, i.e. in making concrete of materials chosen so as to correspond to the specific conditions imposed.

Even if we disregard the complexity of the actual conditions, we are faced when studying the principal deteriorating factors (alternate frost, aggressive waters, alternate moisture, reinforcement corrosion, etc.) with a number of incompletely clarified relations, despite the fact that in some cases we know of suitable measures (air entrainment, appropriate composition of cement, choice of aggregates, etc.) that could reduce the unfavourable effects to an allowable minimum. Taken individually, the matter in question involves whole complexes of problems and relations that had been solved and reported in literature the world over.

I do not, therefore, deem it necessary to dwell here on either an analysis or a survey of the existing findings of world research not even for the selected most important cases of concrete deterioration.

As to the relation between research and practice: at the present time we are confronted with a very exacting but responsible question of intentionally, systematically ensuring concrete durability adequate to the given conditions, by the selection of suitable materials, composition and technology of concrete. This task bring us face to face with the necessity of determining the durability by accelerated tests relative to the important initial physical and mechanical properties of concrete. Simple tests of the fundamental properties of concrete and their changes based on scientific analyses of the deteriorating processes should afford us—jointly with the elucidation of the relations that exist between graudal deterioration and the loss of ultimate strength—the necessary data for forecasting and designing concrete of the required durability.

Safety and Durability of Concrete Structures

The safety of concrete structures is primarily given by the ratio of concrete strength to stress caused by loading. The design of concrete structures is usually based on the 28-day strength. As both concrete strength and load are functions of time, the safety of concrete structures, too, is a very complicated function of time (31, 117).

Although it is generally the compressive strength that is used for a measure of concrete strength, the tensile and shear strengths, the bond with reinforcement as well as deformation leading to unstable equilibrium between external and internal forces or attaining an inadmissible value, can also decide about structure failure. This considerably complicates the question of safety, and a distinction is, therefore, made, in the design of concrete structures, between three kinds of safety expressed by: reaching the concrete strength, state of dangerous cracks (particularly from the point of reinforcement corrosion and thus actually of the structure durability), and finally, limit deformation.

So long as a concrete structure or its components are acted on by no deteriorating factors, its safety without decreasing, increases due to gradual hydration of concrete after 28 days. Such is the case of a concrete structure exposed to no harmful effects of its environment, for instance a protected concrete structure of an above-ground building (Fig. 2).

As soon as a concrete structure begins to be acted upon by deteriorating factors in arbitrary time (age of concrete) T_x, a gradual loss of its strength and in turn, of its safety starts to take place so that after a time within the range T_{min} and $T_{r\,max}$, its strength is likely to drop below the value of the load and the structure might collapse (Fig. 3).

Such a drop in strength cannot be permitted under actual conditions. The degree of safety given by the strength-load ratio must not fall below a certain minimum value corresponding to the minimum strength æ.

The simplest though not the most economical solution to the given real case would consist in using concrete capable of long time resistance to aggressive agents in a way that the required minimum safety of

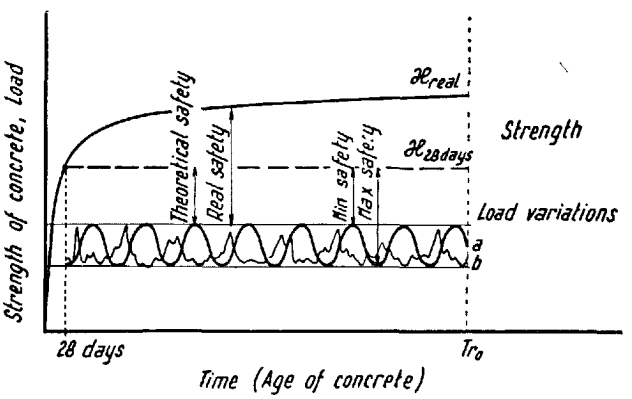

Fig. 2. *Long-time development of safety in favourable conditions*

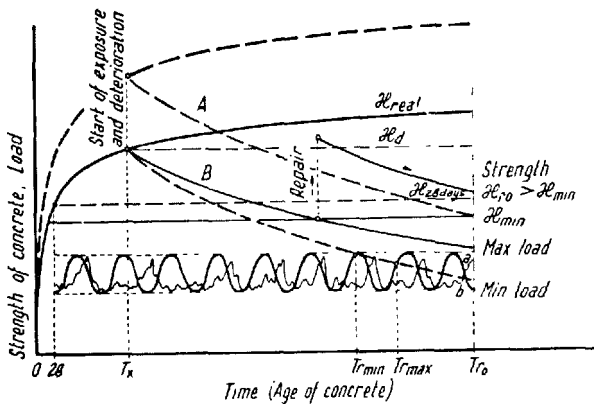

Fig. 3. *Long-time development of safety in adverse conditions*

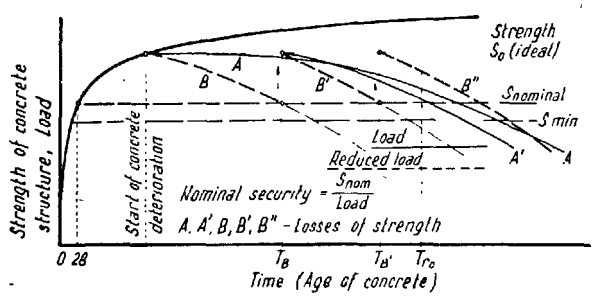

Fig. 4. *Securing the necessary concrete strength for the durability of the structure*

the structure—the concrete strength-to-stress ratio—would be ensured even after losses occurring in the structure during the time of economical durability of concrete T_{r_0}, have taken place (Fig. 4). This can generally be achieved by overdrawing the sections and the whole structure as well. While in the case of concrete deterioration following curve A, the requisite safety would be ensured during the whole of time T_{r_0}, it would be necessary in case B to:

either repair the structure in times T_B, $T_{B'}$, so that at the subsequent stages concrete weakening would proceed according to curve B' (or other B'') until the reduced strength would be higher in time T_{r_0} than $S_{nominal}$. Several such repairs might be required,

or reduce the load, for instance in time $T_{B'}$ so that the nominal safety would again be ensured in time T_{r_0},

or after the repair in time T_B has been made, protect the structure (e.g. on its surface) in a way that makes concrete lose its strength at a slower rate (e.g. according to curve A'), and thus again ensure that $S_{T_r} > S_{nominal}$ in time T_{r_0},

or finally, allow (e.g. after the structure was restored for the first time—curve B') a reduced safety with a higher risk of failure p_r under the same load for the time period $T_{B'}$ to T_{r_0}.

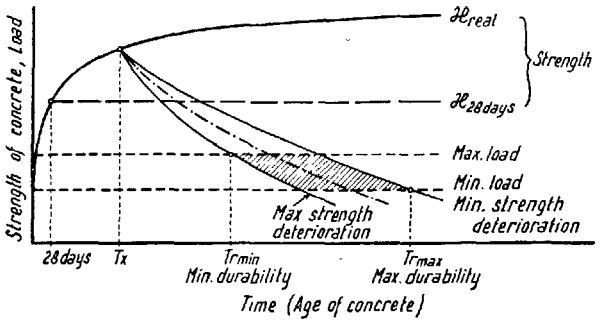

Fig. 5. *Probability factor in the durability of concrete structures*

Although each of the alternatives is likely to lead to the same engineering effect, it is clear at first sight that this is not so in the way of cost.

From the engineering point the relation shown in Fig. 4 in terms of curves A, A', B, B', B'' represents the time effect of a set of external aggressive agents, on strength or other important mechancical or physical properties of concrete. The difficulty we have to cope with is that such curves should be known in advance, before we start to build the structure, or or mastered to a degree that would allow us to create them by technological means and thus satisfy the design requirements similarly as we do in the case of for instance the 28-day strength of concrete.

This rational approach offers new criteria for an economic analysis of concrete structures, and places the initial investment cost in correct relation with the set of total costs.

Taking account of the complicated relations between concrete strength and the external factors and their combinations, the dependence of strength can be expressed in terms of a certain (say 90%) reliability or probability. This necessarily leads to a certain probable durability of the structure delimited by the minimum and the maximum probable durability (Fig. 5).

As this brief analysis clearly suggests, the relationships figuring in the solution of the durability of concrete (and other) structures are very complicated. They must, however, be borne in mind whenever a solution of the durability of concrete proper is attempted.

Significance of the Homogenity of Concrete for its Durability

Generally speaking the action of aggressive agents exert on concrete and its components depends on the following:

a) properties of the aggressive agent, its intensity or

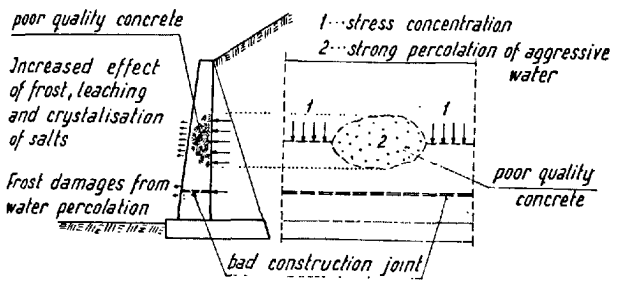

Fig. 6. *Adverse effect of concrete heterogeneity on the action of aggressive agents and the durability*

concentration,

b) properties of concrete and its components from the point of the relation between the aggressive agents and the mechanical properties of concrete and its ingredients, which are undergoing gradual deterioration,

c) the intensity of contact between the aggressive agent and concrete given by: the specific surface of the body, nature, quantity and accessibility of pores, removal of deteriorated parts of concrete from the surface, and supply of fresh aggressive agent.

So far as concrete proper is concerned, the adverse effect is given by: permeability, porosity, moisture absorption, reduced bond between ingredients, and strength—mainly the tensile one—of concrete.

While with respect to forces and stresses, the non-homogeneity of concrete leads to stress concentration in sections of high-quality (more compact, high-modulus-of elasticity and deformability) concrete, deteriorating processes usually concentrate in the weakest, most inferior parts of concrete. From this stems the *great significance of concrete homogeneity for its durability.*

In some cases the effect of concrete non-homogeneity can manifest itself in several ways, as indicated for instance by the sketch of an abutment wall in Fig. 6. Unfavourable seepage of water also intensively wets the adjacent high-quality concrete which is thus exposed to stronger action of aggressive water and frost on the wall face.

The homogeneity of concrete is a resultant of the homogeneities of its materials (cement, aggregates, admixtures), their proportioning, and of manufacture and placing of concrete. Even though the compressive strength of concrete is not a safe index of its durability, an evaluation of the various factors and their effects may well start out from the variability of this property of normal concretes (105). With respect to their effects on the variability of concrete strength, those factors are assigned the following rating:

Cement quality	50%
Aggregate grading	25%
Sand bulking	10–25%
Proportioning—by weight	8%
—by volume	16–100%
Compaction (poor)	50%

As to cement: its quantity relative to voids and surface of aggregates plays a more important role in concrete durability than does its strength. In sufficient filling of voids and covering of aggregate grains lead on the one hand to porosity and permeability, on the other to imperfect joining of aggregate grains (inferior bond). For these reasons the grading and variability of aggregates are of major importance in case of durable concrete. To ensure a dense concrete texture, proportioning of cement must start out from the most unfavourable grading of aggregates, and it is just in this that the high variability of aggregates manifests itself to disadvantage. It is, therefore, necessary, *to accord due attention to the grading of aggregates, variability of their fractions as well as to the proportioning of the fractions and cement.* This holds equally true for the placing (compacting in particular) of concrete. The relations between concrete workability, compacting means and compacting proper are eventually the decisive factors for the homogeneity of concrete in a structure.

In very close connection with concrete homogeneity is the quality of joints, mainly that of construction joints. Even when concreting is done very carfully, construction joints are usually a typical source of deterioration of concrete structures due to external agents. Poor quality of joints between old and fresh concrete is a regular source of deterioration by the action of waters and weather (Fig. 7). The importance of such joints increases still further in the case of reinforced concrete because of higher danger of reinforcement corrosion.

From the point of permeability, the non-homogeneity of concrete also asserts itself adversely by creating conditions conductive to electrolytic and chemical corrosion of the reinforcement.

The foregoing discussion was concerned with the statistical homogeneity of concrete expressing uniform distribution of heterogeneous concrete components in its mass or in each section.

Concrete is essentially a heterogeneous material in which consideration must be given to the important relations that exist between hardened cement paste, aggregates and reinforcement.

In regard to the durability of concrete, cement,

hardened cement paste and their properties play a decisive role also in the relation to the aggregates whose durability is usually higher than that of concrete or of hardened cement paste (Fig. 8). Accordingly it is the following three components that come into play whenever concrete is undergoing deterioration by diverse agents: aggregates, hardened cement paste and their bond ensuring mutual connection and collaboration. The relations shown in Fig. 8 convince us that the bond is actually the weakest link in that system. This circumstance in combination with other facts proving that the bond is the weakest link of concrete structure even from the point of tensile strength and permeability, suggests the way to be followed by basic research in an endeavour to improve the properties of concrete not only from the aspects of the durability but on all counts as well.

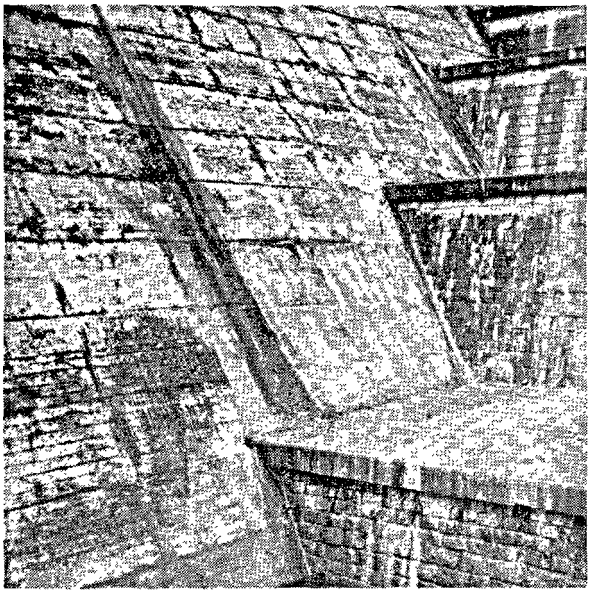

Fig. 7. *Construction joints in a dam as weak points of concrete structure*

Role of Protection in the Durability of Concrete Structures

The durability of concrete, particularly in a strongly aggressive environment, must also be ensured by protecting the material against intensive contact with aggressive agents. Protection of concrete must be considered an inseparable part of the solution to the problem of durability of heavily endangered concrete structures and their parts.

The object of protecting concrete structures is to restrict or completely eliminate the effect of adverse and aggressive external factors either by preventive or by supplemental measures. Timely preventive measures are the most effective and cheapest solution of all. All protective measures can be classified in two groups:

1 *Adjustment of the environment of the structure*, such as: drainage of the foundation soil, ventilation and withdrawal of aggressive vapours and gases, conveying of aggressive agents, weakening or neutralization of aggressive substances within the manufacturing process, neutralization of underground aggressive waters, etc.

As to *conveying of aggressive substances*: special emphasis should be put on the use of the various measures and on ensuring their correct functioning by

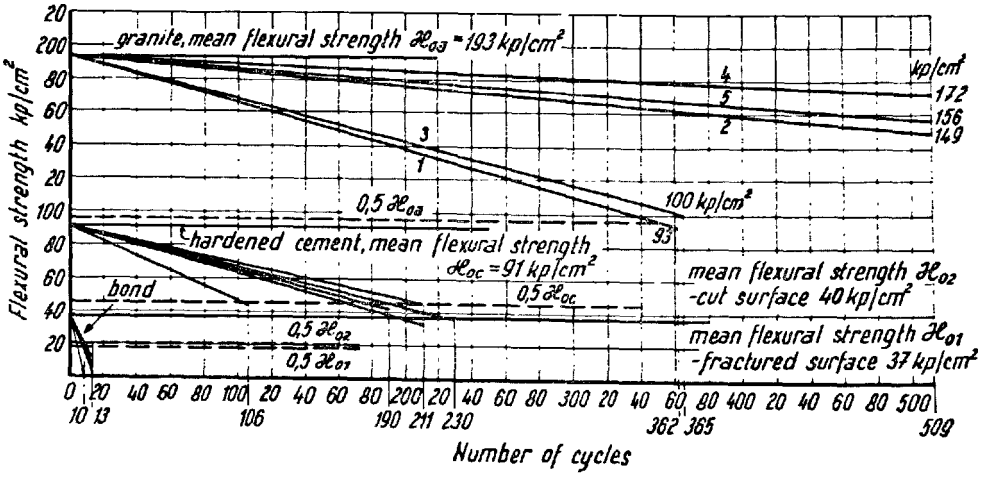

Fig. 8. *Frost resistance of granite, hardened cement paste and their bond (113)*

regular checks and maintenance. These measures include: ventilation and air conditioning, particularly of manufacturing spaces, prevention of steam condensation on concrete structures (ceilings, roofs), efficient drainage of roofs and perfectly functioning—especially in winter time—water withdrawal systems, perfect drainage of pavement, particularly when using de-icing salts, prevention of water flow on facades, a year-round reliable operation of drainage systems of bridge structures, protection of the structure against stray currents, etc.

2 *Treatment and protection of concrete surfaces* such as impregnation and chemical treatment of concrete surfaces (fluoro-silicates, ocratization), impermeable and resistent coatings and membranes (films), impermeable and resistant layers and plasters, impermeable and resistant linings and walling (protection of piles in sea water, of pavement, etc.).

The indispensable condition for a surface insulation to be effective is absolute impermeability.

The effectiveness of surface protection is contingent to: impermeability to gases and liquids, chemical resistance against agents present in the given medium, deformability as relating to the protected structure under all conditions of operation (temperature, humidity), high homogeneity of mechanical, physical and chemical properties, mechanical resistance against impacts and other effects of normal operation, static security, particularly from the point of limiting deformations and eliminating buckling (stability).

While in *conventional insulating materials* (clay, rocks, aggregates, etc.) it is the thickness that matters with regard to the coefficient of permeability, in modern insulating materials (impermeable films), the crucial point is the *absence of defects*. The necessary safety of the latter insulations as regard impermeability is usually obtained through the use of multiple films and of perfect, impermeable joints.

The decisive condition for an effective function of any insulation is high homogeneity and impermeability. This immediately implies high demands on the quality and control of the respective materials, of their technology and of the completed insulation. This leads to increased importance of prefabrication in this field.

The necessity of obtaining by control insulation that would effectively perform during operation of the concrete structure, brings us face to face with the need to separate the function of the insulation from that of the protected structure (factory stacks, tanks, cooling towers, etc.). This is yet another proof of the imperative *need to approach the solution to the problem of the durability of concrete and concrete structures on a complex basis*, particularly in the presence of strong aggressive media.

Correct sharing in the task by the durability or resistance of concrete, and by the protection of concrete structures must be effected with a view to the given specific conditions.

Role of Maintenance and Repair of Concrete Structures

Maintenance and repair of concrete structures are important factors of both physical and economical durability.

The task of systematic maintenance consists in ensuring for a structure the same conditions as have been considered in its static and technologic solutions. Systematic control and regular, timely maintenance can restrict or completely eliminate the usual cuases of pathologic state of a structure. They include: inappropriate foundation and uneven settlement, inferior quality of components, improper composition and placing of concrete, wrong type and insufficient support of formwork, imperfect curing of concrete during hardening, etc.

From the long-time point of view (durability), even isolated overloading of the structure, producing no effect on its instantaneous strength, can be the cause (cracks) of an unfavourable development of reinforcement corrosion and structure durability. Special care should, therefore, be accorded to concrete structures as regard the state and causes of crack formation in concrete.

The durability of structure—even of a high-quality one—is generally threatened in yet another way, namely by excessive wetting of the structure by rain or other water. This risk becomes particularly serious if the structure is periodically exposed to the action of frost. Regular maintenance and control of the draining system play, therefore, an outstanding role in the durability of concrete and concrete structures thus exposed. Bearing in mind that water in concrete is the cardinal factor of almost all deteriorating processes that occur in it (frost, dissolving, chemical reactions), the speediest possible withdrawal of water should be provided for structures built above the ambient water level.

The object of repairs is to stop the progress of deterioration and to restore the structure to its original safety both instantaneous and long-term, as implied by the required durability.

The efficiency of repairs is to a considerable extent dependent on the quality of the bond between old and fresh concrete. The demands made on the tech-

nique and quality of repairs in this respect are very high indeed. Some of the modern materials, such as epoxy resins, offer us hitherto unheard of possibilities of effective repairs of deteriorating concrete structures.

The Bond and its Significance for the Durability of Concrete

Deterioration of concrete by various agents can essentially take place on three fronts: hardened cement paste, aggregates, and the joints.

Deterioration of the texture of concrete depends on: magnitude of the deteriorating action of the medium (internal stresses produced by freezing of concrete, volume changes, osmotic pressure, crystallization pressure; weakening due to dissolution of components), strength of concrete, the tensile one in particular.

The importance of the bond for the durability of concrete can thus be assessed also indirectly, from the properties of the joint relative to those of hardened cement paste or aggregates (rock). Generally speaking, the effect of the aggregate-cement bond is the greater, the larger the specific surface of aggregate grains.

Effect of the Bond on the Mechanical Properties of Concrete

The case that decides about the failure of the joint is that in which it is stressed by tension with shear also coming unfavourably into effect. The importance of the bond is given by low strength of the joint relative to both hardened cement paste and the currently used rocks of aggregates.

Direct tests of flexural strength of various rocks, hardened cement paste and the joint after 28 days afford us a clear picutre of the bond and of the fractured and the cut joint (Fig. 9) (113). This is one of the reasons why aggregate grains separate from cement in the course of concrete disintegration.

Effect of the Bond on Concrete Permeability

Even though the joints between aggregate grains and cement form no continuous channels for the flow of water through the texture of concrete, they can nevertheless substantially affect penetration of water in concrete. As direct tests of the joint permeability in relation to the permeability of the adjacent rock and hardened cement paste have clearly shown, the permeability of the joint is many times greater than that of the other two components. Equivalent breadth of the joint as expressed by hardened cement

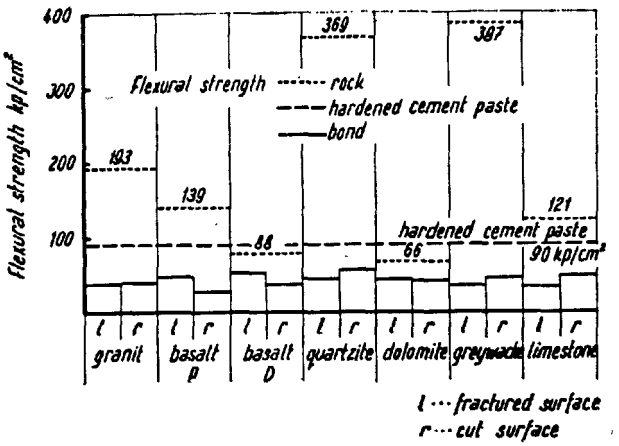

Fig. 9. *Bond of cement with different rocks (113)* .

paste was several cm and grew rapidly by frost action.

Effect of the Bond on the Durability of Concrete

The relatively low strength of the joint and the increased possibility that water can enter it, are the reasons of its low durability whenever moist concrete is exposed to the action of alternate frost.

According to direct durability tests of prisms ($4 \times 4 \times 16$ cm) made in part of rock, in part of cement paste, the frost resistance of the joint under flexure is very low. A typical example of the results obtained for granite is in Fig. 8 (113).

Notwithstanding the fact that in concrete ingress of water in the joint is not so easy as it is in the test prisms, the above is a clear evidence of the important part that the bond between aggregate grains and cement plays as regard the durability of concrete and the mode of its deterioration by alternate frost and other aggressive agents, particularly in the case of aggregate grains with a smooth surface (natural gravel and sand).

The examples of results achieved with various rocks quoted above, bear clear evidence as to the general importance of the aggregate-cement bond and in turn of the necessity of

a) thorough scientific studies of the contact zone and of the conditions for a perfect bond (up to the ultimate strength of one of the components),
b) practical measures that will lead to the creation of favourable conditions for a perfect cement-aggregate grains bond (clean surface, suitable treatment of the surface of grains, etc.).

Analysis of Concrete Deterioration by Aggressive Agents and by Deteriorating Processes

Depending on the purpose for which it is intended and on the local climatic and other conditions, concrete of structures is exposed to the effect of a whole number of aggressive agents and otherwise deteriorating factors. Several such agents combine in their action as a rule. Irrespective of this, a separate analysis of the action of each agent must be made in order to ascertain the basic conditions, kinetics and final effect of each of them on concrete properties in measurable relationships.

The relationships that we are thus attempting to elucidate are both qualitative and—that mostly—quantitative, and we need them to express the degree of deterioration as a function of the intensity and duration of the external action.

External factors of the durability of concrete. Using the main effect on the gradual deterioration of concrete, we can classify them in four groups (Table 1).

Basic Processes of Concrete Deterioration

The effects of various deteriorating factors and processes of mechanical, physical, chemical and biological nature on concrete can be subdivided in three basic categories:

1—*internal or surface stresses* due to non-homogenous volume changes in concrete, or to mechanical action such as impacts, friction, cavitation, etc. This group also includes the effect of temperature and humidity variations, volume changes caused by freezing of water in closed pores.

2—*dissolving and washing away of soluble components*—cement in particular—from concrete. This leads to a loss of strength, especially of tensile strength because of loss of: binder (cement) cross section, and cement-aggregate bond.

3—*chemical reactions and physico-chemical processes* leading to the formation of voluminous salts or to osmotic pressures. Loss of concrete strength mostly in tension is then caused by: reduced strength of concrete components, reduced cement-aggregate bond, and internal pressures (salts, osmotic pressure).

An analysis of deteriorating processes is also important for quantitative observations by appropriate test methods.

Important criteria for the properties of concrete and of its components bearing on the durability, are another of its results. Among them are:

i) tensile strength of hardened cement paste, ii) cement-aggregate bond, iii) permeability (or absorptivity and capillarity) of concrete and iv) chemical resistance of cement (hardened cement paste) to aggressive waters, acids, sulphates, etc.

The processes of concrete deterioration just outlined are related to certain concrete properties that necessarily result from the properties of the components, composition, placing and the resultant mechanical and physical properties of concrete.

It is, therefore, possible to deduce for concrete and its components, the favourable properties they should have and the requirements they shoud meet to resist the above-enumerated basic processes of concrete deterioration (Table 2).

Some of the requirements have general validity and include:

i) homogeneity of concrete, ii) low permeability and absorptivity of the components and of concrete, iii) appropriate system of pores, abundance of binder, air-entrainment, water-cement ratio, compaction, iv) high bond and tensile strength, v) effective protection

Table 1. *Classification of aggressive agents and their action*

Group	Specification	Effect on concrete
mechanical effects	load, overload and shocks	cracks, mainly in binder
	impacts and friction	erosion, crushing
	flow water and air	erosion, cavitation
physical effects	temperature variations and differences	cracks, peeling off, bond failure
	humidity changes and non-uniformity	cracks and bond failure
	frost (alternate)	cracks and bond failure, peeling off
	fire and high temperatures	cracks, chemical changes
	electric current and radiation	reinforcement corrosion, binder dissolution
chemical effects	air and other gases	binder dissolution, H_2S, SO_2, CO_2 and NH_3 reactions
	aggressive waters	binder dissolution, reactions: H_2SO_4 sulphates, carbon waters, chlorides
	chemicals	reactions of acid salts and acids
	soil and soil minerals	reactions of weak acids, sulphate salts, zeolites
biological effects	vegetation	cracks, etching by juices, moisture
	microorganisms (bacteria, microscopic forms of organic life)	formation of sulphates, mechanical weakening of texture

of reinforcement, vi) appropriate curing at the initial stage of hydration (moisture).

Relative Importance of Aggressive Agents

The importance of various aggressive agents or deteriorating processes for the durability of concrete is generally a function of a number of conditions, and after all, of the criterion of evaluation. It is also among others a function of local conditions. Irrespective of this it is necessary to know—from a higher, international aspect—the relative importance of the various causes of concrete deterioration—no matter that they might be evaluated in terms of the extent of failure they produce.

The RILEM Technical Committee for the Durability of Concrete and Concrete Structures in which participate all the principal countries where concrete durability is of major engineering and economical significance, has made an inquiry to determine the

Table 2. *Requirements on the components of durable concrete for different classes of its deterioration*

Concrete	Component	Class of concrete deterioration		
		1 Stresses by mech. effects and nonhomogeneous volume changes	2 Dissolving and leaching	3 Compounds of increased volume, osmotic pressure
Cement	Physical	Reduced fineness	Reduced fineness	—
	Chemical	$C_3S > C_2S > C_3A > C_4AF$	Low CaO content	Low C_3A, C_4AF contents, high C_2S content, low CaO content, low MgO, low alkalies content
Aggregate	Physical	Adequate coef. of thermal volume changes. Low absorption Reduced mica content. Reduced relative volume changes by absorption.	Low permeability and absorption	Low permeability and absorption
	Chemical	—	No soluble components No alterable rocks	No FeS_2 No active SiO_2 (alkali reaction) No $CaMg(CO_3)_2$
Admixtures	Physical	Gas forming admixtures.	Air entraining or combined effect admixtures Waterproofing admixtures.	
	Chemical	Pozzolanas } with air- Blast furnace slag } entrainment	Pozzolanas Blast furnace slag.	Pozzolanas Blast furnace slag, No $CaCl_2$
Hardened cement paste	Physical	Low w/c	Low permeability and absorption	
Bond	Physical		Reduced relative volume changes Rough clean surface, low permeability	
	Chemical	—	—	No active SiO_2 in aggregate No $CaMg(CO_3)_2$
Water			No acid waters, both anorganic and org No polluted waters	
Reinforcement			No chlorides Air entraining or combined effect admix Low permeability and absorption of concrete cover Effective cover thickness Surface treatment of reinforcement—use of corrosion inhibitors	
Composition, placing and condition of hardening of concrete	Physical		Plain concrete with adequate quantity of cement to fill up small pores and cover the grains surface Low w/c for good workability Adequate air content Homogeneity—avoid segregation (in mixing, transport and placing) Impermeable construction joints. Adequate surfacing Avoid loss of water by evaporation (shuttering, impermeable membranes, surface protection) Adequate temperature for hydration	
	Chemical		Avoid excessive carbonation Surface treatment by fluorosilicate	
Mechanical and physical properties of concrete			Homogeneous concrete Low permeability and absorption High tensile strength Adequate air pore system	

relative importance of the various factors. The following criteria were considered:

11 modes of concrete deterioration

alternate wetting	crystallization of salts	sulphates
alternate frost	abrasion	acids
reinforcement corrosion	internal stresses	aggregate reaction
leaching	external stresses	

5 classes of structures according to their exposure
i) indoor concrete with normal atmosphere, ii) indoor concrete with condensation and aggressive vapours or gases, iii) outdoor covered structures, iv) outdoor exposed structures, v) underground structures, structures exposed to chemical effects

3 degrees were used for the classification
0—comparatively little importance
1—some importance
2—general importance

Although this system of the modes of concrete deterioration, the internal and external stresses in structures in particular, could be subject to discussion, the results of the inquiry are of outstanding general significance for the future trend of research and cooperation. This is the sequence of the modes of concrete deterioration resulting from the inquiry:

1 reinforcement corrosion
2 sulphates
3 alternate wetting
4 alternate frost
5 leaching
6 acids
7 internal stresses
8 external stresses
9 crystallization of salts
10 aggregate-cement reactions
11 abrasion

The slight difference between the points given to alternate wetting and alternate frost and leaching is evidently due to the circumstance that the effect of alternate frost like that of leaching is conditioned by the presence of water in concrete.

Physical and Mechanical Properties of Concrete Important for the Durability.

The action of aggressive agents on concrete and its results depend on:

the character of the agents in relation to concrete and its components (chemical nature, concentration, etc.),
the possibility of their action (permeability, porosity, capillarity, etc.),
the resistance of concrete and its components to stresses produced by the majority of disintegrating process (tensile strength, cement-aggregate bond).

The presence of water and the possibility of its ingress in concrete is the decisive factor of most deteriorating processes.

Of the physical properties of concrete (and of its components), the following are the most important: *porosity*, *permeability*, *capillarity* and *absorptivity*.

Porosity of concrete and its components

Porosity of concrete is given by the porosity of concrete components and by pores in the cement paste-aggregate joint. Generally speaking, systems of pores differ one from another and are very closely linked with mechanism of formation of the texture of each component. Considering the possibility of water and gas penetrating in concrete, two general classes of pores (Fig. 10) may be distinguished:
open or accessible pores connected to the remaining pores and to the surface; they may be accessible from one or from both sides;
closed, inaccessible pores, without connection to the remaining pores or to the surface.

Closed pores come into play only in the mechanical properties of concrete. Open pores are a very important factor in permeability, capillarity, absorptivity and durability of concrete.

According to their form and origin, pores can be classified in the following three kinds:
cells (bubbles)—characterized by three roughly equal dimensions,
cracks or lentils—with two predominant dimensions,
channels—with just one predominant dimension.

The way pores affect the mechanical and physical properties (tensile strength, permeability, absorptivity,

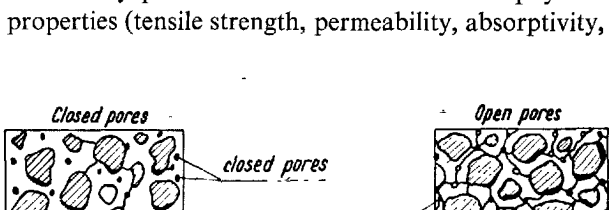

Fig. 10. *Porosity of concrete*

capillarity) essentially differs from one kind to another. The most unfavourable from mechanical aspects are cracks. Continuous channels sometimes linking onto cracks, play the biggest part of all as regard permeability inasmuch as they appreciably facilitate flow of water through the texture. Pores accessible from one side as well as discontinuous channels, exert their effect mostly by air cushions during expansion of freezing water.

To be in a position to exactly estimate the effect of porosity on mechanical and physical properties, we must acquire detailed knowledge of pore morphology, size and distribution. Tests of directional permability, absorptivity and capillarity are likely to afford us at least integrated data on the properties of the system of pores under study; Experimental data of this sort depend, however, also on the effect of applied pressure and accordingly, water pressure, too, becomes an important criterion in pore system studies. The phenomenon is exploited in modern engineering practice of air-entrained concrete. These phenomena should be taken into account in research and test methods which must be based on physical properties independent of those factors whose effect is to be expressed by physical laws of general validity.

Whereas the porosity of aggregates (rocks) can merely be determined and taken in consideration when choosing the aggregates, we are in a position—partially at least—to adjust the porosity of cement paste and the joint. This the basis of the successful technique of air-entrained concrete (90).

If air bubbles are to play a role favourable from the point of concrete frost resistance, they must be connected into the spatial system of capillary channels, be uniformly distributed in the texture of cement paste, have adequate (small) spacing. The length of and the flow conditions in the channels eventually decide about the inner pressure (tension) in concrete and about the suitability of the system of pores, exert highest possible effect at small total air content.

Air bubbles can play their favourable role only in the space taken up by cement paste. As their spacing varies in reality, we should consider that corresponding to a uniform bubble distribution. The size and hence also the number of air bubbles per unit volume of air bubbles is under otherwise identical conditions a function of surface tension and thus of the properties—efficiency—of air entraining admixtures. The total air content of hardened cement paste, and the more so of concrete with aggregates of diverse size, is therefore, not an adequate criterion of efficient air entrainment.

Neither is the total air content of concrete a suitable criterion of the actual degree of air entrainment. T. C. Powers has correctly referred his spacing factor to the volume of cement paste. In this way specification of air entrainment of concretes with different aggregate skeletons could be set on a logical comparable basis.

The main effect of air entraining admixtures and of artificial air entrainment of concrete consists in modification of the system of pores; this has been proved by research work carried out in the United States (6, 7, 90, 91) and resulting in the establishment of the main characteristics of pore systems of ordinary and air entrained concretes (Table 3).

Detailed data on pore distribution from the point of their sizes in air entrained concretes, and the effect of water-cement ratio, nature of the admixture and the effect of vibrations are summarized in Fig. 11.

It is a pity that the tests made in the USA do not contain detailed information on the nature of the pore systems of ordinary and air entrained concretes, which would make it possible to estimate the effect of air entraining admixtures on the pore system still more clearly and specifically.

The predominant size of pores as shown in Fig. 11 indicates the necessity to also elucidate the effect of fineness of cement on the formation of the pore system in relation to those fractions of sand that are designated as most efficient for air entrainment. Several research studies (21, 47, 95, 123) especially those of postwar years have proved sand grain sizes between 0.30 and 0.60 mm to be the decisive ones for the content of entrained air.

It also follows from Fig. 11 that pores larger than 0.120 mm dia. are rather random in occurrence. They are pores of air entrapped in concrete.

Further studies of the effect of a system of pores on the durability of concrete are also fully justified from the point of improving the resistance of air entrained concrete to sulphates, sea water, alkali reactions, and with volume unstable rocks.

Another problem that deserves clarification in relation to the character of the pore system (size of air bubbles at equal total air content) is the loss of mechanical properties of concrete (tensile strength in particular).

Table 3. *Nature of pores in ordinary and air entrained concrete*

Kind of concrete	Air content %		Specific surface of pores cm^2/cm^3		Spacing factor cm	
	Range	Avg.	Range	Avg.	Range	Avg.
Ordinary	0.2–5.7	2.0	42–435	175	0.023–0.155	0.064
Air entrained	2.4–10.6	4.4	242–615	387	0.005–0.020	0.013

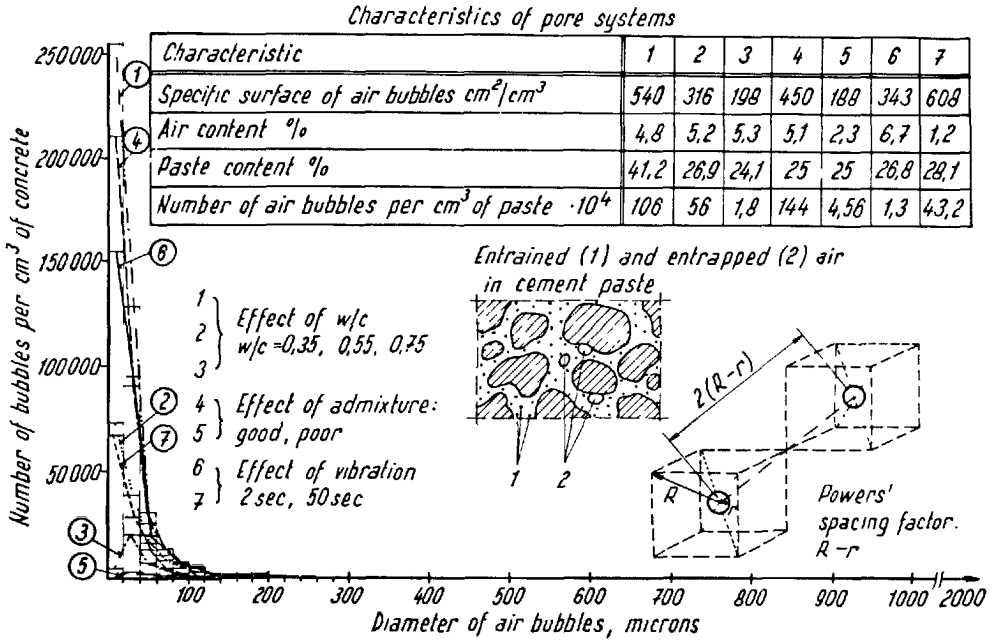

Fig. 11. *Influence of various factors on the quantity and distribution of pores in air-entrained concrete*

Very important for the mechanical and physical properties of concrete are pores contained in the cement-aggregate joint. They are usually larger pores cuased by air adhering to rough surface of the aggregates. In this sphere of research we meet a number of complex problems of utmost theoretical and practical significance.

Relation between porosities of cement paste and aggregates (rocks)

The relation between the properties of the pore system of aggregate grains and that of hardened cement paste bears decisively on the course of physical, physico-mechanical and physico-chemical processes that lead at later stages to deterioration of the texture of the two components and of their joint.

We can judge as to this relationship from the familiar, usually experimentally verified properties: absorption (total), permeability. As only sound, unweathered rocks are employed for aggregates, and from natural gravels the strongly weathered parts are usually eliminated, permeability and absorption of aggregates are relatively low. A proof of this is offered in Table 4 (62, 85).

The unfavourable effect of water-cement ratio and specific surface of aggregates is evident from the case of cement mortar. This phenomenon is clearly in very close connection with high permeability of the aggregate-cement joint, also determined experimentally by direct tests (115). The motion of water in concrete follows the path of least resistance and the relatively high permeability of the joint creates conditions leading to strong action of hydraulic pressures, ice, dissolving effect of waters and acids, as well as to that of aggressive salts in the joints.

It is logical to presume that the nature of the pore system of aggregates (rocks in particular) will be in close connection with their "technology"—process of their formation. We may, therefore, assume essentially different systems of pores in igneous rocks, sedimentary rocks and metamorphic rocks.

The mechanics of frost action in wet rocks undoubtedly follows the same basic mechanico-physical laws, and for this reason it will be necessary to study the basic properties of rocks important for their frost resistance, by the same means.

A certain connection between the system of pores in and the frost resistance of rocks was proved in France (65). The studies have proved the utmost importance of calcite moisture for volume changes (Fig. 12) and deterioration. They have at the same time pointed out the significance of the nature and size of pores for absorptivity and frost resistance of the rock. A mercury porosimeter facilitated the determination of the size distribution of the pores and helped to explain the causes of different frost resistance (Fig. 13) after the unlike nature of the pores became

Table 4. *Permeability and absorptivity of concrete components and mortar*

Material	Coefficient of permeability k cm/sec	Absorptivity volume (%)
Cement paste hardened (w/c = 0.7)		—
age— 5 days	4.10^{-8}	—
6 days	1.10^{-8}	—
8 days	4.10^{-9}	—
13 days	5.10^{-10}	—
24 days	1.10^{-10}	—
Granite	$7.48.10^{-10}$	1.2
Quarzite	$1.15.10^{-10}$	—
Limestone	$1.72.10^{-12}$	0.27–4.3
Diorite	$1.15.10^{-12}$	—
Dolomite	—	18
Basalt	$3.45.10^{-13}$	6.7
Sandstone	$1.72.10^{-9}$	—

Material	Coefficient of permeability k cm/sec	Absorptivity volume (%)
Cement mortar 1/3, w/c = 0.71	—	13.6
1/4, w/c = 0.73 1)	—	17.4
1/5, w/c = 1.18 1)	—	21.4
1/6, w/c = 1.95	—	21.5
1/4, w/c = 0.61	—	8.4
1/5, w/c = 0.71 2)	—	9.9
1/6, w/c = 0.89 2)	—	12.1
1/7, w/c = 1.05	—	13.3
Granite slightly weathered	6.10^{-7}	—
Sandstone siliceous slightly weathered	$8.6.10^{-3}$	—
Limestone slightly damaged	$1.9.10^{-3}$	—
Granodiorite slightly damaged	1.10^{-3}	—
Basalt slightly damaged	$5.0.10^{-3}$ to $1.0.10^{-6}$	—
Sandstone slightly damaged	$1.7.10^{-4}$	—

1) 60% of grains to 0.2 mm. 2) 30% of grains to 0.2 mm.

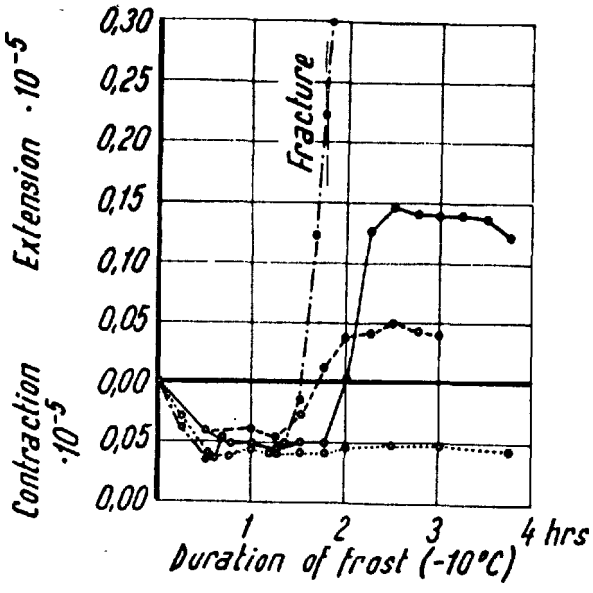

Fig. 12. *Effect of limestone's humidity on its volume changes by frost* (−10°C) (65)

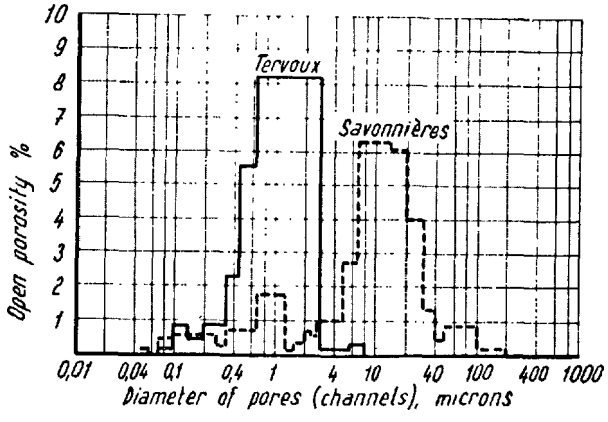

Fig. 13. *Difference of pore system (histograms) of two limestones (S, T) with different frost resistance* (65)

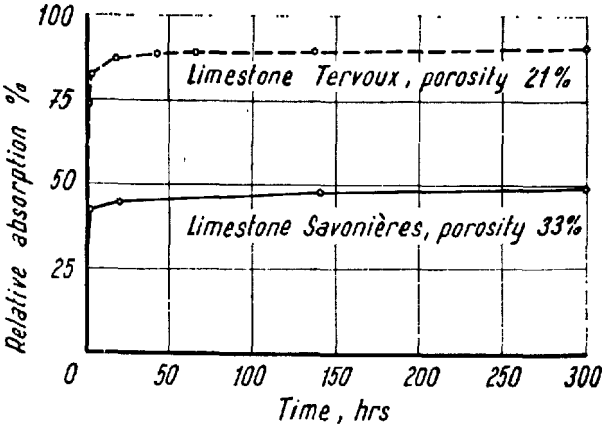

Fig. 14. *Water absorption of two limestones (S, T) with different frost resistance* (65)

evident from the rate and degree of relative absorption of two calcites on their immersion in water (Fig. 14). Fine open pores (capillary channels to 5μ dia.) of the Tervoux calcite are the reason for rapid penetration of water in its texture, and hence of the higher relative degree of saturation, decisive for the unfavourable effect of frost.

Concrete permeability

Permeability of concrete decides about the pos-

sibility of water and substances contained in it to penetrate in concrete through interconnected open channels. It is defined by the permeability coefficient k in the Poiseuille-Darcy law for the rate of water flow through a porous medium, viz. $v = kI$. So long as no complete penetration of water through concrete had taken place (Fig. 15), the water head must also include the effect of capillarity. The relative head is then given by the relation

$$J = \frac{h + h_0}{x} \tag{2}$$

where

h—the actual height of water column above concrete surface

h_0—the capillary elevation

x—the thickness of concrete (depth to which water had penetrated).

The permeability coefficient k is not a time constant. It depends on gradual cement hydration and on the effects of water flowing through the capillary channels (swelling of channel walls, clogging with or washing off of fine particles including air bubbles).

At the initial stage larger pores connected to the channels cause by their filling up the flow to decelerate. After water had penetrated through concrete, these pores lose their effect on the apparent (resultant) velocity and outflow (Fig. 16). Surface cracks also cause changes in percolation of water through concrete. This is the reason why the permeability of concrete is usually expressed in terms of completed percolation and of the amount of water that had flowed through. Even though simple such a procedure is usually time consuming. The permeability coefficient however, be determined (with some approximation) from the relation for unsteady percolation

$$k = \frac{x^2}{2th_r} \tag{3}$$

where

x—the actual depth to which water had penetrated,

t—the time,

h_r—the height of water head ($h_r = h + h_0$)

At large enough h, h_0 may be neglected.

The above relation is approximate in that it disregards the time necessary for filling up large pores on the flow channels. Nevertheless, the permeability coefficient k thus obtained is a measure of the possibility of water penetrating in concrete.

Concrete absorptivity

Absorptivity of concrete or of another substance is usually understood to mean the quantity of water that penetrates in the specimen during a certain time of immersion in water (Fig. 17). It is a measure of the open porosity. Penetration of water occurs due to simultaneous action of hydrostatic pressure h and capillary forces that can be expressed in terms of the height of water column h_0, the capillary elevation. So far as specimens completely immersed are concerned, the counterpressure of air contained in

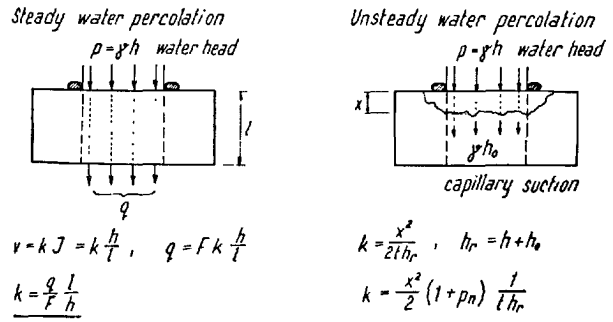

Fig. 15. *Percolation of water through the concrete*

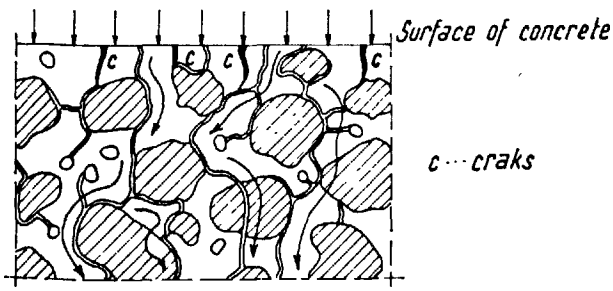

Fig. 16. *Concrete pore system and percolation of water*

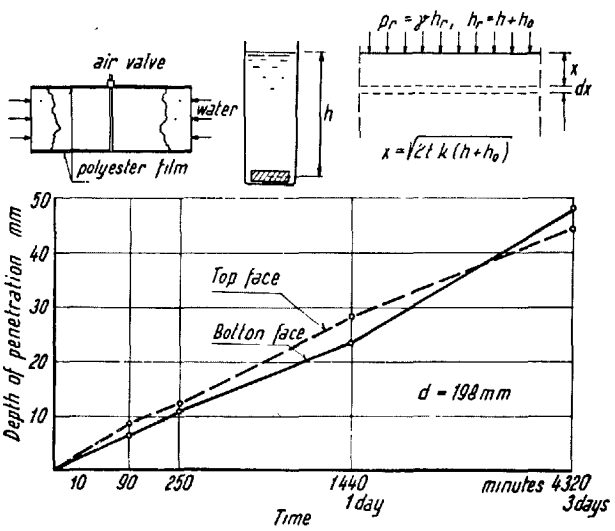

Fig. 17. *Absorption of water by concrete*

concrete pores should be considered, too.

The depth of absorption can be expressed by the relation

$$x = \sqrt{2tk(h + h_0)} \qquad (4)$$

which holds on the assumption that all the pores (channels) are open to flow and directly contribute to water percolation in the principal direction. What actually happens is that water penetrates through transverse channels and simultaneously to no-through channels. The resultant percolation is slowed down by the time necessary to fill the volume of both.

After time t the amount of water that had penetrated in the specimen is given by the relation

$$Q = F_0, x, \pi_0 = F_0\pi_0\sqrt{2tk(h + h_0)} \qquad (5)$$

where

F_0—the free surface of the specimen,
π_0—the (relative) open porosity.

For a statistically homogeneous material the relation between the weight increases of the specimen is given by the relation between percolation depths from the initial state (Table 5).

The linear dependence of the relative percolation depth on $\sqrt{t/t_0}$ ($t_0 = 10$ min in our case) can be used to advantage in the determination of the smoothed value of the permeability coefficient k (Fig. 17).

Capillary elevation

In penetration of water in concrete and its components, capillarity asserts itself as an additional water pressure head. If we wish to express the permeability coefficient k from formula 4, h_0 must be measured by a suitable test (Fig. 18).

Time, permeability coefficient k and capillary elevation are bound together by the relation

$$t = \frac{h_0}{k}\left(lg\frac{h_0}{h_0 - x} - \frac{x}{h_0}\right) \qquad (6)$$

Given experimental values (two at least), both the permeability coefficient k and the capillary elevation h_0 can be determined. Both values can be ascertained more accurately from a larger number of experimental values.

But in all cases the process calls for further analysis.

Table 5. *Rate of water penetration into specimen*

Absorption time	10 min.	40 min.	90 min.	160 min.	250 min.	360 min.	24 hrs.
Relative depth of penetrat. or relat. weight increase	1/12	1/6	1/4	1/3	5/12	1/2	1

While in the action of direct hydrostatic pressure the resultant permeability coefficient k is related to all the pores—no matter what their cross section, the situation changes once capillary forces—also bound to the dimensions of the capillary channels or cracks—come into action. Accordingly, the distribution of water flow among the different size groups of channels will be different (Fig. 18).

This alone is already a good indication of the high demands imposed on a test method capable of determining the fundamental properties of the pore system, and the resistance of the texture to specific aggressive processes.

In all the cases, i.e. unsteady percolation, absorption of water in concrete and capillary elevation, we must furthermore consider the effect of flow-ineffective channels and partially open pores, on the values of: t, x and k.

The possibility of using these physical criteria as a measure of concrete capability to resist the effect of alternate frost or of aggressive substances contained in water in relation to the 10 mins and 24 hrs

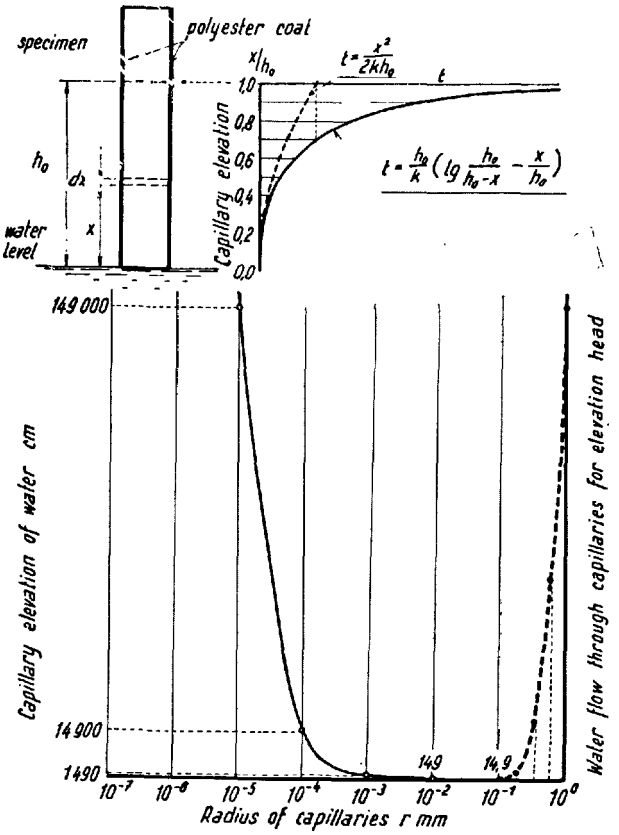

Fig. 18. *Capillary elevation of water in concrete (mortar, paste)*

absorptivity and frost resistance was successfully verified in Great Britain. A characteristic dependence between frost resistance and capillary absorption of standard mortars (ISO- 1/3) was also determined in France (120). Volume changes of the test specimens ($4 \times 4 \times 16$ cm) of various cement mortars used as an index of frost resistance and capillary absorption have proved the importance of the pore system for frost resistance (Fig. 19).

Tensile strength and bond of concrete components

The tensile strength of hardened cement paste and its bond with aggregates are decisive as regard the crack formation and deterioration proper of the texture by internal forces (ice, crystals, etc.). Concrete in the immediate vicinity of a tensile reinforcement is stressed in tension to failure by a system of cracks. In most cases these cracks do not affect the ultimate strength of sections but their effect on unfavourable action of aggressive media on concrete and its reinforcement in particlar, is of a decisive character.

Even though the danger of cracks in the covering layer of reinforcement is reduced by suitable prestress, as little as an isolated overloading there can give rise to harmful cracks.

The tensile strength and high aggregate-cement bond are of essential importance for the mechanical properties and durability of concrete and concrete structures; it is up to research to seek new ways towards their improvement.

The Function of Cement and Hardened Cement Paste in the Durability of Concrete

Hardened cement paste—though occupying but a small fraction (15 to 30%) of the total volume of concrete, holds a decisive position marked out by its task. It is at the same time a component of concrete that can most and best of all be affected by technology. Implied in this is the decisive effect of cement on all the properties as well as on the durability of concrete.

Depending on the circumstances, cement plays a role in the durability of concrete both by its chemical properties (composition) and by the physical and mechanical properties in hardened cement paste. Very important, too, is its relation to aggregates.

The *chemical aspect* involves the relation of cement components to aggressive agents of chemical nature which can either dissolve some of them, or through chemical reactions create new products that give rise to an internal state of stress by physico-chemical processes or crystallization.

The *physical aspect* refers to some of the physical properties that are of importance for:

the possibility of ingress of water and aggressive agents in concrete (chemical, physico-chemical processes),

the magnitude of stress in concrete (aggregates) and its eventual deterioration by cracks.

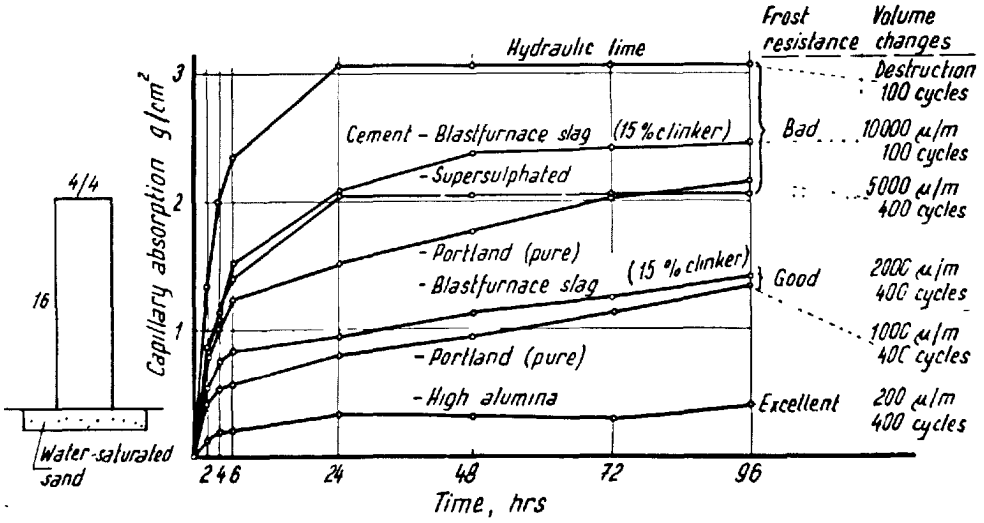

Fig. 19. *Capillary absorption of mortars* ISO (*1/3*) *with different cements* (*120*)

The physical properties in question include: porosity, permeability, absorption capillary elevation.

The *mechanical aspect* is concerned with tensile strength and bond of cement (rock) grains.

So far as the durability of concrete is concerned, the point in question is the relative capability of hardened cement paste and aggregate grains to resist the effect of various factors of the aggressive medium. Deterioration of concrete structure, however, always proceeds along the path of least resistance.

Effect of Cement Properties on the Durability of Cement and Concrete

Cement plays a role in these three ways: chemical and mineralogical composition; the properties of hardened cement paste; its relation to the aggregate, or to its components.

As to the *chemical and mineralogical composition of cement*: we are mostly interested in the relative content of the principal mineralogic components (C_3A, C_3S, C_2S and C_4AF), content of free lime (CaO), MgO and alkalies (Na_2O and K_2O). An important practical role is also played by hydraulic admixtures added to cement, which assert themselves also by their hydraulic capability (blast furnace slag, fly ash, trasses, tuffs, etc.).

The general criteria based on the existing results of world research are reviewed in Table 2. As a general rule it is necessary to verify them experimentally for the given specific conditions. A verification of that sort should start out from the decisive mechanical and physical properties of hardened cement paste: tensile strength, porosity, permeability, absorptivity.

Frost resistance of young, fresh concrete

Young concrete is very sensitive to the action of frost for the following reasons; a) it generally contains in its pores a large amount of chemically free water due to excess mixing water which only gradually combines with cement components or evaporates; b) the bond between the components (aggregate grains and cement) is weak and leads to low strengths, particularly in tension; c) high permeability facilitates motion of water and in turn formation of ice lenses in insufficiently solidified concrete structure.

As regard processes taking place in concrete during its cooling and deterioration by internal stresses: the tensile strength (bond) is the best indicator of the the resultant deterioration in the structure (eventually of its prestress).

The humidity of young concrete is given by mixing water. The water-cement ratio thus becomes a suitable index of the amount of water that is likely to turn to

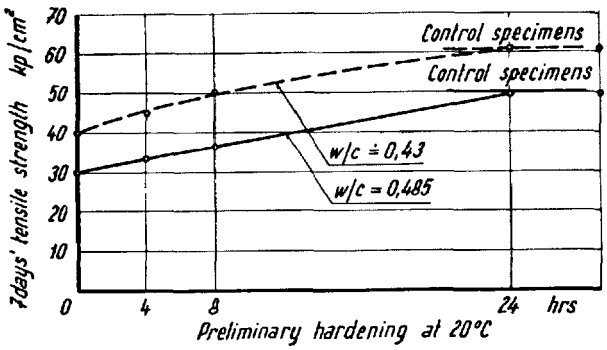

Fig. 20. *Effect of one frost (24 hrs, −14°C) on the 7 days' tensile strength of concrete for different ages at frost (0, 4, 8, 24 hrs) (65)*

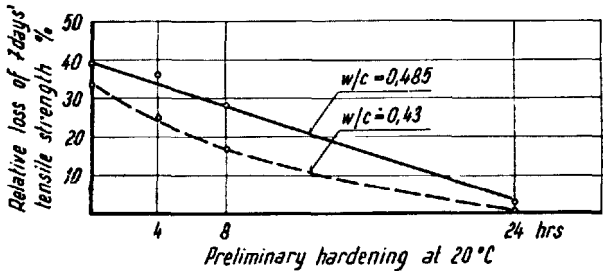

Fig. 21. *Effect of W/C ratio on the relative loss of concrete strength at 7 days by a single frost (−14°C) (65)*

ice in concrete cooled below 0°C. Another such index is the actual tensile strength or cement-aggregate bond at the instant of the first frost. This is corroborated also by the results of work done by M. Mamillan (Fig. 21).

Fig. 21 shows the effect of concrete age (degree of hydration) before the action of frost of −14°C/24 hrs/ on the 7-day tensile strength. The lower the previous temperature (< 20°C), the lower was the degree of hydration achieved and the higher the final loss of concrete strength. Not only the nature of cement (strength, rate of hardening, heat of hydration) but the water-cement ratio, too, come into play here (Fig. 22).

The mechanics of chemically free water contained in concrete and in hardened cement paste in particular, turning to ice under the action of frost continues to remain an unclarified clue to perfect understanding and explanation of the effect of alternate frost on wet concrete and its mechanical properties. Equally unclarified relations and processes accompany the temporarily favourable properties of frozen concrete (high tensile strength especially); their elucidation would help to better understanding of the effect of

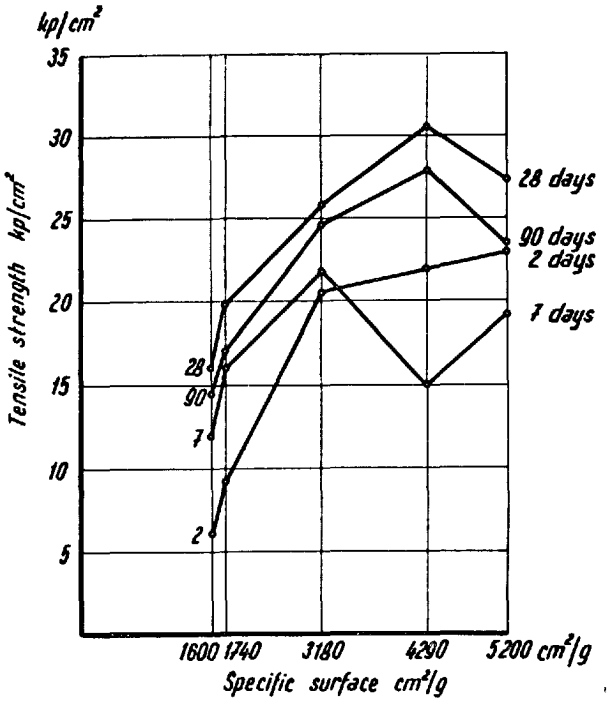

Fig. 22. *Effect of cement fineness on the tensile strength of concrete* ($W/C = 0.51$, 350 kg/m², $v = 50\%$, $T = 20°C$) (*118*)

frost on concrete—wet concrete in particular (116).

The *physical properties of cement*—fineness of grinding, granulometry and the relation surface to water, too, play a part here. These properties assert themselves predominantly through the amount of water bound by the surface of cement grains and through the resultant system of pores.

The favourable effect of greater fineness on frost resistance is clearly conditioned by an adequate increase in the amount of gypsum ($CaSO_4 \cdot nH_2O$) with respect to the extent of the reaction proceeding on the surface of grains (120). Surplus gypsum and coarse grinding (together with cement) act unfavourably on texture formation and limited durability of hardened cement paste, clearly because of these two factors: limited bond and tensile strength, unfavourable changes of the system of pores and higher absorptivity.

These results are at variance with earlier findings which had proved coarse grain cements favourable for concrete frost resistance (13). It is obvious that the relations are more complicated by far, and that next to porosity, the tensile strength—bond with aggregates—and deformability of hardened cement paste assert themselves in them. It we consider hardened cement paste as porous system of grains of partially hydrated clinker, we may assume that there exists an optimum grain size that leads—depending on the degree of intergrowth and the tensile strength of grains—to maximum tensile strength of hardened cement paste.

The size of cement grains influences the size and nature of pores in hardened cement paste in the same way as does the water-cement ratio. A coarse grain, porous texture leads to higher absorption and thus to limited frost resistance. Equally unfavourable will this property assert itself in resistance to aggressive agents and in moisture dependent reactions (e.g. alkali reactions).

The properties of hardened cement paste and mortar should, however, be also judged in relation to aggregates (their size). The fissurability tests signal higher danger of crack formation in case of restrained shrinkage with unfavourable consequences for tensile strength, permeability, absorptivity and hence also durability of concrete. A proof of this is offered by the dependence of tensile strength of concrete on the fineness of cement grinding (Fig. 22).

Cement admixtures

Various cement admixtures employed to obtain most diverse effects must, too, be always evaluated from the point of their influence on long-term properties of hardened cement paste, mortars and concretes. This requirement in itself indicates the necessity of knowing the composition of the various admixtures so as to exclude beforehand any unfavourable secondary effects, especially those on reinforcement corrosion.

Of particular importance are *inorganic components* which in combination with cement act like an active part of the binder: blast furnace slag, various pozzolanes of volcanic or orgaic origin, and a number of artificial pozzolanes such as fly ash, burnt clay, slag, etc.

Considering the durability of concrete, these components exercise the following favourable effects on the properties of cement and concrete:

Increase the resistance to aggressive waters (acidic or sulphatic); this is due to their chemical composition and binding of $Ca(OH)_2$ released by cement (clinker) hydration. The relation between the amount of free lime and the capacity of the pozzolanic component to bind it is of importance. Therefrom results the importance of the composition and relative amount of the two components: clinker and pozzolana;
reduce the permeability and the possibility of lime leaching;
increase the relative tensile strength;
eliminate harmful reactions between cement com-

ponents (Na_2O, K_2O) and some aggregates (SiO_2, dolomitic limestone).

A condition of the development of these favourable properties is sufficient humidity for hardening. Otherwise large volume changes, lower rate of strength increase and reduced frost resistance—unless ensured by suitable air entraining—will come into play on a broad scale.

As to frost resistance: the results of existing studies are not consistent. This has surely something to do with the different composition and nature of natural and artificial pozzolanas.

With respect to the *properties of hardened cement paste*: those mainly involved are:

physical properties—porosity, permeability, absorptivity and capillary elevation, coefficient of thermal expansion, volume changes due to humidity changes; *mechanical properties*—tensile and shear strengths, modulus of compressibility and elasticity, bond with aggregates and reinforcement.

The principal of these properties was analyzed in previous Section (Physical and Mathematical Properties of Concrete Important for the Durability). Next to the properties of cement, their formation is affected by technology (water-cement ratio, admixtures) and conditions of mortar and concrete hardening.

Among the other factors one should include the *water-cement ratio* and the fissurability of hardened cement paste given by the relation between volume changes and growth of tensile strength during cement hydration in mortar or concrete. This cement property is designated as fissurability and verified by a test based on simplified modelling of hardened cement paste on rigid core. Crack formation in the texture of concrete—in cement paste—for various reasons is of decisive importance for the action of deteriorating factors and for the durability of concrete.

The unfavourable effect of a high water-cement ratio on the mechanical and physical properties of cement paste and concrete—its durability under adverse conditions in particular—is generally known today.

Susceptibility of hardening concrete to cracking—fissurability

The fact that hardening and usually also shrinkage of cement paste take place in concrete in the aggregate skeleton and on aggregate grains creates conditions leading to crack formation in cement paste. The spatial system of such cracks unfavourably affects the resultant tensile strength and far more so, permeability and absorptivity of concrete.

A simple test to verify this cement property was introduced in France. The criterion of cement suitability is the occurrence of the first crack during storage (after 24 hrs) in controlled atmosphere ($T = 20 + 2°C$, $v = 50\%$). From the point of their suitability for structures exposed to adverse effects of external agents in liquid or gaseous form, cements are classified according to the interval between mixing and crack formation.

It would be of interest to verify to a greater detail the effect of restricted shrinkage of cement on the formation and properties of the texture of cement paste with respect to both mechanical and physical properties closely connected with the durability of concrete.

As to the relation of cement to aggregates: the hitherto research has mainly been concerned with detrimental reactions leading to concrete deterioration, viz. alkali-silica or alkali-carbonate reactions.

Great attention was given to the alkali-silica reaction by research in countries with natural conditions for its occurrence (USA, Denmark). Its principles were explained and convenient preventive measures stated. Alkali-carbonate reactions are being studied mainly in Canada (35).

Concerning the outstanding importance of bond for the durability of concrete, it seems to the point to study with increased interest the long-time relations between cement and different minerals of rocks used in concrete aggregates.

Formation of Cracks in Cement and Concrete and Their Relation to Concrete Durability

Cracks and their formation are of decisive importance for the durability of all concretes. They reduce the effective strength of concrete (in tension and bond), and facilitate ingress of aggressive agents of liquid and gaseous (but also of solid) nature in concrete and eventually to reinforcement. It is, therefore, necessary to accord due attention to crack formation in concrete structures, study its causes and introduce measures that would eliminate or at least alleviate it. According to their causes cracks in concrete or in hardened cement paste may be classified in four groups, viz.:

a) cracks caused by normal shrinkage and hydration heating,
b) cracks initiated by the effect of normal stresses (flexure, tension, principal tension),
c) cracks due to pathology of concrete structures
d) cracks arising in the texture of concrete by the action of aggressive agents and deteriorating processes.

The danger of cracks for the durability of concrete increases with the humidity of the environment.

Cracks caused by normal shrinkage and hydration heating

These cracks arise in cement paste, mortar and concrete by volume changes during hardening whose natural course is restricted by external and internal conditions such as anchorage, friction (concrete pavement), aggregates, reinforcement, etc. High rate of volume changes at the initial stage of cement hardening caused by loss of water in dry conditions leads to intensive formation of surface cracks (Fig. 23). The ensuing shrinkage of concrete is smaller by far than that of hardened cement paste (Fig. 24), so that local stresses in cement paste near aggregate grains are substantially larger (stress concentration).

This fact has been proved by T. C. Hsu (38) in his studies of the effect of shrinkage on stresses in binder between aggregate grains. As theoretical studies of a model of the texture of mortar and concrete and experimental verifications made on two-dimensional models have shown, the following three kinds of cracks can form in cement paste between aggregate grains:

1 tensile cracks in reduced cross section of cement paste between grains,
2 diagonal tensile cracks in cement paste,
3 tensile cracks in the cement-aggregate joint.

The relation between tensile stresses in cement paste between the grains, and tensile stresses in the joint depends on the spacing of grains (Fig. 25).

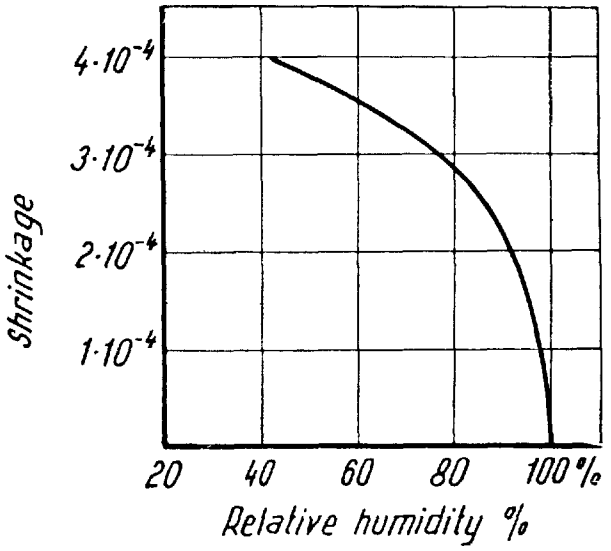

Fig. 23. *Effect of air relative humidity on drying shrinkage.* (58)

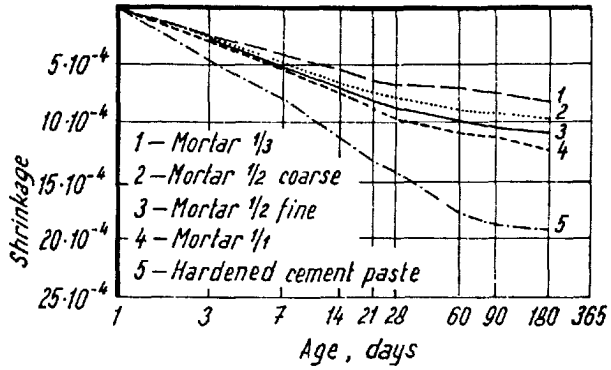

Fig. 24. *Effect of cement content on the shrinkage of mortar* (55)

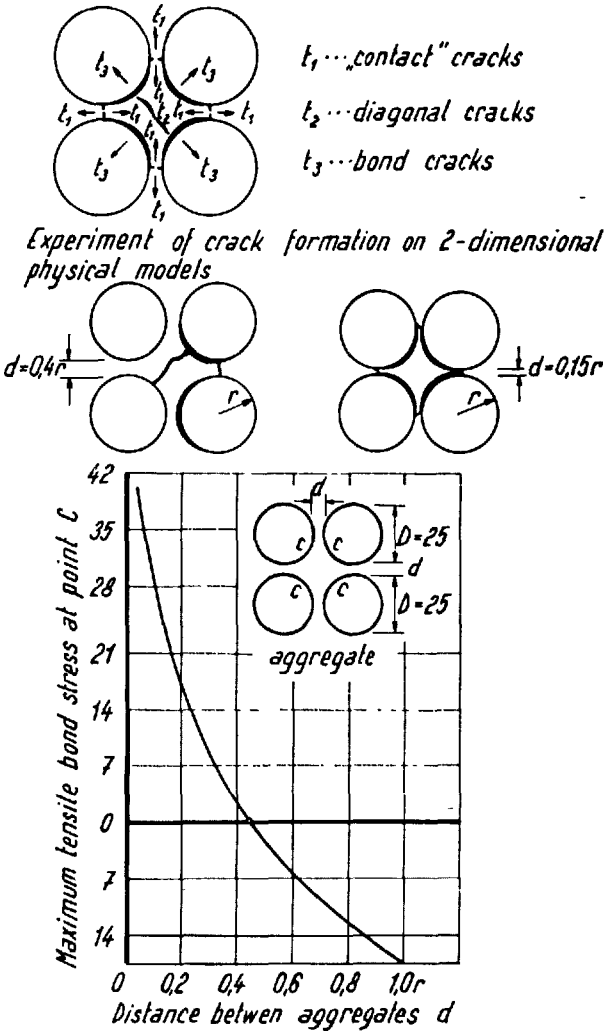

Fig. 25. *Tensile bond stresses and crack formation between aggregate grain skeleton* (38)

Even though the results of Hsu's study must of necessity be considered—from the quantitative aspects—as general indices of conditions, for no account was taken of the deformational, plastic in particular, properties of fresh and hardened cement paste, they clearly point out the principle of this important process.

Microscopic studies of concrete of cylindrical specimens before test and after application of a certain load (deformation 0 to 30×10^{-4}) have proved the existence of a whole system of cracks around the aggregate grains (joint) before loading, and gradual develop of cracks with loading. It was the cracks on the contact surface between binder and aggregate grains (38) that predominated in every case. This is another proof of the importance of the cement- aggregates bond. While development of such cracks may seem favourable from the point of view of stress distribution in the texture of concrete, the situation becomes completely different when judged from the point of concrete capability to resist aggressive factors of a most diverse nature.

Heat of hydration concrete is contingent on the nature and composition of cement, ambient temperature and other factors (admixtures, heat removal, etc.). A change of temperature leads to different thermal expansions of concrete components and thus also to internal stresses whose nature and range are given by the change of temperature, and thermal and mechanical properties of the components. In ternal stresses in concrete are also caused by differences of temperature of the core and the surface of concrete body. Unlike those produced by normal shrinkage, cracks due to temperature changes are much deeper (several m) and wider (1 mm), and spaced farther apart (44). They mostly occur in bulky structures where the temperature differences are greater, and their danger grows with the quantity, fineness and rate of cement hydration.

In this case, too, the relation between cement deformability and tensile strength is of importance for crack formation.

Actual conditions representative of size, stress distribution and concentration in hardened cement paste are highly complex. Even though surface cracks exert no serious effect on static behaviour of concrete, they represent a weakening from the point of the effect of aggressive agents.

Tensile prestressing of hardened cement paste resulting from its shrinking differently that the aggregates is the cause of reduced effective tensile strength of concrete as well as of crack formation on a dried surface. *Restriction of shrinkage-induced stresses is one of the ways toward increased relative strength of hardened cement paste, and above all, of concrete*, not to mention the secondary stresses in structures and the necessity to consider them in structure design.

It is, therefore, imperative from the point of the durability of concrete structures, not only to study the possibilities of reducing shrinkage of cement in its manufacture but also to control this cement property by a suitable test.

Cracks due to normal loading of structure

Structural members or parts of cross sections under tension are always liable to crack formation once the effective tensile strength of concrete has been exceeded. This happens even in cases when all tension is assigned to reinforcement.

Even under normal load crack formation depends on several factors: steel quality (stress in reinforcement), reinforcement bond, rigidity, effective height and shape of section, tensile strength of concrete, thickness of protective concrete layer, etc.

Crack formation due to load of reinforced concrete is of decisive importance mostly because of the possibility of reinforcement corrosion, the depth and width of cracks playing the cardinal role in that.

The possibility of dangerous crack formation is restricted in design by calculation and limitation of the theoretical width of cracks specified by various authors from 0.05 to 0.40 mm according to the environment. Even a minute, narrow crack is a source of locally different moisture of concrete, and at its contact with reinforecement a likely cause of electrochemical corrosion. The question to be tackled is that of under what conditions is it necessary to properly seal the tensile parts of concrete structure sections and thus exclude the possibility of corrosion since it is practically impossible at present to eliminate crack formation in general (except prestress).

In prestressed concrete structures cracks in concrete are unlikely to appear under normal load, and if they do after accidental limited overload, they close up again. So long as such a structure is in no direct contact with water (capillary elevation, permeability) or humid air containing aggressive gases, the cracks spell no danger.

Cracks of pathological character

Cracks of this sort are caused by the difference between the assumed action of the structure and the actual possibilities and conditions of structure behaviour. There are several causes for this: inappropriate foundation of the structure, deficiencies in design and construction, imperfect maintenance and

unsuitable operation of the structure.

As we see, they are all consequences of technical imperfections which though distant by their nature from the complex problem of durability of concrete and concrete structures, are apt to exercise a decisive influence on the durability of an otherwise high-quality structure. It is generally a system of larger, wider and deeper cracks, particularly dangerous in case of reinforced concrete.

In sufficient survey of foundation conditions and *inappropriate foundation* lead to unfavourable settlement and deformation of the structure and thus also to extraordinary stresses, mainly tensile, and in the ultimate stage to crack formation.

Similar consequences are brought about by *deficiencies of design* mainly consisting in selection of an inappropriate structural system, imperfect design, poor structural details and inadequate measures against the effect of external agents (insulation).

Advances in automatic computer techniques offer us the possibility of speedily effecting complicated calculations—but it is up to the designer and researcher to provide the basic conception of a suitable structure and the requisite physico-mechanical data, particularly those relating to long-time behaviour.

Many seemingly minor design details are of importance for concrete durability: *rapid removal of water* (rain or other, especially aggresive) from the structure, suitable position and execution of working joints (Fig. 7), perfect expansion joints, elimination of crack formation by suitably positioned reinforcement, reinforcement of corners of openings (Fig. 26), etc.

Structural design is greatly deficient in the way of preventive and protective measures devised to ensure the durability of concrete structures mainly under conditions of aggressive underground waters and sewage. A design properly conceived from the point of drainage or neutralization of aggressive agents, especially those of gaseous and liquid nature, can substantially contribute to the durability of concrete structures in industrial buildings. Surface insulation of concrete against excessive attack of aggressive agents must be solved within the framework of the complex questions of the durability of concrete structures.

Deficiencies in the execution of concrete structures are caused by: poor quality of the basic materials,

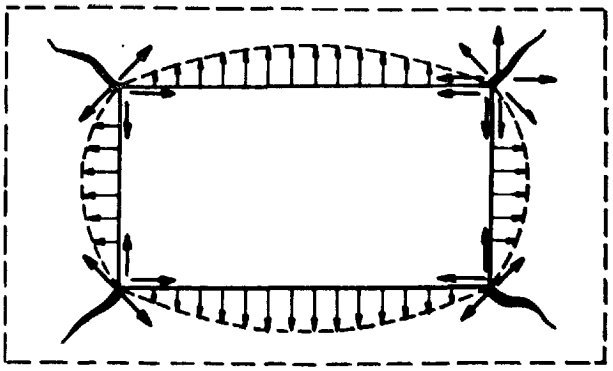

Fig. 26. *Cracks formation in corners of an opening*

inappropriate composition and processing of concrete, defective construction and function of the formwork and supporting structures, improper curing of concrete. Current practice pays no heed to the fact that manufacture of durable concretes calls for somewhat different approach to the selection of basic materials for, and technology of concrete from which high homogeneity and impermeability are required.

Imperfect maintenance and unsuitable operation of a structure are likewise a cause of defects that result in reduced durability be it due to a disproportional effect of aggressive agents when the drainage system has failed, or to crack formation by excessive load. It is in the interest of the durability of a structure in aggressive environment to reliably close all the cracks or renew the original function of continuous concrete.

Cracks due to the action of aggressive factors and deteriorating processes

As pointed out in the foregoing (Section; Effect of Cement Properties on the Durability of Cement and Concrete), aggressive factors according to their action on the texture of concrete may be classified in three groups. Two of those can cause cracks in concrete texture by:

a) producing internal or surface stresses in the texture,
b) giving rise to voluminous salts or to the effects of osmotic or crystallization pressures.

Cracks of this sort can occur either in hardened cement paste or in the cement-aggregate joint.

Methods of Testing Forecasting and Design for the Durability of Concrete

The great importance of concrete durability in numerous cases of concrete application in aggressive environment leads to the necessity of selecting the basic components, designing concrete and ensuring its

correct technology with a *view to the long-time effect of the specified aggressive factors.* This brings about the imperative need for verifying and proving the durability of concrete by accelerated tests. We are thus faced with the necessity of making a quantitative determination of the durability of concrete and an estimate whether or not it will be sufficient for the required safety at the end of the assumed life of the structure. And the tests of the durability of concrete and of its components should be made before the beginning or in the course of construction or on the occasion of any supplementary control—to supply us with reliable data and proofs.

Fundamentals of Test Methods

The requirements imposed on tests methods may be classified in two groups, viz. scientific and technical.

Scientific Requirements

From the scientific point of view every modern test method intended for durability testing must be based on new, advanced findings about the texture of concrete and mechanics of its deterioration, mechanics of its durability even if the technical arrangement of the test makes us seek the simplest possbile ways. These considerations necessarily reveal the fact that every method is subject to development.

Losses of important mechanical and physical properties represent a decisive indication of the durability of concrete and concrete structures. The character and purpose of the structure or of its part, and the type of stressing are then the main factors for the selection of the decisive mechanical or physical characteristics (compressive or tensile strength, modulus of elasticity, permeability, etc).

Al scientific test methods must, therefore, be necessarily *based on a scientific analysis of the individual isolated possible processes and their thorough qualitative and quantitative understanding* with respect to the various components of concrete. It is only on their basis that it is possible to reliably and safely proceed to the study of the complicated interaction between the components of concrete.

The actual processes of concrete deterioration occurring in practice are both very complex and very diverse. This is due to a very large number of possible combinations of the properties of the components of concrete and time sequence or simultaneity of the effect of the most different external factors of aggressive or beneficial character. In particular, structures exposed to weathering or other factors of natural character are practically impossible to compare in this respect.

These facts put the test methods face to face with the important problem of the fundamental approach to the solution of the following complex problems:

a) *Modelling of real conditions*

Test methods based on the endeavour to produce in the test conditions as identical with the actual ones as possible, are fundamentally correct. In the case of the durability of concrete this, however, has one principal drawback: it solves every case separately, independently of the general laws of mechanics, physics and chemistry, and affords, therefore, no generally valid results that could scientifically be applied, approximately in any event, to other at least similar cases. At the same time it cannot by far characterize the complex conditions in actual practice in the case of preliminary tests connected with the design of concrete mix of a suitable durability.

This approach can be compared with an attempt to carry out the structural design of every structure with its particular loading by means of a model without applying generally valid laws of structal mechanics and the strength of materials.

Furthermore, it necessitates costly, long-term tests using even more costly apparatus which can never a priori create a genuine, true-to-life model of reality.

b) *Analysis of deteriorating processes*

This method leads via a consistent analysis of the complex effect of the combined system of various factors, its separation from the point of their character, and an analysis of elementary, basic processes, to simple laws of qualitative and quantitative character.

In connection with an analysis of external conditions based on long-term observations of climatic conditions and considering also the interaction betwen the deteriorating processes in their combined effect, it is possible to acquire scientific data that can be used for an objective and technically true evaluation of the deteriorating effect of the respective environment and its principal factors.

This is seemingly a more complicated and exacting method which, however, offers one *substantial advantage* in that it is *based on the study of basic mechanical, physical and chemical reactions* as regard both the *qualitative and the quantitative aspects* opening the way to a scientific solution of this complex problem.

c) *Use of statistical methods*

The application of non-destructive methods of testing to the inspection of mechanical or physical properties of test specimens and concrete makes the problem easier with respect to the required number of

test specimens and test locations.

At any rate, statistics must help us out in: the determination of the sufficient number of test specimens, measurements or observations on the real structure to ensure the required reliability; the processing of results achieved, particularly in long term observations; the general evaluation of atmospheric or other real conditions of great variability which cannot be processed in any other way.

d) *Use of non-destructive methods*

From the numerous methods of non-destructive testing available for the inspection of the properties of concrete, more than one should be used at the same time. The selection must be based on the following principles:

1. The test method must be simple and quick, must not introduce extraordinary stresses in the test specimen; must be sensitive to the deterioration of structure and afford reproducible results.

2. The test method must not introduce appreciable disturbances in the regime of the durability test (changes of humidity, internal stresses, etc.). Should such changes be used (water absorption, permeability) a suitable procedure must be selected.

3. The use of ultrasonic or sonic methods based on simple measurements of the impulse velocity is not suitable because it is not sensitive enough to the deterioration of the texture of concrete (cracks).

4. For effective studies of the gradual deterioration of the texture of concrete it is necessary to develop new methods, especially such that are based on the damping of energy of ultrasonic or sonic impulses.

5. These methods must be combined with destructive tests for general control.

Technical Requirements

From the technical point of view, every new test method must satisfy a number of requirements including:

a) *Effectiveness*

The condition of effectiveness is given by the same process of concrete deterioration in test specimens and in reality, and by the ability to discern with sufficient sensitivity, between different durabilities due to different character of the components of concrete.

b) *Reliability*

Deterioration of concrete, its state and rate (including that of concrete components) must be controlled by objective methods. In their relation to reality the tests must afford reliable data on the relative durability of tested concretes.

c) *Reproducibility*

The method must ensure high uniformity of test conditions, of humidity in particular, and the rate of heating and cooling.

d) *Acceleration*

Practically all test methods are accelerated. However, they must not introduce new factors in the process of concrete deterioration, and must afford at least informative, reliable results for general information.

e) *Simplicity*

The durability test must be simple, easily checked and capable of mechanization and automation in a relatively simple outfit.

f) *Non-destructive character and effectiveness from the point of view of objective control* of progressive deterioration of concrete in test specimens and structures.

Analysis of the Methods of Testing Concrete Durability

The complexity of the processes of concrete deterioration and the urgent need for timely ensurance of concrete durability lead to an endeavour to utilize experimental results on as large a scale as possible. This brings us logically to an analysis of the test methods used in various countries and to the necessity of their simplification and unification. A suitable comparative test method is the least prerequisite for cooperation.

An analysis of the test methods used or standardized in various countries, made within the framework of RILEM Technical Committee for the Durability of Concrete and Concrete Structures (RILEM-CDC) has shown that:

1 There is generally great inconsistency among the methods used in various countries.

2 No relation exists between the nature of concrete (aggregates, cement paste) deterioration in natural conditions, and the regime of the test method.

3 Generally speaking there is no adequate control of the structural characteristics of test specimens either before or in the course of the tests.

Since the system of pores and its relation to water has a decisive effect on the course of deteriorating processes, and their influence on the texture of concrete depends on other mechanical properties of the material (tensile strength, bond), the nature of the pore system and those mechanical properties must be

ascertained prior to the test proper.

Absorptivity and its rate, permeability and capillary elevation can serve for important indicators of the properties of concrete particularly from the point of aggressive agents action.

4 Greater use should be made of tensile strength together with compressive strength control when testing the durability of concrete and of its components. This also important in relation to the necessary control of concrete durability of structures under actual conditions in case of long term observations.

Determination of the rate of concrete deterioration relative to its specific properties as necessary information for forecasting at least the relative rate of deterioration of concrete in structures should be considered the primary task of laboratory tests of concrete durability under various conditions.

The following important relations should be solved at the same time:

a) between gradual deterioration of concrete in structure and the results of accelerated laboratory tests,

b) between deterioration of concrete of laboratory specimens and of specimens under actual but controlled conditions,

c) between deterioration of concrete in structure and of tests specimens under the same conditions.

An important role in all these cases is played scale. Its formulation requires among others a qualitative as well as a quantitative control of deteriorating processes.

Long-Term Observations and Studies

Long term tests and observations of structures under actual conditions (environment) form an indispensable part of any rational set of methods for testing the durability of concrete, which should be based on the actual mode of concrete deterioration and be systematically verified—as far as its effectiveness and reliability go—by long term tests and scientific observations of structures.

The generally high requirements—be they of scientific, work, material or financial character—*make international cooperation in this field imperative.* This naturally imposes yet higher demands on the perfection of the system both as regard defined conditions of manufacture and placement of specimens or conditions of structures, and as regard the techniques of measurement and observations (of specimens and structures) and the final processing of their results (evaluation, analysis, conclusions).

In either case the essential conditions of success are:

1. Complete documentation concerning the properties of the basic materials, composition, placing and curing of concrete, supplemented by additional tests of mechanical, physical and chemical properties important for long-term effect of external agents (environment);

2. Complete documentation concerning the scope and nature of load, environment and aggressive agents acting on concrete in the course of test or observation;

3. Complete documentation concerning the structure or test specimen from the point of design, testing, overloading, etc.

Besides the usual control tests special tests given by the present-day state of research are used. This makes of the structures under observation long term research objects.

All of this also imposes extraordinary claims as regard the elaboration of a suitable set of methods of controlling concrete in structures and in specimens, which would enable us to continuously deal with a limited number of specimens.

Long Term Field Observations

The task of long term observations of concrete structures from the point of durability consists in part in the determination of the actual rate of concrete deterioration under real conditions, in part in the verification of the durability of concrete made on the basis of short term laboratory tests of durability. Only systematic observations of objects with complete data on concrete, and perfect long term control of external conditions can offer reliable results of scientific nature.

Observations of structures without such a sound basis, without perfect information about the mechanics of concrete deterioration and without modern means for analyzing the mode and degree of concrete deterioration can never furnish us with substantial help in the solution of this complicated problem. If sufficient in number, such observations can only provide data on:

the physical durability of various kinds of structures within a wide range given by the difference in their initial quality;

defects of a general nature which are no functions of the properties of concrete and its components relative to the environment.

The value of the results of an evaluation of the above sort appreciably increases in case of precast standard elements or structures with identical technologic procedure.

Filling of technologic documentation together with design documentation, at least for objects of major economic importance exposed to extraordinary conditions would greatly aid in the evaluation of results of periodic, incomplete inspections.

Main emphasis should be placed on thorough, systematic observations of selected structures using methods based on scientific data on concrete deterioration by various factors and modern means of concrete properties control in suitably chosen time intervals.

Closely connected with this is the need for uniform, clear terminology for phenomenological descriptions of failures that are likely to occur in concrete structures.

And finally, due consideration should be given to properly instructing the inspectors in the way of carrying out inspections, sampling and sample testing, description of phenomena, etc. A system of records should permit machine processing of data.

The high claims of such effective observations of the durability of concrete structures, and the necessity to arrive at reliable conclusions as fast as possible place the need for cooperation on a broad international basis in the forefront of interest.

Long Term Concrete Studies

Long-term tests of concrete and its components are a necessary link in the control of accelerated test methods and deteriorating processes (nature, rate) usually of a slow rate. In every case they offer the possibility of a comparison of concretes of different natures and compositions. Such was for instance one of the conclusions of long term studies of various cements (Long Time Study of Cement Performance in Concrete) organized by Portland Cement Association during the last war: the frost resistance of concrete can substatantially be increased by air entrainment (43).

In concrete cases of large structures long term tests represent an important long in the evaluation of the relation: specimen concrete—structure concrete (effect of scale, different conditions, size and nature of stress).

Long term tests of concrete bodies on exposure sites taken separately, though a good means of concrete and concrete structures control under natural conditions, are not fast enough in affording data for durable concrete technology. Their drawback lies in that the whole process progresses very slowly and thus it is not possible under variable environmental conditions to draw conclusions until after a considerable time. This reason alone would be enough to warrant systematic observations, measurements and recording of the characteristics of external conditions.

Accordingly, it is necessary to establish more such exposure sites to cover the whole scale of climatic and other (industrial) conditions.

This only underscores our justified demand to base research of the durability of concrete and concrete structures on a suitable combination of all the methods, viz. scientific analysis of the mechanics of concrete deterioration by various factors, control of the basic physical, mechanical and chemical properties important for the individual processes, accelerated laboratory tests of the components of, and of concrete, long term studies of concrete specimens and elements on exposure sites, and long term scientific observations of concrete in structures.

Progress of Deteriorating Processes and its Effect on Concrete Durability

Determination of the degree and rate of deterioration of concrete from the point of its effect on the ultimate strength of a concrete section, element and structure, is a fundamental task of great practical importance.

There are two questions involved here:

a) to what depth and extent have deterioration of the texture of concrete and loss of its mechanical and physical properties taken place;

b) what is the effect of this deterioration on the function of the original element or structure.

An important part in this is played by the nature of loading and the main task of concrete. The latter can be static (a section under compression, etc.) or physical, protective (concrete cover of steel).

In the first case—compressive stress—the matter in question is the relative loss of ultimate strength from the point of the whole section (Fig. 27). In the most

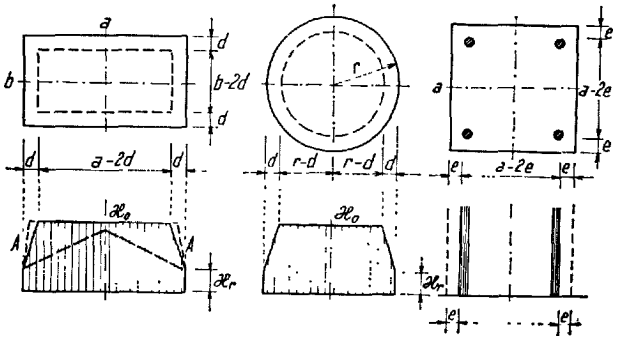

Fig. 27. *Loss of strength of concrete elements and structures*

unfavourable case of an aggressive medium acting from all sides of the element, the weakening of the section is

$$\Delta p = d\frac{a + b - 2d}{ab} \cdot \left(\frac{æ_r}{æ_0} - 1\right) \quad (7)$$

for a rectangular section

$$\Delta p = d\frac{r_0 - \frac{d}{2}}{r_0^2} \cdot \left(\frac{æ_r}{æ_0} - 1\right) \quad (8)$$

for a circular section

The resultant weakening depends on the depth and degree of deterioration, d, $æ_r$, and on the properties of the section (shape and size).

High impermeability of concrete will lead to small d even in the case concrete had completely disintegrated on the surface (A). High permeability, on the other hand, will mean deeper, more dangerous deterioration (B). This again brings out the importance of some of the physical properties of concrete.

In the second case when the main task of concrete is to protect reinforcement against corrosion, it is the ability of concrete to perform such function that is the decisive one. If we disregard the presence of random cracks, the degree of reinforcement protection is a function of the product $(e \cdot 1/k)/k$—the coefficient of permeability. In this case, however, we are not interested so much in the loss of the mechanical as in *the loss of the physico-chemical properties of concrete*: impermeability and chemical nature (pH). Hence *impermeability of protective concrete has double significance*—one, for the gradual deterioration of concrete, same as in the previous case, and two, for the reinforcement corrosion proper.

Taking into consideration the possibility of rapid reinforcement corrosion (pitting corrosion in particular) and very difficult and costly remedial action, the safety requirements must be formulated by excluding the conditions of reinforcement corrosion for the reason of ineffective protection by concrete. This raises the demands on the impermeability of the concrete protective layer, its homogeneity and durability proper relative to the environment.

The time necessary for water to penetrate to reinforcement can be expressed by the relation

$$t_e = \frac{e^2}{2kh} \quad (9)$$

where

k—the coefficient of permeability,
h—the head of water column.

Up to that time no appreciable corrosion should be likely to occur at all.

Otherwise, considering the general reinforcement corrosion (uniformly distributed on the section surface), the relations that come into play here are those deduced for gradual corrosion of circular sections of concrete, and the requirement that a smaller number of larger sections of steel should be preferred from the point of safety.

In structural elements subjected to bending moment or tension the conditions are made worse by the necessity of accounting for cracks in the cover concrete and for the possibility of local corrosion due to different humidity.

As the foregoing notes suggest, the task facing research in the way of ensuring data for a rational solution of the durability of reinforced concrete and reinforced concrete structures is a great one indeed.

Cooperation in Testing and Research

The need for cooperation and coordination of research activities relating to complex problems of concrete durability under conditions concomitant to the broad field of applications and great economic significance of this material, follows logically from the general interest in and the difficulties encountered along the way to a successful solution.

Such cooperation on a national scale in testing frost resistance was realized in practice in the United States under the sponsorship of Highway Research Board, National Research Council and National Academy of Science. Three series of tests were made within the framework of this coordinated research:

a) the first in 1936, with the aim to determine the effect of various portland cements;

b) the second in 1944, with the aim to determine the relation between a comparative test method and the methods employed by various laboratories;

c) the third in 1959, with the aim to compare four ASTM test methods:

C 290–52 T—Rapid freezing and thawing in water,
C 291–52 T—Rapid freezing in air and thawing in water,
C 292–52 T—Slow freezing and thawing in water or brine,
C 310–53 T—Slow freezing in air and thawing in water, using three kind of concrete with both sound and poor aggregates and different degree of air entrainment. Thirteen research institutes participated in these tests. (34)

The International RILEM Symposium held in Prague in 1961—Durability of Concrete and Concrete Structures—has clearly shown the international need for as well as willingness based on mutual interest,

to close organized cooperation in research relating to the difficult problems of concrete structure durability. RILEM Technical Committee for the Durability of Concrete and Concrete Structures which has taken upon itself to carry out this task in a general way, is attempting to gradually ensure its fulfilment on the basis of an analysis of the present state of world research, endeavouring to prepare optimum conditions for an organized international cooperation both in scientific laboratory studies of the basic questions of the mechanics of the durability of concrete and its components, and in providing scientific and technical data for a rational design and manufacture of concretes having specified durability expressed in terms of the physical durability of concrete structures. This preparatory work includes moreover the organization of systematic long term observations of the durability of various concrete structures and exposure sites so that the outlay for this costly work summarized on an international basis would yield maximum possible amount of high-quality findings of a general nature.

The accomplishment of this task will call for close cooperation with all national and international organizations and research institutes engaged in serious studies of concrete durability.

Quick, regular interchange of data, contact between specialists and periodic exchange of opinions at international meetings and conferences are other important conditions for a successful international cooperation.

Conclusions

The durability of concrete structures is a highly complicated problem whose solution must be based on a scientific analysis of and research into the various mechanical, physical and chemical processes that cause gradual loss of the basic physical and mechanical properties of concrete. It should also be ensured on a basis in daily practice, from the design through construction methods to the maintenance of structures.

Similarly as in mechanics where theory has passed from empiric knowledge to calculations based on the understanding of the laws of mechanics, we are facing today the problem of durability in concrete technology, with the need for *conscious, intentional selection of materials, creation of the texture and of the whole technologic process with a view to the specifically required durability of concrete under given conditions.*

The durability of concrete and concrete structures is at the present time a measure of structure quality same as is the strength of concrete. It unquestionably is an expression of a long time quality of concrete given by the required durability of the structure, as well as one of a long term economic solution of concrete and structure technology.

Even though our analysis has indicated how significant is a complex solution of the durability of concrete structures, the crucial point of our task and of the measures to fulfil it continues to lie in concrete proper, its technology in particular.

Air entrainment, a technique introduced in the United States a quarter of a century ago, must be designated a valuable contribution to ensuring the durability of concrete, particularly under the action of alternate frost in humid environment and everywhere elsewhere new voluminous products arise through unfavourable reactions. Further work, above all that relating to *efficient control of the system of pores* produced by various admixtures, will of course be required before the technique is safely established in practice.

Irrespective of the fact that some of the principal questions of durability mechanics, e.g. concrete deterioration by alternate frost have not been fully elucidated so far, we should on the basis of the present-day knowledge endeavour to create conditions for ensuring high durability of concrete, at least for the characteristic, essential exposure conditions of structures. In doing so we must start out from the mechanics of the various deteriorating processes of concrete due to diverse agents, and from its connection with the fundamental mechanical, physical and chemical properties of concrete and its components. *Results of this scientific analysis of the processes should, therefore, be utilized, qualitatively at least, in the technology of concrete structures:* choice of materials, composition, placing and curing of concrete. In the exceptional case of a very strong attack of aggressive agents we should utilize to the full such preventive measures—drainage, protection of concrete—that lead a priori to a limited action of the aggressive agents on concrete.

In close connection with this is the need for a reliable, scientific formulation of provisional recommendations for the production of durable concrete and concrete structures based on the present state of our knowledge. By its nature and urgency, the technique of gradual introduction of ever more perfect

technological procedures and ever more suitable materials for concrete structures under unfavourable conditions imposing high requirements on the durability, combined with systematic control of selected structures and its reciprocal impact on laboratory research, is the only possible way towards a solution of this difficult task.

Despite a number of partial tasks whose object is a complete clarification of the mechanics of concrete deterioration by various agents, especially as it concerns the relation to hardened cement paste and its bond with aggregates, and which pertain to all concrete components, admixtures including, we should direct our activities towards obtaining reliable scientific and experimental data for a rational design of concrete of the required durability.

Present-day findings, above all an analysis of the main deteriorating processes in concrete, already indicate some of the important requirements on the properties of concrete, such as impermeability, absorptivity, capillary elevation, tensile strength of hardened cement paste, cement-aggregate bond. Besides further elucidation—quantitative in particular—of their relations to concrete durability, the matter to concentrate on is the search for suitable technologic measures and cement properties (fineness of grinding) ensuring them. We have to search for new, suitable admixtures, or for new materials that would reliably provide the required properties of concrete.

A speedy and successful solution to this complex of intricate problems should and must be sought in broad but close international cooperation and coordination of reserach work that would ensure maximum effect—basic relations of general validity capable of furnishing reliable data for the technology of durable concretes.

This fact logically leads to the need for suitable, uniform test methods which as the only ones will permit uniform evaluation of concrete durability under laboratory conditions, and for more intensive utilization of results achieved on a world scale.

Quantitative evaluation of laboratory tests, of the accelerated ones especially, in relation to reality and from the point of designing concretes with the required durability under conditions defined in advance, has become a task of first magnitude. Every means—no matter how small—of rendering concrete technology more exact has an enormous economic and engineering significance considering the present day volume of cement and concrete production and the ever growing quantity of cement per inhabitant. Mastering this relation together with a rational technology of durable concretes will provide a sound basis from which to tackle the optimalization of the solution given by minimum overall costs.

Advances in civil engineering and concrete technology bring along some new tasks concerning the long term concrete quality—concrete durability. Among the most important ones we should include the durability of concrete and reinforced concrete prefabricates of all kind, and of structures built of them. Mass production, high degree of technologic control and a broad field of application under most diverse circumstances create conditions highly conducive to the solution of the questions of concrete durability.

It is just in this instance that the properties of cement as a binder play a very important part, and we should exploit to full the possibilities that cement manufacture has to offer by way of improving conditions relative to the deteriorating processes, both from the mechanical (tensile strength), the physical (fineness of grinding, grain size) and chemical aspects. Contradictory requirements, especially under combined effects, will of necessity call for specialization in cements. Great possibilities are offered by new materials of suitable properties, appropriately introduced in the texture of cement paste having already a satisfactory durability of its own.

The scope of the tasks that confront us, their outstanding economic importance and great complexity, as well as the high claims they make on scientific capacity, time and materials, convert them into a fitting subject of wide international cooperation.

References

1. ACI Committee 212: Admixtures for concrete, ACI J. Nov. (1963).
2. ACI Committee 306: Proposed ACI Standard Recommended Practice for Cold Weather Concreting, ACI J. Sept. (1965).
3. N. Altner: Einflüsse der Porosität des Zementsteines auf die Frostwiderstandsfähigkeit des Betons. Baustoffindustrie 8, (1965).
4. ASTM Standards:
   C290–63T—Method of Test for Resistance of Concrete Specimens to Rapid Freezing and Thawing in Water.
   C291–61T—Method of Test for Resistance of Concrete Specimens to Rapid Freezing in Air and Thawing in Water.
   C292–61T—Method of Test for Resistance of Con-

crete Specimens to Slow Freezing and Thawing in Water or Brine.
C310–61T—Method of Test for Resistance of Cements to Slow Freezing in Air and Thawing in water.
5. S. Aoki, Z. Murata, S. Hozumi and Y. Ishii: The effect of surface active agents on the durability of concrete, Proc. Jap. Cement. Eng. Ass., (1964).
6. J. E. Backstrom, E. W. Burrows, R. C. Mielenz and V. E. Wolkodoff: Origin, evolution and effects of the air void system in concrete, Part 2—influence of type and amount of air-entraining agent, ACI J. Aug. (1958).
7. J. E. Backstrom, R. W. Burrows, R. C. Mielenz and V. E. Wolkodoff: Origin, evolution and effects of the air void system in concrete, Part 3—influence of *W/C* ratio and compaction, ACI J. Sept. (1958).
8. Balasz and Kunszt: Causes for deterioration of steam-cured concrete structures, Magyar Epitörpari, No. 9, 98–99, (1965).
9. A. Basalla: Über die Widerstandsfähigkeit des jungen Betons gegen Frosteinwirkung, Der Bauingenieur, No. 4, (1964).
10. I. A. Benjamin and G. D. Jr. Ratliff: The Effect of early freezing on low density aggregate type concrete, ASTM Proc. (1960).
11. R. H. Bogue: The Chemistry of Portland Cement. New York, (1947).
12. J. Bonzel: Beton mit hohen Frost- und Tausalzwiderstand. Beton, No. 11, (1965).
13. H. W. Brewer and R. W. Burrows: Coarse-ground cement makes more durable concrete. ACI J. Jan. (1951).
14. H. E. Brown: Interim Report—An investigation of the durability of steam-cured concrete, Virginia Council of Highway Investigation and Research 23 p., bibl. 23, Charlottenville, (1966).
15. G. M. Bruere: Rearrengement of bubble sizes in air-entrained cement pastes during setting, Australian Jour. of Appl. Science, No. 3, (1962).
16. A. D. Buck and W. L. Dolch: Investigation of reaction involving nondolomitic limestone aggregate in concrete, ACI J., July, (1966).
17. Building Reaearch Station. Shrinkage of natural aggregate in concrete, Digest No. 35, June, (1963).
18. M. Buisson: Lois régissant la circulation de l'eau dans les corps poreux. Bull. Tech. Veritas, (1950).
19. F. Campus; R. Dantine, M. Dzulynski, K. Gamski, F. Pirotte and R. Baus: Journée CERES sur la durabilité du béton et du béton armé, Memoires No. 16, Université de Liège. Sept. (1966).
20. C. C. Carlson: Fire resistance of prestressed concrete beams. study A—influence of thickness of concrete convering over prestressing steel strand, PCA Res. Dev. Lab. Bull. 147, July, (1962).
21. M. A. Craven: Sand grading influence on air entrainment in concrete, ACI J., Nov., (1948).
22. W. Danilecki: Quelques observations sur l'effet exercé par la forme et les dimensions des éléments de construction sur leur résistance a la corrosion, Symp. RILEM, Durability of Concrete, II part, Prague (1961).
23. R. Dutron and A. Mommens: Corrosion des Armatures dans le béton armé, Centre Nat. Rech. Scient. et Tech., (1964).
24. J. Farran: L'altérabilité des roches, ses facteurs, sa prévision, Annales ITMTP, Nov., (1965).
25. V. K. Gouda and G. E. Monfore: A rapid method for studying corrosion inhibition of steel in concrete, P.C.A. Res. Bull. 187, Sept. (1965).
26. D. W. Hadley: Alkali reactivity of dolomitic carbonate rocks, HR Res. No. 45, (1964), PCA Res. Dev. Bull. 176.
27. P. de Haller: Der Austrocknungsvorgang von Baustoffen. Zurich, (1942).
28. W. C. Hansen: Porosity of hardened portland cement paste, ACI J. Jan., (1963).
29. W. C. Hansen: Twenty-year report on the long time study of cement performance in concrete, PCA Res. Rew. Lab., May, (1965).
30. E. Hartmann: Frost testing methods. Beton Herstellung, Verwendung, Dec. (1964). (In German).
31. R. P. Haviland: Engineering reliability and long life design, Van N. Y. Nostrand, (1964).
32. E. C. Higginson: Effect of steam curing on the important properties of concrete, ACI J., Sept. (1962).
33. Highway Research Board: Report on Cooperative Freezing-and-Thawing Tests of Concrete, HRB, Spec. rep. 47 (1959).
34. Highway Research Board: Report on Cooperative Freezing-and Thawing Tests of Concrete. Spec. rep. 47, (1959).
35. Highway Research Board: Symposium on alkali-carbonate rock reactions, (15 reports), Highway Res. Rec. No. 45, (1964).
36. A. W. Hill: La corrosion des aciers dans le béton contenant de Chlorure de calcium. Rév, des Mat. de Constr., Mars (1964).
37. T. T. C. Hsu; F. O. Slate, G. M. Sturman and G. Winter: Microcracking of plain concrete and the shape of the stress-strain curve, ACI J., Feb. (1963).
38. T. T. C. Hsu: Mathematical analysis of shrinkage stresses in a model of hardened concrete, ACI J., March (1963).
39. T. T. C. Hsu and F. O. Slate: Tensile bond strength between aggregate and cement paste or mortar, ACI J., April (1963).
40. G. M. Idorn: Durability of concrete structures in Denmark, Copenhagen (1967).
41. Institut für Baustoffe und Physik: Betonkorrosion-Tagung, Leipzig 1967. Baustoffindustrie 9, (1967).
42. A. W. Isberner: Durability studies of exposed aggregate panels, PCA, Res. Dev. Lab. J., May (1963).
43. F. H. Jackson: Long-time study of cement performance in concrete. Chapter 9—correlation of the results of laboratory tests with field performance under natural freezing and thawing, ACI J., S159, (1955/56).
44. A. Joisel: Note sur la gélivité du béton. Rév. des Mat. de Constr. April (1961).
45. M. F. Kaplan: Strains and stresses of concrete at initiation of cracking and near failure, ACI J., July, (1963).
46. L. A. Keiser, N. B. Marjamn and L. I. Panfilova: Temperature gradients in concrete of precast structures subjected to steam-curing and their influence on concrete quality and durability, RILEM,

Moskva (1964).
47. H. L. Kennedy: Entrained air—its effect on the constituents of portland cement concrete, ASTM Proc. (1944).
48. P. Klieger: Some aspects of durability and volume change of concrete for prestressing, PCA Res. Dev. Lab. J. Sept. (1960).
49. P. Klieger and J. A. Hanson: Freezing and thawing tests of lightweight aggregate concrete, ACI J. Jan. (1961).
50. P. Klieger: Extensions to the long-time study of cement performance in concrete, PCA Res. Dev. Lab. J., Jan. (1963).
51. P. Klieger and W. Perenchio: Silicone influence on concrete resistance to freeze-thaw and de-icer damage, HRB, No. 18 (1963).
52. Y. Koh, T. Goto, Y. Yamazaki, E. Imamura and M. Makimizu: The effect of freezing and thawing on the bond strength between lightweight aggregate concrete and reinforcing Bar, Proc. Jap. Cement Eng. Ass. (1963).
53. B. Kroone and D. N. Crook: Studies of pore size distribution in mortars, Wag. Con. Res., Nov. (1961).
54. W. H. Kuenning: Resistance of portland cement mortar to chemical attack. A progress report. PCA Res. Bull. 204, (1966).
55. H. Lafuma: Retrait et fissuration des ciments et bétons, AITBTP, Dec. (1956).
56. R. Landgreen and J. Tatman: Outdoor concrete exposure test plot at Skokie, PCA Res. Dev. Lab. Bull., 202, (1966).
57. T. D. Larson, J. L. Mangasi and R. R. Radowski: Preliminary study of the effects of water-reducing retarders on the strength, air void characteristics and durability of concrete, ACI J. Dec. (1963).
58. F. M. Lea: The Chemistry of Cement and Concrete, London (1956).
59. F. M. Lea and C. M. Watkins: The durability of reinforced concrete in sea water, Nat. Building Studies, Res. paper No. 30, HM Stat. Office, London, (1960).
60. A. E. Lentz and G. E. Monfore: Thermal conductivity of concrete at very low temperatures, PCA Res. Dev. Lab. J., May (1965).
61. F. W. Locher and H. Pisters: Beuteilung betonangreifender Wässer, Zement-Kalk-Gips, No. 4, (1964).
62. G. M. Lomize: Filtratsiya v treshcinatykh porodakh. Moskva, (1961).
63. H. Lossier: Pathologie therapeutique du béton armé. Dunod, Paris (1955).
64. I. D. Mackenzie: Inspection and maintenace of concrete in ACI J. Nov. (1964).
65. M. Mamillan: La gélivité des matériaux. Annales IPBTP, Juillet-Août, (1967).
66. A. Markestad: Attack of concrete floors by chemical agents, Nord. Beton, No. 1 (1966).
67. B. Mather: Effects of sea water on concrete. HRB Rep., Dec. (1964).
68. R. C., Mielenz V. E. Wolkodoff, J. E. Backstrom and H. L. Flack: Origin, evolution and effects of the air void system in concrete. Part 1—entrained air in unhardened concrete, ACI J. July (1958).
69. R. C. Mielenz, V. E. Wolkodoff, V. E., Backstrom and R. W. Burrows: Origin, evolution and effects of the air void system in concrete. Part 4—The air void system in job concrete, ACI J., Oct. (1958).
70. A. I. Minas: K voprosu o prognoze dolgovechnosti stroitelnykh konstrukcii, nakhodyashchikhsya v agressivnoi srede, Trudy Kazakh. Fil. Akademii Stroitelstva i arkhitektury SSSR. Sbornik 4 (1962).
71. A. I. Minas: Mechanismus der Korrosion von Baustoffen durch Salze und Laugen, Baustoffindustrie No. 7 (1966).
72. A. I. Minas: Metod opredeleniya dolgovechnosti konstruktsii nakhodyashchikhsya v agressivnoi srede, Alma- Ata (1967).
73. D. E. Monfore and G. J. Verbeck: Corrosion of Prestressed wire in concrete, ACI J., Nov. (1960).
74. G. E. Monfore, and A. E. Lentz: Physical properties of concrete at very low temperatures, PCA Res. and Dev. Lab. Res. Bull. 145, (1962).
75. G. E. Monfore and B. Ost: Corrosion of aluminium conduct in concrete. PCA Res. Dev. Lab. J., Jan. (1965).
76. V. M. Moskvin and A. M. Podvalnyi, Issledovanie korrozionnykh protsessov v nagruzhennom betone, Izv. ASA-UUSR, No. 4, (1962).
77. J. D. Mozer, A. C. Bianchini and C. E. Kesler: Corrosion of reinforcing bars in concrete, ACI J., Aug. (1965).
78. J. Murata: Studies on the permeability of concrete, Bull. RILEM, Dec. (1965).
79. R. Nagano: On the durability of concrete using cement admixtures and AE agent against freezing and thawing under various curing conditions and ages, Proc. Jap. Cement Eng. Ass. (1964).
80. R. W. Nurse: Assesment of concrete durability, Symp. Concrete Quality, Nov. (1964).
81. B. Ost and G. E. Monfore: Corrodibility of prestressing wire in concrete made with Type 1 and Type 1S cements. PCA J. May (1963).
82. B. Ost and G. E. Monfore: Penetration of chloride into concrete, PCA Res. and Dev. Lab. J., Jan. (1965).
83. W. Perenchio: Effect of surface grinding and joint sawing on the durability of paving concrete, PCA Res. Dev. Lab. J., Jan. (1964).
84. T. C. Powers and T. L. Brownyard: Studies of physical properties of hardened portland cement paste. ACI J., Oct.-Dec. (1946). Jan.-April (1947).
85. T. C. Powers, L. E. Copeland, J. C. Hayes and H. M. Mann: Permeability of portland cement paste, PCA Res. Bull. 53, (1955).
86. T. C. Powers: Résistance au gel du béton jeune, ITBTP, Paris (1957).
87. T. C. Powers, L. E. Copeland and H. M. Mann: Capillary continuity or discontinuity in cement pastes, PCA Res. Dev. Lab. J., May (1959).
88. T. C. Powers: Prevention of frost damage to green concrete, Bull. RILEM 14, March (1962).
89. T. C. Powers: Protection du béton au premier âge contre le gel, Bull. RILEM, Mars (1962).
90. T. C. Powers: Characteristics of air void systems, PCA Res. Bull. 174, Topics in Concrete Technology (1965).
91. T. C. Powers: The mechanism of frost action in con-

crete, Stanton Walker lecture No. 3. University of Maryland (1965).
92. J. D. Richards: The effect of various sulphate solutions on the strength and other properties of cement mortars at temperatures up to 80°C, Mag. Con. Res., June (1965).
93. M. H. Roberts: Effect of calcium chloride on the durability of pretensioned wire in prestressed concrete, Mag. Con. Res., Nov. (1962).
94. E. C. Roshore: Durability of prestressed concrete beams, Jour. Prestressed Concrete. Oct. (1965).
95. E. W. Scripture, F. B. Hornibrook and D. E. Bruyant: Influence of size grading of sand on air-entrainment. ACI J., Nov. (1948).
96. Silaenkov E. S.: Ob otsenke dolgovecnhosti autoklavnykh yacheistykh betonov. Sbornik, No. 7. Akad. Stroit. i Arkhit. SSSR, (1962).
97. E. S. Silaenkov, G. V. Tikhomirov, A. D. Ulyanova and G. M. Zakharikova: Vliyanie karbonizatsii avtoklavnykh yacheistykh betonov na ikh dolgovechnost. Sbornik No. 7 Akad. Stroit. i Arkhit. SSSR, (1962).
98. E. S. Silaenkov, G. V. Tikhomirov and T. A. Skobeleva: Stoikost yacheistykh betonov pri poperechnom uvlazhenii i vysušivanii, Sbornik No. 7, Akad. Stroit. i Arkhit. SSSR, (1962).
99. E. S. Silaenkov: A study of durability of cellular concretes and units made of these (in Russian), Sverdkovsk (1962).
100. E. S. Silaenkov: Dolgovechnost krupnorazmernkh izdelii iz avtoklavnykh yacheistykh betonov, Moskva (1964).
101. F. O. Slate and S. Olsefski: X-rays for study of internal structure and microcracking of concrete, ACI J. May (1963).
102. T. Sneck: Corrosion of iron and steel embedded in concrete, Helsinki (1961) (in Finnish).
103. L. C. Snowdon: The moisture movement of natural aggregate and its effect on concrete, RILEM Inter. Symp.—Durability of Concrete, Prague (1962).
104. L. C. Snowdon and A. G. Edwards: The moisture movement of natural aggregate and its effect on concrete, Mag. Con. Res. No. 41. July (1962).
105. E. N. Sparkes: The control of concrete quality—a review of the present position, Symposium: Mix Design and Quality Control of Concrete, London (1954).
106. H. H. Steinour: Influence of the cement on the corrosion behaviour of steel in concrete, PCA Res. Dev. Lab. J., May (1964).
107. E. G. Swenson: The durability of concrete under frost action. Tech. paper. No. 26, Div. Building Res. Nat. Res. Council, June, (1955).
108. T. Thorwaldson: Chemical sapect of the durability of cement products.—Proc. 3rd internat. Sympos.: Chemistry of Cement, (1952).
109. S. Tsumura, R. Nagano and K. Nakano: Shrinkage and freezing-and-thawing test of lightweight concrete, Proc. Jap. Cement Eng. Ass., (1964).
110. I. L. Tyler: Long-time study of cement performance in concrete—Ch. 12.: concrete exposed to sea water and fresh water. ACI J., March (1960).
111. F. Vaessen: Korrosionsfrage beim Spannbeton, Bet. u. Stahlbet. 11, (1966).
112. O. Valenta: International Working Centre for Concrete of Hydraulic and Transport Structures in Prague. Acta Technica, No. 1, (1957).
113. O. Valenta: The significance of the aggregate-cement bond for the durability of concrete, RILEM Symp. Durability of Concrete, Prague, (1961).
114. O. Valenta: Die Bedeutung der Haftung zwischen Zuchlagstoffen und Zement für die mechanischen und physikalischen Betoneigenschaften, Wissenschaftliche Zeitschrift der Hochschule für Bauwesen, Leipzig (1963).
115. O. Valenta: The significance of aggregate-cement bond for mechanical and physical properties of concrete, Congress on Large Dams, Edinburgh, (1964).
116. O. Valenta: The physical and mechanical effects of moisture on constructional materials—mainly concrete—under the action of frost, Symp. RILEM/CIB, Helsinki (1965).
117. O. Valenta: Durability of concrete and concrete structures, SNTL, Prague (1965) (in Czech).
118. M. Vénuat: L'influance de la granulométrie des ciments sur les propriétés physiques et mécaniques des mortiers et bétons, Rév. des Mat. de Constr., Juillet-Oct. (1961).
119. M. Vénuat: Ciments aux cendres volantes. Influence de la proportion de cendre sur les propriétés des ciments, Rév. des Mat. de Constr., Oct.-Déc. (1962).
120. M. Vénuat: Compte rendu de la résistance au gel du ciment, Rév. des Mat., Juin-Août, (1963).
121. G. Verbeck and R. Landgren: Influence of physical characteristics of aggregates on frost resistance of concrete, ASTM Proc. (1960).
122. E. N. Vershinina: Adsorbtsionnaya aktivnost—kharakteristika morozotoikosti stroitelnoi keramiki. Stroit. i Arkh. 11, (1965).
123. S. Walker and B. L. Bloem: Studies of concrete containing entrained air, ACI J, June (1946).
124. K. Walz and R. Springenschmid: Betonstrassen und Tausalzeinwirkung, Beton, 12, (1962).
125. K. Walz und J. Bonzel: Ausblühungen auf Betonflächen. Beton, 12, (1962).
126. K. Walz und H. Helms-Derfert: Schutz von jungen Strassenbeton gegen Tausalzeinwirkung, Beton, 5, (1965).
127. B. Warris: The influence of air-entrainment on the frost-resistance of concrete. proc, No. 35, Swedish Cement and Concrete, Res. Inst., Stockholm (1963).
128. V. G. Zolotukin: Zhestkost i treschinostoikost konstruktsii iz avtoklavnogo penozolobetona, Sbornik No. 7, Akad. Stroit. i Arkhit. SSSR, (1962).

Oral Discussion

Hoshagrahar C. Visvesvaraya

May I start by expressing our congratulations to the author for his excellent paper in which he has not only given a vast amount of useful information on the durability of concrete but also brought out very clearly the important issues connected with this highly complicated subject.

The author has rightly divided the principal aspects of durability into two groups—the *physical* and the *economical*. The *physical durability* is expressed in terms of the decisive mechanical and physical properties of concrete; what properties are decisive depends on a given situation and so the physical durability of the same concrete could be different in different situations of use depending on the performance expected of it. Similarly the economic durability expressed by equation 1 in the authors' paper takes into account only the direct costs; the indirect costs such as having to do either without a structure in case of collapse (Ex: collapse of a rail bridge) or with an unsatisfactory structure in case of damage (Ex: damaged highway pavement) as well as the economic consequences of the collapse of a structure have also been kept in view in the overall assessment (Ex: Bursting of dam).

There cannot be any two opinion on the significance of the homogenity of concrete which the author has discussed in the paper; the non-homogeneity of concrete leading to stress concentration should perhaps be qualified as in sections of low deformability in stead of *high* modulus of elasticity and *deformability*.

The importance of a proper understanding of the cracking phenomenon in the durability studies of concrete has already been well emphasised in the paper.

Cracking can occur in concrete when it is still fresh and/or after it has set and hardened. Cracking in fresh concrete could result from a rapid evaporation of moisture leading to excessive plastic—shrinkage, or differential settlement over obstacles such as aggregate particles or the reinforcement, or separation of cement mortar from aggregate caused by local bleeding. These cracks have been variously defined as "plastic", "plastic—shrinkage", "settlement", "presetting" "prehardening" or "surface" cracks and the author appears to be in favour of the last mentioned word. The term "surface cracks" could be misleading, in that, such cracks have been found to be not only on the surface but also extending all the way through slabs. Ravina and Shalon (1), in a very recent report, have mentioned the observation of plastic cracks up to depths of 23 cm. The cracks were of a width of 0.1 to 3.0 mm and had lengths ranging from a few centimeters to 1 or 2 meters.

Cracking of hardened concrete could result from shrinkage restrained internally (when bond cracking between aggregates and mortar may develop) or externally (when larger cracks may form), or from severe fluctuations in the temperature (causing differential expansions of the aggregate and matrix or concrete and steel in reinforced sections) and humidity (resulting in excessive shrinkage on drying and in reduction of surface tension on wetting) or application of stress.

Regarding the development of cracks induced due to shrinkage, the author has rightly considered the result of the investigations of T. C. Hsu (2) in which the possibility of the formation of three types of cracks (viz. tensile cracks in reduced cross section of cement paste between grains, diagonal tensile cracks in cement paste and tensile cracks in the cement—aggregate joint) have been found. In structures of reinforced concrete, the internal stresses developed in a cross-section due to fluctuations in temperature arising from differences in the thermal expansion properties of concrete and steel are not usually accounted for and the resulting simplifications in the analysis appears to be the major reason for this. In the discussions that arose over a paper by Vetter (3), it was pointed out that the thermal coefficient of concrete may vary from 4×10^{-6} to 6×10^{-6} per degree Fahrenheit (depending on the composition), where as that of steel from 6.3×10^{-6} to 6.8×10^{-6} which may give a difference sufficient enough to cause a rather wide variation in the stresses. This appears to be a point which requires a more serious attention and investigation, especially for such conditions which introduce tensile stresses in concrete.

Cracking is also induced in concrete due to the stress which is brought on it by the application of external loads. Hsu, Slate, Sturman and Winter (4) studied the micro-cracking in concrete in relation to the stress-strain curve and the type, location and extent of progress of the cracking with the increasing stress and strain on the cross section. Bond cracks (resulting from shrinkage) were found to exist even before the application of load, and with increase in stress, the cracks increased in length width and number. This increase was negligible up to stresses less than 30 per cent of ultimate stress and above which matrix cracks also developed, and at about 70 to 90

per cent they increcased noticeably and formed continuous crack patterns. Sturman, Shaw and Winter (5) have extended the investigations by Hsu et. al. (4) to the study of the influence of flexural strain gradient on microcracking, by comparing the behaviour of eccentrically loaded specimens with that of concentrically loaded specimens. By observations based on sonic method, Jones (6) also finds that the micro-cracking (from stress) starts in concrete when the stress on it reaches about 30 per cent of the ultimate. The limitations of sonic and ultrasonic methods in these studies which the author has mentioned are also brought out here. The true ultimate strength of concrete when it is subjected to sustained loading represented by the stage at which extensive internal cracking occurs in concrete, is about 70 to 90 per cent of the short term ultimate strength. Estimation of the sustained load strength of concrete from micro-cracking and other methods have been recently reviewed in detail (7). According to Glucklich (8), up to 30 per cent of stress negligible bond cracks occur, between 30 and 50 per cent slow growth of bond cracks occurs, between 50 and 75 per cent slow growth of matrix cracks and bond cracks occurs, and between 75 and 100 per cent fast growth of matrix cracks occurs. Glucklich has also discussed in detail the effect of micro-cracking on time-dependent deformations and the long-term strength of concrete. For an understanding of the cracking and the conditions under which progressive cracking occurs in concrete, the theory of fracture mechanics is also being applied (9).

Research on concrete cracking should ultimately lead to the realisation of the various factors by which cracks in concrete could be minimized if not eliminated altogether. The plastic-shrinkage cracks could be minimized to a considerable extent by taking proper care and necessary precautions as given by Lerch (10). Regarding this aspect, an engineer incharge of a construction job could benefit much from the tips given by Jellic (11) also. The attempts at reducing the shrinkage cracking in hardened concrete could be through the use of expanding cements which is already mentioned in the paper.

Probably the micro-cracking of concrete resulting from stress is the one type of cracking which cannot be avoided in concrete as the concrete section has to sustain a stress. However the extent of this cracking could be minimized by keeping the stress on it to within 30 per cent of the short term ultimate load. This aspect of study becomes more complex because a balance is to be struck between the adoption of smaller stresses and the resulting increased expense or reducing the expenses by using higher stress when the micro-cracking from stress will be more which will affect the durability of the structure. In any case this discussion emphasises the effect of overloading on durability; a structure overloaded over a length of time, having developed micro-cracks, even if the overload is removed could lead to lower durability of the concrete.

The use of prestressed concrete in reducing the cracks that may develop in concrete structures from any occasional overloading is already given in the paper. The closing up of cracks an unloading in a prestressed structure is a well known phenomenon but this is not universally applicable at all sections under all conditions. There are many prestressed structures known to have developed cracks which did not respond to reduction of superimposed load; in fact a case recently brought to our notice in India regarding the cracking observed in the prestressed concrete girders of a railway bridge. Gracks are noticed to have formed in the end blocks of these girders and through these cracks rain and other water has been gaining access to the high tensile and other steel in the ends of the girder. This could have set in the rusting of steel and hence affect the strength and durability of the structure and the problem is now being investigated. Obviously, the prestress acting on the girder cross section has not been of use in preventing these cracks; similarly the prestressing might not be of assistance in so far as microcracking due to stresses caused by overloading are concerned.

The authors conclusions that the complex problem of durability is to be studied on the basis of long-term observations in the laboratory as well as long-term field observations on the basis of uniform test methods should be fully endorsed.

The few comments given above are an only by way of elaboration of certain points briefly brought in the excellent paper presented by the author and not as criticism or comment.

References

1. D. Ravina and R. Shalon, "Plastic shrinkage cracking", Journal of the American Concrete Institute, Proc. Vol. 65, No. 4, April 1968. pp. 282–292.
2. T. C. Hsu—Ref. (38) of the paper.

3. C. P. Vetter, "Stresses in reinforced concrete due to volume changes", Transactions of the American Society of Civil Engineers, Vol. 98, pp.1039–1079.
4. T. C. Hsu, et al—Ref. (37) of the paper.
5. G. M. Sturman, S. P. Shah and G. Winter, "Micro-cracking and inelastic behaviour of concrete", Proceedings of the ASCE-ACI International Symposium on Flexural Mechanics of Reinforced Concrete, Nov. 1964, pp. 473–499.
6. R. Jones, "A method of studying the formation of cracks in a material subject to stress", British Journal of Applied Physics, Vol. 3, No. 7, July 1952, pp. 229–233.
7. D. Prakash and C. S. Viswanatha, "True ultimate strength of plain concrete", RILEM Bulletin (Paris), No. 36, September 1967, pp. 163–173.
8. J. Glucklich, "The effect of micro-cracking on time-dependent deformations and the longterm strength of concrete", International Conference on the Structure of Concrete (Imperial College, London), 1965, 14 pp.
9. M. F. Kaplan, "The application of fracture mechanics to concrete", International Conference on the Structure of Concrete (Imperial College, London), 1965, 7 pp.
10. W. Lerch, "Plastic shrinkage", Journal of the American Concrete Institute, (Journal Vol. 28), Proe. V. 53, 1957 pp. 797–802.
11. Jellic, Journal of the American Concrete Institute, (Journal Vol. 28), Proc. V. 53, No. 3, September 1965, p. 321.

Author's Closure

Oldřich Valenta

Mr. Visvesvaraya has rightly pointed to the high complexity of concrete and concrete structures durability. This state of things led me only to the try of giving to the participants of this symposium a framely picture of actual state of research as well as of general direction for future research and international cooperation in it.

Mr. Visvesvaraya has also rightly pointed to the necessity to consider *also indirect costs* in the analysis of concrete structure durability. Complete analysis of every individual case must be done. Any timely repair of the structure must be covered by the 2nd member of the equation No 1. Increased probability of collapse must be dealt with as probability of collapse admitted and accepted by normal design regulations.

Many causes and effects *of cracks in concrete* have got to be considered when analysing their effect on the durability of concrete and concrete structures.

No complete analysis could be included in the paper. We are actually very far from using at least the same definitions in describing them. When considering the durability of concrete we must concentrate especially on their consequencies: *increased permeability and nonhomogeneity of concrete* when water, aggressive solutions or liquids, vapor and gases may penetrate into concrete easily and rapidly. This refers also to prestressed structures endangered even by isolated overloading. Load carrying capacity has not been necessarily reduced—but penetration to liquids or gases has been increased with due unfavourable effect on corrosion processes and durability of concrete and reinforced concrete.

Homogeneity of concrete has different consequences depending on the forces or agents acitng on concrete: *Concrete section with increased porosity* generally has:

a) *reduced strength and rigidity* (modulus of elasticity or deformation)—leading to reduced stresses,
b) *increased permeability* leading to increased deteriorating action due to easier penetration of agents.

This remark had *to stress the fact that increased care should be given to concrete technology* as to obtained homogeneity in cases of its exposure to aggressive agents than in cases of structures not exposed or protected.

Supplementary Paper III-24 Behaviour of Mortars and Concretes in the Temperature Range from +20°C to −196°C

Giampietro Tognon*

Synopsis

Results of an investigation on specimens of cementitious mortar and of concrete cast with different types of aggregates and cement, as well as on specimens of lapidary materials for comparison, are reported.

Two cryogenic chambers, with temperatures adjustable in the treating cell respectively from +20°C to −100°C and from −100°C to −180°C, were used and for the temperature of −196°C a thermostatic container with liquid nitrogen.

Performed tests showed an increase of compression, bending, tensile strengths and of modulus of elasticity as the treating temperature was decreased.

Strengths are neither influenced by the type of cement nor—it seems— by the nature of aggregates, but by the content of free water in the specimen.

This last fact is the cause of an anomalous behaviour of strength trend which appears about in −35C° and −60°C range.

The trend of the thermal contraction coefficient was also determined and the existence of above indicated the singular zone.

Tests were performed to know the behaviour of concrete to the impact at very low temperatures.

Repeated cycles of freezing and thawing from ambient temperature down to −196°C and vice versa, showed that concretes do not undergo significant degradation.

Then, following direct investigation on water-ice system, and on the ground of thermometric measurements and of distribution of porosity, one tried to explain the behaviour of hardened concrete at lower and very low temperatures through a thermodynamic interpretation and to justify strength values reached with a triaxial stress.

Introduction

Rather recent and still limited in their numbers are the studies about the behaviour of concrete at very low temperature (1) (2).

On the other hand, it is not long since the opportunity has arisen, to bring the concrete into contact with fluids or in ambients that are at temperatures about 180 ~ 200°C below zero. This is the case of tanks used to hold liquid gases: methane for instance, that boils just at −178°C.

This report has the purpose to bring a contribution to the knowledge of the specific physical properties that mortars and concretes hardened in a normal ambients assume, when the temperature of their mass is brought in equilibrium to values decreasing little by little to approximately −200°C.

First Part

At the moment to program the investigation, it has been thought right to soon have an idea about the fundamental characteristics of the phenomenon which had to be studied, to free it from the variables which might have proved to have no influence on it and to bring it, if possible, back to its essence.

Consequently, the first plan of research was made, to establish the influence of the type of cement on the behaviour of the respective hardened concrete subjected to extremely low temperature.

*Central Chemical Laboratory, Italcementi S. p. A., Bergamo, Italy.

Materials

Cements and Pozzolanas

As far as cements are concerned, it seems to be useful to point out the reasoning which led to choose, for this first investigation, pozzolanic cements rather than portland cements.

As everybody knows, the Italian pozzolanas, which constitute with the clinker the fundamental component of our pozzolanic cements, consist of a vitreous mass containing crystals (of feldspar, leucite, augite, and so on) and they had their origin, according to the most accepted hypotheses, in an explosive volcanic eruption, during which, the gases, when liberated pulverized the melted magma and impeded by the sudden cooling that followed, its complete crystallization. The evolution of dissolved gases produced a fine texture of canals or bubbles so that the consolidated vitreous particles have a high internal surface area. This particular physical state is called "aerogel", namely a gel in which the liquid phase has been replaced by a gas (3) (4).

With reference to the physical characteristics of pozzolanas and in particular to their constitutional porosity and to their large internal surface, it was deemed important to verify, whether the hardened concretes of pozzolanic cements could results more suitable than concretes of portland cement, to stand the mechanical stress arising when the free water turns into ice during the tests.

In conclusion, three groups of cements, all of industrial production, have been chosen:

I Group—consisting of No. 19 pozzolanic cements, Class 325 (plastic mortar according to the recommended project ISO 771–775) with an average percentage of pozzolana equal to 36%. These 19 cements were produced in as many works, and consequently with clinkers having different chemical composition. On the contrary, the types of pozzolana are three and their origin, as well as the corresponding values of their average porosity and internal surface are indicated in Table 1. The strengths at 20°C of the respective concretes for which we give the composition at the following point, vary in a range included between 270 and 390 kg/cm²;

Table 1. *Physical properties of the pozzolanas*

Denomination of the pozzolana and origin	Average porosity cm^3/g measured on 58 mm granules	Specific surface m^2/g measured on $< 200\ \mu m$
(BC) Bacoli (Campania)	0.3528	9.300
(BR) Barbarano (Lazio)	0.4090	10.500
(SL) Salone (Lazio)	0.0547	38.700

II Group—consisting of No. 11 cements, still of the pozzolanic type, Class 425, that is high strength cements. The average percentage of pozzolana of the qualities already described, is equal to 30%. The clinkers are included in the set of the first group. The strengths of concretes at 20°C vary between 380 and 450 kg/cm²;

III Group—consisting of No. 4 high strength portland cements, Class 425, which have given, in concrete, strengths included between 480 and 550 kg/cm².

Concretes

The cubes, having 10 cm of side, and 10 × 10 × 50 cm prisms were cast, settling by vibration concretes having the following compositions:

aggregate: of siliceous and calcareous nature consisting of sand and gravel after the Fuller's ideal curve with max 30 mm;
cement: of different types as already described, in the quantity of 300 kg/m³
w/c ratio: 0.5 (constant).

The concretes differed therefore with the difference of the cements.

After curing for two months in conditioned room at 20°C and 100% R. H. (fog), from the 10 × 10 × 50 cm prisms, specimens of the following dimensions were obtained by cutting: 4 × 4 × 16 cm and 2 × 4 × 25 cm. The curing in room has been protracted for 6 months and then the treatments and tests were started.

Experimental Procedures

The experimental procedures adopted at this first stage of the research have been simplified; in particular, the conditions of temperature and humidity, chosen for the treatment of the specimens, were as follows:

+100°C—in climatic cabinet until a constant weight is reached, in order to obtain specimens having the same % value of residual humidity;

+20°C—R.H. 85%—in climatic cabinet for 48

hours:

+10°C—R.H. 85% in climatic cabinet for 48 hours; at the end of this treatment the free water contained in the specimens is around an average value equal to 3.72% (see Table 2, forward);

−78°C—in thermostatic container in constant contact with dry ice for 48 hours;

−196°C—in thermostatic container, steadily immersed in liquid nitrogen, for 48 hours.

The compressive strength have been determined for each type of concrete and for each of the above mentioned conditions, on three cubic specimens having sides of 10 cm, as well as on the couples of pieces obtained after breakage by bending of three $4 \times 4 \times 16$ cm prisms, which as already said, had been previously obtained in their turn, by cutting, from $10 \times 10 \times 50$ cm prisms. Before the breakage by compression, care was taken to bring the pieces again to the pre-established temperature.

The dynamic Young's modulus was measured on three specimens, for each type of mix, in the dimensions of $2 \times 4 \times 25$ cm, using the flexural resonance method.

Moreover: on three specimens having the dimensions just given above and conveniently provided with pins, the linear variations for thermal contraction were executed by means of an apparatus equipped with a comparator having a sensibility of ± 5 μm.

Experimental Results

Table 2 groups the values of the strengths, shrinkage, and the Young's modulus of elasticity obtained on the basis of the tests already described. Some additional remarks are given on this subject.

Mechanical Strengths

a) The compressive strength are rising as the temperature of treatment falls, as it appears from the diagrams of Fig. 1, which were drawn with the average values for each group of cements.

It is to notice, that the increase in strength is higher for the first drop in the temperature (+20°C, −78°C), than for the second one (−78°C, −196°C). The pertinent ratios are diminishing as the initial strengths of concrete rise, owing to the fact that the increases remain pratically constant in each interval, independently from the initial strengths of the concrete.

In the case of bendings the test was made only for the greater drop in the temperature, obtaining trends corresponding to those of compression.

b) As the increases of strength of the concretes due to the fall in temperature result to be pratically constant, at least in each of the two intervals taken into consideration, and as it is the case of concretes that differ only with the characteristics of the cement, the deduction is that the type of cement does not influence the trend of the phenomenon which is being considered. In particular, also the type of pozzolana as well as its quantity in the pozzolanic cement do not modify the above mentioned conclusion. The only thing that could be said is, that the pozzolana of Salone, which has an average porosity of one time and a half lower and a specific surface B. E. T., almost four times higher than those of the remaining two types, causes increases tending to be inferior to those that may be found with the pozzolanas of Bacoli and of Barbarano, which result to be less finely porous.

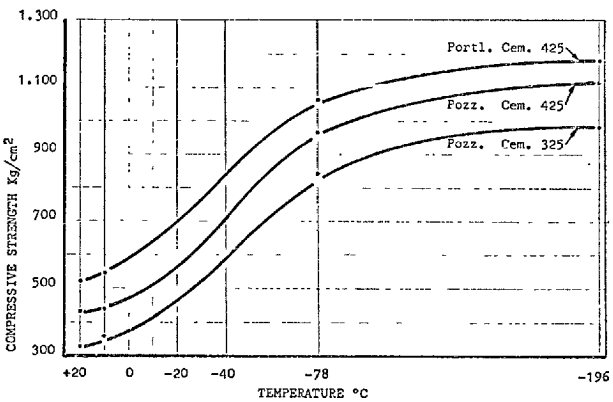

Fig. 1. *Relation between compressive strength of concretes with different types of cements and treatment temperature*

c) Independently from the group of cements, the set of the values of the compressive and bending strengths of the concretes at +20°C can be statistically put in correlation with the corresponding set of values obtained at −78°C and −196°C. This constitutes a further confirmation, in quantity terms, of the fact that the increases are connected with the values of the initial strengths of the concretes and of the fact that, surely such increases do not depend, at least in the sense of a connection of significant probability

Tabel 2. *Concretes with different types of cements—physical characteristics*

Cements	No.	Pozzolana type	%	Concrete cubes 10 × 10 × 10 cm: Compressive strengths kg/cm² +20°C	+10°C	−78°C	−196°C	Concrete prisms 4 × 4 × 16 cm: Flexural strengths kg/cm² +20°C	−196°C	H_2O free %	Concrete prisms 4 × 4 × 25 cm: Dynamic Young's modulus kg/cm² +20°C	−196°C	+20°C	Thermal contraction μm/m from +20°C to −196°C
1st Group pozzolanic cements type 325	1	BC	31	273	267	747	802	58.5	95.5	3.25	—	—	—	—
	2	BC	32	285	353	780	871	71.8	137.7	3.67	—	—	—	—
	3	SL	33	293	335	863	945	81.7	120.8	4.30	—	—	—	—
	4	SL	36	294	363	690	906	55.–	112.4	3.32	356.000	415.000	345.000	−1.148	+30
	5	BC	38	304	345	892	1006	56.4	134.9	3.97	—	—	—	—	—
	6	BR	38	305	337	784	1074	66.–	174.2	3.82	—	—	—	—	—
	7	BR	40	314	333	740	885	74.9	92.7	3.60	346.000	421.000	339.000	−1.397	−36
	8	BR	40	316	345	773	893	58.–	151.7	3.95	—	—	—	—	—
	9	BC	38	319	322	828	954	64.8	146.1	3.90	—	—	—	—	—
	10	BC	35	320	330	864	990	60.4	123.6	3.27	353.000	438.000	330.000	−1.430	−150
	11	SL	38	320	347	794	978	56.4	179.8	3.88	—	—	—	—	—
	12	BC	32	324	349	859	1002	69.3	143.3	2.51	—	—	—	—	—
	13	BC	35	322	371	866	1000	65.3	165.8	3.59	338.000	422.000	320.000	−1.282	−96
	14	BC	35	333	340	926	1095	67.4	174.2	N.D.	—	—	—	—	—
	15	BC	35	334	333	953	1033	N.D.	179.8	N.D.	374.000	441.000	346.000	−1.170	−100
	16	BR	40	354	383	920	1106	70.1	205.1	N.D.	—	—	—	—	—
	17	BC	35	367	375	943	1161	90.6	154.6	4.10	358.000	431.000	335.000	−1.338	−72
	18	BR	38	387	385	926	1034	70.–	134.9	N.D.	316.000	336.000	335.000	−1.226	−92
	19	SL	38	—	—	—	—	—	—	—	335.000	394.000	318.000	−1.214	+30
$\bar{X}$			36.1	320.2	345.2	841.6	985.3	66.9	146.–	3.65	347.000	412.250	333.500	−1.276	—
C.V.				8.84	7.80	9.29	9.38	14.26	20.91	12.33					
2nd Group pozzolanic cements type 425	1	SL	30	375	416	837	987	60.8	112.4	3.97	—	—	—	—	—
	2	BC	32	390	388	1023	1161	87.5	165.8	3.95	—	—	—	—	—
	3	SL	29	414	379	791	909	68.1	137.7	3.60	—	—	—	—	—
	4	BC	30	417	420	873	1092	71.3	129.3	3.26	—	—	—	—	—
	5	BR	30	417	444	957	1153	70.7	154.6	4.47	—	—	—	—	—
	6	BC	27	423	444	1128	1222	79.6	182.7	4.18	—	—	—	—	—
	7	BR	32	423	439	1026	1041	76.5	165.8	4.42	—	—	—	—	—
	8	BC	30	430	426	888	1073	71.7	179.8	3.73	—	—	—	—	—
	9	BC	30	443	403	931	1024	65.–	115.2	3.62	—	—	—	—	—
	10	BC	30	444	449	1118	1337	92.–	241.7	4.17	—	—	—	—	—
	11	BC	27	449	490	1065	1302	75.3	146.1	4.56	—	—	—	—	—
$\bar{X}$			29.7	420.5	427.1	967.–	1118.3	74.4	157.4	3.99	—	—	—	—	—
C.V.				5.34	7.31	11.76	11.79	12.45	23.35	10.28	—	—	—	—	—
3rd Group portland cement type 425	1			482	482	1051	1173	86.3	168.6	3.71	378.000	400.000	358.000	−1.000	+20
	2			515	512	1034	1041	82.1	151.7	3.47	—	—	—	—	—
	3			515	566	990	1163	93.6	174.2	3.31	407.000	474.000	390.000	−1.396	+4
	4			554	596	1170	1347	86.8	134.9	3.54	—	—	—	—	—
	5			—	—	—	—	—	—	—	377.000	446.000	367.000	−1.258	−34
$\bar{X}$				516.5	539.–	1061.3	1181.–	87.2	157.4	3.51	387.333	440.000	371.666	−1.218	—
C.V.				5.70	9.55	7.25	10.66	5.46	11.28	4.56	—	—	—	—	—

on the type of cement and therefore on its composition; and they also do not depend on its components: clinker and pozzolana chosen of different origin and having different chemical and mineralogical characteristics.

Young's Modulus of Elasticity

The dynamic modulus of elasticity that, as everybody knows, is bound to the mechanical strengths of the concrete, shows as increase in value included between 14–19% as the temperature is decreased from +20°C to −196°C. By returning to the normal temperature, values are found, on average, slightly lower than the values measured at the beginning.

Thermal Contraction

The thermal contraction measured for the greatest drop in the temperature (+20°C, −196°C) is around 1250 μm/m in the concretes with pozzolanic cements as well as in those with portland cements. By returning to the normal temperature, the presence of a residual deformation (hysteresis) is revealed, sometimes of positive sign and sometimes of negative sign.

Thermal Cycles

It appeared to be useful to investigate already at

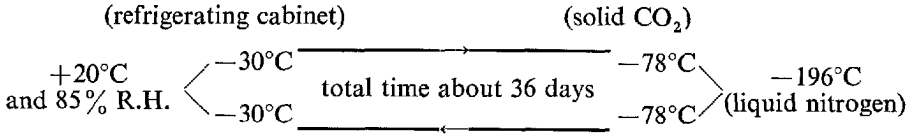

this first stage of the research, about the behaviour of concretes after they have been submitted to the repetition, for ten times, of the thermal cycle, the scheme of which is given hereunder:

The time of stay of the specimens at each stage of the cycle was varying, owing to technical necessity, from 5 to 7 days; this period of time was of course more than enough to obtain the equilibrium of temperature; the passage from a temperature value to the other one took place suddenly.

The concretes on which the investigation has begun, after two months of curing in a room at +20°C and 100% R. H. and after that they had been put subsequently in equilibrium at +20°C and 85% R. H., had the composition already described and different for the type of their cement: nine of them have been made with normal strength pozzolanic cements (type 325) and three were made with high strength portland cements (type 425).

Strengths

The Table 3, that follows, shows the single values and the average values of compressive and bending strength determined on the respective types of concrete on completion of the tenth cycle. For the comparison, also the strengths are shown, which were obtained by testing twin specimens, not submitted however to the cyclic treatments and that during the whole corresponding period have been cured in conditioned room.

The results obtained, and above all the comparison between the two series of data prove, that the concretes have not suffered a significant degradation, as a consequence of the cyclic treatment. It may be stated in addition that, on the 10 × 10 cm cubes, after they had been subjected to the cycles, an increase may be found of about 6% in the strengths, in comparison with the strengths measured on the untreated specimens. On the contrary, the bending strength determined on specimens having a thinner section: 4 × 4 × 16 cm, have likewise a reduction of about 14%. It must be taken into account on the other hand, that for all the time the specimens remain at low or very low temperature (about 80% of the total employed for the cycles) it is not possible to think that the strengths may increase, contrary to what is to be expected for specimens cured in a normal ambient. This last comment is not valid in the case it is deemed

Table 3. *Strengths of concretes submitted to cycles of freezing and thawing*

Cements	No.	Pozzolana type %	Concrete cubes 10 × 10 × 10 cm — Compressive strengths kg/cm²		Concrete prisms 4 × 4 × 16 cm — Flexural strengths kg/cm²	
			Specimens submitted to 10 cycles from +20°C to −196°C	Specimens kept in the conditioned room to 20°C and 85%R.H. for the same period	Specimens submitted to 10 cycles from +20°C to −196°C	Specimens kept in the conditioned room to −196°C and 85%R.H. for the same period
Pozzolaniccements type 325	1	BC 35	344	325	34.4	52.2
	2	BC 35	387	406	51.5	50.8
	3	BC 35	388	353	36.–	46.3
	4	BC 35	391	417	60.8	67.1
	5	BR 38	396	380	60.4	56.2
	6	SL 35	408	402	72.8	62.2
	7	SL 36	434	413	48.–	66.5
	8	BR 35	441	429	58.5	66.4
	9	BR 40	446	402	57.3	68.6
$\bar{X}$			403.9	391.9	53.3	60.7
Portland cement type 425	1		526	441	46.8	77.–
	2		542	527	62.2	76.5
	3		619	511	87.5	87.–
$\bar{X}$			562.3	493.–	65.5	80.2
$\bar{X}$ general			443.5	417.2	56.4	65.6

that it is possible to justify increases or anyhow not excessive decreases in strength in connection with the effect called "hibernation", consisting of the fact that a concrete cured for some time in an ambient with a temperature lower than normal, when brought again in a normal ambient shows, at the end, higher strengths than a concrete cured uninterruptedly in a normal ambient.

Finally it is to mention that on completion of the cyclic tests and before breakage tests were carried on, it was not remarked in spite of a scrupulous visual inspection any deformation, cracks, breakage of edges or any other damage on the surfaces of the specimens.

Trend of the Young's Modulus of Elasticity

The dynamic modulus of elasticity has been measured at the beginning (+20°C) and half-way through each cycle (−196°C); the average trends, in connection with the number of cycles, are represented

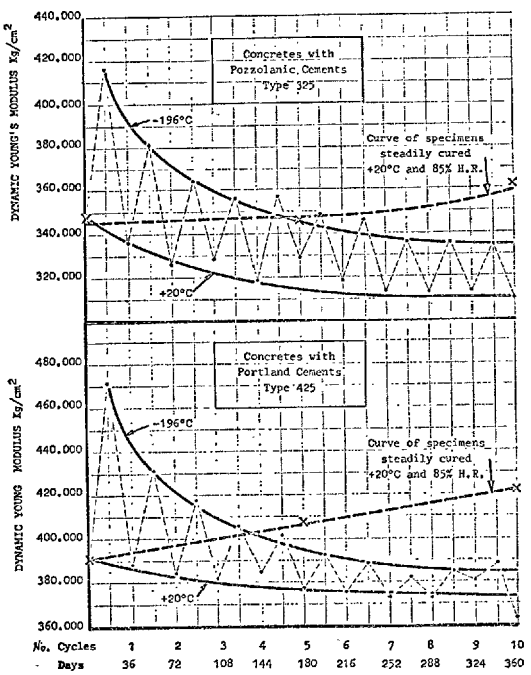

Fig. 2. *Trend of Young's modulus with cycles of freezing and thawing*

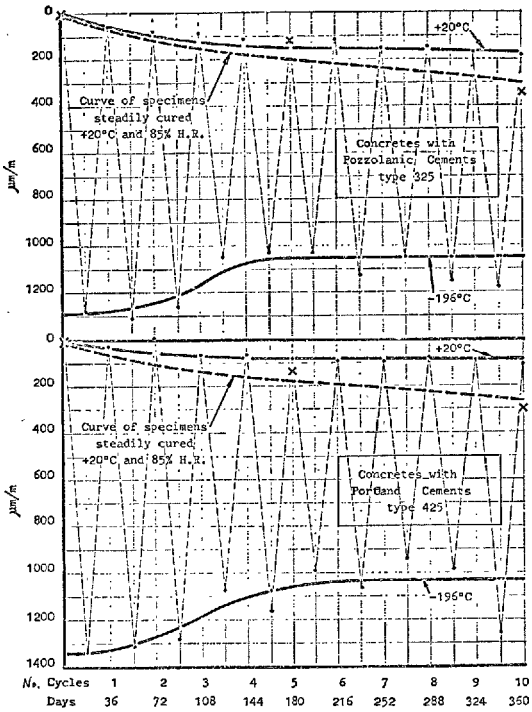

Fig. 3. *Trend of thermal contraction with cycles of freezing and thawing*

respectively for the group of pozzolanic cements and the group of portland cements, in the diagrams of Fig. 2.

In conclusion, on the specimens submitted to cycles it has been observed, when they were each time in equilibrium with the normal conditions, that there was a progressive slow decrease of the modulus of elasticity, whereas on the specimens cured steadily at +20°C and 85% R. H., it has been verified on the contrary (see again Fig. 2), in a corresponding time, an equally slow increase: on an average equal, in absolute value, to the above mentioned decrease.

The modulus of elasticity measured on the specimens, when half-way through each cycle they were in equilibrium with the temperature of −196°C, is rapidly decreasing up to the fourth or fifth cycle, and then it decreases very slowly for the subsequent cycles, until it reaches a trend parallel to the one of the +20°C.

Trend of the Contraction

The trends are shown on the diagrams of Fig. 3.

About the specimens subject to cycles, at the moment they were at +20°C, is noted a progressive increase of the contraction, but this increase is inferior to the one that can be measured on the specimens which have been cured for a corresponding time in a conditioned room.

It is therefore evident that the linear variations measured on the specimens brought again to a normal temperature are not ensuing only from the cyclic treatment, but they are the result due to the addition on another effect, in spite of the handicap constitution by the curing at low temperature, that is, the effect of hygrometric shrinkage still acting due to the relatively limited age of the specimens (2 months) at the beginning of the test.

The measurements taken at −196°C show, going towards the third and fourth cycle, a reduction of the contraction which seems then, to fix itself, although with a great dispersion of values, on a trend which remains parallel to the one of the +20°C.

Second Part

What we reported in the first part confirmed that the cement concrete is a material fit for being usefully

employed also when it is brought down to extremely low temperatures. In particular we established:

—that the type of cement, as regards the nature both of the clinker of origin and of the pozzolana as a possible component of the mix, does not influence the behaviour of the concrete at the very low temperatures;

—that the concrete can support, without any degradation, the effects of repeated cycles of freezing down to temperatures reaching −196°C and warming to room temperature.

Consequently we went on with our research, investigating on concretes with different characteristics. So we made plans for additional types of tests, as well as refining the testing procedures, and explain the causes of its characteristic trend.

Materials

Cements

Six types of cement have been taken into consideration and their characteristics are shown in Table 4, hereunder (the numbers correspond to those of Table 2).

It is to point that the cements, within each group, have mechanical strength comparable with one another. The clinkers of origin result, on the contrary to have rather different mineralogical compositions, particularly as regards the C_3A contents; the pozzolanas are present in the three types already described.

Table 4. *Properties of the cements*

Cements	No.	Specific surface Blaine cm²/g	Mineralogic composition of respective clinkers				Strengths of plastic mortars kg/cm² at 28 days, 20°C	
			C_2S	C_3S	C_3A	C_4AF	flexion	compression
Pozzolanic cements type 325	4	3970	19.4	60.7	4.4	11.4	64	327
	7	4820	18.9	56.4	13.1	7.5	60	365
	17	4520	20.9	54.8	9.4	10.2	63	353
	18	4670	24.8	52.5	10.6	6.9	65	350
Portland cements type 425	1	3700	15.5	62.0	0.8	14.1	83	485
	3	3790	23.5	53.6	9.3	9.8	82	470

Aggregates

Cubes having 10 cm of side and 4 × 4 × 16 cm prisms were cut from blocks of 5 mineralogically different types of aggregates. Table 5 indicates their main mineralogical and physical characteristics.

The materials in question can be considered as non porous, that is very compact, and having consequently a very reduced possibility of absorbing water.

Tests were made also with light aggregates, that is, with granular roundish products, obtained by expansion, through thermic treatment of schistous clays.

Such aggregates (complying with ASTM C330) have a density included between 600 kg/m³ for the size 0–3 mm and 450 kg/m³ for the max. size 8–15 mm.

Table 5. *Physical properties of the aggregates*

Type of aggregate	Petrographic features		Density g/cm³	Cumulative pore volume cm³/g	Adsorbed water content % by wt	Strength tests kg/cm² at 20°C	
	Type of rock-texture	Mineralogic composition				flex	compress
Limestone	Sedimentary microcrystalline with light diagenetical alteration	calcite	2.684	0.0009	0.16	180	1870
Granite	Igneous-granitic	feldspars, amphiboles	3.056	0.0015	0.75	200	1930
Porphyry	Hypoabyssal microgranulatic	feldspars, quartz, micas	2.665	0.0009	0.46	295	2000
Basalt	Volcanic-ophitic	feldspars, augite, olivine	2.885	0.0002	0.30	450	3230
Silica	Sedimentary microgranulatic	quartz, with amorphous cement	2.622	0.0082	0.72	The material was crumbly and no strength test was allowed	

Concretes

$10 \times 10 \times 50$ cm prisms were made for each of the 6 types of aggregate, employing 6 types of cement. The composition of concretes was:

aggregate: obtained by means of crushing and then subdivided by a sieve, in four granulometric sizes, in order to obtain the Fuller's continuous line with max. 20 mm;

cement: quantity: 300 kg/m³;

water: w/c ratio: 0.5 (constant).

We made a set of concretes differentiated by the type of aggregate, which are putting themselves on two classes of strength, considering that as already said, the cements, in their respective type show pratically equal strengths.

After 5–6 months of curing in conditioned room at 20°C and 100% R. H. (fog) from the $10 \times 10 \times 50$ cm specimens, cubes of 10 cm of side and prisms having the dimensions $4 \times 4 \times 16$ and $2 \times 4 \times 25$ cm were obtained by cutting. Before starting the treatments and the tests, we protracted the curing of the specimens in that room for another year, owing to necessities of program.

Two types of light concrete were made with the aggregates of expanded clay: one of them consisting of light aggregate only (divided into three sizes) and the other consisting of light aggregate completed by a certain quantity of fine siliceous sand, in order to make it more compact.

The mix proportions of the dry aggregates in % of weight, are as follows:

	Concrete "A"	Concrete "B"
sand 0.4–0.6	—	22
aggregate 0–3	45	35
aggregate 3–8	30	23
aggregate 8–15	25	20

The quantity of cement (portland type 425) has been 300 kg/m³, while the w/c ratio was 0.66 and 0.50 respectively for concrete "A" and concrete "B" to obtain mixes equally workable.

As regards the curing and the shape of the specimens, all we said for the normal concretes is confirmed.

The specific weights at the moment of breakage resulted to be: 1100–1150 kg/m³ and 1300–1350 kg/m³ respectively for the concretes "A" and "B". Considering the object of this work, it is interesting to point out that, whereas for the concretes containing the different aggregates taken into consideration, having anyhow a normal specific weight, the coefficient of thermal conductivity λ is ranging around 2.0 kcal/m, h, °C (oven dry specimens), for the concretes of expanded clay it may be mentioned a value about four times lower, that is $\lambda = 0.5$ kcal/m, h, °C (oven dry specimens).

Plastic Mortar

In order to reduce the effects due to the variability of the peculiar characteristics of materials, and in particular of concretes, we decided to test also specimens of plastic mortar, the mix of which results to be evidently more homogeneous than the mix of a concrete. In this way we intended to use an additional means to improve the research in particular situations and particular test, in the case the experimental trends could appear doubtful or at least not in accordance with the expectation.

Consequently homogeneous sets of $4 \times 4 \times 16$ cm specimens were made in plastic mortar, using the same portland cement type 425. Sets of specimens in the figure of "eight" were prepared with the same type of mortar, suitable for breakage by a simple tensile stress.

Equipment and Test Conditions

For the execution of the second part of the work, the most important apparatus employed in addition to those already mentioned, consisted of:

—*a thermostatic unit* for low temperatures consisting of No. 3 boxes. The temperature of the box No. 1 may be regulated between +20 and −100°C. The temperature of the box No. 2 may range down to −180°C. The box No. 3, made in cupper, consists of a hollow space, where is possible the storage of liquid nitrogen, so to fix the temperature at −196°C. The sensitivity of regulation of the temperature, within the respective fields in the three boxes is ±3°C. The real test temperature was measured by means of a thermometric feeler, sensitive at ±0.5°C, immersed in a witness specimen having physical and geometrical characteristics similar to those of the specimens on which the investigation was made.

—*an equipment for shock tests:* at the first we used an impact machine similar to the one used for testing

toughness of steels. The results were unsatisfactory and it seemed that this might depend on the technique of the test. Tests of shock strength, were therefore carried out using another equipment (8) (9). The apparatus consists of a frame on which a hammer of 25 kg, with a terminal of hemispherical shape, is free to fall from a changeable height, striking the upper face of the cubic specimen.

The height of fall increased each time by 1–2 cm until the specimen submitted to this test breaks.

The above mentioned test has been made for each value of temperature, on 3 specimens: from the first one we obtained the indication of the most probable height of fall to cause breakage; on the remaining two specimens the most approximate value of the height of breakage was determined and confirmed, by making a reduced number of shocks in order to avoid damage of the specimen.

The breakage by shock is considered to have taken place when the falling hammer does no more rebound on the specimen. Planes of breakage subdivide the specimen into two or more prisms.

—*we covered the specimens* with layers of expanded polystyrene in order to avoid losses of temperature. The time necessary to carry out the tests varied from 30 to 90 seconds. The departures of temperature at the surface of the specimen could be contained around 0.5–2.5°C under the worst conditions.

—*the specimens submitted* to special curing in order to maintain a pre-established degree of humidity, were jacketed with polyethylene film.

—*the specimens were maintained* in the box at test temperature for about 24 hours; this time has proved to be more than sufficient to reach the equilibrium value.

Test Results

Mechanical Strength

The aggregates, as the temperature decreases, show increases both in bending and in compressive strength as indicated by the diagrams of Fig. 4.

The trend of the curves is regular enough, taking into account the difficulty to find samples of stones free from defects, like microcracks. We don't indicate the bending strengths of the different aggregates in the range of temperature −60 and −80°C. The diagrams would have announced, in this range, a particularly irregular trend. The compressive strength shows, in correspondence, except for the basalt, a regular increasing trend also within that field.

The concretes, made with different types of aggregates show both at compression and at bending strength trends, on the average, an increase (about 45% at compression and 50% at bending, changing from +20 to −180°C) as the temperature is lowered (see Fig. 5).

We find a certain dependence, that we cannot call a correlation, between the strength of concretes and the corresponding aggregates, on the contrary, we note a clear dependence between strengths of concretes and the relative cements. We point out an interesting trend in bending of concretes: there are some irregularities, and exactly a decrease in strength, when a temperature about −50 ~ −60°C is reached. We note again an increase, after the minimum correspondence to −80 ~ −90°C has been reached.

We cured for 3 years in fog-room a set of concrete samples. These were made with calcareous aggregate and high ratio in cement (450 kg/m³); this is a rapid hardening and high strength cement. Half of them were submitted to a drying treatment in a stove at

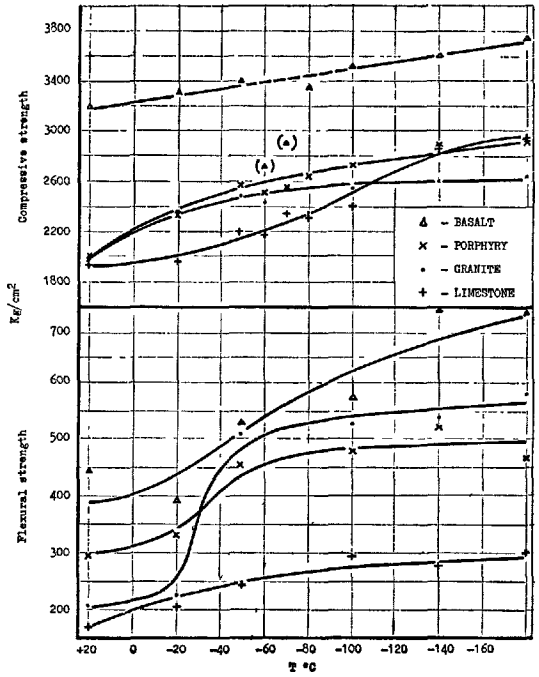

Fig. 4. *Relation between strength of stone and temperature of treatment*

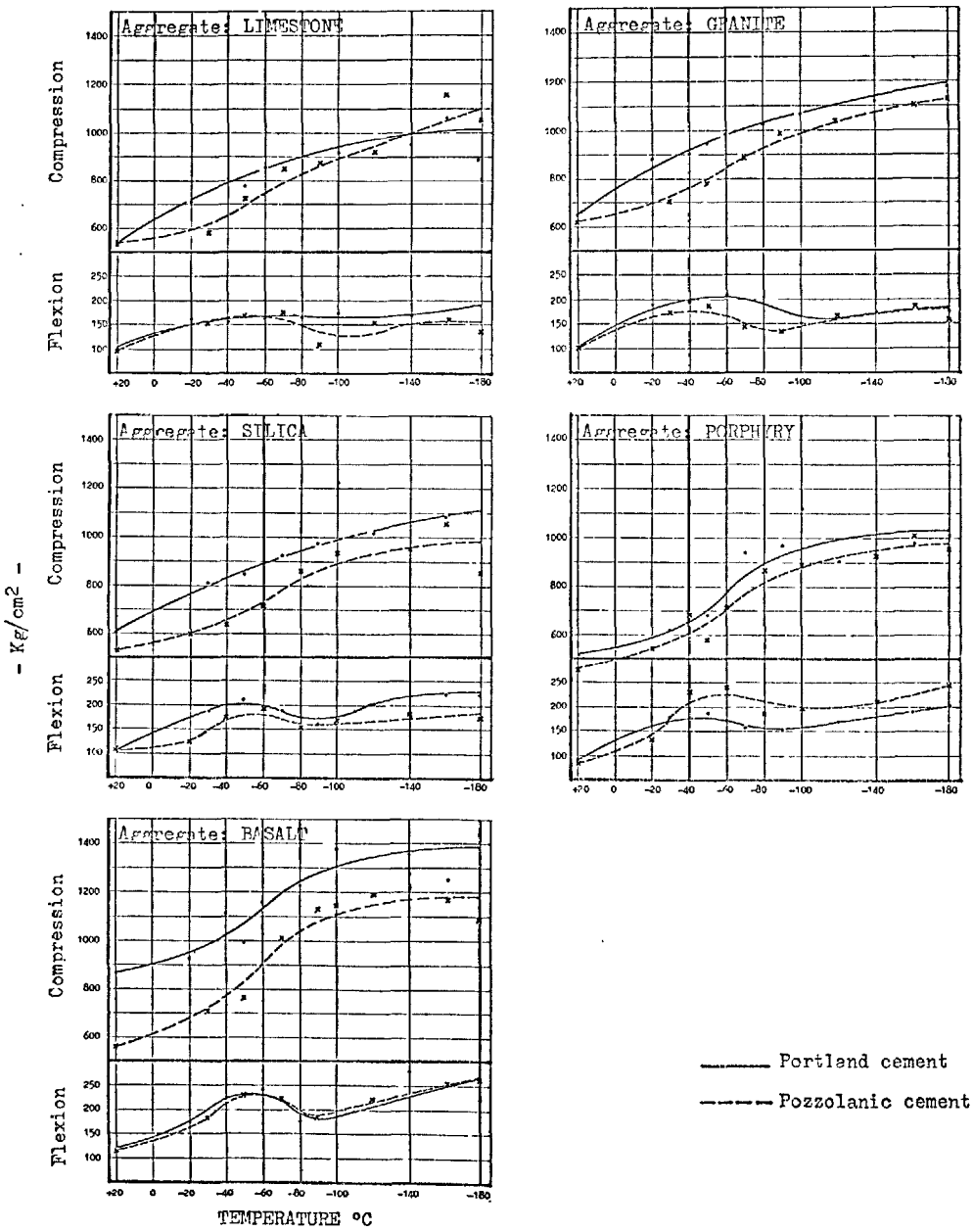

Fig. 5. *Strengths of concretes made with different aggregates and two types of cement at various temperatures*

110°C. Then they were treated together with the specimens at the moist state, at low temperatures. The results of the compression strengths are shown in the diagram of Fig. 6.

In this diagram is put in evidence the influence of the quantity of the free water contained in the concrete on the trend of the strength as the temperature decreases.

We notice increases of strength of concretes containing expanded clay, previously cured in fog-room, when the temperature decreases (see Fig. 7).

Plastic Mortar

The availability of a large number of specimens having homogeneous characteristics gave us the possibility to carry out a particularized investigation on the trend of the strengths. In this test, we put down

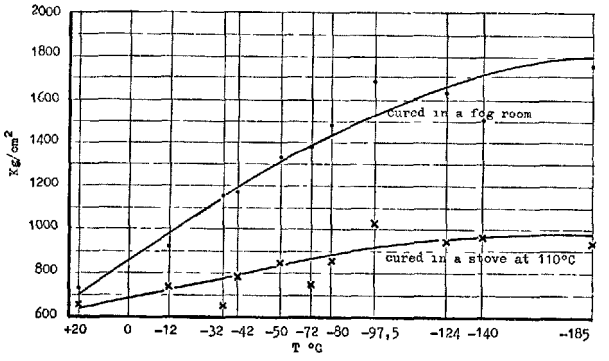

Fig. 6. *Relation between compressive strength of concrete and temperature of treatment*

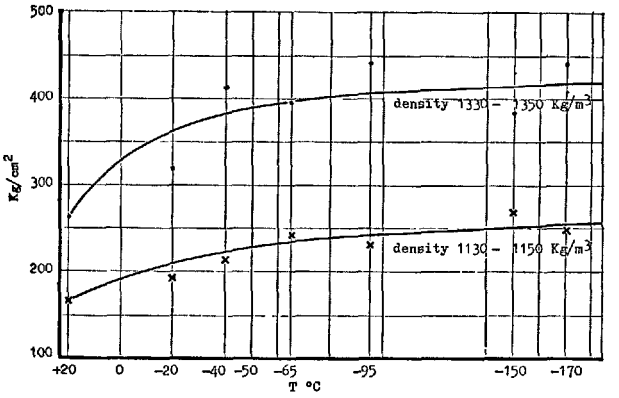

Fig. 7. *Relation between compressive strength of concrete made with expanded clay and temperature of treatment*

the temperature 5°C every time. The diagrams of Fig. 8 indicate the trends of tensile, bending and compressive strength of specimens cured in water up to the moment of the test. In the same diagram we indicate the strength found on specimens dried in a stove at 110°C. It is evident that the presence of free water in the specimen is necessary for increasing strength.

We notice, as it is evident in the Figures, an inflection in every types of strength of the saturated specimens in the range of temperature from −50°C to −100°C. We have hatched in Fig. 8 the area included between the interpolated line and that of the experimental values to lay particular stress to the phenomena.

Shock Strength

The results with the impact machine on samples made with plastic mortar have been very dispersed and we don't think opportune to relate them. The apparatus provided with a beating hammer has been

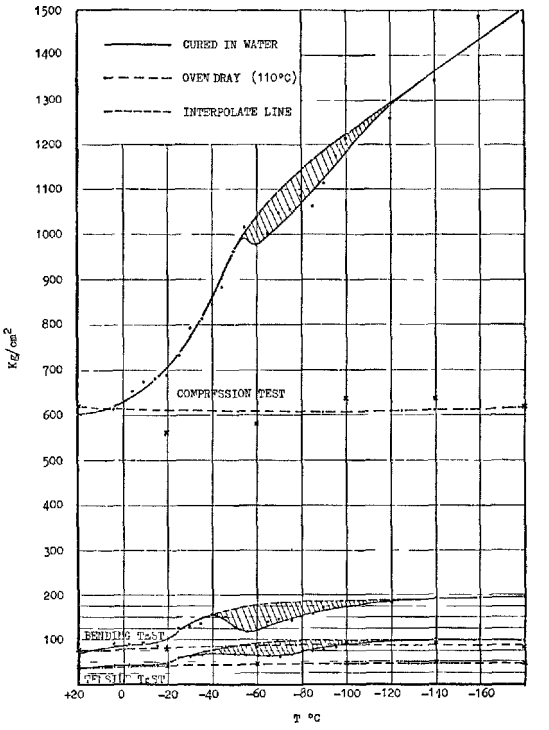

Fig. 8. *Relation between strength of plastic mortar and treatment temperature*

used on shock tests on concrete made with various aggregates. Fig. 9 shows the respective diagrams.

The procedure of the test justifies the dispersion of results. We think the shock strength of concretes, brought to very low temperature, to be strongly bound to their behaviour at bending and compression.

Dimensional Variations due to Thermic Effect

The investigation about thermic contraction, very characteristic for the materials that now we consider, has been made by some authors (2) (10) (11), but they did not include very low temperatures, and different types of cement mixes. Our results on testing lead to find some anomalies in behaviour.

Thermic Contraction

Aggregates

The curves representing the trend of linear thermal contractions are parabolic (see Fig. 10a), and consequently the respective contraction coefficient changes linearly with the temperature.

The respective average values in the field from +20 to −180°C are shown hereinafter in Table 6,

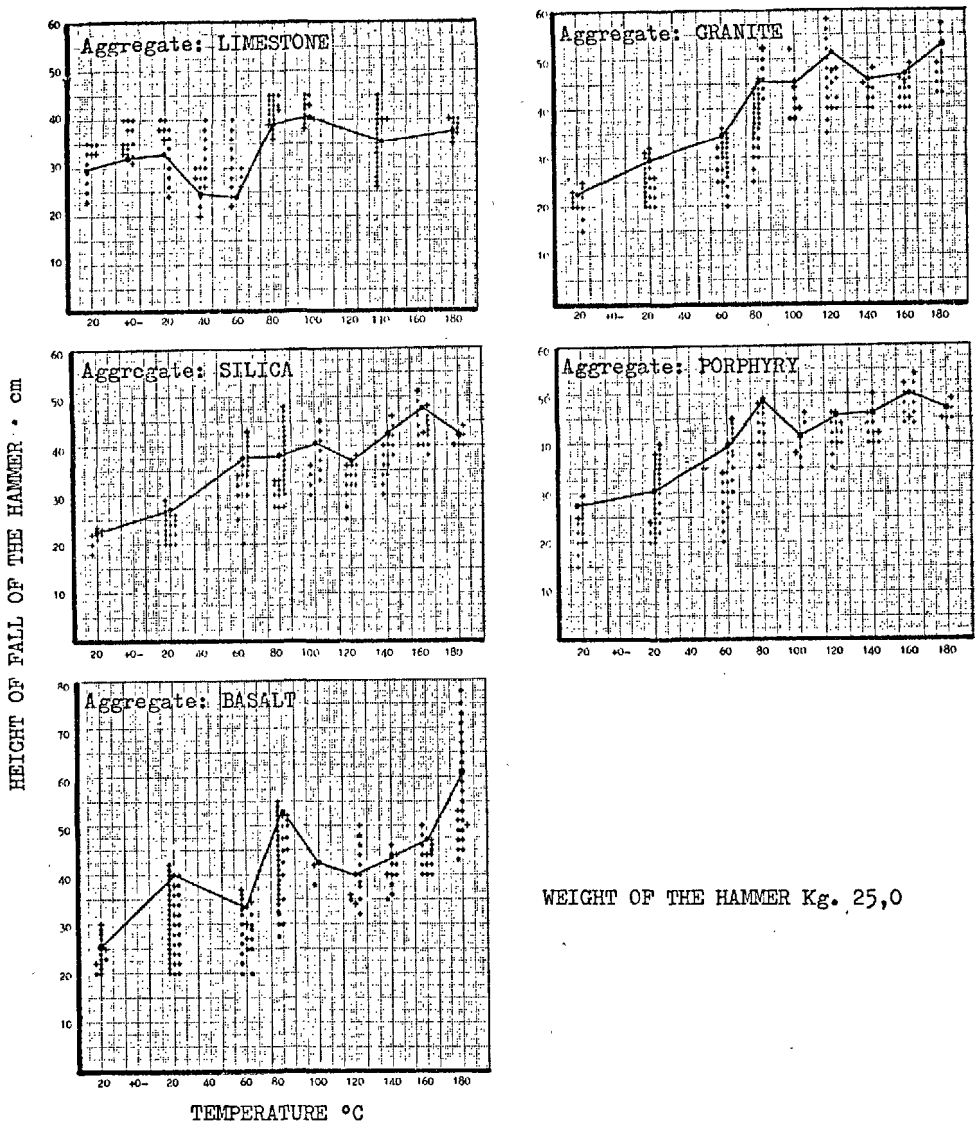

Fig. 9. *Relation between shock strength of concretes with different types of aggregates and treatment temperature*

Table 6. *Thermal contraction ($\cdot 10^{-6}/°C$) of aggregates and respective concretes for $0 < T < -160°C$*

	Aggregate			Concrete		
	$\lambda = \lambda(T)$	λ T = 0°C	λ T = −160°C	$\lambda = \lambda(T)$	λ T = 0°C	λ T = −160°C
Limestone	5.224 + 0.030T	5.224	0.424	6.901 + 0.036T	6.901	1.141
Granite	4.395 + 0.018T	4.395	1.515	5.195 + 0.028T	5.195	0.715
Porphyry	8.740 + 0.026T	8.740	4.580	8.875 + 0.030T	8.875	4.075
Basalt	8.480 + 0.026T	8.480	4.320	9.571 + 0.032T	9.571	4.451

On account of their very low coefficient of water imbibition, negligible are the differences between the linear deformations of specimens cured in a humid and in a dry room.

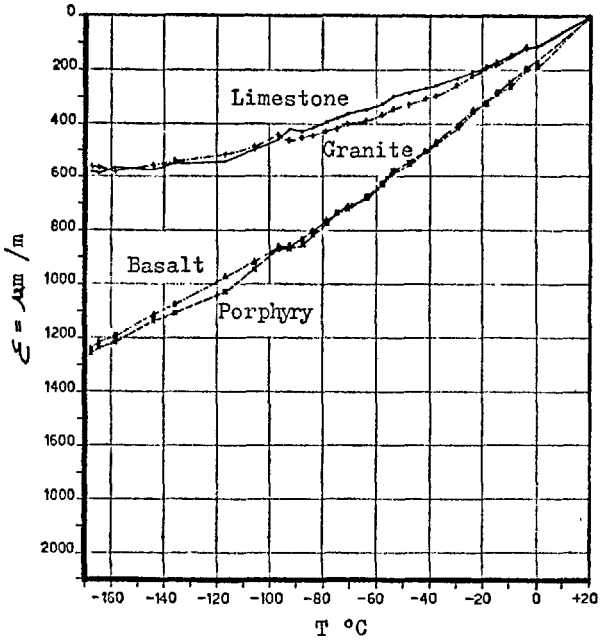

Fig. 10a. *Linear deformations of aggregates*

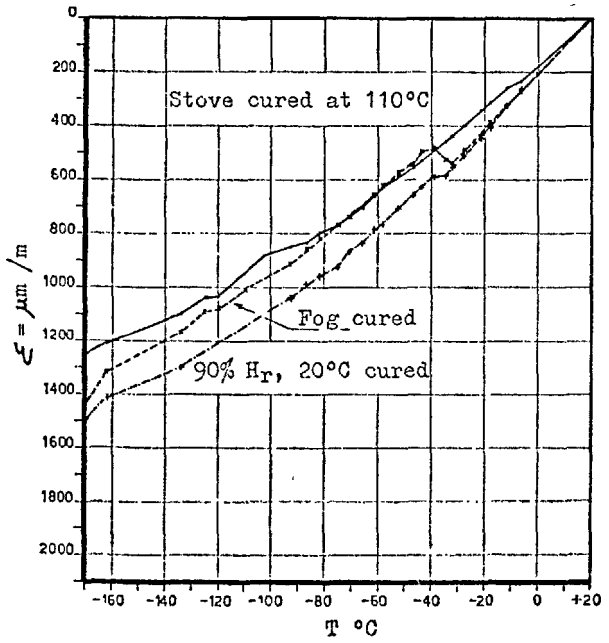

Fig.10b. *Linear deformations of concrete made with porphyric aggregate*

Concretes

Before carrying out tests, some specimens were dried in a stove at 110°C, others were stored in a room almost saturated with water (90% R.H., 20°C), others were stored in a fog-room (20°C).

The thermic contraction of the dried concretes has a regular trend and the respective average shrinkage coefficients are indicated in Table 6.

The specimens cured at 90% R. H., 20°C, shrink since the beginning more than the dried specimens and go on, with the exception of a slight interruption at about −37°C, with a regular trend. In Fig. 10b it is shown the trend of the concrete made with porphyritic aggregate.

The specimens stored in a fog-room, and therefore saturated with water, shrink at first as much as those which were brought in equilibrium at a humidity of 90%. But at a little below −10°C, their curve deviate upwards in comparison with the curve of 90%, at first slightly, then rapidly, at a little below the temperature of −30°C, owing to a rather sudden expansion, the curve continues with a variable trend till −60°C ~ −65°C, and then puts itself, till the end, along a line parallel to the line of the non-saturated samples.

Paste and Mortar

The dried paste takes a trend of contraction almost rectilineal. If it is moist, the average coefficient of shrinkage is greater and it reaches $19.6 \cdot 10^{-6}$/°C, in comparison with the $10 \cdot 10^{-6}$/°C, reached when it is dry. The phenomenon of expansion is noticed also for plastic mortar, as found for the paste, when the specimen had been stored in a room having a humidity $\geqslant 60 \sim 70\%$ R. H. (20°C). In Fig. 11a, the curves refer respectively to the specimens immersed in water, cured in a room having 90% of R. H., 20°C and cured in a fog-room.

The effect of expansion becomes stronger when passing from a type of curing to the other one as the specimen absorbs more water, or is able to fill those porosities on which the expansion is depending. The filling of porosities is more full in moist atmosphere rather than in water.

The curves in Fig. 11b which correspond to specimens dried at 110°C, cured in rooms having 22 and 30% of R. H., 20°C, confirm by their trend that only the presence of free water can cause the expansion in question.

The experimental results show concordantly that the specimens previously dried, contract less than the corresponding moist specimens as the temperature decreases, from the beginning of the test. On the first ones the test is started after the samples have already undergone the shrinkage, characteristic of the loss of humidity, ensuing the drying treatment. The changes in length, continuously measured on them, are exclusively due to contraction on account of the thermic effect.

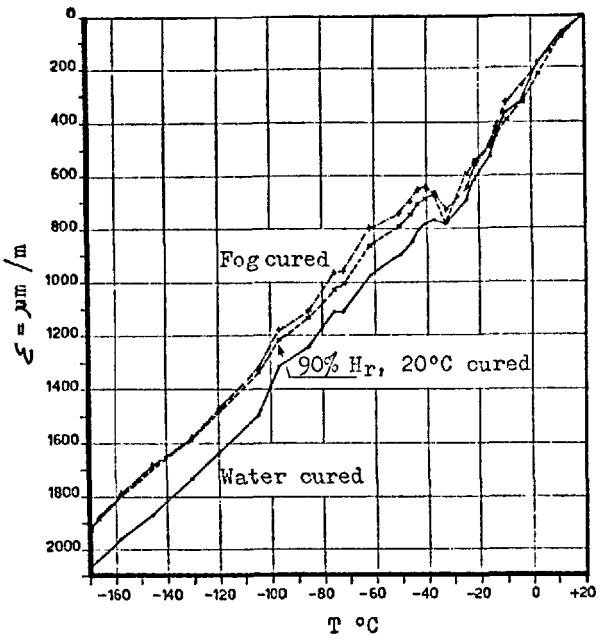

(a)

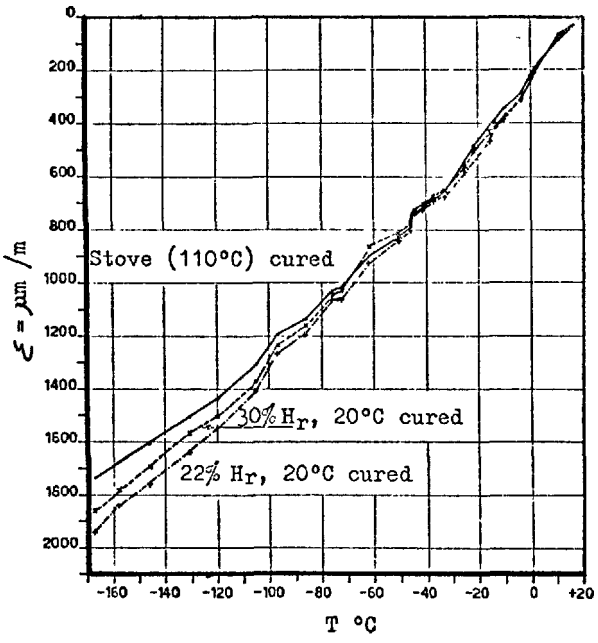

(b)

Fig. 11. *Linear deformations of mortars*

On the moist specimens, there is the superimposition of the thermic contraction on the hygrometric shrinkage. The nature of this shrinkage is quite different from the one due to the evaporation of the free water.

Table 7. *Thermic contraction of ice*

Temper. °C	μm/m	Temper. °C	μm/m
−25	673	−65	2248
−30	1043	−70	2371
−35	1273	−75	2584
−40	1523	−80	2745
−45	1554	−85	2892
−50	1636	−90	2052
−55	1839	−95	3222
−60	2104		

In a cement paste the freezing of the free water takes place at first in the coarsest porosities, which are not, in general, at critical filling, so it does not arise an expansion of the mass. At the same time, some additional water migrates from the finer, completely filled porosities, towards the coarsest ones. This water freezes, in its turn. The capillaries undergo, thus, a loss of water, and consequently a hygrometric shrinkage arises.

As the temperature decreases more and more, also the water contained in the capillaries freezes (about −30°C). As this temperature we observe stopping of the shrinkage and the appearance of the sudden expansion; when all the free water has frozen (about −70°C) the contraction continues as the thermic effect.

The Water-Ice System

Owing to the fundamental influence of water and ice on the appearance and trend of the phenomena under consideration, we wanted to measure the coefficient of contraction of ice. The results, which are in good accordance with those of the literature (12), are shown in Table 7.

In Fig. 12 it is also shown the trend of the specific volume of the water-ice system.

Hysteresis Curves

Concretes and Mortars

Specimens of these materials containing different quantities of humidity, have been submitted to cooling and warming cycles and their respective variations in length were observed.

Fig. 13 indicates the trends referring to concretes submitted for three times consecutively, without any interval, to changes in temperature with start from +20°C down to −150°C and vice-versa. The fog cured specimens show a very clear hysteresis effect; such an effect is very little noticeable on specimens having 90% of R. H. and it is pratically inexistent on specimens dried at 110°C.

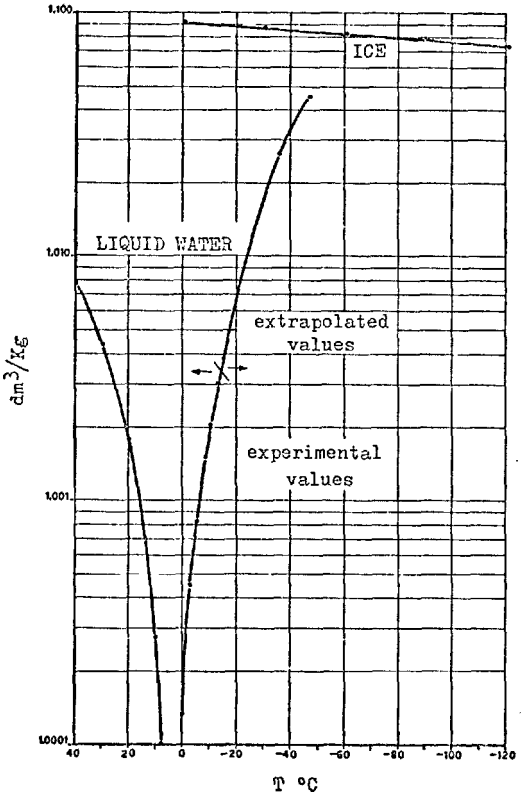

Fig. 12. *Relation between specific volume of water and temperature*

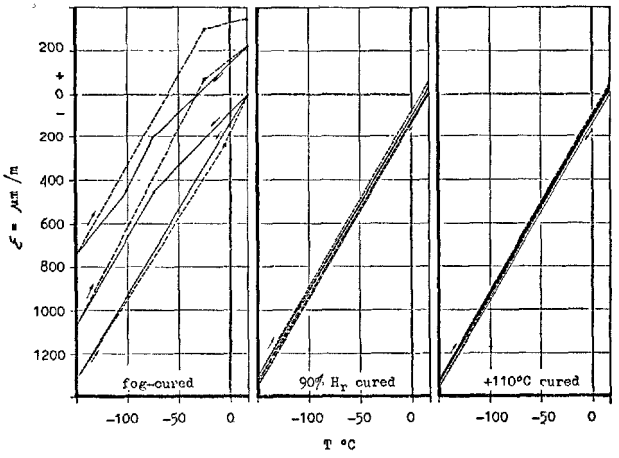

Fig. 13. *Relations between linear deformations of concrete and temperature for three cycles of freezing and thawing*

The results of tests made on specimens of plastic mortar, are indicated in the diagram of Fig. 14 and fully confirm the existance of the hysteresis as well as its trend.

It is necessary to point out, that for cooling and warming cycles between −50 and −90°C no hysteresis effect was noticed. The moist cement paste undergoes a deformation beyond its elastic limit, owing to water freezing in the capillaries. If a warming happens, some water will migrate from the coarse porosities to the deformed capillaries. So, at the room temperature, we will find an hysteresis, that is an increase of dimensions in comparison with the ones measured at the beginning.

On repeating the freezing, the process of subsequent expansion in the capillaries happens again, at least as long as there is sufficient water in the coarse pores for their previous saturation. There will be, at the end, a further increase in the permanent deformation.

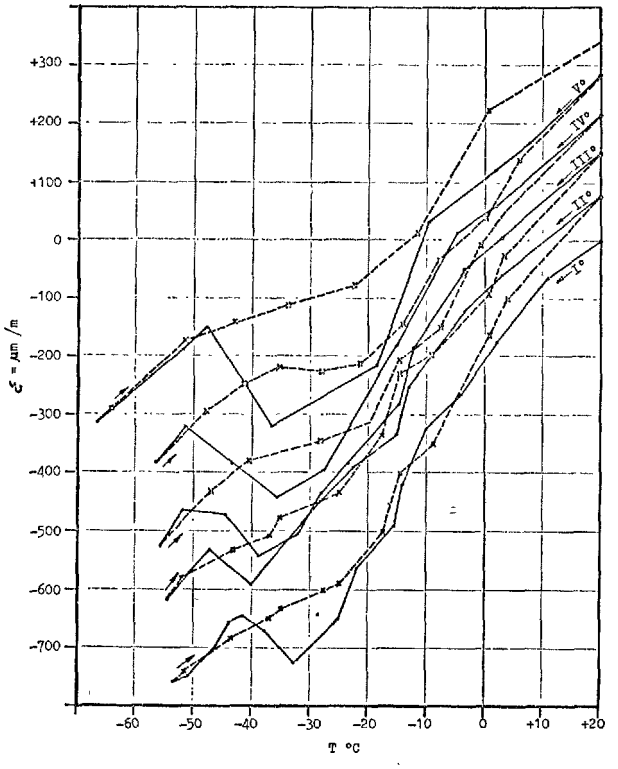

Fig. 14. *Relation between linear deformations of fog cured mortar and temperature (for five-cycles of freezing-thawing)*

Complementary Investigations

Calorimetric Tests

The object of this investigation is the research, through calorimetric tests, of the temperature or of the interval of the temperature at which the water contained in a paste freezes.

Choice and Preparation of Samples

Samples of pure paste, prepared with high strength cement, w/c = 0.45, cured for 300 days in water were used.

The samples were heated in a stove at 110°C, after cooling in a drying container, and were weighed on an analytical balance. Some samples were tested in this condition and their water content (determined as loss of ignition) was 0.1139 g/g of dried paste equal to 16.56% (this accords with the theoretical value of the non evaporable water, wn) (12).

Other samples cured after having been put in water for 24 hours, were kept into a box, saturated with water at 20°C, for 48 hours. The absorption of humidity was examined, by weighing again the samples on an analytical balance.

After the treatment described above, the average value of the content of water of the samples determined as loss on ignition was: 0.18056 g/g of moist paste $w_0 = 31.62\%$ of which 16.56% non evaporable water (wn) 15.06% evaporable water (we).

Equipment

For cooling samples, different freezing apparatus were employed according to the interval of temperature under examination.

The temperatures of the cooled samples were measured with I/RO thermocouple connected with a millivoltmer (Class 0.1). A multiple jackets calorimeter was used. The proper calorimetric container is plastic made, tightly jacketed with copper (shield against convective movements), contained in a stainless steel jacket. The whole is immersed in a thermostatic bath at a temperature of 25.2 $\pm$0.01°C.

The thermometer consists of a thermometric feeler provided with platinum resistance connected with a branch of a Wheatstone's bridge. The loss of balance of the bridge, which is proportional to the variation of the temperature, is continuously registered by means of a galvanometric recorder with a sensitivity of 0.00758°C per mm.

Results

The warming of the samples from the initial temperature T_i to the final one T_f involves a variation of enthalpy ΔH_0

$$\Delta H_0 = \frac{\Delta a \times c}{P}$$

where:

Δa = thermic change in mm

c = calorimetric equivalent of the calorimeter cal/mm

P = weight of the samples in grams

Tables 8 and 9, respectively for wet and dried samples, give the values of ΔH_0 and the values of $\Delta H_{corr.}$, because the temperature T_f show a dispersion of 22°C $\pm$ 1.5°C and for this reason a correction is made, in order to refer always to a final temperature of 22°C.

Table 8. *Samples with 31.62% of water*

Test number	Temperature of the sample (°K)	T_f(°K)	Enthalpy change ΔH_0	ΔH corr.
1	88.16	294.98	53.1927	53.2464
2	98.16	294.29	52.3566	52.6179
3	107.16	295.15	51.7200	51.7233
4	110.41	295.69	50.9368	50.7754
5	119.36	295.02	48.3317	48.3749
6	133.16	295.33	45.9168	46.1555
7	143.16	295.65	44.5869	44.4414
8	147.36	295.29	44.7777	44.7393
9	167.96	295.31	41.5207	41.0754
10	177.66	295.51	40.1034	40.1508
11	188.96	296.29	37.6532	38.3124
12	190.16	295.66	37.2940	37.1440
13	201.36	294.94	35.4947	35.5610
14	202.96	296.35	34.8845	34.5275
15	203.91	296.28	33.0073	32.6725
16	212.91	296.00	32.8323	32.5782
17	218.96	295.06	30.7916	30.8216
18	227.04	295.58	29.2588	29.1331
19	235.66	295.35	26.8864	26.8303
20	237.16	295.15	24.7248	24.7284
21	239.66	294.97	24.3245	24.3793
22	247.66	295.65	22.7445	22.5978
23	253.66	296.78	21.1968	20.7117
24	257.16	295.55	19.1005	18.9877
25	257.91	295.58	18.5971	18.4423
26	263.66	294.89	15.5649	15.6452
27	265.91	295.01	14.4838	14.5294
28	266.86	295.05	14.3380	14.3710
29	268.91	295.21	9.0316	9.0151
30	269.16	295.64	9.1071	8.9637
31	271.16	295.27	9.9380	7.9056
32	271.26	294.95	8.0199	8.0829
33	272.16	294.85	8.9348	9.0267
34	273.60	295.11	7.2235	7.2385
35	274.76	295.74	6.6626	6.4880
36	277.16	295.29	6.3023	6.2645
37	277.36	295.19	6.0057	5.9967
38	277.96	296.22	6.1442	5.8247
39	278.96	294.82	5.3941	5.4967
40	280.96	295.20	4.7856	4.7727
41	282.36	295.27	4.0690	4.0063

Table 9. *Samples with 16.56% of water*

Test number	Temperature of the sample (°K)	T_f(°K)	Enthalpy change ΔH_0	ΔH corr.
1	131.16	195.53	29.2012	29.1372
2	179.06	185.06	21.6371	21.6061
3	204.41	196.28	17.5098	17.3156
4	228.16	197.89	13.1313	13.0951
5	255.96	184.83	7.1290	7.0209

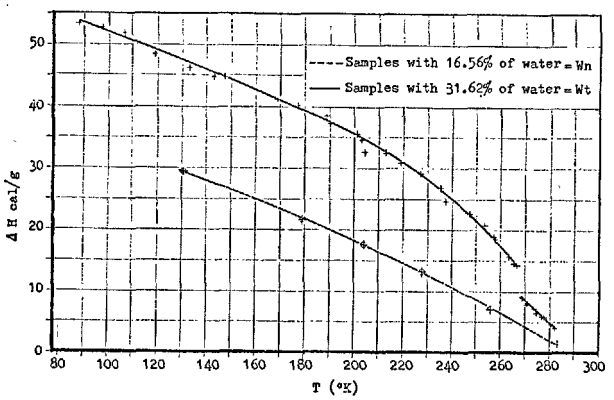

Fig. 15. *Enthalpy changes of cement pastes with variable water content from 295°K to T °K*

It is possible to draw the diagram of the $\Delta H = \Delta H(T)$ of the dried samples showing a water content (determined as loss of ignition) equal to 16.56% and of the wet samples showing water content (determined as loss of ignition) equal to 31.62% (Fig. 15).

As it may be noticed, the trend $\Delta H = \Delta H(T)$ is regular and continuous for the dried specimens and it may be well represented by a parabola:

$-\Delta H_{295°K}^{T_i°K} = 42.00662 - 5.9079 \cdot 10^{-2} T - 3.00173 \cdot 10^{-4} T^2$

It is now to consider the trend of ΔH of the moist specimens.

It is possible to see a clear discontinuity for $T = 269.16$°K which is attributable to the change of the state from ice to water. Following to this transformation, the calories involved are:

$\Delta H = 5.1$ cal/g

Referring to the melting heat of water under normal conditions $\Delta H_m = 79.71$ cal/g, the result obtained is, that at this temperature, 0.0639 g of water freezes per g of paste, which is equivalent to 35% of the evaporable water.

The decrease of the freezing point may be attributed to the presence of dissolved salts.

If we want to evaluate the temperature at which all the water is frozen, we can usefully examine the diagrams $C_p = C_p(T)$.

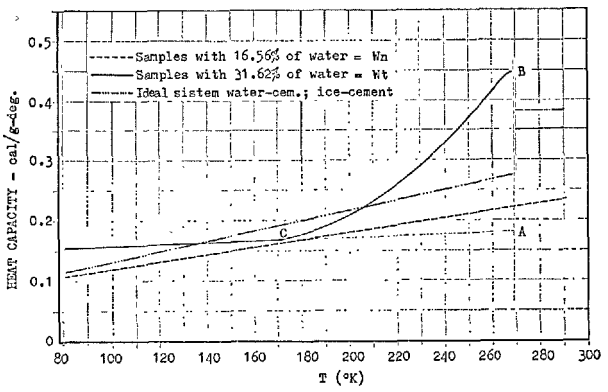

Fig. 16. *Heat capacity of cement pastes with variable water content from 80°K to 290°K*

Such diagrams (14) can be obtained by derivation: $C_p = \partial \Delta H / \partial T$

The trend $\Delta H = \Delta H(T)$ for the wet samples can be analytically represented by three parts of curve:

for $80 < T_k < 170$

$-\Delta H_{295°K}^{T_i°K} = 67.2300 - 0.14788T - 5.28293 \cdot 10^{-5} T^2$

for $170 < T_k < 269$

$-\Delta H_{295°K}^{T_i°K} = 101.812 - 0.77023T + 3.76696 \cdot 10^{-3} T^2 - 7.89380 \cdot 10^{-6} T^3$

for $269 < T_k < 282$

$-\Delta H_{295°K}^{T_i°K} = 103.220 - 0.35070T$

and the $C_p = C_p(T)$ will be respectively:

for $80 < T_k < 170$ $C_p = 0.14788 + 1.05658 \cdot 10^{-4} T$

for $170 < T_k < 269$ $C_p = 0.77023 - 7.53393 \cdot 10^{-3} T + 2.36814 \cdot 10^{-5} T^2$

for $269 < T_k < 282$ $C_p = 0.35070$

The quantities of water that freeze at temperatures inferior to the transition point (269.16°K), lead to an excess of specific heat.

The difference between the behaviour of wet samples and the behaviour of the dried samples may be attributed to a progressive change in the state of water.

At this point, we represent graphically the trends of $C_p = C_p(T)$ (Fig. 16).

In addition to the experimental behaviour, the graph represents also the trend of the specific heat of the ideal system of "ice-dried paste" and "water-dried paste".

By extrapolating the trend of the curve of the specific heats valid for $T < 170$°K down to the temperature of $T = 269.16$°K (which is equivalent to the admission of a total freezing at this temperature) the area ABC is isolated. This area, when measured in

heat terms, represents the calories involved in the progressive freezing of water for $T < 269.16°K$. The measurement of the area graphically executed has given a value of 10.2 cal/g of paste.

Supposing as a first approximation, that the latent heat of melting does not change considerably with the temperature, by the following ratio we obtain:

$$\frac{10.2 \text{ cal}}{79.62 \text{ cal/g.}} = 0.1278 \text{ g.}$$

which means that 0.1278 g., that is about 70% of the evaporable water, freeze in this interval.

The change of state of such a system is quite different from a normal one for the reason that the water absorbed by the paste is contained in microcapillaries.

Other authors have studied similar effects (15); for instance, water absorbed by the gel of silica, nitrogen by dioxide of titanium. Thermodynamic explanations have been put forward, but the incomplete knowledge of the superficial conformation of the paste and the presence of collateral effects do not allow to reach a whole explanation of the phenomenon.

We can affirm consequently by this peculiar investigation, that evaporable water freezes gradually from $-4°C$ to $-95°C$.

Some anomalies in the trend of concretes in this range of temperature are so explained.

Triaxial Tests

The concraction phenomena help us to explain the increase of strengths as temperature decreases.

Freezable water is essential for the increment of strength.

The ice in the capillary net raises a state of stress in the surrounding mass because its contraction coefficient is the highest among the coefficients of the other materials. We think it is not right to consider ice like an inert solid filling porosities. In mechanical terms we can figure it like a diffused reinforcement pre-stressing the surrounding material.

We deemed interesting to identify the internal stress state with the stresses produced it in a specimen when submitted to triaxial stress and where $\delta_x = \delta_y \neq 0$. The δ_z of breakage increase on increasing of the stresses acting on the plane x,y. The results of the tests are shown in Fig. 17. In the same figure we put in relation the value of the lateral stress and the consequent value of the δ_z with the value of the temperature at which the same compressive strength is corresponding.

It appears finally opportune to point out the varia-

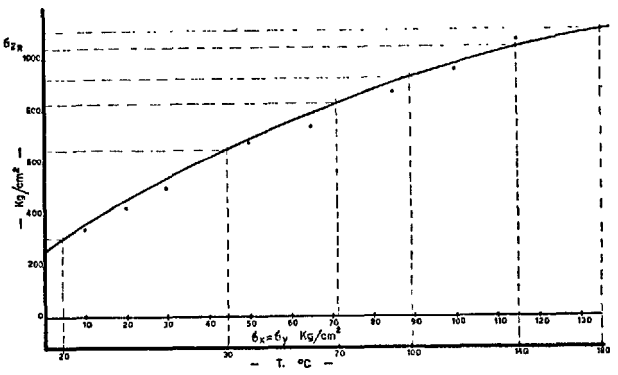

Fig. 17. *Relation between the temperature of treatment and $\delta_x = \delta_y \neq 0$ stress of a triaxial test*

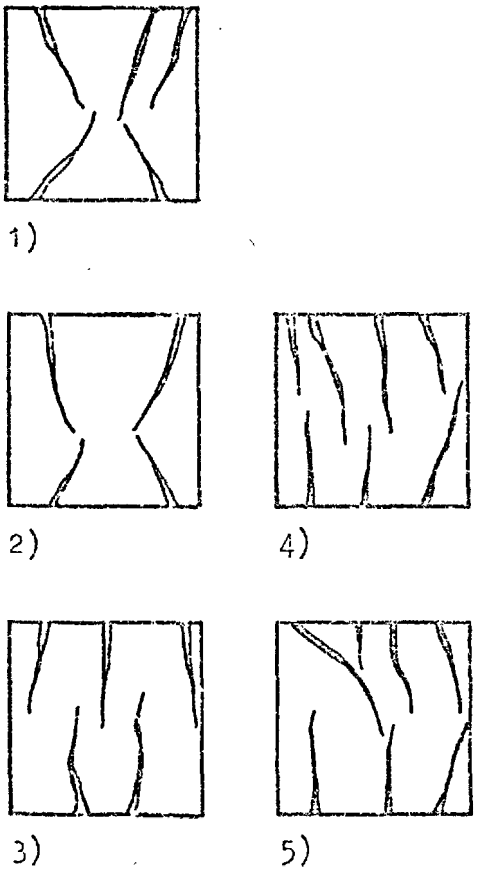

Fig. 18. *Breakage lines of concretes with different water contents at different temperatures*

1) Test at +20°C (cured at R.H. 100%, +20°C) $\delta R = 356$ kg/cm²
2) Test at −70°C (cured at R.H. 100%, +20°C) $\delta R = 820$ kg/cm²
3) Test at −180°C (cured at R.H. 100%, +20°C) $\delta R = 1125$ kg/cm²
4) Test at +20°C (dried at +110°C) $\delta R = 384$ kg/cm²
5) Test at −160°C (dried at +110°C) $\delta R = 474$ kg/cm²

tion of fracture planes in which specimens break as temperature decreases (see Fig. 18).

The kind of fracture is pointed out by some authors (16) (17) as a peculiar characteristic of the strength values.

Conclusions

—The fog-cured, hardened concrete, increases its mechanical strengths when it is cooled from room to low temperatures, even down to −196°C.

—The concrete, cured at 110°C so to eliminate its free water, when cooled doesn't show increases in strength.

—Cement type and nature of the pozzolana, in the case of pozzolanic cement, do not modify trends of the phenomenon. The same can be said in regard to the seven different types of aggregates with which the concretes were made (including also the aggregates of expanded clay). The highest strength, found at low temperatures, is bound to the room temperature strength of the concrete; so it depends on all the variables which condition a concrete (strength of the cement, its quantity, type of aggregate, curing, and so on).

—The shock strength of cooled concretes depends on their respective bending and compressive strength.

—Degradation of no significance was found in the physical and mechanical characteristics on concretes treated cyclically from +20 to −196°C with a long curing at the test temperature.

—The dynamic modulus of elasticity, that at room temperature follows the trend of strengths, increases as temperature decreases.

—The thermal contraction coefficient of concrete at low temperatures, depends on the type of aggregate and feels the effects of the respective water contents. In connection with water content hysteresis curves appear on specimens submitted, without interruption, to warming and cooling treatments.

—The enthalpy variation referred to cooling temperature on cement paste specimens, indicates that the free water freezes progressively from −4°C down to −90°C.

—Inflections on mechanical strengths in the range −10°C ~ −60°C can be explained on the basis of what written at the preceding point. In the moist specimens, the migration of water, during the freezing, from the capillaries to the coarsest porosities causes a hygrometric shrinkage, in addition to the thermal contraction; the corresponding dried specimens are subject only to the effect of thermal contraction. The progressive and complete freezing of the water contained in the porosities causes a deformation: hence the hysteresis.

—The freezing of the water contained in the capillaries induces in the mass of the paste an internal stress, more and more diffuse and intense. When all the free water is frozen and the temperature still falls down, paste and ice go on with their thermal contraction. The contraction coefficient of ice is higher than the one of paste and of the aggregate, and consequently the ice contained in the porosities and in the capillaries consists of a sort of pre-stressed reinforcement immersed in the paste. By means of triaxial compressive tests, we found the values of the lateral stresses, to which the values of the temperature are corresponding, to obtain the same monoaxial breakage strengths in the cooled moist specimens.

Acknowledgements

The author wants to express his gratitude to the Chairman and Managing Director of "Italcementi" S.p.A. Cav. Lav. Dr. Ing. Carlo Pesenti, who understood widely and deeply the problem of scientific research and encouraged the Central Laboratory of the Company in its activity of study and practical and technical experimentation.

He is grateful also to Prof. Dr. F. Massazza, director of the Laboratory for the contribution he gave in the discussions concerning this work. He thanks Dr. Ing. P. Ursella for the very help he performed during the experimentation and the interpretation of the results, as well as during the drafting of the present paper, and finally he thanks Dr. Costa, Mr. Martinelli and Mr. Morlotti for their co-operation.

References

1. G. E. Monfore and A. E. Lentz, "Physical properties of concrete at very low temperatures", Journal of the P.C.A. Res. Develop. Lab. **4**, No. 2, 33–39 (May 1962).
2. V. M. Moskvin, H. M. Kapkin and B. M. Mazur, "Deformations at subzero temperatures of concretes subjected to different hardening conditions", Proc. International Conference RILEM, Moscow (July 1964).
3. B. Tavasci, "Struttura della Pozzolana di Segni", Il Cemento **42**, 4–10 and 25–29 (1946).
4. B. Tavasci, "Struttura della malta di calce e pozzolana di Bacoli", Il Cemento **45**, 114–120 (1949).
5. H. F. W. Taylor, "The chemistry of cements", Vol. 2, 1st Ed. 72 (Academic Press Inc., London England, 1964).
6. A. E. Lentz and G. E. Monfore, "Thermal conductivity of concrete at very low temperatures", Journal of the P.C.A. Res. Develop. Lab. **7**, No. 2, 39–46 (May 1965).
7. A. E. Lentz and G. E. Monfore, "Thermal conductivities of portland cement paste, aggregate and concrete down to very low temperatures", Journal of the P.C.A. Res. Develop. Lab. **8** No. 3, 27–33 (September 1966).
8. A. Guttmann und F. Wenzel, "Beitrag zur Stossfestigkeit von Beton", Zement **23**, No. 36, 528–534 (September 1934), Zement **23**, No. 37, 545–551 (September 1934).
9. A. Guttmann und K. Seidel, "Über die Druckfestigkeit, Stossfestigkeit und Absuntzbarkeit von Beton", Zement **25**, No. 14, 233–240 (April 1936).
10. R. A. Helmuth, "Dimensional changes of hardened portland cement pastes caused by temperature changes", Highway Research Board, Proceedings **40**, 315–335 (1961).
11. A. Palmieri, "Ricerche sperimentali sui coefficienti di dilatazione di inerti, calcestruzzi, malte e paste di cemento", L'Energia Elettrica **25**, No. 12, 1195–1215 (1958), **27**, No. 5, 381–392 (1961), **42**, No. 10, 681–685 (1965).
12. N. E. Dorsey, "Properties of ordinary water substance" (Reinhold Publ. Corp. New York, U.S.A., 1940).
13. T. C. Powers and T. L. Brownyard, "Studies of the physical properties of hardened portland cement paste", Res. Lab. of the P.C.A., 250, (March 1948).
14. O. Kubaschewski and E.L.L. Evans, "Metallurgical thermochemistry" Vol. 1, (Pergamon Press, London, England, 1965).
15. A. R. Ubbelohde, "Melting and crystal structure", 25–30, (Clarendon Press, London, England 1965).
16. H. W. Hayden and M. G. Moffatt, "The structure and properties of materials", Vol. III (John Wiley and Sons, New York, U.S.A., 1966).
17. N. H. Polakowsky and E. J. Ripling, "Strength and structure of engineering materials", (Prentice Hall, Inc., Englewood Cliffs, N. J. U.S.A., 1966).

Oral Discussion

Rolf F. Feldman

The experimental results of the author are very interesting. The result that the specimens which were dried before cooling contract less than the corresponding moist specimens should, however, be further discussed.

The resultant length change that occurs when a saturated sample of hydrated portland cement is cooled may involve many factors and it is the purpose here to discuss a few of them separately with the view of further understanding the results.

We will initially consider hydrated portland cement as a relatively inert high surface area material and consider it as saturated with water at 0°C. As cooling takes place (We assume that equilibrium is maintained, kinetic effects not playing a role.), one of the effects we might except is a change in the surface free energy change due to interaction of the adsorbate (H_2O) with the adsorbent (hydrated cement).

The above phenomena is considered here as small and more so because the amount of physically adsorbed water in cement is not very large. However, in the above case, we have ignored any effect due to menisci forces and freezing. When cooling takes place to temperatures below 0°C and water in some large pores freezes, a new equilibrium will be set up; the vapour pressure required to maintain the saturated state of the sample will be that of supercooled bulk water at the temperature of the sample. Below zero, and in the presence of bulk ice, this will be impossible to maintain and the system will attain equilibrium at a new p/p_0 value, where p is the vapour pressure of bulk ice at the temperature of the sample and p_0 is the vapour pressure of bulk water at the same temperature. Thus there will be an effective reduction in vapour pressure as the sample is cooled and a shrinkage due to menisci forces in the small pores of the specimen.

In the discussion above, we have considered the solid (hydrated portland cement) to be inert, but immediately we can see that this assumption is not correct. When hydrated is first dried, an irreversible

shrinkage is obtained and it has already been shown how cooling can effectively reduce the relative humidity of the specimen. At −15°C the relative humidity would be 86 per cent, and it is considered here that the irreversible shrinkage phenomenon would represent a larger portion of the shrinkage observed on cooling than capillary effects which have been observed on stabilized cement paste (1, 2).

One last area of importance is the effect of the cooling on the interlayer hydrate water. It has been shown (1) how this water plays a very important role in length change phenomena at low vapour pressures and one might wonder if the low temperatures could cause a further change in order and mobility of this water, resulting in a length change.

References

1. R. F. Feldman, Sorption and length-change scanning isotherms of methanol and water on hydrated portland cement. Submitted to V International Symposium on the Cement Chemistry.
2. R. A. Helmuth, and D. M. Turk, The reversible and irreversible drying shrinkage of hardened portland cement and tricalcium pastes. J. Portland Cement Assoc., Res. and Rev. Lab., **9**, 8–21, 1967.

Author's Closure

Giampietro Tognon

The results of the experiment, set forth in our supplementary paper and further demonstrations on the same subject, are still being worked out.

We therefore agree that a thorough examination thereof would be well-advised; and we deem of interest and, moreover, useful the suggestion put forth by Mr. Feldman regarding break-down of the components of the basic occurrence, i.e., the lower contraction taking place further to cooling applied to previously dryed test specimens, as compared to contraction noted on comparable moist test specimens.

In the first place, it is important to bear in mind that, in the part of testing where we would observe freezing effects most accurately, the test specimens are to be considered, at least theoretically speaking, immersed in a closed system. Their mass has certainly achieved the temperature levels that we have pointed out, without having the possibility, though, of reaching the point of equilibrium at the respective temperatures, as like as the necessary adsorptions or desorptions of water.

It therefore arises that any consideration as regards equlibrium adjusted by the Gibbs' equation, the menisci forces and the effects on the interlayer hydrate water may be well applied in the case of a system in a condition of well definable equilibria, but in our investigation method, we would work out them in a particular way in order to put them valid.

The type of investigation according to procedures recommended by Mr. Feldman, a result of his importand works, is definitely to be applied.

Supplementary Paper III-25 The Influence of Temperature on Sulphate Attack on Portland Cement Mortars

J. H. P. van Aardt*

Synopsis

The paper discusses various aspects concerning corrosion of portland cement products in sulphates. Some reactions at 5°C and 25°C of the relevant calcium aluminate hydrates are considered with special reference to early ages. Various calcium sulpho-aluminate hydrates are dealt with in relation to rate of reaction at the two temperatures and the various products formed when both the sequence of mixing of the reactants and their quantities are varied. The stability of calcium aluminate hydrates and calcium sulpho-aluminate hydrates at these temperatures is considered with a view to explaining some of the observations in practice as regards sulphate attack on portland cement products. Experiments with mortars and observations on their behaviour in sodium sulphate solutions at 5°C and 22°C are considered. Two of the important findings are:—(1) cubic calcium aluminate hexahydrate is unstable at low temperatures and more so in the presence of $Ca(OH)_2$; (2) under some circumstances a calcium mono-sulpho-aluminate with a basal spacing at 8.5 Å is the reaction product of C_3AH_6, $Ca(OH)_2$ and $CaSO_4 \cdot 2H_2O$ at 25°C.

Introduction

The entire issue of sulphate corrosion of portland cement products is complicated by physical factors such as the density and the permeability of the product. In other words, durability depends also on the cement content, the grading and type of aggregate, the degree of compaction, the water/cement ratio and the thoroughness of curing; in short the higher the quality of a cement product, the better its resistance to sulphates. The influence of these physical factors can be so marked that in some instances they may obscure the influences on corrosion of differences in chemical composition of various portland cements. Nevertheless, the chemical composition of portland cement, especially the alumina content, determines to a large extent its resistance to the sulphate ion. Although much is known about sulphate attack there are still some doubts about certain aspects of the mechanism involved when calcium aluminates react with sulphate to cause deterioration in portland cement products. It is known, for instance, that the reactions are affected by temperature but there is as yet no clear understanding of the matter. In this contribution, experiments concerning the nature and behaviour of some calcium aluminates at 5°C and 25°C are described; reactions at early ages are considered. The behaviour of portland cement mortars in sulphate solutions at these temperatures is also discussed.

Some Reactions of Tricalcium Aluminate Hexahydrate and Tricalcium Aluminate at 5°C and 25°C

Working with suspensions of C_3AH_6 in water and of C_3A in water, van Aardt and Visser (1) have shown that both the substances behaved differently at 5°C and 25°C. In the presence of $Ca(OH)_2$, the two aluminates gave the same reaction product at 5°C. Fig. 1 shows that the reaction product at 5°C of (i) C_3AH_6 (1.89 g) plus $Ca(OH)_2$ (0.37 g) plus H_2O (50g) and (ii) C_3A (1.35 g) plus $Ca(OH)_2$ (0.37 g) plus water, has *d*- spacings at 10.6 Å and 5.3 Å, similar to C_4AH_{19} described by Jones and Roberts (2). This indicates that C_3AH_6 is unstable at 5°C and more so in the presence of $Ca(OH)_2$. Furthermore, C_3AH_6 plus $Ca(OH)_2$ at 25°C seemed to react partially to form a compound

*National Building Research Institute, South African Council for Scientific and Industrial Research, Pretoria, South Africa.

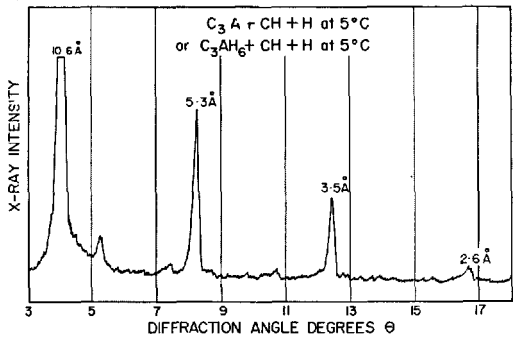

Fig. 1. *X-ray diffractogram of tetracalcium aluminate hydrate at* 5°C

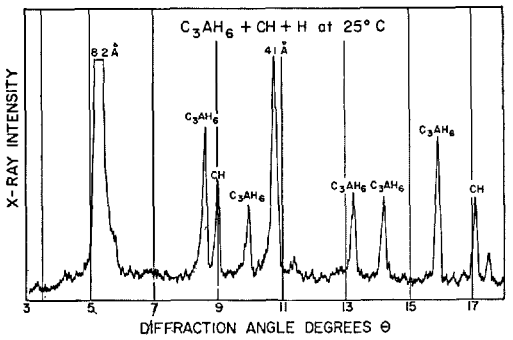

Fig. 2. *X-ray diffractogram of* C_3AH_6 *and* $Ca(OH)_2$ *in water at* 25°C

with *d*- spacings at 8.2 Å and 4.1 Å. The 10.6 Å compound was unstable above 30°C; at this temperature, the suspension showed *d*- spacings for C_3AH_6, $Ca(OH)_2$ and the 8.2 Å compound. The filtered wet 10.6 Å compound behaved in a similar way on heating to 50°C in an enclosed space, the silky appearance of the paste disappeared and it was changed into a very wet paste; water was clearly set free. Fig. 2 is an X-ray diffraction diagram of the substance obtained in this way; it is similar to a diagram of a suspension of C_3AH_6 plus $Ca(OH)_2$ at 25°C, i.e. the 8.2 Å, 4.1 Å substance plus $Ca(OH)_2$ plus C_3AH_6. When the suspension containing the 8.2 Å substance was kept at a temperature above say 70°C for a period, only C_3AH_6 and $Ca(OH)_2$ were detected on the X-ray diffraction diagram .

The course of the reactions when C_3A was added to water can be summarized as follows:

$$2C_3A + H_2O \xrightarrow{\text{approx. } 25°C} C_4AH_{19} + C_2AH_8 \qquad (1)$$

The two types of hydrates could be detected by the basal spacings at 10.6 Å and 10.7 Å. Two types of

Fig. 3. *X-ray diffractogram of cubic* C_3AH_6 *in water at* 25°C

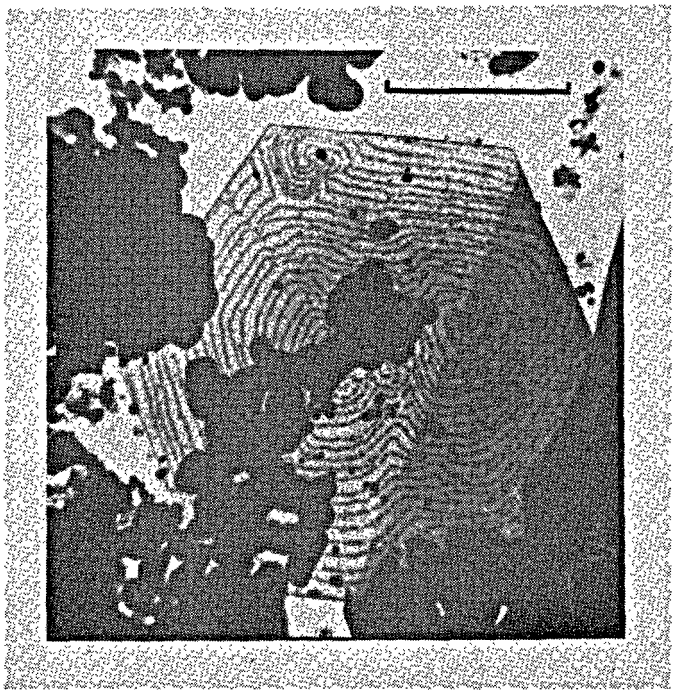

Fig. 4. *Electron micrograph showing zoning during reaction between* $C_2AH_8 + Ca(OH)_2$

hexagonal plates could also be observed under the electron microscope. When the temperature was raised, the aluminates were converted to cubic C_3AH_6 and some hexagonal substance with a basal spacing at 7.6 Å. The X-ray diffractogram was identical to that of a suspension of C_3AH_6 in water at 25°C (see Fig. 3).

When $Ca(OH)_2$ was added to the suspension at 25°C, the C_2AH_8 reacted with it and C_4AH_{19} was produced.

$$C_4AH_{19} + C_2AH_8 \text{ (eqn. 1)} + 2Ca(OH)_2 \xrightarrow{+H_2O,\ 25°C \text{ and lower}} 2C_4AH_{19} \qquad (2)$$

When (2) was heated to about 50°C it changed into cubic C_3AH_6 and a hexagonal substance with a basal spacing at 8.2 Å, (see Fig. 2). On cooling to 5°C, this again formed the 10.6 Å substance.

When $Ca(OH)_2$ was added to the suspension (1) above and the mixture was examined under the electron microscope soon after the addition, hexagonal crystal showing the zoning as in Fig. 4 were observed. It is assumed that this was a reaction between C_2AH_8 and $Ca(OH)_2$. A similar observation but with the zoning even more pronounced was made when C_3A and C_3S were mixed in water and the temperature of the suspension kept in the vicinity of 25°C. The zoning disappeared on storage.

Reaction Products at Early Ages of C_3A and of C_3AH_6 with Calcium Sulphate

Having established the behaviour as described above of C_3A and of C_3AH_6 in water and in the presence of $Ca(OH)_2$ in water at 5°C, and 25°C, the reactions of $CaSO_4$ with the calcium aluminate hydrates were investigated.

Reactions at 25°C

Suspensions containing essentially the 10.6 Å hexagonal hydrate and the 8.2 Å substance were prepared as follows:

C_3A (1.35 g) or C_3AH_6 (1.89 g) was reacted for seven days with $Ca(OH)_2$ (0.37 g) in water (100 g) at 5°C to give the 10 .6 Å hydrate and C_3AH_6 (1.89 g) plus $Ca(OH)_2$ (0.37g) in water (100 g) was used at 25°C to give the 8.2 Å substance.

The reaction products obtained when one mole or three moles $CaSO_4 \cdot 2H_2O$ was added to these calcium aluminate hydrates and the reaction mixtures kept at 25°C were described by van Aardt and Visser (3). The addition of one mole of sulphate to the 10.6 Å compound produced a phase with *d*- spacings 9.6 Å, 4.77 Å at early ages, i.e. one hour to seven days (see Fig. 5(A)).

This substance changed to a phase with *d*- spacings 8.9 Å, 4.4 Å at equilibrium. When three moles of sulphate were added, only the 9.6 Å compound and $CaSO_4 \cdot 2H_2O$ were observed at one hour: the equilibrium phase was ettringite. The presence of excess $Ca(OH)_2$ tended to retard the reaction rate. In brief:

$$10.6\text{ Å} \xrightarrow{+1\ CaSO_4 \cdot 2H_2O} 9.6\text{ Å} \xrightarrow{Ca(OH)_2 + \text{time}} 8.9\text{ Å}$$

$$10.6\text{ Å} \xrightarrow{+3\ CaSO_4 \cdot 2H_2O} 9.6\text{ Å} + CaSO_4 \cdot 2H_2O \longrightarrow \text{ettringite}$$

One mole of sulphate added to the 8.2 Å compound, produced a phase with *d*- spacings 8.5 Å, 4.23 Å and ettringite: gypsum was also present at an early age, i.e. one hour, but was not detected at seven days (see Fig. 5(B)). The 8.5 Å compound changed to ettringite and finally at equilibrium the 8.9 Å compound was observed; the change from ettringite to 8.9 Å appeared to pass through the 9.6 Å substance. When three moles of sulphate were added the 8.5 Å phase and gypsum were observed at one hour; the equilibrium phase was ettringite. The presence of $Ca(OH)_2$ tended to retard the reaction rate. In brief:

$$8.2\text{ Å} \xrightarrow{+1\ CaSO_4 \cdot 2H_2O} 8.5\text{ Å} + E \longrightarrow E + \text{aluminate} \longrightarrow 9.6\text{ Å} \longrightarrow 8.9\text{ Å}$$

$$8.2\text{ Å} \xrightarrow{+3\ CaSO_4 \cdot 2H_2O} 8.5\text{ Å} + CaSO_4 \cdot 2H_2O \longrightarrow \text{ettringite}$$

In the presence of gypsum, a suspension containing both the 10.6 Å and 8.2 Å compounds gave the intermediate phase 9.6 Å and 8.5 Å at early ages (see Fig. 5(C)).

When all the reactants, i.e. C_3A (1.35 g) or C_3AH_6 (1.89 g) and $Ca(OH)_2$ (0.37 g) and $CaSO_4 \cdot 2H_2O$ (0.86 g) were added at once, C_3A and $CaSO_4$ rapidly formed ettringite; the latter then reacted with more calcium aluminate to form the 9.6 Å compound within one day. C_3AH_6 reacted with the $CaSO_4$ to again produce ettringite; in this instance the ettringite was only slowly changed to the 9.6 Å substance. The equilibrium phase was again the 8.9 Å compound in both instances. Three moles of sulphate gave only ettringite at early ages while unreacted sulphate and aluminate were present.

With one mole of calcium sulphate and C_3A, in the absence of added $Ca(OH)_2$, the 9.6 Å phase was predominant after one day (see Fig. 6(A)), but with C_3AH_6, ettringite was predominant (see Fig. 6(B)); at later ages both suspensions contained the 9.6 Å compound. In the presence of saturated $Ca(OH)_2$

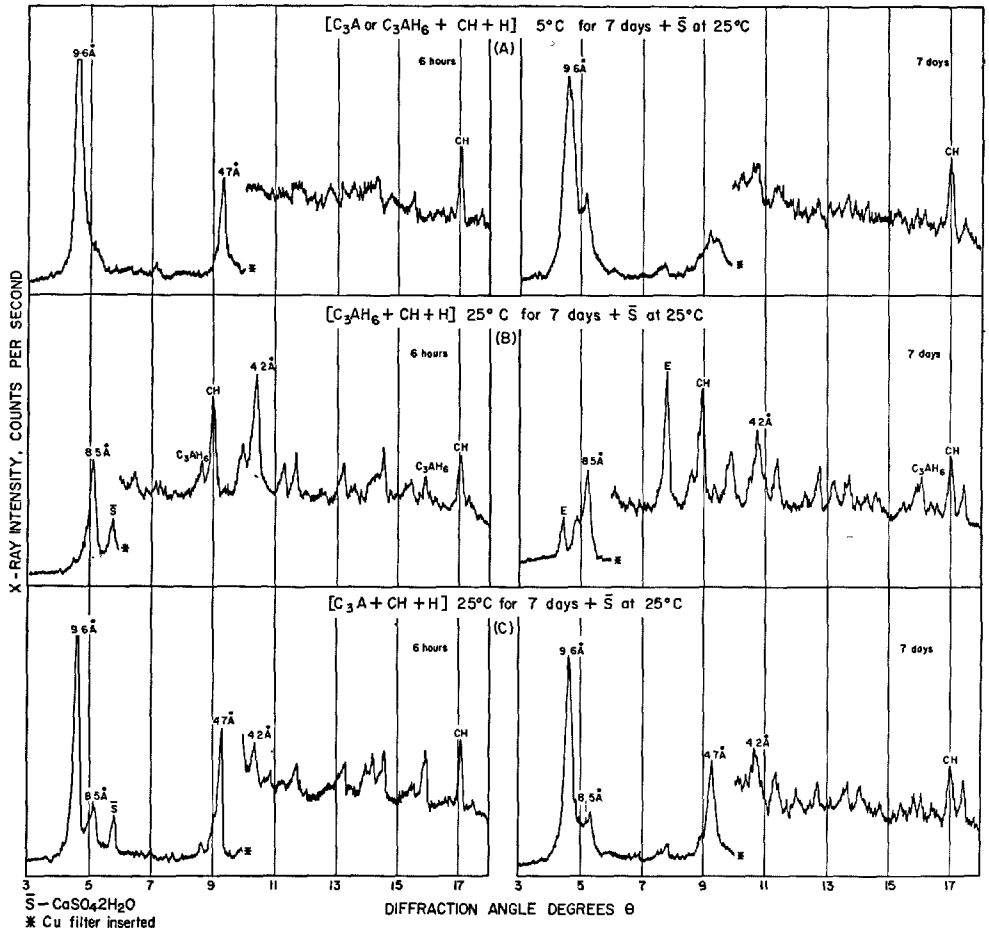

Fig. 5. *X-ray diffractograms of various calcium sulpho-aluminate hydrate at* 25°C

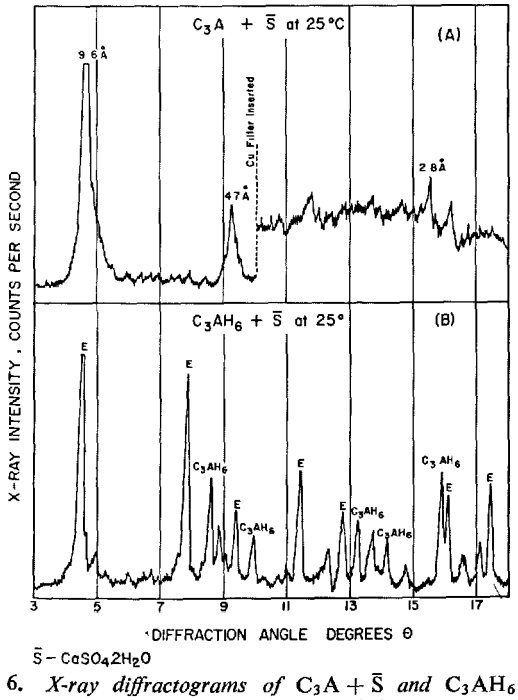

Fig. 6. *X-ray diffractograms of* $C_3A + \bar{S}$ *and* $C_3AH_6 + \bar{S}$ *after one day in water at* 25°C

solutions, the 8.9 Å phase was detected at equilibrium. Ettringite was the only phase observed when three moles of gypsum were added to the aluminates.

Reactions at 5°C

The following reaction mixtures in the form of suspensions in 100 g of water were examined:

(1) C_3A (1.35 g) plus $CaSO_4 \cdot 2H_2O$ (0.86 g)

(2) C_3AH_6 (1.89 g) plus $CaSO_4 \cdot 2H_2O$ (0.86 g)

(3) C_3A (1.35 g) plus $Ca(OH)_2$ (0.37 g) plus $CaSO_4 \cdot 2H_2O$ (0.86 g)

(4) C_3AH_6 (1.89 g) plus $Ca(OH)_2$ (0.37 g) plus $CaSO_4 \cdot 2H_2O$ (0.86 g)

(5) C_3A (1.35 g) + $Ca(OH)_2$ (0.37 g) reacted at 5°C for 7 days } plus $CaSO_4 \cdot 2H_2O$ (0.86 g)

(6) C_3A (1.35 g) + $Ca(OH)_2$ (0.37 g) reacted at 25°C for 7 days } plus $CaSO_4 \cdot 2H_2O$ (0.86 g)

(7) C_3AH_6 (1.89 g) + $Ca(OH)_2$ (0.37 g) reacted at 25°C for 7 days } plus $CaSO_4 \cdot 2H_2O$ (0.86 g)

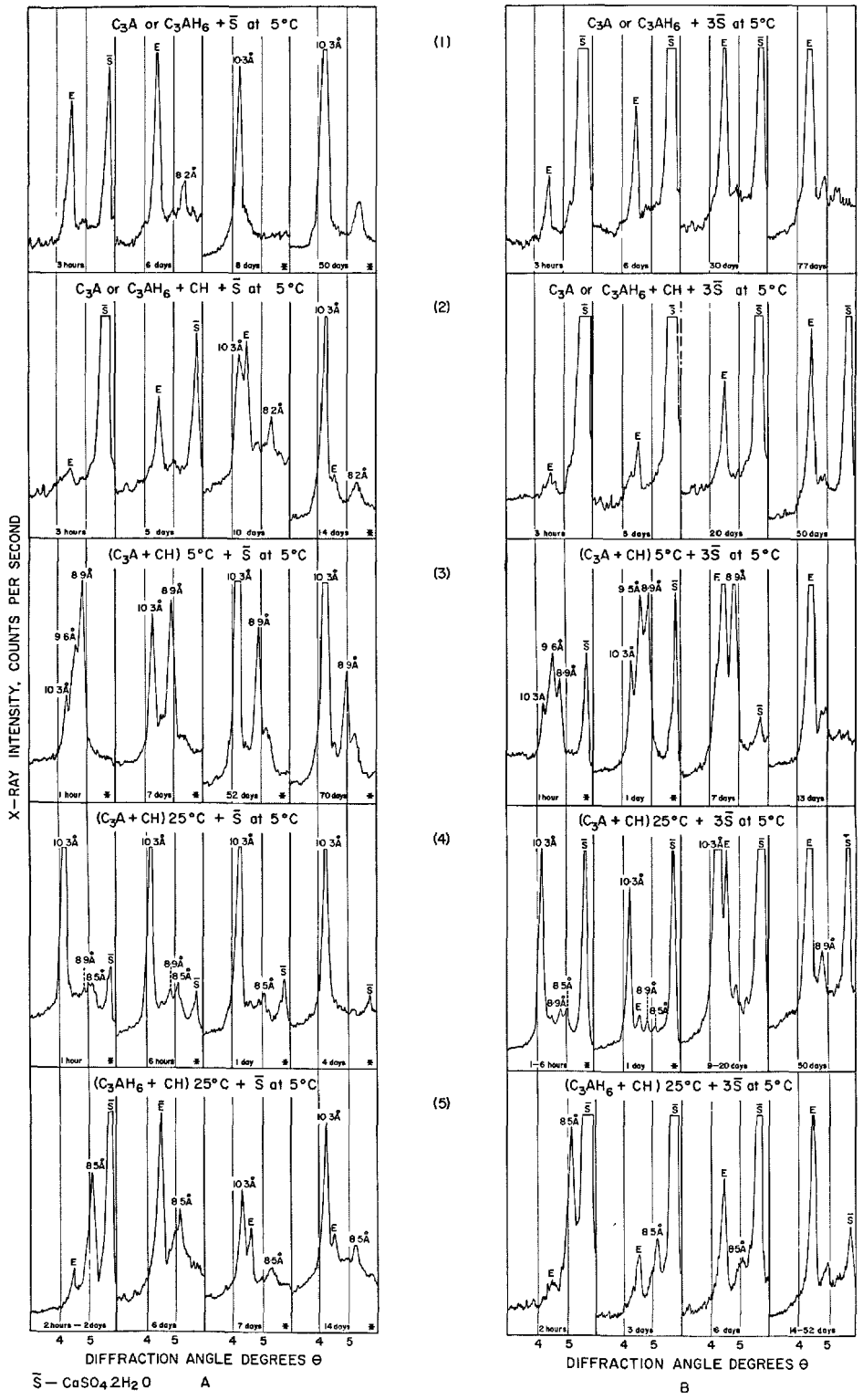

Fig. 7. *X-ray diffractograms of various calcium sulpho-aluminate hydrates at* 5°C

These experiments were repeated with three moles of $CaSO_4 \cdot 2H_2O$ added instead of one mole.

It was observed that when either C_3A or C_3AH_6 was mixed with one mole of $CaSO_4 \cdot 2H_2O$ and sus-

pended in water the first reaction product was ettringite and at a later stage some 8.2 Å substance was also present. Hydrated aluminates then reacted with ettringite to produce a substance with a basal spacing at 10.3 Å. This reaction appeared to be faster with C_3AH_6 than with C_3A. Thus with ettringite as an intermediate product the final product was the 10.3 Å substance. A similar position existed when $Ca(OH)_2$ was also present in the suspension, but the $Ca(OH)_2$ appeared to retard the rate of reaction as can be seen from Figs. 7A(1) and 7A(2).

When C_3A (and also C_3AH_6) was first reacted with $Ca(OH)_2$ for 7 days at 5°C before the addition of $CaSO_4 \cdot 2H_2O$ the course of the reactions was quite different, little ettringite was formed, gypsum appeared to react fast with the aluminate, which in this instance was C_4AH_{19}, to produce the monosulphate compounds 9.6 Å and 8.9 Å. These changed to the 10.3 Å calcium monosulpho-aluminate, i.e. the stable calcium, mono-sulpho-aluminate hydrate at 5°C. Eventually after a few months, only this substance and $Ca(OH)_2$ were detected in the suspension (see Fig. 7A(3)).

When C_3A plus $Ca(OH)_2$ were first reacted for seven days at 25°C before the addition of $CaSO_4 \cdot 2H_2O$ at 5°C, a complex mixture of calcium sulpho-aluminate hydrates formed rapidly (see Fig. 7A(4)). Little ettringite was produced and the 10.3 Å substance formed soon after the addition of $CaSO_4 \cdot 2H_2O$.

As was expected the conditioned mixture at 25°C of C_3A and $Ca(OH)_2$ contained both the 10.6 Å and some 8.2 Å calcium aluminate hydrates and these reacted with $CaSO_4 \cdot 2H_2O$ as described under the reactions at 25°C, but the reaction products then changed to the 10.3 Å material which is a stable phase at 5°C.

When C_3AH_6 and $Ca(OH)_2$ were mixed and kept at 25°C for seven days before the addition of $CaSO_4 \cdot 2H_2O$ at 5°C, the reaction follows a completely different course (see Fig. 7A(5)). Much of the substance with a basal spacing at 8.5 Å was formed in the initial stages and much of the 8.2 Å calcium aluminate hydrate and C_3AH_6 were present. Large quantities of ettringite were formed and there were no 9.6 Å and 8.9 Å materials. The 8.5 Å substance, the ettringite and aluminate hydrates slowly reacted finally to produce the 10.3 Å material.

As was expected, the use of three moles of $CaSO_4 \cdot 2H_2O$ instead of one gave only ettringite at equilibrium. The 10.3 Å calcium mono-sulpho-aluminate was an intermediate phase when the three moles of $CaSO_4 \cdot 2H_2O$ were added to the C_4AH_{19} hydrate. Figs. 7B(1)–7B(5) gives an indication of the course of the reactions.

The Influence of Heating and Cooling on the 10.3 Å, the 9.6 Å and the 8.9 Å Calcium Mono-Sulpho-Aluminate Hydrates

Turriziani and Schippa (4) have reported the existence of a 10.3 Å hydrate at 1°C and a mixture of 9.6 Å and 10.3 Å hydrates in the 12–17°C region. As can be seen from Fig. 8 this is the stable phase when suspensions formulated to give the mono-sulphate hydrates were cooled and kept at 5°C for long periods. These suspensions were filtered and the solid X-rayed in a damp condition out of contact with carbon dioxide. During the X-ray work the sample was at a relative humidity of 100 per cent. By merely raising the temperature of the solid on the X-ray machine to above 20°C, it was possible to change the substance into the 9.6 Å hydrate, and when ice water was passed through the cell containing the solid, (the water did not come in contact with the sample) the 9.6 Å hydrate was immediately changed back to the 10.3 Å hydrate; this conversion 10.3 Å $\underset{\text{(cool, ice water)}}{\overset{\text{heat 20°C}}{\rightleftharpoons}}$ 9.6 Å could be performed repeatedly at will (see Fig. 9).

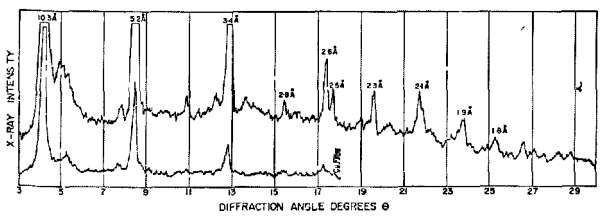

Fig. 8. *X-ray diffractogram of the* 10.3 Å *calcium mono-sulpho-aluminate hydrate at* 5°C

However, when a wet solid consisting essentially of 9.6 Å, prepared from aluminates and $CaSO_4 \cdot 2H_2O$, was cooled on the X-ray machine, it did not change rapidly to 10.3 Å as described above; the 8.9 Å substance appeared and this changed only slowly to 10.3 Å. The 8.9 Å substance appeared to be formed from 9.6 Å preferably in the presence of $Ca(OH)_2$ at temperatures between 15°C and 25°C. When a sus-

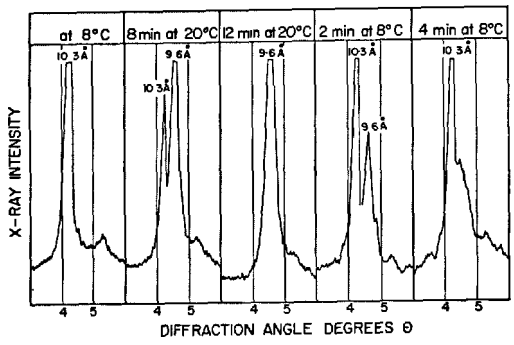

Fig. 9. *X-ray diffractogram showing the behaviour of the* 10.3 Å *and* 9.6 Å *hydrate during heating and cooling*

pension containing the 8.9 Å hydrate was heated to above 30°C, it was changed to the 9.6 Å hydrate. On cooling, the 9.6 Å hydrate apparently changed through the 9.8 Å hydrate to the stable 10.3 Å hydrate at 5°C.

The relationships between the 8.9 Å, the 9.6 Å and the 10.3 Å hydrates is not clearly understood at this stage; it is not clear why, when once the 10.3 Å hydrate was formed, it could be easily changed to the 9.6 Å hydrate and back to the 10.3 Å hydrate, but when fresh 9.6 Å hydrate (not obtained by heating the 10.3 Å hydrate) was cooled, it changed slowly through the 8.9 Å hydrate to the 10.3 Å hydrate.

The Influence of Temperature on the Sulphate Resistance of Portland Cement Containing Tricalcium Aluminate

It has long been known that the resistance of concrete and mortar made with portland cement containing C_3A can be improved or rendered immune to attack by the sulphate ion if they are autoclaved in saturated steam at temperatures above 100°C; higher temperatures are beneficial but even relatively low temperatures, say from 40°C upwards, appear to induce some resistance although not rendering the products completely resistant to attack by the sulphate ion (see for instance the work by Richards (5)).

It is, however, not quite clear why autoclaving should render the aluminates resistant to sulphate attack, because the stable cubic calcium aluminate hexahydrate phase, produced at the temperatures normally used, is also attacked by sulphates and changed into ettringite, the substance generally accepted to be responsible for the expansion of cements containing C_3A. It is often argued that the resistance is due to the reduction of the $Ca(OH)_2$ content as some $Ca(OH)_2$ which aids expansion, reacts with silica in the mortar or concrete to form hydro-calcium-silicates, which are resistant to sulphate attack. Some investigators are of the opinion that during autoclaving some complicated hydrogarnets are produced and that they are resistant to sulphate corrosion. Furthermore it is likely that the physical state of the autoclaved product and the nature of the calcium silicate hydrates have some influence on the matter; it is known that the gel-like tobermorite normally found in water-cured cement products is changed somewhat to a more crystalline state in the autoclaved product. There are many arguments for and against these theories, for example, in connection with the reduction of the $Ca(OH)_2$ content due to reaction with silica. It has been found (6) that when an aggregate that contains no silica is used for concrete or mortar and the material is autoclaved, the resultant product is also resistant to sulphate attack. In this instance there is no question of a reduction of the $Ca(OH)_2$ content due to reaction with silica.

Recently Chatterji and Jeffery (7), (8) have put forward a new hypothesis as regards sulphate attack, in which they doubt the accepted theory that the mere formation of ettringite is responsible for the sulphate expansion. Their hypothesis has since been criticized by other workers in this field (9), (10). Whatever the mechanism of the deterioration or expansion one should not lose sight of the fact that expansion need not necessarily be the prime cause of deterioration. There can be breakdown of the structure before actual expansion takes place and, once breakdown or deterioration has occurred, only a small force is required to produce expansion. However, the forces involved, when a portland cement contains alumina or aluminates and calcium sulphate, can be tremendous; Fig. 10 shows how a steel mould was ruptured when portland cement was mixed with a few per cent of kaolinite and gypsum. Note that although much expansion has occured, there is little lowering of the quality of the hydrated product. It has been shown (6) that the rate of expansion has a marked influence on the quality of the expanded product; a slow expansion of a homogenous body can be considerable without disintegrating the body, but a rapid expansion leads to distintegration. Furthermore it is possible to limit or stop the expansion of a body containing ingredients that cause sulphate expansion by means of steaming; the expansion of expanding cements can be controlled

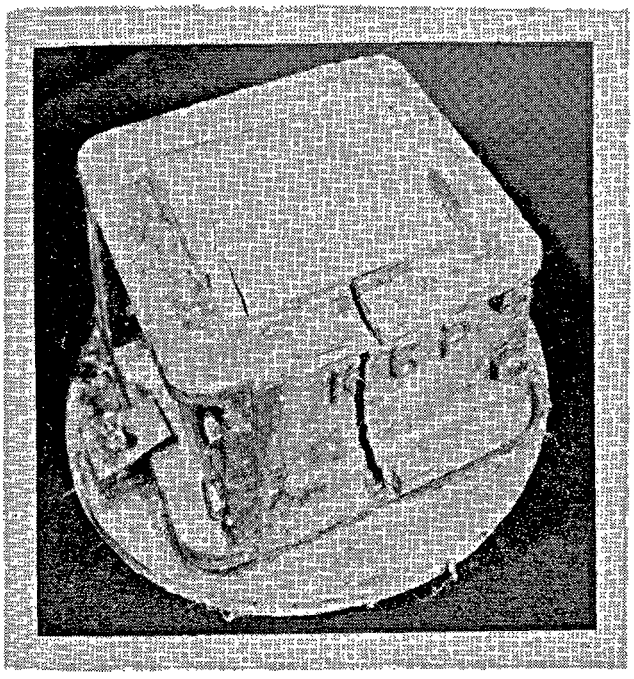

Fig. 10. *Large forces develop during the formation of calcium sulpho-aluminates (4 in cube steel mould)*

somewhat by steaming at atmospheric pressure at the appropriate time after casting.

The above discussion deals with the influence of temperature during the curing period on the subsequent sulphate resistance of portland cement products, but it is also conceivable that temperature changes after curing and during the use of cement products could have an effect on their durability; temperature changes can be of importance by causing changes in the aluminate hydrates and sulpho-aluminate hydrates already in the product, or it can determine the type of sulpho-aluminate hydrate produced when sulphate enters the product from an external source. One is inclined to get the impression that sulphate corrosion of portland cement products is more common and serious in colder climates than in warmer regions. Freezing and thawing may be one of the reasons for this because it is likely that freezing and thawing will weaken the structure and create favourable conditions for further deterioration by sulphate attack. However, the fact that different aluminates and sulpho-aluminates are the stable phases at different temperatures, and that there is a backwards and forwards shift of equilibrium, may have a considerable influence on durability. This may be of much importance in products such as expanding cements that could contain appreciable quantities of aluminates and sulpho-aluminates. It appears that if sufficient sulphate is present to change all the aluminates into ettringite, no trouble would be experienced because ettringite is stable also at low temperatures in the absence of aluminates, but should mono-sulpho-aluminate hydrates and free aluminate hydrates be present, the equilibrium will change with temperature changes at the low level. That such equilibrium shifts are likely is clearly indicated by the work described in the former half of this paper.

In an attempt to investigate the influence of low temperatures on the sulphate resistance of portland cement mortars, experiments were undertaken in which mortars were exposed to sulphates at 5°C and 22°C. In these experiments the following variables were examined:

1. C_3A-content;
2. high pressure steam curing;
3. water curing;
4. exposure in sodium sulphate at 5°C;
5. exposure in sodium sulphate at 22°C.

Specimens were prepared, exposed and examined by procedures described by van Aardt (11).

Crushed, fresh dolomitic rock was used as aggregate in the mortars with a view to eliminating possible pozzolanic reaction in the autoclave between $Ca(OH)_2$ and fine silica; the intension was to prevent the lowering of the $Ca(OH)_2$-content of the specimens during autoclaving. Some specimens were cured under water for 28 days while others were autoclaved at 150 lb/in² saturated steam pressure for 3 hours. The portland cement used had a C_3A-content of approximately 7 per cent and, where it was increased to 14 per cent in the specimen, finely ground C_3A prepared separately was mixed in a mechanical mixer with the required quantity of cement.

After curing, the specimens were immersed in 5 per cent sodium sulphate solution as follows:

1. A set of specimens was stored in the solution at 22°C;
2. A set of specimens was stored in the solution at 5°C.

Table 1 reflects the condition of the specimens after storage for 300 days in the sulphate solution. It can be seen that the autoclaved specimens stored in sulphate solution at 5°C deteriorated rapidly while those stored at 22°C remained sound and unaffected. Fig. 11 illustrates the nature of the deterioration of the specimen in the foreground, i.e. the one that was stored in a sulphate solution at 5°C, while the other one, stored at 22°C in the solution, was unaffected

Table 1. *The influence of temperature on corrosion*

Description of specimen		Treatment during immersion in 5% Na_2SO_4 solution	Period of storage in Na_2SO_4	Observations as regards expansion and deterioration
C_3A content %	Curing			
7	Water-cured	kept at 5°C	300 days	Very rapid deterioration
7	Water-cured	kept at 22°C	300 days	Rapid deterioration
7	Autoclaved	kept at 5°C	300 days	Cracking started after 200 days, bad cracking after 300 days
7	Autoclaved	kept at 22°C	300 days	No cracking or expansion after 300 days of exposure
14	Water-cured	kept at 5°C	300 days	Very rapid deterioration
14	Water-cured	kept at 22°C	300 days	Very rapid deterioration
14	Autoclaved	kept at 5°C	300 days	Expansion started after 100 days, complete disintegration at 300 days
14	Autoclaved	kept at 22°C	300 days	No cracking or expansion after 300 days of exposure

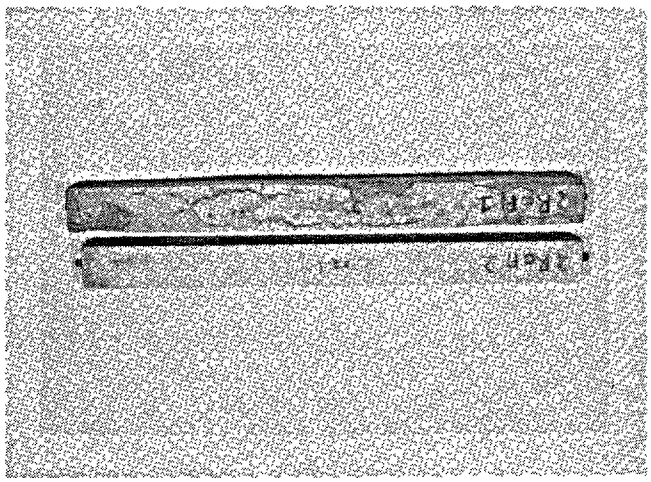

Fig. 11. *Specimens showing the influence of temperature of the sulphate solution on the behaviour of outclaved specimens* ($1'' \times 1'' \times 11\frac{1}{4}''$)

and sound in every respect. These mortars are generally of very high quality and of low permeability and it normally takes a considerable time for liquids to penetrate to the interior. For this reason the ones under consideration were dried, evacuated and the sulphate solution admitted under vacuum. It is not known at this stage whether specimens made with quartzitic aggregate would behave in a similar way or not as the latter experiments have been started only recently. However, the indications are that a similar trend can be expected.

Working with portland cement mortar specimens to which C_3A, C_3AH_6, the 10.6 Å hydrate and the 8.2 Å hydrate were added when the mortars were prepared for moulding and curing, it was observed that in sodium sulphate solutions, the ones containing C_3A or the 10.6 Å hydrate appeared to deteriorate much more rapidly than the ones to which C_3AH_6 or the 8.2 Å hydrate was added.

The work on mortars appears to substantiate the belief that if portland cement products are subjected to sulphate solutions at low temperatures, i.e. temperatures below say 10°C, there is a likelihood of more severe deterioration than at higher temperatures and that autoclaved products are not immune to sulphate attack at low temperatures especially if the portland cement contains much alumina or calcium aluminates.

Acknowledgement

The Author wishes to thank Miss S. Visser for her assistance and Mr. G. R. Basson for the electron microscope work. Both are of the National Building Research Institute of the South African Council for Scientific and Industrial Research.

References

1. J. H. P. van Aardt and S. Visser, "Some reactions of tricalcium-aluminate-hexahydrate at medium temperatures". Cem. Lime Mf., *XL*, 7–11 (Jan. 1967).
2. F. E. Jones and M. H. Roberts, "The system CaO–Al_2O_3–H_2O at 25°C". Research Seriesl, Building Research Station, Garston (1962).
3. J. H. P. van Aardt and S. Visser, "Reaction products at early Ages of C_3A and C_3AH_6 with calcium sulphate". To be published in Cem. Lime Mf.
4. R. Turriziani and G. Schippa, "Riconoscimento all'ATD ed ai Raggi X dei Solidi Quaternari CaO–Al_2O_3–$CaSO_4$–H_2O". Ricerca Scient., **25**, 2895–8 (1955).
5. John D. Richards, "The effect of various sulphate solutions on the strength and other properties of cement mortars at temperatures up to 80°C". Mag.

Concr. Res., **17**, 69–76 (June 1965).
6. Chemistry of Cement (Proc. 4th int. Symp., vol. II, Natn. Bur. Stand. Monogr. 43, Government Printing Office, Washington 25, D.C. p. 835–53, 1962). See paper by J.H.P. van Aardt entitled "Deterioration of cement products in aggressive media".
7. S. Chatterji and J. W. Jeffery, "New hypothesis of sulphate expansion". Mag. Concr. Res., **15**, 83–6 (July 1963).
8. S. Chatterji and J. W. Jeffery, "Further evidence relating to the 'New hypothesis of sulphate expansion'". Mag. Concr. Res., **19**, 185–9 (Sept. 1967).
9. M. H. Roberts. Contribution to discussion of paper by S. Chatterji and J. W. Jeffery on "A new hypothesis of sulphate expansion". Note E1361, Building Research Station, Garston, England (1963).
10. Symposium on Structure of Portland Cement Paste and Concrete (Highway Research Board Special Report no. 90, Washington, p. 328–52, 1962). See paper by P. K. Mehta and A. Klein entitled "Investigations on the hydration products in the system $4CaO \cdot 3Al_2O_3 \cdot SO_3$–$CaSO_4$–$CaO$–$H_2O$".
11. J. H. P. van Aardt, "Acid attack on hydraulic cement mortars with special reference to the use of calcareous aggregates" (In German). Zement-Kalk-Gips, **50**, 440–7 (Oct. 1961).

Supplementary Paper III-30 The Frost Resistance of Cement Grouts for Prestressed Concrete Applications

Cameron MacInnis*

Synopsis

This paper is a summary of an extensive, three-stage experimental program carried out to study the factors affecting the frost resistance of cement grouts for prestressed concrete applications.

In Part I, the expansive tendencies, during a freezing cycle, of seventeen different cement grout mixtures (at a variety of maturities) were investigated. The length change patterns exhibited in the Part I tests are grouped into a number of categories and a short theoretical section is devoted to the interpretation of these patterns. The Part I experimental results provided a good comparative picture of the frost resistance of the various cement mixes at different maturities.

In Part II, a limited number of mixes were subjected to a freezing cycle in a restrained condition ("tube" tests) and resultant pressures were measured. In Part II experimental results provided an indication of the pressures developed by the various grout mixtures during freezing (at different maturities) and these were found to correlate very well with the various expansion patterns exhibited in the Part I tests.

In Part III, selected mixes were chosen for freezing tests in grouted beams of various dimensions. These tests demonstrated in a practical way the validity of the findings in Parts I and II and showed that only mixes exhibiting continuous expansion after freezing starts can produce enough pressure to crack beams.

The estimated curing periods required, for both air-entrained and non-air-entrained cement grouts of various water-cement ratios, to achieve frost-resistance, are presented. Cement composition was found to be of minor importance compared with the provision of air-entrainment and low water-cement ratios for the achievement of frost resistance.

Introduction

The factors affecting the frost resistance of grouts for prestressed concrete applications are to a large extent the same as those which apply to concrete in general, i.e. (a) water-cement ratio, (b) maturity of grout, (c) cementing materials and (d) admixtures, especially air-entraining agents. Provided that the general quality of the cementing materials being used is satisfactory, there is no doubt that frost-resistant grouts can be produced by the use of a low water-cement ratio and purposely entrained air voids of adequate spacing, together with the provision of favourable curing conditions for a sufficient period of time before the grouts in question are subjected to frost action. However, although there is considerable knowledge and agreement about the various factors affecting the frost-resistance of grouts, little attempt has previously been made to assess the relative importance of these factors. This, therefore, was the purpose of this program of studies.

Outline of Investigation

The frost-resistance of a given post-tensioned prestressed member will be a function of the frost-resistance of the grout itself plus what might be called "beam factors", e.g. amount of restraint, dimensions of beam, duct sizes, maturity of concrete in the beam, strength. Because of the large number of "beam factors" involved in the frost-resistance of a grouted member it was decided that initially

*University of Windsor, Ontario, Canada.

the studies should be limited to the grout itself—to be followed later with studies of grouted beams. A three-stage approach, as follows, was adopted:

Part I—Evaluation of the relative frost-resistance of a variety of grout mixes in an unrestrained condition, by obtaining an accurate measurement of expansive tendencies during a freezing cycle.

Part II—Study of a limited number of selected mixes (and maturities) in a restrained condition to measure the forces involved and, if possible, the effect of restraint on the pressure generated.

Part III—Study of a limited number of selected mixes (and maturities) in freezing tests of grouted beams of various dimensions. These should demonstrate in a practical way the validity of the findings of Parts I and II.

Test Programme—Part I

Since sand is not commonly used in grouting mixtures for prestressed concrete because of the danger of segregation and blockages during the grouting operation it was decided to deal only with non-sanded grouts in this study. The various factors to be investigated were dealt with as follows in the experimental program:

Maturity of Grout

The frost resistance of all mixes investigated were studied at six different maturities—1, 2, 3, 4, 7 and 28 days of standard laboratory curing.

Cements

Although ordinary portland cement is most commonly used in grouting mixtures it was decided because of their potential beneficial effect on frost-resistance, to include air-entraining and rapid-hardening portland cements as well. In all, three ordinary portland cements, one air-entraining portland cement and two rapid-hardening portland cements were included in the program.

Admixtures

Preliminary tests were conducted to evaluate the effectiveness of a number of water-reducing and air-entraining agents, as a result of which one agent from each class was chosen for the main test programme. The water reducing agent chosen was a lignin type and was utilized in grout mixes with each class of cement in the program. The air-entraining agent chosen was a neutralized Vinsol resin and was used in mixes with ordinary portland cement and in one mix with rapid-hardening portland cement.

Water-Cement Ratios

The minimum water-cement ratio will largely be governed by the fluidity required for pumping and will therefore, in the absence of a water-reducing agent be more or less fixed for a given cement. This forms a lower limit to the experimental values. Thus, a fluidity of 30-40 sec (using the German Immersion Apparatus) served as a guide for the minimum water-cement ratio mix made up with each cement. Higher water-cement ratio mixes were also included using both the ordinary portland and air-entraining portland cements.

In all, seventeen different mixes were included in the Part I experimental programme, as shown in Table 1, Summary of test results.

Table 1. *Summary of test results—Part I*

Cement	Mix design-nation	W/C ratio	Admix-ture	Flu-idity* secs.	Air content (%)	Age at which there is no	
						Transi-tory expansion displayed	Ultimate expansion displayed
OPC	0–1	0.45	—	33	—	7	7
	0–2	0.40	WRA	32	—	3–4	3
	0–3	0.50	AEA	40	13.5	7	1
	0–4	0.50	—	11	—	28	28
	0–5	0.50	AEA	18	5.0	7	1
	0–6	0.55	—	12	—	28	28
RH	RH–1	0.52	—	34	—	7	4
	RH–2	0.55	AEA	35	5.0	7	1
	RH–3	0.51	WRA	33	—	3	3
AE	AE–1	0.45	—	33	6.6	7	1
	AE-2	0.40	WRA	60	5.5	2–3	1
	AE-3	0.40	WRA	60	8.0	4	1
	AE–4	0.50	—	18	6.2	7	1
2–OPC	2–0–1	0.45	—	43	—	7	3
	2–0–2	0.50	—	23	—	7	4
2–RH	2 RH–1	0.69	—	34	—	28	7
3–OPC	3–0–1	0.50	—	35	—	28	28

*Using the German immersion apparatus in which a measurement is made of the time required for a bullet-shaped plunger to fall a specified distance through a tube filled with grout,

Freezing Test Procedure—Part I

The freezing test procedure used in the Part I program is based on the premise that "length measurements can be used to tell whether or not at any given time a specimen is vulnerable to frost action. If it shrinks normally in the freezing range it is immune; if it dilates it is not immune—the process that eventually causes disintegration has begun" (1). Also it has been pointed out that test conditions fundamentally different from field conditions must be avoided if valid results are to be obtained in freezing tests (1). The freezing cycle chosen, therefore, was a relatively slow lowering of temperature from 65°F to 5°F (+18°C to −15°C) over a period of nine hours. Length measurements were made on the specimens (in the freezing chamber) at regular intervals during the freezing cycle using a mechanical length comparator which could be read to 0.0005 in.

The freezing test specimens were prisms, 1-1/2 × 1-1/2 × 10 in., which had a suitable stainless steel insert embedded in each end to facilitate the taking of length measurements. The specimens were cured at a temperature 65°F (18°C) from time of casting until *subjected* to the freezing test. Suitable precautions were taken to prevent the loss or gain of moisture from the time specimens were cast until *completion* of the freezing test.

Interpretation of Freezing Test Results

On examining the length change patterns exhibited by the specimens from the various mixes when subjected to the freezing test, it was possible to detect a range of patterns which could conveniently be grouped into a number of categories. It seems appropriate therefore, before dealing with the merits of the various mixes, to discuss briefly the interpretation of these patterns, which are presented in idealized form in Fig. 1.

In Case A (Fig. 1) there is a normal thermal contraction until the freezing temperature is reached, followed by a distinctive continuous expansion as the temperature is lowered further, This obviously represents a great vulnerability to damage by frost.

In Case B, there is a sudden expansion at the freezing point followed by a transitory contraction and then expansion at a lower rate as the temperature is reduced further. Case B, it is felt, also represents a serious vulnerability to damage by frost.

In Case C there is transitory expansion at the freezing point followed by contraction at an increased rate. This latter phenomenon was also noted by Powers (2) and is claimed to occur after ice crystals begin to form in the air voids of the paste. Once crystals have formed, they tend to attract water from the cement gel pores on further cooling, causing the cement gel to shrink. As long as the ice crystals have space available for expansion in the air voids the net result is a contraction at a rate greater than that due to the thermal coefficient alone. If the transitory expansion in a case such as C were very great it is believed that this would represent a considerable vulnerability to frost action.

In Case D, normal thermal contraction is followed by a period of no length change and then contraction at an increased rate. The period of no expansion is,

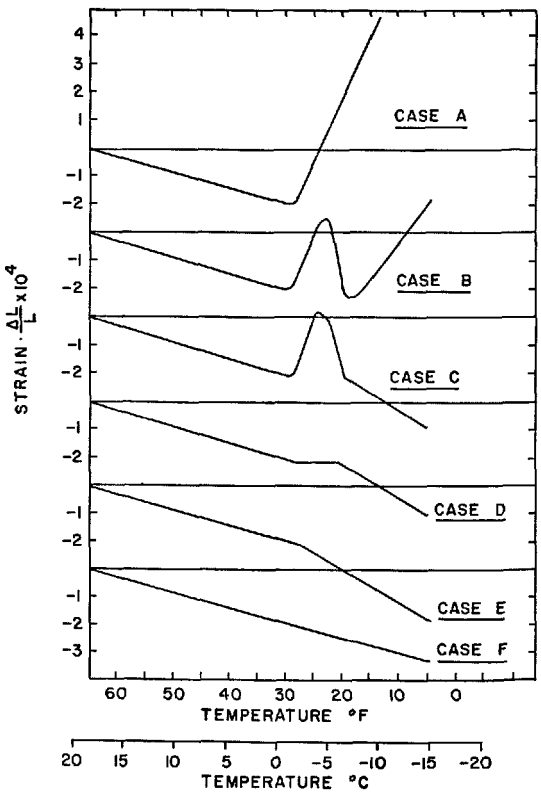

Fig. 1. *Typical "Idealized" length change patterns exhibited during freezing cycle*

according to Powers (2), due to a cancelling out of opposite effects, i.e. "the tendency to expand from the freezing of water in capillary cavities is about equal to the thermal contraction plus the tendency to contract due to diffusion of water from the gel pores to the ice bodies". The explanation of the subsequent increased rate of contraction is the same as for Case C. Case D, it is believed, represents a frost-resistant condition. Although a tendency to expand exists in some regions during the no length change period, no irreparable damage is likely to occur to the grout.

In Case E there is normal temperature contraction followed by increased contraction after freezing starts. The explanation for the increased rate of contraction is the same as for cases C and D. This also represents a frost-resistant condition.

In Case F there is a constant rate of contraction throughout the thermal range. Only in virtually dry grouts will the relationship be constant over the whole range of temperature. This also represents a frost-resistant condition.

To summarize, it would appear that A and B represent grouts that would be vulnerable to frost action; D, E and F represent grouts that would be frost-proof. Condition C is the doubtful one and the magnitude of the transitory expansion should be taken into consideration when assessing the possibility of frost damage.

Discussion of Test Results—Part I

The experimental results are presented in Table 1 and Figs. 2 to 8. It is proposed in this discussion to deal in turn with the various factors investigated. The important effect of maturity of grout on frost-resistance was well demonstrated by all mixes and need not be discussed separately as it will come up in discussion of the other factors.

Type of Cement

The first three mixes investigated (0–1, RH-1 and AE-1) demonstrated the effects of these different types of cement and the duration of curing, on frost-resistance. These three mixes were all made to the same consistency. The average freezing test results for these mixes are presented in Fig. 2.

As would be expected, the air-entraining cement performed most satisfactorily, producing a length change pattern similar to Case C at an age of one day. Even this cement, however, showed a significant amount of transitory expansion and it was not until the age of 7 days that the transitory expansion was eliminated. The rapid-hardening cement produced intermediate results, showing a Case C length change pattern at the age of 4 days while at 7 days it no longer exhibited the transitory expansion. In the case of the ordinary portland mix (0 –1) it was not until the age of 7 days that both the transitory expansion at the start of freezing and the ultimate expansion at the lower temperature were eliminated.

In mix 0–2 the use of the water reducing agent, allowed reduction of the water-cement ratio from 0.45 (mix 0–1) to 0.40 without affecting the fluidity, Table 1. This in turn reduced the age at which expansive tendencies were no longer exhibited from 7 days to the 3-day age.

Using the water-reducing agent with the rapid-hardening cement, however, it was possible to reduce the water-cement ratio only from 0.52 (mix RH-1) to 0.51 (RH-3) and still achieve the same fluidity, Table 1. Nevertheless, this did appear to have a significant affect on frost resistance, reducing the age at which ultimate expansion was no longer exhibited from four days to three days. However, if mixes 0–2 and RH–3 are now compared (Fig. 3) it is seen that their performance in the freezing test are practically identical, both indicating immunity from frost action after 3 days curing.

Water-Cement Ratio

The effect of water-cement ratio is demonstrated very well in Fig. 4 where No. 1 -OPC is used in mixes of 0.40, 0.45, 0.50 and 0.55 water-cement ratios. It can be seen that the 0.40 water-cement ratio mix indicated frost-resistance at the 2-3 day age, the 0.45 mix at the 7-day age, and the 0.50 and 0.55 mixes at the 28 day age. To demonstrate better the difference in frost-resistance of the 0.50 and 0.55 water-cement ratio mixes it would have been desirable to have freezing tests run between the 7 and 28 day ages; however, even at the 28 day age the 0.55 water-cement mix exhibited a case D length change pattern compared with a case F pattern for the 0.50 mix.

The effect of water-cement ratio can also be seen in the mixes made with No. 2-OPC, i.e. 2-0-1 and 2-0-2, also in the rapid-hardening cement mixes RH-1 and RH-3 (see Table 1). In the air-entraining cement

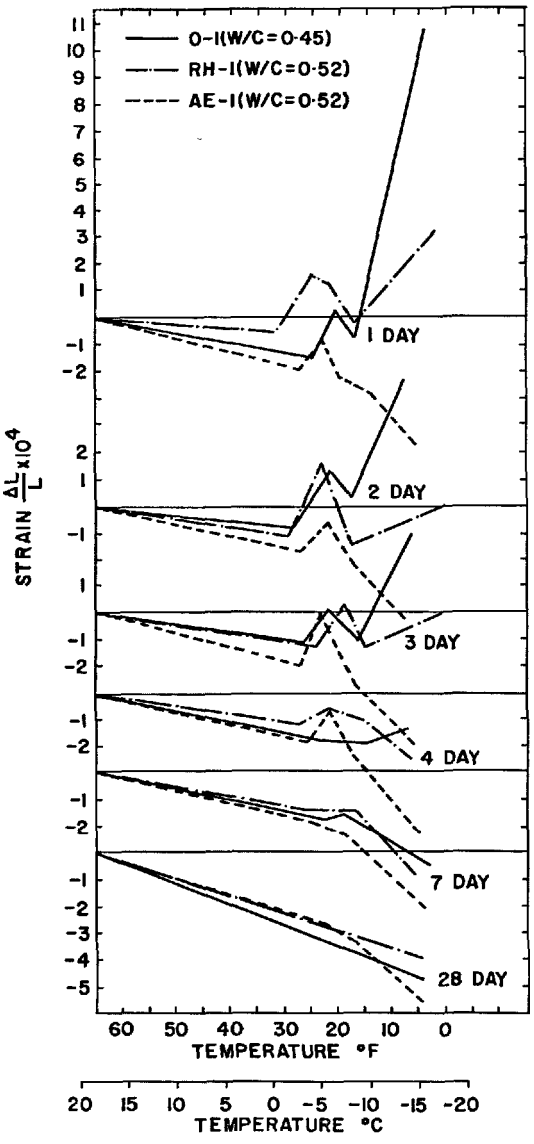

Fig. 2. *Effect of type of cement on length change patterns exhibitad during freezing cycle*

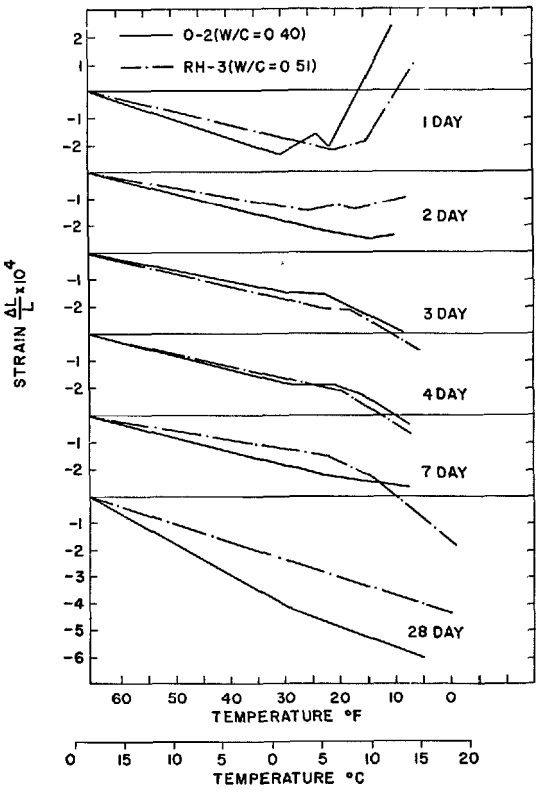

Fig. 3. *Effect of water-reducing agent on length change patterns of both ordinary and rapid-hardening portland cement mixes*

mixes (AE-1, 3, 4) the effect of the water-cement ratio on frost-resistance seems to be clouded by the much greater effect of the entrained air itself, so that there was no significant difference in frost-resistance indicated by air-entrained mixes of 0.40, 0.45 and 0.50 water-cement ratios (see Table 1).

Differences between Cements of Same Type

In addition to the differences in performance between the various types of cement there was significant differences shown by the cements within each group. In Fig. 5, for example, freezing test results are presented for 0.50 water- cement ratio mixes made with each of the three ordinary portland cements used in the programme. It can be seen that mixes 0-4 and 3-0-1 exhibited strong expansive tendencies up to and including the 7-day age which were equivalent to patterns exhibited by mix 2-0-2 specimens at the age of 2 days. Similarly, significantly different freezing test results were exhibited by the two 0.45 water-cement ratio mixes, 0-1 and 2-0-1.

It is interesting to note in Fig. 6 that if the cements 1-OPC and 2-OPC are compared at the same fluidity (but different water-cement ratios, 0.45 and 0.50) there is little difference in frost behaviour. Similarly, the two RH cements, when compared at the same fluidity, are very similar in frost resistance although the water requirements are vastly different (0.52 versus 0.69 water-cement ratio for mixes RH-1 and 2RH-1 respectively).

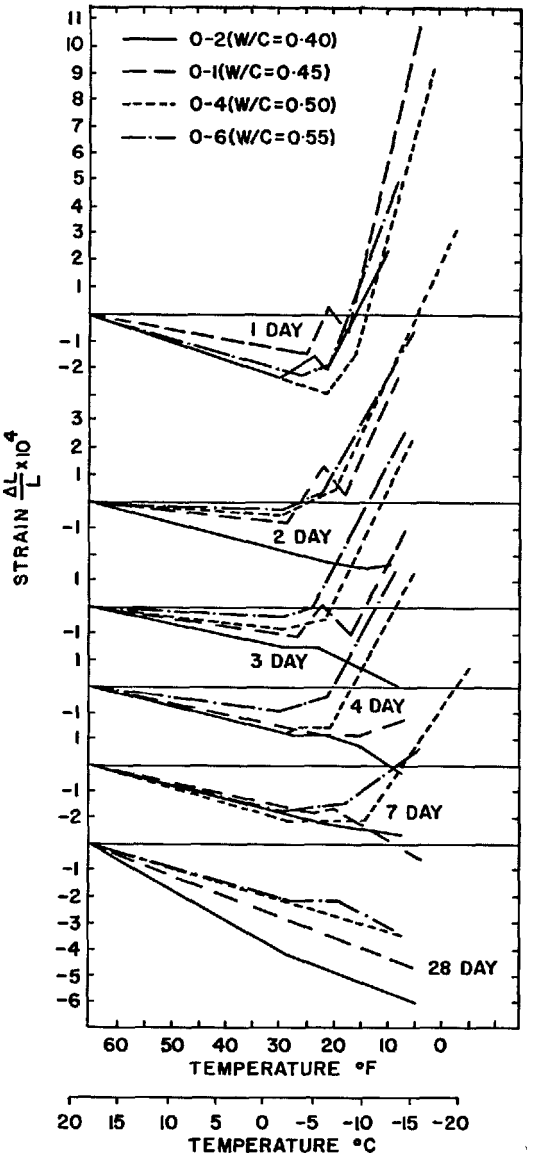

Fig. 4. *Effect of water-cement ratio on length change patterns exhibited during freezing cycle*

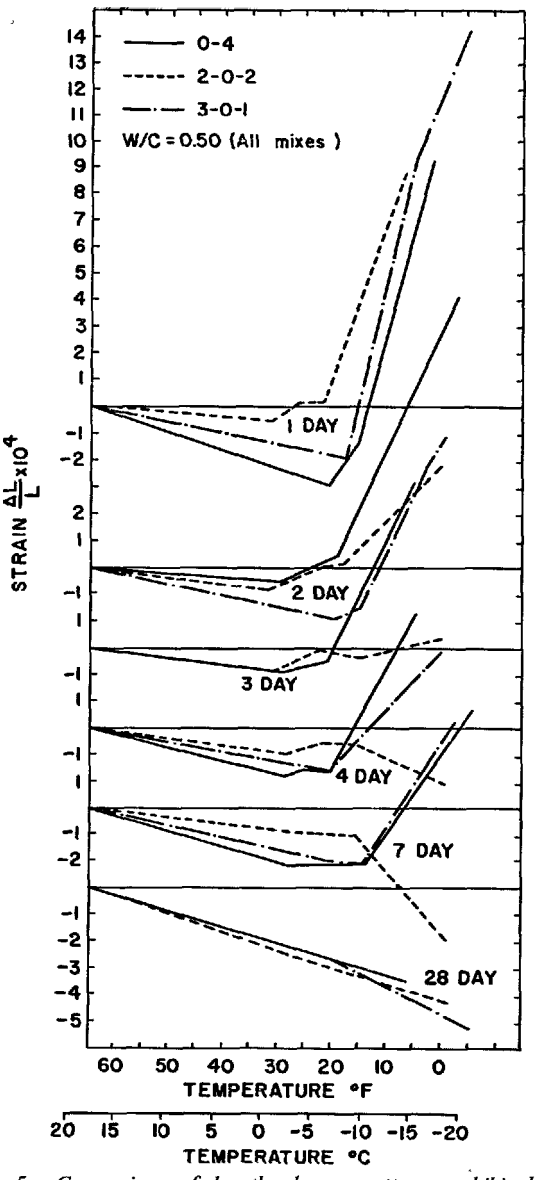

Fig. 5. *Comparison of length change patterns exhibited by different ordinary portland cements during freezing cycle*

Air-Entrainment

The significant effect of entrained air on frost-resistance was already indicated when the performance of the air-entraining cement was compared with normal and high-early portland cements. Similar results were produced by using an air-entraining agent in the ordinary and rapid-hardening cement mixes. In Fig. 7 a plain mix at a water-cement ratio of 0.50 is compared with mixes of the same water-cement ratio containing 5.5 and 13.5% air respectively. Both of the air-entrained mixes eliminate the ultimate

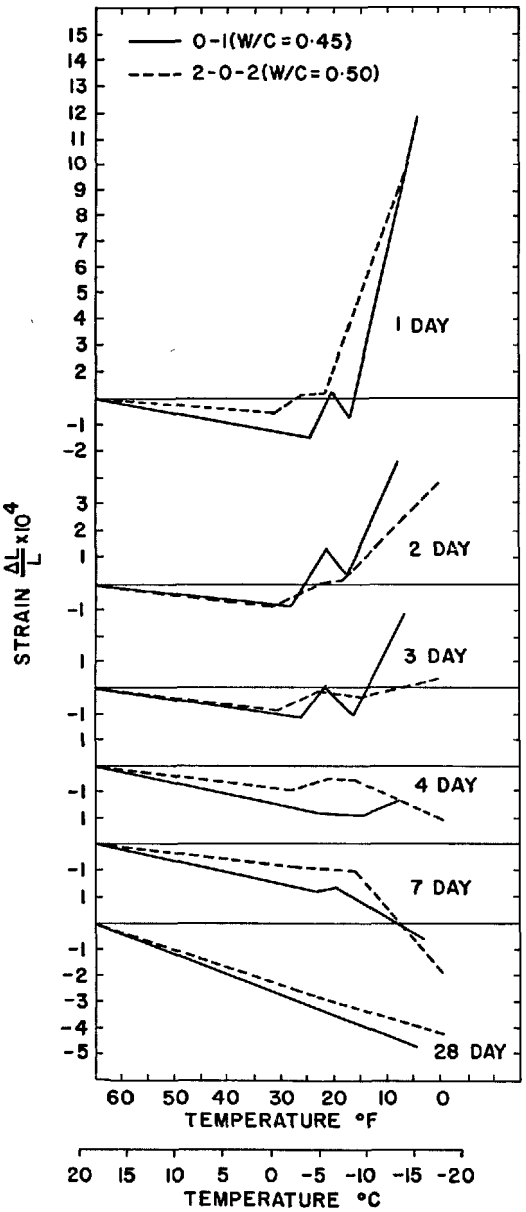

Fig. 6. *Comparison of length change patterns exhibited by different ordinary portland cements at same fluidity*

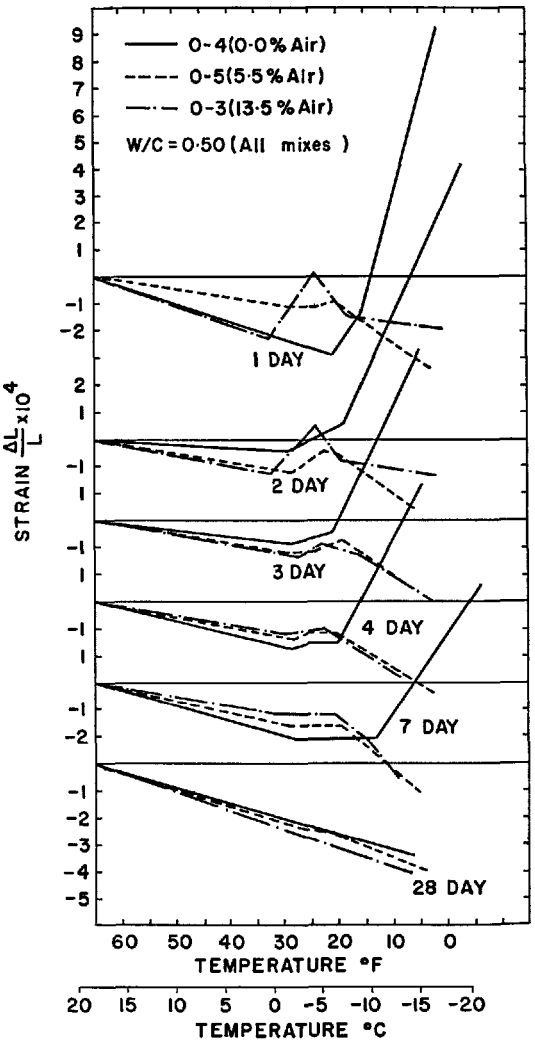

Fig. 7. *Effect of air-entrainment on length change patterns exhibited during freezing cycle*

expansive effects at all test ages, although transitory expansions are noticeable up to the age of 4 days. Probably of most significance is the fact that the 5.5% air mix appears to be equally as effective as the 13.5% air mix. In the air-entrained high-early cement mix ultimate expansions were eliminated at all ages, but some transitory expansions were noted up to the 4-day age. This same pattern of performance also holds for all mixes made with the air-entraining cement (mixes AF-1, 2,3 and 4).

It is interesting to compare mixes AE-2, AE-1 and 0-3. In Fig. 8 it can be seen that mix AE-2 containing

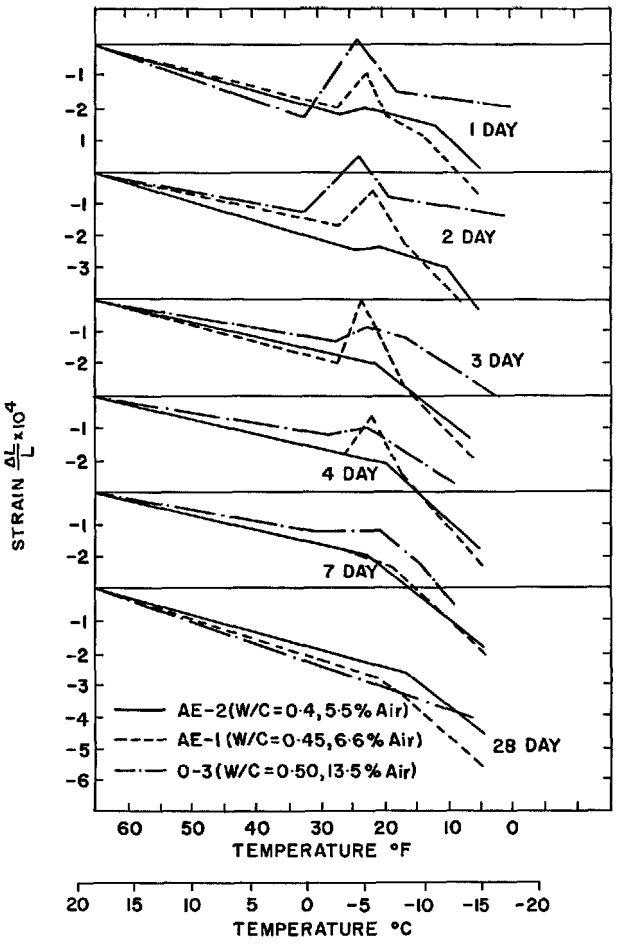

Fig. 8. *Effect of air-entrainment and W/C ratio on length change patterns exhibited during freezing cycle*

5.5% air at a water-cement ratio of 0.40 exhibited smaller transitory expansions and for a shorter period than either mix AE-1 containing 6.6% air at a water-cement ratio of 0.45 or even mix 0-3 containing 13.5% air at 0.50 water-cement ratio. Thus, providing a mix contains a certain minimum of entrained air (say 5 per cent) a lower water-cement ratio seems more effective than additional air in increasing frost-resistance.

Test Programme—Part II

The test method used in Part I (unrestrained tests) provides a sensitive assessment of the expansive tendencies during freezing of a grout specimen. However, it was realized that a completely quantitative assessment of the frost resistance of the various grouts was not provided; and there was some difficulty in interpreting some of the data, especially mixes that showed transitory expansions during the freezing test. Also, this data was obtained on unrestrained specimens, whereas, in practice, the grout is contained in ducts in the prestressed member.

As a next stage, therefore, the effect of freezing on restrained grout specimens was studied by measuring the strains developed in grouted steel tubes during a freezing cycle. Aside from providing information on the effect of restraint, this test procedure has the advantage of ensuring no moisture loss and provides data which can be related to potential damage to a prestressed member.

The aims of Part II can be briefly summarized as follows:

1. To determine the magnitude of the forces developed by the freezing grouts.
2. To determine if there is a direct relationship between the results of tests on restrained and unrestrained grouts.
3. To determine if the degree of restraint affects the magnitude of the forces developed by the freezing grout.

Selection of Mixes for Investigation

The results obtained in Part I were taken into account in deciding which mixes and maturities to

test in Part II. mix 0-1 was a natural choice since in the Part I experimental programme it exhibited excessive expansions for maturities up to 3 days, minor expansions for the 4 and 7 day maturities and complete immunity to frost action at 28 days. It was also decided to test a mix of a higher water-cement ratio (mix 3-0-1 at water-cement ratio of 0.50) and to include an air-entrained mix at a relatively high water-cement ratio (AE-4 at water-cement = 0.50).

To determine the effect of restraint on the generation of expansive forces three different tube wall thicknesses were included in the program, i.e. 0.128 in., 0.09 in., and 0.06 in. An outline of the program carried out is shown in Table 2.

Test Procedures—Part II

Selection and Preparation of Tubes

The tubes used in this part of the programme were solid drawn steel tubing of similar interior diameter to the ducts provided in prestressed concrete members and the wall thicknesses chosen were such that strains would be in the same range as that exhibited by concrete in service. Tubing of 1-3/4 in. O.D. and 10 gauge (0.128 in.) thickness was chosen for the maximum size. Wall thicknesses of 0.09 in. and 0.06 in. for the other two sizes were obtained by machining the 10 gauge tube down to these values.

The tube specimens were cut to 2 ft. lengths, which was considered to be long enough to eliminate end effects. The ends of the specimens were threaded to accommodate an end cap and adaptor required in the pressure calibration of the tubes.

Strain Measurement of Grouted Tubes

One-quarter inch foil strain gauges were used for strain measurement of the grouted tubes during the freezing test. Six gauges were mounted at approximately the centre of each tube-four circumferentially and two longitudinally, diametrically opposite each other. As a preliminary, pressure-strain relationships were established for each tube, so that the strains recorded in the subsequent tests could be related to pressures being generated by the grouts during the freezing cycle. The tubes of 0.128 and 0.09 in. wall thickness were calibrated to a maximum pressure of 3000 lb/in^2 while the tubes of 0.06 in. wall thickness were calibrated to a maximum pressure of 2000 lb/in^2.

Freezing Regime

The freezing regime was similar to that used in Part I except that the minimum temperature of 0°F was maintained for 8-10 hours. Strain readings were taken on the grouted tubes at regular intervals during the freezing cycle. Prisms (as used in Part I) were provided for subjection to the freezing test at the same time as the grouted tubes. This was to assist correlation of the restrained and unrestrained tests.

Disccuion of Test Results—Part II

Comparison of Different Mixes

In Table 2 a summary is provided of the average maximum pressures indicated by the gauges for all mixes (and maturities) tested in the program. It can be seen that in the restrained tests, mix 3-0-1 (water-cement = 0.50) produced the highest pressures, mix 0-1 (water-cement = 0.45) intermediate values and mix AE-4 (water-cement = 0.50) the lowest pressures. With mix 0-1, increasing maturity in the grout resulted in decreasing pressures being developed in the grouted tubes, ranging from 1500 to 2000 lb/in^2 at the 1 day maturity down to zero lb/in^2 for the 28 day maturity. On the other hand, mix 3-0-1 exhibited a consistent level of pressure (in the range of 2000 to 2200 lb/in^2) for all maturities up to 7 days, and the relatively small pressure of 90 lb/in^2 at 28 days. Mix AE-4 exhibited the relatively low level of 200-270 lb/in^2 pressure for all ages tested (1, 7 and 28 days).

Effect of Degree of Restraint on Pressures Developed

It can be seen from Table 2 that four sets of grouted tubes (three wall thicknesses) were provided for studying the effect of degree of restraint on the generation of expansive forces. In general, the greater the restraint, the lower is the pressure developed, but this

Table 2. *Summary of test results—Part II*
Pressure measurements of grouted tubes during freezing

Age of grout before freezing	Average maximum pressures produced in grouted tubes — lb/in.²								
	Mix 0–1 W/C = 0.45			Mix 3–0–1 W/C = 0.50			Mix AE–4 W/C = 0.50		
	Tube wall thickness-in.			Tube wall thinkness-in.			Tube wall thickness-in.		
	0.128	0.09	0.06	0.128	0.09	0.06	0.128	0.09	0.06
1	1750	1525	1965	1340	2170	2695	50	260	205
2					2000				
3	760	630	890						
7		165			2250			205	
28		0			90			270	

pattern is by no means consistent. With mix 3-0-1, this pattern of decreasing pressure for increasing wall thickness was most pronounced. The tube of 0.06 in. wall thickness exhibited an average maximum equivalent pressure of 2695 lb/in² followed by 2170 lb/in² for the tube of 0.09 in. thickness and 1340 lb/in² for the tube of 0.128 in. thickness. With mix 0-1 tubes at both the 1 and 3-day maturities it can be seen that the thin-walled tubes exhibited higher pressures than the thick-walled tubes, but in both cases the tubes of intermediate thickness exhibited the lowest pressures. It is also significant that the differences in pressures between the different tubes were much smaller for mix 0-1 than for mix 3-0-1. With mix AE-4 tubes, the thin-walled tube exhibited a higher pressure than the thick-walled tube, but the tube of intermediate thickness exhibited the highest pressure. However, all pressures for the AE-4 tubes were relatively low (50 to 260 lb/in²).

Correlation between Restrained and Unrestrained Test Results

It is interesting to compare the test results for the grouted tubes with the length change patterns exhibited in the freezing test by unrestrained prism specimens of the same mixes.

Mix 0-1 in the unrestrained tests, Fig. 2, exhibited case "A" length change patterns (normal temperature contraction initially, followed by distinctive continuous expansion as the temperature was lowered further) for the 1 and 3-day specimens, a case "D" length change pattern (normal temperature contraction, followed by a period of no length change, then contraction at an increased rate) for the 7-day specimens and a case "F" length change pattern (practically constant rate of contraction throughout the thermal range) for the 28-day specimens. Corresponding to these in the restrained tests, Table 2, were pressures of 1500–2000 lb/in² for the 1-day tests, values of 600–900 lb/in² for the 3-day tests, a value of 165 lb/in² for the 7-day test and zero pressure for the 28-day test. The tube test has thus served to provide an indication of pressures corresponding to the expansion patterns exhibited by this mix at various maturities in the unrestrained test. It is interesting to note that although the three-day test on the unrestrained prisms exhibited expansions somewhat less severe than the 1-day specimens, the pressures in the 3-day tubes were less than 50 per cent of the 1-day test values.

Mix 3-0-1 in the unrestrained tests, Fig. 5, exhibited case "A" length change patterns (normal temperature contraction followed by distinctive continuous expansion as temperature was lowered further) for maturities of 1, 2, 4 and 7 days. It will be noted, however, that the magnitude of the expansions exhibited decreased with increasing maturity of grout. In spite of this, the pressures indicated in the tube tests, Table 2, remained the same, i.e. about 2000–2200 lb/in² for all 0.09 in. tubes tested up to the age of 7 days. The 28-day unrestrained specimens showed a case "F" length change pattern (continuous contraction rate throughout) and the 28-day tube test produced the relatively low pressure of 90 lb/in².

Mix AE-4 in the unrestrained tests exhibited case "C" length change parterns (transitory expansion at freezing point, followed by contraction at an increased rate) for both the 1 and 3-day maturities and case "E" length change patterns (normal temperature contraction followed by increased contraction after freezing starts) for the 7 and 28-day maturities. In the tube tests, however, there was little difference in the pressures generated at maturities 1, 7 and 28 days, Table 2. Indeed, the pressures indicated at all maturities of AE-4 tested (ranging from 200 to 270 lb/in²) are so small that they are not likely to be of practical importance.

Conclusions—Part II

The test results for the restrained grout specimens ("tube" tests) have provided an indication of pres-

sures developed by the various grout mixtures during freezing and hence, serve as a calibration for the expansion patterns exhibited by the unrestrained grout specimens in the freezing test (Part I). Probably the most interesting aspect of the test results for the restrained specimens is the extent to which they correlate with the freezing test results for the unrestrained grout prisms. The main conclusions follow:

1. The test results for the restrained grout specimens have confirmed the usefulness of length change measurements on unrestrained specimens as a means of determining the probable frost resistance of a given grout mix.

2. The restrained tests confirmed the benefit of air-entrainment for frost resistance. Only relatively low pressures (50 to 270 lb/in^2) were exhibited by the tubes grouted with AE-4 (6.2% air) which had a relatively high water-cement ratio (0.50).

3. Only those mixes (and maturities) that exhibited a case "A" length change pattern (normal temperature contraction initially, followed by continuous distinctive expansion as the temperature was lowered further) in the unrestrained prism tests produced significant pressures in the tube freezing test. Mixes exhibiting transitory expansions in the unrestrained test did not produce significant pressures in the tube test.

4. The test results indicated that the importance of water-cement ratio in determining the frost behaviour may be even greater than was indicated in the unrestrained test. This is because higher water content mixes tend to expand slightly as hydration proceeds and hence at later maturities fit more tightly into the grout duct than would a lower water-cement ratio mix. Hence expansive pressures are exerted immediately freezing starts provided there is still free water available to freeze.

5. In general, the greater the restraint (the thicker the wall of the tube) the lower was the pressure developed in the tube; but this pattern was not consistent and more testing would be required to confirm this pattern.

Test Programme—Part III

In Part III, selected mixes were chosen for freezing tests in grouted beams. The basic aim of these studies was to demonstrate in a practical way the validity of the findings of Parts I and II.

The three mixes studied in Part II (mixes 0-1, 3-0-1 and AE-4) were included in the programme of freezing studies on grouted beams. A rapid-hardening cement mix (2-RH-1) was also included. The maturities at which each mix was tested were determined as the programme proceeded, on the basis of the results obtained from the first beams tested, and taking into consideration the performance of these mixes in Parts I and II. In all, 15 sets of grouted beams were subjected to the freezing test, as shown in Table 3.

Table 3. *Freezing test results on grouted beams*

Age of grout	Mix 0–1 (W/C = 0.45)			Mix 3–0–1 (W/C = 0.50)			Mix AE–4 (W/C = 0.50)			Mix 2–RH–1 (W/C = 0.69)		
	Concrete cover			Concrete cover			Concrete cover			Concrete cover		
	1 in.	1–½ in.	2 in.	1 in.	1–½ in.	2 in.	1 in.	1–½ in.	2 in.	1 in.	1–½ in.	2 in.
0 hr.							○	○	○			
12 hr.							○	○	○			
1 day	×	×	○	×	×	×	○	○	○	○	○	○
2 〃	○	○	○	×	×	○						
3 〃	○	○	○							○	○	○
4 〃				×	×	○						
5 〃				×	×	○						
7 〃				×	×	○						
14 〃				○	○	○						
28 〃				○	○	○						

Design and Fabrication of Beams

Beams were used which had three different thicknesses of concrete cover over the grouted tubes, i.e. 1 in. 1-1/2 in. and 2 in. Ducts were formed with thin-wall rigid plain steel tubing with lock joint seams, 1-5/8 in., I.D. The beams were 2 ft. long and 6 in. in depth; the ducts were centrally spaced so that the minimum cover was at the sides of the beams.

The concrete for the beams was designed to provide a nominal minimum 28-day strength of 6,000 lb/in^2 at a "very low" degree of workability. The moulds were stripped from the beams after 1 day and the beams were cured in water (at 65°F) for 7 days, and then remained in the laboratory for approximately 6 months before being grouted and subsequently subjected to the freezing tests.

Test Procedures—Part III

The freezing regime was the same as that used in Part II. In fact for some of the early maturities, the tube specimens (of Part II) and grouted beams were subjected to the freezing test at the same time.

To confirm that freezing temperatures were being attained in the grout of the beam specimens, temperature records (using thermistors) were obtained for one set of beam specimens (mix 0-1, 1-day maturity) during the freezing test. The temperature readings were obtained in the centres of the grouted ducts.

Discussion of Test Results

The results of the freezing tests on the grouted beams are presented in Table 3. An "X" denotes that the beam cracked during the freezing cycle; an "O" indicates that no cracking occurred.

Grout mix 3-0-1, it can be seen, produced cracks in beams of 1 in. and 1-1/2 in. concrete cover for maturities up to 7 days, but produced no cracks at the 14 and 28-day maturities. Mix 0-1 produced no cracks beyond the 1-day maturity. Mix 2-RH-1 procuced no cracks at the two maturities tested. Mix AE-4 produced no cracks even when the beams were subjected to the freezing cycle immediately after the grout was injected in the beams. However, the concrete cover afforded a significant protection for the grout so that it was about 12 hours old before freezing temperatures obtained in the grout.

After the freezing test, several beams (including some that showed cracking externally and some that did not) were sawn in two. In all cases where a crack showed on the surface it extended to the grouted duct, and where no crack was visible on the surface no cracking was noted in the sawn cross-section.

Correlation between Unrestrained Tests and Beam Tests

If the beam test results are compared with the length change patterns shown by the unrestrained grout prisms, it is seen that only those mixes (and maturities) that exhibited case "A" length change patterns (continuous expansion after freezing started) in the unrestrained freezing tests, produced cracks in the grouted beams. And *not all* mixes that exhibited case "A" length change patterns produced enough pressure to cause cracks. For example, mix 2-RH-1 exhibited case "A" expansive patterns at maturities up to 3 days, but did not produce cracks in the beams at either the 3-day or 1-day maturities. Similarly mix 0-1 exhibited case "A" expansive patterns at the 3-day maturity, but did not produce beam cracks at this maturity. Nevertheless, if a criterion of frost-resistance is desired on the basis of length change tests during the freezing cycle, then any mix (and maturity) that does not produce a continuous expansion as the temperature is lowered below the freezing point can be considered not dangerous.

Correlation between Tube Tests and Beam Tests

By comparing the results obtained in the tube tests with those obtained on the grouted beams an indication of the pressure required to produce cracks can be obtained, as well as an indication of the correlation between the two test methods. Mix 0-1 at the 1-day maturity exhibited equivalent pressures of 1500–2000 lb/in^2 in the tube test (Table 2), and produced cracks in the beams having 1 and 1-1/2 in. of concrete cover but not in the beam of 2 in. concrete cover (Table 3). At the 3-day maturity this mix exhibited equivalent pressures of 630 to 890 lb/in^2 in the tube test, but produced no cracks in the beam tests.

Mix 3-0-1, at the 1-day maturity, exhibited pressures ranging from 1340 to 2695 lb/in^2 in the tube tests and produced cracks in all three beams. At the 2 and 7-day maturities the tube tests exhibited average equivalent pressures of 2000 and 2250 lb/in^2 and produced cracks in the beams having 1 and 1-1/2 in. of concrete cover but not in the 2 in. concrete cover beams. Hence, there appears to be a reasonable correlation between the tube and the beam tests. Indicated pressures of 1340 lb/in^2 or higher in the tube tests represented mixes (and maturities) that produced cracks in grouted beams. Indicated pressures as high as 890 lb/in^2 represented mixes and maturities that did not produce cracks, even in beams of 1 in. concrete cover.

No tube tests were conducted on the AE-4 mixes at the zero and 12-hour maturities, but the pressures produced in the beams were not great enough to produce cracks, and hence would probably be less than 1000 lb/in^2.

Conclusions—Part III

The results obtained in this section demonstrated in a practical way the potential danger from frost action on grouted beams and provided a yardstick for interpretation of the test methods in Parts I and II. The main conclusions are:

1. The beam tests confirmed the validity of the unrestrained test method used in Part I and showed that only mixes exhibiting case "A" length change patterns (continuous expansion after freezing starts) can produce enough pressure to crack beams. Transitory expansions do not appear to be serious.

2. There was also a good correlation between the tube tests and the beam tests. It would appear that equivalent pressures in excess of 1000 lb/in^2 as determined in the tube test are required to cause cracks in beams of minimum concrete cover (1 in.).

3. The beam tests demonstrated that with certain grout mixes (3-0-1, at water-cement = 0.50 e.g.) it is possible to crack beams even when they possess concrete cover in excess of that often required by Codes of Practice for Prestressed Concrete.

Final Discussion and Conclusions

In this research programme the basic aim has been to find out how to produce frost-resistant cement grouts for use in prestressed concrete applications. On the basis of the results obtained in Parts I, II and III, it is possible to draw several conclusions of general application.

Danger of Frost Damage

Beams cracked with a grout of 0.50 water-cement ratio, cured for 7 days at 65°F. Thus, frost damage can be a real danger, even in the absence of free water —and hence a much greater danger exists if free water is available in the ducts.

Air-Entrainment

Air-entrainment was found to be the most effective method of preventing expansion and cracking by freezing temperatures. The introduction of entrained air, even at a low percentage (5%) in a mix of high water-cement ratio (0.50) was effective in eliminating all but transitory expansions at all maturities tested. It also prevented cracks in the grouted beams, even when the beams were subjected to the freezing cycle immediately after injection of the grout. Thus air-entrainment is effective as a protection against frost even in fresh grout; however, this is considered to be mainly of academic interest, for it would seem unwise to grout beams if there was danger of early frost and no protective measures were undertaken for at least the first 24 hours after injection.

Five percent air appeared to be just as effective as air contents as high as 13.5 per cent in producing frost-protection.

Water-Cement Ratio

Water-cement ratio is next in importance to air-entrainment in providing frost-protection for grouts. Provided a mix contains 5% of entrained air, a lower water-cement ratio seems more effective than additional air in increasing frost-resistance.

Curing Period

If no entrained air is employed, the estimated curing periods required for mixes of various water-cement ratios to achieve adequate protection to prevent cracks in a beam (of 1-1/2 in. concrete cover) are given below for two curing conditions.

Cement	Water-cement ratio	Curing period required—days @ 65°F (18°C)	Curing period required—days @ 40°F (4°C)
Ordinary portland	0.40	3	6
〃 〃	0.45	7	14
〃 〃	0.50	14	28
〃 〃	0.55	14+	28+
Rapid-hardening	0.52	2	4
Fine grained RH	0.69	2	4

The indicated curing period required for curing at 65°F (18°C) are based on the results of this research programme; the indicated periods required at 40°F (4°C) were calculated according to a maturity factor relationship due to Saul (3).

Type of Cement

Type of cement used is of minor importance compared with air-entrainment or water-cement

ratio in the achievement of frost-resistant grouts. Although, one can normally expect the development of frost-resistance at an earlier age with rapid-hardening portland cement than with ordinary portland cement, it has been shown that a water-reducing agent can so reduce the water requirement of an ordinary portland cement mix to make its performance equal to that of rapid-hardening cements in frost-resistance.

Recommendations

On the basis of results obtained in this research programme, the following recommendations are made regarding the achievement of frost-proof grouts for prestressed concrete.

1. The use of an air-entraining or gas-forming agent to provide at least 5 per cent voids is strongly recommended for grouts injected in the winter time. Even with the provision of such an agent the grout should not be injected if the air temperature is below freezing or is likely to fall below freezing during the next 24 hours, unless suitable precautions are taken to protect the fresh grout for at least 24 hours.

2. If entrained air is used the water-cement ratio of the mix will not be critical. However, if for some reason there is objection to the use of void-producing agents then the water-cement ratio should be the minimum possible consistent with achieving adequate fluidity; and if grouting is carried out during freezing weather adequate measures should be taken to provide curing in line with the requirements laid down in the final conclusions.

Acknowledgements

The author wishes to thank Professor W. Fisher Cassie, Head of the Department of Civil Engineering, University of Newcastle-upon-Tyne, for his advice and encouragement and for providing the facilities for carrying out this research; Professor J.D. Geddes of the Welsh College of Advanced Technology (formerly Senior Lecturer at Newcastle-upon-Tyne) for helpful discussions and suggestions throughout the research program; the Cement and Concrete Association who awarded a fellowship to the author for three years; and G & T Earle Ltd., of Hull, for generously providing the cements used in the investigation and particularly Mr. Hunter Rose, their Technical Manager, for his interest and assistance.

References

1. T. C. Powers, "Basic considerations pertaining to freezing and thawing tests", PCA Research Department Bulletin 58, 20–24 (1955).
2. T. C. Powers and R. A. Helmuth, "Theory of volume changes in hardened portland cement paste during freezing," Highway Research Board Proceedings, 33, 184 (1953).
3. A. G. Saul, "Principles underlying the steam curing of concrete at atmospheric pressure," Magazine of Concrete Research, 3, No. 6, 127–40 (1951).

Supplementary Paper III-31 Chemical Reactions of Strong Chloride-Solutions with Concrete

Heinz G. Smolczyk*

Synopsis

For the purpose of filling a gap within the numerous investigations on resistance against chemical attack and to suggest new points of view concerning seawater action and deicer scaling, the behaviour of concrete in strong chloride-solutions has been investigated.

Test specimens: Small concrete cubes 4 × 4 × 4 cm, quartz aggregate 0/5 mm, w/c 0.5 and 0.7

Cements
Z 1 = blastfurnace slag cement with 75% slag
Z 2 = portland cement with <1% C_3A
Z 3 = portland cement with 12% C_3A

Solutions:
Solution I = $MgCl_2$ 3 mol/l
Solution II = $CaCl_2$ 3 mol/l
Solution III = NaCl saturated
Solution IV = H_2O (for comparison)

The changes in the visible conditions and, after a period of 2 years, the compressive strengths were measured. Furthermore the reaction products were investigated by a special method of X-ray analysis.

All the three chloride solutions reacted chemically with all concrete cubes.

Nevertheless, only I and II attacked the concretes with Z 2 and Z 3 seriously which were destroyed within different periods, each of less than 16 weeks. At this the denser concrete (w/c 0.5) did not behave better than the poor quality (w/c 0.7). The expanding reaction products of Z 2 and Z 3 were

in Solution I: $MgO \cdot Mg(OH)Cl \cdot 5H_2O$

in Solution II: $CaO \cdot CaCl_2 \cdot 2H_2O$

which formed out of the reaction with free $Ca(OH)_2$ followed by a total loss of the alkalinity of paste.

In all other cases the concrete was not attacked and the alkaline reaction with phenolphthalein was not reduced although the afterhardening in IV was always stronger than in I and III.

With III all three cements formed

$$3CaO \cdot (Al, Fe)_2O_3 \cdot CaCl_2 \cdot 10H_2O$$

which had very little if any affect on the very strong afterhardening of Z 1, whereas the other two cements did only obtain about 60% of their full strengths.

Even with I and II the blastfurnace slag cement did not show any visible alterations. The strengths have been measured with only I so far. They had remarkably increased during 2 years of immersion and reached about 40% (w/c 0.7) and even about 70% (w/c 0.5) of the very strong afterhardening in III and IV.

The results of X-ray investigation stood in full agreement with the other test results.

Introduction

Papers about the resistance of concrete against aggressive waters mostly deal with the attack of strong aggressive chemicals in relatively low concentrations. Well known are the numerous tests with diluted sulfate-solutions which have been leading to the development of sulfate-resisting cements (portland cements without C_3A, blastfurnace slag cements with more than 70% slag, supersulfated cements and high alumina cements).

*Forschungsinstitut für Hochofenschlacke, Rheinhausen, West Germany.

In solutions of higher concentration, however, the chemical reactions in many cases are of different types: e.g. seawater already reacts much less than a sulfate solution of equal concentration. On concrete exposed to the daily tidal range, however, seawater action is very strong. Under this severe condition in several long time tests blastfurnace slag cements with more than 60% slag have shown very good performance without exception (1), (2), (3), (4), (5). This high resistance against seawater attack cannot be explained neither by the higher sulfate resistance only, nor by a higher resistance against frost action. Other causes must be present in addition.

Substances known as rather uneffective can eventually become very aggressive if their concentrations are high enough. Only few papers deal with this matter (6), (7), (8), (9), (10). In this field strong chloride solutions are of special interest. They certainly have a far greater importance on seawater action and also on frost-deicer action than is generally assumed.

Experimental Part

Experiments

For completion and control of earlier investigations (13) the behaviour of small concrete cubes (4 × 4 × 4 cm) should be compared in

Solution I:	$MgCl_2$	3 mol/l
Solution II:	$CaCl_2$	3 mol/l
Solution III:	NaCl	saturated
Solution IV:	H_2O	

The following 3 cements bought from commercial sources were tested:

Z 1: Blastfurnace slag cement "Z 275" with 75% slag
Z 2: Portland cement "Z 275" with < 1% C_3A
Z 3: Portland cement "Z 375" with 12% C_3A

The legend of concrete was

Aggregate: Quartz 0/0.2 mm = 15%
" 0.2/1 " = 25%
" 1/3 " = 32%
" 3/5 " = 28%
Mix: Cement/aggregate = 1/3
Water: w/c = 0.5 good quality
w/c = 0.7 poor quality

Curing conditions

before immersion: 10 days water (Cond. D)
3 days water + 7 days moist air (Cond. E)

The changes in the visible conditions of the concrete cubes and their compressive strengths were measured. Furthermore the reaction products were investigated by X-ray analysis.

Test Results

The changes in the visible conditions of the concrete cubes in the $CaCl_2$-solution up to 16 weeks are shown in Fig. 1. The two different precuring conditions (10 days water or 3 days water + 7 days moist air) had no significant if any influence on their behaviour. After 16 weeks the cubes have not suffered any further deteriorations since 1½ years. Cement Z 1 shows no alteration. The two other cements Z 2 and Z 3 are seriously attacked. At this the poor quality (w/c 0.7) has proved slightly better than the dense concrete (w/c 0.5).

A very similar behaviour was observed with the $MgCl_2$-solution, as is shown in Fig. 2.

Fig. 3 is a photograph of these small cubes after 4 months immersion in 3 mol $MgCl_2$. This picutre had not changed until the strength-test was taken after 2 years.

Immersion in saturated NaCl-solution up to 2 years did not create visible alterations on any concrete cube.

After 2 years of immersion the compressive strengths of the cubes were measured and compared with the compressive strengths measured after 10 days of water curing. Table 1 shows the results for H_2O, NaCl and $MgCl_2$. (The time of immersion in $CaCl_2$-solution has not reached 2 years yet.)

Evidently in all cases after 2 years' water curing the compressive strengths were higher than after 2 years' immersion in the chloride-solutions. With the cements Z 2 and Z 3 no compressive strengths could be measured after 2 years' immersion in $MgCl_2$. (And also after immersion in $CaCl_2$. See Fig. 1, Fig. 2 and Fig. 3.)

On the other hand, compared with the compressive strengths immediately before chemical attack (10 days water), the cements Z 2 and Z 3 showed in NaCl-solution no loss in strength, and Z 2 even showed increases of 60% to 80%. The very large increase in the compressive strength of Z 1 after 2 years NaCl-immersion was nearly as high as by curing in water and even after $MgCl_2$-immersion increases of 40% to 70% were measured

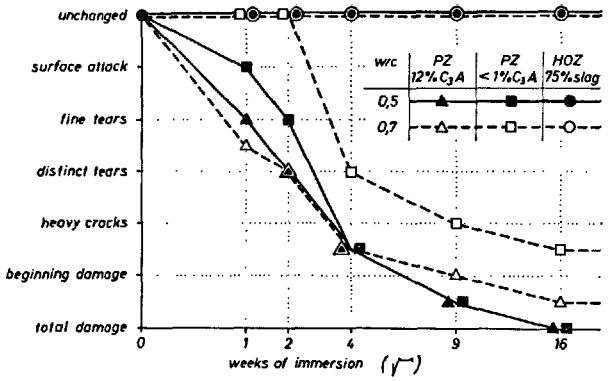

Fig. 1. *Changing visible conditions of small concrete cubes with time of immersion in 3m* $CaCl_2$*-solution*

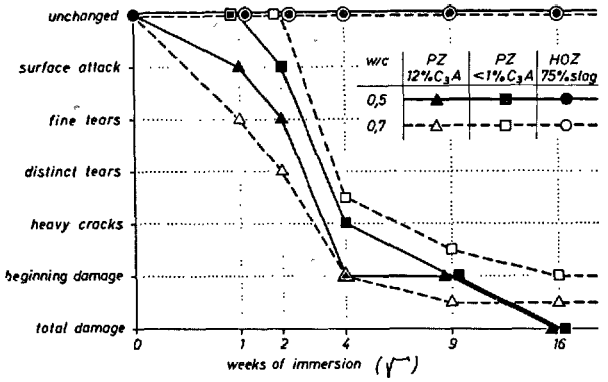

Fig. 2. *Changing visible conditions of small concrete cubes with time of immersion in 3m* $MgCl_2$*-solution*

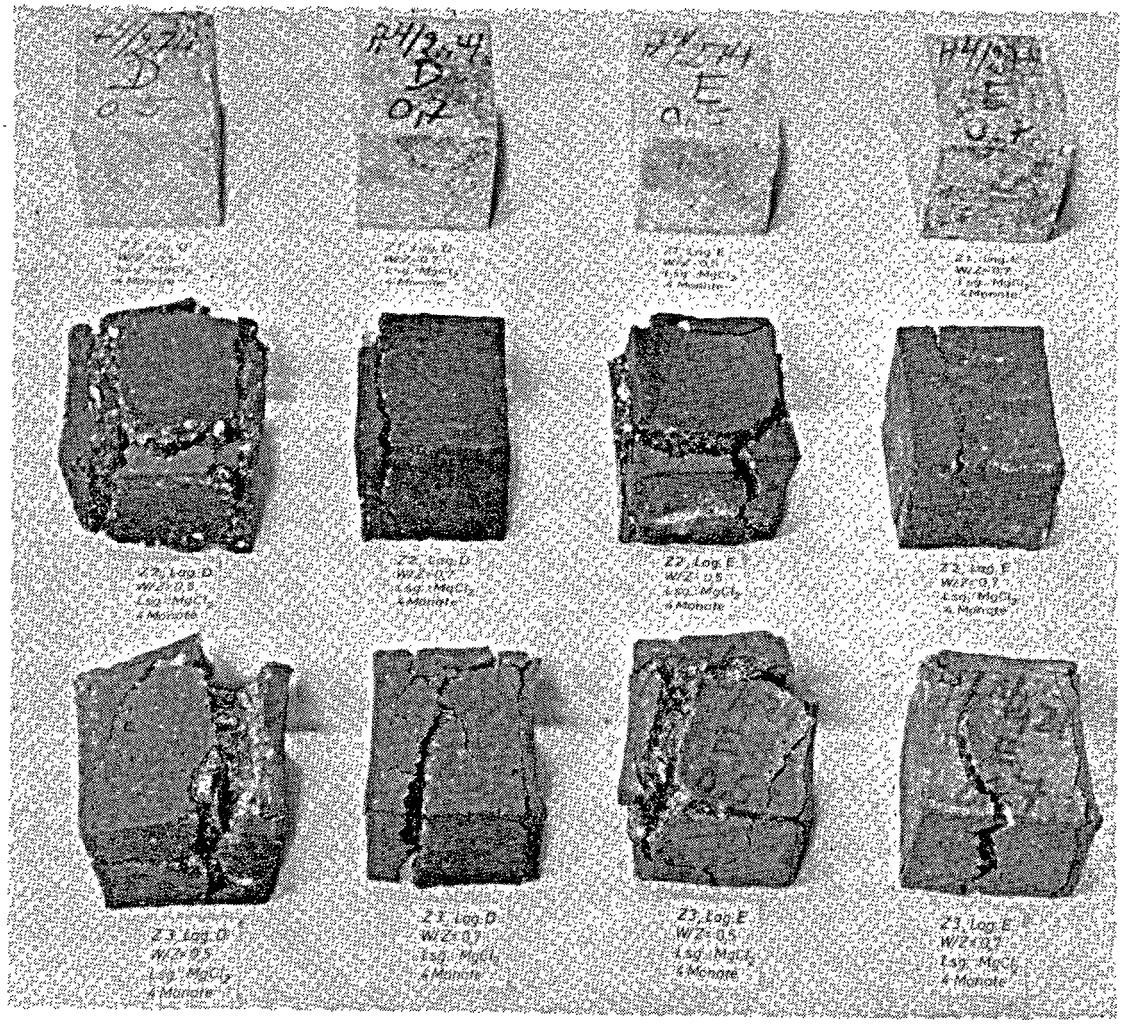

Fig. 3. *Influence of strong* $MgCl_2$*-solutions on concrete*
Small concrete cubes (4 × 4 × 4 cm) after 4 months of immersion in 3 mol M_3Cl_2

Table 1. *Compressive strength of small concrete cubes after 2 years of immersion*

Preceding curing condition:			10 days H_2O	10 days H_2O		10 days H_2O		3 days H_2O +7 days moist air	
Immersion in solution:			H_2O	NaCl-saturated		$MgCl_2$-3 mol/l		$MgCl_2$-3 mol/l	
Cement	w/c	Age	kg/cm²	kg/cm²	%	kg/cm²	%	kg/cm²	%
PZ375 with 12%C_3A	0.5	10 days	385		98		0		0
		2 years		378		0		0	
		2 years	633		60		0		0
	0.7	10 days	185		115		0		0
		2 years		213		0		0	
		2 years	382		56		0		0
PZ275 with <1%C_3A	0.5	10 days	272		164		0		0
		2 years		447		0		0	
		2 years	674		66		0		0
	0.7	10 days	114		184		<10		<10
		2 years		209		<10		<10	
		2 years	376		56		<3		<3
HOZ275 with 75% slag	0.5	10 days	238		243		173		170
		2 years		579		413		406	
		2 years	589		98		70		69
	0.7	10 days	128		291		142		137
		2 years		373		182		176	
		2 years	412		91		44		43

Reaction Products

The causes of these great differences were investigated by X-ray analysis. On this behalf small mortar specimen were made with w/c 0.5 and plastic-sand as aggregate. Plastic-aggregate is very advantageous for this purpose because it can very easily and completely be separated from the hardened paste. Thus an X-ray diagram of pure paste is performed without disturbing residues of quartz (11).

These plastic-cement-mortars were also cured in water for 10 days and then stored in the chloride solutions. They were investigated by X-ray analysis for different times of immersion. For control X-ray diagrams of the pastes of the concrete cubes and of several reaction products were taken after 2 years of immersion.

All the powder specimens for X-ray analysis were prepared in the same way according to earlier publications (11), (12):

Drying of paste at 20°C and 1 Torr = mmHg—grinding 40 min in cyclohexane—drying 2 min in faintly streaming air—firm pressing of the very fine powder ($\sim 5\mu$m) into the specimen holder.

This method constantly results in a homogeneous and very dense surface of the powder specimen. No precautions were taken against preferred orientation.

Among the X-ray diagrams more than 50 could be evaluated accurately and this work resulted in rather a clear picture of the chemical reactions. Here only those diagrams shall be shown that are essential and sufficient for understanding the problem.

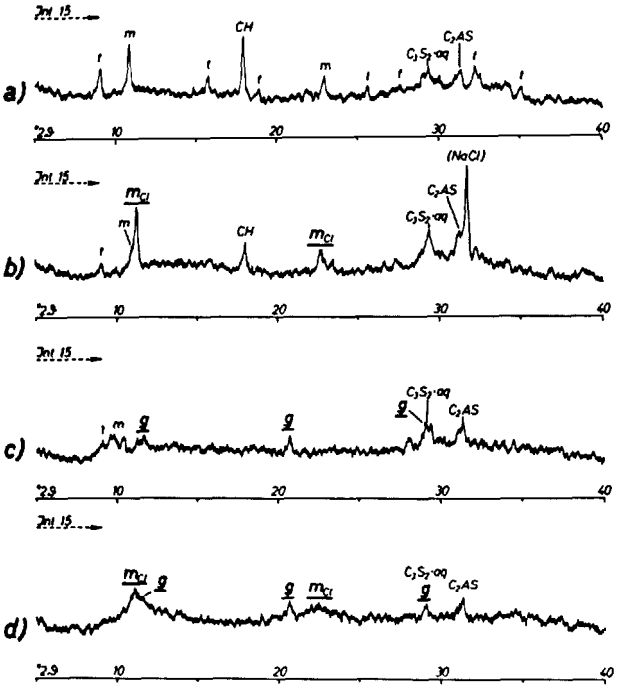

Fig. 4. *Reaction of blastfurnace cement (75% slag) with chloride solutions*

X-ray diagrams of paste, CuK_α
Mortars, plastic aggregate, w/c 0.5
Curing condition: 10 days in H_2O

a) H_2O—10 days
b) NaCl—saturated—8 weeks
c) $CaCl_2$—3 mol/l—8 weeks
d) $MgCl_2$—3 mol/l—1 year

Hydration products:
$C_3S_2 \cdot aq$ = Tobermorite
C_2AS = Trace of crystallized slag
$CH = CaO \cdot H_2O$
$t = 3CaO \cdot (Al, Fe)_2O_3 \cdot 3(CaSO_4, CaO) \cdot aq$
$m = 3CaO \cdot (Al, Fe)_2O_3 \cdot (CaO, CaSO_4) \cdot aq$

Reaction products:
$m_{Cl} = 3CaO \cdot (Al, Fe)_2O_3 \cdot CaCl_2 \cdot 10H_2O$
$g = CaSO_4 \cdot 2H_2O$

Fig. 4 clarifies the behaviour of the blastfurnace slag cement in water and in the three chloride solutions. The least alterations are visible in the NaCl solution. Here by partial inversion of the already present AFm-phase (m) only the adequate chloride-containing member (m_{Cl}) of the solid solution is formed. Simultaneously the AFt-phase (t) and the free calcium hydroxide are decreasing slightly.

In the other two solutions the alterations are slightly more distinct. The calcium hydroxide disappears totally, and the sum of calciumaluminate-

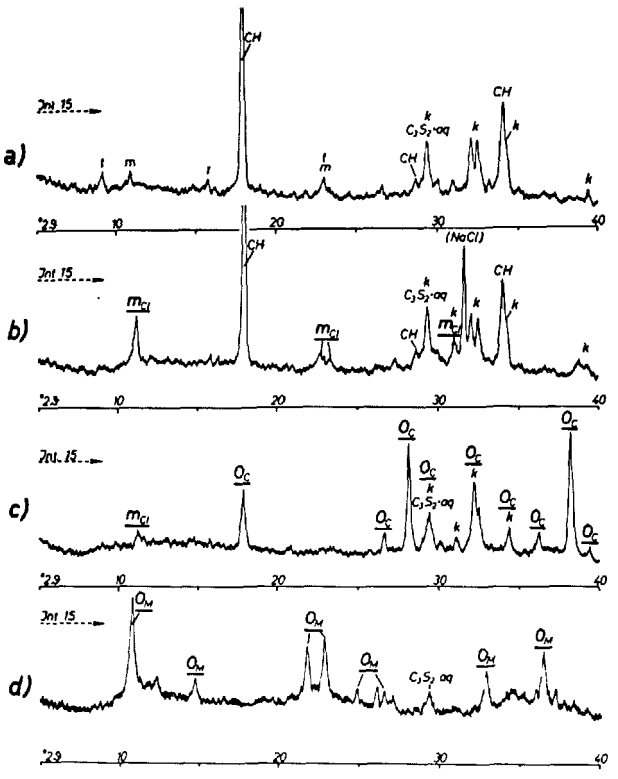

Fig. 5. *Reaction of portland cement* (12%C_3A) *with chloride solutions*

X-ray diagrams of paste, CuK_α.
Mortars, plastic aggregate, w/c 0.5.
Curing condition: 10 days in H_2O.

a) H_2O—10 days
b) NaCl—saturated—8 weeks
c) $CaCl_2$—3 mol/l—2 weeks
d) $MgCl_2$—3 mol/l—1 year

Hydration products:
C_3S_2·aq = Tobermorite
CH = $CaO \cdot H_2O$
k = rest of klinker
t = $3CaO \cdot (Al, Fe)_2O_3 \cdot 3(CaSO_4, CaO) \cdot aq$
m = $3CaO \cdot (Al, Fe)_2O_3 \cdot (CaO, CaSO_4) \cdot aq$

Reaction products:
m_{Cl} = $3CaO \cdot (Al, Fe)_2O_3 \cdot CaCl_2 \cdot 10H_2O$
O_C = $CaO \cdot CaCl_2 \cdot 2H_2O$
O_M = $MgO \cdot Mg(OH)Cl \cdot 5H_2O$

hydrates decreases. Moreover some gypsum (g) is formed. On the average the alterations of the slag cement mortar are small and all observed reaction products are well known products of cement hydration, too (11).

Compared with these results the reactions of the portland cement mortar are much stronger, as is shown in Fig. 5. In NaCl-solution the same amount of chloride-containing AFm-phase (m_{Cl}) has formed as with the slag cement, although in the portland cement mortar before immersion only very little C_4AH_{13} (m) was present. In the two other solutions about 20% of calcium hydroxide disappear totally and as for cement paste odd reaction products very distinctly appear by immersion in $CaCl_2$-solution appears

$$CaO \cdot CaCl_2 \cdot 2H_2O$$

and by immersion in $MgCl_2$-solution

$$MgO \cdot Mg(OH)Cl \cdot 5H_2O$$

The portland cement with $< 1\%$ C_3A behaved similarly and the same reaction products were observed as are to be seen in Fig. 5.

The X-ray diagrams of the concrete cubes were less distinct but otherwise in full agreement with Fig. 4 and Fig. 5.

Comparison and Summary of Results

The behaviour of the concrete cubes and the results of X-ray investigation add up to the following picutre:

In water storing all the three cements show a strong afterhardening from 10 days to 2 years. With the portland cement with $< 1\%$ of C_3A and with the blastfurnace slag cement the compressive strengths of the concretes with w/c 0.5 increase by nearly 150% and the compressive strengths of the concretes with w/c 0.7 by more than 200%. Since after 10 days of hydration the blastfurnace slag cement shows no residues of clinker phases any more, its very strong afterhardening can only be due to hydration of the slag. The afterhardening of the portland cement with 12% of C_3A (and higher early strength) is less than half as strong in all cases. These facts are important for valuating the further results.

By immersion in NaCl-solution the high alkalinity of paste remains unchanged and all the three cements form

$$3CaO \cdot (Al, Fe)_2O_3 \cdot CaCl_2 \cdot 10H_2O$$

well known as "Friedel'sches Salz".

This reaction has practically no influence on the concrete with blastfurnace slag cement, for it obtains nearly the same strength as by water-curing. The hydration of the slag is not disadvantageously influenced because similar hydration products are formed by water-curing, too.

In case of the two portland cements, however, it seems that rather a constant proportion of the clinker is hampered with respect to its hydration. Although the strengths of the concretes increase in NaCl-solution too, all test specimens reach, in a rather equal degree, only about 60% of their maximum strength they obtained when cured in water for 2 years.

Fundamentally different are the reactions of the two other chloride solutions. By reaction with the free $Ca(OH)_2$ they form expanding oxychlorides which within a short time destroy concretes with high contents of $Ca(OH)_2$. This reaction is accompanied by a total loss of the high alkalinity of paste. Unexpectedly this danger appears slightly greater in case of dense concrete than in case of less dense concrete. Similar observations during several experiments with various strong salt-solutions are already reported by W. H. Kuenning (7) and also by H. Berndt and E. Würth (10).

Although even the test specimens with the blastfurnace slag cement show greater alterations of their X-ray diagrams in $CaCl_2$-solution and $MgCl_2$-solution than in NaCl-solution, they do not form expanding oxychlorides and thus remain sound. This result stands in full agreement with earlier experiments (13):

6 blastfurnace slag cements with slag contents of 47% to 80% remained unaffected during 2 years immersion in 3 mol $MgCl_2$-solution. Furthermore, a steady increase in the resistance of the small mortar specimens was measured with increasing slag contents.

Using concrete cubes, moreover, in the $MgCl_2$-solution within 2 years all the strengths increase in case of the blastfurnace slag cement. At this they obtain with w/c 0.7 about 140% and with w/c 0.5 even about 170% of the compressive strengths before immersion. Furthermore the alkaline reaction with phenolphthalein is not reduced. The normal very strong afterhardening of this cements, however, is disturbed in any case. The concretes with w/c 0.5 reach about 70% and the concretes with w/c 0.7 only about 40% of their maximum strength they obtained when having been cured in water for 2 years. As there is no expanding influence, the dense concrete in this case behaves definitely better than the less dense concrete.

It can be assumed that in the case of the $CaCl_2$-solution the strengths of the concretes with blastfurnace slag will show similar tendencies.

Final Conclusions

Strong solutions of NaCl, $CaCl_2$ and $MgCl_2$ react chemically with concrete.

Nevertheless, destroying chemical attacks occur only with $CaCl_2$ and $MgCl_2$ if the concrete possesses too much free $Ca(OH)_2$. At this a higher density of the concrete does not pay out in a much better protection as otherwise has been proved in most of the other chemical attacks.

In all other cases the concrete will not be attacked, but its afterhardening will at worst be only reduced, whereas the alkaline reaction with phenolphthalein is not reduced.

Blastfurnace slag cements with more than 60% of slag are resistant against all the three chloride-solutions. e. g. a blastfurnace slag cement with 75% of slag proved, when immersed in saturated NaCl-solution, the same very strong afterhardening as it did by curing in water.

These unexpected facts are apt to provide new points of view with respect to the resistance of concrete against deicer scaling, to the durability against seawater action and also to connected problems especially the qualification of suitable concretes to protect the reinforcement against steel corrosion.

References

1. A. Eckhardt and W. Kronsbein: "Beton und Zement im Seewasser" Deutscher Ausschuß für Stahlbeton, Schriftenreihe, Heft 102, Berlin 1950.
2. A. Hummel and K. Wesche: "Beton im Seewasser", Deutscher Ausschuß für Stahlbeton, Schriftenreihe, Heft 124, Berlin 1956.
3. F. M. Lea and C. M. Watkins: "The durability of reinforced concrete in sea water" National Building Studies Technical Paper 30, HMSO, London, 1960.
4. F. Campus: "Essais de résistance des mortiers et bétons à la mer (1934–1964)" Silicates ind. **28**, 79–88 (1963).
   F. Campus, R. Dantienne et M. Dzulynski: "Constatations effectées après trente années d'immersion marine d'éprouvettes de mortier, des bétons et des bétons armés dans la mer du Nord" International Symposium on the "Behaviour of Concretes Exposed to Sea Water", Palermo, May 1965; Tagungsbericht von H.-G. Smolczyk, Betonsteinzeitung **31**,

465–470 (1965).
5. O. E. Gjoerv, I. Gukild and H. P. Sundh: "Investigation of concrete piles under varying conditions in sea water" RILEM-Bulletin No. 32, 305–322 (1966).
6. B. Kopyczinski: "Communication sur la durabilité du béton dans un fleuve pollué par les déchets industriels" International Symposium "Durability of Concrete" Prag 1961, Preliminary Report (Prag 1961). 331–338.
7. W. H. Kuenning: "Resistance of portland cement mortar to chemical attack—a progress report" Highway Research Record No. 113, 43–87 (1966) Reprinted as PCA Research Bull. No. 204.
8. W. Riedel, Ch. Göhring and H. Sprenger: "Einfluß des Hochofenschlackenanteils bei Huttenzementen auf die Korrosionsbeständigkeit des Zementsteins in Endlaugen der Kaliindustrie" Baustoffindustrie **9**, 272–276 (1967).
9. N. Ewers: "Wirkung von Magnesiumchloridsole of Straßenbeton" Baustoffindustrie **10**, 281–283 (1967).
10. H. Berndt and E. Würth: "Einfluß von Tausalzlösungen auf Beton" Dyckerhoff & Widmann KG, HV-Laboratorium Utting/Ammersee, Laborbericht Juli 1967—unpublished so far.
11. H. G. Smolczyk: "Die Hydratationsprodukte hüttensandreicher Zemente" Zement-Kalk-Gips **18**, 238–246 (1965).
12. H. G. Smolczyk: "Grundsätzliche Fragen zur Anwendung der Röntgen-Phasenanalyse in der Zementchemie" Zement-Kalk-Gips **14**, 391–99 (1961).
13. H. G. Smolczyk: "Some observations and new aspects concerning sea-water action on concrete in the tidal zone" RILEM-Bulletin No. 32, 299–304 (Sept. 1966)

Supplementary Paper III-39 A Durability Study of Concrete Using Monte Carlo Simulation

Kenneth R. Lauer and Callin W. Gray*

Synopsis

This paper deals with a durability study of a hypothetical bridge deck. The durability study is accomplished by employing the Monte Carlo method of analysis utilizing a digital computer. It consider such stochastic variables as compressive strength, air content, curing, freeze-thaw cycles, and salt scaling. Laboratory data was used to establish the relationships used in the study.

The ultimate goal of this study is to be able to predict how long a bridge deck will be in service before resurfacing or rebuilding of the deck is necessitated.

Air-entrained and non-air-entrained concrete are used in different cases of the bridge deck. The influence of air-entrained concrete on durability is observed.

The bridge deck is placed in a climatic environment comparable to that of South Bend, Indiana. Consideration is given to placing the bridge deck in April and in August and the effects of placement time are observed.

Introduction

The purpose of this paper is to introduce the Monte Carlo method of analysis as a valid approach in studying the durability of concrete in service.

The majority of concrete technology research in the last twenty five years has been orientated toward laboratory experiments. Traditional methods of reach have been to compare similar concretes or comparison of dissimilar concretes for similar purposes. While the above mentioned research was good, it gave only qualitative results. For example, in the late 1940's and early 1950's, many investigators showed that air-entrained concrete is much more frost resistant than non air-entrained concrete. Investigators studied, in the laboratory, one or two variables at a time holding all other parameters constant.

The investigators have payed little or no attention to what actually happens to the concrete when it is in service. That is to say, what happens to the concrete when the combined effect of temperature, chemical attack (interor and exterior), freezing and thawing, traffic, etc. are acting on the concrete simultaneously? Since many of these factors which influence the durability of concrete are stochastic variables, the formulation of an exact mathematical expression for durability becomes impossible. In order for an analysis to be meaningful, a mathematical approach such as Monte Carlo simulation must be utilized.

In this paper, the mathematical simulation has been formulated on the basic ideas of durability obtained predominantly from laboratory investigations and some field investigations. The temperature and precipitation data are from the South Bend, Indiana area.

Monte Carlo Method

Historical

As the name implies, Monte Carlo involves a system or process which concerns an element of chance (1). That is, the input to the system is random variables.

Monte Carlo was first called "model sampling" before 1948 when Fermi, Metropolis and Ulam used the method for obtaining estimates of the eigenvalues associated with the Schrodinger equation (2).

The use of the Monte Carlo method at the end of the second world war in relation to problems concerned

*Department of Civil Engineering, University of Notre Dame, Notre Dame, Indiana, U.S.A.

with random neutron diffusion in fissionable material brought to light the mathematical power of the method (3). Computers were used to carry out the computation of the above mentioned problem.

The method came into prominence about 1957 with the advent of the high-speed digital computer. The method without a high-speed computer would be impractical because of the time involved to carry out the numerous simulations.

Scope

Definition

Monte Carlo simulation is a technique which utilizes the probabilities of possibilities of occurrence of the pertinent stochastic variables by imitating the occurrence of the states of nature that interact with the different designs under investigation through the use of random number generation. Each simulated design is observed until it fails to meet the requirements for which it was originally intended. After a number of simulations have been completed for one design, that design's life may be predicted.

The probabilities of the possibilities of occurrence of the various stochastic variables are usually grouped in a two-dimensional matrix notation. This two-dimensional ordered array is used when one dependent variable is known to be essentially a function of one stochastic variable. A three-dimensional matrix may be used if one dependent variable is known to be a function of two stochastic variables.

The probabilities of the possibilities of occurrence of the various stochastic variables are determined from field and/or laboratory investigations.

Types

Problems to which this method of analysis is applicable are of two types: deterministic and probabilistic.

The deterministic type has no direct association with random processes; but when theory has exposed the underlying structure of the problem, it may be possible to recognize that this structure or formal expression also describes some apparantly unrelated random process, and, therefore, the solution of the deterministic problem is accomplished numerically by Monte Carlo simulation of an accompanying probabilistic problem.

The probabilistic type of Monte Carlo problem is essentially the observation of random numbers chosen in such a way that they directly simulate the physical random process of the original problem and infer the desired solution from the behaviour of these random numbers.

This direct simulation of a probabilistic problem is the type of Monte Carlo used in studying the durability of concrete in this paper.

Random Number Generation and the Computer

Random numbers may be obtained from random number tables or they may be pulled out of a hat full of slips of paper with various numbers on them. But the quickest method which can be used to generate a sequence of numbers, one at a time so devised that no reasonable statistical test will detect any significant departure from randomness is by the congruential or midsquare method using the digital computer. The numbers generated on the computer by either of the above methods are called pseudorandom numbers since the next number to be generated can be predicted from the last number which the computer generated. La Russo (4) has thoroughly checked out the congruential pseudorandom number generator at the University of Notre Dame Computer Center and has reported it satisfactory. This subroutine was used for generation of the "random" numbers for the simulation model.

Application of the Monte Carlo Method to a Concrete Durability Study

Introduction

Durability of concrete has been defined as its resistance to deteriorating influences which may through inadvertence or ignorance reside in the concrete itself or are inherent in the environment to which it is exposed (5).

Of the many factors influencing the durability of concrete in service, the following major ones are considered: (1) probability of occurrence for compressive strength, (2) probability of occurrence for air content, (3) compressive strength loss due to air-entrainment, (4) loss in compressive strength due to improper curing and compaction, (5) time, and temperature effects on gain in strength, (6) dynamic modulus of elasticity and freeze-thaw cycles, (7) compressive strength and dynamic modulus of elasticity, (8) compressive strength and pulse velocity, and (9) de-icing scale rating

and the number of scale cycles. These factors are considered primarily because of their importance relative to the durability of concrete bridge decks and because of the data available in these areas for the simulation model.

The concrete mix used in the model represents the most homogenous data available. In some instances relationships were adjusted to be more applicable. The following mix proportions and properties were used.

	Non-air entrained mix	Air entrained mix
W/C, wt	0.50	0.50
Cement factor, bags/cu yd	6.4	6.0
Slump, inches	2–4	2–4
Max. aggregate size, inches	1	1
Air content, % entrained	0.0	4.5

The variables in the model are assumed to be linearly independent thereby making the principle of superposition applicable.

The model has been formulated in the same sequence as the various parts of the model are explained.

Compressive Strength

The variability of the strength of the concrete is characterized in the relationship of probability of occurrence for a given strength versus strength. Implicitly implied in the above mentioned curve is all the possible variations in the concrete mix before it is placed in the field.

For reasonable field control, and no radical changes in mix proportions, the curve of percentage frequency of occurrence versus strength is approximately bell-shaped. That is, if a bar chart or histogram of per cent frequency of occurrence versus strength is plotted, see Fig. 1, the histogram or "parent" distribution may be approximated by the theoretical Gaussian or "normal" distribution curve.

Two significant properties of the normal curve are the following. The total area under the normal curve is equal to one and the area under the curve between any two points A and B is the probability of occurrence of a value in that interval. Therefore, if the specific strength distribution for a certain mix being produced at a certain batch plant is known, then, for that certain mix, the probability of a certain strength being produced at that plant can be determined.

It is assumed in this study that the probability curve is a normal curve and is given in Fig. 1. The concrete is non-entrained. The average 28 day compressive strength is assumed to be 4500 psi. From the data in

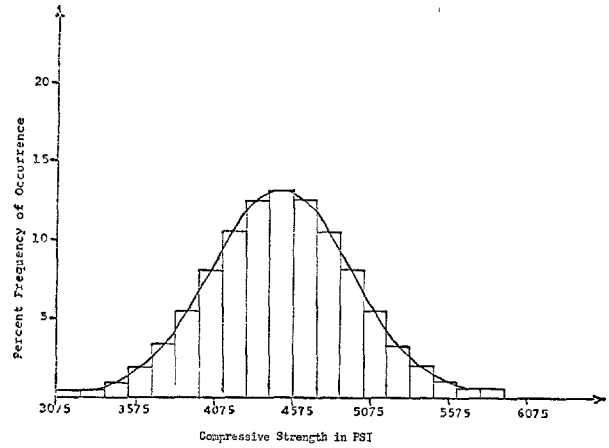

Fig. 1. *Percent frequency of occurrence versus compressive strength for 4,500 psi non-air-entrained concrete*

Newlon's (6) paper, the standard deviation for 4500 psi concrete is approximately 450 psi. This gives a coefficient of variation of 10%. A coefficient of variation of 10% infers good quality control procedures.

One way of using the normal curve in the simulation model is to approximate the curve by its corresponding histogram as in Fig. 1. A cell interval of 150 psi and nineteen cells were used in order to approximate the normal curve. Theoretically, the furthest extents of the ordinates of a normal curve never terminate on the abscissa axis. Therefore, some of the values of compressive strength, even though they may have a very, very small probability of occurrence still have a chance of occurring. If the range of strength varies from a value of three times the standard deviation in either direction from the average strength, then 99.73% of all the strength values will lie in this range.

In Table 1, the average cell strength values are

Table 1. *Average cell strength values, their probabilities of occurrences, and their specific number designations*

Average cell strength psi	Probability of occurrence, per cent	Specific number designation
3150	.3	1–3
3300	.4	4–7
3450	.9	8–16
3600	1.8	17–34
3750	3.3	35–67
3900	5.5	68–122
4050	8.1	123–203
4200	10.6	204–309
4350	12.5	310–434
4500	13.2	435–566
4650	12.5	567–691
4800	10.6	692–797
4950	8.1	798–878
5100	5.5	879–933
5250	3.3	934–966
5400	1.8	967–984
5550	.9	985–993
5700	.4	994–997
5850	.3	998–1000

listed with their probabilities of occurrence and their specific number designations for indicating what strength the concrete will have when the random number selection is made. The range of random numbers is 1 to 1000 inclusive.

Now, the computer picks a random number which will determine what non-air-entrained strength the concrete will have. If the computer picked 501, the strength of that batch of concrete would be 4500 psi.

Air Content

Air content has a very marked effect on the durability of concrete. The lack of sufficient entrained air in concrete can considerably decrease the durable life of a structure exposed to frost action.

Klieger (7) has shown that the "optimum" air content for a given mix is a function of the maximum size of the aggregate, workability of the mix, and the cement factor for the mix. Optimum air content is considered by Klieger (7) to be that minimum air content beyond which further increases in air result in only a small decrease in expansion due to freezing and thawing.

Since the exact relationship between strength and air content probability distribution has not been fully investigated, it is assumed that the probability distribution of air content remains constant for the whole range of strength variation. That is to say, one air content probability curve is used for the whole range of strength variation, 3150 psi to 5850 psi. The average air content was chosen as the optimum air content according to Klieger's (7) work. For the specific mix under study, the optimum air content is 4.5%. The air content probability curve is assumed to be a normal curve. From Newlon's (6) work the average standard deviation for air content is assumed to be 0.70%. This gives a coefficient of variation for air content of about 15.6%. A cell interval of .30% was used for the approximation of the normal curve.

In Table 2, the average cell values are given with their probabilities of occurrence and their specific number designations. These values and the previously mentioned strength values were calculated using a mathematical probability table.

It may be shown from Klieger's (7) results that the average percentage change in strength for each 1% of entrained air for total amounts of entrained air up to 6% is approximately linear. This is true if the cement factor, slump, and maximum size of aggregate are maintained constant.

For the specific mix in question the plot of loss in strength versus the air content is given in Fig. 2. This relation is used in the model.

Table 2. *Average cell air content values, their probabilities of occurrences, and their specific number designations*

Average cell air content, %	Probability of occurrence, per cent	Specific number designation
2.4	.1	1
2.7	.7	2–8
3.0	2.8	9–36
3.3	3.0	37–66
3.6	7.6	67–142
3.9	11.8	143–260
4.2	15.5	261–415
4.5	17.0	416–585
4.8	15.5	586–740
5.1	11.8	741–858
5.4	7.6	859–934
5.7	3.0	935–964
6.0	2.8	965–992
6.3	.7	993–999
6.6	.1	1000

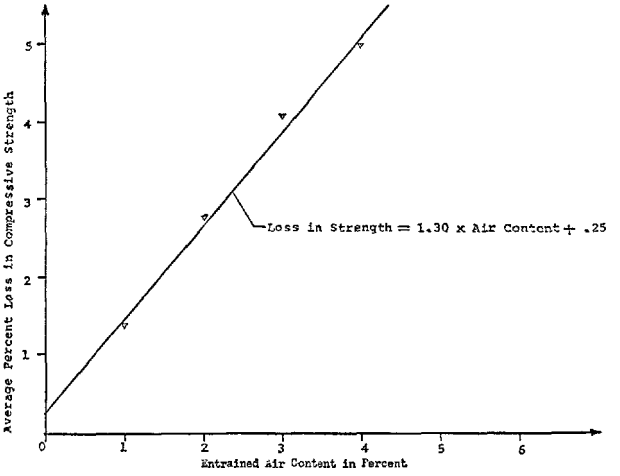

Fig. 2. *Loss in strength versus percentage entrained air content (Points plotted are from Klieger's (7) data)*

After a strength is selected an air content is picked by having the computer choose a random number. Suppose this number is 200. From Table 2, the air content for the previously selected 4500 psi batch is 3.9%. One per cent of air is deducted from 3.9% to take into account the entrapped air content. The assumption of one per cent entrapped air was used for all air-entrained simulations. The computer calculates the loss in strength due to air entrainment by the equation in Fig. 2. The loss in strength is subtracted from the original compressive strength to give a new compressive strength.

The above steps are omitted in the simulation model for the non-air-entrained concrete.

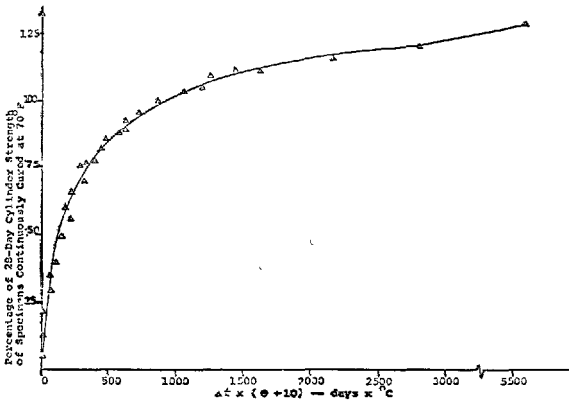

Fig. 3. *Percentage compressive strength as a function of age and temperature (Saul and Nurse (8))*

Moisture Loss and Compaction

The computer, next, modifies the compressive strength in order to account for moisture loss due to less than perfect curing conditions and imperfect compaction of the concrete in the field. A loss in strength of five per cent is deducted from the compressive strength to give the updated compressive strength of the concrete.

In the non-air-entrained case, the five per cent loss is computed with respect to the non-air-entrained strength which the computer chose first.

A loss of five per cent would indicate good compaction in the field and a relatively good membrane type of curing method. For some jobs, the loss due to the above mentioned factors may be as high as 20 per cent.

When the effect of compaction and moisture loss on compressive strength are better understood, these relationships may be incorporated into the simulation model.

Time, Temperature, and Strength Gain Relationship

The relationship of temperature to the rate of concrete hardening and gain in strength is of importance in concrete durability. As a rule, for moist curing conditions, high temperatures accelerate strength gain and low temperatures reduce strength gain.

Most investigators (8, 9, 10) agree that strength gain is proportional to the product of time and temperature. The approach of Saul and Nurse is a good method of estimating strength gain from time-temperature relations (8, 9).

This relationship using Price's data is shown in Fig. 3. Price's (11) data is for concrete cured in a moist environment at 100°F, 73°F, 50°F, 33°F and 16°F and tested in compression at 3, 7, 14, 28, 90 and 180 days. In Fig. 3, it may be seen that the gain in strength, after a certain time-temperature period, approaches the constant value of approximately 128% of the 28 day, 73°F, moist cured laboratory test specimen strength.

For this study it is assumed that the concrete gains compressive strength according to the above mentioned curve. Also, the maturity factor, $\Delta t \times (\theta + 10)$, is assumed to be the summation of the individual maturity factors. The average temperature effect on the concrete is assumed to be equal to that of the average daily temperature of the air everyday for 90 days after the concrete is placed. That is to say, the concrete is observed to see what gain in strength due to temperature occurred during the first 90 days of its existence. Then, the concrete is observed on a monthly average temperature basis in order to calculate the further gain in strength of the concrete. If and when the concrete reaches the value of 128% of the laboratory strength, the concrete is not permitted to gain any more strength.

In order to use this relationship some means of obtaining temperatures which are most likely to occur in the field is necessary. Since temperature is also a random variable, it was necessary to determine the probability of occurrence of temperature on a daily and monthly basis. The South Bend, Indiana, area weather data (12) was used for the analysis. For the daily basis, twenty-seven years of continuous records were available and analyzed. For the monthly data, sixty-seven years of data was available and was analyzed. The method of analysis was to sort the temperatures out according to a predetermined number of cell sizes. The cell sizes used were 10, 11, 12, 13, 15 and 20 cells. In order to conserve computer time, only the 10, 15 and 20 cell data was used in the simulation study.

In Table 3, the analyzed average daily temperature data for May third, for ten cells, is given.

Now, the computer picks a random number, 401, and for example, if the concrete was placed on May third, then the average daily temperature for that day was 54.5°F. Therefore the maturity factor for that day is calculated by the equation, Maturity Factor $= \Delta t \times (\theta + 10)$ where $\Delta t = 1$ day and $\theta =$ the average daily temperature determined by the random number selection, in degrees centigrade.

The above process is then repeated using the temperatures and specific number designations of

Table 3. *Average daily cell temperature values, their probabilities of occurrences, and their specific number designations for May 3rd. 10 cells*

Average daily cell temperature °F	Probability of occurrence, per cent	Specific number designation
39.2	7.4	1–74
43.0	11.1	75–185
46.7	11.1	186–296
50.5	3.7	297–333
54.5	14.8	334–481
58.0	11.2	482–593
61.8	14.8	594–741
65.6	7.4	742–815
69.3	11.1	816–926
73.1	7.4	927–1000

Table 4. *Precipitation probabilities and their specific number designations for the first ten winter days*

Winter day	Precipitation probability, per cent	Specific number designation
1	30.8	1–308
2	34.6	1–346
3	26.9	1–269
4	19.2	1–192
5	19.2	1–192
6	26.9	1–269
7	30.8	1–308
8	42.3	1–423
9	30.8	1–308
10	26.9	1–269

May fourth, May fifth, etc. until 90 days have been observed. The cumulative maturity factor is constantly being updated during this process.

After ninety days, the concrete is studied on a monthly average temperature basis in a similar manner. Then, after the winter months are over the concrete's gain in strength is computed and added to the former compressive strength to give the updated compressive strength. The gain in strength is computed from the equations of the straight line relationships obtained when the percentage strength gain is plotted against the log of the maturity factor using Price's data.

Freezing and Thawing Cycles and Compressive Strength Relationship

In order to simulate the freezing and thawing cycles which occur in nature it was necessary to analyze the daily low and daily high temperature values for the winter months in the same manner as the daily average temperatures and the monthly average temperatures were analyzed as described in the previous section. The winter days in this study were assumed to be 150 in number and extended from November first to March thirtieth, inclusive.

To have a freezing and thawing cycle in nature which will damage the concrete to some degree structurally, precipitation in the form of melting snow or freezing rain is essential to provide the required saturation in order to cause hydraulic pressure to build up in the capillary cavities when the temperature of the concrete drops below freezing. The amount of precipitation necessary to cause frost distress was assumed to be .20 inches of snow or greater and/or .05 inches of freezing rain or greater. The precipitation probabilities for the winter days were computed from twenty-six years of continuous record for the South Bend area. In Table 4, the precipitation probabilities for the first ten winter days are listed along with their corresponding specific number designations.

First, the computer pulls a random number which corresponds to some specific high temperature for the given day. Then, the computer pulls another random number corresponding to a specific low temperature for the same day. It is assumed that this temperature occurs after the high temperature and at night before 12 o'clock midnight. Then the computer chooses another random number and this number specifies whether a sufficient amount of precipitation was available to cause frost distress. For example, suppose on the third day of winter, the computer pulled the random number 300. Then it did not rain or snow, see Table 4, in sufficient amounts to cause frost distress in the bridge deck even if the concrete was beginning to freeze. If the computer had pulled the random number 200 for the third winter day instead of 300, from Table 4, the concrete was exposed to sufficient moisture that day to be damaged by frost distress provided that the high and the low temperatures of that day were sufficient to cause a freezing cycle.

It is generally aggreed that $E_D = Kf^n$ where $E_D =$ the dynamic modulus of elasticity, $K =$ a constant depending on the mix components, $n =$ an exponent, and $f =$ the compressive strength of the concrete (13, 14, 15, 16, 17, 18).

Laboratory freezing and thawing tests are based on an "accelerated" freeze-thaw cycle. The measure of deterioration is loss in dynamic modulus of elasticity after a prescribed number of cycles have been completed or linear expansion or weight loss of the specimen after a prescribed number of cycles have been completed.

The loss in dynamic modulus of elasticity indicates a structural weakening of the concrete due to frost distress. Conventionally, a plot of relative dynamic modulus of elasticity in per cent versus number of freeze-thaw cycles is made. See Fig. 4. If the concrete

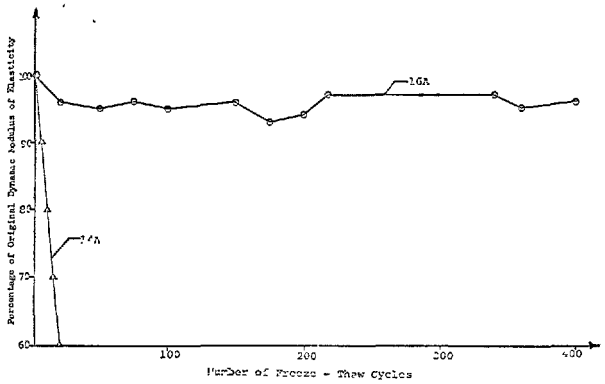

Fig. 4. *Relative dynamic modulus of elasticity as a function of freeze-thaw cycles (Hussell (21))*

is fairly frost resistant, the curve will resemble curve 16A. If the concrete is fairly non-front resistant, it will resemble curve 14A. If a core sample was taken from a structure exposed to frost action with concrete in it like that of curve 14A, the compressive strength of the core would be significantly less than that of a core taken from a structure made with concrete, exposed to frost action, of the type of curve 16A. Therefore, a correlation should exist between strength and dynamic modulus of elasticity when concrete has been subjected to frost action. Whitehurst (19) and Cheesman (2) report good correlation between laboratory resonance frequency measurements of the modulus of elasticity and that calculated from the pulse velocity which was obtained in the field. The equation relating the pulse velocity to the dynamic modulus of elasticity is

$$E = \frac{V^2 d(1 + u)(1 - 2u)}{(1 - u)}$$

where

E_D = the dynamic modulus of elasticity of the concrete
V = the pulse velocity
d = the density of the concrete
u = Poisson's ratio

Now if the calculation of the dynamic modulus of elasticity from the field data corresponds to that measured in the laboratory on a core of the field concrete and there is a correslation between the laboratory modulus of elasticity and compressive strength, then the following is most likely to be true.

Let

$$E_R = \frac{E_p}{E_0}$$

where

E_R = relative dynamic modulus of elasticity
E_p = the present dynamic modulus of elasticity
E_0 = the original dynamic modulus of elasticity before the "accelerated" freezing and thawing cycles commenced

Since $E_D = Kf^n$, and assuming K to remain constant

$$E_R = \frac{(Kf_p)^n}{(Kf_0)^n} = \frac{f_p^n}{f_0}$$

where

f_p = the present compressive strength
f_0 = the original compressive strength before the freezing and thawing cycles commenced.

Also, the part of the original compressive strength which the concrete presently possesses $= f_p/f_0 = E_R^{1/n}$ or the present loss in strength due to freezing and thawing in per cent of the original strength of the concrete $= (1.0 = E_R^{1/n}) \times 100$.

The ordinates of the curves given in Fig. 4 were converted by the last equation stated above. Fig. 5 shows the linear least squares fit plot of the converted data points.

It would be possible to measure the approximate loss in strength of concrete exposed to frost action if the exposure cycles in the field were comparable to those of the "accelerated" freeze-thaw tests. In the simulation model, an adjustment of the requirements for a frost deteriorating freeze-thaw cycle in the field is used in order to utilize the "accelerated" laboratory freeze-thaw cycle results. It is felt that the "accelerated" laboratory freeze-thaw test which most nearly approximates the freeze-thaw cycles in the field is ASTM Designation C291–57T. This procedure is based on rapid freezing in air and thawing in water. In order to assure that at least the top 1 inch of concrete is thawed out, it was considered necessary that the high air temperature of any given day be at least 35°F. A low air temperature at night of at least 29°F and sufficient precipitation had to have fallen before the computer tailed a freeze-thaw cycle. A low temperature of 29°F was also chosen to insure that the top 1 inch of concrete was frozen. By using the above two temperatures as part of the criterion for a frost deteriorating cycle, the laboratory "accelerated" freeze-thaw test is approximated as much as is possible. The major fault of the field criterion for tailing freeze-thaw cycles is the fact that the intensity of the cycles in the field are not uniform as they are in the laboratory. No way was devised to take into account the variable intensity of the freeze-thaw cycles in the field.

After the computer goes through all the winter days tabulating the number of frost deteriorating cycles, the loss in compressive strength due to freeze-thaw cycles is computed from the equations which are repre-

sented graphically in Fig. 5.

After the loss in compressive strength due to freeze-thaw cycles is calculated, for the air-entrained mix, the air content of the concrete of the particular simulation run is compared to the air content of the mix from which the equations were approximated. In this case, the air content is 5.0%. If the air content of the particular run is between 4 to 6%, it is assumed, considering Klieger's optimum air content of 4.5% for this concrete, that no adjustment in the loss in strength due to frost deteriorating cycles is required. Also from Klieger's work (7), if the air content of the particular batch is greater than 6.0%, the loss in strength due to freezing and thawing is decreased by 5% of the previously computed loss. If the air content of the batch is less than 4.0% then the originally computed loss in strength is increased by 10% of the original value.

Finally, the loss in strength is subtacted from the present compressive strength and the new updated compressive strength is tabulated.

In the non-air entrained concrete model, the loss in strength due to deteriorating freeze-thaw cycles is calculated and immediately deducted from the present compressive strength.

Pulse Velocity, Dynamic Modulus of Elasticity and Compressive Strength Relationships

Klieger's work (22), presents the relationship between compressive strength and dynamic modulus of elasticity, as measured by the resonance method, for different types of cements for a non A/E mix having a cement factor of 6 bags/cu. yd. The test ages were 1, 7, 28 days, 3 months, 1 and 3 years. The ordinates of this curve were reduced by 6% in order to approximately convert this curve to the 6 bags/cu. yd., air-entrained mix curve having an average air content of 4.5%.

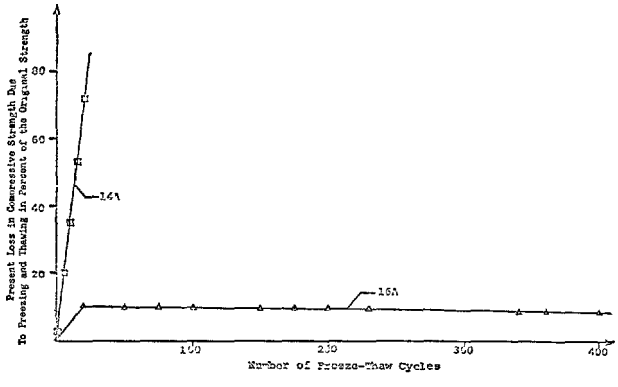

Fig. 5. *Loss in strength due to number of freeze-thaw cycles*

The values of the non-air entrained case and the air entrained case were then plotted on 2 × 2.4 cycle logarithmic paper (Fig. 6). On this paper, the curves were straight lines in the area which was applicable to the simulation model. The equations of the straight line relationships are of the form

$$E_D = Kf^n$$

where E_D, K, f and n are as previously defined.

It was then assumed that the value of the dynamic modulus of elasticity of the concrete under study at any instant of time may be approximated by one of the above equations.

The computer then calculates the present value of the dynamic modulus of elasticity. This step simulates the obtaining of a core sample from the bridge deck and the subsequent laboratory resonant testing of the core in order to ascertain the dynamic modulus of elasticity of the concrete.

Again, Klieger's work (22) presents the relationship between compressive strength and pulse velocity for a

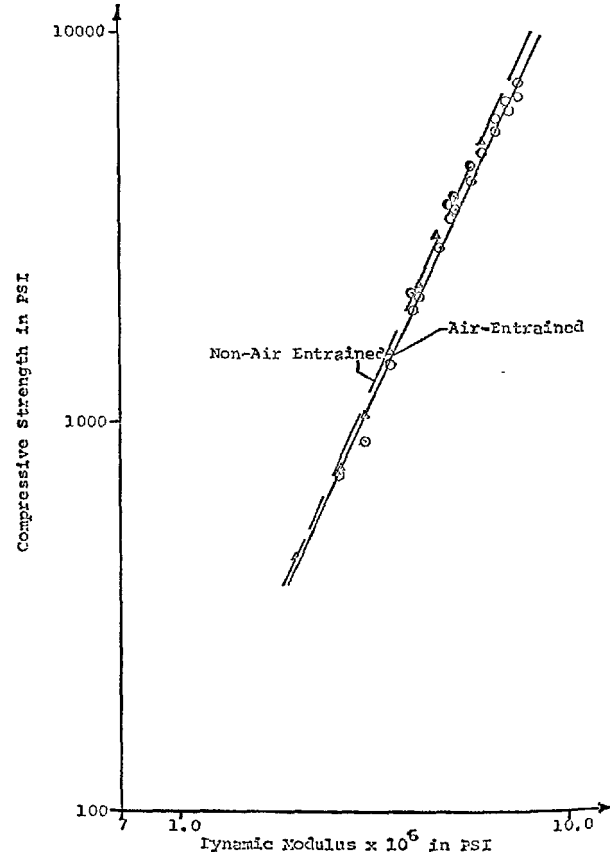

Fig. 6. *Compressive strength—Dynamic modulus of elasticity relationship on log- log paper (Points plotted are from Klieger's (22) data)*

6 bags/cu. yd., non-air entrained, mix using different types of cement. Test ages for this relationship were the same as the above mentioned dynamic modulus-strength relationship. The pulse velocity was determined by the soniscope. If these points are plotted on 2×2.4 cycle logarithmic paper, the relationship is found to be linear (Fig. 7). It is assumed that the pulse velocity of the concrete at any time may be computed from the equation of the linear portion of the logarithmic plot.

The computer, now, calculates the pulse velocity of the batch of concrete in the deck. The calculation of the pulse velocity simulates the taking of a core sample from the specifically placed batch in the bridge deck and determining the pulse-velocity in the laboratory or using the soniscope directly in the field in order to determine the pulse velocity for the specific area of the deck in which the batch was placed. It is further assumed that in either of the just mentioned interpretations the pulse velocity is determined on a specimen of concrete in which the reinforcement steel, either longitudinal or tranverse has no effect on the value of the measured pulse velocity. This asumption was made because the data used for the pulse velocity—strength relationship was for plain concrete. The pulse velocity is higher in reinforced concrete due to the fact that steel is denser than concrete.

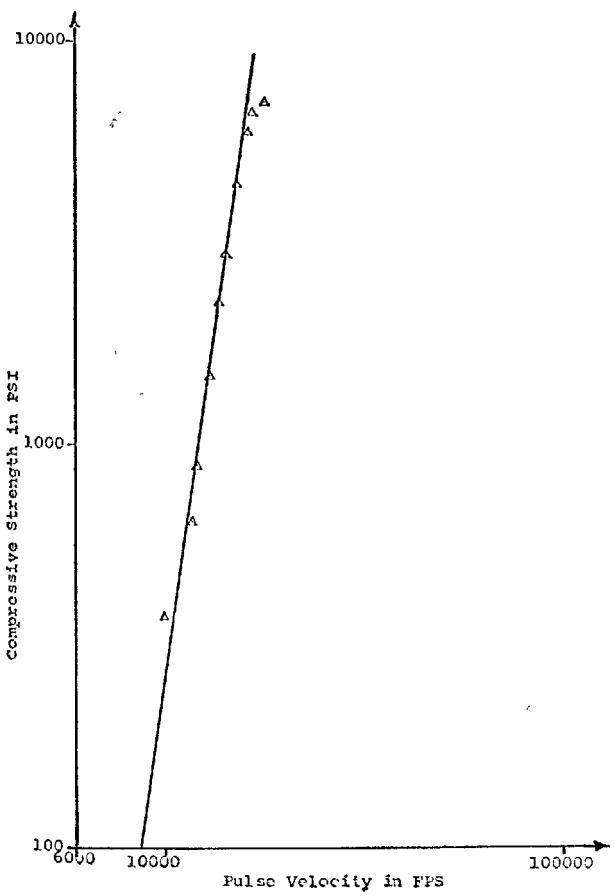

Fig. 7. *Compressive strength-pulse velocity relationship on log-log paper (Points plotted are from Klieger's (22) data)*

In both the dynamic modulus-strength and pulse velocity-strength relationships, the compressive cube strength was used in Klieger's original work (22). The compressive cylinder strength was obtained by multiplying the compressive cube strength by 0.75 after the suggestion by Jones (23) and the British Standard 1881, 1952.

Structural Failure Criteria

The propagation of an ultrasonic wave through concrete, either in the field or in the laboratory, and the subsequent calculation of the velocity of propagation or pulse velocity is a means of evaluating the overall quality of the concrete. If the concrete is of good structural quality it will be dense and the pulse velocity will be high. If the concrete is structurally poor its pulse velocity will be low.

According to Leslie and Cheesman (24), the quality of concrete in service may be rated from the following pulse velocity measurements.

Pulse velocity, ft per sec	General condition
above—15,000	excellent
12,000—15,000	good
10,000—12,000	questionable
7,000—10,000	poor
below— 7,000	very poor

The above listed pulse velocities give an indication of the structural integrity of the concrete. Whitehurst (25) reports that the above categories are based on normal concrete having a unit weight of approximately 150 lb/cu ft. Cheesman (20) states that although concrete having a pulse velocity between 16,000 to 12,000 f.p.s. is generally structurally sound, some tranverse cracking, a very few popouts, and non-progressive light scaling may be present on the surface. The above is possible since the concrete just below the surface probably is in excellently good condition. If the pulse velocity is less than 12,000 f.p.s., the concrete is probably not in good structural condition.

It is assumed that a structural failure is imminent if the pulse velocity calculated by the above mentioned equation is less than or equal to 12,000 f.p.s.

The computer then checks the computed pulse velocity of the concrete against the value of 12,000

f.p.s. If the value is less than or equal to 12,000 f.p.s. the computer prints out the life of the present concrete batch in years, its failure pulse velocity, the dynamic modulus of elasticity at failure, the average life of the concrete which is equal to the summation the individual lives of the previous batches including the present batch divided by the number of simulations just completed, the compressive strength of the concrete at failure, and the average compressive strength of the concrete at failure which equals the summation of the individual compressive strength at failure up to and including the most recent simulation divided by the number of simulations just completed. The computer also prints out the scale rating when the concrete failed and the non-air entrained strength which the concrete theoretically possessed at its inception.

The computer then begins the next simulation by choosing a random number corresponding to the non-air-entrained strength of the next batch of concrete. The previously mentioned steps are then repeated.

If the computed pulse velocity is greater than 12,000 f.p.s. then the numerical scale rating is calculated as described below.

Relation of Salt Scaling to Durability

The problem of salt scaling of bridge decks is probably the primary cause why most bridge decks need resurfacing (26).

In the salt scale test, the salt solution is placed on the specimen and frozen and then thawed for a specific length of time. Sometimes water is placed on the specimen and salt pellets or flakes are placed on the specimen and allowed to remain there for a prescribed time period before the specimen is allowed to be frozen. After a certain predetermined number of scale cycles, the surface of the specimen is rated qualitatively on the percentage of surface area scaled and the depth of scaling. The scale cycles are repeated until a specific scale rating is reached or until a certain number of cycles is achieved. Then a plot of numerical scale rating versus the number of scale cycles is made. Fig. 8 is one such plot for a scale resistant concrete (curve 46A) and a scale susceptible concrete (curve 26A). According to Klieger (27) classification, the numerical scale ratings are as follows:

0—no scaling
1—very slight scaling
2—slight to moderate scaling
3—moderate scaling
4—moderate to bad scaling
5—severe scaling

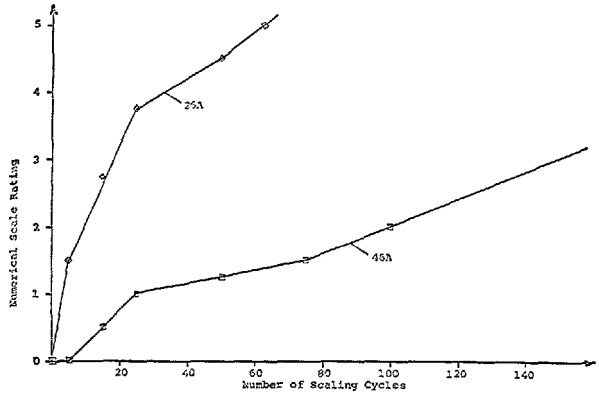

Fig. 8. *Scale rating versus number of scaling cycles (Hussell (21))*

Scaling Failure Criteria

Good maintenance practice would dictate that the time to resurface a bridge deck would be before the scaling and cracking becomes too severe, approximating the numerical scale rating 3.

It is assumed that everytime the conditions necessary to cause a frost deteriorating freeze-thaw cycle are satisfied; a salt application is also made on the bridge deck. This assumption also supposes fairly good maintenance practices. If is further assumed that 3 per cent sodium chloride solution (by weight) is placed on the deck everytime the salting is done. This assumption is not entirely correct since the rate of salt application is variable. Three per cent sodium chloride was used in the laboratory salt scaling tests which are used as the data (21) in this study. It is further assumed that the numerical scale rating expected in the field may be calculated from the equations of the straight line segments in Fig. 8. These curves are based on 14 days moist plus 21 days dry curing, then freezing with the salt solution on the surface of the slab. This procedure and specific salt concentration presents the most severe condition possible and a condition which may exceed field conditions. The curing conditions of the salt scaling tests are not the same as those assumed for the bridge deck, but the mix proportions of the concrete with the above mentioned curing came closer to the rest of the mix properties of the other relationships which were utilized in the study.

The computer calculates the scale rating in real number form from one of the above mentioned equations. The scale rating, for the air-entrained concrete, is modified to take into account the actual air content of the concrete. The measured air content for the air-entrained curve 46A is 4.1%. Using Klieger's work (27, 28) as a guide, it is assumed that if the actual air content is greater than or equal to 3.1% and less than

or equal to 5.1% no adjustment in scale rating is necessary. If the actual air content is greater than 5.1%, then the scale rating is decreased by 30%. If the actual air content is less than 3.1%, the scale rating is increased by 50% of its computed value.

For the non-air-entrained case, no modification of the initially computed rating is made.

In order to use Klieger's (27) numerical integer scale rating the computer rounds off the real number form of the scale rating to the nearest whole integer value. The computer, then, compares the computed scale rating with the scale rating of three. If the scale rating is less than three, the computer continues to calculate the cumulative maturity factor for the concrete and the compressive strength is updated and additional freezing and thawing cycles are taken into account. The constant updating of the cumulative maturity factor, compressive strength, and the age of the concrete batch is repeated until the concrete fails structurally, or failure is caused by moderate salt scaling. After a failure by scaling occurs, the same parameters at failure as those listed after a structural failure are printed out by the computer.

Expected Simulation Results

A number of simulations are run in the manner described. The specific number of simulations which are run corresponds to the number of simulations which are needed to cause the average life of the concrete to approach and maintain a relatively constant value. This expected value is then predicted as the average life of the concrete bridge deck before it will have to either be rebuilt or resurfaced. The average life of the bridge deck may be obtained by observing what happens to a number of the randomly placed batches of concrete in the deck, since the average life is the summation of the lives of each batch of concrete in the deck including that of the most recently completed simulation divided by the cumulative number of simulations completed.

The average compressive strength at failure should also approach and maintain a relatively constant value after a specific number of simulations. This value of average compressive strength at failure should approximately equal the compressive strength of a core sample taken from the bridge deck when its expected average life is reached.

Results and Discussion

Introduction

Air-entrained and non-air-entrained concrete with approximately the same mix proportions were studied.

The effect of the placement time was studied by placing the concrete, hypothetically, on April first and on August first.

Since an exact analysis was not attempted to determine the theoretical probability curves for the temperature data, the effect of varying the cell number was observed. Only the results for 10 cell temperature data are shown in this paper.

Average Life—Number of Simulation Results

In Fig. 9 and 10 the plots of the average life of the bridge deck versus the number of simulations completed may be seen for the air-entrained concrete and the non-air-entrained concrete. In the above mentioned plots the first value of the average life and every tenth value of the average life is plotted thereafter.

It may be seen that the non-air-entrained cases damp out or approach a relatively constant value after a fewer number of simulations than the air-entrained cases. This is due to the greater complexity of the air-entrained model.

It is, also observed that the air-entrained concrete

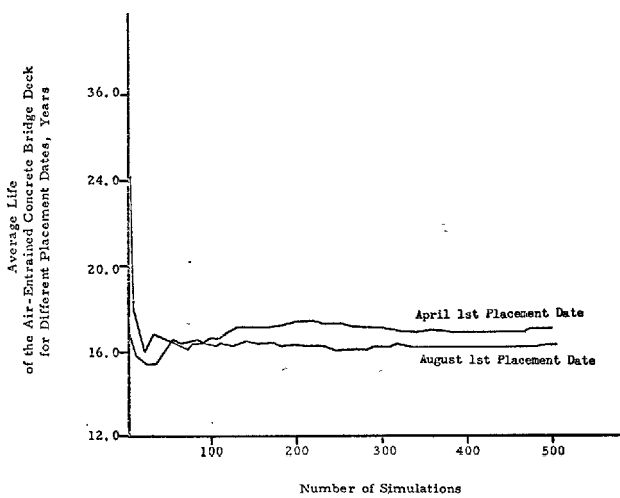

Fig. 9. *Average life versus number of simulations*

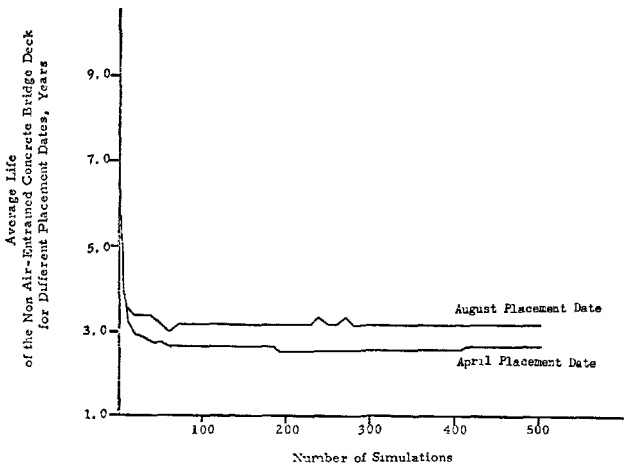

Fig. 10. *Average life versus number of simulations*

Table 5. *Expected average life parameters of the bridge deck depending on placement date*

Air entrained concrete		
	Placement date	
	April 1st	August 1st
Expected average life, years	16.9	16.2
Number of simulations	501	501
Standard deviation, years	3.8	3.7
Variance, years squared	14.7	14.0
Coefficient of variation, per cent	22.8	23.1
Predominant method of failure	Salt scaling	Salt scaling
Computer time utilized	1h 8m 59s	1h 7m 42s

Table 6. *Expected average life parameters of the bridge deck depending on placement date*

Non air-entrained concrete		
	Placement date	
	April 1st	August 1st
Espected average life, years	2.6	2.1
Number of simulations	501	501
Standard deviation, years	.6	.6
Variance years squared	.4	.3
Coefficient of variation, per cent	24.2	27.5
Predominant method of failure	Salt scaling	Salt scaling
Computer time utilized	0h 13m 10s	0h 12m 28s

has an average life of about 8 times that of the non-air-entrained concrete.

Tables 5 and 6 list the expected average life parameters of the bridge deck for the various cases.

The predominant method of failure for all cases is scaling. This is reasonable since bridge deck concrete with a mean 28 day laboratory strength of 4500 psi will most likely not fail structurally.

The concrete placed in April lasted approximately 7 months longer than the concrete placed in August because both fail after approximately the same number of winters of exposure. The above statement is true for both the air-entrained and non-air-entrained concrete cases.

Average Compressive Strength—Number of Simulation Results

The plots of the average compressive strength of the bridge deck versus the number of simulations completed are of the same general shape as the plots of the average life of the bridge deck versus the number of simulations completed.

In Table 7 the expected average compressive strength of the bridge deck, is given at the average life expectancy.

The expected value of the average compressive strength should be approximately equal to the compressive strength of a core sample taken from the hypothetical bridge deck when it reaches a state of structural deterioration or moderate salt scaling.

It may be seen from Table 7 that the date of placement has a marked effect on the value of the expected average compressive strength for the air-entrained mix. It is observed that the value of the expected average compressive strength for the April first placement

Table 7. *Expected average compressive strength of the bridge deck when the average life expectancy is reached*

Air entrained concrete	
Placement date	Compressive strength psi
April 1	3610
August 1	4650
No. of simulations (Same for both placement dates)	501
Non air-entrained concrete	
Placement date	Compressive strength psi
April 1	2640
August 1	2230
No. of simulations (Same for both placement dates)	501

data is approximately 1000 psi lower than that of the August first placement date.

For the air-entrained cases, the 90 days following the August first placement date are generally on an average daily temperature basis for the South Bend area considerably warmer than those 90 days following the April first placement date. This implies that there will be a considerable greater strength gain after the August first placement data than the April first placement date provided that an adequate continuous moist curing procedure is employed as assumed in this analysis.

It can be seen from Table 7 that the values of the expected average compressive strength for the air-entrained cases are between 1000 and 2400 psi greater than the expected values of average compressive strength for the non-air-entrained concrete. This difference is due to the dissimilarity in the loss in strength—number of freeze-thaw cycles relationship for the air-entrained and non-air-entrained cases as shown in Fig. 5.

For the non-air-entrained cases, it may be seen that the April first placement date yields a higher value of expected average compressive strength than the August first placement date. No plausible explanation is apparent to explain the greater value of approximately 350 psi in the expected average compressive strength of the April first placement date in relation to that of August first. Since the difference is only about 2 times the probability distribution for strength cell width of 150 psi, it may be possible that this difference is due to the random fluctuations of the variables in the simulation model.

The results of the study show that the expected average compressive strength of the air-entained concrete is much greater than that of a similar non-air-entrained concrete if both are exposed to the same type of climatic conditions.

It also appears that the placement date has a marked effect on the expected average compressive strength of the air-entrained concrete bridge deck; whereas the placement date does not have as great an effect on the expected average compressive strength of the non-air-entrained concrete bridge deck.

Conclusions

The most important conclusion to be drawn from the analysis is that the Monte Carlo simulation approach to a concrete durability study is highly feasible. However, to make the results of the mathematical model most meaningful, it is imperative to have the proper combination of laboratory and field data available for input to the model. At present all of the essential knowledge for the most meaningful use of the simulation model has not been thoroughly developed. As this knowledge becomes available the simulation model can be readily modified to incorporate the findings.

It may also be concluded that, since the values of the expected average life of the bridge deck appears to be of the proper magnitude, the initial assumption of the application of the principle of superposition to the many variables involved in the durability of concrete may not be in serious error.

The simulation model is very flexible. As a result if enough time, money and effort are expended on the procurement of input data for the simulation model, the results will make possible the most durable type of concrete for a given structure in any given environmental situation for given economic considerations.

References

1. I. Miller and J. E. Freund, Probability and Statistics for Engineers, Prentice-Hall, Inc., Englewood Cliffs, New Jersey, 1965, p. 5.
2. A. H. Herbert Meyer, Editor, Symposum on Monte Carlo Methods, John Wiley and Sons, Inc., New York, 1956 P. vii and p. 4.
3. J. M. Hammersley and D. C. Handscomb, Monte Carlo Methods, Methuen and Co. Ltd., London, 1964, p. 40.
4. R. S. LaRusso, Analysis of Seepage and Groundwater Flow by Monte Carlo Methods, Ph. D. Dissertation, Dept. of Civil Engineering, University of Notre Dame, Indiana, June, 1967.
5. "Durability of Concrete in Service," Reported by ACI committee 201, Hubert Woods, Chairman, Proceedings of the American Concrete Institute, Vol, 59, No. 12, p. 1771.
6. H. H. Newlon, Jr., "Variability of portland cement concrete," Paper presented at the Conference on Statistical Quality Control Methodology in Highway and Airfield Construction, Charlotteville, Virginia, May 3–5, 1966.

7. P. Klieger, "Studies of the effects of entrained air on the strength and durability on concrete made with various maximum sizes of aggregates," Portland Cement Association Bulletin, No. 40, October 1952.
8. S. G. Bergstrom, "Curing temperature, age and strength of concrete," Magazine of Concrete Research, No. 14, Dec. 1953, London.
9. C. Brunet, "Influence of the (time-temperature) parameters on the hardening of concrete," Copenhagen Symposium, RILEM Bulletin, No. 32, 1956, pp. 22–43.
10. J. M. Plowman, "Maturity and the strength of concrete," Magazine of Concrete Research, Vol. 8, No. 22, March 1956.
11. W. H. Price, "Factors influencing concrete strength," Proceedings of the American Concrete Institute, Vol. 22, Sept.—June 1950–1951, pp. 417–431.
12. "Local climatological data," U. S. Depertment of Commerce, St. Joseph County Airport, Sourth Bend, Indiana, 1940–1966 daily basis, 1900–1966 monthly basis.
13. Chefdeville, "Vibration testing of concrete-second part," RILEM Bullein, No. 15, August 1953, pp. 61–77.
14. S. Takano, "Determination of concrete strength by a non-destructive method," RILEM Proceedings, International Symposium on Non-Destructive Testing of Materials and Structures, Vol. 1, 1954.
15. S. Ohgishi and T. Uchida, "A study on the properties of concrete by the ultrasonic method," Proceedings of the Fourth Japan Congress on Testing Materials, Kyoto, Japan, 1961. pp. 104–106.
16. S. Ohgishi, "On the relations between compressive strength, pulse velocity, dynamic E and logarithmic decrement of concrete," Proceedings of the Fifth Japan Congress on Testing Materials, Kyoto, Japan, 1962, pp. 123–130.
17. S. Ban, H. Muguruma and K. Yasui, "Static and dynamic moduli of elasticity of concrete," Proceedings of the Second Japan Congress on Testing Materials, Kyoto, Japan, 1958, pp. 161–173.
18. K. Kohno, K. Emura and K. Kinoshiro, "Investigation into the early strengths and the dynamic modulus of elasticity of concrete containing different types of cement," Proceedings of the Ninth Japan Congress on Testing Materials, Kyoto, Japan, 1966, pp. 110–120.
19. E. A. Whitehurst, "Pulse velocity techniques and equipment for testing concrete," Highway Research Board Proceedings, 1954, pp. 226–240.
20. W. J. Cheesman, "Dynamic testing of concrete with the soniscope apparatus," Highway Research Board Proceedings, Vol. 29, 1949, pp. 176–183.
21. D. J. F. Hussell, "Freeze-thaw and scaling tests on silicone-treated concrete," Highway Research Board Record, No. 18, 1962, pp. 13–33.
22. P. Klieger, "Long—time study of cement performance in concrete—chapter 10," Portland Cement Association Bulletin, No. 39.
23. R. Jones, "Testing of concrete by ultrasonic pulse technique," Highway Research Board Proceedings, Vol. 32, 1953, pp. 258–275.
24. J. R. Leslie and W. J. Cheesman, "An ultrasonic method of studying deterioration and cracking in concrete structures," Journal of the American Concrete Institute, Vol. 26, 1950, pp. 17–36.
25. E. A. Whitehurst, "Soniscope tests concrete structures," Proceedings of the American Concrete Institute, Vol. 47, 1951, p. 434.
26. "States escalate bridge deck repair battle," Engineering News-Record, May 4, 1967 edition, pp. 47–52.
27. P. Klieger, "Curing requirements for scale resistance of concrete," Portland Cement Association Bulletin, No. 82, June 1957.
28. G. J. Verbeck and P. Klieger, "Studies of "Salt" scaling of concrete," Portland Cement Association.

Supplementary Paper III-59 Measuring Gas Diffusion for the Valuation of Open Porosity on Mortars and Concretes

Hans E. Schwiete, H. J. Böhme and Udo Ludwig*

Introduction

Together with water, cement and its aggregate (sand, gravel and broken material) form mortar or concrete which is damp to plastic in consistency, according to the amount of water added, and which hardens by the reaction of the water with the cement.

The denseness of hardened mortar or concrete depends upon

1. the ratio of cement : aggregate : water
2. the quality of the cement
3. the type and particle size distribution of the aggregates
4. the degree of compaction
5. and upon the type and duration of subsequent treatment of the fresh mortar or concrete.

Cement in combination with water increases the denseness of the mixture because the hydration products (calcium silicate hydrate, calcium aluminate ferrite hydrate, calcium aluminate ferrite sulphate hydrate and free calcium hydroxide) have a higher specific volume than the unhydrated cement.

Measurement of the Gas Diffusion

The amount of gas which diffuses independant of time through samples of mortar or concrete was measured by the application of Fick's first law:

$$\dot{S}_0 = -D_0 \cdot q \cdot \frac{dc}{dx}$$

The amount of the substance ($\dot{S}_0$) which in the time (t) diffuses through a cross-section (q) is proportional to the diffusion gradient (dc/dx), and the proportionality factor is D(cm²/sec.). In the case of porous media the sum of the permeable cross-sections (Σq) should be introduced into the diffusion equation, however only the cross-section of the sample (F) is known. The texture of the material must also be taken into account, i.e. the pores are variable in width and length. However only the thickness (L) of the investigated body is known. Furthermore if the pore width is equal to or smaller than the free path length of the diffusing particles, the normal volume—or gas type of diffusion is replaced by Knudsen's capillary diffusion (molecular diffusion). One must also reckon with the effect of Volmer's surface diffusion particularly in the case of hydration products with highly active surfaces. Thus it seems appropriate to define an effective diffusion coefficient (D_{eff}), as Wicke (1) has done. This is:

$$-\dot{S} = D_{\text{eff}} \cdot F \cdot \frac{dc}{dx}$$

If one relates the concentration gradient to the measurable thickness L, the following equations define the diffusion coefficient:

$$D_{\text{eff}} = \frac{S \cdot L}{F \cdot t \cdot (C_0 - C_L)} = \frac{V \cdot p \cdot L}{F \cdot t \cdot (p_0 - p_L)}$$

The "specific permeability" is defined according to Manegold (2):

$$\psi = \frac{D_{\text{eff}}}{D_0}$$

It should be noted that D_{eff} and D_0 refer to the same conditions of temperature and pressure.

Measurement of the Effective Diffusion Coefficient

To determine the diffusion coefficient we built a simple apparatus (3) which uses oxygen as the measuring medium (Fig. 1). The paramagnetism of oxygen is used to determine the oxygen content in a stream of nitrogen. The apparatus consists essentially of two measuring tubes, a sample container with sample, a differential manometer and a gas analyser. In addition there is a burette to calibrate the volume of the measuring tubes. Subsequently another apparatus was built in which the total pressure could be lowered to 150 Torr so that it was possible to distinguish the various types of diffusion (volume, molecular and surface diffusion), qualitatively at least, by their different

*Institut für Gesteinschtenkunde, Technische Hochschule Aachen, Aachen, West Germany.

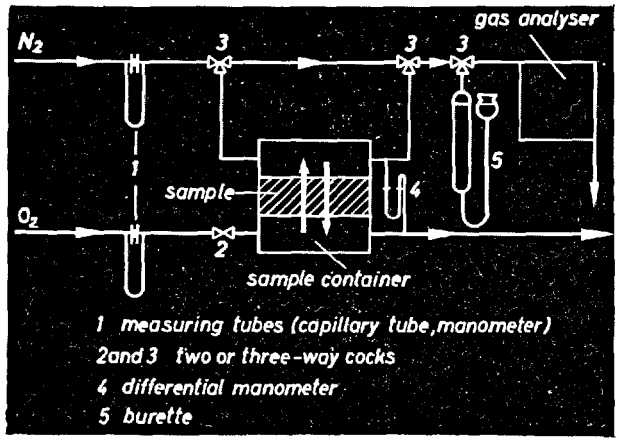

Fig. 1. *Measurement of gas diffusion*

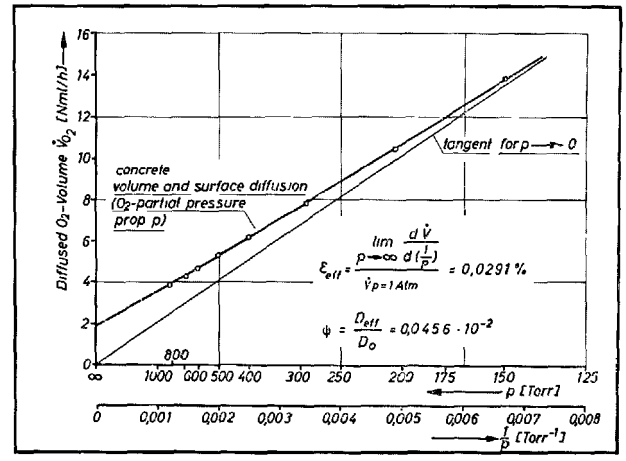

Fig. 2. *Diffusion measurement on concrete*

response to pressure. The gas analyser uses electrochemical principles and allows measurement in the range from 0 to 0.1, 0.01 and 0.001% oxygen. With four different sample holders cylindrical samples 3, 6, 5, 8 and 15 cm in diameter and 1 to 3 cm high could be measured.

Interpretation of the Measurements

As the gas diffusion measurements are "stationary" i.e. independant of time, the oxygen content can be given the value 1 where the gas enters the sample and the value 0 where it leaves it.

Thus:

$$D_{eff} = \frac{\dot{S} \cdot L}{c \cdot F}$$

where

D_{eff} = effective diffusion coefficient in cm²/sec.
L = thickness of the sample in cm
F = cross section of the sample in cm²
$\dot{S}$ = the amount of oxygen in cm³/sec. which diffuses through the sample

As the analyser gives the oxygen content in % and as the amount of the transporting medium, nitrogen, is measured in cm³/sec., this yields

$$\dot{S} = \frac{n \cdot \%\, O_2}{100}$$

with n = the amount of nitrogen in cm³/sec.

Thus:

$$D_{eff} = \frac{n \cdot \%\, O_2 \cdot L}{F} \quad (cm^2/sec.)$$

The diffusion coefficient of N_2–O_2 without specimen has been determined as 0.203 cm²/sec. (between 11.7°C and 13.1°C and 756 – 761 Torr) and using this value the specific permeability at 20°C and 760 Torr is

$$\psi = \frac{D_{eff}}{D_0} = \frac{D_{eff}}{0.211}$$

Mean Error of the Measurements

The mean error comprises the individual errors in determining the sample dimensions, the amount of nitrogen present and the concentration of oxygen. We estimate this error to be in the range $\pm 3 - 7\%$. For large samples with a high specific permeability it is small, and in the case of small samples with a low specific permeability, it is large. Žagar (4), who investigated the method for determining the "apparent diffusion coefficient" reckons with a relative error of $\pm 5\%$. We remounted the specimens repeatedly and found, in agreement with Žagar, that the reproducibility lies below this limit of error. Furthermore the error is affected by uneven or insufficient drying of the specimens. We dried ours at 50°C to constant weight. This ensures sufficiently quick drying but does not alter the hydration products too much.

Results of the Measurements

Analysis of the Types of Diffusion Occuring in Concrete

Normally, Knudsen and Volmer diffusion can be distinguished by their characteristic response to pressure. Following the experiments of Wicke and Kallenbach (5) we carried out similar measurements on concrete samples and have established that even in dense concretes volume diffusion is predominant (Fig. 2). At pressures up to 150 Torr molecular diffu-

sion was not observed.

The curves, however, show that surface diffusion is present. The curve for $p \longrightarrow \infty$ does not run through the origin but instead cuts the ordinate. If one eliminates the effect of Knudsen diffusion by applying infinitely high pressure, and the effect of Volmer diffusion by a parallel shift of the curve measured, one arrives at a definition for the "effective porosity" which shows, quantitatively, in the slope of the curve, only the stereometric influence of texture. The effective porosity can therefore be formulated mathematically as follows:

$$\varepsilon_{\text{eff}} = \frac{\lim\limits_{P\to\infty} \dfrac{d\dot{S}}{d\left(\dfrac{1}{P}\right)}}{\dot{S}_0\,(P = 1\ \text{atm.})}$$

If neither Knudsen nor Volmer diffusion contribute to material transport, then the specific permeability (ψ) is equal to the effective porosity ε_{eff}:

$$\psi = \frac{D_{\text{eff}}}{D_0} = \varepsilon_{\text{eff}} \quad \text{for} \quad \begin{cases} D_{\text{eff}} \sim \dfrac{1}{P} & \text{and} \\ \dfrac{d\varepsilon_{\text{eff}}}{d\left(\dfrac{1}{P}\right)} = \dfrac{D_{\text{eff}}}{D_0} \end{cases}$$

It is apparent from the results above that one must reckon with an appreciable amount of surface diffusion in cemented building materials and therefore

$$\psi \neq \varepsilon_{\text{eff}}$$

In the case of these materials, however, there is the possibility that a proportionality exists between ψ and ε_{eff} and this means that to a given permeability a certain effective porosity can be assigned.

In contrast to the measurements of Wicke and Kallenbach, in our case the partial pressure of oxygen was not kept constant. As it varies with the total pressure one can approximately determine ε_{eff} from the tangent to the curve at $p \longrightarrow 0$, and from the difference

$$\psi_{\text{total}} - \varepsilon_{\text{eff}} = \psi_0$$

the contribution of surface diffusion can be calculated.

For concrete we determined:

$$\left.\begin{aligned} \varepsilon_{\text{eff}} &= 0.028\,\% \\ \psi_{\text{total}} &= 0.044 \cdot 10^{-2} \\ \psi_{\text{surface}} &= 0.016 \cdot 10^{-2} \end{aligned}\right\} \quad 760\ \text{Torr},\ 0°\text{C}$$

Laminar flow was observed during the gas permeability measurements. Thus from the equation

$$\vartheta_s = \frac{r_{\text{eff}}^2 \cdot \varepsilon_{\text{eff}}}{8}$$

the value of r_{eff}^2 can be calculated. When $Ds = 11 \cdot 10^{-2}$ cm^2 and $\varepsilon_{\text{eff}} = 2.8 \cdot 10^{-4}$, $r_{\text{eff}} = 5.5 \cdot 10^{-4}$ cm $= 5.5\ \mu$m.

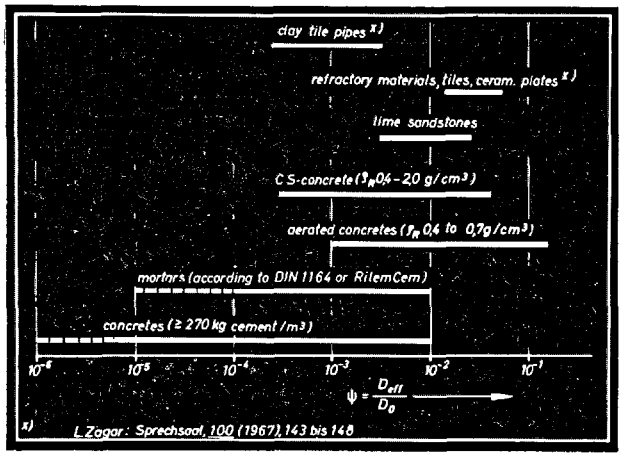

Fig. 3. *Specific permeability of inorganic building materials*

Žagar (4) made comparative measurements of the electrical conductivity, the ionic diffusion, the gas diffusion and the replacement of air by water in ceramic tiles, roofing tiles, earthenware pipes and refractory bricks (chamotte, silica and magnesite) and he found that the later two methods were a reliable means of determining the effective porosity of fine-pored ceramic materials.

The Specific Permeability of Sintered and Cement-Bonded Building Materials

Fig. 3 is a compilation of the specific permeabilities of some inorganic building materials which have been determined by the gas diffusion method. The values for mortar and concrete show a wide spread which ranges from 10^{-2} to 10^{-6} or 10^{-5} respectively, depending upon the age of the samples, the composition of the mixture and the degree of compaction. It should be noted that only those mortars and concretes which can be drilled (with a compressive strength of more than about 100 kg/cm^2) have been tested. This means that in the very early stages of hardening the specific permeability is probably 10 to 100 times higher. The practical application of these results shows the importance of a sufficient duration for the after-treatment of concrete in order to prevent premature drying-out.

Normal aerated concretes or lime sandstones do not reach denseness of high-grade mortars and concretes.

For comparison, Žagar's values (4) for sintered ceramic building materials have been listed. For them

$$\varepsilon_{\text{eff}} = \psi \cdot 100(\%)$$

In the following it is shown on the basis of measurements, that, at least partially, a good proportionality must exist between ε_{eff} and ψ for mortars and concretes. Otherwise the relationships which have been found in investigations of the material strength, frost resistance and carbonation would not be so pronounced.

Influence of the Specific Permeability on Compressive Strength and Frost Resistance

A further example shows the influence of specific permeability on the compressive strength and the freeze-thaw resistance for cement mortars in which the cement fraction is replaced by cement raw material up to a value of 30%. The raw material was made up of 15% montmorillonitic, kaolinitic or illitic clay components, 10% quartz and 75% limestone.

Fig. 4 shows that there is a nearly linear relationship between the compressive strength measured and the specific permeability of the mortar, irrespective of the time of ageing. This means that the compressive strength measured after 3, 7 and 28 days can be directly correlated with the specific permeability measured at these intervals.

In order to determine the resistance to freeze-thaw action the linear expansion and the resonance frequency were used. After being stood for 28 days in water the samples were frozen at −15°C for 4 hours and then thawed for 1 hour in a water bath at 20°C.

Fig. 5 shows the relationship between the linear expansion of the mortar samples, measured according to Rilem-Cem, after 30 freeze-thaw cycles, and the specific permeability after 28 days in water. It can be seen that with increasing amounts of raw material the specific permeability and the linear expansion increase. It appears that the differences arise from the constituent clay components. Thus with even 10% of raw material the unfavorable influence of the clay minerals becomes apparent. As one would expect, the montmorillonite-bearing material are worse in effect than the kaolinitic ones.

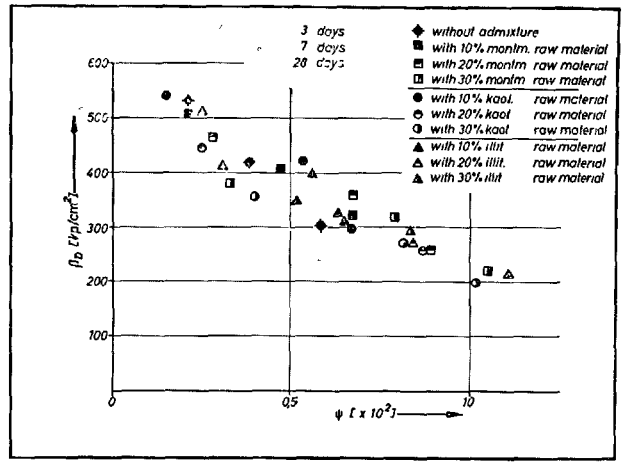

Fig. 4. *Specific permeability of mortars and compressive strength according to Rilem-Cem*

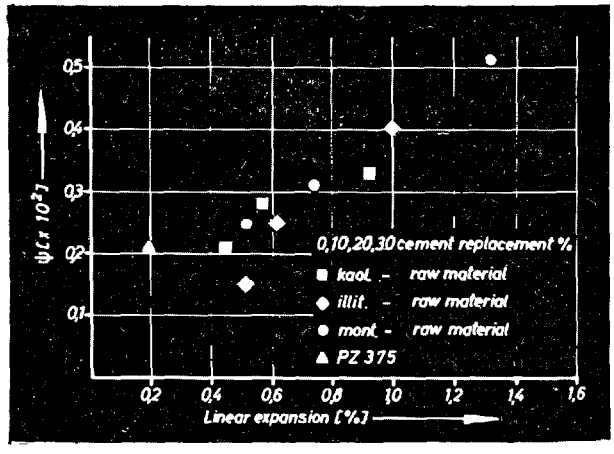

Fig. 5. *Influence of specific permeability on freeze-thaw-resistance*

Influence of the Specific Permeability on the Carbonation of Concretes

To study the carbonation we had 7-year old samples from bending strength tests and section of the same age taken from beams for measuring shrinkage. These are samples left over from the sea water experiments carried out by the German Committee for Reinforced Concrete. The bending strength samples were kept moist for one day and then stored in water up to the day of investigation. The bending test was carried out at earliest after 7 days, and at latest after 90 days of preliminary storing. Thus all the samples were stored in water for different lengths of time. The beams for measuring shrinkage were kept wet for one day and subsequently stored in an air conditioning chamber for one year at 20°C and a relative humidity of 65%. Then the samples were kept in a bunker for $4\frac{1}{2}$ years at about 8°C and 62% relative humidity. Thus this beams suffered a very rapid drying so that, at least at the surface, sufficient strength could not develop and the closing of the open pores by the formation of hydrates could not take place. Fig. 6 shows the relationships obtained between the average depth of carbonation (determined with phenolphthalein) and the specific permeability for the two kinds of concrete. The minimum specific permeability for the beam is 0.1% and at most 0.9% and the corresponding

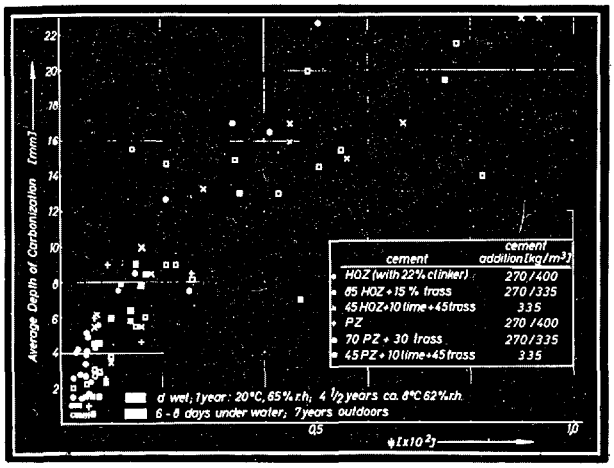

Fig. 6. *Influence of the specific permeability on the depth of carbonation of concretes*

depths of carbonation are 2 mm and 23 mm respectively. The specific permeabilities for the bending test samples are only 0.02 and 0.26% with a maximum average carbonation depth of only 10mm. This means, however, that the carbonation depth for the bending test samples fall on one line with those for the beams for measuring shrinkage.

These results show that the measurement of the specific permeability of mortars and concretes can give an important indication about what depth of carbonation can be expected after a given time. As the carbonation is purely a diffusion process accompanied by ad—and absorption, the amount of lime available, and the kind and amount of the bonding medium which is added, must also exert an influence, apart from that of the specific permeability.

It should be added that we have successfully used the specific permeability to estimate the influence of the addition of plastic dispersions and puzzolanic materials on the properties of mortars.

Furthermore gas diffusion measurements have shed light on the following problems: the waterproofing of concrete with skins of plastic, the chemical resistance of cement mortars and concretes, and hydrate alterations in aluminous cements.

Summary

From the data presented it is apparent that besides normal gas diffusion surface diffusion also occurs in cement-bonded building materials. Only with further measurements of the gas diffusion at varying total pressures it will be possible to determine the effective porosity which plays a role in any transportation effects in the material, and hence allow the labyrinth factor (χ) and the effective pore radius (r_{eff}) to be calculated, using the equation

$$\chi = \frac{\varepsilon_{eff}}{P_{total}} \quad \text{and} \quad D_S = \frac{r_{eff}^2 \cdot \varepsilon_{eff}}{8}$$

Measurements of the gas diffusion at normal pressure have already shown a close connection between the texture and useful technical properties.

References

1. E. Wicke: Kolloid-Z. **93** 127 (1940).
2. E. Manegold: Kolloid-Z. **82** 26 (1938).
3. H. E. Schwiete and U. Ludwig: "On the determination of open pores in cements stone", Tonind.-Ztg. **90**, 562–574 (1966).
4. L. Žagar: "Pore size distribution in ceramic materials" Sprechsaal 100 (1967) H. 1, 3 and 4.
5. E. Wicke and R. Kallenbach: "Surface diffusion of CO_2 in activated carbon" Kolloid,-Z. 97 (1941) 135–151.

Supplementary Paper III-99 The Behaviour of Concrete Subjected to Freezing and Thawing as a Reference for Frost Resistivity of Concrete

Yoshiro Koh and Eiji Kamada*

Synopsis

The length change of concrete during freezing and thawing was recorded continuously and automatically with the aid of differential transformers. Test specimens were 10 by 25 cm cylinders under oven-dry and saturated conditions and sealed with water proofing paint after storage in water for four weeks. The tensile strength and moisture content of the specimens were measured after 13 alternate freezing and thawing cycles within the range from 20°C to −30°C.

Four water-cement ratios were applied to concrete mix. Coarse aggregates were gravel, crushed stone and several kinds of artificial lightweight aggregates.

Oven-dry specimens give uniform thermal expansion, however, saturated specimens show different behaviors on the length-temperature curve. The saturated specimens using high water absorptive aggregates show abnormal expansion during freezing, and the residual expansion after 13 alternate freezing and thawing cycles is about 0.1 to 0.3 per cent. In this case, the decrease in the tensibl strength exceeds 50% of the initial strength. In case of low water absorptive aggregates, no expansion during freezing is observed, and increase in the residual expansion and decrease in the tensile strength are very small.

The grade of transitional and residual expansions depends upon the difference of water-cement ratio and degree of moisture content of concrete due to absorptive aggregates.

The residual expansion will suggest the grade of frost damage of concrete, as there is a relation between the residual length change of specimens and the decrease of splitting tensile strength.

To make clear the relation between frost resistivity of concrete and transitional and residual expansion, we made slow and rapid freezing and thawing tests for finding out the relation between the residual expansion and the behavior of decrease of dynamic elastic modulus, and water permeability test.

Introduction

The durability of concrete is always one of the important properties as well as the strength of concrete for structures and the workability of concrete at a time of placing. We have to make effort to clarify what is the best way to know the behavior of concrete exposed to natural weathering.

Many researchers made the freezing and thawing test of concrete according to the standard methods such as ASTM Designation C290 or C291 to make clear the behavior of concrete exposed to freezing and thawing action. A few of them carried out their special investigations on the behavior of concrete, especially on the volume change of concrete during freezing. There are, for example, Valore's paper in 1950 and Wills' study in 1963 according to Powers' proposed method in 1955.

In Japan, many papers on the resistance to freezing and thawing were presented at the General Meetings of the Japan Cement Engineering Association in recent ten years from 1957 to 1966. Almost of all researchers turned their investigations to the effect of cements, aggregates and admixtures on the resistance to freezing and thawing comparing the properties of concrete with each other by applying ASTM C290 or C291 methods. The remainder aimed at investigating the resistance of green concrete to freezing and thawing soon after placing, as a reference to winter concreting.

The investigation herein described was intended to study the expansion when concrete was exposed to severe freezing action, however, our method will also be a measure for the resistance to freezing and thawing.

Test method by Powers (1) and a paper written by Valore (2) encouraged us to start our effort to study the behavior of concrete frozen down to −30°C. Up to

*Hokkaido University, Sapporo, Japan.

this time we made various freezing and thawing tests of concrete in accordance with the method defined in our laboratory or ASTM C290. The freezing temperature was fixed to $-15 \sim -20°C$ or $-7 \sim -10°C$, the latter was mainly applied to the study on the frost resistance of early age concrete as a reference for winter concreting.

We intended to clarify the abnormal expansion of concrete expected during freezing and thawing, when concrete was made with undesirable aggregates with soft particles such as so-called "bad" aggregates, either artificial or volcanic lightweight aggregates, which might show rather low resistance to frost action.

Description of the Investigation

Test Procedure

The investigation consisted of measuring the resistance to freezing and thawing of concretes made with two natural aggregates and seven artificial lightweight aggregates and with or without air entraining agent. Three moisture conditions were applied; (1) oven-dry, (2) wet and (3) supplying water. Another test series was carried out as preliminary test in 1966 for two moisture conditions of oven-dry and wet. The three freezing and thawing methods were our new method, described in detail later and hereafter referred to as the "medium cycle", our conventional method of slow freezing and thawing, shown in the second line of Table 1 and hereafter called the "slow cycle", and the ASTM Designation C290, hereafter called the "rapid cycle".

We know that fast cooling and lower temperature cause severe damage to concrete or mortar, as mentioned in papers of many researchers and mine. However, we made an attempt to prepare an apparatus for "medium cycle" capable to cool air temperature down to $-40°C$ and to heat air up to $40°C$.

Medium Cycle

The medium cycle consisted of cooling of the $10\phi \times 25$ cm cylinder specimens from $20°C$ to $-30°C$ for a period of about 6.5 hours and heating up to $20°C$ for a period of about 5.5 hours (Table 1). Temperature at the center of the specimens was measured and recorded by thermocouple, which was embedded when concrete was placed, and by recorder. This medium cycle was repeated 13 times and 5 times in the principal test and the preliminary test respectively.

Subject to moisture conditions, the specimens were prepared for the test before freezing. In case of oven dry condition, five or two days before freezing and thawing test, the specimens were removed from water and dried in oven at $105°C$ for four days in the principal test and for one day in the preliminary test respectively. In both cases of wet and water supplying conditions, the specimens were removed from water one day before the end of curing period.

The length and weight of the concrete cylinders were measured before preparing the specimens for the test. The cylinders first had been applied with neoprene water proof paint, then were wrapped in non-woven fabric made from polyvinylalcohol to minimize drying through pin-hole of the paint, and they again had the paint applied except on two tiny dented round areas in the center of the both ends of cylinders, where the measuring rods were adhered with epoxy-resin adhesive. The measuring rod was made of quartz glass and the diameter of the rod was approximately 12 mm. The length of the rods was 250 mm and 50 mm at the top and bottom ends respectively. An additional

Table 1. *Method of freezing and thawing*

Method	Specimen	Condition of moisture	Freezing		Thawing		Age when test was started	Measurement
			Temp. °C	Cooling period hr.	Temp. °C	Heating period hr.		
Medium cycle	Sealed after water curing	1) Oven dry 2) Wet 3) Supplying water	−30	6.5	20	5.5	28 (14)*	Length change Splitting tensile strength
Slow cycle	Water curing	in water	−18	21~22	5	2~3	28 (14)*	Length change Dynamic modulus of elasticity
Rapid cycle C290	Water curing	in water	−18	about 1	5	about 2	28	Dynamic modulus of elasticity

*Preliminary test

thermocouple was fixed on the surface of concrete for measurement of temperature during freezing and thawing at the surface of the specimens (Fig. 1). Ring shape foam polystylene insulations were attached to both ends of the concrete to minimize the cooling of the concrete along vertical axis and the temperature effect to the quartz glass rods. The depth of the insulations was 4 cm and the diameter was the same as that of concrete specimens. The clearance between the measuring rods and the insulation was greased to avoid restriction due to the frost by cooling of the surface of rod. And then the specimens were wrapped by two layers of butyl rubber sheet, 33 cm in width, to eliminate the difference between the temperatures at the surface and the center of the cylinder (Figs. 2 and 3).

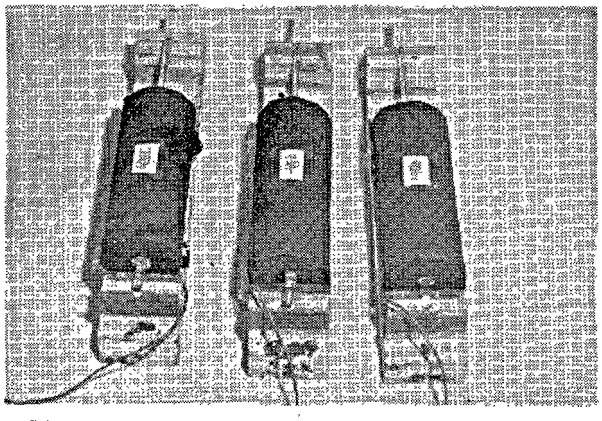

Fig. 1. *Specimens after waterproofing by paint and fabric*

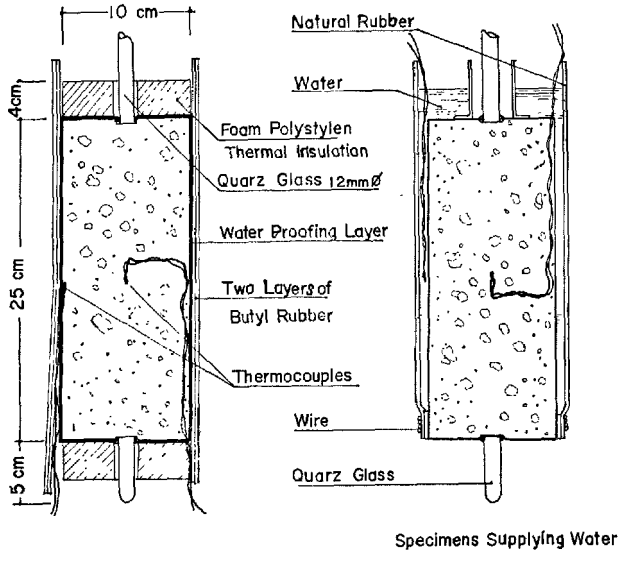

Fig. 2. *Specimens for medium cycle*

In case of the specimens for water supplying condition, no foam insulation and waterproofing layers of paint and non-woven fabric were applied. The concrete cylinder was put in a rubber pipe and the bottom was tightly bound with wire. We made a narrow space for pouring water around the cylinder by using rubber strips (Fig. 4). When set up in the testing chamber, sufficient water to cover the top end of cylinder was poured into the space.

The specimens were placed on a vertical electric comparator in the freezing chamber. The ambient air temperature was controlled at 20°C before cooling. The specimens were cooled down to −30°C and warmed up to 20°C by air in chamber. No program control of temperaure was applied in this test. Temperature (Fig. 5), expansion and contraction were recorded automatically.

Slow Cycle

The slow cycle of freezing and thawing in water, which was conventional in our laboratory, was made

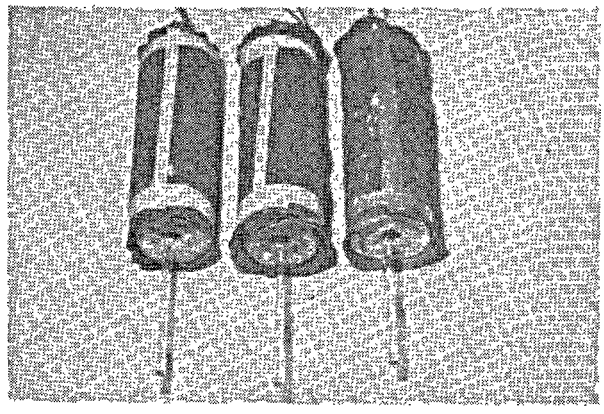

Fig. 3. *Specimens wrapped with butyl rubber sheet*

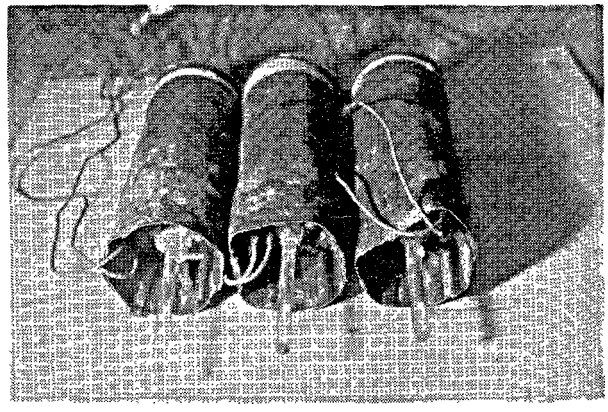

Fig. 4. *Specimens for test under condition supplying water*

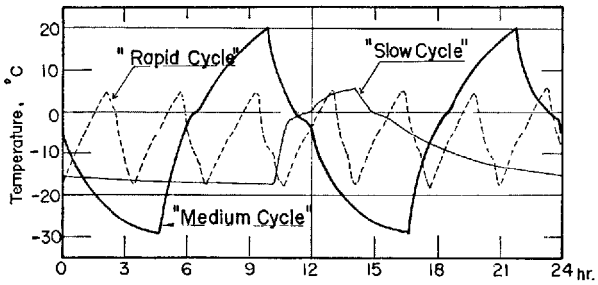

Fig. 5. *Typical temperature curves*

by using 7.5 × 7.5 × 40 cm square beam type specimens as shown in Table 1. Specimens were frozen in water at—18°C for 22 hours and thawed in water at 5°C for 2 hours in this test (Fig. 5). That is one cycle of freezing and thawing per day. Freezing and thawing was started after curing in water for 28 days at 20°C and was terminated when specimens had lost more than 50 per cent of their initial dynamic modulus. Two brass gage plugs were embedded at each end along the longitudinal axis, and the dynamic modulus of elasticity, the total residual length change and weight loss were measured at every six or ten cycles of freezing and thawing. However, in the preliminary test, slow cycle was started after curing in water for 14 days at 20°C, and no gage plug was embedded for the measurement of length change. And three types of beam specimens were used, i.e. 10 × 10 × 40 cm, 7.5 × 7.5 × 40 cm and 4 × 4 × 40 cm.

Rapid Cycle

The conventional rapid cycle of freezing and thawing in water was made in accordance with ASTM Method C290 at the laboratory of the Hokkaido Building Research Institute. Specimens were the same with those of slow cycle and were frozen and thawed in water with approximately seven or eight cycles per day (Fig. 5 and Table 1). Weight loss and fundamental frequency measurements were made on all specimens. No rapid cycle was carried out in the preliminary test.

Materials

The coarse aggregates were a diluvial gravel, a crushed andesite and seven kinds of artificial lightweight aggregates including some trial products as shown in Table 2. The diluvial gravel contains considerable per cent of soft particles, however, it is used in our district due to the lack of good aggregates in the vicinity of Sapporo city. In the preliminary test,

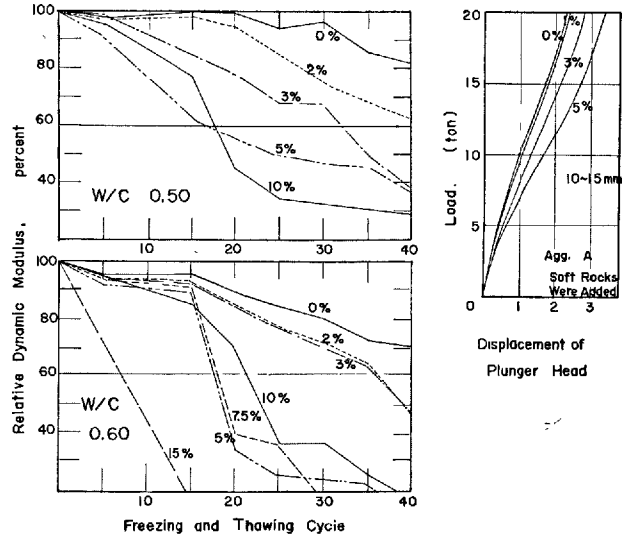

Fig. 6. *Hattori's test results*

only the gravel was used without any treatment (content of soft particles is approximately 5% by volume, i.e. 3.6% by weight), however, the soft and light particles were picked out by hand to avoid the effect of them on the frost resistance of concrete in this test, and the content of them was considered less than 2% by volume.

The content of soft particles shows a considerable effect on the resistance of concrete to freezing and thawing, and the curves of displacement of plunger versus load, obtained by crushing test of coarse aggregates, are not only a measure of hardness but also of the quality of aggregates for durable concrete, as shown in Fig. 6 and mentioned in my previous paper with aid of Hattori (5) for the RILEM Symposium on the Durability of Concrete held in Prague in 1961. In the conclusion of the paper, I mentioned that the soft particles should be less than 3% by volume based on the test results considering frost action.

Fig. 7 shows the crushing test results of the artificial coarse aggregates by Hashimoto (4), by using Hattori's apparatus (5), consisted of cylinder, of which inside diameter is 10 cm and effective depth is 20 cm, and plunger.

Well graded diluvial sand from the same source was used as fine aggregate. A little effect of soft and light particles in sand on the strength of concrete is inevitable. Aggregates in surface dry condition were used for making concrete.

A normal portland cement used widely in our district was used. A neutralized Vinsol resin solution was used as air entraining agent for a part of concrete mixes.

Table 2. *Characteristics of aggregates*

	Aggregate		Specific gravity		Water absorption %	Unit volume weight kg/m³	Solid volume percentage %	Percentage of passing sieves mm					
			Surface dry	Oven dry				5	10	15	20	25	
Coarse	Diluvial	A	2.59	2.50	2.64	1658	66.2	6	42	69	76	100	
	Crushed stone	C	2.75	2.70	1.46	1657	61.5	5	19	35	54	100	
	Artificial lightweight aggregate	D	1.40	1.23	14.6	780	63.4	2	38	100	—	—	
		B	1.44		12.2			—	40	90	100	—	
		G	1.36	1.23	8.7			—	40	90	100	—	
		E	1.44	1.32	9.0	832	63.3	4	41	86	95	100	
		J	1.25	1.22	2.8	803	65.8	0	40	88	96	100	
		S	1.18	1.08	8.1	717	66.4	21	62	80	100	—	
		M	1.26	1.18	7.1	761	64.6	5	34	93	98	100	
Fine	Diluvial	A	2.54					0.15	0.30	0.60	1.2	2.5	5
								2	20	46	75	90	100
Coarse	Diluvial	Ap	2.57		2.68	1699	65.3	2	37	—	85	100	

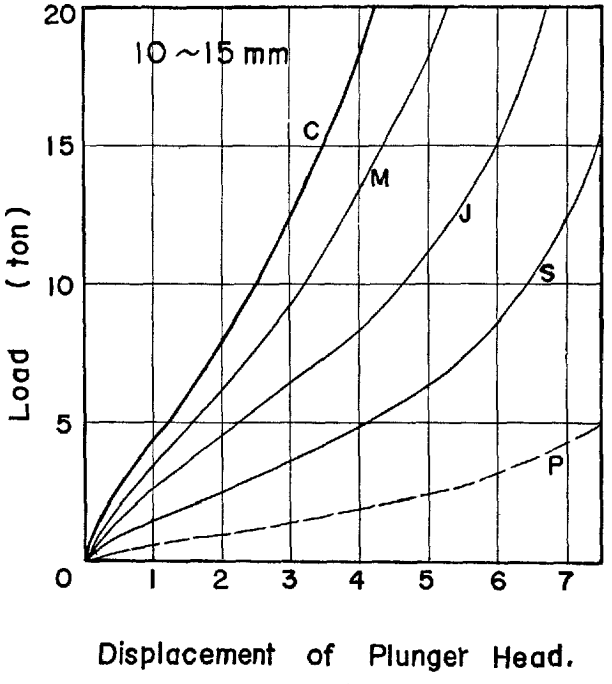

Fig. 7. *Hashimoto's data by using Hattori's apparatus*

Concrete

Concrete mixes were decided after trial mix to have a slump of 18 cm. Three kinds of water cement ratio were chosen to apply to the principal test, i.e. 0.50, 0.70 and 0.90 by weight. Three kinds of slump, 8, 18 and 22 cm, and five variations of water-cement ratio, i.e. 0.4, 0.5, 0.6, 0.7, 0.9, and 1.1, were chosen for the preliminary test (Table 3).

Four $10\phi \times 20$ cm cylinders and one $10\phi \times 25$ cm cylinder for the medium cycle were made from the same batch. The former was used for testing compressive and splitting tensile strengths at the end of curing period, when freezing and thawing was started. The splitting tensile strength and moisture content were also measured after defined repetitions of medium cycle by using $10\phi \times 25$ cm specimens. Three $7.5 \times 7.5 \times 40$ cm square beam type test specimens for slow or rapid cycle and three $10\phi \times 20$ cm cylinders for compressive strength test were made from each batch. The compressive strength test was made at the end of curing period (Table 4).

When concrete was placed in molds, thermocouples were installed in the geometric center of each of the cylinder specimens for medium cycle and of the specimens for measuring temperature for slow or rapid cycle (Fig. 3).

All specimens, except those tested under oven-dry conditions, were cured in water for 28 days and 14 days, respectivley for the principal and the preliminary, at 20°C, including the first day in molds in room air and the final day for preparing of the medium cycle specimens in air.

Table 3. *Testing plan for three methods*

Condition	Agg.	W/C	Medium cycle non AE	Medium cycle AE	Slow cycle non AE	Slow cycle AE	Rapid cycle non AE	Rapid cycle AE
Wet	A	0.50	○		○		○	○
		0.60			○			
		0.70	○		○	○		
		0.90	○		○			
	C	0.70	○					
	D	0.50	○	○			○	○
		0.70	○	○	○	○		
		0.90	○					
	B	0.50	○					
		0.70	○					
	G	0.50	○					
		0.70	○					
	E	0.50	○				○	○
		0.70	○		○	○		
	J	0.50	○				○	○
		0.70	○		○	○		
	M	0.50	○					
		0.70	○		○	○		
	S	0.50	○				○	○
		0.70	○		○	○		
Oven dry	A	0.50	○					
	B		○					
	S		○					
Supplying water	A	0.50	○					
		0.70	○					
	D	0.50	○					
		0.70	○					

Preliminary test

Condition	Agg.	W/C	Medium cycle Slump. cm 8	Medium cycle Slump. cm 18	Medium cycle Slump. cm 22	Slow cycle Slump. cm 8	Slow cycle Slump. cm 18	Slow cycle Slump. cm 22
Wet (Dry)	Ap	0.40		○			○	
		0.50	○	○	○	○	○	○
		0.60	○	○	○	○	○	○
		0.70	○	○	○	○	○	○
		0.90		○			○	
		1.10		○			○	
Wet	A	0.40		○				
		0.50		○				
		0.60		○				
		0.70		○				
		0.90		○				

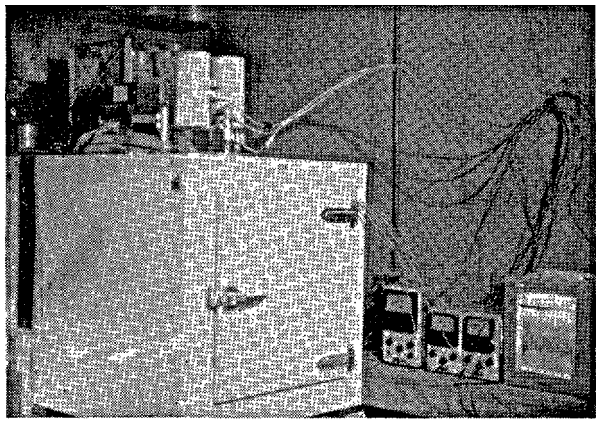

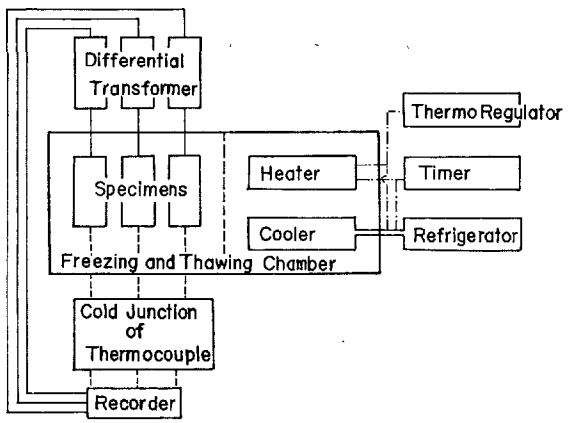

System of Apparatus for "Medium Cycle"

Fig. 8. *Apparatus for "medium cycle"*

Testing Apparatus

The parts of measuring apparatus for medium cycle were composed of electric comparator and recorder (Fig. 8). Three differential transformers were installed in a stand with three quartz glass legs to eliminate the effects of temperature on the comparator (Fig. 9).

Three 10 by 25 cm cylinder specimens (Figs. 2 and 3) were placed on the comparator, and the expansion and contraction during freezing and thawing in air chamber were continuously recorded with the aid of differential transformer and recorder. From the record we can find the relation between temperature and linear expansion of the specimens. Freezing and thawing procedures at the center of the specimens are shown in Fig. 5.

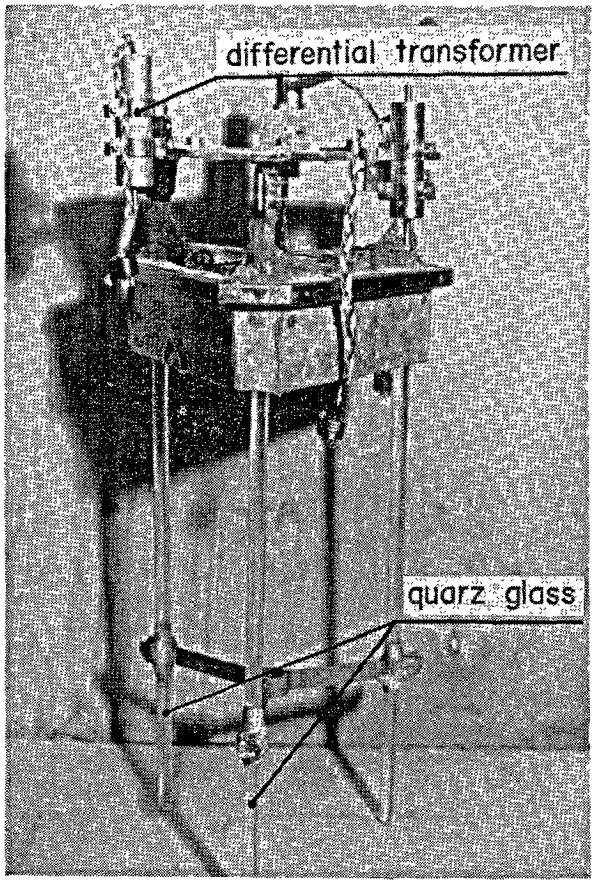

Fig. 9. *Electric comparator*

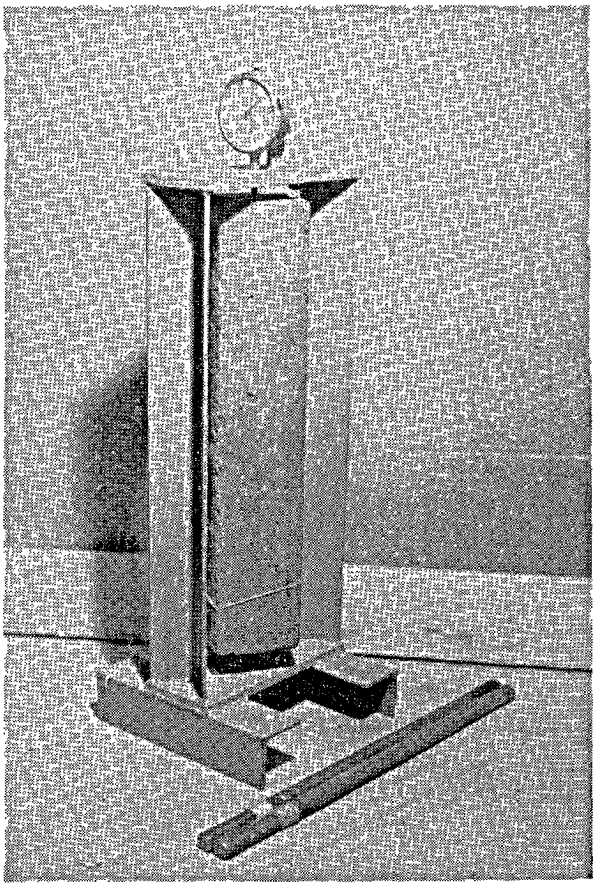

Fig. 10. *Comparator for measurement of total residual expansion in "slow cycle"*

Both the apparatus at the laboratory of Hokkaido Building Research Institute, capable to test according to ASTM C290, and our apparatus were used for rapid and slow cycles respectively.

And we prepared another comparator for the slow cycle, consisting of a dial gage with 1/1000 mm divisions mounted on a stand designed to hold the specimen vertical along its longitudinal axis. All parts of the comparator were made of mild steel as the comparator was used only in room air where the air temperature was controlled at 20°C (Fig. 10).

Discussion of Data

Preliminary Test

A part of the results obtained by the preliminary test is shown in Figs. 11 and 12. As shown in Table 3, the aggregates were limited to diluvial sand and gravel, and concrete mixes were chosen so those that water-cement ratio might vary from 0.4 to 1.1 and the value of their slump was changed as to give 8, 18 and 22 cm. Only non-air-entraining concrete was applied and wet and oven dry conditions were compared.

The fluctuation of data, we observed, was probably caused by use of diluvial coarse aggregate in the vicinity of Sapporo, which contained about 5% of soft and light particles by volume as mentioned above.

Fig. 11 shows the results of our conventional slow freezing and thawing test. In this test, we intended to compare the effect of the size of specimens by using $4 \times 4 \times 40$ cm, $7.5 \times 7.5 \times 40$ cm and $10 \times 10 \times 40$ cm prisms.

In the same repetitions of freezing and thawing, 4 cm square beam specimen give the largest reduction of dynamic modulus. Our conventional $7.5 \times 7.5 \times$

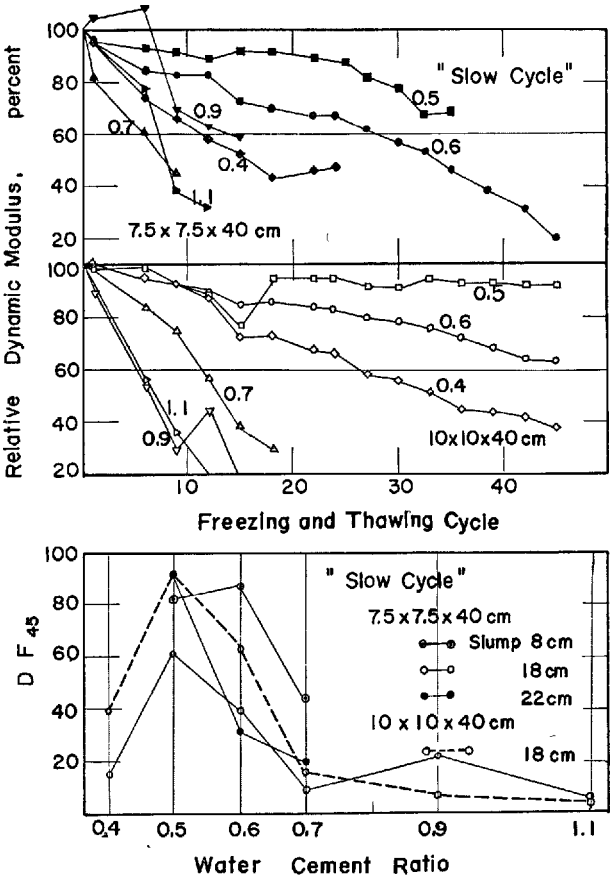

Fig. 11. *Results of preliminary test (slow cycle)*

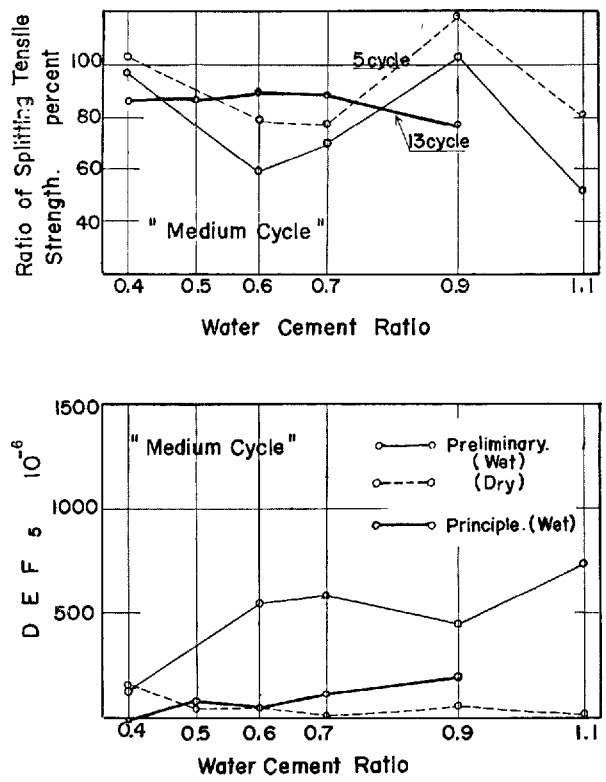

Fig. 12. *Results of preliminary test (medium cycle)*

40 cm prism gives moderate results between the results of 4 cm and 10 cm square beams as shown in Fig. 11. Specimens, of which the water-cement ratio is 0.40, show rather bad results in spite of the low value. The reason for the inversion of order by water-cement ratio seems to be that the age of concrete at the start of test was insufficient for comparison of the effect of water-cement ratio, as the test was started after 14 days of water curing. The recovery of strength during thawing period will be considerable for specimens of higher water-cement ratio, however, as for the low water-cement ratio, such as 0.40, the growing of dynamic modulus was not considered even at the young age of concrete such as 14 days. Moreover, the high content of soft particles in the coarse aggregate might have an influence on the above mentioned inversion of order by water-cement ratio and on the different results derived from the size of specimen.

In Fig. 12, we compare the results by medium cycle of the preliminary test by using coarse aggregate without treatment and those of the principal test by using treated aggregate. There is a difference of the cycle of freezing and thawing between the preliminary and the principal test. However, the ratios of splitting tensile strength after freezing and thawing to the initial strength and the relation between the DEF by the medium cycle and the water-cement ratio were largely affected by picking out of the soft particles. The remarkable role played by soft particles on the frost resistance is again recognized by these results (Figs. 12 and 6).

Principal Test

The data obtained by the principal test are presented in Table 4 and Figs. 13 ~ 22. The concrete mixes tested and their data of compressive and splitting tensile strengths at age of 28 days, when freezing and thawing cycles started, are shown in Table 4.

Concrete, of course, contracts as it is cooled. When highly saturated concrete is cooled to low temperature, however, the formation of ice results in expansion which may exceed the contraction due to cooling as mentioned in several papers published in USA. This expansion has been called dilation in Powers' paper (1).

The typical curves of contraction and expansion are shown in Fig. 13. They have a tendency different from

Table 4. *Proportion of concrete and strength*

Concrete	W/C	Sand percent	Absolute volume. l/m³			Water content l/m³	Cement content kg/m³
			Cement	Fine agg.	Coarse agg.		
non AE	0.50	40.3	124	270	400	196	391
	0.60	42.9	100	301		189	315
	0.70	44.1	85	316		189	268
	0.90	44.6	70	322		197	216
AE	0.50	34.4	115	263	400	181	362
	0.70	42.9	81	300		179	255

Condition	W/C	Agg.	Strength of concrete							
			non AE				AE			
			Medium cycle		Slow	Rapid	Medium cycle		Slow	Rapid
			Comp. kg/cm²	Tensile kg/cm²	Comp.	Comp.	Comp.	Tensile	Comp.	Comp.
Wet	0.50	A	377	30.8	355	346				296
		D	362	28.5			305	26.0		366
		B	352	30.1						
		G	329	28.5						
		E	399	32.6		401				323
		J	375	32.6		389				250
		M	307	28.0						
		S	360	28.6		331				180
	0.60	A			240					
	0.70	A	229	24.4	205				192	
		C	218	23.6						
		D	195	24.4	200		190	21.6	181	
		B	218	21.2						
		G	155	20.9						
		E	178	25.6	219				194	
		J	233	25.0	215				174	
		M	213	24.3	205				179	
		S	234	23.3	204				165	
	0.90	A	111	15.3	118					
		D	105	13.5						
Oven Dry	0.50	A	373	27.3						
		B	326	29.7						
		S	337	30.1						
Supplying water	0.50	A	368	29.1						
		D	343	28.0						
	0.70	A	206	21.3						
		D	200	20.0						

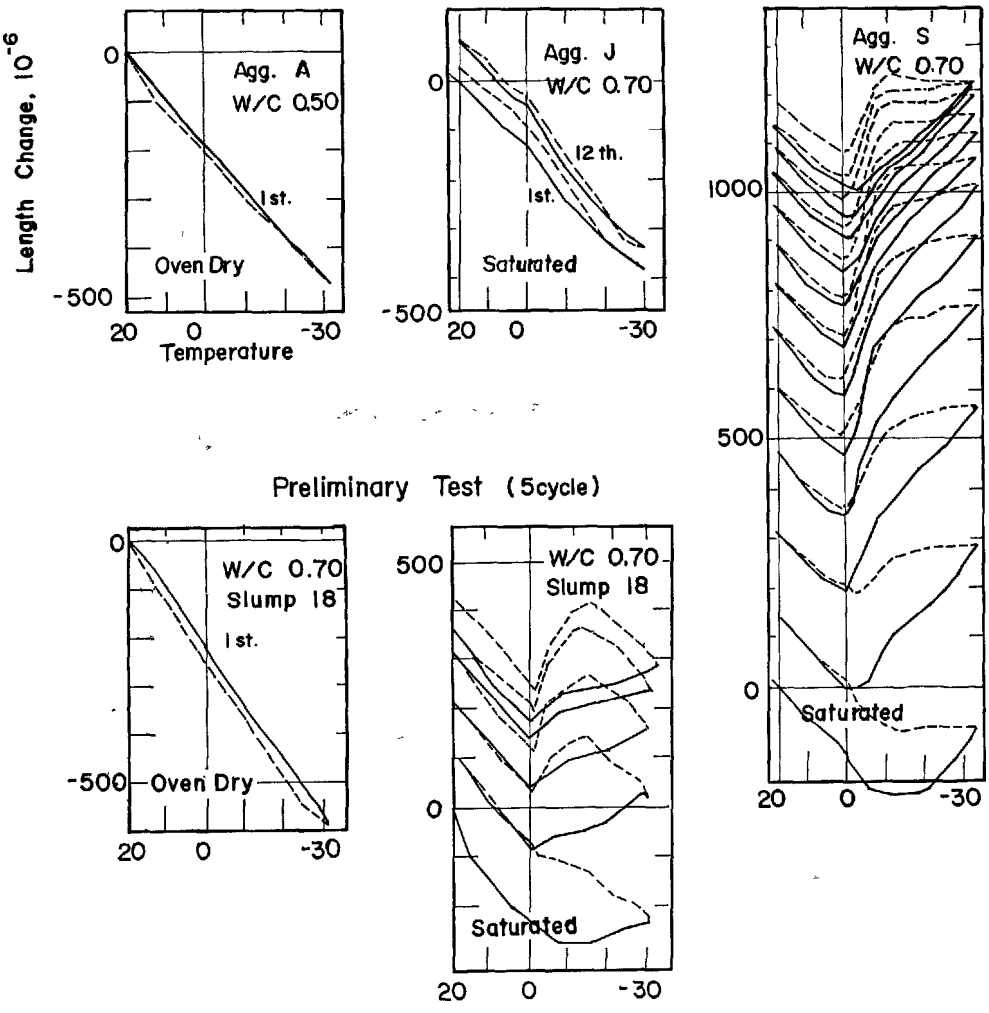

Fig. 13. *Typical curves of contraction and expansion*

that shown by the typical cooling curves for limestone concrete in the Powers' slow cycle carried out by Wills et al (3). There are many different factors such as aggregates, water-cement ratio, slump, cooling rate and range of temperature, curing conditions etc., between Wills' test and ours, however, it seems, the cooling rate will be the most effective factor.

The specimens under oven-dry condition in the preliminary test and made from diluvial gravel without treatment showed no dilation and left no residual length change. However, we observed abnormal expasion and contraction during freezing and thawing respectively, and considerable total residual length change after five repetitions of medium cycle in case of the specimens under saturated conditions as shown in Fig. 13.

The similar behavior was observed in case of the artificial lightweight aggregates which showed high water absorption, Aggregate S, as seen in Fig. 13. Aggregate J, which was low water absorptive one, showed little total residual length change after thirteen repetitions of medium cycle. This total residual length change is called by us "the degree of expansion by frost". As the notation to simplify the words, we used DEF for this new term. The designation of this term is the degree of expansion caused by freezing and thawing, and expressed by the ratio of total residual length change of the specimens subjected to medium cycle in millionth of the initial unit length. Another similar notations are used in this paper hereafter. They are,

DEF_n: Degree of expansion caused by n cycles of medium cycle,

DEF_s: Degree of expansion caused by slow cycle.

The former is calculated from the record of electric

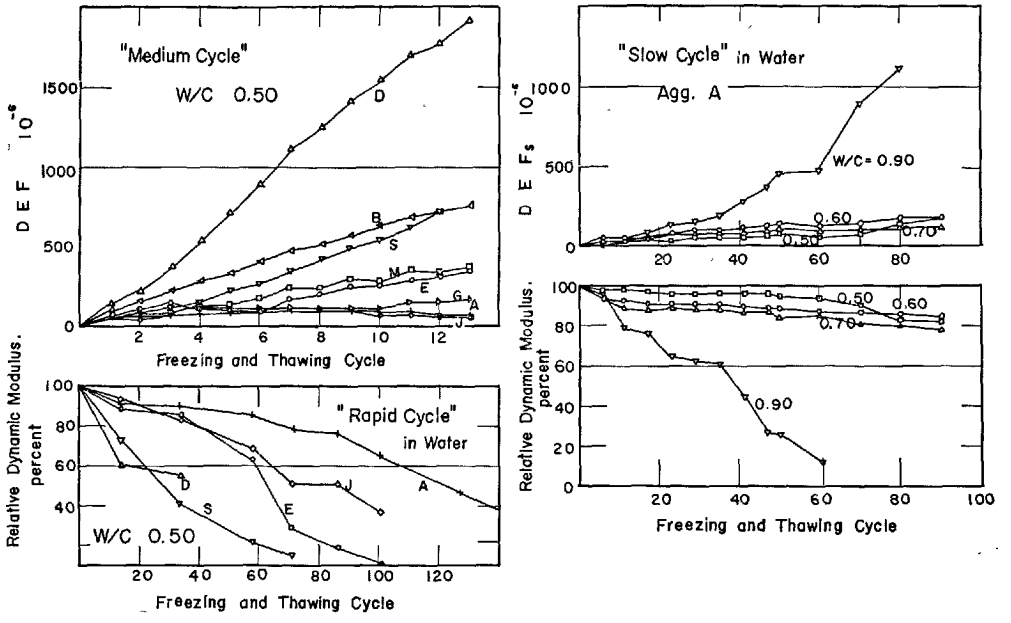

Fig. 14. *DEF, DEFs and rapid cycle*

comparator and the latter is measured by any suitable comparator after any cycle of thawing of the slow cycle.

Fig. 14 shows that the larger the DEF of medium cycle, the larger the reduction of dynamic modulus of elasticity tested by rapid cycle. The left half of the figure shows the different behavior of aggregates, of which water absorption vary as shown in Table 2. The effects of soft particles in the diluvial coarse aggregate, aggregate A, are eliminated by picking out of the soft particles before mixing concrete as mentioned above (Fig. 12). The right half of the figure shows the difference of concrete mix, i.e. the difference of water-cement ratio. The higher the value of the water-cement ratio, the weaker the resistance to freezing and thawing.

DEF versus Splitting Tensile Strength

The splitting tensile strength is reduced by freezing and thawing. There is a good relation between the value of DEF and the corresponded ratio of tensile strength as shown in Fig. 15. This means DEF_n will be one of good measure for the decrease of strength by freezing and thawing action. Fig. 16 shows the relation between DEF and moisture percent in concrete by volume when the test by medium cycle was terminated. It seems, DEF is not distinctly in proportion to moisture percentage of concrete by volume.

DEF by Medium Cycle, DEF_s and Relative Dynamic Modulus by Slow Cycle

DEF_n, DEF_s of each cycle and the relative dynamic modulus are shown together in Fig. 17 to compare with each other. The similar tendency is shown in both DEF and DEF_s by medium cycle and slow cycle respectively. The medium cycle accelerate the expansion compared with slow cycle. The reduction of dynamic modulus is proportional to DEF_s as shown in Figs. 17 and 18.

Moisture Condition of Test Specimens

The growing behavior of DEF of sealed specimens under wet condition by medium cycle is compared with that of specimens under the condition supplying water in Fig. 19. The termination of medium cycle is only 13 cycles in the test, however, we can observe the different tendency of growing expansion expressed by DEF. The residual length change under moisture condition supplying water is more than that of specimens under wet condition in each medium cycle. The DEF curves of the former turn upwards as the number of cycle by repetitions of freezing and thawing increases, however, the curves of the latter show gentle slope and it seems to approach a definite value. In case of air-entraining concrete, the DEF curves goes

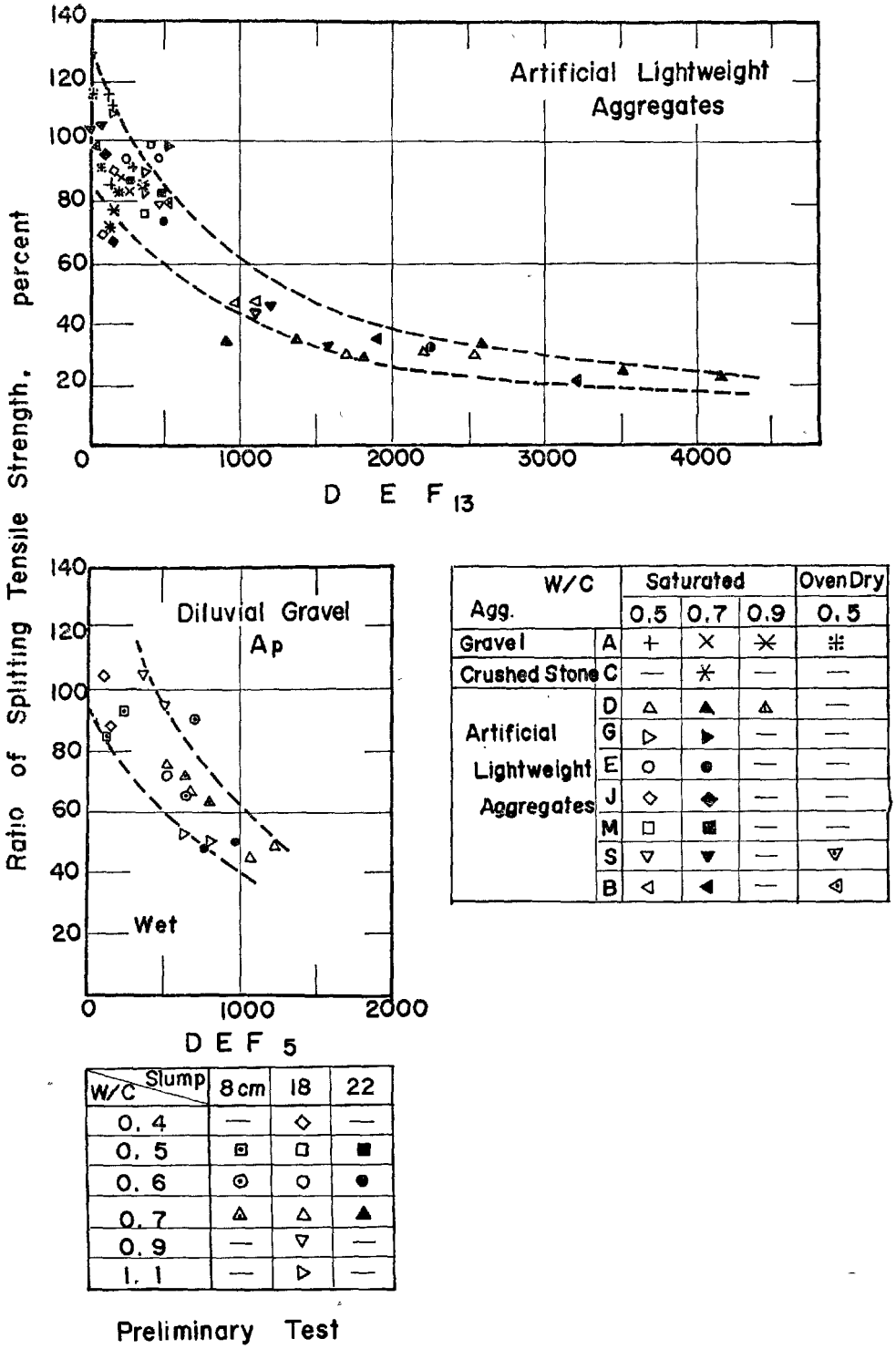

Fig. 15. *Splitting tensile strength and DEF*

up gradually and their total values are small compared with non air-entraining concrete,

Wills' Slow Cycle versus Our Slow Cycle

Fig. 20 compares the Willls' and our methods of

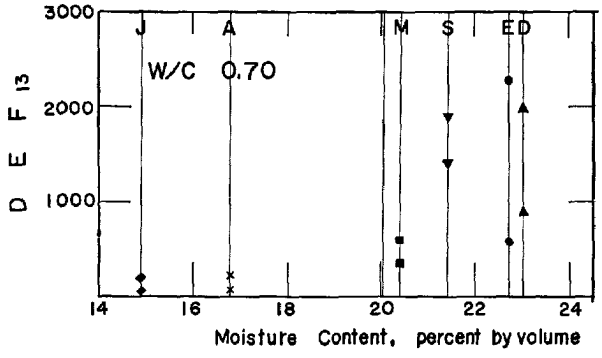

Fig. 16. *Moisture content and* DEF_{13}

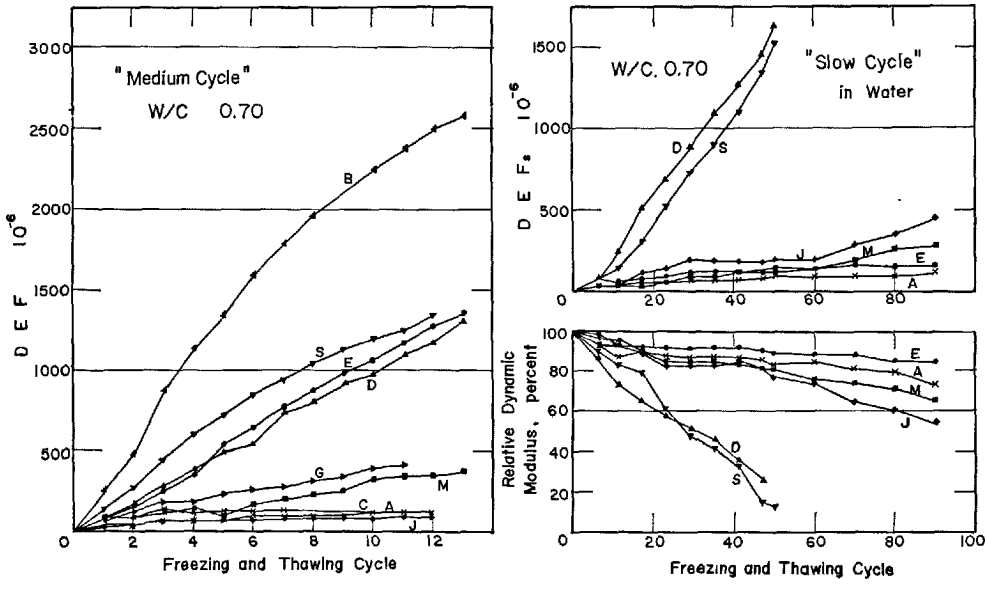

Fig. 17. *Comparison between "medium cycle" and "slow cycle"*

slow cycle. The results of our test by slow cycle (DEF_s) is remarkably similar to the relation between Wills' cumulative length change and reduction in dynamic modulus, in spite of the difference of test method, aggregates, water-cement ratio and cooling rate of both "slow cycle" methods.

Water Permeability Test

Water absorption of concrete is considered as an important factor to the resistance of concrete to freezing and thawing. We made water permeability test after four weeks of water curing followed by oven drying for 7 days in air at 80°C, by using $15\phi \times 4$ cm disc specimens. Water pressure of 2 kg/cm² was applied to the round area of 5 cm in diameter on the center for 1 hour. The quantity of permeable water is shown in Fig. 21. After the permeability test followed by drying again at 80°C, we made vacuum water absorption test of the specimens. Both results are shown in Fig. 22. The difference between vacuum saturated water absorption test results and moisture content after curing for four weeks is small in case of the diluvial gravel, however, all concretes made with artificial lightweight aggregates show large difference, probably caused by internal pores of coarse aggregates.

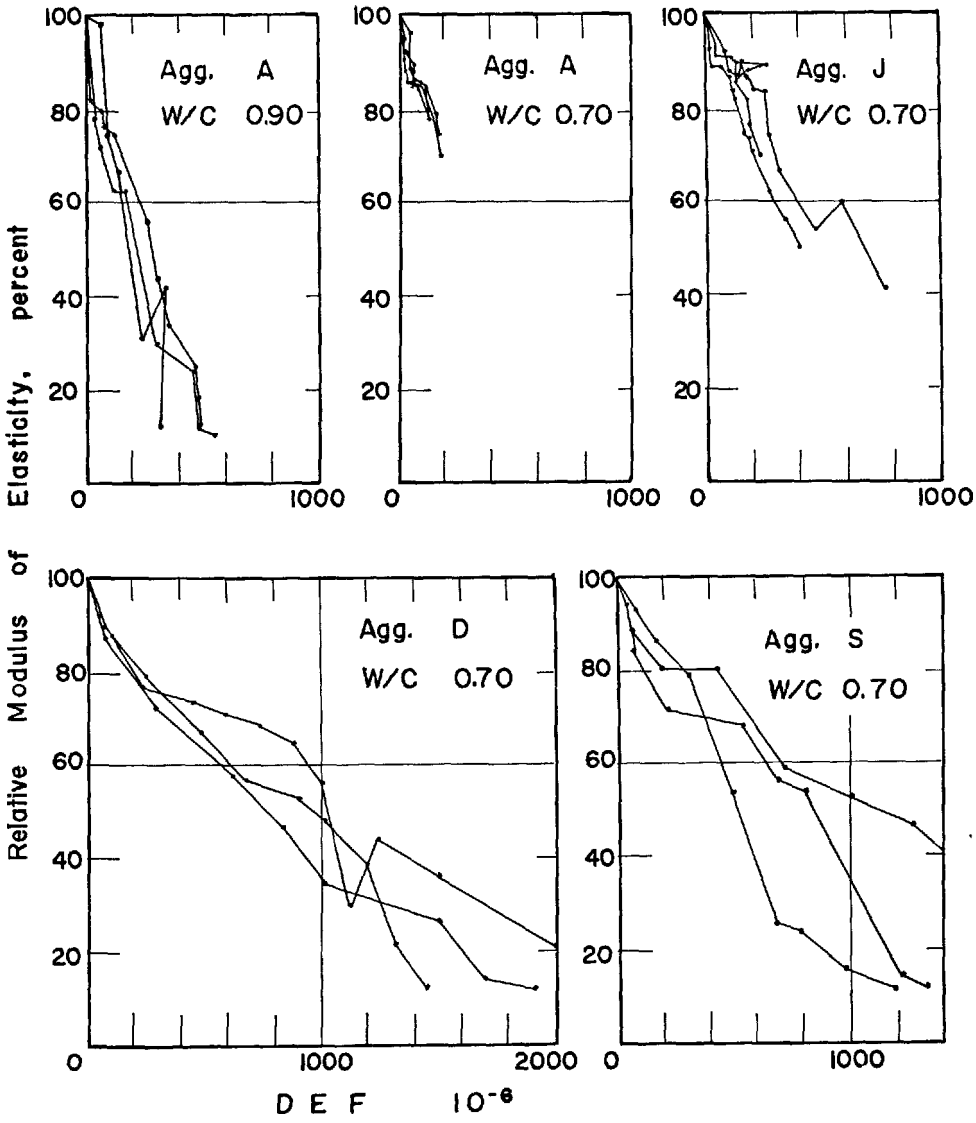

Fig. 18. *Relative dynamic modulus and degree of expansion caused by "slow cycle"*

Conclusion

These data, based on the tests of concretes made with several kinds of artificial lightweight aggregates which show various resistance to freezing and thawing, appear to support the following conclusions:

1. The degree of expansion by frost, either DEF or DEF_s, which is designated in this paper, is a good measure of the resistance of concrete to freezing and thawing action. Medium cycle reduces the period of getting the same order of DEF and is easy to test compared with slow cycle.

2. The measurement of total residual length change of the specimens used in slow cycle test is a good measure of the reduction of dynamic modulus of elasticity when the definite concrete mix is used for the test. It appears the measurement of the length change will be also a good measure for the rapid cycle.

3. How many repetitions of medium cycle will be a good measure for proper judgment of the resistance of concrete to freezing and thawing is to be decided by studies in future.

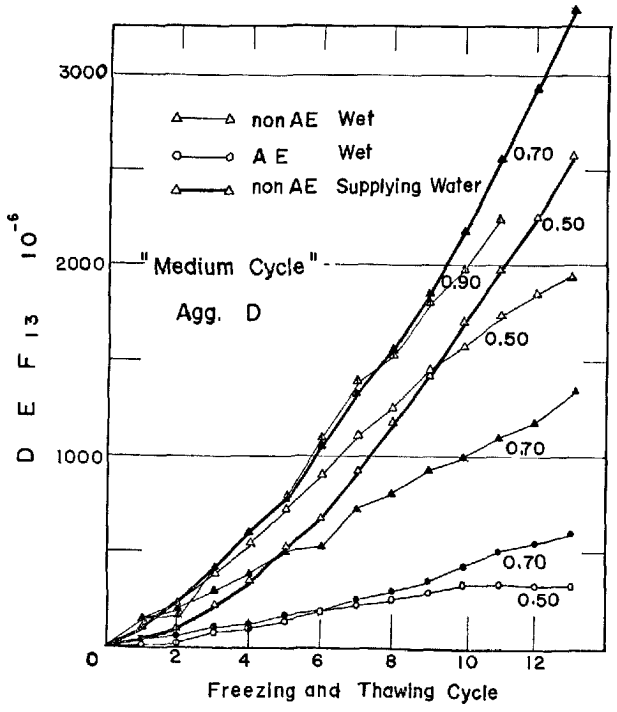

Fig. 19. *Moisture conditions and DEF_{13} by using aggregate D*

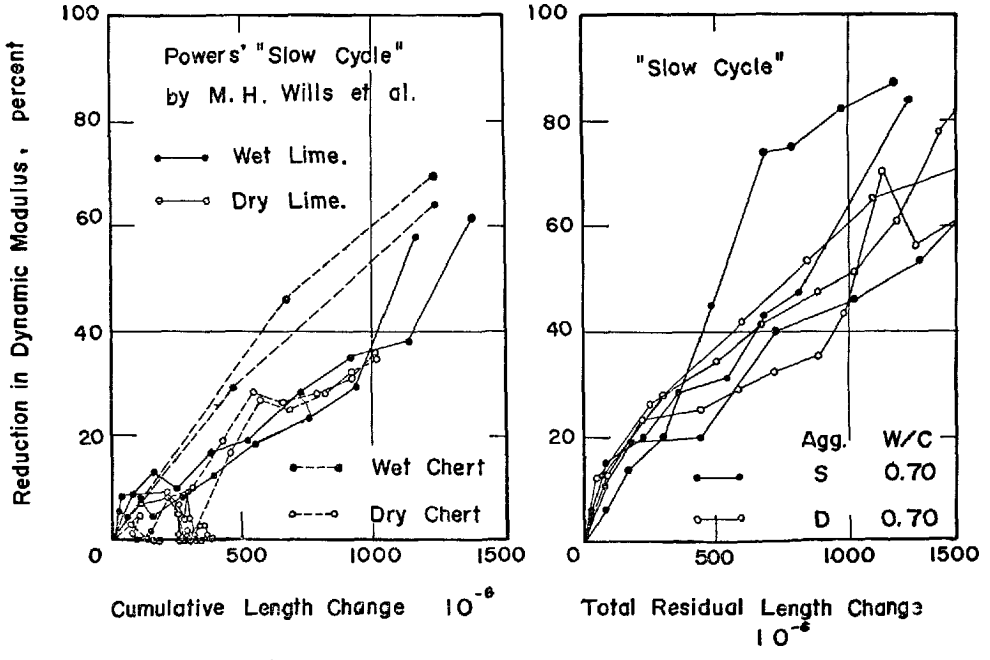

Fig. 20. *Wills' test results and our results obtained by "slow cycle"*

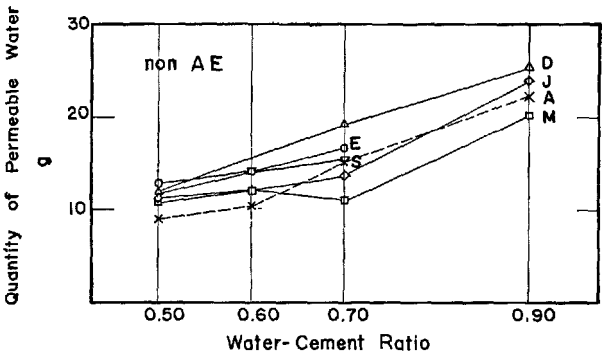

Fig. 21. *Results of water permeability test*

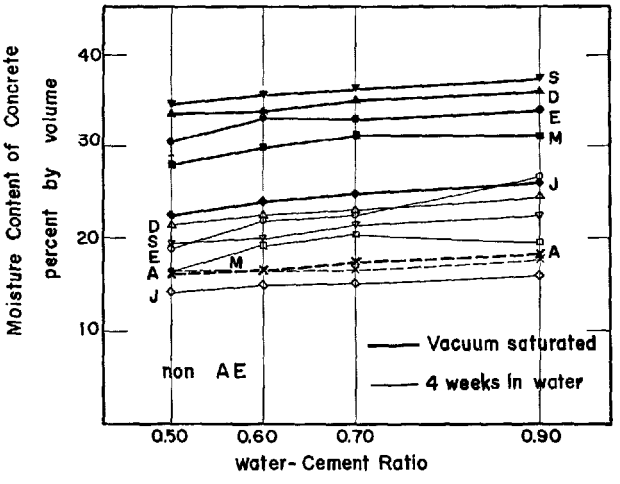

Fig. 22. *Water absorption by vacuum saturation and moisture content after 4 weeks curing*

References

1. T. C. Powers, "Basic considerations pertaining to freezing and thawing test", Proceedings, Am. Soc. Testing Materials, **55**, 1955, p. 1132.
2. R. C. Valore, Jr., "Volume changes in small concrete cylinders during freezing and thawing", Proceedings, American Concrete Inst., **46**, 1950, p. 417.
3. M. H. Wills, Jr., H. A. Lepper, Jr., R. D. Geynor and S. Walker. "Volume change as a measure of freezing and thawing resistance of concrete made with different aggregates", Proceedings, Am. Soc. Testing Materials, **63**, 1963, p. 946.
4. Y. Koh, T. Goto and Y. Hashimoto, "An experimental study on the artificial lightweight aggregate concrete, Cement Gijutsu Nempo XIX, 1965, p. 455. (in Japanese), Synopsis is reviewed in Review of the General Meeting of Japan Cement Engineering Association 1965, No. 78, p. 220.
5. Y. Koh and T. Hattori, "Effect of coarse aggregate on the durability of concrete", Preliminary Report of RILEM International Symposium, Durability of Concrete, Praha 1961, p. 135.

Supplementary Paper III-123 Effect of Conversion on Properties of Concrete Using High-Aluminous Cement

Ryuichi Tsukayama*

Synopsis

Properties of high-aluminous cement concrete after conversion were investigated by accelerated test. The following two methods to accelerate the conversion of hydration product were employed:

(1) curing in water at 50°C after the age of 1 day,
(2) placing large specimen in which temperature rise of concrete due to heat of hydration is permitted.

Two kinds of cement were used. The percentage of Fe_2O_3 in cements were 2.5% and 16% respectively. Both cements were free of SO_3.

As the result of test, it was observed that the following changes in the properties of high-aluminous cement concrete took place due to conversion.

(1) Strength lowers to some value at which it would be kept for long period.
(2) Durability of freezing-thawing action is remarkably deteriorated.
(3) Permeability is increased.
(4) Secondary temperature rise and expansion is produced during conversion.

To make clear the cause of these phenomena, the distribution of open pores was measured by Mercury Pressure Porosimeter. The total volume of pore increased and the peak of pore distribution moved from about 100 Å (radius of pore) to about 1000 Å. This means that conversion multiplies the quantity of larger pores. This increase of pore seems to have a close relation to the change of properties in converted high-aluminous cement concrete.

From the practical point of view, the above experimental results lead to the conclusion that the concrete of satisfactory strength after conversion can be obtained by selecting smaller water-cement ratio. But it is not suitable to decide mix proportion on the strength base only, when durability of concrete is required.

Introduction

Although high-aluminous cement is a very useful material for rapid work of construction, the amount of consumption is far less than portland cement. Besides an economical reason, this is mainly because of such an unfavorable properties as reduction in strength with age due to conversion.

A number of researches gave knowledge on these properties. For example, beneficial summarization was given by Robson (1), and comprehensive data from laboratories and fields were collected and analysed by Neville (2). But a lack of the decisive testing method which affords a reliable estimation of final or residual properties is, even now, responsible for the very limited consumption.

In this report, an accelerated conversion test method by curing at higher temperature was investigated. Since the effect of higher temperature differs according as whether a specimen gets warmed after suffiecient hydration period under normal temperature or soon after mixing, two methods corresponding to each condition were examined.

Properties of concrete with high-aluminous cements which were studied by these methods include porosity, heat of hydration, and volume change. Tests were also conducted to determine the effect of conversion on compressive strength, bending strength, tensile strength, permeability, and resistance to freezing and thawing action. Concrete mixes for the tests contained two different types of high-aluminous cement.

*Research Laboratory, Nihon Cement Co., Ltd., Tokyo, Japan.

Materials

Concrete was prepared from two different types of high-aluminous cement, domestic cement produced by sintering in a rotary kiln (cement A), and one imported cement produced by fusion (cement B). The chemical compositions, shown in Table 1, were quite different in both cements. Cement A contains more than 50 per cent of Al_2O_3 and less than 3 per cent of Fe_2O_3, whereas cement B less than 40 per cent of Al_2O_3 and more than 15 per cent of Fe_2O_3. Natural sand and gravel from a river were used for all concrete mixes, and the maximum size of gravel was 25 mm.

Table 1. *Chemical composition of cement* (%)

	cement A	cement B
ig. loss	0.2	+0.5
insol.	4.8	0.2
SiO_2	2.3	3.4
Al_2O_3	56.2	39.8
Fe_2O_3	2.8	16.6
CaO	35.0	37.7
MgO	0.4	0.9
TiO_2	2.3	1.9

Accelerated Coversion Test Procedure

In trying to investigate the effect of conversion on several properties of concrete, it was necessary to find out the conditions of curing, so as to get fully-converted concrete in a short period. For this purpose, the curing at temperature above normal seemed suitable, because the conversion of high-aluminous cement hydration product has a tendency of being accelerated with increasing temperature. The details of the curing conditions in the following two methods were determined by experiments.

Method-1; Curing in water at higher temperature,

Method-2; Curing at raised temperature caused by heat of hydration,

Method-1

This method aimed at converting the sufficiently hydrated concrete in water at higher temperature. In this method, compressive strength was mainly examined. Specimens were 10 cm in diameter and 20 cm in height.

Fig. 1 shows the effect of the length of standard curing under water at 20°C prior to curing at higher temperature. The concrete mixes were designed for a 40 per cent water-cement ratio and a 10 cm slump. The initial temperature of concrete was controlled at 20°C. The specimens were removed from the mould in 3–4 hrs. after casting, placed in water at 20°C till the age of 6 hrs., 1 day and 28 days, respectively, and then stored in water at 50°C. By curing in water at 50°C, the strength of concrete fell to a stable lower value in 7 days, irrespective of the duration of the pre-curing at 20°C.

The effect of curing temperatures is clearly shown in Fig. 2. Concrete mixes of two different water-cement ratios, that is, 40 per cent and 60 per cent were used in this test. Specimens were cast at 20°C and cured in water at the same temperature for 1 day, thereafter they were stored in water at 40, 50 and 60°C, respectively. The higher the temperature, the more rapid the reduction of strength. It took 28 days for the concrete cured at 40°C, 7 days at 50°C, and 2 days at 60°C until it reached the minimum value. Hereafter, the strength showed a little gain and then maintained a constant level. This slight

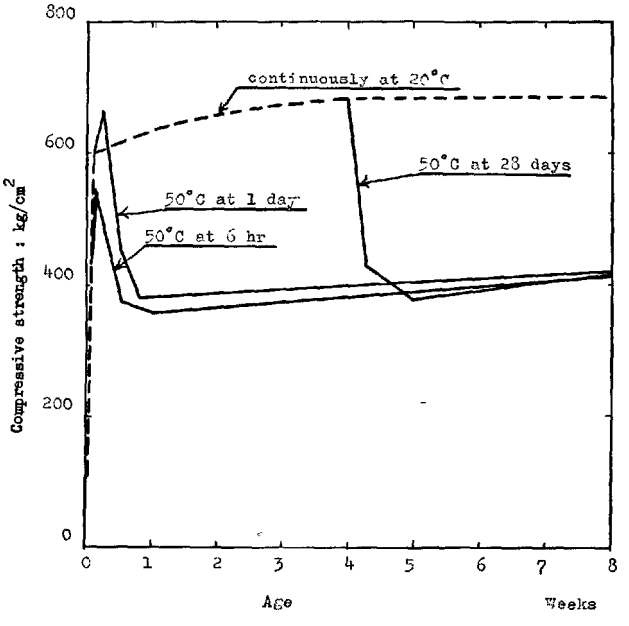

Fig. 1. *Effect of duration in water at 20°C before placing at 50°C*

increase in strength is to be ascribed to hydration of unhydrated cement. Increased pore and dehydrated water due to conversion seemed to provide a favourable condition for this delayed hydration.

To find out any difference of strength at higher temperature between continuous curing and alternate one, concrete specimens were stored in each water at 20°C and at 50°C for 7 days, reciprocally. The result of strength tests, in Fig. 3, shows that there is no difference between them.

Based on the above tests, the following details of the test method seemed to be suitable:

initial temperature of concrete is controlled at 20°C;

for 1 day after casting, cure in water at 20°C;

from 1 day to 7 days, cure in water at 50°C.

X-ray analysis of neat cement paste cured by this method is shown in Table 2, indicating nearly complete change, taken place as below.

Therefore, fully-converted specimens of

$$3CAH_{10} \longrightarrow C_3AH_6 + 2AH_3 + 18H$$

concrete can be obtained by this method from the concrete initially cured at normal temperature. However, the fully-converted concrete which had been at a higher initial temperature or in which a greater temperature rise due to heat of hydration occured, showed a lower strength. Method-2 was devised for such cases.

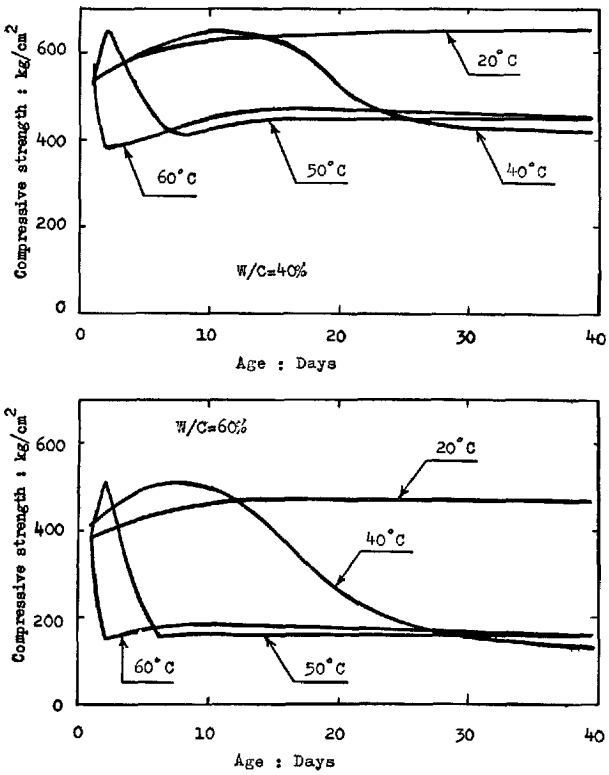

Fig. 2. *Effect of curing temperature*

Method-2

Owing to a very rapid rate of heat generation in a initial stage of hardening, the concrete made from high-aluminous cement often shows a remarkable temperature rise.

In this method, concrete was cast in a cylindrical container, 34 cm in diameter and 32 cm in height, and then placed in a adiabatic calorimeter. The heating equipment in a calorimeter was not operated, so that a natural curves of temperature rising and falling similar to an actual change in a structure could be obtained. Since the conditions of heat leakage of the calorimeter were constant, checking of repeated tests showed a good agreement. As typical examples, temperature curves are shown in Fig. 4.

Table 2. *Result of X-ray analysis of hydrated cement paste*

Temperature of curing	Water-cement ratio	Unhydrated cement			Hydration product		
		CA	C_2AS	CT	CAH_{10}	AH_3	C_3AH_6
20°C	40%	○	○	△	◎	△	×
	60%	○	○	△	◎	△	×
50°C	40%	△	○	△	×	◎	×
(Method-1)	60%	×	○	△	×	◎	◎

◎: strong, ○: moderate, △: weak, ×: none

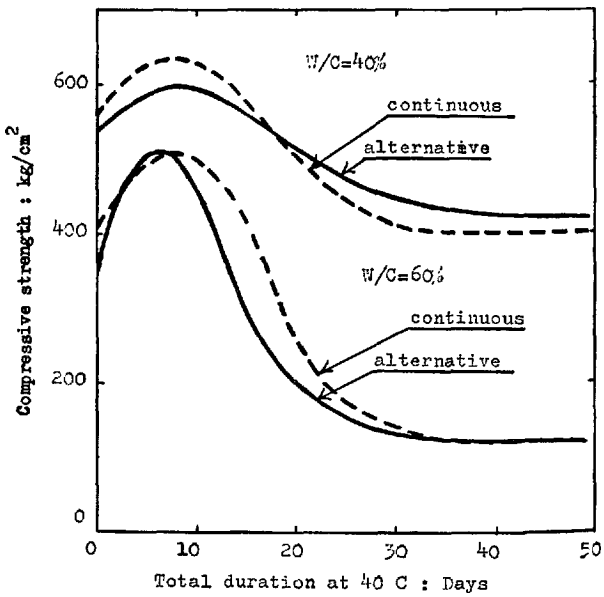

Fig. 3. *Difference between continuous and alternative curing at higher temperature*

Table 3. *Result of X-ray analysis of concrete*

Cement	Curing condition	Unhydrated cement				Hydration product			
		CA	C_2AS	C_4AF	CT	CAH_{10}	C_2AH_8	C_3AH_6	AH_3
A	20°C, in water	○	○	×	△	◎	×	×	×
	Method-2	×	○	×	△	△	×	◎	◎
B	20°C, in water	○	×	○	×	◎	△	×	×
	Method-2	×	×	×	×	×	×	◎	◎

◎: strong, ○: moderate, △: weak, ×: none

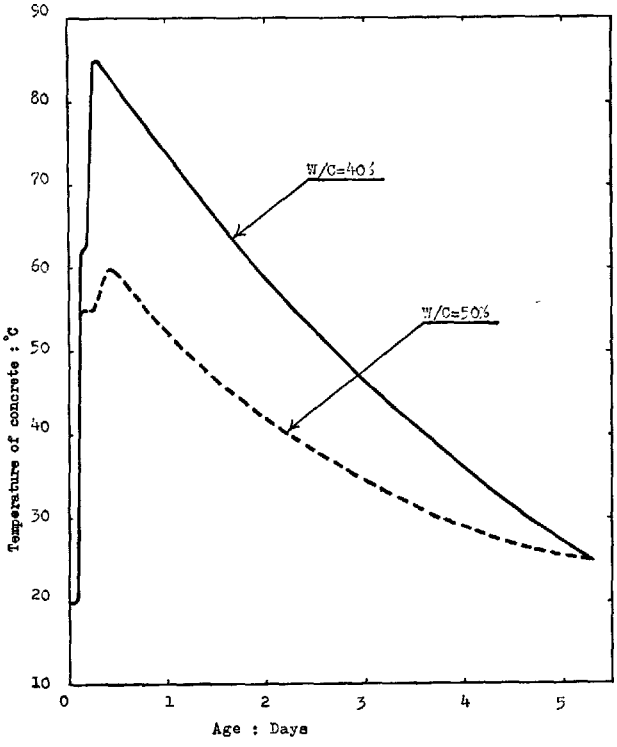

Fig. 4. *Typical temperature change of concrete in Method-2*

Table 4. *Comparison of strength between Method-1 and Method-2 (cement B, W/C = 40%)*

Curing condition of specimen	Age in days	Compressive strength (kg/cm²)
in water at 20°C	1	614
for 1 day at 20°C and then for 6 days at 50°C (in water)	7	402
core specimen cured by Method-2	2	312
	4	303
	6	310

Concrete specimen was taken out at the age of two days, from which two or three specimens of core were cut. By X-ray detection, it was confirmed that the concrete had been completely converted (Table 3). A result of strength test indicated that the strength did not vary with a longer storage in the calorimeter than two days. The fully-converted strength by this method was a little lower than that obtained by Method-1.

Pore Size Distribution

Many previous publications have pointed out an increase in porosity due to conversion and a close relationship between the reduction in strength and the increase in porosity.

Lea (3) determined densities of high-aluminous cement hydration product cured at normal and higher temperature. Neville (2), based on Lea's data, deduced the increase in porosity corresponding to conversion from hexagonal CAH_{10} to cubic C_3AH_6. Schwiete and Ludwig (4) verified the close relation between porosity measured by gas penetration method and several properties such as resistance to chemical action,

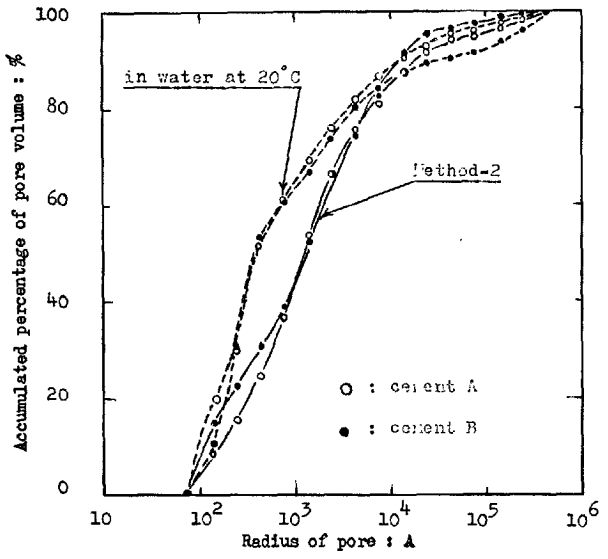

Fig. 5. *Pore size distribution curve, W/C = 50%*

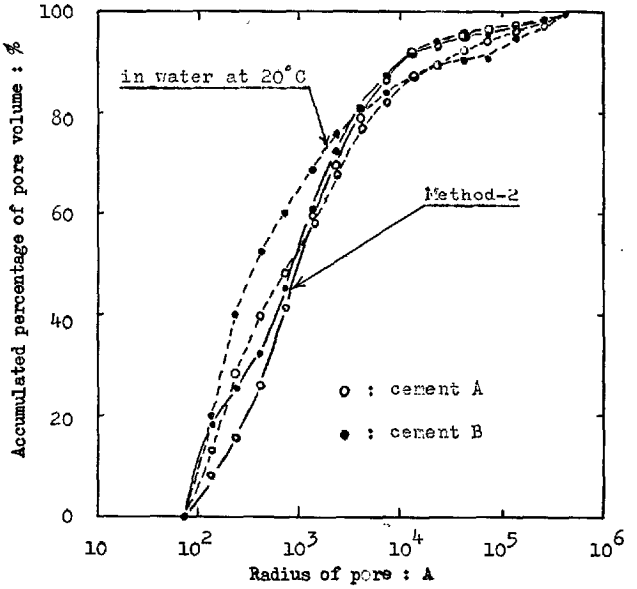

Fig. 6. *Pore size distribution curve, W/C = 40%*

resistance to freezing and thawing action, and carbonation due to air, on mortar and concrete. In the recent symposium on structure of portland cement paste and concrete, there were many presentations concerning to porosity and its effect (5, 6, 7). But all these works contained no result on high-aluminous cement.

Since the measurement of porosity provides a useful means for investigation on the effect of conversion, distribution of open pores in high-aluminous cement concrete was tried to measure by a mercury pressure porosimeter. As the size range of pores by this apparatus is limited between 75 Å–75000 Å, the result includes no gel pores (8). Samples were taken from concrete cured at normal temperature and at higher temperature (Method-2). Gravels in concrete were removed.

In Table 5, increase in porosity due to conversion can be seen. Further, the distribution of pores shifted to a larger side as shown in Figs. 5 and 6. The changes in the distribution occurred mainly between 100 Å–1000 Å. The average radius at 50 per cent point was around 400 Å for cured at normal temperature and around 1000 Å for cured at higher temperature. The distribution curves showed no difference for the two types of cement. These changes in the distribution of pores seemed to have a conclusive effects on properties of concrete made from high-aluminous cement, especially concerning to conversion, but insufficient data were obtained to establish relationships between them.

Table 5. *Porosity in concrete measured by mercury pressure porosimeter*

Cement	W/C %	Curing condition	Porosity $\times 10^{-4}$ cm³/g.
A	40	20°C, in water	284
		Method-2	476
	50	20°C, in water	472
		Method-2	488
B	40	20°C, in water	300
		Method-2	534
	50	20°C, in water	459
		Method-2	620

Micro-structure in hardened high-aluminous cement paste were observed with the aid of electron microscope. Broken surface of the paste was reproduced by replica method. The surface texture of the paste cured in water at 60°C for 5 days (Fig. 7.2) formed outstanding contrast to that cured in water at 20°C for 1 day (Fig. 7.3). The former had very ragged surface with many small granules, while the latter had flat surface. The details of the former can be observed in Fig. 7.3. In such a granular system, porosity of hardened paste should be greatly increased. The capillary pore existing in paste cured in water at 20°C for 1 day is shown in Fig. 7.4. In converted paste, capillary pore could not be found out clearly, because of the very granular texture of the surface.

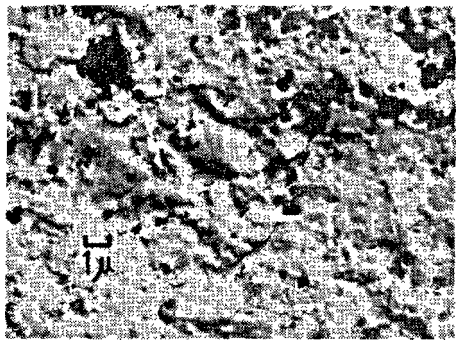

(1) converted cement paste, W/C = 40%

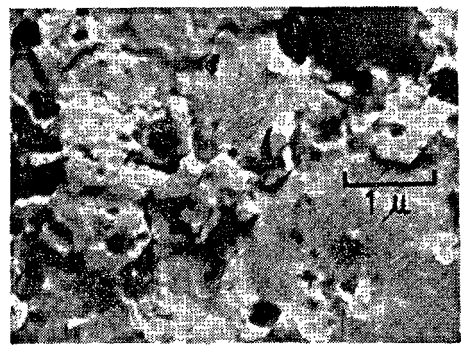

(3) detail of Fig. 7.1

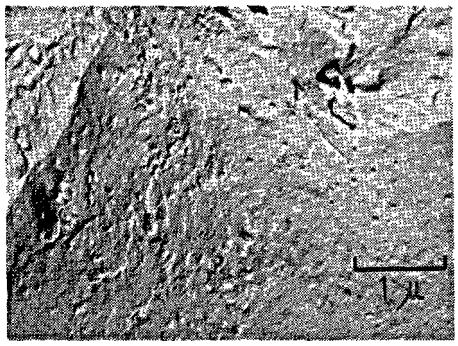

(2) normaly cured cement paste, W/C = 40%

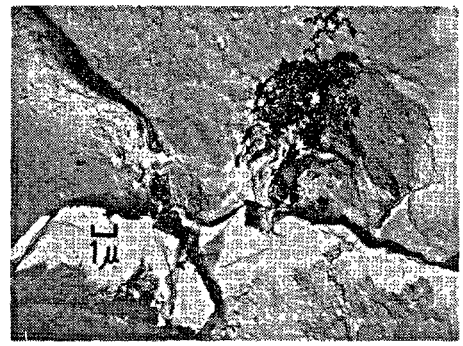

(4) capillary pore in normaly cured cement paste W/C = 60%

Fig. 7. *Electron micrograph of hydrated high-aluminous cement paste* (*cement A*)

Temperature Rise and Volume Change

Temperature Rise

As one of the method for determining the effect of conversion Method-2 was proposed. By this method of curing, concrete showed a remarkable temperature rise during the earlier stage of hardening. Although the general tendency could be observed in Fig. 4, more details of the temperature curves are to be examined in Fig. 8. The most conclusive features for the curves were that there existed two steps in the course of the temperature rise. Beginning the evolution of heat in 2–3 hrs after mixing, the temperature of concrete increased very rapidly. In about 4–5 hrs the speed of temperature rise abruptly slowed down, and then showed again the second step of rising. For concrete with a water-cement ratio of 60 per cent, even a temporary fall in temperature was observed at this point. Similar features were found in a previous publication, but any explanation was not given. Probably, this is due to the hydration of unhydrated cement, and this secondary hydration could not occur until the early hydration product was converted.

When concrete was cooled positively, a curve of temperature rise has only one step. These phenomena were likely to give certain influence on the strength of concrete, but enough data have not been obtained at present.

Volume Change

Volume change of high-aluminous cement concrete cured under water at normal and higher temperatures were tested. For measurement, Carlson Strain Meter was embedded within a concrete specimen, which was 10 cm in diameter and 20 cm in height. Specimens were removed from molds in about 4 hrs after casting, and placed in water at 20°C for 7 days, thereafter in water at 50°C. This procedure

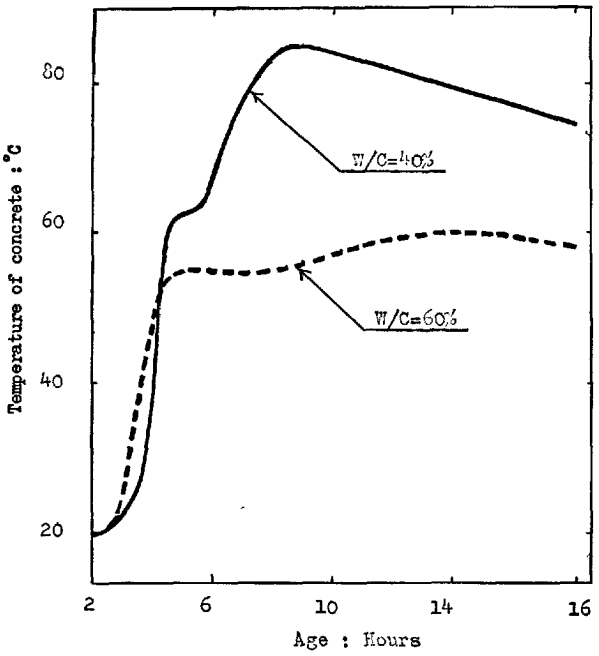

Fig. 8. *Distinctive feature of temperature change*

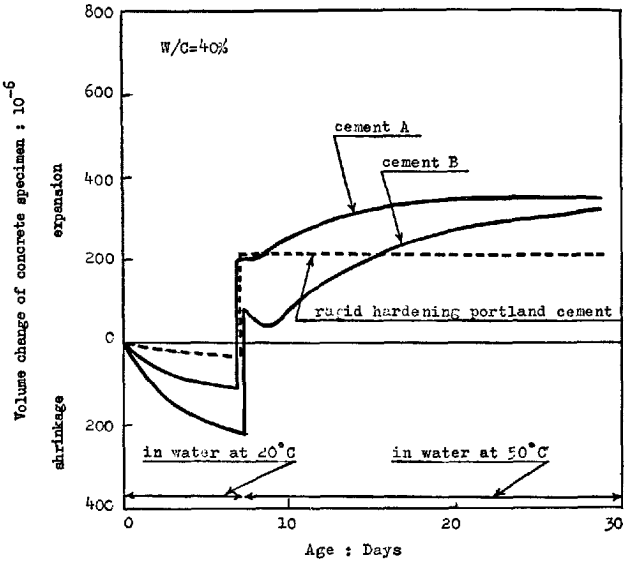

Fig. 9. *Volume changes of concrete during conversion in water*

was just the same as Method-1. Volume change was measured from soon after casting. Results are shown in Fig. 9. During the initial curing in water at 20°C, some shrinkage took place, while after moved into water tank at 50°C considerable expansion occurred. The expansion did not ceased until 23 days after placing at 50°C for cement A and 15 days for cement B. The tendency quite differed for a reference specimen made from rapid-hardening portland cement. The volume of the latter was invariable in water at 50°C.

This behavior of high-aluminous cement does not appear to have been sufficiently well known. The conversion might be contributory factor in the expansion of concrete.

Effect of Conversion on Properties of Concrete

Strength

Compressive strength, bending strength, and tensile strength of concrete were tested with specimens which were cured under two different conditions. One group of the specimens were cured in water at 20°C for 1 day, and another group was cured for 1 day under the same condition as the former and then in water at 50°C for 6 days (Method-1). The temperature of concrete at placing was 20°C. Mix proportions were selected to give the three different slumps, 3, 10 and 18 cm for each water-cement ratio of 37, 43, 49 and 55 per cent.

Test data indicating the relationship between cement-water ratio and strength are shown in Figs. 10, 11 and 12. Because of a small variation between mixes having different value of slump, all of the data were expressed in a single linear function. Almost all the functions were calculated with a small error of correlation.

In every kind of strength test a reduction in strength due to conversion became greater with the increase in water-cement ratio. If the ratio was 40 per cent or less, the reduction was fairly small, and at 40 per cent of the water-cement ratio, concrete with compressive strength over 300 kg/cm², bending strength over 40 kg/cm², and tensile strength over 30 kg/cm² seemed to be safely obtained. These values would satisfy the designed strength for wide range of purposes.

The difference in strength resulting from types of high-aluminous cement appeared to be more distinctive for converted strength than for normally cured strength.

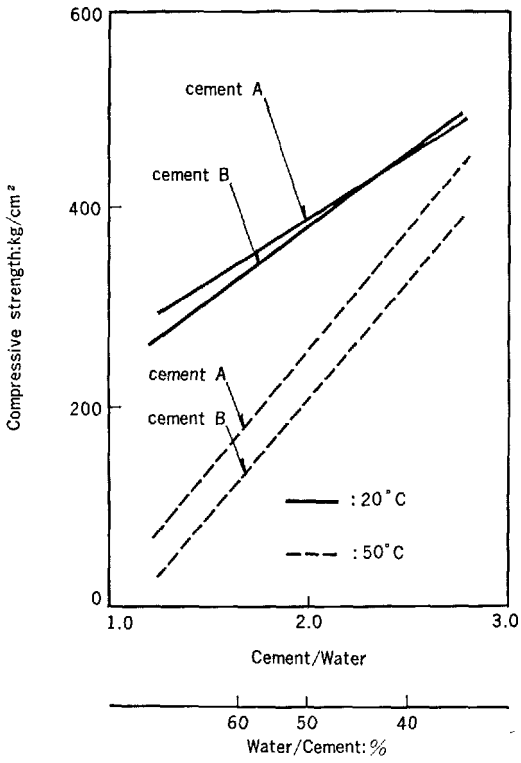

Fig. 10. *Relation between water-cement ratio and compressive strength*

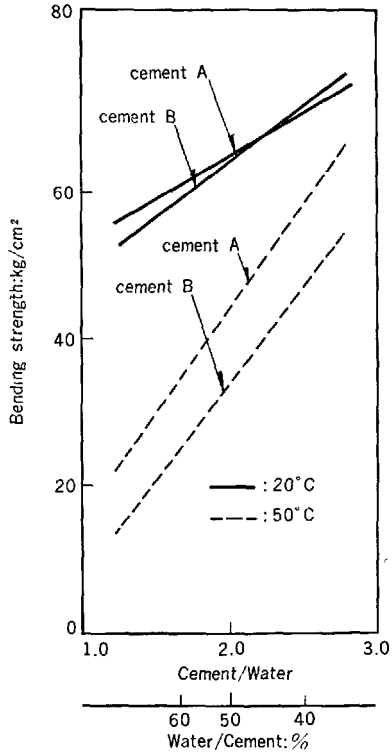

Fig. 11. *Relation between water-cement ratio and bending strength*

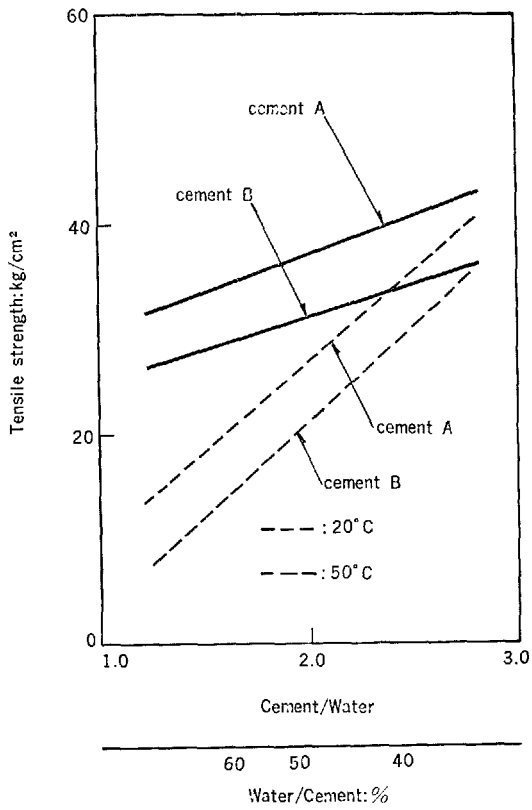

Fig. 12. *Relation between water-cement ratio and tensile strength*

Permeability

Effect of conversion on permeability of concrete with water-cement ratio of 35, 45, 55 and 65 per cent was tested. A cylindrical specimen, 15 cm in diameter and 30 cm in height was cast and cured under water at 20°C for 1 day, and was divided into six disks of 4 cm thick by concrete saw. After curing in water at 50°C for 6 days more, specimens were dried in a room of constant humidity at 55 per cent. Drying was continued for 35 days till the weight became nearly constant. The reference specimens were dried for the same period just after dividing. Under the pressure of 3 kg/cm², water was forced into a disk for 30 minutes. Permeability was indicated by the difference in weight before and after adding pressure.

Fig. 13 shows a percentage loss in weight after drying for 35 days. Converted specimens gave greater loss of weight than reference specimens. The relationship between water-cement ratio and an amount of water penetrated into concrete are plotted in Fig.14. However, the permeability of converted specimens did not differ so greatly from that of normally cured,

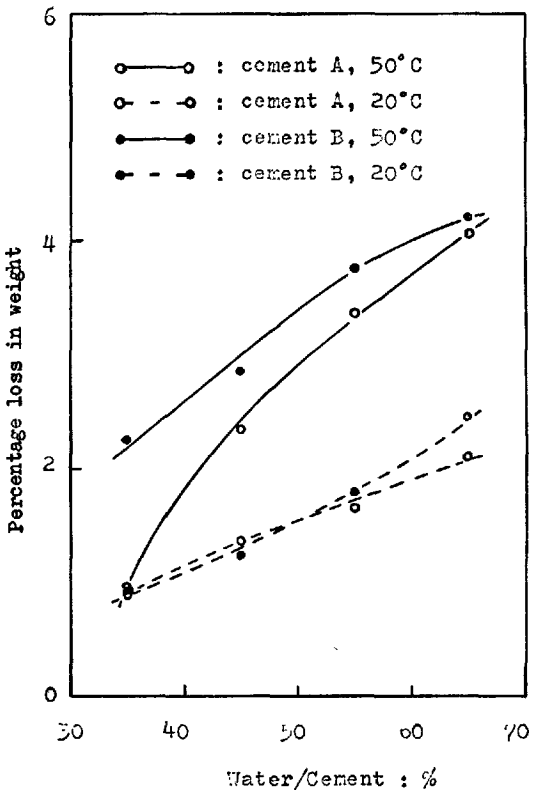

Fig. 13. *Percentage loss in weight after drying for 35 days*

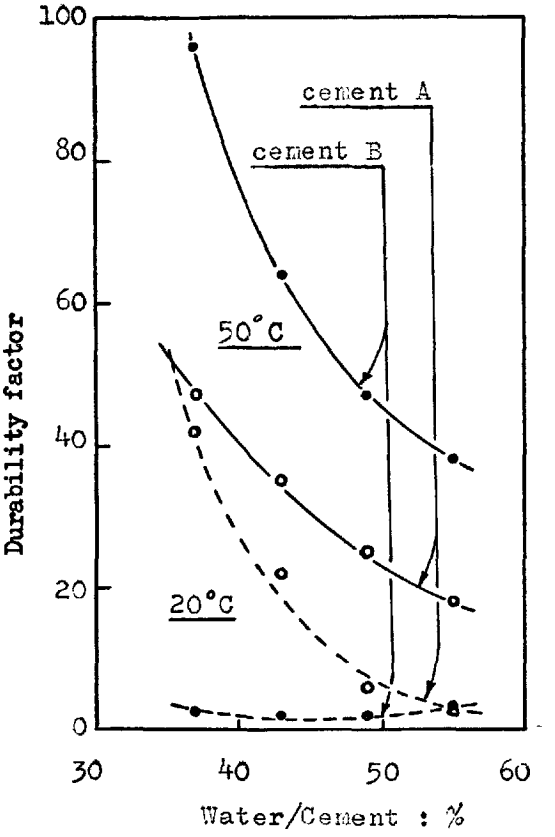

Fig. 15. *Result of freezing and thawing test*

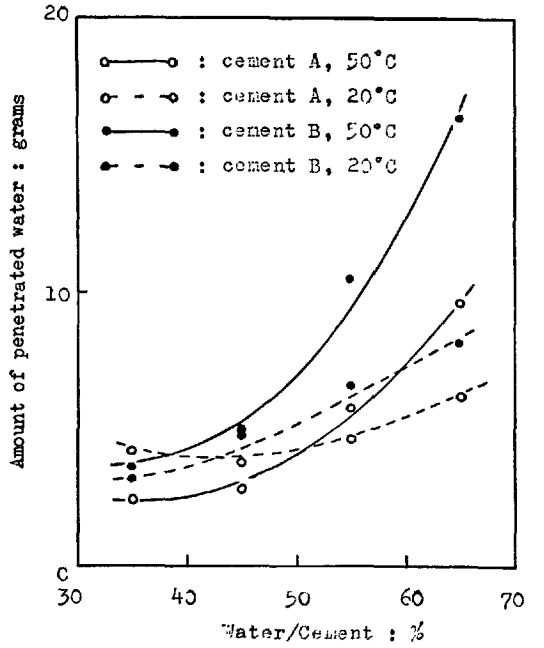

Fig. 14. *Amount of water penetrated into concrete under pressure of 3 kg/cm² in 30 minutes*

there seemed to be a general tendency of the increase in permeability due to conversion. In this result, the increasing amount of capillary pores may be implicit.

Resistance to Freezing and Thawing Action

Freezing and thawing tests were performed on 7.5 × 10 × 40 cm beam specimens. After casting, specimens were cured in water at 20°C for 2 days and then in water at 50°C for 7 days. Reference specimens were cured in water at 20°C for 9 days. The accelerated freezing and thawing test procedure consists of subjecting saturated specimens to 2 hrs freezing at −17°C and 1 hr thawing at 5°C. Dynamic modulus of elasticity and weight change were often measured. Durability factors were calculated when percentage of elasticity dropped to 60 per cent of the initial or at 300 cycles of freezing and thawing.

In Fig. 15, significant decrease in durability of

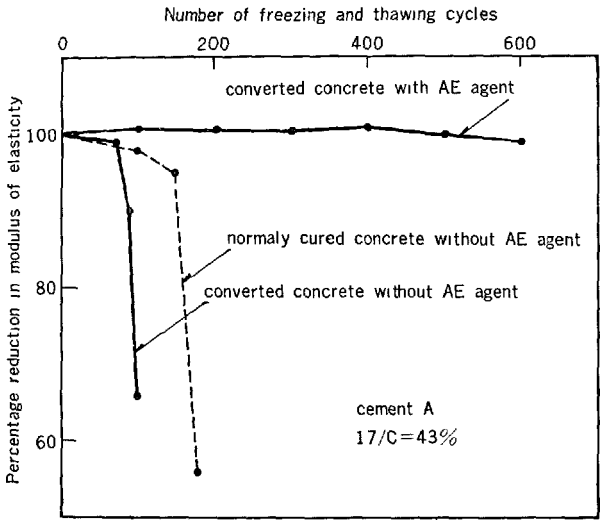

Fig. 16. *Effect of AE agent on durability of high-aluminous cement concrete*

converted concrete was observed. But, as with portland cement, air entraining agent enabled the converted concrete to withstand 300 cycles and over of freezing and thawing. Fig. 16 clearly shows this effect. The variation of durability with the type of cement, as shown in Fig. 15, seemed to imply the difference in characteristics of pores. Further research should be needed for this problem.

Effect of Conversion Observed in Field Test

To investigate the long term behavior in field, high-aluminous cement concrete was placed in a part of concrete pavement. In order to make a test under the severest condition, the placement was conducted in summer, the temperature of concrete at placing being about 30°C.

Table 6 gives the mix proportion used in this test. The size of the test slab was $0.2 \times 0.8 \times 3.4$ m For each type of cement, two slabs were cast, one being cured by watering on the surface, and one being left without watering. A Carlson Strain Meter was embedded in concrete. Core specimens for compression test, 10 cm in diameter and 17 cm in height were cut out at the age of 1, 7, 28, 91 and 182 days.

Among these four slabs, two showed gradual reduction in strength (cement A without watering and cement B with watering), one showed no reduction till 182 days (cement A with watering), and one showed remarkable reduction from 1 day (cement B without watering). The test result of the first two are shown in Figs. 17 and 18. The maximum temperature caused by heat of hydration within 1 day after placing,

Table 6. *Mix proportion of concrete used in field test*

Cement	Slump (cm)	Max. size of aggregate	W/C (%)	Unit weight of materials (kg/m³) C	W	S	G
A	2–5	25 mm	40	368	147	703	1201
B	2–5	25 mm	40	365	147	773	1163

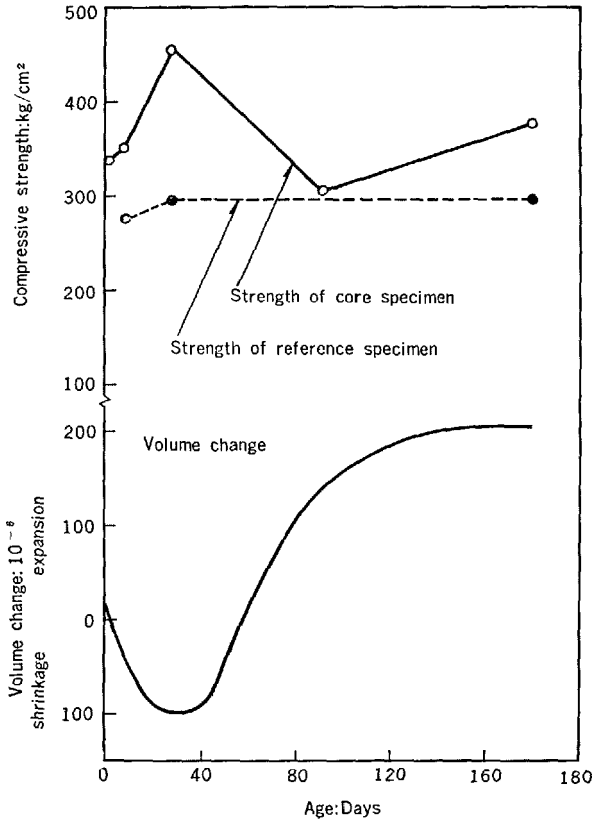

Fig. 17. *Results of field test*
(1) cement A, without watering

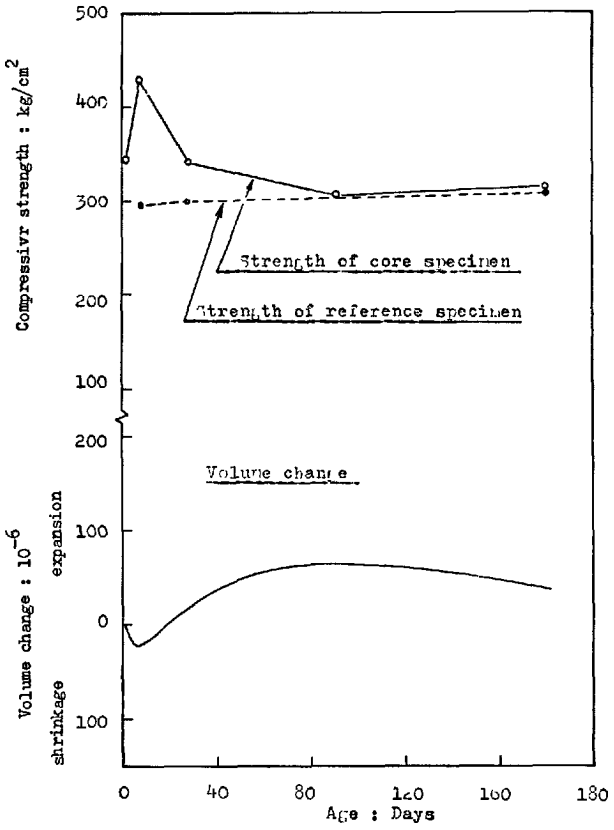

Fig. 18. *Results of field test*
(2) cement B, with watering

was 76.5°C for cement A without watering (Fig. 17) and 62.0°C for cement B with watering (Fig. 18). The strength of core specimen reduced gradually and reached the minimum in 90 days. Comparing with the strength of reference specimen which was cured at the site of the test slab, and then immersed in water at 50°C for 7 days before testing, the minimum value of the core was nearly equal to the reference specimen. From the age of 91 days on, the strength showed slight increase similar to the result in Fig. 2.

In their lower part, Figs. 17 and 18 contain the results of volume change testing. Volume change was calculated by subtracting thermal volume change from apparent volume change, on the assumption that the coefficient of thermal expansion of concrete being 10×10^{-6}. The parallelism between the reduction in strength and the expansion of concrete was observed. The same phenomena as this were observed in laboratory and already shown in Fig. 9.

Conclusion

As early as 1930, it was of common knowledge that the deterioration of concrete using high-aluminous cement was caused by conversion. To keep the damage at a minimum, use of low water-cement ratio has been recommended. But any decisive method to test residual or final strength has not been established. And the effect of conversion on properties of concrete other than strength has not been well known.

At the start of this study, the proposed method of accelerated conversion test, which covers two typical cases of conversion, was examined. One method is for conversion in concrete placed and cured at normal temperature, and the other is for conversion due to heat of hydration in concrete soon after placing. It was made clear that residual or final strength can be estimated in a short period by these methods. Further study is still needed to clarify the effect of placing temperature of concrete.

As a result of applying these method to some other properties than strength, it was observed that permeability and resistance to freezing and thawing are much influenced by conversion, and that, even if strength of converted concrete is nearly equal, there is considerable difference in above mentioned properties resulting from type of cement. One of them showed very low resistance to freezing and thawing action whereas the proportion of concrete was selected for a mix with a water-cement ratio less than 40 per cent.

In order to study the mechanism of deterioration caused by conversion, micro-structure in hydrated high-aluminous cement was surveyed by a porosimeter and an electron microscope. Increase in porosity and change in pore size distribution were found. Also outstanding transformation in internal structure produced by conversion was recognized. The average radius of pores was about 400 Å for specimen cured at normal temperature and about 1000 Å for cured at higher temperature. The texture of broken surface in hydrated cement paste cured at higher temperature was more ragged than that cured at normal temperature. Aggregation of many small granules, which seemed to be products of conversion, was observed

on the surface.

Summarizing the results of X-ray analysis, electron microscope observation, heat of hydration, volume change, and strength test, the phenomena of conversion could be explained as follows: The transformation, $3CAH_{10} \rightarrow C_3AH_6 + 2AH_3 + 18H$, leads to the increase in porosity and free water, which easily make residual unhydrated cement hydrated. By this secondary hydration, C_3AH_6 is directly produced and a slight gain in strength and generation of heat occurred. Expansion of concrete taken place at the same time may be ascribed to the pressure of water derived from dehydration of CAH_{10}. Micro structure of converted hydration product becomes ragged aggregation of C_3AH_6 embedded in crystallized AH_3. At the boundary between them, greater amount of pore may exist.

Acknowledgements

The author is indebted to Prof. R. Kondo, Tokyo Insitute of Technology, for his kind permission to use porosimeter and to Dr. K. Chujo, Dr. J. Yamada and Dr. K. Yamazaki, Nihon Cement Co., for thier guidance. Thanks are also due to Mr. T. Hashimoto for his assistance in microscopy. The author wishes gratefully to acknowledge the assistance given by Messrs. J. Morii, K. Kobiki, A. Miyoshi, I. Yamashita, T. Tateiba, N. Kamigaki, T. Minabe and H. Miyaji.

References

1. T. D. Robson, "High-alumina cements and concrete", Contractors Record Limited, (1962).
2. A. M. Neville, "A study of deterioration of structural concrete made with high-alumina cement", The Institution of Civil Engineers, Vol. 25, 287–324, (July, 1963).
3. F. M. Lea, "The effect of temperature on high-alumina cement", Trans. Soc. Chem. Ind., Vol. 59, 18–21, (Jan., 1940).
4. H. F. Schwiete and U. Ludwig, "Determination of open pores in hydrated cement", Tonind.-Ztg., 90, No. 12, 562–574, (1966). (in Germany).
5. R. Helmuth and D. H. Turks, "Elastic moduli of hardened portland cement and tricalcium silicate pastes: Effect of porosity", Highway Research Board; Symposium on Structure of Portland Cement Paste and Concrete, 135–144, (1966).
6. R. H. Mills, "Effect of sorbed water on dimentions, compressive strength and swelling pressure of hardened cement paste", *ibid*, 84–111,
7. C. Cesareni and G. Frigione, "Some researches on the physical properties of hardened pastes of portland cements containing granulated blast furnace slag", *ibid.*, 48–57.
8. G. Verbeck, "Pore structure", Concrete and Concrete-Making Materials, ASTM. STP 169-A, (1966).

Supplementary Paper III-124 Influence of Chloride and Hydrocarbonate on the Sulphate Attack

Friedrich W. Locher*

Synopsis

Earlier storage tests have shown that concrete is attacked less by sea water than by pure sodium- or magnesium sulphate solutions of the same concentration. Therefore it has been examined if chloride and hydrocarbonate which are contained in sea water as active substances beside sulphate, are responsible for the decrease of the sulphate attack. For that purpose storage tests have been performed in solium- and magnesium sulphate solution with 2500 mg SO_4^{2-}/*l* without and with additions of 30 g NaCl/*l* or of 0.19 g $NaHCO_3$/*l*. Small prisms (1 × 1 × 6 cm) and flat primss (1 × 4 × 16 cm) of mortar according to the German standard specification have been used as test specimens. Three portland cements with calculated contents of tricalcium aluminate of 12%, 8% and 0% as well as three blast-furnace cements with 50%, 65% and 77% granulated blast-furnace slag have been chosen as cements. It is shown more clearly by the expansion of the flat prisms than by the decrease in relative bending strength of the small prisms, that magnesium sulphate attacks more intensely than sodium sulphate. The sulphate attack is generally increased by the addition of chloride to the sulphate solution, whereas it is clearly reduced by the addition of sodium hydrocarbonate. X-ray diffraction analysis and microscopic investigations indicate that the formation of calcite on the surface of the test specimens may be responsible for this result.

Introduction

Experiences and tests have shown that concrete is attacked less by sea water than by pure sodium- or magnesium sulphate solutions of the same sulphate concentration. This is generally attributed to the influence of the high concentration of chloride. It effects, that less trisulphate (ettringite), $3CaO \cdot Al_2O_3 \cdot 3CaSO_4 \cdot 32H_2O$, is formed, because its solubility is increased by chloride (1) and a part of the aluminate is combined as monochloride (tricalcium aluminate monochloride hydrate, Friedel's salt), $3CaI \cdot Al_2O_3 \cdot CaCl_2 \cdot 10H_2O$ (2). Besides, there is assumed that the trisulphate crystallizes from the solution when chloride is present, because of the higher solubility of trisulphate in chloride containing solutions and so it does not cause expansion. But our own tests which attended to the examination of the sulphate resistance of cement, have shown, that the sulphate attack is not diminished by an addition of chloride to sodium- or magnesium sulphate solutions, but it is often strengthened. These tests have shown, that fibrous and nodular separations of calcite, aragonite and vaterite are formed on the surface of concrete prisms, which were exposed to the attack of synthetic sea water.

The composition of synthetic sea water in which the concrete prisms were stored, is given in Table 1. It corresponds to the composition of natural sea water with a total salt concentration of 33.25 g/*l*. Therefore the small concentration of hydrocarbonate is responsible for the formation of calcium carbonate on the surface of the concrete. Although the carbonate concentration of sea water cannot influence the reaction between the aluminate of the cement and the sulphate of the sea water, it is to assume that the penetration of the sulphate is restrained by the calcium carbonate, formed on the surface of the concrete.

Table 1. *Composition of the artificial sea water for the concrete storage tests*

cations	mg/l	anions	mg/l
sodium, Na^+	10,470	chloride, Cl^-	18,920
potassium, K^+	380	sulphate, SO_4^{2-}	2,650
magnesium, Mg^{2+}	1,280	hydrocarbonate, HCO_3^-	140
calcium, Ca^{2+}	410		

*Forschungsinstitut der Zementindustrie, Düsseldorf, West Germany.

Accordingly the chemical influence of the components of the solution on the reaction between aluminate and sulphate is not important to the degree of attack of the sea water on concrete, but the increasing of the resistance against diffusion by separation of calcium carbonate on the surface and in the pores of the hardened cement. It results from tests about the sulphate resistance of cement (3) that the resistance of the hardened cement against diffusion has a decisive influence on the sulphate resistance of the cement. It appears that portland cement, poor in tricalcium aluminate, has a high sulphate resistance, because its hydration products cannot react with sulphate. During the hydration of blast-furnace cements there are always formed hydration products which are susceptible to sulphates. Nevertheless, blast-furnace cements with at least 65% granulated blast-furnace slag are sulphate resistant, because their hardened paste is so impermeable that neither sulphate nor other non aggressive ions can penetrate into it (4).

In order to confirm if the hydrocarbonate concentration of sea water is significant for the attack of sea water on concrete there were carried out storage tests with 6 cements, i.e. 3 portland cements with different contents of tricalcium aluminate and 3 blast-furnace cements with different contents of granulated blast-furnace slag. The hydrate phases and the compounds which are formed in the reaction thereof with the different sulphate solutions were identified by X-ray analysis. In addition the changes on the surfaces of the mortar specimens were tested microscopically.

Tests

For the investigation 6 cements of the type Z275 were chosen, i.e. 3 portland cements with 12%, 8% and 0% tricalcium aluminate and 3 blast-furnace cements of 50%, 65% and 77% granulated blast-furnace slag. The composition and the specific surfaces of the cements are given in Table 2. The phase composition of the portland cements are calculated from the chemical analysis. The slag contents of the blast-furnace cements are ascertained by microscopic counting of the sieve fraction 30–40 μm and correction of the counting results by analytically determined concentrations of CaO, MnO and S^{2-} in the sieve fraction and in the whole cement. The specimens for storage tests—small prisms 1 × 1 × 6 cm (5) and flat prisms 1 × 4 × 16 cm (6)—are made of mortar in accordance with DIN 1164 with 1 part by weight of cement, 1 part of standard sand I (fine), 2 parts of standard sand II (coarse) and 0.6 parts of water. The prisms have been cured for 1 day in moisture saturated air and then suspended in water. Some remained in water until they were tested for flexural strength. Other at the age of 21 days were suspended in the different sulphate solutions. After a sulphate storage of 4, 8, 12, 18, 26, 38 and 52 weeks the flexural strength (B_s) of the small prisms was examined and compared with the flexural strength of water stored test specimens (B_w) of the same age. The expansion of the flat prisms was measured in time intervals of 4 weeks. The length change of adequate water stored prisms was taken into account. The relative flexural strength B_s/B_w of the small prisms and the expansion of the flat prisms were taken as a criterion for the aggressive effect of the different sulphate solutions.

Table 2. *Composition (%) and fineness (cm^2/g) of the test cements*

	PZ 12	PZ 8	PZ 0	HOZ 50	HOZ 65	HOZ 77
loss on ignition	1.6%	1.9%	0.6%	1.2%	1.3%	0.8%
insoluble residue	0.1	0.3	0.1	0.2	0.3	0.2
SiO_2	19.0	21.7	20.7	25.8	26.5	29.2
$Al_2O_3 + TiO_2 + P_2O_5$	6.5	4.5	3.5	10.4	11.1	12.5
Fe_2O_3	3.4	2.1	6.6			
FeO				1.7	0.9	1.1
Mn_2O_3	0.1	0.1	0.1			
MnO				0.3	0.9	0.6
CaO	63.2	65.5	64.7	53.9	49.7	44.7
MgO	1.6	0.8	0.6	3.1	4.9	5.8
SO_3	2.9	2.5	2.6	2.3	3.1	2.7
C_3S	57	63	65			
C_2S	13	16	11			
C_3A	12	8	0			
C_4AF	11	7	17			
C_2F	0	0	2			
slag content				50	65	77
fineness (Blaine)	2800	2570	3390	3650	3860	3930

Pure sodium- and magnesium sulphate solutions with the same sulphate concentration of 2500 mg SO_4^{2-}/l (0.026 m) are chosen as aggressive solutions. Besides, sodium- and magnesium sulphate solutions of the same sulphate concentration with additions of sodium chloride or sodium hydrocarbonate are included in order to test the influence of chloride and hydrocarbonate on the sulphate attack. The concentrations of the additions corresponded with 18.200 mg Cl^-/l and 140 mg HCO_3^-/l to the concentration of sea water.

4 small prisms produced in the same kind and tested at the same time, were stored in a solution of 600 m*l* and adequate 6 flat prisms were stored in a solution of

4000 ml. The solutions of the small prisms were restored every 4 weeks, of the flat prisms every 8 weeks.

The X-ray diffraction analysis which should give informations about the influence of the chloride and hydrocarbonate additions on the formation of trisulphate were carried out on mortar prisms (1 × 1 × 16 cm) as already described (3). Plastic sand which consisted of polyethylene globules with an average diameter of 0.7 mm was used as aggregate instead of quartz sand. The small prisms were produced of mortar with 1 part by weight of cement, 1.33 parts of plastic sand and 0.6 parts of water. After 1 day of moist curing and further water curing they were exposed to the attack of sulphate solutions at the age of 21 days. After 8 weeks of sulphate storage the test specimens were crushed, the plastic sand was separated by sieving and portion of the cement was investigated by X-ray diffraction analysis (CuK_α-radiation).

The microscopic test should give informations about alterations on the surface of the prisms. For that purpose the phase composition and the nature of surface layers were examined with a polarisation microscope on thin sections cut parallel to the 1 × 1 cm top area of the small prisms with quartz sand and as aggregate after 28 days of sulphate storage.

Results

Storage Tests

The results of the storage tests are compiled in Tables 3 and 4. The Tables 3a and 3b contain the relative flexural strength of the small prisms and the Tables 4a and 4b the expansion of the flat prisms.

The flexural strength of the small prisms composed of portland cement (Table 3a) indicates the known influence of the content of tricalcium aluminate. The prisms composed of portland cement with 12% tricalcium aluminate disintegrate after 12 weeks at the latest, the prisms of portland cement with 8% tricalcium aluminate after 1 year, whereas the prisms of portland cement free of tricalcium aluminate even did not change after one year. An essential difference in the effect of sodium- and magnesium sulphate is not to realize. The additions of sodium chloride and sodium hydrocarbonate do not have a remarkable influence on the degree of attack of the sulphate solutions.

The small prisms consisting of blast-furnace cement with 65% and 77% granulated blast-furnace slag (Table 3b) are not attacked by sulphate solutions. Differences in the effect of the various solutions are only to observe at prisms of blast-furnace cement with 50% slag, which are destoryed after 18 weeks of sulphate storage. In this case the addition of sodium hydrocarbonate does reduce the aggressive effect of the sodium sulphate solution, but not the aggressive effect of the magnesium sulphate solution.

Table 3a. *Relative bending strength of the small prisms with portland cements*

C_3A-content	solution	sulphate storage, weeks						
		4	8	12	18	26	38	52
12%	Na_2SO_4	0.86	0	0	0	0	0	0
	+ NaCl	0.77	0.28	0	0	0	0	0
	+ $NaHCO_3$	0.68	0.36	0.21	0	0	0	0
	$MgSO_4$	0.54	0.07	0	0	0	0	0
	+ NaCl	0.14	0	0	0	0	0	0
	+ $NaHCO_3$	0.70	0.20	0	0	0	0	0
8%	Na_2SO_4	1.10	1.16	1.03	1.05	0.96	0.92	0.77
	+ NaCl	0.94	0.85	0.97	0.85	0.94	0.84	0
	+ $NaHCO_3$	1.04	1.09	1.18	1.02	1.10	1.14	0
	$MgSO_4$	0.96	0.96	0.91	0.96	0.94	0.91	0.69
	+ NaCl	0.86	0.89	0.89	0.80	0.80	0.81	0
	+ $NaHCO_3$	1.13	1.22	1.17	1.22	0.99	0.94	0
0%	Na_2SO_4	1.03	1.04	0.99	1.06	1.08	1.14	1.05
	+ NaCl	0.94	0.88	0.84	0.85	0.99	0.87	0.87
	+ $NaHCO_3$	1.13	1.12	1.15	1.14	1.17	1.20	1.05
	$MgSO_4$	1.15	1.10	1.13	1.20	1.08	1.15	1.18
	+ NaCl	0.88	0.80	0.81	0.80	0.73	0.80	0.75
	+ $NaHCO_3$	1.24	1.16	1.19	1.18	1.18	1.13	1.12

Teble 3b. *Relative bending strength of the small prisms with blast-furnace cements*

slag-content	solution	sulphate storage, weeks						
		4	8	12	18	26	38	52
50%	Na_2SO_4	1.02	0.90	0.66	0	0	0	
	+ NaCl	0.93	0.80	0	0	0	0	
	+ $NaHCO_3$	1.02	1.08	1.06	0.96	1.00	0.90	
	$MgSO_4$	1.14	0.98	0.44	0	0	0	
	+ NaCl	0.92	0.63	0.29	0	0	0	
	+ $NaHCO_3$	1.06	0.80	0.30	0	0	0	
65%	Na_2SO_4	1.23	1.29	1.18	1.18	1.20	1.01	
	+ NaCl	1.10	1.05	1.06	1.06	1.02	1.08	
	+ $NaHCO_3$	1.15	1.20	1.16	1.29	1.15	1.27	
	$MgSO_4$	1.29	1.32	1.15	1.19	1.15	0.89	
	+ NaCl	1.16	1.00	0.94	0.95	0.96	0.95	
	+ $NaHCO_3$	1.29	1.30	1.23	1.27	1.25	1.02	
77%	Na_2SO_4	1 01	1.02	1.01	1.03	1.03	1.10	
	+ NaCl	0.98	0.98	0.96	0.93	1.00	0.94	
	+ $NaHCO_3$	0.98	1.05	1.00	1.00	0.99	1.07	
	$MgSO_4$	1.22	1.09	1.12	1.20	1.13	1.28	
	+ NaCl	1.12	1.07	1.07	1.03	1.03	1.08	
	+ $NaHCO_3$	1.16	1.10	1.08	1.20	1.13	1.35	

Table 4a. *Expansion (mm/m) of the flat prisms with portland cements*

C_3A-content	solution	sulphate storage, weeks							
		4	8	12	20	28	36	44	52
12%	Na_2SO_4	0.73	1.52	2.53	d	d	d	d	d
	+ NaCl	0.64	2.41	4.24	10.20	d	d	d	d
	+ Na HCO_3	0.05	0.09	0.09	0.09	0.32	1.35	1.99	3.50
	$MgSO_4$	0.89	2.67	d	d	d	d	d	d
	+ NaCl	2.41	3.22	d	d	d	d	d	d
	+ Na HCO_3	0.74	1.38	d	d	d	d	d	d
8%	Na_2SO_4	0	0	0	0	0	0	0.15	0.10
	+ NaCl	0	0	0	0	0	0	0.04	0.10
	+ Na HCO_3	0	0	0	0	0	0	0	0.12
	$MgSO_4$	0.36	0.39	0.59	0.90	1.37	2.32	3.33	4.01
	+ NaCl	0.34	0.40	0.59	0.92	0.98	1.09	1.26	1.41
	+ Na HCO_3	0.49	0.56	0.56	0.84	1.29	2.07	2.92	3.99
0%	Na_2SO_4	0	0	0	0	0	0	0.12	0.17
	+ NaCl	0	0	0	0	0	0	0.19	0.19
	+ Na HCO_3	0	0	0	0	0	0	0.12	0.12
	$MgSO_4$	0	0	0	0.09	0.09	0.15	0.38	0.49
	+ NaCl	0	0	0	0.15	0.27	0.36	0.43	0.48
	+ Na HCO_3	0	0	0	0	0	0	0.17	0.23

d = destroyed

Teble 4b. *Expansion (mm/m) of the flat prisms with blast-furnace cements*

slag-content	sotution	sulphate storage, weeks							
		4	8	12	20	28	36	44	52
50%	Na_2SO_4	0.12	0.18	0.69	2.71	4.70	d	d	d
	+ NaCl	0.10	0.49	3.91	d	d	d	d	d
	+ Na HCO_3	0	0	0	0.09	0.09	0.19	0.25	0.31
	$MgSO_4$	1.72	9.18	d	d	d	d	d	d
	+ NaCl	1.22	7.87	d	d	d	d	d	d
	+ Na HCO_3	0	0	0.13	0.30	0.52	1.07	1.84	3.04
65%	Na_2SO_4	0	0	0	0	0	0.28	0.34	0.34
	+ NaCl	0.04	0.04	0.21	0.47	0.47	0.73	0.88	0.88
	+ Na HCO_3	0	0	0	0	0	0.11	0.23	0.23
	$MgSO_4$	0.17	0.17	0.32	0.59	0.84	1.19	1.49	1.65
	+ NaCl	0.20	0.20	0.37	0.52	0.64	0.89	1.06	1.12
	+ Na HCO_3	0.03	0.03	0.08	0.30	0.30	0.36	0.52	0.52
77%	Na_2SO_4	0	0	0	0	0	0	0	0
	+ NaCl	0	0	0	0	0	0	0	0
	+ Na HCO_3	0	0	0	0	0	0	0	0
	$MgSO_4$	0	0	0	0	0	0.07	0.07	0.07
	+ NaCl	0	0	0	0	0	0.12	0.24	0.24
	+ Na HCO_3	0	0	0	0	0	0	0.10	0

d = destroyed

The expansion behaviour of the flat prisms which are shown in Table 4 reveals more clearly than the decrease in strength of the small prisms, the influence of the sulphate resistance of the cement as well as the differences in the aggressive effect of the sulphate solutions. Nevertheless both methods yield nearly the same sequence in sulphate resistance of the 6 cements.

The test specimens of all cements are attacked much more by the magnesium sulphate solution than by

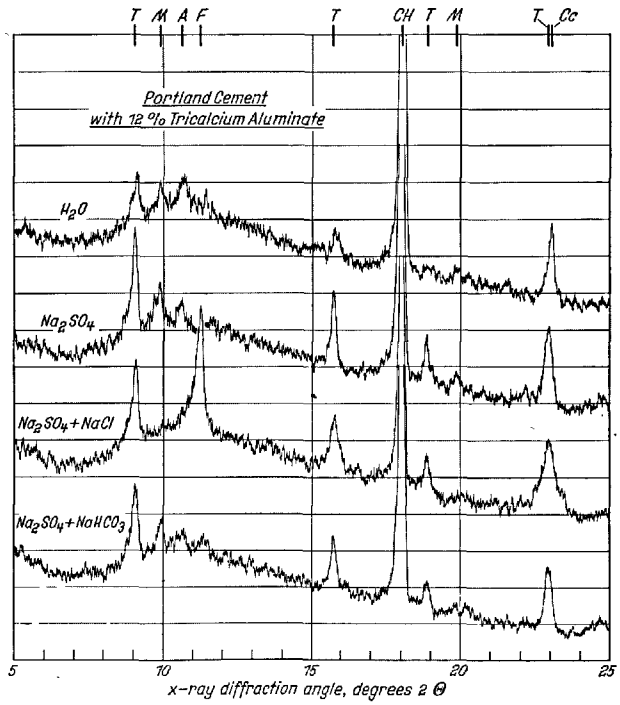

Fig. 1a. *X-ray diffraction diagrams of the hardened portland cement with 12% tricalcium aluminate after a storage of 8 weeks in distilled water and in sodium sulphate solutions without and with additions of sodium chloride and of sodium hydrocarbonate.*
T = *trisulphate (ettringite)*, M = *monosulphate*, A = *tetracalcium aluminate hydrate*, F = *monochloride (Friedel's salt)*, CH = *calcium hydroxide*, Cc = *calcite*

the sodium sulphate solution. The addition of sodium chloride has a small reducing effect, but only when test specimens of portland cement with 8% tricalcium aluminate are stored in a magnesium sulphate solution. In any other case the aggressive effect of the sulphate solution does not change or even it is intensified. An addition of hydrocarbonate reduces the aggressive effect of the sulphate solutions, especially on the prisms of cement with a smaller sulphate resistance.

X-ray Tests

The X-ray investigations are limited on the cements with the smallest sulphate resistance, i.e. the portland cement with 12% tricalcium aluminate and the blast-furnace cement with 50% granulated blast-furnace slag. The corresponding X-ray diffraction diagrams are shown for portland cement on Fig. 1a and 1b and for blast-furnace cement on Fig. 2a and 2b.

The water cured prisms consisting of portland cement contain trisulphate (ettringite), monosulphate

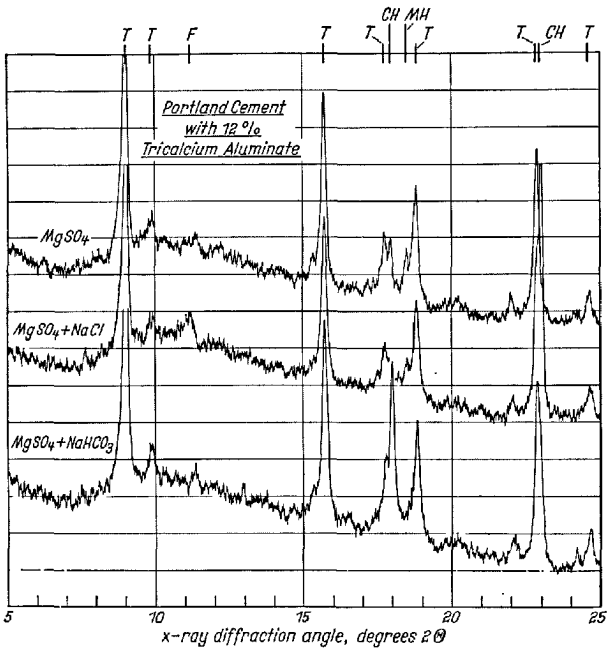

Fig. 1b. *X-ray diffraction diagrams of the hardened portland cement with 12% tricalcium aluminate after a storage of 8 weeks in magnesium sulphate solutions without and with additions of sodium chloride and of sodium hydrocarbonate.* T = *trisulphate (ettringite)*, M = *monosulphate*, A = *tetracalcium aluminate hydrate*, F = *monochloride (Friedel's salt)*, CH = *calcium hydroxide*, MH = *magnesium hydroxide*, Cc = *calcite*

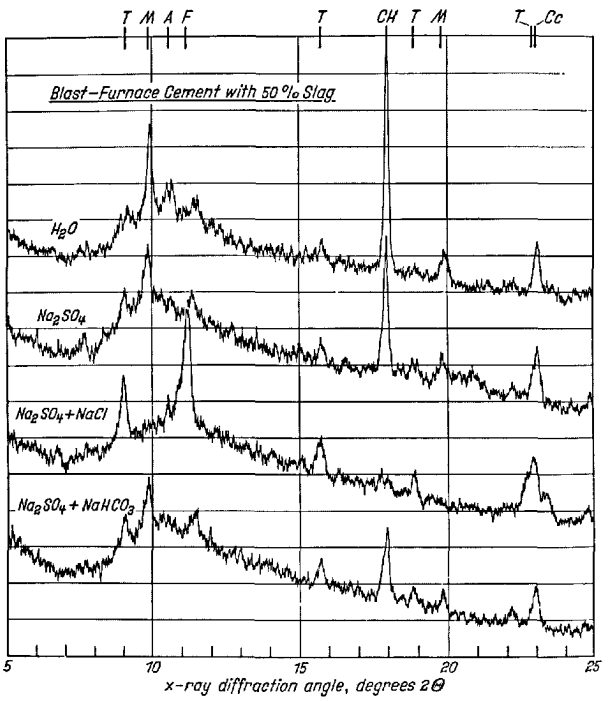

Fig. 2a. *X-ray diffraction diagrams of the hardened blast-furnace cement with 50% granulated blast-furnace slag after a storage of 8 weeks in distilled water and in sodium sulphate solutions with and without additions of sodium chloride and of sodium hydrocarbonate.*
T = *trisulphate (ettringite)*, M = *monosulphate*, A = *tetracalcium aluminate hydrate*, F = *monochloride (Friedel's salt)*, CH = *calciumhydroxide*, Cc = *calcite*

and tetraclacium aluminate hydrate as aluminate bearing hydration products (Fig. 1a, diagram uppermost). After storage in sodium sulphate solution the trisulphate content has increased (Fig. 1a, 2. diagram). If the solution contains sodium chloride in addition to sodium sulphate, monochloride (Friedel's salt), $3CaO \cdot Al_2O_3 \cdot CaCl_2 \cdot 10H_2O$ (Fig. 1a, 3. diagram), is formed besides the trisulphate. The addition of sodium hydrocarbonate results in a diminution of trisulphate content in comparison with storage in a pure sodium sulphate solution (Fig. 1a, 4. diagram). Aluminate carbonate hydrates could not be identified, calcite only in small quantities because the carbonate is precipitated only in a thin surface layer so that the calcite concentration of the total sample remains small (see microscopic investigations).

The prisms stored in the magnesium sulphate solution contain much bigger quantities of trisulphate (Fig. 1b), because the prisms containing portland cement with a high content of tricalcium aluminate are vigorously attacked and damaged within 8 weeks and consequently the magnesium sulphate solution could react with the compounds of the hardened cement without any difficulties. Accordingly the calcium hydroxide concentration, originally very high, has been nearly completely consumed. Probably the magnesium sulphate solution has reacted with the calcium hydroxide to form solid magnesium hydroxide and calcium sulphate solution which on its side reacts with the still available aluminate hydrate to trisulphate (7). Additions of sodium chloride (Fig. 1b, 2. diagram) or sodium hydrocarbonate (Fig. 1b, 3. diagram) do not have any influence on the course of the reaction perceptible by X-ray diffraction. Nevertheless the stronger calcium hydroxide line on the 3. diagram points out, that in presence of sodium hydrocarbonate the reactions are not so far advanced. The high calcite content of the specimen stored in the magnesium sulphate solution with sodium chloride is due to its rapid disintegration and subsequent precipitation of the liberated lime by the carbon dioxide of the air which is permanent dissolved in the sulphate solution.

In the hydration of blast-furnace cements the same aluminate hydrates are formed as in the hydration of

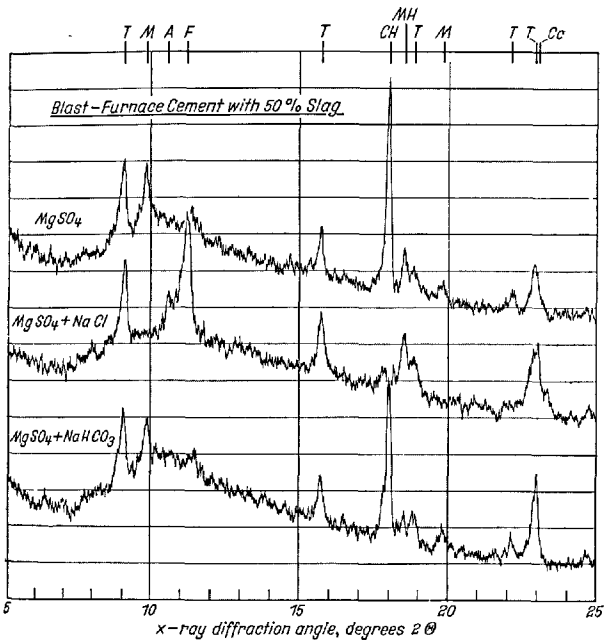

Fig. 2b. *X-ray diffraction diagrams of the hardened blast-furnace cement with 50% granulated blast-furnace slag after a storage of 8 weeks in magnesium sulphate solutions without and with additions of sodium chloride and of sodium hydrocarbonate.*
T = *trisulphate (ettringite)*, M = *monosulphate*, A = *tetracalcium aluminate hydrate*, F = *monochloride (Friedel's salt)*, CH = *calcium hydroxide*, MH = *magnesium hydroxide*, Cc = *calcite*

portland cement, but there is much more monosulphate and less trisulphate (Fig. 2a, diagram uppermost). The trisulphate content is increased a little by storage in the sodium sulphate solution (Fig. 2a, 2. diagram). But the evident decrease in calcium hydroxide content indicates that a reaction with the sulphate solution took place. When sodium chloride is present, the monochloride is formed (Fig. 2a, 3. diagram), analogous to the behaviour of the portland cements. Besides, the diagram exhibits an increased formation of trisulphate and a complete consumption of calcium hydroxide. An addition of sodium hydrocarbonate (Fig. 2a, 4. diagram) does not yield any alteration compared with the pure sodium sulphate solution, excepting a further decrease in calcium hydroxide content.

In the case of magnesium sulphate attack (Fig. 2b) trisulphate is formed to a greater extent. But there is no difference between the influence of the pure magnesium sulphate solution (Fig. 2b, diagram uppermost) and the magnesium sulphate solution with addition of carbonate (Fig. 2b, 3. diagram). In the presence of chloride monochloride is formed again (Fig. 2b, 2. diagram), without any influence on the trisulphate content and with complete reaction of the calcium hydroxide.

Microscopic Inspections

During storage in water or in various sulphate solutions coatings are formed on the surfaces of the small prisms. The microscopically determined composition of the coatings depends on the kind of solution but not on the type of cement. When stored in water or in sodium sulphate solution the coating is composed of calcite, $CaCO_3$, and when stored in magnesium sulphate solution it consists of brucite, $Mg(OH)_2$ with only a very small admixture of calcite.

The surface coatings of the water cured prisms with a mean thickness of 2 to 3 μm are very thin compared with the 15 to 20 μm thick coatings on prisms stored in the various sodium sulphate solutions. An addition of sodium chloride has no influence on the thickness of the calcite coating, an addition of sodium hydrocarbonate effects a small increase only.

The brucite coating formed during storage in magnesium sulphate solution, has an average thickness of 5 μm. It increases significantly up to 30 μm, when sodium chloride is present in the solution. If the magnesium sulphate solution contains sodium hydrocarbonate, the surface coating has a thickness of 2 or 3 μm and is composed of a mixture of brucite and calcite.

Discussion

The storage tests especially those by the flat prism method, mainly indicated that

1. solutions of magnesium sulphate attack the mortar prisms of all cements more vigorously than solutions of sodium sulphate,

2. an addition of sodium chloride to the sulphate solution does not diminish the rate of attack but even increases it in some cases and

3. an addition of sodium hydrocarbonate diminishes the rate of attack of the sulphate solution.

These results agree with those of the X-ray diffraction investigations, that means that the test specimens

which are more vigorously attacked, show the higher content of trisulphate. That is particularly valid for the attack of magnesium sulphate solution too.

When chloride is present trisulphate has an increased solubility according to investigations mentioned by W. W. Kind (2), consequently it is to crystallize either in a small quantity only or in the harmless formation in the pores of the hardened cement paste. The above-mentioned X-ray diffraction investigations indicate however, that the formation of trisulphate is not hindered by addition of chloride. Moreover monochloride is formed but always by consumption of monosulphate and tetracalcium aluminate hydrate. The fairly large quantities of monochloride indicate that the sodium chloride added to the solution, also reacts with the nonhydrated tricalcium aluminate.

Furthermore it is remarkable that the prisms which were not heavily attacked, contain much more monochloride than the disintegrated prisms. Hence it follows that the chloride ions penetrate the hardened cement more quickly than the sulphate ions and react there with monosulphate, tetracalcium aluminate hydrate and probably with the nonhydrated tricalcium aluminate, too, forming monochloride. But as the monochloride is not stable in presence of sulphate, it gets converted later on into trisulphate when sulphate attack proceeds. Hence it is unlikely that in a sulphate solution containing chloride less trisulphate is formed than in a sulphate solution without chlorides. The assumption that in presence of chloride the harmless form of trisulphate crystallizes in the pores of the hardened cement does not correspond to results of the storage tests. In sulphate solutions containing hydrocarbonate the trisulphate is formed significantly slower than in solutions without carbonate. As there is no difference in the kind of the chemical reaction the retarded formation of the trisulphate can only be attributed to the increase of the diffusion resistance. So it can be assumed that the hydrocarbonate together with the calcium hydroxide forms calcite, which grows upon the surface and in the pores near the surface of the hardened cement and hinders penetration of the solution. The microscopic inspections show, however, that in solutions of sodium sulphate without addition of hydrocarbonate coatings of calcite are formed, too, but which, as the results of the storage tests show, do not diminish sulphate attack. So it seems to be important that the solution always contains a sufficient quantity of carbonate to form a calcite coating also on the surface in cracks arisen by sulphate expansion. In solutions without admixture of carbonate, the supply of carbon dioxide dissolved from the air, obviously is very slow and consequently the calcite coating is formed not quickly enough to prevent penetration of sulphate when sulphate susceptible cements are used and the sulphate attack proceeds quickly.

The brucite coatings of various thicknesses formed during storage in magnesium sulphate solutions with and without chloride have no influence on sulphate attack. The aggressive effect is significantly diminished however, when the coating consists of a mixture of brucite and calcite.

The results of the investigations point out the fact that the high content of chloride in the sea water has no essential effect on the sulphate attack. A significantly greater influence is exerted by the content of hydrocarbonate. But it is still doubtful, whether the comparatively weak aggressive effect of the sea water can be explained in this way only.

Summary

Experiences and investigations showed that sea water has a significantly less aggressive effect on concrete than pure sodium or magnesium sulphate solutions of the same sulphate concentration. So it has been examined whether chloride and hydrocarbonate, the other efficaceous components in the sea water besides sulphate, are responsible for the diminution of the sulphate attack. For that purpose storage tests have been performed with solutions of sodium and magnesium sulphate with 2500 mg SO_4^{2-}/*l* with and without additions of 30 g NaCl/*l* or of 0.19 g $NaHCO_3$/*l*. Small prisms (1 × 1 × 6 cm) and flat prisms (1 × 4 × 14 cm) of mortar according to the German standard specification with 3 portland cements with calculated contents of tricalcium aluminate of 0%, 8% and 12% and 3 blast-furnace cements with 50%, 65% and 77% slag were used as test specimens. The decrease in bending strength of the small prisms and the expansion of the flat prisms tested in certain time intervals were taken as a criterion for the aggressive effect of the solutions. Microscopical inspections of the small prisms gave informations about the character of the surface coatings formed during the sulphate storage, and the nature of chemical reactions between the hydration products and the consistuents of the solutions were illustrated by X-ray diffraction analysis. The expansion of the flat prisms showed more significantly than the decrease in strength of the small pri-

sms, that magnesium sulphate is a more aggressive media than sodium sulphate. The sulphate attack is either not changed or increased by an addition of chloride to the sulphate solution, whereas it is clearly reduced by the addition of sodium hydrocarbonate. X-ray diffraction investigations reveal that in any case the formation of trisulphate (ettringite) is the cause for the detrimental effect of all sulphate solutions tested. The formation of trisulphate is not diminished by sodium chloride, retarded however by sodium hydrocarbonate. Microscopic examinations showed that on the surface of the prisms coatings are formed, which are composed of calcite ($CaCO_3$), when prisms have been in water and in sodium sulphate solutions and the coatings are composed of a mixture of brucite ($Mg(OH)_2$) and calcite when the prisms have been stored in magnesium sulphate solutions. An addition of hydrocarbonate increases the formation of calcite. Thus the assumption has been made that the calcite crystals grow upon the surface and in the pores near the surface of the hardened cement and hinder the penetration of the sulphate solutions.

References

1. F. M. Lea, "The chemistry of cement", 2nd ed., p. 297, (Edward Arnold, London, 1956).
2. W. W. Kind, "The problem of the influences of chloride on the velocity of the sulphate attack" (in Russian), Zement **1**, 3–6 (1956).
3. F. W. Locher, "The problem of the sulphate resistance of slag cements" (in German), Zement-Kalk-Gips **19**, No. 9, 395–401 (1966).
4. Verein Deutscher Zementwerke E. V., Tätigkeitsbericht, p. 68 and 72 (1965/66) (in German).
5. A. Koch and H. Steinegger, "A rapid method for testing the resistance of the cements to sulphate attack" (in German), Zement-Kalk-Gips **13**, No. 7, 317–342 (1960).
6. W. Wittekindt, "Sulphate resistant cements and their testing" (in German), Zement-Kalk-Gips **13**, No. 12, 565–572 (1960).
7. H. zur Strassen, "Survey about the reactions at the setting of the cement" (in German), Tagungsberichte der Zementindustrie No. 21, Part 1, 71–87 (1961).

Oral Discussion

Arthur W. Brown

Dr. Locher will be interested to know that in similar work in connection with sodium chloride contaminated aggregates, it was found that the incorporation of sodium chloride in an ordinary portland cement mortar mix, at a level of 2% on the cement, imparted considerable sulphate resistance to the O.P.C. based specimens in solutions containing up to 24,000 mg. SO_4^{2-}/litre. Could this perhaps be due to the appearance of sodium as bicarbonate, following the complexing of some chloride as chloro-aluminate? I feel that in view of his findings this may well be the case. Using sulphate resisting portland cement no differences due to the incorporation of sodium chloride have been detected up to date, that is in 9 months.

Author's Closure

Friedrich W. Locher

The reduction of the sulphate attack by an addition of chloride to the cement is perhaps to be attributed to the quick formation of aluminate chloride hydrates during the early hydration reactions. At lower chloride concentrations the monochloride is formed, at higher chloride concentrations the trichloride, too, according to recent results of W. Richartz (will be published). The monochloride reacts with the later penetrating sulphate solutions to ettringite, but it does not generate a crystallization pressure. The trichloride is resistant against sulphate. An addition of chloride to cement effects that a bigger quantity of aluminate will be already bound as aluminate chloride hydrates during the setting of the cement and consequently less aluminate can react to form trisulphate.

Supplementary Paper III-138 Mechanisms of Sulphate Expansion of Hardened Cement Pastes

Susanta K. Chatterji*

Synopsis

The expansion of cement motars or concrete due to sulphate attack can be ascribed to (i) the formation of sulphoaluminate, (ii) the formation of gypsum, and (iii) other reactions catalyzed by the sulphate ions. It has been shown that of the two sulphoaluminates which may form, monosulphate formation form C_4AH_{13} explains the observed expansions under different conditions better than the formation of ettringite. This mechanism of sulphate expansion also opens up a method of improving the sulphate resistance of ordinary portland cement by adding finely ground calcium carbonate. The formation of gypsum may lead to an expansion of the concentration of sulphate solution is such that a supersaturated solution of gypsum is formed. It has been proposed that recrystallization of X-ray amorphous calcium hydroxide, which is catalyzed by sulphate ions, may lead to some expansion. The cations, present though not contributing to expansion directly, may influence the rate of sulphate attack.

Introduction

It has been observed by the earliest users of portland cement that structures made with portland cements are not very stable when exposed to water containing sulphate ions. A large number of research workers have studied this problem in order to elucidate the mechanism of the deterioration, arriving at different conclusions. The action of water containing sulphate ions on the hardened cement pastes or mortar etc. had been followed either by measuring the rate of expansion or loss of strength (tensile or compressive) or by ultrasonic resonance vibration. It has generally been agreed that the main reason for the deterioration of structures is due to the expansion of the hardened cement and that the alteration of mechanical properties occurs as a result of this expansion. In recent years a series of papers has been published from this laboratory on the volume stability of cementitious pastes. The main object of this paper is to collect together the various ideas, put them in perspective and compare them with other theories.

The reactions between hardened cement paste and sulphate ions (disregarding the effects of cations for the present) can be broadly divided into three categories, in order of descending importance:

(i) formation of sulphoaluminates,
(ii) formation of gypsum,
(iii) other reactions catalyzed by the sulphate ions.

The effects of these reactions on the volume stability of hardened cement pastes will be discussed in the following sections. At the end, the effects of different cations on the rate of sulphate attack on hardened pastes will be discussed.

*Department of Crystallography, Birkbeck College, London, United Kingdom.

Formation of Sulphoaluminates

There are two types of sulphoaluminates that can form by the reaction between C_3A and sulphate ions in the presence of excess Ca^{2+} ions; these are $C_3A \cdot 3CaSO_4 \cdot 32H_2O$ (ettringite) and $C_3A \cdot CaSO_4 \cdot 11H_2O$ (monosulphate). In both the structures part or the whole of the Al^{3+} ions can be replaced by Fe^{3+} ions. Of these two sulphoaluminates, ettringite is stable in the presence of excess sulphate ions. Monosulphate forms when the sulphate ion concentration falls below the value at which ettringite is stable.

Two theories have been proposed connecting the formation of different sulphoaluminates with the volume expansion of hardened cement pastes. According to the earlier theory of Lafuma (1) the volume expansion is due to the formation of ettringite. It has been assumed that the ettringite formation can take place by two mechanisms. If the liquid phase containing sulphate ions is saturated with respect to $Ca(OH)_2$, the ettringite formation occurs through a solid state reaction between C_3A and SO_4^{2-} and Ca^{2+} ions from solution. A simple molar volume calculation shows that this reaction is accompanied by a volume increase of about 815% calculated on the basis of C_3A volume. But if the liquid phase is unsaturated with respect to $Ca(OH)_2$ the reaction goes through the liquid phase and the ettringite crystallization occurs in the pores present in the structure without causing any expansion. Until recently this was the only accepted theory of sulphate attack involving sulphoaluminate formation.

In 1963 another mechanism of sulphate attack was proposed, which does not involve ettringite formation as the cause of expansion (2). In this mechanism the expansion is attributed to the conversion of *pre-existing* C_4AH_{13} to monosulphate by reaction with SO_4^{2-} ions present in the liquid phase. The main experimental basis of this mechanism was an observation that in a $C_3A + Ca(OH)_2 + CaSO_4 \cdot 2H_2O$ paste, expansion had occurred when ettringite was disappearing and monosulphate was forming. This observation is very difficult to explain on the basis of Lafuma's theory. This observation has recently been confirmed by Seligmann and Greening (3). In a paste of $C_3A + Ca(OH)_2 + CaSO_4 \cdot 2H_2O$, having gypsum to aluminate molar ratio of $\frac{1}{4}$, they observed that most of expansion occurred during the disappearance of ettringite and formation of monosulphate.

The new mechanism can be put in the following terms. During hydration of cements the alumina bearing compounds first go into solution and then precipated out as hydrated compounds. The actual nature of the hydration compounds depends on temperature and concentrations of other ions present in the liquid phase. Taking the case of freshly ground portland cement, containing no CO_2 and hydrating at room temperature, the main alumina bearing compound will be ettringite as long as the sulphate ion concentration is high. When the sulphate ion concentration falls below the value necessary for ettringite formation, monosulphate may be precipitated if the sulphate ion concentration is high enough for monosulphate stability otherwise C_4AH_{13} will be precipitated. As the above reactions proceed through the liquid phase the reaction products will form in the pores present in the structure without causing any expansion. If the structure containing C_4AH_{13} is subsequently exposed to sulphate solutions, sulphate ions will start to diffuse inwards. When the sulphate ion concentration reaches a critical value monosulphate will start to form from C_4AH_{13} by an ion exchange process. This mode of monosulphate formation leads to volume expansion. On further increase in sulphate ion concentration, monosulphate will be converted to ettringite by a 'through-solution' process. These secondary ettringite crystals will be precipitated in the pores present in the structure without causing any significant expansion.

The volume expansion due to the formation of monosulphate from C_4AH_{13} may or may not be accommodated in the structure depending on the $Ca(OH)_2$ concentration in the liquid phase. If the $Ca(OH)_2$ concentration is low a part of the expanding C_4AH_{13} crystals will dissolve (being under compression) and diffuse out to other parts of the structure, thereby accommodating the expansion. If the concentration of $Ca(OH)_2$ is high in the liquid phase the solubility of C_4AH_{13} will be depressed, thereby making the accommodative process inoperative, and as a consequence there will be disruptive expansion.

It is to be noted that the formation of monosulphate by itself does not necessarily give rise to volume expansion. Volume expansion occurs only when it forms from C_4AH_{13} by an ion exchange process. It seems that some confusion has arisen by not noting this distinction (4). It follows from the above discussion that an anhydrous compound with SO_3/Al_2O_3

molar ratio 1 or less, e.g. C_4A_3S, will form monosulphate during dissolution and precipitation processes without causing any expansion.

One of the basic assumptions of this new mechanism is the formation of C_4AH_{13} in the paste, instead of C_4AH_{19} as is found in the phase equilibrium studies (5). The validity of this assumption has been confirmed by taking X-ray diagrams of moist clinker pastes in which the proportion of aluminate phase had been increased by adding C_3A. The X-ray diagram of these pastes showed the existence of C_4AH_{13} in the pastes (6).

Another assumption is that the formation of monosulphate from C_4AH_{13} is an ion exchange process. If this assumption is true then it should be possible to replace the SO_4^{2-} ions from the monosulphate structure by other ions / by placing the monosulphate crystals in a suitably concentrated solution of the appropriate ion. Take the case of portland cement paste containing both ettringite and monosulphate, in $CaCl_2$ solution of fairly high strength. Soon after placement of the paste in the chloride solution, the chloride ions will start to diffuse inwards from outside. When the concentration of chloride ion has reached the appropriate value monosulphate will be converted to monochloroaluminate, thereby releasing sulphate ions in the liquid phase. These freshly released sulphate ions can then migrate to other places and can convert any C_4AH_{13} crystals available to monosulphate causing further expansion; provided the sulphate ion concentration can reach the appropriate value. The chances of reaching this sulphate ion concentration will be more in a low w/c paste than in a high w/c paste, simply because the amount of diluting liquid phase present in the paste is less in the former than in the latter. In other words, the richer paste is expected to expand more, notwithstanding its higher strength, than the lean paste when placed in $CaCl_2$ solution. Recently, Heller and Ben-Yair (7) have published some results which seemed to corroborate the above expectations. In this work the authors exposed paste prisms made from (a) ground clinker and (b) portland cement to 3.5% calcium chloride solution and also to distilled water. They also made prisms from portland cement with w/c ratios of 0.3 and 0.5 which were also exposed to 3.5% calcium chloride solution. The authors found that "expansion of cement clinker exposed to chloride solutions ... resemble that in distilled water. Bars of normal portland cement, however, expand more in chloride solutions than in distilled water." From this they concluded that "addition of gypsum to ground clinker causes increased expansion in chloride solutions". Thus the chloride solutions, though themselves not giving rise to any expansion, cause expansion in the presence of sulphate. Furthermore, they also found that the portland cement prisms with low w/c expanded more than those with higher w/c ratio. Both these observations are in accordance with the proposed mechanism.

It follows from the proposed mechanism of sulphate expansion that if C_4AH_{13} can be converted to a more stable compound with a lower basal spacing then monosulphate, which changes directly to ettringite when exposed to sulphate solution, this should result in lower expansion. Monocarboaluminate (monocarbonate) seems to fulfil all these requirements (8,9). It is expected that the addition of finely ground $CaCO_3$ to portland cement will result in the formation of monocarbonate at the expense of C_4AH_{13}, and this should result in lower sulphate expansion on subsequent exposure to sulphate solutions. This corollary of the proposed mechanism has been verified recently (10).

It is evident that none of the above results are easily explained by Lafuma's theory. Another observation, which is also difficult to explain from the ettringite formation theory is that the same amount of ettringite formation in sulphate resistant cement causes less expansion than in the case of ordinary portland cement (11). This is easily explained by the proposed mechanism as a monosulphate type of compound does not seem to form in sulphate resistant cement (6).

Taking all the evidence it is clear that if sulphoalminate formation has anything to do with sulphate expansion, then monosulphate formation explains the observations better than ettringite formation.

Formation of Gypsum

Portland cement always liberates $Ca(OH)_2$ during its hydration. Matured portland cement pastes generally contain about 14% $Ca(OH)_2$. When these pastes are exposed to sulphate solutions, if the concentration of Ca^{2+} and SO_4^{2-} ions exceed the solubility product of gypsum, gypsum will be precipitated. As the

gypsum crystals are surrounded by a supersaturated solution they will grow even when they are under constraint, provided the constraining force is not higher than the 'crystal growth pressure' (12). The crystal growth pressure is a function of supersaturation. Thus if the conditions are appropriate, i.e. the supersaturation is high, the formation of gypsum may lead to expansion. Lea has earlier discussed the possibility of cement expansion due to gypsum formation on the tacit assumption that the gypsum formation is a reaction between solid $Ca(OH)_2$ and sulphate ions present in aggressive solutions (13). The assumption of a reaction between solid $Ca(OH)_2$ and SO_4^{2-} ions from solution is questionable in view of the fact that the structures of $Ca(OH)_2$ and $CaSO_4 \cdot 2H_2O$ are so different and the explanation in terms of crystal growth pressure seems preferable. This type of expansion assumes importance in the presence of magnesium sulphate solution, because of the low solubility of $Mg(OH)_2$.

Other Reaction Catalyzed by Sulphate Ions

From the above discussion it will appear that mortar prisms made from pure C_3S should not expand when exposed to gypsum solution. But Thorvaldson has found that even these mortars expand when exposed to gypsum solution for a long time (14). This result is rather difficult to explain as there is no possibility of any sulphoaluminate or gypsum formation. One possible explanation has been suggested by an observation that $Ca(OH)_2$ crystals grow more readily in the presence of gypsum (15). It is known that during C_3S hydration a certain amount of X-ray amorphous $Ca(OH)_2$ forms (16). In the presence of SO_4^{2-} ions these X-ray amorphous $Ca(OH)_2$ will start to recrystallize into bigger crystals, at the same time developing an expansive force (12). As this recrystallization process depends on double diffusion of SO_4^{2-} and $Ca(OH)_2$ it will be slow. It seems probable that in the case of portland cements similar expansion will also occur.

It is possible that other reactions may contribute to expansion under certain circumstances and investigation of this field is far from exhausted.

Effect of Cations

So far only the effects of sulphate ions have been discussed. Though these provide the basic reasons for expansion, the course of reaction is also effected by the cations. These cations can be divided into three general classes: (i) those forming very soluble hydroxides, e.g. Na^+, K^+ (ii) those forming sparingly soluble hydroxides, e.g. Mg^{2+}, Fe^{2+}, and (iii) those forming volatile or neutral compounds e.g. NH_4^+ or H^+.

The metal sulphates of the first group will form gypsum and highly soluble metal hydroxides. Depending upon the initial concentration of the metal sulphate, formation of gypsum may or may not develop an expansive 'crystal growth pressure'. But the formation of metal hydroxide will increase the OH^- ion concentration in the liquid phase; in a closed system equilibrium will soon be reached. This increase in OH^- ion concentration will firstly depress $Ca(OH)_2$ concentration in the liquid phase thereby bringing the expansion accommodative process into play. Secondly, this increase of OH^- ion concentration may attack other constituents of the structure thereby decreasing the strength of the whole. Thus two opposing forces will be brought into play if the system is a closed one. If on the other hand, the system is an open one, i.e. there is a continuous flow of sulphate solution, the concentration of OH^- ion in the liquid phase may not reach a high value and as a consequence the expansion accommodative process will not be operative and expansion may be severe.

The second group of metal sulphate solutions are very corrosive. None of the cementing materials is stable in their presence, the final products being gypsum, sparingly soluble metal hydroxide, silica and aluminium hydroxide gels. As against this extreme corrosiveness, these metal hydroxides form a protective coating by being precipitated all over the structure and thereby hindering further transport of ions to the reacting surfaces. Thus in the case of rich pastes this type of metal sulphate may be less aggressive than the other two types.

The third group of sulphates consist of $(NH_4)_2SO_4$ and H_2SO_4. In this case neither the accommodative process nor the protective coating formation can

occur. The attack is very vigorous and is not limited only to expansion but also includes weakening the strength of the paste by dissolving out the cementing components.

Acknowledgements

The author would like to thank Professor J. D. Bernal for his continued interest and encouragement in cement research. It is a pleasure for the author to acknowledge the help, advice and encouragement from Dr. J. W. Jeffery.

References

1. H. Lafuma, Rev. Mat. Const. No. 243, p. 441 (1929); No. 244, p. 4, (1930).
2. S. Chatterji and J. W. Jeffery, Mag. Conc. Res., Vol. 44, p. 83, (1963).
3. P. Seligmann and N. R. Greening, Highway Res. Record, No. 62, p. 80, (1964).
4. P. K. Mehta and A. Klein, Highway Research Record, Special Report, 90, p. 328, (1966).
5. M. H. Roberts, J. Appl. Chem. Vol. 7, p. 543, (1957).
6. S. Chatterji and J. W. Jeffery, Mag. Conc. Res., Vol. 16, p. 236, (1964).
7. L. Heller and M. Ben-Yair, J. Appl. Chem., Vol. 16, p. 223, (1966).
8. S. Chatterji and J. W. Jeffery, J. Amer. Ceram. Soc., Vol. 46, p. 268, (1963).
9. M. H. Roberts, Building Research 1964, p. 55, H. M. S. O. (1965).
10. S. Chatterji and J. W. Jeffery, In the press.
11. L. Heller and M. Ben-Yair, J. Appl. Chem., Vol. 14, p. 20, (1964).
12. S. Chatterji and J. W. Jeffery, Trans. Faraday Soc., Vol. 60, p. 1947, (1964).
13. F. M. Lea, Canadian J. of Res. No. 27B, p. 297, (1949).
14. T. Thorvaldson, Proc. 3rd Inter. Symp. Chem. Cement, 1952, p. 436, (1954).
15. S. Chatterji and J. W. Jeffery, J. Amer. Ceram. Soc., Vol. 45, p. 536, (1962).
16. D. L. Kantro, et al. J. Coll. Sci., Vol. 14, p. 363, (1959).

Oral Discussion

Arthur W. Brown

Dr. Chatterji proposes the theory that he and Dr. Jeffery initiated some 5 years ago, and does so with considerable supporting evidence.

Nevertheless I do not find it possible to accept this theory in the light of our experience to date. I would ask Dr. Chatterji what mechanism he suggests for sulphate attack on the many cements with tricalcium aluminate contents around 8% or less, where, after ettringite formation and its conversion to the mono-sulphoaluminate during hydration, there is little or nothing left to form the C_4AH_{13} as a basis for his mechanism of attack?

Our experience is that serious specimen damage occurs only after the appearance of ettringite in significant quantity.

After disagreeing with Dr. Chatterji I feel I must perhaps suggest some evidence in favour of his theory. We have found, as I believe have others, that the longer a specimen is cured in water before immersing in sulphate solutions, the more decisive is the effect of the sulphate. We also know that cements with high C_3A and therefore a good potential for the formation of C_4AH_{13} are attacked much more in relation to their C_3A contents than the O.P.C.'s with lower C_3A contents mentioned earlier. Is this perhaps significant?

Author's Closure

Susanta K. Chatterji

It is unfortunate that Mr. Brown did not specify either the nature of sulphate solution used in his experiments or the type of damage that resulted. As I have tried to show in my paper, there may be more

than one type of mechanism operation in any given situation. Without any further information it is impossible to suggest which mechanism was operative in the experiments carried out by Mr. Brown.

I would like to thank Mr. Brown for supplying me with some evidence in favour of one of the proposed mechanisms.

SESSION III-3 CARBONATION OF CONCRETE

Principal Paper Neutralization (Carbonation) of Concrete and Corrosion of Reinforcing Steel

Minoru Hamada*

Synopsis

Reinforced concrete structures have extremely long lives, but there have been cases of the reinforcing steel being corroded even in ordinary atmospheric environments. The purpose of this paper lies in defining the phenomena related to life spans of reinforced concrete structures, providing a guide for building high quality structures of long life and contributing to the sound development of reinforced concrete structures. The contents of the paper consist of a summarization of long-term studies carried out by the author and its group. The paper begins with a description of the experiments which motivated this research and with the theme presented by the author that neutralization (carbonation) of concrete has a relation with corrosion of reinforcing steel as the basis, considers the various factors influencing the rate of neutralization of concrete, describes through experiments the methods of determining neutralization connected with rusting of steel, introduces surveys made of actual buildings and further comments on the result of studies on special cases which have an effect on the life spans of reinforced concrete structures.

1. Purpose and Significance of the Study

Reinforced concrete structures, barring cases of dynamic failure or special types of chemical corrosion, are generally said to be of a semi-permanent nature.

In looking at actual reinforced concrete buildings, the first of which date back to about 70 years age, corrosion of steel has been noticed in recent years in relatively old buildings which have existed in normal atmospheric and other environmental conditions. It is desirable that the causes of such phenomena be pursued, if possible to place a numerical evaluation on the so-called semi-permanent life, and if occurrence of such phenomena is the fate of reinforced concrete, to find a method of prolonging the life.

In Japan, as a result of investigations of the Great San Francisco Earthquake of 1906, it became to be considered ideal for future buildings to be of reinforced concrete. However, in a country like Japan where the humidity is high, especially in the hot summer months, there is a question regarding the susceptibility of reinforcing steel to rusting, and therefore, durability tests under the conditions of natural exposure as described later were begun. The author, after twenty years of outdoor exposure tests, investigated the results obtained up to that time, the first study of its kind in the world.

From the results, it was ascertained that over the years the alkali of concrete is neutralized from the surface by carbon dioxide gas in the atmosphere, rusting beginning to take place when the neutralization reaches the reinforcing steel. Having determined that neutralization of concrete has a great influence on rusting of reinforcing steel, numerous studies were carried out centered around this problem. Method of evaluating the life of a building and of prolonging that life have been suggested to contribute to the sound development of future reinforced concrete structures. This paper is a summary of these many studies.

*Tokyo University of Science, Tokyo, Japan.

2. Origin of Studies

The experiments were motivated by the reasons stated in the preceding section and consisted of two groups.

2.1 Experiment No. 1 (1)

This experiment first began in the autumn of 1907 by the late Dr. Riki Sano. Specimens consisted of untreated steel and steel coated with rust preventive material. Also, these steels were embedded in concretes of various mix proportions and with varying coverages. These specimens numbered in the hundreds were placed outdoors in the atmosphere, indoors, in the earth and in ponds, and rusting of the steel was examined.

Unfortunately, there were a number of the specimens lost in later years and those which will be described hereafter were mainly specimens which had been placed outdoors in air.

Place of Exposure: A corner of a spacious inner court of a two-storied brick building of the Department of Architecture, Faculty of Engineering, University of Tokyo.

Steel: Round bars of 1/2-inch diameter, polished and embedded in the centers of various concretes.

Concrete: The mix proportions used were the six varieties given in Table 1 and the concrete was cast in prisms 15 cm × 15 cm × 60 cm. Some of the 1:3:6 mixes were 6 cm × 6 cm × 60 cm and 60 cm × 60 cm × 90 cm.

The mix proportions were by volume and although the concrete was relatively stiff no detailed records such as kept today were taken as this was in the early days of concrete technology. Neither was compaction of the concrete complete.

Survey: Of the several specimens, of each type remaining 20 years after manufacture, three or four each were broken and examined. The remainder were left for further long-term tests and presently a number of them still exist after 60 years.

Table 1. *Types of concrete in corrosion test*

No.	Mix proportion				
	Cement	Lime	Sand	Gravel	Cinder
1	1	0	1	2	0
2	1	0	2	4	0
3	1	0	3	6	0
4	1	0	5	10	0
5	1	2	4	8	0
6	1	0	2	0	4

Rusting: Results show that richness or leanness of concrete mix proportions and the degree of compaction have an important relation with the outcome.

2.2 Relation between Alkalinity Retained in Concrete and Rusting

It was well known at that time that steel would not rust if its environment was alkaline, but if this environment were neutralized, the steel would tend to rust. As it was readily assumable that the alkali of the concrete would gradually be neutralized from the surface inward by penetration of carbon dioxide gas in the atmosphere, the fractured surfaces of all of the specimens tested were examined by application of phenolphthalein reagent. This examination showed there was no rust to be seen when concrete in contact with steel was colored red while rusting had occurred without fail when the concrete in contact did not become colored. Table 2 shows that after 20 years the steel was mainly rusted in parts where compaction of concrete was inadequate and neutralization had progressed deep into the interior of the concrete at such parts.

Estimation of Time of Rusting of Steel in Reinforced Concrete: Judging from the above, even should

Table 2. *Rusting of steel in reinforced concrete at 20 years*

No. of type of concrete	Width of concrete prism		
	6 cm	15 cm	60 cm
1	—	No corrosion except for partial rusting at voids caused by poor compaction.	—
2	—	Ditto	—
3	Completely rusted concrete cracked longitudinally by expansion.	Ditto	Approximately 10% of surface of steel covered with red rust. Rusting where honeycombing existed.
4	—	Approximately 30% of surface of steel rusted. Mostly at parts of poor constitution.	—
5	—	Approximately 10% of surface of steel rusted. Mostly at parts of poor constitution.	—
6	—	Completely rusted.	—

Note: indicates no applicable test specimen.

the compaction of concrete be complete, when penetration of carbon dioxide gas reaches the steel, it is thought possible that rust can form at this time, a fact which provides an important basis for evaluation of the life of reinforced concrete.

The average depths of neutralization of 15-cm prisms included in the above-mentioned group of specimens are given in Table 3.

With rich mixes, the concret tends to be dense so that penetration of carbon dioxide gas is lessened and since the content of calcium hydroxide in the concrete is greater, the depth of neutralization is naturally less.

As the above specimens were not adequately compacted, it is assumable that the depth of neutralization would have been less if complete compaction had been obtained.

In the following, theorizing simply with the inclusion of some bold assumptions that for a given concrete the quantity of carbon dioxide gas reaching a depth, x, in a given time is proportionate to $\frac{1}{x}$, then the time, t, required for the depth, x, to be neutralized is $t = kx^2$, with k a constant based on mix proportions and placing practices. Considering water-cement ratio to be 0.60 in normal cases of concrete for buildings, and determining the constant, k, from results of concretes of the same quality as those in the specimens of the before-mentioned tests, $t = 7.2x^2$ (t: years, x: coverage in centimeters) is obtained. This, of sorts, is the equation for estimating life of reinforced concrete. (2)

Table 3. *Concrete mix proportions and depth of neutralization at 20 years*

Mix proportion	Depth of neutralization (cm)
1 : 1 : 2	0.65
1 : 2 : 4	1.4
1 : 3 : 6	3.3
1 : 5 : 10	4.3

2.3 Experiment No. 2 (3)

Since compaction of concrete in the above test had been unsatisfactory, Prof. Shozo Uchida, five years later, began similar tests in which placement of concrete was carried out as perfectly as possible. The results of these tests were extremely good and a similar equation, $t = 167x^2$, was formulated based on these tests. In other words, at the same water-cement ratio, merely the difference in constitution produces a life $167/7.2 \fallingdotseq 23$ times longer showing how much it is necessary to improve the constitution.

3. Test Studies of Neutralization of Concrete

3.1 Test Studies in Taiwan (4)~(9)

In Taiwan, corrosion of steel in reinforced concrete is more rapid than in Japan and the author upon conducting a survey pointed out high temperatures and influence of salt air as external conditions, and poor gradation of sand and use of too much water as internal conditions for this phenomenon. Later, the author planned and directed the making of 15 cm × 15 cm × 30 cm prisms of various mix proportions which were placed in the vicinity of Takao (Kaoshun) Lighthouse and in the city of Taipei upon which 1-year, 4-year and 9-year results were studied.

Table 4. *Tests in Taiwan*

Test location		Takao (Kaoshun)			Taipei			
Test period (yrs.)		1	4	9	1	4	9	19
Depth of neutralization (mm)	Portland cement	1.5–2.5	1.1–3.3	2.5–6.5	0.5	0–0.8	1–3.5	2–9.5
	Blast furnace slag cement	2.0–4.5	1.8–5.3	5.0–14.5	1–2.5	0.8–3.5	1.5–7.5	2.5–6.5*

*Maximum depth 36 mm

The results summarized are as follows:

a. The depths of neutralization of specimens at Takao were greater than those at Taipei, i.e., the rate of neutralization differs with climate.
b. Neutralization was considerably retarded in the case of dry-consistency concrete adequately compacted, i.e., neutralization progresses along voids.
c. Depth of neutralization is increased the greater the water-cement ratio.
d. A comparison of blast furnace slag cement and portland cement showed depth of neutralization of concrete using the former to be about twice that using the latter. This is due to less free $Ca(OH)_2$ in blast furnace slag cement.

These tests in Taiwan were carried out after thorough planning and were conducted on a very large scale. The carefully collected data provided valuable

information for later studies.

However, the specimens at Takao were evidently lost at the end of World War II and only those at Taipei now remain. Measurements of depths of neutralization after 19 years were recently carried out by Chinese engineers (10). It is reported that depths of neutralization have increased and the neutralization of blast furnace slag cement concrete has become extremely irregular.

3.2 Comparative Study of Various Concretes in Relation to Neutralization under Accelerated and Natural Conditions (Part 1) (11)

Outline

These experimental studies were conducted with the purpose of comparing various reinforced concrete specimens neutralized under identical conditions.

Accelerated tests were carried out along with natural exposure tests. The acceleration of neutralization was secured in an apparatus containing 15% carbon dioxide gas. Results of one year of accelerated tests and 4 measurements during $6\frac{1}{2}$ years of natural exposure tests establish the appropriateness of this method of accelerated testing which closely approximate the results obtained from exposure in the atmosphere.

It was also ascertained that use of surface-active agents markedly reduced the rate of neutralization and also that use of these agents in lightweight concrete made it possible to restrict neutralization in this type of concrete to about the same degree as in normal concrete.

Test Specimens

Test specimens were 40 cm × 40 cm × 15 cm in size each having three parallel ϕ — 9 mm steel bars covered with mill scale embedded in it. In order to be able to measure neutralization from the direction of the steel bars only, all surfaces of the specimens other than the surfaces perpendicular to the reinforcing steel were thoroughly coated with an asphalt-based paint. The types of specimens are listed in Table 5.

Method of Testing

The testing room was an air-tight chamber as shown in Fig. 1, into which carbon dioxide gas was directly introduced. The air inside the chamber was agitated with a fan. Regulation of the concentration of carbon dioxide gas was performed manually once every day. Outdoor exposure tests were carried out in the open air on the roof of the building of the Department of Architecture, Faculty of Engineering, University of Tokyo.

Table 5. *Types and general descriptions of test specimens*

Code	Type of concrete	General description
A I	Normal	W/C = 75% } Slump 21 cm, gravel 20 mm
A II	Ditto	W/C = 65% } sand 0.6 mm and under
A III	Ditto	W/C = 55% }
B I	Pozzolanic cement	W/C = 65%, other conditions same as above
C I	Air-entrained	AEA pozzolith } Other conditions
C II	Ditto	AEA vinsol resin } same as A II
D I	Pumicite	Asama pumicite, slump 21 cm, gravel 20 mm, sand 2.5 mm, diotomaceous earth 25 kg/m³
F I	Pumicite air-entrained	AEA pozzolith } Same as D I, no diotomaceous earth
F II	Ditto	AEA vinsol }
G I	Cinder	According to standard mix proportions for pumicite concrete, sand 2.5 mm, gravel 20 mm

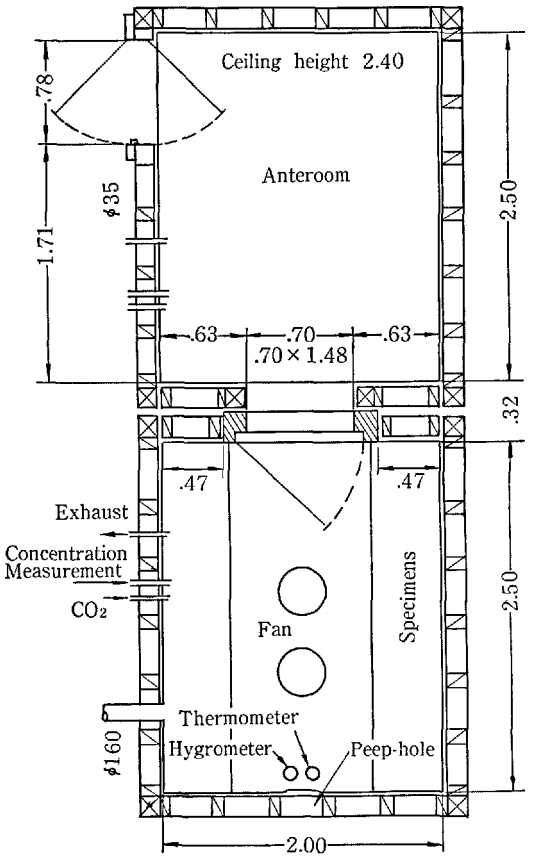

Fig. 1. *Carbon dioxide gas accelerated neutralization test chamber*

Test Results

Measurements were made three times, at 1 month,

Table 6. *Neutralization of specimens in accelerated tests* (1 year)

Code	Depth of neutralization (mm)			Observations
	Max.	Min.	Av.	
A I	30.0	18.0	25.0	Depth of neutralization irregular
A II	23.0	10.0	18.0	Depth of neutralization slightly irregular
A III	15.0	8.0	12.0	Depth of neutralization extremely irregular
B I	25.0	15.0	22.0	Generally uniformly neutralized
C I	10.0	2.0	6.0	Ditto
C II	17.0	5.0	12.0	Ditto
D I	50.0	30.0	40.0	Generally uniformly reutralized, slight alkali remaining
F I	15.0	7.0	12.0	Generally uniformly neutralized
F II	25.0	10.0	17.0	Slightly irregular
G I	50.0	40.0	45.0	Rust formation on reinforcement at neutralized parts

Table 7. *Neutralization of specimens in outdoor natural exposure tests (6 1/2 years)*

Code	Depth of neutralization (mm)			Observations
	Max.	Min.	Av.	
A I	11.0	5.0	7.5	Neutralization progressed along surfaces of gravel, extremely irregular
A II	7.0	2.0	3.0	Slightly irregular
A III	3.0	0.5	1.5	Uniformly neutralized
B I	10.0	3.0	6.2	Neutralization progressed along surfaces of gravel, extremely irregular
C I	3.0	0.5	1.5	Uniformly neutralized
C II	4.0	1.0	1.8	Ditto
D I	19.0	6.0	13.0	Neutralization through aggregate, extremely irregular
F I	9.0	2.0	4.6	Slightly irregular
F II	10.0	4.0	6.2	Slightly irregular, neutralization through aggregate
G I	26.0	7.0	14.2	Extremely irregular, neutralized portion slightly whitened

6 months and 1 year for the accelerated tests, and at 6 months, 1 year and $6\frac{1}{2}$ years for the outdoor tests. The results given here are for 1 year of accelerated tests and $6\frac{1}{2}$ years for the outdoor exposure tests. Tables 6 and 7 give the results of measurement of neutralization. Comparisons of depths of neutralization between accelerated-test specimens and exposure-test specimens are given in Table 8. A study of these comparisons shows the following:

a. Normal concrete is more readily neutralized the greater the water-cement ratio. Specimen AI, especially, showed extremely irregular depth of neutralization indicating the non-uniform constitution of the concrete. It was noticeable that neutralization had progressed along the surfaces of gravel which was probably because the cement paste at the undersides of gravel was more porous than at other parts due to bleeding and other causes.

b. The depth of neutralization of pozzolanic cement concrete was naturally greater than that of portland cement concrete because of less free $Ca(OH)_2$, being one and a half to two times greater. Concrete containing surface-active agents showed extremely small depth of neutralization. This was probably because of smaller water-cement ratios and consequently denser cement paste and also because of dispersion of cement particles. In lightweight aggregate concrete, neutralization was extremely great when diatomaceous earth was contained. Especially, in concrete using coal cinders, the neutralized portions had reached the reinforcement and rust had already formed. It was found that addition of surfactants to lightweight concrete will provide improvements to a level equal to or better than normal concrete.

In considering the acceleration rate in tests using carbon dioxide gas it is generally necessary to know the acceleration rate over the natural exposure tests.

Table 8. *Neutralization ratios of specimens (1-year acceleration, 6 1/2-year natural exposure)*

Type of concrete	Code of concrete compared									
	AI	AII	AIII	BI	CI	CII	DI	FI	FII	GI
AI (Portland cement, normal concrete)		1.39 2.50	2.08 5.00	1.14 1.21	4.16 5.00	2.08 4.17	0.63 0.58	2.08 1.63	1.47 1.21	0.56 0.53
AII (Portland cement, normal concrete)	0.72 0.40		1.50 2.00	0.82 0.48	3.00 2.00	1.50 1.67	0.45 0.23	1.50 0.65	1.06 0.48	0.40 0.21
AIII (Portland cement, normal concrete)	0.48 0.20	0.67 0.50		0.55 0.24	2.00 1.00	1.00 0.83	0.30 0.12	1.00 0.33	0.71 0.24	0.27 0.11
BI (Pozzolanic cement, normal concrete)	0.88 0.83	1.22 2.06	1.83 4.13		3.66 4.13	1.83 3.44	0.55 0.48	1.83 1.35	1.29 1.00	0.49 0.44
CI (Portland cement, AE concrete, Pozzolith)	0.24 0.20	0.33 0.50	0.50 1.00	0.27 0.24		0.50 0.83	0.15 0.12	0.50 0.33	0.35 0.24	0.13 0.11
CII (Portland cement, AE concrete, vinsol resin)	0.48 0.24	0.67 0.60	1.00 1.20	0.55 0.29	2.00 1.20		0.30 0.14	1.00 0.39	0.71 0.29	0.27 0.13
DI (Pumicite, diatomaceous earth)	1.60 1.73	2.22 4.33	3.33 8.66	1.82 2.10	6.67 8.66	3.33 7.22		3.33 2.82	2.35 2.10	0.89 0.92
FI (Pumicite, AE concrete, Pozzolith)	0.48 0.61	0.67 1.53	1.00 3.07	0.55 0.74	2.00 3.07	1.00 2.55	0.30 0.35		0.71 0.74	0.27 0.32
FII (Pumicite, AE concrete, vinsol resin)	0.68 0.83	0.95 2.06	1.42 4.13	0.77 1.00	2.83 4.13	1.42 3.44	0.43 0.48	1.42 1.35		0.38 0.11
GI (Cinder)	1.80 1.90	0.25 4.74	3.75 9.45	2.04 2.29	7.50 9.45	3.75 7.89	1.12 1.09	3.75 3.09	2.65 2.29	

Note: Upper figures neutralization ratios for tests in carbon dioxide chamber. Lower figures for outdoor exposure tests. Examples of comparisons: Depth of neutralization of pumicite concrete (DI) in carbon dioxide is 1.6 times AI, 2.22 times AII, in open air 1.73 times AI, 4.33 times AII, etc.

The relation between the rate of neutralization in air containing 15% carbon dioxide gas adopted for these

tests and that of open air containing 0.02 to 0.05% was thus investigated. In regard to this, there was a formula induced by the author with the assumption that the rate of neutralization is proportionate to the concentration of carbon dioxide gas. This formula may have been appropriate when the concentration was low, but in accelerated tests such as considered, in which the concentration of the gas would be high, the formula was thought to be inapplicable. Interpolating linearly to obtain the results for 2 months from the accelerated test data for 1 month and 6 months and comparing with the results of $6\frac{1}{2}$ years of natural exposure a good approximation can be seen. In other words, in these accelerated tests with carbon dioxide gas, it was found there was an acceleration of approximately 40 times expressed in terms of the period required for neutralization. Since natural exposure tests of this kind require a long time the practical significance of accelerated tests is great.

3.3 Comparative Study of Various Concretes in Relation to Neutralization under Accelerated and Natural Conditions (Part 2) (12)

Outline

Following on the tests conducted as described in 3.2, various concretes were similarly tested for neutralization under identical conditions and compared. This time, the condition of exposure indoors was added and neutralization of concrete under the three conditions of accelerated tests, outdoor tests and indoor tests were measured.

The accelerated tests were conducted for 6 months and the outdoor and indoor tests for 5 years. The results were generally the same as those described in 3.2. It was noted that there was considerable difference in neutralization occurring indoors and outdoors and the ratios of depth of neutralization for the different conditions were studied.

Table 9. *Comparison between estimated and natural exposure value of neutralization*

Type of concrete	AI	AII	AIII	BI	CI	CII	DI	FI	FII	GI
Estimated value of neutralization at 2 month acceleration	5.6	4.1	2.2	8.6	1.8	2.7	13.2	4.0	7.0	12.6
Neutralization at 6 1/2 years of outdoor exposure	7.5	3.0	1.5	6.2	1.5	1.8	13.0	4.6	6.2	12.5

Materials

Four types of cement were used. These were normal portland cement, high-early strength portland cement, blast furnace slag cement and pozzolanic cement.

The aggregates used were river sand, volcanic pumicite and coal cinders. Among other materials, 4 types of surface-active agents, Pozzolith, Lissapol, Vinsol Resin and Darex were used, each in standard amounts.

Test Specimens

The test specimens were 15 cm × 15 cm × 30 cm prisms each with a ϕ–13 mm steel bar embedded in the center. Mill scale was removed from the steel bars with sandpaper after which the bars were thoroughly washed with hydrochloric acid and again with water before they were embedded. The varieties of specimens tested are given in Table 10. The specimens were cured for 4 weeks in moist sand and for another 4 weeks indoors in the air. The tests began from the age of 8 weeks. To measure neutralization only from the top and bottom surfaces of the concrete placed, polyvinyl chloride paint was applied to the sides of the specimens to prevent neutralization from these two surfaces.

Methods of Testing

a. Outdoor Exposure: Rooftop of Building. No. 1,

Table 10. *Types of specimens*

No.	Code	Type of concrete	General description
1	A	Normal (wet mix)	Cement content 300kg, W/C = 70% } Slump 21cm
2	B	Ditto	Cement content 350kg, W/C = 60% } Slump 21cm
3	C	Ditto	Cement content 400kg, W/C = 50% } Slump 21cm
4	D	Normal (dry mix)	Cement content 350kg, W/C = 60%, Slump 10cm
5	E	Blast furnace slag cement	Cement content 350kg, W/C = 60%, Slump 21cm
6	F	Pozzolanic cement	Cement content 350kg, W/C = 60%, Slump 21cm
7	G	High-early strength cement	Cement content 350kg, W/C = 60%, Slump 21cm
8	H	AE	Pozzolith 5.3g (per 1kg cement) } Cement content 350kg, Slump 21cm
9	I	Ditto	Lissapol-N 0.4cc (per 1kg cement) } Cement content 350kg, Slump 21cm
10	J	Ditto	Vinsol resin 0.6cc (per 1kg cement) } Cement content 350kg, Slump 21cm
11	K	Ditto	Darex 0.4cc (per 1kg cement) } Cement content 350kg, Slump 21cm
12	L	Light-weight	No air-entraining agent
13	N	Light-weight, AE	Pozzolith No. 5 } Cement content 350kg, Asama pumicite, Slump 21cm, equal volumes of fine and coarse aggregates
14	O	Ditto	Lissapol-N } Cement content 350kg, Asama pumicite, Slump 21cm, equal volumes of fine and coarse aggregates
15	P	Ditto	Vinsol resin } Cement content 350kg, Asama pumicite, Slump 21cm, equal volumes of fine and coarse aggregates
16	Q	Ditto	Darex } Cement content 350kg, Asama pumicite, Slump 21cm, equal volumes of fine and coarse aggregates
17	R	Cinder	Cement content 320kg, lime 40kg } Slump 21cm, equal volumes of fine and coarse aggregates
18	S	Ditto	Cement content 350kg, no lime } Slump 21cm, equal volumes of fine and coarse aggregates
19	T	AE cinder	Pozzolith No. 5 added to Mix R } Slump 21cm
20	U	Ditto	Lissapol-N added to Mix R } Slump 21cm
21	V	Cinder (water-proofed)	1:3 and 1:2 (0–4cm) finish coat of waterproof mortar on Mix S

Department of Architecture, Faculty of Engineering, University of Tokyo. (Concentration of carbon dioxide gas: 0.02–0.03%)

b. Indoor Exposure: Interior of room facing inner court of Building No.1, Faculty of Engineering, University of Tokyo, not too frequently entered by people. (Concentration of carbon dioxide gas: 0.04–0.05%)

c. Accelerated Carbon Dioxide Gas Test: Accelerated neutralization test chamber described in 3.2, 15% carbon dioxide gas concentration, 85% humidity, normal temperature.

Test Results

The depths of neutralization at 6 months of acceleration were as shown in Table 11. The results of outdoor and indoor exposure for 5 years are given in Table 12. The results of accelerated tests as clearly shown in the table indicate that:

a. The general trend of the extent of resistance to neutralization was approximately the same as the results described in 3.2.

b. Concretes containing surface-active agents, both normal and lightweight, had slow neutralization rates indicating their high resistance to neutralization. There were differences according to the types of surface-active agents, those with high dispersing effects producing better results than those which were simple foaming agents.

c. There were no differences in depths of neutralization between surfaces which were at top and bottom of concrete at the time of placement. This was because the height of the placement was not very great.

The comparison of rate of neutralization caused by outdoor and indoor exposure is as given in Table 13. The following may be said from the results:

a. The neutralization rate of various normal concretes using river sand and gravel as aggregates were approximately the same for outdoor, indoor and accelerated tests. On the other hand, in the case of lightweight concrete, the rate was approximately the same for indoor and accelerated tests whereas in outdoor testing there were many cases where the rates were higher. This is considered to be because lightweight concrete is porous and absorptive, and therefore, in the case of these tests in which no cover was provided on the concrete against the outdoor exposure, such things as the leaching of lime from the concrete by rainwater were disadvantageous in respect to neutralization.

b. From the above, it can be said that in the case of normal concrete, the accelerated tests using carbon dioxide gas agree well with both outdoor and indoor tests, but in the case of lightweight concrete the accelerated test agrees well with indoor tests, but not always with outdoor exposure tests. However, with lightweight concrete containing a surface-active agent with good dispersing qualities, the results of carbon dioxide gas accelerated tests agree well with both outdoor and indoor test results.

c. Throughout the three types of tests, the concretes in order from the slowest rate of neutralization were normal concrete containing a surface-active agent, high-early strength cement concrete, normal concrete for dry consistency, normal concrete, lightweight concrete with a surface-active agent, blast furnace slag cement concrete and pozzolanic cement concrete.

d. In general, blended cements are neutralized more quickly than portland cements. Although the ratio of neutralization depth differs according to tests, it is roughly between 1.1 and 2.3 depending on the type of cement and the various conditions of the concrete.

In comparing neutralization from outdoor and indoor exposure, it was found the neutralization indoors had progressed more than that outdoors, being 1.0 to 3.0 times deeper. This is because of the influence of rainwater in the case of outdoor natural exposure in which the voids in the concrete are filled with water making it difficult for carbon dioxide gas to penetrate the concrete, and also because the concentration of carbon dioxide gas indoors is slightly higher. This tendency has been found in investigations of neutralization in actual buildings.

From the above, the following conclusions are obtained:

Table 11. *Depth of neutralization at 6 months acceleration*

Code	Type of concrete	Depth of neutralization (mm)		
		Surface A	Surface B	Average
A	Normal	10	17	13.5
B	Ditto	8	12	10.0
C	Ditto	4	3	3.5
D	Ditto (dry mix)	2	3	2.5
E	Slag cement	10	12	11.0
F	Pozzolanic cement	15	10	12.5
G	High-early strength cement	5	3	4.0
H	Normal, AE	2	1	1.5
I	Ditto	2	4	3.0
J	Ditto	8	5	6.5
K	Ditto	3	5	4.0
L	Lightweight	30	20	25.0
N	Lightweight, AE	10	10	10.0
O	Ditto	10	15	12.5
P	Ditto	20	15	17.5
Q	Ditto	15	20	17.5
R	Cinder	25	35	30.0
S	Ditto	25	30	27.5
T	Cinder, AE	25	15	20.0
U	Ditto	20	30	25.0
V	Waterproof	3*	5*	4.0*

*Value not including thickness of waterproof mortar.

Table 12. *Results of 5 years outdoor and indoor exposure tests*

Code	Type of concrete	Surface measured*	Depth of neutralization at 5 yrs. of outdoor Exposure (mm)			Depth of neutralization at 5 yrs. of indoor Exposure (mm)			Ratio of indoor to outdoor depth of neutralization
			Max.	Min.	Av. (Av. of 2 surfaces)	Max.	Min.	Av. (Av. of 2 surfaces)	
A	Normal	Top	6.0	1.5	3.5 (2.8)	12.0	4.0	9.0 (7.8)	2.6 (2.9)**
		Bottom	5.5	0.5	2.0	9.0	5.0	6.5	3.2
B	Ditto	Top	5.5	1.0	3.4 (2.6)	12.0	4.0	9.6 (6.9)	2.8 (2.6)
		Bottom	3.5	0.5	1.8	9.0	0.5	4.2	2.3
C	Ditto	Top	5.0	1.0	2.3 (1.6)	8.0	0.5	4.1 (3.8)	1.8 (2.4)
		Bottom	5.0	0.5	0.9	5.0	2.0	3.5	3.8
D	Normal (dry mix)	Top	3.0	0.5	1.2 (1.6)	8.5	1.0	4.1 (4.2)	3.4 (2.6)
		Bottom	4.0	1.0	1.0	6.0	0.5	4.2	2.2
E	Blast furnace slag cement	Top	8.5	2.0	3.5 (2.9)	15.0	6.5	9.2 (8.7)	2.6 (3.0)
		Bottom	6.0	1.0	2.3	11.0	5.0	8.1	3.5
F	Pozzolanic cement	Top	10.5	5.0	3.7 (3.4)	17.0	5.0	10.5 (9.9)	2.8 (2.9)
		Bottom	8.5	2.0	3.1	10.5	4.0	9.2	3.0
G	High-early strength cement	Top	4.0	1.0	1.0 (1.5)	10.0	1.0	5.4 (4.6)	2.8 (3.1)
		Bottom	3.0	0.5	1.1	9.0	0.5	3.8	3.5
H	Normal, AE (Pozzolith)	Top	3.0	0.5	1.1 (1.1)	8.0	1.0	4.2 (2.7)	3.8 (2.4)
		Bottom	3.0	0.5	1.1	3.0	0.5	1.1	1.0
I	Ditto (Lissapol)	Top	4.0	1.0	1.9 (1.5)	8.0	0.5	4.6 (3.3)	2.4 (2.1)
		Bottom	3.0	0.5	1.1	5.0	0.5	1.9	1.7
J	Ditto (Vinsol)	Top	3.0	1.0	1.9 (1.8)	9.0	4.0	6.5 (5.3)	3.4 (2.9)
		Bottom	5.0	0.5	1.7	13.0	2.0	4.1	2.4
K	Ditto (Darex)	Top	4.0	1.9	1.9 (1.7)	5.0	2.0	4.2 (3.3)	2.2 (1.9)
		Bottom	4.0	1.9	1.5	6.0	0.5	2.3	1.5
L	Lightweight	Top	16.0	4.0	8.5 (9.5)	25.0	10.0	16.3 (15.8)	1.9 (1.7)
		Bottom	18.0	5.0	10.5	20.5	3.5	15.3	1.5
N	Lightweight, AE (Pozzolith)	Top	5.0	1.0	2.7 (2.7)	18.0	5.0	7.5 (7.1)	2.8 (2.6)
		Bottom	6.0	1.0	2.7	15.0	3.0	6.7	2.5
O	Ditto (Lissapol)	Top	12.0	5.0	8.0 (5.2)	17.0	5.5	9.7 (7.7)	1.2 (1.7)
		Bottom	5.0	1.0	2.3	18.0	4.0	8.7	3.3
P	Ditto (Vinsol)	Top	13.0	4.0	8.3 (7.4)	20.0	6.0	11.3 (10.7)	1.4 (1.5)
		Bottom	12.0	1.5	6.2	19.5	8.5	10.1	1.6
Q	Ditto (Darex)	Top	10.0	4.0	7.4 (8.3)	22.0	7.5	9.7 (9.5)	1.3 (1.1)
		Bottom	13.0	6.0	9.2	15.0	4.0	9.3	1.0
R	Cinder (lime)	Top	34.0	8.0	21.7 (20.3)	26.0	20.5	23.0 (20.9)	1.1 (1.0)
		Bottom	36.0	1.0	18.9	27.0	15.0	18.8	1.0
S	Ditto (plain)	Top	25.0	3.0	15.0 (13.5)	25.0	16.0	20.8 (17.9)	1.4 (1.3)
		Bottom	36.0	1.0	11.9	20.0	11.0	15.0	1.3
T	Ditto (Pozzolith)	Top	22.0	2.5	6.5 (6.8)	19.0	12.0	14.8 (16.8)	2.3 (2.5)
		Bottom	20.0	3.0	7.0	23.0	18.0	18.8	2.7
U	Ditto (Lissapol)	Top	16.0	7.0	11.6 (10.3)	20.0	7.0	16.4 (18.6)	1.4 (1.8)
		Bottom	15.0	5.0	9.6	26.0	13.0	20.8	2.2

* "Top" and "Bottom" indicate top and bottom surfaces respectively at time of concrete placement.
**Figures in ( ) indicate ratio of average of two surfaces.

a. In normal concrete, there is less tendency of neutralization the lower the water-cement ratio and the higher the cement content.

b. Surface-active agents for concrete markedly reduce the rate of neutralization. However, the effect will differ according to the type of agent, the results being better the higher the dispersing action.

c. Neutralization occurs more rapidly with blended cements than with portland cements. The ratio of the depth of neutralization differs considerably according to the variety of cement and the conditions under which the cement is used.

Table 13. *Neutralization ratios*

Type of concrete	Test		
	Outdoor (5 yrs.)	Indoor (5 yrs.)	Accelerated (6 mos.)
Normal	1.0	1.0	1.0
Ditto (dry mix)	0.62	0.61	(0.25)
Blast furnace slag cement	1.11	1.26	1.10
Pozzolanic cement	1.31	1.44	1.25
High-early strength cement	0.58	0.67	0.40
Normal, AE (Pozzolith)	0.42	0.39	(0.15)
Normal, AE (Lissapol)	0.58	0.48	0.30
Normal, AE (Vinsol)	0.69	0.77	0.65
Normal, AE (Darex)	0.65	0.48	0.40
Lightweight	(3.65)	2.29	2.50
Ditto, AE (Pozzolith)	1.04	1.03	1.00
Ditto, AE (Lissapol)	2.00	1.26	1.25
Ditto, AE (Vinsol)	(2.85)	1.55	1.75
Ditto, AE (Darex)	(3.19)	1.38	1.75
Cinder (lime)	(7.80)	3.03	3.00
Cinder	(5.20)	2.59	2.75
Ditto (Pozzolith)	2.62	2.43	2.00
Ditto (Lissapol)	(3.96)	2.69	2.50

Table 14. *Types of concrete*

	Unit cement content (kg/m³)	Fly ash (kg/m³)	Water reducing agent	W/C (%)	Slump (cm)
A-1	350	0	None	57	15
B-1	350	50	None	60	15
C-1	320	50	None	55	8
D-1	320	50	None	60	15
A-2	350	0	Used	52	15
B-2	350	50	Used	55	15
C-2	320	50	Used	50	8
D-2	320	50	Used	55	15

d. The neutralization of plain lightweight concrete is rapid, but when surface-active agents are used, the resistance is greatly improved. The surfactants are better the higher the dispersing qualities.

e. The neutralization of cinder concrete is rapid. Considerable improvement can be obtained by use of a dispersing agent, but even this is not sufficient. Also, there is fear of corrosion of reinforcing steel from sulphur compounds contained in the aggregate.

f. The neutralization ratios of various concretes under the three conditions, acceleration, natural exposure and deposit indoors, roughly approximate each other in the case of normal concrete, but with lightweight concrete, the ratio is somewhat different for natural exposure.

g. In the case of natural exposure, neutralization is more rapid indoors than outdoors.

3.4 Tests of Influence of Fly Ash on Neutralization of Lightweight Aggregate Concrete (13)

Outline

The poor workability of lightweight concrete can be improved by the use of fly ash. However, it is conceivable the calcium hydroxide produced by the hydration of cement will react with the fly ash to form an insoluble compound. The tests conducted were for the purpose of studying this point. It was found that the use of a water-reducing agent along with the fly ash would result in neutralization of roughly the same extent as lightweight concrete without fly ash, but from the viewpoint of durability it is desirable to use a water-reducing agent alone for the improvement of workability of lightweight concrete.

Test Specimens

The specimens were 15 cm × 15 cm × 30 cm prisms with ϕ–13 mm polished steel bars embedded at a depth to obtain a 3-cm coverage. The concretes were as shown in Table 14. Normal portland cement was used as cement, Asama natural pumicite as lightweight aggregate both fine and coarse, and Pozzolith as a water-reducing agent. The specimens were cured for 2 weeks in water after which they were air-cured to the ages of 4 and 13 weeks.

Method of Testing

As described previously, measurements were made at 1 month and 6 months of accelerated testing with carbon dioxide gas and at 4 years of outdoor and indoor testing.

Test Results

The test results are shown in Tables 15 and 16. These tables give the results of 4 years of natural outdoor exposure, 4 years of deposit indoors, 1 month and 6 months of acceleration. The neutralization ratios obtained from the study of these data are given in Table 17, while the comparison by condition in order to see the difference according to conditions of the test is shown in Table 18. As is clearly seen from the

Table 15. *Depth of neutralization*

(Unit : mm)

Code	1-Month acceleration						6-Month acceleration					
	4-week curing			13-week curing			4-week curing			13-week curing		
	Max.	Min.	Av.	Max.	Min.	Av.	Max.	Min.	Av.	Max.	Min.	Av.
A-1	6	0.5	3	5	1	3	8	2	5	8	3	5
B-1	7	2	4	7	1	4	9	3	6	12	4	9
C-1	8	0.5	5	8	2	6	10	2	8	20	5	15
D-1	9	2	5	9	2	7	12	3	8	15	3	12
A-2	4	0.5	2	5	0.5	2	5	1	3	6	1	3
B-2	5	0.5	2	5	0.5	3	6	1	3	7	1	5
C-2	6	0.5	4	7	1	5	8	1	5	10	2	8
D-2	6	0.5	4	7	1	5	7	1	6	10	2	8

Table 16. *Depth of neutralization*

(Unit: mm)

Code	Type of concrete	Outdoor exposure (4 yrs.)				Indoor deposit (4 yrs.)			
		Max.	Min.	Av.		Max.	Min.	Av.	
A-1	Cement 350kg, plain, no fly ash	12.0 9.0	2.0 1.5	6.7 4.1	5.4	20.0 15.0	10.0 8.0	13.2 11.8	12.5
B-1	Cement 350kg, plain, fly ash 50kg	16.0 12.0	1.0 2.0	6.8 4.5	5.7	17.0 25.0	11.0 5.0	13.2 13.2	13.2
C-1	Cement 320kg, plain, fly ash 50kg	13.0 20.0	2.5 3.0	10.4 8.2	9.3	22.0 18.0	11.0 10.0	15.4 14.1	14.8
D-1	Cement 320kg, plain, fly ash 50kg	28.0 21.0	2.5 2.0	9.5 10.9	10.2	15.0 19.0	11.0 8.0	13.6 13.6	13.6
A-2	Cement 350kg, dispersing agent, no fly ash	4.0 5.0	1.0 1.0	2.6 2.3	2.5	14.0 12.0	7.0 5.0	10.5 9.2	9.9
B-2	Cement 350kg, dispersing agent, fly ash 50kg	5.0 10.0	2.0 1.0	3.2 5.0	4.1	19.0 14.0	7.0 7.0	13.6 9.5	11.6
C-2	Cement 320kg, dispersing agent, fly ash 50kg	15.0 15.0	2.0 3.0	6.3 9.5	7.9	16.0 16.0	9.0 8.0	13.4 10.9	12.2
D-2	Cement 320kg, dispersing agent, fly ash 50kg	8.0 11.0	1.0 1.0	7.8 4.5	6.2	13.0 17.0	8.0 8.0	10.9 12.3	11.6

Note: All specimens measured for neutralization from side surface perpendicular to direction of concrete placement.

Table 17. *Ratios to normal concrete of depths of neutralization*

Test condition	A-1	B-1	C-1	D-1	A-2	B-2	C-2	D-2
Outdoor exposure (4 yrs)	1.0	1.1	1.7	1.9	0.5	0.8	1.5	1.2
Indoor deposit (4 yrs)	1.0	1.1	1.2	1.1	0.8	0.9	1.0	0.9
Acceleration (18 mos.) Complete neutralization	1.0	1.3	1.4	2.3	0.8	0.9	0.9	1.1
Acceleration (18 mos.) Neutralization in progress	1.0	1.3	1.4	2.0	1.0	1.0	1.1	1.2
Acceleration (6 mos.)	1.0	1.2	1.6	1.6	0.6	0.6	1.0	1.2
Average	1.0	1.2	1.5	1.8	0.7	0.8	1.1	1.1

Table 18. *Ratios of depths of neutralization according to differences in test conditions*

Test condition	A-1	B-1	C-1	D-1	A-2	B-2	C-2	D-2	Av.
Outdoor exposure (4 yrs)	1.0	1.0	1.0	1.0	1.0	1.0	1.0	1.0	1.0
Indoor deposit (4 yrs)	2.3	2.3	1.6	1.3	3.9	2.8	1.5	1.9	2.2
Acceleration (18 mos) Complete neutralization	2.2	2.7	1.8	2.7	3.7	2.7	1.4	2.1	2.4
Acceleration (18 mos) Neutralization in progress	4.0	4.8	3.3	4.3	8.9	5.3	3.0	4.2	4.7
Acceleration (6 mos)	0.9	1.1	0.9	0.8	1.2	0.7	0.6	1.0	0.9

results:

a. When fly ash is added without the use together with a water-reducing agent, the rate of neutralization is 1.1 to 2.3 times more rapid than plain lightweight concrete for all conditions.

b. When both fly ash and a water-reducing agent are added, the rate of neutralization is slightly slower. This indicates the beneficial effect of the water-reducing agent. However, when cement content is reduced, the neutralization is great.

c. Compared with the case of addition of a water-reducing agent only, the addition of fly ash with the water-reducing agent results in more rapid neutralization under all conditions.

d. Parenthetically, when fly ash is to be used, the use of a water-reducing agent together with the fly-ash will slow down neutralization to an extent.

e. The depths of neutralization for 6 months of acceleration and 4 years of outdoor exposure are about the same. Therefore, the acceleration factor for lightweight concrete is 8. The neutralization of specimens left standing indoors is more rapid than those subjected to outdoor exposure, being approximately 2.2 times faster.

3.5 Relation between the Factors of Concrete Materials and Mix Proportions and the Rate of Neutralization (14)

Various combinations of factors are now studied centered about the experiments of the author.

Variety of Cement and Neutralization

As contemplated in 3.1 to 3.4, the rate of neutralization differs considerably between portland cement and blended cement. The comparison of neutralization of these cements as obtained from various test results is as shown in Table 19. When blended cement or a pozzolanic admixture is used, the neutralization is rapid so that for the improvement of durability of reinforced concrete structures, portland cement should be used. Of portland cements, high-early strength portland cement produces slower neutralization than normal portland cement for even better results.

Variety of Aggregate and Neutralization

Of the aggregates used for concrete, normal river sand, river gravel and crushed stone are dense and hard so that they are less air-permeable than the cement paste and neutralization will therefore progress through the paste. However, in the case of lightweight aggregate for lightweight concrete, the aggregate itself has large voids and the permeability is great so that neutralization will progress through the aggregate also. Therefore, neutralization is generally more rapid than in normal concrete. The test results may be summarized as shown in Table 20. It is seen that neutralization of lightweight aggregate concrete is extremely more rapid than normal concrete and that the use of pozzolanic admixtures is of great disadvantage from the standpoint of durability. However, this neutralization can be slowed down by the use of water-reducing agents and air-entraining agents.

Table 19. *Scopes and averages of depths of neutralization ratios using mixed cement*

Test condition	Portland cement		Blast furnace slag cement		Pozzolanic cement	Fly ash mixture (Cement replacement 15–20%)
	Normal	High-early strength	Slag (30–40%)	Slag (60%)		
Carbon dioxide gas acceleration	1	0.4	1.1–2.3 1.8	2.1–2.2 2.2	1.2–2.8 1.9	1.6–2.8 2.3
Outdoor exposure	1	0.6	1.1	—	1.3–2.1 1.7	1.9–2.4 2.2
Indoor deposit	1	0.7	1.3	—	1.4	1.1–1.2 1.2
Average	1	0.6	1.4	2.2	1.7	1.9

Types of Surface-Active Agents and Neutralization

There are various advantages of using surfactants such as airentraining agents and water-reducing agents. The water-cement ratio is reduced, cement particles are dispersed and dense concrete is obtained to slow down neutralization so that the use of a surface-active agent would be highly beneficial in improving the durability of reinforced concrete buildings. A gross summarization of these studies would be somewhat as given in Table 21. In other words, when a surface-active agent is used, the neutralization of normal concrete and lightweight concrete both become slower by about the same ratio. Compared with plain concretes, it may be considered the ratio is 0.6 for air-entraining agents and 0.4 for waterreducing agents. Therefore, if a high-performance water-reducing agent is used, concrete of good durability can be obtained even with reduction in cement content.

Water-Cement Ratio and Neutralization

In general, neutralization of concrete is slower the lower the water-cement ratio. This is because the cement paste is more dense. This is clearly seen from Tables 22 and 23 which summarize the relation between water-cement ratio and neutralization ratio.

The author, from the tests described in 2.1 and from some amount of theoretical considerations, has induced the following formula for progress of neutralization. (2)

Table 20. *Scopes and averages of depths of neutralization ratios of lightweight concrete (Cement used; normal portland)*

Test condition	Normal concrete (plain)	Lightweight concrete (Pumicite fine and coarse aggregate)			
		Pumicite, plain or with diotomaceous earth	Cinder, plain	Pumicite, AEA	Pumicite, dispersing agent
Carbon dioxide gas acceleration	1	2.2–4.0 2.9	2.5–4.0 3.1	0.9–2.0 1.6	0.7–1.5 1.1
Outdoor exposure	1	3.0–4.3 3.6	3.0–5.2 4.3	1.5–3.2 2.5	1.0–1.5 1.2
Indoor deposit	1	2.3	2.6	1.4	1.0
Average	1	2.9	3.2	1.8	1.1
			River sand, pumicite gravel, AEA 0.8		

Table 21. *Scopes and averages of depths of neutralization ratios using surface-active agents*
(Using normal portland cement and no other additives)

Test condition	Plain concrete*	Normal concrete		Pumicite fine and coarse aggregate concrete	
		AEA	Dispersing agent	AEA	Dispersing agent
Carbon dioxide gas acceleration	1	0.3–0.7 0.6	0.2–0.3 0.3	0.4–0.7 0.6	0.3–0.6 0.4
Outdoor exposure	1	0.6–0.8 0.7	0.3–0.5 0.4	0.5–0.9 0.6	0.3–0.5 0.4
Indoor deposit	1	0.5–0.8 0.6	0.4	0.5–0.7 0.6	0.4–0.8** 0.6
Average	1	0.6	0.4	0.6	0.4

* "Plain concrete" indicates no additives in controls for respective concretes.
**This figure not included for calculation of average because of extreme discrepancy with other values.

Table 22. *Ratios of depths of neutralization according to water-cement ratios*
(Normal concrete, depths of neutralization in mm, figures in parentheses denote ratio to water-cement ratio of 60%)

Type of concrete		Carbon dioxide gas acceleration		Outdoor exposure	
W/C	Admixture	6 months	1 year	1 year	6-1/2 yrs
0.69	None	20 (1.3)	25 (1.4)	4 (2.0)	7.5 (2.5)
0.60	None	15 (1)	18 (1)	2 (1)	3.0 (1)
0.50	None	10 (0.7)	12 (0.7)	1 (0.5)	1.5 (0.5)
0.55	AEA	10 (0.7)	12 (0.7)	1.5 (0.8)	1.8 (0.6)

Note: Cases of use of dispersing agents not included.

Table 23. *Ratios of depths of neutralization according to water-cement ratios*
(Normal concrete, depths of neutralization in mm, figures in parentheses denote ratio to water-cement ratio of 60%)

Type of concrete		Test condition		
W/C	Admixture	6 mos. carbon dioxide gas acceleration	5 yrs. outdoor exposure	5 yrs. indoor deposit
0.71	None	13.5 (1.4)	2.8 (1.1)	7.8 (1.1)
0.60	None	10.0 (1)	2.6 (1)	6.9 (1)
0.52	None	3.5 (0.4)	1.6 (0.6)	3.8 (0.6)
0.54	AEA	3.0(0.3)	1.5 (0.6)	3.3 (0.5)
0.55	AEA	6.5 (0.7)	1.8 (0.7)	5.3 (0.8)
0.54	AEA	4.0 (0.4)	1.7 (0.7)	3.3 (0.5)

Note: Cases of use of dispersing agents not included.

$$t = kx^2$$

where

$$k = \frac{0.3(1.15 + 3w)}{(w - 0.25)^2}$$

for plain concrete using portland cement and normal aggregates,

w: water-cement ratio
t: period of time (years)
x: depth of neutralization (cm)

Ratio of Neutralization according to Factor of Concrete

The effects on neutralization of various materials used in concrete obtained from the tests of 3.2 to 3.4 and expressed as ratios are as shown in Table 24.

Introducing these in the equation in 3.5, the following is obtained:

$$t = \frac{k}{R^2}x^2$$

where

$R = r_c \times r_a \times r_s$ (see Table 24)

This may be used to calculate the depths of neutralization and the periods required for neutralization of various concretes.

Table 24. *Depth of neutralization ratio by factor*

Type of cement	Portland cement		Blast furnace slag cement		Pozzolanic cement	Fly ash cement (Fly ash 20%)
	Normal	High-early strength	Slag 30–40%	Slag 60%		
(r_c)	1	0.6	1.4	2.2	1.7	1.9
Type of aggregate	River sand, river gravel		River sand, pumicite gravel		Pumicite sand, pumicite gravel	Cinder (fine, coarse)
(r_a)	1		1.2		2.9	3.3
Surface-active agent	Plain		AEA		Dispersing agent	
(r_s)	1		0.6		0.4	

4. Investigations of Reinforced Concrete Buildings

4.1 Case No. 1 (A Bank Building) (14)

The building in this investigation was well built with adequately thick surface finish and appreciately great coverage provided for the reinforcing steel. A period of 37 years had elapsed since completion during which time maintenance and upkeep of the building had been satisfactory. The concrete had been proportioned by volume at a ratio of about 1: 2: 3.3 and had been of a wet consistency causing a great amount of laitance to occur at construction joints.

Table 25. *Outline of investigations*

Case investigated		1	2	3	4	5
Outline of building	Use	Bank	Apartment house	Elementary school	Office	(Various)
	Scale	Reinforced concrete, 5 stories, 1 basement	Reinforced concrete, 3 stories, 1 basement	Reinforced concrete, 3 stories	Reinforced concrete, 3 stories, 1 basement	22 buildings
	Floor area m²	4451	446	1246	3580	
	Location	Tokyo	Tokyo	Yamagata	Hokkaido	Tokyo
	Completion	1921	1924	1937	1938	1912–1940
Year of investigation		1958	1958	1947	1959	1950–1952
Years from completion		37	34	10	21	10–38
Portions of buildings investigated		Entire building	Basement	Above ground level	Entire building	Columns, walls
Investigator		K. Kishitani	K. Kishitani	M. Hamada	T. Nishi, T. Koh	S. Takenouchi
Remarks		Concrete containing silicate admixture $F_c = 200 - 300$ kg/cm² Mix ratio by volume, 1:2:3.3 Good workmanship in finish	$F_c = 320$ kg/cm² Adjacent to river estuary	Lean mix containing pozzolanic cement Structural strength inadequate Dimensions of members less than designed Heavily snowbound	Use of building frequently altered	Various buildings subjected to fire damage

The depths of neutralization of concrete at various parts of this building were as are shown in Table 26. The summarization according to thickness of finish is given in Fig. 2. Generally speaking, columns, partition walls and interior surfaces of outer walls showed less neutralization the greater the thickness of the finish. The considerable scatter in the values is thought to be due to the quality of surface finish (for example, whether or not painting had been performed), the quality of concrete, and the conditions under which the building was used.

The exterior surfaces of outer walls were covered with polished granite slabs so that the thickness of the finish was not less than 30 mm. In this case, the depth of neutralization was only 10 mm regardless of the thickness so that it may be said the finish was good for durability. However, wherever neutralization had progressed to reinforcing steel, the steel in almost all cases showed formation of rust.

4.2 Case No. 2 (The Basement of an Apartment House) (14)

The building investigated had a road in front and a levee wall of the Sumida River estuary approximately 1.5 meters behind the back wall. There was evidence of river water (salt water) having entered the basement during floods.

The depth of neutralization of the interior concrete was of an ordinary degree as seen from a comparison of the measurement values in Table 26 with an average value of about 21 mm* for a period after completion of approximately 34 years. No rusting at all could be observed on the steel in concrete above ground, but in the basement, the corrosion of steel in columns and ends of undersides of beams was severe with large cracks formed in the concrete coverage. Upon measuring the salt content in the finish plaster and concrete, it was found to be extremely high as shown in Table 27. In general, the allowable limits for salt contained in concrete materials are 0.04% for water and 0.01% for sand. This converted to salt in oven dry concrete is 0.004%. Therefore, it was seen in the basement of this building that although the neutralization was of a normal extent, there was severe rusting of reinforcing steel due to salt.

The thickness of the plaster coating was from 10 to 20 mm which is considered to have been relatively ineffective in preventing neutralization of concrete.

4.3 Case No. 3 (An Elementary School Building)

The building in this case was constructed in a snowy region and already after 10 years from construction the concrete had been neutralized to depths of 50 to 90 mm. The mortar on the outside was loosened, the reinforcing steel was rusted to push the concrete cover outwards and cracks could be seen everywhere. However, the main reinforcement in the frame, even where the concrete was almost entirely neutralized, was not rusted on the inner side. The reasons for such extremely rapid neutralization are thought to be the following:

1) Use of pozzolanic cement in the concrete mix
2) Extreme infiltration of water from snowfall

*$t = 7.2x^2$; when $t = 34$ years then $x = 2.1$ cm.

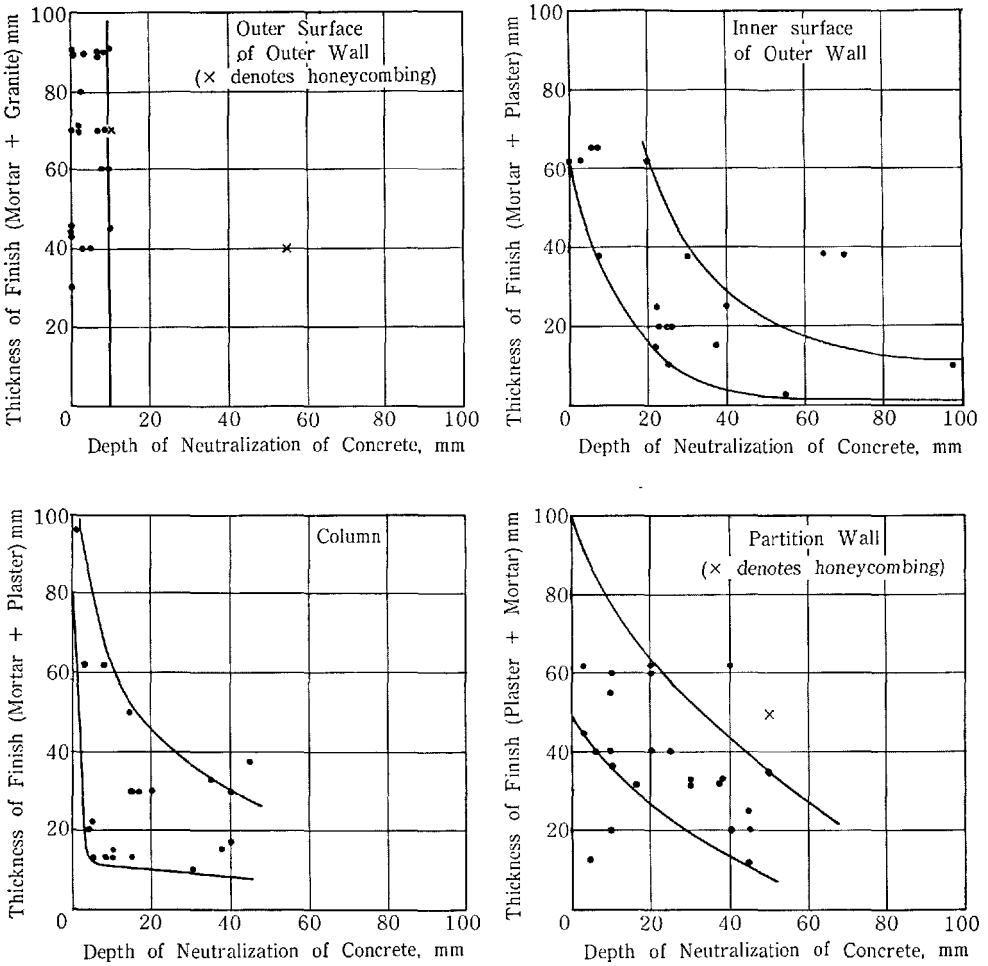

Fig. 2. *Relation between depth of neutralization of concrete and thickness of finish*

4.4 Case No. 4 (An Office Building) (15)

The building in this case had been constructed in Hokkaido, an area of cold climate.

The purposes for which the rooms in the building had been used had been frequently changed during the 21 years from completion. The average depth of neutralization was 34.5 mm with averages of the various rooms ranging between 21.7 mm and 47.5 mm.

The depths of neutralization by purpose of use of room are given in Table 28. According to the investigation, the rooms with histories of use with a great many prople working in them tended to show greater neutralization. Due to the geographic conditions, this building was heated for long periods in the wintertime so that the air in the interior was dry while ventilation was inadequate and it is considered concentrations of carbon dioxide were high. Therefore, the depth of neutralization was great overall. It was indicated that such methods of finish as coating plaster with paint of low air-permeability or covering concrete with air-tight material are effective in hindering neutralization.

4.5 Case No. 5 (Fire-Damaged Buildings) (16)

Twenty-two reinforced concrete buildings subjected to fire in World War II were selected at random and about 10 parts of each building on the average, mostly interior columns and walls, ranging from undamaged by fire to heavily damaged by fire were measured for

Table 26. *Depths of neutralization of concrete in buildings investigated, cases 1 to 4*

Case	Portion of building	Story	Location	Main finish	Depth of neutralization (mm)	Remarks
No. 1 Office building	Outer wall	1–4	Inner surface	Mortar & plaster	22–70	Thickness of mortar: 5–30mm Thickness of plaster: 5–30mm
		1–4	Ditto	Mortar, Plaster & paint	20–30	
		1st basement	Ditto	Mortar & plaster	0–40	
		1–5	Outer surface	Mortar & granite facing slab	0–10	
	Column	3–4	Inner surface	Mortar, plaster & paint	1–38	
		1–2	Ditto	Mortar & plaster	10–30	
		1st basement	Ditto	Ditto	3–45	
	Partition wall	1–4	Inner surface	Mortar & plaster	1–45	
		1st basement	Ditto	Ditto	0–50	
	Floor slab	1–4	Upper surface	Terrazzo finish	0–2	
No. 2 Apartment house	Column	1st basement	Top	Plaster	10–20	Thickness of plaster: 12–13mm
		Ditto	Middle	Ditto	15–25	
		Ditto	Bottom	Asphalt waterproofing	0–5	
	Beam	1	Middle underside	Plaster	15–45	
	Wall	1st basement	Inner surface	Plaster	12–20	
	Slab	1	Underside	Plaster	35	
No. 3 Elementary school	Outer wall & column	1–3	Inner & outer surfaces	Mortar or plaster	50–90	
No. 4 Office building	Column	1st basement	Inner surface	Plaster	5–28	
		1	Ditto	Ditto	8–85	
		1	Ditto	Plaster & mortar	10–50	
		2	Ditto	Plaster	0–60	
		3	Ditto	Ditto	0–60	
	Beam	1–3	Underside	Plaster	20–60	
		1–3	Side surface	Ditto	16–80	
	Wall	1st basement	Inner surface	Plaster	20–70	
		1–3	Ditto	Ditto	30–55	
		1–3	Ditto	Mortar	4–25	
	Slab	Roof slab	Underside	Plaster	15–100	
			Top surface	Lignoid, etc.	0–27	

Table 27. *Salt content in the finish plaster and concrete*

Location	Specimen	Salt content (%)
1st story column	Finish plaster	0.09
	Finish plaster	0.38–0.60
Basement column	Concrete coverage	0.39–0.75
	Concrete inside of reinforcing steel	0.17
Beam	Underside concrete coverage	0.70–0.87
Wall	Various portions	0.40–0.56
Slab		0.09–0.36

Table 28. *Depth of neutralization by purpose of room (Investigation case No. 4)*

No.	Purpose of room		Measurement of depth of neutralization		
	Previous purpose	Current purpose	Points of measurement	Av. depth-mm	Overall av. mm
1	Recreation room Japanese room → office room	Japanese room Ditto	6 5	43.3 52.6	47.5
2	Office room Conference room Reception room	Office room Ditto Ditto	14 5 4	46.1 31.0 39.5	41.7
3	Office room	Clinic, barber shop	14	41.2	41.2
4	Corridor	Battery room	3	40.8	40.8
5	Corridor Office room Conference room Document storage room → conference room Reception room	Document storage room Ditto Ditto Ditto Ditto	5 15 2 3 2	25.2 46.0 35.0 46.7 37.5	40.8
6	Office room Executive offices	Reception room Executive offices	8 17	38.9 33.7	35.4
7	Japanese room Corridor Japanese room → office room	Conference room Ditto Ditto	18 6 3	29.9 37.7 34.3	32.1
8	Office room Japanese room	Business machines room Ditto	7 17	57.7 18.9	29.8
9	Corridor Stairway Toilet room	Corridor Stairway Toilet room	11 10 11	35.2 26.0 22.0	27.8
10	Anteroom	Telephone operator room	8	25.5	25.5
11	Kitchen	Kitchen	6	22.5	22.5
12	Dry area	Dry area	5	21.7	21.7

depth of neutralization.

As a result of the investigation, the items described below were brought to light.

Fire-Damage and Neutralization

The black dots in Fig. 3 indicate portions of concrete considerably damaged by fire. The finish coat on

reinforced concrete such as mortar or plaster, if damaged to some extent during a fire, will be loosened from the concrete and will then drop off in many cases. Most of the black dots represent portions of concrete where this had happened so that the concrete surfaces were directly subjected to fire and heat to a considerable degree becoming discolored and crazed with hair cracks. These portions were distributed over wide areas and in every building the neutralization at these portions had distinctly progressed to a much greater extent than portions unharmed by fire. Since the investigation was conducted several years after suffering damage, and the buildings had been left in fire-gutted condition, it should be considered that the damaged portions were even more neutralized during this time.

The dots crossed with bars represent portions which had been subjected to some degree of fire damage with the surface finishes still existing so that fire damage to concrete was extremely light. The neutralization was extremely light compared to the black dots.

The open dots indicate portions completely escaping fire damage and in general neutralization had occurred to an even lesser degree than the portions represented by dots crossed with bars.

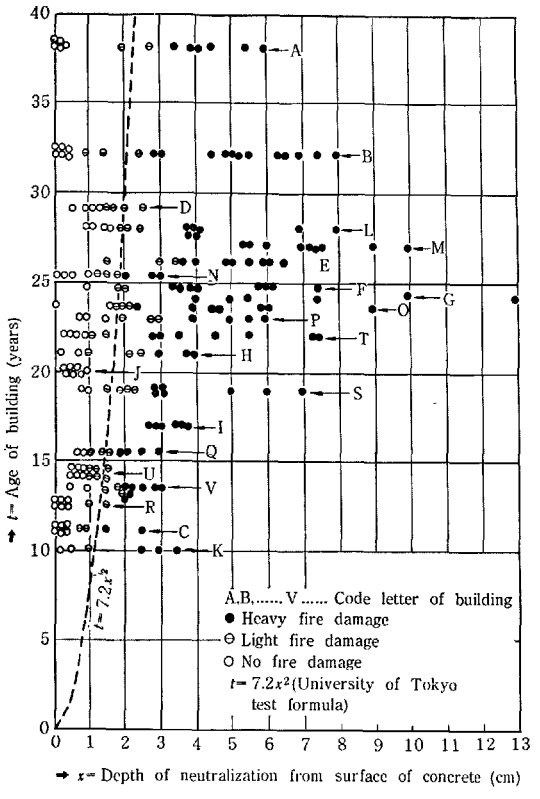

Fig. 3. *Fire-damage and neutralization*

Neutralization and Lapse of Time

The relation between depth of neutralization and age based on Fig. 3 on concrete completely escaping fire damage modified to neglect the thicknesses of surface finishes would be as is given in Fig. 4. It should be kept in mind, however, that the protective effect of the same thickness of surface finish will differ according to the material and the quality of the work. Almost all of the buildings investigated had concrete covered with ordinary finishes, mortar or plaster. The trend in the case of finish thicknesses of 1 to 2 cm was as is indicated by the broken lines in the figure.

Corrosion of Reinforcing Steel

Little corrosion of steel could be seen in parts which had escaped fire even when the depth of neutralization had progressed to near the location of the steel. In portions subjected to fire damage, since neutralization had progressed to considerable depths and because concrete had been cracked and made porous by fire, formation of rust could be seen in many cases. It appeared that in portions exposed to rain and wind the rusting was especially rapid.

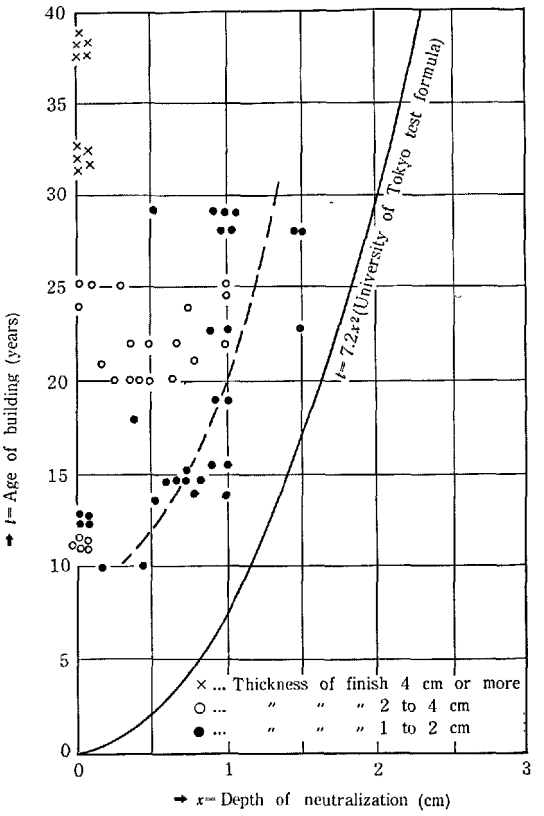

Fig. 4. *Relation between depth of neutralization and age on concrete escaping fire damage*

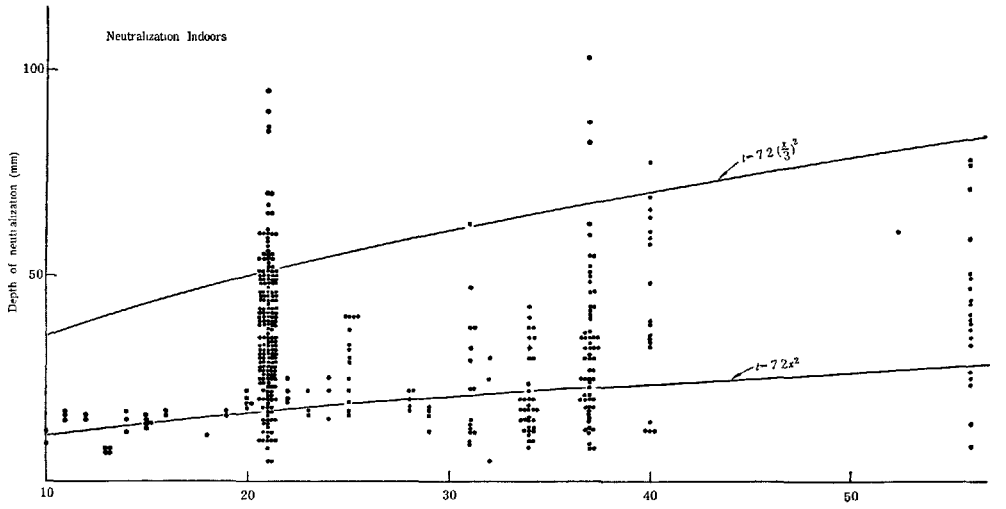

Fig. 5. *Relation between depth of neutralization indoors and age*

In investigations conducted by other researchers, which are not many, there was a case of an office building constructed in 1910 which was well-built for that time and was maintained in good condition. Although there were portions on the interior which had been neutralized to depths of 25 to 80 mm, it is reported no formation of rust could be recognized.

4.6 Neutralization of Concrete and Rusting of Reinforcing Steel as seen from Cases Investigated

1) Neutralization is rapid when the concrete is of a poor mixture. Neutralization of concrete containing blended cement such as pozzolanic cement is especially rapid.

2) Plaster is not effective against neutralization while mortar is effective.

3) When concrete is covered with materials impermeable to water or air, such as tile and stone, the rate of neutralization is reduced.

4) Neutralization occurs more rapidly indoors than outdoors.

5) The relation between depth of neutralization indoors and age according to the investigations and other references can be illustrated as in Fig. 5. It is readily seen that neutralization is 1 to 3 times greater indoors than outdoors as described in Chapter 3.

6) As special cases, when there is action of salt, reinforcing steel in concrete will be heavily rusted without regard to neutralization, and when the concrete is subjected to fire, neutralization is accelerated and the steel will be rusted.

7) When concrete is neutralized, the reinforcing steel in the neutralized portion is rusted in many cases, but this is not always true depending on the conditions. These conditions are, for example, that the concrete is relatively dense and of low air-permeability and furthermore faces a relatively dry interior of a building.

5. Functions of Neutralization and Steel Corrosion

5.1 Function of Neutralization

In order to study the function of neutralization of concrete it would appear first necessary to consider the constitution of hardened concrete. Meyers (17) stated that certain types of aggregates will release alkalis when subjected to the action of carbon dioxide to raise the possibility of alkali-aggregate reaction. However, since most aggregates are inert against carbon dioxide, it may be said that of the components of concrete, only the hydration products of cement have a relation with neutralization. According to Copeland and Kantro, (18) calcium hydroxide, tobermorite gel, ettringite, calcium aluminate monosulphate hydrates, calcium aluminum hydrates, calcium ferrite hydrates, hydrogarnets, etc. are contained in hydration products

of portland cement. Of these hydration products, calcium hydroxide, when subjected to action of carbon dioxide in the presence of a suitable amount of moisture, will readily react with the carbon dioxide to produce calcium carbonate and water. Although it may be thought that the hydration products other than calcium hydroxide are relatively unaffected by carbon dioxide, according to the studies of Meyers, Lieber and Blakey (19), and Verbeck (20), it was indicated that all hydration products of portland cement will react with carbon dioxide subjected to pressures of one atmosphere or more. Also Steinour (21) concluded from results of experiments and physicochemical considerations it is possible for the hydration products of portland cement even in normal atmosphere to be decomposed by minute quantities of carbon dioxide contained in them to be changed into calcium carbonate, hydrous silica, alumina and ferric oxide.

However, the degree and rate of carbonation of concrete will depend not only on the concentration and pressure of the carbon dioxide in the surrounding atmosphere, but also very much on such factors as the cement content, moisture content, porosity, permeability, internal relative humidity, etc. of the concrete.

Verbeck, using $1 \times 1 \times 1\frac{1}{4}$ inch mortar specimens in studying the relation between relative humidity and the rate of carbonation, reported that rate of carbonation is extremely high at relative humidities of 50 and 75% and low at 100 and 25%. He explains the low rate of carbonation at relative humidity of 100% to be because the pores of cement paste are filled with water at such high humidity so that carbon dioxide must first be dissolved in the water and then gradually be dispersed into the interior, this dispersion being slower than when the pores are not filled with water so that carbon dioxide is able to be dispersed into the interior in the form of gas. As for the low rate of carbonation at relative humidity of 25%, this is explained by the scarcity of relatively free water necessary for carbonation.

Powers (22) states that when the moisture in hydrated cement paste is 45% or less the water in the paste loses the characteristics of liquid water so that it is incapable of dissolving calcium hydroxide making it impossible for the latter to be spread through the gel pores thus slowing the rate of carbonation. Powers also assumes that the hydration products other than calcium hydroxide in hydrated cement paste contain two kinds of calcium ions, one of which is relatively susceptible to the action of carbon dioxide and the other relatively insusceptible to such action, and the relatively susceptible calcium ions at the outer parts are combined topochemically with carbon dioxide, but are not broken off from the gel structure.

The question of whether one of the components of the hydration products of cement in concrete reacts with carbon dioxide or whether many components react in parallel is answered by Powers that calcium hydroxide easily reacts with carbon dioxide, but only part of the other hydration products is reactive while the remainder does not readily react, so that at the beginning of carbonation calcium hydroxide and a part of the other hydration products react with carbon dioxide.

5.2 Neutralization and Steel Corrosion

The author, as one method of learning of the formation of rust on steel in reinforced concrete, studied whether rusting could be predicted by spontaneous electrode potentials immersing steel bars in calcium hydroxide solutions of differing hydrogenion concentrations and measuring the spontaneous electrode potentials and amounts of corrosion of the steel. The steels used were ϕ–5 × 100 mm bars polished with emery paper and washed thoroughly with alcohol and ether to remove adhering organics and ϕ–9 × 100 mm unpolished bars with mill scale from which organics were removed in the same manner.

The polished bars were immersed in 10 different solutions varying between pH of 7.0 to 12.0 adjusted with calcium hydroxide and the spontaneous electrode potentials were measured. The unpolished bars were immersed in 7 different solutions varying between pH to 7.0 to 12.0 and again the spontaneous electrode potentials were measured.

The amount of corrosion was measured only on polished bars. The method of measurement was to take out the polished bars from the solutions at the designated ages, wash them in hot solutions of 10% ammonium citrate, washing again with alcohol and

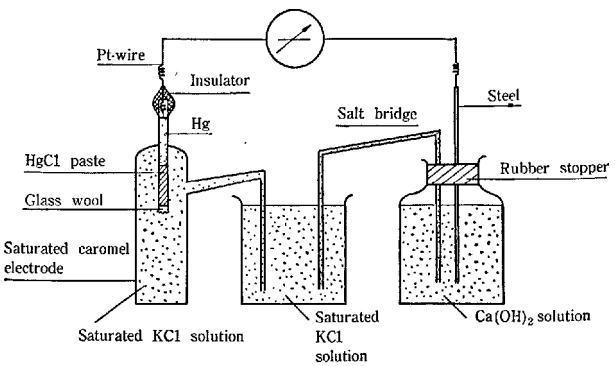

Fig. 6. *Spontaneous potential measuring apparatus*

drying to measure the weight loss. The amount of corrosion was expressed by the weight loss per unit area.

Test Results and Considerations

The changes in electrode potentials of polished steel in calcium hydroxide solutions of different hydrogen ion concentrations are given in Table 29 and Fig. 7 while the changes for unpolished steel are given in Table 30 and Fig. 8. In looking at the electrode potential variation of polished steel, no drop could be seen in calcium hydroxide solution with pH of 12.0; even after 96 hours the electrode potential still had not dropped. In solution of pH 11.0, there was a slight rise at 30 minutes after which the potential began to drop and a clear tendency of the steel to corrode could be seen. In solution of pH $\leqq$ 10.5, there was a very rapid drop in electrode potential with elapse of time. To summarize, in solutions of pH $>$ 11, there was no corrosion of steel, in solutions of 10 $<$ pH $\leqq$ 11 a slight trend of corrosion could be seen, while in solutions of pH $\leqq$ 10 the corrosion of steel was extremely great. In the case of unpolished steel, since there was corrosion at spots where the mill scale was broken the results of measurements of spontaneous electrode potential were roughly the same as for polished steel. Looking at Table 31 and Fig. 9, the tendency of corrosion agrees quite well with the tendency for rust formation as seen from the spontaneous electrode potential.

Table 29. *Results of potential measurements of polished steel*

pH of corrosion testing solution	Potential (−mV)						
	0 min	30 min	6 hrs	1 day	2 days	3 days	4 days
12.0	298	250	200	175	178	174	180
11.0	295	280	305	390	430	480	535
10.5	300	376	570	610	625	635	643
10.0	302	385	571	610	630	640	644
9.5	303	393	555	675	715	740	745
9.0	305	403	586	664	710	750	750
8.5	305	404	597	685	724	762	764
8.0	302	404	620	697	750	769	780
7.5	308	424	630	708	761	789	805
7.0	305	416	610	704	744	780	794

Table 30. *Results of potential measurements of unpolished steel*

pH of corrosion testing solution	Potential (−mV)						
	0 min	30 min	6 hrs	1 day	2 days	3 days	4 days
12.0	297	295	252	245	234	235	225
11.0	303	295	290	292	302	304	310
10.5	305	309	317	339	356	388	425
10.0	304	325	354	452	480	554	628
9.0	303	398	551	603	698	753	800
8.0	308	424	568	675	713	787	813
7.0	305	450	650	702	750	800	814

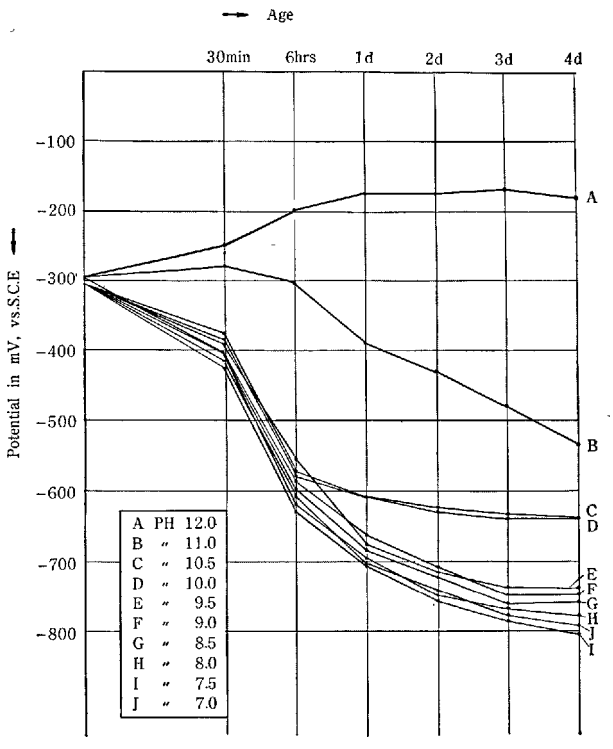

Fig. 7. *Time-potential curves of various corrosion testing solutions (Polished steel)*

Table 31. *Corrosion of polished steel*

pH of corrosion testing solution	Period of corrosion (hrs)	Corrosion in weight loss ($\times 10^{-5}$ g/cm^2)	pH of corrosion testing solution	Period of corrosion (hrs)	Corrosion in weight loss ($\times 10^{-5}$ g/cm^2)
12.0	24	3.13	9.0	48	16.60
11.0	〃	4.67	8.5	〃	16.90
10.5	〃	7.20	8.0	〃	19.90
10.0	〃	7.71	7.5	〃	21.70
9.5	〃	10.39	7.0	〃	21.80
9.0	〃	11.59	12.0	120	4.21
8.5	〃	12.71	11.0	〃	15.10
8.0	〃	13.30	10.5	〃	22.40
7.5	〃	13.50	10.0	〃	24.20
7.0	〃	13.65	9.5	〃	25.00
12.0	48	3.02	9.0	〃	25.40
11.0	〃	5.91	8.5	〃	25.50
10.5	〃	13.80	8.0	〃	26.30
10.0	〃	14.40	7.5	〃	27.10
9.5	〃	16.00	7.0	〃	32.40

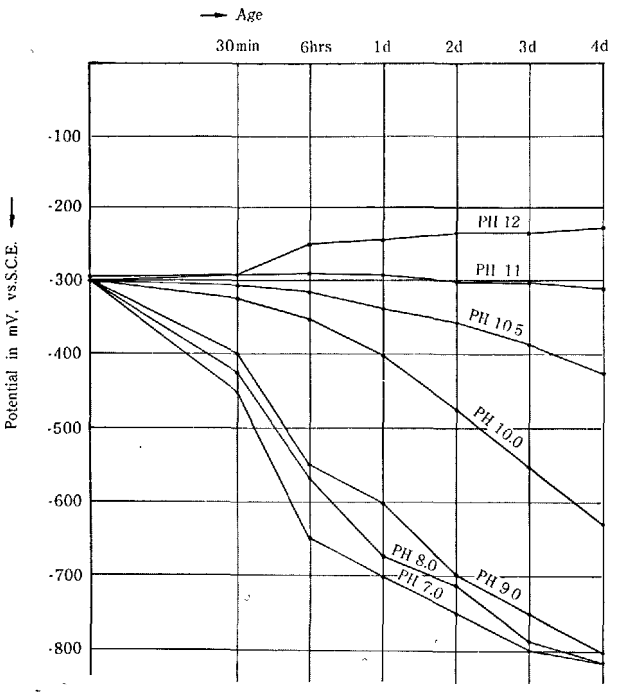

Fig. 8. *Time-potential curves of various corrosion testing solutions (unpolished steel)*

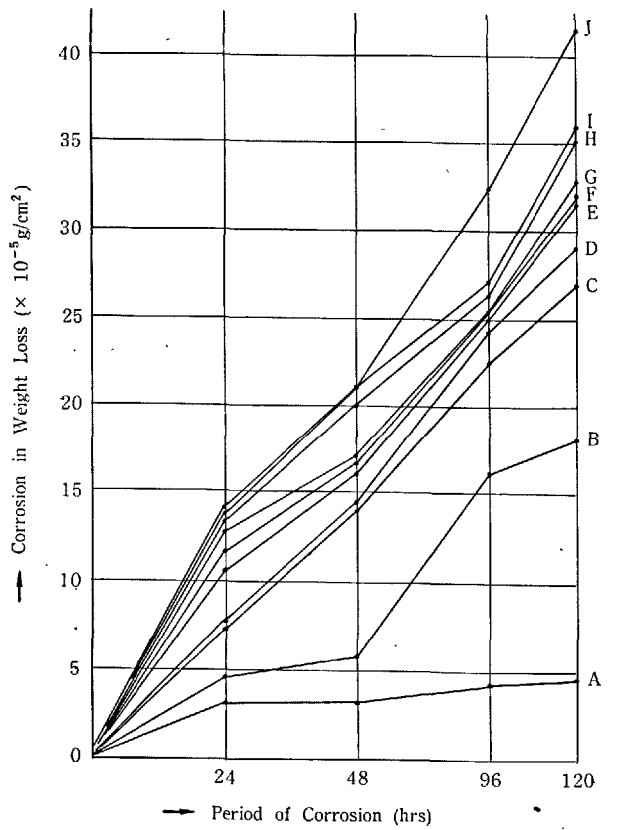

Fig. 9. *Corrosion in weight loss of polished steel in various testing solutions*

Summarizing the above, the corrosion of steel in reinforced concrete has a close relationship with neutralization of the concrete. Empirically, it had been said from the past that reinforcing steel in neutralized parts of concrete was liable to be corroded. From the foregoing conclusion and the conclusion obtained from measurements of hydrogen ion concentrations in neutralized and unneutralized parts of concrete described later—the hydrogen ion concentration of neutralized portions is 10 or less and there is a great difference with the concentration in unneutralized portions—it is further concluded that the reinforcing steel in concrete in the presence of oxygen and water will be corroded in neutralized areas while it will not be corroded in unneutralized areas substantiating the concept which had been recognized empirically.

5.3 Considerations on the Method of Determining Neutralization by Phenolphthalein

Measurement of the depths of the so-called neutralized layers of mortar and concrete is generally performed by spraying phenolphthalein solution on the specimens and determining the thicknesses from the surfaces of the specimen remaining uncolored which are considered as the depths of neutralization. However, contemplating on the above method from a common sense point of view, a question will arise whether there would not be considerable differences in the depth of neutralization values depending on the moisture content of mortar and concrete and the variety of phenolphthalein solution which may or may not contain water. The present circumstances are that no quantitative measurement is made of calcium carbonate and calcium hydroxide in the neutralized and unneutralized portions of specimens and there is no certain proof that phenolphthalein is appropriate for use in determination of neutralization of mortar and concrete. The author's cooperators carried out various studies on whether or not the phenolphthalein was appropriate for use in concrete neutralization determination tests. Firstly, regarding the phenolphthalein solution to be used in the determination of neutralization, 1% anhydrous phenolphthalein solution and 1% hydrous solution (5% of ethyl alcohol replaced with water) were prepared and painted on non-autoclaved cellular concrete of 15% moisture content. The results were that hydrous phenolphthalein indicated great coloring capability immediately after painting which in a few minutes changed to the same degree of coloring as the anhydrous phenolphthalein so that there was no difference in respect to determina-

tion of depth of neutralization. Therefore, it can be said there would be no difference in the results whether hydrous or anhydrous phenolphthalein solution is used for determination of depth of neutralization.

Next, the quantitative measurements of calcium carbonate and calcium hydroxide and the measurements of hydrogen ion concentrations in neutralized and unneutralized portions of specimens with varying moisture contents are described below.

Non-Autoclaved Cellular Concrete

The specimens consisted of 20 cm × 20 cm × 50 cm cellular concrete left outdoors for 10 years and divided into 4 equal parts with the procedure below followed for each of the specimens.

Specimen 1 was immersed 48 hours in water of 20°C temperature, Specimen 2 was immersed 10 hours in water of 20°C temperature, Specimen 3 was left in the same condition as when cut up and Specimen 4 was dried 24 hours in vacuum. After this, each of the specimens was cut in two at the middle, wiped thoroughly with a dry cloth and painted with 1% anhydrous phenolphthalein. Samples were taken from each of the specimens from the 4 portions indicated in Fig. 10 and quickly ground roughly in a porcelain mortar. In order to prevent carbonation of the samples, they were immediately vacuum-dried and after drying removed to an agate-mortar and pulverized to an extent that particles could not be sensed with the finger-tips and then placed in a tube-bottle and stoppered tightly to be used as samples for quantitative measurement of calcium carbonate and calcium hydroxide.

The quantitative measurement of calcium carbonate was calculated by using a Schrötter carbon dioxde measurement apparatus and measuring the quantity of carbon dioxde gas formed from decomposition by hydrochloric acid.

As for the methods of quantitative measurement of calcium hydroxide, there are the Lerch-Bogue Method, (23) Schlöpter-Bukowski Method, (24) Fujii Method, (25) Franke Method, (26) etc., but all of these methods have their disadvantages along with the advantages and it cannot be considered that quantitative measurement values of high reliability can be obtained.

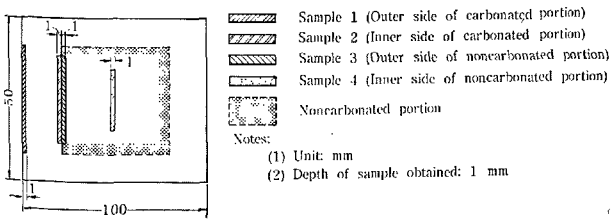

Fig. 10 *Portions of specimens from which samples were obtained*

In these tests, as quantitative measurement values of high accuracy are required because comparisons must be made of the calcium hydroxide from the same specimen, it was thought to make combined use of the Lerch-Bogue Method and X-ray diffraction. In the Lerch-Bogue Method the completion time of extraction is not clear and has the fault of also measuring the calcium hydroxide loosely combined in the hydration products. By using the combination method, the extraction completion time is accurately determined by X-ray diffraction to minimize the error from overmeasurement of calcium hydroxide so that quantitative measurements of high accuracy are obtained.

In this combined method, the sample was dispersed in a solvent and calcium hydroxide extracted for a given period and measured quantitatively. After extraction for the given time the extraction residue was thoroughly washed with ethyl alcohol and ether, vacuum-dried and used as the sample for X-ray diffraction. The extraction was performed over a hot water both of 90 to 95°C, titrating every 15 minutes. At the same time, X-ray diffraction was performed on the extraction residue and the calcium hydroxide quantity obtained from the quantitative measurement value of the Lerch-Bogue Method at the point when calcium hydroxide reflection at the surface (001) could no longer be recognized.

The measurement of hydrogen ion concentration was performed by using the extraction completion time of the respective samples determined by the combined Lerch-Bogue and X-ray diffraction method, extracting the calcium hydroxide in the samples using glycerin ethyl alcohol, quickly filtering after completion of extraction, diluting the filtrate 4 times with distilled water and measuring with a pH-meter.

On one hand, 50 g each were taken from the samples before vacuum drying and these were vacuum-dried, weighed after drying and the moisture contents of the samples before drying were calculated from the equation below.

$$\text{Moisture content } (\%) = \frac{\text{Weight of sample before drying (g)} - \text{Weight of sample after drying (g)}}{\text{Weight of sample after drying}} \times 100$$

5.3.2 Ordinary Concrete

The specimens were taken from ordinary concrete

60 cm × 60 cm × 90 cm placed outdoors for 60 years, cut in half at the middle and painted with 1% anhydrous phenolphthalein with samples taken from each of the specimens from the 4 portions indicated in Fig. 10. In preparing the samples, aggregate was removed as much as possible and the procedure for preparation and the methods of quantitative measurement were according to the preceding paragrapy. However, before making the quantitative measurements of calcium hydroxide and calcium carbonate, the insoluble residue and the calcium oxide of the samples were measured quantitatively, the cement portion in the samples accurately calculated, and the analysis values of the calcium hydroxide and the calcium carbonate converted into equivalent of cement and tabulized.

Test Results and Considerations

The results of quantitative measurement in the case of cellular concrete are given in Table 32. The result of X-ray diffraction on extraction residues of major points on various samples from Specimen 3 are indicated in Fig. 11. The results of quantitative measurement on ordinary concrete are given in Table 33. As can be seen from Tables 32 and 33, when the moisture content of the specimens is comparatively high being 20 to 30%, it becomes difficult to discern the neutralized and unneutralized portions using phenolphthalein due to the dispersion phenomenon of the calcium hydroxide at the surface of the specimen. Even when straining to distinguish the neutralized portion by the shade of the area colored by phenolphthalein, as can be seen from the analysis results in Table 32, a great amount of calcium hydroxide was measured from the neutralized area and thus, in this case, it cannot be considered that the neutralized area is correctly indicated chemically. However, when the moisture content of the specimen is 15% or less, it is possible to clearly define between the neutralized and unneutralized areas with phenolphthalein, while a considerable difference between neutralized and unneutralized areas is seen in the quantitative measurement results. On one hand, as seen in Fig. 12, there is a great difference in the hydrogen ion concentration on either side of the borderline between the neutralized and unneutralized areas, and as described in 5.2, since the corrosion of reinforcing steel depends greatly on the before-mentioned hydrogen ion concentration, it may be considered that neutralized and

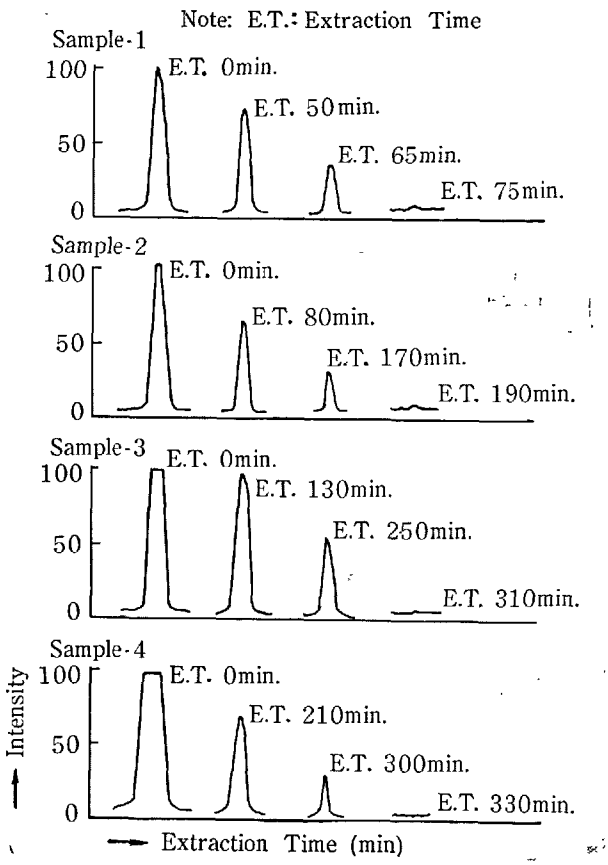

Conditions of Diffraction:
Voltage 35 KV, Current 15mA, Ratemeter 8, Multiplier 1, Time Constant 4

Fig. 11. *X-ray diffraction of free* $Ca(OH)_2$ *extraction residue of specimen 3*

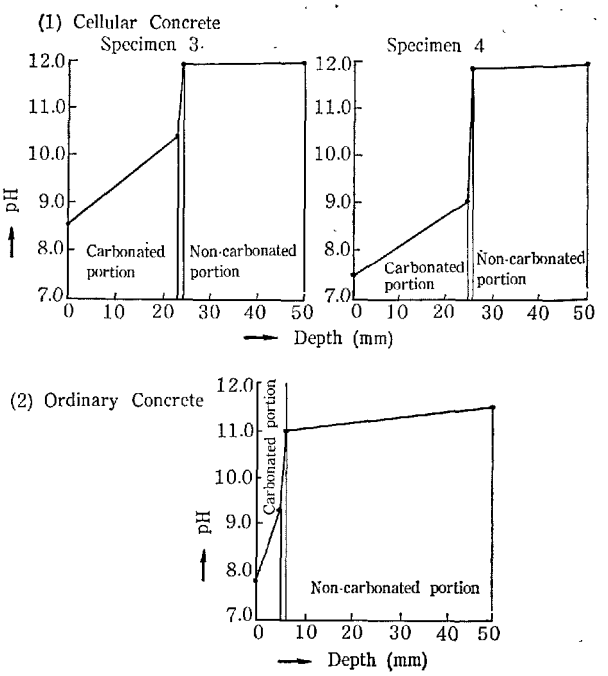

Fig. 12. pH *of carbonated and non-carbonated portions*

unneutralized portions can be indicated with considerably high accuracy using phenolphthalein.

Table 32. *Results of analysis (Cellular concrete)*

(1) Specimen 1 (Moisture content 31.5%)
Depth of carbonation: Entire area painted with phenolphthalein colored and impossible to determine area neutralized. Difficult to obtain Samples 2 and 3, therefore, samples obtained from location 10mm from surface of specimen.

Sample 1				Sample taken 10mm from surface				Sample 4			
Period of extraction of $Ca(OH)_2$	$Ca(OH)_2$	$CaCO_3$	pH	Period of extraction of $Ca(OH)_2$	$Ca(OH)_2$	$CaCO_3$	pH	Period of extraction of $Ca(OH)_2$	$Ca(OH)_2$	$CaCO_3$	pH
300 min	12.9%	9.2%	11.2	310 min	13.5%	8.8%	11.4	330 min	14.3%	8.5%	11.7

(2) Specimen 2 (Moisture content 21.5%)
Depth of carbonation: Entire area painted with phenol phthalein colored but neutralized area distinguished by intensity of color. 11mm

Sample 1				Sample 2				Sample 3				Sample 4			
Period of extraction of $Ca(OH)_2$	$Ca(OH)_2$	$CaCO_3$	pH	Period of extraction of $Ca(OH)_2$	$Ca(OH)_2$	$CaCO_3$	pH	Period of extraction of $Ca(OH)_2$	$Ca(OH)_2$	$CaCO_3$	pH	Period of extraction of $Ca(OH)_2$	$Ca(OH)_2$	$CaCO_3$	pH
260 min	12.2%	11.8%	11.0	300 min	12.3%	10.5%	11.1	315 min	15.0%	8.2%	11.5	330 min	14.3%	7.9%	11.8

(3) Specimen 3 (Moisture content 15.2%) Depth of carbonation: 23mm

Sample 1				Sample 2				Sample 3				Sample 4			
Period of extraction of $Ca(OH)_2$	$Ca(OH)_2$	$CaCO_3$	pH	Period of extraction of $Ca(OH)_2$	$Ca(OH)_2$	$CaCO_3$	pH	Period of extraction of $Ca(OH)_2$	$Ca(OH)_2$	$CaCO_3$	pH	Period of extraction of $Ca(OH)_2$	$Ca(OH)_2$	$CaCO_3$	pH
75 min	4.0%	25.2%	8.5%	190 min	7.7%	21.3%	10.4	310 min	18.3%	5.2%	11.8	330 min	18.9%	5.0%	11.9

(4) Specimen 4 (Moisture content 1.7%) Depth of carbonation: 25mm

Sample 1				Sample 2				Sample 3				Sample 4			
Period of extraction of $Ca(OH)_2$	$Ca(OH)_2$	$CaCO_3$	pH	Period of extraction of $Ca(OH)_2$	$Ca(OH)_2$	$CaCO_3$	pH	Period of extraction of $Ca(OH)_2$	$Ca(OH)_2$	$CaCO_3$	pH	Period of extraction of $Ca(OH)_2$	$Ca(OH)_2$	$CaCO_3$	pH
60 min	3.2%	28.8%	7.5	170 min	5.8%	24.2%	9.1	320 min	19.5%	6.2%	11.8	340 min	20.0%	5.8%	11.9

Table 33. *Results of analysis (Ordinary concrete)*

Depth of carbonation: 5mm

Sample 1 (Moisture content 1.4%)				Sample 2 (Moisture content 1.8%)				Sample 3 (Moisture content 2.2%)				Sample 4 (Moisture content 2.4%)			
Period of extraction of $Ca(OH)_2$	$Ca(OH)_2$	$CaCO_3$	pH	Period of extraction of $Ca(OH)_2$	$Ca(OH)_2$	$Ca(OH)_3$	pH	Period of extraction of $Ca(OH)_2$	$Ca(OH)_2$	$CaCO_3$	pH	Period of extraction of $Ca(OH)_2$	$Ca(OH)_2$	$CaCO_3$	pH
49 min	0%	25.4%	7.8	70 min	0%	21.6%	9.3	300 min	17.0%	3.6%	11.0	313 min	17.9%	0%	11.3

6. Special Cases

6.1 Reinforced Concrete Chimneys (Influence of High Temperatures and Gases)

Reinforced concrete chimneys are subjected to the actions of heat and gases so that from a durability standpoint these chimneys are placed at a disadvantage. The author, in order to clarify the condition of this type of chimney investigated 7 chimneys which fell down in the First Muroto Typhoon of September 1934 and 2 chimneys at public bath-houses in Tokyo. For instance, a factory chimney 15 years after construction was completely neutralized for 10 cm on

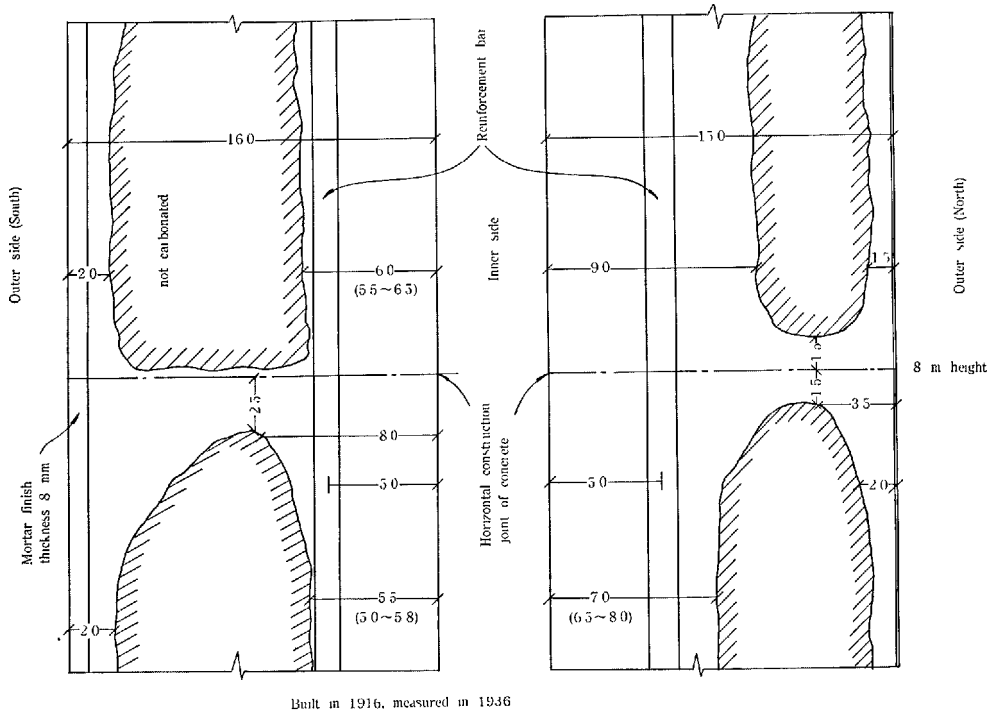

Fig. 13. *Chimney for heating wooden dormitory building in Tokyo*

both outer and inner sides, and the main reinforcement, ϕ–9 mm bars, had been reduced to less than half their diameters. In the case of the bath-house chimneys, such results as $t = 6.2x^2$ for exterior surfaces and $t = 1.7x^2$ for interior surfaces were seen, while at construction joints the conditions were even worse and the reinforcing bars had become rusted at 10 to 20 years. (Fig. 13)

The concrete of almost all reinforced concrete chimneys are uncovered and although a great deal depends on the lining, the interior concrete is exposed to heat and smoke with high concent rations of carbon dioxide and sulphur dioxide gas while the exterior is subject to some extent of concentrated gases and to minute cracking caused by temperature stresses. Therefore, the life of a reinforced concrete chimney is short, especially at construction joints. After experimental and theoretical studies, it was pointed out that special care should be exercised in design and construction, and that it would be beneficial to use high early strength portland cement. (27), & (28)

Later, in 1936, the author ascertained the weak points of construction joints in a study of a chimney for heating of a dormitory. In 1950, in an investigation of 2 chimneys at Sapporo Thermal Power Station conducted by Koh, (29) the difference in neutralization depending on height and the relation with the interior lining were studied and it was found that the coverage on the interior for several meters from the top was insufficient.

In 1956 to 1958, Fukuchi (30) investigated 9 chimneys damaged by earthquake and 14 chimneys which went undamaged at public bath-houses in Tokyo and it was indicated that the coefficient of x^2 in the beforementioned equation should be selected at 1.0 or less. This figure substantiates to a considerable extent the appropriateness of the 0.77 coefficient induced in 1937 for cases of good concrete workmanship in which considerations were given to the concentration of gas.

The results of investigation on a chimney at a hospital in Sapporo carried out by Koh in 1961 also show that chimneys which are continuously used are neutralized rapidly, that interior lining is necessary and that concrete mixtures must be improved. It was indicated that the top portion of a chimney is especially liable to be damaged, The investigations by the author on a locomotive shed in Niigata Prefecture in 1948 and by Nishi on a locomotive shed in Hokkaido in 1955 also point out examples of corrosion by smoke from locomotives and show the durability of dense concrete of a good quality mix.

In the case of thermal power plants, there are cases in which the coefficient of x^2 must be taken at 0.1.

In summary, although depending on various conditions, the corrosion of reinforcing steel in chimneys is fairly rapid and there is a need for close observation.

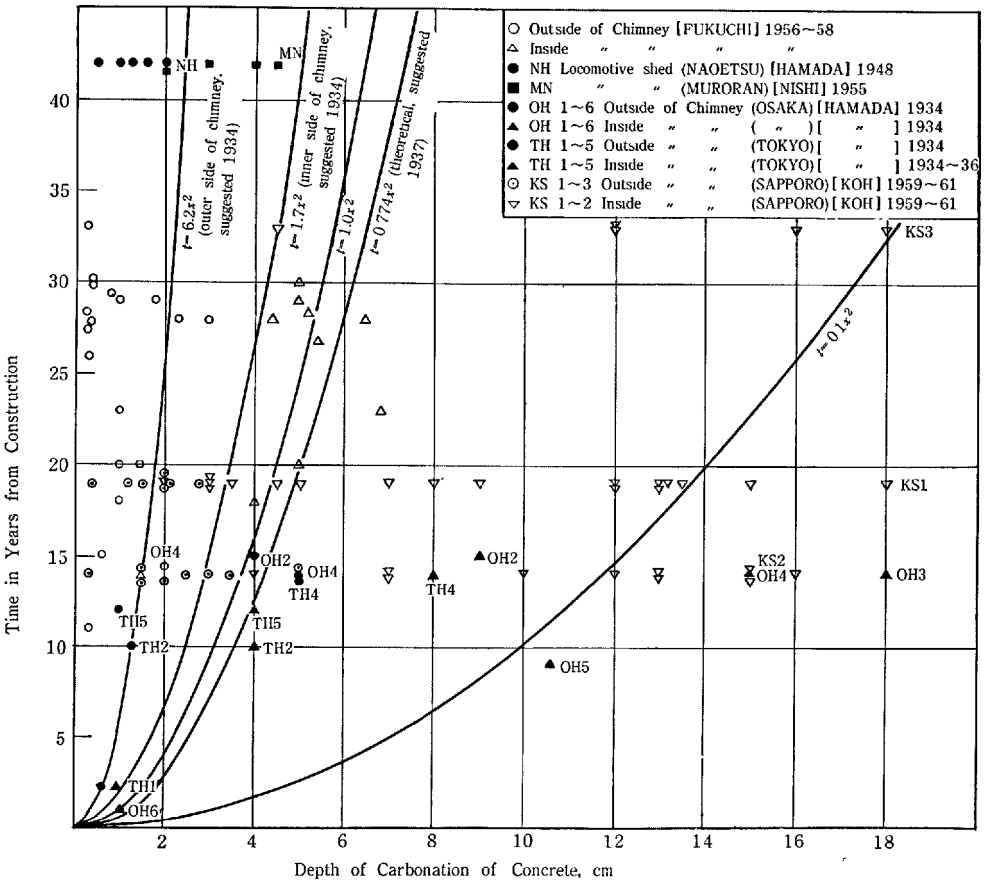

Fig. 14. *Depths of carbonation measured on chimneys and locomotive sheds. Curved lines with formulae are suggested by Hamada based on measured date and hypothetical studies*

Fig. 14 gives an illustrative summary of the relation between age and depth of neutralization and indicates that a diagnosis of deterioration should be made within 20 years.

6.2 Fire-Damaged Buildings

The investigation by Takenouchi in 1952 on buildings damaged by fire during the war conducted mainly on neutralization of interior columns and walls produced the result that neutralization progresses greatly from fire damage. (16) According to Kimura, (31) up to 600°C, neutralization is not different from that at normal temperature, but from 700°C and above, the situation changes completely and neutralization progresses 2.5 cm or more in 2 hours of heating.

6.3 Cold Weather Regions

In regions of cold climate, the neutralization is considerably different from that seen in other regions. When concrete is dry, the air-permeability is raised so that it would appear neutralization would become accelerated. The neutralization indoors would be severer than in warm regions because of drying occurring from heating throughout half the year. The results of experiments for a 3-year period on specimens placed outdoors in the cold and in the corridor of a heated building showed about 2.5 times neutralization indoors over outdoors.

Comparing this neutralization with the data on neutralization according to thickness of finish obtained by the beforementioned Takenouchi on portions of buildings not subjected to fire damage, it is found to be considerably greater.

Even when there is a finish on the exterior, the concrete at corner portions of a building will become more air-permeable from frost damage so that examples of some acceleration of neutralization have been seen.

6.4 Rusting of Reinforcing Steel under Special Conditions such as Chemical Factories and Countermeasures

Tatsumi (32) carried out a number of experiments in 1934 having noticed the corrosion of concrete at factories which have electrolytic processes and the electrolytic corrosion from direct current in subways, etc. With the same point of view, the author conducted tests (33) in 1938 on concrete containing electrolytic materials such as calcium chloride which are used as accelerators in cold weather concreting.

In such cases the rusting of reinforcing bars is severe. This is because when small amounts of electrolytic material enter the concrete, although there may be little difference in the specific resistance, the rusting of steel is extremely severe due to the Cl^- gathering at the anode.

In chemical plants, there is much corrosion of concrete from sulphur dioxide gas and various other acids and in 1955 a guide to prevention of corrosion of reinforced concrete (34) was prepared by the Committee on Countermeasures for Corrosion of Concrete based on both previous studies and a new survey which had been conducted.

Also, Nagano (35) reported in 1958 on a systematic study on electrolytic corrosion affected by type of cement, concrete mix proportion and whether or not admixtures had been used.

Acknowledgements

The author wishes to express his deepest gratitude to Dr. Tadao Nishi, Professor, University of Tokyo, Dr. Koichi Kishitani, Associate Professor, University of Tokyo, Dr. Yoshiro Koh, Professor, Hokkaido University, Dr. Katsuro Kamimura, Building Research Institute, Ministry of Construction, Mr. Hideo Teramoto, Research Laboratory, Nihon Cement Co., Ltd., and Mr. Tsuruyoshi Saito and Mr. Koretoshi Hitotsuya of the Central Research Laboratory, Onoda Cement Co., Ltd. for their invaluable cooperation in preparation of this paper.

References

1. R. Sano, "Corrosion tests of steel (Report No. 1)" (in Japanese), Report of the Committee for Investigation of Earthquake Damage Prevention, No. 74 (Jun. 1911).
2. S. Uchida and M. Hamada, "Durability tests of steel and concrete" (in Japanese), Journal of Architecture and Building Science, No. 516 (Oct. 1928).
3. S. Uchida, "Corrosion tests of steel (Report No. 2)" (in Japanese), Report of the Committee for Investigation of Earthquake Damage Prevention, No. 76 (Sept. 1913).
4. M. Hamada, K. Ono and I. Nakamura, "Reinforced concrete in buildings in Taiwan" (in Japanese), Pamphlet of the Japan Portland Cement Manufacturers Association (Apr. 1937).
5. K. Ohno, "Weathering tests of concrete in Taiwan (No. 1)" (in Japanese), Bulletin of the Cement World (Apr. 1938).
6. K. Ohno, "Weathering tests of concrete in Taiwan (No. 2)" (in Japanese), Bulletin of the Cement World (May, 1938).
7. I. Nakamura, "Weathering tests of concrete in Taiwan (No. 3)" (in Japanese), Bulletin of the Cement World (Mar. 1942).
8. M. Hamada, "Prevention of weathering of reinforced concrete in Taiwan" (in Japanese), Journal of Architecture and Building Science (Apr. 1942).
9. H. Takahashi, "Weathering tests of concrete in Taiwan (No. 4)" (in Japanese), unpublished (1946).
10. Li Yih Shing and Renn Jong Yeuan, "Weathering tests of concrete in Taiwan (No. 5)" (in Japanese), Proceedings of Japan Cement Engineering Association (1956).
11. K. Kishitani, "Weathering of concrete (Parts 1 & 2)" (in Japanese), Transactions of Architectural Institute of Japan, No. 46 and 48 (Mar. 1953 & 1954).
12. K. Kishitani, "Durability of reinforced concrete" (in Japanese), Transactions of Architectural Institute of Japan (Oct. 1954).
13. K. Kishitani, "Durability of lightweight concrete containing fly ash" (in Japanese), Transactions of Architectural Institute of Japan (May, 1955).
14. K. Kishitani, Durability of reinforced concrete (in Japanese), (Publishing Dept., Kajima Institute of Construction Technology, Tokyo, Japan, Feb. 1963).
15. T. Nishi and Y. Koh, "Neutralization measurement of twenty-year old reinforced concrete buildings" (in Japanese). Proceedings of Japan Cement Engineering Association (1959).

16. S. Takenouchi, "Investigation of neutralization of concrete in fire-damaged buildings" (in Japanese), Research Report No. 20. Architectural Institute of Japan (Oct. 1952).
17. S. L. Meyers, Rock Products, **52** (1) 96–98 (1949).
18. L. E. Copeland and D. L. Kantro, The Chemistry of Cements (1964).
19. I. Lieber and F. A. Blakey, Journal of ACI, **28**, 295–308 (1956).
20. G. Verbeck, Special Technical Publication No. 205, 17–36 (1956).
21. H. H. Steinour, Journal of ACI, **30**, No. 8, 905–907 (1957).
22. T. C. Powers, PCA Research Department Bulletin No. 146 (1962).
23. W. Lerch and R. H. Bogue, Industrial Engineering & Chemistry, 18, 739 (1926).
24. P. Schlöpter and R. Bukowski, Eidgenössische Materialprüfungsanstalt an der E. T. H. Zurich, Report No. 63, Zurich (1933).
25. K. Fujii, Proceedings of Japan Cement Engineering Association, III (in Japanese), 93 (1949).
26. B. Franke, Zeitung für anorganische und allgemeine Chemie, 247 (1941).
27. M. Hamada, "Life spans of reinforced concrete chimneys" (in Japanese), Bulletin of the Cement World, No. 323 (Feb. 1935).
28. M. Hamada, "Properties of reinforced concrete chimneys of bath-houses" (in Japanese), Transactions of Architectural Institute of Japan, No. 5, 72–81 (Mar. 1937).
29. Y. Koh, "Results of measurements of neutralization of thermal power stations and chimneys" (in Japanese), Transactions of Architectural Institute of Japan No. 66, 141–144 (Oct. 1960).
30. T. Fukuchi, "Investigation of public bath-house chimneys in Tokyo" (in Japanese), Proceedings of Japan Cement Engineering Association XII, 410–416 (1958).
31. S. Kimura, "Heat resistance of concrete of varying ages" (in Japanese), Proceedings of Japan Cement Engineering Association XI, 336–340 (1957).
32. J. Tatsumi, "Influence of electric current on strength of reinforced concrete structures (Parts 1 and 2)" (in Japanese), Transactions of the Architectural Institute of Japan, 268–279 (Apr. 1934), and 35–44 (Mar. 1936).
33. M. Hamada, "Problems of steel corrosion and its prevention in concrete containing calcium chloride" (in Japanese), Transactions of the Architectural Institute of Japan, No. 9, 51–60 (Apr. 1938).
34. Japan Construction Materials Association, Prevention of Corrosion of Reinforced Concrete, (in Japanese), p. 160 (Nov. 1955).
35. R. Nagano and S. Yamawaki, "Study on the resistibility to electrolytic corrosion of reinforced concretes made of various concrete by an automatic constant apparatus" (in Japanese), Proceedings of Japan Cement Engineering Association, XII, 463–470 (1958).

Written Discussion

Heinz G. Smolczyk

Synopsis

In addition to the widely interesting part of Mr. Hamada's paper on the very extensive Japanese long time studies on carbonation the results of five years' experiments of three German laboratories are described, evaluated and compared with various publications of other authors.

The evaluation proved the following results for mortars and concretes with dense aggregate:

a) Carbonation does not depend on the quantity of free $Ca(OH)_2$ in the paste.

b) Carbonation increases the strength of normal concretes in any case. Exceptions are the supersulphated cements.

c) The equation

$$\text{carbonation} \sim \sqrt[2]{\text{time of carbonation}}$$

is an approximation, which becomes suitable for extrapolation only after a longer period of carbonation i.e. with older concretes.

d) Carbonation of older mortars and concretes with portland cements and with ortland blastfurnace slag cements can be expressed in terms of the formula

$$\text{carbonation} \sim (1/\sqrt{\text{compressive strength}}) \times \sqrt{\text{time}}$$

e) Following d) carbonation must decrease with an increase of afterhardening of concrete. Thus greater differences in initial carbonation between cements with lower initial strength and high afterhardening and cements with higher early strength and low afterhardening gradually disappears with growing age of the older concretes.

f) With respect to carbonation it is safer to use rich mixes with normal hardening cement than leaner mixes with higher early strength cement.

The Problem

The principal paper of Mr. Hamada especially the first part "Carbonation of Concrete" is a widely interesting summary mainly of the very extensive Japanese work on this field, which represents the basis of our knowledge of the carbonation of various types of concrete (1) and (2). Thus the impression could occur that nearly all the questions are answered, and the supplementary papers also seem to confirm this opinion.

But there are also other tests and facts, which clearly do not agree with some of these theories: e. g. distinct differences to the $\sqrt{\text{time}}$—relation, carbonation of calciumsilicatehydrates and calciumaluminatehydrates in the paste, cases with stronger carbonation of lime-rich cements than those lower in lime, extremely strong influence of the precuring conditions on carbonation rate etc. Many of these observations have already been reported in (3), (4), (5), (6), (7), (8), (9), (10), (11), (12) and (13).

Our Laboratory has evaluated these questions for about seven years (14). The experiments and long-time studies will not be finished in the near future, but it nevertheless seems to be necessary to report on part of these tests which are apt to put another point of view on the subject and could possibly clarify some apparent contradictions (15).

Test Results (Experimental Results)

Cements

The following studies have been carried on by several laboratories (14) with

3 "Hochofenzementen" (HOZ): slag cements > 30% slag

2 "Eisenportlandzementen" (EPZ): slag cements < 30% slag

4 "Portlandzementen" (PZ): portland cements

1 "Sulfathüttenzement" (SHZ): supersulphated cement

All the cements were bought from commercial sources and selected in such manner that specimens with all variations in strength could be compared.

Three laboratories made mortar-prisms 4 × 4 × 16 cm and labor "F" also mortar-prisms 5 × 5 × 25 cm and concrete-prisms 5 × 5 × 25 cm with aggregate 0~15 mm. Up to now, for five years the progress in carbonation has been tested with phenolphthalein and partly the maximum binding of CO_2 and furthermore some compressive strengths of carbonated specimens.

The interesting data of the cements and of the test specimens are to be seen in Table 1. The compressive strengths of the concretes were only measured after 7 days and 28 days. The strengths after 14 days are interpolated according to the formula of G. Sadran (16).

Table 1. *Composition of cements and strengths of mortars and concretes*

No.	Cements Type	CaO %	SiO_2 %	slag resp. C_3A %	w/c	Compressive strengths in kg/cm² mortars 7 days	28 days	90 days	concretes w/c 0.45 7 days	14 days	28 days
1	HOZ	49.9	28.1	74	0.76	113	225	313	314	435	538
					0.50	246	459	595			
2	HOZ	53.7	26.4	55	0.76	94	199	304	322	446	551
					0.50	213	436	645			
3	HOZ	57.1	24.3	43	0.76	165	298	378	502	625	710
					0.50	383	563	687			
4	EPZ	59.7	21.9	15	0.76	123	252	360	414	549	655
					0.50	283	581	723			
5	EPZ	59.9	25.4	29	0.76	154	240	303	456	602	707
					0.50	358	541	645			
6	PZ	64.5	20.7	8	0.76	168	267	311	474	581	657
					0.50	355	525	616			
7	PZ	63.5	21.7	<1	0.76	95	182	278	—	—	—
					0.50	252	428	653			
8	PZ	63.6	21.0	2	0.76	86	149	213	—	—	—
					0.50	246	375	452			
9	PZ	63.1	22.4	13	0.76	154	247	308	463	581	669
					0.50	356	506	640			
10	SHZ	45.3	25.4	85	0.76	328	427	489	—	—	—
					0.50	506	624	711			

$$\frac{1}{B} \sim \frac{1}{t_w} \qquad [1]$$

B = compressive strength

t_w = time of water-curing

The mortar have been stored indoors (65% RH, 20°C) after 28 days of water-curing, the concretes in a seldom used room (50% RH, ~ 20°C) after 7 days of moist treatment.

Some further tests (prestressed piles, heat treatment, outdoors storage, CO_2 storage) (14) shall not be reported here.

Results of the Carbonation of Mortars

In this report the test results of each experimental step are generally shown in tables.

With respect to the mortars, however, the number of single tests has been so great that the exact equations of carbonation progress could be established.

For this purpose the measured depths of carbonation 'X_v' and the time of carbonation 't' were drawn to double logarithmic scale as is to be seen in Fig. 1 (cement Z8) and Fig. 2 (cement Z1). The logarithms

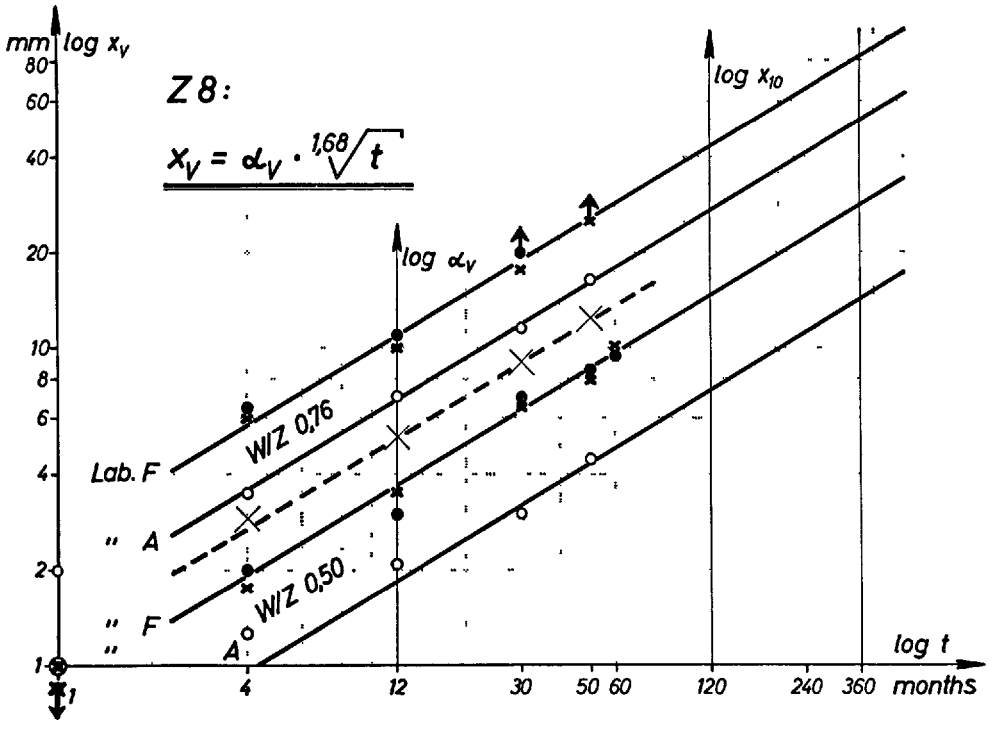

Fig 1. *Calculation of genuine carbonation progress for portland cement Z 8*
– – – × – – –trend line of overaged log-values

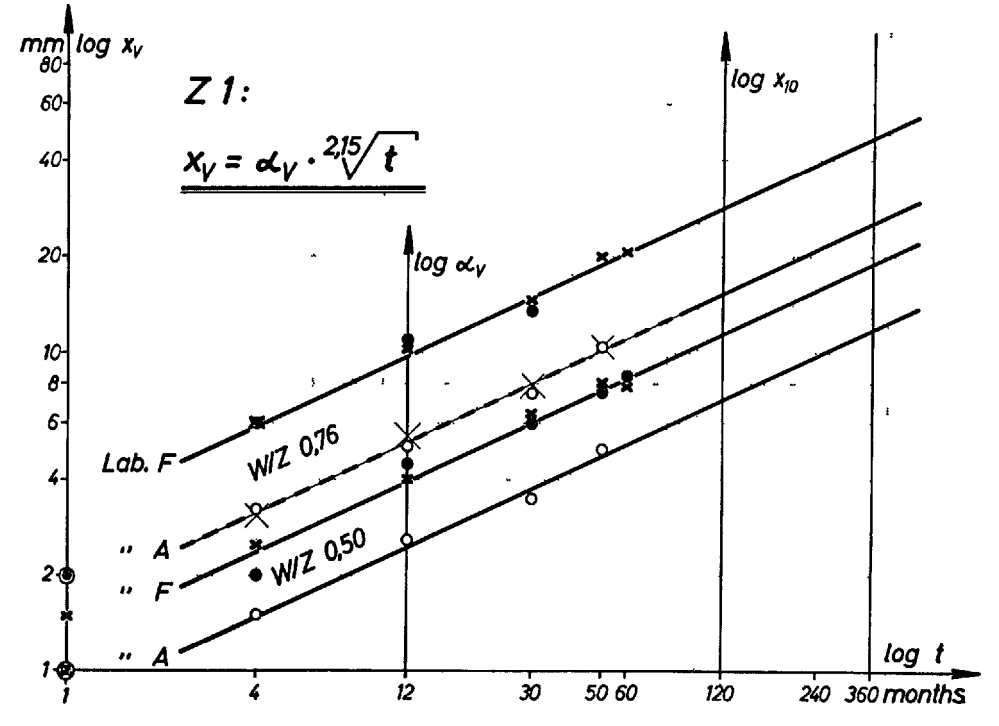

Fig 2 *Calculation of genuine carbonation progress for portland blastfurnace slag cement Z 1*
– – – × – – –trend line of averaged log-values

of all the 6 test series were averaged at 4, 12, 30 and 50 months. The slope of the average values (---- in the diagrams) then equals the value 'v' in the general equation

$$X_v = \alpha_v \sqrt[v]{t - t_0} \qquad [2]$$

't_0' being a relative short period of retardation

Equ. [2] becomes [3] already within 4 to 6 months

$$X_v = \alpha_v \cdot \sqrt[v]{t} \qquad [3]$$

Knowing the 'v' for a given cement, it is possible to calculate for each tested mortar of this cement the exact speed constant 'α_v' and to interpolate or also extrapolate carbonation depths 'X_v'. Table 2 shows these values 'v' and 'α_v' and also the carbonation 'X_{v10}' after 10 years as results for further evaluating.

The carbonation depth after 10 years was chosen, because only after this period an approximaitve formula

$$X \sim \sqrt[2]{t}$$

is possible, as is to be seen in Fig. 3. Here, for mortars of w/c 0.76 (Laboratory F) the experimental carbonation-curves (see Table 2)

of $\quad Z1: X_v = 9.7 \cdot \sqrt[2.15]{t}$

and $\quad Z9: X_v = 7.6 \cdot \sqrt[1.74]{t}$

are drawn on a graph with $\sqrt{t}$-axis in thick curves. The thin lines show that even after 1 year a linear adjustment can lead to very great deviations by extrapolating (14).

The best adjustment is possible in case of 't' being great enough according to the formula

$$X_q = X_o + \alpha_q \cdot \sqrt[2]{t} \qquad [4]$$

This function (— — — — — in the diagram) does not start from the origin. But X_o only represents a mathematical correction and must not be mistaken for the experimental time of retardation or induction period 't_o' in equ. [2].

This 'X_o' is very awkward with respect to further calculations and it is possible to calculate within the range from 5 to 30 years with only little divergence by using the formula

$$X \cong \alpha \cdot \sqrt[2]{t} \qquad [5]$$

Table 2. *Carbonation of mortars with $\sqrt[v]{time}$ (experimental) and $\sqrt[2]{time}$ (calculated)*

Cements No.	Laboratory	w/c = 0.50 (RILEM CEM) Experimental values v	α_v*	x_{v10} ($\equiv x_{10}$) mm	α**	Calculated values for v ≡ 2 $\frac{x_{30}}{x_{v30}}$	w/c = 0.76 Experimental values α_v*	x_{v10} ($\equiv x_{10}$) mm	α**	Calculated values for v ≡ 2 $\frac{x_{30}}{x_{v30}}$
1	A	2.15	2.5	7.2	2.3	12/12	5.2	15.1	4.8	26/25
	F		4.0	11.6	3.7	20/19	9.7	28.2	8.9	49/47
2	A	1.88	2.4	9.3	2.9	16/15	6.4	22.0	6.9	38/39
	F		3.7	12.3	3.9	26/22	9.1	30.5	9.6	53/54
3	A	1.99	1.0	3.3	1.0	6/6	3.4	11.0	3.5	19/19
	F		1.9	6.0	1.9	10/10	6.0	19.3	6.1	33/34
4	A	1.78	0.8	2.8	0.9	5/5	4.2	15.1	4.8	26/28
	F		1.8	6.5	2.1	11/12	7.7	27.8	8.8	48/52
5	A	1.99	1.6	5.2	1.6	9/9	5.1	16.2	5.1	28/28
	F		3.0	9.6	3.0	17/17	7.9	25.1	7.9	44/44
6	A	1.73	1.1	4.3	1.4	7/8	3.9	14.8	4.7	26/28
	F		2.0	7.7	2.4	13/14	7.1	26.2	8.3	45/49
7	A	1.73	1.7	6.3	2.0	11/12	6.3	24.1	7.6	42/46
	F		3.2	11.9	3.8	21/22	9.5	35.2	11.1	61/67
8	A	1.68	1.9	7.3	2.3	13/14	6.9	26.5	8.0	46/52
	F		3.7	14.5	4.6	25/28	10.8	42.0	13.3	73/83
9	A	1.74	1.4	5.3	1.7	9/10	5.2	20.0	6.3	35/37
	F		2.5	9.5	3.0	16/18	7.6	28.5	9.0	49/54
10	A	1.48	6.3	30.0	9.5	52/63	10.6	53.0	16.7	92/110
	F		8.5	40.0	12.6	69/85	17.8	83.0	26.2	144/175

* $x_v = \alpha_v \cdot \sqrt[v]{t}$ (t = time in years)
** $x_{v10} \equiv x_{10}$
$x \cong \alpha \cdot \sqrt[2]{t}$

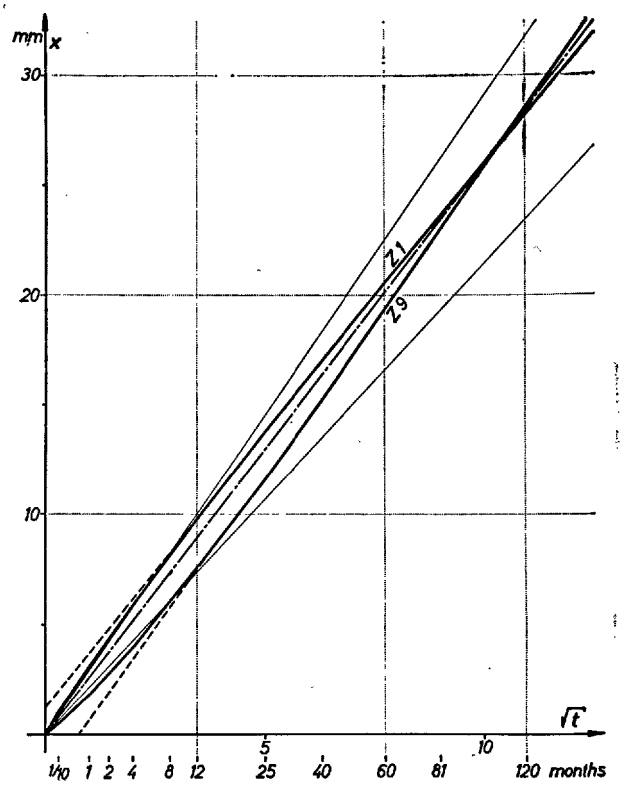

Fig. 3. *Genuine carbonation progresses of Z 1 and Z 9 and trend lines of $\sqrt[2]{t}$-approximation*
– – – – – –best approximation
— — — — —good long-time approximation
————wrong approximation

provided that 'X_v' in equ. [2] and 'X' in equ. [5] are taken the same value not earlier than after 10 years.

This approximative adjustment [5] is also drawn in Fig. 3. It is in case of Z1 and Z9 very nearly the same (— · — ·). Likewise in Table 2 besides the experimental values 'v', 'α_v' and 'X_{v10}' according to equ. [3] also the adjusted values 'α' according to equ. [5] are calculated and further the deviations

$$\frac{X_{30}}{X_{v30}} = \frac{\alpha}{\alpha_v} \cdot 30^{v/2} \qquad [6]$$

which are to be expected after 30 years.

Additional Test Results

Table 3 shows the carbonation depths and the compressive strengths of the corresponding concrete prisms after 5 years. The evident test deviations are put in parenthesis. Nevertheless, even the other results show that exact values of carbonation of a precisely defined concrete are not to be obtained easily.

In Table 4 the compressive strengths of completely carbonated mortars (in normal air and in 3% CO_2) are compared to the initial strengths after 28 days of water-curing. The columns "S_A/S_W%" and "S_C/S_W%" show the strengths after carbonation given in % of the strengths immediately before carbonation.

Of numerous sufficiently carbonated mortar prisms (normal air and 3% CO_2) the CO_2-contents of the carbonated paste were analyzed, chemically and by X-ray analysis. Of several just slightly carbonated specimens the CO_2-contents of the thin carbonated layer could be measured with X-ray analysis only. For this purpose the contents of calcite and vaterite of the mechanically enriched paste were measured quantitatively. Fig. 4 shows the X-ray diagrams of the completely carbonated mortars of Z7 and Z2 (enriched paste).

All CO_2-contents were calculated as carbonated CaO/cement and are listed in Table 5.

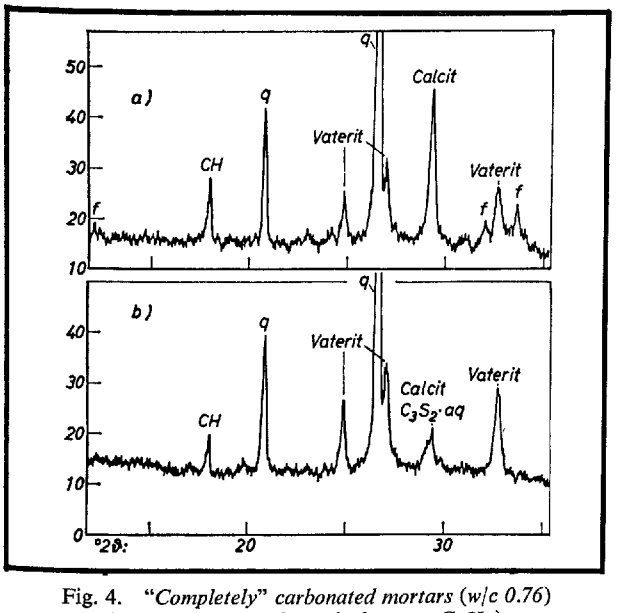

Fig. 4. *"Completely" carbonated mortars (w/c 0.76) (X-ray diagrams of enriched pastes,* CuK_α)
a) Portland cement (Z7)
b) Portland blastfurnace slag cement (Z2)

Evaluation

Alterations Due to Carbonation

Besides lowering the alkalinity of concretes, car-

Table 3. *Carbonation and compressive strength of concrete prisms 5 × 5 × 25 cm after 5 years*

Cement No.	Carbonation X_5 in mm	average	Compressive strength in kg/cm²	average
1	8.5 7.8	8.2	(839) 670	670
2	6.0 6.8	6.4	657 672	665
3	2.8 3.6	3.2	689 770	720
4	4.8 4.4	4.6	596 707	652
5	(6.5) 4.3	4.3	689 755	722
6	5.1 3.8	4.5	587 676	632
9	4.1 3.8	4.0	677 657	667

Table 4. *Compressive strength of cement mortars after total carbonation in air or* CO_2. *Mortar bars 4 × 4 × 16 cm, w/c 0.76*

No.	Cements Type	Slag C_3A %	28 days in water (S_w)	Compressive strength in kg/cm² 50 months in air 20°C, 65% r.h. Lab. F	Lab. H	S_a/S_w%	6 months in 3%CO_2 Lab. A	S_c/S_w%
1	HOZ	74	225	350	330	151	456	203
2	HOZ	55	199	356	320	170	396	199
3	HOZ	43	298	474	418	150	708	238
4	EPZ	15	252	497	384	175	708	281
5	EPZ	29	240	428	380	168	592	247
6	PZ	8	267	520	384	169	648	243
7	PZ	<1	182	397	336	202	482	265
8	PZ	2	149	318	350	224	442	296
9	PZ	13	247	426	396	166	516	209
10	SHZ*	85	427	232	194	50	190	45

*SHZ = Supersulphated cement

Table 5. *Carbonated* CaO *in mortars after total carbonation in air or 3% CO_2*

Cement No.	CaO	w/c	Paste of mortars Carbonated CaO in % in air chem.	in air X-ray	in air average	in 3% CO_2 chem.	in 3% CO_2 (X-ray)
1	49.9	0.76	22.5	23.2	22.9	29.6	24.7
		0.50	—	21.6		28.1	22.4
2	53.7	0.76	27.0	28.2	27.6	32.6	28.6
		0.50	—	26.2		29.0	25.2
3	57.1	0.76	36.8	34.5	35.7	39.1	34.5
		0.50	—	31.2		36.6	29.2
4	59.7	0.76	37.3	35.8	36.6	—	—
5	59.9	0.76	35.5	36.8	36.2	39.7	37.3
		0.50	—	34.7		(41.1)	34.0
6	64.5	0.76	38.1	36.3	37.2	—	—
7	63.5	0.76	35.4	36.8	36.1	43.3	40.6
		0.50	—	34.9		42.6	34.8
8	63.6	0.76	34.5	35.9	35.2	—	—
9	63.1	0.76	33.2	33.5	33.4	44.4	40.1
		0.50	—	31.3		43.3	35.4
10	45.3	0.76	14.5	14.7	14.6	—	—

bonation changes also the strength—probably the permeability too—and the composition of the paste.

Table 3 and especially Table 4 show that the compressive strengths of all the HOZs and PZs and remarkably increased. An exception is the SHZ (also the high alumina cements!), which behaves differently in many respects. Therefore the SHZ must not be compared to the other cements.

The binding of CO_2 of the mortars is drawn on a graph "carbonated CaO versus CaO-content of the cements" in Fig. 5 (see Table 5). Obviously the capacity of the slag cements to neutralize CO_2 increases linear with their CaO-content and is far greater than the free $Ca(OH)_2$ of the paste could be accounted for. On the average HOZs carbonate in air as long as there is left more than 25% noncarbonated CaO in the paste. Only then they can be called "completely carbonated". The PZs reach this point with 30% noncarbonated CaO already. Nearly all of the carbonated mortars without any alkaline reaction showed rests of free $Ca(OH)_2$.

Theories, based upon a neutralization of CO_2 or a resistance against carbonation only by the free $Ca(OH)_2$ of paste are disproved by these experimental results! (17)

After carbonation in 3% CO_2 the chemical analysis results in 5%~10% more carbonated CaO though the X-ray analysis proved nearly the same $CaCO_3$-contents as after carbonation in normal air. Up to now

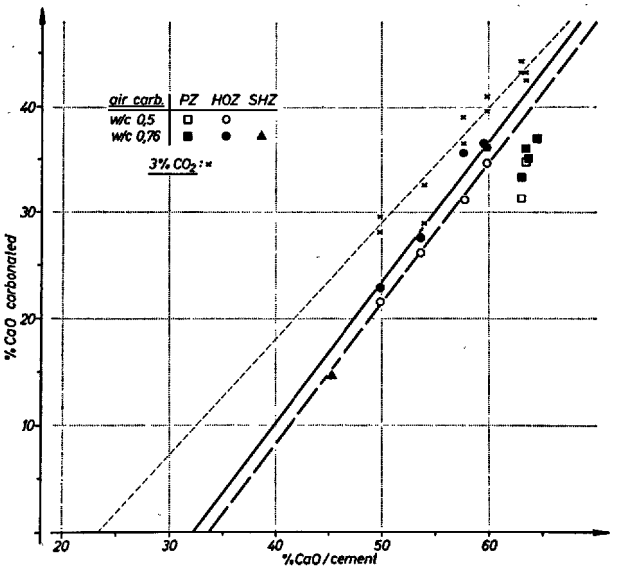

Fig. 5. *Carbonated* CaO *of completely carbonated cements (paste of mortars) versus total* CaO *of cements*

this "missing CO_2" could not be explained.

Rate of Carbonation

In the approximative function [5]

$$X \cong \alpha \cdot \sqrt{t}$$

α determins the speed of carbonation which depends on the storage or weathering conditons and on the properties of the concrete.

The Tables 1, 2 and 3 show that constant ratios X_{HOZ}/X_{PZ} or $X_{W/C=0.76}/X_{W/C=0,50}$ do not exist. Other tests have meanwhile proved that these ratios can be altered at pleasure just by varying the precuring conditions. For this reason the parameters 'storage condition', '*w/c*-ratio' and 'type of cement' do not suffice to postulate the progress of carbonation and this way of representation requires too many exceptions and therefore is far too complicated (14).

Surely, the decisive parameter is the permeability (18). But the permeability is difficult to measure and even more difficult to predetermine. As, however, the easily measurable compressive strength is to a certain extent connected with the porosity and permeability of a concrete, an empirical relation was detected after thorough investigations and numerous evaluation tests (19).

In Fig. 6 for all the PZs, EPZs and HOZs and for *w/c* 0.76 and *w/c* 0.50 the carbonation depths 'X_{10}' of the mortars and their factors '$1/\sqrt{B}$' are drawn on a plot (see Tables 1 and 2). B is the compressive strength after 28 days of water-curing i. e. at the begin

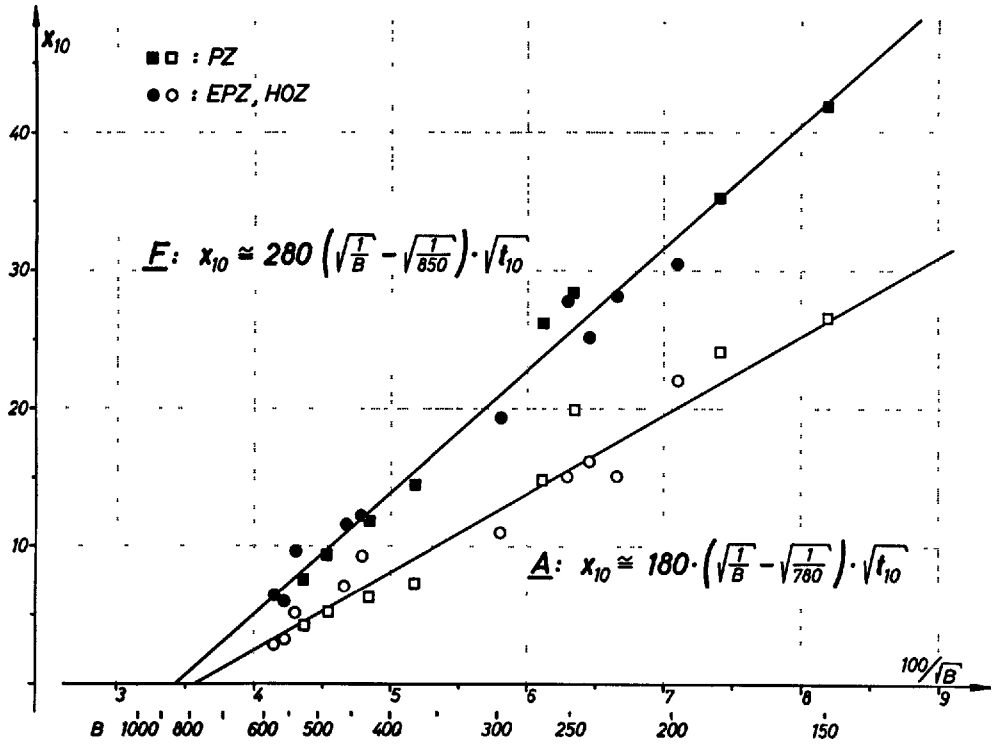

Fig. 6. *Carbonation of mortars "Indoors"*
X_{10} = *carbonation after 10 years in mm*
B = *compressive strength after 28 days of water-curing in kg/cm²*
t_{10} = *10 years*

of carbonation. With these straight lines the speeds of carbonation for the different conditions of Laboratory A and Laboratory F can be calculated and equ. (5) becomes

$$X \cong a \cdot \left(\frac{1}{\sqrt{B}} - \frac{1}{\sqrt{B_G}}\right) \cdot \sqrt{t} \qquad [7]$$

This equation has only the two constants 'a' and 'B_G' which depend on the storage conditions alone:

'a' is the speed constant

'B_G' is the strength limit of carbonation i. e. a concrete with a compressive strength $>$ 'B_G' does not carbonate.

This diagram is based on ~200 test values (Labor. F) and. ~100 test values (Labor. A) respectively.

Inquiries proved that the storing room of Laboratory Fhad been used more frequently than the one of Laboratory A. Thus the CO_2 content of the air was in Labor. F somewhat higher than in Labor. A. The relative humidity had been ~65% RH in both cases. It is clearly to be seen that little differences such as these result in a strong influence on the rate of carbonation.

Fig. 7 is a similar diagram of the concrete prisms after 5 years storage indoors at 50% RH (see Tables 1 and 3). Because of the still very steep strength increase at the beginning of carbonation (7 days), in this case the 14 days' strengths were put in as 'B'.

The constant 'B_G' for the concretes is greater than it is in the case of the mortars, according to the lower relative humidity of the room. This diagram is based on 14 test values only.

Comparison with Other Published Data

The carbonation of all the alkaline components of paste and not only that of the free $Ca(OH)_2$ is based on a fundamental chemical law and this fact was published by several authors (5), (8), (9), (12), (14), (17), (19), (20) and (21).

Meanwhile only few authors report on the altera tion of strength due to carbonation. A. Meyer, H.-J. Wierig and K. Husmann investigated tiny cylinders (12 mm) which are undoubtedly not suitable for comparisons with concretes or even mortar prisms (15).

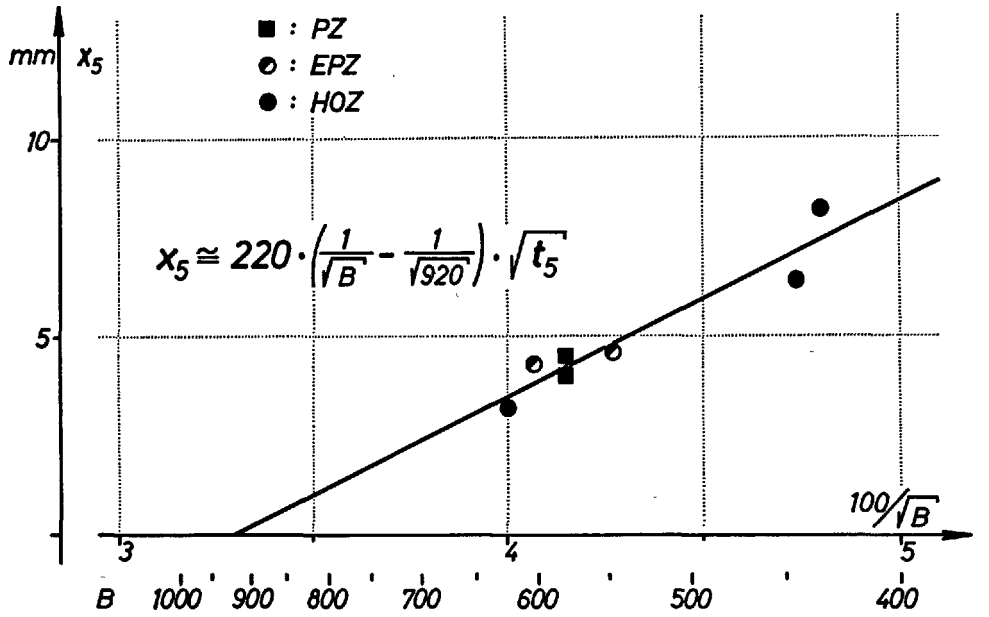

Fig. 7. *Carbonation of concretes "Indoors"*
X_5 = *carbonation after 5 years in mm*
B = *compressive strength after 14 days of moist treatment in kg/cm²*
t_5 = *5 years*

W. Manns and O. Schatz investigated the carbonation of completely dried mortar prisms 4 × 4 × 16 cm in 9% CO_2 and report on losses of strength not only with SHZ but also with HOZ containing more than 60% slag (22).

As with the exception of the SHZ and the PZ these experiments disagree completely with our results, we searched for the cause:

In Fig. 8 for 5 PZ, 7 HOZ and 2 SHZ all the available compressive strengths 'B' and flexural tensile strengths 'F' measured by the Laboratories A, F and H and by Manns and Schatz (Laboratory I.f.B.) are drawn to double logarithmic scale. Only those specimens are represented which has been water-cured or completely dried (40°C and 105°C) or completely carbonated.

According to a well known formula (24) the strength characteristic of mortars 4 × 4 × 16 cm is

$$F = B^{0.70-0.73}$$

Fig. 8 shows that the following specimens fit well in this equation

a) Water-cured prisms (3 to 91 days) of all the laboratories.
b) All the dried prisms (40°C and also 105°C each) and all the carbonated prisms of Laboratories A, F and H.

On the other hand the dried prisms and the carbonated prisms of Laboratory I.f.B. do not obey this law any more. Using the 4 mean values of the dried specimen (7 single results) and the 4 mean values of the carbonated prisms (39 single results) a compensating computation resulted in the (trend line) average equation

$$F \cong 0.0005 \cdot B^{1.9}$$

The drying conditions in Laboratory I.f.B. had completely destroyed the strength characteristic of normal mortars. For this reason these results can not be compared with the results of the other laboratories. Moreover, they cannot be brought in any relation to the behaviour of a normally treated concrete structure which will never be completely dried at 40°C or 105°C.

The relation between the rate of carbonation and the initial compressive strength has not specially been reported yet, but many published results provide an excellent proof.

A. Meyer, H.-J. Wierig and K. Husmann tested the carbonation of mortars 4 × 4 × 16 cm after 7 days' water-curing using 4 different cements and 5 different *w/c* factors (Test series 4) (15).

Here again—as in the case of our own concrete prisms—not the 7 days' but the 14 days' strength

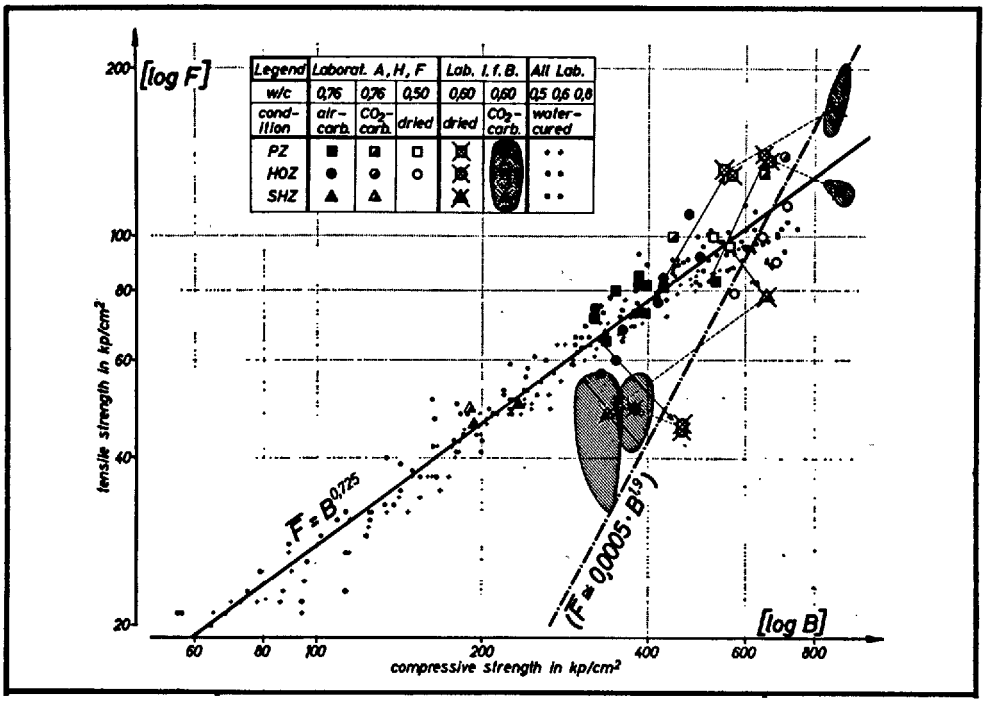

Fig. 8. *Relation between compressive strength and flexural tensile strength of mortars 4 × 4 × 16 cm after various treatments. Well knownstatistic equation of normal treated mortars:*

$$F = B^{0.70-0.73}$$

Table 6. *Compressive strengths of mortars and carbonation after 2 1/2 years (According to test results of A. Meyer, H.-J. Wierig and K. Husmann)*

w/c ratio	Remarks about calculation of 14 days' strengths		PZ (Z 21) B_{14d} kg/cm²	PZ (Z 21) $x_{2.5}$ mm	HOZ (Z 22) 50% slag B_{14d} kg/cm²	HOZ (Z 22) 50% slag $x_{2.5}$ mm	HOZ (Z 23) 75% slag B_{14d} kg/cm²	HOZ (Z 23) 75% slag $x_{2.5}$ mm	HOZ (Z 24) 65% slag B_{14d} kg/cm²	HOZ (Z 24) 65% slag $x_{2.5}$ mm
0.6	measured strengths after	7 days	295		244		204		176	
		28 days	420		410		344		316	
	interpolated acc. to Sadran	14 days	368	8	344	9	281	10.5	250	11.5
0.4	calc. factor	1.5	552	4	501	4.5	421	7	375	7
0.5	calc. factor	1.3	478	6	434	6	365	9	325	9
0.8	calc. factor	0.6	221	13	200	15	168	14.5	150	> 20
1.0	calc. factor	0.4	147	17	133	18.5	112	> 20	100	> 20

must be set for 'B'. With use of the published 7 and 28 days' strengths (Test series 3) these 14 days' strengths have been calculated and were together with the also published carbonation after $2\frac{1}{2}$ years specified in Table 6. Fig. 9 proves that the relation

$$X \sim 1/\sqrt{B}$$

is excellently confirmed. Furthermore it is to be seen that the carbonation conditions had been extremely strong in this laboratory (50% RH).

With tests on old structures this accuracy cannot be expected due to the lack of information about the exact weathering conditions during the length of time (14).

The concretes being best comparable must be those which had been stored outdoors sheltered from rain and which are old enough for a statistical survey without inaccurate extrapolation of carbonation

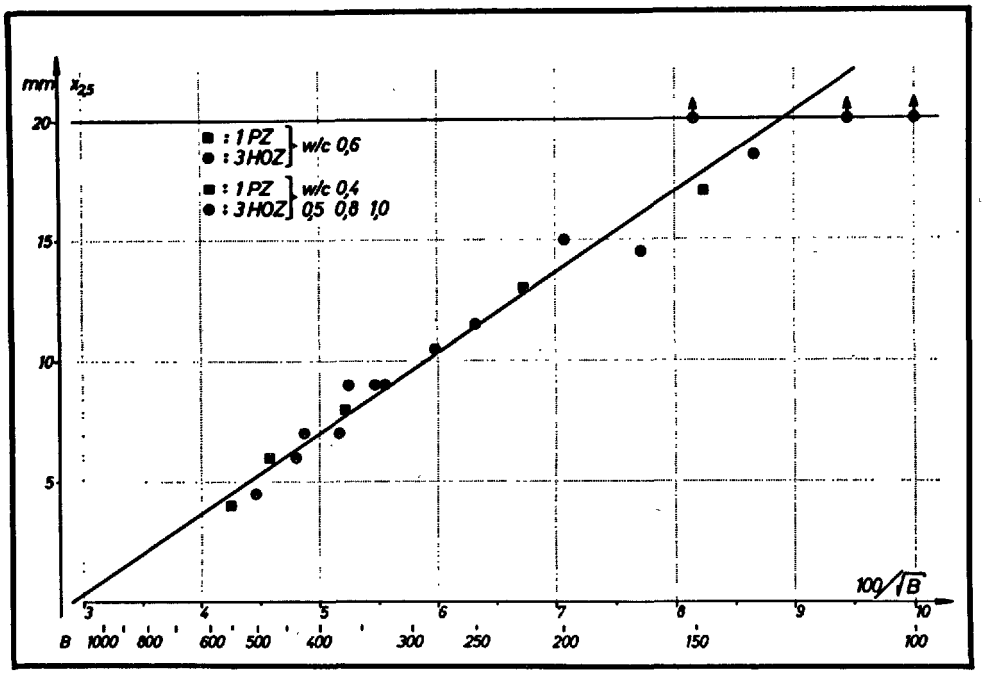

Fig. 9. *Carbonation of mortars "Indoors"*
$x_{2.5}$ = *carbonation after 2.5 years in mm (published)*
B = *compressive strength after 14 days' watercuring (w/c 0.6 published, the other w/c calculated)*
(Calculated with test results of A. Meyer, H.-J. Wierig and K. Husmann)

Table 7. *Carbonation of very old construction-concretes*
Age: > 20 years; weathering condition: 'Out-doors, without rain'

Authors	Construction	specimen	Type of cement	Strength B kg/cm²	Age years	Carbonation mm x	Carbonation mm x_{25}	Marks in Fig. 10
A. Meyer, H.-J. Wierig and K. Husmann	LS-Bunker, Köln	B 4	PZ	360	23	5	5.2	■
	Bunker, Dülmen	B 17	PZ	250	26	25	24.6	■
	T-Laner, Dülmen	B 18	PZ	400	26	12	11.8	■
	"	B 20	PZ	370	26	8	7.9	■
	Molkerei, Bielefeld	B 63	PZ	230	40	26	20.6	■
	Chem. Werke Hüls	B 34	HOZ	280	21	20	21.8	●
	Bunker, Wilhelmshaven	B 35	HOZ	310	23	5	5.2	●
	LS-Bunker, Wilhelmsh.	B 41	HOZ	260	23	18	18.8	●
	Bunker, Wilhelmshaven	B 57	HOZ	420	23	10	10.4	●
	"	B 58	HOZ	400	23	6	6.3	●
	LS-Bunker, Wilhelmsh	B 59	HOZ	400	23	15	15.6	●
	Brücke, Bottrop	B 61	HOZ	130	25	55	55.0	●
	"	B 62	HOZ	130	25	50	50.0	●
	Brücke, Oberhausen	B 88	?	180	23	40	41.7	▲
	"	B 90	?	270	22	19	20.3	▲
G. Rehm and H. Moll	Aachebrücke, Bregenz		PZ	540	41	0	0	□
	Mendener Brücke, Stütze 1		HOZ	190	31	32	28.8	○
	" 2		HOZ	150	31	55	49.4	○
	Mendener Brücke, Wand außen, 3		HOZ	290	31	23	20.6	○
	" " 4		HOZ	290	31	25	22.4	○
H.-J. Kleinschmidt	Brücke Edersee		PZ	366	50	~11	~8	⊠

depths.

Using the reports given by G. Rehm and H. Moll (25) by H.-J. Kleinschmidt (26) and A. Meyer, H.J. Wierig and K. Husmann (15) in Table 7, all the concrete structures (without exception) are listed which firstly met this storage condition, secondly were older than 20 years, and thirdly were published with strength data. The carbonation after 25 years was calcu-

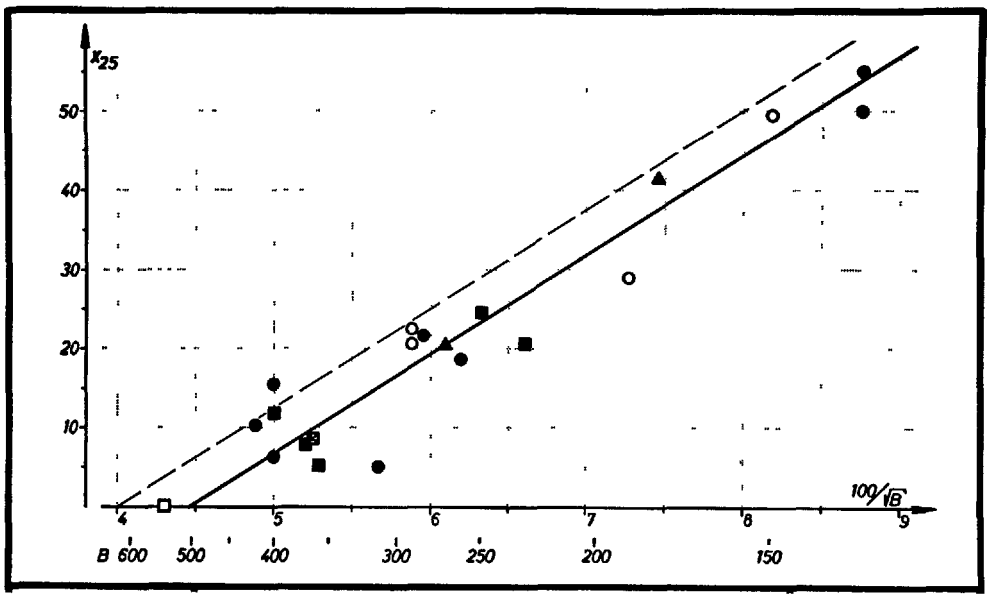

Fig 10 *Carbonation of old concrete structures "outdoors sheltered from rain" (age > 20 years)*
x_{25} = *reduced carbonation after 25 years in mm*
B = *published compressive strength in kg/cm²*
■⊠□ = *PZ* ●○ = *HOZ* ▲ = *Cement unknown*
(According to A Meyer, H-J. Wierig, K Husmann ■●▲, *G. Rehm, H Moll* □○ *and H-J Kleinschmidt* ⊠)

lated according to the formula

$$X_{25} \cong X_t \cdot \sqrt{\frac{25}{t}} \qquad [8]$$

Though the strength data are probably not very exact, even these concretes show the same tendency as Fig. 10 proves. The dotted line in this diagram is calculated according to results of another very comprehensive German longtime study with > 15 cements and three *w/c* factors.

These examples sufficiently demonstrate the fact that the so far recommended—and several exceptions including—parameters "type of cement" and "*w/c* factor" and "precuring condition" are to be represented much better by the single summarizing factor $1/\sqrt{B}$ (23).

Conclusions

By comparing numerous carbonation studies in several laboratories for the storage condition "outdoors without rain" the average constants

$$a \cong 250 \quad \text{and} \quad B_G \cong 625$$

were estimated. Thus equ. [7] becomes

$$X \cong 250 \cdot \left(\frac{1}{\sqrt{B}} - \frac{1}{\sqrt{625}}\right) \cdot \sqrt{t} \qquad [9]$$

This relation is drawn on a graph in Fig. 11 for

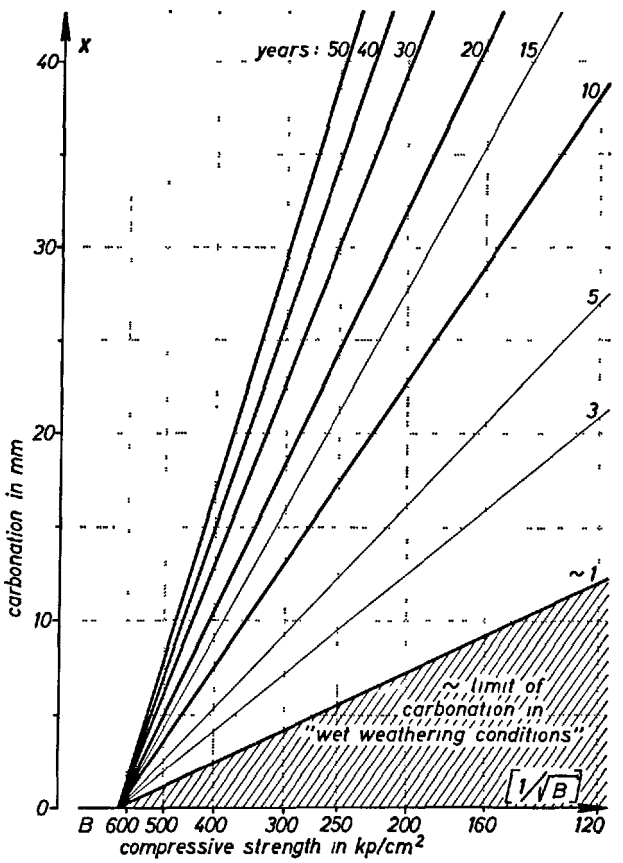

Fig 11. *Approximative carbonation of concretes "outdoors sheltered from rain" without afterhardening*

carbonation periods up to 50 years. This diagram stands for the very unfavourable case that the concretes have only little if any afterhardening.

$$X = 250 \cdot \left(\frac{1}{\sqrt{B}} - \frac{1}{\sqrt{625}}\right) \cdot \sqrt{t}$$

On the other hand it is well known that concretes with slowhardening cements generally develop slow but high afterhardening (27)

$$N = B_\infty - B_w$$

even in air of natural humidity conditions. In this case equ. (1) can be slightly altered in

$$\frac{1}{B} = \frac{1}{B_\infty} + \left(\frac{1}{B_w} - \frac{1}{B_\infty}\right) \cdot \frac{n \cdot t_w}{t + n \cdot t_w} \qquad [10]$$

B_∞ = final strength
B_w = strength after water curing (= B_0)
t_w = time of water curing
n = retarding factor
t = time of air storage (and carbonation)

The calculation of the relation between equ. [9] and equ. [10] is only possible by means of a rather difficult integration. Nevertheless the problem can be solved accurately by graphical constructions. As a final result Fig. 12 shows the carbonation progress of concretes "B 250" (kg/cm²) with afterhardening 'N = 250' (kg/cm²) and 'B 350' (kp/cm²) with afterhardening 'N = 100' (kp/cm²). (Constants of afterhardening according to [10] are $t_w = 1$ month and $n = 4$.)

It is to be seen that after 30 to 40 years the two concretes will reach quite the same carbonation as a 'B 425' without afterhardening. Furthermore this diagram demonstrates clearly another fact: It is impossible to calculate or extrapolate the carbonation of an old concrete by only using the carbonation of the present young concrete and without at least knowing its strength development (14) and (19).

Fig. 13 is a similar diagram like Fig. 11 for carbonation periods from 10 to 30 years without afterhardening (N = 0) and also taking into consideration two slow ($n = 4$) afterhardenings N = 100 kg/cm² and N = 250 kg/cm². This diagram provides an explanation for the experience that the relation

$$X \sim \frac{1}{\sqrt{B}} \cdot \sqrt{t}$$

is to be proved less accurately with old concretes

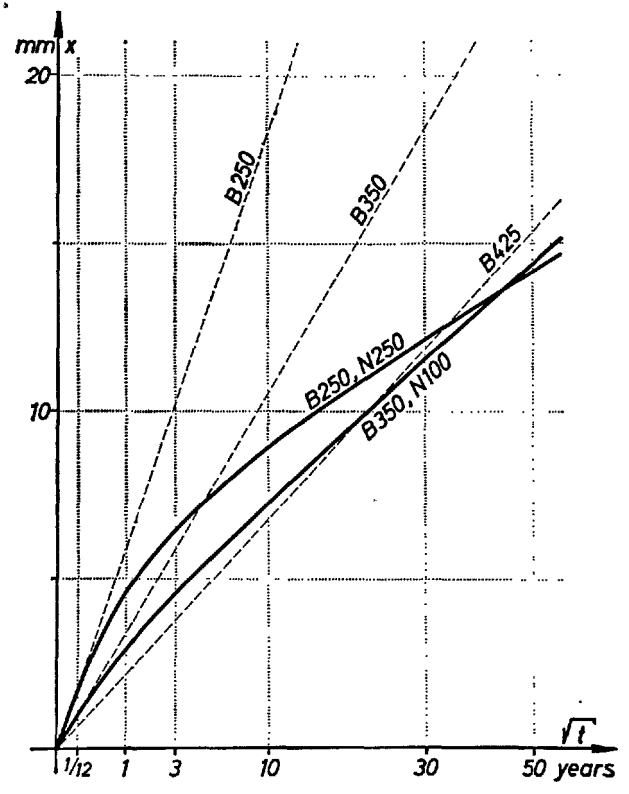

Fig. 12. *Approximative carbonation progress of different concretes with different afterhardening*
B = initial compressive strength in kg/cm²
N = afterhardening in kg/cm²
($a = 250$, $B_G = 625$, $n = 4$)

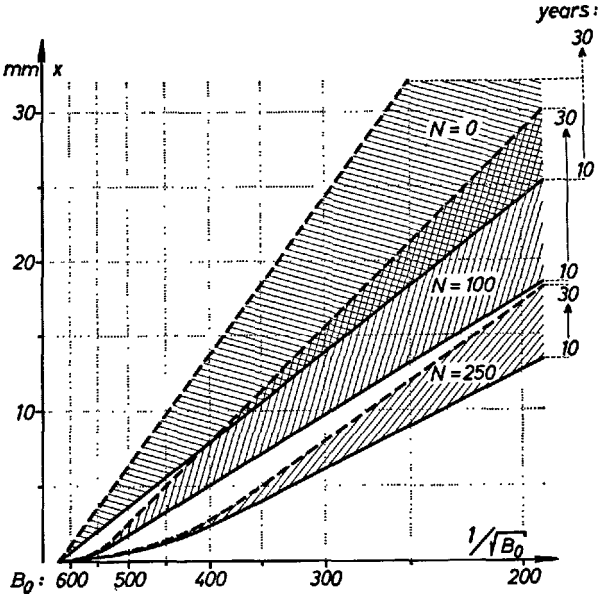

B_0 = initial compressive strength in kp/cm²
N = slow afterhardening in kp/cm²
x = carbonation depth in mm

Fig. 13. *Approximative carbonation of concretes "outdoors sheltered from rain" with afterhardening*
($a = 250$, $B_G = 625$, $n = 4$)

(see Fig. 10) than with mortars in a laboratory.

Following Fig. 12 and Fig. 13 grater differences in initial carbonation between cements with lower initial strength and high afterhardening and cements with higher early strength and low afterhardening will gradually disappear with growing age of older concretes. This corresponds exactly with the general results of extensive studies on old and very old concrete structures (4), (6), (11) and (14).

Summary

A high content of free $Ca(OH)_2$ cannot protect any concrete against carbonation.

In case of portland cements and blastfurnace slag cements the carbonation progress is practically entirely determined by the permeability of the concrete. Thus under constant storage conditions the entire carbonation behaviour can be calculated in first approximation by means of the initial strength and the afterhardening of the concrete only.

For this, not the knowledge of the chemical composition of the cement is necessary but the knowledge of the complete strength development of the concrete under certain distinct storage conditions.

At any rate it is safer to make a concrete with a sufficiently high content of normal or even with slow hardening cement than a concrete with similar initial strength but a lower content of high early strength cement.

Acknowledgements

The author is very indebted to Dr. F. Schröder, Dr. K. Habel and Dr. W. Kayser for the extensive basic experimental work and several supplementary tests, carried out accurately whenever they seemed to be necessary, and were performed in their laboratories

Labor. F Forschungsinstitut der Forschungsgemeinschaft Eisenhüttenschlacken, Rheinhausen

Labor. A Hauptlabor. der August Thyssen-Hütte AG, Duisburg-Hamborn

Labor. H Zementwerk der Fried. Krupp Hüttenwerke AG, Bochum, Werk Rheinhausen

References

1. M. Hamada: "Neutralisation (carbonation) of concrete and corrosion of reinforcing steel" V-ISCC, III–3, 1–89, Tokyo (1968).
2. K. Kishitani and K. Hamada: "Dauerhaftigkeit des Stahlbetons in Zusammenhang mit der Neutralisierung durch CO_2" (in Japanese) Bericht des 'Kajima Institute of Constr. Technology' Tokyo (1963).
3. P. E. Halstead: "Corrosion of metals in buildings" Chemistry and Industry 1957, 1132–1137.
4. T. Soda and K. Yamazaki: "Long time study (20 years) on the neutralisation of concrete and the rusting of reinforcement in concrete", Japan Cem. Engin. Assn. **12**, 91–93 (1958).
5. B. Kroone and F. A. Blakey: "Reaction between carbon dioxide gas and mortar", J. Amer. Concrete Inst. **31**, 497–510 (1959).
6. F. Gille: "Ueder die Tiefe der karbonatisierten Schicht von alten Betonproben" beton **10**, 328–330 (1960).
7. K. Kosaka: "Durability (especially carbonation) test of concrete" Intern. Symp. 'Durability of Concrete' (Prag 1961) Final Report (Prag 1962).
8. S. Asano, M. Ozu and Y. Inoue: "The hydration and carbonation of various kinds of cement and cement compounds" Japan Cem. Engin. Assn. **16**, 68–69 (1962).
9. H.-G. Smolczyk: "Die roentgenographische Beurteilung von Beton aus Tonerdezement", Betonsteinzeitung **30**, 573–579 (1964).
10. T. Mori, K. Shirayama and A. Yoda: "The neutralization of concrete, the corrosion of reinforcing steel and the effects of surface finish", Japan Cem. Engin. Assn. **19**, 249–255 (1965).
11. B. Wedler: "Vorwort" zu diversen Arbeiten über Karbonatiserung alter Betone (Zusammenfassung) Deutscher Ausschuß für Stahlbeton, Heft 170, 3–4 und 50 (Berlin 1965).
12. Y. Inoue and S. Asano: "On the carbonation of hydrates of hydraulic compounds", Japan Cem. Engin. Assn. **20**, 66–67 (1966).
13. St. Soretz: "Korrosionsschutz im Stahlbeton und Spannbeton", Betonsteinzeitung **33**, 52–63 (1967).
14. F. Schröder, H.-G. Smolczyk, K. Grade, R. Vinkeloe and R. Roth: "Über den Einfluß on Luftkohlensäure und Feuchtigkeit auf die Beschaffenheit der Betone als Korrosionsschutz für Stahleinlagen", Rheinhausen 1964. Deutscher Ausschuß für Stahlbeton, Heft 182 II Berlin (1967), 1–28.
15. A. Meyer, H.-J. Wierig and K. Husmann: "Carbonatisierung von Schwerbeton", Beckum 1964. Deutscher Ausschuß für Stahlbeton, Heft 182/I, 1–32, Berlin (1967) (und Heft 170, 40–58, Berlin 1965).
16. G. Sadran and R. Dellyes: "Representation lineaire de la resistance mecanique des ciments en fanction du temps", Revue Mater. Constr. Nr. 606, 93–106 (1966).
17. H.-G. Smolczyk: "Zur Röntgen-Feinstrukturbeugung

als mineralogisch-analytischem Verfahren" Z. Phys. Chemie **53**, 123–134 (1967).
18. H.-E. Schwiete: "Über die Bestimmung der offenen Porosität im Zementstein", Tonindustriezeitung **90**, 562–574 (1966).
19. F. Schröder and H.-G. Smolczyk: "Zum Einfluß der Zementart auf die Karbonatisierung von Beton", Proceedings of RILEM-Techn. Comm. 'Corrosion of Reinforcement of Concrete' (CRC), Wexhem Springs in 1965, 95–96 (1968).
20. H. H. Steinour: "Influence of the cement on the corrosion behaviour of steel in concrete", PCA Res. and Dev. Lab. Bull. 168, May 1964.
21. E. G. Swenson and P. J. Sereda: "A mechanism for carbonation, shrinkage of lime and hydrated cement". To be published in the Journal of Appl. Chemistry (Revised June 1967).
22. W. Manns and O. Schatz: "Über die Beeinflussung der Festigkeit von Zementmörteln durch die Karbonatisation", Betonsteinzeitung **33**, 148–156 (1967).
23. F. Schröder and H.-G. Smolczyk: "Carbonation and protection against steel corrosion", V-ISCC, IV-3 "Slags and slag cements", 83–91, Tokyo (1968).
24. A. Hummel: "Das beton-ABC" 11th edition, p. 13 Ed. W. Ernst & Sohn, Berlin (1951).
25. G. Rehm and H. Moll: "Beobachtungen an alten stahlbetonteilen hinsichtlich Carbonatisierung des Betons und Rostbildung an der Bewehrung". Deutscher Ausschuß für Stahlbeton, Heft 170, 6–20, Berlin (1965).
26. H.-J. Kleinschmidt: "Untersuchungen über das Fortschreiten der Carbonatisierung an Betonbauwerken". Deutscher Ausschuß für Stahlbeton, Heft 170, 24–36, Berlin (1965).
27. E. Spohn: "Gedanken zum Geldbruck DIN 1164 Zement" Zement-Kalk-Gips **21**, 105–108 (1968).

Oral Discussion

Heinz G. Smolczyk

At first sight a direct relation between strength and carbonation rate (see my written discussion) seems to be strange, but this fact is proved by too many experimental results—once again by the supplementary papers III-16 of W. Manns and K. Wesche (see Fig. 1) and III-52 of A. Meyer (see Table 1).

And there is a theoretical explanation for this surprising result because of the relation between compressive strength B and capillary porosity ε_c in connection with the chemical composition of the cement. The tendency of this very relation is partly being reported of at this Symposium.

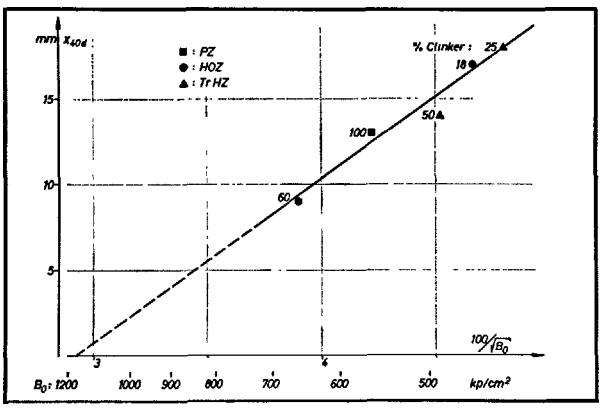

Fig. 1. *Carbonation of completely dried mortars after 40 days' storage in 9%CO_2*
B_0 = *compressive strength after heat-treatment (40°C or 105°C)*
x_{40d} = *carbonation depth*
(According to test results of K. Wesche)

According to R. Helmuth and G. Verbeck—principal paper III-1—compressive strength is proportional to 1-capillary porosity. We found an even better linearity—also with the test results of Helmuth and Verbeck—by plotting compressive strength against 1-capillary porosity, but the difference is only slight.

The results of R. Mills—supplementary paper III-46—show an increase in capillary porosity with increasing CaO/SiO_2—ratio at constant strength.

The studies of our laboratory with a mercury porosimeter showed the same tendency. Some results are to be seen in Fig. 2, where compressive strengths after 90 days' watercuring. Four cements with very different chemical composition and two water-cement

Table 1. *Investigations on building constructions*
Average results of carbonation, age and compressive strength according to test results of A. Meyer, H. J. Wierig and K. Husmann

Type of cement	Number of specimens	Mean age (years)	Mean carbonation (mm)	Mean compressive strength (kg/cm²)	Mean carbonation after 20 years (mm)
PZ	27	25	10.8	384	9.7
HOZ and EPZ	36	21	14.6	335	14.2
Experimental difference				49	4.5
Theoretical difference according to the difference in compressive strength from 335 to 384 kg/cm²					≅ 5 ± 1 mm

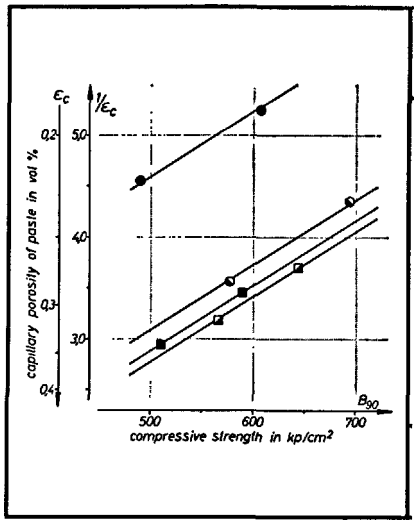

Fig. 2. *Relation between capillary porosity and strength Mortar prisms 4 × 4 × 16cm, w/c 0.50 and 0.60, 90 days' watercuring*

Chemical data in %

	slag	C/S	CaO	CO_2 max
■	0	3.3	66.4	~29
◪	25	2.7	60.4	~28
◓	50	2.2	54.5	~22
●	75	1.7	48.5	~16

ratios were tested, see the table beside the diagram. The general slope of the curves is the same for all cements, but the porosity decreases distinctly with decreasing clinker content, CaO/SiO_2 ratio, CaO content or maximum amount which could be expected after complete carbonation.

All these results lead to the tendency

$$\text{strength} = \frac{\text{f(CaO)}}{\text{f(capillary porosity)}}$$

and the empirical formula

$$\text{carbonation} \sim \sqrt{\frac{1}{\text{strength}}}$$

receives the theoretical explanation

$$\text{carbonation} \sim \sqrt{\frac{\text{f(capillary porosity)}}{\text{F(CaO)}}}$$

And this—on the other hand—corresponds very closely to the formula of R. Kondo, M. Daimon and T. Akiba—supplementary paper III-116.

Many precise experimental studies will be necessary to establish the exact mathematical relation but I think the validity of the general tendency is proved sufficiently by the great number of quite different test results published by quite different authors.

Author's Closure

Minoru Hamada

First of all, I wish to thank Dr. Smolczyk for having gone to the trouble of reading the many Japanese papers on the subject in order to prepare his very detailed discussion.

Dr. Smolczyk's opinions are based on tests carried out for 5 years at 3 research institutes in Germany, using portland cement, eisenportland cement and blast furnace slag cement.

I first with to explain that my standpoint is research has been to take reinforced structures above ground to clarify the relationship between rusting of steel and carbonation of concrete, as a reference for producing structures of long life, and therefore my ovservations are based on a broad point of view.

1. Very broadly speaking, I am in general agreement with his opinion that carbonation is unrelated to the free $Ca(OH)_2$ in paste. In other words, there are in the range of concrete of extremely high strength using high-early strength cement to concrete which is very porous such as cellular concrete, and taken as one group, it may be said that free $Ca(OH)_2$ and carbonation are unrelated.

Dr. Smolczyk's pinpointing of gross CaO rather than free $Ca(OH)_2$ is no doubt one way of considering the matter. However, the quantity of free $Ca(OH)_2$ resulting from hydration of CaO depends greatly on the degree of hydration, and the prevention of rusting of steel with which I am concerned is dependent on free $Ca(OH)_2$.

Further, the comment that there is $Ca(OH)_2$ remaining in neutralized portions is quite correct, but the question is whether this amount of $Ca(OH)_2$ will contribute towards prevention of rusting of steel.

I am not discussing whether or not free $Ca(OH)_2$ exists as a chemical component. My viewpoint is that steel in the portion of concrete which is not colored by phenolphthalein will rust.

2. It has been pointed out that carbonation will increase strength. This is naturally so, and I have no arguments against this.

3. Dr. Smolczyk states that depth of carbonation proportional to the root of the time of carbonation is suitable only with very old concretes. My concern is with the rusting of steel in concrete and therefore, naturally considers long-time age, and limited to this regard, both Dr. Smolczyk and I are basically in agreement.

4. Dr. Smolczyk suggests a method of expressing

depth of carbonation for various cements by a formula with not only age in years, but also early strength as factors. In contrast, I am of the thought that it would be more commonly applicable to indicate depth of carbonation with concrete materials-cement, aggregates, admixture—and water—cement ratio, cement paste quantity, etc. which are deeply related to the structure of concrete, as factors.

5. The depth of carbonation when using high early strength cement and long-term strength-gaining cement are discussed and an interesting analysis of data has been made. However, without going into the case of underground structures, it may be said that long-term strength gain at concrete in ordinary building structures cannot be expected.

In short, as to substantiate the point I emphasize in my paper, Dr. Smolczyk mostly aptly states at the end, manufacture of a dense and impermeable concrete comes before all else.

Supplementary Paper III-16 Variation in Strength of Mortars made of Different Cements Due to Carbonation

Wilhelm Manns and Karlhans Wesche*

Synopsis

By carbonation strength is varied in the area of the concrete surface: in the case of portland cement strength is increased, on the other hand, it was suggested that with slag sulphate cement strength is reduced by carbonation.

This has been confirmed by researches on structural concrete at an age of 4 to 10 years. Due to the considerable decrease in strength of concrete made of slag sulphate cement caused by absorption of atmospheric carbon dioxide which must be equalized with the known phenomenon of concrete corrosion, it should be considered whether this corrosion is confined to the slag sulphate cement only or whether it can be observed with other cements. Therefore, researches on the carbonation of mortar prisms made of six types of cements were carried out, namely on specimens of 1 portland cement, 1 slag sulphate cement, 2 blast furnace cements, 2 trass blast furnace cements.

The specimens were cured after drying in an air current enriched by 9% CO_2 and their strengths were compared with specimens cured at 20°C at a relative humidity of 65%. The influence of the absorption of carbon dioxide proved to be dependent on the type of cement, essentially on the content of portland cement clinker and thus on the content of $Ca(OH)_2$ produced by hydration: at a content over 40% clinker strength increased by up to 70%, at a content below 40% of clinker it decreased by up to 50%. The variation in strength is accompanied by a variation in the modulus of elasticity and in weight. The variation in weight is linear to that in strength so that it is possible to estimate by the variation in weight whether carbonation will induce an increase or decrease in compressive strength. The investigations will be continued.

Introduction

By carbonation, i.e. the reaction of carbon dioxide of the air, the alkalinity of cement paste and thus the rust protection of the reinforced and prestressed concrete structures is reduced. Particular attention has been devoted to this question and to the researches interconnected with the carbonation depth and the rate of carbonation in Japan and the Federal Republic of Germany during the last years. The question whether the strength characteristics of concrete will be changed and to which extent has not been followed, however, on a larger scale so far.

Previous Investigations

According to the American researches by Leber and Blakey (1), Kroone and Blakey (2), and Cole and Kroone (3) strength of concrete made of portland cement (PC) is increased by carbonation by about 40 to 100% which, according to Toennis (4), can be economically utilized for production of concrete blocks.

Mußgnug (5) found, however, that concretes made of slag sulphate cement (SSC) stored at room temperature developed strengths reduced by about 30 to 40% compared with those stored under water or in open air. Gaede (6) also observed on long term tests on 10 cm concrete cubes of blast furnace cement (BFC) and of SSC considerable decreases in strength which are, however, statistically verified for SSC only with about 20 to 35%, whereas for PC the already stated increase in strength could be deter-

*Institut für Bauforschung Technische Hochschule Aachen, Aachen, West Germany.

mined although somewhat reduced.

Basing on the results of Gaede, investigations have been made on 4 to 10 years old SSC concretes. For this purpose, cores with a diameter of 10 and 15 cm were taken from buildings and, if possible, three test specimens were made thereof. A height of 4 cm of the upper specimen was chosen to prevent an influence of the carbonated layer on the results of the successive specimens. The mean specimen had the usual specimen size with a slenderness ratio of $h/d = 1$, the height of the lower specimen was chosen with 4 cm to compare the strengths of the upper and lower specimens. The test results are summarized in Table 1.

Table 1. *Strength results of test specimens made of cores of SSC concrete*

	Slenderness ratio	Strength (mean value) kg/cm²	Standard deviation kg/cm²	Sample size
upper specimen	0.25–0.40	636	106	20
mean specimen	1	580	59	19
lower specimen	0.25–0.40	798	106	14

Because of the influence of the specimen height the strengths of the upper and lower layers can be compared only. A statistical check of the characteristic values of the random test showed that the compressive strength values of the two random tests differed significantly. The difference between these compressive strengths is given with a statistical safety of S = 95% within a range of 85 to 235 kg/cm².

If the compressive strengths of the surface layer, i.e. specimens with carbonated concrete, are plotted against the carbonation depth the correlation coefficient points to a significant relation between the two variables, so that it can be assumed that the significant difference in strength between external and internal concrete is also due, besides other influences, to the influence of carbonation causing decrease in strength.

Manns and Sasse (8) found by ball penetration tests according to DIN 4240 that, on 20 cm concrete cubes made of SSC, the penetration measuring instruments indicating the strength of the surface layer only could be assigned to a strength which had a mean value of about 30% below the destructively tested strength.

Induced by the somewhat contradictory behaviour of PC and SSC reported of in previous papers, Manns and Schatz (14) carried out carbonation tests on cement mortar prisms of different cements in the Institute of Building Research of the Technical University Aachen.

Tests

Six cements of different compositions were tested and the magnitudes influencing carbonation such as there are temperature, humidity, cement content, water/cement ratio, compaction, and surface of specimen were kept invariable. The following cements were chosen: 2 blast furnace cements (BFC I and II), 2 trass blast furnace cements (TBFC I and II), 1 slag sulphate cement (SSC), and 1 portland cement (PC).

Some cement characteristics are shown in Table 2.

Table 2. *Several characteristics of cements used for carbonation tests*

Type of cement	Test acc. to DIN	Constituents			Retains on a 0.09 sieve DIN 4188	Begin of setting	End of setting	Modulus of rupture		Compressive strength after	
		cement clinker	slag sand	trass				7d	28d	7d	28d
		M%	M%	M%	M%	h	h	kg/cm²	kg/cm²	kg/cm²	kg/cm²
BFC I	1164	ab. 18[1]	ab. 82	—	0.28	5.00	7.15	49	65	211	329
BFC II	1164	ab. 60[1]	ab. 40	—	0.10	3.30	4.20	69	83	308	516
TBFC I	1167	50[1]	35	15	0.70	3.15	4.35	39	69	166	361
TBFC II	1167	25[1]	50	25	0.95	3.50	5.15	31	61	115	305
PC	1164	100[1]	—	—	4.40	3.25	4.15	61	78	320	413
SSC	4210	2–3	82–83	ab. 15 anhydrite	—	—	—	80–85[2]	91–94[2]	410–440[2]	560–590[2]

[1] without calcium sulphate
[2] values which do not belong to the Institute of Building Research

For the tests according to DIN 1164 standard cement prisms were made and cured for 28 days according to the Standards and then dried at 40°C up to constant weight (By mistake, the PC prisms were dried at 105°C.).

The storage temperature of 40°C was chosen for two reasons: firstly to prevent a liberation of crystalline bound water, and secondly to anticipate a postponed hardening of the mortar. Storage of water saturated cement mortar prisms at 40°C has accomplished this effect since the compressive strength values given below of specimens stored under constant air conditions did not indicate any tendency to an increase in strength.

After drying part of the specimens was stored under constant air conditions at 20°C and at a relative humidity of 65% (air curing). The remaining test specimens were cured in a CO_2 apparatus. The CO_2 apparatus consisted of two superimposed sheet steel boxes connected on their ends by semi-circular tubes. Circulating air was provided by a built-in ventilator, a thermostat was adjusted for an equal temperature of 25°C, the relative humidity measured by a hygrometer varied between 65 and 70%. Through test gas meters 3.3 l air/min. and 0.33 l CO_2/min. were supplied to the CO_2 apparatus. The test gas meters were adjusted semi-diurnally to exclude any irregularities in the supply of air and CO_2 so that the air was enriched by an average of about 9% CO_2. The apparatus was not gas tight so that an excess pressure could not arise (CO_2 curing).

In given intervals, two specimens, each of which was taken out of the CO_2 apparatus and one specimen out of the air-conditioning room and, after determining the weight, were tested for modulus of rupture and compressive strength according to DIN 1164. Between the modulus of rupture and compressive strength tests the common phenolphthalein test was carried out. With the exception of PC, the phenolphthalein test distinguished colourless zones sharply from coloured ones. If a specimen showed no longer a red colouring, it was designated as completely carbonated. The carbonation depth of PC could presumably not be clearly determined since the hydration of PC was abruptly stopped by drying at 105°C and continued by CO_2 curing so that calcium hydroxide was freed continuously over the whole section also influenced by CO_2.

Test Results

Compressive Strength

In Fig. 1 the compressive strength is plotted against the time by determining the terminated drying as starting point. It can be seen that strength development of

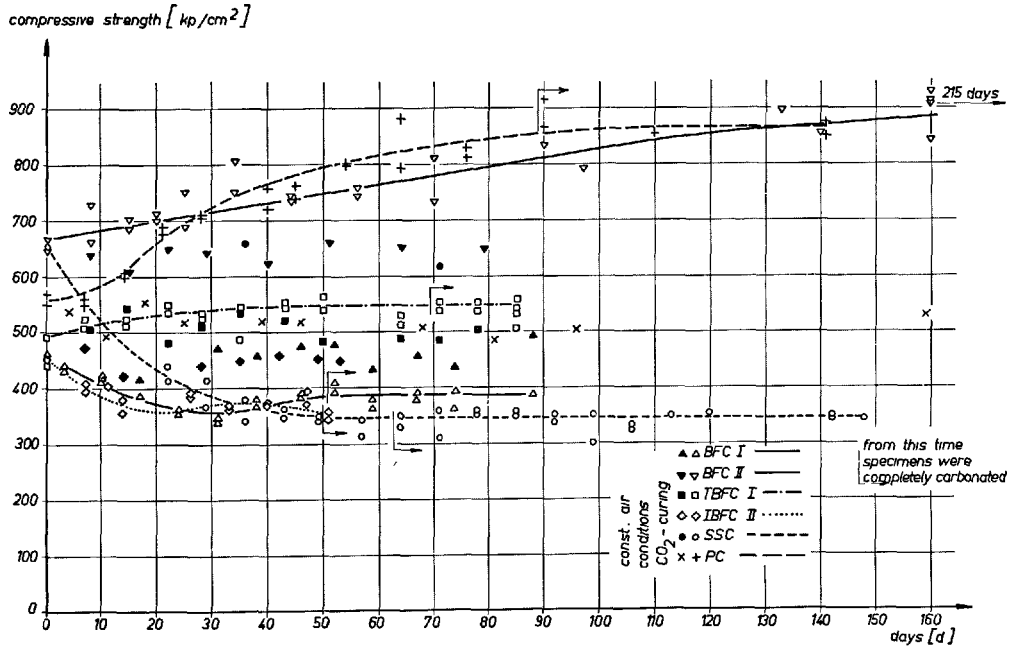

Fig. 1. *Relation between compressive strength and the duration of CO_2 curing and under constant air conditions resp.*

the individual cements differed considerably. This is still more obvious when instead of the absolute strength values the relative strength values are chosen as percentages of the compressive strength upon starting the CO_2 curing and curing under constant air conditions respectively (Fig. 2). The strength values

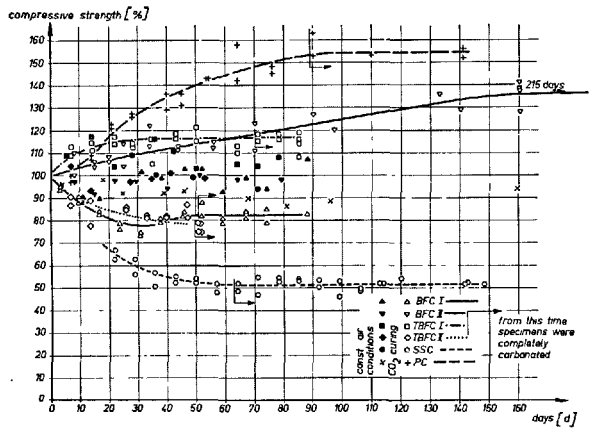

Fig. 2. *Change in compressive strength at CO_2 curing and under constant air conditions resp.*

under constant air conditions do not show any tendency: they vary in accordance with the natural scattering about the mean value of 100%. The strength values of the CO_2 curing have either an increasing or a decreasing tendency for the individual cements, however, they change any more after reaching a limit value different for each cement. This limit value was attained when carbonation of the specimen was completed and for PC specimens the first remarkable change in colour became obvious in the centre of the specimen. For PC, BFC II and TBFC I test specimens compressive strength values of carbonated mortar were above and for BFC I, TBFC II and SSC test specimens below the strengths upon starting the CO_2 curing.

A further insight into the relationship between compressive strength and carbonation provides the relation of the compressive strength as a function of the carbonation depth. The tendency of the relations is the same for the individual cements as shown in Fig. 1. The values, however, form a S-shaped curve. It should be added to this that a change in compressive strength cannot be discovered up to a carbonation depth of 5 mm and at a carbonation depth of about 15 mm, strength does not increase nor decrease any

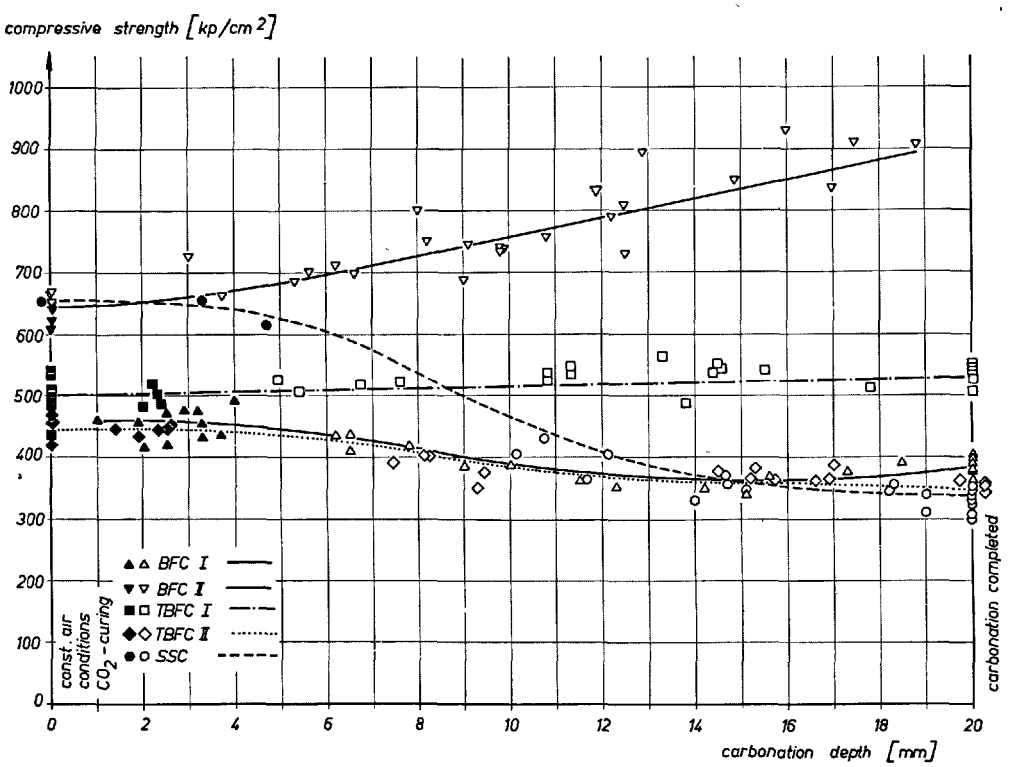

Fig. 3. *Relation between compressive strength and carbonation depth*

more. Since the latter can be presumably explained by the form of the fracture of the specimen it is difficult and not logical to draw up a mathematical relationship between compressive strength and carbonation depth which is based on these tests. The compressive strength as a function of carbonation is, however, well expressed if the absolute strength values are substituted by those refering to CO_2 curing and curing under constant air conditions respectively (Fig. 4).

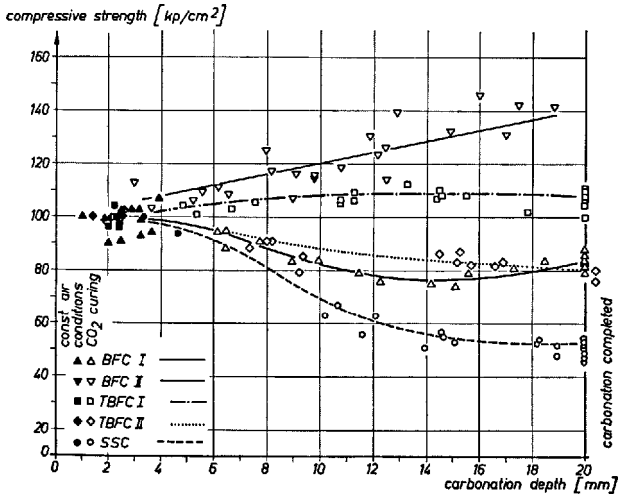

Fig. 4. *Relation between compressive strength and carbonation depth (at K = 0 mm, β_D = 100%)*

Modulus of Rupture

In Fig. 5 the modulus of rupture is plotted as a function of the time and in this diagram the end of drying is given as the starting point. At first, the modulus of rupture of all cement types decreases considerably during CO_2 curing and it increases after some time of storage to a greater or lesser extent to adjust, after the specimens are completely carbonated, to a value which is above or below the initial values depending on the type of cement. A still better insight into the relationship between modulus of rupture and carbonation is given by plotting the modulus of rupture against the carbonation depth (Fig. 6). Here is also shown the decrease of the modulus of rupture of all cements, however, for a carbonation depth up to 6 to 10 mm only, thereupon the modulus of rupture increases in a greater or lesser extent up to the completed carbonation of the specimens. This irregularity in the development of the modulus of rupture can be explained by the shrinkage process caused by carbonation which has been investigated by Powers (9), Leber and Blakey (1), and Verbeck

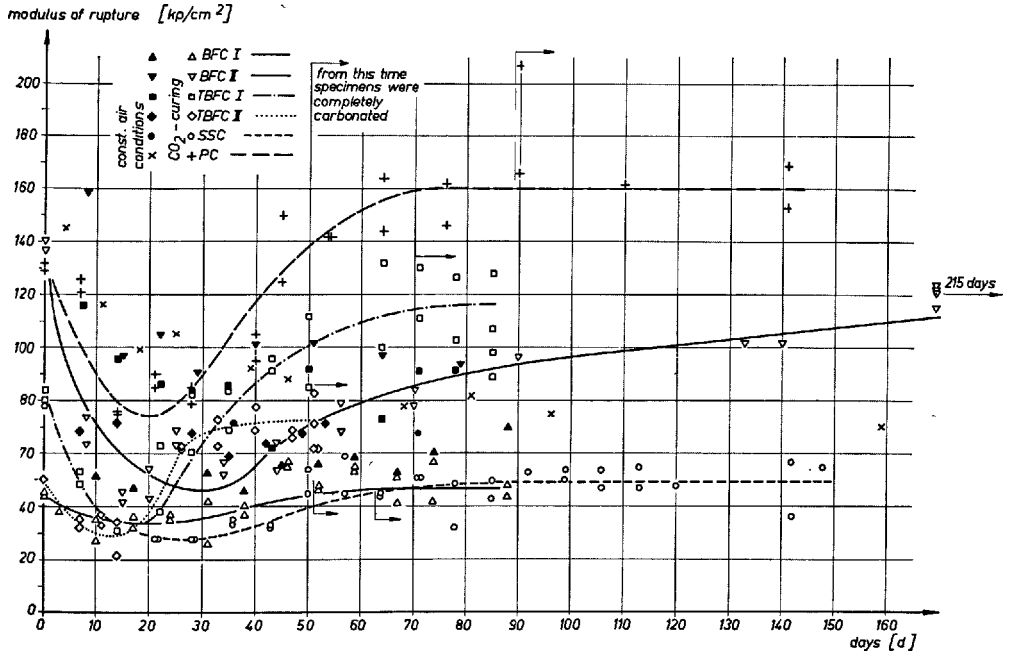

Fig. 5. *Relation between modulus of rupture and time of CO_2 curing and under constant air conditions resp.*

(11). Hereby, compressive stresses occur in the core and tensile stresses in the carbonated zone which reduce the modulus of rupture determined by the flexural test. This initial tensile stress of the tensile zone reaches probably its highest value at a carbonation depth of 6 to 10 mm which is then reduced with progressing carbonation and which will become zero when the carbonation process is completed. Then, the modulus of rupture determined in this phase cannot be falsified by shrinkage stresses caused by carbonation. The internal stresses caused by the carbonation process can be estimated from Fig. 6, however, it must be taken into account that the elastic behaviour may be changed with carbonation. Tests give rise to assume that changes in strengths and in the elastic behaviour are alike.

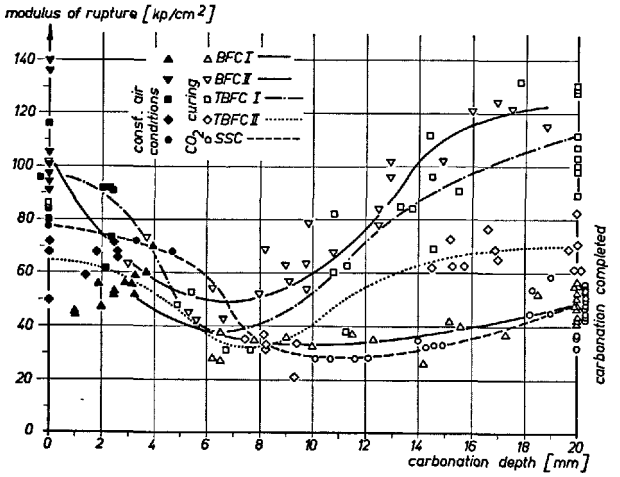

Fig. 6. *Relation between modulus of rupture and carbonation depth*

Change in Weight

In Fig. 7 the change in weight is plotted as a function of the time with the end of drying as zero point. It can be seen that the mortar prisms of PC, BFC II and TBFC I have increased in weight, those of SSC, however, decreased in weight, those of BFC I and TBFC II first increased in weight and afterwards decreased. When carbonation is completed, a considerable change in weight does not occur emphasizing that the chemical process is finished. In comparing the time behaviour of the change in weight and the compressive strength (Fig. 2) it can be noted that both follow the same tendency and that the termination of weight change nearly coincide with the change in compressive strength. It is, therefore, obvious that there is a correlation between change in weight and

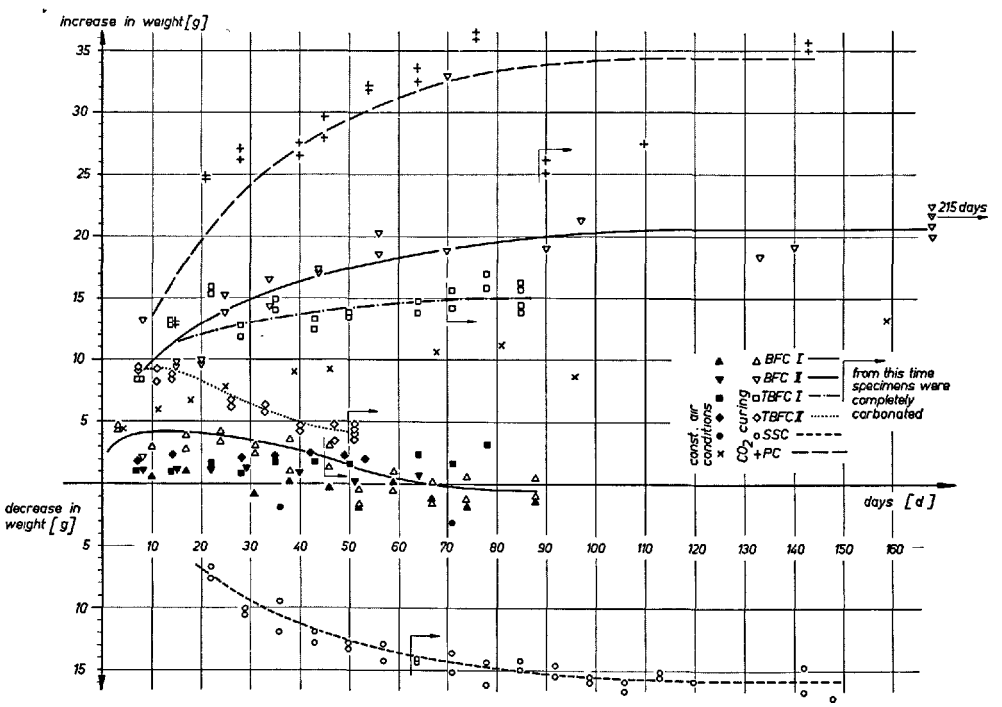

Fig. 7. *Change in weight at CO_2 curing and under constant air conditions resp.*

change in compressive strength. It should be considered, however, that the test specimens increase in weight after drying at 40°C (specimens of PC at 105°C) in the CO_2 apparatus at a relative humidity of 65 to 70% up to reaching equalized moisture. PC specimens increased in weight by about 11 g, all other specimens by 1 to 2 g. Thus two processes were interacting at the change in weight: the increase in weight caused by taking up humidity and the change in weight caused by carbonation. This fact explains the course of curves for specimens of TBFC II and BFC I. In plotting the relation between change in weight and change in compressive strength in Fig. 8, the change in weight caused by taking up humidity is eliminated up to equilibration. By the method of least error squares the correlation line was determined in the form of

$$\Delta\beta_D = a \cdot \Delta G_K + b$$

The following equation was developed with $a = 13.0$ and $b = -15.1$:

$$\Delta\beta_D = 13.0 \cdot \Delta G_K - 15.1$$

$\Delta\beta_D$ = change in compressive strength in per cent
ΔG_K = change in weight in per cent caused by carbonation.

The confidence limit of the determined straight line was also calculated and is shown in Fig. 8. The precision equivalent for the equation was $B = 0.84$. It can be seen from the diagram that the values for PC deviate somewhat from the straight line which probably depends on the different drying method. However, a valuable information is given by this unintentional difference in treatment that probably different preliminary treatment, even though unessential, may modify the found relation. The test for linearity, i.e. the evidence whether the assumption of a linear relation is justified, resulted in a statistical security of S = about 95% if the PC specimens were included, if they were excluded, however, it resulted in S = about 99% (Fig. 9). If the PC specimens were not considered, the values resulted in $a = 10.8$ and $b = -18.5$ for the constant of the straight line equation at a precision equivalent of $B = 0.92$.

The change in weight due to carbonation may be caused by

a) the carbonation of the calcium hydroxide in releasing 1 mol H_2O from 1 mol CO_2. Even if it is assumed that the water is completely evaporated, a considerable increase in weight remains;

b) the carbonation of crystal and gel connections. Some mols H_2O are released by 1 mol CO_2 from which at least one part must evaporate since the specimens had an equilibration humidity. D'Ans and Eick (12) for instance, give for carbonation of ettringite the following reaction equation:

$$C_3A \cdot 3CaSO_4 \cdot 32H_2O + 3CO_2 \longrightarrow$$
$$3CaCO_3 + 2Al(OH)_3 + 3CaSO_4 \cdot 2H_2O + 23H_2O$$

According to this reaction 4 mols CO_2 are taken up whereas 23 mols water are released. Even if it is assumed that only part of the water is diffused out and changed over into the evaporable form, a considerable decrease in weight is still remaining.

This assumption is strengthened by the fact that PC specimens released considerable more calcium hydroxide in hydration, contrary to the other tested specimens, and developed the highest increase in weight, whereas SSC specimens developing less free calcium hydroxide but containing large quantities of ettringite showed the highest loss in weight. It is uncertain whether the decrease in compressive strength along with a loss in weight may be connected with the reduced strength of the forming products or

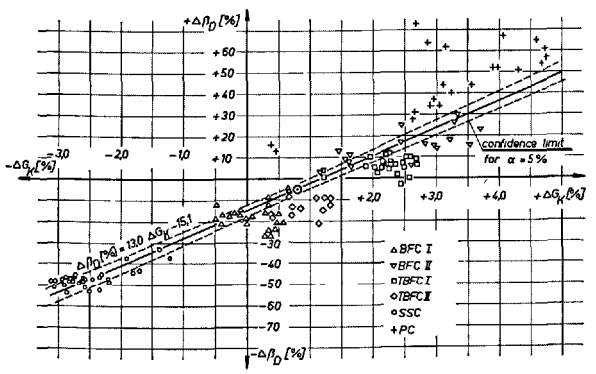

Fig. 8. *Relation between change in compressive strength* ($\Delta\beta_D$) *and change in weight* (ΔG_K)

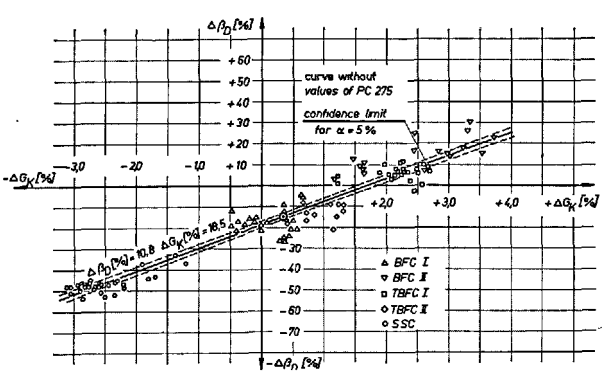

Fig. 9. *Relation between change in compressive strength* ($\Delta\beta_D$) *and change in weight* (ΔG_K)

with an inferior density of cement paste.

Change in Compressive Strength and Clinker Content

The assumption that change in compressive strength depends on the quantity of released calcium hydroxide which is highly affected by the clinker content of the cement, points to the conclusion that there is a regression between clinker content of cement and changes in compressive strength. Change in compressive strength after completed carbonation in relation to the strength at 28 days (upper values) and the strength after heat treatment (lower values) is shown in Fig. 10 as a function of the clinker content. Mean values were plotted only. It is noted that regression of these test values can be approximated by a straight line, even so, if the value of the change in strength of SSC in relation to the 28 days strength deviates considerably. For calculation of the regression straight lines mean values only were used, since the number of the individual values for each cement was different. In using the equilibration calculation, the following equations and precision values can be given:

$$\frac{\beta_{DK}}{\beta_{D28}} = 1.44\,A + 76.5 \quad \text{with } B = 0.94$$

$$\frac{\beta_{DK}}{\beta_{D\infty}} = 1.16\,A + 54.8 \quad \text{with } B = 0.96$$

β_{DK} = compressive strength in the state of completed carbonation

β_{D28} = compressive strength prior to drying

$\beta_{D\infty}$ = compressive strength after drying (this strength corresponds nearly to the ultimate strength)

A = clinker content in % (PC = 100%)

β_{DK}/β_{D28} and $\beta_{DK}/\beta_{D\infty}$ resp. = 100 give the clinker content, a falling below of which results, following these tests, in a decrease in strength which gives in the first case about 20% and in the latter ab. 40%.

Rate of Carbonation

In practice, the rates of carbonation determined by these tests cannot be assigned to atmospheric conditions nor can be used for a prediction of carbonation depths, nevertheless they should be given for completion's sake. In Fig. 11 carbonation depths are a linear function of the time. In Fig. 12 they are given on a double logarithmic scale. It may be of interest, however, to note that the rates for specimens of BFC I, TBFC I and II and SSC do not differ considerably, the specimens of BFC I, however, is carbonated at a much slower rate.

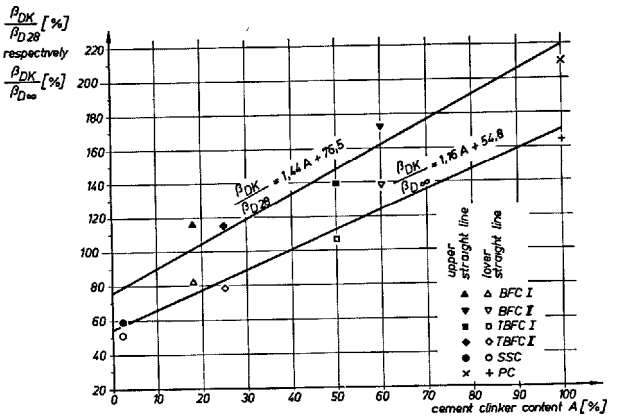

Fig. 10. *Relation between carbonation and cement clinker content*

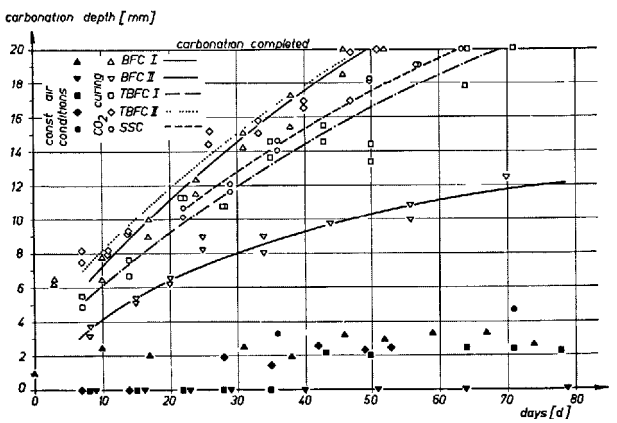

Fig. 11. *Relation between carbonation depth and time at CO_2 curing and under constant air conditions on a linear scale*

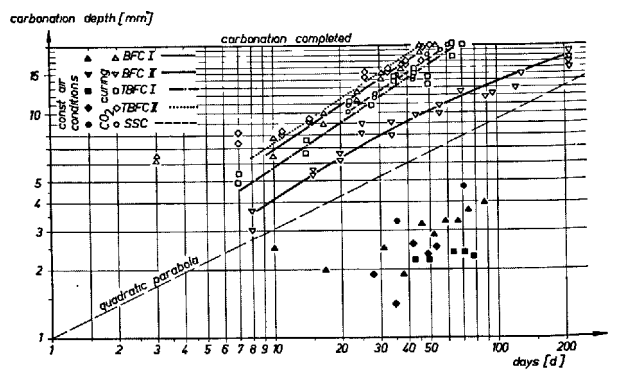

Fig. 12. *Relation between carbonation depth and time at CO_2 curing and under constand air conditions on a double logarithmic scale*

Conclusions

As stated, conditions of temperature and humidity, cement content, water/cement ratio, compression, surface of specimens, and CO_2 enrichment were kept constant so that the results relating to other conditions have limited validity only. Further researches are being made in the Institute of Building Research and are directed to the above mentioned magnitudes. The compressive strength results correlate well with American results (1, 2, 4, 10, 11, 13). The difference in strength observed by the authors on 4 to 10 years old SSC concretes of partly carbonated and non carbonated specimens can, according to the test results, be fully related to decrease in compressive strength caused by carbonation. Similar results have been found by investigators (1, 2, 4, 11) for flexural tensile strength and increase in weight.

The conclusion of Toennis (4) that weight control is a solid method in determining the magnitude of carbonation can be supplemented in so far as for all cements the change in weight is linear to the change in compressive strength and that it allows an estimation whether carbonation affects an increase or decrease in compressive strength.

Furthermore, it is questionable whether the problem of a decrease in compressive strength is of any significance in practice. If under normal conditions the carbonation processes at such a slow rate that a structural member cannot completely be carbonated, due to its life or due to its dimensions, or even if carbonation is stopped because of environmental conditions after reaching a maximum depth, it cannot be expected, in general, that a building may loose its stability. This statement can, however, be considered as secured only by profound investigations into all questions, the more as with thin bending members the carrying capacity determining the compression zone is only some centimeters in height. If, however, surface requirements are to be met as to hardness and wear, the test results will give valuable hints for practical works. Linear regression between PC clinker content and change in compressive strength caused by carbonation resulted in an increase in strength at a clinker content $>40\%$ and a decrease in strength at a clinker content $<40\%$. Whether this limit of 40% of the clinker content will be also confirmed under other conditions must be clarified by further researches.

References

1. I. Leber and F. A. Blakey, "Some effect of carbon dioxide on mortars and concrete", Journal of American Concrete Institute, Title No. 53–16 No. 16, 295 (1956).
2. B. Kroone and F. A. Blakey, "Reaction between carbon dioxide gas and mortars", Journal of American Concrete Institute, Title No. 56–32 No. 6, 497 (1959).
3. W. F. Cole and B. Kroone; "Carbon dioxide in hydrated portland cement", Journal of American Concrete Institute, Title No. 56–64, 1275 (1959/60).
4. H. T. Toennies, "Artificial carbonation of concrete masonry units", Journal of American Concrete Institute, Title No. 56–42 No. 8, 737, (1959/60).
5. G. Mußgnug, "Einige charakteristische Eigenschaften des Gipsschlackenzementes", Zement-Kalk-Gips **8**, 208 (1951).
6. K. Gaede, "SO_3-Gehalt der Zuschlagstoffe, Langzeitversuche", Deutscher Ausschuß für Stahlbeton **126** (1957).
7. K. Wesche and W. Manns, "Betone aus Sulfathüttenzement in höherem Alter", Deutscher Ausschuß für Stahlbeton **186** (1966).
8. W. Manns and H. R. Sasse, "Über die Auswertung der Kugelschlagprüfung bei Beton aus Sonderzementen", beton **2**, 63 (1966).
9. T. C. Powers, "A hypothesis on carbonation shrinkage", Journal of the Portland Cement Association **2**, 40 and Zement-Kalk-Gips **9**, 416 (1962) resp.
10. F. M. Lea and C. H. Desch, "The chemistry of cement and concrete", 2nd ed., p. 475, (Edward Arnold Ltd., London, England, 1956).
11. G. I. Verbeck, "Carbonation of hydrated portland cement", Journal of the Portland Cement Association **2**, Bulletin 87, **17** (1958).
12. J. D'Ans and H. Eick, "Untersuchungen über des Abbinden hydraulischer Hochofenschlacken", Zement-Kalk-Gips **12**, 449 (1954).
13. C. H. Hunt and L. A. Tomes, "Reaction of hardened porltand cement paste with carbon dioxide", Journal of Research of the National Bureau of Standards **6**, 473 (1962).
14. W. Manns and O. Schatz, "Über die Beeinflussung der Festigkeit von Zementmörteln durch Karbonatisation", Betonstein-Zeitung **4**, 148 (1967).

Supplementary Paper III-52 Investigations on the Carbonation of Concrete

Adolf Meyer*

Synopsis

Tests carried out on concrete and mortar under defined conditions showed that the age, the composition of the concrete and the conditions of storage are to be considered as the main factors influencing the progress of carbonation. An investigation of concrete samples taken from 53 old building constructions had longly confirmed the tendency of the interdependence found under definrd conditions. The test results allowed, to predict approximatively the depth of carbonation for a certain concrete. The carbonation resistance of a fully compacted and normal cured concrete is essentially determined by its water/cement ratio and by the type of cement used.

Introduction

Concrete exposed in air will release more or less of its free water. This drying process involves primarily the layers next to the surface. The progress and the degree of the evaporation depend upon the conditions of storage and the structure of the concrete. During the evaporation the pore-water in the concrete is replaced by air, and from this time on, carbon dioxide can react with the alkaline compounds of the concrete. This transformation that reduces the initial alkalinity of the concrete is called carbonation. The carbonation may have an undesirable influence on the protection of the steel in reinforced concrete against corrosion. It is therefore interesting to know under what conditions a profound carbonation of the concrete will occur, and what depth the carbonated layer will reach.

In the present paper tests made in the Laboratory of the Westphalian Cement Industry are briefly dealt with. In these tests Dr.-Ing. H.J. Wierig and Dr.-Ing. K. Husmann took part besides the author.

Methods to Demonstrate the Reaction of Carbon Dioxide in Concrete

The depth of the carbonated layer in mortar and concrete can be determined by various methods. The microscopic detection of the calcium carbonate is a precise method. As a rule, a distinct border between the unchanged hydrated phases of clinker and the newly formed calcium carbonate is clearly to be seen in thin sections. The calcium carbonate with its pronounced double refraction in polarized light differs clearly from the almost isotropic cement gel and the less double-refractive calcium hydroxide.

In serial tests, the use of pH-indicators has proved well. These indicators do not allow to determine the exact pH of the concrete, they merely indicate the depth of the modified concrete layer. Comparative tests made on thin sections have confirmed that a 2% solution of phenolphtalein in ethyl-alcohol makes visible the border zone between the carbonated and the not carbonated concrete. Besides phenolphthalein thymolphthalein and alizarin yellow R are used as indicators. The zones dyed by these indicators are virtually identical to those coloured by phenolphthalein, see Fig. 1. However, in practice the colouring properties of these indicators are often less distinct than those of phenolphthalein.

The concrete to be tested should be broken or cut two days before the determination of the depth of the carbonation by pH-indicators take place. In cutting the concrete not hydrated cement particles are layed bare, that might interfere with the determination of the carbonation level.

Due to the presence of porous aggregates, cavities and cracks in the concrete, the carbonation level seldom appears as a straight line parallel to the surface

*Portland-Zementwerke Heidelberg AG, Forschungs und Beratungsstelle Heidelberg, West Germany.

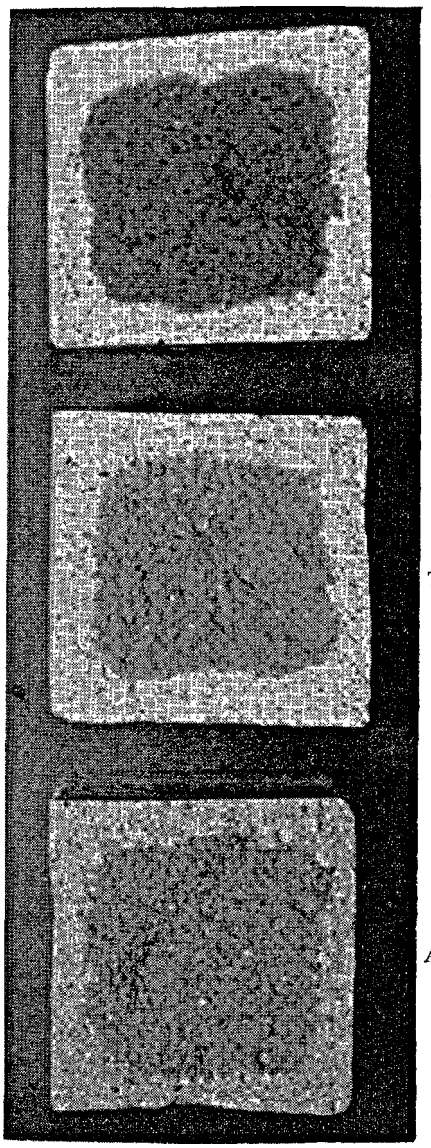

Fig. 1. *Surfaces of a broken prism 4 × 4 × 16 cm of standard mortar (DIN 1164) coloured by 3 indicators*

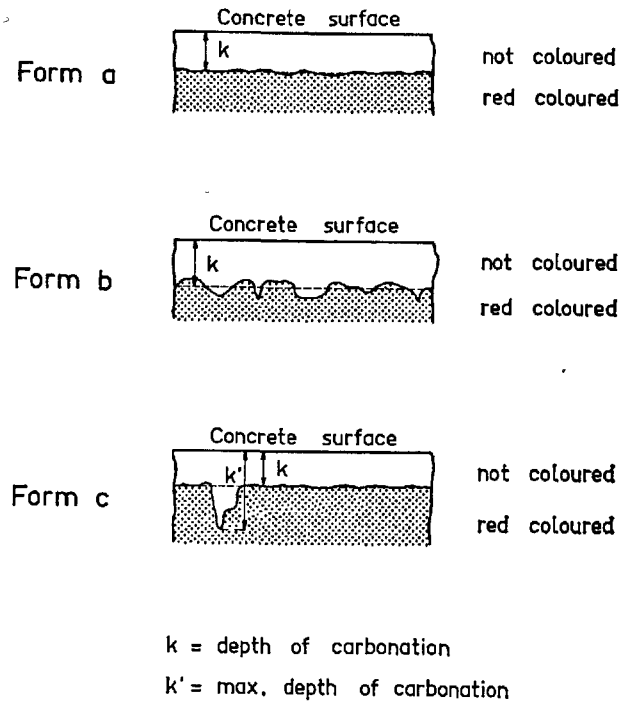

Fig. 2. *Definition of the depth of carbonation*

of the concrete. One observes irregularities of that borderline that render difficult the precise determination of the depth of carbonation. Fig. 2 shows our definition of the depth of carbonation. In the cases *a* and *b* only the measured value *k* is indicated, in case *c*, the maximun value k_{max} is stated additionally.

Properties of Concrete Affected by Carbonation

Protection of the Reinforcement against Corrosion

It has been found out by appropriate tests that the passivation ensuring the protection of the steel against corrosion is neutralized by carbonation (1, 2). As a result, the steel in a carbonated concrete will undergo corrosion as soon as two other conditions are present: access of oxygen and of moisture. In a dairy we have had some years ago the opportunity to study the effect of the passivation of steel in reinforced concrete. In this dairy the steels of a reinforced beam were partially embedded in carbonated concrete and partially in non-carbonated concrete, see Fig. 3. The depth of the carbonation was after about 40 years 26 mm. The steel was covered with 15 mm of concrete. In the near of the wall the concrete cover was thicker. Here in the non-carbonated zone—red coloured by phenolphtalein—the steel showed no sign of corrosion while in the grey carbonated zone severe corrosion had

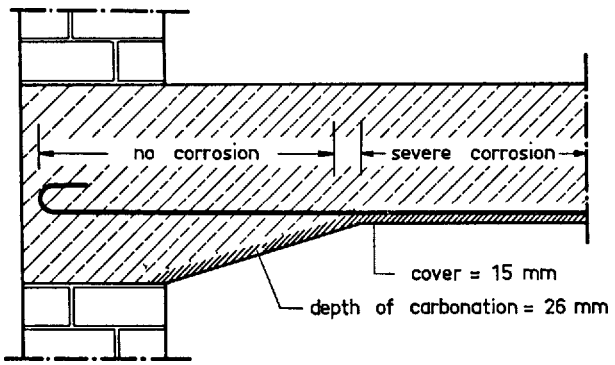

Fig. 3. *Reinforced beam about 40 years old in a dairy*

Table 1. *Compressive strength of mortar*

No.	Cement Type	Percentage of blastfurnace slag by weight	Compressive strength in kg/cm² storage condition a	b
1	Portland cement	0	528	778
2	"	0	449	711
3	"	0	474	701
4	Portland blast-furnace cement	20	480	725
5	"	25	485	733
6	Blastfurnace cement	45	542	695
7	"	50	440	540
8	"	75	432	377
9	"	75	424	421
10	Supersulphated cement	n.b.	595	371
11	Aluminous cement	n.b.	608	749

occurred.

Strength

The influence of carbonation on the strength was studied by cylinders 11.3 mm in height and in diameter. The mix of the mortar was cement: sand: water 1: 3: 0.4 by weight. The small cylinders were made from 11 different cements and stored as follows:

a) 56 days under water
b) 28 days under water, 21 days exposed in air at 10% CO_2 and 80% of relative atmospheric humidity, then 7 days under water.

In storage a non-carbonation of the mortar occurred. In storage *b* all samples were completely carbonated. The results of the strength tests after 56 days are summarized in Table 1.

The effect of carbonation was by no means identical in all cases. In mortars of portland cement and of portland blastfurnace cement the compressive strength increased significantly, while in mortars of blastfurnace cement containing approx. 50% of blastfurnace slag and in mortars of aluminous cement the increase was not significant. The strength of mortars made from blastfurnace cement with a high slag content remained almost unchanged. In mortars made from supersulphated cement the strength decreased clearly.

Permeability

Cores of 15 cm in diameter were extracted from 6 concrete building constructions presenting a rather deep carbonation. Slices of 3 cm were cut out from the carbonated and the non-carbonated zones of these cores. These specimens were tested as to their permeability for water vapour by the method described in (3). In these tests the carbonated specimens were almost as impermeable as the non-carbonated ones.

Similar results were obtained in partially carbonated mortar specimens stored 4 months in water and then exposed to an atmosphere enriched with for carbon dioxide. In these tests the differences of the permeability of the carbonated and the non-carbonated specimens remained within the limits of the margin of error.

As far as the progress of carbonation is concerned, an eventual difference of permeability between non-carbonated and carbonated zones would be of minor importance since the carbon dioxide of the air will always pass through carbonated concrete on its way from the surface of the concrete to the level of carbonation.

Moisture Movement

3 concrete specimens 15 cm in diameter and 2 cm thick, were extracted from the carbonated and the non-carbonated zones of a 43-year old concrete. The sides and the bottom of the specimens were sealed and the specimens were saturated several days with water. Then the specimens were stored in air 20°C, 65% of relative humidity. In Fig. 4, the loss of water in kg/m² is plotted as a function of the time. It was found out that the carbonated concrete dried faster at the beginning than the non-carbonated concrete.

Shrinkage

We did not perform tests to study the shrinkage of mortar and concrete due to carbonation. We refer however to the numerous papers dealing with this subject (4) (5). The carbonation results in a slow ir-

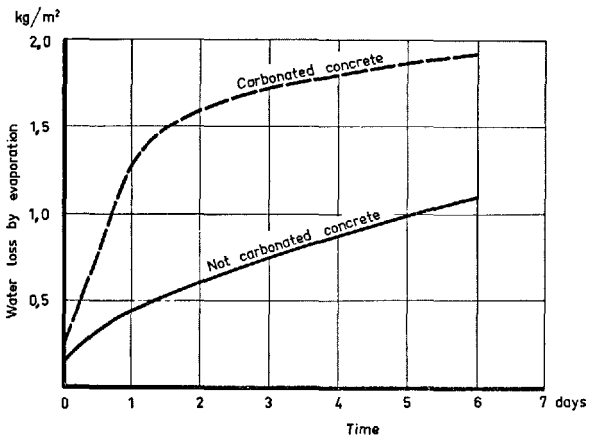

Fig. 4. *Water loss of wet concrete in air (20°C and 65% relative humidity)*

reversible contraction.

Test Series

The main factors bearing on the progress of carbonation are being studied in 5 test series. Moreover, we have determined the depth of carbonation in 60 different concretes, the age, the composition and the storage conditions of which were known to us. These tests are called "test series 6".

In all the test series the depth of carbonation was determined by spraying the breakage or cutting surface with phenolphtalein. All the concretes and mortars described in the following part were stored in normal atmosphere.

In some tests carried out simultaneously in an atmosphere enriched with carbon dioxide the progress of carbonation was considerably accelerated. However, this result is true only as long as the progress of the carbonation is determined by the diffusion of carbon dioxide, while it does not apply to the progress due to the migration of the evaporation level. It is therefore advisable to dry the samples prior to the exposure to air enriched with carbon dioxide, so that the level of humidity is almost the same in all samples. By the way, it is well possible that other chemical equilibria will occur when mortar and concrete are exposed to higher pressures of carbon dioxide. This fact might disturb the interpretation and the evaluation of the results.

Influences on the Progress of Carbonation

Test series 1

Specimen: Concrete beams $10 \times 15 \times 50$ cm
Cement : aggregate : water = 1 : 5.4 : 0.53 per weight (mix)
Type of Cement: 4 Portland cements, 3 Blast-furnace cements
Storage condition: 4 weeks wet, then placed on the small side and submerged to half its height in water, the other half being exposed to normal room air.
Age: 8 years up to now

Test series 2

Specimen: Concrete cubes $10 \times 10 \times 10$ cm
Water/cement ratio: 0.4 to 0.8
Type of Cement: Portland cement Z275
Storage condition: a) 1 day wet, then exposed to normal room atmosphere
b) like a), but once a week submerged in water for 1 hour
Age: 4 years up to now

Test series 3

Specimen: Concrete beams $10 \times 15 \times 70$cm
Water/cement ratio: 0.4, 0.5, 0.6, 0.7 and 0.8
Type of Cement: 1 Portland cement, 3 Blast-furnace cements, 1 Pozzolanic cement
Storage condition: 7 days wet, then in an airconditioned room: 18°C/50% of relative atmospheric humidity
Age: 3 years up to now

Test series 4

Specimen: Mortar prisms $4 \times 4 \times 16$ cm
Water/cement ratio: }
Type of Cement: } see test series 3
Storage condition: }
Age: 3 years up to now

Test series 5

Specimen: }
Water/cement ratio: } see test series 3
Type of Cement: }
Storage condition: like in test series 3, but once a week submerged in water for 2 minutes
Age: 3 years up to now

Effect of Age

Fig. 5 shows the average depth of carbonation in % as related to the age (test series 1 and 2). The depths of carbonation measured on the last day of the test were considered as 100%. These values are medium values for different concretes, the values of each concrete differ more or less from the average. The measuring points of each test series form almost a straight line. Since on the abscissa the age is plotted as a radical value, an almost quadratic function exists between the depth of carbonation and the age of the concrete stored in air. Theoretically we get the same relation between depth of carbonation and age by using Fick's first diffusion law for the diffusion of carbon dioxide in concrete.

The two curves of Fig. 5 do not cross the abscissa at the end of the curing period, but somewhat later. Obviously, carbonation starts after a certain induction time, but this time is of minor importance when long periods are considered. The relations between the depth of carbonation and the age apply only to concretes in which the evaporation of the free water is faster than the diffusion of the carbon dioxide into the concrete. In concretes exposed to atmospheric precipitations, the progress of carbonation is slowed down by the absorption and evaporation of water. In this case the depth of carbonation may be limited by the depth of drying.

Effect of Composition of Concrete

In a fully compacted concrete with dense aggregates and without air-entraining admixture the progress of carbonation depends largely upon the water/cement ratio and the type of cement used.

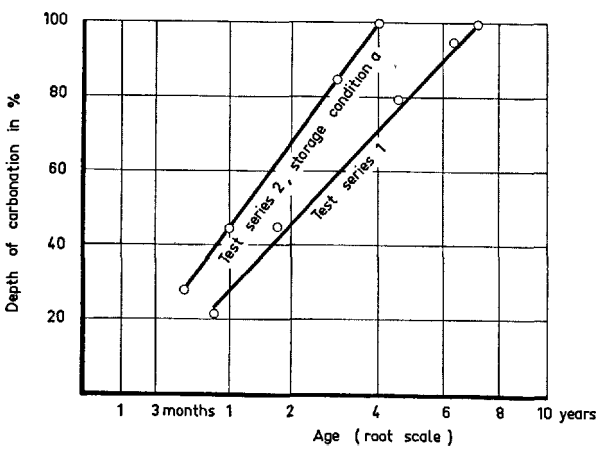

Fig. 5. *Effect of age on the progress of carbonation*

Water/Cement Ratio

Fig. 6 interprets the test series 3, 4 and 5. The depth of carbonation in concrete and mortar $2\frac{1}{2}$ years old having a water/cement ratio of 0.6 is = 100%. The depths of carbonation measured at different water/cement ratios are related in percent to that value. Between the water/cement ratio and the depth of carbonation existed nearly a linear function. In trials made at a relative atmospheric humidity of 65%, the depth of carbonation depended more on the water/cement ratio when the latter was low. That means, that the curve in Fig. 6 is a little steeper geometrically.

Type of Cement

In Fig. 7 the results of test series 1 are indicated, in

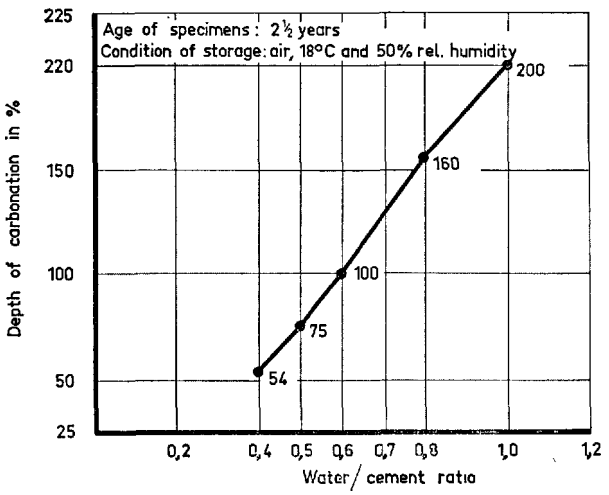

Fig. 6. *Effect of water/cement ratio on the progress of carbonation (results of test series 3, 4 and 5)*

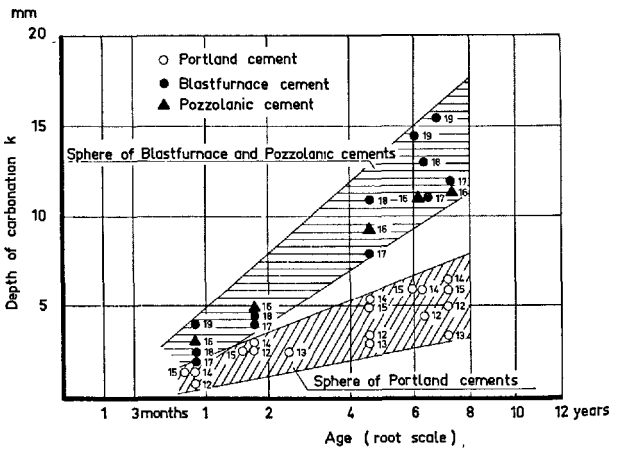

Fig. 7. *Effect of cement type on the progress of carbonation (results of test series 1)*

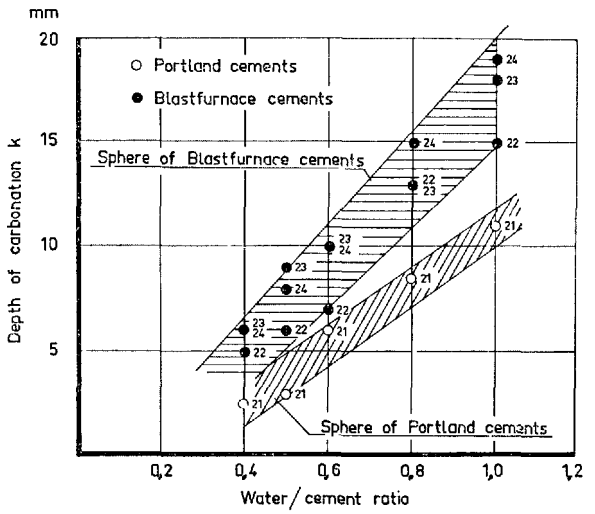

Fig. 8. *Effect of water/cement ratio and cement type on the depth of carbonation of concrete 2 1/2 years old (results of test series 3)*

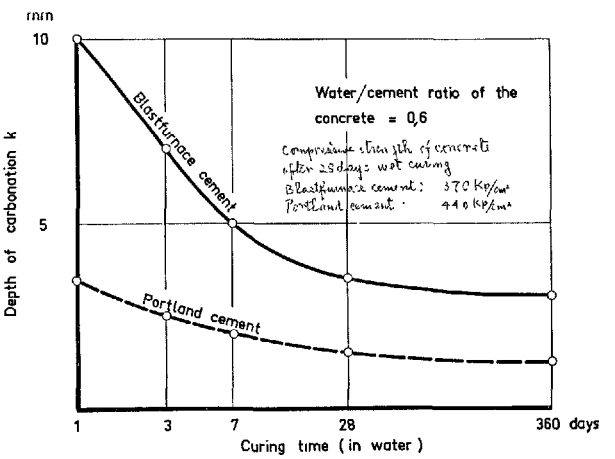

Fig. 9. *Effect of the curing time on the depth of carbonation. Concrete storaged after wet curing for 1 year in open air protected from rain*

Fig. 8 those of test series 3. The concretes made of portland cement showed lower depths of carbonation under the same conditions, than the concretes made from blastfurnace cement and pozzolanic cement. In concrete made of blastfurnace cement, the depth of carbonation increased with an increasing percentage of blastfurnace slag. At a percentage of approx. 50% of blastfurnace slag the carbonation was 1.5 times as deep as in portland cement concrete, while it was 2 times as deep when the percentage of blastfurnace slag amounted to 70%. In mortar tests (test series 4 and 5) the influence of the type of cement used upon the depth of carbonation was less pronounced than in concrete trials. That difference might be due to the fact that the shrinking behaviour of small mortar prisms is not identical to that of concrete test cubes.

The fact that the resistance of a concrete to carbonation is a function of the cement type used, seems to be due to the difference in the percentage of carbonatable substances and especially of free calcium hydroxide. Owing to the high diffusion resistance of the concrete, only limited quantities of carbon dioxide can diffuse through the concrete in the unit of time, thus transforming carbonatable substances. This is the reason why the progress of carbonation depends upon the presence of carbonatable substances, all other conditions being identical.

Storage Conditions

Concrete *constantly stored under water or away from the air* will not carbonate.

Concrete *constantly exposed in room air* after curing will release the free water. Simultaneously the air penetrates into the concrete. Concrete constantly stored in air will undergo the strongest carbonation. As long as the level of carbonation did not reach the drying level under those storage conditions an approximately quadratic function exists between the depth of carbonation and the age of the concrete. In concrete cured under water for a longer period the progress of carbonation is reduced, see Fig. 9.

*Concretes *exposed to open air* and *moistened* from time to time in their shell zones by precipitations will carbonate less rapidly. In this case the depth of carbonation will not surpass the two uppermentioned limits. The progress of carbonation depends primarily upon the chronological order of the periodical moistening and drying of the concrete. In the test series 2 the depth of carbonation in concrete specimens 4 years old, moistened regularly once a week, amounted only to 30–60% of the depth of carbonation in concrete stored in the air.

Fig. 10 shows the influence of the storage conditions upon the progress of carbonation generally.

Results of Test Series 6

The 60 concretes of test series 6 differ from each other as to their age and their composition. On the other hand they were stored under almost identical

*The portland cement used for these concrete tests was a nomal portland cement with appr. 12% C_3A. The slag content of the blastfurnace cement was appr. 70%.

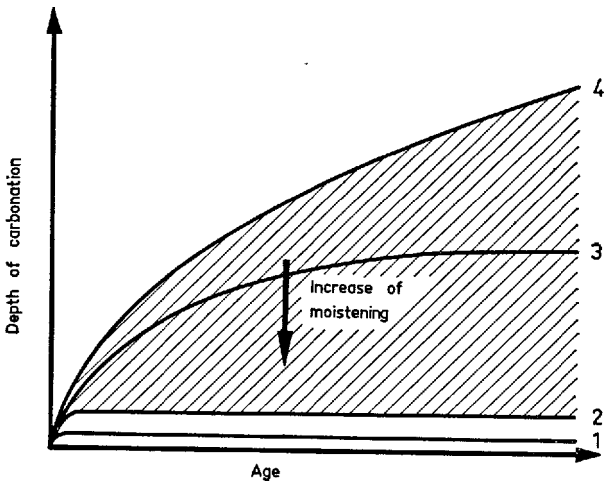

Fig. 10. *Effect of storage conditions on the progress carbonation (model)*

1. Constantly under water or in moist air
2. Horizontal concrete surfaces out door in wet climate
3. Out door in air not protected from rain and snow
4. Constantly exposed in room air or out doors protected from rain and snow

conditions, that means that all these concretes were stored to normal room air after a short moist curing.

Different types of cements were used for the concrete specimens. The ages of the concrete specimens ranged from 1 to 12 years, medium age approx. 5 years. In Fig. 11 the depth of carbonation $k'_t = 10$ related to the age of 10 years is plotted against the water/cement ratio. It was calculated on the base of the quadratic function between the depth of the carbonation k and the age t indicated in the test series 1 to 5 by equation

$$k'_{t=10} = k \cdot \sqrt{\frac{10}{t}}$$

Fig. 11 shows clearly that there exists a linear function between the depths of carbonation related to an age of 10 years and the water/cement ratio in concretes made from portland cement, although concretes of different consistency and different granulometry of the aggregate were compared. In concretes made from blastfurnace cement the linear function between the depth of carbonation and the water/cement ratio is less clearly visible due to the fact that the percentage of blastfurnace slag has not been taken into consideration.

Investigations on Old Building Constructions

In 1962 and 1963, 53 old concrete or reinforced concrete building constructions were examined in

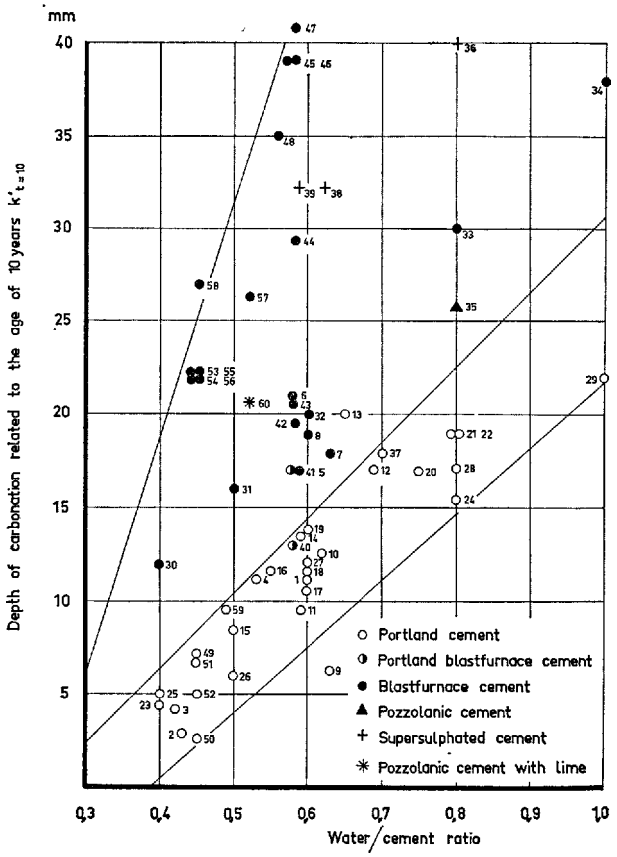

Fig. 11. *Effect of water/cement ratio and cement type on the depth of carbonation related to the age of 10 years (Results of test series 6–60 different concretes)*

order to determine the depth of carbonation in the concrete as a function of the age, the composition of the concrete and of the storage conditions. The building constructions has been erected between 1910 and 1955. The results of these investigations are published already (6).

63 concrete samples were tested. It was found out that the depths of carbonation in these concretes depended essentially on the age and the composition of the concrete as well as on the storage conditions.

The relations stated in the chapter "Influences on the progress of carbonation" existing between these values and the depth of carbonation could be confirmed as a whole in the samples taken from these old building constructions. Some marked variations are due to the fact that the technical data of the concretes could not be reproduced exactly, and that the conditions of storage were not fully known as far as their nature, their intensity and their chronological order are concerned.

Summary and Conclusions

Concrete and mortar tests made under well known conditions have proved that the age and the composition of the concrete as well as the conditions of storage are the main factors that act on the progress of carbonation.

Effect of Age

In concretes stored in air but protected from rain and snow the depth of carbonation increased more rapidly in the beginning than later on. A simple relationship between the depth of carbonation and the age could be established that applied to the period of the investigations of about 10 years. Supposing that this relationship is also applicable to older concretes, the depth of carbonation reached after 10 years will have doubled in at least 50 years. Concrete is carbonated less rapidly, if his outer zone is moistened from time to time for instance by rain.

Effect of Concrete Composition

In concretes having a water/cement ratio of 0.50 the depth of carbonation is only approx. half the depth of carbonation in concrete stored under the same conditions but having a water/cement ratio of 0.80. The depth of carbonation of concrete of portland cement having a water/cement ratio of 0.50 stored 50 years in open air protected from rain will be probable 10 — 15 mm. In concretes made from blastfurnace cement or pozzolanic cement greater depths of carbonation could be measured than in concrete made from portland cement, all other conditions being identical.

Effect of Storage Conditions

Concrete soaked with water is practically free from carbonation. In concretes stored at normal room atmosphere the greatest dephts of carbonation were measured. Periodical moistening of the concrete for instance by rain hampers the progress of carbonation noteworthily. In this case the depth of carbonation can be limited by the depth of evaporation.

Investigations in Building Constructions

The investigation of 63 concrete samples taken from old building constructions have largely confirmed the results of our tests as to the relation existing between the depth of carbonation, the age, the composition of the concrete and the storage conditions.

Carbonation and Reinforcement

In case the steel in reinforced concrete is endangered by corrosion due to unfavorable environmental conditions, care must be taken to prevent the carbonation from reaching the steels. In this respect are important the thickness of the cover and its resistance against carbonation. The carbonation resistance of a fully compacted and normal cured concrete is essentially determined by its water/cement ratio and by the type of cement used.

References

1. B. Zschokke "The corrosion of steel in reinforced concrete" (in German) Schweiz. Bauzeitung **67** (1916).
2. H. L. Moll "The corrosion of steel in concrete" (in German) Deutscher Ausschuß für Stahlbeton Vol. 169, Berlin (1964).
3. H. J. Wierig "A simple method of measuring the water vapour permeability of mortar and concrete" (in German) Zement-Kalk-Gips, **16,** 125–130 (1963).
4. J. J. Shideler "Carbonation shrinkage of concrete masonry units" Journal PCA **5** (1963).
5. G. Verbeck, "Carbonation of hydrated portland cement" PCA Bulletin **87** (1958).
6. Forschungsinstitut für Hochofenschlacke, Rheinhausen Laboratorium der Westfälischen Zementindustrie, Beckum "The depth of the carbonation in building constructions" (in German) Deutscher Ausschuß fur Stahlbeton, Vol. 170 Berlin (1965).

Supplementary Paper III-116 Mechanisms and Kinetics on Carbonation of Hardened Cement

Renichi Kondo, Masaki Daimon and Tokuji Akiba*

Synopsis

Carbonation of mortar or concrete is the reaction between cement components, either unhydrated or hydrated, and carbon dioxide in the air. Studies were made on carbonation under simplified and accelerated experimental conditions to clarify the mechanisms and kinetics. These are discussed in regard to the data of carbonation, neutralized depth and also the pore size distribution. Carbonated products are concentrated especially near the surface at shorter period, but distributed afterward to the deeper part. The slope of the degree of carbonation to the deepness becomes gradually more gentle with the lapse of time. While neutralization does not occur immediately even at the surface in contact with CO_2 gas. The length of the induction period which appear in the neutralization varies with the type of specimen, and these differences are mainly dependent on lack of uniformity in the pore structure. The rate of neutralization can be expressed as $L^2 = kt$ or $(L + l)^2 = kt$ in the first approximation where L is the neutralized depth and t is the time of carbonation. On this rate the water-cement ratio and curing time show the greater effect, and the greater the pore volume, the faster the rate. The above equations suggest that the rate determining process is diffusion. Nevertheless a boundary between parts, carbonated and un-carbonated, is ambiguous, carbonation is assumed to occur at a boundary which corresponds to the neutralized depth. Thus we can apply the following equation:

$$k_t = \frac{2D_0\varepsilon\Delta P T^{0.75}}{273^{1.75}RC_0\rho},\quad k_e = \frac{k_t}{f}$$

Then, the rate constant of neutralization is calculated in consideration of the material transfer of either CO_2 or H_2O in order to determine which diffusion controls the rate of reaction. In consideration of the magnitude of the f value, the species of diffusion which controls the rate of neutralization is infered to be CO_2, H_2O or both of them depending on the pore structure of the specimens. Thus the above rate equations seem to be reasonable to the rate of neutralization in assumptions, and applicable to the practice.

Introduction

Studies on the carbonation of cement mortar and concrete have been made mainly in connection with shrinkage and cracks in European countries, and in connection with corrosion of reinforcing steel in Japan. Studies of carbonation has been made by chemists on each pure cement hydrated or unhydrated compound, while on the rate of neutralization of concrete by building engineers. Some studies seem necessary to fill the gap between them.

As the cement mortar and concrete are porous materials consisting of cement hydrates, carbonation seems to be unavoidable. However, its resistivity should be taken into account. Carbonation is regarded as an example of the reaction of porous solid with gas or liquid which diffuses into the former. Metal refining by the pellet method, sulfate attack on concrete, etc., are also reactions of this type. One of the authors has studied the rate of oxidation of carbonaceous matters contained in shale or clay, in relation to the bloating mechanisms of lightweight aggregates, and found a relationship between the rate and the pore structure.

In a similar way, studies were made on carbonation under simplified and accelerated experimental conditions to make clear the mechanisms and kinetics. As carbonation is concerned with the diffusion of CO_2 gas, examination of the pore size distribution must be important. As the pore size distribution of concrete other than lightweight concrete can be estimated from that of mortar, specimens in the form of mortar were prepared.

*Research Laboratory of Engineering Materials, Tokyo Institute of Technology, Tokyo, Japan.

The degree of carbonation, neutralized depth and pore size distribution were measured under accelerated conditions. In this experiment portland cement and portland blastfurnace cement were used in comparison. The rate of neutralization and the carbonation mechanisms were discussed.

Carbonation and Neutralization

Nevertheless, the carbonation of mortar or concrete is unavoidable because the hydraulic cements and their hydrates are calcarious and reactive with CO_2, the rate of reaction is the most important aspect to be investigated in practice.

Carbonation is the reaction of cement hydrates or unreacted cement with carbon dioxide, and it is a kind of gas solid reaction. However, the existence of adsorbed water or the drying condition influences the rate of carbonation. Maximum rate was found by Hunt and Tomes (1) in a certain drying condition. Accurate control in the relative humidity is, accordingly, important in the carbonation experiment.

Although the mechanism of carbonation of hydrated cement is complex, one molecule of water should be liberated by the reaction of one molecule of carbon dioxide with calcium hydroxide. Hunt and Tomes (1), however, found experimentally that the decreasing of non-evaporable water is less than the increasing of carbon dioxide in carbonation of hardened cement, so that other phases also react with carbon dioxide while calcium hydroxide is still present.

Inoue and Asano (2) found that not only calcium hydroxide but also unhydrated C_3S decreased in carbonation, and that hydrated C_3S tends to produce calcite, but unhydrated C_3S produces vaterite. Formation of vaterite was also reported by Schröder (3) to form by a topochemical reaction between moist CO_2 gas and calcite in the surface layer of concrete.

On the other hand, cement hydrates are originally basic, but neutralized by the carbonation. The neutralization of mortar or concrete is expressed with the depth of the neutralized layer or its rate of increase, which is described by Hamada (4) in this symposium. It is, however, difficult to distinguish a spot in a specimen as neutralized or not, because the carbonation advances continuously; for example, it is probable that only certain species are reacted while others are not, or only the surface of each particle of reactant is carbonated, while the core remains unchanged. The depth of neutralization of specimens is determined conveniently by phenolphthalein as an indicator in connection with the fact that the reinforcing steel in concrete is reported (5) in a passive state when the latter maintains an alkalinity greater than 10.5 in pH value. In the later part of this paper, the relationship between the depth of neutralization and carbonation will be discussed.

Experimental

Preparation of Specimens

In this experiment, portland cement and portland blastfurnace cement of compositions as shown in Table 1 are used in comparison, while the sands put to use are of different fineness, as illustrated in Fig. 1. Both sands were previously treated with 10% HCI for 2 hrs to remove the carbonates. The conditions of the mortar preparation are given in Table 2. The size of the specimens molded is 2 cm × 2 cm × 8 cm. After being cured in saturated $Ca(OH)_2$ solution for 7 or 28 days, the specimens are dried with a rotary pump for 24 hrs and then put into a desiccator maintaining RH 44% for more than 7 days to approach an equilibrium. Five surfaces of each specimen are sealed with the epoxy-resin and one surface, 2 × 2 cm in size, is exposed to CO_2 gas. The specimens previously cured are exposed to CO_2 gas to carbonate

Table 1. *Chemical analysis of cement used*

	L.O.I.	Insol.	SiO_2	Al_2O_3	Fe_2O_3	MnO	CaO	MgO	SO_3	S	Na_2O	K_2O	Total
Portland cement (P)	0.5	0.6	22.3	4.4	3.1	—	64.5	1.5	1.8	—	0.37	0.61	99.8
Portland blastfurnace cement (S)	0.7	0.3	25.8	9.8	2.2	0.5	54.7	2.8	2.3	0.4	—	—	99 5

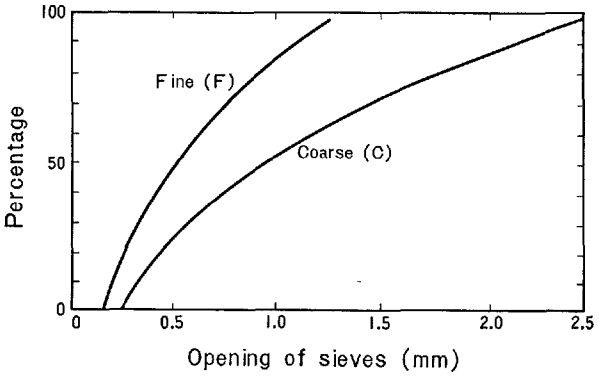

Fig. 1. *Fineness of sands used*

Table 2. *Conditions on the preparation of mortar specimens*

Group	A				B				C				D				E
No.	1	2	3	4	1	2	3	4	1	2	3	4	1	2	3	4	
Kind of sand	C	F	C	F	C	F	C	F	C	F	C	F	C	F	C	F	
Sand ratio	2																3
A.E.R.*	×	○	○	×	○	×	×	○	○	×	×	○	×	○	○	×	
W/C	0.65				0.5				0.65				0.5				
Kind of cement	P		S		P		S		P		S		P		S		
Curing days	28								7								

*0.3 cc of Vinsol resin for 1 kg of cement was added in mixing water

at 20 ± 1°C. The specimens are laid to avoid contact with each other in a desiccator of sufficient size. CO_2 gas is led from a bomb through 3 bottles to the desiccator. And the saturated $Zn(NO_3)_2$ solution is put in 2 of the 3 bottles, and the desiccator is put to maintain CO_2 gas at 44% relative humidity.

Analytical Methods

Carbonated specimens are cut lengthwise with a diamond cutter and the neutralized depth is determined with 1% phenolphthalein solution. Some of the carbonated specimens were sliced into 1 mm thickness perpendicularly to the direction of diffusion, using a grinding wheel of 0.5 mm thickness. And each slice is crushed for such tests as the quantification test by X-ray diffraction, fixed CO_2 by the micro diffusion method (6) and free $Ca(OH)_2$ by a modified Franke method (7) using isopropanol as the solvent. The pore size distribution of several specimens were also measured with a mercury pressure porosimeter.

Results

Results of Carbonation

The degree of carbonation was determined by various methods such as X-ray diffraction analysis, chemical analysis for fixed CO_2 and free $Ca(OH)_2$. The analytical results are given in Fig. 2. The amount of calcium hydroxide quantified by X-ray diffraction is in good accordance with the results by the Franke method. But the amount of calcite estimated by X-ray diffraction does not correspond to the fixed carbon dioxide chemically obtained. This discrepancy is remarkable in the sample taken from the deeper position from the surface. This result is an evidence that amorphous carbonate is likely to form in the deeper part. X-ray diffraction intensity of calcite also decreases steeply especially near the surface of specimens carbonated for a long period, due to the formation of vaterite. The modification of $CaCO_3$ produced is calcite in the early stage of carbonation, but is vaterite in the later stage where carbonation of unhydrated cement components must take place as reported by Inoue and Asano (2). At the early stage, the carbonation occurs only near the surface, but in the deeper part at the later stage. In comparison of A2 and C2, the slope of the carbonation ratio is steeper in case of A2 than in case of C2, and the rate of C2 is larger than of A2. This difference is important in view of the rate of neutralization in connection with the pore size distribution.

The amounts of free $Ca(OH)_2$ of uncarbonated specimens are 0.038, 0.019 and 0.033g CaO/g specimen for A2, A4 and C2 respectively. The amount of free $Ca(OH)_2$ is larger in portland cement mortar than in portland blastfurnace cement mortar. In a comparison between A2 and A4, in which portland cement and portland blastfurnace cement are used respectively, fixed carbon dioxide in the specimens carbonated for 7 days are 0.00303 and 0.00267 mole/g specimen. Therefore, these values are equivalent to 0.645 and 0.547 each of the total CaO of cement. It is considered from these results that all of the CaO in cements is effective for the fixation of CO_2.

The molar ratio of fixed carbon dioxide to free $Ca(OH)_2$ are about 0.2 regardless of different depth from the surface. This result reveals that the there is no great difference in the case of carbonation between the calcium hydroxide and the other phases.

In Fig. 2, the arrow shows the neutralized depth, where some free $Ca(OH)_2$ still remains.

Results of Neutralization

The neutralization rate of the specimens are shown in Fig. 3. An explanation of why the neutralization could not be detected in such specimens as D3, D4 and E is that the carbonation takes place imperfectly and unneutralized part remains even near the surface, in spite of the carbonation progress in the deeper part at the same time. Though the slope of the lines in Fig. 3 tends to become steeper in the later stage, the rate of neutralization can be expressed as $L^2 = kt$, in the first approximation, where L is the neutralized depth, t is time and k is a constant. Therefore, the value k shows the ease of neutralization. The difference in sands and the addition of A. E. R. seem to have no significant effect. The curing time and

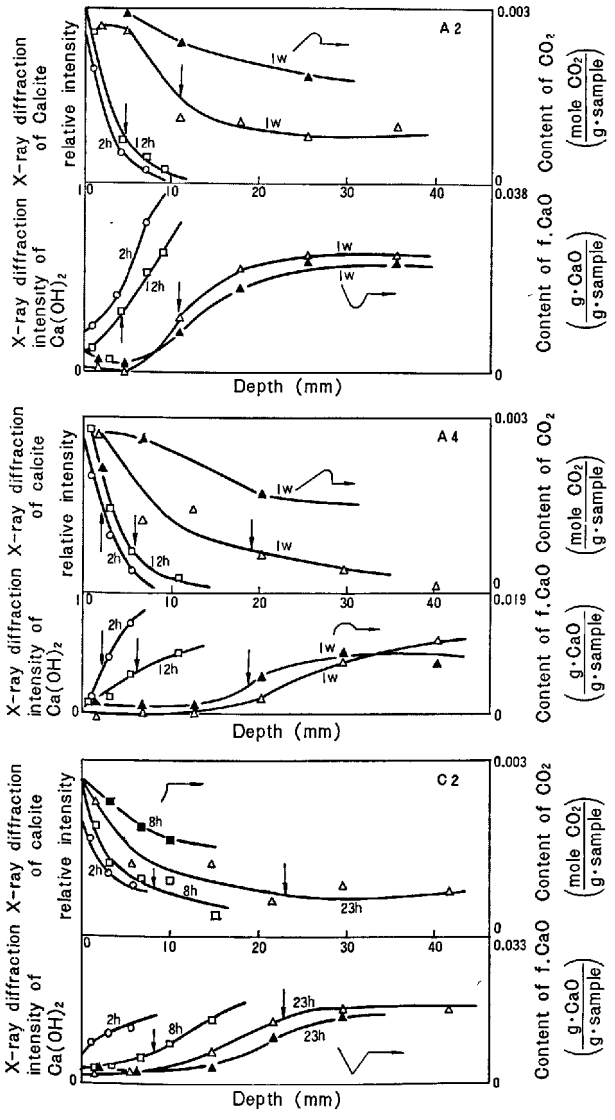

Fig. 2. *Experimental results on carbonation*
↓ : *showing the neutralized depth*
■, ▲ : *obtained by chemical analysis*
Time of carbonation is taken as parameter

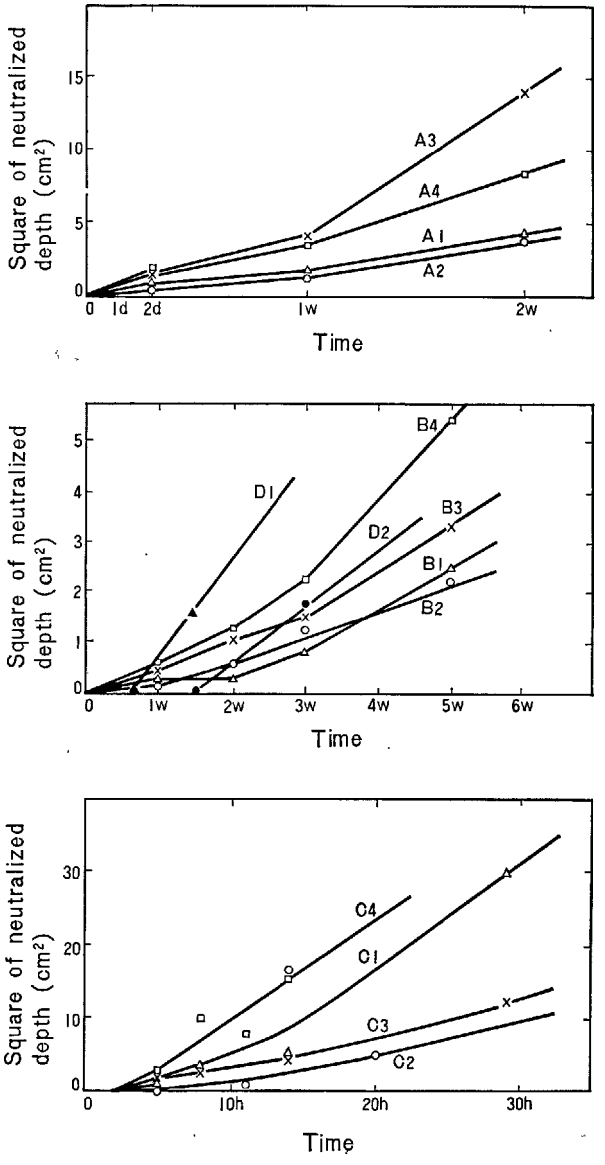

Fig. 3. *Relationship between neutralized depth and time of carbonation*

the water-cement ratio show the greatest effect and portland blastfurnace cement seems to be easily neturalized at least in this accelerated conditions.

Pore Size Distribution

The determination of the pore size distribution is useful in consideration of the rate of neutralization. The pore size distribution of various samples are compared in Fig. 4. The shorter the curing time, the larger the size and total volume of pores. The pores existing at the beginning must be gradually filled with produced hydrates. But this trend is not clearly observed in the cases of B2 and D2, in which the W/C ratio is as low as 0.5 and cement particles are compactly packed. Even though in the case of D4 the W/C ratio is 0.5, it has a large pore volume. This seems to be due to the low degree of hydration of portland blastfurnace cement not filling the pores enough with hydrates, in the case of curing for 7 days. While in the specimens cured for 28 days, even with such a high W/C ratio as 0.65, the total of the pore volume is nearly equal in both case of portland cement and portland blastfurnace cement. As the pore volume of C specimen is greater than that of B, the rate of neutralization is faster in case of the former. E2 is the specimen containing portland cement, with W/C = 0.65 and sand-cement ratio of 1 : 3, cured for 28 days. The rate of neutralization of such specimens as D3, D4 and E could not be measured as inducated previously. This fact seems to be due to the existence of large pores where CO_2 gas preferentially diffuses and carbonation takes place at the peripheries of large capillaries. As some reduction in pore volume is generally observed, accompanied by carbonation, it suggests that the volume of reaction procucts including carbonate is increased.

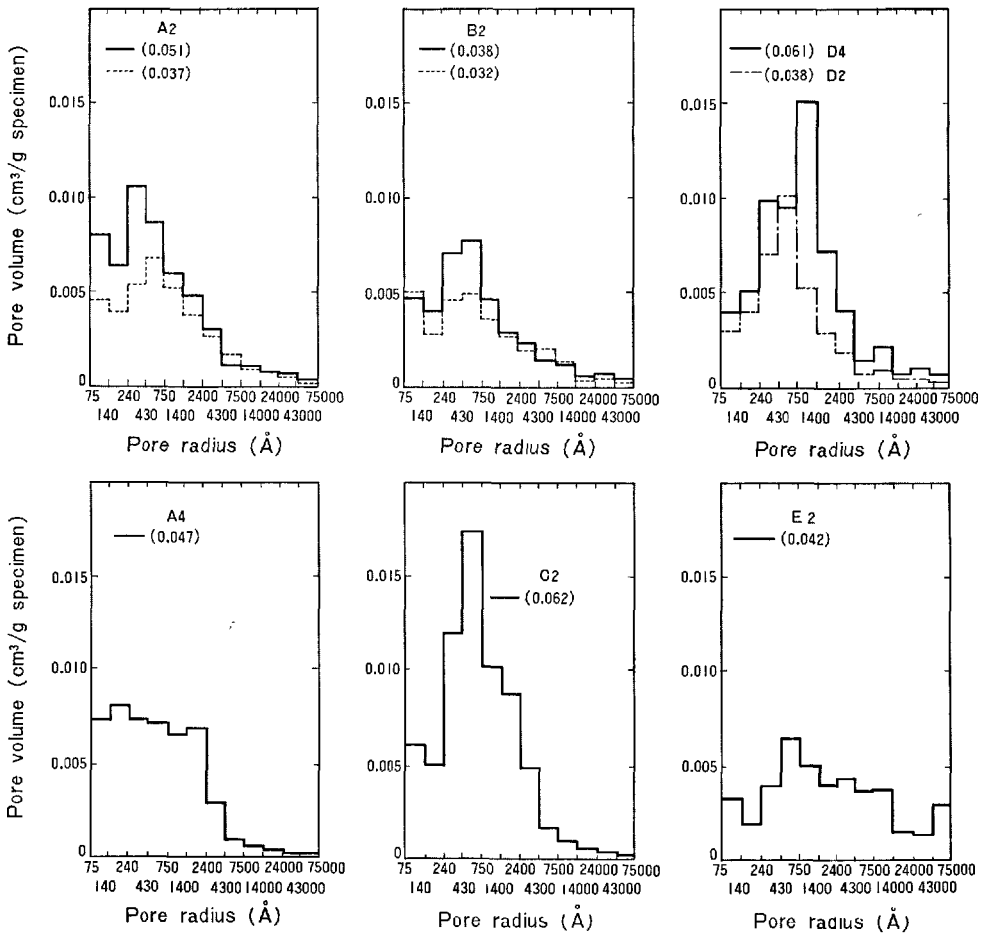

Fig. 4. *Pore size distribution of specimens*
—, —·—: *showing the unneutralized part*
·····: *showing the neutralized part*
( ): *showing the total pore volume*

Induction Period in Neutralization

Neutralization does not occur immediately even on the surface which is in direct contact with CO_2 gas. The length of the induction period varies with the type of specimen as follows: almost 0 hr for A group; about 15 hrs for B group, 2 hrs for C group and even several days for D1 and D2. These differences occur depending chiefly on their pore structure. The induction period is considered to be attributable to the lack of uniformity in the pore structure. The induction period of the specimens cured for 7 days are longer than those for 28 days. This fact seems to be partly due to the existence of unhydrated cement components which react more slowly with CO_2 gas than the hydrates. In other words, the pore structure must be more uniform and the cement components must be more extensively hydrated in the case of the specimens cured for 28 days than in those for 7 days.

Rate Equation on Neutralization

The rate of neutralization of various specimens are shown in Fig. 3. In the first approximation, the rate can be expressed by the equation,

$$L^2 = k_e t \tag{1}$$

or

$$(L + l)^2 = k_e t \tag{2}$$

where

- L: the neutralized depth
- t: the carbonation time
- k_e: the neutralization rate constant experimentally obtained
- l: the constant to be related with induction period

These equations suggest that the rate determining process is diffusion, because this type of equation can be derived when the rate of reaction is controlled by diffusion. The rate of diffusion is shown as

$$N_0 = \frac{D\Delta C}{L} \tag{3}$$

and thus the rate of reaction is expressed as

$$\frac{dL}{dt} = \frac{N_0}{C_0 \rho} = \frac{D\Delta C}{C_0 \rho L} \tag{4}$$

Therefore, the following equations result:

$$L^2 = kt, \quad k = \frac{2D\Delta C}{C_0 \rho} \tag{5}$$

where D is the diffusion constant, ΔC is the difference in concentration, C_0 is the amount of reactant in unit weight of specimen and ρ is the density.

Nevertheless, the boundary between the two parts, neutralized and unneutralized, can not be clearly distinguished, carbonation is assumed to occur at the boundary. In Fig. 5, an idealized model of neutralization is shown. Thus, we can apply the following equations, in view of counter diffusion, inward and outward, and that diffusion coefficient of gas is written as $D_T = D_0 \times (T/T_0)^{1.75}$

$$k_t = \frac{2D_0 \varepsilon \Delta P T^{0.75}}{273^{1.75} R C_0 \rho} \tag{6}$$

where

- D_0: the diffusion constant at 0°C (cm^2/sec)
- ΔP: the difference of pressure (atm)
- C_0: the maximum amount of fixed CO_2 or produced H_2O (mole/g specimen)
- ρ: the density of the specimen (g/cm^3)
- T: temperature (°K)
- R: gas constant (= 22400/273),
- ε: the porosity of the specimen (cm^3/cm^3)
- k_t: the theoretical neutralization rate constant

$$k_e = \frac{k_t}{f} \tag{7}$$

where f is the tortuosity.

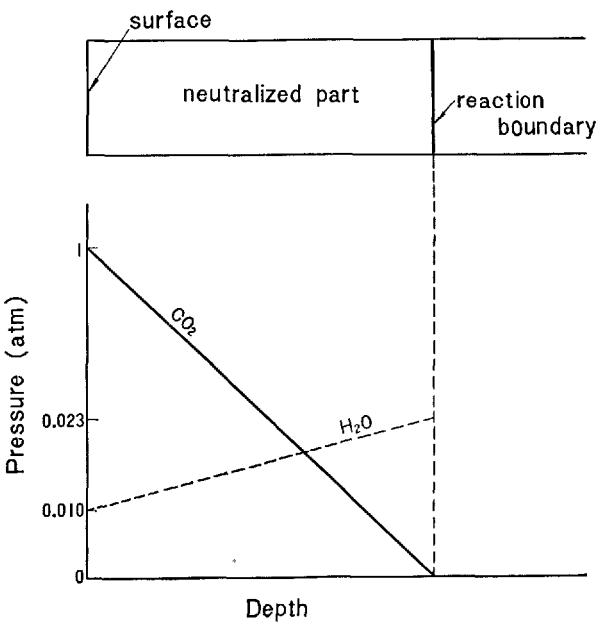

Fig. 5. *The model of neutralization in which the rate determining process is assumed to be the diffusion of* CO_2 *or* H_2O

Rate Constant of Neutralization

In this system, there are three kinds of gas species. CO_2 diffuses inward the specimen, and air and H_2O produced by carbonation diffuse outward. The rate constant of neutralization is calculated in consideration of the material transfer of either CO_2 or H_2O, in order to determine which diffusion controls the rate of reaction. Calculated values for specimens A2, B2, C2 and D2 were shown in Table 2.

Experimental values of ε/ρ in Fig. 4 are not to be used because the diffusion constant of diffusion in the smaller pore than the order of mean free path decreases proportionally to the radius according to Knudsen's Law. Therefore the experimental values were corrected and the effective values obtained were 0.0394, 0.0299, 0.0583 and 0.0320 for the unneutralized specimens of A2, B2, C2 and D2 respectively.

The partial pressure of CO_2 and that of air varies from 0 to 1 atom, where as in case of H_2O it varies only between 0.010 atom (= RH 44%) and 0.023 atom (= RH 100%). Thus, the value, ΔP in equation (6) is 1.0 for CO_2 diffusion, and 0.013 for H_2O diffusion.

Diffusion of CO_2 gas in air must be considered in the neutralization under atmospheric condition. However, the diffusion of CO_2 in H_2O is taken into account in the case of accelerating condition, in which diffusion of H_2O in CO_2 gas must also be considered. Regardless of the kind of diffusions concerned, their diffusion coefficients are approximately the same value, $D_0 = 0.14$, which is then used in the calculation.

Table 3. *Rate constant and tortuosity*

In the case of CO_2 diffusion (ΔP = 1 atm)

	A2	B2	C2	D2
C_0	0.0030	0.0027	0.0024	0.0024
k_e	0.25×10^{-5}	0.041×10^{-5}	4.7×10^{-5}	0.16×10^{-5}
k_t	1.8×10^{-4}	1.5×10^{-4}	3.3×10^{-4}	1.8×10^{-4}
f	72	370	7.0	110

In the case of H_2O diffusion (ΔP = 0.013 atm)

	A2	B2	C2	D2
C_0	0.0015	0.0014	0.0012	0.0012
k_e	0.25×10^{-5}	0.041×10^{-5}	4.7×10^{-5}	0.16×10^{-5}
k_t	4.7×10^{-6}	3.9×10^{-6}	8.6×10^{-6}	4.7×10^{-6}
f	1.9	9.5	0.18	2.9

As for the value of C_0, analytical data were adopted. In the case of H_2O diffusion, however, analytical value is multiplied by 0.5, because the molar ratio of reduced non-evaporable water to increased carbonate is about 0.5 according to Hunt and Tomes. In spite of this, the ratio must be 1 in the carbonation of $Ca(OH)_2$.

In consideration of the magnitude of the f value, the type of diffusion which controls the rate of neutralization seems to be both of CO_2 and H_2O for A2, H_2O for B2, CO_2 for C2, and CO_2 and H_2O for D2 respectively, as the f value is empirically expected to be approximately in the order of 5 to 10.

Discussion

Carbonation occurs partly in the deeper position caused by diffusion through large pores, while the degree of carbonation is not greatly increased until the smaller pores are filled with CO_2 gas in spite of the peripheries of the large capillaries being rapidly carbonated. The degree of neutralization is expressed in terms of the depth where a small amount of $Ca(OH)_2$ still remains. All components of the cement, not limited to $Ca(OH)_2$, either hydrated or unhydrated, react with CO_2 gas, and the easiness of carbonation of $Ca(OH)_2$ is not greatly different from that of the other phases.

The tendency of the lines in Fig. 2 becoming steeper at the later stage seems in part to be due partly to an experimental error, if any, caused by some permeation of CO_2 gas through the epoxy-resin coating and also to the following facts: the pore size has a distribution, the rate of carbonation of every components can not be neglected in the diffusion of CO_2 gas, and the size of specimen is limited.

The rate of neutralization of concrete was measured by Hamada (4) and formulated as follows;

$$t = \alpha x^2$$

where,

t: expressed in years
α: a constant and determined as 7.3
x: the depth of neutralization in cm

The value, k_e can be derived as 0.043×10^{-7} from the value α. While, the value $k_t = 0.54 \times 10^{-7}$

is calculated from equation (6), if A2 mortar is to be carbonated in the air. In this case, the value f is to be about 13, but it must be reduced to about 10 for the mortar part in consideration of the difference in the proportion of specimens. Thus, the equations (6) and (7) seem to be applicable in practice and also reasonably assumed as the rate equations of neutralization.

References

1. C. M. Hund and L. A. Tomes, Reaction of hardened portland cement paste with carbon dioxide, J. Research N. B. S. **66,** 473–481 (1962).
2. Y. Inoue and S. Asano, On the carbonation of hydrates of hydraulic compounds, Semento Gijutsu Nenpo **20,** 80–85 (1966).
3. F. Schröder, Vaterit das Metastabile Calciumkarbonat als Sekundäres. Zementsteinmineral, (in German) Tonindustrie-Zeitung **86,** 354–360 (1962).
4. M. Hamada, Carbonation of Concrete, Proceedings of the 5th International Symposium on the Chemistry of Cement, Tokyo, 1968.
5. R. W. Nurse, "Slag cement" The Chemistry of Cements II, Edited by H. F. W. Taylor, Academic Press, London and New York (1964).
6. E. J. Conway, "Micro diffusion analysis & volumetric error" 176, 4th Ed. Crosby Lockwood & Son Ltd., London (1957).
7. B. Franke, A new method for determining calcium oxide and calcium hydroxide in the presence of hydrous and anhydrous calcium silicate, (in German), 2, Anorg. u. Allgem. Chem. **247,** 180–184 (1941).
8. A. Wheerer, "Advances in catalysis III" 266 Academic Press Inc., New York (1951).

SESSION III-4a HYDRATION OF PORTLAND CEMENT PASTE AT HIGH-TEMPERATURE UNDER ATMOSPHERIC PRESSURE

Principal Paper Hydration of Portland Cement Paste at High Temperature under Atmospheric Pressure

Gunnar M. Idron*

Synopsis

Literature of the hydration of portland cement at elevated temperatures under atmospheric pressure is reviewed. The discussion is broadly introduced in pointing to the increasing importance in practice of accelerated hardening of concrete. Principles applied in studies of slow hydration at low temperatures are briefly mentioned.

Heating shortens the induction period of the course of hydration, and increases the rate of the early hydration. There are indications that temperatures above 80 ~ 90°C may result in decreased ultimate degrees of hydration. Studies of volume change, strength and elasticity mostly point to the same direction. Ultrasonic velocity measurements have proved useful. Measurements of heat evolution at high temperatures seem to have met considerable difficulties, but improvements are under way.

The detailed steps of reaction in the hydration process have not been found described in available papers. Adsorption, dissolution, mass-transfer and crystallization are emphasized with reference to room-temperature hydration, as useful subjects of studies to elucidate the kinetics of high temperature reactions. Empiric models of the overall reaction kinetics for hydration at varying temperatures are mentioned, but much more work is avowedly needed before the decisive features are revealed.

High temperature hydrates evidently differ from room-temperature hydrates, particularly in that the CaO/SiO_2 ratio is greater, and that less separates of aluminates, ferrites and sulphoaluminates are formed at high temperatures. Small amounts of crystalline calcium silicates have been found to result from heat curing. Considerable uncertainties remain in interpreting hydration of pure compounds with regard to cement-water systems.

Heat curing has been found to influence the morphology and agglomeration of the hydrates in cement paste; recent studies point towards increased heterogeneity. This effect may be utilized to gain ultimate strength. The need is emphasized for considering temperature a paramount parameter in future studies of cement hydration.

Introduction

The hydration of portland cement paste at high temperatures at atmospheric pressure is a topic of current interest as steam curing of concrete has proved an important innovation in the establishment of the manufacture of large precast concrete units for house-building and civil engineering purposes in many countries, although so far predominantly in Eastern and Western Europe.

The immense market demand has enforced the introduction and development of accelerated manufacture of concrete in factories as replacement for traditional curing at ordinary temperature of concrete

*Concrete Research Laboratory, Karlstrup, Denmark.

cast in situ, and heating with low pressure steam has been found an easy and cheap way of achieving the accelerated hardening, strength development etc.

It may be found surprising, that hydration at elevated temperatures has not been the subject of comprehensive studies in the past. However, 'room-temperatures', i.e. 18°C to 25°C, was considered a convenient and almost universal standard condition in cement and concrete research laboratories, and in most respects the field behaviour of concrete in structures was not significantly different from the behavious found by measurements under simplified laboratory exposure. Moreover, the important development took place in north-temperate, climatic regions without excessive exposures, and development of research and practice had the character of a harmonious evolution, in the 'thirties even involving the introduction of both high-early-strength, rapid-hardening and slow-hardening, low-heat portland cements. The long-sighted, fundamental studies on the basic nature of the hydration of portland cement paste at room-temperature commenced in the same period and was advanced particularly in the USA.

The first studies announcing the benefit of temperature as a parameter in research concerning cement hydration appeared in the late 'forties, if we exclude a few eclectic pre-war studies, particularly referring to block manufacture problems in some countries. In the introduction of this new era the hydration in the temperature range 0°C to 20°C attracted much more interest than acceleration by means of heating. This is due to the immense post-war demand for building at all seasons, that is to say, also throughout the winter. By research it was demonstrated that this could be done by means of precautions in winter-concreting based upon the then sufficiently established understanding of the nature of hardening and hardened cement paste, including the influence of varying temperature on the rate of hydration etc. The applications were especially helpful for practice in countries with moderate winter climates, where site construction proved possible and economic in the 0°C to minus 20°C range.

In regions of more severe winters the tremendous demand for housing etc. in the same period created the prefabrication concrete industry, where plant manufacture of large concrete units was speeded up by means of accelerated hardening, predominantly by means of hydration of portland cement paste at elevated temperatures under atmospheric pressure. The breakthrough of this industry came in the USSR and other Eastern countries in the 'fifties, and the development was excellently reviewed and summarized during the RILEM symposium: *Accelerated hardening of concrete in manufacturing precast reinforced concrete units* in 1964 in Moscow.

Today, prefabrication of concrete is neither confined to particular climatic regions nor to house building, but is an integral part of the magnificent growth of the building industry all over the world. Low-pressure steam curing has become one important possibility among others for increasing the rate of production. But the basic technology of accelerated hydration of portland cement is still much in the dark, in contrast to the situation when concreting about 20 years ago needed and obtained the application of knowledge of the hydration at ordinary and low temperatures.

This paper attempts to summarize the present state of knowledge and to outline some important fields of further studies which may counteract the unsatisfactory economy of an empiric development. In this concept, it seems appropriate to mention that an adequate theoretical understanding of the technology of hydration at elevated temperatures will enable systematic applications in the dry polar regions as well as in the humid-temperate regions, and also in excessively moist and arid warm belts of the earth. Without the support of a scientific approach, practice will still need expensive and incompatible field experi ences under each of these different conditions, which are all becoming important for future building activity.

Steam curing of concrete has been found to influence the strength development and the final strength level of concrete. Various authors have discussed how the different thermal expansion of the solid, liquid and gaseous phases results in the development of internal stresses in the concrete, thus possibly creating interior fracturing. These problems are merely touched upon in the present paper. A discussion in more detail of the mechanics of the fracturing by steam curing of concrete, and therefore also of the beneficial effects of prehardening or other precautions which can prevent expansive forces from causing internal disruption and other mechanical effects, is considered to be beyond the scope of this paper which concentrates upon the influence of temperature ($20 \sim 100$°C) on the hydration of portland cement.

It is appropriate to examine whether high temperature (up to 100°C) treatment might possibly change the characteristics of the cement compounds. However, the transformation temperature of the polymorphs concerned are orders of magnitude higher than 100°C, and no evidence has been found of significant transformation below 100°C. Therefore, the cement compounds are considered unaltered within the range of

reaction temperatures dealt with. Gypsum, however, which is a constituent part of ground cement may be altered into hemihydrate as described by among others W.C. Hansen and J.S. Offutt (1). This alteration will affect the initial hydration reactions as the different types of calcium sulphate have different solubilities. Moreover the solubilities are affected differently by the temperature as shown in Fig. 1. For the sake of completeness, it must also be mentioned that K. Takemoto, M. Kanaya, T. Tashiro and T. Shimoda (2) described changes of cement during high-temperature storage. They concluded that the gypsum will dehydrate when cement is stored for a long time at 55°C to 85°C, and that the cement minerals will hydrate, taking water from the gypsum. (This observation may well deserve attention in modern cement storage practice).

When temperature at first was considered a parameter in studies of cement hydration it was assumed that the reaction process was not influenced by temperature except with regard to the rate of the reactions. On this basis maturity functions were made an important aid in calculations of strength development etc. A.G.A. Saul (3) defined the maturity of concrete as its age multiplied by its average temperature above 0°C, and concluded that concrete of the same mix will have approximately the same strength at the same maturity, whatever combination of time and temperature produced that maturity. Modifications of this principle and applications on other characteristics than strength, e.g. heat of hydration, have been worked out by S.G. Bergstrøm (4), E. Rastrup (5), (6), A. Nykänen (7) and others. These studies proved to be important for investigations of the physical properties of concrete, see e.g. P. Nerenst (8), and for the establishment of the optimum technological conditions for the manufacture of concrete under special conditions, RILEM symposium 1956 (9), J. Jessing (10) and other authors.

In more recent investigations the approximations necessary for the calculation of maturity functions have been found to possess much uncertainty, see e.g. K. M. Alexander and J. H. Taplin (11), and (12). U. Danielsson (13) examined maturity functions by means of the conduction calorimeter and recommended caution with regard to their use as more than rough approximations. Thus, it is not to be expected that maturity functions covering the 20°C to 100°C range of hydration temperatures can readily be established, despite their proved validity for practical purposes in the 0°C to 20°C range of hydration temperatures. In fact, it seems more fruitful to search for descriptions in more detail of hydration phenomena in the 20°C to 100°C range in order to ascertain how the processes involved change with temperature with regard both to the rate of hydration and to the compositions and the characteristics of the reaction products.

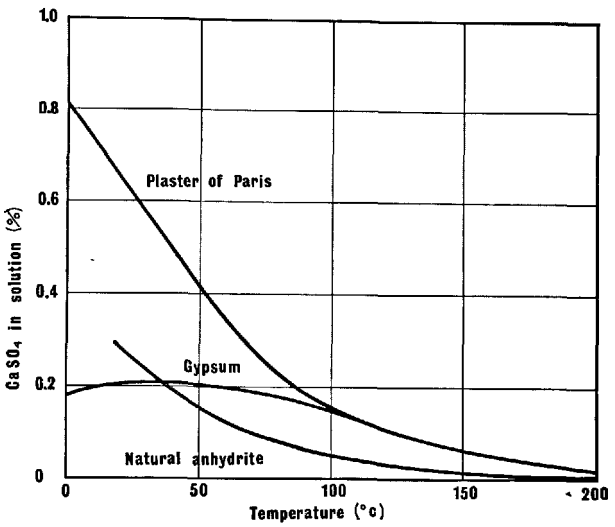

Fig. 1. *Water solubility of different forms of calcium sulphate. From L. E. Copeland and D. L. Kantro (57)*

Rather much of the information referred to below has been found in studies referring to concrete as the experimental material. Such studies are discussed when observations regarding the hydration process and the reaction products have been found, but evaluations with regard to the technology of steam curing of concrete have been omitted, because this topic is treated elsewhere. This limitation covers also the influence of surrounding atmosphere on the hydration, for instance of the relative humidity and of carbon dioxide.

The Course of Hydration

The hydration of portland cement is accompanied by phenomena like i) conversion of reactants (cement and water) into hydration products; ii) heat evolution; and iii) formation of a solid structure exhibiting strength and rigidity. Continuous recording of these phenomena has been used in many investiga-

tions to describe the course of hydration.

The Conversion of Reactants

The amount of cement and water converted into hydration products at any given stage of hydration are determined in various ways, for instance by the intensity of a significant peak in an X-ray diffractogram, by the amount of non-evaporable water, etc. In the literature, either of these characteristics has been used to define what is termed the 'degree of hydration'. For the sake of convenience this term will be used in the following:

The effect of temperature on the temporal changes in the degree of hydration was studied by G. Verbeck (14) (in the temperature range 50°C to 80°C), J. H. Taplin (15) (in the range 5°C to 82°C), D. L. Kantro, S. Brunauer and C. H. Weise (16) (in the rage 5°C to 50°C), U. Danielsson (13) (in the range −2°C to 40°C), P. P. Budnikov, S. M. Royak, J. S. Malinin and M. M. Mayants (17) (in the range 20°C to 90°C), P. P. Budnikov and E. Erschler (18) (at temperature levels 20°C and 80°C), and J. Gebauer and I. Odler (19) (at temperature levels 20°C and 80°C).

From these studies it may be concluded that the rate of hydration increases with increasing temperature level at the early stages of hydration and at moderate hydration temperatures (below 60 ~ 80°C). However, G. Verbeck (14), J. H. Taplin (15) and N. C. Ludwig and S. A. Pence (20) found that curing of higher temperatures (above about 80°C) results in a reduction of the degree of hydration at later age as compared with degree obtained by curing at room-temperature. This phenomenon is illustrated in Fig. 2 (unpublished data obtained at the Concrete Research Laboratory Karlstrup (21)). The tests reported by J. Gebauer and I. Odler (19) on cement pastes with a water-cement ratio of 0.30 and cured at 20°C and 80°C, however, did not reveal a similar reduction.

The possible reason for the reduction will be discussed later on, but the following observations are of interest in this respect:

1. L. E. Copeland, D. L. Kantro and G. J. Verbeck (22) showed that at room-temperature, the quantity of hydrated cement was proportional to the amount of non-evaporable water. No data have been found in the literature to illustrate whether this is true also at higher temperatures.

2. The 'degree of hydration' curve is strongly influenced by the water-cement ratio as demonstrated among others by J. H. Taplin (15), and by the chemical and mineralogical composition of the cement as shown among others by P. P. Budnikov and E. Erschler (18).

The conversion of portland cement and water into hydration products is accompanied by a contraction which is due to the fact that the total volume of the hydrates formed is less than the sum of the volumes of the anhydrous phases and the water involved in the reaction.

W. Czernin (23) used a volumenometer to measure the contraction as a function of time and illustrated the course of hydration by means of data obtained in this manner. As shown also by J. S. Malinin, L. J. Lopatnikova, V. I. Guseva and N. D. Klishanis (24), contraction vs. time curves at room-temperatures are characterized by an initial period (lasting a few hours) of low contraction rate. Then the rate increases, passes through a maximum, and then decreasing slowly towards zero.

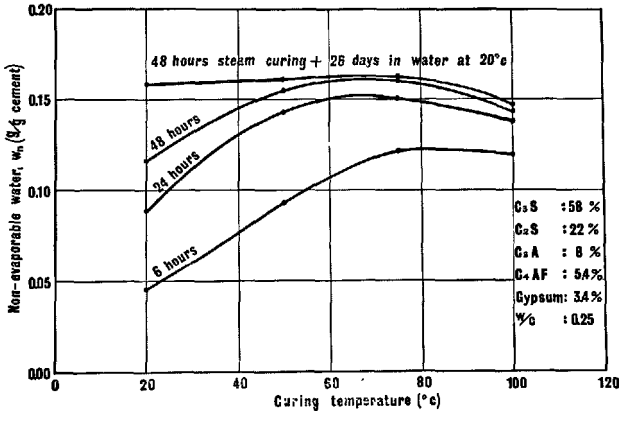

Fig. 2. *Non-evaporable water content in portland cement pastes as a function of curing temperature, measured at the indicated ages (from water addition). Data from (21), not published*

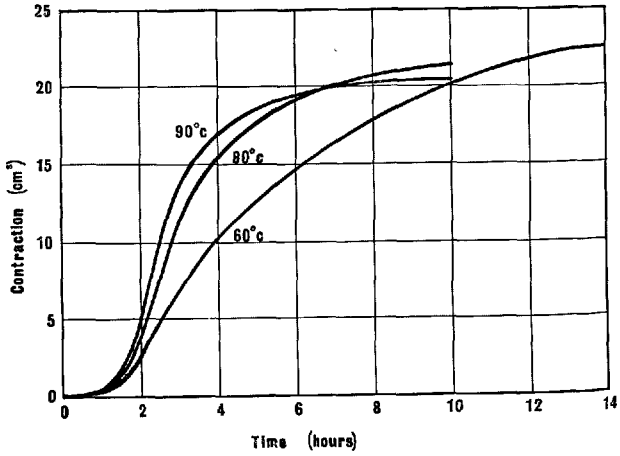

Fig. 3. *Contraction of portland cement mortars versus curing time under isothermal conditions. From L. A. Sil'chenko, M. V. Mikhailov and P. A. Rehbinder (26)*

R. Malinowski (25) used the same technique as Czernin to measure the volume changes of cement paste hydrating at 80°C. L.A. Sil'chneko, M. V. Mikhailov and P. A. Rehbinder (26) described an ingenious but simple apparatus which allowed them to study the effect of temperature on the contraction of hydrating portland cement mortars. As appears from Fig. 3, they observed that the rate of contraction, in the early hydration stages, increased with increasing temperature. The total contraction, however, at an age of about 12 hours, was higher with a curing temperature of 60°C than with temperatures of 80°C and 90°C. (The contraction dealt with above does not imply that a hydrating specimen of cement paste undergoes a decrease in its outer dimensions during hydration. On the contrary, a slight expansion of moist-cured specimens is usually observed).

Heat Evolution

Various calorimeter techniques have been applied to measure the heat which is liberated during the the hydration of portland cement. The heat of solution method is used to obtain figures of the total heat of hydration at the later age stages. The conduction calorimeter technique provides information on the rate of heat evolution and is particularly suited for investigations of the early stages of hydration. Thus, this latter technique is also best suited for studies of temperature effects, since in such studies the early hydration stages are of particular importance.

W. Lerch (27) and others in studies at room-temperature found that the rate of heat evolution curve has two or more peaks. The first peak occurs a few minutes after mixing with water and represents, according to Lerch, initial rapid dissolution of aluminates and rapid crystallization of hydrated calcium aluminates. This peak is followed by a period of low activity, lasting usually 2 to 3 hours and named the induction or 'dormant' period. At the end of the induction period, the rate increases again, passes through a maximum (second peak) and decreases then slowly towards zero. The second peak usually occurs 6 to 10 hours after mixing. Mainly, it represents heat evolution associated with the reaction of calcium silicates with water to form calcium silicate hydrates. A third peak may occur, depending generally on the contents of C_3A, gypsum, and alkalies in the cement as well as on the ratio between them.

Data on the effect of the temperature level under isothermal curing conditions on the heat evolution during hydration are presented by a number of authors. In the low temperature ranges (below about 40°C), the temperature effect was studies by H. Yokomichi (28), E. Rastrup (5), (6), L. E. Copeland, D. L. Kantro and G. J. Verbeck (22), H. Lehmann and W. Roesky (29) and U. Danielsson (13) and others. Some of Danielsson's results are reproduced as Figs. 4 and 5. Studies of the effect of higher temperatures (in the 40°C to 100°C range) were reported by N. C. Ludwig and S. A. Pence (20), L. E. Copeland, D. L. Kantro and G. J. Verbeck (22), Jo Gebauer and I. Odler (19), (30), and P. P. Budnikov and E. Erschler (18).

From these studies it appears that the temperature level strongly influences the evolution of heat of hydration. In general, the effect of increasing temperature consists in a reduction of the induction period and an increase of the rate of heat evolution, As seen in Fig. 4, this effect manifests itself as a displacement of the main peak towards zero time and as an increase of the height of the peak.

In the low-temperature range (below about 40°C), L. E. Copeland, D. L. Kantro and G. J. Verbeck (22), H. Lehmann and W. Roesky (29), and U. Danielsson (13) found that the total heat of hydration, at any stage of hydration, is proportional to the degree of hydration as defined above, irrespective of the temperature level. However, J. Gebauer and I. Odler (30) in their experiments found the ratio between non-evaporable water and heat of hydration to be less in pastes cured at 20°C than in pastes cured at 80°C, this difference being particularly pronounced at later ages (28 days).

As appears from the above, only a few data are reported on isothermal heat evolution at high temperature levels (above about 60°C). This may be due to

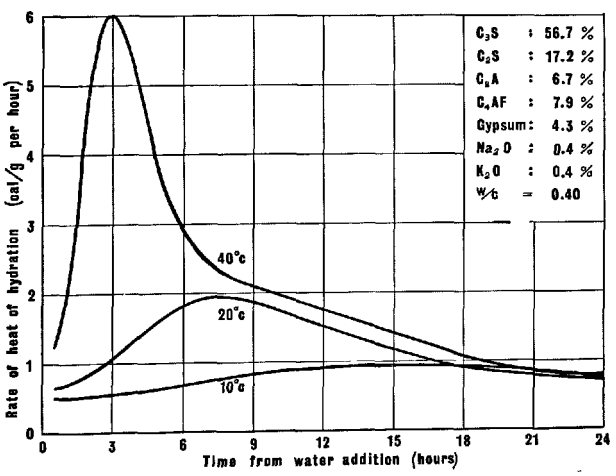

Fig. 4. *Rate of heat of hydration for portland cement pastes cured continuously at 10°C, 20°C, and 40°C, respectively. From U. Danielsson (13)*

experimental and instrumental difficulties. However, for future investigations, the microcalorimeter developed by E. Calvet (31) and used by M. de Tournadre in his studies of the hydration of calcium aluminates (32) and calcium sulphate (33) seems to be a suitable instrument for accurate measurements of heat evolution under isothermal conditions.

Strength and Elasticity

With a given cement and with given mix proportions, the development of strength and stiffness in cement paste and concrete proceeds in a manner similar to that of the degree of hydration.

Thus, as shown for instance by R. Malinowski (25), the rate of strength growth increases initially, then it passes through a maximum, after which it decreases slowly towards zero. Unfortunately, however, rather few experimental data are reported in the literature on the strength development during the very early stages of hydration.

Early changes in elasticity, on the other hand, were studied by means of ultra sonic methods by A. E. Whitehurst (34), J. Andersen and P. Nerenst (35), L. Palotas, D. Balazs and I. Gemesi (36), M. Lystbæk (37), and others who calculated the dynamic modulus of elasticity from continuously measured values of the ultrasonic velocity.

Numerous test series are reported in the literature concerning the effect of the level of curing temperature on the strength and stiffness development. They all show that the rate of strength (and stiffness) growth at the early stages of hydration increases strongly with increasing curing temperature. With increasing age, however, this effect of temperature becomes less pronounced, and it is even frequently observed, see e.g. J. A. Hanson (38), that strength and modulus of elasticity at later ages (for instance at 28 days) are greater for specimens cured at moderate temperatures (below about 40°C to 50°C) than for specimens cured at the highest temperature (about 80°C to 100°C). This applies whether high temperature curing was used continuously during the whole curing period or only during the first few hours of curing. This phenomenon is demonstrated in Fig. 6 (data from J. Gebauer and I. Odler (19)).

The ultrasonic technique has been taken in use at the Concrete Research Laboratory Karlstrup (see Fig. 7) to study the effect of temperature on the growth of modulus of elasticity during the very early stages of hardening of concrete. Preliminary results are presented in Fig. 8. The plateau which is observed on both curves has not yet been interpreted.

The reduction of strength at later ages which is often observed with steam curing, has not been fully explained. W. Czernin (39), J. A. Hanson (38), H. H. Bache and P. Dragsholt (40), and P. P. Budnikov and E. Erschler (18) showed that structural disintegration, due to different thermal expansion of solid material and water and vapor phases, could occur under certain unfavourable conditions. This would be expected to cause strength losses. H. H. Bache and P. Dragsholt (40), however, concluded from their results that structural disintegration could account for only part of the strength reduction observed. It is worth mentioning in this connection that P. P. Budnikov, S. M. Royak,

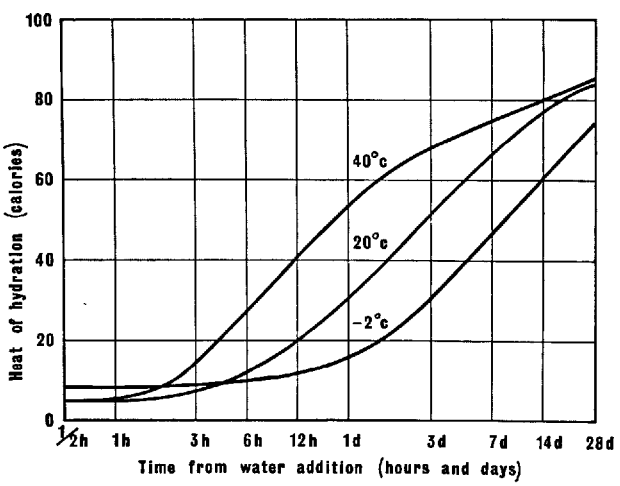

Fig. 5. *Heat of hydration versus curing time (log scale) for portland cement pastes cured continuously at −2°C, 20°C, and 40°C, respectively. Cement composition as indicated at Fig. 4. From U. Danielsson (13)*

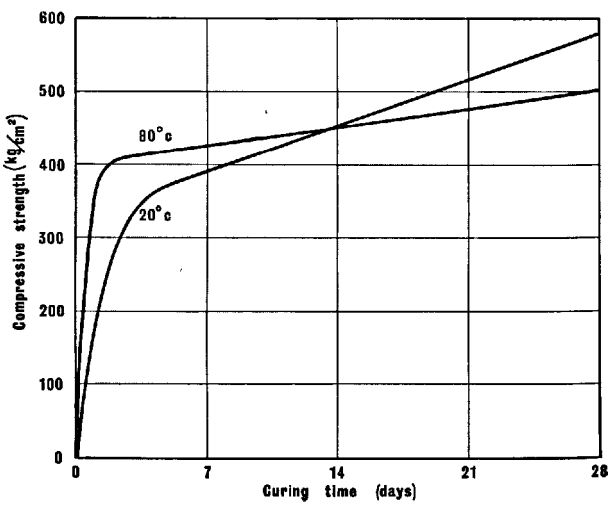

Fig. 6. *Evolution of compressive strength for cement pastes cured isothermally at 20°C and 80°C, respectively. Data from J. Gebauer and I. Odler (19)*

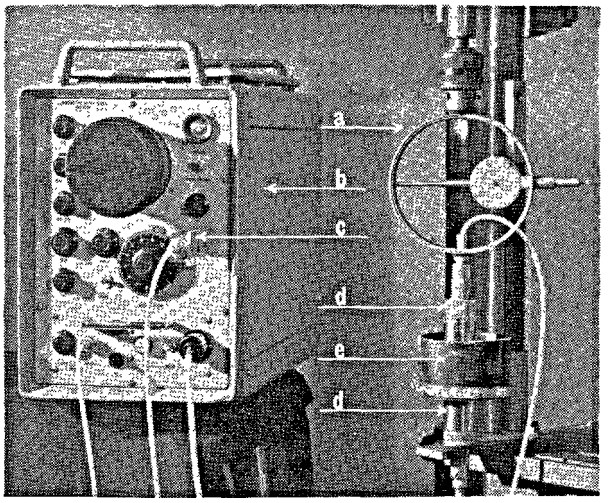

Fig. 7. *Setup for continuous measurement of ultrasonic velocity in cement paste, mortar or concrete during hardening: a) pressure device with dynamometer (it is often useful to apply a certain pressure to the specimen in order to facilitate the propagation of sonic pulses through the specimen, particularly at the early stages of hydration); b) ultra sonic apparatus; c) switch by means of which the transmission of pulses may be switched off between readings; d) transducers (the upper transducer is in direct contact with the surface of the specimen); and e) mould containing the concrete specimen (the bottom is made of steeel, the cylindrical shaft of rubber, while the part of the upper surface of the specimen, which is not in touch with the transducer, is covered with a steel plate). From M. Lystbæk (37)*

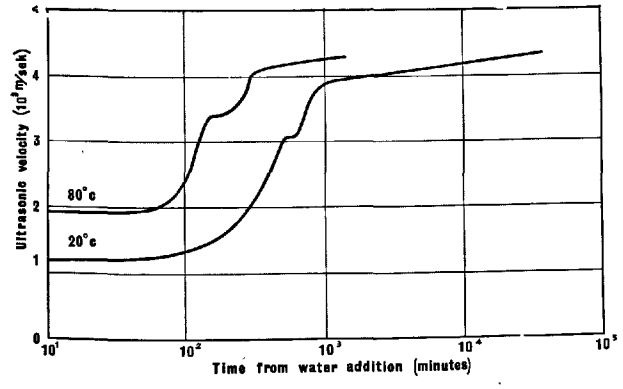

Fig. 8. *Ultrasonic velocity in portland cement concrete cured permanently at the temperature levels indicated. Preliminary data from the Concrete Research Laboratory Karlstrup*

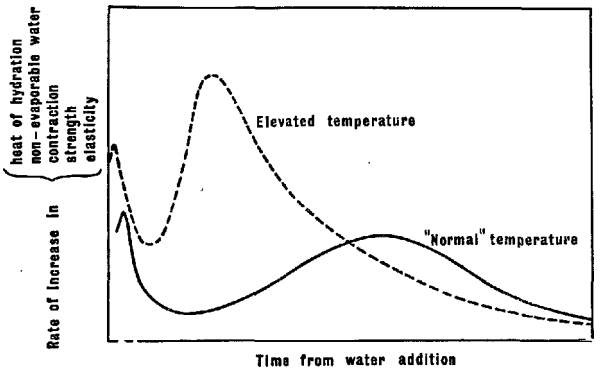

Fig. 9. *Qualitative picture of the effect of a temperature increase on the rate of development of the phenomena indicated*

J. S. Malinin and M. M. Mayants (17) in experiments with pure C_3S pastes found that with equal degree of hydration, specimens hydrated at about 50°C obtained much less strength than specimens hydrated at temperatures below and above 50°C. They attributed the phenomenon to the formation of a special, metastable hydration product which formed only at about 50°C.

The various methods mentioned provide a somewhat indirect and incomplete picture of the hydration process, and observations on hydration at elevated temperature levels must accordingly be interpreted with singular caution. With reasonable certainty, however, the following can be said:

1. Whether degree of hydration, volume change, heat of hydration, strength or elasticity are used to characterize the hydration process, a temperature increase manifests itself in the same manner: The length of the induction period decreases and the early stage rate of hydration increases with increasing temperature. This is qualitatively illustrated in Fig. 9.

2. At later ages, curing temperatures above about 60°C to 80°C are frequently found to result in a reduction of the degree of hydration, contraction, strength, and modulus of elasticity as compared with what is obtained at lower temperature levels. However, there is also experimental evidence pointing in the opposite direction.

Mechanisms of Reaction

The hydration of portland cement is a heterogeneous, stepwise reaction.

From numerous investigations of hydration at room temperatures it appears that the reaction steps should be sought within such topics of physical chemistry as adsorption, dissolution, mass-transfer, and crystallization. Several models have been suggested to describe the individual steps or combinations of steps

involved in the hydration process. A few examples of such models are presented in the following:

Adsorption

W. C. Hansen (41) suggested a hydration mechanism of C_3A, C_2S, and C_3S based on the chemi-sorption of OH^- and H_2O^+ ions from water by Ca^{2+} and O^{2-} ions in the surfaces of crystals. A. K. Chatterji and R. S. Rawat (42) stated that the reaction between cement clinker and water is a semiconducter surface reaction, and the hydration of clinker minerals therefore is a chemi-sorption process occuring on the surface of clinker crystals. Whether physical adsorption occurs is not mentioned.

Dissolution

S. A. Greenberg and T. N. Chang (43) in investigations on the hydration of C_3S at 30°C considered dissolution of calcium silicate to be one of the processes occuring. N. Kawada and A. Nemoto (44) in a detailed description of mechanisms of the reaction between C_3S and water showed that the initial step is a dissolution of approximately half of the calcium from the surface of the C_3S particles. This mechanism is in agreement with the one suggested by J. S. Malinin, L. J. Lopatnikova, V. I. Guseva and N. D. Klishanis (24).

Mass-Transfer

Diffusion of hydrated ions away from surfaces of unhydrated minerals is one of the steps discussed by S. Brunauer and S. A. Greenberg (45). V. B. Ratinov and A. P. Lavut (46) derived an equation which describes the hydration kinetics assuming convection and diffusion to take place. N. Kawada and A. Nemoto (44) described transfer through solution, of the amorphous coating formed on unhydrated calcium silicate to nucleii of more crystalline calcium silicate hydrate.

Mass-transfer (either by diffusion or by Poiseuille flow) through coating of hydration products on surfaces of unhydrated minerals is described by H. N. Stein (47), H. zur Strassen (48), T. C. Powers (49) and others.

Crystallization

S. A. Greenberg and T. N. Chang (43) demonstrated that after the initial surface reaction between C_3S and water the solution was only slightly supersaturated with respect to hydrated calcium silicate but highly supersaturated with respect to calcium hydroxide, and they stated that the rate of crystallization of the hydrated silicate was much faster than the rate of hydration. H. E. Schwiete, U. Ludwig and P. Jäger (50) suggested that the topochemically formed ettringite coating on C_3A grains later on is bursting off due to crystallization pressure. V. YA. Khaimov-Mal'kov (51) derived an equation for crystallization pressure.

In order to elucidate the reaction kinetics at elevated temperatures it would be desirable to establish i) the steps involved in the hydration, and ii) the influence of temperature and degree of hydration upon the reaction scheme and the velocity of the steps. Hence, the various 'rate determining steps' could possibly be found.

However, since no model, accounting in detail for the complete course of the hydration process, has so far found sufficient support in experimental data to be generally accepted and since no indication of the effect of temperature on the particular reaction steps possibly involved was found in the literature reviewed, the following literature survey is limited to investigations dealing only with measurements of the overall rate of reaction and its variation with temperature. In some of these investigations, calculation-models have been used to correlate experimental data to kinetical theories; these models, naturally, are more or less realistic. For instance, the fact that the individual cement grains consist of a mixture of the cement minerals is rarely taken into consideration, see Fig. 10.

V. B. Ratinov, A. P. Lavut (46), V. B. Ratinov, G. D. Kucheryaeva, G. G. Melent'eva and S. M. Pimenova (52), and V. B. Ratinov, T. I. Rozenberg and I. A. Smirnova (53) stated that the kinetics of hydration may be divided into two stages. In the earliest stage (1 ~ 3 days), transfer of materials proceeds through convection and diffusion. In the second stage, which occurs after the formation of a rigid skeleton, the transfer of materials is a diffusion only. They derived equations describing the hydration kinetics within the first stage, and they presented experimental

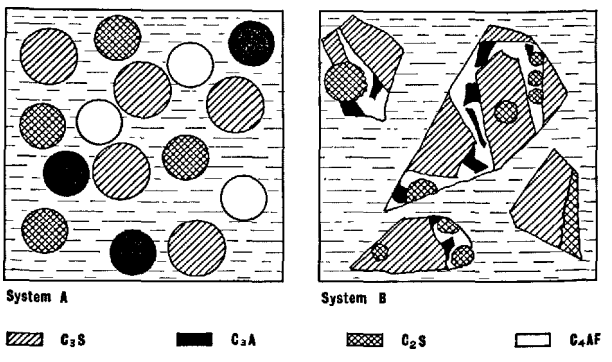

Fig. 10. *Models of water-cement systems. System A contains grains of pure clinker minerals. System B contains grains of a mixture of clinker minerals*

evidence for the validity of the equation:

$$m_\tau^{1/3} - m_0^{1/3} = -K \cdot D^{2/3} \cdot C \cdot \tau,$$

where m denotes the amount of unhydrated material at time τ and $_0$, respectively, K a constant, D the diffusion coefficient, and C the solubility of the anhydrous phase. The temperature affects the solubility C and $K \cdot D^{2/3}$. The theoretical and experimental results were used to calculate the ratios of the hydration rate and the dissolution rates of C_3S and β–C_2S at various temperatures. It was shown that increasing temperature results in increasing solubility of β–C_2S and C_3S, and a decrease in the ratio between the reaction rates of C_3S and β–C_2S. Some of the data are presented in Table 1.

P. P. Budnikov, S. M. Royak, Y. S. Malinin and M. M. Mayants (54), (17) measured the degree of hydration (by means of X-ray investigations) of cement minerals and mixtures of them at various ages and at various temperatures. For all the materials investigated they found that the empiric equation

$$L = K \cdot \log\tau - B$$

covered the test results with reasonable accuracy within the range $20\% < L < 80\%$, see Fig. 11. In this equation, L denotes the degree of hydration, τ time, and K and B constants which depend on the type of clinker mineral or mineral mixtures and the temperature. B is related to the induction period. The effect of temperature was described by the following equations:

$$\log B = A - n \log T,$$

and

$$K = cT + d,$$

in which T is the absolute temperature in °K. A, n, C, and D are constants distinctly related to each kind of binding materials.

T. M. Berkovltch, D. M. Kheiker, O. I. Grachva, O. S. Volkov and E. S. Mikhalerskaya (55) concluded from their investigations that the kinetics of the hydration process can be described by the first order

Table 1. *The effect of temperature on hydration rates and on solution rates of* C_3S *and* β-C_2S. (*From V. B. Ratinov and A. P. Lavut* (46)).

Temperature °C	Ratio between hydration rates of C_3S and β-C_2B		Ratio between solution rates of C_3A and β-C_2S
	24 hours	72 hours	
20	4.1	4.7	2.4
35	3.7	2.8	2.0
50	2.5	2.4	1.9
65	2.4	2.4	1.8

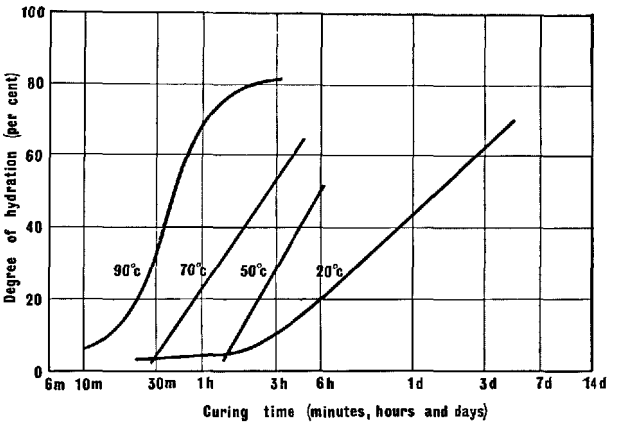

Fig. 11. *Kinetics of hydration of the clinker mineral* C_3S *at different temperatures. From P. P. Budnikov, S. M. Royak, Y. S. Malinin and M. M. Mayants* (54)

equation:

$$-\log c = K \cdot \tau + \text{const},$$

where c is the amount of unhydrated cement, τ time, and K a rate constant. Plots of $\log c$ versus τ showed two rectilinear portions corresponding to two different values of the rate constant K. Thus, they suggested the hydration process to be divided into two periods. The effect of temperature was said to consist in an increase of the rate of hydration, but the fundamental regularities of the process were not considered to be greatly affected. Data were presented for the hydration of C_3S and β–C_2S within the range $25° \sim 175°C$, and it was demonstrated that the rate constants vary with temperature according to Arrhenius' law within each of the two periods.

Values of the activation energy which is a constituent part of Arrhenius equation, have been used to describe the effect of temperature on cement hydration. G. Verbeck (56) showed that the Arrhenius equation is valid within the temperature range $4° \sim 110°C$. The activation energy found has the same value for different types of cement. L. E. Copeland and D. L. Kantro (57) on the other hand showed that the activation energy depends on the degree of hydration. H. E. Schwiete, H. Knoblauch and G. Ziegler (58) found in investigations on the kinetics of hydration of C_3S and β–C_2S that the hydration of C_3S is a reaction of third order with an activation energy of 2.1 Kcal/mol, and that the hydration of β-C_2S is a reaction of 1.5 order with an activation energy of 1.8 Kcal/mol. J. H. Taplin (59) found, however, activation energies of about 10 Kcal/mol for the hydration of C_3S and 18 Kcal/mol for the hydration of β–C_2S. In investigations on composition of the

liquid phase during the hydration of cement, C. D. Lawrence (60) found the activation energy for the reaction between C_3A and sulphate to be 9.0 Kcal/mol.

R. F. Feldmann and V. S. Ramachandran (61) studied the effect of temperature (from 2°C to 52°C) on the hydration of C_3A/gypsum mixtures. They concluded, that gypsum decreases the reactivity of C_3A by sorption of SO_4^{2-} ions and that gypsum reduces the rate of conversion of hexagonal to cubic hydroaluminate by sorption of SO_4^{2-} ions. At the highest temperature (52°C), a large amount of gypsum may have an accelerating effect, as the gypsum prevents the growth of impermeable C_3AH_6 films on the surface of C_3A.

Hydration Products

Observations on the influence of the temperature upon rate of hydration and on the final strength of cement paste indicate that the hydration products formed at elevated temperatures differ from those at room temperature. The identification of the various hydration products is not simple, as the type of hydration products found depends on the identification-criteria (chemical composition, X-ray pattern, DTA-temperatures, IR-traces, etc.) and on the conditions (relative humidity, CO_2-concentration, etc.), under which the investigations are carried out. This may explain the fact that a distinct picture of the phase-composition of cement hydrated at elevated temperature has not been found in the literature.

System $CaO–Al_2O_3–Fe_2O_3–CaSO_4–H_2O$

Equilibria in the ternary system $CaO–Al_2O_3–H_2O$ was reviewed by F. E. Jones (62). He concluded that the only aluminates appearing in the temperature range 20 ~ 100°C are C_4AH_{19} and C_2AH_8 which, however, both are metastable with respect to C_3AH_6. O. P. Mchedlov-Petrosyan (63) used calculated values of thermodynamic functions to predict the components which might be expected to form under various hydration conditions and to predict the energetics of the reactions involved. These included reaction of formation of the various hydrated components from solutions, hydration reactions of anhydrous cement compounds, and transformation reactions. Concerning the system $C_3A–H_2O$ and the system $CA–H_2O$ as well, he concluded that the only thermodynamically stable compound in the temperature range 25 ~ 125°C is C_4AH_{19}. M. de Tournadre (32), (64) and P. Longuet and M. de Tournadre (65) studied the hydration of calcium aluminate by means of a microcalorimeter. They found that C_3A at 30°C hydrated into C_3AH_6 only.

E. T. Carlson studied the hydration of calcium aluminate ferrites (66) and properties of the hydrates (67). He concluded that the hydrogarnet phase $C_3(A, F)H_6$ is a stable phase above 35°C. At 70°C a solid solution of C_3AH_6, in which one-tenth of Al_2O_3 is replaced by Fe_2O_3, is precipitated. Moreover, he found that all the aluminoferrite hydrates reacted with calcium sulphate solution forming mixtures of the monosulphate and the trisulphate types, the latter predominating at later stages.

O. P. Mchedlov-Petrosyan (63) concluded concerning the system $CaO–Al_2O_3–CaSO_4–H_2O$ that trisulphate is the thermodynamically stable product up to 70°C, and that monosulphate is the stable compound above 70°C. H. Kühl (68) considered that the formation of ettringite above 40°C is not possible, whereas W. Lieber (69) obtained ettringite from aqueous solutions up to 90°C. This is in agreement with Y. M. Butt, A. A. Maier and B. G. Varshal (70), who found transformation temperatures for ettringite to monosulphate in the temperature range 125°C to 175°C. On the other hand, they found monosulphate to be stable in contact with its saturated solution in the temperature range 50°C to 200°C.

System $CaO–SiO_2–H_2O$

O. P. Mchedlov-Petrosyan (63) treated the hydrothermal main-reactions and side-reactions in the system $Ca(OH)_2–SiO_2–H_2O$ from a thermodynamical point of view as previously described. He found that amount the compounds having C: S = 2: 1 (and 3: 1, 4: 1, 5: 1, and so on) hillebrandite ($2CaO \cdot SiO_2 \cdot 1.17H_2O$) is the stable phase. For compounds having C: S between 3: 2 and 4: 3 foshagite ($4CaO \cdot 3SiO_2 \cdot 1.5H_2O$) is the stable one. With a C: S ratio of 1: 1 14 Å tobermorite ($5CaO \cdot 6SiO_2 \cdot 10.5H_2O$) is stable up to about 80°C, 11 Å tobermorite ($5CaO \cdot 6SiO_2 \cdot 5.5H_2O$) up to about 100°C and above that xonotlite ($6CaO \cdot 6SiO_2 \cdot H_2O$) is stable. 14 Å tobermorite is the stable phase by C: S = 5: 6 up to 50°C, xonotlite stable above 50°C. With a C: S ratio of 2: 3, 1: 2, 1: 3, 1: 4, and so on, gyrolite ($2CaO \cdot 3SiO_2 \cdot 2.5H_2O$)

is the stable phase. Using an isothermal solution calorimeter J. E. Taylor (71) determined the heats of formation of a number of calcium silicate hydrates. The results obtained were very close to those calculated by O. P. Mchedlov-Petrosyan (63).

O. P. Mchedlov-Petrosyan (63) in a description of the thermodynamics in the hydration of β–C_2S and C_3S concluded that the most stable endproduct up to 100°C in both cases is hillebrandite. Other products, however, such as for instance foshagite and tobermorite are possible endproducts due to kinetical and structural conditions.

D. L. Kantro, S. Brunauer and C. H. Weise (72) reported that calcium hydroxide and a tobermorite-like product is found during hydration of β–C_2S at the temperatures 5°C, 25°C, and 50°C. They found an increase in the final CaO/SiO_2-ratio with increasing temperature. Such increase in CaO/SiO_2-ratios are also found in products hydrated at temperatures up to 100°C, as described by H. Funk (73). D. L. Kantro, S. Brunauer and C. H. Weise (72) moreover found an increase in H_2O/SiO_2-ratios with increasing temperatures. Concerning hydration of C_3S they found no unidirectional changes with temperature in the ultimate ratios of CaO/SiO_2 and H_2O/SiO_2. H. Funk, B. Schreppel and E. Thilo (74) found that hydrated intermediate products with water contents up to $H_2O/SiO_2 = 1.5$, and β–C_2S-like structures occur. The intermediate products are also formed by interaction between β–C_2S and gaseous water at 100°C. In this case the porous final products have compositions of $1.8 \sim 2CaO \cdot SiO_2 \cdot 1 \sim 2H_2O$, and structures which are still similar to that of β–C_2S.

P. P. Budnikov, S. M. Royak, S. J. Malinin and M. M. Mayants (17) found that the 'basicity' of the hydrosilicate phase in specimens of hydrated C_3S increases up to a temperature of about 50°C and decreases slightly in the range 50 ~ 90°C. At 90°C, however, the 'basicity' is still higher than at 20°C. Specimens of hydrated C_2S showed no change in 'basicity' by change in temperature.

E. R. Buckle and H. F. W. Taylor (75) showed that when C_3S is hydrated at temperatures above 50°C small amounts of tricalcium silicate hydrate are formed together with tobermorite gel and calcium hydroxide.

H. Funk and F. Zimmermann (76) stated that below a hydration temperature of 120°C only the ill-crystallized phases of calcium silicate hydrate exist.

Natural Minerals

Investigations on the characteristics of the cement paste are difficult due to small size and low order of crystallinity of the components. Larger pieces of natural minerals, which are more or less identical to the cement paste components have sometimes been examined and their characteristics have been compared with the cement paste components. Recently two such investigations, which are of interest to the present problems, have been published.

V. C. Farmer, J. Jeevaratnam, K. Speakman and H. F. W. Taylor (77) studied the thermal decomposition of 14 Å tobermorite from Crestmore. The composition is considered to be $Ca_5Si_6O_{18}H_2 \cdot 8H_2O$ with small amounts of CO_2 and B_2O_3. At 55°C there is a sharp change to 11.3 Å tobermorite $Ca_5Si_6O_{18}H_2 \cdot 4H_2O$. The 11.3 Å tobermorite looses most of its water gradually, at 55°C to 200°C, apparently without undergoing fundamental change in structure.

At Crestmore a new mineral has been found. The mineral was described by K. Speakman, R. A. Chalmers, J. A. Gard, H. F. W. Taylor and A. B. Carpenter (78) and it was named jennite. Jennite seems to be very similar to the C–S–H I phase found in cement paste (H. F. W. Taylor (79)). Jennite has a composition $Na_2Ca_8(SiO_3)_3(Si_2O_7)(OH)_6 \cdot 8H_2O$.

On heating, jennite remains stable up to 70°C, but at 70°C to 90°C there is a sharp loss of water, which amounts to about 7% of the initial weight. The product thus formed is called meta-jennite; its composition is thought to be $Na_2Ca_8(SiO_3)_3(Si_2O_7)(OH)_6 \cdot 5H_2O$.

It is of interest in this connection that T. Yoshii and G. Sudoh (80) in studies of the system Na_2O–CaO–SiO_2–H_2O at 20°C found, that when C_3S and C_2S initially hydrated in contact with a Na^+-containing liquid, the hydrated solid phases after 98-days are $N_{0.26}C_{1.60}SH_n$ and $N_{0.15}C_{1.40}SH_n$.

Hydration Products in Cement Paste

Study of pure few-component-systems can give an idea of the compounds which would be expected to appear during the hydration of cement. Cement paste, however, is a multi-component system in which formation of meta-stable compounds and solid solution series is possible, and as equilibrium is possibly not reached, the hydration-pattern obtained from pure-system investigations may very well be very much different.

A. E. Sheikin and N. I. Oleinikova (81), in X-ray investigations of steam cured cement paste, found the presence of low intensity lines of trisulphate and lines of monosulphate of much higher intensity, as well as

lines of C_2AH_8 and diffuse lines of C_4AH_{13} and gypsum. The presence of C_3AH_6 was not established. They concluded that the hydration products of steam cured cement paste are similar to those of ordinary cement paste at long duration of hydration, which may point out the formation of more stable compounds at steam curing.

P. P. Budnikov and E. Erschler (18) concluded from studies of low pressure steam curing of concrete that in the course of steam treatment, formation of hydrosulpho-compounds in cement paste takes place up to 60°C. At higher temperatures these are transformed into compounds of lower sulphate content, and free calcium sulphate is released.

L. Hjorth (82) found monosulphate to be present and ettringite to be absent in a cement sample initially hydrated 7 hours at 100% RH and 80°C, and thereafter stored for two months at 100% RH and room-temperature. The ettringite phase seems to disappear at about two hours of hydration. The presence of ettringite and the absence of monosulphate was found in a similar sample cured at room-temperature and 100% RH for two months.

G. L. Kalousek (83) investigated by means of DTA the amount of the different SO_3-containing compounds in cement hydrated at the temperatures 24°C, 55°C, and 82°C. He found that some SO_3 was 'missing' and he suggested that SO_4^{2-} is incorporated in the tobermorite gel substituting SiO_4^{4-}. The solid solution formed is called phase X. The effect of the temperature is considered to be an acceleration of the reaction: Ettringite → monosulphate → solid solution of monosulphate and calcium aluminate hydrate → phase X. He found it reasonable to assume that the constituents Al_2O_3, SO_3, and Fe_2O_3 have solid solution saturation levels in phase X. Once the saturation values are exceeded, such constituents would become parts of other phases.

In X-ray investigations of cement hydrated at 100°C, A. Aitken and H. F. W. Taylor (84) found no hydrated aluminate or sulfoaluminate phases. P. P. Budnikov, S. M. Royak, J. S. Malinin and M. M. Mayants (17), however, found monosulphate by means of DTA in a cement hydrated 24 hours at 90°C.

From electron microscopic observations Å. Grudemo (85) stated that there is no fundamental change in the C–S–H gel phase at temperatures of about 100°C or a little higher.

There are some indications that small amounts of crystalline hydrated silicates are formed during the hydration of cement at elevated temperature besides the formation of tobermorite gel. A. Aitken and H. F. W. Taylor (84) found that some tricalcium silicate hydrate was formed at 50°C to 75°C, and G. L. Kalousek and A. F. Prebus (86) reported that hillebrandite was formed at 50° to 120°C.

I. Odler and J. Gebauer (19), (30) found in an investigation of cement hydrated at different temperatures that a phase characterized by a DTA-peak at 450°C occured in cement paste hydrated at 80°C. This phase was considered to be α–C_2SH.

P. P. Budnikov, S. M. Royak, J. S. Malinin and M. M. Mayants (17) in a review of literature mentioned that the presence of C_2SH_2, $C_2SH_2 + C_3S_2H$, and C_3SH_3 in high-temperature hydrated cement has been reported.

It can be concluded that the reaction products of cement hydrated in the temperature range 50°C to 100°C differ from the products formed at room-temperature as follows:

1. The calcium silicate gel obtained probably has a higher content of Al^{3+}, Fe^{3+}, and SO_4^{2-} ions. By analogy with results from investigations on pure clinker minerals the calcium silicate gel, moreover, is considered to have a higher CaO/SiO_2-ratio and a different H_2O/SiO_2-ratio.
2. Small amounts of some other, more crystalline calcium silicate hydrates may be formed.
3. Less amounts of separate hydrated aluminate, ferrite or sulfoaluminate phases will be formed, if formed at all. The ratio between the amounts of trisulphate and monosulphate will probably be lower.

Moreover, it seems well established that increasing temperature does not promote the transformation of hexagonal calcium aluminate hydrates into cubic calcium aluminate hydrates when these products are present in cement paste.

The Structure Formation

Many authors have stated that curing of concrete at elevated temperatures results in lower ultimate strength than curing at room-temperatures. Studies reporting curing at elevated temperatures without loss of ultimate strength have appeared only exceptionally, see e.g. R. Malinowski (87). Thus, a certain loss of ultimate strength is often considered the payment for the acceleration of hardening of concrete.

However, recent experiments at the Concrete Research Laboratory Karlstrup have demonstrated that under certain conditions more than 50 % increase of ultimate strength can be achieved by means of steam curing. These apparently contrasting observation call for a brief discussion of the nature of the strength determining factors and their dependence on temperature.

The strength of cement paste, mortar and concrete is controlled by the building up of a structure composed of hydration products (here designated the *microstructure*) and their interaction with grains of unhydrated cement and fillers, which together with the microstructure constitute the *macrostructure*, as shown schematically in Fig. 12. The strength and rigidity of the macrostructure is influenced by the temperature through its influence upon:

1. Interatomic forces within the individual particles which are formed during the hydration.
2. Interfacial atomic forces which bind the individual particles together and to grains of hydrated cement and fillers.
3. Size and morphology of the hydrated particles as well as their intergrowth and agglomeration.
4. The distribution of microstructure, i.e. its geometrical arrangement and its density distribution.

The contribution of intrinsic particle strength and interfacial forces to the strength of the microstructure was discussed by S. Chatterji and J. N. Jeffery (88) who explained the difference between tensile and compressive strength on the basis of a model of the structure of set cement, provided through examinations of electron micrographs. The effect of temperature on crystal growth was discussed by P.P. Budnikov and E. Erschler (18) who suggested that the ratio between the amount of crystalline hydration products and the amount of gel increases and that the crystal size increases with increasing temperature. They further suggested that this temperature effect on the microstructure would lead to decreasing strength with increasing temperature. The same effect was suggested by F. Keil (89) in his review on the hardening of hydraulic binders. Measurements of the specific surface area of hydration products rather consistently show that the specific surface area decreases with increasing temperature at the late age stages of hydration (see e.g. N. C. Ludwig and S. A. Pence (20), P. P. Budnikov, S. M. Royak, Y. S. Malinin and M. M. Mayants (17), O. Matsuda and S. Ishimura (90), and S. Brunauer and D. L. Kantro (91)) indicating that coarser particles are formed at elevated temperatures than at room-temperatures.

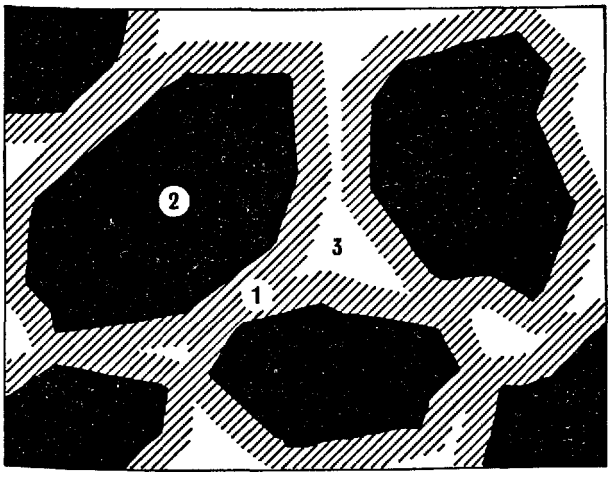

Fig. 12. *Model of structure of hardened cement paste. The microstructure (1) consisting of particles of hydrated compounds of varying shape and size (typical size 10–100 Å) is located in the space between particles of unhydrated cement and filler (2), gluing these solid particles together to form a solid macrostructure. The pore space in the macrostsucture is marked (3).*

Unfortunately, the available information about these matters is insufficient to provide a synthesis by means of which the influence of curing temperature on the strength of cement paste may be interpreted. However, some comments concerning the microstructure distribution shall be made in the following.

Studies of hardened cement paste in the electron microscope have demonstrated that the microstructure is of a complex and highly heterogeneous character, see e.g. Å. Grudemo (85) and Portland Cement Association (92), and recent observations on fracture surfaces of hardened cement paste by means of the scanning electron microscope, see Fig. 13, have similarly demonstrated the heterogeneity of the microstructure. The possible significance of this fact, as regards the strength of the macrostructure, does not seem to have been recognized in many earlier investigations.

G. Verbeck (14), however, suggested a heterogeneous distribution of the microstructure of cement paste to be the cause of the decrease of ultimate strength which is generally observed with steam curing. He assumed, thus, that in the case of curing at elevated temperatures, a condensed coating of hydrates is formed on unhydrated grains, leaving the remaining structure relatively open, while in the case of curing at room-temperatures a more homogeneous microstructure is formed, see Fig. 14 (1 and 2). According to Verbeck's theory, the relatively open microstruc-

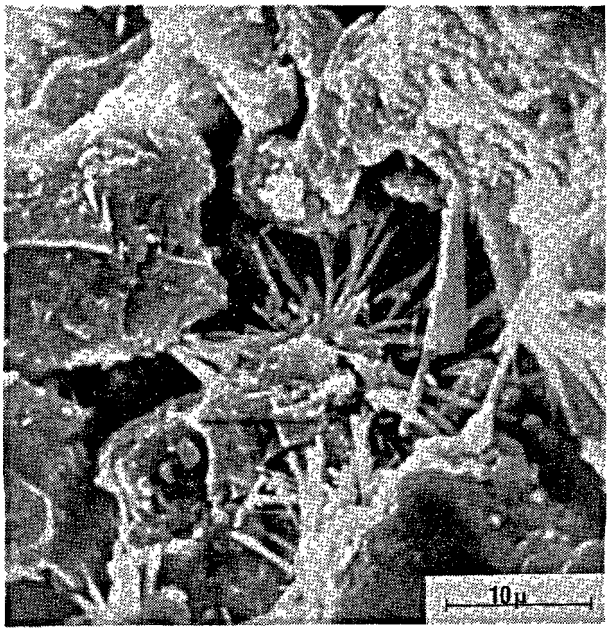

Fig. 13. *Scanning electron micrograph showing fracture surface of steam cured cement paste. The cement paste has been cured under water for 24 hours at 90°C and then cured under water for 28 days at 20°C prior to examination. The specimen was prepared by pressing in almost dry condition followed by impregnation with water. The porosity of the paste prior to hydration was 0.40. A portland cement of 3740 cm²/g Blaine was used. Investigation by the Concrete Research Laboratory Karlstrup.*

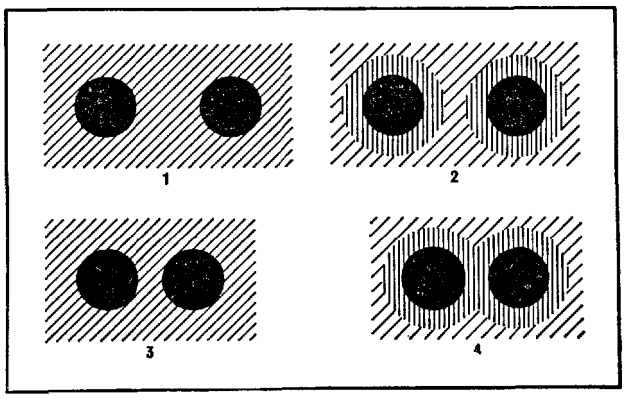

Fig. 14. *Effect of heterogeneity of microstructure on the strength of cement paste. Particles of unhydrated cement (black) are surrounded by a microstructure, which in case (1) and (3) is uniformly distributed. In case (2) and (4) the microstructure is heterogeneous as the cement grains are surrounded by a denser coating. With loose packing (1) and (2), the cement paste is strongest, when the microstructure is homogeneous, while the opposite is the case with dense packing (3) and (4). In the latter case the dense microstructure coatings (4) around the cement particles glue the particles together.*

ture around the denser zones which is formed at elevated temperatures is responsible for the lower strength of the macrostructure. In experiments at room-temperature, P. A. Rehbinder (93) found that cement paste adjacent to aggregate particles exhibited much higher strength (measured as microhardness) than paste forming the mass of matrix in between particles.

From these studies it seems reasonable to expect that improvement of the strength of hardened cement paste may be achieved by condensation of the agglomerate of the solids of fresh paste, thus utilizing the higher strength of the microstructure adjacent to hydrating cement grains or inert fillers. In fact, this principle has, for room-temperature hydration, already been applied successfully in the USSR, see G. M. Khutortsov, N. V. Mikhailov and P. A. Rehbinder (94) and N. B. Ur'ev, N. V. Mikhailov and P. A. Rehbinder (95). This beneficial effect of the heterogeneity of the microstructure, obtained in the case of densely packed pastes or mortars, should probably be even more pronounced with curing at elevated temperatures, as shown schematically in Fig. 14 (3 and 4).

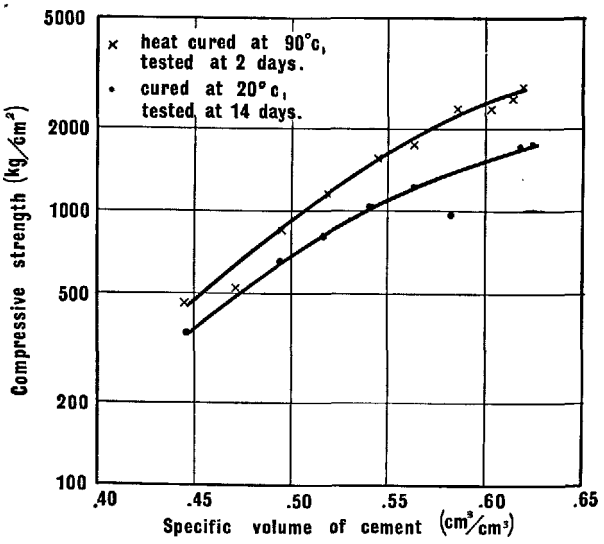

Fig. 15. *Compressive strength (log scale) of Portland cement paste specimens cured at 20°C and 90°C, respectively, versus fractional cement content (by volume). The specimens were small cylinders (11.3 mm high and 11.3 mm in diameter), prepared by pressing. Specific surface area of cement: 5100 cm²/g Blaine. The heat cured specimens were cured under water at 90°C for approximately 24 hours; during the next 24 hours they were air dried at 90°C, cooled down to 20°C, and then tested. The specimens cured at 20°C were cured under water for 7 days, dried in 65% relative humidity for 7 days, and then tested. Data from the Concrete Reseach Laboratory Karlstrup.*

Experimental evidence which is in agreement with this conclusion has been obtained at the Concrete Research Laboratory Karlstrup, where studies have been commenced on the effect of temperature on the strength of portland cement paste and mortars prepared with finely ground quartz sand. Small cylinders (11.3 mm by 11.3 mm) are prepared by mechanical compaction of almost dry mixtures followed by impregnation with water. Compressive strength levels up to five times of those obtained with traditional preparation methods have been obtained. The effect of steam curing (90°C) is an overall increase of approx. 50% in ultimate strength, see Fig. 15. It is believed that this strength gain is due to the existence of a condensed microstructure which glue together the closely packed solid particles (cement and filler) into a strong macrostructure.

It seems promising by means of further experimental and theoretical research to pursue these possibilities for utilizing steam curing, not only to accelerate the hardening of concrete, but also—contrary to practice of today—to increase the quality of the manufactured products considerably.

Concluding Remarks

The importance for the building industry of acceleration of the manufacture of concrete by means of curing at elevated temperatures has been stressed in the introductory remarks. The presented survey of knowledge on the hydration of portland cement paste at high temperature under atmospheric pressure shows that much fundamental knowledge on this subject is still lacking. This means that technical progress in the coming years to a large extent must still rely upon empiric development work, to be advanced by means of modern instrumentation and data processing methods.

The hydration of portland cement has been found strongly influenced by temperature. It has not been possible to establish a synthesis of the interdependence which has proved to be widely varying with different cement-water systems. Moreover, most of the information available concerns rather incommensurable investigations, and in many studies elevated temperatures have been a factor of only minor emphasis.

In the writer's opinion the hydration temperature ought to be considered a paramount parameter in future investigations, and room-temperature should be referred to as a special, modified condition in the broader picture.

It is a challenge to further development, that recent studies have shown a considerable gain of final strength as the result of heating during hydration.

The writer is indebted to his associates Messrs H. H. Bache, L. Hjorth, P. Nepper-Christensen and N. Thaulow for valuable assistance and co-operation by the compilation of literature and the preparation of this paper.

References

1. W. C. Hansen and J. S. Offutt, "Gypsum and anhydrite in portland cement", (United States Gypsum Co., Chicago, USA, 1962).
2. K. Takemoto, M. Kanaya, T. Tashiro and T. Shimoda, "The changes in the qualities of portland cement under high-temperature storage", (Japan Cement Engineering Ass., Tokyo, Japan, p. 96–99, 1965).
3. A. G. A. Saul, "Principles underlying the steam curing of concrete at atmospheric pressure", Magazine of Concrete Research **3**, 127–140, (1951).
4. S. G. Bergström, "Curing temperature, age and strength of concrete", Magazine of concrete Research **5**, 61–66, (1953).
5. E. Rastrup, "The temperature function for heat of hydration in concrete", Proc. RILEM Symposium on Winter Concreting Theory and Practice, DNIBR, Copenhagen, Denmark, Session B II, p. 3–20 (1956).
6. E. Rastrup, "Heat hydration in concrete", Magazine of Concrete Research **6**, (1954).
7. A. Nykänen, "Hardening of concrete at different temperatures, especially below the freezing point", Proc. RILEM Symposium on Winter Concreting Theory and Practice, DNIBR, Copenhagen, Denmark, Session B II, p. 3–12 (1956).
8. P. Nerenst, "Computation of freezing resistance of concrete at early ages", Proc. RILEM Symposium on Winter Concreting Theory and Practice, DNIBR, Copenhagen, Denmark, Session C, p. 1–33, (1956).
9. "RILEM Symposium—Winter concreting theory and practice, Copenhagen 1956—Proc." (DNIBR, Copenhagen, Denmark, 1956).
10. J. Jessing, "Safe combinations of mix proportions, temperature and protection time in winter concreting", Proc. Symposium on Structure of Portland Cement Paste and Concrete, Highway Research

Board, Washington, USA, p. 425–430, (1966).
11. K. M. Alexander and J. H. Taplin, "Concrete strength, paste strength, cement hydration, and the maturity rule", Australian J. of App. Sc. **13**, 277–284 (1962).
12. "Onderzoek betreffende het stomen van beton", (Commissie voor Uitvoering van Research, The Hague, 1962).
13. U. Danielsson, "Conduction calorimeter studies of the heat of hydration of a portland cement", (Cement- och Betong-institutet, Stockholm, Sweden, 1966).
14. G. Verbeck, "Cement hydration reactions at early ages", (Portland Cement Ass., Skokie, USA, Res. Dept. Bull. 189, 1965).
15. J. H. Taplin, "The temperature dependence of the hydration rate of portland cement paste", Australian J. App. Sc. **13**, 164–171, (1962).
16. D. L. Kantro, S. Brunauer and C. H. Weise, "Development of surface in the hydration of calcium silicates, II: extension of investigations to earlier and later stages of hydration", (Portland Cement Ass., Skokie, USA, Res. Dept. Bull. 151, 1962).
17. P. P. Budnikov, S. M. Royak, Y. S. Malinin and M. M. Mayants, "Investigations into hydration processes of portland cement in heat-moist treating at the temperature up to 100°C", Preprint from RILEM Symposium, Moscow, USSR, Session 1/7, (1964).
18. P. P. Budnikov and E. Erschler, "Studies of the processes of cement hardening in the course of low-pressure steam curing of concrete", Proc. Symposium on Structure of Portland Cement Paste and Concrete, Highway Research Board, Washington, USA, p. 413–446, (1966).
19. I. Older and J. Gebauer, "Zementhydratation bei der Warmbehandlung, I", Zement-Kalk-Gips **55**, 276–281 (1966).
20. N. C. Ludwig and S. A. Pence, "Properties of portland cement pastes cured at elevated temperatures and pressures", J. of ACI **52**, 673–687 (1956).
21. F. R. Wegener Olsen, "Rapport over teknisk-kemiske øvelser. Concrete Res. Lab. Karlstrup (1964), (unpublished).
22. L. E. Copeland, D. L. Kantro and G. J. Verbeck, "Chemistry of hydration of portland cement", (Portland Cement Ass., Skokie, USA, Res. Dept. Bull. 153, 1960).
23. W. Czernin, "Zementchemie fur Bauingenieure", (Bauverlag, Wiesbaden, Germany, 1960).
24. Y. S. Malinin, L. J. Lopatnikova, V. I. Guseva and N. D. Klishanis, "On hydration and hardening of portland cement", Preprint from RILEM Symposium, Moscow, USSR, Session I/14, (1964).
25. R. Malinowski, "Inverkan av temperaturen på betongens hårdning", Cement och Betong **40**, 251–273 (1965).
26. L. A. Sil'chenko, M. V. Mikhailov and P. A. Rehbinder, "The kinetics of the hydration of cement in concrete at elevated temperatures", Dokl. Akad. nauk SSSR **167**, (1966).
27. W. Lerch, "The influence of gypsum on the hydration and properties of portland cement pastes", (Portland Cement Ass., Chicago, USA, Res. Dept. Bull. 12, 1946).
28. H. Yokomichi, "Influence of high temperatures of mixing water on setting, consistency, strength and heat of hydration of concrete", Proc. RILEM Symposium on Winter Concreting Theory and Practice, DNIBR, Copenhagen, Denmark, Session D. p. 3–16 (1956).
29. H. Lehmann and W. Roesky, "Festigkeitsentwicklung und Hydration von Portland- und Hüttenzementen bei 20°, 5° und 1°C", Tonindustrie-Zeitung **89**, 337–350 (1965).
30. J. Gebauer and I. Odler, "Zementhydratation bei der Warmbehandlung, II", Zement-Kalk-Gips **55**, 303–308 (1966).
31. E. Clavet and H. Prat, "Recent progress in microcalorimetry", (Pergamon Press, London, England, 1963).
32. M. de Tournadre, "Effets thermiques liés a l'hydratation des aluminates de calcium", Revue des Matériaux, 432–444 (1965).
33. M. de Tournadre, "Etude microcalorimétrique de l'hydratation du sulfate de calcium anhydre. Effets des inhibiteurs de cristallisation", Compte Rendus des Académie des Sciences **246**, 947–949 (1958).
34. E. A. Whitehurst, "Evaluation of concrete properties from sonic tests", (American Concrete Institute, Detroit, USA, Monograph No. 2, 1966).
35. J. Andersen and P. Nerenst, "Wave velocity in concrete", J. of ACI **48**, 613–635 (1953).
36. L. Palotas, D. Balazs and I. Gemesi, "Investigation of concrete hardening during steam curing by non-destructive tests", Preprint from RILEM Symposium, Moscow, USSR, Session II/7, (1964).
37. M. Lystbæk, "Lydhastighed i frisk beton", (Concrete Research Laboratory, Karlstrup, Denmark, 1967).
38. J. A. Hanson, "Optimum steam curing procedure in precasting plants", J. of ACI **60**, 75–100, (1963).
39. W. Czernin, "Einige Bemerkungen über das Verhalten der Zement bei Dampf-Behandlung", Betonstein-Zeitung **24**, 24–28 (1958).
40. H. H. Bache and P. Dragsholt, "Varmehærdning af beton, II", (Concrete Research Laboratory, Karlstrup, Denmark, 1966).
41. W. C. Hansen, "Actions of calcium sulfate and admixtures in portland cement pastes", (Am. Soc. Test. Mat., Philadelphia, USA, p. 3–37, 1960).
42. A. K. Chatterji and R. S. Rawat, "Hydration of portland cement", Nature, 711–715 (1965).
43. S. A. Greenberg and T. N. Chang, "The hydration of tricalcium silicate", J. Phys. Chem. **69**, 553–561 (1965).
44. N. Kawada and A. Nemoto, "Calciumsilikate im frühen Verlauf der Hydratation", Zement-Kalk-Gips **56**, 65–71 (1967).
45. S. Brunauer and S. A. Greenberg, "The hydration of tricalcium silicate and β-dicalcium silicate at room temperature", (Portland Cement Ass., Skokie, USA, Res. Dept. Bull. 152, 1960).
46. V. B. Ratinov and A. P. Lavut, "Hydration kinetics of minerals of portland cement clinker", Dokl. Akad, nauk SSSR-Chimiji **146**, 642–645 (1962).
47. H. N. Stein, "Some characteristics of the hydration of $3CaO \cdot Al_2O_3$ in the presence of $CaSO_4 \cdot 2H_2O$", Silicates Industries **28**, 141–145 (1963).

48. H. zur Strassen, "Zur Frage der nicht-selektiven Hydration der Zementminerale", Zement und Beton, 32–34. (1959).
49. T. C. Powers, "Some physical aspects of the hydration of portland cement", (Portland Cement Ass., Skokie, USA, Res. Dept. Bull. 125, 1961).
50. H. E. Schwiete, U. Ludwig and P. Jäger, "Investigations in the system $3CaO \cdot Al_2O_3$–$CaSO_4$–CaO–H_2O", Proc. Symposium on Structure of Portland Cement Paste and Concrete. Highway Research Board, Washington, USA, p. 353–367, (1966).
51. V. YA. Khaimov-Mal'kov, "The growth conditions of crystal in contact with large obstacles", (Growth of Crystals, New York, USA, Vol. II, p. 20–28, 1959).
52. V. B. Ratinov, G. D. Kucheryaeva, G. G. Melent'eva and S. M. Pimenova, "The thermodynamics and diffusion properties of the principal constituents of cement during their hydration", (Building Research Station, Garston, England, 1962).
53. V. B. Ratinov, T. I. Rozenberg and I. A. Smirnova, "Über den Mechanismus der Wirkung der Erhärtungsbeschleunigungszusätze für Beton", (Deutsche Bauakademie, 1965).
54. P. P. Budnikov, S. M. Royak, Y. S. Malinin and M. M. Mayants, "Investigations of the kinetics of hydration of portland cement clinker minerals during hydrothermal treatment", (Building Research Station, Garston, England, 1965).
55. T. M. Berkovltch, D. M. Kheiker, O. I. Grachva, O. S. Volkov and E. S. Mikhalerskaya, "Hydration process in the accelerated hardening of cement", Preprint from RILEM Symposium, Moscow, USSR, Session I/16, (1964).
56. G. Verbeck, "Energetics of the hydration of portland cement", Proc. 4th Internat. Symp., Chemistry of Cements, Washington, USA, Vol. I, p. 453–465, (1960).
57. L. E. Copeland and D. L. Kantro, "Chemistry of hydration of portland cement at ordinary temperature", (The Chemistry of Cements, Vol. I, Academic Press, London, England, p. 313–370, 1964).
58. H. E. Schwiete, H. Knoblauch and G. Ziegler, Forschungsber, Landes Nordrhein-Westfalen, No. 784, p. 1–56, (1959).
59. J. H. Taplin, "The temperature coefficient of the rate of hydration of β-dicalcium silicate" Proc. 4th Internat. Symp., Chemistry of Cements, Washington, USA, Vol. I, p. 263–266, (1960).
60. C. D. Lawrence, "Changes in composition of the aqueous phase during hydration of cement pastes and suspensions", Proc. Symposium on Structure of Portland Cement Paste and Concrete, Highway Research Board, Washington, USA, p. 378–391, (1966).
61. R. F. Feldman and V. S. Ramachandran, "The influence of $CaSO_4 \cdot 2H_2O$ upon the hydration character of $3CaO \cdot Al_2O_3$", Magazine of Concrete Research **18**, 185–196 (1967).
62. F. E. Jones, "Hydration of calcium aluminate and ferrites", Proc. 4th Internat. Symp., Chemistry of Cements, Washington, USA, Vol. I, p. 204–242, (1960).
63. O. P. Mchedlov-Petrosyan (ed.), "Thermodynamik der silikate", (VEB Verlag, Berlin, Germany, 1965).
64. M. de Tournadre, "Contribution a l'étude de l'hydratation des aluminates de calcium au moyen de la microcalorimétrie", (Université d'Aix-Marseille, France, 1964).
65. P. Longuet and M. de Tournadre, "Hydration des aluminates de calcium en présence de vapeur d'eau", Comptes Rendus Académie des Sciences **256**, (1963).
66. E. T. Carlson, "Action of water on calcium aluminoferrites", J. of Research of the NBS **68A**, 453–363 (1964).
67. E. T. Carlson, "Some properties of the calcium aluminoferrite hydrates", (U.S. Dept. of Commerce, NBS, Washington, USA, 1966).
68. H. Kühl, "Der Baustoff Zement", (VEB Verlag, Berlin, Germany, p. 242, 1963).
69. W. Lieber, "Ettringit-Bildung bei höheren Temperaturen", Zement-Kalk-Gips **52**, 364–365 (1963).
70. Y. M. Butt, A. A. Maier and B. G. Varshal, "Stability of hydrated calcium sulphoaluminates", (Building Research Station, Garston, England, 1961).
71. J. E. Taylor, "The heat of formation of some calcium silicate hydrates", Preprint from the 9th Conference on the Silicate Industry, Budapest, Ungarn, (1967).
72. D. L. Kantro, S. Brunauer and C. H. Weise, "Development of surface in the hydration of calcium silicates", (Portland Cement Ass., Skokie, USA, Res. Dept. Bull. 140, 1961).
73. H. Funk, "Die produkte der Wassereinwirkung auf β–Ca_2SiO_4 bis 120°", Zeitschrift für anorganische und allgemeine Chemie **291**, 276–293 (1957).
74. H. Funk, B. Schreppel and E. Thilo, "Über primäre Zwischenprodukte bei der Hydration von β–Ca_2SiO_4 und über den Bildungsmechanismus des kalkreichen, tobermoritähnlichen Calciumsilicathydrates", Zeitschrift für anorganische und allgemeine Chemie **304**, 12–24 (1960).
75. E. R. Buckle and H. F. W. Taylor, "The hydration of tricalcium and β-dicalcium silicates in pastes under normal and steam curing conditions", J. of Appl. Chem. **9**, 163–172, (1959).
76. H. Funk and F. Zimmermann, "Schlecht kristallisierende Calciumsilikathydrate (mit 1 CaO/SiO_2) und ihre Umwandlung in den eigentlichen Tobermorit", Tonindustrie-Zeitung **88**, 40 (1964).
77. V. C. Farmer, J. Jeevaratnam, K. Speakman and H. F. W. Taylor, "Thermal decomposition of 14 Å tobermorite from Crestmore", Proc. Symposium on Structure of Portland Cement Paste and Concrete, Highway Research Board, Washington, USA, p. 291–299, (1966).
78. K. Speakman, R. A. Chalmers, J. A. Gard, H. F. W. Taylor and A. B. Carpenter, "Jennite, a new mineral", Am. Min. **51**, 56–74 (1966).
79. H. F. W. Taylor, "A review of autoclaved calcium silicates", Proc. Symposium on Autoclaved Calcium Silicate Buildihg Products, Soc. of Chem. Ind., London, England, p. 195–205, (1967).
80. T. Yoshii and G. Sudoh, "Influence of Na_2O on the formation of calcium silicate hydrate", (Japan Cement Engineering Ass., Tokyo, Japan, p. 16–19,

1959).
81. A. E. Sheikin and N. I. Oleinikova, "Effect of hydrothermal treatment and fineness of grinding of cement on the structure and properties of cement stone", Preprint from RILEM Sympsoium, Moscow, USSR, Session I/17, (1964).
82. L. Hjorth, "Studieophold ved Building Research Station, England—Røntgendiffraktometri, cements hydratisering, I & II", (Concrete Research Laboratory, Karlstrup, Denmark, 1966).
83. G. L. Kalousek, "Analyzing SO_3-bearing phases in hydrating cements", Mat. Res. & Stand. **5**, 292–302 (1965).
84. A. Aitken and H. F. W. Taylor, "Hydrothermal reactions in lime-quartz pastes", J. of Appl. Chem. **10**, 7–15, (1960).
85. Å. Grudemo, "The microstructure of cement gel phases", (Cement- och Betonginstitutet, Stockholm, Sweden, 1965).
86. G. L. Kalousek and A. F. Prebus, "Crystal chemistry of hydrous calcium silicates: III, morphology and other properties of tobermorite and related phases", J. Am. Ceram. Soc. **41**, 124–132, (1958).
87. R. Malinowski, "Försök med accelererad härdning av pressad betong i tättslutande formar", (Chalmers Tekniska Högskola, Göteborg, Sverige, 1966).
88. S. Chatterji and J. W. Jeffery, "Strength development in calcarious cements", Nature **214**, 559–561 (1967).
89. F. Keil, "Gedanken zur Theorie der hydraulischen Erhärtung", Zement-Kalk-Gips **56**, 201–213 (1967).
90. O. Matsuda and S. Ishimura, "Effect of initial curing temperature and admixture upon the hydration of cement—especially upon the specific area of hydrated cement", (Japan Cement Engineering Ass" Tokyo, Japan p. 32–33, 1957).
91. S. Brunauer and D. L. Kantro, "The hydration of tricalcium silicate and β-dicalcium silicate from 5°C to 50°C", (The Chemistry of Cements, Vol. I, Academic Press, London, England, p. 287–309, 1964).
92. "Carbon replica work in electron microscopy", J. of the PCA **6**, 53–55 (1964).
93. T. Y. Lyubimova and P. A. Rehbinder, "Peculiarities of the crystallization hardening of cement in the zone of contact with various solid phases (Fillers)", Doklady Akademii nauk SSSR **163**, 1439–1442 (1965).
94. G. M. Khutortsov, N. V. Mikhailov and P. A. Rehbinder, "Optimum structure of concrete and the conditions of its formation", Doklady Akademii nauk SSSR **170**, 648–651 (1966).
95. N. B. Ur'ev, N. V. Mikhailov and P. A, Rehbinder, "The structure-forming role of solid surfaces in the adhesive action of water-cement suspensions", Doklady Akademii nauk SSSR **164**, 626–628 (1965).

Written Discussion

Roman Malinowski

Synopsis

The influence of various heat curing conditions on temperature increase, irreversible expansion and contraction of cement paste and of strength was studied. Mortar of proportion cement: sand: water = 1: 1: 0.3 was used. Various holding periods of 0, 3 and 6 hours, curing temperatures of 60°, 80° and 98°C and various curing times of 1 1/4, 3 1/4, 5 1/4 and 6 hours were proved. In additional tests the influence of higher temperature of concrete (when placing), heating immediately by higher ambient temperature, the influence of the pressure of closed forms on the strength and the influence of various water-cement ratios (0.25, 0.35, and 0.45) was proved. The relations strength: irreversible expansion: contraction were analysed and general remarks presented.

Introduction

The contraction is a fundamental phenomenon in the hydration process of cement (1) and in the creation of the structure of the cement paste (2), (3).

The chemically bound water (Wn) decreases its volume about 1/4 (2) creating the contraction pores in the gel. The contraction water which fills the pores can be checked by simple volumenometric test (2), (3).

Many authors connect the properties of hardened cement paste and concrete such as strength, drying shrinkage, water permeability and durability, with contraction (2), (3). The contraction is actually a

resultant of simultaneously occurring internal (in the microstructure of cement paste) and smaller external (in the dimensions of tested specimens) volume changes (4), (5).

The contraction is accelerated in higher temperatures, especially in the first heating period and increases insignificantly after a heating period of 10~14 hours (6, 7, 8). The likeness of both processes: as well of contraction as of increasing of strength enables to fix the optimal heat curing procedure for concrete based on contraction tests (9).

In the above mentioned works (6)~(9) the connection between the contraction and the thermal expansion was not analysed. This problem seems to be of great importance because of the volume changes caused by higher temperatures (10), (11), (12).

Experiments

Testing Conditions and Procedure

Expansion, contraction and strength of mortar were tested simultaneously during and after the heat curing process. Changes of temperature were recorded.

The volumenometer for the expansion and contraction test consisted of a glass bottle (200 cc) with a measuring pipe and a rubber stopper (Fig. 1). The temperature of mortar was recorded in cubes 10^3 cm cast in steel forms. For strength tests mortar prisms 2.5 × 2.5 × 16 cm were prepared in steel forms.

The mortar was made of standard portland cement, sand of fineness modulus 1.8 in a proportion 1: 1. The water-cement ratio in the main series was 0.3.

The mortar was mixed in a RILEM laboratory mixer, then placed and compacted on a Vebe vibration table.

The specimens for expansion—contraction tests were cured in a heating vessel in water. The specimens for strength tests were cured in steam in steel forms without covering.

The curing cycle consisted of:

—rising of temperature

—heating at constant temperature

—cooling in water to 20°C and then water curing up to 28 days.

The expansion and contraction were measured by changes of the water level (above the mortar) in the volumenometer.*

The irreversible expansion of the fresh mortar ($\varepsilon_{m.\,ir.}$) is

$$\varepsilon_{m.ir.} = \varepsilon_{\Sigma} - \varepsilon_{w} - \varepsilon_{m.r.} \text{ in cm}^3/100 \text{ g cement}^{**}$$

when ε_{Σ} — is the total expansion of the volumenometer (water + paste)

ε_{w} — the expansion of the water (above the mortar) in the volumenometer

$\varepsilon_{m.r.}$ — the thermal expansion of the mortar measured by deflectometer

$\varepsilon_{m.r.} = \alpha_{m} \cdot \Delta t^{\circ}$

α_{m} = thermal expansion coefficient of fresh mortar (approximately 0.0001 in volume)

The contraction (C) is

$$C = V_0 - V_x \text{ in cm}^3/100 \text{ g cement}^{**}$$

When V_0, V_x is water level before curing and after cooling (at 20°C).

The contraction was tested for each curing cycle immediately after cooling, at the age of 1 and 28 days.

Scheme for the expansion-contraction tests is given in Fig. 1.

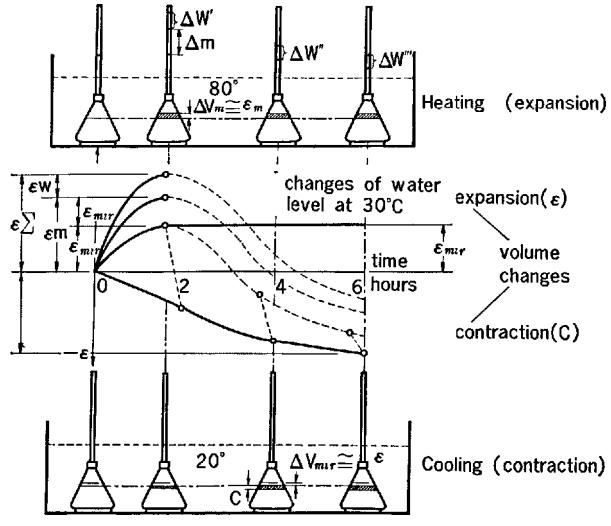

Fig. 1. *Scheme for the expansion—contraction test of heat cured mortar*

Symbols: Δw^{1}, Δw^{11}, Δw^{111}-*expansion of the water in cm³/100 g cem.** ΔV_{m}, $\Delta V_{m.r.}$, $\Delta_{m.ir.}$—*expansion of mortar total, reversible, irreversible in cm³/100 g cement.** ε_{Σ}, ε_{w}, ε_{m}, $\varepsilon_{m.r.}$, $\varepsilon_{m.ir.}$—*expansion in % (volume) total in the volumenometer, of water, of mortar-total, -reversible, -irreversible.*

*or in % (volume) when multiplying by $\frac{1}{1/3.1 + w/c}$ for the main serie × $\frac{1}{0.623}$.

* Additionally the expansion was controlled by deflectometer in the cubes for temperature records.

**For the main series (mortar 1: 1: 0.3) this value is approximately cm³/100 cm³ mortar (% in volume) or cm³/62.3 cm³ cement paste.

The changes in the water level measured during the isothermal and the cooling periods show besides contraction an additional absorbtion of water by mortar (Fig. 1).

Strength was tested for each curing cycle immediately after cooling of the specimens in water and at the age of 28 days. Contraction and strength tests of the same mortar cured after remoulding (in water—20°C) were also made.

Results

Series No. 1—The influence of various holding periods, curing temperatures and curing times on expansion, contraction and strength Table 1.

The results of the expansion-contraction tests and the compressive strength of mortar are presented in Fig. 2.

The temperature in the center of the specimens 10^3 cm becomes after 1 1/2 ~ 2 hours higher than the external heating temperature. For the external temperature 98°C about 15°C after 1 1/2 hour, for 80°C about 12°C after 1 3/4 hour and for 60°C about 10°C after 2 1/4 hour. Similar results were achieved for all holding periods.

The irreversible expansion takes place only under the first 90 minutes of heating. It increases at higher temperatures (80°C and 98°C) and decreases when adapting a holding period. There were not noticed any significant changes in the external dimensions after achieving the maximum expansion.

The contraction is accelerated remarkably at higher curing temperatures. The contraction immediately after curing at 98°C was much higher than at other temperatures. At longer curing time, at later age (1 and 28 days), especially when adapting longer holding periods the differences between the contraction values diminish.

Higher temperature accelerates the strength in-

Table 1. *Temperature, irreversible expansion, contraction and compressive strength of heat cured mortar. Proportions, cement: sand: water = 1:1:0.3*

°C curing temp.	Holding period h-hours	Testing time h-hours d-days	Maximal temperature °C after	h-hours (in 10^3cm)	Irreversible expansion after curing of 1 1/2 hours	Contraction cm³/100 g cement* of paste after curing—hours**					Compressive strength of mortar							
											kg/cm²				% σ_{28} normal			
	h	h(d)	°C	h	cm³/100g cem.*	1 1/4	3 1/4	5 1/4	6***	Average	3 1/4	5 1/4	6***	Average	3 1/4	5 1/4	6***	Average
60	0	im h	68	2 3/4	0.41	0.2	0.7	1.2	1.8	—	46	210	284	—	5	23	31	—
		24 h				2.0	2.1	2.2	2.4	—	—	—	—	—	—	—	—	—
		28 d				3.4	3.3	3.4	3.5	3.4	710	760	770	747	78	84	85	82
	3	im h	70	2 1/2	0.26	0.4	1.3	1.5	1.5	—	146	305	390	—	16	33	43	—
		24 h				1.9	2.0	2.0	1.9	—	—	—	—	—	—	—	—	—
		28 d				3.3	3.1	3.2	3.2	3.2	725	821	780	775	80	90	86	85
	6	im h	69	2 1/4	0.09	0.4	1.4	1.7	1.9	—	156	217	350	—	17	24	43	—
		24 h				1.9	2.1	2.1	2.2	—	—	—	—	—	—	—	—	—
		28 d				3.2	3.1	3.0	3.1	3.1	826	820	847	831	91	90	93	92
80	0	im h	90	2	2.15	0.4	1.5	1.6	1.8	—	198	295	355	—	23	32	39	—
		24 h				2.3	2.2	2.4	2.5	—	—	—	—	—	—	—	—	—
		28 d				3.4	3.3	3.2	3.2	3.3	735	750	775	753	81	82	85	82.5
	3	im h	92	1 3/4	0.45	0.6	1.2	1.5	1.7	—	245	430	507	—	27	47	56	—
		24 h				2.1	2.1	2.2	2.1	—	—	—	—	—	—	—	—	—
		28 d				3.0	2.8	2.9	3.0	2.9	854	832	932	873	94	91	102	95.3
	6	im h	92	1 1/2	0.26	0.8	1.5	1.7	1.8	—	365	434	530	—	40	47	58	—
		24 h				2.1	2.1	2.1	2.2	—	—	—	—	—	—	—	—	—
		28 d				3.0	3.0	3.1	3.0	3.0	808	780	790	793	89	86	87	87
98	0	im h	113	1 1/4	2.40	1.5	2.2	2.9	—	—	217	323	370	—	24	36	41	
		24 h				2.1	2.9	3.6	—	—	—	—	—	—	—	—	—	—
		28 d				3.6	3.7	3.9	—	3.7	680	654	595	643	74	72	65	70
	3	im h	115	1.15	0.90	1.8	1.9	2.1	2.5	—	300	365	443	—	33	40	49	—
		24 h				2.7	2.8	3.0	3.0	—	—	—	—	—	—	—	—	—
		28 d				3.0	3.1	3.0	3.2	3.1	906	830	797	844	99	91	87	92
20		3 h	35					0.15					—				—	
		6 h						0.3					45				5	
		24 h						1.8					310				33	
		29 d						3.0					910				100	

* Irreversible expansion and contraction value in % volume (of the paste) should be multiplied by 1/0.623.
** Heating 1 hour, cooling 1/4 hour.
***Heating and cooling 1 hour each.

crease. The strength at the age of 28 days diminishes by rapid heating, especially at higher temperatures (98°C). After adapting a suitable holding period the 28 days strength heat cured mortar was only insignificantly less than of the normally cured.

Estimated optimal conditions (for minimum expansion, high-, early- and 28 days strength) in the tests were:holding period of 3 hours, temperature 80°C and curing time 5 1/4 hours.

Series No. 2—Influence of different initial temperatures of the mortar (20°C and 60°C) and of the environment (20°C and 98°C) on expansion contraction and strength (Table 2).

Mortar 1: 1: 0.35 (cement: sand: water) was used. The specimens were cured without holding period 1 1/4 and 4 1/4 hours at the temperature of 98°C.

There was observed increased expansion by rapid heating and when using hot mortar.

Also a remarkable contraction of rapidly heated specimens and of hot mortar was noted immediately after curing, at the age of 24 hours and at the age of 28 days.

A significant decrease of strength for heated specimens and for warm mortar was noted, especially when the surfaces of specimens were uncovered. In closed forms the losses in strength were less.

Series No.3—The influence of different water cement ratios (0.25, 0.35 and 0.45) on expansion, contraction and strength (Tables 3 and 4).

Mortar 1: 1 (cement: sand) was cured at 80°C during 4 and 6 hours (heating time 2 hours, cooling time 1/2 hour).

Higher expansion was noted at higher water-cement ratios.

The contraction of paste in % (volume) is higher immediately after curing for less water-cement ratios, approximately the same for all water-cement ratios at the age of 24 hours and higher at 28 days for high water-cement ratios.

Similar tendencies are notified for the strength tests.

Analysis-General Remarks

1. The simultaneously occurring at heat curing irreversible expansion, the accelerated contraction

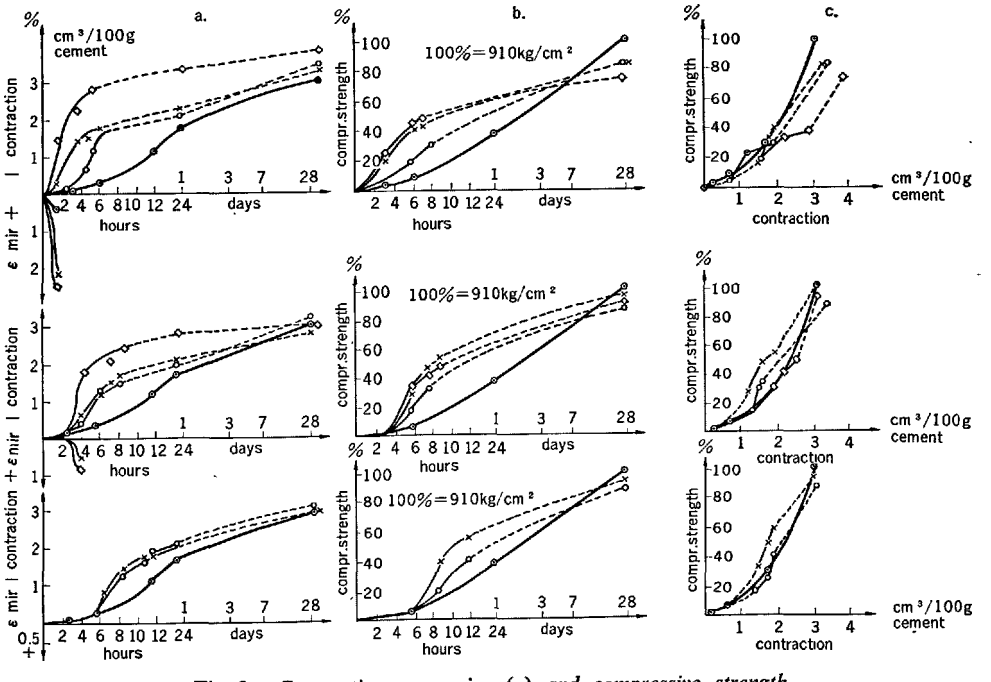

Fig. 2. *Contraction, expansion (a) and compressive strength (b) of mortar cured in various temperatures and after different holding periods. Cement: sand: water = 1: 1: 0.3 by weight. The relation strength: contraction is given in (c). Symbols: Curing temperatures, ⊙—20°C, ○—60°C, ×—80°C, ◇—98°C, ————continuous curing, - - - - - - - - additional water curing at 20°C.*

Table 2. *Expansion, contraction and compressive strength of cement mortar cured at various initial temperatures of paste and the chamber. Curing without holding period at temperaturs up to 98°C. Water-cement ratio 0.35. Cement:sand proportion = 1:1 by weigth.*

Initial of temperatures		Curing periods hours heating isothermal period cooling	Irreversible expansion approx. 1 1/2 hours	Contraction measured at 20°C cm³/100 g			Compressive strength kg/cm² at age of	
Cement mortar	Chamber			Immediately after curing	At age of 24 hours	At age of 28 days	Immediately after curing	28 days
20°	20°	2–0–1/2 2–2–1/2	1.6	1.5 2.0	2.8 2.9	3.6 3.5	280 1) 420 2) 460	750 1) 705 2) 755
		Average	1.6	—	2.85	3.55	—	—
20°	98°	0–2–1/2 0–4–1/2	2.4	2.0 2.4	3.1 3.1	4.4 4.2	— 1) 156 2) 375	— 1) 355 2) 657
		Average	2.4	—	3.1	4.3	—	—
60°	98°	2–0–1/2 2–2–1/2	> 4.5	2.4 3.0	3.9 4.0	5.4 5.6	— 1) 70 2) 258	— 2) 135 2) 340
		Average	> 4.5	—	3.95	5.5	—	—

1) open form
2) closed form

Table 3. *Expansion, contraction and compressive strength of cement mortar with different water-cement ratios. Curing at 80°C in curing chambers without holding period and at various curing times. Cement: sand proportion = 1:1 by weight.*

W/C ratio	Curing period hours heating isothermal period cooling	Irreversible swelling after 1 1/2 hours curing in cm³/100 g cement	Contraction after curing, cm³/100 g cement			Irreversible swelling after 1 1/2 hours curing in % of cement paste volume	Contraction after curing in % of cement paste volume			Compressive strength after curing, kg/cm²	
			Immediately	At age of 24 hours	At age of 28 days		Immediately	At age of 24 hours	At age of 28 days	Immediately	At age of 28 days
0.25	2–0–1/2	0.9	1.6	2.6	3.1	1.6	2.8	4.4	5.4	264	827
	2–2–1/2	0.8	2.1	2.5	2.9	1.45	3.7	4.4	5.0	508	855
	2–4–1/2	0.9	2.3	2.6	3.0	1.6	4.0	4.5	5.2	608	768
	Average	0.9	—	2.6	3.0	1.55	—	4.4	5.2	—	816
0.35	2–0–1/2	1.5	1.5	2.9	—	2.2	2.2	4.3	—	70	710
	2–2–1/2	1.7	2.1	2.7	3.8	2.5	3.1	4.0	5.6	410	812
	2–4–1/2	1.6	2.5	2.8	—	2.4	3.7	4.15	—	490	766
	Average	1.6	—	2.8	3.8	2.4	—	—	5.6	—	763
0.45	2–0–1/2	2.5	1.6	3.1	4.6	3.23	2.07	4.0	5.9	50	550
	2–2–1/2	2.4	2.3	3.5	4.8	3.1	2.97	4.5	6.2	158	534
	2–4–1/2	2.7	2.7	3.5	4.6	3.5	3.4	4.5	5.9	176	576
	Average	2.5	—	3.4	4.7	3.3	—	4.4	6.0	—	553

Table 4. *Contraction and compressive strength of cement mortar cured at 20°C. After 24 hours the remoulded specimens were cured in water. Cement: sand proportion = 1: 1 by weight.*

W/C ratio	Contraction cm³/100 g cement after hours			days	Compressive strength kg/cm² after 24 hours	28 days
	6	12	24	28		
0.25	0.4	0.7	2.0	3.0	455	945
0.35	0.4	0.75	2.3	3.6	250(?)	865
0.45	0.5	0.9	3.3	4.9	137	603

and increase in strength have great influence on the structure and strength of the cement paste at the cement paste at the later age.

2. The irreversible expansion which lasts 1 ~2 hours is caused mainly by the thermal expansion of the fluid and gas phase of the paste. The thermal expansion coefficient of water is approximately 10 and that of air and steam 100 times higher than of the solids of mortar (sand). The rapidly hardened

paste makes this increased volume of pores stable (Fig. 3), (11), (12).

3. The irreversible expansion is increased by higher temperature and is diminished by longer holding periods (Figs. 2 and 3). During the holding period the binding forces, the contraction and the strength are growing. Other factors and conditions which diminish the expansion under the heat curing process are: less water-cement ratio (stiff consistency) external hydraulic pressure or the form pressure (14), (15).
4. The function strength: contraction valid for normal curing conditions (water—20°C) (3) shows irregularities and discontinuities in heat curing. Different strength: contraction values are noted for various curing conditions and at various age of the tested mortar (Fig. 2c).

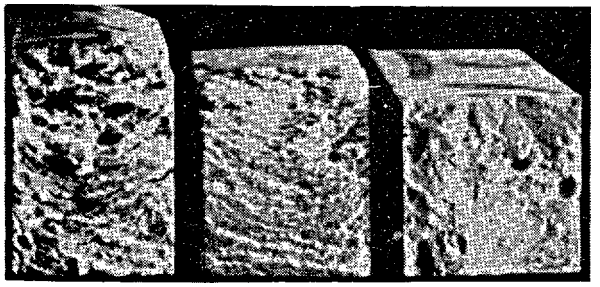

Fig. 3. *Irreversible expansion of cement paste (W/C = 0.3) cured immediately without holding period at 98°C. a—in closed form, b—in open form, c—warm paste placed in form before heating. Section 2.5 × 2.5 cm.*

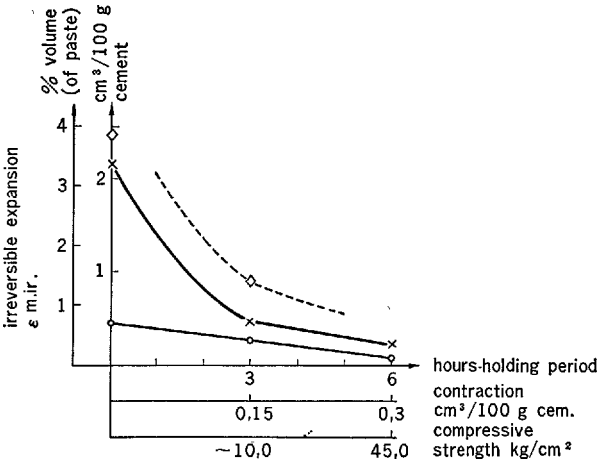

Fig. 4. *Expansion as function of curing temperature and holding period simultaneously (initial contraction and early strength).*

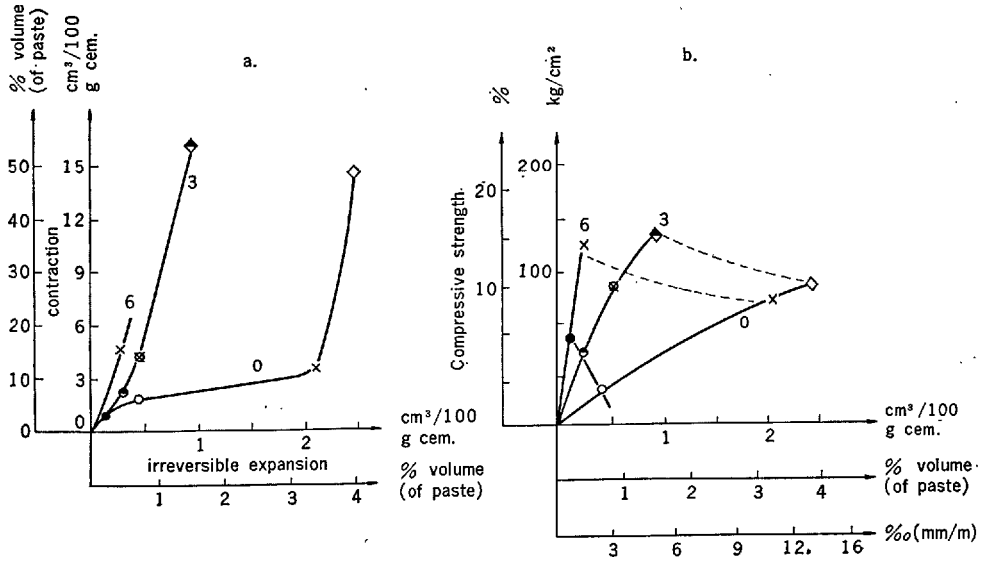

Fig. 5. *The relation contraction: irreversible expansion (a) and the relation strength: irreversible expansion (b) at the time of maximum expansion after approximately 1 1/4 hour heat curing. Various curing temperatures:*

60°C—○ ◓ ● holding period 0, 3, 6, hours
80°C—× × × " " 0, 3, 6, "
98°C—◇ ◈ — " " 0, 3 – "

100% is the contraction and strength of the normally cured mortar at the age of 28 days.

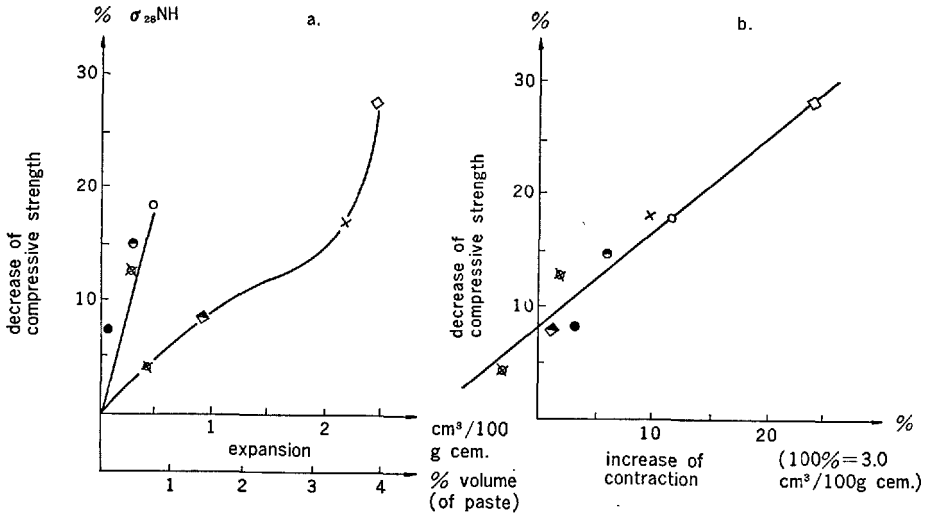

Fig. 6. *The relation decrease of strength: expansion (a) and the relation decrease of strength: contraction (b) for the heat cured mortar at the age of 28 days.*
Various curing temperatures:
60°C—○ ◓ ● holding period 0, 3, 6 hours
80°C—× × × " " 0, 3, 6 "
98°C—◇ ◈ — " " 0, 3 – "
100% is the contraction and strength of the normally cured mortar at the age of 28 days.

The relation early strength: contraction for mortar immediately after curing in 60°C and 80°C without holding period is approximately similar to the normally cured. At 100°C higher contraction occurs and no significant changes in strength are noted (Fig. 2c). For longer holding periods at 80°C the strength is higher for the same contraction (Fig. 2c).

The relations the expansion: contraction and the strength: contraction after 1 1/4 hour heat curing (at the moment when maximum expansion occurred) are not synonymous.

For both the expanded and not expanded mortar approximately the same contraction for a constant temperature was achieved. The contraction was for 100°C much higher than for 80°C while the strength was approximately the same (Figs. 5a and 5b).

At the age of 28 days the relation strength: contraction is mostly influenced by the expansion which takes place during the curing process. The relative decrease in strength (in %) corresponds with the relative increase of the contraction.* Both are caused by expansion (Fig. 6).

5. Presented tests show general tendencies for the relation expansion—contraction—strength of heat cured pastes and mortars. For more complete analyses there should also be used other cement types, mortars of different water-cement ratios. Further tests should include measuring of changes in porosity and pressure in the paste during and after the expansion—contraction test and be completed by microscopical investigations.

This work was carried out at the Construction Division of Chalmers University of Technology by grant of the Swedish Governmental Building Research Committee.

Part of this work was published in Cement & Betong No. 3, 1965.

The author thanks engineer G. Linden, civil engineer L. Berntsson and civil engineer E. Aas-Jakobsen for help in executing the experiment of this work.

*As 100% is the strength and contraction of normally cured mortar at 28 days.

References

1. H. Kühl, Zement Chemie V, III VEB Berlin 1952, p. 277–314.
2. T. C. Powers, P. C. A. Bulletin No. 22. Chicago III, 1948.
3. W. Czernin, Zement Chemie für Bauingenieure. Bauverlag Wiesbaden 1964.
4. R. L'Hermite, Nouvelle contribution a l'etude du retrait de ciment. Ann. de L'Inst. Techn. du Bat. et des Trav. Public. No. 106. December 1949.
5. K. Eyman, Wiazanie Cementow portlandzkich. I. T. B. Warszawa Nr 136–1952.
6. J. S. Malinin and M. M. Kapkin, Izmierienie metodom kontrakcji processa twierdienia cementa pri propariwanii. Cement 1963.
7. B. G. Skramtajew, T. J. Gortshakow and M. M. Kapkin, Accelerated hardening of concrete, RILEM 1964, Moskwa.
8. S. A. Mironow, Accelerated hardening of concrete, RILEM 1964, Moskwa.
9. R. O. Krasnowskij and others, Beton i Shelesobeton. Moskwa, Nr. 2–1967.
10. Mchedlow-Petrosyan and Bunakow. Silicattechnik 12–1961.
11. R. Malinowski, Cement och Betong Nr. 3–1965.
12. S. A. Mironow and L. A. Malinina, Uskorjenie twerdienia betona. Moskwa 1964.
13. W. Czernin, II Intern. Kongress der Betonstein Industrie. Wiesbaden, juni 1957. (Zementstein Zeitung 1958).
14. Z. Franjetic, Zementstein Zeitung Nr. 12–1963.
15. R. Malinowski, Cement och Betong Nr. 1–1968.

SESSION III-4b HIGH TEMPERATURE CURING OF CONCRETE UNDER ATMOSPHERIC PRESSURE

Principal Paper High-Temperature Curing of Concrete under Atmospheric Pressure

Yu. M. Butt, V. M. Kolbasov and V. V. Timashev*

Synopsis

The curing of concrete with saturated water steam at atmospheric pressure and the temperature range of 60–100°C is now a basic and most wide accelerated method for concrete hardening in commercial scale. This method, which is widely used in many countries to intensify the process of manufacture, optimal use of plant equipment and plant facilities, is based on the acceleration of the hydration reactions of portland cement clinker. This acceleration, in its turn, brings to the accelerated hardening of the hardened cement paste in concrete. Along with, the hydration chemical reactions, taking place during hydrothermal curing of concretes, are followed by a number of physico-chemical and physical reactions, which assert a complicated influence on the properties and the structure of the concrete. The way the sequence and the degree of completeness of the said processes, the way these factors influence both on the formation and the resulting qualities of the concrete are due to a lot of factors-primary due to the chemical and compound compositions of the cementing material in concrete, W/C ratio, the rate of homogenization, the rate of the concrete tamping, the quality of aggregates, the hydrothermal curing of the concrete (including the precuring time, the rate of temperature rise, the isothermal curing and its temperature, the excess pressure, the rate of cooling), as well as the conditions of consequent hardening of concrete articles (temperature, humidity, gaseous composition of the environment etc).

The strengthening of the hardened cement paste during the steam curing of a concrete lies in the process of the structure forming, this process are caused by the hardening of cement. Meanwhile the destructive processes, bringing about decreasing of the concrete strength, are connected with the physical change, alteration of its structure due to the heat— and moisture transfer, and to the expansion of the concrete forming components depend on the influence of temperature. The efficiency of the present ways of accelerated concrete hardening depends on the optimal ratio of forming and destructive processes these ways provide, since it is known (1), that destructive processes do always follow the hardening of the cement paste, though in various degree and in various stages.

Introduction

The curing of concrete with saturated water steam at atmospheric pressure and the temperature range of 60–100°C is now a basic and most wide accelerated method for concrete hardening in commercial scale. This method, which is widely used in many countries to intensify the process of manufacture, optimal use of plant equipment and plant facilities, is based on the acceleration of the hydration reactions of portland cement clinker. This acceleration, in its turn, brings about the accelerated hardening of the hardened cement paste in concrete. Along with, the hydration chemical reactions, taking place during hydrothermal curing of concretes, are followed by a number of physico-chemical and thermo-physical reactions, which assert a complicated influence on the properties and the structure of the concrete. The way the sequence and the degree of completeness of the said processes, the way these factors influence both on the formation

*The Moscow Mendelleyev's Institute of Chemical Technology, Moscow, U.S.S.R.

and the resulting qualities of the concrete are due to a lot of factors primary due to the chemical and compound compositions of the cementing material in concrete, W/C ratio, the rate of homogenization, the rate of the concrete tamping, the quality of aggregates, the hydrothemal curing of the concrete (including the precuring time, the rate of temperature rise, the isothermal curing and its temperature, the excess pressure, the rate of cooling), as well as the conditions of consequent hardening of concrete articles (temperature, humidity, gaseous composition of the environment etc.)

The strenthening of the hardened cement paste during the steam-curing of a concrete lies in the process of the structure forming, this process are caused by the hardening of cement. Meanwhile the destructive processes, bringing about decreasing of the concrete strength are connected with the physical change, alteration of its structure due to the heat—and moisture transfer, and the expansion of the concrete forming components due to the influence of temperature. The efficiency of the present ways of accelerated concrete hardening depends on the optimal ratio of forming and destructive processes these ways provide, since it is known (1), that destructive processes do always follow the hardening of the cement paste, though in various degree and in various stages.

The Mechanism and the Kinetics of Cement Hydration

The Mechanism of Hydration

The mechanism of portland cement hydration at elevated temperatures is just the same as at 20–25°C. It is but the kinetics of the process, the sequence and the completeness of the phase transformations suffer the change. The ions, forming up a crystal dissolving when interacted with water, during the fluctuations periodically take positions, in which the strength of their bond with the lattice is of the least value. The ions of the surface layer of crystals, especially those on the edges and the apexes of the crystals more easily (as to compare with the ions inside the crystals) enter into chemical interaction with water and hydrate, i.e. "catch" attract H^+ or H^- ions. Partially hydrated ion is in a less strong bond with the lattice and almost immediately transfers into solution where its hydration ends. The outcome of a part of ions out of the lattice brings to deformation of a surface layer of crystals. Then a destruction of a surface layer of crystals comes, this lessening the "break-out" energy of the break-off of the rest of crystals from the remnants of the lattice. Since such fluctuation migrations are constant, the process of water "corrosion" of a crystal should run consequently and constantly. The depth of the reaction frontage depends on the crystal density and—in case of an "ideal" crystal might correspond to the depth of the monomolecular layer of water. The ions, hydrated on the surface of a crystal immediately transfer to the solution. During the destruction of a surface layer of a crystal there might happen a break-off of not only separate single crystals, but so well the "blocks" of them—counting hundreds and thousands ions. Hydration of such "blocks" in the solution is similar to that of a "starting" crystal. Most of the workers admit now the possibility of a reaction by means of a joint of anhydride grains with water with consequent precipitation of the particles, transferred into the solution (2~7).

The process of cement grains corrosion by water is of a decreasing rate, this being excited both with the formation on their surface of protecting films consisting from reaction products and with the decrease of dimensions of hydrating particles in the course of time. One of the reason of the quick formation of protecting films on hydrating grains is the exfoliation of some ions "blocks" from a crystal and these "blocks" can not easily move in a liquid phase and group together near the surface of a "matrix" crystal. Their consequent hydration brings to the consolidation of the film. The formation of the film is also contributed by a various speed of the diffusion of the ions in the solution, this variance bringing to the selective expulsion from the reaction zone of some moleculae (e.g. of calcium oxide hydrate) and to the concentration of other moleculae (e.g. of orthosilicic acid) on the surface of a crystal. As a result of such an incongruent dissolution of the compounds in the zone of reaction, low basic crystallic hydrates form at first; further these hydrates can increase their basicity due to subsequent recrystallization in the environment, saturated with the calcium hydroxide.

Development of the surface reaction of the direct joining of water to anhydrides greatly depends on the energetic state of the rigid body surface. It is possible that the lessening of the chemical bond in the lattice of dissolving crystals and the increase of the rate of the electrolytic association on the H^+ and OH^- ions

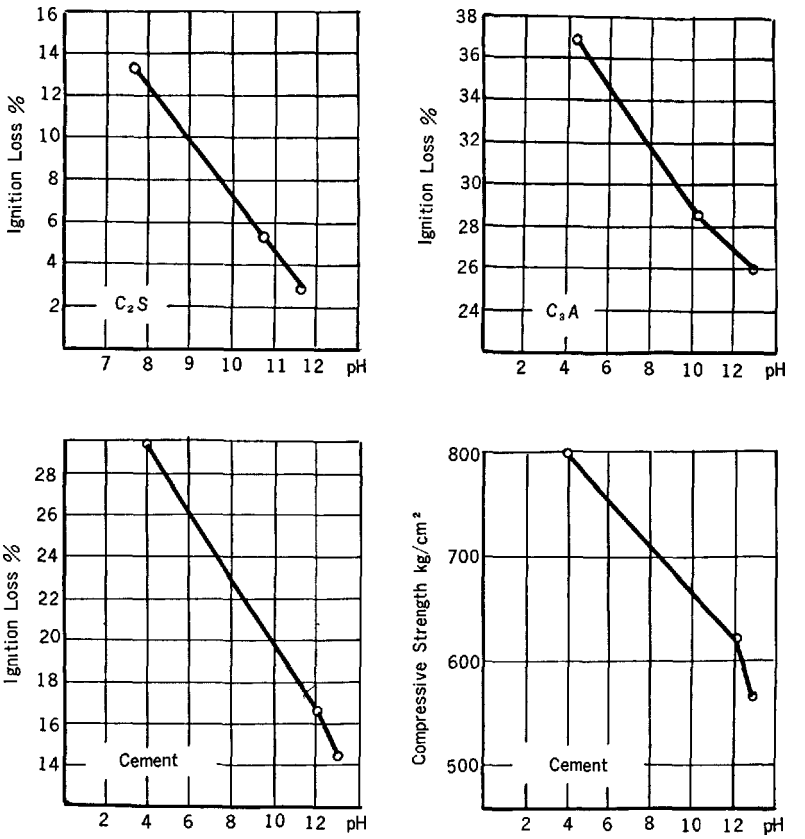

Fig. 1. *Hydration rate and the strength values of compounds and cement depending on pH of water solution*

should bring up to the acceleration of the hydration processes. And indeed, the increase of the H^+ ions concentration in the water solution, obtained by adding of the salts-electrolytes, was accompanied with an increase of hydration rate of separate compounds and of the cement as a whole (Fig. 1). The change of the rate of water moleculae dissociation (decrease of $(H_2O)_n$ groups), taking place in the magnetic field, this being of 2000–2500 ersted intensity, might attain such a rate of hydrogen bonds' break-up, when their break-off is possible. The change of the physical features of water, the breaking up its associates and the appearance of some amount of free H^+ and OH^- ions, positively affected both the rate of the cement hydration and the strength of units made from this cement (Fig. 2). Such a positive influence was also observed when water was influenced by the X-rays and slow neutrons' stream. The water temperature increase at the 0–100°C range evenly decreases down the viscosity of water. The change of the features and the qualities of water as the temperature rises, influences hydration and hardening kinetics of the compounds

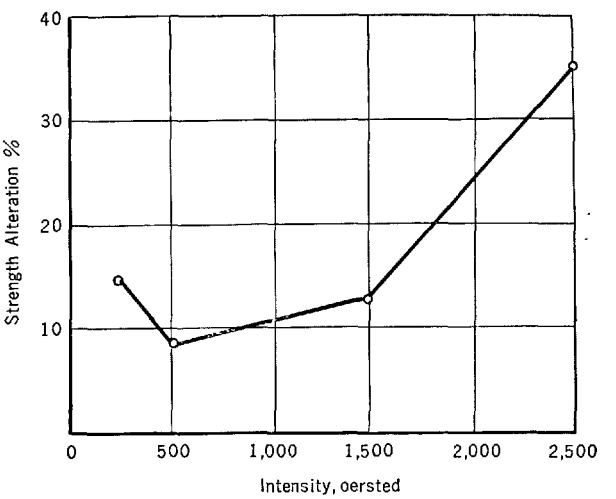

Fig. 2. *The influence of a constant magnetic field intensity on relative values of the strength of a hardened cement paste of 1:0 composition; 7 days age*

mixed with water of different temperature. The highest C_3S hydration rate and strength are found

when this compound was mixed with water of 60°C (Fig. 3). C_3S and C_4AF hydration rate increased 1.5–2.0 times mixed with water of 20 and 40–80°C respectively. The strength of samples made from these compounds practically didn't rise, however. The portland cement with Saturation Factor SF = 0.96; Silicate Modulus = 2.00; Alumina Modulus = 1.3 mixed with water of 60–80°C temperature also has higher hydration rate and strength (Fig. 4).

The Kinetics of Hydration

The kinetics of polycompounded cement grains' hydration, which is of a heterogenodiffuse character, is limited by the inner mass transfer through the shells of hydrated products, appearing around these grins in the course of time. The exact quantity description of the speed of this process is rather difficult, though its general regularities have been described elsewhere (8 ~ 14). Some of the offered equations of the kind $dV/d\tau = f(V)$, (where $dV/d\tau$—hydration speed, V—hydration rate and τ—hydration time), listed in the Table 1. The constant coefficients in these equations do not reveal the process nature and, therefore cannot find out which features of the "matrix" material define the hydration kinetics. The use of these equations brings about various results, and this shows that they could be used just for description of some separated stages but not the process as a whole.

A more satisfactory description of the kinetics process is given by the equations of A. Polak (15, 16),

Table 1. *Equations of hydration process rate*

Author	$dV/d\tau$
1. E. N. Gapon (14)	$dF/\delta_0 \cdot V$
2. S. Brunauer, L. E. Copeland and R. H. Bragg (8)	$K(1-V)^{3/2}$
3. P. P. Budnikov, S. M. Royak, Yu. S. Malinin, M. M. Mayants (37)	$K' \cdot \exp \frac{K''-V}{K'''}$
4. T. M. Berkovich, D. M. Kheiker O. I. Gracheva, O. S Volkov, E. S. Mikhailevskaya (39)	$K(1-V)$
5. Gimsvert	$KV(1-V)$
6. M. I. Ridge (10)	KV
7. A. F. Polak (16)	$\frac{3V^{2/3}(1-V)^{2/3}V_0^{1/3}(1-V_0)^{1/3}}{A_1V^{2/3}V_0^{1/3}+B_1(1-V)^{2/3}(1-V_0)^{1/3}}$
8. K. Schiller (18)	$\frac{3V^{2/3}(1-V)^{2/3}}{B_3V^{2/3}+(1-V)^{2/3}}$

Note:

$$A_1 = \frac{1}{K_x S_{0x}}; \quad B_1 = \frac{1}{K_y S_{0y}};$$

S_{0x}, S_{0y}—specific surface of dissolving and crystallizing phases

$K_x = \frac{\mathscr{D}}{\delta_x}$; $K_y = \frac{\mathscr{D}}{\delta_y}$—the constants of dissolution and crystals growth rates

$\mathscr{D}$—D—coefficient of diffusions

$\delta_x u \delta_y$—conditional thickness of respective diffusion layers

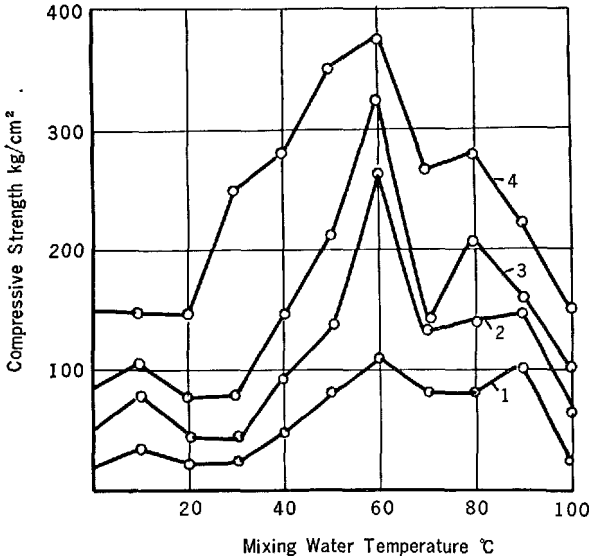

Fig. 3. C_3S *specimens' strength, depending on the mixing water temperature. 1–1 day; 2–3 days; 3–7 days; 4–28 days*

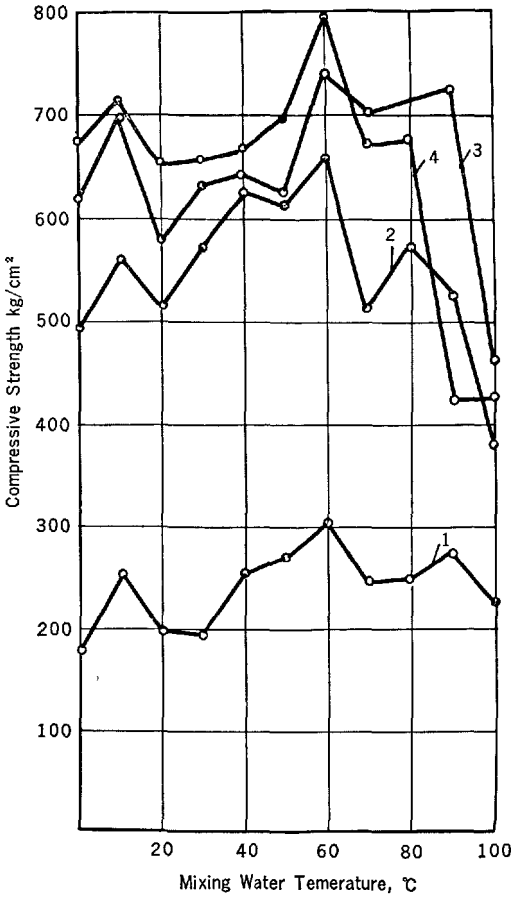

Fig. 4. *Portland cement specimens' strength, depending on the mixing water temperature. 1–1 day; 2–3 days; 3–7 days; 4–28 days*

V. Ratinov and A. Lavut (17) and K. Schiller (18). These authors make following assertions. The dissolution process of the binding material and the growth of crystals of the newly formed compounds run simultaneously and both these processes are connected with each other by the mass balance conditions. The surfaces of the binding material and of its hydrates are not constant ones, though the powders are of a monodisperse nature. The "nuclei" of hydrates appear just during the beginning of the process (during the induction period) and the time counting starts from the moment the nuclei formation ends. During the initial period of hydration the process speeds up; in the range of $V = 0.4 - 0.6$ it attains its maximum value and then decreases. The absolute values of the reaction rate depend on the concentration and the oversaturation on the depth of diffusion layers of the dissolving grains, on the constants both of the dissolution rate and of the crystal growth and on many other factors.

The rise of the process temperature rises up the rate of the process, though doesn't change the basic phenomenae of its run (Fig. 5). As well as at the normal temperature, there are two distinct periods of the process: a quick and a slow one. With the increase of the temperature, the duration of all the hydration periods decreases, while the hydration rate of the binding material increases—at the main stage of the process (Table 2). The activation energy of a given compound is similar at 40–80°C temperature range (Fig. 6). C_3A and C_4AF strongly respond the temperature rise and at 50°C they are almost completely hydrated to 1–3 days age. At these conditions both C_2S and C_3S hydration rates increase.

The coefficient of the reaction temperature (γ) decreases with the temperature rise: $\lg \gamma^{\tau} \simeq 10E/2.3RT^3$ showing the lowering of the influence of the temperature on the hydration rate of the binding material at the increasing of the time of hydrothermal treatment. Decrease of the γ-value with the temperature increase is specific to heterogeneous processes. The retardation of the binding material hardening and hydration during its hydrothermal curing at the second period of the process can be explained by the

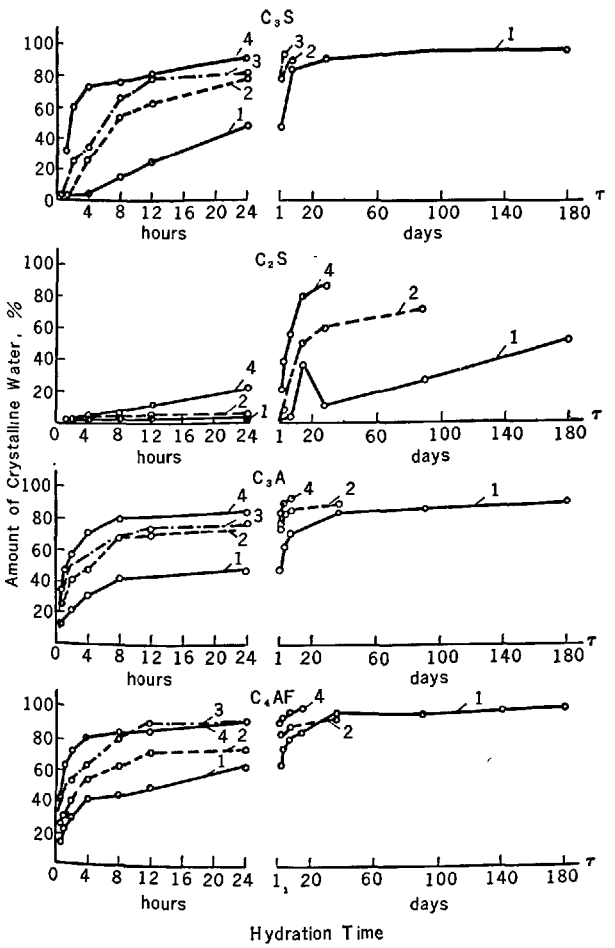

Fig. 5. *Hydration rate of compounds depending on the temperature (data of M. M. Mayants). Hardening temperature, °C: 1–20; 2–50, 3–70; 4–90.*

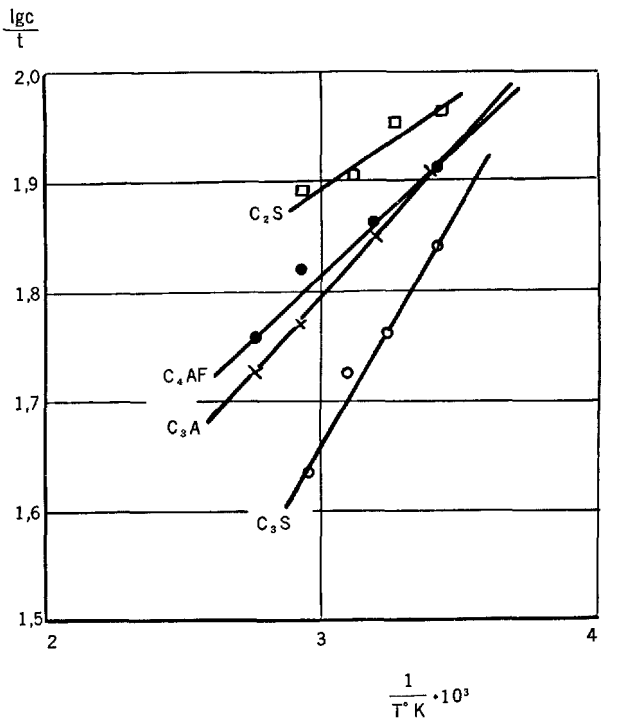

Fig. 6. *Graph of the function. $lgc/\tau = f(1/T)$ (τ-days)*

Table 2. *The rate of hydration of compounds at various temperature*

Compound	Temperature, °C	Hydration rate, per cent, age, days							Authors
		1	3	7	28	90	120	360	
C_3S	20	—	36	46	69	93	94	—	Yu. M. Butt (4)
	20	—	64	—	78	91	—	—	R. Nurse (13)
	20	—	48	—	75	87	—	97	G. J. Verbeck (9)
	20	—	51	65	82	91	95	—	O. S. Volkov (28)
	20	—	31	44	63	—	81	—	S. A. Mironov (52)
	20	31	45	56	78	86	92	—	H. Knoblauch (25)
	35	42	48	58	78	87	92	—	〃
	50	47	53	61	80	89	—	—	〃
	50	78	—	90	—	—	—	—	M. M. Mayants (12)
	65	57	64	71	85	88	—	—	H. Knoblauch (25)
	90	90	—	—	—	—	—	—	M. M. Mayants (12)
β-C_2S	20	—	7	10	—	29	—	—	Yu. M. Butt (12)
	20	—	10	—	42	51	—	—	R. Nurse (13)
	20	—	19	—	40	68	—	87	G. J. Verbeck (9)
	20	—	7	15	32	46	60	—	O. S. Volkov (28)
	20	—	10	15	25	—	50	—	S. A. Mironov (52)
	35	10	19	26	48	81	91	—	H. Knoblauch (25)
	50	20	25	31	55	86	92	—	〃
	65	23	32	40	60	88	92	—	〃
	90	22	41	57	87	—	—	—	M. M. Mayants (12)
C_3A	20	—	54	63	72	—	86	—	S. A. Mironov (52)
	20	—	58	—	90	96	—	—	R. Nurse (13)
	20	—	65	67	73	81	87	—	O. S. Volkov (28)
	50	75	83	86	89	—	—	—	M. M. Mayants (12)
	90	84	90	92	—	—	—	—	M. M. Mayants (12)
C_4AF	20	—	48	55	62	—	76	—	S. A. Mironov (52)
	20	—	32	—	87	95	—	—	R. Nurse (13)
	50	92	94	—	—	—	—	—	M. M. Mayants (12)

formation of a compact protecting film consisting from a well crystallized products of hydration. This film serves as a protective shell of unhydrated grains of the cement and prevents the access of water molecules to such grains. So, the film decreases the rate of the inner mass transfer.

The Phase Composition of the Newly Formed Compounds, the Structure of the Hardened Cement Paste and of the Concrete

Phase Composition of the Newly Formed Compounds

It is widely known, that hydrothermal curing of cements up to 100–200°C shows no any serious influence on the phase composition of the newly formed compounds. According to some authors (19~22), the hydration products, forming at the steam curing, do not differ from the hydrate compounds appearing when hardening of cements at normal temperature conditions. That is why different features of the cement paste hardened at normal and elevated temperature can not be explained just only by the change of the composition of the newly formed compounds.

The present data concerning the change of calcium silicates' basicity during the hydrothermal curing of the hardened cement paste (23~24, 37) as well as concerning the stability of the high sulphate form of calcium sulphoaluminate hydrate and its role in the hardening process (35~40) are quite contradictory and unsufficient. Therefore on the base of these data one cannot judge the influence of this change on the strength and durability of the hardened cement paste.

In any case there is but a few data to consider the change of the silicate hydrates' composition to be the main reason of the hardened cement paste qualities change. We can count one of the recent work in this field—the work of J. Gebauer and I. Odler (41). These authors point out the appearance of a noticeable amount of $C_2SH(A)$ in the cement hydration products (6 hours, 80°C), this hydrate being identified on the thermograms by endothermal effect at 450°C. The presence of this hydrate instead of silicate hydrates having fibrous pattern (C_2SH_2, CSH(B)) results to a very serious disattaintment of strength of the hardened systems (42). At the same time there are some data (38) proving the possibility to intensify the process of the cement paste hydration during the steam curing

through a desired formation of calcium sulphoaluminate hydrates.

It is possible, however, just when special cements are used, these containing admixtures of alumina compound. For it is found, that a considerable fraction of alumina in the portland cement clinker cannot be used to form calcium sulphoaluminate hydrates in the course of the first stage of hardening, when the appearance of this compound aids the strengthening of the hardened cement paste. Beside this, it is known that the frame, consisting of calcium sulphoaluminate hydrates, is the base of an early strength gain of the hardened cement paste even at the normal temperature of hardening. That is why this factor cannot be considered as responsible for the quality changes of the hardened cement paste, these changes resulted hydrothermal treatment. Up to the present, there is not yet any generally accepted and well grounded opinion concerning the real strength making factors of the hardened cement paste forming at 30–100°C. Silicate hydrates C_2SH_2, CSH(B), aluminate hydrates C_3AH_6, C_4AH_{11-19} and $Ca(OH)_2$ with $CaCO_3$ are considered to be the main products of portland cements hydration in this temperature range. Following compounds have been revealed in the systems: afwillite, xonotlite, calcium aluminate hydrates and various complex salts based on aluminum oxide hydrate. It is necessary to stress that the formation of hydrates of any composition, in the strict meaning of it, does depend on the temperature and humid conditions of the environment of the hydration process. First of all, the temperature of the environment determines the solubility of the binding material in water. Along with it determines the concentration and the oversaturation rate of the liquid phase, the correlation of the oxides dissolved in it (CaO, SiO_2, Al_2O_3 etc.), the viscosity of water, the rate of association of water moleculae, the quantity and the pattern of the newly formed crystallization nuclei. And, at last, the temperature of the environment influences the character of the processes in the solid phase, these processes taking part on the surface of the hydrated binding material. However, the phase composition changes of the hydrates which form at 30–100°C temperature range due to the reasons listed, bring to both the minor calcium silicate hydrates basisity and to some changes of the quantitative correlation of the forming phases, this leading to neither any serious change of the structure nor to the structure and the features of the hardening cement paste.

It is rather possible to make some changes of the phase composition of the newly formed compounds by bringing into the mixing water electrolytes preventing the polymerisation of the silicic acid. Indeed, in the presence of Na^+, K^+ and Li^+, in the "$C_3S + H_2O$" system at 100°C highly basic calcium silicate hydrates—$C_2SH(B)$ and $C_2SH(A)$ more readily formed than low basic ones. Alkali cations by themselves can serve as crystallization "nuclei". N. V. Belov (44) has shown that there are active hydrate "areas" of a certain form in the liquid phase and these "areas" might serve as crystallization nuclei. It is necessary to say that cations Ca^{2+}, Mg^{2+}, Ma^+, K^+, Li^+ as well as the water moleculae associates play an important role in forming these areas. Such active areas often define the type and the structure of the resulting compounds in the hardening material, since for every given concentration of these ions in the solution, there are crystallization areas of definite geometric and crystallic forms.

Crystalline Structure

The first stage of forming of a crystalline structure of a hardened cement paste new compounds presents the appearing of various areas ("nuclei") of crystallization. These are as follows: 1—hydration areas; 2—crystallization nuclei of a new phase—due to the accumulation of the pertinent ions, and—3—crystallization areas on different colloid films used for being "dusted" with a compound under investigation. The nuclei appeared tend to grow and to coalesce.

The process of a consequent coalescence of crystals is yet not a clear one. Even concerning the base limiting factor of this process the oversaturation rate of the water media—there are quite contradictory opinions. Some workers suppose that, in accordance with thermodynamic data, the coalescence should take place even at the lowest oversaturation rates of the solution (16). However, some others workers (45, 46) think that the coalescence of crystals can take place just only at the highest oversaturated rates of the solutions, at a great amount of crystals in the newly formed compounds. In these conditions the probability of the appearing of contacts when growing crystals draw together, increases and is the more, the higher is the oversaturation rate and the longer its "lifetime". The coalescence takes more vigorous character after the inductive period is over (during this period the solution oversaturation reaches its highest peak). Afterwards, as for as the surface of new hydrate phase increases and the oversaturation decays, hydration process takes even higher rate though it is already followed not by the crystals coalescence but by their dimensional increase. In other words, the crystalline framework appeared during the first stage of the process, overgrows. If to break down the crystallic con-

struction, the crystals of which have exceeded its critical dimensions, then the crystals developing during the further hydration, would not coalesce any more, forming but coagulation compound of relatively small strength.

So the crystals of gypsum having two H_2O moleculae and attained approximately one millimeter size practically did not form coalescent "buildups". So well the formation of contacts bringing to such "buildups" to form, slows down in the case if both the form and dimensions of the crystals of a hydrate have attained the equilibrium of a given conditions. And indeed, various types of crystals of calcium silicate hydrates, which grew up at hydrothermal synthesis with $P = 2000$ atm. both at normal and steam curing, made no "buildups" during a prolonged storing in different solutions. This was true for the two groups of samples—for a non loaded group and for a constantly compressed one—with an approximate charge of 100 g/mm².

Besides, regular crystalline "buildups" can form only at some very definite conditions necessary for isomorphism to display. Theoretically, not all the crystalline hydrates of a hydrated cement paste can make regular "buildups" with each other since a lot of them belong to different structural pattern. The highest ability in this respect belongs to crystalline hydrates of the same pattern, though practically it might occur that, in forced conditions, crystals of different pattern make contacts.

The picture of a buildup, forming between the crystalline hydrates of a similar pattern might be as follows: In a narrow gap between some crystals, neared together due to some reasons (e.g. crystalline pressure, convective shifts etc.) the concentration of an entrained solution arises, this bringing to oversaturation, and the crystallization occurs. Active parts of the surface of coalescing grains play the role of the new crystals growth. The direction of the growth of crystals is parallel to the surface of an opposite grain. The crystals reach this surface and make a "buildup" with the body of a matrix crystal. The heat released during this process is being spent to make up for the decrease of the solution concentration, this being done by bringing of some ions from the surface layers of coalescing crystals into a dissolved state. Resulting such a transfer of the substance, takes place the filling up the gap between the crystals closing together. The crystalline lattice of an appearing "seam" is nearly similar to the lattices of the both coalescing crystals, though the zone of contact might contain a number of dislocations lessening the strength of the "seam".

When crystals of the different structural pattern are coalescing, the structure of the "seam" serves as a transfer zone between one lattice and another one—and is of quite a larger dimension as to compare with the contact zone between the isostructural crystals.

The contacts of coalescing were studied in preparations consisting from calcium sulphoaluminate and silicate hydrates. These hydrates, obtained through the hydrothermal recrystallization, were put in ampules made from molybdenum glass with an oil lock. In order to bring the crystals up to the distance of hk minim at which the coalescing takes place, the crystals were being compressed with the force of 100 g/mm². The liquid phases of real hardening cements were used as a media. The temperature of the test was 20–80°C.

Fig. 7 shows the "buildup" of a hexagonal ($a = 11.43$ Å) and a prismatic ($a_0 = 10.98$ Å) crystals of calcium aluminate hydrate. The closeness of the cells parameters of the two coalescent crystals, found by the microdiffractography method, shows that in this case the coalescing can run along the flat nets similar by their form and almost equal by their dimensions (at parameters difference of the coalescing crystals lattices up to $\Delta = 15 - 16$ per cent). In this

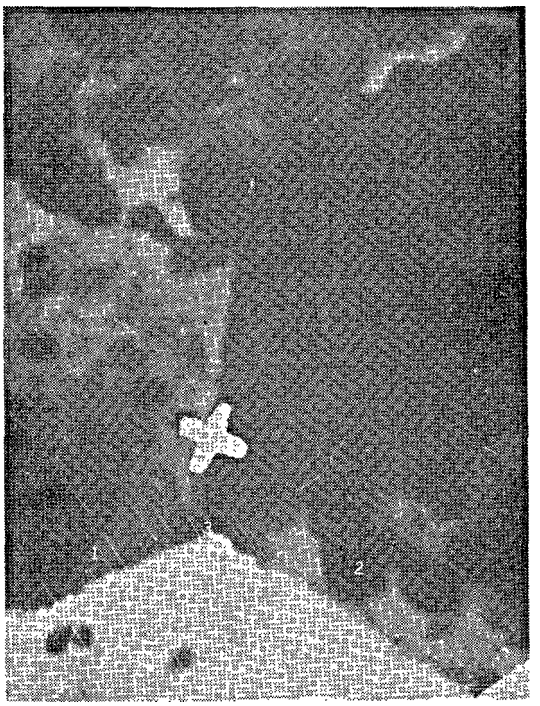

Fig. 7. *Electron microscopic picture of two coalescent crystals of calcium aluminates hydrates* (×9,000); *x—the point, where microdiffractogram was taken.*
1—prismatic crystal of calcium aluminate hydrate;
2—hexagonal crystal of calcium aluminate hydrate;
3—the area of coalescence.

case $\Delta = 4.5$ per cent. The analysis of the microdiffractogram obtained in the point located in the zone of the coalescence of crystals (Fig. 8) shows that $a_0 = 11.11$ Å. The proximity of a_0 values for all the three zones shows that the process of coalescence runs without any noticeable change of the parameters of coalescing crystals lattices in the plane of their conjugation. In other words, an isomorphous mixing takes place, this resulting from the crystallographic similarity, from the closeness of the composition and from the ability of aluminate hydrates to form isostructural phases of changeable composition. Table 3 shows possible planes and angles of coalescence between the crystals. The angle of the turn of plane nets of the coalescing crystals in the plane of conjugation is 22°.

Calcium silicate hydrates formed some accumulation of fine crystals of the same habitus (needles, fibres, prisms). It was not possible to obtain any

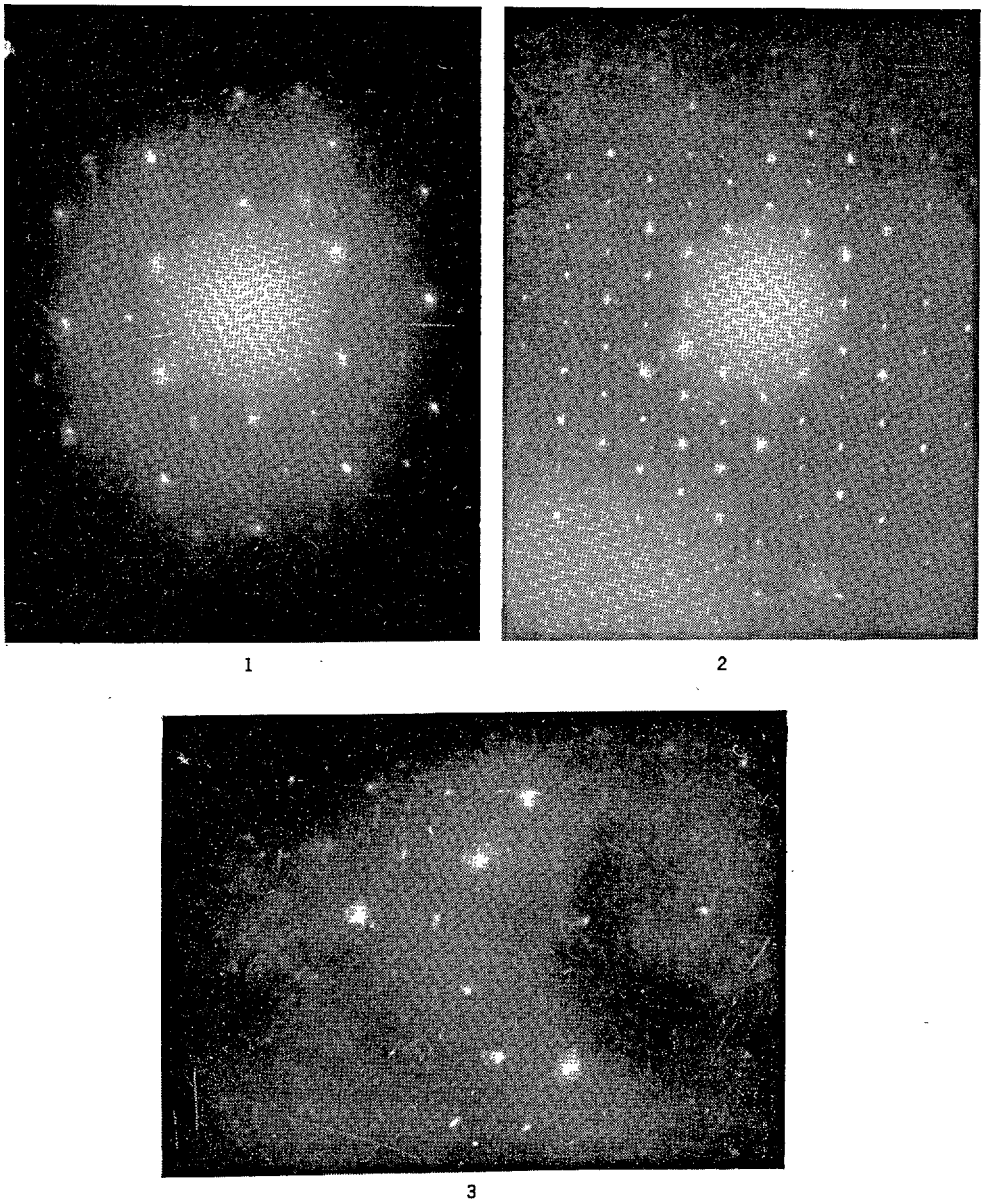

Fig. 8. *Electron microdiffractograms*
1—prismatic crystal of calcium aluminats hydrate;
2—hexagonal crystal of calcium aluminate hydrate;
3—the area of coalescence.

Table 3. *The possible planes and angles of coalescence*

Electronogram of a crystal having $a_0 = 11.43$Å	Electronogram of a crystal having $a_0 = 10.98$Å	[cos α]	$\sim\alpha$
$(6\bar{2}0)$	$(\bar{2}40)$	0.727	44
$(\bar{6}20)$	$(\bar{7}10)$	0.981	11
$(\bar{3}30)$	$(\bar{5}10)$	0.835	33
$(\bar{3}10)$	(620)	0.900	25
(330)	(620)	0.900	25

valuable microdiffaction from the contact zones in such conglomerations. The possibility of coalescence of needle-like, fibrous and prismatic calcium silicate hydrates of the same structural pattern is evident. The composition of the phase on Fig. 9a, is C_6S_3H–$C_2SH(C)$. Probably the coalescence between calcium silicate hydrates of differen habitus is also possible (Fig. 9b).

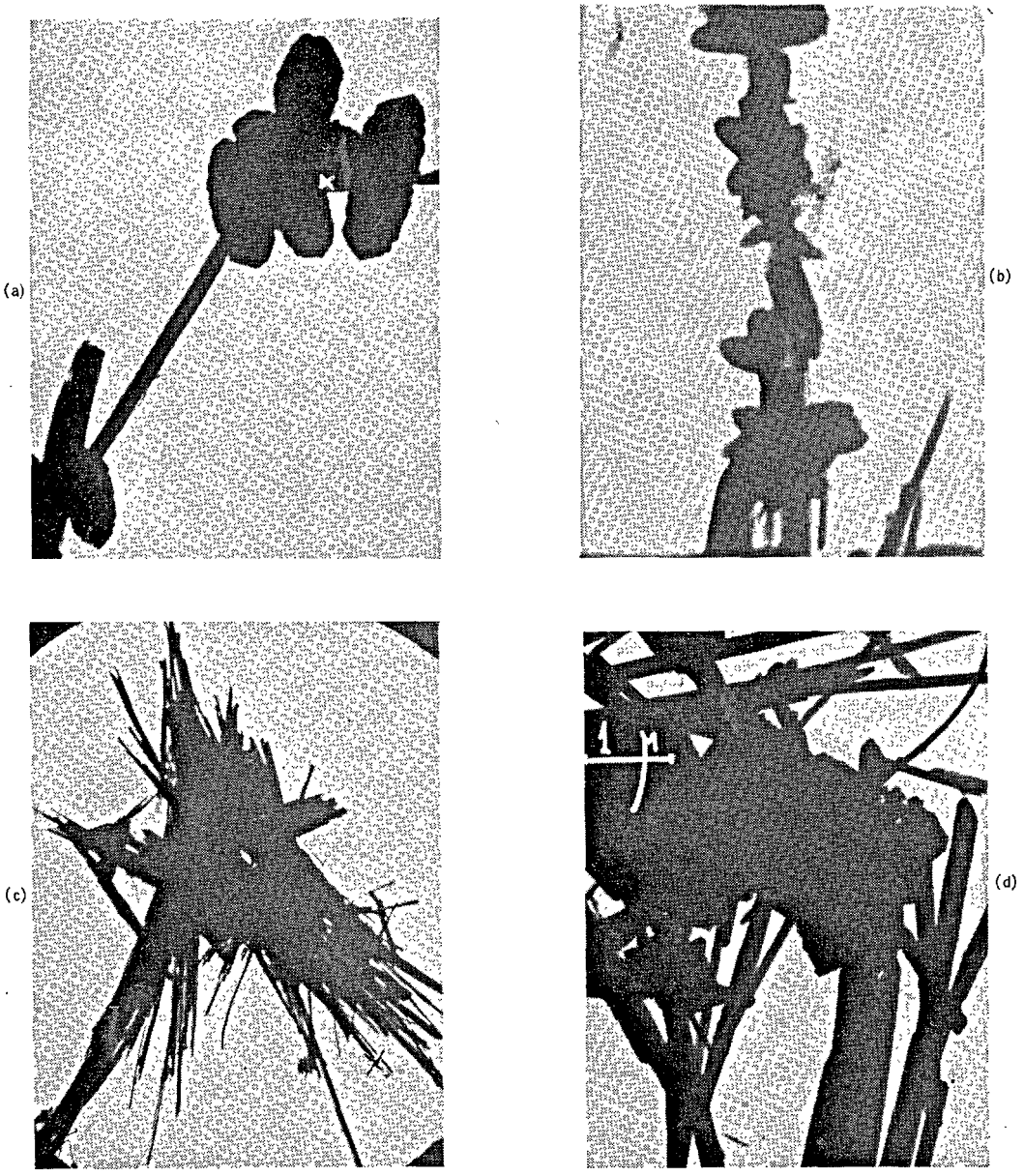

Fig. 9. *Electron microscopic pictures of crystals of calcium silicate hydrates*
a, b) C_6S_3H–$C_2SH(C)$ (×6,000); c) hillebrandite; d) xonotlite (×7,5000)

Distinct coalescences between calcium silicate hydrates and calcium aluminate hydrates were not found. The coalescence process between calcium silicate hydrates and portlandite runs easily.

The investigation of the influence of crystalline hydrates of various kind on the kinetic of portland cement hardening was conducted in the following manner. Plate-like crystals of $Ca(OH)_2$, of tobermorite and of calcium aluminate hydrate C_4AH_{12}, acicular crystals of $CaSO_4 2(H_2O)$ and of calcium aluminate sulphate, and cubic crystals of C_3AH_6, synthesized by a well known methods, were added to the binding material in dry form, 15 per cent by weight. In the most of the cases, the introduction of the said crystalline hydrates was not accompanied with an increase of an initial strength of the hardening samples. Therefore, the admixture to the cement of various preliminary synthesized crystalline hydrates, which form during the hardening of the binding material, not always brings to the formation of a rigid crystalline frame in the hardened cement paste. The efficiency of the influence of various crystalline hydrates as the "centres" of crystallization depends on the type of a given crystalline hydrate, on the size of its crystals, on the amount of the admixture and on the way this admixtures is being introduced.

Calcium silicate hydrate having $C/S \simeq 1$ and with the particle size nearly 10^{-7} cm, and the same hydrate but having $C/S \simeq 2$ with the particle size $10^{-6} - 10^{-5}$ cm, brought to a considerable acceleration of the portland cement hardening at 100°C steam curing (Fig. 14). Calcium silicate hydrates precipitation was used just immediatelly after it had been prepared—without drying—and was added into a ready cement paste, this mix was additionally mixed. Positive influence of calcium silicate hydrate of both dispersity values results from a minor size of the crystals and from their ability to grow.

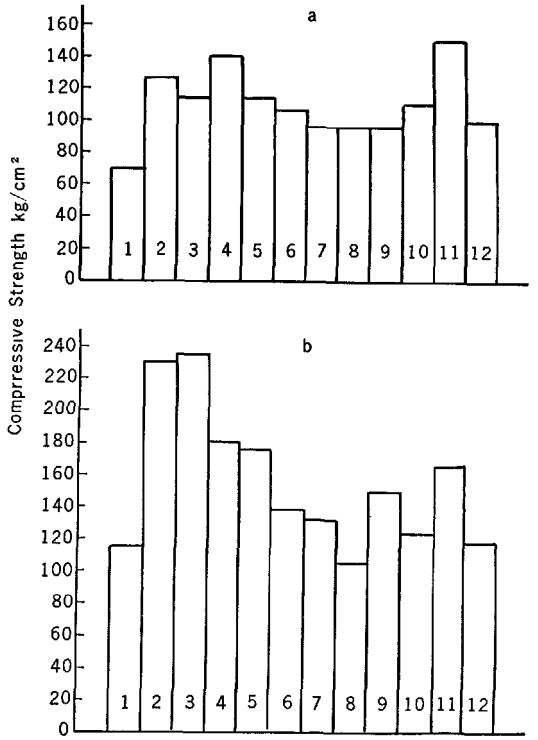

Fig. 14.a, b. *The effect of various crystalline and non-crystalline compounds on the strength of a cement mortar (1: 3, W/C ratio = 0.3) immediatelly after the steam-curing (a) and at the age of 28 days after the steam-curing (b). (The steam-curing pattern: 1.5–8–1.5; 90°C; sealed moulds).*

1—neat cement.
2—1% of calcium silicate hydrate having $C/S \simeq 2$ added.
3—2% of calcium silicate hydrate having $C/S \simeq 2$ added.
4—3% of calcium silicate hydrate having $C/S \simeq 2$ added.
5—CaO, 0.1% added.
6—$Ca(OH)_2$, 0.1% added.
7—$Ca(OH)_2$, 1% added.
8—silica sand, 3,000 cm^2/g, 1% added.
9—silicic acid gel, 1% added.
10—silicic acid gel (aerosol), $S_0 = 200\ m^2/g$, 1% added.
11—the mixture "sand + CaO", 1: 1, 1% added.
12—the mixture "silicic acid + CaO", 1: 1, 1% added.

Physical Structure and the Factors of Destruction

Hydrothermal treatment of a concrete at atmospheric pressure shows a considerable influence on its physical structure. It brings about the change of a general porosity, pore structure of the hardened cement paste, and to the change of both the dispersity and the rate of crystallizing of hydrate phases.

The components of the concrete: solid (cement, aggregate), liquid (mixing water) and a gaseous one (entrained air) tend to expand in various degree under the influence of heat. The distortion of the primary structure of a freshly—laid concrete first of all is due to a volume expansion both of free water and entrained air (47 ~ 51). This expansion is many times larger than that of solid components of the concrete. By S. A. Mironov and L. A. Malinina (52), common concrete contains 2–4 per cent of air entrained during the making of the concrete mix, its placing and tamping. The water content of a freshly made concrete mix is usually many times higher. Taking into consideration that the temperature expansion of water and air (53) is dozens and hundreds times higher than that of solid components of a concrete, the cardinal role of these phases in both reversible and non-reversible deformations of the hardening cement paste at the steam curing is quite clear. Non-reversible volume changes of

concrete resulting its expansion after the steam curing proves a destructive process in the structure of the hardened cement paste (54, 55). The amount of residual expansion of a steam—cured concrete depends not only on the rate of expansion of liquid, solid and gaseous phases of concrete. It also depends on the intensity of the heat—and mass exchange processes. In capillary—porous colloid bodies, to which concrete also belongs, the phenomenon of the moisture transfer, resulted from the gradients of temperature and humidity, follows the main law of the transfer of a substance (56). Migration of water is a typical factor during the process of the concrete structure formation during its steam curing. Migration of water and the changing capillary pressure in the hardening concrete turn to be, at some definite conditions, the main reason of the so called "directed" porosity formation of the hardened cement paste. In the upper layers of concrete units, where the highest change of temperature and of conditions in moisture take place, these processes have very intensive character (47).

The microstructure of the hardening cement paste is different, this resulted from the change of dispersity of the newly formed hydrate compounds—depending on the hardening temperature. This difference is described elsewhere (1, 2, 3, 57 ~ 60). At the steam curing the number of geleous components in the products of hydration decreases, while the amount of crystalline phase and the size of its crystals regularly increases. The compactness of the hydration products forming at the steam curing is 15–20 per cent higher as to compare with normal hardening (1). With the increase of both the duration and the temperature of isothermal heating of concrete units at the steam curing, appearing of newly formed compounds having even more coarse disperse pattern is noticed (58, 59, 61). In this connection it is necessary to remind that physical and physicochemical patterns of the structures, formed during the hardening of a binding material in many respects do depend on the dispersity of the particles of the newly formed compounds and on their concentration in a unit of volume (43). The higher is the dispersity and the concentration of hydrate particles in a unit of volume, the more contacts appear between them—and the higher their interconnection resulted from the actions both of van der Waals and friction forces. Therefore the higher is the strength of the system as a whole. One of the reasons of unsufficient strength during the steam curing as to compare with those of common hardening is the enlargement of hydrate particles (along with simultaneous decrease of contact points)—due to the dissolution of the said particles from their being the most unstable elements of the structure. Due to the reasons listed, the lessening of adhesion between the newly formed crystalline formations and between the said formations and other structural components of the hardening cement paste, the appearance of inner stretching forces resulted from the pressure of the crystals growing at the a steam treatment might be accompanied by the change of the structure and by its weakening. So, the structure of the hardened cement paste is constantly changing during the steam curing of concrete. And these changes have both positive effect (the strengthening of the hardened paste) and a negative one (formation of defects in the paste and decrease of its strength).

Formation of defected structure at the hydrothermal treatment of concretes lies in the influence of some physico-chemical factors, these being as follows disintegration and the transformation of the metastable phases formed earlier, re-crystallization of hydrated products and packing and re-packung of the particles of the hardening system—this accounted for more quiet crystals growth condition at the decrease of the liquid phase oversaturation, contraction shrinkage of the hardening system, osmosis etc.

The most of these processes and their role in the hardened cement paste destruction have not yet been studied enough, however, due to the complexity and versatility of the processes, and their manysided influence on the qualities of cements and concretes.

One of the displays of the physical constitution of a hardened cement paste, this constitution depending on the conditions of hydration, is the formation of the pore structure. During the recent years there appeared a considerable number of scientific works (22, 62–76), devoted to the study of the influence of hydrothermal treatment at atmospheric pressure on the pore structure of the cement paste.

A sound means to appraise the physical structure of a material is its both the general and differential porosity. And indeed, the above mentioned destructive process of the cement paste, recrystallization and the size-enlargement of hydrated phases, contraction shrinkage of the system, specific to the hardened cement paste, distinctly reveal in the form of the changes of both the general porosity; and the faults of the structure of the paste. It also takes the form of re-distribution of the general pore structure and pore sizes. So, by measuring these parameters, one can trace the character and the rate of destruction of the cement paste in a hardening concrete this revealing in the change of its pore structure. It is experimentally proved (68), that the physical features, and durability of concretes are directly related to the general pore volume and to the porosity pattern of hardened ce-

ment paste. Table 4 shows the composition of the cements investigated.

Table 5 shows the connection between the general amount of pore volume and the compressive strength of a steam—cured cement paste made on cements of various chemical and compound compositions. As seen from Table 5, the general amount of pore volume is one of the most important factors influencing the strength of the hardened cement paste and the rate of the change of the strength in the course of time.

It is also known that the pore volume of the hardened cement paste in a steam—cured concrete as a rule is higher than that in a commonly hardened concrete. The relation between these two porosities depend on the compound composition of the cement, the pattern of hydrothermal treatment, the character subsequent hardening and W/C, Table 6 contain the data concerning the influence of a steam—curing and of subsequent hardening on the general porosity of the hardened cement paste made from clinkering compounds and cements.

Hydrothermal treatment shows also great influence on pore size distribution and it is of great importance for the durability, strength and for the thermophysical features of concrete. On the data available one cannot draw a conclusion concerning the pore structure change of the hardened cement paste due to the hydrothermal treatment, since these date are scare and contractionary. Some workers (62, 66) assert, that the hardening of cement paste at elevated temperature (80–100°C) brings to the pore volume increase to increase of the macro-pore fraction ($r > 1 \cdot 10^{-4}$ cm) and, quite naturally, to decrease of micro-pore fraction ($r < 5 \cdot 10^{-5}$ cm). Other works (22, 67) contain the data showing the increase of micropore fraction—along with an increase of the general volume of porosity.

The investigations of the authors of work show that the steam-curing tends to a preferable increase of the porosity of the hardened cement paste along with a decrease of micropore phase (r = less than 100 Å). However, the change of the hardened cement paste pore structure at the hydrothermal treatment depends on some other factors—first of all the composition and the properties of cements.

Table 4. *The data of the cement used*

Cements, No.	Compound composition, %				SF	Silica modulus	Alumina modulus
	C_3S	β-C_2S	C_3A	C_4AF			
1	54.35	19.62	11.11	12.49	0.91	1.90	1.66
2	55.88	14.85	5.47	18.18	0.91	1.67	1.01
3	48.33	21.15	7.59	18.27	0.88	1.58	1.12
4	43.52	32.24	10.64	6.66	0.83	3.13	2.46
5	63.0	14.7	4.4	13.1	—	—	—
6	23.4	57.4	4.5	12.2	—	—	—
7	18.7	51.5	12.2	13.4	—	—	—
8	62.1	10.8	9.6	13.1	—	—	—

Table 5. *The effect of porosity of a hardened cement paste on its strength*

Cement, No.	W/C	Compressive strength, kg/cm²			General porosity, %		
		Pre-curing prior to the steam-curing, min.					
		0	30	120	0	30	120
1	0.4	41	54	93	46.4	43.4	42.3
	0.3	277	316	380	25.1	25.3	24.5
2	0.4	70	87	103	39.0	37.0	37.5
	0.3	201	259	256	29.6	28.1	27.0
3	0.4	0	0	50	49.8	47.5	42.8
	0.3	17	55	143	39.6	36.6	31.8

Table 6. *The influence of the steam-curing on the amount of the general porosity of specimens made from separate compound and from cements*

Hardening conditions	Age of specimens		General porosity, %, of specimens made from,					
	normal hardening	after steam-cutting	C_3S	C_2S	C_3A	C_4AF	cement 1	cement 4
Normal hardening	28 days	—	17.7	35.6	41.4	16.9	16.0	24.0
Steam-curing, 2+3+8+1 hours, at 80°	—	2 hours	27.9	42.9	43.3	22.1	19.4	26.7
	—	28 days	26.3	31.0	41.5	20.0	16.1	22.1

The Influence of the Binding Material Composition on the Structure and the Properties of Hardened Paste and of Concrete

One of the main ways to increase the efficiency of the concrete steam-curing is the use of cements having

optimum properties, which provide formation of a necessary composition and the structure of the cement paste this giving both necessary qualities and the durability of concrete. In this respect of the main importance are the compound composition and crystallic pattern of the clinker, the composition and the fineness of a given cement.

Compound Composition

It has been found (68), that the chemical and compound compositions of binding material shows a considerable effect on the strengthening of a hardening system—since the very beginning of the process. Figs. 10 and 11 show the kinetics of the strength gain of various hardening cement pastes of normal consistency during the first hours of hardening. The samples are prepared from separate compounds and from polycompounded cements of various chemical and compound composition (Table 4). These data show that both structural and mechanical properties of the cement paste of a concrete do depend during an early term of hardening, on the chemical and compound compositions of cement. It is necessary to say that there are great variations in the kinetics of developing systems' hardening. And in its turn all this shows a great influence of compound composition both on developing structures strength and on the rate of a hardening cement paste destruction during the temperature rise when hardening. All the aforesaid shows the necessity to consider, (when choosing the optimal duration of a pre-curing before steam-treatment) the structural and rheological properties of cement pastes in concretes, these properties being defined by the chemical and compound compositions of the binding material.

As far as steam-curing is considered, cements of high hydraulicity with an increased C_3S content are referred to as having optimum compound composition.

The reason of this point of view is, firstly, the higher physical test data of steam-cured concretes made on such cements and, secondary, the optimum structural and rheological properties of alite cements as to liability of being heated.

Figs. 10 and 11 show that tricalcium silicate and cement with higher alite content have retarded gain of plastic strength at the first hours of hardening and it does conform with an induction period at the kinetics of tricalcium silicate hydration process (69).

Keeping the paste made from tricalcium silicate and cements with higher content of said silicate in the plastic, non-consolidated, "form-filling" state for a short period of time before steam-curing, can serve as one of the reasons to weaken the destruction of the

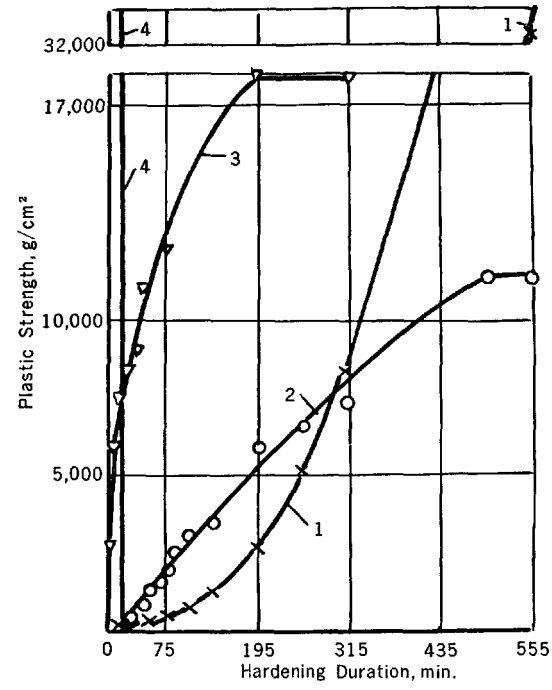

Fig. 10. *The kinetics of the plastic strength gain of a normal consistency paste made from clinker compounds at normal hardening*
1. C_3S_1 2. β-C_2S 3. C_3A 4. C_4AF

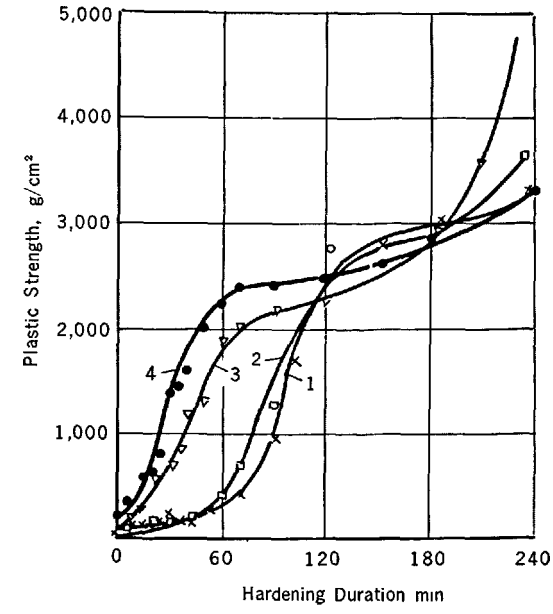

Fig. 11. *The kinetics of the plastic strength gain of a normal consistency paste made from cements of various compound composition; temperature—20°C*

hardening system when heated during the steam-curing. Despite this, the increase of pre-curing of the paste made from tricalcium silicate up to 12–30 hours (69) increases the strength of hardened samples. The reasons of these are as follows. During the pre-treatment at normal temperature, the products of hydration of higher dispersity have more points of coalescence. This, in its turn brings to the formation of an optimum structure, providing higher strength after the steam-curing and during the subsequent normal hardening.

Table 7 shows the data of strength and hydration rate tests of samples made from separate compounds and from cements of various compound composition. Hydration rate tests were conducted on an "ignition loss" basis. The samples hardened in normal conditions as to the temperature and humidity. The heating pattern was 1.5 + 8 + 1.5 hours; isothermal temperature of 90°C. Pre-treatment of moulded specimens before steam-curing was 10–12 hours. Tests were conducted on specimens 1.41 × 1.41 × 1.41 cm made from normal consistency paste. The specimens of normal hardening were kept in air-humid environment at room temperature. Steam-curing was performed in forms covered with metallic plates. Cements No 3,5 and 7 were burned on a pilot rotary kiln from the same raw materials and the same conditions, while cement No. 8 was a commercial one. Cements and separate compounds were ground in laboratory mills up to 3,000 cm²/g (by air-permeability method). When grinding, gypsum was added to cements and to alumina-bearing compounds. Tables 8 and 9 contain the porosity data of the same samples, the data being obtained by means of a hydrargyrum porosimetry. This method was used to measure the pore volume in the range of 20 microns—40 Å. For convenience to discuss the results, the pores are divided into four subdivisions as to their sizes. Pores having $r_1 > 10^4$ Å —"coarse" pores; those having 10^4 Å $> r_2 > 10^3$ Å—capillary macropores; those having $r = 10^3$ Å $> r_3 > 10^2$ Å—"intermediate" pores and those having r 10^2 Å $> r_4 > 40$ Å—micropores.

Table 7. *Compressive strength (kg/cm²), and hydration rate (ignition loss, %) of samples made from separate compounds and from cements of normal hardening and steam-cured at 1.5 + 8 + 1.5 hours, at 90°C*

Compound or cement	Normal hardening, age				After the steam-curing, at the age of			
	7 days		28 days		30 minutes		28 days	
	$R_{compr.}$	Ign. loss	$R_{compr.}$	Ign. loss	$R_{compr.}$	Ign. loss	$R_{compr.}$	Ign. loss
C_3S	300	10.9	520	13.6	200	10.0	265	11.3
β-C_2S	55	2.6	320	6.4	100	2.7	410	6.7
C_3A	—	—	65	27.1	15	22.9	10	24.8
C_4AF	—	—	380	13.9	280	17.2	345	17.5
Cement 5	—	—	950	10.1	710	8.0	860	11.7
Cement 6	—	—	775	9.9	570	8.6	760	11.2
Cement 7	—	—	760	7.9	375	7.1	600	10.7
Cement 8	—	—	900	10.3	540	9.9	630	11.4

These data show that the strength value of tricalcium silicate is next to that of tricalcium aluminoferrite. However, to distinct from C_3AF, the steam-curing of C_3S brings to unsufficient use of its binding properties, and the steam-cured samples of C_3S are of 2–2.5 times lesser strength as to compare with 28 days' normal hardening.

Subsequent hardening of C_3S steam cured samples at normal temperature and humid conditions brings about a noticeable strength gain; the kinetics of this process depends on the pattern of hydrothermal

Table 8. *Structural porosity of specimens made from separate compounds*

Compound	Specimen age		General porosity, cm³/g	The distribution of pores by their radii and volumes							
	after the steam-curing	normal hardening		$r_1 > 10^4$ Å		10^4 Å $> r_2 > 10^3$ Å		10^3 Å $> r_3 > 10^2$ Å		10^2 Å $> r_4 > 40$ Å	
				cm³/g	%	cm³/g	%	cm³/g	%	cm³/g	%
C_3S	30 min.	—	0.1792	0.0195	10.9	0.0900	50.2	0.0475	26.5	0.0222	12.4
	28 days	—	0.1406	0.0095	6.7	0.0530	37.7	0.0480	34.1	0.0301	21.4
	—	7 days	0.1397	0.0140	10.0	0.0500	35.8	0.0477	34.2	0.0280	20.0
	—	28 days	0.0775	0.0070	9.1	0.0036	4.6	0.0394	50.8	0.0275	35.5
β-C_2S	30 min.	—	0.2155	0.0107	5.0	0.1120	52.0	0.0808	37.5	0.0120	5.5
	28 days	—	0.1406	0.0080	5.7	0.0290	20.6	0.0802	57.1	0.0234	16.6
	—	7 days	0.2233	0.0080	3.6	0.1253	56.0	0.0707	31.7	0.0193	8.7
	—	28 days	0.1444	0.0054	3.6	0.0316	21.9	0.0815	56.4	0.0249	17.1
C_3A	30 min.	—	0.2888	0.1850	64.0	0.0810	29.2	0.0100	3.5	0.0128	4.5
	28 days	—	0.2831	0.1808	63.9	0.0760	26.9	0.0200	7.0	0.0063	2.2
	—	28 days	0.2201	0.0282	12.9	0.1273	57.8	0.0423	19.2	0.0223	10.1
C_4AF	30 min.	—	0.0928	0.0025	2.7	0.0460	49.5	0.0250	27.0	0.0193	20.8
	28 days	—	0.0754	0.0024	3.2	0.0191	25.4	0.0280	37.1	0.0259	34.3
	—	28 days	0.1041	0.0062	6.0	0.0338	32.5	0.0521	50.0	0.0120	11.5

Table 9. *Structural porosity of specimens made from polycompounded cements*

Cements, No.	Specimen age		General porosity, cm³/g	The distribution of pores by their radii; their volumes							
	after the steam-curing	normal hardening		$r_1 > 10^4$ Å		10^4 Å $> r_2 > 10^3$ Å		10^3 Å $> r_3 > 10^2$ Å		10^2 Å $> r_4 > 40$ Å	
				cm³/g	%	cm³/g	%	cm³/g	%	cm³/g	%
5	30 min.	—	0.0903	0.0044	4.9	0.0096	10.6	0.0490	54.3	0.0273	30.2
	28 days	—	0.0398	0.0028	7.0	0.0051	12.8	0.0125	31.4	0.0194	48.8
	—	28 days	0.0401	0.0095	23.7	0.0039	9.7	0.0086	21.4	0.0181	45.2
6	30 min.	—	0.0996	0.0060	6.0	0.0055	5.5	0.0700	70.3	0.0181	18.2
	28 days	—	0.0488	0.0026	5.3	0.0046	9.4	0.0150	30.8	0.0226	54.5
	—	28 days	0.0430	0.0035	8.1	0.0039	9.1	0.0222	51.6	0.0134	31.2
7	30 min.	—	0.1213	0.0044	3.6	0.0466	38.4	0.590	48.6	0.0113	9.4
	28 days	—	0.0764	0.0062	8.1	0.0041	5.4	0.0433	56.7	0.0288	29.8
	—	28 days	0.0510	0.0045	8.8	0.0064	12.5	0.0188	36.9	0.0213	41.8
8	30 min.	—	0.0889	0.0039	4.4	0.0080	9.0	0.0580	65.2	0.0190	21.4
	28 days	—	0.0551	0.0039	7.0	0.0023	4.2	0.0248	45.0	0.0241	43.8
	—	28 days	0.0418	0.0104	24.9	0.0022	5.3	0.0092	22.0	0.0200	47.8

curing. The softer are the conditions of hydrothermal during, the more efficient the subsequent hardening is, and the more complete is the use of the binding features of this compound. However it is necessary to say, that the softer is the hydrothermal curing, the lower is the strength gain of C_3S samples just immediatelly after the steam-curing (see Tables 7 and 10). The strength data of C_3S samples attained at different conditions hardening, well correlate with their cumulative porosity and the pore size distribution (by sizes). So, the less strength corresponds to increased values of cumulative porosity and to relative more coarse pore structure. All this well agrees with the present views. Concerning the coarse crystallization of new hydrated compounds during the steam-curing of cements. It is quite naturally that C_3S samples having nearly the same porosity have similar cumulative porosity and the same distribution of pore volumes (by their radii).

As to compare with β-dicalcium silicate, the tricalcium silicate just after the steam-curing gives the structure of lower porosity and higher strength. This is probably the answer of why so many workers preferably recommend alite cements for steam-curing. It is necessary to say however, that the efficiency of hydrothermal curing, β–C_2S—as to compare with common hardening,—has quite distinct advantages over tricalcium silicate (3), since it is belite cements, which more completely reveal their binding qualities when steam-cured, especially when to consider their kinetics of their subsequent hardening. As seen from Tables 7 and 10, steam-cured samples of dicalcium silicate show maximum relative strength gain during the subsequent hardening; the strengthening of the "β–C_2S + water" system corresponds to the sharp

Table 10. *Strength of specimens made from separate compounds, hardened at various conditions (by S. A. Mironov and L. A. Malinina (52))*

Compound	Compressive strength, kg/cm²					
	at normal hardening during				after the steam-curing at 2 + 6 + 2 hours, 80°C, at the age of	
	7 days	28 days	180 days	365 days	3 hours	28 days
C_3S	322	466	512	584	98	409
β-C_2S	24	42	193	325	19	154
C_3A	118	124	0	0	0	0
C_4AF	300	384	493	595	440	546

drop of the cumulative porosity (this drop being one and half times during 28 days) and redistribution of the pore volume resulting to the decrease of their sizes (Table 8). Similar regularity is observed in case of polycompounded cements (Table 7 and 9). Though this regularity is of less distinct character through mutual influence of all hydrating compounds. Intensive hardening after steam-curing, typical for concretes made with alite cements in many cases brings these concretes to attain (at 28 days) the strength values of concretes of similar composition but hardened in common condition. This is rarely observed in case of concretes on alite cements. Nevertheless one can agree with the opinion (70–72), that higher β–C_2S content in cements destined for steam-curing, is undesirable since these cements give just after the steam-curing, low strength values—especially at shortened periods of hydrothermal treatment. The strength increase of such concretes is possible through a more prolonged pre-curing (at shortened steam-curing) and through a prolonged isothermal heating. In the last case the strength of belite cements amounts

to 70 per cent of a standard compressive strength (73) or lower—depending on the content of other compounds—first of all C_3A (Table 7). Higher C_3A content sharply lowers the strength of steamed alite cements (No. 5 and 8) and belite cements (No. 6 and7) and practically doesn't influence their strength when hardening at normal temperature and humid conditions. Immediately after the steam-curing, the strength of low-alumina cements No. 5 and 6 amounted 73–75 and of high-alumina cements—50–60 per cent of the strength of 28 days normally hardened samples. After 28 days of steam-curing, the relative strength of these cements amounted respectively 90–98 and 70–79 percent of the said strength. As a rule, the steam-cured concretes with higher C_3A content have increased porosity. The above said is in accordance with the recommendations (70, 71, 73) concerning the perferable use of alite cements with lower content of tricalcium aluminate (up to 4–5 per cent) for hydrothermal treatment, the lowest content of C_3S in these cements being 45 $\sim$ 60 per cent. Hydrothermal treatment of low alumina cements along with sufficient isothermal curing provides for high strength with a well pronounced trend to a subsequent strength gain at normal temperature and humid conditions. The use of these cements is obligatory when it is necessary to fabricate concrete articles of higher durability and of higher resistance to the influence of the environment.

However, at accelerated steam-curing of concretes one would recommend the use of cements with higher content of tricalcium aluminate along with moderate or higher content of alite (1, 30, 37, 70, 72). In this case tricalcium aluminate can be referred to as a compound, increasing the speed and the rate of C_3S hydration (57). From another point of view, C_3A can also be referred to as a phase taking an independent part in making high strength of the hardening cement paste—at the condition of an optimum increased as to compare with usual content of sulphuric anhydrid in the cement of a sufficient fineness (72).

There are some works (74, 75) in which the allowed tricalcium aluminate content in cements able to efficient hardening when steam-cured, is considered in connection with alite content. The authors (74) think, that for the steam curing at 100°C during 3 hours, cements having more than 55 per cent of C_3S and up to 4–5 per cent of C_3A are suitable. If the alite content is near 50 per cent, then the C_3S content might be increased up to 11 per cent. In other words some increase of C_3A in clinker to some extend allows to decrease the alite content in a concrete subjected to a short-termed steam-curing (75).

The most harmful changes give the steam-curing of samples made from neat tricalcium aluminate. In this case the steam-curing brings to sharp decrease of strength of the compound-this being of a lower strength even without steam-curing. It cannot be explained by a lesser hydration rate, basing on the amount of combined water in samples (Table 7), since the cubic calcium aluminate hydrate makes loose structures and can not form dense protective films around the remnants of unhydrated grains, these films preventing the further hydration of the said grains. The increased amount of combined water in C_3A samples of natural hardening is probably the result of the presence in them of some hexagonal crystalline hydrates containing some higher amount of water. This supposition can be proved by a higher content of micropores in normally hardened C_3A samples—as to compare with steam-cured samples. Low strength of C_3A samples corresponds to their higher (as to compare with other compounds) cumulative porosity and to their prevailing content of coarse and macropores ($r_1 + r_2$). Hydrothermal treatment aids a considerable change of the pore structure of tricalcium aluminate. In these conditions the content of coarse and macro-pores (over 90 per cent in steam-cured samples as to compare with 70 per cent in normally hardened samples). It is necessary to say that pore sizes in steam cured samples are 10 times larger and the general value of the cumulative porosity is 25 per cent higher as to compare with C_3A samples of normal hardening. Therefore the low strength of C_3A and detrimental influence of hydrothermal curing might be well explained through the structural features of hydrated phases of this compound.

And indeed, the main reason of the low strength of this compound lies in the formation of a coarse crystalline frame composed from the cubic tricalcium aluminate hydrate (having six moleculae of water) of a higher homogenity of pores and in the loose bond between its separate crystals. The cases when said compound is of any noticeable strength coincide with the presence in the hydration products of hexagonal crystalline hydrate phases, these providing the formation of a more strong crystallic structure.

Subsequent storing of steam-cured samples of C_3A at air-humid conditions does not bring about any noticeable changes in the structure developed during the steam-curing.

The highest strength during the steam-curing of clinkering compounds gives the C_4AF (Table 7 and 10). The strength of steam-cured samples made from this compound turned to be some lower as to compare with the normally hardened samples. This is in

accordance with the most of the earlier data. High strength of C_4AF samples well agrees with minimum cumulative porosity and with minimum pore fraction having radius more than 10^3 Å ($r_1 + r_2$)—as to compare with other compounds. The pores of the said dimension ($r > 10^3$ Å) might be considered as a factor lowering the strength of the hardened cement paste. In any case it refers more to the said pore dimension rather than to the smaller pores. It has been found (76) that destructive phenomenae during the steam-curing bring to the pore sizes' enlargement.

It is specific for C_4AF steamed samples that they, as to compare with those of normal hardening, have increased content of micropores (10^2 Å $> r_4 >$ 40 Å) and of combined water. It agrees well with the supposition that iron component of C_4AF hydrates more completely, this being accompanied—as it is known—by the formation of geleous products. These products can contribute to the compensation and healing of structural defects of aluminate carcass which appear at C_4AF steam-curing. Our ealier data show that at C_4AF steam-curing, the newly formed compounds are of more disperse pattern as to compare with those of normal hardening. It agrees with the supposition expressed. Specific surface data obtained by low temperature adsorption of nitrogen were 12.4 and 9.6 m^2/g respectively—i.e. two times higher than that for newly formed phases of the samples of other compounds. Table 9 shows that there is no unfavourable change of C_4AF structural porosity as a result of hydrothermal curing of this compound. It is necessary to say however that the presence of this compound in clinker (10–15 per cent usually) makes no material influence on the strength of a steam-cured concrete (72, 77). Moreover, there are some data (77) that at higher C_4AF content in clinker (20 per cent), the strength of a steam-cured concrete lowers significally.

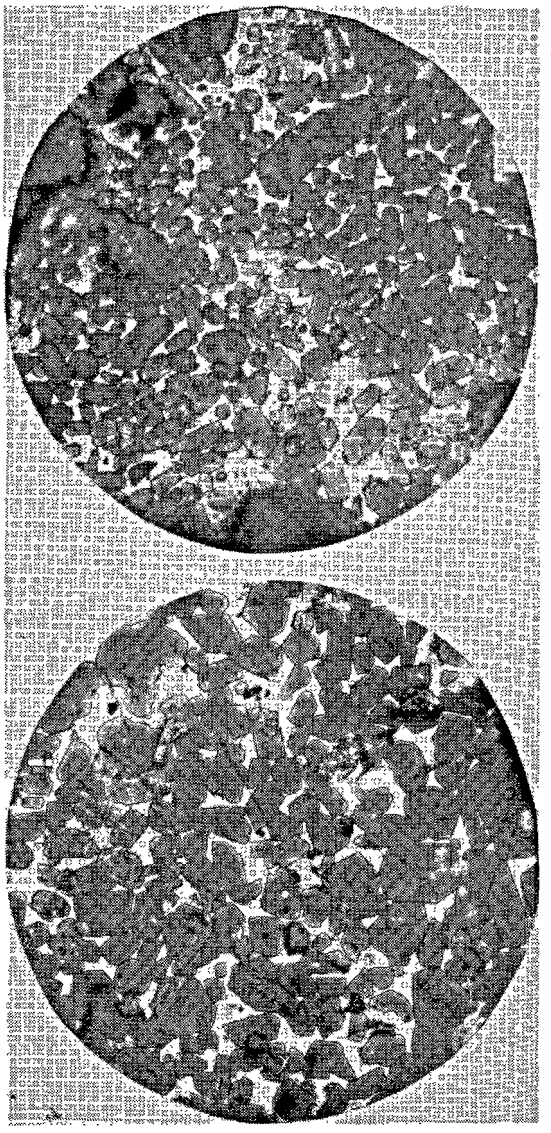

Fig. 12. *Microscopic structure of a laboratory burnt clinker; the structure is near to an optimum one. (Reflected light, ×400)*

Crystalline Structure

Considering that the form of crystals and the crystalline structure of alite and belite, these being main phases of portland cement, strictly depend on their crystallic lattices, one can judge the hydraulicity of a cement by the crystalline pattern of said compounds in it.

Based on a long year experience in the quality control of clinkers and cements of the USSR, the authors (78–80) came to conclusion that regular form of crystals of the main compounds of clinker corresponds to higher quality of cement. Fig. 12 shows the optimum microstructure of clinker. However, if either distorted or partly broken crystals prevail, then the cement made on this clinker would have decrease strength. This dependence has been traced by the authors on clinkers of 80 cement plants. Cements made with these clinker hardened in usual steam-curing on 1.5–3–1 hours pattern—at 95–96°C.

Polyhedral and poorly developed crystals of alite and granular or strongly hatched crystals of belite more oftenly bring about lower hydraulicity. The presence on alite crystals of a "boarder" consisting from the secondary crystals of belite and appeared as a result of C_3S disintegration, is also both the reason and the sign of a slow hardening of cement—during the first period at least. However, the macrodefects cannot

Table 11. *Compressive strength of specimens made from cement consisting from a clinker with various admixtures*

Deformation admixture	Amount of the admixture, %	Air-humid storing, age, days				After the steam-curing at 1.5 + 8 + 1.5 hours, 100°C	
		0.5	1	3	28	age, 30 min	age, 28 days
—	0.0	29	91	156	82	144	153
Cr_2O_3	0.5	22	70	127	131	121	155
	1.0	16	56	105	126	105	128
	1.5	14	56	87	81	184	133
	2.0	38	93	171	163	123	236
P_2O_5	0.5	17	61	140	171	123	182
	1.0	12	56	163	128	156	158
	1.5	7	48	200	200	219	169
	2.0	7	33	136	132	106	128
SO_3	0.5	53	103	170	201	161	170
	1.0	53	94	141	211	151	162
	1.5	66	111	179	192	150	188
	2.0	48	88	125	128	116	171

be considered as a sufficient sign of the hydraulicity of cement. The main role in changing the hydraulicity of crystals of compounds and of the binding material as a whole belongs to the structure of crystalline lattices of separate compounds. Depending the character of the change in lattice composition, defects can result to either decrease or increase of the hydraulicity of a compound. For example, the defects appeared during the occlusion of aluminium oxide, titania, sulphuric anhydride and of some other compounds into the C_3S lattice, contribute to the acceleration of the surface reaction and to the strength gain of the system. Of course, besides providing for pertinent defect, it is necessary to provide for their optimum concentration in crystals. The excess of different (by type) and opposite (by sign) defects in a crystal can bring about the lowering of its interconnection with H^+ and OH^- of water. Table 11 contains data showing complex character of the hardening of cements containing the admixtures which deform crystals at 20–100°C temperature range. So, 0.5–2.0 per cent of Cr_2O_3 results to a small decreased of samples' strength immediatelly after steam-curing; at the age of 28 days the articles of cements, having 0.5 and 2.0 per cent of chromium oxide show higher strength. The addition of 2 per cent of Cr_2O_3 is of the most efficient influence. For normal conditions of hardening L. D. Yermakov (81) and M. M. Sychev (82) recommend 0.15–0.30 per cent of Cr_2O_3 admixture. The addition of 1.0–1.5 per cent of P_2O_5 and 0.5–1.5 per cent of SO_3 also positively influence the steam-curing.

When providing for the conditions in clinker to form alite and belite crystals, optimum as to their size and structure, it is also helpful to provide for the conditions to form these phases as particles of a definite size. Some articles (83–84) point out positive influence of fine crystalline pattern of clinker on the hydraulicity of cement. Along with there are some works (78) mentioning about the obtaining of high-strength cements from coarse-crystalline clinkers. Such contradictory data are conditioned by the fact that the researchers, when studying the influence of alite crystals on the properties of cement, considered neither the structure of crystals nor the fineness of clinker ground. It is rather probable, that the conclusion concerning influence of alite crystals' size on the properties of cement can be drawn just in case when the particle size of the given cement is commeasurable with the size of C_3A crystals. In all other cases it is necessary to consider many attendant factors—for example: 1) the character and the rate of a coarse crystals grinding; 2) aggregative character of fine crystals in the particles of cement; 3) the rate of coverage of alite crystals' surface with the interstitial phase; 4) compound composition of separate cement particles; and some other factors.

At the steam-curing, the hydraulicity of cements having nearly the same compound compositions, and made with clinkers of some 3,000 cm^2/g specific surface, these clinkers consisting from different sized crystals of alite and belite, was commeasurable. 3—hours steam-curing at 95–100°C of cements of the like compound composition, made from clinkers having approximately 3,000 cm^2/g fineness and consisting from alite and belite crystals of various sizes, showed very similar strength. Therefore size of alite and belite crystals is not the factor of a noticeable influence on the strength of steam-cured units. It is at 4,500–6,000 cm^2/g fineness of cement the positive influence of the clinker fine crystalline pattern reveals more distinctly. 20–40 microns are optimum for the change of the size of alite crystals for the similar conditions.

Fineness of Cement

Hydration kinetics of cement rises as its fineness increases. Table 12 contains data showing the hydration rate of various fractions of clinker powder.

The rise of hydration rate when their fineness increased, brings about some higher density of the forming hardening cement paste due to the formation of a great amount of hydration products. Further increase of the fineness of cement over a certain limit brings, however, to a decrease of the hardened cement paste density due to the increase of both the water consump-

tion of the binding material and of contraction shrinkage of the "water—cement" system.

The study of a hardened cement paste physical structure shows its some definite relation to the fineness of cement. The increase of the specific area of cements within the range of 3,000–6,000 cm^2/g tends to some decrease of the summary porosity and to the re-distribution of the hardened cement paste pores volumes, namely—to the increase of the coarse pores volume—on the account of the volume of micropores. Table 13 shows that the change of properties of a steam-cured hardened cement paste, this change being connected with the fineness of these cements, is also defined by the compound composition of said cements. The fineness increase of belite cements proved to be more efficient than that of alite cements.

The fineness of cement shows noticeable effect on the character of structural changes in the steam-cured hardened cement paste at its subsequent hardening at normal temperature and moisture conditions. In this case the increasing of cement fineness brings to a more coarse-voided structure of the hardened cement paste to form. The process of the re-distribution of the pore structure of the hardened cement paste during its ageing is probably connected with the crystallization process and with the densification of the geleous phase of hydration products. The influence of a cement fineness on the process of the re-distribution is in accordance with the pertinent changes of cements hydration rate.

The Material Composition of Cement

The problem of using cements containing finely ground mineral for making concretes subjected to steam-curing is a disputable one. Some authors think (85, 86) that for such concretes only "netclinker" cements should be used, which contain no any mineral admixtures but gypsum. Such an assertion is based on the fact that the addition of more oftenly used admixtures such as ground silica sand, blast-furnace slags and hydraulic products lowers the strength of concrete, though in separate cases the improvement of some other features is noticed—e.g. the resistance

Table 12. *The kinetics of hydration of the fractions of a clinker powder*

Size of a clinker powder grains, microns	The amount of water combined during						
	1 hour		3 days		7 days		28 days
	%, weight	%, to compare with 28 days	%, weight	%, to compare with 28 days	%, weight	%, to compare with 28 days	%, weight
0–7.5	10.71	58	14.63	79	15.02	81	18.45
0–20	6.58	37	9.39	53	11.02	62	17.65
20–42	1.85	19	4.8	50	7.8	82	9.5
42–63	1.18	17	3.32	48	4.71	69	6.86
63–80	1.02	20	2.67	52	3.28	64	5.12
80–200	0.60	16	1.9	51	2.73	74	3.69

Table 13. *The effect of the cement fineness on the properties of a steam-cured hardened cement paste*

Cement, No.	Specific surface, cm^2/g	Specimen age after the steam-curing	General porosity, cm^3/g	Pores distribution by their radii and their volume								Compressive strength, kg/cm^2	Amount of combined water, %
				$r_1 > 10^4$ Å		10^4 Å $> r_2 > 10^3$ Å		10^3 Å $> r_3 > 10^2$ Å		10^2 Å $> r_4 > 40$ Å			
				cm^3/g	%	cm^3/g	%	cm^3/g	%	cm^3/g	%		
5	2500	30 min	0.0903	0.0044	4.9	0.0096	10.6	0.0400	54.3	0.0273	30.2	710	8.03
		28 days	0.0398	0.0028	7.0	0.0051	12.8	0.0125	31.4	0.0194	48.8	860	11.67
	3500	30 min	0.0906	0.0052	5.7	0.0061	6.7	0.0537	59.3	0.0256	28.3	690	10.86
		28 days	0.0303	0.0047	15.5	0.0036	11.9	0.0096	31.6	0.0124	41.0	800	—
	4500	30 min	0.0825	0.0021	2.5	0.0046	5.6	0.0446	54.1	0.0312	37.8	715	12.18
		28 days	0.0281	0.0050	17.8	0.0041	14.6	0.0099	35.2	0.0091	43.4	750	—
6	2500	30 min	0.0996	0.0060	6.0	0.0055	5.5	0.0700	70.3	0.0181	18.3	570	8.55
		28 days	0.0488	0.0026	5.3	0.0046	9.4	0.0150	30.8	0.0266	54.5	760	11.6
	3500	30 min	0.0753	0.0028	3.7	0.0020	2.7	0.0472	62.7	0.0233	30.9	700	10.46
		28 days	0.0375	0.0034	9.1	0.0045	12.0	0.0087	23.1	0.0209	55.8	950	—
	4500	30 min	0.0817	0.0043	5.3	0.0040	4.9	0.0485	59.3	0.0249	30.5	750	11.54
		28 days	0.0286	0.0051	17.8	0.0044	15.4	0.0107	37.4	0.0084	29.4	810	—

against agressive solutions etc. At the same time many studies in the recent years (87 ~ 89) have shown that the use of a high quality blast-furnace portland cement for steam-curing gives a concrete of high technical values and excellent durability.

Table 14 contains data considering the efficiency of the steam-curing of concretes with various cements. These data show that the steam-cured portland blast-furnace slag cement is not much inferior to a "neat" portland cement—as their absolute strength values and the strength gain are concerned.

The study of the hardening of the portland blast-furnace slag cement at steam-curing (88) has shown that the best results are obtained when this cement is steam-cured at elevated temperature. The increase of duration of the steam-curing is more favourable for the blast-furnace portland cement rather than for portland cement (See Table 15).

It is specific for portland blast-furance slag cement concretes that they have a less shortage of the strength gain during the steam-curing and at subsequent hardening as to compare with portland cement concretes.

Table 14. *The influence of a kind of cement on the steam-curing effect of concrete (1.5 + 8 + 1.5 hours, at 80°C) (by S. A. Mironov and L. A. Malinina data (52))*

Cement, kind	Compr. strength, 28 days norm. hard., kg/cm²	Cement consumption, kg per m³ concrete	W/C	Compressive strength, kg/cm²	
				Compressive strength, kg/cm²	age 28 days
Pozzolanic portland cement	446	340	0.42	233 / 68	326 / 95
Portland blast-furnace slag cement	412	320	0.42	330 / 72	424 / 93
Portland cement	430	275	0.4	333 / 74	485 / 107

Note: numerator: compressive strength, kg/cm²; denominator, per cent of the standard strength.

The main difference between the portland blast-furnace slag cement and the portland cement—both having hardened at the steam-curing—is that the portland blast-furnace slag cement contains less of hydrolytic calcium hydroxide and more of low basicity silicate hydrates. These silicate hydrates in the hardening blastfurnace portland cement paste are mainly represented by a unibasic silicate hydrate of the tobermorite group with a trace of silicate hydrate, C_2SH/A/(89).

To obtain portland blast-furnace slag cement of an efficient hardening while steam-cured, it is advisable to use clinker of increased C_3S and C_3A contents. The contents of clinker, granulated blast-furnace slag and of gypsum should be designed in consideration of the features of these materials. Blast-furnace portland cement should have higher fineness.

Good results to intensity the hardening of concretes while steam-curing are obtained (38) by designing the material composition of cement, The authors of this work have advanced an idea that cements whose hardening is mainly based on the formation of calcium aluminate sulphates, should increase their strength at steam-curing more rapidly than the portland cement whose hardening is mainly based on the formation of silicate hydrates bond. On this idea the authors have offered a "four-component" cement consisting from portland cement (58 ~ 65) per cent, aluminous cement (or high alumina metallurgical slags) (3–7 per cent), $CaSO_4 \cdot 2H_2O$ (7–10 per cent) and hydraulic admixture (23–28 per cent).

Both aluminous compound and increased amount of $CaSO_4 \cdot 2H_2O$ are added to increase the amount of calcium aluminate sulphate hydrates during the first stage of hardening. It is known that this crystalline hydrate forms at the hardening of portland cement but its amount is not sufficient to provide for a substantial strengthening of the hardened cement paste while its steam-curing. Calcium aluminates contained in portland cement clinker reveal insufficiently during

Table 15. *The influence of a kind of cement on the efficiency of various steam-curing pattern (W/C = 0.56; cement consumption—280 kg/m³) (by S. M. Royak, A. F. Cherkasova and E. T. Yashina data (88))*

Cement, kind	Amount of additions in a cement slag (tripoli earth)	Compressive strength, 28 days norm. hard., kg/cm², "GOST 310-41"	Compr. str. (kg/cm²), 1 hour age after the heating by patterns, hours								
			3 + 4 + 2			3 + 6 + 2			3 + 8 + 2		
			Isothermal heating, t, °C								
			80	90	100	70	80	90	70	80	90
Portland cement	0/5	564	146	144	139	123	148	159	170	—	132
Portland blast furnace slag cement	33/15	436	144	161	176	134	161	184	140	171	185

the grinding of cements and therefore the main amount of these aluminates can react with gypsum only at the later stages of the hardening. According to some data (38) only 30–50 per cent of alumina content of portland cement can be used for calcium aluminate sulphate to form during the first period of hardening.

The solubility of calcium aluminates in the liquid phase is suppressed by the calcium oxide hydrate, formed at the C_3S hydrolysis. Hydraulic admixture introduced into the above-mentioned cement aims to lower the CaO concentration in the mortar, thus increasing the solubility of calcium aluminates and—therefore—increasing the rate of formation of calcium aluminate sulphate hydrate.

The Influence of Various Technological Factors on the Structure and on the Properties of the Hardened Cement Paste and of Concrete

Water-Cement Ratio and the Method of Moulding

The water content in a moulded concrete article is of the primary influence as to the quality of concretes of both normal hardening and even in a grater rate at steam-curing. The presence of water is necessary for a normal hydration and hardening of the cement in a concrete; the content of water immensely influences the kinetics and the completenes of these processes (91 ~ 94). It also influences the workability of a concrete mix. Besides, water is a concrete mix component, which takes part in destructive processes of a concrete during its hydrothermal treatment. Considering this, it is necessary to obtain maximum lessening of the water content in a concrete mix. The free water, which evaporates during the hardening, as well serves as the main factor of the pore structure of the hardened cement paste along with the entrained air and with the pores of contraction. When steam-curing, the W/C ratio influences the qualities and the durability of concrete. It also influences the optimum duration of separate periods of hydrothermal treatment. The lowering of the W/C ratio allows to shorten the pretreatment and to increase the rate of temperature rise during the steam-curing of the concrete. It also provides for the possible shortening of an isothermal heating of concrete and increasing its temperature (95). When freshly moulded concrete is being heated, the role of water in increasing the porosity of the hardened cement paste depends on the thermic expansion of the water. It also depends on the migration of highly disperse droplets and vapours through the capillary pores as a result of the temperature and moisture gradients of the concrete body. W/C ratio is also of a great importance for the kinetics of the structural and mechanical consolidation of the hardened cement paste. Accelerated consolidation of the hardened cement paste structure at lowered W/C (Fig. 13) is one of the reasons permitting to intensify hydrothermal treatment.

There is a spread opinion (52) that high strength concretes with low W/C made from stiff concrete mixes can be steam-cured using shorter time-patterns as to compare with low-strength concretes of plastic consistency. But even in case of stiff mixes the lowered rate of temperature rise is possible. The lowering of W/C in a concrete mix increases its absolute strength and provides for its more rapid hardening (75). When considering the W/C ratio, it is necessary to remember that its change brings about the change of the workability (stiffness) of a concrete mix and, therefore, it defines the method of tamping when moulding the concrete articles. In commercial scale the use of lean concrete mixes is restricted with the difficulty of their tamping. Efficient tamping of stiff concrete mixes requires for special equipment; along with, it complicates the technological process and rises up its

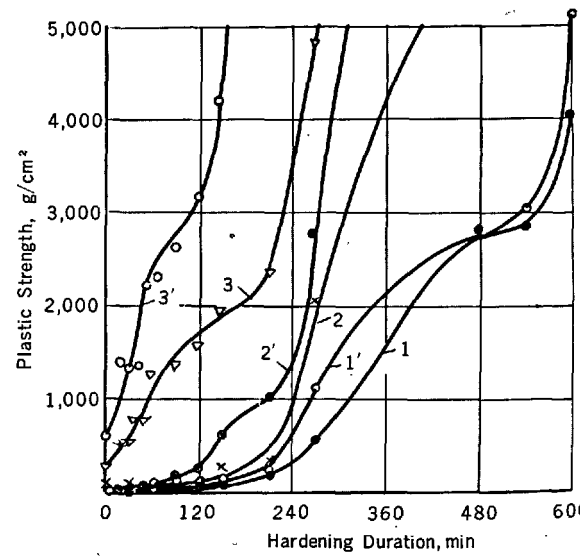

Fig. 13. *The effect of the W/C ratio on the cements plastic strength. Curves 1, 2, 3—cement 1, W/C ratio—0.4, 0.3, 0.2 respectively.*
Curves 1', 2', 3'—cement 3, W/C ratio—0.4, 0.3, 0.2 respectively

Table 16. *Strength, porosity, bulk weight and moisture content of a steam-cured hardened cement paste*

W/C	$R_{compr.}$ kg/cm²		General porosity, %		Bulk weight g/cm³		Moisture content %		The way of moulding
	Cements No.								
	1	3	1	3	1	3	1	3	
0.60	72	0	45.4	52.2	1.43	1.26	19.2	27.1	Pouring
0.50	71	12	43.0	49.2	1.46	1.36	21.6	23.9	
0.40	93	50	42.3	42.8	1.46	1.54	18.0	20.5	Jolting, 100 times
0.30	380	143	24.5	31.76	1.95	1.77	10.6	14.7	
0.25	417	246	23.2	27.14	1.98	1.96	10.5	12.9	Vibration, 30 seconds
0.20	565	377	20.6	17.53	2.04	2.28	7.5	7.7	
0.15	580	190	14.3	23.29	2.17	2.14	6.3	10.4	Pressing, force
0.10	616	202	15.6	23.86	2.16	2.20	7.3	10.2	= 600 kg/cm²

cost. Therefore a commercial concrete should be not lower than 0.3.

Table 16 shows the influence of the W/C ratio and of the method of concrete tamping on the strength and physical data of a steam-cured hardened cement paste. One can see from these data that the lowering of W/C ratio brings to the sharp of the hardened cement paste strength, to a favourable change of its general porosity, of its bulk weight, of its moisture content after the steam-curing. In other words, the parameters, reflecting the structure of the hardened cement paste immensely and favourably change.

It is of a great importance that the increase of W/C ratio immensely changes the structural porosity of a steam-cured hardened cement paste. In such a case the volume of coarse capillary pores increase (Table 17) and this is one of the main reasons of lower durability and lower frost resistance of steam-cured concretes made at high W/C ratios. High content of coarse pores and macropores in a hardened cement paste of higher W/C ratio is, as it was previously said, due to the fact that during the steam-curing, free water increases the pores' sizes in a steam-cured hardened cement paste. Moreover, B. G. Skramtaev, T. I. Gorchakov and M. M. Kapkin (76) show that the pattern of the change of a hardened cement paste during the steam-curing is greatly defined by the W/C ratio. In other words the hardened cement paste of low W/C ratio (0.3–0.4) is turning to be more dense during the steam-curing, while that of higher W/C (0.5–0.6) is turning to be more porous.

The W/C ratio greatly influences the residual water content (i.e.—after the steam-curing) of a hardened cement paste (Table 16) which, in its turn, greatly defines the hardening of the paste at normal temperature and humid conditions. Table 18 contains data showing the strength gain of steam-cured cements

Table 17. *Pore size distribution in cement specimens at 100°C by "0 + 2 + 0 hours" pattern 1*

W/C	General porosity	Distribution of the pores sizes by their radii		Notes
		over 10^3Å	over 10^4Å included	
0.50	46.9	56.0	26.3	For the 100%-porosity serves that one of specimens tested by the kerosene oversaturation method. Samples tested at the age of 30 minutes after the steaming
0.25	25.5	15.0	10.9	
0.20	22.2	13.0	8.6	
0.15	16.4	19.0	11.5	

Table 18. *The W/C ratio effect on the strengthening of a steam-cured hardened cement paste at subsequent hardening at normal temperature-humid conditions*

W/C	Rate of the strength gain, age 28 days, multiplicity factor		Mode of moulding	Notes
	cement 1	cement 3		
0.60	3.9	—	Pouring	The strength of specimens, age 30 minutes after the steaming, is taken for the rerefence
0.50	4.2	—		
0.40	3.7	4.9	Jolting, 100 times	
0.30	1.7	2.82		
0.25	1.60	2.3	Vibration, 30 sec.	
0.20	1.52	2.14		

during the subsequent air and humid curing-depending on the W/C ratio. Great difference in strength correlations shows some more intensive strengthening of steam-cured hardened cement pastes of higher water content during subsequent hardening. But even more rapid strength gain of the steam-cured samples of higher W/C ratio does not allow them to attain strength level of cement samples at lower W/C.

Practically to obtain rapid hardening of steam-cured articles, as well as to obtain more complete use of binding features of the binding material, in some cases one can provide for an additional wetting of the steam-cured articles (96~97). It allows to obtain intensive hardening of the article after their steam-curing without any increase of the W/C ratio. For an efficient use of this method an additional amount of water supply is necessary—at a definite moment, namely prior to the appearing of solid diffusion shells on the grains of clinker—but after the forming of a minimum strength structure, which is able to withstand washout (96). At the same time it is necessary to take into consideration, that in many cases technical standards limit the residual moisture content of the steam-cured articles. In such cases the low W/C concretes are highly desirable.

So, the W/C ratio increase in steam-cured concretes, despite making favourable conditions for an intensive hydration of the binding material, negatively influences the strength, the hardening kinetics of the cement paste especially on the early stages of the process.

Conditions of Hardening

At present there is not yet a generally accepted opinion concerning the optimum pattern of a concrete steam-curing. There is a spread trend to shorten the steam-curing of concrete in order to speed-up the manufacturing process and for this one would use strictly shortened pattern of steam-curing. However, the physical defects thus appearing in the structure of the cement paste, lower the concrete strength and durability. This in turn calls for an additional cement consumption per cubic meter of concrete.

The efficiency of the steam-curing depends on the duration of separate periods of the process and of their respective conformity, to the properties, and the composition of the cements used and on the composition of the concrete, on the W/C ratio as well as on some other factors. Hydrothermal treatment of concrete consists of the following cardinal periods.

1. Pre-treatment, which starts from the time of mixing of a concrete components with water up to the temperature rise of a moulded article due to an external heating.

2. The period of the temperature rise, during which the article is being heated from the temperature of the environment up to the temperaure ordered.

3. Isothermal heating, during which the article is being kept in a steam environment at the constant temperature ordered.

4. The period of temperature lowering, during which the article cools down the environment temperature.

Each of the said periods plays its important role to form the qualities of the hardened cement paste and of the concrete.

a) Pre-Treatment

One of the ways to increase the stability of the hardened cement paste during the temprature increase and, therefore, improving the qualities of the steam-cured concrete, is the pre-curing of the concrete mix prior to the steam-curing. This pre-curing is performed prior to and after the moulding of articles (75~98). There are some ideas (91, 98~101) that during a long pre-curing at normal temperature, an intensive hydration of cement particles, the lessening of uncombined water amount (which most readily evaporates during the heating), the formation of geleous hydration products and the filling of "free water zone" with the said products. Higher concentration of calcium hydroxide in the liquid phase is also of some importance due to its higher solubility at normal temperature, as to compare its solubility at the steam-curing temperature. Packed structure of the hardened cement paste formed during the temperature rise, prevents water migration in concrete thus preventing its loosening and warping which otherwise would lead to the strength disattainment. Besides, during a prolonged curing the concrete attains its initial strength, sufficient to withstand temperature deformations and stresses, developing in a steam cured articles. According to V. A. Fedorov (55), increasing the pre-treatment before a steam-curing at 80°C from 15 min to 24 hours admitted to lower the residual deformation of a hardened cement paste from 3 mm/meter down to 0.2 mm/meter. It can be of a great importance that during a pre-treatment, highly disperse hydrates of well developed surface form, these sorbing water in capillary pores thus preventing its untimely evaporation during a steam-curing. There is also some opinion (91) that untimely temperature rising of a hardening concrete helps to a hardening of shells around the particles of cement. These shells made from newly formed compounds can lead to the retardation—and even to the full cessation—of "water-cement" chemical interaction. According to the aforesaid, certain prolongation of a normal temperature pre-treatment of concrete articles before they are steam-cured, is helpful. Some other authors think however, that the prolongation of a pre-treatment above a definite short term is not only disadvantageos but even can bring about negative results. It has been found (102) that the

strength of a concrete of 2 hours pre-treatment was higher than the same concrete of 4 hours pre-treatment. The steam-curing after a short termed precuring brings about a relatively higher deformations though does not bring about a serious strength drop. According to the authors, feeble structure in an early age and at new conditions of hardening is able to get a "self-healing" of the defects appeared. It does not take place however after the 4 hours pre-treatment, when more rigid and less plastic structure form.

Some authors also think (103, 104) that for articles made from a cement mortar it is advisable to have a 3-hours pre-curing before steam-curing. According their data, however (103), the strength of mortar specimens with cement having 3,800 cm^2/g and steamed without a pre-curing, is similar to those steamed at 3 hours and made of mortar with cement having 3,300 cm^2/g surface. It has also been shown (101) that concrete steam-cured at 85°C without a pre-curing was of equal strength with that one which had a 6-hours pre-curing before the steam-curing.

All the abovesaid proves that there is no generally accepted opinion concerning the optimum time for a pre-curing of a concrete prior to its steam-curing. It is quite understandable to take into consideration that the efficiency of a pre-treatment of a concrete with normal temperature and destined for a steam-curing also depends on the composition of the concrete and cement, on the W/C ratio, on the environment temperature etc. According to some data (52), the optimum time of a pre-curing of concretes made from portland cement can vary in the range of 2–10 hours—depending on the above listed factors. Some authors think (105, 106) that optimum duration of a pre-curing period of concretes prior to their hydrothermal curing corresponds to the moment of transition of a coagulated structure of a "mortar" part of these concretes (i.e.—"cement-sand-water") into a crystallo-coagulated phase. Other authors assert (107, 108) that hydrothermal curing of a concrete should be coordinated with the kinetics of the cement heat release and the beginning of this process should not coincide with the period of maximum heat release.

The beginning of a concrete setting can be considered as the optimum time of pre-curing (52).

There are some data of a considerable interest (109, 110) showing that the breaking down of a cement paste structure during its formation does not influence the hardened cement paste strength. Meanwhile the break down of the structure during its consolidation lowers down the specimens' strength sharply. All this admits to think that the most dangerous structure during the temperature rise is—(considering defects' formation and hardened cement paste strength lowering)—such a structure which has already lost its plasticity and ability to "self-healing", but has not yet attained the necessary strength to withstand stresses arising from the volume change of the components of a concrete and from the mass-transfer. In other words, optimum time for pre-curing of a concrete depends on its structural and mechanical state, attained to the beginning of hydrothermal curing. It is due to the difference in these properties (Figs. 10 and 11) that alite cements admit a shorter pre-curing time as to compare with belite cements. Table 19 shows the change of strength and of other properties of various compound composition, depending on the pre-curing period of samples prior to their steam-curing.

Duration of a pre-curing, as well as duration and temperature of isothermal heating influence the hardening of a cement paste after the steam-curing. The shorter the stages of hydrothermal curing and the lower its maximum temperature, the more efficient is the subsequent hardening and the more strength gain is obtained to 28 days after the steam-curing (Table 20). This corresponds to the data concerning the structure formation of a hardening cement paste during the hydrothermal curing (76). These data show that the most efficient hardening and hydration products accumulation take place at the

Table 19. *The effect of a pre-curing time on the properties of the cement mortar specimens (1: 3) steamed at 100°C by a 0 + 2 + 0 hours pattern*

Cements, No.	Precuring time prior to steaming	W/C	Strength, kg/cm²				General porosity, %	Bulk weight, g/cm³	Moisture content, %
			compressive		tensile				
			30 min.	28 days	30 min.	28 days	30 min		
1	0	0.3	142	280	20	53	22.5	1.97	4.3
	30	0.3	230	297	29	54	20.4	2.06	3.4
	120	0.3	237	310	30	55	19.3	2.06	3.1
3	0	0.3	69	221	13	49	22.5	2.00	4.2
	30	0.3	109	281	19	50	20.7	2.01	3.4
	120	0.3	163	302	24	52	20.1	2.04	3.2

Table 20. *The effect of a pre-curing time on the hardened cement paste after steaming (2 hours, 100°C)*

Pre-curing time, prior to steaming, min	Compressive strength, kg/cm², after the steaming, age	
	30 minutes	28 days
0	64	255
120	199	260

first period of the steam-curing, i.e.—during 4 hours. After this period hydration process retards and the processes of re-crystallization prevail. One can naturally suppose that the structures, formed by less crystallized newly formed compounds, are more liable to an additional structure at subsequent hardening due to their greater mobility and greater solubility of highly disperse hydrates. Therefore, reduced steam-curing on account for a shortened pre-curing and-mainly-on · account for shortened isothermal heating seem to be more advantageous to avoid (or to reduce) the strength disattainment, which is specific to the steam-cured concretes.

The principal ways to reduce the pre-curing of concrete articles prior to their steam-curing are either the use of high early strength alite cements or the use of concrete mix with reduced W/C ratio. It is also possible to perform pre-curing of the concrete mix prior to its moulding and the use of rigid, tightly sealed moulds in order to prevent temperature expansion of the concrete and to restrict the moisture exchange with the environment.

b) The Rate of Temperature Rise

Main defects and distortions of a hardened paste physical structure arise during the heating of concrete articles, when the hardened cement paste has not yet attained the strength necessary to absorb thermal stresses without any change of monolithic character of the structure. Destruction of a hardened cement paste during the temperature rise takes the form of a developing and increasing of the volume of capillary and coarse pores, this resulting from the migration of highly disperse water and steam-air mixture, which is filling the pores.

The said migration in its turn results from a temperature and humid gradient in a concrete and this gradient attains its maximum value during the heating of the concrete. Temperature expansion of water and of an entrained air also of a great importance for the defects and tensile stresses to appear. The negative influence of free water and of entrained air increases as their amount increases. It also increases with the temperaure rise. At the negative influence of these factors destructive processes of moisture migration and of temperature expansion of liquid and of gaseous phases of the hardened cement paste develop more strongly. During the same period, hydration process of a cement runs most vigorously. This process, as it is known, is being accompanied with contraction phenomenae, which condition contracting stresses in the hardened cement paste. That is why the period of the temperature rise at a concrete hydrothermal curing is one of the cardinal factors of this process.

There are various points of view concerning the rate of the temperature rise. According to our opinion, the most grounded of these points of view are those which can coordinate the heating rate of a concrete mix with its rheological and structural properties during the heating. In connection with this, the coordination of the rate of temperature rise with the duration of a concrete pre-curing prior to its steaming is evident. There are some interesting data (III) showing that, irrespective of the kind of a cement, the pre-curing at slow temperature rise does not give the effect necessary. In other words, the slow temperature rise prior to the steam-curing can compensate the absence of a pre-curing. However, quick temperature rise (up to 80°C of isothermal heating) can lead, at the conditions of insufficient pre-curing, to a considerable loss of strength of a concrete.

To obtain a least stressed but most dense structure of a hardened cement paste of a concrete while steam-cured, the temperature rise should have such a rate so as an additional pore volume, appeared as a result of air and water migration and temperature rise, be compensated, rather than supplemented by a pore volume formed as a result of the contraction shrinkage of a hardening system "cement-air". To achieve this, it is necessary to express quantitatively and to bring to conformity the hardened cement volume changes resulted from the said phenomenae. So, the rate of a hardened cement paste destruction during the temperature rise when steam-crued, depends on structural and mechanical features of the paste at the start of heating of a concrete, on the rate of the temperature rise, on the water content of the concrete mix and on the content of the entrained air. In their turn, the structural and mechanical features of a hardened cement paste depend on material and compound compositions of the cement, on its fineness and on a pre-treatment duration. A concrete mix water content can be reduced by means of the reduction of mixing water. The amount of an entrained air depends on the amount of an air-entraining agent and on the rate of a concrete mix tamping when moulding the concrete articles.

In order to speed up the temperature rise when steam-curing, one can use rigid moulds with covers (better with sealed ones). Such forms fix the dimensions of a moulded article, prevent its surface from evaporation by condensing steam and from residual expansion. Use of well-tamped (and therefore having

minimum of an entrained air) stiff mixes of low W/C ratio is also helpful. The so called "step-by-step temperature rise" during the steam-curing of a concrete (52) is a vey effective one. This method consists of an accelerated temperature rise up to 35–40°C. Then comes the curing at such temperature during 1.5–2.5 hours, which is followed by further accelerated rise up to the isothermal temperature ordered. Such a method provides for no any serious temperature deformation or the deformation of a concrete structure during an accelerated heating up to 35–40°C. The curing at such temperature provides a concrete for the strength necessary to remain dense with a least defects at subsequent heating up to the temperature of an isothermal curing. The efficiency of a low temperature rise at a steam-curing of concrete can be probably explained similarly.

c) The Temperature and Duration of an Isothermal Heating

At the isothermal heating of concrete, the hydration process of a cement continues. During this the structural defects, appeared at some earlier stages of hardening of a concrete, turn to be more stable. At the same time, the process of re-crystallization of hydrate phases takes place, this being accompanied with further "reconstruction" of the newly formed compounds, which, in its turn, can stipulate either strengthening or weakening of a hardened cement paste. The alteration of the properties of a concrete during the isothermal heating when steam-curing depends on the temperature and duration of this period. Practically the isothermal heating runs at various temperatures ranging from 60 to 100°C. It also has various duration —from 0 to 24 hours. Both these parameters show independent influence on the hardening kinetic and on the features of steam-cured concrete articles.

With the increase of isothermal curing temperature, the maximum strength of any given condition is mostly attained for a shorter period. According to S. A. Mironov and L. A. Malinina data (52), in order to attain 70 per cent of the standard strength of a concrete having W/C ratio of 0.4, the duration of isothemal heating, amounted to: at 60°C–9 hours, at 80°C–5 hours and at 100°C–4 hours respectively. However, the absolute value of maximum strength at elevated temperatures, is less as to compare with lower temperature of steam-curing. According to the studies conducted by the authors of this work and at the conditions they have chosen, the steam-curing at 60°C would give maximum compressive strength of 360 kg/cm² after 16 hours of isothermal curing; however the "steaming" of a concrete of similar composition at 100°C reduces both the time to attain maximum strength (up to 2 hours) and absolute compressive strength (up to 290 kg/cm²). The data of Table 21 show that even at similar duration of the steam-curing, a more higher temperature of isothermal curing results to the higher strength disattainment at subsequent hardening. These phenomenae can be explained with the increase of defects of a hardened cement paste at higher temperatures of the steam-curing, due to a higher volume alterations of its water and entrained air, an immense role in this respect can play following factors: a) lower rate of hydration at elevated temperature due to a more complete crystallization and to a more "packing" of the newly formed compaction, these making "shells" around unhydrated grains of cement; b) strong evaporation of a concrete mixing water (up to 60–70 per cent) (102).

With the increase of isothermal curing duration, the strength gain of a concrete sharply lowers (113) and the higher the isothermal temperature, the more sharp is the drop of the strength gain. Table 22 shows that the prolongation of isothermal curing ever 4 hours does not give any sufficient rise of a concrete strength. During a prolonged isothermal curing even at 80°C, the drops of a hardened cement paste strength are observed. Probably this is a result of the formation of a low strength calcium silicate $C_2SH(A)$ (52) and of the

Table 21. *The influence of the isothermal curing temperature on the efficiency of a concrete steam-curing (by C. A. Mironov and L. A. Malinina data (52))*

Cement consumption, kg/m³	W/C	Compressive strength, after steaming at "2 + 8 + 2 hours" pattern			
		at 80°C		at 100°C	
		immediatelly after the steaming	age 28 days	immediatelly after the steaming	age 28 days
250	0.6	158/65	285/116	183/75	194/80
440	0.36	279/68	404/99	250/64	341/84

Note: numerator-strength, kg/cm²
denominator—% of the standard strength

Table 22. *The effect of an isothermal curing duration while steam-curing on the strength of a concrete*

Steam-curing pattern, hours, 80°C	Compressive strength	
	immediatelly after the steaming	age 28 days
1.5 + 4 + 1.5	561/94	688/115
1.5 + 8 + 1.5	560/94	704/118
1.5 + 12 + 1.5	586/96	710/119
1.5 + 18 + 1.5	596/100	702/118
1.5 + 24 + 1.5	559/93	656/110

Note: numerator—strength, kg/cm²
denominator—% of the standard strength

change of the structure of newly formed compounds. All this is accompanied with the weakening of an "intercrystallic bond" and with a developing crystalline pressure and inner strain forces.

Practically the duration and the temperature of the steam-curing should be such as to fit the given conditions of manufacture. It is necessary to remember that the efficiency of these parameters of the hydrothermal curing depend on the chemical and compound compositions of the cement, on its hydraulicity and hardening kinetics, on the concrete water content and its consistency, on the composition and the compactness of the concrete, on the thickness of the concrete article etc. When choosing the steam-curing patterns, the isothermal curing should be the shorter, the higher is the temperature of the process.

The Rate of the Temperature Drop and the Subsequent Hardening

Unfavourable effect of the sharp cooling of concrete units, i.e. the temperature gradient in the body of concrete, brings about the formation of stretching stresses in the surface layers of the unit. At some definite conditions (big difference between the unit temperature and that of its environment, draughts etc.) it is accompanied with disturbance of the monolithic structure of the unit and with the formation of micro- and macrocracks. These defects lower both the strength and the durability of a concrete units. According to some various authors, the maximum admitted difference between the temperature of a surface of a steam-cured article and that of its environment varies in the range of 40–75°C (52, 114, 115). S. Reinsdorf (114) shows that the cooling pattern after the hydrothermal curing greatly influences the strength of concrete unit at early ages of the hardening. Too rapid cooling intensifies the drying of a steam-cured concrete (112) and this is mostly considered to be the negative factor, resulting to a retarded hardening of such a unit. Some loosening of a concrete due to the intensive evaporation of sharp water cooling of the units is probable. However, the degree of this loosening on this stage of the steam-curing is negligible, since to this time the hardening cement paste attains sufficient strength. Therefore, the main deformations and disturbance of a concrete structure taking place at this period, can be regarded as a result of internal stresses, arising from the temperature gradient while its cooling. A steam-cured concrete, having residual water in its pores, is able to the further hardening. The kinetic of this process depends on the hydraulic properties of the cement used, on the temperature and humid conditions of the environment and on the pattern of a preceded hydrothermal curing. At shortened isothermal curing, the slow cooling of concrete units is, as a rule, an effective one, since in these conditions the "maturing" of the concrete occures on account of the heat this concrete has accumulated.

The humidity of the environment is of a great importance for the hydrothermal curing of a concrete unit and for its subsequent hardening. After the steam-curing, at the conditions of humid environment, the process of a concrete hardening is of rather intensive character. According to some data (116), the strengthening of a steam-cured hardened cement paste while

Table 23. *Properties and porosity of a steam-cured hardened cement paste*

Cements, No.	Hardening conditions	Curing time prior to the steaming, min	Specimens' age after the steam-curing	Compressive strength, kg/cm²	Ignition loss, %	Specific surface, m²/g	General porosity, %	Pore size distribution, by their radii			
								$r_1 > 10^4$Å	10^4Å $> r_2 > 10^3$Å	10^3Å $> r_3 > 10^2$Å	10^2Å $> r_4 > 40$Å
I	steaming at 100°C, 0 + 2 + 0 hours	0	30 min	321	8.17	4.04	25.53	11.77	3.81	77.37	7.05
		180	30 min	430	9.86	5.70	23.90	7.46	0.28	78.98	13.28
		0	28 days	563	13.30	4.68	15.30	9.11	27.14	60.36	3.39
		180	28 days	636	13.88	2.17	14.38	31.15	3.65	47.59	17.61
	steaming at 80°C, 3 + 8 + 1 hours	120	60 min	667	10.91	2.74	19.43	9.32	9.23	73.13	8.32
		120	28 days	885	13.59	1.40	16.08	11.66	2.65	65.20	20.48
	natural	—	28 days	841	12.12	3.40	16.04	19.79	6.34	57.88	15.99
II	steaming at 100°C, 0 + 2 + 0 hours	0	30 min	189	7.47	8.50	35.76	1.44	27.30	69.06	2.20
		180	30 min	224	7.91	9.06	34.52	5.61	3.17	86.46	4.76
		0	28 days	575	13.07	6.70	25.36	45.03	12.83	35.80	6.34
		180	28 days	654	15.40	6.05	23.50	3.62	3.88	82.87	9.63
	steaming at 80°C, 3 + 8 + 1 hours	120	60 min	426	7.63	6.69	26.73	2.18	1.36	85.54	10.92
		120	28 days	606	16.70	7.70	22.12	15.99	0.98	75.85	7.18
	natural	—	28 days	601	12.85	5.85	24.00	3.88	1.55	88.62	6.35

its subsequent storing in a humid-air environment results from several factor such as: the compacting of its structure, the lowering of its general porosity and the re-distribution of its pores' volume, thus forming a more favourable structure (Table 23). This is very interesting, since it shows the possibility of a considerable reconstruction of a hardened cement paste structure formed during the hydrothermal treatment at atmospheric conditions favourable for hardening. It is also interesting, that the hardened cement paste structure attains its respective greater value when steaming at an accelerated pattern (2 hours at 100°C) and at shorter terms of the pre-curing. As we have already said, it can be explained by less crystallinity and metastability of a hardening cement paste structure, forming at these conditions.

References

1. И. В. Кравченко, И. Т. Власова, "О структуре цементного камня при ускоренном пропаривании", научные сообщения НИИЦемента, 8 (39) (1960)
   (I. V. Kravchenko, and I. T. Vlasova "On the structure of cement stone in accelerated steaming", Scientific Bulletin of All-union State Research In stitute of Cement Industry, 8 (39) (1960).)
2. W. C. Hansen, "Porosity of hardened portland cemente paste", Journal American Concrete Institute, No. 1, "Proceedings", v. 60. 141–156, (1963).
3. Ю.М. Бутт, В.В. Тимашев, Л.А. Лукацкая, "Влияние ионного состава воды на скорость гидратации портландцемента", Сборник "Проблемы прогрессивной технологии строительных материалов". Красноярск, 276-293, (1965).
   (Yu. M. Butt, V. V. Timashev, and L. A. Lukatskaya "Influence of ionic compound on hydration speed of portland cement". Collection "The problems of progressive technology of building materials". Krasnoyarsk, 276–293, (1965).)
4. Ю.М. Бутт "Исследование скорости гидратации портландцементов и составляющих их соединений". Журнал прикладной химии, т. 22, No. 3, 223-224 (1949).
   (Yu. M. Butt "Research on hydration speed of portland cements and their component compounds". The Journal of Applied Chemistry, V. 22, No. 3, 223–224, (1949).)
5. И.П. Выродов, "К диффузионной кинетике реакций". Кинетика и катализ, Т. 5, вып. 4, 706–715 (1964).
   (I. P. Vyrodov, "On diffusion kinetics of reactions". Kinetics and Catalysis, V. 5, Issue 4, 706–715, (1964).)
6. Т. Пауэрс, "Физические свойства цементного камня и теста", Proceedings of the Fourth International Symposium on the Chemistry of Cement, Washington, 1960, Москва, Стройиздат, 402–438, (1964).
   (T. Powers, "Physical properties of cement stone and Paste". Proceedings of the Fourth International Symposium on the Chemistry of Cement, Washington, 1960. Moscow, Stroiizdat, 402–438, (1964).)
7. R. Kelli, "Твердо-жидкие реакции", Canadian Journal of chemistry, V. 38, 1209–1216, (1960).
   (R. Kelli "Solid and liquid reactions". Canadian Journal of Chemistry, V. 38, 1209–1216, (1960).)
8. S. Brunauer, L. E., Copeland and R. H. Bragg, "The stoichiometry of the hydration of tricalcium silicate at room temperature II. hydration in paste form", Journal of Physical Chemistry, v. 60, No. 1, 116–120, (1965).
9. G. J. Verbeck and C. W. Fotter, "The heats of hydration of the cement", Journal American society for testing materials", v. 50, "Proceedings", 1235–1262 (1950).
10. M. I. Ridge, Journal of Applied Chemistry, 10, 218 (1956).
11. В.Б. Ратинов, Я.Л. Забежинский, Т.И. Розенберг, "К вопросу о теории твердения минеральных вяжущих", Труды ВНИИЖелезобетона, вып. I, 3–36, (1957).
    (V. B. Ratinov, Ya. L. Zabezhinsky and T. I. Rosenberg "On the problems of the theory of hardening of mineral bindings". Proceedings of All-union Research Institute of Rearticles & Non-metallic Materials, Issue 1, 3–36 (1957).)
12. М.М. Маянц, "Исследование особенностей физико-химических процессов гидратации портландцемента в условиях тепловлажностной обработки при температуре до 100°С". Кандидатская диссертация, СССР, Москва, НИИЦемент, (1965).
    (M. M. Mayants, "Research on the properties of physicochemical processes of hydration of portland cement during steam treatment at a temperature to 100°C". The Candidates' Dissertation, USSR, Moscow, All-union State Research Institute of Cement Industry, (1965).)
13. Р. Нэрс, "Фаза трехкальциевого силиката", "Proceedings of the third international Symposium" on the chemistry of cement, London, 1952, Москва, Стройиздат, 27–56 (1958).
    (R. Nurse, "Phase of tricalcium silicate". Proceedings of the Third International Symposium on the Chemistry of Cement, London, 1952, Moscow, Stroiizdat, 27–56 (1958).)
14. Е.Н. Гапон, "Гидратация ионов и молекул", Журнал Русского физико-химического общества, серия химическая, т. 40, вып. I, 235–248 (1928).
    (E. N. Gapon, "Hydration of ions and molecules". The Journal of Russian Society of Physical Chemistry, Chemical Series, V. 40, Issue 1, 235–248 (1928).)
15. А. Ф. Полак, "Кинетика гидратации и развитие кристаллизацион-нойструктуры срастания монominеральных вяжущих веществ типа полуводного гипса", Коллоидный журнал, т. 22, No. 6,

689-701, (1960).
(A. F. Polak, "Kinetics of hydration and development of crystallizational growth structure of monomineral binding materials of semi-water gypsum type". The Colloid Journal, V. 22, No. 6, 689–701, (1960).)

16. А. Ф. Полак, Тверцение мономинеральных вяжущих веществ, Стройиздат, Москва, (1966).
(A. F. Polak, "Hardening of monomineral binding materials", Stroiizdat, Moscow, (1966).

17. В. Б. Ратинов, А. П. Лавут, "Исследование кинетики гидратации минералов портландцементного клинкера", ДАН СССР, т. 146, No. 1, 151–155, (1962).
(V. B. Ratinov and A. P. Lavut "Research on hydration kinetics of minerals of portland cement clinker". Reports of Academy of Science of USSR, V. 146, No. 1, 151–155, (1962).)

18. K. Schiller, "Mechanism of re-crystallisation in calcium sulphate hemihydrate plasters", Journal of Applied Chemistry, 12, 3, 135–144, (1962).

19. H. F. W. Taylor. "Гидротермальные реакции в системе $CaO–O_2–H_2O$ и автоклавная обработка цемента и цементно-кремнеземистых продуктов". Proceedings of the Fourth International Symposium on the Chemistry of Cement, Washington, 1960, Москва, Стройиздат, 159–200, (1964).
(H. F. W. Taylor, "Hydrothermal reactions in $CaO–O_2–H_2O$ system and autoclave processing of cement and cement-silicic products". Proceedings of the Fourth International Symposium on the Chemistry of Cement, Washington, 1960, Moscow, Stroiizdat, 159–200, (1964).)

20. С. А. Миронов, "Некоторые обобщения по теории и технологии ускорения твердения бетона", Доклады Rilem, Москва, (1964).
(S. A. Mironov "Some generalizations on the theory and technology of concrete hardening acceleration". Reports of Rilem, Moscow, (1964).)

21. W. Czernin. Zement und Beton, No. 2, 12 (1955).

22. А. Е. Шейкин, Н. И. Олейникова, "Влияние тепловлажностной обработки и тонкости помола цемента на структуру и свойства цементного камня", Доклады Rilem, Москва, (1964).
(A. E. Sheikin and N. I. Oleinikova "Influence of steam treatment and fineness of cement grinding on the structure and properties of cement stone". Reports of Rilem, Moscow, (1964).)

23. J. D. Bernal, "Структуры продуктов гидратации цемента", Proceedings of the Third International Symposium on the Chemistry of Cement, London, 1952, Москва, Стройиздат, 137–176, (1958).
(J. D. Bernal "Structures of cement hydration products". Proceedings of the Third International Symposium on the Chemistry of Cement, London, 1952, Moscow, Stroiizdat, 137–176, (1958).)

24. Т. М. Беркович. Д. М. Хейкер, О. И. Грачева, Н. И. Купреева, "Процессы автоклавного твердения асбестоцемента", Труды ВНИИАсбестцемента, вып. 8, 25–65, (1958).
(T. M. Berkovich, D. M. Kheiker, O. I. Gracheva and N. I. Kupreeva "Proceesss of the autoclave hardening of asbestos cement". Proceedings of All-union Research Institute of Asbestos Working Industry, Issue 8, 25–65, (1958).)

25. H. Knoblauch, "Uber die Hydratationsgeschwindigkeit der Zementklinker-mineralien C_3S und C_2S", Tonindustrie-Zeitung, 82, No. 3–4, 36 (1958).

26. E. R. Buckle and H. F. W. Taylor, "The hydration of tricalcium and β-dicalcium silicates in paste under normal and steam-curing conditions", Journal of Applied Chemistry, 9, No. 3, 163–172 (1959).

27. H. Schwiete and H. Müller-Hesse, "Neuere Ergebnisse über die Hydratation von Kalziumsilikaten", Zement- und Beton, No. 16, 25–29 (1959).

28. О. С. Волков, П. Н. Соколов, "К вопросу о гидратации твердении индивидуальных клинкерных минералов и влияние на эти процессы добавки асбеста." Труды ВНИИАсбестцемента, вып. 14, 3–23, (1962).
(O. S. Volkov and P. N. Sokolov "On the problem of hydration and hardening of individual clinker minerals and the influence of adding asbestos on these processes". Proceedings of All-union Research Institute of Asbestos Working Industry, Issue 14, 3–23, (1962).

29. L. E. Copeland, E. G. Schulz and S. Brunauer, "Die hydratation von trikalziumsilikat und ß-dikalziumsilikat bei Raumtemperatur", Silikattechnik, 11, No. 8, 367–373 (1960).

30. Э. Я. Эршлер, "Поведение цементного камня при пропаривании", Бетон и железобетон, No. 6, 279–282, (1964).
(E. Ya. Ershler, "Properties of cement stone on steaming". Concrete and Reinforced Concrete, No. 6, 279–282, (1964).)

31. К. Э. Горяйнов, Б. Д. Тринкер, "Влияние тепловой обработки на прочнисть и морозостойкость бетона". Бетон и железобетон, No. 6, 265–267, (1964).
(K. E. Goryainov and B. D. Trinker "Influence of thermal treatment on strength and frost-resisting property of concrete". Concrete and Reinforced Concrete, No. 6, 265–267, (1964).)

32. A. Van-Bemst, "Hydratisierung von kalziumsilikaten: Bestimmung der chemischen Zusammensetzung der gebildeten Hydrosilikaten", Industrie Chemie Belge, 20, 67–70 (1955).

33. H. Funk, "Der Hydratationsverlauf von ß-Dikalziumsilikat unter Bildung von nagelförmigem Tobermoritahnlichem Kalziumsilikathydrat", Silikattechnik, 11, No. 8, 373–375 (1960).

34. Л. Г. Шпынова, В. А. Тихонов, Сборник "Исследования, вяжущих веществ и изделий на их основе", вып. 1, 54–79, Львов, (1961).
(L. G. Shpynova and V. A. Tikhonov, Collection "Research binding materials and products, manufactured on their base.

35. G. Kalousek, and M. Adams, "Hydration products formed in cement pastes at 25 to 175°C", Journal of American Concrete Institute, 23, No. 1, 77–90, (1951).

36. Ю. М. Бутт, А. А. Майер, Б. Г. Варшал, "Устойчивость гидросульфоалюминатов кальция" ДАН СССР, 136, No. 2, 398–400, (1961).
(Yu. M. Butt. A. A. Maier and B. G. Warshal, "Stability of calcium hydrosulfoaluminates". Re-

ports of Academy of Sciences of USSR, 136, No. 2, 398–400, (1961).)

37. П. П. Будников, С. М. Рояк, Ю. С. Малинин, М. М. Маянц, "Исследование процессов гидратации портландцемента при тепловлажностной обработке при температуре до 100°С", доклады Rilem, Москва, (1964).
(P. P. Budnikov, S. M. Royak, Yu. S. Malinin and M. M. Mayants, "Research on hydration processes of portland cement during steaming treatment at a temperature to 100°C". Report of Rilem, Moscow, (1964).)

38. И. В. Кравченко, Ю. Ф. Кузнецова, Г. И. Чистяков, "Новый быстротвердеющий при пропаривании цемент для сборного железобетона и перспективы его использования". Доклад на Всесоюзном совещании по современным проблемам технологии бетона в промышленности сборного железобетона, Москва, Стройиздат, (1965).
(I. V. Kravchenko, Yu. F. Kuznetsova and G. I. Chistyakov, "New rapid-hardening-in steaming cement for prefabricated reinforced concrete and prospects of its application". Report on the All-union Symposium on the Recent Problems of Concrete Technology in Prefabricated Concrete Industry, Moscow, Stroiizdat, (1965).)

39. Т. М. Берковнч, Д. М. Хейкер, О. И. Грачева, О. С. Волков, Е. С. Михалевская, "Процессы гидратации при ускорении твердения цемента". Доклады Rilem, Москва, (1964).
(T. M. Berkovich, D. M. Kheiker, O. I. Gracheva, O. S. Volkov and E. S. Mikhailevskaya, "Hydration processes in acceleration of hardening of cement". Reports of Rilem, Moscow, (1964).)

40. О. М. Астреева, Л. Я. Лопатникова, В. И. Гусева, Изучение процессов гидратации цементов, Москва, (1960).
(O. M. Astreeva, L. Ya. Lopatnikova and V. I. Guseva, "Research on cement hydration processes", Moscow, (1960).)

41. J. Gebauer and I. Odler, "Zementhydratation bei der Warmebehandlung, Teil II", Zement-Kalk-Gips, 19, No. 7, 303–308, (1966).

42. Ю. М. Бутт, Л. Н. Рашкович, Твердение вяжущих при повышенных температурах, Москва, Стройиздат, (1965).
(Yu. M. Butt and L. N. Lashkovich "Hardening of bindings at raised temperatures". Stroiizdat, Moscow, (1965).)

43. А. В. Волженский, "О зависимости структуры и свойств цементного камня от условий его образования и твердения". Строительные Материалы, No 4, 10–13, (1964).
(A. V. Volzhensky, "On the relation of structure and properties of cement stone of the conditions of its formation and hardening". Building Materials, No. 4, 10–13, (1964).

44. Н. В. Белов, В. С. Молчанов, Н. Прихолько, "Синтез и строение гидросиликатов, содержащих катионы тяжелых металлов", Трудыпятого Всесоюзного Совещания по экспериментальной и технической минералогии и петрографии, Москва, 1956, изд. АН СССР, 38–43, (1958).
(N. V. Belov, V. S. Molchanov and N. Prikhod'ko, "Synthesis and formation of hydrosilicates containing cations of heavy materials". Proceedings of the Fifth All-union Symposium on Experimental and Technical Mineralogy and Petrography". Moscow, 1956, Publishing House of Academy of Sciences of USSR, 38–43, (1958).

45. П. А. Ребиндер, "Физико-химическая механика дисперсных систем". Издательство "Наука", Москва, 9–16, (1966).
P. A. Rehbinder "Physicochemical mechanics of dispersing system". Publishing House "Nauka", Moscow, 9–16, (1966).)

46. М. И. Стрелков, "Изменение истинного состава жидкой фазы, возникающей при твердении вяжущ их веществ и механизм их твердения", Труды совещания по химии цемента, Москва, Стройиздат, 183–200, (1956).
M. I. Strelkov "Change of actual composition of liquid phase rising on setting of steaming materials and mechanism of their setting". Proceeding of Symposium on the Chemistry of Cement, Moscow, Stroiizdat, 183–200, (1956).)

47. Н. И. Подуровский, "Пропаривание цементных бетонов в средечистого насыщенного пара", Кандидатская диссертация, СССР, Москва, МИСИ им, В. В. Куйбышева, (1961).
N. I. Podurovsky "Steaming cement concretes in the medium of pure saturated vapour". Candidate Dissertation, USSR, Moscow, Moscow Institute of Building after V. V. Kybyshev, (1961).)

48. Л. А. Малинина, В. А. Федоров, "Деформация бетона в процессе пропаривания и при дальнейшем хранении в воздушно-влажных условиях", Известия АС и А СССР, Ио. 1, 24–27, (1962).
(L. A. Maliniva and V. A. Fedrov, "Deformation of concrete as it is steamed and on its further keeping in air-moisted conditions". Report of AS and A of USSR, No. 1, 24–27, (1962).)

49. З. Райнсдорф, "Усовершенствование пропаривания бетона при атмосферном давлении пара и прогрева бетона при температуре до 100°С", Доклады Rilem, Москва, (1964).)
(Z. Rainsdorf, "Improvement of concrete steaming at atmospheric pressure of vapour and at a temperature to 100°C", Reports of Rilem, Moscow, (1964).)

50. В. П. Ганин "Выбор сокращенных режимов электропрогрева бетона", Бетон и железобетон, Ио. 12, 547–550, (1960).
(V. P. Ganin, "Selection of short-cut procedures of electric concrete heating". Concrete and Reinforced Concrete, No. 12, 547–550, (1960).)

51. К. Э. Горяйнов, Е. С. Векслер, "Деструкция в твердеющем бетоне раннего возраста при нагреве и способы уменьшения ее интенсивности", Доклады Rilem, Москва, (1964).
(K. E. Goryainov and E. S. Veksler "Destruction in setting concrete of early rise on steaming and methods of decreasing its intensity". Reports of Rilem, Moscow, (1964).)

52. С. А. Миронов, Л. А. Малинина, Ускорение твердения бетона, Стройиздат, Москва, (1964).

(S. A. Mironov and L. A. Malinina "Acceleration of concrete hardening". Stroiizdat, Moscow, (1964).)

53. Л. А. Малинина, Е. И. Малинский, "Исследование деформации бетонов в процесе автоклавной обработки", Доклады Rilem, Москва, (1964).
(L. A. Malinina and E. I. Malinsky "Research on deformation of concretes as they are treated with high pressure steam". Reports of Rilem, Moscow, (1964).)

54. С. А. Миронов, Л. А. Малинина, В. А. Федоров, "О нарастании прочности и линейных деформаций бетона при пропаривании", Бетон и железобетон, Ио. 4, 170–174 (1961).
(S. A. Mironov, L. A. Malinina and V. A. Feodrov, "On the growth of strength and linear deformations of concrete on its steaming". Concrete and Reinforced Concrete, No. 4, 170–174, (1961).)

55. В. А. Федоров, "Влияние режимов и условий пропаривания на морозостойкость бетонов", Доклады Rilem, Москва, (1964).
(V. A. Fedorov, "Influence of procedures and conditions of steaming on frost-resisting property of concretes". Reports of Rilem, Moscow, (1964).)

56. А. В. Лыков, Явление переноса в каппилярно-пористых телах, Москва, (1954).
(A. V. Lykov, "Transfer phenomenon in capillary-porous bodies". Reports of Rilem, Moscow, (1954).)

57. Т. М. Беркович, "К вопросу о физико-химических основах тепловлажностной обработки цементных материалов". ДАН СССР, 133, Ио. 5, 1140–1142, (1960).
(T. M. Berkovich, "On the problems of physico-chemical bases of steam treatment of cement materials". Reports of Academy of Sciences of USSR, 133, No. 5, 1140–1142, (1960).)

58. R. Nurse, "Curing concrete of elevated temperatures", Building Research Congress, (1951).

59. N. C. Ludwig and S. A. Pense, "Properties of portland cement pastes cured at elevated temperatures and pressures", Journal of American Concrete Institute, No. 1, 673–705 (1956).

60. H. F. Thomson, "Warn concrete-jower strength", Pit and Quarry, 49, No. 9, 319–321, (1957).

61. Т. М. Беркович, "О кинетике цроцесса гидратапии цемента". ДАН СССР, 149, No. 5, 1127–1130, (1963).
(T. M. Berkovich "On kinetics of cement hydration process", Reports of Academy of Sciences of USSR, 149, No. 5, 1127–1130, (1963).)

62. Ф. М. Иванов, Т. Г. Красовская, В. Л. Солнпева, "Влияние тепловлажностной обработки на структуру и свойства цементных растворов", Доклады Rilem, Москва, (1964).
(F. M. Ivanov, T. G. Krasovskaya and V. L. Solntseva, "Influence of steam treatment on the structure and properties of cement solutions". Reports of Rilem, Moscow, (1964).)

63. О. П. Мчедлов-Петросян, Ю. Л. Воробьев, Д. А. Учингус, А. В. Ушеров-Маршак, "Влияние комплекса химических добавок на синтез свойств бетона при термообработке", Труды ХИИТа, вып. 73, Харьков, 31–43, (1965).
(O. P. Mchedlov-Petrosyan, Yu. L. Vorobiev, D. A. Uchingus and A. V. Usherov-Marshak, "Influence of a group of chemical admixtures on synthesis of properties of concrete as it is thermally treated". Proceedings of Khar'kov Institute of Railway Transport Engineers after S. M. Kirov, Issue 73, Khar'kov, 31–43, (1965).)

64. В. Ф. Хворостянский, "Влияние некоторых физических факторов на формирование структуры и прочности мелкозернистого бетона при пропаривании его при 100°С", Труды НИИЖБа, вып. 32, 77–87, (1963).
(V. F. Khvorostyansky, "Influence of some physical factors on forming of structure and strength of fine-grained concrete as it is steamed at a temperature of 100°C". Proceedings of Research Institute of Concrete and Reinfroced Concrete, Issue 32, 77–87, (1963).)

65. Г. И. Горчаков, М. М. Капкин, Б. Г. Скрамтаев, "Повышение морозостойкости бетона". Москва, Стройиздат, (1965).
(G. I. Gorcharkov, M. M. Kapkin and B. G. Skramtaev "Increase of frost resisting properties of concrete". Stroiizdat, Moscow, (1965).)

66. П. П. Ступаченко, "Структурная пористость и ее связь со свойствами цементных, силикатных и гипсовых материалов". Трупы ДВПИ, 63, вып. 1, 3–62, Владивосток, (1964).
(P. P. Stupachenko, "Structural porosity and its Connection with properties of cement, silicate, and gypsum materials". Proceedings of Far East Polytechnical Institute after V. V. Kybyshev, 63, Issue I, 3–62, Vladivostok, (1964).)

67. С. А. Миронов, Л. А. Малинина, О. Е. Королева, В. Ф. Хворостянский, "Методы кратковременной тепловлажностной обработки бетона". Доклады Rilem, Москва, (1964).
(S. A. Mironov, L. A. Malinina, O. E. Koroleva and V. F. Khvorostyansky, "Methods of short-cut steam treatment of concrete". Reports of Rilem, Moscow, (1964).)

68. М. К. Имащев, Ю. М. Бутт, В. М. Колбасов, "К вопросу о формировании структуры и прочности цементного камня в условиях ускоренной тепловлажностной обработки", Труды МХТИ им. Д. И. Менделеева, вып. 45. 34–37, (1964).
(M. K. Imashev, Yu M. Butt and V. M. Kolbasov, "On the problem of formation of structure and strength of cement stone in the conditions of steam treatment". Proceedings of Moscow Institute of Chemical Technology after D. I. Mendeleev, Issue 45, 34–37, (1964).)

69. С. М. Рояк, Ю. С. Малинин, М. М. Маянц, "Исследование процессов гидратации трехкальциевого силиката при тепловлажностной обработке", Труды НИИЦемента, Вып.17, 64–75, (1962).
(S. M. Royak, Yu. S. Malinin and M. M. Mayants "Research on hydration processes of tricalcium silicate on steam treatment". Proceeding of All-union State Research Institute of Cement Industry, Issue 17, 64–75, (1962).)

70. Л. А. Кайсер, "Кинетика твердения портландцементов в условиях пропаривания", Доклады

Rilem, Москва, (1964).
(L. A. Kaiser "Kinetics of hardening of portland cements in steaming conditions". Reports of Rilem, Moscow, (1964).)
71. Д. Е. Горбачев, "О выборе режима пропаривания бетонов на различных портландцементах", Бетон и железобетон, Ио. 10, 470–472, (1959).
(D. E. Gorbashev "On selection of steaming procedure of concrete with variable portland cements". Concrete and Reinforced Concrete, No. 10, 470–472, (1959).)
72. З. Райнсдорф, "Влияние состава портландцементов на результат пропаривания", Доклады Rilem, Москва, (1964).
(Z. Rainsdorf "Influence of composition of portland cements on the result of steaming". Reports of Rilem, Moscow, (1964).)
73. Л. А. Семенов, М. И. Подуровский, Н. Н. Волковский, "Тепловлажностная обработка бетона в безнапорных камерах пропаривания", Доклады Rilem, Москва, (1964).
(L. A. Semenov, M. I. Podurovsky and N. N. Volkovsky, "Steam treatment of concrete in nonpressure steaming chamber". Reports of Rilem, Moscow, (1964).)
74. М. Т. Власова, З. Л. Данюшевская, И. В. Кравченко, "О выборе состава цементов для бетонов и растворов, подвергаемых картковременной термовлажностной обработке". Цемент, Ио. 2, 22–26, (1960).
(M. T. Vlasova, Z. L. Danyushevskaya and I. V. Kravchenko, "On selection of composition of cements for concretes and solutions subjected to short-cut steam treatment". Cement, No. 2, 22–26, (1960).)
75. С. А. Миронов, Л. А. Малинина, О. Е. Королева, В. Ф. Хворостянский, Методы кратковременной тепловой обработки бетона и перспективы их применения при производстве сборного железобетона. Москва, Стройиздат, (1964).
(S. A. Mironov, L. A. Malinina, O. E. Koroleva and V. F. Khvorostyansky, "Methods of temporary steam treatment of concrete and prospects of their application on prefabricated reinforced concrete production". Stroiizdat, Moscow, (1964).)
76. Б. Г. Скрамтаев, Т. И. Горчаков, М. М. Капкин, "Повышение морозостойкости пропаренного бетона". Доклады Rilem, Москва, (1964).
(B. G. Skramtaev, T. I. Gorchakov and M. M. Kapkin, "Increase of frost-resisting properties steamed concrete". Reports of Rilem, Moscow, (1964).
77. J. Kilian, "A klinkerösszetetel hatasa a höerlelt betonok szilardnlasara", Epitöanyag, 17, No. 8, 288–294 (1965).
78. Ю. М. Бутт, В. В. Тимашев, "Портландцементы с заданной кристаллнческй структурой и получение на их основе высококачественных цементов", Журнал Всесоюзного химического общества им. Д. И. Менделеева, т. 10, Ио. 5, 551–558, (1965).
(Yu. M. Butt and V. V. Timashev, "Portland cement with fixed crystall structure and production of high quality cements on their basis". The Journal of All-union Society of Chemistry after D. I. Mendeleev, V. 10, No. 5, 551–558, (1965).)
79. И. В. Кравченко, М. Т. Власова, Б. Э. Юдович, "Фазовый состав и структура высокопрочных и особобыстротвердеющих цементов", Труды НИИЦемента, вып. 20, 3–23, 26–40, (1964).
(I. V. Kravchenko, M. T. Vlasova and B. E. Yudovich, "Phase composition and structure of high-strength and extra-rapid-hardening cements". Proceedings of All-union State Research Institute of Cement Industry, Issue 20, 3–23, 26–40, (1964).)
80. Л. Я. Лопатникова, "К петрографии цементного клинкера", Эксперимент в технической минералогии и петрографии, изд. Наука, Москва, 120–126, (1956).
(L. Ya. Lopatnikova, "On petrography of cement clinker". Experiment in Technical Mineralogy and Petrography, Publishing House "Nauka", Moscow, 120–126, (1956).)
81. Л. Д. Ершов, Высокопрочные цементы, Гостехиздат, УССР, (1952).
(L. D. Ershov "High strength cement". Gostekhizdat, Ukrainian Soviet Socialist Republic, (1952).)
82. М. М. Сычев, В. И. Корнеев, "Дегируюшие добавки улучшают свойства цемента", Цемент, Ио. 5, 3–5, (1964).
(M. M. Sychev and V. I. Korneev "Dehydrating admixture improves cement's properties". Cement, No. 5, 3–5, (1964).)
83. В. Н. Юнг, Основы технологии вяжуших веществ, Промстройиздат, Москва, (1951).
(V. N. Yung, "Foundations of technology of binding materials". Promstroiizdat, Moscow, (1951).)
84. А. Е. Шейкин, С.М.Рояк, "Высокопрочые быстротвердеющие цементы", Новое в химии и технологии цемента, Стройиздат, Москва, 93–111, (1962).
(A. E. Sheikin and S. M. Royak, "High-strength rapidhardening cements". News in Chemistry and Cement Technology, Stroiizdat, Moscow, 93–111, (1962).)
85. А. Е. Шейкин, А. Я. Либман, Гун Цзя-Сэнь, Ц. Д. Урьева, Л. А. Хапанцева, "Быстротвердеющий портландцемент для производства сборного железобетона", Бетон и жедезобетон, Ио. 2, 68–71, (1959).
(A. E. Sheikin, A. Ya. Libman, Gun Tszya-Sen, Ts. D. Ur'eva and L. A. Khapantseva, "Rapid hardening portland cement for prefabricated reinforced concrete production". Concrete and Reinforced Concrete, No. 2, 68–71, (1959).)
86. З. Райнсдорф, "Влияние состава портландцемента на результат пропаривания", Доклады Rilem, Москва, (1965).
(Z. Rainsdorf, "Influence of composition of portland cement on the result of steaming". Reports of Rilem, Moscow, (1965).)
87. С. А. Миронов, "Некоторые обобщения по теории и технологии ускорения твердения бетона", Доклады Rilem, Москва, (1964).
(S. A. Mironov "Some generalizations on the theory and technology in concrete hardening acceleration".

Reports of Rilem, Moscow, (1965).)

88. С.М. Рояк, А.Ф. Черкасова, Е.Т. Яшина, "Влияние тепловлажностной обработки на твердение *шлакопортландцемента*", Доклады Rilem, Москва, (1964).
(S. M. Royak, A. F. Cherkasova and E. T. Yashina, "Influence of steam treatment on the hardening of portland slag cement". Reports of Rilem, Moscow, (1964).)

89. В. Н. Попко, "Твердение шлакопортландцемента при пропаривании", Цемент, Ио. 1, 7–9, (1967).
(V. N. Ponko "Hardening of portland slag cement". Cement, No. 1, 7–9, (1967).)

90. H. Funk, "Über Kalk reiche Tobermoritphasen", *Silikattechnik*, 11, No. 8, 375–377 (1960).

91. А. Е. Шейкин, "Пути получения высокопрочных бетонов", Бетон и железобетон, Ио. 4, 113–118, (1957).
(A. E. Sheikin "Method of obtaining high-strength concretes". Concrete and Reinforced Concrete, No. 4, 113–118, (1958).)

92. R. W. Carlson and L. R. Forbrick, "Correlation of methods for measuring heat of hydration of cement", Industrial and Engineering Chemistry, vol. 30, No. 7, 382–386 (1938).

93. L. E. Copeland and R. H. Bragg, "Self-desication in portland-cement pastes", American Society for Testing materials Bulletin, No. 204, 34–39, (1955).

94. G. H. Taplin, "A Method for following the hydration reaction in portland cement paste", Australian Journal of Applied Science, 10, No. 3, 329–345, (1959).

95. Н. Карапчинский, А. Пеев, "Исследование некоторых вопросов в области пропаривания бетонов", Доклады Rilem, Москва, (1964).
(N. Karapchinsky and A. Peev, "Research of some problems in the field of concrete steaming". Reports Rilem. Moscow, (1964).)

96. Т. М. Беркович, "Физико-химические основы интенсификации процесса твердения портландцементного асбестоцемента", Труды НИИАсбестоцемента, вып. 15, 3–30, (1962).
(T. M. Berkovich, "Physicochemical foundations of intensification of hardening process of portland-asbestos cement". Proceedings of Research Institute of Asbestos Working Industry, Issue 15, 31–37. (1962).)

97. Е. С. Михалевская, О. С. Волков, Л. П. Буланова, Т. М. Беркович "Влияние водоцементного фактора на кинетику гидратации цемента и асбестоцемента", Труды НИИАсбестоцемента, вып. 15, 31–37, (1962).
(E. S. Mikhailevskaya, O. S. Volkov, L. P. Bulanova and T. M. Berkovich "Influence of water-cement factor on kinetics of hydration of cement and asbestos cement". Proceedings of Research Institute of Asbestos Working Industry, Issue 15, 31–37, (1962).)

98. А.С. Миронов, Температурный фактор в твердении бетона, Москва, (1948).
(A. S. Mironov "Temperature factor in hardening of concrete". Moscow, (1948).)

99. А. С. Паителеев, В. В. Тимашев, "Об ускорении твердения бетона в условиях вибропроката", Труды МХТИ им. Д. И. Менделеева, Москва, вып. 36, 116–128, (1961).
(A. S. Panteleev and V. V. Timashev, "On acceleration of concrete hardening in the conditions of vibration rolling". Proceedings of Moscow Institute of Chemical Technology after D. I. Mendeleev, Moscow, Issue 36, 116–128, (1961).)

100. Э.Я. Эршлер, "Исследование процессов твердения портландцемеитов при пропаривании бетонов", Кандидатская диссертация, Москва, МХТИ им. Д. И. Менделеева, (1963).
(E. Ya Ershler, "Research on hardening processes of portland cements in steaming concretes", Dissertations of Candidates, Moscow, Moscow Institute of Chemical Technology after D. I. Mendeleev, (1963).)

101. Реферат содоклада Чернина, "К вопросу о поведении цементов при пропаривании", Второй Международный конгресс по бетону в Висбадене, Госстройиздат, Москва, 16–22, (1960).
(Report from the Lecture by Chernina, "On the problem of behaviour of cements in steaming", 2nd International Congress on Concrete at Wiesbaden, Gosstroiizdate, Moscow, 16–22, (1960).)

102. Н.И. Подуровский, Е.С. Савин, "К вопросу оценки качества тепловлажной обработки бетона", Сборник трудов РИСИ, Ростов/Дон, вып. ХУ, (1958).
(N. I. Podurovsky and E. S. Savin, "On the problem of appreciation of quality of steam curing concrete" Collection of Proceedings of RISI, Rostov/Don, Issue XV, (1958).)

103. С. М. Рояк, Х. М. Лейбович, "О цементе для ускренного производства предварительно напряженных бетонных конструкций", Труды НИИЦемента, Москва, вып. 13, 63–72, (1960).
(S. M. Royak and Ha. M. Leibovich, "On cement for accelerated production of the prestressed concrete constructions", Proceedings of All-Union State Research Institute of Cement Industry, Moscow, Issue 13, 63–72 (1960).)

104. Реферат доклада Ольсона, "Влияние температуры на твердение бетона", II Международный конгресс в Висбадене по бетону, Госстройиздат, Москва, 11–15, (1960).
(Report from the Lecture by Olson, "An influence of temperature on hardening of concrete", 2nd International Congress on Concrete at Wiesbaden, Gosstroiizdat, Moscow, 11–15 (1960).)

105. Л. А. Сильченко, Н. В. Михайлов, П. А. Ребиндер, "Выбор, оптимального времени выдерживания бетона перед гидротермальной обработкой", ДАН СССР, 162, Ио. 6, 1342–1345, (1965).
(L. A. Silchenko, N. V. Mikhailov and P. A, Rehbinder, "Selection of optimum aging time for concrete before hydrothermal treatment", Report of the Academy of Sciences of the USSR, 162, No. 6 1342–1345, (1965).)

106. Ю. С. Малинин, М. М. Капиин, "Измерение методом контракции процессов твердения цемента при пропаривании", Цемент, Ио. 6, 23–26, (1958).
(Yu. S. Malinin and M. M. Kapin, "A measuring

method of contraction process of hardening cement in steaming", Cement, No. 6, 23–26, (1958).)
107. О Т. Мчедлов-Петросян, А. Г. Бунаков, Ф. А. Латышев, Г. В. Чеснок-Смотрич, "О выборе технологии автоматизированного изготовления крупноразмерных строительных изделий", Строительные материалы, Ио. 8, 16–18, (1961). (O. T. Mchedlov-Petrosyan, A. G. Bunakov, F. A. Latyshev and G. V. Chesnok-Smotrich, "On selection of technology of automatic production of large-sized building articles", Building Materials, No. 8, 16–18, (1961).)
108. T. C. Powers, Journal Portland cement Accociation Research Developm. Labs, No. 28, (1961).
109. Н. В. Михайлов, Е. Е. Калмыкова, "Исследование структурно-механических свойств цементныхх паст при помощи эластовискозиметра", ДАН СССР, 99, Ио. 4, 573–576, (1954). (N. V. Mikhailov and E. E. Kalmykova, "A research of structure-mechanical properties of cement pastes by elasto viscosimeter", Report of the Academy of Sciences of the USSR, 99, No. 4, 573–576, (1954).)
110. В. Б. Черногоренко, И. Г. Гранковский, "Исследование структурномеханических и других свойств цементного теста при его переходе от вязко-пластичного состояния в упругохрупкое", Коллоидный журнал, 25, Ио. 5, 600–605, (1963). (V. B. Chernogorenko and I. G. Grankovsky "Research on structural, mechanical and other properties of cement paste as it turns from plastic condition into elastobrittle condition". The Kolloid Journal, 25, No. 5, 600–605, (1963).)
111. Aurich Bauingenieur Heinz, "Zum Einflüß der vorlagerungszeit bei der wärmebehandlung von beton", Betonstein-Zeitung, 29, No. 3, 143–149 (1963).
112. G. Y. Kunsrt, "Küeso tenyezök hatasa a görölessel szibarditott betonra", Epitoanyag, 14, No. 11, 382–396 (1962).
113. J. Riha, "Schnellverfahren zur Beschleunigung der erhärtung von beton, II. Teil", Baustoffindustrie, 6, No. 3, 71–73 (1963).
114. S. Reinsdorf, "Warmebehändlung von beton bei niedrigen temperatur", Baustoffindustrie, 4, No. 11, 282–284, (1961).
115. Л. А. Кайсер, Н. Б. Марьямов, Л. И. Панфилова, "Температурные градиенты в бетоне сборных конструкций, подвергаемых пропариванию, и их влияние на качество и долговечность бетона", Доклады Rilem, Москва, (1964). (L. A. Kaiser, N. B. Mar'yanov and L. I. Panfilova, "Temperature gradients in concrete of prefabricated constructions subjected to steaming and their influence on quality and durability of concrete". Reports of Rilem, Moscow, (1964).)
116. М. К. Имашев, Ю. М. Бутт, В. М. Колбасов, "Влияние предварительной выдержки на формирование структуры пропаренных образцов из клинкерных минералов", Труды МХТИ им. Д. И. Менделеева, вып. 50, 96–100, (1966). (M. K. Imashev, Yu. M. Butt. and V. M. Kolbasov, "Influence of preliminary keeping of steamed articles of clinker minerals for structure forming". Proceedings of Moscow Institute of Chemical Technology after L. I. Mendeleev, Issue 50, 96–100, (1966).)

Written Discussion

Jørn Jessing and Poul Nerenst

In the principal paper by Butt, Kolbasov and Timashev (1) it is clearly demonstrated, that data from practice or research on accelerated hardening of concrete often are conflicting. This is not surprising, as experience has only been collected during a relatively short period. It shall be attempted in the following to perform a systematic discussion of these factors, even if it is not based on experimental research.

Rate of the Hydration Process

The curing of concrete at elevated temperature results in an acceleration of the hardening, i.e. the physical and chemical reactions in the cement-water-aggregate system proceed at a higher rate. The direction and rate of reaction are in general controlled by the driving potentials of the system. The hydration of cement depends primarily on

the chemical potential,
the temperature and
the pressure.

The chemical potential is determined by the nature and concentration of the reacting components, i.e. of the cement type and of the ratio of water to cement. For a given concrete mix these parameters will be constant.

The temperature history of the system (temperature as function of time) will depend on several factors: the initial temperature of the concrete mix, the amount of heat generated by hydration, the temperature difference between the system and its sur-

roundings and the thermal characteristics of the system.

As to the pressure, we are concerned only with thermal curing at temperatures below 100°C, i.e. the pressure is considered constant and equal to the atmospheric pressure, unless the curing takes place in closed, rigid forms.

It seems an established fact, that the course of the hydration reaction and the end products are substantially the same within a temperature range from 20°C to 100°C (1), (2). Although the temperature might influence the habit of the hydrated compounds (size and form of particles etc.), these problems have only in part been clarified, and we shall in the following assume identical hydration products at all temperatures below 100°C.

Destructive Processes

The mechanical properties of hardening concrete depend on the new structure formed during the hydration. Changes in the thermodynamic potentials may give rise to other physical processes, which may damage the formation of new structure in cement paste.

Two causes of harmful processes in concrete hardening at elevated temperatures are considered:

a. changes of temperature,
b. cnanges of water vapour pressure.

Changes of Temperature

A temperature change will cause volume changes in concrete. As the concrete components have rather different coefficients of thermal expansion (water about 10 times those of solids), they dilate differently. The resulting strain differences may damage the structure of concrete, if its internal cohesion and adhesion have only attained low values.

If the temperature change occurs, because the ambient temperature is higher than that of the concrete body, heat will be transferred to concrete, predominantly to its surface layers. This may cause temperature gradients and an uneven stress distribution, leading to crack formation.

If the temperature of the surrounding atmosphere is below the concrete temperature, heat transfer from concrete may reverse the mechanism just described, which in a similar way could damage the concrete.

Changes of Water Vapour Pressure

Changes in the pressure of water vapour may have detrimental effects, when cement paste or aggregate contain air-filled pores or bubbles of entrained air. In that case water may change phase within the system, i.e. evaporate or condense, which in turn entail consumption or liberation of heat.

Pressure changes caused by differences between the external and the internal vapour pressure may have more serious consequences:

If the relative pressure of water vapour is higher in the surroundings than in concrete, vapour will condense on its surface. Directly this may only be an advantage, but as condensation liberates heat, it may be harmful indirectly, by increasing the surface temperature and producing temperature gradients in the concrete body.

If vapour pressure is higher in concrete than in the curing medium (as it will be, if both are saturated, but the temperature of concrete the highest one), evaporation will take place at the concrete surface. This produces gradients of vapour pressure within the concrete and lead to transport of water (by flow or by diffusion) through the structure. The displacement of water will produced a hydraulic pressure, which the paste may not be able to resist.

Classification of Variables

In order to understand the physical processes and treat them mathematically, it is necessary to discuss the factors, which determine the temperature history of the concrete body and those, which determine the vapour pressure history. In practice it is possible to accelerate the hardening process by varying a great number of factors. Some of these are given by the characteristics of the materials and their mix proportions, i.e. the chemical and geometrical properties and the state of the concrete. Other factors are inherent with the curing conditions, i.e. the resistance to heat and moisture flow through the boundary of the concrete body and the temperature and humidity of the surrounding medium. The variables are listed systematically in Table 1.

Discussion of Variables

Among the parameters in Table 1 those directly related with the structure will be treated separately. Air content and aggregate content are omitted as they can be considered constant. The parameters directly influencing heat and mass transfer are dealt with more comprehensively.

Cement Types

Cements differ with respect to clinker compound

Table 1. *Classification of variables*

Materials	Chemical and physical properties of the system: Cement type (compound composition and fineness) Volume fraction of cement, Volume fraction of water } initial paste* porosity Volume fraction of air Volume fraction of aggregate Geometrical characteristics of the system: Volume of concrete body, Surface of concrete body } shape factor Initial state of the system: Temperature Vapour pressure
Curing	Boundary conditions: Heat insulation of concrete Moisture insulation of concrete External conditions: Initial temperature of surrounding medium Initial vapour pressure of surrounding medium Temperature changes as function of time Vapour pressure changes as function of time

*paste defined in accordance with T. C. Powers.

composition and fineness. It is rather well known how the hydration rate may be increased by selecting a optimal combination of these characteristics. Whether it may also be possible to obtain cement types especially suitable for thermal curing seems not sufficiently clarified; there are indications, that C_3A becomes unfavorable as temperature is raised (3), but this may result also indirectly from excessive temperature differentials due to the rapid hydration and heat development of the aluminate compounds.

The Volume Fraction of Cement

The cement content if of importance absolutely as well as in relation to the amount of water. A high cement content will generate more heat (and vice versa) and a high *w/c* ratio will in general accelerate hydration (4). The *w/c* ratio on the other hand will also change the mechanical properties of the paste, which may or may not enable the structure to withstand destructive forces.

The Volume Fraction of Water

The volume fraction of water shall initially and during hydration be sufficient to make continuous reaction with cement possible. The amount of free water will change due to chemical and physical adsorption during gel formation. The content of free water, its temperature, and the structure of the cement-water system determines the water vapour pressure in concrete, which in turn is responsible for a possible vapour transfer to or from environments. The increasing fineness of the structure connected with the gel formation will lead to lowering of the vapour pressure (self-desiccation).

The Temperature History

The temperature of a concrete member as function of time is determined by its geometrical and thermal properties and the heat development during hydration. Under certain assumptions the rate of temperature changes within a body placed at an environmental temperature different from its own can be calculated by means of the time constant defined as

$$\tau = \frac{V \cdot c_b \cdot R_b}{\Sigma k F}$$

when V = volume of concrete member
c_b = specific heat of concrete
R_b = density of concrete
$k \cdot F$ = coefficient of heat transmission multiplied by surface area

A method for a successive computation of the concrete temperature was developed by Nerenst, Rastrup and Idron (5):

$$N = N_b + \frac{C}{c_b \cdot R_b}(Q - Q_0) - \sum_0^t \frac{1}{\tau}(N - N_u)\Delta t$$

where N = concrete temperature
N_b = initial concrete temperature
N_u = temperature of surroundings
C = cement content
t = time
Q = heat development of cement $Q(t)$

The heat development must be known (as a table or a curve) $Q = Q(t)$ at constant temperature. By means of a time-temperature function it is possible to convert curing time at one (constant or varying) temperature into curing time at another (constant) temperature, see e.g. Rastrup in (6).

The Vapour Pressure History

The history of vapour pressure in concrete will depend on its water content in relation to its changing pore volume (coefficient of saturation). The pore volume comprises capillary capacity of paste, the possible porosity of aggregate and the content of air. As water is consumed by hydration and, simultaneously, the capillary capacity of paste is changing, a mathematical formulation of the vapour pressure history will be rather difficult to arrive at.

The problems of moisture transfer are in many ways analogous with heat transfer. It might, therfore, be possible to use an approach similar to that referred to above in connection with the temperature history, in order to calculate the vapour pressure history. Several important aspects of moisture transfer in connnection with the drying of concrete have been

treated by Pihlajavaara (7), (8). For the moisture loss by evaporation, for the moisture loss due to fixation of water by hydration and for the moisture gain due to carbonation expressions are derived, which might be used for calculation under certain conditions.

Protection against Destructive Processes

Whether a potentially destructive mechanism will actually damage the mechanical properties of the concrete will depend on the newly formed structures ability to accommodate the stress and strain produced by the mechanism in question. As paste structure is gaining in strength and rigidity, it seems possible to avoid or disminish the adverse consequences if the harmful processes can be delayed or postponed to a later stage of the hydration. At a certain degree of hardening damage is prevented because the mechanical properties have reached a sufficiently high level, i.e. the concrete has become immune against the destructive processes. This is also in agreement with the empirically established rules of maximum heating rates and necessary preheating periods (9), (10).

On the other hand it should be noticed that some properties of cement paste will develop in a direction, which will not make it easier for the solid structure to accommodate the influences which may be exerted. Flow or diffusion of water through the paste caused by vapour pressure differences may thus be met with increasing resistance as the permeability of cement paste decreases during hardening. The pressure gradient will become greater and the hydraulic pressure in paste may grow to a value, which leads to rupture.

The negative effects can, however, also be counteracted by external means, in the first place by using different form types. The form of the concrete member will always mean that concrete and curing medium is separated, i.e. a certain isolation against heat and moisture transfer is obtained. As most of the damaging processes are caused by temperature and vapour pressure differences the mould will provide some protection. In principle 4 different cases can be met with as shown in Table 2.

It shall be mentioned, that the application of a highly effective heat insulation has little sense as we are dealing with hardening of concrete at elevated temperatures.

Further, it will be possible to avoid harmful processes by using closed, rigid forms, which show no thermal expansion. By this means the water vapour exchange is excluded and the damage due to the too rapid and different dilations of the components under temperature rise in concrete can largely be avoided.

Table 2. *Influence of form type on heat and mass transfer*

		Heat	
		exchange	no exchange (adiabatic)
Moisture	no exchange	impermeable elastic covering	impermeable heat insulation
	exchange	no form	vapour permeable heat insulation

Combined Effect of Accelerating and Destructive Processes

It will appear from the above, that the temperature history of concrete is controlling both the rate of hydration and destructive processes; the vapour pressure within the concrete is decisive for another potentially destructive mechanism. The combined effect of accelerating and destructive processes may be illustrated by using a superposition principle introduced by Nerenst and Plum (11) in a discussion of the effect of freezing on green concrete:

The increase in hydration rate, which may be obtained at elevated (constant) curing temperatures, is illustrated in part (a) of Fig. 1. As the reactions are supposed to be the same in all cases, an identical degree of hardening will eventually give the same mechanical properties, if destructive processes are prevented.

In Fig. 1b is shown, how the hardening proceeds, if the temperature is increased from e.g. 20°C to 80°C after a preheating period of some hours. If the temperature is raised at rate of 20 deg/hour, it is assumed that the actual temperature history can be substituted by a stepwise temperature increase of 20 deg. every hour. We may now construct the resulting hardening curve by using parallel bits of the appropriate hardening curves valid for constant curing temperatures. We are still assuming the absence of harmful processes.

In practice such processes are often difficult to avoid. According to the foregoing discussion they may be avoided if curing takes place in impermeable, rigid forms. At the time of form removal, however, the energy stored in concrete, because expansion was suppressed, will be released, and damage may occur, if the strength is not sufficient to prevent it. This is depicted in Fig. 1c, where the different curves show, that different reductions in mechanical strength must

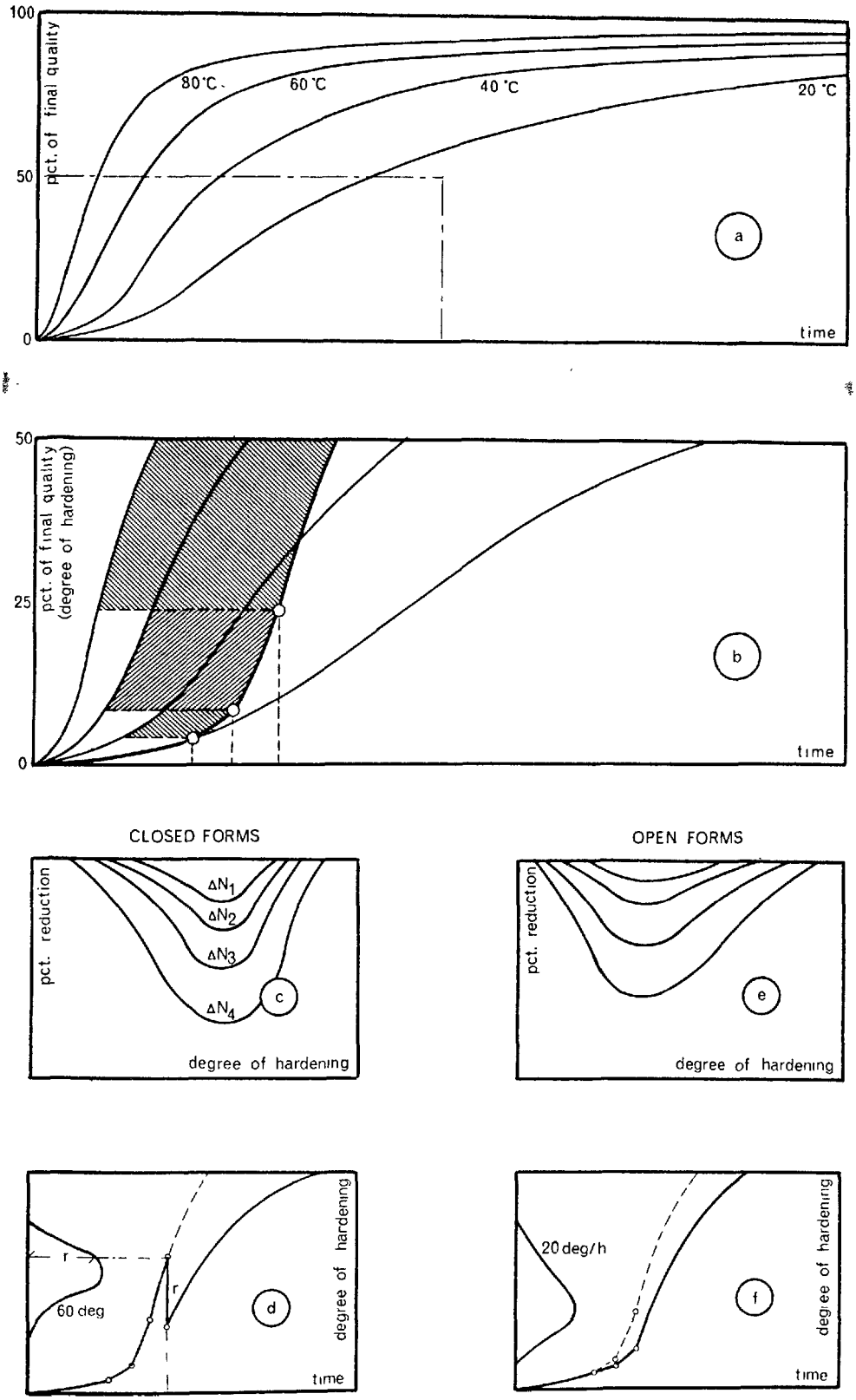

Fig. 1. *Combined effect of accelerating and destructive processes*

be expected in dependence of the total temperature increase (ΔN) during the heat treatment. The reduction will further be a function of the degree of hardening obtained at the moment of form removal. The point at which the reduction becomes zero, indicates, the degree of hardening, at which the concrete has obtained immunity to destructive processes. In a rather formal way Fig. 1c may be used to predict the final part of the hardening curve after moulds have been removed: The curve corresponding to the actual temperature increase (ΔN) from Fig. 1c is placed along the abscissa in Fig. 1d. At the time for form removal the reduction r is to be expected. The hardening curve is then lowered a corresponding amount and may after this procese after the appropriate curve from Fig. 1a.

Concrete moulds will normally be open or partly open. In this case the amount of destruction will depend on the rate of temperature increase. In Fig. 1e is shown how the quality reduction will depend on the heating rate and be a function of the degree of hardening attained, when heating starts. The construction of a resulting hardening curve is in this case more complicated, as the quality will be reduced continuously during the whole period of temperature raise. An example is shown in Fig. 1f.

Conclusion

The inconsistency of the great amount of information, which is available on high temperature curing of concrete, might in the authors opinion be overcome, if the many parameters are dealt with according to the physico-chemical nature of their influence. It might even be possible to handle the problem mathematically, if the development of certain properties can be established at different temperatures (isotherms) and if it can be proved, that these properties are identical, when destructive processes are prevented, e.g. by hardening in impermeable, rigid moulds. It is further a necessity, that temperature functions are formulated for the range $20°C \sim 100°C$, and to clarify the effect of harmful mechanisms.

The increasing use of prefabricated concrete elements makes it important, that research within this field is carried out with a similar intensity as earlier in the field of concreting at low temperatures.

References

1. Y. M. Butt, V. M. Kolbasov and V. V. Timashev: "High temperature curing of concretem under atmosperhic pressure". V-ISCC, Principal Paper, Session III-4-b (preprint). Tokyo, (1968).
2. The Chemistry of Cement, Vol. I (Academic Press, London and New York, 1964), edited by G. F. W. Taylor. See chapter 11 by H. F. W. Taylor: "Steam curing of portland cement products".
3. P. Freiesleben Hansen, J. Jessing, K. Mønsted and E. Trudsø: "Physical and chemical properties of cement mortar cured at elevated temperatures". V-ISCC, Supplementary Paper, Session III-4-b. Tokyo 1968.
4. L. E. Copeland, D. L. Kantro and G. Verbeck: "Chemistry of hydration of portland cement", Chemistry of Cement, Vol. I, p. 429–465, U. S. Department of Commerce, National Bureau of Standards, Washington, 1962.
5. P. Nerenst, E. Rastrup and G. M. Idorn: "Betonstøbning om vinteren". SBI Anvisning 17, 108. p. Teknisk Forslag. Copenhagen (1953).
6. E. Rastrup: "Heat of hydration in concrete". Mag. of Concr. Res., vol. 6, No. 17, p. 79–92. London (1954).
7. S. E. Pihlajavaara: "On the main features and methods of investigation of drying and related phenomena in concrete". VTT publication 100. 142 p. Helsinki (1965).
8. S. E. Pihlajavaara and M. Väisänen: "Numerical solution of diffusion equation with diffusivity concentration dependent". VTT Report, Series III—Building 87. 22 p. Helsinki (1965).
9. A. C. A. Saul: "Principles underlying the steam curing of concrete at atmospheric pressure". Mag. of Concr. Res., vol. 2, no. 6, p. 127–140. London 1951).
10. J. Riha: "Smernice pre Urychlovanie Tvrdnutia Betónvých Stavebných Diekov Rychloohrevom do 100°C" CS VTS, 30 p. Zilina 1965.
11. P. Nerenst and N. M. Plum: "Freezing and thawing tests on green concrete". Session BI, Proc. RILEM Symposium Winter Concreting. Danish National Institute of Building Research. Special Report. Copenhagen (1956).

Authors' Closure

Yuri M. Butt, V. M. Kolbasov and V. V. Timashev

I consider the material of this written discussion to be a very important and interesting addition to our investigations as it is closely connected with problems of our paper. I have no other remarks.

Supplementary Paper III-65 Influence of Cement Characteristics on Mix Proportion for Steam Cured Prestressed Concrete

R. K. Lewis and Frank A. Blakey*

Synopsis

In the production of prestressed concrete it is required in Australia that a minimum strength of 4000 lb/sq.in. on cylinders be obtained before transfer of prestress is permitted. Where steam curing is used the concrete is proportioned to give this strength at the end of the steam-curing cycle. For a given steam treatment variations in the cement characteristics result in a wide range of cement factors necessary to achieve this strength.

This report relates the cement factor required to satisfy the above strength requirement to the phase composition of the cement used.

An empirical relation is also obtained between the cement properties and the rate of development of strength under fog curing for up to 91 days, and the gain in strength of steam-cured concrete with subsequent fog curing to 28 days.

Introduction

Previous papers (1, 2, 3) have reported the results of a study of the optimum steam-curing conditions for high strength concrete. In the latter paper (3) the influence of cement characteristics was reported. To obtain a predetermined compressive strength after a particular steam-curing cycle it was found necessary to adjust the mix proportions to suit the cement used. It was also found that the 28-day compressive strength of concrete cured with steam, then with fog ranged from 98 to 124 per cent of the strength of concrete continuously fog cured.

An estimate of the cement factor necessary to meet the specification requirements was obtained from the standard 7-day tests for cement strength. A more accurate relationship was desired and to this end an analysis was made of the rates of strength development in relation to the chemical properties of the cement.

Mix Proportions of Concrete

Table 1. *Chemical and phase composition of the cements tested* (%)

	Chemical composition										Phase composition			
Cement No.	SiO_2	Al_2O_3	Fe_2O_3	CaO	MgO	SO_3	Na_2O	K_2O	Loss on ignition	Total alkalies	C_4AF	C_3A	C_2S	C_3S
1	19.9	6.8	3.4	65.5	0.7	2.0	0.03	0.26	1.5	0.2	10	12	12	59
2	20.5	6.2	4.2	64.5	0.7	2.1	0.02	0.20	1.5	0.15	13	9	19	53
3	22.7	5.0	5.2	63.2	0.6	1.7	0.02	0.17	1.3	0.13	16	4	36	39
4	20.8	4.5	4.3	62.9	2.0	2.8	0.52	0.57	2.2	—	13	5	14	48
5	21.7	4.1	3.7	64.4	1.95	2.33	—	—	0.88	—	11.2	4.4	18.6	58
6	23.0	3.6	4.3	64.4	0.85	2.35	0.15	0.53	0.81	—	13.1	2.2	27.7	50.6

Tables 1 and 2 show the chemical and physical properties of the cements tested. These represent cements from four Australian States.

The target compressive strength at the end of the steam treatment chosen was the minimum transfer strength of 4000 lb/sq.in. on cylinders, (5000 lb/sq.in. on 4-in. cubes), as required by the Code of Prestressed

*Division of Building Research, C. S. I. R. O., Highett, Victoria, Australia.

Concrete CA 35 (Standards Association of Australia 1963). The slump of these mixes was maintained at around 2 in. The steam cycle chosen had a delay period of 4 hr from mixing, a 10 degC/hr temperature-time gradient, and an isothermal (constant temperature) period of 6 hr at 80°C.

Table 3 sets out the compositions of the mixes that satisfy the above requirements. The cement factor ranged from 575 to 842 lb/cu.yd. The former value was that obtained for a "high early strength" cement and the latter for a "low heat cement".

The specimens were compacted for 10 sec on a table vibrator having a frequency of 3000 cycles/min.

It is usually considered desirable to reduce the sand content as the cement content is increased. Fig. 1 shows the relationship between the absolute volumes of the cement and sand used in this work, where a unit increase in the absolute volume of cement was balanced by a unit reduction of the sand content.

Table 3 also shows the grading of the sand and basalt aggregate used, and the compresseve strength of the concrete at the end of the steam treatment.

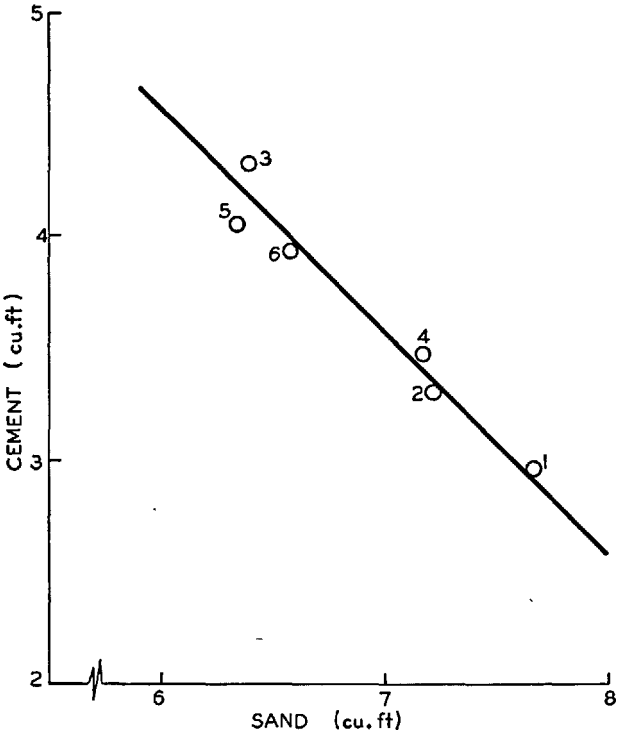

Fig. 1. *Relationship between the absolute volumes of cement and sand*

Table 2. *Physical properties of the cement tested*

Cement No.	Specific surface area (sq. cm/g)		Normal consistency of paste (%)	Setting time (min)		Standard mortar compressive strength (lb/sq. in.)			
	As supplied by association†	As measured by authors		Initial	Final	1 day	3 day	7 day	28 day
1	3300	3820	25.5	105	165	—	6550	8900	10450
2	3500	3560	24.5	90	150	—	6100	8000	9700
3	3650	3700	23.5	90	165	—	4350	5800	8550
4	3650	3510	25.2	150	210	3940*	6580*	7300*	8660*
5	3080	3100	—	120	225	—	5250	6600	8500
6	2990	3000	—	175	225	—	6250	7700	9200

*As tested by authors †Cement and Concrete Association of Australia

Table 3. *Composition of concrete mixes and compressive strength after steam treatment*

Cement No.	Mix proportions to make 1 cu. yd of concrete (dry weight, lb)			Water/cement ratio, W, by weight	Compressive strength (lb/sq. in.)	Grading of aggregate		
	Cement	Sand	5/8-in. Stone		After steam treatment*	B.S.S. Sieve No.	% Passing, by weight	
							Sand	Stone
1	575	1265	2030	0.542	5160	3/4 in.	—	100
2	646	1190	2000	0.486	5150	3/8 in.	—	0
3	842	1051	2020	0.37	5220	4	—	—
4	676	1182	2005	0.49	4820	7	100	—
5	791	1043	1990	0.45	4960	14	93.4	—
6	766	1084	1985	0.425	5200	25	59.6	—
						52	23.2	—
						100	4.5	—

*Average of two replicates

Fig. 2 shows the development of compressive strength with fog curing up to 91 days for three of the cements tested. These results are tabulated in the previous report (3). With up to 7days of fog curing there was little difference between the compressive strengths obtained from each cement, but with longer periods wide variations occurred. Inspection of the plotted results suggested that they could be represented by two straight lines on a log-linear plot, except for cement No. 5 for which the graph was one straight line to 91 days. The two cements high in C_2S (No. 3, 6) have a second gradient steeper than the initial gradient. That is, they gained strength faster than if the initial gradient had continued, but because the function is a log-linear one, the absolute gain in strength in a given time interval is lower than that obtained during the early period.

The prediction of the strength at any age is dependent on the knowledge of these gradients, the age at which one gradient is replaced by the other, and the strength at particular age. In Table 4 the actual values of the parameters of the concrete strengths are set out for each of the six cements tested.

Abrams (4) made predictions of the 28-day compressive strength based on the ratio $K/7^w$, where w was the water/cement ratio by apparent volume. Taylor (5) suggests that nowadays the relationship is closer to $K/5^w$. The terminology of apparent-volume is not completely satisfactory and it is more appropriate to think of the exponent as 1.5 W, where W is the water/cement ratio by weight.

From trial mixes, and also from those reported in this paper, the value of K was found to vary from 21,200 to 30,600 lb/sq.in. depending on the cement used, strength being determined from 4-in. cubes. The variation for any one cement was of the order of ± 1000. A correlation between the value of K and the chemical composition of the cement was sought, but there appeared to be no unique relationship. This could be expected from the strength-age relationships,

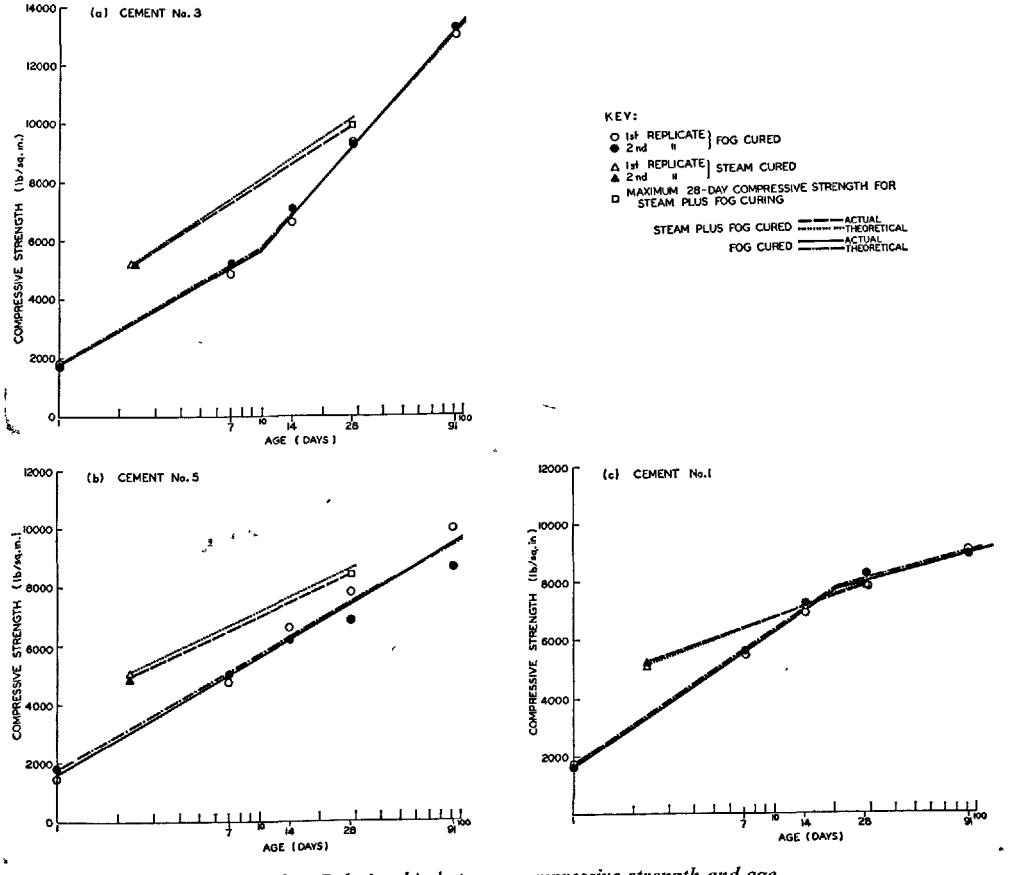

Fig. 2. *Relationship between compressive strength and age*

in that the 28-day strength lies sometimes along the initial gradient portion and sometimes along the second gradient portion.

Table 4. *Values of parameters in concrete strength relations*

Cement No.	$5^{1.5W}$	Compressive strength (lb/sq. in.) A (1 day)	Compressive strength (lb/sq. in.) B (91 day)	K_1 (lb/sq. in.)	$\sqrt{\frac{S}{3500}}$	SO_3/C_3A	Gradient constants L (Initial)	Gradient constants M (Second)	Gradient constants F (Steam & Fog)
1	3.71	1670	9000	6200	1.044	0.167	4660	1850	2530
2	3.24	1800	9730	5820	1.009	0.234	4380	3200	2850
3	2.44	1770	13180	4320	1.028	0.425	3900	7800	4400
4	3.27	1510	8460	4940	1.0	0.560	4300	2900	2960
5	2.96	1650	9450	4880	0.941	0.530	4000	4000	3200
6	2.79	1770	10140	4940	0.926	1.07	4130	4730	4050

Compressive Strength at 1 Day

It was therefore assumed that the above form of relationship between strength and water/cement ratio should be related to a time prior to the change of gradient, and the strength at 1 day was chosen. Values of K_1 were obtained from the expression $K_1 = A5^{1.5W}$, where A is the compressive strength at 1 day, and these values were systematically compared to the other characteristic parameters. The best correlation was established between K_1 and the initial gradient constant, the straight line obtained (Fig. 3) having the form:

$$K_1 = 2.25L - 4300 \qquad [1]$$

where L is the initial gradient constant.

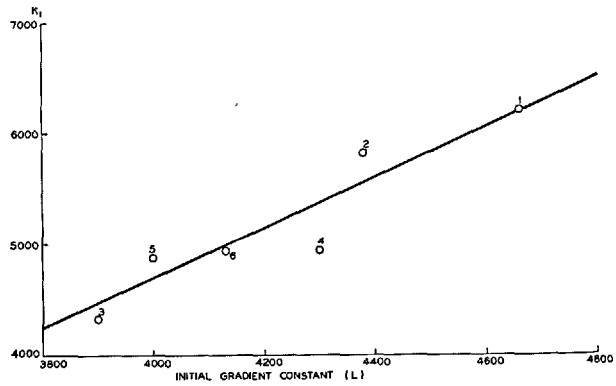

Fig. 3. *Relationship between* K_1 *and initial gradient constant*

Further investigation was then done to relate this gradient to the phase composition.

Lerch (6) studied the influence of additions of SO_3 to mortar mixes made from a wide range of cement types in order to establish optimum SO_3 contents. The optimum amount depended not only on the amount of C_3A present, but also on the alkali content of the cements. As the SO_3 content was increased up to the optimum, the compressive strength at 1 day and subsequent ages increased.

The SO_3 contents in the cements used in this work were close to optimum values. The results obtained must be considered with this in mind. Deviations in SO_3 content from those given in this report may vary Equation [1]. In normal cement manufacture it is unlikely that large deviations would in fact occur and therefore the formula should generally hold for the grade of concrete made in this work.

Another fact arising from the work of Lerch is that the ratio of the optimum SO_3 content to the C_3A content varies in his work from 0.21 for a C_3A content of 14.3 per cent, to 0.79 for a C_3A content of 2.4 per cent. That is, as the C_3A content decreases, the optimum SO_3 content decreases at a slower rate.

Initial Gradient Constant

The initial gradient constant was believed to be related to the proportions of C_3S, C_3A, C_2S, and to the specific surface area of the cement. By successive variations in the constants appropriate to each

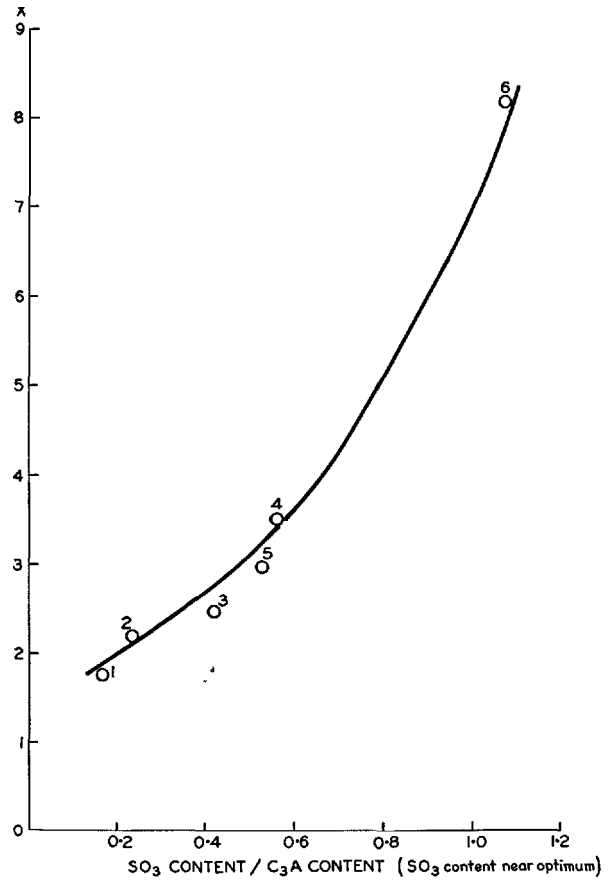

Fig. 4. *Relationship between* X *and* SO_3/C_3A *ratio*

phase component, the following was obtained.

Initial gradient constant =

$$L = 50(C_3S + (X)C_3A + 0.75C_2S)\sqrt{\frac{S}{3500}} \quad [2]$$

where (X) is a function, (see Fig. 4), of the ratio of SO_3 to C_3A, (for optimum or near-optimum values of SO_3 content), and S is the specific surface area, measured by Rigden air-permeability apparatus.

The formula is a 'rate' expression and as such the coefficients of the components do not mean that only a portion of the constituent is acting, but rather that the activity of the various constituents differs. Thus the most active phase is the C_3A (since (X) is greater than 1), followed by the C_3S and then the C_2S.

Second Gradient Constant

A direct relationship between the second gradient constant and the chemical phase composition was not immediately found. When the ratios of the second/initial gradients were compared with the cement composition, however, a linear relationship was established, as shown in Fig. 5.

$$\text{Gradient ratio, } M/L, = 6R - 2.36 \quad [3]$$

where

$$R = \frac{50(C_2S + 0.5C_3S)\sqrt{\frac{S}{3500}}}{L}$$

Expanding the above expression, and substituting for L from Equation [2] we obtain:

Second gradient constant =

$$M = 300\frac{S}{3500}(C_2S + 0.5C_3S) - 2.36\left\{50\sqrt{\frac{S}{3500}}(C_3S + (X)C_3A + 0.75C_2S)\right\}$$

$$= 50(0.64C_3S + 4.23C_2S - 2.36(X)C_3A)\sqrt{\frac{S}{3500}} \quad [4]$$

Thus for the second stage of the strength development the activity of the C_2S is seven times as large of the C_3S, whilst the influence of C_3A is negative.

Although the initial and second gradient constants, and the 1-day compressive strength may be calculated from Equations [1], [2] and [4], it is impossible to predict the strength development completely since the time at which the former gradient gives way to the latter is still unknown. Various attempts to relate the change-over point directly to the phase composition failed. Another approach was to relate the ratio of the 91-day and 1-day compressive strengths to the phase composition.

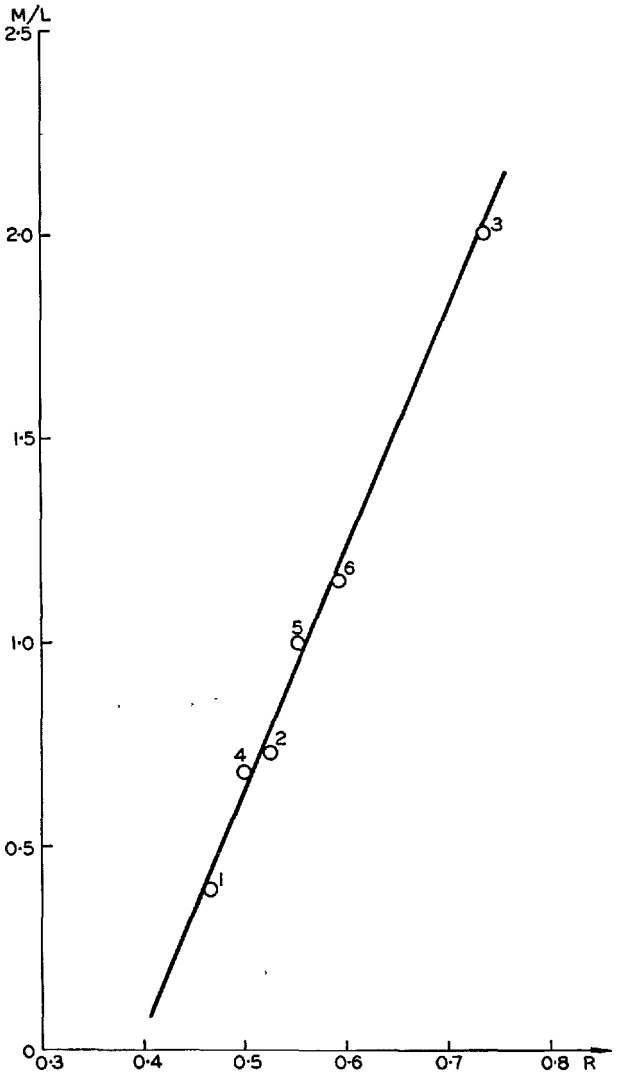

Fig. 5. *Relationship between* M/L *and* R

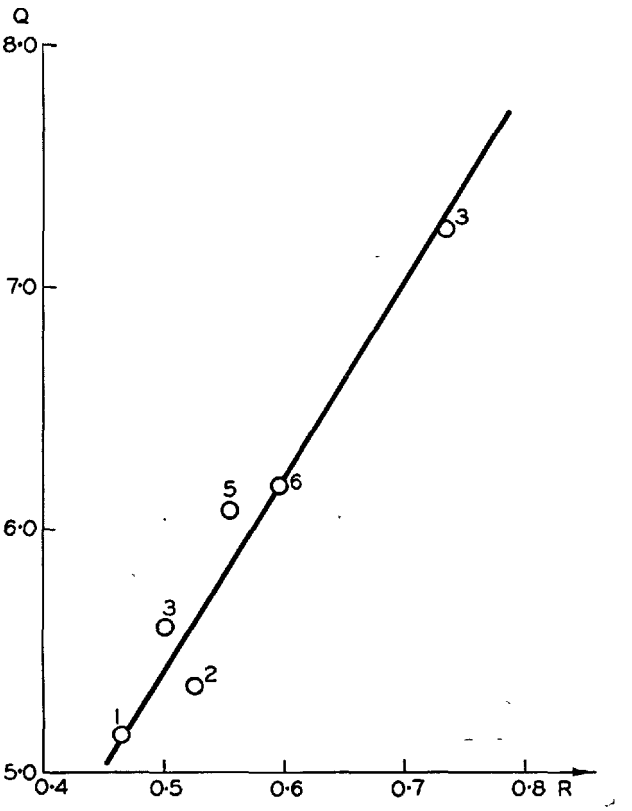

Fig. 6. *Relationship between* Q *and* R

Compressive Strength at 91 Days

To obtain a relationship it was necessary to first divide the ratio of 91-day to 1-day compressive strength, B/A, by the term $\sqrt{S/3500}$. The result is designated by Q. It was found (Fig. 6) that Q is related to R by the expression:

$$Q = 8.2R + 1.3 \qquad [5]$$

where R is as defined above. Thus, substituting for Q, the 91-day compressive strength, B, was found to be:

$$B = A(8.2R + 1.3)\sqrt{\frac{S}{3500}} \qquad [6]$$

where A is the compressive strength at 1 day.

Prediction of Cement Factor

Fig. 7 shows the relationship between the cement factor and the initial gradient constant. The higher the initial gradient, the lower the cement factor necessary to achieve the grade of concrete specified in the

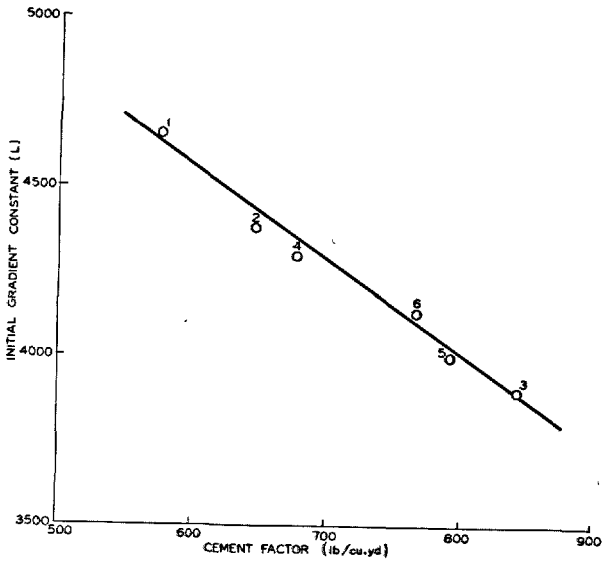

Fig. 7. *Relationship between initial gradient constant and cement factor*

work. The equation of the straight line relationship is:

$$\text{Cement Factor} = 2230 - 0.357L \qquad [7]$$

Prediction of Water/Cement Ratio

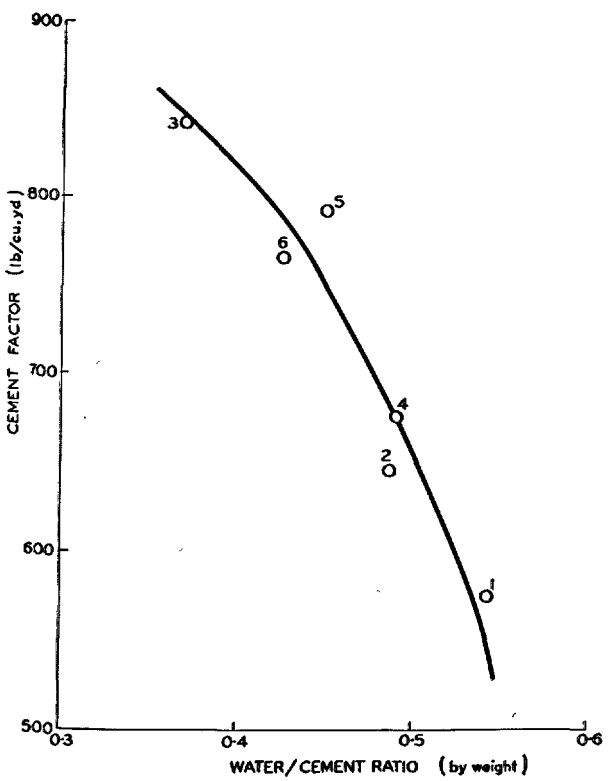

Fig. 8. *Relationship between cement factor and water/cement ratio*

From Table 3 it can be seen that as the cement factor increases the water/cement ratio required (under the circumstances of decreasing sand content) is decreased. This relationship is shown in Fig. 8. For mixes having a cement factor of 800–900 lb/cu.yd, a decrease of 100 lb/cu.yd in cement resulted in an increase of about 0.1 in the water/cement ratio, whereas for the leaner concretes (600 lb/cu.yd cement factor) a similar decrease necessitated an increase of only 0.05 in the water/cement ratio.

From the information on the chemical composition of the cement it is possible, using the above expressions, to calculate the cement factor and water/cement ratio necessary to produce a concrete having the properties specified for this work.

Compressive Strength of Steam-Plus-Fog-Cured Concrete

As mentioned earlier in the report, the 28-day compressive strength of steam-plus-fog-cured con-

crete ranged (depending on the cement) from 98 to 124 per cent of the strength of concrete continuously fog-cured for 28 days.

The steam-cured concrete had a steam maturity of about 1200 deg Chr (based on 0°C) which is equivalent to about 2.3 days at 21°C. If the compressive strength following steam curing is plotted on Fig. 2 at this age, then the rate of development of strength during the subsequent fog-curing to 28 days is, for cements No. 1, 2 and 4 approximately the same as the secondary rate development of the continuously fog-cured specimens. For those cements high in C_2S (No. 3 and 6) the rate of development during the fog curing is lower than the secondary rate of development of continuously-fog-cured specimens, but higher than the initial rate. The gradient constant for the steam plus fog curing condition has been designated by F.

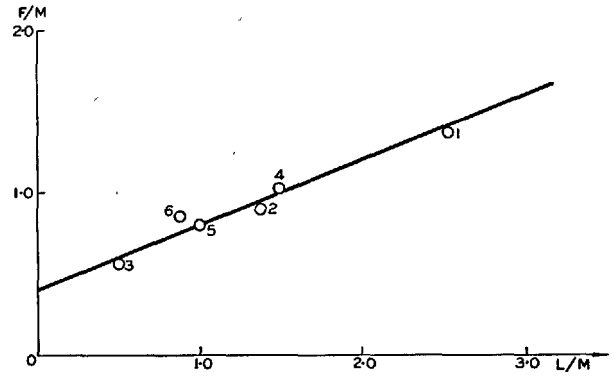

Fig. 9. *Relationship between F/M and L/M*

Fig. 9 shows the relationship between F/M and L/M, from which Equation [8] has been obtained.

$$F = 0.4(L + M) \qquad [8]$$

Accuracy of Strength Prediction

Table 5 sets out the various physical constants of the mixes used in this work, calculated from the above equations. Comparison with the actual values used shows that the prediction of the concrete properties is very good. The cement factor was predicted to within ±5 per cent, the 1-day compressive strength to within +11.2, −6.1 per cent, and the 91-day compressive strength to within +7.1, −4.8 per cent.

The greatest difference between the theoretical and the actual strength values occurred in the case of cement No. 4. In Table 3 it will be noted that the compressive strength after the steam curing is 280 lb/sq.in. below the average value of 5100 lb/sq.in, taken in this work. Thus if in this case the original mix proportion had been adjusted to obtain the higher "ex-steam" compressive strength, then the difference between the theoretical and actual strength development would have been less.

Table 5. *Calculated values of properties of concrete*

Cement No.	Gardient constants L		Gardient constants M		Gardient constants F		K_1 (lb/sq. in.)		Compressive strength (Fog cured) (lb/sq. in.) 1 day		Compressive strength (Fog cured) (lb/sq. in.) 91 day		Cement factor (lb/cu. yd)	
	Theo-retical	Error %	Theo-retical	Error %	Theo-retical	Error %	Theo-retical	Error %	Theo-retical	Error %	Theor-retical	Error %	Theo-retical	Error %
1	4710	+1.1	1890	+2.2	2640	+4.3	6300	+1.6	1700	+1.8	9020	+0.1	550	−4.3
2	4340	−0.9	3560	+11.2	3160	+10.9	5470	−6.0	1690	−6.1	9610	−1.2	680	+5.3
3	3960	+1.5	7750	−0.64	4680	+6.4	4610	+6.7	1770	0	13100	−0.6	818	−2.9
4	4270	−0.7	2820	−2.8	2840	−2.0	5320	+7.7	1680	+11.2	9140	+7.1	705	+4.3
5	4040	+1.0	3880	−3.0	3170	−0.95	4790	−1.8	1720	+4.2	9460	0	790	0
6	4110	−0.5	5010	+5.9	3650	−11.0	4950	+0.05	1690	−4.6	9650	−4.8	760	−0.8

Limitations of Empirical Formula

The expressions obtained in this work apply only to concrete mixes having the same type of ingredients. Variations in the grading of the sand aggregate, the maximum particle size of the stone, the strength level after steam curing and the workability desired will all affect the relationship.

Although the six cements tested cover a wide range of chemical and physical properties, they all have one

aspect in common and it is that the change-over point, from the initial to the second gradient, occurs at ages later than one day. If a cement is so chemically constructed to produce a rapid early strength growth in the first 24 hours, followed by a lower rate of strength growth thereafter, then it is anticipated that such a cement would not follow the pattern of results outlined in this report.

Conclusions

Although the expressions are purely empirical, it is believed that they may provide the basis for some theoretical explanations at a later date.

It is possible to predict with reasonable accuracy the strength-age relationship of fog-cured concrete, proportioned to give a compressive strength of 5100 lb/sq.in. after a steam cycle giving a maturity of about 1200 degChr. Prediction can also be made of the development of strength of steam-cured concrete with subsequent fog curing to 28 days.

The cement factor necessary to produce the above strength can be predicted from the chemical characteristics.

The important characteristics of the cement, from the point of view of the above predictions, are the proportions of C_3S, C_3A, C_2S, the specific surface area and the SO_3/C_3A ratio.

References

1. R. K. Lewis, "Steam curing of lightweight concrete. The effect of delay prior to steaming and of temperature-time gradient", Const. Review, **36**, No. 2, 20–25 (1963).
2. R. K. Lewis, "The effect of maximum temperature and maturity on the steam curing of lightweight concrete", Const. Review, **37**, No. 4, 23–29 (1964).
3. R. K. Lewis, "A summary of investigations of steam curing of concrete related to cement characteristics", Const. Review, (In press).
4. D. A. Abrams, "Design of concrete mixtures", Structural Materials Research Laboratory, Lewis Institute, Chicago, Bulletin No. 1, Dec. 1918.
5. W. H. Taylor, Concrete Technology and Practice, 2nd ed., p. 30 (Angus and Robertson Ltd., Sydney, Australia, 1965).
6. W. Lerch, "The influence of gypsum on the hydration and properties of portland cement pastes", A.S.T.M. Proc. **46**, 1252–1292 (1946).

Supplementary Paper III-91 Heat of Hydration of Portland Cement during Steam Curing under Atmospheric Pressure

Hideo Teramoto and Naoya Kawada*

Synopsis

The hydration processes of cement during steam curing are so complicated that it has not been made clear as yet. As a clue for solving the problem, the authors tried to measure the rate of heat liberation of cement paste taking place during steam curing.

The calorimeter used for this purpose consisting of a pair of conduction calorimeters; one for sample and other for dummy. As both calorimeters are equal in heat capacity, effects on change of curing temperature can be canceled and only the heat of hydration of cement paste during steam curing can be measured.

Using the calorimeter, the influence of various curing cycles on the rate of heat liberation of cement was investigated. The relation between peaks of heat liberation and strength, and the mechanisms of hydration at every peak were studied.

Introduction

As the steam curing of concrete is one of the methods effective for hardening acceleration, for obtaining the high strength at early ages, for reducing drying shrinkage and so on, it has become popularly employed in the manufacture of precast concrete. The properties of steam cured concrete are affected by many factors, e.g. time of presteaming, rate of heating, etc. At present, the conditions of steam curing process are determined only by experience alone. While physical properties of steam-cured concrete have been described in detail by many authors, hydration process of cement during steam curing has not been made clear as yet. In order to find suitable steam curing conditions for manufacturing concrete products of excellent quality, it is necessary to clarify the hydration process of cement taking place during steam curing.

The conduction calorimeter is a very useful apparatus for studying hydration process at room temperature, but it cannot be used during steam curing because it is so designed as to determine the heat of hydration at a constant temperature. In order to measure the rate of heat liberation of cement during steam curing, two twin-type calorimeters were designed and tested.

The heat liberation curves were obtained by the calorimeters and the characteristics of reactions occurring at every step of steam curing were investigated.

Calorimeter

The conduction calorimeter developed by Lerch (1) has such a structure as is shown in Fig. 1 and it is useful for studying the kinetics of hydration of cement at early ages.

A sample container made of copper was packed with fresh cement paste, placed on a conduction tube and it was then covered with a Dewar's vessel. The heat of hydration evolving in the sample container flows down through the conduction tube and is released subsequently into the water which is kept at a constant temperature by means of thermo bath. At the top side (A) and the bottom side (B) of the conduction tube, thermodetectors were placed and the difference of temperatures between A and B, which is in proportion to the rate of heat evolution of cement, was determined.

When the curing temperature rises during steam

*Research Laboratory, Nihon Cement Co., Ltd., Tokyo, Japan.

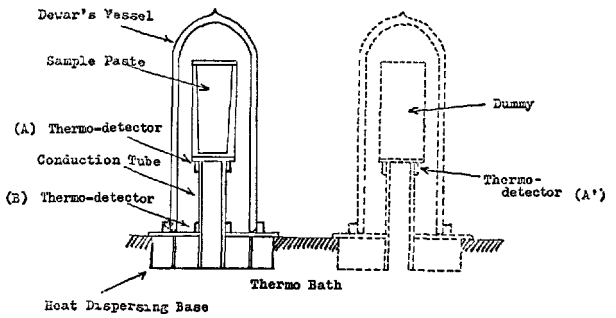

Fig. 1. *Schematic structure of conduction calorimeter and twin-type conduction calorimeter*

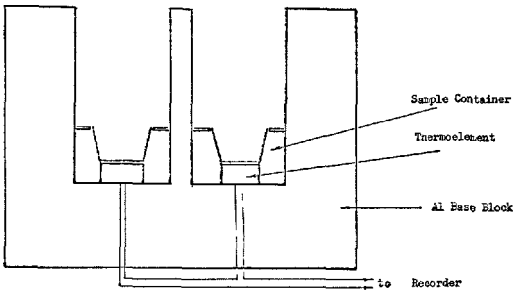

Fig. 2. *Microcalorimeter*

curing, which is the rise of the temperature of water in the thermo bath, heat flows from B to A. Hence, it gives us false information as if endothermic reaction is occurring in the cement paste during the heating period.

In order to remove the structural defect of the conduction calorimeter, an additional conduction calorimeter having the same thermal properties was set in parallel. The container was packed with inactive substance which was equal to the sample in heat capacity, and this was used as a dummy. By detecting the diference of temperature between A and A', the rate of heat liberation of the cement can be obtained without being disturbed by the temperature change. Twin-type calorimeters such as Calvet's calorimeter, the conduction calorimeter designed by Danielsson (2) and the microcalorimeter designed by the Oyo-Denki Lab. (3) are reported. The authors, however, designed two kinds of twin-type calorimeters as follows:

(1) The Oyo-Denki Lab.'s microcalorimeter of special design

The Oyo-Denki Lab.'s microcalorimeter consists of (1) an Al base block about 28 kg in weight similar to the block of DTA apparatus, (2) an insulator to keep the block at uniform temperature and (3) covers with mixing parts. The authors' microcalorimeter consists of only an Al block as shown in Fig. 2. Sample containers are ϕ 54 $\times$ 35 mm in size and are made of copper. The one for a dummy was filled with about 27 g of fly ash paste and the other was filled with about 25 g of cement paste. Each containers were placed on each thermoelement in the Al block. The calorimeter was set in a steam curing bath. As measurement was disturbed by water drops falling on the containers, which condensed on the ceiling of the steam curing bath, covers were placed over the openings of the Al block to shut out water drops.

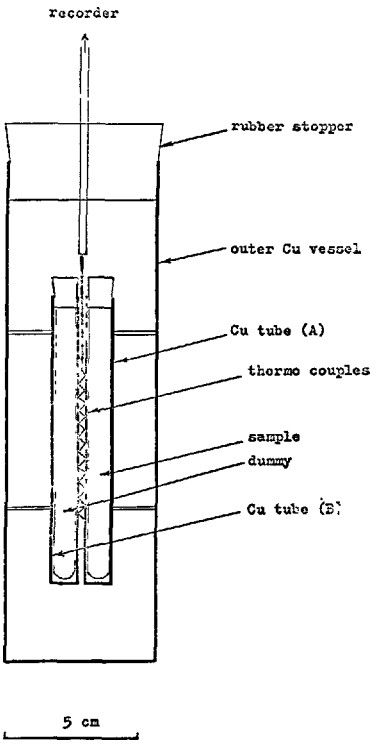

Fig. 3. *Structure of twin-type calorimeter*

This calorimeter, however, has one weak point. Water condenses on the sample container and thermoelement during cooling period of steam curing and disturbs the measurements of the heat liberation.

(2) Twin-type calorimeter devised by the authors

Another twin-type calorimeter as shown in Fig. 3 was designed and tested.

A glass test tube was filled with cement paste, sealed with a rubber stopper and placed in a Cu tube (A). Another glass test tube was filled with

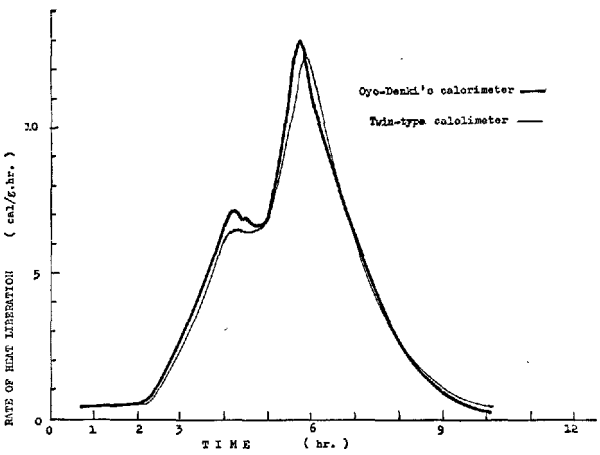

Fig. 4. *Comparison between the two calorimeters*

an inert substance used as a dummy, which had almost the same heat capacity as the cement paste, and was placed in a Cu tube (B). At the space between the Cu tubes (A) and (B), 10 thermocouples arranged in series were installed and were connected with a recorder. The Cu tubes were set in an outer large Cu vessel. The relation between electromotive force of the thermocouples and the rate of heat liberation was determined by standardized electric heater and it showed linear relation up to about 500 cal/hr., but lost its linearity when over 500 cal/hr. This is probably due to the temperature difference between the tube B and the outer vessel, which is caused by the accumulation of heat in tube B, into which much more heat flows from the tube A than that which flows from the tube B to the outer vessel when the heat generation in the tube A is high.

At the period in which curing temperature rises at high rate, e.g. at the rate of 40°C/hr, the temperature difference between the outer and the inner Cu vessel reaches as much as 2°C. If the diameter of outer vessel can be decreased, the temperature difference between the outer and the inner vessels being reduced, the relation between the electromotive force of the thermocouples and the rate of heat liberation can be improved.

(3) Comparison between both calorimeters

Curves of the rate of heat liberation shown in Fig. 4, were obtained by each calorimeters using the same program of steam curing. The results obtained were almost the same. According to the test results, whether the air surrounding the cement paste is saturated with water vapour or not seems to be of little importance to the rate of hydration of cement.

Measurement of Volume Changes of Cement Pastes during Steam Curing

Much has been reported on the volume change of cement paste at early ages during constant temperature curing, but there are only a few reports on that occurring during steam curing.

The volume of cement paste decreases by early hardening process, which is called "intrinsic shrinkage" or "autogenous shrinkage". But, the volume increases with the rise of curing temperature. As both shrinkage and expansion take place during steam curing, complicated volume changes were noted.

Homma's method (4), which is available for determining volume changes of cement paste at constant temperature, was applied to obtain the informations on the volume changes taking place during steam curing. Fresh cement paste was filled in a thin rubber container having a capacity of about 20–30 ml, taking cares not to bring air bubbles into the container, and this was sealed tightly with a bakelite stopper having a curved surface so as to prevent occurrence of void between the stopper and cement paste, as shown in Fig. 5. The sample thus prepared was suspended in water kept at a given temperature and was connected with a chemical balance, and its weight in water was measured. When the sample paste shrinks, its weight in water increases. The contracted volume of cement paste can be obtained by multiplying density of water at a given temperature by the increased weight of sample in water. During steam curing, the surface of water in the thermo bath was

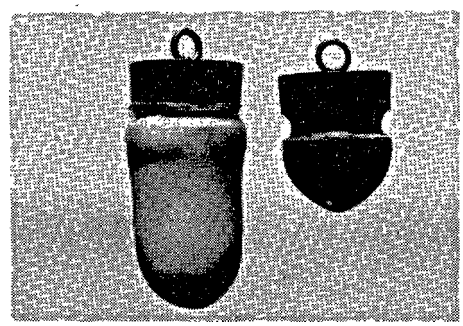

Fig. 5. *Rubber container and bakelite stopper for measuring volume change*

Fig. 6. *Apparatus for measuring the rate of heat liberation and the volume change*

covered with liquid paraffin so as to keep it at constant level. Water which had been boiled to expel dissolved air was filled in the thermo bath, so as to prevent the clinging of air bubbles on the sample by heating and causing thereby a decrease of weight of the sample in water. By an automatic recording thermal balance reconstructed for this purpose, changes of weight in water were determind. The apparatus is shown in Fig. 6.

Effects of SO_3 Contents in Cement on the Heat Liberation Curves during Steam Curing

By mixing gypsum with normal portland cement clinker, cements having various SO_3 contents (1.8, 2.3, 2.8 and 3.3%) were prepared. The fineness of the cements was about 3600 cm^2/g by the Blaine method. After the cement paste with W/C = 0.4 was cured at 25°C for 5 hours, it was heated at the rate of 20°C/hr up to 75°C and cured at this temperature thereafter.

The results are shown in Fig. 7.

The heat liberation curve of the sample cured at 20°C is also shown for reference. As the cements of four kinds gave nearly the same heat liberation curves at 20°C, the curve representing them is that of the cement with 1.8% SO_3 content.

Just after beginning of heating, the rates of heat liberation curve showed lower values than the one cured at 20°C, but a little later it increased rapidly in every case of cements.

Eleven hours after mixing, the rate of heat liberation of cement paste cured at 20°C reached the highest peak and this figure was 2.2 cal/g.hr. During steam curing, the peaks of heat liberation curve appeared at the hours 8 to 9 after mixing, and their heights were about 12 or 13 cal/g.hr., which were 5 to 6 times higher than that of sample cured at 20°C.

After passing the peaks, the rate of heat liberation of steam cured sample decreased rapidly and fell below 0.5 cal/g.hr. at 15 hours.

Sample paste prepared from cement with 1.8% SO_3 showed two peaks of heat liberation at 7 and 9.5

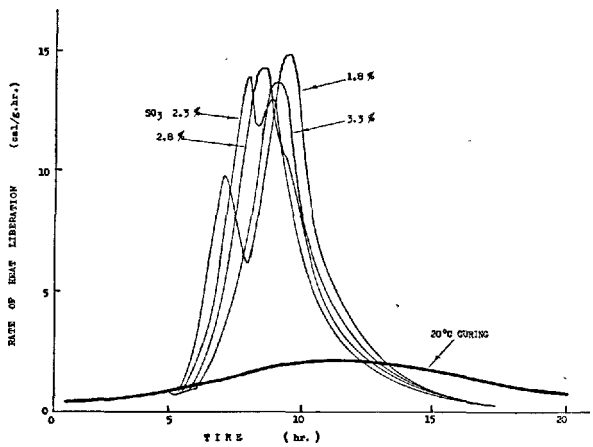

Fig. 7. *Effects of* SO_3 *contents in cement on the heat liberation curves during steam curing*

hours after mixing, and that with 2.3% SO_3 also showed two peaks at 8 and 9 hours after mixing. They had two different hydration steps. The first peak may be dependant on rapid hydration of aluminate phase in cement and this will be discussed later. The latter peak depends on hydration of alite. The samples prepared from cement with 2.8% and 3.3% SO_3 showed only one peak, because the two hydrations occurred almost simultaneously.

Effects of Time of Presteaming on Strength and Heat of Hydration

The time of presteaming is one of the most important factors which affects the strength of steam cured concrete products. O.P. Mchedlov-Petrosyan, A.G. Bunakov and Ju. L. Vorodyov (5) stated that the optimum preheating time would be determined from the heat liberation curve of concrete, and that the time immediately after the curve passes the peak should be chosen. In this section, the relation between

the rate of heat liberation and compressive strength of specimens cured at various presteaming times and by the same steam treatment is discussed.

Specimens for strength test ($\phi 5 \times 10$ cm) were prepared by molding a mixture of 1241 g of portland cement, 2308 g of natural sand and 517 ml of water, and for the calorimeter test the same mixture was filled in a test glass tube. The specimens for strength test in molds and the specimens for heat liberation test placed in the twin type calorimeter mentioned above were cured at 20°C for a given period of time, and then heated in a steam curing bath. Conditions of steam curing were as follows;

Temperature of presteaming	20°C
Time of presteaming (hours)	1/4, 1/2, 1, 2, 4, 8 and 16 (7 levels)
Rate of heating	20°C/hr.
Temperature of isothermal curing	85°C
Time of isothermal curing	5 hr.
Rate of cooling	20°C/hr.

When the temperature fell to 30°C in the cooling period, the specimens were brought out of the steam curing bath, taken out of the molds and then cured in water at 20°C. The compressive strength was examined 1 hour after the specimens were brought out of the steam curing bath and 28 days after mixing.

Fig. 8 shows the results of the strength test and Fig. 9 gives the rate of heat liberation.

The thick line in Fig. 9 shows a heat liberation of cement hydrated at 20°C. According to the view of Mchedlov-Petrosyan et al., the presteaming time of 8 to 9 hours seems to be most appropriate, because the heat liberation curve at 20°C shows the maximum at 8 hours. Compressive strength at 28 days increased with the increase of presteaming time up to 4 hours, and decreased when presteaming time was longer. Compressive strength at 1 hour after steam curing showed higher value with the increase of the presteaming time. Considering the above results, it may be concluded that the presteaming time should be determined in accordance with the conditions necessary for practical performances instead of heat liberation curve of concrete.

The heat liberation curves of the test samples cured with presteaming time shorter than 4 hours had two sharp peaks appearing at a intervals of 1 to 2 hours, the first peak being due to the hydration of aluminate and the second due to the hydration of silicate. With 4 hours' presteaming, both reactions occurred almost

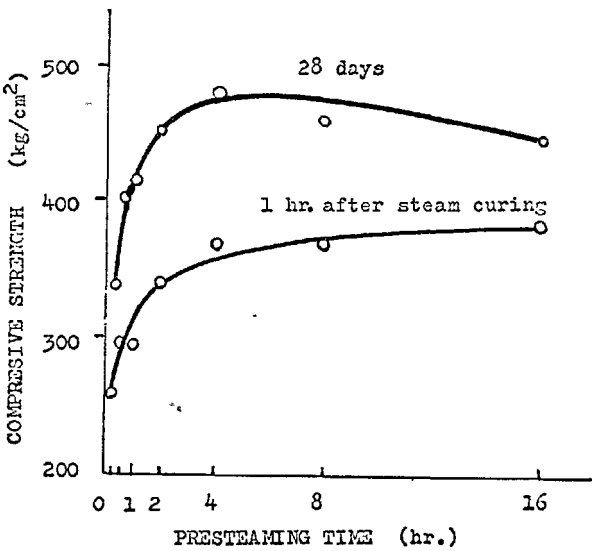

Fig. 8. *Effect of the time of presteamig period on strength*

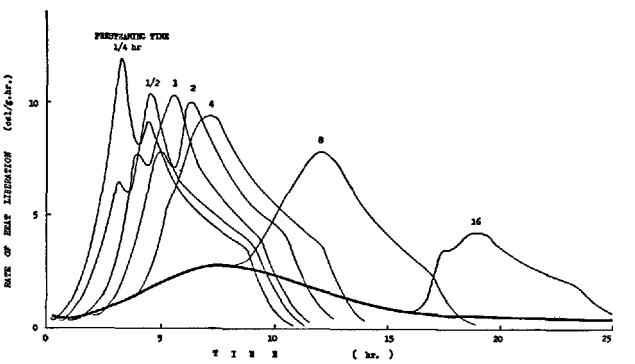

Fig. 9. *Effect of time of presteaming period on the rate of heat liberation*

at the same time. With longer presteaming period, a low and gentle peak appeared. With 16 hours curing at 20°C, the hydrated products covered the surface of the unhydrated cement particles, the rate of diffusion of water through the film of the hydrated products fell, and the rate of heat liberation of cement decreased to almost zero. When the sample was heated at this condition, the diffusion of water through the film of hydrated products was activated by rising temperature and the hydration became active again. But the rate of heat liberation decreased again in a short time, presumably due to filling up of the capillary pores of cement paste with hydration products appearing as a result of the hydration. This may be the reason why a steam cured mortar showed high strength immediately after steam curing, but exhibiting relatively low strength development at the later stage.

Hydration of C_3S during Steam Curing

C_3S used in this investigation was made from the mixtures of chemical reagents heated repeatedly in an electric furnace until free CaO content fell below 0.1 %. It was pulverized to the fineness of 3600 cm^2/g by the Blaine method, and the sample paste was prepared with $W/C_3S = 0.4$. The pastes were cured under following conditions;

No.	1	2	3	4	5
Presteaming period (hr)	cured at 20°C	2	5	2	5
Rate of heating (°C/hr)		20			
Temperature of isothermal curing (°C)		60		80	
Time of isothermal curing (hr)		17.5	14.5	15.5	12.5
Rate of cooling (°C/hr)		20			

The results are shown in Figs. 10-14.

The rate of heat liberation of C_3S cured at 20°C (No. 1), began to rise from about 3 hours after mixing, passed through the maximum about 10 hours after and decreased gradually thereafter. The volume of C_3S-paste continued to shrink until 24 hours after mixing and it was high in proportion to the rate of heat liberation.

The rate of heat liberation in curing No. 2 was closely equal to that of No. 1 until 1.5 hours after start of heating. It may be concluded from the results that nucleation process of calcium silicate hydrate is not accelerated by heating. After the paste had reached the potential sufficient for nucleation, the hydration of C_3S was accelerated by the rising temperature and the rate of hydration increased rapidly. At 4.9 hours after mixing, the rate of heat liberation reached the maximum and its peak was 18.1 cal/g.hr., which was 3 times as high as No. 1. The rate of heat liberation then dropped rapidly and 9 hours after mixing it was less than 2 cal/g. hr. The C_3S-paste expanded after the beginning of heating, but shrank after the end of the dormant period.

With longer presteaming time, (No. 3 and No.5) the rate of heat liberation increased as soon as the heating began.

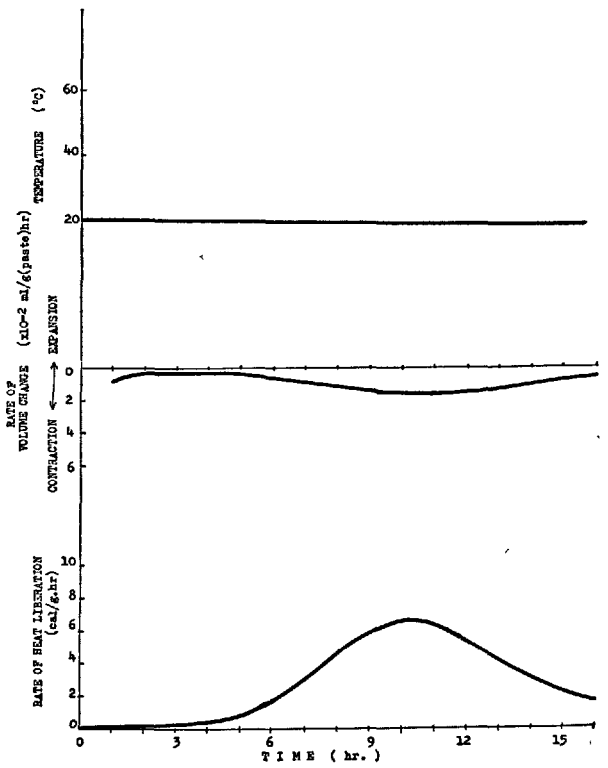

Fig. 10. *Hydration of C_3S cured at 20°C (No. 1)*

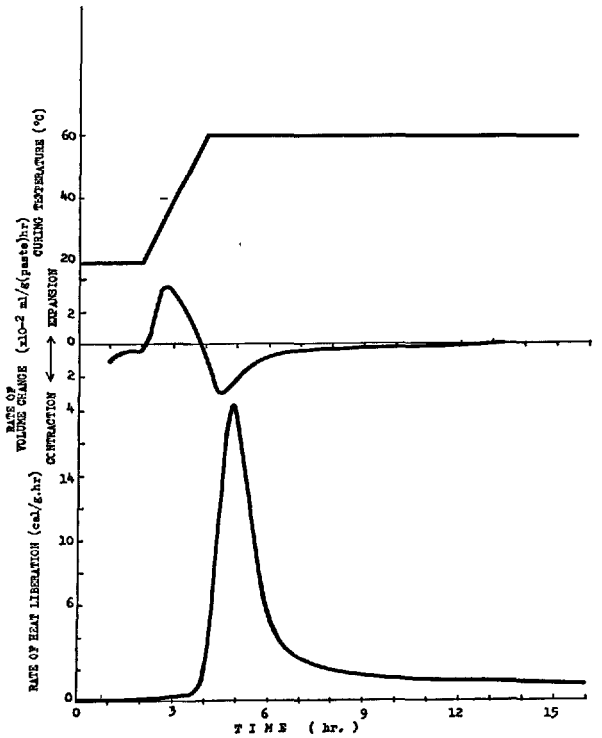

Fig. 11. *Hydration of C_3S, presteaming time 2 hrs, curing temperature 60°C (No. 2)*

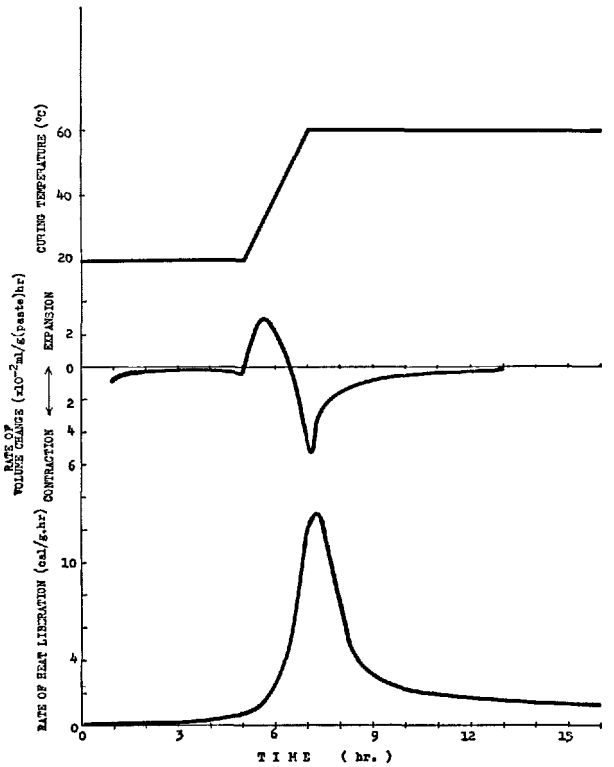

Fig. 12. *Hydration of* C_3S, *presteaming time 5 hrs, curing temperature 60°C (No. 3)*

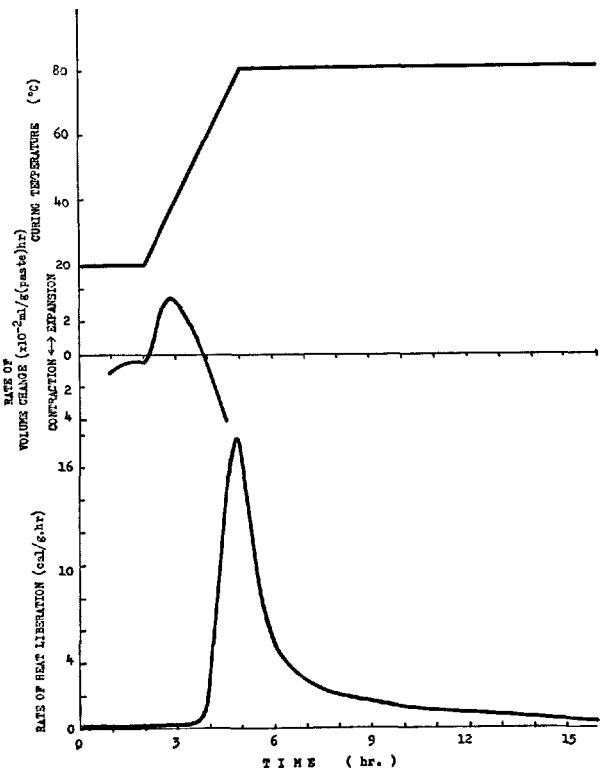

Fig. 13. *Hydration of* C_3S, *presteaming time 2 hrs, curing temperature 80°C (No. 4)*

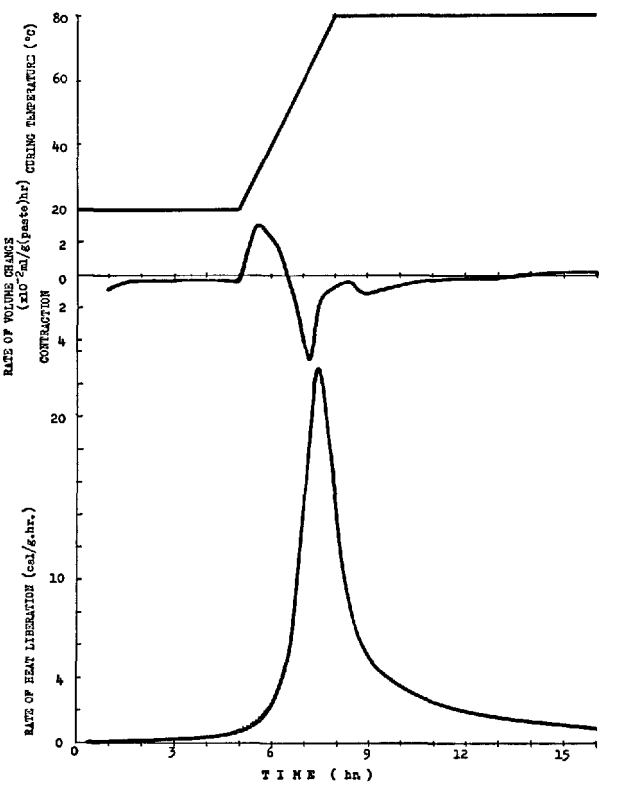

Fig. 14. *Hydration of* C_3S, *presteaming time 5 hrs, curing temperature 80°C (No. 5*

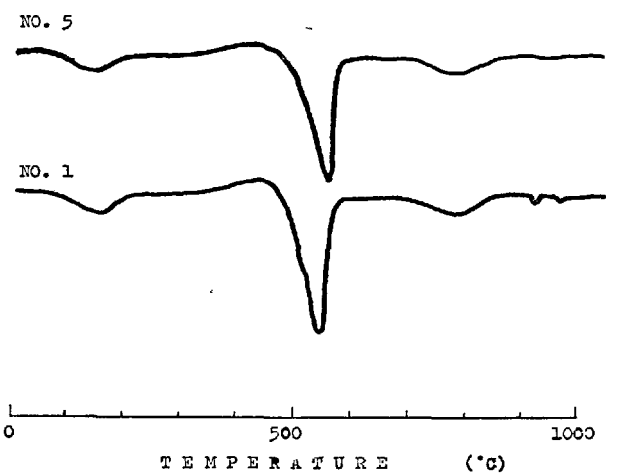

Fig. 15. *DTA curves of* C_3S *paste curves at 80°C (above) and 20°C (below) (24 hours aftermixing)*

The highest rate of heat liberation was 23.0 cal/g.hr. of No.5. The height of the peak of No.3 was nearly equal to that of No.2. With isothermal curing at 60°C, the height of the peak of heat liberation curve de-

creased proportionally to the length of presteaming time, but the situation was quite contrary at 80°C.

Amounts of nonevaporable water of C_3S-paste at 24 hours after mixing were as follows, and practically no difference was observed among them; No. 1 10.5%, No. 2 9.1%, No. 3 10.1%, No. 4 11.2% and No. 5 11.6%.

The hydration products in the pastes occurring when cured at the raised temperature were thought to be of the same kind as those occurring when cured at 20°C according to DTA (see Fig. 15).

Hydration of β–C_2S during Steam Curing

β-C_2S having 1% Cr_2O_3 content as stabilizer was prepared by heating a mixture repeatedly until free CaO disappeared and was ground to the fineness of 2800 cm^2/g by the Blaine method. Sample paste prepared with $W/C_2S = 0.4$ was cured in accordance with the program shown in Fig. 16.

It shows that the rate of heat liberation was increased by heating but it did not reach 1 cal/g.hr. even when heated at 80°C, and that the sample pastes did not harden in 24 hours. It may be concluded therefore that the steam curing has only a small effect on the rate of hydration of β-C_2S.

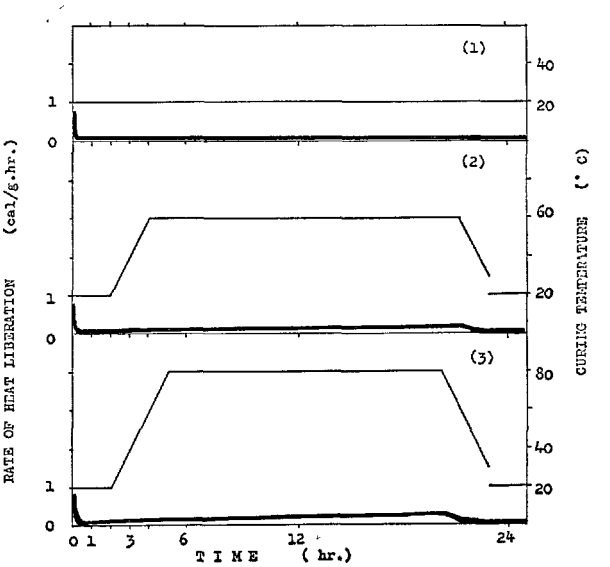

Fig. 16. *Rate of heat liberation of* C_2S *at various curing conditions*

Hydration of C_3A during Steam Curing

C_3A prepared by burning a mixture of chemical reagents in an electric furnace was ground to the fineness of 3100 cm^2/g by the Blaine method. Mixing of 800 g of C_3A and 160 g of gypsum (88μ under) was made. In consideration of the fact that low W/solid-ratio may possibly hinder perfect hydration owing to lack of water, the sample pastes were prepared with W/solid = 1. The prepared samples were cured at 20°C (Fig. 17) and treated in accordance with the programs shown in Fig. 18 and Fig. 19.

The reaction of C_3A with gypsum was accelerated with the rising temperature and all gypsum in the mixture were spent at early ages. After the gypsum in the mixture were totally consumed, the hydration proceeded rapidly and the paste hardened. Results of DTA (Fig. 20) shows that the hydration product formed before the disapperance of gypsum was trisuphate hydrate and this later became monosulphate and C_3AH_6. W. Lieber (6) reported that C_3A reacts with gypsum at high temperature and forms trisulfate hydrate. The results of DTA show that the formation of trisulphate hydrate will take place as long as gypsum remains in paste.

The paste was expected to expand with the formation of trisulphate hydrate, but it showed contraction through the curing period except at the time of 10 hours after mixing. This may be due to the presence of large amount of water in the paste.

The paste expanded at the beginning of steam curing because of the expansion of free water in the paste. When the rapid hydration occurred with the disapperance of gypsum, the volume of paste contracted at a high rate. After that, the rate of contraction gradually decreased in case of 60°C curing, but the paste expanded in case of 80°C curing and the rate of expansion gradually decreased with the

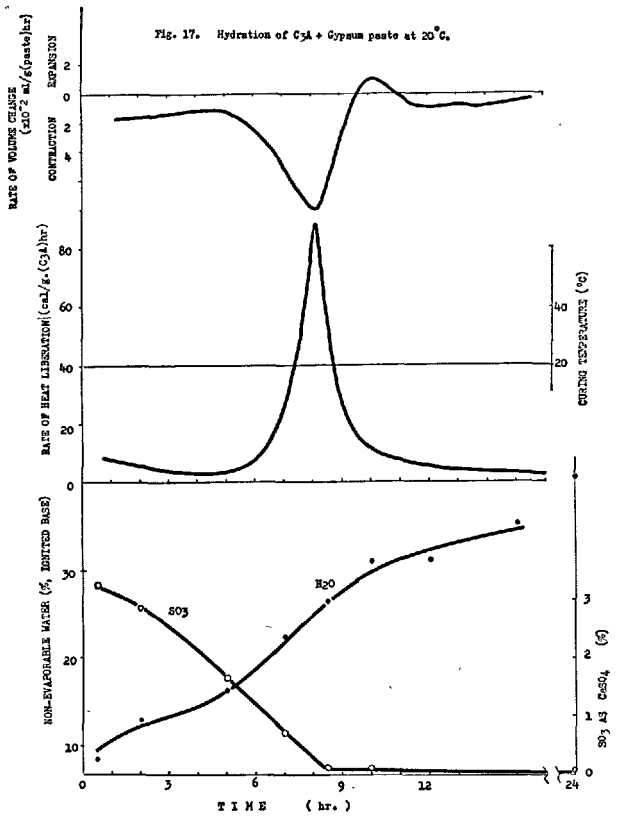

Fig. 17. *Hydration of* C_3A + *Gypsum paste at 20°C*

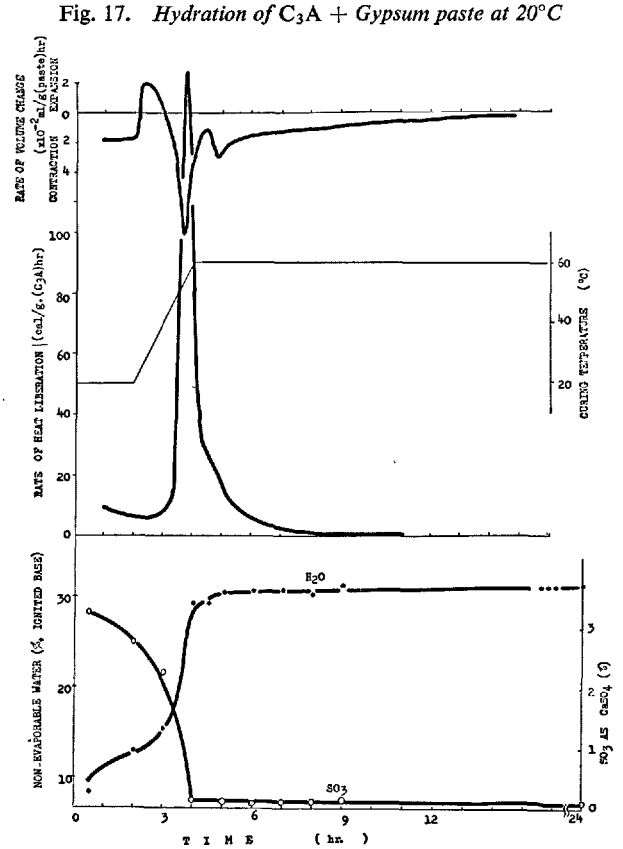

Fig. 18. *Hydration of* C_3A + *Gypsum paste, presteaming time 2 hours, curing temperature 60°C*

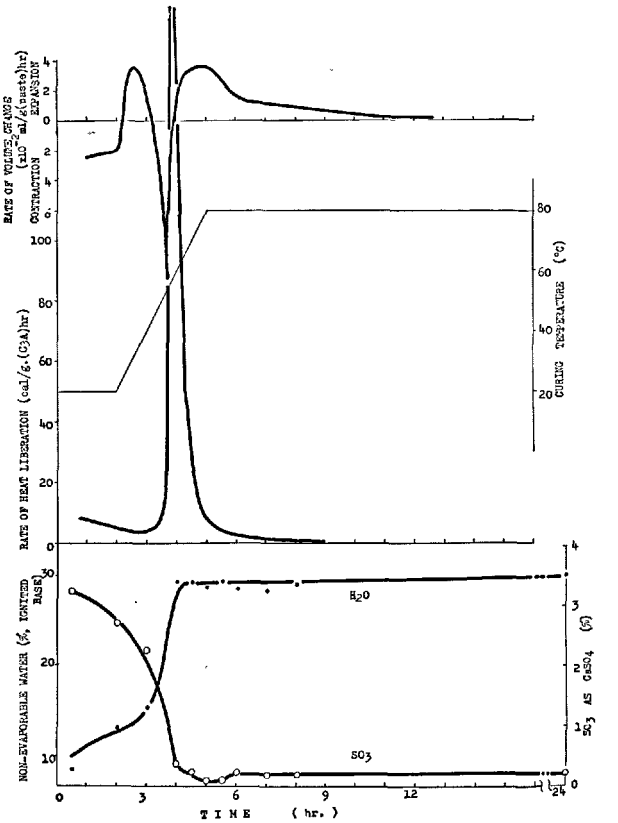

Fig. 19. *Hydration of* C_3A + *Gypsum, presteaming time 2 hrs, curing temperature 80°C*

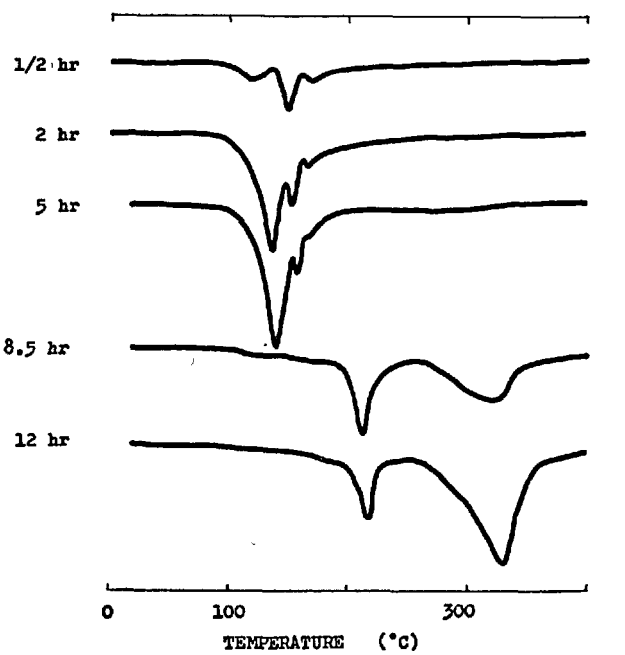

Fig. 20–1. *DTA curves of* C_3A + *Gypsum cured at 20°C*

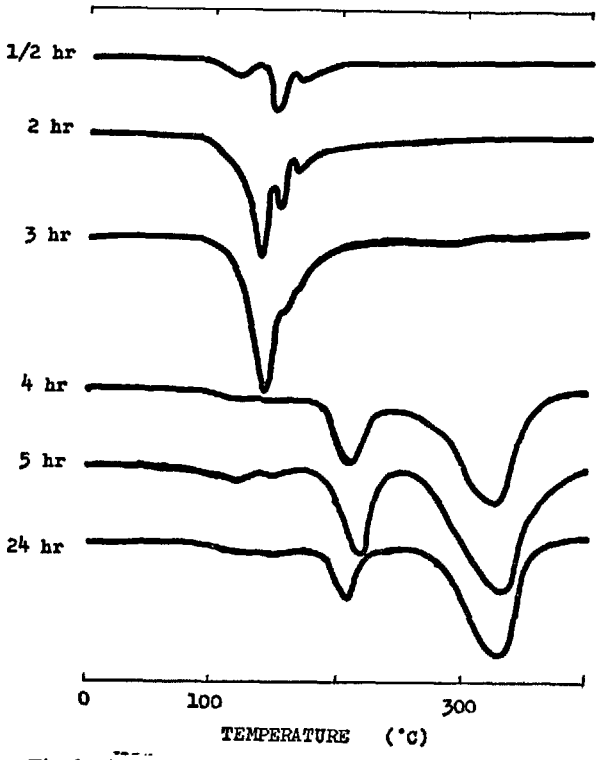

Fig. 20–2. *DTA curves of* C_3A + *Gypsum cured at 60°C*

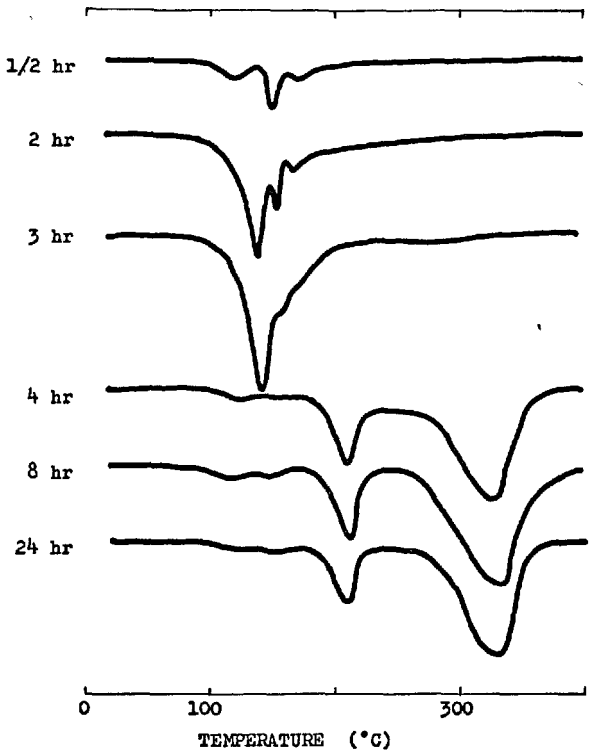

Fig. 20–3. *DTA curves of* C_3A + *Gypsum cured at 80°C*

lapse of time.

The degrees of hydration of C_3A after 24 hours were 75, 65 and 63% with curing temperatures of 20, 60 and 80°C respectively. It shows that the rate of hydration of C_3A after 24 hours decreases with the rise of temperature. The amount of non-evaporable water has the same tendency as the rate of hydration; 40.7% for 20°C, 31.4% for 60°C and 30.1% for 80°C (on ignited base). The difference between the amounts of non-evaporable water for 20°C curing and that for 60°C and 80°C was probably due to the difference in ratios of monosulphate-C_4AH_n solid solution to C_3AH_6 of these samples.

Hydration of C_4AF during Steam Curing

C_4AF prepared by burning a mixture of chemical reagents in an electric furnace was ground to the fineness of 4200 cm^2/g by the Blaine method.

In the hydration of system C_4AF + gypsum, the formation of trisulphate hydrate decreases the calcium concentration in the liquid phase. It seems that the hydration of C_4AF in portland cement was different from that of the mixture of C_4AF and gypsum, because the former proceeded in the solution of high calcium concentration and the latter in low concentration. For this reason, 360g of C_4AF was mixed with 54 g of $Ca(OH)_2$ and 108 g of gypsum ($<88\mu$).

The sample pastes were prepared with W/solid = 0.5. The prepared samples were cured under three kinds of heat treatment as shown in Figs. 21-23.

The rate of heat liberation for curing temperature of 20°C is small until 24 hours, except for a certain period after mixing when rapid reaction takes place. The pastes contracted at nearly constant rate. The DTA curve of the paste at 24 hours shows that large amount of gypsum still remains (see Fig. 24) (endothermic peaks at 150° and 180°C).

The rate of heat liberation of paste cured at 60°C increased as soon as heating started. When it reached to 6 or 7 cal/g.hr., the heat liberation curve kept a constant level until 10 hours. At 11 hours, a steep peak appeared. It was caused by the rapid hydration of C_4AF taking place immediately after the gypsum

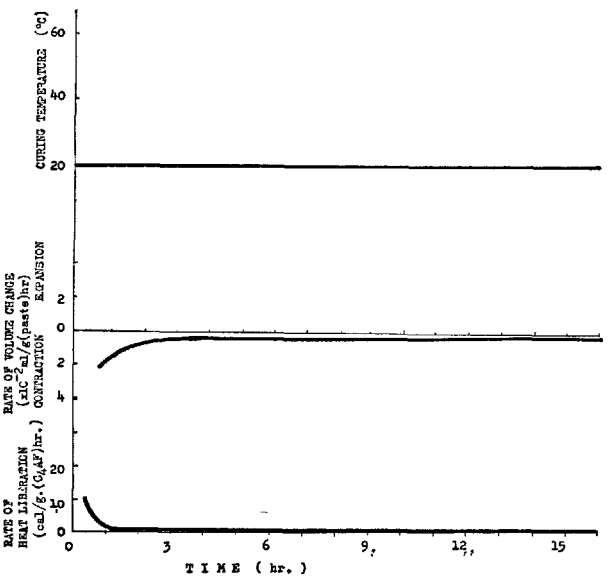

Fig. 21. *Hydration of* C_4AF + *Gypsum* + $Ca(OH)_2$ *cured at 20°C*

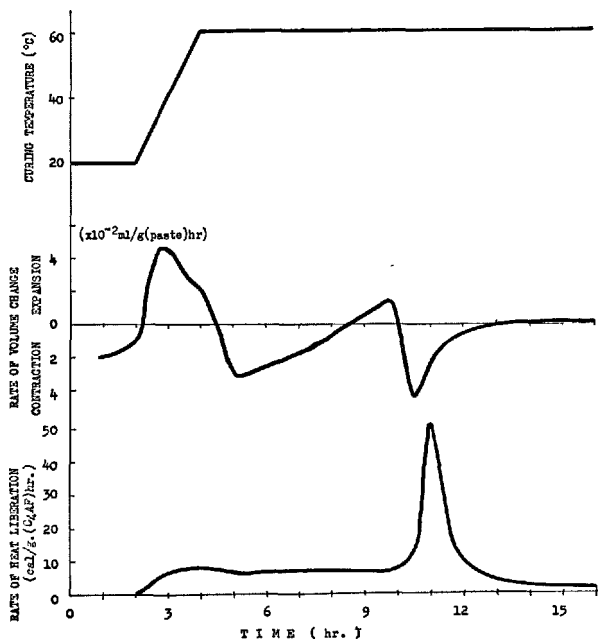

Fig. 22. *Hydration of* C_4AF + *Gypsum* + $Ca(OH)_2$ *paste, presteaming time 2 hrs, curing temperature 60°C*

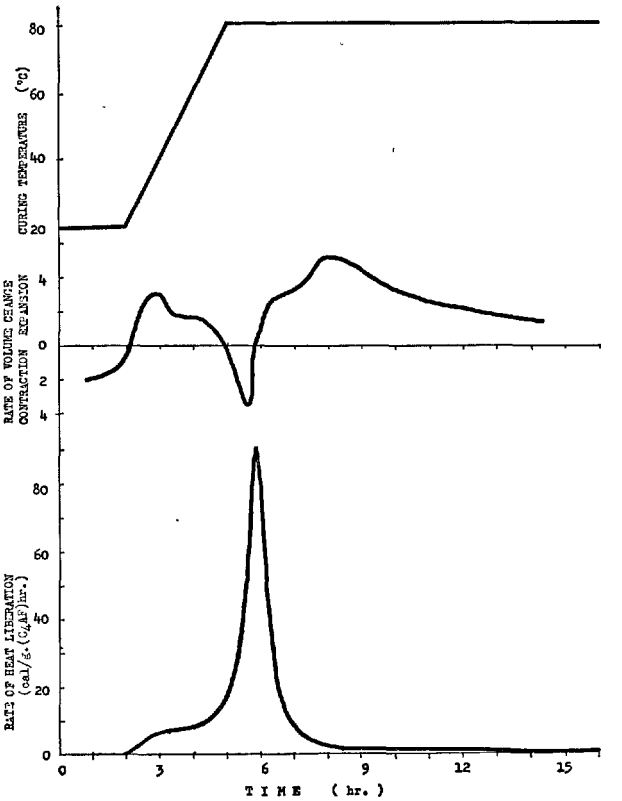

Fig. 23. *Hydration of* C_4AF + *Gypsum* + $Ca(OH)_2$ *paste, presteaming time 2 hrs, curing temperature 80°C*

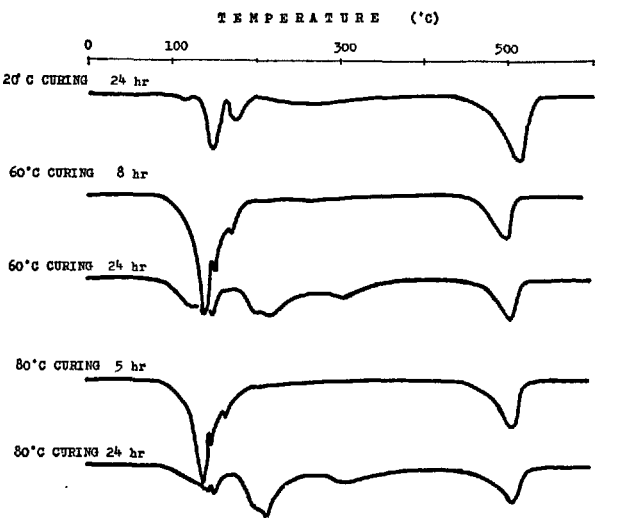

Fig. 24. *DTA curves of* C_4AF + *Gypsum* + $Ca(OH)_2$ *paste*

in the mixture had been spent for the formation of trisulphate hydrate. The paste hardened at this hydration. While the gypsum remained in the paste the

hydration product was trisulphate hydrate, but after the disappearance of gypsum trisulphate hydrate was decomposed and formed $C_3(A, F)H_6$ and monosulphate-$C_4(A, F)H_n$ solid solution. The paste expanded during the heating period and shrank at the early period of isothermal steam curing. The rate of volume contraction decreased gradually with the lapse of time and at 8.5 hours the paste began to expand. It may have been caused by the formation of trisulphate hydrate. The rapid hydration of C_4AF caused by the disappearance of gypsum brought about the volume contraction of the paste. After the peak of heat liberation, the rate of volume contraction fell rapidly to almost zero.

The reaction of C_4AF with gypsum was more accelerated at 80°C than at 60°C curing, and the peak of heat liberation closed by the disappearance of gypsum in the paste occurred at early ages. After the appearance of the peak, the rate of heat liberation fell down to 1 or 2 cal/g.hr. The hydration product was trisulphate hydrate at first but after reaching the peak monosulphate-$C_4(A, F)H_n$ solid solution hydrate and $C_3(A, F)H_6$ resulted. The paste expanded during the heating period and contracted after the rapid reaction owing to the disappearance of gypsum in the mixture took place. The cycle of contraction and expansion and contraction occurring in 60°C curing, expansion first by heating and contraction caused by rapid hydration, did not take place in 80°C curing. After reaching the peak of heat liberation the paste expanded. After the disappearance of gypsum in the paste, the hydration of the phase containing alumina caused contraction of the paste by 60°C curing and expansion of the paste by 80°C curing.

Hydration of Normal Portland Cement during Steam Curing

Studies of hydration process of normal portland cement during steam curing were made from the scopes of the heat liberation and volume change. It was studied in relation to the results of hydration of each compounds mentioned above.

Normal portland cement used for the experiments had components of 48% C_3S, 28% C_2S, 9% C_3A, 9% C_4AF and 3.1% $CaSO_4$ according to Bogue's formula. Sample pastes were prepared with W/C = 0.4 at 20°C. The pastes were cured by 8 kinds of heat treatments as follows;

No.	1	2	3	4	5	6	7	8
Time of presteaming (hr)	cured at 20°C	2	5	1/2	1	2	5	10
Rate of heating (°C/hr)		20						
Temperature of isothermal curing (°C)		60		80				
Time of isothermal curing (hr)		17.5	12.5	17.0	16.5	15.5	12.5	7.5
Rate of cooling (°C/hr)		20						

The heat liberation of sample No. 1 cured at 20°C, was small during the dormant period which lasted for about 2 hours, but it increased after that period and reached the maximum at 9.5 hours. Its peak was 2.8 cal/g.hr. The rate of heat liberation decreased gradually thereafter. The sample contracted continuously up to 24 hours after. When the rate of heat liberation reached the peak, the contraction rate of volume also reached the maximum. SO_3 as calcium sulphate contained in the cement paste decreased with the lapse of time and was almost completely spent for the formation of trisulphate hydrate at 12 hours. In the paste of C_3A + gypsum mentioned above, the rapid hydration occured when gypsum in the paste was totally spent for the formation of trisulphate hydrate. In the paste prepared from portland cement, however, a peak which should have been caused by the disappearance of gypsum did not appear.

In the heat treatment of No. 2, the heat liberation curve of the cement paste showed that the hydration

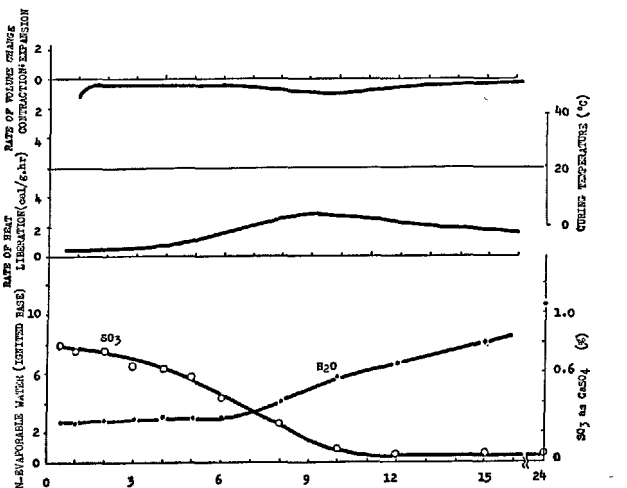

Fig. 25. *Hydration of normal portland cement cured at 20°C (No. 1)*

of cement still remained in the dormant period after the beginning of heating.

The paste expanded due to the thermal expansion of water. After 3 hours, curing temperature rose to above 40°C, the rate of heat liberation increased rapidly and the hydration of cement changed from the dormant period to the active period. The change of volume altered from expansion to contraction. At 5 and 6.5 hours after the mixing two peaks of heat liberation occurred. The first was the sharp and high peak (17 cal/g.hr.) accompanied by the contraction of the paste. It appears to be that this peak of heat liberation was caused by the hydration of aluminate owing to the disappearance of gypsum. Gypsum in the cement paste decreased rapidly during the period of 2 to 5 hours after mixing and SO_3 as calcium sulphate dropped to only 0.05% at 5 hours (as shown in Fig. 26). The latter peak was gentle and shaped like a shoulder of the first. It seems that this peak arose from the hydration of silicate. The hydration of silicate in C_3S-paste caused the volume of paste to contract as described above, but in the case of portland cement paste, it caused a slight expansion. Results of DTA show that before the appearance of the first peak, trisulphate hydrate (endothermic peak at 120°C) was formed, but this product decreased in course of time to form monosulphate-C_4AH_n solid solution hydrate (endothermic peak at 220°C). Both of the endothermic peaks became broad and indistinct after 1 week.

In case of No. 3, the rate of heat liberation and the rate of volume change showed the same tendency as those in No. 2. The height of earlier peak caused by absence of gypsum was lower than that of No. 2.

A notable difference between hydration processes at 60°C curing and at 80°C curing is shown by the heat liberation curves of No. 2 and No. 6. Three peaks appeared in the heat liberation at 80°C curing, the first at 4.8 hours, the second at 5.1 hours and the last at 6 hours. The former two were not so sharp as the last, and these peaks appeared successively one after another. As free $CaSO_4$ dropped to the minimum at 4.5 hours, it seems that the first peak came to appear by the rapid hydration of aluminate owing to the absence of gypsum. SO_3 as calcium sulphate increased again at 5 hours. At this time the temperature of curing was 80°C. DTA curves show that trisulphate hydrate was found formed up to 4.5 hours and at 5 hours trisulphate hydrate and monosulphate hydrate appeared. After 5.5 hours, endothermic peaks became indistinct. P.P. Budnikov and Ya. Erschler (7) reported that the transition of hydrosulpho-

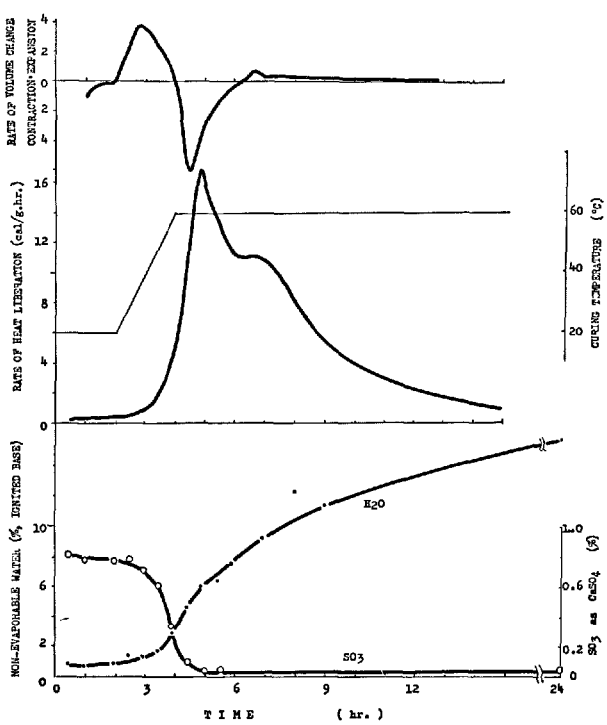

Fig. 26. *Hydration of normal portland cement. presteaming time 2 hrs, curing temperature 60°C (No. 2)*

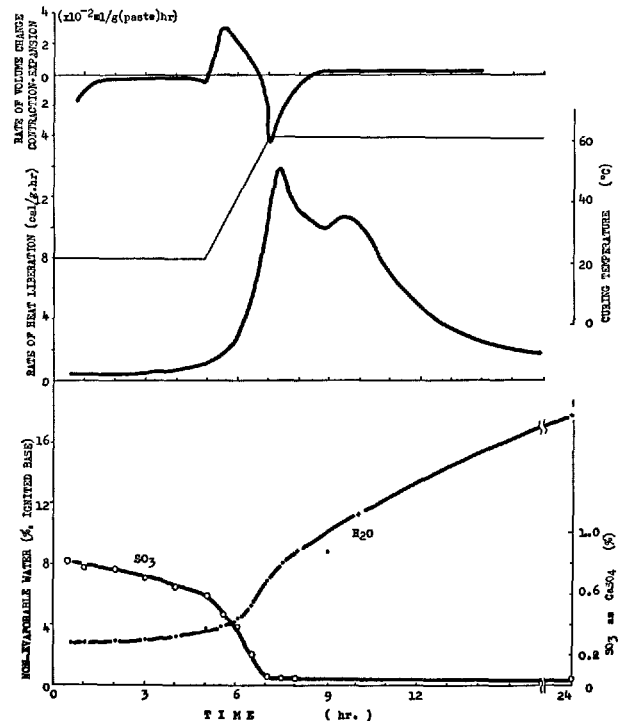

Fig. 27. *Hydration of normal portland cement, presteaming time 5 hours, curing temperature 60°C (No. 3)*

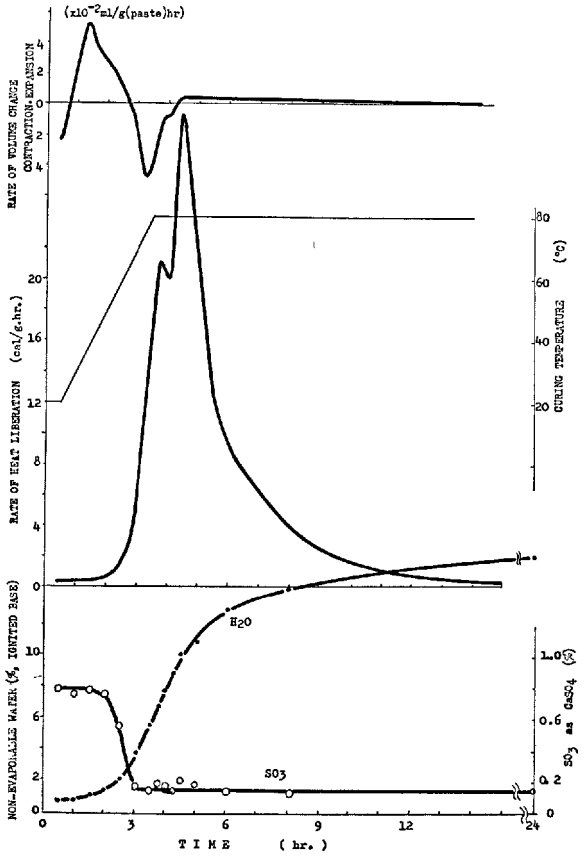

Fig. 28. *Hydration of normal portland cement, presteaming time 0.5 hr, curing temperature 80°C (No. 4)*

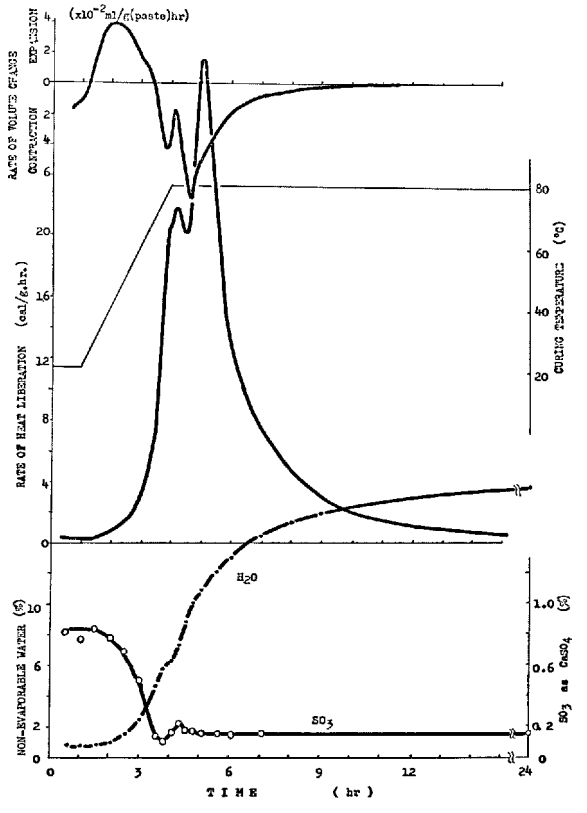

Fig. 29. *Hydration of normal portland cement, presteaming time 1 hr., curing temperature 80°C (No. 5)*

compounds into the low sulphate takes place; this was accompanied with the release of free $CaSO_4$ under the influence of high temperature and a liquid phase saturated with $Ca(OH)_2$. From the facts of increase of free $CaSO_4$ and disappearance of tri-and mono-sulphoaluminate hydrates as shown by DTA, it may be concluded that the second peak appeared owing to the partial decomposition of aluminate hydrates.

The third peak was the highest of all and it was caused by the accelerated hydration of silicate phase.

At every step of hydrations, the volume contracted in high rate. After the occurrence of the third peak, the volume expanded for a while, but thereafter the paste maintained its constant volume.

In both cases of shorter and longer presteaming period than that of No. 6, two peaks appeared. With shorter presteaming period (No. 4 and No. 5), the amount of SO_3 as gypsum decreased with the lapse of time, but as the release of SO_3 occurred before SO_3 in cement was spent for the formation of trisulphate hydrate, a peak of heat liberation due to the disappearance of gypsum did not appear. Therefore, the first peak is considered as showing the hydration owing to the release of SO_3 and the second as showing the hydration of silicates.

With longer presteaming period (No. 7 and No. 8), gypsum in cement was used up for the formation of trisulphate hydrate during the heating period and a peak of heat liberation caused by the rapid hydration of aluminate appeared. When the curing temperature was raised up to 80°C, trisulphate hydrate formed should have decomposed, as was shown in the case of No. 8, that is, SO_3 as gypsum dropped to the amount less than 0.1% at 12 hours and increased to 0.2% at 13.5 hours. The peak of heat liberation was accompanied with the decomposition of trisulphate hydrate, perhaps overlapped with a large and sharp peak caused by the hydration of silicate.

In all of the cases except No. 7, the paste con-

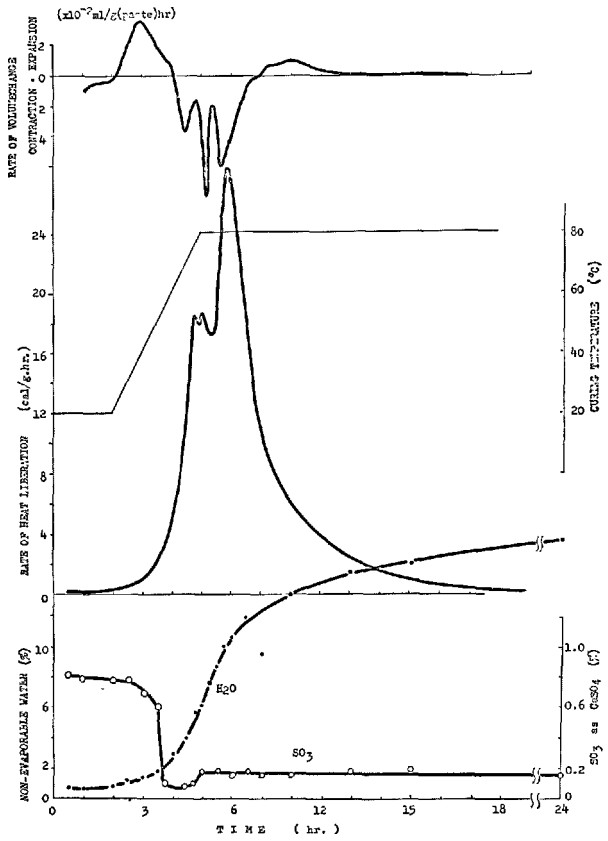

Fig. 30. *Hydration of normal portland cement, presteaming time 2 hrs, curing temperature 80°C (No. 6)*

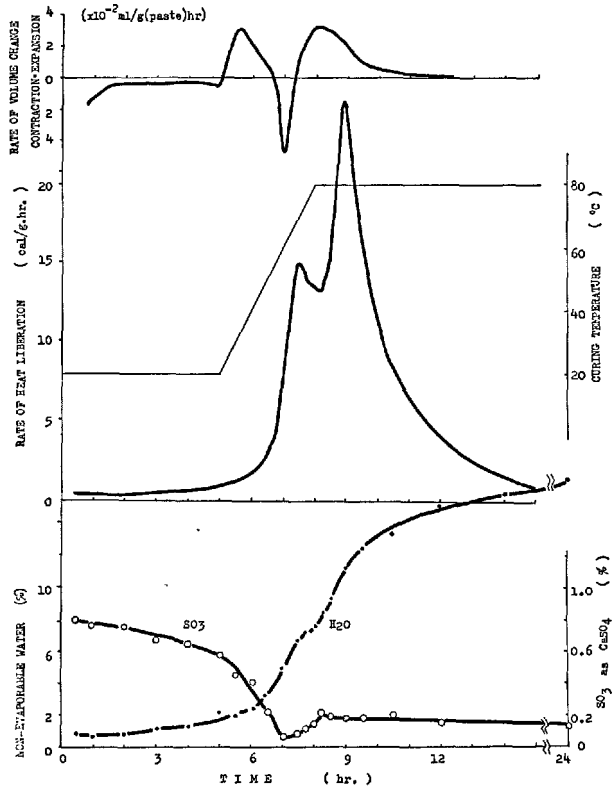

Fig. 31. *Hydration of normal portland cement, presteaming time 5 hrs, curing temperature 80°C (No. 7)*

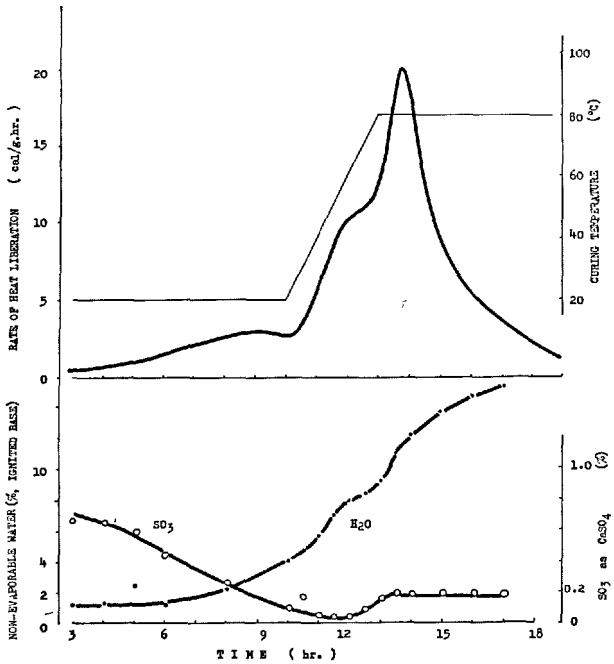

Fig. 32. *Hydration of normal portland cement, presteaming time 10 hrs, curing temperature 80°C (No. 8)*

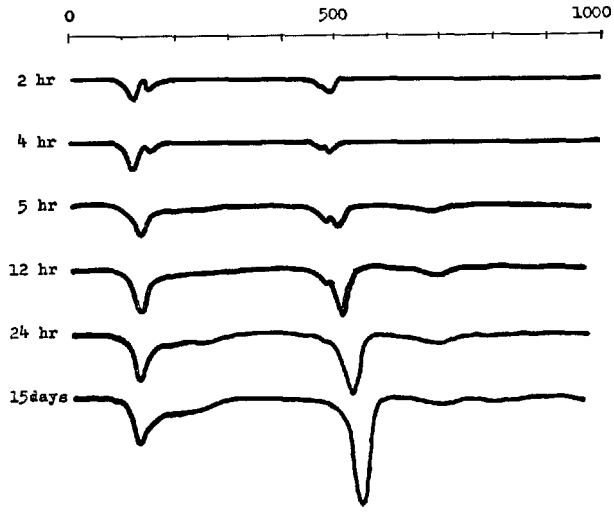

Fig. 33–1. *DTA curves of normal portland cement paste cured at 20°C (No. 1)*

tracted when the hydration of silicate took place, and in case of No. 7, it expanded. This expansion may be attributed to the hydration of silicate taking

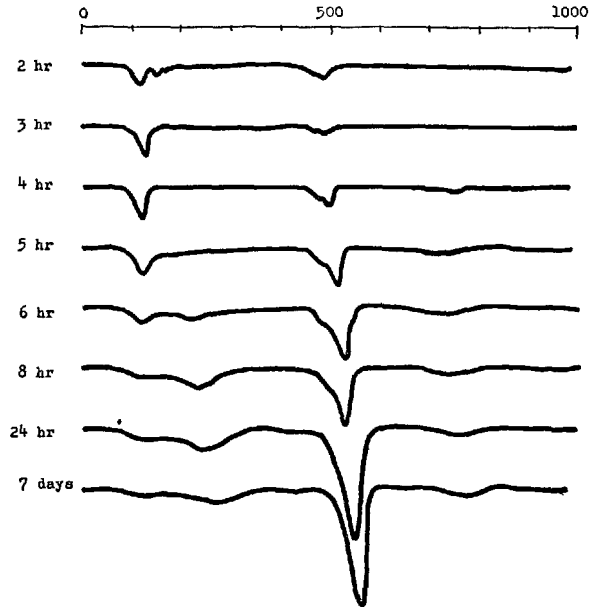

Fig. 33–2. *DTA curves of normal portland cement paste cured at 60°C (No. 2)*

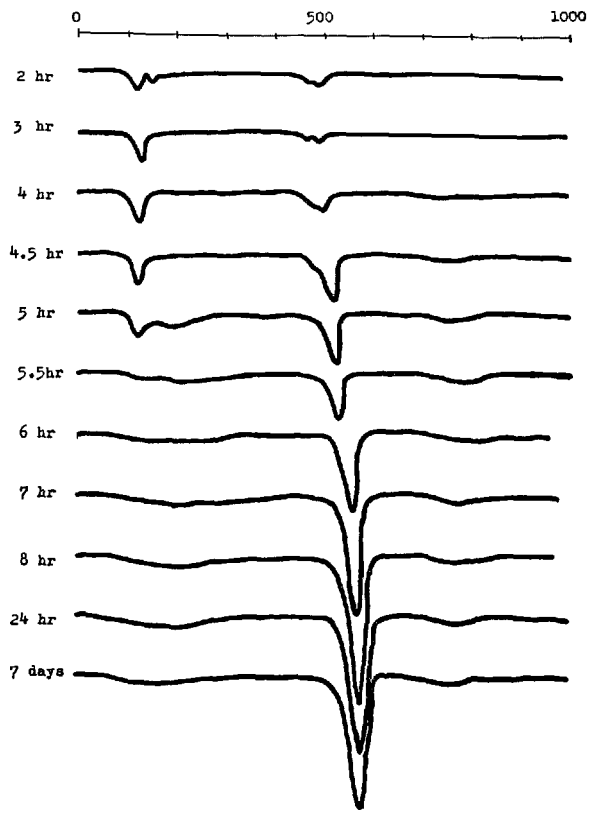

Fig. 33–3. *DTA curves of normal portland cement paste cured at 80°C (No. 6)*

place after the hardening of the paste.

Shorter presteaming time brought about a heat liberation curve with a sharp and eminent peak, but sharpness and height of the peak decreased with length of presteaming time. This may be due to the extent of early hydration of cement.

By 60°C isothermal curing, a heat liberation curve having one sharp and high peak and another gentle peak were obtained, the first owing to the disappearance of gypsum and the latter due to the hydration of silicate. At the temperature of 80°C, a heat liberation curve having a low peak, due to the disappearance of gypsum, and a high peak, due to the hydration of silicate, were obtained.

General Conclusion

For a better understanding of the hydration process of cement taking place during steam curing under atmospheric pressure, the authors tried to determine the rate of heat liberation, and were able to obtain useful informations on the effects of steam curing on the rate of hydration, the steps of hydration and so on. For this purpose, twin-type calorimeters were designed and tested. In addition, they tried to determine the volume change taking place during steam curing.

The rates of heat liberation were measured under various conditions of steam curing, and the hydrations occurring during process which caused to reveal peaks of heat liberation were studied.

Generally speaking, one or two peaks of heat liberation took place. These peaks were caused by the hydration of silicate, which was accelerated by heating 3 or more times higher than when cured at 20°C, and by the hydration of aluminate which was caused by the disappearance of gypsum. In some cases, these hydrations took place simultaneously. In the case of isothermal curing at 80°C, another peak of heat liberation appeared by the hydration of aluminate which may have been caused by a partial decomposition of trisulphate hydrate into an unknown phase.

The paste cured at 20°C continued contracted at a low rate for 24 hours. During the steam curing period, it expanded as soon as heating started, but it again began to contract with the appearance of

the first peak of heat liberation. The rate of volume change during steam curing was greater than that when cured at 20°C.

Acknowledgement

The writers wish to express their appreciation to the management of the Nihon Cement Co. Ltd. for granting the permission to publish this paper and thank Mr. M. Shimokawa and Mr. A. Nemoto for their assistances which made the preparation of this report possible.

References

1. W. Lerch, "The influence of gypsum on the hydration and properties of portland cement pastes", Proc. Amer. Stand. Test. Mater., **46**, 1252–1292 (1946).
2. U. Danielsson, "Conduction calorimeter studies of the heat of hydration of a portland cement", Swedish Cement and Concrete Research Institute at the Royal Institute of Technology. No. 38, (1966) (Stockholm).
3. K. Fujii, T. Watanabe and S. Hagiwara, "Immediate heat liberation of portland cement as mixed with water", Semento Gijutsu Nenpo, **14**, 120–125 (1964) (in Japanese).
4. E. Homma and I. Hida, "Early volume change of portalnd cement paste caused by hydration", Semento Gijutsu Nenpo, **16**, 121–125 (1962) (in Japanese).
5. O. P. Mchedlov-Petrosyan, A. G. Bunakov and Ju. L. Vorodyov, "Physicochemical fundamentals of directed structure-formation in accelerated concrete units". Preprint from RILEM Symposium, Moscow, USSR, Session 1/15, (1964).
6. W. Lieber, "Ettringit-Bildung bei höheren Temperaturen", Zement-Kalk-Gips, **52**, 364–365 (1961) (in German).
7. P. P. Budnikov and E. Erschler, "Studies of the processes of cement hardening in the course of low-pressure steam curing of concrete". Proc. Symposium on Structure of Portland Cement Paste and Concrete, Highway Research Board, Washington, USA, pp. 413–446 (1966).

Supplementary Paper III-108 Physical and Chemical Properties of Cement Mortar Cured at Elevated Temperatures

P. Freisleben Hansen, John Jessing, Karen Mønsted and Erik Trudsø*

Synopsis

In order to investigate the laws governing the acceleration of concrete hardening at elevated curing temperatures, the course of a number of physical and chemical properties of cement mortar was followed. At four levels of curing temperature, the compressive strength, sound velocity, internal damping, electrical resistance, alkalinity, and content of non-evaporable water were determined intermittently or continuously at ages from ½ hour to 24 hours.

The data obtained show that the effect of temperature on the development of mechanical properties can with moderate accuracy be accounted for by means of concrete maturity, but only within certain intervals. When the curing temperature exceeds 45°C, the mechanical properties seem to be impaired and after 24 hours lower values than those obtained by curing at 25°C can result.

The rates by which physical and chemical properties develop have been examined by differentiating the basic curves. This has revealed certain relations between the hydration processes and the mechanical properties and has permitted identification of the reaction of water with C_3S and C_3A, respectively. The methodology applied appears promising for future studies of concrete hardening.

Scope

The use of curing methods, which accelerate the hardening of concrete, becomes increasingly important for the building industry. For ordinary concrete, acceleration is most frequently achieved by an increase in the curing temperature. The investigation reported in this paper was undertaken in order to obtain knowledge on the influence of temperature on the course of the hardening process, especially as regards such properties which are of immediate practical importance.

Four temperature levels were chosen: 25°C, 45°C, 60°C, and 80°C, as it was desirable to cover as wide a range as possible with the equipment at hand.

For practical production, the most pertinent properties are the workability of fresh concrete, the setting time, and the strength and rigidity of the hardening concrete. As no apparatus for measuring strictly reological properties was available, one settled for determining the dynamic modulus of elasticity as well as the internal damping immediately after mixing and moulding and intermittently during the rest of the experiment. Strength was measured at certain intervals by compression tests of cylinders.

The intension was to explain the effect of the curing temperature by the changes it produces in the chemical and physical processes during hydration; therefore, it was attempted to follow these by different means. The content of non-evaporable water was determined in two ways: 1) by subtracting the content of evaporable water found by drying and weighing of broken pieces of test cylinders from the original content of water and 2) by intermittent observation of volume contractions caused by the chemical fixation of water. Temperature and electrical resistance were recorded continuously during the whole test. Also the pH-value was recorded continuously, but only during the first stages of hydration.

*Danmarks Ingeniørakademi, Bygningsafdelingen Copenhagen, Denmark.

Materials and Techniques

Materials

A cement mortar, made as specified by RILEM-Cembureau in the method of testing strength of cement (1), was used in the investigation. The cement was of the rapid-hardening portland type with a fineness of 3930 cm^2/g (Blaine) and a chemical composition as shown in Table 1. Setting time determined by the Vicat method was about 180 min (initial set) and 290 min. (final set). The mechanical strength of prisms made of standard mortar (according to RILEM-Cembureau) is shown in Table 2. Danish standard sand and destilled water was used. The ratio of water to cement was 0.5, and the ratio of paste to sand also 0.5 (by weight).

Mixing and Curing

The ingredients were mixed in accordance with the specification, and the mortar was introduced directly from the mixing bowl into the moulds, which were mounted on a vibrating table. The mortar was placed in three layers, each being compacted by a steel rod under simultaneous vibration. Moulding lasted about. 4 min. The acrylic moulds consisted of 14 cylinders ($4\phi \times 8$ cm) and a rectangular box ($5 \times 10 \times 20$ cm).

Table 1. *Chemical analysis and compound composition (per cent) of cement used in test*

SiO_2	20.8	$CaCO_4$	4.1
Al_2O_3	4.86	C_4AF	6.7
Fe_2O_3	2.19	C_3A	9.2
CaO	64.7	C_3S	54
MgO	1.20	C_2S	19
SO_3	2.42		
loss on ignition	2.72		
	98.89		
Free CaO	2.03		
K_2O	0.75		
Na_2O	0.31		

Table 2. *Mechanical strength of cement used in test determined by the RILEM-Cembureau method (data from 4 series)*

	Bending strength			Compressive strength		
age, days	1	3	7	1	3	7
mean value, kg/cm²	38.6	71.4	74.8	139	357	453
standard deviation	1.6	0.8	1.3	4	6	4

The 14 cylinders were used as follows (Fig. 1): 12 for the determination of compressive strength at ages from 30 min to 24 hours, 1 for measuring the electrical resistance between two copper electrodes mounted at top and bottom, and 1 cylinder finally for temperature recording by means of a thermistor inserted into the center of the cylinder. The box was used to determine wave velocity and damping, but also a thermistor was introduced, because the bigger dimensions of the box would make it more difficult to avoid deviations from the prescribed temperature level. All cylinders and the box were placed in a waterfilled tank (see Fig. 2), where the temperature

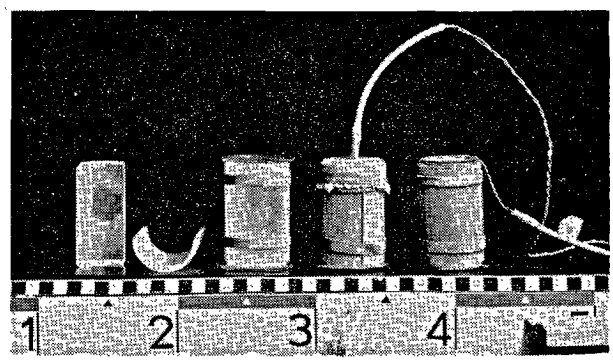

Fig. 1. *Mounting of mortar cylinders (from left to right):*
Acrylic moulds (lined with PVA-sheet before filling)
Moulds closed with glass plates (specimen for strength test)
Mortar cylinder with thermistor (specimen for recording of temperature)
Moulds provided with copper plates (specimen for recording of electrical resistance)

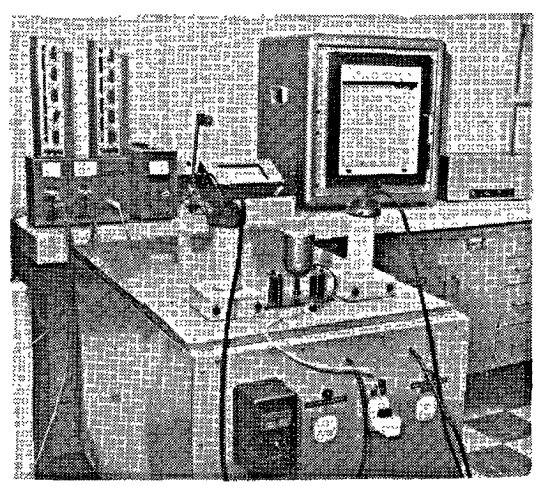

Fig. 2. *Storage tank with thermostat and agitator for circulation of water. In the background the pH-meter and the multiple-channel recorder can be seen*

was held constant by a thermostat. Mixing, moulding, mounting and placing in the bath was completed within 15–17 min. after cement and mixing water was brought into contact.

Compressive Strength

When the mortar cylinders had reached the prescribed age, they were taken out of the curing tank, demoulded with care, and subjected to compression at room temperature within 2–3 min after the end of the curing period. A beam testing machine with the loading brought about by shot flowing into a pan (see Fig. 3) was used to determine compressive strength values below 5 kg/cm²; the loading rate was about 10 kg/cm² per sec. At failure, the flow stopped automatically, and the compressive strength was calculated by weighing the amount of shot. When cylinders had attained higher strength, a hydraulic Mohr and Federhaff compression machine was used, ajusted to the same loading rate as above. The cylinders failed distinctly in shear, even at very early ages.

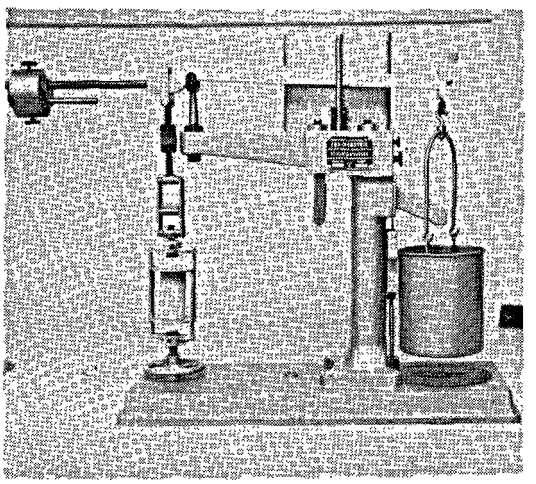

(a)

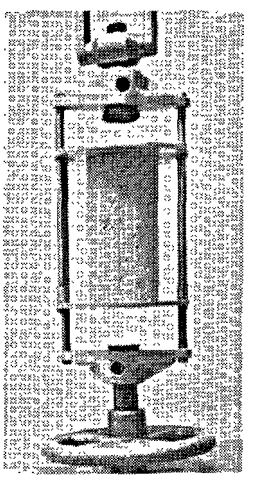

(b)

Fig. 3. *Compressive test for low strength mortar cylinders*

Wave Velocity and Damping

Fig. 4 shows two electro-acoustic transducers lowered 20 mm into the rectangular moulding box to which were glued on both sides hollow cylindrical liners, closed against the mortar by a "window" of 1.0 mm thick acrylic sheet. One transducer acts as a transmitter, the other one as a receiver, both of them operating by virtue of the piezo-electric effect of barium titanate. 50 times per second, an electrical condenser is discharged across the crystal of the transmitter, the resonant frequency of which is 100 kc per sec. A short train of longitudinal waves of this frequency is thereby transmitted through the mortar and, on the arrival to the receiver, forces the crystal here to vibrate in its fundamental frequency, identical with that of the transmitter, thus producing an electrical signal in step with the short wave train.

On the electrically produced time scale of an oscilloscope, this signal is used repeatedly (50 times a second) as a trigger of an arrival mark, and the distance, in micro-seconds, is read from here to a starting mark, caused on the same scale by a signal at every one of the repeated onsets of the transmitter crystal.

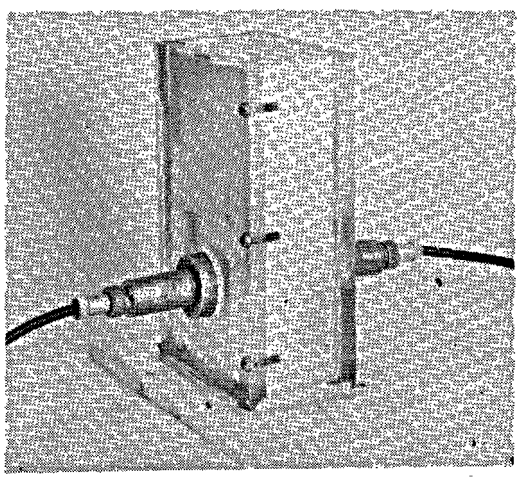

Fig. 4. *Electro-acoustic transducers in contact with mortar in acrylic box*

By subtracting from this figure the passing time of a wave directly from the transmitter to the receiver and with only two thin acrylic sheets, as those forming the windows of the box, placed in between—the net passing time through the mortar is found. Dividing this passing time into the local thickness of mortar ($26\frac{3}{4}$ mm), yields the sound velocity c, which is related to the dynamic modulus of elasticity E_{dyn} by the equation

$$c = \sqrt{\frac{E_{dyn}}{\rho}}$$

where ρ is the mass of a unit volume of mortar. Figs. 8 and 11 below show E_{dyn}, calculated on this basis, versus curing time. Intervals between readings of passing times were of 5–15 min. in the beginning; later on they were increased to $\frac{1}{2}$–1 hour or more.

As a basis for relative evaluation of damping capacities was measured the strength of the electrical signal from the receiver, the transmitter being at all times driven with one and the same fixed voltage of the apparatus (Cawkel).

Provided that the maximum receiver voltage V is proportional to the amplitude of the first wave of the arriving wave train, the parameter $\log(1/V)$ should be a growing function of the damping which this wave has undergone by passing through the mortar, and eventual changes in it should be ascribed to gradual hardening of the cement paste. Now, certain contributions to total internal damping will be constant and independent of the mortar such as: the resistance against transmission of acoustical energy from transmitter through contact with vaseline to thin acrylic sheet, from here to mortar, and from this material to the corresponding layers on the receiver side. In this brief investigation, no correction has been attempted for these complications, and as is seen from Fig. 11, rather sudden and characteristic changes are obvious in "damping expression" $\log(1/V)$ as a function of curing time.

When possible, the damping capacity of the mortar was measured and calculated at the same times as the sound velocity.

Alkalinity (pH-Value)

The alkalinity of the cement mortar was determined by means of the cell:

Glass electrode | mortar pH | saturated calomel electrode.

The sample was taken directly from the mortar mix and put into an acrylic tube ($3\phi \times 5$ cm). On the pH-meter, single values are read to calibrate indications on the recorder (see Fig. 5).

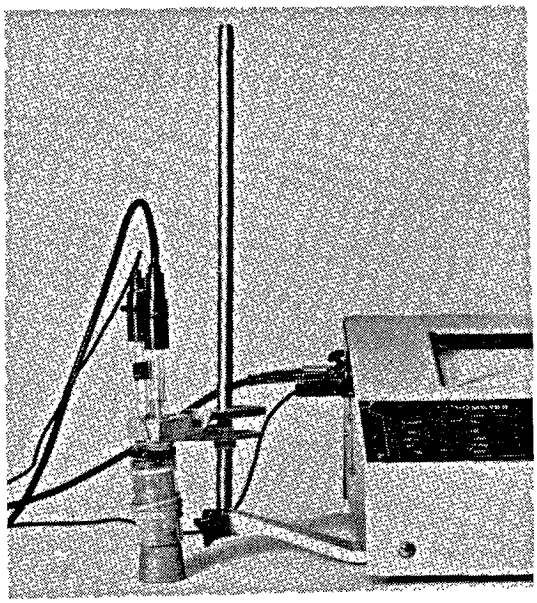

Fig. 5. *Electrodes inserted in mortar for registration of pH-value*

The curves cannot be used for an absolute determination of the alkalinity, as the pH-meter was not stable during the entire experiment. In order to save the electrodes, the recording was switched off after a few hours, when the mortar had set.

Non-Evaporable Water

The content of non-evaporable water in the cement paste was calculated on the basis of evaporable water content in the mortar.

From the center of cylinders crushed in the strength test two samples of about 10 g were taken and their weight determined by means of an analytical balance. The sample was pounded if necessary and immersed in alcohol to stop hydration. After evaporation of water and alcohol, the sample was dried for 24 hours at 105°C and the weight loss determined.

Volume Contraction

It has been suggested by W. Czernin (2) that the degree of hydration in cement paste may be determined by observation of the contraction which results from the increase in density accompanying the chemical fixation of water. To avoid the volume changes of water, which may be difficult to control during the temperature rise, the original procedure was modified and a special device developed.

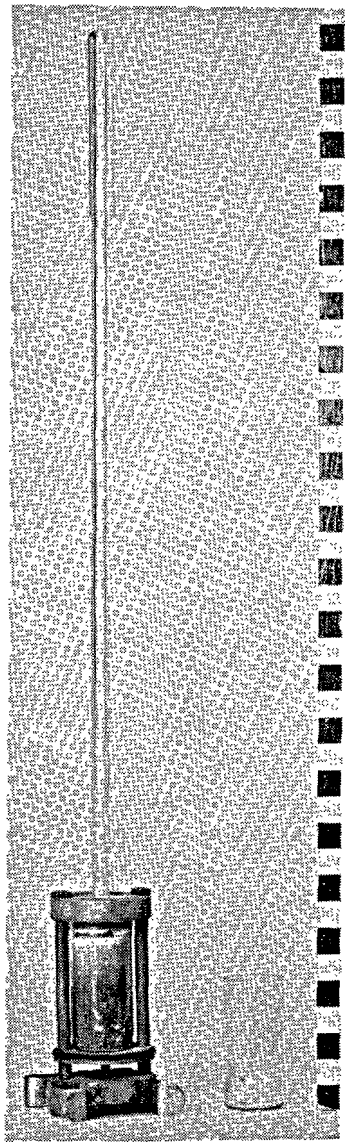

Fig. 6. *Device for determination of volume contraction in cement paste*

Water and cement was mixed by hand with a w/c-ratio of 0.5. Paste with 20–25 g cement was filled into a glass cylinder, evacuated during 15 min. hand compacted, and weighed. The cylinder was mounted in a holder with a graduated dilatometer tube (see Fig. 6), and submerged in water, the temperature of which was controlled by thermostat and did not deviate more than 1/10–1/20°C from the curing temperature aimed at (in the 80°C test, however, differences about 1/2°C occurred at the end of the curing period). The tube was loosely covered with a glass cap to reduce evaporation. It was calibrated along its length in hundredths of a ml, which allowed estimation of thousandths by means of a magnifying glass.

Observations

For each temperature level, three identical test series were carried out in order to ensure reproducibility. For those measurements which were undertaken at fixed times (strength and evaporable water), the three results were averaged, and mean values are used in the diagrams. For other quantities, which were recorded continuously or read at convenient intervals, averages have been formed when appropriate; in illustrations, however, typical curves selected among the three possibilities at hand have been used. Mean curves would not have been suitable, as interesting details might escape by the procedure.

Compressive Strength

Mortar cylinders were tested for compressive strength at the following ages: $\frac{1}{2}$, 1, $1\frac{1}{2}$, 2, $2\frac{1}{2}$, 4, 6, 8, 10, 12, 16, and 24 hours. At curing temperatures 60°C and 80°C the 8 and 10 hours measurements were omitted, and tests were made at 3 and 9 hours' age instead. In Table 3 are presented mean values and standard deviations from a statistical treatment, and the means are plotted in Fig. 7. It appears for curing at all 4 levels that after initiation of the strength development, the early stages of the hardening process

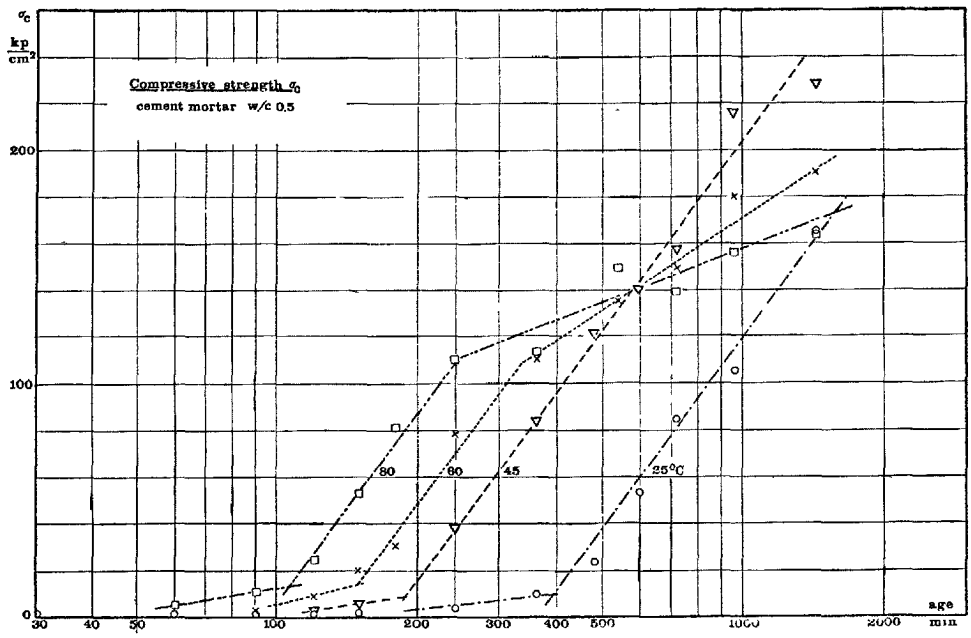

Fig. 7. *Development of compressive strength at different curing temperatures (indicated points are average of three observations)*

Table 3. *Compressive strength of mortar cylinders cured at different temperature levels;* m = *average;* s = *standard deviation* (kg/cm^2)

age	25°C		45°C		60°C		80°C	
(hours)	*m*	*s*	*m*	*s*	*m*	*s*	*m*	*s*
½	0.66	0.07	0.72	0.04	0.84	0.03	1.18	0.18
1	0.75	0.06	0.93	0.05	1.26	0.07	4.98	0.18
1½	0.89	0.07	1.35	0.12	2.38	0.16	10.7	0.5
2	0.98	0.09	2.73	0.16	8.1	1.7	24.3	0.9
2½	1.21	0.07	5.49	0.4	19.2	1.4	52.4	1.3
3					29.3	2.6	81	4
4	2.92	0.07	38.0	0.7	78	10	110	6
6	8.7	0.6	84	4	110	11	113	6
8	23.1	1.1	121	8			149	6
9					135	3		
10	53.1	0.6	140	11				
12	84	6	157	4	149	15	139	4
16	105	6	216	6	180	11	156	2
24	165	4	228	17	190	11	164	4

may fairly well be approximated by exponential growth curves (straight lines in diagram with logarithmic abscissa). At first the lines are parallel, but for the specimens cured at 60°C and 80°C the curves deflect, which results in strength values at 24 hours' age not much higher than those obtained by curing at 25°C.

Dynamic Modulus of Elasticity and Damping

Readings of the travelling time for sound waves were carried out with regular intervals as soon as a signal transmitted through the mortar could be picked up. As is seen in Fig. 11 it was possible at the lower temperatures to take readings of passing times as early as 15–25 min. after mixing. At the higher temperatures it lasted somewhat longer before signals from the transmitted wave were strong enough to affect the arrival mark trigger. This difference in sensibility may be explained by the decreased piezoelectric effect of the transducers at elevated temperatures; if this physical explanation were not realistic, it would look paradoxical that quicker hardening, as a result of higher temperature, should give increased internal damping in the mortar. After a relatively short period the readings gave a constant value, probably because contact failed between hardening mortar and form. Curves of the damping capacity

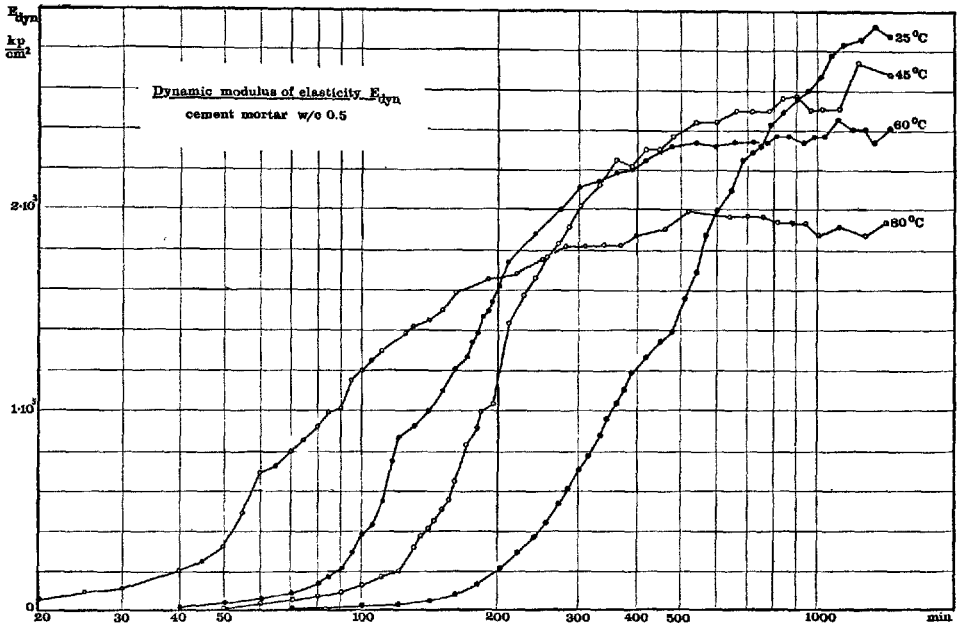

Fig. 8. *Typical curves for the development of dynamic modulus of elasticity at different curing temperatures*

are presented in a later section of this paper.

Typical curves of the development of E_{dyn} at the four temperature levels are shown in Fig. 8 (because of their abundance, not all observations are marked). From the 25°-curve it may be noticed, that the growth is rather regular within the first 24 hours, but the development, maybe, takes place within two separate periods: before and after curing in about 400 min. (this graduation is discernible in all three identical test series). The depicted curves for higher curing temperatures show similar features. Moreover, all of the curves seem simply to be parallel in the beginning. The transition from the first to the second part of the E_{dyn} development occurs at still earlier ages and at still lower values of E_{dyn} as the temperature rises. The second part of the elasticity increase, further, seems to be less intense at higher temperatures, which results in an obviously lower modulus at 24 hours' age.

Electrical Resistance

From typical graphs of the electrical resistance of the mortar cylinder, as produced by the recorder for each temperature level, a number of single points were selected and plotted in Fig. 9a-d as resistivity (ohm cm).

The four curves show some common characteristics: an initial slight decrease of the resistance is superseded by an increase, which becomes less and less pronounced as the curing temperature is raised. The subsequent local maximum appears to occur at a time which is particularly sensitive to temperature changes: it moves from about 450 min. at 25°C to 180 min at 45°C, 90 min. at 60°C and about 60 min. at 80°C. The decrease in resistance following the maximum point, results in a second minimum, and a final increase covers the rest of the examined curing period.

Volume Contraction and Non-Evaporable Water Content

Typical curves for the volume contraction in cm^3 per 100 g cement is shown in Fig. 10 for the 4 temperature levels. At 25°C the readings were continued beyond the 24 hours' period in order to facilitate comparison. It is noted that the curve at 45°C show a perceptible parallelism with that at 25°C, but this is not the case for those at 60°C and 80°C. The 60°-curve is roughly parallel with the foregoing for curing times below 150 min., but turns off and is at times beyond 1000 min. lower than the 45°-curve.

The 80°-curve hardly shows any tendency to parallelism at all, at the most during the first 50 min. The

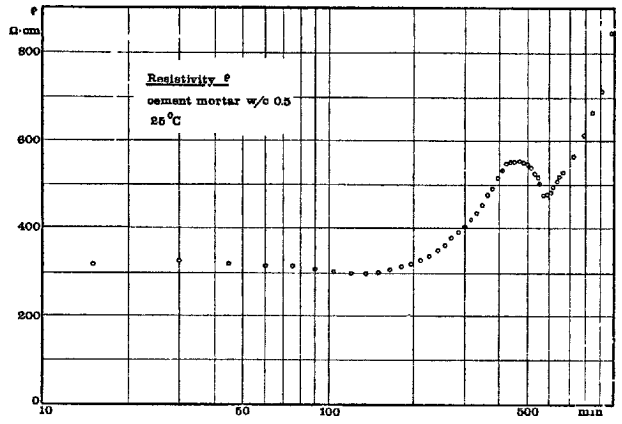

Fig. 9a.
cured at 25°C

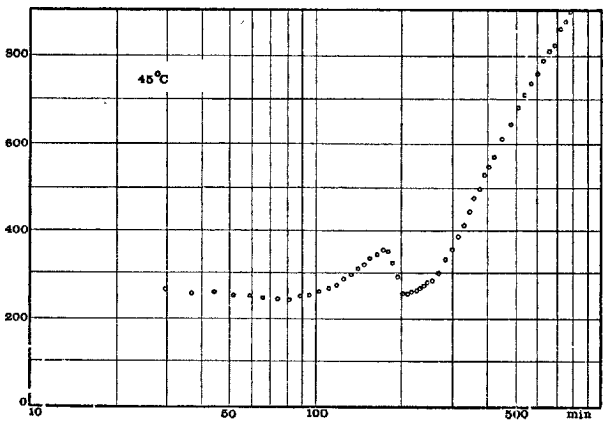

Fig. 9b.
cured at 45°C

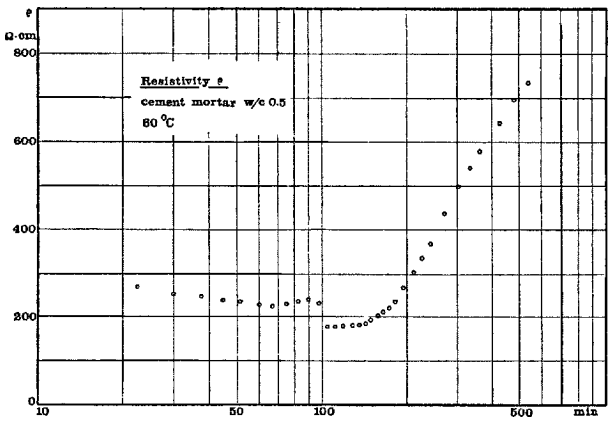

Fig. 9c.
cured at 60°C

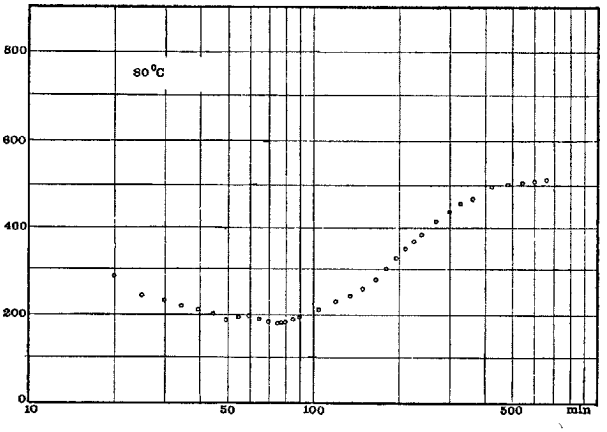

Fig. 9d.
cured at 80°C

Fig. 9. *Typical curves for the variation in electrical resistivity of cement mortar*

increase is then impaired during the next 50 min, is again intensified for a period, but merges slowly with the 60°-curve along the rest of its course.

The volume contraction can be used as a measure of the degree of hydration. According to Powers and Brownyard (3), the specific volume of the non-evaporable water is reduced by 24 per cent. The amount of non-evaporable water is, therefore, related directly to the volume contraction; the reduction of the specific volume of adsorbed water is negligible in comparison. The amount of non-evaporable water at complete hydration can be calculated from the clinker composition of cement as indicated by Copeland, Kantro and Verbeck (4):

$$\frac{w_n}{c} = 0.226(C_3S) + 0.194(C_2S: 0.982) + 0.510(C_3A) + 0.097(C_4AF) + 0.149(CaCO_4) = 0.219 \text{ g water per } g \text{ cement}$$

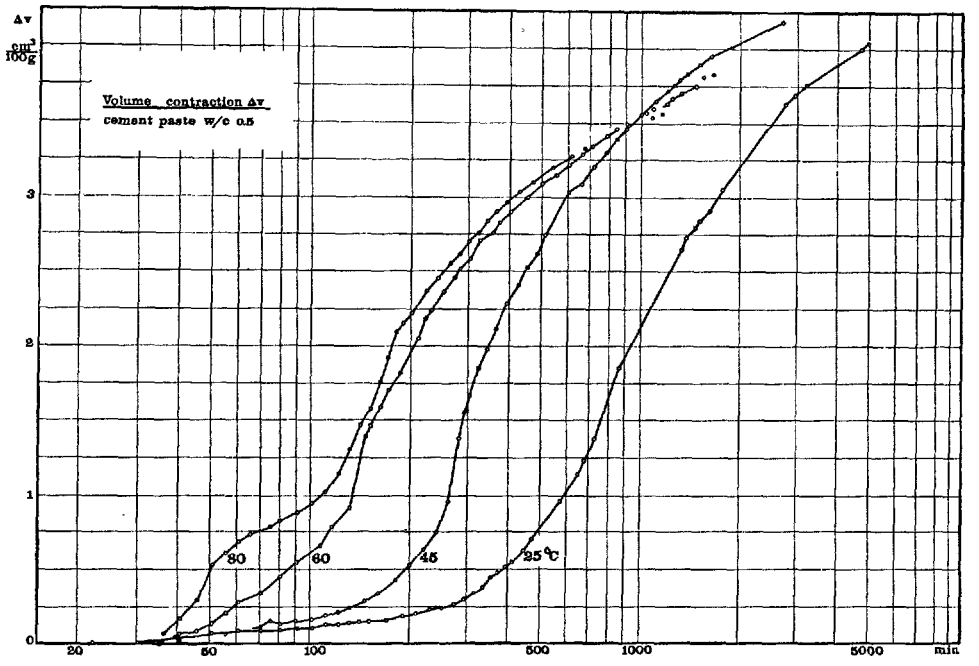

Fig. 10. *Volume contraction of cement paste cured at different temperatures*

Table 4. *Content of non-evaporable water in cement mortar after curing at different temperatures;* m = *average,* s = *standard deviation (per cent by weight of fresh mortar)*

age	25°C		45°C		60°C		80°C	
(hours)	*m*	*s*	*m*	*s*	*m*	*s*	*m*	*s*
½	0.62	0.09	0.82	0.18	0.92	0.15	1.75	0.32
1	0.69	0.10	0.42	0.09	0.83	0.11	1.53	0.17
1½	0.66	0.03	0.51	0.14	0.79	0.07	1.87	0.22
2	0.46	0.08	0.45	0.12	1.61	0.09	2.40	0.15
2½	0.55	0.08	0.48	0.14	1.90	0.24	3.07	0.21
3					2.22	0.15	2.79	0.12
4	1.24	0.08	0.67	0.30	2.82	0.16	3.39	0.36
6	1.22	0.18	1.98	0.07	3.03	0.31	3.38	0.28
8	1.23	0.06	2.73	0.14			3.98	0.24
9					3.61	0.29	3.43	0.09
10	2.11	0.13	2.64	0.09			3.22	0.60
12	2.02	0.19	2.58	0.19	3.38	0.11	3.93	0.18
16	2.20	0.14	2.65	0.25	3.75	0.22	3.38	0.23
24	3.69	0.15	3.70	0.10	4.03	0.17	4.45	0.23

This corresponds to a volume contraction of 5.25 cm³ per 100 g cement. The y-axis in Fig. 10 could therefore have been calibrated also in degree of hydration, with curves aiming at an asymptote $\Delta v = 5.25$ cm³ per 100 g.

The content of non-evaporable water determined by weighing and drying mortar samples, ought to result in values comparable with those obtained indirectly by the volume contraction. The sources of error inherent in the later method are, however, so significant that only the magnitude in general and the main tendency can be confirmed. Average values and standard deviations are presented in Table 4. The amount of non-evaporable water in the units used in the table (per cent by weight of fresh mortar) should at complete hydration be 4.87 per cent.

Discussion and Results

The methods used in this investigation have brought about some novel features of the hardening process and the effect of temperature. The determination of initial set, the development of mechanical properties in consequence of the chemical reactions during hydration, and time-temperature functions for concrete cured at temperatures between 20°C and 100°C, are particularly interesting and seem to indicate fruitful fields of future research.

The Setting Time

The development of rigidity in cement paste or mortar is usually characterized by the setting time determined e.g. by the Vicat needle or a similar penetration test. Physically, the initial set may be interpreted as the emergence of a continuous solid structure from the original dispersion of coarse solid particles in an aqueous solution.

Therefore, a determination of wave velocity and damping was aimed at as soon as possible after mixing, in order to detect early changes in these properties. Typical curves are shown in Fig. 11a-d, and it appears that the dynamic modulus of elasticity in the beginning remains on a low, fairly constant level corresponding to the low rigidity of water. The moment, when the rigidity with certainty starts to grow, can be determined rather precisely, and it is believed that a through network of solid matter exists in the paste at that time.

The internal damping is plotted in the same figures. As long as setting has not begun, the mobility of the system causes a considerable loss of energy. When continuity is established in the paste by formation of hydrates, this should be reflected by a decrease in the damping curve, as is actually the case in Fig. 11a and b, where the deflection points of damping are even more distinct than those of the elasticity. As damping became smaller with rising temperature it was increasingly difficult to obtain a discernible early signal, which is evident in Fig. 11c and d.

Another interesting detail may be observed from the damping curves: in the interval observed, the decrease markedly takes place at two different rates. The age at which the rate changes is 140 min at 25°C, 105 min at 45°C, and 70 min at 60°C (at 80°C the point could not be determined).

Chemical Reactions and Mechanical Properties

As concrete hardens, several chemical reactions are in progress in the cement paste. The reactions result in the formation of new solid compounds with mechanical properties depending on the structure of the hydrates. Because of the complex nature of the hydration, it has been considered rather difficult to interprete the mechanical properties of hardening cement paste in detail as regards the processes going on between water and single clinker compounds. Usually, the broader concept of relations between net fractions of reacted cement and physical properties is accepted. In order to throw some light on these matters, the principle of comparing rates was put to use. As readings for a number of properties had been made continuously or with short intervals, it was possible to calculate differentials with respect to time for the dynamic modulus of elasticity, for the electrical resistivity, and for the volume contraction. Maxima and minima on the differentiated curves will correspond to inflection points on the basic curves.

The results are interesting.

Firstly, the differential curves are reproducible. This is demonstrated in Fig. 12, where the changes in resistance, for the three parallel test series run at 45°C are shown as an example. It should be noticed that all the main features are repeated in each of the 3 curves. For the volume contraction, the reproducibility was only ascertained by a few duplications.

Secondly, it is possible to identify several chemical reactions and establish their connection with the development of mechanical properties. In the identification, also the observations of mortar temperature (see Fig. 13) and of alkalinity proved useful.

The Differential of the Dynamic Modulus of Elasticity

The differential of the dynamic modulus of elasticity is at 25°C clearly developing during two stages (A and B) separated by a minimum, approximately 450 min after mixing (Fig. 14a). The first stage (A) is subdivided with a local minimum at about 230 min and peaks after curing in 210 and 300 min. One may further notice that the beginning of the temperature rise (which occurs somewhat later in the box than in the cylinders due to the size effect) coincides with the second maximum after curing in 590 min.

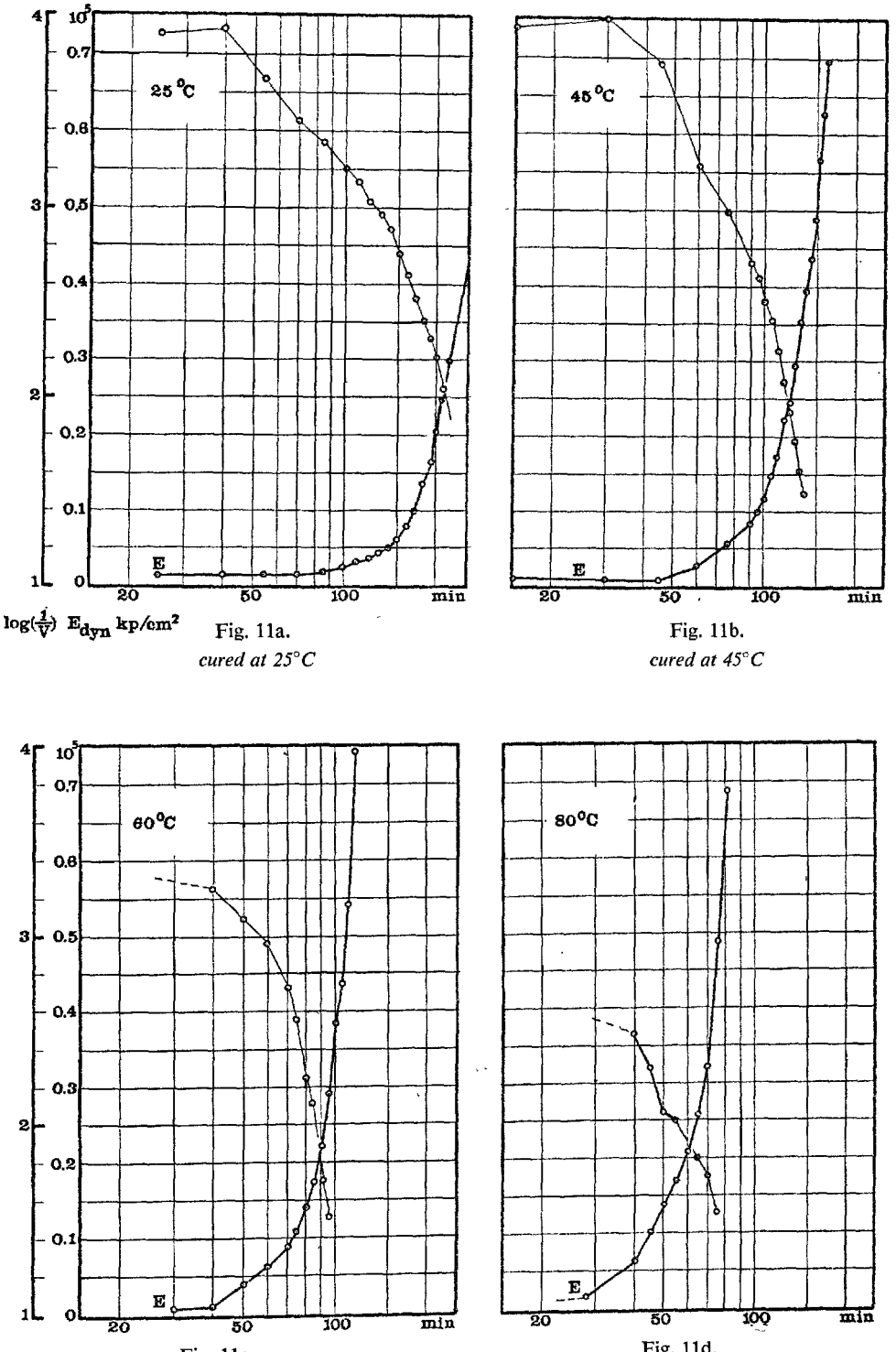

Fig. 11a. *cured at 25°C*

Fig. 11b. *cured at 45°C*

Fig. 11c. *cured at 60°C*

Fig. 11d. *cured at 80°C*

Fig. 11. *Typical curves of dynamic modulus of elasticity and internal damping of cement mortar*

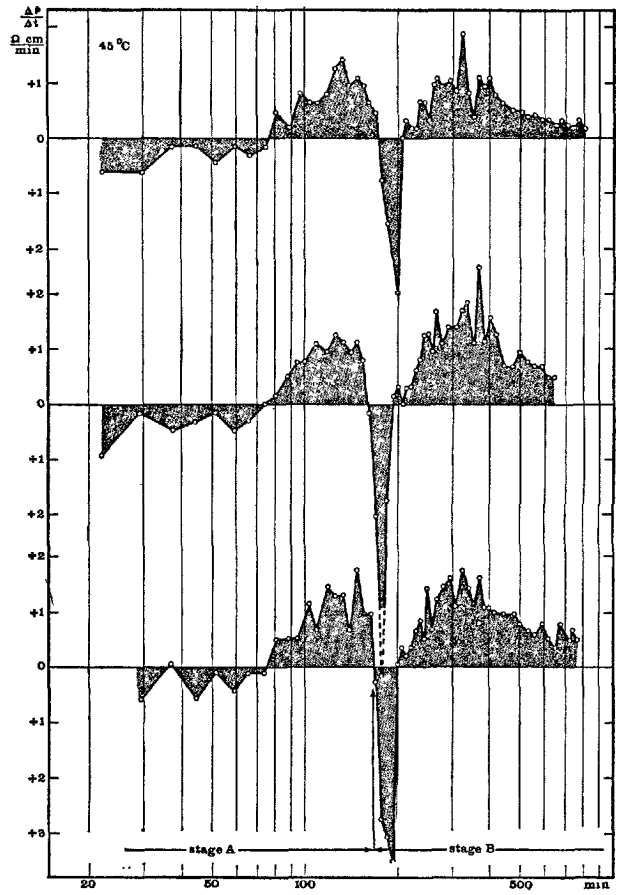

Fig. 12. *Differentials of the electrical resistivity as determined in three mortar cylinders cured at 45°C*

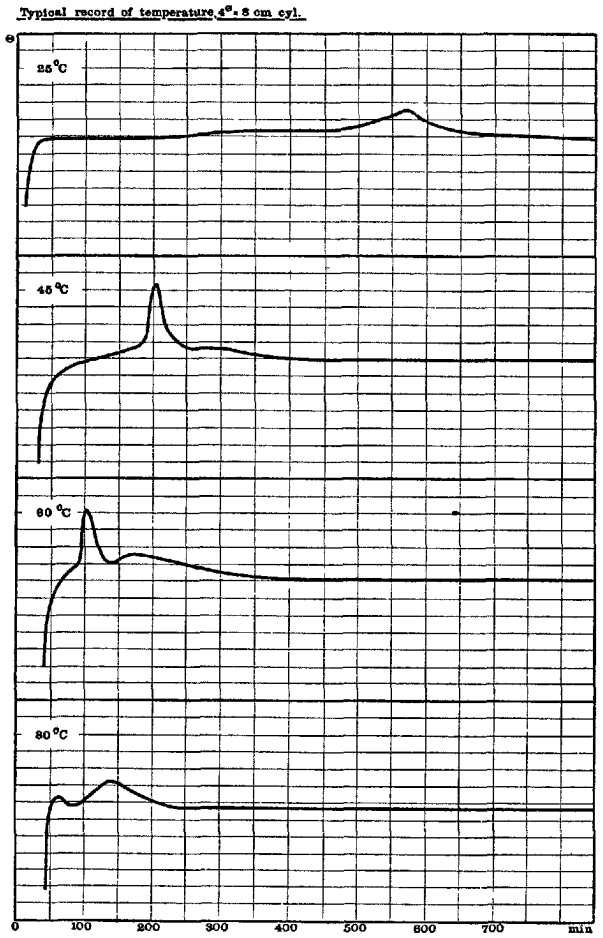

Fig. 13. *Typical recordings of temperature in mortar cylinders cured at different temperatures*

At 45°C the picture has not changed principally, the events only happen a little earlier, and peaks are more pronounced (Fig. 14b).

The first stage (A) has its maxima approximately after 125 and 165 min.; the separating minimum arrives after 185 min., and the peak in the second stage (B), which is now the highest one, comes after 200 min. Here, again, it seems that the temperature rise starts shortly after the highest peak. A very early peak (about 100 min.) and a rather late one (about 350 min) may be distinguished.

Important changes are noted at 60°C (Fig. 14c): the highest peak (in stage B) occurs after curing in only 115 min. That this peak actually corresponds to the one about 200 min at 45°C, is substantiated by its position relative to the temperature peak. The two stages are divided by the minimum at 125 min., and the second stage (A) is still characterized by 2 peaks, situated at app. 150 and 180 min. The final decrease now precedes a second, rather faint peak on the temperature curve.

The early peak and the late secondary one may still be discerned.

At 80°C (Fig. 14d), the first peak occurs after 75 min., the separating minimum after 85 min, and the two smaller peaks after 115 and 170 min. The two temperature maxima arrive shortly after the declines of the differential curves.

The curves shown in Fig. 14a-b are typical, and the values mentioned above refer to these curves. The ages at which the extreme values of elasticity differential and temperature occurred are summarized in Table 5. These times are averages of 3 observations, if available.

The Differential of the Electrical Resistivity

The differential of the electrical resistivity at the four temperature levels is illustrated in Fig. 15a-d, on which recordings of the pH-value are also shown.

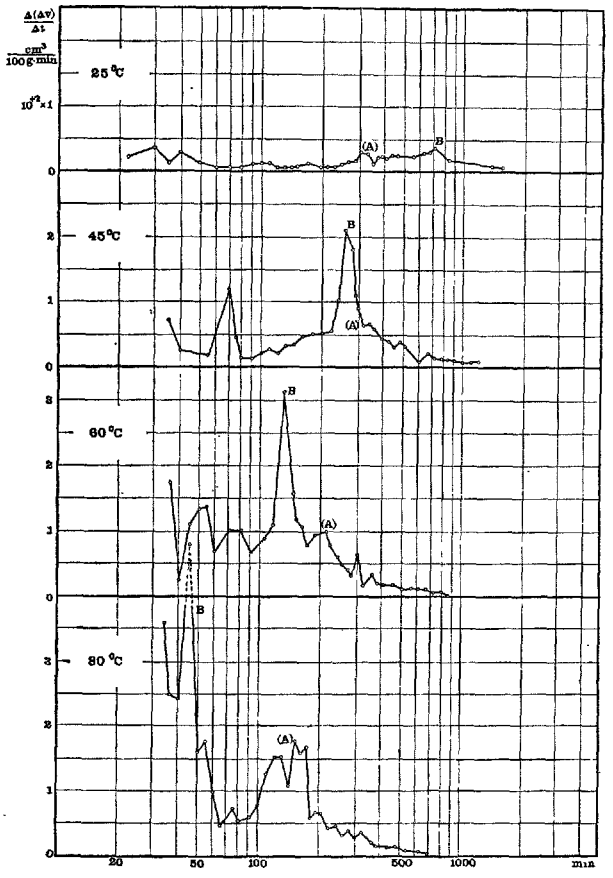

Fig. 14. *Differentials of dynamic modulus of elasticity for cement mortar cured at different temperatures*

Table 5. *The occurrence of characteristic values of the elasticity differential; temperature in mortar box and strength indicated for comparison (min after mixing)*

	Curing temperature	25°C	45°C	60°C	80°C
Stage A	Start of $\frac{\Delta E}{\Delta t}$	100	60	37	38
	Start of temperature rise	(165)	(130)	110	90
	Maximum 1 of $\frac{\Delta E}{\Delta t}$	203	128	153	112
	Minimum 1 of $\frac{\Delta E}{\Delta t}$	223	138	183	148
	Maximum 2 of $\frac{\Delta E}{\Delta t}$	285	163	201	164
Separating minimum of $\frac{\Delta E}{\Delta t}$		470	183	138	90
Stage B	Strength = 10 kg/cm²	390	190	150	105
	Start of temperature rise	450	210	125	75
	Peak of $\frac{\Delta E}{\Delta t}$	585	212	122	75
	Temperature maximum	610	250	145	90

The curve for curing at 25°C consists of 4 parts in which indications of the two stages A and B may be found. The resistivity is reduced during the first 125 min., but some change is perceived a little earlier (after curing in 100 min.); this is approximately at the same time as the first increase in elasticity is noticed. The resistance subsequently grows untill an age of 460 min. (A), but the change starts some 80 min. before and leads to a second negative area (i.e. falling resistivity) with a marked peak (B) at 540 min, which coincides with the temperature maximum. The resistivity increases once more during the rest of the observed period, but the differential seems to fall off at an age about 960 min. In this case the recording of alkalinity was discontinued rather early and does not supply much information.

At 45°C, the course is largely the same, but some acceleration is obvious. The negative part ends at 76 min. and the first maximum is reached at 130 min. The negative peak (B) covers the period from 170 to 205 min. and corresponds to the temperature maximum. The second maximum is situated at 330 min. and is more pronounced. The pH-value increases as the differential decreases and assumes negative values, i.e. corresponds to rising conductivity.

At 60°C, the first negative differential comes to an end after 56 min., and the positive area (A) hardly starts to build up, at 73 min., before the steep decline begins and results in a peak (B) at about 96 min.; again coincidence with the temperature maximum is noted. In the second positive region, a faint deflection point (or perhaps a secondary minimum separating A and B) is observed after curing in 170 min., and at this age the second temperature maximum is found. In the positive region a first maximum lies at 210 min and maybe a second one at 270 min. The pH-value rises as the negative peak occurs, i.e. from 90 to 110 min.

Finally, for curing at 80°C, the resistivity differential starts with low negative values at a minimum about 45 min after mixing, but increases rapidly to a narrow positive maximum at 52 min. The negative peak (B) is broader and less intense, setting in from 58 to 76 min. The second positive area shows two distinct maxima (B and A) and maybe more. The negative peak (B) corresponds still to the first temperature maximum and the relative minimum in the positive area to the second temperature maximum.

The alkalinity increases at the peak after (45 min and) after 60 min. Averages of the extreme values for the three curves at each temperature level is presented in Table 6.

The Differential of the Volume Contraction

The differential of the volume contraction is shown

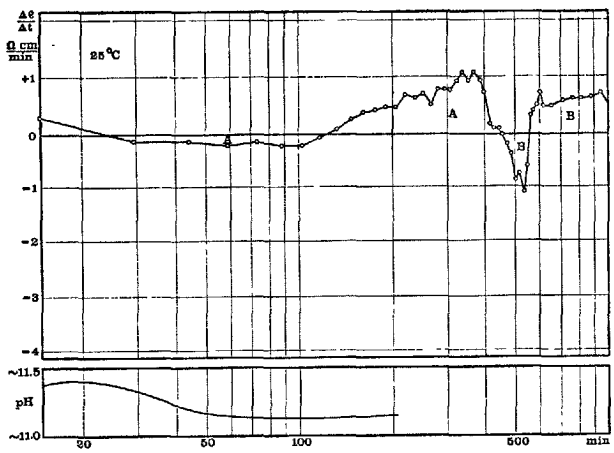

Fig. 15a.
cured at 25°C

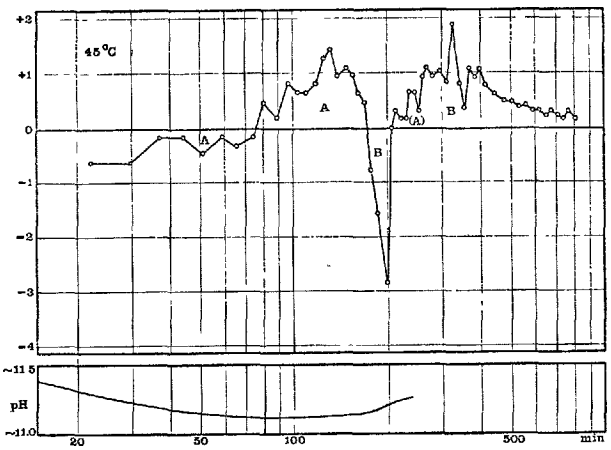

Fig. 15b.
cured at 45°C

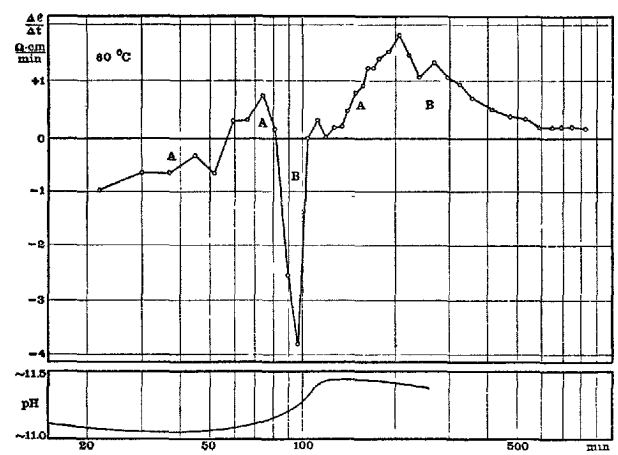

Fig. 15c.
cured at 60°C

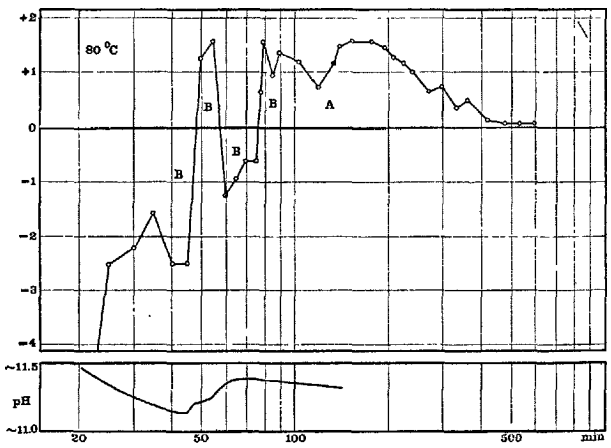

Fig. 15d.
cured at 80°C

Fig. 15. *Differentials of the electrical resistivity and the alkalinity both determined for cement mortar*

Table 6. *The occurrence of characteristic values of the resistivity differential; temperature in mortar cylinder indicated for comparison (min. after mixing)*

	Curing temperature	25°C	45°C	60°C	80°C
Stage A	$\frac{\Delta\rho}{\Delta t} = 0$	120	76	59	50
	Start of temperature rise	140	85	75	70
Stage B	Start of temperature rise	470	165	83	68
	$\frac{\Delta\rho}{\Delta t} = 0$	465	169	83	55
	Negative peak of $\frac{\Delta\rho}{\Delta t}$	555	192	96	64(42)
	Temperature maximum	585	202	105	57
	$\frac{\Delta\rho}{\Delta t} = 0$	585	203	104	74

in Fig. 16 for the four curing temperatures. They are perhaps—at least with the technique used in this investigation—less informative than the previous differentials, but some remarkable features were found.

At 25°C, the most intense hydration produces a peak at 710 min (stage B). The most distinct peak is at 45°C after 170 min., at 60°C after 130 min. and at 80°C after 45 min. This peak seems to move from right to left across a region (stage A) with a relatively high hydration rate. The region is probably characterized by two smaller peaks, which also increase

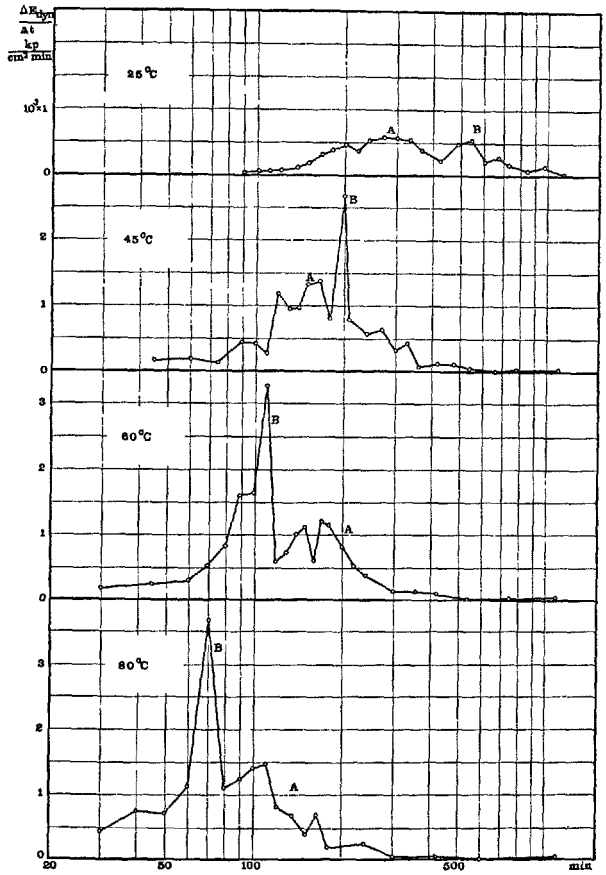

Fig. 16. *Differentials of the volume contraction of cement paste cured at different temperatures*

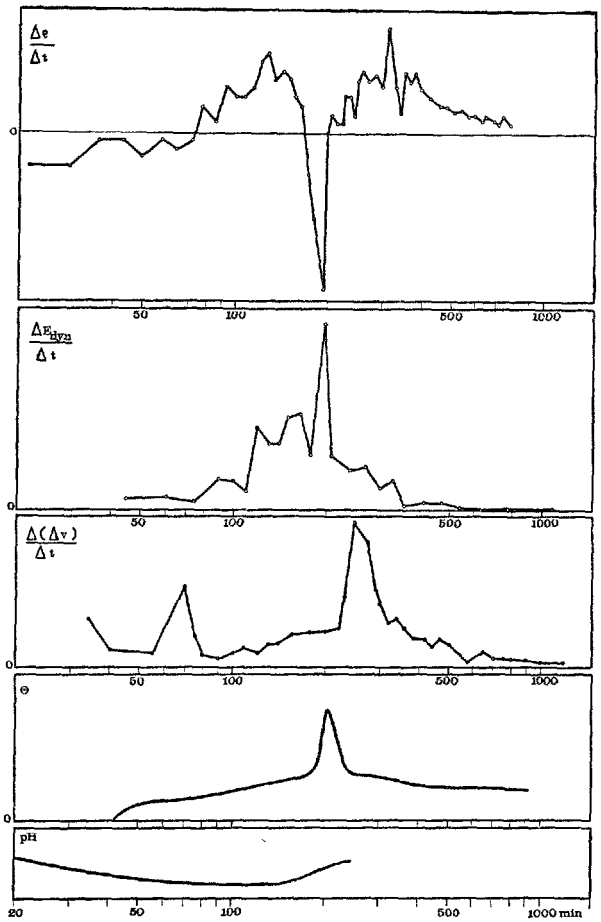

Fig. 17. *Mutually corresponding curves for resistivity differential, differential of modulus of elasticity, differential of volume contraction, temperature, and alkalinity for mortar cylinders cured at 45°C*

Table 7. *The occurrence of characteristic values of the volume contraction differential; temperature in mortar cylinders indicated for comparison (min. after mixing)*

	Curing temperature	25°C	45°C	60°C	80°C
Stage A	Maximum of $\frac{\Delta(\Delta v)}{\Delta t}$	320	280	180	140
	Maximum temperature	380	270	175	145
Stage B	Peak of $\frac{\Delta(\Delta v)}{\Delta t}$	710	260	135	45
	Maximum temperature	585	202	105	57

somewhat in intensity and also move from right to left, but more slowly than the highest peak. The region in question is, at 25°C, found after curing in 300–350 min., at 45°C after 150–350 min., at 60°C after 100–250 min., and at 80°C after 90–180 min. In Table 7 are presented the times when the maximum and the peak occur at the four curing temperatures.

Interpretation

Interpretation of the findings is based on Copeland and Kantro's account of the early reactions in cement paste (5): When cement is mixed with water, the "immediate" heat of hydration causes a temperature rise, which is not observed in this experiment, as mounting etc. lasted about 15 min. After a period extending from 1 to 3 hours (presumably at room temperature), 1 or 2 subsequent temperature peaks may be expected, caused by the hydration of the clinker minerals.

It was possible in the three differentiated curves to ascertain at least two different stages or processes, each characterized by its maximum rate and with a certain sensitivity to temperature changes. This is illustrated by Fig. 17 which shows in one diagram five curves obtained by curing at 45°C.

Considering first the course of events at 25°C, it may be assumed, that the first reaction at the end of the dormant period takes place between C_3A and water; this will cause a heat development, which can

be perceived as a slight, but lengthy temperature increase (Fig. 13). The formation of hydrates gives the system some rigidity, which is seen from the modulus of elasticity (Fig. 14), but the solid matter will decrease the mobility of ions, i.e. the electrical resistivity will increase (Fig. 15a). When C_3S begins to react, calcium hydroxide is formed, i.e. the alkalinity will grow (which is not covered by Fig. 15a), the temperature shows a marked peak (Fig. 13), the electrical resistivity falls rapidly in consequence of the ion activity, but increases again as new solid matter is formed (Fig. 15a), which is also reflected in a second, different increase in the modulus (Figs. 8 and 14) and in the strength increment, manifest only at this age (Fig. 7).

As the temperature is raised this sequence of the processes changes. At 45°C, the order is largely the same (see Fig. 17), but at 60°C the C_3S reaction appears prior to the C_3A reaction. This picture is repeated at 80°C, but there are indications of three reactions: the resistivity shows 2 negative minima, one at 40–45 min. and another at 60–70 min. (Fig. 15d). As both C_3S and C_2S produces calcium hydroxide during hydration, this seems a reasonable explanation also of the small changes in the pH-curve, which can be distinguished. Hereby may further be explained, why the temperature rise (start to maximum) in stage B, which for curing at lower temperatures coincides almost exactly with the negative peak in the resistivity differential (See Table 5), at 80°C seems to be somewhat displaced to the left—as it ought to be because the hydration of C_3S and C_2S will both release heat.

Time-Temperature Functions and Reaction Rates

By definition a time-temperature function is a variable $f(\theta)$ by which the duration t of a process at one temperature θ can be converted to the duration t_a of the same process at another temperature Θ_a:

$$t_a = f_a(\theta) \cdot t$$

For concrete hardening at low and normal temperatures, the effect of the temperature level on concrete properties is often taken into account by the use of time-temperature functions, and this has also been attempted for accelerated hardening at curing temperatures not exceeding 100°C. Different forms of time-temperature functions have been proposed, some empirical (6) and some based more or less on the Arrhenius equation (7). Much seems to indicate, that at least two processes govern the early stages of hydration; therefore, a time-temperature function derived from the Arrhenius equation cannot be expected in detail to give an accurate description of properties dependent on these processes.

If one wants, nevertheless, to apply a time-temperature function, it is necessary either to consider only phenomena resulting from a single process or to accept certain deviations. Both approaches have been tried on data obtained in the present investigation.

It was attempted to find the reaction rates by applicating the Arrhenius equation on such characteristics of the hydration process which seemed to depend on only one reaction. Characteristic points belonging to three different properties, but depending, presumably, on the same reaction (C_3S hydration) were chosen: the peak of the E_{dyn}-differential, the peak of the ρ-differential, and the peak of the Δv-differential. At the higher curing temperatures, some of these events occurred before the mortar temperature had reached the presupposed level. It was decided in such instances to transform the periods, during which acceleration was achieved at all, in time at the proper temperature, by means of the Nurse-Saul maturity concept, and to discount the period, when no acceleration took place. In Tables 8–10 are shown the observed time, the correction and the "reaction rate" taken as the reciprocal of the time.

Table 8. *Determination of reaction rate by means of the E_{dyn}-differential peak*

$\frac{\Delta E}{\Delta t}$-peak	25°C	45°C	60°C	80°C
Observed occurrence	585	212	122	75
Corrected time	565	173	88	35
Reaction rate (nominal)	1.77	5.75	11.4	28.6

Table 9. *Determination of reaction rate by means of the p-differential peak*

$\frac{\Delta \rho}{\Delta t}$-peak	25°C	45°C	60°C	80°C
Observed occurrence	555	192	96	64
Corrected time	535	170	72	34
Reaction rate (nominal)	1.87	5.90	13.9	29.4

Table 10. *Determination of reaction rate by means of the Δv-differential peak*

$\frac{\Delta(\Delta v)}{\Delta t}$-peak	25°C	45°C	60°C	80°C
Observed occurrence	710	260	135	45
Corrected time	680	233	103	16
Reaction rate (nominal)	1.47	4.29	9.7	62.5

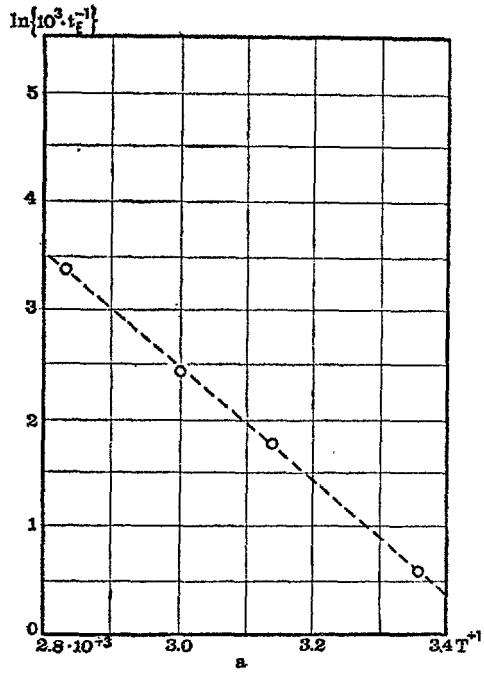

Fig. 18a.
peak of elasticity differential

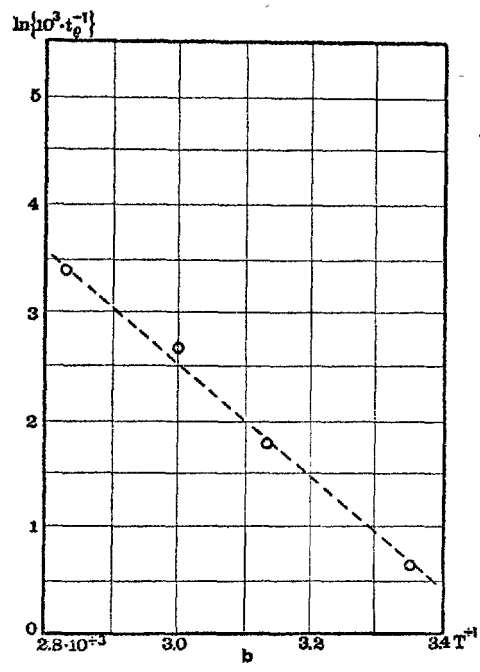

Fig. 18b.
peak of resistivity differential

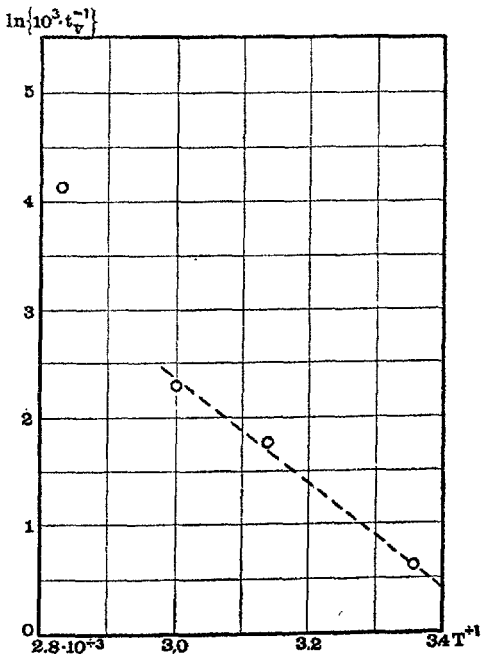

Fig. 18c.
peak of volume contraction differential

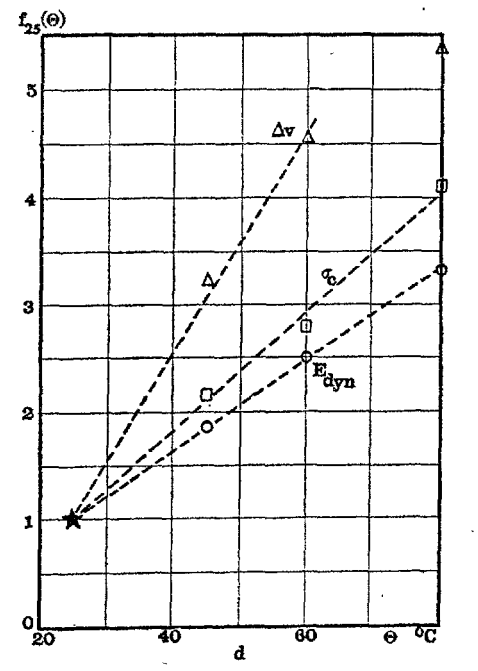

Fig. 18d.
different maturity functions

Fig. 18. *Reaction rates and time-temperature functions*

The logarithms of the rates are plotted in Fig. 18 versus the inverse of the absolute temperature. The almost straight lines obtained indicate a fairly good agreement with the Arrhenius formula

$$\text{rate} = \text{constant} \cdot e^{-Q/RT}$$

in which Q is the activation energy, R is the gas constant and T is the absolute temperature.

The elasticity line and the resistivity line give by calculation the same slope from which the activation energy is found to $Q = 29.6$ kcal/mol. The three points from the volume contraction, which forms a straight line, gives $Q = 28$ kcal/mol. This is not inconsistent with the reaction energy of C_3S.

In the following, a range of variation about 25% ($\pm 12.5\%$) is regarded as acceptable.

For the compressive strength it is possible to convert the curing times at 45°C, 60°C and 80°C to curing time at 25°C within limited ranges of the compressive strength (see also Fig. 7):

25°C: $f_{25}(25) = 1.00$ (by definition)
45°C: $f_{25}(45) = 2.15$ (valid for all observed values)
60°C: $f_{25}(60) = 2.81$ ($\sigma_c < 120$ kg/cm²)
80°C: $f_{25}(80) = 4.15$ ($\sigma_c < 110$ kg/cm²)

The values of the time-temperature function are shown in Fig. 17d.

For the dynamic modulus of elasticity, the following values of a time-temperature function may be found under the same conditions (see also Fig. 8):

45°C: $f_{25}(45) = 1.87$ ($E_{dyn} < 2.35 \cdot 10^5$ kg/cm²)
60°C: $f_{25}(60) = 2.47$ ($E_{dyn} < 2.05 \cdot 10^5$ kg/cm²)
80°C: $f_{25}(80) = 3.30$ ($E_{dyn} < 1.60 \cdot 10^5$ kg/cm²)

Finally, it was attempted to apply the principle in the same way on the volume contraction, but with less success because only intermediate intervals could be used without excessive variations:

45°C: $f_{25}(45) = 2.76$ ($1.1 < \Delta v < 3.7$ cm³/100 g)
60°C: $f_{25}(60) = 4.52$ ($0.5 < \Delta v < 2.8$ cm³/100 g)
80°C: $f_{25}(80) = 5.35$ ($0.8 < \Delta v < 2.6$ cm³/100 g)

Also the time-temperature functions obtained by the modulus of elasticity and by the volume contraction are depicted in Fig. 18d.

With good approximation, the calculated points are on a straight line, with the exception of the one corresponding to Δv at 80°C. This confirms that the development of concrete properties by curing at temperatures from 25°C to 80°C can be described by means of maturity functions (sum of products time and temperature).

Conclusion

It was possible to establish a series of facts, which allow the following interpretations:

1. Curing at elevated temperatures below 100°C accelerates the development of mechanical properties. The acceleration can be accounted for by means of the concrete maturity, but at ages of about 24 hours the quality obtained by curing above 45°C may be impaired due to other influences.

2. By curing at temperatures above 45°C it seems that the hydration of C_3S is accelerated in particular, and in cases where this process starts before the hydration of C_3A, the mechanical properties may be injured.

3. A comparison of the development of physical and chemical properties during the hardening of concrete—according to the applied rather simple methods—already appears promising. Further detailed insight in hydration processes will no doubt result from a more refined technique based on the same principles.

Additional Investigation

The investigation reported in supplementary paper III-108 has been supplemented with a test series carried out by Mrs. Karen Mønsted, in which the gypsum content of the cement was increased. This retarded and flattened peak B. The original interpretation of the reactions A and B as, therefore, not correctly. When peak B occurs later with higher gypsum contents, it must represent a reaction with C_3A. This interpretation provides, in addition, an explanation of the strength decrease at high curing temperatures: the formation of solid structure by the hydration of C_3S might be disturbed, because the ettringite is not stable at high temperatures, but is transformed into monosulphate.

References

1. "On the testing of cement", p. 44, (Cembureau, Malmö, Sweden 1956).

2. W. Czernin, "Zementchemie für Bauingenieure", 2nd ed., p. 78 (Bauverlag, Wiesbaden-Berlin, Germany 1964).
3. T. C. Powers and T. L. Brownyard, "Studies of the physical properties of hardened portland cement paste, Part 5", J. Am. Con. Inst., Proc. **43**, p. 669–712 (1947).
4. L. E. Copeland, D. L. Kantro and G. Verbeck, "Chemistry of hydration of portland cement", Chemistry of Cement, Vol. I, p. 429–465, U.S. Department of Commerce, National Bureau of Standards, Washington, U.S.A. 1962.
5. L. E. Copeland and D. L. Kantro, "Chemistry of hydration of portland cement at ordinary temperature", The chemistry of Cement, Vol. I, p. 313–370 (Edited by H. F. W. Taylor, Academic Press, London and New York 1964).
6. R. W. Nurse, "Steam curing of concrete", Mag. of Concr. Res., **1**, p. 79–88 (1949).
7. E. Rastrup, "Heat of hydration in concrete", Mag. of Concr. Res., **6**, p. 79–92 (1954).

Oral Discussion

Hideo Teramoto

Generally, before high-temperature curing to accelerate hardening of concrete, pre-curing is performed at normal temerature for several hours. Also, the temperature rise is made to be gradual. It is considered raising temperature without precuring or suddenly raising temerature will have adverse effects on strength and other properties of concrete.

The authors cure mortar specimens immediately after molding by placing them in water tanks maintained at 25°C to 80°C. It is wished to know the reason or purpose of these tests in which curing methods which are rarely used in actual practice were adopted.

Author's Closure

John Jessing

The remarks by Mr. H. Teramoto touches upon a important question, and I am happy for this opportunity to discuss it.

The purpose of our investigation was *not* to imitate curing conditions in practise, because the procedures which are used generally will confuse the different influences on the hydration process. Our purpose was—as a first step—to investigate the influence of the temperature *level* on the hydration process and mechanical properties. The next step might be to find the influence of temperature *changes* on the hydration process and mechanical properties. A more detailed presentation of the principal point of view is given in the written discussion in session III by Jessing and Nerenst, and I beg to refer to this.

SESSION III-5 HIGH-TEMPERATURE CURING OF CONCRETE UNDER HIGH PRESSURE

Principal Paper High-Temperature Steam Curing of Concrete at High Pressure

George L. Kalousek*

Synopsis

H. F. W. Taylor reviewed the science of hydrous calcium silicates and, more recently, some practical applications of the findings. With this background, this paper is developed partly around the results of examinations of 24 commercially produced autoclaved products. The binders were strongly to poorly crystallized tobermorite, $C_5S_6H_5$. Some contained a low lime tobermorite gel designated $C_{5-6}S_6$ Hn for given reasons. Laboratory tests to explain the difference between Taylor's C–S–H(I) and $C_{5-6}S_6$ Hn lead to a tentative conclusion (with reservations) that C–S–H(I) is a poorly to well-crystallized variety of tobermorite. On the other hand, $C_{5-6}S_6$ Hn is the precursor of the Lock Eynort tobermorite, the phase found as a binder in the commercial products.

The gel-crystal phase composition of the binder relates to physical properties of the products. This is an area of future fruitful research. The possible important effects of ion (Al^{3+}, Fe^{3+}, SO_4^{2-}, etc.) substitution in the lattice of tobermorite on properties is discussed. Possible techniques of differentiating between gel and crystal phases in a binder are reviewded.

Introduction

The chemistry of autoclave curing of concrete is essentially the chemistry of the reaction of CH with S and/or silicates in high-temperature steam at high pressure. Portland cement may supply all the C and part of the S or silicates. Any additional S required is supplied as ground quartz or other reactive siliceous materials such as fly ash, shale fines, oil shale ash, aggregate fines, etc. The CH for production of sand-lime brick, fine grain (sand) concrete, and similar products is available as quicklime, hydrated lime, by-product lime including nepheline slurry (largely βC_2S), etc. The principal requirements of lime and S are that both be sufficiently reactive to yield binders of satisfactory quality and at competitive costs.

Autoclave curing according to Bessey (1) was first applied in Germany in 1898 for curing sand-lime brick. The new industry grew rapidly in several countries. About two to three decades after this start, autoclave curing extended into commercial production of concrete block and products, asbestos-cement products, cellular concrete, thermal insulation and structural light weight calcium silicates, calcium silicate fillers and other products. Concrete now being developed for the upper temperatures of evaporator chambers in sea water desalting plants is another autoclaved material.

The growth of the industry, worldwide, was especially rapid in post World War II years. A large variety of products made from several different raw materials are being produced in large volume in the Soviet Union. The status of the industry there was reported in a Rilem Symposium (2). A review of that symposium including comparison of the autoclave curing industries in the Soviet Union and the United States was published (3). Proceedings of a symposium (4) in London in 1964 documents the status of the autoclaved calcium silicates especially of sand-lime brick. The report of ACI Committee

*Concrete Department of the Interior, Bureau of Reclamation, Denver Federal Center, Denver, Colorado, U.S.A.

516, High Pressure Steam Curing (5), describes modern practices and properties of autoclaved products mostly in the United States and Canada. Taylor (6) reviewed the importance of the chemistry in the industry. Important relations between properties and chemical nature of the binders were summarized by Hansen (7). Volzhensky (8) reported on the impact of autoclave curing on the structural concrete industry in the Soviet Union. These relatively recent reports reflect the strong sustained growth of, and progress within, the industry. Bessey (9) predicted further extensive increase in use of autoclave curing in the field of concrete structural products.

Undoubtedly chemistry will play an increasingly important role in the advances to be made. During the first three to four decades of the industry, chemistry made only small contributions. In 1929, Thorvaldson and Shelton (10) discovered αC_2SH in autoclaved cement pastes, but the significance of the discovery remained obscure for over 20 years. The earlier attempts to identify the binders of sand-lime brick by optical microscopy and XRD (11, 12) were unsuccessful. These research tools lacked sufficient resolution. Also, reference phases prepared under controlled laboratory conditions were not always available. In 1952, Taylor (13) identified by XRD the binder of a commercially produced sand-lime brick which later was recognized as tobermorite. This and other investigations were the forerunners of the chemistry of autoclaved products.

The early practical advances were achieved almost entirely through empirical approaches. Correlations of physical properties, generally strength and shrinkage, with the kinds and compositions of the raw materials and conditions of autoclaving supplied information applied in the production. The contribution of chemistry to the technology, however, has made sizable advances during the past 10 to 20 years. Projections based on these accomplishments indicate increasing usefulness of basic chemical research in the industry. This paper is a review of the contributions of chemistry to the technology. An attempt is made to direct attention to areas of chemical research which appear to have considerable promise.

The rather extensive basic chemical research on hydrated calcium silicates conducted during the past 20 years, and areas of related technology, is given in excellent review reports by Taylor (6, 14, 15, 16) and by Heller and Taylor (17).

A new mineral addition to the family of hydrous calcium silicates is jennite, $NC_8S_3H_{11}$, recently described in detail (18).

Background Relating to Binders

The first laboratory experimental results showing effects of high-pressure steam on strengths of portland cement specimens were published in 1911 by Wig (19). Several similar studies on cement with and without additions of silica (20, 21, 22, 23, 24, 25) were conducted. Woodward (21) and Menzel (24) demonstrated that drying shrinkage was markedly reduced by autoclaving. Miller (20) and Thorvaldson (23) reported that specimens cured in the autoclave had significantly better resistance to sulfate attack than normally cured products. Menzel (24) developed the optimum silica replacement for cement for maximum strength and minimum shrinkage, this being about 40% silica and 60% cement by weight. Mironov and Malinina (25) reported extensive results of tests on various proportions of different cements and pure clinker phases with silica for different steam pressures and times of curing. Their results showed that the binders having highest strengths had C/S ratios of 0.9 to 1.0. They demonstrated that the optimum $\bar{S}$ content of specimens autoclaved at 175°C was 1.0 to 1.5%. With exception of results by Bozhenov and Kavalerova (26), to be discussed, the binder compositions most frequently reported were 0.9–1.0 C/S. The mineral of the binder was generally not identified.

The XRD reexamination of tobermorite from Tobermory, Scotland, by Claringbull and Hey (27) supplied data on a most important reference standard. Data like Taylor's (13) showed the binder of an industrial product was tobermorite. The XRD data on a lime-silica product disclosed in a U.S.A. patent (28) was in complete agreement with the Claringbull-Hey data. The exact formula, $C_5S_6H_5$ was deduced by McConnell (29). The average values of complete analysis of several preparations (showing the complete tobermorite pattern) for C,S,$\bar{C}$, free C and free S (30, 31) gave a C/S ratio of 0.83 in excellent agreement with the 5C:6S (0.833) value reported by McConnell.

An application of chemistry was made (32) in the interpretation of the minimum and maximum

strength in Menzel's strength vs silica replacement relation. The low strength was attributed to αC_2SH and the maximum strength to a phase of 0.9 to 1.0 C/S. Butt and Krzheminski (33) and Butt, Rashkovich, and Danilova (34) reported similar findings on autoclaved calcium silicates made of calcium silicates and silica. Malinina (35) associated low strength with αC_2SH and high strength with a phase of 0.8–1.0 C/S.

The C/S ratio, generally reported 0.9–1.0, is substantially higher than the 0.83 C/S ratio of tobermorite. Further, the 0.9–1.0 C/S binder reported in one investigation (32) exhibited an exotherm at about 830–840°C which pure tobermorite does not show. These inconsistencies were reconciled by studies (31), to be discussed, showing that 1.18% S was replaced by 1.00% A in the tobermorite lattice. In a 1.0 C/S raw mix containing 4.0% A the actual C/(S+A) ratio is close to 0.83. The A-substituted tobermorite, unlike pure C-S tobermorite, exhibited an exotherm at about 830–840°C. The XRD patterns of tobermorite and A-substituted bobermorite were identical except for a small increase of the basal spacing at 11.3Å to about 11.5–11.7Å by A substitution.

In order to develop reference standards from raw materials used commercially, pastes of cement and ground quartz, shale, pumice or slag fines were autoclaved (36) following a plant cycle with 8 hours at 175°C. The sample having C/(S+A) ratios of 0.8–0.9 gave satisfactory XRD patterns for tobermorite. It was, therefore, assumed that the commercially produced counterparts also contained tobermorite as binder.

The most readily synthesized calcium silicate using CH and ground quartz is xonotlite, C_5S_5H. It forms rapidly at 200°C and higher temperatures. At temperatures around 200°C, xonotlite would be expected to be the binder in many commercially produced products. Most raw materials contain sufficient Al_2O_3 to stabilize tobermorite, and only a few tenths of a percent of Al_2O_3 retard xonotlite formation. Tobermorite forms first and is stabilized by the Al_2O_3 in the lattice. Xonotlite has very low drying shrinkage compared to tobermorite (37) and has been patented (38) as a high-temperature thermal insulation. Xonotlite may form in sand-lime brick made with pure silica sand and pure CH and cured at temperatures around 200°C. Bessey (1, 39) reported some very low drying shrinkage of samples of sand-lime brick in which he found microscopically long needle-like crystals (morphologically similar to xonotlite crystals). Based on similar observations including XRD, it was suggested the binder was xonotlite (40).

Other calcium silicate hydrates beside tobermorite and xonotlite have capabilities as binders and were discussed by Taylor (6). Bozhenov and Kavalerova (26) autoclaved nepheline slurry, CH and $C\bar{S}H$ mixtures of 2.3 C/S. At temperatures of 225°, 265°, 310°C they reported presence of tobermorite gel, gyrolite, xonotlite, αC_2SH and C_3SH_2, with highest strength obtained on products autoclaved at 265°C. It is not known if so high a temperature (265°C) is economically feasible using cement and quartz.

The equilibria involving gyrolite and the related phase truscottite (or reyerite), Z-phase of Assarsson (41) and other phases as xonotlite and tobermorite were described by Harkins (42). Taylor (6) reported that gyrolite and the Z-phase can be synthesized at pressures used commercially. It may be speculated, however, that a relatively high silica concentration in solution would be required (6, 40, 42, 43, 44).

The high costs of silica gel or silica glass to supply silica for solution may militate against gyrolite and related phases as binders for commercial products. Taylor (6) discussed other possible related binders but technological results are still too limited to permit drawing conclusions about practical use of these.

Identification of Binders in Commercial Products

Results of XRD examinations of binders of 22 commercially produced autoclaved products, two deep oil well cements autoclaved in the laboratory and several reference samples have been published (45, 46). Out of the total of 24 commercial products, the binders of 22 were reported to be tobermorite in different degrees of crystallinity and some contained $C_{5-6}S_6Hn$ (the formula, CSHn, previously used has been modified for reasons to follow). The two unidentified binders might have been poorly crystallized tobermorite and $C_{5-6}S_6Hn$ but interference of aggregate and calcite lines in the XRD patterns precluded positive identification.

Only two of the samples contained a phase other than tobermorite or $C_{5-6}S_6Hn$ in more than trace amounts. One asbestos-cement product contained

in the order of 7–12% αC_2SH. A sand-lime brick contained a significant, but not major, amount of $C_3SH_{1.5}$. Information was not available on raw materials, and proportions, or autoclaving conditions and, therefore, no explanation can be advanced for the presence of these extraneous phases. Other phases were present in some of the samples but on basis of very weak intensities of the strongest XRD lines of such phases, the amounts were regarded as traces generally less than 1%. Among these were cement clinker phases, CH (0.0–0.7%), gyrolite, $C_3SH_{1.5}$, αC_2SH and perhaps others. The hydrogarnets were not detected. The trace amounts of CH, coexisting with residual silica (which always was present as excess fines or aggregate), may appear surprising. It has been observed (47) that residual clinker phases persisted in autoclaved asbestos-cement samples immersed in saline water for 20 years. The explanation is that the residual clinker phases are completely surrounded by impervious hydration products. This explanation may also apply to the presence of the phases named above, and still others. Aitken and Taylor (48) detected several phases in cement or cement-silica pastes autoclaved for different periods of time. The time of autoclaving was less for some samples, and more for others, than usually used in commercial production. Kennerley (49) examined nine grout samples exposed to temperatures up to 225°C in geothermal bores. Exclusive of $C\bar{C}$ and CH, the binders of the cement grouts were largely αC_2SH and, of cement-pozzolan grouts, one or more of the "tobermorite family" depending on C/S ratio. Xonotlite, hillebrandite, and γC_2SH were detected in lesser amounts.

The identification (45, 46) of tobermorite was based on the three strongest XRD lines of this phase, 11.3, 3.07, and 2.97Å. A second parameter, the ratio of intensities of the 2.97/3.07Å lines, was introduced for purpose of differentiating between Taylor's C–S–H(I) (intensity ratio equal to 0.0) and tobermorite (intensity ratio equal to 0.70–0.80). Also this parameter was useful in identifying tobermorite in samples containing calcite. Low-lime tobermorite gels were described by Kalousek (50, 30) and Neese (51) as a series of solids of composition C_4S_5Hn (actually revised later to C_5S_6Hn), CSHn, C_5S_4Hn, and C_4S_3Hn. The C_4S_3Hn, synthesized only at room temperature, decomposed into C_5S_4Hn and αC_2SH in an autoclave at 175°C (52). Not being a stable autoclave product, it is not considered further in this paper.

The C_5S_6Hn and CSHn were prepared as separate solids characterized only by composition and an exotherm at 830 ± 5°C. The only difference between the two, detectable instrumentally, was in the much stronger intensity of the exotherm exhibited by CSHn. The intensity difference is of little diagnostic value in the examination of samples under consideration. Because of the uncertainty relating to separate identification of these two phases, and because they frequently coexist, the formula $C_{5-6}S_6Hn$ has been adopted for use in this paper. The possibility of a solid solution between the two has not been established but cannot be excluded.

C_5S_4Hn exhibits a characteristic exotherm at 860 ± 5°C and is readily detected when present with the other gel phases of the series. Furthermore, the 3.0–3.1Å spacing was exhibited at 3.02–3.03Å by C_5S_4Hn and at 3.04–3.05Å by $C_{5-6}S_6Hn$, both products having been synthesized hydrothermally. In the earlier report (30) attention was not directed to this difference because of the coincidence of the strong 3.035Å line of calcite with the corresponding line of $C_{5-6}S_6Hn$. A compilation of XRD data by Glen (53) for tobermorite and related phases shows the 3.0–3.1Å spacing at 3.06–3.08Å for tobermorite and C–S–H(I), and at 3.02–3.03Å for related gel-like phases. The hazard and uncertainty of differentiating between C_5S_4Hn and $C_{5-6}S_6Hn$ by XRD are recognized. However, because of the extensive DTA results characterizing these two solids, it seemed desirable to direct attention of possible application of XRD for this purpose. This differentiation applies explicitly to samples prepared by autoclaving.

In recent tests (54), CH and tripoli in a 0.83 C/S were used in following the sequence of reactions starting with C_5S_4Hn and terminating with tobermorite at 175°C. In another series, the formation and crystallization of C-S-H(I) was followed using a Type I portland cement and tripoli mix, the C/(S + A) ratio was 0.83 in most tests and the mixes were autoclaved at 175° and 205° C for different periods of time.

The DTA results of the representative samples of the CH-tripoli mix are included in Fig. 1 (curves 1, 2, 3, 4) and the XRD results are given in Fig. 2. The 5-hour sample (curve 1, Fig. 1) exhibited an exotherm at 860°C and an XRD spacing at 3.02Å. The binder was considered to be essentially C_5S_4Hn. In Fig. 2, XRD curve 1 is of a 4-hour sample and curve 2 is of a companion 4-hour specimen made with a mix containing 2% added $C\bar{C}$. The XRD curves are the same except for a small peak of calcite at 3.035Å. The 3.02Å spacing is that of C_5S_4Hn, the presence of which was confirmed by DTA (the curve being nearly the same as that of the 5-hour sample). The 6-hour

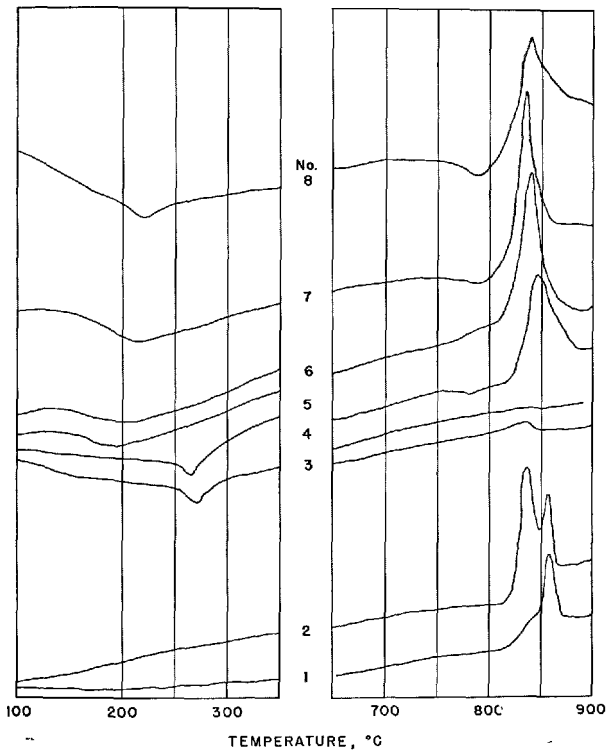

Fig. 1. *DTA results, No. 1, 2, 3, and 4, on* CH–S *mixes autoclaved at 175°C for 5, 6, 6-1/3, and 8 hours, respectively; and No. 5, 6, 7, and 8 on cement-S mixes autoclaved at 175° for 4 and 8 hours, and at 205°C for 24 and 96 hours, respectively*

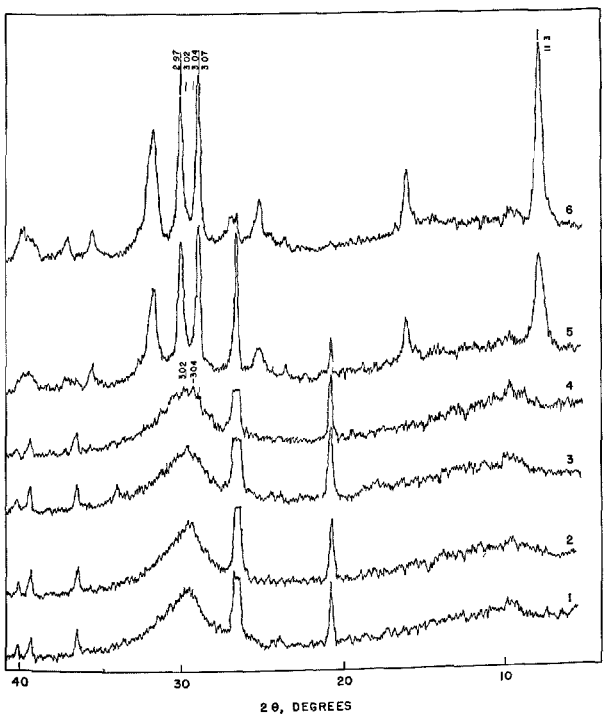

Fig. 2. *XRD tracings on* CH–S *mixes No. 1, 2, 3, 4, 5, and 6 autoclaved at 175°C for 4, 4, 5, 6, 6-1/3, and 8 hours, respectively. No. 2 contained 2 percent* $\overline{CC}$

sample showed exotherms at 860° and 835°C indicating presence of both C_5S_4Hn and $C_{5-6}S_6Hn$. This result was confirmed by the 3.02Å and 3.04Å peaks in the XRD patterns. In an attempt to obtain essentially pure C_5S_6Hn, the mixes were removed from the autoclaves at 20-minute intervals. The 6-1/3-hour sample was essentially well-crystallized tobermorite, not C_5S_6Hn. DTA indicated presence of a little C_5S_6Hn and XRD measurements revealed 4.5% quartz. The composition of this tobermorite, corrected for the free S, was 0.92 C/S. The 8-hour sample contained no residual C_5S_6Hn and only a trace of quartz and, therefore, the sample was essentially pure tobermorite.

The Type I cement-tripoli mix autoclaved at 175°C showed early formation of C–S–H(I) gel as indicated by the 3.09Å line in the XRD pattern (curve 1, Fig. 3). The C–S–H(I) persisted as a phase over broad variations in autoclaving conditions, 175°C for 4 to 96 hours and 205°C up to 96 hours, with change of C (S + A) from 0.83 to 0.60, with increase in W/S ratio to 0.8 from 0.6, and with replacement of tripoli by quartz. The only variation was changes in intensities of the XRD spectrum, the line intensity increased with increase in time and temperature of autoclaving. Representative XRD patterns are compiled in Fig. 3. The DTA results are included in Fig. 1 as curves 5, 6, 7, and 8. Only Sample 8 (curves at 205° for 96 hours) showed a small endotherm at

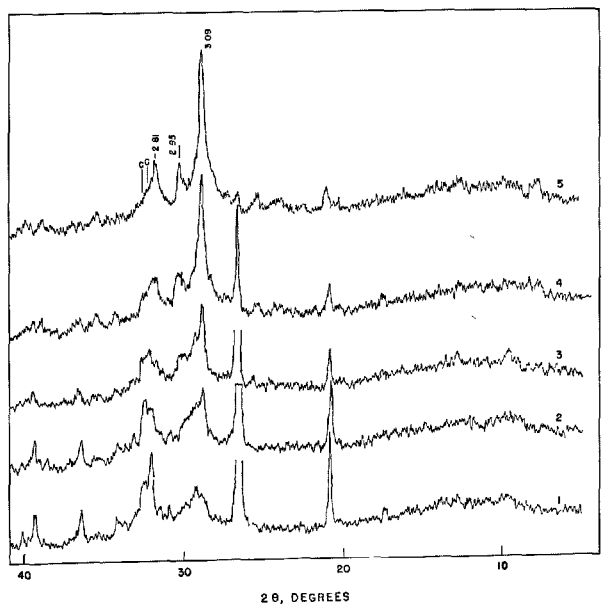

Fig. 3. *XRD tracing on cement-S, mixes No. 1, 2, and 3 autoclaved at 175°C for 4, 8, and 24 hours and No. 4 and 5 at 205°C for 24 and 96 hours*

200°C, compared to the 260-270°C endotherm of tobermorite. The exotherm at 850°C in the 4-hour sample (curve 5) decreased to 835°C after 8-hour curing at 175°C. This behavior is also shown by well-crystallized A-substituted tobermorite.

Present results showing that $C_{5-6}S_6Hn$ is a precursor of tobermorite of the Lock Eynort type substantiate the earlier results (30). The C–S–H(I) in present tests appeared to be a sinlge phase occurring in different degrees of crystallinity, depending on curing conditions and other variables mentioned.

Applying the above considerations, representative results on the commercially produced products and reference sample made with a Type I cement-ground quartz mixes are discussed. In Fig. 4 are presented XRD results on a 62.5% cement: 37.5% S samples autoclaved for 8 and 16 hours at 163°C by tracings No. 1 and 2, respectively. Samples No. 3 and 4 are commercial asbestos-cement products showing the weakest (No. 3) and strongest (No. 4) XRD patterns on these products. (These combinations of cement and quartz caused nucleation of tobermorite crystals unlike the combinations discussed in previous paragraphs in which C–S–H(I) was formed. All attempts, some already mentioned, to determine the cause of nucleation of C–S–H(I) were unsuccessful.) Sample No. 5 is a laboratory product made with a 50% Type I cement: 50% S mix and No. 6 is the same mix with 20% asbestos fiber replacement. The more intense XRD lines of Sample No. 6 suggests that asbestos promoted crystal growth. All six samples (1-6) were considered to be tobermorite, No. 1 and 3 being poorly crystallized and also probably contained significant amount of $C_{5-6}S_6Hn$.

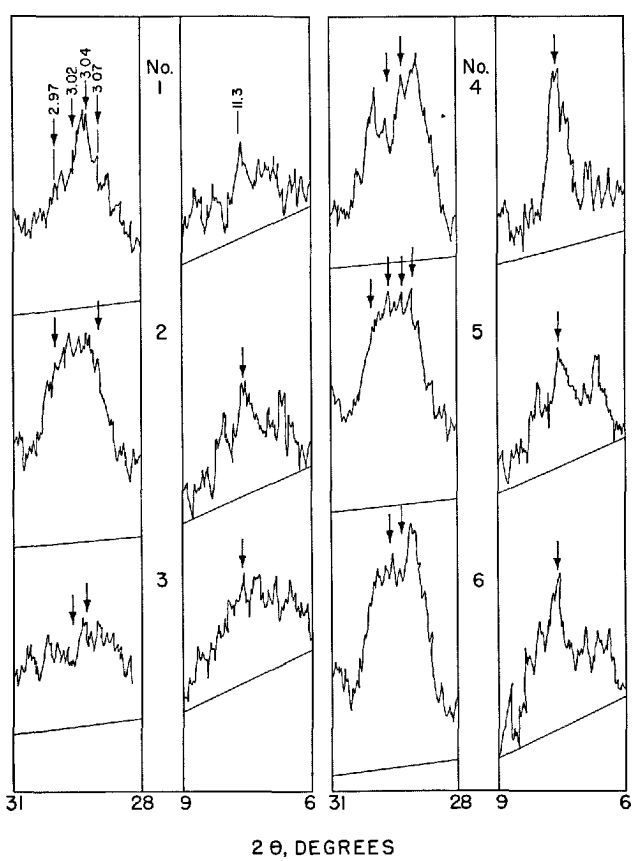

Fig. 4. *XRD tracings (No. 1 and 2) on 62.5: 37.5 cements: S autoclaved at 163°C for 8 and 16 hours, respectively, No. 3 and 4 on commercial products and No. 5 and 6 on 50: 50 cement: S and 50: 30: 20 cement: S: asbestos autoclaved 16 hours at 163°C*

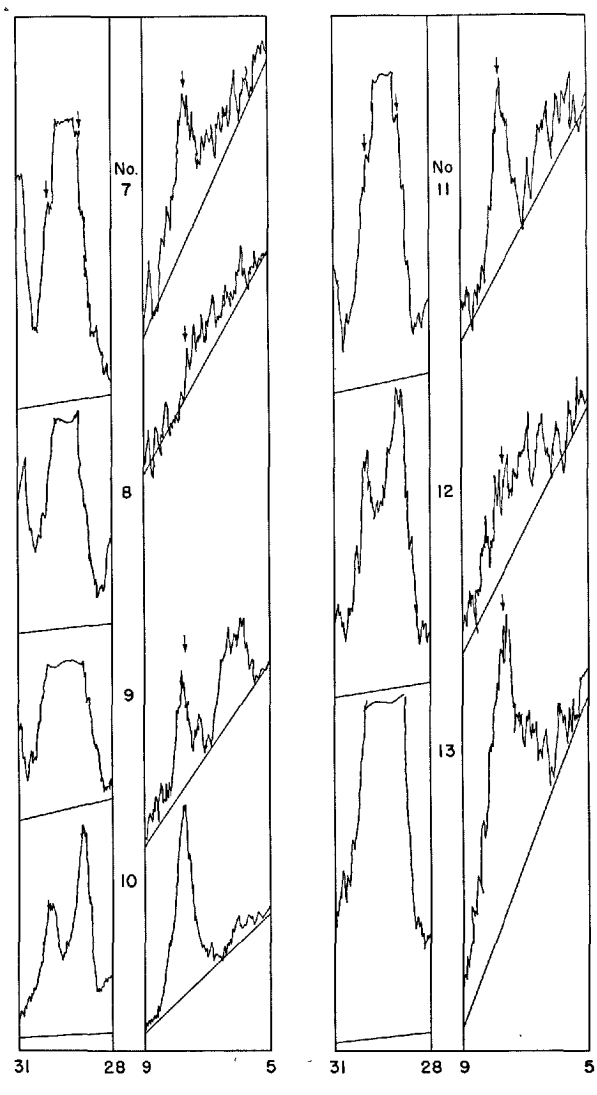

Fig. 5. *XRD tracings of concrete block (No. 7 and 8), concrete brick (No. 9), cellular concrete (No. 10), sand-lime brick (No. 11) and calcium silicate thermal insulation (No. 13)*

Present results on the 3.04Å line permits some modification of previous interpretations on the phase compositions of the binders. In laboratory samples prepared with care to prevent carbonation, it may be assumed that the 3.04Å line was due to $C_{5-6}S_6Hn$, not $C\bar{C}$. On this basis, Sample No. 1 contained a relatively large amount of $C_{5-6}S_6Hn$ which is not surprising, considering the relatively mild extent of autoclaving, 8 hours at 163°C. The XRD result on Sample No. 3 (commercial product) compared to that of No. 1 suggests that $C_{5-6}S_6Hn$, probably in significant amount, was also present in Sample No. 3, provided that the latter was not contaminated with $C\bar{C}$. At the present state of knowledge it may be assumed that if tobermorite is poorly crystallized, some $C_{5-6}S_6Hn$ may be present. However, before any conclusion to this effect can be drawn, more critical methods of testing for the crystalline tobermorite and $C_{5-6}S_6Hn$ will be required.

In Fig. 5, the patterns of concrete blocks (No. 7 and 8), concrete brick (No. 9), cellular concrete (No. 10), sand-lime brick (No. 11), deep oil well cement (No. 12) and calcium silicate thermal insulation (No. 13) are representative of autoclaved products. Large calcite contaminations in most samples tended to mask, or masked, the 3.07 and 2.97Å lines. Samples exhibiting the 11.3Å line, such as Sample No. 13, were considered to contain tobermorite even though the 3.07 and 2.97Å lines were completely submerged in the strong calcite line. In this pattern other lines of tobermorite were apparent. The binder of Sample No. 8 could not be even tentatively identified because of absence of the 11.3Å line and the masking of the 3.07 and 2.97Å lines, if present.

Application of the intensity ratio, 2.97/3.07 of 0.70-O.80, as a test for tobermorite, assuming absence of C–S–H(I), is misleading on "over autoclaved" CH–S products. A partial transformation of tobermorite to xonotlite causes a drop of this ratio to values of 0.5 and less as illustrated by results of Soo-Lee and Gon-Chen (55).

The apparent absence of C–S–H(I) in the group of 24 commercial products is surprising. Its occurrence as a binder should not be precluded in other products. Still incomplete current studies on binders (for possible commercial application) made with cement and fly ash showed presence of C–S–H(I). C–S–H(I) is apparently another modification of tobermorite. Another modification was reported by Grothe, Schimmel, and zur Strassen (56) in a laboratory produced sand-lime brick. As mentioned, attempts to ascertain cause of nucleation of C–S–H(I) were unsuccessful. This may not be due to the R_2O_3 in the cement or fly ash. Sauman (57) obtained C–S–H(I) in autoclaved mixtures of βC_2S and quartz powder.

Ionic Substitutions in Lattice of Tobermorite

Basic Studies

In studies of substitution of Al^{3+} in the lattice of tobermorite, the compositions of the mixes were computed generally to a 0.83 C/(S + A) ratio. On a weight basis 1.00% A replaced 1.18% S. The tobermorite with substituted A exhibited the same XRD pattern as the A-free tobermorite except for a small increase in values of the basal spacing with increasing amounts of A. Up to 5–6% A was substituted before a hydrogarnet, C_3ASH_4, was detected by XRD as a second phase. Diamond (58) in similar experiments reported A substitution up to 10%; A in excess of 10% and up to 15%, however, did not appear as a hydrogarnet. In autoclaved pastes, made from CH and shale, a hydrogarnet was not detected with 10% addition of A (36). Glenn (53) reported A substitution in tobermorite made with CH and bentonite.

Diamond (58) also substituted several percent of F, using goethite as source of F, into tobermorite. Later experiments (59) with new starting materials of same apparent descriptions lead to substitutions of less F than in the previous tests. Unpublished results by the writer on samples prepared with C_2F and C_4AF (the latter supplying equal amounts of A and F) led to a tentative conclution that F was substituted in tobermorite. Reproducibility of results, however, was poor. Furthermore, using mix compositions computed on assumption that the F substituted for the C yielded indirect evidence that some of the Fe^{3+} assumed octahedral coordination and occupied Ca^{2+} positions. The difficulty in attempts to substitute F may be due to the larger ionic radius, 0.64Å, of the Fe^{3+} compared to 0.50 and 0.41Å of Al^{3+} and Si^{4+}, respectively. More recent tests (60) on pastes made of CH, tripoli and goethite in C/(S + F) ratio of 0.83 and autoclaved at 175°C for 8 and 16 hours again yielded uncertain results. More intensive curing,

72 hours at 200°C of a mix having a 0.83 C/(S + F) which was equivalent to a C/S ratio of about 1.0, resulted in formation of well-crystallized xonotlite and goethite. In this experiment the F did not stabilize the tobermorite lattice as A does. The F-bearing tobermorite or the precursor gel which presumably formed was entirely decomposed by the prolonged autoclaving at 200°C. The DTA tracing showed no exotherm at 835°C, a result previously reported (59).

At room temperature, Copeland, Bodor, Chang, and Weise (60) reacted high-lime tobermorite gel with aluminates, ferrites, and sulfates. The F substituted in amount of 7.1% and the product had a C/S ratio of 1.52. A in amount of 5.0% substituted in a solid of 1.50 C/S ratio. It is apparent that tobermorite and high-lime tobermorite gel have approximately the same capacities for Al^{3+} but different capacities for Fe^{3+}. On basis of present knowledge on substitution of F, it may be speculated that the F enters the lattice of the intermediate gel in the course of the reactions. In the recrystallization of tobermorite gel to low-lime gel and then to tobermorite some or all of the F, depending on intensity of autoclaving may be expelled. Obviously, no definite conclusion may be drawn, and more research is required on Fe^{3+} substitution.

Diamond (58) reported substitution of several percent of M into tobermorite. The results (58, 59) tended to be somewhat erratic, perhaps for some such reason as relates to F substitution.

At room temperature, Copeland, Bodor, Chang, and Weise (60) substituted 7.4% $\bar{S}$ into high-lime tobermorite gel and the product had a C/S ratio of 1.76. Studies (61) on autoclaved pastes of CH, tripoli and $C\bar{S}H$ cured at 175°C and 205°C for 8 to 72 hours indicated that 1.2 to 1.9% $\bar{S}$ (presumably as SO_4^{2-} substitution for SO_4^{4-}) entered the lattice. The average amount was 1.6% S.

Phases other than Tobermorite in the Pastes

The A, etc., in a paste not substituted in the tobermorite lattice obviously appears as some other phase. The most probable second phase with A and F is a member or members of the hydrogarnet solid solution of composition, $C_3((A_{1-x}\cdot F_x)(H_{6-2y}\cdot S_y))$. As mentioned, C_3ASH_4 formed as the second phase with substituted tobermorite of composition $C_5(S + A)_6H_5$ and another unidentified hydrogarnet (31) formed in pastes having a composition of 6C/6 (S + A). A hydrogarnet was not detected in any of the 24 commercially produced products (45, 46). Akaiwa and Sudoh (62) autoclaved pastes of Type I cement, 55% Type I cement: 45% slag, and Type I cement: 40% quartz flour. Hydrogarnet was found only in the pastes made with slag and autoclaved at 250°C. Aiken and Taylor (48) detected hydrogarnet sporadically and in small amounts in autoclaved cement and cement-silica pastes. Kalousek, Curtis, and Schmertz (63) and Kalousek (52) reported only a trace amount of hydrogarnet in one clinker paste cured at room temperature, as a metastable phase. Copeland, Kantro, and Verbeck (64) detected a hydrogarnet in small amount in a Type V cement paste cured for 14 years at room temperature.

The distribution of F in autocalved products is not definitely known because of uncertainties about the amounts substituting. The possibility that some of the F may appear as goethite of hematite has been indicated in scattered tests. Further experimental evidence is required for ascertaining distribution of this constituent in autoclaved products.

The conclusion that hydrogarnets do not form in autoclaved products except sporadically and in small amounts may be made with one exception. A hydrogarnet can generally be expected in products made with fly ash, slag, etc., of high A content and used in relatively large amount.

The $\bar{S}$ in excess of about 1.6% has been observed to appear as either anhydrite or a substituted apatite in pastes autoclaved at 120° to 200°C (61). The apatite is the mineral ellestadite with composition of $C_{10}S_3\bar{S}_3H$.

Applied Studies

Published data on the effects of substituted ions on properties of tobermorite are still small in number. The results on optimum $\bar{S}$ content of steam-cured products has been reviewed (61). The amounts of $\bar{S}$ for optimum strength have not been published, but scattered results including extrapolation indicate that less than 1% $\bar{S}$ might be the amount for optimum performance.

Noorlander (65) reported data showing that drying shrinkage of autoclaved sand-lime brick decreased progressively with increasing amounts of kaolin or gibbsite added to the raw mix. Based on experience described in this report, it may be assumed that the A substituted in the lattice of tobermorite. The data are reproduced in Fig. 6 as drying shrinkage vs A content computed as percentage of tobermorite using a value of 9% of C added to the sand. The

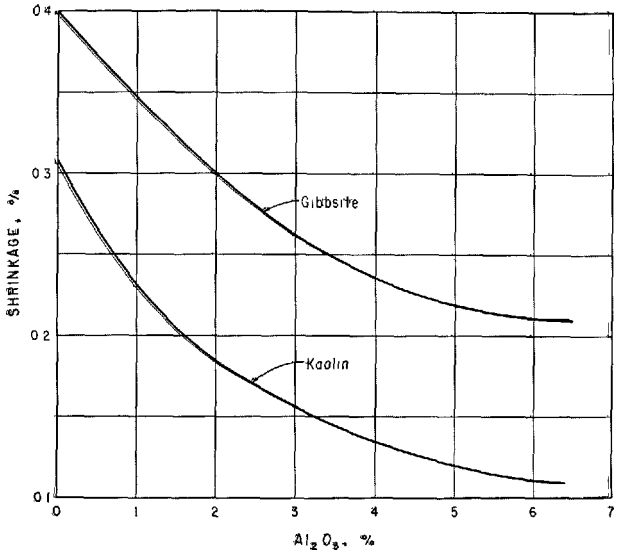

Fig. 6. *Drying shrinkage vs* Al_2O_3 *content in tobermorite (Noorlander (66))*

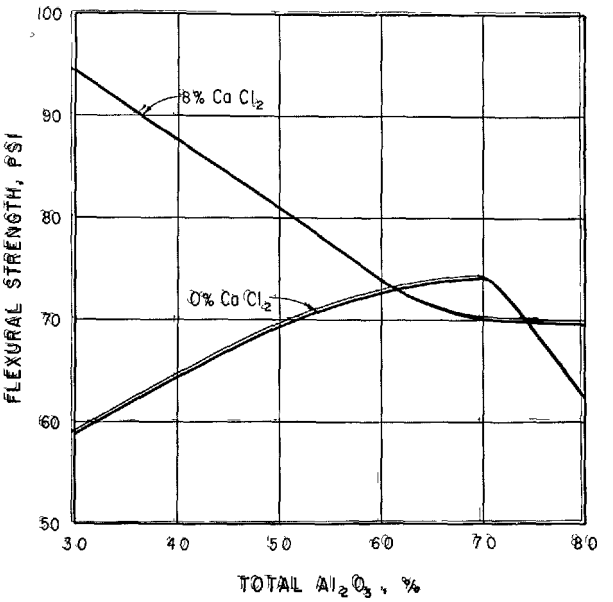

Fig. 7. *Flexural strength vs* Al_2O_3 *content with and without added* $CaCl_2$

shrinkage decreased with increasing amount of A. The lowest shrinkage reported occurred at 6% A on basis of the assumed composition. This result suggests that minimum shrinkage may be associated with an optimum A content. The shrinkage reduction from 0.3% (zero A) to 0.11% with an optimum A addition is significant.

Data reported in a patent (66) on effect of A substitution on reduction of drying shrinkage at high temperatures (108° to 649°C) of calcium silicate thermal insulation are reproduced in this paper. The results, in turn, are compared with results of similar products containing chloride. The experiments were designed on the assumption that drying shrinkage at these high temperatures might be reduced by substitution of $C\bar{l}$ for the $O\bar{H}$ in the crystal lattice. The mixes made of CH, diatomite, tripoli, kaolinite and $CaCl_2$ had a C/(S + A) ratio of 0.83. The amount of $C\bar{l}$ was not counted, it being assumed that $C\bar{l}$ replaced $O\bar{H}$. Autoclaving was at 186°, 192°, 198°, 203°, and 208°C. Only at 208°C was drying shrinkage reduced. This reduction amounted to 50% for specimens containing a total A content of 7% and $C\bar{l}$ of 5.1%. Tests for free $CaCl_2$ were negative. XRD patterns were the same for samples with and without added $CaCl_2$.

The flexural strength (Fig. 7) was at an optimum value at 7% A content in specimens containing no $CaCl_2$. The strength of the sample containing 5.1% $C\bar{l}$ and 7% A was about the same as that without $C\bar{l}$ (the variations are apparent in Fig. 7). Drying

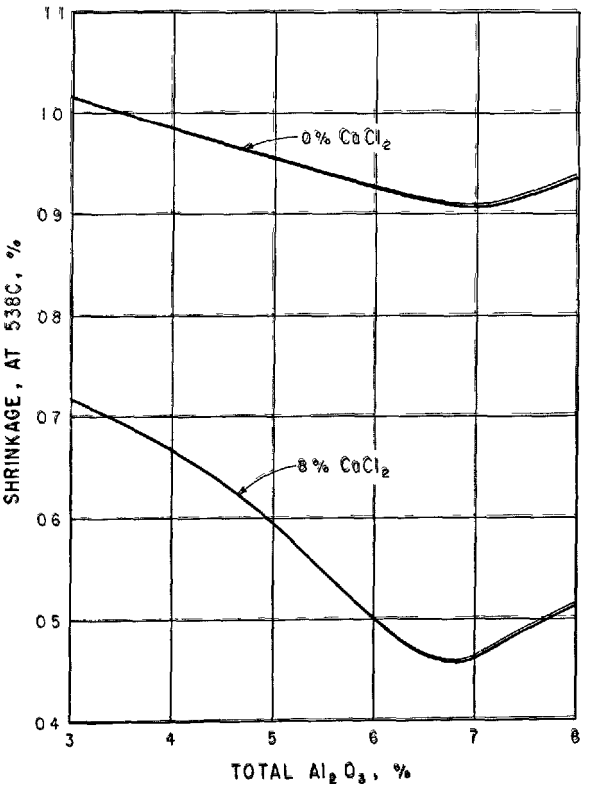

Fig. 8. *Drying shrinkage at 538°C vs* Al_2O_3 *content, with and without added* $CaCl_2$

shrinkages at 538°C of the 0.0 and 5.1% $C\bar{l}$ specimens cured at 208°C are shown in Fig. 8. Shrinkage

of the 0.0% $\bar{Cl}$ specimens decreased only slightly with increasing A contents to 7.0% and then increased slightly with more added A. The 5.1% $\bar{Cl}$ addition caused a large shrinkage reduction compared to the 0.0% $\bar{Cl}$ samples. The lowest shrinkage occurred with 7% A addition.

Actual proof was not developed, nor is such conclusion drawn, that the $\bar{Cl}$ substituted for the $\bar{OH}$. The unusual effect of $\bar{Cl}$ on drying shrinkage at elevated temperature appears to merit further study.

The probable modification of properties of tobermorite products by lattice substitution to obtain optimum properties appears to be a potentially rich area for basic and applied research.

Kinetics

In an aqueous dispersion of CH and S, the CH dissolves rapidly and Ca^{2+} are available immediately for reaction. The S dissolves slowly at room temperature but the rate of solution increases with increasing temperatures. Greenberg (67), and Halstead and Lawrence (68) used solubility data of CH and S in studying the kinetics of the reaction. Both reached the conclusion that rate of solution of S, or more specifically the availability of the silicate ions in the reaction zone, was the rate-determining step.

The manner of deposition of films of reaction products on the S grains and properties of such encapsulating deposits have been studied in recent years. Moorehead and McCartney (69) exposed large crystals of quartz to a solution saturated with CH in an autoclave at 235° and 335°C. They deduced the following sequence of reactions: (1) The S dissolved as $H_3SiO_4^-$, (2) the silicate and Ca^{2+} formed a deposit of a calcium silicate hydrate on the quartz surface, (3) xonotlite crystals nucleated on the reaction product film and the deposit of this phase grew outwardly into the liquid phase, and (4) the rate of reaction was governed by the rate of diffusion of the silicate ions through the deposit surrounding the quartz crystal. The solution of the quartz finally destroyed the initial quartz-calcium silicate hydrate interfacial bond and the residue of the quartz crystal was likened to a nut in a shell. Kondo (44) reacted quartz and silica glass of 5–10 micron size with CH at temperatures of 80° to 216°C. From analytical data collected, he computed the thickness of the films to be 0.5 and 1.0 microns for the silica glass and quartz, respectively. The rate of diffusion of the ions through the deposit was considered to be the rate-determining step. Krzheminski, Rashkovich, Sudina, and Varlamov (70) using a specially designed XRD spectrometer placed over the CH–S mixture in an autoclave obtained a continuing record of the reaction. The nature of the calcium silicate hydrate was reported to vary with increasing distance from the surface. Only at later periods of reaction did the rate of diffusion through the film of reaction product become the rate-determining step. Logginov, Rehbinder, and Abrosenka (71) reported that the rate of formation of the reaction products decreased with increasing thickness of the film deposit. After a certain lapse of time the thickness of the film became uniform and the rate of reaction was then governed by the rate of diffusion. Assarsson (72) autoclaved CH with S, silica gel and different silicate minerals. He reported the films of reaction products nucleated on the surface of the silica and silicates. The subsequent rate of reaction depended on the availability of the Ca^{2+} and silicate ions to the surfaces of the reaction products already formed.

There is general agreement that the rate-determining step in the reaction of CH and S is the diffusion of ions through the reaction products surrounding the S grains. Direct evidence of the occlusion of CH crystals by surface deposits is not so well documented as is that of S grains. Kalousek (73) compared the relative rates of reaction of large crystals of CH, up to 85 microns across, to freshly slaked C (the crystals being submicron in size) with sodium silicate at 25°C. The small crystals reacted rapidly, but the reaction with the large crystals proceeded to completion very slowly. Microscopic examinations revealed that the large CH crystals, although etched, remained surrounded by presumably nearly impervious reaction products for months. Dry mixtures of C and S, with subsequent addition of mixing water were compared (74) to mixtures prepared by addition of the S to CH suspensions freshly prepared by slaking C in hot water. The latter gave more uniform and reproducible results in autoclave curing. These and similar experiences indicated that unless the CH is thoroughly dispersed, it tends to form agglomerates. Such CH agglomerates may become surrounded by deposits of reaction products and behave like large individual crystals of CH. The Soviets practice (2) of fine grinding of CH with silica sand for improving quality of fine grain concrete may relate to a greater

availability of CH for reaction by preventing the occlusion of agglomerates of CH by deposits of reaction products.

It has been observed (6, 30, 44, 50, 51, 70, 75, 76) that reaction of CH and S at temperatures of about 125°C to 200°C proceeds through stages. The first reaction product is a lime-rich phase generally called lime-rich tobermorite gel of probable composition of C_7S_4Hn (30, 51, 52, 77). The phase reacts with residual S to form C_5S_4Hn and further reactions with residual S results in formation of CSHn followed by C_5S_6Hn provided the raw mix had a 5C:6S composition. If the C:S is less than 5:6, residual silica remains. Kalousek (30) using a 0.83 C/S (5C/6S), 4.0 W/S mix and curing at 175°C, and Neese (51) with a 0.33 C/S, 1.85 W/S mix, and curing at temperatures of 140° to 200°C reported highly similar results. The sequence of reactions was: $7C + 4S + Hn \longrightarrow C_7S_4H_3 \xrightarrow{S} C_5S_4Hn \xrightarrow{S} CSHn \xrightarrow{S} C_5S_6Hn \longrightarrow C_5S_6H_5$, Neese's final product coexisted with S. The time of formation of the different compositions varied between the two investigations. This difference is attributed to effect of W/S ratio. The lower the water content, the slower is the rate of formation of the products. Others (30, 55, 78) have reported similar effects of W/S on rate of reaction. In CH–S mixes of 0.8 C/S made with 4.0–20.0 W/S, compared to a 1.0 W/S, the rate of reaction was markedly increased (55). The effects of W/S have not been as systemically studied on CH–S as with portland cement pastes. A W/S ratio of 1.0 using CH and S gives a stiff paste due to the large surface area of the CH and such value of W/S would be considered low. An early attempt (36) to produce lime-cement-sand and gravel block on a concrete block machine was unsuccessful due to high water requirements with attendent low strengths. The Soviets (2) have surmounted this problem by using dead burnt lime and retarders to prevent hydration of the C until after the products were molded and heat applied to the forms.

The preceding discussions do not apply fully to silica gel, compared to quartz. Replacement of silica gel for quartz in a 0.8 C/S mix (30) increased the time of formation of tobermorite to 72 hours, compared to 8 hours for quartz. Increasing the C/S to 0.83 of the silica gel mix reduced the time from 72 hours to 24 hours. It was postulated that C_5S_6Hn, the precursor of tobermorite, was stabilized by the higher silica concentration in solution in the 0.8 C/S mixes due to persistence of free silica gel. Soo-Lee and Gon-Chen (55) using C/S ratios of 0.80 and 0.85 obtained essentially the same results mentioned for silica gel. Gaze and Robertson (79) in parallel experiments using ground quartz in one mix and diatomite in the other obtained tobermorite and $C_{5-6}S_6Hn$, respectively. The difference could have been due to a higher silica concentration in the CH-diatomite mix.

Nucleating agents are surfaces of solids possessing cell-size domains of about the same size as that of the solid to be nucleated. As already discussed, quartz surfaces (69) may become a substrate on which nucleating points may form, such as those for xonotlite. The number of nucleating points in such case would be obviously proportional to the surface areas of the quartz.

Funk (80) measured qualitatively the rate of hydration of βC_2S with and without addition of lime-rich tobermorite gel and αC_2SH at temperatures of 25° to 120°C. The mixture of βC_2S with the added gel hydrated more rapidly than in absence of the gel and the product was high-lime tobermorite gel. The mix containing the added αC_2SH also hydrated more rapidly and the product of hydration was only αC_2SH. Funk reported that hydration of βC_2S without addition was a solid-state reaction; and with the additions a through-solution mechanism applied. Sauman (57) reported marked acceleration of the hydration of βC_2S in a 50% βC_2S: 50% quartz powder by additions of CH, C_3S and γC_2S. He offered no explanation, but it may be inferred that the CH, as such or originating from hydrolysis of C_3S, reacted with the quartz to form the lime-rich gel, and this, as in Funk's test, served as nucleating agent. It is not apparent how γC_2S accelerated hydration unless its lattice as such served to nucleate the reaction product. The simplest explanation of the acceleration of hydration of βC_2S by nucleating agents is the diffusion of the Ca^{2+} and silicate ions away from the surfaces of the βC_2S crystals. The thickness of reaction deposit around the βC_2S crystals would thereby be decreased. The dissolving ions with a thinner deposit to permeate, would diffuse from the residue crystals of βC_2S at a faster rate with attendant acceleration of hydration.

The formation of αC_2SH by hydrothermal reaction of CH and S is erratic and unpredictable; other lime-rich products frequently form (74). A patented process (81) describes selective formation of αC_2SH by additions of NaOH or NaF to the raw mix. The mechanism was not described, but both additions decrease concentration of CH in the solution, and this may be a factor in formation of αC_2SH.

The mechanism of nucleation, either spontaneously from super-saturated solution or by epitaxial crystallization, of the different calcium silicate hydrates is not understood. The process may be governed by

the species of the ions formed and their concentrations under the conditions of the experiments. Information on concentrations of both ions at room temperatures has been published. Very little is known definitely of the species of the ions formed at hydrothermal temperatures. Taylor advanced some speculative interpretations which merit mention here as a guide to further research in a neglected area. The Ca^{2+} may exist as such, or as $Ca(OH)^{+}$ or $Ca(H_2O)(OH)^{-}$. The silicate ions may be present as $H_3SiO_4^-$, $H_2SiO_4^{2-}$, $HSiO_4^{3-}$ or condensed polysilicates. The species of ions and concentrations of these undoubtedly have an effect on the type of phase that uncleates either spontaneously or epitaxially. Taylor's (6) suggestions on relations between kind of silicate ion in solution and types of product are presented diagrammatically in Fig. 9. For example, $H_3SiO_4^-$ forms the intermediate products which recrystallizes to gyrolite. The methods of analysis for kind and amounts of silicate ions developed by Lentz (82), and Funk and Frydrych (83) would appear to be means for testing Taylor's hypothesis.

Only at temperatures up to about 200°C, the phase C_7S_4Hn forms initially in reaction between CH and S. At temperatures above 200°C, this phase may no longer form. Bozhenov and Kavalerova (26) reported formation of gyrolite at 225°C from a 2.3 C/S mix. Kondo (44) observed gyrolite formation at 216°C as the initial reaction product. The experimental data are still too few to define the temperature above which the CH and S form species of ions favoring the nucleation of a product other than C_7S_4Hn.

The preponderance of evidence relating to the kinetics of reactions of CH and S points to through-solution mechanisms. Solid state reactions in hydrating cements were discussed by Hansen (8) and of βC_2S by Funk (80). Steinour (85) and Mielenz and Peppler (86) critically reviewed Hansen's hypothesis, particularly the improbability of diffusion of such ions as H_3O^+ and OH into the structures of the solid reactants.

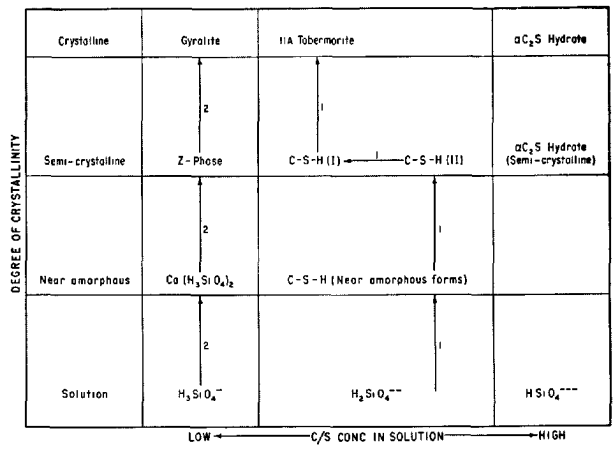

Fig. 9. *Taylor's (6) diagrammatic relation between degree of crystallinity and* C/S *ratio of solution*

Most generally the binders in commercially autoclaved products are metastable phases. The only exception appears to be xonotlite. Peppler (87) in study of the system C–S–H at 180°C allowed up to 6 months for attainment of equilibrium starting with both saturated and undersaturated solutions of the starting materials. He concluded that only two ternary phases were stable, xonotlite and hillebrandite. Roy and Harker (88) presented compatibility diagrams of the system C–S–H at temperatures up to 1,000°C. They cautioned about the uncertainties on the attainment of equilibrium, especially at the lower temperatures used in commercial autoclaving.

The preceding discussions were concerned with the kinetics of CH and S. No comparable research results are available on cement and S. This system is more complex because the cement clinker grains become encapsulated by reaction products. Further the calcium silicates form initially as lime-rich phases which later become reactants with S so long as it is available. When S availability for reaction is decreased, as it appears to be at times, the lime-rich gel may crystallize as αC_2SH.

Relation of Binders and Properties

Most of the commercially prepared samples which were examined were made with cement and ground quartz or perhaps some other siliceous fines. Mixes prepared with cement require substantially less water than those made with lime. This larger water requirement for CH–S mix may be surmounted partly by forming the stiff mixes under high pressure.

Taylor, Moorehead, and Cole (78) compressed CH–S mixes with 0.23 W/S under high pressures and obtained very high strengths. XRD and electron microscopy revealed the binder to be possible $C_{5-6}S_6Hn$ (89) of fibrous habit. Very dry mixes, 0.06 W/S, of CH and S contained (90) some free CH and some C_5S_4Hn (as suggested by reported DTA

results) and other phases after curing at 180°C for 16 hours. In such very dry mixes, water may be exhausted by self-desiccation and, therefore, the hydration reactions may stop.

Very little data appears to have been published showing the effects of $C_{5-6}S_6Hn$ in a binder consisting partly of tobermorite on strength of dense products. Sanders and Smothers (91) published results indicating increasing strength with increasing amount of tobermorite formed in dense products made with cement and S. In highly watered suspensions of CH and S, 3.0 to 6.0 W/S, used in manufacturing lightweight thermal insulation and structural products, strength was markedly higher with tobermorite as binder compared to $C_{5-6}S_6Hn$ (92). No reason can be advanced to explain why a highly compacted product with $C_{5-6}S_6Hn$ has high strength and the same phase in a product of low density gives inferior strength, far less than due to effect of increased water content.

Strength results were not available on the commercial products examined (45, 46). Because all products were marketed, many under specifications, there was no reason to believe that any had poor strengths independently of binder phase composition. Sauman (93) on basis of detailed tests concluded that optimum strength was obtained for product containing a binder consisting of tobermorite and "CSH" (presumably $C_{5-6}S_6Hn$).

Correlation of type of binder with strength of product requires attention to possible "overautoclaving" of the product. Prolonged autoclaving of dense products may cause strength reduction from an optimum value. Bessey (94) suggested that either a change in crystal form of the tobermorite or an inversion of one phase into another (for example, tobermorite to xonotlite) could cause strength reduction. The destruction of the quartz-calcium silicate hydrate interface through solution of the S and diffusion outwardly of the silicate ion (69) would be another factor causing strength loss. This effect has not been established for quartz-tobermorite or other aggregate-binder interfaces. However, until proven or disproven, the Moorehead-McCartney effect is a factor suspect of causing strength reduction of "overautoclaved" products.

The beneficial effect of increasing autoclave temperature for accelerating formation of binder of satisfactory strength in the approximate temperature range of 140–200°C is well documented. Much less is known about the effect of increasing temperatures between 200–225°C to 350°C on cement-silica or lime-silica products. Binders prepared by autoclaving a raw mix of 2.3 C/S gave maximum strength at 265°C (26). At temperatures above 265°C, the phases were more strongly crystallized, and those below this temperature were more gel-like. The reaction products differed in phase makeup at different temperatures. The two effects mentioned by Bessey (94) and that by Moorehead and McCartney (69) may have contributed to the strength decreases at temperatures above 265°C. It does not necessarily follow that a given binder if well crystallized may have lower strength than if poorly crystallized. Xonotlite may be such an example. On the other hand, the composition of the tobermorite—$C_{5-6}S_6Hn$ binder may relate to the relative amounts of these two phases present.

Effects of temperatures at 260° to 300°C have been reported (95) on a 1:2 mix of hydrated lime and quartz fines mixed with 8% of water. Time to temperature (300°C) in the autoclave was 20 minutes. After holding times of 1 minute and 100 hours at 300°C, the compressive strengths were 23,800 and 18,500 psi, respectively. The CH was combined in the total autoclave time of 21 minutes at this temperature. XRD revealed no recrystallization of the binder in 100 hours. Strength loss was attributed to the Moorehead-McCartney effect.

Another factor which will have to be considered in relating strengths to degree of crystallinity will be the amounts of substituent ions in the lattice. Properties may relate to amount of substituent ions while the binder retains approximately a constant crystal size so far as differentiation between gel-like and crystalline phases is concerned.

Frost resistance relates to porosity of autoclaved products. The Soviets (2) report that binders consisting of gel and crystals, or gels alone, have lower porosities, and therefore higher frost resistance, than well-crystallized binders. Control of porosity is amenable through control of intensity of autoclaving.

The markedly better resistance of autoclaved products to sulfate attack compared to normally cured products, has been recognized for some time (23, 96, 97). Such improvement is of a particular interest in application of asbestos-cement and concrete pipe in soils containing sulfate. The improvement in part has been attributed to removal of CH by combination with the S or silicates during autoclaving. The inactivation of the A-bearing phases to reaction with $\bar{S}$ to form ettringite has been attributed to several mechanisms, no one of which has been substantiated experimentally. Autoclaved Type I and Type V cement products tend to show equal resistance to sulfate attack. The assumption that hydrogarnets,

known to be immune to sulfate attack, are formed does not appear to be tenable. It is doubtful that hydrogarnets are usually present in significant amount, if at all. It is well established that sulfate resistance is increased by decreased permeability of the cement paste. If the A-substituted tobermorite, as such, is resistant to $\bar{S}$ attack low permeability of the autoclaved product or concrete would not be a requirement. Some of the samples of autoclaved asbestos-cement pipe that were examined contained well-crystallized tobermorite and others contained poorly crystallized tobermorite with some $C_{5-6}S_6Hn$. It would be interesting to compare such products for sulfate resistance and also for strength.

In the United States and Canada, autoclaving as a method of curing gained favor because of drying shrinkage reduction (4). Tobermorite shrinks about one-half as much as tobermorite gel.

A further improvement due to autoclaving, and inferred from Noorlander's (66) results, is the shrinkage reduction by substitution of A in tobermorite. The effects of optimum $\bar{S}$ and F for minimum shrinkage and maximum strength remain to be explored experimentally. Tobermorite is not the binder of lowest shrinkage among autoclaved calcium silicate hydrates. αC_2SH undergoes much less shrinkage but at the cost of sizable strength loss. The effects of reactive siliceous additions, W/C ratios, and curing time and temperature may be summarized in a generalization (4): "Those factors which increase strengths of cement-silica pastes also increase drying shrinkage."

Effects of autoclaving on other properties (creep, porosity, adsorption, etc.) have been described in the Rilem (2) and ACI reports (4).

Determination of dependable relations between nature of the binder, principally gel-crystal composition, and physical properties of the products should prove highly useful in advancing the technology. The gel-crystal composition should be amenable to control through predetermined autoclave cycles and choice of starting materials. No single method is yet established for this purpose. XRD appears to give a qualitative indication of degree of crystallinity. Usefulness of this method should increase as differentiation between gel and crystals is more fully resolved by other methods in conjunction with XRD. BET nitrogen surface areas of 38, 38, 45, 70, and 86 m^2/g were reported (98) for binders of autoclaved blocks made with pumice, sintered shale, shale, cinders and silica sand and gravel, respectively. The nitrogen surface areas were 43 (36) and 50 m^2/g (30) for tobermorite, and about 160–180 m^2/g (30) for $C_{5-6}S_6Hn$. The surface area results suggest that the binder of the sand and gravel, and cinder blocks contained some high surface area phase, presumably $C_{5-6}S_6Hn$. A substituted tobermorite exhibits a higher surface area than pure tobermorite (59) and this factor would have to be considered in application of surface area results for the suggested purpose.

DTA might prove useful only in examining products containing little or no A. The A-substituted tobermorite shows an exotherm at about the same temperature as $C_{5-6}S_6Hn$.

Uncertainties still exist on usefulness of electron microscopy for defferentiation between gel and crystals on the grid collected from liquid suspensions of the test sample. The sample on the grid is not necessarily representative of the major phase. This difficulty may be subject to correction by application of the scanning microscope (99) in conjunction with a replication method (60). Techniques of preparing the surface for replication offer opportunities for innovations. An earlier report (30) that $C_{5-6}S_6Hn$ was of fibrous morphology was later revised on bases of new results (92) that the morphology was of a crinkled foil variety in agreement with observations by Grudemo (100). Now recently, (89) the crystal habit of this phase was reported to be fibrous. It is not certain which of the two habits represent $C_{5-6}S_6Hn$. Perhaps both are present and method of sample preparation for examination is a factor as to which is collected. On the other hand, excessive illumination, even though of minimal intensity required for resolution, may account for the crinkled foil habit. Examinations of various phases (92) using minimal and intensive illumination showed the crinkled foil crystals unaffected by intense illumination while other were altered, some significantly. The possibility that the crinkled foil may be an artifact cannot be excluded. Budnikov and Strelkov (101) discussed similar difficulties experienced in electron microscopic examination of cement pastes.

Summary

1. A large background of scientific information has been developed on hydrous calcium silicates as binders of concrete products during the past 20 years.

2. Results on 24 autoclaved commercial products indicate the binder to be well to poorly crystallized tobermorite. The latter (in some samples) coexists with $C_{5-6}S_6Hn$ gel, proposed to be the precursor of tobermorite.
3. Lattice substitution in tobermorite of Al^{3+}, Fe^{3+}, SO^{2-}, etc., may significantly affect the properties.
4. The gel-crystal composition of the binders appears to be an important area for research for explaining and controlling properties.
5. Kinetics of the reactions of CH and S are closely dependent of the rate of diffusion of the ions through the reaction products encapsulating the S grains.
6. More remains to be learned about the effects of W/S ratios on properties of CH-S products.
7. Results suggest that Taylor's gel, C–S–H(I), may differ from the low-lime gels described by Kalousek and Neese.

References

1. G. E. Bessey, "Sand-lime bricks," National Building Studies, Special Report No. 3, DSIR, Building Research Station, London, HMSO (1948).
2. Proceedings of the RILEM Symposium on Accelerated Curing of Concrete (Section on High Pressure Steam Curing), Moscow (1964).
3. G. L. Kalousek, "Autoclave curing of concrete in Soviet Union and United States," ACI Proceedings **63,** pp. 817–833 (1966).
4. Proceedings of the International Symposium on Autoclaved Calcium Silicate Building Products, London (1965).
5. ACI Committee 516 Report, "High pressure steam curing: Modern Practices and Properties of Autoclaved Products," ACI Proceedings **62,** pp 869–908 (1965).
6. H. F. W. Taylor, "A review of autoclaved calcium silicates," Proceedings of the International Symposium on Autoclaved Calcium Silicate Building Products, London (1965), preprint.
7. W. C. Hansen, "Autoclave cycles and reactions," National Concrete Masonry Association Seminar, Washington (1962).
8. A. V. Volzhensky, "Autoclave treatment of heavy and lightweight concretes," Proceedings of the Rilem Symposium on Accelerated Curing of Concrete (Section on High Pressure Steam Curing), Moscow (1964), preprint.
9. G. E. Bessey, "The history and present day development of the autoclaved calcium silicate building products industry," Proceedings of the International Symposium on Autoclaved Calcium Silicate Building Products, London (1964), preprint.
10. T. Thorvaldson and G. R. Shelton, "Steam curing of portland cement mortars, a new crystalline substance," Canadian Journal of Research **1,** p. 148 (1929).
11. G. Grime and G. E. Bessey, "The cementing material of sand-lime bricks. an X-ray and microscopical investigation," Ceram. Soc. Trans. **32,** pp 14–20 (1933).
12. E. P. Flint, H. F. McMurdie and L. S. Wells, "Formation of hydrated calcium silicates at elevated temperatures and pressures," Journal Research NBS **21,** pp 617–638 (1938).
13. H. F. W. Taylor, Journal Appl. Chem. **2,** p. 3, London (1952).
14. H. F. W. Taylor, "Hydrothermal reactions in the system $CaO–SiO_2–H_2O$ and the steam curing of cement and silica products," Chemistry of Cements Proceeding of the Fourth International Symposium, **1,** pp. 167–190, Washington (1960).
15. H. F. W. Taylor, "The Chemistry of Cement," **1,** p. 417 (Academic Press Inc., London, England, and New York, U.S.A.) (1964).
16. H. F. W. Taylor, "The chemistry of cement hydration," Proceedings of the Seventh Conference on the Silicate Industry (Siliconf), Budapest (1963), pp. 199–220.
17. L. Heller and H. F. W. Taylor, "Crystallographic data for the calcium silicates," HSMO, London (1956).
18. A. B. Carpenter, R. A. Chalmers, J. A. Gard, K. Speakman and H. F. W. Taylor, "Jennite, A New Mineral," American Mineralogy **51,** p. 56074 (1966).
19. R. J. Wig, "Effect of high pressure steam on crushing strength of portland cement mortar and concrete," Tech. Paper 5, Bureau of Standards, September 5, 1911.
20. D. G. Miller, "Strength and resistance to sulfate waters of concrete cured in steam at 100 to 350°F," Proc. ASTM **30,** p. 636 (1940).
21. P. M. Woodworth, "Some tests of concrete masonry units cured with high pressure steam," ACI Proceedings **26,** pp. 504–512 (1931).
22. J. C. Pearson and E. M. Brickett, "Studies of high pressure steam curing," ACI Proceedings **28,** pp. 537–550 (1932).
23. T. Thorvaldson, Discussion of Reference 22, ACI Proceedings **29,** (1933).
24. C. A. Menzel, "Strength and volume change of steam cured portland cement mortar or concrete," ACI Proceedings **31,** pp. 125–149 (1934).
25. S. A. Mironov and L. A. Malinina, "Autoclave cured concrete," State Publishing Office of Literature of Structural Engineering, Architecture and Structural Materials, Moscow, 1958 (English Translation).
26. P. I. Bozhenov and V. I. Kavalerova, "Cements of autoclave curing," Proceedings of the RILEM Symposium on Accelerated Curing of Concrete (Section on High Pressure Steam Curing), Moscow

(1964), preprint.
27. G. F. Claringbull and M. M. Hey, "Re-examination of tobermorite," Mineralog. Mag. **29,** pp. 960–962 (1952).
28. U. S. Patent No. 2,665,996, January 12, 1954, "Hydrous calcium silicates and method of preparation," George L. Kalousek, assignor to Owens—Illinois Glass Company, Toledo, Ohio.
29. J. D. C. McConnell, "The hydrated calcium silicates, riversideite, tobermorite and plombierite," Mineralog. Mag. **30,** pp. 293–305 (1954).
30. G. L. Kalousek, "Tobermorite and related phases in the system CaO–SiO_2–H_2O," ACI Proceedings **51,** pp. 989–1011 (1955).
31. G. L. Kalousek, "Crystal chemistry of hydrous calcium silicates: I, substitution of aluminum in lattice of tobermorite," Journal American Cer. Soc. **40,** pp. 74–80 (1957).
32. G. L. Kalousek and Milton Adam, "Hydration products formed in cement pastes at 25 to 175°C," ACI Proceedings **48,** pp. 77–90 (1951).
33. Yu. M. Butt and S. A. Krzheminski, "Study of the formation of calcium hydrosilicates and hydroaluminates under hydrothermal treatment," Doklady Akad. Nauk SSSR **89,** pp. 709–712 (1953).
34. Yu. M. Butt, L. N. Rashkovich, and S. G. Danilova, "Reaction of calcium silicates with SiO_2 in hydrothermal curing," Doklady Akad. Nauk. SSSR **107,** pp. 571–574 (1956).
35. L. A. Malinina, "Composition of portland cement and optimum steam pressure of autoclave treatment of concrete," Beton i Zhelezobeton, pp. 65–68 (2) (1957).
36. G. L. Kalousek, "Studies on the cementitious phases of autoclaved concrete products made of different raw materials," ACI Proceedings **50,** pp. 365–378 (1954).
37. G. L. Kalousek, "Fundamental factors in the drying shrinkage of concrete block," ACI Proceedings **51,** pp. 233–248 (1954).
38. U. S. Patent No. 2,547, 127, April 3, 1951, "Calcium silicate of microcrystalline lathlike structure," George L. Kalousek, Assignor to Owens—Illinois Glass Company.
39. G. E. Bessey, Discussion of Report, "Cement hydration at elevated temperatures," by G. L. Kalousek, Proceedings of the Third International Symposium on the Chemistry of Cement, pp. 357–361, London (1952).
40. G. L. Kalousek, Ibid, pp. 364–367.
41. G. O. Assarsson, Discussion of Report, "Hydrothermal reactions in the system CaO–SiO_2–H_2O and the steam curing of cement-silica products," by H. F. W. Taylor, Chemistry of Cement, Proceedings of the Fourth Interantional Symposium, **1,** pp 190–194, Washington (1960).
42. R. Ian Harker, "Dehydration series in the system $CaSiO_3$–SiO_2–H_2O," J. Amer. Cer. Soc. *47,* pp 521–529 (1964).
43. D. A. Buckner, D. M. Roy and Rustum Roy, "Studies in the system CaO–Al_2O_3–SiO_2–H_2O: II, The system $CaSiO_3$–H_2O," Amer. J. Sci. **258,** 132–147 (1960).
44. R. Kondo, "Kinetics study on hydrothermal reaction between lime and silica," Proceedings of the International Symposium on Autoclaved Calcium Silicate Building Products, London (1965), preprint.
45. G. L. Kalousek, F. V. Camarda, J. E. Kopanda and Z. T. Jugovic, "Analysis of asbestos-cement binders," Materials, Research and Standards **6,** pp 169–179 (1966).
46. G. L. Kalousek and J. E. Kopanda, "Binders of autoclaved products," Publication Pending.
47. P. W. Manson and L. R. Blair, "Sulfate resistance of asbestos-cement pipe," Materials, Research and Standards **2,** pp 828–835 (1962).
48. A. Aitken and H. F. W. Taylor, "Steam curing of cement and cement-quartz pastes," Chemistry of Cement Proceedings of the Fourth International Symposium **1,** pp 285–290, Washington (1960).
49. R. A. Kennerley, "Products of hydrothermal hydration of cements from geothermal bores," New Zealand Jour. of Sci. *4,* pp 453–468 (1961).
50. G. L. Kalousek, "Application of differential thermal analysis in a study of the system lime-silica-water," a discussion of the report, "Cement hydration at ordinary temperature," by H. H. Steinour, Proceedings of the Third International Symposium on the Chemistry of Cement, pp 296–311, London (1952).
51. von Hugo Neese, "zur Kenntnis der Entstehungsbedingungen der Calciumhydrosilikate im System CaO–SiO_2–H_2O," Tonindustrie Zeitung **83,** pp 124–125 (1959).
52. G. L. Kalousek, "The reactions of cement hydration at elevated temperatures," Proceedings of the Third International Symposium on the Chemistry of Cement, pp 334–355, London (1952).
53. G. Rembert Glenn, "X-ray studies of lime-bentonite reaction products," Jour. Amer. Cer. Soc. **50,** pp 312–316 (1967).
54. E. J. Benton, Unpublished data.
55. Tun Soo-Lee and Loo Gon-Chen, "The Formation of tobermorite-like calcium silicate hydrates," Proceedings of the Seventh Conference on the Silicate Industry (Siliconf), pp 293–310, Budapest (1963).
56. H. Grothe, G. Schimmel and H. zur Strassen, Discussion of Paper, "Hydrothermal reactions in the system CaO–SiO_2–H_2O and the steam curing of cement and cement-silica products," by H. F. W. Taylor, Chemistry of Cement Proceedings of Fourth International Symposium **1,** pp 194–196, Washington (1960).
57. Z. Sauman, "Study of the hydration rate of dicalcium silicate in the mix with quartz under hydrothermal conditions," Proceedings of the International Symposium on Autoclaved Calcium Silicate Building Products, London (1965), preprint
58. S. Diamond, "Tobermorite and tobermorite-like clacium silicate hydrates: their properties and relationships to clay minerals," No. 24, PhD Dissertation, Purdue University, Lafayette, August 1963.
59. S. Diamond, Joe L. White and W. L. Dolch, "Effects of isomorphous substitution in hydrothermally synthesized tobermorite," The Amer. Mineral **51,** pp. 388–401 (1966).

60. L. E. Copeland, E. Bodor, T. N. Chang and C. H. Weise, "Reactions of tobermorite gel with aluminates, ferrites and silicates," Journal PCA Research and Development Laboratories, **9,** pp 61–67 (1967).
61. E. J. Benton and G. L. Kalousek, "Sulfatebearing phases in steam cured cement pastes," Publication Pending.
62. S. Akaiwa and G. Sudoh, "Strength and microstructures of hardened cement pastes cured by autoclaving," Symposium on Structure of Portland Cement Paste and Concrete. Special Report 90, Highway Research Board Publication 1389, pp 36–47, Washington (1966).
63. G. L. Kalousek, C. W. Davis, Jr and W. E. Schmertz, "An investigation of hydrating cements by differential thermal analysis," ACI Proceedings **45,** pp 693–712 (1949).
64. L. E. Copeland, D. L. Kantro and G. Verbeck, "Chemistry of hydration of portland cement," Chemistry of Cement Proceedings, Fourth International Symposium **1,** pp 429–468, Washington (1960).
65. A. Noorlander, "Reducing the shrinkage of calcium silicate bricks," Proceedings of the International Symposium on Autoclaved Calcium Silicate Building Products, London (1964), preprint.
66. U. S. Patent No. 2,875,075, February 24, 1959, "Hydrous calcium silicates," G. L. Kalousek, Assignor by mesne assignments, to Owens-Corning Fiberglas Corporation, a Corporation of Delaware.
67. S. A. Greenberg, "Reaction between silica and calcium hydroxides solutions," J. Phys. Chem. **65,** pp 12–16 (1961).
68. P. E. Halstead and C. D. Lawrence, "Kinetics of reaction in the system $CaO–SiO_2–H_2O$," Chemistry of Cements Proceedings of the Fourth International Symposium **1,** pp 321–325, Washington (1960).
69. D. R. Moorehead and E. R. McCartney, "Hydrothermal formation of calcium silicate hydrate," J. Am. Cer. Soc. **48,** pp 565–569 (1965).
70. S. A. Krzheminski, L. N. Rashkovich, N. K. Sudina and V. P. Varlamov, "Influence of the composition of the mixture and the temperature of hydrothermal treatment on the kinetics of interaction of lime and quartz," Proccedings of the International Symposium on Autoclaved Calcium Silicate Building Products, London (1964), preprint.
71. G. I. Logginov, P. A. Rehbinder and V. F. Abrosenka, "Interaction of calcium hydroxide with sand of different dispersities at ordinary temperatures," Colloid Jour. (English Translation) **21,** pp 429–434 (1959).
72. G. O. Assarsson, "Hydrothermal reactions between calcium hydroxide and amorphous silica, reactions between 120 and 160°C," J. Phys. Chem. **62,** pp 223–228 (1958). "Hydrothermal reaction of calcium hydroxide quartz at 120–122°C," ibid **64,** pp 328–331 (1960). "Hydrothermal reaction between calcium hydroxide and muscovite and feldspar at 120–220°C," ibid **64,** pp 626–632 (1960).
73. G. L. Kalousek, "Studies of portions of the quaternary system soda-lime-silica-water at 25°C," Jour. Res. NBS **32,** pp 285–302 (1944).
74. G. L. Kalousek, J. S. Logiudice and V. H. Dodson, "Studies on the lime-rich crystalline solid phases in the system lime-silica-water," J. Am. Cer. Soc. **37,** pp 7–13 (1954).
75. T. M. Berkovich, D. M. Kheiber, O. I. Gracheva and N. I. Kupreeva, "Properties of calcium silicate hydrates," Doklady Akad. Nauk. SSSR **120,** pp 853–856 (1958).
76. V. Satava, "A study of the process of hardening of lime and silica at 175°C—the relation between structure and strength of hardened materials," Proceedings of the International Symposium on Calcium Silicate Structural Building Products, London (1965), preprint
77. S. A. Greenberg and T. N. Chang, "Investigation of colloidal hydrated calcium silicates II: solubility relationships in the calcium oxide-silica-water system at 25°C," Jour. Phys. Chem. **69,** pp 182–188 (1965).
78. W. H. Taylor, D. R. Moorehead and W. F. Cole, "High-strength calcium silicate hydrate: 1. strength tests," Proceedings of the International Symposium on Autoclaved Calcium Silicate Building Products, London (1965) preprint.
79. R. Gaze and R. H. S. Robertson "Some observations on calcium silicate hydrate (I)—tobermorite," Mag. of Concrete Research **8,** pp 7–12 (1956).
80. H. Funk, "Two different ways of hydration in the reaction of βC_2S with water at 25 to 120°C," Chemistry of Cement Proceedings of the Fourth International Symposium **1,** pp 291–295, Washington (1960).
81. U. S. Patent No. 3,131, 024 (April 28, 1964), "Method of producing dicalcium silicate alpha hydrate," James P. Leineweber, Assignor to John Mannville Corporation, N. Y., N. Y.
82. C. W. Lentz, "The silicate structure analysis of hydrated portland cement paste," Symposium on Structure of Portland Cement Paste and Concrete, Special Report 90. Highway Research Foard Publ. 1389, pp 269–283, Washington (1966).
83. H. Funk and R. Frydrych, "The degrees of anion condensation in silicic acids and silicates," ibid, pp 284–290.
84. W. C. Hansen, "Actions of calcium sulfate and admixtures in portland cement pastes," A.S.T.M. Special Technical Publication No. 266, pp 3–25 (1959).
85. H. H. Steinour, Discussion of Hansen's Report, ibid, pp 25–33.
86. Mielenz and R. B. Peppler, Discussion of Hansen's Report, ibid, pp 35–37.
87. R. B. Peppler, "The system of lime, silica and water at 180°C," Jour. Res. NBS **54,** 205–211 (1955).
88. D. M. Roy and R. I. Harker, Discussion of Report, "Hydrothermal reactions in the system $CaO–SiO_2–H_2O$ and the steam curing of cement and cement-silica products," by H. F. W. Taylor, Chemistry of Cement Proceedings of the Fourth International Symposium, pp 196–201, Washington (1960).
89. W. F. Cole and D. R. Moorehead, "High strength calcium silicate hydrate: II. X-ray, DTA, chemical and electron microscope results, Proceedings of the

International Symposium on Autoclaved Calcium Silicate Buildings Products, London (1964), preprint.
90. H. G. Midgley and S. K. Chopra, "Hydrothermal reactions between lime and aggregate fines," Mag. of Concrete Res. **12**, pp 73–82 (1960).
91. Dean L. Sanders and W. J. Smothers, "Effect of tobermorite on the mechanical strength of autoclaved portland cement-silica mixtures," ACI Proceedings **54** (1957).
92. G. L. Kalousek and A. F. Prebus, "Crystal chemistry of hydrous calcium silicates: III morphology and other properties of tobermorite and related phases," American Cer. Soc. **41**, pp 124–132 (1958).
93. Z. Sauman, "Calcareous hydrosilicate component—an important factor influencing strength of porous concrete," Chem. Abs. **66**, No. 10, p. 3878n (March 6, 1967) (Stavivo **44** (9), pp. 336–340 (1966), Czech).
94. G. E. Bessey, "Hydrated calcium silicate products other than hydraulic cements," The Chemistry of Cement II, p 101, Academic Press, London and New York (1964).
95. Patent Specification 1,043,015, Patent Office, London (September 21, 1966), "Method of manufacturing building structural and paving products using a calcium silicate hydrate bonding matrix".
96. T. Thorvaldson, "Portland cement and hydrothermal reactions," Symposium on Chemistry of Cement, pp 246–267, Stockholm (1938).
97. T. Thorvaldson, "Chemical aspects of the durability of cement products," Proceedings of the Third International Symposium on Chemistry of Cement, pp 436–466, London (1952).
98. L. Gleysteen and G. L. Kalousek, "Simplified method for determination of apparent surface area of concrete products," ACI Proceedings **51**, pp 437–447 (1955).
99. L. H. Pruden, E. J. Korda and J. P. Williams, "Characterization of surface topography with the scanning electron microscope," Jour. Amer. Cer. Bull **46**, pp 750–754 (1967).
100. A. Grudemo, "Electron study of morphology and crystallization of calcium silicate hydrates," Svenska Forskningsinst. Cement Betong vid Kgl. Tek. Hogskol. Stockholm, Handl, No. 26, pp. 1–103 (1955).
101. P. P. Budnikov and M. I. Strelkov, "Some recent concepts on portland cement hydration and hardening," Symposium on Structure of Portland Cement Paste and Concrete, Special Report 90, Highway Research Board Publ. No. 1389, pp 447–464, Washington (1966).

Written Discussion

Waldemar C. Hansen

This is to be limited to a discussion of through-solution reactions and the reactions which have been referred to, by various authors, by such terms as topochemical, solid-state, solid-liquid and in situ reactions. Kalousek, concludes that the preponderance of evidence points to a through-solution mechanism for the reaction of silica with calcium hydroxide and he refers to a paper published by me in 1959 pertaining to solid-state reactions in portland cement pastes. Two, more recent, papers (1 and 2) review some of the literature on such reactions. From these reviews, and from other literature which was not included in those papers for example (3 and 4), it seems that one must conclude that compounds such as silica and the cement minerals cannot dissolve in an aqueous medium without undergoing a reaction with the ions of water and possibly other ions from the medium. That is, a reaction must occur at the surface of the solid particle which overcomes the ionic forces that bind the ions to one another in the solid. For example, when sllica reacts with water the surface of the particle is converted to a silicic acid. The ions of this acid, probably by further hydration, can separate from the unreacted solid and diffuse into the liquid. In other words, the silicic acid dissolves in the water and any silicic acid that precipitates from the solution was formed by a through-solution mechanism. However it was not formed by the dissolution of silica which, after dissolving, reacted with the water to form silicic acid.

The evidence in the literature points to the conclusion that compounds such as calcium oxide and the cement minerals, which form reaction products with water having relatively low solubilities, become coated with a layer of the reaction product; which, after reaching some thickness, ruptures or spalls forming a number of small particles or crystallites. This exposes fresh surfaces of the reactant to the liquid phase. These colloidal sized particles, because of their size and probably because of an almost amorphous nature, have higher solubilities than the solubility of larger and more nearly perfect crystals of the reaction product. Hence they tend to dissolve and recrystallize as relatively large and perfect crystals. It seems reasonable to assume that some of these colloidal

particles act as nuclei for the crystallization of the dissolved material.

According to Kalousek, Funk found that additions of either a lime-rich tobermorite gel or alpha-C_2SH to pastes of beta-C_2S accelerated the rate of hydration of the C_2S. Also that the final product in each case was the same as the added material. It seems that this acceleration can be explained on the basis that the solubility of the topochemical product formed on the surfaces of the C_2S grains was greater than that of either of the additives. Accordingly these materials acted as nuclei to remove the dissolved calcium silicate and prevented the solution from becoming saturated with respect to the topochemical coating. It seems that under such conditions the coating might be dissolved almost as rapidly as it formed, whereas, in the absence of added nuclei, no nuclei were present until the topochemical layer formed its own, probably after a layer ruptured.

According to Vyrodov, supplementary paper, "On some aspects of theory of solidification and strength formation of cement-stone and concrete," Baikov believed that the cement minerals reacted topochemically with water and that these more or less amorphous reaction products were the binder of the cement paste. Some dissolution and recrystallization of these products occurred, but this was not essentially a part of the mechanism which caused hardening and the development of strength.

Taylor, principal paper, "The calcium silicate hydrates," suggests the following in the formation of C-S-H. A high C/S product is formed on the surfaces of the crystals of C_3S and C_2S. This probably is composed initially of Ca^{2+}, $H_2SiO_4^{2-}$, and OH^- ions and H_2O molecules and has a C/S ratio close to that of the starting material. A second product is formed by dissolution and reprecipitation of this product. Further anion condensation may occur within this material, either by *in situ* transformation or by repeated dissolution and reprecipitation. It is seen from this that Taylor believes that it is possible for these reaction products to develop better crystallinity without dissolving and recrystallizing from solution. It seems that there may be no need to postulate that the original topochemical product has to dissolve before it can improve its crystallinity. When the cement minerals react in the presence of relatively large amounts of water and possibly also under high-pressure steam curing much of the topochemical reaction product probably dissolves and recrystallizes, but with W/C ratios of practice and at atmospheric temperatures probably very little of this product dissolves. However there might be considerable in situ rearrangement of the structure as the cement paste ages.

It seems that cement technologists should accept the conclusions that (a) the cement minerals react topochemically with water and possibly other ions from the liquid phase of the cement paste, (b) these reaction products will dissolve to some limited extent to yield relatively large and nearly perfect crystals and (c) the second step is of relatively little importance in the development of the properties of the hardened paste cured at atmospheric pressure but may be of greater importance for pastes cured at elevated pressures.

References

1. W. C. Hansen, "Solid-liquid reactions in portland cement pastes," Materials, Research and Standards **2**, 490–493 (1962).
2. W. C. Hansen, "Basic chemistry of reactions of aggregates in portland-cement concrete," Journal of Materials **2**, 408–431 (1967).
3. H. E. Schwiete, U. Ludwig and P. Jäger, "Investigations on the system $3CaO \cdot Al_2O_3$–$CaSO_4$–CaO–H_2O," Zement-Kalk-Gips No. 6, 229–236 (1964). In German.
4. J. G. M. de Jong, H. N. Stein and J. M. Stevels, "Hydration of tricalcium silicate," Journal of Appllied Chemistry **17**, 246–250 (1967).

Written Discussion

Jaromir Jambor

Synopsis

The aim of the research project discussed in this paper was to find a relationship between phase constitution and strength of hardened cementitious pastes. Specimens of

hardened pastes containing different types of binding new-formations were used for the investigation. These cementitious pastes were made of mixes of $Ca(OH)_2$, C_3A and C_3S with ground siliceous materials and were left to harden for different periods of time at temperatures 20°C, 80°C and 175°C.

The phase constitution of hardened cementitious pastes was studied by X-ray phase analysis, by a complex thermal analysis, by electron microscopy and by chemical analysis. Over-all porosity and compressive strength of specimens were determined by usual methods.

The results have shown that the strength of hardened cementitious pastes is given by the type and the volume of binding new-formations developed in the pastes.

Among the pastes containing the same volume of binding new-formations the highest strength was developed by those, in which the tobermorite—like phases were found as binding new-formations. The drop of relative strength (P) of pastes, depending on the type of binding new-formations developed in the pastes, is characterized by the following sequence:

Tobermorite-like phases (100% P) → CSH I (56 to 62% P) → mixture of 70 to 80% gehlenite hydrate and 20 to 30% CSH I (28 to 32% P) → mixture of 70 to 80% of hydrogarnet phase and 20 to 30% of CSH I (13 to 20% P) → C_3AH_6-hydrogarnet phase (3 to 4% P).

The strength of pastes containing the same type of binding new-formations is given by a power function of volume-θ occupied in the paste by the binding new-formations and may be expressed by the general formula:

$$P = a\theta^3 + b\theta^2 + c\theta$$

The relationship between the strength and the phase constitution of cementitious pastes may be in practice biased by internal flaws of their macrostructure developing, as a rule, in the early stage of their hardening.

Introduction

In his principal paper "High temperature steam curing of concrete at high pressure" (Part III, Session 5) G. L. Kalousek (1) discusses the present knowledge of interrelations between the type or constitution of the binder, developed in autoclaved products and their physico-mechanical properties. The results of research work made by W. H. Taylor, D. R. Moorehead and N. F. Cole (2), further by W. F. Cole and D. R. Moorehead (3), by D. L. Sanders and W. J. Smothers (4), by G. L. Kalousek and A. F. Prebus (5), by Z. Šauman (6) and by others justify the opinion that the value of strength of autoclaved products depends to a considerable extent on the development and contents of tobermorite as well as on the relative presence of tobermorite and $C_{5-6}S_6H_n$ in binding new-formations, developed in these products in the course of autoclave treatment. G. L. Kalousek points out in this connection several factors, which may influence the strength of autoclaved products—it is above all the overautoclaving, the degree of crystallinity and the surface area of the binding new-formations, the amounts of substituent ions in the lattice etc. At the same time Kalousek stresses the fact, that the determination of dependable relations between the constitution of the binder and/or the binding new-formations and the physico-mechanical properties of autoclaved products is of great importance for further progress in the technology of their production.

The statements, pronounced in the general report are in principle correct, however they should be supplemented by the statement that the elucidation of interrelationships between the over-all phase constitution and the physico-mechanical properties becomes an important presupposition of the future improvement of technology of production not only of autoclaved products but also of cementitious pastes and concretes, hardening at normal temperature, and/or under higher temperature, and under normal pressure.

Among the other papers, dealing with these problems, it is necessary to recall the work of T. C. Powers (7, 8, 9), who found that the strength of cement paste is a power function of the volume of hydration products developed in the paste and summarily denoted as cement gel, and that with increasing volume of cement gel the strength of the paste increases too approximately according to the cubical relationship. Similar results have been obtained by Giertz—Hedström (10), J. Jambor (11, 12), F. M. Lea and F. F. Jones (13) and others.

Owing to the importance of this problem, the presented paper contains some new data concerning the relationship between crystallo-chemical phase consitution and strength of hardened cementitious pastes, which supplement the data of principal paper report presented by G. L. Kalousek and elucidate

further this problem. These data have been determined by a long-time research program carried out by the Institute of Construction and Architecture of the Slovak Academy of Sciences in the course of the recent years.

Methods Used

For the purpose of study of relationships between the phase constitution of hardened cementitious pastes and their compressive strength a selection has been made from a large number of test specimens which had been used for the study of the influence of different curing on the strength of cementitious pastes of different composition. But for insignificant exceptions, all specimens showing visible cracks or other damage capable of influencing the compressive strengths were excluded from the selection.

Preparation of Test Specimens

For the preparation of cementitious pastes homogenized mixes of convenient siliceous powdered materials with 34%, 50% and 64% by weight of powdered $Ca(OH)_2$ were used. Further, mixes of the same siliceous materials with 50% by weight of C_3A and/or of C_3S were used. The mixing water was added in a quantity necessary to prepare a paste of normal consistency (according to the Czechoslovak standard CSN 72 2110). After a 3 minute homogenization cube specimens with 2 cm edge were moulded. These specimens were compacted by rodding and were left to set in moist air of 97 to 100% relative humidity and under the temperature of 20°C. The subsequent curing of the specimens proceeded in one of the following three ways.

a. The test cubes were demoulded and left to harden in water at the temperature 20–21°C for a period 90 and/or 180 days. In the case of some of the pastes it was necessary to prolong the period of humid atmosphere curing of specimens before their immersion in water.

b. The test cubes (in moulds) were put into a steam chamber and cured in a saturated steam medium at the temperature 80°C. The temperature rise was controlled so as to let the temperature attain the value of 80°C during 120 minutes. The total period of steam curing was 24 hours.

c. The test cubes (in moulds) were put into a pressure vessel and cured in a saturated steam medium at the temperature 175°C and under the overpressure about 8 atm. The heating process was controlled so as to let the temperature attain the value of 175°C in the pressure vessel in the course of 120 minutes. The total period of high temperature steam curing was 24 hours.

After the conclusion of the curing period 6 test specimens of each paste were dried at 100°C and their bulk density (unit weight) and compressive strength were determined. The crushed specimen fragments were further disintegrated, homogenized and used for determination of the true density (specific weight) and of the over-all phase constitution of the hardened paste.

Testing Methods

The chemical composition and the approximate specific surface of the initial materials, used for the preparation of cementitious pastes, as well as the compressive strength, the bulk density and the true density specimens were determined by usual methods.

In order to determine the over-all crystallo-chemical phase constitution of hardened pastes a combination of the following methods was used:

a. X-ray powder diffraction (XRD) analysis, used for the determination of the type of binding new-formations contained in the hardened paste, of the presence of unbound $Ca(OH)_2$ and $CaCO_3$ and of the contents of nonhydrated C_3A and/or C_3S.

b. Complex thermal analysis used for the determination of the contents of the free $Ca(OH)_2$ and $CaCO_3$ in the hardened paste and at the same time as a check of the XRD analysis.

c. Electron microscopy used as a check of the XRD and thermal analyses.

d. Chemical analysis used for the determination of the approximate content of the unreacted siliceous admixture and in combination with the previously listed methods for the determination of the approximate over-all content and the composition of the binding new-formations.

Diffractograph Micro 111 made by the company C. H. F. Müller in Hamburg was used for the XRD analysis. The apparatus consists of a strictly stabilized source of X-rays, of a precision goniometer with a proportional counter and of a transistorized measuring and registration equipment. Quantitative determination of non-hydrated C_3A and C_3S in the hardened pastes was obtained by the method of the internal standard.

Thermal analyses were made by means of a complex thermoanalytic equipment, namely the Derivatograph, delivered by the company MOM, Budapest. This equipment allows a simultaneous differential thermal analysis (DTA), a thermogravimetric analysis (TG)

and a derived thermogravimetric analysis (DTG) on the same specimen. The equipment includes a precision registration device allowing a reliable quantitative evaluation of the thermogravimetric analysis. A sufficiently accurate determination of the weight reduction due to the decomposition of $Ca(OH)_2$ or $CaCO_3$ was possible owing to a simultaneous evaluation of the DTG record.

The electron microscope used for the microscope analysis was a Czechoslovak Tesla BS-242 table model. Specimens were prepared by the normal techniques from dilute water suspensions of finely ground samples on collodium films. Ultrasound treatment was chosen for perfect disintegration of the samples in suspension.

Modified Steopoe's method (14) was used for the chemical analysis of hardened pastes. This method is based on the fact that when solving a hardened paste in HCl with $d = 1.12$ (under simultaneous cooling) the unreacted siliceous admixtures separates in the form of an unsoluble residue whereas the other components of the specimens enter into the solution. From the contents of CaO, SiO_2 and Al_2O_3 assessed in the solution the share of the above mentioned oxides bound in $Ca(OH)_2$, $CaCO_3$, C_3A and C_3S was subtracted. The remaining parts of soluble CaO, SiO_2 and Al_2O_3 give the approximate composition and over-all contents of the binding new-formations, contained in the paste. This method is not perfectly accurate due to the fact that in solving the finely ground paste in HCl a certain share of the unreacted siliceous admixture mainly R_2O_3 enters into the solution too. This must be taken into account mainly in the case of cementitious pastes made of siliceous admixtures with higher R_2O_3 content and with low contents of the binding new-products.

Materials Used

The following siliceous materials were used for the preparation of the cementitious pastes:

1. dacite tuff (pozzolanic material of high activity);
2. fly ash (pozzolanic material);
3. activated kaolin made by burning for 2 hours at 650°C of washed kaolin (pozzolanic material of high activity);
4. ground washed siliceous sand (practically pure β-quartz).

All the used siliceous materials were ground to the maximum grain size of 90 microns.

The following binders were used for the preparation of the pastes:

a. Powdered calcium hydroxide-$Ca(OH)_2$ made of selected lumps of pure quicklime slaked with 45% of water and passed through a 200-micron aperture sieve;

b. Tricalcium aluminate—C_3A—prepared by five times repeated burning of granules pressed of chemically pure $CaCO_3$ and Al_2O_3 mixed in molecular proportion 3: 1. The burning temperature was 1380°C

c. Tricalcium silicate–C_3S–prepared by five times repeated burning of granules pressed from a mixture of chemically pure $CaCO_3$ and SiO_2 mixed in molecular proportion 3: 1, to which 0.5% admixture of fine CaF_2 was added as mineralizer. The burning temperature was 1380°C.

After the last burning of C_3A as well as C_3S were ground to the maximum grain size of 90 microns and their composition was checked both by chemical and XRD analysis.

The results of the chemical analysis as well as of the XRD analysis and of the microscope examination of the original samples of materials used for the preparation of the pastes are given in Table 1.

Results and Discussion

Phase Constitution of Hardened Pastes

The results of the study of phase constitution of hardened pastes, as well as the approximative composition of binding new-formations, calculated on the basis of chemical analysis, are given in Tables 2 to 5.

Among the non-binding phases in the studied pastes in the first place the unreacted residue of the siliceous admixture and $CaCO_3$ were identified. In most of the pastes the free $Ca(OH)_2$ was found, too. This free $Ca(OH)_2$ was, however, not identified only in pastes prepared of mixes containing C_3A and was present only in smaller quantities in pastes prepared of a mix of activated kaolin with 34% by weight of $Ca(OH)_2$, as well as of a mix of activated kaolin and C_3S. In the pastes made of mixes of siliceous materials and clinker minerals residues of non-hydrated C_3A and/or C_3S have been identified in addition to the above mentioned non-binding phases. Exceptions were only pastes made with C_3A which were subjected to autoclave treatment (pastes No. 133, 233, 333 and 433). In these pastes no non-hydrated C_3A has been found by XRD—analysis and hence its perfect hydration may be assumed.

The binding new-formations identified in pastes of similar constitution and subject to the same treatment have mostly shown considerable similarity. Disregarding some secondary binding phases, which were present in some of the pastes in smaller quantities, the

Table 1. *Chemical and mineralogical composition of the used materials*

Material	Chemical composition (%)										Results of XRD—and microscopic analysis	Specific surface according to Blaine (cm^2/g)
	Ignition loss at		Insoluble residue	SiO_2	Al_2O_3	Fe_2O_3	CaO	MgO	SO_3	Undetermined residue		
	100°C	1000°C										
Dacite tuff	4.68	8.51	—	65.07	11.12	1.74	5.80	2.19	0.47	0.42	Partially decomposed vitreous phase 65–75%, cristobalite + chlorite + biotite < 20%	14,061
Fly ash	0.32	1.10	—	53.67	25.28	7.83	7.79	1.98	1.48	0.53	Vitreous globular particles often hollow 75–85%; mullite + β-quartz < 35%; carbon	2,743
Activated kaolin	0.12	1.41	—	53.61	44.02	0.22	0.26	0.15	—	0.21	Amorphous phase + residues of damaged kaolinite crystals 85–90%; β-quartz < 10%	17,294
Ground silicious sand	0.16	0.07	—	98.34	1.29		traces	—	—	0.14	β- quartz > 98%	2,160
Powdered calcium hydroxide	0.36	23.58	0.16	—	0.57		73.40	1.81	traces	0.12	Practically $Ca(OH)_2$ only	—
Tricalcium aluminate- C_3A	—	—	0.55	—	37.32	—	62.10	—	—	0.03	Practically C_3A only	3,972
Tricalcium silicate- C_3S	—	—	1.54	25.92	2.12		70.20	—	—	0.22	Practically C_3S only + 0.52% free CaO	3,842

Table 2. *Approximate phase constitution of cementitious pastes hardening under different conditions and approximate composition of their binding new-formations*

Paste number	Paste composition	Curing		Type of binding new-formations (determined by XRD-analysis)	Approximate phase constitution of hardened pastes (% by weight)					Approximate over-all composition of binding new-formations (calculated on basis of chemical analysis)
		Temperature (°C)	Time (days)		Unreacted share	C_3A resp. C_3S	$Ca(OH)_2$	$CaCO_3$	Binding new-formations	
101	Dacite tuff 66% $Ca(OH)_2$ 34%	20	90	II	36.2	—	8.9	4.5	49.7	$C_{0.97}:S:R_{0.10}:H_{1.59}$
102			180	II	31.1	—	6.5	8.7	53.0	$C_{0.88}:S:R_{0.07}:H_{1.58}$
103		80	1	II	43.2	—	12.8	18.7	24.8	$C_{0.89}:S:R_{0.10}:H_{2.16}$
104		175	1	I	32.2	—	1.2	15.4	50.7	$C_{0.89}:S:R_{0.09}:H_{0.81}$
111	Dacite tuff 50% $Ca(OH)_2$ 50%	20	90	II	23.2	—	17.3	11.3	47.4	$C_{1.13}:S:R_{0.11}:H_{1.75}$
112			180	II	18.7	—	14.8	14.8	51.0	$C_{0.96}:S:R_{0.08}:H_{1.69}$
113		80	1	II	29.2	—	14.3	25.3	30.8	$C_{1.33}:S:R_{0.08}:H_{2.41}$
114		175	1	I–II	17.2	—	6.2	23.1	53.2	$C_{1.13}:S:R_{0.08}:H_{0.90}$
131	Dacite tuff 50% C_3A 50%	20	90	V	35.3	5.0	—	6.6	52.5	$C_{2.48}:A:S_{0.19}:H_{6.28}$
132		80	1	V	35.3	10.0	—	4.9	49.4	$C_{2.53}:A:S_{0.15}:H_{6.88}$
133		175	1	V	32.4	—	—	5.1	62.2	$C_{2.56}:A:S_{0.34}:H_{5.70}$
141	Dacite tuff 50% C_3S 50%	20	90	II	31.3	8.0	7.6	6.7	45.9	$C_{1.08}:S:R_{0.10}:H_{1.75}$
142		80	1	II	33.7	15.0	6.3	7.1	37.5	$C_{1.13}:S:R_{0.15}:H_{1.29}$
143		175	1	I	32.1	15.0	3.3	9.0	39.9	$C_{1.11}:S:R_{0.17}:H_{1.36}$

following five characteristic types of new-formations have been established in the studied pastes:

Type I. The binding new-formations were constituted mostly by tobermorite and/or by its mixture with CSH I. This type of binding new-formations, referred to on the subsequent pages by a sum-

Table 3. *Approximate phase constitution of cementitious pastes hardening under different conditions and approximate composition of their binding new-formations*

Paste number	Paste composition	Curing: Temperature (°C)	Curing: Time (days)	Type of binding new-formations (determined by XRD-analysis)	Approximate phase constitution of hardened pastes (% by weight): Unreacted share	C_3A resp. C_3S	$Ca(OH)_2$	$CaCO_3$	Binding new-formations	Approximate over-all composition of binding new-formations (calculated on basis of chemical analysis)
201	Fly ash 66%	20	90	II	41.1	—	12.9	9.5	36.1	$C_{0.95}:S:R_{0.33}:H_{2.02}$
202	$Ca(OH)_2$ 34%		180	II	38.5	—	13.9	7.4	39.4	$C_{0.96}:S:R_{0.34}:H_{2.52}$
203		80	1	II	46.4	—	14.2	16.4	22.7	$C_{1.10}:S:R_{0.32}:H_{1.75}$
204		175	1	I	27.5	—	7.5	9.6	55.0	$C_{0.84}:S:R_{0.21}:H_{1.18}$
211	Fly ash 50%	20	90	II	28.4	—	22.2	15.3	33.6	$C_{1.06}:S:R_{0.26}:H_{2.36}$
212	$Ca(OH)_2$ 50%		180	II	23.7	—	16.2	15.5	43.8	$C_{1.15}:S:R_{0.31}:H_{2.59}$
213		80	1	II	33.3	—	17.9	17.3	31.1	$C_{1.70}:S:R_{0.21}:H_{1.61}$
214		175	1	I–II	14.2	—	18.4	5.7	61.3	$C_{1.04}:S:R_{0.20}:H_{1.29}$
231	Fly ash 50%	20	90	V	38.8	5.0	—	5.4	49.9	$C_{2.61}:A:S_{0.24}:H_{5.40}$
232	C_3A 50%	80	1	V	37.4	10.0	—	4.5	47.7	$C_{2.51}:A:S_{0.26}:H_{5.31}$
233		175	1	V	34.9	—	—	4.8	59.9	$C_{2.70}:A:S_{0.25}:H_{5.20}$
241	Fly ash 50%	20	90	II	32.5	8.0	8.7	7.4	43.0	$C_{1.09}:S:R_{0.17}:H_{1.91}$
242	C_3S 50%	80	1	II	38.5	15.0	7.7	7.4	31.0	$C_{1.35}:S:R_{0.24}:H_{1.56}$
243		175	1	I	35.3	15.0	5.3	8.7	35.3	$C_{1.17}:S:R_{0.22}:H_{1.23}$

Table 4. *Approximate phase constitution of cementitious pastes hardening under different conditions and approximate composition of their binding new-formations*

Paste number	Paste composition	Curing: Temperature (°C)	Curing: Time (days)	Type of binding new-formations (determined by XRD-analysis)	Approximate phase constitution of hardened pastes (% by weight): Unreacted share	C_3A resp. C_3S	$Ca(OH)_2$	$CaCO_3$	Binding new-formations	Approximate over-all composition of binding new-formations (calculated on basis of chemical analysis)
301	Activated kaolin 66%	20	90	III	34.1	—	1.9	8.1	55.3	$C_{1.87}:A:S:H_{6.00}(69\%) + C_{0.80}:S:H_{1.57}(31\%)$
302	$Ca(OH)_2$ 34%		180	III	30.6	—	0.6	7.9	60.4	$C_{1.71}:A:S:H_{6.00}(82\%) + C_{0.80}:S:H_{0.89}(18\%)$
303		80	1	III	42.6	—	5.1	10.2	41.6	$C_{2.00}:A:S:H_{4.68}(80\%) + C_{0.80}:S:H_{0.60}(20\%)$
304		175	1	IV	35.4	—	0.7	7.6	55.9	$C_{2.05}:A:S:H_{4.00}(78\%) + C_{0.80}:S:H_{0.63}(22\%)$
311	Activated kaolin 50%	20	90	IV	17.0	—	6.9	11.6	64.8	$C_{2.29}:A:S:H_{4.90}(71\%) + C_{0.80}:S:H_{2.50}(29\%)$
312	$Ca(OH)_2$ 50%		180	IV	16.0	—	4.6	11.2	67.3	$C_{2.25}:A:S:H_{4.70}(79\%) + C_{0.80}:S:H_{2.50}(21\%)$
313		80	1	IV	28.2	—	9.6	13.0	48.6	$C_{3.00}:A:S:H_{4.00}(74\%) + C_{1.10}:S:H_{1.51}(26\%)$
314		175	1	IV	11.9	—	0.6	12.0	75.0	$C_{2.34}:A:S:H_{4.00}(77\%) + C_{0.80}:S:H_{0.65}(23\%)$
321	Activated kaolin 34%	20	90	IV	8.3	—	20.6	13.9	56.8	$C_{2.78}:A:S:H_{5.90}(67\%) + C_{1.00}:S:H_{2.50}(33\%)$
322	$Ca(OH)_2$ 66%		180	IV	8.1	—	16.0	15.4	60.3	$C_{2.78}:A:S:H_{5.00}(79\%) + C_{1.00}:S:H_{2.50}(21\%)$
323		80	1	IV	12.6	—	16.9	20.2	50.0	$C_{3.00}:A:S:H_{4.00}(75\%) + C_{1.61}:S:H_{1.11}(25\%)$
324		175	1	IV	5.0	—	2.6	23.7	68.4	$C_{3.00}:A:S:H_{3.72}(74\%) + C_{1.46}:S:H_{0.50}(26\%)$
331	Activated kaolin 50%	20	90	V	38.5	5.0	—	5.5	50.5	$C_{2.54}:A:S_{0.24}:H_{5.65}$
332	HC_3A 50%	80	1	V	38.1	10.0	—	4.3	47.0	$C_{2.33}:A:S_{0.18}:H_{6.25}$
333		175	1	V	37.2	—	—	3.8	58.8	$C_{2.59}:A:S_{0.26}:H_{5.57}$

Table 5. *Approximate phase constitution of cementitious pastes hardening under different conditions and approximate composition of their binding new-formations*

Paste number	Paste composition	Curing: Temperature (°C)	Curing: Time (days)	Type of binding new-formations (determined by XRD-analysis)	Approximate phase constitution of hardened pastes (% by weight): Unreacted share	C_3A resp. C_3S	$Ca(OH)_2$	$CaCO_3$	Binding new-formations	Approximate over-all composition of binding new-formations (calculated on basis of chemical analysis)
341	Activated kaolin 50% C_3S 50%	20	90	III	21.2	8.0	0.7	4.4	65.4	$C_{1.81}:A:S:H_{3.00}(68\%) + C_{0.80}:S:H_{0.70}(32\%)$
342		80	1	IV	33.6	15.0	2.3	3.1	45.8	$C_{2.56}:A:S:H_{4.00}(74\%) + C_{0.80}:S:H_{2.10}(26\%)$
343		175	1	IV	35.3	15.0	1.0	4.7	43.6	$C_{2.08}:A:S:H_{2.55}(76\%) + C_{0.80}:S:H_{0.55}(24\%)$
402	β-SiO_2 sand 66% $Ca(OH)_2$ 34%	20	180	III	59.4	—	19.5	15.1	5.3	$C_{1.07}:S:R_{0.26}:H_{2.22}$*
403		80	1	III	61.3	—	17.5	9.1	11.5	$C_{2.70}:S:R_{0.19}:H_{4.21}$*
404		175	1	I	46.8	—	2.3	11.8	38.6	$C_{0.95}:S:R_{0.02}:H_{0.97}$
412	β-SiO_2 sand 50% $Ca(OH)_2$ 50%	20	180	III	46.3	—	33.9	13.3	5.9	$C_{1.80}:S:R_{0.24}:H_{2.88}$*
413		80	1	III	44.5	—	20.0	19.4	15.7	$C_{3.70}:S:R_{0.17}:H_{3.97}$*
414		175	1	I	30.2	—	19.1	8.8	41.5	$C_{0.92}:S:R_{0.02}:H_{0.84}$
431	β-SiO_2 sand 50% C_3A 50%	20	90	V	42.3	5.0	—	4.9	47.5	$C_{2.65}:A:S_{0.09}:H_{5.23}$
432		80	1	V	42.5	10.0	—	3.3	43.8	$C_{2.73}:A:S_{0.11}:H_{5.45}$
433		175	1	V	40.9	—	—	4.4	54.4	$C_{2.76}:A:S_{0.11}:H_{5.43}$
441	β-SiO_2 sand 50% C_3S 50%	20	90	III	45.2	6.5	9.3	8.6	30.4	$C_{1.45}:S:R_{0.07}:H_{1.92}$
442		80	1	III	45.8	15.0	8.7	6.6	23.6	$C_{1.38}:S:R_{0.08}:H_{1.75}$
443		175	1	I	38.9	13.0	3.3	8.1	36.6	$C_{1.07}:S:R_{0.06}:H_{1.08}$

* In the case of these pastes the calculation is subject to relatively great error.

marizing name of "tobermorite-like phases", gave diffractometer traces showing in addition to the CSH I diffraction lines also distinct characteristic diffraction lines of tobermorite, especially 11.3 Å; 3.07 Å and 2.97 Å, and/or diffraction lines 5.5 Å; 2.27 Å and 2.14 Å. The binding new-formations of this type have been identified even in pastes prepared of mixes of siliceous materials with $Ca(OH)_2$ and with C_3S and subjected to autoclave treatment under a pressure of 8 atm. and at 175°C for 24 hours. Exceptions were pastes prepared of activated kaolin (i.e. No. 304, 314, 324 and 343) in which the tobermorite-like phase have not been found.

Type II. The binding new-formations were mostly produced by CSH I and/or by its mix with CSH II. This type of binding new-formations has been identified by the characteristic diffraction lines 3.02–3.06 Å; 2.76–1.81 Å; 1.82 Å and other as well as by differential thermal analysis and electron microscopy. CSH I and/or its mixture with CSH II has been identified as the principal binding phase in most of the studied pastes hardening at the temperature of 20°C and 80°C, except the pastes prepared with C_3A as well as pastes made with activated kaolin.

Type III. The binding new-formations, which were mostly constituted by a mixture of about 70 to 80% of gehlenite hydrate-C_2ASH_n and 20 to 30% CSH I. In the diffractometer traces this type of binding new-formations was characterized by diffraction line of gehlenite hydrate 12.4 Å; 6.2 Å; 4.16 Å; 2.48 Å etc. in addition to the CSH I diffraction lines. The presence of gehlenite hydrate in binding new-formations was proved by electron microscopy, too. The binding new-formations of this type have been identified only in hardened pastes made of a mix of activated kaolin with 34% of $Ca(OH)_2$ and hardening at 20°C and 80°C (paste No. 301, 302, 303) as well as in the paste made of activated kaolin with 50% of C_3S hardening at 20°C (paste No. 341).

Type IV. The binding new-formations, which were mostly constituted by a mixture of about 70 to 80% of hydrogarnet phase $C_3AS_nH_{6-2n}$ with 20 to 30% CSH I. This type of binding new-formations was characterized by the diffractometer traces, apart from CSH I diffraction lines, by diffraction lines approximately 9.8 Å; 5.0 Å; 3.31 Å; 3.01 Å; 2.77–2.71 Å; 2.26 Å; 2.01 Å and other. It may be inferred from the foregoing values, that the constitution

of the hydrogarnet phase varied between the constitution of C_3AH_6 and that of plazolite-$C_3AS_2H_2$ and hence its approximate constitution may be assumed to be C_3ASH_4. The binding new-formations of this type have been established in all pastes prepared of mixes of activated kaolin with 50% and 66% by weight of $Ca(OH)_2$ and further, in the paste made of activated kaolin with 34% of $Ca(OH)_2$ autoclaved at 175°C (No. 304), as well as in pastes made of activated kaolin with 50% of C_3S, hardening at 80 and 175°C (No. 342 and 343).

Type V. The binding new-formations, which were mostly constituted by C_3AH_6 and/or the hydrogarnet phase with a small contents of SiO_2 the constitution of which came very near C_3AH_6. This type of binding new-formations has been identified by the characteristic diffraction lines 5.09–5.13 Å; 4.41–4.44 Å; 3.32–3.25 Å; 3.12–3.14 Å; 2.78–2.80 Å; 2.28–2.30 Å; 2.026–2.04 Å and 1.67–1.68 Å. The lowing of the above values of spacings were established for pastes prepared of active siliceous materials whose SiO_2 took a more pronounced part in the reaction processes and further in pastes hardening under higher temperatures. The binding new-formations of this type were identified in all pastes in which C_3A was used as the cementitious substance.

Typical instances of diffractometer traces of pastes containing individual types of binding new-formations, as described above, are shown in Fig. 1. and 2. The complex thermoanalytic records of some pastes are shown in Fig. 3 to 6.

In the pastes prepared of mixes consisting of siliceous sand with $Ca(OH)_2$, hardening at the temperaure 20 and 80°C (pastes No. 402, 403, 412 and 413) the identification of the type of the binding new-formations could not be carried out quite reliably. The results of the XRD-analyses justify, however, even in this case the opinion, that the new-formations in question are a mix of CSH I and CSH II.

Some diffraction lines in the diffractometer traces of the studied pastes as well as the results of electron microscopy have shown that in addition to the above mentioned main types of binding phases even some secondary binding phases are found in most of the studied pastes in smaller quantities. In the pastes made of mixes with C_3A the presence of C_2AH_8 as well as of the gel-like $Al(OH)_3$ could be found. In the pastes made of mixes with fly-ash and hardening at a temperature of 20°C solitary crystals of ettringite have been identified. In a number of cases the identification of these secondary phases was not feasible owing to their low content.

The results of chemical analyses as well as the composition of binding new-formations and their over-all contents in the pastes, as obtained by calculation on the basis of the former, are in good agreement with the above described results of XRD, microscopic and thermal analyses. Certain differences of the calculated over-all composition of the binding new-formations from the theoretical values should be accounted for by the limited accuracy of the applied chemical analysis and further by the fact that the eventual presence of secondary phases was not taken into consideration. For the same reasons it is necessary to admit certain error of the calculated values of the over-all contents of the developed binding new-formations. These errors do not have, however, any relevant influence on the conclusions of the investigation.

Compression Strengths and Their Relation to the Phase Constitution of the Hardened Pastes

The obtained values of bulk density, true density and compression strength of the studied hardened pastes are given in the first part of Tables 6 to 9.

Compressive strength as well as bulk density of individual pastes vary within wide limits depending on the composition and method of curing of these pastes. Highest values of strength have been attained by pastes made of mixes of siliceous materials with C_3S and on the contrary the lowest were the values of strength of the pastes made with C_3A. Strength of the pastes autoclave-treated at 175°C exceed in most cases highly the values of strength of corresponding pastes hardening at a temperature of 20°C or 80°C. In the case of pastes made of mixes of siliceous materials with $Ca(OH)_2$ and hardening at a temperature of 20°C their strength is usually proportional to the activity of the siliceous admixture. All these statements show that compressive strength of hardened cementitious pastes essentially depends on the same factors as their phase constitution.

In order to clarify the mutual relation between the phase constitution and compressive strength of hardened cement pastes, the over-all porosity of individual pastes was computed and their phase constitution expressed in % by weight has been converted to % by volume, with respect to their over-all porosity and/or to their over-all volume of solid phases. The following values of true density were used for the calculation of volume occupied by individual solid phases contained in the pastes: $C_3A = 3.00$ g/cm³, $C_3S = 3.13$ g/cm³, $Ca(OH)_2 = 2.23$ g/cm³, $CaCO_3 = 2.71$ g/cm³, unreacted residue of dacit tuff 2.16 g/cm³, fly-ash = 2.13 g/cm³, activated kaolin = 2.46 g/cm³,

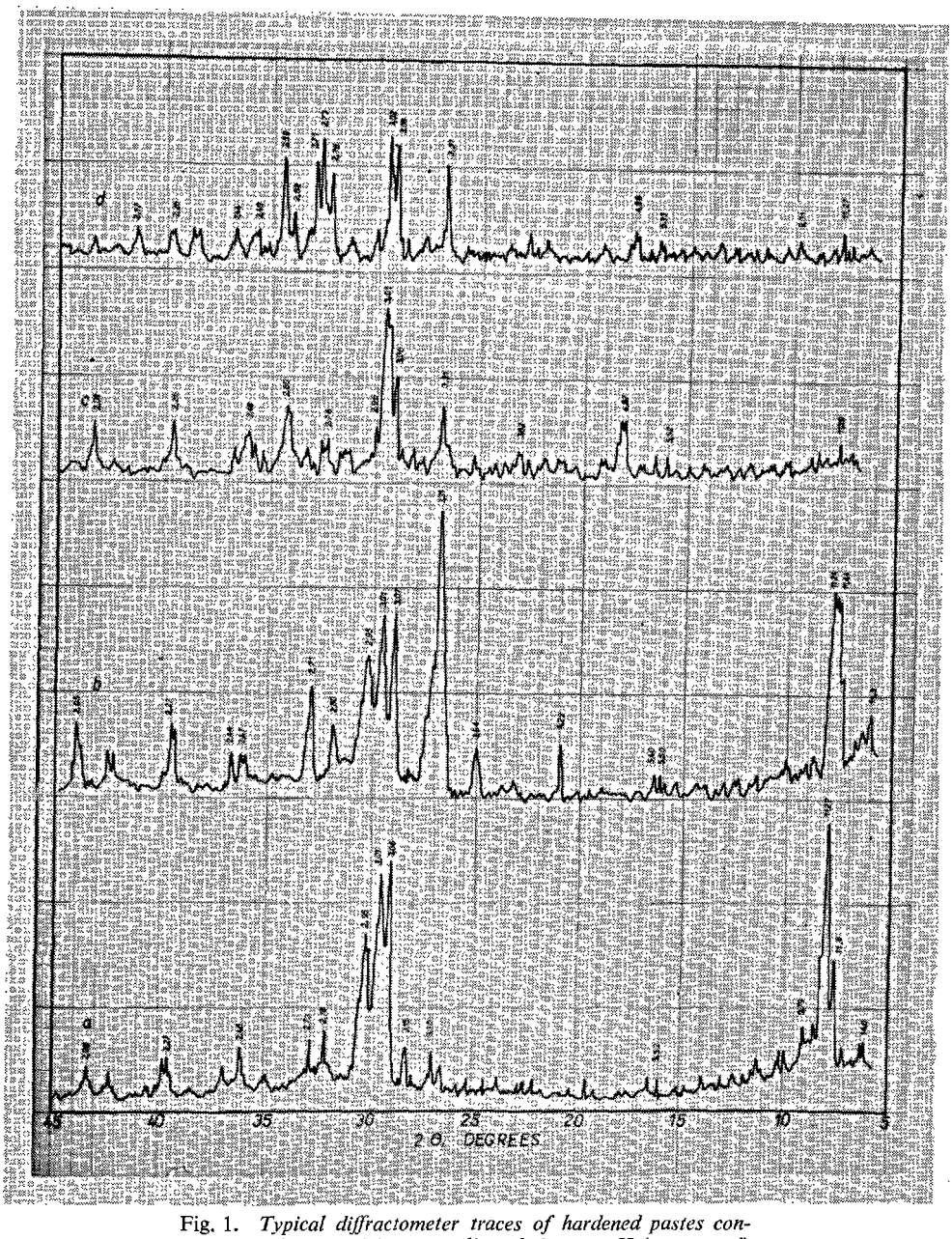

Fig. 1. *Typical diffractometer traces of hardened pastes containing the type I (traces a, b) and the type II (traces c, d) of binding new-formations:*
a—paste No. 104; b—paste No. 404; c—paste No. 203; d—paste No. 241.

β-SiO_2 sand = 2.62 g/cm³, CSH I = 2.25 g/cm³, tobermorite-like phases = 2.45 g/cm³, mixture of gehlenite hydrate and CSH I = 2.32 g/cm³, mixture of hydrogarnet phase and CSH I = 2.50 g/cm³ and the C_3AH_6-hydrogarnet phase = 2.52 g/cm³. The over-all constitution of the studied pastes, expressed in % by volume is shown in the second part of Tables 6 to 9.

As a result of mutual comparison of values presented in Tables 6 to 9 and apparent relationship may be found between the compressive strength and the type as well as volume of the binding new-formations developed in the studied pastes. This relationship is represented in Fig. 7 in which the values of compressive strength of all studied pastes are given in dependence on the over-all volume of the binding new-formations developed in the pastes. If the negative influence of macrostructure flaws in the hardened paste (e.g. cracks) is disregarded the obtained results

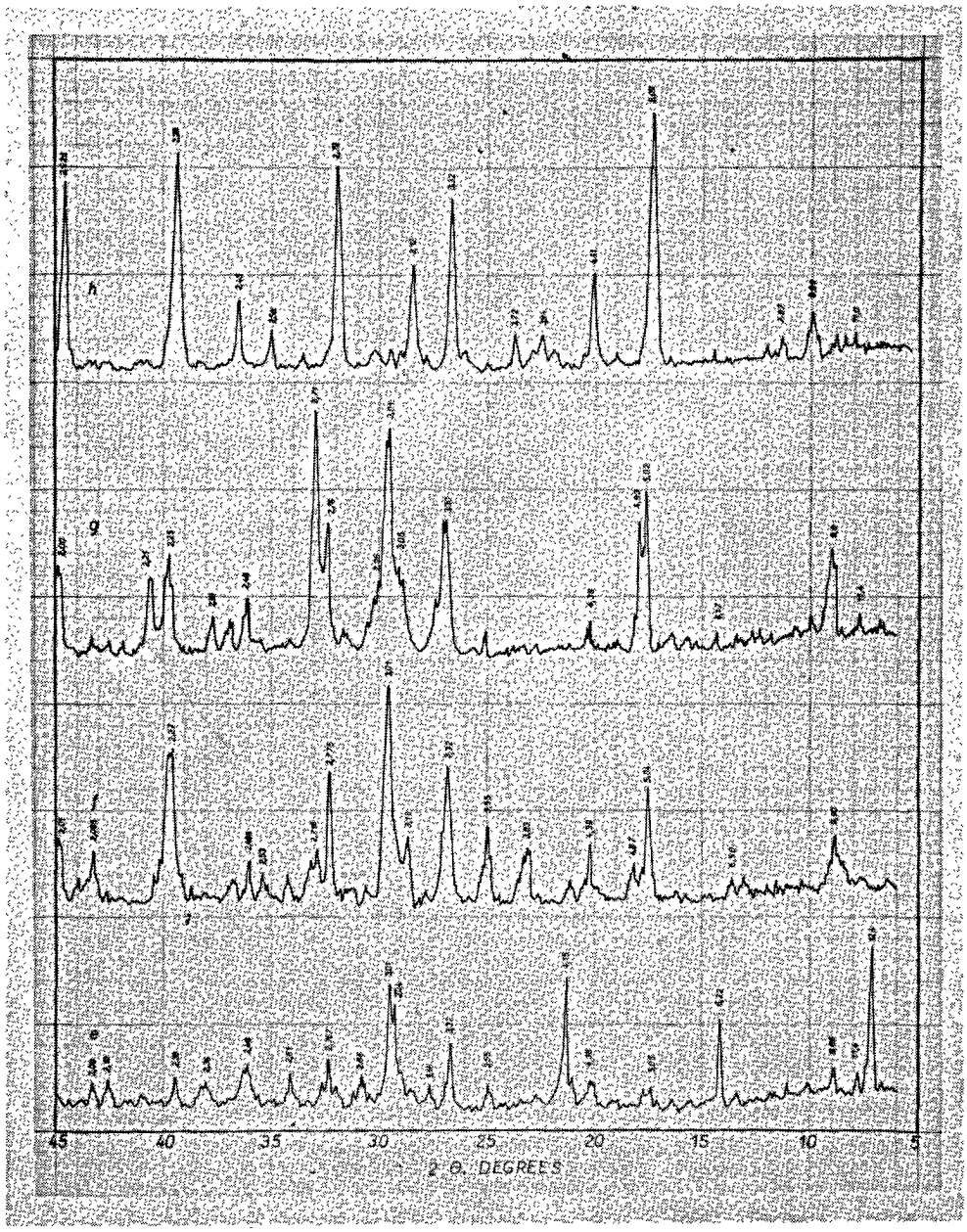

Fig. 2. *Typical diffractometer traces of hardened pastes containing the type III (trace e), the type IV (traces f, g) and the type V (trace h) of binding new-formations:*
e—paste No. 302; f—paste No. 313; g—paste No. 314; h—paste No. 133.

entitle to the opinion, that the compressive strength of a hardened cementitious paste is given only by the type and by the over-all volume of the binding new-formations contained therein, regardless of the initial composition of the paste and of the method of its curing.

An intensive influence of the type of binding new-formations developed in the paste on its compressive strengths is shown by the comparison of compressive strength of pastes having almost the same over-all contents of binding new-formations, only of different type. The highest values of strength have been obtained

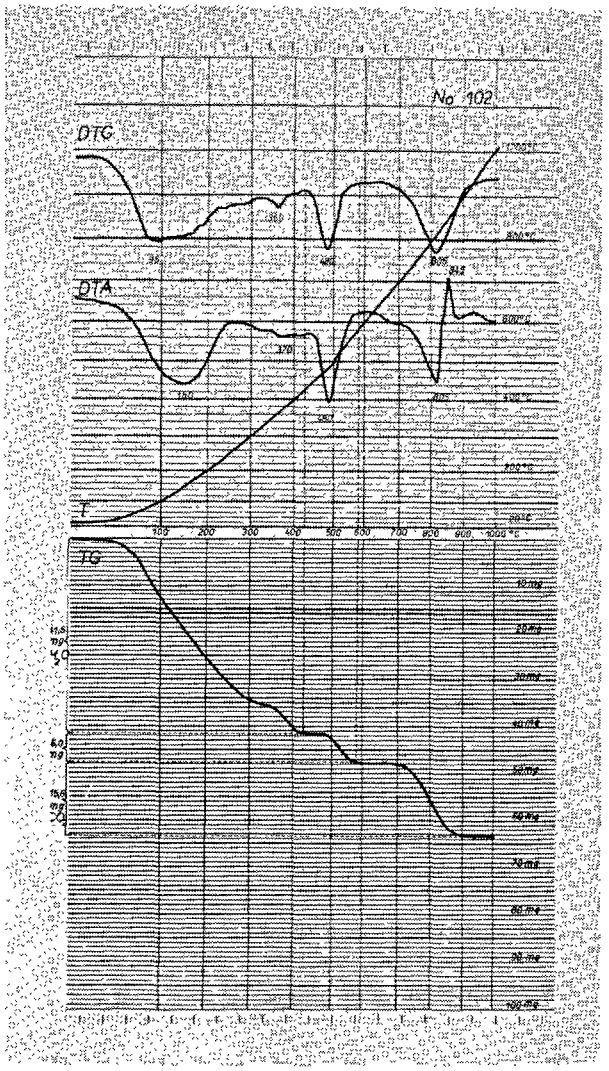

Fig. 3. *Original derivatograph trace of paste No. 102 (dacite tuff 66% + $Ca(OH)_2$ 34%—cured for 180 days at 20°C)*

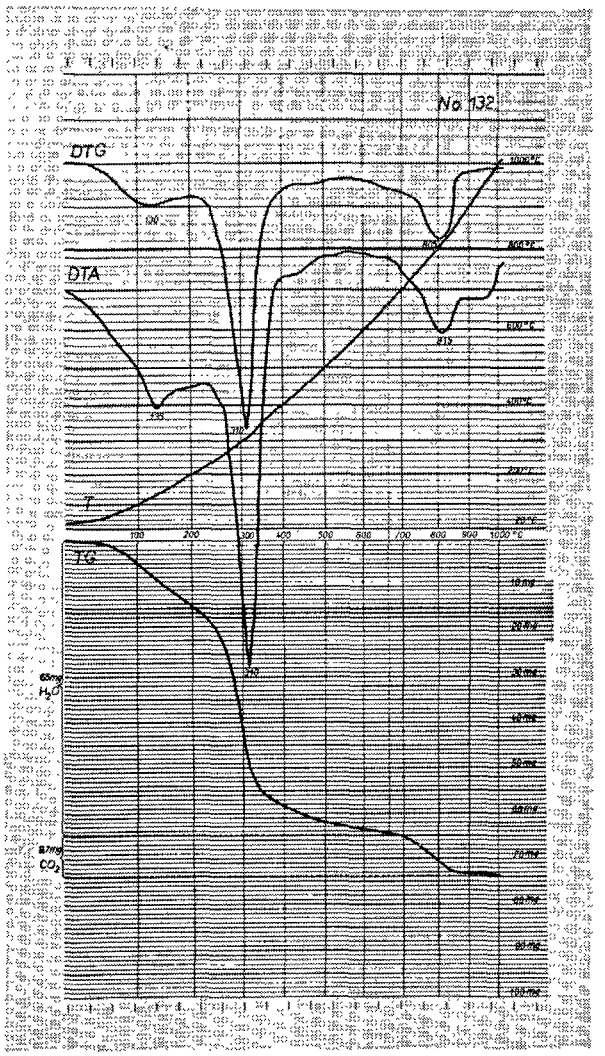

Fig. 4. *Original derivatograph trace of paste No. 132 (dacite tuff 50% + C_3A 50%—steam-cured for 24 hours at 80°C)*

for pastes, in which tobermorite-like phases have been identified as the binding new-formations. If strength of this type of pastes is taken as basis and evaluated by 100%, then the pastes containing approximately the same over-all volume of binding new-formations, only of different type, have the following values of compressive strength.

Type of binding new-formations developed in the paste:	Compressive strength (per cent):
Type I. Tobermorite-like phases	100
Type II. CSH I	56–62
Type III. Mixture of about 70 to 80% gehlenite hydrate and 20 to 30% CSH I	28–32
Type IV. Mixture of about 70 to 80% of hydrogarnet phase and 20 to 30% CSH I	13–20
Type V. C_3AH_6-hydrogarnet phase	3–4

The above given values of strength of pastes with different types of binding new-formations apply only to pastes containing an over-all quantity of binding new-formations up to about 30% by volume. It is, however, probable that the same relative values of strength would result for pastes with a higher over-all content of binding new-formations. The presented comparison proves anyway a fundamental influence of the type of binding new-formations developed in the paste on its strength. The clarification of the proper cause of the different influence of individual types of

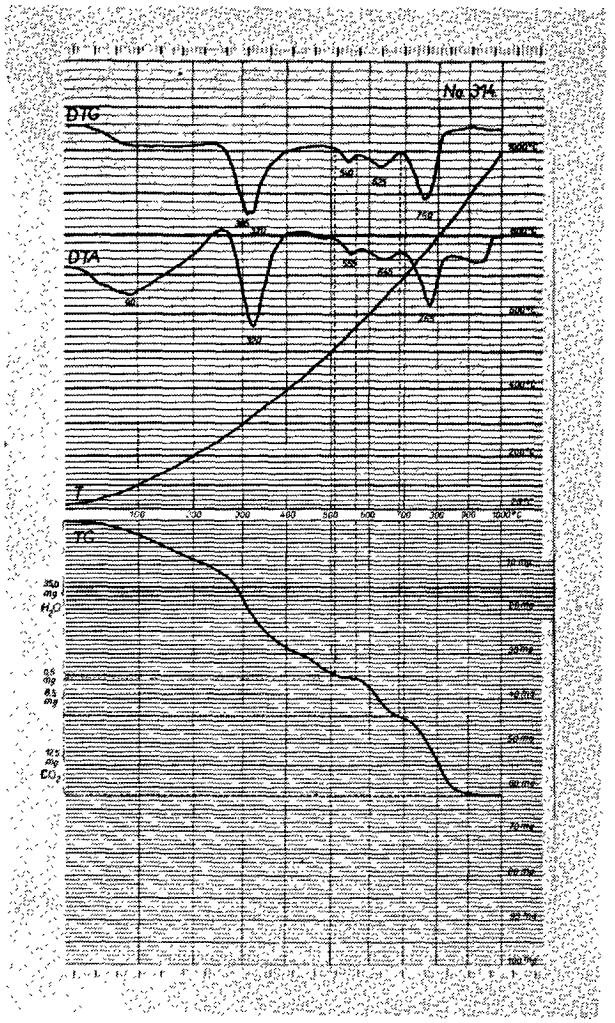

Fig. 5. *Original derivatograph trace of paste No. 314 (activated kaolin 50% + $Ca(OH)_2$ 50%—autoclaved for 24 hours at 175°C)*

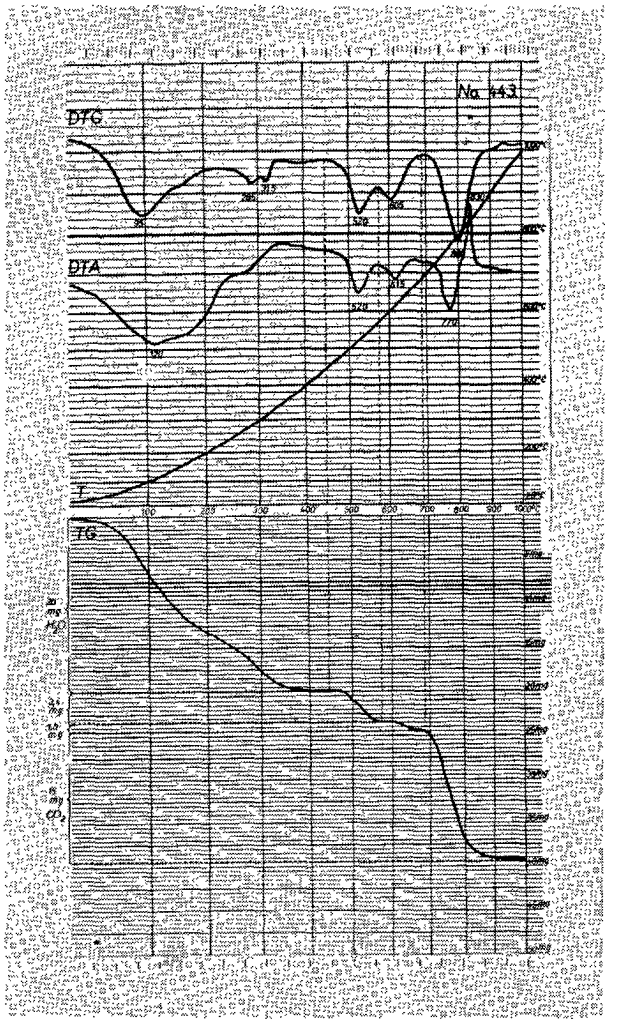

Fig. 6. *Original derivatograph trace of paste No. 443 (β-quartz sand 50% + C_3S 50%—autoclaved for 24 hours at 175°C)*

binding new-formations on strength of hardened cementitious pastes exceeds the frame of this paper and will be discussed in a special paper.

The strength of pastes, containing the same type of binding new-formations is in the first place a function of volume occupied by the binding new-formations in the paste. The functional relationship of the compressive strength and the volume of binding new-formations is different for pastes with different type of binding new-formations. Fig. 7 shows characteristic curves plotted by graphical fitting of values corresponding to pastes, containing the same type of binding new-formations. These curve express functional relationships of compressive strength depending on volume of binding new-formations of Type I to V, as specified above.

Although the functional relationships of compressive strength and volume of binding new-formations differ from each other for pastes with different types of binding new-formations, the relationships in general may be expressed with sufficient accuracy by a function of third degree

$$P = a\theta^3 + b\theta^2 + c\theta$$

where P = compressive strength

θ = volume of binding new-formations developed in the paste, expressed as a percentage of volume of the paste

a, b, c = constants describing the variation of the curve, the value of which depends of the type of binding new-formation.

After substitution of the corresponding values the following formulae have been derived for the suggested functional relationships and/or for the calculation of strength of pastes with binding new-formations of Type I to V:

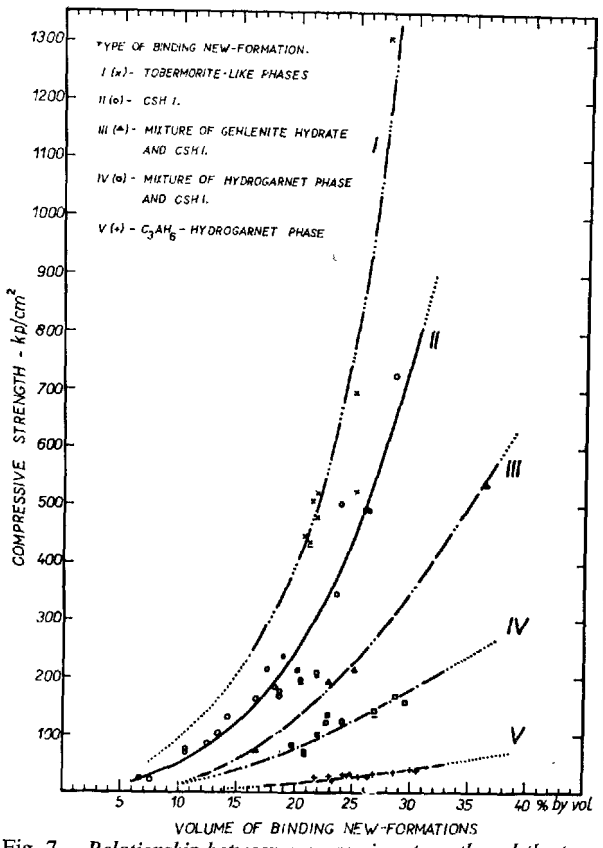

Fig. 7. *Relationship between compressive strength and the type as well as volume of binding new-formations developed in the pastes*

I. For pastes containing binding new-formations of type I (tobermorite-like phases);

$$P = 0.18\theta^3 - 5.093\theta^2 + 50.15\theta$$

II. For pastes containing binding new-formations of Type II (CSH I);

$$P = 0.0275\theta^3 - 0.05\theta^2 + 2.25\theta$$

III. For pastes containing binding new-formations of Type III (mixture of about 70 to 80% of gehlenite hydrate and 20 to 30% CSH I);

$$P = 0.0011\theta^3 + 0.4675\theta^2 - 3.54\theta$$

IV. For pastes containing binding new-formations of Type IV (mixture of about 70 to 80% of hydrogarnet phase and 20 to 30% CSH I);

$$P = -0.005\theta^3 + 0.475\theta^2 - 3.75\theta$$

V. For pastes containing binding new-formations of Type V (C_3AH_6-hydrogarnet phase);

$$P = 0.00327\theta^3 - 0.1252\theta^2 + 2.146\theta$$

The determined values of strength of most of the studied pastes correspond to the reported functional relationships of the compressive strength and the volume of the binding new-formations. Some deviations from these relationships may be explained by the

Table 6. *The physico-mechanical properties and approximate phase constitution of hardened pastes (in % by volume)*

Paste number	Paste composition	Curing: Temperature (°C)	Curing: Time (days)	Type of binding new-formations (determined by XRD-analysis)		Bulk density (g/cm³)	True density (g/cm³)	Compressive strength (kg/cm²)	Approximate phase constitution of hardened pastes (% by volume): Overall porosity	C_3A resp. C_3S	$Ca(OH)_2$	$CaCO_3$	Unreacted share	Binding new-formations
101	Dacite tuff 66%	20	90	II	CSH I	0.915	2.270	214.2	59.7	—	3.7	1.6	14.9	20.1
102	Dacite tuff 66%	20	180	II	CSH I	0.924	2.271	207.3*	59.3	—	2.7	3.0	13.1	21.9
103	$Ca(OH)_2$ 34%	80	1	II	CSH I	0.941	2.299	76.2	59.1	—	5.4	6.5	18.5	10.5
104	$Ca(OH)_2$ 34%	175	1	I	Tobermorite related phases	0.921	2.325	446.2	60.4	—	0.5	5.2	13.3	20.6
111	Dacite tuff 50%	20	90	II	CSH I	0.889	2.325	167.4	61.8	—	6.8	3.7	9.2	18.5
112	Dacite tuff 50%	20	180	II	CSH I	0.896	2.320	197.4	61.4	—	5.9	4.8	7.6	20.3
113	$Ca(OH)_2$ 50%	80	1	II	CSH I	0.909	2.351	87.1	61.3	—	5.8	8.5	12.0	12.4
114	$Ca(OH)_2$ 50%	175	1	I–II	Tobermorite related phases	0.890	2.341	437.4*	62.0	—	2.5	7.6	6.9	21.0
131	Dacite tuff 50%	20	90	V	C_3AH_6-hydrogarnet phase	1.161	2.403	28.9	51.6	2.0	—	2.9	18.9	24.6
132	Dacite tuff 50%	80	1	V	C_3AH_6-hydrogarnet phase	1.166	2.412	21.4	51.6	4.0	—	2.2	18.9	23.3
133	C_3A 50%	175	1	V	C_3AH_8-hydrogarnet phase	1.153	2.404	36.2	52.1	—	—	2.2	17.0	28.7
141	Dacite tuff 50%	20	90	II	CSH I	1.379	2.315	725.4	40.4	3.6	4.7	3.3	19.8	28.2
142	Dacite tuff 50%	80	1	II	CSH I	1.375	2.372	347.0	41.8	6.6	3.9	3.6	20.8	23.3
143	C_3S 50%	175	1	I	Tobermorite related phases	1.362	2.336	695.6	41.6	6.6	2.1	4.6	20.3	24.9

*Test specimens showed individual very fine cracks.

Table 7. *The physico-mechanical properties and approximate phase constitution of hardened pastes (in % by volume)*

Paste number	Paste composition	Curing		Type of binding new-formations (determined by X-ray analysis)		Bulk density (g/cm³)	True density (g/cm³)	Compressive strength (kg/cm²)	Approximate phase constitution of hardened pastes (% by volume)					
		Temperature (°C)	Time (days)						Overall porosity	C_3A resp. C_3S	$Ca(OH)_2$	$CaCO_3$	Unreacted share	Binding new-formations
201		20	90	II	CSH I	1.042	2.254	164.3	53.7	—	6.0	3.6	20.3	16.4
202	Fly ash 66%		180	II	CSH I	1.047	2.250	183.0	53.4	—	6.4	2.8	19.3	18.1
203	$Ca(OH)_2$ 34%	80	1	II	CSH I	1.055	2.292	70.1	54.0	—	6.1	6.1	23.2	10.5
204		175	1	I	Tobermorite related phases	1.061	2.311	524.6	54.0	—	3.5	3.7	13.7	25.1
211		20	90	II	CSH I	0.969	2.322	132.0	58.3	—	9.4	5.3	12.9	14.1
212	Fly ash 50%		180	II	CSH I	0.977	2.324	175.3	58.0	—	6.9	5.5	11.0	18.6
213	$Ca(OH)_2$ 50%	80	1	II	CSH I	0.984	2.339	101.0	57.9	—	7.6	6.1	15.2	13.2
214		175	1	I–II	Tobermorite related phases	0.992	2.341	492.4	57.7	—	7.9	2.0	6.5	25.9
231		20	90	V	C_3AH_6-hydrogarnet phase	1.253	2.327	29.7	46.2	2.1	—	2.5	23.8	25.4
	Fly ash 50%													
232		80	1	V	C_3AH_6-hydrogarnet phase	1.270	2.365	33.2	46.3	4.3	—	2.1	23.1	24.3
	C_3A 50%													
233		175	1	V	C_3AH_6-hydrogarnet phase	1.250	2.335	46.2	46.5	—	—	2.3	21.2	30.0
241		20	90	II	CSH I	1.350	2.279	492.2	40.7	3.4	5.2	3.7	21.0	26.0
242	Flay ash 50%	80	1	II	CSH I	1.367	2.350	237.0	41.8	6.4	4.6	3.6	24.8	18.8
	C_3S 50%													
243		175	1	I	Tobermorite related phases	1.345	2.320	479.6	42.0	6.4	3.2	4.2	22.8	21.4

limited accuracy of methods used for the determination of the phase constitution of the pastes and/or for the determination of the over-all volume of binding new-formations developed in the paste. The second cause of some of the deviations may be internal microscopic flaws (cracks) in the macrostructure of hardened pastes. These flaws did not appear visibly on the specimens, but their existence and their eventual negative influence on the obtained values of compressive strength of some of the pastes cannot be excluded.

Conclusion

The reported results of studies concerning the influence of the type and volume of binding new-formations developed in the cementitious paste on its compressive strength explain and overcome to a certain extent the differences of opinion of various authors as to what is the proper cause of high strength of hardened cementitious paste and what are the measures to be taken to attain this strength.

The statement that the type of binding new-formations developed in the paste is of a decisive influence on their strength and that the values of strength (P) of various pastes decrease depending on the type of the developed binding new-formations according to the sequence: tobermorite-like phases (100% P) → CSH I (56–62% P) → mixture of gehlenite hydrate and CSH I (28–32% P) → mixture of hydrogarnet phase and CSH I (13–20% P) → C_3AH_6-hydrogarnet phase (3–4% P), is in good agreement with the results obtained by G. L. Kalousek, M. Adams, A. F. Prebus, L. D. Sanders, W. J. Smothers, W. H. Taylor, Z. Šauman and others (1, 2, 3, 4, 5, 6). Most of these authors attribute the decisive influence on the strength of hardened paste precisely to the type of the developed binding new-formation, usually to tobermorite.

On the other hand, the statement that the strength of the cementitious paste, the type of the binding new-formation being the same, is a power-function of volume occupied in the paste by the binding new-formations and which may be expressed by the

Table 8. *The physico-mechanical properties and approximate phase constitution of hardened pastes (in % by volume)*

Paste number	Paste composition	Curing		Type of binding new-formations (determined by XRD-analysis)	Bulk density (g/cm³)	True density (g/cm³)	Compressive strength (kg/cm²)	Approximate phase constitution of hardened pastes (% by volume)					
		Temperature (°C)	Time (days)					Overall porosity	C_3A resp. C_3S	$Ca(OH)_2$	$CaCO_3$	Unreacted share	Binding new-formations
301		20	90	III Gehlenite hydrate + CSH I	0.950	2.401	194.2	60.5	—	0.8	2.8	13.0	22.8
302	Activated kaolin 66%		180	III Gehlenite hydrate + CSH I	0.952	2.396	214.3	60.2	—	0.3	2.8	11.7	25.0
303	$Ca(OH)_2$ 34%	80	1	III Gehlenite hydrate + CSH I	0.920	2.416	72.2	61.9	—	2.2	3.5	15.8	16.6
304		175	1	IV Hydrogarnet phase + CSH I	0.922	2.428	103.1	62.0	—	0.3	2.6	13.1	21.9
311		20	90	IV Hydrogarnet phase + CSH I	0.985	2.411	146.2	59.2	—	3.1	4.2	6.7	26.8
312	Activated kaolin 50%		180	IV Hydrogarnet phase + CSH I	0.988	2.390	167.2	58.7	—	2.1	4.1	6.5	28.6
313	$Ca(OH)_2$ 50%	80	1	IV Hydrogarnet phase + CSH I	0.952	2.415	78.2	60.6	—	4.2	4.6	10.8	19.8
314		175	1	IV Hydrogarnet phase + CSH I	0.927	2.425	159.2	61.8	—	0.3	4.1	4.4	29.4
321		20	90	IV Hydrogarnet phase + CSH I	0.936	2.373	120.6	60.5	—	8.8	4.9	3.1	22.7
322	Activated kaolin 34%		180	IV Hydrogarnet phase + CSH I	0.942	2.367	125.0	60.2	—	6.9	5.5	3.1	24.3
323	$Ca(OH)_2$ 66%	80	1	IV Hydrogarnet phase + CSH I	0.929	2.407	81.6	61.4	—	7.1	7.0	4.7	19.8
324		175	1	IV Hydrogarnet phase + CSH I	0.927	2.432	141.2*	61.9	—	1.1	8.2	1.9	26.9
331		20	90	V C_3AH_6-hydrogarnet phase	1.127	2.521	27.6	55.3	1.9	—	2.3	17.5	23.0
322	Activated kaolin 50%	80	1	V C_3AH_6-hydrogarnet phase	1.162	2.560	29.5	54.7	3.9	—	1.9	17.7	21.8
333	C_3A 50%	175	1	V C_3AH_6-hydrogarnet phase	1.158	2.550	32.7	54.6	—	—	1.6	17.0	26.8

*Test specimens showed individual very fine cracks.

general formula

$$P = a\theta^3 + b\theta^2 + c\theta$$

which is in good agreement with the results of T. C. Powers as well as other authors who have considered the increasing quantity and hence the volume of the binding new-formations as the principal cause of the strength's growth of hardened cementitious pastes (7, 8, 9, 10, 11, 12, 13).

The obtained results have confirmed that both groups of opinions are justified, although their validity is limited by certain conditions. The statement that the strength of hardened cementitious paste is given both by the type and by the over-all volume of the binding new-formations contained therein, is in full agreement with the theory of P. A. Rehbinder (15, 16, 17).

The obtained results concerning the relationship between the phase constitution and the strength of hardened cementitious pastes apply, as stated earlier, only to pastes in which no apparent or hidden flaws of macrostructure are present, capable of affecting negatively the values of strength. According to our experience these internal flaws of macrostructure of cementitious pastes made in practice appear very frequently. They appear usually as a consequence of internal stresses developing in hardening pastes in the course of recrystallization of phases, under thermal shocks and often also as a consequence of an inconvenient control of hydration kinetics of binders, etc. An important influence on the possibility of propagation of cracks in macrostructure of hardened cementi-

Table 9. *The physico-mechanical properties and approximate phase constitution of hardened pastes (in % by volume)*

Paste number	Paste composition	Curing: Temperature (°C)	Curing: Time (days)	Type of binding new-formations (determined by XRD-analysis)	Bulk density (g/cm³)	True density (g/cm³)	Compressive strength (kg/cm²)	Approximate phase constitution of hardened pastes (% by volume): Overall porosity	C_3A resp. C_3S	$Ca(OH)_2$	$CaCO_3$	Unreacted share	Binding new-formations
341		20	90	III Gehlenite hydrate + CSH I	1.240	2.356	536.5	47.3	3.2	0.4	2.1	10.8	36.2
342	Activated kaolin 50%	80	1	IV Hydrogarnet phase + CSH I	1.120	2.430	135.2	53.8	5.6	1.1	1.3	15.4	22.8
343	C_3S 50%	175	1	IV Hydrogarnet phase + CSH I	1.076	2.436	71.3*	55.8	5.4	0.5	1.9	15.5	20.9
403		20	180	II Probably CSH I + CSH II	1.072	2.512	< 5.0	57.2	—	9.5	6.0	24.7	2.6
403	β-SiO_2 sand 66%	80	1	II Probably CSH I + CSH II	1.296	2.510	26.4	48.3	—	10.2	4.4	30.5	6.6
404	$Ca(OH)_2$ 34%	175	1	I Tobermorite related phases	1.283	2.529	521.4	49.3	—	1.3	5.4	22.4	21.6
412		20	180	II Probably CSH I + CSH II	1.013	2.473	< 5.0	59.0	—	15.4	5.0	17.9	2.7
413	β-SiO_2 sand 50%	80	1	II Probably CSH I + CSH II	1.079	2.484	24.2	56.6	—	9.7	7.7	18.6	7.4
414	$Ca(OH)_2$ 50%	175	1	I Tobermorite related phases	1.170	2.440	507.6	52.0	—	9.8	3.7	13.3	21.2
431		20	90	V C_3AH_6	1.377	2.588	27.4	46.8	2.3	—	2.5	22.3	26.1
432	β-SiO_2 sand 50%	80	1	V C_3AH_6	1.417	2.610	32.4	45.7	4.8	—	1.7	23.0	24.8
433	C_3A 50%	175	1	V C_3AH_6-hydrogarnet phase	1.408	2.565	38.0	45.2	—	—	2.3	22.0	30.5
441		20	90	II CSH I	1.666	2.401	502.6	30.7	3.6	7.3	5.5	29.2	23.7
442	β-SiO_2 sand 50%	80	1	II CSH I	1.654	2.560	214.5	35.3	8.0	6.5	4.0	29.1	17.5
443	C_3S 50%	175	1	I Tobermorite related phases	1.651	2.466	1307.4	33.0	7.0	2.5	5.0	25.0	27.5

*Test specimens showed individual very fine cracks.

tious paste due to the developing internal stresses is exerted by the contents, by the character and the distribution of the non-binding phases present in the paste. The possibilities of a spectacular restriction or even elimination of flaws development in the macrostructure of hardened cementitious pastes will require further research.

References

1. G. L. Kalousek, "High temperature steam curing of concrete at high pressure", V-ISCC, Principal paper, Part III, Session 5, Tokyo (1968), preprint.
2. W. H. Taylor, D. R. Moorehead and W. F. Cole, "High-strength calcium silicate hydrate: I. Strength tests," Proceedings of the International Symposium on Autoclaved Calcium Silicate Building Products, London (1965), preprint.
3. W. F. Cole and D. R. Moorehead, "High-strength calcium silicate hydrate: II. X-ray DTA, chemical and electron microscope results", Proceedings of the International Symposium on Autoclaved Calcium Silicate Buildings Products, London (1965), preprint.
4. L. D. Sanders and W. J. Smothers, "Effect of tobermorite on the mechanical strength of autoclaved portland cement-silica mixtures", J. Amer. Concrete Inst. Proc., **54**, pp. 127–139 (August 1957).
5. G. L. Kalousek and A. F. Prebus, "Crystal chemistry of hydrous calcium silicates: III. Morphology and other properties of tobermorite and related phases", J. Amer. Ceram. Soc., **41**, pp. 124–132 (April 1958).
6. Z. Šauman, "Calcareous hydrosilicate component—an important factor influencing strength of porous concrete", (in Czech/, Stavivo, **44**, pp. 336–340 /September 1966).

7. T. C. Powers and T. L. Brownyard, "Studies of the physical properties of hardened portland cement paste", J. Amer. Concrete Inst. Proc., **18**, Nos. 2–8 (October 1946–April 1947)
8. T. C. Powers, "The physical structure of cement and concrete", Cement and Lime Manuf., **29**, pp. 13–24 (March 1956).
9. T. C. Powers, "Structure and physical properties of hardened portland cement paste", J. Amer. Ceram. Soc., **41**, pp. 1–6 (1958).
10. S. Giertz-Hedström, "The physical structure of hydrated cements", Symposium on the Chemistry of Cement, Stockholm 1938 (1939).
11. J. Jambor, "The influence of phase constitution and macrostructure of hardened lime-pozzolanic pastes on their strength", (in Slovak), Stavebnícky časopis SAV, **11**, pp. 115–136 (1963).
12. J. Jambor, "Relation between phase composition, over-all porosity and strength of hardened lime-pozzolana pastes" Mag. Concrete Res., **15**, No. 45, pp. 131–142 (November 1963).
13. F. M. Lea, "The chemistry of cement and concrete", Rev. edition, p. 637 (E. Arnold London, 1956).
14. A. Steopoe, "Investigation concerning reactivity of Roumanian trasses in trass-lime and trass-cement mortars", Zurich, International Association for Testing Materials, **1**, p. 918 (1931). See also: Tonindustrie Zeitung, **52**, No. 80, p. 1609 (1928); **55**, No. 30, p. 346 (1931); Zement, **29**, pp. 193–194 (1940).
15. E. E. Segalova and P. A. Rehbinder, "Present-day physicochemical theories of the hardening process of cementitious materials", (in Russian), Stroitel'nye Materialy, **6**, pp. 21–25 (January 1960).
16. G. M. Khutortsov, N. V. Mikhailov, P. A. Rehbinder, "Optimum structure of concrete and the conditions of its formation", Dokl. Akad. Nauk SSSR, **170**, pp. 648–651 (1965).
17. J. Jambor, "Physico-chemical mechanics and its contribution to the problems of hydration of mortar materials and of hardening of cementitious pastes, mortars and concretes", (in Slovak), Stavebnícky časopis SAV, **12**, pp. 321–337 (1964).

Written Discussion

Surinder K. Chopra

Kalousek's excellent review bring out important gaps in the existing knowledge on the relations between binders and strength properties of autoclaved products prepared from lime and siliceous fines. A study on this topic is reported below and a probable mechanism of strength development in autoclaved products moulded under pressure has been suggested.

Five different mixes of lime and fines, designated as E, F, G, H and I were prepared from pure hydrated lime and a high purity ground quartz sand, raw and calcined fly ash samples, granulated slag (Indian) and foamed slag (British) respectively. The two samples of fly ash, raw and calcined, had a fineness of 2763 and 3466 sq. cm. per g. (Blaines) respectively while the remaining three materials had a specific surface of 3200 ± 50 sq.cm per g. The ratio of hydrated lime to fines in the mixes E, F, and G was 30: 70 parts by weight. In the other two mixes, e.g. H and I, the ratio of lime to slag fines was 10: 90. These mix ratios had been selected in the light of the earlier work of Midgley and Chopra (1) except that a ratio of 10: 90, instead of 5: 95, was chosen for lime-slag mixes as the Indian slag has a CaO/SiO_2, ratio lower than that of the British granulated slag.

In order to analyse the respective effects of factors such as porosity, degree of hydration, and nature of hydration products etc. on the strengths of mixes of lime with fines, preparation of cylindrical compacts from the moist mixes at a uniform porosity was considered desirable. Earlier Midgley and Chopra had moulded their specimens from different lime-fines mixes at a uniform pressure of 2 tons per sq.in. Since this process does not ensure a uniform degree of compaction of the different lime-fines mixes, which in turn may influence the strengths of autoclaved specimens, the effects of moulding pressure on deformation (i.e. degree of compaction), density and porosity of cylinderical compacts prepared from the moist mixes at varying W/S ratios were studied after Lecnazar (2). Relationships between moulding pressure and deformation, and porosity were determined for each of the five mixes at varying W/S ratios (0 to 0.24) and were interpreted in the form of curves. The moulding pressure for each mix corresponding to a W/S ratio of 0.12 (commonly employed in practice for sand-lime bricks) was chosen from the curves so that all the moulded compacts (3 in. ht $\times$ 2 in. dia), were at the same final porosity. The data in Table I show that the average final porosity was $0.33 \pm .02$ (a lower variation in porosity was not found practicable). The data further revealed that if a uniform pressure of 2 tons per sq.in. is employed for moulding compacts from these moist mixes at a W/S ratio of

Table 1.

Mix No.	Mix composition by wt.	Porosity (before autoclaving)	Properties of compacts after autoclaving			
			Porosity	Non-evaporable	Surface area of solids	Density of solids
		Average	Average	mg/g	sq m/g	g/cc
E	30 L*: 70 Quartz sand	0.32	0.318	0.059	78	2.49
F	30 L: 70 Fly ash (R)	0.35	0.341	0.122**	71	2.51
G	30 L: 70 Fly ash (C)	0.32	0.354	0.089	68	2.64
H	10 L: 90 Slag (g)	0.33	0.311	0.062	38	2.73
I	10 L: 90 Slag (f)	0.31	0.38	0.025	18	2.93

* L stands for lime, R for raw, C for calcined, g for granulated and f for foamed slag.
** Not reliable because of presence of unburnt carbon.

0.12, the porosity of the compacts may vary within wide limits i.e. 0.193 to 0.319 in the series under consideration.

The green compacts were autoclaved in a laboratory autoclave (Cenco) at a pressure of 160 psi for 16 hours and were tested for water absorption, compressive and tensile (splitting) strengths. Compacts were crushed and lightly pounded to prepare a granular sample passing No. 30 and retained on No. 80. U.S. Sieves. The granular samples were dried under vacuum (3) for the determination of non-evaporable water by determining loss in weight up to 650°C in a thermogravimetric balance. The other determinations made on the granular samples were density using Kerosine oil and B. E. T. surface areas by water vapour absorption after Ludwig and Pence (4). The autoclaved products were also examined with the help of X-ray powder diffraction and differential thermal analyses for identifying the hydration products formed.

The data on compressive strengths, non-evaporable water contents, surface areas, porosities etc. of compacts of different autoclaved lime-fines mixes are summarized in Tables 1 and 2 and show that strength development does not bear any simple relationship either with the B. E. T. surface areas or nonevaporable water contents. Though the data in Tables 1 and 2 indicate in a general way that strengths are low when total porosity is higher, the explanation of strength development in terms of porosity values also suffers from limitations as shown little later.

11.4 Å-tobermorite was the main cementitious phase in lime-fly ash mixes F and G; and poorly crystallized tobermorite was present in lime-quartz and lime-granulated/foamed slag mixes in order of decreasing amount. Xonotlite was detected only in lime-quartz mixes. Some CSH (probably $C_5S_4H_n$ according to Kalousek) was also present in lime-quartz and lime-granulated slag mixes. α C_2SH was present in both mixes (H and I) of lime and slag; the quantity being more in lime and foamed slag mix. A hydrogarnet, C_3ASH_4, was formed in both the mixes of lime and fly ash (F and G). The composition of hydrogarnet phase in the lime-slag mixes was $C_3AS_2H_2$ thus confirming earlier results of Midgley and Chopra. In all the mixes $Ca(OH)_2$ had been consumed almost completely.

As in the past, it is difficult to correlate strength with the formation of calcium silicate hydrate phases except that poor strengths of lime-foamed slag mix are probably due to the formation of αC_2SH. The problem of choosing between tobermorite and "CSH" phase for high strengths has been discussed by Kalousek in the principal paper and the data of this study is also not conclusive. Interpretation has to wait till more is known about the gel-crystal composition of the binders. The densities of the C_3ASH_4 and $C_3AS_2H_2$ are 3.00 (by calculation) and 3.13 g/cc respectively (5) and are higher than those of lime and fly ash or slag fines from which they are formed. If hypothetical equations are written after Hansen (6), it is found out that their formation from their components results in an increase in porosity of the compacts which could affect strengths adversely. Since according to Satava (7) porosity is a more important factor than the nature of solid phase formed by a hydrothermal reaction, the final total porosities of the autolcaved compacts were calculated on the assumption that the specific volume of combined water is not different from that of evaporable water and are reported in Table 1. The data show that an increase in porosity on autoclaving is probably an important cause of lower strengths in lime-fly ash/foamed slag mixes.

The principal stress, which in the case of unconfined compression is the compressive strength, is known to increase rapidly with an increase in cohesion and also with an increase in the friction angle. Cordon and Gillespie (8) believe that in high strength concrete the total bond strength between aggregate particles and

paste controls the cohesive value and as the quality of paste increases, failure in bond controls the strength of concrete.

Mixes of lime and aggregate fines could be likened to those of cement and fine aggregate. Presence of smaller-sized particles is known to increase both cohesion and angle of friction. On application of high moulding pressure little water was found to squeeze out from lime-fines mixes even at water/solid ratios above 0.12 and lower than 0.24. It may therefore be inferred that most of the added water was held tightly by lime (having internal surface as well) and therefore its contribution towards promoting deformation and thereby adhesion could be a variable factor. Since the compacts for compressive strength test were prepared at a W/S ratio of 0.12 and different loads were applied for achieving the same value of porosity, and adhesion between particles is improved by application of pressure, differences in degree of adhesion could have arisen at the stage of moulding the compacts themselves. All the above mentioned factors account for the green strength of the compacts.

As a result of hydrothermal reactions the strengths of compacts increased manifoldly. For example, the compressive strength of compact H(10 lime: 90 slag) was about 950 psi after curing in 99 per cent relative humidity for 28 days and 9,203 psi after autoclaving at 160 lbs per sq. in. for 16 hours, the increase being ten times. Similarly, Midgley and Chopra had found the strengths of compacts containing 95–100 parts of slag fines with 0 to 5 parts of lime ranging between 3,780 to 8,589 psi. Surely, presence of this small quantity of lime cannot result in the formation of hydration products in any large quantity and it alone cannot account for this manifold increase in strength. The increase in strength could be primarily due to the strengthening of the primary bonds resulting from bridging between particles in contact, where surfaces are under pressure or deformed, and hydrate or react more readily. Solid state reactions are postulated for the formation of primary bonds. The formation of Bernal's welds by intergrowth of the lattices of crystals in contact due to some re-arrangement of the lattice as postulated by Lea (9) in explaining bond of cement to aggregate is also quite likely. The adhesional strength of the interparticulate bridges (10) and the number and strength of welds seem to be important factors in governing the strength and other properties of the compacts. Though difficult to assess, some information on this was obtained by subjecting the cylindrical compacts to direct tensile stresses by performing the splitting test (11). The results are reported in Table 2, together with the ratios of compressive to splitting strengths under columns 5. The ratios in mixes F, G and H are different from those of E and I.

Table 2. *Water absorption and strength of cylindrical specimens (Autoclaved for 16 hours at a pressure of 160 psi)*

Specimen designation		Water absorption after 48 hours per cent	Crushing strength lb/in²	Splitting strength lb/in²	Ratio 3/4
1		2	3	4	5
E	(i)	7.67	11,614	907	
	(ii)	7.71	12,445	901	
	(iii)	7.39	10,666	770	13.4
	Av.	7.59	11,545	859	
F	(i)	12.52	3,899	416	
	(ii)	12.06	4,413	398	
	Av.	12.54	4,156	407	10.2
G	(i)	7.59	4,743	630	
	(ii)	8.47	4,566	703	
	(iii)	10.37	4,636	771	
	Av.	8.81	4,648	701	6.6
H	(i)	5.18	8,418	980	
	(ii)	6.53	10,486	861	
	(iii)	4.91	8,704	1141	
	Av.	5.54	9,203	994	9.2
I	(i)	10.54	2,780	230	
	(ii)	6.44	2,568	211	
	(iii)	—	—	288	
	Av.	8.49	2,674	243	11.0

A lower ratio (Table 2) indicates comparatively a better adhesion of cementitious phase particles to other particles in the system (excluding those of calcium hydroxide if present). Because in the present study, the fineness of reactants, W/S ratio and porosity etc. of the compacts were nearly the same, the major factors responsible for differences in adhesional strengths would be the nature of surfaces, shape and surface texture of particles and their mutual orientation etc. It is therefore not surprising to find better adhesional strengths of reactive solids i.e. two samples of fly ash and a granulated slag against ground quartz and foamed slag. The reason of the relative inactivity of the latter has been explained earlier by Assarson (12). Briefly, the explanation of strength development in pressure-moulded lime-fines products could be as follows:

Application of pressure improves the adhesion between particles by formation of primary interparticulate bridges. Strengthening of the latter forms an initial framework during early periods of autoclaving. Increase in strength can take place by a further conversion of the reactants into reaction products of high specific surface i.e. by increasing the cohesion. Alternatively, the strengths can also be increased by increasing the number and strengths of welds i.e. working through adhesion, through a judicious choice of materials and methods both the approaches can

lead to high strengths. However, the practical limitation in either case is the aggregation which beyond a certain degree will reduce strength through an increase in porosity.

References

1. H. G. Midgley and S. K. Chopra, "Hydrothermal reactions between lime and aggregate fines", Mag. of Concrete Res. **12** pp. 73–82 (1960).
2. F. J. Lecnazar, "Reactivation of prematurely hydrated portland cements", J. Sci. and Industr. Res. **21** D, No. 2 pp. 33–38 (1962).
3. L. E. Copeland and John C. Hayes, "The determination of non-evaporable water in hardened portland cement pastes", Research & Development Laboratories of the Portland Cement Association, Bulletin 47, pp. 1–9 (1953).
4. N. C. Ludwig and S. A. Pence, "Properties of portland cement pastes cured at elevated temperatures and pressures", Proc. Am. Concrete Institute, **52**, pp. 673–687 (1956).
5. C. O. Smith, "Identification and qualitative chemical analysis of minerals", D. Van. Norstand Company Inc. 1953. pp. 283.
6. W. C. Hansen, Discussion of the paper "Portland-pozzolana cement by G. Malquori", Chemistry of Cements, Proceedings of the Fourth International Symposium, **2**, pp. 1000 Washington (1960).
7. V. Satava, "A study of the process of hardening of lime and silica at 175°C. The relation between the structure and strength of hardened materials", International Symposium on Autoclaved Calcium silicate Building Products, Society of Chemical Industry, London (1965). (preprint).
8. W. A. Cordon and H. A. Gillespie, "Variables in concrete aggregate and portland cement paste which influence the strength of concrete", J. Am. Con. Inst., **60** no. 8, pp. 1029–52 (1953).
9. F. M. Lea, "Cement Research: Retrospect and prospect", Chemistry of Cements, Proceedings of the Fourth International Symposium, **1**, pp. 5–8, Washington (1960).
10. S. J. Gregg, "The surface chemistry of solids", Chapman and Hall Ltd., London, 1961, p. 168.
11. C. K. Romesh and S. K. Chopra, "Determination of the tensile strength of concrete and mortar by split test", Indian Concrete Journal **34**, no. 9, pp. 359–57 (1960).
12. G. O. Assarson, Discussion of the paper "Hydrothermal reactions in the system $CaO–SiO_2–H_2O$ and the steam curing of cement and cement-silica products", Chemistry of Cements, Proc Fourth International Symposium. **1**, pp. 190–194, Washington (1960).

Author's Closure

George L. Kalousek

Dr. Jambor has presented a remarkable paper. The numerous quantitative results on kinds and amounts of binder phases, densities, etc. (and the compounding of these data for construction of Fig. 7), is a monumental achievement. The results either supply, or suggest, answers to several important questions on relation of type and volume of binder to strength.

Curve I in Fig. 7 representing tobermorite, or tobermorite plus some C–S–HI, shows this binder to have higher strength than the poorly crystalized C–S–H of Curve II for the "binder-space ratios" studied. (The term binder-space ratio is analogous to Power's gel-space ratio and is adopted for this discussion as a matter of simplification and consistence with Powers' term.) Dr. Jambor's equations relating strength to binder-space ratio shows that strength is approximately proportional to the cube of the binder-space ratio (expressed in percent). In this respect his relations' are in argument with that of Powers and Rehbinder. Type II binder, mostly poorly crystalized C–S–H, is more closely related to cement gel than the other four binders under discussion. A direct comparison (not made) of the curves for Type II binders and cement should prove interesting and informative. Allowance would have to be made for the volume of CH and small amounts of other hydrates per cent with C–S–H in cement gel. Jambor included only the binding phases in computing the binder-space ratio.

The Type II binder is C–S–HI or C–S–HI plus some C–S–HII. Presence of $C_{5-6}S_6Hn$ in some of the samples is suspect but not in others. The presence of $C_{5-6}S_6Hn$ in the pastes of low binder-space ratios seems improbable on basis of strength results (zero or near zero) discussed in the principal paper. Comparable strength of C–S–HI at binder-space ratios of 7.5- to 15.0-per cent range from 20 to 100 kg/cm^2. On the other hand, extraordinarily high strengths have been reported (references 78 and 95 in P. P. III-5) for lime-silica specimens formed under high pressure

of which the binder was probably $C_{5-6}S_6Hn$. It follows that $C_{5-6}S_6Hn$ is a binder of superior strength in dense products and an inferior one in products of low density.

It is possible that Curve II is a composite of several curves, one not differing much from the other except as mentioned for $C_{5-6}S_6Hn$ and C–S–HI. A direct comparison of C–S–HI—space ratio curve with the C–S–HII—space ratio curve and in turn with the gel-space ratio curve (the latter corrected for free CH, etc.) should prove informative. The techniques developed by Sereda and associates at the Division of Building Materials, National Research Council of Canada using compacts with controlled porosities should be found highly effective.

Comparison of Curve IV (C–S–HI—hydrogarnet) and Curve V (hydrogarnet) permits evaluation of additiveness of strength of the two binders. Hydrogarnet (Curve V) is a binder of very low strength. The values presented in related tables of data, and which were applied in construction of Curve IV, were used to compute the C–S–HI—space ratio of the Type IV binders; these ranged from about 5 to 8 per cent. Similarly the hydrogarnet-space ratios had computed values of about 15 to 20 per cent. Over these binder-space ratios, the strength of C–S–HI ranges from about 20 to 50 kg/cm², and hydrogarnet from about zero to 20 kg/cm². The sums of the strengths of these binders at any given binder-space ratio are only a small fraction of the strengths shown by Curve IV. This observation is interpreted to mean that the C–S–HI binds together the particles of the hydrogarnet.

Dr. Jambor's technique should prove especially usedul in clarifying the relation of binder-space ratio to strength of calcium aluminate cements. These cements form two composite binders: The metastable CAH_{10}–C_2AH_8 which possesses high strength, and the equilibrium hydrogarnet-alumina gel/gibbsite composite which is generally thought to be of low strength. Manufactures urge lowest possible water content to avoid strength retrogression due to transformation to the stable phase. Limited data obtained by the writer indicate that using very low-water contents and curing at relatively high temperature, the pastes contained the stable phases as binder and had superior strength. The question arises: Did not many structures made with calcium aluminate cement with low-water content undergo transformation or partial transformation to the stable phases without serious strength loss?

Dr. Chopra's results on binders of different porosities and consisting of different phases are an interesting addition to the data already reported. His hypothesis on the effects of pressure forming for securing high strength is also of interest.

Drs. Soroka and Sereda (supplementary paper No. III-34) studies on pressure molding of hydrated cement and gypsum compacts, and corresponding in situ hydrated samples of different porosities appear to contribute much to the understanding of interparticulate bonds. The hypotheses presented are expected to be useful in explaining the third power increase in strength with increasing values of binder-space ratio.

The technology of pressure forming, long known to the sand-lime industry, should become increasingly more sophisticated and important to the industry as knowledge of the fundamentals of high binder-space ratios is increased. The opportunities in the field of autoclave curing of precast ware, allowing a variety of single and composite binders, appear especially bright.

Dr. Hansen's discussion directs attention to an apparent contradiction of through-solution vs topochemical reactions. The term through-solution is often used loosely in the sense that it does not include steps in the overall reaction between a solid and solution such as quartz and CH solution. The following hypothesis is mentioned, not as an explanation, but rather to direct attention to a sequence of reactions which may occur.

The Si^{4+} in quartz is a part of a crystalline lattice and is strongly bonded to 0^{--}. The surface of a quartz grain is disordered to some depth due to breakage of interionic bonds during grinding and subsequent redistribution of surface charges. According to Weil the disordered surface consists of 0^{--} screening the Si^{4+}. A solution of CH supplies Ca^{2+} to combine with the 0^{--} and OH^- with the Si^{4+}. This may be regarded the first step of the reaction. Some of the Si–O bonds in the surface "layer" of the quartz would not yet be broken. The surface complex of randomly orientated Ca^{2+}, Si^{4+} and OH^-, called the "quartz-CSH complex," would be firmly bonded to the quartz through the still unbroken Si–O bonds. As the reaction continues with the Ca^{2+} and OH^-, the remaining Si–O bonds in the surface layer are broken. A C–S–H, possibly C_7S_4Hn is formed. During the formation of this hydrate, a new layer of the quartz-CSH complex is formed. The C_7S_4Hn remains bonded through surface charges to the underlying layer of the quartz-CSH complex. Partial hydrolysis of the C_7S_4Hn would supply silicate ions to solution. The reactions in the two suggested steps would continue with Ca^{2+} and OH^- diffusing inwardly through the reaction products.

The presence of free CH assures high Ca^{2+} concentration and continued formation of C_7S_4Hn. After the free CH is depleted, the reaction of the residual quartz continues. The C_7S_4Hn becomes the supply of Ca^{2+} ions.

The C_7S_4Hn in the interior of the reaction products and at the interface with the quartz-CSH complex supplies through solution the Ca^{2+} and OH^- to continue the reaction with the quartz. Eventually in this zone, which extends outwardly, the composition of the C–S–H reaches the stable ratio of 5C: CS and supply of Ca^{2+} is depleted. At this stage actual solution of the quartz may begin.

This alternate reaction of direct solution of the quartz is suggested by studies of Moorehead and McCartney (reference 69, p. p. III-5). The silicate ions diffuse outwardly through the reaction products to continue formation of C–S–H of successively lower C/S ratios. This reaction would occur through solution.

It is recognized that the model just presented is highly speculative even though consistent in gross features with results on kinetics studies. Some evidence in the literature supports a through-solution mechanism, others a topochemical reaction. It is probable that the condition of the test and stage of the reaction are factors determining the type of reaction occurring. Obviously, more direct evidence (which is difficult to obtain) will be required for an entirely acceptable conclusion.

Dr. Hansen's explanation of the mechanism of Funk's seeding experiments appears logical to the writer.

Supplementary Paper III-80 Hydroxyl Ellestadite Produced by Hydrothermal Reaction Containing Calcium Sulphate

Kunihiro Takemoto and Hajime Kato*

Synopsis

Mechanical strength of hydrated calcium silicate cured in autoclave is affected by the contents of calcium sulphate in the raw mixtures and the optimum content was around 2% of SO_3. The possibility of introduction of sulphur into tobermorite at the elevated temperatures was examined.

Sulphur tends to be separated from the substituted tobermorite gel to form $CaSO_4$.

In the hydrothermal reaction products of the hardened mass of which raw mixture contains calcium sulphate, there exists a mineral, hydroxyl ellestadite $Ca_{10}(SiO_4)_3(SO_4)_3 \cdot (OH)_2$, known as a mineral of apatite group.

The condition in which hydroxyl ellestadite is formed was revealed. When the CaO/SiO_2 molar ratios of mixtures exceed 1, hydroxyl ellestadite is produced coexisting with xonotlite, hillebrandite, portlandite and anhydrite according to the chemical composition of the mixtures.

However, when the ratios were less than 1, anhydrite was the only SO_3-bearing phase coexisting with quartz, xonotlite and gyrolite. Some properties of the synthesized hydroxyl ellestadite were measured by means of optical, X-ray and thermal analysis and so on, and compared with the results of the earlier investigators. Formation of hydroxyl ellestadite and its relation with the coexistence with alumina were discussed. Chemical composition and thermal decomposition of this mineral were also discussed.

Introduction

Calcium sulphate is usually added to portland cement clinker as a form of gypsum to control its setting time.

When cement is mixed with water at ordinary temperatures below 100°C, the calcium sulphate reacts with tri-calcium aluminate to form calcium sulphoaluminate hydrates, $C_3A \cdot 3CaSO_4 \cdot 32H_2O$ and $C_3A \cdot CaSO_4 \cdot 12H_2O$. Kalousek (1) reported that the SO_3 content calculated from both calcium sulphoaluminate hydrates determined by D. T. A. could not account for all the SO_3 in the paste and suggested the introduction of sulphur into tobermorite gel in the paste, perhaps as SO_4^{2-}.

Copeland, Bodor, Chang and Weise (2) observed the formation of substituted tobermorite in the reaction of tobermorite gel with aluminate, ferrite and sulphate after bottle-shaking and ball-milling. The measured maximum amount of substitution was one atom of substituents, such as Al, Fe and S, to 6 atoms of Si.

Above 100°C, calcium tri-sulphoaluminate hydrate decomposes to monosulphoaluminate hydrate and calcium sulphate hemi-hydrate and at higher temperatures to calcium aluminate hydrate and anhydrite.

However, the influence of SO_3 on the mechanical strength of autoclaved building materials and the reaction of SO_3 in the autoclave hydration are not clear so far (3, 4).

The present authors (5) tested the mechanical strength of the autoclaved mass of various mixes of portland cement, quartz sand, slag and gypsum and examined the SO_3-bearing phases in the mass by X-ray diffraction, D.T.A., I. R. and so on. The authors made clear the conditions of formation of hydroxyl ellestadite in the hydrothermal reaction in this paper.

*Central Research Laboratory, Onoda Cement Co., Ltd., Tokyo, Japan.

Mechanical Strength of Autoclaved Concrete

In the course of the investigation of autoclaved concrete, the authors (5) examined various mixes, considering many factor such as CaO/SiO_2 molar ratio, alumina content, SO_3 content, curing temperature and time, etc.

The authors found that the SO_3 content affected the mechanical strength of the hardened mass, and discovered that the optimum content of SO_3 was around 2% in the raw mixture.

A few examples are shown in Fig. 1.

The materials used and the treating conditions were as follows:

Materials:

White portland cement clinker—pulversized to the fineness of Blaine 3870 cm^2/g.

Quartz sand—pulverized to the fineness of Blaine 5260 cm^2/g.

Gypsum—chemical reagent calcium sulphate di-hydrate.

Table 1. shows chemical compositions of these materials.

Treating Condition

Specimens of 10 × 10 × 70 mm. were set in a 17*l* autoclave. The temperature was raised to 179°C (saturated steam pressure 10 kg/cm^2) in 2 hrs., and then kept at the same temperature for the following 5 hrs. and lowered to room temperature in the next 2 hrs.

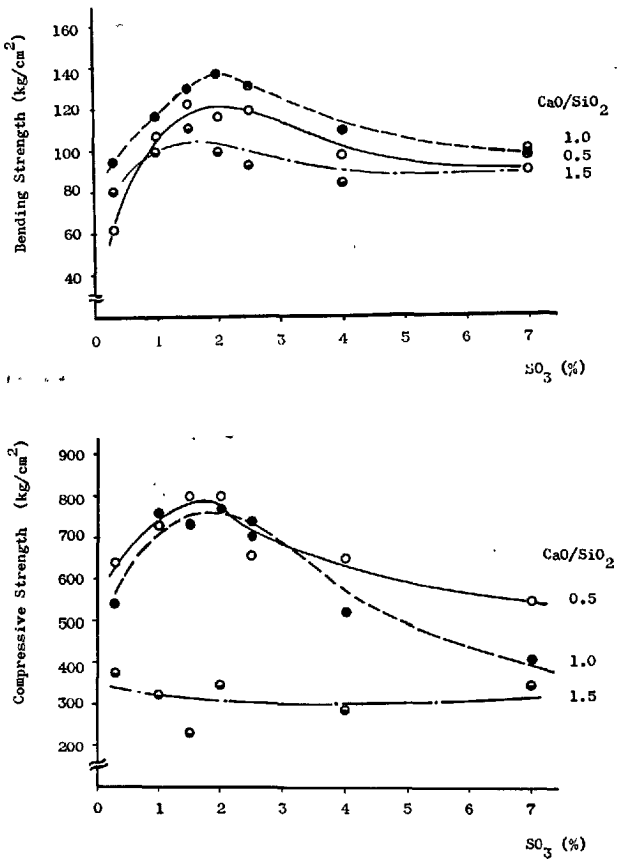

Fig. 1. *Mechanical strength of the autoclaved mass in connection with* SO_3 *content*

Table 1. *Chemical compositions of raw materials*

Material	Chemical composition (%)									Fineness Blaine (cm^2/g)
	ig. loss	insol. res.	SiO_2	Fe_2O_3	Al_2O_3	CaO	MgO	SO_3	Total	
white cement clinker	0.9	0.3	24.1	0.2	4.8	67.1	1.5	0.3	99.2	3,870
quartz sand	−0.4	—	96.1	2.2	1.3	—	—	—	99.3	5,260
gypsum	20.99	—	—	—	—	32.52	—	46.59	100.10	—

Introduction of Sulphur into Tobermorite Lattice

Tobermorite gel of which CaO/SiO_2 molar ratio was 1.2 prepared from burnt lime and silica gel at 60°C, then the mixture of the gel and about 6% of gypsum was ball-milled with 9 parts of distilled water for 6 days, as previously stated (2). Then the product was filtered and dried in a vacuum desiccator.

X-ray examination shows no crystal other than tobermorite gel. According to the chemical analysis this tobermorite contained the SO_3 of 6.08% on ignited base, i.e., SO_3/SiO_2 molar ratio was 0.156. The substituted gel was treated at 133°C, 158°C and 179°C respectively in an autoclave. X-ray diffraction patterns of the treated gel were shown in Fig. 2.

From these experiments, at the elevated temperatures, sulphur seems to be separated from the substituted tobermorite gel to form $CaSO_4$.

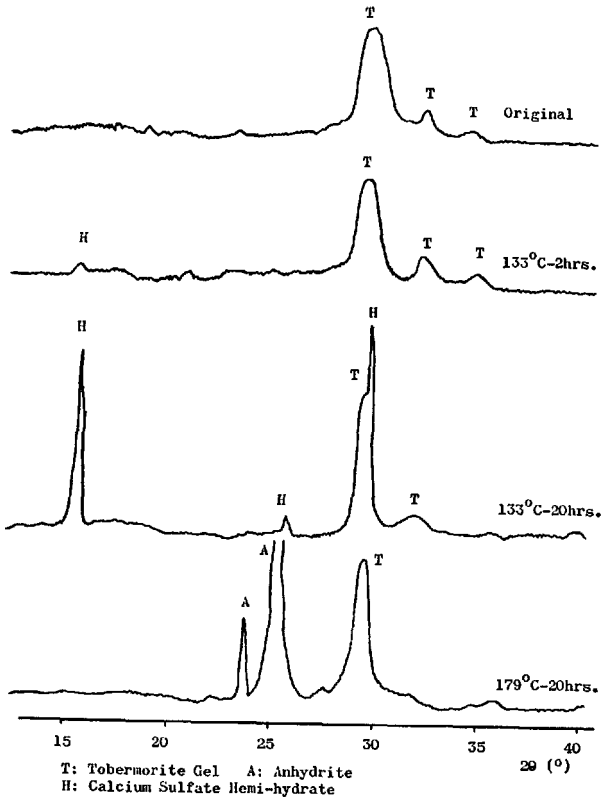

Fig. 2. *X-ray diffraction patterns of the substituted tobermorite gel, original, and after autoclaved at 133°C, 179°C, respectively*

Formation of Hydroxyl Ellestadite

In the preliminary experiments of hydrothermal reaction, starting with any combination of raw materials containing calcium and silica, such as portland cement clinker, C_3S, C_2S and calcium oxide or calcium hydroxyde with quartz or silica gel, and one of calcium sulphates, such as gypsum, hemi-hydrate and anhydrite, hydroxyl ellestadite is easily formed if the chemical composition of the raw mixture and the reaction temperature are suitable. So, the present authors conveniently used the followings as raw materials for determining the conditions of formation of hydroxyl ellestadite.

Lime: Analytical grade chemical reagent calcium carbonate was burnt at 1200°C for 20 hrs.

Silica: Two kinds of silica were used. One was fine quartz ($<2\mu$) and the other was silica gel. The main difference is that the quartz requires higher temperature than silica gel to react. The quartz was mainly used because of its easy detection by X-ray. Table 2 gives analytical data of these silica.

Gypsum: Chemical reagent calcium sulphate di-hydrate.

The raw mixtures, composition of which were stoichiometric to those of the circles shown in Fig. 3, were kept in Ni-crucibles with small amounts of distilled water and treated in a 17*l* autoclave.

Hydrothermal Treatment

It was recognized by the present authors that hydroxyl ellestadite was formed at temperatures a little higher than 100°C, but not at just 100°C even

Table 2. *Chemical composition of silica*

Material	Chemical composition (%)				
	ig. loss	SiO_2	$Al_2O_3 + Fe_2O_3$	CaO	$K_2O + Na_2O$
quartz	1.55	97.00	0.18	trace	—
silica gel	11.23	86.12	0.58	trace	0.55

by the long treatment of 2 months.

It is difficult to establish the phase equilibrium under 200°C, because of the slow rate of formation of the minerals appearing in the system CaO–SiO_2–$CaSO_4$–H_2O at such temperatures.

Therefore, a temperature of 235°C (saturated steam pressure 30 kg/cm²) was chosen with the reaction time of 100 or 200 hrs. The reaction temperature of the autoclave was controlled within ±1°C.

Detection

The reaction products obtained were dried in vacuum desiccator. Detection of the phases in the products were made by X-ray diffraction analysis and infrared absorption analysis.

Results

The results are shown in Fig. 3. The SO_3-bearing phases detected are as follows:

Anhydrite, when the CaO/SiO_2 molar ratio of the raw mixture is below 1.

Hydroxyl Ellestadite, when the CaO/SiO_2 molar ratio of the raw mixture is larger than 1. This mineral is known as a mineral of apatite group (6).

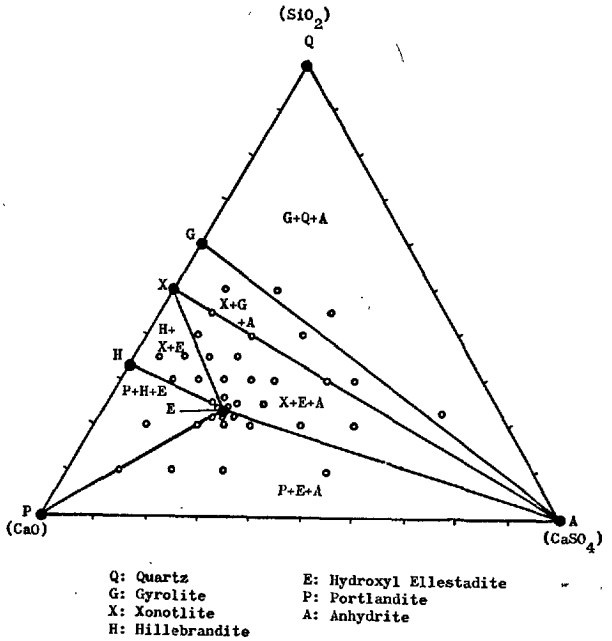

Fig. 3. *Hydrothermal reaction products in the system* CaO–SiO_2–$CaSO_4$–H_2O *at 235°C*

Properties of Hydroxyl Ellestadite

A sample of hydroxyl ellestadite was prepared from the raw materials mentioned before.

According to the X-ray diffraction examination, it contained a small amount of residual quartz. The properties of this synthesized sample were as follows:

Optical and X-ray Properties

Average refractive index: $\bar{n}_D = 1.632 \pm 0.002$
Birefringence: $B \leqq 0.002$
Shape: hexagonal prism with pyramidal ends
Extinction: parallel extinction
Elongation: negative
Space group: C^2_{6h}, $P6_3/m$
Unit cell: $a = 9.48^4$ Å
$c = 6.92^7$ Å

Table 3 shows X-ray data of hydroxyl ellestadite synthesized by the authors.

Density

$d = 2.96 \pm 0.01$ g/cm³

Chemical Composition

Table 4 gives the analytical data of the sample.

Table 3. *X-ray powder diagrams of the synthesized hydroxyl ellestadite* (Cu Kα)

No.	$d_{obs.}$	$d_{calc.}$	hkl	I	No.	$d_{obs.}$	$d_{calc.}$	hkl	I
1	8.23	8.213	100	1	21	2.075^5	2.076	113	1
2	5.31	5.295	101	1	22	2.054^0	2.054	400	w
3	4.75	4.742	110	w	23	2.012^7	2.013	203	1
4	4.11	4.107	200	1	24	1.957^2	1.956^6	222	3
5	3.92	3.914	111	1	25	1.905^6	1.903^1	132	2
6	3.54	3.534	201	w	26	1.885^0	1.884^2	230	1
7	3.466	3.465	002	3	27	1.852^6	1.852^8	123	3
8	3.194	3.192	102	1	28	1.818^5	1.818^5	231	2
9	3.109	3.105	120	2	29	1.793^2	1.792^3	140	2
10	2.835^5	2.833	121	10	30	1.767^8	1.766^3	402	2
11	2.799	2.797	112	5			1.766^5	303	
12	2.739	2.738	300	6	31	1.731^4	1.732^0	004	2
13	2.650	2.648	202	3	32	1.693^7	1.694^6	104	w
14	2.550	2.546	301	1	33	1.655^9	1.654^2	223	1
15	2.314	2.312	122	1			1.655^2	232	
16	2.280^5	2.278	130	3	34	1.621^8	1.621^8	133	1
17	2.245	2.244	221	w	35	1.598^8	1.598^4	501	w
18	2.221	2.223	103	w	36	1.553^2	1.552^3	240	1
19	2.167^2	2.164	131	1	37	1.545	1.544^1	331	1
20	2.15	2.14^8	302	w					

Table 4. *Chemical composition of the synthesized hydroxyl ellestadite*

Material	Chemical composition (%)					
	insol. res.	ig. loss	CaO	SiO_2	SO_3	total
Hydroxyl ellestadite	1.90	3.71	51.96	17.76	24.71	100.04

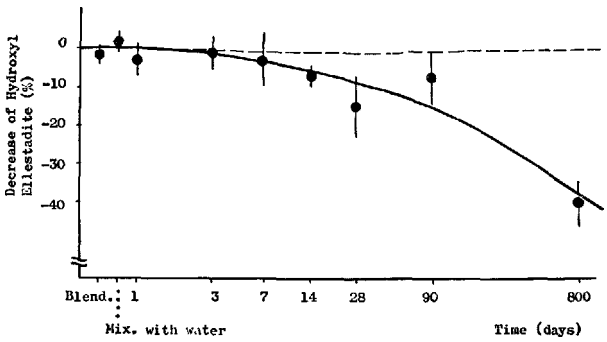

Fig. 4. *The stability of hydroxyl ellestadite in hydrating cement*

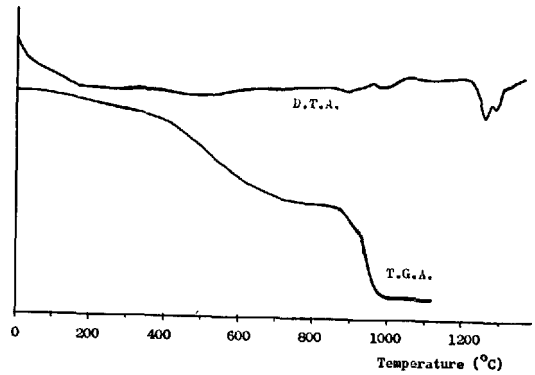

Fig. 5. *D.T.A. and T.G.A. curves of the synthesized hydroxyl ellestadite*

Stability in the Hydrating Cement

The mixture of portland cement, 16% of the synthesized hydroxyl ellestatite and 4% of quartz (5–10μ) was hydrated at room temperature. Quartz was used as an internal standard. The water-cement ratio was 0.5. After various length of time, hydroxyl ellestadite, in the hydrating mixture, was pursued by X-ray diffraction analysis. The results are shown in Fig. 4.

Thermal Properties

Fig. 5 shows D. T. A. and T. G. A. curves of the synthesized hydroxyl ellestadite.

Discussion

Mechanical Strength

Almost all of the specimens measured of their mechanical strength, contained 11 Å tobermorite, CSH(I), or tobermorite gel, Of course, the conditions at which the specimens were treated were far from the equilibrium. As a result, unreacted clinker minerals, quartz and slag remained in the hardened mass.

The reason why the strength showed a maximum of around 2% of SO_3 content in the raw mixtures was not clear. But, the formation of hydroxyl Ellestadite tends to reduce the strength of the specimens.

Hydroxyl Ellestadite in CaO–SiO_2–$CaSO_4$–H_2O

At the saturated steam temperature of 235°C, hydroxyl ellestadite coexists with portlandite, hillebrandite, xonotlite and anhydrite, but not with gyrolite and quartz, while anhydrite coexists with gyrolite, xonotlite, portlandite and hydroxyl ellestadite, but not with hillebrandite. At lower temperatures, hydroxyl ellestadite will coexist with tobermorite, CSH(I), CHS (II), tobermorite gel and α–C_2S hydrate, as seen in the hydrothermal products (5) the mechanical strength of which were measured.

Hydroxyl Ellestadite coexisting with Hydrogarnet

(i) A synthesized hydroxyl ellestadite was treated with C_3A in an autoclave at the temperature of 235°C for 100 hrs. The phases detected were hydroxyl ellestadite, hydrogarnet and a small amount of anhydrite.
The cell dimension of the hydrogarnet type mineral shows little substitution of SiO_2 occured.

(ii) The mixture of silica gel, burnt lime, gypsum and C_3A the stoichiometry of which is the same as that of the former experiment, was also treated in the same way.
The reaction products were anhydrite, hydrogarnet portlandite and hydroxyl ellestadite.
The cell dimension of the hydrogarnet shows the composition of about $C_3AS_{0.7}H_{4.6}$
From these results, it is concluded that hydroxyl ellestadite is considerably stable coexisting with hydrogarnet, and both minerals could exist in the autoclaved mass of raw materials which contain Al_2O_3 and SO_3 components.

Stability in the Hydrating Cement

Experiments about the stability of hydroxyl ellestadite in the hydrating cement at room temperature up to 800 days show that this mineral is unstable in the hydrating cement.

X-ray Diffraction and Chemical Composition

The properties of the synthesized hydroxyl ellestadite should be compared with those reported by the previous investigators.

Dihn and Klement (7) reported the unit cell dimension as $a = 9.54$ Å $c = 6.99$ Å. These values are somewhat different from those measured by the authors.

The density calculated from the cell dimension and the ideal formula of $Ca_{10}(SiO_4)_3(SO_4)_3(OH)_2$ is 3.07 g/cm³.

The formula calculated from the chemical composition of the sample synthesized by the authors is $Ca_{9.4}(SiO_4)_3(SO_4)_{3.1}(OH)_{4.2}$

The deviation from the ideal formula is commonly observed in the formations of hydroxyl apatite $Ca_{10}(PO_4)_6(OH)_2$ (8).

Thermal Properties

D.T.A. Curve of the hydroxyl ellestadite is smooth as usually observed on the mineral of the apatite group.

From the T. G. A. curve of the synthesized hydroxyl ellestadite, two types of water seem to exist.

At the temperatures from 200°C to 800°C, this mineral loses progressively one of two types of water, and loses the other at 860°C. X-ray diffraction patterns and infra-red absorption of the original sample of the synthesized hydroxyl ellestadite and the sample heated at 800°C, 900°C and 1,300°C, respectively are shown in Fig. 6.

The comparison between the infra-red absorption of the original sample and that of the sample heated at 800°C shows slight difference in the regions around 1,450 and 3,400 cm^{-1}. The former is related to the contamination of CO_2. The later is related to OH vibration and the absorption of the original seems broader than that of the other.

The second stage in the T.G.A. curve is of course the thermal decomposition of this mineral as seen in Fig. 6. Hydroxyl ellestadite decomposes on heating in the air to $Ca_nSi_2O_{n+7}$ ($n = 5 - 6$), anhydrite and water at 860°C, then to dicalcium silicate and anhydrite with or without calcium oxide at 1230°C.

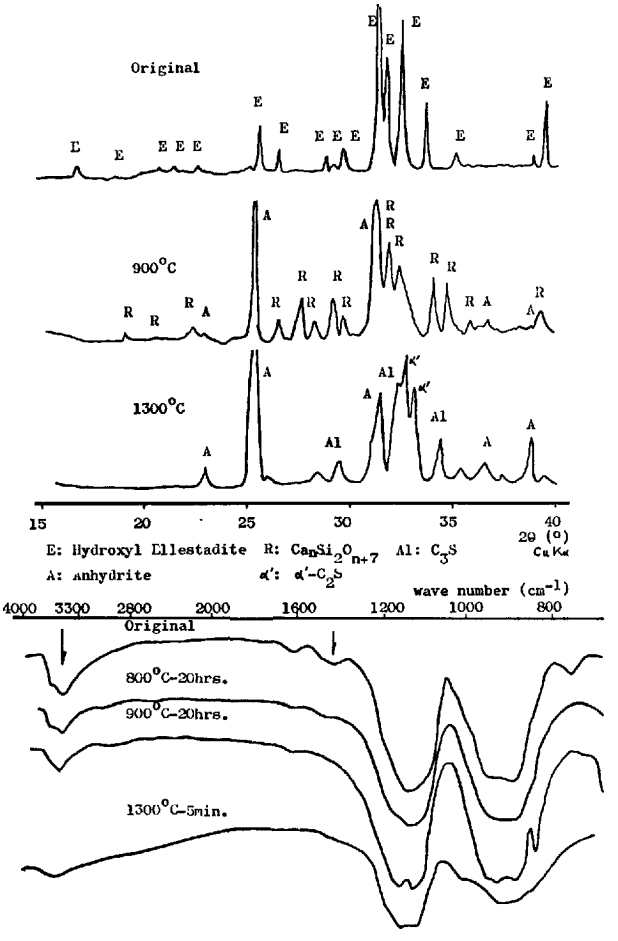

Fig. 6. *X-ray diffraction patterns and infra-red absorption of the synthesized hydroxyl ellestadite, original and heated at 800°C, 900°C and 1300°C*

$$Ca_mSi_3S_3O_{m+15}(OH)_2 \rightarrow Ca_nSi_2SO_{n+7} + 3CaSO_4 + H_2O$$

$$Ca_nSi_2SO_{n+7} \rightarrow Ca_2SiO_5 + CaSO_4(+CaO)$$

$Ca_nSi_2O_{n+7}$ is a mineral which is commonly observed in sulphate ring of the rotary kiln for cement burning (9), (10).

References

1. G. L. Kalousek, "Analyzing SO_3-bearing phases in hydrating cements", Material Res. and Stand., **5**, 292–304 (1965).
2. L. E. Copeland, E. Bodor, T. N. Chang and C. H. Weise, "Reactions of tobermorite gel with aluminates, ferrites and sulfates", J. of P.C.A. Res. and Dev. Lab., **9**, 61–74 (1967).
3. G. Pohl, "Die Bedeutung des Schwefels in Kalk bei der Herstellung von Kalksandsteinen", Zement-Kalk-Gips, **14**, 468–469 (1961).
4. N. Djabarov and W. Slatanov, "Die Wirkung des Gipses auf die Festigkeit der Kalksanderzeugnisse",

Zement-Kalk-Gips, **16**, 104–107 (1963).
5. K. Takemoto, Y. Saiki and H. Kato, "Effect of gypsum on the strength of the autoclaved paste of blended portlnad cement", Proc. of Japan Cement Eng. Assoc., **19**, 168–172 (1965)., or, Rev. 19th Gener. Meeting Tech. Sess. p. 112–113 (1965).
6. D. McConnell, "The substitution of SiO_4- and SO_4- groups for PO_4- group in the apatite structure; ellestadite, the end-member", Amer. Min., **22**, 977–986 (1937).
7. P. Dihn and R. Klement, "Isomorphe Apatitarten", Z. Elektrochem., **48**, 331–333 (1942).
8. W. A. Deer, R. A. Howie and J. Zussman, Rock-Forming Minerals, vol. **5**, p. 329, (Longmans, Green and Co., Ltd., London, England, 1962).
9. W. Gutt and M. A. Smith, "A new calcium silicosulphate", Nature, **210**, 408–409 (1966).
10. Y. Ono, M. Amafuji and T. Okumura, "Double salt from sulfate-rings adhered to the wall of rotary kiln", J. of Res. Onoda Cement Co., **17**, 245–259 (1966).

Supplementary Paper III-87 Some Physical Properties of Aerated Concrete under Autoclave Process

Koh-hei Ono and Kōzō Ojiri*

Synopsis

The physical properties of aerated concrete under the autoclave process were investigated on the basis of (i) heat transfer (ii) linear changes and (iii) mechanical properties.

The apparent thermal diffusivities K were derived from the measurement results on temperature profile of a cylinder by using Fourier's heat flow equation. The average value of K during the heating-up period with a rate of 0.75 ~ 1.0°C/min to 180°C and the early stage of soaking at the temperature was approximately 4 times as large as that determined for the final product.

The values of K and their variation with the autoclave time schedule and with the position in the specimen suggested that heat transfer in concrete was promoted both by the presence of liquid water and by the movement of vapor or liquid in the specimen.

By the application of these values to Fourier's equation again, the temperature profiles of a slab of 20 cm thickness at successive time were determined. The temperature difference between surface and center was 120°C when the surface was heated up to 180°C with a rate of 1°C/min. Seven hours soaking at this temperature was required for this difference to become less than 5°C.

A simple apparatus by the "Differential Optical Lever Method" was devised for successive measurement of linear change of specimen under autoclave process.

In a specimen without additives, almost the same expansion-shrinkage phenomena were observed for various compositions (cement-siliceous sand-blastfurnace slag), Specimen sizes (2.5 cmϕ × 10 cm and 20 × 20 × 60 cm) and bulk densities (0.5 g/cm^3, 1.8 g/cm^3), and the mean coefficient of expansion during heating-up period to 180°C was 9 ~ 10 × 10^{-6}/°C.

Augmented expansion was observed in the heating-up period for the specimen added with light-burnt MgO, but it was observed in the soaking period when dead-burnt MgO was added. This tendency was irrespective of other factors, whereas the amount of expansion somewhat influenced by compositions, sizes and bulk densities of the specimen. The excessive addition of MgO led to disruption of the specimen.

In view of thermal stress, it is concluded that the thickness of 20 cm was approximately estimated to be the upper limit for a slab to be securely produced under the autoclave condition carried out in this study.

Introduction

The use of autoclaves is an essential process in the manufacture of aerated concrete.

Many difficulties during this process are encountered which are ascribed to the fact that young age concrete is subjected to water vapor having high temperature and high pressure and their comparatively rapid changes with time. Unsuitable conditions produce various kinds of defects in the product i.e., cracks of various shapes within or on the surface of the product and nonhomogeneity of mechanical strength in its inside. For purposes of improving such phenomena, and in addition, determining the best autoclave time schedule, it is essential to investigate chemical and physical properties through the autoclave process.

There have been many reports about the chemical reactions, especially hydration mechanisms and their equilibriums. In the case of physical properties, however, only a few papers have been written. The reasons seem to be as follows:

1) Difficulties in the measuring technique under the condition of saturated steam at high temperature filled in an autoclave.
2) The effect of the material size is one of the important factors to measure these properties. The specimen of fairly large size must be subjected to the

*Research Laboratory, Asahi Glass Co., Ltd., Yokohama, Japan.

test so that the results are applied to concrete of manufactured size.

The gradients of temperature, vapor pressure and moisture content along a cross-section of concrete, which are very important problems for manufacturing, are developed only when the specimen is large enough. Size effect on the volume change also must be discussed.

Physical properties concern with the problems on defects of product and determination of best autoclave condition on the basis of the relationships in the following categories:

i) Mechanical properties
ii) Volume change
iii) Heat transfer
iv) Movement of moisture

Several investigations concerned with these subjects were recently reported.

N. I. Dybrovna, et al. (1) and C. A. Mironov, et al. (2) followed the volume changes due to hydraulic movement during the autoclave process by the differential voltage transformer (DVT). Weight changes were measured by also N. I. Dybrovna, et al. (1) and K. F. Lomunov, et al. (3) by using a balance equiped to an autoclave.

A. I. Avakov, et al. (4) followed also the volume changes by strain gauge buried in concrete.

In addition, temperature profiles were determined by the C–A thermocouple for a cubic or a slab in these investigations.

The relationships of these informations to the mechanical properties were discussed by C. A. Mironov (2) and A. I. Avakov (4).

P. Smallwood (5) calculated temperature distributions for a brick during autoclave process assuming that the relevant properties of the specimen are constant during autoclaving.

Also at the Research Laboratory of Asahi Glass Co., Ltd. some studies of these subjects under steam curing condition have been carried out in these few years. Then some ideas of the methods for measurement will be submitted and the several results obtained will be discussed in this paper.

Heat Transfer in Concrete

Most of the products at factories are slabs and blocks of various sizes. The slabs are not suited to laboratory work due to their large width and length. Therefore any expedient experimental method must be devised.

Heat transfer in concrete under steam curing depends on two mechanisms, i) heat conduction in solids and ii) the movement of moisture. Either can be dealt with by Fourier's equation. The latter is, however, more complicated because of the condensation—vaporization mechanism of water in concrete. Therefore, one way is, as a first approximation, to assume only the mechanism i) for heat transfer phenomena observed experimentally. Then, by the deviations from the theory, mechanism ii) might be presumed.

The testing results from a long cylinder can be applied to the treatment of a large slab and satisfactory results may be derived. The reason is that the thermal diffusion is unidirectional in a cross-section perpendicular to a longitudinal direction for both cases. On the basis of such a concept, the heat transfer phenomena are investigated in this paper.

Method of Measurement

A cylindrical specimen of 20 cmϕ × 60 cm was moulded which was designed so as to be a product with bulk density of 0.5 g/cm^3 after autoclave curing. At the same time C–A thermocouples were buried in concrete, along the longitudinal axis and the center cross-section perpendicular to the axis (Fig. 1). This specimen was preliminarily cured at 40°C, and above 90% R. H. for 15 hrs.

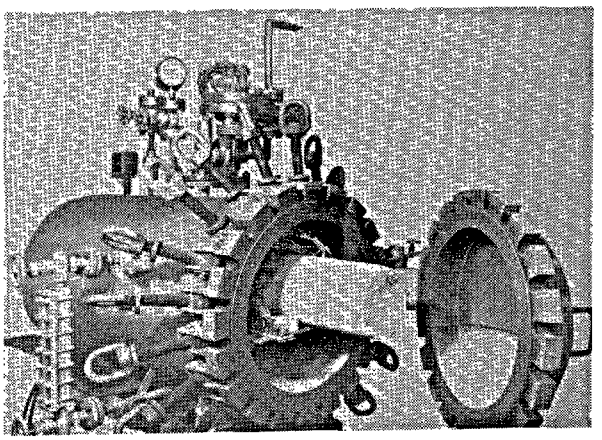

Fig. 1. *Long cylindrical specimen of aerated concrete set in autoclave having 200 lit. in content. CA-thermocouples are buried in concrete and drawn out of autoclave through flange*

The joints through which the thermocouples are drawn out of the autoclave had to be of the same material as the thermocouples to prevent the development of a contact potential.

Before heating-up, the autoclave was evacuated to −500 mmHg.

The specimen was heated in the autoclave to a temperature of 180°C and a vapor pressure of 10 atm (heating-up period) and kept under this condition for 8 hrs (soaking period). Then the water vapor in the autoclave was blown off through a leakage value in order to cool to 100°C and atmospheric pressure in approximately 30 min (blow-off period), and the autoclave was opened and the specimen was immediately removed from the autoclave in the atmosphere at 20°C (cooling-period). Variations in temperature over this whole cycle was recorded.

Computation Procedure

From the data on the temperature distribution along the longitudinal direction, it was confirmed that thermal diffusion along that direction near the center cross-section was completely negligible.

The apparent thermal diffusivities K were computed as a function of the time, the temperature and the position along the radial direction of the cylinder by the analytical solution of Fourier's heat flow equation (6). The values of K obtained were applied again to the analytical solution of Fourier's heat flow equation for a infinite slab of 20 cm thickness, so that the temperature profile of the slab under the autoclave process was derived.

The values of K were computed by the application of the respective datum on temperature at a desired time and position in the cross-section to heat flow equation under the following initial conditions for each period.

Heating-up period: Temperature in the whole body is constant (25°C) at initial time ($t = 0$).

Soaking period: The initial temperature distribution is adapted in itself to be parabolic in a range of $r = 0 \sim 7.5$ cm at initial time ($t = 0$).

Cooling period: Temperature in the whole body is constant (100°C) at initial time ($t = 0$).

Therefore the results given in Table 1-a, b, c, mean the average values from each initial time to the desired time.

The reason why such computations were carried out are as follows:

1) Heat flow equation is analytically solved only for the cases of simple initial conditions.
2) Average value of K has the advantage for the practical application.
3) The results by this method give suggestions for one of the purposes of this study which is to know qualitatively the mechanism of heat transfer.

Most of these computations were carried out by IBM 360.

The values of film thickness of heat transfer were derived from the experimental data by the following ordinary procedure:

This value is equal to a distance from the surface of a cylinder or a slab to the point at which the tangent line of temperature-distribution curve at the surface intersects with a horizontal line showing ambient temperature.

Table 1-a. *Thermal diffusivity K (cm²/min), during heating-up period at rate of 1°C/min.*

t = heating time
r = distance from center of cylinder along radial direction.

t (min)	Temperature of vapor (°C)	r (cm) 7.5	5.0	2.5	0
30	55	0.41	0.29	0.19	0.12
60	85	0.51	0.41	0.29	0.27
90	115	0.70	0.50	0.33	0.29
120	145	0.80	0.52	0.37	0.34
150	175	1.19	0.56	0.41	0.40
155	180	1.38	0.57	0.42	0.40

Table 1-b. *Thermal diffusivity K (cm²/min), during early stage of soaking period.*

t = time soaked at 180°C.

t (min)	Temperature of vapor (°C)	r (cm) 5.0	2.5	0
20	180	0.15	0.20	0.25
40	180	0.16	0.26	0.29
60	180	0.22	0.31	0.32
80	180	0.31	0.40	0.42
85	180	0.33	0.40	0.42

Table 1-c. *Thermal diffusivity K (cm²/min), during cooling period.*

t = cooling time

t (min)	Surface temperature (°C)	r (cm) 10	7.5	5.0	2.5	0
15	62	0.22	0.57	0.91	1.08	0.92
30	52	0.23	0.43	0.61	0.67	0.63
60	45	0.20	0.27	0.37	0.42	0.42
120	36	0.18	0.22	0.24	0.26	0.46
240	28	0.14	0.15	0.15	0.15	0.15

Results

The results of measurement of temperature distri-

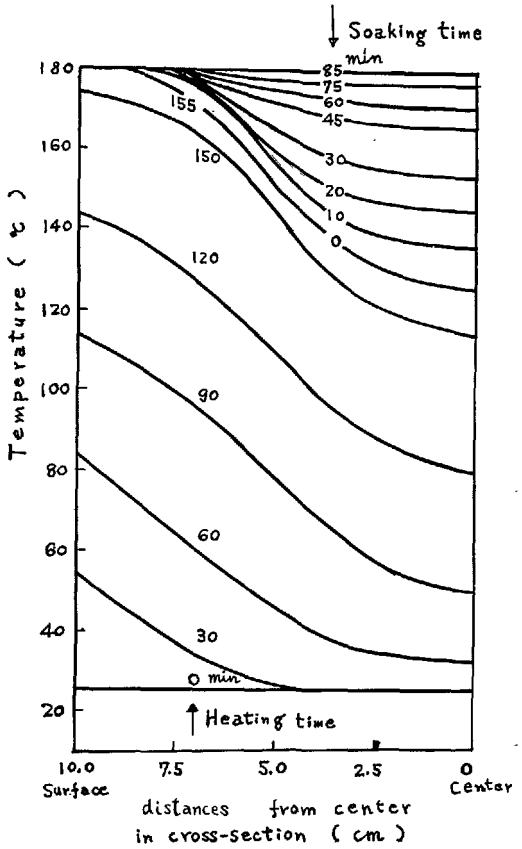

Fig. 2a. *Temperature profiles during heating-up and soaking period when long cylinder of 20 cmϕ is heated at rate of 1°C/min*

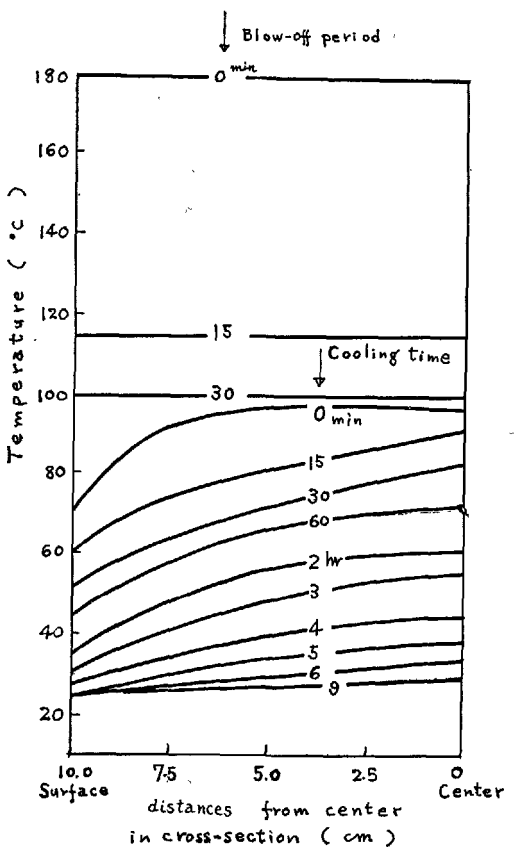

Fig. 2b. *Temperature profiles for long cylinder of 20 cmϕ during blow-off and cooling period*

bution for a cylindrical specimen are illustrated in Fig. 2-a, b. The surface temperature of the cylinder was equal to that of ambient saturated steam at any time of heating and soaking period, whereas for cooling period it was higher than the ambient temperature. Therefore the film thickness of heat transfer was treated as zero for heating and soaking period, and for cooling period it was determined to be approximately 2.0 cm as a mean value for this period by the method described before. It should be noticed, however, that this value would be largely varied by the ambient condition of cooling.

During the heating-up period, K increased with the temperature or with the time and was larger near the surface than at the center of the cylinder. The average value of K for the whole cross-section during heating-up period with a heating rate of 1°C/min was 0.40 cm^2/min as shown in Table 1-a.

Heating rate of 0.75°C/min resulted in approximately the same values of K and the same tendency of the variation.

At the initial stage of the soaking period, K decreased once, but gradually increased again to reach 0.42 cm^2/min (Table 1-b).

For the blow-off period no temperature difference in the cylinder was observed. Then K value is considered to be infinite. After the specimen was removed from the autoclave, however, temperature gradient in a specimen developed again.

The values of K at the initial stage of the cooling period were relatively high and gradually decreased with time.

For an infinite slab of 20 cm thickness the following results were computed.

1) The heating-up period and the early stage of the cooling period: Assuming that heating rate = 1°C/min from room temperature to 180°C and average thermal diffusivity K = 0.40 cm^2/min, temperature at the center reaches 60°C at the end of heating period, and 7 hrs soaking at 180°C is required for the temperature difference to be less than 5°C.

2) The cooling period: Assuming that $K = 0.6$ cm²/min at 30 min after the specimen is removed from the autoclave, temperature difference between the surface and the center is 40°C, which is a maximum temperature difference during this period.

Discussion

Thermal diffusivities K of the final product having a bulk density of 0.5 g/cm³ have been determined to be 0.10 cm²/min at room temperature, and it somewhat increases with temperature to a value 0.13 cm²/min at 200°C (7). Therefore the average values of K in a specimen during heating-up period obtained above corresponded to 4.0 times of the value of the final product. Their variations with time, temperature and location are also extraordinarily large.

The moisture movement phenomena which consist of the three mechanisms shown below may be assumed from such a tendency.

i) The driving force for the movement of water vapor is its pressure gradient attributed to temperature gradient which has been at first originated from the time lag of heat conduction in solids.

The water vapor which reaches lower temperature field condenses there to raise the temperature by the heat of condensation.

ii) If the heat is transfered to any low temperature field by the heat conduction process, the liquid water which had been stored there evaporates for the reestablishment of the equilibrium water vapor pressure, thus the rate of temperature rise is reduced by the heat of vaporization.

For the above two cases the condensed liquid water may also diffuse in a specimen due to the gradient of water content and play a role of heat transfer.

iii) If at any time, capillaries connecting a pore to the others are sealed with condensed water to some degrees and in addition temperature of that region rises further, the pressure of the air which has permeated into the pores by that time increases, and forces condensed water to come out of the capillaries or of the pores.

During the heating-up period, the mechanism i) is superior to ii), whereas at the early stage of the soaking period ii) is superior to i). The water content in the specimen gradually increases up to 180°C. On the contrary at the early stage of the soaking period mechanism ii) plays a significant role, since only inside temperature increases with time.

In addition, the moisture movement from inside to outside of the specimen will be derived from the mechanism iii) at the later stage of the heating-up period and the early stage of the soaking.

These movements of moisture will appear more distinctly near the surface than at the center because of a larger temperature and pressure gradient at the surface. Therefore values of K vary more significantly there.

The phenomena of the inside pressure increase and the weight diminution at the end of the heating period or at the early stage of the soaking period have been observed by K. F. Lomunov, et al. (3). The differences in K along the radial direction decrease as the temperature differences disappear after a few hours' soaking at 180°C.

During the blow-off period, a violent movement of water vapor from inside may also be suggested by the fact that no temperature difference in a specimen was observed. At an early stage of cooling, relatively high values of K indicate that the water vapor continue to move towards the outside.

Then, values of K approach to that of the final product as the specimen continue to be cooled and dried for long hours.

The violent moisture movement in concrete may have a influence upon the mechanical properties under autoclave process.

Linear Change during Autoclave Process

As mentioned in the "Introduction", two kinds of methods have been reported on the continuous measurement of linear change during the autoclave process. The DVT method is rather simple and precise, whereas the method by straingauge needs a special adhesive agent having an endurance for moisture at high temperature, and a correction for such a condition. Common difficulty for both methods lies rather in their expensiveness as equipment.

The linear changes during steam curing are a function of i) thermal expansion of solid part of concrete, ii) hydraulic movement and iii) hydration reaction. Linear changes by hydration reaction of usual silicates are not so large as compared with ther-

mal expansion or hydraulic movement, but some hydration reactions, for example the reaction of MgO + H_2O = $Mg(OH)_2$ dealt with in our investigation, are known to show extraordinarily high expansion. If such a reaction is contained in the usual system of silicates, it sometimes becomes an origin of fracture.

Augmented expansion of this reaction, however, can be used effectively for balancing the expansion of the concrete part with that of the reinforcement part or sometimes for manufacturing prestressed concrete.

In this section a simple apparatus for measurement of linear change is presented and some results are discussed concerning the above problems.

Apparatus and Method

An apparatus was devised by which the linear change of concrete in an autoclave could be measured successively on the basis of the principal "Differential Optical Lever Method". Fig. 3-a, b, c show this apparatus, Its principal features are as follows:

The linear change of the specimen placed horizontally in a quartz tube is transfered to the rotation angle of a mirror through a quartz rod and a stainless steel part. At the same time, the linear changes of the quartz rod and the stainless steel part are cancelled by those of another quartz rod and stainless steel part with same lengths. This dilatometer is set in an autoclave.

A small pyrex-glass window is attached through the flange of the autoclave. Light is allowed to come into the autoclave through this window, to be reflected by the mirror and to focus on a scale placed outside. The location of the light spot on the scale is recorded automatically by taking a photograph at regular intervals.

The mirror was made of the Pt-Rh alloy, which was the only material that could withstand corrosion by water vapor at high temperature. Both the mirror and the window glass were heated by two nichrome heaters which were fitted inside and outside the window glass.

Before the measurements, the accuracy of this apparatus was calibrated by a rod of steel of which expansion coefficient was already known. The linear change of the specimen of 2.5 cmϕ × 10 cm in a whole cycle of autoclaving was measured by this dilatometer. The same method can be applied easily to a specimen of larger size. In our investigation, however, only a maximum expansion of the larger specimen of 20 × 20 × 60 cm during the autoclaving cycle was measured by the simple method of recording

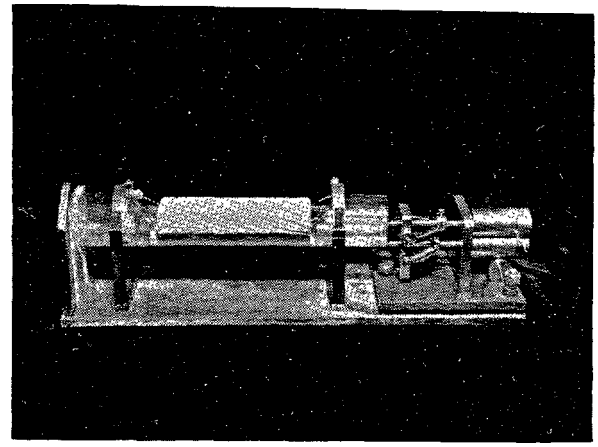

Fig. 3a. *Dilatometer in which specimen of 10 cm in length is inserted. It is consisted of quartz tube and rod, stainless steel part and Pt-Rh minor*

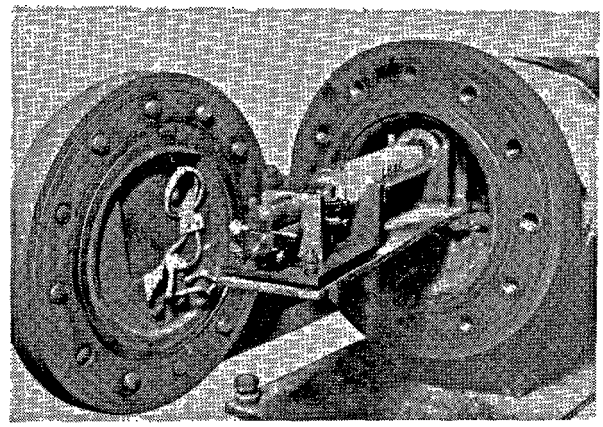

Fig. 3b. *Dilatometer set in autoclave of 5 lit. in content and Pyrex-Glass window through flange. The window is fitted with nicrome heater on each of its inside and outside.*

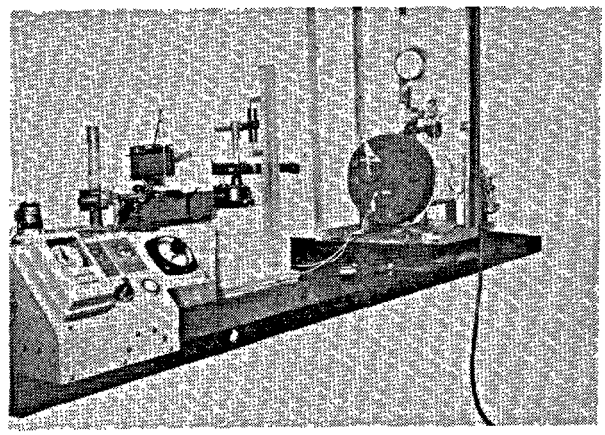

Fig. 3c. *Overall apparatus for successive measurements of linear change of concrete in autoclave. Location of light spot focused on scale placed outside of autoclave, which corresponds to rotation angle of mirror shown in Fig. 3-a, b, is photographed at regular intervals*

the linear change of the specimen on a ground glass plate by a carbon rod previously attached to the specimen. By this method, the information on the size effect of the specimen could be obtained satisfactorily. The specimens for both methods were previously stored under 40°C above 90% R. H. for 12 hrs. Autoclaves of 5.0 liters and 200 liters content were used for a small size and a large size specimen respectively. The specimen in an autoclave was heated to 180°C, 10 atm vapor pressure at a rate of 1°C/min, soaked under this condition for the desired period and cooled to room temperature.

The influences of the addition of MgO on volume change were investigated both for batch compositions (cement-siliceous sand-blastfurnace slag) and for bulk densities (0.5 g/cm^3, and 1.8 g/cm^3). The starting materials were ground to approximately 3000 cm^2/g. The bulk densities were controlled both by the additives and by water-cement ratio. Two kinds of MgO were used, one was light-burnt MgO (900 ~ 1000°C), another was dead-burnt MgO (1700°C).

Results and Discussion

Characteristic of Expansion-Temperature Curve

As seen in Fig. 4 the expansion-temperature curve without MgO during heating-up period is almost linear, but has a slightly S-shaped characteristic. The average coefficient of expansion is 12.5 × 10^{-6}/°C for the temperature range of 80° ~ 150°C, whereas it is 8.0 × 10^{-6}/°C for both in lower and higher temperature range.

The average value up to 180°C from room temperature is 10 × 10^{-6}/°C (9 × 10^{-6}/°C for cement-sand system), which is almost the same order as the coefficient of thermal expansion of the starting material, i.e., that for cement 14 × 10^{-6}; siliceous sand 11 × 10^{-6}; concrete with crushed slag 10.6 × 10^{-6} (9).

From these data it may be said that the expansion-temperature relation depends mainly on the thermal expansion of the solid part in concrete and secondarily is slightly deformed to an S-shaped characteristic by the other mechanisms. To account for this characteristic, it seems necessary to describe the hydraulic movement in concrete.

The effects of the moisture behavior on thermal expansion of concrete have been investigated by several authors. According to them, there is a maximum of the thermal coefficient at an intermediate state of wetness, which is 70% R. H.. Powers (8) explained this mechanism by saying that there are capillary water and a water fixed in the gel that is constituted

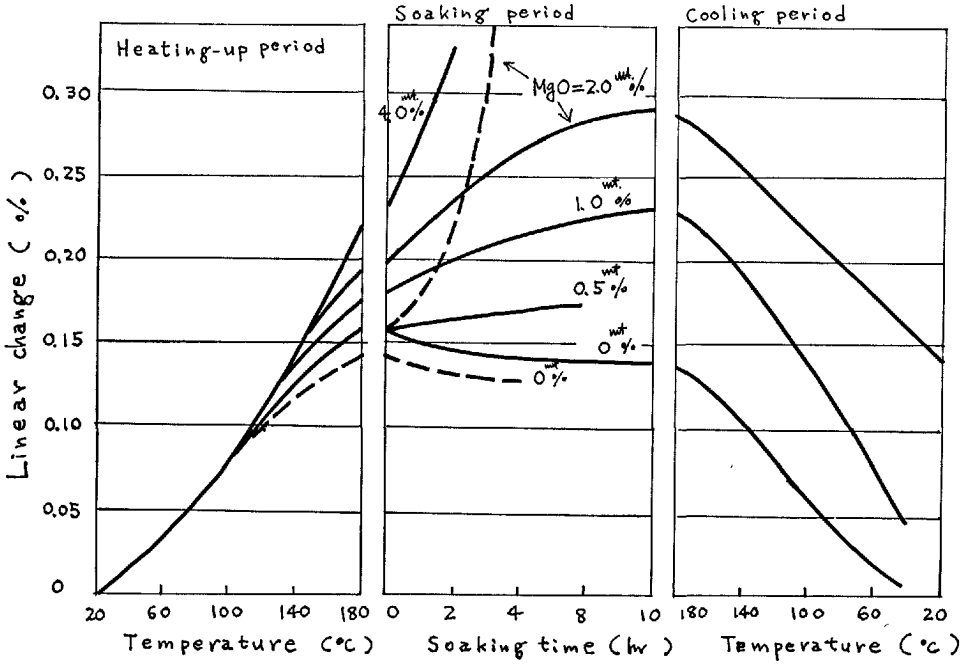

Fig. 4. *Linear change during a whole autoclave cycle Conditions: heating rate 1°C/min; specimen size 2.5 cmφ × 10 cm; bulk density 0.5 g/cm^3; burning temperature of* MgO, *dead-burnt* MgO *(1700°C); composition, slag rich system (——) and siliceous sand or cement rich system (- - - -)*

by the hydration phase; a change in temperature destroys the equilibrium between two kinds of water, then requires a transfer of water between the two phases. The delay in this transfer results in the additional dilation that disappears after reestablishment of the equilibrium.

L. Hermite (9) and Honma (10) suggested that the reduction of the surface tension of the capillary water with the temperature increase diminishes the shrinkage pressure which results in additional expansion.

In the present study, the specimens absorb water to achieve a highly humid situation in their interior in the heating period as previously mentioned and, in addition, continuously change their quality by hydration reaction. These conditions seem to be explained by the several theories above.

The slight shrinkage in the early stage of the soaking period also seems to be connected with the moisture movement in concrete.

The Effect of bulk Densities and Sizes

The amount of expansion and its tendency to vary with time elapsed during the autoclave process were almost the same for the specimen of density of 0.5 g/cm³ and 1.8 g/cm³ in the case of no addition of MgO (Fig. 6). The larger size specimen of 20 × 20 × 60 cm also showed the same amount of expansion and variation tendency as the smaller one (2.5 cmϕ × 10 cm) (Fig. 5). The following assumptions are based on these informations.

i) Moisture movement in concrete has scarcely any significant role for expansion phenomena in the autoclave process, although it should be remembered that there may be a little influence of it as mentioned in the former section, namely overall linear change in autoclave process depends on the thermal expansion coefficient of the solid part of concrete.

In other words, it can be said that the concrete under autoclave process has permeability and Young's modulus large enough for moisture movement and its force in concrete respectively.

ii) The summed-up length of the solid parts along the linear direction is a base length for calculating the amount of expansion or shrinkage as long as the solid parts are continuously linked. Then the amount of expansion or shrinkage is independent of the porosity of the concrete.

The Effect of the Addition of MgO

Augmented expansion effect of dead-burnt MgO was observed mainly in the early stage of the soaking period at 180°C. This tendency was irrespective of the various compositions, bulk densities or the specimen sizes, but the sensibilities of MgO were somewhat different for each case. In the case of the speci-

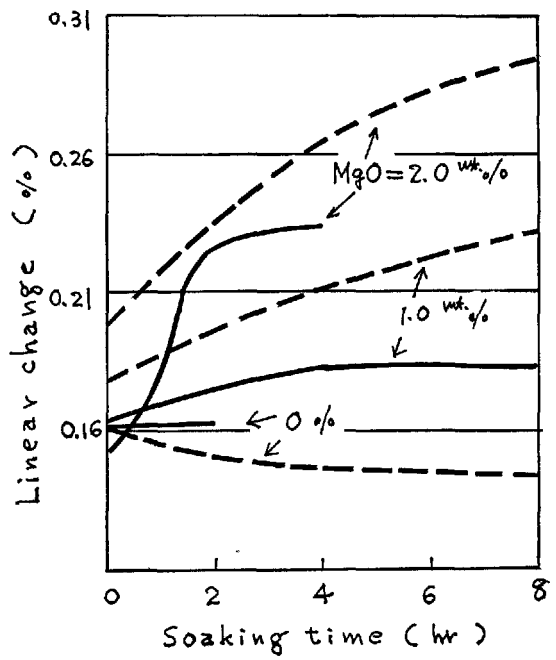

Fig. 5. *Size effect developed during the soaking period Conditions: composition, slag rich system; specimen sizes, 20 × 20 × 60 cm (——) and 2.5 cmϕ × 10 cm (- - - -) the others are the same with Fig. 4*

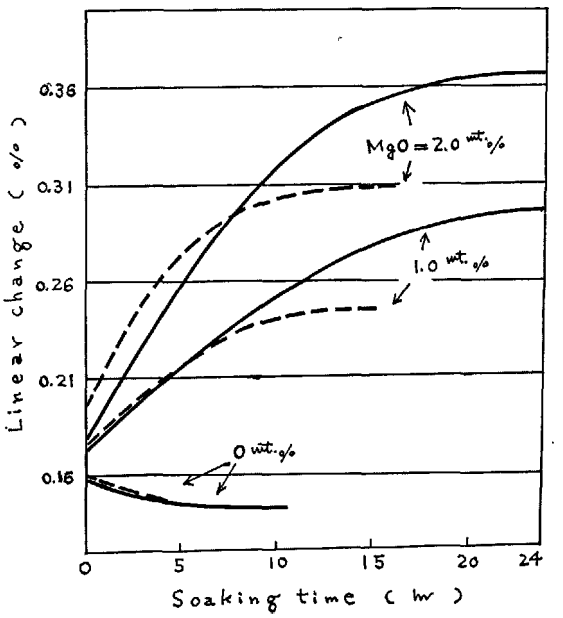

Fig. 6. *Influences of bulk density during the soaking period Conditions: composition, slag rich system; bulk densities 1.8 g/cm³ (——) and 0.5 g/cm³ (- - - -); the others are the same with Fig. 4*

men having a bulk density of 0.5 g/cm³, the addition of more than 2% of MgO led to extraordinarily high expansion. An addition of 4% of MgO caused fine cracks across each other or disruption, and 10% of MgO caused dusting (Fig. 4). These are typical damages arising from the differences in the expansion characteristics of the different phases. In view of compositions, the specimens having a large percentage of blastfurnace slag showed a higher resistibility to expansion effect by MgO than siliceous or cement rich compositions (Fig. 4). Compared with that of 0.5 g/cm³, the expansion of MgO in the specimen having a bulk density of 1.8 g/cm³ continued to develop for a longer period of 20~24 hrs (Fig. 6).

A large size specimen reduced the expansion effect of MgO (Fig. 5).

The expanding effect by light-burned MgO was completed during the heating-up period to 180°C as seen in Fig. 7.

From the above data, some practical and useful informations could be drived.

1) The time when augmented expansion of MgO develops is controlled mainly by the selection of its burning temperature.
2) The amount and type of MgO has to be changed with the compositions, densities and dimensions of the specimen.
3) Too much addition of MgO causes cracks due to difference in the expansion characteristics of different phases.
4) The coefficient of shrinkage during the cooling period is approximately equal to that of the specimen without addition of MgO irrespective of the amount of MgO added to the specimen.

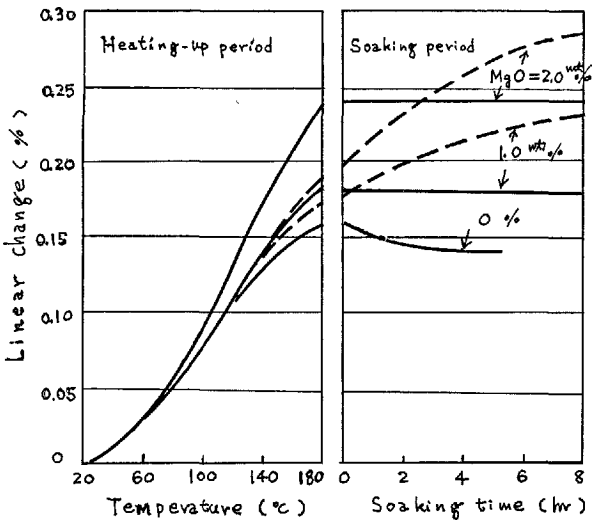

Fig. 7. *Influences of burning temperature of* MgO
Conditions: composition, slag rich system; burning temperatures of MgO, *light-burnt* MgO (*900–1000°C*) (——) *and dead-burnt* MgO (*1700°C*) (- - - -)*; the others are the same with Fig. 4*

There develops, then, the accumulated compressive stress due to the augmented expansion of MgO in the case of a reinforced concrete product.

It is considered to be advantageous also in reducing the tensile stress which develops during the cooling period due to thermal stress.

Mechanical Properties and Thermal Stress

Investigation of the process of development of mechanical properties during autoclave reaction is conclusively important for determining the time schedule of autoclaving.

Moreover determination of the actual stress in a concrete material under a given condition of heat transfer requires data on mechanical properties. In the previous sections we treated heat transfer and linear change of concrete. Therefore in this section the problem of thermal stresses will be discussed by using the some results of measurement on Young's modulus and mechanical strength.

Experimental Method

The blocks having the same shape and dimensions as that used for the test on the temperature distribution were subjected to measurement of mechanical properties in room condition. The blocks had been soaked for 0~8 hrs at 180°C and 10 atm.

The test pieces of 3.5 × 3.5 × 16 cm were cut at several locations along the radial direction in an original block so that direction of the longitudinal axis of the test piece coincides with that of the original block and also the center cross-section perpendicular to the longitudinal axis of the test piece coincides with that of the original block.

Young's modulus and mechanical strengths of these test pieces were determined. Sound velocities were measured and from the data, Young's modulus E (kg/cm²) was calculated by the following equation.

$$E = \rho u^2/g \qquad [1]$$

where, ρ = bulk density of specimen (kg/cm³)
u = sound velocity in concrete (cm/sec)
g = acceleration of gravity (cm/sec²)

The strengths for 0 hr soaking specimens were estimated from the experimental data on the Young's modulus by the empirical equation [2], since the specimen was too fragile to subject to usual mechanical strength test.

$$E = 4500\sqrt{0.9Fc} \qquad [2]$$

where, Fc = compressive strength (Kg/cm²)

This equation was obtained by the revision of Purins's empirical equation for ALC products (7), $E = 3000\sqrt{0.9Fc}$, on the basis of the experimental data on E and Fc of 2 hrs soaking specimens. Tensile strengths Ft (kg/cm²) were calculated by the Kano's equation (7) for concrete.

$$Fc = 2.66Ft^{1.44} \qquad [3]$$

This equation has been shown to be in good coincidence with ALC products.

From the data on expansion coefficient, temperature distribution and Young's modulus, the thermal stress both in a cylinder of 20 cmϕ and in a large slab of 20 cm thickness were estimated by the equation given in Table 2, where Poisson's ratio was assumed to be 0.3.

In the case of the initial stage of cooling period, the possibility of the surface crack due to sudden change in temperature was discussed also on the basis of the values of Biot's modulus and nondimentional time.

Table 2. *Computation equation for surface and center stresses.*(11)

Shape	Surface	Center
Long cylinder	$\frac{E\alpha}{1-\mu}(Ta - Ts)$	$\frac{E\alpha}{2(1-\mu)}(Ta - Tc)$
Infinite slab	$\frac{E\alpha}{1-\mu}$	$\frac{E\alpha}{1-\mu}$

E = Young's modulus.
α = coefficient of thermal expansion.
Ta, Ts, Tc = average, surface and center temperature, respectively.
μ = Poisson's ratio.

Table 3-a,b,c,d. *Experimental and calculated results of mechanical properties of cylinder*

a. Soaking time = 0 hr.

Distance from center, r (cm)	Young's modulus, E(kg/cmr) × 10^{-4}	Compressive strength, Fc (kg/cm²)	Tensile strength, Ft (kg/cm²)
0	0.33	0.6*	0.35**
4	0.33	0.6*	0.35**
8	0.33	0.6*	0.35**

b. Soaking time = 2 hrs.

0	1.54	12.8	3.3**
4	1.78	19.3	4.0**
8	1.97	20.6	4.2**

c. Soaking time = 4 hrs.

0	1.99	32.5	5.7**
4	2.01	31.8	5.6**
8	2.16	33.0	5.7**

d. Soaking time = 8 hrs.

0	2.01	35.1	6.0**
4	2.09	34.2	5.9**
8	2.30	35.5	6.0**

*Calculation from equation (2)
**Calculation from Kano's equation.

Results and Discussion

Mechanical Properties

Experimental and calculated results are given in Table 3-a, b, c, d. Variations in mechanical properties (Young's modulus and mechanical strength) along the cross-section were most distinct in the block soaked for 2 hrs at 180°C after the end of the heating-up period. It should be remembered that temperature difference in like size specimen disappeared at 1.5 hrs' soaking (Fig. 2-a). These variations decreased in the specimen at longer soaking time. This tendency means that the time lag for heat transfer in concrete is accompanied by that for the development of mechanical properties.

Thermal Stress and Failure

If the specimen was perfectly elastic, the inner tensile stress of 0.8 kg/cm² for a cylinder (20 cmϕ) and 1.8 kg/cm² for a slab (20 cm thickness) should be developed at the end of the heating-up period, which were considerably larger than the tensile strength of the material at that time (0.35 kg/cm² for cylinder as seen in Table 3-a). Then the inner crack might be predicted to arise for both shapes.

The stress, however, must be relaxed more or less during hardening process, then the values of 0.8 kg/cm² and 1.8 kg/cm² may be somewhat reduced.

The surface tensile stresses of the cylinder and the slab at the initial stage of the cooling period, 6.0 kg/cm² and 9.0 kg/cm², respectively, were approximately comparable to the tensile strength at that time.

If the stress is completely relaxed only during heating-up period and after that the specimen is perfectly

elastic, the surface tensile stress of 0.8 kg/cm² for the cylinder and 1.8 kg/cm² for the slab should be developed at the time at which the temperature distribution in the specimen disappear. These values are certainly noticed to be lower than the tensile strength at that time (4.2 kg/cm² for cylinder). Therefore the possibility of the inner crack during hardening process (heating-up and early stage of soaking period) is reduced. In addition, these tensile stresses are accumulated to the tensile stresses developed at cooling period and the possibility of the surface crack slightly increases.

On a basis of these approximate estimation concerning thermal stress, it is concluded that the thickness of 20 cm is the upper limit for a slab to be securely produced under the autoclaving condition carried out in this investigation.

Furthermore it should be noticed that failure phenomena under autoclaving process might be affected also by the drastic movement of moisture in concrete, or heterogeneous linear changes due to the different phases contained in concrete as pointed out in previous sections.

Summary

(1) For a cylindrical specimen of 20 cmϕ, average value of apparent thermal diffusivity K during the hardening process (the heating-up period and the early stage of the soaking period) under the heating rate of 1.0~0.75°C/min in autoclave process was determined to be approximately 4 times as large as that determined for the final product.

(2) From the values of K and their variation with autoclave time schedule and the position in the specimen, it was presumed that heat transfer in concrete was affected both by the presence of liquid water in concrete and by movement of vapor or liquid in concrete.

(3) The temperature profiles of a slab of 20 cm thickness at successive times were determined. The temperature difference between surface and center was 120°C when the surface was heated up to 180°C with a rate of 1°C/min. Seven hours soaking at this temperature was required for this difference to be less than 5°C.

(4) By the application of the principal "Differential Optical Lever Method", a simple apparatus was devised for successive measurements of linear change of specimen under autoclave process.

(5) Almost the same expansion-shrinkage phenomena in the case of no addition of MgO were observed for various compositions (cement-siliceous sand-blastfurnace slag), specimen sizes (2.5 cmϕ × 10 cm and 20 × 20 × 60 cm) and bulk densities (0.5 g/cm³ and 1.8 g/cm³).

(6) Augmented expansion was observed in the heating-up period for the specimen added with light-burnt MgO, but it was observed in the soaking period when dead-burnt MgO was added. This tendency was irrespective of other factors, whereas the amount of expansion somewhat influenced by compositions, sizes and bulk densities of concrete. Excessive addition of MgO caused disruption of the specimen.

(7) In view of thermal stress, it is concluded that the thickness of 20 cm was approximately estimated to be the upper limit for a slab to be securely produced under the autoclaving condition carried out in this study.

Acknowledgement

The writters express their sincere thanks to Mr. J. Nakayama and Mr. Y. Nakamura at the Research Laboratory, Asahi Glass Co., Ltd., for helpful discussions, and to Mr. O. Kida of this Laboratory for his assistance in the experimental work.

References

1. N. I. Dybrovna, V. S. Pinskii and B. S. Petrov, "Qualities of starting materials and resistivity to cracks of aerated concrete under autoclave process" (in Russian), Stroitel Materialy **11** (8) 25–27 (1965).
2. C. A. Mironov, M. Ya. Krivitskii and A. N. Schastnyi, "Temperature distribution and deformation of aerated concrete under autoclave process" (in Russian), Stroitel Materialy **12** (11) 17–19 (1966).
3. K. F. Lomunov, V. K. Runov and A. F. Shchurov, "Cracks of aerated concrete product under autoclave process" (in Russian), Beton i Zhelezobeton **12** (4) 41–44 (1966).

4. A. I. Avakov, L. T. Yakovlev and K. E. Goryainov, "Method for experimental investigation on stress of aerated concrete under autoclave process" (in Russian), Stroit i Arkhitekt **9** (9) 133–137 (1966).
5. P. Smallwood, "Some thermal aspects of autoclaving calcium silicate building products" Preliminary paper for International Symposium on Autoclaved Calcium Silicate Building Products in London (1965).
6. H. S. Carslaw and J. C. Jaeger, "Conduction of heat in solids" Oxford University Press (1959).
7. ALC Research Committee Report (in Japan), (1965).
8. T. C. Powers, "The physical structure and engineering properties of concrete" Research and Develop. Labs. Portland Cem. Assoc., Research Dept. Bull., No. 90 (1958).
9. R. G. L'Hermite, "Volume changes of concrete" Proc. 4th International Symposium Chem. Cement, 659–694 (1960).
10. A. Honma, "Study on thermal expansion of hardened cement paste" Annual report of cement technique, XV 92 (1961) (in Japan).
11. W. D. Kingery, "Introduction to ceramics" John Wiley & Sons, Inc., New York. London (1960).

Supplementary Paper III-111 Influence of Minor Components on the Strength of Calcium Silicate Hydrate Synthesized by Hydrothermal Reaction

Gunji Shikami*

Synopsis

In the present investigation, it was studied about the influence of the addition of the foreign components, such as beryllium, zinc, and alkaline compounds, on the strength and the reaction rate of hydrothermal synthesized products.

Addition of beryllium and zinc even in quantities up to 0.1–0.4 per cent, can appreciably delay the progress of hydrothermal reaction, deteriorating seriously the development of the strength of the reaction product at the usual hydrothermal condition (160–180°C, 3–6 hours). They, however, do not entirely stop the hydrothermal reaction, but merely lower the rate of the reaction. The manner of the hydrothermal reaction does not be changed substantially by the addition of the poisoning compounds, as recognized from the molar ratios of the hydrated substances.

The addition of alkali in minor quantities can promote the reactivity as well as the strength development of the product. The promotion of the strength may be explained by the increased reactivity of quartz and the formation of a compound of system R_2O–SiO_2–H_2O in the hardened product. Alkalies added in quantities above 0.3 per cent, however, generally tend to retard the reaction and deteriorate the development of the strength of the reaction product. Addition of alkali causes a marked decrease of the water absorbing capacity of the hydrothermal product.

Introduction

Many investigators have studied about the factors affecting the strength of hydrothermally synthesized calcium silicate hydrate (1), namely,

i) CaO/SiO_2 molar ratio
ii) the temperature and the duration of an autoclaving
iii) the physical properties of the starting materials, especially crystalline modifications, crystallinity, and fineness of the siliceous material
iv) the compacting pressure and the amount of mixing water applied at the moulding
v) the addition of some foreign components

Of these, we were interested particularly in the factor (V). Since these were already some studies on the influence of Al_2O_3 (2) and MgO (3), the present investigation was undertaken to determine the influence of the addition of beryllium, zinc, lithium, sodium and potassium on the strength of the hydrothermally synthesized products. The presence of them even in minor quantities was known to have rather remarkable influence, either favourable or unfavorable, on the strength of the products of hydrothermal synthesis. The results of these experiments are reported below.

Methods and Conditions of Experiment

Material

The principal components, CaO and SiO_2, were obtained from slaked lime of analytical reagent and high-purity quartz respectively, whose chemical compositions and physical properties are shown in Table 1. By X-ray and thermal analysis, it was shown that this slaked lime was contaminated with a little amount of calcium carbonate.

Preparation of Specimen

Autoclaved specimens were prepared by the follow-

*Osaka Cement Co., Ltd., Osaka, Japan.

Table 1. *Properties of raw materials*

	ig. loss	SiO_2	Al_2O_3	Fe_2O_3	CaO	MgO	Na_2O	K_2O	Total	Surface area (cm^2/g)
Quartz powder	0.2	97.2	1.2	0.2	0.6	0.0	0.1	0.6	100.1	2200[1]
Hydrated lime	23.2	n.e.	n.e.	n.e.	76.7	n.e.	n.e.	n.e.	99.9	313002

[1] by air permeability.
[2] by water vapour adsorption.

ing method. Slaked lime and quartz powder were weighed out in quantities corresponding to a CaO/SiO_2 molar ratio of 0.60 and these were thoroughly mixed up with prescribed amounts of the selected foreign components, e.g. BeO, ZnO. Then water was added to the mixed powder in a quantity corresponding to a water-powder ratio of 0.55, followed by thorough kneading.

The paste thus prepared was placed into a mould $2 \times 2 \times 8$ cm. After 8 to 12 hours the paste was autoclaved under the prescribed conditions, followed by demoulding.

Analysis of Free Lime and Quartz

Quantitative Analysis for Free Lime

According to the method of quantitative analysis for free lime in portland cement clinker, the specimen prepared by the procedure described above was treated in glycerine-ethanol solution with $Sr(NO_3)_2$ as catalyst and titrated with ammonium acetate solution. Thus the amount of unreacted lime in the specimen was determined.

Quantitative Analysis for Unreacted Quartz

In the analysis for unreacted silica, following the method of Steope, a pulverized sample was rapidly dissolved in 1 N HCl solution containing 5 per cent NaCl, then washed with a solution of 5 per cent Na_2CO_3 and 5 per cent NaCl by weight, and finally washed in succession with 1 per cent HCl solution and hot water. The ignited residue represented the amount of unreacted silica.

Analysis in a blank test of slaked lime-quartz mixture prior to hydrothermal synthesis gave a result of 56.9 per cent which was considered to be satisfactory against the calculated value of 57.5 per cent.

Determination for Combined Water of the Hydrate

In the determination for combined water of hydrothermal hydrate, there are three factors which make the result inaccurate, namely the crystalline water due to unreacted slaked lime, the error due to contamination with carbon dioxide and the water physically adsorbed by calcium silicate hydrate. Therefore, for accurate determination of combined water in the hydrate, the errors resulting therefrom had to be corrected against the result of a thermal gravimetric analysis. Namely, the loss due to slaked lime at 500°C and that of calcium carbonate over the range of 690 to 850°C were deducted from the weight loss over the temperature range of 100 to 850°C and the remain was recorded as the amount of combined water. The correction of physically adsorbed water was carried out by keeping the specimen in vacuum for 8 to 10 hours. In a thermal analysis (DTA and TGA) the temperature was raised at a rate of 10°C/min.

Influence of Addition of Beryllium and Zinc

The presence of beryllium or zinc compounds in the system even in minor amounts or trace can rather seriously retard the progress of hydrothermal synthesis, as seen from Table 2 showing the result of synthesis 180°C—6 hours. As seen from the tabulated data, beryllium and zinc, added in quantities up to 0.1–0.4 per cent either in the form of oxide or sulphate, retard the hardening reaction and lower the development of the strength. The lowering effect, however, depends on the conditions of the hydrothermal treatment, as it is shown in Fig. 1.

To clarify the retarding effect due to such components, an experiment was made with some zinc compounds, whose result is shown in Table 3. To make easy identifing the reaction product, the experiments were carried out with a CaO/SiO_2 ratio of 1.0 and

Table 2. *Chemical compositions and physical properties of the hydrates synthesized with addition of beryllium and zinc compounds*

Composition of mixture (%)				Reacted amounts (%)		Molar ratio of hydrate		Compressive strength (Kg/cm^2)	Surface area (m^2/gr)	Apparent sp. gravity
CaO	SiO_2	Minor components		CaO[2]	SiO_2	CaO/SiO_2	H_2O/SiO_2			
36.24	63.75	—		36.17	26.05	1.49	1.46	253	68.7[1]	2.17
36.19	63.76	BeO	0.06	36.19	24.76	1.55	1.31	261	62.5	2.03
36.17	63.72		0.11	10.88	1.79	5.48	2.72	0	3.2	n.e
36.09	63.58		0.33	13.95	0.74	—	—	0	3.6	n.e
36.10	63.61	$BeSO_4$	0.29	36.10	22.86	1.68	1.34	190	48.1	2.08
36.00	63.43		0.57	33.82	18.00	1.98	1.82	120	28.9	2.03
35.59	62.71		1.70	21.41	5.48	4.09	2.65	117	21.1	2.12
36.17	63.72	ZnO	0.11	36.17	25.14	1.53	1.46	247	75.9	1.91
36.13	63.65		0.22	36.13	23.18	1.66	1.60	200	54.8	2.00
36.05	63.51		0.44	12.37	0.61	—	—	0	5.2	n.e
36.13	63.51	$ZnSO_4$	0.22	36.13	26.31	1.47	1.46	231	53.0	1.95
36.05	63.51		0.44	34.55	21.95	1.66	1.63	215	45.3	2.00
35.89	63.24		0.87	3.36	0.00	—	—	0	4.8	n.e

[1] Surface area of starting mixture; 2.6 m^2/gr.
[2] These figures contain the amounts of CaO contaminated by CO_2 (up to 0.6% in most cases). The ratio CaO/SiO_2 is corrected as to CO_2 contamination.

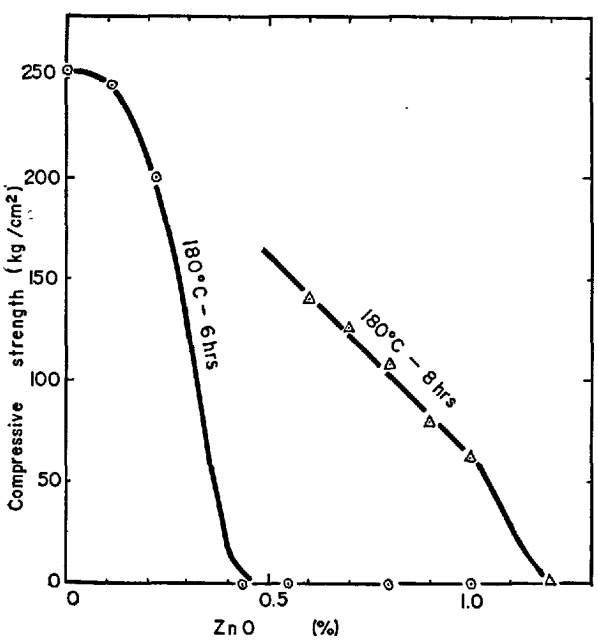

Fig. 1. *Effect of adding zinc oxide on the strength of autoclaved products*

with a larger proportion of mixing water (water/solid = 1) in a stainless steel container.

The amount of unreacted silica in the products synthesized at 200°C was difficult to be determined, because there were many troubles in the filteration called for by the Steope method. According to the results from X-ray analysis, some amounts of quartz (unreacted silica) were recognized in the products at 200°C-6 hours, but in the case of 200°C-12, 24 hours treatments the trace of quartz was not found. These results were also confirmed from the curve in Fig. 2. The compositions of the hydrates formed at 200°C-6 hours were not calculated, because the amount of unreacted quartz could not be estimated by X-ray analysis from the point of accuracy.

The progress of hydrothermal reaction can be discussed from the amount of the reacted silica and tobermorite gel formed, the degree of crystallization of tobermorite, the converting rate of tobermorite into xonotlite, and the surface area etc., the data of which were shown already in Table 2 and 3. The details of such findings are summarized in Fig. 2 to Fig. 8 and will be explained below.

Fig. 2 shows the influence of a presence of zinc compound on the reaction rate. From Fig. 2 it is noted that the reactivity of quartz is lowered remarkably when the reaction temperature is lower and reaction time shorter. These results are important from the industrial point, because these conditions are usual in autoclaved concrete industry. These lowering effect, however, decreases with increasing maturity of autoclaving. The dependence of silica's reactivity on the kind of zinc compound added has not been confirmed yet.

The typical change of hydrate phase with increasing maturity of hydrothermal treatments ,determined by X-ray analysis, is shown in Fig. 3. The diffraction pattern by X-ray alters from (1) through (2) and (3) to (4) with increasing hydrothermal treatments. In the figure, (1) is the X-ray pattern of tobermorite gel

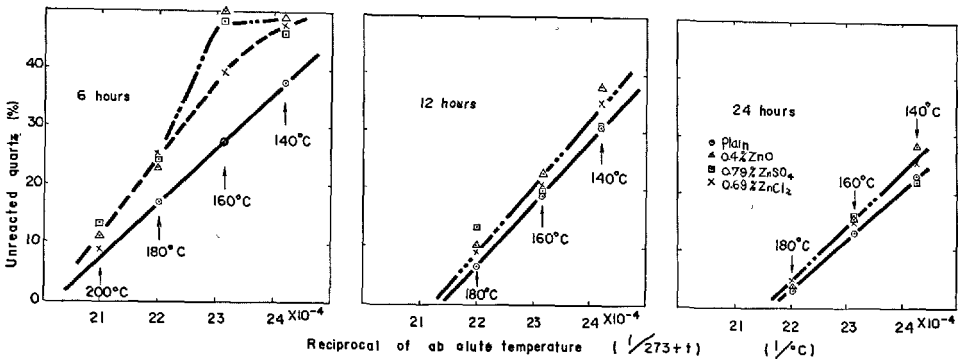

Fig. 2. *Influence of addition of zinc compounds on the reactivity of quartz. The molar ratio of starting mixture is* CaO: SiO_2 = *1.0*

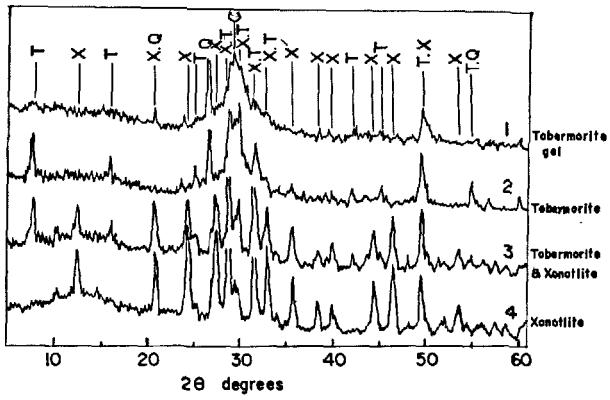

Fig. 3. *Typical X-ray diffraction patterns of the autoclaved products. Notations in the figure are as follows; T: tobermorite, X: xonotlite, Q: quartz, C: calcite. The patterns vary from 1, through 2, 3 to 4 with increased autoclave*

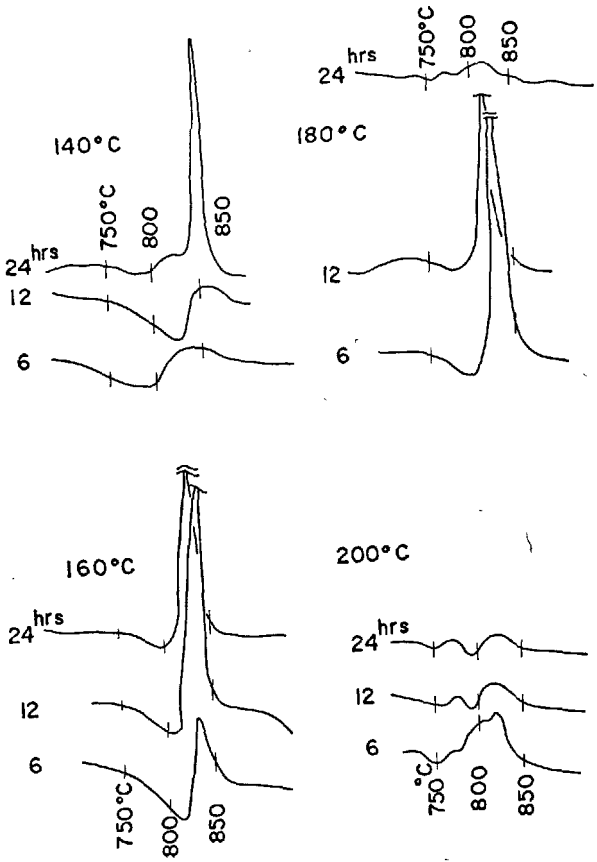

Fig. 4. *Differential thermal analysis curves of hydrothermal products not containing poisoning compounds. Molar ratios of the starting mixtures are* CaO: SiO_2 = *1*

(near amorphous tobermorite), (2) that of semi-crystalline tobermorite with the peak of 11 Å, (3) that of crystalline tobermorite in coexistence with xonotlite and (4) that of xonotlite. The results of identification of hydrate are tabulated in the final column of Table 3. From Table 3 it is known that the addition of zinc compound results in delaying the crystallization of tobermorite and conversion of tobermorite into xonotlite.

In a differential thermal analysis, as seen from Fig. 4, the formation of tobermorite in hardend product is indicated by a characteristic peak, resulting from the exothermic reaction due to β-wollastonite. The said peak appeared at a temperature range 810–830°C. The peak grows higher with increasing amount of tobermorite. Then the peak drops rather sharply with conversion of tobermorite into xonotlite and continues dropping until the said conversion is completed. The analysed results of DTA, not shown here, well agreed with that of X-ray analysis.

The evolution of the combined water in a thermal gravimetric analysis is plotted in Fig. 5. The gradual

Table 3. *Chemical compositions and physical properties of the hydrates synthesized with addition of zinc compounds* ($CaO/SiO_2 = 1.000$)

Hydrothermal condition		Amounts of Zn-compd[1] (%)		Unreacted amounts (%)[1]		Properties of hydrate				
						Molar ratio[3]		Temp. of peak[2]	Surface area	
Temp.	Duration (hr)			SiO_2	CaO	CaO/SiO_2	H_2O/SiO_2	(°C)	(m^2/gr.)	Phases[5]
140°C	6	—		37.8	24.7	1.83	1.44	824	n.e.	$Ca(OH)_2$, Q
		ZnO	0.04	49.1	38.7	4.60	3.32	840	〃	$Ca(OH)_2$, Q
		$ZnSO_4$	0.79	46.5	38.7	2.23	2.34	n.e.	〃	$Ca(OH)_2$, Q
		$ZnCl_2$	0.69	48.0	39.0	3.22	1.97	845	〃	$Ca(OH)_2$, Q
	12	—		30.8	11.5	1.85	2.23	846	34.2	$Ca(OH)_2$, Q, Tob-gel
		ZnO	0.40	38.0	38.5	—	—	846	3.9	$Ca(OH)_2$, Q
		$ZnSO_4$	0.79	31.0	9.7	1.99	1.81	846	4.0	$Ca(OH)_2$, Q, Tob-gel
		$ZnCl_2$	0.69	35.3	17.0	2.04	2.30	855	4.2	$Ca(OH)_2$, Q, Tob-gel
	24	—		22.7	3.36	1.69	1.62	853	47.8	Tob-gel, Q, $Ca(OH)_2$
		ZnO	0.40	28.0	13.0	1.58	1.65	843	35.5	Tob-gel, Q, $Ca(OH)_2$
		$ZnSO_4$	0.79	21.6	3.29	1.55	1.55	850	55.4	Tob-gel, Q, $Ca(OH)_2$
		$ZnCl_2$	0.69	25.2	2.48	1.90	1.99	843	50.8	Tob-gel, Q, $Ca(OH)_2$
160°C	6	—		26.8	9.53	1.61	1.68	850	55.3	$Ca(OH)_2$, Q, Tob-gel
		ZnO	0.40	50.2	38.1	—	7.22	815	4.0	$Ca(OH)_2$, Q
		$ZnSO_4$	0.79	48.4	38.7	3.32	3.86	830	5.5	$Ca(OH)_2$, Q, Tob-gel
		$ZnCl_2$	0.69	39.6	24.9	2.09	2.89	n.e.	23.7	$Ca(OH)_2$, Q, Tob-gel
	12	—		19.0	0.99	1.552	1.490	842	49.8	$Ca(OH)_2$, Q, Tob-gel
		ZnO	0.40	22.8	0.68	1.785	1.740	839	63.7	$Ca(OH)_2$, Q, Tob-gel
		$ZnSO_4$	19.9	19.9	1.84	1.587	1.493	840	42.9	$Ca(OH)_2$, Q, Tob-gel
		$ZnCl_2$	0.69	20.2	0.72	1.654	1.614	826	55.5	$Ca(OH)_2$, Q, Tob-gel
	24	—		12.9	0.09	1.341	1.210	829	67.8	Tob-gel, Q
		ZnO	0.40	15.6	0.37	1.436	1.276	827	63.5	Tob-gel, Q
		$ZnSO_4$	0.79	16.0	0.51	1.447	1.340	824	60.0	Tob-gel, Q
		$ZnCl_2$	0.69	15.1	0.33	1.417	1.330	820	60.7	Tob-gel, Q
180°C	6	—		17.2	0.51	1.489	1.560	827	67.9	Q, Tob-gel
		ZnO	0.40	23.0	5.40	1.552	1.500	846	39.0	Tob-gel, Q, $Ca(OH)_2$
		$ZnSO_4$	0.79	24.3	5.96	1.608	1.510	846	27.0	Tob-gel, Q, $Ca(OH)_2$
		$ZnCl_2$	0.69	25.4	3.69	1.776	1.820	836	29.3	Tob-gel, Q, $Ca(OH)_2$
	12	—		6.74	0.00	1.167	1.030	820	59.6	Tob., Q
		ZnO	0.40	10.4	0.14	1.168	1.123	820	71.0	Tob-gel, Tob., Q
		$ZnSO_4$	0.79	13.8	0.14	1.382	1.285	820	60.0	Tob., Tob-gel, Q
		$ZnCl_2$	0.69	9.53	0.13	1.241	1.066	820	52.5	Tob., Q
	24	—		3.19	0.00	1.055	0.344	820	24.4	Tob., X
		ZnO	0.40	3.85	0.00	1.076	0.575	808	30.9	Tob., X
		$ZnSO_4$	0.79	3.60	0.00	1.083	0.599	818	32.4	Tob., X
		$ZnCl_2$	0.69	4.50	0.00	1.098	0.648	824	33.1	Tob., X
200°C	6	—		n.e	0.00	n.e	n.e	821	35.0	X, Tob., Q
		ZnO	0.40	n.e	0.00	n.e	n.e	815	62.7	Tob., X, Q
		$ZnSO_4$	0.79	n.e	0.00	n.e	n.e	805	40.8	Tob., X, Q
		$ZnCl_2$	0.69	n.e	0.00	n.e	n.e	810	29.6	X, Tob., Q
	12	—		0.0[4]	0.00	1.00	0.222	793	21.0	X, Tob. (trace)
		ZnO	0.40	0.0	0.00	1.00	0.406	806	20.0	X, Tob.
		$ZnSO_4$	0.79	0.0	0.00	1.00	0.262	797	20.0	X, Tob. (trace)
		$ZnCl_2$	0.69	0.0	0.00	1.00	0.320	801	26.2	X, Tob. (trace)
	24	—		0.0	0.00	1.00	0.222	800	16.5	X
		ZnO	0.40	0.0	0.00	1.00	0.350	797	15.9	X, Tob.
		$ZnSO_4$	0.79	0.0	0.00	1.00	0.236	800	13.9	X, Tob.
		$ZnCl_2$	0.69	0.0	0.00	1.00	0.247	798	21.8	X

1) These figures in ignited base.
2) Exothermic peak relating to the formation of β-woollastonite.
3) Corrected values as to CO_2 contamination.
4) Estimated from X-ray analysis
5) Q.; quartz, Tob-gel; tobermorite in low crystalinity, Tob; tobermorite with 11Å peak, X; xonotlite.

loss of weight over the range of 100 to 800°C increased with increasing amount of tobermorite formed and begins to decrease as the formed tobermorite is converted into xonotlite. Since, as shown later in Fig. 8, CaO/SiO_2 ratios intimately relate to the amount of hydrated silica, it can be used as a measure for the progress of the reaction. But, when the conversion of tobermorite into xonotlite begins, H_2O/SiO_2 ratios change sharply, while CaO/SiO_2 ratios are indifferent to the progress. It is clear that a progress of synthesis can be known reasonably from both ratios, as shown in Fig. 6. Considering these ratios tabulated in Table 3,

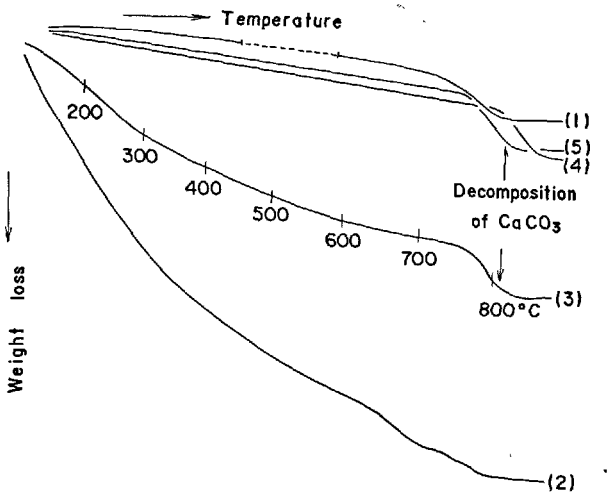

Fig. 5. *Thermogravimetric curves of hydrothermal products not containing posioning compounds. Molar ratio of the starting mixtures is* CaO: $SiO_2 = 1$. *Autoclaved conditions as follows;* (1) *140°C — 6 hrs,* (2) *160°C — 12 hrs,* (3) *200°C — 6 hrs,* (4) *200°C — 12 hrs,* (5) *200°C — 24 hrs. Dashed line was extrapolated by substracting the weight loss due to* $Ca(OH)_2$ *from the original one*

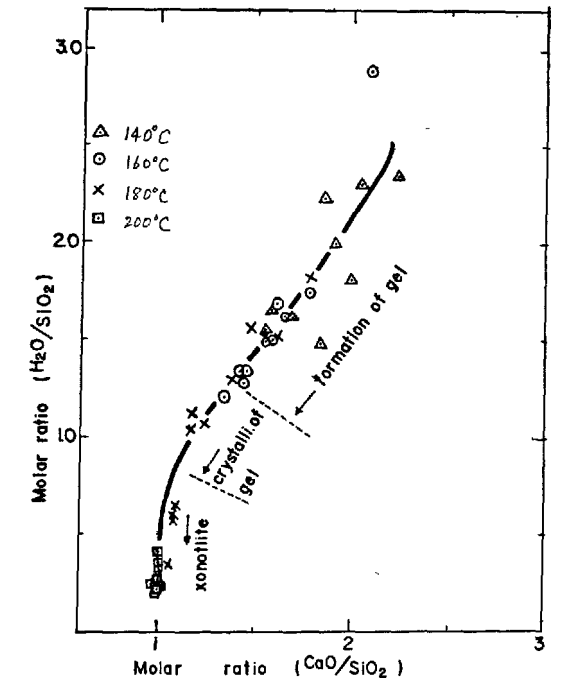

Fig. 6. *Change in morlar ratio of the hydrates with the progress of the reaction. These results were obtained with the autoclaved products containing or not containing zinc compound*

it is also concluded that an addition of zinc lowers the rate of hydrothermal reaction and conversion of tovermorite into xonotlite.

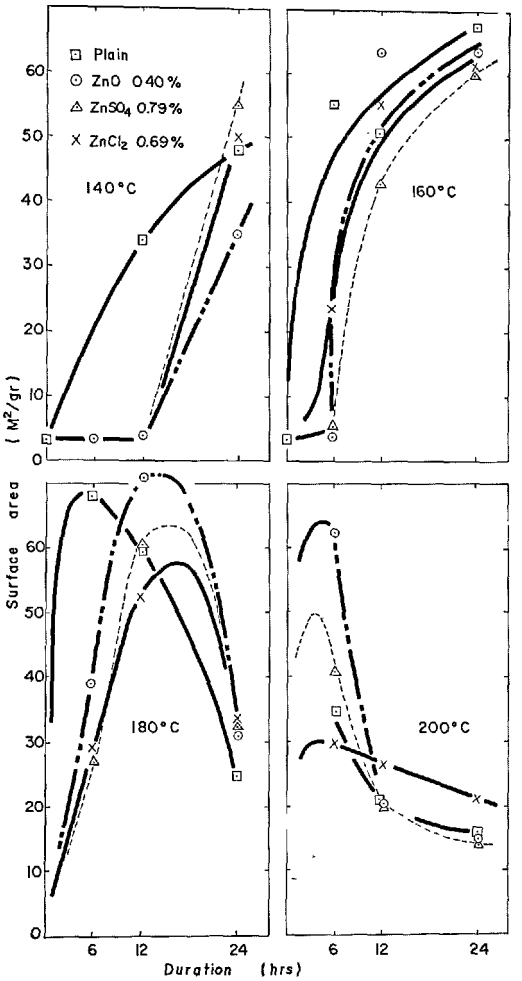

Fig. 7. *Change in surface area of the products. Surface area was determined by vapour adsorption with the aid of BET equation*

Fig. 7 shows the change in the surface area of the hardened product. Comparing these results with that of the X-ray analysis and differential thermal analysis, it is known that the surface area of the hardened product increases with progressive formation of tobermorite and starts decreasing sharply as it is converted into xonotlite.

Fig. 8 shows the relationship between CaO/SiO_2 ratio of the formed hydrates and the amount of hydrated silica in the product. It is recognized that this relationship can be plotted in a curve regardless of a presence of zinc and beryllium compounds. Since either CaO/SiO_2 ratios or H_2O/SiO_2 ratios of the hydrate formed are not influenced by the addition of zinc compounds, it comes to the conclusion that zinc compounds do not have any effects on the composition of the hydrates formed in the products. Only to be noted is that the result of differential thermal analysis

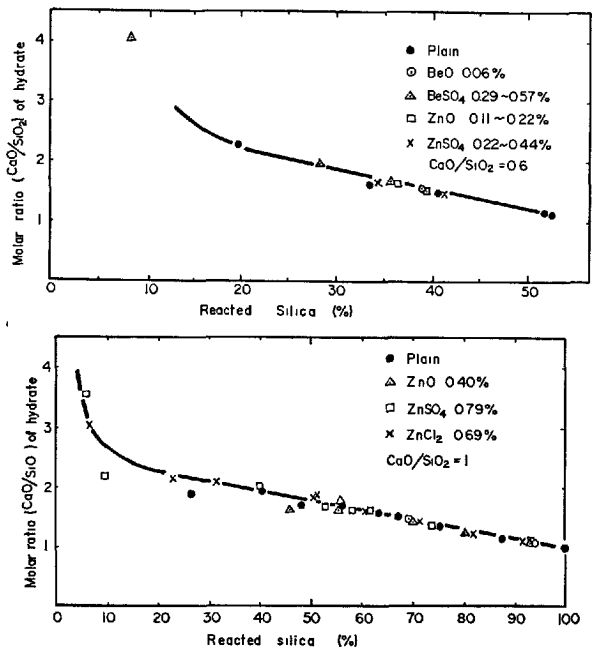

Fig. 8. *Relation between the reacted silica and molar ratio of the hydrate. Molar ratios of the starting mixture are* CaO: $SiO_2 = 0.6$ *in upper experiment and 1.0 in lower one respectively*

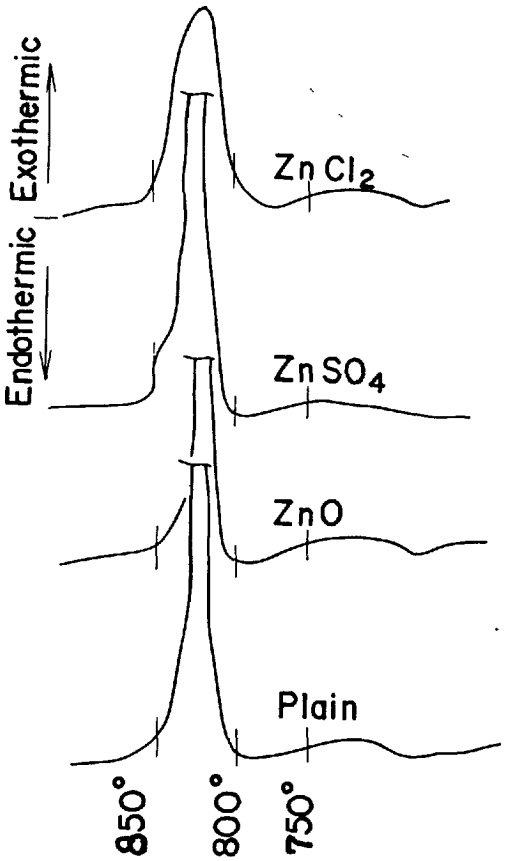

Fig. 9. *Change in the DTA curve caused from the kind of the added compounds. Broader peak is recognized in the case of* $ZnCl_2$

of the products containing $ZnCl_2$ indicated a somewhat broader peak at 820°C compared with the hardened products of other systems (Fig. 9) and the change in surface area was of somewhat different pattern, suggesting somewhat different physical properties of the formed hydrates.

From the results of the experiments above mentioned, it is known that by addition of zinc or beryllium compounds

i) the rate of the reaction between CaO, SiO_2, and H_2O is decreased appreciably with resultant drop in strength of the reaction product under usual hydrothermal condition,

ii) but the substantial pattern of the reaction and the compostion of the hydrate are not affected,

iii) and the growth of tobermorite and xonotlite as well as crystal phase conversion thereof is interfered in some degrees.

Influence of Addition of Alkali

The addition of alkalies shows remarkable influence on the properties of the hydrothermally hardened products as well as zinc and beryllium compounds. To be noted, however, is that alkalis, unlike beryllium or zinc, can promote the hydrothermal synthetic reaction in some cases.

Table 4 shows the results of this series of experiments. In this experiments lithium was added in a form of oxide, sodium and potassium in a form of hydroxide, which were prepared in a form of aqueous solutions of fixed concentrations, for the convenience of the procedure.

The influence of an addition of alkalies on the reactivity of quartz is as illustrated in Fig. 10. While the addition of alkalies in minor quantities can somewhat promote the reactivity of quartz, but it lowers reactivity if it is added in larger quantities (above 0.3 per cent). The lowering effect is least significent with lithium and becomes stronger with potassium and sodium. As already mentioned above, important is the fact that the addition of alkalies in minor quantities can promote reactivity between CaO and SiO_2.

Table 4. *Chemical composition and physical properties of the hydrate synthesized with the addition of* R_2O

Temperature	Duration	Composition of mixture (%)			Properties of hydrate							
					Reacted amount		Molar ratio[1]		Temp. of peak (°C)	Compressive strength (Kg/cm²)	Bulk density	App. sp. gravity
		SiO_2	CaO	R_2O	SiO_2	CaO[1]	CaO/SiO_2	H_2O/SiO_2				
160°	3 hrs	63.83	36.17	—	11.74	22.18	2.02	1.98	811	105	1.14	2.08
		63.74	36.11	Li_2O 0.13	13.98	23.28	1.78			138	1.24	1.94
		63.61	36.04	0.34	13.30	25.06	2.02	1.98	787	199	1.42	1.64
		63.17	35.79	1.02	14.70	21.46	1.56			149	1.43	1.76
		63.72	36.10	Na_2O 0.17	11.88	20.69	1.98			114	1.32	1.91
		63.56	36.01	0.42	10.18	18.38	1.93	2.09	800	109	1.44	1.62
		63.02	35.70	1.27	7.16	15.85	2.37			29	1.47	1.85
		63.71	36.09	K_2O 0.18	12.10	21.78	1.93			125	1.28	1.84
		63.53	35.99	0.46	11.91	20.75	1.87	1.65	832	100	1.26	1.84
		62.95	35.66	1.37	9.30	17.40	2.00			68	1.41	1.70
	6 hrs	63.83	36.17	—	16.92	26.44	1.67	1.47	843	175	1.20	2.06
		63.74	36.11	Li_2O 0.13	17.56	26.80	1.64			209	1.25	1.92
		63.61	36.04	0.34	19.44	27.34	1.51	1.42	793	240	1.40	1.61
		63.17	35.79	1.02	18.27	24.18	1.42			169	1.41	1.61
		63.72	36.10	Na_2O 0.17	14.53	23.75	1.75			165	1.31	1.86
		63.56	36.01	0.42	13.44	20.65	1.65	1.66	803	121	1.41	1.62
		63.02	35.70	1.27	8.47	14.24	1.80			31	1.41	1.82
		63.71	36.09	K_2O 0.18	16.93	27.26	1.73			155	1.24	1.94
		63.53	35.99	0.46	16.20	25.42	1.68	1.57	838	156	1.32	1.83
		62.95	35.66	1.37	10.61	18.13	1.83			84	1.37	1.64
180°	3 hrs	63.83	36.17	—	23.78	34.70	1.56	1.44	821	194	1.12	2.05
		63.74	36.11	Li_2O 0.13	24.94	31.99	1.37			320	1.25	1.73
		63.61	36.04	0.34	22.39	29.25	1.40	1.18	772	235	1.35	1.57
		63.17	35.79	1.02	24.21	28.00	1.24			168	1.31	1.57
		63.72	36.10	Na_2O 0.17	22.98	31.82	1.48			300	1.34	1.75
		63.56	36.01	0.42	21.01	29.28	1.49	1.20	819	265	1.41	1.63
		63.02	35.70	1.27	11.07	21.28	2.06			83	1.40	1.58
		63.71	36.09	K_2O 0.18	26.48	34.92	1.41			210	1.18	1.89
		63.53	35.99	0.46	23.85	33.70	1.51	1.35	824	275	1.36	1.75
		62.59	35.66	1.37	14.72	27.04	1.97			150	1.41	1.59
	6 hrs	63.83	36.17	—	26.05	36.17	1.49	1.46	821	247	1.16	2.09
		63.74	36.11	Li_2O 0.13	30.76	35.46	1.24	1.33	802	352	1.45	1.66
		63.61	36.04	0.34	26.14	34.23	1.40	1.51	827	248	1.45	1.59
		63.17	35.79	1.02	23.78	30.60	1.38	1.49	769	191	1.37	1.65
		63.72	36.10	Na_2O 0.17	29.72	35.36	1.27	1.12	820	330	1.34	1.59
		63.56	36.01	0.42	23.03	32.46	1.51	1.40	803	300	1.41	1.55
		63.02	35.70	1.27	12.65	23.40	1.98	2.09	774	118	1.44	1.57
		63.71	36.09	K_2O 0.18	29.37	36.09	1.32	1.31	821	294	1.19	1.87
		63.53	35.99	0.46	25.45	35.62	1.79	1.48	818	300	1.29	1.73
		62.95	35.66	1.37	17.42	29.69	1.90	2.12	833	174	1.40	1.59

[1] Not corrected values as to CO_2 contamination. Molar ratios of CaO/SiO_2 and H_2O/SiO_2 will be lowered by the correction up to 0.01–0.03.

Fig. 11 shows the relationship between the bulk density and the apparent specific gravity (by an immersing method in water) of the hardened products. A marked difference between the products containing and not containing alkali is noted from the figure. While the bulk densities increase progressively with increasing addition of alkali (see Table 4), the tendency is reversed with regard to the apparent specific gravities which decrease with increasing addition of alkali. This phenomenon comes from the fact that the alkali containing products are more compact and less water permeable (less absorbent). As seen from Fig. 12, the apparent specific gravities of the hardened products decrease with increasing amount of alkali added and with increasing amount of the reacted silica. Therefore, this tendency may be attributed to the formation of the hydrate in the system R_2O–SiO_2–H_2O, which is likely to impart water impermeability to the

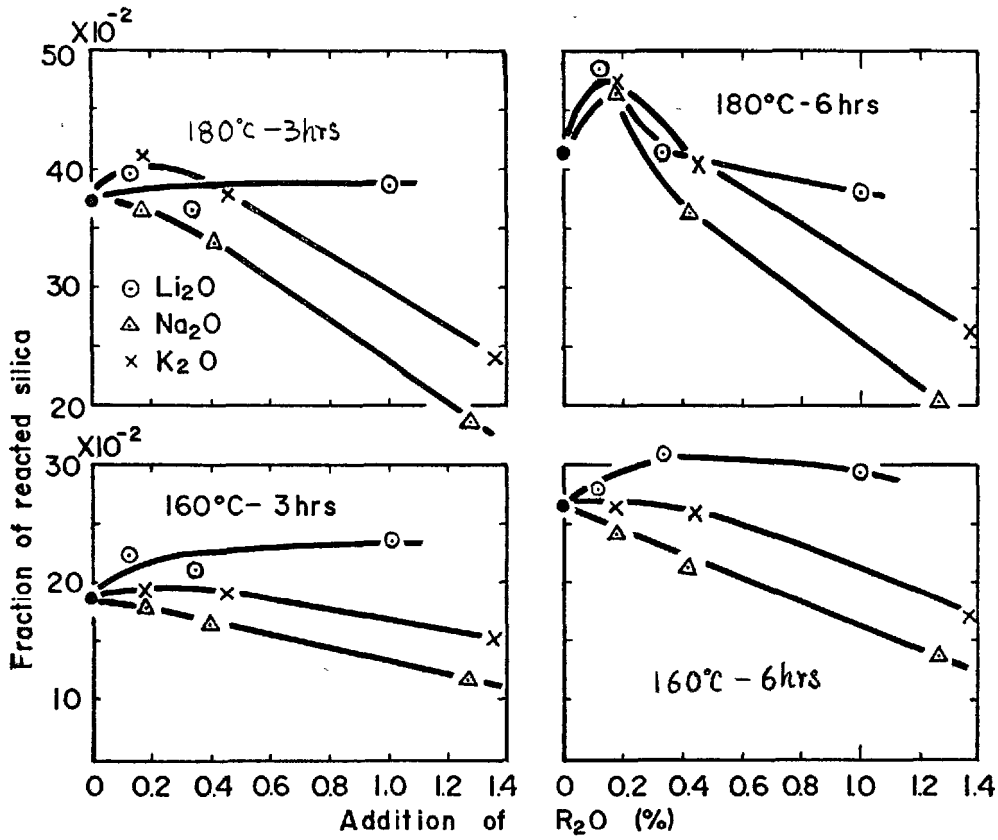

Fig. 10. *Influence of adding alkalies on the reactivity of quartz*

product. (see also Fig. 14).

From Table 4 it is clear that alkali containing products have substantially higher strength than expected from the amount of reacted silica. For instance, Na_2O containing product synthesized under condition of 180°C-3 hours is stronger than plain product, although the amount of reacted silica is smaller than that of the corresponding ones. Supposing that this phenomenon had something to do with the apparent specific gravity or bulk density of the hardened product, we plotted in Fig. 13 the strength of the hardened products as function of the ratio of the amount of reacted silica by apparent specific gravity. Since apparent specific gravity intimately relates to the bulk density (see Fig. 11), the said relation may as well be plotted with the product of reacted silica and bulk density on the axis of abscissa.

Judging from the results of Fig. 12, Table 4 and Fig. 13, it is clear that an addition of alkalies has considerable influence on the physical properties of the product synthesized by hydrothermal reaction.

The curve in Fig. 14 is the relationship between the CaO/SiO_2 ratio of the formed hydrate and the amount of reacted silica in the products. It is noted from the figure that the CaO/SiO_2 ratios of the hydrate formed in the products containing alkali are $0 \sim 0.2$ lower than that of the hydrate not containing alkali at the same amount of reacted silica. These differences are larger with potassium, sodium and lithium in this order and also with increasing amount of alkali added. This means that the said differences are roughly proportional to the molar fraction of alkali in the products. It is then apparent that the hydrate of the system R_2O–SiO_2–H_2O, in addition to calcium silicate

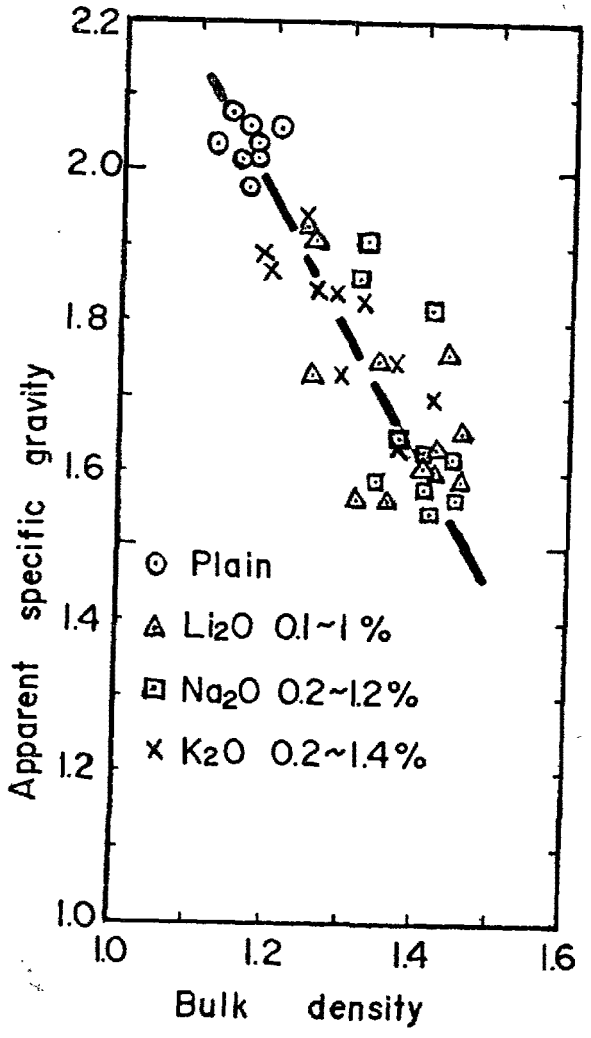

Fig. 11. *Relation between bulk density and apparent specific gravity of the products*

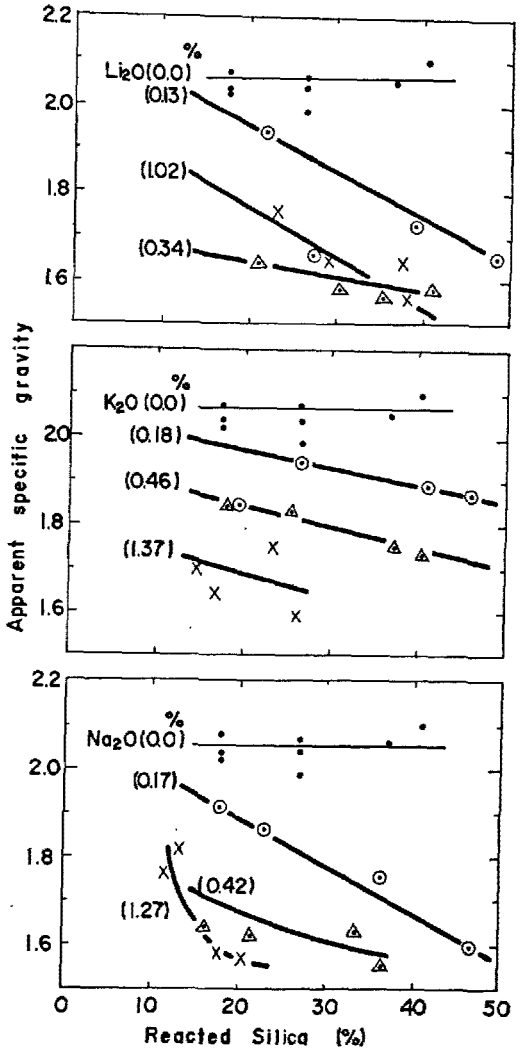

Fig. 12. Decrease of apparent specific gravity caused from the increasing addition of alkalies and the increased amount of reacted silica

hydrate, is likely to be formed in the products.

Assuming the formation of alkali silicate hydrate, there rises the suspicion that the increase of silica's reactivity by addition of alkali in a minor quantity, as shown in Fig. 10, is due to the reaction of R_2O on SiO_2. This suspicion, however, can be denied on the ground that the reactivity of silica decreases with increasing addition of alkali beyond a certain limit and that the increase of silica's reactivity with addition of minor amounts of alkali is by far more remarkable than might be expected from the reaction with the added alkali.

So, taking all these into consideration, it is concluded that an addition of alkali up to 0.3 per cent:

i) promotes silica's reactivity,

ii) imparts a high degree of water impermeability to the hardened products, substantially improving the strength of the products even if the amount of reacted silica remains the same,

iii) appears to give rise to formation of a hydrate of system R_2O–SiO_2–H_2O, besides calcium silicate hydrate, in the hardened products and accordingly results in lower CaO/SiO_2 ratios of the hydrate compared with that of the hydrate not containing alkali.

An addition of alkali in larger quantities above 0.3 per cent, however, is generally detrimental, causing a drop of the strength of hardened product.

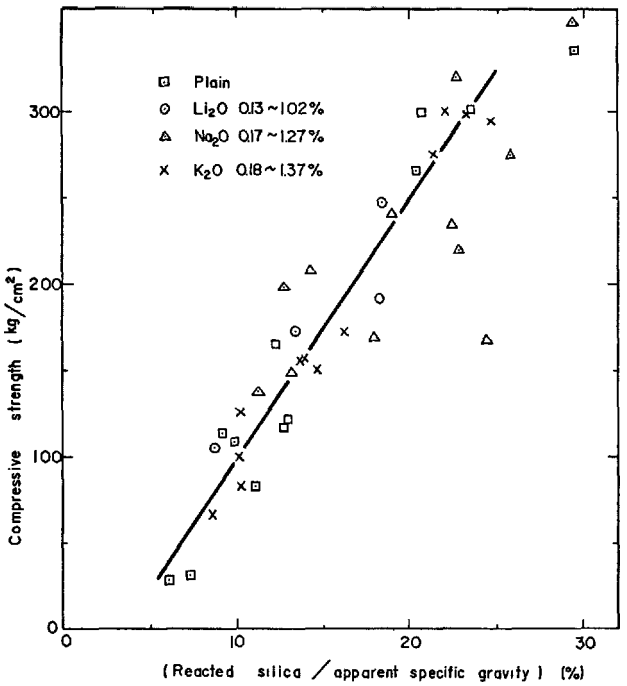

Fig. 13. *Relation between the compressive strength and the ratio (amount of reacted silica/apparent specific gravity)*

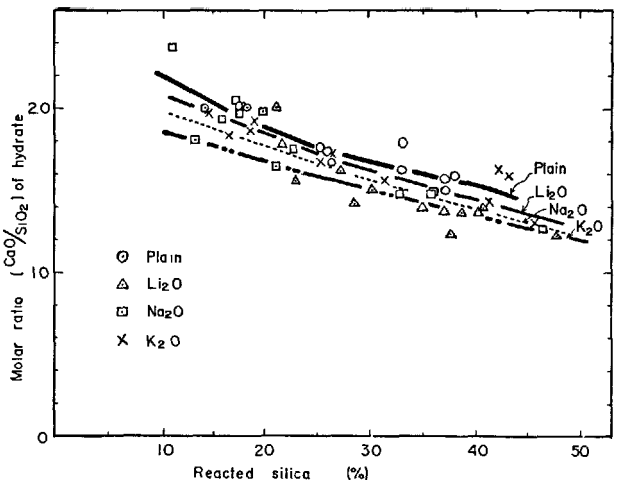

Fig. 14. *Relation between reacted silica and molar ratio (CaO/SiO_2) of the hydrate*

Discussion

Reaction in the Presence of Beryllium and Zinc

Oxides of beryllium and zinc are almost insoluble in water (solubility of BeO and ZnO are 5–20 $\times$ 10^{-6} g/100g water and 4.2 $\times$ 10^{-4} g/100g water respectively) but are soluble as hydroxide in alkaline solutions. On the other hand their salts are water soluble but react with base quantitavely precipitating their hydroxide. For instance, according to Hazel et al (4), zinc sulphate titrated with sodium hydroxide or sodium silicate produces the precipitation of hydrated zinc oxide. Under the conditions of his study, no zinc silicates were formed, but peptizing effect of silica on the zinc precipitates was observed, and also observed the mutual coagulation of hydrated zinc oxide and silica. A similar example of reaction is observed by Britton (5). When 0.02 M $BeSO_4$, 0.02 M $ZnSO_4$, and 0.02 M $CaCl_2$ solution were titrated with 0.102 N Na_2O: 2.16 SiO_2 solution, precipitation of their hydroxide took place at pH 5.31, 5.25 and 10.07 respectively. As may be seen from these examples, oxide or sulphate of beryllium and zinc is converted in the alkaline solution containing silica into the corresponding hydroxide which precipitates at lower pH of 5 to 6 compared with calcium. At the beginning of hydrothermal reaction, hydroxide of beryllium or zinc is supposed to be adsorbed in a form of insoluble colloid onto the surface of quartz prior to the reaction between lime and silica and thus seriously interfers with dissolving of quartz. There appears no chemical reaction to take place between zinc hydroxide and silica, the apparent combination accounted for by mutual adsorption. It is presumed that the progress of the hydrothermal reaction is apparently retarded by a thin film of hydroxide formed by said mutual adsorption and the normal reaction rate is restored when this thin film has been destroyed under progress of reaction. The facts that the drop in reactivity of quartz appeared seriously in low temperature and short duration and decreased with rising temperature and prolonged duration (see Fig. 2), is reasonably understood by the hypothetic film of hydroxide mentioned above.

Acceleration of Reaction by Addition of Alkali

According to Kalousek (6), there is a close relation between Na_2O concentration and the solubility of

CaO and SiO_2 in the solution. For instance, in aqueous solution containing 20 g Na_2O/l, the solubility of CaO is lowered to 0.02–0.03 g/*l* compared to 0.5–0.6 g/*l* in lime water. On the other hand, the solubility of SiO_2 increases gradually as Na_2O concentration of the solution increases. This tendency is maintained essentially even at still higher temperatures.

In the present series of experiments, the addition of alkali amounted up to 1.5 per cent which corresponds to about 15 g/*l* mixing water. Within this range the solubility of CaO decreases sharply with increasing addition of alkali, whereas the solubility of SiO_2 increases slightly. The observed influence of the addition of alkali on the rate of hydrothermal reaction may, therefore, be explained by the fact that the solubility of silica is raised by addition of alkali in minor quantities (up to 0.3 per cent), whereas addition in larger quantities of alkali retards the rate of the reaction through lowering of the solubility of lime.

As to hydrates of system R_2O–SiO_2 formed with addition of R_2O, it is reported by Kalousek (6) that Na_2O/SiO_2 ratios can vary from 0 to 0.25 according to Na_2O concentration. While accurate molar ratios of R_2O/SiO_2 could not be obtained from the present series of experiments, it was observed that R_2O/SiO_2 molar ratios were almost common with Li_2O, Na_2O and K_2O, in most cases ranging from 0.0 to 0.2.

It has been already pointed out that the strength of the hardened product is promoted rather remarkably by addition of alkali and this may be attributed to the binder-like function of sodium silicate hydrate, resulting from addition of alkali, for calcium silicate hydrate.

Conclusion

By the present study on the influences of the addition of beryllium, zinc and alkali compounds on the rate of hydrothermal synthetic reaction of calcium silicate hydrate, it is concluded as follows:

i) An addition of beryllium and zinc even in quantities up to 0.1–0.4 per cent, can appreciably delay the progress of hydrothermal reaction, deteriorating seriously the development of strength of the reaction product at the usual hydrothermal condition (160–180°C, 3–6 hours). The deteriorating effect is not affected by the kind of the compounds e.g. oxide or sulphate.

ii) An addition of beryllium and zinc, however, does not entirely stop the hydrothermal reaction, but merely delay the progress of the reaction. This is supported from the results that the mixtures containing the poisoning compounds can hydrate as well as the one not containing them at an increased autoclaving. The hydrothermal reaction is not changed substantially by the addition of the poisoning compounds, as known from the molar ratio of the formed hydrate. But from the identification of the existing phase by X-ray analysis, it is found that the addition of them has some retarding effects on the crystallization of tobermorite and the conversion of tobermorite into xonotlite. Its retarding effect on the reaction rate may be attributable to its tendency to form hydroxide over quartz surface and to interfere with the dissolving of quartz. This will explain the fact that the said retarding effect is less significent when the reaction temperature is higher and the reaction time is longer.

iii) The addition of alkali in minor quantities can promote the reactivity as well as the strength development of the reaction product. The promotion of the strength of the product by addition of alkali may be explained by the increased reactivity of quartz and the formation of a compound of system R_2O–SiO_2–H_2O in the hardened product. Added alkali in quantities above 0.3 per cent, however, generally retards the reaction, deteriorating the strength development of the product. In this case, the retardation of the reaction is explained by the effect of added alkali to lower the solubility of CaO.

iv) The addition of alkali causes a marked decrease of the water absorbency of the hydrothermal reaction product, while the bulk density of the product increases with its addition. This fact is very interesting from the point of view of the autoclaved product which is less permeable to the water than the conventional one.

References

1. G. E. Bessey, The chem. of cement, "Hydrated calcium silicate products other than hydraulic cements"

II, p. 101–134 (Academic Press Inc., London and New York, 1964).
2. K. Takemoto, "Hydration of cement in autoclaved curing". (in Japanese), Jour. Cera . Assoc. Japan, **73** c91–97 (1965).
3. K. Miyazawa and H. Kamao, "Strength development by autoclave treatment of lime-siliceous materials mixtures" (in Japanese), Proc. of Japan Cement Eng. Association, **17**, 205–209, (1963).
4. J. F. Hazel, W. M. McNabb and P. E. Machemer, Jour. Electrochem. Soc., **99**, (July 1952), or "Soluble silicate" vol. 1, p. 233–234, (The Waverly Press Inc., USA, 1953).
5. H. T. S. Britton, "Hydrogen ions" 3rd ed., vol. 2, p. 106, London, or "Soluble silicate" vol. 1, p. 156, (The Waverly Press Inc., USA, 1953).
6. G. L. Kalousek, "Studies of portions of the quaternary system soda-lime-silica-water at 25°C", Jour. of Research of N.B.S., **32**, (1), 285–302, (1944).

Author Index

For Volume III

Subject Index

For Volume III

Proceedings of
The Fifth International Symposium
on the
Chemistry of Cement
Tokyo, 1968

PART IV
ADMIXTURES AND SPECIAL CEMENTS
(Volume IV)

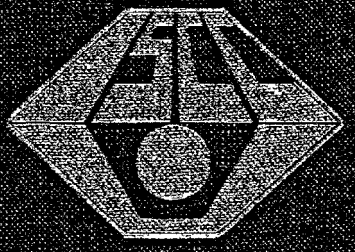

The Organizing Committee
for the Fifth International Symposium
on the Chemistry of Cement

The Cement Association of Japan

Proceedings of
The Fifth International Symposium
on the
Chemistry of Cement
Tokyo, 1968

PART IV
ADMIXTURES AND SPECIAL CEMENTS
(Volume IV)

Symposium held October 7-11, 1968 at the
Tokyo Metoropolitan Festival Hall, Tokyo

Proceedings published in 4 volumes December 31, 1969

Explanatory Notes

Abbreviations.

The following symbols, which have been universally recognized by cement chemists for formulating more complex compounds, are used interchangeably with the respective oxide formulas throughout this book:

$C = CaO$, $S = SiO_2$, $A = Al_2O_3$, $F = Fe_2O_3$, $M = MgO$, $N = Na_2O$, $K = K_2O$, $H = H_2O$,

Less common abbreviations of this type are defined as they occur.

Commonly used abbreviations of more general nature are as follows:

DTA = differential thermal analysis
EPMA = electron probe micro analysis
IR = infrared
NMR = nuclear magnetic resonace
psi (or p.s.i.) = pounds per square inch
rh (or RH) = relative humidity
w/c (or W/C) = water – cement ratio
XRD = X-ray diffraction

Identification Number of Supplementary Papers

Example: Supplementary Paper III—50, III is session III and 50 is the arrival number of contribution. This number coincides with the number used in the preprint of papers distributed in advance of the symposium.

Contents

Volume IV

Part IV Admixtures and Special Cements

Session IV-1 Use of Surface-Active Agents in Concrete

Session IV-2 Fly Ash and Fly Ash Cement

Session IV-3 Slags and Slag Cements

Session IV-4 Expansive Cement

Session IV-5 By-product Gypsum from Various Chemical Industries, as a Retarder for the Setting of Cement

Principal Paper

SESSION IV-1 USE OF SURFACE ACTIVE AGENTS IN CONCRETE

Principal Paper Use of Surface-Active Agents in Concrete

Richard C. Mielenz*

Synopsis

This report summarizes use of surface-active organic substances in portland cement concrete to cause air entrainment, reduce water requirement, control rate of setting and hardening, and otherwise modify properties of the fresh and hardened product. Surface-active substances causing air-entrainment are positively adsorbed at air-water interfaces and may be adsorbed at water-solid interfaces, particularly on granules of cement. Widely used air-entraining admixtures are anionic. Complex relationships determine the efficiency of air entrainment, void size distribution, and effects on viscosity in fresh concrete. Data show the importance of interchange of air among bubbles prior to stiffening of the concrete. A separate relationship of durability factor and air-void spacing factor occurs for each cement-admixture combination in air-entrained concrete as water-cement ratio and water content are varied.

Water-reducing, set-controlling admixtures employed to substantial extent in concrete construction are salts of sulfonated lignin, water-soluble hydroxy acids and their salts, and carbohydrates. They can be combined with accelerators, catalysts, air-entraining compounds, or other substances for specific purposes. Water-reducing, set-controlling admixtures modify the properties of fresh and hardened concrete primarily by activity at the interface of mixing water and cement, but the mechanisms are not understood completely. Engineering properties of concrete containing water-reducing, set-controlling admixtures can be evaluated by standard testing procedures. Expanded research on use of surface-active organic substances as admixtures is recommended as a part of continued progress in the technology of portland cement concrete.

Introduction

Technical and scientific application of organic, surface-active additives and admixtures in portland cement mixtures was initiated about 1936 with the introduction of air-entraining agents and organic materials that reduce water requirement for given consistency, change time of setting, and modify other properties of concrete (1). These materials are surface-active agents. This paper summarizes knowledge of their function and use in concrete. Most applications of these agents are based on empirical tests and experience because basic data and theory are too sparse to permit quantitative prediction of the effects that will be produced in concrete. Ultimately, research data should provide a quantitative basis for their selection and control as additives and admixtures for concrete.

The scope of this paper is as follows: Application of water-soluble organic materials to entrain air or to reduce water requirement and control setting and hardening of portland cement concrete through physical-chemical activity at air-water and water-solid interfaces.

*Product Development, Master Builders, Division of Martin Marietta Corporation, Ohio, U.S.A.

Air-Entraining Admixtures for Concrete

Materials for Air Entrainment

Air-entraining agents for concrete are organic substances that promote formation of minute air bubbles in concrete during the mixing operation and subsequently inhibit coalescence, dissolution, or escape of the bubbles until stiffening of the matrix has occurred. The active constituents of the agents are positively adsorbed at air-water interfaces and may be adsorbed or chemisorbed at the surface of portland cement and aggregate in an aqueous medium. Air-entraining admixtures marketed in the United States of America have been classified into seven groups (2):

Group A—Salts of wood resins
Group B—Synthetic detergents
Group C—Salts of sulfonated lignin
Group D—Salts of petroleum acids
Group E—Salts of proteinaceous materials
Group F—Fatty and resinous acids and their salts
Group G—Organic salts of sulfonated hydrocarbons

Surface-active agents in general may be classified as follows by their physical-chemical properties (3):

1. Anion-active compounds
2. Cation-active compounds
3. Nonionic compounds

In the first class, the hydrocarbon structure contains negatively charged hydrophilic groups, such as COO^-, SO_3^-, and OSO_3^-, so that large anions are released in water. Conversely, if the hydrocarbon ion is positively charged, the compound is cation-active. Compounds composed of positively and negatively charged organic ions are said to be amphoteric. Nonionic compounds release no ions into aqueous solutions. Surface-active compounds of all these classes can cause air entrainment in concrete, but their efficiency and the characteristics of the air void system vary widely.

Use of Air-Entraining Admixtures

Anionic surface-active agents are the most widely used as air-entraining admixtures in concrete mixtures for general construction. All of the products tested by the Bureau of Public Roads (4) are of this type. In concrete mixtures at plastic consistency, anionic surface-active agents are used at rates about 0.002 to 0.5 per cent by weight of the cement content[1] to produce air content of 5 to 6 per cent, or a cement paste-air void ratio of about 3.5 to 6 by volume. Salts of wood resins, synthetic detergents, salts of fatty and resinous acids, and organic salts of sulfonated hydrocarbons, which are most widely used as air-entraining agents, typically are employed at rates of 0.002 to 0.06 per cent, based upon the active constituents of the admixture. In tests of diverse anionic detergents, including both sodium and organic salts, in concrete with water-cement ratio about 0.45 by weight[2] and slump of 3 to 4 in., air content of 5 to 6 per cent was achieved by use of the admixture at rates of 0.002 to 0.006 per cent.

When an air-entraining admixture is used in concrete simultaneously with a water-reducing admixture, the rate of use of the air-entraining agent is less than that otherwise required to produce the same air content, even when the water-reducing admixture does not cause air entrainment when used alone. For example, in tests of water-reducing retarders, Grieb, Werner, and Woolf (5) found that the requirement for the air-entraining admixture was reduced 14 to 100 per cent at constant cement content and slump.

So far as the author is aware, no commercial air-entraining admixtures for concrete are based upon cationic surface-active compounds; data on their effects in concrete are scanty. Bruere (6) gives data on dodecyl trimethyl ammonium bromide as an air-entraining agent in cement pastes. Satisfactory void systems were developed with its use at rates of 0.010 to 0.075 per cent. Unpublished data are available on a group of seven cationic surfactants tested in concrete with a calcium lignosulfonate used at the rate of 0.16 per cent. Water-cement ratio was 0.47 and slump was 3 to 4 in. The air content of concrete containing the lignosulfonate as the only admixture was 3.0 per cent. When the cationic agents were added at rates of 0.0015 to 0.0067 per cent, air content was 5.2 to 5.7 per cent. The agents were a fatty amide, a fatty amine, dodecylamine acetate, dodecyl trimethyl ammonium chloride, and hexadecyl trimethyl ammonium chloride. The air-void system was not evaluated microscopically, but the properties of the fresh concrete indicated that the air bubbles were stable. Conversely, cationic n-alkyl dimethyl amines from two sources produced air content of 1.7 to 3.2 per cent when used at rates as high as 0.033 per cent.

---

[1] Rate of use of the admixture will be expressed as per cent by weight of the cement content unless otherwise noted.

[2] Water-cement ratio is expressed by weight throughout this report.

Nonionic surface-active agents comprise natural products, condensation products of fatty substances and their derivatives with ethylene oxide, products obtained by condensation of phenolic compounds having side chains with ethylene oxide, and miscellaneous nonionic compounds possessing solubilizing polar groups (3). Condensation products of phenolic compounds having lateral chains with ethylene oxide have been used as admixtures for concrete, especially in non-plastic mixtures, such as are used in the molding of concrete products, to which they impart a plasticizing effect without substantial entrainment of air. However, nonionic surface-active agents generally are not effective as air-entraining agents for concrete because of instability of the bubbles in the fresh mixture (6–8).

Bubble Formation and Dissolution

Because of the presence of hydrophobic and hydrophilic portions in the molecule of the surface-active compound, an air-entraining compound is concentrated at air-water interfaces, with the hydrophobic portion preferentially oriented toward the air (9, p 68; 10, p 99). The process is a dynamic one during and following mixing of concrete because the volume of bubbles increases as air is supplied from several sources, and the air-water interface is subject to many influences (11). The amount of air originally incorporated in the mixture can be decreased by escape of bubbles, and Landgren (12) detected consumption of a part of the oxygen by oxidation reactions, such as with metallic iron, ferrous iron, or sulfide sulfur in the cement.

As each air-water interface develops, the surface-active agent is concentrated there at a rate characteristic of the substance, its concentration in solution, and environmental conditions, such as temperature. The adsorbed film decreases surface tension, possibly by 20 dynes/cm or more, decreasing the rate at which the bubbles dissolve, the tendency of bubbles to coalesce, and the work necessary to produce bubbles of given surface area.

However, the stability of the bubbles is not related directly to the surface tension, at least as measured at equilibrium. Maximum stability is obtained at a concentration of surface-active substance such that the ratio of instantaneously developed surface tension to the equilibrium surface tension is at a maximum (13). Important factors in foam stability are low equilibrium surface tension, moderate rate of attainment of surface tension, and high viscosity. Important also in determining the rate of coalescence of bubbles is the like electrostatic charge that exists at the interface containing ionic surfactants; the charge tends to repell such bubbles from one another (14). These factors have not been related quantitatively to air entrainment in concrete. Examination of a series of three concrete mixtures that differed only in the proportion of an anionic surface-active agent necessary to produce nominal air content of 3.0, 6.5, and 8.8 per cent showed that air content increased with increased concentration of the agent, and specific surface (α) of the void system increased from 603 to 737 to 1112 $in.^2/in.^3$ (8). The increased concentration of agent allowed increased bubble formation and stabilized more very small bubbles.

In water solution, the surface-active agent is soluble to varying degree in the bulk of the liquid and individual molecules are interchanged between the adsorbed film and the liquid (9). When the surface of the bubble is stretched, as with distortion of the bubble, surface tension is increased and additional molecules of the agent move into the interface. Because this process is not instantaneous, the increased surface tension tends to restore the bubble to its original surface area. Hence, the bubbles can sustain short-time loads. The adsorbed film formed in water at concentrations ordinarily used in production of air-entrained concrete is highly permeable to air (11); hence, in an air-water system, bubbles dissolve at rates related to the excess of pressure to which the air is subjected. At diameters less than 50μ, the rate of dissolution is very rapid. In solutions containing a high concentration of calcium ion, many anionic surfactants will precipitate as calcium salts. Such salts precipitated in the adsorbed film further stabilize bubbles and, if present in sufficient concentration, may prevent the complete dissolution of the bubble.

Although the principles stated above are universally accepted for water-air systems, their application to air-entrained concrete has been questioned on the basis that distances between bubbles in air entrained concrete are too great and solubility of air in water is too low to allow transmission of appreciable amounts of air between bubbles. Bruere (15) concluded that cement pastes mixed at a water-cement ratio of 0.45, using a high-speed (1000 rpm) electric mixer, showed no evidence of rearrangement of bubbles of air after cessation of mixing. The void system was compared among pastes with normal stiffening time, pastes caused to stiffen in about three minutes by addition of ammonium carbonate, and pastes caused to remain fluid for four hours by addition of citric acid. Similar pastes prepared in an atmosphere of nitrous oxide contained a coarser void system than that produced

by air entrainment, but the specific surface did not vary significantly with two hour variation in the period during which the pastes remained fluid. Bruere concluded that interchange of nitrous oxide occurred among bubbles of nitrous oxide during mixing but not following fabrication of specimens. He concluded also that the differing results obtained with nitrous oxide and air relate to the higher solubility of nitrous oxide in water.

The latter conclusion is not justified inasmuch as the transmission of gas between bubbles is controlled by the rate at which the gas molecules diffuse through the aqueous solution and the surface tension relationship characteristic of the two gas-liquid systems, rather than by the solubility of the gases in water. In both instances, the aqueous phases in the cement pastes prepared by Bruere were saturated for nitrous oxide or for air, respectively; hence, rearrangement of bubble sizes is controlled by net transfer of gas, rather than by net uptake of gas by the solution.

Several factors distinguish cement pastes from concrete. Most important are the relatively low water-cement ratio (0.45) used by Bruere, the mixing procedure, and the lack of aggregate to entrap bubbles large enough to escape from cement pastes. The relationship establishing the rate of interchange of air is (11):

$$\frac{dB}{dt} \alpha \frac{aD\gamma}{T}\left[\frac{1}{d_1} - \frac{1}{d_2}\right] \qquad (1)$$

where d_1 and d_2 are respective diameters of a small bubble losing air and a large bubble gaining air, B = mass of air transported, a = area of the surface of the small bubble, D = a diffusion coefficient, γ = surface tension at the gas-solution interface, and T = average distance between the surface of the bubbles.

Hence, significant transfer of air requires juxtaposition of small bubbles possessing high internal pressure and large bubbles, such as those greater than 100μ in diameter, in which excess pressure is negligible. Values of α observed by Bruere in rapidly stirred pastes are 1900 to 2500 in.^{2}/in.^{3}, magnitudes that are not observed in normally compacted concrete and that show the virtual absence of large bubbles that could effectively produce high values for the factor $\left[\frac{1}{d_1} - \frac{1}{d_2}\right]$.

On the contrary, α in neat cement pastes mixed in a drumtype concrete mixer at water-cement ratio of 0.30 to 0.60 was 570 to 1330 in.^{2}/in.^{3} and spacing factor ($\bar{L}$) (16, 17) was 0.0127 to 0.0063 in., values that are common in concrete of that water-cement ratio (11). Air content determined microscopically was always higher than that indicated by pressure meter to be in the fluid cement paste and the difference in these values increased as the water-cement ratio increased. These relationships indicate significant interchange of air between bubbles following casting of the specimens, since transmission of air from a small bubble of high internal pressure to a large bubble of lower internal pressure causes an increase in air-void volume. Any change of level of the top of the fresh specimen before hardening might be partially or wholly offset by bleeding and settlement. In fact, such increase of air-void volume may be a mechanism by which air entrainment decreases bleeding and settlement of concrete.

To examine these concepts on bubble rearrangement, two series of three air-entrained concrete mixtures were prepared using Type I portland cement, crushed dolomite coarse aggregate of nominal 1-inch maximum size, and neutralized Vinsol resin as an air-entraining admixture to entrain 5–6 per cent of air as determined by pressure meter on the fresh concrete (Table 1). Water-cement ratio was 0.41—0.49, 0.61—0.67, and 0.81—0.87, respectively. Each series included four mixtures as follows: Concrete with no other admixture, concrete with calcium chloride added at the rate of two per cent by weight of the cement, and two mixtures containing mucic acid to achieve retardation of setting as determined by bond pin pull-out procedure (18). In the intermediate series, the desired retardation was not achieved. In two of the series, extended retardation was achieved at the higher rate of use of the mucic acid, but the concrete was hard at 24 hr. and developed strength normally thereafter.

Parameters of the air-void system were determined by the modified point-count procedure (17) on small slabs sawed from 6-inch cube specimens (Table 1.). As has been established previously (8) α decreases markedly as water-cement ratio increases (Fig. 1.). So strong is this relationship that other factors influencing α can be discerned only at relatively constant water-cement ratio.

The series prepared at the lowest water-cement ratio shows a relationship of α and rate of hardening that is consistent with qualitative predictions of the air-diffusion concept. α for the accelerated concrete was 930 in.^{2}/in.^{3}, whereas that of the reference mixture was 851 in.^{2}/in.^{3}, in contrast to a value of 690 in.^{2}/in.^{3} for the two retarded mixtures. Conversely, the other two series show essentially constant values of α regardless of time of setting,[3)] the values being 580 to 625 in.^{2}/in.^{3} for the intermediate series and 373 to 444 in.^{2}/in.^{3} for the series of highest water-

Table 1. *Relation of time of setting of concrete to specific surface of the air-void system*

Series and mixtures		AEA,[1] ml per 100 lb cement	Chemical admixtures, per cent by wt. of cement		Water-cement ratio by weight	Slump (in.)	Air content[2] (%)	Time of setting[3] (hr.)	Slump after 45 min.[4] (in.)	Specific surface[5] (in.$^{-1}$)
			$CaCl_2$	Mucic acid						
I	A	56.9	2.0	—	0.49	5–1/4	5.0	1–1/2	1/4	930
	B	56.9	—	—	0.47	5	4.6	5–3/4	2–1/4	850
	C	46.3	—	0.053	0.42	5	5.8	7	2–3/4	690
	D	42.5	—	0.106	0.41	6	6.0	—[6]	1	690
II	A	41.5	2.0	—	0.65	4	5.4	3–1/2	3/4	625
	B	47.3	—	—	0.67	5–1/2	6.2	8	3–1/2	580
	C	41.5	—	0.027	0.63	5–1/4	6.6	7–1/2	3–1/4	590
	D	35.7	—	0.053	0.61	5–1/2	6.4	8–1/2	3	615
III	A	42.5	2.0	—	0.85	5–1/4	6.4	4–1/2	1–1/2	370
	B	34.0	—	—	0.87	6	4.2	8	1–3/4	645
	C	25.5	—	0.053	0.85	6	5.2	8–1/2	2	395
	D	25.5	—	0.106	0.81	6	5.0	—[6]	1–1/4	445

[1] 12 per cent neutralized Vinsol resin solution.
[2] Determined by pressure meter (ASTM C 231) (19)
[3] Time following mixing to attain bond pin pull of 5 psi.
[4] Slump cone specimen cast immediately following mixing; cone lifted after 45 min.
[5] Modified point-count procedure (ASTM C 457) (17)
[6] Excessively retarded, but hard at 24 hr.

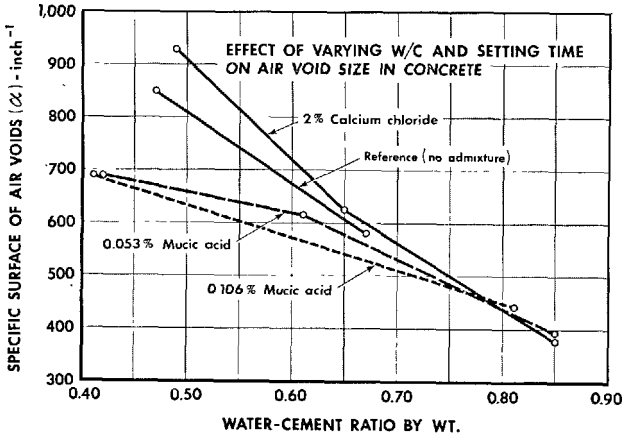

Fig. 1. *Effect of varying w/c and setting time on air void size in concrete.*

Table 2. *Effect of vibration time and type of agent on the air-void system of concrete*[1] *(Data from Zipparro (21))*

Type of agent	Time of vibration (sec.)	Air content (%)[3]	Void parameters determined by microscopical linear traverse procedure[2]		
			Air content (%)	Specific surface (in.$^{-1}$)	Spacing factor, (in.)
Saponin	0	6.07	6.09	994	0.0047
	60	6.07	4.89	1004	0.0051
	180	6.07	4.14	863	0.0064
Nonionic	0	5.67	6.49	480	0.0094
	60	5.67	5.03	467	0.0108
	180	5.67	4.23	429	0.0127
Cetyl trimethyl ammonium bromide	0	5.87	7.08	797	0.0054
	60	5.87	5.44	662	0.0073
	180	5.87	5.05	570	0.0088
Na dodecyl sulfate	0	6.07	6.29	772	0.0059
	60	6.07	4.69	793	0.0066
	180	6.07	4.26	841	0.0065

[1] 3/4-in. nominal maximum size sand and gravel aggregate; water-cement ratio = 0.49.
[2] ASTM Designation: C 457 (17)
[3] Determined gravimetrically on the fresh concrete compacted by rodding.

cement ratio. These relationships appear to relate to the magnitude of $\frac{dB}{dt}$ in equation 1, particularly as it is influenced by the pressure gradient, namely, the factor $\left(\frac{1}{d_1} - \frac{1}{d_2}\right)$. This effect is most notable for the third series for which very low values of α prevail, indicating values of bubble size in which excess pressure is virtually nil. An α of 400 in.^{2}/in.^{3} corresponds to an average bubble diameter of about 300μ. In void systems of this specific surface diffusion of gas is very slow even in gas-water systems because of the limited pressure gradient. In these concrete mixtures, the stable end value of α appears to be about 600 in.^{2}/in.^{3} at a water-cement ratio of about 0.65 and about 400 in.^{2}/in.^{3} at a water-cement ratio about 0.85.

Tests along similar lines were conducted by O'Neill (20) and by Zipparro (21). The air-entraining admixtures used by Zipparro were sodium dodecyl sulfate (anionic), cetyl trimethyl ammonium bromide (cationic), and a polyethyleneoxy derivative (nonionic); supplementary tests were performed on concrete containing purified saponin, Vinsol NVX, and Darex AEA. Some of Zipparro's data are shown in Tables 2 and 3.

The specific surface (α) of the air voids in concrete

[3] *Data for the reference mixture in the high water-cement ratio series (Mix III B) are not considered (and are not include in Fig. 1.) since the desired air content was not achieved and α is anomalously high for the indicated water-cement ratio.

Table 3. *Effect of time of initial set and type of agent on the void system of concrete*[1] *(Data from Zipparro (21))*

Air-entraining admixture	Time of initial set, (hr.)[2]	Air content (%)[3]	Void parameters determined by microscopical linear traverse procedure[4]: Air content (%)	Specific surface (in.$^{-1}$)	Spacing factor (in.)
Vinsol NVX	4	5.87	6.41	1013	0.0045
	15	6.07	7.48	663	0.0061
Darex AEA	4	5.67	6.63	866	0.0051
	15	6.48	6.79	579	0.0076
Saponin	4	6.48	5.90	1171	0.0040
	15	6.48	5.27	1229	0.0040

[1] 3/4-in. nominal maximum size sand and gravel aggregate; water-cement ratio = 0.49 by weight; retardation achieved by use of citric acid as an admixture.
[2] ASTM C 403. (19)
[3] By gravimetric method on the fresh concrete.
[4] ASTM C 457.

containing the two non-ionic or the cationic agents decreases immediately with vibration or after initial vibration but for the concrete containing the anionic agent increases consistently with vibration. Whether these effects are characteristic of these classes of admixtures cannot be stated on the basis of the available data. Increasing α or decreasing void size is the trend that would be expected from prior work on anionic agents (23). The contrary change observed in the mixtures containing the non-ionic or the cationic agent can be explained only by coalescence of bubbles (an unlikely possibility) or differential dissolution of small bubbles and passage of the air into larger bubbles.

Table 3 shows the effect of retardation of setting upon α, namely, an increase in average void size.

Table 4. *Calculated rate of air diffusion in selected concrete mixtures*[1] *(Data from O'Neill (20))*

Item	Concrete mixture 1	2	3	4
Water-cement ratio by wt.	0.49	0.75	0.49	0.49
Type of agent	Vinsol NVX	Vinsol NVX	Vinsol NVX	Dodecyl Na Sulfonate
Concentration of agent, per cent by wt. of cement	0.0154	0.0152	0.0302	0.0053
Air content, per cent	7.18	10.22	10.71	9.39
Specific surface, in.$^{-1}$	823	698	966	1046
Spacing factor, in.	0.0055	0.0037	0.0031	0.0032
Surface tension of filtrate, dynes/cm.	69.57	65.54	69.57	71.37
Average diameter of voids losing air, microns	70	58	63	64
Average diameter of voids gaining air, microns	220	232	255	255
Relative rate of air transfer, gm/sec $\times 10^{-15}$	55	32	97	149

[1] 3/4-in. nominal size sand and gravel aggregate

Table 5. *Effect of time of setting on air-void parameters of concrete*[1] *(Data from O'Neill (20))*

Admixture	Water-cement ratio by wt.	Accelerated, normal retarded[2]	Void parameters determined by linear traverse procedure[3]: Air content (%)	Specific surface (in.$^{-1}$)	Spacing factor (in.)
Vinsol NVX	0.49	Accelerated	8.76	738	.0050
		Normal	7.18	823	.0055
		Retarded	9.46	633	.0055
Vinsol NVX	0.75	Normal	10.22	698	.0037
		Retarded	12.35	567	.0037
Triton X-100	0.49	Normal	10.71	966	.0031
		Retarded	12.51	608	.0042
Triton X-100	0.49	Normal	8.27	577	.0068
		Retarded	8.19	624	.0063
Dodecyl Na Sulfate	0.49	Normal	9.39	1046	.0033
		Retarded	9.33	669	'0052

[1] 3/4-in. nominal maximum size sand and gravel aggregate.
[2] Acceleration achieved by use of ammonium carbonate at the rate of 0.60 per cent; retardation obtained by use of citric acid at the rate of 0.275 per cent (w/c = 0.49) or 0.395 per cent (w/c = 0.75). Time of initial setting 4 hr. without set-controlling admixture and 15 hr. with the retarder (ASTM C 403) (19); setting time of accelerated mixture was not reported.
[3] ASTM C 457. (17)

This effect is not observed with use of saponin, possibly because of the extraordinarily thick adsorbed film at the air-water interface (6).

O'Neill (20) compared air-void parameters among concrete mixtures in which varying time of setting was achieved by use of ammonium carbonates as an accelerator or citric acid as a retarding admixture. He reports that air content determined gravimetrically on the fresh concrete was consistently lower than that determined microscopically. He concludes that this effect relates to diffusion of air from small bubbles to larger bubbles before setting of the cement paste matrix.

Using the diffusion rate relationship (equation 1) and surface tension values determined on filtrates extracted from the fresh concrete mixtures, O'Neill gives estimates relative to rates of diffusion of air for four of his mixtures (Table 4), but the results cannot be expressed as weight or volume of air involved in the diffusion process for any given quantity of concrete. The parameters of the air-void systems in the hardened concretes are shown in Table 5. The effect of type of agent upon chord size distribution is shown in Fig. 2 and the effect of retardation or acceleration is shown in Fig. 3 for representative mixtures.

The data are consistent with the concept that diffusion air from small bubbles to large can effect a significant change in the parameters of the air-void system. Apparently, α about 600 in.^{2}/in.^{3} at a water-cement ratio of 0.49 is a stable end value. In other words, interchange of air apparently occurs at an insignificant rate if the average void size is larger than about 250 μ at this water-cement ratio. O'Neill found (Table 4) that the average diameter of air bubbles gaining air was 220 to 254 μ. Hence, if the average size of all the voids is in this range, further transfer of air is extremely slow.

The values found by O'Neill for the diameter of bubbles losing air (58 to 70 μ), corresponding to α of 2630 to 2180 in.^{2}/in.^{3}, may be compared with α found by Bruere (15) for rapidly stirred cement pastes in which no diffusion of air was indicated. His values were 1500 to 2500 in.^{2}/in.^{3} at water-cement ratio of 0.45. This comparison supports the conclusion that the range of void sizes in those cement pastes was insufficient to permit measurable transfer of air under the conditions of testing. A conclusion that diffusion of air between bubbles of various sizes can occur in concrete under ordinary conditions is consistent also with some of the findings of Larson, Mangusi and Radomski (23), who observed decrease in specific surface of the voids with retardation of setting in two of three series of tests. The stable end value of α achieved after a 35-hr delay in setting was 641 in.^{2}/in.^{3} at a water-cement ratio of 0.397.

The extent to which α at cessation of mixing is controlled by water-cement ratio in contrast to interchange of air among the air bubbles is undecided. Moreover, any quantitative evaluation of these factors presents a difficult experiment inasmuch as they are not independent. High water-cement ratio and water content of concrete contribute to reduction of α because shearing action during mixing is less and they likewise facilitate diffusion of air through the matrix. These factors are considered in detail by Powers (24).

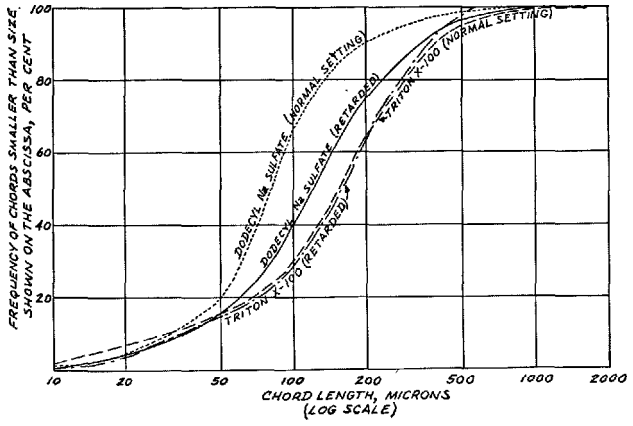

Fig. 2. *Effect of setting time of concrete on distribution of chord lengths of air voids determined by microscopical linear traverse. Dodecyl Na sulfonate and Triton X-100 used as the air-entraining admixtures. After O'Neill (20).*

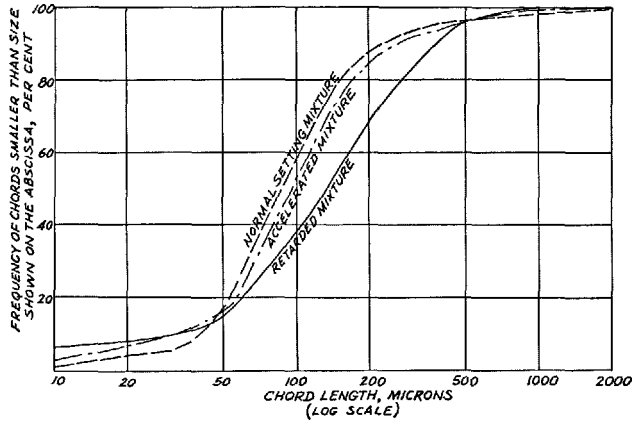

Fig. 3. *Effect of setting time of concrete on distribution of chord lengths of air voids determined by microscopical linear traverse. Neutralized Vinsol resin used as the air-entraining admixture. After O'Neill (20).*

Adhesion of Bubbles to Cement and Aggregate

The three classes of air-entraining agents cause generation of bubbles having differing ionic charge relationships: anionic surface-active agents produce bubbles that are negatively charged; cationic agents cause bubbles to be positively charged; and nonionic agents do not induce an appreciable charge on the bubble. Development of an ionic charge is considered to be an important factor promoting resistance of bubbles to coalescence (14).

Moreover, various types of surface-active agents respond differently to surfaces of cement granules or particles of aggregate that carry ionic charges. Anionic surface-active agents are positively adsorbed at the surface of particles of cement (11, 25, 26). Those including a large hydrophobic anion free from closely spaced polar groups are bound to the surfaces, probably through calcium ions that in turn are held ionically in the silicate or aluminate structure of the cementitious compounds. As a result, the surface is rendered hydrophobic and adherence of air bubbles is facilitated. Mielenz, Wolkodoff, Backstrom and Flack (11) reported contact angles of 46°00′ and 81°30′ for bubbles formed in aqueous slurries of portland cement in the presence of either of two common anionic air-entraining agents of this type.

Surfaces of aggregate particles may carry either net positive or negative charge in aqueous suspensions, depending upon the composition and molecular structure of the constituent minerals, the pH of the aqueous phase, and any contamination of the surfaces, but a net negative charge is typical of quartz and common rock-forming silicates (9). Bruere (6) has shown that finely ground quartz does not adsorb sodium dodecyl sulfate or sodium abietate from water solution, but adsorption was observed in the presence of calcium hydroxide and the quartz adhered to entrained air bubbles. This effect is thought to be the result of adsorption of calcium ions onto negatively charged locations on the mineral surfaces, followed by interaction of the calcium ions and the organic anions.

Unlike the anionic organic ions just discussed, in which closely-spaced polar groups are absent, the anion of some anionic surface-active agents includes or is composed of polar groups that can interact with charged sites in surfaces of cement granules or constituents of aggregates (26). In fact, the adsorption or chemisorption so effected may dominate, leaving a net residual negative charge at the surface of the solid particles (27). The like charge causes a decrease in interparticle attraction and possibly a net repulsion, which in turn causes a decrease in degree of flocculation or dispersion of the finely divided solids. Air bubbles in such a slurry do not adhere to particles of cement because the adsorbed organic anion is likewise negatively charged. Also, with sufficient concentration of polar groups within the anion, the surfaces of the affected solids are hydrophilic and so are not conducive to preferential displacement of water by air. The outstanding surface-active agents in this class from the standpoint of wide use are salts of sulfonated lignin.

Bruere (6) demonstrated that the cation from cationic surface-active agents likewise is adsorbed by portland cement in aqueous mixtures, presumably at negatively charged sites in the surface. Tetradecyl ammonium bromide and some alkylamine hydrochlorides effect flotation of finely ground quartz in aqueous slurries, freshly ground quartz being negatively charged in neutral or alkaline media (9). When Bruere used tetradecyl ammonium bromide at rates less than 0.05 per cent, the surfaces of cement were rendered hydrophobic. At higher concentration, a second layer of cations apparently is adsorbed, with the polar end oriented toward the aqueous phase. The cement granules then are hydrophilic and adhesion of bubbles decreases as the concentration of the agent is increased.

Nonionic surfactants may or may not be adsorbed on particles of cement or aggregate. Bruere (6) found that saponin is adsorbed by cement in aqueous mixtures whereas a condensation product of ethylene oxide with a nonionic alkyl phenol apparently was not adsorbed appreciably. The cement granules remained hydrophilic and no bubble adherence occurred.

Adsorption and bubble adherence modify viscosity and bleeding of cement pastes. Anionic surface-active agents that make cement hydrophobic increase viscosity of the paste even in the absence of air entrainment apparently because of an increase in interparticle attraction (6). This effect is more pronounced in the presence of air bubbles in part because of the linkage that is established between cement granules and air bubbles. The increase in viscosity is greater than is expected from the increase in surface area of the system resulting from the entrainment of air. A cationic air-entraining agent increased the paste viscosity to a maximum as its concentration increased, but at higher concentration the viscosity decreased. These effects apparently were caused by initial formation of a hydrophobic surface, followed by development of hydrophilic surfaces when a second layer formed. In the absence of air entrainment, both saponin and calcium lignosulfonate decreased paste viscosity

because of the development of hydrophilic surfaces and decrease of interparticle attraction; this effect was overcome by entrainment of air. The factors that contributed to increased paste viscosity likewise decreased bleeding of pastes.

Except for anionic air-entraining agents that render cement hydrophilic, most notably soluble salts of sulfonated lignin, which are usually used at rates of 0.10 to 0.50 per cent, air-entraining admixtures appear to effect insignificant change of hydration reactions because of the low rate at which they are used relative to the cement content. Kelly and Bryant (18) noted small differences in rate of hardening of concretes containing either of two anionic air-entraining agents. Kreijger (28) detected small changes in heat of hydration for both C_3S and C_3A in the presence of anionic agents. He observed no significant change in heat of hydration with use of nonionic surface-active agents.

Geometry of the Air-Void System

The bulk of air voids in air-entrained concrete mixed to a plastic consistency are spherical or nearly so, especially in sizes less than about 1000 μ, because the air bubbles were enclosed within the viscous matrix that was under hydrostatic head imposed by the superimposed concrete. In well proportioned concrete of plastic consistency, voids of irregular shape molded against particles of aggregate are infrequent.

Air voids are retained within unhardened concrete by viscosity of the cement paste matrix, adherence to granules of cement and, to some extent, to particles of aggregate, and mechanical entrapment. Comparing the air void system in concrete with that of cement paste at the same water-cement ratio and compacted similarly, Mielenz, Wolkodoff, Backstrom and Flack (11) concluded that over half of the air content of entrained air concrete may be retained by entrapment among the aggregate. For two anionic agents of good quality, the average void size in the hardened concrete and hardened cement paste was the same or nearly so, whereas for an anionic agent of intermediate quality, the average void size in the concrete was significantly greater than that found in the cement paste. Hence, for these agents, air entrainment depended to differing degree upon the entrapping effect of aggregate.

The average size of air voids is affected by other factors, notably the kind and concentration of surface-active agent, water-cement ratio, and the kind and amount of compaction (6, 11, 8, 22, 29). Increased roughness of surface of aggregate, increased temperature, and decreased slump are reported to decrease average void size (22). Bruere (30) showed that mixing time and speed are important factors; mixing time, type of cement, and presence of calcium chloride did not greatly modify void size in pastes. Grading of fine aggregate produced minor change of average air void size in concrete, although the effect in mortars undoubtedly is appreciable.

Bruere (29) studied the effect of combinations of surface-active agents upon air entrainment in rapidly stirred cement pastes. He concluded that particular combinations could be employed to produce bubble systems of especially high α under given conditions of mixing. However, the findings are not applicable directly to concrete mixtures because of the high proportion of air bubbles that are retained in concrete by entrapment among the aggregate.

Contrary effects can be produced by introduction of surface-active chemicals that decrease the stability of adsorbed films of air-entraining admixtures. Table 6 comprises data on three concrete mixtures containing an air-entraining portland cement (ASTM Type IA) (31). Addition of a water-reducing admixture based upon calcium lignosulfonate (0.266 per cent) and reduction of cement content increased air content of the fresh concrete as indicated by the pressure meter from 6.8 to 8.6 per cent and that of the hardened concrete as determined by the microscopical point-count procedure from 9.49 to 11.98 per cent. An aliphatic alcohol 1-decanol was added to an equivalent concrete mixture at the rate of 0.008 per cent, the air content being reduced to 6.4 per cent as determined by the pressure meter or 6.25 per cent as determined by the point-count procedure. α was decreased (average void size increased) and spacing factor ($\bar{L}$)

Table 6. *Effect of an aliphatic alcohol on air-void system of concrete*[1]

Item	Concrete mixtures[2]		
	1	2	3
Cement content, lb/yd[3]	520	441	448
Water content, lb/yd[3]	257	233	246
Water-cement ratio by wt.	0.49	0.53	0.55
Air content, per cent[3]	6.8	8.6	6.4
Slump, in.	4½	4½	4
28-day compressive strength, psi[4]	4000	3230	4480
Microscopically determined parameters of the air-void system[5]			
Air content, per cent	9.49	11.98	6.25
Specific surface, in.$^{-1}$	734	700	635
Spacing factor, in.	0.0048	0.0044	0.0065

[1] Type IA cement (ASTM C 175) (31); sand and gravel aggregate of 1-in. nominal maximum size.

[2] Mixture No. 1 contains no admixture; Mixture No. 2 contains a calcium lignosulfonate water-reducing admixture (0.266 per cent); Mixture No. 3 contains calcium lignosulfonate admixture (0.266 per cent) and 1-decanol (0.0008 per cent).

[3] ASTM C 231 (19)

[4] ASTM C 39 (19)

[5] Modified point-count procedure (ASTM C 457) (17)

increased, although not critically. A higher rate of use to further reduce the air content might increase $\bar{L}$ above the range that should correlate with satisfactory freezing and thawing resistance of concrete.

Data show that within narrow limits $\bar{L}$ is an inherent characteristic of a given air-entrained concrete mixture following completion of mixing (8, 22). Little change in the $\bar{L}$ is observed in concrete mixtures sampled before application of any compactive effort and after differing modes of compaction, even though the air content is decreased substantially. In concrete that was vibrated internally for 2 and 50 seconds, Backstrom, Burrows, Mielenz and Wolkodoff (8) found that air content was decreased from about 7 per cent to 6.60 and 1.20 per cent, respectively. The decrease was accomplished by reduction in the number of air voids in all sizes from 20 to 4000 μ; there was no evidence of disruption of large bubbles into smaller ones. Since bubbles whose diameter after 2 seconds of vibration is less than 80 microns are unlikely to escape from concrete, the data appear to show that the internal vibration promoted dissolution of the smallest bubbles.

Effect of Air Entrainment on Some Engineering Properties of Concrete

Air entrainment is employed for two main reasons in modern construction: (1) improved resistance of the concrete to freezing and thawing and (2) improved working qualities of the fresh concrete. Optimum use of air entrainment requires change in the proportioning of the mixture. Powers (24, 32) recently dealt with the factors influencing the proportioning of air-entrained concrete. Consequently, no detailed discussion of these matters is required here. Using data from actual concrete mixtures containing neutralized Vinsol resin, Powers (32) shows that the change in water content effected with change of air content at constant consistency and aggregate grading is a linear function of the cement content. At cement content less than about 835 lb per cubic yard, each one per cent of air replaces 20 to 25 per cent of that volume of water (about 3.4 to 4.2 lb), the remainder being compensated by a decrease in the aggregate content. Warris (33) found that air entrainment reduces water content of concrete at given consistency at an average rate of 0.3 times the increase of air content. The change decreases as cement content increases, becoming nil at 400 kg per cu. m. (674 lb per cu. yd.) or above.

Powers (32) contrasts such behavior in equivalent mixtures in which air entrainment is effected by use of calcium lignosulfonate, showing that the relative volume of water displaced at given consistency is increased 6 to 50 per cent over that effected by neutralized Vinsol resin. The net reduction in water requirement increased with increased cement content. Independent data obtained in a large series of concrete mixtures containing a Type I portland cement (about 440 lb per cu. yd.) and 1-inch nominal maximum size sand and gravel aggregate together with a calcium lignosulfonate water-reducing admixture (0.266 per cent) show a consistent reduction of water content with increasing air content, the typical value being about 8.3 lb per cubic yard for each one per cent of air entrained by any of a wide variety of air-entraining admixtures.

Powers (32) notes that the water-content *vs* air content relationship for the mixtures containing neutralized Vinsol resin is like that characterizing the mixture containing no air-entraining agent, whereas the locus representing concrete containing the calcium lignosulfonate is displaced from the position representing the mixture containing no surface-active agent. He concludes that the effect is caused by adsorption of lignosulfonate and change of interparticle attraction. The findings do not deny adsorption of neutralized Vinsol resin; rather, the adsorption does not modify the water-cement-air content relationship to appreciable degree.

The kind and extent of the changes produced in concrete mixtures by air entrainment depend upon many factors. To evaluate some of these effects in a particular combination of cement and aggregates, three series of concrete mixtures were prepared, as follows:

Series I	Constant slump (3 to 4 in.) and air content (5.5 ± 0.5 per cent by pressure meter) with varying cement content and water-cement ratio (nominally 0.44 to 0.62).
Series II	Nominally constant cement content (about 525 lb per cu. yd.) and air content (5.5 ± 0.5 per cent by pressure meter) with varying slump (2 to 7 in.)
Series III	Constant proportion of air-entraining admixture and cement content (about 525 lb per cu. yd.) and varying slump (2 to 7 in.)

Each series comprised eight concrete mixtures:

Air-entraining admixture	Water-reducing admixture
1. Neutralized Vinsol resin*	None
2. Neutralized Vinsol resin*	Calcium lignosulfonate
3. Alkyl aryl sulfonate	Calcium lignosulfonate

*12 per cent solution

Each group of mixtures included two concretes containing neutralized Vinsol resin as the only admixture, three concretes containing neutralized Vinsol resin and the calcium lignosulfonate, and three concretes containing the alkyl aryl sulfonate and the calcium lignosulfonate (Table 7). All of the concrete mixtures contained a Type I portland cement from a single source, nominally 1-in. maximum size, crushed and graded dolomite coarse aggregate, and natural sand, all meeting applicable specifications of the American Sosiety for Testing and Materials. Specimens were prepared from each concrete mixture as follows:

Table 7. *Data on concrete mixtures relating water-cement ratio, water content, and air-void parameters*[1]

Series[2]	Mix[3]	Air-entraining admixture[4]		Cement content (lb/cu.yd.)	Water content (lb/cu.yd.)	Water-cement ratio by wt.	Slump (in.)	Air content,[5] (%)	28-day compressive strength (psi)[6]
		Agent	Amount						
I	A	VR	45 ml	596	269	0.45	3	5.4	5530
	B	VR	13 ml	524	234	0.45	4	5.8	5950
	C	AAS	.060 lb	528	236	0.45	3-1/2	5.0	6390
	D	VR	11 ml	434	234	0.54	3	5.8	4850
	E	AAS	.045 lb	442	237	0.54	4	5.5	4850
	F	VR	31 ml	428	266	0.62	4	5.6	4020
	G	VR	9 ml	377	236	0.63	3-1/2	5.2	3840
	H	AAS	.045 lb	378	237	0.63	3	5.0	3820
II	A	VR	45 ml	522	247	0.47	2	5.2	5700
	B	VR	12 ml	518	218	0.42	2	5.6	5980
	C	AAS	.211 lb	524	221	0.42	2	4.3	6650
	D	VR	10 ml	518	230	0.44	4-1/4	5.4	5600
	E	AAS	.045 lb	517	231	0.45	4-1/2	5.8	6120
	F	VR	30 ml	522	275	0.53	6-1/4	5.1	4830
	G	VR	9 ml	517	235	0.45	6-1/2	6.0	5250
	H	AAS	.038 lb	516	238	0.46	6-3/4	5.9	5230
III	A	VR	34 ml	533	238	0.45	1-3/4	4.0	6390
	B	VR	10 ml	533	225	0.42	1-1/2	3.2	6930
	C	AAS	.045 lb	533	221	0.41	2	3.5	6490
	D	VR	10 ml	516	233	0.45	4-3/4	5.4	5610
	E	AAS	.045 lb	517	230	0.45	4-3/4	5.4	5620
	F	VR	34 ml	509	271	0.53	6-1/2	5.8	4700
	G	VR	10 ml	510	242	0.47	6-3/4	5.6	5120
	H	AAS	.045 lb	510	235	0.46	6-3/4	6.0	5140

[1] 1-in. nominal maximum size crushed dolomite coarse aggregate, natural sand, and Type I portland cement.
[2] Series I: Nominally constant slump and air content; varying cement content and water-cement ratio.
Series II: Nominally constant cement content and air content but varying slump.
Series III: Constant proportion of air-entraining admixture; varying slump.
[3] Mixes A and F in all of the series include neutralized Vinsol resin (VR) as the only admixture (12 per cent aqueous solution).
Mixes B, D, and G include neutralized Vinsol resin (VR) (12 per cent solution) and calcium lignosulfonate (0.266 per cent).
Mixes C, E, and H include alkyl aryl sulfonate (AAS) and calcium lignosulfonate (0.266 per cent).
[4] per 100 lb of cement
[5] ASTM C 231 (19).
[6] ASTM C 39 (19).

Size	Number	Test
6- by 12-in. cylinder	3	28-day compressive strength (ASTM C 39) (19)
3- by 4- by 16-in. prism	3	Freezing and thawing resistance (ASTM C 290) (19)
4- by 6- by 6-in. prism	1	Microscopical determination of the air-void system (ASTM C 457) (19) (magnification 150 dia.)

Series I shows the effect of air entrainment when water-cement ratio and cement content vary over a wide range (Table 8). Durability factor (DF) and compressive strength decline as water-cement ratio is increased. For the concretes containing the calcium lignosulfonate, spacing factor ($\bar{L}$) decreased greatly as water-cement ratio increased from about 0.44 to about 0.53, this change being related mainly to a simultaneous increase in specific surface (α) of the voids. As the water-cement ratio increased to about 0.62, α decreased and $\bar{L}$ increased. However, these changes were not reflected in the DF. The effect of varying water-cement ratio upon the void system in the concrete containing neutralized Vinsol resin as the only admixture cannot be discussed as well because only two concretes were prepared in this series. However, the results demonstrate that $\bar{L}$ decreased slightly as water-cement ratio increased from about 0.44 to about 0.62, whereas DF decreased significantly.

No general correlation is indicated between $\bar{L}$ and

Table 8. *Air-void parameters and freezing and thawing durability factor for concrete relating water-cement ratio, water content, and air-void parameters*[1]

Series	Mix	Microscopically determined parameters[2] Air content (%)	Change of air content[4]	Specific surface (in.$^{-1}$)	Spacing factor (in.)	Durability factor[3]
I	A	5.03	−0.4	957	0.0050	49
	B	5.54	−0.3	543	0.0079	67
	C	4.96	−0.0	501	0.0091	66
	D	5.95	+0.2	694	0.0053	46
	E	5.48	−0.0	630	0.0065	49
	F	6.74	+1.1	760	0.0046	28
	G	6.44	+1.2	476	0.0068	25
	H	5.19	+0.2	512	0.0080	31
II	A	5.06	−0.1	1047	0.0044	46
	B	6.17	+0.6	839	0.0044	42[5]
	C	2.82	−1.5	539	0.0107	31
	D	6.43	+1.0	800	0.0045	42
	E	5.38	−0.4	658	0.0066	41[6]
	F	6.21	+1.1	860	0.0049	34[5]
	G	8.02	+2.0	772	0.0038	51
	H	6.95	+1.0	599	0.0057	45
III	A	3.95	0.0	778	0.0065	31
	B	3.83	+0.6	575	0.0088	52
	C	4.62	+1.1	543	0.0085	59
	D	6.33	+0.9	746	0.0050	51
	E	4.89	−0.5	680	0.0060	49
	F	6.64	+0.8	774	0.0050	34
	G	5.86	+0.3	668	0.0061	42
	H	6.16	+0.2	672	0.0057	33

[1] See Table 7 for mixture proportions, and 28-day compressive strength.
[2] Modified point-count procedure, ASTM C 457 (17)
[3] Rapid freezing-thawing in water, ASTM C 290(19); durability factor computed after 250 cycles; average of 3 specimens except as noted. The specimens in each series were tested simultaneously.
[4] Difference obtained by subtracting air content of fresh concrete determined by ASTM C 231 (19) from air content of hardened concrete determined microscopically.
[5] Average of two results; for Mix II-B one specimen having durability factor of 2 and for Mix II-F one specimen having durability factor of 6 were disregarded.
[6] One specimen only; two specimens broken in handling.

DF such as would be predicted from the theory covering the function of air voids during freezing of concrete (34). Rather, each combination of admixtures produces its own relationship between $\bar{L}$ and DF. Any value of DF correlates with values of $\bar{L}$ which are least for concrete containing neutralized Vinsol resin alone, maximum for concrete containing the alkyl aryl sulfonate and the calcium lignosulfonate, and intermediate for concrete containing neutralized Vinsol resin and the calcium lignosulfonate.

Another interesting phenomenon is the relationship of air content of the fresh concrete as determined by the pressure meter to that of the hardened concrete determined microscopically. For the concretes at a water-cement ratio close to 0.44, the hardened concrete contains less than 0.4 per cent less air than is indicated by the pressure meter test of the fresh concrete. At water-cement ratio of about 0.62, the hardened concrete contains 0.2 to 1.2 per cent more air than indicated by the presure meter in the fresh concrete. The relationship of these factors at water-cement ratio of 0.53 is intermediat .

In Series II, slump was fixed at about 2, $4\frac{1}{2}$, and $6\frac{1}{2}$ in., whereas the proportions of the air-entraining admixture were adjusted to produce air content of 5.5 ± 0.5 per cent while cement content was held nominally constant. The desired air content was not achieved for the concrete containing the alkyl aryl sulfonate with the calcium lignosulfonate when the slump was 2 in. Water-cement ratio ranged from 0.42 to 0.53.

In Series II, water-cement ratio and water content increased as the slump was increased from 2 to 6–3/4 in. Air content of the hardened concrete and the difference between the air content of the fresh concrete indicated by the pressure meter and that of the hardened concrete also increased (Fig. 4). The latter effect was more pronounced than in Series I. Again, the maximum divergence was found in the mixtures containing neutralized Vinsol resin. As slump increased, α decreased when neutralized Vinsol resin was used (with or without the calcium lignosulfonate) but increased slightly in the concrete containing the alkyl aryl sulfonate and the calcium lignosulfonate. Simultaneously, $\bar{L}$ for the concrete containing the calcium lignosulfonate decreased, whereas that for the concrete containing neutralized Vinsol resin as the only admixture increased slightly.

As slump increased, DF in each group of concretes changed, increasing when the concrete contained the calcium lignosulfonate and decreasing when neutralized Vinsol resin was the only admixture. Again, no general relationship was exhibited between $\bar{L}$ and DF (Fig. 5). Within each group of mixtures containing the same admixtures, a consistent correlation is indicated, DF increasing with decrease of $\bar{L}$. For the concrete containing the alkyl aryl sulfonate and the calcium lignosulfonate and gauged to a slump of 2 in., the air content was 4.3 per cent as determined by pressure meter in contrast to the specified range of 5.5 ± 0.5 per cent and the air content determined microscopically was only 2.82 per cent.

Series III simulates a condition in which water content and slump are increased without purposeful modification of cement content or rate of use of the air-entraining admixtures. The quantity of air-entraining admixture employed was that necessary to produce air content of 5.5 ± 0.5 per cent when slump was $4\frac{1}{2}$ in. Water content was increased 33 lb to increase the slump of the concrete containing neutralized Vinsol resin as the only admixture from 1–3/4 to $6\frac{1}{2}$ in., whereas the increase required for similar change of slump when the calcium lignosulfonate was present was only 14 to 17 lb per cubic yard.

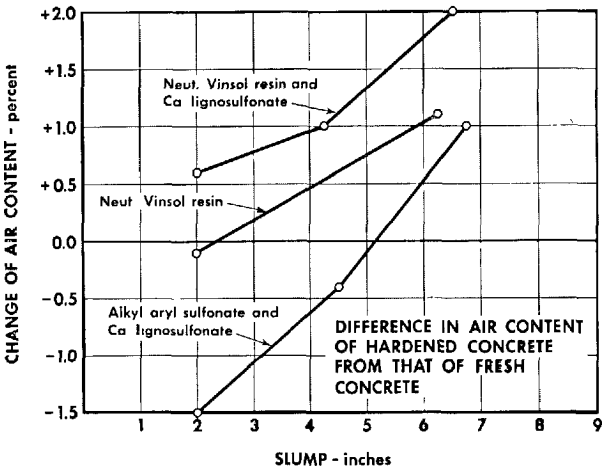

Fig. 4. *Difference in air content of hardened concrete from that of fresh concrete.*

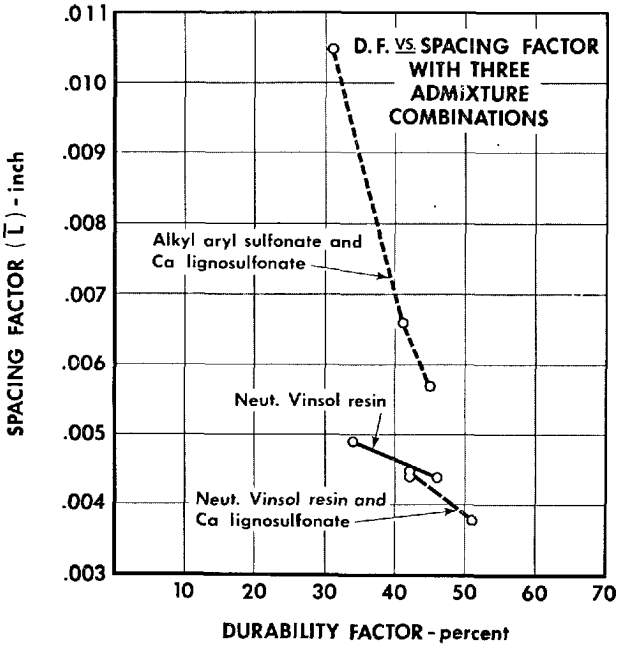

Fig. 5. *D.F. vs. spacing factor with three admixture combinations.*

As the water content and slump were increased, air content indicated by the pressure meter increased. However, no consistent increase occurred in the difference between the indicated air content of the fresh concrete and that determined microscopically on the hardened concrete. With increase in slump under the stipulated conditions, $\bar{L}$ tended to decrease, in part because of the increase in air content. α tended to increase when the calcium lignosulfonate was present, whereas no change was observed when neutralized Vinsol resin was used as the only admixture. Compressive strength decreased considerably as the slump was increased.

DF remained essentially constant over the range of slump when neutralized Vinsol resin was used as the air-entraining admixture, regardless of the presence or absence of calcium lignosulfonate. Conversely, DF of the concrete containing the alkyl aryl sulfonate and the calcium lignosulfonate decreased linearly as slump was increased, although DF at the highest slump was essentially equal to that of the concrete containing neutralized Vinsol resin as the only admixture. Again, individual relationships were established between $\bar{L}$ and DF for each admixture system.

Water-Reducing and Set-Controlling Admixtures for Concrete

Hansen (35) concluded that organic water-reducing retarders include the configuration H–C–OH and that their effect results in large part from adsorption of the molecule or large anions on exposed surfaces of cement granules. He suggested that the anions may be adsorbed by Ca^{++} ions in the solid surfaces, and that large anions and molecules of appropriate structure and composition also may be adsorbed by hydrogen bonding through OH groups to O^- ions in the solid surfaces (36). He proposes that salts analogous with the $C_3A \cdot 3C\bar{S} \cdot 32H$ and $C_3A \cdot C\bar{S} \cdot 12H$ can form with substitution in their crystal structure of organic molecules, such as salts of hydroxy acids and lignosulfonates (36, 37). Although such action probably occurs for retarding compounds of smaller molecular size, such isostructural analogues of the sulfoaluminates cannot develop by intracrystalline accommodation of lignosulfonates, whose molecular weights range from about 2,000 to 100,000 (38).

According to Steinour (39, 40), the effective molecular configuration is a stable OH group that is not subject to ionization or ionizes only slightly, and he found a relation between degree of retardation and the number of un-ionized or undissociated OH groups per molecule of the admixture. He concluded that their action in retarding hydration of cement is mainly or entirely adsorption by hydrogen bonding on both the calcium silicates and tricalcium aluminate. In a study of cement pastes containing each of 13 calcium salts of simple organic acids, Danielsson (41) concluded that retardation of setting is the result of adsorption of molecules on surfaces of the cement and that the

retarding capacity increases exponentially with the number of groups capable of forming hydrogen bonds with surfaces of the cement grains.

According to Taplin (42), the group HO–C–C = O is an important compound of some organic substances that retard hydration of portland cement. He concluded that for an organic substance to retard portland cement hydration and setting the molecule must contain at least two oxygen atoms each bound to a single but different carbon atom in such a way that the oxygen atoms can approach each other. Conversely, a few organic substances, such as oxalic acid, were found not to retard hydration of portland cement even though the specified atomic grouping is present. Effectiveness of the individual components varied widely with location and arrangement of the OH groups in the molecule. Kennerley, Williams and St. John (43) concluded that retardation of setting appears to be associated with presence of OH groups, particularly if two carboxyl groups are present also. They note that when the carboxyl groups of tartaric acid are changed to alcohol groups, an accelerating action is produced. They suggest that at least four carbon atoms are necessary in order that significant retardation will be effected.

A widely used classification of water-reducing and set-controlling admixtures for concrete comprises four groups (44) based upon hydroxylated, organic substances.

1. Lignosulfonic acid and its salts
2. Modifications and derivatives of lignosulfonic acid and its salts
3. Hydroxy acids and their salts
4. Modification and derivatives of hydroxy acids and their salts

To these classes may be added:

5. Carbohydrates and polyols
6. Modifications and derivatives of carbohydrates and polyols

Classes 1 and 2 constitute the largest volume of use in construction to this time. The products are based mainly upon calcium or sodium, less commonly, magnesium or ammonium, salts of sulfonated lignin resulting from the sulfite process of paper manufacturing. Calcium lignosulfonates are the most common. The lignosulfonate usually will have been processed by any of several methods to partially or completely remove wood sugars that are a constituent of raw sulfite liquor. However, the lignosulfonates used as admixtures for concrete are a complex mixture of many substances resulting from the degradation of the wood. Kennerley, Williams, and St. John (43) concluded that a large part of the set-retarding action of lignosulfonates is due to the presence of wood sugars, and they found that unrefined lignosulfonates often produce excessive air content.

Products of Class 3 include organic acids and their salts, such as sodium, calcium, potassium, or triethanolamine salts of gluconic acid. Hydroxyacetic acid, hydroxylated adipic acid, tartaric acid, citric acid, mucic acid, and the like, together with their water-soluble salts, are included in this class.

Class 5 includes such substances as simple sugars, disaccharides, and water-soluble polysaccharides as well as some sugar derivatives, such as sorbitol.

Classes 2, 4, and 6 are modified by processing or are blended with organic or inorganic accelerators, catalysts, air-entraining agents, or, rarely, air-detraining agents. Accelerators or catalysts can completely overcome the retarding effect of the main constituent so that the admixture performs in concrete as a water-reducing agent or water-reducing accelerator (Types A and E, respectively, of ASTM Designation: C 494) (19).

This classification does not include materials that have been used to limited extent in concrete as water-reducing and set-controlling admixtures for concrete, such as hydroxyethyl cellulose and related polymers and various water-soluble silicones, such as salts of methyl- and ethyl-siliconates. These materials are not discussed because of the meager information that is available. Some data on silicone admixtures are given in the recent International Symposium on Admixtures for Mortar and Concrete (45–48), and elsewhere (49).

Mechanism in Cement Hydration

The mechanism through which water-reducing, set-controlling admixtures modify the hydration, setting, and hardening process in hydraulic cement mixtures is believed most widely to be adsorption or chemisorption of the organic molecule at the solid-water interface on particles of cement and products of hydration (35, 36, 39). This action is accompanied by others if the admixture includes supplementary materials and, moreover, the modification of the course of cement hydration effected by the formation of the adsorbed film at the solid-liquid interface will itself generate secondary changes in the hydration and setting process. Suzuki and Nishi (50) concluded that organic substances that retard hydration of portland cement do so by reaction with the cement to form insoluble compounds that precipitate in the cement paste and on surfaces of the cement granules. Differences in effects of various compounds were thought to arise in differing stability, solubility, and mor-

phology of the precipitated substances. Those substances whose calcium salts are only slightly soluble delay or stop hydration and retard setting of concrete as a result of formation of an insoluble layer on the cement grains. Organic substances whose calcium salts are highly soluble do not cause substantial change in hydration and setting of portland cement. They recognize the possibility of adsorption or chemisorption of the organic compound or ions on surfaces of cement or hydration products. In reality, the processes of adsorption and precipitation are hardly separable if the organic phase interacts with intact surfaces of the solid phases.

The effects that are to be expected from adsorption or chemisorption of hydroxylated organic compounds or precipitation of insoluble organic compounds on cement granules include:

1. Change of rate of hydration of constituents of the cement.
2. Change of rate of interaction of sulfate with constituents of the cement.
3. Change of concentration of substances in the mixing water, including change of pH value.
4. Change of rate of formation of hydration products.
5. Change of particle size and crystal habit of hydration products.
6. Formation of products of reaction of the admixture and the cement or the hydration products.

The hydroxylated admixtures are adsorbed to differing degree by the constituents of portland cement. For example, Blank, Rossington and Weinland (51) show maximum uptake of calcium lignosulfonate from water solution by C_3A and much smaller uptake by C_4AF, C_3S, and C_2S, the amounts decreasing in that order. Seligmann and Greening (52) found that 99 per cent of sucrose was removed from 5 cc. of one per cent aqueous solution in seven minutes by one gram of C_3A. Similar conclusions and data are given by other workers (27, 51, 53, 54).

The results obtained in water differ from those obtained in other media, such as alcohol, wherein no hydration of the cement has occurred. The preferential order of uptake of salicylic acid in ethyl alcohol solution is

$$C_3S > C_2S > \text{Type I portland cement} > C_3A = C_4AF = 0 \quad (51).$$

Addition of small amounts of water to the alcohol solution greatly increases the uptake in the presence of the aluminates, showing that the adsorptive power of the aluminates in water is caused primarily by the hydration products. The amount of salicylic acid taken up in the presence of C_4AF increases as the proportion of water increases, presumably because more hydration product is formed in given time. With C_3A, C_2S and C_3S, maximum uptake of salicylic acid occurs with minor proportions of water in the alcohol solution, from which Blank, Rossington and Weinland (51) concluded that water and salicylic acid compete for adsorption on calcium aluminate hydration products, C_3S, and C_2S. They state: "Certain modified properties of cement due to admixture addition are a result of preferential adsorption of the admixture by the hydration products of tricalcium aluminate and tetra-calcium aluminoferrite, thereby rendering them inactive and allowing the main cementing compounds (C_3S and C_2S) to control the reaction."

Manabe and Kawada (55) found that the amount of lignosulfonate removed from solution in aqueous suspensions of portland cement increased as the concentration of the lignosulfonate increased. Equilibrium was established rapidly when the lignosulfonate was used in amounts less than 0.5 per cent, but the uptake continued over the course of 30 minutes at high concentrations. Multimolecular adsorption occurred, the amount of calcium lignosulfonate adsorbed being 350, 470, 510, and 540 mg per 100 g. of cement at water-cement ratio of 0.4, 0.5, 0.6, 0.7, and 1.5, respectively. The amount easily adsorbed as a monolayer is provided by use of calcium lignosulfonate at the rate of 0.3 per cent; at higher concentrations the monolayer is completed and multimolecular layer adsorption occurs with still higher concentrations of the lignosulfonate.

Crepaz and Raccanelli (54) and Russian workers (53, 56–58) also emphasize the uptake of hydroxylated admixtures by hydration products. Any such action must be an important factor in cement hydration since it will slow down crystallization, alter the extent of supersaturation of the solution phase, and change the form of the hydration products. Crepaz and Semenza (59) and Young (60) show by electron microscopy change of habit of hydration products of C_3A in the presence of a lignosulfonate and the former show that the calcium-aluminoferrite phase in the presence of the admixture characteristically produces small agglomerations of crystals. Earlier work in this field is reviewed by Young. Crepaz and Raccanelli (54) postulate that these changes result from preferential adsorption of the lignosulfonate on certain crystallographic planes of the crystals.

Feldman and Ramachandran (61) suggest that the rate of hydration of C_3A is decreased by adsorption

of SO_4^{-2} ions on exposed surfaces of the crystal, and further that adsorption of SO_4^{-2} ions on hexagonal hydroaluminates inhibits their conversion to cubic hexahydrate. Both of these mechanisms will retard the hydration of C_3A. They correlate these concepts with earlier conclusions of Russian workers (62–64), who studied the effect of surface-active agents on hydration of C_3A, and the observation by Sersale (65) that, at room temperature, a small amount of calcium lignosulfonate retards the conversion of the hexagonal hydro-aluminates to C_3AH_6.

Roberts (66) found that sucrose (0.1 per cent) decreased the amount of calcium and alkali hydroxide released in cement pastes initially, but a slight increase was observed at one day and no change thereafter. A slight increase in concentration of Al_2O_3 and Fe_2O_3 was detected at six hours (with one per cent addition of sucrose appreciable quantities of these substances were found in solution), suggesting formation of a soluble complex with the sucrose. Similar results have been reported for saccharose (50). The concentrations of calcium and sulfate were increased significantly to age 7 days, except that at 7 days the concentration of calcium was slightly decreased relative to the filtrate from the reference paste.

Seligmann and Greening (52) observed great acceleration of the reaction of gypsum with C_3A in an aqueous mixture with sucrose, causing formation of large amounts of the high-sulfate calcium sulfoaluminate. They concluded that solid C_3A sorbs sucrose to produce a surface that does not permit formation of an impermeable layer of the sulfoaluminate. Thus, the usual immediate retarding effect of gypsum on the reaction of C_3A did not occur. After the initial accelerated reaction, further reaction of gypsum and C_3A was somewhat retarded.

Calcium lignosulfonate increases calcium and sulfate concentration during the early period of hydration of cement; supersaturation with respect to $Ca(OH)_2$ and $CaSO_4 \cdot 2H_2O$ commonly occurs (66–68). With delay in time of addition of the admixture to the paste during mixing, the composition of the solution is intermediate between that obtained from the untreated cement paste and that obtained from the paste to which the admixture was added at the start of mixing (66, 68). Similar results are reported by Farkas and Dodson (68) and by Goetz (69) for a salt of a hydroxy acid.

Seligmann and Greening (52) examined pats of pulverized C_3S and water containing small proportions of lignosulfonate admixtures by X-ray diffraction to determine the rate of calcium hydroxide formation. Hydration was delayed indefinitely. In the presence of alkalies, delayed set occurred. The alkali appeared to react with the lignosulfonate on surfaces of C_3S to destroy the hydration-inhibiting effect. Such an action is consistent with Swenson and Thorvaldson's observation (70) of early degradation of lignosulfonate in cement pastes and concrete.

Study of mixtures of sodium calcium aluminate, C_3S, CaO, $Ca(OH)_2$, and gypsum provides valuable information on the action of a calcium lignosulfonate admixture (52). The particular commercial admixture selected by the authors is reported elsewhere (71) to include about 12 per cent of residual wood sugars. The effect of the lignosulfonate anion in contrast to the effect of the sugars is not distinguishable in the data. The ability of the admixture to inhibit release of Ca^{++} from C_3S was found to be an important factor in its effect on hydration of the aluminate. In the presence of $Ca(OH)_2$, the admixture produced only slight retarding effect initially and substantial retardation at 17 hr. Substitution of C_3S for $Ca(OH)_2$ resulted in acceleration of hydration of the aluminate in the presence of the admixture, and the acceleration was increased greatly by agitation of the mixture, presumably because of exposure of fresh surfaces of the aluminate to continued reaction. This acceleration was accompanied by considerable heat generation.

The author concludes that C_3S will not produce setting in the presence of a lignosulfonate unless some minimum quantity of sodium or potassium is present. In the absence of appreciable concentration of dissolved $Ca(OH)_2$ lignosulfonate produces accelerated hydration of C_3A comparable to the initial effect of sucrose. The immediate acceleration is decreased by delayed addition of the admixture so as to permit initiation of the hydration reactions, and the setting of the mixture typically is retarded more than would result from earlier addition of the same proportion of the admixture.

Available data show that water-reducing, set-controlling admixtures do not change significantly the nature of the hydration reactions or the composition of the reaction products (44). The rates of the reactions are modified, the reactions of the calcium aluminates being accelerated or retarded initially as outlined above, and the silicate hydration and setting retarded unless the retardation effect is compensated, as by use of accelerating chemicals or application of heat.

The relative importance of interaction of the hydroxylated admixtures with anhydrous constituents of portland cement in lieu of interactions with hydration products is conjectural. The data of Blank,

Rossington and Weinland (51) indicate the importance of the latter reactions whereas others emphasize uptake of the admixture by the unhydrated cement, especially C_3A. Bruere (72) explained the increased effectiveness of water-reducing, set-retarding agents when added to portland cement mixtures after a preliminary mixing period as being the result of diminished availability of anhydrous surfaces upon which adsorption could be accomplished because of accumulation of immediately-formed hydration products. Contrariwise, sorption of the admixture upon the hydration products formed on surfaces of the cement granules might be more effective in delaying additional hydration than is their direct adsorption on anhydrous surfaces, and sorption on separate particles of hydration products may modify the development among the hydration products of the adhesive forces that otherwise would lead to setting.

Effect of Cement Composition

Chemical and compound composition of the cement influences the effects that are produced by hydroxylated admixtures in concrete (43, 73–75). The factors involved are not well understood nor are they quantitatively predictable. Consequently, concrete containing the proposed materials should be tested to select the admixtures and rate of use that will yield optimum results in the work. Such testing should be conducted in concrete, preferably utilizing the mixing facilities that are proposed for use in the construction.

The content of aluminates is the most important factor influencing the effectiveness of hydroxylated admixtures in terms of water-reduction, retardation, and strength development of concrete (58, 73, 74). The effectiveness generally decreases as the content of C_3A increases. However, inasmuch as the content of C_3A in commercial cements typically decreases as the content of the calcium-aluminoferrite phase increases, and *vice versa*, tests performed upon cements of varying Al_2O_3/Fe_2O_3 ratio do not permit easy determination of the relative significance of the content of C_3A and of the ferrite phase. Crepaz and Raccanelli (54) conclude from tests of ground clinkers of varying Al_2O_3/Fe_2O_3 ratio that the effect of a lignosulfonate admixture on hydration of C_3S in producing extended retardation relates more to the amount of the ferrite phase than to the amount of C_3A. They believe the ferrite phase produces gelatinous hydration products that accumulate on surfaces of the calcium silicates under some conditions, with resulting prolonged retardation of setting in the manner described by Lerch (76) for under-sulfated low alkali cements of high C_4AF content. This process may explain the prolonged retardation produced by a lignosulfonate admixture on setting of concrete containing a low-alkali cement of high C_4AF and low C_3A content that caused problems in tunnel lining construction in California (71).

Kawada and Nishiyama (77) show that C_2F takes up much less calcium lignosulfonate from aqueous solution than does C_4AF, except at concentrations of the admixture less than about 100 mg/cc.

The efficiency of hydroxylated admixtures in water reduction and retardation depends also upon alkali content of the cement, their effectiveness decreasing with increased alkali content (74). However, Seligmann and Greening (52) conclude that some, as yet undetermined proportion of alkalies must be available to overcome the retardation of hydration and setting that otherwise could be caused among the calcium silicates. Apparently, the alkalies promote breakdown of the adsorbed film of the hydroxylated compounds so that hydration can proceed. The admixture can control the availability of alkalies to the extent that sodium is combined in calcium aluminate or sodium and potassium are components of the silicates; if hydration of these compounds is retarded, the concentration of alkalies in the solution phase will be decreased.

The effect of hydroxylated admixtures upon early hydration reaction and setting is influenced also by the type and amount of calcium sulfate that is present in the cement as an interground addition. The relationships are complex (37, 78). In a cement-water mixture, the immediately developed concentration of sulfate can be low because of deficient quantity of calcium sulfate or because the calcium sulfate is in the form of the slowly-soluble natural anhydrite. Conversely, the immediately developed concentration of sulfate can be higher than the saturation concentration for gypsum because of the presence of substantial amounts of the hemihydrate or soluble anhydrite phases. The excessive concentration of calcium sulfate will lead to false setting tendency of the mixtures if precipitation of gypsum occurs following cessation of mixing and prior to completion of placing of the concrete. The time of precipitation depends not only upon the degree of supersaturation but also upon the presence of gypsum crystals or other particles that can serve as crystallization nuclei. With complete destruction of original gypsum during the cement manufacturing operation, no nuclei suitable for immediate precipitation of gypsum remain so that the precipitation and consequent stiffening may be delayed until after removal of the concrete from the mixer, with resulting

problems in handling and placing of the concrete (72). Conversely, if suitable nuclei of gypsum remain, the precipitation usually will occur in the mixer, stiffening will be overcome by continued mixing, and no ill effects or only some increase in water requirement for given consistency may be the practical result. Manabe (67) concluded that granules of portland cement might also serve as crystallization nuclei for gypsum, and Hansen (37) suggested that crystallites of calcium sulfoaluminate might serve a similar role.

Addition of a hydroxylated admixture to the cement-water system can effect any of several changes relative to these phenomena. The previously noted increase in concentration of calcium sulfate that typically occurs in the presence of a lignosulfonate and (at least some) salts of hydroxy acids may lead to premature stiffening or an aggravated degree of stiffening as the result of precipitation of gypsum in the cement paste matrix. Loss of slump of concrete associated with use of these admixtures has been reported by several authors (52, 79, 80). In other instances, these admixtures may decrease or eliminate loss of slump; Goetz (69) shows for a particular combination of cement and a salt of a hydroxy acid that false setting of the cement paste is delayed, apparently because the admixture reduced the ability of solids in the mixture to serve as nucleii for precipitation of gypsum. Seligmann and Greening (52) show the effectiveness of sucrose in decreasing false set of cement paste, this result being due to consumption of calcium sulfate in an accelerated production of high-sulfate calcium sulfoaluminate from C_3A.

Seligmann and Greening (52) and Palmer (81) cite an instance of early stiffening that is akin to flash set of the C_3A induced in a low-sulfated cement as a result of early depletion of the available calcium sulfate; this action is apparently the result of acceleration of initial reaction of C_3A by a lignosulfonate. In this instance, as is reported above, setting of the silicates did not occur normally, possibly because of insufficient alkalies to remove adsorbed lignosulfonate from the silicates or because of precipitation of iron-bearing hydration products on the silicates. Their data suggest that sucrose would produce an effect similar to that of the lignosulfonate. But a salt of hydroxy acid apparently did not cause abnormal retardation of setting under these conditions (91).

Reduction of Water Requirement

ASTM Specifications C 494 (19) require that a water-reducing admixture for concrete reduce water requirement by five per cent or more with respect to the water requirement of the comparable concrete mixture not containing the admixture. At rates of use typically employed in construction, commercially available water-reducing admixtures allow 5 to 12 per cent of water reduction at equal air content, the average being 6 to 8 per cent.

The physical-chemical causes for reduction of water requirement are not completely understood, apart from the mechanical results of entrainment of air bubbles. Powers (32) concluded that it is a consequence of adsorption of the admixture upon surfaces of the cement grains. Bruere (6) shows that calcium lignosulfonate used at rates ranging from about 0.020 to 0.080 per cent progressively reduces viscosity of cement pastes in which air entrainment was avoided by imposition of a vacuum during the mixing operation. He believed this effect to be the result of adsorption of the lignosulfonate on the cement granules with consequent development of hydrophilic surfaces.

Ernsberger and France (27) described the uptake of lignosulfonate anions by portland cement and the development in dilute aqueous suspensions of a high degree of dispersion of the cement as indicated by increased time of sedimentation. Maximum dispersion was obtained with 0.5 g of calcium lignosulfonate per 100 g of cement, and amounts ranging from 0.2 to 0.4 g/g were highly effective. Electrophoretic observation of cement-water suspensions demonstrated that cement particles in distilled water did not migrate in an electrical field whereas cement particles suspended in a calcium lignosulfonate solution moved toward the anode, indicating existence of a negative charge on the particles. They attributed the negative charge to adsorbed lignosulfonate anions, and the dispersion of cement to mutual repulsion of the particles. Similar observations were made with respect to salts of hydroxy acids in unpublished work. Scripture (82) concluded that reduction of water requirement results from the dispersion; mixing water that otherwise would be trapped among the flocculent cement is made free to contribute to fluidity of a mortar or concrete mixture.

Prior and Adams (44) point out that acquisition of an electrical potential by a particle with adsorption of an ion will orient water dipoles around the particle to form a sheath which acts mechanically to prevent close approach of adjacent particles. In concrete mixtures, the adsorption may effect only a reduction of interparticle attraction, rather than development of forces of repulsion. Hence, each cement particle is not free to act independently of others but the decrease in interparticle attraction permits greater mobility of particles. They conclude that water freed from the

flocculated system is available to lubricate the mixture. Another or a supplementary concept may be that to achieve the same level of interparticle forces of attraction, a lesser distance of separation is required when the forces of attraction are reduced through adsorption of the hydroxylated admixture; hence, a lesser proportional volume of interstitial water is required for given viscosity.

Cordon (83) shows that a lignosulfonate admixture reduces the amount of water that is required to change slump of concrete to given extent, as was discussed previously in this report (Table 7). That is, by introduction of the admixture, the concrete mixture is made more sensitive to water content in relation to consistency.

Workability

Workability of concrete cannot be measured by a single parameter since it is an expression of diverse properties, namely, (1) compactibility, (2) mobility, and (3) stability of the fresh mixture (84). An evaluation of workability should consider not only the magnitude of these properties, but also the relationship of their magnitude to time after completion of mixing and to the properties of the hardened concrete.

By use of a retarding admixture, the period of time following completion of mixing and preceding the onset of setting can be extended (85). Purposeful retardation in excess of a week has been produced by use of a water-reducing retarder so as to permit continuity of placing operations under special conditions. Wallace (86) concluded that a lignosulfonate water-reducing retarder "appeared to loosen the mix and improve mobility of the concrete during vibration. However, the greatest benefit from a workability viewpoint was obtained through lengthing the hardening period. This kept underlying layers alive longer and enabled them to be knitted together with subsequently placed concrete."

Whether use of a water-reducing admixture will improve workability of concrete as apart from effects of delay of setting and aside from the effects of accompanying air entrainment has been the subject of critical discussion (79) even though numerous reports of observations of such effects in practice have been published (87). Pertinent technical data are meager.

Desov (46) found that a lignosulfonate greatly reduced viscosity of cement paste relative to that of cement paste without a chemical admixture. The effect considerably exceeded that produced by soaps of wood resins used as an air-entraining admixture. Nishi (7) shows that for concretes of equal slump and water-cement ratio, with and without a lignosulfonate admixture, mortar screened from the concrete containing the admixture had substantially greater flow than did mortar screened from the reference mixture, even at equal air content and lower cement paste content of the mortar. Ashworth (75) reported that sucrose improved workability of concrete as measured by compacting factor when used at the rate of 0.05 per cent.

Conversely, as is noted above, consistency of concrete as measured by slump can decrease more rapidly with use of a water-reducing admixture, regardless of its effect on time of setting, than occurs in an equivalent mixture without such an admixture. To the extent that slump is a measure of workability in these instances then workability will be decreased, at least after some period of time during which the concrete has been handled. Hughes and Bahramiam (88) concluded that the Vebe test (89) is a very satisfactory measure of the ease with which the concrete can be vibrated into place, this method being superior to the slump test for this purpose. Della Libera (90) reported that slump loss of concrete containing a water-reducing admixture may be more or less than that of the equivalent concrete without the admixture, but loss of workability as indicated by the Vebe apparatus is less. He illustrates observations for a concrete containing a lignosulfonate admixture for which slump loss during the first two hours after mixing was about 3 cm whereas no appreciable change occurred in the Vebe measurement of workability.

Skeen (91) evaluated workability of concrete containing each of four surface-active agents: (1) an anionic air-entraining agent, (2) a nonionic agent consisting of condensation products of polyethylene oxide with substituted phenols, (3) an air-entraining agent consisting of a triethanolamine salt of sulfonated hydrocarbons, and (4) an impure calcium lignosulfonate. Mixing of the concrete was conducted under reduced atmospheric pressure to hold air entrainment at a minimum. Workability was measured as a "compacting factor", that is, the ratio of the weight of the fresh concrete in a test vessel after compaction in a standard manner to the maximum weight attainable by vibration (92). Skeen concluded that agent 2 above, improves the working qualities and agent 4 provided marked improvement in working qualities of the concrete when used at rates of 0.15 and 0.30 per cent.

Heat of Hydration

Forbrich (73) experimented with mixtures of cal-

cium lignosulfonate, orthohydroxy benzoic acid, and calcium chloride to determine their effect upon hydration of C_3A, C_3S, and portland cement. He classified orthohydroxy benzoic acid and other substituted hydroxy benzoic acids as catalysts in the hydration and setting of portland cement mixtures inasmuch as the small rates of use to achieve such action preclude the possibility that the effect is a consequence of direct combination with any phase of the cement.

Calcium lignosulfonate used alone delayed the time of rapid heat evolution by C_3A and greatly retarded heat liberation from C_3S. Orthohydroxy benzoic acid slightly retarded heat liberation of portland cement and C_3S, whereas that of C_3A was slightly accelerated. Calcium chloride increased the maximum rate and amount of heat liberated by portland cement and C_3S during the first 24 hours, but had little effect on C_3A. By combination of the three agents in various proportions, early heat liberation of portland cement could be controlled in almost any direction.

Combinations containing calcium chloride typically had little effect upon total heat liberation from a group of portland cements after seven days. Conversely, a combination of calcium lignosulfonate and the catalyst, used at the rate of 1.065 per cent, slightly decreased heat release at three days but at 28 days six of seven cements showed increased heat generation up to 12 per cent with respect to heat evolved by the cement without admixture. Moreover, Forbrich observed that use of the formulated admixtures increased compressive strength of concrete at given age and increased the ratio of strength of concrete to heat released from cement pastes. That is, the admixture appeared to increase the efficiency of the cement in producing strength per unit of hydration as expressed by heat generation.

Danielsson (41) found that heat of hydration at 28 days was not notably altered by the use of a group of calcium of simple organic acids, in spite of retardation of setting and initial heat release.

Polivka and Klein (74) concluded that setting time of mortar as determined by a penetration test can be calculated as a function of the time required for a paste of the same cement to reach maximum heat of hydration. Kennerley, Williams and St. John *et al* (43) found also that the maximum rate of increase in temperature of cement paste correlates with physical hardening of the paste. Consequently, setting of portland cement mixtures with and without water-reducing, set-controlling admixtures seems to be determined by the degree of hydration attained. In view of the interaction of chemical admixtures and hydration products of cement, the rate of hydration and the rate of setting could be quite different.

Bleeding and Settlement

Water-reducing, set-controlling admixtures influence the rate and capacity of fresh portland cement mixtures to bleed and settle under the influence of gravity. Lignosulfonates typically reduce the rate and capacity of bleeding even when the air content of the test mixture is equal to that of the reference mixture not containing a chemical admixture (93, 94). Conversely, hydroxy acids and their salts commonly increase the rate and capacity of portland cement mixtures to bleed and settle at given air content and degree of retardation of setting (91, 93, 94).

Kreijger (28) studied the effect of surface-active agents on the bleeding properties of cement pastes and mortars. He concluded that at given water-cement ratio anionic water-reducing, set-controlling admixtures reduce bleeding rate more than can be accounted for by air entrainment, whereas anionic air-entraining admixtures reduce bleeding rate and capacity in closer relation to the effect of air content as deduced by Powers (95). Kreijger gives the following equations for cement pastes at water-cement ratio = 0.5.

For anionic, water-reducing admixtures:

$$\frac{Q_x}{Q} = 1 - 10x \qquad (2)$$

$$\frac{H_x}{H} = 1 - 10x \qquad (3)$$

For anionic air-entraining agents (rendering cement granules hydrophobic) and nonionic water-reducing admixtures:

$$\frac{Q_x}{Q} = 1 - 4.0x \qquad (4)$$

$$\frac{H_x}{H} = 1 - 4.0x \qquad (5)$$

where:

Q and Q_x are respectively bleeding rate for cement pastes without and with the admixture; H and H_x are respectively bleeding capacity of cement pastes without and with the admixture; and x is the air content. Equation 4 is considered to be valid to maximum air content of 14.5 per cent, whereas equation 2 is considered to be valid to air content of 4.1 per cent.

Equations 2 and 4 are compared by Kreijger with that calculated for his cements from the theoretical formula given by Powers (95) in which no account is taken of any physical-chemical effects of the admix-

tures. The resulting formula is stated as

$$\frac{Q_x}{Q} = 1 - 2.45x \qquad (6)$$

Hence, for the cement admixture combinations used by Kreijger both types of admixtures produced effects other than mere incorporation of air bubbles. In view of other data, it is questionable whether Equations 2 and 3 can be applied to the broad spectrum of hydroxylated anionic water-reducing compounds.

Kreijger (28) concluded also that bleeding rate of concrete can be calculated from bleeding rate of cement paste when an admixture is employed, provided the same concentration of admixture is used in each mixture.

Manabe and Kawada (55) found that portland cement is dispersed by addition of calcium lignosulfonate to aqueous suspensions in amounts up to 0.3 per cent, this concentration corresponding to that necessary to produce the readily formed portion of a monomolecular layer over the cement granules. At this concentration, maximum stability of the suspension (10 g. cement in 15 ml. of aqueous solution) was attained. At higher concentrations further dispersion of the cement occurred and coarse particles separated from the suspension, causing progressive decrease in volume of the suspension at given time following cessation of shaking.

Bruere and McGowan (96) evaluated several polyelectrolytes that produce flocculation through increased particle attraction in cement pastes, mortars, and concrete. Discussion of admixtures of this type is outside the scope of this paper.

Stress-Strain Relationships

When used at rates that provide reduction of water requirement and the time of setting appropriate for general construction, water-reducing, set-controlling admixtures typically increase compressive strength of concrete significantly (97). Unless setting is unusually retarded, the increase in compressive strength is apparent at 24 hours and at 7 and 28 days the increase is in the range from 10 to 20 per cent, and may be substantially higher. The strength increase, expressed in proportion to the strength of the reference concrete not containing the admixture, usually is greater at 3 and 7 days than at 28 days and later. The improvement in compressive strength is related in part to the reduction in water-cement ratio, but the increase in strength typically exceeds that expected from change in water-cement ratio (98). The effect of calcium lignosulfonate used at 0.266 per cent is shown in Table 7 for air-entrained concretes of differing cement content, water-cement ratio, air content, and slump. Based upon analysis of data obtained by testing of a lignosulfonate admixture in concrete in combination with 26 portland cements and 36 combinations of aggregates, Mielenz (87) adduced the following relationships of 28 day compressive strength and void cement ratio:

$$Sa = 8518 - 1830Va \qquad (7)$$

$$Sp = 8190 - 1992Vp \qquad (8)$$

Where Sa = 28 day compressive strength of the admixture concrete, psi; Sp = 28 day compressive strength of the concrete without admixture, psi; Va and Vp = void-cement ratio by volume of the concretes. These relationships indicate that on the average, at constant air and cement content, an increase of 19 per cent in 28 day compressive strength can be expected even if the water reduction effected is only 5 per cent. If a water-reducing retarder is used at rates sufficient to effect extended retardation, early strength may be decreased but later strength will be increased, provided the concrete is properly cured and protected and provided the air content is in the proper range.

Flexural strength of concrete at given cement and air content typically is increased by use of water-reducing, set-controlling admixtures, but the improvement is proportionally less than that effected in compressive strength. Similar conclusions may be reached relative to their effects upon tensile strength, shearing strength, and modulus of elasticity (80). Abrasion resistance of surfaces and bond with reinforcement are related to compressive strength of concrete, and so typically are likewise improved.

Only very limited data are available on the effect of water-reducing, set-controlling admixtures on creep of concrete. Some recent data are given by Hope, Neville and Guruswami (99) for normal weight concrete and by Jessop, Ward and Neville (100) for concrete containing lightweight aggregate. Each report is based upon tests in which only one portland cement (Type III, high early strength) was used. Use of a water-reducing retarder based upon either lignosulfonate or salts of a hydroxy acid was found apparently to cause an increase in creep of the normal weight concrete. In the tests of the lightweight concrete, a lignosulfonate retarder appeared to increase creep whereas a retarder based upon a salt of a hydroxy acid seemed to reduce creep under most of the conditions applied. The authors recommend caution in generalization of their observations in consideration of other cement-admixture combinations.

Available information on the effect of hydroxylated admixtures upon the structure, texture, and composition of the cement paste matrix of concrete and upon development of bond of cement paste to aggregate particles is insufficient to explain quantitatively the observed changes in stress-strain relationships that are induced. Except for changes in the composition of calcium aluminate hydration products that may occur under some circumstances, such as formation of analogues of the high-sulfate calcium sulfoaluminate (36), the hydration products of portland cement appear to be the same in spite of the presence of the surface-active admixture, but rates of hydration of the several constituents, sequence of formation of the hydration products, and crystal habit and size distribution of the hydration products are changed. Therefore, the change in properties of concrete may arise in large part in the altered texture and structure of the hydrated cement paste. This concept is consistent with conclusions of several workers who observed by electron microscope change of crystal size and habit of hydration products of tricalcium aluminate and of calcium aluminoferrites and changes in the morphology of hydration products of C_3S and C_2S (54, 57, 60, 101–103). Hope, Neville and Guruswami (99) cite the observation of change in size and shape of crystals formed by hydration of C_3A in the presence of lignosulfonate to account for the indicated changes in magnitude of creep of concrete.

Although these modifications within the matrix undoubtedly affect stress-strain relationships in hardened concrete, the possibility of modification of boundary relationship among the hydration products and between the hydration products and aggregate particles should not be overlooked.

Drying Shrinkage

The effect of water-reducing, set-controlling admixtures upon drying shrinkage of concrete is a matter of concern with respect to performance of the concrete in service. Standard tests of drying shrinkage, such as ASTM Designation: C 157 (19), typically specify use of unrestrained specimens of small size that are cured initially in moist air in the molds, then briefly in moist air or lime water, and then are dried in air, usually at 23.0 $\pm$ 1.1°C. and 50 $\pm$ 4 per cent relative humidity. These conditions cause more rapid drying and greater shrinkage than occurs in structural members and slabs in service, and they produce an optimum environment for shrinkage of the cement paste matrix by carbonation (104). Moreover, such procedures neglect any internal cracking that would be an important manifestation of shrinkage stress yet will reduce the indicated shrinkage strain. Della Libera (90) reported lesser cracking of concrete pavements and structures with use of a lignosulfonate admixture.

Water-reducing, set-controlling admixtures produce varying results in such accelerated tests. For no admixture of these types is any substantial reduction of drying shrinkage shown consistently. Some hydroxylated admixtures cause an increase in drying shrinkage even when water content is reduced. At early periods, the increase may be 100 per cent or more relative to the length change of the reference concrete. However, the changes are most pronounced at early ages and they decrease with passing time, possibly with reversal of the relationship to the reference concrete after several months of drying. Increases in early drying shrinkage are greatest when the admixture includes constituents that accelerate the hydration and setting process, so as to partially or completely overcome the set-retarding action of the hydroxylated component. The resulting change in drying shrinkage depends on many factors, most important of which are the characteristics of the cement and aggregate (105).

Bruere and Newbegin (106) determined the effect of various water-reducing, set-controlling admixtures on accelerated drying shrinkage of concrete beam specimens. The admixtures included calcium lignosulfonate, mixtures of calcium lignosulfonate and calcium chloride, mixtures of calcium lignosulfonate and triethanolamine, sodium gluconate, and sucrose. After seven days of drying at 50 $\pm$ 3 per cent relative humidity, the drying shrinkage of the concrete containing the admixtures was increased 30 to 110 per cent (for one cement-aggregate combination) and 0 to 50 per cent (for a second cement-aggregate combination), whereas after 168 days of drying the respective changes in drying shrinkage were -6 to 6 per cent and -8 to 0 per cent. The authors conclude that "the effects of admixtures on shrinkage (of concrete) after 14 days of drying are not indicative of their effects after longer periods of drying."

Helmuth and Turk (107) showed that drying shrinkage of portland cement pastes in a carbon dioxide-free atmosphere is dependent upon how the drying is carried out and how long the pastes were stored moist after hydration was substantially complete. For example, ultimate drying shrinkage at a low relative humidity was greatly reduced by prior storage at intermediate relative humidity, rather than direct exposure to the low humidity following curing. Also, they found that prolonged moist curing can substantially reduce the shrinkage that occurs on first drying at low relative

humidity. They conclude that irreversible changes occur in the structure of the hydration products during moist curing with the result that shrinkage upon drying is reduced. These results indicate the error that can arise in extrapolation of results obtained in accelerated drying of small specimens to predict performance of structures and pavements in service. An important contribution would result if the Helmuth-Turk studies were repeated to evaluate the effect of water-reducing, set-controlling admixtures on the magnitude of delayed drying shrinkage.

The cause of any increase in drying shrinkage that may relate to use of a water-reducing, set-controlling admixture is not understood completely. The effect may result from increased proportion of cement that is hydrated at given time, this possibility being most pertinent to performance of admixtures containing an accelerator or catalyst. The magnitude of shrinkage does not correlate directly with loss of water when concretes with and without a water-reducing, set-controlling admixture are compared. For example, in a series of concrete mixtures containing 511 to 516 lb of cement per cu. yd. and 5.4 to 5.8 per cent of air with slump of $3\frac{1}{2}$ to 4 in., drying shrinkage during 180 days was 0.045 per cent linearly for the concrete containing no water-reducing admixture whereas that of five concretes containing lignosulfonate water-reducing retarders was 0.054 to 0.058 per cent; yet weight loss was 3.31 per cent for the reference concrete and 3.04 to 3.20 per cent for the specimens containing the water-reducing admixtures. The ratio of lineal shrinkage to weight loss increased consistently as the water-cement ratio decreased. The test was performed in accordance with ASTM Designation: C 157 (19), using 3- by 4- by 16-in. beams.

The relationship appears to be like that shown by Roper (108) for cement pastes with water-cement ratio of 0.35 and 0.50, respectively. For given weight loss expressed as a percentage of the weight of the paste at given relative humidity, substantially greater shrinkage occurs in the paste of lower water-cement ratio. The loss of weight occurring at relative humidity down to about 90 per cent is accompanied by little shrinkage. At relative humidity from 90 to 40 per cent, a substantial increase takes place for each increment of weight loss. Roper concludes that the first type of water is that contained in macropores of the cement paste, whereas the second type of water is held by capillary condensation so that its loss creates capillary compression of high magnitude.

In other words, considering the case in which the water-reducing admixture is incorporated in the concrete mixture without reduction of cement content, the water-cement ratio is reduced thereby. Presumably, the excess of water that is present in the reference concrete to provide the specified consistency, will exist in larger openings (Roper's macropores) in the cement paste. Loss of this water will effect little shrinkage and the time required for its movement through and out of the concrete will delay the initiation of loss of water from the small capillaries in which significant capillary tension can develop. Meanwhile, the relative smaller proportion of water that is present in macropores of the cement paste within the concrete containing the admixtures is lost sooner and loss of water within capillaries is initiated quickly, with resulting early development of relative humidity within the concrete at levels in which high capillary tension can develop. In tests of water-reducing and air-entraining admixtures Kondo and Hideshima (109) found that drying shrinkage of concrete is less with use of water-reducing admixtures based upon calcium lignosulfonate than for the reference concrete or concrete containing conventional air-entraining admixtures; in these tests drying was accomplished at an ambient relative humidity of 70 to 80 per cent.

If the use of the admixture is accompanied by a reduction of cement content so as to maintain the water-cement ratio constant or nearly so, decrease of relative humidity within the concrete still will be more rapid than within the reference concrete because of the higher water content of the latter concrete.

Although the above conditions and processes are qualitatively valid and germane to explanation of the effect of hydroxylated admixtures on drying shrinkage of concrete, they cannot afford a complete comprehension of the mechanical and physical-chemical processes involved because of the effects of such admixtures upon the texture and structure of the cement paste as well as upon its physical properties such as permeability, tensile strength, and creep characteristics. For example, Stupachenko (47) studied pore size distribution and porosity of hardened cement pastes and mortar by absorption of benzol and use of the mercury porosimeter. He reported that use of a lignosulfonate admixture at the rate of 0.25 per cent did not significantly change the total porosity, but the volume proportion of pores with radius of 500 to 1000 Å was decreased 8 per cent in the mortar (water-cement ratio = 0.5) and 30 per cent in the cement paste (water-cement ratio = 0.25) whereas the proportion of pores measured by the mercury porosimeter (radius = 100 to 65,000 Å) was increased about 11 per cent in each instance. For the reference mortar without admixture, pores with diameter greater than 1 μ constitute about 21 per cent of the total porosity

in contrast to 25 per cent for the mortar with the lignosulfonate admixtures, and pores having diameter greater than 1000 Å constitute 40 per cent and 52 per cent of the two mortars. Stupachenko concluded that the cement paste containing the admixture should be more permeable to water and other fluids than is equivalent cement paste without the admixture; this conclusion would not necessarily relate to the concrete as a whole. These factors also will influence the rate and magnitude of drying shrinkage under given conditions of exposure.

Wallace and Ore (80) found that so-called autogenous shrinkage of concrete, that is, shrinkage occurring in sealed specimens for which no moisture loss is permitted, is reduced by use of a lignosulfonate admixture. The reduction was observed at all periods to an age of five years.

Resistance to Freezing and Thawing

Resistance of concrete to the effects of freezing and thawing depends mainly upon the air content, distribution of air voids in the cement paste matrix, and the degree of saturation of the aggregate and the matrix (34, 110). However, the quality of the cement paste as defined by water-cement ratio and extent of hydration is an important factor both because of the physical properties of the hardened matrix and because of the influence of the fresh cement paste upon the geometry of the air-void system. Also, as has been noted (Table 8), the specific relationship of the parameters of the air-void system, such as the air-void spacing factor, and resistance to freezing and thawing is affected by the composition and rate of use of the air-entraining agent and any chemical admixtures that may be present. Wallace and Ore (80) found that the average freezing and thawing resistance of concrete containing any of several water-reducing, set-controlling admixtures was 39 per cent greater than that of comparable reference concretes. In studies by the Bureau of Public Roads (5), concretes containing each of 22 water-reducing retarders were about equally resistant or more resistant to freezing and thawing as were the comparable reference air-entrained concretes without a water-reducing admixture. Concretes containing each of the three remaining admixtures of the 25 tested showed somewhat less resistance to freezing than did the reference concretes. Other reports also show reduced resistance to freezing and thawing of concrete containing individual water-reducing admixtures (111, 112). So far as the present author is aware, such instances of reduced resistance to freezing and thawing correlate with deficiencies of parameters of the air-void system, such as excessive spacing factor (or unprotected paste volume) and deficient air content.

Additional research is necessary to establish quantitatively the parameters of the air-void system and the cement paste matrix that control the resistance of the matrix of concrete to effects of freezing and thawing. Larson, Cady and Malloy (113) concluded that Philleo's protected paste volume concept (114) evaluated by a new procedure that they propose, provides the best indication of resistance to freezing and thawing. Price (115) found that total air content determined microscopically does not correlate significantly with dilation of concrete in a freezing and thawing test but that air content based upon voids less than 1000 μ in diameter correlates at the 90 per cent confidence level, and a higher degree of correlation results with elimination of all voids larger than 500 μ.

Warris (116) emphasizes the importance of the degree of saturation of concrete at time of freezing, including the partial or complete filling of air-voids, as a basic factor in the resistance to distress. This condition is not contemplated in the several analyses noted in the previous paragraph. Moreover, consideration should be given to the ease with which air voids of differing size are filled by water under conditions of capillary absorption and hydraulic flow. Bache, Idorn, Nepper-Christensen and Nielson (117) show from observation of deposits of calcium hydroxide in air voids that voids near surfaces in contact with water can readily fill with water; however, the deposits were virtually restricted to voids larger than 50 μ in diameter. Noting that small voids should fill with water faster than do larger voids because of the pressure-solubility relationship of air contained in a bubble (11), these authors suggest that the cement paste adjacent to large voids may be less dense and more permeable than that close to small voids. Slate (118) suggests that the hydrophobic film at the interface of entrained air bubbles impedes entry of water into the voids after hardening of the concrete. These are matters for further study.

Considering the above factors, it appears that air voids that are most important for protection of the cement paste of concrete from damaging effects of freezing are those of intermediate size, such as 50 to 500 μ, that are less likely to fill with water prior to freezing than are smaller voids, yet are small enough to provide efficient distribution of the available air volume and a relatively large specific surface for entry of water into the voids during freezing.

Urgently Needed Research

Air-Entraining Admixtures

1. Techniques for measurement of bubble size, proportional volume, and distribution in fresh concrete.

2. Further evaluation of factors controlling the proportional volume and geometry of the air-void system in hardened concrete, including effects during mixing and following mixing, particularly bubble dissolution and enlargement.

3. Evaluation of parameters determining the freezing and thawing resistance of concrete that is saturated with water or nearly so, including geometry of the void system in relation to the cementitious matrix of the concrete and properties of the matrix.

4. Determination of properties and composition of air-entraining admixtures that will provide optimum effects on workability, bleeding, and settlement of fresh concrete and yet will produce a satisfactory air-void system in hardened concrete.

5. Discovery of the properties and composition of air-entraining admixtures that will produce air-void systems of optimum efficiency in hardened concrete, that is, adequate protection of the matrix at minimum air content.

6. Evaluation of factors controlling the rate and degree of filling of air voids prior to freezing, including such factors as void size, structure of the cement paste and its variation with proximity to voids, and the nature of the void-cement paste interface.

7. Determination of the mechanism by which air entrainment in concrete affects permeability and absorption of water, such as improved uniformity by reduction of bleeding and segregation, change of capillary structure of the matrix, and properties of the interface between air voids and the matrix.

Water-Reducing, Set-Controlling Admixtures

8. Development of water-reducing admixtures that accelerate setting and early strength development of concrete, without introduction of adverse effects on other properties.

9. Development of water-reducing admixtures to further improve and maintain working qualities of fresh concrete, including avoidance of undesirable stiffening, control of time of setting, minimizing bleeding and settlement, and improvement in placing and finishing qualities.

10. Development of water-reducing admixtures that will reduce appreciably the volume change of hardened concrete, including drying shrinkage and creep.

11. Evaluation of the effect of water-reducing admixtures on bond of the cement paste matrix and the surface of aggregate particles.

12. Definitive studies on effects of admixtures upon stress-strain phenomena in concrete, including such properties as strength, elasticity, creep, and resistance to cracking, in relation to changes of composition, texture, and internal structure of the matrix and physical-chemical processes at matrix-aggregate boundaries.

References

1. R. F. Blanks and H. F. Kennedy, The technology of cement and concrete, Vol. I, Concrete Materials, John Wiley and Sons, Inc., New York, N. Y., 422 p. (1955).
2. F. H. Jackson and A. G. Timms, "Evaluation of air-entraining admixtures for concrete," Public Roads, **27**, 259–267 (1954).
3. J. P. Sisley and P. J. Wood, Encyclopedia of surface-active agents (Chemical Publishing Co. Inc., New York, N. Y., U.S.A., 1952).
4. W. J. Halstead and B. Chaiken, "Chemical analysis and sources of air-entraining admixtures for concrete", Public Roads, **27**, 268–278 (1954).
5. W. E. Greib, G. Werner and D. O. Woolf, "Water-reducing retarders for concrete—physical tests", Public Roads, **31**, 136–152 (1961).
6. G. M. Bruere, "Fundamental actions of air-entraining agents," RILEM intern. Symp. on Admixtures for Mortar and Concrete, Brussels, Topic III/1, 5–23 (1967).
7. T. Nishi, "On the recent studies and applications in Japan concerned to admixtures in use of building concretes and mortars (Part I)—effects of surface active agents upon fresh concretes and mortars," RILEM Intern. Symp. on Admixtures for Mortar and Concrete, Brussels, Topic III/4, 41–62 (1967).
8. J. E. Backstrom, R. W. Burrows, R. C. Mielenz, and V. E. Wolkodoff, "Origin, evolution and effects of the air void system in concrete. Part 2—influence of type and amount of air-entraining agent", Proc., Am. Concrete Inst., **55**, 261–272 (1958).

9. A. M. Gaudin, "Flotation," 2nd Ed., McGraw-Hill, Inc., New York, N. Y. (1957).
10. J. J. Bikerman, Surface Chemistry, 2nd Ed., Academic Press, Inc., New York, N. Y. (1958).
11. R. C. Mielenz, V. E. Wolkodoff, J. E. Backstrom and H. L. Flack, "Origin, evolution, and effects of the air void system in concrete, Part 1—entrained air in unhardened concrete", Proc., Am. Concrete Inst., **55**, 95–121 (1958).
12. J. R. Landgren, Personal Communication.
13. T. G. Jones, K. Durham, W. P. Evans and M. Camp, "The stability of foams", Proc. 2nd Intern. Congr. of Surface Activity, Vol. 1, 225–230 (1957).
14. J. J. Bikerman, "Foams and emulsions: formation, properties, and breakdown," Chem. and Physics of Interfaces, Am. Chem. Soc., 58–64 (1965).
15. G. M. Bruere, "Rearrangement of bubble sizes in air-entrained cement pastes during setting", Australian J. Appl. Sci., **13**, 222–227 (1962).
16. T. C. Powers, "The air requirement of frost resistant concrete," Proc., Am. Concrete Inst., **29**, 184–202 (1949).
17. American Society for Testing and Materials, Designation: C 457, "Air void content in hardened concrete," ASTM Book of Stds., Part 10, 315–327 (1967).
18. T. M. Kelly and D. E. Bryant, "Measuring the rate of hardening of concrete by bond pullout pins," Proc., Am. Soc. Testing Mater., **57**, 1029–1040 (1957).
19. American Society for Testing and Materials, ASTM Standards, Part 10, 1967.
20. C. P. O'Neill, "The effect of surface-active agent and water-cement ratio on the diffusion of air in the air void system of portland cement concrete", MS Thesis, Univ. of Notre Dame, Notre Dame, Indiana (1965).
21. V. J. Zipparro, Jr., "The effects of vibration and air diffusion on the air void system of air-entrained concrete" MS Thesis, Univ. of Notre Dame, Notre Dame, Indiana (1964).
22. J. E. Backstrom, R. W. Burrows, R. C. Mielenz, and V. E. Wolkodoff, "Origin, evolution and effects of the air void system in concrete. Part 3—influence of water-cement ratio and compaction", Proc., Am. Concrete Inst., **55**, 359–375 (1958).
23. T. D. Larson, J. L. Mangusi, and R. R. Radomski, "Preliminary study of the effects of water-reducing retarders on the strength, air void characteristics, and durability of concrete", Proc., Am. Concrete Inst., **60**, 1739–1753 (1963).
24. T. C. Powers, "Topics in concrete technology—part 4", J. Portland Cement Assn. Res. and Devel. Lab., **7**, 23–41 (1965).
25. G. M. Bruere, "Air entrainment in cement and silica pastes," Proc., Am. Concrete Inst., **51**, 905–919 (1955).
26. P. C. Kreijger, "Action of AE agents and water-reducing agents and the difference between them", RILEM Intern. Symp. on Admixtures for Mortar and Concrete, Brussels, Topic II/2, 31–37 (1967).
27. F. M. Ernsberger and W. G. France, "Portland cement dispersion by adsorption of calcium lignosulfonate", Ind. and Eng. Chem., **37**, 598–600 (1945).
28. P. C. Kreijger, "Effect of surface active agents on the bleeding properties and on the heat of hydration of cement paste and mortar," RILEM Intern. Symp. on Admixtures for Mortar and Concrete, Brussels, Topic III/2, 25–31, (1967).
29. G. M. Bruere, "Bubble characteristics in air-entrained cement pastes containing various mixtures of surface-active agents," Aust. J. Appl. Sci., **14**, 204–212 (1963).
30. G. M. Bruere, "The relative importance of various physical and chemical factors on bubble characteristics in cement pastes", Aust. J. Appl. Sci., **12**, 78–86 (1961).
31. American Society for Testing and Materials Book of Standards, Part 9 (1967).
32. T. C. Powers, "Topics in concrete technology—part 3", J. Portland Cement Assn. Res. and Devel. Lab., **6**, 19–42 (1964).
33. B. Warris, "Influence of water-reducing and air-entraining admixtures on the water-requirement, air-content, strength, modulus of elasticity, shrinkage and frost-resistance of concrete," RILEM Intern, Symp on Admixtures for Mortar and Concrete, Brusscls, Topic III/IV/1, 5–16 (1967).
34. T. C. Powers and R. A. Helmuth, "Theory of volume changes in hardened portland cement paste during freezing," Proc., Highway Res. Bd., **32**, 286; issued as Bull. No. 46, Portland Cement Assn., Res. and Devel. Labs.
35. W. C. Hansen, Discussion of Proc. of the Third International Symposium on the Chemistry of Cement, London Cement and Concrete Assn., 318–321 (1952).
36. W. C. Hansen, "Actions of calcium sulfate and admixtures in portland cement pastes," Am. Soc. Testing Mater. Spec. Tech. Publ. No. 266, 3–25 (1960).
37. W. C. Hansen, "SO_3 abstracts and newletter", U.S. Gypsum Co., Chicago, Ill., 4 p. (Aug. 1967).
38. R. C. Mielenz and R. B. Peppler, Discussion of W. C. Hansen Paper on "Actions of calcium sulfate and admixtures in portland cement pastes," Am. Soc. Testing Mater. Spec. Tech. Publ. No. 266, 35–37 (1960).
39. H. H. Steinour, "The setting of portland cement. A review of theory, performance and control", Portland Cement Assn. Res. Lab. Bull. 98, Chicago, Ill. (Nov. 1958).
40. H. H. Steinour, Discussion of Paper by W. C. Hansen, "Actions of calcium sulfate and admixtures in portland cement pastes", Am. Soc. Testing Mater. Spec. Tech. Publ. No. 266, 25–37 (1960).
41. U. Danielsson, "Studies of the effect of simple organic admixtures on the properties of cement paste", RILEM Intern. Symp. on Admixtures for Mortar and Concrete, Brussels, Topic II/4, 57–68 (1967).
42. J. H. Taplin, Discussion of Paper by H. E. Vivian, "Some chemical additions and admixtures in cement paste and concrete", Proc. 4th Intern. Symp. on Chemistry of Cement, Natl. Bur. of Stds. Monograph 43, **II**, 924–925 (1960).
43. R. A. Kennerley, A. L. Williams and D. A. St. John, "Water-reducing retarders for concrete," Domi-

nion Lab. Rpt. 2026, Dept. of Sci. and Ind. Res., Lower Hutt, N.Z., 66 p. (1960).
44. M. E. Prior and A. B. Adams, "Introduction to producers' papers on water-reducing admixtures and set-retarding admixtures for concrete," Am. Soc. Testing Mater. Spec. Tech. Publ. No. 266, 170–179 (1960).
45. V. M. Moskvin and V. G. Batrakov, "Increase in concrete durability by addition of silicones", RILEM Intern. Symp. on Admixtures for Mortar and Concrete, Brussels, Topic IV/6, 71–83 (1967).
46. A. E. Desov, "The effect of silica organic compound GKZ-94 (Polyhydrosilican) on the physico-technical properties of concrete and mortars," RILEM Intern. Symp. on Admixtures for Mortar and Concrete, Brussels, Topic IV/7, 85–94 (1967).
47. P. P. Stupachenko, "The influence of admixtures SSB, GKZh and $Ca(NO_3)_2$ on structural porosity of a mortar portion of concrete," RILEM Intern. Symp. on Admixtures for Mortar and Concrete, Brussels, Topic IV/8, 95–107 (1967).
48. L. N. Dyagileva, I. A. Iochinskaya, E. E. Melamed and V. B. Ratinov "The mechanism of effect of complex admixtures on the processes of hardening of cement" RILEM Intern. Symp. on Admixtures for Mortar and Concrete, Brussels, Topic II/7, 97–109 (1967).
49. B. C. Carlson, D. F. Curtis and R. C. Hedlund, "Development of a concrete admixture to improve freeze-thaw durability", Highway Res. Bd. Highway Res. Record No. 62, 13–28 (1964).
50. S. Suzuki and S. Nishi, "Influence of saccharides and other organic additives on the hydration of portland cement," Rev. 13th Gen. Meeting, Japan Cement Eng. Assn., 34–35 (1959).
51. B. Blank, D. R. Rossington, and L. A. Weinland, "Adsorption of admixtures on portland cement", J. Am. Ceram. Soc. **46**, 395–399 (1963).
52. P. Seligmann and N. R. Greening, "Studies of early hydration reactions of portland cement by X-ray diffraction", Highway Res. Bd. Highway Res. Record No. 62, 80–105 (1964).
53. O. I. Luk'yanova, E. E. Segalova, and P. A. Rebinder, "Effect of hydrophilic plasticizing admixtures on the properties of concentrated cement suspensions," (in Russian), Kolloidnyi Zhurnal, 19, No. 1, 82–89, Moscow (1957). (Trans. from Slavic Languages Assn. Translation Center).
54. E. Crepaz and A. Raccanelli, "Contribution to knowledge of the action of calcium lignosulfonate on hydration of cements" (in Italian), L'Industria Italiana del Cemento, 819–826 (Sept. 1964).
55. T. Manabe and N. Kawada, "Effect of calcium lignosulfonate addition on the properties of portland cement paste at initial hydration period," Rev. of the 13th Gen. Meeting, Japan Cement Eng. Assoc., Tokyo, 40 p. (1959).
56. B. D. Trinker, "Time-strength increment in mortars and concretes after addition of surface-active materials and electrolytes," (in Russian), Betony i Rastvory, Issledovaniya Nauk, Issledovatel. Inst. po Stroitel'stvu, 73–112 (1957). Chem. Abstr. **53**, 1959 (2) 1671.h.
57. E. E. Segalova, E. S. Solv'eva and P. A. Rebinder, "Structure development in suspensions of tricalcium aluminate by crystallization," (in Russian), Doklady Akad. Nauk SSSR, **113**, 134–137 (1957). Chem. Abstr. **51**, No. 13350 (1957).
58. O. I. Luk'yanova, E. E. Segalova and P. A. Rebinder, "Nature of the induction period of portland cement hydration if a hydrophilic plasticizer is added," (in Russian), Doklady Akad. Nauk SSSR, **117**, 1034–1036 (1957). Chem. Abstr. **52**, No. 7652.f (1958).
59. E. Crepaz and C. Semenza, "The action of plasticizing and air entraining admixtures on cement hydration," Sixth Congress on Large Dams, Int. Comm. on Large Dams, Question 23, 23–32 (1958).
60. J. F. Young, "Hydration of tricalcium aluminate with ligno-sulphonate additives", Concrete Res., **14**, No. 42, 137–142 (Nov. 1962).
61. R. F. Feldman and V. S. Ramachandran, "The influence of $CaSO_4 \cdot 2H_2O$ upon the hydration character of $3CaO \cdot Al_2O_3$," Concrete Res., **18**, No. 57, 185–196 (1966).
62. P. P. Budnikov and R. D. Azelitshaya, "Effect of electrolyte additions on hardening process of tricalcium aluminate," (in Russian), Zhurn. Priklad, Khim. **32**, 1181–1185 (1959). Chem. Abstr. **53**, No. 17469.g (1959).
63. P. P. Budnikov, R. D. Azelitskaya and S. S. Rozhdestvenskii, "Hydration of $4CaO \cdot Al_2O_3 \cdot Fe_2O_3$ and its relation to small additions of electrolytes," (in Russian), Silikattechnik, 12, 288–291 (1961). Chem. Abstr. **56**, No. 12546.b (1962).
64. E. S. Solv'eva and E. E. Segalova, "A study of the kinetics of supersaturation in aqueous suspensions of tricalcium aluminate and the determination of its metastable solubility" (in Russian), Kolloidnyi Zhurnal, **23**, 306–314 (1961).
65. R. Sersale, "The crystalline habits of calcium aluminate hydrates", La Ricerca Scientifica, **27**, 777–790 (1957).
66. M. H. Roberts, "Effect of admixtures on the composition of the liquid phase and the early hydration reactions in portland cement pastes," RILEM Intern. Symp. on Admixtures for Mortar and Concrete, Brussels, Topic II/1, 5–29 (1967).
67. T. Manabe, Discussion on Paper by W. C. Hansen, "False set in portland cement," 4th Intern. Symp. on Chem. of Cement, Washington, D.C., Proc., I, 404–408 (1960).
68. W. H. Dodson and E. Farkas, "Delayed addition of set retarding admixtures to portland cement concrete," Proc., Am. Soc. Testing Mater., **64**, 816–826 (1964).
69. H. W. Goetz, "False set of cement as influenced by hydroxylated carboxylic-acid-type admixture" Am. Soc. Testing Mater., Mater. Res. and Stds., **7**, 246–249 (1967).
70. E. G. Swenson and T. Thorvaldson, "Detection of lignosulfonate retarder in cement suspensions and pastes," Am. Soc. Testing Mater. Spec. Tech. Publ. **266**, 159–169 (1960).
71. L. H. Tuthill, R. F. Adams, S. H. Bailey and R. W. Smith, "A case of abnormally slow hardening

concrete," Proc., Am. Concrete Inst. **32**, 1091–1109 (1961).
72. G. M. Bruere, "Importance of mixing sequence when using set-retarding agents with portland cement," Nature, **199**, No. 4888, 32–33 (1963).
73. L. R. Forbrich, "The effect of various reagents on the heat liberation characteristics of portland cement", Proc., Am. Concrete Inst., **37**, 161–184 (1940).
74. M. Polivka and A. Klein, "Effect of water-reducing admixtures and set-retarding admixtures as influenced by portland cement composition," Am. Soc. Testing Mater. Spec. Tech. Publ. **266**, 124–139 (1960).
75. R. Ashworth, "Some investigations into the use of sugar as an admixture to concrete," Proc., Inst. Civil Eng., **31**, 129–145 (1965).
76. W. Lerch, "The influence of gypsum on the hydration and properties of portland cement pastes," Proc., Am. Soc. Testing Mater., **46**, 1251–1292 (1946).
77. N. Kawada and M. Nishiyama, "Actions of calcium lignosulfonate upon portland cement clinker compounds," Rev. of the 14th Gen. Meeting, Japan Cement Eng. Assoc., Tokyo, 25 p. (1960).
78. W. C. Hansen, Discussion of Paper by H. W. Goetz, "False set of cement as influenced by hydroxylated carboxylic-acid-type admixture," Mater. Res. and Std., Am. Soc. Testing and Mater., **7**, 249–250 (1967).
79. L. H. Tuthill, R. F. Adams, and J. M. Hemme, Jr., "Observations in testing and use of water-reducing retarders," Am. Soc. Testing Mater. Spec. Tech. Publ. **266**, 97–117 (1960).
80. G. B. Wallace and E. L. Ore, "Structural and lean mass concrete as affected by water-reducing, set-retarding agents," Am. Soc. Testing Mater. Spec. Tech. Publ. No. 266, 38–96 (1960).
81. K. E. Palmer, Discussion of Paper by L. H. Tuthill *et al*, "A case of abnormally slow hardening concrete," Proc., Am. Concrete Inst., **58**, 1828–1831 (1961).
82. E. W. Scripture, Jr., "Cement dispersion and concrete quality," Eng. News-Rec., 127: 23, 81–84 (1941).
83. W. A. Cordon, Discussion of Paper by E. L. Howard, K. K. Griffiths, and W. E. Moulton, "Field experience using water-reducers in ready-mixed concrete," Am. Soc. Testing Mater. Spec. Tech. Publ. **266**, 149–155 (1960).
84. K. Newman, "The use of workability tests for concrete mix design and quality control," Res. Rept. **6**, Imperial College of Science and Technol., London, 23 (1960).
85. L. H. Tuthill and W. A. Cordon, "Properties and uses of initially retarded concrete," Proc., Am. Concrete Inst., **52**, 273–286 (1955).
86. G. B. Wallace, Discussion on Paper by L. H. Tuthill, R. F. Adams, and D. R. Michell, "Mass concrete for oroville dam," Symp. on Mass Concrete, Am. Concrete Inst. Spec. Publ. **Sp-6**, 195–196 (1963).
87. R. C. Mielenz, "Water-reducing admixtures and set-retarding admixtures for concrete: uses; specifications; research objectives", Am. Soc. Testing Mater. Spec. Tech. Publ. No. **266**, 218–239 (1960).
88. B. P. Hughes and B. Bahramiam, "Workability of concrete: a comparison of existing tests", J. Maters., **2**, Am. Soc. Test. Maters., 519–536 (1967).
89. V. Bahrner, "Report on consistency tests on concrete made by means of the V. B. consistometer," Rept. 1, Joint Res. Group on Vibration of Concrete, Swed. Cement Assn., Malmo, Stockholm, 23 (1940).
90. G. Della Libera, "Durability of concrete and its improvement through water reducing admixtures," RILEM Intern. Symp. on Admixtures for Mortar and Concrete, Brussels, Topic IV/11, 139–176 (1967).
91. J. W. Skeen, "Effect of vacuum mixing on concrete containing surface-active agents," Proc., 31st Inter. Congr. Ind. Chem., Liege, Sept. 1958 (Reprinted by the Bldg. Res. Sta., England, as Reference QL-622).
92. W. H. Granville, A. R. Collins, and D. D. Matthews, "The grading of aggregates and workability of concrete," Road Research Tech. Paper 5, 2nd Ed., Her Majesty's Stationery Office, London, 38 (1947).
93. John Ryell, "An unusual case of surface deterioration on a concrete bridge deck", Proc., Am. Concrete Inst., **62**, 421–440 (1965).
94. C. A. Vollick, "Effect of water-reducing admixtures and set-retarding admixtures on the properties of plastic concrete," Am. Soc. Testing Mater. Spec. Tech. Publ. **266**, 180–200 (1960).
95. T. C. Powers, "The bleeding of portland cement paste, mortar, and concrete", Portland Cement Assn. Res. Lab. Bull. 2, Chicago, Ill. (1939).
96. G. M. Bruere and J. K. McGowan, "Synthetic polyelectrolytes as concrete admixtures", Australian J. Appl. Sci., **9**, 127–140 (1958).
97. American Concrete Institute Committee 212 Report, "Admixtures for concrete," Proc., Am. Concrete Inst., **60**, 1481–1524 (1963).
98. B. Foster, "Summary", Am. Soc. Testing Mater. Spec. Tech. Publ. **266**, 240–246 (1960).
99. B. B. Hope, A. M. Neville and A. Guruswami, "Influence of admixtures on creep of concrete containing normal weight aggregate," RILEM Intern. Symp. on Admixtures for Mortar and Concrete, Brussels, Topic IV/2, 17–32 (1967).
100. E. L. Jessop, M. A. Ward and A. M. Neville, "Influence of water-reducing and set-retarding admixtures on creep of lightweight aggregate concrete," RILEM Intern. Symp. on Admixtures for Mortar and Concrete, Brussels, Topic IV/3, 33–46 (1967).
101. V. A. Tikhonov and L. A. Tikhomirova, "The effect of surface-active substances on changes in cement rock structure," (in Russian) Zhurnal Prikladno Khimmi, **27**, No. 10, 1067–1081 (1954).
102. A. B. Shekhter, N. N. Serb-Serbina and P. A. Rebinder, "Investigation with the electron-microscope of the effect of a surface admixture on the crystallization of hydrated minerals of cement clinker," (in Russian), Doklady Akad, Nauk SSSR, **89**, 129–132 (1953). Chem Abstr. **49**, 12809.d (1955).
103. A. N. Adamovich, "Electron-microscope investigation of crystal formation in hydration of

cement-clinker minerals, and their modification by adsorption effects of surface-active additions," (in Russian), Trudy Soveshch. po Khim. Tsementa, Moscow, 394–400 (1956). Chem. Abstr. **52**, 6751.d (1958).
104. G. Verbeck, "Carbonation of hydrated portland cement," Am. Soc. Testing Mater. Spec. Tech. Publ. **205**, 17–36 (1958).
105. B. Tremper and D. L. Spellman, "Shrinkage of concrete—comparison of laboratory and field performance", Highway Res. Bd., Highway Res. Record **3**, 30–61 (1963).
106. G. M. Bruere and J. D. Newbegin, "Some aspects of the drying shrinkage of concrete containing chemical admixtures", RILEM Intern. Symp. on Admixtures for Mortar and Concrete, Brussels Topic IV/5, 61–69 (1967).
107. R. A. Helmuth and D. H. Turk, "The reversible and irreversible drying shrinkage of hardened portland cement and tricalcium silicate pastes", J. PCA Res. and Develop. Labs., **7**, No. 2, 8–21 (1967).
108. H. Roper, "Dimensional change and water sorption studies of cement paste," Symp. on Struct. of Portland Cement Paste and Concrete, Highway Res. Bd. Spec. Rept. **90**, 74–83 (1966).
109. Y. Kondo and S. Hideshima, "Experimental researches on air-entrained concrete" (in Japanese), *Proc.*, Japan Cement Eng. Assn., 177–182 (1956).
110. U. Danielsson and A. Wastesson, "The frost resistance of cement paste as influenced by surface-active agents", Proc., Swed. Cement Concrete Res. Inst., Stockholm, **30**, 3–38 (1958).
111. T. Nishi, "On the recent studies and applications in Japan concerned to admixtures in use of building concretes and mortars (Part II)—effects of surface active agents upon hardened concretes and mortars", RILEM Intern. Symp. on Admixtures for Mortar and Concrete, Brussels, Topic IV/9, 109–125 (1967).
112. D. L. Ivey and T. J. Hirsch, "Effects of chemical admixtures in concrete and mortar", Texas Transportation Inst. Res. Rept. 70–3 (Final) (March 1967).
113. T. D. Larson, P. D. Cady, and J. J. Mallory, "The protected paste volume concept using new air void measurement and distribution techniques," J. Mater., **2**, Am. Soc. Test. Mater., 202–224 (1967).
114. R. E. Philleo, "A method of analyzing void distribution in air-entrained concrete," Unpublished paper, Portland Cement Assn., Res. and Develop. Div., Skokie, Ill. (May 1955).
115. J. T. Price, "The effect of entrapped air on air-void system parameters in hardened concrete," MS Thesis, Dept. Civil Engineering, Penna. State University (1967).
116. B. Warris, "The influence of air-entrainment on the frost-resistance of concrete. Part B. Hypothesis and freezing experiments," Proc. No. 36, Swed. Cement Concrete Inst., Stockholm, (1964).
117. H. H. Bache, G. M. Idorn, P. Nepper-Christensen, and J. Nielson, "Morphology of calcium hydroxide in cement paste", Symp. on Struct. of Portland Cement Paste and Concrete, Highway Res. Bd. Spec. Rept. 90, 154–174 (1966).
118. F. O. Slate, "A qualitative hypothesis to explain entrainment of air in concrete", Cornell Engineer, Cornell University, Ithaca, N. Y. (Jan. 1966).

Oral Discussion

Norihiro Kudo

Dr. Mielenz states that the activity of surface-active agents as set-controlling agent is due to the formation of insoluble film by their adsorption or chemisorption to the surface of cement grains.

There is a set-retarding agent, on the Japanese market, which is the mixture of water-soluble silicofluoride and some acids. It is probable that this retarder also makes insoluble film or layer on the surface of cement grains by the reaction of its ingredients and Ca-ion of cement, and the thickness of this laver is proportional to the dosage, subsequently the retarding effect of this retarder is proportional to the dosage.

Fig. 1 shows the initial set of concrete containing three types of retarding agents. The silicofluoride type retarder indicates the proportional retarding action, which is quite preferable property as set-controlling agent. Though the retarding effect of these retarding agents reduces slightly, this inclination does not change at 30°C.

Compressive strength of these concretes at 7 days is shown in Fig. 2. This tendency does not change at 28 days of age. As shown in this figure, the overdosage of the organic type retarding agents, say, more than 1.0% of cement weight, makes fatal defect in concrete structure.

Since surface-active agents are originally used as water-reducing and/or air-entraining agent, it must be thought that their set-retarding effect is a sort of "side-effect", that is to say, there are some doubts and anxiety to use such kind of surface-active agents as set-controlling agents. I'd like to ask Dr. Mielenz for some comments on this point.

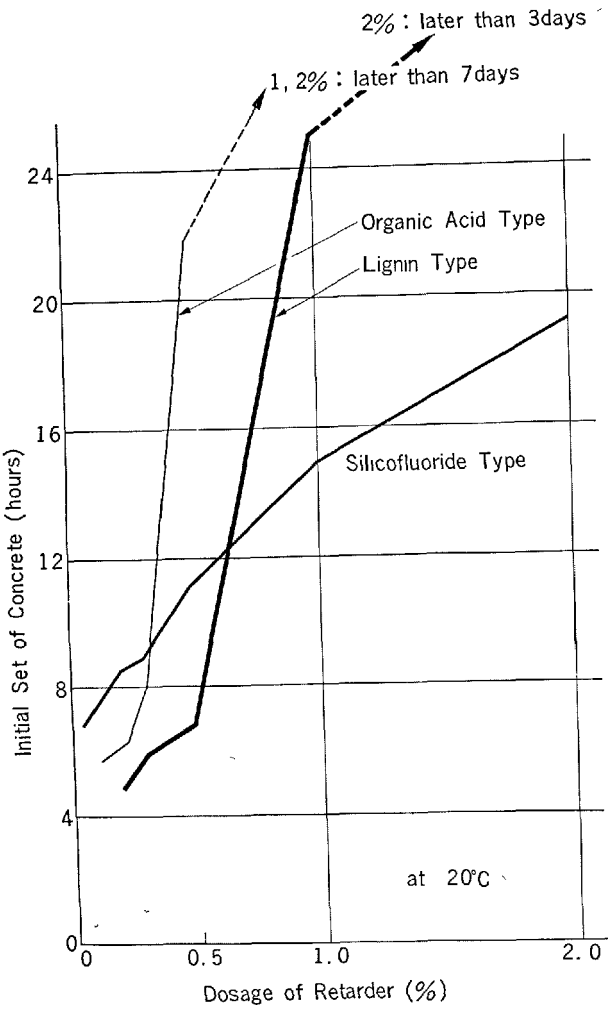

Fig. 1.

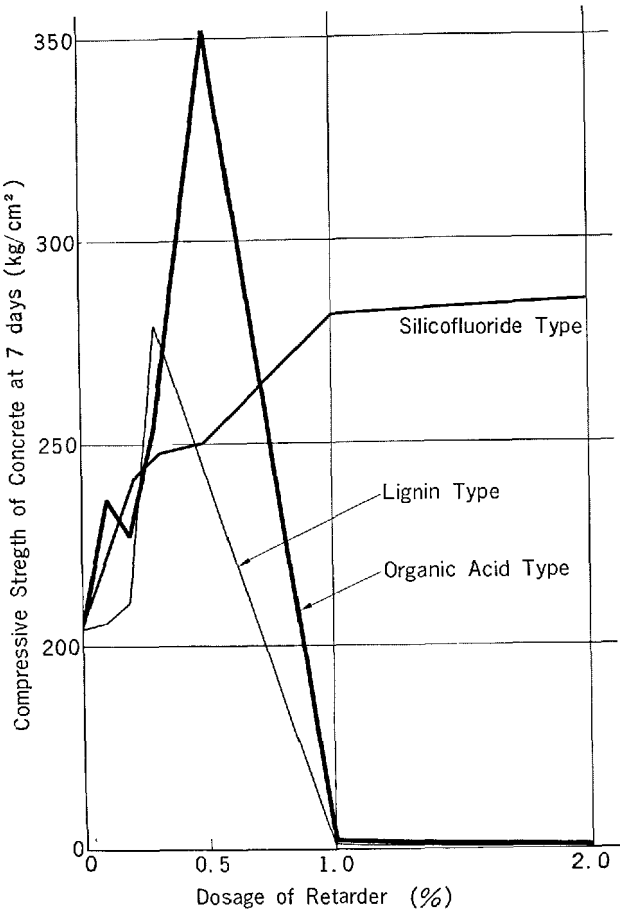

Fig. 2.

Oral Discussion

Udo Ludwig, Hans E. Schwiete and K. Seiler

1. During the study on the reaction mechanism of some special retarders we found out that with silicofluorid type retarders after short time the reaction products with lime ($Mg(OH)_2$, CaF_2 and $C_{2-3}S \cdot aq$) had a surface area that is equal to that of the unhydrated cement. Therefore we are in the opinion that in this case the retardation is due to a coating of reaction products on the surface of the clinker grains or on the active centers of the clinker surface.

2. With organic additives (hexites and polyhydroxy carbonic acids) lime reacts in solutions under formation of less solid phases with less surface area (Table 1). Therefore we assume an addition reaction of the organic molecules on the clinker surface or on the active centers. Proving this idea we mixed the portland cement with optimum addition of retarder and W/C = 0.35. As a function of the time we made a suspension with a total water content of 200 ml. By filtration the water was seperated from the solid phase. The organic substances were determined by a method from Springer (2). The results are given in the following Table 2.

From Table 2 you see the rapid initial decrease of the retarder concentration and here with the fixation of retarding molecules on the clinker surface. The general aspect of the retardation on the beginning of cement hydration is for the silico-fluorid and the organic retarders the same: less lime liberation and sulphate and water fixation. From special interest is that retarded mortars and concretes must be wetted thoroughly for a longer time for they have initially a higher open porosity.

The chemical measurement of fixation of organic molecules by Springer-method was conducted by Dr. K. D. Pohl.

Table 1. *Reaction of retarders with lime saturated solutions*

Research No.	Starting mixture retarder	[ml]	CaO [g]	Reaction time [h]	CaO (filtrate) [g/l]	C/S-ratio of CSH-phase	Weight of the solid [g]	Spec. surface [m²/g]	pH (filtrate)
1	MgSiFe 5%	10.5	3.4	0.5	0.575	2.25	5.3782	109.0	13.00
2		10.5	4.1	0.5	1.040	2.70	5.6476	100.7	
3		10.5	3.4	24	0.580	2.25	5.3538	116.0	13.00
4		10.5	4.1	24	1.051	2.70	5.6700	102.6	
5	"R"	10.0	4.1	0.5	0.564	2.70	6.6782	60.5	12.77
6	"R"	10.0	4.5	0.5	0.805	2.97	7.0104	83.9	
7	"R"	10.0	4.1	24	0.673	2.49	6.5272	61.3	12.81
8	"R"	10.0	4.5	24	0.834	2.90	6.8325	81.6	
9	"N"	6.0	3.79	0.5	1.280		3.3433	10.7	13.03
10	"N"	6.0	4.00	0.5	1.349		3.5506	11.2	
11	"N"	6.0	3.79	24	1.364		3.2323	11.5	13.03
12	"N"	6.0	4.00	24	1.321		3.5697	11.6	
13	"P"	15.0	3.90	0.5	1.180		4.3464	32.1	13.01
14	"P"	15.0	4.00	0.5	1.194		4.3948	33.4	
15	"P"	15.0	3.90	24	1.126		4.4216	33.2	13.00
16	"P"	15.0	4.00	24	1.133		4.5830	35.3	

"R" industrial retarder (main compound: $MgSiF_6$)
"N" industrial retarder (main compound: Hexite)
"P" industrial retarder (main compound: Polyhydroxy carbonic acids)

Table 2. *Combination of the retarders "N" and "P" on the portland cement as a function of the hydration time*

Retarder	Hydration time [min]	Used ml of $\frac{\text{In } K_2Cr_2O_7}{50 \text{ ml solution}}$ [ml]	Content of retarder in the filtrate [%]
"N"	—	3.53	100.0
"N"	5	0.97	27.5
"N"	15	0.80	22.7
"N"	30	0.72	20.4
"N"	240	0.38	10.8
"P"	—	3.62	100.0
"P"	5	2.05	56.5
"P"	15	1.61	44.5
"P"	30	1.20	33.2
"P"	240	0.80	23.8

References

1. K. Seiler: "The influence of retarders with special view on silico-fluoride containing retarders" Thesis Inst. f. Gesteinshüttenkunde der RWTH Aachen 1968.
2. U. Springer: "Quantitative determination of organic substances in clays" (in German), Zeitschr. f. Pflanzenkunde, Düngung und Bodenkunde **40** (1948) 166.

Oral Discussion

Richard A. Kuntze and P. Hawkins

Dr. Mielenz has indicated that several effects must be expected when hydroxy compounds are added to portland cement. For example, a change in the rate of interaction between sulfate and C_3A may result in an increased or decreased formation of calcium sulfoaluminate (ettringite). This is of particular interest with respect to false set, since our own work has indicated that ettringite contributes to this type of early stiffening of cement paste (1).

Seligmann and Greening (2) reported that the formation of ettringite is increased by sucrose whereas ligonsulfonates have a negligible effect. In contrast, Goetz (3) has found that hydroxy acids decrease the formation of ettringite even if hemihydrate is present in the cement. Our own work has shown that some hydorxy acids are capable of delaying the crystallization of gypsum by direct retardation of the hydration of hemihydrate (Fig. 1). Consequently, false set of cement may be affected by these materials by reducing the amount of ettringite formed and by delaying the crystallization of gypsum.

Hydroxy acids differ widely in their effect on the crystallization of gypsum depending not only on their molecular configuration, but also on the concentration of $Ca(OH)_2$ (Figs. 2 and 3). Therefore, if the effect of the hydroxy acids is just sufficient to produce gypsum crystallization after the mixing is completed, false set may be obtained with a cement that otherwise does not show this behaviour. Alternatively a false setting cement may appear to behave normally, if the crystallization of gypsum is delayed until testing is completed.

In contrast to hydroxy acids, little or no effect on the crystallization of gypsum has been observed with sucrose or lignosulfonates. In view of this difference in the behaviour between hydroxy acids and other hydroxy compounds such as lignosulfonates, we would like to ask Dr. Mielenz if observations made in prac-

tice support or disagree with the results obtained by us.

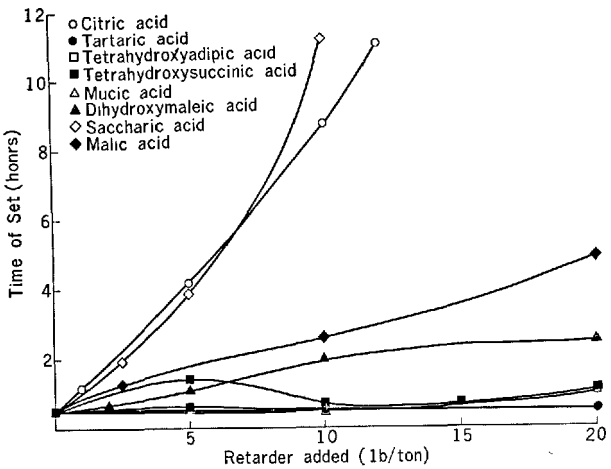

Fig. 1. *Effect of hydroxypolycarboxylic acids on the hydration of* $CaSO_4$ $1/2H_2O$

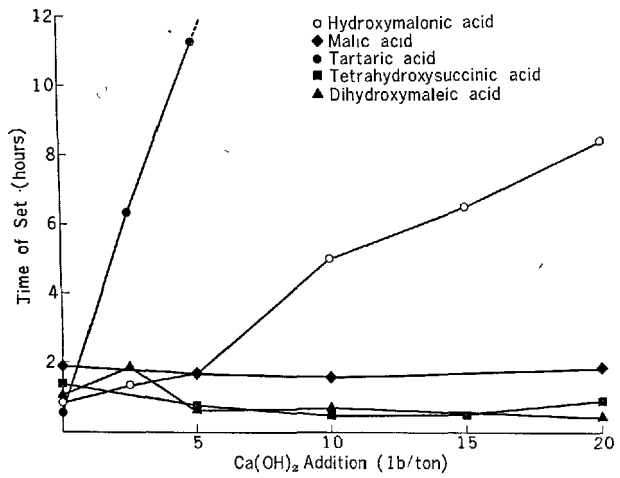

Fig. 2. *Effect of* $Ca(OH)_2$ *on the retarding efficacy of hydroxypolycarboxylic acids.*

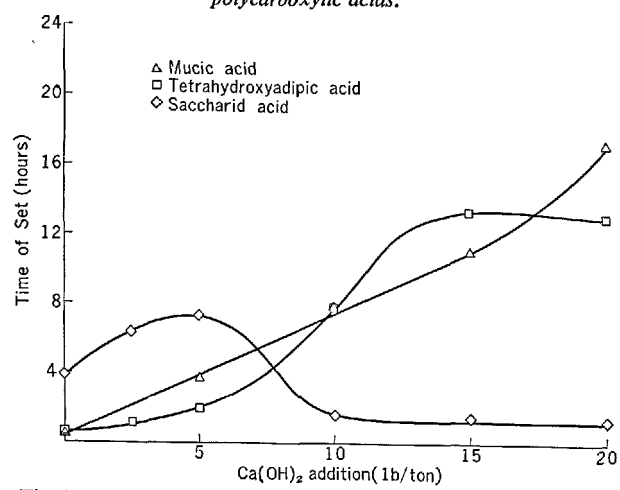

Fig. 3. *Effect of* $Ca(OH)_2$ *on the retarding efficacy of hydroxycarboxylic acids.*

References

1. R. A. Kuntze and P. Hawkins, "The effect of hydration characteristics of hemihydrate on the false set of portland cement". Written discussion (No. IV-16) on "Utilization of chemical gypsum for portland cement" by K. Murakami (Session IV-5), Fifth Int'l Symposium on the Chemistry of Cement, Tokyo, 1968.
2. P. Seligmann and N. R. Greening, "Studies of early hydration reactions of portland cement by X-ray diffraction". Highways Res. Bd. Highway Res. Record No. 62, 80–105 (1964).
3. H. W. Goetz, "False set of cement as influenced by hydroxylated-carboxylic-acid admixture". Mater. Res. and Stds., 7, 246–249 (1967).

Oral Discussion

Geoffrey J. Frohnsdorff

Since the understanding of the mechanism of hydration of C_3S and alite is of great interest to us all, I would like to make some comments on this subject and to ask Dr. Mielenz if he agrees with them.

Since C_3S, unlike C_3A, does not normally react rapidly and continuously on being mixed with water, it seems reasonable to consider its hydration to be "self-retarded". This suggests that an understanding of the mechanism of the self-retardation is a prerequisite to understanding the retarding or accelerating effects of surface active agents and other additives.

The study of the mechanism is difficult because it appears that a number of consecutive and concurrent reactions are involved and, even when present in minute amounts, the products of the reactions may have large retarding effects on the reactions in which they are formed. A continuing need in studying the effects of additives on the hydration of C_3S or cement is to design experiments which, at least partially, separate the reaction steps. Some ways in which this may be done are illustrated by:

1) The work of Dr. Kondo (1) in which the hydration of C_3S in water extracted from a C_3S paste was compared with the hydration carried out in distilled water.
2) The work of Drs. Dolch and Compbell (2) in which they studied the earliest reactions of C_2S in a very large quantity of water or aqueous solution (W/C = 2000) so as to avoid the complications caused by formation of new solid products; this technique might prove valuable in studies of surface active agents or other

admixtures by helping to show their effects on initial rates of hydrolysis of cement compounds.

3) The work of Dr. Bruere (3) who showed the effects on cement hydration of delayed additions of retarders.

I would like to suggest that understanding of the effects of the retarders and accelerators would be significantly aided by extensions of methods to which I have just referred. I would like to ask Dr. Mielenz if he agrees with this point of view.

References

1. Kondo, R. and Ueda, S., "Kinetics and mechanisms of the hydration of cements", Fifth International Symposium on the Chemistry of Cements, Tokyo, (1968).
2. Campbell, L. E., "Some orthosilicates and their hydrates", Ph.D. Dissertation, Purdue University (1967).
3. Bruere, G. M., Nature, **199**, 32 (1963).

Oral Discussion

John H. Taplin

Would Dr. Mielenz care to make a comment on the suggestion that I made to Dr. Lieber in session II, namely, that retarders may act by delaying the nucleation of a calcium silicate hydrate and that the adsorption of retarders on anhydrous clinker mineral surfaces may be unnecessary for retardation.

Author's Closure

Richard C. Mielenz

Mr. Kudo has provided data on time of setting and compressive strength of concrete containing each of three types of set-retarding chemical admixtures that are identified as silicofluoride, organic acid, and lignin types, respectively. By their nature water-soluble salts of hydroxy acids and of lignosulfonic acid are water-reducing retarders for portland cement mixtures; hence, it is not appropriate to designate their set-retarding action as a "side-effect." Although the retardative action of these types of organic admixtures can be partially or completely overcome by suitable intermixture with accelerating agents, salts of hydroxy acids and lignosulfonates are widely and successfully employed as set-retarding admixtures in construction.

In his tests, Mr. Kudo extended the rate of use of the organic admixtures well beyond the proportions in which they normally are used in portland cement mixtures for general construction. Unfortunately, he has not identified the chemical composition of the two organic admixtures so that it is not possible to state an optimum rate of use for these products to meet the requirements of typical construction. In particular, note should have been made as to whether the rates of use indicated are for the active constituent or an aqueous solution. However, calcium lignosulfonates usually are used at rates in the range 0.15 — 0.40 and salts of hydroxy acids in the range 0.05 — 0.10 percent by weight of the cement content of concrete.

The low maximum strength reported for the concrete containing the lignosulfonate relative to that for the concrete containing the organic acid type admixture probably relates to air entrainment. The air-entraining efficiency of differing lignosulfonates varies widely and may be a basis for selection of a product for use in concrete. In any event, comparative tests like those shown should be conducted at equivalent air content or the air content and proportioning of each concrete mixture should be stated for the reader.

Mr. Kudo refers to "doubts and anxiety" about use of organic surface active agents in concrete. There is no basis for such concern provided the product approved for use conforms with carefully prepared specifications, such as A.S.T.M. Designation: C 494, Standard Specifications for Chemical Admixtures for Concrete, and provided proper dispensing procedures are employed so as to control the rate of use of the admixture within close limits, usually ± 3 percent of the amount required.

Kuntze and Hawkins have summarized valuable information on the effect of various hydroxy acids on time of setting of plaster of Paris, and they apply this information to an interpretation of reactions of calcium sulfate in portland cement mixtures. They note the report of Seligmann and Greening (52)* on accelerated ettringite formation in the presence of sucrose. Not noted is the observation by Seligmann and Greening of similar behavior in the presence of a lignosulfonate in the absence of appreciable amounts of calcium hydroxide. These latter authors also confirm the observation of others that calcium lignosulfonate retards the setting of plaster by delaying the precipitation of gypsum.

In any event, as is stated in the principal paper,

*Numbers in parentheses refer to references appended to the principal paper.

numerous factors influence the development of a stiffening tendency (or lack thereof) in concrete. Practical experience is in accord with the findings of scientific work in this field. The C_3A content and alkali content of the cement, the form and amount of calcium sulfate addition, any aeration of the cement, the composition and rate of use of any chemical admixtures and the sequence of addition of the concrete-making materials and the mixing cycle employed in preparation of the concrete, ambient conditions, such as temperature, and job conditions, such as distance of haul and timing of placing and finishing operations—all together determine whether loss of working qualities will occur in specific concrete construction. Under particular circumstances, either a hydroxy acid salt or a lignosulfonate may alleviate or aggravate premature stiffening of concrete. If the action is a false setting tendency, the problem may arise either because early precipitation of gypsum that otherwise would occur during mixing of the concrete is delayed to the interval when the concrete is being handled and worked, or because precipitation of gypsum that otherwise would be delayed until after completion of placing is caused to occur during the period when the concrete is being handled and worked. Inordinate delay of stiffening, combined with premature finishing of unformed surfaces, can lead to unsoundness of the surfaces because of interference with normal process of bleeding and settlement of the concrete (93). In cements that are deficient in available calcium sulfate, either because of low SO_3/Al_2O_3 ratio or because the calcium sulfate is in the form of slowly soluble anhydrite, a flash setting related to inadequate retardation of C_3A may induce an irreversible stiffening of the concrete prior to completion of placing. These matters have been discussed by Seligmann and Greening in relation to practical problems.

The data supplied by Ludwig and his coworkers are interesting but they cannot be discussed in detail because they do not provide complete information on the systems and procedures utilized in the investigation. Presumably, the mixtures referenced in Table 1 do not include portland cement or ground portland cement clinker, but the text of the discussion is confusing in this respect. The condition of dryness of the solids should be known in order that the significance of the reported weight of precipitated material can be established. Likewise, their statement that the specific surface of reaction products of lime and magnesium silicofluoride is equal to that of unhydrated portland cement is surprising considering their reported values of $100 - 116\ m^2/g$ in contrast to usual values of $0.3 - 0.5\ m^2/g$ for commercial portland cement. I am unable to identify the substance designated as "hexite." Can it be a hexose or hexatol?

Ludwig *et al* conclude from their data that the retardative action of the silicofluoride and of the organic agents arises from deposition or interaction at the anhydrous surfaces of granules of portland cement. On the contrary, the data provided with the discussion do not separate such effects from those that would arise if the admixtures interact with hydration products that either are plated over the surfaces of the clinker components or are dispersed in the mixing water. Such distinction requires carefully developed experiments that involve delayed addition of the admixtures, use of non-aqueous media, and detailed study of the composition and morphology of the resulting cement paste matrix. Such procedures have been explored, as is noted in the principal paper, and such work is now in progress in several laboratories.

I agree with the comments of Dr. Frohnsdorff relative to the techniques that should be applied in the study of hydration of C_3S or alite. The recommended procedures should be supplemented by study of cement-admixture reactions in non-aqueous or partially aqueous systems, as was initiated by Blank *et al* (51). Moreover, the solid products and solutions should be studied chemically and the morphology of the solid products should be established, as by scanning electronmicroscopy.

I agree with Dr. Taplin's suggestion that chemical retarders may act by delaying the nucleation of a calcium silicate hydrate. However, the reactions and physical-chemical effects of the surface-active agents are considerably more complex than can be explained by a single mechanism.

Likewise, adsorption of chemical retarders on anhydrous surfaces of clinker compounds may not be an essential aspect in the cement-admixture interaction. However, this concept does not deny the probable significance of uptake directly upon such anhydrous surfaces. Data by Blank *et al* (51) indicate that water molecules and molecules of hydroxylated chemical admixtures compete for sites on anhydrous surfaces, a situation that will always give water the statistical advantage in a practical concrete mixture. In this connection it is worthwhile to recall the independent work of Polivka and Klein (74) and of Kennerley *et al* (43), who found close correlation between release of heat of hydration and time of setting of portland cement pastes, regardless of the presence or absence of a water-reducing, set-controlling admixture. Their data indicate that setting is determined largely by the

quantity of hydration products produced, a conclusion that, if confirmed, will depreciate the significance of any action of chemical retarders on nucleation of the products of hydration.

Supplementary Paper IV-5 Possible Mechanisms of Influence of Admixtures on Creep of Cement Paste

Emlyn L. Jessop, Michael A. Ward* and Adam M. Neville**

Synopsis

Creep data under conditions of drying of neat cement pastes with two water-reducing and set-retarding admixtures are presented. To find the possible mechanism of action of the admixtures the following factors have been investigated experimentally and are discussed: the magnitude and rate of loss of water from the given pastes at higher temperatures, density of hydrated cement paste, surface tension of the solution of admixture in water, and morphology of the hydrated paste as revealed by electromicrographs. Some relation between the ease with which water can move within and out of the paste and creep is shown to exist, but it is suggested that all the other factors be further studied, too.

Introduction

Admixtures have been used in concrete for some time with many beneficial effects (1, 2). Not all the effects are, however, understood or even well-known: among these is the influence of admixtures on creep, a property of considerable, and indeed increasing, importance in the design and performance of concrete structures.

At the 1967 RILEM International Symposium on Admixtures for Mortar and Concrete there were presented two papers (3, 4), arising from work at The University of Calgary on the influence of water-reducing and set-retarding admixtures on creep of concrete made with lightweight and normal weight aggregates. Little other work in this area has been published. The earlier two papers (3, 4) dealt with the creep behaviour of concrete at the phenomenological level. In the present paper, an attempt is made to study the mechanism through which two selected water-reducing and set-retarding admixtures affect the creep of neat cement paste under conditions of drying.

There is an important limitation of the present work that should be mentioned. The behaviour of admixtures, insofar as influence on the properties of concrete is concerned, is not simply related to the ASTM classification (1) of the admixture and is often sensitive to the properties of the actual cement used. As far as creep is concerned, earlier work (3, 4) showed that admixtures, even when belonging to the same ASTM classification, vary widely in their influence. Thus no generalization from the present experiments is possible: the paper describes no more than the effects of the particular admixtures.

Previous Work

In earlier tests (3, 4) creep of concretes containing four water-reducing and set-retarding admixtures was studied. The effects of an admixture were determined by a comparison with an admixture-free, or plain mix, which had the same workability and the same compressive strength at the time of application of the sustained load; such mixes were termed corresponding mixes. Thus the concrete with an admixture had a reduced cement content as well as a reduced water content compared with the corresponding plain mix. As a result, the volumetric content of cement paste in the concrete with an admixture was lower, too.

*Department of Civil Engineering. The University of Calgary, Alberta, Canada.

**Department of Civil Engineering. The University of Leeds, Leeds, United Kingdom.

Now, the influence of cement paste content on creep is such that a concrete with a lower paste content (i.e. with an admixture) would be expected (5) to exhibit less creep than the corresponding plain mix. In fact, in nearly all the tests the opposite was the case. Thus the quantity of the cement paste per unit volume of concrete cannot account for the influence of admixtures on creep. Furthermore, tests on four admixtures have indicated that there is no simple correlation between creep and the chemical group to which the admixture belongs. It appears, therefore, that an explanation of the influence of admixtures on creep must be sought in the quality of the paste, viz. the physical structure of the gel or the properties of the water.

Theoretical Considerations

Cement paste has been shown to be the seat of creep in concrete, the influence of the aggregate being mainly a restraining one (6). Although creep occurs under conditions of hygral equilibrium between the concrete and the ambient medium, such creep being known as basic creep, additional creep takes place if moisture is lost from the concrete while under sustained load; this is known as drying creep (7). While the exact mechanism of creep is still under discussion, it seems likely that creep is closely associated with movement of moisture in the cement gel, this movement being induced by the applied load. Support to this statement is lent by the fact that cement paste containing no evaporable water does not creep (8).

Powers (9) suggested that diffusion of moisture within the cement gel gradually dissipates mechanically induced swelling. The situation is that within the gel there exist voids of different sizes, on the surfaces of which there are formed films some 13Å thick, providing wide enough space is available between adjacent solid surfaces. When this is not the case, adsorption is hindered, and when a compressive stress is applied to a cement paste specimen, the films in the areas of hindered adsorption are subjected to an additional pressure which is brought to a state of equilibrium by diffusion of water from these wedge-shaped crevices into wider spaces. A part of creep can be explained by this diffusion process.

It could be postulated that if moisture movement is the essential element in creep, then the speed or ease of this movement is a factor in creep. It follows that changing the characteristics of moisture movement in cement paste might change its creep behaviour. One way of effecting such a change is to alter the properties of water in the cement paste, e.g. the surface tension of the water. Another way would be to alter the physical structure of the gel in which the moisture movement takes place, i.e. of the solid-water interface. It should be explained that the term water is taken to mean in reality a solution of salts such as exists in hydrated cement paste.

The presence of admixtures can affect the surface forces existing between the water and the gel, with the result that, under an applied sustained stress, the movement of moisture will be facilitated. It is known that some admixtures reduce the surface tension of water, and this could result in an increased magnitude and rate of creep. However, it is also possible that admixtures affect the morphology of the gel so that the surfaces along which moisture has to move are changed.

A morphological change was observed by Young (10) in the case of hydrated C_3A when calcium lignosulphonate was added: instead of the usual hexagonal platey structure there were acicular interwoven crystals. This behaviour was, however, not confirmed (11) in the case of hydration of C_3S with the same admixture.

Even if the behaviour of C_3A with an admixture were the same under conditions existing in a hydrating cement paste as in Young's tests on pure C_3A, the presence of an acicular crystal structure of C_3A may not be important. Tamas (12) points out that aluminates represent only a minor part of portland cement and their hydration products are not only small in absolute amount but also have a specific surface negligible in comparison with the products of hydration of the silicates. He believes, therefore, that it is the hydration of the silicate phase that is changed by admixtures. More specifically, there is activation or de-activation of the reaction between the silicate phase and water, so that with a retarder there is a lower amount of tobermorite gel formed at a given time. Such behaviour represents a change in structure which may be responsible for a variation in creep characteristics of the paste.

Another type of structural change which could occur in hydrated cement paste due to the presence of an admixture is that associated with the geometry and distribution of pores. These properties influence

permeability and strength and may well affect drying creep, which involved movement of moisture from the gel. If this is correct, then the paste with a higher creep should also show a higher loss of water due to a sustained load than a nominally similar paste without an admixture and with a lower creep. Furthermore, high-temperature drying should lead to a differential loss of water in the two pastes, if the admixture indeed affects the size and distribution of pores in the hydrated paste.

To resolve the mode of influence of admixtures on creep, it would be useful to answer the following questions.

1. Do the admixtures used in the previous tests on concrete (3) alter the surface tension of the mixing water?
2. Do the admixtures alter the structure of the cement gel in a manner likely to influence creep? Specifically,
   (a) do they affect the density of the gel?
   (b) do they affect the morphology of the gel?
3. Does either of the changes under 1 or 2, or both, lead to a more rapid or a higher loss of moisture from the specimen of hydrated paste?

Experimental

The tests consisted basically of a comparison of the properties of 6 by 12 in. cylinders of neat cement paste with and without an admixture; two admixtures were used. The properties involved were: the modulus of elasticity of the paste, creep under conditions of drying, density of the hydrated paste, morphology as revealed by a scanning electron microscope. In addition, the surface tension of the mixing water for a series of admixture concentrations was determined.

The same cement was used as in the previous investigation (3); this was a Type III high early strength portland cement, whose properties are given in Table 1. Two commercially produced admixtures were used. According to the ASTM classification, they are water-reducing and set-retarding. Admixture A belongs to Class 3 (hydroxylated carboxylic acid) and admixture B to Class 1 (lignosulphonic acid). The descriptions A and B refer to the same admixtures which were used in the earlier investigations (3, 4). The admixtures were used in amounts prescribed by the manufacturers to achieve normal water-reducing and set-retarding effect.

The mixing water was ordinary tap water at a temperature of approximately 21°C.

The water-cement ratio of the plain mix specimens was 0.4. For the specimens containing an admixture the ratio of the weight of water plus admixture to the weight of the cement was 0.4.

All the specimens were demoulded at the age of 24 hours and thereafter stored in water at a temperature of 21°C. The creep specimens were loaded at the age of 28 days, the nominal stress-strength ratio at loading being 0.50. The load was applied in a testing machine incorporating a load-maintaining device and sustained for 12 hours. The test environment had a relative humidity of 50 ± 5 per cent and a temperature of 21°C. Thus the specimens were drying while undergoing creep so that both basic and drying creep took place. The extent of the latter is, however, not known as the water first lost from a specimen exposed to load and to drying for so short a time (12 hours) is capillary water. Such removal of capillary water may, however, facilitate the movement of gel water, pos-

Table 1. *Properties of cement*

Bogue compound composition, %				Alkali content, %		SO_3 %	Blaine specific surface, cm^2/g
C_3S	C_2S	C_3A	C_4AF	Na_2O	K_2O		
56.0	17.0	9.0	6.0	0.12	0.38	2.75	5060

Table 2. *Creep data*

Time since loading, hours	Admixture					
	Nil		A		B	
	Creep, 10^{-6}	Rate of creep, 10^{-6} per hour	Creep, 10^{-6}	Rate of creep, 10^{-6} per hour	Creep, 10^{-6}	Rate of creep 10^{-6} per hour
1	560		415		680	
		185		125		260
2	745		540		940	
		120		75		150
3	865		615		1090	
		105		65		120
4	970		680		1210	
		80		70		100
5	1050		750		1310	
		75		35		75
6	1125		785		1385	
		65		50		80
7	1190		835		1465	
		65		40		80
8	1255		875		1545	
		55		40		70
9	1310		915		1615	
		55		30		75
10	1365		945		1690	
		55		30		75
11	1420		975		1765	
		50		35		60
12	1470		1010		1825	

Table 3. *Strength, stress-strength ratio, secant modulus of elasticity, density, and void content*

Property	Admixture		
	Nil	A	B
Strength, psi, at 28 days	10,650	10,880	11,100
Stress-strength ratio	0.52	0.51	0.50
Secant modulus of elasticity at a stress-strength ratio of 0.5 × 10^6 psi	2.28	2.34	2.06
Density at age of 25 min., g/cm³	1.921	1.867	1.835
Void content, per cent	1.5	4.2	5.9

Table 4. *Relative loss of water on heating*

Time since start of heating, hours	Relative loss of water for admixture		
	Nil	A	B
1	1.000*	1.000	1.000
2	1.719	1.423	1.744
5	1.999	1.819	2.026
10	2.064	1.940	2.102
50	2.120	2.018	2.178

*represents saturated surface dry condition.

Table 5. *Relative surface tension of water with admixture*

Admixture content in water by weight, per cent	Relative surface tension with admixture	
	A	B
0	100	100
0.006*	99.9	—
0.06*	—	96.9
50	98.5	79.8
100	97.3	74.5
Benzene, on same scale	39.7	

*as prescribed by the manufacturer and used in the actual mix.

sibly by inducing a state of tension in the liquid.

The results of the creep tests are given in Table 2. Table 3 lists the strength, the actual stress-strength ratio at application of load, and the secant modulus of elasticity at a stress-strength ratio of 0.50, determined at the same time.

In the moisture loss tests, specimens cured in fog at a relative humidity of 100 per cent for 28 days were dried in an oven at 105°C. The results are presented in Table 4.

Additional tests were made on the density of the fresh cement paste. Here a known volume of compacted fresh paste, 25 minutes old, was weighed with a sensitivity of 10^{-5}. The results are presented in Table 3.

Table 5 gives the surface tension of water with the admixtures in different concentrations. An arbitrary scale is used in which the surface tension of pure water is 100 and that of benzene is 39.7. The surface tension was determined using a capillary rise and fall technique.

Discussion of Results

From Table 2 it can be seen that, compared with the plain mix, admixture A decreases and admixture B increases creep for the 12-hour period under test. When the same admixtures were used in concrete (3, 4) a qualitatively similar effect was observed for periods under load up to 150 days.

Table 5 shows that for the concentration of admixtures used in the present tests the effect of admixture B is to reduce the surface tension of the water by about 3 per cent; admixture A appears to have no effect. While the creep of the paste with admixture B is higher than that of the plain mix, in the case of admixture A there is no accord between the effect of the admixture on the surface tension and on creep. It seems thus that the surface tension effect can do no more than contribute to the influence of the admixtures on creep.

The data on density (Table 3) are of interest: both admixtures cause a decrease in the density of the hydrated paste: about 3 per cent in the case of admixture A, and approximately 4 per cent for B. The difference between the two admixtures may be due to the slight air-entraining properties of admixture B (about 1 per cent in excess of the plain mix). A reduction in density can be interpreted to mean a less well-packed gel which may permit easier movement of moisture, and hence a higher magnitude or rate of creep. However, the decrease in density was not accompanied by a decrease in strength, compared with the plain mix, and may mean increased hydration of the mixes with an admixture. Since the main product of hydration—gel—is responsible for creep, the presence of more gel could account for higher creep. This possibility does not, however, explain the difference between the creep behaviour of mixes with admixture A and B. In any case, the amount of gel present should be checked by measurement of the degree of hydration—a test which was not performed.

The electron micrographs showed no significant morphological difference between the mixes with and without an admixture. The magnification was 15,000 times, which is inadequate to resolve the changes in the gel structure; for this, a magnification ten times greater would be necessary. An indirect indication of the structure of the hydrated paste is

obtained from the values of the secant modulus for the different mixes. Specifically, in comparison with the plain mix, the mix with admixture A has a higher secant modulus and a lower creep; the converse is the case with admixture B. This behaviour was previously found also to exist in concretes with and without the same admixtures, both with lightweight and normal weight aggregates (3, 4).

Perhaps the most significant results obtained in the present investigation concern the moisture loss from the different mixes when subjected to higher temperature. Table 4 shows that, relative to the plain mix, the mix with admixture A loses less moisture (and exhibits less creep); the opposite is the case with admixture B. As pointed out earlier, the water actually lost is probably mostly capillary water but its movement may well affect the internal movement of gel water—a factor in creep.

Summary of Possible Effects of Admixtures

It is possible that the increased creep of the mix with admixture B, compared with the plain mix, can be accounted for by a greater ease of moisture movement within and out of the paste and a lower surface tension of water with this admixture. These two phenomena are likely to be related to one another. There is also a possibility of a change in the gross morphological structure when this admixture is used.

In the case of admixture A, the creep is lower than in the plain mix. The moisture loss of the mix with the admixture was lower than for the plain mix, but the rate of loss was higher in the former case. If this trend continues, it is possible that the ultimate loss of water will be higher in the mix with the admixture. There is no comparable rate-effect in the creep of the two mixes, but it is interesting to recall that in the earlier tests (3, 4) on concrete with admixture A, the rate of creep decreased only slowly with time so that the long-term creep was in most cases higher than for the plain mix. It is conceivable, therefore, that the presence of admixture A leads to a similar increase in creep as in the case of admixture B but with a delay. The reason for this still unconfirmed behaviour of cement paste with admixture A is not known.

Tentative Conclusions

1. There appears to exist a relation between the ease with which water is lost from hydrated paste on heating and the magnitude of creep of mixes with and without the admixtures used in the present tests.
2. The influence of admixture B on the surface tension of water appears to be in accord with the influence on the magnitude of creep; there is, however, no such relation in the case of admixture A. It is, therefore, not possible to correlate the surface tension effect with creep.
3. The density of paste 25 minutes old and creep are related in the case of the mix with admixture B, as compared with the plain mix, but again no such relation exists for admixture A. Thus, the density and creep cannot be correlated.
4. It is possible that admixtures affect the gross morphology of the hydrated paste, and therefore the shape of the stress-strain curve and the creep. A confirmation at the level of gel particle size is still required.
5. It seems from the above that the mechanism through which admixtures influence creep is still uncertain. The present paper has suggested some of the possible mechanisms, which it is proposed to examine in more detail in the future.

Acknowledgements

The authors would like to thank Mr. D. R. Morgan for his help in the experimental work. The project was supported by a grant from the National Research Council of Canada, which is gratefully acknowledged.

References

1. American Society for Testing Materials, "Symposium on effect of water-reducing and set-retarding admixtures on properties of concrete", Special Technical Publication No. 266, 1959.
2. RILEM, "International symposium on admixtures for mortar and concrete", Brussels, Aug. 30 to Sept. 1st, 1967.
3. Jessop, E. L., Ward, M. A., Neville, A. M., "Influence of water-reducing and set-retarding admixtures on creep of lightweight aggregate concrete", Published in the Symposium listed in ref. 2, 33–46.
4. Hope, B. B., Neville, A. M., Guruswami, A., "Influence of admixtures on creep of concrete containing normal weight aggregate". Published in the Symposium listed in ref. 2, 17–32.
5. Neville, A. M., "Creep of concrete as a function of its cement paste content", Magazine of Concrete Research, Vol. 16, No. 46, March 1964, 21–30.
6. Neville, A. M., "Properties of concrete", Sir I. Pitman and Sons, London, 1963, and John Wiley and Sons, New York, 1964, Reprinted Nov. 1965, 532.
7. Ali, I., Kesler, C., "Mechanisms of creep in concrete", American Concrete Institute, Special Publication No. 9, 1964, 35–57.
8. Glucklich, J., Ishai, O., "Creep mechanism in cement mortar", Journal of the American Concrete Institute, Proc. Vol. 59, July 1962, 923–948.
9. Powers, T. C., "Mechanisms of shrinkage and reversible creep of hardened cement paste", International Conference on the Structure of Concrete, London, 1965.
10. Young, J. F., "Hydration of tricalcium aluminate with lignosulphonate additives", Magazine of Concrete Research, Vol. 14, No. 42, November 1962, 137–142.
11. Young, J. F., Private communication.
12. Tamas, F. D., "Acceleration and retardation of portland cement hydration by additives", Highway Research Board, Special Report No. 90, Symposium on Structure of Portland Cement Paste and Concrete, 1966, 392–397.

Supplementary Paper IV-45 Effects of Organic Compounds on the Hydration Reactions of Tricalcium Aluminate

Kenneth E. Daugherty and Milton J. Kowalewski, Jr.*

Synopsis

At one time it was believed that the hydroxyl-carbon groups found in many organic admixtures might be responsible for the retardation of the reaction of water molecules with cement compounds. It was theorized that the reduced rates and the associated set-delays were a result of hydrogen bonding of the hydroxyl-carbon groups to cement compound surfaces.

A more modern theory stated that the α-hydroxyl carbonyl groups was responsible for the set-delay produced in portland cement on the basis that many set-retarding agents contain or hydrolyzed to give this functionality.

In order to investigate reactions of compounds containing α-hydroxyl carbonyl groups with cementitious materials, the effects of 13 well-characterized, interrelated organic compounds on the hydration reactions of tricalcium aluminate were examined at 25°C. The organic compounds contained various types and numbers of hydroxyl groups and carbonyl groups. The compounds were: acetic acid, glycolic acid, DL-mandelic acid, glyceric acid, ketomalonic acid di-sodium-salt, ethylene glycol, glycol aldehyde, sucrose, D-(+)-trehalose, D-(+)-glucose, fructose, mannitol and sorbitol.

The principal means of investigation was to study the disappearance of tricalcium aluminate and the appearance of new hydrated phases by X-ray diffraction. The method employed in this paper of using a C_3A-C_3AH_6 calibration curve appeared to be a useful method for quantitatively following the course of the hydration of C_3A, both in the presence and absence of organic compounds. For each organic compound, results were obtained covering the period from 22 minutes to 64 days. Sucrose was investigated more intensively as compared to the other organic compounds.

It was found that the hydroxyl groups tend to retard the hydration of tricalcium aluminate and carbonyl groups tend to accelerate the hydration of tricalcium aluminate. The α-hydroxyl carbonyl group itself does not appear to be important in retarding the hydration of tricalcium aluminate though it may be for other cement compounds. Various effects of the blocking action of organic compounds preventing the hexagonal hydroaluminates from forming the cubic hexahydroaluminate are discussed.

Possible mechanisms for the hydration of tricalcium aluminate in the presence of hydroxyl and carboxyl groups are considered.

It has been shown in many investigations that compounds containing hydroxyl and carbonyl groups are important factors in influencing hydration rates and possibly the hydration products of portland cement and its constituents. This paper is concerned with the effects of organic compounds on the hydration reaction of C_3A, and also the role of hydroxyl and carbonyl groups on the hydration of C_3A to the hexagonal hydroaluminates, C_2AH_8 and C_4AH_n, and then subsequent conversion to the cubic hydroaluminate, C_3AH_6.

This paper examines the effects of 13 well-characterized, interrelated organic compounds on the hydration reactions of C_3A in the absence of other ions such as sulphate and calcium. The organic compounds contain various types and numbers of hydroxyl and carbonyl groups. The compounds studied were: acetic acid, glycolic acid, DL-mandelic acid, glyceric acid, ketomalic acid di-sodiumsalt, ethylene glycol, glycol aldehyde, sucrose, D-(+)-trehalose, D-(+)-glucose, fructose, mannitol and sorbitol. Sucrose was investigated more intensively than the other organic

*Technical Center, American Cement Corporation, Riverside, California, U.S.A.

compounds.

The hydration of C_3A in the absence of organic compounds was also studied to provide a control against which to measure the effects of organic compounds. Reactions in which C_3A hydrated more rapidly than C_3A alone were considered to be accelerated by the organic compound. Conversely, those in which C_3A hydrated more slowly than C_3A alone were considered to be retarded by the organic compound.

This investigation is part of a broader study aimed at understanding the interaction of selected organic compounds with inorganic compounds found in cementitious materials.

Forbrich (1) stated that calcium lignosulfonates delayed the time of rapid heat evolution of C_3A, and that orthohydroxybenzoic acid (salicylic acid) had a slight accelerating effect on the hydration of C_3A. Prior and Adams (2) listed some categories of set-retarding admixtures such as lignosulfonic acids and hydroxylated carboxylic acids that are designed to delay initial and final set in a controlled manner. Vivian (3) found that carbohydrates such as sugars, starches, cellulose and hydroxylated carboxylic acids had marked retarding actions on the hydration of portland cement.

Stein (4) observed that in the early stages of the hydration of C_3A at normal temperatures, the formation of C_2AH_8 and C_4AH_{13}, rather than of C_3AH_6, was favored. The conversion of the hexagonal hydroaluminates (C_2AH_8 and C_4AH_{13}) to C_3AH_6 could accelerate the hydration of C_3A by removal of the layer of products formed around the C_3A grains by a solution mechanism. The rate of reaction at the surface and passage of H_2O through the layer of hexagonal hydroaluminates controls the overall reaction. Stein indicated that dislocations intersecting a surface have a significant influence on the hydration rates.

Segalova, Selovéva and Rebinder (5) observed that polar ions in solution can retard the reaction by adsorbing on sites formed by defects and dislocations in the crystalline structure.

Blank, Rossington and Weinland (6) found that calcium lignosulphonate and salicylic acid in aqueous solution were more strongly adsorbed on C_3A and C_4AF than on C_3S and C_2S. This also confirmed the previous work of Ernsberger and France (7).

According to Young (8), lignosulphonates favored the formation of C_2AH_8 and C_4AH_{13} with respect to C_3AH_6 and modified their crystal habit. Such a morphological change can be regarded as a physical consequence of adsorption as postulated by Rebinder (5). Young demonstrated that lignosulphonates definitely inhibited the change from the hexagonal hydroaluminates to C_3AH_6 under normal conditions. Additions of gypsum and lime did not alter the sequence of reactions.

Chatterji (9) has commented that (i) pure salts of lignosulphonic acids were inferior retarders to commercial lignosulphonates; (ii) the reducing sugars were the main active ingredients of the commercial calcium lignosulphonates; and (iii) a mixture of reducing sugars and the pure lignosulphonates was a better retarder than either of the compounds alone. Chatterji also found that higher strength development and a lower rate of hydration went hand in hand with the thinness of hexagonal hydroaluminates.

Feldman, Ramachandran and Sereda (10,11) studied the influence of gypsum and calcium carbonate upon the hydration character of C_3A. They found that the degree to which gypsum retarded the hydration of C_3A at a particular temperature was affected by (i) the concentration of SO_4^{2-} ions on and around the surface of the C_3A; (ii) the rate of reaction of SO_4^{2-} ions with the hexagonal hydro-aluminates; and (iii) the reaction of the hexagonal hydroaluminate layer around the C_3A grains. They have also observed that during hydration the C_2AH_8 and C_4AH_{13} are stabilized if the temperature was low and that increased amounts of $CaCO_3$ progressively inhibited C_3AH_6 formation.

Van Aardt and Visser (12) have shown that C_3AH_6 is unstable at low temperatures and, in the presence of $Ca(OH)_2$ at 5°C, a metastable compound thought to be C_4AH_{19} was formed.

Hansen (13) pointed out that the organic materials used for prolonging the period during which a cement slurry remains sufficiently fluid for transporting by pumps at elevated temperatures generally contained one or more hydroxyl carbon groups. Hansen (14) also suggested that these organic compounds were adsorbed on the cement surfaces so that they retarded the adsorption of hydronium ions on the cement mineral surfaces and slowed down the setting reaction.

Steinour (15) suggested that the activity of retarding was due to hydrogen bonding of the hydroxyl groups. Hydroxyl carboxylic acids such as tetrahydro-adipic acid may undergo intermolecular association by hydrogen bond formation whereby a hydroxyl group in one molecule may react with a hydroxyl group in another molecule. Steinour also suggested that compounds with several hydroxyl groups appeared generally to be strong retarders in portland cement pastes.

Stein (17) concluded that all polyalcohols exhibited a retarding action on portland cement hydration. With the use of gypsum, ettringite coatings on the C_3A were replaced by C_4AH_{19} formations that created

heat. Eventually the C_4AH_{19} formation dissipated and more hydration occurred toward the final C_3AH_6 phase.

Seligmann and Greening (16) have found that materials which cause retardation of set, such as sucrose or lignosulfonates, can also produce a large initial acceleration of the hydration reactions of portland cement paste. They found that 1 g of C_3A will remove 99% of the sugar from 5 cc of a 1% sucrose solution within 7 minutes. Gypsum or $Ca(OH)_2$ did not interfere with the process. They also showed that if the C_3A were allowed to hydrate for several minutes in the absence of sucrose and then sucrose was added, the sorption of the sucrose was reduced.

Taplin (18) studied a wide range of set-retarding agents on portland cement. Surprisingly, he found that they nearly all contained the α-hydroxyl carbonyl group.

Bruere (19) found that α, α-trehalose (D-(+)-trehalose) possessed only weak retarding properties in portland cement pastes whereas all of the other sugars studied in his investigation were powerful set-retarding agents. D-(+)-trehalose did not contain the α-hydroxyl carbonyl group nor did it form this group in an alkaline medium. Bruere found that the other sugars either contained the α-hydroxyl carbonyl

Table 1. *List of the organic compounds used.*

#	Compound name	Empirical formula	Compound structure	Molecular weight
1	Acetic acid	$C_2H_4O_2$	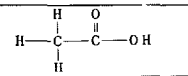	60.05
2	Glycolic acid	$C_2H_4O_3$	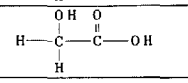	76.05
3	DL-mandelic acid	$C_8H_8O_3$	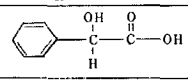	152.14
4	Glyceric acid	$C_3H_6O_4$	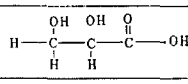	106.08
5	Ketomalonic di-Na-salt	$C_3Na_2O_5$	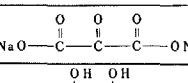	162.01
6	Ethylene glycol	$C_2H_6O_2$	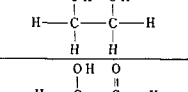	62 07
7	Glycolic aldehyde	$C_2H_4O_2$	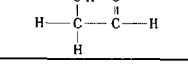	60 05
8	Sucrose	$C_{12}H_{22}O_{11}$	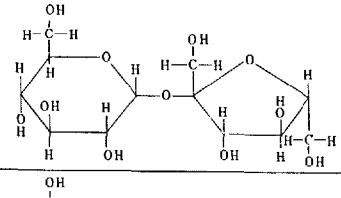	342.30
9	D-(+)-trehalose	$C_{12}H_{22}O_{11}$	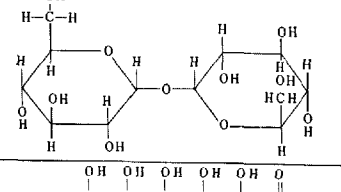	342.30
10	D-(+)-glucose	$C_6H_{12}O_6$	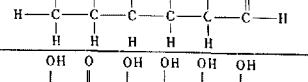	180.16
11	Fructose	$C_6H_{12}O_6$	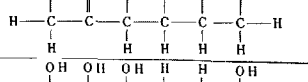	180.16
12	Mannitol	$C_6H_{14}O_6$	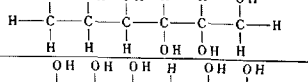	182.17
13	Sorbitol	$C_6H_{14}O_6$	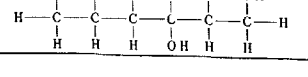	182.17

group or were capable of forming it in an alkaline medium, such as exists in portland cement paste. Bruere (20) supported Taplin's (18) beliefs that the α-hydroxyl carbonyl group was the active adsorbing group in many set-retarding agents in portland cement paste.

From a review of the literature mentioned above, it was thought that the adsorption of α-hydroxyl carbonyl groups on C_3A might play a major role in governing the effectiveness of retardation. Also, it was of interest to the authors to determine the relationships of carbonyl and hydroxyl groups relative to the set-retardation of C_3A hydration in the absence of sulphate and calcium ions. With this in mind, the effects of simple, well-characterized, interrelated, water-soluble organic compounds containing varying numbers and types of hydroxyl and carbonyl groups were studied in the hydration reactions of C_3A. (See Table 1). Special emphasis was placed on sucrose because it is the best characterized and best known of the common retarders.

Reagents

C_3A Preparation

Many methods have been suggested for the preparation of C_3A. Among them are those of Van Aardt and Visser (20), and Seligmann and Greening (21). However, the following method was found to be more effective in yielding high purity C_3A with little difficulty:

Two moles of $Al(OH)_3$ and a 1/1000 mole excess of $Al(OH)_3$ and 3 moles of $CaCO_3$, all of Baker analytical reagent grade, were blended in a ball mill for approximately 12 hours. The blended powder was transferred to platinum crucibles (100 gram capacity) and heated in an electric furnace for 2 hours at 900°C. The crucilbes containing the calcined material were then transferred to a Leco electric furnace for at least 6 hours at 1455°C. The material was air-cooled to room temperature and ground to −200 mesh (−74 microns) in an agate ball mill. It was felt that the use of a glove box was unnecessary. Some material was also ground to −325 mesh (−43 microns). The sieves used throughout this investigation were Tyler Standard Screen Scale Sieves.

The X-ray powder diffraction analysis showed no trace of CaO or $C_{12}A_7$ or other impurities. (Fig. 1). The pattern was in excellent agreement with the C_3A pattern of Swanson, Gilfrich and Ugrinic (22). The C_3A was also analyzed by Diamond (23) and his analysis was in excellent agreement with the authors. The free lime chemcial analysis by the method described by Lea and Desch (24) showed less than 0.1% CaO.

The C_3A was stored under desiccation using Ascarite and Anhydrone. The C_3A is believed to be of the highest purity available. The −200 mesh C_3A had a surface area of 0.46 m^2/g. The surface areas were determined by N_2 adsorption using a Perkin-Elmer-Shell Model 212 Sorptometer (BET method). The −200 mesh material was used throughout the investigation unless otherwise noted.

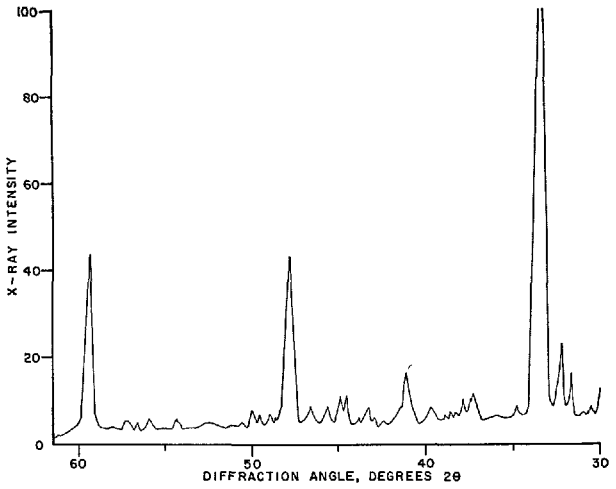

Fig. 1. *X-ray powder diffraction pattern of pure* C_3A.

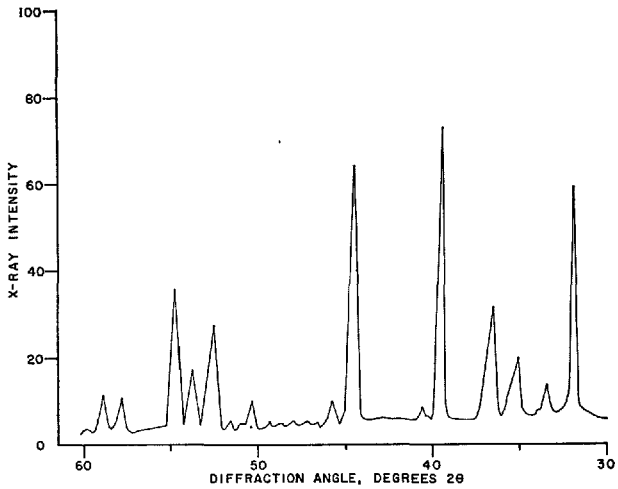

Fig. 2. *X-ray powder diffraction pattern of pure* C_3AH_6.

C_3AH_6 Preparation

A number of methods have been suggested for the preparation of C_3AH_6 including those of Stein (25), and Van Aardt and Visser (26). The following method was found to be particularly effective in yielding high purity C_3AH_6 with little difficulty:

C_3A was mixed with distilled H_2O and ice chips at a H_2O/C_3A ratio of greater than 10 for 60 minutes at 25°C in a Spex mill. The ice had melted by this time and the container was placed in a 15°C chamber for 16 hours. The samples, which were completely hydrated, were then heated to 150°C for 2 hours in order to drive the intermediate metastable C_2AH_8 and C_4AH_n compounds to C_3AH_6.

X-ray powder diffraction analysis showed that the material was completely hydrated with no detectable traces of C_3A, C_2AH_8, C_4AH_n or other impurities. The X-ray pattern was in excellent agreement with the pattern described by Thorvaldson, Grace and Vigfusson (29) (Fig. 2).

The C_3AH_6 had a surface area of 1.7 m^2/g as determined by N_2 adsorption.

Organic Compounds

The compounds used in this study were well-characterized and of reagent grade purity (See Table 1). Acetic acid (No. 1), glycolic acid (No. 2), glyceric acid (No. 4), ketomalonic acid di-sodiumsalt (No. 5), ethylene glycol (No. 6), D-(+)-trehalose (No. 9), mannitol (No. 12) and sorbitol (No. 13) were obtained from Aldrich Chemical Company. DL-mandelic acid (No. 3) and fructose (No. 11) were obtained from Matheson, Coleman and Bell. Glycol aldehyde (No. 7), sucrose (No. 8), and D-(+)-glucose (No. 10) were obtained from Allied Chemical Corporation.

Instrumentation

X-ray Diffraction Analysis

The X-ray diffraction analyses conducted throughout this investigation were at 25°C using nickel-filtered copper Kα radiation at 45KV and 35 mA and a Norelco proportional counter and diffractometer. The X-ray scanning was conducted at a rate of 2° 2θ/min with a 2° divergence slit, a 2° scatter slit, a 0.006 inch receiving slit and a time constant of 4 seconds. An automatic sample changer described in the paper by Berger, Frohnsdorff, Harris and Johnson (28) was employed for routine sample analysis.

Method of Analysis

Preparation of Standard Calibration Curves

A series of 16 samples (Table 2) were prepared ranging from 100 mole % C_3AH_6 and 0 mole % C_3A to 0 mole % C_3AH_6 and 100 mole % C_3A. The samples were weighted to a 1/10 of mg, blended in an agate mortar, funneled to produce a homogeneous material, blended again, funneled again, and blended again in order to produce the samples for X-ray powder diffraction analysis. The loss in the overall preceding operation was less than 1%.

X-ray diffraction patterns were run on each smaple. An example of the pattern produced with 35.27 mole % C_3A and 64.73 mole % C_3AH_6 is found in Fig. 3. The intensities were determined for the 33.3°2θ, 47.7°2θ and 59.7°2θ peaks of C_3A and the 39.3°2θ, 44.4°2θ and 54.6°2θ peaks of C_3AH_6. The preceding

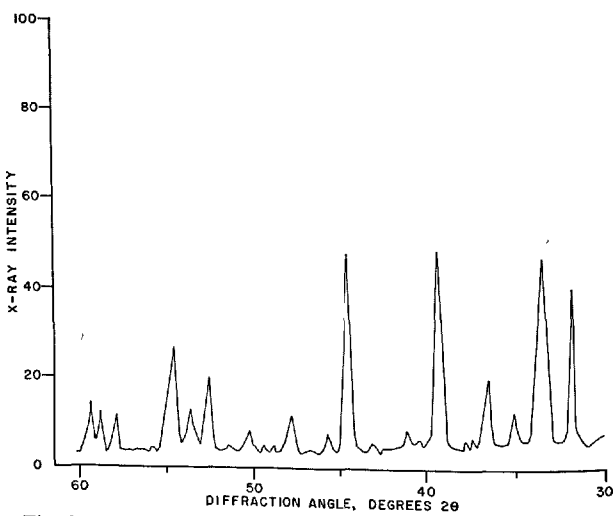

Fig. 3. *X-ray powder diffraction pattern of 35.27 mole% C_3A and 64.73 mole % C_3AH_6.*

Table 2. *Data collected from X-ray diffraction patterns of samples containing varying mole percentages of* C_3A *relative to* C_3AH_6. *Data plotted in Fig. 4.*

No.	% C_3A Relative to % C_3AH_6		Relative intensities of C_3A and C_3AH_6 peaks						Ratios of C_3A to C_3AH_6				
	% C_3A	% C_3AH_6	① C_3A 33.3°	② C_3A 47.7°	③ C_3A 59.3°	④ C_3AH_6 39.3°	⑤ C_3AH_6 44.4°	⑥ C_3AH_6 54.6°	① / ④	② / ⑤	③ / ⑥	Average	Average ×3.333
1	0	100	6	0	0	67.5	59.5	31.5	0.089	0	0	0.030	0.100
2	3.48	96.52	6.5	3.0	2.5	55.5	53.5	29.0	0.118	0.056	0.087	0.087	0.290
3	7.88	92.12	9.5	4.0	4.0	45.5	45.0	25.0	0.209	0.088	0.160	0.152	0.507
4	13.45	86.55	20.0	5.0	6.5	56.5	55.5	28.25	0.354	0.090	0.23	0.225	0.750
5	17.36	82.64	22.5	6.5	7.5	46.5	45.5	24.5	0.485	0.143	0.306	0.311	1.037
6	20.73	79.27	26.0	8.0	9.5	51.5	49.5	27.0	0.505	0.162	0.352	0.340	1.133
7	30.51	69.49	40.0	8.0	12.0	44.0	43.5	22.5	0.91	0.184	0.533	0.542	1.807
8	45.14	54.86	61.0	17.0	17.0	34.0	32.5	17.5	1.795	0.523	0.970	1.096	3.653
9	55.14	44.86	73.5	23.0	26.5	31.0	32.0	16.0	2.37	0.72	1.66	1.58	5.267
10	64.73	35.27	72.0	23.5	22.0	23.0	25.5	12.0	3.13	0.921	1.83	1.96	6.533
11	72.33	27.67	74.5	20.0	25.0	18.0	19.5	9.5	4.15	1.025	2.64	2.605	8.683
12	78.83	21.17	45.0	15.5	19.0	8.0	10.0	4.75	5.62	1.55	4.00	3.72	12.40
13	89.32	10.68	93	34.5	31.5	4.5	8.25	3.0	20.7	4.18	10.5	8.79	29.30
14	92.96	7.04	93	29.5	35.5	4.0	7.5	2.25	23.3	3.94	15.8	14.35	47.83
15	97.04	2.96	93	29.5	30.0	3.5	5.0	1.0	26.6	5.90	30.0	24.20	80.67
16	100	0	123	38.5	40.0	3.0	6.0	0	41.0	6.4	00	00	00

100% C_3AH_6 and 0% C_3A and 100% C_3A and 0% C_3AH_6. The theoretical curve can be seen as a dotted line in Fig. 4.

C_3A/C_3AH_6 ratios were then calculated from the intensity ratios $^{1}33.3°2\theta/^{1}39.3°2\theta$, $^{1}47.7°2\theta/^{1}44.4°2\theta$, and $^{1}59.3°2\theta/^{1}54.6°2\theta$. The three ratios were then averaged and, for convenience, multiplied by a constant 3.333 in order to produce a graph of per cent unhydrated C_3A vs ratio of C_3A/C_3AH_6 with 0.01 in the lower left hand corner (Fig. 4). The calculations were greatly facilitated by the use of a time-sharing computer which saved many hours of calculations.

The calibration curve (Fig. 4) was then used for computing from X-ray diffraction data the per cent hydration of C_3A in samples hydrated in the presence of the organic compounds.

The calibration curve agreed well with the theoretical curve based on mass absorption coefficients for peaks were selected because of their high intensities and little interference.

Preparation of C_3A Samples with Organic Compounds

A series of 7 samples was prepared for each organic compound (Table 1). Each sample contained 10 mg of organic compound, 1 g of C_3A and 0.6 ml of distilled H_2O. A standard solution was prepared for each organic compound containing 167 mg of organic compound and 10 ml of distilled H_2O. A volume of 4.2 ml of this solution was added to 7 g of C_3A in a 25 ml beaker and mixed by hand for 2 minutes with a glass stirring rod.

The resulting mixture had a H_2O/C_3A ratio of 0.6 and contained 1% by weight of organic compound to C_3A. A H_2O/C_3A ratio of 0.40 is the stoichiometric ratio necessary to hydrate C_3A to C_3AH_6. The samples were divided immediately into 7 equal-sized portions and placed in 7 ml glass vials and capped with plastic snap-top lids. The samples were then transferred to an environmental chamber held at 25°C. The quantity of H_2O evaporated from these vials was less than 1.5 weight % of sample in the first 5 days.

The samples were stored in the chamber for 22 minutes, 90 minutes, 6 hours, 24 hours, 4 days, 16 days and 64 days. The samples were desiccated immediately upon removal from the chamber using a Welch vacuum pump, a glass vacuum desiccator and an Anhydrite drying tower. The samples were desiccated for 12 hours and the hydration reactions were

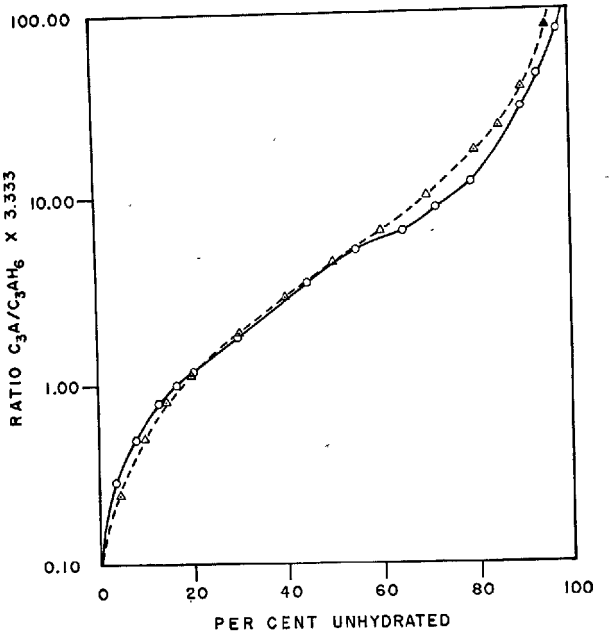

Fig. 4. *Calibration curve used in the analysis of* C_3A–C_3AH_6 *mixtures.*

—— Plot of the X-ray peak intensity ratio of $C_3A/C_3AH_6 \cdot 3.333$ for different molar ratios of C_3A and C_3AH_6 (0 mole % unhydrated to 100 mole % unhydrated). Data taken from Table 2.

---- Plot of the theoretical curve for different molar ratios of C_3A and C_3AH_6 computed from mass absorption coefficients for pure C_3A and pure C_3AH_6.

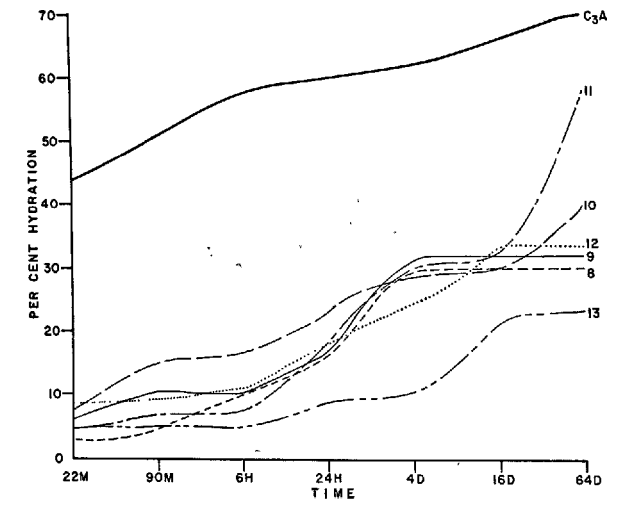

Fig. 6. *Plot of the per cent hydration of* C_3A *samples mixed with organic compounds vs time in minutes* (*M*), *hours* (*H*), *and days* (*D*).

The numbers refer to the following compounds found in Table 1 in order of decreasing hydration:

C_3A = normal hydration with no organic compounds
11 = fructose
10 = D-(+)-glucose
12 = mannitol
9 = D-(+)-trehalose
8 = sucrose
13 = sorbitol

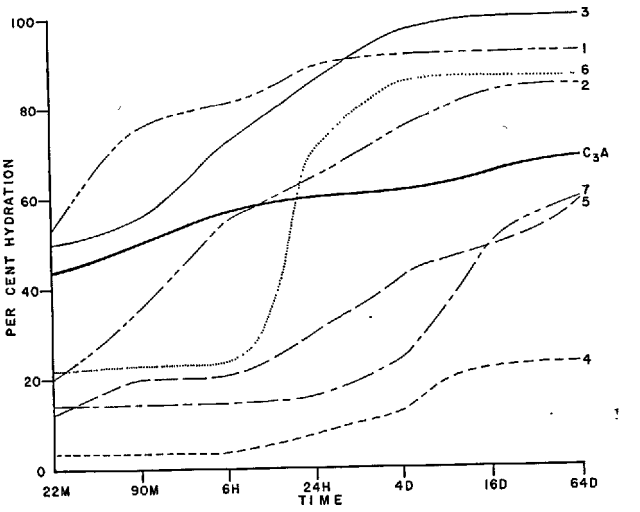

Fig. 5. *Plot of the per cent hydration of* C_3A *samples mixed with organic compounds vs time in minutes* (*M*), *hours* (*H*), *and days* (*D*).

The numbers refer to the following compounds found in Table 1 in order of decreasing hydration:

3 = DL-mandelic acid
1 = acetic acid
6 = ethylene glycol
2 = glycolic acid
C_3A = normal hydration with no organic compounds
7 = glycol aldehyde
5 = ketomalonic acid di-sodium-salt
4 = glyceric acid

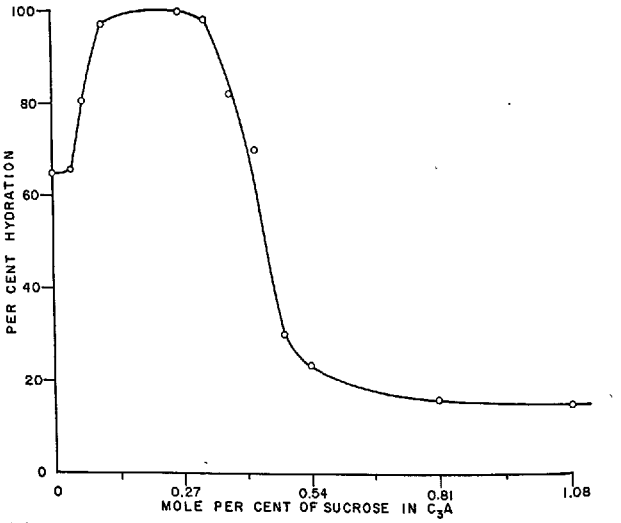

Fig. 7. *Effect of varying concentrations of sucrose on the hydration of* C_3A *after 24 hours hydration at 25°C.*

arrested. The samples were ground to —325 mesh in an agate mortar and analyzed by X-ray diffraction. The samples before and after grinding were kept in the glass vials with the lids in place. The samples in the glass vials with the lids removed were then heated to 160°C in an oven for 12 hours in order to convert any hexagonal hydro-aluminates to the stable

cubic C_3AH_6. Lea and Desch (29) have stated that the metastable hexagonal hydroaluminates convert more rapidly with rising temperature to the stable cubic C_3AH_6. The samples were again analyzed by X-ray diffraction without grinding. The extent of the hydration of the C_3A to C_3AH_6 after the heat treatment is found in Fig. 5 and 6. The hydration of C_3A in the absence of other organic compounds is also plotted in Figs. 5 and 6. These curves were obtained in an identical manner as the C_3A samples containing organic compounds.

Preparation of C_3A Samples with Sucrose

The effect of sucrose on the hydration of C_3A was studied in greater detail than for the other compounds because of wide interest in this particular compound.

Sucrose was dissolved in distilled H_2O and added to C_3A in a series of different molar concentrations at a H_2O/C_3A ratio of 1.0. This was done in the manner described in the previous section.

The samples were stored for 24 hours in the chamber at 25°C, vacuum desiccated as described previously, heated as described previously and analyzed by X-ray diffraction. (Fig. 7).

Results and Discussion

Quantitative X-ray diffraction has been found to be a convenient method for following the hydration of C_3A with time (Fig. 4). The results following these hydration reactions have been found to be reproducible to within $\pm 3\%$ of the quantity present.

The results of the data in Fig. 5 and Fig. 6 are self-explanatory for the per cent hydration of various organic compound-C_3A mixtures with time on a log 4 basis. However, it should be pointed out that during the first 22 minutes the hydration of the organic compound-C_3A mixtures was very rapid. C_3A hydrated 43%, the sugars and sugar derivatives hydrated less than 10% and a couple of the acids hydrated better than 50%. It is interesting that mandelic acid which contains an α-hydroxyl carbonyl group is an accelerator and sucrose which forms an α-hydroxyl carbonyl group as an alkaline medium (19) is a retarder of C_3A hydration.

The hydration of C_3A is believed to proceed through the initial formation of the metastable phases of C_2AH_8 and C_4AH_n followed by their subsequent transformation to the more stable phase, C_3AH_6, which is the only stable aluminate hydrate existing over a wide range of temperatures (30).

$$2C_3A + (n + 8)H_2O \longrightarrow C_2AH_8 + C_4AH_n \longrightarrow 2C_3AH_6 + (n - 4)H_2O$$

Some of the organic compounds block the hydration at the metastable phases while others permit the reaction to proceed to C_3AH_6. In general, the accelerators (acids) permit the hydration to proceed to C_3AH_6 while the retarders (sugars and sugar derivatives) block the reaction at the metastable phases. Table 3 lists the organic compounds and indicates their effectiveness in blocking the hydration of C_3A at 1 day of hydration and at 64 days of hydration.

Table 3. *Interpretation of data listed for compounds in increasing effectiveness of blocking the formation of C_3A hydrates based on data taken from X-ray powder diffraction patterns at a H_2O/C_3A ratio of 0.6 and a temperature of 25°C.*

$$2C_3A + (n + 8)H_2O \longrightarrow C_2AH_8 + C_4AH_n \longrightarrow 2C_3AH_6 + (n - 4)H_2O$$

Based on effectiveness of hydration evaluated in 2 ways:
(1) at 1 day
(2) at 64 days

Compound No.	Compound name	1 Day	64 Days
3	DL-mandelic acid	–	–
1	acetic acid	–	–
2	glycolic acid	–	–
4	glyceric acid	–	–
	C_3A (no organic addition)	–	–
6	ethylene glycol	+	–
7	glycol aldehyde	+	–
12	mannitol	+	–
11	fructose	+	–
5	ketomalonic acid (di-Na-salt)	+	+
8	sucrose	+	+
10	D-(+)-glucose	+	+
13	sorbitol	+	+
9	D-(+)-trehalose	+	+

Symbols:
+ Organic compound blocks the hydration of C_3A at the metastable phases C_2AH_8 and C_4AH_n.
– Organic compound does not block the hydration of C_3A at the metastable phases C_2AH_8 and C_4AH_n and the stable phase C_3AH_6 is formed.

The −325 mesh C_3A hydrated more rapidly than the −200 mesh C_3A. The hydration increase was on the order of 7%.

Fig. 7 clearly demonstrates that sucrose in small concentration acts as an accelerator and in higher concentration acts as a retarder. Sucrose in a concentration of 0.27 mole % corresponds to 0.34 weight %. Sucrose was found to effectively retard the hydration of C_3A at concentration levels as high as 20 mole %

in C_3A.

The initial acceleration effect in Fig. 7 for sucrose has been observed for all of the sugars and sugar derivatives found in Table 1 at concentration levels of 0.25 mole % relative to C_3A.

Additions of 0.2 mole % free lime relative to C_3A to the sucrose-C_3A samples shifted the curve in Fig. 7 to the right.

A possible explanation for the preceding results might be the following: In concentrations of 0.3 mole % or less relative to C_3A the organic materials complex or chelate with available calcium ions (and other cations) in solution and on the surface of the C_3A. These reactions might affect the rates of solution of C_3A and the solution, precipitation or nucleation of the hydration products in a manner which accelerates hydration.

After the available calcium is tied up, the organic material is adsorbed on the surface of the C_3A. This adsorption may be chelation with calcium in the C_3A, complexation, or surface adsorption depending upon the type of organic molecule. In general, chelates and complexes at high pH levels are stable and have low solubilities in water if they are relatively free of groups that can be hydrated. The greater the size of the hydrocarbon groupings, the lower will be the solubility in water (31). These concepts might prove useful in determining the effectiveness of organic compounds as retarders and accelerators.

Organic compounds with more insoluble calcium salts would be expected to form more closely packed, more impervious sheaths around the C_3A. This might prevent H_2O from further attacking the C_3A. The organic layers could prevent the intermediate products, C_2AH_8 and C_4AH_n, from transforming to C_3AH_6. Retardation of hydration would be the result.

Sucrose can form many different complexes with calcium and similar organic molecules can be expected to behave similarly. Among the calcium complexes of sucrose that can form in lime solutions are $C_{12}H_{22}O_{11} \cdot CaOH$, $(C_{12}H_{22}O_{11})_2$ Ca and $(C_{12}H_{22}O_{11})$ Ca–O–Ca$(C_{12}H_{22}O_{11})$ (32).

Some compounds such as ethylene glycol appear to be effective retarders in early hydration reactions and accelerate hydration in later stages.

The mechanism of retardation and acceleration of organic compound-C_3A systems is open to speculation and further work is aimed at examining these phenomena. It is without question that the type of organic compound and the rates of solution, nucleation and precipitation of the various species in the hydrating system are important.

Various instrumental means of investigating organic compound-C_3A reactions were considered. For this particular study X-ray diffraction was found to be more directly applicable, however, it is to be expected that the supplementary use of calorimetry, electron microscopy, and other techniques will lead to a better understanding of the mechanism of hydration of organic-cementitious materials.

Conclusions

The following conclusions apply to a temperature of 25°C, a H_2O/C_3A ratio of 0.6 and 0.1 weight % to 1.0 weight % additions of organic compounds to C_3A:

1. Water-soluble organic compounds containing hydroxyl, carboxyl or carbonyl groups act as either accelerators or retarders for the hydration of C_3A depending upon their concentration levels and composition.
2. The α-hydroxyl carbonyl group itself does not appear to be especially important in the hydration of C_3A, though it may be for other cement compounds.
3. The carboxyl group (acids) tends to accelerate C_3A hydration and the hydroxyl group (sugars) tends to retard hydration.
4. Mandelic acid is a strong accelerator for the hydration of C_3A.
5. Of the compounds examined, sorbitol is the most effective retarder of C_3A hydration on a weight basis.
6. Some organic compounds appear to block the conversion of C_2AH_8 and C_4AH_n to C_3AH_6 while others permit the C_3AH_6 to be formed readily:
   (a) In general, the organic acids permit the hydration of C_3A to proceed to C_3AH_6.
   (b) In general, sugars and their derivatives, block the hydration reactions at C_2AH_8 and C_4AH_n.
7. A simple organic compound containing a carboxylic acid group and zero or one hydroxyl group will accelerate C_3A hydration and a simple organic compound containing two or more hydroxyl groups will retard C_3A hydration.

Acknowledgment

The authors wish to express their thanks to Mr. James P. Giles, President of American Cement Corporation, for granting permission to publish this paper.

The authors wish to express their appreciation to Mr. Jay Waddell for his help on some phases of the X-ray diffraction work, to Mr. William Fryer for his help with the time-sharing computer system, and to Dr. Geoffrey Frohnsdorff for his help, encouragement and stimulating discussions.

References

1. L. R. Forbrich, "The effect of various reagents on the heat liberation characteristics of portland cement", Proc., Am. Concrete Inst., **37**, 180 (1940).
2. M. E. Prior and A. B. Adams, "Introduction to producer's papers on water-reducing admixtures and set-retarding admixtures for concrete", Am. Soc. Testing Mater., Spec. Tech. Publ., No. 226, 172 (1959).
3. H. E. Vivian, "Some chemical additions and admixtures in cement paste and concrete", Proc. Fourth Intern. Symp. Chem. Cement, Wash. 926 (1960).
4. H. N. Stein, "Influence of quartz on the hydration of $3CaO \cdot Al_2O_3$", Highway Res. Board, Spec. Rept. 90, 368–377 (1966).
5. E. E. Segalova, E. S. Solovéva and A. A. Rebinder, "Structure development in suspensions of tricalcium aluminate by crystallization", (In Russian), Dokl. Akad, Nauk S.S.S.R., **113**, 134–137 (1957).
6. B. Blank, D. R. Rossington and L. A. Weinland, "Adsorption of admixtures on portland cement", J. Am. Ceram. Soc., **46**, 395–399 (1963).
7. F. M. Ernsberger and W. G. France, "Portland cement dispersion by adsorption of calcium lignosulphonate", Ind. Eng. Chem., **37**, 598–600 (1945).
8. J. F. Young, "Hydration of tricalcium aluminate with lignosulphonate additives", Mag. Concrete Res., **14**, 137–142 (1962).
9. S. Chatterji, "Electron-optical and X-ray diffraction investigation of the effects of ligonosulphonates on the hydration of C_3A", Indian Concrete J., **41**, 151–160 (1967).
10. R. F. Feldman, V. S. Ramachandran and P. J. Sereda, "Influence of $CaCO_3$ on the hydration of $3CaO \cdot Al_2O_3$", J. Am. Ceram. Soc., **48**, 25–30 (1965).
11. R. F. Feldman and V. S. Ramachandran, "The influence of $CaSO_4 \cdot 2H_2O$ upon the hydration character of $3CaO \cdot Al_2O_3$", Mag. Concrete Res., **18**, 185–196 (1966).
12. J. H. P. Van Aardt and S. Visser, "Some reactions of tricalcium aluminate hexahydrate at medium temperatures", Cement Lime Manuf., **40**, 7–11 (1967).
13. W. C. Hansen, Proc., Third Intern. Symp. Chem. Cement, London, 598–627 (1952).
14. W. C. Hansen, "Actions of calcium sulphate and admixtures in portland cement pastes", Am. Soc. Testing Mater., Spec. Tech. Publ., No. 266, 23 (1959).
15. H. H. Steinour, Discussion on "Action of calcium sulphate and admixtures in portland cement pastes" by Hansen, W. C., Am. Soc. Testing Mater., Spec. Tech. Publ., No. 266, 25–37 (1959).
16. P. Seligman and N. R. Greening, "Studies of early hydration reactions of portland cement by X-ray diffraction", Highway Res. Board, Highway Res. Record Number 62, 80–105 (1964).
17. H. N. Stein, "Influence of some additives on the hydration reactions of portland cement, II. electrolytes", J. Appl. Chem. (London), **11**, 482–492 (1961).
18. J. H. Taplin, Proc. Fourth Intern. Symp. Chem. Cement, Wash., 924–925 (1960).
19. G. M. Bruere, "Set-retarding effects of sugars in portland cement pastes", Nature, **212**, 502–503 (1966).
20. Ibid., p. 7.
21. Ibid., p. 97.
22. H. E. Swanson, N. T. Gilfrich and G. M. Ugrinic, Nat. Bur. Std. (U.S.), Circ. 539, ASTM Std. Cards 8–5, 8–6, No. 5, 10 (1955).
23. S. Diamond, Purdue Univ., School of Civil Eng., private communication.
24. F. M. Lea and C. H. Desch, The chemistry of cement and concrete, Second Edition, p. 103–105, (Edward Arnold Publishers Ltd., London, England, 1956).
25. H. N. Stein, "Mechanism of the hydration of $3CaO \cdot Al_2O_3$", J. Appl. Chem. (London), **13**, 228–232 (1963).
26. Ibid., p. 7.
27. T. Thorvaldson, N. S. Grace and V. A. Vigfusson, Can. J. Res., **1**, 201 (1929).
28. R. L. Berger, G. J. C. Frohnsdorff, P. H. Harris and P. D. Johnson, "Application of X-ray diffraction to routine mineralogical analysis of portland cement", Highway Res. Board, Spec. Rept. 90, 235 (1966).
29. Ibid., p. 174.
30. T. D. Robson, High alumina cement and concretes, p. 52, (John Wiley & Sons, Inc., New York, U.S.A., 1962).
31. A. E. Martell and M. Calvin, Chemistry of the metal chelate compounds, (Prentice-Hall Inc., Englewood Cliffs, New Jersey, U.S.A., 1952).
32. I. A. Sheka, M. M. Polyachenko and I. I. Sokova, "Cryoscopic investigations of lime-sugar-water systems", Tr. Tekhnol. Inst. Pishchevoi Prom.,

16, 227–34 (1956).

Oral Discussion

Shigeaki Koide

A discussion of influences of some organic groups on the hydration process of tricalcium aluminate is of much interest. The actions of the groups, however, for the hydration of CA are different from that just mentioned in the paper. We have found that the carboxyl group has always retarded the hydration process of CA irrespective of its concentration and the species of compounds, and lowered the heat liberation during hardening. The effect is especially marked when the group were contained in the chelate compounds, for instance, EDTA which produces the sexadentates with a high stability constant. On the other hand, such chelate compounds that produce tetradentates or sexadentates with rather low stability constants have been less effective. On the basis of the results, the retarding action of the group is considered to be due to the ligand compounds temporarily produced between Ca^{++} or aluminum ion and carboxyl group.

On the retarding or accelerating mechanism of the hydration process of tricalcium aluminate in the presence of the organic groups, we should like to ask the author's opinion.

Authors' Closure

K.E. Daugherty and M.J. Kowalewski, Jr.

We appreciate the comments of Mr. Shigeaki Koide.

We agree that the reactions of various organic groups are different for monocalcium aluminate (CA) as compared to tricalcium aluminate (C_3A). In this paper, only the results of our studies with C_3A are described. The work that we have done with CA also indicates that the carboxyl and hydroxyl groups generally retard hydration. We have some evidence, however, that this is not always true.

The retarding action of the organic functional groups on C_3A, CA and other similar compounds is considered to be due to the ligand compounds produced between the calcium ions, aluminate ions and the organic groups. The concentration and type of hydroxyl and carboxyl groups will determine the stability constants, as well as complex or chelate formation.

In our paper we have considered complexes to be those which are produced when a metal ion combines with an electron donor. A chelate is a substance that has combined with a metal and contains two or more donor groups so that one or more rings are formed. Our views on the retarding and accelerating mechanism of the hydration process of C_3A in the presence of organic groups are found in the results and discussion section of our paper. We have found no reason to alter our views and they correlate well with the thoughts of Mr, Shigeaki Koide.

Supplementary Paper IV-51 Abnormally Delayed Setting of a Low-Heat Portland Cement with Calcium Lignosulphonate Admixtures

René J. Bauset*

Synopsis

Abnormally long setting times occurred in the concrete at two sites of the Quebec Hydro-Electric Power Commission's project on the Manicouagan River. The project was supplied at the time with a low-heat portland cement from three manufacturers.

Data is presented showing field performance tests and preliminary tests undertaken for acceptance of the admixture. Data outlining the history of cement supply is reviewed.

A conclusion is reached that the slow setting was due to an overdosage of calcium lignosulphonate admixture with a low SO_3 type of portland cement.

Introduction

Full development of the Manicouagan and Outardes rivers was begun in the autumn of 1959. These rivers flow parallel and close to one another, emptying into the Gulf of St. Lawrence near Baie-Comeau, a seaport located about 400 miles' northeast of Montreal, Canada. The development comprizes seven power-houses with a total installed capacity of 5.5 million kW.

Manicouagan 5 is a multiple-arch dam requiring over 2,900,000 cubic yards of high strength concrete for its construction. The Manicouagan 2 dam is a hollow-joint gravity structure requiring a little under 1,000,000 cubic yards of lean concrete in its mass, and 3,000 psi concrete on its faces.

Because of the logistics of the entire development project, the same low-heat portland cement was used for both dams.

Field Observations at Manic 2

In September 1963, the green-cutting crew noticed that sections of a 1,000 cubic yard monolith had not yet set. Inspection indicated that concrete had stopped hardening at the initial set while adjacent concrete had hardened normally. Field laboratory tests showed that with the cement we had in stock in the laboratory, long delays in the time of set were obtained only by quadrupling the dosage of the water reducing retarder (Table 1).

Table 1. *Effect of a calcium lignosulphonate admixture on the compressive strength development of an air-entrained concrete made with a low-heat portland cement (LAB No 631017)*

Pounds per yd³ Cement	Water	% wt. cement admix	Inches slump	% Air	Compressive strength, psi 3-day	7-day	28-day	91-day
360	232	0.3	1	4.2	*	*	3210	4400
360	230	0.45	1 1/2	4.3	*	*	2725	3485
360	225	0.6	2	3.0	755	1335	3025	4070
360	206	1.2	2 3/4	1.2	Nil	60	*	3800
250	205	0.3	2 1/4	5.2	*	*	1295	1920
250	210	0.45	3	4.0	*	705	1455	2330
250	197	0.6	1 1/4	2.7	655	995	1930	2035
250		1.2	2 1/2	1.5	Nil	60	1195	2515

*Cylinders not taken.
Field tests at Manic 2, September 1963.

*Hydro-Quebec, Montreal, Canada.

Since the field personnel were positive that no more than double dosage had occurred, investigations were then directed to the cement. Attention was also directed to a similar case of slow-hardening concrete reported by Tuthill (1).

Further studies made during the winter slack season showed that difficulties corresponded to arrivals of cement from one of the three suppliers.

Field Observations at Manic 5

The commercial grade, de-sugarized, calcium lignosulphonate type of water-reducing agent used at Manic 2 having been proved unsatisfactory, a proprietary mixture with a long history of successful application was accepted for use at this site. Batching of concrete with this admixture started on the 18 th of May, 1964.

On the 20th, it was noticed that standard cured samples of concrete were not setting. But the accelerated cured concrete sample showed normal results averaging 4,995 psi after 48 hours in a water bath maintained at 170°F $\pm$ 2°. At the end of two weeks, all the standard-cure cylinders showed a potential strength of almost 4,200 psi.

The concrete placed in the field was observed for the next 9 days with no apparent development of set. Because production delays were becoming intolerable, the field staff proceeded to remove 620 cubic yards of "soft" concrete at a total cost (direct cost and lost production time) of six times the original in-place cost.

Performance Tests, Manic 5

The first series of tests evaluated the admixture in mixes used for compressive strength testing of cement (2). Results are shown in Table 2. It can be seen that mixes prepared with cement A had a long hardening period and the compressive strength after 5 days was extremely low. But a reduction of dosage to 0.15% of admixture restored considerably the rate of strength gain. The compressive strengths with the reduced dosage for cement A were similar to those with 0.3% addition to cement B. Subsequently, tests were done on over 50 samples of cement A that were taken from three 6,500-ton shipments received from manufacturer A during the period under review. All showed excess retardation of around $4\frac{1}{2}$ days with relatively low compressive strength obtained at 7 days. But the 90-day strengths were all well above our specified values.

Table 2. *Effect of a calcium lignosulphate proprietary admixture on compressive strength development for two different low-heat cements*

Cement source	Admixtures, % wt. cement		Compressive strength 2″×2″ cubes, 1:2.75 mortar.	
	air	water reducing	age	p.s.i.
A-1	nil	nil	3d	1495
A-1	0.1	nil	3d	1250
A-2	nil	nil	3d	1535
A-1	nil	0.15	3d	1000
A-2	nil	0.15	3d	925
A-1	nil	0.3	5d	112
A-1	0.1	0.3	5d	172
B	nil	nil	3d	1745
B	nil	0.3	3d	925

Discussion

Performance tests prior to these setting "failures" had shown that low-heat cement showed excess retardation with admixtures. One potential supplier of admixtures had reported early in 1963 that his product, although satisfactory from the standpoint of strength benefit, would not be acceptable on the basis of the rate of hardening results. His graph of Proctor penetrometer results with cement No. 630110 shows an 8-hour retardation for the final set.

Further studies on 5 different admixtures were done and it was found that all retarded the hardening of concrete for approximately the same period. Since this retardation was acceptable to the field staff, one of the admixtures reported on Fig. 1 was accepted and was the one eventually involved in the excess retardation reported at Manic 5.

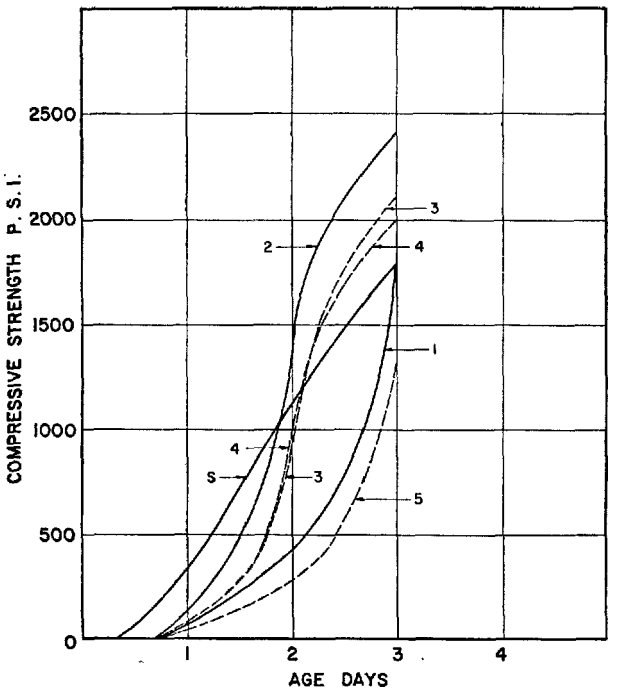

Fig. 1. *Effect of five different lignosulphonate admixtures on early age strength development.*

When the admixtures were tested in 1963, the characteristics of cements were as shown in Tables 3 and 4. All are low C_3A, moderately-high alkali cements ground to an average 3290 cm²/gm fineness. The low heat of hydration requirement combined with high strength also dictates low additions of gypsum to the clinker (3). It is therefore probable that the time for initial set is determined by the exhaustion of the gypsum (4). Fig. 2 shows the effect of gypsum on the setting time of a cement made by manufacturer A. In order to stay within the specified setting times, lower percentages than needed for optimum performance were most probably used, as is indicated by the physical data of these cements shown in Table 5.

Effect of Calcium Lignosulphonate on the Setting Characteristics of Low Heat Portland Cement from Plant A.

Further tests on the setting characteristics of cements P–143–1–to–6 showed that the retarding effect of the admixture was very pronounced for cements contain-

Table 3. *Physical characteristics of low-heat portland cements*

Test	Quebec hydro specification	Cement No. 621115	Cement No. 630110	Cement No. 631017	Table 2 A–1	Table 2 A–2	Table 2 B
Blaine fineness cm²/g	3200 ± 200	3170	3170	3279	3474	3376	3270
Autoclave expansion, %	0.1 max.	0.1	0.09	0.03	0.08	0.05	0.07
Heat of hydration cal/g 7 d.	62 ± 3 max.	59.7	60.0	61.3	62.4	61.9	59.2
Vicat initial set	3½ hrs ± 45 min.	3:00	3:10	5:20	4:20	4:25	3:15
Vicat final set	5½ hrs ± 45 min.	5:30	5:30	6:00	4:25	6:00	5:50
Compressive strength 2" × 2" mortar cubes p.s.i.							
3 day	1400 min.	1607	1710	1823	1548	1675	2030
7 "		2210	2370	2700	2435	2525	3000
28 "		4208	4170	5040	4775	4813	5010
91 "	5600 min.	6277	6380	5975	6075	5825	6550

Table 4. *Chemical characteristics of low-heat portland cements*

Test %	Quebec hydro specification	Cement No. 621115	Cement No. 630110	Cement No. 631017	Table 2 A–1	Table 2 A–2	Table 2 B
SiO_2		23.5	23.4	23.4	22.7	22.8	23.1
Al_2O_3		4.6	4.7	4.4	4.5	4.8	4.7
Fe_2O_3		4.2	4.2	3.4	4.5	4.4	3.9
CaO		61.5	61.5	62.3	63.1	62.8	62.3
MgO		2.9	2.9	2.4	2.7	2.8	2.6
SO_3		2.08	2.05	2.06	1.27	1.31	2.01
Loss on ignition		0.6	0.6	0.2	0.6	0.5	0.5
Na_2O		0.28	0.28	0.25	0.16	0.15	0.24
K_2O		0.78	0.78	0.68	0.55	0.65	0.80
Insoluble residue		0.29	0.29	0.23	0.26	0.59	0.26
Free lime	0.7 max	0.26	0.26	0.09	0.49	0.34	0.31
Water soluble alkali		0.79	0.79	0.70	0.52	0.58	0.77
C_2S		46.	45.	41.	32.	35.	40.
C_3S		29.	29.	35.	44.	40.	35.
C_3A	5%	5.1	5.3	4.9	4.4	5.3	5.7
C_4AF		13.	13.	12.	13.	13.	12.

Note: Compound compositions determined by method shown in ASTM Standard C–150–65

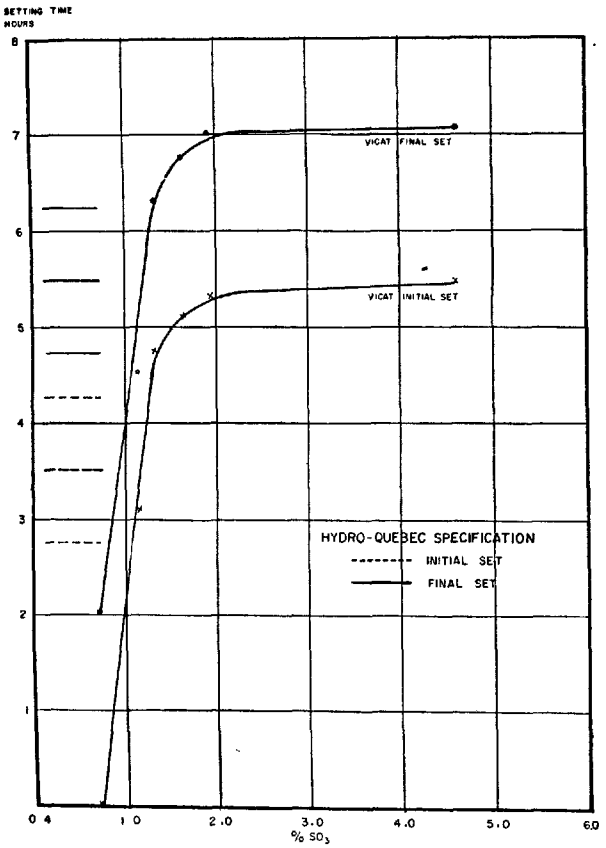

Fig. 2. *Influence of gypsum on setting properties of low heat portland cements from manufacturer "A".*

ing 1.1% SO_3. It was concluded that the dosage of the admixture should not exceed 0.2% for cements containing less than 1.6% SO_3 and that the normal dosage of 0.3% could be used with cements around 2% SO_3.

Having discounted the possibility of a high sugar content lignosulphonate being used, and the possibility of overdosage of the admixture and delayed addition of the admixture, then the SO_3 content of these cements determined the dosage of the retarding admixtures. Seligmann & Greening (5) reported that, for the similar case reported in California (1):

"The observed excessive retardation resulted from a combination of factors and a chain of events that ultimately caused a lack of sufficient alkali release during the early hydration of the cement."

Table 4 illustrated a significant drop in alkalies for cements A-1 and A-2, which could be a contributory factor in this instance.

Table 5. *Physical characteristics of cements from manufacturer A used in laboratory investigation of effect of gypsum content*

Cement no.		P-143-2	P-143-4	P-143-1	P-143-5	P-143-6	P-143-3
SO_3, %		0.72	1.15	1.33	1.67	1.97	4.61
Time of set							
Vicat initial (hrs)		0:01	3:05	4:45	5:10	5:20	5:25
Vicat final (hrs)		2:00	4:35	6:20	6:45	7:00	7:05
Autoclave expansion, %		—	0.06	0.07	0.05	0.04	0.03
False set		10, 0, 0, 0, x	50+, 50+, 50+, 48+,	50+, 50+, 48+, 45+, 50+	50+, 50+, 50+, 50+, 50+	50+, 50+, 50+, 50+, 50+	50+, 50+, 50+, 50+, 50+
Compression strength (psi) of mortar cubes	3 days	1530	1515	1568	1683	1975	1753
	7 days	2518	2338	2150	2339	2688	2353
	28 days	4250	4733	4442	4513	4492	4050
	90 days	4675	5238	5339	4988	4950	5100
Heat of hydration cal/g	7 days	64.6	63.1	58.2	56.9	60.0	52.2

Conclusion

Whenever preliminary studies show a tendency for an admixture to retard excessively the set of a cement, careful consideration should be given to its use in the field. If used with low C_3A and low SO_3 cements, each shipment of these sensitive cements should be checked in order to avoid delays in construction due to excessive retardation.

When very long retardation periods are required, the effect of overdosages of the retarder should also be tested in order to establish a limit. The required dosage should be well within this limit in order to allow for field errors.

Post Scriptum

Both of these dams were completed without the use of retarding admixtures. The cement specification was also changed to allow wider latitude in setting times, thus permitting optimum addition of gypsum. This cement has since been used successfully in concretes with admixtures.

Acknowledgements

The author thanks the Quebec Hydro-Electric Power Commission for its cooperation in the presentation of this supplementary technical paper. He also wishes to express his appreciation to cement manufacturers in the Province of Quebec for the advice and data given in the preparation of this paper.

References

1. Tuthill, Adams, Bailey & Smith: "A case of abnormally slow hardening concrete for tunnel lining." ACI Journal title 57–51 page 1091–1109, March 1961.
2. Canadian Standards Association, Standard A5-1961 "Portland cements" clause 7, 8, 4.
3. Lerch W. "The influence of gypsum on the hydration and properties of portland cement pastes." A.S.T.M. proceedings, Vol. 46, page 1252 (1946).
4. Steinour, H. "The setting of portland cement" November 1958 Page 34. Portland Cement Association. R.D. bulletin 98.
5. Seligmann, P., Greening N. "Studies of early hydration reactions of portland cement by X-ray diffraction," Highway Research Record No 62, PP80–105 (1964).

Supplementary Paper IV-89 Investigations on the Method of Test for Setting Time of Concrete Especially of Concrete Containing Water Reducing Admixture

Jiro Okabe, Koji Nakajima and Takuji Yoshihara*

Synopsis

Time of setting is one of the most important properties of concrete. Setting time of concrete depends upon the hydration velocity of the cement in concrete. Therefore, the rate of the setting of cement has a much significance for the use of cement in mortar and concrete. However, the setting time of cement is determined by the tests on cement paste and have not much significance for the estimation of the setting time of concrete.

In order to determine the setting time of concrete, the penetration resistance method is being used widely. This method requires concrete whenever the setting time is determined. For convenience, use of mortar in lieu of concrete is being tried sometimes. However, it has not been clarified whether or not the mortar sieved from concrete and the mortar prepared by a mortar mixer give the same setting time.

In order to establish the testing method by using mortar in lieu of concrete, the accuracy of this method is examined and the effects of the change in proportion, mixing condition and temperature on the setting time are studied. The following results are obtained.

(1) The setting time of concrete can be determined by using the mortar prepared by a mortar mixer.

(2) The setting time of the mortar is influenced by various factors, especially when the admixtures are used.

(3) Therefore, the test should be performed as follows: 1) The water-cement and sand-cement ratio shall be identical with that of the concrete, 2) The same materials as in the concrete shall be used, 3) The same mixting sequence shall be used, 4) The mixing period of the mortar shall be determined depending upon the kind of the mixer used.

The effects of various factors on the setting time of the concrete or the mortar containing the admixture are also discussed.

Introduction

Time of setting is one of the most important properties of concrete. The acceleration of the time of setting and hardening of concrete is required in the precast concrete industries, and in cold weather concretings, while the retardation of the time of setting and hardening of concrete is also required for the manufacture of the massive concrete and in hot weather concretings. Consequently, set controlling admixtures for accelerating and retarding the setting time have been widely used in concrete manufacture.

Setting time of concrete depends upon the hydration velocity of the cement in concrete. Therefore, the rate of the setting of cement has a much significance for the use of cement in mortar and concrete. In the specification of cement, the requirements for the initial and final set of cement are prescribed. Initial and final set of cement are defined by the methods of testing that determine the time when neat cement paste shows an arbitrary defined resistance to a particular deformation (1). However, setting time of cement is determined by the test on cement paste made with a water-cement ratio and a mixing condition which are completely different from that of concrete. Indeed, this test is normally made for the purpose of finding out the false set of cement. Therefore, the setting time of cement have not much significance for the estimation of the setting time of concrete. Especially for the concretes containing water reducing and set controlling admixtures, it is impossible to know the time of setting of concrete from the test for cement paste (2). The reaction velocities of the process of setting can be determined by many other methods. These include the measurements of change in electrical conductivity (3), electrical potential (4), heat evolu-

*General Research Laboratory, Sanyo Pulp Co., Ltd., Iwakuni, Japan.

tion (5), etc. However, these are not being used as the practical method to determine the setting time. In order to determine the setting time of concrete, the penetration resistance method (6) is being used widely. This method provides a procedure for determining the times of initial and final setting of concrete by measuring the penetration resistance of the mortar sieved from the concrete mixture (Concrete method). Unfortunately, the concrete test requires great quantities of materials and a long time. And the results obtained vary widely with the change in the places and dates of testing, materials used and mixing conditions.

As a more convenient method, use of mortar in lieu of concrete has been tried occasionally (Mortar method). However, it has not been clarified whether or not the mortar sieved from concrete and the mortar prepared by a mortar mixer give the same setting time. It was observed in our laboratory that, when water reducing admixtures are used, the setting time of the concrete differed widely from that of mortar prepared by a mortar mixer.

Hence, the investigation on the use of mortar in lieu of concrete is carried out when lignosulphonate water reducing admixture, water reducing and retarding admixture and water reducing and accelerating admixture are added to cement.

Furthermore, the effects of various factors on the setting time are investigated by using mortar test.

Experimental

Materials

Cement

Normal portland cement is used. The quality conforms to the specification of normal portland cement in JIS (Japan Industrial Standard) R 5210 (7). In Table 1, the composition and the physical properties of the cement is shown.

Table 1. *Composition and physical properties of cement*

Ignition loss (%)	Tricalcium silicate (%)	Tricalcium aluminate (%)	Initial set (hr-min)	Final set (hr-min)
0.6	50.0	9.0	2–40	3–58

Fine Aggregate

River sand at Nishiki river (Iwakuni, Japan) is used. Specific gravity, absorption, fineness modulus and maximum size of the sand is 2.59, 1.80%, 3.04 and 5.0 mm, respectively.

Coarse Aggregate

River gravel at Nishiki river is used. Specific gravity, absorption, fineness modulus and maximum size of the gravel is 2.64, 1.20%, 7.10, 25 mm, respectively.

Admixtures

Three kinds of lignosulphonate water reducing admixtures which conform to the specifications of Type A (Normal), Type D (Retarding) and Type E (Accelerating) water reducing admixture in ASTM C494–65T, respectively, are used.

Test for Setting Time of Concrete (Concrete Method)

The initial and final setting time of concrete are determined with the penetration resistance apparatus (Proctor penetration resistance needle) according to ASTM C403–65T.

Test for Setting Time by Using Mortar in Lieu of Concrete (Mortar Method)

The mortar mixer used is of the ASTM C305 type (8). Mortar is mixed by the following methods.

1. Saturated surface dry fine aggregate, cement and water or an admixture solution are placed in the bowl, then mixed at the slow speed (140 rpm) for three minutes (Method M1).

2. Saturated surface dry fine aggregate and cement are placed in the bowl and premixed at the slow speed for 1 minute, the mixer is stopped and water or an admixture solution is added to the mixture, then mixed again at the slow speed for three minutes (Method M2).

The initial and final setting time of the mortar are determined by the method prescribed in ASTM C403–65T.

As the amount of the mortar prepared by this mixer is not enough to prepare the specimen, the mixing is performed twice and the first mortar mixture is placed in the lower part of the test container.

Preparation of Concrete

A revolving drum tilting mixer (size is 2 ft^3) is used. Proportions of the concretes are indicated in

Table 2. The concretes are mixed by two methods as follows.

1. Fine aggregate, coarse aggregate and cement are placed in the mixer, then water or an admixture solution is added. After all the materials have been introduced into the mixer, the concrete is mixed for three minutes (Method C1).

2. Saturated surface dry fine aggregate, dry coarse aggregate and cement are mixed for 1 minute without water addition, then water or an admixture solution is added and mixed for three minutes (Method C2).

Table 2. *Proportions of concretes*

Kind of admixture	Slump (cm)	Air (%)	Water/Cement (%)	Sand/Aggregate (%)	Sand/Cement (%)	Cement (kg/m³)
none	7.3	2.0	52.7	40	254	300
Type A	7.9	4.8	45.0	37	233	300
Type D	8.7	4.2	45.0	37	233	300
Type E	7.9	4.2	45.0	37	233	300
none	18.4	1.3	63.3	44	268	300
Type A	18.1	3.8	53.1	41	250	300
Type D	18.0	4.4	53.1	41	250	300
Type E	17.3	4.0	53.1	41	250	300

Results and Discussions

Applications of the Testing Method by Using Mortar in Lieu of Concrete

It was observed occasionally that the setting time determined by using the mortar in lieu of concrete (Mortar method) was not identical with that determined by using the mortar sieved from the concrete (Concrete method). Therefore the factors affecting the setting time was studied. After the extensive work, it is concluded that both methods give the same results when the same proportion, mixing sequence, mixing period and temperature are used.

The initial and final setting times of concretes are determined by testing mortars sieved from the concrete mixtures in accordance with ASTM C403–65T. The proportions of concretes are shown in Table 2, and the times of setting are shown in Table 3.

In this method, the mixing of concrete is carried out according to the Method C1. That is, after all the materials has been introduced into mixer, the mixing is started. The mixing is continued for 3 minutes. The materials are kept at 20°C and the experiment is carried out at 20°C.

The setting time of mortars is determined by the Mortar method. The same cement and fine aggregate, the same water-cement, sand-cement ratio and the same temperature as those used in the Concrete method are used, and after all the materials have been introduced into the mortar mixer, the mixing is started and continued for 3 minutes. The results are shown also in Table 3.

In order to find out the causes of discrepancies which were observed occasionally between the setting times in both methods, the effects of proportions, mixing sequence, mixing period and temperature on the setting time of the concrete are investigated in details.

Influence of Mixing Sequence

The influence of the mixing sequence on the setting time of concrete is studied. In Table 4, the results are shown.

Table 3. *Setting time of concrete determined by the concrete method and mortar method*

Kind of admixture	Slump (cm)	Time of setting (hr-min) concrete method initial	concrete method final	mortar method initial	mortar method final
none	7.5	5–16	7–17	5–20	7–15
Type A		5–18	7–10	5–10	7–10
Type D		6–26	8–30	6–35	8–40
Type E		4–15	6–05	4–15	6–05
none	18.0	5–45	7–35	5–50	7–45
Type A		6–00	8–05	6–03	8–10
Type D		7–10	9–25	7–10	9–15
Type E		5–00	7–00	5–30	7–00

Concretes and mortars are mixed by the Method C1 and M1.
Proportions of concretes are shown in Table 2.
Proportions of mortars are the same water-cement and sand-cement ratios as that of corresponding concretes.

Table 4. *Influence of mixing sequence on the setting time of concrete.*

Kind of admixture	Mixing method	Slump (cm)	Air (%)	Time of setting (hr-min) initial	Time of setting (hr-min) final
none	C1	7.2	2.1	5–16	7–17
	C2	8.0	1.9	5–23	7–20
Type A	C1	5.5	4.7	5–18	7–10
	C2	8.0	5.0	7–10	9–00

Proportions of concretes are the same as that shown in Table 2.

The change in the mixing sequence brings about an unexpected remarkable effects on the setting time. That is, when the cement and the aggregate are premixed before the admixture solution is added, the setting time of the concrete is delayed by two hrs. for the Type A admixtures.

The effect of the mixing sequence on the setting time of mortar is shown in Table 5.

Table 5. *Influence of mixing sequence on the setting time of mortar.*

Kind of admixture	Mixing method	Water/Cement (%)	Sand/Cement (%)	Time of setting (hr-min) initial	final
none	M1	52.7	254	5–55	8–30
	M2			6–40	9–05
Type A	M1	45.0	233	6–25	9–05
	M2			9–20	11–50
Type D	M1	45.0	233	7–50	10–20
	M2			12–10	15–10
Type E	M1	45.0	233	5–05	6–45
	M2			6–40	8–40

In the Mortar method, the same phenomena as in the Concrete method are observed. When the cement is premixed with fine aggregate before the admixture solution is added, the setting time of the mortar is delayed by two to five hrs. depending upon the kind of admixture used.

In our preliminary experiment, the same delaying phenomena are observed for the mortar containing other kinds of Type A admixture (β-naphthalene sulphonic acid-formaldehyde condensation product) and retarders (sugar, glucose etc.). V. H. Dadson and E. Farkas studied (9) on the delayed addition of set retarding admixtures to the concrete. The addition of lignosulphonate and hydroxylated carboxylic acid to concrete two minutes after the mixing has been started, increases their efficiency as retarder. G. M. Bruer studied (10) on the set retarding effects of calcium lignosulphonate and citric acid in cement paste made with water-cement ratio of 0.35 by weight, and showed that when the cement was premixed with water, then mixed again with the retarder solution, the setting time of the paste were considerably longer than when the retarder was added to the dry cement with the mixing water. These authors pointed out that the effect of delayed addition is much greater in cement with higher tricalcium aluminate content. Bruer explained these phenomena as follows. When cement was premixed with water for a few minutes, gypsum in cement had ample time to dissolve and coat the tricalcium aluminate. Consequently, when the retarder was added to the premixed cement, the tricalcium aluminate is unable to absorb it and a large amount of the retarder was available to retard the silicate hydration reaction. Dadson and Farkas also supported this theory.

The delaying phenomena observed in this study may relate to the delayed addition. During the premixing, the cement reacts with a small quantity of water which is absorbed in the sand. This can be proved by the fact that when the oven dry sand is used in place of the saturated surface dry sand, no delaying phenomenon is observed. It is very interesting that such a minute amount of water brings about the delayed addition phenomenon and not only retarding admixture but Type A and Type E admixtures also exhibit the delaying of the setting time.

In the performance of the testing by the method using mortar in lieu of concrete, the effects of the mixing sequence on the setting time should be recognized. This premixing method (Method M2) is being used as the mixing method for the preparation of mortar in JIS R5201 (11). But this mixing method should be avoided in the test for the setting time by using mortar, if the concrete is not prepared by the premixing method (Method C2). It is concluded that, as concretes are usually mixed by Method C1, the mortar used in the Mortar method shall be mixed by Method M1 in order to know the setting time of the concrete.

Influence of Mixing Period

Influence of mixing period on the setting time is studied. The concrete is mixed by the Method C1 for three and six minutes. The results shown in Table 6 indicate that the extension of the mixing period brings about a decrease in the setting time by about 25 to 45 minutes.

Table 6. *Influence of mixing period on the setting time of concrete*

Kind of admixture	Mixing period (min)	Slump (cm)	Air (%)	Time of setting (hr-min) initial	final
none	3	7.2	2.1	5–16	7–17
	6	6.8	2.1	4–55	6–45
Type A	3	5.5	4.7	5–18	7–10
	6	6.8	4.8	4–50	6–55

Proportions of concrete are the same as that shown in Table 2. Concretes are mixed by the Method C1.

The effect of the mixing period on the setting time is also studied by the Mortar method. The results are shown in Table 7.

In the Mortar method (Method M1), the mixing period shall be decided so that the setting time of the mortar may reach to the same setting time as that obtained by the Concrete method. In our experiment, the same mixing period as in the concrete mixing is necessary for the Mortar method (three minutes). This period, however, shall be varied depending upon the kind of the mixer used.

Table 7. *Influence of mixing period on the setting time of concrete*

Kind of admixture	Mixing period (min)	Time of setting (hr-min) initial	final
none	1	5–55	7–55
	3	5–10	7–10
	6	4–50	6–30
Type A	1	5–55	8–10
	3	5–10	7–10
	6	4–50	6–35
Type D	1	7–50	10–35
	3	6–35	8–40
	6	5–35	7–30
Type E	1	5–05	6–50
	3	4–10	6–05
	6	3–50	5–20

Proportions of mortar: W/C = 52.7%, S/C = 252% for no admixture mortar
W/C = 45.0%, S/C = 233% for admixture mortar
Mortars are mixed by the Method M1.

Influence of Proportions of Concretes

Table 3 indicates that the setting times of concretes vary with change in the proportions and the concretes with higher consistencies give longer setting times.

The influences of the changes in water-cement ratio and sand-cement ratio of the mortar on the setting time are studied by the mortar test. The results are shown in Fig. 1.

The setting time varies widely when the proportions of the mortar are varied. It seems to be seen a linear correlation between the setting time and the consistency of the mortar.

In the Mortar method, the proportions of the mortar shall be identical with that of the concrete.

Influence of Temperature

Influence of temperature on the setting time is studied by the Mortar method. The results are shown in Fig. 2.

The effect of the temperature on the setting time of the mortar is remarkable. The mortars containing the type D and E admixtures exhibit greater deviation in the setting times from the mortar without admixture when the temperature of the mortars is lowered.

In the Mortar method, the same temperature shall be used as in the Concrete method.

Effects of Various Factors on the Setting Time of the Concrete or the Mortar Containing the Admixtures

In Table 8, the specified requirements for the setting times of the concretes containing various types of admixtures are summarized.

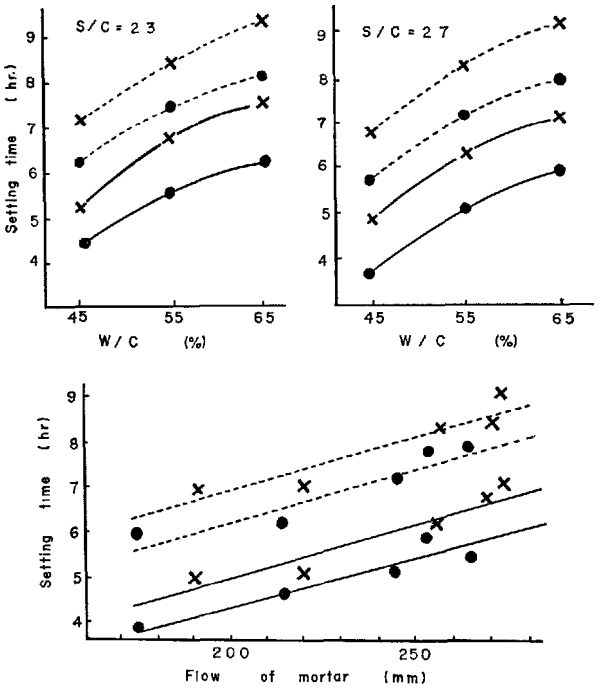

—●— Initial setting time of the mortar without admixture
—×— Initial setting time of the mortar containing type A admixture
--●-- Final setting time of the mortar without admixture
--×-- Final setting time of the mortar containing type A admixture

Fig. 1. *Influence of the proportion and concistency of mortar on the setting time.*

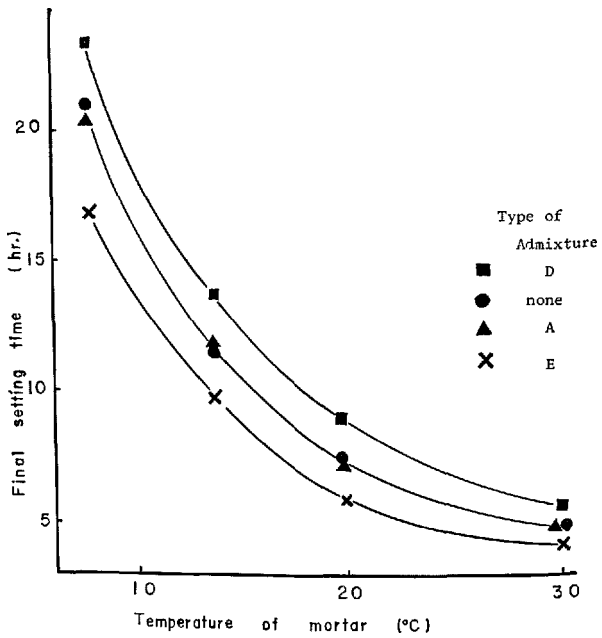

Fig. 2. *Influence of temperature on the setting time of mortar.*

Table 8. *Specifications for the setting time of water reducing admixtures for concrete*

	ASTM C 494–65T			BR*	JSMS**		
	Type A	Type D	Type E		Type B	Type C	Type D
	Normal	Retarding	Accelerating	Retarder	Normal	Retarder	Accelerating
Initial							
max.	±1	+3	−3	+4	±1	+3	−3
min.	...	+1	−3	+1	...	+1	−0.5
Final							
max.	±1	+3	...	+3	±1	+3	−0.5
min.	...	...	−1	...	...	...	...

Figs. in the Table indicate the deviations of the setting time from reference concrete without admixture, in hr.
* see reference (12)
** see reference (13)

In these specifications the setting time of concrete is determined as prescribed in ASTM C403–65T. Proportions and mixing methods are specified in the respective specification. The effects of the retarding and accelerating admixtures are expressed as the deviations of the setting time of the concrete or mortar containing the admixtures from the standard concrete or mortar without admixture. As the setting time of concrete is affected by the various factors as mentioned above, the deviation of the setting time is also affected by the factors such as proportions, mixing sequence, mixing period and temperature. In order to exhibit the effect of the proportions, the deviations of the setting times of the concretes containing the admixtures from concrete without admixture are calculated from Table 3 and shown in Table 9.

With increasing the slump of the concrete, the deviation of the setting time increases for Type A and D admixtures and decreases for Type E admixture. This fact indicates that the efficiency of the set accelerating admixture decreases with increasing the consistency of the concrete.

The effect of the mixing sequence is very important as shown in Tables 4 and 5. When the concrete is mixed by Method C2, the setting time of the concrete containing the admixture is delayed by more than 2 hrs. than that of the concrete mixed by Method C1. While, the concrete without the admixture is affected by the change in the mixing method to a much smaller extent. Accordingly, when the concrete is mixed by Method C2, the qualities of the admixtures expressed as the deviation of the setting time do not conform to the requirements in the specification.

The effect of the mixing period is shown in Fig. 3.

When the mixing period is varied, the deviations of the setting times of the mortars are constant for the Type A and E admixtures, but for the Type D admixture, the deviation decreases with the extension of the mixing period.

The effect of the temperature is also remarkable as shown in Fig. 2. The Type E admixture can be used more effectively in the lower temperature.

Table 9. *Deviation of the setting time from no admixture concrete.*

Slump of concrete	Deviation of the setting time of the concrete (hr-min) containing					
	Type A admixture		Type D admixture		Type E admixture	
	initial	final	initial	final	initial	final
7.5	0–02	0–07	1–10	1–30	1–01	1–12
18.0	0–15	0–28	1–25	1–48	0–45	0–37

Proportions of concretes are shown in Table 2.

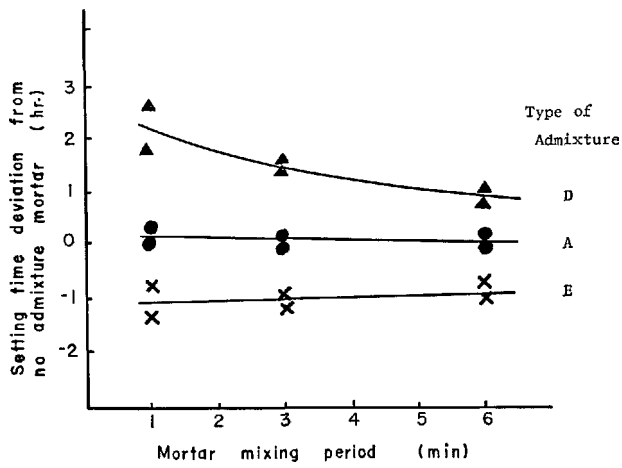

Fig. 3. *Influence of the mixing period on the deviation of the setting time of the mortar containing various admixtures from the mortar without admixture.*

These results indicate that the efficiency of these admixture varies with the change in the various factors mentioned above. In establishment of the specification for chemical admixture, the testing method for the setting time should be decided under the consideration of these factors.

On the other hand, in the use of the admixture it must be recognized that the efficiency of the set con-

trolling admixture varies with the change in the proportions, mixing method and temperature in actual job condition and in some case, the quality of the admixture may not conform to the requirement in the specification.

Conclusion

In order to determine the setting time of concrete, especially of the concrete containing various types of admixtures, the method using mortar in lieu of concrete (Mortar method) is studied.

When the admixtures are used, the results obtained by this method are influenced profoundly by various factors. Therefore, the mortar test should be performed as follows.

1. The proportions of the mortar for the test shall be identical with that of the concrete.
2. The same materials as in the concrete shall be used.
3. The same mixing sequence as in the concrete shall be used.
4. The mixing shall be continued until the setting time of the mortar reaches to the setting time obtained by the concrete test.

This method is more convenient than concrete test and gives the practical information on the setting time of concrete, and gives more accurate and reproducible results than concrete test. This method can be used for determining the effects of various variables such as cement, mixture proportion, mixing method, temperature and admixtures upon the setting time of the concrete.

The effect of the retarding and accelerating admixture on the setting time of the concrete are investigated and it is clarified that the efficiency of these admixture varies with the change in proportions, mixing sequence, mixing period and temperature. The significance of the effect of the mixing sequence is pointed out.

Therefore, in establishment of the specification for chemical admixture, the testing method for the setting time should be decided under consideration of these factors.

References

1. JIS R 5201–1964, "Physical testing methods of cement", 8. Test for setting. ASTM C 191–58, "Time of setting of hydraulic cement by Vicat needle". ASTM C 266–58T, "Time of setting of hydraulic cement by Gillmore needle".
2. K. Kosaka, "Test for setting of cement with practical water-cement ratio" (in Japanese), Cement and Concrete No. 217, 18–20 (March 1965).
3. R. H. Bogue, The chemistry of portland cement, 2nd ed., p. 647, (Reinhold Publishing Corp., New York, U.S.A., 1955).
4. N. Aschan, "Determining the setting time of cement paste, mortar and concrete with a copper-lead electrode", Magazine of Concrete Research No. 56, [18], 153–159 (1966).
5. H. F. W. Taylor, The chemistry of cements, **1**, p. 327, (Academic Press Inc., London and New York, U.S.A., 1965).
6. ASTM C 403–65T, "Test for time of setting of concrete mixtures by penetration resistance".
7. JIS R 5210, "Portland cement".
8. ASTM C 305–59T, "Tentative method for mechanical mixing of hydraulic cement pastes and mortars of plastic consistency".
9. V. H. Dadson and E. Farkas, "Delayed addition of set retarding admixtures to portland cement concrete", ASTM Proceedings **64** 816–826 (1964).
10. G. M. Bruer, "Importance of mixing sequence when using set retarding agents with portland cement", Nature **199**, 32–33 (July 6, 1963).
11. JIS R 5201–1964, "Physical testing methods of cement", 10. Strength of Cement.
12. United States Department of the Interior Bureau of Reclamation, Concrete Manual, 7th ed., p. 604, (U.S. Government Printing Office, Washington, 1963).
13. Comittee on Admixture for Concrete, JSMS, "The classification and specifications for admixtures for structural concrete" (in Japanese), J. Soc. Materials Science, Japan **16** No. 167, 581–588 (1967).

Supplementary Paper IV-107 Study on the Admixture for Aerated Concretes Including Maleic Anhydride Modified

Kenji Akutsu*

Synopsis

Various kinds of surface active agents are now used as air-entraining agent (AE agent) or dispersant for cement, but there are few which are effective as foaming agent, one of admixtures for aerated concrete. Various basic tests have been performed on the foaming agents, in which a maleic anhydride modified resin, a product of recent synthetic chemistry, is utilized.

Utilization of Maleic Anhydride Modified Resin in Foaming Agent

Well known as surface active agents for the cement admixture are salts of resin acids, salts of alkylbenzene sulphonic acids, salts of lignin sulphonic acids, non-ionic agents, etc., but since the foaming agent is different from the ordinary air-entraining agent (AE agent) and thus requires introduction of a large amount of air (5% to 80% larger than the air-entraining agent requires), the foaming agent must have a high foam stability and consequently must have a good effect in reducing the bleeding of concrete. For this purpose it seems that, if there is a higher surface activity in the cement paste and further, if there is a group of atoms capable of forming a primary bondage with calcium ion, Ca^{2+}, in the paste, the stability of foam film would be more effective.

On the basis of the foregoing concept, an attempt has been made to utilize as a foaming agent a maleic anhydride modified resin prepared by adding maleic anhydride to abietic acid, a main component of resin acid of the anionic surface active agent, to introduce carboxyl groups (–COOH), that is, hydrophilic groups, into a molecule.

That is, total three carboxyl groups (–COOH) are involved in a molecule by the maleic anhydride modification, and thus the electronegativity is increased and the ability for bonding Ca^{2+}, Al^{3+}, etc. is enhanced.

Maleic anhydride modified resin

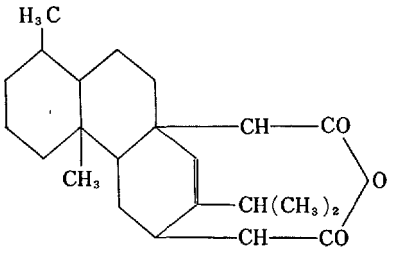

In that case, it is also possible to allow the abietic acid to react with other unsaturated polybasic acid than maleic anhydride, for example, fumaric acid.

Said resulting maleic acid copolymer is saponified, and after addition of a foam stabilizer thereto, is uniformly emulsified, whereby an admixture is prepared.

Heretofore used as foaming mixtures have been a glue-resin mixture, saponine-resin mixture, protein-hydrolysate, etc.

In addition, a foam stabilizer, such as sodium silicate, has been added thereto, but there have been problems in the stability and storability of the product. However, the foaming agent of maleic anhydride modified resin is hardly deteriorated in quality even if it should be stored for a long time, for both main component and additive are the products of synthetic chemistry.

*Taisei Construction Co., Ltd., Tokyo, Japan.

Basic Property Test

The basic property tests of maleic anhydride-modified resin (M.R.) foaming agent were conducted according to the test procedure for the surface active agent for concrete. That is, these tests were to determine the correlation of the foaming agent with its utility by conducting the tests as itemized below prior to the concrete test.

(i) Quantitative determination of solid matters (evaporation residue)
(ii) Specific gravity
(iii) pH (hydrogen ion concentration) of dilute solution
(iv) Viscosity
(v) Surface tension (specific surface tension and specific boundary tension)
(vi) Foaming capacity and stability
(vii) Dispersibility (rate of bleeding)

Among the foregoing items, the solid matters, specific gravity, viscosity, etc. relate to workabilities, such as dilution, mixing, etc., and the surface active actions has an important correlation with foaming, wetting, emulsification, dispersion, etc. Further, as to the hydrogen ion concentration, the pH that is very far from the neutral point (pH-7) must be avoided. The concentration, at which the AE agent or foaming agent can demonstrate its characteristics to a maximum as a cement admixture, resides around the so-called critical micelle concentration (C.M.C), which can be inferred from a surface tension-concentration curve. In the testing procedure for the surface active agent for concrete the specific surface tension or specific boundary tension is determined according to the testing procedure for the synthetic detergent, JIS K3362 (drop count meter), but in the present test, Du Noüy's surface tension balance (Photo 1) was used. To determine the viscosity viscotester (Photo 2) was used.

Fig. 1 shows a surface tension-concentration curves obtained by testing 4 kinds of commercially available typical surface active agents for cement.

Resin acid chloride, non-ionic agent, alkylbenzene suphonic acid chloride, and lignin sulphonic acid chloride were used as said four kinds of surface active agents.

As to the relations between concentration and surface tension, the M.R. foaming agent has a large percentage decrease in surface tension next to the non-ionic agent, and salt of alkylbenzene sulphonic acid, and its normal applicable concentration as foaming agent ranges between 0.05 and 0.2%.

As to the dispersibility test, Fig. 2 shows a result of determination on the amount of water separated from the cement paste having a water-cement ratio, w/c, of 65%.

The result reveals that the M.R. foaming agent has the least bleeding capacity.

Results of the research for basic properties of maleic anhydride modified resin and other commercially available surface active agents are shown in Table 1.

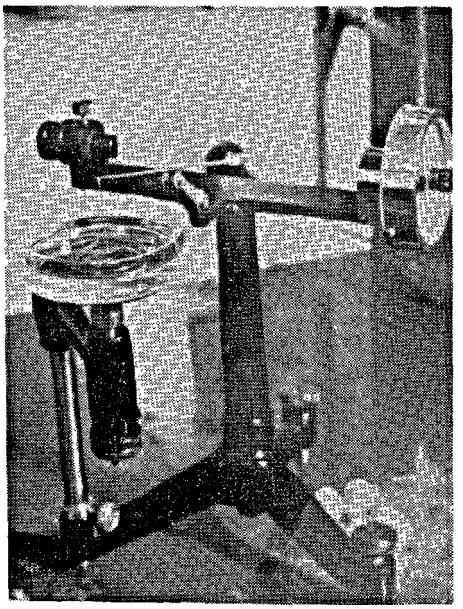

Photo 1. *Du Noüy's surface tension balance*

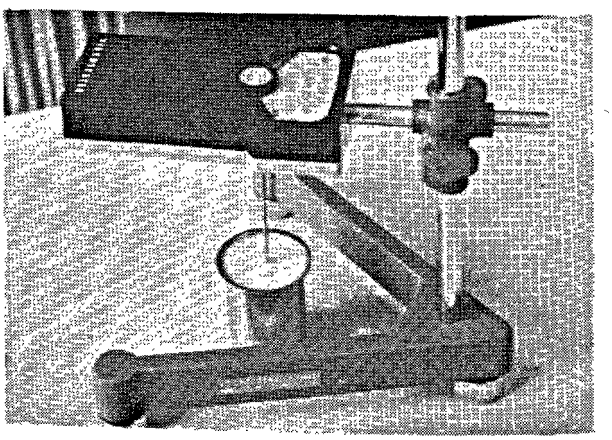

Photo 2. *Viscotester*

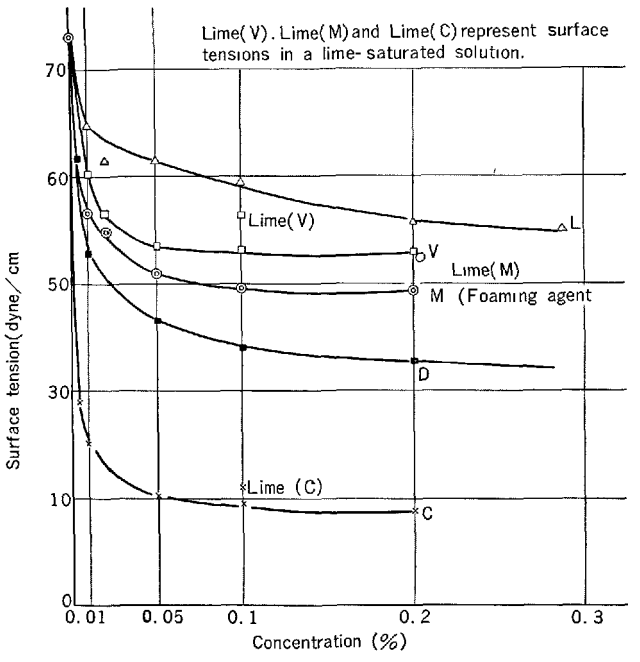

Fig. 1. *Change in surface tension with concentration.*

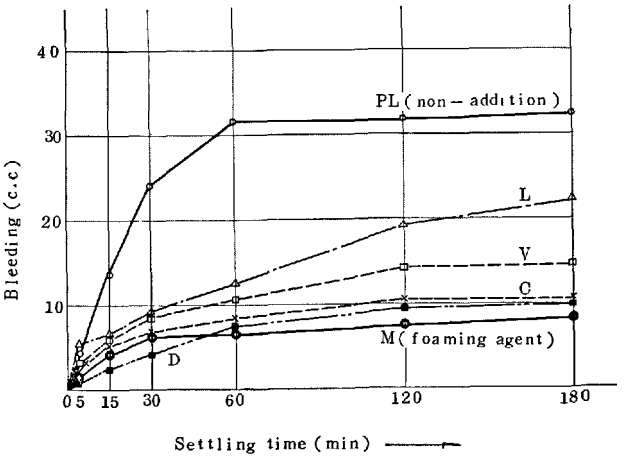

Fig. 2. *Bleeding of cement paste using a surface active agent (w/c = 65%).*

Table 1. *Basic properties of M.R. foaming agent and other surface active agents*

	M.R foaming agent	Surface-active agents			
		V	D	C	L
Color	Yellowish liquid	Brown liquid	Brown liquid	Yellow viscous solution	Yellow powder
Solid matter(%)	14.1	20.5	10.7	23.1	91.1
S.G (g/cc)	1.028	1.065	1.027	1.025	50% solution 1.229
pH	8.4	11.4	9.4	7.2	5.7
Viscosity (c.p)	30	92	5	600	10

Setting Test

Admixture for aerated concrete, either foaming agent or gas forming agent, must not contain any substance that retards the setting of lime or cement, because if the setting or hardening is retarded, there is a fear of disintegration of the formed foams.

Influences of M. R. foaming agent and said four kinds of surface active agents for concrete upon the setting time of the cement were comparatively studied. The result is shown in Fig. 3.

In addition, change in setting time when the M. R. foaming agent was employed together with calcium chloride or sodium fluoride as accelerating agents, and the influence of methylcellulose (MC) water-soluble polymer, which has been recently used as an admixture for cement, and further the influence of organic acid (succinic acid) when used as a retarder, were studied. The results are shown in Figs. 4–7.

The setting test was conducted according to the cement physical test procedure, JIS R 5201. The

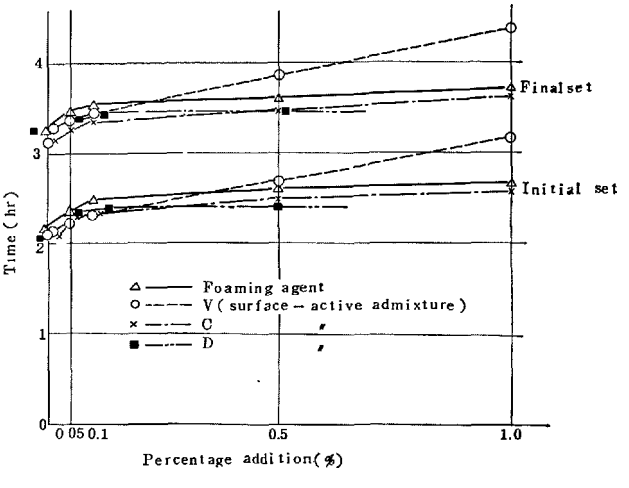

Fig. 3. *Relation between percentage addition and setting time*

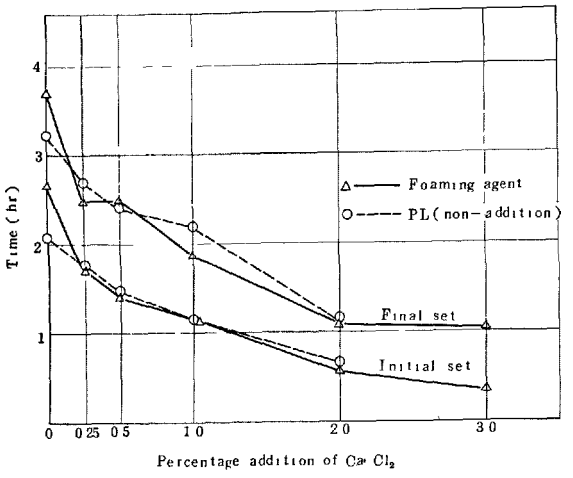

Fig. 4. *Influence of calcium chloride on set.ing tme*

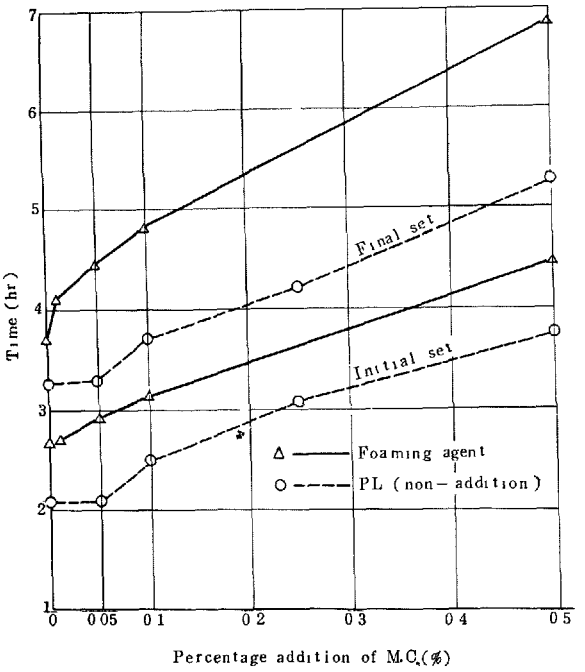

Fig. 6. *Influence of methylcellulose on setting time*

result of quality test of the cement used is the same as that of the cement used in the following section 4, aerated Mortar Test.

As shown in Fig. 3, when the M.R. foaming agent and other commercially available surface active agents for concrete were used alone one by one, the relations between percentage addition, % wt. (percent by weight of cement) and setting time did not greatly influence the setting phenomena of cement in more or less normally usable amount, except for the lignin sulphonic acid agent.

At 1% addition, both the initial and the final setting

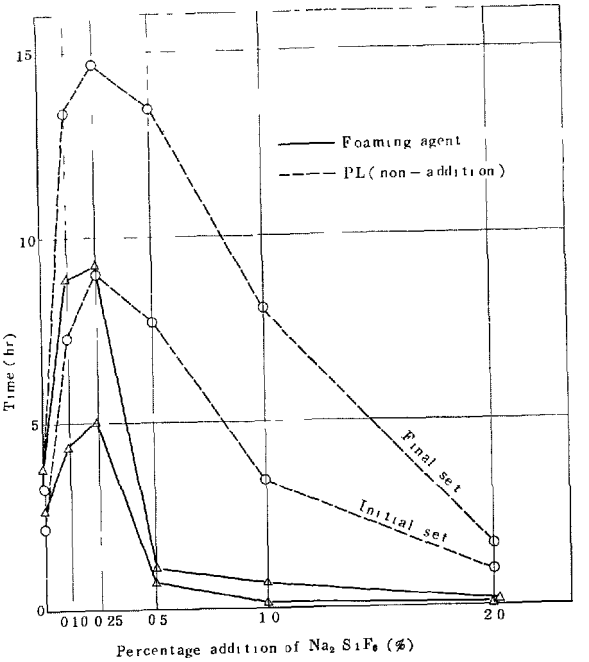

Fig. 5. *Influence of sodium silico-fluoride on setting time*

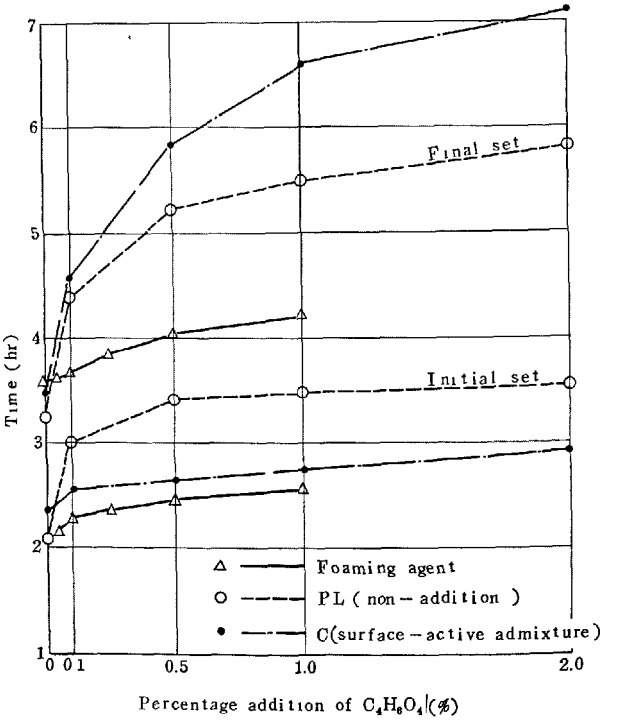

Fig. 7. *Influence of succinic acid on setting time*

were about 30 minutes retarded by use of the M. R. foaming agent as well as the C and D surface active agent, but when the V surface active agent was used, the setting was further retarded.

In the case where the M.R. foaming agent was used together with an accelerating agent, the initial and the

final setting were accelerated by increasing the percentage addition when calcium chloride, $CaCl_2$, was used, but in case sodium silico-fluoride was used, considerably retarded setting was observed, to the contrary, up to 0.5% addition and an almost instantaneous setting was attained with increasing the percentage addition. Further, when succinic acid, $C_4H_6O_4$, $\begin{matrix}CH_2\text{–}COOH\\ |\\ CH_2\text{–}COOH\end{matrix}$, was added as an organic retarder, the retarded setting was observed with the increase of the percentage addition. When succinic acid was used together with non-ionic surface active agent, a more retarding effect was obtained than that when the M.R. foaming agent was used.

When methylcellulose, M.C., which has been recently used especially as an admixture for masonry mortar, was added, somewhat retarded setting was observed as shown in Fig. 6, but such a phenomenon is a general trend observable when a hydrating substance is added. As an exception, an abnormal setting reaction was observed when the lignin surface active agent was simultaneously used. In addition, when the foaming agent was used together with silicate material bentonite as a pouring material, no influence was observed up to about 2% addition.

Aerated Mortar Test

The maleic anhydride modified foaming agent can be used both in an aerated concrete, wherein the lightweight aggregates are used (the ordinary aggregates may be used together), and in a heat-insulating aerated mortar, wherein only fine aggregates are used. But the amount of the maleic anhydride modified foaming agent to be added must be decided in view of the specific weight or strength of the desired concrete or mortar, and a required amount of air must be introduced therein.

In the present test, a M.R. foaming agent was added to the standard sand mortars in various mixing proportions, and the amount of M.R. foaming agent to be added was varied from 0.01 to 1.0% wt. Bending strength, compressive strength, drying shrinkage, air amount, etc. were studied as a basic test for aerated concrete for concreting at site or precasting.

Materials Used

Cement: ordinary portland cement (quality test result is shown in Table 2).
Fine aggregates: standard sands obtainable at Toyoura, Yamaguchi-prefecture, Japan
Admixture: maleic anhydride modified resin foaming agent

Mixing

Mix proportion used in the present test is shown in Table 3.

Table 3. *Mixing proportions of aerated mortar*

Mixing proportion	Cement (g)	Standard sand (g)	Water (cc)	W/C (%)	Percentage addition of foaming agent (%)
1:2	520	1,040	312	60	0, 0.01, 0.05 0.1, 0.2, 0.3
1:3	400	1,200	320	80	0.1, 0.2, 0.3 0.5, 1.0
1:4	350	1,400	350	100	(Total 8 kinds)

Testing Procedure

The test was conducted according to the cement physical testing procedure, JIS R 5201, and an asphalt mixer (experimental use; volume: about 10 l) was used for mixing. After determination of flow value,

Table 2–1. *Chemical compositions of cement used*

	Ig. Loss (%)	MgO (%)	SO_3 (%)	$3CaO\cdot SiO_2$ (%)	$3CaO\cdot Al_2O_3$ (%)
Ordinary portland cement	0.7	1.5	2.0	45	9

Table 2–2. *Physical properties of cement used*

Specific gravity	Fineness		Setting times			Flow	Bending strength (kg/cm²)			Compressive strength (kg/cm²)		
	Blaine's specific surface (cm²/g)	Residue on 88μ sieve (%)	Water content (%)	Initial (hr-min)	Final (hr-min)	(mm)	3 days	7 days	28 days	3 days	7 days	28 days
3.16	3,350	2.0	27.2	2–16	3–20	243	31.6	47.6	70.2	130	232	409

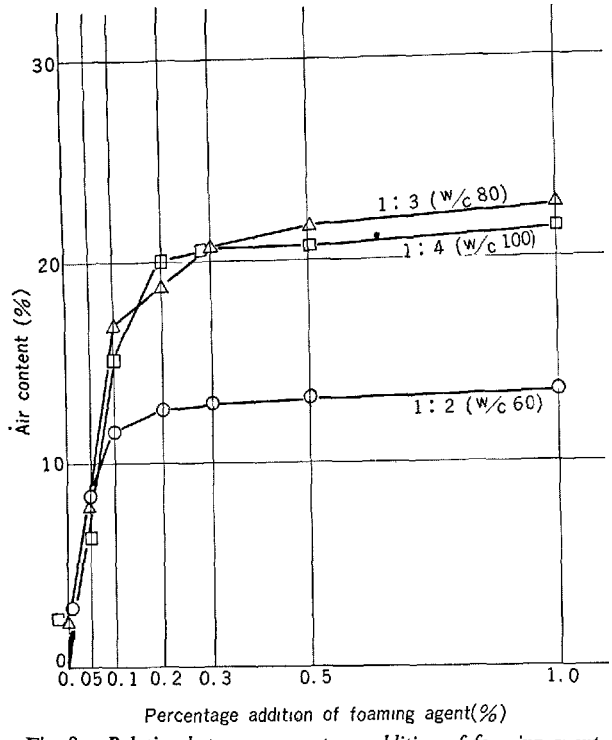

Fig. 8. *Relation between percentage addition of foaming agent and air content*

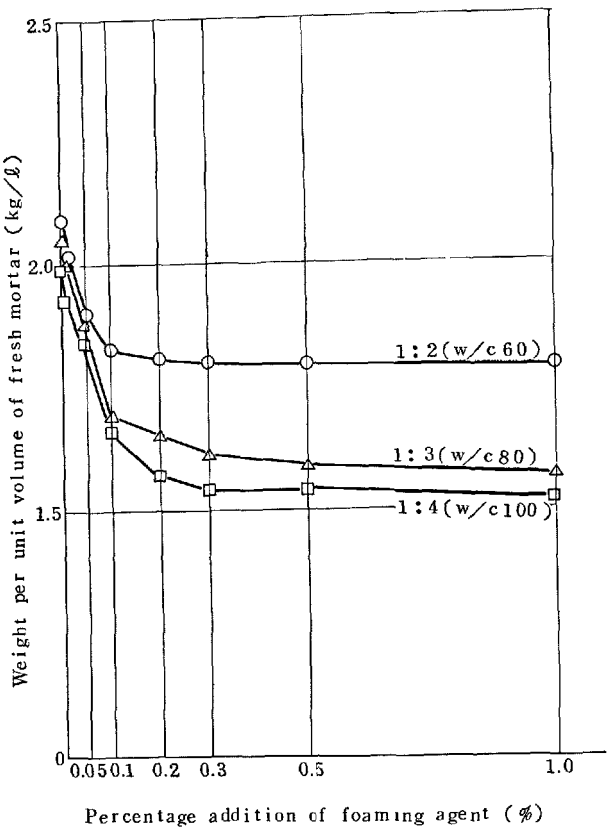

Fig. 9. *Relation between percentage addition of foaming agent and weight per unit volume of fresh mortar*

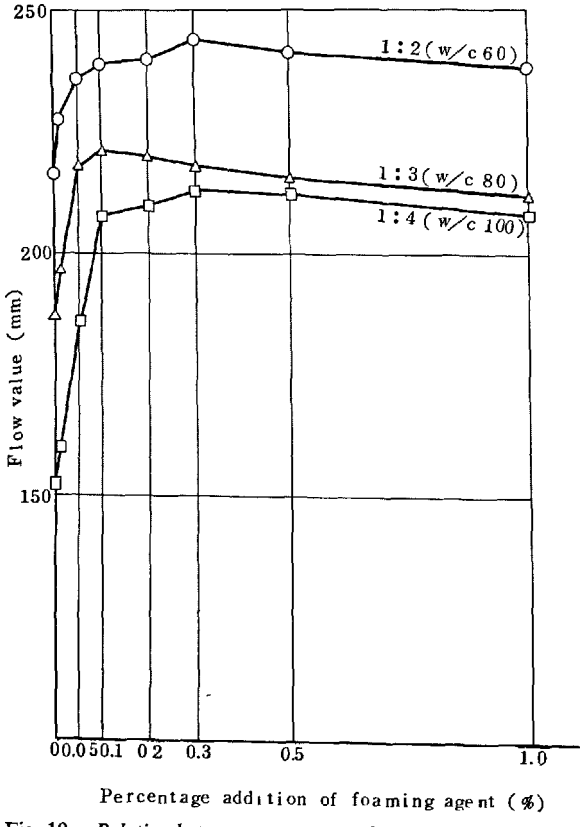

Fig. 10. *Relation between percentage addition of foaming agent and flow value*

a standard mortar specimen ($4 \times 4 \times 16$ cm) was prepared. As to the curing, both high humid air curing (humidity: 80%, temperature: 20°C) for the strength test and low humid air curing (humidity: 50%, temperature: 20°C) for the drying shrinkage test were carried out.

Results and Discussion

(i) The relation between the amount of added foaming agent, amount of air, and the weight per unit volume of fresh mortar are shown in Figs. 8 and 9.

With the increased amount of M.R. foaming agent, the amount of air was increased, and a point of flection corresponding to the critical micelle concentration (C.M.C.) was observed around 0.1 — 0.2% addition of M.R. foaming agent. The relation between the percentage addition (concentration) of the M.R. foaming agent and the amount of air was in an exponential curve, and the increase in the amount of air was in proportion with the amount of adsorption at the boundary and accorded with the Freundlich's adsorption isotherm formula.

(ii) As to the relation between the amount of M.R.

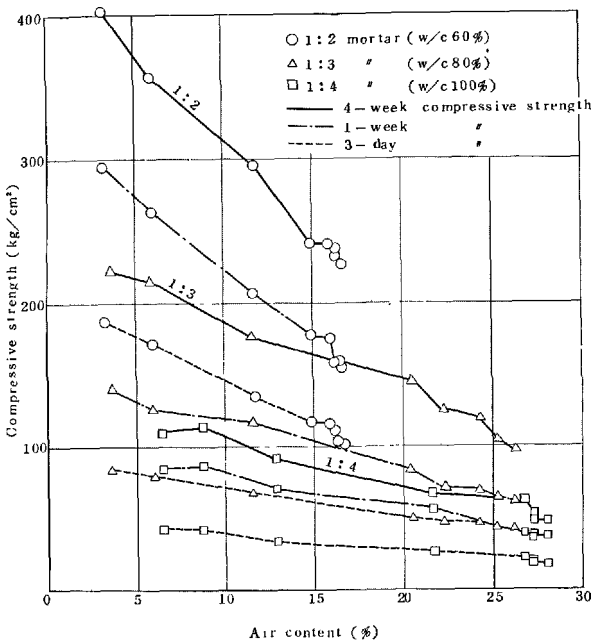

Fig. 11a. *Relation between air content and compressive strength*

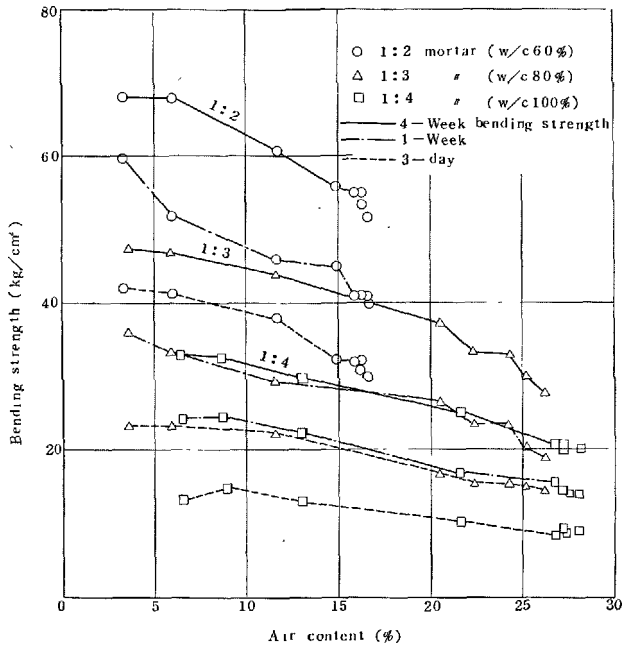

Fig. 11b. *Relation between air content and bending strength*

foaming agent and the flow value, the flow value considerably increased with increasing amount of M.R. foaming agent up to 0.1 — 0.2%, but on the contrary decreased with further amount of M.R. foaming agent, as shown in Fig. 10. Such a phenomenon seems to be due to an increase in viscosity of cement paste with increasing amount of foaming agent.

(iii) The relation between the change in the amount of air and the compressive or bending strength are shown in Fig. 11-a, 11-b.

In every mixture, the strength decreased with increasing amount of air. The higher the amount of air, the higher the percentage decrease in strength. However, the change in strength was small when the percentage addition of M.R. foaming agent exceeded 0.1%.

(iv) As to percentage drying shrinkage and percentage decrease in weight, the larger the amount of cement used, or the larger the amount of air in the mortars at the same mixing proportion, the higher the percentage shrinkage in proportion with the amount of M.R. foaming agent added, as shown in Figs. 12–14.

(v) One example (1: 3 mortar) of the test result of percentage water absorption is shown in Fig. 15. The standard mortar specimen was dried until it reached a constant weight, and was dipped into water at a constant temperature of 20°C, whereby the relation between the time and the percentage water absorption was determined. The results reveal that at not

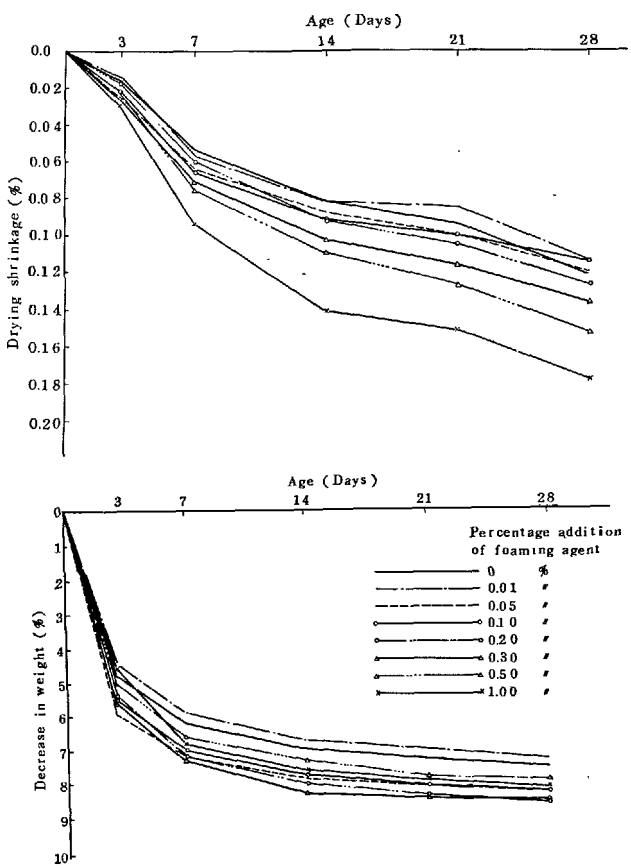

Fig. 12. *Drying shrinkage and decrease in weight of aerated mortar (1: 2)*

less than 0.5% addition of M.R. foaming agent,

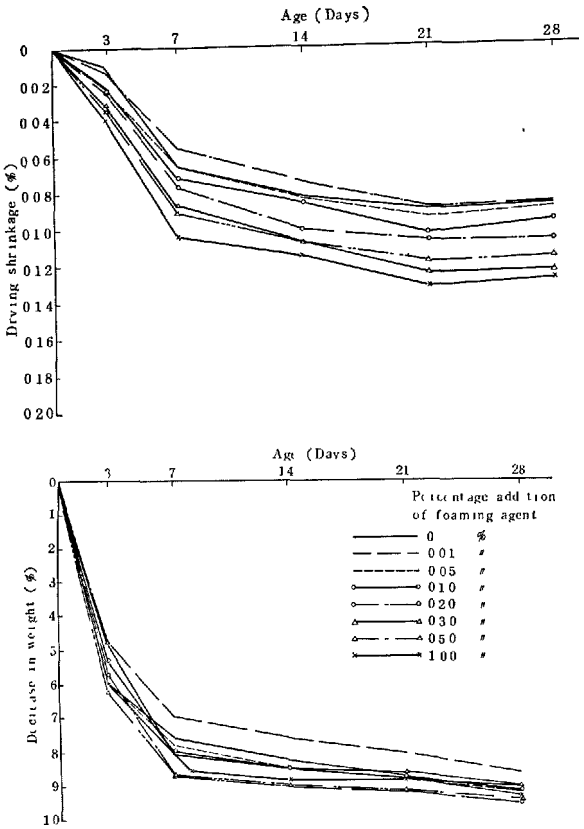

Fig. 13. *Drying shrinkage and decrease in weight of aerated mortar (1: 3)*

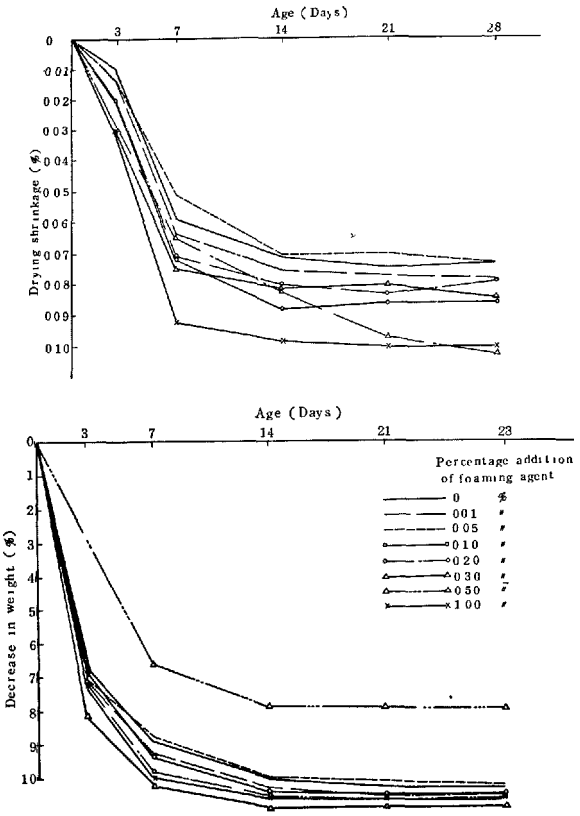

Fig. 14. *Drying shrinkage and decrease in weight of aerated mortar (1: 4)*

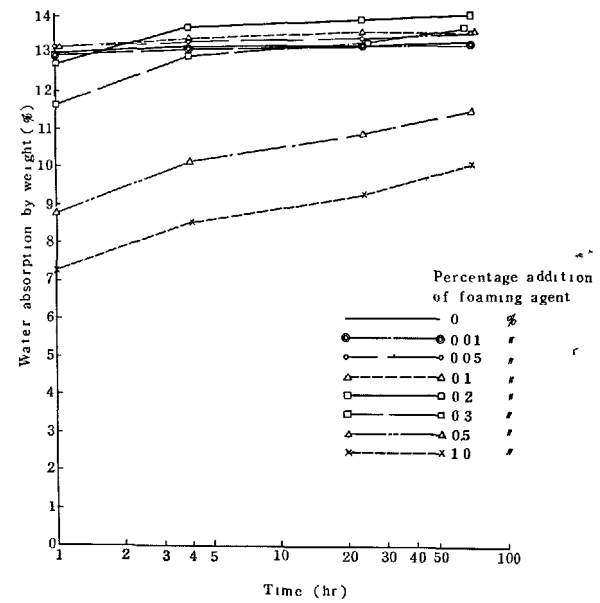

Fig. 15. *Relation between dipping time and water absorption of aerated mortar (1: 3)*

a considerable water proof effect was obtained. Further, the mortar having 0.05 — 0.2% of foaming agent, when about 10 — 20% of air was introduced, shows the same percentage water absorption similar to that of the plain mortar where no foaming agent was added. Such a phenomenon seems to be due to the fact that insoluble metal salts are formed between maleic anhydride modified resin and calcium hydroxide in the paste as mentioned above.

Conclusion

As discussed above, the results of research of the basic property, setting and mortar tests of maleic anhydride modified resin having a special molecular structure when the maleic anhydride modified resin is utilized as a foaming agent reveal that it is effective as an admixture for aerated concrete.

References

1. Gyula Rudnai, Light weight concrete, 1st ed., p. 42 (Academy of Sciences, Budapest, 1963).
2. Lloyd I. Osipow, Surface chemistry, 1st ed., p. 7 (Reinhold Pub. Corp., New York, 1962).
3. R. H. Bogue, The chemistry of cement, 2nd ed., p. 463 (Reinhold Pub. Corp., New York, 1955).
4. A. C. I. Committee 212, "Admixture for concrete", J. Am. Concrete Inst., 60, p. 1486 (1963).
5. Rudolf C. Valore, "Cellular concrete part I–II", J. AM. Concrete Inst., 51, p. 779 & p. 817 (1954).

SESSION IV-2 FLY ASH AND FLY ASH CEMENT

Principal Paper Fly Ash and Fly Ash Cement

Masatane Kokubu*

Synopsis

Classifying various researches regarding fly ash, the author first describes the chemical composition and physical properties such as particle shape, specific gravity and fineness of various fly ashes and discusses the influence of fly ash on workability, strength, volume change, heat of hardening, watertightness, durability, abnormal expansion due to alkali-aggregate reaction, etc. of concrete and establishes the practical limits of the effect of fly ashes in improving these properties of concrete. Next, as a result of summarization taking into consideration the various studies of chemical behavior of fly ash, it is found appropriate to theorize that the superior characteristics imparted to concrete by fly ash are due not only to the smooth, spherical particle shape, fine grain size and pozzolanic activity, but also to the acceleration of hydration reaction caused by replacement of fly ash particles in the floc structure of cement particles.

Although pozzolanic reaction is extremely complicated, it was possible to ascertain that the glass phase is the chief part of the phase composition contributing to pozzolanic reaction, the latter being governed by the surface area of the glass phase, and that increase in concrete strength from pozzolanic reaction has a close relationship with the $SiO_2 + Al_2O_3$ content of fly ash, while other fruits of research which offer clues to the explanation of pozzolanic reaction are recognized. Also, the reasons for the marked effect in increase of long-term strengths of concrete even with pozzolanic reaction of a degree not reflected in test values of non-evaporable water and heat of hydration are discerned.

Further, from results of studies, practical methods of solving the problems involved in actual use of fly ash such as pack setting during storage, fluctuation of air content in air-entrained concrete, etc. are suggested. The problems relevant to fly ash cement are also discussed.

Introduction

The idea of using the ash produced at the time of combustion of finely pulverized coal as a pozzolan for concrete has been in existence for a long time, research results having been published as early as 1914. (1) The term "fly ash" first appeared in literature in 1937 (2) and it is from this time that research related to this material began to be actively conducted. Parenthetically, as it became possible to collect fly ash of high fineness, greater pozzolanic effect could be expected and the use of fly ash in concrete began to be seriously studied.

With the progress in research on facilities for economically collecting good quality fly ash (3)(4)(5) the studies became even more intense, almost all of them being conducted in the United States. After the performance data of fly ash used at Hungry Horse Dam were published by the U.S. Bureau of Reclamation, (6) the use of fly ash in concrete for hydraulic structures and various other structures spread all over the United States and in 1954 an ASTM standard on fly ash (See Appendix 1) was established.

In Japan, studies on fly ash were begun around 1950. This was a period when the demand for electric power showed a sudden growth and along with this there was great activity in constructing both hydroelectric and thermal power stations so that studies connected with fly ash were advanced rapidly. In 1958 a standard on fly ash (See Appendix 1) was established. The utilization of fly ash in European countries came at

*Faculty of Engineering, The University of Tokyo, Tokyo, Japan.

about the same time as in Japan. In France, a standard on fly ash cement (See Appendix 2), in the U.S.S.R. and Great Britain, standards on fly ash (See Appendix 1) were approved in 1963 and 1965 respectively.

Fly ash, besides being used as an admixture for cement and concrete, is used in considerable quantities as an additive in celluar concrete, artificial lightweight aggregate, refractory materials, brick, in soil improvement and in asphalt as well as in abrasives, purifiers for polluted water, fertilizer and medicines, and there has been data from research in these fields published, but it is not within the scope of this paper to discuss these subjects.

It is difficult to say how much fly ash is being used as an admixture for cement and concrete in various countries of the world, but it is estimated the annual consumption in recent years has been around 1,500,000 tons in the U.S.A., 1,000,000 tons each in Japan, France and Germany and 500,000 tons in Great Britain.

Since fly ash is a by-product of the combustion of pulverized coal, it is first necessary to have facilities for collection which will economically assure uniformity of quality in order for the advantages of the material to be truly demonstrated. The advantages of good quality fly ash are the improvement of workability of concrete, improvement of strength, watertightness and durability of concrete at advanced ages, alleviation of heat of hardening of concrete and reduction of drying shrinkage, although probably, the foremost advantage of fly ash lies in the economy resulting from reduction of cement. When considering the fact that thermal power stations are going to great expense in disposing of the material as waste, the advantages of utilizing fly ash are even more marked.

These advantages of fly ash can be said to offset the shortcomings of portland cement. In concrete work, the qualities most desirable for the cement to possess will differ somewhat with the type of structure and peculiarities of the work. However, when it is attempted to obtain special portland cements which will completely satisfy the requirements of each project, it will generally be extremely uneconomical.

Under such circumstances, it is possible to obtain the properties desired of a concrete by modifying its nature through the use of a good quality fly ash as an admixture. Therefore, the true worth of a good quality fly ash is in economical improvement of the qualities of cement.

It is natural that fly ash cement should appear on the market for the reasons stated above. "Fly ash cement" is a term not yet generally accepted internationally, but since "portland-pozzolan cement" would allow pozzolans other than fly ash to be included, this term will be used purposely according to the custom in Japan in order to avoid confusion in the discussions here.

It is natural for the quality of fly ash to differ according to quality, fineness and method of burning of the pulverized coal, collecting facilities, etc., and the chemical composition of fly ash varies considerably according to country. Still, it is extremely interesting that papers from various countries all list the beforementioned advantages of fly ash.

Past research on pozzolans has been summarized and introduced by Lea (7) at the International Symposium on the Chemistry of Cement in 1938, theASTM Symposium (8) of 1949 and the symposium of 1953 of the Italian Chemical Society. Malquori (10) also introduced such research at the International Symposium on the Chemistry of Cement of 1960. These naturally include researches on fly ash.

The purpose of this paper is to summarize the results of research published in various countries, list the physical and chemical properties of fly ash, endeavor to solve the problems involved and clarify the various precautions to be taken in using the material.

There are almost 700 research reports on fly ash which have been published to date. As it will be impossible to cover all of these reports in this paper, only the representative ones of each topic discussed here will be referred to. It should be mentioned there do exist excellent papers which are not referred to due to lack of space.

Chemical Composition of Fly Ash

In the standards on fly ash of the U.S.A., Japan, U.S.S.R. and Great Britain, there are provisions for the amounts of silica (SiO_2), moisture content, loss on ignition, etc. Although it is said the active portion of fly ash consists of silica and alumina, the pozzolanic activity cannot be judged by chemical composition alone. On the other hand, it is a fact that pozzolanic activity differs greatly with the SiO_2 content and it is natural for the quantity of SiO_2 to be specified in the various countries. In the ASTM standard, the total amount of $SiO_2 + Al_2O_3 + Fe_2O_3$ is specified.

Examples of chemical composition of fly ash in various countries are given in Table 1 which shows there are great differences according to the country. These are only isolated examples, the data coming from different periods so that there may be little significance in making detailed comparisons. As far as Table 1 is concerned, the average values by country are 58–40% for SiO_2, 27–21% for Al_2O_3, 17–4% for Fe_2O_3 and 6–4% for CaO. These variations are due to the great difference in quality of coal between the various countries, the fly ash of Japan being conspicuously high in SiO_2 content compared with

Table 1. *Example of test results of fly ash in various countries*

Country		Number of composite samples	Chemical composition (%)										Molecular ratio $\frac{SiO_2}{Al_2O_3}$	Specific gravity	Specific surface (cm²/g)	Reference
			Loss on ignition	SiO_2	Al_2O_3	Fe_2O_3	CaO	MgO	SO_3	Na_2O	K_2O	Total				
Japan	Av	12	0.73	57.96	25.86	4.31	3.98	1.58	0.34	1.49	2.15	98.40	3.83	2.14	3090	
	Max		1.23	63.27	28.35	5.90	6.74	2.09	0.81	2.36	3.15	99.27	4.31	2.23	4150	
	Min		0.06	53.41	22.88	2.82	1.04	1.00	0.02	0.88	1.73	97.48	3.47	1.96	1220	
	R		1.17	9.86	5.47	3.08	5.07	1.09	0.79	1.48	1.42	1.79	0.84	0.27	2930	
	$\sqrt{s}$		0.36	2.94	1.32	0.81	1.64	0.44	0.26	0.44	0.38	0.57	0.29	0.08	890	
U.S.A.	Av	34	7.83	44.11	20.81	17.49	4.75	1.12	1.19	0.73	1.97	99.73	3.71	2.40	3673	(17)
	Max		18.0	51.9	28.3	31.3	12.0	1.4	2.8	2.10	2.98	100.55	5.76	2.69	4795	
	Min		1.0	32.7	14.6	8.5	11.1	0.7	0.3	0.22	1.28	97.94	2.93	2.14	2430	
	R		17.0	19.2	13.7	22.8	0.9	0.7	2.5	1.88	1.70	2.61	2.83	0.57	2365	
	$\sqrt{s}$		4.75	4.52	3.67	6.07	2.91	0.33	0.79	0.51	0.46	0.53	0.67	0.14	750	
Great Britain	Av	14	3.86	46.16	26.99	10.44	3.06	1.96	1.59	0.90	3.26	98.22	2.92	2.10	5180	(11)
	Max		11.70	50.70	34.10	13.50	7.70	2.90	6.80	1.90	4.20	102.90	3.19	2.33	8100	
	Min		0.60	41.40	23.90	6.40	1.70	1.40	0.60	0.20	1.80	96.10	2.52	1.90	2500	
	R		11.10	9.30	10.20	7.10	6.00	1.50	6.20	1.70	2.40	6.80	0.67	0.43	5600	
	$\sqrt{s}$		3.62	2.53	2.50	2.11	1.49	0.41	1.58	0.51	0.72	1.60	0.16	0.13	1780	
France	Av	17	3.72	48.45	25.89	8.07	5.95	2.36	1.01	n=15 0.64	n=15 3.94	100.3	3.38	—	—	(12), (60), (64), (66), (73), (74), (84), (85), (86)
	Max		15.15	54.05	33.40	15.30	38.75	4.45	7.00	0.85	6.00	—	7.38	—	—	
	Min		0.30	29.90	10.80	5.80	1.48	1.10	0.10	0.15	0.70	—	2.58	—	—	
	R		14.85	24.15	22.60	9.50	37.27	3.35	6.90	0.70	5.30	—	4.80	—	—	
	$\sqrt{s}$		4.01	5.81	6.03	2.20	9.31	0.91	1.73	0.19	1.23	—	1.11	—	—	
Germany	Av	9	9.65	41.13	24.39	13.93	5.06	1.85	0.77	—	—	96.78	2.88	—	—	(87), (88)
	Max		20.10	49.54	29.35	20.88	11.81	4.26	2.10	—	—	98.35	3.57	—	—	
	Min		1.48	34.10	21.06	8.37	2.18	0.75	0.12	—	—	94.33	2.59	—	—	
	R		18.62	15.44	8.29	12.51	9.63	3.51	1.98	—	—	4.02	0.98	—	—	
	$\sqrt{s}$		7.14	5.38	3.43	4.64	3.37	1.15	0.62	—	—	1.25	0.30	—	—	
U.S.S.R.	Av	15	—	55.08	25.97	7.83	5.08	1.81	n=11 1.63	—	—	97.40	3.70	—	—	(72), (77), (89), (90)
	Max		—	62.08	37.15	12.01	10.62	2.90	3.78	—	—	—	5.09	—	—	
	Min		—	47.90	20.71	3.08	1.10	0.28	0.20	—	—	—	2.20	—	—	
	R		—	14.18	16.44	8.93	9.52	2.62	3.58	—	—	—	2.89	—	—	
	$\sqrt{s}$		—	5.20	4.57	2.49	2.77	0.79	1.39	—	—	—	0.75	—	—	

R: Range
$\sqrt{s}$: Sample standard deviation

Table 2. *Chemical composition and phase composition of representative fly ashes of Japan*

Samples		Chemical composition (%)									
Notation	Classification	Moisture content	C	SiO_2	Al_2O_3	Fe_2O_3	CaO	MgO	SO_3	Na_2O	K_2O
A	Fly ash	0.10	0.93	59.30	24.99	3.77	3.27	1.69	0.12	0.88	2.53
B	〃	1.09	0.10	63.27	26.08	2.82	1.04	1.00	0.18	1.51	3.15
C	〃	0.05	0.06	59.93	25.97	3.50	4.39	1.12	0.02	1.06	2.21
D	〃	0.16	0.70	53.41	25.54	5.07	6.74	2.00	0.61	1.74	1.89
E	〃	0.19	1.23	53.82	25.63	4.68	5.80	1.90	0.58	2.15	2.03
F	〃	0.11	0.69	55.61	26.06	4.46	4.98	2.09	0.37	1.65	2.13
G	〃	0.18	0.98	55.52	26.43	4.72	3.81	1.78	0.81	2.36	2.02
H	〃	0.09	0.52	60.75	26.14	4.37	2.49	1.12	0.25	1.32	2.31
I	〃	0.15	1.12	59.86	27.21	3.70	2.59	1.20	0.28	1.31	1.73
J	〃	0.20	0.77	57.68	28.35	4.08	2.68	1.05	0.65	1.50	1.90
K	Coarse fly ash	0.10	0.97	58.20	25.02	4.67	4.52	2.09	0.04	0.98	2.04
L	〃	0.08	0.69	58.19	22.88	5.90	5.47	1.89	0.14	1.45	1.89
Average		0.21	0.73	57.96	25.86	4.31	3.98	1.58	0.34	1.49	2.15

Table 2. (*continued-2*)

Samples	Chemical composition (%)										
Notation	S	TiO_2	P_2O_5	Li_2O	SrO	MnO	BaO	PbO	ZnO	NiO	As_2O_3
A	0.00	0.86	0.52	0.02	0.10	0.03	0.13	0.004	0.00	0.014	0.000
B	0.00	0.62	0.13	0.00	0.01	0.02	0.07	0.003	0 00	0.007	0.016
C	0.00	0.75	0.22	0.03	0.05	0.04	0.06	0.005	0.00	0 012	0.032
D	0.00	0.97	0.90	0.02	0.14	0.05	0.20	0.006	0.00	0.021	0.024
E	0.00	0.97	0.89	0.02	0.14	0.04	0.17	0.005	0.01	0.022	0.040
F	0.00	0.86	0.98	0.02	0.18	0.03	0.18	0.004	0.01	0.022	0.036
G	0.00	0.97	0.31	0.02	0.06	0.04	0.13	0.004	0.00	0.015	0.046
H	0.00	0.85	0.13	0.03	0.06	0.03	0.09	0.006	0.00	0.007	0.004
I	0.00	1.07	0.13	0.04	0.05	0.03	0.08	0.030	0.00	0.009	0.036
J	0.00	0.93	0.13	0.01	0.05	0.03	0.08	0.004	0.10	0.010	0.010
K	0.00	0.77	0.70	0.03	0.11	0.04	0.13	0.003	0.02	0.017	0.000
L	0.00	0.63	0.70	0.02	0.17	0.05	0.12	0.003	0.01	0.017	0.000
Average	0.00	0.85	0.48	0.02	0.09	0.04	0.12	0.006	0.01	0.015	0.020

Table 2. (*continued-3*)

Samples	Chemical composition (%)			Molecular ratio	Phase composition (%)				
Notation	B_2O_3	Ga_2O_3	Total	$\frac{SiO_2}{Al_2O_3}$	Quartz	Mullite	Quartz + Mullite	Glass	Iron compounds
A	0.13	0.022	99.41	4.02	11.5	15.0	26.5	71.1	2.4
B	0.09	0.024	100.23	4.27	9.3	13.3	22.6	76.9	0.5
C	0.17	0.026	99.70	3.92	11.0	15.7	26.7	72.9	0.4
D	0.32	0.022	100.53	3.55	5.4	7.8	13.2	84.4	2.4
E	0.26	0.022	100.60	3.56	7.2	9.2	16.4	80.9	2.7
F	0.25	0.013	100.74	3.62	7.0	8.0	15.0	82.7	2.3
G	0.29	0.021	100.52	3.56	7.9	9.8	17.7	79.6	2.7
H	0.15	0.018	100.74	3.94	7.5	12.0	19.5	78.7	1.1
I	0.15	0.012	100.79	3.73	7.2	13.3	20.5	79.5	1.9
J	0.18	0.022	100.42	3.47	11.0	18.2	29.2	69.4	1.4
K	0.15	0.022	100.62	3.97	11.8	12.7	24.5	72.4	3.1
L	0.16	0.021	100.48	4.31	8.6	13.9	22.5	72.2	5.3
Average	0.19	0.020	100.47	3.83	8.9	12.4	21.1	76.7	2.2

Note 1. The fily ashes listed in Table 1 are identical to those in this table. The 10 varieties, A to J, are representative fly ashes widely marketed in Japan for use in concrete.
2. The trace elements of fly ashes were quantitatively analysed by the method proposed by Funato (91)
3. The quantitative analysis method of phase composition was as follows:
Quartz and Mullite: directly measured by intensities of X-ray diffraction tests.
Iron compounds : calculated from chemical components.
Glass : 100—(Quartz + Mullite + Iron compounds)

the fly ash of the U.S. and European countries.

The SO_3 exists mainly in the form of calcium sulfate and according to recent studies, it has been ascertained that the pack setting of fly ash during storage is due to the influence of calcium sulfate.

It is thought the reason the MgO content is specified in the ASTM standard is the considerations of harmful effects as in cement. Also, the alkali content is specified in ASTM, but in Japan there is almost no aggregate which may cause alkali-aggregate reaction and therefore there is no provision for alkali in the Japanese standard.

The loss on ignition is a measure of the carbon content and in this respect also there is a great difference according to the country, the average values ranging between 10 and 0.7%. In the early reports, the necessity for moderately low carbon content is emphasized, but the effect on the properties of hardened concrete is negligible even when the carbon content of fly ash is high to a certain extent. However, when fly ash of high ignition loss is used for air-entrained concrete, control of air content becomes difficult in many cases and for practical reasons the amount of ignition loss must be carefully considered.

Along with chemical analysis, quantitative measurement of the phase composition of fly ash has been given importance in recent years.

The major phases composing fly ash are quartz,

mullite and a comparatively large amount of glass. Of the chemical components, SiO_2 exists in the form of quartz and glass phases while part of the Al_2O_3 exists as mullite and the remainder is contained in the glass phase. Needless to say, the mineral composition will differ in a complex manner according to the quality and fineness of the pulverized coal, method of burning and other factors.

The results of analyses of 10 representative fly ashes now being marketed in Japan and 2 coarse fly ashes are given in Table 2. Table 2 also gives the phase compositions. A comparison of these with 7 out of 14 British fly ashes reported by Watt and Thorne (11) is given in Table 3.

Table 3. *Example of comparison of phase composition of Japanese and British fly ashes*

	Japanese fly ash	British fly ash
Quartz	11.8–5.4%	8.5–2.2%
Mullite	18–8%	14–6.5%
Glass	84–69%	88–71%

Physical Properties of Fly Ash

Particle Shape of Fly Ash

Although the particle shape of fly ash differs somewhat with size, the great part consists of spherical glass, in which quartz, small needle-shaped fragments of mullite and minute quantities of hematite or magnetite are contained. In some cases the spheres exist linked together.

Most fly ash consists of fine and dense spherical particles, but there are cases of relatively large particles having voids in the interiors. Some of the large particles are hollow spheres with openings which on occasion contain minute spherical particles resembling the form of fish eggs. There are also shell forms and other irregularly formed particles interspersed in the fly ash.

It will be convenient to discuss particle shape of fly ash by the 4 classifications of spherical and rounded, rounded, irregular, and angular.

Fig. 1 shows fly ash photographed by Terrier and Moreau (12) with an ore microscope while Fig. 2 shows fly ash photographed by a scanning electron microscope.

The ratio of the mixture of porous particles with internal voids and irregular shaped particles differs with the fly ash. One Japanese fly ash contained approximately 12% porous particles while a coarse fly ash contained approximately 20% (13). In any case it is an outstanding feature of fly ash that most of the particles are spherical, something which is not seen in other pozzolans. This is thought to be the principal reason for the improvement of workability of concrete obtained with fly ash.

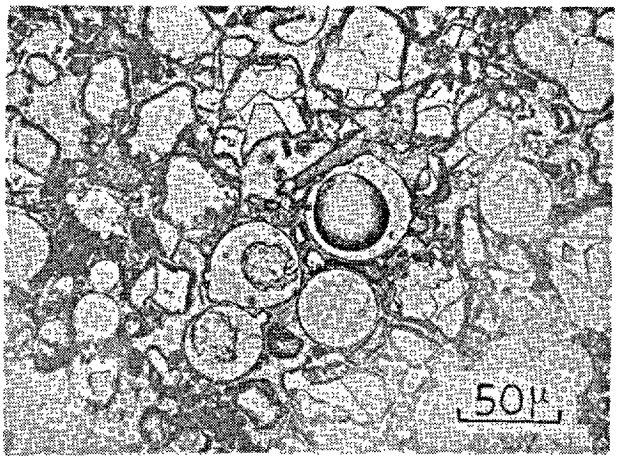

Fig. 1. *Example of fly ash photographed by ore microscope*

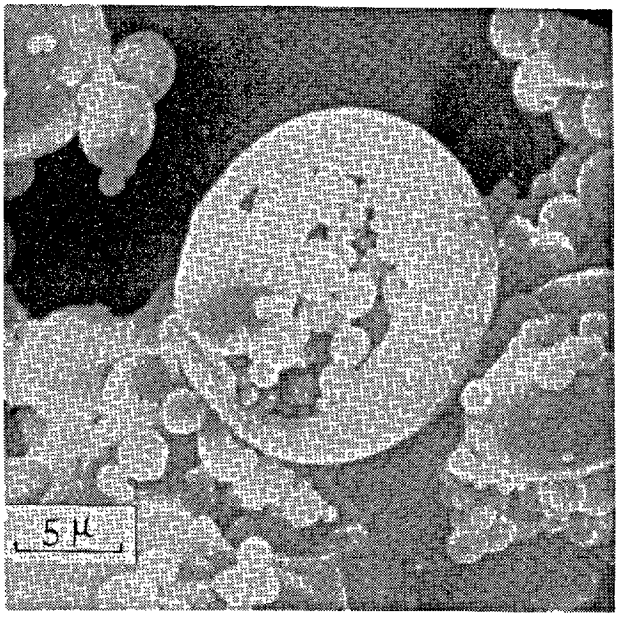

Fig. 2. *Example of fly ash photographed by electron scanning microscope*
Courtesy Japan Electron Optics Laboratory Co., Ltd. News (in Japanese), p. 7, No. 1 (1967).

Specific Gravity of Fly Ash

The results of measurement of specific gravities of

fly ash in the U.S., Japan and Great Britain are given in Table 1. Naturally, the specific gravity is higher the higher is the Fe_2O_3 content and the average values by country range between 2.10 and 2.40.

There is a report that the specific gravities of individual particles differ according to particle shape with apparent specific gravity being higher the smaller the particle (14). This substantiates the fact that porous particles are distributed in the fly ash. However, there is a report of greater specific gravity in the case of coarse-particled fly ash (15).

Fineness of Fly Ash

As fineness of fly ash is an important factor governing pozzolanic activity along with the SiO_2 content and also greatly affects the workability of concrete, all of the countries have attached importance to this aspect and specified limits and uniformity of fineness.

Regarding the procedure for determining fineness, there has been great discussion on whether sieving or the specific surface method measured by the air permeability apparatus should be used. At present most researchers use the specific surface method. This is because of the simplicity of this method and because it is possible to estimate the mean particle size (See Appendix 1, ASTM). When discussing the quality of fly ash from one plant, the specific surface area obtained by the air permeability method is highly reliable. However, when comparing with other fly ashes, it is thought there is a necessity for examining the reliability of the values as there are cases of deviation of test values due to differences in specific gravity, particle distribution, particle shape, carbon content, etc. There are a number of papers reporting it difficult to recognize a correlation between pozzolanic activity of fly ash and test values obtained by the air permeability method of measuring fineness (16)(17)(18). However, Brink and Halstead (17) state there is a relation between the quantity passing 44μ sieves and pozzolanic activity, while Watt and Thorne (11) surmise there may be a close relationship between fineness measurement values and pozzolanic activity in the case of disagglomerated ashes. Fig. 3 gives the results of tests on the 10 fly ashes listed in Table 2, these fly ashes considerably resembling each other in chemical composition. The compressive strength ratios obtained on mortar specimens at the age of 13 weeks and the fineness values (See Appendix 1, JIS) present a comparatively clear correlation except for one fly ash.

Although there is disagreement on the above, there is no question that the fineness value of a fly ash is one guide to its quality. Also, the standard value of fineness is significant in providing a criterion in planning fly ash collecting facilities.

Table 1 also gives examples of the specific surface areas of fly ashes in various countries. In this case also, a wide difference is seen between countries, the average values being between 5,180 and 3,090 cm^2/g.

Japanese coal is generally high in content of ash and volatile matter while low in coking properties. Therefore, when this is burned in the form of pulverized coal, thermal explosion occurs within the flame and combustion gases and there is a tendency for the individual particles to become finely divided. It is thought that in the case of Japan, fly ash of high fineness and low carbon content can be obtained comparatively readily because of this. On the other hand, it might be considered that coal of other countries are higher in coking properties compared with Japanese coal with less volatile matter so that the abovementioned fine division does not occur when the pulverized form is burned and there is a smaller ratio of finely divided powder to be contained in the ash. This and the fact that the SiO_2 content is high as mentioned before are the distinguishing features of Japanese fly ash and as a result there are cases when there is considerable difference in the influence of fly ash on the properties of concrete between Japan and various other countries.

Therefore, it is conceivable there would be considerable differences in the fly ashes of other countries which will complicate the discussions, but since fly

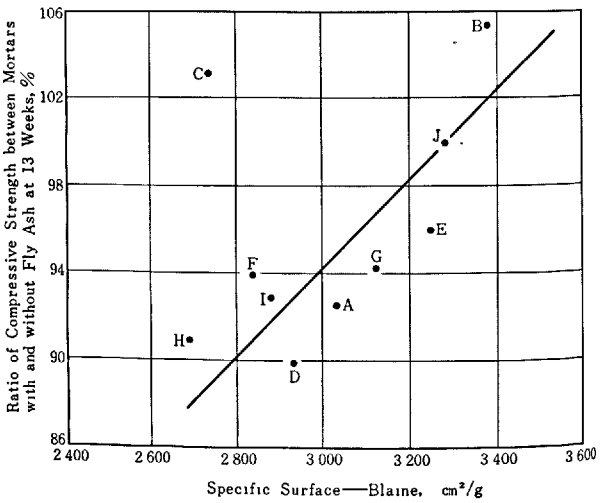

Fig. 3. *Relation between specific surface of fly ash and relative compressive strength of mortar at 13 weeks. Relative compressive strength indicates ratio to compressive strength of mortar without fly ash. Fly ash replacement ratio, 25%.*

ash is after all a by-product, this is inescapable.

The comparatively close resemblance of the Japanese fly ashes is because of identical periods of formation of coal strata and identical component plant material so that all coal mined in the country are the same in quality and also since only the portions meeting JIS specifications are sold on the market except in the case of coarse fly ash.

Strength and Other Properties

When discussing the physical properties of fly ash it is highly necessary to have test values of unit water content and strength when the fly ash is used in mortar or concrete, and all of the countries clearly designate the standards for these aspects (See Appendix 1). However, since the testing methods differ, direct comparison of the values will be avoided here.

Influence of Fly Ash on Various Properties of Concrete

Influence of Fly Ash on Workability of Concrete

That replacement of a portion of the cement with a suitable amount of fly ash when mixing concrete would improve workability was made clear in a paper by Davis et al (2) as early as 1937. It was suggested in this paper that suitable replacement ratios would be 30% or less for ordinary construction. Viewed in the light of present day common knowledge, however, the paper attributes surprisingly little to fly ash for the reduction in unit water content necessary to obtain a concrete of a given consistency. This probably is due to the fact that fly ash in those days were inferior to present day fly ash in quality and especially in fineness.

It is though that with the use of fly ash in the great volume of concrete in Hungry Horse Dam (arched-type concrete dam, construction begun in 1948, height 172 m, concrete volume 2,360,000 m^3) as an impetus, exceptional progress was made in the techniques of collecting and producing fly ash in the United States. The interior concrete of this dam was a lean air-entrained concrete with a unit cement content of 111 kg/m^3, unit fly ash content of 56 kg/m^3 (a replacement ratio of 33% of cement with fly ash), air content of 3.7% and slump of approximately 5 cm and the unit water content was only 88 kg/m^3 (19). The reduction in unit water content was of course due to entrained air to a great extent, but nevertheless this was an epoque-making project in the use of fly ash in concrete.

The rate of reduction in the unit water content necessary for a given consistency obtained by replacing a part of the cement with fly ash will differ depending on the mix proportions of the concrete, the particle shape and fineness of fly ash, the fly ash replacement ratio, gradation of fine aggregate, etc. The results of tests on 20 varieties of fly ash marketed in Japan with a replacement ratio of 25% ranged between 11 and 4% water reduction or an average of 7% (18).

It was not possible to ascertain the unit water content reduction ratios for fly ashes of the various countries, but it is thought that a reduction of about 5% can well be expected if the fly ash is of a suitable fineness.

The shape and surfaces condition of particles, and fine particle size are some of the reasons which can be thought of for the reduction of unit water content due to fly ash. It has been said from before, citing examples of microscopic photographs, that the main reason was the smooth spherical shape (6). Yamazaki also conducted studies of these factors (20) and applying the immobile water factor proposed by Powers (21) and Steinour (22) regarding cement particles, or the factor related to the amount of water lying immobile on the surfaces of finely divided particles, rearranged the test results of bleeding rates of fly ash slurries to indicate the relation between shape and surface condition of fly ash and other finely divided particles and the water retention factor in discussing the effects of fly ash, and ascertained that the smooth spherical shape was the most important reason for the improvement of workability of concrete due to fly ash. When the fineness of fly ash increases, the effect of reducing unit water content of concrete is generally great. This is thought to be due to the higher rate of spherical particles with smooth surfaces the higher the value in fineness.

Yamazaki further states that the particles of fly ash in a dry state often present a floc structure from the mutual attraction of the particles, while some fly ashes are agglomerated, and establishes that when concrete is mixed using fly ash which present floc structures or agglomerates, the particles of fly ash are floculated and difficult to disperse (20). (See Fig. 4) If this flocculation were to be prevented, it is conceivable the effect of fly ash on the workability of concrete would be improved further. As a practical means of prevention, there is the method of using fly ash in slurry form by mixing vigorously with water beforehand instead of using it as a powder. This method is

described later. There are many reports that state bleeding of concrete is reduced by replacement of a part of the cement with a good quality fly ash, but there are cases when rather the bleeding is increased.

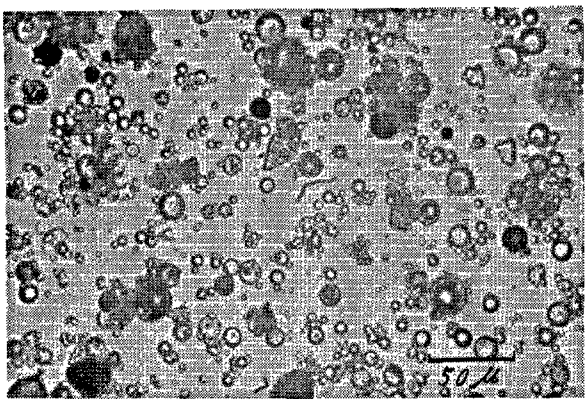

(a) Fly ash particles dispersed in pure water.

(b) Flocculated fly ash particles in supernatent liquid of cement paste.

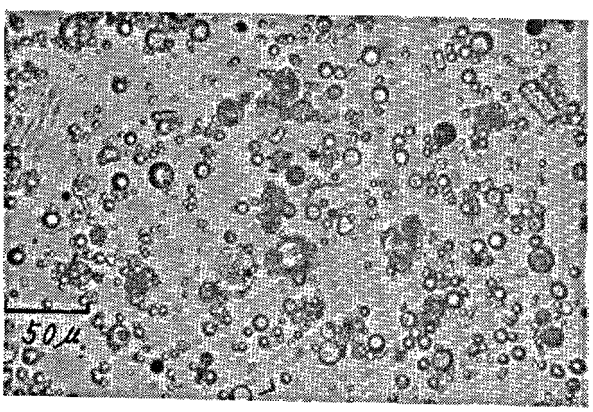

(c) Fly ash particles in supernatent liquid of cement paste containing suitable amount of cement dispersing agent.

Fig. 4. *Flocculation and dispersion of fly ash particles in water and supernatent liquid*

Influence of Fly Ash on Strength of Concrete

Although with some difference in degree, the pozzolanic effects of fly ash, or the improvements in long-term strength, watertightness and durability, have been described in almost all reports since the advent of the material, which fact has been instrumental in causing it to be used in dam concrete and other concrete. These pozzolanic effects of fly ash will not only differ extremely according to the quality of the fly ash and the amount used, but also with the quality of cement, the mix proportion, the age and curing conditions, but when about 25% of normal portland cement is replaced with good quality fly ash and the concrete is cured at normal temperature in the presence of adequate moisture, it is not seldom that the strength of the concrete will become greater than that of concrete without fly ash within the age of 6 months.

It is a characteristic of concrete containing fly ash to demonstrate strength increases over long periods, and especially, it appears there is a tendency for tensile strengths to be improved. (23) Fig. 5 is an example of the relation between compressive strength and tensile strength of concrete containing fly ash correlated to age (24) which shows tensile strength to be improved over that of concrete without fly ash at advanced ages. This can be said to be an advantage of fly ash offsetting to some degree the defects of normal portland cement.

One disadvantage of fly ash when cement content is reduced is that the strength of concrete at early ages is reduced. One method of covering this disad-

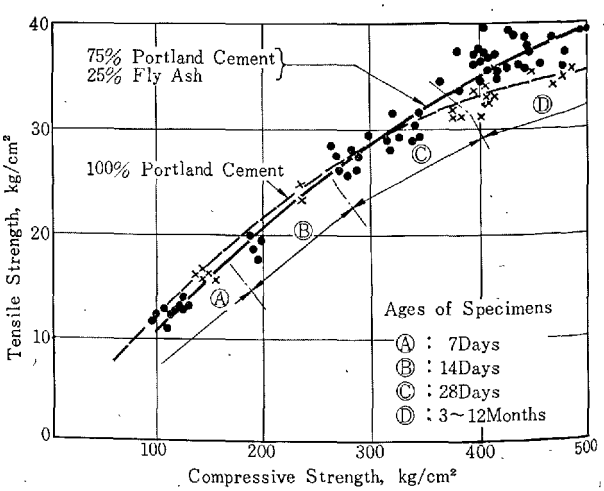

Fig. 5. *Example of relation between tensile strength and compressive strength of concrete (Max. size coarse aggregate, 25 mm; cement factor, 300 kg/m³; slump, 6–7cm; specimens cured in water maintained at 21°C; test ages, 7 days–12 months).*

vantage is to use more fly ash than the amount of cement reduction, the unit cement content and unit fly ash content being selected in a manner to obtain the required strength at the designated age (25). This is done in many cases in concrete pavements and other members, although of course the concrete mix must be selected in consideration of cost.

When fly ash is used for ordinary members, the members, unlike hydraulic structures, will gradually become dried and there will be a fear that strength increases at advanced ages cannot be expected. Stingley and Peyton (26) have reported on 1- to 10-year test results of beam specimens job-cured in exactly the same manner as concrete of an experimental pavement in Kansas in which flexural strengths of beams reached maximum values at about 1 year in the case of concrete without fly ash, while for concrete with fly ash, the strength increased for 3 to 4 years exceeding 70 kg/cm^2 after 3 years.

Tsukayama and Miyoshi (27) have reported on tests of cores and beams cut out of test pavement slabs at the age of 10 years. When the amount of fly ash used was adjusted to obtain 28-day compressive strength (curing in water at 21°C) equal to that of concrete without fly ash (curing in water at 21°C), the compressive strength of the fly ash concrete pavement slab which was approximately 100% of that of the concrete pavement slab without fly ash at 3 months, had increased to 120% at the age of 10 years. Further, the flexural strength ratio which was approximately 80% at the age of 3 months had increased to approximately 150% at 10 years. In these tests also, it is indicated that the effect of fly ash is more pronounced in flexural strength than compressive strength.

Kokubu and Ito (28), on testing compressive strength of core specimens taken from concrete pavement slabs of first class national highways with 30% replacement of cement with fly ash have reported that strengths which were 370 kg/cm^2 at 3 months had increased to 610 kg/cm^2 at the age of 9 1/2 years.

However, Legg (29) has reported that as a result of testing compressive strengths of core specimens cut out from concrete pavement slabs at ages of 28 days to 5 years, the strength of concrete with fly ash which was more than 250 kg/cm^2 at 28 days increased to more than 400 kg/cm^2 at 5 years, but were still poorer than the strength of concrete without fly ash.

The strength of concrete containing fly ash is accompanied by complicated factors as described previously and it is not surprising that uniform results cannot be obtained in field tests. However, it is thought there have been no reports that the use of fly ash in an actual project has had bad effects, except in cases of especially high water-cement ratios of concrete.

The pozzolanic reaction of fly ash differs greatly with the temperature of the concrete, being more active the higher the temperature. Therefore, when fly ash is used for massive concrete the strength of concrete will be considerably greater than in the case of curing at normal temperature making fly ash advantageous from the viewpoint even of only strength. (2) Takano (30) on testing compressive strengths when a part of normal portland cement was replaced with fly ash and mixing and curing of the concrete was performed at temperatures of 10°C, 21°C and 30°C, states that strengths at 3 months or later are lower the higher the curing temperature in the case of concrete without fly ash whereas they are higher the higher the curing temperature in the case of concrete containing fly ash. In other words the use of fly ash alleviates the drop in the long-term strength gain ratio produced by high-temperature curing of concrete.

Stolnikov and Kind (31), in consideration of precast concrete, has reported on normal pressure steam curing of concrete containing fly ash. This research was conducted with the thought to augment the reduction in short-term strength when fly ash is used. In the intake pressure tunnel of Kurobegawa No. 3 Power Station which passes through hot bedrock of temperatures 100°C or higher, the cement in the tunnel lining concrete was replaced 25% with fly ash and excellent results were obtained (32).

Influence of Fly Ash on Volume Change of Concrete

There is an extremely great number of papers which report that by replacing part of the cement with good quality fly ash, drying shrinkage of mortar and concrete is reduced. Blanks (33) for example, has obtained test results as shown in Fig. 6. Blanks also states that autogenous shrinkage is somewhat reduced. These are features of fly ash different from other pozzolans which are said to be due to the reduction in unit water content necessary for the required consistency. There are, however, reports (34) which say that drying shrinkage increases somewhat more than for concrete without fly ash when fly ash of high carbon content and low fineness is used.

In performing tests of drying shrinkage with concrete specimens, it is normal for reduction in the amount of drying shrinkage not to be very pronounced in proportion with replacement of cement with fly ash, even when the fly ash used is of good quality. When beams of 10 cm × 10 cm cross sections are dried severely for 6 months and more, the reduction

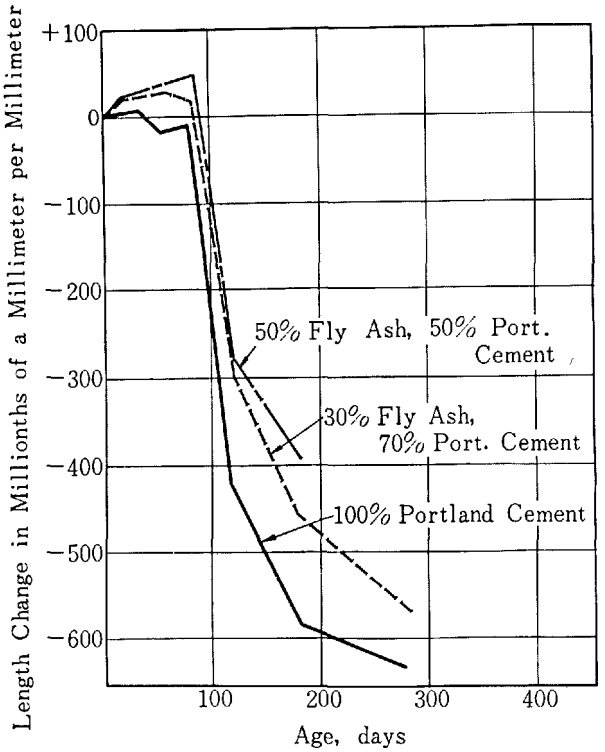

Fig. 6. *Drying shrinkage of concretes. Measurements made on 10 × 10 × 75 cm beams fog cured 90 days, then dried at 50% humidity, 21°C.*

in drying shrinkage barely reaches 15 to 20%. For a shorter period, at about a month of drying, there is very little difference seen, the reduction in drying shrinkage of concrete containing fly ash being only about 5% of that of concrete without fly ash. It is not possible for concrete members exposed to outdoor air to be dried as severely as in the above tests. Nevertheless, it is clearly seen in experience with projects using fly ash that cracks accompanying drying are reduced. In other words, the degree to which the detrimental effects of drying shrinkage are reduced is much more prominent than indicated by the drying shrinkage values obtained with concrete specimens. One of the reasons for this is that in almost all tests the shortening in length of a specimen due to drying shrinkage is measured along the central axis of the specimen. When this is done, it is impossible to obtain the shrinkage at the surface portion occurring with the drying.

Davis et al (2) sealed off 15-cm cube specimens on five sides allowing drying to occur from only one surface and measured shrinkage not only at the central axis, but also along an axis near the surface in discussing shrinkage in the interior of the specimens. Nagataki (35) also sealed five sides of beam specimens and measured shrinkage at each of the surfaces that accompanied drying. Nagataki also studied tensile stresses occurring when drying shrinkage is restrained. As a result he has ascertained that when concrete with part of the cement replaced with fly ash is dried at relatively early ages, the difference in moisture content between surface portion and interior is alleviated and the tensile stresses produced by drying is reduced. This is thought to happen because in young concrete containing fly ash, the free water slightly to the interior from the surface is in a readily evaporable condition. Therefore, it is thought even if the effect of fly ash in concrete indicated by drying shrinkage values obtained in normal methods of testing is small compared with the effect in cement paste or mortar, the role that good quality fly ash plays in preventing cracking of concrete is surprisingly great.

The above is an indication that it will often be reasonable to use fly ash not only for concrete in hydraulic structures, but also in various members in general.

Influence of Fly Ash on Heat of Hardening of Concrete

When concrete is made replacing a portion of the cement with fly ash, the rate of evolution of heat of hardening of the concrete is retarded. The U.S. Bureau of Reclamation has conducted numerous experiments concerning heat of hardening of concrete containing fly ash. (19) Davis et al (2) state that the value of the rate of reduction in heat of hardening of concrete at 28 days when fly ash is used is equal to approximately one-half of the percentage figure of fly ash replacement. The reason that the rate of reduction does not equal the percentage figure of fly ash replacement is the finely divided powder effect of fly ash, a matter to be discussed later.

One of the reasons for the extensive use of fly ash in dam concrete is this alleviation of heat of hardening, which makes it easier to regulate the temperature of the concrete reducing the fear of cracking from thermal stresses (24)(36).

Influence of Fly Ash on Watertightness and Durability of Concrete

Unless curing conditions are especially poor, the watertightness of concrete containing fly ash is improved. This is only natural when pozzolanic activity is considered. Davis (34) compared permeability coefficients of concretes of unit cement contents of 225 kg/m³ at the age of 6 months, and states that the coefficient of concrete with 30% of cement replaced

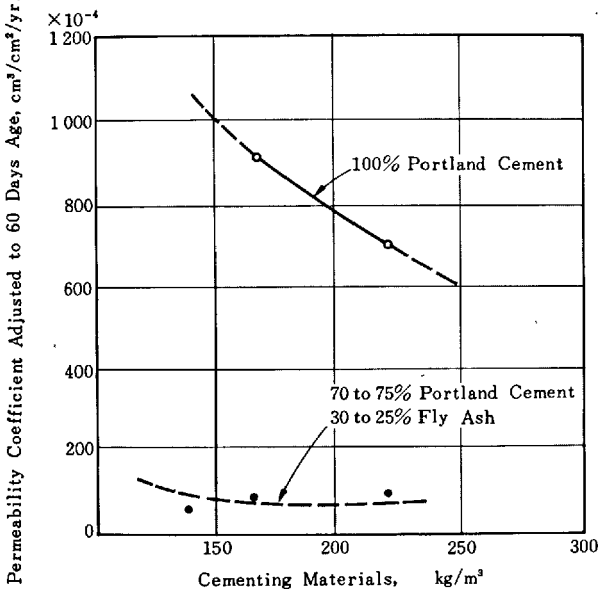

Fig. 7. *Permeability of concrete with and without fly ash.*

with fly ash was 1/5 of that of concrete without fly ash, while with 50% replacement, the coefficient was reduced to 1/12. The U.S. Bureau of Reclamation and the Corps of Engineers have tested watertightness of lean concrete containing large-sized coarse aggregate and both have shown the effectiveness of fly ash in this respect. Fig. 7 illustrates the test results reported by Higginson (37) which indicate the marked improvement in watertightness obtained by use of fly ash. Yoshikoshi (38) has also carried out wide studies of fly ash, and especially in regard to watertightness, originated a simple method of testing permeability in which a concentric hole of small diameter was provided in a cylinder to obtain a thick-walled specimen and hydraulic pressure was applied from outer surface, and discusses in detail the effect of fly ash on watertightness of concrete. Going by this method, the same relation between the direction of concrete placement and the direction of permeation of water as seen in the field is obtained.

Fundamentally, the watertightness and durability of concrete structures depend a great deal on defects in workmanship at joints and other parts of concrete whenenver these defects exist. Therefore watertightness of a concrete structure will be greatly affected by whether or not workability of concrete is good. Other than in cases of grossly inferior quality of concrete or especially severe exposure conditions, the quality of concrete does not necessarily determine watertightness. When a good quality fly ash is suitably used, workability of concrete is improved to aid in reducing defects occurring at the time of concrete placement so that it is thought watertightness of concrete members will be improved even more.

By proper use of pozzolans in concrete, resistance to various kinds of aggressive waters is improved. It is even said that this is the principal reason for pozzolans to have become used so actively. From the viewpoint only of resistance to action of aggressive water, there are other pozzolans which are superior to fly ash. However, there are many reports which state that this type of durability was improved by replacement of a part of the cement with fly ash (2)(23)(39)(40).

Even when workable concrete is carefully consolidated, about 1% of air bubbles is generally contained in the concrete, and depending on the cement and aggregate, the air may be as high as 2% or more. These bubbles of air are not entrained air, but are effective to some degree in providing durability against freezing and thawing. When concrete is mixed with the addition of fly ash, the air bubbles are reduced due to the influence of the fine particles so that the air content of the concrete is reduced to about 0.5% after consolidation. Therefore, when fly ash is used in concrete which is not air-entrained, it is customary for the performance of the concrete in freezing and thawing tests to be somewhat impaired. (23) However, there is a report saying that at an age of 5 months better results were obtained in freezing and thawing tests with a non air-entrained concrete containing fly ash compared with non air-entrained concrete without fly ash (41). This is believed to be due to the influence of pozzolanic effect of the fly ash.

It is needless to say that durability of concrete against freezing and thawing action will be vastly improved by entrainment of a suitable amount of air using a good quality admixture. Larson (42) established that this principle can be applied to concrete containing fly ash. Parenthetically, as a result of measurement of the size and distribution of air voids on the surface of a sawed section of concrete containing fly ash and from results of freezing and thawing tests, Larson states that fly ash has no ill effects on air voids of hardened concrete and in comparison of concretes of equal strength and air content there was no difference between concretes with and without fly ash.

The freezing and thawing tests mentioned above are an extremely severe test of concrete differing greatly from the meteorological conditions to which concrete in the field is exposed. As the correlation between the results of these laboratory tests and durability of field concrete is a great problem which has not yet been solved, no attempt will be made here to discuss this

matter. Even limiting the discussion to comparison tests for estimating the effect of fly ash, there are problems remaining regarding test methods such as the age of concrete at which freezing and thawing should be commenced, the method of curing during this period, and the moisture conditions of specimens during freezing and thawing (34)(43).

Influence of Fly Ash on Alkali-Aggregate Reaction

Alkali-aggregate reaction is mostly considered a problem in North America and apparently in Australia there has been some trouble (44), but it appears there have not been many cases in other parts of the world which have been reported.

The use of pozzolans to prevent alkali-aggregate reaction has been recommended by Stanton (45), Hanna (46), Lerch (47) and others. In many studies that have followed, it has been indicated that certain natural or artificial pozzolans are effective in reducing alkali-aggregate reaction while some other pozzolan have almost no effect.

Meissner, as a result of comparative experiments of the effect of fly ash and 10 other pozzolans in controlling alkali-aggregate reaction, reported that fly ash, although not as much as opal and calcined shale, had considerable merit (48). Blanks (49) and Lerch (50) have also produced results of experiments which enable comparison to be made of the effect of fly ash versus other pozzolans.

Brinks and Halstead (17) experimented with 10, 20, 35 and 50% replacements respectively of cement using 17 out of 34 varieties of fly ash listed in Table 1. Fig. 8 is an example of the test results which shows that a high percentage of replacement with fly ash (e.g., about 35% replacement of cement) is effective in controlling expansion from alkali-aggregate reaction in the case of all fly ashes. However, it is indicated at the same time that there is a pronounced difference according to the fly ash in the relation between the fly ash content and the effect in controlling expansion.

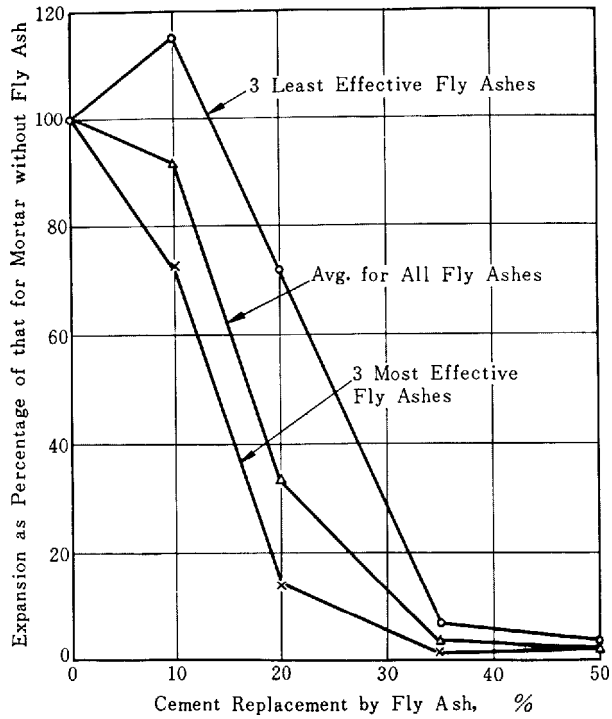

Fig. 8. *Effect of fly ash on expansion of alkali-reactive mortar at age of one year.*

As described above, although fly ash is not the most suitable admixture for prevention of alkali-aggregate reaction, there is no question that it has a practical effect. It is a fact, however, that the effect of fly ash on alkali-aggregate reaction differs to some extent not only according to the aggregate and cement, but also the quality and the amount of fly ash used.

In testing the effect of admixtures in controlling alkali-aggregate reaction, the ASTM method (51) is widely used. However, this is an accelerated test using mortar specimens so that there are many questionable points remaining and it is desirable that progress be made in studies regarding correlation to concrete in the field.

Chemical Behavior of Fly Ash in Concrete

Chemical Characteristics of Fly Ash in Concrete at Early Ages

The chemical composition and fineness of fly ash, as described previously, differ greatly according to country and even within the same country there are considerable differences according to the plant. Therefore, it is difficult to accurately describe the chemical characteristics of fly ash within concrete and it is especially so at early ages.

Yamazaki (52) disclosed that in concrete with fly ash cured at normal temperature, the strength of the concrete estimated from the void-cement ratio calculated considering fly ash not to be part of the cement

is somewhat higher even at early ages when hardly any pozzolanic reaction has occurred. For example, Fig. 9 shows the results of compressive strength tests of concrete made to a given consistency adding fly ash while maintaining unit cement content at 290 kg/m³. Although water-cement ratio is slightly increased with increasing addition of fly ash, the concrete strength is clearly greater at the age of 7 days when very little pozzolanic reaction has occurred. Also, similar increases in concrete strengths are found when adding limestone powder which has no pozzolanic reactivity at all. The same phenomenon was seen with finely divided powders of gray wacke and silicious sand which too are considered to cause hardly any chemical reaction in cement paste. Yamazaki further experimented on the non-evaporable water in the cement paste portion of mortar in which finely divided mineral powders were used and pointed out these mineral powders, even when hardly causing any chemical reaction within the cement paste, brought about an increase in non-evaporable water per unit amount of cement equivalent to the increase in strength, in other words increased the amount of cement hydrated from early ages. Regarding the reason for this, Yamazaki theorizes that replacement by fly ash or other finely divided mineral powders in the floc structure constructed of cement particles expands the available space in which hydration products are precipitated to increase the hydration of cement. This effect was named "finely divided powder effect."

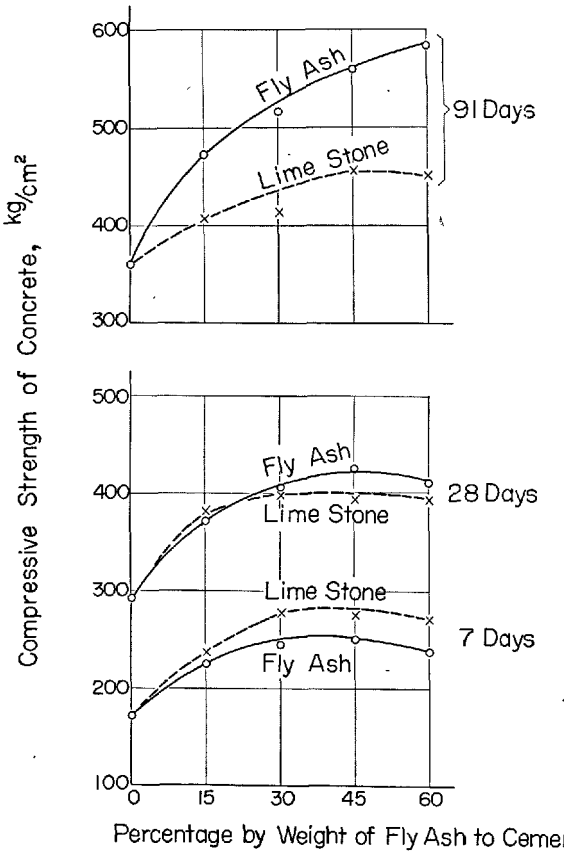

Fig. 9. *Compressive strength of concrete made by replacing part of fine aggregate with fly ash. (Unit cement content of concrete maintained at 290 kg/m³, and therefore finely divided powder was added and was not replacement for cement.)*

Kawada (53) studied the hydration of cement paste at early ages when fly ash is added. As the actual water-cement ratio is changed by replacement of cement with fly ash, Kawada measured the rate of heat evolution of cement pastes (without fly ash) at various water-cement ratios for reference (See Figs. 10 & 11). According to the results, there is no great change in the time required for the rate of heat evolution curve to reach a peak according to water-cement ratio, but the rate of heat evolution per gram of cement is higher the lower the water-cement ratio. Further, up to one hour of addition of water, the amount of hydration heat shows almost no change with variation in water-cement ratio, but at 24 hours, the amount of heat is reduced when the water-cement ratio is increased. Next, Kawada took pastes with a constant water-cement and fly ash ratio of 0.4 in which a part of the cement was replaced with fly ash from which soluble components were removed by washing with water and measured the rate of heat evolution and the amount of heat evolution per gram of cement (See Figs. 11 & 12). With the increase in the fly ash replacement ratio, the time at which the rate of heat evolution reaches a peak is somewhat quickened and also the peak is at a higher point. The fact that the heat of hydration per gram of cement is constant at one hour regardless of the amount of fly ash indicates that the amount of hydration reaction occurring within a short period of time after addition of water is not governed by the quantity of water or fly ash. The heat of hydration of paste without fly ash becomes lower with increased water-cement ratio at 24 hours, but in paste in which there is a replacement of cement by fly ash, the heat of hydration per gram of cement is conversely greater with the increase in the amount of fly ash. This appears to substantiate the appropriateness of Yamazaki's theory of finely divided powder effect of fly ash.

In the above experiments, fly ash washed with water was used to exclude influence of the soluble components of fly ash. In the case of unwashed fly ash, the peak of heat evolution is only heightened a little and the time at which the maximum is reached is slightly retarded (See Fig. 12). The soluble components of fly ash consist mostly of calcium sulphate, but the

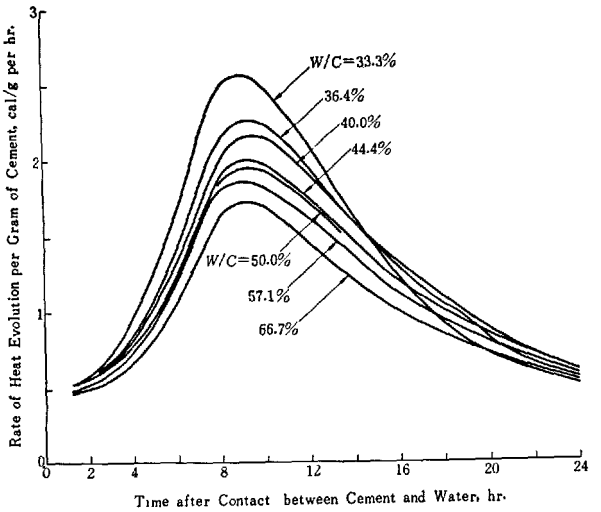

Fig. 10. *Effect of water-cement ratio on rate of heat evolution.*

content is extremely small while the rate at which they are leached out is slow, so that it is assumed the influence of the soluble components on initial chemical behavior of fly ash in concrete is of a negligible degree. Therefore, it is thought the effect of fly ash on cement hydration at early ages, is limited to the finely divided powder effect or the increase of cement hydration through the increase of available space for hydration products.

Method of Testing Pozzolanic Activity

Methods of testing pozzolanic activity of pozzolans have been studied by many researchers for more than one hundred years. However, since the varieties of pozzolans used in concrete are so myriad with pronounced differences in quality, and since the purposes of use of these pozzolans are also varied, it is extremely difficult to establish an appropriate test method for pozzolanic activity.

Lea (7) summarized and discussed the various methods of testing pozzolanic activity at the International Symposium on the Chemistry of Cement held in 1938, while Malquori (10) also discussed test methods at the Fourth International Symposium on Chemistry of Cement held in 1960. These reports and the discussions thereof all comprise information of great value, part of which are useful guides to research on methods of testing pozzolanic activity even today.

Moran and Gilliland (54) have discussed methods of testing pozzolanic activity dividing their studies into the 3 categories of tests on pozzolan alone, tests on pozzolan-lime mixtures and tests on poz-

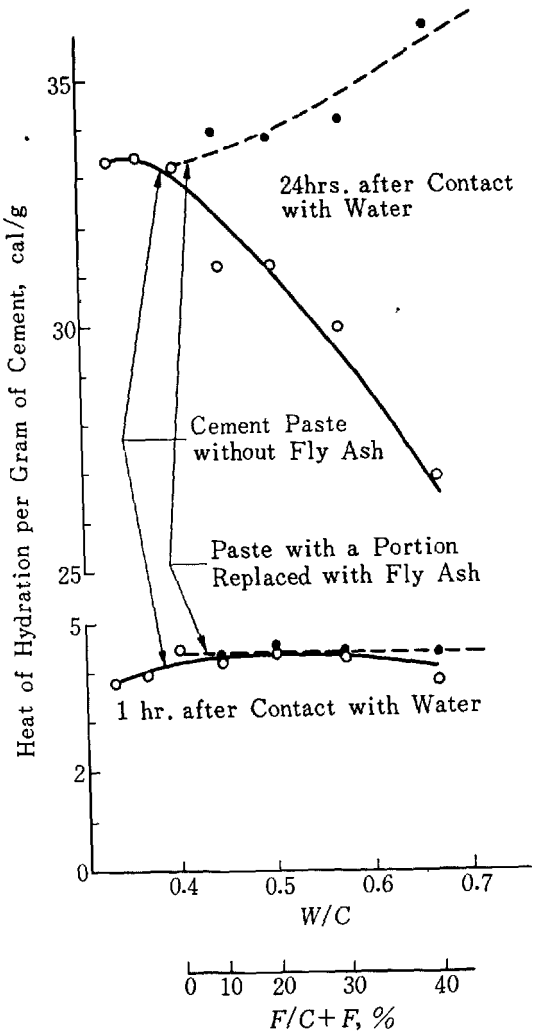

Fig. 11. *Heat of hydration per gram of cement per various water-cement and fly ash ratios. Thoroughly washed fly ash with water-cement fly ash ratio maintained at 0.4.*

zolan-portland cement blends. Although today, when research and testing techniques have progressed further and methods have been suggested which are combinations of various methods so that establishing of distinct classifications is difficult, if an attempt were to be made to classify the methods of testing pozzolanic activity which can be considered to be commonly used, it would result in the form given in Table 4.

Forest and Demoulian (60) compared Steopoe's method, (62) the method suggested in AFNOR P 15-301, (65) the method in ASTM Designation: C 379-56T (61) and the method of Poliet and Chausson (60) using 6 pozzolans including 4 fly ashes. As a result, they have pointed out that the AFNOR

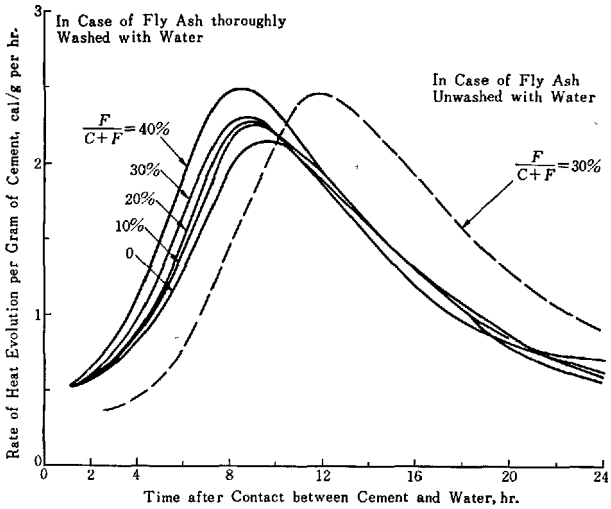

Fig. 12. *Rate of heat evolution for cement per gram in paste with portion of cement replaced with fly ash. Water-cement fly ash ratio maintained constant at 0.4.*

Table 4. *Classification of methods of testing pozzolanic activity considered to be relatively frequently used*

Classification		Example of test method
Method testing strength by accelerated curing of pozzolan-lime mortar or pozzolan-portland cement mortar		ASTM C 593–66T(55) ASTM C 402–65T(56)
Method adding pozzolan to lime solution	Quantitative measurement of lime	Chapelle's method(57) Moran and Gilliland's method(54)
	Quantitative measurement of lime and alkali	AFNOR P 15–462(58) Italian standards ISO recommendation No 1156(59)
Method treating pozzolan or pozzolan-lime mixture with acid or alkali	Quantitative measurement of SiO_2	Florentin's method(60)
	Quantitative measurement of $SiO_2 + Al_2O_3$	ASTM C 379–56T(61) Poliet and Chausson's method(60) Austrian standards Charisius' method(66)
	Quantitative measurement of $SiO_2 + Fe_2O_3$	Steopoe's method(62)
	Quantitative measurement of $SiO_2 + Al_2O_3 + Fe_2O_3$	Sestini and Santarelli's modification of Baire's method(11) Feret-Florentin method(63)
	Quantitative measurement of insoluble residue	Guillaume's method(64) AFNOR P 15–301(65)
Method measuring development of dissolution heat of pozzolan		Jambor's method(66)

Remarks Besides the above, there are Lea's method(67) of measuring electrical conductivity of pozzolan-lime solutions, a method of combining insoluble residue and development of dissolution heat of pozzolan (66) and Devillard's method (68) of quantitatively measuring lime by exposing mixtures treated with carbolic acid to ultra-violet rays. Also, petrographic analysis, X-ray analysis and differential thermal analysis are sometimes effective.

P 15–301 method is a method of quantitatively measuring insoluble residue, and due to a portion being dissolved by acid at the beginning, it is not effective in predicting pozzolanic activity, that the method of ASTM Designation: C 379 is not sensitive enough for comparison of pozzolanic activity between various pozzolans, while the method of Poliet and Chausson showed a good correlation with results of strength tests.

Jarrige and Darques (69) examined Devillard's method (68) in regard to fly ash and state that a good relation was obtained with results of strength tests at 3 months.

Watt and Thorne, (11) using the 14 fly ashes listed in Table 1 carried out detailed tests with the Feret-Florentin method (63) and the lime solution method, an application of the Feret-Florentin method to lime solutions. At the same time they compared testing methods using Sestini and Santarelli's modification of Baire's method, (11) Lea's electrical conductivity method (67) and Moran and Gilliland's method. (54) As a result, they found the Feret-Florentin method and the lime solution method to have good reproducibility and the best correlation with strength results of lime mortars at equal ages and curing temperatures. The correlation with strength at the age of 3 months was especially good. However, it is stated that no correlation could be seen at advanced ages of one year or more. As one means of acceleratedly testing pozzolanic activity within a short period of time, it is conceivable to raise curing temperatures, but in the two methods above, there was very little relationship between 28-day to 1-year strengths of lime mortars tested after accelerated curing at temperatures maintained at 50°C and at 20°C, and it is stated that there is hardly any correlation between short-term chemical testing methods and long-term strengths of mortar. Watt and Thorne further concluded that chemical methods of testing were not suitable for estimating long-term strengths when fly ash is used in construction.

In the widely used standards of various countries, chemical methods of testing pozzolanic activity are specified, but these would more be criteria for judging acceptability of various pozzolans. Because of the extremely great number of pozzolans, it cannot be helped if the standards are inadequate in some respects.

The values of SiO_2, Al_2O_3, Fe_2O_3, etc. often specified in standards are provided as a first-line limit of the chemical components necessary for a pozzolan and cannot be considered as having much significance in evaluating pozzolan and cannot be considered as having much significance in evaluating pozzolanic

activity.

Needless to say, the value of a method of testing pozzolanic activity of a pozzolan does not depend only on reproducibility, speed and simplicity; the correlation with strength of standard-cured concrete or mortar is an important yard-stick.

Taking fly ash into consideration, since it can be thought it is used more frequently in concrete when strength is important compared to other pozzolans, the correlation with long-term strength especially becomes even more important. Thinking in such terms, the most effective method of testing pozzolanic activity of fly ash would be a method based on strength of mortar or concrete obtained by accelerated curing. Even were this method of testing strength to be adopted, a problem remains regarding the relationship with strength of concrete cured at normal temperature. For example, in ASTM Designation: C402–65T, (56) the pozzolanic activity index with portland cement is tested with accelerated curing, but it is noted that the index is for evaluating the degree to which fly ash contributes to longer strength development of concrete and is not a measure of the compressive strength of concrete containing the fly ash.

The purpose of using fly ash is not solely to increase long-term strengths, but at times it will be to increase resistance of concrete to sulphate attack or to decrease leaching by soft water. Needless to say, it will then be necessary to perform pozzolanic activity tests which are in accordance with such purposes.

The Pozzolanic Reaction of Fly Ash

The pozzolanic reactions of various pozzolans have been studied by a great number of researchers from quite some time ago (7)(8)(9)(10). Regarding these studies, reference has already been made, but it is worthy of note that Malquori cites the crystalline chemical soundness of glass as governing pozzolanic activity of natural pozzolans. The major reports on pozzolanic reaction of fly ash made public since the Fourth International Symposium on the Chemistry of Cement may be summarized as in the following.

Guillaume (70) quantitatively measured CaO produced by hydration in cement paste containing fly ash, discussed the relationship between decrease in CaO with age and progress of pozzolanic reaction and suggested that pozzolanic reaction of fly ash began from an age of about 14 days.

Jambor (66) states that pozzolanic reaction is defined as an reaction of SiO_2 and Al_2O_3 in fly ash with $Ca(OH)_2$ to form calcium silicate hydration products and calcium aluminate hydration products and that evaluation of pozzolanic reaction must take into consideration not only the fixing capacity of CaO, but the process of reaction between fly ash and $Ca(OH)_2$.

Shikami (71) tested reactions of various fly ashes added to CaO and $CaSO_4$ suspensions and together with results of tests by Florentin's method and other factors, demonstrated that fly ash was most reactive in a combined solution of lime and gypsum and also that besides calcium silicate hydration products, other reaction products, such as aluminates like $C_3A \cdot 3CaSO_4 \cdot 32H_2O$ also can be considered to be produced. The production of calcium sulphoaluminate hydrates have been proven in electron microscope observations by Saji as will be described later (See Fig. 19).

Pyachev (72) shows the results of strength tests on mortars made by adding fly ash to C_3S, C_2S, C_3A, C_5A_3 and C_4AF respectively and states that the extent to which fly ash contributes to strength is governed by the C_3S and C_2S content in cement. Among other things, Pyachev also states that the reaction between C_3S or C_2S with fly ash differs greatly with curing conditions and that the amount of addition of fly ash to obtain maximum strength will be markedly different for standard curing and steam curing.

Terrier and Moreau (12) stated that pozzolanic reactivity of fly ash is governed by the latent heat of devitrification of fly ash in differential thermal analysis and at the same time suggested that EPMA (Electron Micro-Probe Analyzer) would be a suitable apparatus to determine the composition of pozzolanic reaction products at fly ash surfaces.

Venuat (73) conducted wide-scale experiments using 2 different clinkers, 3 different fly ashes and gypsum in various mix proportions corresponding to F/(C + F) ratios of 20, 30, 40, 70 and 90%. Applying Feret's coefficient (equation below) to strength test values of 1:3 mortar in discussing pozzolanic reaction of fly ash, he has stated that pozzolanic reaction begins to appear from about the age of 28 days.

$$S = K\left(\frac{C_V}{C_V + V + A}\right)^2$$

$$K \fallingdotseq S\left(\frac{\frac{C}{W} + \rho_c}{\frac{C}{W}}\right)^2$$

where K: Feret's coefficient
S: Compressive strength
$\frac{C}{W}$: Cement-water ratio by weight
ρ_c: Specific gravity of cement
C_V: Absolute volume of cement

V: Volume of water

A: Volume of air

An example of the relation of the addition rate of fly ash to compressive strength is given in Fig. 13 in which it is shown that in comparison to strength in the case when fly ash is considered inert, the strength of mortar is slightly higher at 7 days and greatly higher at 90 days.

Ducreux and Jarrige (74) separated fly ash by sieving to obtain several fractions according to particle size and further in some cases crushed these fractions to obtain fly ashes of various finenesses. Using these fly ashes the strengths of 1:3 mortars were investigated and the respective pozzolanic reactions were discussed by application of Feret's coefficient and as a result it is stated among other things that fly ashes of 5 to 30μ particle size were highest in acitivity.

Sakurai et al (13) tested compressive strength of 1:2 mortras made using 12 fly ashes listed in Table 1 with 25% replacement of cement by weight as well as the reactivity of fly ash to lime saturated solutions in which case the mol values at various ages of SiO_2, Al_2O_3 and Fe_2O_3 which had reacted with lime solutions were measured.

From the test results, Sakurai showed that Feret's coefficient at ages of 28 days to 6 months had a close relationship with the mol values of $SiO_2 + Al_2O_3 + Fe_2O_3$ as illustrated in Fig. 14 and that the calculated value of the specific surface area of the glass phase, computed by multiplying the specific surface area of the fly ash obtained by the air-permeability method by the ratio of the glass phase content, also had a close relationship with Feret's coefficient (See Fig. 15). Further, comparing the results of X-ray analysis of the residue after removal of reaction products from samples in which reaction with lime had occurred with results of X-ray analysis on the original fly ash, it was found that the ratios between quartz contents and mullite contents were exactly identical in both, but the percentages of the quartz and mullite contents were markedly higher in the residue than in the original fly ash (See Fig. 16). Similar tests were conducted on pulverized quartz sand in which case only 1.9% of the SiO_2 reacted with lime.

These test results demonstrate that the glass phase is the major part of the phase composition of fly ash contributing to pozzolanic reaction in concrete with very little reaction on the part of the crystalline phases. It has also been ascertained that the SiO_2/Al_2O_3 value of the glass phase in the original samples of fly ash is very close to the ratio in the reaction products. This suggests that the products of pozzolanic reaction of fly ash contain not only calcium silicate hydrates

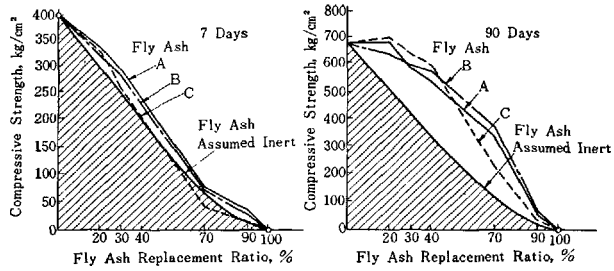

Fig. 13. *Evaluation of pozzolanic properties of fly ash.*

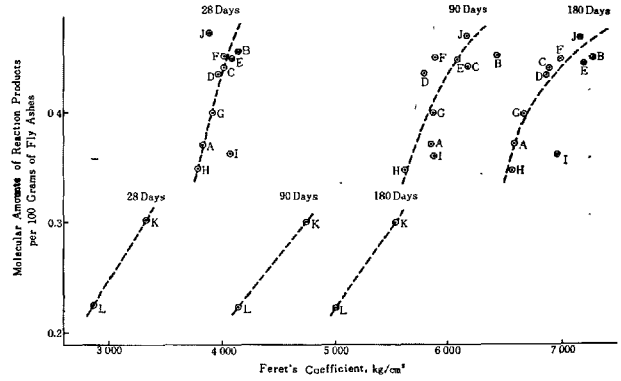

Fig. 14. *Relation between Feret's coefficient of mortar containing fly ash and molecular amounts of reaction products of fly ash in saturated lime solution.*

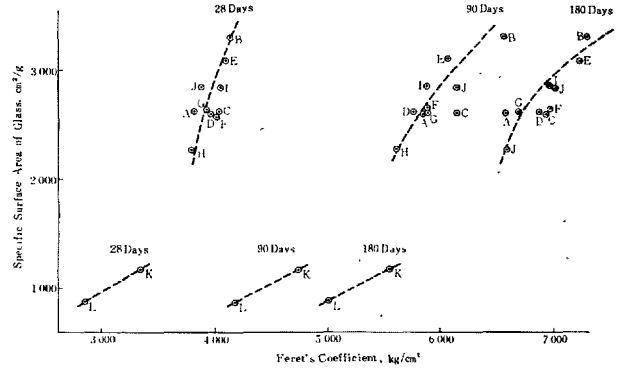

Fig. 15. *Relation between Feret's coefficient and specific surface area of glass. Specific surface area of glass calculated from glass content of original fly ash. Curve inclined gradually with age becoming vertical at 7 days, but not shown in diagram. Curves illustrated show pozzolanic reaction progress at various ages. Deviation of Feret's coefficient at same age and specific surface area of glass indicates difference of reactivity of each glass.*

but also calcium aluminate hydrates.

Thorne and Watt (11) tested crushing strength of lime mortar using 14 varieties of fly ash listed in Table 1 (proportions by weight: fly ash 2.50, sand 2.0, lime 1.0) as well as the amount of acid-soluble material ($SiO_2 + Al_2O_3 + Fe_2O_3$) by the lime solution method. Prior to the tests, the fly ashes were all washed exhaustively with water. This was in consideration of prevent-

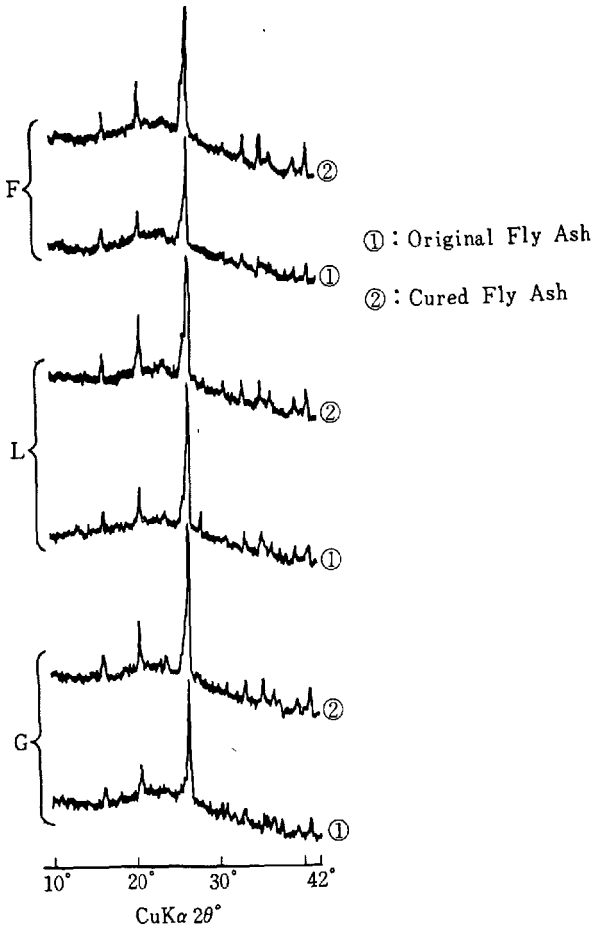

Fig. 16. *Variation of intensity of X-ray diffraction. Relative intensity of crystal phases in each pair, ① and ②, invariable, but absolute intensity increases from ① to ② with dissolution of glass phase.*

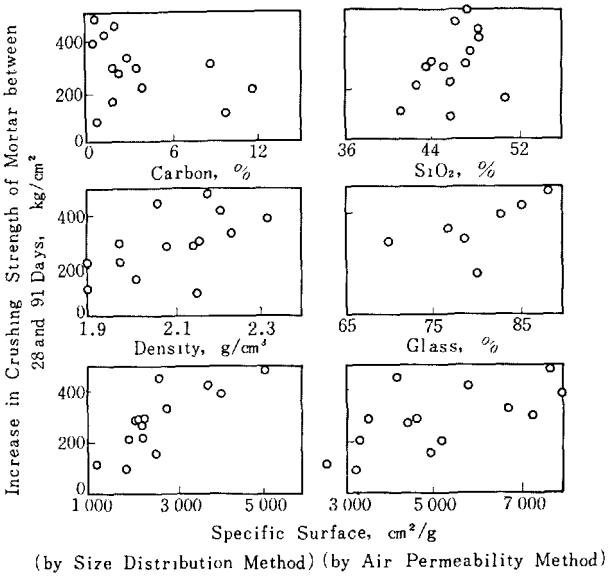

Fig. 17. *Crushing strength of fly ash mortars in relation to various characteristics of fly ashes.*

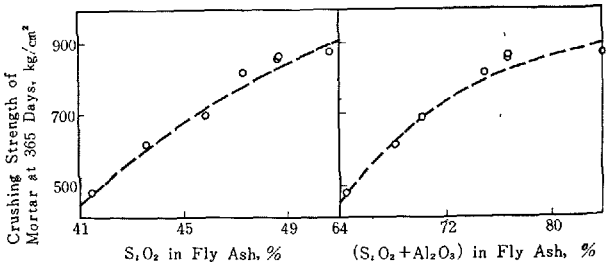

Fig. 18. *Crushing strenth of mortars at 365 days in relation to* SiO_2 *and* $SiO_2 + Al_2O_3$ *contents of fly ashes.*

ing increase in error from agglomeration of fly ash particles.

As a result of the tests, little relationship was seen between increase in crushing strength from 28 days to 91 days and the silica content, alumina content, glass content, carbon content and density of fly ash, while the best correlation was found with the specific surface as determined by particle size analysis. On the other hand, no relationship whatsoever was recognized with the specific surface determined by the air-permeability method (See Fig. 17). It is also stated there was a close relationship between acid-soluble increments and specific surfaces and it is concluded that pozzolanic reaction occurring during this period is dependent on the surface area of the fly ash contributing to reaction.

It was also shown that the relationships between specific surface and acid-soluble increments with crushing strengths at advanced ages of 1 to 2 years were weakened, these strengths being closely related to the SiO_2 content or the $SiO_2 + Al_2O_3$ content of the original fly ash (See Fig. 18) and that pozzolanic activity was governed by the content of reactive components in the fly ash.

Saji (75) broke hardened cement-fly ash pastes at certain designated ages and preparing replicas by deposition from the fractured surfaces at which fly ash particles were exposed, made observations using electron microscopes. Fig. 19 shows electron microscope photographs of specimens cured in water at 20°C with the left photographs indicating the surfaces of fly ash particles and the right photographs the surfaces of cement hydration products with which fly ash had been in contact. These photographs clearly show the progress of pozzolanic reaction with elapse of time, but it is worthy of note that before 140 days, the surfaces of fly ash particles are comparatively simple while the concave surfaces on the side of the hydration products in contact with the fly ash present a complex condition so that there is little symmetry in appearance

Age	Fly ash particles embedded in cement paste	Hydrated cement substances in contact with fly ash
28 days	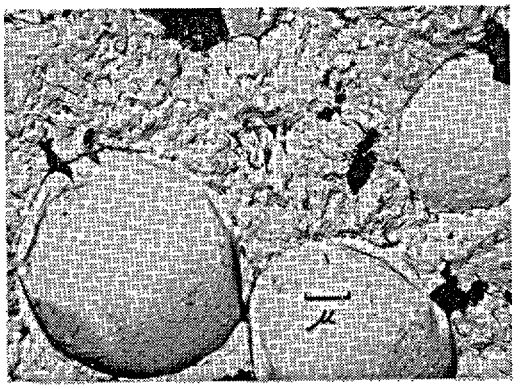	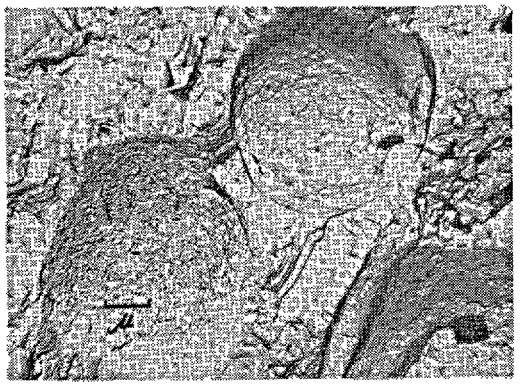
42 days	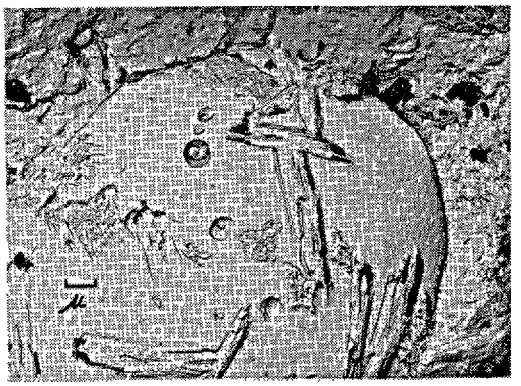	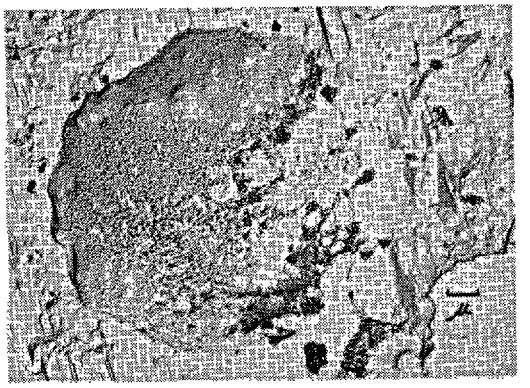
140 days	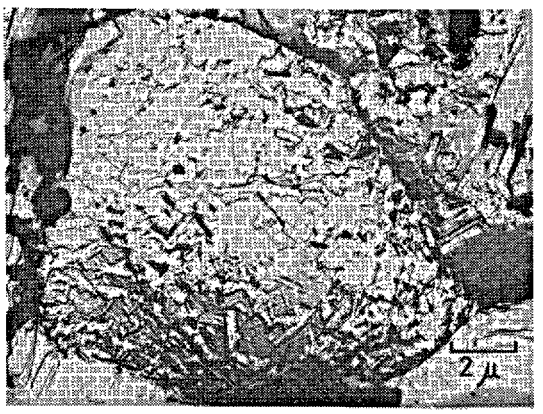	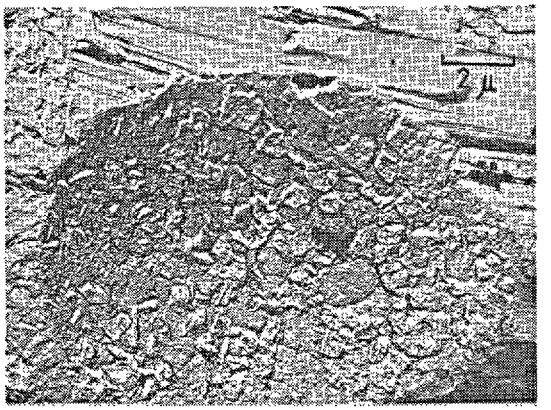

Fig. 19. *Electron micrograph of ruptured surface of hardened cement paste containing fly ash.*

between the two. This is thought to be because at early ages there is a rim between fly ash particles and cement hydration products, with pozzolanic reaction taking place in this rim, it being filled with reaction products as pozzolanic reaction progresses.

When concrete containing fly ash is adequately cured, there is marked increase in long-term strengths, but normally, even in these cases there are surprisingly little increases in non-evaporable water and heat of hydration. As an explanation for this, Yamazaki (52) points out that the products of pozzolanic reaction at advanced ages are formed in the thin rim between fly ash particles and cement hydration products, so that even with reaction of an extent which does not affect the non-evaporable water and heat of hydration values, the pozzolanic reaction will serve to strengthen the bond between fly ash particles and cement hydration products. Fig. 20 shows the increase in strength accompanying increase in nonevaporable water to be higher the greater the age, which agrees with the abovementioned theorization. Yamazaki suggests that in discussing the relationship between mix proportions and strengths of mortars, if the volume of the solid phase of a unit volume of the cement paste portion is taken as a parameter, the latter's relationship with strength may be expressed with a single curve regardless of whether different types of cement are used, whether admixtures are used or whether curing temperatures and ages differ. It is stated that when fly ash particles and cement hydration products are strongly bound together, it is more reasonable to consider the unreacted portion of fly ash as a solid phase which governs the strength of mortar just as the unreacted portion of cement.

Homma and Kikuchi (76) tested flexural strengths, compressive strengths, and non-evaporable water at various ages of 1 : 2 mortar made with 10 to 30% replacement of cement with fly ash cured at temperatures of 20° and 40°C and also performed X-ray diffraction of hardened mortar. They also took hardened specimens of cement paste mixed at a ratio of 70 (cement) to 30 (fly ash) and conducted tests by the BET Method for specific surface area to which N_2 was adsorbed and for non-evaporable water. The Feret's coefficient corresponding to the mortar strengths at various ages were obtained and the respective ratios to the Feret's coefficient corresponding to strengths of mortar without fly ash were calculated in discussing the influence of fly ash on the strength

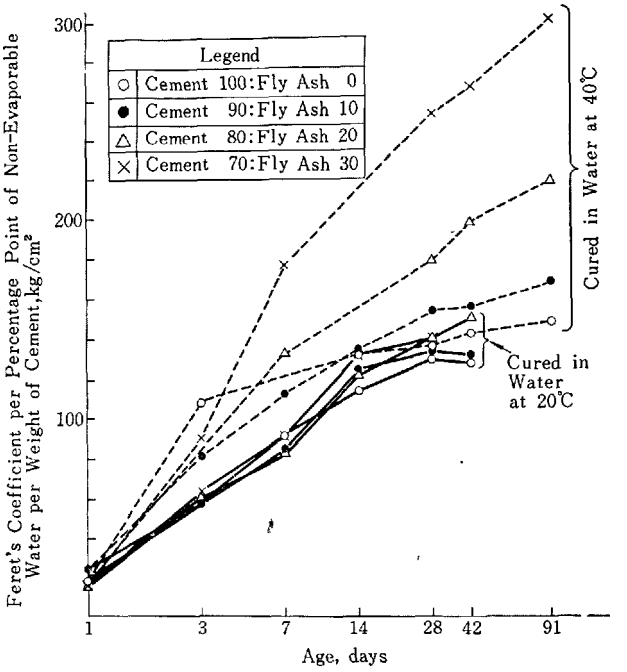

Fig. 20. *Development of Feret's coefficient per non-evaporable water of hardened cement paste.*

of mortar. It is stated that the age at which the Feret's coefficient ratio exceeds 1 is around 20 days for curing at 20°C and around 5 days for curing at 40°C. The specific surface area of the hardened cement paste increased slowly with age when fly ash was not used, but when fly ash was added it reached a maximum value at a certain age and thereafter grew smaller. The age at which the maximum value is reached agrees generally with the age at which the effect of fly ash on strength began to appear as indicated by the Feret's coefficient. It was also demonstrated that the quantity of non-evaporable water was increased when fly ash was used and that the increase was greater in the case of curing at 40°C than at 20°C. The Feret's coefficient per percentage point of the non-evaporable water is as given in Fig. 20 showing that the strength gain per percentage point is greater when fly ash is used. The results of these experiments offer a key to the search for the structure of pozzolanic reaction products. However, it should be mentioned it is thought that at the beforementioned ages at which the effect of fly ash becomes pronounced, the finely divided powder effect of the fly ash plays a part along with the pozzolanic effect.

Problems in Use of Fly Ash as a Concrete Admixture

Influence of Carbon Content of Fly Ash

As mentioned before, even when a certain amount of carbon is contained in fly ash, so long as the carbon particles are not weak, it is not thought the difference in carbon quantity will have much effect on the various properties of hardened concrete.

Fedynin (77) tested 5 varieties of fly ash with ignition loss of 6, 12, 15, 25 and 28%. The results showed very little influence of high carbon content on strength, durability, wear resistance, etc. of concrete and Fedynin explains the reason for this to be the semi-coking or coking of pulverized coal so that the fly ash itself is strong and hard. Also, there is an example of a test pavement in the U.S.A. on which it is reported a fly ash of approximately 13% ignition loss was used without any trobule. (29)

The reason the use of fly ash of small carbon content has been emphasized in a great number of reports in the past is probably because as the combustion in boiler furnaces is incomplete in the case of fly ash of high carbon content, the proportion of minute and smooth spherical particles is low and the effect on the various properties of concrete is weakened.

However, when air-entrained concrete using fly ash is made, a considerable amount of the air-entraining agent is adsorbed on the active carbon in the fly ash during mixing of concrete so that the effect of the agent is reduced. As a result, in order to obtain the required air content, it becomes necessary to increase the unit quantity of agent and it is not rare for this quantity to become several times the quntity sufficient when fly ash is not used (18)(23). There is an example of a project in which this quantity was increased by 11 times (29). Fine mineral powders have the characteristic of adsorbing admixtures by nature so that the increase in unit admixture content required is not restricted to the case of fly ash, but with the latter, the influence of active carbon is added to the abovementioned effect.

The ignition loss of fly ash has a close relationship with carbon content and there is a report which states that ignition loss and required unit admixture content are proportionate and suggests a method of calculating required unit admixture content from ignition loss test values (42). However, the carbon content and required unit admixture content are not necessarily proportionate when the source plant of fly ash differs. When pulverized coal is burned and fly ash is produced, it is thought that in the uncombusted portion of coal maintained at high temperature the carbon will have been changed to various forms in which there would be portions with weak adsorption even in uncombustioned portions. Also since the fineness of uncombustioned carbon is not uniform, carbon content and required unit admixture content would not necessarily be proportionate.

A further inconvenience is that the amount of air-entraining agent adsorbed by carbon differs with slight fluctuations in carbon content, which increases fluctuation in air content and in turn workability to make the control of air-entrained concrete difficult. There are countries in which adsorption quantities of methylene blue are measured by colorimetric tests to obtain an indication of admixture to be adsorbed by fly ash during mixing of concrete (18). Since adsorption of methylene blue and required unit AEA content are roughly proportionate, this method has proved useful in control of air-entrained concrete construction.

Pack Setting of Fly Ash during Storage

There are fly ashes which become pack set during storage. This tendency is stronger in the case of fly ash of high fineness. When pack setting occurs during storage, conveying and weighing is made difficult in the case of bulk fly ash, while in the case of bagged fly ash weighing is difficult. This is the second of the problems involved in the use of fly ash. Since Japan is a country of high humidity, the tendency for pack setting is pronounced, but it is unlikely that this is a problem limited to Japan. The pack setting of fly ash is a complicated phenomenon, hardening occurring with some fly ashes while not occurring with others.

Homma and Taniguchi (78) and Nagasako Homma (79) investigated the causes of pack setting in the case of various fly ashes and discovered that pack setting occurred because minute quantities of calcium sulphate existing on the surfaces of fly ash particles absorbed moisture from the atmosphere to act as a binder. Nagasako and Homma (79) also state that with the addition to fly ash of minute quantities of water of about 0.1%, calcium sulphate adhering to the particle surfaces is transformed into gypsum which will prevent pack setting, and that crushed coarse fly ash also would not pack set. Furthermore, it was found that fly ash blended with 20%

or more of crushed coarse fly ash is not readily pack set.

Use of Fly Ash in Slurry Form

Since fly ash is after all a by-product of combustion of pulverized coal, it is conceivable there is fear of some fluctuation in quality. Therefore, there are many standards of fly ash which contain provisions for uniformity of quality. When such provisions are not clearly understood, some fluctuation in quality of fly ash will occur and this will constitute a cause of fluctuation in the quality of concrete. This is the third problem encountered when fly ash is to be used as an admixture.

Even when the quality of fly ash meets the requirements on uniformity, as previously described, some amount of fluctuation in carbon content is unavoidable unless the conditions under which fly ash is produced are extremely good and it will be difficult to control air content and workability of air-entrained concrete. These and pack setting during storage pose the difficulties in using fly ash as an admixture.

Testing and research (80) were conducted to overcome these difficulties on the job at Okutadami Dam (gravity dam, height 157 m, concrete volume 1,630,000 m^3, period of concrete placement 1958–1961). As a result it was established that when fly ash was first vigorously mixed with water to form a slurry of a water-fly ash ratio of about 50% for storage in large quantities and then was used as necessary in this slurry form, it was splendidly made uniform to facilitate control of concrete and that even a mixture of two different fly ashes could be used. Also, since pack set fly ash could be readily used, all of the abovementioned difficulties were all nicely overcome. Furthermore, the workability of concrete was improved prominently over the case of use of fly ash in powder form and it was even found that durability was somewhat improved. In addition, when the slurry method was adopted, the equipment required was limited to the slurry mixing tank, slurry storage tank, air compressor, slurry pumps and slurry pipes eliminating the need for such equipment as screw conveyors, air sliders, bucket elevators and fly ash silos so that equipment on the job could be reduced drastically. Also, the concrete batching plant is no longer soiled by scattering of fly ash in the air. Following Okutadami Dam, this method of using fly ash was adopted at a number of dam projects other than gravity-type, such as arched types and hollow-gravity types, all with good results.

The reasons workability and durability of concrete is improved when the slurry method is adopted are thought to be that the individual particles of fly ash are released by the breaking up of agglomerates and that air entrapped in the agglomerates is released. Thorne and Watt (11) demonstrated that crushing strength of lime mortar containing fly ash which was first exhaustively extracted with water was two to three times greater than the case when fly ash was used without treatment after collection and cited the increase in the surface area of fly ash made available for reaction by the breaking up of agglomerates. The ratio of this strength increase cannot be applied immediately to the ratio of strength increase obtained when fly ash is used in slurry form for concrete, but the results of the tests do suggest that the slurry method will at times be effective in increasing strength of concrete.

Problems Involving Fly Ash Cement

Apart from its role as an admixture for concrete, fly ash has been in use for some time as an additive to cement. The U.S. Bureau of Reclamation has been having fly ash cement manufactured under special specifications and has been using it in concrete dam construction. Some of the portland-pozzolan cements presently being marketed in the U.S.A. contain fly ash. In Japan, a Japanese Industrial Standard on fly ash cement was established in 1960 (See Appendix 2), and presently 3 types of such cement are on the market. In France, standards on fly ash cement were established in 1959 (See Appendix 2) and 6 types are now being marketed. The consumption of this type of cement is extremely large and comprises approximately 1/3 of the cement manufactured in France.

The question of whether it would be better for fly ash to be used as an admixture for concrete or in the form of fly ash cement will depend on the economic structure and customary practice and is not a matter to be decided lightly. When in the form of fly ash cement, there is an advantage in that uniformity of fly ash is more easily secured. However, there are many cases in which it is more economical for fly ash to be used as a concrete admixture in power company construction and in other work. Also, since there is considerable difference in the quality of fly ash pro-

duced at various plants, unless as a concrete admixture, it will generally be impossible to use good quality fly ash in the most suitable manner to compensate for defects in portland cement, or to increase or decrease as necessary the amount used according to type of member, dimensions of member, temperature and other factors.

The influence of fly ash on the various properties of concrete is basically the same whether it is used as an admixture when making concrete or whether it is used in the form of fly ash cement. The technical problems involved in fly ash cement can be listed as the chemical composition and fineness of cement clinker and the method of blending the fly ash and the amount to be mixed in the cement.

There are numerous reports which state that the effect of fly ash differs with the type of cement when the fly ash is used to replace part of the cement. Davis (81) states that fly ash is more effective with normal portland cement and moderate heat portland cement than low heat portland cement, the reason being that these two types are high in C_3S content.

Brink and Halstead (17) taking 10 cements of greatly different alkali content, tricalcium silicate content and mortar strength, compared strengths of 1 : 2 mortar made replacing 50% of cement with fly ash and reported that at the earlier ages (e.g., 28 days or less) the alkali in cement appeared to accelerate the reaction between cement and fly ash, but at the greater ages (e.g., one year or more) the strength was higher the higher the C_2S content. Timms and Grieb (23) using two portland cements greatly different in alkali content, tested concretes made replacing part of the cement with fly ashes and reported that the effect of fly ash on strength and durability of concrete differed with cement.

In the studies of Stingley and Peyton (26) and Tsukayama and Miyoshi (27) on pavement concrete, it is reported that the effect of fly ash on strength was less in concrete made with moderate heat portland cement than in concrete made with normal portland cement.

There are reports (82)(83) which have stated that concrete made replacing a part of portland blast-furnace slag cement with fly ash demonstrated long-term strength equal to that of concrete without fly ash when the fly ash used was of good quality.

The chemical reaction in concrete between portland cement clinker and fly ash as mentioned previously is very complicated and differs not only with the quality of fly ash and the chemical composition of the clinker, but also greatly with fineness of the clinker. Judging from the fact that in all countries with the exception of France the production of fly ash cement is far less in comparison to the production of portland cement, it is doubtful that a portland cement clinker made esepcially for fly ash cement is being produced in any of the countries. It is thus natural that research in this direction has not progressed and it is extremely difficult to clarify a chemical composition of clinker suited to fly ash cement. At present, except for special cases, it is believed that so-called normal portland cement clinker is being used as material for fly ash cement.

The second problem of fly ash cement is whether in manufacture fly ash should be blended with ground portland cement clinker or whether clinker and coarse-particled fly ash should be mixed and ground together.

When coarse fly ash is ground, there is a fear that the smooth spherical shape will be lost. However, according to the work by Yoshikoshi (38). the part of the fly ash crushed when ground together with clinker is limited to the relatively larger particles so that the finer fly ash particles retain their smooth spherical shapes. Since the effect of fly ash in improving the various properties of concrete depends on the minute particles, it is believed the features of fly ash are retained even in the case of combined grinding. Actually, in this study by Yoshikoshi, it was shown that at the same degree of fineness, fly ash cement made by grinding coarse fly ash and clinker together, displayed roughly the same behavior as a blend of fine fly ash of the same chemical composition and a clinker ground separately in advance.

Venuat (84) has conducted a detailed study regarding finenesses of portland cement clinker and fly ash when manufacturing fly ash cement. Clinker ground to four different finenesses ranging between 2,500 and 6,400 cm^2/g and fly ash ground to three finenesses between 3,000 and 8,000 cm^2/g were blended to make fly ash cements and mortar specimens were made of the respective strengths in 3 classes of mix proportions. From the results, Venuat points out the existence of a certain fineness of fly ash suited to a given fineness of clinker and that fineness of fly ash has a great influence on strength at early ages, but little on strength, drying shrinkage and durability at advanced ages.

Summarizing the abovementioned and other studies, it appears that the difference in the method of manufacturing, whether by grinding fly ash and clinker separately or together, has a negligible effect on the various properties of fly ash cement. The fineness to be aimed for in grinding or the amount of fly ash to be blended should be determined upon testing to obtain cement of the required quality. In such a case,

it is important that fly ash cement of the required quality should be economically obtained, at times this being the governing consideration in manufacture of fly ash cement.

Conclusions

It is of course a difficult matter to gather every piece of literature throughout the world, and especially, in the case of fly ash which is a by-product and moreover a material which has come into use only comparatively recently, this difficulty becomes even greater. However, summarizing the various researches on fly ash and fly ash cement made public in various countries which it has been possible to obtain up to the present, it is believed the following can be said:

(1) As a result of reviewing the chemical compositions, phase compositions, and physical properties such as particle shape, specific gravity and fineness of various fly ashes, it has been found that this material differs greatly by country and by plant within each country. As examples, in chemical composition, SiO_2 ranged between 63 to 30%, Al_2O_3 between 34 to 11%, Fe_2O_3 between 31 and 3% while CaO ranged between 39 to 1%. Specific surface areas were between 8,100 to 1,200 cm^2/g. This is apparently due to differences in quality of coal, methods of burning, methods of collecting fly ash and other factors.

(2) On making an investigation of researches on the influences of various fly ashes with respect to workability, strength, volume change, heat of hardening, watertightness, durability against freezing and thawing, durability against aggressive waters and abnormal expansion from alkali-aggregate reaction of concrete, it was found that the reports from all countries agree in emphasizing although with some difference in degree, that a fly ash of suitable chemical composition and high fineness, or in other words a good quality fly ash, will influence these properties benefitially. The marked effects with respect to workability, drying shrinkage, heat of hardening, watertightness and durability against agressive waters have already become common knowledge. The age at which the strength of concrete with about 25% of the portland cement replaced with good quality fly ash exceeds that of concrete without fly ash is 3 to 6 months at 20°C moist curing. This age is reduced further when moist curing at higher temperatures is carried out indicating clearly that fly ash is of even greater advantage at high temperatures. It is also shown that the effect of fly ash is more pronounced in tensile strength and flexural strength than in compressive strength.

However, in the reports of all countries, it is pointed out that these effects differ considerably depending on the quality of fly ash and there are even examples cited in which prominent effects were not noted.

(3) It has been made clear that entrained air introduced by the use of an admixture in concrete containing fly ash is the same in size and distribution as entrained air in concrete without fly ash. Therefore, the durability against freezing and thawing of air-entrained concrete with fly ash is governed by concrete strength and air content as in the case of normal air-entrained concrete.

The amount of admixture required to obtain the desired air content often is increased extremely when fly ash is used. The reason for this is the adsorption of the admixture by carbon contained in the fly ash. Since it is impossible to maintain fineness and carbon content of fly ash perfectly uniform, it is stressed that special attention must be given to air content, and in turn workability, when fly ash is used with air-entrained concrete and there are simple testing methods which have been conceived for obtaining criteria for unit admixture content required to yield the specified air content.

However, it has been established by experience that when fly ash is first mixed vigorously with water to form a slurry and is stored in large quantities to be used as necessary instead of using it in powder form, the uniformity of fly ash will not only be maintained surely, but it will pose no difficulty to use pack set fly ash. On top of this, workability of the concrete is improved and also the method will result in more economy in many cases.

As mentioned above, the quantity of carbon content will greatly affect fresh concrete but there is little influence on the various properties of hardened air-entrained concrete.

(4) The excellent properties imparted to concrete by fly ash are not due only to the smooth, spherical particle shape, the high fineness and pozzolanic activity. The theorization that replacement of fly ash particles in the floc structure of the cement particles to increase the available space around the cement particles thus accelerating the hydration reaction also contributes to an extent has been indicated to be appropriate. When a finely divided powder such as fly ash is added, the strength of concrete becomes higher to some extent than the strength corresponding to the void-cement ratio even at early ages when there is

still no pozzolanic reaction. Since it has also been indicated that the soluble components of fly ash are of minute quantity and the rate at which they are leached out is slow, the reason for this strength increase can be explained brilliantly by the above theorization.

(5) Pozzolanic reaction, even when limited to that of fly ash, is an extremely complex phenomenon which has not yet been fully explained. However, it has been clarified that the phase composition of fly ash related to pozzolanic reaction is chiefly the glass phase, that the pozzolanic reaction depends on the surface area of the glass phase, that the strength increase of concrete due to pozzolanic reaction has a close relationship with the $SiO + Al_2O_3$ content of fly ash, and that calcium aluminate hydrates are contained in the pozzolanic reaction products as well as calcium silicate hydrates. These are research results which provide a key to the explanation of pozzolanic reactivity.

(6) The effects of pozzolanic reaction seen in concrete containing fly ash is somewhat different from the effects of other types of pozzolan. In concrete using fly ash, even with pozzolanic reaction of a degree not affecting the test values of non-evaporable water and heat of hydration, the strength of concrete at advanced ages is markedly increased when this reaction occurs. It has been established the reason for this is that the pozzolanic reaction products are formed in the rims between fly ash particles and cement hydration products so that even a weak pozzolanic reaction is extremely effective at long-term ages in causing fly ash particles and cement hydration products to be strongly bonded together.

(7) In regard to the manner of testing pozzolanic activity of pozzolans, there have been a great many methods which have been suggested from the past, each with its special features. In spite of this, at the present stage, there is still no test method with a close relationship to the long-term strengths of concrete or mortar containing fly ash. However, if the objective is limited to fly ash, it is a fact that various studies on the properties of fly ash have progressed to a considerable degree, and there are many actual examples of use of fly ash in the field with results of long-time tests already published, and therefore, in the case of fly ash, there is not very much necessity to discuss the values of the various methods of testing pozzolanic activity from a broad point of view. It should be adequate for a suitable method to be selected and applied in accordance with the circumstances of each country.

(8) Fly ash cement is already widely used practically, and good results have been reported. However, there is no generally accepted theory regarding the problems with respect to the chemical composition and fineness of cement clinker to be used in manufacture of fly ash cement, the method of blending fly ash, the quantity of fly ash to be blended, etc. This may appear strange, but probably is due to the different circumstances of each country.

To summarize, fly ash is already being used in many areas as an important ingredient of concrete, the purpose of its use being not only economy, but also the improvement of the various properties of portland cement concrete. Parenthetically, a good quality fly ash will even augment the defects of portland cement. Therefore, the concept of fly ash as a by-product is already becoming something of the past. It is necessary to seriously consider collecting methods so that good quality fly ash can be made available economically. The day when even greater lustre is added to these pearls born from coal through such efforts is looked forward to with great anticipation.

Acknowledgements

The sincerest gratitude of the author is extended to Dr. Kimbe Chujo, Dr. Junji Yamada and the engineers of the Nihon Cement Company Laboratory for their untiring aid in writing this paper and for their performance of supplementary tests whenever found necessary, and to the engineers of the Ministry of Construction for conducting field tests in connection with this paper.

References

1. "An investigation of the pozzolanic nature in coal ash", Eng. News Rec., Vol. 71, No. 24, 1334–1335, (1914).

2. R. E. Davis, R. W. Carlson, J. W. Kelly and H. E. Davis, "Properties of cements and concretes containing fly ash", Proc. Amer. Concrete Inst., 33,

577–612, (May–June, 1937).
3. "Fuel panel discussion on cinder catchers", Trans. Amer. Society of Mechanical Eng., **59**, 355–371, (1937).
4. N. W. Elmer, "Profitable fly ash handling", Steel, **106**, 64–65, (Feb. 12, 1940).
5. C. M. Weinheimer, "Evaluating importance of the physical and chemical properties of fly ash in creating commercial outlets for the material", Trans. Amer. Society of Mechanical Eng., **66**, 551–561, (Aug. 1944).
6. H. S. Meissner, "Pozzolans used in mass concrete" Symp. on Use of Pozzolanic Materials in Mortars and Concretes, Special Technical Publication No. 99, ASTM, 16–30, (1949).
7. F. M. Lea, "The chemistry of pozzolans", Proc., International Symp. on the Chemistry of Cements, Stockholm, 460–483, (1938).
8. Symposium on Use of Pozzolanic Materials in Mortars and Concretes, Special Technical Publication, No. 99, ASTM, (1949).
9. Symposium on Pozzolans and Their Use, Rome, Italian Chemical Society, Ann. Chim., **44**, 569–768, (1954).
10. G. Malquori, "Portland-pozzolan cement", Proc. of the 4th Int. Symp. Chem. of Cement, Washington, 983–1000, (1960).
11. J. D. Watt and D. J. Thorne, "The composition and pozzolanic properties of pulverised fuel ashes", J. Appl. Chem., **15**, 585–594, (Dec. 1965), **15**, 595–604, (Dec. 1965) and **16**, 33–39, (Feb. 1966).
12. P. Terrier and M. Moreau, "Study on the mechanism of pozzolanic reaction of fly ash with cement", Rev. Mater. Constr. Trav. Publics, **613**, 379–396, (Oct. 1966) and **614**, 440–451, (Nov. 1966) (in French).
13. T. Sakurai, T. Sato, M. Hashimoto and M. Fukunaga, "Pozzolanic reactivity of fly ash", Proc. of the 21st General Meeting, Cement Assoc. of Japan, 101–109, (1967) (in Japanese).
14. M. Kajii and K. Usui, "Relation between particle size and specific gravity of fly ash", Cement and Concrete, **170**, 11–13, (April 1961) (in Japanese).
15. W. I. Luke, "Nature and distribution of particles of various sizes in fly ash", U.S. Army Eng. Waterways Experiment Station Technical Report No. 6–583, 1–21, Nov. (1961).
16. L. J. Minnick, "Investigation relating to the use of fly ash as a pozzolanic material and as an admixture in portland cement concrete", Proc. ASTM, **54**, 1129–1158, (1954).
17. R. H. Brink and W. J. Halstead, "Studies relating to the testing of fly ash for use in concrete", Proc. ASTM, **56**, 1161–1206, (1956).
18. M. Kokubu, T. Kawahara and S. Dazai, "Collective test of various fly ash", Trans. Japan Society of Civil Eng., No. 68, Extra Paper (1–1), 1–27, (May 1960) (in Japanese).
19. W. H. Price and W. A. Cordon, "Development of high quality concrete of low cement content for large dams built by the Bureau of Reclamation", Trans. 5th Int. Congress on Large Dams, Paris, Vol. IV, Q. 19, R-4, 57–71, (1955).
20. K. Yamazaki, "Fundamental studies of the effects of mineral fines on the workability of concrete", Trans. Japan Society of Civil Eng., **84**, 98–118, (Aug. 1962) (in Japanese).
21. T. C. Powers, "The bleeding of portland cement paste, mortar, and concrete", PCA Research Bull. No. 2 (1939).
22. H. H. Steinour, "Rate of sedimentation", PCA Research Bull., No. 3, (1944).
23. A. G. Timms and W. E. Grieb, "Use of fly ash in concrete", Proc. ASTM, **56**, 1139–1157, (1956).
24. M. Kokubu, M. Yoshikoshi, N. Tashiro and K. Ohashi, "Design of concrete mixtures using fly ash in various types of large dams", Trans. 8th Int. Congress on Large Dams, Edinburgh, Vol. 3, Q. No. 30, R-8, 139–160 (1964).
25. C. E. Lovewell and G. W. Washa, "Proportioning concrete mixtures using fly ash", Proc. Amer. Concrete Inst., **54**, 1093–1102, (June 1958).
26. W. M. Stingley and R. L. Peyton, "Use of fly ash as admixture in an experimental pavement in Kansas", Highway Research Record, No. 73, Symposium on Fly Ash in Concrete, Highway Research Board, 26–31, (1965).
27. R. Tsukayama and A. Miyoshi, "Ten years test on pavement concrete ontaining fly ash", Review of the 22nd General Meeting, Cement Assoc. of Japan, 117–121, (1968).
28. M. Kokubu and S. Ito, "Investigation on experimental concrete pavement using various cements and fly ash", Cement and Concrete, **269**, (Jul. 1969) (in Japanese).
29. F. E. Legg, Jr., "Experimental fly ash concrete pavement in Michigan", Highway Research Record, No. 73, Symposium on Fly Ash in Concrete, Highway Research Board, 1–12, (1965).
30. M. Kokubu, I. Miura, S. Takano and R. Sugiki, "Effect of temperature and humidity during curing on strength of concrete containing fly ash", Trans. Japan Society of Civil Engineers, No. 71, Extra Papers (4–3), 1–10, (Dec. 1960) (in Japanese).
31. V. V. Stolnikov, and V. V. Kind, "Cements and concretes with fly ash and methods for accelerating their hardening", RILEM International Conference on the Problems of Accelerated Hardening of Concrete in Manufacturing Precast Reinforced Concrete Units, Moscow, II-21, (1964).
32. M. Kokubu, H. Yoshida, S. Matsui, K. Kadowaki and K. Yamazaki, "Investigation on execution of concrete lining in hot temperature tunnel", Review of the 16th General Meeting, Japan Cement Eng. Assoc., 136–140, (1962).
33. R. F. Blanks, "Fly ash as a pozzolan", Proc. Amer. Concrete Inst., **46**, 701–707, (May 1950).
34. R. E. Davis, "Use of pozzolans in concrete", Proc. Amer. Concrete Inst., **46**, 377–384, (Jan. 1950).
35. S. Nagataki, "Study on shrinkage stress in concrete for pavement", Collected Papers, No. 1, Department of Civil Engineering, Univ. of Tokyo, No. 6405, 1–15, (1964) (in Japanese).
36. M. Jirsak and A. Kraus, "Durability of hydrated concrete with fly ash", Final Report, RILEM Symp. Durability of Concrete, Prague, 323–330,

(1961) (in French).
37. E. C. Higginson, "Mineral admixture", Significance of Tests and Properties of Concrete and Concrete Making Materials, ASTM Special Technical Publication, No. 169–A, 543–555, (1966).
38. M. Yoshikoshi, "Investigation on fly ashes as pozzolanic admixture", Trans. Japan Society of Civil Engineers, No. 31, 1–62, (Nov. 1955) (in Japanese).
39. G. W. Washa and N. H. Withey, "Strength and durability of concrete containing Chicago fly ash", Proc. Amer. Concrete Inst. **49**, 701–712, (Apr. 1953).
40. G. Babatchev, and P. Pentchev, "Resistance of cement mixture to corrosion", Final Report, RILEM Symp. Durability of Concrete, Prague, II, 79–92, (1961) (in French).
41. R. E. Davis, H. E. Davis and J. W. Kelly, "Weathering resistance of concrete containing fly ash cements", Proc. Amer. Concrete Inst., **37**, 281–293, (Jan. 1941).
42. T. D. Larson, "Air entrainment and durability aspects of fly ash concrete", Proc. ASTM, **64**, 866–886, (1964).
43. J. Navratil, "Durability of hardened fly ash cement paste", Final Report, RILEM Symp. Durability of Concrete, Prague, II, 161–164, (1961).
44. A. R. Alderman, A. J. Gaskin, R. H. Jones and H. E. Vivian, "Australian aggregates and cements in relation to cement-aggregate reaction", Proc. Amer. Concrete Inst., **46**, 613–616, (Apr. 1950).
45. T. E. Stanton, O. J. Porter, L. C. Meder and A. Nicol, "California experience with the expansion of concrete through reaction between cement and aggregate", Proc. Amer. Concrete Inst., **38**, 209–236, (Jan. 1942).
46. W. C. Hanna, "Unfavorable chemical reactions of aggregates in concrete and a suggested corrective", Proc. ASTM, **47**, 986–999, (1947).
47. W. Lerch, "Discussion" on the above paper, Proc. ASTM, **47**, 1005–1008, (1947).
48. H. S. Meissner, "Expansive cracking in concrete dams caused by reactive aggregate and high alkali cement", 3rd Int. Congress on Large Dams, Stockholm, Vol. II, Q. No. 11, R. 47, 1191–1202, (1948).
49. R. F. Blanks, "The use of portland-pozzolan cement by the Bureau of Reclamation", Proc. Amer. Concrete Inst., **46**, 89–108, (Oct. 1949).
50. W. Lerch, "Studies of some methods of avoiding expansion and pattern cracking associated with the alkali-aggregate reaction", Symp. on Use of Pozzolanic Materials in Mortars and Concretes, Special Technical Publication, No. 99, ASTM, 153–177, (1949).
51. ASTM C441–67, Standard Method of Test for Effectiveness of Mineral Admixtures in Preventing Excessive Expansion of Concrete Due to the Alkali-Aggregate Reaction.
52. K. Yamazaki, "Fundamental studies of the effects of mineral fines on the strength of concrete", Trans. Japan Society of Civil Engineers, No. 85, 15–44, (Sept. 1962) (in Japanese).
53. N. Kawada and A. Nemoto, "On early hydration phenomenon of cement as mixed with fly ash," Proc. of the 22nd General Meeting, Cement Assoc. of Japan (124–128), (1968) (in Japanese).
54. W. T. Moran and J. L. Gilliland, "Summary of methods for determining pozzolanic activity", Special Technical Publication, ASTM, No. 99, 109–130, (1949).
55. ASTM C593–66T, Tentative Specification for Fly Ash and Other Pozzolans for Use with Lime.
56. ASTM C402–65T, Tentative Spec. for Raw or Calcined Natural Pozzolans for Use as Admixtures in Portland Cement Concrete.
57. M. Papadakis and M. Venuat, "Fabrication and utilization of hydraulic materials", 2nd Edition, (1966) (private publication, in French).
58. AFNOR FD P15–462, Test Method of Pozzolanic activity, (in French).
59. ISO Recommendation, Pozzolanicity Test for Pozzolanic Cements, No. 1156, (Sept. 1964).
60. J. Forest and E. Demoulian, "Appreciation of the activity of fly ash and pozzolans", Rev. Mater. Constr. Trav. Publics, **577**, 312–317, (Oct. 1963) (in French)
61. ASTM C379–56T, Tentative Spec. for Fly Ash for Use as a Pozzolanic Material with Lime, Discontinued 1966-Replaced by C593.
62. A. Steopoe, "On the determination of the hydraulic activity of pozzolans", Rev. Mater. Constr. Trav. Publics, **492**, 210–212, (Sept. 1956) (in French).
63. R. Feret, "Researches on the nature of pozzolanic reaction and materials", Rev. Mater. Constr. Trav. Publics, **281**, 41–44, **282**, 85–92, **288**, 293–298, (1933) (in French).
64. L. Guillaume, "Simple control of pozzolanic fly ash added to portland cement", Rev. Mater. Constr. Trav. Publics, **517**, 272–273, (Oct. 1958) (in French).
65. AFNOR P15–301, Test Method of Cement, (Mar. 1946) (in French).
66. J. Jambor, "A new method for determination of pozzolanic activity", Rev. Mater. Constr. Trav. Publics, **564**, 240–256, (Sept. 1962) (in French).
67. F. M. Lea, "Investigation on pozzolans", Tech. Paper, No. 27, Department of Scientific and Industrial Research, (1940).
68. L. Alviset, "Contribution to the report of efflorescence", Rev. Mater. Constr. Trav. Publics, **499**, 99–112, (Apr. 1957) (in French).
69. A. Jarrige and V. Darques, "Fixation of lime in cement by fly ash", Rev. Mater. Constr. Trav. Publics, **594**, 144–148, (Mar. 1965) (in French).
70. L. Guillaume, "Pozzolanic activity of fly ash in portland cement and slag cement", Silicate Inds., Vol. 28, No. 6, 297–300, (1963) (in French).
71. G. Shikami, "On pozzolanic reaction of fly ash", Proc. Japan Cement Eng. Assoc., X, 221–227, (1956) (in Japanese).
72. V. A. Pyachev, "Relation between mineral component of clinker and strength of portland fly ash cement", Cement (Tsement), **30**, No. 2, 9–10, (1964) (in Russian).
73. M. Venuat, "Fly ash cement, influence of the proportion of fly ash on properties of cement", Rev. Mater. Constr. Trav. Publics, **565**, 271–279, **566**, 315–324, **567**, 349–356, (Oct., Nov. and Dec. 1962)

(in French).
74. R. Ducreux and A. Jarrige, "Influence of fineness of fly ash on behavior of fly ash cement", Silicate Inds., **27**, No. 11, (1962) (in French).
75. K. Saji, "The electron microscopy of hardening cement pastes", Zement-Kalk-Gips, **12**, No. 9, 418–423, (Sept. 1959) (in German).
76. E. Homma and Y. Kikuchi, "On the development of strength in fly ash cement", Review of the 22nd General Meeting, Cement Assoc. of Japan, 82–84, (1968).
77. N. I. Fedynin, "Characteristics of unburned coal ash and its influence on properties of ash concrete", Construction Material (Stroitelnye Materilg), **9**, No. 4, (1963) (in Russian).
78. A. Homma and K. Taniguchi, "Effect of soluble component in fly ash on its pack setting property", Cement and Concrete, **240**, 19–23, (Feb. 1967) (in Japanese).
79. N. Nagasako and M. Homma, "On characteristics and method of prevention against pack setting of fly ash", Cement and Concrete, **270**, (Aug. 1968) (in Japanese).
80. M. Kokubu, "Mass concrete practices in japan", Symp. on Mass Concrete, Amer. Conc. Inst., Publication SP-6, 127–150, (Mar. 1963).
81. R. E. Davis, "A review of pozzolanic materials and their use in concrete", Symp. on Use of Pozzolanic Materials in Mortars and Concretes, Special Technical Publication No. 99, ASTM, 3–15, (1949).
82. W. E. Grieb and D. O. Wolf, "Concrete containing fly ash as a replacement for portland blast-furnace slag cement", Proc. ASTM, **61**, 1143–1153, (1961).
83. W. Kobayashi, "Blended cement containing slag and fly ash", Cement and Concrete, **210**, 19–25, (Aug. 1964) (in Japanese).
84. M. Venuat, "Fly ash cement, influence of fineness of the constituents on properties of cement", Rev. Mater. Constr. Trav. Publics, **595**, 208–212, (Apr. 1965) (in French).
85. J. Forest and E. Demoulian, "Research on method of rapid appreciation of reactivity of fly ash and pozzolans used as admixture for cement", Silicate Inds., **29**, No. 7, 265–278, (1964) (in French).
86. M. Venuat and J. Alexander, "Study on rheologic behavior of fly ash", Rev. Mater. Constr. Trav. Publics, **615**, 481–495, (Dec. 1966) (in French).
87. W. Krausbein, "Hydraulic behavior of fly ash and its influence on sulphate resistance of portland cement", Zement-Kalk-Gips, **4**, No. 5, 123–127, (May 1951) (in German).
88. W. Knauts, "Sintering technology of ash", Silicatechnik, **11**, No. 7, 308–311, (July 1960) (in German).
89. G. N. Babachev and P. S. Penchev, "Chemical resistance of cement containing fly ash collected by cottrell in power station", Hydraulic Engineering and Construction (Gidrotekh Stroitel), **30**, No. 10, 26–31, (1960) (in Russian).
90. N. S. Dubovskaya and P. G. Usov, "Electron microscope investigation of the products of hardening of lime-ash binder", Construction and Architect, (Strt. i Arkhitect) **8**, No. 4, 85–88, (1965) (in Russian).
91. M. Funato, "Determination of trace elements in fly ash", Review of the 21st. General Meeting, Cement Assoc. of Japan, 87–89, (1967).

Appendix 1 Standard Specifications for Fly Ash in Various Countries

1. Specifications

Country	Designation of standard	Year
Japan	JIS A 6201 FLY ASH[a]	1958
U.S.A.	ASTM C350–65T Tentative Specifications for FLY ASH FOR USE AS AN ADMIXTURE IN PORTLAND CEMENT CONCRETE[b]	1965 (First established in 1954)
Great Britain	B.S. 3892 Specifications for PULVERIZED-FUEL ASH FOR USE IN CONCRETE[a]	1965
U.S.S.R.	GOST 6269–63 BINDER ACTIVE MINERAL ADDITIVES	1963
Others	[c]	

a. Methods of sampling and testing are included.
b. Methods of sampling and testing are determined in accordance with the requirements of the ASTM Designation C311 and C402.
c. In the other countries, there exist specifications for fly ash only manufactured in case of artificial pozzolans, and these are not included in this appendix.

2. Chemical Requirements

	Japan JIS A 6201	U.S.A. ASTM C350–65T	Great Britain B.S. 3892	U.S.S.R. GOST 6269–63
Silicon dioxide (SiO_2), min. percent	45	—	—	40.0
Silicon dioxide (SiO_2) plus aluminum oxide (Al_2O_3) plus iron oxide (Fe_2O_3), min. percent	—	70.0	—	—
Magnesium oxide (MgO), max. percent	—	—	4	—
Sulfur trioxide (SO_3), max. percent	—	5.0	2.5[a]	3
Moisture content, max. percent	1	3.0	1.5	—
Loss on ignition, max. percent	5	12.0	7.0[b]	10
Available alkalies as Na_2O, max. percent	—	1.5[c]	—	—

a. Where the weight of pulverized-fuel ash to be used in the mix is equal to or greater than the weight of cement in the mix, a limit of 1.5 percent on the maximum sulphate content of the pulverized-fuel ash to be used shall apply.
b. Unless otherwise agreed between purchaser and vendor.
c. Applicable only when specifically required by the purchase for use in concrete containing reactive aggregate and cement required to meet a limitation on content of alkalies.

3. Physical Requirements

	Japan JIS A 6201	U.S.A. ASTM C350–65T	Great Britain B.S. 3892	U.S.S.R. GOST 6269–63
Fineness:				
Mean particle diameter, microns, max.	—	9.0	—	—
Amount retained when wet-sieved on No. 325 (44-micron) sieve, max. percent	25	—	—	—
Specific surface, (Air permeability test), min. cm^2/g	2700	—	Zone A. 1250[a] up and to and including 2750 Zone B. Above 2750 and up to and including 4250 Zone C. Above 4250, subject to a range not greater than 1500	
Compressive strength of mortar:				
Percentage of control at 7 days, min.	—	100	—	—
Percentage of control at 28 days, min.	63	100	—	—
Percentage of control at 91 days, min.	80	—	—	—
Increase of drying shrinkage of mortar bars at 28 days, max. percent	—	0.03	—	—
Water requirement, max. percent of control	100	105	—	—
Soundness:				
Autoclave expansion of mortar bars, max. percent	—	0.50	—	—
Pozzolanic activity index:				
With portland cement, at 28 days, min. percentage of control	—	85	—	—
With lime, at 7 days, min. psi	—	800	—	—
Reactivity with cement alkalies:				
Mortar expansion at 14 days, max. percent	—	0.020[b]	—	—
Uniformity requirements:				
Fineness and specific gravity	c	d	—	—
Water requirement	e	—	—	—
Air entrainment	—	f	—	—

a. By agreement between the purchaser and the vendor any other range of specific surfaces may be supplied.
b. The indicated test for reactivity with cement alkalies is optional and to be applied only at the purchaser's request. The test need not be requested unless the fly ash is to be used with cement containing 0.60 percent or more of alkalies calculated as sodium oxide and aggregate that is regarded as deleteriously reactive with alkalies in cement.
c. In tests on individual samples, the specific surface shall not vary more than 450 cm^2/g from that of the preceding sample.
d. In tests on individual samples, the specific surface shall not vary more than 15 percent, nor shall the specific gravity vary more than 5 percent, from the average established from the tests on ten preceding samples, or by all preceding tests if less than ten.
e. In tests on individual samples, the water requirement shall not vary more than 5 percent from that of preceding sample.
f. In addition, when air-entraining concrete is specified, the quantity of air-entraining agent required to produce an air content of 18.0 percent by volume of mortar shall not vary from the average established by the ten preceding tests, or by all preceding tests if less than ten, by more than 20 percent.

Appendix 2 Standard Specifications for Fly Ash Cement in Various Countries

1. Specifications

Country	Designation of standard	Year	Year first established
Japan	JIS R 5213 FLY ASH CEMENT	1964	1960
France	NF 15–302 PORTLAND CEMENT WITH SECONDARY CONSTITUENT	1964	1959
Others	a		

a. In the other countries there exist specifications for fly ash cement only manufactured in case of pozzolanic cement, and these are not included in this appendix. The countries are as follows: Bulgaria, China, Czechoslovakia, West Germany, Greece, Hungary, Italy, Mexico, Netherlands, Portugal, Rumania, Spain, U.S.A. (ASTM and Federal), U.S.S.R., Yugoslavia.

2. Descriptions and Characteristics of Manufacture

	Japan JIS R 5213		
Denomination	Fly ash cement		
Quality	A class	B class	C class
Symbol	—	—	—
Content of fly ash, percent	Under 10	Above 10 and up to and including 20	Above 20 and up to and including 30
Content of blast-furnace slag and fly ash, percent	—	—	—
Ratio of blast-furnace slag/fly ash	—	—	—

	France NF 15–302					
Denomination	Fly ash cement			Blast-furnace slag and fly ash cement		
Quality	250	325	400	250	325	400
Symbol	CPAC 250	CPAC 325	CPAC 400	CPALC 250	CPALC 325	CPALC 400
Content of fly ash, percent	15±5	15±5	7.5±2.5	15±5	15±5	7.5±2.5
Content of blast-furnace slag and fly ash, percent	—	—	—	15±5	15±5	7.5±2.5
Ratio of blast-furnace slag/fly ash	—	—	—	2/3–3/2	2/3–3/2	2/3–3/2

3. Chemical Requirements

	Japan JIS R 5213		
	Fly ash cement		
	A class	B class	C class
Magnesium oxide (MgO), max, percent	5.0	5.0	5.0
Sulphur trioxide (SO_3), max, percent	2.5	2.5	2.5
Insoluble residue, max, percent	—	—	—
Loss on ignition, max, percent	4.0	—	—

	France NF 15–302					
	Fly ash cement			Blast-furnace slag and fly ash cement		
	CPAC 250	CPAC 325	CPAC 400	CPALC 250	CPALC 325	CPALC 400
Magnesium oxide (MgO) max, percent	5	5	5	5	5	5
Sulphur trioxide (SO_3), max, percent	3.5	3.5	3.5	3.5	3.5	3.5
Insoluble residue, max, percent	19[a]	19[a]	11[a]	12.5	12.5	5.5
Loss on ignition, max, percent	6.5	6.5	5	8	8	4.75

a. In case of using coal ash, these are as follows:
CPAC 250 and 325 . . . 7.5, CPAC 400 . . . 4

4. Physical Requirements (Major items only)

	Japan JIS R 5213		
	Fly ash cement		
	A class	B class	C class
Fineness: Specific surface, cm^2/g, min	2700	2700	2700
Time of setting (Vicat test): Initial set, min, not less than	60	60	60
Final set, hr, not more than	10	10	10
Tensile strength: 1 day in moist air, 6 days in water, kg/cm^2, min	—	—	—
1 day in moist air, 27 days in water, kg/cm^2, min	—	—	—
Bending strength: 1 day in moist air, 6 days in water, kg/cm^2, min	25	24	23
1 day in moist air, 27 days in water, kg/cm^2, min	40	38	36
Compressive strength: 1 day in moist air, 6 days in water, kg/cm^2, min	110	100	90
1 day in moist air, 27 days in water, kg/cm^2, min	220	210	200

4. Physical Requirements (continued)

	France NF 15-302					
	Fly ash cement			Blast-furnace slag and fly ash cement		
	CPAC 250	CPAC 325	CPAC 400	CPALC 250	CPALC 325	CPALC 400
Fineness: Specific surface, cm^2/g, min	—	—	—	—	—	—
Time of setting (Vicat test): Initial set, min, not less than	30	30	30	30	30	30
Final set, hr, not more than	—	—	—	—	—	—
Tensile strength: 1 day in moist air, 6 days in water, kg/cm^2, min	35	40	55	35	40	55
1 day in moist air, 27 days in water, kg/cm^2, min	50	55	65	50	55	65
Bending strength: 1 day in moist air, 6 days in water, kg/cm^2, min	—	—	—	—	—	—
1 day in moist air, 27 days in water, kg/cm^2, min	—	—	—	—	—	—
Compressive strength: 1 day in moist air, 6 days in water, kg/cm^2, min	160	210	315	160	210	315
1 day in moist air, 27 days in water, kg/cm^2, min	250	325	400	250	325	400

Remarks

Preparation of specimens for strength test:

JIS: Natural Toyoura sand to pass 297-μ and be retained on 110-μ sieve. Specimens $4 \times 4 \times 16$ cm. Mix 1:2. Water/cement ratio 0.65. Compressive strength tests on broken prisms from bending strength test. The strength at any age shall be higher than the strength at the preceding age.

NF: Sand from Leucate (Aude) equal parts (tol. 10%). 0.5 – 1 mm, 1 – 1.6 mm, 1.6 – 2 mm. Specimens for tensile strength tests, eight shaped specimens, section 5 cm^2, for compressive strength tests, 5-cm side cubes. Mix 1:3, water according to normal consistency of neat cement paste. Mortar pressed in by means of iron pestle (8 mm diam. by 20 cm) with round end.

Written Discussion

Hirotoshi Abe, Shigeyoshi Nagataki and Ryuichi Tsukayama

The Sub-Committee on Fly Ash was set up in 1957 by Japan Society of Civil Engineers for the purpose of investigating the quality of fly ash and the method of its use. Since 1962, thirteen laboratories of the members in the committee has carried out the long term research upon neutralization of concrete containing fly ash and corrosion of steel bar embedded in the concrete specimens exposed to in natural conditions. The reason the committee took up this problem was because a discussion whether fly ash had a bad effect on neutralization and corrosion or not occured at a period when the demand of fly ash for reinforced concrete structure began to grow rapidly. Some of researchers eagerly stated that neutralization and corrosion would proceed faster in concrete containing fly ash.

This research project is being performed under the leadership of Prof. Kokubu, the chairman of the committee. However, when Prof. Kokubu prepared the P.P. IV-2, this research could not be referred to because the test data had been obtained only up to the age of 2 years. Afterwards, the data at the age of 5 years were studied, and many knowledges about the influence of fly ash on neutralization of concrete were made clear. The object of this discussion is to supplement the principal paper with these new data. Hereafter, the same tests are scheduled to be conducted at the ages of 10 and 20 years.

Materials and Test Method

Cement and Fly Ash

The laboratories joining in the long term test made specimens with two types of cement, normal portland cement and moderate-heat portland cement, each being supplied from the same lot of a factory. Fly ash was also supplied from a single lot. The test results are shown in Table 1 and Table 2, indicating the typical products in Japan used in the test.

Table 1. *Physical and chemical properties of cements (JIS R 5201, 5202)*

Type	Fineness cm^2/g	Bending strength 3d.	7d.	28d. kg/cm^2	Comp. strength 3d.	7d.	28d. kg/cm^2	Chemical composition SiO_2	Al_2O_3	Fe_2O_3	CaO %
N	3220	32.9	48.1	72.8	132	227	416	22.5	5.3	3.0	63.6
M	3250	28.0	41.3	63.3	98	156	283	23.2	4.2	3.3	63.4

N = normal portland cement
M = moderate-heat portland cement

Table 2. *Physical and chemical properties of fly ash (JIS A 6201)*

Fineness cm^2/g	Bend. str. ratio 7d.	28d. %	91d.	Comp. str. ratio 7d.	28d. %	91d.	Chemical composition SiO_2	Al_2O_3	Fe_2O_3	CaO %
3500	79	82	92	74	78	97	56.0	28.5	4.2	4.4

Aggregate

River gravel and sand were used, which were employed for daily work in each laboratory. The maximum size of the gravel was 25 mm. and the fineness moduli of the sands were 2.65–2.79. Specific gravities were 2.62–2.68 for gravels and 2.49–2.69 for sands. Absorptions were 0.8–1.9% for gravels and 1.8–2.7% for sands.

Mix Proportion of Concrete

Sixteen mixtures of concrete proportioned by combining four factors, per cent replacement of cement with fly ash, unit cement-fly ash content, type of cement and slump were used. Besides these factors, concretes containing air-entraining agents or water-reducing agents were also tested in some laboratories. In the case of replacing 30% of cement with fly ash, the reduction of unit water content ranged from 5% to 9% for normal portland cement and from 6% to 7% for moderate-heat portland cement. The amount of reduction depended on unit cement-fly ash content and slump.

Size and Type of Specimen

Cylinderical specimens, 15 cm. in diameter and 30 cm. in height were used. In order to investigate the problem of corrosion, three polished steel bars, 9 mm. in diameter, were embedded in concrete. The coverage of steel bars were 20, 30, and 50 mm., respectively. To keep the coverage accurate during placement of concrete, special metal fittings were used.

Manufacturing of Specimen

Concrete was mixed in a tilting drum type mixer used for daily work in each laboratory. Concrete was carefully placed and compacted so as to keep the correct location of steel, and not to make a defect in upper part of specimen due to bleeding.

Curing

One or two days after placing, specimens were demoulded and then cured in water at 18–24°C till the age of 14 days. Subsequently, the specimens were stored in an outdoor exposing space of individual laboratory. All spaces were in good condition for sunshine and ventilation. The outer part of specimen was temporally moistened by rain, and dried by sunshine. Under these condition, the rate of neutralization of concrete was slower than continuously dry condition. The temperatures in the exposing spaces, although depending on the location, were between −5°C and 35°C.

Neutralization Test

The neutralization of concrete and the corrosion of steel bar were scheduled to be tested at 2, 5, 10, and 20 years. The depth of neutralized part from the outer surface was measured on inner surfaces exposed by cutting a specimen. A specimen was cut along two cross sections, 7 cm. apart from both top and bottom surfaces. Then the middle part was cut again along a vertical section including the center of the cylinder (See Fig. 1). The maximum and the minimum depth of neutralization and the area of neutralized part were determined by means of spraying phenol phthalein solution on the surface. The mean depth of neutralization was calculated according to the following formula.

cross section,

$$d = R - \sqrt{B/\pi}$$

vertical section,

$$d = \frac{1}{2h}(A - B)$$

where,

d = mean depth of neutralization, cm.
R = radius of specimen, cm.
h = height of specimen, cm.
A = total area of section, cm^2.
B = area of colored part, cm^2.

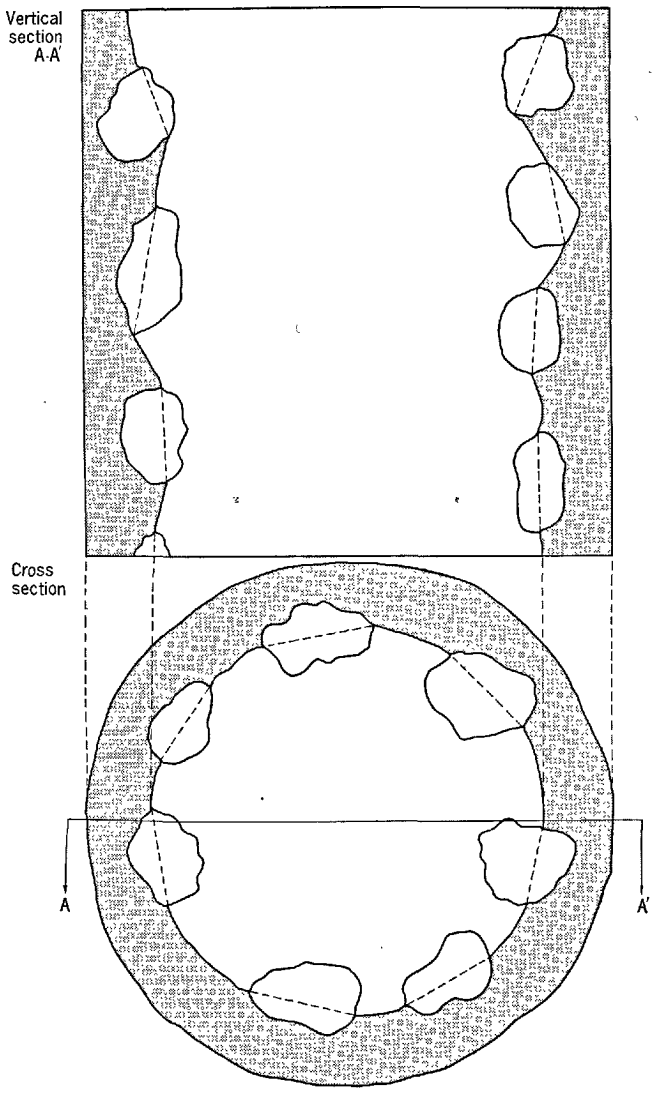

Fig. 1. *Sections of specimen for measuring the depth of neutralization*

Observation of Corrosion

Taking out steel bars from the specimen after measurement of neutralization, the extent of rusting was observed. In case of finding a corroded part, the area was measured and surrounding concrete was carefully investigated.

Compressive Strength Test

Compressive strength was also tested at the age of 28 days and 2 years on specimens manufactured simaltaneously with the specimens for neutralization test. The formers were cured in water at 20°C, and the latters were cured in the same procedure as the specimens for neutralization test.

Effect of Types of Cement, Use of Fly Ash, Cement-Fly Ash Content and Slump

Table 3 shows the test results at the ages of 2 years and 5 years. The clear relation between corrosion of steel and neutralization of concrete was not found out, because only small number of specimen showed the occurence of rust up to the age of 5 years. Accordingly, Table 3 contains only the mean depth of neutralization. Since the difference between laboratories due to the quality of aggregate and the location of exposure space are relatively small, Table 3 shows the average value of all laboratories.

The results show the influence of four factors, that is, type of cement, use of fly ash, unit cement-fly ash content and slump, on neutralization of concrete. Since some of the total combinations of these four factors were omitted, the influence of a special single factor could be known by averaging the data of pairs in which other three factors were kept constant. Fig. 2 shows the effect of each factor. The arrow line indicates the range of the data. Among the four factors use of fly ash and unit cement-fly ash content had major effect on neutralization of concrete. The type of cement and slump had only a slight influences on it.

Effect of Fly Ash

Effect of fly ash on neutralization are shown in Fig. 2–1. The mean depth of neutralization for concrete without fly ash was 0.24 cm. at 2 years and 0.49 cm. at 5 years, while for concrete replaced 30% of cement with fly ash was 0.33 cm. at 2 years and 0.68 cm. at 5 years. By replacing 30% of cement with fly ash neutralization of concrete progressed double as deep as concrete without fly ash.

Effect of Unit Cement-Fly Ash Content

In Fig. 2–2, the depth of neutralization showed marked decrease with the increase of unit cement-fly ash content.

Effect of Slump

Fig. 2–3 shows the effect of slump. The trend of slight increase with slump was observed, however, the increase was merely 0.1–0.2 cm. per 10 cm. variation in slump.

Effect of Cement Type

Fig. 2–4 shows the effect of the type of cement. The concrete which used moderate-heat portland cement showed a little greater increase in the depth of neutralization than the case of concrete which used normal portland cement. But, the difference between them which was less than 0.1 cm., appeared to be no essential importance.

(2-1) Percent of replacement

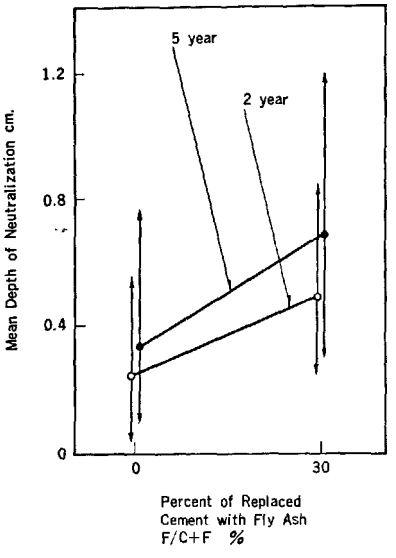

(2-2) Unit cement-fly ash content

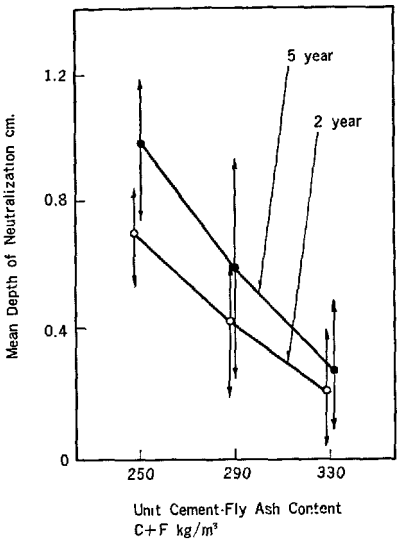

(2-3) Slump

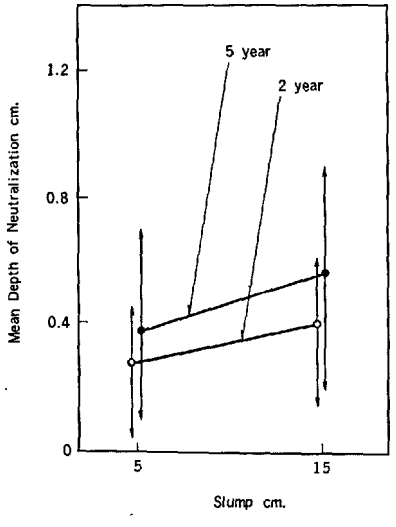

(2-4) Type of cement

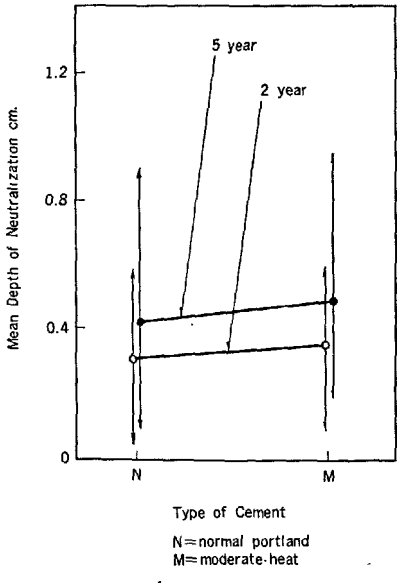

Fig. 2. *Effect of percent of replacement, unit cement-fly ash content, slump and type of cement on mean depth of neutralization of concrete*

Table 3. *Summerization of test results at the age of 2 and 5 years average of 8 laboratories*

Cement	C + F	Slump	F/C + F	W	W/C (W/C + F)	Comp. str. 28 days	Mean depth of neutralization	
	kg/m³	cm.	%	kg/m³	%	kg/cm²	2 year cm.	5 year cm.
N	330	15	0	177	54	348	0.15	0.20
			30	165	72	271	0.40	0.50
					(50)			
		5	0	158	48	414	0.05	0.10
			30	149	65	318	0.25	0.30
					(45)			
	290	15	0	177	61	283	0.30	0.40
			30	161	79	210	0.60	0.90
					(56)			
		5	0	155	53	336	0.20	0.25
			30	146	72	257	0.45	0.60
					(50)			
	250	15	0	176	70	203	0.55	0.75
			30	165	94	147	0.85	1.20
					(66)			
M	330	5	0	152	46	328	0.10	0.20
			30	143	62	253	0.30	0.30
					(44)			
	290	15	0	173	60	206	0.35	0.45
			30	160	79	169	0.60	0.95
					(55)			
		5	0	155	53	250	0.25	0.35
			30	145	71	196	0.50	0.70
					(50)			

Effect of Water Cement Ratio

The previously described results showed independently the effect of each four factors. The depth of neutralization in an actual concrete mix consisted of the combination of these four factors could not be estimated from Fig. 2. Therefore, the data were analysed again as a function of water cement ratio. In case of using fly ash, the ratio of water to cement (W/C) was adopted instead of the ratio of water to cement and fly ash ($W/C + F$), because of the short period of curing in water.

Between the mean depth of neutralization and water cement ratio (W/C), a strongly linear correlation was verified as in Table 4. (coefficient of correlation ranged from 0.976 to 0.995). The relation between water cement ratio and mean depth of neutralization, and between water cement ratio and the compressive strength at 28 days are shown in Fig. 3.

The trend observed in this figure could be summarized as follows:

(1) The relation between water cement ratio (W/C) and the mean depth of neutralization might be expressed by different straight lines depending on use of fly ash and type of cement.

(2) The mean depth of neutralization was smaller for concrete with fly ash than for concrete without fly ash so long as the comparison was made on the basis of equal water cement ratio.

Table 4. *Experimental formula for the relation between water-cement ratio and mean depth of neutralization of concrete*

Cement	$F/C + F$ %	Experimental formula for neutralization 2 years	5 years
N	0	$d = 2.20\ W/C - 1.00$ (0.984)	$d = 2.89\ W/C - 1.36$ (0.976)
	30	$d = 2.05\ W/C - 1.05$ (0.923)	$d = 3.14\ W/C - 1.68$ (0.976)
M	0	$d = 1.79\ W/C - 0.95$ (0.994)	$d = 1.79\ W/C - 0.62$ (0.978)
	30	$d = 1.78\ W/C - 0.79$ (0.992)	$d = 3.83\ W/C - 2.07$ (0.995)

in parenthesis; coefficient of correlation
d; mean depth of neutralization, cm.
W/C; water-cement ratio by weight,
N; Normal portland cement
M; Moderate-heat portland cement

(3) The difference in the gradient of the line in this figure, which is steeper for the data at 5 years than for the data at 2 years, indicates that the effect of water cement ratio increases with age.

(4) Irrespective as to whether using fly ash or not, the concrete of normal portland cement having the same compressive strength at 28 days showed the nearly equal depth of neutralization. For example, the mean depth of neutralization of the concrete having

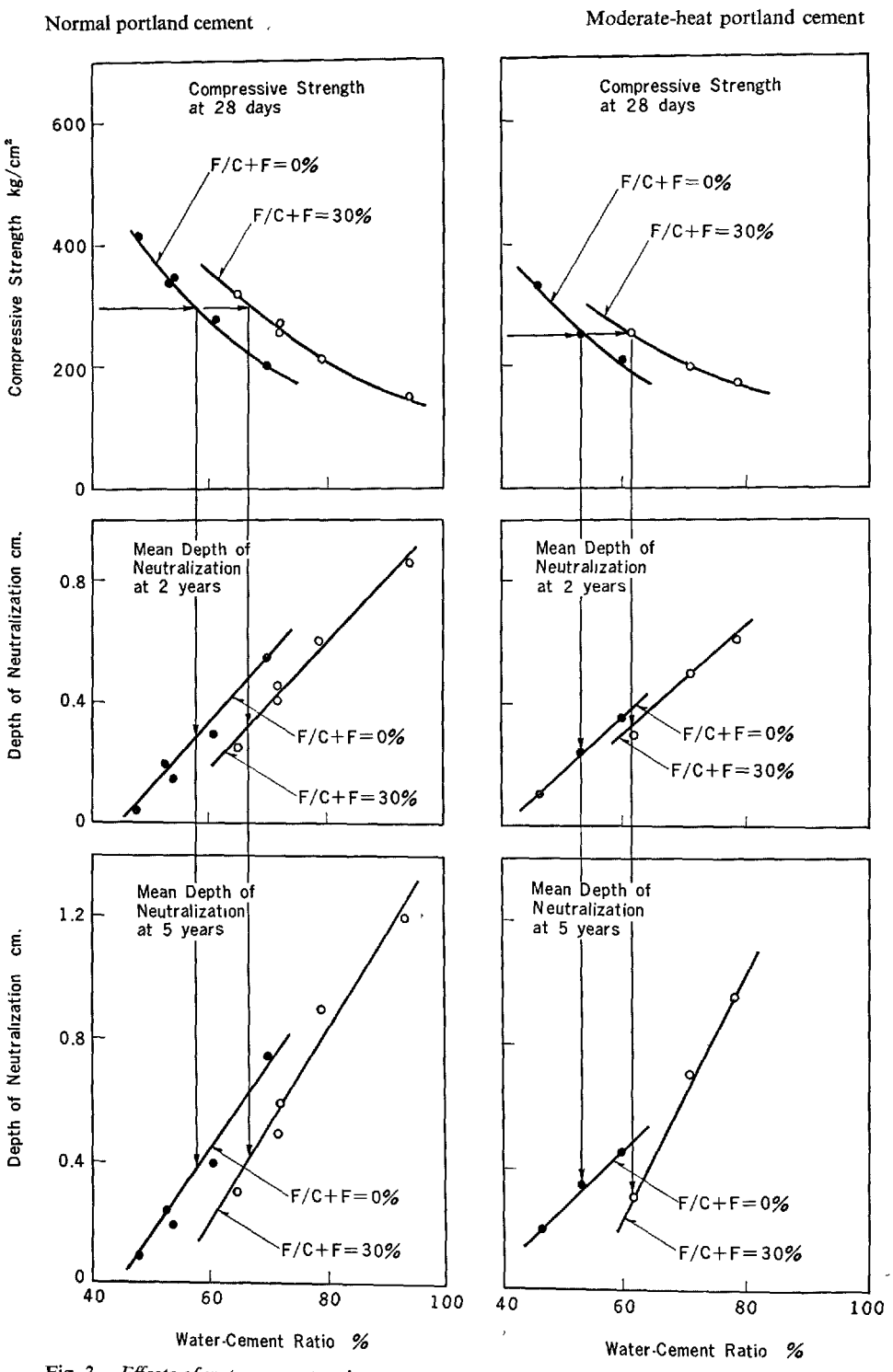

Fig. 3. *Effects of water-cement ratio on compressive strength and mean depth of neutralization*

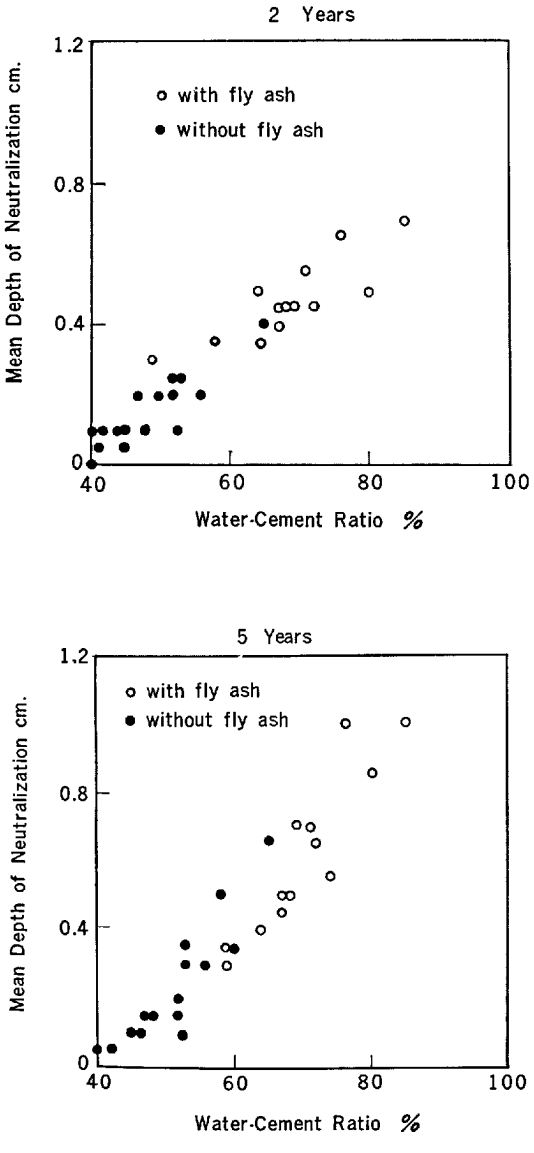

Fig. 4. *Effect of water-cement ratio on mean depth of neutralization of concrete containing air-entraining agent and water-reducing agent*

300 kg/cm² of 28 days strength was 0.30 cm. for concrete without fly ash and 0.32 cm. for concrete with fly ash at 2 years, and at 5 years 0.40 cm. and 0.42 cm. respectively. The data for moderate-heat portland cement demonstrated the similar trend to those shown above.

Effect of Air-Entraining Agent and Water-Reducing Agent

The neutralization test of concrete using air-entraining agent or water-reducing agent are conducted at several laboratories. The tests results at 2 years and 5 years showed that the mean depth of neutralization was slightly reduced by use of air-entraining agent or water-reducing agent. The relation between water cement ratio and the depth of neutralization are shown in Fig. 4. Since the separate data in each of three laboratories are plotted in this figure, some scattering of the data due to the difference in quality of aggregate and in the condition of exposure are observed. Nevertheless, the linear relation can be seen between water cement ratio and mean depth of neutralization. The reason of the reduction in the depth of neutralization by use of these agents is considered to be mainly due to the reduction in water content and water cement ratio.

Neutralization of Concrete Containing Fly Ash

The results of the exposure test described previously indicate that there is a close relationship between water cement ratio and mean depth of neutralization. On the basis of this relationship, the depth of neutralization can be predicted. A survey of the relation between compressive strength and the mean depth of neutralization revealed that there was no essential difference for both concrete with and without fly ash, having the same 28 days strength. Consequently, the restriction to the use of fly ash in a reinforced concrete structure in fear of the increase of neutralization of concrete and corrosion of steel bar appeared to be unnecessary so far as the concrete mix is proportioned on the basis of 28 days strength, regardless of fly ash itself having the character of increasing the neutralization. But, since the above conclusion was obtained from the data on concrete cured in alternately wet and dry condition, different behaviors might appear with concrete placed indoors and kept dry.

Written Discussion

Toshio Sakurai

It was my thesis that pozzolanic reactivity was to be attributed to the solubility of the glass of fly ash (1). Moreover I considered that the strength of mortar or concrete containing fly ash could possibly be due to

the amount and structure of the outer product formed mainly by the dissolution of the glass. In this paper, as an extension of this consideration, I have formulated a conception regarding the relationship between the strength of mortar or concrete and the quantity of glass, that is, the effective surface area of fly ash.

I have attempted to explain the relationship between the Feret's coefficient of mortar containing fly ash K and the curing time t in the following equation:

$$K = A \log t + C$$

According to the result obtained, K vs t is a straight line as is shown in Fig. 1. The sample of higher early strength seems to indicate a higher later strength, with no intersection of the lines. Accordingly, a factor A seems to show the effect of fly ash on the strength.

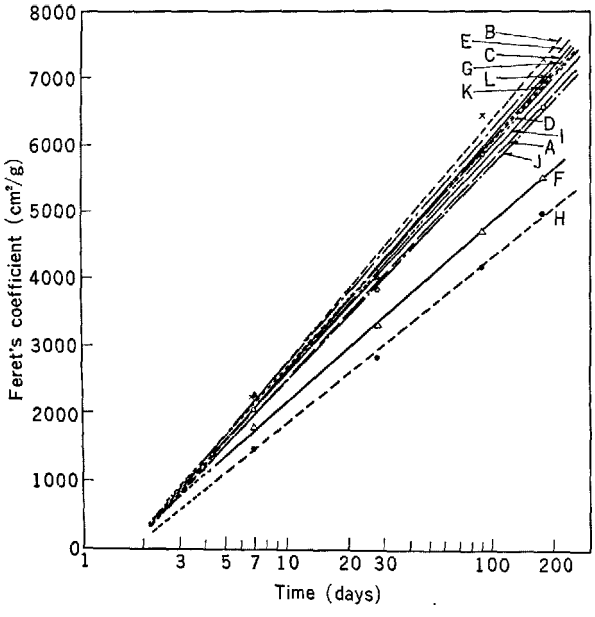

Fig. 1. *Relationship between Feret's coefficient of mortar containing fly ash and curing time.*

Table 1. shows the surface area of each fly ash measured by the air permeability method (second column) and the coefficient of pozzolanic reactivities given by Sakurai et. al. (1) (third column). The fourth column is the product of the second and third columns. This product may be considered to be the effective surface area of fly ash. The relationship between slope A obtained from Fig. 1 and this product, S_{eff}, is indicated in Fig. 2.

These two are in an almost straight line relationship, as is shown in the Fig. Accordingly, it is possible to estimate the mortar strength after an arbitrary curing time if the effective surface area of fly ash is known.

As stated above, it is clear that the properties of mortar or concrete containing fly ash are determined by the effective surface area of the fly ash.

Table 1. *The properties of fly ashes.*

Sample	Surface area	Coefficient of pozzolanic reactivity	Seff
A	3650	1.35	4928
B	4290	1.36	5834
C	3560	1.60	5696
D	3100	1.65	5115
E	3800	1.45	5510
F	1620	2.53	4099
G	3200	1.60	5120
H	1230	2.47	3038
I	3290	1.49	4902
J	2870	1.50	4305
K	3570	1.26	4498
L	4070	1.60	6512

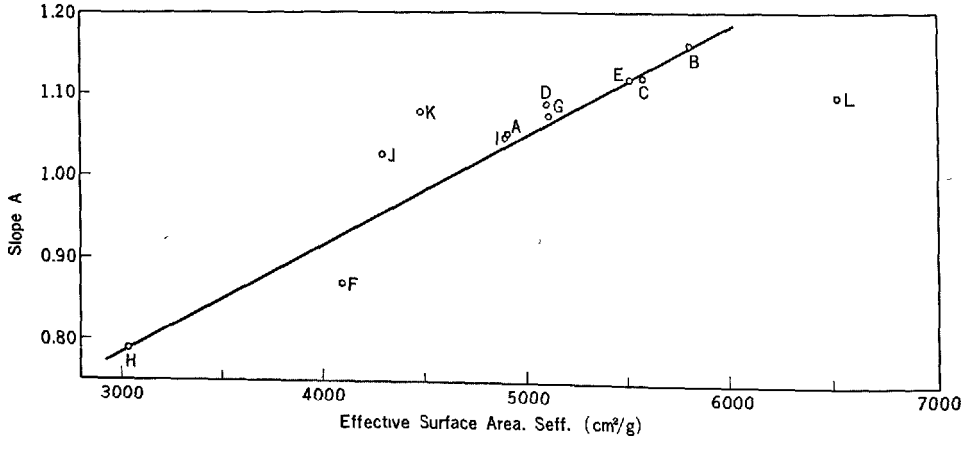

Fig. 2. *Relationship between slope A obtained from Fig. 1 and effective surface area S_{eff}.*

Reference

1. T. Sakurai, T. Sato, M. Hashimoto and M. Fukunaga, "Pozzolanic reactivity of fly ash", Review of the 21st General Meeting, Cement Assoc. of Japan, (1967).

References

1. B. Mather, "Portland-pozzolan cement made with Tennessee Valley authority fly ash." USAEWES, TR 6–541, May 1960, Vicksburg, Miss., USA; 40 pp-table.
2. W. I. Luke, "Nature and distribution of particles of various sizes in fly ash." USAEWES, TR 6–583, November 1961, Vicksburg, Miss., USA; 21 pp-illus.

Oral Discussion

Bryant Mather

Kajii and Usui (14) are cited as having found that specific gravity increases with decreasing particle size. I found (1) that by *grinding* fly ash from a surface area of 1855 to 5860 cm^2/g (air permeability) the specific gravity increases as follows:

Surface Area, cm^2/g,	Specific Gravity
1855	2.44
3565	2.70
4250	2.74
4660	2.75
5860	2.78

In other work by Luke (2), where two fly ash samples were separated into size fractions by use of an air classifier, the results were as follows:

	Fly Ash A		
	Specific Gravity	Fineness (a.p.), cm^2/g	Fe_2O_3, %
As received	2.41	2817	24.33
"Fine"	2.47	6061	19.87
"Medium"	2.60	1846	38.23
"Coarse"	2.92	1230	43.46
	Fly Ash B		
	Specific Gravity	Fineness (a.p.), cm^2/g	Fe_2O_3, %
As received	2.52	8,824	19.63
"Fine"	2.53	10.714	16.46
"Medium"	2.64	3,030	37.38
"Coarse"	3.02	1,846	53.35

This reversal of the relationship resulting in increasing specific gravity with increasing particle size is believed to reflect the differences in composition of the fractions, especially the increase in iron content with increasing particle size.

Author's Closure

Masatane Kokubu

Messrs. Abe, Nagataki and Tsukayama, based on results of experiments on concrete of equal compressive strength in which depths of neutralization with time were equal whether or not fly ash was used, have concluded that the depth of neutralization from the surface of suitably placed concrete exposed to the atmosphere is dependent on the quality of the concrete. In other words, they have concluded it is not necessary to restrict the use of fly ash in consideration of rusting of reinforcing steel in the case of suitably placed concrete.

Although only one variety of fly ash was used in this work, since the fly ashes marketed in Japan are all similar, it may be considered the test results are representative of Japanese commercial fly ash.

Since the test period of the above research is still short, it may not be proper to induce a decisive conclusion from the results. However, the author is in complete agreement with the conclusions of Messrs. Abe, Nagataki and Tsukayama and is looking forward with great expectation to the results of these tests which will be carried out for another 15 years.

The effective surface area of fly ash introduced by Dr. Sakurai is a factor which is thought to be useful in estimating the general outline of pozzolanic reactivity of fly ash by mineralogical means and his research work is of interest in this sense.

The author has heard with great interest Mr. Mather's discussion in relation to the particle size and specific gravity of fly ash and agrees with his opinion that when Fe_2O_3 contents of fly ashes differ the specific gravity of the coarser fly ash can be greater. Since the iron contents of Japanese fly ashes are much less than those of other countries, we were unaware of this point.

Supplementary Paper IV-7 Hydrated Phases after Reaction of Lime with "Pozzolanic" Materials or with Blast Furnace Slags*

Riccardo Sersale and Paolo Giordano Orsini*

Synopsis

Products of reaction between saturated lime solutions and several materials, natural or synthetic, have been studied with different experimental techniques for a better understanding of the hydraulic binders hydration process.

Natural glasses (true pozzolanas), artificial glasses (blast furnace slags, industrial or synthetic), zeolites (herschelite, analcite), volcanic tuffs (neapolitan yellow tuff, rhenish trass, which are zeolitized equivalents of the corresponding pozzolanas), have been considered.

Maximum amount of lime fixed by each material has been determined. Reaction products have been identified as follows:

1) Tobermorite-like calcium silicate hydrate and gehlenite hydrate from flegrean pozzolana. 2) Calcium silicate hydrate, tetracalcium aluminate and gehlenite, from neapolitan yellow tuff and rhenish trass. 3) Calcium silicate hydrate and gehlenite from zeolites. From herschelite also tetracalcium aluminate is produced. 4) Tetracalcium aluminate hydrate, calcium silicate, gehlenite and, probably, small amounts of hydrogarnets from blast furnace slags.

As it concerns the evolution of alumina contained in the reactants, an high content of Al_2O_3 and CaO favours hydrogarnet formation. An increase of silica, corresponding to medium contents of SiO_2 and Al_2O_3 favours gehlenite hydrate formation. Tetracalcium aluminate prevails when a silica rich glass, with small amounts of alumina, is used as reactant.

Identification of phases originated from different pozzolanic materials and from basic blast furnace granulated slags, after contact with lime, has been attempted by different investigators (1). It is well known, in fact, that composition, structure and relative abundance of new formed phases, influence technical behaviour of hydrated and hardened pastes.

In our Institute, emphasis has been given to the following topics:

—observation and identification of products;

—influence of reactants on the nature of hydrated phases;

—influence of environment, when reaction is carried either in excess liquid ("suspension") or in conditions comparable with practical use (paste).

In this note we shall refer on the whole of our experimental results and on their interpretation.

Pyroclastic Materials: Products of Reaction with Lime (Suspension)

Reaction between lime and the following pyroclastites, whose analyses are reported in Table 1, has been studied first:

1) Light pozzolana from Bacoli Naples, Italy; (2nd Flegrean volcanic period).
2) Dark pozzolana from Segni (Colli Albani volcanic region, Italy) (2).
3) Yellow neapolitan tuff from Ponti Rossi Naples, Italy; (2nd Flegrean volcanic period); zeolitized equivalent of flegrean pozzolana. Zeolite term prevailing in the groundmass is *herschelite* (3).

*Istituto Chimica Industriale, Fac. Ingegnerio, Università di Napoli, Napoli, Italy.

Table 1. *Chemical composition of pyroclastic materials examined (wt%; 105°C dry)*

	1	2	3	4
SiO_2	57.80	45.05	54.68	54.88
Al_2O_3 (+ TiO_2 + Mn_3O_4)	18.34	17.46	17.70	19.55
Fe_2O_3	2.20	8.73	3.82	3.00
FeO	2.14	2.34	0.29	0.30
CaO	3.15	10.02	3.66	3.37
MgO	0.97	4.10	0.95	1.63
K_2O	8.05	6.67	6.38	4.78
Na_2O	4.18	2.22	3.43	4.23
H_2O (T > 110°C)	3.75	3.90	9.11	8.28
	100.58	100.49	100.02	100.02

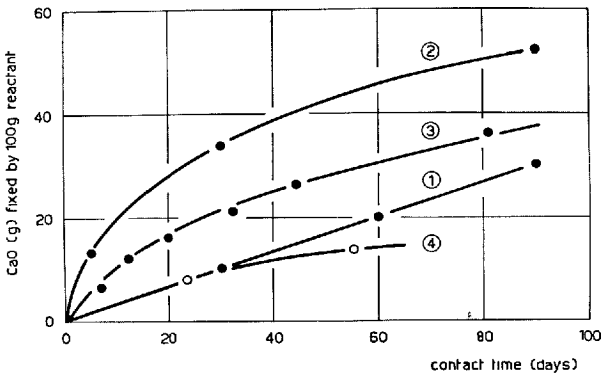

Fig. 1. *Lime uptake of four pyroclastites:*
1) Light pozzolana.
2) Dark pozzolana.
3) Yellow tuff.
4) Trass.

4) Trass from Krets (Andernach/Rhein, Germany; zeolite term prevailing in the groundmass is *analcite* (4).

These products, powdered to 230 mesh, have been kept in contact, at room temperature, with a saturated lime solution according to a standard procedure already described in a previous work (5). The plot of their lime uptake has been reported in Fig. 1.

In Table 2 are reported hydration products identified with X-ray diffraction analysis; interplanar spacings correspond to the strongest reflections.

Examination of this table confirms the existence of

Table 2. *Products of reaction between pyroclastic materials (see Table I) and saturated lime solution. Interplanar spacings (Å) correspond to strongest reflections.*

	1	2	3	4
C–S–H	3.05	3.07	3.05	3.05
	1.83			1.82
	1.66			1.67
C_2ASH_8	12.62		12.51	12.61
	4.18		4.20	4.24
	2.80		2.88	
C_4AH_{13}			7.92	7.92
			2.88	2.92
			2.79	2.80
$C_3A.\ CaCO_3.\ 12H_2O$		3.80		
		7.67		
C_3AS_3–C_3AH_6		2.02		
		5.05		

a relation between products and reactants. In the case of pozzolanic glass, considering that the excess liquid phase cancels any variation of total alkalinity (due to alkalies released from pyroclastic materials in correspondence with the lime uptake), it can be deduced that, alumina content being constant, an increase of silica favours formation of gehlenite hydrate. This result will be confirmed in the case of synthetic glasses. In the case of zeolitized glasses (numbers 3 and 4 in Table 2) contemporary presence of gehlenite and tetracalcium aluminate among hydration products cannot be explained on the basis of initial composition only (see analyses 1 and 3 in Table 2) but must be ascribed to the role of alkalies, even in dilute solutions. The larger amounts of alkalies released from zeolitic groundmass lowers lime concentration and favours formation of gehlenite hydrate.

Zeolites: Products of Reaction with Lime (Suspension)

Two zeolites, namely *Herschelite* from Aci Castello (Catania, Italy) and *Analcite* from Nova Scotia (North America) (8) have been studied with the same experimental procedure already described. These minerals have been selected because the zeolitic terms are prevailing in the volcanic tuffs previously investigated (yellow neapolitan tuff and Rhenish trass).

Chemical composition of specimens studied has been reported in Table 3. Products after reaction with lime, as identified by X-ray diffraction analysis, have been reported in Table 4. The plot of lime uptake, in Fig. 2, shows that amount and rate of lime fixation are higher for herschelite than for analcite in accordance with the corresponding results already reported in Fig. 1 concerning yellow neapolitan tuff and Rhenish trass.

Considering the nature of hydrated phases, obtained by action of saturated lime solution on pure minerals (Table 4), experimental conditions being equal, no tetracalcium aluminate was formed from analcite. This can be ascribed either to the higher silica content in analcite or to a larger amount of alkalies liberated which reduces lime concentration in equilibrium solution.

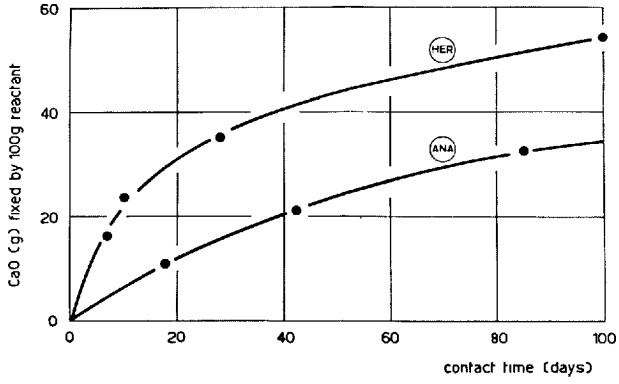

Fig. 2. *Lime uptake of two zeolites: Herschelite; Analcite.*

Table 3. *Chemical composition of zeolite minerals examined (wt%; 105°C dry)*

	Herschelite	Analcite
SiO_2	44.73	54.02
Al_2O_3	21.18	22.93
Fe_2O_3	tr.	0.32
FeO	—	—
CaO	1.65	0.78
MgO	—	—
K_2O	8.04	—
Na_2O	4.53	13.05
H_2O (T > 110°C)	19.62	8.40
	99.75	99.50

Table 4. *Products of reaction between pyroclastic materials (see table 3) and saturated lime solution*

	Herschelite	Analcite
C–S–H	3.04	3.06
	1.82	1.83
	1.65	1.64
C_4AH_{13}	8.00	
	2.89	
	2.69	
C_2ASH_8	12.40	12.51
	4.12	4.25
	2.89	2.92

Synthetic Glasses: Products of Reaction with Lime (Suspension).

With the same experimental procedure already described, hydration reaction of synthetic glasses with different composition, has been followed in order to ascertain the influence of chemical composition of reactants (only major constituents are involved in this case) on the nature of products.

Attention has been particularly given to the evolution of alumina contained in reactants, which is difficult to follow because reaction products are not easily identifiable (9).

Three synthetic glasses have been prepared, with composition predisposed to formation of different hydration products (10).

Composition of different glasses has been reported in Table 5. Specimen No. 5, with mol ratio SiO_2: Al_2O_3: CaO = 1: 1: 1 is predisposed to formation of gehlenite hydrate, after fixation of suitable amount of "external" lime (lime from the $Ca(OH)_2$ saturated solution).

Specimen No. 6, with a mol ratio 0. 4: 1: 2 is predisposed to formation of terms in the isomorphous series *Grossularite*-Tricalcium aluminate hexahydrate (C_3AS_3-C_3AH_6) (11), after fixation of suitable amount of "external" lime. Specimen No. 7, with mol ratio 0. 6: 1: 3. 5, is predisposed to the formation of terms in the same series, even without fixation of lime.

Lime uptake of three synthetic glass specimens is plotted in Fig. 3. Hydrated phases, identified by means

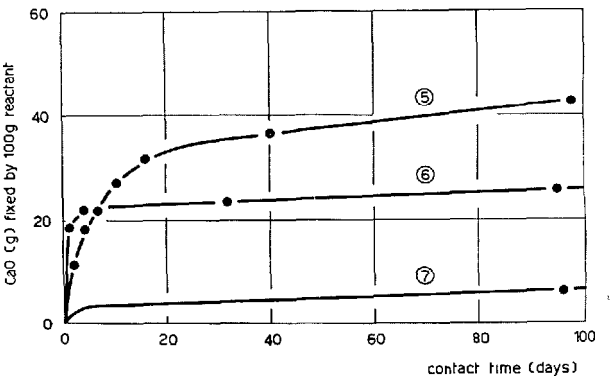

Fig. 3. *Lime uptake of three synthetic glasses with different mol ratio* SiO_2: Al_2O_3: CaO
5) 1 : 1 : 1
6) 0.4 : 1 : 1
7) 0.6 : 1 : 3.5

Table 5. *Chemical composition of synthetic glasses examined (wt%; 105°C dry)*

	5	6	7
SiO_2	27.35	10.01	10.70
Al_2O_3	47.40	45.43	30.82
CaO	25.05	44.53	58.40
	99.80	99.97	99.92

Table 6. *Hydration products of synthetic glasses (see table 5) after contact with water*

	6	7
C_2ASH_8	12.44	
	4.16	
	2.87	
	2.49	
C_3AS_3–C_3AH_6	5.04	5.04
	2.76	2.76
	2.26	2.26
	2.01	2.01
$Al(OH)_3$ minor amounts	4.85	
	4.37	
	4.32	

Table 7. *Products of reaction between synthetic glasses (see Table 5) and saturated lime solution*

	5	6
C–S–H minor amounts	3.09	
	2.76	
	1.81	
C_2ASH_8	12.44	
	4.16	
	2.87	
	2.49	
C_3AS_3–C_3AH_6	5.04	5.04
	2.76	2.76
	2.26	2.26
	2.01	2.01

of X-ray diffraction analysis, formed after reaction of different specimens with water or with saturated lime solution, have been reported respectively in Tables 6 and 7.

Absence of tetracalcium aluminate among these products confirms its formation from alumina poor reactants only (12). High alumina content, on the contrary, causes formation of gehlenite hydrate if silica is correspondingly high, or hydrogarnets if, even at room temperature, lime content (constitutional or external) is high.

Blast Furnace Slags: Products of Reaction with Lime (Suspension)

Three blast furnace specimen have been considered. Their composition is reported in Table 8.

As these specimen show equal lime uptake, only one plot has been reported in Fig. 4.

Compounds, identified by X-ray diffraction analysis, formed during reaction of each specimen with lime are shown in Table 9.

Table 8. *Chemical composition of blast furnace slags examined (wt%; 105°C dry)*

	8	9	10
SiO_2	32.23	29.94	28.57
Al_2O_3 (+TiO_2)	14.27	15.43	16.18
Fe_2O_3	1.87	1.64	5.12
Mn_3O_4	0.21	0.79	0.44
CaO	41.63	41.31	36.29
MgO	5.17	6.51	7.91
Stot	0.86	1.24	1.39
Na_2O	2.09	0.66	0.50
K_2O	0.62	0.73	0.20
H_2O (T > 110°C)	1.03	1.34	3.37
	99.98	99.59	99.97

Table 9. *Products of reaction between blast furnace slags (see Table 8) and saturated lime solution*

	8	9	10
C–S–H	3.04	3.04	3.04
	1.82	1.83	1.83
C_4AH_{13}	7.83	7.74	7.79
	3.89	3.87	3.89
	2.86		2.87

Among these products, besides tobermorite like calcium silicate hydrate and tetracalcium aluminate hydrate, it has been possible to identify some terms in the hydrogarnet isomorphous series (reflections at 3.37 to 3.39 Å and 2.29 to 2.30 Å). Presence of these terms cannot be taken as certain. In any case their presence is not fundamental in order to explain the well known resistance of blast furnace cements to sulphate rich waters.

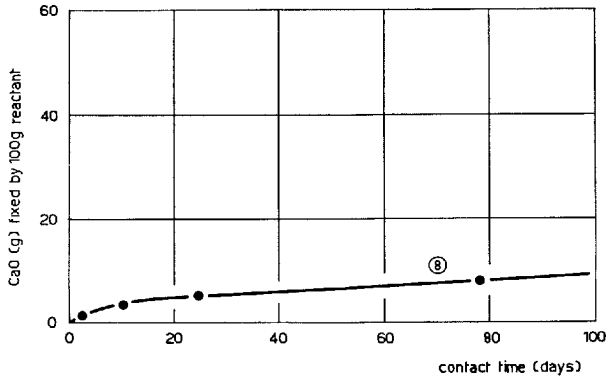

Fig. 4. *Lime uptake of blast furnace slags. Composition reported in Table 8.*

Pyroclastic Materials: Products of Reaction with Lime (Paste)

Same specimen reported in Table 2, mixed with 40% lime, have been used to prepare pastes. 40% water was added to the dry mixture. Homogeneous paste has been formed under pressure into small cylinders. These, after setting in a CO_2 free atmosphere, have been kept at room temperature, under distilled and reboiled water. After five years the core of cylinders, isolated after crushing, has been ground avoiding atmospheric contamination. The powder has been analysed with the methods of X-ray diffraction.

Substances identified have been reported in Table 10. Gehlenite hydrate and calcium aluminate (or

Table 10. *Products of reaction between pyroclastic materials (see Table 1) and lime, in paste.*

	1	2	3	4
C–S–H	3.04	2.96	3.02	3.01
	2.75	2.78	2.78	2.79
	1.82	1.83	1.82	1.86
C_2ASH_8	12.69	12.10	12.39	12.37
	4.19	2.87	4.20	4.21
	2.87		2.49	
C_4AH_{13}				7.82
				3.83
				2.79
$C_3A \cdot CaCO_3 \cdot 12H_2O$	7.69	7.43	7.56	
	(2.87)	3.76	3.77	
		2.78	2.78	

Value in parenthesis is common to other phases.

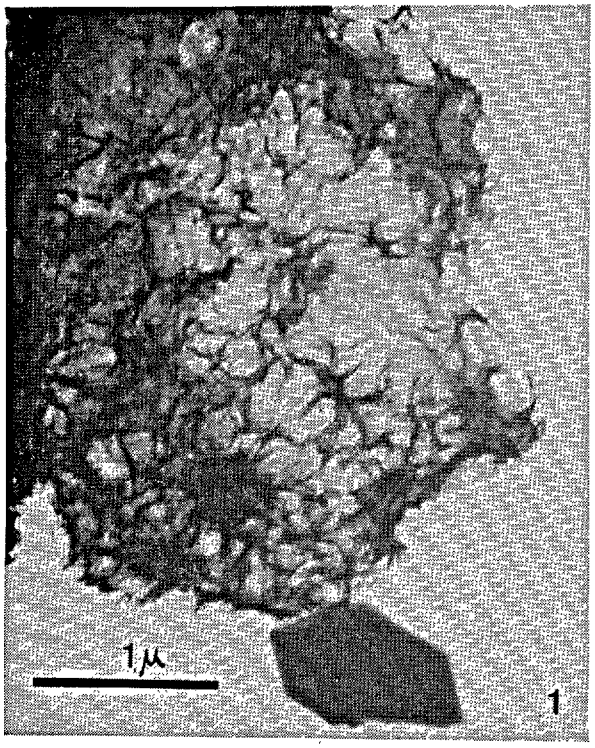

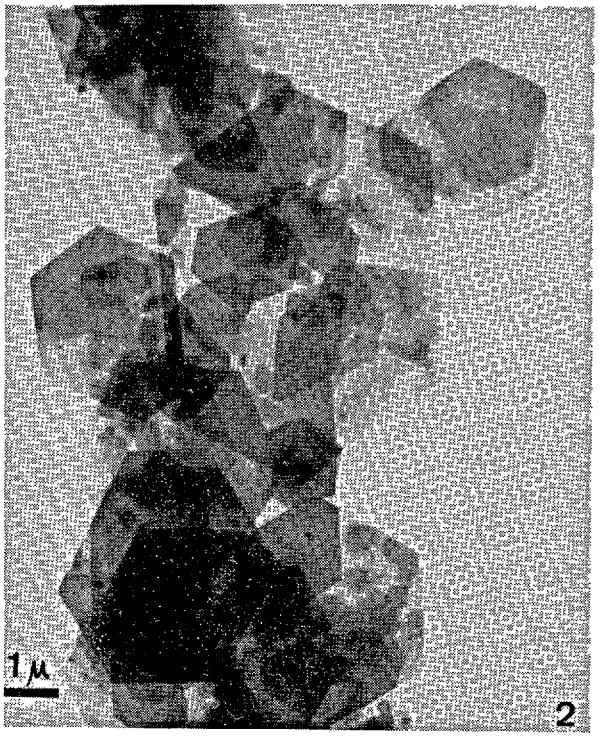

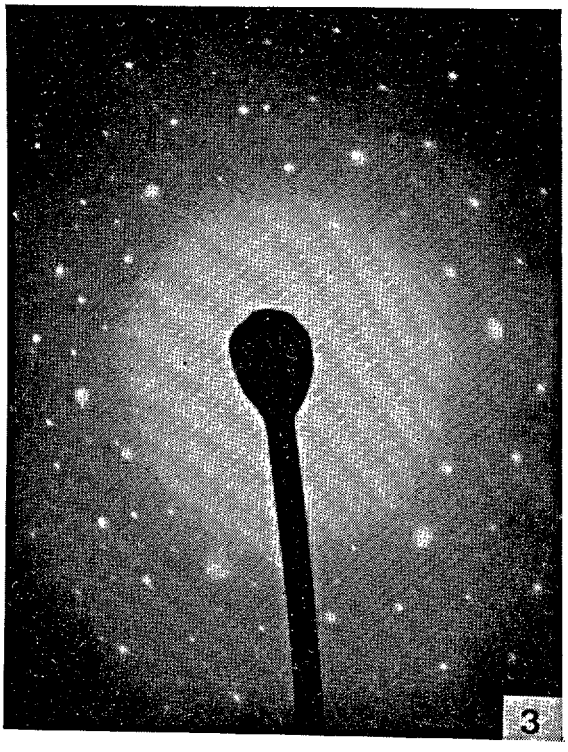

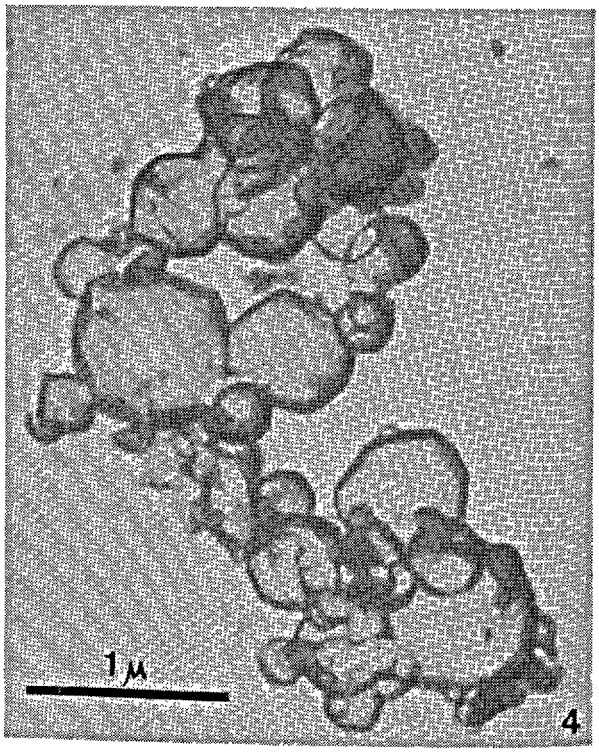

Photo 1

1. Crinkly foils of tobermorite.
2. Hexagonal thin plates of gehlenite and of tetracalcium aluminate hydrate
3. E.D. pattern from a plate in 2.
4. Isometric crystals of hydrogarnet series term (from synthetic glass No. 6) Carbon replica.

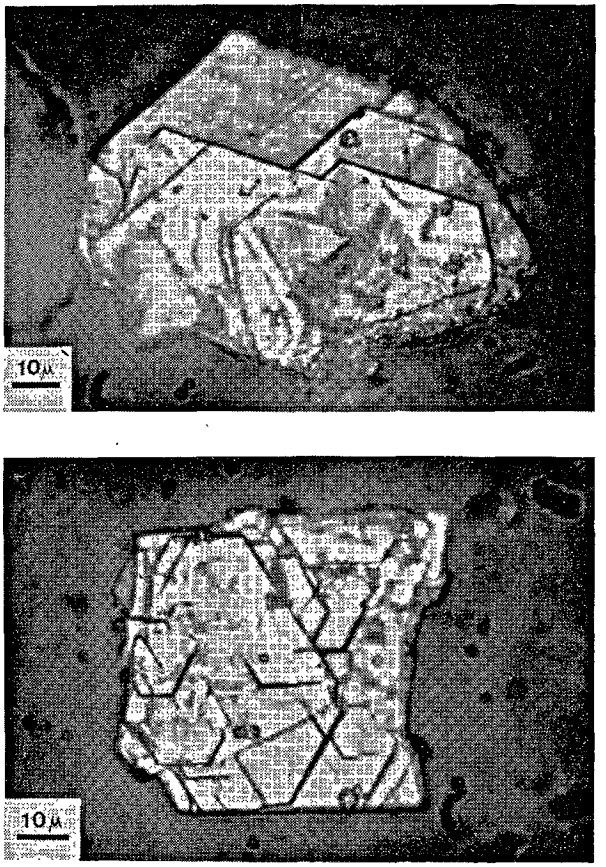

Photo 2
1. Hexagonal plates from pozzolana (reaction in paste)
2. Hexagonal plates from yellow tuff (reaction in paste)

carbo-aluminate) hydrate are constantly present besides tobermorite.

Products in Table 2, corresponding to reaction in suspension, when compared to products in Table 10, corresponding to reaction in paste, reveal a close analogy between the two types of reaction, at least within the limits of specimens and of conditions experienced. A slight difference concerns pozzolanic glasses. Pozzolana from Segni, for instance, reacting in paste has given also gehlenite hydrate (6). This confirms that the relative amounts of gehlenite and calcium aluminate (or carbo-aluminate) besides chemical composition of reacting glass, is influenced by lime concentration in the environment.

Besides X-ray diffraction analysis, specimens have been subjected to microscope observation and to differential thermal analysis. Results obtained with these techniques are reported hereafter.

Microscope Examinations

Micrographs in Photo 1 show solid phase obtained after reaction (in suspension) of some material investigated, with lime solution.

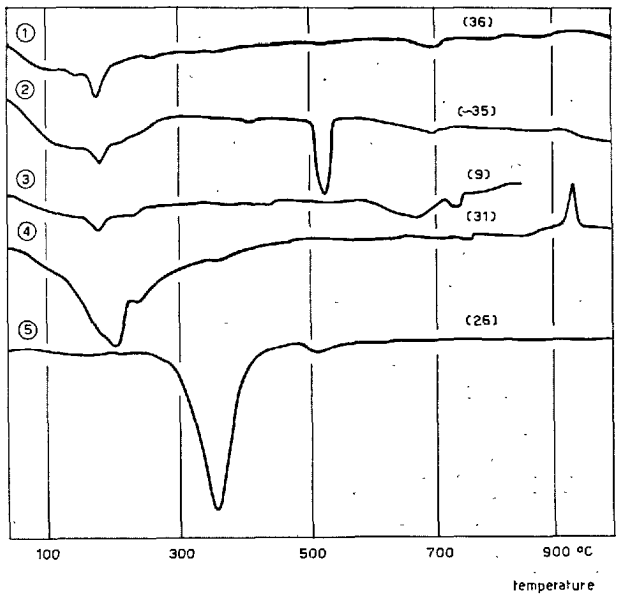

Fig. 5. *Differential thermal curves of:*
1) Pozzolana after reaction in suspension
2) Pozzolana after reaction in paste
3) Blast furnace slag.
4) Synthetic glass No. 5 (Table 5).
5)Synthetic glass No. 6 (Table 5).

Micrograph No. 1 shows crinkly foils of tobermorite, other forms of tobermorite have been observed elsewhere (14).

Micrograph No. 2 shows hexagonal crystals with basal lattice constant (see electron diffraction pattern No. 3) $a_0 = 5.73$ Å (15). This value being common to both gehlenite and tetracalcium aluminate, further discrimination between these compounds, with X-ray analysis, is necessary.

Micrograph No. 4 shows monometric crystals of terms in hydrogarnet series produced after reaction of synthetic glass No. 6 with lime.

In Photo 2, optical micrographs concerning pastes from pozzolana (Bacoli) and from yellow tuff (Naples) are reported. In both cases, No. 5 and No. 6, packed hexagonal plates can be observed at high magnification. Specimens were obtained evaporating on the glass slide a drop of xylene suspension containing small fragment of pastes. Dispersion of fragments in xylene has been achieved by treatment with ultra-acoustic waves.

Differential Thermal Analysis

Differential thermal curves were obtained with a

model D-200 Deltatherm analyzer (Technical Equipment Corp. U.S.A.) (16) on different reaction products and are reported in Fig. 5.

Curves No. 1 and No. 2 refer to pozzolana (Segni, No. 2 in Table 1) after reaction with lime, in suspension and in paste respectively (Numbers between brackets indicate the amount of lime taken up). Their profiles are much alike if the peak at 550°C, due to non combined lime, is not taken in consideration. The most significant thermal effect is the exothermic one with maximum between 150°C and 200°C due to free water and fundamentally to tobermorite. A weaker endothermic effect follows slightly over 200°C, probably due to tetracalcium aluminate (or carboaluminate).

No peak corresponding to terms in the series of hydrogarnets has been found between 300°C and 400°C. Curve No. 3 refers to a blast furnace slag (specimen No. 8 in Table 8) which has taken up around 10% lime. A first endothermic effect due to water, tobermorite and ettringite (17) between 150°C and 200°C is followed by a peak, at 200°C to 220°C, due to tetracalcium aluminate hydrate (or to its solid solution with sulphate). Also in this curve thermal effects due to hydrogarnets between 300°C and 400°C are absent.

Curve No. 4 refers to synthetic glass No. 5 in Table 5. Besides an endothermic effect with maximum at 200°C due to free water, tobermorite and mainly to gehlenite hydrate and a weaker effect with maximum around 225°C probably due to tetracalcium aluminate hydrate (or to the corresponding carbo-aluminate), a third effect, exothermic, with maximum between 900°C and 950°C can be attributed to the crystallization of gehlenite.

Curve 5 of glass No. 6 (Table 5) shows typical shape of terms of hydrogarnet series, considering that endothermic peak at 550°C is due to lime.

Results obtained with differential thermal analysis thus correspond to those obtained with X-ray diffraction and microscope methods.

Conclusions

The whole of experimental results points out that:
—Reactivity of zeolitized glasses (volcanic tuffs) to comparable to that of pozzolanic glasses (true pozzolanas).
—Stable hydrates originated after reaction of all pyroclastic products examined are: tobermorite-like calcium silicate, gehlenite, tetracalcium aluminate (or the corresponding carboaluminate). Formation of one or two alumina containing compounds depends upon composition of reactant and is influenced by the amount of alkalies released in correspondence with lime take up.
—Formation of tetracalcium aluminate hydrate is favoured when alumina poor glasses are used as reactant. Alumina rich reactants produce gehlenite or hydrogarnets. Formation of former or latter product depends upon silica and lime content of reactants.
—Among hydration products of blast furnace slags tobermorite and tetracalcium aluminate have been recognized. Neither gehlenite nor hydrogarnet have been detected via X-ray diffraction so that alumina in reactant slag seems to be in excess to the quantity engaged for reaction products. The problem of alumina collocation after reaction needs thus further investigation.
—Stable hydrated phases after reaction with saturated lime solution are qualitatively the same as obtained after reaction in pasty state. Reaction in suspension has, obviously, an higher rate and an higher degree of completeness, while crystals, better shaped and with regular faces, are more suitable for identification.

References

1. J. Jambor, "Hydratationsprodukte der Kalk-Puzzolan-Bindemittel", Zement-Kalk-Gips **5**, 177 (1963).
   U. Ludwig, H. E. Schwiete, "Kalkbindung und Neubildungen bei den Trass-Kalk-Reaktionen", Zement-Kalk-Gips **10**, 421 (1963).
   H. G. Smolczyk, "Die Hydratationsprodukte huttensandreicher Zemente", Zement-Kalk-Gips **5**, 258 (1965).
2. R. Sersale, "Precisazioni sulla Costituzione della Pozzolana di Segni", Ind. Ital. Cem. **32**, 169 (1962).
3. R. Sersale, "Genesi e Costituzione del Tufo Giallo Napoletano", Rend.Acc.Sc.fis. e mat., Napoli, [4], **25**, 181 (1958).
4. R. Sersale and R. Aiello, "Genesi, Costituzione e Reattività del "Trass" Renano", Atti Acc.Sc.fis. e mat., Napoli, [3], **5**, No. 1, 1 (1965).
5. R. Sersale and P. G. Orsini, "Idratazione e Trasformazione della Loppa d'Alto Forno per Contatto con Soluzione Satura di Idrossido di Calcio", Atti Acc.Sc.fis. e mat., Napoli, [3], **9**, 1 (1960).
6. R. Sersale, P. G. Orsini and R. Aiello, "Sulla Costituzione dei Prodotti di Reazione di talune Zeoliti e Piroclastiti, con Soluzione Satura di Calce", Nota II. "Roentgenografia dei soli di di Neo-formazione", Rend. Acc.Naz. Lincei, Cl.Sci. fis.mat. e nat. [8], **36**, No. 2, 162 (1964).
7. The chemistry of cements, vol. II (Academic Press Inc., London, England, and New York, USA 1964), edited by H.F.W. Taylor. See chapter by R. Turriziani entitled "Aspects of the chemistry of

pozzolanas".
8. R. Sersale, V. Sabatelli, "Sull'attivita 'Pozzolanica' delle Zeoliti", Nota I. "Reattività dell'Herschelite con Soluzione d'Idrossido di Calcio", Rend.Acc. Sc.fis. e mat., Napoli, [4], **27**, 263 (1960). Nota II. "Reattività dell'Analcime con Soluzione d'Idrossido di Calcio", ibidem, [4], **28**, 45 (1961).
9. R. Sersale, P. G. Orsini and R. Aiello, "Analogie Struttu rali fra Alluminato Tetracalcico Idrato e Gehlenite Idrata", Rend. Acc. Naz. Lincei, Cl. Sc.fis.mat. e nat. **34**, 274 (1963).
10. V. Amicarelli, R. Sersale and V. Sabatelli, "Sull'Idratazione di Vetri del Sistema SiO_2–Al_2O_3–CaO. Influenza della Composizione Iniziale sulla Natura delle Fasi Idrate", Rend.Acc.Naz. Lincei, Cl.Sc.fis. mat. e nat. **40**, 858 (1966).
11. G. Malquori, R. Sersale and R. Aiello, "Sul Comportamento della Gehlenite Idrata in Soluzione Satura d'Idrossido di Calcio", Rend.Acc.Naz. Lincei, Cl. Sc.fis.mat. e nat. **36**, 3 (1964).
12. F. W. Locher, "Hydraulic properties and hydration of glasses of the system CaO–Al_2O_3–SiO_2", Proc. 4th Int. Symp. Chem. Cement, Washington 1960, N.B.S. Monograph 43, vol. II (1962).
13. R. Sersale, P. Vitagliano, R. Aiello, V. Amicarelli, "Sulla Presenza di Idrogranati fra i Prodotti d'Idratazione in Presenza di Calce, delle Loppe d'Alto Forno Granulate", Ric. Sci. **7**, 600 (1966).
14. Å. Grudemo, "The microstructure of cement gel phases", Trans. Royal Inst. Techn. No. 242. Stockholm (1965).
15. R. Sersale, P. G. Orsini and R. Aiello, "Sulla Costituzione dei Prodotti di Reazione di Talune Zeoliti e Piroclastiti, con Soluzione Satura di Calce", Nota I. "Microscopia Elettronica dei Cristalli di Habitus Esagonale", Rend.Acc.Naz. Lincei **34**, 537 (1963).
16. W. W. Wendlandt, "Thermal methods of analysis", p. 200 (Intersicence Publ., New York, USA (1964).
17. V. S. Ramachandran, R. F. Feldman and P. J. Sereda, "Application of differential thermal analysis in cement research", N.R.C. Div. Building Res., paper No. 249. Ottawa (Canada).

Supplementary Paper IV-17 Study of Reactions between CaO or $3CaO \cdot SiO_2$ and β-$2CaO \cdot SiO_2$ and Power Station Fly Ashes under Hydrothermal Conditions

Zdeněk Šauman*

Synopsis

The author investigated the reactivity of ten types of power station fly ashes with CaO in a 3:1 ratio (by weight) under hydrothermal conditions—175°C/8 atm. The character of hydrosilicate, as well as of further reaction components formed during the 16-hour hydrothermal process, was determined. The relative quantity of the tobermoritic phase was compared for the individual fly ash mixtures with the achieved strength values of porous silicate shapes; in the majority of cases an unambiguous relationship was found.

It was shown on the basis of C_3S—fly ash reactions in various weight ratios that the maximum quantity of the tobermoritic phase was formed in the case of equal weights of both starting components. The reaction of β-C_2S with fly ash was stopped at its very beginning due to coating layers of silica gel around the β-C_2S grains or their agglomerations.

The author also studied the reaction of mullite with CaO or C_3S and β-C_2S during the autoclave process, as most investigated fly ashes contain a significant quantity of mullite. In the first case is formed exclusively the hydrogarnet phase, in the second phase the hydrogarnet component with a smaller quantity of tobermorite. It was found that the main factor influencing the hydraulic properties of fly ashes is, beside α-quartz, the quantity and composition of the glass phase, but above all the SiO_2 content.

Introduction

The manufacturing technology of porous concretes employing power station fly ash as one of the main raw materials has until recently been based on empirical methods which made it in certain cases difficult to explain anomalies directly during the production of these materials. The reaction of various forms of SiO_2 with CaO under hydrothermal conditions has received relatively very great attention from many authors during the last 10 or 15 years. The field of the reactions of fly ashes of different compositions with CaO in the course of autoclaving has, however, with regard the narrowly specialized subject, been given substantially less attention. Déry (1) studied the reaction products formed in the autoclaved mixture fly ash—lime exclusively with the aid of X-ray diffraction. Apart from other components, hillebrandite was determined.

Butt, Majer and Varshal (2) studied the phases formed during the autoclaving of fly ashes with lime at 8 and 16 atm. Apart from hydrosilicate components, belonging to the tobermorite group, there was determined at a pressure of 16 atm. a phase corresponding with its composition to the mineral plazolite—$3CaO \cdot Al_2O_3 \cdot 2SiO_2 \cdot 2H_2O$.

Tun Soo-lee and Wang Yan-mou (3) investigated, chiefly by means of X-rays, the formation and character of the tobermoritic phase in mixtures fly ash—lime during the autoclave process.

The reactions of clinker minerals, mainly $3CaO \cdot SiO_2$ and β-$2CaO \cdot SiO_2$, with quartz sand in the course of the autoclave process were systematically studied by Bozhenov and Kavalerova (4), Kravchenko et al. (5) and further workers.

Volkov et al. (6) found by comparing the ratios of starting mixtures of alite and β-C_2S with quartz that maximum strength values were obtained—with the application of sand having a specific surface around 3,000 cm^2/g—for the case of a 50% addition of alite and a 20% addition of belite to the sand at 8 atm.

Šauman (7) studied the anomalous hydration of β-C_2S in a mixture with quartz sand of a different

*Research Institute of Building Materials, Brno, Czechoslovakia.

fineness during the autoclave process.

Relatively little attention was given to the reaction of fly ashes with clinker minerals.

Watt and Thorne (8) compared the mineralogical composition of 14 British fly ashes with compressive strength data for their mixtures with lime stored at normal temperature.

Simons and Jeffery (9) and Minnick (10) studied the relationship between the hydraulic properties of power station fly ashes and their mineralogical composition and pointed out the importance of the composition of their glass fraction and of further minerals. The last author determined especially the influence of the carbon content and the ignition loss of fly ashes on their pozzolana activities.

Šauman (11) compared compressive strength values for porous concrete blocks and found that the main factor influencing the strength of these materials is above all tobermorite and the CSH(I) phase, respectively.

Owing to the fact that already in a previous paper (12) of the author it was not possible to find at least an approximate correlation between the obtained strength values of porous concretes with specific surface, granulometric composition, fly ash porosity, combustible fraction content, etc., further factors were studied which could contribute to the evaluation of power station fly ash and which could also explain at least partly some anomalous phenomena in the technology of porous concrete production.

Experimental

Methods and Materials

X-ray Investigations

For the identification of reaction components, as well as for the quantitative determination of the appropriate phases was employed the Müller "Mikro 111" X-ray diffractograph, in all cases with CuKα radiation. The samples were comminuted, passed through a 400 mesh sieve and mixed with 10% $Mg(OH)_2$ used as an internal standard. The lines 2.36 Å or 4.76 Å were used.

To prevent preferential orientation a similar technique of preparation was employed as described by Copeland and Bragg (13).

As far as other physical methods are concerned, use was made of electron microscopy including diffraction, differential thermal analysis, and in certain cases infrared spectral analysis (Perkin-Elmer Infracord 337 instrument).

Chemical Methods

For the determination of uncombined $Ca(OH)_2$ was used the modified Franke method (14). The soluble SiO_2 form was determined by means of the method (15) derived from the Steopoe process.

Synthetic Preparation of Clinker Minerals and Mullite

The preparation of $3CaO \cdot SiO_2$ and β-$2CaO \cdot SiO_2$ has been described in detail by the author in another paper (16).

For studying the reactivity of mullite with CaO and clinker minerals, two samples of the mullite phase were used which were obtained by two different processes: by a solid state reaction from starting materials and by electromelting. In the first case the content of corundum did not exceed 1%, in the second one 2 to 3% in addition to a certain amount of glass phase.

The specific surface of the mullite sample prepared by solid-phase reactions was 4,760 cm^2/g and that of the mullite sample prepared by electromelting was 4,530 cm^2/g. The corresponding values for C_3S were 3,670 cm^2/g and for β-C_2S 3,160 cm^2/g. In all cases the Blaine method was used.

Selection of Starting Materials—Fly Ashes

For the actual experiments was employed a total of 10 types of Czechoslovak fly ashes from 10 Czechoslovak electric power stations, 8 samples being brown coal fly ashes and 2 hard coal fly ashes. The complete chemical analysis is given in Table 1.

The specific surface was determined by the Blaine method, as well as with the aid of the BET instrument. The results are presented in Table 2.

At the same time an X-ray analysis of the given fly ash types was carried out.

Each fly ash contains a fluctuating quantity of α-quartz and mullite, besides a very small quantity of haematite. The ER sample contains anatase and the TI fly ash a smaller quantity of anatase and rutile.

Actual Preparation of Samples for Hydration

To the mixtures intended for the hydrothermal process was added approximately 25% boiled distilled water and using a mould cubes with a 10 mm edge were prepared.

Instead of an autoclave small pressure vessels with an inner diameter of 25 mm were employed; these

Table 1.

Determined component in %	Type of fly ash									
	NO	ER	BR	MA	NH	TR†	MO	PC†	PH	TI
H_2O	0.26	0.66	0.63	0.18	0.09	0.36	0.16	0.07	0.19	1.96
C	1.47	5.46	6.08	2.00	8.80	7.55	1.10	2.61	4.86	6.41
SiO_2	53.88	52.45	51.60	54.10	46.98	51.41	52.09	57.55	52.88	39.62
Al_2O_3	28.16	23.42	28.67	30.35	24.55	24.70	27.14	24.99	28.90	31.20
Fe_2O_3	6.44	7.37	6.40	6.70	9.89	6.26	10.90	6.15	6.42	7.27
TiO_2	0.66	1.72	1.43	1.62	0.86	0.94	1.21	1.41	1.78	6.48
CaO	5.39	5.77	2.05	2.25	5.04	4.25	4.96	3.70	3.90	5.60
MgO	0.90	1.15	0.98	0.99	0.80	1.02	trace	0.42	trace	trace
K_2O	2.34	0.95	1.53	1.56	2.71	2.94	1.68	3.05	1.28	0.56
Na_2O	0.10	0.12	0.29	0.28	0.53	0.57	0.49	0.34	0.21	0.26
SO_3	1.08	0.65	0.54	0.26	0.29	0.26	0.20	0.14	0.16	2.34
S^{--}	0.05	trace	trace	trace	trace	trace	trace	trace	trace	trace

† hard coal fly ash

Table 2.

Designation of fly ash	Specific surface (cm^2/g) measured by method	
	Blaine	BET
NO	3,700	71,000
ER	2,940	194,000
BR	3,490	118,000
MA	3,600	101,000
NH	2,640	40,000
TR	3,900	78,000
MO	2,700	23,000
PC	2,400	8,000
PH	4,900	94,000
TI	6,400	62,000

were filled to 1/3 of their content with boiled distilled water. Immediately above the water level was placed on a holder the cube of the investigated sample. The pressure vessels of each sample series were placed in an electrically heated thermostat with forced air circulation, usually at a temperature of 175°C (8 atm.), for different periods of time. It took about 30 minutes to reach the given temperature. After the termination of the hydrothermal process, the samples were dried at 100°C in a nitrogen stream for a period of 7 to 8 hours.

Results and Discussions

Hydrothermal Reaction of Power Station Fly Ashes with CaO

The individual fly ash samples were homogenized with CaO in a 3: 1 weight ratio and autoclaved in the form of a moistened mixture in the small pressure vessels for a period of 16 hours at 175°C.

Evaluation of X-ray Measurements

In mixtures with NO fly ash it was possible to determine considerable quantities of tobermorite, since the interference lines of this phase ~11.3, 3.07, 2.97 Å and others exhibit a considerable degree of intensity. Also interferences corresponding to still unreacted α-quartz and mullite can be seen. Visible are also relatively intense diffractions of the hydrogarnet component which are not overlapped by lines of the remaining components—5.04, 2.75, 2.25, 2.00 Å, and others.

The mixture with the ER fly ash already contains a significantly smaller quantity of the tobermoritic component, besides the hydrogarnet phase and the still unreacted components—α-quartz and mullite. The quantity of the hydrogarnet component is somewhat smaller than in the previous case.

In mixtures with the BR fly ash the tobermorite content has again increased approximately to the value of the content of the first mixture. Here can again be seen interferences of the hydrogarnet component and of the still unreacted α-quartz and mullite.

Conditions are similar also in the mixture with the MA fly ash; the differences lie exclusively in the integral intensity of the individual diffractions.

The mixture with the NH fly ash contains approximately the same quantity of the hydrogarnet and of the tobermoritic phase.

The diffraction diagram of the mixture with the TR fly ash exhibits a similar character. In accordance with the integral intensity of the tobermorite diffractions, the content of this component is somewhat lower.

In the mixture with the MO fly ash a steep increase of the tobermorite content was noted; on the other hand, a very small quantity of the hydrogarnet phase is present.

In the next mixture with the PC fly ash was observed a very considerable quantity of tobermorite, besides a relatively small quantity of the hydrogarnet phase.

In the mixture with the PH fly ash is apparent a considerably lower tobermorite content (in relation to the previous case).

It seems that the altogether smallest quantity of tobermorite is present in the mixture with the TI fly ash, since the diffractions ~11.3 Å, 2.98 Å, and others display a minimum degree of integral intensity.

Fig. 1 presents X-ray diffraction diagrams of CaO mixtures with the fly ashes NO, ER, PC and TI.

In the studied mixtures no significant quantities of still uncombined $Ca(OH)_2$ were determined.

Apart from the above experiments, also autoclaving of the fly ashes in the identical weight ratio with CaO was carried out using shorter periods of time—2, 4 and 8 hours at 175°C/8 atm. In the investigated mixtures of the individual fly ashes was formed already in the course of a 2—4 hour reaction a significant quantity of the tobermoritic phase. With a prolonged hydration period (8 hour reaction) the content of this phase rises steeply and reaches in the majority of cases its maximum value, since the difference in the tobermorite content in mixtures autoclaved for 8 and 16 hours is very small.

Apart from tobermorite is formed as the first reaction component the hydrogarnet phase. The formation of this component takes place during the first periods of the hydrothermal process, since already after a 2 hour reaction this phase can be identified reliably by X-ray methods. It can be assumed that this component exhibits a composition which approaches the formula $3CaO \cdot Al_2O_3 \cdot SiO_4 \cdot 4H_2O$. It is, however, possible to speak only about an approximate composition, since in connection with the Fe-ions in the fly ash glass the hydrogarnet phase can contain also a small quantity of iron; its composition is given by the general formula: $C_3A_{1-n}F_nS_xH_{6-2x}$.

It appears that the reactivity during the first two hours of the hydrothermal process is, among other things, influenced by the value of the specific surface; after the above period of two hours, this influence becomes apparently considerably smaller.

Differential Thermal Analysis

The DTA-curves do not exhibit significant anomalies and are therefore not presented here.

Electron Microscopy

The conclusions derived from electron microscopy and electron diffraction correspond to the data obtained by means of micro-structural X-ray measurements. After a 4 hour hydrothermal period it is already possible to determine the typical platy tobermorite crystals, the number of which reaches its maximum after 8 or 16 hours of the reaction. Fig. 2 presents an electronmicrograph of a mixture with the TR fly ash autoclaved for 8 hours.

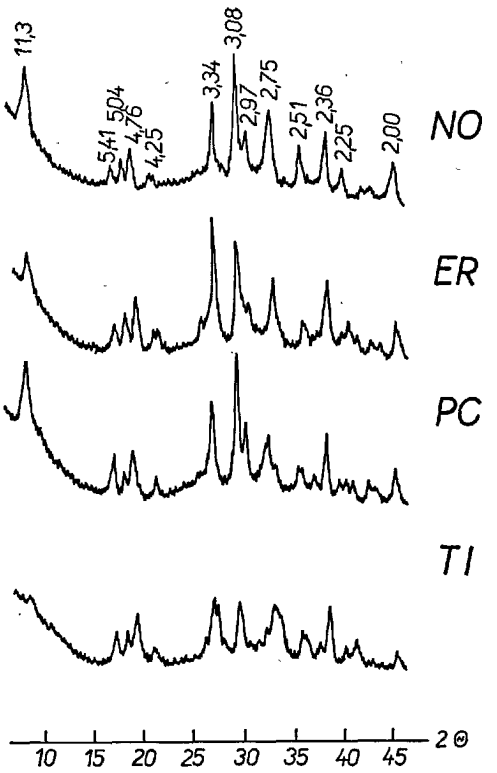

Fig. 1. *X-ray diffraction diagrams of power station fly ash samples with CaO (3: 1) after 16 hours of hydrothermal process (175° C/8 atm.).*

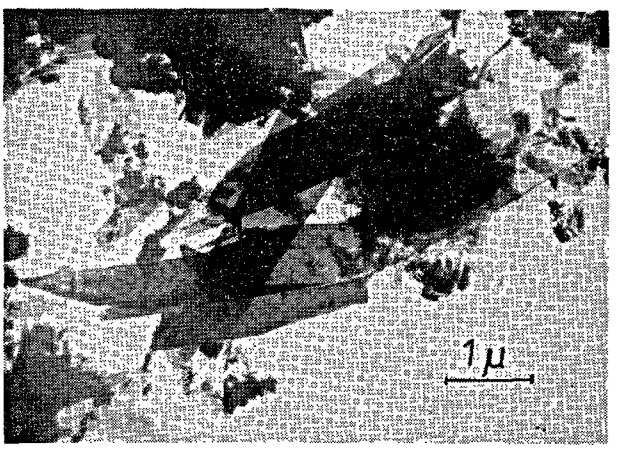

Fig. 2. *Electronmicrograph of the mixture TR fly ash with CaO (3: 1) after 8 hours of hydrothermal process (175°C).*

Evaluation of Fly Ashes with Regard to Formed Tobermoritic Phase

For assessing the quality of the investigated fly ashes will be mainly considered their capability of forming in the course of the hydrothermal process with CaO the maximum quantity of the binding component—the tobermoritic material. It was found on

the basis of preliminary experiments that the actual tobermoritic phase, 11.3 Å—tobermorite, exhibits the highest binding qualities. For the above reasons were prepared mixtures fly ash—lime (3 parts to 1 part) which were autoclaved in the form of moistened samples in small pressure vessels for a period of 12 hours. Each mixture was autoclaved twice, in order to obtain more objective results. The approximate relative quantity of the tobermoritic phase was expressed by the ratio of the integral intensity values of the relevant diffractions of tobermorite and brucite employed as the internal standard: $\frac{I \sim 11.3\,Å}{I\,4.76\,Å}$. This data was compared with the determined strength values for test porous silicate shapes (cubes with a 10 cm edge) prepared from the individual fly ashes (75 parts fly ash, 22 parts CaO, 3 parts $CaSO_4 \cdot 2H_2O$ and a small quantity of Al-powder). The technology of the laboratory production of porous silicate shapes was controlled in such a way as to obtain a minimum scatter of density values. This density fluctuated for the individual types between 680 and 700 kg/m³.

It is readily apparent from the diagram in Fig. 3 that the values of the relative quantity of the tobermoritic phase correspond approximately to the compressive strength data. Only minor differences can be seen for fly ashes BR and PH.

Reaction of Fly Ashes with $3CaO \cdot SiO_2$ under Hydrothermal Conditions

For a more detailed study and clarification of the reactivity of C_3S and β-C_2S with fly ashes was employed the mixture of three fly ash samples—TR, ER and MO. Moistened mixtures were prepared with graded C_3S quantities, as shown in Table 3. Hydration was carried out at 175°C for a period of 16 hours and 72 hours.

X-ray Evaluation

16 Hour Reaction

Mixture 1 contains a very small quantity of the tobermoritic phase with regard to the diffuse interference line ~3.06 Å. The quantity of this component is already substantially higher in mixture 2. This contains a certain quantity of CSH(I) apart from a small quantity of tobermorite, since the ~11.3 Å diffraction almost merges with the background of the X-ray record. In mixture 3 the ~11.3 Å diffraction is already highly pronounced, the further characteristic tobermorite line (2.98 Å) also exhibits a higher degree of intensity.

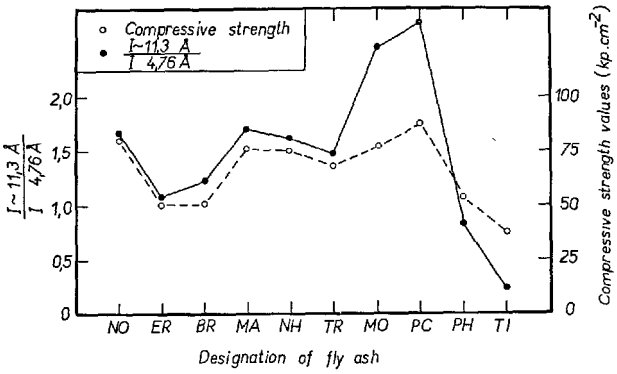

Fig. 3. *Comparison of the relative tobermorite quantity with the achieved compressive strength values.*

Table 3.

Mixture number	Quantity of $3CaO \cdot SiO_2$ or β-$2CaO \cdot SiO_2$ (%)	Quantity of fly ash (%)
1	10	90
2	20	80
3	30	70
4	50	50
5	70	30
6	80	20
7	90	10

In mixture 4 can again be noted an increase of the diffractions which are typical for tobermorite (11.3, 3.08, 2.98, 2.81 Å, and others). The lower intensity diffractions (2.73, 2.23, 1.97 Å) probably correspond to the hydrogarnet phase.

The X-ray diffraction diagram of mixture 5 already exhibits a decreased intensity of tobermorite diffractions. Here is also apparent the presence of a certain quantity of the $C_2SH(A)$ phase. On the basis of the 4.98, 3.25, 2.73 Å and even other diffraction it is possible to assume the formation of the hydrogarnet component.

In the remaining mixtures the contents of the tobermoritic phase are rapidly reduced, whereas the $C_2SH(A)$ quantity is increased. It is possible to determine also a small quantity of unhydrated C_3S besides C_3S-hydrate and liberated $Ca(OH)_2$. The presence of the hydrogarnet phase can be identified only with great difficulties, since the most interferences are overlapped by lines corresponding to the starting minerals or to the newly formed products.

72 Hour Reaction

Mixture 1 contains a very small quantity of the tobermorite group phase. In the other mixtures the tobermorite contents again grow, the maximum being reached in mixture 4, in which there is in the unhydrated, original form the same weight ratio of C_3S and fly ash. The presence of the hydrogarnet phase is indicated by the lines 4.98, 4.33, 2.73 Å, etc. The next

mixture 5 contains already a certain quantity of the $C_2SH(A)$ phase, besides the tobermoritic hydrogarnet component and the uncombined $Ca(OH)_2$ and undecomposed C_3S.

In the previous and also in the following mixtures the tobermorite content rapidly decreases and simultaneously the quantity of the $C_2SH(A)$ component grows. Apart from the liberated calcium hydroxide there is present also a very small quantity of still undecomposed C_3S and C_3S-hydrate.

A comparison with X-ray diffraction diagrams of mixtures hydrated for 16 hours brings out the fact that through further hydration the contents of CSH(I) and tobermorite are increased, besides an increased quantity of the $C_2SH(A)$ component. Conversely, in the course of the prolonged hydration (72 hours), the quantity of C_3S-hydrate and of the unhydrated C_3S fraction is reduced.

Based on the integral intensity degree of the diffraction ~11.3 Å of the tobermorite, it was possible to assess the relative content of this phase in the sample. By plotting along the vertical axis of the diagram the ratios of the integral intensity values $\frac{I \sim 11.3\ Å}{I\ 4.76\ Å}$ and along the horizontal axis C_3S data (%) in the original, unhydrated mixtures, it is possible to express at least theoretically the relative quantity of the tobermorite (Fig. 4).

The curve representing the relative quantity of the tobermorite exhibits in both cases a steep rise and reaches its maximum approximately for a 50% C_3S content in the original, unhydrated mixture.

Reaction of Fly Ashes with β-2CaO·SiO₂

Mixtures with a graded β-C_2S content were prepared by the same method.

During the 16 or 72 hour reaction, no more pronounced hydration of β-C_2S took place, and thus no hydrosilicate components were formed. This phenomenon was also observed with quartz sand of extreme fineness which was the subject of other papers published by the author (7, 17).

It was shown that in the course of hydrothermal reactions of β-C_2S with fly ash, very fine quartz sand (specific surface higher than 4,500 cm^2/g), blast furnace slag, quartz glass, or even other materials with a significant SiO_2 content, the silica gel is liberated and coats the β-C_2S grains or their agglomerations with a protective layer and reduces or almost completely inhibits its own hydration of β-C_2S.

In order to study in greater detail the reactions between β-C_2S and power station fly ash, mixtures of power station fly ash with β-C_2S were hydrated in a weight ratio 65: 35. Samples in the form of moistened mixtures were hydrated for periods of 2, 4, 8, 16, 24, 72 hours and 7 days at 175°C/8 atm. It was found that not even during the 7 day hydrothermal process there occurs a more pronounced hydration of β-C_2S, since the integral intensity of the β-C_2S diffractions exhibits an almost unchanged intensity with respect to the original, unhydrated mixture.

Also the content of the soluble SiO_2 form is increased only slightly in the course of the hydrothermal process, as is clearly shown by the reaction mechanism diagram (Fig. 5). This graphical representation of the approximate reaction mechanism indicates an almost unchanging integral intensity value of the line ~3.04 — 3.06 Å which seems to represent only the β-C_2S diffraction. The slight increase is probably caused by an almost negligible rise of the integral intensity value of this line owing to the formation of a slight quantity of the tobermoritic phase.

It is not without interest that it was found during investigations of the hydration of mixtures β-C_2S—power station fly ash that a quantity of 8—10% power station fly ash, added to β-dicalciumsilicate, prevents its own hydration, and thus also inhibits the formation of binding hydrosilicate components of the tobermorite group. On the other hand, however, an addition of a small quantity of calcium hydroxide (1—3%) to the unhydrated mixture β-C_2S—fly ash causes its own hydration of β-dicalciumsilicate, since the formed silica gel is bound by the present calcium hydroxide to the tobermoritic material. Similar effects were obtained with a small addition of C_3S or the phase $C_2SH(A)$.

Reaction of Mullite with Ca(OH)₂ under Hydrothermal Conditions

Owing to the fact that the employed power station fly ashes contain apart from quartz also a certain quantity of mullite, the reactivity of the latter was investigated with calcium hydroxide and finally with the main clinker minerals—$3CaO \cdot SiO_2$ and β-$2CaO \cdot SiO_2$.

In order to clarify more closely the above type of reactions, mixtures were prepared with graded quantities of both components. The selected weight ratios of the mixtures mullite: CaO are summarized in Table 4.

Apart from a synthetically prepared mullite sample M-S also mullite M-B was used; the latter was obtained by electromelting. Hydration was again carried

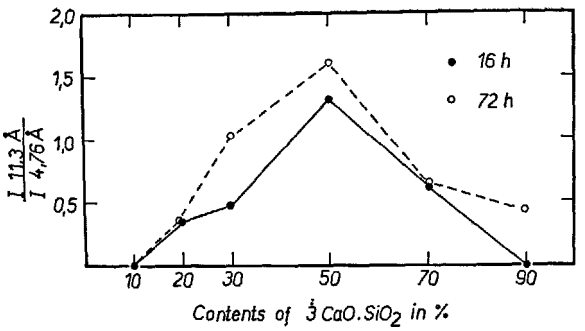

Fig. 4. *Graphical representation of the relative quantity of tobermoritic material against C_3S content.*

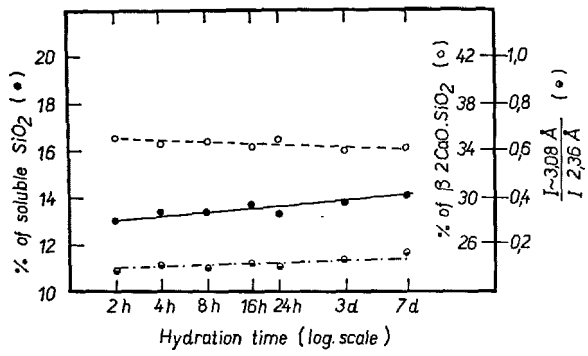

Fig. 5. *Representation of reaction mechanism power station fly ash –β-2CaO·SiO₂ (175° C/8 atm.).*

Table 4.

Mixture number	Ratio of CaO (C_3S of β-C_2S): Mullite
1	1:1
2	1:2
3	1:3
4	1:5
5	1:10
6	2:1
7	3:1
8	5:1
9	10:1

out in the form of a moistened paste for periods of 16 and 72 hours at 175°C.

Evaluation of X-ray Measurements

Reaction of Mullite M-B with CaO

The X-ray diffraction diagram of mixture 1 shows relatively intense diffractions of still unreacted $Ca(OH)_2$ besides diffractions 5.04, 2.75, 2.00 Å and others which correspond to the hydrogarnet phase.

In the X-ray diffraction diagram of mixture 2 the diffractions of the hydrogarnet phase display a somewhat lower intensity.

With an increasing quantity of mullite and a decreasing CaO content, the hydrogarnet phase is reduced. In mixture 5 only a very small quantity of this component is present. Similar results were obtained for the mixtures 6—9; the quantity of unreacted $Ca(OH)_2$ increases and the content of the hydrogarnet component is reduced.

The series of samples hydrated for a period of 72 hours contains larger quantities of the hydrogarnet component—with respect to the previous samples. The contents of free $Ca(OH)_2$ and mullite have been somewhat reduced.

Reaction of Mullite M-S with CaO

In the X-ray diffraction diagram of mixture 1 can readily be seen very intense diffractions of the hydrogarnet component 5.03, 4.36, 2.75, 2.25, 2.00 Å and others. The diffractions of unreacted mullite exhibit a relatively very low intensity. Interferences of $Ca(OH)_2$ are no longer apparent, in contrast to the identical mixture with mullite M-B which still contains a significant quantity of this phase.

In further mixtures the quantity of the hydrogarnet phase is gradually decreased, as was shown in the case of the mixtures 2 and 3; the content of unreacted lime does not, however, reach the limiting quantity which is essential for X-ray identification. Similarly also in the further mixtures the contents of the hydrogarnet component are reduced; the lowest quantity of the latter was recorded in the mixtures 5 and 9.

In the course of the 72 hour hydrothermal process the content of the hydrogarnet component is increased in all cases. The highest quantity of this component was again identified in the mixture with CaO in a 1:1 ratio.

It follows from the results of X-ray measurements that the largest quantity of the hydrogarnet phase is contained in mixtures with CaO in a 1:1 ratio in the course of a 72 hour reaction; when mullite M-S was employed, a significantly larger content was noted.

In Fig. 6 are reproduced X-ray diffraction diagrams of mixtures mullite—CaO in a 1:1 ratio after a 72 hour reaction.

Differential Thermal Analysis

The differential thermal analysis curves of mixtures with mullite M-B, autoclaved for 72 hours, are shown in Fig. 7. The thermogram of mixture 1 exhibits two crater-shaped peaks with maxima around 350° and 480°C, the latter corresponding to the decomposition of $Ca(OH)_2$. The peak at the lower temperature is caused by the decomposition of the hydrogarnet component. As can readily be seen from the slope of the difference curves of further reaction mixtures, the period corresponding to the hydrogarnet com-

ponents is gradually reduced, in the 1: 10 mixture it is an almost insignificant bending of the difference curve.

DTA curves of autoclaved mixtures with mullite M-S are of a similar character as has been observed for the case of the previous mixtures. In Fig. 8 are reproduced DTA curves of mixtures after 72 hours of hydration. The sample mullite: CaO = 1: 1 is characterized by a deep valley with a maximum around 360°C which corresponds to the hydrogarnet component. With an increasing mullite content, the content of this phase is rapidly reduced; the lowest quantity in all the studied mixtures can again be noted in the 1: 10 sample. The thermogram of the 3: 1 mixture exhibits two deep valleys with maxima around 340°C and 520°C, the first of which corresponds to the decomposition of the hydrogarnet phase and the second to $Ca(OH)_2$. With an increasing CaO content in the original, unhydrated mixture, the quantity of the hydrogarnet component decreases and the $Ca(OH)_2$ content increases.

From the above observations also follows a substantially lower reactivity of mullite M-B with CaO under the employed experimental conditions.

Reaction Mullite M-S—$3CaO \cdot SiO_2$ Evaluation of X-ray Measurements

16 Hour Reaction Period

Mixture 1 is characterized by intensive diffractions of still unreacted mullite besides relatively pronounced diffractions of the hydrogarnet phase—4.99, 3.26, 3.05, 2.73, 2.60, 2.50, 2.40, 2.23, 1.98 Å and others.

It may not be without interest that a certain quantity of tobermorite is present, i.e. on the basis of diffractions 11.3, 2.98, 2.81 Å and others. Mixture 2 also contains a significant quantity of the hydrogarnet phase besides a smaller quantity of tobermorite. The quantity of both components does not differ too much with respect to the previous case.

In mixture 3 can be observed a reduction of the contents of the hydrogarnet phase and tobermorite. Conditions are similar in the next two mixtures—4 and 5. In the X-ray diffraction diagram of mixture 6 can be seen tobermorite diffractions of a low intensity, beside interferences of the hydrogarnet component.

The X-ray diffraction diagram of mixture 7 is characterized by already less intensive diffractions of the tobermoritic phase, conversely the interferences corresponding to the hydrogarnet component exhibit an increased degree of intensity. The mixture contains also a smaller quantity of the $C_2SH(A)$ phase on the basis of the interferences 4.22, 3.90, 3.54, 3.27 Å and

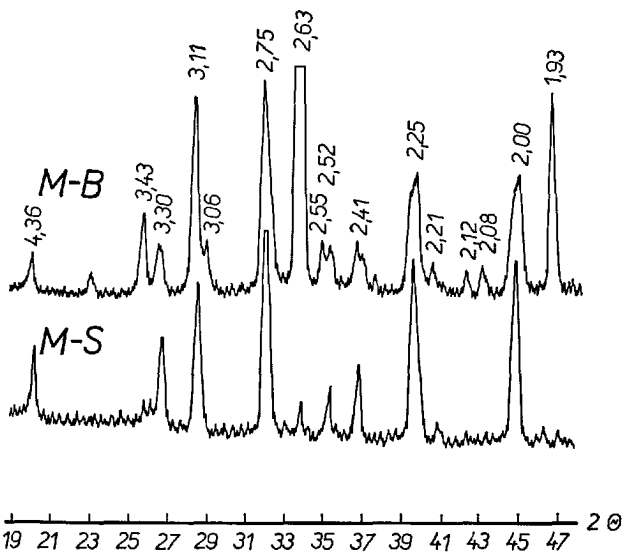

Fig. 6. *X-ray diffraction diagrams of mixtures mullite-CaO (1: 1) after a 72 hour hydrothermal process.*

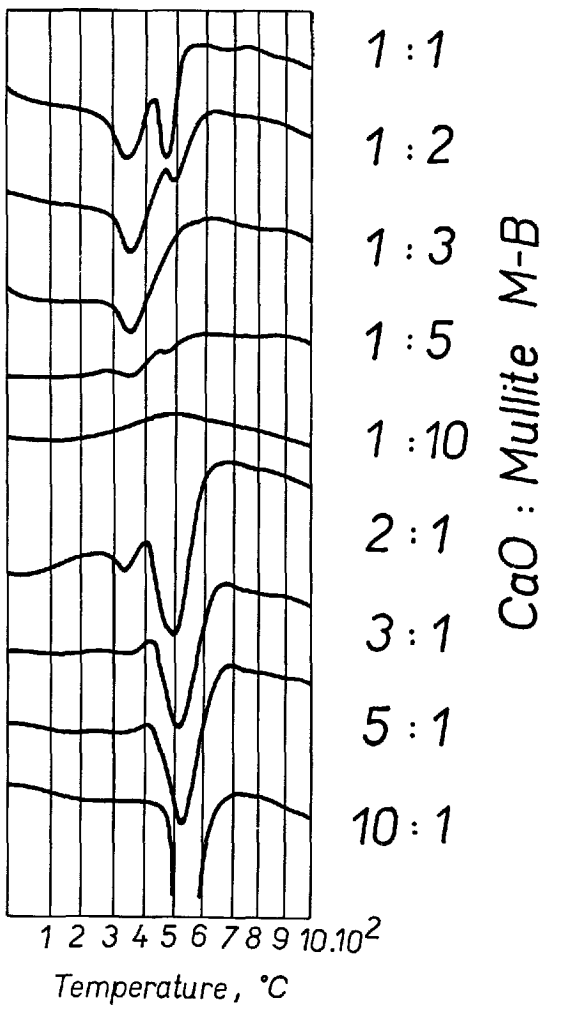

Fig. 7. *DTA curves of the mixtures mullite M-B with CaO; 72 hours/175°C.*

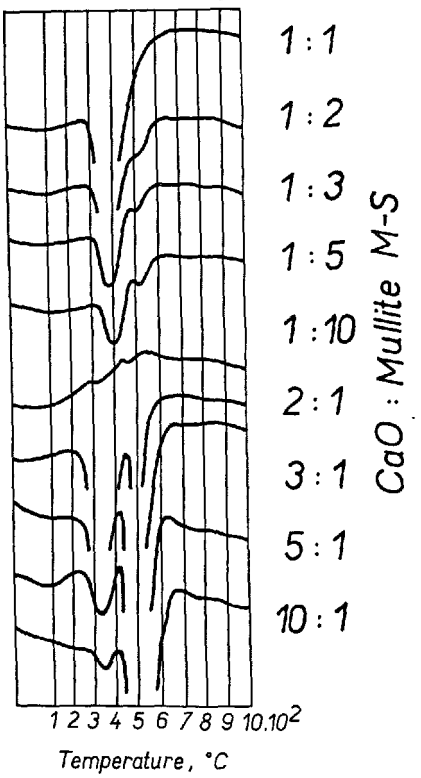

Fig. 8. *DTA curves of the mixtures mullite M-S with CaO; 72 hours/175°C.*

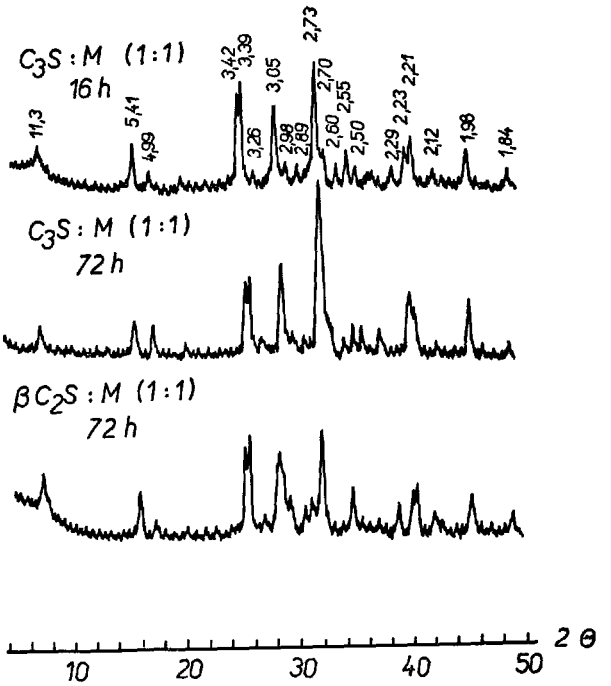

Fig. 9. *X-ray diffraction diagrams of mixtures—3CaO·SiO₂ or β-2CaO·SiO₂ with mullite.*

others.

In the next mixture of mullite with C_3S (1 : 5), the content of the $C_2SH(A)$ phase has risen rapidly; at the same time can be noted a certain quantity of unreacted $Ca(OH)_2$. The content of the hydrogarnet phase has been somewhat reduced. In the X-ray diffraction diagram of mixture 9 can be seen very intensive $C_2SH(A)$ diffractions besides interferences of unreacted $Ca(OH)_2$. The sample contains a small quantity of the hydrogarnet component and of the unhydrated C_3S fraction, besides a small quantity of C_3S-hydrate.

72 Hour Hydrothermal Reaction

Mixture 1 contains a considerable quantity of the hydrogarnet phase which is significantly larger than in the identical mixture hydrated for 16 hours. Apart from a more pronounced tobermorite quantity, there are also present unreacted mullite and a very small quantity of the $C_2SH(A)$ phase.

The maximum content of the hydrogarnet component can readily be seen in mixture 2. In mixture 3 and in the next mixtures 4 and 5, the quantity of the hydrogarnet component decreases rapidly, and simultaneously there is an increase in the contents of the $C_2SH(A)$ component and uncombined calcium hydroxide, besides a small quantity of C_3S-hydrate. The presence of tobermorite can also be noted in mixture 3, in the remaining mixtures the tobermorite quantity is below the limit essential for X-ray determinations.

Mixture 6 contained besides a significant quantity of tobermorite the hydrogarnet phase and a considerable quantity of unreacted mullite. In the next sample 7 it is no longer possible to identify quite positively tobermorite, the content of the hydrogarnet component has been rapidly reduced. The reduction of the quantities of the above reaction components takes place in further mixtures 8 and 9.

Fig. 9 shows X-ray diffraction diagrams of mixture 1 after 16 and 72 hours of hydration.

Differential Thermal Analysis

The DTA curves show endothermal peaks within the temperature range 180°–600°C corresponding to the decomposition of tobermorite, and hydrogarnet phase eventually to that of other components ($Ca(OH)_2$, $C_2SH(A)$).

Reaction Mullite—β-2CaO·SiO₂

Evaluation of X-ray Measurements

In the course of the 16 hour reaction in the mixtures

1 and 2 to 5 none of their own hydration of β-C_2S takes place, and thus no formation of the tobermoritic and hydrogarnet phases can be observed, since the hydration of dicalciumsilicate is suppressed as a consequence of protective layers around the β-C_2S grains or their agglomerations. Only through the addition of 2—3% C_3S or 1—2% CaO to the starting mixture mullite—β-C_2S, or by prolonging the hydration period to 72 hours, there occurs the hydration of β-C_2S and the formation of the tobermoritic and hydrogarnet phases. In the first case this is the consequense of binding the formed silica gel with $Ca(OH)_2$ to the tobermoritic material, in the second case this is due to the ageing of the protective gel layers and thus to an increased diffusion of water molecules to the actual β-C_2S particles.

In Fig. 9 is shown the X-ray diffraction diagram for mixture 1 after 72 hours of hydration.

The DTA curves are of a similar nature as has been observed for the mixtures mullite—C_3S.

Determination of Composition of Hydrogarnet Phase

To an approximate composition at least of the hydrogarnet components were prepared $3CaO \cdot Al_2O_3$ glasses with a graded quantity of SiO_2 (0.5, 1.0, 1.5 and 2.0 mol.). Glass samples were autoclaved at 218°C for a period of 5 hours and after drying and comminution, the process was further repeated another five times.

The obtained values for the edge (a) of the elementary cell approach data published by Locher (18). It was found on the basis of the values thus obtained that the hydrogarnet phase formed by the reaction between mullite and CaO corresponds basically to the component $3CaO \cdot Al_2O_3 \cdot SiO_2 \cdot 4H_2O$, in contrast to the phase formed by the reaction of mullite with C_3S or β-C_2S the composition of which corresponds approximately to the formula $3CaO \cdot Al_2O_3 \cdot 1.5SiO_2 \cdot 3H_2O$.

Influence of Hydrogarnet Phase on Obtained Strength Values

From the moistened mixture of mullite M-S with CaO in a 1 : 1 ratio test cubes with a 20 mm edge were prepared; these were autoclaved at 175°C for a period of 16 hours. It was found that the test cubes practically do not exhibit more pronounced compressive strength values. It can thus be assumed that the hydrogarnet phase (C_3ASH_4) exerts no significant influence on the compressive strength values of porous silicate shapes made from power station fly ash and lime.

Determination of Quantity and Character of Glass Phase of Power Station Fly Ashes

On the basis of a qualitative and semi-quantitative X-ray analysis of the individual fly ashes, as well as with regard to the results in quantity and type of the hydrosilicate and hydrogarnet phases, there can be assumed a considerable influence of the actual petrographic composition of the fly ashes on the character of hydrothermal reactions with CaO. For this reason it appeared essential to carry out a quantitative X-ray determination of the main crystalline components—mullite, α-quartz, haematite, anatase and rutile, and to determine the quantity and character of the glass phase of the fly ashes. The results of the X-ray determinations are summarized in Table 5.

The α-quartz content in the studied fly ashes fluctuates between 4.7% NH and 12.6% ER. Also the mullite content exhibits a considerably wide range: 2.0% NO—29.3% MA.

On the basis of the X-ray determination of both major and minor mineralogical components and from data contained in the overall chemical analysis was calculated the probable composition of the glass phase of the individual fly ashes (Table 6). The glass of the MA fly ash contains the highest quantity of SiO_2, whereas the lowest SiO_2 content was observed in the glass of the fly ash TI. The greatest Al_2O_3 quantity is present in the glass phase of fly ash NO, whereas conversely the lowest Al_2O_3 content was noted in the glass of the fly ash MA.

The knowledge of the SiO_2 quantity in the glass phase of the fly ashes makes it possible to carry out a comparison of the compressive strength values of porous silicate shapes with a glass SiO_2 content. It follows from the enclosed graphical representation (Fig. 10) that there exists in almost all cases a certain proportionality between the compressive strength values and data about the SiO_2 content in the glass. This proportionality is somewhat less pronounced in the case of comparing the contents of glass SiO_2 and the quantity of α-quartz contained in the fly ashes, with the achieved strength values. Analogically it is possible to compare data about the relative quantity of the hydrogarnet phase with the Al_2O_3 content in the glass phase of the individual types of investigated fly ashes (Fig. 11). The relative quantity of the hydrogarnet phase is given by the ratio of the integral intensity of the diffractions $\frac{I \sim 2.75\,Å}{I\,2.36\,Å}$ and $\frac{I \sim 5.05\,Å}{I\,4.76\,Å}$. The numerical data in the numerator of both fractions

Table 5.

Designation of fly ash	α-quartz (%)	Mullite (%)	Anatase (%)	Rutile (%)	Haematite (%)	C (%)	Glass phase (%)
NO	7.9	2.0	—	—	4.6	1.47	84.0
ER	12.6	15.4	1.34	—	2.5	5.46	62.7
BR	10.1	22.9	—	—	3.2	6.08	57.7
MA	9.4	29.3	—	—	3.1	2.00	56.2
NH	4.7	9.4	—	—	3.6	8.80	73.5
TR	11.9	17.2	—	—	1.8	7.55	61.5
MO	7.0	22.9	—	—	5.3	1.10	63.7
PC	7.5	18.0	—	—	2.4	2.61	69.5
PH	5.9	23.3	—	—	1.7	4.86	64.2
TI	5.2	24.1	0.87	0.50	2.7	6.41	60.2

Table 6.

Designation of fly ash	Composition of the glass phase (%)									
	SiO_2	Al_2O_3	Fe_2O_3	TiO_2	CaO	MgO	K_2O	Na_2O	SO_3	S^{--}
NO	53.75	31.61	2.17	0.78	6.38	1.06	2.76	0.12	1.27	0.06
ER	57.08	19.86	7.83	0.61	9.27	1.85	1.53	0.19	1.74	trace
BR	61.16	21.34	5.59	2.50	3.57	1.72	2.67	0.50	0.94	trace
MA	64.69	16.53	6.40	2.87	3.99	1.77	2.76	0.50	0.46	trace
NH	53.59	24.07	8.51	1.16	6.82	1.08	3.66	0.72	0.39	trace
TR	56.41	20.10	7.26	1.52	6.92	1.65	4.78	0.92	0.43	trace
MO	60.87	16.86	8.82	1.90	7.82	trace	2.64	0.77	0.31	trace
PC	64.41	17.28	5.32	2.02	5.29	0.60	4.36	0.48	0.20	trace
PH	62.52	18.82	7.30	2.75	6.04	trace	1 98	0.32	0.25	trace
TI	46.03	23.20	7.63	8.53	9.35	trace	0.93	0.42	3.90	trace

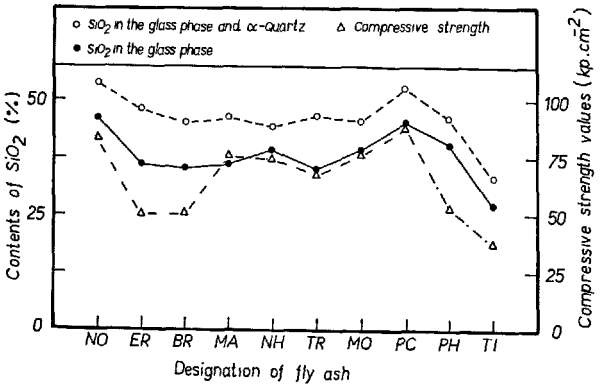

Fig. 10. *Comparison of compressive strength values of porous concrete shapes which contain α-quartz and SiO_2 in the glass phase.*

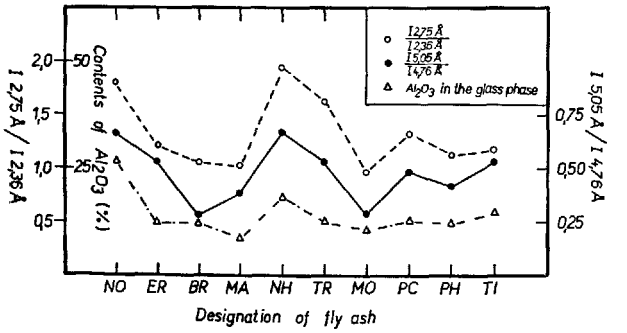

Fig. 11. *Comparison of the relative quantities of the hydrogarnet phase with the Al_2O_3 contents in the glass.*

correspond to the diffraction of the hydrogarnet component. The values of both ratios follow at least approximately the Al_2O_3 content data in the glass phase of the individual fly ashes. A more significant difference was found only in the case of the integral intensity value of diffraction 5.05 Å of the hydrogarnet component in the hydrated mixture of the MA fly ash.

It appears from the above that the main part of the hydrogarnet component was formed by the reaction of Al contained in the glass phase of the fly ash, with CaO. An already substantially smaller quantity of this component was formed by the hydrothermal reaction of mullite with lime.

Finally were prepared synthetically glasses which approach in their composition the glass phases of the studied fly ashes in which, however, the content of the individual components was graded in suitable ranges.

By autoclaving samples of synthetic glasses with CaO and by the determination of their reaction products, the influence of the individual components on the formation of tobermorite was investigated. It was found that apart from the SiO_2 quantity, which plays a basic part, a growing K_2O content exhibits a certain positive influence on the formation of tobermoritic material.

Conclusion

Reactions of 10 power station fly ashes with CaO in a 3: 1 weight ratio were studied at 175°C (8 atm.) for a period of 16 hours. Apart from tobermorite and probably the CSH(I) phase was determined the hydrogarnet phase—probably C_3ASH_4. By comparing the relative quantities of tobermorite with the achieved compressive strength values of porous silicate shapes was obtained a satisfactory tolerance which indicates that tobermorite exerts on the former a fundamental influence.

By the reaction of fly ash with C_3S is formed besides tobermorite again the hydrogarnet component; the maximum quantity of tobermorite was noted for a starting ratio of 1: 1. β-C_2S does not react with fly ash even in the course of a 7 day hydration as a consequence of protective coating layers of silica gel around the β-dicalciumsilicate grains or their agglomerations which prevent the diffusion of water molecules to the β-C_2S particles.

By the reaction of mullite with $Ca(OH)_2$ is formed the hydrogarnet component, the composition of which probably corresponds to the formula $3CaO \cdot Al_2O_3 \cdot SiO_2 \cdot 4H_2O$, whereas when C_3S or β-C_2S is used instead of CaO, there is formed, besides a smaller fraction of tobermorite, a hydrogarnet phase, whose composition corresponds probably to the formula $3CaO \cdot Al_2O_3 \cdot 1.5SiO_2 \cdot 3H_2O$. On the basis of comparisons of the SiO_2 content in the glass phase of the individual fly ashes with the achieved compressive strength values of porous silicate shapes, as well as with due regard to experiments with synthetically obtained glasses, there appear the content and character of the glass phase as the most important criteria for the assessment of power station fly ashes for the manufacture of porous concretes. It was shown simultaneously that the formed hydrogarnet phase does not significantly contribute to the achieved strength values of autoclaved building materials.

References

1. M. Déry, "X-ray analyses of Hungarian fly-ashes and binding materials with CaO produced on their basis" (in Hungarian), Építöanyag **13**, No. 6, 201–205 (1961).
2. Yu. M. Butt, A. A. Majer and B. G. Varshal, "Reaction between lime and fly-ashes in autoclave process at 8 and 16 atm." (in Russian), Sbornik trudov, "Rosniims", **17**, 55–64 (1960).
3. Tun Soo-lee and Wang Yan-mou, "The hydrated compounds of the lime-pulverized coal ash products" (in Chinese), Guisuanyan Xuebao **3**, No. 4, 242–254 (1964).
4. P. I. Bozhenov and V. I. Kavalerova, "About mutual reactions of C_3S and beta-C_2S with the additive of CaO and SiO_2 in hydrothermal processing" (in Russian), Dok. Mezvuzovskoj konf. po izuceniju avtokl. mater. i ich primeneniju v stroit., 187–194 (1959).
5. I. V. Kravchenko, A. M. Dmitriev, O. S. Volkov and D. M. Kheiker, "Hydration products of clinker minerals under the conditions of ultradeep oil wells" (in Russian), Trudy Niicementa, 35–50 (1960).
6. O. S. Volkov, O. I. Gracheva and D. M. Kheiker, "Study of clinker minerals reaction with quartz in autoclave process by the method of X-ray phase analysis" (in Russian), Trudy naučnoissled. inst. sljudy, asbestocem. izdelij II, 68–79, (1961).
7. Z. Šauman, "Hydration rate of dicalcium silicate in mixes with quartz under hydrothermal conditions", Proceed. of the Intern. Conference on Autoclaved Silicate Building Products (London 1965), p. 101–109 (The Society of Chemical Industry, London 1967).
8. J. D. Watt and D. J. Thorne, "Composition and puzzolanic properties of pulverised fuel ashes", J. appl. chem. **15**, No. 12, 585–604 (1965).
9. H. S. Simons and J. W. Jeffery, "An X-ray study of pulverised fuel ash", J. appl. chem. **15**, No. 12, 328–336 (1960).
10. L. J. Minnick, "Investigations relating to the use of fly-ash as puzzolanic material and as an admixture in portland cement concrete", Proceed. of the American Society for Testing Materials **54**, 1129–1164 (1954).
11. Z. Šauman, "Limy hydrosilicate components, an important factor influencing the strength of porous concrete" (in Czech), Stavivo **44**, No. 9, 336–340 (1966).
12. M. Matoušek and Z. Šauman, "Defining and determining of fly-ash influence on the properties of porous concrete" (in Czech), Research Report, Research Institute of Building Materials, Brno (1966).
13. L. E. Copeland and R. H. Bragg, "Preparations of samples for the geiger counter diffractometer", Bull. No. 92, PCA Research Dept. (Skokie).
14. E. E. Presler, S. Brunauer, D. L. Kantro and C. H. Weisse, "Determination of free calcium hydroxide contents of hydrated portland cements and calcium silicates", Anal. Chemistry **33**, No. 7, 877–882 (1961).
15. J. Jambor, "Chemical analyses in building engineering" (in Czech), p. 393 (SAV Bratislava, 1953).
16. Z. Šauman, "Study about the possibilities of synthet-

ical clinker minerals preparation and their X-ray identification in industrial clinkers of portland cement" (in Czech), Technologie silikátu III, 20–41 (1959)
17. Z. Šauman, "Anomalies in the hydration of beta-$2CaO \cdot SiO_2$ in quartz sand mixtures under hydrothermal conditions", Proceed. of Eight Conference on the Silicate Industry, p. 275–283 (Akadémiai Kiadó, Budapest, 1966).
18. F. W. Locher, "Hydraulic properties of glass materials rich in lime of $CaO–Al_2O_3–SiO_2$ system", (in German), p. 21. (Habilitation and Disertation Work, Bergakademie, Clausthal, 1959).

Supplementary Paper IV-63 Investigations on the Behaviour of Natural and Artificial Puzzolans

Hans E. Schwiete, P. Kastanja, Udo Ludwig and Peter A. Otto*

Synopsis

The chemical, mineralogical and physical data of 10 trasses from the Rhineland, 6 from Bavaria, one Austrian trass, 2 puzzolanas from Italy, a calcined molererde from Denmark, and 3 samples of granulated slags from power stations have been determined. The lime bonding and the resulting formation of hydrates has been investigated as well as the reactivity of these stone flours in mixtures with lime, portland- and slag cement.

All the natural puzzolanas were found to contain varying amounts of glassy groundmass which, in the case of the Rhine trasses, was 55 ~ 60% and for the Bavarian trasses constituted 62 ~ 67%. In the Austrian trass and the molererde the amorphous silica-rich groundmass shows signs of adopting the cristobalite lattice. The artificial puzzolanas, namely the slags from power stations, are almost completely glassy. The crystalline components of the puzzolanas have been identified microscopically and by X-rays.

Of the puzzolanas of volcanic origin the Bavarian trasses show the highest content of SiO_2, ranging from 59.2 ~ 66.0%, whilst the Italian puzzolana from Salone only contains 48.1%. The Al_2O_3 content varies between 13.8% for the Bavarian trass to 20.6% for the Italian puzzolana from Bacoli. Accompanying the low SiO_2 content, the puzzolana from Bacoli has the highest amounts of CaO and MgO, namely 10.0% and 5.7% respectively.

The highest loss by ignition was found for the Austrian trass with 15.3%; this sample contains 1.96% SO_3.

The molererde consisting of a mixture of silicified diatoms and clays contained 14.3% SiO_2 and 13.4% Al_2O_3. With smaller silica contents of 47.5 ~ 51.8%, the granulated slags contain larger amounts of Al_2O_3 (26.8 ~ 33.1%) and Fe_2O_3 (6.6 ~ 13.3%).

The specific weights of the puzzolanas have been determined and also their specific surfaces. Whilst the specific surfaces of natural puzzolanas lie between 0.7 and 2.7 m^2/g, according to Blaine, the values obtained by the adsorption method according to BET were between 4.4 and 95 m^2/g. These great differences in the areas are caused by partial alteration of the glassy fraction to zeolites and montmorillonite.

The surface areas of the granulated slags were found to be 0.5 m^2/g by Blaine's method but only 1.01 ~ 1.27 m^2/g by BET.

The combination with lime was determined in suspensions of puzzolanas and lime of which the W/S factor (water/solid) was 5. The greatest affinity for lime was shown by the molererde. After 90 days 591 mg CaO/g molererde were bonded. The lime combination of the artificial puzzolanas lies in the range of the Bavarian trasses and the Italian puzzolanas showing values between 228 and 283 mg CaO/g granulated slag.

After 90 days the newly-formed hydrates in the residues of these samples were examined. CSH phases formed as well as C_4AH_{13} (tetracalcium aluminate), $C_3(A, F)S_nH_{6-2n}$, n = 0 – 3, (these are mixed crystals in the hydrogarnet series), and occasionally C_2ASH_8 (gehlenite hydrate). In addition the formation of $C_3(A, F)Cs_3H_{32}$ (ettringite) was observed for the sulphate-bearing Austrian trass. If extra sulphate was added ettringite and monosulphate hydrate formed from all the puzzolanas.

Investigations of the strengths of lime-rich cements (e.g. trass cement 30/70) showed that the contribution of the natural puzzolanas with a high specific surface (according to BET) is overshadowed in the early stages of hardening by the high requirement of water.

In contrast, for lime-poor bonding materials a contribution to the strength was observed even at an early stage, in particular if anhydrite was added.

If a granulated slag with a low specific surface (after BET) but which has been sufficiently finely ground is used, an improvement in the final and also partly in the initial strength is observed. This occurs even with additions as small as 30% as the water requirement is not increased.

*Institut für Gesteinshüttenkunde, Technische Hochschule Aachen, Aachen, West Germany.

Introduction

This work continues earlier investigations (1, 2) into the properties of natural puzzolanas of volcanic origin (3). We investigated molererde calcined at 800°C, which originated from silicified diatoms; this is a very reactive puzzolana (4, 5). The behaviour of granulated slags from power stations shows that these materials also posses the properties of natural puzzolanas (5).

Chemical, mineralogical and physical data of puzzolanas were determined. The reactivity of these stone flours in mixtures with lime, portland and slag cements have been investigated, as well as their combination with lime and the hydrates thus formed.

The Chemical Composition of Puzzolanas

As Table 1 shows, the chemical composition of puzzolanas varies over a wide range. We investigated 10 trasses from the Rhineland, 6 from Bavaria, 1 from Austria, 2 puzzolanas from Italy, molererde and 3 samples of granulated slag from power stations. Of the puzzolanas of volcanic origin, the Bavarian trasses show the highest content of SiO_2, ranging from 59.17—65.97%, whilst the puzzolana from Salone only contains 48.13%. The Al_2O_3 content varies between 13.77% for a Bavarian trass and 20.58% for the puzzolana from Bacoli. Accompanying the low SiO_2 content the puzzolana from Salone has the highest amounts of CaO and MgO, namely 9.96 and 5.70% respectively. The highest loss by ignition was from the Austrian trass (15.29%); this sample contains 1.96% SO_3.

With somewhat smaller silica contents of 47.46—51.82% the granulated slag contain larger amounts of Al_2O_3 (26.84—33.09%) and Fe_2O_3 (6.60—13.26%).

Table 1. *Chemical composition of puzzolanas*

	Rhine trasses	Bavarian trasses	Austrian trasses	Italian puzzolanas		Molererde	Granulated slags
				Salone	Bacoli		
loss of ignition	4.62–11.84	6.05–8.80	15.29	4.32	3.53	2.80	–
SiO_2	51.00–57.73	59.17–65.97	57.13	48.13	58.92	74.26	47.46–51.82
Al_2O_3	17.19–19.08	13.77–16.59	17.51	18.25	20.58	13.42	26.84–33.09
TiO_2	n.d.	n.d.	0.80	0.73	0.50	traces	0.84–1.32
Fe_2O_3	1.80–5.81	3.07–5.38	3.28	7.30	0.82	2.73	6.60–13.26
CaO	3.13–5.81	3.33–7.83	0.22	9.96	4.07	1.74	2.09–3.81
MgO	1.10–1.75	0.94–2.85	0.08	5.70	1.49	2.26	1.95–4.56
Na_2O	0.84–5.45	1.69–2.18	0.44	0.88	2.86	0.52	0.20–0.80
K_2O	2.80–6.36	1.55–2.52	2.74	4.41	6.61	1.41	3.30–4.40
SO_3	traces	traces	1.96	traces	traces	0.25	0.01–0.10

The Mineralogical Composition of the Puzzolanas

The mineralogical composition was determined by X-ray diffraction. All natural puzzolanas contain varying amounts of a glassy groundmass which, in the case of the Rhine trasses, was 55—60% and for the Bavarian trasses constitutes 62—67%. In the Austrian trass and the molererde the amorphous groundmass consists of opal, which shows signs of adopting the cristobalite lattice. The slag from power stations are completely glassy.

The Rhine trasses contain larger amounts of quartz and feldspar, and varying amounts of chabasite, analcime, mica, illite and kaolinite, whereas for augite and hornblende amounts only up to 1% were determined.

Similarly in the Bavarian trass larger amounts of quartz and feldspar were found. The augite content was in many cases under 1%. In addition amounts of montmorillonite up to 7% were found. The Austrian trass contains cristobalite, alunite, kaolinite, analcime and small amounts of quartz as well as augite. The high ignition loss of this material is explained by the presence of opal, alunite and kaolinite.

Augite, analcime and leucite are the principal crystalline phases in the puzzolana from Salone; in addition, small amounts of quartz and chabasite were found.

The main components of the puzzolana from Bacoli are feldspar and analcime, whilst only small amounts

of augite and quartz were found.

The molererde contains cristobalite, montmorillonite, illite and haematite as crystalline phases.

In contrast to the natural puzzolanas, the artiffcial ones, namely the granulated slags, contain a very small crystalline fraction amounting to 3%, which could not be identified more closely.

The Physical Data of the Puzzolanas

As Table 2 shows, the specific weights of the puzzolanas, with exception of the molererde, lie between 2.42 and 2.69 g/cm³. The specific surfaces of the volcanic puzzolanas, which were determined by the nitrogen-absorption method of BET, show a strikingly wide range. Great differences in surface area are caused by partial alteration of the glassy fraction to zeolites and montmorillonite.

Table 2. *Specific weights and specific surfaces of the puzzolanas*

Puzzolana	Spec. weight (g/cm³)	Spec. surface (m²/g) after Blaine	after BET
Rhine trass	2.42—2.60	0.70—1.18	19.6—95.0
Bavarian trass	2.52—2.63	0.71—0.95	8.3—39.0
Austrian trass	2.44	0.92	60.5
Italian puzzolanas			
Salone	2.69	0.89	17.4
Bacoli	2.45	0.90	4.4
molererde	2.25	2.70	12.0
slag granulated	2.58—2.68	0.50	1.01—1.27

Lime Bonding of Puzzolanas

The combination with lime was determined in suspensions of puzzolana and lime of which the W/S factor (water/solid) was 5. In Table 3 the degree of combination of the various puzzolanas with lime after periods of 56 and 90 days is shown.

Table 3. *The amount of lime combined with puzzolana after 56 and 90 days*

Puzzolana	Combined lime in mgCaO/g puzzolana 56 days	90 days
Rhine trass	264—335	270—373
Bavarian trass	186—241	192—254
Austrian trass	400	417
Italian puzzolanas		
Salone	248	254
Bacoli	262	266
Molererde	570	591
slag granulated (spec. surface = 5000 cm²/g Blaine)	210—272	228—283

The values† show that, among the volcanic puzzolanas, the Bavarian trasses combine with the least amount of lime (192—254 mgCaO/g trass) after 90 days, whereas the Austrian trass combines with the largest amount (417 mgCaO/g trass); this is a consequence of its reactive opal groundmass.

The greatest affinity for lime is exhibited by the molererde with 591 mgCaO/g molererde. This can also be related to the high opal content of this puzzolana. The lime combination of the artificial puzzolanas lies in the range of the Bavarian trass and the Italian puzzolanas, with a lime content of 228—283 mgCaO/g granulated slag.

Formation of New Hydrates in the Puzzolanas

After 90 days the following hydration products were observed in suspensions of CaO and puzzolanas shaken together; the residues were examined by X-ray analysis and in the electron microscope. In the case of the volcanic puzzolanas, CSH phases form as well as C_4AH_{13} (tetracalcium aluminate), $C_3(A, F)S_nH_{6-2n}$ (where $n = 0 - 3$; these are mixed crystals in the hydrogarnet series) and occasionally C_2ASH_8 (gehlenite hydrate). In addition the formation of $C_3(A, F)Cs_3H_{32}$ was observed for the sulphate-bearing Austrian trass.

The hydration products of the molererde were only CSH phases. In spite of the Al_2O_3 content of 13.4% no aluminous phase occurs which indicates that the aluminate is taken into the CSH phase.

In the experiments with granulated slag the formation of CSH phases, hydrogarnet and small amounts of gehlenite hydrate was observed.

If extra sulphate is added, ettringite and monosulphate hydrate occur in all the puzzolanas.

†In order to examine free lime we used Franke-method. This method gives too high values specially if C_4AH_{13} is formed.

The Reactivity of the Puzzolanas with Lime or Cement

For puzzolana-lime mixtures (70: 30) we have observed, in the case of the natural puzzolanas, that the strength of the mortar increases with increasing affinity of the puzzolana for lime. Thus the molererde which has the greatest affinity for lime yields mixtures that have the highest strength (of 127 kg/cm²) despite their greater requirement of water.

For the granulated slags the strength of the mortar is directly dependant on the specific surface.

Even after 4 years the strengths of cements containing up to 30% German trasses were less than that of pure cement. This fact can be explained by their greater internal surface and the correspondingly higher water requirement. However, taking into account the various W/C factors (water: cement) it becomes apparent that the volcanic puzzolanas do contribute to the strength of the mortar.

Mixtures of up to 30% granulated slag with portland cement had a lesser initial strength but after 90 days it was higher than that of pure portland cement if granules with a specific surface of 5000 cm²/g (Blaine) were used.

A considerable increase in strength was observed if puzzolana was added to cement poor in lime. Thus the 3-day strength of slag cement containing 70% slag sand was improved by up to 100% if 15% of the slag sand was replaced by molererde. The role of molererde in the hydraulic hardening could be demonstrated by the combination of lime and sulphate, and also by the earlier appearance of a thermic reaction.

Investigations (6) using mixed bonding materials with trass reveal the same tendency, as the Fig. 1 shows. The influence of the trass on the strength is evident after only 7 days, if anhydrite is used to provide sulphate.

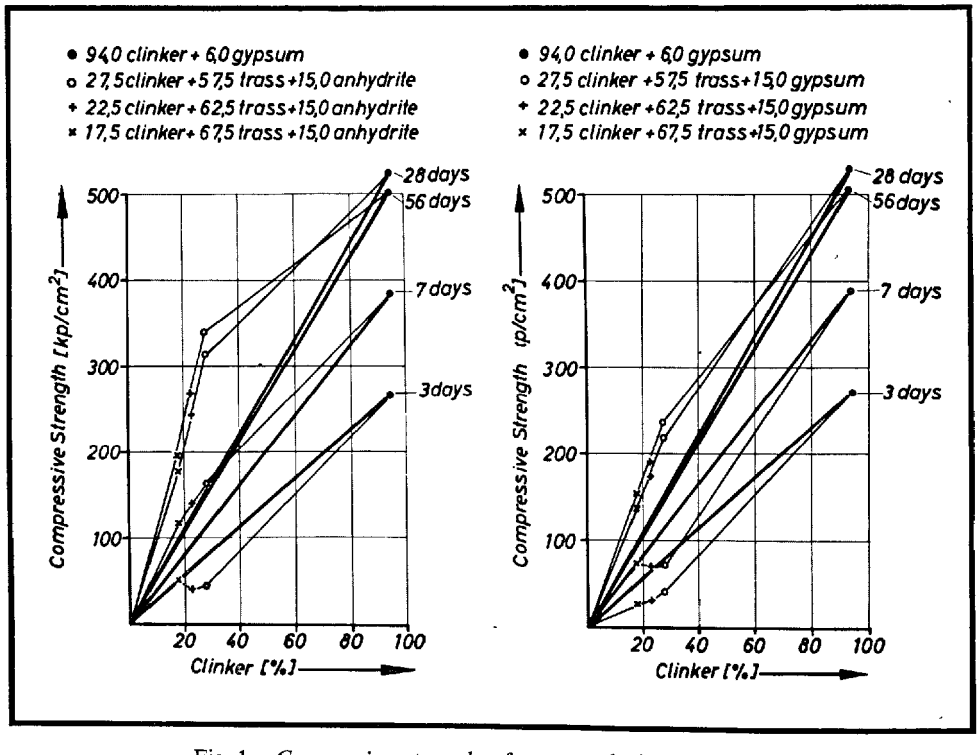

Fig. 1. *Compressive strength of mortars high in trass and sulphate content.*

Summary

All the silicate stone flours which have been investigated form compounds with lime. The pronounced reactivity of natural and artificial puzzolanas is due:

1) to their chemical and mineralogical composition
2) to the high amount of glassy or amorphous phases

3) and to their large reactive surface

The same hydrate phases which occur in the hydration of standard cements appear as reaction products when these puzzolanas react in aqueous solution with calcium hydroxide and calcium sulphate.

In contrast to granulated slags, the contribution that natural puzzolanas make to the strength in the early stages of hardening is disguised by the high requirement of water in the case of the lime-rich cements (trass cement 30/70). In the case of bonding materials poor in lime, an increase of strength is shown even at an early stage, in particular if anhydrite is used.

References

1. U. Ludwig and H. E. Schwiete: "Research on the hydration of trass-cements" Chemistry of Cement, Washington, Vol II 1093–1098 (1960).
2. U. Ludwig and H. E. Schwiete: "The mortar-technological properties and the chemical and mineralogical behaviour of trass-cement and trass-lime-mixtures and the comparision with puzzolanas and stone flours" Presented at the Symposium on "Puzzolanas—their Survey, Manufacture and Utilisation", New Delhi, India, December 1964.
3. H. E. Schwiete, P. Kastanja and U. Ludwig: "The chemical and mortar-technological properties of different puzzolanas and stone flours and their reaction with $Ca(OH)_2$ in aqueous solution" (in German), Forschungsbericht des Landes NRW No. 1441 (1965).
4. H. E. Schwiete, U. Ludwig and P. Otto: "The influence of molererde on the technological properties of slag rich blast furnace cement" (in German). Part I Forschungsbericht des Landes NRW No. 1550 (1965); Part II (will be published).
5. H. E. Schwiete, P. Kastanja and U. Ludwig: "The puzzolanic properties of granulated slags from power stations", Unpublished Investigations, Aachen (1967).
6. H. E. Schwiete and U. Ludwig: Unpublished Investigations, Achen (1961).

Supplementary Paper IV-135 The Different Action Mechanism of Pozzolanic Materials and Slags in the Hydraulic Binders

Adriano Celani, Pietro A. Moggi and Arturo Rio*

Synopsis

In order to outline the different action mechanism of pozzolanic materials and slags in the hydraulic binders an investigation was carried out on the equilibrium relations of these materials with lime solutions and free calcium hydroxide from portland cement.

The experimental results point out that the amount of fixed $Ca(OH)_2$ is much higher for pozzolanas than for slags. They show furthermore the different lime retention force of both materials, which force results in a lower lime concentration of the liquid in contact with the solid mass, when its pozzolana amount is sufficient, as well in a greater resistance to the leaching action of an aqueous solution.

Such a different behaviour is due to the different nature of the calcium silicate hydrates formed by reaction between lime and pozzolanas or slags.

Introduction

As it is known, true pozzolanas are materials of volcanic origin which, though not hydraulic in themselves, combine with the lime at ordinary temperature and in the presence of water to give compounds possessing hydraulic properties.

On the contrary, granulated blast furnace slags, which are principally constituted of a vitreous material with variable composition depending on the pig iron production process, possess its own latent hydraulic properties which need only a simple alkaline activation, generally promoted by lime, to reveal themselves.

Whilst pozzolanas combine progressively with lime to give silicate and aluminate hydrates by chemical fixing of its quantities appreciable in respect of their reactive silica and alumina contents, slags, on the other hand, absorb only small amounts of lime, whose main function, as F. M. Lea (1) pointed out, is to promote the hydration. The reaction course does not depend on the further combination with the lime, but on the hydration of the slag itself, though it could not be excluded, in agreement with other authors (2), that there is a moderate reaction with lime when this is present in excess.

However, the quantitative differences in the lime absorption require a different proportioning of these materials when pozzolanic and slag cements are prepared.

Besides the different quantity of lime susceptible to be combined, there is another quantitative point of view of this combination on which the attention should be recalled: the compounds which are formed during the hydration of pozzolanic cements, in consequence of the reaction between the hydrolysis lime of clinker and the constituents of pozzolana, are chemically different from the compounds formed during the hydration of high slag content cements.

In the first case little basic and then chemically more stable compounds are formed: consequentially there is a sharp increase of the chemical resistance with a remarkable improvement of the physical and mechanical characteristics.

In the second case, on the contrary, the reaction between lime and slag gives rise to more basic hydrated compounds which will be more attackable, though their formation is followed by the increase of strengths.

In the literature it is possible to find several works in which comparison is made between the relative lime absorption capacity of pozzolanas and that of slags; on the contrary, as far as we know, never pointed out was the different force by which the above materials fix and retain lime.

In a first stage of our research (3) we studied the quantitative relations between the concentration of

*Soc. Calci e Cementi di Segni, Laboratorio Centrale, Roma, Italy.

lime in solution and the amount of lime combined with pozzolanas and slags, in equilibrium with the solution itself. The tests were performed on mixtures with different lime/material ratio. The experimental results confirmed that the combined lime amount is much higher for the pozzolanas than for the slags. They have furthermore proved the different stability of the compounds formed from the combination of the lime with the examined materials.

Successively the research was extended to the behaviour of pozzolanas and slags towards the lime developed during hydration of portland cement.

The tests, carried out on mixtures with different cement/material ratio, covered the observation of the following characteristics:

—Proportioning of the material, mixed with cement, which is required to absorb quantitatively the hydrolysis lime of portland cement.
—Quantity of the hydrolysis lime fixed by the material in function of the time and of the cement/material ratio.
—Equilibrium relations with the lime concentration of the contact solution.
—Chemical-physical constitution of the hydration products and of the lime combination products with the examined materials.
—Lime retention power of the combination products.

Experimental

Materials and Research Methods

The compositions of the used materials are reported in Table 1. The slags No. 1 and No. 2 come from two different countries and have been chosen from those commonly used for the industrial production of blast furnace cements. The pozzolanas No. 1 and No. 2 also belong to the types commonly used for the production of pozzolanic cements; they differ in the reactive silica amount which highly affects pozzolanic activity. The sand was chosen in order to have comparison value with a material of practically negligible pozzolanic activity.

The clinker, the composition of which is reported in Table 1, is also of usual industrial production. It has been always used mixed with 5% of gypsum. Finally, standard mixture were prepared with an absolutely inert material. To this aim $BaSO_4$, pure for analysis, was used.

Mixtures of the various materials with cement in variable ratio were prepared.

The performed tests, which will be described later in detail, are the following:

—Pozzolanic activity determination.
—Hydrolysis lime absorption.
—Specific surface measurements.
—X-ray analysis.
—Leaching with diluted lime solution.

Pozzolanic Activity Determination

The pozzolanic activity determination was carried out according to the test as specified by Italian Standards 1966, which has been proposed by I.S.O. for international application.

According to this test, which covers the determination of the lime concentration and of the total alkalinity of the contact solution with the cement paste at 40°C after 8 days, are "positive" those cements with their representative points lying under the isotherm of the lime-alkalies solubility (Fig. 1).

The test was carried out on cements with 30, 70 and 80% of one of the two slags, which are similar in their behaviour, (points L_3, L_7, L_8); with 30 and 40% of the pozzolana No. 1 (points P_3, P_4) and with 20 and 30% of the pozzolana No. 2 (points P'_2, P'_3); finally with 30, 70 and 80% of sand (points S_3, S_7, S_8) and on the cement without additions as comparison.

The test results are "positive" only with slag contents above 70%, while addition of 30% of pozzolana No. 1 and of 20% of pozzolana No. 2 are sufficient to reach the same result. The sand, as it was to be expected, does not present any pozzolanic activity.

Hydrolysis Lime Absorption

Cement mixtures were prepared with 20, 30, 50 and 70% of the slags, of the two pozzolanas, of sand and of $BaSO_4$. They were hydrated with a water/cement ratio = 12.5, on keeping them in a polyethylene bottle under agitation in a thermostat at 40°C up to the fixed ages of 1, 7, 28 and 60 days.

At the end of the curing the suspension was filtered in CO_2 free atmosphere, the solid was washed with alcohol and ether and then overdried at 105°C in CO_2 free air stream. On the liquid, the alkalinity was determined by titration with HCl and methyl orange as indicator and the lime concentration by com-

Table 1. *Chemical composition (%) and fineness of grinding of materials*

	Loss on ignition	SiO_2	Al_2O_3	Fe_2O_3	CaO	MgO	SO_3	$CaCO_3$	Na_2O	K_2O	S^{--}	Residue > 40 micron
Slag N. 1	0.43	33.45	14.42	1.42	42.20	6.14	traces	3.71	0.72	0.69	1.52	14.6
Slag N. 2	1.17	30.80	17.51	1.46	43.40	5.23	—	3.47	0.66	0.74	1.35	14.2
Pozzolana N. 1	4.59	46.72	18.94	9.96	9.70	4.78	traces	nil	0.72	4.58	—	25.4
Pozzolana N. 2	6.67	88.60	3.19	0.17	0.43	nil	nil	nil	0.02	0.06	—	24.0
Sand	0.75	90.70	2.05	3.25	1.11	0.30	—	—	0.76	0.87	—	21.0
Clinker	0.12	22.56	3.84	3.99	66.85	1.00	0.63	—	—	—	—	10.0

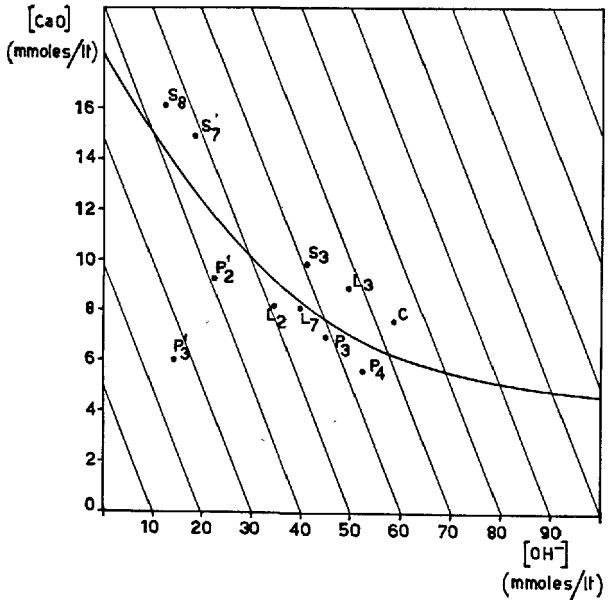

Fig. 1. *Solubility isotherm of $Ca(OH)_2$ in presence of alkalies at 40°C.*

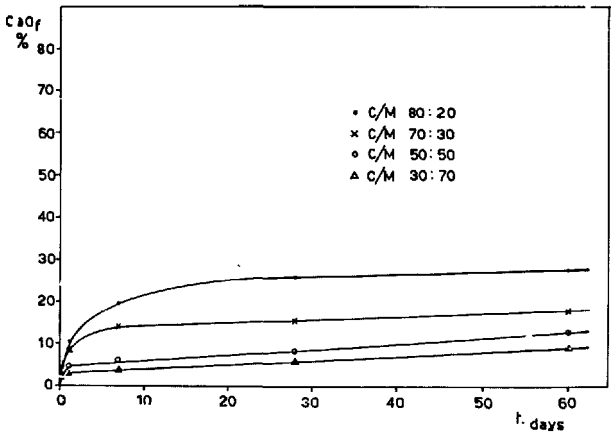

Slag 1

Fig. 2. *Fixed CaO vs. time and cement/material ratio*

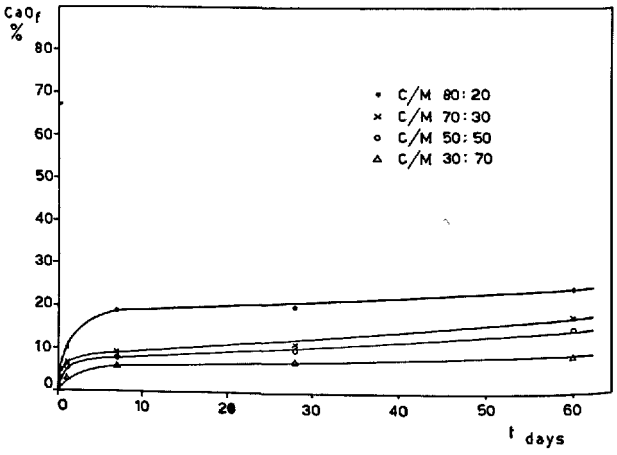

Slag 2

Fig. 3. *Fixed CaO vs. time and cement/material ratio*

plessometric titration with EDTA and calconcarbonic acid as indicator.

On the solid the free lime was estimated according to the T.V.M. method (4) and the ignition loss at 950°C. The concentration of the lime in solution and of the free lime in the solid phase have been referred as percentage to the anhydrous original mixture.

From the tests performed on the mixtures with $BaSO_4$, the lime available at various ages for each cement/material ratio was derived and then the absorbed lime was estimated by the difference between available lime and the total free lime in solution and in the solid phase, the cement/material ratio being equal.

The diagrams in Figs. 2, 3, 4, 5, 6 plot the lime absorbed by 100 g material versus time and cement/material ratio.

In Tables 2, 3, 4 are reported the percentages of the lime absorbed by the various materials, in function of the cement/material ratio, to the lime-available at different ages, 1, 7, 28 days, respectively.

The obtained results clearly show the different activities of slags and pozzolanas in the absorption of hydrolysis lime.

—Slags present an activity which, on the whole, differentiate very little from that of an inert material

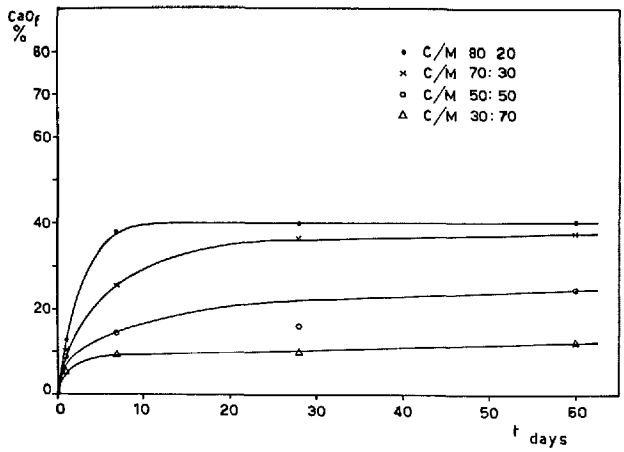

Pozzolana 1

Fig. 4. *Fixed CaO vs. time and cement/material ratio*

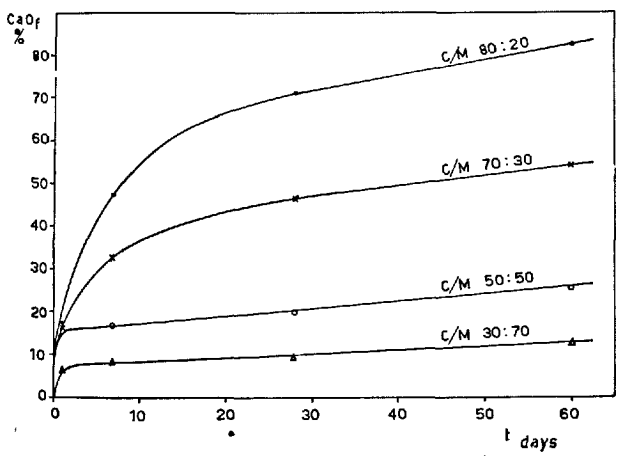

Pozzolana 2

Fig. 5. *Fixed CaO vs. time and cement/material ratio*

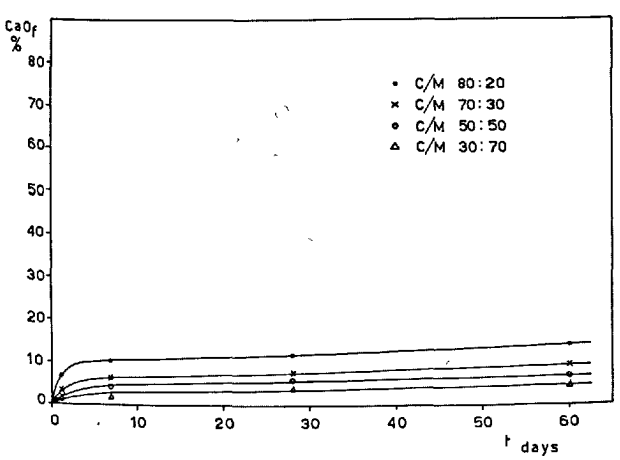

Sand

Fig. 6. *Fixed CaO vs. time and cement/material ratio*

Table 2. *Fixed* CaO *as percent of available* CaO *at 1 day*

C/M	80:20	70:30	50:50	30:70
Slag N. 1	17.7	22.3	31.9	37.3
Slag N. 2	17.0	18.1	24.6	28.2
Pozzolana N. 1	22.2	31.8	47.8	72.2
Pozzolana N. 2	28.9	44.7	83.7	89.0
Sand	5.8	8.3	11.6	18.7

Table 3. *Fixed* CaO *as percent of available* CaO *at 7 days*

C/M	80:20	70:30	50:50	30:70
Slag N. 1	19.0	23.5	39.3	52.7
Slag N. 2	18.3	18.5	27.2	45.2
Pozzolana N. 1	39.6	45.2	68.8	90.2
Pozzolana N. 2	47.4	81.8	90.0	94.4
Sand	7.1	11.3	18.0	26.9

Table 4. *Fixed* CaO *as percent of available* CaO *at 28 days*

C/M	80:20	70:30	50:50	30:70
Slag N. 1	19.6	23.9	47.2	61.8
Slag N. 2	18.9	18.9	38.0	59.5
Pozzolana N. 1	40.1	61.9	90.3	95.3
Pozzolana N. 2	71.2	92.1	96.0	99.2
Sand	10.6	12.8	24.5	37.6

such as sand. On the contrary pozzolanas, especially pozzolana No. 2, that results more active than No. 1, present a clearly higher activity.

If a scale should be made for the activity on the basis of the results of this test, it should be somewhat as this:

sand < slag No. 2, slag No. 1 < pozzolana No. 1
1 : 2 : 4
< pozzolana No. 2
: 7

—The two slags have similar behaviour, the slag No. 1 is somewhat more active than the No. 2, and in 28 days they fix 60%, at the most, of the available lime in the mixture with the higher slag content.

—The pozzolana No. 2 can absorb already after 1 day 90% of the available lime in the mixture in which it is contained in higher amount. At 7 days also pozzolana No. 1 attains such a yield and at 28 days the lime absorption is almost quantitative for both pozzolanas, even for the mixture with 50% of pozzolana.

—Likewise the rate of lime absorption is higher for the pozzolanas, specially for the No. 2 than for the slags.

Results of particular interest have been obtained

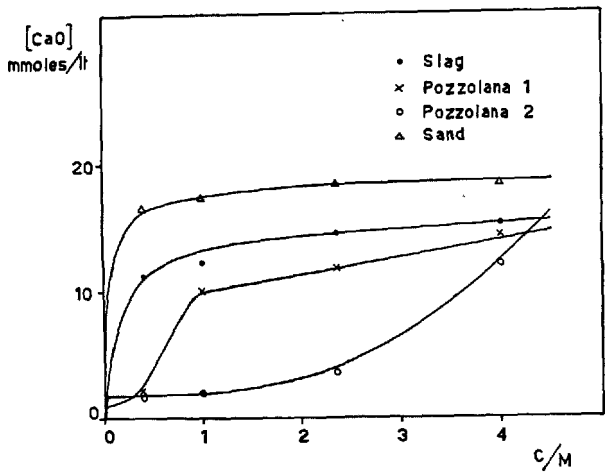

Fig. 7. *CaO concentration in equilibrium with mixtures cement-materials at 7 days*

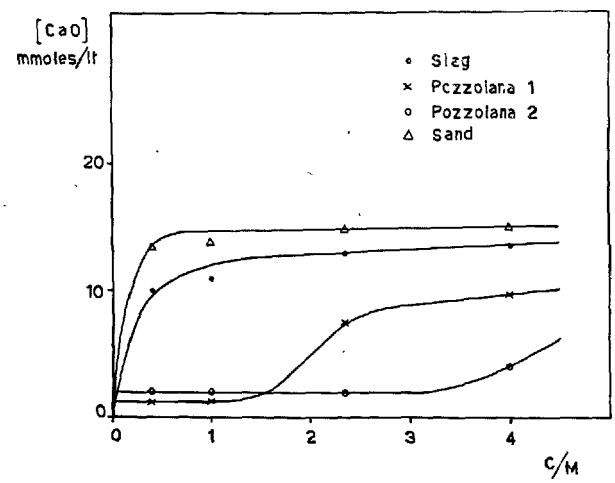

Fig. 8. *CaO concentration in equilibrium with mixtures cement-materials at 28 days*

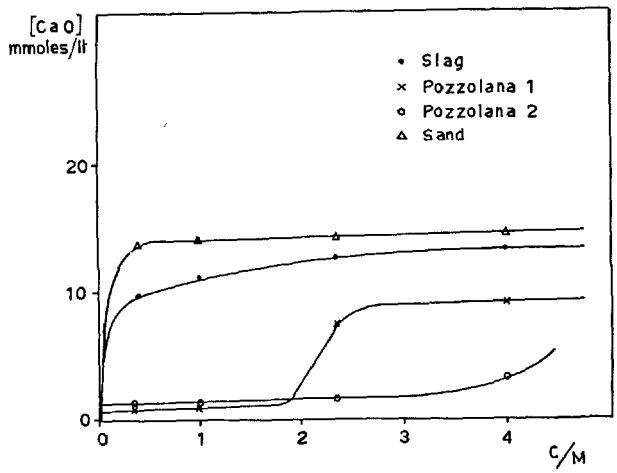

Fig. 9. *CaO concentration in equilibrium with mixtures cement-materials at 60 days*

also from the determination of the lime concentration in the contact solution with the solid.

In the diagrams of the Figs. 7, 8, 9 the concentration in mmols/l of the lime in the contact solution is plotted in function of the cement/material ratio at ages of 7, 28 and 60 days respectively. Because of the similarity of their behaviours, only one slag of the two has been reported, that is the No. 1, a little more active.

The overall development of the curves points out to the different forces with which lime is retained by the reactive silica of the materials under examination. Indeed, the lower is the lime concentration in the contact solution, the stronger is the retention power.

From Fig. 9 it is noted that for sufficiently high pozzolana content in mixture with cement, the lime concentration in the contact solution is under 2 mmols/l. This equilibrium concentration of the lime in solution occurs, in the system $CaO–SiO_2–H_2O$, in correspondence to the coexistence zone among silica, CSH(I) and the liquid phase (5). The value of nearly 9 mmols/l obtained for cements with lower pozzolana content corresponds, on the contrary, to the equilibrium concentration of the lime in the presence of the alkali amount developed from the material.

Slags present a completely different course from that of the pozzolanas, and analogous one to that of the sand. There is no evidence of stable and well defined compounds, not even for mixtures with higher slag cement. In fact the lime concentration of the contact solution is always greater than the equilibrium value corresponding to the alkalinity of the solution.

Specific Surface Measurements

The specific surface of the cements with 30 and 70% of slag No. 1 and of the pozzolana No. 1 after 1, 7 and 28 days of curring according to the test procedure for hydrolysis lime absorption, has been measured.

The measurement was carried out by nitrogen adsorption from nitrogen-helium mixture, after degasing the samples for two hours at 105°C in helium stream: the specific surfaces, calculated according to the B.E.T. method (6), are given in Table 5.

The cements with pozzolana give rise to hydration products of higher specific surface than those containing an equal amount of slag. The difference is more remarkable for the mixtures with much addition

Table 5. *Specific surfaces of hydration products of mixtures cement-slag or pozzolana*

Mixture	Specific surface m²/g		
	1 day	7 days	28 days
70% Cement + 30% Slag	18.06	46.24	110.31
70% Cement + 30% Pozzolana	25.71	69.49	116.87
30% Cement + 70% Slag	23.59	54.63	115.44
30% Cement + 70% Pozzolana	42.68	83.09	129.99

Table 6. *Absorption of lime in mixtures of slag and pozzolana with calcium hydroxide*

Mixture	Absorbed CaO by 100 gr of material	Absorbed CaO in percent of available CaO
50% $Ca(OH)_2$ + 50% slag	21.50	28.40
35% $Ca(OH)_2$ + 65% slag	16.25	39.90
25% $Ca(OH)_2$ + 75% slag	13.60	53.80
20% $Ca(OH)_2$ + 80% slag	12.36	65.30
15% $Ca(OH)_2$ + 85% slag	9.33	70.10
50% $Ca(OH)_2$ + 50% pozzolana	43.66	57.80
35% $Ca(OH)_2$ + 65% pozzolana	36.20	88.70
25% $Ca(OH)_2$ + 75% pozzolana	24.17	95.80
20% $Ca(OH)_2$ + 80% pozzolana	18.24	96.30
15% $Ca(OH)_2$ + 85% pozzolana	12.93	96.80

material, in which the difference of constitution of the reaction products of lime with the two materials produces a more remarkable effect.

X-ray Analysis

For better investigation of the nature of the combination compounds between lime and slag, or pozzolana, some mixtures of pure calcium hydroxide with 50–65–75–80 and 85% of slag No. 2 and of pozzolana No. 1 were prepared. These mixtures were hydrated for 15 days under the same conditions as for the hydrolysis lime absorption test. On the solution the alkalinity and the lime concentration were determined, on the solid the free lime and the ignition loss.

In Table 6 there are given the lime amounts absorbed by the two materials in the different mixtures.

Finally the solids were analyzed by X-ray diffraction.

From the development of the X-ray diffraction diagrams the following observations can be made:

—The lines of $Ca(OH)_2$ at 4.90 and 2.63 Å are always present in the mixtures containing slag, even with high percentages of this material. Comparison of the diagrams of the same mixtures before their hydrating shows that the lime absorption is only of little extent, which let us suppose that this absorption is of mostly physical nature, even if high percentages of absorbed lime result from the analysis.

In the case of pozzolanas the lines of $Ca(OH)_2$, on the contrary, have been found to be already quite absent with mixtures containing 25% $Ca(OH)_2$ and 75% material. According to the results of the chemical analysis this confirms the quantitative absorption of the available lime which, moreover, results to be wholly combined with the material to give new compounds.

—For all mixtures with slag the lines of the tetracalcium aluminate hydrate, C_4AH_{13}, at 7.9 and 3.95 appear very clear together with the less strong lines at 2.86 Å. These lines are completely absent for the mixtures with pozzolana.

—In the diffraction diagrams of the hydrated mixtures of lime and slag the lines of the hydrated dicalcium aluminate silicates, C_2ASH_8 (gehlenite), appear as well, the line at 4.18 Å being more evident, while the one at 2.87 Å is hardly distinguishable on account of the near line of the C_4AH_{13}.

—In the case of mixtures with slag the lines of calcium hydrosilicate with high CaO/SiO_2 ratio, CSH(II), at 9.8, 3.07 and 2.80 Å are visible. They appear stronger for mixtures with higher material content and therefore it seems clear that this compound is derived directly from the hydration of the hydraulic compounds of the slag, whereas hardly probable is its formation from combining of lime with slag.

—All mixtures containing pozzolana show also the lines at 3.07 and 2.80 Å, while at 9.80 no line is present. Thereafter the calcium hydrosilicate formed must be supposed as belonging to the type CSH(I) with low CaO/SiO_2 ratio, even if in the various mixtures the line at 12.5 Å, proper to such compound, seems to be hardly distinguishable because of the low value of the diffraction angle θ.

Leaching with Dilute Lime Solution

With the tests previously described, the quantitative differences in the hydrolysis lime absorption as well as the diversity of the compounds formed by the action of the lime on slags and on pozzolanas were pointed out.

A very important aspect of such phenomenon, on which the attention must be recalled, is the different binding power with which the lime can be retained by the two examined materials.

To this aim, the samples derived from the lime absorption test at 28 days have been submitted to a treatment, which may be told to as leaching, with a dilute lime solution.

A prefixed quantity of sample was mixed with 100 ml

Table 7. *Leaching action of a* $Ca(OH)_2$ *0.002m solution on hydrated cements with slag or pozzolana*

Mixture	free CaO	fixed CaO	total CaO	leached CaO	ΔCaO fixed
80% cement + 20% slag N. 1	15.17	3.93	19.10	+15.67	−0.50
70% cement + 30% slag N. 1	12.68	4.23	16.91	+13.07	−0.39
50% cement + 50% slag N. 1	6.41	6.49	12.90	+ 7.12	−0.71
30% cement + 70% slag N. 1	2.23	4.61	6.84	+ 2.37	−0.14
80% cement + 20% slag N. 2	15.29	3.79	19.08	+16.21	−0.92
70% cement + 30% slag N. 2	13.46	3.35	16.81	+14.20	−0.74
50% cement + 50% slag N. 2	3.62	9.33	12.95	+ 5.00	−1.38
30% cement + 70% slag N. 2	2.31	4.43	6.74	+ 2.74	−0.43
80% cement + 20% pozzolana N. 1	11.30	8.04	19.34	+11.03	+0.27
70% cement + 30% pozzolana N. 1	6.20	10.98	17.18	+ 5.64	+0.56
50% cement + 50% pozzolana N. 1	1.23	12.40	13.63	− 0.30	+1.53
30% cement + 70% pozzolana N. 1	1.00	6.36	7.36	− 0.28	+1.28
80% cement + 20% pozzolana N. 2	4.65	14.30	18.95	+ 3.35	+1.30
70% cement + 30% pozzolana N. 2	1.03	16.33	17.36	+ 0.25	+0.78
50% cement + 50% pozzolana N. 2	0.47	11.96	12.43	− 0.60	+1.07
30% cement + 70% pozzolana N. 2	0.37	6.11	6.48	− 0.21	+0.58

of a 0.002 M $Ca(OH)_2$ solution in a polyethylene bottle and kept in a thermostat at 40°C under agitation. After 8 days the suspension was filtered in CO_2 free air. On the solution the alkalinity and the new lime concentration, while on the solid free lime and ignition loss were determined.

Of each mixture, the lime content being known from the previous tests, such an amount was weighed that, were all the free lime passed into the leaching solution, the latter should have a concentration of 0.010 M. In this way, if the final concentration resulted higher than this value, also a partial going into solution of the lime previously combined would be proved; in the contrary case a further lime absorption would be proved.

In order to take into account any possible ulterior hydration of cement during treatment with leaching solution, a first test was carried out with cement-$BaSO_4$ mixtures and for each of them was calculated the amount of hydrolysis lime passed into solution.

The results of the leaching test are reported in Table 7. All values are given as percent of the initial anhydrous mixture.

The first three columns show respectively the free and fixed lime concentration of the sample before the test, as well as their sum.

In the fourth column there is reported the difference between the total amount of lime passed into solution during leaching and the lime passed into solution owing to further hydration of cement, that is the true leached lime. A negative variation will then indicate a lime absorption from the solution.

In the fifth column the difference is given between the true leached lime and the free lime in the solid before testing. This value, if negative, will indicate the quantity of the previously combined lime drawn off during leaching; it will, on the contrary, indicate the quantity of lime further fixed by the material, if it is positive.

The difference in the behaviour of the two kinds of cement is evident. While for the cement containing slag all free lime and some of the lime previously combined is passed into solution, for the cements containing pozzolanas no leaching of the previously combined lime occurs, not only, but rather, for the mixtures with higher amount of such material, a further lime absorption from the solution was observed.

Discussion of Results

The experimental results, on the whole, may be so summarized:

—The pozzolanic activity test, carried out according to Italian Standards 1966, gives positive result only with cements containing more than 70% slag, whilst it is sufficient an addition of 20–30 per cent of pozzolana.

—During the hydration of cements containing additions of the two examined materials, both slags and pozzolanas may react with the lime developed by hydrolysis from portland cement.

However, the amount of lime absorbed by the slag is, at each age and for whatever cement/material ratio, by far inferior to that absorbed by poz-

zolana. Slag contents of 70% in the cement absorb, after 28 days hydration, at the most 60% of the lime available through hydrolysis, whilst at the same age the lime absorption is practically quantitative for cements containing 30–50% of pozzolana.

—The contact solution with the pozzolanic cements tends, with the hydration development, to assume a lime concentration inferior to 2 mmols/l, corresponding to an equilibrium concentration with the products of the lime-silica combination of tobermoritic type, CSH(I). In the case of cements containing slag there is, on the contrary, no evidence of the formation of well defined compounds, and the contact solution reaches a lime concentration equal or superior to the equilibrium value for the amount of alkalies developed by the material.

—The products of combination between lime of hydrolysis and pozzolana present high specific surface, whilst, at the same age and material/cement ratio the contribution of the corresponding products of the lime-slag combination is smaller.

—The X-ray analysis of mixtures of $Ca(OH)_2$ with different quantities of both materials shows the different constitution of the combination products. In the case of pozzolana the $Ca(OH)_2$ is fixed almost qusntitatively and the obtained compounds are of tobermoritic type, CSH(I). In the case of slag, on the contrary, there is formation of tetracalcium aluminate hydrate, C_4AH_{13}, hydrated gehlenite, C_2ASH_8, and calcium hydrosilicates of the type CSH(II), which present higher CaO/SiO_2 ratio. All these compounds seem to be derived directly from the hydration of the hydraulic compounds in the slag, whereas the lime absorption seems to be mostly of physical nature and the formation of combination products of lime with slag is not evident.

—The products of the combination of lime with slag or with pozzolana which are formed during the hydration of the cements added with such materials show a different stability in regard to the leaching action of a very dilute lime solution. Whilst in the case of the cements containing slag, all free lime and some of the combined lime pass into contact solution, in the case of the cements containing pozzolana it occurs, on the contrary, that during the test, further lime combines.

The results, on the whole, demostrate that slags and pozzolanas are not equivalent in view of their action on the hydrolysis lime of portland cement. The amount of the lime fixed by pozzolanas is much higher than in the case of slags and by far stabler reaction products are obtained.

This is due to different nature of the lime hydrosilicates formed from the reaction of hydrolysis lime with pozzolanas or with slags. In the first case compounds of tobermoritic type, CSH(I), are formed, with a low CaO/SiO_2 ratio, therefore scarcely basic and chemically more stable compounds. In the case of slag, on the contrary, the formed products present a higher CaO/SiO_2 ratio and are then more basic and chemically less stable.

The different stability of the compounds from the combination of lime with pozzolanas or with slags, that is, the different power with which the lime is retained from both materials, is proved by the lower lime concentration of the solution in contact with the solid phase when a sufficient quantity of pozzolana is present, as well as from the different behaviour towards the leaching action of an aqueous solution.

Lime is only weakly retained by slag and a part of it is easily given to the contact solution, whilst the compounds from the combination with pozzolana appear absolutely stable to the action of the leaching solution.

References

1. F. M. Lea, The Chemistry of Cement and Concrete, 2nd Ed., p. 419 (Arnold Publ., London, England, 1956).
2. F. W. Locher, J. Wuhrer and K. Schweden, "Effect of the finesses of grinding and the particle size distribution on the properties of portland and blast furnace cement and hydraulic limes" (in German). Tonind. Ztg. Keram. Rundschau **90**, 547–554 (1966).
3. A. Celani, M. Collepardi and A. Rio, "Different mechanism of action of lime on pozzolanic materials and slags" (in French), Rev. Mater. Constr. Trav. Publics **614**, 433–439 (1966).
4. E. E. Pressler, S. Brunauer, D. L. Kantro and C. H. Weise, "Determination of the free calcium hydroxide contents of hydrated portland cement and calcium silicates". Anal. Chem. **33**, 877–882 (1961).
5. R. H. Bogue, The Chemistry of Portland Cement, 2nd Ed., p. 520 (Reinhold Publ. Co., New York, U.S.A., 1955.
6. S. Brunauer, P. H. Emmett and E. Teller, "Adsorption of gases in multimolecular layers". J. Am Chem. Soc. **60**, 309–319 (1938).

SESSION IV-3 SLAGS AND SLAG CEMENTS

Principal Paper Blastfurnace Slags and Slag Cements

Fritz Schröder*

Synopsis

Blastfurnace slags continuously grow in importance for the manufacture of cements. Type and quantity of the blastfurnace slag produced are intimately connected with the trend and measures taken to economize the blastfurnace processes. One of these measures is to decrease the volume of slag referred to 1 ton of pig iron produced. The results of research work evaluated in this connection covered the chemical composition changed for this purpose, especially the increased MgO content and the dependence on temperature and viscosity of slag melts of optimum composition.

By appropriate granulation, the liquid condition of these melts is frozen in and settles the latent hydraulicity of the granulated glassy slags. Some studies dealt with the application of the ion theory of solutions on slag melts. The structure of the liquid slags and their behaviour in frozen-in condition can best be explained by a liquid structure which, in an ternary system with Frenkel type, Stewart type and Bernal type fluids as corners, is closer to the Frenkel type corner. The participation of the Frenkel type fluid indicates that the glassy state of granulated slags can be described neither by the glass structure model of Zachariasen nor by that of Porai-Koshits alone.

Further studies—e. g. on the separation of different slag phases and on fluorescence properties—substantiate the views on structure and hydraulicity of glassy slags.

The composition of both slag cements and their individual components—slag, clinker and sulphate components—largely influence the properties of cement, such as setting, volume stability, and evolution of mechanical strength.

The particular properties of slag cements can be attributed to the properties of granulated blastfurnace slag and are, therefore, most pronounced in slag cements having high contents of blastfurnace slag:

Good elasticity on account of a relatively high ratio of flexural strength/compressive strength.

Very low heat of hydration, high after-hardening and good suitability for heat or steam treatment.

High resistance to sulphate solutions and some other aggressive media. Especially the durability against sea water has been proved by several long-time studies.

The behaviour of slag cements during carbonation is, as a physical property, largely influenced by the type of precuring of the concrete. On sufficient moist after treatment, no difference from cements without slag can be found. In slag cements the strength increases considerably during carbonation, in supersulphated cements it decreases. As a protection of steel reinforcement, concrete made with slag cements has for decades proved satisfactory and, in cases of simultaneous chemical attack, even highly satisfactory.

For these reasons, slag cements rich in granulated blastfurnace slag have been used successfully in many important concrete structures, especially in massive structure elements or where action of chemically aggressive waters had to be expected.

*Forschungsinstitut für Hochofenschlacke, Rheinhausen, West Germany.

Introduction

The 100th anniversary of slag cements (slag in this context applying only to blastfurnace slag as yielded by modern coke furnaces) happens to have fallen in the period between the 4th and 5th International Symposium on the Chemistry of Cement (Washington 1960 and Tokyo 1968). It may be remembered that on March 12th, 1863, E. Langen, the chief director at the time of the Friedrich-Wilhelm Iron and Steelworks at Troisdorf near Bonn (Germany) first produced cements from granulated blastfurnace slag (1). These first slag cements were well homogenised mixtures of finely ground granulated slag and hydrate of lime. In quality standards they were the equal of the portland types made at the time.

Though the invention did not at the time give an impetus to the use of granulated blastfurnace slag in cement production in Germany itself—in contrast to its neighbours, such as Belgium, France, Austria and Switzerland—yet Langen had laid the foundation for intensive research into its latent hydraulic hardening properties. In addition to a number of engineers from the cement industry, leading cement chemists, such as W. Michaelis, L. Tetmeyer, E. Dietrich, later H. Passow and H. Kühl to name only a few, carried out research into the suitability of slag granulated by quick water quenching. It is on these early investigations that the development of present-day "portland blastfurnace slag cements" or "ciments metallurgiques" or "Hüttenzemente" and the "supersulfated" is based. Today these are made and used all over the world.

Output of slag cements activated with portland cement clinker—or calcium sulphate—has registered a further increase in countries with major cement and iron and steel industries in the years since the 4th International Symposium on the Chemistry of Cement (Washington 1960). A few statistical data will illustrate the point. According to the returns of the Cement Statistical and Technical Association "CEMBUREAU" in Malmö (2), the number of plants producing slag cements rose from 117 in 1961 to 179 in 1965.

Since the figures are based on answers to a questionnaire, they may not be wholly accurate. But if we consider that in West Germany alone the number of portland cement factories producing slag cements rose during the period from 41 to 48, we realise that they cannot be far wrong.

The proportion of slag cements in the overall production of some leading industrial nations in 1966 was as follows: USSR over 35 percent, Federal Republic of Germany over 28 percent, Belgium over 25 percent, Italy over 16 percent, France over 14 percent, Japan over 6 percent.

The growing use of granulated blastfurnace slag is also evident from the fact that various countries, such as the USSR, France etc., have meanwhile permitted the addition of up to 15 percent ground slag to portland cements.

In France, for instance, portland cements (class 160/250 and class 210/325) accounted for 71.1 of total production in 1962 and 71.2 percent in 1965 (3). This proportion was made up as follows, taking the figure of 71.2 percent (resp. 71.1) as 100:

		1962	1965
CPA	Portland cement without addition	25.3%	20.4%
CPAL	Portland cement with < 15% granulated slag	44.1%	45.1%
CPACL	Portland cement with < 15% granulated slag + fly ash	18.3%	19.2%
CPAC	Portland cement with < 15% fly ash	12.2%	15.4%

The growing use of blastfurnace slags in cement production is merely indicated by these few figures. Side by side we have seen the introduction of modern, highly perfected research methods and test instruments and the effects of the far-reaching modernisation and greater efficiency of blastfurnaces on the properties of furnace slag in general, granulated slags in particular and hence on slag cements, a drive which has continued unabated in industrialised countries since 1960. All these considerations prompted cement chemists to examine and deepen the knowledge gained so far and to tackle the remaining problems.

At the 4th International Symposium on the Chemistry of Cement (Washington 1960), W. Kramer (4) reported on "Blastfurnace slags and slag cements", and I. I. Kholin and S. M. Royak (5) on "Blastfurnace cement in the USSR".

For a discussion on the results of research published since 1960, we will find useful points of departure in several major publications issued after the Symposium. I cite first the second edition of the well known monograph "Hochofenschlacke" by F. Keil in 1963 (6), second the chapter "Slag cements" by R. W. Nurse in H. F. W. Taylor's "Chemistry of Cement", 1964, (7) and third the extensive survey contained in the paper "Caracteristiques et emplois des laitiers de hauts fourneaux" by P. Javelle and P. Ponteville (8). Other instructive accounts of the same theme are given by

R. H. Bogue (9), H. Kühl (10) and F. M. Lea and C. H. Desch (11).

Slags in Modern Blastfurnace Processes

World steel production, like that of cement, continues to expand steadily. Steel is today made mainly by the open-hearth (SM) and the converter method (Thomas, LD, LDAC processes). The open-hearth method today uses 50 to 70 percent of basic pig iron won from ore, the modern converter process 70 to 90 percent. This high proportion of basic pig has become necessary because the supply of scrap has not kept pace with the rise in steel output.

Moreover, in the last ten years the more modern LD and LDAC processes have increasingly superseded the open-hearth method, so that pig iron production must rise in step with steel output. In 1966, a world output of over 400×10^6 tons of steel consume 340×10^6 tons of crude pig and 60×10^6 tons of scrap. Failing other and equally economic methods, these huge quantities will continue to come mainly from blastfurnaces for the foreseeable future. The rise of 160% registered between 1950 and 1966, accompanied by a marked shift of emphasis from Thomas to stahleisen production, called for new modern blastfurnace plants as well as new developments in process technology to obtain substantially higher output from existing installations.

The present high level of capacity was achieved by the following means:

In new plants by units of greater size with throughputs up to 3,000 tons per day;

By feeding 100% classified burden (ore + fluxes + coke) or pellets of virtually limited grain size spread (6 — 30 mm) and the wide use of ore concentrates;

By using high blast temperatures (1,000 to 1,300 centigrade), with partial enrichment of the wind with oxygen and higher top pressures;

By injecting oil, coal breeze, methane, partly in water vapour, into the tuyeres;

By reducing the quantity of slag per ton of pig.

These measures and their success in improving blastfurnace technology and economy are due to the growing volume of theoretical and practical work carried out since 1950, and particularly as from 1960, in the major industrial nations, sometimes by international cooperation (12), (13), (14), (15), (16) and (17). Their results, with special emphasis on the properties of molten slags, may be summed up as follows:

In modern blastfurnace processes a reduction of the slag volume is of decisive importance. The heat exchange of a blastfurnace proceeds on the counterflow principle. To obtain ideal heat exchange conditions, the interaction of the ascending current of gases and the descending iron and slag melts in the stack should be kept to the minimum. Due to its lower density, a quantity of slag equal by weight to that of the iron melt has about three times its volume. Consequently, the larger the slag component—more or less irrespective of its viscosity—the slower will be the rise of the gas current, and the reduction process it produces, as well as the rate of melt descent (14).

For this reason the reduction of the slag volume per ton of pig is a decisive factor in the efficient operation of large furnaces. Less slag means a larger gas flow per unit of time, permitting a more efficient utilisation of fuels at higher blast temperatures. Whatever the furnace run and fluxes may be, a low volume of slag puts less strain on heat efficiency than a large one and so permits considerable reductions in the required coke charges.

Yet even a low volume of slag does not do away with the need for a suitable chemical slag composition to keep the furnace run trouble-free and obtain pig iron of uniform composition at a steady output rate.

According to W. Oelsen and H. G. Schubert (18) low quantities of slag react more fully, i. e. they foster the transfer of Fe and Mn into the pig melt. With a reduced slag volume, a small increase in its basicity will already improve the degree of sulphur and nitrogen extraction. There are few steel plants in the world today where, due to their dependence on poorer ore deposits, the volume of slag amounts to 400 to 1,000 kilogrammes per ton of pig iron. In most mills employing modern techniques in the mass production of pig, particularly in the USA, USSR, Japan and Western Europe, the average ratio today is 280 to 340 kilogrammes per ton of pig.

Increasing basicity by an addition of limestone alone can under otherwise identical conditions not be carried out at will over the customary furnace temperature range of 1,350 to 1,550 centigrade. A higher limestone content alone quickly makes the slag highly viscous and would give rise to operating troubles which could only be eliminated by substantial increase in temperature. In the past, no irregularity in the furnace run were observed where large quantities of slag were used and their basicity raised by the addition of dolomitic limestone. This led to the conclusion that a rise in the MgO content at the same time as that of CaO, or an

exchange of CaO against MgO improves the flow properties of basic slags within certain limits. The favourable metallurgical effect of increasing slag basicity in this way is limited by a low Al_2O_3 content. Raising the alumina content of low-lime slags does not improve their efficiency. Slags rich in lime, on the other hand, are given better flow properties by raising the Al_2O_3 component to between 15 and 18 percent. This will also facilitate desulphurisation of the bath. Viscosity can be further lowered by increasing furnace temperature or MgO content.

The connections between the chemical composition of slags and optimal working conditions, temperature, viscosity and desulphurisation capacity had already been largely established (4) before the 4th International Symposium on the Chemistry of Cement was held at Washington 1960. The change-over to low slag volumes during the last 10 years has given rise to fresh investigations in laboratories and full-scale production plants of the sequence and speed in the reaction between Fe bath and slag (19), (20), (21), (22), (23), (24), (25) and (26). A number of investigations was devoted in particular to the influence of higher MgO content on viscosity and desulphurisation capacity in the temperature range between 1,350 and 1,600 centigrade and in general on the control of slag run and uniformity of the pig iron produced (27), (28), (29), (30), (31), (32), (33), (34), (35), (36), (37) and (38).

Within the scope of this paper it is impossible to deal in detail with the many conclusions reached. Evaluation of the results obtained shows that the conclusions reached differ, as yet, regarding an optimum content of MgO for the lowest viscosity and the highest degree of desulphurisation. However, the discrepancy still existing is understandable if one considers that both different testing conditions and working hypotheses and slags of different pig iron melts have served as starting points for the relevant research work.

However, as a common result of the various investigations, it can be confirmed that the most favourable slag compositions for the production of different pig iron grades are not solely governed by the amount of the MgO content. One must rather consider all, but at least the four most important components CaO—MgO—Al_2O_3—SiO_2 that make up 93 to 95 weight percent of the composition (33), (37).

Tables 1a and 1b give a survey of the chemical composition of blastfurnace slags from different countries. A comparison of the MgO figures in the two tables shows the general tendency to apply higher MgO contents (38), (39), (40), (41), (42), (43), (44), and (45).

With regard to slag composition, blast furnace operators, especially in countries where,—in the absence of national ore bases—the burden consists of various ores, follow the suggestions of E. F. Osborne, R. C. deVries, K. H. Gee and H. N. Kraner (46). Table 2a shows optimum slag compositions; the values are taken from cit. lits. (46) and (47). Also the indications on composition, temperatures and viscosities in Table 2b are taken from these sources (46) and (47).

Slags of this composition require only low melting temperatures. Already below 1,500 centigrade their viscosity is very low and their sulphur absorption

Table 1a. *Chemical composition (per cent) of blastfurnace slags (Analysis samples from 1962–1967)*

	SiO_2	Al_2O_3	FeO	MnO	TiO_2	CaO	MgO	Na_2O	K_2O	S	CaO/SiO_2
Ruhrgebiet	28–40	10–18	0.2–2.1	0.1–4.2	0.1–1.5	38–46	5–12	0.4–2.3	0.3–1.3	0.9–2.2	1.07–1.49
Niedersachsen	34–39	12–16	0.3–1.2	0.9–2.0	0.5	32–42	5–10	1.1–1.2	1.3–1.5	0.7–1.0	0.83–1.21
Saargebiet	34–35	13–16	0.4–2.0	0.5–1.1	0.5–1.1	37–43	4– 8	0.4–1.0	0.6–0.8	0.6–1.0	1.08–1.25
France	30–38	13–22	0.5–3.8	0.1–1.0	.0.5	35–48	2– 8	0.3–0.5	0.6–0.8	0.4–1.5	1.20–1.50
England	32–40	14–22	0.3–1.2	0.1–2.6	0.4–1.0	33–43	2–16	0.3–0.5	0.4–1.4	0.7–2.7	0.97–1.31
USSR†	34–35	5–23	0.3–2.4	0.1–2.1		29–48	0–18			1.1	
South Africa††	28–36	12–22	0.6–2.5	0.2–0.9		28–36	13–21			0.7–1.4	0.85–1.12

*From (39); **From (40); ***From (7), (39), (41); †From (29), (42), (43), (44); ††From (38), (45).

Table 1b. *Composition (per cent) of blastfurnace slags*

Source	Type	CaO	SiO_2	Al_2O_3	MgO	FeO	MnO	S
German*	Hematite	44–48	34–36	9–14	2–6	0.2–0.4	0.4–0.8	1.8–2.4
	Thomas	41–45	31–34	8–13	4–6	0.6–1.5	2.0–4.0	1.5–2.0
	Foundry	43–45	32–34	13–16	3–5	0.2–0.9	0.4–0.8	1.9–2.5
	Stahleisen	40–45	31–36	8–14	4–8	0.3–1.0	2.5–4.5	2.1–2.7
British**	Hematite	49–53	29–32	8–10	3–6	0.7–1.1	0.1–0.5	1.5–1.7
	Basic	40–42	32–33	17–18	3–4	0.5–0.9	1.2	0.6–1.4
	Foundry	38–41	33–35	17–22	2	0.4–0.8	0.2–1.8	0.6–1.9

* From F. Keil (6)
**from F. M. Lea and C. H. Desch (11)

capacity at optimum level.

A comparison of these most effective slag compositions clearly shows that smaller fluctuations in CaO and MgO content or a moderate raising or lowering of the Al_2O_3/SiO_2 ratio will have a limited bearing on the properties listed. In other words, suitably formulated slag compositions will not produce sudden increases in viscosity and thus no trouble in the furnace run, even if their composition alters a little in line with the unavoidable fluctuations in the burden.

The influence of Al_2O_3 and especially MgO content on viscosity (and desulphurisation capacity) becomes apparent from the space diagram (Fig. 1) of O. Farkas (33). This author infers from it that, for all slags of any Al_2O_3 percentage, an MgO content of 10 to 12 percent may be considered an optimum. If the points of optimum slag compositions, based on $CaO + MgO + Al_2O_3 + SiO_2 = 100$ weight percent, are plotted at the 10-percent-MgO-level of the quaternary system silica-alumina-calcium oxide—magnesium oxide (Fig. 2), these points, according to O. Farkas (33), lie in the area shown in the phase fields of Merwinite and Melilithe.

However if, for plotting optimum slags in this quaternary system, one for instance selects the levels of equal Al_2O_3 contents (10, 15, 20 weight percent), the points come also into the phase fields of merwinite aud melilithe.

Fig. 3 shows the range of compositions of optimum slags for equal contents of 15 weight percent of Al_2O_3.

With a view to taking into account possible losses of temperature when filling the ladles, it is indispensable to know the liquidus temperature of the slag melts selected for being fed to the granulation plant for cement slag production. Due to their functions in the blastfurnace, blastfurnace slags are among those materials which are most often chemically analysed. For their chemical composition which is thus always well known the relevant liquidus temperature can be calculated from the figures given by (46). The liquidus temperature can be ascertained direct on small samples by means of the high-temperature microscope according to J. H. Welch (48), (49). In this connection the high-temperature microscope

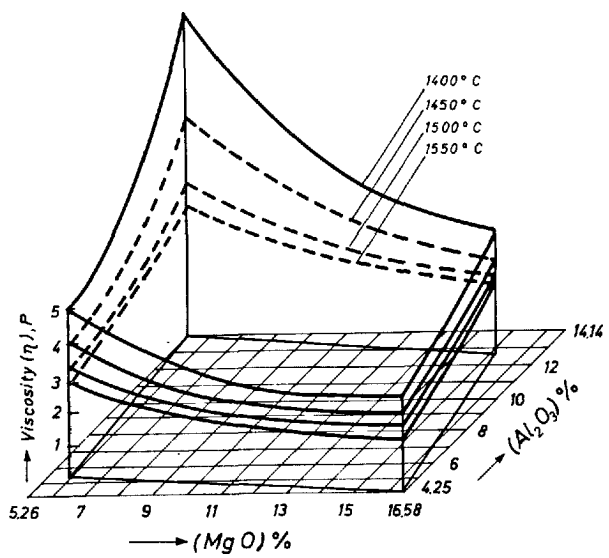

Fig. 1. *Viscosity of blast furnace slag by different weight-% of Al_2O_3 and MgO at 1400°C, 1450°C, 1500°C, and 1550°C (by O. Farkas [33])*

Table 2. *Optimal slag compositions for different proportions of Al_2O_3 for 1400°C—1600°C*
a) figures by E. F. Osborn, R. C. deVries, K. H. Chee and H. H. Kraner (46)

	Chemical composition				Liq. p.	Viscosity (Poise) by °C				First	Refractive index
	Al_2O_3	SiO_2	CaO	MgO	°C	1500	1450	1400	1350	crystall.	of glass (n)
1	5	35	44	16	1589 ± 4					Periclase	1.644
2	10	33	44	14	1518 ± 4					C_3MS_2	1.648
3	15	29	44	12	1502 ± 2					C_2S	1.648
4	20	24	45	11	1531 ± 6					C_2S	1.654
5	10	35	40	15	1464 ± 3					C_3MS_2	1.642
6	15	34	41	10	1437 ± 2					Melilite	1.641
7	15	36	35	14	1405 ± 3					Spinel	1.629

b) figures by P. Kozakevitch and G. Urbain (47)

1	10	35	45	10		2.3					
2	10	35	40	15		2.1					
3	15	35	45	5		3.0	4.6	7.0			
4	15	35	40	10		2.7	3.9	6.0			
5	15	35	35	15		2.6	3.6	5.3	8.3		

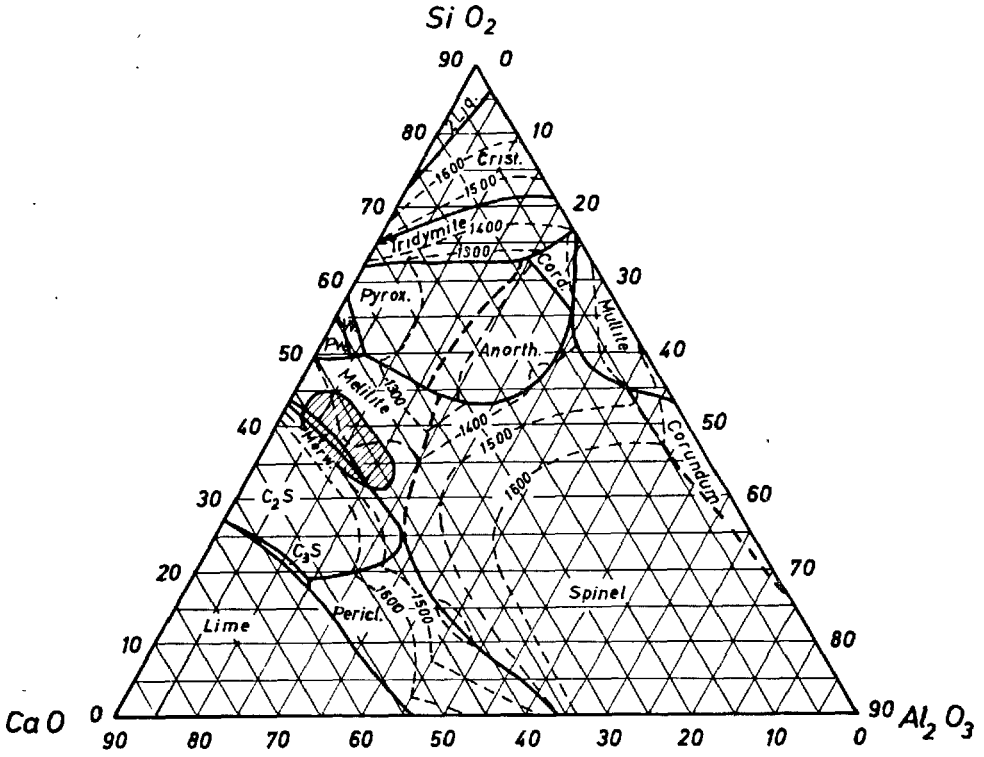

Fig. 2. *Optimum composition of blast furnace slag in the quaternary system CaO-MgO-Al_2O_3-SiO_2 in the plane for 10% MgO*

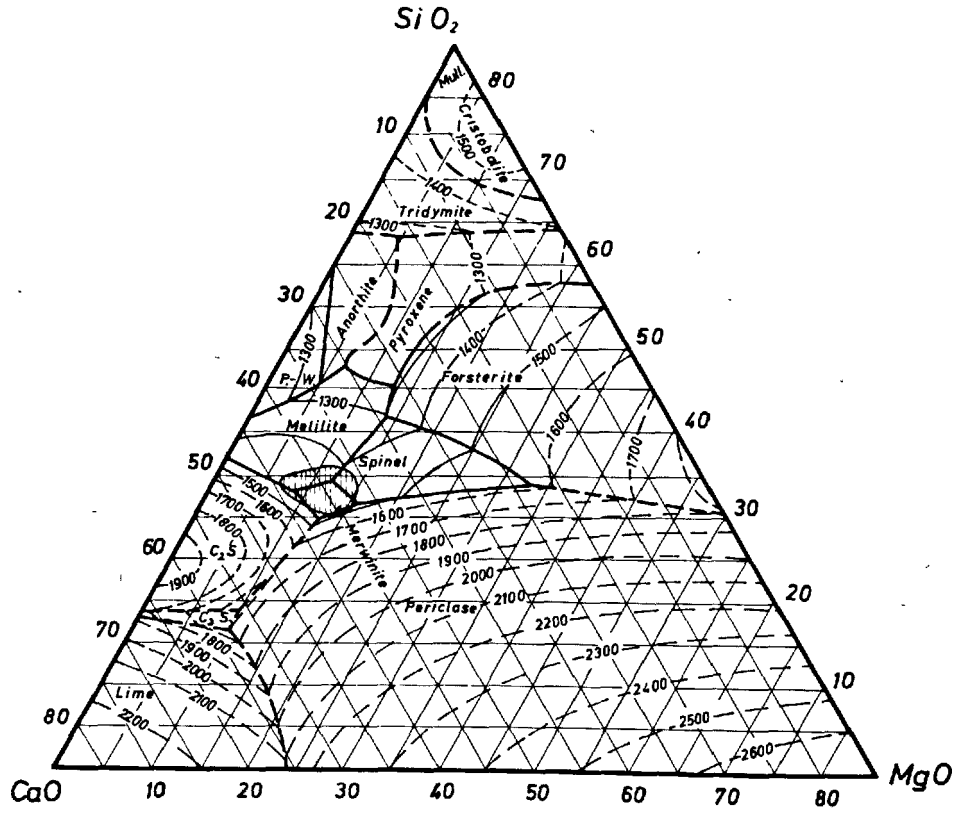

Fig. 3. *Optimum composition of blast furnace slag in the quaternary system CaO-MgO-Al_2O_3-SiO_2 in the plane for 15% Al_2O_3*

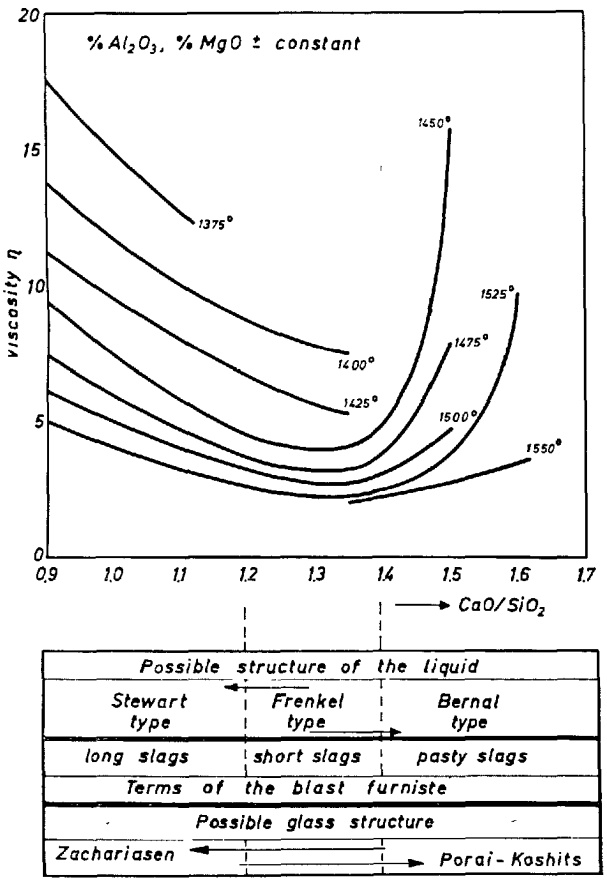

Fig. 4. *Viscosity of slag melts (Basic) vs. CaO/SiO_2-ratios. The graph above according to P. Kozakevitch (54). Supplementary scheme by F. Schröder.*

indicates also the kind of the primary mineral phases and admits estimations of the viscosity.

S. Klemantaski (17) describes the method of E. T. Turkdogan and P. M. Bills (32) to determine the viscosity after computation of the mole fractions of the silicic acid (N_{SiO_2}) and that of the silicic acid equivalent alumina (N_a) from a diagram that indicates the $\log \eta$ of viscosity in function of the sum $N_{SiO_2} + N_a$. (The silicic acid equivalent of alumina is the difference silicic acid-mole fractions in the composition of melts of identical viscosity of the systems $CaO - SiO_2$ and $CaO - Al_2O_3 - SiO_2$.

The relations between chemical compositions, the temperature and the viscosity shows the graph published by P. Kozakevitch (54) on Fig. 4. The supplementary scheme on this graphe by F. Schröder may serve as an illustration of detections in the next chapter.

The Problems of the Liquid Slags and their Glassy State

The Ion Theory and the Structure of the Liquid Slags

The results of earlier comparative investigations (50) (51) and (37) showed that the latent hydraulic properties of granulated slags depend on virtually the same conditions which make for optimum slag runs in blastfurnaces. They are temperature, viscosity and the chemical composition of the silicate melts. In the past chemical analysis was mainly employed to elucidate the factors which governed the selection of slag composition for the type of pig iron to be obtained, on the one hand, and the further use of the solid slag on the other. Meanwhile, the application of modern physical and electro-chemical methods to research into the melting processes producing slag has modified our views on the structure of liquid slags as well. Since this change also effects the explanation of the hydraulic properties of vitreous slag, we have included in our bibliography the publications of the following authors, representative of the large volume of work done: P. Herasymenko and G. E. Speight (52), H. Flood and K. Grjotheim (53), P. Kozakevitch (54), R. Kammel and H. Winterhager (55), M. Frohberg (56), H. P. Schulz (24), and R. E. Boni and G. Derge (57).

Earlier ideas of metallurgists on the "constitution" of slags which considered the melts as result of mutual solutions of melt-resistant oxide molecules were originally formulated by H. Schenck (58). On them are based the deliberations by F. Keil (6) on the transition of liquid slags into the vitreous state, and H. E. Schwiete and F. C. Dölbor (59) still mention molecules as components of vitreous slags.

Research into the electrolytic properties and surface tensions at high temperatures have increasingly displaced this molecular theory.

It is now widely held that the oxide components of

slag melts are disproportionately bound into complex ion compounds of smaller or larger size. According to the ion-theory on the structure of silicates in solid and liquid form, the more or less regular arrangement of the ions in coordination lattices is attributed to electrovalent and covalent binding forces. Si^{4+} as the central ion of a tetrahedron, surrounded by four oxygen ions, can actuate valencies to neighbouring Si^{4+} ions via oxygen bridge links. In this way, an open lattice of unlimited space form into which the metallic cations are built by virtue of their coordination trend and following the laws of electro-neutrality.

The tetrahedral SiO_4^{4-}-complex anion is produced during the melting from the silicic acid of the gangue, fluxes and coke ash. It also forms during dissociation, e.g. of the orthosilicates (Fe_2SiO_4, $CaSiO_4$) produced before the meltdown of the burden, as per $R_2SiO_4 = 2R^{2-} + SiO_4^{4-}$.

The decreasing viscosity (growing liquefication) of silicates with increasing temperatures is attributed, on the one hand, to a rising number of thermal linkage fractures. On the other hand, the addition of metallic oxides (alkaline, alkaline earth and other metal oxides) which foster the coordination trend of the SiO_4^{4-} anion also promotes chemical linkage fractures.

The division of a spatially unlimited SiO_4^{4-} tetrahedra-lattice or network into complex silicate anions of smaller size as the basic oxide component rises is assumed to be governed by the equations shown in Table 3.

Since blastfurnace slag melts never consist exclusively of neso-silicates (O/Si = 4), so that a situation similar to the formation of orthosilicates (Ca_2SiO_4, Mg_2SiO_4) cannot occur, the more complex-anion structures form in line with the O/Si ratio obtaining at any time, such as $(Si_8O_{20})^{8-}$ or $(Si_3O_9)^{6-}$. The ratio O/Si governs their dimensions which have an important influence on slag flow properties.

J. O. M. Bockris and J. D. Kitchener (60) are of the opinion that in melts with metal oxide content of 10 — 60 mol-%, $(Si_3O_9)^{6-}$-rings form the basic unit, while complexes of formula $(Si_nO_{2n+1})^{6-}$ determine the viscosity.

Table 3. *Reactions for the disproportionation of a spatially unlimited SiO_2-lattice According to R. Kammel and H. Winterhager (55)*

Basicity		Silicate Structure	Relationship O/Si	Viscosity η
acid	SiO_2	Tekto-Silicates	2.0	diminishing
	$2SiO_2 + O^{2-} = Si_2O_5^{2-}$	Phyllo-Silicates	2.5	
	$Si_2O_5^{2-} + O^{2-} = 2SiO_3^{2-}$	Ino-Silicates	3.0	
	$2SiO_3^{2-} + O^{2-} = Si_2O_7^{6-}$	Soro-Silicates	3.5	
basic	$Si_2O_7^{6-} + O^{2-} = 2SiO_4^{4-}$	Neso-Silicates (Single-Tetrahedra)	4.0	

According to O. Farkas (33), a base oxide content of 25 mol-% leads to the formation of larger complex anions, such as $(Si_9O_{21})^{6-}$ or $(Si_{12}O_{28})^{8-}$, at 33 mol-% those of $(Si_6O_{15})^{6-}$ or $(Si_8O_{20})^{8-}$. Only at a base oxide content of 50 mol-% are complex anions with structures such as $(Si_3O_9)^{6-}$ or $(Si_4O_{12})^{8-}$ said to form. The concentration limit of orthosilicate lies within the range of 66 to 70 mol-% base oxide. In this case, the slags would contain practically only freely moving $(SiO_4)^{4-}$-anions surrounded with the metal cations.

In the most effective blastfurnace slags the CaO + MgO content generally lies above 50 mol-%, mainly between 54 and 57. In this base concentration range, according to (60), small complex anions of the general composition $(Si_nO_{3n+1})^{2n+2-}$ (example: $(Si_2O_7)^{6-}$) are formed. The cations present in the liquid slag surround the complex anions and saturate their free negative charges. In this way, 2 Ca^+ and 1 Mg^{2+} will be found in the hollow spaces of the $(Si_2O_7)^{6-}$ anion in the structure of the akermanite ($Ca_2MgSi_2O_7$) which is of great importance in blastfurnace slags.

In the even more important structure of the merwinite ($Ca_3MgSi_2O_8$) the Ca^{2+} and Mg^{2+} cations are said to hold together the single tetrahedrons of $(SiO_4)^{4-}$ anions present in it.

In the gehlenite structure ($Ca_2Al_2SiO_7$), where a $(SiO_4)^{4-}$ tetrahedron of the $(Si_2O_7)^{6-}$ anion can be replaced by an $(AlO_4)^{4-}$ tetrahedron as a lattice component, the free valencies of complex anion $(SiAlO_7)^{7-}$ are assumed to be saturated by the two Ca^{2-} cations and the one Al^{3+} ion.

In the transition of slag melts into the vitreous state, we must consider the important fact that the binding link fractures produced by the thermal agitation are reversible. This means that during the cooling down fissures in the lattice close again. Bearing this in mind, the production of glassy blastfurnace slags with optimum hydraulic properties would call for a faster rate than the speed at which the lattice fragments recombine.

In melts at temperatures of 1,500 to 1,600 centigrade, the binding forces acting between cations and anions are weakened by the thermal agitation, and the disproportionate development of smaller and larger complex silicate structures (e.g. as neso-silicates and soro-silicates) is fostered.

It may be assumed that in these processes Ca^{2+} and Mg^{2+} cations behave in different ways. For the same valency, the ion radius of Mg^{2+} is smaller than that of Ca^{2+}. The Mg^{2+} consequently has a higher ion

potential and stronger covalency forces. Possibly, the Mg^{2+} cation promotes the enrichment (cluster formation) of small, more mobile structural units between larger coherent silicate complexes or lattice fragments and so contributes to the lowering of viscosity.

Research into structure models for molten liquids has made contributions to this subject which raise the probability of the conclusions drawn from the ion theory as applied to slag melts.

According to the atomistic interpretations of the structure of liquids by W. A. Weyl (61) such silicate melts can be described by using a ternary diagram whose corners represent the extreme models of liquids, outlined by J. D. Bernal (62), J. Frenkel (63), and G. W. Stewart (64). The exact location therein of slag melts cannot yet be stated. A number of electron-microscope investigations on melt phase separation seem to indicate that slag melts in particular have a relatively high proportion of the "Frenkel"-model, as compared with the other two liquid models.

Frenkel's liquid no longer has any structural relation to the configuration of the corresponding crystal phases. Rising temperatures result in faulty arrangements (empty sites, displacements) which form centers of assymetry exerting an influence on the binding forces in their vicinity. The cristalline substances melt at a disproportionate binding energy rate. Stronger forces may be lead to temporary clusters and weaker forces to fluctuating fissures. Therefore the structure of such a melt alters continuously.

Already a few centigrade above their thermodynamically and kinetically well defined melting point the liquid has a very low viscosity. The temperature coefficient of the viscosity is small. Such a melt may at any point of time be described by the presence of variable clusters separated by fluctuating fissures. Liquids of the Frenkel-type cannot be supercooled sufficiently to form a glass.

The Bernal liquid has a structure free of faulty arrangements and similar to the crystal from which it has originated during the rise in temperature. Mostly such crystals can be strongly overheated. The melting process takes place progressively. The liquid remains still stable above the melting point. Such melts are of very high viscosity and have also a high temperature coefficient of viscosity. Melts having "Bernal structure" can just as well as "Stewart liquids" be easily undercooled to form glass.

An essential characteristic of the Stewart liquid is its ability to be drawn out into long fibres, i.e. that contrary to the clusters of the Frenkel liquid the structural elements are arranged into groups capable of orientation, e.g. to chainlike or ringlike shape. For this type of substances exists no relation between the average bond energy and the lattice energy, nor between the melting point and the viscosity.

The slag melts rich in basic oxides (mainly CaO + MgO) cannot straight away be blown into fibres. This is only possible by increasing their proportion of Stewart liquid after being melted together with fine quartz sand. Lime basic blastfurnace slags will only become very highly fluid a few degrees above melting point by adding other oxides, viz magnesia.

The MgO thus influences increasing of their portion in Frenkel liquid. There is also another fact which points to the proportion of Frenkel liquid, viz optimal effective slag melts with 10 ± 4 wt% of magnesia and 16 ± 4 wt% of alumina. They cannot normally be undercooled, but have to be very rapid quenched during the granulation process. Other indications for the participation of the "Frenkel type" in liquid slags are the extraordinary crystallization capacity below liquidus and the often found heterogeneity of the slag glasses in micro range by separation of liquid phases (see photos No. 7–11).

Last not least also the intensive violet, blue and red fluorescence radiations (65) may be signs for the participation of the Frenkel liquid, it will be considered that this liquid type melts are favoured by formation of assymetry centers. The last will be surely multiplied by the O^{2-} of variable polymerisation degree, introduced by CaO and MgO.

The employ of the ion-theory (52) (55) (56) and of the atomistic conception of the phase relations due to the complex structure of liquids (61) on the hot slag melts may lead us to the opinion that: the amount of the oxygen content depending on the increasing sum of CaO + MgO up to ~56 wt%, the great number of the silicate anions with a low polymerisation degree, and the participation of liquid of the Frenkel type capable of a fluctuating formation of clusters and fissures, determine the very low viscosity a few centigrades above liquidus and the desulphurization rate of slag melts.

The Glassy State

Most of what has been said so far also applies to granulated vitreous blastfurnace slags, because the melt structure has been frozen into them by very rapid quenching.

The degree of latent hydraulic hardening properties of granulated slags is governed by the extent to which this quick quenching freezes in the disproportionate structure of the melt.

In addition to the tapping temperature the viscosity

and the chemical composition of the melts, the granulation temperature and the granulation speed determine thereby mainly the glass-structure and glass content, resp. the latent hydraulicity, resp. the quality of the cement slags.

The above statements are also apt to facilitate the answer to the question of the structure of the slag glasses and their properties. In 1964 R. W. Nurse (7) in his explanations on the crystal-chemical structure has compared the glass structure models elaborated by W. H. Zachariasen (66) and E. A. Porai-Koshits (67).

Based on the interpretations of a number of deductions from glass properties and referring to further results of investigations R. W. Nurse reaches the conclusion that the differences between the network theory and the crystallite theory in its modern form will vanish.

According to the present state of our knowledge, it can be assumed from the still "hypothetical" position of the slag melts in the ternary diagram (Frenkel—Bernal—Stewart) that the structure of the slag glasses forms a solid solution in a chain whose final links may be the two mentioned structure models.

Whether the glassy state of slags corresponds more to the one or to the other of the two glass-structure types will probably depend on the proportion of Frenkel-liquid which was able to be transformed into the solid glass state. According to R. W. Nurse, he and his coll. F. W. Parker, T. Tanaka, T. Sakai and J. Yamane as well as R. Kondo assume that the network theory is more convenient (7), whilst de Langavant (7) and S. Solacolu (7) prefer the crystallite theory. F. Keil (6) and H. E. Schwiete and F. C. Dölbor (59) plead also for the network theory.

The Granulation

Slag melts as they are nowadays preponderant in blastfurnace processes are liquids that easily crystallize by normal cooling down. The liquidus temperatures of these slags are situated—dependent on their composition—between 1320 and 1450°C (56). From heating-up tests carried out on slags (45) (68) we know that nucleation and growth of crystallites starts with temperatures > 840°C. When freezing in the structure of the slag melts it is, therefore, necessary to very quickly undercool the range of the liquidus temperature and the range up to below 800°C in order to avoid formation of undesirable heterogeneities, e.g. the separation of melilite crystals.

Granulation of slag melts, i.e. their transformation into a granular solid sand which can be easily evacuated from the blastfurnace zone is about ten years older than the discovery of the hydraulic properties of this product. The various processes developed to this purpose have simultaneously a double function: splitting the slag to the size of sand grains, and cooling it quickly down to 100°C. In nearly all cases water is used as a cooling means. In view of good cement properties it is convenient, according to P. Großstück (69) to granulate currently with fresh water instead of using circulatory water system. In the latter case the water will heat up so as to favour devitrification. Often the use of abundant water already results in the required splitting. With a view to reducing the amount of water required, compressed air, pressure water, or specific mechanical devices are used to intensify the splitting process. F. Keil (6) has recently described the different granulation processes.

Running slags have the highest possible temperatures. Therefore running slag granulation always provides very reactive cement slags. With this process the melt after leaving the slag mold flows over a short fire-proof runner or spout and then drops ~ 20 cm down into a pressure water jet. This causes splitting and quick cooling and conveys the more or less porous-foamy granulated product into provided Talbot-cars. From these the excess water can run off at once.

Due to the flowing-off of the running slags, the height of the slag layer is reduced above the bath raising between two tappings. According to A. Send (26) this phenomenon handicaps the desulphurization. For this reason, recently with very large furnace units the slags are drawn off together with the pig iron.

It depends on local space conditions whether the large volume of tapping slags will be granulated directly at the furnace or at a more distant centralised plant. If granulation takes place at the furnace, the melt flows on to a runner at the track-free head of the furnace platform. At the runner end it drops into a sufficiently long water runner positioned below, where it is seized, separated, quenched and flushed on into a concrete basin. The quality of the granulated slag with regard to splitting off and glass content depends on the length of the water runner. On the bottom of the basin there is an 80—100 cm thick sand-gravel filter layer (70) which in turn is covered by a framing of steel rails. The granulated slag drains into the sand-gravel layer and can be lifted up by the grab excavator without thereby destroying the filter layer. By means of tubes perforated at the base of the filter layer, it is possible to flush the latter so as to remove any accumulated slag fines.

Also in central granulation plants grain separation

and quenching is accomplished in the runner with or without pressurised water. Here granulation may be improved by fitting spraying heads through which the pressurised water for granulation and the cooling and convoying water arrive in two super-imposed levels. According to I. I. Kholin and S. Royak (5) the U.S.S.R. formerly preferred granulation with and without runners into basins. But already before 1960 they gradually changed over side by side with this wet granulation to the "semi-dry" granulation. The terms "wet" and "semi-dry" referring to the water content of the granulated slag. In the latter process, granulation proceeds in a drum in two stages: at first quenching and foaming with little water under pressure. At second the still hot and highly porous slag is mechanically splitted off, and expelled out of the drum. The advantage of this method consists in: decomposing less sulphide, and forming less hydrogen sulphide. This reduces corrosion of concrete and steel of the granular plants.

In 1963 V. F. Krylov (71) stated in a comparative report on these two granulation processes that wet granulation in the runner is the most efficient; except for very hot slag melts it is suitable for any acid and basic slag.

In the United States S. P. Kinney and F. Osborne (72) have introduced a splitting and quenching process. This is characterized by the slag jet being torn by means of steam-air jets in a fixed wide steel tube and blown at high pressure through an atomized water curtain. The steam, air and water nozzles are arranged in a semi-circle at the rear of the tube. This process is capable of producing granulated slag and foamed slag.

According to W. Altpeter (73) granulated slag can be safely conveyed hydraulically if the slag- (15% in volume) water- (85% in volume) mixture is carried in rubber conduits. A report by W. Hahn and S. Geron (74) inform both on the wear of tubes made of other materials and of the pumps, as well as on the minimum transportation speed.

Granulated Slag for Cements

(by F. Schröder and K. Grade)

Condition and Characteristics

By a suitable granulation process the slag melts are converted into a vitreous granular sand 0—5 mm, which is more or less porous. In connection with the systematic study of the qualities of granulated slags, the Forschungsinstitut für Hochofenschlacke, Rheinhausen (Research Institute for Blastfurnace Slags) has also currently made grain size analyses. As during these investigations (76) also air-granulated slags and slags quenched in granulation mills were screened, the results are summarily represented by the attached diagram (Fig. 5). The scattered range of variations of the wet granulated slags of the diagram corresponds with the results obtained by E. Prandi (75), testing 54 slag samples.

Photos No. 1—6 demonstrate the petrographic condition of cement slag grains of good hydraulicity. A high percentage of porous grains (Photos 1 and 2) is an advantage for the production of blastfurnace slag cements with relatively high initial strength. Dense vitreous grain portions (Photos 3, 4 and 5) stimulate the development of high final strengths and favour above all the post-hardening. Photo No. 6 shows a vitreous grain with interspersed melilite crystals. Those crystals and skeleton crystals, e.g.

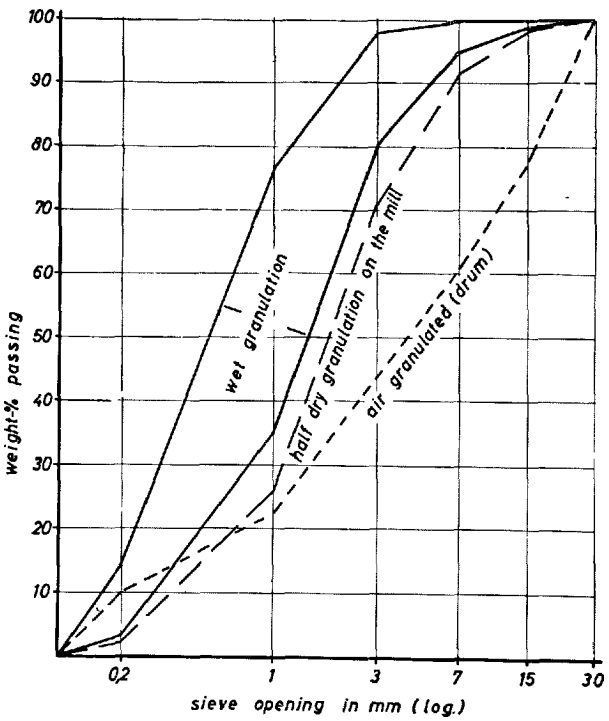

Fig. 5. *Grading of granulated slags. Interpretation of test-results (1961–1966) by F. J. Rheinhausen (76)*

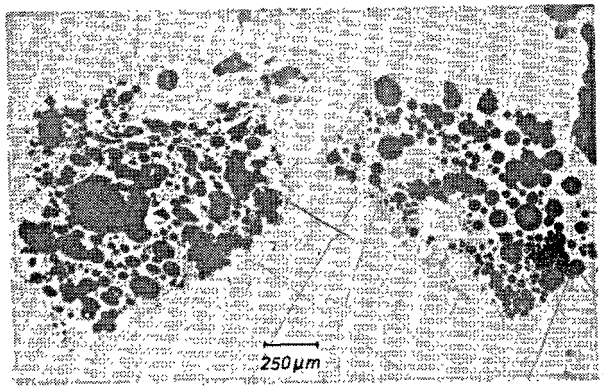

Etched with HF-vapor Reflected light

Photo. 1. *Vitreous slag—foam texture mill-granulated, easily grindable*

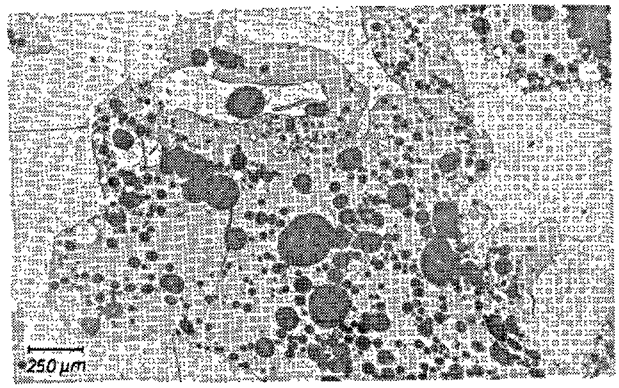

Etched with HF-vapor Reflected light

Photo. 2. *Vitreous slag—splinterlike porous texture wetgranulated, easily grindable*

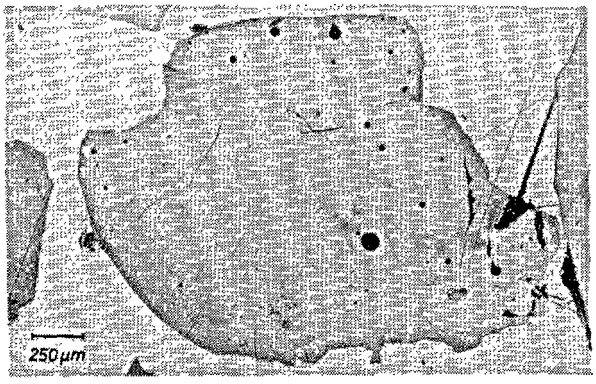

Etched with HF-vapor Reflected light

Photo 3. *Vitreous slag—dense texture wet-granulated, poorly grindable*

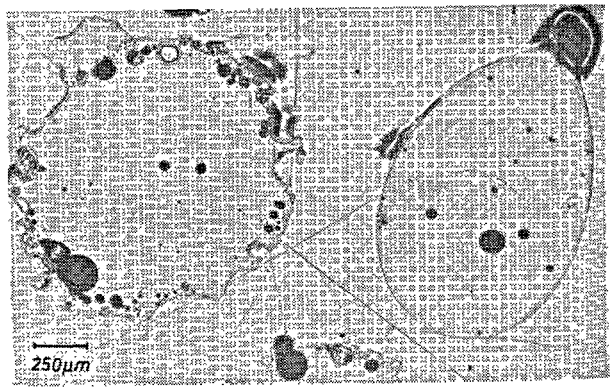

Etched with HF-vapor Reflected light

Photo 4. *Vitreous slag—dense texture air-granulated in the drum, poorly grindable*

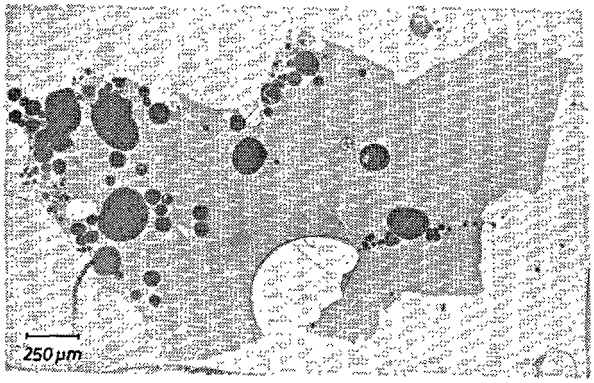

Etched with HF-vapor Reflected light

Photo 5. *Vitreous slag—poor porous, dense and splinterlike texture wet-granulated, rel. easily grindable*

Etched with HF-vapor Reflected light

Photo 6. *Vitreous slag with enclosures of melilite-crystals wet-granulated, dense, texture, poorly grindable*

C_2S-C_3MS_2- and CS-like, grow below the liquidus by too slowly cooling rate.

Foamy-porous granulated slags form during granulation of running slags or hot tapping slags resulting from the production of stahleisen, foundry and hematite and hot operated basic pig iron.

Dense-vitreous grain mixtures are generally obtained from cold-blast stahleisen slags and normal Thomas pig iron slags. Blastfurnace cement works connected to blastfurnace plants with two or more blastfurnaces have thus the possibility, by cutting different granulated slags, of producing cements with high initial and final strength.

P. Aitcin (68) and S. L. Kolhatkar and T. V. Cherian (77) report on the influence of high tapping or granulating temperatures on the color.

While the first (68) elucidates the change of the color, in function of the tapping temperature, from dark grey-brown to brownish-white, the last (77) related the brightening to the increasing liquidus temperature of synthetic, modified, high-alumina slag glasses. These vitreous slags have simultaneously been investigated in respect of temperature influences on other physical properties, such as bulk density, porosity and water retention potential. The results attained are similar to the findings of H. E. Schwiete and F. C. Dölbor (59) testing the relations between granulation conditions and properties of granulated hematite slags on numerous technical specimens.

The results obtained from the investigations of the dependence of the bulk density, the water and vitreous content on the slag temperature and in particular on the granulating conditions confirm the previous findings: the bulk density decreases and the amount of retained water increases as the temperature becomes higher.

Quality of granulation is characterized by the amount of vitreous grains. H. E. Schwiete and F. C. Dölbor (59) modified the quenching conditions by using molds with varied calibers so as to obtain between 6 and 98% glass contents. The strength development of test cements selected from 30 technical slags specifically granulated for this purpose showed a dominant dependence on the glass content measured by microscope.

According to a generally accepted view increasing contents of crystalline components in vitreous slags considerably reduce the quality of their hydraulicity but not to such an extent that slags with only 30—40% vitreous constituents can no more be used for the production of cements with low strength specifications. I. I. Kholin and S. M. Royak (5) make the same statements, however, with the difference that they regard part of the mineral formations as hydraulically active. According to the findings of F. Keil and F. Gille (78) that akermanites react hydraulically without activator, this opinion is justified, and, no doubt, certain orthosilicate formations in vitreous slag will behave analogously.—

P. P. Budnikov and V. S. Gorskov (79) are of the same opinion. It has incited them to carry out investigations with a view to increasing the hydraulicity by a controlled crystallization. The results obtained show that by repeated re-melting at different temperatures and cooling to 1,000 centigrades via unstable crystallizations the ratio merwinite/gehlenite can be so varied that the more reactive component is preponderant.

In the Research Institute for Blastfurnace Slags, Rheinhausen, the glass content and the content of crystalline portions in granulated slags are determined as follows: the specimen reduced to a particle size of 40—60 μ is bedded into a plastic material and a polished section is made. The latter is etched with 1% alcoholic HNO_3 and HF-vapour, and subsequently the amount of vitreous and crystalline components (the latter possibly separated according to minerals) are counted by means of an integration ocular.—When checking the vitreous content of granulated slags in blastfurnace slag cements, a cement dispersion specimen (grain size 30—40 μ) is bedded into Canadabalsam and with the aid of the polarizers one ascertains the proportion of purely vitreous grains, of grains differing in respect of their crystal content and of entirely crystalline grains.

In a previous section of this report we have pointed out that the structure of vitreous slag cannot be described solely by the crystallite-theory of Porai-Koshits (67) nor by the network theory of Zachariasen (66). By means of electronic-optical investigations, by analysis of the X-ray small-angle scattering as well as on the basis of the diffuse light dispersion, a drop-shapped separation of melting phases could be demonstrated in many slag glasses, viz. a micro-heterogeneity not caused by crystal growth.

It is known, however, that often certain blastfurnace slags with a low liquidus temperature after cooling present an enamel-type condition. By microscopic examinations of such slags the writer could find droplet-like separation areas more than 1,000 Å in diameter. In the meantime, F. Schröder and K. Grade (80) examined many specimens of vitreous slags by light-microscopic and fluorescent-microscopic methods in respect of such separations and other petrographic textures which are indicative of phase separations in the melt.

Photo No. 7 shows a vitreous slag grain with a "schlieren-" or streak-chaped separation of different glass-phases. Fluorescence has shown in a glass-matrix (pink fluorescing; greyish white on the photo) streaks of orthosilicatic glass (blue fluorescing; grey on the photo;—the grey color is produced by etching with HF-vapour).

Photo No. 8: In a melilite glass matrix (red fluorescing) there are embedded drop-shaped roundish separation areas of orthosilicatic glass (intense bright blue fluorescing, thus mainly C_2S)—between polarizers showing only tensio birefringence; further a crystallite with myrmekitic eutectic texture consisting of melilite (crystalline, fluorescing violet, white on the photo) and of merwinite-glass-like particles(irregular rounded, partly crooked in the melilite, bright blue fluorescing; grey on the photo by etching with HF-vapour) and some needle-shaped wollastonite crystallites (fluorescing red, very weak; white on the photo).

Photo No. 9: Myrmekitic eutectic textures there are embedded in the melilite glass matrix (fluorescence color: salmon; dark grey on the photo). These textures consist of merwinite (fluorescence color: blue; on the photo lighter grey) and melilite (violet fluorescing; on the photo white). These textures can only be explained by separated melting phases in the beginning crystallization.

Photo No. 10: The vicor—glasslike matrix (rend-

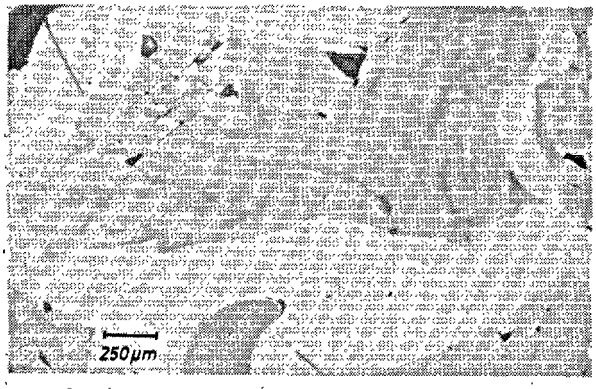

Etched with HF-vapor Reflected light

Photo 7. *Vitreous slag—cord texture*

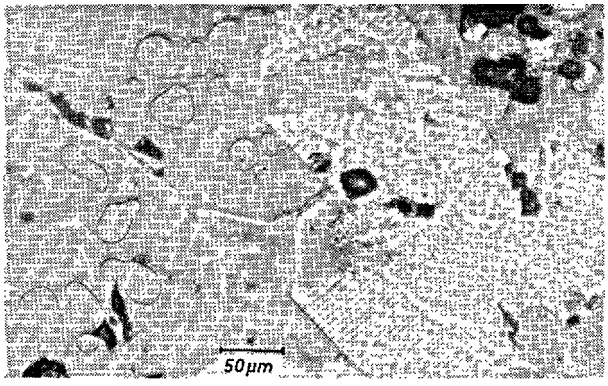

Etched with HF-vapor Reflected light

Photo 8. *Vitreous slag with enclosures: ortho-silicates (drop-like, medium-grey), melilite-crystal with myrmecitic eutect texture (white—melilite; grey—ortho-silicates)*

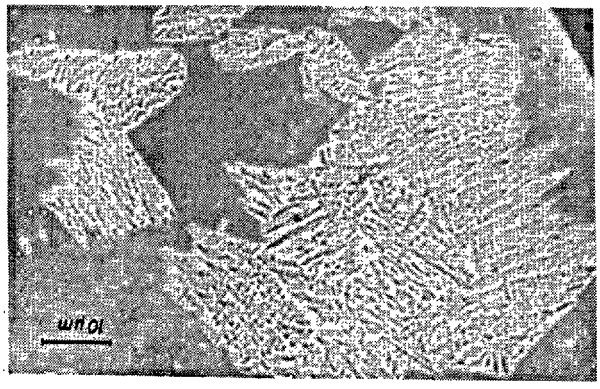

Etched with HF-vapor Reflected light

Photo 9. *Vitreous slag with myrmecitic enclosures of melilite (white) and merwinite (medium-greay)*

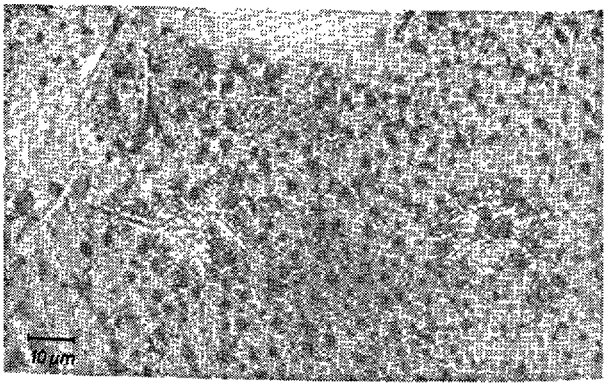

Etched with HF-vapor Reflected light

Photo 10. *Vitreous slag with separation of glassic ortho-silicates (dark-grey to black) and single merwinite-aggregations (white)*

ered visible by etching with HF-vapour; pink fluorescing; on the photo light grey) consists of statistically distributed mervinite droplets (blue fluorescing) and melilite glass (red fluorescing). A mixture of red and blue radiation results in pink fluorescence. In this matrix moreover occur: partly still roundish droplets, partly with needle-like crystallites, of orthosilicatic separations (bright blue fluorescing, black on the photo). These were confirmed also by W. Gutt (81).

On the occasion of paper read in Leipzig on "the hydraulic properties of vitreous blastfurnace slags" H. Busch (82) has pointed out, based on electron—optical representations of smallest vitreous slag splinters, that in a silicate glass matrix are embedded separated droplets of another vitreous silicate phase. As the relevant examination report is not available as yet, we are attaching hereto Photo No. 11 which is reproduced from a publication by H. Peyches (83) and which exactly shows what H. Busch (82) indicates in his electron—optical figures on the structure of the slags examined.

In air-cooled blastfurnace slags the melilites, members of the solide solution series akermanite (C_2MS_2)-gehlenite (C_2AS) are the predominant minerals. From optimum slag melts with an akermanite/gehlenite-ratio 1.2 up to 0.8. In addition to a very high nucleation capacity they have an extremely high speed of growth.

Melilite crystals fluoresce deep violet. If, therefore, in the above mentioned vitreous slag matrix a formation of melilite nuclei starts already at or a few centigrades below the liquidus temperature, such start of nucleation, however, not being detectable either by X-ray-diffraction or by microscopic examination,

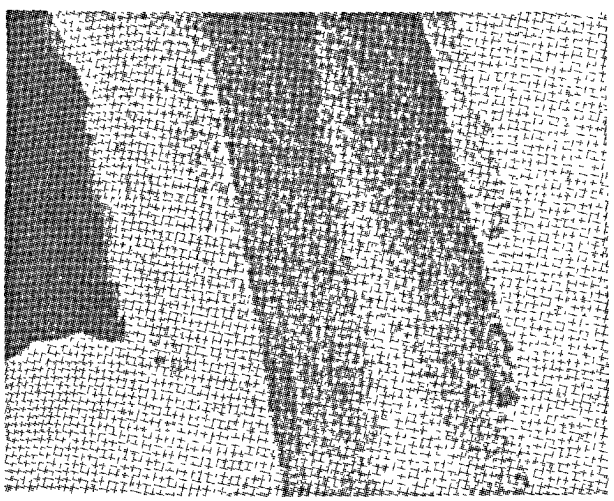

Photo 11. *Thin splinters of glass (electron micrographs by Peyches, 82). Demonstration o j dark droplets within a lighter glass-matrix*

yet the modification of the fluorescence with all the transitions between red and violet point to this submicroscopic heterogeneity of vitreous slags. It takes place essentially in lime—alumina—silica slags lower in MgO.

Microscopic examinations of vitreous slags give little information on where the sulphur of the molten slag remains. The fact is known that part of the sulphides is leached by granulation water. In thin sections of less basic vitreous grains, small skeleton crystals of CaS are seen very rarely. Glass grains obtained by quenching of cold operated slags have yellow-brown to dark-brown colors and remaind of the brown color of technical glasses containing sulphide-sulphur. CaS having a low content of MnS fluoresces orange. A mixture of the red fluorescence radiation with the orange fluorescence the writer calls "salmon". Such a fluorescence is radiated from $CaO—Al_2O_3—SiO_2$ slag glasses with only a few % (< 5) of MgO and $\sim 1.0\%$ S^{2-}.

Better information on the behaviour of sulphur in slags is supplied by microscopic examinations on air-cooled blastfurnace slags (84). Aggregates of CaS-droplets, partly occuring oriented are found in more vitreous parties on the ladle walls. Frequently twisted wormlike inclusions are embedded mainly in the rim zones, rich in akermanite, of melilites. These intergrowths of akermanite and sulphides must be interpreted as being myrmekitic segregations. Furthermore, sulphide segregations occurred in wedges, especially between merwinite crystal aggregates, hence rich in basic oxide. Here one sees isolated myrmekitic eutectic textures of oldhamite and potassium iron sulphide, deep-brown skeleton crystals, accumulations of sodium iron manganese sulphide and amorphous masses of sodium polysulphides. A number of the textures visible under the microscope indicate that in the course of the first cooling stage, molten sulphide is separated from the molten silicate. If further studies on thin sections substantiate these findings of the existence of a sulphide melt—the replacement of O^{2-} ions by S^{2-} ions in silicates has not been proved as yet—this would mean that, at very high temperatures, structural components of the molten sulphide are distributed in the molten slag, between the silicate structure components. They have a liquidifying effect, since, according to R. E. Boni and G. Derge (57) sulphides lower the interfacial tensions of base oxide-alumina-silica melts. Sulphides lower the surface tensions of alumina-silicate melts containing MgO more than those of melts containing CaO and BaO. This might explain the influence of MgO on viscosity, as described above.

For the vitreous slag this behaviour of the sulphides

in slag melts means: The faster quenching is effected or the more the sulphide melt remains distributed between the cluster like structure components of the liquid slag frozen in, the higher the reacting surface during hydration.

This view at the same time offers an explanation of the finding that vitreous slags having C/S-ratios of 1.1—1.2 and higher MgO content show a more favourable hydraulic behaviour than those having a higher degree of basicity, and confirms the author's opinion that a decline in the degree of basicity may be compensated to a certain extent by higher granulation temperatures (85).

The occurrence and the distribution of the sulphides—especially of the CaS—therefore must be considered as a hydraulicity factor. This view was last taken by I. I. Kholin and S. M. Royak (5).

The Chemical Composition

The chemical composition of the molten slags is responsible for the liquidus temperature, the degree of liquidity above this temperature and, thus, also for the selection of the granulation conditions.

However, as figures on these different physical characteristics are rarely available the values of chemical analysis, for the time being, mostly represent those magnitudes that are taken account of for the appraisal of the hydraulicity of vitreous slag. From the period under review, there also exist studies on the influence of the chemical composition of granulated slags on the properties of slag cements. The view generally held that high CaO contents and at the same time higher alumina contents under otherwise equal conditions constitute the most important active chemical components has been established as a confirmation of the findings obtained in the previous decades by (4) and (5) at the 4th International Symposium on the Chemistry of Cement, Washington 1960. This view is also held in special publications (6) (7) and (8).

In recent years several scientists (37) (38) (86) (87) (88) (89) (90) (91) (92) (93) (94) (95) and (96) reported on the influence of the chemical composition and of various chemical components, respectively. Special attention was devoted to MgO with a view to the strength of cement (37) (86) (87) (88) and to the soundness (38) (89) (90).

Its effect on hydraulicity is rated differently. So D. Heyl (37) when increasing at the same time the MgO content from 8 to 12% and the C/S-ratio from 1.2 to 1.3, did not find any clearly recognizable improvements in quality. A. Oelschläger (86) found improvements in strength by increasing the MgO content (up to 10%), when the degree of basicity remained constant. When the MgO content increased, while the degree of basicity dropped, there resulted a decrease in strength which partly was very high. For C/S 0.88, mixes with 9% MgO in the granulated slag showed poor hydraulic properties only. Thus, according to this author, the MgO content affects the strength less than does the C/S-ratio. J. Janowski (87) considers slags as rich as possible in MgO, but with Al_2O_3 contents not exceeding 11%, better suited than slags rich in lime. According to A. Schillak (88), MgO as a constituent of the vitreous phase is harmless up to contents of 7%, but at the same time the slag should contain more than 12% Al_2O_3. To increase the initial strength of cements made from granulated slags with higher MgO-content Schwiete (89) recommends an increase of the Al_2O_3/SiO_2-ratio.

An adverse influence of higher MgO contents on the soundness has not been found as yet. N. Stutterheim (38) studied the properties of slag cements which contained granulated slag with 13 to 20% MgO. All cements show good technical properties, the expansion in the autoclave was extremely low. J. G. D. Steyn and M. D. Watson (90) find, by microscopy, in the slags with 5 to 22% MgO, a maximum of 2.3% by volume of periclase crystals, but of very small dimensions. With these samples, too, the expansion in the autoclave remained within the limits established by cement standards. E. Mariani and G. Schippa (91) find that higher MgO contents in granulated slags are harmless, since only with contents exceeding 20 to 25% there is a precipitation of periclase.

According to J. Janowski (87), a high content of lime is desirable with a view to hydraulicity. Tests on subsequent enrichment in lime of slags were carried out by A. Achillak (88) and the "Iron and steel Orsk-Chalilovo" (92). At Ors-Chalilovo, enrichment of the slag (C/S = 1.12) in lime was carried out up to a degree of basicity of 2.0. The product obtained proved valuable for cement manufacture. According to A. Schillak (88), very high CaO contents decrease the share of the metastable vitreous phase, which remains a prerequisite for hydraulic setting.

M. Venuat (93), in studying test cements (85% slag—15% clinker) of granulated slags with CaO/SiO_2-ratios of 1.01—1.21 finds an increase in strength with increasing basicity.

The favourable effect of higher Al_2O_3 contents was found by A. Schillak (88), J. Janowski (87), H. Sopora (94), M. Venuat (93) as well as H. E. Schwiete and F. C. Dölbor (59). They confirm the view held hitherto that with equal basicity an increase in Al_2O_3 content considerably increases strength. An increase

to 11% Al_2O_3 may with a low CaO/SiO_2-ratio compensate for the loss of strength to be expected by a decrease of basicity.

According to H. Sopora (95), a higher FeO content indicates trouble in the blastfurnace run and, thus, corresponding quality declines of the slags. A quality decrease is also brought about by a higher MnO share, since then there is more formation of manganese sulphide, which, however, has an adverse effect on the quality of the slag and may possibly make slags unusable for cement manufacture. S. Solacolu and P. Balta (96) study the influence of manganese and of sulphur on the hydraulicity of slags of the system $CaO—MgO—Al_2O_3—SiO_2$. They find—depending on the position of the slag in the four-component-system, varying effects of Mn and S on hydraulicity. An adverse effect occurs especially when at the same time Mn and S exist in higher quantities and when MnS is formed. An adverse influence of MnO, especially with slags of low basicity and low Al_2O_3 content is also assumed by I. I. Kholin and S. M. Royak (5).

Factories producing slag cements are highly interested in being supplied with slags of uniform quality. In connection with this, the research institute at Rheinhausen has for years checked the compositions of the slags of two blastfurnaces producing different pig irons. An impression of the uniformity of the slag produced will be given by Table 4.

Criteria for Evaluation of Hydraulicity Properties

The continuosly growing importance of granulated blastfurnace slags as raw materials for cement has kept alive the interest of cement chemistry in methods permitting rapid appraisal of their hydraulic properties. The relevant methods indicated in the past have since 1960 been applied, checked and critically reviewed with respect to the value of their results (95), (65), (97), (98), (68), (59) and (99).

F. Keil (6) and R. W. Nurse (7) have again discussed all testing methods that provide a) various chemical indices, b) physico-chemical and c) physical reference values.

Also all these indices and reference values have, either on account of the method used or due to the properties of the material, only a limited or doubtful value, they are nevertheless characterized as valuable means of a rapid and rough appraisal. The reason for this lies in the fact that, in deriving them, one has considered the slag melts as homogeneous liquids. According to F. Schröder (65) no account has been taken of the fact that by chemical analysis all interstructural components are destroyed, that exact data on the various factors influencing the energetic condition of the vitreous slag are not supplied, and that, furthermore, the physical parameters proper, such as content of glass, refractive index or specific gravity, always represent statistic averages only.

The uncertainty of chemical indices and of the criteria derived from them will be seen in Table 5 (100). It contains, of technical cement slags, the chemical analysis, the CaO/SiO_2 ratios, the "F-values" in part a), and in part b) the compressive strength values of test cements made from these slags. According to the added criterion of the "F-values", the slag samples No. 12 and No. 37 having F-values > 1.9 (2.02 and 1.91 resp.), as slags of very satisfactory hydraulic properties, should have considerably higher compressive-strength values after 28 days, if the information supplied by the F-value is related to the whole strength evolution.

For appraising the adverse effect of FeO and MnO on the strength evolution separately, H. Sopora (95) has proposed to square the MnO content and to extend the formula as follows:

Table 4. *Uniformity of the chemical slag composition*

	Blastfurnace No. I				Blastfurnace No. II			
	CaO	SiO_2	Al_2O_3	MgO	CaO	SiO_2	Al_2O_3	MgO
1964								
Mean value	41.40	31.58	15.34	6.29	41.28	31.65	15.35	6.29
Highest value	43.17	32.25	16.83	8.07	42.92	32.66	16.29	7.93
Lowest value	39.07	30.70	13.69	5.15	39.47	30.63	13.99	5.29
Standard deviation s	1.200	0.418	0.570	0.319	1.001	0.596	0.560	0.802
Coefficient of variation V i.%	2.90	1.30	3.72	5.07	2.42	1.88	3.65	12.75
1965								
Mean value	40.59	32.54	14.58	6.52	40.57	32.51	14.61	6.60
Highest value	41.75	33.40	15.56	7.03	41.52	33.11	15.46	7.14
Lowest value	39.26	31.85	13.94	5.93	39.44	31.66	14.07	5.83
Standard deviation s	0.732	0.418	0.397	0.319	0.688	0.441	0.310	0.373
Coefficient of variation V i.%	1.80	1.28	2.72	4.89	1.70	1.36	2.12	5.65

Table 5a. *Chemical composition of blastfurnace slags and clinker from H. Knoblauch (100)*

Slags No.	SiO_2 %	CaO %	Al_2O_3 %	S %	MgO %	FeO %	MnO %	K_2O %	Na_2O %	SO_3 %	fr. CaO %	$\frac{CaO}{SiO_2}$	F-Value*
12	34.0	37.6	20.64	1.54	3.08	0.63	0.24	1.13	0.43	—	—	1.11	2.02
27	36.5	41.8	12.79	2.09	4.16	0.38	0.19	0.80	0.75	—	—	1.14	1.58
37	33.1	44.5	15.92	1.79	6.37	0.38	0.70	0.40	0.43	—	—	1.34	1.91
49	34.1	49.8	10.70	1.76	2.88	0.50	0.20	0.36	0.38	—	—	1.46	1.82
50	35.7	47.6	9.30	1.67	2.57	0.55	1.34	1.01	0.71	—	—	1.34	1.60
Clinker	20.9	65.0	5.95	—	2.30	3.10 (Fe_2O_3)	0.42 (Mn_2O_3)	0.23	0.38	0.88	1.06	—	—

Bogue's formula: C_3S: 61.32% C_3A: 10.52% C_2S: 13.67% C_4AF: 9.43%

*F-Value $= \frac{CaO + 0.5MgO + Al_2O_3}{SiO_2 + MnO}$

Table 5b. *Strength development (DIN 1164) of cements, made from the a. m. five slags, containing 20% clinker, 7% anhydrite, 73% granulated blastfurnace slag*

Slags No.	Specific surface in cm^2/g (Blaine)		Setting time hours		Tensile strength after days				Compressive strength after days			
	slag	cement	initial	final	1	3	7	28	1	3	7	28
12	3610	4035	4.00	6.10	22.7	46	54	76	87	264	306	360
27	3640	4060	3.30	5.20	8.7	40	67	79	37	184	316	448
37	3480	3945	3.15	4.40	9.3	45	76	93	37	190	310	435
49	3660	4060	5.40	7.45	11.3	53	83	84	42	230	395	474
50	3450	3870	2.40	4.55	9.2	41	75	95	36	174	296	400

$$F = \frac{CaO + 0.5MgO + Al_2O_3}{SiO_2 + FeO + (MnO)^2}$$

H. E. Schwiete and F. C. Dölbor (59) indicate for the appraisal of granulated hematite slags, on the basis of their chemical composition, a more comprehensive degree of basicity:

$$Bg_{Schwiete\text{-}Dölbor} = \frac{\%CaO + (\%Al_2O_3 - 10)}{SiO_2 + 10Al_2O_3}$$

(Bg = basicity degree).

From theoretical considerations of the glass structure, based on the network theory of W. H. Zachariasen (6), and with due regard to the Al/Si-ratio in potash feldspar, up to 10% Al_2O_3 are supposed to be built as networkformers into the SiO_4^{4+} tetrahedron structure and the surplus, in the case of higher Al_2O_3 contents, is supposed to be present in the form of network modifiers.

This assumption is in contradiction to statements by R. Kondo (101) and to those by H. Schenck and T. E. Gammal (21), according to which, on the basis of physico-chemical studies of the reaction equilibria of molten slag/iron bath, the alumina in slags is active as an acid constituent up to a ratio of $CaO/SiO_2 = 1.3$.

Using the above formula, the authors obtained, by calculation, a higher rate of exactitude (86%) for the relationship between chemical composition and compressive strength than by the formula

$$Bg = \frac{CaO + (x - 10)Al_2O_3 + CaS + Na_2O + K_2O}{SiO_2 + 10Al_2O_3 + MgO + MnO}$$

Recently H. E. Schwiete (89) has held the view that the rate of exactitude of $Bg_{Schwiete\text{-}Dölbor}$ can be increased, if the shares of chemical components occurring in combined form in the crystalline inclusions of the vitreous slag is taken account of, as follows, in the formula:

$$Bg_{Schwiete\text{-}Rivas} = \frac{(\%CaO - C') + (\%Al_2O_3 - A' - 10\%) + (\%MgO - M')}{(\%SiO_2 - S') + 10\%Al_2O_3}$$

In this basicity degree, C', A', M' and S' represent the percentage of CaO, Al_2O_3, MgO and SiO_2 combined in the slag minerals. The inclusion of MgO in the sum of the basic oxydes (network modifier) means a revision of the older view that Mg^{2+} with fourfold coordination operates as a networkformer.

In recent years, for the appraisal of the hydraulic hardening capacity, also index n = refraction of light of vitreous slag (102) and devitrifying heat, determined by DTA and DTK testing methods (98), (45), (97), (68) and (103) as well as glass content determinations have been used. While W. Schrämli (97) rejects the information supplied by the DTA curves, J. E. Krüger (98), in consideration of studies by J. E. Krüger, K. H. L. Sehlke and J. H. P. van Aardt (45) on the devitrification phenomena in South-African vitreous slags, and (103) hold the view that the devitrifying heat values found by means of DTA can be used for appraisal. They think the DTA curves applicable also for determining the content of granulated slag in slag cements.

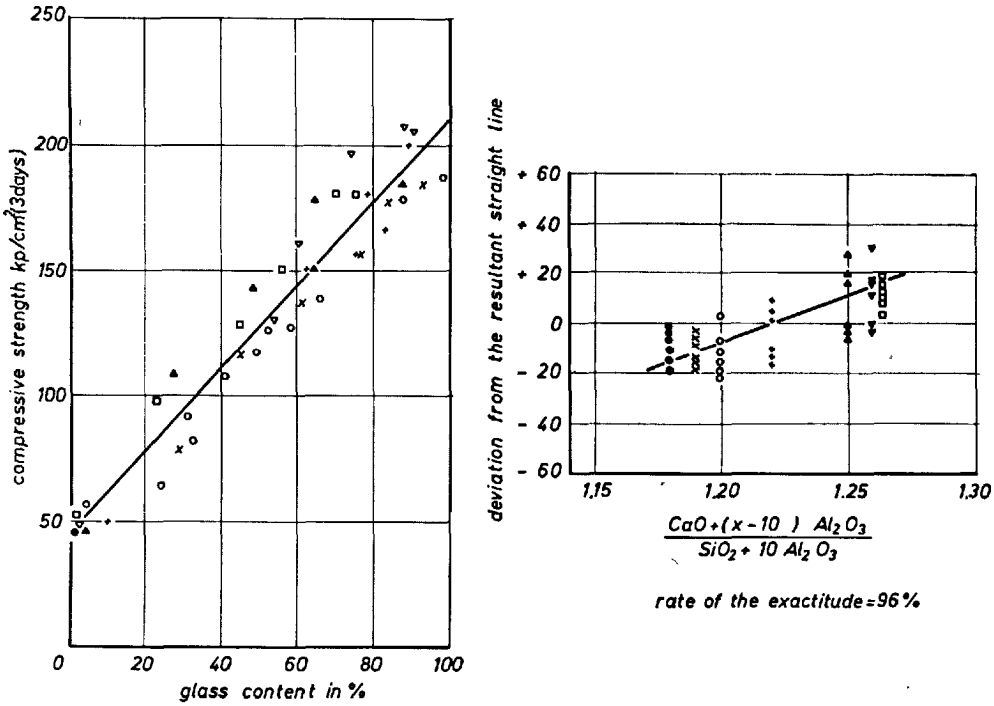

Fig. 6. *Glass content and compressive strength according to H. E. Schwiete & F. C. Dölbor.*

The glass contents, as determined by microscopy, in hematite slags quenched in different ways have been related by H. E. Schwiete and F. C. Dölbor (59) to the strength values of the respective test cements. In comparing content of glass and compressive strength (Fig. 6) they have obtained a rate of exactitude of 96% for the straight line of optimum (as contrasted with 82—86% in the comparison strength—degree of basicity, see above), deviations from the straight line of optimum being related to variations of the degree of basicity.

The evaluation method proposed by F. Schröder (65) and based on the varying fluorescence of vitreous slag is being successfully used at the Research Institute for Blastfurnace Slags, Rheinhausen, as well as at some German blastfurnace cement factories.

At the 4th International Symposium on the Chemistry of Cement W. Kramer (4) reported on the first studies by F. Schröder on the fluorescence and the fluorescence test for the appraisal of vitreous slags. He, furthermore, mentioned the authors view that the index = % red fluorescing glass particles × CaO/SiO_2 ratio may be a reliable one for the comparison of slag hydraulicity for slags of variant origin. Fig. 7 gives an example of such an application.

To the question then raised by J. H. Welch (104) whether such a comparison was justified the following

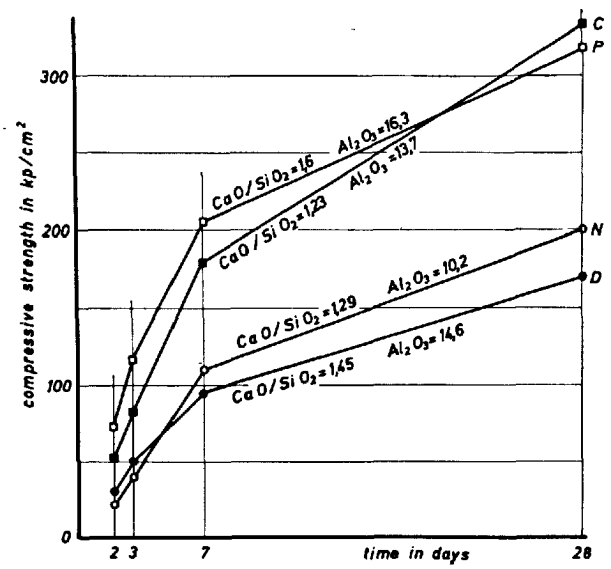

granulated slag No.	% fluorescing material			
	violet	bright blue bluish white	pink	brown
C	4	2	94	—
P	4	20	69	7
N	15	31	54	—
D	8	5	41	46

Fig. 7. *Compressive strength of four granulated foundry pig iron slags with different fluorescence.*

answer may be given:

The fluorescence of basic vitreous slag is a specific property of its vitreous structure. The percentage of red fluorescent vitreous particles gives the quantity of the hydraulically active vitreous slag with statistically homogeneous distribution of the controlling structural constituents. The CaO/SiO_2 ratio is a value that points to the ratio O/Si in the slag. C/S is a measure of the disproportioning of an originally three-dimensional SiO_4 tetrahedron network into smaller complexes with $(Si_3O_7)^{6-}$ anions and single SiO_4^{4-} tetrahedrons.

The nearly linear dependence of the 28-day-compressive strength values obtained of test cements made from 15 slags of different origins (with equal composition of slag, clinker and anhydrite and of equal grinding fineness) on the above index was good confirmation (65).

A comparison between the compressive-strength values of test cements and the fluorescence radiations —divided into color groups—of the slags used confirms, according to (59), the quality of this rapid test (see Fig. 8). The different chemical composition of two slag samples and their variant picked up pink, salmon, blue and violet fluorescing fractions are demonstrated in Fig. 10.

Determinations of the Fluorescence of Granulated Slags (by K. Grade)

Co-worker of the author, has for some time made attempts with a view to quantity determination of the fluorescence colors by measuring their spectral degree of remission. For this purpose the sample crushed to sizes of 0.040 to 0.60 mm is filled into the quartz-glass bulb of spectrophotometer PMQ II with ZFM fluorescence end (Messrs. Zeiss, Heidenheim). The sample is then exposed to ultra-violet radiation (wave length approx. 365 microns) at an angle of 45° and excited to fluorescence. The emitted radiation is resolved into its spectrum, and its intensity is measured at intervals of 10 microns each throughout the spectrum. As a reference value for the respective wave length the degree of remission of MgO exposed to standard light A (white) is used.

From the curves determined by the test data the standard color values X, Y and Z as well as the standard light components x, y and z (107) are calculated by the coordinates method (105) (106). By means of these values the position of the color in the standard color chart and in the identical CIE color chart can be determined and clearly identified.

Fig. 9 shows the positions of the red fluorescence colors radiated by vitreous slag of different origins. The figure shows the variations of the red fluorescence colors pink—red—salmon—red brown in the CIE color chart, the red-brown color being caused by the influence of FeO, MnO and S^{2-}. The range of the granulated slags which were used in the course of 1966 for cement production at a certain factory has been made conspicuous in the diagram by hatching. The portion set out indicates that there was only slight variation in the quality of these granulated slags.

For the visual color impression, an increasing X-value, in the represented portion of the CIE color chart, means an increase in the content of red, whereas, with equal X-values, increasing Y-values means a decrease in color saturation. In the diagram, the light intensity value Y, which, with granulated slags of satistactory hydraulicity, exceeds 35 and may rise to 200, could not yet be plotted. Of the tested slags, the compressive strength values of equal test cements are available. They were related to the results of fluore-

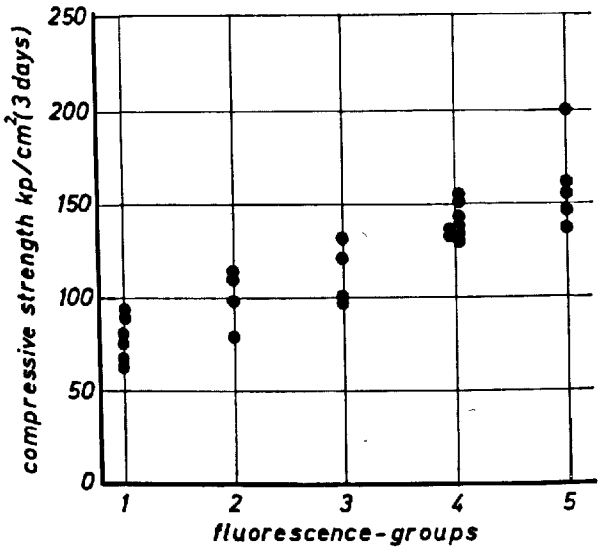

30 slags divided in fluorescence groups	compressive strength in kp/cm² after 3 days
1. violet, blue, single grains brown	67-67-76-80-90-95
2. violet, less reddish brown	78-97-110-112
3. red and reddish brown	98-98-120-130
4. salmon, single grains reddish brown	132-132-133-133-136-136-138-140-150-153
5. salmon, pink	136-145-155-160-200

Fig. 8. *Compressive strength due to fluorescence of the granul. slags. According to H. E. Schwiete & F. C. Dölbor (59)*

scence color measuring. On the basis of the comparison of the two properties, the point cloud in the diagram (Fig. 9) could be divided into areas of high, intermediate and low hydraulicity.

Further attempts will be made to detect the relations between the results demonstrated in Fig. 9, the chemical composition and the compressive strength values.

To be on the safe side, a number of other researchers used, for appraisal of the hydraulic setting capacity of technical and synthetical slags, the time-consuming technological methods of testing the mechanical strength values partly in compliance with the existing standard specifications, partly by leaning on the proposals made by F. Keil and G. Haegermann (108) s.p. (97)–(101), and partly on other technological strength-testing methods (86), (109), (110) and (111).

According to W. Wittekindt (109), the hydraulicity of granulated slags with binding agents (85% slag, 15% lime hydrate, fineness 3,500 cm^2/g Blaine) is to be determined rapidly through the strength of samples heat-treated at 60°C according to the German standard specification for lime, DIN 1060.

Another rapid-testing method, according to A. I. Stepanowa and S. M. Smechowa (110), consists in the four-hour steam curing of standard mortar samples and in the strength test after a cooling time of one hour. Test cements having a specific fineness of 3,000 cm^2/g (Blaine) are supposed to show the 7-day-compressive-strength values, and test cements of 5,000 cm^2/g, the 28-days-compressive-strength figures.

A French rapid-testing method using the compressive-strength test of standard prisms is described by M. Venuat and P. Papadakis (111). The excitation of the latent hydraulicity is caused by NaOH, which is added as mixing liquid (200 gr NaOH granular, dissolved in 1 litre of H_2O). The relationship of solution/cement amounts to 0.5. Testing is performed

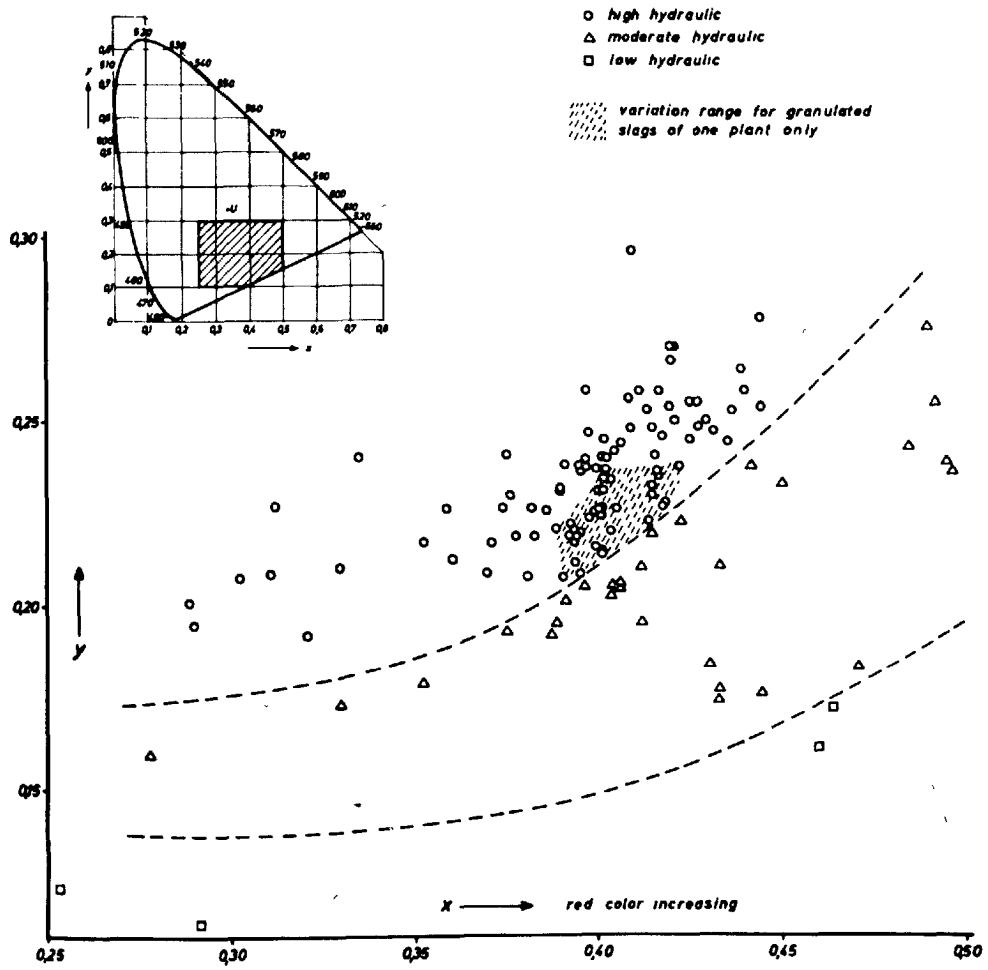

Fig. 9. *Flourescence colors of granulated slags in the CIE standard colorimetric system. (Part of the whole CIE system above on the left.)*

6 hours after forming, and after 24 hours. Vitreous slag of satisfactory hydraulicity must reach values of > 80 kg/cm², and > 125 kg/cm², respectively.

Hydration

Modern methods of research over the last 10 to 15 years have greatly expanded our knowledge of the hydration of hydraulically active, vitreous blastfurnace slag. Yet even today certain points are open to discussion.

The latest work done at the Research Institute for Blastfurnace Slags leads us to assume as a certainty that the calcium silicate hydrates—CSH phases—are the components of the hydration product which govern its strength properties. In considering the other hydrates and the hydration processes, we must distinguish between the hydration which mainly runs off in $CaSO_4$—saturated solution (supersulfated cements) and that which runs off wholly in $Ca(OH)_2$-saturated or almost saturated solution (portland blastfurnace slag cements).

Even without activation by sulfates or $Ca(OH)_2$, blastfurnace slags yield hydration products, in aqueous solutions, according to H. E. Schwiete, U. Ludwig, K. E. Würth and G. Grieshammer (112), but reaction is very weak.

As for sulfate activation of slags, by anhydrite in supersulfated cements, we can assume as certain today that only ettringite and CSH phases will form, (113), (7), (114), and (115) while the pH value of the solution will remain below 12 (7).

During the hardening of supersulfated cements, the ettringite content hardly rises further as from the third to the seventh day, while during the same period compressive strength still increases substantially. So we must assume, contrary to earlier beliefs, that the ettringite makes but a very small contribution to strength properties (114), (116). Moreover, the $CaSO_4$ component added in maximum quantities of 15

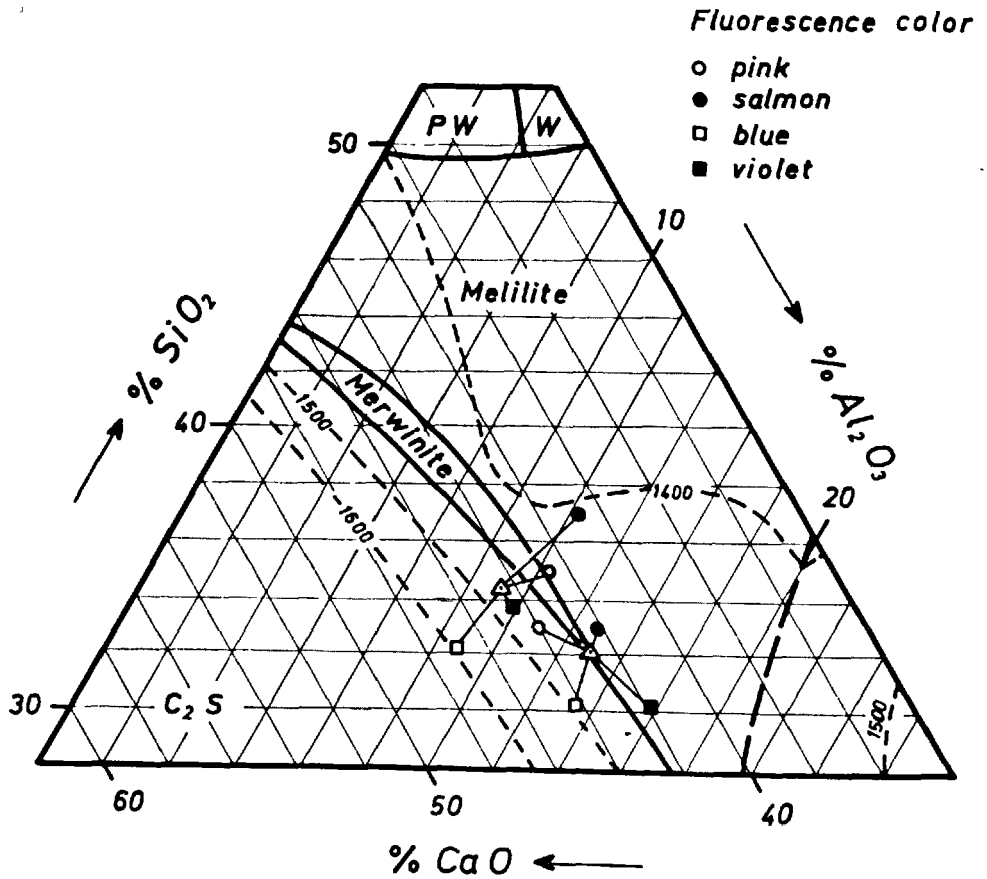

Fig. 10. *Chemical compositions of two granulated slags and their variant fluorescent fractions in the quaternary system CaO-MgO-SiO_2-Al_2O_3 (Plane for 10% MgO)*

percent to the cement can only bind part of the Al_2O_3 in the form of ettringite (116), (117). Consequently, over 90 percent of a slag must react in a different way. According to J. D'Ans and H. Eick (113) the surplus Al_2O_3 separates out as $Al(OH)_3$.

While opinions on the hydration of supersulfated slag cements are fairly unanimous, reports on hydration and hydration products by alkaline activation of slags at pH values above 12 differ in their conclusions. Most of the differences can be attributed to variations in experimental conditions. R. W. Nurse and H. F. W. Taylor (7), as well as R. Sersale and G. Orsini (118) found in hydrated pure cement pastes from blastfurnace slag cements tobermorite phases, ettringite, hexagonal calcium-aluminate-hydrates with and without sulfate, and partly also calcium-hydroxide. F. W. Locher (119) however, in extensive hydration tests with synthetic and technical vitreous slags, partly very rich in Al_2O_3, found detectable quantities of

Gehlenite hydrate C_2ASH_8 and
Hydrogarnet $C_3A(S, H_2)_3$.

F. W. Locher prove larger quantities of these two hydrates in slags with very high Al_2O_3 contents (over 20 percent) or those activated with $Ca(OH)_2$ only (but without sulfate), or those which were not hydrated in paste form but in saturated calcium-hydroxide solutions.

Pursuing the question to what degree these results may be applied to the hydration of cements, rich in granulated slag, in mortars and concretes, H. G. Smolczyk (114) evaluated some 3,000 X-ray diagrams of numerous mortars, made with extremely different slag cements having hydration periods ranging from 1 day to 4 years. The observed hydration products are listed in Table 6.

Table 6. *Hydration products of cements containing high proportions of blastfurnace slag*

Distinctly proved main phases:	
$C_3(A, F)\cdot 3(CaSO_4, Ca(OH)_2)\cdot aq$	AFt-phases
$C_3(A, F)\cdot(CaSO_4, Ca(OH)_2, CaCO_3, CaCl_2)\cdot aq$	AFm-phases
Calciumsilikatehydrates	CSH-phases
Calciumhydroxide	
Very rare or undistinctly observed phases:	
C_2ASH_8	Gehlenite hydrate
$C_3(A, F)\cdot 3(S, H_2)$	Hydrogarnet
C_2AH_8	Dicalcium aluminate hydrate

Clearly, in full agreement with the authors mentioned above, we have here the four main phases of high lime content which also occur in the hydration of portland cements. The complicated composition of the calcium-aluminate-hydrates may be summed up for simplicity's sake in the phases:

AFt for (Aluminate-Ferrite-tri-sulfate, hydroxide, etc.)

and

AFm for (Aluminate-Ferrite-mono-sulfate, hydroxide, chloride, carbonate, etc.)

It was also observed that the sulfate in supersulfated cements was present in the AFt phase only, while in blastfurnace slag cements in some cases the AFt phase reacted with other aluminates forming sulfate-containing AFm phases. H. E. Schwiete, U. Ludwig and P. Jäger (120) noted the same.

In partial agreement with the results of F. W. Locher, formation of C_2ASH_8 after 28 days of water curing was definitely shown in a case of a blastfurnace slag cement extremely rich in Al_2O_3. Within one year this C_2ASH_8 had turned into hydrogarnet.

A semi-quantitative evaluation of the results led to the safe conclusion that in the hydration of slag cements only the four main phases of high lime content are of any importance. W. Richartz (121) arrives at the same conclusion based on further examinations, partly by electron microscopy.

These experimental results lead to two difficulties in the stoichiometric calculation of hydration processes in blastfurnace slag cements.

a) The lime contents of all hydrates are always greater than those of the slags;
b) The slag is always richer in alumina than is the average of all observed hydration products.

The explanation for a) may be found in the fact that the $Ca(OH)_2$ freed by clinker hydration is partly consumed by slag hydration.

This lime binding effect of the slag has meanwhile been proved by many authors (116), (118), (122), (123), (124), (7) and (125). Fig. 11 shows the results obtained by E. W. Nurse and H. G. Midgley.

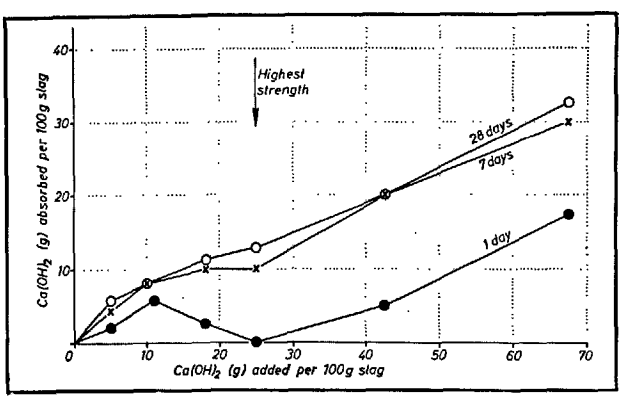

Fig. 11. *Relation between lime added and lime absorbed in slag pastes. Nurse and Midgley*
Water: binder ratio 0.3
Slag analysis: 39.7% CaO; 34.5% SiO_2
15.9% Al_2O_3; 3.9% MgO

Saturation of $Ca(OH)_2$ and NaOH in the paste of cements with high slag content (over 70% ground slag) is partly lowered in the hydration process, (126), but the pH value remains above 12, so that high calcareous calcium silicate hydrates are formed. In supersulfated cements, $Ca(OH)_2$ does not appear as solid component, the pH value remains below 12, so that less calcareous calcium silicates result.

Explanation of point b) is much more difficult. The presence of free aluminium hydroxide is possible only in hardened cement paste having no free $Ca(OH)_2$ as solid component, such as supersulfated cements (113), (7) and (114). In the high alkaline paste of portland blastfurnace slag cements, on the other hand, the entire Al_2O_3 content must be bound in some form in the hydration products. On the basis of quite different experiments carried out by G. L. Kalousek (127), H. G. Smolczyk (114) believes that these "missing alumina" have been incorporated into the calcium silicate hydrate phase.

This assumption has recently received strong support from a paper by L. E. Copeland, E. Bodor, T. N. Chang and C. H. Weise (128). They showed that tobermorite phases can bind subsidiary components, such as Fe^{+++}, Al^{+++} and SO_4^{--}, firmly into the intermediate layers of their crystal lattice. This theory is also apt to explain differences between the quantitative X-ray determination of calcium-aluminate-sulfate hydrates and the SO_4^{--} contents of paste.

Further H. E. Schwiete, U. Ludwig, K. E. Würth and G. Grieshammer (112) reported on MgO-containing tobermorite like phases which have been observed in hydrated slags rich in MgO.

On behalf of a definite solution of the problem of all the hydration products of blastfurnace slag cements the calcium silicate hydrate phases will have to be object to very accurate and thorough investigations.

Blastfurnace Slag Cements

(by F. Schröder and R. Vinkeloe)

Definition and Composition

Today, there exist standard specifications for blastfurnace slag cements in more than 15 countries. These comprise cements to which

Portland cement clinker
Calcium sulphate plus portland cement clinker
Hydrated lime

is added for activation of the latent hydraulic hardenability of granulated blastfurnace slag, and which, furthermore, conform to the minimum strength requirements of the national standards.

Slag cements consisting of granulated slag and 15 to 20% hydrated lime are today manufactured in very few countries only and in very small quantities (example: Ciment de laitier au Portland, in France). Since a number of years in some countries "ternary"-cements composed of slag, pozzolan and portland cement cliker are manufactured (6). Seen from the point of view of strength-properties, these cements do exceed the minimum strength requirements, but are not yet always included in the standards, as for instance in Germany.

Looking at the stipulations on the composition of slag and activator given in the national standards it can be noted that today blastfurnace slag cements are regarded as those consisting of

slag and portland cement clinker,
slag and calcium sulphate + up to 5% portland cement clinker.

Since the standards also specify the mixing ratio of slag and portland cement clinker, the result is, particularly in countries having slag cement industries for more than 30 years, a multitude of types of slag cements with their pertaining definitions. A summary is given by F. Keil (6). It would be very welcome if for the purpose of adjusting the requirements as to the composition on the sector of cement standards, in order to facilitate comparisons and to establish a better basis for the understanding between cement chemists, and in the development and preparation of new or in the modification of existing standard specifications, the recommendations made by International Standards Organisation (ISO) were followed.

The ISO-recommendations for the composition of the present slag cements stipulate the following (7):

Types Proportion of slag in % of the sum slag + portl. cement clinker	Standard Specification
< 35*	Portland blastfurnace cement Ciment de fer Eisenportlandzement
35—80*	Blastfurnace slag cement Ciment de haut fourneau Hochofenzement
possible subdivision:	
35—60*	Blastfurnace slag cement 35–60
60—80*	Blastfurnace slag cement 60–80
> 85	Ciment de laitier au clinker

* According to national standards the limits may vary at ±5%.

Composition of supersulphated cement "Sulfathüttenzement": Supersulphated cement is made from blastfurnace slag, calciumsulphate and a small portion of lime, portland cement clinker or portland cement. The SO_3-contents must be > 5%.

The specific properties mainly attributed to cements with a high slag contents, as for instance the very small heat development and the high resistance against chemical aggressive natural water, sea water, industrial and other waste water, have very much added to the development of this type of cement (129), (123), (130) and have secured them a rather remarkable share in production. About 10 years ago, Japan also started with the production and application of this cement type (131), (132).

Supersulphated cement has a particular place in the range of cements with high slag contents. With a very high initial strength and a very low heat of hydration at the same time, it stands out against others because of its special capability of resisting against sulphate-bearing waters and soils, and also to sea water (133), (134), (135), (136) and (137). However, at low temperatures it does not harden as quick as other cements. Heat treatment is not suitable for this cement type (134), and it does not keep as good as the other types (134), (138) and (139).

Determination of Composition

The determination of the content of slag in blastfurnace slag cements is required for certain aspects, as for instance for the control of production, for the control of the standard requirements, and for the control of long-term supplies for mass-concrete-structures or hydraulic engineering. Applicable test methods base on the physical, the mineralogical and the chemical differences of clinker and granulated slag. A summary and review is made in a report by K. Grade (140).

When the basic components clinker and granulated slag are available, as for instance in the cement plants, then the chemical analysis of clinker, granulated slag and cement, and the following comparison of the concentration of usefull chemical components, as for instance CaO, MnO according to the formula % slag is $\frac{c-k}{s-k}$ times 100, is suitable. In the formula, c is the weight-% of the chemical component in cement, s weight-% in the slag, and k the weight-% in the clinker.

A rapid method advisable for cement laboratories is described by E. Vogel (141). The cement is dissolved with NH_4Cl solution and the ammonia which develops, is titrimetrically determined. The determination of the existing contents of slag is effected by means of calibration curves, which will be drawn with defined mixtures of the slag and clinker used. A determination of the contents of slag by means of the DTA and/or thermogravimetry is, besides others, suggested by J. E. Krüger (98), O. P. Mtschedlow-Petrossian, N. A. Lewtschuk and I. S. Strelkova (103) and by N. S. Zargorodnij, O. P. Mchedlov-Petrosyan, I. M. Sidocenko and I. S. Strelkova (99). In these methods, in which for purposes of comparison the slag and the clinker must be separated, the surface of the exothermic peaks caused by the devitrifying of the slag at a temperature of 860°C, and the increase in weight caused by oxidation of the sulphides, are used for determination. For such cases where clinker and slag are not available separately for comparison, different methods of determination were suggested.

J. Brocard (142) and M. Duriez and M. Cl. Houlnik (143) made use of the differences in the specific weight existing between clinker and granulated slag for a quantity separation of the cement into clinker and granulated slag by heavy liquids.

Combined microscopic and chemical tests on concentrates of varying density are recommended by F. Keil and F. Gille (144) whereas R. E. Cromarty (145) tests fractions of varying magnetic susceptibility. Both use sulphide sulfur as a chemical element for comparison.

Manganese is recommended by P. Catharin (146)

and K. Bleher (147) to serve as reference value, whereby the procedure adopted by P. Catharin meets that of F. Keil and F. Gille, whereas K. Bleher compares the MnO contents of different grain fractions and those of cement.

Detailed studies made by the working group "Mikroskopie" in the "Verein Deutscher Zementwerke" (VDZ) in the years 1966/67 intended for the revision of the cement standard DIN 1164 led to a method of analysis (148) in which the grain particles 30—40 μ are sieved out from the cement and the contents of granulated slag is determined microscopically with reflected light after the clinker grains have been polish-ground and etched.

By analysing chemically CaO and MnO it is tested, whether the grain fraction and the cement are of the same composition, and possible whether the microscopically defined contents of granulated slag is to be corrected.

Strength Properties

Influence of the Testing Method

Strength as a symbol of the quality of the cements to a great extent depends on the specifications prevailing for testing. For this reason it is only possible here to make relative comparisons or to say as far as numerical values are given, these cannot easily be transferred to other cases. An example of the influence of the testing method on the strength is tried in the following.

In 1942 the present form of the standard specification, the DIN 1164, was issued by decree in Germany. In the years before, the compressive strength of the cements was determined from 7 cm test cubes consisting of earth moist mortar, whereas after 1942 testing was carried out on cubes consisting of plastic mortars. R. Grün and K. Obenauer (149) taking 330 different portland cements and 294 blastfurnace slag cements found out which factors must be applied in order to be able to transfer the strength values so far obtained from 7 cm cubes to those of plastic mortar in conformity with DIN 1164. From mean values derived from these tests the following conversion factors resulted:

Cement type	Testing age	Conversion factor
Portland cement	3 days	0.500
	7 days	0.620
	28 days	0.792
Blastfurnace slag cement	3 days	0.376
	7 days	0.466
	28 days	0.622

As can easily be seen from these factors, the plastic mortars had a considerably less compressive strength than the conventional type earth moist mortars. Furthermore, it became obvious that the drop of strength caused by the testing method is not the same for all types of cements. Actually, the blastfurnace cements suffered most, particularly at their early stage of hardening.

At present a new issue of stadard specifications for cement as recommended by RILEM-CEMBUREAU is available for introduction, where as regards the test regulations mainly the composition of mortar and the compaction of the test cubes is changed. This change in the specifications also leads to varied strength results, whereby, however, everybody involved is of the opinion that this testing method allows the best comparison of cement types.

The granulometric composition of the test sand of the ruling German standard specification, the DIN 1164, is not very favourable. So, especially in the case of coarsely ground cements the water/cement-ratio is, for a part, very different from that specified at 0.60. The consequence of this is, that mainly the more coarsely ground portland cements attain higher strength which can no longer be called typical. The effective water/cement ratio in individual cases was determined at 0.52, thus, it was considerably under the theoretical value of 0.60 and also led to substantial increases in strength. Extensive tests have prove that this disadvantage does not longer apply to the new test method of RILEM-CEMBUREAU; here only slight differences in the effective water/cement-ratio and the theoretical value of 0.50 have been observed. From this it can be understood that the increases in strength, which the cement shows because of this new test method, cannot be the same for all cements. A comprehensive summary of the standard specifications on the testing of cement at present available in 35 countries has been published by A. Meyer (150). As it is likely that these are discussed elsewhere, the present indication should be sufficient.

Influence of the Granulated Blast Furnace Slag

The strength properties of the blastfurnace slag cements show certain particularities against portland cements. The German "Eisenportland" cements, which are cements with a relatively small contents of slag, hardly differ from the portland cements with regard to strength. As is explained in the paragraph on the heat of hydration, a small addition of blastfurnace slag will definitely increase the initial strengths. Cements having a high contents of slag, however, show a difference against portland cements with regard to

the increase in strength depending on the age at the time of testing. The evolution of strength here is no longer determined by the properties of the clinker, but by the properties of the slag. Cements which have a high slag contents are such cements which contain much silica; when the final strength is very high and hardening after 28 days is constant and lasting then the initial hardening is smaller (151). Some very good example for this are the tests made with the 20 years old concrete of the navigation lock in Wilhelmshaven/ Germany. A concrete with blastfurnace slag cement with high slag contents, which at the time of pouring

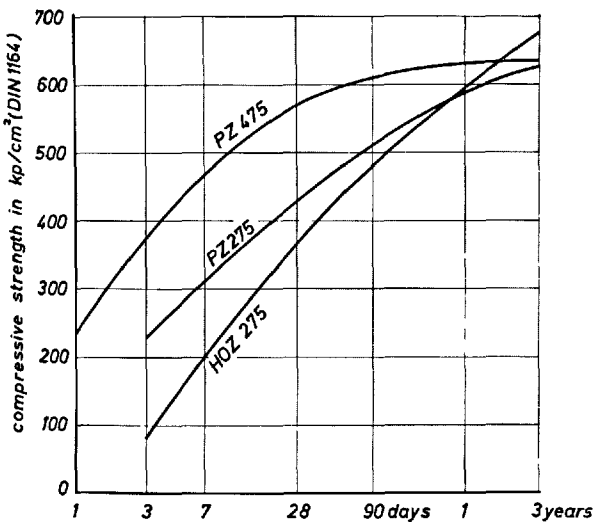

Fig. 12. *Evolution of compressive strength of commercial cements in West Germany acc. E. Spohn 1961 (153)*

is to come up to the specifications of class B 160, i.e. a compressive strength of 160 kg/cm² after 28 days, showed after 20 years a compressive strength of 700 kg/cm² and more. Even presuming that at that time the compressive strength of the concrete could have been 300 kg/cm², it still proves the considerable after-hardening of these type of cements (152).

As comparison with portland cements H. Spohn (153) gives the development of strength for blastfurnace slag cements of class Z 275 as shown in Fig. 12. His statement firstly confines to cements from certain plants. The absolute value of the strengths indicated, therefore, cannot be applied to other cements. The curves, however, show the typical tendency of the increase in strength in case of blastfurnace slag cements with a higher contents of slag, that is to say in such cements for which the development of strength is mainly determined by the behaviour of the slag. Where the initial strengths are low, the final strengths are high (153), (154) and (155).

Fig. 13 illustrates the development of strengths typical for blastfurnace slag cements with three different types of slags. It shows the influence of the type of slag and at the same time the fineness of grinding of the cement made therefrom. Practically both influences cannot be separated, and therefore they shall be explained together as follows.

Influence of Fineness

As for all cements, an increase in the fineness of grinding also in blastfurnace slag cements results in an in-

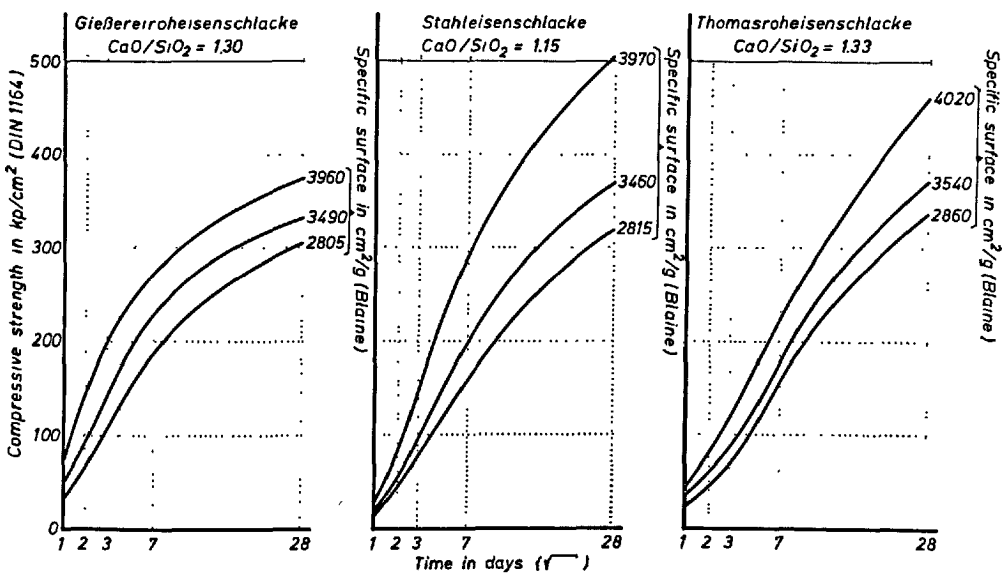

Fig. 13. *Influence of different slags and different fineness on compressive strength vs. time of blastfurnace slag cements (slag 75%)*

crease of strength. The increase of strength is substantially determined by the type of slag involved as may be seen from Fig. 13. The data given in this figure derive from very extensive studies and tests carried out by the Research Institute for Blastfurnace Slag, Rheinhausen, during the past five years; they may be called as typical, they reveral the specific behaviours of the individual slags. For the cements shown in the left part of the illustration a hot foundry pig iron slag with a CaO/SiO_2-ratio of 1.30, and a moderately hot, but relatively acid stahleisen-slag with CaO/SiO_2-ratio 1.15, and for the cements at the right side of the figure a cold Thomas pig iron slag with a favourable CaO/SiO_2-ratio of 1.33 were ground. From Fig. 13 it can be seen, that the cement consisting of foundry pig iron slag increases in strength, such as

after	1 day	from	25 to	60 kg/cm²	} = > 100%
"	2 days	"	50 "	150 "	
"	3 "	"	90 "	190 "	
"	7 "	"	165 "	270 "	= 60%
"	28 "	"	305 "	370 "	= 20%

are obtained by increasing the fineness from about 2,800 to 4,000 cm²/g (Blaine).

In case of a very acid stahleisen-slag the same increase in the fineness only after three days causes an increase in strength from 65 to 125 kg/cm²—so about 100%—but only after 28 days an increase from 320 to 500 kg/cm², which is about 56%. The increased fineness in this case of slag has quite a different effect on the development of strength than the foundry slag. When the increase of initial strengths after one and two days is less, the final strength is raised to a much greater degree. The reason for this is not the chemical composition (here C/S 1.15), but the physical condition. To this point also the results obtained from cements made of cold basic slag. Despite of the better C/S-ratio (1.33) the increase in the fineness as illustrated at the right side of the Fig. 13 has an effect on the blastfurnace slags from cold basic pig iron slag, but a smaller increase in the strength must be expected at all days of testing. These results also show that it is possible, provided the slags are properly cut, to influence the hardening curves of the blastfurnace cements with high slag contents. Furthermore, it can be expected from these test results that primarily the good dispersion of the slag component, namely a very high fineness, is of importance for the development of strength.

This is mainly demonstrated in the following results, which have been chosen from the test results obtained by the Research Institute to serve as examples. Clinker and slag were ground separately to different specific surfaces, and homogeneously mixed to blastfurnace

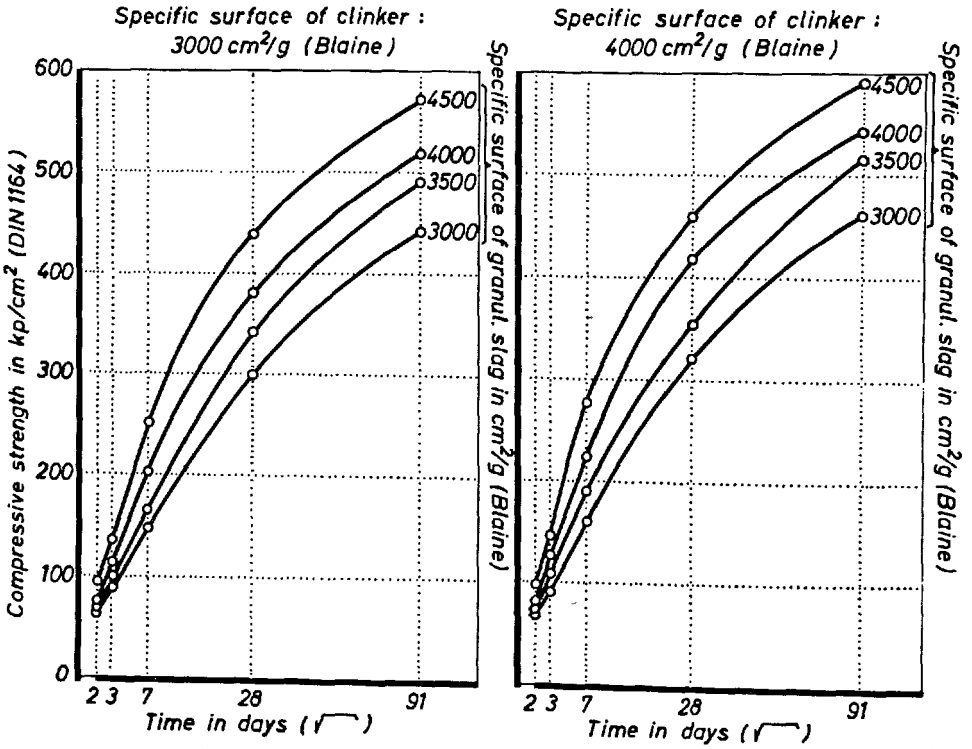

Fig. 14. *Test slag-cements; compressive strength vs. time as a function of fineness (slag 75%)*

slag cement with slag content of as much as 75%. The values of strength as shown in Fig. 14 indicate that the fineness of clinker has attained only little influence on the development of strength, whereas the higher fineness of the slag has led to an increase in strength, as applies to the result shown in Fig. 13.

Further investigations in the Research Institute have shown, moreover, that due to the properties of clinker of standard composition, the development of strength of blastfurnace slag cement with high slag content is influenced only to a minor degree, Tables 7 and 8. However, the test series for the development of strength of blastfurnace slag cements with high slag contents quite early show the influence of the quality of granulated slag. The evolution of strength of the cements made of well granulated slags (No. 1–3 and 5–9) stand out distinctly against those of badly granulated slags (No.11, 10, 4). In the well granulated slags slight differences in the CaO/SiO_2-ratio have a minor effect only on the strength at a later age of the cement. However, they become noticable at the early stage of strengths, just like the tapping temperatures to be derived from the individual types of slag. These results correspond very well to those obtained by H. E. Schwiete and F. C. Dölbor (59).

Influence of the Portland Cement Clinker

Some authors consider also the influence which the composition of the clinker has on the properties of strength of the blastfurnace slag cements. Whereas the average composition of clinker in the Tables 7 and 8 show slighter influences of these components on the strength of blastfurnace slag cements, it must be taken from other analysis that clinker with higher C_3S contents are more advantageous. So according to H. Sopora (94) slightly basic slags attain the best strength with clinkers having a high lime contents. Granulated slags which he examined are relatively slow in reaction and have F-values below 1.5.

V. F. Krylov, V. L. Pankratov and V. M. Kolosovskaja (44) with acid slags (SiO_2 34–37%, CaO 29–38%, Al_2O_3 9–23%, MgO 5–18%) obtain good properties of strength with a clinker having very high C_3S- and C_3A-contents.

K. Goto, M. Hanada and H. Miyairi (156) found out that the early strength is so much the more, the higher the C_3S contents of the clinker used. Simultaneously, the share in strength of the granulated slag increases with the use of clinker with high C_3S-contents.

Against this, the influence of C_3A is smaller, a higher C_3A-contents merely causes negative effects in respect to the rate of the hydration heat.

Influence of Calcium-Sulphates

The effect of the various calcium-sulphate-modifications on the strength and setting of blastfurnace cements is being dealt with by a number of cement chemists in the period under review, H. E. Schwiete and F. C. Dölbor (59), M. Hanada and H. Miyairi (157) R. Nagano and S. Yamawaki (158) and H. Sopora (94).

In general it was found that the use of anhydrite, artificial as well as natural, has the best effect on the early and on the final strengths. H. E. Schwiete and F. C. Dölbor (59) in the range of 0.5 to 4% SO_3, found an increase of the compressive strength in the order semi-hydrate—dihydrate—artificial anhydrite—natural anhydrite—where the compressive strength curves of the test cements (30% clinker) with semihydrate and dihydrate for all ages showed definite maxima with low SO_3-contents (0.5—1%) whereas artificial anhydrite contents constantly improve the early strengths at 3 and 7 days. As concerns the strengths at later ages the compressive strength curves for artificial anhydrite show maxima at about 3—3.5% SO_3, and those for natural anhydrite at about 1% SO_3. Tests carried out with mixing of dihydrate and anhydrite showed that in the range of 0.5 to 4% SO_3, with varying sulphate additions, a mix containing 25% dihydrate and 75% anhydrite provides the most uniform development of compressive strength. Also with regard to the setting, a modification of the calcium sulphate is of importance. Semihydrate according to R. Nagano and S. Yamawaki (158) and also H. E. Schwiete and F. C. Dölbor (59) is not suitable, since it is likely to cause false set. The slightest change in the setting occurs (59) with mixing of 55% dihydrate and 45% anhydrite.

It can be taken from the studies that blastfurnace slag cements do very well agree to contents of 4% SO_3, except in the form of semihydrate.

Separate Grinding

For cements which are made of components having a varying grindability and a varying hydraulic behaviour, the grinding procedure may play an important role for attaining maximum hydraulic properties. The effect of the grinding on the strength-properties of the product to be ground has, therefore, been investigated by several authors in the period under review.

So F. W. Locher, J. Wuhrer and K. Schweden (159) have tested the influence of the fineness and W. Kayser (160) that of particle size distribution on the strength-properties of cement. Both authors found that for blastfurnace slag cements with slag contents

Table 7. *Influences of granulated blastfurnace slag and clinker on blastfurnace cements with low clinker contents*

Composition: granulated slag 65%
clinker 30%
gypsum 5%
Spec. surface (Blaine) 3,500 ± 100 cm²/g

Test No.	Origin of granulated slag and CaO/SiO_2-relationship	Clinker	Compressive strength in kg/cm² after days 2	3	7	28
1	hot basic pig iron self-fluxing burden CaO/SiO_2 1.48	I	72	102	217	371
		II	61	111	246	403
		III	110	150	280	464
2	hot basic pig iron CaO/SiO_2 1.44	I	78	103	214	369
		II	76	120	214	400
		III	75	101	221	376
3	hot basic pig iron CaO/SiO_2 1.30	I	70	125	211	360
		II	67	124	224	380
		III	83	116	218	375
4	basic pig iron 35% cryst. portions CaO/SiO_2 1.31	I	55	70	120	260
		II	50	65	115	275
		III	40	65	120	275
5	stahleisen CaO/SiO_2 1.13	I	50	85	230	395
		II	45	85	195	420
		III	40	90	215	395
6	stahleisen CaO/SiO_2 1.43	I	77	115	210	326
		II	82	128	234	350
		III	91	134	234	340
7	hematite pig iron CaO/SiO_2 1.38	I	80	115	200	330
		II	90	125	210	345
		III	90	130	225	345
8	foundry pig iron CaO/SiO_2 1.23	I	70	105	200	335
		II	60	115	240	410
		III	80	110	215	365
9	foundry pig iron CaO/SiO_2 1.45	I	90	135	230	365
		II	105	155	250	360
		III	115	160	260	360
10	foundry pig iron wet granulation CaO/SiO_2 1.30	I	45	55	130	250
		II	40	85	145	295
		III	45	75	150	295
11	foundry pig iron semidry granulation CaO/SiO_2 1.29	I	50	80	155	250
		II	60	85	165	260
		III	35	90	180	270

Table 8. *Characteristics of the three clinker types for test cements in table 7*

Clinker	X-ray analysis				Amorphous in X-ray analysis	Chemical analysis			
	C_3S	C_2S	C_3A	C_xA_yF		MgO	free CaO	SO_3	K_2O plus Na_2O
I	61	14	7	9	6.0	0.7	1.5	—	0.95
II	51	22	7	12	4.5	1.4	0.80	0.70	0.80
III	50	20	14	6	2.0	4.0	2.8	1.10	0.60

Clinker	Lime factor	Hydraulic modulus	Silicate modulus	Alumina modulus	As portland cement* compressive strength in kg/cm² after days 2	3	7	28
I	103.57	2.33	2.37	1.55	101	145	235	445
II	98.18	2.12	1.90	1.80	120	185	270	430
III	104.67	2.37	2.17	2.91	140	195	300	465

*SO_3-contents of test cements = 2,5%; Spec. surface (Blaine) 2,900 ± 100 cm²/g.

of 50 and 60% the early strength is mainly determined by the fineness of the clinker, and the later process of hardening by the fineness of the granulated slag. In the case of cements with high slag contents, the fineness of the slag and its hydraulic properties are of decisive importance. W. Kayser (160), furthermore, found that the strength-properties of blastfurnace slag cements with a tight grain distribution of the same specific surface exceed that of blastfurnace slag cements with wide-spread grain distribution. Both authors consider a separate grinding to be the most advantageous method.

J. Birthelmer (161) shares this opinion, he found that separately ground cements attain the same strength as those which are ground together with greater specific surfaces.

Separate grinding is also advised by N. Stutterheim (38) for cements made of South African slags with high magnesia contents; these show a much greater resistance to grinding than clinker. Separately ground cements with 50% granulated slag with high magnesia contents provided the same strength-properties as portland cements and were resistant to autoclave test.

H. E. Schwiete and F. C. Dölbor (59) support a separate grinding in such cases where the granulated slag in the cement has higher contents than the clinker, and where it is more difficult to grind than the clinker. They ascertained that with clinker a grinding of 3,500 cm^2/g is of minor, but with granulated slag is of major importance. Regarding to the fineness H. Sopora (94), in the case of combined grinding, finds the strongest dependency of the strength on the fineness in the range 2,500 to 3,200 cm^2/g.

F. Guye (162) recommends a higher fineness for Southafrican cements consisting of clinker with a high MgO-contents (16–25%) and for granulated slag containing much magnesia (up to 22% MgO) for improvement of volume stability of such cements.

Special Properties of Blastfurnace Slag Cements

Elastic Properties

It is known that particularly blastfurnace slag cements with high slag contents show a very high bending strength (123). Cement or concrete test prisms are generally much less resistant against bending- or flexural stresses than against compressive stresses. In blastfurnace slag cements, however, the slag component has a positive influence on the bending strength. With an increase in the content of slag the bending strength grows likewise. Thus, the relation of bending- to compressive strength of the blastfurnace slag cements with less clinker contents explains the good elastic properties of the concretes made from this type of cement (163).

M. J. Challier (164) has made up a brittleness factor K for this;

$$K = \frac{E}{\sqrt{W}}$$

E = dynamic modulus of elasticity
W = compressive strength of the concrete.

The modulus of elasticity (E-module) is a measure for the resistance against deformation which a specimen produces when being subjected to loading.

A high value for E means a small deformation, a low value, however, means a big deformation with equal loading. When the factor K is high, fracture occurs with relatively less deformation. This, however, meets the definition of the brittleness. In other words, the smaller the K-factor, the more elastic is the test specimen. M. J. Challier (164) sets up the following standard of values referring to the test after 28 days:

K = 23,000—26,000 for concretes of medium quality
K = 20,000—23,000 " " " good quality
K = < 20,000 " " " best quality.

The Research Institute for Blastfurnace Slag, Rheinhausen, for instance, has determined values for the K-factor, which are even below 18,000, by taking gravel concretes with blastfurnace slag cements with minor clinker contents and medium cement content between 250 and 300 kg/m^3 mixed concrete after 28 days.

A further reference to the favourable elastic properties of blastfurnace slag cements is made by S. Härig (165) in which especially the values of E-module are set against the bending strength.

Besides other properties such as the high resistance against chemical attack and the low heat development, the elastic properties of the blastfurnace slag cement concrete are of importance for marine- and mass-concrete constructions (166), (167) and (168).

Heat of Hydration

The heat of hydration of slag cements is as specific as the strength evolution. For portland blastfurnace cement (< 35 slag) they do not differ essentially from that of pure portland cements. The hardening of the

blastfurnace cements (> 60 slag) is characterized by more colloidal reaction runs (10). Therefore it seems that/the heat development of these slag cements in the first two to three days is essentially more definite with the portland clinker component and that furhter heat evolution is due to the proportion of granulated slag.

R. Dietrich (155) found that, independently of the slag content, all cements, on full hydration, i.e. after a long time, develop approximately the same amount of heat. Cements, however, differ very much in the process of heat development as referred to the time factor (169), (170), (171), (172), (173), (174), (175) and (176).

H. Lehmann and W. Roesky (170) pointed out that with slag cements the heat of hydration developed per kg/cm² is less than with cements without additional slag, i.e. that for achieving equal strength values on cements with high (> 60%) slag additions less heat is developed. Interesting in connection with this conclusion is the information by H. Lafuma (177) that the maximum increase in temperature in 4 × 4 × 16 cm prisms of pure cement and mortar (1/3 ISO) was measured as follows:

Cements	High alumina	Portland	Ciment de laitier au clinker slag content > 80%
Pure cement paste	14.8°C	5.4°C	0.50°C
Mortar 1/3 ISO	5.6°C	1.65°C	0.13°C

The very low heat of hydration is a specific property of blastfurnace slag cements (with slag > 60%). An example of the decrease in heat development of cements with increasing addition of granulated slag is given by R. Alegre (175) (Table 9). However, a function apparently so linear as shown in this table, does not always exist.

Table 9. *Influence of slag content on heat of hydration publ. by R. Alégre (175)*

Slag content (%)	0	30	50	70	85
Age	Heat of hydration (cal/g)				
12 hours	27	16	11.5	8	6
1 day	62	40	30	23	18
2 days	75	54	43	36	27
3 days	79	60	48	40.5	30
4 days	82	64	52	43	32.5
5 days	85	68	55.5	45.5	34
6 days	87	71	59	47.5	35.5
7 days	90	—	62	49	36.5

Specific surface 3000-3100 cm²/g

H. E. Schwiete and K. H. Karsch (174) and U. Ludwig and K. Rakel (173) have established that the heat of hydration increases with the w/c-value. Referred to the clinker portion in cements containing much slag, the w/c-value is always higher than that of the test mixture. The clinker component, therefore, in combination with a slower reactable slag, reaches faster high hydration degrees (123) and, therefore, positively influences the heat evolution during the first hardening stages.

On account of these facts, the heat of hydration of some cement with a small slag share, e.g. that of an "Eisenportlandzement", can be higher in the early stages of hardening than that of a portland cement containing 100% of the same clinker. A considerable decrease in the hydration heat released during the first days can be observed only on cements containing more than 70% slag.

The low heat of hydration is a great advantage of these particular cements (Table 10), which, on account of their high resistance to aggressive media, is well-suited for all tasks of hydraulic engineering in cases of mostly very large cross sections of solid structures.

As opposed to slim reinforced-concrete structures in building construction, where the heat developed is dissipated sufficiently fast, the high increase in temperature in solid concrete structures of large cross section may be responsible for the formation of fissures. On this problem, test results of our Research Laboratory (178), (168) as well as of other authors (179) (171), (180) and (181) are available. These permit a very good evaluation of the temperature increases to be expected in structure, when the heat of hydration of the cement used is known.

The heat of hydration of cement can be measured adiabatically or by means of a heat-flow calorimeter (182) (in simplified form, vacuum flask method) or from the difference in heat of dissolution. The last mentioned, indirect method is very unsatisfactory for both slag-containing and puzzolanic cements (7), (183), (172), (175) and (182). Most of these cements contain slowly soluble constituents that may render the determination of the heat of dissolution very difficult and inaccurate. Likewise the determination

Table 10. *Heats of hydration of portland and portland blastfurnace cements publ. by R. W. Nurse (7)*

Cement	Heat evolved (cal/g)		
	1 day	2 days	3 days
Ordinary portland	23—42	42—65	47—75
Rapid-hardening portland	35—71	45—89	51—94
Portland blastfurnace	18—28	30—50	33—67

of the loss on ignition cannot be effected directly. F. Gille (183) proposes a determination of the loss on ignition through the CaO content. This method is adopted by the German standardization proposal (184).

Since the heat of hydration is obtained from the difference in heat of dissolution, inaccuracies in the determination of the heat of dissolution may considerably influence the final result.

In solution calorimetry, cement is hydrated under isothermal curing conditions. These results, therefore, are mainly of scientific interest, because they permit drawing conclusions with regard to exact, but also varying curing conditions.

In the U.S.A. and in Italy also conduction calorimetry is used for measuring heat of hydration. In the Research Institute for Blastfurnace slags, Rheinhausen, a process based on heat flow has been used in the last few years. By this method the heat of hydration can be determined directly under isothermal curing conditions. The advantage of this process is that by insoluble residues or loss on ignition no difficulties in measuring occur. This test may be carried out also with mortar and with different w/c-values. The heat evolution is obtained in the form of a curve. The process can be used properly up to a curing time of 28 days.

The heat of hydration, just like the curing of cement, is a function of temperature.

For practical structural engineering purposes, thus, the adiabatic (155) and (185) method gain special importance. Partly, however, also the vacuum flask method, simpler to employ, give useful results for practical purposes (172), (179) and (182), for which either the increase in temperature of a mortar or pure-cement sample is tested, or the heat dissipated through the walls of accurately gauged vacuum flasks is measured, and the heat of hydration determined from it.

The vacuum flask method is generally employed in France (177). Its advantages and drawbacks are described by R. Alegre (175). Also the results obtained are not quite precise, they, nevertheless, constitute a valuable help for the constructional engineer.

Fig. 15 graphically shows the results of the various measuring methods obtained on altogether 325 cement samples in the Research Institute. The influence of temperature on the heat evolution of hydration can be seen from the positions of the scatter bands for the various test methods after 1 to 7 days. The relationships shown in the diagram are in accordance with the data given by R. Alegre (175).

It can be seen that the heat of hydration, as measured by the isothermal method, after 28 days, corresponds approximately to that measured adiabatically after 7 days; the values measured by the isothermal method after 7 days correspond to the adiabatic values after 2 to 3 days (155), (185), (172) and (175). The vacuum flask methods partly give lower results than the adiabatic methods and at the same time show a greater scattering.

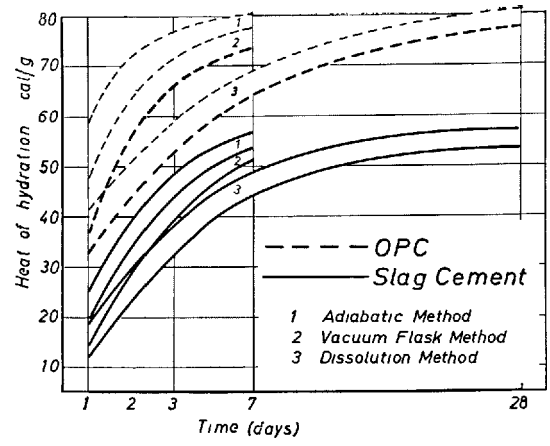

Fig. 15. *Heat of hydration determined by different methods dispersion ronge of values obtained from 325 cement samples*

Influence of Curing Temperature

The reaction speed of blastfurnace slag cement is as much dependent on the curing temperature as is portland cement. At low temperatures the cements—"Eisenportlandzement" and blastfurnace slag cements with < 50 weight-% slag act similar to portland cement. The reaction of cement with high slag contents, however, is partly a little more delayed at temperatures of $+5$°C or below (170).

With temperatures exceeding 20°C, especially in case of heat treatment or steam curing, blastfurnace slag cements generally show very favourable strength results (186), (187) (188), (44), (189) and (190). Firstly, the increase in strength, which can be attained by heat treatment, rises with growing slag contents, and simultaneously the after-hardening is maintained better when the contents of slag is increased. The final strength of blastfurnace slag cements will be lowered only little or not at all with an initial heat treatment.

Behaviour in Aggressive Solutions (by F. Schröder and H. G. Smolczyk)

General Survey

There is ample literature on the behaviour of slag cements in aggressive solutions—especially in sul-

phate solutions and in sea water—as well as on the testing methods. As this group of subjects is assigned to another principal paper (III—2), this paper is to give only a general survey and to deal only with some very recent results.

A great number of laboratory tests—mostly with mortars—have been carried out. This paper, however, refers mainly to all long-time studies that were made, and comments on their results, the reasons for which are the following:

Short-term tests, mortar tests and rapid tests are highly dependent on specific test conditions and especially on the treatment of the samples, mostly very small ones, prior to the chemical attack. Large-size concrete samples are generally more indifferent to such variations.

Moreover, in some cases unsuitable mixtures of clinker and very slightly hydraulic slag were made for such tests and called "blastfurnace slag cement". If, in such tests, the indication of the strength characteristics is missing, i.e. if the mixtures are not qualified as cement, their results are of very little value with respect to the comparison of cement types. The same applies by analogy to all the other cements having several components. P. Pirotte (191) has put emphasis on these facts.

A very critical appraisal must be made of the results of comparisons between fast-setting and slow-setting cements, which after 1 to 3 months may very well have the same strength. For rapid tests, however, they are subjected to chemical reaction mostly at a very early stage, at which the slow-setting cement still has a much lower strength than the fast-setting cement. The behaviour of the sample—e.g. concerning strength —after long-time chemical reaction is frequently, however, not related to the strength which this sample had at the beginning of its immersion, but to the mostly very high strength which another sample, immersed in plain water all the time, has acquired in the meantime. In our opinion, it is misleading to speak in such cases of "loss of strength" or of "increase in strength". In these cases one should at least use the terms "*relative* loss" or "*relative* increase". Many cases can be established in which samples consisting of slow-setting cement, in spite of a *relative loss in strength*, showed a greater *increase in strength*, during the chemical reaction, than the sample of fast-setting cement.

These facts explain why a few papers on laboratory tests also report poorer resistance of slag cements against chemical attack, as compared to portland cement (192), (193), (194) and (195) or an equal behaviour (196) and (197).

The vast majority of all laboratory tests, on the contrary, have shown a higher stability—especially of blastfurface slag cements and supersulphated cements, rich in granulated slag—in sulphate solutions (7), (116), (198), (199), (200), (201), (202), (203), (189), (204), (135), (205), (206) and (207), in chloride solutions (198), (207), (208) and (209), and in acid waters and against leaching (7), (198), (200), (189), (210), and (211) as well as in sea-water solutions (200), (189), (212) and (213).

Likewise during all the long-time studies, known to us, of concrete in sulphate solutions and in sea-water the slag cements have shown a more favourable behaviour than standard portland cements, and the blastfurnace slag cement rich in granulated slag (189), (212), (214), (215/16), (217), (218), (219) and (220) have proved without any exception a better durability.

Results of Long-Time Studies Including Slag Cements

F. Campus (215) reports on immersion of mortars, concretes and reinforced concretes, consisting of altogether 10 cements, in $MgSO_4$ solution (4870 mg SO_3/litre) and in the tidal zone of the North Sea near Ostend up to a period of 30 years. During these studies, the 4 tested slag cements have shown a very good behaviour in either solution—especially in the form of concrete cubes having a mixture ratio of 1: 5.4 and a w/c-factor of 0.45. Concretes consisting of some other cements—especially high calcareous types—had after 20 years in the $MgSO_4$ solution deteriorated to such an extent already that a compressive-strength comparison with the concretes immersed in water was no longer possible. Likewise in sea water the edges and corners of samples with nonresistant cements were very strongly deteriorated.

Experiments carried out by the "Deutscher Ausschuß für Stahlbeton" with the storage of concrete cubes with 13 cements in the tidal zone of the North Sea near Wilhelmshaven for up to 25 years led to virtually the same results. However, these tests will have to be investigated in detail once again, for although experimental conditions and results are accurately known, some confusing facts have lately come to light.

The evaluations so far made by A. Eckhardt and W. Kronsbein (221) after a period of 19 years, and by A. Hummel and K. Wesche (214) after 25 years, had established that durability increased in the following order:

1st Portland cement
2nd "Erzzement"
3rd "Eisenportlandzement"

4th Blastfurnace slag cement
5th High-alumina cement.

Binders with trass additives were comparable with the first three cements and in no case attained the stability of blastfurnace slag cements.

Based on the subsequent determination of the cement content and the pore volume of the paste for test specimen which had not yet been wholly destroyed by sea water after 25 years, K. Wesche (222) tabulated a new sequence. This attributed identical behaviour to portland cement, "Eisenportland" cement and blastfurnace slag cement, while only slag cements with trass additives and high-alumina cements are said to attain a higher durability.

In an attempt to investigate the reasons for these markedly contradictory views, Tables 11 a, b and c list all measured values so far published which may help to elucidate the matter (214), (221) and (222). Three series of concrete cubes, each with 13 binders, were made in the mixing ratios 1:3 (Table 11a), 1:4 (Table 11b) and 1:5 (Table 11c). All cements were mixed with plain freshwater, (methods a) a few extra ones with sea water (method b). The table lists the compressive strengths of the concrete cubes after 28 days and after 2 and 19 years immersion in sea water. Already after 19 years, 25 concretes of cements without or with little slag were no longer in any condition to be tested. Consequently, after 25 years, cubes of 9 cm were cut out of all specimens which had not yet been wholly destroyed. On these the compressive strength of the still undamaged concrete was measured. After 19 years, the loss in weight was determined for three cubes, each, after 25 years the loss of volume for one cube, each of the concrete still intact.

From this summary of the published measurements, we can easily draw the following conclusions:

All concretes with high-alumina cement proved stable, though some loss of strength was noted on some of the cubes mixed with sea water.

On all concretes with the three blastfurnace slag cements (approx. 50%, 60% and 70% slag), even with the lean mixing of only 260 kg/m³, very high strengths were measured after 19 years. After 25 years, they still remained durable as witnessed by the low loss of substance.

The "Erzzement" and the two "Eisenportland" cements (approx. 25% and 35% slag) attained a durability comparable to blastfurnace slag cements only at a cement content around 300 kg/m³. For the three normal portland cements, a content of 350 kg/m³ was clearly required to obtain the same level.

Fig. 16 shows the average behaviour of these 5

Table 11a. *Sea water test of DAfSt* *a) Mix, 1 : 3*

Specimen		Concrete composition			Compressive strength in kg/cm²				Loss of substance in %	
20 cm-cubes		Cements	Cement content kg/m³	w/c ratio	20 cm-cubes			Sawn out c. (9–15 cm) 25 years	Loss in weight (3 spec.) 19 years	Loss in volume (1 spec.) 25 years
No.	kind				28 days	2 years	19 years			
DAfSt.	No.	102	168	102	102			124	102	124
1	a	PZ A	363	0.45	358	539	attack	584	6	13
1	b	PZ A 10–13%	379	0.45	360	539	attack	536	5	11
2	a	PZ H C_3A	367	0.43	332	510	496	521	1	3
3	a	PZ G	375	0.44	347	545	486	608	3	9
4	a	EPZ M 25–35%	370	0.43	380	514	425	526	2	4
4	b	EPZ M slag	378	0.43	405	521	480	592	0	2
5	a	EPZ L	373	0.43	360	486	418	512	2	4
6	a	HOZ M M: ~ 50%	378	0.45	279	476	455	512	1	3
6	b	HOZ M R, F: > 60%	377	0.45	295	529	525	577	0	2
7	a	HOZ R slag	377	0.44	371	513	497	526	0	4
8	a	HOZ F	377	0.42	322	535	517	538	1	2
9	a	Erz-Z	387	0.41	459	653	548	723	1	3
9	b	Erz-Z	387	0.41	391	693	607	718	1	3
10	a	TSZ	392	0.40	537	721	673	760	0	2
10	b	TSZ	396	0.42	617	779	642	573	0	0
11	a	PZ A	256	0.64	217	384	attack	436	11	23
		+ Trass	+110	0.45						
11	b	PZ A	259	0.65	202	392	339	394	7	14
		+ Trass	+112	0.44						
12	a	EPZ M	242	0.63	212	416	370	408	9	10
		+ Trass	+104	0.44						
13	a	HOZ M	249	0.64	173	374	327	396	8	11
		+ Trass	+107	0.45						

Table 11b. *Sea water test of DAfSt b) Mix, 1 : 4*

Specimen		Concrete composition			Compressive strength in kg/cm²				Loss of substance in %	
20 cm-cubes		Cements	Cement content kg/m³	w/c ratio	20 cm-cubes			Sawn out c. (9–15 cm) 25 years	Loss in weight (3 spec.) 19 years	Loss in volume (1 spec.) 25 years
No.	kind				28 days	2 years	19 years			
DAfSt.	No.	102	168	102	102			124	102	124
1	a	PZ A	—	0.56	280	355	attack	—	43	—
1	b	PZ A 10–13%	—	0.55	251	434	attack	—	64	—
2	a	PZ H C_3A	286	0.55	227	378	attack	481	22	38
3	a	PZ G	294	0.56	271	426	attack	601	16	20
4	a	EPZ M	292	0.55	289	403	attack	473	8	20
4	b	EPZ M 25–35% slag	296	0.55	258	427	attack	424	10	16
5	a	EPZ L	294	0.53	281	427	attack	538	9	25
6	a	HOZ M	287	0.56	217	376	387	418	3	3
6	b	HOZ M M: ~ 50%,	292	0.56	206	421	436	492	1	4
7	a	HOZ R R, F: > 60%	293	0.55	270	398	389	418	3	6
8	a	HOZ F slag	291	0.55	274	432	436	465	2	3
9	a	Erz-Z	304	0.53	371	535	attack	512	12	16
9	b	Erz-Z	306	0.55	279	552	515	628	2	4
10	a	TSZ	308	0.56	521	643	504	635	1	2
10	b	TSZ	312	0.59	533	626	408	437	1	3
11	a	PZ A	200	0.79	145	312	attack	332	24	38
		+ Trass	+ 86	0.55						
11	b	PZ A	206	0.80	141	338	attack	359	20	34
		+ Trass	+ 89	0.56						
12	a	EPZ M	196	0.78	145	346	352	426	10	17
		+ Trass	+ 84	0.55						
13	a	HOZ M	203	0.78	132	286	324	384	13	19
		+ Trass	+ 87	0.55						

Table 11c. *Sea water test of DAfSt c) Mix, 1 : 5*

Specimen		Concrete composition			Compressive strength in kg/cm²				Loss of substance in %	
20 cm-cubes		Cements	Cement content kg/m³	w/c ratio	20 cm-cubes			Sawn out c. (9–15 cm) 25 years	Loss in weight (3 spec.) 19 years	Loss in volume (1 spec.) 25 years
No.	kind				28 days	2 years	19 years			
DAfSt.	No.	102	168	102	102			124	102	124
1	a	PZ A	—	0.67	205	285	attack	—	destr.	—
1	b	PZ A 10–13%	—	0.65	197	336	attack	—	destr.	—
2	a	PZ H C_3A	—	0.66	160	284	attack	—	84	—
3	a	PZ G	—	0.66	206	345	attack	—	40	—
4	a	EPZ M	—	0.65	213	331	attack	—	57	—
4	b	EPZ M 25–35% slag	—	0.65	175	307	attack	—	42	—
5	a	EPZ L	250	0.66	228	357	attack	430	28	64
6	a	HOZ M	250	0.67	150	286	280	317	10	22
6	b	HOZ M M: ~ 50%,	251	0.65	138	363	332	412	6	10
7	a	HOZ R R, F: > 60%	248	0.64	240	372	365	407	4	4
8	a	HOZ F slag	249	0.66	236	386	361	421	3	6
9	a	Erz-Z	257	0.67	232	397	attack	502	25	30
9	b	Erz-Z	252	0.65	182	431	attack	420	20	34
10	a	TSZ	265	0.63	303	433	382	471	1	5
10	b	TSZ	258	0.63	384	431	358	234	4	7
11	a	PZ A	167	0.93	124	220	attack	attack	68	85
		+ Trass	+ 72	0.65						
11	b	PZ A	171	0.93	101	220	attack	283	46	72
		+ Trass	+ 74	0.65						
12	a	EPZ M	173	0.92	119	262	268	312	13	30
		+ Trass	+ 74	0.64						
13	a	HOZ M	176	0.92	98	214	275	318	21	30
		+ Trass	+ 76	0.64						

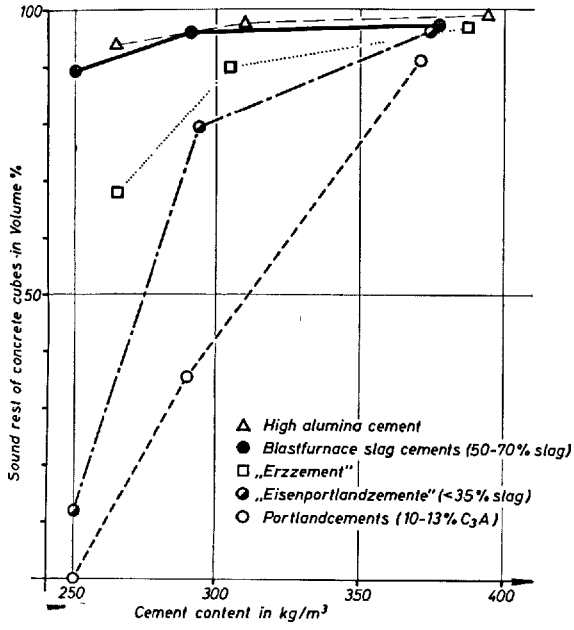

Fig. 16. *Condition of concrete after 25 years exposure in sea-water (tidal zone)*
(According to test results of A. Hummel and K. Wesche)

cement groups.

Portland cements and "Eisenportland" cements with trass substitute gave poorer results in rich mixing and somewhat better ones in lean mixing than the same cements without trass additive.

The excellent properties of blastfurnace slag cements were in all cases impaired by trass substitution.

A further longtime study extending over 27 years was carried out in Norway near Trondheim (220). Here, reinforced concrete piles from 9 different cements—among them a blastfurnace slag cement with over 60% slag content and a "Eisenportland" cement with less than 30%—were exposed upright in the tidal zone. For the main test, cement content was 313 kg/m³ and the w/c-factor approx. 0.6.

The concrete with blastfurnace slag cement (w/c 0.64) and with portland cement with 3% C_3A (w/c 0.56) showed high stability, while those with portland cement with 11% C_3A (w/c 0.61) were destroyed. The "Eisenportland" cement behaved better than this portland cement, but not as well as another with 6% C_3A, which attained the durability of the lean mixing with blastfurnace slag cement only when the cement content was raised from 313 to 417 kg/m³ (w/c 0.47).

In this long-time study, the specimens were attacked by a combination of sea water, frost and steel corrosion, and the assessment also takes the degree of steel corrosion into account.

In another longtime study carried out in England over 23 years, reinforced concrete piles were exposed in the tidal zone of the Thames estuary near Sheerness and half-immersed in three-fold sea water concentration near Watford. F. M. Lea and C. M. Watkins (212) reported on these experiments. Eleven cements—among them one blastfurnace slag cement—were tested in mixture of 1:2.6; 1:5 and 1:9. Here the order of increase in resistance to chemical attack was again:

1st Portland cement
2nd Trass cement and blastfurnace slag cement
3rd High alumina cement

The same order applies to the resistance against corrosion of the reinforcement. A comparable degree of corrosion protection was achieved for the following mixing and concrete covers of the steel.

Blastfurnace slag	mix.	1:2.6	and	2.5	cm cover
cement:	"	1:5	"	5	" "
Portland cement:	"	1:2.6	"	5	" "

Excellent behaviour of blastfurnace slag cement was also noted on concrete blocks weighing about 10 tons which had been immersed as bulwarks in the North Sea tidal zone on the island of Heligoland (208) and (217). Today after over 50 years their surfaces are rough, corners and edges are lightly rounded, whereas similar blocks of other cements show deep fissures and soft spots and have sustained severe partial damage.

Resistance of Slag Cements against Sulfate Action

Satisfactory behaviour in sea water has often been attributed to the well-known resistance of blastfurnace slag and supersulphated cements to sulfate solutions. But this cannot be the only reason. For "Eisenportland" cements with slag contents up to 30% already show an increase in their resistance to sea water, while resistance against pure sulfate solutions (for instance Na_2SO_4) only rises at slag contents above 50%, as has been shown in an extensive study by F. W. Locher (205).

Using the method developed by Koch and Steinegger (195), F. W. Locher investigated the sulfate resistance of slag cements consisting of portland cement clinker with 0.8% and 11% C_3A and granulated slag with 11 and 17.7% Al_2O_3. He found that for slag contents above 60% sulfate resistance improved in all cases compared with slag-free cements. Where slag

content was below 60%, a difference between the two slags was noted. While the low-alumina slag at contents above 20% brought about an increase in sulfate resistance in every case, the high-alumina slag at first had a negative influence. Sulfate-resistant cements were only obtained when slag contents were raised to over 60%. Fig. 17 shows six diagrams taken from this study which, in our opinion, adequately define the sulfate resistance of blastfurnace slag cements, a question which has sufficiently been discussed for decades.

Other Aggressive Media

Less attention has so far been paid to behaviour in the presence of chloride solution. Unlike the sulfates these have no effect in low concentrations but in concentrated solutions they can cause deterioration or complete destruction of concretes with high-calcareous cements (198), (207), (208), (209) and (223). H. G. Smolczyk (209) was able to show that saturated NaCl solution does not impair the development of compressive strength in blastfurnace slag cements containing over 70% slag, in contrast to portland cements with and without C_3A. In solutions of 3 mol/l $MgCl_2$ or 3 mol/$CaCl_2$ concretes of the latter cements were even destroyed within weeks, while those from blastfurnace slag cements with a slag content above 70% remained resistant. Even in the $MgCl_2$ solution, increases about 70 percent in compressive strength were measured after 2 years.

Clearly, these findings indicate that blastfurnace slag cements are not specially sensitive to the Mg^{++}

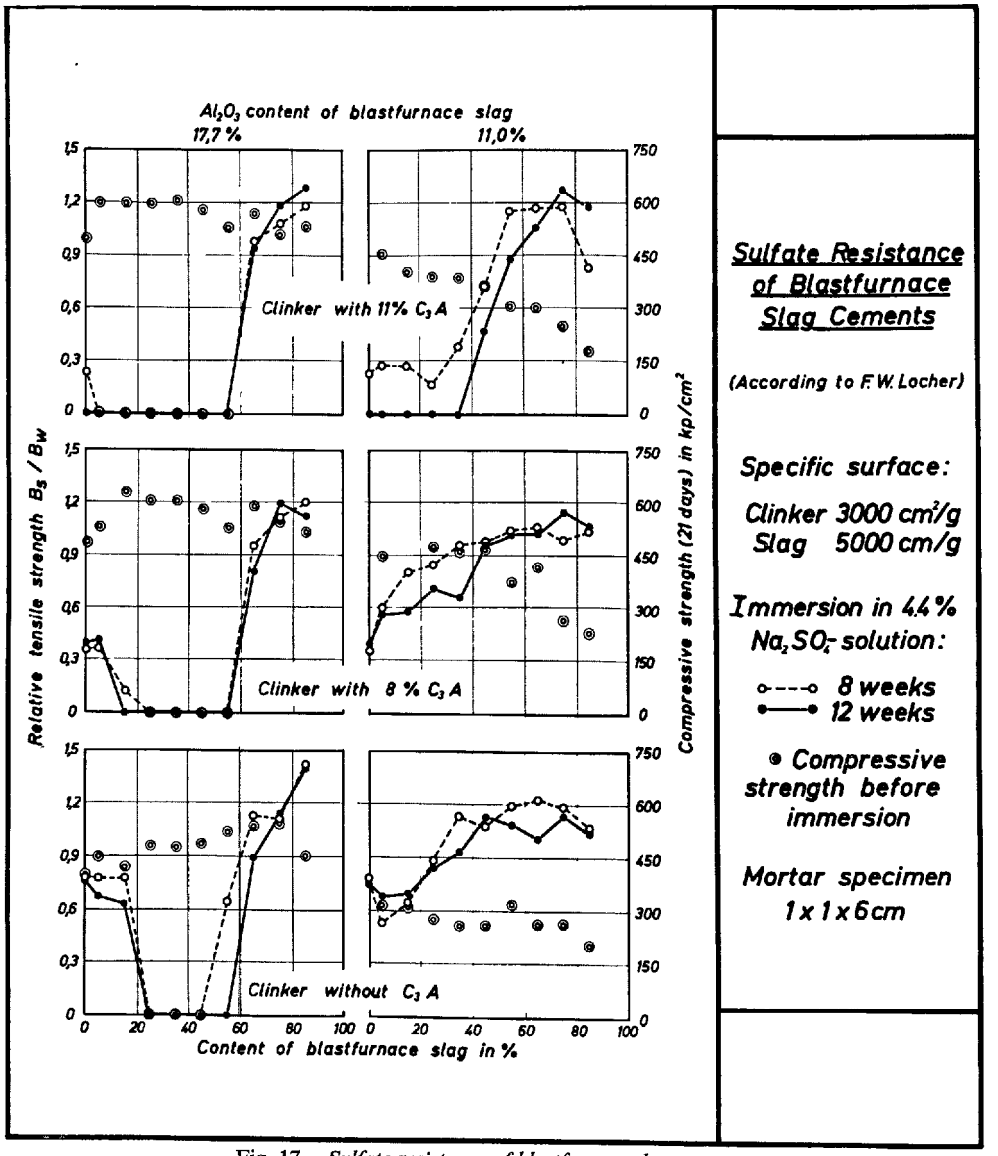

Fig. 17. *Sulfate resistance of blastfurnace slag cements*

ion. Long-time tests in $MgSO_4$ solutions by F. Campus (215/16) produced the same result. Apparently, the term "basic change" coined by E. Burke (224) has only a limited application to slag cements.

Bearing in mind that sea water has a high chloride content and that in tidal zone we must allow for marked increases in concentration within the concrete or on its surface (217) and (11), (see p. 539–553,) we may assume here a direct connection between the resistance of blastfurance slag cement to sea water and chloride solutions. We may also expect blastfurnace slag cements to resist the chemical attack of defrosting salts. Clearly, there is a wide field here for further investigations.

All concretes being strongly alkaline, their resistance to acid waters is comparatively low. Neutral water with very low salt content can also leach out porous concretes in the course of time. In this case, concrete density is a far more important factor than the selection of any given cement type (211). But, here, too it is reported that blastfurnace slag cements have shown rather a better performance than cements of higher lime content without slag (11) (see p. 539–553), (225) and (10) (see p. 710 (Vol. II) and p. 636 (Vol. III)).

Some Reasons for the Resistance of Slag Cements

There must be some fundamental reasons for the good resistance of cements with higher slag content against various solutions aggressive to concrete. A number of authors attribute it to the low CaO content. But this alone cannot explain pronounced differences in behaviour. We can be reasonably certain today that the greater durability of slag cements to given chemical reactions, such as acid waters, sea water or strong chloride solutions, is not merely due to the CaO in the cement, but is largely attributable to the lower content of free $Ca(OH)_2$ in the paste (7), (116), (123) and (225). Blastfurnace slag cements in contrast to supersulphated cements still contain free $Ca(OH)_2$ and have pH values above 12 (7), (126) and (226), but direct chemical attack causes this $Ca(OH)_2$ to be quickly converted, so that the leaching out or diffusion of the $Ca(OH)_2$ bound in the hydrates then proceeds very slowly. Moreover, this reaction leaves behind low-calcareous hydrate gels of lesser permeability which soon arrest many types of chemical attack (227).

These considerations also explain the apparent contradiction that we find the cements with greatest sulfate resistance just among the blastfurnace slag types with the highest Al_2O_3 content. The richer the slag in Al_2O_3, the lower the amount of clinker needed in the cement without any impairment of strength (123). In these cements with high contents of granulated slag, however, little additional ettringite can form under the influence of sulfate, as the ratio of diffusion-inhibiting hydrate gels to free $Ca(OH)_2$ is much greater than in other cements (116) and (228).

In the case of sulfate attack, two further factors must be considered. In the hardened paste of blastfurnace slag cements only a small part of the Al_2O_3 is available for additional ettringite formation, since the larger share has already been bound into the calcium-aluminate-sulfate hydrate phases or can evidently be very firmly bonded into the calcium-silicate hydrate phases (115), (114), (127) and (128). In addition, H. G. Smolczyk (116) established by microscopic examination that the ettringite crystals formed in the paste of cements with high slag contents are so tiny (about 5 micron) that they are not likable to set up any friction.

Effect of Mineral Oils

While the action of mineral oilds on concrete is certainly not in the nature of a chemical reaction, it should be briefly mentioned to complete the picture. Here, we have a very recent comparative experiment by W. Steinbach (229) available. Cement mortars from a portland cement with 12% C_3A and a blastfurnace slag cement with 70% slag were stored for one year in heavy oil, diesel oil and gasoline. The mortar prisms (w/c 0.5 and w/c 0.8), were cured in water for

Table 12. *Compressive strength of cement-mortars after 1 year of immersion in mineral oils. (According to results of W. Steinbach)*

Immersion in	w/c	Portland cement		Blastfurnace slag cement	
		kg/cm²	%	kg/cm²	%
Immediately before immersion	0.5	627	100	531	100
	0.8	330	100	234	100
Heavy oil	0.5	596	95	557	105
	0.8	289	88	219	94
Disel oil	0.5	621	99	600	113
	0.8	305	92	238	102
Petrol	0.5	556	89	619	117
	0.8	285	86	312	133
Air (20°C, 65% r.h.)	0.5	649	104	584	110
	0.8	377	114	271	116
Water (20°C)	0.5	671	107	721	136
	0.8	357	108	352	150

7 days, then in the open air for 21 days and them immersed in the 3 oils with control specimens further exposed to open air and a 5th series cured in water.

Compressive strengths immediately before curing and after one year are compiled in Table 12. It will be seen that while the blastfurnace slag cement registered the highest strength increase in water curing, a higher growth rate was also measured for all other storage methods—including open air curing—than for the portland cement.

In summing up it can be stated that slag cements—and in particular the types with high contents of blastfurnace slag and the supersulphated cements—provide a relatively high resistance against various media which would either attack or weaken concrete of different composition. Admittedly, care must be taken to given them the sufficient wet after-treatment required for all hydraulic binding agents, as laid down in the concrete specifications of practically all countries.

Carbonation and Protection against Steel Corrosion
(by F. Schröder and H.G. Smolczyk)

Carbonation

The carbonation of concrete and possible differences between slag cements and portland cements have been investigated particularly in Germany over the last eight years with often contradictory results.

The research was sparked off by earlier carbonation tests carried out in Japan. Here, K. Kishitani and K. Hamada (230) found that the depth of carbonation rises without limit with the square root of time and that carbonation rate is lowest for pure portland cement. T. Soda and K. Yamazaki (231) noted after five to ten years storage an arrest of carbonation up to altogether 20 years and found no difference in the carbonation depth of blastfurnace slag cements and portland cements. According to K. Kosaka (232) the differences were small. The results of measurements by T. Mori, K. Shirayama and A. Yoda (233) do not show consistently better performance by portland cements.

This work was followed up in Germany during the years 1962 to 1964 by various authors who investigated old and very old concrete structures. Individual results and their interpretations varied to some extent, but on an average no significant differences between slag cements and portland cements were noted (234).

Carbonation tests with mortars and laboratory concrete batches did, however, show very marked differences in both results and their interpretations (235), (236) and (237).

According to A. Meyer, H. J. Wierig and J. Husmann (236), the conditions of storage have a considerable bearing on carbonation, but carbonation speed obeys in all cases the law:

$$\text{Carbonation depth} = \text{const.} \sqrt{\text{time}}$$

In addition, slag cements are said in principle to carbonate faster than portland cements.

F. Schröder, H.G. Smolczyk, K. Grade, R. Vinkeloe and R. Roth (237) by contrast found that this approximate carbonation law was obeyed only under dry storage conditions (20 centigrade and 65% relative humidity) and even then by all the cements not in the same way. Carbonation functions differ in different cement types, particularly at the start of the process. Thus, blastfurnace slag cements with high slag contents tend to carbonate quicker at the start, but are then caught up by portland cements of the same compressive strength. It appears that concrete quality and its after-treatment before carbonation have a far greater influence. In addition, determination of CO_2, X-ray and microscopic investigations of carbonated concrete brought experimental proof that the free $Ca(OH)_2$ content of the paste has virtually no effect on carbonation rate, since all other hydration products of cement are alkaline and carbonate too (238) and (239). Calcite, Vaterite and partly also Aragonite appear as carbonation products (240), (241), (242) and (243).

Why results and interpretations are partly so much at variance may probably be explained by the following reflections as well as recent measurements:

a) So far we have too few long-time carbonation studies with concrete available, so that we too often extrapolate the results of few years on to much longer time spans. All we know about carbonation functions so far can only be regarded as rough approximations and so quite inadequate for extrapolated conclusions and the exact definition of different behaviour.

b) The experimental conditions of many tests are not strictly comparable. Since concrete quality, e.g. its density, is a decisive factor, it must be kept uniform if we want to measure the influence of chemical cement composition. We can roughly approximate this requirement if we compare test specimen of equal compressive strength. In short, we must use cements of comparable compressive strength and store the test specimen in water for a sufficiently long time.

Frequently, however, slag cements with more than 70% slag and portland cements "Z 375" are compared in the form of 4 × 4 × 16 cm mortar prisms, which

are already exposed to ambient atmosphere carbonic acid after 3 to 7 days. Small mortar shapes dry out very fast, so that the start of open-air storage must be directly taken as the reference strength, i.e. not that strength ratio of roughly 1: 1.3 between blastfurnace slag cement "Z 275" and portland cement "Z 375", which correspond to cement quality after 20 days water storage. As blastfurnace slag cement "Z 275" has a different compressive strength increase rate than a portland cement "Z 375", we must, in fact, take a ratio of approximately 1: 1.9 for 7 days pre-storage, and at 3 days only about 1: 2.2. And the square root of these ratios roughly correspond to the carbonation speed ratios, measured and compared in these reports. However, these measurements do not compare types of cement, but merely compressive strengths of test specimen.

Numerous measurements we have carried out ourselves have shown that carbonation depth on mortars and concretes of portland cements, "Eisenportland"-cements and blastfurnace slag cements, stored under identical conditions, after a few years becomes closely proportional to the factor $1/F_0$, where F_0 is the compressive strength of the test specimen at the start of carbonation and includes the influences of the water/cement ratio, the type of cement, its quality class and the after-treatment of the specimen. Any dependence of carbonation on the chemical composition of the cement has so far been noted only for high alumina and supersulphated cements. These carbonate at a markedly faster rate than their factor $1/F_0$ indicates.

These results also provide an answer to the chemically well founded theoretical reflections of H. Steinour (244). But though he points out the reserves of alkalinity of the cement paste, in addition to the free $Ca(OH)_2$, he assigns no significant importance to the degree of this overall alkalinity.

This assumption probably applies only to such cements which do not form any free $Ca(OH)_2$ and so also develop hydrates which are leaner in lime content. Carbonation speed of all other concretes, on the other hand, seems to be governed to all practical purposes exclusively by their physical properties which may be roughly summed up in their compressive strength. Probably, carbonation in concretes containing $Ca(OH)_2$ is not governed by the high speed of chemical reaction but by the slower rate of drying out.

These findings agree with the results of H. E. Schwiete and U. Ludwig (245) who recognised the open porosity of the concrete as a decisive factor and developed suitable testing methods.

Future carbonation tests should, therefore, include the measurement of pore distribution and development of compressive strength in the test specimen. Above all, in order to obtain a basis for valid assessments, we must know the strength of each specimen *immediately before* it starts to dry out and carbonate.

These initial strengths are also required in order to measure the changes in strength as carbonation proceeds. Here again, opinions differ. A. Meyer, H. J. Wierig and J. Husmann (236) state that compressive strength of portland cements rises considerably as a result of carbonation, while that of blastfurnace slag cements containing less than 50% slag remains unchanged. But in their experiments they enforced carbonation by storing tiny cylinders (1 cm) in 10% CO_2 and then compared these minute bodies with others which were stored over 56 days in water. This comparison is inadmissible, because of the marked final hardening of slag cements in water storage, so that it does not tell us the real changes in strength by carbonation. Therefore, it is not surprising that a different experiment, carried out in the same laboratory, produced entirely different results (229). Here, the $4 \times 4 \times 16$ cm test specimen of a blastfurnace slag cement with 70% slag increased in strength to 110% and 116% after only one year's storage in the ambient air (see Table 12).

According to W. Manns and O. Schatz (246) carbonation will only increase the strength of slag cements if they contain more than 40% clinker. In this test, the specimens were first dried at 40 centigrade and then carbonated in 9% CO_2.

These test conditions again do not correspond to practical reality. Extensive tests at the Research Institute for Blastfurnace Slag and two other laboratories of the slag cement industry have yielded results completely different from the ones mentioned above. They are shown in Table 13. Here, lean mortars of 10 cements were stored in water for 28 days and then carbonated completely by 50 weeks open-air storage (20°C, 65% r. h.) or 6 months in 3% CO_2 (20°C, 65% r. h.).

Except for the sulphate slag cement, considerable increases in compressive strength were measured on all samples. The increase in strength, when the samples are exposed to air, range between 50 and 120%, and when they are exposed to CO_2, between 100 and 200%. With blastfurnace slag cements containing more than 50% of slag, the average values were somewhat lower than those of the other cement types, and the portland cement types with $< 3\%$ C_3A showed the greatest increase in strength. Only the supersulphated slag cement lost half of its strength, when exposed either to air or to CO_2.

Table 13. *Compressive strength of cement mortars after total carbonation in air or CO_2*
Mortar bars 4 × 4 × 16 cm, w/c 0.76

Cements		Compressive strength in kg/cm²					
Type	Slag C_3A %	28 days in water (*Sw*)	50 months in air 20°C, 65% r.h.			6 months in 3% CO_2	
			Lab. F	Lab. H	S_A/S_W%	Lab. A	S_C/S_W%
HOZ	74	225	350	330	151	456	203
HOZ	55	199	356	320	170	396	199
HOZ	43	298	474	418	150	708	238
EPZ	15	252	497	384	175	708	281
EPZ	29	240	428	380	168	592	247
PZ	8	267	520	384	169	648	243
PZ	<1	182	397	336	202	482	265
PZ	2	149	318	350	224	442	296
PZ	13	247	426	396	166	516	209
SHZ*	85	427	232	194	50	190	45

* SHZ = Supersulfated cement

These tests were carried out with standard cement types bought from commercial sources, and moreover several laboratories obtained the same results. It will be necessary to discuss the reason why some of the results obtained by other authors are different.

Protection of Reinforcement against Corrosion

Many authors see a direct relationship between carbonation of concrete and protection of reinforcing steel against corrosion, and it is certainly true that the safest protection of the steel against corrosion is afforded by the alkaline-reacting concrete. For this, however, the concrete must be compact and resistant to substances that generally attack the concrete itself.

Therefore, it is probably safer to say that a non-compact or unstable type of concrete gives less protection against steel corrosion and also carbonates more rapidly, when exposed to air (237). It is difficult to check by experiment whether steels, if sufficiently covered with carbonated, but compact concrete, may corrode to such an extent that damage occurs, for carbonation of compact concrete takes very long.

This question also could not be clarified definitely during the colloquium of the RILEM Technical Committee on "Corrosion of Reinforcement of Concrete" at Wexham Springs in September 1965. Considerations on this specific subject will be found in the two "General Reports" by P. Halstead (247) and C. A. Lobry de Bruyn (Chairman of the colloquium) (248).

The testing of very old structures has shown that in non-compact concrete types or insufficient concrete covering, damage due to corrosion has often occured, whereas on steels, in compact concrete types which had carbonated very slowly, only traces of rust have been found, even if the concrete contained chloride (249). In this connection, some authors report a lesser rust prevention by slag cement types (234) and (236), other did not find that there was any difference compared to portland cement types (234), (237) and (250).

On the influence of chloride additives and on the behaviour of steam-treated concrete types, extensive concrete tests have been carried out in Belgium, about which R. Dutron and A. Mommens (251) have reported in detail. During these tests great differences with varying test conditions were established, but no systematic differences between slag cement and portland cement.

In old structures near the sea, and in reinforced concrete immersed for decades in sea water in England, Belgium, Italy, France and Norway, the protection of the reinforcing steel against corrosion was clearly better with blastfurnace slag cements than with ordinary portland cements (212), (215/16), (218), (219) and (220).

Discussion on Slag Cement Types in Prestressed Concrete

More recently apprehensions repeatedly have been expressed in Germany that the sulfide in slag cement, harmless for normal reinforcing steel, may, with certain prestressing steels subject to high stresses, lead to cathodic hydrogen embrittlement and to stress corrosion fracture.

These discussions have been brought about by a number of cases of corrosion damage on prestressed prefabricated concrete consisting of sulfide-containing high alumina cement (252).

However, F. K. Naumann and A. Bäumel (253), who had already described this type of stress corrosion, have clearly pointed out in their publication that hydrogen embrittlement cannot occur within alkaline concretes and that, even in high alumina cements, previous conversion and decrease in volume of the hydration products are a prerequisite for it. According to H. G. Smolczyk (243) this decrease in volume alone is not sufficient to explain the fundamentally different and very disadvantageous behaviour of converted concrete consisting of high alumina cement. He rather points to the decisive role of the water of crystallization in the stoichiometric computation of the conversion in % by volume:

$$3CAH_{10} \longrightarrow C_3AH_6 + 2AH_3 + 18H$$

100% by volume ~48% by volume ~55% by volume

This means that after the conversion about half of the previously solid hydrate exists as free water, which may evaporate and leave pores. The same results were

obtained also by H. E. Schwiete, U. Ludwig and P. Müller (254). This conversion is well known (11) (see p. 437-444,) (255) and can be very well established by X-ray analysis, as is shown in Fig. 18 (243).

Since blastfurnace slag cements form the same hydration products as portland cements (7), (114) and (118), such conversions are not possible, and a comparison with high alumina cement is fundamentally wrong (243). Furthermore we do not know of any case of stress corrosion faillure in concrete consisting of slag cement.

Corrosion tests by B. Ost and G. E. Monfore (256) with prestressing steels in mortars of 3 types of portland cement and 5 types of slag cement (slag up to 77%, sulfide up to 0.8%) with and without chloride additive have not shown any difference between portland cement and slag cement.

Two extensive long-time tests with prestressed concrete piles were started at 6 different places by "Arbeitsgemeinschaft Hochofenschlackenforschung" in 1963, and by "Deutscher Ausschuß für Stahlbeton" in 1964. Moreover a prestressed-concrete testing program (257) with samples half-immersed in sea water has been carried out in France since 1961. It may be expected that in 5 to 10 years significant results from these 3 long-time studies will be available.

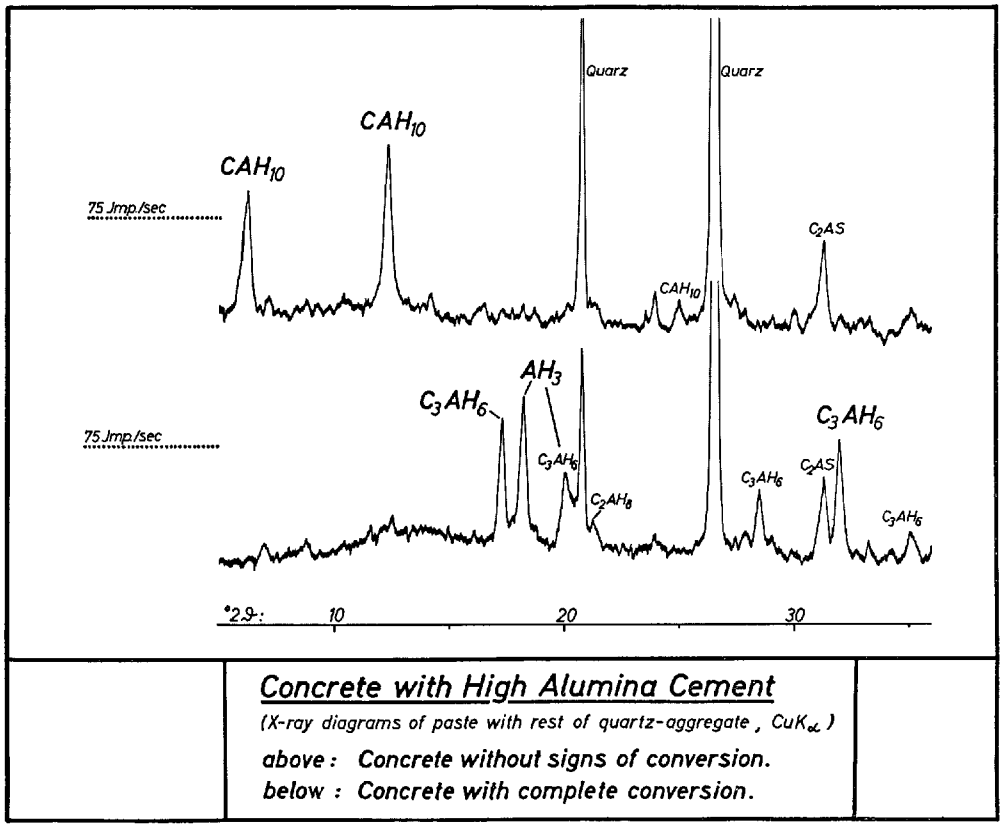

Fig. 18. *Concrete with high alumina cement*

Technical Application of Blastfurnace Slag Cements

Blastfurnace slag cements are used in all branches of concrete and reinforced concrete construction, in civil engineering and building construction, in hydraulic engineering, bridge construction and in the concrete block industry.

There are practically no restrictions on their use in reinforced and prestressed concrete constructional work (189). Only in West Germany high slag cements containing more than 50% by weight are—for the time being—excluded from use in prestressed concrete with direct bonding—i.e. without enveloping tubes. A table showing preferred applications of various cements has been prepared in France (111).

Due to their specific properties, slag cements, mainly those high in slag content are particularly suitable for steam-curing. Steam-cured concretes made from slag

cement are often superior to those without such treatment, but at least equivalent.

A special field of application is moreover the range of concrete for building structures for which cements with a low heat of hydration and/or high resistance to chemical attacks are demanded. Numerous structures in many countries witness the good use of the specific characteristics of slag cements. The following examples are representative for many others:

Bridges: partly prestressed concrete: over the "Oosterschelde"/Netherlands (258), to the Isle Oleron/France (259), along the highway "Autostrada del sole"/Italy (260) and e.g. the motorcar-roads and highways at Düsseldorf/Germany (261);

Marine structures: harbour-locks "Baudoin" Anvers/Belgium (189), "Haringsvliet"/Netherlands (262), "Wilhelmshaven"/Germany (152), and the dams and tides-power station at the Rance/France (263);

Hydraulic engineering structures: Pumping power-station Vianden/Luxembourg (267), Metro-tunnel Rotterdam (268) and airport Shiphol (269), (270) and (271), the canal-locks at the "Mosel"-navigation-way (264), (265) and (266), Montblanc-tunnel/France/Italy (274), barrage "Roselend"/France (272) and (273) and the atom- and nuclear research-center Jülich/Germany (277).

References

1. A. Guttmann, "Die Verwendung der Hochofenschlacke" 2. Aufl., Düsseldorf, Verlag Stahleisen (1934)
2. CEMBUREAU, "The cement statistical and technical association" World Cement Directory, Malmö, Schweden (1961 und 1965)
3. Syndicat National des Fabricants de Ciments et Chaux Hydrauliques, "La situation de l'industrie des chaux et ciments en France, en Europe et dans le monde en 1964" Rev. Mater. Constr. Nr. 586/87, 224–227 (1964) Nr. 598–99, 346–352 (1965)
4. W. Kramer, "Slag and slag cements" Proceedings of the Fourth International Symposium on the Chemistry of Cement, Washington 1960, U.S. Department of Commerce, National Bureau of Standards, Monograph 43, Vol. II, 957–973.
5. I. I. Kholin und S. M. Royak, "Slag cements in the USSR" Proceedings of the Fourth International Symposium on the Chemistry of Cement, Washington 1960, U.S. Department of Commerce, National Bureau of Standards, Monograph 43, Vol. II, 1057–1065.
6. F. Keil, "Hochofenschlacke" 2. Aufl. Düsseldorf, Verlag Stahleisen (1963).
7. R. W. Nurse, "Slag cements" in H. W. F. Taylor's 'The chemistry of cements', Vol. 2, 37–67, Academic Press, London and New York (1964).
8. P. Javelle und P. Ponteville, "Caracteristiques et emplois des laitiers de hauts fourneaux" Association technique de la Siderurgie Francaise, Comm. des Ingenieurs de Hauts Fourneaux, IRSID, VSP 66—RL 04, (Fevrier 1966).
9. R. H. Bogue, "The chemistry of portland cement" 2. Edition, Reinhold Publ. Corp., New York (1955).
10. H. Kühl, "Zement-Chemie", 3. Aufl., VEB Verlag Technik, Berlin, Bd. I—III (1956,/1961).
11. F. M. Lea and C. H. Desch, "The chemistry of cement and concrete" 2. Edition, Edward Arnold Publ. Ltd, London (1956).
12. A. Michel, "Wandlungen in der Eisen- und Stahlindustrie" Stahl und Eisen **83**, 10–17, (1963).
13. G. Heynert and J. Willems, "Neuere Entwicklungen bei der Roheisenherstellung im Hochofen" Die Umschau 67, 689–692 (1967).
14. M. Michard, "Evolution possible des caracteristiques des laitiers de haut fourneau en Lorraine" Rev. Mater. Constr. **602**, 472–484 (1965).
15. L. von Bogdandy and R. Wartmann, "Rechnerische Erfassung der Reduktion im Gegenstrom als Grundlage eines mathematischen Hochofenmodells" Arch. f.d. Eisenhüttenwesen **36**, 221–236 (1965).
16. R. L. Stephenson, "The future of ironmaking and its effect on blast-furnace slag" Pit and Quarry **58**, Nr. 9, 133–134 (1966).
17. S. Klemantaski, "Silicates in the iron and steel industry" (An outline of research on slags at the British Iron and Steel Research Assn.) Sil. Ind. **28**, 513–516 (1963).
18. W. Oelsen and H. G. Schubert, "Die Gleichgewichte zwischen Roheisenschmelzen und Kalk-Kieselsäure-Tonerde-Schlacken bei reagierendem Kohlenstoff" Arch. f.d. Eisenhüttenwesen **35**, 1039–1057 (1964).
19. R. G. Ward and K. A. Salmon, "The kinetics of sulphur transfer from iron to slag" J. Iron and Steel Inst. **196**, 393–403 (1960).
20. H. Schenck, M. G. Frohberg and T. El Gammal, "Das Schwefelgleichgewicht zwischen flüssigem kohlenstoffgesättigtem Eisen und Kalk-Kieselsäure-Schlacken" Arch. f.d. Eisenhüttenwesen **31**, 11–17 (1960).
21. H. Schenck and T. El Gammal, "Untersuchung über den Mechanismus der Reaktionen von Sehwefel und Mangan in kohlenstoffgesättigtem Eisen unter CaO-SiO_2- und CaO-SiO_2-Al_2O_3-Schlacken" Arch. f.d. Eisenhüttenwesen **37**, 539–540 (1966).
22. M. R. Kalyanram, T. G. McFarlane and H. B. Bell, "The activity of calcium oxide in slags in the systems CaO-MgO-SiO_2, CaO-Al_2O_3-SiO_2, CaO-MgO-Al_2O_3-SiO_2 at 1500°C" J. Iron and Steel Inst. **195**, 58–64 (1960).
23. H. J. Langhammer and H. G. Geck, "Viskositätsmessungen an Schlacken" Arch. f.d. Eisenhüttenwesen **38**, 691–699 (1967).
24. H. P. Schulz, "Grundlagen der Schwefelreaktionen" Arch. f.d. Eisenhüttenwesen **35**, 803–819 (1964).
25. W. Oelsen, H. G. Schubert and K. Klein, "Eisenschmelzen und Hochofenschlacken im Graphiet-

tigel bei langerer Schmelzdauer" Arch. f.d. Eisenhüttenwesen **38,** 675–684 (1967).
26. A. Send, G. Winzer and K. Grebe, "Die Entschwefelung im Hochofen und ihre Beeinflussung durch die Abstichfolge" Stahl und Eisen **87,** 1296–1304 (1967).
27. I. P. Bardin, I. S. Kulikow, W. M. Sudin, L. M. Zyliew, G. A. Sokolow, A. L. Galatonow, N. N. Babarykin and I. I. Gultjaj, "Herstellung von schwefelarmen Roheisen unter den Betriebsverhältnissen des Magnitogorsker Kombinates" Stal in Deutsch **1,** 105–110 (1961).
28. V. J. Miller and N. M. Babuschkin, "Physikalisch-chemische Eigenschaften von titanmagnesiahaltigen Schlacken mit hohem Tonerdegehalt" Stahl in Deutsch **1,** 853–859 (1961).
29. N. L. Zilo and L. I. Bol'Sakowa, "Einfluß eines Austausches von Kalk durch Magnesia auf die physikalischen Eigenschaften von Hochofenschlacken" (russisch) Izvest. vyssich ucebnych Zavedenij (Moskva), cernaja matallurg. **7,** Nr. 8, 25–27 (1964).
30. G. Cavalier and M. Sandrea-Deudon, "Laitiers quaternaires CaO-MgO-Al_2O_3-SiO_2: Temperature de cristallisation commencante et champs de cristallisation sur plans a magnésie constante" Rev. Metallurg. **57,** Nr. 12, 1143–1157 (1960).
31. Sagajdak, N. L. Zilo and L. I. Bolsakova, "Viskosität von Hochofenschlacke des Hochofenwerks Magnitogorsk" (russisch) Izvestija Akad. Nauk SSSR, OTN, Metall. i. Gornoc Delo, Nr. 3, 50–57 (1963).
32. E. T. Turkdogan and P. M. Bills, "A critical review of viscosity of CaO-MgO-Al_2O_3-SiO_2 melts" Amer. Ceram. Soc. Bull. **39,** 682–687 (1960).
33. O. Farkas, "Untersuchungen zur Ausbildung der Zusammensetzung von Hochofenschlacken mit hohem Entschwefelungsvermögen und niedriger Viskosität" Freiberger Forschungshefte, Reihe B, **106,** 43–75.
34. V. M. Zudin, N. N. Babarykin, A. L. Galatonow and I. S. Kulikow, "Einfluß des Magnesiumoxyds auf das Entschwefelungsvermögen von Hochofenschlacken" Stahl in Deutsch **1,** Nr. 9, 847–853 (1961).
35. A. L. Galatonov, "Einfluß der Basizität und der Viskosität auf das Entschwefelungsvermögen der Schlacke im Hochofen" Stahl in Deutsch, **4,** Nr. 10, 896–902 (1964).
36. G. I. Zhmoidin and I. S. Kulikov, "The physical properties of blastfurnace slags and the effect on them of magnesium oxyde, sulphur, manganese and iron" Russian Metall. **5,** 12–13 (1960).
37. D. Heyl, "Einfluß des MgO-Gehaltes der Schlacke auf die Betriebsdaten des Hochofens, insbesondere auf die Entschwefelung" Diplom-Arbeit, Bergakademie Clausthal, TH (1959).
38. N. Stutterheim, "Properties and uses of high-magnesia portland slag cement concretes" Journ. Amer. Concr. Inst. 1027–1045 (1960).
39. Forschungsinstitut für Hochofenschlacke, Rheinhausen, "Chemische Analysen" not published.
40. M. Thibault, "Situation actuelle de la production de traitement et du transport des laitiers utilisés en construction routière" Bulletin de liaison des laboratoires routiers ponts et chaussees, Special C, 31–51 (1965).
41. W. Gutt, W. Kinniburgh and A. J. Newman, "Blastfurnace slag as aggregate for concrete" Magazine of Concr. Research **19,** Nr. 59 (1967).
42. P. S. Semenov and J. D. Krucinin, "Der Einfluß der Kristallisation auf das Schäumen der Hochofenschlacken" Stal in Deutsch **10,** 925–926 (1962).
43. R. A. Cheraskow and G. K. Petrenko, "Die Verwendung granulierter Schlacken für die Herstellung von Portlandzement" (russisch) Zement **30,** 18–19, (1964).
44. V. F. Krylov, V. L. Pankratov and V. M. Kolosovskaja, "Schnellerhärtender Hüttenzement mit sauren Hochofenschlacken" (russisch) Zement **31,** 15–16 (1965).
45. J. E. Krüger, K.H.L. Sehlke and J.H.P. van Aardt, "High-temperature studies on blastfurnace slags" Cement and Lime-Manufact. **37,** No. 4 und 5, (Sept. und Juli 1964).
46. E. F. Osborne, R.C. de Vries, K.H. Gee and H.M. Kraner, "Optimum composition of blastfurnace slag as deduced from liquidus data for the quaternary system CaO-MgO-Al_2O_3-SiO_2" J. Metals, N. Y. **6,** 33–45 (1954).
47. P. Kozakevitch and G. Urbain, "Viscosité et structure des laitiers liquides" Gahair du CESSID—Physique et Chimie des Laitiers.
48. W. Gutt, "Some applications of high-temperature microscopy" Sil. Ind. **27,** 285–296 (1962).
49. B. G. Baldwin, "The liquidus- and high-temperature properties of blastfurnace slags" J. Iron und Steel Inst. **186,** S. 388–395 (1957).
50. O. Vorwerk and W. Kramer, "Neuere Forschungsarbeiten auf dem Gebiet der Hochofenschlacke" Zement-Kalk-Gips **6,** 319–324 (1953).
51. P. Hüttemann, "Betriebsuntersuchungen zur Schlackenführung und Schlackenverwertung bei der Thomas- und Stahlroheisenerzeugung" Techn. Mitteilg., Hüttenwerk Rheinhausen AG **3** (1955).
52. P. Herasymenko and G. E. Speight, "Ionic theory of slag-metal equilibria" J. Iron and Steel Inst. **166,** 169–183 und 289–304 (1950).
53. H. Flood and K. Grjotheim, "Thermodynamic calculation of slag equilibria" J. Iron and Steel Inst. **171,** 64–70 (1952).
54. P. Kozakevitch, "Quelques propriétés des laitiers de hauts fourneaux à l'état liquide susceptibles d'influencerleur utilisation ultérieure" Rev. du Tarmacadam **8,** 27–38 (1955).
55. R. Kammel and H. Winterhager, "Struktur und Eigenschaften von Schlacken der Metallhüttenprozesse" Teil I Erzmetall **9,** 207–214 (1956).
56. M. Frohberg, "Die Anwendung der Ionentheorie auf metallurgische Schlacken unter besonderer Berücksichtigung der Sauerstoff- und Schwefelverteilung" Arch. f.d. Eisenhüttenwesen **32,** 597–606 (1961).
57. R. E. Boni and G. Derge, "Surface structure of non-oxidizing slags containing sulphur" Trans. AIME, J. of Metals 59–64 (Jan. 1956).
58. H. Schenck, "Physikalische Chemie der Eisenhüttenprozesse" Verlag Springer, Berlin, (1932).
59. H. E. Schwiete and F. C. Dölbor, "Einfluß der Ab-

kühlungsbedingungen und der chemischen Zusammensetzung auf die hydraulischen Eigenschaften von Hämatitschlacken" Forschungsberichte des Landes NRW Nr. 1186 (1963).
60. Bockris and J. D. Kitchener, "Viscous flow in silica and binary liquid silicates" Glastechn. Ber. **31**, 98 (1958).
61. W. A. Weyl, "Eine atomistische Deutung der Phasenbeziehungen in Alkali-Kieselsäure-Systemen" Glastechn. Ber. **34**, 301–311 (1961).
62. J. D. Bernal, "A geometrical approach to the structure of liquids" Nature **183**, 141–147 (1959).
63. J. Frenkel, "Kinetic theory of liquids" Oxford, Clarendon Press (1946).
64. G. W. Stewart, "Physical concepts of ionic and other aqueous solutions" Amer. J. Phys. **12**, 321–323 (1944).
65. F. Schröder, "Über die hydraulischen Eigenschaften von Hüttensanden und ihre Beurteilungsmethoden" Tonind. Zeitg. **85**, 30–44 (1961).
66. W. H. Zachariasen, "The atomic arrangement in glass" J. Amer. chem. Soc. **54**, 3841–3851 (1932).
67. E. A. Porai-Koshits, "Submikroskopische Struktur einiger komplexer Gläser" Glastechn. Ber. **32**, 450–459 (1959).
68. P. C. Aitcin, "Sur les propriétés minéralogiques et l'utilisation dans les mortiers et bétons des laitiers de hauts fourneaux de fonte Thomas" Rev. Mater. Constr. **608** und **609** (Mai/Juni 1966).
69. P. Großstück, "Verfahren zur Herstellung von Schlackensand" Stahl und Eisen **74**, 1011–1016 (1954).
70. A. Köhler and R. Ehrhardt, "Trennung von Wasser und granulierter Hochofenschlacke" Protokoll über die Sitzung des Arbeitsausschusses für Verwertung der Hochofenschlacke des VDEh am 25.11.1959.
71. V. F. Krylov, V. L. Pankratov and V. S. Zlodeeva, "Über das Wasserstrahl- und das Wasserrinnenverfahren zur Granulierung von Hochofenschlacke" Stahl in Deutsch **3**, 233–236 (1963).
72. S. P. Kinney and Fred Osborne, "Profitable returns from expansion of blast furnace slag for light weight aggregate" Blast Furn. **43**, 493–501 (1955).
73. W. Altpeter, "Erfahrungen mit der hydraulischen Förderung von Hochofenschlackensand und anderen Feststoffen in Hüttenwerken" Stahl und Eisen **81**, 1006–1014 (1961).
74. W. Hahn and H. Geron, "Hydraulische Hüttensandförderung" Protokoll über die Sitzung des Arbeitsausschusses für Verwertung der Hochofenschlacke des VDEh am 25.11.1959.
75. E. Prandi, "Stabilisation au laitier granulé" Rev. Gen. Routes **33**, 376, 101–104 (1963).
76. Forschungsinstitut für Hochofenschlacke, Rheinhausen, Interner Bericht (August 1965)—not published—
77. S. L. Kolhatkar and T. V. Cherian, "Granulation and hydraulic properties of high alumina blast furnace slag" TISCO **12**, Nr. 2, 66–75 (1965).
78. F. Keil and F. Gille, "Hydraulische Eigenschaften basischer Gläser mit der chemischen Zusammensetzung der Gehlenits und Åkermanits" Schriftenreihe der Zementindustrie, **15**, 47–54 (1954).
79. P. P. Budnikov and V. S. Gorskov, "Steigerung der Wasseraktivität von Hochofenschlacken durch eine gerichtete Kristallisation" —russisch— Sowj. Fachz. "Stroiteljnye materialy" **9**, 22–23 (1964).
80. F. Schröder and K. Grade, "Untersuchungen über Hochofenstückschlacken" Untersuchungsbericht Nr. 1966/254 aus dem Forschungsinstitut für Hochofenschlacke, Rheinhausen—not published—
81. W. Gutt, "High-temperature phase equilibria in the partial system $2CaO \cdot SiO_2$–$2MgO \cdot SiO_2$–Al_2O_3 in the quaternary system CaO–SiO_2–Al_2O_3–MgO" J. Iron and Steel Inst. **201**, 532–536 (1963).
82. H. Busch, "Über die hydraulischen Eigenschaften glasiger Hochofenschlacken" Vortrag Symposium 'Petrographie von Schlacken und Zementen', Leipzig (Okt. 1967).
83. I. Peyches, "Nouvelles études sur la structure des états vitreux" Sil. Ind. **28**, 223-229 (1963).
84. F. Schröder, "Die Wirkung von Auslaugewässern auf Grund-und Oberflächengewässer sowie auf Baustoffe" Vortrag beim VDEh "Ausschuß für Verwertung der Hochofenschlacke" am 24.10.1967.
85. F. Schröder, "Chemische und mineralische Zusammensetzung von Stückschlacken—Einfluß auf Grund- und Oberflächenwässer—" Vortrag Symposium 'Petrographie von Schlacken und Zementen', Leipzig (Okt. 1967).
86. A. Oelschläger, "Hochofenschlacke mit hohem Magnesium-oxydgehalt für die Herstellung von Hüttenzementen" Silikattechn. **15**, 288–292 (1964).
87. J. Janowski, "Gesichtspunkte für die Verwendbarkeit von Hochofenschlacken zur Zementherstellung" Cement-Wapno-Gips **16**—polnisch—, 89–97 (1961).
88. A. Schillak, "Die Verbesserung der hydraulischen Eigenschaften von Hochofenschlacken durch Aktivierung der Schlacken und Ausnutzung ihrer Abfallwärme" Bergakademie **11**, 594–599 (1959).
89 H. E. Schwiete and K. H. Kühle, "Über die Möglichkeiten der Verwendung von Hochofenschlacke mit hohen MgO-Gehalten für die Zementerzeugung" Vortrag beim VDEh "Ausschuss für Verwertung der Hochofenschlacke" am 24.10.1967.
90. J. G. D. Steyn and M. D. Watson, "Liquidus properties of high magnesia blastfurnace slags and crystalisation of periclase from them" J. Iron and Steel Inst. **203**, 445–453 (1965).
91. E. Mariani and G. Schippa, "Alcune considerazioni sugli idraulici ad alto tenore in magnesio" L-Ind. Ital. del Cemento **34**, 1021–1026 (1964).
92. "Kalksättigung von Hochofenschlacken" Stahl in Deutsch **4**, 363 (1963).
93. M. Venuat, "Recherches sur quelques laitiers particuliers" Rev. Mat. Const. **602**, 494–502 (1965).
94. H. Sopora, "Die Zementschlacken der DDR" Baustoffind. **7**, Nr. 4, 114–118 (1964).
95. H. Sopora, "Bewertung von Hochofenschlacken für die Zementherstellung im Betriebslaboratorium" Silikattechn. **10**, Nr. 7, 361–363 (1959).
96. S. Solacolu and P. Balta, "Les propriétés hydrauliques des laitiers de haut fourneau du système MgO-CaO-Al_2O_3-SiO_2 contenant du manganèse et du soufre" Rev. Mat. Constr. **583**, 95–110 (1964).
97. W. Schrämli, "Zur Charakterisierung von Hochofen-

schlacken mittels Differentialthermoanalyse" Zement-Kalk-Gips **16,** 140–147 (1963).
98. J. E. Krüger, "The use of D. T. A. for estimating the slag content of mixtures of unhydrated portland cement and ground granulated blastfurnace slag" Cement & Lime Manuf. G. B. **35,** 104–108 (Nov. 1962).
99. N. S. Zargorodnij, O. P. Mtchedlow-Petrosyan, I. M. Sidocenko and I. S. Strelkova, "Bestimmung der Schlacken und Gipsmenge in Zementen nach einer thermographischen Methode"—russisch— Zement **28,** 13–15 (1962).
100. H. Knoblauch, "Untersuchung der flüssigen Phase des Zementleims von Hochofenzementen und der zu ihrer Herstellung verwendeten Schlacke" Tonind. Zeitg. **86,** 449–460 (1962).
101. R. Kondo, "On the structure of high-lime glass" Proceedings of the IV. Intern. Symposium on the Chemistry of Cement, Washington 1960, 973–975.
102. B. Jankowski and J. Kuckert, "Bestimmung der Lichtbrechung von Schlacken. Schnellmethode zur Schlackenuntersuchung" Neue Hütte **11,** 418–420 (1966).
103. O. P. Mtchedlow-Petrosyan, N. A. Lewtschuk and I. S. Strelkova, "Thermische Untersuchung der Schlackenqualität und Beurteilung der Schlackenzugabe zu Zement" Silikattechn. **13,** 153–156 (1962)
104. J. H. Welch, "Discussion" to (4) Chemistry of Cement, proceedings of the IV. Intern. Symposium, Washington 1960, 981.
105. C. Zeiss, "Grundlagen der Farbmessung" Druckschrift 50–669/I–d.
106. "Handbook of Colorimetry" Cambridge (Mass.) (1936).
107. Deutsche Normen, "Farbmessung, Normvalenzsystem, Farbmaßzahlen" DIN 5033 Blatt 2 und 3 (Augs. 1954).
108. F. Keil, "Zur Bewertung der Zementschlacken" Zement **33,** 90–93 (1944).
109. W. Wittekindt, "Zur Qualitätsbeurteilung von Hochofenschlacken und Puzzolanen" Zement-Kalk-Gips **16,** 314–320 (1963).
110. A. I. Stepanowa and S. M. Smechowa, "Eine Schnellmethode zur Bestimmung der Schlackenaktivität" —russisch—Zement **29,** 20–21 (1963).
111. M. Venuat and M. Papadakis, "Controle et essais des Ciments, Mortiers, Bétons" Éditions Eyrolles, Paris (1961).
112. H. E. Schwiete, U. Ludwig, K. E. Würth and G. Grieshammer, "Neubildungen bei der Hydratation von Hochofenschlacken" Vortrag an der Karl Marx-Universität, Leipzig, Nov. 1965; ref. Tonind. Zeitg. **88,** 419–420 (1964).
113. J. D'Ans and H. Eick, "Das System CaO-Al_2O_3-$CaSO_4$-H_2O bei 20°C" Zement-Kalk-Gips **6,** 302–311 (1953).
114. H. G. Smolczyk, "Die Hydratationsprodukte hüttensandreicher Zemente" Zement-Kalk-Gips **18,** 238–246 (1965).
115. U. Ludwig and H. E. Schwiete, "Die Hydratation eines Sulfathüttenzementes" Tonind. Zeitg. **89,** 174–176 (1965).
116. H. G. Smolczyk, "Die Ettringitphasen im Hochofenzement" Zement-Kalk-Gips **14,** 277–284 (1961).
117. R. W. Nurse, "Slag composition and its effect on the properties of super-sulfate cement" Atti del Convegno sulla Prodizioni dei Cementi Siderurgici, Napoli 1960, 178–195 (Stabilimento Tipografico, G. D'Agostino, Napoli).
118. R. Sersale and G. Orsini, "Idratatzone et trasformazione della Loppa d'alto forno per constatto con soluzione d'idrossido di calcio" Ric. sci. **30,** 1230–1237 (1960).
119. F. W. Locher, "Hydraulische Eigenschaften von kalkreichen Gläsern des Systems CaO-Al_2O_3-SiO_2" Schriftenreihe der Zementindustrie, Heft 25 (1960), (VDZ eV, Düsseldorf).
120. H. E. Schwiete, U. Ludwig and P. Jäger, "Untersuchungen im System $3CaO \cdot Al_2O_3$-$CaSO_4$-CaO-H_2O" Zement-Kalk-Gips **17,** 229–236 (1964).
121. W. Richartz, "Über die Bildung tonerdehaltiger Hydratphasen bei der Zementerhärtung" Tonind. Zeitg. **90,** 449–457 (1966).
122. V. Rodt, "Das Verhalten von Hochofenschlacken gegenüber gesättigter Kalkhydratlösung" Zement **30,** 247–250, 259–263 (1941).
123. W. Kramer and H. G. Smolczyk, "Die Entwicklung der Hüttenzemente in Deutschland" Atti del Convegno sulla Prodizioni dei Cementi Siderurgic, Napoli 1960, 249–274 (Stabilimento Tipografico, G. D'Agostiono, Napoli).
124. C. H. Schmitt, "Über die Kalk-Bindung durch Hochofenschlacke bei der hydraulischen Erhärtung von Schlackenzementen" Zement-Kalk-Gips **16,** 321–324 (1963).
125. H. E. Schwiete, U. Ludwig and J. J. Rivas Roz, "Das hydraulische Reaktionsvermögen von Hüttensand in Bindemittelmischungen und die entstehenden Hydratationsneubildungen" Sonderdruck des GHI Aachen, TH Aachen (1966).
126. R. Roth, "Chemisch-analytische Untersuchungsmethode zur Bestimmung der intergranularen. Lösung von abbindenden Zementen" Tonind. Zeitg. **86,** 267–271 (1962).
127. G. L. Kalousek, "Crystal chemistry of hydrons calcium silikates I. Substitution of aluminium in lattice of tobermorite" J. Amer. Ceram. Soc. **40,** 74–80 (1957).
128. L. E. Copeland, E. Bodor, T. N. Chang and C. H. Weise, "Reactions of tobermorite gel with aluminates, ferrites and sulfates" Journ. of the PCA, **9,** 61–74 (January 1967).
129. W. Kramer and F. Schröder, "Über den Aufbau und die Eigenschaften klinkerarmer Hochofenzemente" Techn. Mitteilg. **10** (Okt. 1959).
130. L. Blondiau, "Qualite et application des ciments de haut fourneau belges" Sil. Ind. **25,** 545–550 ff. (1960).
131. "Yawata portland blast-furnace cement" Yawata Chemical Industry Co., Ltd.
132. "The cement industry in Japan" The Cement Association of Japan (1967).
133. R. Kondo, "New types of sulfated slag cement suitable for soil stabilization" Rev. **14,** Gen. Meet. Tokyo 1960, 76–77.

134. S. Reinsdorf, "Eigenschaften und Verwendung von Sulfathüttenzement (SHZ)" Bauplanung-Bautechnik **16,** 230–234 (1962).
135. L. Blondiau, "Aptitude de ciment sursulfaté à la construction des égouts" Rev. Mat. Constr. **535,** 91–98 (1960) und **536,** 113–118 (1960).
136. L. Blondiau, "Bétonnage sous l'eau. Comportement du ciment sursulfaté, du ciment de haut fourneau et du ciment portland" Rev. Mat. Constr. **532,** 7–11 (1960).
137. J. H. P. van Aardt, "Säureangriff auf Beton bei kalkhaltigen Zuschlagstoffen" Zement-Kalk-Gips **14,** 440–447 (1961).
138. L. Blondiau, "Conversation du ciment sursulfaté" Rev. Mat. Constr. **559,** 103–114 (1962).
139. F. K. Schlünz, "Hydrophobe Zemente" Silikattechnik **10,** 556–559 (1959).
140. K. Grade, "Die Bestimmung des Hüttensandgehaltes in Hüttenzementen" Schriftenreihe d. Zementindustrie, **29,** 113–140 (1962).
141. E. Vogel, "Schnellmethode zur angenäherten betriebsmäßigen Bestimmung des Schlackengehaltes in Eisenportland- und Hochofenzementen" Silikattechnik **3,** 559–560 (1952).
142. J. Brocard, "Le dosage du laitier de haut fourneau dans les ciments" Rev. Mat. Constr. **424,** 10–17 (1951).
143. M. Duriez and M. C. Houlnick, "Contrôle des proportions de laitier pour cimenteries et de portland entrant dans la composition d'un ciment" Rev. Mat. Constr. **422,** 323–331 (1950) und **423,** 351–357 (1950).
144. F. Keil and F. Gille, "Die Bestimmung des Schlackensandes im Zement" Zement **27,** 541–546 (1938).
145. R. E. Cromarty, "The use of a magnetic separator and sulphide determination in the determination of the slag content of portland blastfurnace cement" Cement and Lime Manuf. **38,** (1965).
146. P. Catharin, "Über die quantitative Schlackenbestimmung in Mahlprodukten aus Portlandzement und Hochofenschlacke" Zement und Beton **8,** 14–19 (1957).
147. K. Bleher, "Bestimmung des Anteils der Hochofenschlacke in Hüttenzementen" Zement-Kalk-Gips **13,** 156–158 (1960).
148. Verein Deutscher Zementwerke eV, "Entwurf DIN 1164, Blatt 3—Bestimmung der Zusammensetzung—vom 27. 4. 1967.
149. R. Grün and K. Obenauer, "Über die Eigenschaften von Deckenzementen, Beziehungen zwischen neuen und alten Normen" Zement **31,** 101–108 (1943).
150. A. Meyer, "Normen für die Festigkeitsprüfung von Zement" Zement-Kalk-Gips **17,** 1–14 (1964).
151. K. Okada, S. Nishibayashi and T. Tomisawa, "Physical properties, especially creep, of portland-blast furnace slag cement" Rev. 14 Gen. Meet. Tokyo 1960, 65–66.
152. W. Ferck, "Die Stahlbetonarbeiten beim Bau der vierten Hafeneinfahrt in Wilhelmshaven" Deutscher Betonverein eV, Vorträge auf dem Betontag 1963.
153. E. Spohn, "Ist die Zementnorm DIN 1164 reformbedürftig?" Zement-Kalk-Gips **14,** 202–207 (1961).
154. W. Mandry, "Über das Kühlen von Beton" Springer Verlag, Berlin (1961).
155. R. Dietrich, "Untersuchungen über die Wärmetönung und andere für Massenbeton wichtige Eigenschaften von Beton aus Zementen mit unterschiedlichem Klinker- und Schlackengehalt" Dissertation TH Stuttgart (1959).
156. K. Goto, M. Hanada and H. Miyairi, "Studies on portland blast-furnace slag cements. Mainly about the influence of the chemical composition of the clinker used in portland blast-furnace cement" Rev. **15,** Gen. Meet. Tokyo 1961, 61–62.
157. M. Hanada, "Studies on the portland blast-furnace slag cement" Chiefly on the effects of calcium sulfates Rev. **16,** Gen. Meet. Tokyo 1962 (81–83).
158. R. Nagano and S. Yamawaki, "Effect of modification of gypsun, properties of portland blastfurnace slag cement" Rev. **14,** Gen. Meet. Tokyo 1960, 62–63.
159. F. W. Locher, J. Wuhrer and K. Schweden, "Einfluß der Mahlfeinheit und Kornverteilung auf die Eigenschaften von Portland- und Hüttenzementen sowie von hydraulischen Kalken" Tonind. Zeitg. **90,** 547–554 (1966).
160. W. Kayser, "Über den Einfluß der Korngrößenverteilung auf die Eigenschaften von Hütten- und Portlandzementen" Dissertation TH Karlsruhe (1965).
161. J. Birthelmer, "Gemeinsame oder getrennte Vermahlung" Silikattechnik **6,** 76–77 (1965).
162. F. Guye, "Ciments à haute teneur en magnésie stables à l'essai à l'autoclave" Rev. Mat. Constr. **567,** 333–348 (1962).
163. C. Cesareni, F. Parissi and V. Vignoli, "Das Schlacke-Klinker-Verhältnis und die physikalischen Eigenschaften von Hüttenzementen"—polnisch—Cement-Wapno-Gips **18,** 159–167 (1963).
164. M. J. Challier, "L'auscultation dynamique du beton" Annales des ponts et chaussees, 6 (1954).
165. S. Härig, "Die Beeinflussung des E-Moduls von Beton durch Zemente mit unterschiedlichem mineralischem Aufbau und durch natürliche und künstliche Zuschlagstoffe" Dissertation TH Stuttgart (1964).
166. R. Vinkeloe, "Prüfverfahren zur Ermittlung des dynamischen Elastizitätsmoduls von Beton-prismen" Tonind. Zeitg. **86,** 272–276 (1962).
167. R. Vinkeloe, "Beton als Reaktorwerkstoff" Berichte Deutsche Keram. Gesellschaft **40,** 103–108 (1963).
168. R. Vinkeloe, "Temperaturverteilung im Beton als Folge der Abbindewärme des Zementes—Beitrag zur Klärung der Rißschäden im Massenbeton" Betonsteinzeitg. **31,** 681 (1965).
169. F. Keil, "Zemente in der neuzeitlichen Bautechnik" Beton **11,** 163 (1961).
170. H. Lehmann and W. Roesky, "Festigkeitsentwicklung und Hydratation von Portland- und Hüttenzementen bei 20, 5 und 1°C" Toind. Ztg. **89,** (1965) 337–350.
171. A. Basalla, "Wärmeentwicklung im Beton" Zementtaschenbuch 1964/65, 275 ff.
172. C. J. de Langavant, "L'emploi de la méthode Thermos

pour la calorimétrie continue des réactions lentes a caractère évolutif et pour la calorimétrie des réactions tres faibles" Publ. techn. CERILH **67.**
173. H. E. Schwiete, U. Ludwig and K. Rakel, "Die Hydratations-wärme von Zementen" Tonind. Zeitg. **89,** 166–169 (1965).
174. K. H. Karsch and H. E. Schwiete, "Adiabatisches Kalorimeter zur Bestimmung der Hydratationswärme eines Zementes" Zement-Kalk-Gips **16,** 165–169 (1965).
175. R. Alègre, "La calorimétrie des ciments au CERILH" Rev. Mater. Constr. **544, 546, 547, 548** und **549** (1961).
176. N. Sato, T. Shigeta and S. Ito, "Measurement of the heat of hydration of portland blast-furnace slag cement" Rew. **14,** Gen. Meet. Tokyo 1960, 60–61.
177. H. Lafuma, "Caracteristiques des ciments a forte teneur en laitier de haut-fourneau" Convegno sui cementi siderurgici, Neapel (1960).
178. H. Engler and R. Vinkeloe, "Vorteil geringer Betontemperaturen" Beton **12,** 496–500 (1962).
179. O. Eisenmann, "Zur Vermeidung von Temperaturrissen im Massenbeton" Die Bauwirtschaft **14,** 523–527 und 546–549 (1960).
180. G. Wischers, "Betontechnische und konstruktive Maßnahmen gegen Temperaturrisse in massigen Bauteilen" beton **14,** 22–26 und 65 ff. (1964).
181. A. Stucky and M. H. Derron, "Problèmes thermiques posés par la construction des barrages-réservoirs" Publ. **38** der Ecole Polytechnique, Lausanne (1957).
182. L. Santarelli and E. Fonda, "La mesure de la chaleur d'hydratation avec la methode thermométrique a dispersion prédéterminée" Rev. Mater. Constr. **544,** 13 (1961).
183. F. Gille, "Erreurs dans la mesure de la chaleur d'hydratation des ciments par la methode de dissolution d'après la norme ASTM C 186" Compte rendus du XXXI[e] Congres de Chimie Industr., Liege, Vol. II, 51–56 (Sept. 1958).
184. Normenvorschlag des Arbeitskreises VDZ 'Hydratationswärme' Zement-Kalk-Gips **19,** 191–194 (1966).
185. A. Basalla, "Ein adiabatisches Kalorimeter zur Bestimmung der Wärmeentwicklung im Beton" Zement-Kalk-Gips **15,** 136–140 (1962).
186. K. Walz, "Der Einfluß einer Wärmebehandlung auf die Festigkeit von Beton aus verschiedenen Zementen" Beton **10,** 222–232 (1960).
187. M. Lesage, "Etude sur létuvage des ciments à addition de laitier" Rev. Mat. Constr. **594,** 163–172 (1965).
188. L. Duhoux, "Influence de la température sur le ciment de haut fourneau 'Ulysse'" Rev. Mat. Constr. **594,** 149–152 (1965).
189. P. Pirotte, "Hüttenzemente und ihre Anwendung in Belgien" Tonind. Zeitg. **89,** 156–159 (1965).
190. L. Blondiau, "Etuvage et autoclavage des bétons de ciment portland, ciment de haut fourneau et ciment sursulfaté" Rev. Mat. Constr. 4–14, 52–63, 82–97, 125–139, 163–167, 204–210, 300–302, 382–387 und 400–414 (1963).
191. P. Pirotte, "Diskussion über Hochofenzemente" —französisch— International Symposium 'Durability of Concrete' Prag 1961; Finat Report, 183–184 (Prag 1962).
192. W. Gaca, "The durability of hydrotechnical concretes made with some polish cements" International Symposium 'Durability of Concrete' Prag 1961; Preliminary Report, 8–20 (Prag 1961).
193. K. Goto, M. Hanada and H. Miyairi, "Studies on portland blast-furnace slag cements" Japan Cem. Engin. Assn. **16,** 80–81 (1962).
194. J. Brocard and R. Cirodde, "Recherches sur le comportement du béton en Méditerranée" RILEM-Bulletin No. **32,** 323–329 (Sept. 1966).
195. A. Koch and H. Steinegger, "Ein Schnellprüfverfahren für Zemente auf ihr Verhalten bei Sulfatangriff" Zement-Kalk-Gips **13,** 317–324 (1960).
196. A. Meyer, "The resistance of portland cement and slag cement to sulphate solutions" International Symposium 'Durability of Concrete' Prag 1961; Final Report, 429–434 (Prag 1962).
197. R. Nagano, "A part of a ten year study by sonic method on resistivity of concrete immersed in sulfate solutions" Japan Cem. Engin Assn. **17,** 172–174 (1963).
198. B. Kopyczinski, "Communication sur la durabilité du béton dans un fleuve pollué par les déchets industriels" International Symposium 'Durability of Concrete' Prag 1961; Preliminary Report, 331–338 (Prag 1961).
199. G. Babatchew and P. Pentchev, "Résistance à la corrosion des ciments mixtes" International Symposium 'Durability of Concrete Prag 1961; Final Report, 79–92 (Prag 1962).
200. F. Ohama, "Effect of acid solution or sea water on the resistance to corrosion of concrete used for canal lining" Japan Cem. Engin. Assn. **17,** 111–114 (1963).
201. W. Kobayashi, "A study on the blended cements containing blast-furnace slag and fly ash" Japan Cem. Engin. Assn. **18,** 83–85 (1964).
202. S. Reinsdorf, "Die Sulfatbeständigkeit der Zemente der DDR" Silikattechnik **15,** 147–151 und 192–195 (1964).
203. P. Bardet, "La pathologie des mortiers et bétons" Rev. Mat. Constr. **585,** 167–173 (Juin 1964).
204. J. D. Richards, "The effect of various sulfate solutions on the strength and other properties of cement mortars at temperatures up to 80°C" Mag. of. Concr. Res. **17,** 69–76 (1965).
205. F. W. Locher, "Zur Frage des Sulfatwiderstandes von Hüttenzementen" Zement-Kalk-Gips **19,** 395–401 (1966).
206. U. Ludwig and H. E. Schwiete, "Einfluß der offenen Porosität auf die Beständigkeit von Mörteln und Betonen gegen aggressive Lösungen" Baustoffind. **9,** 265–271 (1967).
207. W. Riedel, Ch. Göhring and H. Sprenger, "Einfluß des Hochofenschlackenanteils bei Hüttenzementen auf die Korrosionsbeständigkeit des Zementsteins in den Endlaugen der Kali-Industrie" Baustoffin **9,** 272–276 (1967).
208. H. G. Smolczyk, "Some observations and new aspects concerning sea-water actions on concrete in the tidal-zone" RILEM-Bulletin **32,** 299–304 (Sept. 1966).

209. H. G. Smolczyk, "Chemical reactions of strong salt-solutions with concrete" Supplementary Paper to V-ISCC.
210. F. Parissi, P. Barone and R. Marotta, "Laugungsversuche an Probekörpern aus Hüttenzementen" —polnisch— Cement-Wapno-Gips **17,** 325–331 (1962).
211. F. W. Locher, "Chemischer Angriff auf Beton" Beton **17,** 17–19 und 47–50 (1967).
212. F. M. Lea and C. M. Watkins, "The durability of reinforced concrete in sea-water" National Building Studies Technical Paper **30,** HMSO, London (1960).
213. K. Wesche and S. Mängel, "Influence of temperature on concrete attacked by sea water" RILEM-Bulletin **32,** 295–297 (1966).
214. A. Hummel and K. Wesche, "Beton im Seewasser" Deutscher Ausschuß für Stahlbeton, **124,** Berlin (1956).
215. E. Campus, "Essais de résistance des mortiers et Bétons à la mer (1934–1964)" Silicates ind. **28,** 79–88 (1963).
216. F. Campus, R. Dantienne and M. Dzulynski, "Constatations effectuées après trente années d'immersion marine d'éprouvettes de mortier, des bétons et des bétons armés dans la mer du Nord" International Symposium on the 'Behaviour of Concretes Exposed to Sea Water' in Palermo, Mai (1965).
217. H. G. Smolczyk, "Hochofenzemente in chemisch angreifenden Wässern" Tonind. Zeitg. **89,** 159–165 (1965).
218. F. Parissi and R. Marotta, "I cementi d'altoforno nei Lavori marittimi" International Symposium on the 'Behaviour of Concretes Exposed to Sea Water' in Palermo, Mai 1965 Tagungsbericht von H. G. Smolczyk, Betonsteinzeitg. **31,** 465–470 (1965).
219. L. Duhoux and A. Tessier, "Usine marémotrice de la Rance. Composition des bétons" RILEM-Bulletin **32,** 268–278 (1966).
220. O. E. Gjoerv, I. Gukild and H. P. Sundh, "Investigation of concrete piles under varying conditions in sea water" RILEM-Bulletin **32,** 305–322 (1966).
221. A. Eckhardt and W. Kronsbein, "Beton und Zement im Seewasser" Deutscher Ausschuß für Stahlbeton, **102,** (Berlin 1950).
222. K. Wesche, "Der Einfluß der Zementsteinporen auf die Widerstandsfähigkeit von Beton im Seewasser" Deutscher Ausschuß für Stahlbeton, **168,** 34–44 (Berlin 1965).
223. N. Ewers, "Die Wirkung von Magnesiumchloridsole auf Straßenbeton" Baustoffind. **10,** 281–283 (1967).
224. E. Burke, "Discussion about 'basic change" International Symposium on the 'Behaviour of Concretes Exposed to Sea Water', Palermo, Mai 1965; Tagungsbericht von H. G. Smolczyk, Betonsteinzeitg. **31,** 465–470 (1965).
225. I. Biczok, "Beton-Korrosion, Betonschutz" Deutsche Ausgabe, VEB Verlag für Bauwesen, Berlin, 44-47 und 63–65 (1960).
226. A. Bereczky, "Über die Dauerheftigkeit des Betons" Baustoffind. **5,** 330–301 (1962).
227. A. Stepoe, "Allgemeine Betrachtungen über die Betonkorrosion" Baustoffind. **10,** 258–264 (1967).
228. H. Lehmann and A. Mields, "Über die ettringitähnliche Phase einiger Zemente unter Einfluß hoher Calciumsulfatzusätze" Tonind. Zeitg. **87,** 73–81 (1963).
229. W. Steinbach, "Über die Einwirkung von Mineralölen auf die Festigkeit von Zementmörtel" Betonsteinzeitg. **33,** 462–469 (1967).
230. K. Kishitani and K. Hamada, "Dauerhaftigkeit des Stahlbetons im Zusammenhang mit der Neutralisierung durch CO_2" —japanisch— Bericht des Kajima Institute of Constr. Technology, Tokyo (1963).
231. T. Soda and K. Yamazaki, "Long time study (20 years) on the neutralization of concrete and the rusting of reinforcement in concrete" Japan Cem. Engin. Assn. **12,** 91–93 (1958).
232. K. Kosaka, "Durability (Especially carbonation) test of concrete" International Symposium 'Durability of Concrete' Prag 1961; Final Report (Prag 1962).
233. T. Mori, K. Shirayama and A. Yoda, "The neutralization of concrete, the corrosion of reinforcing steel and the effects of surface finish" Japan Cem. Engin. Assn. **19,** 249–255 (1965).
234. Diverse Arbeiten über Karbonatisierung alter Betone. Deutscher Ausschuß für Stahlbeton, **170,** 1–59 Berlin (1965) B. Wedler: 'Vorwort' (Zusammenfassung der Arbeiten, **170,** 3–4.
235. F. Gille, "Über die Tiefe der karbonatisierten Schicht von alten Betonproben" Beton **10,** 328–330 (1960).
236. A. Meyer, H. J. Wierig und K. Husmann, "Karbonatisierung von Schwerbeton" Beckum 1964 Deutscher Ausschuß für Stahlbeton, **182,** Berlin (1967).
237. F. Schröder, H. G. Smolczyk, K. Grade, R. Vinkeloe and R. Roth, "Über den Einfluß von Luftkohlensäure und Feuchtigkeit auf die Beschaffenheit der Betone als Korrosionsschutz für Stahleinlagen" Rheinhausen 1964 Deutscher Ausschuß für Stahlbeton, **182,** Berlin (1967).
238. H. G. Smolczyk, "Zur Röntgen-Feinstrukturbeugung als mineralogisch-analytischem Verfahren" Z. physik. Chemie **53,** 123–134 (1967).
239. Y. Inoue and S. Asano, "On the carbonation of hydrates of hydraulic compounds" Japan Cem. Engin. Assn. **20,** 66–67 (1966).
240. B. Kroone and F. A. Blakey, "Reaction between carbon dioxide gas and mortar" J. Amer. Concr. Inst. **31,** 497–510 (1959).
241. F. Schröder, "Vaterit, das metastabile Kalziumkarbonat, als sekundäres Zementsteinmineral" Tonind. Zeitg. **86,** 254–260 (1962).
242. S. Asano, M. Ozu and Y. Inoue, "The hydration and carbonation of various kinds of cement and cement compounds" Japan Cem. Engin. Assn. **16,** 68–69 (1962).
243. H. G. Smolczyk, "Die röntgenographische Beurteilung von Beton aus Tonerdezement" Betonsteinzeitg. **30,** 573–579 (1964).
244. H. H. Steinour, "Influence of the cement on the corrosion behaviour of steel in concrete" PCA Research and Development Lab. Bull. **168,** (May

1964).
245. H. E. Schwiete and U. Ludwig, "Über die Bestimmung der offenen Porosität im Zementstein" Tonind. Zeitg. **90,** 562–574 (1966).
246. W. Manns and O. Schatz, "Über die Beeinflussung der Festigkeit von Zementmörteln durch die Karbonatisation" Betonsteinzeitg. **33,** 148–156 (1967).
247. P. Halstead, "Depth and rate of carbonation" (General Report) CRC RILEM Technical Committee Colloquium at Wexham Springs, (Sept. 1965).
248. C. A. Lobry de Bruyn, "Theory of corrosion—electrochemical tests" (General Report) CRC RILEM Technical Committee Colloquium at Wexham Springs, (Sept. 1965).
249. P. E. Halstead, "Corrosion of metals in Buildings" Chemistry and Industry, 1132–1137 (1957).
250. St. Soretz, "Korrosionsschutz im Stahlbeton und Spannbeton" Betonsteinzeitg. **33,** 52–63 (1967).
251. R. Dutron and A. Mommens, "Corrosion des armatures dans le béton-armé" R. R. CRIC m 4, Bruxelles (Décembre 1964).
252. G. Rehm, "Schäden an Spannbetonbauteilen, die mit Tonerdeschmelzzement hergestellt wurden" Betonsteinzeitg. **29,** 651–661 (1963).
253. F. K. Naumann and A. Bäumel, "Bruchschäden an Spannbetondrähten durch Wasserstoffaufnahme in Tonerdezementbeton" Arch. f.d. Eisenhüttenwesen **32,** 89–95 (1961).
254. H. E. Schwiete, U. Ludwig and P. Müller, "Untersuchungen an Kalziumaluminathydraten" Betonsteinzeitg. **32,** 141–149 und 238–243 (1966).
255. H. Lehmann and K. J. Leers, "Reaktionen bei der Erhärtung von Tonerdezementen" Tonind. Zeitg. **87,** 29–41 (1963).
256. B. Ost and G. E. Monfore, "Corrodibility of prestressing wire in concretes made with Type I and Type IS cements"PCA Research and Development Lab., Bull. **159,** (May 1963).
257. Y. Saillard, Diskussionsbemerkung: International Symposium on the 'Behaviour of concretes exposed to sea water' Palermo, May 1965; Tagungsbericht von H. G. Smolczyk, Betonsteinzeitg. **31,** 465–470 (1965).
258. R. T. Hoving, A. C. Krijn and J. H. Loenen, "Brug over de Oosterschelde" Cement **16,** 685–693 und 760–764 (1964).
259. "Brücke zur Insel Oléron" Beton **17,** 217–219 (1967).
260. L. Sala, "Bemerkenswerte Viadukte im Abschnitt Bologna-Florenz der 'Autostrada del Sole'" Vorträge auf dem Betontag in Berlin, 133–155 (1961).
261. E. Beyer, "Hochstraßen" Betonverlag GmbH, Düsseldorf (1960).
262. P. Blokland, "Der Deltaplan und die Entwässerung im Haringvliet" Zement und Beton, **26,** 6–11 (Mai 1963).
263. H. Christaller, "Der Bau des Gezeitenkraftwerkes an der Rance" Wasserwirtschaft **55,** 65–72 (1965).
264. "Die Moselkanalisierung, eine Glanzleistung moderner Bautechnik" Die Bauwirtschaft **18,** 551–554 (1964).
265. H. Kunze, "Tiefbauarbeiten bei der Schiffbarmachung der Mosel" Techn. Mitteilg. Krupp-Werksberichte **21,** 215–219 (1963).
266. O. Selting, "Die Bauarbeiten zur Schiffbarmachung der Mosel" Die Bauwirtschaft **17,** 424–427 (1963).
267. K. Böhler, "Das Pumpspeicherwerk Vianden" Die Wasserwirtschaft **51,** 317–325 und **52,** 8–22 (1962).
268. G. Plantema, H. van Dijk, J. van Herk and Ch. Dekker, "Metro Rotterdam" Cement **15,** 353–355, 407–415, 465–473 und 593–599 (1963).
269. G. H. Kellersmann, "Een voorgespannten betonplatform op Schiphol" Cement **18,** 594–599 (1966).
270. Griffioen, "De Schipholtunnel" Cement **18,** 108–117 (1966).
271. A. van Herk, "Fundering niew stationsgebouw Schiphol" Cement **17,** 21–25 (1965).
272. W. Wunderlich, "Die Talsperre Roselend" Wasserwirtschaft **52,** 242–245 (1962).
273. R. Hemmleb, "Große Ingenieurbauten in den Westalpen" Die Bauwirtschaft **16,** 11–14 (1962).
274. W. Schwarz, "Der Montblanc-Tunnel und die Ausbauarbeiten auf der französischen Seite" Die Bauwirtschaft **6,** 14–24 (1952).
275. W. Zerna, "Experimentelle Festigkeitsuntersuchungen von hyperbolischen Kühltürmen" Bauen macht Freude, Festschrift Firma Heitkamp, 7–25 (1967).
276. K. Walz and G. Wischers, "Beton als Strahlenschutz für Kernreaktoren" Beton **11,** 179–192 (1961).
277. "Die Kernforschungsanlage Jülich des Landes Nordrhein-Westfalen" Hochtief-Nachrichten **40** (Febr. 1967).

Written Discussion

Alfredo Negro

In this principal paper Mr. Schröder makes evident the various possibilities of ionic structure of the silicates in the vitreous slags, which can be identified by the structure itself after devitrification.

A prominent place is given to the silicates of the melilite group, having the general formula $A_2^{2+}\ B^{2+}\ X^{4-}\ O_7^{2-}$ which are considered as solid solutions in the crystalline state; as is known, usually the two main minerals of this solutions are gehlenite $Ca_2\ Al(AlSi)O_7$, and akermanite $Ca_2\ Mg\ Si_2\ O_7$; having a tetragonal lattice which encloses the ions Ca^{2+} with coordination eight, at the centre or irregular polyhedrons, which are made up of oxygen atoms.

In relation to the experimental results of Goldsmith (1), Nurse (2) and other researchers and to the relative interpretation of Christie (3), we carried out some research with X-ray (4) on the introduction of NaF into gehlenite lattice, in order to break the bonds

Ca–O, putting Na^+ in place of Ca^{2+}, and retaining the electroneutrality by the monovalent unity F^-.

These are the results of our works. It has been found that, when a low quantity of NaF is put into gehlenite, a slight deformation of lattice with increase of the unit cell occurs; when a 3.75 NaF percentage is over, a superstructure is originated; a slight lattice contraction, instead, is found when the NaF approaches to five per cent. Decomposition of the gehlenite is obtained using greater additions.

In successive work (5), in order to examine the possibility of the substitution of F^- with OH^-, the above modified gehlenites were hydrated with a lime-saturated solution: we have found that the 3.75 NaF gelenite, although crystalline, presented the typical interferences of the hydrates C_2ASH_8, the stratal hexagonal compound.

The only reported case of hydration of the crystalline gehlenite is that of Carlson, who operated in steam and obtained the cubic compound C_2ASH.

Another set of researches have been carried out on vitreous melilites at different temperatures and pressures, in order to obtain different hydration compounds and to characterize them using X-ray, I.R., and differential-thermal analyses.

The main results are the following: at 50°C (6), glasses in gehlenite-akermanite system present a decrease of reactivity with increasing the akermanite content; when this content is higher than 25%, no reaction occurs. The principal hydration product is C_2ASH_8 and, increasing the akermanite content, only the a_0 parameter in hexagonal lattice decreases from 9.96 Å to 9.93 Å.

Together with the above specified compound, the C_3AH_6 is present which is transformed with time into the successive terms of the hydrogarnets series.

Successive experiments (7, 8) of autoclave hydration on glasses at a higher content of akermanite (from 75% to 100%) have been carried out; the following results have been obtained: at pressure between five and twentyfive atmospheres in almost all the specimens with above specified composition, has been found αC_2SH with small quantities of compounds of tobermorite group, and in some cases with plazolite and xonotlite; anyway, no magnesium hydroxide was found; the interpretation of these results are in according to the specialized literature, that the magnesium takes the place of calcium in the hydrated silicates; in addition a tobermorite 11 Å has been seen, where aluminium partly substitutes the silicon; similar results, starting with other materials are obtained by Kalousek and Diamond (9).

References

1. J. R. Goldsmith "Some melilite solid solutions" J. Geol. **56,** 437–447 (1948).
2. R. W. Nurse and H. G. Midgley "Studies on the melilite solid solutions" J. Iron Steel Inst. **174,** 121–131 (1953).
3. O. H. J. Christie, A contribution to the mineralogy of melilite group, Universitetsforlagest, Oslo (1964).
4. A. Negro and M. Regourd "On the modifications carried out from NaF in lattice of gehlenite" (in French) Silicates Industriels **33,** 137–141 (1968).
5. C. Goria and A. Negro "Hydration of gehlenite with addition of sodium fluoride" (in Italian) Ind. Ital. del Cemento **37,** 757–760 (1967).
6. A. Negro "Hydration experiments at 50°C of glasses corresponding to the gehlenite-akermanite system" (in Italian) Atti Accad. Sci. Torino **102,** 187–193 (1967).
7. A. Negro "On the autoclave treatment of akermanite glass" (in Italian) Atti Acca. Sci. Torino **101,** 649–657 (1967).
8. A. Negro "Autoclave treatment of glasses beloging to the gehlenite-akermanite system" (in Italian). To be published in Ind. Ital. del Cemento.
9. G. L. Kalousek "Crystal chemistry of hydrous calcium silicates: I, Substitution af aluminium in lattice of tobermorite" J. Am. Ceram. Soc. **40,** 74–80 (1957).
   S. Diamond, J. L. White and W. L. Dolch "Effects of isomorphous substitution in hydrothermally-synthesized tobermorite" Amer. Mineral. **51,** 388–401– (1966).

Oral Discussion

Niko Stutterheim

In his paper, Dr. Schröder quotes Guye as recommending a higher fineness for South African cements consisting of clinker with high MgO contents (16-25%) and for granulated slags containing up to 22% MgO for improvement of volume stability. These high MgO clinkers were purely experimental. No portland cements of abnormally high MgO contents (above 5%) are made in South Africa.

On the other hand, slags with MgO of up to 22% are used extensively for slag cements: although such slags are finely ground, this is not done to improve volume stability—they are stable; soundness of such high magnesia slags was the theme of my paper to the 1960 Washington Symposium."

Oral Discussion

Jean Forest

It is desirable first of all to review the interpretation of published data, extracted from a work concerning particular cements bonded with orthophosphoric acid (1), concerning industrial and synthetic blast furnace slags.

The D.T.A. and S.T.A. of these slags which give identical starting temperatures θ°C of devitrification, and knowledge of analytical results from C. Malquori, R. Pinault (2) and Poliet et Chausson, made possible the use of the statistical method.

Applied to 34 slags without Ba and with little alkali content, it reveals a significant correlation between θ°C and $\frac{Ca^{2+} + Mg^{2+}}{Al^{3+}}$ with $r = 0.62$, for a probability threshold of 0.01 read on student's table.

The linear regression can be written:

$$\theta°C = 715.5 + 10.96 \frac{Ca^{2+} + Mg^{2+}}{Al^{3+}} \text{ (Fig. 1).}$$

Justification of this deduction can be found in the work of G. W. Morey (3) who studied the crystallization of a glass 1.11 N-0.95 C-6S in which Al_2O_3 is substituted for CaO.

The effect (Fig. 2) is marked by an increase of devitrification temperature which diminishes nevertheless when the composition permits the appearance of a new mineral.

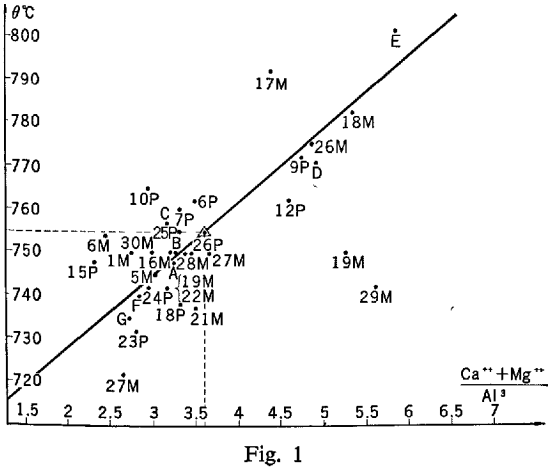

Fig. 1

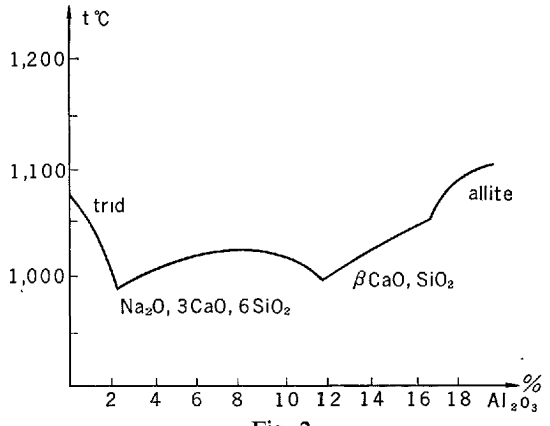

Fig. 2

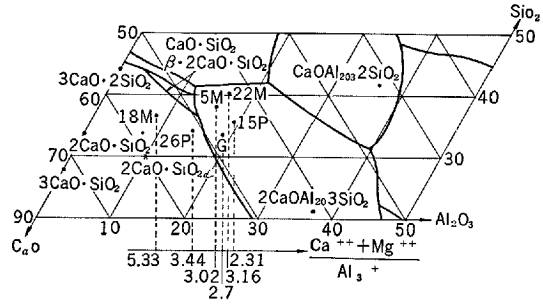

Fig. 3

When $\frac{Ca^{2+} + Mg^{2+}}{Al^{3+}}$ decreases, the representative point of the slag, placed on a Rankin Diagram, considering only the 3 elements Si, Ca, Al, is displaced from the primary stability field of α C_2S to that of C_2AS, passing through the eutectic line (Fig. 3).

The analogy with the preceding case leads us to suppose that the observed correlation results from this transition.

In practice and considering that blast furnace slags high in alumina content are valued, the θ°C knowledge should be one of the basis on which to predict their hydraulic properties.

This observation which wanted explaining concurs with the conclusions of F. Keil and F. W. Locher (4) about the hydraulic properties of glass in the C–A–S. system.

The authors show in fact that the activation with clinker of MgO containing slags, pushes the field of high resistance values of compressive strength up to elevated values of Al_2O_3.

References

1. J. Forest, Contribution to the knowledge of cements bonded with orthophosphoric acid and to the study of some aluminium phosphates (in French) Technical Publication of the C. E. R. I. L. H. No. 145.

2. G. Malquori, R. Sersale and E. Gregorio, The appreciation of the hydraulic value of the blast furnace slags (in Italian) Industr. Ital. cemento 10–10 232–7, 256–68 October-November 1951.
R. Pinault, Physico-chemical study of slags (in French) Thesis of the conservatoire National des Arts et Metiers 1949.
3. G. W. Morey, J. Am. Ceram. Soc. 13, 714–24 1930.
4. F. Keil and F. W. Locher, Zement-Kalk-Gips (in German) 6–245–53 Juli 1958.

Oral Discussion

R. R. Hattiangadi

Dr. Schröder's paper had brought out that portland blast furnace cement had extraordinary good properties in respect of sulphate resistance and was highly recommended. Dr. Hattiangadi asked if there was any correlation between the sulphate resistance of portland blast furnace cement and the alumina content of the slag. In his own experience in India where the blast furnace slag had a very high alumina content, (over 22%), they had found that the sulphate resistance as measured by standard methods was hardly as good as the parent portland cement itself. Dr. Hattiangadi added further that he would be glad to furnish such information as was necessary in this connection. In the general reply to the various points, he got the impression that Dr. Schröder did not touch upon this particular point.

Oral Discussion

Udo Ludwig
Peter A. Otto
Hans E. Schwiete

Some interesting facts during hydration of supersulphated cement are shown in the following Fig.

1. The decrease in anhydrite is corresponding with the increase in heat liberation and strength development. That means that ettringite formation will give in this special case of supersulphated cement a part to strength.
2. In context we measured a decrease in open porosity by means of O_2-diffusion.

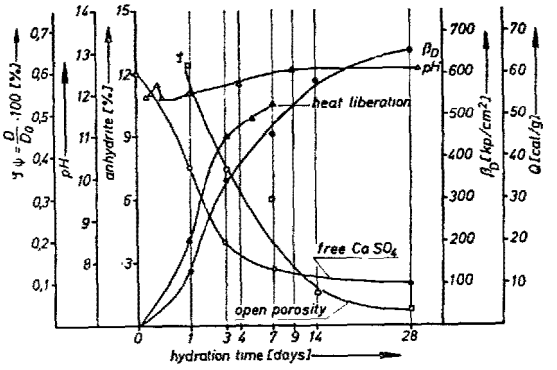

Fig. 1. *Hydration of SHZ*

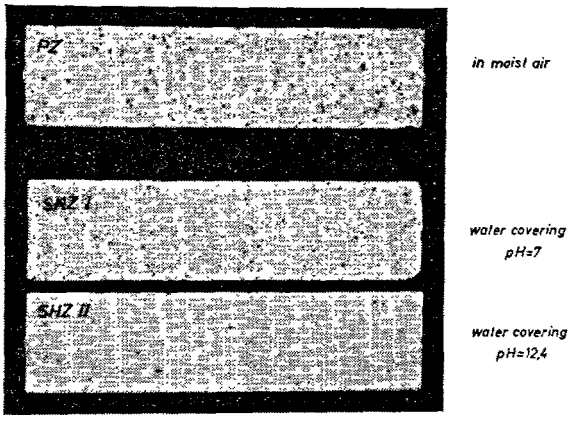

Fig. 2. *Surface abrasion of mortar specimen*

3. The pH-value firstly rises up to 4 hours hydration than decreases and rises again. At least the value lies in the range of 12.6.
4. The following Fig. 2 shows three motar surfaces with portland and supersulphated cement after 3 days hardening brushed with a steel brush.

SHZ I was covered with normal water during the one-days moulding time whilst SHZ II was covered with lime solution of pH = 12.4 by which the surface abrasion was put to zero. This means that by the water fixation during the first hydration and the resulting contraction of volume the open surface becomes poor in lime solution so that only slight hydration reaction can start. Open porosity remains large and CO_2 from air will neutralize the cement.

5. By the carbonation of ettringite ($d = 1.75$ g/cm³) under formation of calcite ($d = 2.71$ g/cm³), gypsum ($d = 2.32$ g/cm³), gibbsite ($d = 2.42$ g/cm³) and evaporation of free water the rest volume becomes 51% of solids and 49% of pores. This increase of porosity explains a loss in strength (3). But wet or moist stored supersulphated cement is in our opinion the best sulphate resisting cement.

References

1. U. Ludwig and H. E. Schwiete: "Hydration of supersulphated cement" (in German), Tonin.-Ztg. **89** 174–176 (1965).
2. U. Ludwig, P. Otto and H. E. Schwiete: "Research on supersulphated cements" (will be published).
3. W. Manns and O. Schatz: "Influence of carbonation on the strength of cement mortars" (in German) Betonstein-Ztg. **33** 148–156 (1967).

Author's Closure

Fritz J. Schröder

Reply to A. Negro

The replacement of CaO by CaF_2 as a fluxing material for lowering the viscosity of slags has been utilized for many years. Thereby an exchange of oxygen ions by twice the number of fluorine ions takes place. It is obvious that this exchange increases the anion to cation ratio in silicate melts. This improves not only a lowering of the viscosity but it also accelerates the crystalisation.

In the case of the replacement of CaO by NaF according to the investigations by A. Negro the F-ions seem also to have acted as a mineralizer.

This can be deducted from the proof of the deformation of the gehlenite-lattice and the formation of a superstructure, and the decomposition of the gehlenite-crystals. The X-ray-diagrams by A. Negro and M. Regourd (1) show the formation and inclusion of wollastonite- and nepheline-crystalites (which was to be expected according to the investigations made by R. W. Nurse and H. G. Midgley (2)), Negro and Regourd assume moreover the inclusions of Na-silicate and Na-aluminate.

Due to these findings, one can assume, that by addition of NaF, gehlenite-lattices with a greater lot of empty sites are being built up. But the strict coordination requirements of the Si^{4+}-ions makes it difficult for silica to form vacant anion sites and therefore the alumina-tetrahedra are essentially disproportionated.

A. Negro's statement that by introducing of minor quantities of NaF the modified and microheterogenic gehlenite-crystals are more reactive than better ordered ones, is therefore not surprising. Due to the surely disturbed coordination requirements and the increased inner surface such gehlenite-crystals, if brought together with $Ca(OH)_2$ or other alkaline solutions will set and harden by capturing hydroxyl-ions and by binding water.

A. Negro's findings on hydration in water and under hydrothermal conditions of gehlenite- and melilite-glasses with an increasing akermanite content confirm some wellknown results, viz. that thereby can build up, besides tobermorite phases, gehlenite-hydrate, plazolite, xonotlite and hydrogarnets as at least I. C. Yang (3) has found under similar conditions.

A. Negro's statement that "at 50°C, glasses in gehlenite-akermanite system present a decrease of reactivity increasing the akermanite content; when this content is higher than 25%, no reaction occours" is in contradiction to F. Keil and F. Gille's (4) findings, and also to the actual experience gained over a period of many years in curing mortars and concrete at temperatures from 40 to 60°C.

References

1. M. A. Negro and M. Regourd "Sur les modifications apportées par NaF dans le réseau de la gehlénite" Silicates Industriels **33** (1968) S. 137–141
2. R. W. Nurse and H. G. Midgley "Studies on the melilite solid solutions" Journ. Iron and Steel Inst. **174** (1953) S. 121–131
3. J. C. Yang "Chemistry of slag-rich cements" V-ISCC, Tokyo 1968, Supplementary Paper IV/128
4. F. Keil and F. Gille "Hydraulische Eigenschaften basischer Gläser mit der chemischen Zusammensetzung des Gehlenits und Akermanits" Zement-Kalk-Grips **2** (1949) S. 229–232

Reply to N. Stutterheim

Considering the discussion remarks on Session IV-3 firstly I thank Mr. Stutterheim for his explanations.

Because of an uninteded shortening which occurred during translation, the reference text on page 64 does indeed give an inexact interpretation of F. Guye's findings.

The text in question should read: By means of a very interesting laboratory investigation, carried out at the "Centre Technique Holderbank" on request of the "Societe Anglo-Alpha, Johannesburg", F. Guye (162) proved the favorable influence of blast-furnace slag on the soundness of high magnesia cements.

The test blastfurnace cements consisted of laboratory clinkers with high MgO-content (16–25%), burned from South African dolomites, and of blast-

furnace slags from a South African iron and steel plant (ISCOR); the slags containing up to 22% MgO. The fineness of these test cements was 4000 to 4500 cm^2/g (Blaine), as usual for blastfurnace cements.

These test blastfurnace cements were found to pass the autoclave test (ASTM C151) under the following conditions: clinker content of the cement: maximum 30 vol.-%; MgO content of the clinker: maximum 17 vol.-%.

Reply to J. Forest

Further I thank Mr. Forest for informing me about his explanations concerning the estimation of the hydraulicity of slag in one of his publications (1).

Investigating a great number of slag samples, Mr. Forest found a relation between the chemical composition, expressed as an atomic ratio Ca + Mg/Al, and the devitrification temperature of slag-glasses.

Forest's relation allows it to valuate relatively well the hydraulic behaviour of granulated slag by means of the chemical analysis, or by measuring the devitrification temperature. This investigation completes the number of research-work done by other authors to estimate the hydraulic capacity of granulated slag by D.T.A. and S.T.A. analysis or by chemical formulas.

After a first review the above relation seems to allow, with the aid of the devitrification temperature, a more secure evaluation of the hydraulic behaviour of granulated slags than the "Hydraulic Potential" according to L. Blondiau (2).

I would, therefore, be glad if Mr. Forest could recheck on the slag samples—provided they are still existing in sufficient quantity—the relation between the "Hydraulic Potential" (that means the difference: solution heat of glassy slag minus solution heat of devitrificated slag) and the atomic ratio Ca + Mg/Al.

Reply to R. R. Hattiangadi

Answering to Mr. Hattiangadi I consider that a strict correlation between the sulphate resistance of portland blastfurnace cements and the Al_2O_3 content of the granulated slag used for their manufacture cannot be stated.

The Indian Standard No. 455–1968 permits only the production of PBFS cements with slag content from 25% to 65%, with a maximum percentage of 3% SO_3. Taking into account the investigations of F. W. Locher (3) (see also principal paper and Fig. 17) the low resistance to sulphate of those cements is obvious.

Since it is, however, possible—as proved by T. Tanaka, T. Sakai and I. Yamane (4) and by H. Williams and S. K. Chopra (5)—to make supersulphated cements from Indian slags (20%-30% Al_2O_3), I hold the view that it should also be feasible to produce from the alumina rich Indian slag sulphate-resisting portland blastfurnace cements with slag content >65 wt. % and somewhat higher SO_3 content. According to F. W. Locher (6) those slags should contain more than 5% MgO.

In many investigations it has again and again been ascertained that those slag rich cements are sulphate resistant without any limitation.

Reply to U. Ludwig

Mr. Ludwig has shortly presented some results from comprehensive investigations on hydration and properties of supersulphated cements (SSC). But his statement that the ettringite formation contributes decisively to the strength development is in contradiction to the results of longtime studies by F. Schröder, H. Schürmann and H.-G. Smolczyk (7).

These authors have pointed out that in general there is no direct influence of the ettringite formation. But such an influence could be seen when relating the strength values to the X-ray determined quantities of hydration products or to the unhydrated cement components. For example, an influence of the ettringite formation could result if when comparing strength values with decreasing anhydrite content the fact is not taken into consideration, that sulphate can be built into the CSH-phases, as shown by L. E. Copeland, E. Bodor, T. N. Chang and C. H. Weise (8).

According to (7) during hydration of SSC, the formation of CSH-phases starts nearly simultaneously with the formation of ettringite. Due to the composition of SSC, especially due to the anhydrite content, the quantity of the built up ettringite (12% to 14% according to our experience) remains nearly constant from the fourth, or from the seventh day latest, whilst the strength increases rapidly up to 28 days and than slower up to 12 or 18 months. Therefore, in the opinion of the a.m. authors (7) the formation of CSH-phases is the decisive factor for the hardening of the SSC.

The decrease in open porosity during hydration of SSC, as measured by Mr. Ludwig (9) is in good accordance with the above said findings, as well as the pH-values, determined by these authors correspond to the formation of CSH-phases.

The dusting of the surface-skins of lean SSC mortars and concretes due to drying out or due to the carbonation especially of the ettringite crystals, is a wellknown fact. In Germany the process of moistening or drizzeling SSC concrete structures with half-saturated lime solutions (pH $\sim$ 12.4) has been used for some 20 years.

Mr. Ludwig's assertion that in his opinion SSC is the most resistant to sulphate ion attack is very valuable, this all the more since it confirms the test results of numerous other authors. (At least see V-ISCC supplementary paper No. IV-130 by George H. Thomas.)

References

1. J. Forest: "Contribution à la connaissance de ciments liés par l'acide orthophosphorique et à la etude de certains phosphates d'aluminium"—Revue Mater. Constr. No. 580, 581, 582 and 583 (January—April 1964).
2. L. Blondiau: "Du côntrole des laitiers granules utilisés en cimenterie" Revue Mater. Constr. 1951, p. 6–9 and p. 42–46.
3. F. W. Locher: "Zur frage des Sulfatwiderstandes von Hüttenzementen" Zement-Kalk-Gips **19**, 395–401 (1966).
4. T. Tanaka, T. Sakai and J. Yamane: "Die Zusammensetzung Japanischer Hochofenschlacken für Sulfathüttenzement" Zement-Kalk-Gips **11**, 50–55 (1952).
5. H. Williams and S. K. Chopra: Discussion to Paper VIII-2, Fourth Internat. Symp. on the Chemistry of Cement, Washington 1960, Proceedings—Monograph No. 43 of National Bureau of Standards, Vol. II, p. 979–981.
6. F. W. Locher: "Hydraulische Eigenschaften von kalkreichen Gläsern des systems CaO–Al_2O_3–SiO_2" Habilitationsschrift Clausthal 1959,—Schriftenreihe der Zementindustrie, Heft 25 (1960).
7. F. Schröder, H. Schürmann and H.-G. Smolczyk: "Die Bedeutung der AFt- und AFm-Phasen bei der sulfatischen Anregung tonerdehaltiger Silikatgläser" (will be published).
8. L. E. Copeland, E. Bodor, T. N. Chang and C. H. Weise: "Reactions of tobermorite-gel with aluminates, ferrites and sulfates" Journ. Res. Lab. PCA **9**, 61–74 (1967) No. 1.
9. U. Ludwig, P. Otto and H.-E. Schwiete: "Hydration of supersulphated cement" (unpublished).

Closure

First of all I wish to thank all the relevent authors and general reporters who represented certain investigations and discussed them in supplementary papers, or dealed with them in written or oral discussions.

Also since 1960 (IV-ISCC, Washington) much research work was done to elucidate the useful characteristics of granulated slags and slag cements (BLFC). Many newer informations—obtained with modern scientific test methods—about the latent hydraulic properties of slags and about the characteristics of the BLFC's are now available, contributing to confirm known statements or to consolidate less secure knowledge.

Nowadays there is only a small lot of unsolved problems and of apparent contradictions.

Firstly there remains the heavy problem of comparing objectively test results, because the standards in addition to national, historic and economical aspects contain different demands and testing methods. Therefore, for laboratory studies all the involved scientists and engineers should use BLFC's corresponding to the draft ISO recommendation no. 771 and test them according to the RILEM-CEMBUREAU methods. And especially the BLFC subtype 60/80 should be used only for valuating the hydraulic capacity of the slag. Furthermore, attention must be paid to the fact that this type of cement only should be compared with an ordinary portland cement, made of the parent clinker.

For a rapid valuating of the hydraulicity of slag the use of moduli or indices—got by combining the chemical components (wt %)—are unsuitable because there is no scientific basis.

Meanwhile, there are undertaken some investigations to combine the physico-chemical properties with the chemical composition. Here the statement of S. K. Chopra and C. A. Taneja (1) and also of T. Rogozinski (2) are remarkable that in slag melts (resp. glassy slags) the Al-ion only have the coordination number 4.

Today it can be taken for sure that for the slag metls besides from their chemical composition the height of the temperature during furnace operation and the high temperature treatment until granulation process are decisive factors. To study this influence the fluorescence radiation of the glassy slag seem to be the simplest aid. Further investigations in this field should proceed from the statements of F. Schröder (3) that there is a shifting of the fluorescence

radiation from UV or dark violet over violet-blue to pink—red for completely crystallized over badly crystallized to completely glassy slag samples of the same chemical composition, or, the release of energy of the fluorescence radiation seems to be related to the disproportioning of the crystal lattices and of the glass constitution, due to the high temperature treatment.

With regard to the strength properties—as well as others—there are no, or only minor differences between PC's and BLFC's containing less than 50% slag. On the contrary, minor slag contentes can improve certain PC properties.

To obtain an explanation for the deviating strength development of the BLFC subtype 60/80 slag we (4) have investigated—among others—the relation between open porosity and mechanical strength of mortars and concretes from different BLFC types. The results obtained from various curing conditions, for the pore size distribution show similar but clear differences depending on the slag content, resp. on the ratio C/S, as demonstrated in the two Figs.

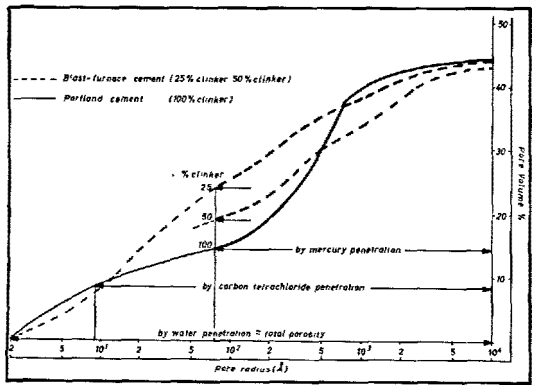

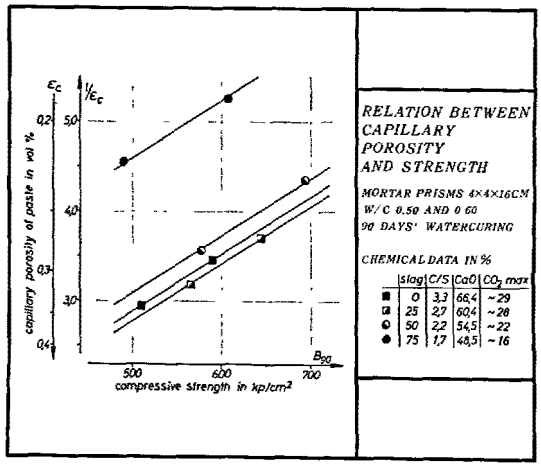

In all test series rising slag content causes a decreasing content of capillary pores.

These results explain the steeper rising strength curves of the slag-rich BLFC and its further hardening over several years, as well as the high density of BLFC concretes and its very high resistance against chemical attack. Moreover, these results explain for what reason the BLFC concretes in spite of their lower content of free $Ca(OH)_2$ don't carbonate faster at later ages than PC concretes of the same quality. And based on these results the formula for carbonation rule

$$= \text{carbonation} \sim \sqrt{1/\text{compressive strength}}$$

—supposed by H.-G. Smolczyk (5) comparing many carbonation test results—obtains a theoretical explanation.

Further investigations about the relations between the ratio C/S, the mechanical strength and other cement properties, e.g. the carbonation, should therefore especially deal with the proportion of low-lime CSH-phases and its detailed properties among the first and the later hydration products of BLFC.

Starting from some cases of corrosion damage on prestressed prefabricated concrete made of sulphide containing high alumina cement, more recently apprehensions have expressed that the sulphide in BLFC—harmless for normal reinforcing steels—may subject to high stresses with prestressed steels leading to cathodic hydrogen embrittlement and to stress corrosion fracture. F. K. Naumann and A. Bäumel (6) clearly have pointed out that hydrogen embirttlement cannot occur within alkaline concretes. Although BLFC form the same hydration products as PC—and therefore a comparison with high alumina cement is fundamentally wrong—the development of H_2S in BLFC concretes is said to be possible due to neutralization in presence of carbonic acid. Although we do not know of any case of stress corrosion failure, since two years we are investigating whether humid carbonic acid may develope H_2S from sulphides in BLFC mortars and concretes. The first part of this investigation (7) shows that only very small quantities of H_2S will be developed by the reaction with unhydrated cement powder, resp. upon the specimen surface during the first hours after demolding. Until today it was impossible to detect any traces of H_2S inside of the partly or completely carbonated specimen.

In the second part we investigate now whether CaS, resp. $Ca(SH)_2$ will be bound during first hydration period into the solid solution compounds of the system $C_3A\bar{S}H$–C_4AH_{13}.

Equal studies in other laboratories would be desi-

rable and would enable the cement-chemists to refute scientifically unsifficient cleared up apprehensions, and would also help to solve several so far unexplained problems and apparent contradictions.

References

1. S. K. Chopra and C. A. Taneja: "Coordination state of aluminium, magnesium and manganese ions in synthetic slag glasses" V-ISCC IV-3, Suppl. Paper No. IV-48.
2. T. Rogozinski: "Über die Konstitution der Hochofenschlacken" Schriften der Hochschule für Architektur und Bauwesen, Weimar, 1968, Heft 3 (C1), S. 62–75.
3. F. Schröder: "Slags and slag cements" V-ISCC Principal Paper IV-3, pp. 28–30 and 41–44.
4. H. Romberg, F. Schröder and R. Vinkeloe: "Einfluß der Zementart auf die Porigkeit sowie Ausbildung der Poren in Mörtel und Beton" (will be published).
5. Written Discussion on Neutralization (Carbonation) of concrete and corrosion of reinforced steel (Carbonation of Concrete) by M. Hamada (Session III-3) submitted by H.-G. Smolczyk, W. Germany.
6. F. K. Naumann and A. Bäumel: "Bruchschäden an Spannbetondrähten durch Wasserstoffaufnahme in Tonerdezementbeton" Archiv f.d. Eisenhüttenwesen **32**, 89–95 (1961).
7. P. Gunkel, F. Schröder and H.-G. Smolczyk: "Einwirkung von sauren Gasen und Dämpfen auf die in verschiedenen Zementen enthaltenen Sulfide und die Möglichkeit der Bildung von Schwefelwasserstoff in Beton" (will be published).

(A) Paper regarding Slag

Supplementary Paper IV-11 A Method of Utilizing Blast-Furnace Slag as a Strength-Improving Agent for Concrete

Tohru Iwai, Toru Mori, Akihiko Yoda and Masaaki Oshima*

Synopsis

Blast-furnace slag, when processed with a special treatment, can be used as an accelerating admixture for portland cement. The special treatment comprises;

a) forming a slurry which consists of water, blast-furnace slag and anhydrite,

b) grinding the slurry sufficiently in a vibrating ball mill and

c) admixing the ground slurry to the cement mix.

Accelerated strength development of cement with the admixture is brought about by rapid crystal growth of calcium sulpho-aluminate which is formed through a reaction between alumina in slag, anhydrite and calcium hydroxide consequent to the hydration of calcium silicate.

Making use of a low grade slag, of which oxides' ratio deviated considerably from the ideal one, the optimum mixing proportion of cement, slag and anhydrite to achieve the highest initial strength was found to be about 80/15/5. A part of anhydrite in the slurry could be replaced by sodium sulphate, which resulted a further acceleration of strength development.

When grinding the slurry, a ball mill of vibrating type with a large capacity was employed. Although an effective accelerating admixture could be produced through sufficient grinding, it was observed that a milling time longer than 25 minutes gave no noticeable improvement of admixture's quality.

Increased strength of cement with the ground admixture was especially in evidence at very early stage (1 to 3 days), and it was also measurable at later stage (7 to 28 days). The later stage improvement of cement strength is attributable to normal slag reaction in which silicate content of slag plays a major role.

Introduction

In construction works rapid strength development of concrete is necessary when formwork is to be removed quickly for re-use or when sufficient early strength for further works is to be obtained; the use of aluminous cement, which offers a very high rate of strength development, however, is kept within narrow bounds because of its high price.

The high rate of strength development of aluminous cement is attributable to the prompt hydration of monocalcium aluminate, while the main component of portland cement is a slow hydrating calcium silicate. Tricalcium aluminate, the secondary component of portland cement, is hydrated rather rapidly, permitting development of initial strength.

The amount of aluminate comprised in portland cement is relatively small but its effects on cement hydration make it of importance. The hydration of tricalcium aluminate itself proceeds too violently, leading to an immediate stiffening of cement paste. To control this phenomena, gypsum is added to cement clinker. Tricalcium aluminate, gypsum and water combined react by forming calcium sulpho-aluminate hydrate, of which crystal grows rapidly and develops the initial strength of cement. The rapid reaction was confirmed by Schwiete, Ludwig and Niel (1), who identified the crystal of the hydrate in a very fresh cement paste.

The initial strength of portland cement can be increased by adding a small amount of aluminous

*Research Institute, Kajima Construction Co., Tokyo, Japan.

cement and extra sulphate. The cement, however, has such defect as making setting time too short and the final strength too low. It was the recognition that pozzolanic materials or latent hydraulic materials contain considerable amount of alumina that the present authors chose them as a low cost alumina additive to portland cement. These admixing materials have been normally utilized not as an alumina source but as a silica source.

Fly ash, which is pozzolanic material, has about 25% alumina, while the alumina content in portland cement is about 5%. If portland cement and fly ash are mixed in proportion of 75 to 25, the mixed cement should contain 10% of alumina. Thus the alumina contents in cement can be doubled.

Pozzolanic materials or latent hydraulic materials are known to be hydrated slowly to release silica or alumina. Therefore, as a rule, mixed cements made of these materials gain strength very slowly. The present study deals with a method of activating these materials by employing a mechanical and chemical treatment.

Activation of Slag through Wet Grinding

As the hydration of cementitious material proceeds on the surface of the particles, it is the total surface area that represents the hydraulic properties of the material with a given composition. In other words, the activity of the material depends on the fineness of the particles, and for a rapid hydration a high degree of fineness is desired.

The conventional blast-furnace cement is made by mixing portland cement and granulated blast-furnace slag. As the usual practice dry granulated slag is fed into a grinding mill with portland cement clinker and gypsum. There is a Belgian method which is called as the Trief process, in which wet-ground granulated slag is fed in the form of a slurry direct into the concrete mixer, together with portland cement and aggregate. Grinding in the wet state results in a greater fineness than would be obtainable with dry grinding.

There are various mills in existence for wet grinding, which are being classified into two types, rotary ball mill and vibrating ball mill. Rotary ball mill possesses a simpler mechanism but is of a lower grinding efficiency compared with vibrating ball mill. In order to obtain a great quantity of materials to be used for practical concreting works, a ball mill of large capacity is necessary. In the present study a vibrating ball mill with a capacity of 60 *l* (vibration frequency: 1,200 c.p.m., maximum amplitude: 5 mm) was employed.

Grinding efficiency of the mill was determined by observing the particle size reduction through an optical microscope. The maximum particle size of slag used for this study was about 50 microns, as seen on Fig. 1-A. When slag was treated with the mill for 30 minutes, the maximum particle size was reduced to about 10 to 15 microns, and for 90 minutes to less than 5 microns, as shown respectively on Fig. 1-B and on Fig. 1-C. In consideration of the processing speed for practical works, the present study chose the wet grinding time of 25 minutes, as will be explained later.

Activation of slag through the wet grinding was confirmed by the preliminary test, in which unprocessed slag with the maximum particle size of 50 microns and processed one with the maximum particle size of 10 to 15 microns were respectively added to rapid hardening portland cement, in which the mixing ratio of slag was 15% to the total amount of the blended cement. The compressive strength was measured in the form of mortar. All mortar specimens for strength measurement in this study were made with w/c ratio of 65% and c/s ratio of 1/2, unless otherwise specified. Up to two months, mortars having unprocessed slag gained a lower strength than mortars composed entirely of portland cement. On the other hand, the development of strength was found to be greater after one week when mortars with processed slag was used than with mortars composed entirely of portland cement. The result, however, was unsatisfactory for the present study, which aimed at an increased strength of hydrated cement in such an accelerated speed as 1 to 3 days.

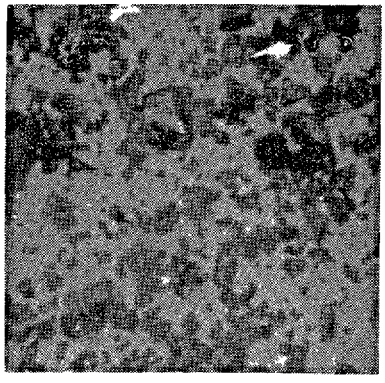

Fig. 1. (*A*) *Before grinding*

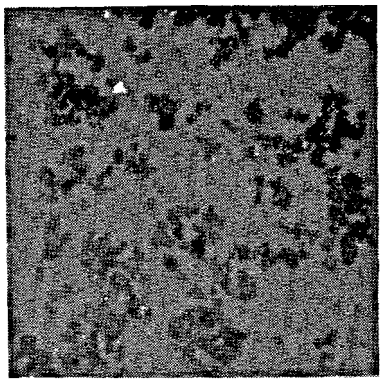

100μ

(B) *After 30 min. grinding*

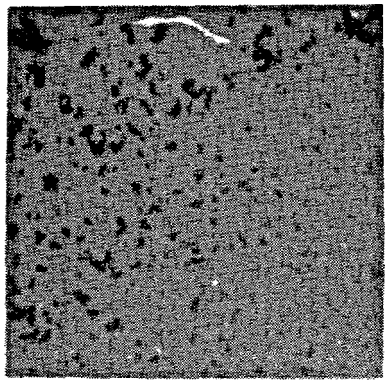

100μ

(C) *After 90 min. grinding*

Fig. 1. *Slag particles*

Activation of Slag through Sulphate Stimulation

Slag, a waste product in the manufacture of iron, is composed of lime, silica and alumina; i.e., the same oxides which make up portland cement, but not in the same proportion. It was reported by various researchers as Tanaka (2) or Locher (3) that the hydraulic properties of slag are greatly influenced by its oxide composition. The ideal slag, according to these researchers, should have the following oxide proportion; $CaO/SiO_2/Al_2O_3 = 50/30/20$. Now the slag used for the present study possessed an oxide proportion which was greatly deviated from the ideal, as shown in Table 1.

Table 1. *Composition of blast-furnace slag*

	CaO	SiO_2	Al_2O_3	MgO	TiO_2	MnO	S
wt. %	41.8	32.6	15.6	6.1	1.8	1.2	0.9

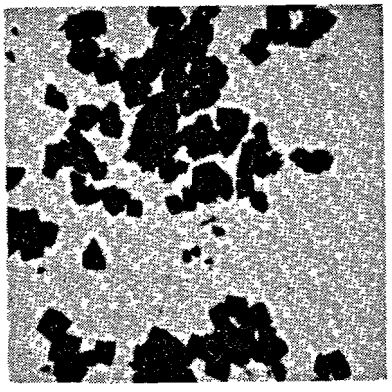

10μ

(A) *with lime*

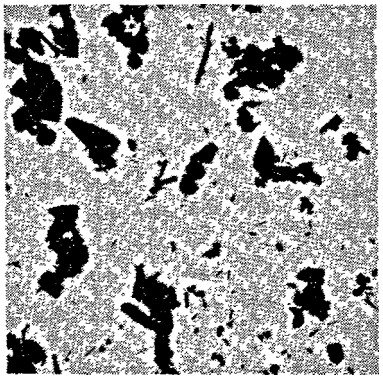

10μ

(B) *with anhydrite*

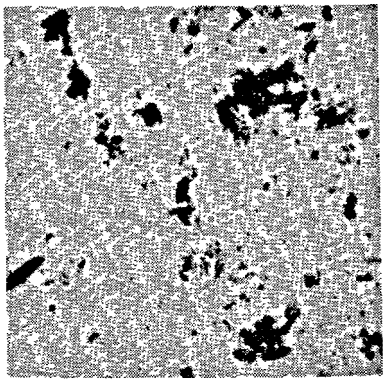

10μ

(C) *with* Na_2SO_4

Fig. 2. *Stimulated slag*

There are two methods for activating slag chemically; sulphate stimulation and lime stimulation. In the hydration of conventional portland blast-furnace cement, slag is stimulated by calcium sulphate and also by lime which is released from calcium silicate. Hydrate formed by slag and lime consists of C–S–H phase and C–A–H phase. Reaction of slag and sulphate results in producing calcium sulphoaluminate hydrate on top of the two phases. According to the investigation of Locher (3) in which C–A–S–glasses were stimulated by anhydrite, lime or portland cement clinker, it was found out that strength development of the hydrate was most in evidence with the sulphate stimulation using slag of the ideal composition.

Figs. 2-A, 2-B and 2-C demonstrate the microscopic pictures of slag particles which were placed in solution of saturated lime, gypsum and sodium sulphate. Slag was wet-ground to bring out the maximum particle size of about 5 microns, and 1 gr of the slag sample was aged in 1 *l* of the stimulating medium for three days. As shown in the pictures, the sulphates affected slag more strongly than lime did, reducing the size of slag particles.

The present study adopted the sulphate stimulation for activating slag, using anhydrite and sodium sulphate.

Wet Grinding of Mixture of Slag and Sulphate

As a rule, when slag or cement is wet-ground, the resulting slurry becomes considerably viscous, making it difficult to handle the slurry. The increase of slurry viscosity is especially noticeable when it contains sulphate. In the present study the slurry was diluted with water to give less viscosity, the proportion of powdered mixture to water being fixed at the ratio of 1 to 1 by weight.

Proportioning of the materials was carried out by the following steps. When, for example, the final weight ratio of cement, slag and sulphate should be 70/25/5 and the w/c ratio 65%, then 25 kg of slag, 5 kg of sulphate and 30 kg of water were milled together for 25 minutes, and 60 kg of slurry thus obtained was added to 70 kg of cement together with 35 kg of water. The total weight of the mixed cement amounted to 100 kg, and the total weight of water to 65 kg.

Figs. 3–A, 3–B and 3–C show the microscopic

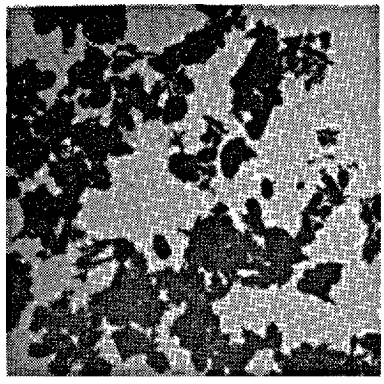

(*A*) *R.H.P.C.*

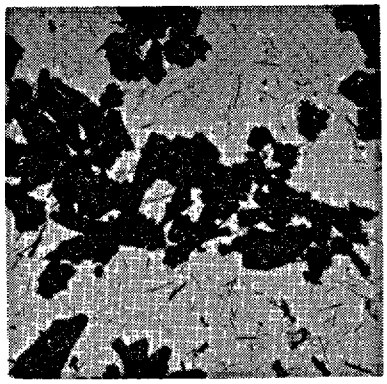

(*B*) *Admixed R.H.P.C.*

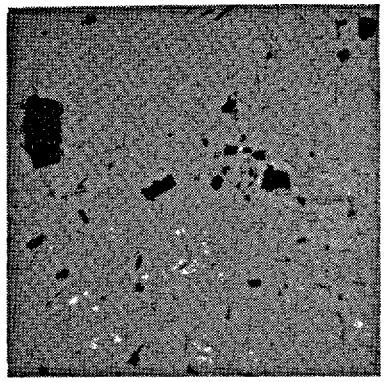

(*C*) *Admixing slurry*

Fig. 3. *One-day-old hydrate*

Table 2. *Slag/Sulphate ratio and mortar strength*

Blending ratio			One-day comp. str. of mortar (kg/cm²)
R.H.P.C.	Ground admix.		
	Slag	Anhydrite	
100	0	0	90
80	20	0	59
80	19	1	86
80	18	2	112
80	17	3	131
80	16	4	140
80	15	5	140
80	14	6	134

Table 3. *Anhydrite/Na_2SO_4 ratio and mortar strength*

Blending ratio				One-day comp. str. of mortar (kg/cm²)
R.H.P.C.	Ground admix.			
	Slag	Anh.	Na_2SO_4	
80	16	4	0	140
80	16	3	1	162
80	16	2	2	190
80	16	1	3	196
80	16	0	4	194

pictures respectively of one-day-old wet-ground portland cement specimen without the admixture, of the same specimen with the admixture and of one-day-old admixing slurry. The X-ray diffraction patterns of these three specimens are presented on Figs. 4–A, 4–B and 4–C, the last two showing the ettringite formation.

Strength of cement with milled admixture could be varied with the ratio of slag/sulphate in slurry. One-day strength of mortar made of 80 parts cement and 20 parts admixture attained the maximum point when the ratio of slag/sulphate was about 15/5, as Table 2 gives.

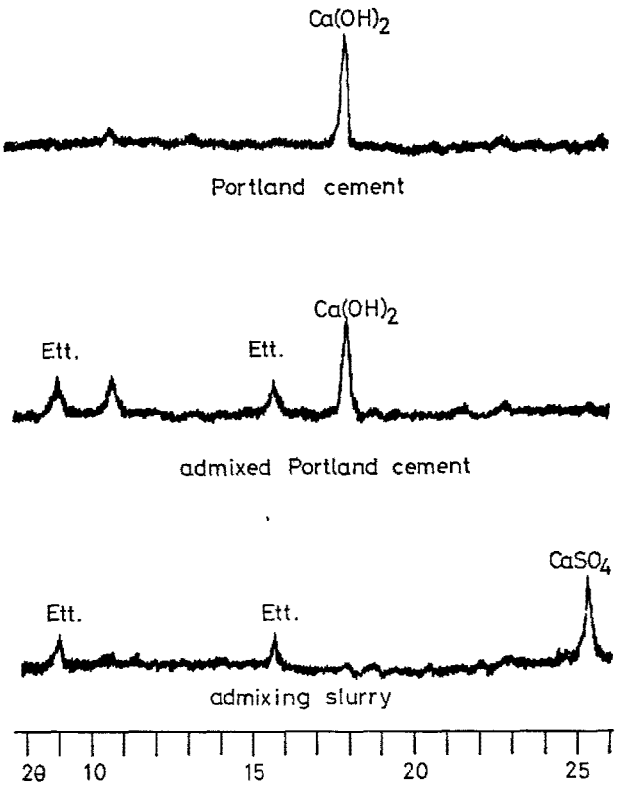

Fig. 4. *X-ray diagrams of hydrate specimens*

Cement with milled admixture gained a higher strength when a part of calcium sulphate was substituted by sodium sulphate. The amount of sodium sulfate to be added to cement, however, should not exceed 2%; for a high contents of sodium sulphate caused efflorescence on the surface of the hardened cement. Table 3 shows the effects of sodium sulfate on one-day strength of mortar.

Grinding Time, Slag Contents and w/c Ratio

Grinding time of slurry could influence the rate of strength development of the mixed cement. Slag, anhydrite, sodium sulphate and water were mixed in the proportion of 16/2/2/20, the slurry being milled for 5 to 40 minutes. Initial strength of the mortars made of 80 parts cement and 20 parts milled admixture are shown on Table 4. Although a sufficiently milled slurry gave a higher mortar strength, a milling time longer than 25 minutes gave no further improvement of mortar strength. In addition, if milling was too prolonged it produced slurry of high viscosity which deteriorated the workability of fresh cement paste.

With a given amount of sulphate to be added, strength of the mixed cement could be varied with the slag contents. Table 5 shows the blending ratio of cement/slag/sulphate, Table 6 and Fig. 5 the initial strength of mortars. The optimum slag content in cement was found to be about 15% with sulphate content of 4%, achieving an increase of initial strength by more than 100%.

Strength increase due to the milled admixture was especially in evidence at the earlier stage of cement hydration and also with the higher w/c ratio. Fig. 6 shows strength (1 to 7 days) of mortar specimens with and without admixture (No. 1 and No. 19 on Table 5). One-day strength of the two specimens with various w/c ratio is compared on Table 7 and Fig. 7.

Generally speaking, higher sulphate content in

cement increases strength at the early stage but causes decreased strength later. A suitable amount of slag in cement, on the other hand, improves the later strength. The mixed cement as presented in this study, containing sulphate and slag, solves both the problems. Pattern of strength development due to each admixture is compared on Table 8 and Fig. 8.

Table 4. *Grinding time of slurry and mortar strength*

Grinding time (min.)	5	10	15	20	25	30	35
One-day comp. str. (kg/cm^2)	109	121	148	178	190	193	194

Table 5. *Blending ratio of cement with admixture*

Sample No.	R.H.P.C.	Ground admix.		
		Slag	Anh.	Na_2SO_4
1	100	0	0	0
2	95	5	0	0
3	90	10	0	0
4	85	15	0	0
5	80	20	0	0
6	99	0	0.5	0.5
7	94	5	0.5	0.5
8	89	10	0.5	0.5
9	84	15	0.5	0.5
10	79	20	0.5	0.5
11	98	0	1	1
12	93	5	1	1
13	88	10	1	1
14	83	15	1	1
15	78	20	1	1
16	96	0	2	2
17	91	5	2	2
18	86	10	2	2
19	81	15	2	2
20	76	20	2	2

Table 6. *One-day comp. strength of mortar (kg/cm^2)*

Anh. + Na_2SO_4 %	Slag %				
	0	5	10	15	20
0	90	89	84	74	59
1	106	120	121	117	104
2	122	138	150	150	144
4	139	166	184	191	183

Table 7. *W/C ratio and one-day comp. strength (kg/cm^2)*

Sample No.	w/c Ratio				
	50	55	60	65	70
1	217	170	129	90	62
	(100)	(100)	(100)	(100)	(100)
19	297	262	230	191	154
	(137)	(154)	(178)	(212)	(248)

(Strength comparison between samples 1 and 19 is made for each w/c ratio, as figures in parentheses.)

Table 8. *1 to 28-days comp. strength of mortar (kg/cm^2)*

Sample No.	Age in days			
	1	3	7	28
1	90	204	293	429
Control	(100)	(100)	(100)	(100)
4	74	192	293	472
15% slag	(82)	(94)	(100)	(110)
16	139	218	264	340
4% sulphate	(154)	(107)	(90)	(79)
19	191	255	316	476
15% slag + 4% sulphate	(212)	(125)	(108)	(111)

(Strength of samples 4, 16 and 19 is compared with that of sample 1 for each age, as figures in parentheses.)

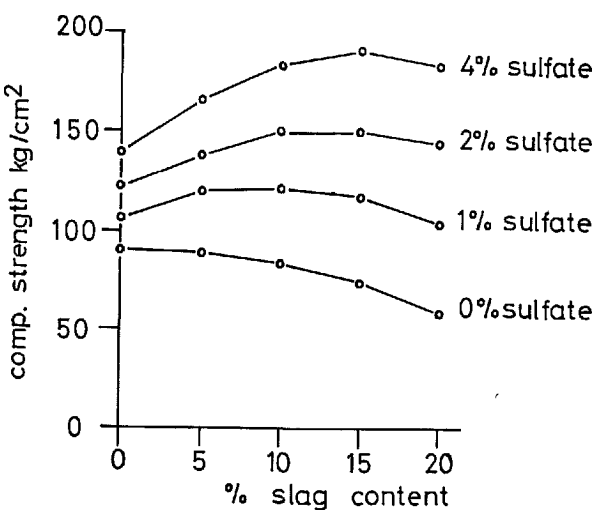

Fig. 5. *One-day strength of mortar*

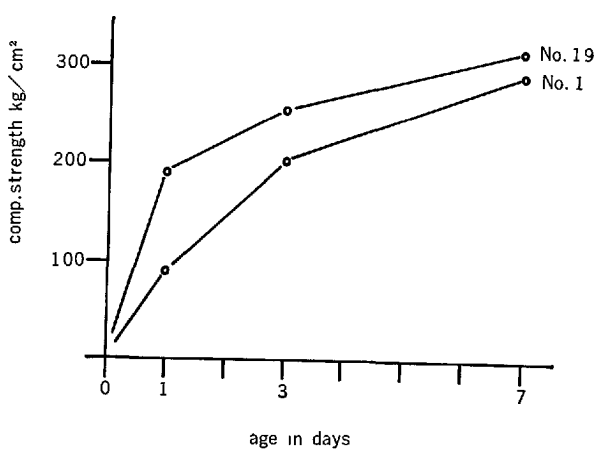

Fig. 6. *Strength development with and without admixture*

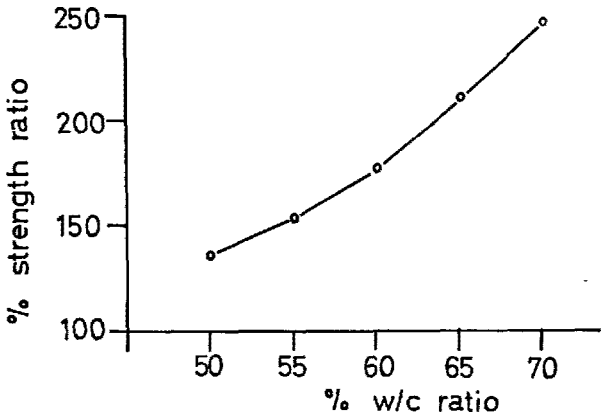

Fig. 7. *Comparison of one-day strength with and without admixture*

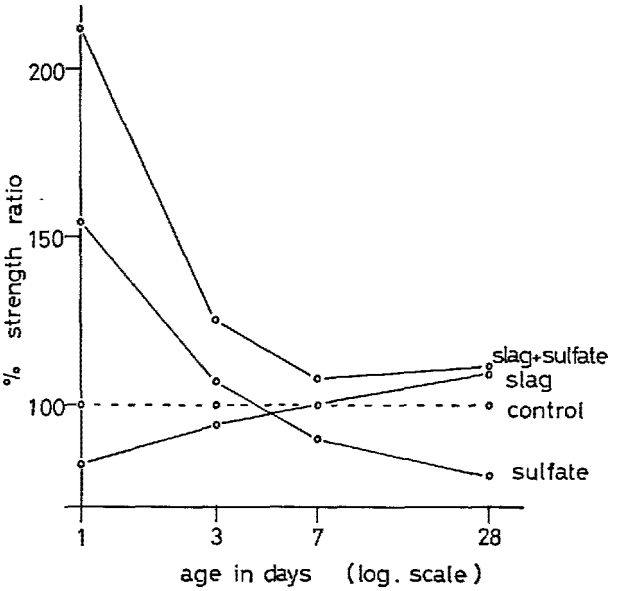

Fig. 8. *Comparison of strength development due to various admixtures*

References

1. H. E. Schwiete, U. Ludwig and E. Niel, "Hydration of portland cement in the early stage", Dissertation Aachen Germany (1962)
2. T. Tanaka, T. Sakai and A. Yamane, "Chemical composition of slag for supersulphate cement", Semento Gijutsu Nempo, 119–124 (1956)
3. F. W. Locher, "Hydraulic properties and hydration of glasses of the system CaO-Al_2O_3-SiO_2", Chemistry of Cement 4th Symp, 267–275 (1960)

Supplementary Paper IV-28 Investigation of the Physicochemical Processes of Hardening of Slag Portland Cement

Vladimir I. Satarin and Yakov M. Syrkin*

Synopsis

Physicochemical investigations of the slag portland cement hardening processes are reported in the paper. Chemical methods of analysis were used for the investigation of the composition of liquid phases and of chemically bound water in hydrated cements.

The morphological structure was defined by electronic microscopy methods. X-ray and thermographic methods were used for the identification of hydrates in the cement stone hardening process.

The complex of theoretical investigations allowed it to find out the ways for the improvement of slag portland cement quality, to work out the parameters of rapid-hardening slag portland cement production technology and to study up its building and technical properties that enable wide use of this new kind of cement in concretes and reinforced concrete constructions produced by the method of hydrothermal treatment.

As a result of the investigations made in the USSR (Institute "Yuzhgiprocement", Kharkov) and aimed at the improvement of the quality of slag portland cement a new type of slag portland cement—rapid-hardening slag portland cement—was created and is now widely produced in industry. The kinetics of hardening of this new type of slag portland cement is equal to that of portland cement of grade 500–600 (in rigid mortars) (1, 2, 3, 4, 5 and 6).

As it is seen from the results of physicomechanical tests of cements (Fig. 1) rapid-hardening slag portland cement is free from the main shortcoming which is inherent to slag portland cements and which is characterized by slower, in comparison with portland cement, strength gain at early stages of hardening.

The technology of manufacturing of slag portland cement is based on finer than usual grinding of the clinker component, in due regard for mineralogical composition and gypsum additions.

For producing such a slag portland cement the following parameters were determined: clinker-slag ratio 60: 40 and 50: 50, fineness of cement grinding 4000 cm^2/g; cement components were ground as follows: clinker—up to 5000 cm^2/g, slag—up to 3000 cm^2/g, addition of gypsum—4–5%.

Investigation of the properties of rapid-hardening slag portland cement in concretes and reinforced concrete constructions had proved its suitableness for use in high-grade concretes and its advantages, in comparison with portland cement, for manufac-

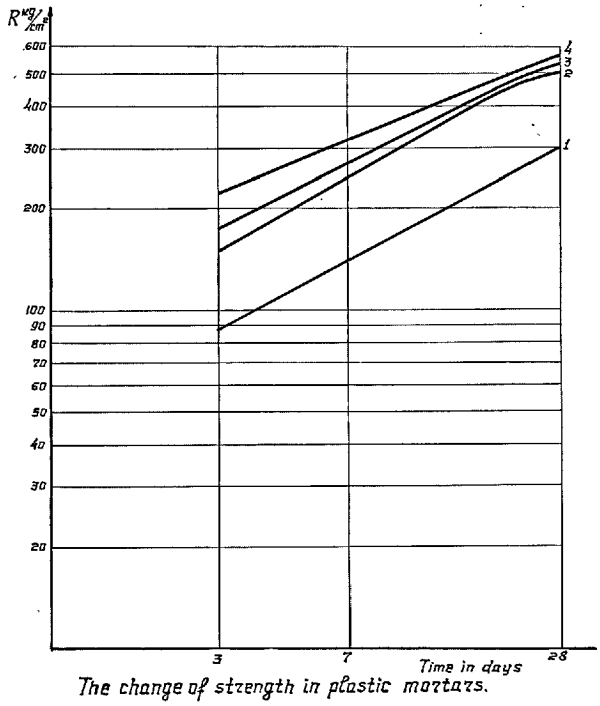

Fig. 1. *Strength changes in plastic solutions*

1—slag portland cement; 2—portland cement of grade 400; 3—rapid-hardening slag portland cement of grade 400; 4—rapid-hardening slag portland cement of grade 500.

*Institute "Yuzhgiprocement," Charkow, U.S.S.R.

turing reinforced concrete products produced by the method of hydrothermal treatment for industrial and civil construction (reduced steam-curing) (7).

For further improvements of rapid-hardening slag portland cement properties complex investigations aimed at studying principal regularities of the hardening process (8) have been carried out at the Institute. Till now nobody studied the hydration process of rapid-hardening slag portland cement. Rapid-hardening slag portland cement was investigated in comparison with portland cement and ordinary slag portland cement.

This report is dedicated to the investigation of structure-forming processes taking place in rapid-hardening slag portland cements. Investigation was carried out by the method of electronic microscopy in combination with electronographical, X-ray, thermographical and chemical methods. In addition to that phase composition and morphological properties of newly formed hydrates were determined and cement stone structure was analysed.

Portland cement and slag portland cements were investigated on the basis of the same clinker and the same granulated blast-furnace slags. For this investigation the following materials were taken: granulated blast-furnace slags from the metallurgical works in Zaporozhye (up to 90% of glass with refractive index 1.67; minerals of the mellilite row, grains C_2S); acid slags from the Novokuznetsk works (up to 95% of glass, 2% of gehlenite and 3% of calcite); clinker from the Belgorod works (65% of alite, 15% of belite and 20% of interstitial substance). The specific surface, determined by the method of air suction through mix bed, equaled: for slag portland cement and portland cement—3000 cm^2/g, for rapid-hardening slag portland cement—4000 cm^2/g. Clinker and slag batching for rapid-hardening slag portland cement was accordingly 50% and 50%; 60% and 40%, for slag portland cement was 30% and 70%. Water/cement ratio for all studied cements was 0.5. Portland cement, rapid-hardening slag portland cement and slag portland cement were also investigated at water/cement ratio which corresponded to normal paste thickness.

The phase analysis of newly formed hydrates was carried out by X-ray and electronic microscopy methods combined with electronographical and thermographical methods. The structure originated and developing as a result of the hardening process was analysed by the electronic microscopy method. As a rule the analysis was carried out after one day, 3 days, 7 days and 28 days of hydration. Besides, several samples were analysed after 4 minutes, 1 hour, 4 hours, 12 hours, 24 hours, 6 months and one year of hydration.

Investigation of Liquid Phases of the Hardening Cement Stone

For the purpose of determining liquid phases of the hardening cement stone cement samples (Table 1) were mixed up with distilled water at a water/cement ratio of 0.5. After 4 minutes, 30 minutes, one hour, 4 hours, 12 hours, one day and 3 days since mixing up liquid phases were extracted by means of a special pressform under pressure of 1500 kg/cm^2 (9, 10). Composition changes in $Ca(OH)_2$, $CaSO_4$ and in R_2O were studied in liquid phases (Fig. 2, 3, 4).

The Fig. 2 shows that after 4 minutes since mixing up the concentration of calcium hydroxide (calcium hydroxide is shown in percentage of CaO) in liquid phases of portland cement and rapid-hardening slag portland cements is much higher (1.63—1.80 g/l) than in the case of the saturated solution of calcium hydroxide. (1.23 g/l). The high concentration of calcium hydroxide is retained up to 4 hours of hydration and in some liquid phases it is retained up to one day hydration and then it falls down.

In portland cement and rapid-hardening slag portland cement containing acid slag, calcium hydroxide content decreases more rapidly because of the higher alkali concentration in the liquid phase (Fig. 3).

By 3 day hydration the concentration of calcium hydroxide in liquid phases of portland cement and rapid-hardening slag portland cements decreases up to 0.14—0.43 g/l which is the evidence of actively proceeding processes of hydrolysis and hydration at

Table 1. *Chemical composition of cements and slags*

Cements	Portland cement	Rapid-hardening slag portland cement with acid slag	Rapid-hardening slag portland cement with basic slag	Slag portland cement with acid slag	Slag portland cement with basic slag	Novokuznetsk slag (acid)	Zaporozhye slag (basic)
SiO_2	21.24	27.18	27.52	37.30	32.91	35.44	39.40
FeO	—	0.65	—	0.66	0.70	—	—
Fe_2O_3	3.48	3.54	2.55	2.88	0.79	0.25	0.35
Al_2O_3	4.91	6.90	4.96	9.28	5.80	12.78	5.34
MnO	0.13	0.70	0.62	0.65	1.01	0.80	1.47
CaO	63.62	54.32	57.57	47.36	52.12	39.65	48.10
MgO	0.80	2.94	1.64	1.30	2.40	6.27	2.77
SO_3	1.90	2.14	2.36	—	1.53	traces	0.50
K_2O	0.14	0.35	0.16	0.47	0.28	0.73	0.39
Na_2O	0.20	0.16	0.12	0.26	0.12	0.25	0.15

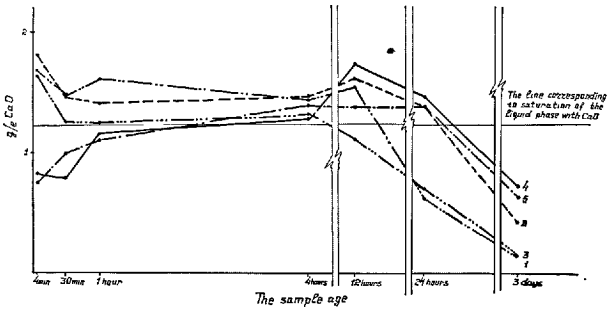

Fig. 2. *The calcium hydroxide content in liquid phases of cement aged up from 4 minutes to 3 days of hardening*

1—portland cement; 2—rapid-hardening slag portland cement with the basic slag; 3—rapid-hardening slag portland cement with the acid slag; 4—slag portland cement with the basic slag; 5—slag portland cement with the acid slag.

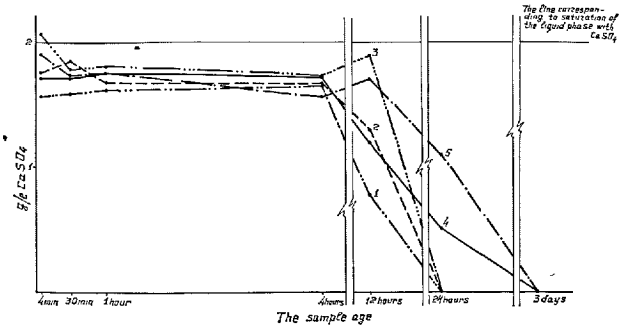

Fig. 3. *The calcium sulphate content in liquid phases of cements aged up from 4 minutes to 3 days of hardening*

1—portland cement; 2—rapid-hardening slag portland cement with the basic slag; 3—rapid-hardening slag portland cement with the acid slag; 4—slag portland cement with the basic slag; 5—slag portland cement with the acid slag.

early stages of hardening.

In spite of that clinker/cement ratio equals 50: 50 in rapid-hardening slag portland cements, the latter as well as portland cement is characterized by substantial activity of hydration processes at early stages (Table 2). This fact is obviously attributed to the high

Table 2. *Changes in chemically bound water content with the age*

Rapid-hardening slag portland cement			Slag portland cement		
The age of the sample	Chemically bound water content, %		The age of the sample	Chemically bound water content, %	
	800°C	1000°C		800°C	1000°C
4 minutes	3.92	3.45	4 minutes	1.38	0.73
30 minutes	4.21	3.79	30 minutes	1.38	0.63
1 hour	4.73	4.31	1 hour	1.54	0.75
4 hours	5.41	4.99	4 hours	2.25	1.68
12 hours	5.85	5.45	12 hours	3.44	2.66
1 day	8.19	8.04	1 day	6.48	5.90
3 days	11.06	10.99	3 days	9.45	9.16

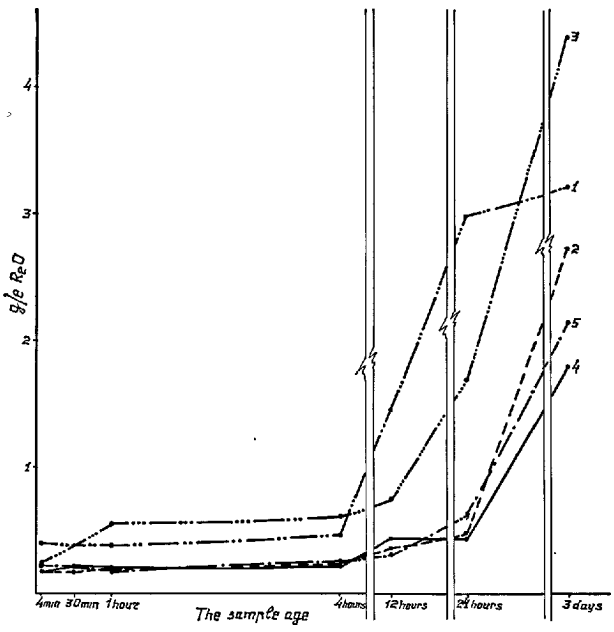

Fig. 4. *The alkali content in liquid phases of cements aged up from 4 minutes to 3 days of hardening.*

1—portland cement; 2—rapid-hardening slag portland cement with the basic slag; 3—rapid-hardening slag portland cement with the acid slag; 4—slag portland cement with the basic slag; 5—slag portland cement with the acid slag.

fineness of the clinker fraction of rapid-hardening slag portland cement.

In difference from portland cement and rapid-hardening slag portland cement the concentration of calcium hydroxide in liquid phases of slag portland cement, produced either with basic or acid granulated slags, after 4 minutes since mixing up with water is much lower (0.75—0.82 g/l) than in the case of the saturated solution of calcium hydroxide. The saturation is reached only in about 4 hours of hydration. The high calcium hydroxide concentration in liquid phases is retained up to one day of hydration, then by 3 days it falls down to 0.64—0.72 g/l.

As above-mentioned experimental data show hydrolysis and hydration processes in slag portland cements at early stages of hydration are somewhat inhibited because of rougher grinding of cement clinker, on the one hand, and because of less clinker content in cement, on the other hand, in comparison with rapid-hardening slag portland cement.

The gypsum concentration in liquid phases of portland cement, rapid-hardening portland cement and slag portland cement produced either with basic or acid granulated slags is high (1.56–1.89 g/l of $CaSO_4$) after 4 minutes since mixing up with water, but however it is lower than that of the saturated solution

(2 g/l of $CaSO_4$) (Fig. 3). The exception to this fact is the rapid-hardening slag portland cement with the acid granulated slag where the gypsum concentration after 4 minutes of hydration is 2.06 g/l of $CaSO_4$.

In portland cement and rapid-hardening slag portland cements gypsum disappears from the liquid phase in one day of hardening and in slag portland cements it disappears in 3 days of hardening. The disappearance of gypsum from the liquid phase is the evidence of completing the reaction with forming a high-sulphate form of calcium hydrosulphoaluminate. Thus, hydration and hardening processes are somewhat inhibited in slag portland cement in comparison with portland cement and rapid-hardening slag portland cements.

The concentration of alkalies in liquid phases increases with the increase of the sample age and by 3 days reaches 1.79–4.40 g/l of R_2O (Fig. 4). With the increase of the quantity of alkalies in liquid phases the solubility of calcium hydroxide decreases. The alkalies, passing into the solution, limit the calcium hydroxide solubility.

Determination of Chemically Bound Water in Rapid-Hardening Slag Portland Cement

Till now there is no single technique of determining chemically bound water; probably it is attributed to inhomogeneous properties of newly formed products of hydration and to complication of dividing chemically bound and non-bound water in hydrated cement.

The determination of chemically bound water in rapid-hardening portland cements is complicated by the proceeding of oxidizing processes combined with the presence of protoxydic compounds (in slag fraction of cement). Our technique of determining chemically bound water is described below.

At the earliest stages including 4 minute, 30 minute, one hour, 4 hour hydration when the cement paste has not yet hardened for determining chemically bound water, 8–10 grammes of cement paste are poured with 30–40 ml of absolute alcohol and are mixed well up, then the alcohol is filtered out.

The hydrated cement is washed in a funnel for 3–4 times with 10–15 ml of absolute alcohol. Such a treatment is quite enough for removing non-bound water from the hydrated paste as the alcohol is mixed with water very well and removes it from the reaction. In order to give constant weight to the dehydrated cement powder this powder is double treated in a funnel with 10 ml of ethyl ether. Thus more easily volatilized other vapours are substituted for heavy alcohol vapours and the drying process of hydrated cement powder is accelerated. The powder is dried up to the constant weight in a chamber at room temperature 22–25°C by means of suction of dried air free from carbon dioxide through it.

After the drying of hydrated cement powder to its constant weight chemically bound water is determined. In portland cement this determination is simple. One gramme of hydrated cement powder is calcinated in a muffle furnace at the temperature of 1000°C up to the constant weight. At the same time the original unhydrated cement is also calcinated and the correction is introduced while determining the percentage of chemically bound water.

The calcining temperature of 1000°C was chosen for portland cement on the basis of great experimental material on the dehydration of individual hydrated clinker minerals and portland cement clinkers.

The calcining temperature for determining chemically bound water in cements containing slag was defined more exactly while studying hydrated rapid-hardening slag portland cements and slag portland cements.

Chemically bound water was determined in rapid-hardening slag portland cement and slag portland cement produced with the same basic slag from the Zaporozhye works at the ages from 4 minutes to 3 days of hardening. Chemically bound water was determined at temperatures of 800–1000°C.

The Table 2 shows that chemically bound water content at 800°C reaches its maximum; at 1000°C it decreases both in rapid-hardening and slag portland cements. At early stages of hardening the difference in chemically bound water content at temperatures of 800 and 1000°C is greater by slag portland cement than by rapid-hardening slag portland cement because the slag content in slag portland cement is greater.

Chemically bound water was determined at the temperature range from 100°C to 1000°C in hydrated slag portland cement and rapid-hardening slag portland cement at the age of 28 days of hardening (Table 3).

As the table data show the quantity of chemically bound water in slag portland cement and rapid-hardening slag portland cement increases with the increase of calcination temperature. In this case we do not observe the decrease of chemically bound water which is caused by the oxidation process of slag protoxydic compounds.

Table 3. *Changes in chemically bound water content with the temperature*

Rapid-hardening slag portland cement		Slag portland cement	
°C	Chemically bound water content	°C	Chemically bound water content
100	5.72	100	3.81
200	11.20	200	8.37
300	11.74	300	8.48
400	12.56	400	9.33
500	14.07	500	9.71
600	15.44	600	11.16
700	16.77	700	12.38
800	17.21	800	12.53
900	17.83	900	12.53
1000	17.83	1000	12.53

Above-mentioned phenomena permit to recommend successive calcination at temperatures of 600°C, 700°C and 800°C etc. while determining chemically bound water in slag portland cements. Maximum weight losses are considered as the weight of chemically bound water as in the case of portland cement.

The quantity of chemically bound water in cement paste increases with the increase of the sample age (Fig. 3). This fact is the evidence of the activity of hydration processes at different cement hardening periods because the chemically bound water content in the cement paste is an indirect evidence of the quantitative increase of newly formed products of hydration in the hardened cement paste.

The quantity of chemically bound water in portland cement and rapid-hardening slag portland cement containing acid slags is much higher than in slag portland cement with the same slag (Fig. 5). This fact proves once more a great activity of hydration processes proceeding in rapid-hardening slag portland cement.

As rapid-hardening slag portland cement and slag portland cement are composed of clinker and slag let us to examine the reaction chemism of producing high-sulphate form of calcium hydrosulphoaluminate in the process of hydration and hardening of these cements.

As it is known, this reaction for portland cement can be expressed as follows:

$$3CaO \cdot Al_2O_3 + 3CaSO_4 \xrightarrow{nH_2O} 3CaO \cdot Al_2O_3 \cdot 3CaSO_4 \cdot 31H_2O \quad (1)$$

This reaction proceeds differently for cements containing slag (11).

According to petrographical data, granulated slags from the Zaporozhye and the Novokuznetsk works contain more than 90% of glass. Proceeding from the chemical analyses and assuming that slags are entirely composed of glassy phase we can express their empirical formulae respectively:

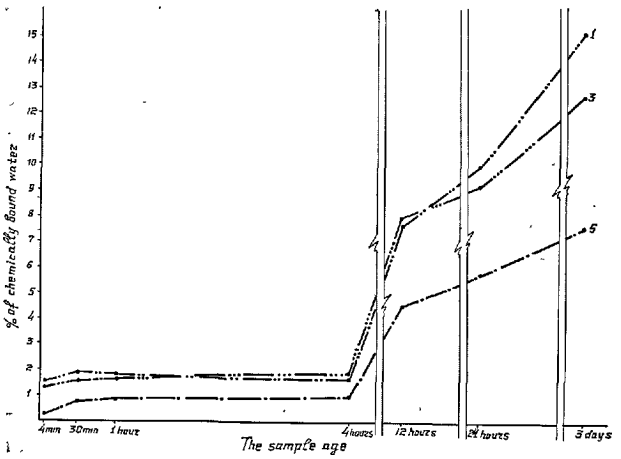

Fig. 5. The chemically bound water content in

Fig. 5. *The chemically bound water content in cement aged up from 4 minutes to 3 days of hardening.*

1—portland cement; 3—rapid-hardening slag portland cement with the acid slag; 5—slag portland cement with the acid slag.

$16CaO \cdot 13SiO_2 \cdot Al_2O_3$ and $6CaO \cdot 5SiO_2 \cdot Al_2O_3$

As appears from formulae above there is no equimolecular ratio C: A = 3: 1 in both of them. Electronic microscopical investigations show that hydrosilicates in hydrated rapid-hardening slag portland cements and slag portland cements are represented in the form of minute low-basic newly formed products of hydration of tobermorite type.

As follows from the above, the reaction chemism of hydration of cements containing slag can be represented as follows.

The clinker fraction of cement is first subjected to hydrolysis and hydration processes and as a result of this calcium hydroxide, gypsum, alkalies and quite small quantities of calcium hydroaluminates, calcium hydrosilicates and calcium hydroferrites are dissolved in the liquid phase. Under the influence of calcium hydroxide and alkalies the slag fraction of cement is excited and glassy slag acquires the reactivity and reacts with gypsum and calcium hydroxide:

$$16CaO \cdot 13SiO_2 \cdot Al_2O_3 + 3CaSO_4 \xrightarrow{nH_2O} 3CaO \cdot Al_2O_3 \cdot 3CaSO_4 \cdot 31H_2O + 13CaSiO_3 \cdot pH_2O \quad (2)$$

$$6CaO \cdot 5SiO_2 \cdot Al_2O_3 + 3CaSO_4 + 2Ca(OH)_2 \xrightarrow{nH_2O} 3CaO \cdot Al_2O_3 \cdot 3CaSO_4 31H_2O + 5CaSiO_3 \cdot pH_2O \quad (3)$$

Hence, the high-sulphate form of calcium hydrosulphoaluminate and calcium hydrosilicate which resembles tobermorite are the reaction products of hydration of slag fraction of cement.

Electronomicroscopical and Electronographical Investigations

While making preparations for direct electronomicroscopical investigations small quantity of cement (0.2–0.3 g) was placed in a test-tube with 2—3 ml of absolute ethyl alcohol. The resulting suspension was dispersed by means of supersound (frequency 2 megs, power—60–70 wt, time of sound action—one minute) and a drop of this suspension was placed on the carbon specimen supporting film located on the objective grid. After evaporation of alcohol the sample was placed either into the column of the electronic microscope for immediate examination or into a vacuum-post where Al as a standard for microdiffraction investigations was sprinkled on it.

The method of electronic microscope replicas was used at the investigation of cement stone structure too.

Together with generally used methods (13, 14) a new method for examination of early stages of structure formation, offered by A. G. Kholodnyi (12), was used. It consists of getting a print from a cement layer stuck to a glass-slide during hardening. The investigations were carried out by means of electronic microscope EM-5.

Electronic microscope analysis of portland cement at 0.5 water/cement ratio showed that at the intial stages of hydration (up to 7 days inclusive) the main hydrate phases were calcium hydrosulphoaluminates of ettringite type and needle-shaped hydrosilicates. The calcium hydrosulphoaluminates were identified by their characteristic elongated and prismatic shape.

The attempts to get diffraction patterns of ettringite crystals have not succeeded as under the influence of electronic eradiation and vacuum the crystals lose water and the inner crystalline structure of the compound gets disordered. The analogous phenomenon was observed by other investigators too (15).

The electronographs of calcium hydrosilicates contain only some wide reflections, the strongest of which lying in the range of 3.0 and 1.8 Å. In connection with it we did not succeed in precise defining of the composition of the needle-shaped calcium hydrosilicates. The diffraction character shows that the hydrosilicates are similar by composition to low-basic calcium hydrosilicates and are characterized by slightly amorphous structure.

As the investigations showed, in the period of portland cement paste setting an intensive formation of crystals of calcium trisulphoaluminate and needle-shaped silicates and also of hexagonal crystals of $Ca(OH)_2$ is observed.

It is characteristic that newly formed products of hydration cover the most of the initial cement grains with a film of hydrates predestining a diffusive character of the solution process and evening by it the rates of hydration of separate phases of portland cement clinker. Thus, it is possible to suppose that to a certain stage of hydration, namely to the stage of the intensive formation of hydrate particles on the surface of the initial clinker grains, the process of hydration of clinker minerals goes at different rates. Thereafter the rates of hydration get equal as a result of formation of hydrate films on the surface of the initial grains. These data agree with the conclusions made by H. Lehmann and V. Roesky (16).

In the process of hardening the structure of portland cement stone gets denser. Crystals of ettringite get localized and the areas appear, formed by the minute particles of calcium hydrosilicates the shape of which resembles the scales of montmorillonite (Fig. 6).

Further the dense hydrosilicate gel becomes the prevailing component of the structure. The process of calcium hydrosilicates formation is accompanied by the development of newly formed hydrosulphoalumi-

Fig. 6. *Portland cement at 0.5 w/c ratio, age-7 days. X 10000*

nates. In portland cement and in rapid-hardening slag portland cements gypsum disappears from the liquid phase in a day hardening, in slag portland cements—in 3 days (Fig. 3). Disappearance of gypsum from the liquid phase shows the completion of the formation of a high-sulphate form of calcium hydrosulphoaluminate.

It is characteristic that hydrosilicate gel and plate-shaped phases of hydroaluminate—hydrosulphoaluminate compounds differ sharply in their morphological characteristics. Therefore the electronic microscope investigations by the method of replicas allow to follow the process of changing of these phases during the hardening process.

The study of portland cement stone at various water/cement ratio (0.5; 0.25) showed that the structure of portland cement stone aged up to one year at higher water/cement ratio was characterized by considerably higher inhomogeneity and by lower desity (Fig. 7, 8).

Crystalline phases occupy considerable volume of the structure both at 0.5 water/cement ratio and at 0.25 water/cement ratio. It is noticed that in the first case the crystals of ettringite having prismatic shape are more frequently met in the structure of cement stone than in the second case (Fig. 8, a). At 0.5 water/cement ratio areas of the structure with considerably lower density than the whole mass of hydrogel are observed. The formation of large crystals is noticed in such areas of the structure (apparently the crystals of calcium hydroaluminate). May be, the pores and areas of less dense hydrosilicate gel are the areas where the large plate-shaped crystals, frequently met in cement structure, arise (Fig. 8, b). The size of these newly formed products of hydration increases in the process of hardening. Evidently the inner tension appears in the places of contact between the large, increasing in their size, plate-shaped crystals and hydrosilicate gel (as a result of pressure of crystalization). Thus the process of hardening of portland cement is accompanied by the rise and development of destructive phenomena finally leading to decrease of strength characteristics of cement stone. The improvement of the material properties comprises the decrease of influence of these phenomena during the process of cement stone hardening. From this point of view it is particularly interesting to follow the hardening process of rapid-hardening slag portland cement and slag portland cement.

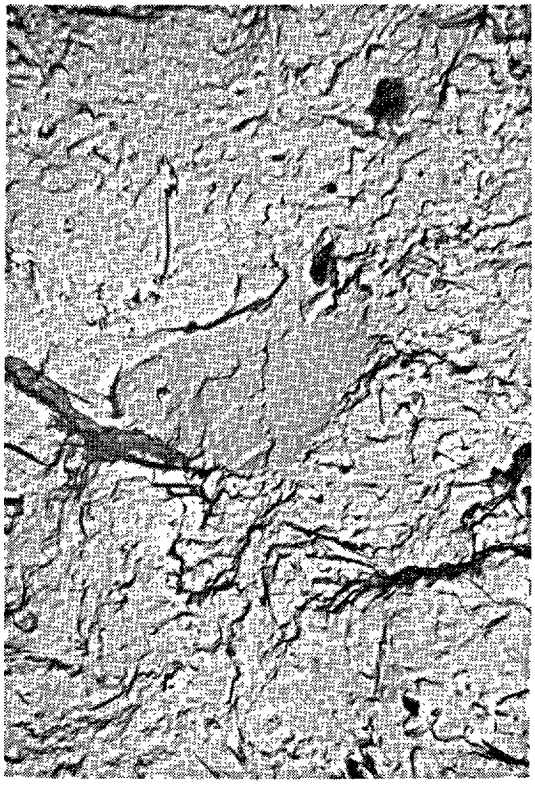

Fig. 7. *Portland cement at 0.25 w/c ratio, age-1 year. X 10000*

The early stages of hydration of these cements are characterized by arising of the same newly formed products of hydration as in the portland cement.

Thus even in the 4-minute samples the particles of calcium hydrosulphoaluminates of ettringite type are observed, but further the calcium hydrosilicates are fixed too. It is characteristic that the content of $Ca(OH)_2$ crystals is smaller comparing with portland cement, what is evidently connected with CaO absorption from the solution in the process of slag excitation. Composition and morphological features of above-mentioned newly formed products of hydration are similar in all studied cements. It is witnessed for example by the fact that the hydrosilicates as a rule give the diffraction of the same type. (2—3 wide reflections in the range of 3.0; 2.8; 1.8 Å). Only in a case of examination of a slag portland cement sample aged up to 28 days and based on the slag from Zaporozhye it was possible to get electronograph with bigger quantity of more distinct reflexes (Fig. 9). The identity of newly formed products of hydration in cement stone of various mineralogical composition, noticed by other scientists too (17), allows it to suppose that the strength charactersistics and other properties of cement stone depend on the intensity of hydration processes and structure formation. From this point of view it is possible to interpret some properties of rapid-hardening slag portland cement.

It is known that slag cements are characterized by

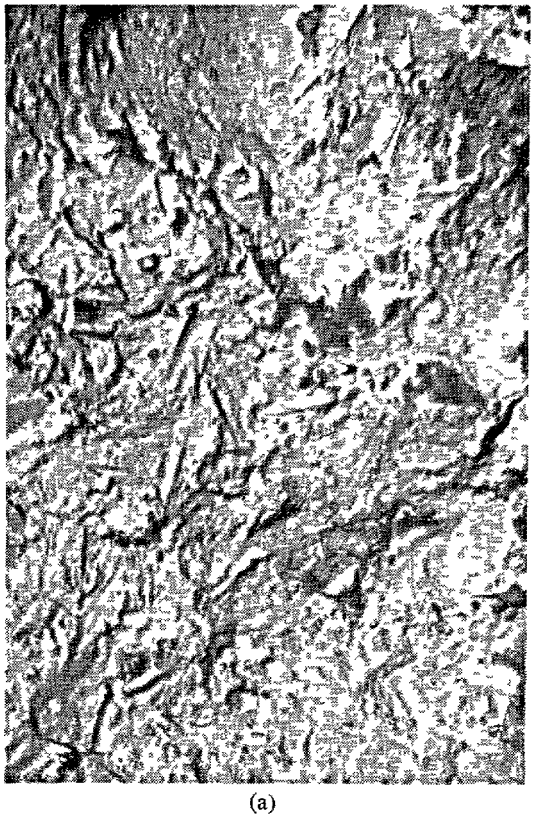

(a)

(b)

Fig. 8. *Portland cement at 0.5 w/c ratio, age-1 year. X 10000*

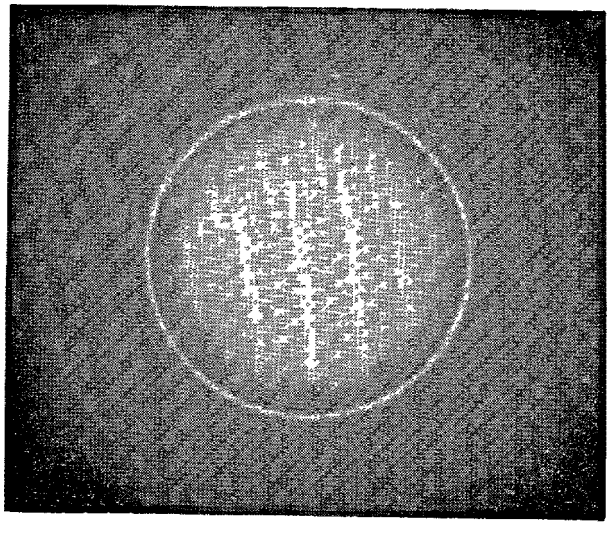

Fig. 9. *Slag portland cement with the slag from the Zaporozhye works at 0.5 w/c ratio, age-28 days.*

considerable strength only after long hardening. Rapid-hardening slag portland cement is characterized by accelerated strength gain at early stages. Electronic microscope examinations indicate that it is caused by intensive formation of calcium hydrosulphoaluminate of ettringite type and lowbasic calcium hydrosilicates.

The processes of structure formation in rapid-hardening slag portland cement and in portland cement proceed similarly, but at early stages a main role of ettringite is marked (Fig. 10). Further, as the investigations of cement stone aged up to a year showed, the calcium hydrosilicates play the main role in the structure of rapid-hardening slag portland cement (Fig. 11). The crystals of ettringite type are observed only episodically. It is characteristic that the size of plate-shaped newly formed products of hydration of hydroaluminate-hydrosulphoaluminate phases in rapid-hardening slag portland cement aged up to a year is considerably smaller than in portland cement. Density of hydrosilicate gel in the samples of rapid-hardening slag portland cement at 0.5 water/cement ratio corresponds approximately to density in the portland cement samples at 0.25 water/cement ratio.

On the basis of the above-mentioned data it is possible to conclude that fineness of clinker component influences the properties of slag portland cement mainly at early stages of hydration when it is necessary to intensify the rise of newly formed

Fig. 10. *Rapid-hardening slag portland cement with the slag from the Almaznyansky works at 0.5 w/c ratio, age-3 days. X 10000*

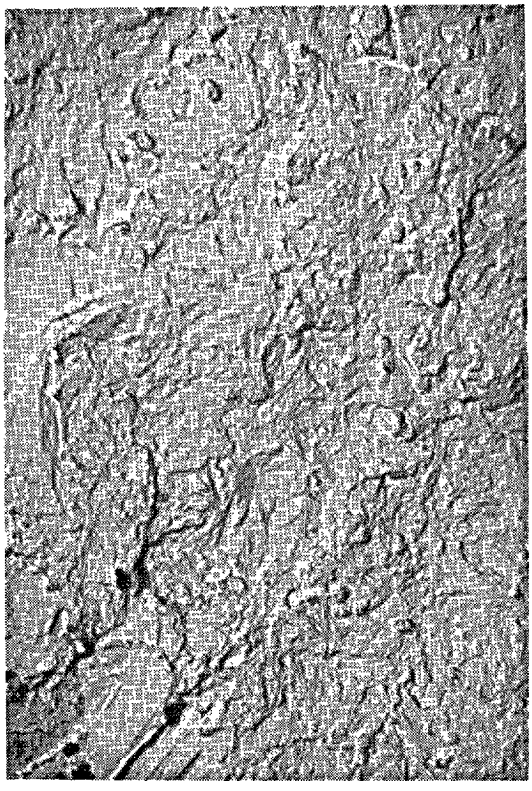

Fig. 11. *Rapid-hardening slag portland cement with the slag from the Novokuznetsk works at 0.5 w/c ratio, age-1 year. X 10000*

hydrates from slag material. Further the hydrosilicate hardening inherent even to the slags without additions proceeds, and probably due to that the influence of destructive phenomena, taking place at the interaction between the hydrosulphoaluminate and hydrosilicate structures of hardening, decreases.

Thus rapid-hardening slag portland cement is a binding material in which the property of portland cement to harden rapidly and the ability of slag cements to form hydrosilicates during a long time luckily combine.

The results of electronic microscope examinations are completed and confirmed by our thermographic and X-ray investigations.

The Thermographic and X-ray Investigations

Differential thermal analysis was carried out by means of automatic thermoweighting device ATVU–8 at a rate of heating 10°C per minute.

Thermographic analysis allowed it to get the average characteristics of hydration process of studied cements. The investigations showed that the character of DTA curves of various cements was identical.

DTA—curves contain mainly 3 endothermic effects connected with the rise of the newly formed hydrates in the process of hydration: the first is in the region of 100–200°C, the second—about 500°C and the third is within the limits of 700°C and 800°C (Fig. 12). The low temperature endothermic effect is the most interesting one (100–200°C). According to the data of our investigations it is a summary effect and is conditioned by water losses by a number of principal minerals of cement stone such as calcium hydrosilicates, hydroaluminates and hydrosulphoaluminates.

According to Midgley's data (18) it is conditioned by water losses by calcium hydrosilicates and high-sulfate form of calcium hydrosulphoaluminates (in the absence of non-bound water in the sample). Our data agree with Midgley's results with the only difference that dehydration temperatures of the above-mentioned hydrate phases coincide in all the cements studied by us.

Intensive increase of the low temperature endothermic effect is characteristic for portland cement at the

initial stages of hardening (up to 7 days at 0.5 water/cement ratio). The increase is mainly attributed to the decomposition of increasing quantity of the calcium hydrosulphoaluminate of ettringite type, being formed in cement stone (Fig. 12). However the growth of low temperature endothermic effect on DTA curves slows up with the increase of sample age what is connected with the decrease of intensity of ettringite formation and its changing into monosulphoaluminate containing smaller quantity of combined water. Then the increase of endothermic effect in the region of 100–200°C is observed again, it is connected with the process of formation of a large quantity of calcium hydrosilicates taking place in this period of hardening. Thus, DTA curves reflect to a certain degree the process of structure formation of portland cement stone. The received DTA curves (Fig. 12, 13) allowed it to find out that in portland cement the process of slowing up of the reaction of ettringite formation and the modification changings of calcium hydrosulphoaluminate in cement stone at 0.5 water/cement ratio took place after about 7 days; in slag portland cement the process is expressed less distinctly and is defined by 1—3 days.

The main feature of the DTA curves of slag portland cements comparing with the curves of portland cement is a smaller value of the endothermic effect caused by the decomposition of $Ca(OH)_2$ (Fig. 13). Evidently the calcium hydroxide is spent on the formation of calcium hydrosilicates.

The question about the nature of the third endothermic effect (700–800°C) has been studied insufficiently. It is characteristic that this effect is especially well expressed on the DTA curves of slag portland cements.

In our opinion the third endothermic effect (700–800°C) is mainly caused by the decomposition of low-basic calcium hydrosilicates and not by that of calcium carbonate. In fact in the opposite case its value would depend on the value of the effect of $Ca(OH)_2$ that is easily carbonated (500°C). However it has not been observed.

It is characteristic that the strength characteristics of rapid-hardening slag portland cements both at the early stages and at the further stages of hardening are higher than the analogous characteristics of portland cement.

The DTA data indicate that this phenomenon is mainly interpreted by more intensive development of hydrosilicate structure of hardening. Thus, the comparing of DTA curves of portland cement and rapid-hardening slag portland cement samples shows that the first endothermic effect in the region of 100–200°C,

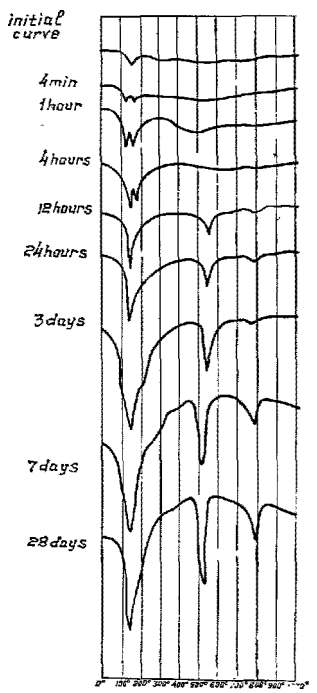

Fig. 12. *DTA-curves of portland cement at 0.5 w/c ratio*

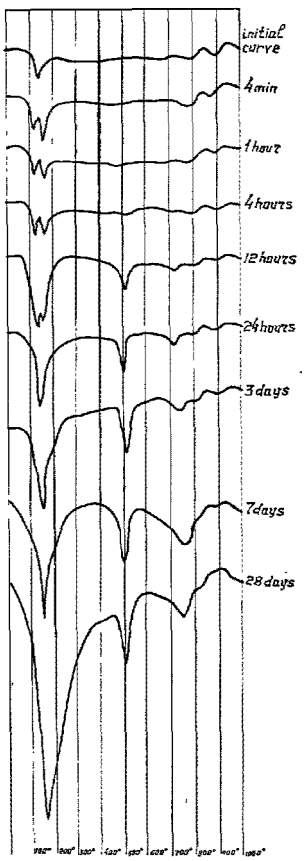

Fig. 13. *DTA-curves of rapid-hardening slag portland cement at 0.5 w/c ratio.*

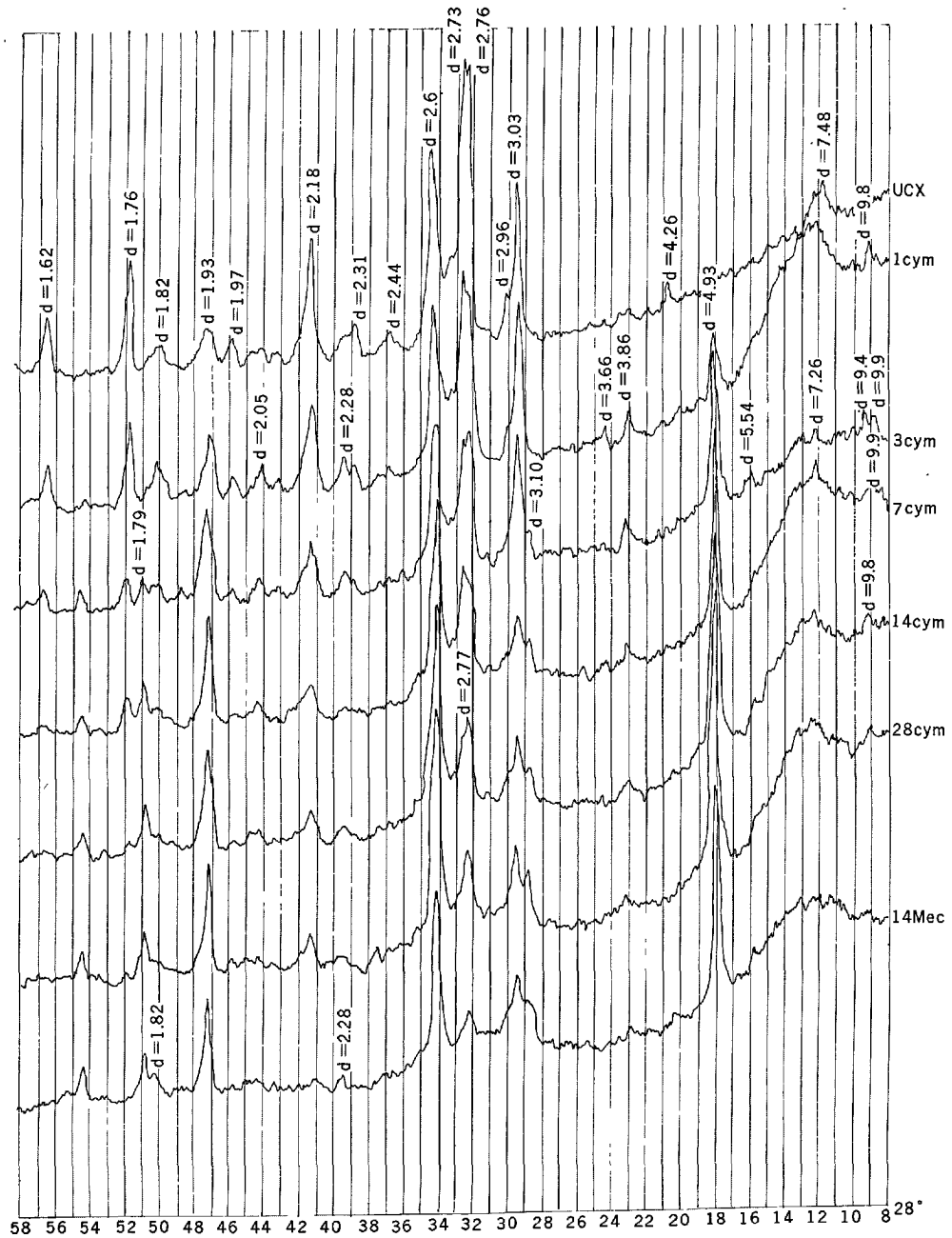

Fig. 14. *X-ray diffraction charts of portland cement at 0.5 w/c ratio.*

characterizing the decomposition of hydrosilicates, is much better developed in rapid-hardening slag portland cement.

X-ray examinations of cement stone samples, together with the data obtained by other methods allowed it to follow the changes in phase composition and in quantity of newly formed products of hydration proceeding in the process of hardening. X-ray examination of the phase composition of the hydrate phases of cement stone is however hindered because of chiefly colloidal character of the greater part of the newly formed products of hydration. It is especially evident at the attempt to estimate the quality and quantity of calcium hydrosilicates produced in the process of hardening; besides the reflexes from them are overlapped by the reflexes of clinker minerals.

The analysis of X-ray diffraction charts obtained from portland cement (Fig. 14) shows that gypsum

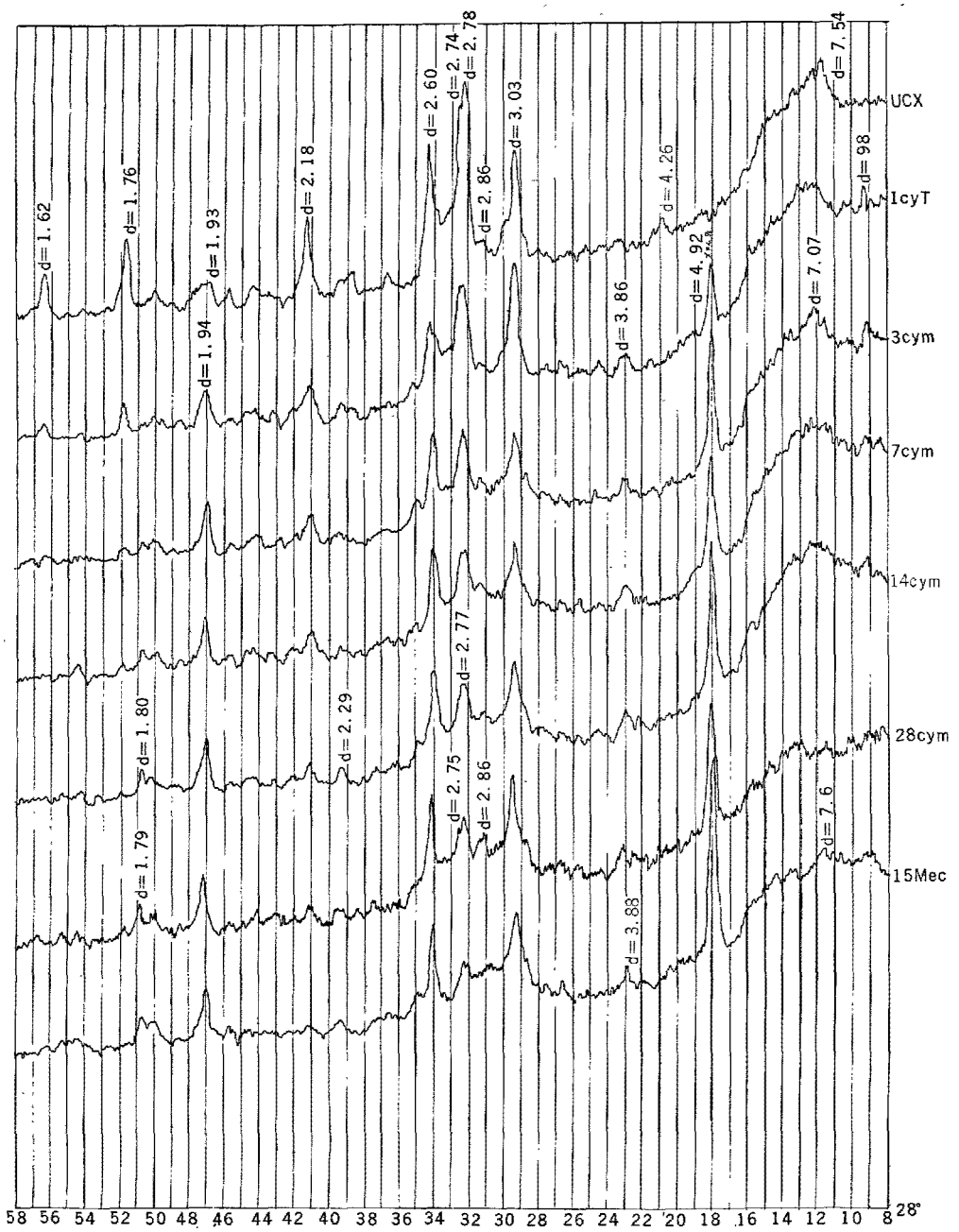

Fig. 15. *X-ray diffraction charats of rapid-hardening slag portland cement at 0.5 w/c ratio.*

aged up to 1—3 days which is present in composition of an initial sample ($d = 7.48$; 4.26 Å) reacts with the aluminate phases of clinker producing a high-sulphate form of calcium hydrosulphoaluminates (hydrosulphoferrites) (reflection with $d = 9.8$; 5.54 Å). In this period the increase of reflex with $d = 4.9$ Å, characterizing crystalline $Ca(OH)_2$, is observed too. The rise and development of this peak show the intensive proceeding even at early stage process of hydrolysis of C_3S, but the produced hydrosilicates don't give distinct reflections on the X-ray diffraction charts because of their amorphous structure and the presence of reflections from the initial clinker phases.

In the process of hardening the X-ray diffraction charts of corresponding samples are characterized by decrease of reflections from the anhydrite phases of clinker and by gradual decrease of reflexions from high-sulphate calcium hydrosulphoaluminates (hydro-

sulphoferrites). The reflection with $d = 3.86$ Å tends to decrease too. In connection with it the reflection should be considered as belonging to the crystals of ettringite type and not to calcium carbonate.

In the samples aged up to 14 months the expansion of reflection is well seen in the region of angles $2\theta = 28–30°$. It may be explained by the going on of hydration process of by that time remaining initial clinker phases and by intensive formation of colloidal compounds of C–S–H gel. To a certain degree this summary reflex is caused by the presence of $Ca(OH)_2$ ($d = 3.10$ Å) in the sample.

The X-ray diffraction charts obtained from rapid-hardening slag portland cement samples (Fig. 15) are similar to the corresponding X-ray diffraction charts of portland cement. Gypsum intensively reacts with aluminates of the initial cement components and is spent on the formation of high-sluphate compounds of ettringite type ($d = 9.8$ Å; 5.6 Å).

The changing of reflection value (401) of tricalcium silicate is characteristic.

Both in portland cement and in rapid-hardening slag portland cement this reflex decreases quite intensively in the period from 3 to 7 days. Consequently, the clinker that is a component of rapid-hardening slag portland cement is hydrated with almost the same intensity as the intensity of hardening of portland cement. However, the calcium hydroxide produced as a result of hydrolysis process partially combines with slag components into colloidal calcium hydrosilicates. That accounts for a smaller value of reflections of $Ca(OH)_2$ on the X-ray diffraction charts of rapid-hardening slag portland cement ($d = 4.9$ Å; 2.61 Å) in comparison with portland cement.

References

1. V. I. Satarin, M. I. Strelkov, Y. M. Syrkin and M. B. Frenkel, "Repid-hardening slag portalnd cement, its technological parameters and some features of technology" (in Russian), The Bulletin of Technical Information of Yuzhgiprocement No. 25 (1958), Kharkov.
2. V. I. Satarin, M. I. Strelkov, Y. M. Syrkin and M. B. Frenkel, "Rapid-hardening slag portland cement" (in Russian), the magazine "Housing Construction and Architecture" No. 7 (1959), Kiev.
3. V. I. Satarin, M. I. Strelkov, Y. M. Syrkin and M. B. Frenkel, "Rapid-hardening slag portland cement" (in Russian), The Proceedings of Yuzhgiprocement **1** (1960), Kiev.
4. Y. M. Syrkin and M. B. Frenkel, "The chemistry and technology of slag portalnd cement" (in Russian), (1962) Kiev.
5. Y. M. Syrkin, M. B. Frenkel, L. G. Novoselskii, N. P. Melnichenko and S. L. Levitova, "Putting into production of rapid-hardening slag portland cement at the Kharkov Cement Works" (in Russian), The Proceedings of Yuzhgiprocement **4** (1963, Moscow.
6. V. I. Satarin, Y. M. Syrikin and L. P. Shatohina, "Concretes based on rapid-hardening slag portland cement" (in Russian), Concrete and Reinforced Concrete No. 2 (1967), Moscow.
7. V. I. Satarin, Y. M. Syrkin and L. P. Shatohina, "Some questions of technology and production of rapid-hardening slag portland cement and its use in the production of reinforced concrete" (in Russian), The Proceedings of Yuzhgiprocement **9** (1967), Moscow.
8. V. I. Satarin, Y. M. Syrkin, L. P. Shatohina, A. G. Kholodnyi and D. S. Lysunkina, "The principles of production and some questions of hardening process of rapid-hardening slag portland cement" (in Russian), The Proceedings of All-Union Symposium on the Chemistry and Technology of Cement in 1965, (1967), Moscow.
9. M. I. Strelkov, "The changes of liquid phase composition appearing in the process of hardening of binding materials and the mechanism of their hardening" (in Russian), The Proceedings of the Symposium on the Chemistry of Cement" (1956), Moscow.
10. V. I. Satarin, U. M. Syrkin and V. M. Mirakyan, "The chemism of rapid-hardening slag portland cement hydration" (in Russian), the magazine "Cement" No. 3 (1967), Leningrad.
11. H.-G. Smolczyk, "The ettringite phases in slag portland cement" (in German), Zement-Kalk-Gips No. 7 (1961).
12. A. G. Kholodnyi, "The electronic microscope method of investigation of structure formation in cement stone" (in Russian), The magazine "Factory Laboratory" No. 11 (1966).
13. Kenjiro Saji, "On the electronic microscopy of hardening cement pastes" (in German), Zement-Kalk-Gips No. 9 (1959).
14. V. R. Garashin and Z. M. Larionova, "Methods of electronic microscope investigation of cement stone and concrete" (in Russian), the magazine "Factory Laboratory" No. 2 (1966).
15. H. E. Schwiete, E. Niel, "Immediately after gaging of a portland cement", Journal of the American Ceramic Society No. 1 (1956).
16. H. Lehmann and W. Roesky, "Strength development and the hydration of portland cement and slat portland cements at 20°, 5° and 1°C" (in German), Tonindustrie-Zeitung und keramische Rundschau No. 15/16 (1965).
17. H.-G. Smolczyk, "The products of hydration of cements with high slag contant" (in German), Zement-Kalk-Gips No. 5 (1965).
18. H. G. Midgley, "The mineralogical examination of set portland cement", The Fourth International Symposium on the Chemistry of Cement, Washington, 1960.

Supplementary Paper IV-48 Co-Ordination State of Aluminium, Magnesium and Maganese Ions in Synthetic Slag Glasses

Surinder K. Chopra and C. A. Taneja*

Synopsis

The states of co-ordination of aluminium, magnesium and manganese ions were determined in slag glasses in the systems $CaO–Al_2O_3–SiO_2$, $CaO–Al_2O_3–SiO_2–MgO$ and $CaO–Al_2O_3–SiO_2–MnO$ respectively by a combination of techniques such as specific volume, molar refractivity, fluorescence and differential thermal analysis. In glasses of composition $10CaO \cdot 8SiO_2 \cdot nAl_2O_3$, where n was varied from 1 to 7 moles (about 9 to 41 percent of Al_2O_3 by weight), the partial molar refraction of alumina ($K_{Al_2O_3}$) was found to be 12.7 which indicates four-fold co-ordination of aluminium ions. This conclusion was also supported by the differential thermal analysis of the glasses $10CaO \cdot (10–n)SiO_2 \cdot nAl_2O_3$ wherein Al_2O_3 replaced SiO_2 in four equal increments. The average partial molar refraction of magnesia (K_{MgO}) was found to be 5.08 and 5.05 in the two glass series having compositions $10CaO \cdot 8SiO_2 \cdot 4Al_2O_3 \cdot nMgO$ and $(12–n)CaO \cdot 8SiO_2 \cdot 4Al_2O_3 \cdot nMgO$ respectively and n varying from 1 to 4 moles (about 2 to 11 percent of MgO by weight). The K_{MgO} values indicate that magnesium ions are also present in four-fold co-ordination. This was confirmed by the fluorescence under UV of glass wherein MgO was replaced by NiO. The data also indicated four-fold co-ordination of magnesium ions. However, in glass compositions $9CaO \cdot 8SiO_2 \cdot 3.5Al_2O_3 \cdot nMnO$ where n was varied from 0.5 to 1.5 moles (about 2 to 7 percent of MnO by weight), the partial molar refraction values of manganese oxide showed six-fold co-ordination of manganese ions. The magnetic suceptibility measurements further revealed that though manganese was present in these glasses both in di- and trivalent states, the former was predominant, being more than 75 per cent.

Introduction

According to the random network theory, glass constituents can be divided into two classes, network formers and network modifiers (1). Oxides such as SiO_2, Al_2O_3, B_2O_3 and P_2O_5 belong to the former class because they are known to provide cations which link together appropriately by sharing of oxygens to form randomized three-dimensional networks of tetrahedra. The oxides of sodium, potassium and calcium are classified as network modifiers because they provide cations which occupy voids in the network. Though this theory is not universally accepted, Parker and Nurse (2), Tanaka, Sakai and Yamane (3), Keil and Locher (4), Kondo (5) and Mchedlov-Petrosyan (6) have employed it successfully to interpret the behaviour of hydraulic glasses corresponding to the blastfurnace slag system.

Granulated blastfurnace slag used commercially for the manufacture of slag cements consists predominantly of $CaO–Al_2O_3–SiO_2–MgO$ glass with a small amount of oxides of manganese and iron. Its hydraulicity is known to be influenced primarily by CaO/SiO_2 ratio and content of each of the oxides of aluminium, magnesium, and manganese etc. (7). Since the stability and the rate of solution of slag glasses, which are so important for hydraulic hardening, are dependent upon glass constitution (4), it is important to know how aluminium, magnesium and manganese oxides are present in the glassy structure. The states of co-ordination of aluminium, magnesium and manganese ions were therefore determined in low-lime synthetic slag glasses, corresponding to the compositions of the Indian blastfurnace slags, in the systems $CaO–Al_2O_3–SiO_2$, $CaO–Al_2O_3–SiO_2–MgO$ and $CaO–Al_2O_3–SiO_2–MnO$ respectively and the main findings of this study are reported in this paper.

*Central Building Research Institute, Roorkee, India.

Experimental

Preparation of Glasses

The synthetic slag glasses were prepared from analytical reagents of highest purity by the Dyckerhoff method (8). Precipitated silica, aluminium oxide, and carbonates of calcium, magnesium and manganese formed the raw materials in this study. Microscopic and X-ray techniques were employed to ensure that each sample was a pure glass. Six different series of glasses of the molecular formulae given below were prepared.

Series	Glass compositions in moles	Variation of 'n' in moles
A	$10CaO \cdot 8SiO_2 \cdot nAl_2O_3$	1 to 7
B	$10CaO \cdot nSiO_2 \cdot 3Al_2O_3$	7 to 10
C	$10CaO \cdot (10-n)SiO_2 \cdot nAl_2O_3$	1 to 4
D	$10CaO \cdot 8SiO_2 \cdot 4Al_2O_3 \cdot nMgO$	1 to 4
E	$(12-n)CaO \cdot 8SiO_2 \cdot 4Al_2O_3 \cdot nMgO$	
F	$9CaO \cdot 8SiO_2 \cdot 3 \cdot 5Al_2O_3 \cdot nMnO$	0.5 to 1.5

Methods of Study of Glass Constitution

The density determinations were made by the displacement method in which samples were weighed in air and in xylene at 27°C and referred to water at 4°C. The refractive index of powdered glass (passing a No. 100 B.S. sieve) was measured by the immersion method employing liquids of known refractive indices and examining the movement of the Becke line under a microscope. The total molecular refractivity of a glass was calculated with the help of Lorentz-Lorenz equation (9).

The synthetic glasses of the series C, D & E were also examined by differential thermal analysis as the latter has been used to deduce information on constitution of slag glasses (10). A heating rate of 10°C per minute was employed to heat the glass sample to about 1100°C. The heating was done in a ceramic holder and the thermocouple used was chromel/alumel. Ignited alumina (α-Al_2O_3) was used as an inert reference material. The glass sample was diluted with an equal amount of periclase of the same fineness (–B.S. Sieve No. 100). The weight of the diluted sample and that of the reference material were equal for each run. Periclase, which is considered to be physically and chemically unreactive (11), was added to prevent sticking of glass at softening temperature to the thermocouple wires.

Of the other methods recommended in the literature X-ray technique was not employed because of its limitations in interpreting complex glasses (12). Infra red absorption spectra was tried but it failed to reveal anything more than the position of Si–O absorption band at 9—10Å in glasses of series A and this did not prove of any help in this study. However, colour fluorescence indicators were found useful and NiO was used on the basis of earlier experience (13).

Magnetic Susceptibility

Magnetic susceptibility measurements were made for determining the state of valence of manganese in glasses of series F. A semi-micro aperiodic balance was used for this purpose. The powdered glass was packed uniformly in a sample holder made of glass of about 0.35 cm diameter and 16 cm length. The sample holder was suspended vertically between the poles of the electromagnet so that its bottom was in uniform field of maximum intensity and the upper portion nearly out of the magnetic field of the electromagnet. Weight of the sample along with the holder was taken before and after exciting the electromagnet with a known rate of current (3 amps.), and the change in weight was noted at 29°C. Ferrous ammonium sulphate was used for calibrating the instrument (29°C). The magnetic susceptibility was calculated from the equation

$$\lambda g = \frac{l}{W}(K_H \Delta W + AK_a)$$

where

λg = the magnetic susceptibility per g of sample in cgs units,
l = the length of the glass sample in cm,
W = the weight of the glass sample in g,
ΔW = the change in weight of the glass sample at a field strength of H Gauss,
A = cross sectional area of the glass sample in sq cm
K_H = the instrument constant for a field strength of H gauss,

and

K_a = the magnetic susceptibility per cc of air in cgs units.

The magnetic susceptibility of ferrous ammonium sulphate per g is $9500 \times 10^{-6}/(T° + l)$ where T is absolute temperature (14). At 29°C, this was found to be 31.35×10^{-6} cgs units. The value of K_H at 29°C was 0.14181×10^{-2}.

Results and Discussions

Co-Ordination State of Aluminium Ions

Aluminium ions can be present in tetrahedral state of co-ordination just like silicons or in octahedral co-ordination just like sodium, potassium or calcium ions. Density, refractive index and molecular refraction (K) are sensitive to a change in the co-ordination state of Al ions. The molecular refraction for visible light is a measure of the deformation of electronic shells in the structural unit. Since aluminium is a small cation of high charge and essentially non-deformable, its contribution to the molecular refraction, ($K_{Al_2O_3}$), is almost entirely due to the refractions of the large and easily deformable oxygen ions. For aluminium in the four-fold co-ordination state, the cation-anion distance is less than that for six-fold co-ordination and the inter-ionic forces are more intense. This causes a greater deformation of oxygen ions and therefore greater molecular refraction than when aluminium is in six-fold co-ordination. Safford and Silverman (15) and Day and Rindone (16) employed the determination of molecular refraction (K) to determine the state of co-ordination of the Al ions in soda-lime-silica glasses containing varying amounts of Al_2O_3.

Keil and Locher (4) maintained calcium oxide at a constant level and studied the effect of increasing alumina contents on the specific gravities and refractive indices of synthetic glasses in the system CaO–Al_2O_3–SiO_2. The molar CaO/SiO_2 ratio was therefore variable. Since the composition of the calcium silicate hydrate phase formed on hydration and activation of slag glasses depends to a great extent on the CaO/SiO_2 ratio in the original slag glass, in the present study the CaO/SiO_2 ratio was maintained constant in glasses prepared with varying alumina content in the part of the CaO–Al_2O_3–SiO_2 system corresponding to Indian slags (17). The results under column 2 in Table 1 show that the glasses cover the entire range of alumina content present in slag glasses. The values in column 3 show that the Zachariasen number of glasses varies from 0.34 to 0.50 thus covering the entire range of compositions which can form glasses (18).

Since the molecular refraction of the parent glass (sample 1) increases in a regular manner (Fig. 1) on incorporating six moles of alumina in six equal increments, it is obvious that the state of co-ordination of aluminium ions remains unchanged in the entire series (A). A similar trend was observed in the corresponding results for samples 8–11 of series B wherein different amounts of silica (7—10 moles) had been added to a glass of CaO/Al_2O_3 ratio of 1.83: 1. The values of density and refractive index decreased as expected because Si^{4+} is known to take up four-fold co-ordination and is a 'network former'.

The partial specific volume of Al_2O_3 in series A was found to be on the average 0.3673 cc/g. The specific volume of α-Al_2O_3 in which Al^{3+} is known to be present in six-fold co-ordination (19) is reported as 0.2525 cc/g (Table 1) and shows no agreement with the observed partial specific volume of this study. Hence, it is inferred that Al^{3+} in the glasses studied does not exist in six-fold co-ordination.

The slope of the linear curve in Fig. 1 represents the partial molar refraction ($K_{Al_2O_3}$) of alumina which

Table 1. *Characteristics of CSA* glass samples*

Sample no.	Glass fromula* (C: S: A)			Zachariasen no.	Glass composition wt. %			Density,	Refractive index	Total refractivity	Partial refractivity	Partial specific volume
					CaO	SiO_2	Al_2O_3	g/cc	n	cc/mole	cc/mole	cc/g
	Series A									K	$K_{Al_2O_3}$	Al_2O_3
	C	S	A									
1	10	8	1	0.34	49.04	42.03	8.93	2.9003	1.634 ± .001	140.79		
2	10	8	2	0.375	45.02	38.59	16.39	2.8866	1.632 ± .001	153.70	12.91	0.3648
3	10	8	3	0.40	41.61	35.67	22.72	2.8749	1.630 ± .001	136.58	12.88	0.3651
4	10	8	4	0.42	38.67	33.15	28.18	2.8650	1.628 ± .001	179.36	12.78	0.3649
5	10	8	5	0.44	30.97	36.13	30.97	2.8517	1.624 ± .001	191.94	12.58	0.3738
6	10	8	6	0.455	33.90	29.06	37.04	2.8423	1.622 ± .001	204.69	12.75	0.3693
7	10	8	7	0.47	31.93	27.37	40.70	2.8357	1.619 ± .001	217.00	12.31	0.3662
											av. 12.70	0.3673
	Series B										K_{SiO_2}	SiO_2
8	10	7	3	0.40	43.55	32.66	23.79	2.8858	1.636 ± .001	159.74		
9	10	8	3	0.40	41.61	35.67	22'72	2.8749	1.630 ± .001	166.54	6.80	0.3758
10	10	9	3	0.405	39.83	38.41	21.76	2.8664	1.625 ± .001	173.42	6.88	0.3720
11	10	10	3	0.41	39.19	40.93	20.88	2.8546	1.618 ± .001	179.94	6.52	0.3842
											av. 6.73	0.3773
	α-Al_2O_3 (crystalline)				—	—	100	3.96	1.764 ± .001		$K_{Al_2O_3}$ 10.63	Al_2O_3 0.2525

*C = CaO S = SiO_2 A = Al_2O_3

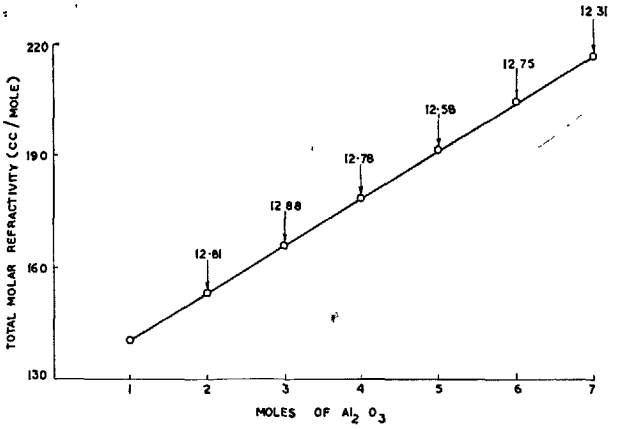

Fig. 1. *Partialmolar refractivity of Al_2O_3 in glasses of composition $10CaO \cdot 8SiO_2 \cdot (1\text{–}7)Al_2O_3$ numerals indicate $K_{Al_2O_3}$ values (average 12.70)*

was found to be 12.70. According to Safford and Silverman (15), Al^{3+} in four-fold co-ordination in glass has a molar refraction contribution of 12.55 (calculated for Al_2O_3), whereas in six-fold co-ordination it is 10.53. Since $K_{Al_2O_3}$ of the glasses of the present study is close to the former value, it is concluded that Al^{3+} in the $CaO–Al_2O_3–SiO_2$ glasses exists only in four-fold co-ordination.

Keil and Locher (4) had believed that aluminium ions existed in six-fold co-ordination in low-lime slag glasses. Chopra and Taneja (20) have examined Keil and Locher's data and calculated the average value of $K_{Al_2O_3}$ for the glasses of CaO/SiO_2 ratio of either 1.06 or 1.24: 1. $K_{Al_2O_3}$ was found to be 12.80 showing four-fold co-ordination. This value should have been between 10.63 and 12.55 if part of Al^{3+} had been present in six-fold co-ordination as believed by Keil and Locher.

Vitreous blastfurnace slags devitrify on heating to temperatures of the order to 800 to 1000°C and the heat evolved during devitrification can be recorded on a differential thermal analysis curve as a single or a set of multiple exothermic peaks. It has been observed that the exothermic effect of devitrification is many a time preceded by a small endothermic peak (21). Yamauchi and Kondo (10) have studied the thermal behaviour of glasses in the $CaO–SiO_2$ and $CaO–Al_2O_3$ systems and have reported correlations between slag compositions and its constitution in terms of peak temperatures in the range 800 to 1,000°C (5). The differential thermal analysis of the synthetic slag glasses of the present study was therefore carried out (Fig. 2). For this purpose glass series C was prepared. In this series increasing amount of SiO_2 was substituted by Al_2O_3 on molar basis. The data show that the peak temperatures of the endothermic effect,

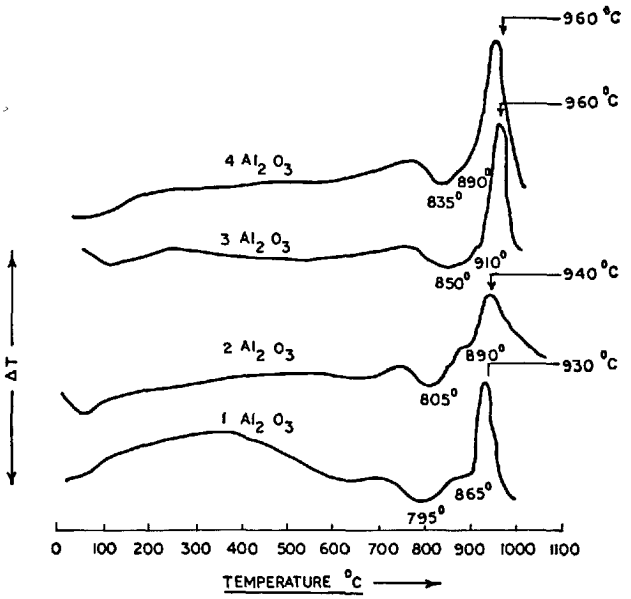

Fig. 2. *DTA curves of synthetic slag glasses of composition $10CaO \cdot (10\text{–}n)SiO_2 \cdot nAl_2O_3$ n varying from 1 to 4*

temperatures of the beginning of the exothermic effect and the exothermic peak temperatures generally show an increase as the number of moles of Al_2O_3 in glass increase. According to Kondo (4) the above mentioned rise in peak temperature indicates tightening of the glass structure by the replacement of silicon-oxygen tetrahedra by unsaturated oxygen in AlO_4 tetrahedra. It may therefore be concluded that the differential thermal analysis support the earlier conclusion of tetrahedral state of co-ordination of aluminium ions in slag glasses in the system $CaO–Al_2O_3–SiO_2$ based on the molecular refractivity data.

Co-Ordination State of Magnesium Ions

Chemical composition and physical characteristics of magnesium glasses of series D and E are reported in table 2.

Magnesium (Mg^{2+}) is a medium size cation having Goldschmidt radius of 0.78Å. It is known to exist in six-fold co-ordination in enstatite ($MgO \cdot SiO_2$) and diopside $CaO \cdot MgO \cdot 2SiO_2$, and four-fold in spinel ($MgO \cdot Al_2O_3$). Roy (22) calculated the molar refractivity of minerals of enstatite and diopside from the published data and determined the same for glasses of the same compositions by employing the Lorentz-Lorenz equation and found an increase of molar refractivity of the glasses by about 0.65. He concluded that the increase was due to a lower state of co-ordination i.e. four-fold assumed by Mg^{2+} ions in the glasses. Galent (23) has also shown that Mg^{2+} ions exist in

Table 2a. *Characteristics of CSAM * glass samples*

Sl. No.	Glass formula* C: S: A: M				Zachariasen no.	Glass composition wt. %				Density	Refractive index	Total refractivity	Partial refractivity of MgO
						CaO	SiO_2	Al_2O_3	MgO	g/cc	n	cc/mole	cc/mole
	C	S	A	M								K	K_{MgO}
1.	10	8	4	—	0.42	38.67	33.15	28.18	—	2.8662	1.626 ± .001	178.70	—
2.	10	8	4	1	0.435	37.63	32.25	27.41	2.71	2.8772	1.629 ± .001	183.81	5.11
3.	10	8	4	2	0.45	36.64	31.40	26.69	5.27	2.8869	1.632 ± .001	188.85	5.04
4.	10	8	4	3	0.46	35.69	30.59	26.01	7.71	2.8970	1.635 ± .001	193.88	5.03
5.	10	8	4	4	0.475	34.81	29.84	25.36	10.02	2.9060	1.638 ± .001	199.00	5.12
													Av. 5.08

Table 2b.

	Minerals									
a.	Periclase	—	—	—	—	100.0	3.576	1.738	4.538	4.538
b.	Spinel	—	—	—	71.68	28.32	3.578	1.719	15.68	5.05
c.	α-Al_2O_3 (crystalline)	—	—	—	100.0	—	3.96	1.764	10.63	

*C = CaO S = SiO_2 A = Al_2O_3 M = MgO

Table 2c. *Characteristics of CSAM* glass samples*

Sl. No.	Glass formula* C: S: A: M				Zachariasen no.	Glass composition wt. %				Density	Refractive index	Total refractivity	Partial refractivity
						CaO	SiO_2	Al_2O_3	MgO	g/cc	n	cc/mole	cc/mole
	C	S	A	M								K	$K_{CaO-MgO}$
6	12	8	4	–	0.40	43.08	30.77	26.16	—	2.8985	1.634 ± .001	192.4	
7	11	8	4	1	0.425	39.89	31.09	26.42	2.61	2.8920	1.633 ± .001	190.6	1.80
8	10	8	4	2	0.45	36.63	31.40	26.69	5.27	2.8869	1.632 ± .001	188.85	1.75
9	9	8	4	3	0.475	33.32	31.73	26.98	7.99	2.8765	1.630 ± .001	187.1	1.75
10	8	8	4	4	0.50	29.92	32.06	27.26	10.76	2.8620	1.627 ± .001	185.3	1.80
													Av. 1.775

*C = CaO S = SiO_2 A = Al_2O_3 M = MgO

Table 2d.

											K_{CaO}
6	12	8	4	–	43.08	30.77	26.16	—	2.8985	1.634 ± .001	192.40 *	6.85
1	10	8	4	–	38.67	33.15	28.18	—	2.8662	1.626 ± .001	178.70 *	
7	11	8	4	1	39.89	31.09	26.42	2.61	2.8920	1.633 ± .001	190.60 **	6.79
2	10	8	4	1	37.63	32.25	27.41	2.71	2.8772	1.629 ± .001	183.81 **	
4	10	8	4	3	35.69	30.59	26.01	7.71	2.8970	1.635 ± .001	193.88 **	6.78
9	9	8	4	3	33.32	31.73	26.98	7.99	2.8765	1.630 ± .001	187.10 **	
5	10	8	4	4	34.81	29.84	25.36	10.02	2.9060	1.38 ± .001	199.00 *	6.85
10	8	8	4	4	29.92	32.06	27.26	10.76	2.8620	1.627 ± .001	185.30 *	
												Av. 6.82

* This difference is for two moles of CaO;
**This difference is for one mole of CaO

four-fold co-ordination in melilite (including akermanite) glasses.

The difference in the total molecular refractivity of spinel ($MgO \cdot Al_2O_3$) and corrundum (α-Al_2O_3) gives the partial molar refractivity of MgO in four-fold co-ordination as magnesium in spinel exists in four-fold co-ordination. This value turns out to be 5.05 against a value of 4.54 for six-fold co-ordination of magnesium ions in periclase (Table 2).

The total molecular refractivity of magnesium glasses of series D was plotted against the number of moles of MgO present in each glass (Fig. 3). The slope of the resulting linear curve represents the partial molar refractivity (K_{MgO}) of magnesia. Since the latter value (K_{MgO}) was found out to be 5.08, it is concluded that Mg^{2+} exists in four-fold co-ordination in these glasses.

In the glass compositions of the series E, CaO was partially replaced by MgO (Table 2c). The maximum percentage of MgO in the substituted glasses is about 10 percent. The data show that the values of density, refractive index and total refractivity decrease on substitution of CaO by MgO. If co-ordination of calcium ions in both the glass series D and E is assumed to be six-fold, the partial refractivity due to CaO can be calculated from the differences in the values of the total refractivity of individual glasses, say No. 6 and 1, 7 and 2, 4 and 9, and 5 and 10. The average K_{CaO} was thus found to be 6.82 (Table 2d) against the reported value of 6.75 (24). If the average differ-

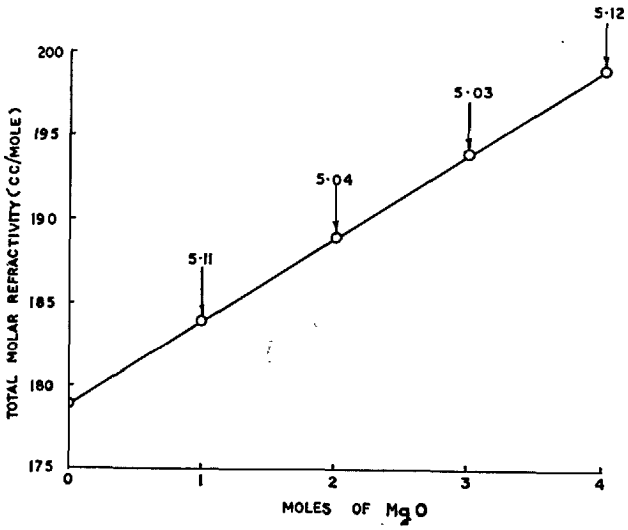

Fig. 3. *Partial molar refractivity of MgO in glasses of composition* $10CaO \cdot 8SiO_2 \cdot 4Al_2O_3 \cdot (0\text{–}4)MgO$ *numerals indicate* K_{MgO} *values (average 5.08)*

ence between K_{CaO} and K_{MgO} is 1.775 (Table 2c), K_{MgO} by difference from glasses of the series E equals 5.045 as against the value of 5.08 for the glasses of the series D. In other words, Mg^{2+} ions exist in four-fold state of co-ordination in the substituted glasses of series E also, thus confirming the earlier conclusions.

Differential thermal analysis of the glasses (series C and D) was also carried out and the pattern of the curves was similar to those given in Fig. 2. The thermal effects were recorded mostly in the range 800 to 1000°C and data are reported in Table 3.

With the addition of 4 moles of MgO to the parent glass of composition $10CaO \cdot 8SiO_2 \cdot 4Al_2O_3$ in four equal increments (series D), a fall was noticed in the temperatures of the endothermic peak, beginning of the exothermic effect and also the exothermic peak due to devitrification. A similar but less pronounced trend was observed in glasses of the series E wherein magnesium oxide substituted CaO in increasing amounts. The data in Table 3 show that the introduction of MgO loosens the structure, and is contrary to expectations on the basis of analogy with tetrahedral state of co-ordination of aluminium ions (Fig. 2).

Weyl and Marboe have reported the work of Petzold Wishman & Kamptz, who had correlated the hardness of glasses with other properties such as softening temperature and molar refractivity, and had found that the molar substitution of MgO for CaO did not fit into a simple pattern (25). Instead of increasing the hardness, as they had expected, the substitution of MgO for CaO on molar basis produced softer glasses. This discrepancy was explained by

Table 3. *Differential thermal analysis data of CSAM glasses*

Glass sample Series	No.	Glass composition C	S	A	M	Peak temperatures in °C endothermic peak	beginning of exother-effect	exothermic peak
D	1	10	8	4	–	850	890	990
W	2	10	8	4	1	840	890	945
W	3	10	8	4	2	825	865	938
W	4	10	8	4	3	820	865	910
W	5	10	8	4	4	820	860	920
E	6	12	8	4	–	842	930	960
W	7	11	8	4	1	835	910	950
W	8	10	8	4	2	825	865	938
W	9	9	8	4	3	790	870	940
W	10	8	8	4	4	862	900	940

Petzold, Wishman and Kamptz on the basis of tetrahedral state of co-ordination of magnesium ions. According to them, the substitution of MgO_4 groups for CaO_4 groups causes the tetrahedral structure to become weaker, because some Si^{4+} ions are replaced by Mg^{2+} ions and the average co-ordination of O^{2-} ions is lowered because the glass structure can accomodate Mg^{2+} but not Ca^{2+} ions in tetrahedral co-ordination. Similarly, the substitution of MgO_4 groups for CaO_6 groups in the slag glasses of series D and E causes the tetrahedral structure to become weaker because tetravalent silicon and trivalent aluminium ions are probably replaced by divalent magnesium ions of bigger size and the average co-ordination of O^{2-} ions is lowered and the structure thus gets loosened as is evident from the data in Table 3.

Mg^{2+} and Ni^{2+} ions are both divalent and have almost equal ionic radii (Goldschmidt). Ni^{2+} has been found to take up a bridging position in the network, and exists in four-fold co-ordination in high alkali borosilicate glasses and in $CaO\text{–}Al_2O_3\text{–}B_2O_3$ and $CaO\text{–}B_2O_3$ glasses containing high CaO (13). The colour of glass under ultraviolet light is purple when Ni^{2+} occurs in four-fold co-ordination. In view of this a part of MgO in glasses No. 8 and 10 was replaced by an equivalent amount of NiO. The glasses when examined under ultraviolet light showed purple colour thus confirming that Mg^{2+} ions exist in four-fold co-ordination in both the series of glasses in the system $CaO\text{–}Al_2O_3\text{–}SiO_2\text{–}MgO$.

Co-Ordination State of Manganese Ions

Since blastfurnace slags are known to contain a small amount of manganese, a few samples of the synthetic slag glasses of the general formula $9CaO \cdot 8SiO_2 \cdot 3.5Al_2O_3 \cdot nMnO$ were prepared in a reducing flame by the Dyckerhoff method. These glasses correspond to the compositions of the Rourkela slag

Table 4. *Characteristics of CSAMn* glass samples (Series F)*

Sl. No.	Glass formula C : S : A : Mn				Zachariasen no.	Glass composition wt. %				Density	Refractive index	Total refractivity	Partial refractivity (K_{MnO})
						CaO	SiO_2	Al_2O_3	MnO	g/cc	n	cc/mole	cc/mole
1	9	8	3.5	—	0.42	37.58	35.79	26.63	—	2.854	1.616	164.3	—
2	9	8	3.5	0.5	0.42	36.61	34.87	25.94	2.58	2.891	1.624	168.1	7.60
3	9	8	3.5	1.0	0.41	35.69	33.99	25.28	5.03	2.920	1.628	172.0	7.80
4	9	8	3.5	1.5	0.41	34.81	33.16	24.67	7.36	2.955	1.636	175.8	7.60
													av. = 7.66

*C = CaO S = SiO_2 A = Al_2O_3 Mn = MnO

(17). The value of n in these glasses (series F) was varied from 0.5 to 1.5 and the corresponding variation of MnO content in the glass was 2.58 to 7.36 percent by weight. The state of co-ordination of manganese ions in these glasses was studied by the partial molar refractivity method and also by investigating fluorescence under UV radiation.

The values of densities, refractive indices and molecular refractivities of the glass samples are reported in Table 4. The average value of partial molar refractivity works out to 7.66 against a value of 7.2 for six-fold co-ordination of manganese reported in the literature (24). The higher experimental value therefore indicates that part of manganese exists either in four-fold state of co-ordination or in trivalent state of valence. According to Weyl and Marboe (26) red fluorescence in manganese glasses under UV radiation is attributed to manganese ions present in interstitial position in the glass network when they are surrounded by six oxygens. The slag glasses of the series containing manganese oxide up to 7.5 percent, when exposed to UV radiations, exhibited red fluorescence thus confirming a six-fold state of co-ordination of manganese ions. This may be presumably due to its greater ionic size. It was therefore inferred that the higher value of partial molar refractivity is probably due to part of manganese occuring in a higher state of valence. This was confirmed as reported below.

It is well known that atoms and ions of transition elements in the free state have unfilled electron shells and hence possess magnetic moments. The magnetic properties of glasses, whose framework is usually slightly diamagnetic, will change substantially by the incorporation of ions of transition elements. It, therefore, follows that measurement of magnetic susceptibilities of the glass samples of the series F could throw light on the state of valence of manganese ions.

The magnetic susceptibility λg of a glass sample can be taken to be the sum of diamagnetic susceptibility $\lambda_0(1 - C_{Mn})$, due to the base glass and the paramagnetic susceptibility, $\lambda_{Mn} \cdot C_{Mn}$, due to the concentration C_{Mn} of manganese present in the glass (27)

Table 5. *Magnetic properties of CSAMn glass samples (Series F)*

Sl. No.	Glass formula C: S: A: Mn				Manganese total percent by wt.	Magnetic susceptibility $\lambda_{Mn} \times 10^{-6}$ in cgs units	Magnetic moment (μ) (Bohr magnetons)	Manganese present in manganic state percent
1	9	8	3.5	—	0	—	—	—
2	9	8	3.5	0.5	2.0	228.24	5.52	18
3	9	8	3.5	1.0	3.9	244.42	5.71	24
4	9	8	3.5	1.5	5.7	232.48	5.58	20

and can be expressed by the equation (1)

$$\lambda g = \lambda_{Mn} \cdot C_{Mn} + \lambda_0(1 - C_{Mn}) \qquad (1)$$

The magnetic susceptibility value λ_{Mn} (at 29°C) for Mn in the synthetic slag glasses of the series F are reported in Table 5 column 4. From λ_{Mn} the paramagnetic moment μ (in Bohr magnetons) due to the manganese in glass was calculated from the equation (2)

$$\mu = 2.83\sqrt{T\lambda_{Mn} \cdot M} \qquad (2)$$

where

M is the atomic weight of Mn (54.93) and
T the absolute temperature.

The magnetic moments due Mn in the synthetic slag glasses are from 5.52 to 5.71 Bohr magnetons (Table 5 column 5). Since the theoretical moment due to spin only, are 5.92 and 4.90 Bohr magnetons for Mn^{2+} and Mn^{3+} respectively, it may be concluded that manganese is predominantly present in the manganous state. The values of $\lambda_{Mn^{2+}}$ and $\lambda_{Mn^{3+}}$ as calculated from equation (2) are 26.38×10^{-5} and 18.07×10^{-5} cgs units respectively.

The relative amounts of divalent (Mn^{2+}) and trivalent (Mn^{3+}) in the glass samples can be calculated from equation (3).

$$\lambda_{Mn} = \lambda_{Mn^{2+}} \cdot C_{Mn^{2+}} + \lambda_{Mn^{3+}}(1 - C_{Mn^{2+}}) \qquad (3)$$

where $\lambda_{Mn^{2+}}$ and $\lambda_{Mn^{3+}}$ are the magnetic susceptibilities and $C_{Mn^{2+}}$ and $(1 - C_{Mn^{2+}})$ are concentrations of the Mn^{2+} and Mn^{3+} ions respectively. By substituting the magnetic susceptibility value, λ_{Mn} in the above equation (3) and the calculated values of $\lambda_{Mn^{2+}}$ and $\lambda_{Mn^{3+}}$

from the equation (2) using the theoretical moments for Mn^{2+} and Mn^{3+} ions, as 26.38 $\times 10^{-5}$ and 18.07 $\times 10^{-5}$ cgs units respectively at 302°K, the amounts of manganous and manganic ions were calculated (equation 3) and are expressed as percentage of total manganese in Table 5. The data indicate that manganese in the synthetic glass sample is predominantly present in bivalent state i.e. from 76 to 82 percent. This is in accord with the knowledge that high temperatures and reducing atmosphere in blastfurnaces promote bivalent manganous state.

Conclusions

The state of co-ordination of aluminium ions in synthetic slag glasses in the system $CaO–Al_2O_3–SiO_2$ was studied by determining the effects of varying the alumina content (from 1 to 7 moles) on the density and refractive indices of glasses of composition $10CaO \cdot 8SiO_2 \cdot nAl_2O_3$ having a CaO/SiO_2 ratio of 1.17: 1. The partial molar refractivity of alumina indicated that aluminium ions are always present in four-fold co-ordination. This was also supported by the value of the partial specific volume of Al_2O_3 and the rise in temperature of the exothermic peak due to devitrification on substituting increasing amounts of Al_2O_3 (moles) for SiO_2 in the glass compositions $10\,CaO \cdot (10–n)\,SiO_2 \cdot nAl_2O_3$. Similarly, the partial molar refractivity of magnesia in glass compositions of general formulae $10CaO \cdot 8SiO_2 \cdot 4Al_2O_3 \cdot nMgO$ and $(12–n)\,CaO \cdot 8SiO_2 \cdot 4Al_2O_3 \cdot nMgO$ where n was varied from 1 to 4, indicated a four-fold state of co-ordination of magnesium ions. This was also confirmed by the purple fluorescence of Ni^{2+} ions in glasses where part of MgO was substituted by NiO. But the average value of partial molar refractivity of manganese oxide in glass compositions of $9CaO \cdot 8SiO_2 \cdot 3.5Al_2O_3 \cdot$ (0.5 to 1.5) MnO showed that manganese ions were present in six-fold co-ordination. This was also indicated by the red fluorescence of manganese glasses in ultraviolet light. The partial molar refractivity data (K_{MnO}), however, indicated further that a part of manganese was present in a higher state of valence and the magnetic susceptibility measurements confirmed that about 18 to 24 percent of manganese was present in trivalent state in the manganese bearing glasses.

Acknowledgement

The authors thank Mr. S. K. Malhotra for his help in the preparation of glasses. The paper is being published with the kind permission of the Director, Central Building Research Institute, Roorkee (U.P.), India.

References

1. W. H. Zachariasen, "The atomic arrangement in glass" Jour. Amer. Chem. Soc. Vol. 54, pp. 3841–3851 (1932)
2. T. W. Parker and R. W. Nurse, "Investigations on granulated blastfurnace slags for the manufacture of portland blastfurnace cement" Technical Paper No. 3, National Building Studies, H. M. S. O., London (1949)
3. T. Tanaka, T. Sakai and J. Yamane, "Die Zusammensetzung Japanischer Hochofenschlacken für Sulfathüttenzement" Zement-Kalk-Gips, **11**, 50–55 (1958)
4. F. Keil and F. W. Locher, "Hydraulic properties of glasses 1. glasses of the system $CaO–SiO_2–Al_2O_3$ without and with MgO", (in German), Zement-Kalk-Gips, 11, 245–253, (1958)
5. R. Kondo, "On the structure of high lime glasses" Chemistry of Cement, Proceedings of the Fourth International Symposium, Washington, USA (1960). National Bureau of Standards Monograph 43 Vol. II, 937 (1962)
6. O. P. Mchedlov-Petrosyan, "Crystalline chemistry of cementing properties" "Reports of symposium on the chemistry of cement" edited by P. P. Budnikov, Yu. M. Butt, S. M. Royak and M. O. Yushkevich p. 71 State Publication of Literature on Structural Materials, Moscow USSR (1956)
7. W. Kramer, "Blast-furnace slags and slag cements" Chemistry of Cement, Proceedings of the Fourth International Symposium, Washington USA (1960) National Bureau of Standards, Monograph 43 Vol. II, p. 962 (1962)
8. W. Dyckerhoff, "Über den Verlauf der Mineralbildung beim Erbitzen Van Genengen aus Kalk, Kieselsaure und Tonerde" Dissertation, Frankfurt/Main (1925)
9. W. A. Weyl, and E. C. Marboe, "The constitution of glasses—a dynamic interpretation", Vol. 1 61 (Interscience Publishers, New York & London, 1962)
10. T. Yamauchi and R. Kondo, "Hydraulic activity of glasses in the $CaO–Al_2O_3–SiO_2–MgO$ system" (in Japanese) J. Ceram. Assoc. Japan, **57**, 486–96 (1951)
11. W. R. Eubank, "Calcination studies of magnesium oxide" J. Amer. Cer. Soc. **34**, 8, 225–29 (1951)
12. Modern Aspects of the Vitreous State, Vol. 1. (Butterworths & Co. London, U. K. 1960), Edited by

J. D. Mackenzie. See Chapter by S. Urnes "X-ray diffraction studies of glass" p. 10–37.
13. (Ref. 9) p. 302
14. P. W. Selwood, "Magnetochemistry" p. 26. (Interscience Publishers, INC, New York & London, 1956)
15. H. W. Safford and A. Silverman, "Alumina-silica relationship in glass", J. Amer. Cer. Soc. No. 7, Vol. 3, pp. 203–211 (1947).
16. D. E. Day and G. E. Rindone "Properties of soda alumina silicate glasses: 1, refractive index, density, molar refractivity and infra red absorption spectra" J. Amer. Cer. Soc. No. 1, Vol. 45, pp. 484–496 (1962)
17. S. K. Chopra, C. A. Taneja and G. S. Mehrotra, "Mineralogy of indian blast furnace slags" Indian Journal of Technology No. 2, Vol. 3, pp. 49–53 (1965)
18. The Chemistry of Cements, Vol. 2 (Academic Press, London and New York USA 1964), Edited by H. F. W. Taylor, See Chapter by R. W. Nurse entitled "Slag Cements" p. 43.
19. A. F. Wells "Structural inorganic chemistry", p. 464 (Clarendon Press, Oxford, UK 1962)
20. S. K. Chopra and C. A. Taneja, "Co-ordination state of aluminium ions in $CaO–Al_2O_3–SiO_2$ glasses", Journal of Applied Chemistry (U. K.), Vol. 15, pp. 175–161 (1965)
21. J. E. Kruger, K. H. L. Sehlike and J. H. P. Van Aardt, "High temperature studies on blast furnace slags", Cement & Lime Manufacture, No. 4 & 5, Vol. 37, (July & Sept 1964)
22. R. Roy, "Magnesium in four-fold co-ordination in glass," J. Am. Chem. Soc. Vol. 72, 3307–8, (July 1950)
23. E. I. Galant, "Co-ordination number of magnesium in glass" (in Russian), Dokl. Akad. Nauk. SSSR, 137 (6), pp. 1424–26 (1961)
24. S. S. Batsanov "Refractometry and chemical structure" pp. 170, 173 (Authorised Translation from the Russian by Paul Porter Sutton, Consultant Bureau, New York, 1961)
25. W. A. Weyl and E. C. Marboe "The constitution of glasses-A dynamic interpretation", Vol. II, Part I, p. 524, (Interscience Publishers, New York and London, 1964)
26. (Ref. 9) pp. 303–304
27. Atma Ram, S. Kumar and Prabhu Nath, "Magnetic & spectrophotometric studies on glasses containin manganese", Central Glass & Ceramic Research Institute Bulletin, Calcultta, India. Vol. 4, No. 4, 182–192 (1957)

Supplementary Paper IV-100 A Contribution to the Study of the Physical Properties of Hardened Pastes of Portland Cements Containing Granulated Blast-Furnace Slag

Cesare Cesareni and Giuseppe Frigione*

Synopsis

This paper wants to bring up a contribution to the study of some fundamental physical properties of the hardened pastes of cement containing granulated blast-furnace slags with the precise intent to put in evidence analogies and differences of the slag under hydrated stage in comparison with the portland cement.

The properties studied, adopting the different methods indiceted by Powers and other Collaborators are:

—Sedimentation process of the fresh pastes.
—Contents of non-evaporable water at a normal temperature.
—Development of the surface area of the pastes.
—Porosity of the pastes.

It has been tempted to find, besides, a relation among the above mentioned properties and the other fundamental physico-mechanical characteristics of the cements for their use.

The experiment has been conducted on a series of cements obtained by mixture of different clinkers, differentiated from the ratio C_3A/C_4AF; and of different industrial samples of slag coming from different blast-furnaces and differentiated by the content of the three fundamental oxides SiO_2-CaO–Al_2O_3.

Clinkers and slags have been mixed in proportions that vary from 10 to 70% and compared with portland cements obtained from the same clinker.

Storage time of 7–28–180–365–630 days and water-cement ratio of 0.30 and 0.50 have been considered.

Introduction

The study of hardened pastes made with portland blast-furnace slag cement acts as a bridge between the chemistry of these cements and their technological application in concrete.

The set of variabilities (chemical composition of the clinker, composition of the slags, physical condition of the same, fineness of the two components, centesimal composition of the mixtures, percentages of gypsum content and of other activating or regulating products) is so vast that a systematic experiment would require many years of work.

It has to be taken into consideration, in particular, that any study on cements containing blast-furnace slag, involves two basic components (clinker and slag) of which one (slag) is in a metastable condition and therefore its behaviour will never be able to be perfectly defined until physico-chemical parameters and therefore an unequivocal consent to the classification of slags are found.

This paper is limited to the illustration of the results obtained by us and a general review on the subject is postponed for later date in order to improve the results by other evidences, to be found in the present experiment.

The main purpose of the work is the enrolment in great lines of the physico-chemical phenomena which charaterizes the process of hydration of hardened cement pastes containing blast-furnace slag.

Since the purpose was to study industrial cements, the slags have been associated with clinkers as they are actually used for the production of blastfurnace cements, i.e., clinkers characterized by high contents of C_3S (1). It follows that since this constituent is in an almost constant quantity, it is possible to study the influence of the other constituents (C_3A and C_4AF) on the hydration of blast-furnace slags.

*Cementir-Cementerie del Tirreno S.p.A. Roma, Italy.

Characteristics of Cements Tested

The clinker and slag used are of ordinary industrial products and have the chemical analyses listed in Table 1.

The slags, by products of three different basic blast-furnace process are granulated directly by pouring in a pit containing sea-water, and located near the furnace.

The values assumed for the three slags from the various formulae in order to evaluate the hydraulic properties of the blast-furnace slags, may be found in Table 2.

Thirty-nine types of cement formed by different percentages of clinker-slag mixture, in ratio of 100/0, 70/30, 50/50, 30/70 and 10/90, from three types of clinker and three types of slag, have been prepared.

The various mixtures have been obtained by mixing in an appropriate mixer the two main components having been ground in a laboratory mill with the addition of a fixed quantity of 4% gypsum, and to a fineness characterized by a Wagner specific surface of about 1850 cm^2/g.

Table 1. *Chemical analyses on starting materials*

	Chemical composition (%)													Ptoential phase composition (%)			
	ig. loss	SiO_2	Fe_2O_3	Mn_3O_4	Al_2O_3	CaO	MgO	SO_3	S	Na_2O	K_2O	BaO	Free CaO	C_3S	C_2S	C_3A	C_4AF
Kl A	0.6	23.0	3.4	—	3.9	65.7	1.3	0.8	—	0.4	0.8	—	0.4	57.6	22.5	4.6	10.3
Kl B	0.5	22.8	2.8	0.1	4.6	66.0	1.5	1.0	—	0.4	0.6	—	0.2	56.7	22.6	7.3	8.8
Kl C	0.7	22.1	2.2	—	5.1	66.1	1.6	0.9	—	0.4	0.8	—	1.5	54.0	21.9	9.7	6.7
Slag 1	0.6	35.9	1.5	0.5	11.6	40.1	6.9	—	1.3	0.7	0.6	—	—	—	—	—	—
Slag 2	0.4	31.2	1.1	0.9	15.5	36.9	10.2	—	1.3	1.1	0.8	0.3	—	—	—	—	—
Slag 3	1.0	31.5	3.7	0.5	13.1	40.7	6.7	—	1.1	0.7	0.7	—	—	—	—	—	—

Table 2. *Evaluation of hydraulic properties of the slags by chemical composition*

			Slag 1	Slag 2	Slag 3
Basicity ratios:					
$p_1 = \frac{CaO}{SiO_2}$			1.12	1.18	1.29
$p_2 = \frac{CaO + MgO}{SiO_2}$			1.31	1.51	1.50
$p_3 = \frac{CaO + MgO}{SiO_2 + Al_2O_3}$			0.99	1.01	1.06
German formula:					
formula I DIN 1164/1917	$\frac{CaO + MgO + 1/3\ Al_2O_3}{SiO_2 + 2/3\ Al_2O_3} > 1$		1.17	1.26	1.29
formula II DIN 1164/1942	$\frac{CaO + MgO + Al_2O_3}{SiO_2} > 1$		1.63	2.01	1.92
formula III F. Keil	$\frac{CaO + CaS + 1/2\ MgO + Al_2O_3}{SiO_2 + MnO}$	Hydraulic properties: < 1.5 medium; 1.5–1.9 good; > 1.9 very good	1.56	1.84	1.83
Belgian formula:					
Blondiau	$\frac{CaO}{SiO_2}$	Hydraulic properties: 1.45—1.54 good	1.12	1.18	1.29
	$\frac{SiO_2}{Al_2O_3}$	1.8—1.9 good	3.09	2.01	2.40
French formula: $i = 20 + CaO + Al_2O_3 + 0.5\ MgO - 2\ SiO_2$ De Langavant		Hydraulic properties: < 12 medium; 12–16 good; > 16 very good	3	15	14

Sedimentation Test on Fresh Pastes

The experiment has been conducted according to the method realized by Valore, Bowling and Baline

(2), (3).

We have verified that the phenomenon has a common procedure for all tested slags, that is, the capacity and bleeding velocity increase continuosly with the increase of slag content.

We have investigated more thoroughly the phenomenon of a group of mixtures, which constitutes clinker A and slag 1.

The characteristics of bleeding tests are listed in Table 3 and shown in Fig. 1.

On the basis of above mentioned characteristics, it has been calculated the value of immobile water W_i: it decreases by increasing the slag content.

The bleeding rate increases with the slag content not only for the decrease of W_i but also for the variations of the fluid density and the fluid viscosity (with an increase of about 2.5% and 6% respectively for the mixture 10/90) which result remarkably enough; and such that they influence, in a great way, the above parameter, as it can be confirmed by the Kozeny-Karman equation adapted for this particular case by Powers (4).

Table 3. *Bleeding characteristics of fresch pastes*

Mix		Specific surface (Wagner)		Density g/cc	W/C ratio		Cement content (absolute volume) C	Water content (absolute volume) W	Bleeding rate ($Q \times 10^6$)	Bleeding capacity ($\Delta H'$)	Porosity sediment (per cent of settled volume)	W_i	Hydraulic radius (microns)
Clinker	Slag	cm^2/g S	cm^2/cc σ		W_i	Vol							
100		1786	5645	3.18	0.30	0.942	0.515	0.485	18	0.0030	48.3		1.661
					0.40	1.26	0.443	0.557	74	0.0190	54.8	0.325	2.192
					0.50	1.57	0.389	0.611	129	0.0456	59.2		2.696
70	30	1825	5675	3.08	0.30	0.923	0.520	0.480	18	0.0038	47.8		1.620
					0.40	1.23	0.448	0.552	72	0.0198	54.3	0.323	2.136
					0.50	1.54	0.394	0.606	153	0.0489	58.6		2.620
50	50	1835	5635	3.04	0.30	0.912	0.523	0.477	22	0.0038	47.5		1.612
					0.40	1.22	0.451	0.549	76	0.0228	53.8	0.318	2.117
					0.50	1.52	0.397	0.603	165	0.0506	58.2		2.602
30	70	1860	5650	3.00	0.30	0.901	0.526	0.474	25	0.0042	47.2		1.588
					0.40	1.20	0.454	0.546	96	0.0280	53.3	0.317	2.078
					0.50	1.50	0.400	0.600	187	0.0589	57.5		2.544
10	90	1890	5665	2.96	0.30	0.887	0.530	0.470	36	0.0051	46.7		1.555
					0.40	1.18	0.458	0.542	124	0.0335	52.6	0.294	2.027
					0.50	1.48	0.403	0.597	219	0.0620	57.0		2.497

(°) The hydraulic radius is calculated from the formula $W/C\sigma$ where W is the water present in the sediment after bleeding and the volume of water corresponds to the porosity of sediment.

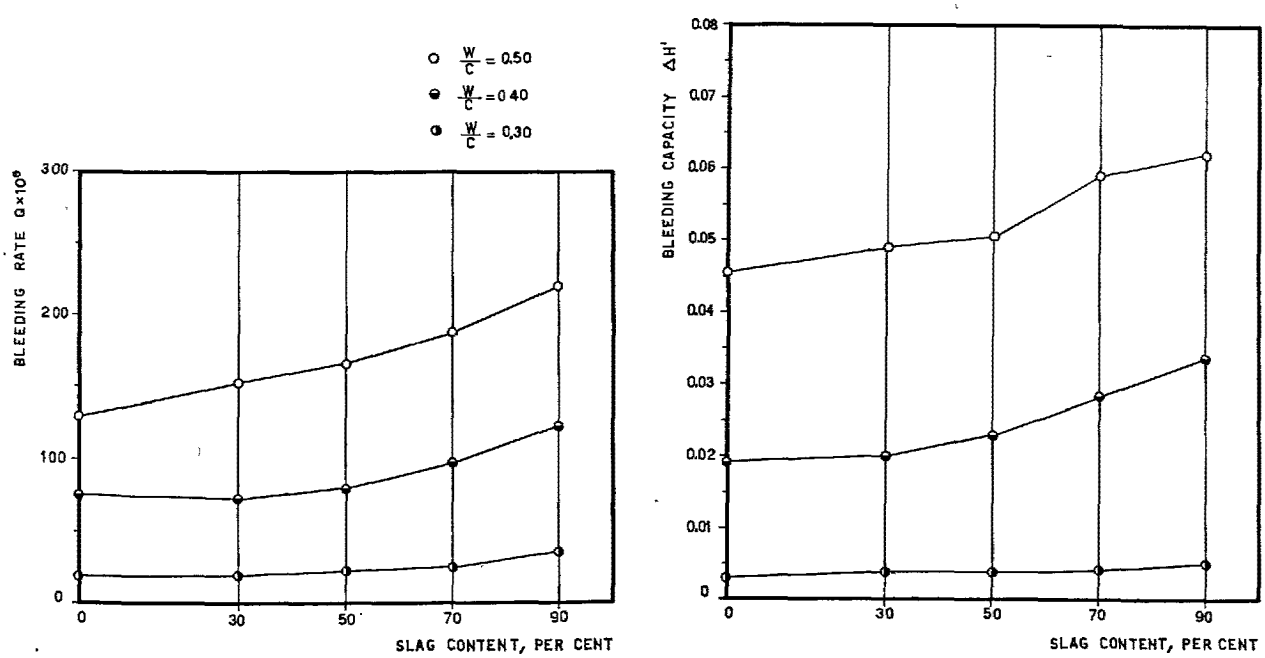

Fig. 1. *Bleeding characteristics as a function of slag content of the cement*

We still ought to consider the flocculation effect which probably is decreased in higher slag mixtures, where the amount of hydrated lime from the clinker, is quite small.

Besides, hydraulic radius have been calculated (already reported in table 3), considering the content of water in fresh pastes equal to the presence of water after the bleeding or, in other words, corresponding to the porosity of the paste sedimentation. From value of hydraulic radius it is possible to evaluate the mean pore size of the paste.

It must be observed that, the hydraulic radius and therefore the mean size of pores, decreases with the increase of the slag content. Such a result does not agree with what was found by Chopra (5).

Tests on Hardened Pastes

Tests on all mixtures were conducted employing two ratios W/C, i.e., 0.30 and 0.50.

The pastes used in this research were mixed free from air as described by Powers, Copeland, Hayes and Mann (6).

The mixtures were immediately poured in test tubes which were accurately corked so that no air could remain between the paste and the cork. Immediately after, the test tube was held in continuous motion attached in a radial position, to a vertical disc rotating at a slow velocity (7 r.p.m.) until the cement has completed its setting. In such a way the bleeding has been avoided obtaining so, for a more vigorous comparison, with pastes having an equal ratio W_0/C.

Successively the test tube was cured in water at $20 \pm 1°C$ until the date of the determinations of the different periods of curing.

The periods of curing considered were: 7–28–180–365 and 730 days.

To appear more evident in the graphic description, in the various diagrams we have limited ourselves in relating the values corresponding to the curing periods of 7–28 and 730 days.

Non-evaporable Water and Free Calcium Hydroxide

Non-evaporable water has been determined by the method described by Copeland and Hayes (7).

The free calcium hydroxide has been determined according to the "time variation method" described by Pressler, Brunauer, Kantro and Weise (8), and following modification (9).

All the mixtures were tested only for the curing periods of 7 days and 2 years.

For the mixture with W_0/C 0.30, the determinations seem, though, affected by a noticeable experimental error, and therefore are not taken into consideration.

In Figs. 2 and 3 are reported the variation bands of Wn/C for the various cement mixture ratios.

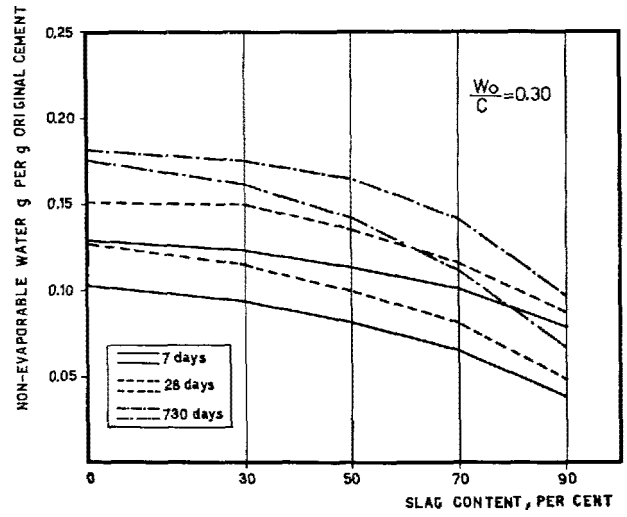

Fig. 2. *Bands of non-evaporable water as a function of slag content of the cement (Wo/C 0.30)*

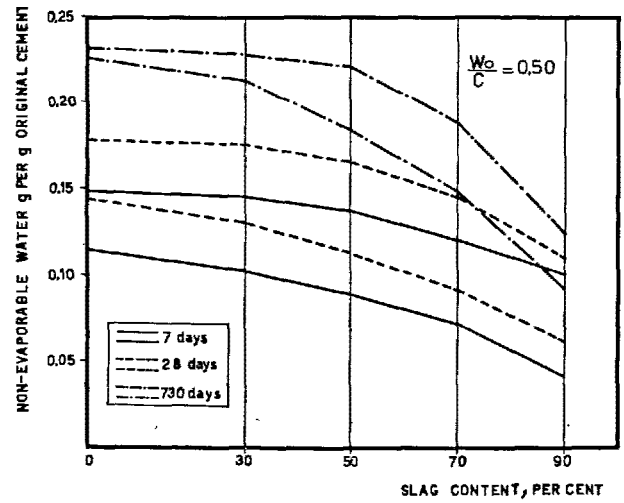

Fig. 3. *Bands of non-evaporable water as a function of slag content of the cement (Wo/C 0.50)*

It is noted that until a cement mixture ratio at 50/50 the values of nonevaporable water are of the

same order as those of portland; while for cement mixtures with 70% to 90% of slag, the values of Wn/C are much inferior and the difference is accentuated with hydration during the time process.

In Fig. 4 are reported the variation bands of CaO extracted. Still in Fig. 5 are reported the bands of CaO absorbed (calculated as a difference between that liberated by the corresponding pure portland cement at the same curing period and the CaO extracted) expressed in grams of lime based on 100 grams of anhydrous slag.

It is observed that the quantity of CaO absorbed for the mixtures 70/30, is of the same order (or even higher) as that of the same slag capable of absorbing if kept in contact and in constant agitation with saturated calcium hydroxide solution; for the mixtures richer in slag, the CaO absorbed is very limited.

In order to evaluate how much non-evaporable water is attributable to water combined in gel, we have also calculated for a series of mixtures the contribution given to Wn/C by the calcium hydroxide and we have obtained the new values of the non-evaporable water (Wn^g/C) always based on 1 g of anhydrous cement (mixtures clinker A—slag 1).

	% clinker	% slag	Wn^g/C
7 days	100	—	0.0634
	70	30	0.0703
	50	50	0.0669
	30	70	0.0604
	10	90	0.0493
730 days	100	—	0.1584
	70	30	0.1767
	50	50	0.1597
	30	70	0.1320
	10	90	0.1099

It is still underlined here that up to 50% of slag, non-evaporable water contained in hydrated products-exclusive of calcium hydroxide-is higher than that of pure portland, and the maximum non-evaporable water content is attained with a cement mixture containing 30% of slag. While the mixtures with higher slag content show an accentuated and progressive Wn^g/C diminution.

The explanation of the above evident phenomena does not appear clear, considering the interaction of the variable; it can be, anyway, hypothesize that with higher slag content:

a) the minor quantity of lime present absolutely in the mixture gives place to more impermeable gel which slows down the hydration reaction and those of "pozzolanic" action; and this occurs due to a topochemical absence of lime.

b) The reaction products have a minor basicity and combine with a minor water quantity.

The confirmation of the validity of both hypotheses or more, probably of the two, requires, according to us, a further experimentation with other and different research methods.

(°) We have indicated non-evaporable water combined with gels with Wn^g/C.

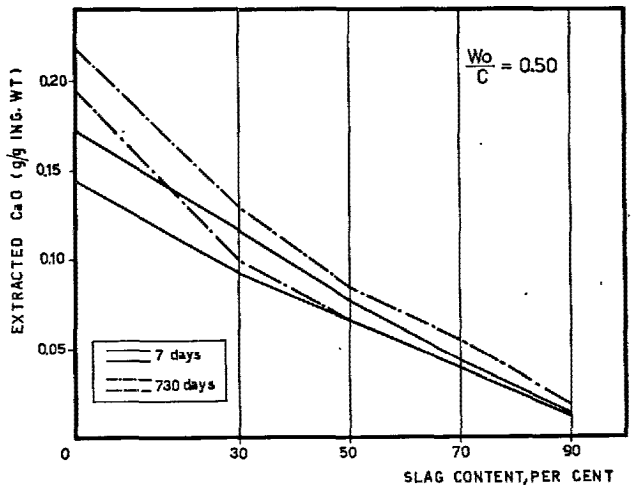

Fig. 4. *Bands of CaO extracted as a function of slag content of the cement (Wo/C 0.50)*

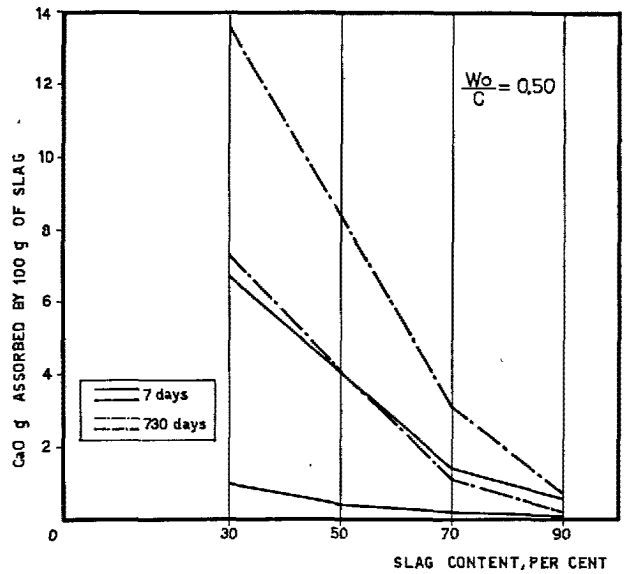

Fig. 5. *Bands of CaO absorbed by 100 g of slag as a function of slag content of the cement (Wo/C 0.50)*

Specific Surface Areas

The specific surface areas and in particular Vm, characteristic parameter of the surface areas to which

it is directly proportional, were evaluated with the method described by Kantro, Brunauer and Weise (10).

The variation bands of the specific surface areas, always relative to 7–28–730 days, are reported in Figs. 6 and 7 (respectively ratio Wo/C 0.30 and 0.50).

This curve trend confirms that the slag hydration products are prevailingly colloids and they contribute significantly to the total surface areas.

In particular it is observed that mixtures of low slag content have areas of the same size as those of pure portland; and attaining a progressively higher surface

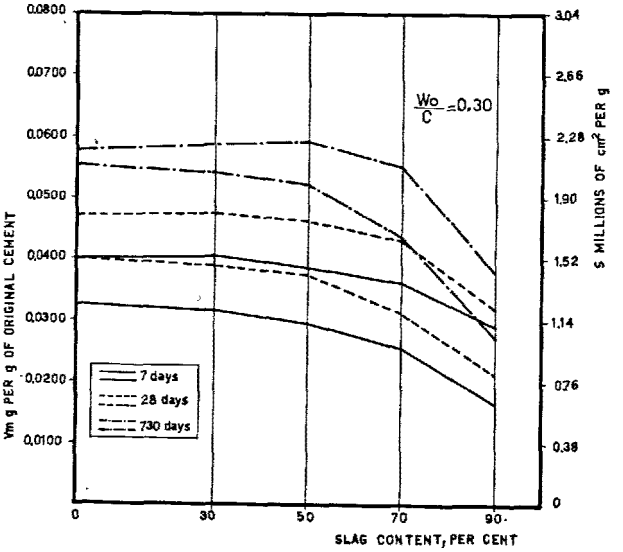

Fig. 6. *Bands of Vm and specific surface area S as a function of slag content of the cement (Wo/C 0.30)*

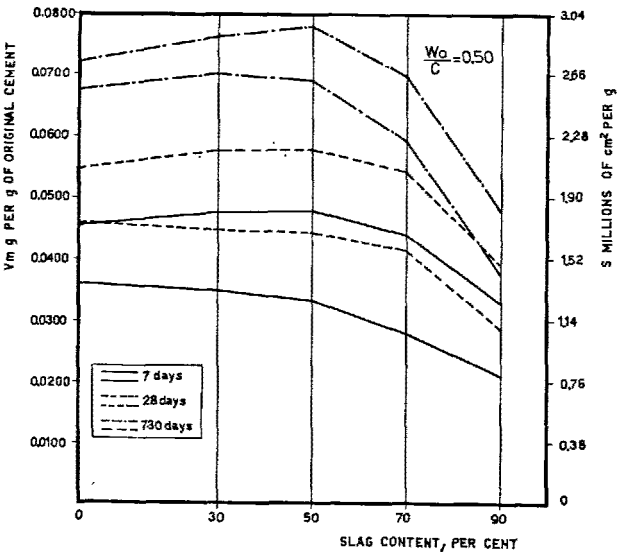

Fig. 7. *Bands of Vm and specific surface area S as a function of slag content of the cement (Wo/C 0.50)*

area during the curing period; and also because of the minor content of calcium hydroxide.

The physico-mechanical characteristics of these cements therefore will be quite similar to the clinkers from which they have been derived and during the curing period these cements have more colloidal new-formations in hardening products; and all those characteristics due to higher quantity of gel will be more conspicuous.

In relation with the above hypothesis, concerning the explanations of the different non-evaporable water content in the cements rich of slag, the surface areas would also show the formation of more compact products and consequently reduced velocity of reaction.

This could give value to Locher's hypothesis (11) according to which the remarkable sulphate resistance of this cement is not due to the chemical properties of the reaction products, but to the capacity of the

Table 4. *Values of Vm × 10⁴ referred to one cubic centimeter of pastes*

Materials		Days	Slag %				
			0	30	50	70	90
Slag 1	Kl A	7	446	430	408	360	254
		28	562	559	517	460	320
		180	710	736	693	580	380
		365	780	804	765	616	422
		730	840	877	831	667	463
	Kl B	7	496	460	420	396	300
		28	615	620	564	520	384
		180	740	762	728	650	460
		365	815	848	803	725	500
		730	860	902	869	775	535
	Kl C	7	524	510	478	425	360
		28	669	646	624	544	436
		180	804	800	763	690	490
		365	837	837	808	720	550
		730	851	869	830	750	562
Slag 2	Kl A	7	446	435	438	384	250
		28	562	560	565	480	293
		180	710	720	714	590	369
		365	780	784	789	648	406
		730	840	874	865	689	437
	Kl B	7	496	468	444	428	308
		28	615	606	590	550	370
		180	740	750	730	656	451
		365	815	787	840	730	511
		730	860	900	904	790	550
	Kl C	7	524	543	524	450	346
		28	669	701	687	590	402
		180	804	845	820	710	450
		365	837	894	862	745	480
		730	851	920	911	774	500
Slag 3	Kl A	7	446	445	426	390	280
		28	562	580	540	500	324
		180	710	728	688	604	378
		365	780	800	780	670	418
		730	840	865	865	715	445
	Kl B	7	496	482	460	450	330
		28	615	632	607	566	410
		180	740	750	745	660	474
		365	815	836	823	750	515
		730	860	890	904	915	534
	Kl C	7	524	568	544	505	370
		28	669	720	690	640	430
		180	804	860	840	760	520
		365	837	887	880	804	545
		730	851	910	904	825	554

hardened cement to avoid the formation of sulphoaluminate, richer in sulphate, in accordance with its particular physical structure.

We have reported in Table 4 the values of Vm in grams developed by one cubic centimeter of paste (Wo/C 0.50).

By such results it appears evident that the chemical characteristics of the clinker have a great influence on the development of the specific surface areas and consequently on the whole hydration process of the cements containing slag and that this influence is practically uniform with the three slags.

Remembering that the content of C_3S and C_2S is almost the same in the three experimented clinkers, it seems quite true that the characteristics which differentiates their actions in the hydration process of the slags are given by the C_3A content.

The different behaviours of the three slags are evident in Fig. 8, where making the value of Vm for one cubic centimeter of portland cement paste equal to 100, the corresponding values of the different mixtures of various curing periods is reported.

By these diagrams, it can be extablished a qualitative classification of different slags which appear independent from the quality of the activating clinker -in decreasing order slag 3, slag 2, slag 1-; which classification, according to the actual experiment, is not capable of having relations with the slag characteristics in spite of the premise about the necessity to find sure parameters for the classification of the slag.

$$K = Vm/Wn$$

Powers and Brownyard (12) put in evidence that the specific surface area BET of gel formed by portland cement pastes as shown in the diagram with respect to the content of non-evaporable water, gives a straight line through the origin, and concludes that this indicates the equality of hydration products in different hydration stages.

The characteristic ratio for each type of cement between specific area and non-evaporable water was indicated with K.

Verbeck and Foster (13) determined the K constant

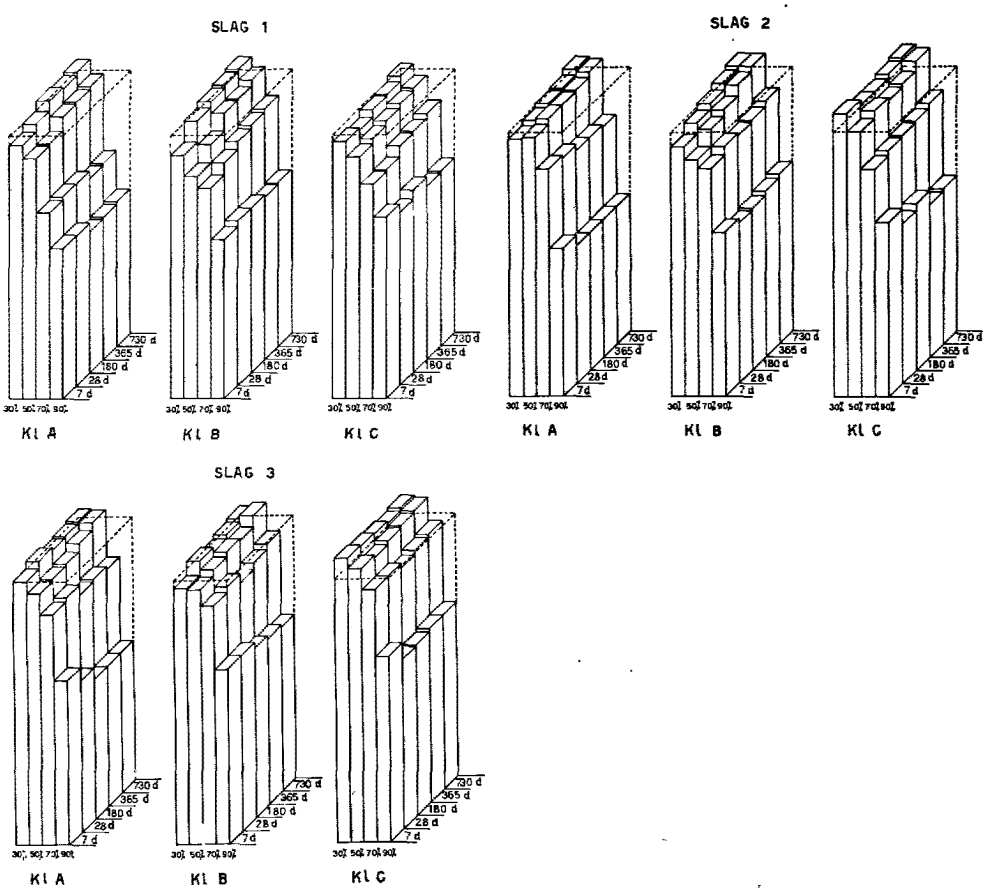

Fig. 8. *Values of Vm (g per cc of paste) expressed in per cent of value of portland cement*

for any given cement with determinations of the heats of hydration, at different curing periods, which were showed to be proportional to the quantity of non-evaporable water (Wn).

Later it was found (8), (14) that K constant applies only for type I ASTM cements.

The constancy of K implies, as already said, that to equal the quantity of non-evaporable water (Wn), one must have equal formation of hydrated compounds. However this is not strictly true with cements containing slags regarding the new-formation of $Ca(OH)_2$, as shown in Fig. 9, and where the calcium hydroxide (expressed as CaO/g ignited cement) is reported in function with Wn/C for a mixture of 70% slag.

For comparison, the correlating line found by Pressler, Brunauer, Kantro and Weise (8) for a cement type I ASTM has also been reported.

It has been observed that in the time interval between 7 to 730 days, although the points are on a straight line, the intersecting line does not pass through the origin.

Anyway the deviation is very little and while it explains why the inconstancy of K is hardly pointed out by the adsorption measurements, it allows to adapt the mean values to K to characterize the cements. The mean characteristics of K in the clinker/slag ratios is shown in Fig. 10.

On the other hand, Lehmann and Roesky (15) have also found for cement containing slag practically a constant ratio between heat of hydration and non-evaporable water quantity along the time interval between 1 to 90 days, and does nothing else but show the modest entity of variation of K.

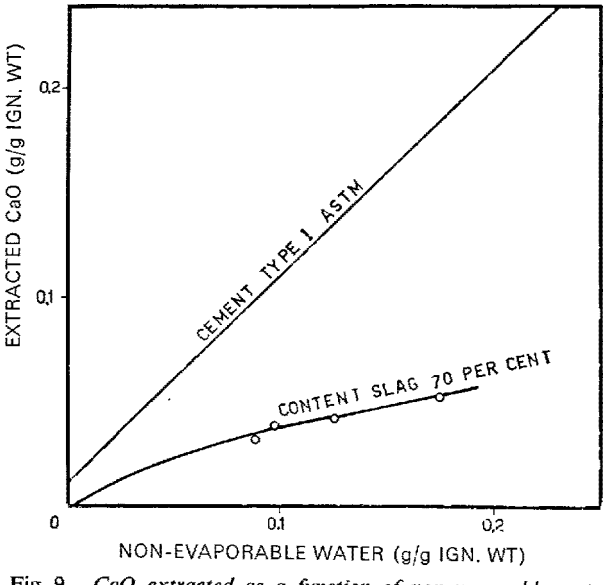

Fig. 9. *CaO extracted as a function of non-evaporable water for hydrated cement containing 70% slag and for hydrated Type I ASTM cement*

Compressive Strength

In Table 5 are shown the values of compressive strength obtained by the various mixtures, in tests done according to the RILEM-Cembureau method, limiting to the curing periods of 7–28–180 days.

Agreeing with what was said by Locher (11) and with what was said by us concerning the variable Vm,

Table 5. *Values of compressive strength (kg/cm²)(Rilem-Cembureau)*

Materials		Days	% Slag				
			0	30	50	70	90
Slag 1	Kl A	7	282	240	210	180	135
		28	413	365	316	277	230
		180	560	538	475	400	280
	Kl B	7	332	260	218	180	140
		28	472	420	355	292	255
		180	575	555	495	400	305
	Kl C	7	309	290	256	215	182
		28	433	408	382	315	258
		180	555	540	500	422	308
Slag 2	Kl A	7	282	245	220	204	150
		28	413	367	330	296	202
		180	560	514	452	392	250
	Kl B	7	332	275	242	212	158
		28	472	415	375	322	210
		180	575	545	482	398	265
	Kl C	7	309	294	258	222	189
		28	433	405	378	347	224
		180	555	532	492	444	266
Slag 3	Kl A	7	282	265	245	210	170
		28	413	386	365	318	250
		180	560	527	477	420	313
	Kl B	7	332	288	260	227	188
		28	472	435	387	333	255
		180	575	548	512	428	320
	Kl C	7	309	310	287	260	190
		28	433	426	400	352	220
		180	555	543	515	448	335

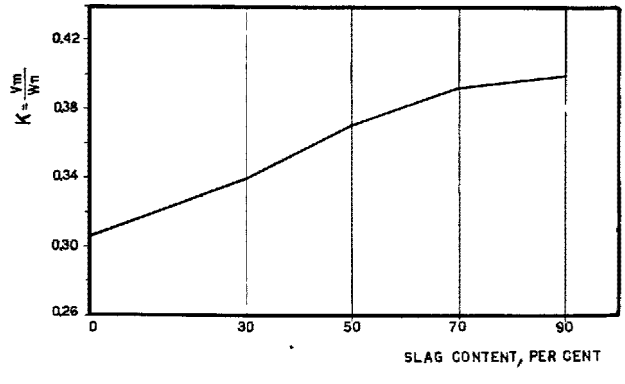

Fig. 10. *The characteristic relationship between Vm and non-evaporable water (Wn) as a function of slag content of the cement*

we confirm that the higher quantity of C_3A contained in the clinker influences positively the slag hydration.

In Fig. 11, the proceeding of Vm referred to cubic centimeter of the paste volume in relation to the compressive strength, has been reported.

Concerning the portland cements, we confirm what was said by Powers and Brownyard (12), i.e., for cements with high C_3A content, you can obtain a deviation of the points from the correlated line.

It is noted that increasing the slag content up to 50%, the slope of the line decrease and i.e., at equal values of Vm, resistances are less.

On the basis of what was found by Powers and Brownyard (12), it can be deemed that adding suitable gypsum in cements, these lines would attempt to put themselves above those of pure portlands.

For mixtures richer in slag, the ratios between strength and surface area become clearly higher, and this would admit once more that we are in front of a hydration characterized by chemical and physical phenomena of different nature.

For these mixtures, however, we have not thought of tracing a characteristic line, being, according to us, necessary to make a further thorough test for clarifying the reason of such a dispersion.

Volume of Capillary Pores

The volume of capillary pores has been calculated according to determinations of total water (16).

In Figs. 12 and 13 are reported the variation bands of the volumes of the capillary pores for the two Wo/C ratios and the curing periods of 7–28–730 days.

It is noted how the volume of capillary pores remains practically constant up to 50% slag content while starting from such value, it denotes a higher increase.

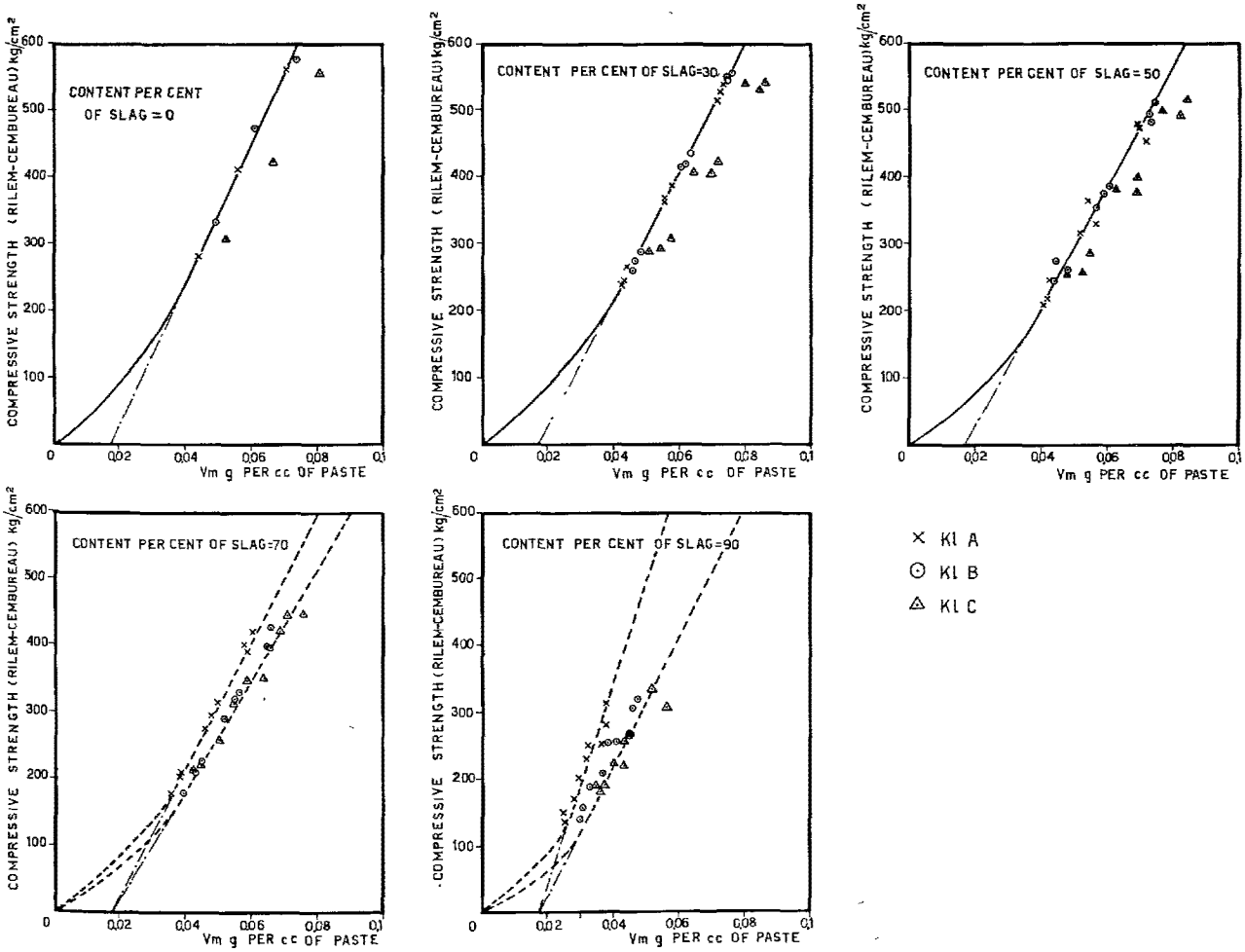

Fig. 11. *Compressive strength versus Vm (g per cc of paste)*

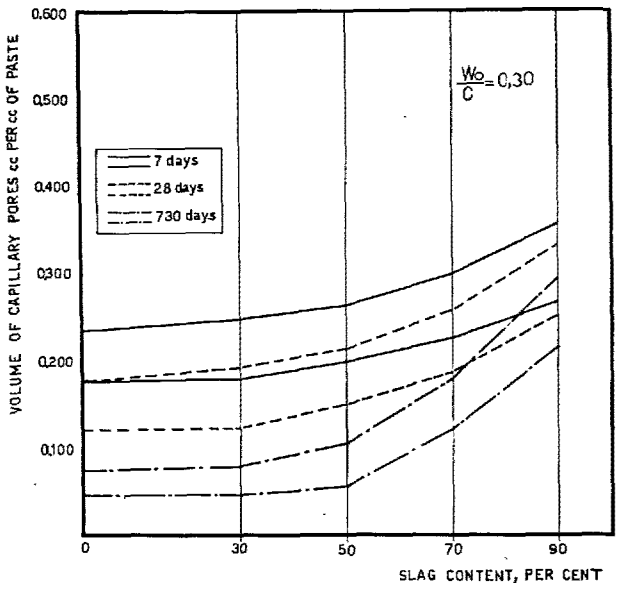

Fig. 12. *Bands of the volume of capillary pores as a function of slag content of the cement (Wo/C 0.30)*

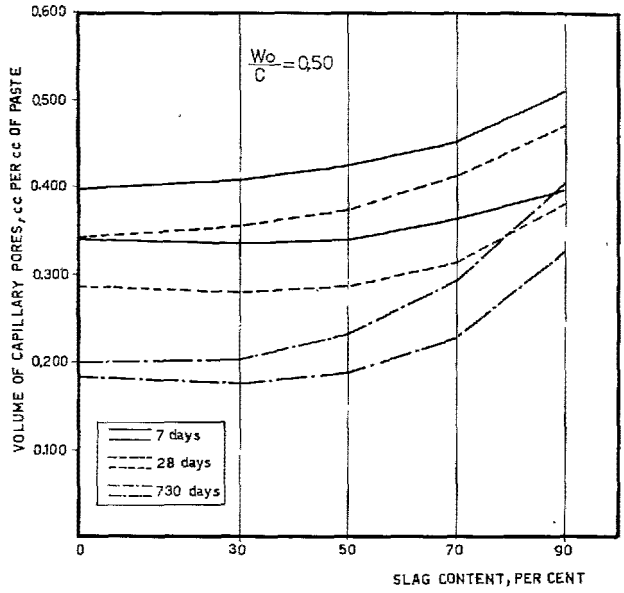

Fig. 13. *Bands of the volume of capillary pores as a function of slag content of the cement (Wo/C 0.50)*

Conclusion

From the entire experiment, it is noted that hydrated pastes of the mixtures containing slag although they give place to a quantity of gel equal or also slightly superior to those produced in clinker portland pastes are, though, all characterized by a small amount of non-evaporable water.

While for the mixtures containing up to a maximum of 50% slag content, the phenomenon can be perfectly explained by the small amount of calcium hydroxide present in relation with the small amount of C_3S in anhydrous cement and of the "pozzolanic" activity of slag. The same explanation is not valid for mixtures richer in slag content whose non-evaporable water content attributed to gel is clearly inferior.

It is also evident that the chemical characteristics of the clinker have a secure influence on the phenomena which characterize the hydration of cements containing slags; and this influence is almost uniform on the three experimented slags.

We can, no doubt, affirm that between the chemical characteristics of the clinker which contribute to differentiate the action on the hydration of slag process the content of C_3A is highly prevailing, naturally at equal contents of C_3A and C_2S.

It is more difficult to find a valid explanation on different behaviours of different types of slags with a same clinker.

Concerning compressive strength, the correlation between the hardening degree measured by the size of mechanical resistance and the hydration degree measured by the physico-structural characteristics of the pastes seem very close; and it is also a fact that the positive action is exerted on the slag hydration by the C_3A content in the activating clinker.

Concerning the properties of fresh pastes, we have realized a behaviour common to all slags namely, that the velocity and the bleeding capacity increase, with an increasing slag content.

From this is derived an effective minor porosity of pastes containing slag in comparison with cements of pure clinker which, practically, brings a lower volume of capillary porosity of pastes containing slag in respect to that noticed by us working for experimental necessities of Wo/C ratio constant.

From the series of tests made on 39 experimented cements, we can convince ourselves that the pace of the physico-chemical phenomena which characterizes the hardening of cement pastes containing granulated blast-furnace slag, are similar to the corresponding portland clinker, at least up to 50% of clinker.

The cements containing high slag percentages seem to form, instead, a type of cement differentiated enough by portland.

In fact, as many times underlined, physical and chemical parameters which characterize hydration do not present congruent values with the mixture arrange-

ments.

If hydration and therefore also the compressive strength have a slower development-that can be corrected, no doubt, industrially, increasing the fineness with the grinding- the different chemical and physical structures of the pastes of these cement exalt its characteristics of sulphate resistance, and render it a cement of election for special uses.

References

1. W. Kramer und H. G. Smolczyk, "Die Entwicklung der Huettenzemente in Deutsch land", Atti della Fondazione Politecnica per il Mezzogiorno d'Italia Vol. V, Convegno sui Cementi Siderurgici, Napoli Italia, p. 249–266 (1960)
2. R. C. Valore, J. E. Bowling and R. L. Blaine, "The direct and continuous measurement of bleeding in portland cement-water mixtures", Amer. Soc. Test. Mater. Proc. **49** 891–908 (1949)
3. ASTM Designation: C 243–58 T, "Tentative method of test for bleeding of cement pastes and mortars", ASTM Standards, Parts 4, American Society for Testing Materials, Philadelphia, p. 55–59 (1958)
4. T. C. Powers, "Physical properties of cement paste", Proc. Fourth Internat. Symposium on the Chemistry of Cement, Washington, p. 577–609 (1960)
5. S. K. Chopra "Physical properties and structure of fresh cementitious pastes", Symposium on Structure of Portland Cement Paste and Concrete" High way Research Board, Washington, p. 9–17 (1966)
6. T. C. Powers, L. E. Copeland, J. C. Hayes and H. M. Mann, "Permeability of portland cement pastes", Proc. Am. Concrete Inst. **51**, 285–298 (1954)
7. L. E. Copeland and J. C. Hayes, "The determination of non-evaporable water in hardened portland cement paste", ASTM Bull. No. 194, 70–74 (1953)
8. E. E. Pressler, S. Brunauer, D. L. Kantro and C. H. Weise, "Determination of the free calcium hydroxide contents of hydrated portland cements and calcium silicates", Anal. Chem. **33**, 877–882 (1961)
9. D. L. Kantro, C. H. Weise and S. Brunauer, "Paste hydration of beta-dicalcium silicate, tricalcium silicate, and Alite", Symposium on Structure of Portland Cement Paste and Concrete, Highway Research Board, Washington, p. 309–327 (1966)
10. D. L. Kantro, S. Brunauer and C. H. Weise, "Dvelopment of surface in the hydration of calicium silicates", Solid Surfaces and the Gas-Solid Interfa ce Advances in Chemistry Series **33**, 199–219 (1961)
11. F. W. Locher, "Zur Frage des Sulfatwiderstands von Hüttenzementen", Zement-Kalk-Gips **19**, 395–401 (1966)
12. T. C. Ppwers and T. L. Brownyard, "Studies of the physical propperties of hardened portland cement paste", J. Am. Concrete Inst. **18**, 101–132, 249–336, 469–504, 549–602, 669–712, 845–880, 933–992 (1946–1947)
13. G. J. Verbeck and C. W. Foster, "Long-time study of cement performance in concrete, chap. 6. The heats of hydration of the cement", Amer. Soc. Test. Mater. Proc. **50**, 1235–62 (1950)
14. The Science of Engineering Materials, Edited by J. E. Goldman, J. Wiley & Sons, Inc., New York, U.S.A. 1957. See Chapter by S. Brunauer entitled "Some aspects of the physics and chemistry of cement"
15. H. Lehmann und W. Roesky, "Festigkeitsentwicklung und Hydration von Portland-und Hüttenzementen bei 20°, 5° und 1°C" Tonind. Ztg. **89**, 337–350 (1965)
16. L. E. Copeland, "Specific volume of evaporable water in hardened portland cement pastes", J. Am. Concrete Inst. **27**, 863–874 (1956).

Supplementary Paper IV-102 Reactive Slag-Like Glasses of the S-A-F-C-M System

V. N. Pai and R. R. Hattiangadi*

Synopsis

The principal and strength-giving product of the portland cement hydration is tobermorite gel with a Ca/Si ratio lower than that of the main ahydrous compounds, C_3S and C_2S. As a result $Ca(OH)_2$, which does not contribute to strength, is also formed during hydration. The less basic crystalline silicates and aluminosilicates are inert, but the lower basicity compositions in the vitreous state are reactive in the presence of portland cement.

This seemed to point to a way of utilizing low-grade limestone (high in silica and magnesia contents) unsuitable for portland cement manufacture.

Since such raw materials ordinarily contain iron and since the processing contemplated is of melting the materials in an oxidising atmosphere, for the sake of fuel economy, Fe^{3+} is a constituent of these glasses.

In order to make the process economical, such compositions were chosen for tests as would melt at temperatures below 1350°C, and strength tests were carried out after intergrinding the same with portland cement clinker.

These experiments prove the feasibility of utilization of these low-grade raw materials to manufacture a cementitious product.

Introduction

Portland cement clinker is a material of high basicity, since its principal mineralogical constituents are tricalcium silicate and dicalcium silicate. As a consequence, the raw mix used in its manufacture must have a high lime saturation value.

It is necessary to start with such a highly basic composition because C_3S and C_2S are perhaps the only crystalline calcium silicates with have an irregular coordination and which have the capacity to chemically react with water and give rise to strength-producing hydrous compounds. These hydrates however have a Ca/Si ratio even lower than that of C_2S. All other crystalline calcium silicates such as merwinite C_3MS_2, akermanite C_2MS_2, monticellite CMS, rankinite C_3S_2, etc. are inert towards water, and their non-reactivity has been explained in terms of the regular coordination of atoms in their crystal structures.

The structure of the hydrous phase, tobermorite gel, obtained by the hydration of the two silicate phases in portland cement has been studied inter alia, by Taylor (1), Kalousek and Roy (2), Brunauer, Kantro and Copeland (3) and others and has been shown to have a variable Ca: Si ratio and it is now generally agreed that a ratio between 1.5 and 2.0 is desirable from the point of view of the mechanical strength of the hardened paste. Bearing in mind the basicity of the tobermorite, one would not start with such a highly basic material as C_3S as a component of the anhydrous cement, were it not for the fact that the C_3S alone reacts with sufficient speed to give commercially acceptable strength at early ages. The rest of the lime, not combined in the tobermorite, forms plates of $Ca(OH)_2$ which make no contribution to mechanical strength. While its presence is required to give a high pH environment for protecting the reinforcing steel, it is at the same time a source of weakness when sulphates are present. It would therefore appear that the use of less basic anhydrous materials could be an advantage, and since this is not possible with crystalline materials, the use of materials in the vitreous state offers a possible solution.

It is indeed well-known that a vitreous or glassy material such as granulated blast-furnace slag containing a lower proportion of lime and a higher proportion of silica than cement clinker can, in conjunction with the latter, hydrate to give similar strength-giving products. Since the product under consideration will be processed from naturally occurring low grade raw materials (such as high-silica, high-magnesia limestone together with bauxite or laterite, where

*Central Research Station, The Associated Cement Cos., Ltd., Thana, India.

necessary) containing iron oxide, it will differ from blast-furnace slag in this respect that whereas only small proportions of iron as Fe^{2+} are present in the slag, this product will contain considerably higher proportions of iron in the Fe^{3+} form. This would be so because the processing method contemplated is one of maintaining an atmosphere with a small excess of O_2, for obtaining maximum fuel effiency, unlike the reducing atmosphere of the blast furnace. An additional difference will be the absence of any sulphide sulphur. The hydraulic properties of such Fe^{3+} containing slag-like glasses are not known, and this investigation was undertaken to study their behaviour when interground with portland cement clinker.

The economic importance of this investigation stems from the fact that in India there are several occurrences of low-grade limestones interspersed among high-grade bands, which are unsuitable for portland cement manufacture, and this appeared to be a means of making cementitious materials out of them.

Experimental

Furnace

A furnace employing butane gas as fuel and castable refractory as furnace material was developed for this purpose. The furnace developed 1550°C in a matter of three hours. The clean hot blue gas flame played directly on the material as in a glass tank or open hearth furnace and served similar function.

The hearth was a shallow dish with smooth surface capable of collecting the molten material. A charge of about 3 kg could be molten at a time and poured out for quenching through a lip provided for the purpose.

A part of the burner equipment reached deep into the wall of the furnace. The burner block was cast out of castable refractory, and the butane and air mixture burnt within the cone of the burner block. The burner head entered the furnace dipping at an angle of 45° and thus facilitating the heating up of the material directly.

Preparation of the Quenched Melts

Nodules of the precalcined raw mix were molten in the furnace and quenched in water. The glass content was estimated with the optical microscope and was generally well above 90%. The quenched melt was interground with portland cement clinker along with 5% gypsum. The clinker had a potential C_3S content of about 35%.

Compressive Strength Tests

The compressive strengths were tested on 2" mortar cubes prepared according to the American Society of Testing Materials Method of Test No. C 109–64 when small quantities of glass were available. Where larger quantities were prepared, 4" concrete cubes made according to British Standard 12–1958 were tested in addition to the mortar cubes above.

Choice of Compositions

Several investigators, notably Osborn et al (4) have carried out studies on blast furnace slag and have reported on the optimum conditions for low liquidus temperature, low viscosities and high desulphurization potential, characteristics that are important in blast-furnace operation. There have also been studies from the point of view of the utilisation of the vitreous slag to produce the highest mechanical strengths when interground with portland cement clinker, and mention should be made of the work of Tanaka (5, 6), Keil (7), Locher (8), Solacolu (9). Solacolu has shown that there is a close relation between the hydraulic activity of vitreous slags and the paragenesis of thermal equilibrium in the completely crystallized state. Mention should also be made of the studies of Nurse and Midgley (10), Gutt (11, 12) on quenching experiments in the system Gehlenite-Akermanite-Merwinite, etc. and of Steyn and Watson (13) on the liquidus properties of high-magnesia blast furnace slags.

The results of Tanaka and Solacolu giving an indication of the compositions where high strengths are to be expected and the equilibrium diagrams of Nurse, Gutt and others showing the liquidus temperatures were utilised in designing mixes, with the difference that Fe_2O_3 is an additional constituent.

The choice of the compositions in the present study was in addition dictated by the requirement that the fusion point should not be in excess of 1350°C so that the actual temperature of the material is not required to be raised beyond about 1450°C which is the temperature ordinarily attained in a cement rotary kiln or in a furnace similar to a glass melting tank furnace with oil or pulverized coal firing. A temperature higher than the liquidus by about 100–150°C was considered desirable to prevent crystallization during the tapping of the melt and quenching with water. Another higher temperature requirement would be more expensive from the point of fuel requirement as well as from the point of the life of the refractories due to the severity of conditions of exposure.

With the above in view more than 30 compositions were chosen around the known low liquidus temperature compositions, and the glasses prepared for strength tests.

Results

A large number of different compositions were tried to investigate as to which among these would be optimum. A few of the results are discussed in the following.

A) Osborn and Schairer (14) have reported a lowest fusion temperature of about 1390°C in the binary system gehlenite-akermanite at 75 mole % akermanite. This composition would have a high MgO content of 11%. Nurse & Midgeley (15) also studied the ternary system C_2AS–C_2MS_2–$C_2A_{1/2}F_{1/2}S$ with iron-gehlenite as the third component. In this system, starting from the above proportion of gehlenite to akermanite, if the iron-gehlenite is increased, the fusion temperature is reduced, and the zone of these lower fusion temperatures is increased. The composition A roughly in this range was tried (Table 1).

The 2″ mortar cube compressive strengths on 75: 25 melt: portland clinker blend ground to 4100 cm²/g (Blaine) are as follows:

3 days	82 kg/cm²
7 〃	181 〃

The strengths were thus rather low.

B) In another experiment the Fe_2O_3 content was reduced, as well as the basicity ratio also was reduced by incorporating a fourth component viz. anorthite (CAS_2) in the system roughly with the composition B (Table 1).

The compressive strengths on 2″ mortar cubes were as follows:

3 days	43 kg/cm²
7 〃	49 〃
28 〃	80 〃

C) Since this gave poor strengths, the Fe_2O_3 was reduced, and CaO and MgO increased (composition C, Table 1).

This composition C gave much higher strengths on 2″ mortar cubes.

3 days	119 kg/cm²
7 〃	171 〃
28 〃	275 〃
91 〃	288 〃

D) If the SiO_2 were increased at the expense of Al_2O_3 as in D (Table 1) roughly corresponding to

C_2MS_2	2 moles
C_2AS	1 mole
$C_2A_{1/2}F_{1/2}S$	0.15 mole

This composition is not far removed from the low melting high magnesia compositions reported by Steyn & Watson (13).

The 2″ mortar cube strengths of a 60: 40 blend of melt: clinker ground to 3800 cm²/g are given in the following along with those for the portland cement alone:

	Melt D blend.	P.C.
3 days	103 kg/cm²	122 kg/cm²
7 〃	129 〃	154 〃
28 〃	219 〃	243 〃

The 4″ concrete cube strengths also are given in the following along with those for the portland cement alone.

	Melt D blend.	P.C.
3 days	147 kg/cm²	155 kg/cm²
7 〃	202 〃	209 〃
28 〃	256 〃	296 〃
3 months	295 〃	

E) Another melt near the ternary system gehlenite-akermanite-iron-gehlenite was:

C_2AS	3 moles
C_2MS_2	2 〃
$C_2A_{1/2}F_{1/2}S$	1 mole
with C_3MS_2	1.1/2 mole

Table 1. *Chemical composition of various quenched melts (%)*

	A	B	C	D	E	F
SiO_2	31.8	30.1	28.2	35.4	26.7	38.8
Al_2O_3	11.6	22.4	19.4	13.3	18.8	18.9
Fe_2O_3	} 10.2	} 6.2	} 3.0	1.4	3.8	1.4
FeO				1.1	1.6	1.9
CaO	39.9	30.6	38.4	39.5	40.4	30.1
MgO	6.0	5.0	10.3	8.6	8.0	7.5

By having merwinite, the acid to base ratio of the composition would increase from 1.5 to 1.6 .(In gehlenite 1/2 the Al^{3+} are tetrahedrally coordinated and considered as acid, while the other half are considered as base).

The actual composition is given under E (Table 1).

The 2" mortar strengths on 60: 40 blend of melt: clinker ground to 3280 cm^2/g are given below:

3 days	91 kg/cm^2
7 "	136 "
28 "	182 "

The corresponding 4" concrete cube strengths were found to be:

	Melt E blend	P.C.
3 days	90 kg/cm^2	96 kg/cm^2
7 "	138 "	138 "
28 "	252 "	238 "
3 months	300 "	353 "
6 "	306 "	377 "
1 year	354 "	430 "

F) De Wys and Foster (16) have reported a binary eutectic between anorthite and akermanite at 1234°C and further reported a ternary eutectic of the above with diopside at 1226°C at the weight proportions 47: 44: 9 of akermanite, anorthite and diopside respectively. This composition works out to

SiO_2	44.7%
Al_2O_3	16.1
CaO	30.5
MgO	8.6

Here the silica is rather high. The alumina may be increased and partly replaced by Fe_2O_3. An increase in the liquidus temperature of the system can be tolerated since the eutectic temperature is rather low. Such a change would be equivalent to having a composition:

CAS_2	1 mole
C_2MS_2	1 mole
$C_2F_{1/2}A_{1/2}S$	1/4 mole

The blend readily melted at a low temperature and was free flowing. The actual composition was found in Table 1.

It was found that the iron had partly reduced to the divalent state.

The melt was interground with portland cement clinker 75: 25 to 4200 cm^2/g with 5% gypsum. The 2" mortar strengths were

3 days	85 kg/cm^2
7 "	130 "
28 "	169 "

This melt F was rather low in lime. The D.T.A. curves of the hydrated cement did not show the presence of free $Ca(OH)_2$. It was therefore felt that this would give better results with a higher clinker content. Therefore another blend was made with melt to cement as 40: 60 ground coarser to 3270 cm^2/g.

The concrete strengths were

	Melt F blend	P.C.
3days	74 kg/cm^2	95 kg/cm^2
7 "	111 "	138 "
28 "	245 "	252 "

The strength thus appears to pick up by 28 days.

A composition around melts C or E was thus regarded as suitable. The following composition was now regarded as the base composition.

SiO_2	29.0%
Al_2O_3	19.0
Fe_2O_3	3.0
CaO	41.3
MgO	7.7

Mixes were prepared by changing the percentage of these oxides by pairs by roughly 2%. These finely powdered mix blends were heated at 1000°C for 2 hrs. rolled into sticks with water, the sticks were melted in an oxy-acetylene flame according to the method of Dyckerhoff and quenched in water. These were ground to 3100 cm^2/g and blended with ground clinker (3100 cm^2/g) and gypsum in the weight proportion 50: 50: 5 and tested for compressive strength according to ASTM 2" mortar cubes (Table 2). The liquidus temperature of these was determined on a hot stage microscope and the values are given in the same table.

The aim of this part of the work was to ascertain the effect of variations in the melt composition on the significant properties, viz. the fusion temperature and the compressive strengths. This should serve as a guide for large scale manufacture.

Products of Hydration

The products of hydration were identified by D.T.A.

Table 2.

Chemical composition %					Liquidus temp.	Compressive strength kg/cm²		
SiO_2	Al_2O_3	Fe_2O_3	CaO	MgO	°C	3 day	7 day	28 day
28.3	20.1	2.7	42.0	7.1	1360	100	138	197
26.4	21.4	2.8	42.2	7.2	1400	112	176	211
30.6	17.4	3.3	41.4	7.1	1400	98	158	253
28.6	19.0	3.1	43.5	5.9	1400	114	156	232
28.9	19.2	3.2	39.8	9.0	1380	114	166	247
28.9	21.1	3.3	39.8	7.1	1450	98	166	253
28.9	17.2	3.1	43.6	7.3	1380	100	154	237
28.4	21.7	3.0	41.0	5.6	1430	108	185	263
28.7	17.6	3.0	41.4	9.2	1390	108	155	245
31.0	19.3	3.0	41.4	5.5	1430	92	149	274
26.8	19.2	3.0	41.5	9.6	1400	124	168	220
30.2	19.5	3.0	39.5	7.5	1420	92	146	260
26.5	19.0	31.	43.4	7.6	1380	118	184	226

and X-ray diffraction. Fig. 1 shows the D.T.A. curves of the melt-cement blends, hydrated for 14 days.

Melt A-cement which contained lower Al_2O_3 and high Fe_2O_3 showed ettringite up to 7 days in addition to tobermorite. C and E which were higher in Al_2O_3 gave monosulphate instead at these ages.

Melt A-cement, which gave poor strengths shows larger exotherm due to the unreacted glass, as well as a fair amount of $Ca(OH)_2$ which has not been taken up by the melt due to its slow hydration.

The other two show only a trace of lime, if at all, indicating that the lime released by the portland clinker has been immediately fixed up by the reactive melt.

Melt cement E, and especially C show some $Mg(OH)_2$. The autoclave tests in all these cements showed an expansion less than 0.3% showing that this

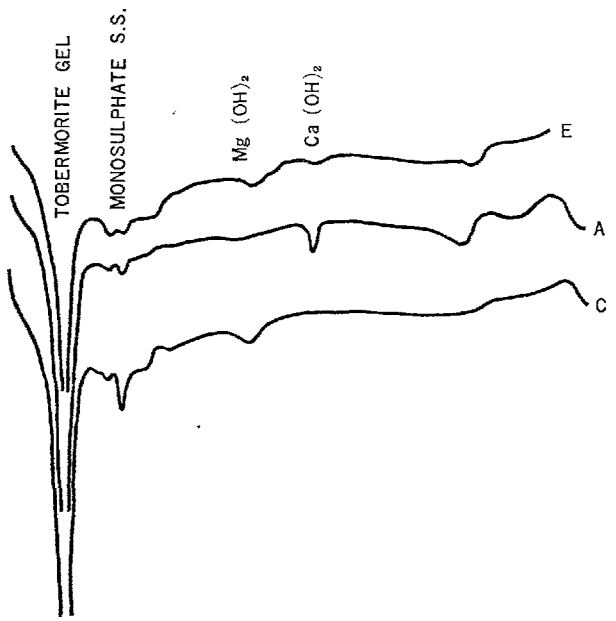

Fig. 1. *D.T.A. curves of melt cements A, C, and E hydrated for 14 days*

$Mg(OH)_2$ had not arisen out of the expansive component viz. periclase, and that these glasses did not contain any periclase as a crystalline component.

Nevertheless $Mg(OH)_2$, similar to $Ca(OH)_2$ is not likely to contribute to strength.

Therefore melts containing MgO greater than 8–10% may not be too desirable.

Discussion

In the present article, some of the results obtained on the iron oxide containing melts, in the S–A–C–M–F system have been reported.

As regards the compositions of these melts the following observations were made from a number of experiments.

1) SiO_2 content much above 30–31% would be undesirable since some compositions with silica content as high as 40% gave low strengths.

2) Al_2O_3 was added to the extent of 20% since much lower Al_2O_3 content was found to give lower early strength, confirming the observations of earlier workers.

3) Fe_2O_3 was a necessary constituent of the melts since it is present in all naturally occurring raw materials used for cement manufacture.

4) CaO as high as in portland cement was considered unnecessary for the reasons given earlier as well as since it increases the fusion temperature. In fact the CaO content was limited to a maximum of about 43% in order to have a reasonably low point of fusion of the raw materials. The optimum composition in the system S–A–C given by Tanaka (6) and by Locher (8) with 50% or more of CaO would require fusion temperatures of about 1500°C and operating temperatures of over 1600°C which are not easy to attain.

5) MgO should give rise to lower fusion temperature. Besides this, the addition of MgO can, in certain composition ranges, yield better strengths. However, the MgO should not be too high so that $Mg(OH)_2$ becomes a product of hydration; since $Mg(OH)_2$—like $Ca(OH)_2$—is not expected to contribute to strength. Again a high MgO content would cause problems of corrosion of refractories during melting. The MgO was therefore limited to a maximum of about 8–10%.

These results have demonstrated that it is possible to process low grade limestone with proportions of

silica and magnesia in excess of those tolerated in portland cement manufacture in order to produce melts which after quenching have properties similar to those of granulated blast furnace slags.

By judicious choice of the compositions it is possible to reduce the fusion point to about 1300°C so that the process can be economical.

Acknowledgements

Thanks are due to Mr. H. V. Kale, Mr. G. R. Amladi, Mr. A. D. Kilpadikar and Mr. S. Viswanathan for the experimental work.

References

1. H. F. W. Taylor, "Progress in ceramic science", Ed. J. E. Burke, p. 89–145 (Pergamon Press, Oxford, U. K., 1961).
2. G. L. Kalousek and R. Roy, "Crystal chemistry of Hydrous calcium silicates 2. characterization of interlayer water", J. Am. Ceram. Soc. **40**, 236–239 (1957).
3. S. Brunauer, D. L. Kantro and L. E. Copeland, "The stoichiometry of the hydration of ß-dicalcium silicate and tricalcium silicate at room temperature" J. Am. Chem. Soc. **80**, 761–767 (1958)
4. E. F. Osborn, R. C. De Vries, K. H. Gee and H. M. Kramer, Trans. Am. Inst. Min. & Metall. Engrs., J. Metals, 33–45 (1954)
5. T. Tanaka "On the hydraulic properties of granulated blast furnace slag." Rock Products **59** (7), 106–110 (1956).
6. T. Tanaka, T. Sakai and J. Yamane, "Composition of Japanese blast furnace slags for supersulphated cements", Zement-Kalk-Gips **11**, 50–55 (1958).
7. F. Keil and F. W. Locher. "Hydraulic properties of glasses, 1. glasses of the system $CaO–SiO_2–Al_2O_3$ without and with MgO", Zement-Kalk-Gips **11**, 245–253 (1958).
8. F. W. Locher, "Hydraulic properties of lime-rich glasses of the system $CaO–Al_2O_3–SiO_2$" (in German), Schriftenreihe der Zementindustrie (Verein Deutscher Zementwerke E. V. Düsseldorf, W. Germany, 1960).
9. S. Solacolu, "Significance of the thermal equilibria of the system $MaO–CaO–Al_2O_3–SiO_2$ with regard to melting and granulation of blast furance slags" Zement-Kalk-Gips **11**, 125–137, (1958).
10. R. W. Nurse and H. G. Midgley, "Studies on the Melilite Solid Solutions", J. Iron Steel Inst. **174**, 121–31 (1953),
11. W. Gutt, "High temperature phase equilibria in the partial system $2CaO·SiO_2–2MgO·SiO_2–Al_2O_3$ in the quaternary system $CaO–SiO_2-Al_2O_3–MgO$", J. Iron Steel Inst. **201**, 532–536 (1963).
12. W. Gutt, J. Iron Steel Inst. **202**, 770–774 (1964).
13. J. G. D. Steyn and M. D. Watson "Liquidus properties of high magnesia blast furnace slags", J. Iron Steel Inst. **203**, 445–453 (1965).
14. E. F. Osborn and J. F. Schairer, "Phase diagrams for ceramists", p. 300, compiled by E. M. Levin, C. R. Robbins and H. F. McMurdie (American Ceramic Society, Columbus, Ohio, U.S.A. 1964).
15. R. W. Nurse and H. G. Midgley, "Phase diagrams for ceramists", p. 318, compiled by E. M. Levin, C. R. Robbins and H. F. McMurdie (American Ceramic Society, Columbus, Ohio, U.S.A. 1964).
16. E. C. De Wye and W. R. Foster, "Phase diagrams for ceramists", p. 299, compiled by E. M. Levin, C. R. Tobbins and H. F. McMurdie (American Ceramic Society, Columbus, Ohio, U.S.A. 1964).

Oral Discussion

Mitsuo Hanada

(1) What are the reagents used for the experiments?
(2) The test results are extremely good. Are there any plans for industrial production, and if so, what is the economical outlook?

Author's Closure

R. R. Hattiangadi

Replying to the first of the two questions by Mr. Hanada, Dr. Hattiangadi first of all stated that he had already ascertained from Mr. Hanada, that by reagents he had meant raw materials used. He assured Mr. Hanada that the raw materials used were representative samples of naturally occurring limestone from some of the quarries obtained in his company's factories in India. The portland clinker used was also commercial clinker. It was explained that there were large quantities of substandard limestone (in terms of calcium values), available in India, which could not be harnessed into use for the manufacture of cement. In soms cases even beneficiation by froth flotation was not possible on account of the very fine crystalline structure of the oxides available. The idea was to find a way of making direct use of this substandard stone for producing a cementing material of suitable quality.

2. Answering to Mr. Hanada's second question, Dr. Hattiangadi stated that it was precisely because there was an urgent economic commercial problem to be solved that the work was undertaken. Based on studies

in reactive slag of SAC and SACM systems by Taylor, Kalousek and Roy, Brunauer, Kantro, Nurse and others, an experimental furnace was erected to carry out pilot scale experiments and it would appear from the results obtained that the economic possibilities of exploitation of this process were good.

Supplementary Paper IV-106 Studies on a Method to Determine the Amount of Granulated Blastfurnace Slag and the Rate of Hydration of Slag in Cements

Renichi Kondo and Shigenari Ohsawa*

Synopsis

A method of quantitative determination of granulated blastfurnace slag not only in unhydrated slag cement but also in hydrated paste as an unreacted part was established by using a salicylic acid, aceton-methanol solution. In this solution, slag hardly dissolves, but most of the hydrated slag, clinker minerals and their hydrates dissolve. By making use of this principle, it is possible to determine the amount of unreacted slag. But in the case of determination of the amount of unreacted slag, it is preferable to make corrections so that most part of aluminate, ferrite and gypsum contained in portland cement also hardly dissolve in this solution.

The experiment to determine the quantity of unhydrated slag on the hydration of portland blastfurnace cement paste and super sulphate slag cement paste were carried out.

The amount of unreacted slag contained in these cement pastes was determined by using the salicylic acid, aceton-methanol solution. The accuracy of this measurement was found to be satisfactory. Unreacted C_3S was quantified and the hydration products were detected by X-ray diffraction. Non-evaporable water, free $Ca(OH)_2$, and free $CaSO_4$ were also determined by chemical analyses, and the hydrated phases were observed under a microscope.

The chemical compositions of the products and the rate of reaction of each component such as slag, C_3S and $CaSO_4$, and the depths of the reacted layer on the particles of slag and C_3S were calculated from the experimental data.

The rate of reaction of slag contained in every type of slag cement was unexpectedly slow. The rate of reaction of slag and also of C_3S was reduced remarkably after about 3–7 days in hydration.

Introduction

The determination of blastfurnace slag is comparatively easy if the slag is in crystalline state, but it is very difficult with glassy slag. The granulated blastfurnace slag is generally in a glassy state and is highly reactive, as it is used for the main constituent of portland blastfurnace cement and super sulphate slag cement. It is necessary to determine the amount of slag when we want to know either the slag content in these cements or the rate of reaction of slag and also the chemical composition of hydration products. In the determination of granulated blastfurnace slag, however, it is difficult to distinguish slag from other cement minerals and their hydrates by an extraction method or the X-ray diffraction method.

Several attempts, listed below, have been proposed to determine the slag content in the protland blastfurnace cement since the beginning of this century.

(1) Dissolution method using acetic acid as the extracting agent (1, 2).
(2) Dissolution method using ammonium chloride-ammonia (3, 4).
(3) Observation under an optical microscope (5).
(4) Separation by using heavy solutions (5).
(5) Determination of Mn content by chemical analysis with sample separated by heavy solution (5).

The experimental error in each of these methods is great and it is impossible to determine the slag content especially in the presence of hydrates. If we would follow the methods (1), (2) and (5) listed above, it is necessary to examine every components of the test cement in isolated forms before blending as reference samples.

Here we found that the determination of granulated blastfurnace slag is possible by an extraction method using salicylic acid, aceton-methanol solution. In this

*Research Laboratory of Engineering Materials, Tokyo Institute of Technology, Tokyo, Japan.

method slag hardly dissolves but most of the hydrated slag, clinker minerals and their hydrates do dissolve. By making use of this phenomenon, with certain corrections if necessary, it is possible to determine the quantity of unreacted slag in cement either unhydrated or hydrated.

This study was made to elucidate the rate of hydration of slag and the chemical composition of the hydration products by a quantitative determination of slag, which has not yet been investigated.

Experiments to Determine the Required Conditions for an Extraction Method

Experiments were carried out as described below to determine the required conditions in which unhydrated slag is practically undissolved, while most of the hydrated slag, clinker minerals and their hydrates are dissolved.

A method established by Takashima and his collaborator (6) utilizes the conditions in which the selective dissolution of such silicates as C_2S and C_3S occurs. These conditions are as follows:

The entirety of a 1 g sample, 6 g of salicylic acid and 40 cc of methanol are put into a beaker and stirred by a magnetic stirrer for 3 hours at room temperature. The filtered residue is then washed with methanol, dried and heated at 850°C for 10 minutes in an electric furnace. Heating conditions were selected by us to avoid a weight increase due to the oxidation of S, Mn and such in the slag.

It was found that 82.7% of slag is insoluble by this method, and that it could not be greatly improved by decreasing the amount of salicylic acid or reduction of treating time.

Another method also established by Takashima (7), is improved by the addition of aceton.

In this method, 0.5 g sample is put into a beaker together with 2.5 g of salicylic acid, 35 cc of aceton and 15 cc of methanol and stirred at room temperature for 1 hour. After being kept motionless for 1 day, it is filtered, and then treated as previously described.

With this method, 99.3% of slag was insoluble. On the basis of the experimental results, the latter method is adopted for the determination of unreacted slag. The tests were made on various samples by this method with results as shown in Table 1.

Table 1. *The amount of inroluble part on various samples treated in a salicylic acid, aceton-methanol solution*

$$\text{Insoluble } \% = \frac{\text{Insoluble part}}{\text{Sample} - \text{Loss on ignition}} \times 100 \text{ (wt.)}$$

Sample	Loss on ignition %	Insoluble %	Remarks
Granulated blastfurnace slag	0.45	99.3	Blaine 4000 cm^2/g
Portland cement	0.53	21.6	" 3100 cm^2/g
C_3S	0.23	4.1	1.3—5.8 μ in radius
C_3S hydrate	21.4	3.4	Hydrated for 6 months, D-dried
βC_2S (Cr-stabilized)	0.13	17.8	In fineness similar to portland cement
C_3A	—	98.6	Blaine 4300 cm^2/g
C_3A hydrate	24.5	99.4	Hydrated for 7 days, P-dried C_3AH_6
C_4AF	—	92.3	Blaine 4230 cm^2/g
C_4AF hydrate	22.6	72.4	Hydrated for 28 days, P-dried
Ettringite	45.0	61.5	Dried by 70% H_2SO_4
Tobermorite	18.7	97.4	Autoclaved at 181°C for 24 hrs.
CaO	—	0.9	$CaCO_3$ was decomposed at 1000°C
$Ca(OH)_2$	24.3	5.9	
$CaCO_3$	44.0	100.0	
$CaSO_4$	0.53	98.8	$CaSO_4 \cdot 2H_2O$ was dead burnt at 750°C
$CaSO_4 \cdot 2H_2O$	20.9	96.3	
MgO (fused)	0.22	91.6	< 10 μ in radius
Fe_2O_3	5.71	99.3	
Al_2O_3	0.52	99.7	

Preparation of Hydrated Samples

Hydration of Low Slag and High Slag Portland Blastfurnace Cements

The compositions of portland cement and granulated blastfurnace slag used are shown in Table 2.

Low slag and high slag portland blastfurnace cements, abbreviated as LC and HC in this paper, were prepared from granulated blastfurnace slag (Blaine

4000 cm^2/g) and portland cement abbreviated as PC (Blaine 3100 cm^2/g). They were blended in the weight ratios of 40: 60 and 70: 30 respectively and hydrated at 20°C in paste form with W/C = 0.4, for 3, 7, 28 and 90 days in glass bottles. The original slag and portland cement were also separately hydrated under the same conditions. The hydration was stopped in such a way that the hydrated samples were ground in an aceton-ether solution in a 1: 1 volumetric ratio for 5 minutes. After the samples were evacuated to eliminate the remaining aceton and ether, they were dried in a condition called P-drying.

Hydration of C_3S-Slag Cement

C_3S-Slag cement was prepared from C_3S and granulated blastfurnace slag in which the particle radii were 1.3–5.8 μ (Blaine 2480 cm^2/g) and 1.35–6 μ (Blaine 4730 cm^2/g) respectively. This powder was obtained with a "Bahco" micro particle classifier. The slag is the same as used in LC and HC. The blended ratio was 50: 50 in weight. The conditions of hydration of this cement were the same as those of LC and HC except the ratio of W/C = 0.5.

Hydration of Super Sulphate Slag Cement

Super sulphate slag cement, abbreviated as SC in this paper, was composed of granulated blastfurnace slag, $CaSO_4$ and C_3S in the weight ratio of 80: 15: 5. The sizes of these components were 1.35–6 μ, 1.35–6 μ and 1.3–5.8 μ in radii, respectively. $CaSO_4$ was obtained by heating gypsum at 750°C. The preparation of hydrated samples was the same as that of C_3S-slag cement.

Table 2. *Compositions of portland cement and granulated blastfurnace slag*

Components	Portland cement	Granulated blastfurnace slag
Loss on ig.	0.5	0.45
Insol.	0.6	—
SiO_2	22.3	32.5
Al_2O_3	4.4	18.5
Fe_2O_3	3.1	0.6
CaO	64.5	41.2
MgO	1.5	4.4
MnO	—	1.1
SO_3	1.8	—
S	—	0.9
TiO_2	0.2	
Na_2O	0.37	
K_2O	0.61	
Free CaO	0.4	
C_3S	53.9	
C_2S	23.4	
C_3A	5.8	
C_4AF	9.5	
$CaSO_4 \cdot 2H_2O$	3.1	
Blaine cm^2/g	3100	4000

Experimental Results

Results of the Extraction Treatment

The conditions of the treatment were followed by the method described above. The results obtained from this treatment are shown in Fig. 1. The data were corrected by the method described in the discussion.

Fig. 2 shows the percentage of reaction of slag in the hardened paste of various types of slag cements.

Determination of Unreacted C_3S by X-ray Diffraction

HC and SC were not examined for the content of C_3S.

MgO as an internal standard was added to the extent of 5% of the samples on an ignited base. The peaks selected for the determinations are 2.10 Å ($2\theta = 43.1°$) for MgO, 1.77 Å ($2\theta = 51.8°$) for alite in LC and 2.19 Å ($2\theta = 41.2°$) for C_3S in C_3S-slag cement. The conditions in the X-ray diffraction were the usual. The area of these peaks was measured with

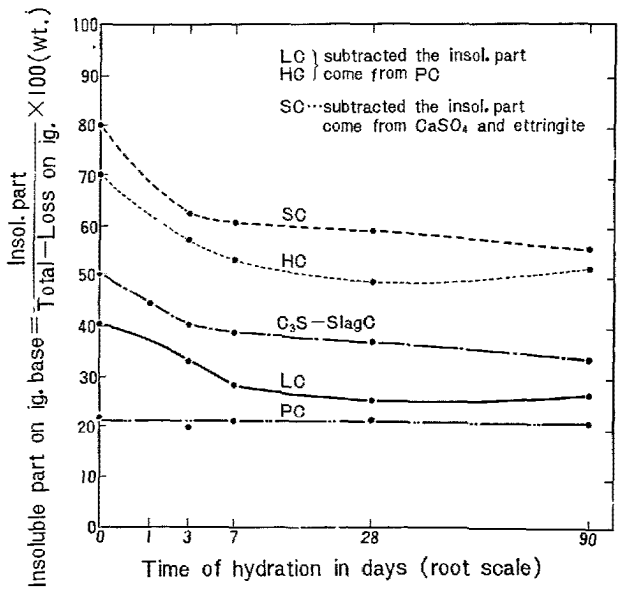

Fig. 1. *Unreacted slag in slag cements or other phases than silicates in portland cement vs. time of hydration.*

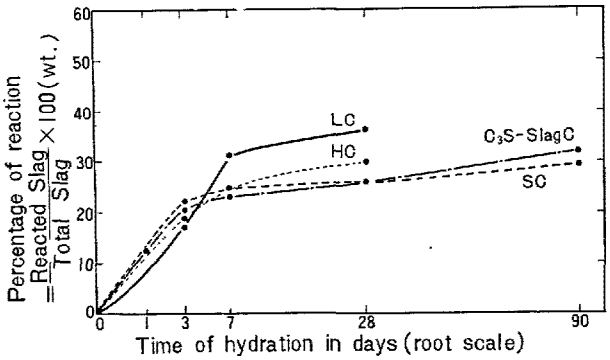

Fig. 2. *Percentage of reaction of slag in slag cements vs. time of hydration.*

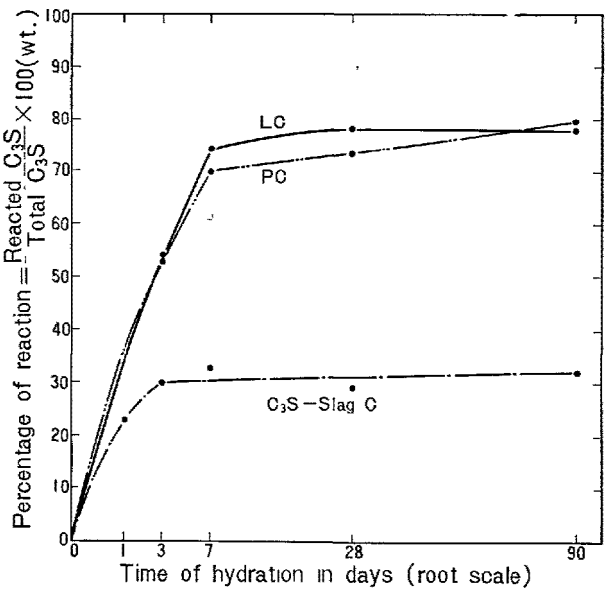

Fig. 3. *Percentage of reaction of C_3S in slag cements or portland cement vs. time of hydration.*

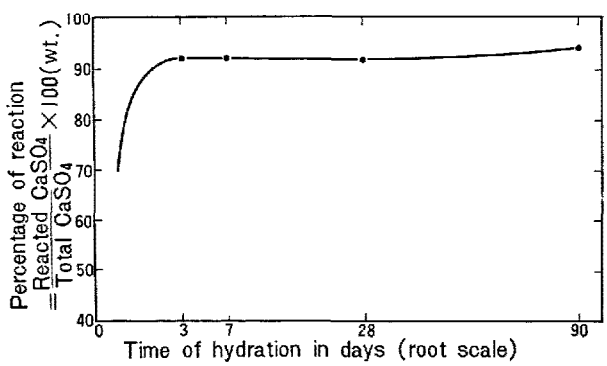

Fig. 4. *Percentage of reaction of C_aSO_4 in super sulphate slag cement vs. time of hydration.*

a planimeter. Fig. 3 shows the percentage of reaction

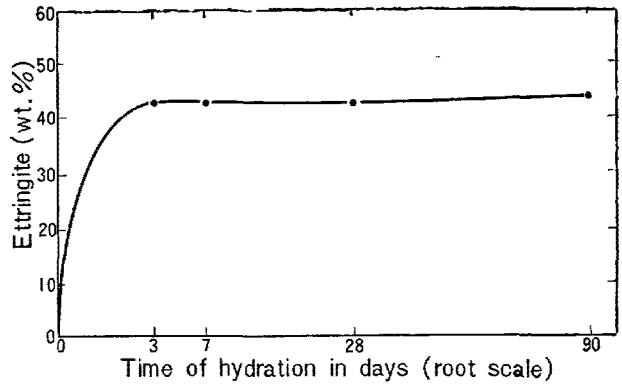

Fig. 5. *Amount of ettringite formed in the paste of super sulphate slag cement vs. time of hydration.*

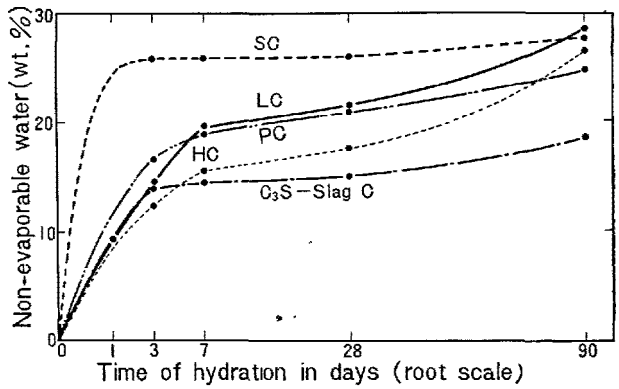

Fig. 6. *Non-evaporable water content in the paste of various cements vs. time of hydration.*

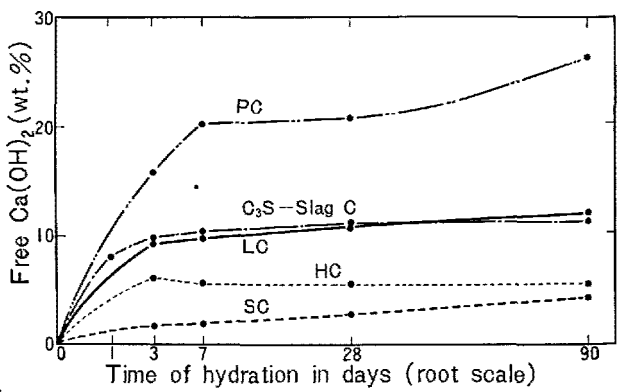

Fig. 7. *Free $C_a(OH)_2$ content formed in the paste of various cements vs. time of hydration.*

in the hardened paste of various types of cements.

Determination of Free $CaSO_4$

Free $CaSO_4$ in the hardened paste of SC was deter-

mined by the method suggested by Forsén (8).

In this experiment 1 g of a powdered sample and 300 cc of half saturated lime water were stirred in a beaker with a magnetic stirrer for 1 hour, at room temperature, and then filtered. The residue was washed with lime water, and then with aceton. As unreacted free $CaSO_4$ dissolves, it was determined by gravimetric analysis with the filtrate, while the residue was P-dried and used for the determination of the unreacted slag. Fig. 4 shows the percentage of reaction of $CaSO_4$ in the hardened paste of SC.

The quantity of formed ettringite was calculated from the data on free $CaSO_4$, and shown in Fig. 5. In this calculation it was assumed that all of the reacted $CaSO_4$ forms ettringite.

Determination of Non-Evaporable Water

Non-evaporable water (9) is that retained in the P-dried sample, and abbreviated as Wn. Wn was determined by ignition of the dried sample at 700°C for 1 hour. The obtained results are shown in Fig. 6.

Determination of Free $Ca(OH)_2$

Free $Ca(OH)_2$ was determined according to the modified Franke method by using ethyl acetoacetate and isopropyl alcohol as the solvent. Fig. 7 shows the results obtained.

Identification of Hydration Products by X-ray Diffraction

In the X-ray diffraction, scanning was operated from 14.7 Å ($2\theta = 6°$) to 1.70 Å ($2\theta = 54°$). Detected phases were described in the discussion.

Microscopic Examination

Observations were made under a polarizing microscope on the polished thin sections of hydrated pastes of slag cements.

In comparison of the number and grain size of $Ca(OH)_2$ in the pastes of PC, LC and HC, both of them were in the same order mentioned above. As for the C_3S–slag cement paste, the diameter of $Ca(OH)_2$ crystals reached about 100 μ even by 24 hrs.

Inner hydration products of C_3S with a lower refractive index were difficult to be observed in the cases of HC and C_3S-slag cement, however, clearly observed in the case of portland cement. While remarkable changes on the surface of slag particles were not observed except the formation of cracks on the large particles

Discussion

The Accuracy of the Extraction Method

The accuracy of the quantitative determination of slag by the extraction method was quite excellent in reproducibility as shown in Table 3, and the coefficient of variations lies within 0.1 to 2%, though this value seems to depend upon the type of slag cement.

It has become clear as the result of this experiment that the determination of slag by this method is, after all, sufficiently effective for estimating the rate of hydration of slag. Moreover, this method can be used for determining the amount of slag contained in unhydrated blastfurnace cement, and further, a similar method may also be adoptable for the pozzolanic reaction.

Corrections in the Determination of Unreacted Slag

The data were corrected in order to quantify a certain reactant such as slag, because a little part of slag is dissolved and a part of the insoluble matter originates from the other phases.

The corrections were made in such a way that 0.7% of unreacted slag is dissolved, and 4.1% of C_3S and 3.4% of C_3S hydrate are insoluble in the extracting solvent. The corrections on C_3S were not made on HC and SC.

In the case of LC and HC, C_3A and C_4AF are almost insoluble so that these amounts should be subtracted from the insoluble matter. Nevertheless, consistent results in the amount of unreacted C_3A and C_4AF could not be obtained by X-ray quantitative analysis. The insoluble part coming from portland cement can be regarded as a constant to be 0.211 at any time of hydration as seen in Fig. 1. Thus the adopted correction is based on this fact instead of the determination of C_3A and C_4AF. Unreacted slag in the hydrated portland blastfurnace cement can now be determined in application of the following relation.

Table 3. *The standard deviations on the mean values obtained by the extraction method*

A. The values are % of insoluble part in the paste of LC

Time in day / Repetition	3	7	28	90
1	44.6	39.9	37.2	40.0
2	46.5	41.1	39.0	38.3
3	44.8	39.3	37.8	
Mean value	45.3	40.1	38.0	39.2
σ	±0.86	±0.75	±0.75	±0.85

B. The values are % of insoluble part in the paste of HC

Time in day / Repetition	3	7	28	90
1	62.9	58.3	55.3	57.8
2	64.3	59.2	56.4	57.3
3	62.8	58.7	54.0	—
Mean value	63.3	58.7	55.0	57.6
σ	±0.69	±0.37	±1.01	±0.25

C. The values are % of insoluble part in the paste of C_3S-slag C

Time in day / Repetition	1	3	7	28
1	45.3	40.7	39.7	38.3
2	45.1	41.1	39.6	38.0
Mean value	45.2	40.9	39.7	38.2
σ	±0.10	±0.20	±0.05	±0.15

Unreacted slag = Insol. part
− Portland cement × 0.211

In the case of SC paste, correction is made on the amount of ettringite which is the main hydration product of this cement and insoluble in the extraction treatment. Therefore, the quantity of ettringite was calculated from the chemical analysis of free $CaSO_4$, and the results are shown in Fig. 5. The amount of unreacted slag in SC paste can be estimated as follows.

Unreacted slag = Insol. part
− Formed ettringite × 0.615

Non-Evaporable Water (Wn)

Concerning non-evaporable water (Wn), Cesareni and others (10) reported that the Wn content of HC is lower than that of PC. On the other hand the content of Wn is formed to be well proportioned to the percentage of reaction of slag, as seen in comparison of Figs. 2 and 6. The Wn content of SC is very large in the early stage, but hardly increases thereafter.

The increase of Wn is remarkable both in LC and HC, but especially so in HC, during the period from 28 days to 90 days.

In case of C_3S-slag C, the increase of Wn in the period between 28 days and 90 days, is seemingly caused by the reaction products of slag, because in this period the hydration of C_3S hardly progresses, and as seen in Fig. 2 the reaction of slag has progressed.

Free $Ca(OH)_2$

The content of formed $Ca(OH)_2$ increases with the time of hydration in case of LC, but in case of HC it gradually decreases as shown in Fig. 7. This result, coinciding with the research of Smolczyk (11), reveals the fact that the $Ca(OH)_2$ produced by hydrolysis of of C_3S is consumed by the pozzolanic reaction of slag.

The $Ca(OH)_2$ content of C_3S-slag C hardly increases on and after 3 days. This is natural because as seen in Fig. 3, the reaction of C_3S has not yet progressed. In case of SC the amount of $Ca(OH)_2$ produced is larger than the theoretical content, though SC contains only 5% of C_3S. A similar tendency has been shown also in Locher's experiment (12).

This fact may have some relation to the fact that the solvent and ettringite react slightly with each other in the modified Franke method, as is referred to by Schwiete and others (13). The present authors, however, could not find the above phenomenon on purely synthesized ettringite. This difference perhaps comes from the fact that the synthesized ettringite grows to a larger crystal than that formed in cement paste.

Effect of Gypsum

In the case of SC containing gypsum anhydrate as the main activator, the hydration of slag is at a high rate in the early stage, but tends to slow down more in the later stage than in other cements. Cesareni and others (10) expected that gypsum, when added to high slag blastfurnace cement, would accelerate the reaction, but the result was contrary to their expectation. And the cause of this was thought to lie in chemical factors so that the amount of lime in the liquid phase is not sufficient in case of HC to complete the hydration of slag.

Formation of Ettringite

From slag comes the Al_2O_3 that composes ettringite rapidly formed in the hydration of SC at early stage. Moreover, judging from the relation between the amount of the reacted slag and the amount of the ettringite thus formed, it is clear that almost all the Al_2O_3 in the reacted slag forms ettringite. Further,

during the first 3 days SC has the highest rate of slag reaction, but on and after 7 days, LC has the highest reaction rate.

If the composition of slag can be simplified as C_4AS_3, SC must produces low lime silicate hydrate such as CS_3Hn besides ettringite in hydration. After consumption of $CaSO_4$, the reaction becomes inert, and thus not a little slag remains unreacted.

The presence of a little alkaline exciter is necessary for Al_2O_3 to dissolve out of slag, but the presence of too much lime renders the product layer on each slag particle denser and so rather hinders the reaction. Nevertheless ettringite is to be dehydrated into an amorphous state when P-dried, the X-ray diffraction peak of ettringite was sharp in our experiment. Thus, the ettringite formed in SC seems to be rather difficult to dehydrate.

Hydration Products Detected by X-ray Diffraction

In the hardened paste of LC, detected hydration products are in addition to C–S–H and $Ca(OH)_2$, C_4AH_{13} and a trace of ettringite after 28 days and C_4AH_{13} and monosulphate hydrate after 90 days.

In the case of HC, monosulphate hydrate is detected as early as after 3 days and both C_4AH_{13} and ettringite are detected on the 90th day.

In the case of C_3S-slag cement, C–S–H, $Ca(OH)_2$ and C_4AH_{13} are detected as early as after 1 day, and unreacted C_3S is clearly detected even after 90 days.

In the case of SC, ettringite and C–S–H are detected on the 3rd day. The shape and height of ettringite peaks are nearly the same regardless of the time of hydration.

Size of Formed $Ca(OH)_2$

There is not much difference between C_3S-slag C and LC in the content of slag, but concerning the other components and particle size distribution. The fact that LC has a higher rate of hydration than C_3S-slag C can be partly explained by the difference in size of $Ca(OH)_2$ formed. Microscopic observation shows that $Ca(OH)_2$ scattered in C_3S-slag C paste is as large as 100 μ in diameter and generally uniform in size, and that on the other hand it is smaller and uneven in size in the case of LC. Thus, a part of particles of slag or of C_3S are surrounded by $Ca(OH)_2$ crystals.

Thickness of the Reacted Layer

Since the rate of reaction of such solid powder as cement largely depends upon the particle size, it is appropriate to compare the reactivities of such reactants as C_3S or slag on the basis of the thickness of the reacted layer. The relationship between the percentage of reaction and the thickness of the reacted layer was determined in accordance with the method already mentioned by Kondo (14). Fig. 8 shows the thickness of the reacted layer of C_3S or slag particles in the hardened paste of various types of cements. The percentage of reaction was obtained by the extraction method for slag, by the X-ray diffraction method for C_3S and by a chemical analysis for $CaSO_4$.

As shown in Fig. 2, slag is hydrated at a high rate during the first 3 to 7 days, but thereafter the reaction is extremely delayed. The thickness of the reacted layer of slag should be a little lowered from the values indicated in Fig. 8, as the original surface area of slag is nearly twice higher than that of C_3S. Simultaneously with this delay, the hydration of C_3S also tends to be delayed as shown in Fig. 3. In the hydration of C_3S alone, the rate of hydration and the thickness of the reacted layer are examined and separately reported by Kondo and Yoshida in this Symposium (15).

According to Cesareni and Frigione (10) one might suggest, concerning the hydration of blastfurnace cement of high slag content, that a sheath of some very compact hydration products wraps around the slag particles and prevents water from penetrating into the particle cores, therefore delaying the reaction.

But this delay in hydration seems to occur not only to HC, but also to various kinds of slag cements investigated. The delay of hydration starts suddenly when this compact sheath has grown to a certain thickness after 3 to 7 days reaction. The thickness of the reacted layer at the beginning time of the reaction

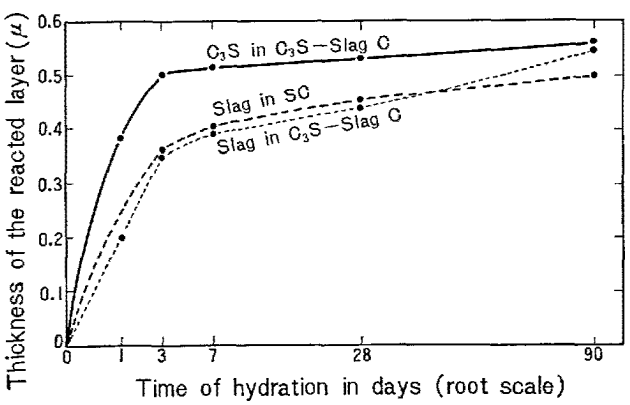

Fig. 8. *Thickness of the reacted layer of slag or C_3S in slag cements vs. time of hydration.*

delay was 0.35 μ and 0.50 μ in cases of the slag and C_3S each contained in C_3S-slag C, and 0.36 μ in case of the slag contained in SC. It seems that also on the surface of C_3S, compact sheath is similarly formed.

Compared with the case of LC, the reaction of C_3S in C_3S-slag C is very slow even before starting of the delay. The reason for this seems to be due to the formation of ettringite in hydration of LC, and because of its comparatively porous quality, the reaction progresses at much the same rate as that of PC until the beginning of the delay.

C_3S in LC as the activator has a higher reaction rate during the first 28 days than in PC. But after 90 days, C_3S in PC has a higher reaction rate. The insoluble part shown in Fig. 1 appears to increase during the period from 28 days to 90 days. This phenomenon seems to be caused by the fact that the hydrates change into less soluble materials, for non-evaporable water and $Ca(OH)_2$ are increased and the reaction having progressed in this period.

Rate of Hydration

As the particles of C_3S and of the slag are coated with the hydration products, the hydration seems to be controlled by the diffusion of the ingredients through the layer of the products. The relationship between the thickness of reacted layer of reactant particles and the reaction rate constant was examined in conformity with the following formula in which $1 - \sqrt[3]{1-\alpha}$ implies the ratio of the thickness of the reacted layer to the radius.

$$(1 - \sqrt[3]{1-\alpha})^N = kt$$

The rate of hydration of slag in C_3S-slag C is expressed as $N = 1.5$ during the first 1 to 3 days, but $N = 7$ in the decay period from 3 to 90 days. As for C_3S, $N = 4$ during the first 1 to 3 days, but indeed $N = 32$ during the period from 3 to 90 days. Concerning the slag in SC, $N = 9$ during the period from 3 to 90 days.

When the reacted layer becomes denser or the pore size smaller, the value N is thought to rise to more than 2 with increasing the resistance to the diffusion (14). Thus it is characteristic that the hydration products formed around the slag particles and the coexistent C_3S particles become denser and denser with lapse of time, and also that the rate of hydration slows down correspondently.

References

1. F. Hart, "Influence of acetic acid on portland cement and blastfurnace slag" (in German), Tonindustrie-Zeitung **28,** 809 (1904).
2. P. N. Grigor'ev and S. E. Chaikina, "Determination of the content of basic slag in portland cement" (in German), Tonindustrie-Zeitung **56,** 1206–1207 (1932).
3. R. Hayden, "Partial decomposition of cement, slag, and related materials by means of ammonium salts" (in German), Zement-Kalk-Gips **4,** 329–332 (1951).
4. E. Vogel, "Rapid method for the approximate operational determination of the slag content in iron-portland and blastfurnace cements" (in German), Silikattechnik **3,** 559–560 (1952).
5. P. Catharin, "On the quantitative determination of slag in powdered product made of portland cement and blastfurnace slag" (in German), Zement und Beton **8,** (2), 14–19 (1957).
6. S. Takashima and M. Kato, "Preparation of standard alite" (in Japanese), Semento Gijutsu Nenpo **15,** 19–23 (1961).
7. S. Takashima, "Selective dissolution of alite by organic acid solution" (in Japanese), Semento Gijutsu Nenpo **12,** 49–55 (1958).
8. L. Forsén, "The chemistry of retarders and accelerators", Proc. of the 2nd Intern. Symp. on the Chem. of Cement, Stockholm, 298–381 (1938).
9. L. E. Copeland and J. C. Hayes, "Determination of non-evap. water in hardened portland cement paste", ASTM Bull. **194,** (12), 70–74 (1953).
10. C. Cesareni and G. Frigione, "Some researches on the physical properties of hardened pastes of portland cements containing granulated blastfurnace slag", Symp. on Structure of Portland Cement Paste and Concrete, 48–57, Highway Research Board (1966).
11. H. G. Smolczyk, "Discussion of paper by G. Malquori", Proc. of the 4th Intern. Symp, on the Chem. of Cement, Washington, 1960 1004–1005 N. B. S. Monog. 43 (1962).
12. F. W. Locher, "Hydraulic properties and hydration of glasses of the system CaO–Al_2O_3–SiO_2", Proc. of the 4th Intern. Symp. on the Chem. of Cement, Washginton, 1960 267–277 N. B. S. Monog. 43 (1962).
13. H. E. Schwiete, U. Ludwig and P. Jäger, "Investigations in the system $3CaO \cdot Al_2O_3$–$CaSO_4$–CaO–H_2O", Symp. on Structure of Portland Cement Paste and Concrete, 353–367, Highway Research Board, (1966).
14. R. Kondo, "Kinetic study on hydrothermal reaction between lime and silica", Symposium on Autoclaved Calicium Silicate Building Products, Society of Chemical Industry, 92–100 (1967)
15. R. Kondo and K. Yoshida, "Miscibilities of special elements in tricalcium silicate and alite and the hydration properties of resulted solid solutions", 5th Intern. Symp. on the Chem. of Cement, Tokyo, 1968.

Supplementary Paper IV-110 Mineral Composition of Blast-Furnace Slag

Hideo Minato*

Synopsis

There is two types in blast-furnace slag. One is water quenched one and the other is slow cooling one, and range of chemical composition in the slag is as follows; SiO_2 30–35, Al_2O_3 13–20, MgO 2–6, CaO 40–50%. Slow cooling blast-furnace slag was constituted with melilite, dicalciumsilicate, pseudowollastonite, anorthite and glass, and had porphyritic texture with phenocrysts of melilite, dicalciumsilicate and pseudowollastonite. Water quenched slag was composed of fine glass bubbles and accompanied with small quantity of minute melilite. In the course of cooling of the molten slag, iron, manganese, alkalies and sulphur were concentrated in the residual liquid, and the melilite crystallized out from these liquid had iron, manganese and alkalies in its components.

Melilite phenocrysts display a characteristic zonal structure under the polarizing microscope. The optical property of the melilite implies that its nucleus is highest in the content of gehlenite molecule, while the rim is lowest. Small idiomorphic crystals of melilite are found in cavites of the slag, in some case. It shows short prismatic shape consisting of a tetragonal prism and the base.

Crystallization on melilite in the course of cooling of molten slag was investigated, also. The chilled margin of slow cooling slag was polished in smooth plane and etched by dilute hydrochloric acid. Globules with diameter of 5–10μ, which were composed of fine short prismatic melilites were observed on the plane under the electron microscope. These globules were the nucleus of dendritic aggregates of melilite needles and the dendrite turned to melilite phenocryst.

Kind of Blast-Furnace Slag

Blast-furnace slag is a by-product of smelting of iron and is classified into two types. One is water quenched slag, the other is slow cooling one. The former is used for raw material of cement and etc., and the latter is used for slag ballast and etc. Mineralogical investigations on these two kinds of slags have been carried out and reported in this paper by this writer.

Water Quenched Slag

Water quenched slag is formed by quenching of molten slag with large amounts of water and used for cement. It has pumice-like appearance and with yellowish gray colour. It was tested its crystalline phase by means of X-ray powder method, observed its texture under the polarizing microscope and analysed by chemical method.

Texture

Thin section of the slag was investigated under the polarizing microscope, many fine glassy bubbles with diameter of 0.05–0.1 mm were observed and in a part of the glassy film, minute crystalline material was observed under crossed nicols. The crystalline material might be fine melilite crystals.

Crystalline Phase

Six powdered slag specimens were tested by means of X-ray powder method and their X-ray powder profiles were shown in Fig. 1. All specimens take glassy phase and two specimens of them are associated with small amounts of melilite crystals. In Fig. 1, X-ray powder pattern of 2.8 Å is derived from melilite. The results of X-ray investigation agree well with that of the observation under the polarizing micro-

*Institute of Earth Science, College of General Education, The University of Tokyo, Tokyo, Japan.

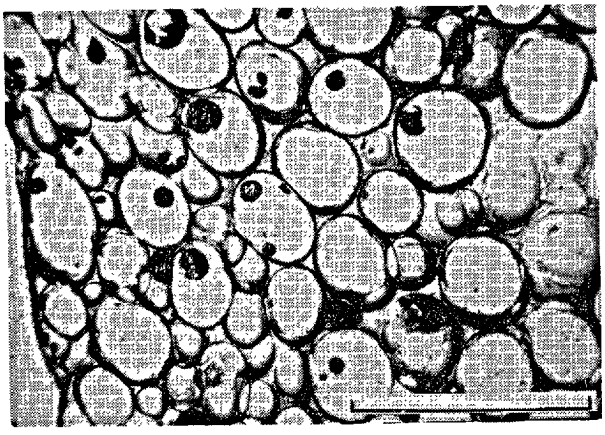

Photo 1. *Water quenched slag. Scale: 1mm*

Table 1. *Chemical composition of water quenched slag.*

No.	1	2	3	4	5	6
	Wt.%	Wt.%	Wt.%	Wt.%	Wt.%	Wt.%
SiO_2	32.9	32.5	32.7	33.7	33.8	34.4
Al_2O_3	17.9	19.5	18.5	16.6	17.4	16.6
Fe_2O_3	0.8	0.9	1.0	1.1	0.9	0.8
MnO		1.1	1.4		0.9	1.0
CaO	42.0	40.6	41.1	41.8	41.9	41.5
MgO	3.7	4.0	3.8	3.1	3.2	3.6
Total	97.3	98.6	98.5	96.3	98.1	97.9

Note: 1-6 correspond to the number of X-ray powder profiles.

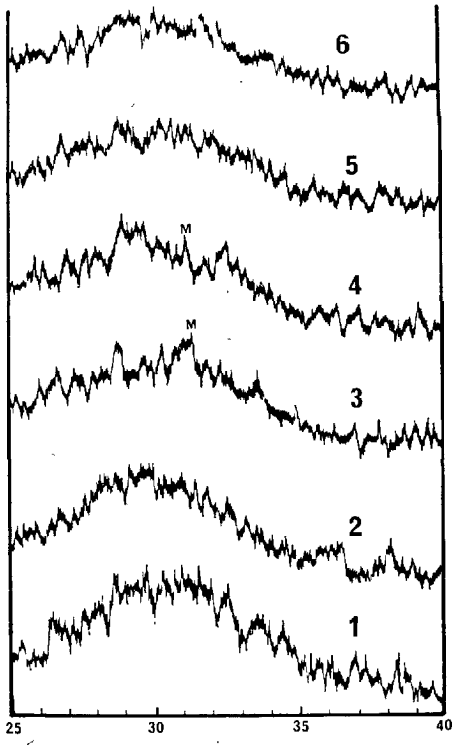

Fig. 1. *X-ray powder profiles of water quenched slag. (Cu K_α radiation) M: X-ray powder pattern of melilite.*

scope.

Chemical Composition

Chemical analyses of six slag specimens are listed in Table 1. Alkalies, sulphur and water were not determined.

Slow Cooling Slag

Slow cooling slag is formed by slow cooling of molten slag in slag yard, and mainly composed of crystalline material. Chemical and mineralogical investigation on the slag have been carried out by the present writer.

Chemical Composition

Chemical compositions of two slags from foundry pig iron and one slag from steel making pig iron are listed in Table 2. Specimens of No. 3 and 4 in the Table 2 are specially made slags of high MgO component. SiO_2, Al_2O_3, MgO and CaO are main components of the slag.

Differentiation of Some Elements in the Course of Cooling of Molten Slag

Differentiation of elements in the course of cooling of molten slag is investigated. Stalactitic glassy bodies were found in a large cavity of throwed slag (Figure 2B). The stalactitic slag was composed of glassy material and associated with small amount of melilite crystals, and formed from the residual liquid of molten slag. The chemical analysis of the slag is listed in No. 5 of the Table 2, and manganese, alkalies and sulphur are concentrated to compared with the chemical analysis of other slags.

Texture

Texture of slow cooling slag was observed under the polarizing microscope and shown in photograph 2. Porphyritic texture is characteristic appearence in slow cooling slag, and melilite and calciumsilicate minerals are phenocrists.

Table 2. *Chemical composition of blast-furnace slags and melilites.*

No.	1	2	3	4	5
	Wt.%	Wt.%	Wt.%	Wt.%	Wt.%
SiO_2	32.17	29.87	31.54	32.07	35.30
TiO_2	0.53	0.86	1.47	1.54	0.52
Al_2O_3	19.48	16.08	16.70	16.51	13.36
Fe_2O_3	0.25	0.46	0.35	0.31	0.37
MnO	0.13	0.44	0.26	0.39	2.00
MgO	3.84	4.02	7.80	7.47	3.74
CaO	42.08	46.60	39.16	40.18	40.64
K_2O	tr.	tr.	tr.	tr.	0.85
Na_2O					0.65
S					2.21
$H_2O(+)$	0.06	0.14	0.67	0.88	0.10
Ig. loss	2.04	2.46	2.52	2.23	0.48
Total	100.58	100.93	100.47	101.58	100.22

No.	6	7	8	9
	Wt.%	Wt.%	Wt.%	Wt.%
SiO_2	33.53	28.37	27.9	28.87
TiO_2		0.14		1.60
Al_2O_3	16.06	26.82	23.2	21.28
Fe_2O_3	0.72	0.60		
MnO		tr.		0.34
MgO	10.73	3.80	4.9	7.15
CaO	36.05	39.99	42.0	39.52
$H_2O(+)$	2.18	0.83	1.0	
$H_2O(-)$	0.96	0.25	0.3	
Total	100.23	100.80	99.3	
Mol. rat.	$Gh_{50}\,Ak_{50}$	$Gh_{73}\,Ak_{27}$	$Gh_{74}\,Ak_{20}$	$Gh_{51}\,Ak_{49}$

No. 1: Slow cooling slag for foundry pig iron.
No. 2: Slow cooling slag for steel making pig iron.
No. 3: Slow cooling slag for foundry pig iron.
No. 4: Water quenched slag of No. 3.
No. 5: Stalactitic glassy slag.
No. 6: Purified melilite crystal in slag No. 1 (Marginal part of crystal).
No. 7: Purified melilite crystal in slag No. 1 (core of crystal).
No. 8: Purified melilite crystal in slag No. 2.
No. 9: Purified melilite crystal in slag No. 3.

Mineral Composition

Melilite

i) Crystal growth of melilite.

Growth of crystalline material from the molten slag was investigated also. Slow cooling slag mass in a iron ladle was used for this investigation. The chilled margin of the mass was composed mainly of glassy material and associated with minute amount of crystalline material (melilite). By the observation under the polarizing microscope with thin section, minute dusty bodies are in glassy material (photograph 3), and the same part is polished to smooth surface and etched by dilute hydrochloric acid, after the process, it is tested under the electron microscope, globules with diameter of 100–150 μ were observed and the globules were composed of minute short prismatic crystal aggregate (Fig. 3 A and photograph 8). The marginal part of crystalline body is composed of dendritic aggregate of elongated melilite crystals. It is observed under the polarizing microscope and the electron microscope (Fig. 3B and photographs 3 and 9). In the core of crystalline body, dendritic aggregate of melilite had same orientation in small area (Fig. 3C), and in the center of the mass, the dendritic mass turn to compact crystal of melilite and is covered with melilite film which is rich in akermanite molecule than that of the center of crystal (Fig. 3D and photograph 4). The early stage of growth of melilite is compared with the crystalline material of water quenched slag and large melilite crystal suggest the growth of zonal structure in melilite.

ii) Zonal structure in melilite crystal.

Zonal structure is characteristic texture in well crystallized melilite and was observed under the polarizing microscope (Fig. 5B and photograph 5). The core (Fig. 5B1) has the highest content of gehlentie molecule and the rim (Fig. 5 B 3) the lowest content of the same molecule. The chemical analyses of the two zones of melilite (Fig. 5 B 2 and 5 B 3) are cited in Table 2–6 and 7, respectively.

iii) Chemical composition of melilite crystal.

Pure melilite grains are separated from slag powder by means of magnetic separater and the method of heavy liquid. Purified materials were analyzed by means of micro method. The results are listed in Table 2 and their molecular ratios of gehlenite and akermanite are calculated too.

iv) Melilite crystals in the cavity of slag

Small idiomorphic crystals of melilite in cavity of the slag which had been left in a ballastyard had been found (Fig. 2 C_1).

Although zonal structure is not so distinct in the melilite crystal from cavities, a thin layer with higher content of gehlenite molecule (Fig. 2A 1) prevails along the border of groundmass, and another layer with lower content of gehlenite molecule (Fig. 2A 3) covers the top of the crystal. The pure material of the melilite in cavities, was easily obtained by hand-picking under the binocular microscope. Clear part of the melilite phenocryst corresponding to 2 in Fig. 5B was obtained from 200–250 mesh fraction of powder slag by using magnetic separator, heavy liquid and binocular microscope.

Both 1 and 2 samples had been examined under the polarizing microscope and they were analysed. The results were listed in 1 and 2 in Table 3.

Crystallization of melilite in cavities. The composition of the melilite crystal in cavities of blast-furnace slag is higher in gehlenite content than the melilite phenocryst from the neighbouring massive part, while the zonal structure of the latter indicates the crystallization course from gehlenite rich to aker-

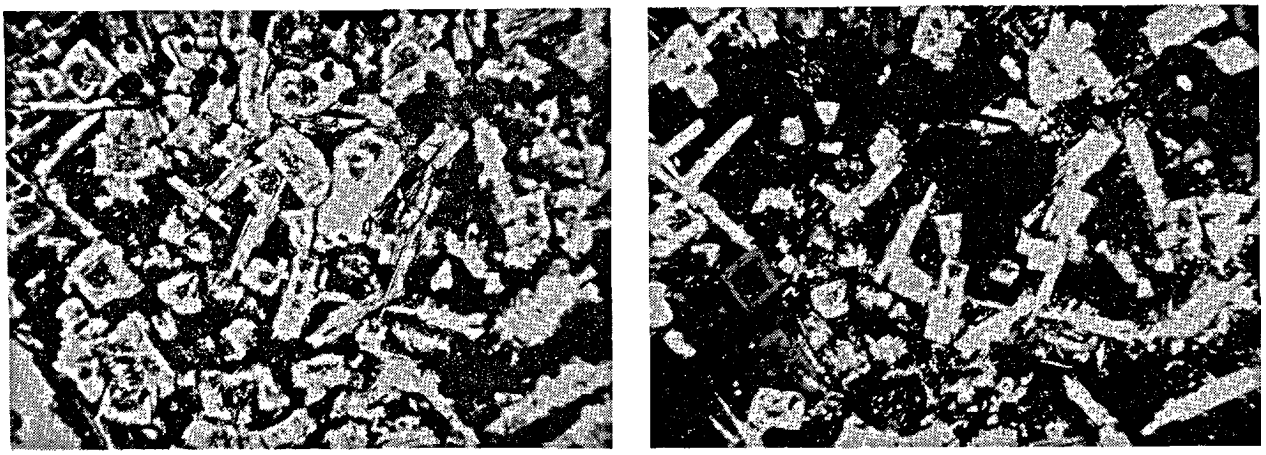

Photo 2. *Porphyritic texture of slow cooling slag.*

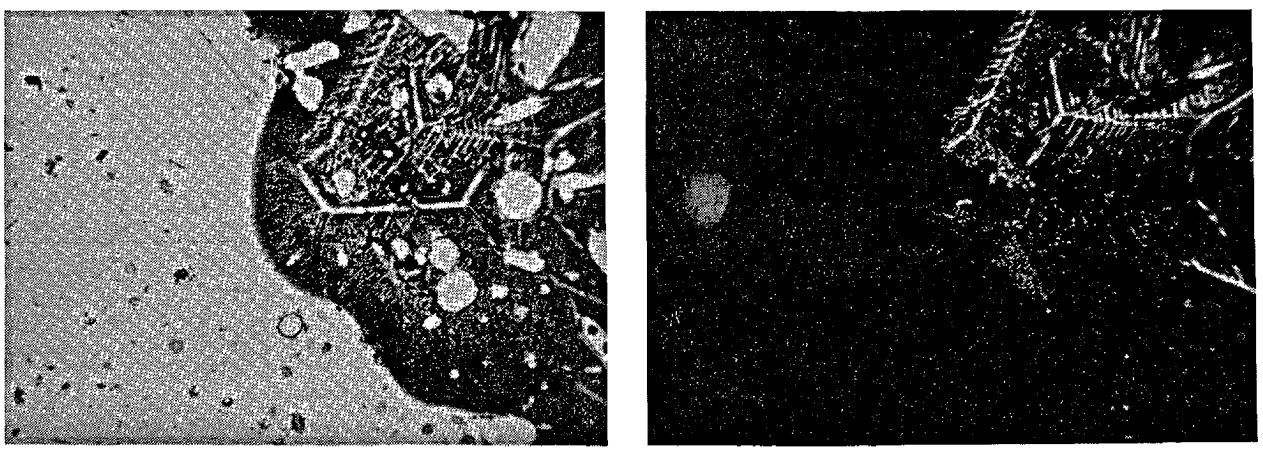

Photo 3. *Dendritic structure in chilled margin of slow cooling slag.*

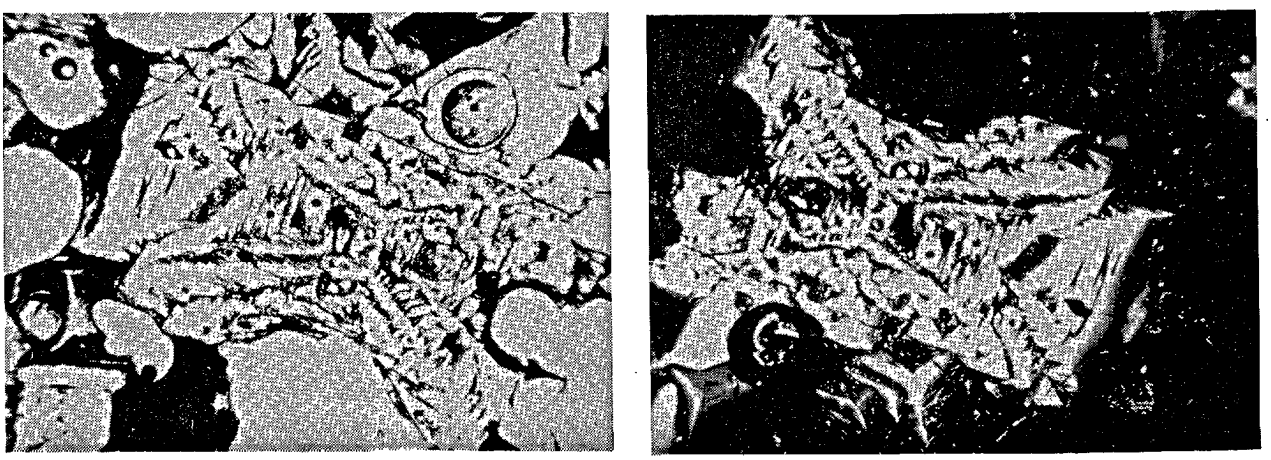

Photo 4. *Crystal growth of melilite.*

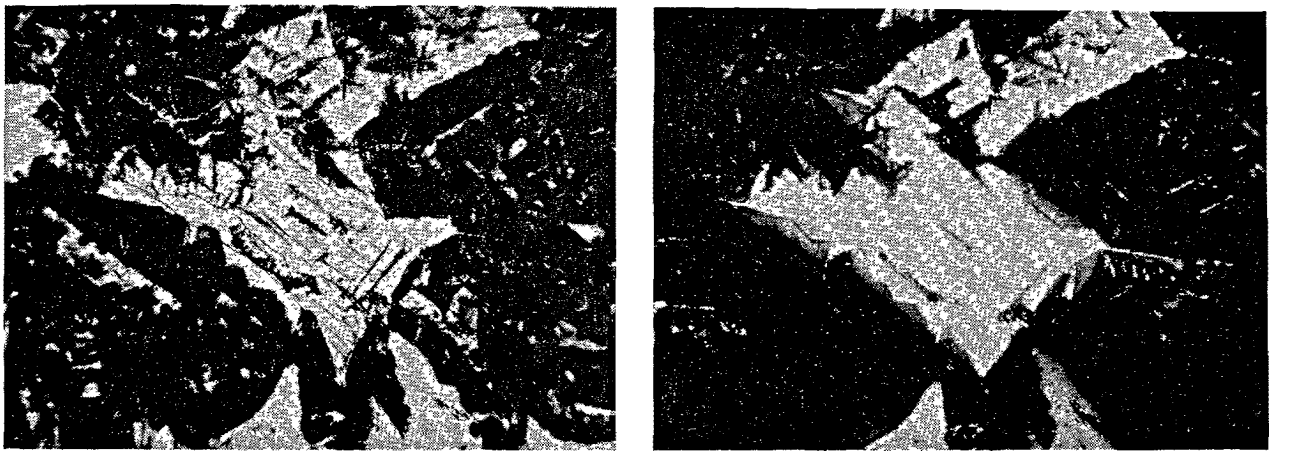

Photo 5. *Zonal structure of melilite.*

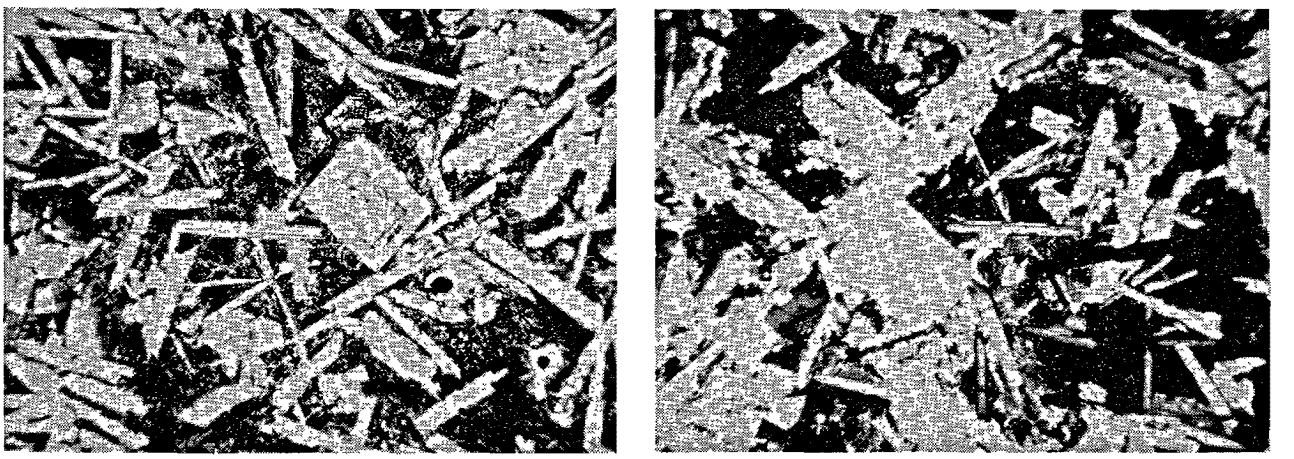

Photo 6. *Pseudowollastonite and melilite.*

Table 3. *Chemical composition of melilites in blast-furnace slag.*

1				2				3			
Wt.%		Atom. rat.		Wt.%		Atom. rat.		Wt.%		Atom. rat.	
SiO_2	28.25	Si	1.31	SiO_2	29.05	Si	1.35	SiO_2	31.31	Si	1.50
TiO_2	1.23	Ti	0.04	TiO_2	0.53	Ti	0.02	TiO_2	0.87	Ti	0.03
Al_2O_3	23.47	Al	1.26	Al_2O_3	20.87	Al	1.13	Al_2O_3	16.68	Al	0.94
Fe_2O_3	1.97	Fe	0.07	Fe_2O_3	2.00	Fe	0.07	Fe_2O_3	0.52	Fe^{3+}	0.02
								FeO	0.32	Fe^{2+}	0.01
								MnO	1.82	Mn	0.10
MgO	4.45	Mg	0.30	MgO	6.64	Mg	0.46	MgO	4.40	Mg	0.31
CaO	40.58	Ca	2.00	CaO	40.20	Ca	2.00	CaO	39.39	Ca	2.02
								K_2O	1.14	K	0.07
								Na_2O	0.74	Na	0.07
$H_2O(+)$	0.84			$H_2O(+)$	0.98			$H_2O(+)$	2.36		
$H_2O(-)$	non.			$H_2O(-)$	non.			$H_2O(-)$	*non.*		
Total	100.79			Total	100.27			Total	100.79		

1: Colourless melilite crystal in cavity.
2: Colourless melilite crystal in massive part.
3: Brownish melilite crystal in cavity.
1 and 2 are derived from same slag.

manite rich melilite, which is reasonable in those range of melilite series from the viewpoint of phase diagram. So, the melilite in cavities cannot be the product of later stage or fractional crystallization of the slag. Possibly, the gas, which had been released from cooling slag to form bubbles played an important role in mineralization in cavities.

Small idiomorphic melilite crystals with brownish colour were found in the cavity of slag collected from the other ballastyard. The chemical analysis of the melilite crystals was listed in 3 of Table 3. This melilite crystals is rich in manganese, alkalies and water. And this characteristic in chemical composition resemble to that of stalactitic glassy slag (5 in Table 2). It may be crystallized out from residual liquid in the course of cooling on molten slag, and will be occurred in a cavity shown in C_2 in Fig. 2.

Dicalciumsilicate and anorthite

The dense fraction of powdered slag which separated by heavy liquid, is investigated by means of X-ray powder method. It is composed of β-dicalciumsilicate and associated with small amount of γ-dicalciumsilicate and anorthite, occasionally. And minute crystals of β-dicalciumsilicate are observed under the polarizing microscope, also.

Pseudowollastonite

There are prismatic minerals which have higher birefringence than that of melilite (photograph 6). This mineral is pseudowollastonite. X-ray powder patterns of 3.24, 2.83 and 1.98 Å are derived from pseudowollastonite.

Perovskite

Minute octahedral crystals with very high refractive index is observed in thin section of slag (photograph 7). This mineral is perovskite and rarely found in slag.

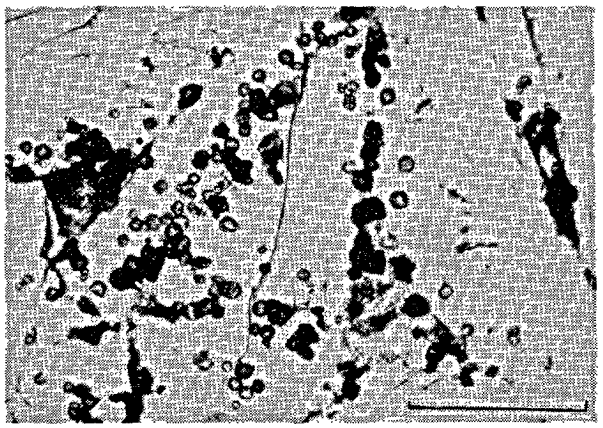

Photo 7. *Perovskite in melilite.*
Scale: 1-6 is 1mm and 7 is 0.3mm.
Electron micrograph:

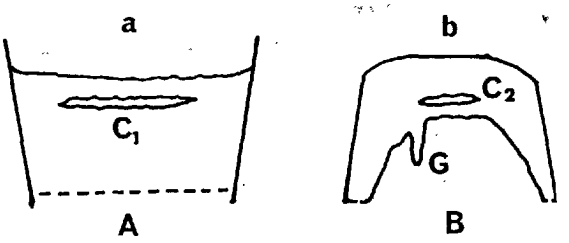

Fig. 2. *Schematic sketches of cinder ladle of slow cooling slag.*

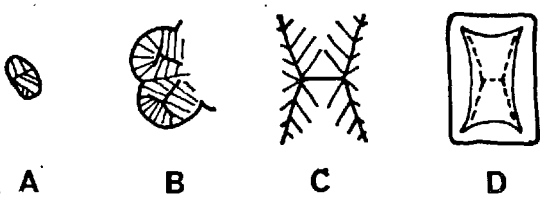

Fig. 3. *Schematic sketches of growth of melilite.*

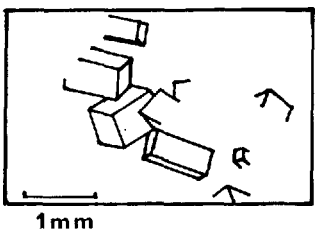

Fig. 4. *Melilite crystals in a cavity of slow cooling slag.*

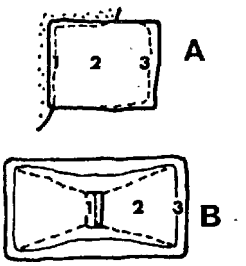

Fig. 5. *Zonal structure of melilite.*
A: Crystal in a cavity, B: Phenocryst.

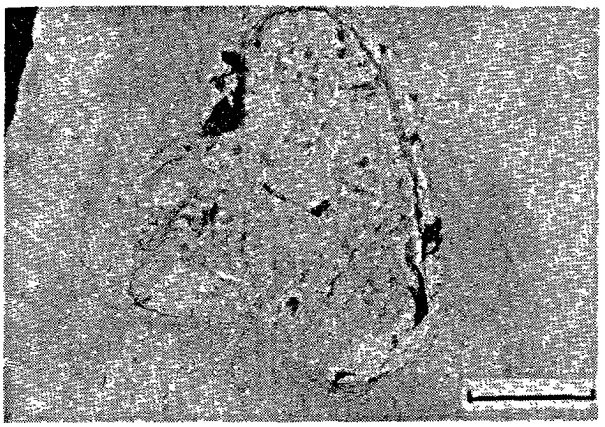

Photo 8. *Globules in glass of chilled margin of slow cooling slag.*

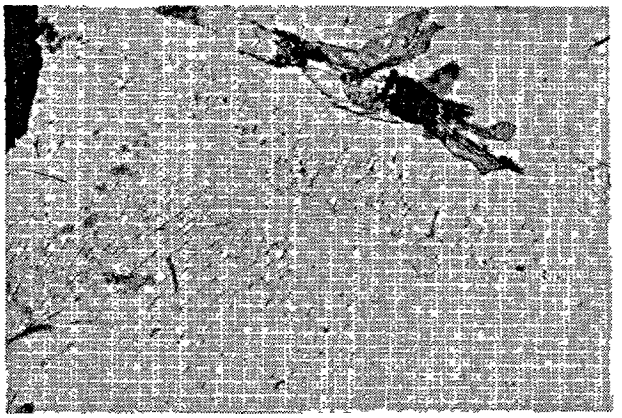

Photo 9. *Dendritic melilite in chilled margin of slow cooling slag.*

Electronmicroscope; scale 3μ

Acknowledgements

The investigater wishes to express his sincere thanks to Yawata Iron and Steel Co. Ltd., Yawata Chemical Industry Co. Ltd., Kawatetsu Iron and Steel Co. Ltd. and Kawatetsu Mining Co. Ltd., whom he owed the specimens used in this study.

References

1. H. Minato, "Melilite crystal in the cavity of blast-furnace slag", Miner, J. **2**, 422–426 (1959).

Supplementary Paper IV-113 Portland Blast-Furnace Cements-A Case for Separate Grinding of Slag

Niko Stutterheim

Synopsis

Portland blast-furnace cement is normally manufactured by grinding together clinker, granulated slag and gypsum. In his review of slag cements for the 1960 Symposium, Kramer dealt, inter alia, with the then current knowledge concerning separate grinding of clinker and slag. He did not deal specifically with blending of the two products in the factory or, with the more novel process of blending at construction site.

In 1948–1952 the author carried out laboratory and pilot plant studies on separate grinding, and blending in the concrete mixing process. He established important advantages for this procedure compared to integral grinding. Separate grinding on an industrial scale was started in South Africa in 1953; although some difficulties were experienced initially by the users due to the novelty of the idea and also because the construction industry was not familiar with portland blast-furnace cements, the demand for the product, and for separately ground slag, has grown impressively. Of the slag more than half was separately ground.

Advantages of separate grinding:—

1. The grinding process is more efficient;
2. Product quality is under better control;
3. Ground slag has much better storage properties than portland cement;
4. Proportions of portland cement and slag is at discretion of user;
5. Workability can be significantly improved or water: cement ratio reduced.

Of special technical and economic interest is the freedom to choose the proportions of slag in the final cement; Portland cement and slag have different properties and by this choice optimum combination for any job can be decided by the user; since slag costs less to produce, this can also yield material economies.

There is therefore a case for all slag intended for use in hydraulic cements to be ground separately and blended with portland cement at construction site. Modern methods of mix design, proportioning and control make this readily possible.

Introduction

In his excellent summary of the state of knowledge of blast-furnace slags and slag cements presented to the Fourth Symposium on the Chemistry of Cement in 1960, Kramer referred, inter alia, to practices then current concerning the grinding of cements containing slag. He pointed out that the great bulk of portland blast-furnace cements were integrally ground, a satisfactory procedure provided that the separate components, cement clinker and granulated slag, had suitable grinding characteristics. This is seldom the case: particularly slag tends to vary considerably in grindability, depending on composition and granulation conditions; moreover, it is generally much harder to grind than portland cement clinker as a result of which the slag component of an integrally ground cement tends to be coarser than the clinker component. As the reactivity of slag is much lower than that of clinker, strength development particularly at early ages is partially inhibited. In fact poor use is made of the latest hydraulicity of the slag.

Consequently cements containing slag like portland blast-furnace cements are commonly regarded as second-grade products which would not be selected where high quality was a prerequisite.

In order to improve quality and reduce variability the possibilities of separate grinding have begun to receive more attention and some manufacturers use separate grinding with subsequent blending before delivery as standard production procedure to ensure greater uniformity of end product. As pointed out by Kramer, each component can then be ground to yield an optimum combination of properties. Developments in the field of mixing of dry powders have made it

*South African Council for Scientific and Industrial Research, Pretoria, South Africa.

possible to ensure intimate blending at no great cost.

In terms of the quality of the product therefore, separate grinding can lead to more economical production.

In the course of experimental studies carried out between 1947 and 1954, reported elsewhere, (1) (2) (3) the author used separate grinding of slag as standard procedure for the preparation of experimental cements containing slag, since only by this procedure could one ensure that fineness of the slag was a controlled variable. This was carried through to the pilot plant stage of the preparation and testing of granulated slags, the blending in this case being done in a concrete mixer, as part of the routine concrete mixing operations. Check tests demonstrated that adequate intermixing could be achieved in this way.

As a result of this pilot plant study it was realized that there were promising possibilities in supplying the construction industry with separately ground granulated slag for on-site mixing with portland cement and the other ingredients of concrete. Such a procedure brought with it two possible disadvantages. Firstly, there was an additional component, viz., the slag, which had to be handled, measured and blended into the concrete. Secondly, there was a risk that users, unacquainted with the necessity to add an activator (such as portland cement) to a finely-ground slag before the latter would develop hydraulic properties, might deliberately or through negligence use the finely-ground granulated slag as sole cementing medium, with possible disastrous results. During the last fifteen years separately ground granulated slag has been used extensively in South Africa without these disabilities having been of any practical consequence. On the contrary, the performance of cements containing separately ground slag as a major constituent has been such that it is now widely accepted as a quality product, as proved by its use in some major construction projects.

Separate grinding and supply of slag has a number of advantages, the most important of which are discussed under the following heads.

Separate Grinding

As already referred to above, separate grinding gives control over fineness and uniformity of quality. There are, however, other advantages; for instance, since the raw materials required for portland cement manufacture are not derived from the same source as granulated slag, the latter being a waste product of blast-furnace operation, there are invariably advantages in grinding products like clinker and slag in geographically separated plants, particularly if there is no case for blending them prior to use on the job. A slag grinding plant should be located in a position which is optimal with respect to the source of the raw slag on the one hand and the consumption centres of the finished product, ground slag, on the other.

Storage

The susceptibility to deterioration in storage of portland cement is well known. Ground granulated slag in the absence of any additive has remarkably good storage properties. In fact, there are cases where this material has not deteriorated after storage in paper bags for three years.

Proportioning

With the integrally ground portland blast-furnace cements the manufacturer pre-determines the proportions of portland cement and slag for the user. Since on most construction works a variety of types of concretes are required, there are obvious advantages in being able to select the proportion of portland cement and of slag to be used for a particular application since this will lead to a more effective utilization of the properties of each component, which can lead to better performance and greater economy. For instance, on many construction works concretes of different quality involving different mix designs and therefore different specifications for instance for strengths, shrinkage, permeability and cost are often required. Blending can be done as part of the concrete mixing operation. Since weigh-batching is now almost universal for well-controlled construction works, batching of an additional component is a simple matter.

Mix Design

If the properties of portland cement and of mixtures of portland cement and slag were identical, the use of mixtures would not affect mix design. However, slag does affect the characteristics of a concrete mix, particularly if it is finely-ground, as should be the practice with separately-ground slag to allow for its lower reactivity. In particular there are two properties which should be taken into account when using portland blast-furnace cements instead of portland cement. The first is that such mixed cements tend to have a lower initial rate of strength gain, leading to lower strengths in the period two to four weeks after casting. It is fairly common experience, at any rate for South African materials, that the mixed cements thereafter develop strengths higher than those for ordinary portland cements. This dictates that if early strengths are important, portland blast-furnace cement concretes should be designed at a lower water-cement ratio, but that if strength at later ages is the important criterion, concretes with a lower cement content could prove acceptable.

The second factor concerns the effect of the use of finely-ground slag on workability or placeability, particularly when using vibrators. It is common experience that these concretes are appreciably more workable as a result of which it is possible to reduce water content compared to the case for portland cement, so leading to higher strengths and lower shrinkage.

These effects are sufficiently large to justify mix design changes.

Two special applications of separately ground slag must be mentioned. The one concerns stabilization of soil for road construction. It has been established that for certain groups of soil types excellent results are achieved by mixtures of ground granulated slag and lime. This is not only a cheaper stabilizer but it has setting properties more suited to the forming and consolidation operations inherent in road foundation construction; experience has shown that the use of this stabilizer leads to reduction in shrinkage cracking of the stabilized soil layers. By having the slag in separately ground form available on the construction site, its rate of application and the proportions of lime to be added can be varied at the discretion of the consulting engineer.

The other special case refers to the process of cementation of rock formations to reduce water penetration and seepage. Under certain circumstances such as for instance those found on the Rand Gold Mines excellent cementation can be achieved with mixtures of 99 parts ground granulated slag and one part calcium chloride, with no addition of any other cementing agent.

Economics

The ex-factory cost of ground granulated slags is appreciably lower than that of portland cements. If all the factors given above are used to best advantage, yielding a concrete in which the slag content is at optimum, the cost will be at a minimum.

In this respect Van Dÿk (4) has done an interesting study; he determined the cost of cement per cubic yard of concrete for different strength levels. The cements used in the study were:—

1. Ordinary portland cement (OPC). (60.1 cent/pocket).
2. High early strength portland cement (HE). (66.4 cent/pocket).
3. Portland blast-furnace cement (interground) (PBFC). (54.7 cent/pocket).
4. 50-50 mixture of OPC and separately ground granulated slag.
5. 50-50 mixture of HE and separately ground granulated slag.
6. Separately ground granulated slag (39.0 cent/pocket).

(Prices are quoted in South African cents. 1 S.A. cent = 1.4 U.S. cent).

The variables were: type of cement and strength at particular ages. No advantage was taken of the greater workabilities possible with cements containing finely ground granulated blast-furnace slag. Some of his results are shown in Fig. 1.

Van Dÿk concludes that the combinaton of 50 percent high early cement and 50 percent slag generally gave the most economical mixes for moist-cured concrete tested at 3, 7 and 28 days.

On the other hand the ordinary portland cement and the portland blast-furnace cement gave the highest costs per unit of strength.

He adds that if concretes of equal placeability had been made for each comparative group, these cost differences would have been accentuated. The ques-

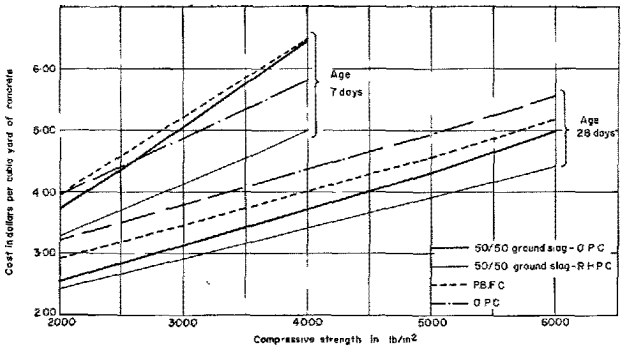

Fig. 1. *Comparative costs of different cements*

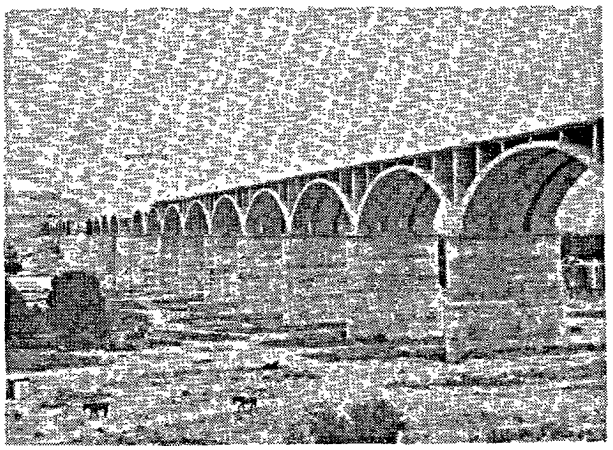

Fig. 2. *Bethulie bridge over Orange River 1,200 metres long.*

toin of the effect of workability is rather complex as it depends upon the criteria of workability to be used. Static workability tests like the slump test are not satisfactory in an age when most concrete is placed by vibration. Moreover, when comparing the workability of concretes made with portland cements on the one hand and portland slag mixes on the other, it becomes particularly important that the workability test used should somehow relate to the placeability obtained in practice with the use of internal vibrators. A start has been made on such studies.

Typical examples of the practical application of concrete mixes designed specifically for combination of portland cement and separately ground granulated slag mixed in the concrete-making operation, are shown in Figs. 2, 3 and 4.

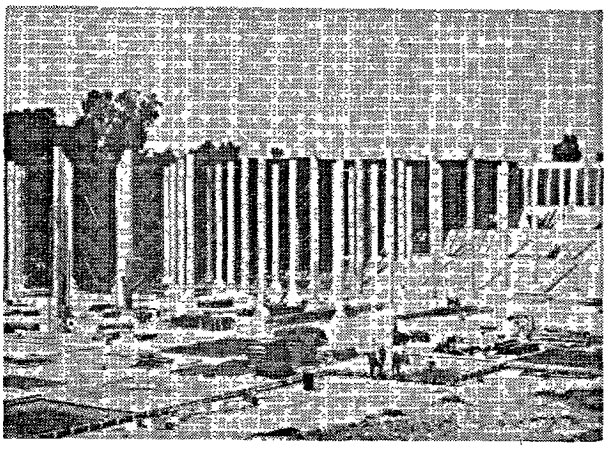

Fig. 3. *Totally enclosed water reservoir under construction—one million cubic metres—Johannesburg.*

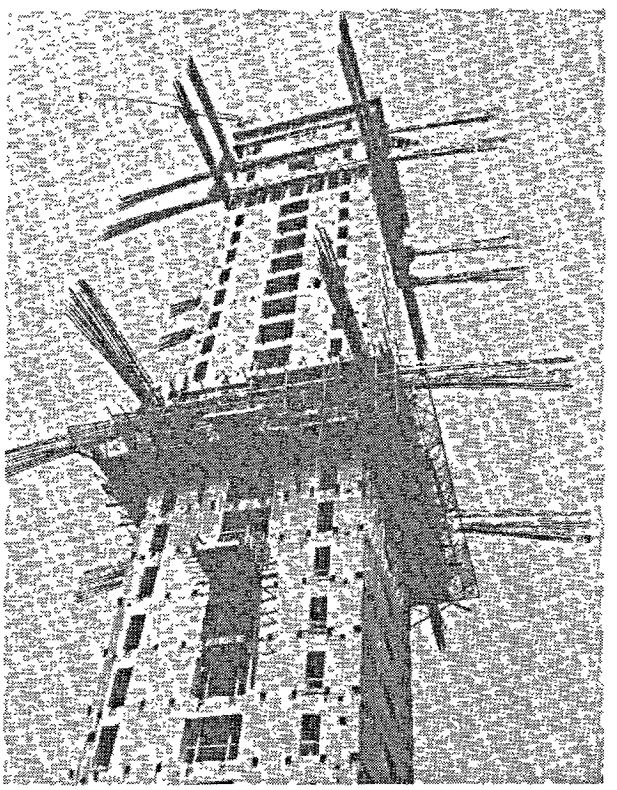

Fig. 4. *Central core of Standard Bank Building under construction with sliding shutter. Ultimate height 170 metres. Johannesburg.*

Conclusion

Blast-furnace slags, being by-products, vary tremendously in quality from place to place. By far the greater bulk of slag produced in the world is not suitable for cement manufacture. Where, however, this product does have physical and chemical properties which allow it to be converted to a potentially hydraulic material, there is scope for using it for constructional purposes. Industries in many countries

have taken advantage of this fact and some have been producing cements containing granulated slag as a major constituent for decades. Most of this cement has been marketed in the form of a product interground with portland cement to give one of the various varieties of portland blast-furnace cements. Recently separate grinding of the slag has become more common but generally only as a preliminary to factory blending to yield a ready-mixed product for sale.

Experience in South Africa with separately-ground granulated high-magnesia slag marketed as such and blended with portland cement or other activator at the point of final use, has shown that this procedure can give very staisfactory results, both technically and from the economic point of view. The resultant product compares favourably with portland cements for certain classes of construction, in particular civil engineering works.

References

1. N. Stutterheim and R. W. Nurse, "Experimental blast-furnace cement incorporating high-magnesia slag". Mag. of Concr. Res., (March, 1952).
2. N. Stutterheim, "Some properties and uses of high-magnesia portland blast-furncae slag cement concretes". J. Amer. Concr. Inst., (April, 1960).
3. N. Stutterheim, "The risk of unsoundness due to periclase in high-magnesia blast-furnace slags". Proc. 4th Int. Symp. Chem. Cement, 1960.
4. J. van Dyk, "Choice of type of cement for optimum economy in concrete". South African National Building Research Institute (unpublished report).

Oral Discussion

Mitsuo Hanada

What are the hydration products when high-MgO slag (such as 15% MgO) is used, especially those of the MgO hydration?

Oral Discussion

Steven Gottlieb

Dr. Stutterheim must be congratulated for strengthening the case for separate grinding of slag, and as this recommendation has far reaching qualitative and economic consequences, I would like to make some comments.

Certain types of blast furnace slags are ground together with portland cement clinker for decades:—in fact, the German cement industry for instance, would hardly exist economically without the substantial quantity of blast furnace cement produced. However, not much has changed in the method of producing blast furnace cements during the past 50 years, though great advances in grinding and classifying technology, particularly during the past 15 years, would have justified such changes for the betterment of quality and economy.

Dr. Stutterheim points out that the higher fineness of the harder slag as achieved by separately controlled grinding, produces more active surface. This is correct, but there is another, perhaps even more important possibility of improvement in regard to the grinding of the clinker constituent, provided that the blast furnace cement is produced at the cement works. With the intended use of blast furnace slag, the clinker can be ground much finer than usual;—utilizing new classifier technology even as high as 7000 cm^2/g Blaine-which normally would be an unreasonable thing to do, not only because of prohibitive costs, but also for many other considerations such as excessive shrinkage and potential instability due to particle attraction leading to agglomeration. However, in a properly designed blending system blending between the very finely ground cement and the finely ground slag is accomplished immediately after the very finely ground clinker and gypsum leave the classifier,—then the disadvantages of excessive fineness disappear, as intimate blending with the slag with increase the average distances between the very small portland cement clinker particles and thus reduce, or even totally eliminate the nuisance attraction forces between these particles.

Surface wetting in such system becomes more uniform due to the absence of particle agglomeration. This could open up ways for further improvement of qualitative and economic performance of clinker and blast furnace slag mixes.

Oral Discussion

Herman Kaiser

I fully agree with Dr. Stutterheim in that separate grinding of slag rather than intergrinding of slag and clinker has a great many advantages.

I understand that one plant here in Japan grinds the slag separately. In Venezuela a plant now under constructon will also grind slag separately, and then blend it with finished portland cement shipped in from another plant.

However, I wonder what the advantages are of leaving the blending to the cement user because quality control can probably better and more reliably be achieved in the cement plant rather than on the construction site.

Furthermore, different customers may require, or want slags ground to different finenesses. This, I fear, might complicate an otherwise quite simple manufacturing process.

Oral Discussion

R. R. Hattiangadi

Congratulating Dr.Stutterheim for bringing to the pointed notice of the delegates that there was, both technically and commercially, a case for separate grinding of granulated blast furnace slag and portland clinker and thereafter blending the same as and when necessary. Dr. Hattiangadi gave a brief resume of his own experiences in India. Dr. Hattiangadi gave figures in respect of a factory where commercial scale experiments had revealed by separate grinding and blending of slag and cement the net saving in power consumption alone, was of the order of 7 to 8 units per tonne of portland blast furnace cement, after making due allowances for power consumption for conveying and blending of the two separately ground materials. In this country (India) the slag which was granulated at some distance from the site of the blast furnace was very much harder to grind than portland clinker and it seemed obvious that it was not correct to intergrind two materials of different grindabilities and of different average diameters.

Dr. Hattiangadi also asked if it was necessary to grind the slag to a greater degree of fineness than the parent portland clinker to which Dr. Stutterheim seemed to say that it would be desirable but not quite necessary.

Author's Closure

Niko Stutterheim

Reply to M. Hanada

"Except in the improbable case for which the high magnesia slag contains some periclase, the hydrates are free of brucite. Searches e.g. by Nurse, Yang, van Aardt, have failed to identify any products other than gel indistinguishable physically from CSH gel. Earlier in this Symposium Prof. Tayler made a case for naming the gel product of portland cement hydration CSH gel, presumably until more is known about. It would therefore be logical to call the product of hydration of a high magnesia slag CMSH gel."

Reply to S. Gottlieb

"I find Dr. Gottlieb's statements about the effect of electrical charges on separately ground slag particles very interesting but must confess lack of knowledge on my part regarding the practical implications of this charged state on blending with portland cement. There may be scope for further study of these phenomena.

As I envisage it, however, separate grinding of slag may well take place at plants geographically distant from portland cement plants; several such plants exist in South Africa. Then blending soon after grinding is of course out of the question. In fact, from other points of view, as set out in may paper, there are overriding technical and economic advantages in blending only at construction site, which may be weeks or months after grinding."

Reply to H. Kaiser

"It is interesting to find confirmation in the experience of Mr. Kaiser in Venezuela for the advantages of separate grinding of slag. Our reasons for believing that separate marketing of the finely ground slag and blending only at the construction site are partly dealt with in my paper. I may add that this procedure allows the user to decide what blend ratios he will use on the job, whereas intergrinding or factory blending puts this decision in the hands of the manufacturer who does not know the requirements for the specific application.

In South Africa about 500,000 tons p.a. of finely ground slag is supplied direct to construction works, and blended with portland cement on site, mostly in the concrete mixer. It is used mainly for large works, e.g. civil engineering constructons; such works are generally under good supervision. We have not had any serious problems with separately marketed slag."

Reply to R. R. Hattiangadi

"The fullscale production trials on integral and separate grinding, respectively, mentioned by Dr. Hattiangadi is further clear indication of the favourable economies of separate grinding. From their work,

Locher *et al* have concluded that the influence of slag fineness on its performance in concrete is decisive; Kayser has stressed the importance of grain size distribution; Birthelmer established that separately ground slag and portland cement attain strengths equal to those for interground cements of higher surface areas. These findings quoted in Dr. Schröder's principal paper to this Symposium reinforce the case for separate grinding."

Supplementary Paper IV-121 The Role of Magnesia and Alumina in the Hydraulic Properties of Granulated Blast-Furnace Slags

Marcel Cheron and Claude Lardinois*

Synopsis

The authors compare the incidence of the Al_2O_3 and especially the MgO content on the hydraulic activity of the iron slags. These slags were prepared from industrial blast-furnace slags to which pure oxides were added covering a large area of chemical compositions limited by the following characteristics:

$$C/S = 0.85 - 1.45; \quad Al_2O_3 = 8.0 - 21.0\%; \quad MgO = 5.0 - 15.0\%.$$

The mixtures were fused at temperatures exceeding 1500°C and quickly cooled, to obtain an almost complete vitrification, which was controlled by X-ray diffraction. These slags were separately ground with gypsum and cements prepared by mixing them with the same proportion of previously ground portland cement. The mechanical strengths of these cements were determined according to the RILEM Cembureau Method.

The representation of the results on triangular diagrams (S-A-M) at constant level of Al_2O_3 showed the beneficial influence of the Al_2O_3 and MgO on the mechanical strengths.

A linear relation between the mechanical strengths and the chemical composition was established and the hydraulic index

$$I_h = \frac{CaO + 1.4MgO + 0.56Al_2O_3}{SiO_2}$$

was proposed.

Tests made on industrial slags showed a good agreement between the hydraulic index of the slag and the mechanical strengths of the corresponding cements.

Introduction

Ten years ago, the cement industry in Belgium, used granulated slags characterized by a CaO/SiO_2 ratio exceeding 1.4 and an almost constant alumina and magnesia content varying between 15-16% for Al_2O_3 and 4-5% for MgO. These slags gave a relatively fair granulation.

During the last ten years, the iron industry of our country as well as of the countries outside, progressed considerably, even regarding the process (preparation of the charge, increase of the blast-furnace size, LD-process), as respecting the raw materials now mostly imported from beyond the seas. This evolution involved many consequences for the slag quality (decrease of the C/S ratio, increase or decrease of the Al_2O_3 percentage, increase of the MgO percentage). Table 1 gives some examples of slags produced currently in 1963-1964. The largest part of the production had a composition similar to that of slags B and C. Slags A, D and E are examples of the extreme compositions encountered. In the same time a fair improvement of the slag vitrification was observed.

The incidence of the qualitative evolution of the slags on its hydraulic value is very important for the cement industry in Belgium and other neighbouring countries such as the Netherlands and the north-east of France, where the average incorporation rate of slag in blast-furnace cements reaches 60–70%.

Table 1.

Slag	CaO/SiO_2	% Al_2O_3	% MgO	% MnO
A	1.65	13.4	4.2	0.7
B	1.27	14.1	4.9	1.2
C	1.21	13.5	7.6	0.9
D	1.18	19.0	8.3	0.5
E	1.06	22.7	13.4	0.5

*Cimenteries CBR, Bruxelles, Belgium.

Literature Survey

All authors agree to consider the non-crystallized state of slags as a strictly necessary condition to their hydraulic activity.

Keil (1) and Kramer (2) synthesized, in 1952 and 1960 respectively, the essential opinions thereabout. L. Santarelli, G. Goggi (3), and more recently H. E. Schwiete and F. C. Dölbor (4) pointed out that strength development appeared as a linear function of the "glass content". S. Solacolu (5) has proposed an explanation of the influence of the vitreous state of slag based on quasi-crystallized phases, namely a molecular preorganization recalling the crystalline phases which should be formed, at equilibrium, by slow cooling of the slag. The hydraulic properties of the slag consequently depend only on the chemical composition within the field of crystallization and there is a discontinuity of properties when passing from one field to the other.

Although some authors, as R. Kondo (6), do not entirely agree with this point of view, it seems self-evident, to admit a certain organization within the glass which is rather difficult to reveal experimentally. But its action on the hydraulic activity is superposed to other essential factors such as the chemical composition of the vitrified part.

According to this last aspect, which has had our full attention in this study, and in the case of basic slags whose composition belongs to the melilite group, the hydraulic activity increases according to the C/S ratio and the alumina content, the part played by the MgO being contested (5) (7) (8) (9).

H. E. Schwiete and F. C. Dölbor (4) obtain a fair statistical concordance between the hydraulic activity and a chemical index where Al_2O_3 is partially associated to SiO_2 as denominator, and partially associated to the lime (% Al_2O_3-10) as numerator.

Other well-known chemical indices (10), more particularly these proposed by F. Keil, C. de Langavant, L. Tetmayer and others consider that the total amount of alumina must be considered as favourable for the hydraulic activity of the slag.

The amphoteric character of alumina cannot be contested; it surely depends on the silica content of the slag and its effect will be more favourable on the hydraulic activity when the C/S ratio of the slag is lower. This point of view has been developed by Hüettemann (8).

The hydraulic value of MgO is accepted by some authors, contested by others. F. Keil and F. W. Locher (9) consider that the slags containing 5% MgO are more active than the slags of similar composition without MgO excepted if the activation is obtained with lime.

E. F. Osborn, R. C. De Vries, K.H. Gee and H. M. Kraner (7) determined the optimum slag compositions with various alumina percentages and pointed out that the optimum magnesium content varied between 16 and 12.5% when the C/S ratio increased from 1.20 to 1.54 and the Al_2O_3 content raised from 5 to 15%. Other authors affirm that until 8%, MgO may replace CaO (1). N. Sutterheim and R. W. Nurse (11) estimate that if MgO reaches 15–16% the slag is less hydraulic; this is probably due to the partial devitrification (spinel); the slags containing a high MgO percentage crystallize fast.

On behalf of structural considerations, H. E. Schwiete and F. C. Dölbor (4) propose a formula of hydraulic index where the magnesia appears as denominator and has an effect opposite to that of the lime.

$$\frac{CaO + (x - 10\,Al_2O_3) + CaS + Na_2O + K_2O}{SiO_2 + 10\,Al_2O_3 + TiO_2 + MnO + MgO}$$

This formula seems however not to have been tested experimentally.

Object of the Study

The main object of this paper will be to specify the incidence of the MgO content for increasing amounts of Al_2O_3 on the hydraulic activity of granulated industrial slags. These slags are characterized by a relatively low C/S ratio and a degree of vitrification higher than 90%. The field of chemical composition covered will be

C/S	from	0.85	to	1.45
Al_2O_3	from	8	to	21%
MgO	from	5	to	15%

The choice of a "quality factor" which permits the evaluation of the hydraulic value of the iron blast-furnace slag is our principal aim; it will be based on the following method as previously proposed (6):

—measure of the degree of vitrification by estimating the crystalline phase amount by X-ray diffraction

—estimation of the hydraulic value by the chemical composition (made for example by the X-ray fluorescence method).

Experimental Part

Industrial Slags

Industrial slags were collected whose chemical characteristics varied in the following way

C/S =	0.72	to	1.65
Al_2O_3 =	13.4%	to	22.7%
MgO =	3.8%	to	16.3%
MnO =	0.2%	to	2.2%
FeO =	0.2%	to	1.0%

The degree of vitrification was controlled by X-ray diffraction and was in all the cases higher than 90%.

The following method was used for this control. First of all were established calibration curves applicable to each group of slags characterized by the same primary crystalline phase e.g. the gehlenite phase. The calibration curve is obtained from mixtures of the vitreous and the crystallized variety of the same sample. The crystallized sample was prepared by heating the slag at 1000°C during 1 hour followed by a very slow cooling. The percentage of the crystallized phase was determined by measuring the intensity of the proper diffraction line (gehlenite at 2.84 Å spacing e.g.).

The Fig. 1 gives an example of the calibration curve. Although the precision of this method is better than 3% we divided for simplicity the examined slags in classes containing 0 to 5, 5 to 10 and 10 to 15% of crystallized material.

The slags with a crystallized phase greater than 10% were discarded. The hydraulic activity of the other slags was measured from cements prepared in the following way

—separate grinding of the slag with gypsum in a laboratory mill to obtain a fineness of 3500 or 4500 cm²/g Blaine and a SO_3 content at 3%.

—separate grinding of a sufficiently large sample of clinker with gypsum to attain a SO_3 content at 3% and a specific surface of 3300 cm²/g Blaine.

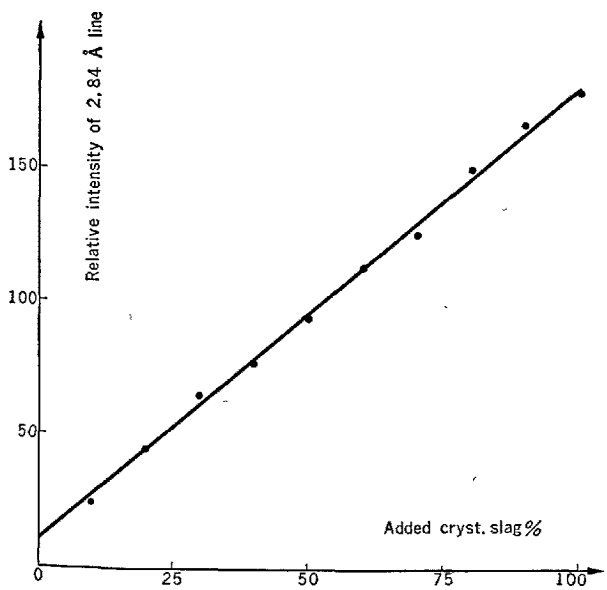

Fig. 1. *2.84 Å line of gehlenite*

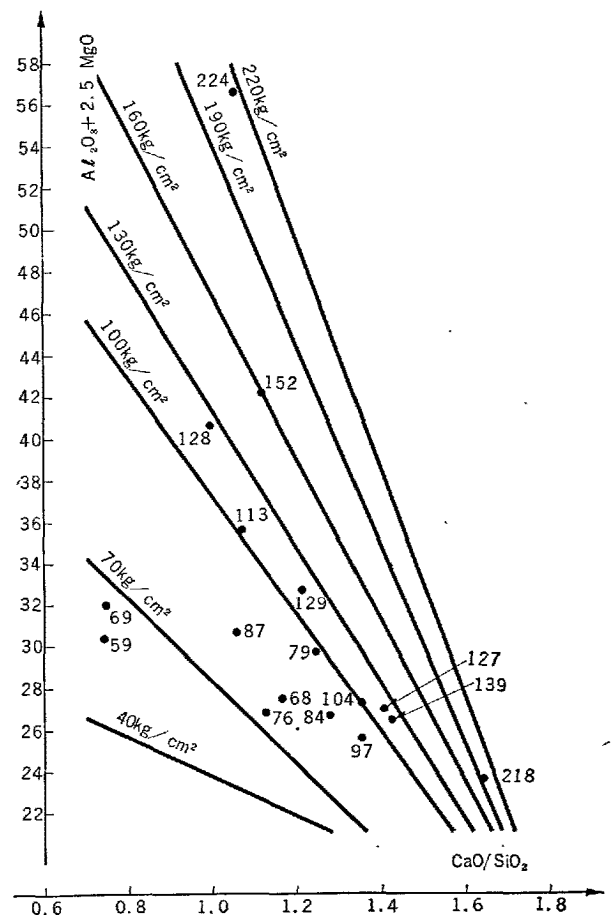

Fig. 2. *Comp. strength of industrial slags at 3 days*

—preparation of the slag/portland cement mixture in three different proportions containing 30–50 and 80% of portland cement.

—test of the mixed cements obtained according to the "RILEM Cembureau" standard testing method for cements (12).

Fig. 2 gives the compressive strengths at 3 days for the cements corresponding to a 70% slag content with a fineness of 4500 cm^2/g Blaine. This graph represents striaght lines of equal mechanical strengths in function of the parameters CaO/SiO_2 and $(Al_2O_3 + 2.5MgO)$. The best correlation was obtained by the choice of a 2.5 coefficient for MgO.

Table 2. *Chemical composition and crystallized phase content of laboratory modified slags.*

Slag No.	Chemical composition				Crystallized phase content %
	% CaO	% SiO_2	% Al_2O_3	% MgO	
1	39.6	44.1	8.9	7.1	—
2	38.2	43.2	10.8	6.4	—
3	37.2	42.0	12.7	6.8	—
4	36.0	39.0	15.9	7.4	—
5	39.0	43.0	9.3	7.5	—
6	37.3	41.2	11.8	9.5	—
7	35.7	40.2	13.4	9.3	—
8	37.3	41.2	12.4	9.1	—
9	35.4	38.9	17.6	9.6	—
10	45.4	40.1	8.5	5.5	—
11	44.2	39.6	10.8	5.3	—
12	43.4	38.3	12.8	5.0	—
13	40.1	35.2	14.0	5.3	—
14	38.1	34.3	9.7	4.8	10–15 (C_2AS)
15	44.2	39.0	8.6	7.6	—
16	43.3	38.6	9.7	7.5	—
17	40.8	36.2	13.1	7.4	—
18	39.3	34.3	14.0	7.5	—
19	37.4	32.7	20.5	7.0	—
20	39.1	34.2	14.1	9.6	—
21	38.2	33.5	14.0	9.7	—
22	36.3	31.4	20.7	9.5	—
23	41.9	37.1	9.1	11.9	10–15 (C_3MS_2)
24	40.6	34.5	10.7	11:6	0–5 (C_3MS_2)
25	40.1	35.2	13.3	11.4	0–5 (C_3MS_2)
26	37.1	32.6	13.9	11.8	—
27	38.4	33.8	11.1	14.3	0–5 (C_3MS_2)
28	37.6	33.2	13.3	14.1	0–5 (C_3MS_2)
29	36.7	31.1	13.6	14.3	0–5 (C_3MS_2)
30	47.2	38.3	8.8	5.3	0–5 (C_3MS_2)
31	45.9	38.0	10.3	5.5	—
32	44.3	37.4	12.4	5.2	—
33	42.5	33.9	14.6	5.1	—
34	39.9	31.6	20.4	4.6	—
35	42.9	34.5	11.9	7.7	—
36	41.7	33.4	14.3	7.1	—
37	38.9	31.4	19.5	6.8	10–15 (C_2AS)
38	44.4	36.5	8.4	10.2	10–15 (C_3MS_2)
39	44.1	36.8	10.7	9.5	10–15 (C_3MS_2)
40	43.7	35.8	12.4	8.9	0–5 (C_3MS_2)
41	40.8	33.0	13.9	9.4	—
42	40.7	32.0	15.8	9.2	0–5 (C_2AS)
43	37.8	29.7	19.8	9.6	—
44	41.3	34.4	9.9	13.4	10–15 (C_3MS_2)
45	38.5	31.7	15.6	13.5	0–5 (C_3MS_2)
46	36.1	29.6	20.2	13.6	—
47	49.7	35.9	8.3	5.1	10–15 (C_3MS_2)
48	48.4	35.2	10.7	5.0	10–15 (C_3MS_2)
49	46.9	34.7	12.0	5.2	0–5 (C_3MS_2)
50	45.0	39.2	13.7	4.8	5–10 (C_2AS)
51	48.8	34.3	8.8	7.2	10–15 (C_3MS_2)
52	47.0	34.6	10.2	7.5	10–15 (C_3MS_2)
53	45.4	32.6	11.3	7.8	—
54	43.5	32.3	14.0	6.9	0–5 (C_2AS)
55	42.6	31.6	14.0	8.8	0–5 (C_2AS)
56	40.8	30.0	13.8	12.0	0–5 (C_2AS)

Similar diagrams were established at the ages of 7 and 28 days and for a slag fineness of 3500 cm^2/g Blaine, and tend to the same conclusions.

Nevertheless, the chemical area covered by the industrial slags was rather small; therefore the composition of some of them was modified in the laboratory to enlarge the investigated field.

Corrected Industrial Slags

We made a choice of four industrial slags with a

Table 3. *Hydraulic index of laboratory modified slags and compressive strengths of cements-mortars made from them.*

Slag No.	Hydraulic index I_h	Compressive strengths after (kg/cm²)	
		3 days	7 days
1	1.26 (a)	35	84
2	1.25 (a)	36	80
3	1.32 (a)	38	90
4	1.42	63	134
5	1.30 (a)	45	117
6	1.39	43	112
7	1.40	58	124
8	1.39	51	124
9	1.51	77	142
10	1.44	39	108
11	1.47	40	97
12	1.50	51	104
13	1.57	90	180
14	1.63	58	188
15	1.53	48	126
16	1.53	48	130
17	1.51	80	190
18	1.67	91	184
19	1.79	153	268
20	1.77	112	232
21	1.78	104	243
22	1.95	165	295
23	1.72	80	157
24	1.82	72	174
25	1.80	99	245
26	1.89	145	303
27	1.91	106	231
28	1.95	104	243
29	2.08	110	253
30	1.55	83	175
31	1.56	86	174
32	1.56	99	185
33	1.70	112	211
34	1.83	124	248
35	1.75	99	199
36	1.79	124	236
37	1.88	102	217
38	1.74	93	184
39	1.72	101	206
40	1.76	101	209
41	1.87	105	222
42	1.95	118	267
43	2.10	172	324
44	1.91	149	243
45	2.09	196	327
46	2.25	212	376
47	1.71	88	170
48	1.74	102	199
49	1.76	122	244
50	1.79	126	234
51	1.86	101	171
52	1.83	105	210
53	1.92	138	295
54	1.89	134	264
55	1.98	170	334
56	2.18	216	377

(a) $I_h = \dfrac{CaO + 1.4\,MgO + 0.70\,Al_2O_3}{SiO_2}$

C/S ratio between 1.16 and 1.41, a Al_2O_3 content of 15%, a MgO content of 5% and a MnO content between 0.6 and 1%.

The chemical composition of these slags were modified by addition of pure oxides, then fused and granulated. The chemical composition of the slags so obtained and their crystalline phase content are given in table 2.

The industrial slags were first ground at 2500 cm²/g Blaine and then intimately mixed with the pure oxides to obtain definite compositions; the mixture was fused by portions of 2 kg, at a temperature exceeding 1500°C, in a graphite crucible protected against oxidation by an outer silimanite crucible and heated in a rotary gas flame furnace.

The fused mass was quickly poured in water to obtain a fine division of the melt. The degree of vitrification was controlled as previously described.

Laboratory cement were prepared by mixing 70% slag separately ground with gypsum to a fineness of 4500 cm²/g Blaine and 30% standard portland cement. These cements were tested according to the RILEM Cembureau method (12). The compressive strength obtained from these samples are reported in Table 3. The compressive strengths at 3 and 7 days are plotted in ternary diagrams (Figs. 3 to 8) resulting from the quaternary diagram ($CaO–SiO_2–Al_2O_3–MgO$) by maintaining the Al_2O_3 content constant at the levels 9–12 and 15%. The slags were divided in three classes according to their Al_2O_3 content: from 7.5 to 10.5, from 10.5 to 13.5 and from 13.5 to 16.5. The first class was projected on the 9% Al_2O_3 level diagram. The second on the 12% level diagram etc . . .

Some of the points of these diagrams correspond to partially crystallized slags; those single-underlined are characterized by a crystalline content lower than 5%, those double-underlined are characterized by a crystalline content between 5 and 15%.

These diagrams prove undoubtedly that an increase in the MgO content improves the mechanical stregnths of the blast-furnace slag cement at least for the area taken on account.

Choice of a Chemical Index for the Hydraulic Activity of the Slag

The chemical index I_h giving the best correlation with the experimental values Figs. 9 and 10 was cal-

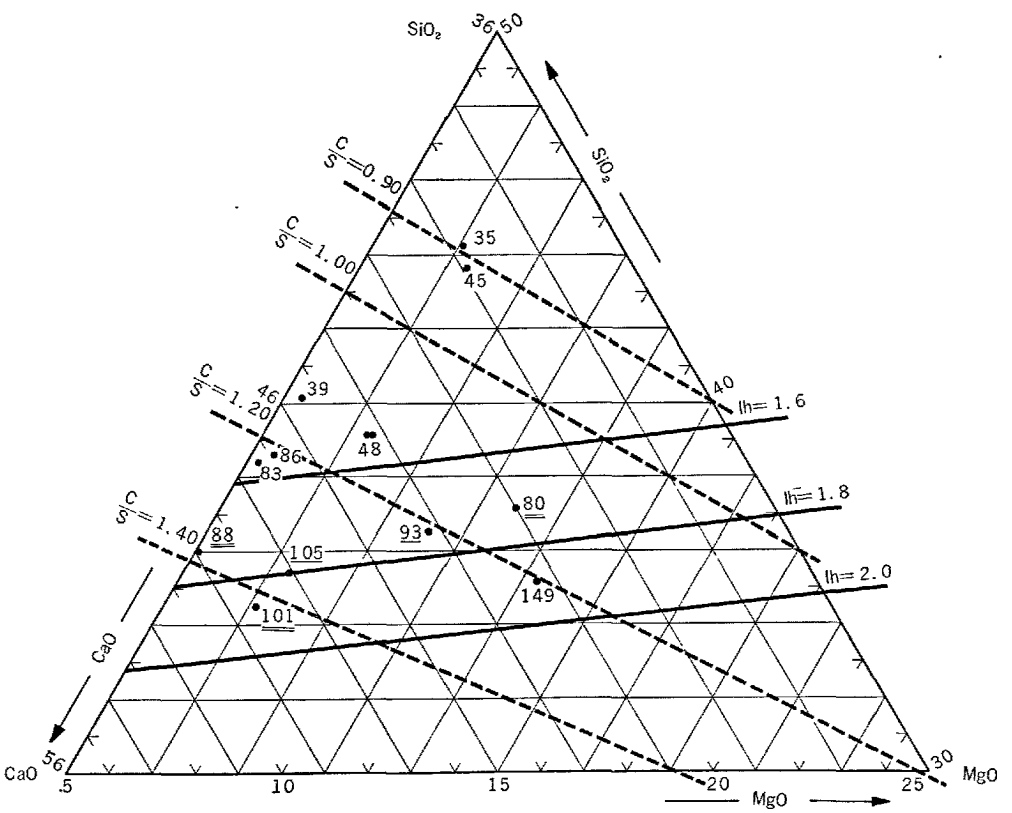

Fig. 3. *9% Al_2O_3 Comp. strength at 3 days*

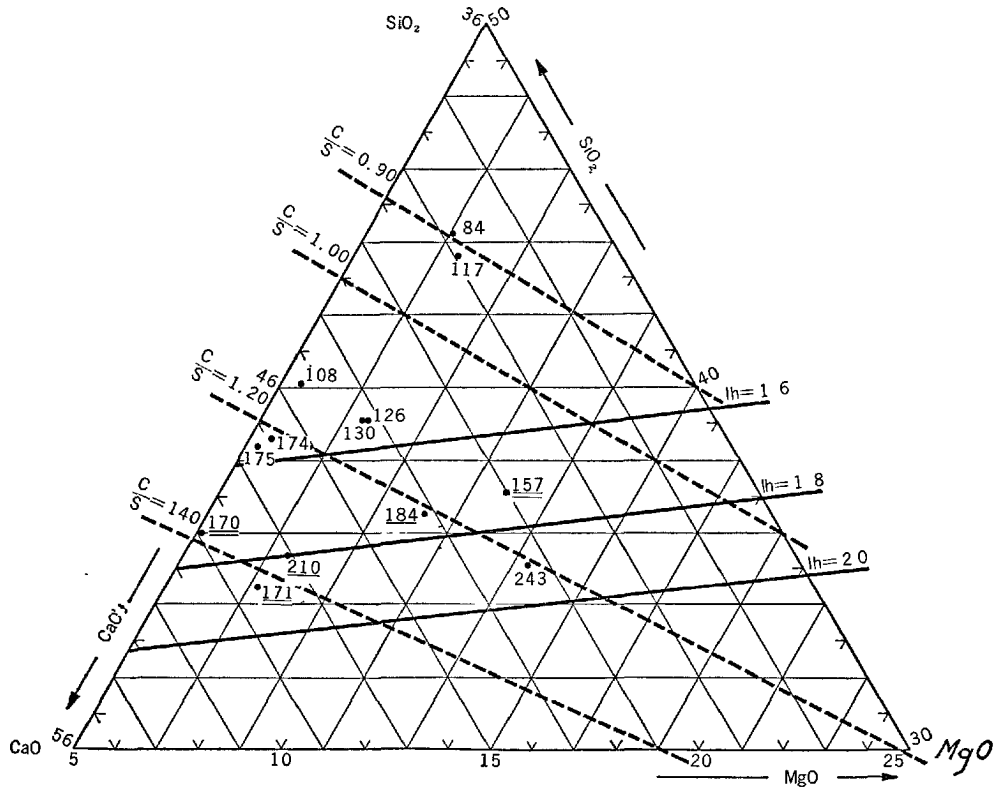

Fig. 4. *9% Al_2O_3 Comp. strength at 7 days*

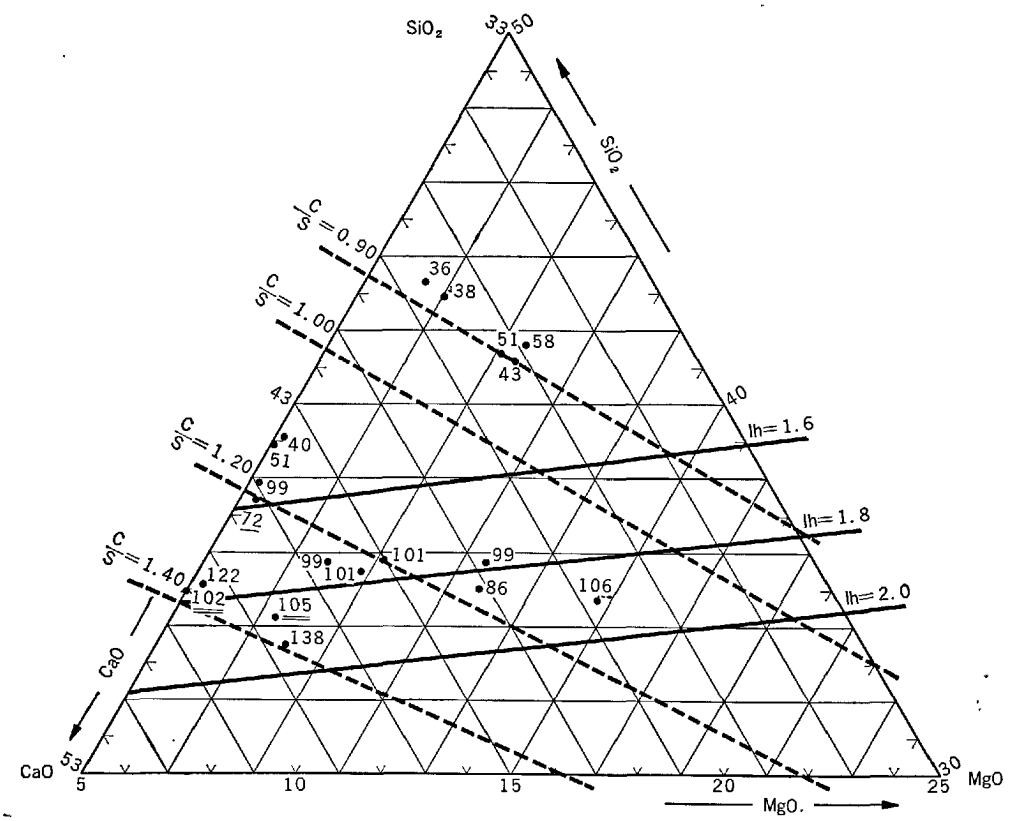

Fig. 5. *12% Al_2O_3 Comp. strength at 3 days*

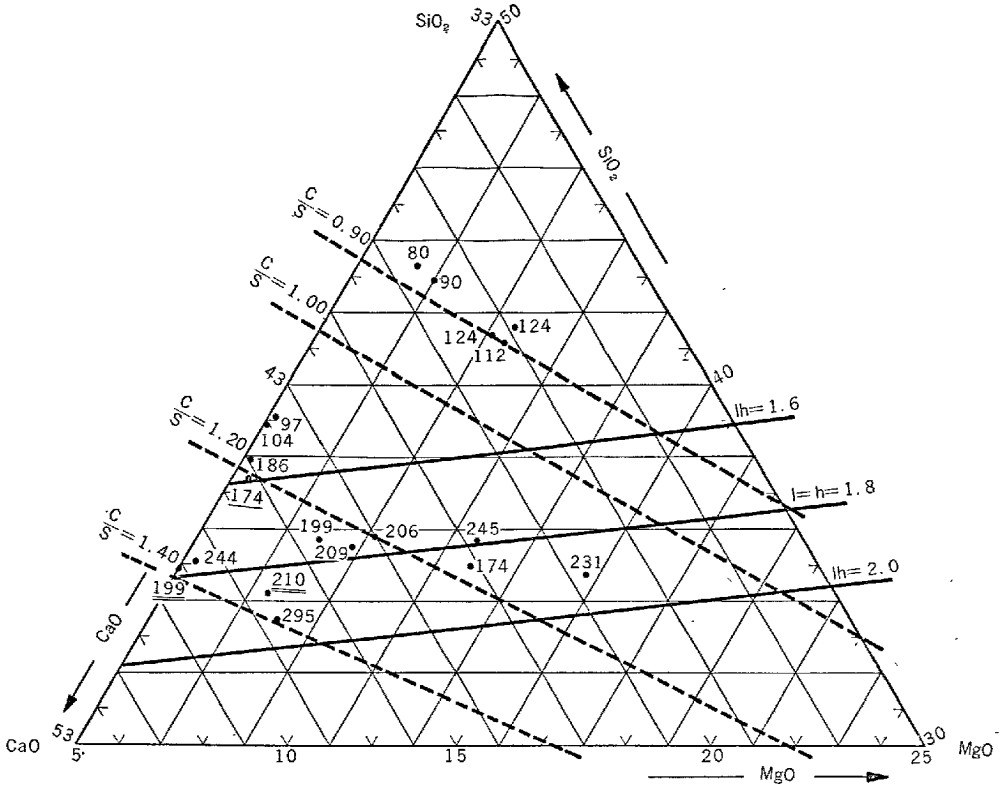

Fig. 6. *12% Al_2O_3 Comp. strength at 7 days*

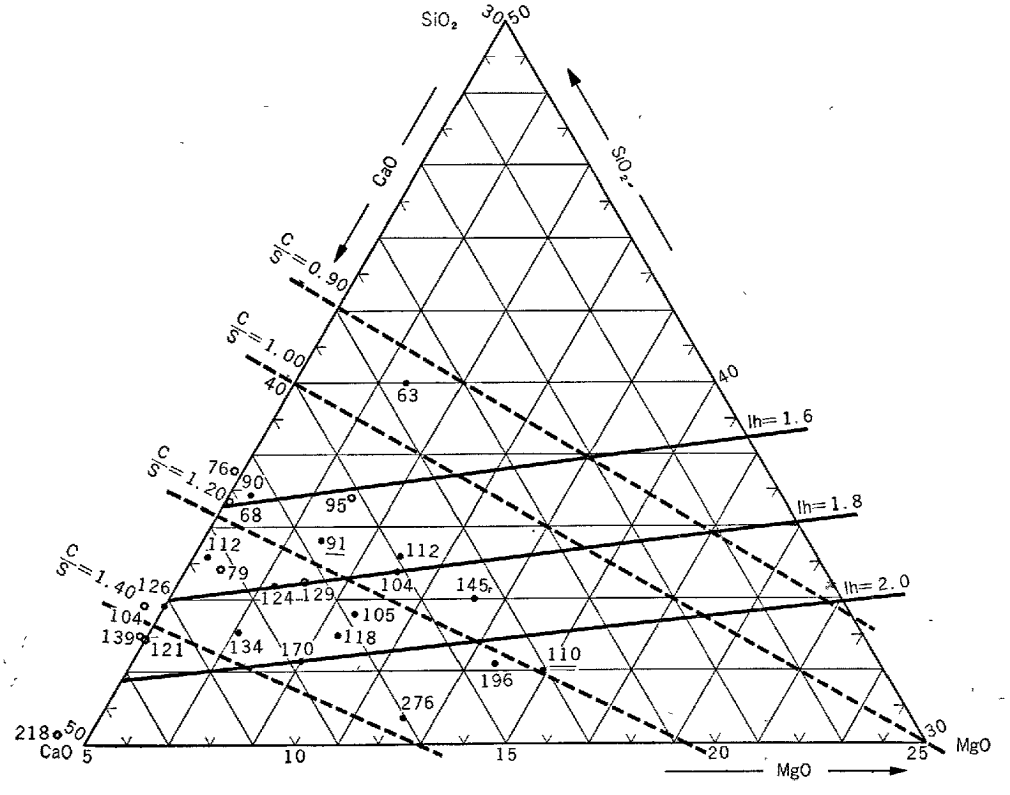

Fig. 7. *15% Al_2O_3 Comp. strength at 3 days*

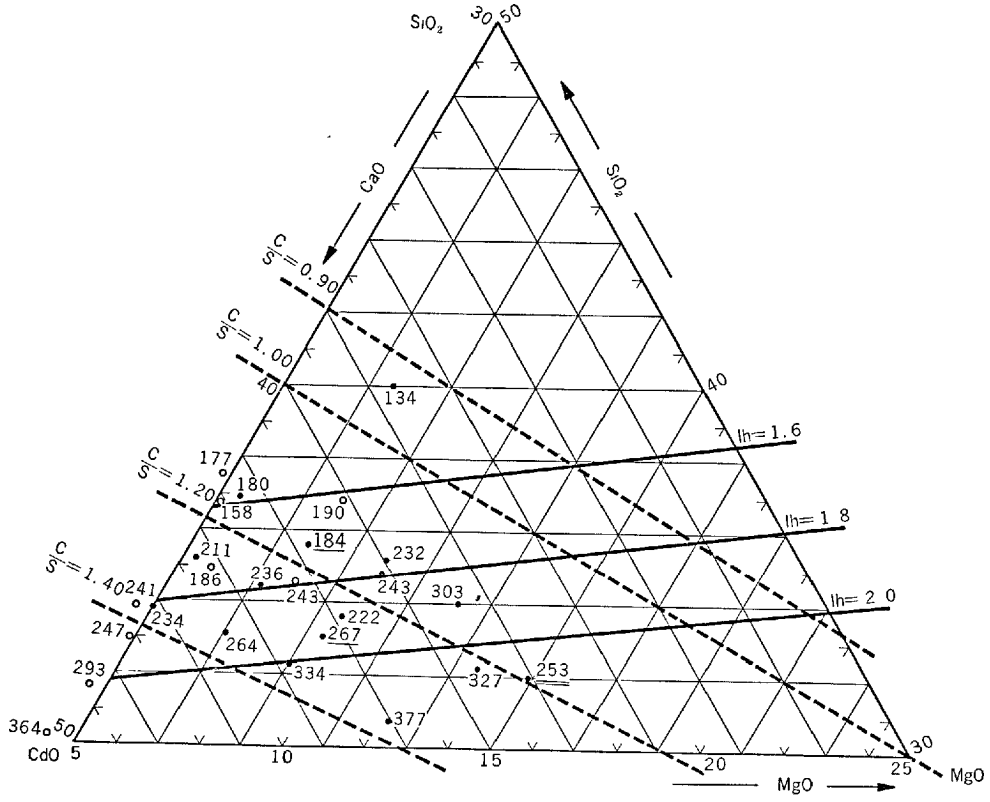

Fig. 8. *15% Al_2O_3 Comp. strength at 7 days*

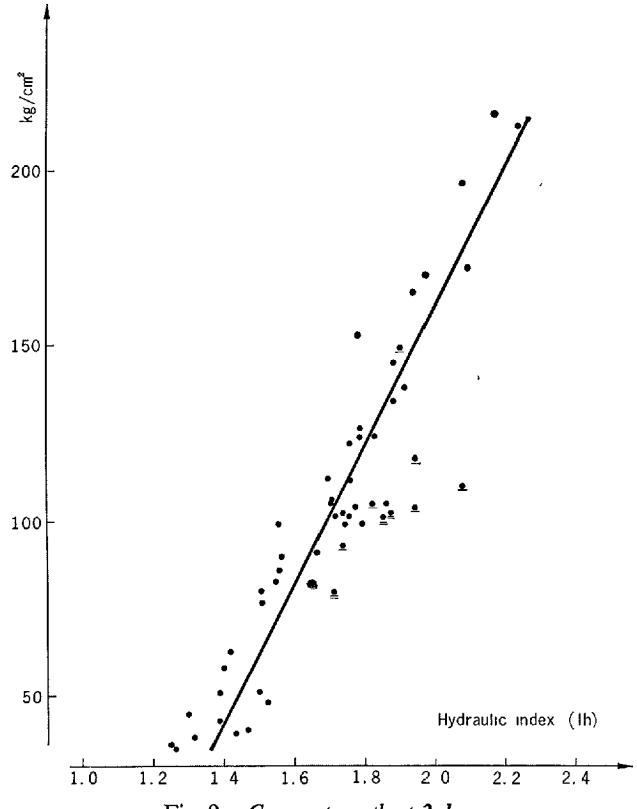

Fig. 9. *Comp. strength at 3 days*

culated and may be expressed as:

$$I_h = \frac{CaO + 1.4\,MgO + 0.56\,Al_2O_3}{SiO_2}$$

For values of I_h lower than 1.4 a better correlation is obtained when the coefficient 0.56 for the Al_2O_3 is replaced by the value 0.70. This formula which was deduced experimentally is in good agreement with the one proposed by Tetmayer for the characterization of the hydraulic vaule of the slags:

$$\frac{\frac{CaO}{56} + \frac{MgO}{40} + \frac{Al_2O_3}{102}}{\frac{SiO_2}{60}} \geqslant 1$$

We plotted on the same figures a certain number of of points corresponding to industrial slags and found a good agreement between the value of the index I_h and the related mechanical strengths. Some of the points coresond to partially crystallized slags and are indicated as previously noted.

On the Figs. 3 to 8 are drawn straight lines corresponding to a constant C/S ratio or to a constant value of the hydraulic index (I_h). These last lines are also the loci of equal mechanical strengths.

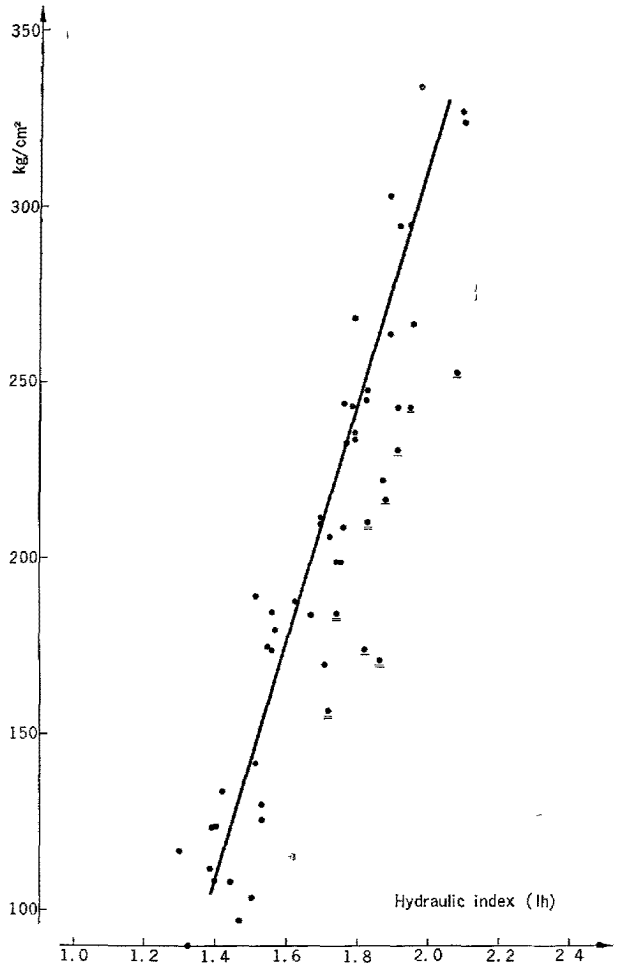

Fig. 10. *Comp. strength at 7 days*

References

1. F. Keil, "Slag cements", Proc. 3d Intern. Symp. Chemistry of Cements, London (1952).
2. W. Kramer, "Blast-furnace slags and slag cements", Proc. 4th Intern. Symp. Chemistry of Cements, Washington (1960).
3. L. Santarelli and G. Goggi, "Expériences sur les Laitiers synthétiques de laboratoire", Silicates Ind. **17**, 52–55 (1952).
4. H. E. Schwiete and F. C. Dölbor, "Einfluss der Abkühlungsbedingungen und der Chemischen Zusammensetzung auf die Hydraulischen Eigenschaften von Hämatitschlacken". Technische Mitteil. No. 1186 Institut für Gesteinshüttenkunde Rhein.-Westf. Hochschule Aachen, 70–83, Köln (1963).
5. S. Solacolu, "Die Bedeutung der Thermischen Gleichgewichte des Systems MgO-CaO-Al_2O_2-SiO_3 für das Schmelzen und Granulieren der Hochofenschlacken", Zement-Kalk-Gips, **4**, 125–137 (1958).
6. R. Kondo, "Blast-furnace slags and slag cements", Discussion, Proc. 4th Intern. Symp. Chemistry of Cements, Washington (1960).
7. E. F. Osborn, R. C. De Vries, K. H. Gee and H. M. Kraner, "Optimum composition of blast-furnace slags, as deduced from liquidus data for the quaternary system CaO-MgO-Al_2O_3-SiO_2". Trans. AIME, J. Metals, 33–45 (1954).
8. P. Hüttemann, "Betriebsuntersuchungen zur Schlackenführung und Schlackenverwertung bei der Thomas- und Stahlroheisenerzeugung", Techn. Mitt. Hüttenwerk Rheinhausen A. G., Heft 3 (March 1955).
9. F. Keil and F. W. Locher, "Hydraulische Eigenschaften von Gläsern. I. Gläsern des Systems CaO-SiO_2-Al_2O_3 mit und ohne MgO", Zement-Kalk-Gips **11**, 245–253 (1958).
10. F. Schröder, "Über die Hydraulischen Eigenschaften von Hüttensanden und ihre Beurteilungsmethoden". Tonindustrie Zeitung **85**, 39–44 (1961).
11. N. Sutterheim and R. W. Nurse, "Experimental blast-furnace cements incorporating high magnesia slags", Mag. of Concrete Research, **9**, 101–106 (1952).
12. Institut Belge de Normalisation. Ciments—Echantillonnage et méthodes d'essais—Essais sur mortier plastique. NBN 178.50, NBN 178.51, NBN 178.52, NBN 178.53 (1959).

(B) Papers regarding High-Sulphate Slag

Supplementary Paper IV-21 Anhydrite Cement

André A. Van Haute*

Synopsis

Anhydrite cement is a synthetic cement composed of anhydrite obtained from residual gypsum and slag. In itself an anhydrite-slag mixture gives a cement of insufficient strength and with too long a setting time. Research aimed at improving this cement will therefore have to be centered on finding the anhydrite-slag ratio producing the greatest strength, on the one hand, and seeking the nature and quantity of components to provide greater strength and to shorten the setting time (catalyst), on the other hand.

A new catalyst has been developed: it consists of a mixture of aluminous cement, K_2SO_4 and $Ca(OH)_2$. After hundreds of tests it has been found that the strongest anhydrite cement is obtained with a 50/40 anhydrite/slag ratio, $\pm 10\%$ catalyst mixture being used. The composition of the mixture can be varied according to whether the purpose is to obtain a cement having the greatest possible compressive strength after 3 days or else after a longer period, say 28 days. Flexion and compression tests were carried out in accordance with the standardized Rilem-Cembureau method; the results are shown in table form in terms of the catalyst composition (3, 7 and 28 days).

From these tests it emerged that the specimens which gave the best results after three days (80 kg/cm² compressive strength) consisted of 6 to 7% aluminous cement, 1.5% $Ca(OH)_2$ and 1.2% K_2SO_4 (that is to say, in all 8.7 to 9.7% catalyst). This anhydrite cement has a normal consistency of 37%; setting begins after 5.15 hours and ends after 7.35 hours; the compressive strength after 28 days attains a value of 400 kg/cm².

On the long term strong specimens require more aluminous cement (8%), less hydrated lime (1.1%), a similar anhydrite/slag ratio (50/40) and the same quantity of potassium sulphate (1.2%). After 28 days a specimen such as this produces a compressive strength of 580 kg/cm².

Anhydrite Cement

This study contains the results of a research to prepare a synthetic cement using anhydrite as the main component. Only the anhydrite obtained by calcining the waste gypsum from the phosphoric acid industry has been used: so that, at the same time, a possible solution to the problem of disposal of waste gypsum from this industry has been found.

Of course, one is immediately faced with the slow setting and the instability to water of the anhydrite. To realize a faster reaction and a waterproof crystal structure a blast furnace slag as well as a mixture of catalyst consisting of K_2SO_4, $Ca(OH)_2$ and aluminous cement has been added.

To be acceptable as a binder, the properties of this new kind of cement must be near those of portland cement and even better: the search for the "optimum composition" of the anhydrite cement to reach the highest possible mechanical resistance, while the other physical properties still conform to the standard specifications of portland cement, has been the main object of this study. At the same time we tried to determine the relative influence of the different components.

*Institute of Industrial Chemistry, University of Louvain, Heverlee, Belgium.

Basic Components

Anhydrite

As raw material residual gypsum was taken from the phosphoric acid industry using Morocco rock. The average composition of the (dry) gypsum waste is as follows:

$CaSO_4$	76%
water	20%
P_2O_5 total	1%
P_2O_5 insoluble	0.15%
Fe_2O_3	0.1%
Al_2O_3	0.15%
F	1%
MgO	0.1%
SiO_2	1%
organic components	rest

This residual gypsum was calcined at a temperature of 850 to 900°C in order to obtain anhydrite II, which was ground to a fineness smaller than 63μ (230 mesh). The specific weight of this anhydrite is 3.04 g/cm^3 and the specific surface (Blaine) 1900 cm^2/g. The porosity of the anhydrite is 0.53.

Because of the already mentioned slow setting of the anhydrite II, an accelerator is needed. The following materials can be considered:

—neutral or weakly acid sulphates: K_2SO_4, Na_2SO_4, $(NH_4)_2SO_4$, $CaSO_4 \cdot 1/2H_2O$, $MgSO_4$, $CdSO_4$, $ZnSO_4$, $FeSO_4$, alum, $CuSO_4$.

—bisulphates: $NaHSO_4$, $KHSO_4$.

—bases: CaO, $Ca(OH)_2$, MgO, $Mg(OH)_2$.

—cement, basic slags . . .

The quantity of accelerator which can be added is mostly restricted from 0.1 to 3% because it can influence the crystal structure and therefore decrease the mechanical strength.

Since the concentrations of the impurities are different according to the rock (apatite), from which the waste gypsum is produced, it ought to be checked in what way these impurities influence the flexural and compressive strengths. It is always preferable not to be dependent on one sole distributor. In nature apatite rock is not found which gives a waste gypsum with larger concentrations of impurities than:

F (in the form of Na_2SiF_6)	4%
Fe_2O_3	3%
P_2O_5 (in the form of H_3PO_4)	2%
Na_2O (in the form of Na_2SO_4)	1%
K_2O (in the form of K_2SO_4)	1%
MgO (in the form of $MgSO_4$)	1%

To conform as much as possible to reality, supplementary tests have been carried out, in which the above mentioned impurities, even in quantities to the maximum possible concentrations in the anhydrite, were recalcined with the latter, and then ground to the above mentioned fineness. We have carried out a series of tests with a well determined composition of the anhydrite cement, which, although it does not completely conform to the "optimum composition" to be found later, is very close to it: we never noticed a drop of more than 10% of the mechanical strength, whereas by adding sulphates and phosphates the final strength even slightly increases.

Slag

Blast furnace slags were used with the following compositions (dry):

CaO	41.60%
SiO_2	31.70%
Al_2O_3	16.70%
MgO	5.70%
MnO	1.10%
FeO	0.80%
S	1.00%
$K_2O + Na_2O$	1.40%

After drying these slags, they were ground also to a fineness smaller than 63μ (230 mesh). The specific weight of the ground slag is 3.0 g/cm^3 and the specific surface (Blaine) 2460 cm^2/g; the porosity has a value of 0.50.

Of course, only "quenched" slags have hydraulic properties. The setting of these slags can be accelerated by adding $Ca(OH)_2$ or portland cement (which liberates $Ca(OH)_2$ during setting). During the setting of the slag the liberated alumina reacts with the hydrated lime, which will therefore be absent in the end product.

Tests have shown that slags for the production of anhydrite cement should have the following composition:

CaO	35 to 45%
SiO_2	preferably 30 to 33%, not more than 35%
Al_2O_3	not less than 15%
S	not more than 1.5 to 1.8%

Catalyst

A mixture of K_2SO_4, $Ca(OH)_2$ and aluminous cement, also ground to a fineness less than 63μ, is used as catalyst.

As mentioned above, K_2SO_4 and a part of the hydrated lime are added as an accelerator for the an-

hydrite: the other part of the lime activates the slag. Also several other sulphates (see above) were tried as accelerators for the anhydrite in the anhydrite cement, but with not so good a result.

As aluminous cement a cement of the English firm "Lafarge Aluminous Cement Co. Ltd.", was used, with the following composition:

Al_2O_3	40%
CaO	37.5%
SiO_2	4.5%
FeO	7%
Fe_2O_3	9%
TiO_2	2%

Crystallographically aluminous cement (with $SiO_2 >$ 5%) consists of $\pm$60% $CaO \cdot Al_2O_3$, the hydration of which will be strongly activated by portland cement, lime and calciumsulphate; it is also composed of 15 to 20% gehlenite, $2CaO \cdot Al_2O_3 \cdot SiO_2$, which sets very slowly, and of 10 to 15% $2CaO \cdot SiO_2$. Furthermore, fibrous structures of $4CaO \cdot Al_2O_3 \cdot Fe_2O_3$ and of $6CaO \cdot Al_2O_3 \cdot 2Fe_2O_3$ are found, and also $CaO \cdot TiO_2$. Not more than 0.5% alkalis may be present, otherwise the setting will be too fast and the full strength will never be developed. The same remark applies to the use of lime.

The main purpose of adding aluminous cement to the catalyst mixture is to increase the final strength of the anhydrite cement.

The optimum composition of the catalyst mixture has to be worked out precisely as a function of the anhydrite-slag ratio, in order to reach the highest mechanical strength of the anhydrite cement, whereas the other physical properties still conform to the standards of portland cement.

Other aluminous cements (for instance the German "Rolandshütte" cement) have a larger percentage of alumina and a lower percentage of ironoxide: the optimum composition will have to be slightly adapted, but tests carried out with "Rolandshütte" show a larger final strength of the anhydrite cement.

Standardization and Accuracy of Tests

Standardization

In order to obtain reliable and reproducible results the following Belgian specifications were accurately used:

—for testing anhydrite cement:

NBN 178.21 for the determination of the fineness. As already mentioned earlier all components were ground to a fineness less than 63μ (230 mesh). Some tests were also carried out with finenesses less than 88μ (170 mesh): the properties of the samples were practically identical.

NBN 178.22 for the determination of the specific weight (approximately 3.0 g/cm^3).

NBN 178.30 for the determination of the consistency of standard cement paste.

NBN 178.31 for the determination of initial and final setting times.

NBN 178.32 for the determination of soundness.

—for testing the corresponding plastic mortars ("Rilem-Cembureau" method):

NBN 178.51 for the preparation and the mixing of the samples.

NBN 178.52 for the curing of the samples

NBN 178.53 for th determination of the flexion and compression strengths.

Two deviations from the specifications have to be noted:

—first of all it was necessary to use only 45% of water for the preparation of the plastic mortars instead of 50% as NBN 178.52 prescribes: indeed, the plastic mortars showed the same plasticity with 45% of water as they did with 50% for plastic mortars made of portland cement.

—secondly, all the samples were cured in saturated humid air at 20°C instead of in water saturated with lime as NBN 178.52 prescribes. Some comparative tests were carried out and we noticed that the two methods of curing were almost equivalent.

Accuracy of Flexion and Compression Tests

In order to have an idea about the accuracy of the whole experiment (going from weighing and mixing of the components to the testing of the mortars) some samples with identical composition were made at different times, following exactly the Belgian specifications mentioned above. The deviations noticed point to inaccuracies inherent to the testing method.

From these "reference" tests the average and the standard deviation were determined. These calculations show on one hand the spreading of the results; on the other hand they offer a criterion for the real meaning of a difference in strength between samples made at different times.

In order to determine the *absolute* standard devia-

tions (S) for each group of results (flexural strengths after 3, 7 and 28 days, and compressive strengths after 3, 7 and 28 days) the differences (d) between each result (n per group) and the corresponding group average are calculated according to the following formula:

$$S = \sqrt{\frac{\sum d^2}{n}}$$

The following *proportional* standard deviations (S') were found:

	3d	7d	28d
flexion	17.7%	10.9%	10.7%
compression	6.9%	8.6%	9.7%

Systematic Investigation about the Influence of the Different Components and about the Optimum Composition

Several introductory tests have shown that the optimum composition has to be found between the following values of the different components:

Anhydrite/slag ratio between 45/45 and 50/40
$Ca(OH)_2$-percentage between 1.0 and 1.5
K_2SO_4-percentage between 0.9 and 1.2
Aluminous cement between 5 and 9%

In order to determine narrower and more precise limits for the optimum composition and to have at the same time a clear picture of the influence of the different components on the strength, the principal combinations of the compositions of the different components, mentioned above, were tested:

A/S: Anhydrite/Slag ratio: 45/45 and 50/40
C: $Ca(OH)_2$-percentage: 1.1%, 1.2%, 1.3% and 1.4% (+1.5% for the A/S ratio 50/40)
K: K_2SO_4-percentage: 0.9%, 1.0% and 1.2%
Al: Aluminous cement: 6%, 7% and 8%.

The samples are numbered X1 to X48 for the A/S ratio 45/45, and X49 to X108 for the ratio 50/40.

Results: Flexion and Compression Strengths (after 3, 7, and 28 days)

Flexural and compressive strengths of the smaples X 1 to X 108 are listed in 9 tables.

Some other tests were made after 56 days: the average increase of the compressive strength with respect to the strength after 28 days was of the order of magnitude of 10%.

Discussion of the Influence of the Different Components

Influence of the Quantity of Aluminous Cement

From the Tables 1 to 9 we can conclude:

Table 1.
A/S: 45/45
$Ca(OH)_2$: 1.1%

No	Composition					Flexural strength kg/cm²			Compressive strength kg/cm²		
	A(%)	S(%)	C(%)	K(%)	Al(%)	3d	7d	28d	3d	7d	28d
×1	46.00	46.00	1.1	0.9	6	9	23.0	49.5	36.6 36.8	105 98	283 312
×2	45.50	45.50	1.1	0.9	7	8.8	24.5	58.4	36.2 37.5	100 104	415 413
×3	45.00	45.00	1.1	0.9	8	8.5	28.3	62.0	39.0 34.0	100 105	410 413
×4	45.95	45.95	1.1	1.0	6	10.7	29.5	61.5	44.6 42.2	117 112	437 433
×5	45.45	45.45	1.1	1.0	7	8.7	25.8	66.0	36.6 37.5	105 103	423 400
×6	44.95	44.95	1.1	1.0	8	9.3	26.8	63.5	37.5 36.5	103 101	462 445
×7	45.90	45.90	1.1	1.1	6	9.3	25.5	64.0	38.7 38.7	110 108	434 414
×8	45.40	45.40	1.1	1.1	7	8.8	28.0	67.6	35.6 35.6	115 119	422 431
×9	44.90	44.90	1.1	1.1	8	8.7	24.5	56.3	35.0 33.8	105 116	435 420
×10	45.85	45.85	1.1	1.2	6	10.5	23	60.0	38.4 32.8	95 104	425 427
×11	45.35	45.35	1.1	1.2	7	11.5	24.5	63.0	41.2 41.2	100 90	456 445
×12	44.85	44.85	1.1	1.2	8	8.5	26.5	62.2	32.8	107	487

—at short term (after 3 days) the best results are obtained with 6% Al, especially in the presence of much lime.

—at long term (after 28 days) the best results are obtained with 8% Al, especially in the presence of not too much lime.

—at medium term (after 7 days) the samples do not show any significant difference in strength according to the content of aluminous cement.

Influence of the Quantity of Hydrated Lime

The effect of the lime seems to be influenced by the anhydrite-slag ratio, so that two cases have to be discerned:

a. 45/45 ratio:

—at short term a maximum strength is obtained

Table 2.
A/S: 45/45
$Ca(OH)_2$: 1.2%

No.	Composition					Flexural strength kg/cm²			Compressive strength kg/cm²		
	A(%)	S(%)	C(%)	K(%)	Al(%)	3d	7d	28d	3d	7d	28d
×13	45.95	45.95	1.2	0.9	6	10.5	29.5	63.5	38.2 38.4	99 104	406 422
×14	45.45	45.45	1.2	0.9	7	9.5	25	74.0	39.2 —	90 94	439 428
×15	44.95	44.95	1.2	0.9	8	9.5	25	60.0	40.6 37.8	93 94	461 435
×16	45.90	45.90	1 2	1.0	6	9.4	25	53.5	36.8 38.4	105 90	419 412
×17	45.40	45.40	1.2	1.0	7	9.3	25	69.0	36.0 38.8	96 91	456 452
×18	44.90	44.90	1.2	1.0	8	9.0	24	58.5	37.2 36.3	95 91	451 (380)
×19	45.85	45.85	1.2	1.1	6	13.6	28.0	51.0	41.0 —	142 137	372 375
×20	45.35	45.35	1.2	1.1	7	11.4	27.5	51.0	40.0 40.6	106 114	353 346
×21	44.85	44.85	1.2	1.1	8	11.1	25.5	56.5	35.6 37.5	114 115	382 400
×22	45.80	45.80	1.2	1.2	6	10.6	31.5	51.2	39.0 38.7	113 121	363 347
×23	45.30	45.30	1.2	1.2	7	11.3	26.5	59.5	42.5 45.0	112 114	414 465
×24	44.80	44.80	1.2	1.2	8	12.8	29.0	58.0	40.0 41.3	135 129	444 422

Table 3.
A/S: 45/45
$Ca(OH)_2$: 1.3%

No.	Composition					Flexural strength kg/cm²			Compressive strength kg/cm²		
	A(%)	S(%)	C(%)	K(%)	Al(%)	3d	7d	38d	3d	7d	28d
×25	45.90	45.90	1.3	0.9	6	13.0	42.5	55.5	67.5 61.5	149 152	366 347
×26	45.40	45.40	1.3	0.9	7	15.4	38.0	64.5	64.0 65.5	154 151	384 378
×27	44.90	44.90	1.3	0.9	8	15.3	37.5	50.5	59.0 57.0	158 168	422 415
×28	45.85	45.85	1.3	1.0	6	17.1	39.2	55.0	73.0 71.2	158 159	332 347
×29	45.35	45.35	1.3	1.0	7	14.1	37.5	60.0	62.8 63.5	146 151	375 369
×30	44.85	44.85	1.3	1.0	8	13.5	33.8	68.5	58.0 57.8	138 133	413 423
×31	45.80	45.80	1.3	1.1	6	14.8	37.5	57.5	62.0 61.1	164 151	372 384
×32	45.30	45.30	1.3	1.1	7	15.0	39.5	60.0	59.5 63.8	151 145	381 390
×33	44.80	44.80	1.3	1.1	8	13.5	40.8	61.5	49.5 51.2	138 150	450 439
×34	45.75	45.75	1.3	1.2	6	12.8	35.5	64.5	50.8 52.0	176 176	450 446
×35	45.25	45.25	1.3	1.2	7	14.8	38.5	70.5	52.0 53.5	172 185	460 475
×36	44.75	44.75	1.3	1.2	8	15.0	40.0	64.0	57.0 58.0	195 182	478 475

with 1.3% $Ca(OH)_2$. Less lime is worse, and also more lime has a weakening effect.

—at long term, no important differences have to be noted, unless a small increase of the strength with decreasing $Ca(OH)_2$-content.

b. 50/40 ratio:

Now, the differences are bigger, but always in the same direction.

—at short term 1.4% $Ca(OH)_2$ gives the best results, particularly in the presence of much K_2SO_4 (1.1 to 1.2%).

—at long term, the use of much lime seems to be fatal. Samples with 1.1% $Ca(OH)_2$ give the best results. The following conclusion can hence be taken: much lime causes high mechanical strengths after 3 days, and small quantities of lime do the same after 28

Table 4.
A/S: 45/45
$Ca(OH)_2$: 1.4%

No.	Composition					Flexural strength kg/cm²			Compressive strength kg/cm²		
	A(%)	S(%)	C(%)	K(%)	Al(%)	3d	7d	28d	3d	7d	28d
×37	45.85	45.85	1.4	0.9	6	14.2	43.0	69.5	59.2	179	410
									56.0	185	438
×38	45.35	45.35	1.4	0.9	7	14.0	39.5	71.5	55.0	185	400
									51.5	186	435
×39	44.85	44.85	1.4	0.9	8	15.5	39.5	68.2	55.0	190	475
									52.0	174	469
×40	45.80	45.80	1.4	1.0	6	12.3	38.8	59.5	53.0	163	420
									55.6	160	418
×41	45.30	45.30	1.4	1.0	7	11.5	34.0	70.5	47.0	169	415
									53.5	182	433
×42	44.80	44.80	1.4	1.0	8	12.0	34.0	63.5	51.2	168	478
									51.0	173	453
×43	45.75	45.75	1.4	1.1	6	11.8	32.5	65.0	54.5	163	413
									54.4	169	428
×44	45.25	45.25	1.4	1.1	7	13.0	33.5	63.5	53.1	173	419
									53.1	175	428
×45	44.75	44.75	1.4	1.1	8	11.2	35.5	70.0	50.5	155	450
									47.5	169	469
×46	45.70	45.70	1.4	1.2	6	10.6	38.0	67.0	47.0	163	433
									48.0	179	469
×47	45.20	45.20	1.4	1.2	7	11.5	31.0	80.0	58.7	168	419
									47.5	165	419
×48	44.70	44.70	1.4	1.2	8	11.0	29.0	80.5	46.9	150	470
									45.0	161	479

Table 5.
A/S: 50/40
$Ca(OH)_2$: 1.1%

No.	Composition					Flexural strength kg/cm²			Compressive strength kg/cm²		
	A(%)	S(%)	C(%)	K(%)	Al(%)	3d	7d	28d	3d	7d	28d
×49	51.11	40.88	1.1	0.9	6	11.5	35.0	88.0	43.7	148	515
									43.7	146	554
×50	51.06	40.84	1.1	1.0	6	11.4	35.5	83.0	45.0	150	544
									45.0	156	531
×51	51.00	40.80	1.1	1.1	6	10.2	38.5	83.5	45.4	159	510
									45.0	160	496
×52	50.94	40.76	1.1	1.2	6	10.1	35.5	80.0	37.5	131	512
									36.9	132	515
×53	50.55	40.44	1.1	0.9	7	11.2	29.5	75.0	40.6	136	546
									41.2	135	528
×54	50.50	40.40	1.1	1.0	7	11.2	36.5	82.0	43.1	149	538
									46.3	159	522
×55	50.44	40.36	1.1	1.1	7	13.0	40.0	83.5	47.5	166	550
									45.0	164	528
×56	50.39	40.31	1.1	1.2	7	12.0	36.0	82.5	44.4	155	328
									42.5	141	534
×57	50.00	40.00	1.1	0.9	8	12.0	39.5	70.5	43.9	149	563
									45.0	137	550
×58	49.94	39.96	1.1	1.0	8	12.3	37.0	76.5	48.8	157	560
									48.8	154	555
×59	49.89	39.91	1.1	1.1	8	13.0	37.0	75.0	47.5	161	575
									52.5	166	544
×60	49.83	39.87	1.1	1.2	8	13.5	33.0	73.5	48.2	150	580
									49.0	153	580

days.

Influence of the Quantity of K_2SO_4

Here also, the effect is somewhat different according to the anhydrite-slag ratio:

a. 45/45 ratio:

—at long term, the strength increases with the K_2SO_4-content.

—at short term, the strength also increases with the K_2SO_4-content, but this time a maximum strength is obtained for 1.1% K. 1.2% K gives worse results.

b. 50/40 ratio:

—at short term 1.2% K is the best percentage to be used, especially in the presence of a high $Ca(OH)_2$-content.

—at long term, there seems not to be an influence of

Table 6.
A/S: 50/40
$Ca(OH)_2$: 1.2%

No.	Composition					Flexural strength kg/cm²			Compressive strength kg/cm²		
	A(%)	S(%)	C(%)	K(%)	Al(%)	3d	7d	28d	3d	3d	28d
×61	51.06	40.84	1.2	0.9	6	15.3	42.5	76.0	54.0 55.5	182 183	536 545
×62	51.00	40.80	1.2	1.0	6	14.1	45.0	77	60.5 59.0	195 189	556 519
×63	50.94	40.76	1.2	1.1	6	13.4	43.5	75	59.0 51.0	182 191	525 544
×64	50.89	40.71	1.2	1.2	6	12.5	37.8	75	58.5 54.5	182 192	519 581
×65	50.50	40.40	1.2	0.9	7	10.9	35.5	59	50.0 48.0	150 146	466 500
×66	50.44	40.36	1.2	1.0	7	12.4	34.0	71	53.2 52.5	137 138	434 456
×67	50.39	40.31	1.2	1.1	7	14.3	36.5	68.0	60.6 63.0	180 176	506 494
×68	50.33	40.27	1.2	1.2	7	15.8	42.5	64.5	65.0 66.2	180 176	512 543
×69	49.94	39.96	1.2	0.9	8	12.8	34.5	75.0	55.6 58.1	154 156	306 347
×70	49.89	39.91	1.2	1.0	8	11.8	41.2	70.5	54.4 60.0	158 165	475 481
×71	49.83	39.87	1.2	1.1	8	13.2	42.0	68.0	54.5 53.7	158 159	512 503
×72	49.78	39.82	1.2	1.2	8	13.2	45.0	56.0	55.0 57.5	169 171	488 363

Table 7.
A/S: 50/40
$Ca(OH)_2$: 1.3%

No.	Composition					Flexural strength kg/cm²			Compressive strength kg/cm²		
	A(%)	S(%)	C(%)	K(%)	Al(%)	3d	7d	28d	3d	7d	28d
×73	51.00	40.80	1.3	0.9	6	16.1	39.0	60.5	64.0 61.2	169 137	428 432
×74	50.49	40.76	1.3	1.0	6	18.2	39.0	66.5	60.5 53.1	179 184	463 466
×75	50.89	40.71	1.3	1.1	6	14.5	37.0	78.5	60.5 60.0	167 164	491 485
×76	50.83	40.67	1.3	1.2	6	16.1	37.1	67.5	66.2 67.0	179 183	463 472
×77	50.44	40.36	1.3	0.9	7	12.0	31.2	62.0	39.4 52.5	153 157	456 419
×78	50.39	40.31	1.3	1.0	7	12.3	39.5	62.5	53.1 58.7	161 169	438 456
×79	50.33	40.27	1.3	1.1	7	8.5	36.5	65.0	53.7 52.8	157 174	453 385
×80	50.28	40.22	1.3	1.2	7	14.1	41.0	77.8	55.5 51.5	171 178	456 459
×81	49.89	39.91	1.3	0.9	8	13.0	40.8	64.5	54.5 57.0	158 161	469 494
×82	49.83	39.87	1.3	1.0	8	13.5	42.0	73.0	47.5 52.8	156 158	463 475
×83	49.78	39.82	1.3	1.1	8	10.0	31.5	72.5	47.2 41.0	134 136	438 447
×84	49.72	39.78	1.3	1.2	8	9.5	33.0	63.0	49.9 45.0	159 164	463 459

the K_2SO_4-content in the presence of 1.1 to 1.2 $Ca(OH)_2$. However, stronger mortars are obtained with increasing K_2SO_4-content in the presence of 1.3 to 1.4% $Ca(OH)_2$.

Conclusion: a large quantity of K_2SO_4 is always favourable, except for an A/S ratio 45/45, tested after 3 days.

Influence of the Anhydrite-Slag Ratio

First of all there is the influence of this ratio on the effect of the other components, as discussed in the previous paragraphs.

On the other hand, we can establish that about 90% of the samples made with a 50/40 anhydrite/slag ratio are stronger than the corresponding samples

Table 8.
A/S: 50/40
$Ca(OH)_2$: 1.4%

No.	Composition					Flexural strength kg/cm²			Compressive strength kg/cm²		
	A(%)	S(%)	C(%)	K(%)	Al(%)	3d	7d	28d	3d	7d	28d
×85	50.94	40.76	1.4	0.9	6	11.8	38.0	65.8	51.9 61.0	153 164	415 388
×86	50.89	40.71	1.4	1.0	6	13.0	41.5	67.8	60.0 55.0	163 171	391 419
×87	50.83	40.67	1.4	1.1	6	13.8	36.5	58.5	58.1 58.5	(139) 172	422 444
×88	50.79	40.62	1.4	1.2	6	14.7	40.0	63.5	60.6 58.8	162 178	469 489
×89	50.39	40.31	1.4	0.9	7	15.0	39.5	69.5	57.5 61.0	164 175	506 494
×90	50.33	40.27	1.4	1.0	7	15.8	35.0	67.5	58.1 58.8	170 159	487 516
×91	50.28	40.22	1.4	1.1	7	11.0	36.0	66.5	54.8 55.3	164 155	453 464
×92	50.22	40.18	1.4	1.2	7	15.1	35.0	66.0	58.1 58.8	162 164	481 491
×93	49.83	39.87	1.4	0.9	8	14.3	41.0	68.5	56.2 53.7	164 161	426 444
×94	49.78	39.82	1.4	1.0	8	11.8	37.0	65.5	53.7 51.8	156 153	462 462
×95	49.72	39.78	1.4	1.1	8	14.5	37.5	66.5	57.5 58.1	173 179	485 481
×96	49.67	39.73	1.4	1.2	8	14.1	32.5	68.2	48.1 50.0	143 148	491 437

Table 9.
A/S: 50/40
$Ca(OH)_2$: 1.5%

No.	Composition					Flexural strength kg/cm²			Compressive strength kg/cm²		
	A(%)	S(%)	C(%)	K(%)	Al(%)	3d	7d	28d	3d	7d	28d
×97	50.89	40.71	1.5	0.9	6	13.5	44.0	54.0	51.2 58.4	133 131	324 290
×98	50.83	40.67	1.5	1.0	6	14.0	42.5	57.5	54.7 52.5	142 147	326 344
×99	50.78	40.62	1.5	1.1	6	12.5	45.5	55.2	55.9 55.6	160 158	316 347
×100	50.72	40.58	1.5	1.2	6	14.2	44.0	60.5	63.8 62.1	154 166	347 349
×101	50.33	40.27	1.5	0.9	7	14.5	44.5	55.0	53.1 53.1	144 153	338 363
×102	50.28	40.22	1.5	1.0	7	12.2	40.2	55.2	54.1 58.1	152 156	349 331
×103	50.22	40.18	1.5	1.1	7	14.0	36.5	62.5	78.8 68.8	188 180	378 370
×104	50.17	40.13	1.5	1.2	7	17.5	44.5	67.5	80.6 83.1	191 198	434 397
×105	49.78	39.82	1.5	0.9	8	11.5	33.0	60.3	52.6 60.8	127 127	448 418
×106	49.72	39.78	1.5	1.0	8	11.6	29.5	63.2	58.9 59.7	135 134	444 428
×107	49.67	39.73	1.5	1.1	8	11.2	25.5	54.0	61.9 61.0	126 125	432 415
×108	49.62	39.68	1.5	1.2	8	11.2	29.0	60.7	59.4 58.9	138 140	427 440

made with a 45/45 ratio. The superiority of the 50/40 samples with respect to the 45/45 samples goes from 20% for a lime content of 1.1% to 5% for a lime content of 1.3%, as can be seen in Fig. 1, which shows the mean value of the compressive strengths after 3, 7 and 28 days as a function of the A/S ratio and the $Ca(OH)_2$-percentage.

The Optimum Composition

If we want to conclude from the previous paragraphs as to the optimum composition, we are faced with two difficulties:

—first of all, the influence of a specific component can not be predicted without taking into account the quantities of the other components in the cement. In other words, as to the strength of the sample, the complete composition has to be seen as a whole.

—secondly, the conditions to have a strong sample at short term contradict those to have a good sample at long term. Very rare are the samples which give good results after 3 and after 28 days. For these reasons, the optimum compositions at short and at long term will be discussed separately.

The Optimum Composition for Strong Samples at Short Term

The highest mechanical strengths after 3 days are obtained with a 50/40 anhydrite/slag ratio, independently of the other components.

—secondly it has been noticed that a small percentage of aluminous cement gives the best results after 3 days. In the systematic research about the influence of the different components not less than 6% aluminous cement has been used. Therefore, later on, some samples with only 5% aluminous cement were made: unfortunately, the mechanical strength decreased at short term, whereas at long term the samples could only be considered equivalent to those with 6% Al.

—by using a 50/40 anhydrite/slag ratio, it has been found advantagous to add up to 1.5% $Ca(OH)_2$. Even compressive strengths of 80 kg/cm² were obtained, which are the highest ones ever gotten during our study of anhydrite cement.

—it can hence be stated that a strong sample at short term should have the following composition:

Anhydrite-slag ratio:	50/40
Aluminous cement:	6 to 7%
$Ca(OH)_2$:	1.5%
K_2SO_4:	1.2%

(the compressive strength after 28 days has a value of 400 kg/cm²).

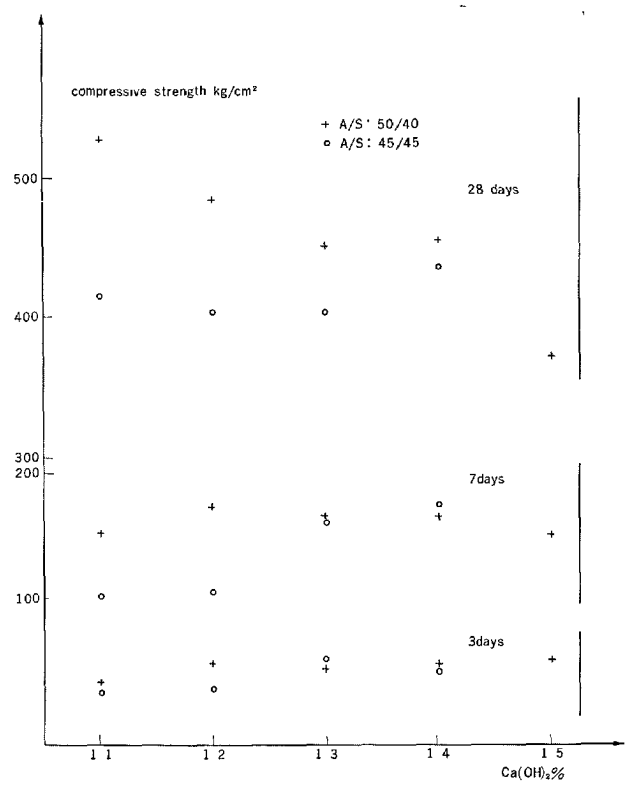

Fig. 1. *Mean value of the compressive strength as a function of the composition of the anhydrite cement.*

The Optimum Composition for Strong Samples at Long Term

According to the tests compressive strengths higher than 550 kg/cm² after 28 days can be obtained with the following composition:

Anhydrite-slag ratio:	50/40
Aluminous cement:	8%
$Ca(OH)_2$:	1.1%
K_2SO_4:	1.2%

The Optimum Composition for Strong Samples after 7 Days

Out of the tables it can be seen that, after 7 days, the compressive strength is higher than 180 kg/cm² for the optimum composition after 3 days, mentioned above, and for the following one:

Anhydrite-slag ratio:	50/40
Aluminous cement:	6%
$Ca(OH)_2$:	1.2%
K_2SO_4:	1.0 to 1.2%

(after 28 days the compressive strength amounts to 540 kg/cm²)

Standard Specifications and Comparisons with Portland Cement

Flexion and Compression Strength

The Belgian standard specifications for flexural and compressive strengths (NBN 178.53) of plastic mortars (Rilem-Cembureau method) on a base of portland cement are formulated for final approval as follows:

	3d	7d	28d
Flexion strength kg/cm²	—	30	50
Compression strength	—	160	300

The following compositions meet the standards: with an A/S ratio of 45/45:

—some with a $Ca(OH)_2$-content of 1.3%, when the K_2SO_4-percentage amounts to 1.2%

—all with a $Ca(OH)_2$-content of 1.4%.

with an A/S ratio of 50/40:

the largest part of the compositions with $Ca(OH)_2$-contents equal to 1.2, 1.3 and 1.4%.

Our results after 7 days are up to 30% higher than the standards as far as the flexural strength is concerned, and up to 20% as far as the compressive strength is concerned; after 28 days the percentages can even reach the values of 50% and 90%, respectively.

Setting Times (NBN 178.31) and Soundness (NBN 178.32)

The proposed Belgian standards stipulate that the initial setting time of portland cement should not be less than 90 minutes, but not be more than 10 hours. As far as the soundness is concerned, the increase of distance separating the indicator points of the apparatus for conducting the "Le Chatelier" test may not exceed 3 mm.

Some figures for anhydrite cement are given below:

	sample X 28	sample X 104 (much lime)
standard consistency		
NBN 178.30: % water	38	37
setting times		
NBN 178.31: initial	5h	5.15h
final	9.35h	7.35h
soundness		
NBN 178.32		
Le Chatelier test	0.9 mm	1.7 mm

Anhydrite cement also conforms to these standards of portland cement.

Supplementary Paper IV-128 Chemistry of Slag-Rich Cements

Julie C. Yang*

Synopsis

The hydration studies of slag-rich cements has been studied with emphasis on the effect of cement composition and curing conditions on strength properties and chemical stability of cement products. Blast furnace slag cement, composed of about 75 per cent finely ground granulated slag powder and 25 per cent portland cement is suggested for structures cured either under high-humidity atmospheric pressure or autoclave conditions including asbestos-cement building products, whereas supersulphated cement is recommended for air-cured massive structures or other applications requiring good sulphate resistance.

Introduction

Granulated blast furnace slag is known to have hydraulic activity. When it is finely ground and mixed with activators, it can be made into a cement for construction work. Slag-rich cements consist of a finely powdered mixture of a high percentage of granulated blast furnace slag, and alkaline activators such as portland cement clinker, portland cement, or calcium hydroxide. In the case of supersulphated cement, dehydrated gypsum (anhydrite) is added with the alkaline activators.

Because of its excellent resistance to chemical attack (1–9), and its low heat of hydration (10–12), many successful structures have been constructed with slag cements in Europe during the past fifty years. Slag-rich cements are claimed to be more resistant to sulphate attack than Type V portland cement (13–15). Its resistance to inorganic acids and food wastes makes it particularly suitable for sewers which carry such effluents, and it also affords some protection against the action of bacteria. Its low heat of hydration makes it particularly suitable for structures requiring large masses of concrete, such as dams, and thick dock walls.

It is intended in this paper to provide basic information on the setting properties and hydration products of slag-rich cements under various curing conditions and an evaluation of its potential in the manufacture of autoclaved building products.

Experimental

Composition

Slag cements employed in this investigation consist of at least 65 per cent by weight granulated blast furnace slag. Two main classes of slag cements are discussed: (a) blast furnace slag cement composed of granulated slag and portland cement, and (b) supersulphated cement. The latter is a mixture of at least 75 per cent of granulated slag, anhydrous calcium sulphate and up to 5 per cent of an activator such as lime, portland cement clinker, or portland cement.

The granulated or quenched slag must consist almost entirely of glass and must have a suitable chemical composition in order to have hydraulic activity. Numerous investigations have been made to correlate the chemical composition and hydraulic activity of slags (16–24). The hydraulic activity of a slag generally rises with increasing contents of CaO and Al_2O_3 and with decreasing contents of SiO_2 and MnO. Parker and Nurse (17) have adopted a formula to determine the quality of slag by a factor M, wherein:

$$M = \frac{CaO + MgO + Al_2O_3}{SiO_2 + MnO} > 1.0 \qquad (1)$$

The oxides are in weight per cent, and the amount of CaO must be corrected for Ca present as CaS. Knowledge of the extent to which MgO can replace

*Research and Engineering Center, Johns-Manville Products Corp., Manville, New Jersey, U.S.A.

CaO and yet maintain a satisfactory cement is rather limited. Stütterheim and Nurse (25) and Stütterheim (26, 27) found that it is possible to make a good hydraulic cement with high-magnesia slags containing 13 to 21 per cent MgO with little or no risk of forming free periclase which might cause disruptive expansion.

Blondiau (28) suggested the composition of a suitable slag for supersulphated cement as one having a CaO/SiO_2 molar ratio of 1.45/1.0 to 1.54/1.0 and a SiO_2/Al_2O_3 ratio between 1.8/1.0 to 1.9/1.0. A SO_3 content of 6 to 9 per cent, corresponding to 10.4 to 15.3 per cent of anhydrite is also desirable for a good supersulphated cement.

Four commercial supersulphated cements and six experimental slag cements made from domestic and foreign slags also were investigated. The commercial supersulphated cements were obtained from Belgium, England, and Germany, respectively. With the exception of the Belgian cement, 3.5 to 5.0 per cent of portland cement was detected in all of the cements. The identification of calcite ($CaCO_3$) and of hydrated lime in trace quantity in the Belgian cement led to the assumption that calcium oxide or hydroxide was the activator.

The experimental blast furnace slag cement was prepared by mixing calculated amounts of preground glassy slag (65 to 95 per cent) and the balance of portland cement. The supersulphated cement composition was 83 per cent slag, 12 per cent anhydrite and 5 per cent portland cement, unless specified. The granulated slags were from Homestead, Pennsylvania; South Works, Illinois (U. S. Steel); Woodward, Alabama (Birmingham Slag Division, Vulcan Materials Company); St. Louis, Missouri (St. Louis Slag Products Company); and Pretoria, South Africa*. These slags were ground to a Blaine fineness of 4200 to 6000 cm^2/g, much finer than regular portland cement, to promote hydration and the development of early strength. The analysis of these slags and of the commercial cements are listed in Tables 1 and 2, respectively.

Table 1. *Chemical composition of commercial supersulphated slag cement*

Chemical composition (%)	Belgian	Belgian	German No. 325	German No. 225
Ignition loss (1000°F)	0.47	0.20	1.59	1.33
CaO	45.30	41.60	42.02	41.80
SiO_2	26.70	30.30	24.96	24.64
Al_2O_3	11.80	14.40	14.54	14.70
MgO	4.20	4.10	5.92	5.78
Fe_2O_3	0.83	0.86	0.41**	0.38**
TiO_2	0.56	0.54	*	*
P_2O_5	0.43	0.10	*	*
Mn_2O_3	0.30	*	1.03	0.92
K_2O	0.49	1.10	0.41	0.42
S--	0.89	0.95	1.12	1.13
SO_3	7.50	5.92	7.77	8.72
Na_2O	0.56	0.34	0.68	0.64
Total (%)	100.03	100.41	100.45	100.46
$CaSO_4$ (Calculated %)	12.75	10.06	13.21	14.82
Blaine fineness (cm^2/g)	6000	4920	3850	3650

* Not determined
**Determined as FeO

Table 2. *Chemical composition of slags and portland cement employed in experimental slag-rich cements*

	Slag composition (%)					
Calculated as oxides	South Works	Homestead	Woodward	St. Louis	Pretoria	Portland cement (Type I)
CaO	43.1	42.4	42.3	41.4	34.1	64.0
SiO_2	34.3	34.3	39.1	33.7	35.4	21.7
Al_2O_3	10.2	11.8	11.5	14.4	10.3	4.8
MgO	6.3	5.2	3.2	5.8	14.6	3.0
Fe_2O_3	2.3	1.6	0.53	0.74	0.2	2.6
TiO_2	0.4	0.55	0.38	0.31	0.4	0.24
P_2O_5	0.15	0.01	0.02	0.01	0.01	0.18
Mn_2O_3	1.60	1.2	0.52	0.47	0.46	—
K_2O	0.19	0.40	0.21	0.99	1.20	0.60
Na_2O	0.19	0.23	0.29	0.19	0.24	0.34
S--	1.41	1.70	1.10	1.39	0.90	—
SO_3	0.09	0.07	trace	0.33	trace	2.1
Ignition loss (1800°F)	0.22	0.31	0.60	0.20	0.11	0.76
Total	100.49	99.77	99.75	99.93	101.20	100.32
Calculated as:						
C_3S						53.63
βC_2S						22.28
C_3A						8.32
C_4AF						7.91
Glass content	>95	>95	>95	>95	>95	
Refractive index of glass	1.66	1.66	1.64	1.64	1.645	
Insoluble residue	0.39	0.34	0.29	0.36	0.17	

Sample Preparation for Hydration Studies at Atmospheric Pressure

Slag cement pastes with a water/solid ratio of 0.60 were prepared with boiled distilled water to minimize the contamination by CO_2. Twenty gram samples were sealed in polyethylene bottles and allowed to hydrate for 24 hours to 60 days at 23 ±2°C in a tumbling device. Other samples were hydrated at various temperatures and times in a CO_2-free atmosphere. After the reaction periods had been completed, the materials were filtered, washed with acetone, and dried in a vacuum desiccator over Ascarite and calcium chloride.

*Courtesy of Dr. N. Stütterheim, South African Council for Scientific and Industrial Research, Pretoria, South Africa.

Sample Preparation for Hydration Studies under Hydrothermal Conditions

A water suspension of 2 grams of slag cement in 40 ml distilled water was placed in a 100-ml capacity stainless steel autoclave. The assembly was closed and the cement was allowed to hydrate at room temperature for 24 hours. Then the assembly was heated to the desired temperature for the required time and quenched. The product was filtered and dried in the same manner as described in the case of atmospheric pressure.

Sample Examination and Identification

X-ray diffraction diagrams of the partially or completely hydrated samples were obtained with a Norelco diffractometer, using copper Kα radiation. The microscopic examinations were made with a Zeiss polarizing microscope. These methods included examination of thin section by transmitted light and with cross-polarization, and similar examination of powders in oil immersion. In addition, polished sections etched in sulphur were examined by reflected light.

Strength Determinations

Compressive Strength

Compressive strength tests were made on 1-in. cube specimens, each of which initially contained 28 grams of solids. Both room-temperature-cured and autoclaved products were formed from 50 per cent by weight slag cement and 50 per cent silica flour (2600 cm^2/g Blaine fineness). The water/cement ratio was 0.60. The procedure for molding the cube specimens was similar to that of ASTM method C109 for 2-in. cubes. The ASTM method was also employed in some tests.

The room-temperature-cured cubes were kept in a humidity chamber at 90 per cent relative humidity for 28 days at 23 $\pm$2°C; the autoclave-cured cubes were kept under the same conditions for 24 hours and then treated hydrothermally for 16 hours at either 170°C or 182°C and their corresponding saturated steam pressures. The specimens were saturated by immersion in water for 24 hours at 23 $\pm$2°C and then broken for their compressive strength on a 60,000-lb Baldwin universal testing machine. Each value was the average of ten cubes.

Flexural Strength

Flexural strength was determined using asbestos-cement specimens 3 × 8 × 1/4-in., prepared from a mixture containing a special chrysotile asbestos fiber blend (from Johns-Manville Jeffrey mine, Quebec, Canada); pulverized sand flour (2600 cm^2/g Blaine); and either portland cement (Type I, 3650 cm^2/g Blaine fineness) or slag-rich cement.

The formulation usually consisted of 20 per cent by weight fiber with the balance varied in composition as specified, but expressed in terms of silica/cement ratio. For example, for a composition with 20 per cent fiber, 30 per cent silica, and 50 per cent slag cement, the silica/cement ratio is 0.60. The weight of the original solids per sample was 150 grams.

A liter of water was added to the premixed dry blend and stirred vigorously for one minute at 500 rpm. The slurry was filtered, tamped, and pressed in a confined mold at 10,000 psi for 10 seconds. The samples were cured in the same fashion as the cubes and tested for flexural strength according to ASTM C223–55 method. For each composition, the modulus of rupture (in psi) was computed from the average of four samples.

Strength Determinations of Asbestos-Cement Pipe

Methods covering the strength tests of asbestos-cement pipe are described in detail in ASTM method C500.

For a 6-inch diameter, 10-ft class 150 pipe, flexural strength was determined on a 9-ft span with third point loading for a 5-second dwell period. Hydrostatic strength was tested to an internal pressure of 525 lb for a 5-second dwell time, and crush strength was determined by crushing 1-ft section under load on a 60,000-lb Baldwin testing machine.

Setting Property Determinations of Asbestos-Cement Compositions

Rate of setting of hydraulic cement is determined by measuring the plasticity of an asbestos cement specimen. The measurement is also an indicator of the shape-retaining characteristics of a product, and is employed to determine the effectiveness of accelerators.

In the laboratory, oblong specimens 3 × 8 × 1/4 inches were prepared as described in the section of flexural strength. An accelerator solution, if needed, was poured over the sample prior to pressing. The pressed sample was then transferred immediately to test equipment which measures the deviation from

horizontal under a given load at a specific time. A span of 6 inches and a load of 140 grams were employed for all the determinations.

For large-diameter pipe, the linear deformation (out-of-roundness) was measured when a 1-ft pipe section of about 2-hour age was placed between two steel plates of a press to which a given load was applied.

Results and Discussion

Cement Hydration and Setting at Atmospheric Pressure

When blast furnace slag cement is in contact with water, glassy slag particles release Ca^{++} ions to the solution. Calcium hydroxide, liberated also from the hydration of the activator portland cement, reacts with the colloidal acid hydrates on the surface of the slag grains to form hydrated calcium aluminates, silicates, and hydrogarnets (29–32). Composition of the calcium silicates depends upon the CaO concentration in the solution. At low CaO concentration, CSH-I* (0.8–1.5 $CaO \cdot SiO_2 \cdot XH_2O$) will form, and if the CaO content exceeds 0.020 mol/liter according to Taylor (33), CSH-II (1.7–2.0 $CaO \cdot SiO_2 \cdot XH_2O$) will be obtained.

Hydration of supersulphated cement takes place when the colloidal acid hydrates react with the available $CaSO_4$ in a high Ca^{++} ion concentration to form calcium sulfoaluminates (31, 32, 34).

X-ray diffraction and microscopic identification of the hydrated products of experimental blast furnace slag cement and a British supersulphated cement at atmospheric pressure are presented in Tables 3 and 4, respectively. In a slag-rich cement concrete or mortar, whether it is composed of a blast furnace slag or a supersulphate cement, if sand or fine quartz powder is added as filler or aggregate, there is no evidence of chemical reaction between the cement components and quartz at room temperature. The data of Table 4 are typical for all the supersulphated cement investigated including the experimental cements.

The main hydration products of the blast furnace slag cement containing 25 per cent portland cement are found to be CSH-I and C_4AH_{13} or its solid solution with 3 $CaO \cdot Al_2O_3 \cdot CaCO_3 \cdot 12H_2O$ at ambient conditions; tobermorite and some hydrogarnet phases at elevated temperatures. The slag cement made with high magnesia slag content of 14.6 per cent (Pretoria Slag) showed no detectable free MgO or $Mg(OH)_2$ upon hydration.

Hydration of supersulphated cement yielded a very poorly crystallized ettringite (3 $CaO \cdot Al_2O_3 \cdot 3CaSO_4 \cdot 31H_2O$) after 15 to 20 minutes which was developed subsequently into a well-crystallized material, probably a mixture of ettringite and its solid solution in which Al^{+3} ions were isomerically replaced by Fe^{+3} ions or $CaSO_4$ replaced by $Ca(OH)_2$ or $CaCO_3$. The monosulphate salt (3 $CaO \cdot Al_2O_3 \cdot CaSO_4 \cdot 12H_2O$) was found in some samples, especially when the hydration was carried out at 75 to 80°C, but not consistently. Gypsum ($CaSO_4 \cdot 2H_2O$) was also found in small quantities in short-term hydrated products. In a 28-day hydrated sample, ettringite was present in fine needle-like crystals, exhibiting a low birefringence, a mean refractive index of 1.48, and a CSH-I binding gel. (Fig.1). An increased amount of ettringite with improved crystallinity was obtained with prolonged reaction time or with increasing temperature up to about 50°C. Unreacted slag particles were still quite abundant in this temperature range.

Table 3. *Hydration of blast furnace slag cement at atmospheric pressure*
Blast furnace slag cement composition:
75% Slag + 25% Portland cement

Slag employed (Blaine fineness)		South Works (4300 cm²/g)	Pretoria (5940 cm²/g)
Hydration condition		Product formed	Product formed
Time	Temp., % RH		
Up to 1 day	20–25°C 90% RH	Amorphous material (C), C_3SH_2*, C_4AH_{13}*, LS	C, C_4AH_{13}, LS*
	70–72°C 90% RH	C, C_4AH_{13}, LS*	C_4AH_{13}, (C), LS*
7 days	20–25°C 90% RH	C, (C_4AH_{13}), LS*	C_4AH_{13}, C, LS*
	70–72°C 90% RH	T, LS*, H*	T, H*
28 days	20–25°C 90% RH	C, (C_4AH_{13})	C, (C_4AH_{13})
	70–72°C 90% RH	T, (H)	T, H*

( ) Denotes minor or intermediate quality
* Denotes trace amount
C = CSH-I = (0.8 – 1.5) $CaOSiO_2 \cdot x\ H_2O$
C_3SH_2 = $3CaO \cdot SiO_2 \cdot 2H_2O$
C_4AH_{13} = $4CaO \cdot Al_2O_3 \cdot 13H_2O$ or its solid solution with $3CaO \cdot Al_2O_3 \cdot CaCO_3 \cdot 12H_2O$
LS = Calcium monosulphoaluminate $3CaOAl_2O_3 \cdot CaSO_4 \cdot 12H_2O$
T = Tobermorite-like CSH-I (good 11.2Å peak)
H = Hydrogarnet solid solution series
$[3CaO \cdot Al_2O_3 \cdot nSiO_2 \cdot 2(3 - n)H_2O]$ where $0 \leq n < 3$

*In this presentation, abbreviations for the formulae of oxides most often encountered in cement chemistry are used, such as C for CaO, A for Al_2O_3, S for SiO_2, F for Fe_2O_3, and H for water. 3 $CaO \cdot SiO_2$ thus becomes C_3S.

Table 4. *Phase identified in a British supersulphated cement hydrated at atmospheric pressure (85–95% RH)*

Time (hr-day) \ Temp. (°C)	20—27	40—50	75—80	95—98
0.25—0.50 hr	A, E*	D, A, E*, (M)	A, D, (M)	A. T, (D), (LS)
1.0 — 3.0 hrs	A, (E), (M) LS*	A, D, (E), (C), LS*	A, C, (E), (M), (D), (LS)	A, T, D, (LS)
5.0 — 7.0 hrs	(A), E, C*	D, A, (E), LS*	A, (E), (LS), (D), T	A, H, T
16 hrs—3 days	(A), E, (C)	D, A, E, C	A, (E), (LS), (D), T	A, H, T
5—20 days	A*, E, C	D, (A), (E), T	A, T, LS*, (D)	A, H, T
28—60 days	A*, E, C	D, A*, (E), T	A, T, (D)	A, H, T

( ) Denotes minor or intermediate quality
T Denotes trace amount
A = Anhydrite ($CaSO_4$)
E = Ettringite ($3CaO \cdot Al_2O_3 \cdot 3CaSO_4 \cdot 31H_2O$)
LS = Calcium monsulphoaluminate ($3CaO \cdot Al_2O_3 \cdot 3CaSO_4 \cdot 12H_2O$)
M = Hydrated calcium sulphate ($CaSO_4 \cdot 2H_2O$, Gypsum)
D = CSH-I (0.8 − 1.5) $CaO \cdot SiO_2 \cdot XH_2O$
T = Tobermorite-like CSH-I (good 11.2Å peak)
H = Hydrogarnet solid solution series $3CaO \cdot Al_2O_3 \cdot nSiO_2 \cdot 2(3-n)H_2O$ where $0 \leq n < 3$

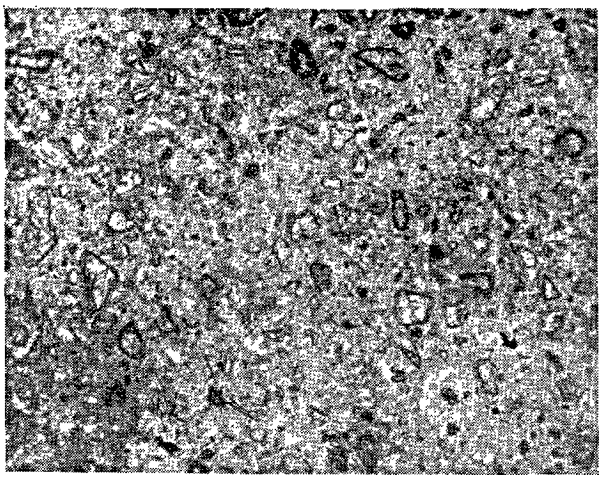

Fig. 1. *An English supersulphated cement hydrated at 23 ± 2°C, 90% RH for 35 days (thin section)* (×200)

Increasing temperature above 50°C resulted in a gradual decomposition of ettringite to calcium aluminate hydrates, probably C_3AH_6 and anhydrous calcium sulphate ($CaSO_4$); no gypsum was detected. Hydration at 95°C resulted in the formation of tobermorite ($C_5S_6H_5$) and also the appearance of poorly-defined hydrogarnets presumably in the solid solution series of C_3AH_6–$C_3AS_nH_{2(3-n)}$ where $0 < n < 3$. Strätling compound (35–37), or gehlenite octahydrate (C_2ASH_8) was not detected in any of the hydrated pastes.

The rate and extent of hydration reactions are determined by the characteristics of the calcium sulphate present (a predominant factor in supersulphated cement), temperature, and rate of release of acid hydrates (hydrated alumina and silica) and other components from the slag cement (38–40).

The good sulphate resistance of the slag-rich cement product is attributed to the absence of free $Ca(OH)_2$ in the set cement and the low C_3A content in the minor portland cement component. Furthermore, the low heat of hydration of the slag cement permits the construction of water-impervious massive structures which are free of cracks—an important feature for structures exposed to sea water or underground aggressive surroundings (41).

Structures made of slag-rich cement should be cured under highly humid conditions, especially the first 2 to 3 days, to prevent surface carbonation and drying out which cause "dusting" (42) and low strength. Most of the well-cured specimens were very dark, usually bluish grey in color when they were freshly cured; and, in aging, the color of these products lightened as a result of oxidation of colored polysulphides to corresponding sulphates.

Blondiau and other researchers (3, 5, 6, 7, 13, 14 and 15) have independently carried out long-term corrosion tests with an air-cured slag-rich cement specimen. They found that in aggresive solutions, such as 2 to 5 per cent solutions of Na_2SO_4, $MgSO_4$ or $(NH_4)_2SO_4$, triple-strength sea water and 0.25 per cent sulphuric acid at a pH of approximately 1.3, slag-rich cements (with slag content greater than 65 per cent) showed better chemical resistance than the portland cement specimens used in the studies. However, the reactivity of ettringite, one of the main hydration products of air-cured, supersulphated cement, in contact with weak inorganic mineral acid of 0.5 per cent concentration or more, or on long period exposure of more than eight years (43), or to high concentration of organic acid generated from food and waste, cannot be ignored.

Previous findings by the author (44) showed that a synthetic ettringite reacted with these media slowly to form insoluble calcium salts such as gypsum ($CaSO_4 \cdot 2H_2O$); calcium citrate tetrahydrate [$Ca_3(C_6H_5O_7)_2 \cdot 4H_2O$]; or partially soluble acetate

$[Ca(C_2H_3O_2)_2]$ and lactate $[Ca(C_3H_5O_4)\cdot 5H_2O]$.

Cement Hydration Reactions under Hydrothermal Conditions

The hydration of slag-rich cements under hydrothermal conditions up to 300°C was investigated to determine the possibility of accelerating the rate of setting, of providing adequate strength in a short period of curing, and of forming compounds of high chemical stability.

When the supersulphated cement paste was subjected to temperatures above 100°C at saturated steam pressure, ettringite and calcium monosulphoaluminate could not be detected by an instrumental method. The slag particles in the cement autoclaved at 170°C, 100 psi or higher temperature and pressure exhibited some thin reaction rims, as shown in Fig. 2. The mean index of refraction of the gel matrix was 1.54. X-ray diffraction examination revealed the presence of $CaSO_4$, tobermorite and a weak pattern of hydrogarnets.

Blast furnace slag cement hydrated under similar hydrothermal condition to form tobermorite and hydrogarnets as shown in Table 5.

Anhydrite ($CaSO_4$), which was originally present in the supersulphated cement, probably reacted partially when the cement was in contact with water to form ettringite prior to the hydrothermal treatment. When the product was autoclaved, ettringite decomposed to yield fine crystalline $CaSO_4$, which recrystallized during the hydration process and grew to crystals up to 20 microns, as observed by microscopic methods.

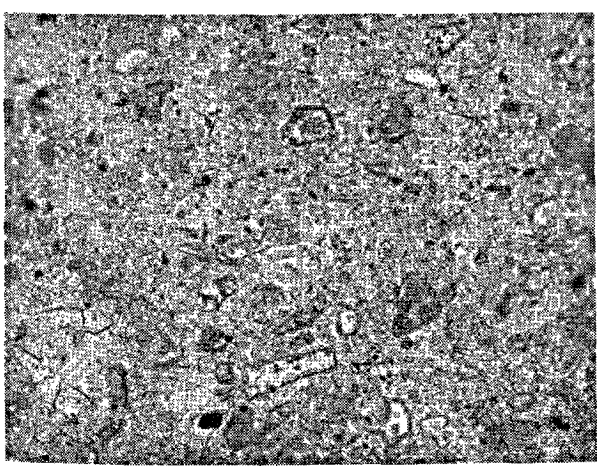

Fig. 2. *An English supersuphated cement autoclaved 5 days at 225°C, 345 psi (thin section)* (×200)

Since anhydrite is not a strength-contributing binder by itself, and ettringite is neither stable nor formed under hydrothermal conditions, the presence of a large amount of $CaSO_4$ in a cement is not desirable if the cement will be subjected to an autoclave cure. In addition, the free $CaSO_4$ present in a set product may slowly react with the hydrated slag components to form ettringite which results in volume expansion and cracking with age. Consequently, blast furnace slag cement is preferred for autoclave-cured products to the supersulphated cement

Hydrogarnet formation is highly desirable for sulphate resistance and high resistance to carbonation (13, 43, 45). The diffraction peaks of the hydrogarnets gradually shifted, indicating a lower cell constant, at higher temperature autoclaving in addition to the improved crystallinity, presumably attributable to a lower water content and higher silica content (46, 47).

Table 5. *Hydration products of slag-rich cement neat pastes and mortars under hydrothermal conditions* (16 hrs at 183°C, 150 psi followed a 24 hr air cure at 23 ± 2°C, 90% RH)

Cement species	Composition (Per cent)		Products identified
	(Per cent)	Silica flour (%) (2600 cm²/g Blaine)	
Portland	100	0	T, X, ($Ca(OH_2)$)
Portland	50–65	35–50	T, (X), Q
British supersulphated	100	0	H, (T), (A), (X)
British supersulphated	80	20	T, H*, (A), (X), (Q)
British supersulphated	50	50	T, G, (A), (Q)
Blast furnace slag	100	0	T, H, (X)
	95	5	(T), H, (X), (Q)
75% South Works slag (4300 cm²/g) +25% portland cement	80	20	T, (H), (X), (Q)
	72	28	T, H*, (X), Q
	63	37	T, G, (X), (Q)
	50	50	T, G, (X), (Q)

( ) Denotes minor quantity
* Denotes trace
T = Tobermorite = $5CaO\cdot 6SiO_2\cdot 5H_2O$
H = Hydrogarnet solid solution series $3CaO\cdot Al_2O_3\cdot (SiO_2)_n\cdot (H_2O)_{2(3-n)}$ where $0 < n < 3$
X = Xonotlite = $6CaO\cdot 6SiO_2\cdot H_2O$
Q = Quartz
G = Gel of hydrated calcium aluminosilicates with mean refractive index n = 1.53 to 1.56

Table 6. *Hydrogarnet formation from a synthetic blast furnace slag cement* treated hydrothermally*

Temperatures (°C) steam pressure and its saturated	Unit cell dimensions of hydrogarnet a_0 (in Å)				
	6 hrs	1 day	2—4 days	7 days	14 days
120	—	—	12.40	12.28	12.28
150	12.28	12.28	12.24	12.23	12.21
170	12.28	12.24	12.21	12.21	—
200	12.25	12.22	12.18	12.13	12.07
250	12.17	12.17	12.13	12.13	12.07
300	12.10	12.07	12.05	12.02	12.02

*Blast furnace slag cement composition
75% South Work slag (4850 cm²/g Blaine fineness)
25% Portland cement

The unit cell dimensions of the hydrogarnets were computed and are listed in Table 6.

As autoclaving temperature approaches 225°C, the gel matrix of the product became coarser and more granular than that of the low-temperature treated specimen. Noted difference in the appearance of the binding gel was observed in Figs. 1 and 2, and the slag grains of the higher pressure autoclaved products were surrounded by thicker reaction rims. X-ray examination showed a distinctive hydrogarnet pattern in the specimen of Fig. 2 which has been reacted 5 days at a temperature of 225°C. The hydrogarnet formed resembled plazolite, $3CaO \cdot Al_2O_3 \cdot 2SiO_2 \cdot 2H_2O$, (48, 51) a cubic mineral which has a unit cell dimension a = 12.14 Å and a refractive index of 1.675. Synthetic plazolite with the same unit cell constant was prepared hydrothermally as a standard for comparison from a pure C_3AS_2 glass autoclaved at 250°C, 580 psi for 12 days.

Few unreacted slag grains remained after autoclaving for 24 hours at 225°C or above. At 300°C and its saturated steam pressure the hydrogarnet formed resembled hibschite, especially at long reaction periods of 10 to 14 days, a natural mineral which has the same theoretical composition and crystal habit as plazolite, but differs in optical properties and unit cell dimensions. The lattice constant of hibschite has been reported as 12.00 $\pm$0.02 Å, the refractive index is (n) = 1.681 (48). Pabst (52) and Cornu (53) observed independently that the cloudy nuclei of hibschite crystals had a higher refractive index than the crust and had slight birefringence. This suggested that the nucleus of hibschite probably contains some iron; otherwise the mineral is nearly identical in composition to plazolite. The chemical analysis by Belyankin and Petrov (54) indicated the presence of about 4 per cent Fe_2O_3 in hibschite. In autoclaving slag-rich cements in this p-t range, it is probable that a small amount of iron, from either the slag or the added portland cement, entered into the hydrogarnet structure and promoted the formation of a hydrogarnet of low unit cell dimension resembling hibschite. Without iron, the hydrothermal treatment of a pure C_3AS_2 glass, even at a higher temperature (354°C, 2500 psi) for 15 days, yields a product with a unit cell dimension a = 12.07 Å (55).

In autoclaved-cured portland cement products, it is a common practice to add silicon flour (quartz) to reduce the free calcium hydroxide content by forming calcium silicate hydrates and to increase strength. Even though the slag-rich cements contain a small amount of free calcium hydroxide which is released by the activator upon hydration, addition of silica to the cement increased strength as well as lowered cost.

Data in Table 5 show that increasing the amount of silica flour of 2600 cm²/g Blaine fineness added to the cement reduced the tendency of forming hydrogarnets. The molar ratio of CaO/Al_2O_3 in the hydrated binding gel decreased gradually with increasing amount of silica because of the ease of interaction of calcium hydroxide and the silica to form CSH compounds. When the added silica exceeded about 30 per cent of the total weight, no hydrogarnet was detected by X-rays, and the CSH compounds were in predominant quantities. The X-ray pattern of the "CASH" gel was very similar to tobermorite; a noted decrease in intensity of 2.81 Å and a shift of 11.1 Å to 11.6 Å were observed. This indicated the introduction of Al_2O_3 into the tobermorite lattice (56), the presence of Al_2O_3 inhibited the formation of xonotlite. Petrographic examination of thin sections of an 100psi, 16-hour autoclaved blast furnace cement mortar showed a very fine-grained binding gel surrounded the quartz and glass particles. The mean refractive index of the binding gel was in the range of 1.53 to 1.56.

Effect of Cement Composition and Curing Conditions on Strength and Possible Applications

The strength of supersulphated cement cured under atmospheric pressure has been discussed in many technical articles, the general consensus indicated that even after seven days moist air and under water curing at 18 to 25°C, the compressive strength of concrete cubes made with supersulphated cement was about 20 to 35 per cent lower than that of the corresponding portland cement specimens, but at the end of 28 days, the supersulphated cement mortar showed high strength (57–60). Our evaluation, as shown in Table 7(a) indicated that even at 28 days, the compressive strength of portland cement is still considerably higher. If the slag with high magnesia content (such as Pretoria slag) is employed to make supersulphated slag cement, it has to be ground to about 6000 cm²/g Blaine fineness in order to have a product of comparable strength to those cements composed of slags of low magnesia content (<6 per cent MgO) at 4500 to 5000 cm²/g, and to pass the ASTM Specification for Type IS portland-blast furnace slag cement (C 205) or (C 358) for Type S cement, or (C 150) for portland cement, since no specification has been set for supersulphated cement

by ASTM.

The possibility of employing supersulphated cement compositions in autoclaved products was also investigated to secure the advantage of a shorter curing period and less storage space for the in-process material. The compressive strength data of Table 7(a) show that for all the mortar tested. the autoclaved products exhibit better strength than the air-cured specimens, but is still 25 per cent or more lower than the corresponding autoclaved portland cement products. This is assumed due to the presence of a considerable amount of non-strength contributing $CaSO_4$.

Compressive strength of 2-in. blast furnace slag cement cube specimens were also evaluated. A composition of 75 per cent slag and 25 per cent portland cement cured for 7 and 28 days showed equal or better strength than that of portland cement. Accelerators can be employed to promote early strength of the slag product and ease of handling in replacing superfine grinding (61–63). Results in Table 7(b) indicate the effectiveness of calcium chloride. Autoclaving of blast furnace cement of the same composition is

Table 7. *Compressive strengths of slag-rich cement mortars*
(*a*) *Supersulphated cement—1-in. cube specimen*
Water/Cement ratio = 0.6 Silica flour used = 2600 cm^2/g Blaine fineness

Cement	Compressive strength MR (psi)					Silica/Cement ratio
	Moist air cure 23 ± 2°C, 90% RH, 24 hrs then in water for			Autoclave cure 23 ± 2°C, 90% RH, 24 hrs then in water for		
	2 days	6 days	27 days	170°C 100 psi 16 hrs	182°C 150 psi 16 hrs	
Portland	—	—	—	8200	—	0.6
Portland	2800	4300	7000	8800	9200	1.0
English	1700	2800	6300	6700	6700	1.0
German (Grade 325)	2200	3620	5380	6300	5700	1.0
German (Grade 225)	2100	3260	5100	6100	6000	1.0
Experimental* No. 1	1500	1600	4500	5000	5600	1.0
Experimental* No. 2	1500	2100	4300	6600	6200	1.0
Experimental* No. 3	1300	2820	3800	5200	5200	1.0
ASTM Specification						
C358-64T	—	600	1500	—	—	—
C205-62T	1200	2100	3500	—	—	—

*Experimental cement composition: 83% slag, 12% $CaSO_4$ and 5% portland cement.
No. 1 Pretoria slag (5940 cm^2/g)
No. 2 Homestead slag (4300 cm^2/g)
No. 3 Woodward slag (4900 cm^2/g)

(*b*) *Blast furnace slag cement—2-in. cube specimens ASTM C-109*

Slag		Cement composition (%)		Accelerator		Compressive strength (psi) 1 day in moist air remaining in water		
Source	Blaine (cm^2/g)	Slag	Portland cement	Species	Weight % (of total mixture)	3 days	7 days	28 days
St. Louis	4300	80	20	0	0	620	2780	3030
		80	20	$CaCl_2$	0.11	785	2800	4680
		80	20	$CaCl_2$	0.267	1225	3190	5050
		73	27	0	0	650	3690	4680
		73	27	$CaCl_2$	0.11	1250	2780	4690
		73	27	$CaCl_2$	0.267	1340	3140	4140
		65	35	0	0	855	3020	3600
		65	35	$CaCl_2$	0.093	1175	3810	5320
		65	35	$CaCl_2$	0.267	1515	3440	—
St. Louis	4300	0	100	0	0	2380	3250	4240
ASTM Specification								
C-205-62T		Type 1S cement				1200	2100	3500
C-358-64T		Type S cement				—	600	1500
						Autoclave cure*		
Portland		0	100	0	0	4800		
South Works	4750	75	25	0	0	4620		
St. Louis	4300	75	25	0	0	4440		

*Autoclaving condition: 24 hrs at 90% RH, 23 ± 2°C, followed by 16 hrs at 170°C, 100 psi

definitely favored, as shown also in Table 7(b); a high-strength product can be achieved.

The application of slag-rich cements in autoclaved asbestos-cement building products was studied. In these products, asbestos fibers are employed for reinforcement and to impart a measure of flexibility to the material. No chemical reaction could be detected by any instrumental means between asbestos fiber and the slag cement, either under air-cured or under hydrothermal conditions, up to 200°C for 24 hours.

Flexural strength was measured for specimens consisting of 20 per cent chrysotile fiber blend, 40 per cent silica flour, and 40 per cent slag-rich cements. The composition was chosen on account of strength properties (as shown in Table 8(a)) and cost considerations. The autoclave conditions studied were in the saturated steam pressure range of 100 to 150 psi. The reference sample was composed of 20 per cent fiber blend, 30 per cent silica and 50 per cent Type I portland cement, (an established optimum formulation for autoclaved product evaluation at Johns-Manville Products Corporation), which has been autoclaved for 16 hours at 100 psi. A photomicrograph, Fig. 3, shows a thin section of an 150-psi autoclaved product. The majority of the slag particles had reacted and disappeared in the gel, and the remaining slag grains showed very distinctive interfacial reaction. By means of point-count determinations, it was estimated that about 75 to 80 per cent of the slag present was reacted in the autoclaved

Table 8. *Flexural strength of autoclaved asbestos cement specimens*

(*a*) *Effect of silica/cement ratio*

Composition (Wt %)			SiO_2 /Cement ratio	Flexural strength MR (psi)*		
Fiber	Cement	Silica		Portland cement	An English super-sulphated C.	Blast furnace** slag cement
20	80	0	0/1	3050	2860	3370
20	66.6	13.4	0.2/1	3100	3020	3410
20	57.2	22.8	0.4/1	4100	3190	3440
20	50.0	30.0	0.6/1	4190	3340	3520
20	44.4	35.6	0.8/1	4000	3400	—
20	40.0	40.0	1.0/1	4050	3310	3700
20	32.0	48.0	1.5/1	3490	3100	3480

* All test specimens were cured at 23 ± 2°C, 90% RH for 24 hrs, then autoclaved for 16 hrs at 170°C, 100 psi.

**The blast furnace slag cement was prepared with 75% South Works slag (4850 cm²/g Blaine fineness) and 25% Type I portland cement.

(*b*) *Effect of curing temperature and duration on asbestos supersulphated cement products*

Cement	Silica /Cement ratio	Curing condition *			Flexural strength MR (psi)
		Temp (°C)	Pressure (psi)	Time (hr)	
Portland cement	0.6/1	170	100	16	4190
Portland cement	1.0/1	170	100	16	4050
A Belgian supersulphated cement	1.0/1	170	100	16	3100
An English supersulphated cement	1.0/1	23 ± 2, 100% RH	Atmospheric pressure	28 days	2300
↑	↑	80	↑	24	2200
		97	↓	48	2150
		97	Atmospheric pressure	72	2250
		130	35	24	1800
		150	55	24	2900
		170	100	16	3310
		183	150	24	3500
		190	170	24	3500
		200	250	24	3300
↓	↓	220	350	24	3200
An English supersulphated cement	1.0/1	250	565	16	2400

*All the autoclaved specimens were air-cured in a humidity chamber 24 hrs at 23 ± 2°C, 90% RH prior to autoclaving.

(*c*) *Effect of blast furnace slag cement compositions and curing conditions on strength of asbestos-cement products**

SiO_2 /Cement ratio	Blast furnace slag cement composition (%)				Autoclaving condition (psi-hr)		
	Slag source	Blaine fineness (cm²/g)	Slag	Portland cement	100-16	125-20	150-16
1.0	South Works	4850	65	35	3590	3670	3890
↑	South Works	4850	75	25	3700	3820	3840
	South Works	4850	85	15	3650	3690	3750
	Homestead	4690	65	35	3520	—	—
	Homestead	4690	75	25	3490	—	—
	Homestead	4690	85	15	3380	—	—
	St. Louis	4300	75	25	3590	—	—
	St. Louis	5200	75	25	3720	—	—
↓	Pretoria	5940	65	35	3600	—	—
1.0	Pretoria	5940	75	25	3510	—	—
1.0	Portland cement control				4050		
0.6	Portland cement control				4190		

*All the asbestos cement formulations contained 20% chrysotile asbestos fiber blend, 40% silica and 40% cement except the last control which contained 30% silica and 50% portland cement; and they were air cured 24 hours at 23 ± 2°C, 90% RH prior to autoclaving.

(*d*) *Effect of accelerators on setting properties of blast furnace slag cement in asbestos cement products*

Cement	Accelerator		Deviation (in.)		Flexural strength** MR (psi)
	Species	Per cent	10 min	60 min	
Slag*	0	—	0.180	0.088	3820
Slag	Na_2SiO_3	1	0.063	0.016	3730
Slag	Na_2SiO_3	2	0.049	0.006	3670
Slag	Na_2CO_3	1	0.101	0.058	3740
Slag	Na_2CO_3	2	0.083	0.037	3720
Slag	NaOH	0.2	0.104	0.048	3740
Slag	$CaCl_2$	1.0	0.028	0.017	3390
Portland	0	—	0.105	0.015	4190

* Blast furnace slag cement composition:
75% South Works slag (4850 cm²/g Blaine fineness) + 25% Type I portland cement (3650 cm²/g)

**Flexural strength determinations were made on the autoclaved product. They were air-cured for 24 hours at 23 ± 2°C, 90% RH then autoclaved for 20 hours at 125 psi 175°C.

Table 9. *Strength data of 6-in. autoclaved asbestos-cement pressure pipes*

Pipe furnish composition (per cent)					Slag cement composition (Slag-portland cement $CaSO_4$)	Autoclaving conditions after 24 hrs at 90% RH 23 ± 2°C	Modulus of rupture—MR (psi)		
Chrysotile fiber	Silica flour (2600 cm^2/g)	Slag*	Portland cement	$CaSO_4$			Flexural	Hydrostatic	Crush
20	30	—	50	—	Control		6000	5100	9200
20	40	32.0	8	—	80-20-0	172°C	4920	4030	7700
20	40	30.0	10	—	75-25-0	110 psi	5530	4820	9480
20	40	30.0	8	2.0 (p)**	75-20-5	24 hrs	5200	4780	8870
20	40	29.6	6.8	3.6 (p)	74-17-9		5520	4670	8410
20	40	32.0	8	—	80-20-0		5230	3390	7660
20	40	30.0	10	—	75-25-0	183°C	5670	4140	9380
20	40	30.9	6.8	2.3 (a)	77-17-6	150 psi	4740	4230	8420
20	40	30.0	8	2.0 (p)	75-20-5	24 hrs	4870	4550	8110
JM Specifications for 6-in. class 150 pressure pipe					—	—	3330	3210	6460

* Slag used: South Works slag (4500 cm^2/g Blaine fineness)
**(p)—denotes plaster of paris ($2CaSO_4 \cdot H_2O$) and
(a)—denotes anhydrite ($CaSO_4$)

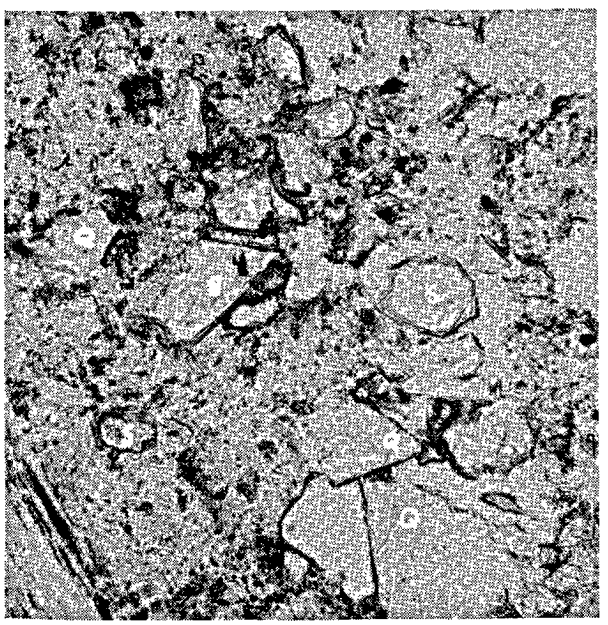

Fig. 3. *An autoclaved asbestos-blast furnace cement product cured for 16 hours at 172°C, 111 psi*
In the thin section unreacted slag grains (S) and quartz (Q) and fiber (F) are noted (×500)

asbestos-cement specimens, and only about 25 to 30 per cent reacted in the 28 day air-cured products.

The data tabulated in Tables 8(b), 8(c), and 8(d) indicated that optimum strength can be achieved with a cement consisting of 75 per cent blast furnace slag powder (4500–5000 cm^2/g) and 25 per cent portland cement at autoclaving pressures 100 to 125 psi. As curing pressure approaches 150 psi, the composition with more portland cement (around 35 per cent) is favored.

Table 10. *Effect of accelerator—sodium silicate on setting properties of asbestos cement pipe (8 ins. in diameter)*

Cement	Na_2SiO_3** (%)	Age of pipe (hour)	Pipe wall thickness (in.)	Load (lb)	Linear deformation (in.)
Slag*	0	2.0	0.40	35.0	Collapsed
Slag	1	2.0	0.40	35.0	0.89
Slag	2	2.0	0.39	35.0	0.59
Slag	0	2.2	0.58	38.8	1.525
Slag	1	2.0	0.63	38.8	0.215
Slag	1	2.2	0.62	38.8	0.209
Portland	0	1.5	0.37	33.5	1.09
Portland	0	2.0	0.38	35.0	0.66
Portland	0	2.0	0.60	38.8	0.14
Portland	1	2.0	0.57	38.8	0.193
Portland	1	2.1	0.59	38.8	0.160

* Blast furnace slag cement composition:
75% St. Louis slag (5200 cm^2/g Blaine) + 25% Type I portland cement (3650 cm^2/g)
**Na_2SiO_3 was sprayed on the wet sheet of asbestos-slag cement-silica furnish at 2.5 gal/min corresponding to 0.8% Na_2SiO_3 based on dry solid. Excess entrained water was removed under reduced pressure prior to the accumulation and integration of rolling layers of materials upon themselves on a mandrel under pressure to form pipe (61).

Effect of intergrinding slag and portland cement clinker was studied. However, due to the abrasiveness and hardness of the granulated slag, portland cement clinker was ground to a much finer size in the process than the slag. As a result a slag cement will have poor hydraulic strength in comparison with a slag cement composed of separately ground components.

The slag-rich cements were further evaluated in pilot plant and production as in an actual asbestos-cement pipe product. The mechanical strength data, as shown in Table 9, and setting property determinations (Table 10) demonstrated that satisfactory autoclaved formulation can be achieved when portland cement is replaced by a blast furnace slag cement.

Chemical abrasion-corrosion tests for soft water and dilute sulphuric acid were conducted. Results in Table 11 and Fig. 4 showed the soundness of using

Table 11. *Abrasion—corrosion resistance of autoclaved asbestos-cement pipe products*

Test group	Asbestos cement pipe composition (%)				Testing condition				Rate of abrasion (inch/24 hr)	X-ray and microscopic identification of inner surface (1-2mm)
	Class	Asbestos fiber	Cement	SiO_2/Cement	Sample	Solution	Time (hr)	Rolling rate (rev/hr)		
1	6 in. 150 Pressure	20	Portland	0.6	Sections cemented together	0.5 N H_2SO_4	336	4800	—	High gypsum content, some swelling
		20	Slag*	1.0						Trace gypsum
2	6 in. 2400 Sewer	20	Portland	0.6	Sections cemented together	0.5 N H_2SO_4	336	4800	—	100% gypsum
		20	Slag	1.0						Trace gypsum
3	6 in. 150 Pressure	20	Portland	0.6	Individual	Distilled water	168	2450	.0011	—
		20	Slag	1.0	Individual	Distilled water	547	2060	.0013	—

*The slag cement composition: 75% South Works slag (4500 cm^2/g Blaine fineness) and 25% portland Type I cement

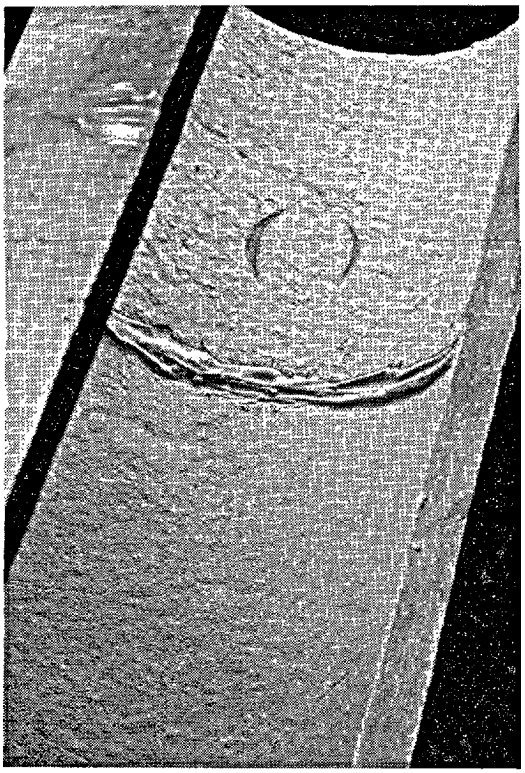

Fig. 4. *Autoclaved asbestos-cement pipe sample after abrasion-corrosion test.*
(Two sections were epoxyed together. Top section—asbestos-portland cement pipe. Bottom section—asbestos-blast furnace slag cement pipe)

blast furnace slag cement in an asbestos-cement product.

Summary

The hydration of supersulphated cement and blast furnace slag cement under atmospheric pressure

and hydrothermal conditions has been investigated. Ettringite and tobermorite-like CSH-I are found to be the main binders in the supersulphated cement hydrated at atmospheric pressure and temperatures below 75°C, whereas tobermorite-like CSH-I and hydrated calcium aluminate (C_4AH_{13} or its solid solutions) are the main hydration products in blast furnace slag cement under the same conditions.

Under hydrothermal treatment or curing temperature above 75°C ettringite decomposes to $CaSO_4$, a non-strength contributing material. Therefore, supersulphated cement is recommended only for air-cured products requiring good sulphate resistance and massive structures. Blast furnace slag cement, with an optimum composition of 70 to 80 percent granulated slag of around 4500 cm^2/g Blaine fineness and the remainder portland cement, yields hydrogarnets and calcium silicate hydrates (tobermorite or xonotlite or a mixture of both depending upon the autoclaving condition) and is recommended for both air-cured and autoclaved products.

The choice of aggregates employed in these systems depends upon the end applications. In the autoclaved compositions hydrogarnets are formed only when the aggregates do not provide an appreciable amount of active silica.

The presence of hydrogarnets presumably improves chemical stability but does not have beneficial effects on strength of the finished material. For high strength requirements, reactive aggregates are preferable. The main binders in the product with the reactive aggregates are hydrated calcium silicates and a tobermorite with aluminum substituted in the lattice.

The results demonstrated the possibility of employing blast furnace slag cement in autoclaved asbestos-cement building products.

Acknowledgement

The author acknowledges Mr. R. L. Blaine of the National Bureau of Standards for providing the German supersulphated cements and to Dr. N. Stütterheim of the South African Council for Scientific and Industrial Research for the supply of high-magnesia slags. Gratitude is expressed also to Dr. W. C. Hansen for his constructive criticisms and to the St. Louis Slag Product Company and Johns-Manville Products Corporation for their permission to make this publication possible.

References

1. W. Kramer, Eigenschaften und Anwendungsmöglichkeiten des Sulfathüttenzements, Betonstein Zeit. No. 11, 405–408 (Nov. 1952).
2. P. P. Budnikov, Instructions concerning the production and the applications of sulphate-slag cements, (in Russion) Cement—Wapno—Gips **13**, No. 22, 289–295 (1957) C. A. **52**, 5782h (1958).
3. L. Blondiau, Aptitude du ciment sursulphaté à la construction des égouts, Rev. materiaux construct. trav. publ. C No. 535, 91–98 (1960); Compatibilité de contact de bétons à base de ciments de natures différentes: Ciments sursulfatés, ciments portland et ciments de haut fourneau, ibid, No. 598–9, 335–345 (July-August, 1965).
4. J. D. Richards, The effect of various sulphate solutions on the strength and other properties of cement mortars at temperature up to 80°C, Mag. Concrete Res. **17**, No. 51, 69–76 (June 1965).
5. H. G. Smolczyk, Slag cement in chemically corroding waters, (in German) Tonind Ztg. Keram. Rundschau **89**, 159–165 (1965) Ceram. Abst. **48**, 274 (Oct. 1965).
6. V. M. Lezhoev and M. G. Kaskperskiĭ, Determining the stability of slag portland cement and slag sulphate cement in mineralized water, (in Russian) Tsement **5**, No. 5, 30–5 (1938) C. A. **33**, 47564.
7. F. W. Locher, zur Frage des Sulfatwiderstands von Hüttenzementen, Zement-Kalk-Gips **55**, 395–401 (Sept. 1966).
8. P. P. Budnikov and V. K. Guzev, Some properties of clinkerless slag cement, (in Russian) Doklady Akad. Nauk. SSSR **73**, 1009–11 (1950).
9. P. P. Budnikov and K. G. Krut, Corrosion of slag portland cements, (in Russian) Z. Prikladnoi Khimy **25**, 211 (1952).
10. T. Yamauchi, R. Kondo and M. Asano, Heat of hydration of slag cements, (in Japanese) Semento Gijutsu Nenpo **6**, 65–9 (1952) Ceram. Abst. **41**, 261 (Oct. 1958).
11. N. Sato, T. Shigeta and S. Ito, Measurement of the heat of hydration of portland—blast furnace slag cement, (in Japanese) Semento Gijutsu Nenpo **14**, 60–1 (1960) (English translation).
12. R. Alégre, Calorimetry of cements at the Centre d'Etudes de Recherches de Industrie des Liants Hydrauliques I, II, III Rev. materiaux construct et trav. publ. C, No. 544, 1–12; No. 546, 181–8; No. 547, 218–229; No. 548 247–262; No. 549 300–314 (1961)
13. D. N. Evans, R. L. Blaine and P. Workman, Comparison of chemical resistance of supersulphated and special purpose cements, "Chemistry of Cements" Proc. 4th Internat'l Sym. U. S. Dept. of Commerce. NBS Monograph 43 Washington D. C. Vol. II,

871–877 (1962).
14. E. Burke, Ibid. 877–879 (1962).
15. R. Kondo, Ibid. 881–6 (1962).
16. F. Keil and F. Gille, Hydraulische Eigenschaften bassicher Gläser mit der chemischen Zusammensetzung des Gehlenits und Åkermanits, Zement-Kalk-Gips **2**, 229–232 (1949).
17. T. W. Parker and R. W. Nurse, Investigations on granulated blast furnace slag for the manufacture of portland blast-furnace cement, National Building Studies, London 1949, Technical paper No. 3.
18. E. F. Osborn, R. C. DeVries, K. H. Gee and H. M. Kramer, Optimum composition of blast furnace slag as deduced from liquidus data for the quarternary system $CaO–MgO–Al_2O_3–SiO_2$, J. Metals, 35–45 (Jan. 1954).
19. T. Yamauchi, R. Kondo and M. Ichikama, Blast furnace slag for the use in supersulphated cement, (in Japanese) Semento Gijutsu Nenpo **8**, 156–160 (1954) Ceram. Abst. **41**, 250j (Oct. 1958).
20. T. Tanaka, On the hydraulic properties of granulated blast furnace slag, Part II. Studies on the synthetic glassy slags in the system $SiO_2–Al_2O_3–CaO$ reveal new data for cement manufacturers, Rock Products **59**, 106 (July 1956).
21. T. Tanaka, T. Sakai and J. Yamane, Die Zusammensetzung japanischer Hochofenschlaken für Sulfathüttenzement, Zement-Kalk-Gips **11**, 50–55 (1958).
22. F. Keil and F. W. Locher, Hydraulische Eigenschaften von Gläsern I. Gläser des Systems $CaO–SiO_2–Al_2O_3$ mit und ohne MgO. Zement-Kalk-Gips **11**, 245–253 (1958).
23. F. W. Locher, Hydraulic properties and hydration of glasses of the system $CaO–Al_2O_3–SiO_2$, "Chemistry of Cements" Proc. 4th Internat'l Sym. U. S. Dept. of Commerce, NBS Monograph 43, Washington D. C. Vol. I, 267–275 (1962).
24. W. Kramer, Blast-furnace slags and slag cements "Chemistry of Cements" Proc. 4th Internat'l Sym. U. S. Dept. of Commerce, NBS Monograph 43, Washington D. C. Vol. II 957–973 (1962).
25. N. Stütterheim and R. W. Nurse, Experimental blast-furnace cement incorporating high-magnesia slag, Mag. of Concrete Research **9**, 10 (March 1952).
26. N. Stütterheim, Properties and uses of high magnesia portland blast-furnace slag cement concretes, J. Am. Concrete Inst. Proc. **56**, 1027–1046 (1960).
27. N. Stütterheim, The risk of unsoundness due to periclase in high-magnesia blast-furnace slags, "Chemistry of Cements", Proc. 4th Internat'l Sym. U. S. Dept of Commerce, NBS Monograph 43, Washington D. C., Vol. II 1035–1040 (1962).
28. L. Blondiau, Le ciment métallurgique sursulfaté, Rev. matériaux construct. trav. publ. C No. 201 (1938); No. 223 (1939).
29. J. D'Ans and H. Eick, Untersuchungen über das Abbinden hydraulischer Hochofenschlacken, Zement-Kalk-Gips **7**, 449–459 (1954).
30. S. Chatterji and D. Lahiri, Eine Notiz über die Aktivierung der granulierten Hochofenschlacken, Science and Culture **22**, 514 (1957). Indian Ceram. **5** (No. 5) 71–2 (1958).
31. L. Blondiau and Y. Blondiau, Action of $CaSO_4$ on the setting properties of sulphate slags and blast-furnace slag cements, (in French) Silicate Industrials **18**, 379–82, 411–416 (1953); Rev. matériaux construct. trav. publ. C No. 435, 165–174 (1953) (in French).
32. H. Eick, Über die Calciumaluminatesulfathydrate, Zement-Kalk-Gips **17**, No. 5, 169–174 (1964).
33. H. F. W. Taylor, Hydrated Calicum Silicates. Part I. Compound formation at ordinary temperatures. J. Chem. Soc. (London) 3682–3690 (1950).
34. H. G. Smolczyk, Die Hydrationsprodukte hüttensandreicher Zemente, Zement-Kalk-Gips **18**, 238–246 (1965).
35. H. zur Strassen and W. Strätling, The reaction between calcined kaolin & lime in aqueous solution. II The reaction products, with reference to the system lime-silica-alumina-water, (in German) Z. anorg. u. allgem. Chem. **245**, 267–278 (1940).
36. N. Fratini and R. Turriziani, A hydrated calcium silicoaluminate (Strätling compound) (in Italian) Ricerca Sci **24**, 1654–1657 (1954).
37. H. zur Strassen, Discussion on "Hydration of calcium aluminates and ferrites" by F. E. Jones "Chemistry of Cements", Proc. 4th Internat'l Sym U. S. Dept of Commerce, NBS Monograph 43, Washington D. C. Vol. I 244–245 (1962).
38. R. W. Nurse, Slag composition and its effect on the properties of supersulfated slag cement, Atti del convenguo sulla produzione e le applicazione dei cementi siderurgici Napoli (May 30-June 2, 1960).
39. H. G. Smolczyk, Die Ettringit Phasen in Hochofenzement, Zement-Kalk-Gips **14**, 277–284 (1961).
40. Shi-Bi Cheng and Chi-Sheng Miou, Formation of calcium sulphoaluminate during the hydration of supersulphated cement as related to the properties of the hardened cement paste (in Chinese) Kuei Suan Yuan Hsueh Pao **4** No. 1, 11–21 (1965).
41. E. Spohn, Discussion on "Chemical resistivities of various types of cements by Renichi Kondo","Chemistry of Cement" Proc. 4th Internat'l Sym. U. S. Dept. of Commerce NBS Monograph 43, Washington D. C. Vol. II 886–887 (1962).
42. T. Yamauchi, R. Kondo and N. Morita, Study on the surface hardening of sulphated slag cement by an orthogonal array experiment, (in Japanese) Yogyo Kyokai Shi **66**, No. 749, 103–110 (1958) Ceram. Abst. **37**, 303h (Nov. 1958).
43. R. Grün, Zemente mit hydraulischen Zuschlägen, Kongressbuch Zürich (1931) des Internationalen Verbandes für Materialprüfung Zürich **1**, 778–845 (1932).
44. J. C. Yang, Studies of a supersulphated slag cement. Part I. Evaluation, modification and possible applications. Johns-Manville Report 492–31 (July 1961).
45. Y. M. Butt, B. G. Varshal and A. A. Maier, The formation of hydrogarnets during the autoclave setting of cement materials, (in Russian) Tr. Shestogo Soveshch. po Eksperim. i Tekhn. Mineralog. i Petrogr., Akad. Nauk SSSR, Inst. Geol. Rudn. Mestorozhd, Petrogr. Mineralog. i Geokhim. Inst. Khim Silikatov, Leningrad, 1961. 203–9 (Pub. 1962) C. A. **58**, 3192a (1963).
46. H. zur Strassen, Die chemischen Reaktionen bei der

Zementerhärtung, Zement-Kalk-Gips 11, 137–143 (1958).
47. D. M. Roy & R. Roy, Crystalline solubility and zeolitic behavior in garnet, phases in the system. CaO–Al_2O_3–SiO_2–H_2O, "Chemistry of Cement" Proc. 4th Internat'l Sym. U. S. Dept. of Commerce, NBS Monograph 43, Washington D. C. Vol. I, 307–314 (1962).
48. W. F. Foshag, Plazolite, a new mineral, Am. Mineral. **5** No. 11, 183–185 (1920).
49. A Pabst, The crystal structure of plazolite, Am. Mineral. **22**, 861–868 (1937).
50. E. P, Flint, H. F. McMurdie and L. S. Wells, Hydrothermal and X-ray studies of the garnet-hydrogarnet series and the relationship of the series to hydration products of portland cement. J. Research, NBS **26**, 13–33 (1941) RP-1355.
51. E. P. Flint and L. S. Wells, Relationship of the garnet-hydrogarnet series to the sulphate resistance of portland cement, ibid., **27**, 171–180 (1941), RP-1411.
52. A Pabst, Re-examination of hibschite, Am. Mineral. **27**, 783–792 (1942).
53. F. Cornu, Hibschite, ein neues Kontaktmineral, Tscherm. min. pet. Mitt. **24**, 327–328 (1095), **25**, 249–268 (1906) and **26**, 457–468 (1907).
54. D. S. Belyankin and V. P. Petrov. the grossularoid group (hibschite and plazolite), Am. Mineral. **26**, 450–453 (1941).
55. E. T. Carlson, Hydrogarnet formation in the system lime-alumina-silica-water, J. Research, NBS **56**, 327–335 (1956) RP-2683.
56. G. L. Kalousek, Crystal Chemistry of hydrous calcium silicates, I. Substitution of aluminum in lattice of tobermorite, J. Am. Ceram. Soc. **40**, No. 3, 74–80 (1957).
57. F. M. Lea and C. H. Desch, The Chemistry of Cement and Concrete, Revised Edition by F. M. Lea p. 421, (St. Martin's press, New York, 1956).
58. The Chemistry of Cements, Vol. II (Academic Press, London and New York, 1964), Edited by H. F. W. Taylor. See Chapter by R. W. Nurse entitled "Slag Cements" p. 58.
59. Supersulphated slag cement, Building Research Digest No. 130 (HMSO London) 1960.
60. M. J. Brocard, Hydration of hydrolysis of calcium silicates and aluminates as a function of temperature (in French) Ann. Inst. Tech. Bâtiment et trav. publ., New Series, No. 12 (1948).
61. J. C. Yang, Method of applying silicate to wet absestos —slag cement sheets after formation but prior to consolidation of such sheets, U. S. Patent 3,269,888 (August 30, 1966) Belgium 655, 381 (May 6, 1965) France 1,422,382 (November 15, 1965) England 1070,700 (September 1967) Italy 741,613 (September 1967).
62. A. V. Volzheuskiĭ and B. V. Sysoev, Effect of additions and autoclave practice on activity of blast-furnace slags, (in Russian) Stroitel. Materialy **5**, No. 5, 27–9 (1959).
63. Cement manufacture from blast furnace slags S. A. "Sofina" Belgium patent 555,216 (March 15, 1957).

Supplementary Paper IV-130 A Comparative Assessment of the Resistance of Super Sulphated, Sulphate Resistant Portland, and Ordinary Portland Cements to Solutions of Various Sulphates and Dilute Mineral Acids

George H. Thomas*

Introduction

The study of the resistance of concrete made with various cements to aggressive solution attack has been the subject of numerous studies which have frequently led to differing conclusions.

The present paper records the results of a specific investigation to determine the relative merits of a supersulphated cement based upon a United Kingdom blast furnace slag so as to assess its value in the manufacture of concretes for use in aggressive environments.

Results from three groups of tests are considered:—

Group 1—A laboratory assessment using concrete specimens.

Group 2—An "on site" assessment in an expermiental sewer exhibiting severe acidic conditions.

Group 3—A laboratory study employing miniature microconcrete techniques.

Group 1 Program

The programme required the comparative assessment of the resistance of three different cements to a range of aggressive solutions. The cements used were:—

(1) A supersulphated cement.

(2) An ordinary portland cement with a relatively high C_3A content.

(3) A "low C_3A" sulphate rsistant portland cement.

All three cements were commercial brands made in the north of England. Some difficulty was experienced in selecting a suitable batch of sulphate resisting portland cement for the tests. Two separate consignments exhibited unusually rapid falling off in workability in preliminary testing and were rejected. The batch finally selected behaved normally.

Chemical analyses of all three cements are recorded in Table 1. "Bogue" constitutions were calculated for the two portland cements and these are listed in Table 2. From the values obtained it was con-

Table 1. *Chemical analysis of cements used in the aggressive solution tests*

	Supersulphated cement	Ordinary portland cement	Sulphate resisting portland cement
Per cent			
SiO_2	30.68	18.84	20.34
Insoluble residue	—	0.78	0.84
FeO	1.22	—	—
Fe_2O_3	—	3.27	5.90
Al_2O_3	13.78	6.50	4.14
TiO_2	0.45	0.27	0.20
CaO	41.08	64.07	62.95
MgO	3.69	1.54	1.19
MnO	0.99	0.03	0.06
SO_3	5.30	2.40	2.47
S	1.07	Nil	Nil
Loss on ignition	0.23	2.00	1.58
Alkalies (by Diff.)	1.51	0.30	0.33
Lime saturation factor	—	0.9954	0.9312
Lime combination factor	—	0.9806	0.9157
Silica ratio	—	1.93	2.03
Alumina/iron ratio	—	1.99	0.70
Free lime	—	0.93	1.01

Table 2. *Calculated constitutions of the portland cements used in the aggressive solution tests*

(Calculation by Bogue's Method)

	Ordinary portland cement	Sulphate resisting portland cement
$3CaO.SiO_2$	53.83	54.40
$2CaO.SiO_2$	9.63	17.28
$3CaO.Al_2O_3$	11.68	1.00
$4CaO.Al_2O_3.Fe_2O_3$	9.93	17.917
$CaSO_4$	4.08	4.20
CaO (Free)	0.93	1.01
MgO	1.54	1.19
MnO	0.03	0.06
TiO_2	0.27	0.20
Insoluble residue	0.78	0.84
Loss on ignition	2.00	1.58
Alkalies (by Diff.)	0.30	0.33

*Swinden Laboratories, United Steel Co., Ltd., Rotherham, United Kingdom.

cluded that the ordinary portland cement was of high quality but with an estimated C_3A conttent which would render it susceptible to sulphatic attack. The sulphate resistant portland cement results indicated that it was a good quality product in its category.

Aggressive Solution Testing Procedure

As concrete made to resist severe aggresive attack is usually of a fairly rich mix, an aggregate cement ratio of $4\frac{1}{2}$:1 was employed. Owing to the differing water requirements of the various cement, it was decided to use a fixed workability and to adjust the water/cement ratio accordingly. The water/cement ratios used were:—

Supersulphated cement— 0.423
Ordinary portland cement— 0.460
Sulphate resisting portland cement—0.455

All the concretes were machine mixed and hand tamped into four inch steel cube moulds. Specimens were damp air stored in the usual way for the first 24 hours and then water cured for a further 27 days prior to immersing in aggressive solutions or water for control.

The solutions used were:—

(1) Na_2SO_4 (3.5% SO_3)
(2) 〃 (0.35% SO_3)
(3) $MgSO_4$ (3.5% SO_3)
(4) 〃 (0.35% SO_3)
(5) $(NH_4)_2SO_4$ (3.5% SO_3)
(6) 〃 (0.35% SO_3)
(7) H_2SO_4 (2.0% W/V)
(8) 〃 (0.25% W/V)

Assessment of attack was by compressive strength supplemented by visual observation. Four specimens from each solution were tested at each test age. To provide an accurate basis for comparison, twelve water control specimens were also tested at the same intervals.

Originally, it was planned to test the concretes at 3 months, 6 months, 12 months, 2 years and 5 years after immersion. After the two years tests had been completed, however, it became clear from visual observation of the specimens that testing beyond 5 years would be necessary in order to establish the relative merits of the two sulphate resisting cements. Final testing of some specimens were, therefore, delayed until after eight or ten years immersion. Results are summarised in Table 3.

In order to facilitate statistical processing of results, selection of concrete specimens for immersion in the various solutions was made on a statistically random basis as was the selection at each age for testing.

The sulphate and acid solutions were prepared from pure chemicals and were replaced by fresh solutions each month. The ratio of solution/concrete at the commencement of the test was approximately 1: 1 by volume but increased as cubes were removed to a maximum of around 9: 1. The cubes were maintained

Table 3. *Summary of mean compressive strengths for group 1 tests*

	Age of test (Years)	Water	Na_2SO_4		$MgSO_4$		$(NH_4)_2SO_4$		H_2SO_4	
			3.5%	0.35%	3.5%	0.35%	3.5%	0.35%	2.0%	0.25%
Supersulphated cement	1/4	8450	8200	8600	8410	8950	7890	8690	8160	8610
	1/2	9160	9340	8930	8610	8860	6300	8510	6130	9100
	1	10160	10610	10380	9350	9520	5810	9870	3700	10050
	2	9860	10430	9260	6240	9800	3740	8580	1170	8760
	5	10100					980			2990
	8	10030	8780		1030			5800		
	10	9960		7400		9510				
Sulphate resisting portland cement	1/4	6930	6990	6500	6570	7170	6300	7440	5820	6620
	1/2	8620	8540	8820	8470	8780	6860	9380	4380	8540
	1	10000	10470	10330	9590	10820	4480	10550	2000	9570
	2	10520	9920	10460	7840	9000	2500	6630	540	6750
	5	9630					40			1620
	8	9340	1740		1240			2150		
	10	9010		5250		6730				
Ordinary portland cement	1/4	9200	8890	9050	8830	9050	8390	8500	7710	8540
	1/2	8970	4760	5950	6860	7810	4660	7460	3960	6620
	1	9320	1360	8220	5180	6930	1820	5920	1410	6620
	2	9320	350	4720	3560	5210	350	2370	490	3080
	5	9130		30	80	730		60		220
	8	8240								
	10									

in solution in sealed glass tanks to eliminate problems arising from evaporation.

Attack by Sulphate Solutions and Sulphuric Acid

Statistical Analysis

The compressive strength results obtained at all ages up to ten years were subjected to statistical analysis. This consisted of three separate operations:—

(1) The removal of "outliers" from water control results by statistical processing (1). It was found to be theoretically unsound to apply this technique to the removal of outliers from the groups of four cubes immersed in aggressive solutions. However, it proved sound and helpful to use the technique on the groups of twelve water cured "control" specimens. Only one test value out of 180 was, in fact, processed out.

(2) An analysis of each cement was carried out separately and a comparison of the results in each aggressive solution at each age was obtained. The method of statistical comparison employed was the Student test. Figs. 1 to 8 illustrate the results of this

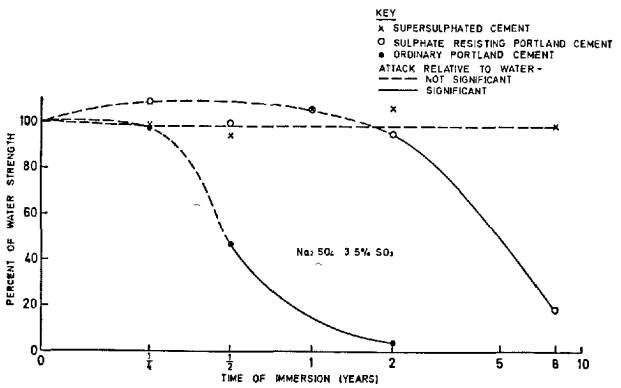

Fig. 1.

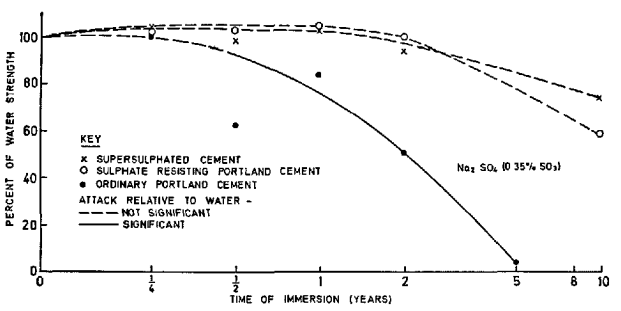

Fig. 2.

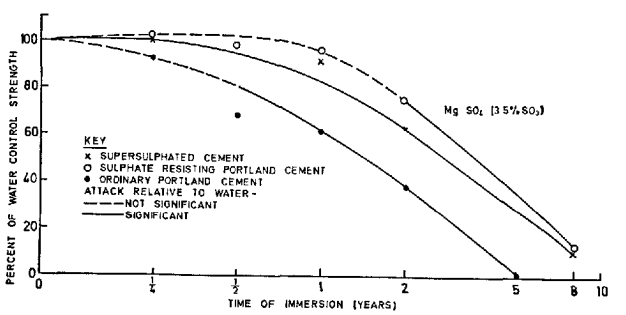

Fig. 3.

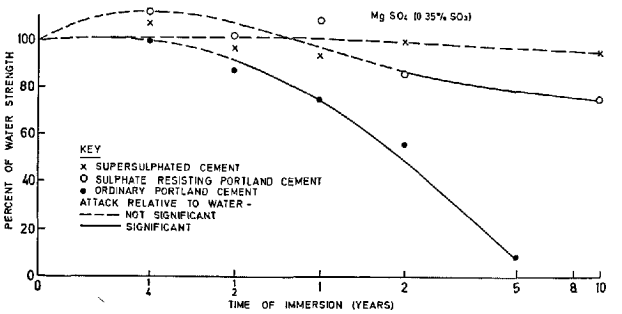

Fig. 4

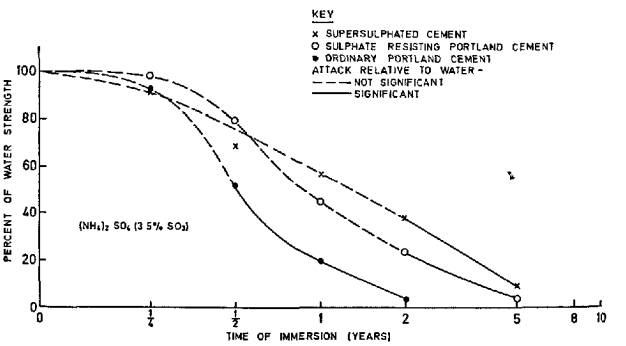

Fig. 5

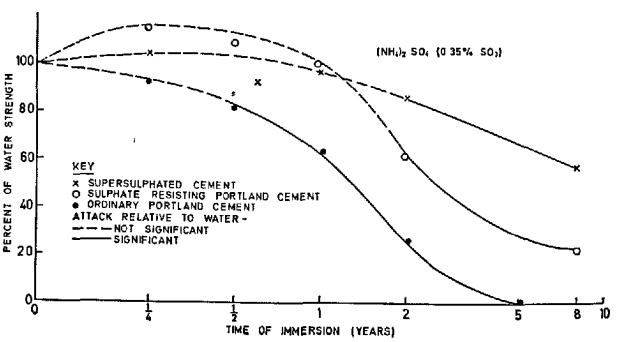

Fig. 6

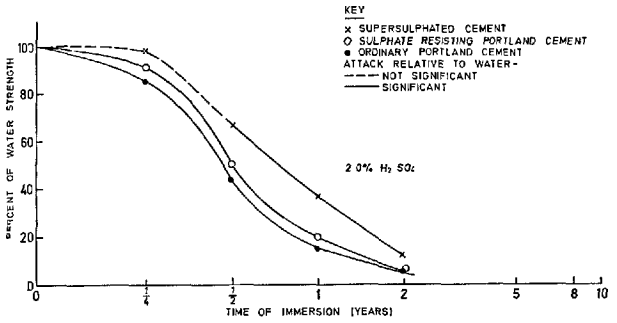

Fig. 7

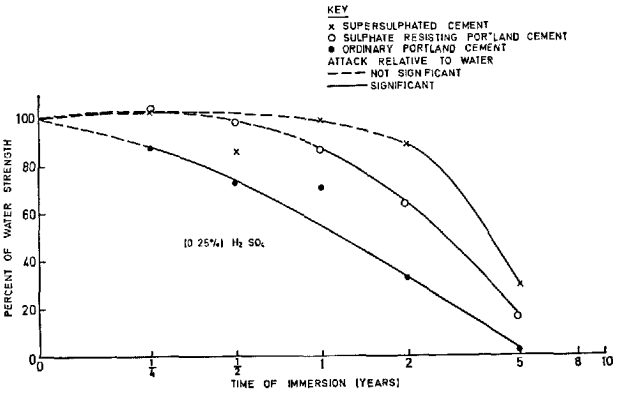

Fig. 8

analysis, the concrete strength in each solution being expressed as a percentage of the equivalent water control strength. The degree of attack expressed in this way is plotted against time on a logarithmic scale and the time at which the attack became significant is indicated.

The comparison is taken one stage further in Table 4. In the first of each pair of columns, symbols are used to indicate when, and to what degree, the attack has become statistically significant. After two consecutive instances of significant attack, the comparison is changed to establish whether or not the attack is continuing and progressive. This is assessed by comparing the respective strengths as a percentage of the water control with the equivalent value for the preceding test age. The results of these statistical tests are summarised in the second of each pair of columns.

(3) For each aggressive solution a comparison was made between the performance of the supersulphated cement and each of the portland cements. The results are summarised in Table 5—a negative sign indicating that supersulphated cement gave an inferior result.

Comparisons within Cements

The main conclusions indicated by analysis of the results may be summarised as follows:—

(1) Ordinary portland cement concrete was attacked by all solutions, in most instances after only a short period of immersion. In each solution the attack had become statistically significant at six months at the latest. In some instances, with the most aggressive conditions, less than half the water control sterngth remained in the solution immersed specimens.

This rapid rate of concrete deterioration was expected and underlines the basic need for cements with a high degree of resistance to sulphates and dilute acidic conditions.

(2) Sulpahte resisting portland cement gave a very much better performance, showing a relatively high degree of resistance to many of the solutions.

Up to two years immersion only the acids and the stronger ammonium sulphate solutions were showing a significant degree of attack but from two years onwards, deterioration became more general and ultimately the concrete was shown to have suffered a significant loss in strength in all test solutions.

(3) The supersulphated cement also demonstrated a high degree of resistance to attack in the early stages. Up to two years, deterioration was only statistically significant in the stronger ammonium sulphate solution and the 2.0 percent W/V acid. Attack by the weaker acid concentration only became significant at two years. It should be noted that although the latter acid concentration may be weak in general chemical terms, it is very much stronger than would normally be encountered in civil engineering.

Again, as with the sulphate resisting portland cement, deterioration became more general after two years immersion. However, even after eight years in the stronger sodium sulphate solution and ten years in the weaker magnesium sulphate solution, no statistically significant attack on the concrete had been recorded.

Comparison between Cements

Supersulphated Cement vs. Ordinary Portland Cement

As may be observed from Table 4, the supersulphated product was significantly superior in resistance to ordinary portland cement in all solutions. After two years immersion and in most instances much earlier, the superiority of the slag based product was obvious.

Supersulphated Cement vs. Sulphate Resisting Portland Cement

Here the position is less clear cut. The main conclusions may be summarised as follows:—

Table 4(1). *Statistical comparison of strengths in solutions versus water control (group 1)*

Cement	Age of test (Years)	Na_2SO_4(3.5%SO_3)		Na_2SO_4(0.35%SO_3)		$MgSO_4$(3.5%SO_3)		$MgSO_4$(0.35%SO_3)	
		V water control	V previous age	V water control	V previous age	V water control	V previous age	V water control	V previous age
Supersulphated	1/4	N	—	N	—	N	—	*S(5)	—
	1/2	N	—	N	—	N	—	N	—
	1	N	—	N	—	N	—	N	—
	2	N	—	N	—	S(0.1)	—	N	—
	5	—	—	—	—	—	—	—	—
	8	N	—	—	—	S(0.1)	S(0.1)	—	—
	10	—	—	S(0.1)	—	—	—	N	—
Sulphate resistant (low C_3A) portland	1/4	N	—	N	—	N	—	N	—
	1/2	N	—	N	—	N	—	N	—
	1	*S(10)	—	N	—	N	—	*S(2)	—
	2	S(10)	—	N	—	S(0.1)	—	S(1)	—
	5	—	—	—	—	—	—	—	—
	8	S(0.1)	S(0.1)	—	—	S(0.1)	S(0.1)	—	—
	10	—	—	S(0.1)	—	—	—	S(0.1)	N
Ordinary (high C_3A) portland	1/4	N	—	N	—	N	—	N	—
	1/2	S(0.1)	—	S(0.1)	—	S(0.1)	—	S(5)	—
	1	S(0.1)	S(0.1)	S(0.1)	(a)S(10)	S(0.1)	N	S(0.1)	S(10)
	2	—	S(0.1)	—	S(10)	—	S(5)	—	N
	5	—	—	—	S(0.1)	—	S(0.1)	—	S(1)

Note: (a) Higher than previous age. When assessing the 2 year value the results was compared with the six month value to give a more legitimate significance level of 5 percent.
* Higher than water control.

Key: N —Not significant. S(2) —Significant at 1—2 percent level.
S(10)—Significant at 5—10 percent level. S(1) — " " 0.1—1 " "
S(5) — " " 2—5 " " S(0.1)— " " 0.1 " "

Table 4(2). *Statistical comparison of strengths in solutions versus water control (group 1)*

Cement	Age of test (Years)	$(NH_4)_2SO_4$(3.5%SO_3)		$(NH_4)_2SO_4$(0.35%SO_3)		H_2SO_4(2.0% W/V)		H_2SO_4(0.25% W/V)	
		V water control	V previous age	V water control	V previous age	V water control	V previous age	V water control	V previous age
Supersulphated	1/4	S(5)	—	N	—	N	—	N	—
	1/2	S(0.1)	S(0.1)	N	—	S(0.1)	—	N	—
	1	—	S(0.1)	N	—	S(0.1)	S(2)	N	—
	2	—	S(0.1)	S(2)	—	—	S(1)	S(5)	—
	5	—	S(0.1)	—	—	—	—	S(0.1)	S(0.1)
	8	—	—	S(0.1)	S(0.1)	—	—	—	—
	10	—	—	—	—	—	—	—	—
Sulphate resistant (low C_3A) portland	1/4	S(5)	—	*S(10)	—	S(1.0)	—	N	—
	1/2	S(1)	S(0.1)	N	—	S(1.0)	S(0.1)	N	—
	1	—	S(0.1)	N	—	—	S(0.1)	S(5)	—
	2	—	S(1)	S(0.1)	—	—	S(0.1)	S(0.1)	S(5)
	5	—	S(0.1)	—	—	—	—	—	S(0.1)
	8	—	—	S(0.1)	S(0.1)	—	—	—	—
	10	—	—	—	—	—	—	—	—
Ordinary (high C_3A) portland	1/4	S(10)	—	N	—	S(1)	—	S(5)	—
	1/2	S(0.1)	S(0.1)	S(2)	—	S(0.1)	S(0.1)	S(0.1)	S(10)
	1	—	S(0.1)	S(0.1)	N	—	S(1)	—	N
	2	—	S(0.1)	—	S(1)	—	S(0.1)	—	S(0.1)
	5	—	—	—	S(1)	—	—	—	S(0.1)

Note: *Higher than water control.
Key: — As in 4(1).

(1) At early ages in three of the solutions, sulphate resisting portland cement displayed a marginal advantage over supersulphated cement. However, in each case, the situation was reversed with time.

(2) In seven out of the eight solutions, supersulphated cement proved to have, sooner or later, significantly superior durability to the sulphate resisting protland product.

(3) In one instance, the stronger magnesium sulphate solution, sulphate resisting portland cement demonstrated superior resistance to the supersulphated cement when assessed by statistical techniques.

Table 5. *Statistical comparison between cements (group 1)*

Cement	Age of test (Years)	Na_2SO_4 (3.5% SO_3)	Na_2SO_4 (0.35% SO_3)	$MgSO_4$ (3.5% SO_3)	$MgSO_4$ (0.35% SO_3)	$(NH_4)_2SO_4$ (3.5% SO_3)	$(NH_4)_2SO_4$ (0.35% SO_3)	H_2SO_4 (2.0% W/V)	H_2SO_4 (0.25% W/V)
Supersulphated versus sulphate resisting (Low C_3A) portland	1/4	−S(5)	N	N	N	N	−S(5)	S(5)	N
	1/2	N	N	N	N	−S(1)	−S(2)	S(10)	N
	1	N	N	N	N	S(2)	N	S(5)	N
	2	N	N	−S(1)	S(10)	S(1)	S(2)	S(1)	S(0.1)
	5	—	—	—	—	S(0.1)	S(0.1)	—	S(0.1)
	8	S(0.1)	—	−S(10)	—	—	—	—	—
	10	—	S(5)	—	S(1)	—	—	—	—
Supersulphated versus ordinary (High C_3A) portland	1/4	N	N	N	S(2)	N	S(1)	S(1)	S(10)
	1/2	S(1)	S(1)	S(5)	S(10)	S(0.1)	N	S(5)	N
	1	S(0.1)	S(10)	S(5)	N	S(0.1)	S(1)	S(2)	S(0.1)
	2	S(0.1)	S(5)	S(1)	S(1)	S(0.1)	S(0.1)	S(1)	S(0.1)
	5								S(0.1)

Note: — ve sign indicates the portland cement better than the supersulphated cement.
Key: — as in Table 4.

Group 2

Acidic Testing in an Experimental Sewer at Burton-on-Trent, the Acidic Resistance of Supersulphated Cements

Acidic conditions in civil engineering environments are usually of a very low concentration. Ground waters rarely reach pH4 unless industrial pollution increases the acidic concentration (2).

Supersulphated cement is generally considered to have an excellent resistance to these conditions, being recommended to give a good life down to at least pH3.5. Laboratory confirmation of such claims is difficult. An acidic concentration of pH3.5 would be neutralized by concretes very quickly. On the other hand, the constant maintenance of an acidic level by the use of pH control equipment is probably creating conditions which are equally far from practice as the acid levels are almost certainly being replaced at a rate far more frequently than is normal in common usage.

The use of higher concentrations such as in the 'Group 1' tests may give results of some comparative value, but clearly the most valuable test for the acidic resistance of a cement is in the kind of environment for which it may be employed.

At Burton-on-Trent the existing sewerage system has been badly attacked and extensive rebuilding is in progress. The attack is usually attributed to dilute sulphurous and sulphuric acid conditions arising from effluent containing waste materials from the brewing industry. As is common in these situations, corrosive conditions are worst above the water level. pH values of below 3.5 are common and values as low as 1.9 have been recorded on the walls (3).

Prior to redesigning the system a testing programme was organised by the Burton-on-Trent Borough Engineer's Department to evaluate materials which might be included in the programme and three different batches of supersulphated cement concrete were subjected to attack below and above the effluent level in an experimental section of the sewer.

Evaluation of test results were again on the basis

Table 6. *Percent of water control strengths of cubes tested in the burton-on-trent experimental sewer*

		Period of immersion (Months)											
		Over the effluent							Below the effluent				
		11	12	19	30	42	64	79	11	12	19	24	30
Supersulphated cement concrete	*Series 1*	96.2		96.2	84.4		75.1	49.0	98.3		95.2		99.8
	Series 2												
	Series 3												
	(a) Gravel					73.6							
	(b) Limestone					78.2							
Ordinary portland cement			72.0							96.0			
Sulphate resisting portland cement			70.0	58.0						92.0		87.0	

of percent of water control and the results are summarised in Table 6.

The results compare very favourably with the portland cement values carried out independently (3) and confirm the superior resistance of supersulphated cement to either ordinary portland or sulphate resisting portland cements. It must be emphasised that the conditions in the experimental sewer are worse than would be expected in applications for which supersulphated cement would normally be specified. However, the superiority in life over both the portland cements tested is definite and confirms the reported applicability of this cement in weak acidic environments, particularly where acid concentrations are at a more typical level than those experienced at Burton.

Group 3

A method of assessing aggressive solution resistance of cements by the use of microconcrete techniques is being developed based on procedures used at the Cement and Concrete Association's Laboratories. These techniques have the following advantages over larger scale testing:—

(i) Smaller quantities of materials are employed.
(ii) Less storage capacity is required.
(iii) Less time is required to prepare specimens.
(iv) Aggressive solution deterioration is more rapid.

The microconcrete techniques have the following disadvantages:—

(i) A higher degree of skill is required in the preparation of specimens.
(ii) The reproducibility of the test is of a lower order and hence more replicate specimens are required.
(iii) The use of half-inch microconcrete cubes is more remote from practice than the conventional four inch concrete cubes.
(iv) The testing of the specimens requires both more time and more precision on the part of the testing machine operator.

One of the reasons for developing the technique is that it promises to provide a rapid means of assessing aggressive solution resistance of cements.

A series of $\frac{1}{2}$" microconcrete cubes made of cements from the same source but of different batches to those recorded in the full scale test have been made. Sufficient specimens were manufactured for testing 5 replicas at each of 3 ages.

The test procedure involved the mixing by hand manipulation of a microconcrete mix consisting of graded washed silica sand, cement and water in a polythene bag. The microconcrete mix was then compacted by vibration into a 10 gang stainless steel precision mould.

The specimens were demoulded after 24 hours and subjected to the same curing procedure as the full scale specimens before immersion in sulphate solutions.

The aggregate cement ratio was 3: 1 and the water/cement ratio fixed as before, by adjusting for constant workability. The workability level was measured by a dropping ball test and the level of penetration fixed at 3 mms.

The water/cement ratios used were:—

Supersulphated cement	0.433
Sulphate resisting portland cement	0.465
Ordinary portland cement	0.465

As a preliminary examination into the possibilities of the test only 2 solutions were employed:—

Na_2SO_4 at 0.5% SO_3
$MgSO_4$ at 0.5% SO_3

To date results have been obtained up to six months and the results are analysed in Tables 7 and 8. Some initial difficulty was experienced in establishing a satisfactory order of test reproducibility. Subsequently, it was found that the use of "soft" tap water for the water control specimens could lead to

Table 7. *Statistical significance of attack with respect to water control*

	Na_2SO_4		$MgSO_4$	
	3 months	6 months	3 months	6 months
Supersulphated cement	N	N	N	N
Sulphate resisting (low C_3A) cement	N	$S^{1.0}$	N	N
Ordinary portland cement	*	*	$S^{0.1}$	$S^{0.1}$

*Specimens in solution completely destroyed.

Table 8. *Statistical significance of attack between cements*

	Na_2SO_4		$MgSO_4$	
	3 months	6 months	3 months	6 months
Supersulphated cement v. ordinary portland cement	*	*	$S^{0.1}$	$S^{0.1}$
Supersulphated cement v. sulphate resisting portland cement	N.S.		N.S	$S^{5.0}$

*O.P.C. specimens compl etely destroyed.

a considerable reduction in strength with time, presumably due to leaching of lime. The latter effect only occurred with the portland cements.

The procedure would appear to be promising as a fairly rapid test of sulphate susceptibility. It is unlikely, however, to be able to define accurately, degrees of resistance.

General Conclusions

In assessing the detailed results, use has been made of statistical techniques in an attempt to differentiate between real effect and experimental variation. It should be noted, however, that statistical superiority or inferiority does not imply satisfactory or unsatisfactory performance or life. In attempting to arrive at the value of a cement for a particular application it is necessary to make use of general trends indicated by the detailed results and to bear in mind not only whether the concrete will be attacked but also its likely residual strength and the rate at which it will deteriorate. From the analysis of results recorded it would appear that the following general guide lines can be drawn as to the applicability of the cements tested:—

(1) In sodium sulphate solutions supersulphated cement gives by far the best performance. It is particularly noteworthy that in the stronger solution, no significant attack was registered even after eight years of continuous immersion. Over the same period the sulphate resisting portland cement had been almost completely destroyed.

(2) In the 0.35% SO_3 Na_2SO_4 solution the advantage for supersulphated cement is less marked but still significant. Clearly either of the two sulphate resistant cements would give a good life.

(3) In strong magnesium sulphate, although the sulphate resisting portland cement gave a statistically significant better performance, in real terms neither cement would appear suitable for use in such high concentrations of this salt.

(4) Magnesium sulphate solution at the 0.35% level is resisted by both cements. Again, the supersulphated cement appears to have a slight advantage in resistance.

(5) In both concentrations of ammonium sulphate, all cements were attacked. Again supersulphated cement gave superior resistance to both the portland cements and in the case of the weaker solution, the order of difference would certainly indicate a considerably extended life.

(6) The reputed superiority of supersulphated cement in weak sulphuric acid concentrations sometimes encountered in civil engineering is confirmed by the results recorded in both Group 1 and 2 tests.

References

1. "Processing data for outliers" by W. J. Dixon, "Biometrics", Vol. 9., No. 1, 1953.
2. "Concrete corrosion, concrete protection" by I.Biczok. p. 242.
3. Corrosion Investigations at Burton-on-Trent; A. M. Douglas, Proc. Inst. Mun. Eng; Vol. 91, No. 4, April, 1964.

SESSION IV-4 EXPANSIVE CEMENT

Principal Paper Expansive Cements

Peter P. Budnikov and Irina. V. Kravchenko*

Synopsis

The existing expanding cements can be divided into those obtained on the base of aluminous cement and on that of portland cement. In respect to their composition and technology of production they differ both as to the form in which exist the compounds of issue necessary to form calcium hydrosulfoaluminate in the hardening cement paste, and to the technology of producing it. Most investigators are inclined to explain the aptitude of cements to expand by the formation in the hardening cement stone of complex compounds having a complex molecule with a great amount of crystallisation water bound with it and by a directed growth of crystals, in particular of calcium hydrosulfoaluminate. But some authors are inclined to see the cause calling forth an expansion of the cement stone during hardening in the action of osmotic forces or in the swelling of solvable films of the hydrate gels.

We are of the opinion that the phenomenon of expansion is inherent to a certain stage of hardening not only of expanding, but also of ordinary cements, but this expansion is distinguished by its intensivity and time of duration. The hydration products form during the hardening of cement first in the shape of finest crystallisation centres which, as they accumulate, grow out into larger semirigid formations. During further hydration the interstices between the particles are filled up by the hydrates formed, what leads on the one part to a condensation of the cement stone, and on the other to an extension and partial destruction of the crystalline semirigid skeleton. This is why a fine expansion of hardening cement is always accompanied by a certain decrease of its strength.

The technology of expanding cements must secure an intensive formation of a quickly growing expanding component during a certain period of hardening of the cement stone which is characterised by the presence in it of a semirigid structure formed by hydrate new formations. The process of expansion of cement can be controlled by acting on all the factors influencing: 1) the velocity of cessation of hydration reactions, 2) the number of crystallisation centres that appear in a volume unity of the hardening cement, and 3) the rate of growth of the expanding components. Such factors are for instance the composition of the cement, the fineness of grind of its components, the temperature of the surrounding medium, the additions-modifiers of structure of hydrate new formations, etc. Practically the period of extensive expansion of cement stone is 1 to 7 days for different variaties of expanding cements. The practice of many years standing of the production and use of expanding cements in construction work in the U. S. S. R. has shown a great perspectivity of the cements suggested by us.

Introduction

When mixing portland, blast-furnace and alumina cement with water, the dissolution of non-aqueous mineral compounds of a cement takes place at first. This is followed by the formation of hydrates, this providing the binding qualities of the cement paste.

During this process the change of the volume of the hardened cement paste takes place (Fig. 1). The primary contraction of the hardened cement on the section of the curve "$a-b$" takes place due to the sedimentation and dissolution of the non-aqueous clinker minerals. Then, on the section "$b-c$" some growth of the volume of the hardening cement takes place, this being connected with the formation of some hydrates (this process will be discussed below). And,

*Moscow Academy of Science, Moscow, U.S.S.R.

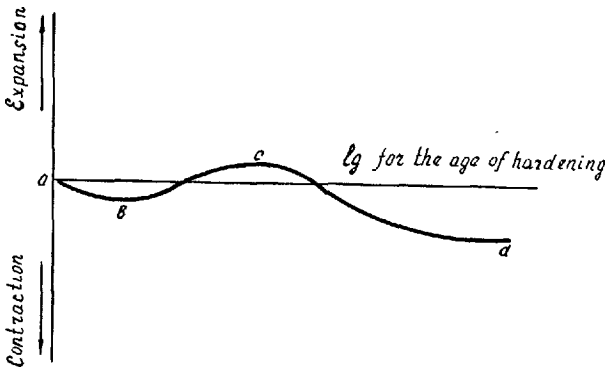

Fig. 1. *The change of volume of cement when hardening*

at last, on the section "$c - d$" the shrinkage of the hardened cement takes place, this being connected with the evaporation of water and consolidation of the geleous mass of the new formations of the hardened cement (1).

As a result of the abovesaid phenomena in mortars and concretes made on ordinary cements, pores, macro- and microcracks form, this worsening the technical qualities of the constructions. The waterproofing of the concrete or mortar, protective features of the concrete layer coating the steel bars, durability and corrosion resistance lower. All this oftenly makes it impossible the use of ordinary shrinking hydraulic cements for monolithic waterproof projects, for rendering joints, hydroisolation, clogging of holes in constructions. Or it brings to the lowering of the quality of construction works.

Therefore it is of no wonder that during the last twenty years a lot of attempts have been made in many countries to develop cements free of the shortage aforesaid, to develop cements not only "non-shrinking" but even expansive ones.

At present there has been a constant, commercial-scale production of three following kinds of expansive cements in the Soviet Union: waterproofing expansive cements (ВРЦ), gypsum-alumina cement (ГГЦ) and expansive portland cement (РПЦ) these having wide spread in construction engineering*.

As far as we know there are two kinds of expansive cements on the U.S. market and deep explorations have been conducted to improve their qualities. In some other countries periodical production of expansive cements and their use in construction takes place as well.

Interesting building qualities of expansive cements, absent in common hydraulic ones, make it profitable for more close consideration of the physiochemical processes taking place during the hardening of these cements and more close study of their features.

Technical Requirements to the Expansive Cements

Various workers in various countries have offered a lot of ways to make expansive cements (3–45). However, the biggest part of these ways has not been commercially introduced through the unreliability and not sufficient reproduction of their technical data, complication of their technology etc.

Principally, the cheapest compounds able to secure the volume increase of the hardened cement paste of expansive cements are the following ones: calcium sulphoaluminate hydrate, magnesium oxide hydrate and calcium oxide hydrate. However, there has not been yet obtained any sound and reliable results when using CaO and MgO as an expansion stimulant and most of the ways offered are based on the formation and rapid growth of the crystals of high sulphate form of calcium sulphaouminate hydrate at the interaction of calcium sulphate with calcium aluminate hydrate.

Various proposals as to the compositions and the ways of making expansive cements differ from each other both by the form the primary compounds exist (these being necessary to form calcium sulphoaluminate hydrate in hardened cement paste) and by the technology of making these cements.

To exemplify this, one may mention that in expansive cements offered in France, Hungary, USA and in some other countries, calcium sulphoaluminate hydrate forms through adding the so called "expanding admixture" in the form of a specially prepared anhydrous calcium sulphoaluminate to the expansive or non-shrinking cement.

One of the expansive cements made in the USSR—is the so called waterproofing expansive cement (ВРЦ), which is obtained by mutual grinding of some components, these containing specially prepared highly basic calcium aluminate hydrate and gypsum hemihydrate. Other kinds of the Soviet expansive cements have no special pre-treatment of their components, this simplifying their technology and lowering the cost.

The method of making expansive cement offered by P.P. Budnikov and B.G. Skramtaev (10) distincts

*Russian letters denote the abbreviations used by the Soviet National Standard—the GOST (ГОСТ)

from the aforementioned methods, this distinction being as follows: alumina cements are ground or blended with either estrich-gypsum or anhydrite cement obtained by mutual grinding of anhydrite with burned dolomite.

W.E. Leyrich has offered the way of making an expansive cement by mutual grinding of alumina and blast-furnace slags with anhydrite and air-slaked lime. Further he, in co-authorship with W. H. Prohorov (7), offered to add the expansive cement of the aforementioned composition to the portland cement and through this process to obtain an expansive portland cement.

V. V. Mikhailov and his co-workers (33), besides his aforesaid waterproofing (hydrophobic) expansive cement (BPLI) have developed a stressing cement, which is made by mutual grinding or blending in a ball mill a mixture containing gypsum, alumina cement and portland cement. The combination of the expansion and the strength growth controlled by the hydrothermal treatment and followed by water curing at normal temperature brings to the stress of reinforcement.

K. Kutateladze, E. Zedhiedze and N. Mamulashvili (44) have offered an expansive cement containing the mixture of the portland cement, gypsum and alunite bearing rock, this mixture burned at 800–900°C.

A. E. Sheikin and T. Yu. Yakub (46) have offered a nonshrinking cement made on the base of a hydrophobized hydrophobic portlanc cement with 5–10 per cent of CaO added.

A. Guttman (3) has offered the way of making of an expansive cement by adding to the cement being ground the admixtures of sulphates and chlorides, i.e.—salts which due to the formation of complex aluminate hydrate bring to the expansion.

G. Bukenbach (25) has offered the making of an expansive cement by the mutual grinding of portland cement clinker with aluminium sulfide.

P. P. Budnikov (USSR) and I. Arens (Poland) have offered the way of making and expansive cement in which, as the source of alumina to form calcium sulfoaluminate hydrate, kaolin burned at 800°C is used.

Keil and Gille (15) have obtained an expansive cement by adding to the mixture of portland cement and blast furnace slags some estrich-gypsum and up to 10 per cent of alumina cement.

A. Lossier (5, 8) has offered some expansive cements contining portland cement, sulphoaluminate cement and blast furnace slags. The amount of the expansion of hardening concrete made with these expansive cements can be, as Mr. Lossier reports, controlled by means of the composition and the dosage of the cement in the concrete and by the curing condition of this concrete.

An expansive cement, containing portland cement and an expansive admixture, this admixture being composed from anhydrous calcium sulphoauminate and gypsum, has been obtained in the University of California (USA). The amount of both the expansive admixture and gypsum is 15–20 per cent.

The U.S. Portland Cement Association (PCA) recommends to make expansive cements by blending various proportion of portland cement, calcium aluminates and gypsum. As distinct from the USSR, where expansive cements are made by mutual blending the PCA recommends the mixing in a concrete mixer some fabricated products: portland cemnt, alumina cements and gypsum—just before the adding of aggregates and water when making the concrete mix.

The authors of this report do not aim to give a comprehensive survey concerning all the patents and proposals as to the compositions and technological layouts for the manufacture of expansive cements. The examples given above should but just outline the main directions of this work which is being intensively conducted in various countries.

The existing expansive cements can be divided those based on alumina cement and those based on portland cement.

The mortars and concretes on expansive cements after the end of the expansion and further drying, give approximately the same contraction as the mortars made with ordinary cements—i.e. 0.1–0.2 per cent. But so far as the expansion taking place before this contraction can reach some per cents, the resulting expansion makes it possible to avoid the harmful consequences of shrinking deformations and—even at the sufficient rate of expansion—to use a considerable resulting expansion for making the prestressing of the concrete reinforcement.

As to the amount of expansion, the expansive cements fall into those ones having a minor value of linear expansion—in the order of some tenths of a per cent—and those with the linear expansion reaching some per cents.

The expansive cements of the first kind are intended for cases where it is necessary to compensate the shrinkage of ordinary concrete; these cements are usually called either "the cements with compensated shrinkage" or "non-shrinking cements".

The cements of the second type are intended to provide for some higher degree of an expansion of the hardened concrete in order to obtain the prestressing of the steel reinforcement. These cements are called

"selfstressing cements". The cements of the first kind prevent the development of shrinkage cracks and pores in concrete while the second ones give concrete providing for the prestressing of the reinforcement. Both the cements have been worked out in the USSR and in the USA as well.

The practice of using expansive cements in construction has shown that, when keeping all the standards, expansive concrete can have quite definite, practically sufficiently stable and reproducible qualities. All this can be achieved without any serious change of the common concrete technology and without any serious deviation from the common practice of construction.

On the base of the experience in production and using expansive cements in construction one can formulate the next basic requirements to the commercial expansive cements:

1. The amount of expansion should be equal or greatly exceed the amount of shrinkage of a common shrinking cement. In the first case there would be a non-contracting cement, while in the second case it would be an expansive one.

2. The expansion of a cement should completely end during the first period of its hardening—without bringing any further stresses in the concrete or in the mortar.

3. The construction qualities of an expansive cement, including its guaranteed amount of expansion, should be sufficiently reliable and completely reproducible.

4. The manufacturing layout of an expansive cement should be simple and commercially expedient.

The Nature of the Expansion of a Hardened Cement Paste

The most of research workers tend to explain the ability of cements to expand by the formation in a hardening cement paste of some complex compounds, these having a complicated molecule with a great amount of combined water and with a definitely directed growth of crystals—particularly calcium sulphoaluminate hydrate (4, 6, 9 et al). However, some authors tend to regard the expansion of a hardening cement paste as a result of either osmotic forces or swelling of the solvable layers of hydrate gels (46).

A. LeChaterier, H. Lafuma, A. A. Baikov and V. V. Mikhailov think that, depending from physicochemical conditions, the formation of calcium sulphoaluminate hydrate in hydrated cement can occur in two ways. At the concentration of CaO in liquid phase above 1.08 g per liter, calcium sulphoaluminate forms as a result of the interaction of the SO_4'' ion with the insoluble solid phase. During this process calcium sulphoaluminate hydrate crystals, forming through the linking to the solid phase of three gypsum moleculae and 19–20 moleculae of water, occupy a greatly larger volume than that of initial compounds, this resulting the expansion of the cement. At the concentration of CaO less than 1.08 g per liter, calcium sulphoaluminate hydrate forms as a result of reactions in the liquid phase—among the compounds dissolved in. During this process the volume, occupied by the calcium sulphoaluminate hydrate, is a little bit less than the sum of the volumes the primary compounds occupied, and thus the expansion of the cement does not take place.

On the base of this conception V. V. Mikhailov has introduced into the technological layout of his waterproof expansive cement which is widely used in the USSR for more than 25 years, the preliminary preparation of highly basic calcium aluminate hydrate and its interaction with gypsum at the high concentration of CaO in liquid phase.

The authors of this work have some other opinion as to the nature of the expansion. The results of the experiments we have conducted make it possible to formulate the following opinion concerning the mechanism of cement expansion phenomenon and of the factors causing to.

First of all it is necessary to say that the expansion, of the first sight a specific phenomenon, is inherent, on a definite stage of hardening, not only to expansive cements but as well to all the other ones. The process taking part at the hardening of expansive cements arises also at the hardening of ordinary contracting cements differing from those ones in expansive cements just by their intensity and duration.

After the mixing a cement with water anhydrous compounds of cement clinker interact with water and convert into hydrates. The products of hydration while hardening of cement paste, at first appear in the form of extremely fine nuclei of crystallization, these nuclei appearing both in liquid phase surrounding a hydration grain and on the surface of such a grain, since the concentration of the solution there is the largest one.

As far as the number of these crystallization nuclei increases, their coalescence into larger formations takes place. It is necessary to point out that in hardened cement paste the crystals of newly formed

compounds do not make a rigid, single whole crystallic coalescence. Along with the microareas where such a rigid frame forms, there are some areas where no rigid coalescence of separate crystals took part. Moreover, if a hardened cement paste were a rigid, single whole crystallic frame, it would break down as a result of continued hydration of the inner part of cement grains, since the newly formed hydration products, during the growth of their crystals, would inevitably assert some pressure on the already formed crystallic coalescence and would, at last, break it down.

It is necessary to say that the break down of the crystallic coalescence formed over some areas of the hardened cement paste do arise and it is due to such "break-downs" that temporary strength drops take place, these drops occuring in all cements-without exception-though in various degree. And the more intensive the cement hydration is, the more probable and the more appreciable these strength drops are.

It is also possible that essential role in these drops to form, take the recrystallization processes: the transition of metastable crystallic hydrates into stable ones and the dissolution of thermodynamically unstable crystallic contacts between separate crystals forming coalescences of crystals. These processes are described by E. E. Segalova and P. A. Rebinder (47).

After the semi-rigid frame in hardened cement paste has been formed, the further hydration of cement brings to both the consolidation of the hardened cements paste, this resulted from filling up the newly formed compounds into the spaces between the cement particles and previously formed hydrates and the moving apart and partial deterioration of the semi-rigid crystallic frame. And it is due to such phenomenon according to the scientists working in the field of expansive cements, a non restricted expansion of hardened cement paste is always followed by some decrease of its strength.

The volume of a hardened cement paste results from the two contrary phenomena occuring in, the first one being the growth of its volume under the influence of continuing crystallization in hydrated newly formed compounds, while the second one being the contraction under the influence of capillary forces.

The ability of a compound to crystallize is mainly defined by two factors: by its ability to spontaneous crystallization (i.e. the number of crystallization nuclei, formed for a unit of time in a unite of volume), and by the linear speed of crystals' growth.

If the number of crystallization nuclei in a unit of the volume is very large or if the speed of the crystals'-growth in newly formed compounds is small, then the dimension of the rigidly framed microareas of the hardened cement paste would be very small—despite a great number of these areas. This is featured by the consolidation of the hardened cement paste accompanied with the full absence or a very small expansion.

On the contrary, if the number of crystallizing nuclei is a little bit less, while the growth of crystals is either having greater speed or is more prolonged, then the dimensions of the areas having rigid crystallation frame would be relatively bigger. Then the growing crystals of newly formed compounds should more often meet some obstacles and move apart surrounding crystallic "Buildups".

On the base of such a conception concerning the nature of cement expansion, the composition and manufacturing layout of any expansive cement should be so designed as to provide for an intensive formation of quickly growing crystals of an expansive compound during a definite period of the paste hardening, this period being characterized by the presence in the hardened paste of a semi-rigid frame formed by the hydrated newly formed compounds.

It also results from this conception that the expansion process can be controlled by regulating all the factors influencing:

1) speed of hydration reactions,
2) the number of crystallization nuclei formed in a unit of volume of the hardening cement per unit of time and
3) the speed of growth of crystals in the expansive compound.

Such factors are, for example, the following ones: the composition of an expansive cement, the fineness of a cement and of its components, the temperature of the environment, the admixtures modifying the structures of newly formed hydrate etc.

The most rapidly crystallized component of the most commonly known expansive cements, able to form quickly growing crystals, is calcium sulphoaluminate hydrate. However, as it was mentioned above, the expansion of a cement depends not only on the amount of this compound in the hardened cement but on the time of its formation as well.

Practically the period for vigorous expansion of the hardened cement paste of various expansive cements lies between one and seven days (see Fig. 2).

If the formation of crystals of calcium sulphoaluminate hydrates occurs too quick (as for example in the case of a very fine expansive cement)—and mainly ends at the first period of hydration, when the hardening cement paste is not yet hard enough, then the amount of expansion would be a small one. At the

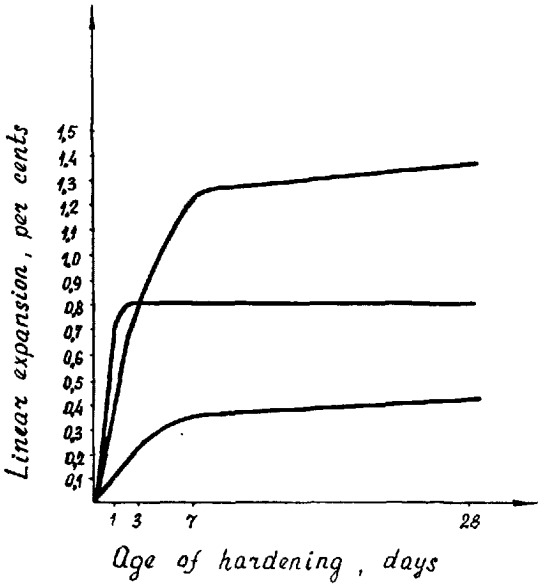

Fig. 2. *The expansion of various expansive cements*

coarser cement the growth of crystals of calcium sulphoaluminate hydrates slows down, this resulting to some greater expansion amount of the cement when hardening. Table 1 below contains the data of the amount of the expansion of alumina expansive cement (ГРЦ) made in the USSR depending on its fineness.

According to our data (20, 38, 45) the control of the amount of the cement expansion when hardening is also possible through the change of CaO concentration in the liquid phase. Increasing the CaO concentration in liquid phase accelerates the crystallization of calcium sulphoaluminate hydrate thus decreasing the amount of the cement expansion. This has been proved by our study of the binding of calcium sulphate into calcium sulphoaluminate hydrate in the systems where the alumina compound is highly basic calcium aluminate $C_{12}A_7$ and less basic one CA.

We have found that the binding of calcium sulphate into calcium sulphoaluminate hydrate in systems containing highly basic calcium aluminate ($C_{12}A_7$), which is hydraulically more active, ends 60–70 times quicker than in systems containing a less basic calcium aluminate (CA). Fig. 3 shows the data concerning the speed of binding of calcium sulphate with various calcium aluminates which we have synthesized.

At the more rapid interaction of highly basic calcium aluminate with calcium sulphate in the liquid phase, the crystals of the formed calcium sulphoaluminate hydrate are of smaller dimensions than those at the slow interaction and it brings to some decrease of the linear expansion. (See Table 2).

Table 1. *The amount of expansion, depending on its fineness*

Specific surface, cm² per gram	Linear expansion, mm per meter					
	1 day	3 days	7 days	14 days	28 days	42 days
2000	0.7	3.2	4.9	8.4	14.1	20.7
2800	1.9	3.0	3.7	4.4	5.4	6.0
3500	1.9	2.9	3.2	3.4	3.7	4.0

Table 2. *Linear expansion of the mixtures of calcium aluminates with gypsum*

Mixture, composition	Linear expansion, per cent			
	1 day	3 days	7 days	28 days
$C_{12}A_7 + CaSO_4 \cdot 2H_2O$	0.08	0.1	0.15	0.30
$CA + CaSO_4 \cdot 2H_2O$	0.20	2.3	5.6	The specimen has greatly elongated, bended and cracked

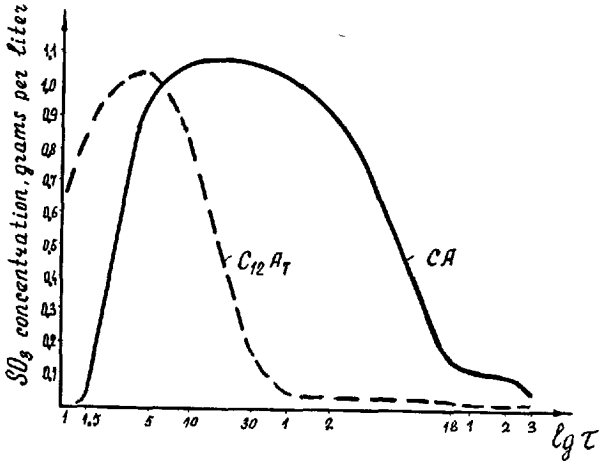

Fig. 3. *The binding of gypsum with various calcium aluminates*

As it is known, the environment temperature makes a serious influence on the hydration processes. We have studied the influence of the temperature of the environment on the speed of the growth of calcium sulphoaluminate hydrates crystals. Fig. 4 shows the photo of calcium sulphoaluminate hydrates formed in the hardened expansive cements at the various temperature of the environment. Table 3 contains the strength data of expansive cements hardened at normal and elevated temperatures.

Our data concerning the influence of the temperature and humidity on the speed of growth of calcium sulphoaluminate hydrates crystals have been used as a basis for designing of a third kind of expansive cement made in the USSR—The expansive portland cement (РПЦ) (27).

We have found that the formation of calcium sulphoaluminate hydrate at the interaction of cal-

a)

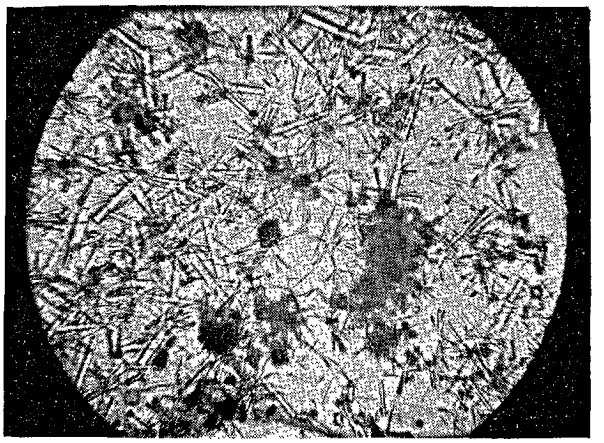

b)

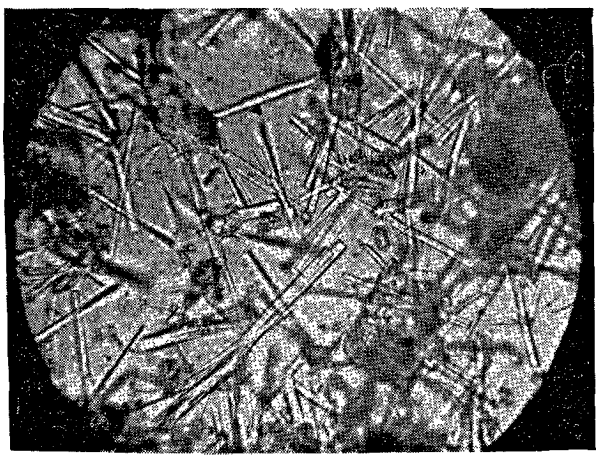

Fig. 4. *The crystals of calcium sulphoaluminate hydrate formed at the hydration of gypsum—alumina cements* (ГГЦ) (×*180*)
a) hydration at 18°C, age 24 hours
b) hydration at 80°C, age 1 hour

Table 3. *The change of strength of expansive cements hardened at various temperatures of the environment*

Cement	Compressive strength, kg/cm²							
	18°C, age				80°C, age			
	6 hours	12 hours	18 hours	24 hours	6 hours	12 hours	18 hours	24 hours
Gypsum alumina expansive cement	75	342	520	602	647	720	887	832
Expansive portland cement	—	17	57	95	387	500	540	596

cium aluminates with gypsum at the temperature 60–80°C occurs with a greater rate exceeding the rate of the formation of calcium silicate hydrates. This gives the base to assume that the rate of strength of cements, whose hardening to a great extent is based

a)

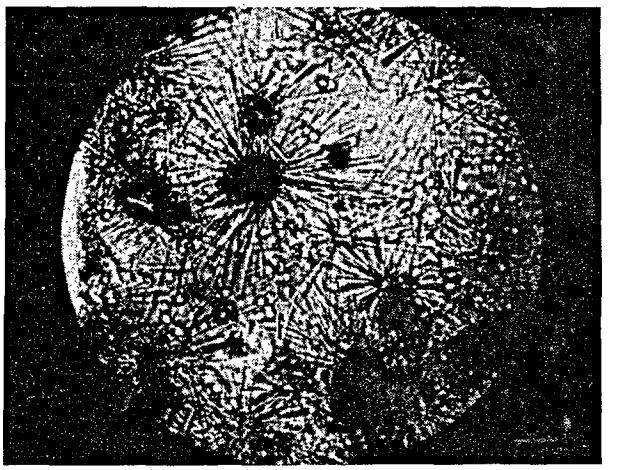

b)

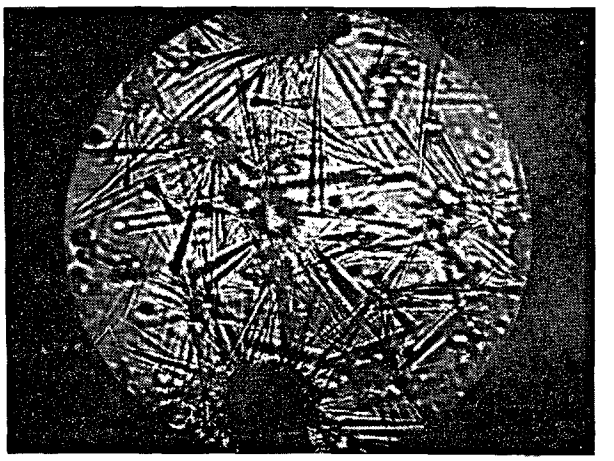

Fig. 5. *The crystals of calcium sulphoaluminate hydrate, formed at the hydration of expansive portland cement* (РПЦ) (×370):
a) hydration at 18°C, age 24 hours
b) hydration at 80°C, age 5 hours

on the formation of calcium sulphoaluminate hydrates, is considerably higher than the rate of strength of cements, whose hardening to a great extent is based on the formation of calcium sulphoaluminate hydrates, is considerably higher than the rate of strength growth of portland cements. On the base of these tests we have designed an expansive portland cement (РПЦ) in which the accelerated strength growth at the steam curing is accounted for a more intensive formation of calcium sulphoaluminate hydrates. After the steam curing is ended, the strength growth continues this accounted for common reactions occuring when hardening portland cements at the common temperature.

Fig. 5 shows the pictures of the crystals of calcium

sulphoaluminate hydrate formed in hardening expansive portland cement (РПЦ) at the normal and elevated temperatures. Fig. 6 contains the data on the strength change of both the ordinary and expansive portland cements at the steam-curing.

The linear expansion of expansive portland cement (РПЦ), that obtained by means of mutual grinding of starting materials, which provide the formation of calcium sulphoaluminate hydrate at the first period of cement hardening, amounts to 2–3 per cent. This expansive portland cement is used in construction technics as a common expansive cement. It is more widely used, however, as a special cement for making reinforced concrete articles in order to speed up their hardening when steam-cured (45). The concrete made of this cement makes no contraction cracks; moreover, it is of high water-proofing values.

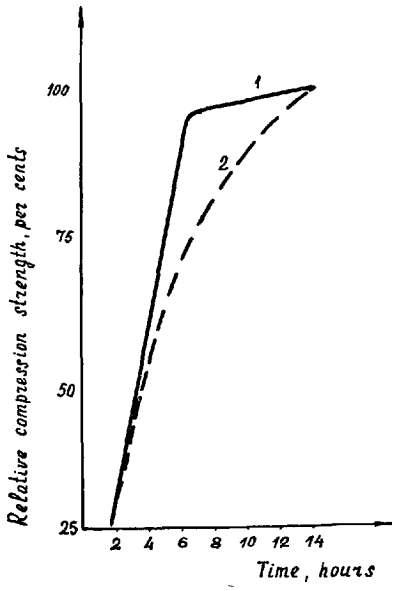

Fig. 6. *The change of strength when steam cured*
1—expansive portland cement
2—ordinary portland cement

The Technical Features of Expansive Cements

Commercial manufacture of expansion cements in the USSR and their wide use was preceeded by the long study of their technical features and numerous tests which have proved the reproduction of the results obtained.

For example, the stability of technical features of the alumina expansive cement (ГРЦ) has been studied by us for twenty years. The strength of cement has been tested in standard mortars of 1: 3 composition in both lean and plastic consistency with normal sand and with common sand used in building in mortars of 1: 2.5 composition; we have also tested cements in concretes of various composition and plasticity. Table 4 contains compression and tensile strength tests data for samples made from alumina expansive cement (ГРЦ) depending on the conditions of five years hardening.

Fig. 7 shows the crystals of calcium sulphoaluminate hydrates extracted from the alumina expansive cement hardened during 11 years.

Alumina expansive cement as well as common alumina cement is a rapid hardening one. The hardening in alternate moisting and drying conditions makes no appreciable adverse influence on it. Its compressive and tensile strength values are higher than those for alumina cement.

Fig. 8 shows the change of linear expansion for expansive alumina cement when hardening in water, in air and at the alternate pattern of hardening. As seen from the data reported, the expansion of an

Table 4. *The change of the strength of expansive alumina cement* (ГРЦ) *depending on the conditions of hardening*

Hardening conditions	Strength, kg per cm²																	
	compression, age:									tensile, age:								
	1 day	3 days	28 days	6 months	1 year	2 years	3 years	4 years	5 years	1 day	3 days	28 days	6 months	1 year	2 years	3 years	4 years	5 years
The specimens of stiff consistency																		
Water	319	341	344	386	522	517	535	543	471	25	20	24	21	34	32	33	29	27
Air	319	386	478	462	477	472	398	366	351	25	25	30	32	33	33	35	32	27
Combined	319	341	563	580	523	590	525	466	420	25	20	35	41	48	60	47	33	37
The specimens of plastic consistency																		
Water	163	212	304	342	325	342	350	286	311	22	15	24	23	22	22	27	30	28
Air	163	180	292	276	315	282	250	236	216	22	22	24	28	31	32	29	25	29
Combined	163	212	359	375	382	390	330	271	241	22	15	32	32	40	36	36	25	28

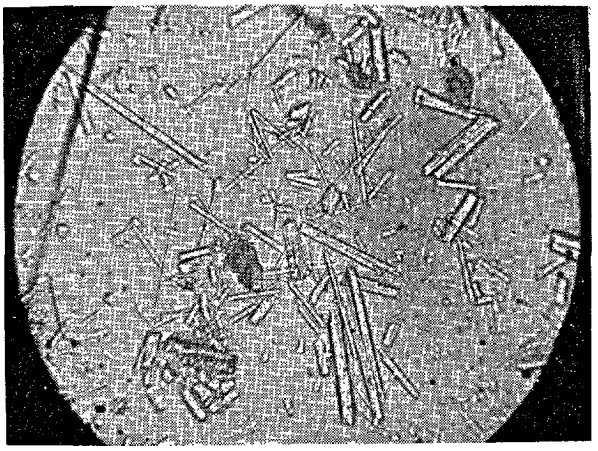

Fig. 7. *The crystals of calcium sulphoaluminate hydrate, formed in gypsum-alumina cement, 11 years of hardening*

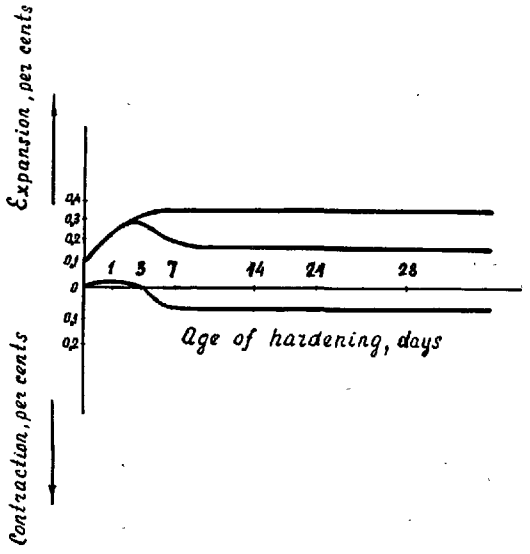

Fig. 8. *The influence of hardening conditions on the amount of expansion of cement*
1—in water
2—at the combined pattern of hardening
3—in air

expansive aluminous cement (ГРЦ) hardened in water during the first day amounts to 50 per cent of the final expansion, this process practically ending at the age of three days. Table 5 contains data concerning the relationship between the expansion amount of a hardened cement and the mortar composition. These data show that the expansion of expansive alumina cement (ГРЦ) decreases proportionally to the decrease of binding agent content in it and inversely proportional to the W/C ratio increase.

The heat release when hardening of alumina expansive cement starts quickly and runs smoothly. The

Table 5. *The amount of the hardening cement expansion depending of the mortar composition*

Mortar composition		Linear expansion, per cent, at various curing age (days), 1	3	7	14	21	28	60
1:0	0.24	0.14	0.26	0.28	0.31	0.31	0.31	0.31
1:0.25	0.26	0.19	0.24	0.26	0.27	0.27	0.27	0.27
1:0.5	0.28	0.17	0.22	0.22	0.22	0.22	0.23	0.23
1:1	0.29	0.12	0.16	0.17	0.18	0.18	0.18	0.18
1:1.5	0.31	0.09	0.14	0.14	0.14	0.14	0.14	0.14
1:2	0.34	0.07	0.12	0.12	0.12	0.12	0.12	0.12
1:2.5	0.41	0.06	0.1	0.1	0.1	0.1	0.1	0.1
1:3	0.43	0.08	0.09	0.09	0.09	0.09	0.09	0.09
1:4	0.67	0.05	0.05	0.05	0.05	0.05	0.05	0.05
1:6	0.77	0	0.01	0.01	0.03	0.03	0.03	0.03
1:8	1.00	0	0.01	0.01	0.01	0.01	0.01	0.01

maximum temperature of its heating is lower than that of alumina cement.

Tests for both the adhesion of expansive alumina cement with reinforcement steel and the safety of the steel were conducted for five years. These tests show that the hardening of concrete and mortars at the constant humidity, expansive aluminous cement bears no corroding action on the reinforcement. At the air hardening, however, when gypsum contained in expansive aluminous cement has no time enough to completely bind into calcium sulphoaluminate hydrate the corrosion of the steels surface takes place.

The studies have shown that concretes and mortars on expansive alumina cement are waterproofing ones at 10 atm. pressure after three days of hardening.

Rich mortars of 1: 2.5 composition and concretes with cement consumption of 350 kg per cubic meter, having W/C = 0.45 and made on expansive alumina cement (ГРЦ) suffer more than 200 alternate freezing-thawing cycles.

The mortars and concretes made from expansive alumina cement are quite stable at alternate watering and drying but cannot be used at temperatures above 80°C since at these temperatures calcium sulphoaluminate hydrate decomposes.

Expansive aluminous cement (ГРЦ) can be used for jointing separate concrete articles into a single unit and for strengthening of articles, for pouring base-plate bolts, for making joints and sockets in water supply tubes having pressure up to 10 atm and sewage in tubes for making hydroisolation and plastering, for building, reservoirs, for jointing large parts of machines and metallic works.

Expansive aluminous cement (ГРЦ) is widely used in the form of gel cements for oil wells and gas wells when sinking into cavernous and cracked rocks.

The study of the technical features of waterproofing expansive cement (ВРЦ) and the inspection of constructions made of this cement have been continued for over twenty five years. This cement is of quick

Table 6. *The technical data of the waterproof expansive cement* (ВРЦ)

Setting hours,		Time, min.	Strength (kg/cm²), specimens made from					Linear expansion when hardening, per cent				The full waterproofing attained in the specimens made from:			
initial		final	paste of normal plastic mortar consistency, age (1 : 2),					in air, age		in water, age		neat cement paste, age		mortar 1 : 2, age	
not earlier than		not later than	6 hours	1 day	3 days	7 days	28 days	1 day	28 days	1 day	28 days	6 hours	1 day	10 hours	1 day
			not less than									pressure, atm.			
4		10	75	120	200	300	500	0.05	0.02	0.2	1.0	1	5	1	5

Table 7. *The technical data of expansive portland cement* (РПЦ)

Fineness, per cent, residue on the sieves:		Specific surface, S, cm²/g	Water for normal consistency, per cent	Setting time, hours-minutes		Compressive strength, kg/cm², age			Linear expansion, per cent, age			The waterproofing of mortars and concretes hardened in various conditions and withstanding the pressure (atms), after:	
No. 02	No. 008			Beginning	End	3 days	7 days	28 days	1 day	3 days	28 days	1-day of water hardening	steam curing
0.1–0.5	6–8	3000–3500	25–29	1.0–2.0	1.5–4.0	200–300	300–400	400–600	0.15–0.50	0.20–0.80	0.20–1.00	8-10	13-15

strength growth value, of short setting time and of high waterproofing value. Table 6 contains the data featuring the technical values of this cement. The widest use of this cement is the joint making of city subways cast sections. The long year service of various Soviet subways has proved high values of the waterproofing expansive cements.

This cement has also been used for repair and restoration, hydroisolation coating, for jointing separate concrete articles into a single unit etc.

Table 7 contains data featuring technical values of expansive portland cement (РПЦ). The study of its features and inspection of construction projects made of this cement have been conducted for thirteen years.

This kind of cement is of high strength, waterproofing and of anticorrosive values. Numerous floating, precast and reinforced construction projects made of this cement some thirteen years ago are still in good service conditions.

This cement has been widely used for making common precast reinforced articles made of precast unit factories since it makes possible to spend half the time for isothermal curing of units when hydrothermally treated as to compare with ordinary portland cement of equal strength.

To add that this cement is of some lesser cost than ordinary portland cement of equal strength.

So, the manufacturing and use of expansive cements in the Soviet Union and in other countries reveal wide prospects for these kind of cements.

To conclude it is necessary to state however, that, despite the broad promise of expansive cements as a building material, their output and their use has not yet attained the volume necessary. And, for their further development, following research work and accumulation of practical experience are necessary concerning:

1. More strict framing of the building features and composition of expansive cements.
2. Working out the optimum compositions and manufacturing layout for expansive concretes of the strictly shaped quality.
3. More strict framing of the optimum areas for use of expansive concretes, specifically for self-stressed one.
4. Finding out the amount of the stress loss in reinforcement work under the influence of the shrinkage and the creep in a long aged concrete.
5. The study of still unexplored features of expansive concretes in order to broaden their use.

References

1. Г.Д. ДИБРОВ, М.С. Остриков. О механизме усадки. 5-ая конференция по коллоидной химии. АН

СССР, стр. 148, М., 1962.
(G. D. Dibrov, M. S. Ostrikov. On Mechanism of Contraction. 5th Conference on Colloidal Chemistry. Academy of Sciences of the U.S.S.R., p. 148 Moscow, 1962.)
2. T. C. Powers. Industrial and Engin. Chem., 27, 790, 1935.
3. A. Guttmann. Zement, 27. Rf. 30, 459, 1938.
4. В.В. Михайлов. Авторское свидетельство Ио 68445 с приоритетом от 12 августа 1942 г. Его же. Бюллетень строительной техники. Стройиздат, Ио 11; М., 1944.
(V. V. Mikhailov. Certificate of Authorship No. 68445 with Priority dated 12th of August 1942. His. Bulletin of Building Technique. Storiizdat, No. 11, Moscow, 1944.)
5. H. Lossier. Le Génie Civil, N 8, 61; N 9, 69, 1944.
6. П.П. Будников. Авторское свидетельство Ио 69600 с приоритетом от 9 апреля 1947 г.; Ио 662240 с приоритетом от 31 мая 1946 г. Бюллетень изобретений Ио 5, 59, 1946.
(P. P. Budnikov. Certificate of Authorship No. 69600 with Priority dated 9th of April 1947; No. 662240 with Priority dated 31st of May 1946. Bulletin of Inventions No. 5, 59, 1946).
7. В.Э. Лейрих. Авторское свидетельство Ио 67697. Бюллетень изобретений Ио 1, 54, 1947.
(V. E. Leirikh. Certificate of Authorship No. 67697. Bulletin of Inventions No, 1, 54, 1947.)
8. M. Lossier. Bulletin de Association Internationale de Congress de Cemiks de Fer., N6, 370, 1948. Его же. Memoires de la Societe de Ingenier Civils, N4, 1948.
9. П.П. Будников, Б.Г. Скрамтаев. Авторское свидетельство Ио 87303 с приоритетом от 10 ноября 1949 г.
(P. P. Budnikov, B. D. Skramtaev. Certificate of Authorship No. 87303 with Priority dated 10th of November 1949.)
10. П.П. Будников, Б.Г. Скрамтаев. Авторское свидетельство Ио 80842 с приоритетом от 12 февраля 1949 г.
(P. P. Budnikov, B. G. Skramtaev. Certificate of Authorship No. 40842 with Priority dated 12th of February 1949).
11. П.П. Шабадин. Авторское свидетельство Ио 74926. Бюллетень изобретений, Ио 5, 66, 1949.
(P. P. Shabadin. Certificate of Authorship No. 74926. Bulletin of Inventions No. 5, 66, 1949.)
12. П.П. Будников, З.С. Косырева. Строительн. материалы, Ио 1, 36, 1949, Их же. Цемент, Ио 4, 11, 1952. Их же ДАН АН СССР, 61, Ио 4, 621 1948.
(P. P. Budnikov, Z. S. Kosyreva. Building Materials, No. 1, 36, 1949. Theirs. Cement, No. 4, 11, 1952. Theirs. Reports of Academy of Sciences of the U.S.S.R., 61, No. 4, 621, 1948.)
13. Э.З. Юдович, Я.Н. Новиков. Расширяющийся Цемент. Промстройиздатб М., 1959.
(E. Z. Yudovich, Ya. N. Novikov. Expanding Cement, Promstroiizdat Moscow, 1959.)
14. В.В. Михайлов, Б.Г. Скрамтаев, Э.З. Юдович. Цемент, Ио 6, 5, 1949.
(V. V. Mikhailov, B. G. Skramtaev, E. Z. Yudovich. Cement, No. 6, 5, 1949.)
15. F. Keil, F. Gille. Zement-Kalk-Gips, 2, Hf. 8, 148,1949
16. A. Hummel, K, Charisius. Zement-Kalk-Gips, 2, Hf. 7, 121, 1949.
17. C. Goria, M. Appiano. Cemento, N7, 1949; N47, 1950.
18. F. Shenker, T. Shunn. Patent of USA, 465, 278, 22, March, 1949.
19. K. Wenkler, F. Shenkler. Patent of England N675.736 от 13 июля 1949.
20. П.П. Будников, И.В. Кравченко, Б.Г. Скрамтаев. Авторское свидетельство Ио 920907 с приоритетом от 6 января 1950.
(P. P. Budnikov, I. B. Kravchenko, B. G. Skramtaev. Certificate of Authorship No. 920907 with Priority dated 6th January 1950.)
21. Б.Г. Скрамтаев, Ю.З. Юдович. Авторское свидетельство Ио 87222 с приоритетом от 12 января 1950.
(B. G. Skramtaev, Yu. Z. Yudovich. Certificate of Authorship No. 87222 with Priority dated 12th January 1950.)
22. В.Г. Гегеле, И.М. Овидовский, В.А. Туманишвили. Авторское свидетельство Ио90135 с приоритетом от 20 марта 1950. Бюллетень изобретений Ио 4, 110, 1951.
(V. G. Gegele, I. M. Ovidovsky, V. A. Tumanishvili. Certificate of Authorship No. 90135 with Priority dated 20th March 1950. Bulletin of Inventions No. 4, 110, 1951.)
23. К.С. Кутателадзе, М.Я. Аласания. Авторское свидетельство Ио 90772 с приоритетом от 1 февраля 1950. Бюллетень изобретений Ио 6, 79, 1951. Его же. Цемент, Ио 3, 18, 1953.
(K. S. Kutateladze, M. Ya. Alasaniya. Certificate of Authorship No. 90772 with Priority dated 1st February 1950. Bulletin of Inventions No. 6, 79, 1951. Theirs. Cement, No. 3, 18, 1953.)
24. В.Г. Скрамтаев. Расширяющиеся цементы. Новые виды цементов, их производство и применение. Промстройиздат, М., 1951.
(V. G. Skramtaev. Expanding Cements. New Kinds of Cements, Their Production and Application. Promstroiizdat, Moscow, 1951.)
25. H. Bickenbach. Bauplanung und Bautechnik. Leipzig, N2, 351, 1951.
26. П.П. Будников, И.Б. Кравченко, Б.Г. Скрамтаев. Авторское свидетельство Ио 92027 с приоритетом от 6 января 1950. Гипсоглиноземистый расширяющийся цемент. Ж. Строительство, Ио 1, 27, 1952.
(P. P. Budnikov, I. V. Kravchenko, B. G. Skramtaev. Certificate of Authorship No. 92027 with Priority dated 6th January 1950. Gypsum Alumina Expanding Cement. Journal "Stroutelsvto (Construction)", No. 1, 27, 1952.)
27. И.В. Кравченко, Ю.Ф. Соломатина. Авторское свидетельство Ио 101675 с приоритетом от 5 ноября 1952.
(I. V. Kravchenko, Yu. F. Solomatina. Certificate of Authorship No. 101675 with Priority dated 5th November 1952.)
28. H. Lafuma. The Third Intern. Symposium on the Chemistry of Cement. London. 1952, p. 581.

29. И. В. Кравченко. Авторское свидетельство Ио 104167 (1953).
(I. V. Kravchenko. Certificate of Authorship No. 104167 (1953).)
30. I. Ahrends. Cement. Wapno. Gips, No. 3, 10, 1953.
31. T. Tanaka, I. Watanabe. Cemento Gijutsu Nenpo, No. 8, 10, 1953.
32. I. Ahrends, B. Dybowska. Cement. Wapno. Gips, No. 4, 82, 1955.
33. В.В. Михайлов. Напрягающийся цемент. Труды совещания по химии цемента. Промстройиздат, М., 1955.
(V. V. Mikhailov. Stressing Cement. Transactions of the Symposium on Cement Chemistry. Promstroiizdat, Moscow, 1955.)
34. I. Dolezsai, I. Kelemen. Epitöanyag/Budapest/, No. 6 196, 1959
35. Дин Шу-Сю. Цзяньчжу Цайляо-Гунье, Ио 3, 34, 1959.
(Din Shu-Syu. Building Materials Industry, No. 3, 34, 1959 (in Chinese.))
36. J. Kazimir. Epitöanyag/Budapest/, N 5, 183, 1960.
37. M. Matousek. Epitöanyag/Budapest/, N 4, 144, 1960.
38. П.П. Будников, И.В. Кравченко. Явления расширения и сбросы прочности при твердении цементов. Журн. Прикл. химии. 33, Ио 11, 2389, 1960.
(P. P. Budnikov, I. V. Kpavchenko. Expanding Phenomena and Breaks of Strength in the Time of Hardening of Cements. Journal "Application of Chemistry", 33, No. 11, 2389, 1960.)
39. П.П. Будников, Чэнь Цзей-лин. Расщиряющийся глиноземистый цемент на основе китайского боксита. Труды химико-технолог. института им. Д.И. Менделеева, 36, 135–143, 1961.
(P. P. Budnikov, Chan Tszei-Lin. Expanding Alumina Cement on the Base of Chinese Bauxite. Transactions of Institute of Chemical Technology after the Name of D. I. Mendeleev, 36, 135–143, 1961.)
40. A. Klein, T. Karby, M. Polivka. J. Amer. Concrete. Inst., 58, No. 1, 59, 1961.
41. P. P. Budnikov. Role of Gypsum in the Hardening of Hydraulic Cements. Fourth Internat. Symposium on the Chemistry of Cement. Washington, 1960, p. 469–477.
42. V. V. Mikhailov. Stressing cement and the mechanism of selfstressing concrete regulation. Fourth Internat. Symposium on the Chemistry of Cement. Washington, 1960, p. 927.
43. О. Мчедлов-Петросян, Д.Г. Филатов. Авторское свидетельство Ио 141092 с приоритетом от 28 января 1961 г.
(O. Mchdlov-Petrosyan, L. G. Filatov. Certificate of Authorship No. 141092 with Priority dated 28th January 1961.)
44. К.С. Кутателадзе, Е, Зедгиедзе, Н. Мамулашвили. Научно-технич. бюллетень Научно-технического Комитета Грузии, Ио 2, 16, 1961.
(K. S. Kutateladze, E. Zedgiedze, N. Mamlashvili. Gruzian Scientific and Technical Bulletin, No. 2, 16, 1961. Scientific and Technical Committee of Georgia)
45. И.В. Кравченко. Расширяющиеся цементы. Госстройиздат, М., 1962.
(I. V. Kravchenko. Expanding Cements. Gosstraizdat, Moscow, 1962.)
46. А.Е. Шейкин. Т.Ю. Якуб. Безусадочный портландцемент, Госстройиздат, М., 1966.
(A. E. Sheikin, T. Yu Yakub. Non-Contraction Portland Cement, Gosstroiizdat, Moscow, 1966.)
47. Е.Е. Сегалова, П.А. Ребиндер. Сб. Новое в химии и технологии цемента. Госстройиздат, 1962.
(E. E. Segalova. P. A. Rebinder. Collection. Recent Achievements in Cement Chemistry and Technology. Gosstroiizdat, 1962.)

Written Discussion

Otar P. Mchedlov-Petrosyan and Dmitrijs A. Ugінčius

The excellent Principal Paper "Expansive Cements" by P. P. Budnikov and I. V. Kravchenko is of great interest for everybody who works in this field of cement and concrete technology. However, the authors say that they do not try to give a complete survey of all the works in this field. That is the reason why we wish to pay attention to some aspects of this problem about which the authors say nothing.

From our point of view the production of expansive compositions on the base of commercial portland cement directly at the construction site or at prefabricated concrete plant, using the simplest technological operations, is a good idea. H. Lafuma backs this idea (1).

Such a composition, in particular, is the same composition which has been already mentioned at this Symposium in connection with other problems (7).

Besides the patent mentioned by the authors of Principal Paper there are some publications giving theoretical basis, ingredients of the compounded additive, structure and properties of materials, obtained while using it (2, 3, 4, 5, 6, 8).

The introduction of this inexpensive additive "reaction accelerator + expander + retarder" in the moment of mixing commercial portland cement proved to provide higher density, strength of cement stone and to reduce its permeability without using manufactured expansive cements.

The using of the action of compounded additive is an example of chemical way of the directed concrete structure formation.

In addition to this we give some data about cement stone structure of expansive compositions on the basis of portland cement.

As thermographic, petrographic and physico-mechanical investigations have shown that cement stone with compounded chemical additive acquires greater density and strength not only during hardening at room temperature but also as the result of steam curing.

The application of additive at the normal (3, 4, 5) and high (2, 6) temperatures proved to be successful and has widely been used during more than seven years.

The additive in consideration may be an example of effectiveness of a radical new trend—the transformation of the expansive composition preparing process from cement technology element to concrete technology element.

References

1. H. Lafuma. Private letter.
2. O. P. Mchedlov-Petrosyan, Iu. L. Vorob'ev, D. A. Uginčius and A. V. Usherov-Marshak. The influence of chemical additives complex on concrete properties while steam curing", (in Russian). Proc. of Kharkov Railway Insti., **73**, Kharkov, USSR, 31–43 (1965).
3. O. P. Mchedlow-Petrosyan, L. G. Filatov, A. W. Uscherow-Marschak. Das Problem der Quellzemente (in German). Baustoffindustrie, N8, 235–241 (1965).
4. O. P. Mchedlov-Petrosyan and L. G. Filatov. "The theoretical foundations of preparing new expansive waterproof compositions on the basis of portland cement" (in Russian). Rep. of Acad. Sci. of USSR, **143**, N2, 380–383 (1962)
5. O. P. Mchedlov-Petrosyan and L. G. Filatov. "Expanding compositions on the basis of portland cement", (in Russian). State Publ. House on Building, Moskow, USSR (1965).
6. O. P. Mchedlov-Petrosyan, A. V. Usherov-Marshak and L. G. Filatov. "Speedhardening expansive compositions on the basis of portland cement for panel house-building", (in Russian). "Building materials", N11, 34–36 (1963).
7. O. P. Mchedlov-Petrosyan and D. A. Uginčius. Supplementary Paper on this Symposium.
8. D. A. Uginčius, O. P. Mchedlov-Petrosyan, R. V. Lutsyk and M. F. Kazansky. "Kinetics of the formation of porous cement structures in the presence of compounded additives." Proc. of the VIII Conf. on the Silicate Ind., Budapest, Hungary, 307–318 (1966).

Written Discussion

Albert Joisel

Introduction

Cement expansions may looks as rather mysterious phenomena. However we intend to indicate that their essential principles are simple; they are based on universally admitted physico-chemical laws; they are strengthened by numerous published results, which we will suppose well known by the readers.

The LeChatelier theory (1887) expresses that the hydraulic constituents of the cement grains go into solution in the mixing water and precipitate as a less soluble hydrated form; it may be stated as follows:

In an *hydraulic cement*, which may be wrote B — X, at least one of its constituents X forms, with the mixing water, an hydrate X — H *molarly less soluble* than the anhydrate in this water.

A solid constituent Y of the concrete (belonging or not to the cement) which forms with the mixing water a hydrate Y — H *molarly as much soluble or much soluble* than the anhydrate in this water, gives an *expansion* (or obviously a simple dissolution, if it is sufficiently soluble and diluted).

Hydraulic Cement

Let us consider (Fig. 1a) the aqueous space between a cement grain B – X, containing a soluble constituent X, and an inert aggregate G.

The X constituent passes into solution in water (Fig. 1b). Its concentration in this water, at first stronger near the cement grain, tends to get more uniform and to reach saturation.

The first precipitation $\boxed{X - H}$ *takes place far*

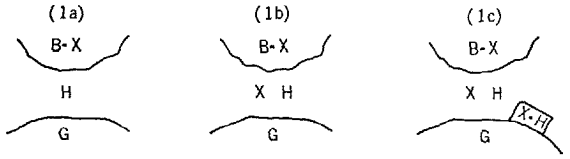

Fig. 1.

from the B — X grain (Fig. 1c). In fact, if it had taken place near the B — X grain, it would mean that a molecule (or an ion) X of the solution could precipitate as an hydrated form $\boxed{X-H}$ in presence of a X, remained anhydrous in the B — X grain. This is not possible as the X constituent is more soluble when anhydrous than hydrated, that is to say: the anhydrous constituent X has a greater affinity for water than has the same X constituent in solution.

The precipitation goes on from the first germs and progressively binds the grains, and particularly the inert grains, each other.

The X constituent is, for instance, a part of the lime of the tricalcium silicate C_3S, which goes into solution almost alone during the hydration. This lime is molarly more soluble than the lime in solution, as we can observe a sursaturation of the mixing water. The initial crystallisation of the portlandite $\boxed{CH}$ is done *at a certain distance from the alite grain.* It goes on afterwards in aqueous interstices.

The X constituent is also the calcium hydroxide of the "fat limes" which is molarly more soluble in water charged with carbonic gas, than the calcium carbonate which precipitate in the interstitial water.

The X constituent is also the part of the silica of a pozzolana which, in the presence of portlandite, goes into solution in the basic water of the interstices and precipitate at a distance from the pozzolana grain in a relatively low calcic form, that is to say, relatively scarcely soluble.

Expansive

Let us consider now an expansive grain Y (Fig. 2a). The Y constituent goes into solution in water (Fig. 2b).

The first precipitation $\boxed{Y-H}$ *takes place near the* Y *grain* (Fig. 2c), as it is there that the concentration is stronger, and as Y has at least as much affinity for water H when it is in solution as when anhydrous.

The Y grain is thus progressively surrounded by a solid layer $\boxed{Y-H}$ (Fig. 2d). At the surface of this layer in contact with water, the interchanges between the water of the (Y, H) liquid and the $\boxed{Y-H}$ solid are possible, if this solid is *somewhat soluble* in the mixing water: the water may enter this hydrate layer, towards the Y anhydrous grain.

On the contrary, the constituent of the Y solid grain, not molarly more soluble in water than the $\boxed{Y-H}$ solid one (that is to say, having no more water affinity when anhydrous than hydrated) cannot take out some water molecule from this solid and so, it cannot go into solution in the aqueous interstice through the Y — H layer. This solid $\boxed{Y-H}$ layer behaves, as we can see, as a *semi-permeable membrane* between the Y solid and the mixing water. (That is what Le Chatelier expressed when saying that the hydration of an expansive constituent is done without dissolution).

The Van't-Hoff's law, derived from the gases's law, applies to the *water osmotic pressure*. This water enters into the membrane, hydrates in situ the Y

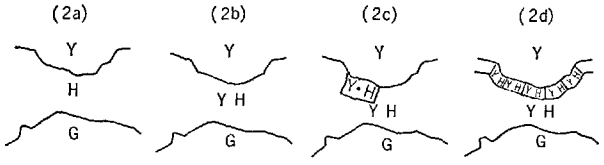

Fig. 2.

constituent, causes high pressures, as it is easy to compute, and breaks out the peripheric part. We are than brought back to the previous process.

The smaller the expansive grain dimension, and the larger Y surface, the lower is the expansion and less dangerous for strength, since the Y part forming the semipermeable membrane is gone into solution and so has not caused expansion.

The expansive constituent Y is, for example, free lime CaO, since we may consider that CaO and $Ca(OH)_2$ have the same molar solubility, or free magnesia MgO. (CaO and MgO are dissolved in water without sursaturation).

Heating at 100° or 200°C, which reduces the lime and magnesia solubilities, but which increases their *dissolution rate*, accelerates the expansion of these two constituents.

Every addition to the portland cement susceptible to form, with the lime (or magnesia) gone into solution,

a lower lime molar solubility product tends to precipitate the lime, for example as an hydrated calcium silico-aluminate, far from the grains, and so to reduce expansion. It is the case for relatively low additions of pozzolana or slag to a cement, which would be unstable because a free lime excess.

The lime and magnesia which are a part of the constitution of vitreous silico-aluminates of slags and pozzolanas cannot promote expansion.

Alkali-Aggregate Reaction

The reactive silica of certain grains, which goes into solution in the alkaline mixing water, leads to local expansions on the peripheral part of these grains, since it forms hydrated mixed silicates or silico-aluminates of alkaline earths and alkalines, which are molarly at least as soluble as the original silica.

The expansion can be reduced either by reduction of alkali content, or largely increasing the reactive surfaces in order to divide the mixed silico-aluminates on thin films through the concrete mass, by the addition of fine pozzolana or grounded slag (Those alkali salts are almost insoluble). For this reason, the grinding of a reactive aggregate reduces the concrete expansion.

Expansion due to Reinforcement Oxidation

Iron, as all metals, is molarly more soluble in the ionised state than in metallic state. If it oxidises, it is then with expansion, unless it dissolves entirely, for example, in acid water.

Hydration of Aluminates

The richer in lime, the more water soluble are the hydrated calcium aluminates; but on the contrary for silicates, the anhydrous aluminates go into solution in their stoechiometric ratio. They form in the aqueous interstices hydrated aluminates with varied molar ratios C/A and *the most stable is the hydrated tricalcium aluminate* C_3AH_6.

The tricalcium aluminate, if used alone, would give an hydrated tricalcium aluminate having the same solubility as the anhydrous one. It would then be expansive. It is effectively observed that the pure tricalcium aluminate hydrates efficiently with expansion; it is not an hydraulic cement; its strength is null.

For the protland cement, in presence of lime freed by the silicate hydration, an aluminate with more than 3 lime molecules may precipitate which is more soluble than tricalcium aluminate and expansive. The final strengths of high tricalcium aluminate cements are then relatively low, chiefly if they are steamed. Autoclave expansion of these cements is frequent; it is diminished if the clinkers are rapidly cooled, because tricalcium aluminate crystals are then smaller (see what is formerly said of the alkali-aggregate reaction).

On the contrary, for an aluminous cement with a C/A ratio <3, a less calcic hydrated aluminate precipitates, then less soluble; it is observed in fact that it remains more lime than alumina in solution. The aluminous cement is not then expansive.

However, if we add a small amount of lime (or of portland) to the aluminous cement, lime richer hydrated aluminate can precipitate in the aqueous interstices (moreover promoting a rapid setting). There is then expansion and the strengths are weakened.

Sulphates Addition to Cements

The tricalcium aluminate, though it is not favorable for final strengths of portland cement, is favorable for early strengths, because it fixes a relatively high amount of water and so contributes to the "squeezing" of the silicates which are the veritable hydraulic constituents of this cement. But for the normal setting cements, we must delay this aluminate hydration by calcium sulphate. This sulphate forms with the alumi-

nate a hydrated *sulphoaluminate which is more soluble, the richer in sulphate.*

If, at the end of the setting, some free calcium sulphate remains, it forms, with the scarcely sulphated hydrated aluminate or sulphoaluminates, *more soluble* hydrated sulfoaluminates, and it promotes an expansion. Therefore, the SO_3 content of portland cement is limited, for example to 3.5%. We can note that this data corresponds for a usual portland cement (with about 12% C_3A), nearly to the potential formula $C_3A\bar{S}CH_n$, that is to say, to the monosulphate.

A raising of temperature at 100°C largely hastens the sulphates dissolution and the silicates hydration (but almost does not change the aluminates hydration rate). The initial distribution of the sulphates against the aluminates is then more *homogenous.* As a result, the expansion due to a high amount of sulphate is less for warm than for cold curing.

We know that at the beginning of hydration, it is a very sulphated hydrated aluminate (trisulphated) that precipitates. Its ulterior transformation into a less sulphated aluminate (monosulphated), then less solu ble, may take place without expansion.

For silico-aluminous cements, alumina richer than portland cements, containing basic slag or certain pozzolanas, the proportion of sulphate may and must be increased (with the high slag content cements and particularly sursulphated cements).

Expansion due to Sulphated Agents

We have just seen that a cement, containing initialy tricalcium aluminate, gives hydrated aluminous or sulphoaluminous products, the mean composition of which is about $C_3A\bar{S}CH_n$. In the presence of sulphate, particularly sulphated waters, it is known that it trisulphated sulphoaluminate that tends to form. Now it is more soluble than the already formed aluminous or sulphoaluminous hydrates of the cement; then it leads to an expansion.

Expansive Cements

As expansive product, free lime CaO, free magnesia MgO, and chiefly varied sulphoaluminates were used. Lime and magnesia must be calcined and ground in definite conditions: particularly the temperature and the duration of calcining have a great influence on the dimension of the expansive grains (and consequently on their porosity). As for the expansion of sulphoaluminates, it should happen or continue after the cement setting (obtained, for instance, through a certain proportion of portland clinker), by the action of a sulphate on hydrated aluminates or sulphoaluminates that are already formed or that are forming. It is then necessary that the sulphate or aluminate does not enter too quickly into solution: high temperature calcined anhydrite and aluminous cement (which must be relatively lime rich, so that the C/A ratio be between 1 and 3), or stoechiometrically analogous mixes, or most often a sulphoaluminous cement, have been used.

The expansion, for a well distribution in the mass, needs a sufficient fineness of the cement, which moreover confers on it a good workability, but which may lead to a relatively important hydraulic shrinkage after expansion, when drying.

At last, it is necessary that the cement contains a high proportion of sound constituents, even in the presence of sulphates. They hydrate relatively slowly and lately consolidate the expanded zones: blast furnace slag, pozzolana, clinker with a low lime saturation rate and low C_3A content.

It can be seen that these principles, concerning in fact:

1)—setting,

2)—time, duration and distribution of expansion,

3)—hardening,

might lead to a large variety of expanesive cements.

As for the structures cracking, if the hydraulic shrinkage is the major cause, the "without shrinkage" cements or "with compensated shrinkage" cements would be of great interest, but the hydraulic shrinkage is never the essential cause of cracking . . .

Oral Discussion

José Calleja

In connection with the Principal Paper Expansive Cement presented by Prof. Budnikov and Prof. Kravchenko, from the Soviet Union, I want to emphasize the interest which the original points of view of the authors should have for future interpretation of expansion phenomena.

Following ideas of the authors, it may be said that, in general variations of volume in the cement paste will cause the weakening of its structure and, consequently, will lower its strength and its durability. These are particularly affected by external and internal microcracking and cracking due to shrinkage.

In this respect, every action which will tend to reduce shrinkage, will equally tend to improve the mechanical strength and the chemical resistance. This is the origin of the so-called "non shrinking cements", or "shrinkage compensated cements", or even "controlled expansion cements".

Spanish research work on such types of cements has been carried out at the "Eduardo Torroja" Institute for Cement and Concrete Research in Madrid, from the year nineteen fifty onwards (1 to 4).

Portland cements were prepared starting from clinkers with a high content of highly basic calcium aluminates and from both, gypsum stone and (or) anhydrite as retarders. A certain amount of free lime was also present in the clinkers, so that conditions were the most favourable for the formation of expansive tricalcium aluminate sulphate hydrates.

Results showed that minimum shrinkage, maximum strength and maximum durability were achieved when the gypsum or anhydrite contents in the resulting portland cements were close to those corresponding to the formation of tricalcium aluminate monosulphate hydrate as final stable sulphated aluminous phase, according to Forsen's point of view (5).

Such amounts of calcium sulphate corresponded also closely to those present in the portland cements called "correctly retarded" by Lerch, years ago (6).

Then, maximum strength in such conditions is most probably the direct or indirect consequence of a minimum change involume (shrinkage compensated as much as possible by expansion), and it seems therefore that the involved calcium sulphate content, i.e., that corresponding to the formation of $C_3A \cdot CaSO_4 \cdot 12H_2O$ from the C_3A of the clinker (leaving aside other influences such as that of the fineness and of the alkali content, etc. in the cements), may provide a limit for separating "shrinkage compensated cements" or "non shrinking cements" from actual "expansive cements" made with the same clinker, as far as the manufacture of such cements is concerned.

I would much ppreciate to know if the authors or any other delegates have had a similar experience and their opinion on this matter.

References

1. J. Calleja, "Influence of the gypsum content in portland cement on the shrinkage of pastes, mortars and concretes". Third International Meeting on the Reactivity of Solids, Vol. III, Sec. V, p. 213–246, Madrid 1956 (in Spanish).
2. J. Calleja, "Improving output and quality in portland cement manufacture". Building Materials (I.E.T.C.C., Spain) Nos. 76 to 78, 1956 (in Spanish).
3. J. Calleja, "Gypsum as a constituent of hydraulic cements". First International Congress on Public Works in Gypsum Soils (I.E.T.C.C., Spain), Madrid, 1962 (in Spanish).
4. J. Calleja, "Points of view on the gypsum content of portland cements". Revista de Ciencia Aplicada (Spain) XIX (6) 107, 494–505, 1965 (in Spanish).
5. L. Forsen, "The chemistry of retarders and accelerators". Proceedings of the Symposium on the Chemistry of Cements, p. 325, Stockholm 1938.
6. W. Lerch, Proceedings A.S.T.M., 46, 1946.

Oral Discussion

Kozo Sugiura

Of the three types of expansive cements industrially produced in the Soviet Union it is stated that expansive portland cement is used mainly for manufacture of precast reinforced articles. Has this type of expansive cement been used for cast-in-situ concrete such as pavements?

For such uses, it is thought that retarding of set would require replacement of gypsum with anhydrite or addition of a retarder. Have such measures been taken?

Supplementary Paper IV-66 Nature of Hydration Products in the System $4CaO \cdot 3Al_2O_3 \cdot SO_3$-$CaSO_4$-CaO-$H_2O$

Alexander Klein and Povindar K. Mehta*

Synopsis.

Commercially made expansive cements in the United States are presently based on the inclusion of an expansive complex in portland cement. The expansive component consists of suitable proportions of $C_4A_3\bar{S}$, $C\bar{S}$ and lime. The hydration products in the systems $C_4A_3\bar{S}$-CS-C-H contain several calcium sulfoaluminate hydrates. Only calcium trisulfohydrates (ettringite) is known to cause expansion under conditions of restraint. For a better understanding of the chemistry of expansive cements, a thorough investigation is undertaken to determine the nature of hydration products from a wide range of anhydrous compositions containing $C_4A_3\bar{S}$, $C\bar{S}$ and lime.

Mixtures of $C_4A_3\bar{S}$, $C\bar{S}$ and lime were made corresponding to $A/\bar{S}$ ratios of 0.25, 0.50, 0.75, 1.00, 1.25 and $C/\bar{S}$ ratios of 2.0, 2.5, 3.0, 3.5, 4.0, 5.0, 6.0, 7.0, 8.0. The hydrating mixtures were studied by X-ray diffraction analysis at 6, 24, 72 and 168 hours.

The results are compared with theoretical predictions, and a phase diagram has been constructed to show the nature of final hydration products in the system.

The utilisation of expansion based on the formation of ettringite has been successfully demonstrated in the U.S.S.R. by Mikhailov(1, 2) and in the United States by Klein and his associates(3, 4, 5, 6). The expansive cements developed at the University of California by Klein and Troxell(3) are blends of portland cement with an expansive component which consists of appropriate proportions of $C_4A_3\bar{S}$, $C\bar{S}$ and lime.

Portland cements containing the "expansive complex" are also being produced commercially from portland cement clinkers containing all the constituents of the "expansive complex". The American Concrete Institute's Committee on Expansive Cements has designated these cements as Type K expansive cements.

Kalousek(7) Jones(8) and D'Ans(9) have made important contributions to our knowledge on the formation of calcium sulfoaluminate hydrate from aqueous solutions of C_3A, $A\bar{S}$, $C\bar{S}$, CH etc., but Mehta and Klein(10) have reported on calcium sulfoaluminate hydrates formed by solid state hydration in the system $C_4A_3\bar{S}$-$C\bar{S}$-C-H.

Mehta and Klein(10) confined their preliminary investigation to reaction mixtures having 2.0 and 4.0 $C/\bar{S}$ mole ratios, and corresponding to $A/\bar{S}$ mole ratios between 0.2 to 1.25. For a better understanding and control of the chemistry of expansive cement, the scope of the present investigation has been enlarged to include mixtures with wider range of $C/\bar{S}$ mole ratios.

Materiais and Experimental Procedure

High-purity $C_4A_3\bar{S}$ was made by intergrinding stoichiometric proportions of reagent grade $CaCO_3$, $CaSO_4 \cdot 2H_2O$ and $Al_2O_3 \cdot 3H_2O$, and thereafter sintering the material at 1350°C in a Globar furnace. High-purity $C\bar{S}$ and lime were made by calcining at 1300°C reagent-grade gypsum and chalk respectively. All the three anhydrous components thus prepared were ground to 3000–4000 cm^2/g Blaine and stored in air-tight bottles.

In Tables 1, 2 and 3 are shown molar compositions of mixes investigated in the present study. In every case weight proportions for a 75 g mix were calculated corresponding to molar proportions of the constituent components. For hydration purposes, 30 g (0.4 water-cement ratio) of chilled distilled water was placed in a porcelain dish, and weighed CaO was the first component to be mixed with water before the weighed portions of other constituents were added. This procedure was adopted in order to offset any detrimental effects of excessive heat of hydration of CaO on the products of hydration. Otherwise the casting,

*University of California, Berkeley, California, U.S.A.

Standard abbreviation used in cement chemistry are followed. Abbreviation $\bar{S}$ stands for SO_3.

Table 1. *Mix proportions, predicted hydration products, and actually present hydration products of mixes having 2.0 to 3.0 C/$\bar{S}$*

Mole ratios		Mix proportions (Molar basis)			Predicted hydration products from the theoretical molar composition	Hydration products at 168 hours, as determined by XRD analysis
C/$\bar{S}$	A/$\bar{S}$	$C_4A_3\bar{S}$	C$\bar{S}$	C		
2.0	0.25	1	11	9	$C_6A\bar{S}_4 \longrightarrow C_6A\bar{S}_3aq + C\bar{S} + CH$	E, C$\bar{S}$, CH
〃	0.50	1	5	3	$C_6A_2\bar{S}_4 \longrightarrow 4/3\ C_6A\bar{S}_3aq + 2/3\ AH_3$	E, AH_3
〃	0.75	1	3	1	$C_6A_3\bar{S}_4 \longrightarrow 4/3\ C_6A\bar{S}_3aq + 5/3\ AH_3$	E, AH_3
〃	1.00	1	2	0	$C_6A_4\bar{S}_4 \longrightarrow 4/3\ C_6A\bar{S}_3aq + 8/3\ AH_3$	E, AH_3
〃	1.25				$C_6A_5\bar{S}_4 \longrightarrow 4/3\ C_6A\bar{S}_3aq + 11/3\ AH_3$	E, AH_3
2.5	0.25	1	11	15	$C_{10}A\bar{S}_4 \longrightarrow C_6A\bar{S}_3aq + C\bar{S} + 3CH$	E, C$\bar{S}$, CH
〃	0.50	1	5	6	$C_{10}A_2\bar{S}_4 \longrightarrow C_6A\bar{S}_3aq + C_4A\bar{S}aq$	E, M_{18} and M_{12}
〃	0.75	1	3	3	$C_{10}A_3\bar{S}_4 \longrightarrow C_6A\bar{S}_3aq + C_4A\bar{S}aq + AH_3$	E, M_{18}, AH_3
〃	1.00	1	2	3/2	$C_{10}A_4\bar{S}_4 \longrightarrow C_6A\bar{S}_3aq + C_4A\bar{S}aq + 2AH_3$	E, M_{18}, AH_3
〃	1.25	1	7/5	3/5	$C_{10}A_5\bar{S}_4 \longrightarrow C_6A\bar{S}_3aq + C_4A\bar{S}aq + 3AH_3$	E, M_{18}, AH_3
3.0	0.25	1	11	21	$C_{12}A\bar{S}_4 \longrightarrow C_6A\bar{S}_3aq + C\bar{S} + 5CH$	E, C$\bar{S}$, CH
〃	0.50	1	5	9	$C_{12}A_2\bar{S}_4 \longrightarrow C_6A\bar{S}_3aq + C_4A\bar{S}aq + 2CH$	E, M_{18} & M_{12}, CH
〃	0.75	1	3	5	$C_{12}A_3\bar{S}_4 \longrightarrow C_6A\bar{S}_3aq + C_4A\bar{S}aq + 2CH + AH_3$	E, M_{18} & M_{12}, $C_xA_yH_z$
〃	1.00	1	2	3	$C_{12}A_4\bar{S}_4 \longrightarrow C_6A\bar{S}_3aq + C_4A\bar{S}aq + 2CH + 2AH_3$	E, M_{18}, $C_xA_yH_z$, AH_3
〃	1.25	1	7/5	9/5	$C_{12}A_5\bar{S}_4 \longrightarrow C_6A\bar{S}_3aq + C_4A\bar{S}aq + 2CH + 3AH_3$	E, M_{18}, $C_xA_yH_z$, AH_3

Table 2. *Mix proportions, predicted hydration products, and actually present hydration products of mixes having 3.5 to 5.0 C/$\bar{S}$*

Mole ratios		Mix proportions (Molar basis)			Predicted hydration products from the theoretical molar composition	Hydration products at 168 hours, as determined by XRD analysis
C/$\bar{S}$	A/$\bar{S}$	$C_4A_3\bar{S}$	C$\bar{S}$	C		
3.5	0.25	1	11	27	$C_{14}A\bar{S}_4 \longrightarrow C_6A\bar{S}_3aq + C\bar{S} + 7CH$	E, C$\bar{S}$, CH
〃	0.50	1	5	12	$C_{14}A_2\bar{S}_4 \longrightarrow C_6A\bar{S}_3aq + C_4A\bar{S}aq + 4CH$	E, M_{18} & M_{12}, CH
〃	0.75	1	3	7	$C_{14}A_3\bar{S}_4 \longrightarrow C_6A\bar{S}_3aq + C_4A\bar{S}aq + 4CH + AH_3$	E, M_{18} & M_{12}, $C_xA_yH_z$, CH
〃	1.00	1	2	9/2	$C_{14}A_4\bar{S}_4 \longrightarrow C_6A\bar{S}_3aq + C_4A\bar{S}aq + 4CH + 2AH_3$	E, M_{18} & M_{12}, $C_xA_yH_z$
〃	1.25	1	7/5	3	$C_{14}A_5\bar{S}_4 \longrightarrow C_6A\bar{S}_3aq + C_4A\bar{S}aq + 4CH + 3AH_3$	E, M_{18}, $C_xA_yH_z$, AH_3
4.0	0.25	1	11	33	$C_{16}A\bar{S}_4 \longrightarrow C_6A\bar{S}_3aq + C\bar{S} + 9CH$	E, C$\bar{S}$, CH
〃	0.50	1	5	15	$C_{16}A_2\bar{S}_4 \longrightarrow C_6A\bar{S}_3aq + C_4A\bar{S}aq + 6CH$	E, M_{18} & M_{12}, CH
〃	0.75	1	3	9	$C_{16}A_3\bar{S}_4 \longrightarrow C_6A\bar{S}_3aq + C_4A\bar{S}aq + 6CH + AH_3$	E, M_{18} & M_{12}, $C_xA_yH_z$, CH
〃	1.00	1	2	6	$C_{16}A_4\bar{S}_4 \longrightarrow 4C_4A\bar{S}aq$	M_{18} & M_{12} + trace of E
〃	1.25	1	7/5	21/5	$C_{16}A_5\bar{S}_4 \longrightarrow 4C_4A\bar{S}aq + AH_3$	M_{18} + AH_3
5.0	0.25	1	11	45	$C_{20}A\bar{S}_4 \longrightarrow C_6A\bar{S}_3aq + C\bar{S} + 13CH$	E + C$\bar{S}$ + CH
〃	0.50	1	5	21	$C_{20}A_2\bar{S}_4 \longrightarrow C_6A\bar{S}_3aq + C_4A\bar{S}aq + 10CH$	E + M_{18} & M_{12} + CH + M_x
〃	0.75	1	3	13	$C_{20}A_3\bar{S}_4 \longrightarrow C_6A\bar{S}_3aq + C_4A\bar{S}aq + 10CH + AH_3$	E + M_{18} & M_{12} + CH + M_x
〃	1.00	1	2	9	$C_{20}A_4\bar{S}_4 \longrightarrow 4C_4A\bar{S}aq + 4CH$	M_{18} & M_{12} + CH + M_x + trace of E
〃	1.25	1	7/5	33/5	$C_{20}A_5\bar{S}_4 \longrightarrow 4C_4A\bar{S}aq + 4CH + AH_3$	M_{12} & M_x + S.S.

Table 3. *Mix proportions, predicted hydration products, and actually present hydration products of mixes having 6.0 to 8.0 C/$\bar{S}$*

Mole ratios		Mix proportions (Molar basis)			Predicted hydration products from the theoretical molar composition.	Hydration products at 168 hours, as determined by XRD analysis
C/$\bar{S}$	A/$\bar{S}$	$C_4A_3\bar{S}$	C$\bar{S}$	C		
6.0	0.25	1	11	57	$C_{24}A\bar{S}_4 \longrightarrow C_6A\bar{S}_3aq + C\bar{S} + 17CH$	E + C$\bar{S}$ + CH
〃	0.50	1	5	27	$C_{24}A_2\bar{S}_4 \longrightarrow C_6A\bar{S}_3aq + C_4A\bar{S}aq + 14CH$	E + M_{18} & M_{12} + CH + M_x
〃	0.75	1	3	17	$C_{24}A_3\bar{S}_4 \longrightarrow C_6A\bar{S}_3aq + C_4A\bar{S}aq + 14CH + AH_3$	E + M_{12} & M_{12} + CH + M_x
〃	1.00	1	2	12	$C_{24}A_4\bar{S}_4 \longrightarrow 4C_4A\bar{S}aq + 8CH$	M_{18} & M_{12} + CH + M_x + trace of E
〃	1.25	1	7/5	9	$C_{24}A_5\bar{S}_4 \longrightarrow 4C_4A\bar{S}aq + 8CH + AH_3$	M_{12} + CH + S.S. phases
7.0	0.25	1	11	69	$C_{28}A\bar{S}_4 \longrightarrow C_6A\bar{S}_3aq + C\bar{S} + 21CH$	E + C$\bar{S}$ + CH
〃	0.50	1	5	33	$C_{28}A_2\bar{S}_4 \longrightarrow C_6A\bar{S}_3aq + 18CH + C_4A\bar{S}aq$	E + M_{18} & M_{12} + CH + M_x
〃	0.75	1	3	21	$C_{28}A_3\bar{S}_4 \longrightarrow C_6A\bar{S}_3aq + C_4A\bar{S}aq + 18CH + AH_3$	E + M_{18} & M_{12} + CH + M_x
〃	1.00	1	2	15	$C_{28}A_4\bar{S}_4 \longrightarrow 4C_4A\bar{S}_3aq + 12CH$	M_{18} & M_{12} + CH + M_x + trace of E
〃	1.25	1	7/5	57/5	$C_{28}A_5\bar{S}_4 \longrightarrow 4C_4A\bar{S}_3aq + 12CH + AH_3$	M_{18} + CH + S.S. phases
8.0	0.25	1	11	81	$C_{32}A\bar{S}_4 \longrightarrow C_6A\bar{S}_3aq + C\bar{S} + 25CH$	E + C$\bar{S}$ + CH
〃	0.50	1	5	39	$C_{32}A_2\bar{S}_4 \longrightarrow C_6A\bar{S}_3aq + C_4A\bar{S}aq + 22CH$	E + M_{18} & M_{12} + CH + M_x
〃	0.75	1	3	25	$C_{32}A_3\bar{S}_4 \longrightarrow C_6A\bar{S}_3aq + C_4A\bar{S}aq + 22CH + AH_3$	E + M_{18} & M_{12} + CH + M_x
〃	1.00	1	2	18	$C_{32}A_4\bar{S}_4 \longrightarrow 4C_4A\bar{S}aq + 16CH$	M_{18} & M_{12} + CH + M_x + trace of E
〃	1.25	1	7/5	69/5	$C_{32}A_5\bar{S}_1 \longrightarrow 4C_4A\bar{S}aq + 16CH + AH_3$	M_{12} + CH + S.S. phases

curing and XRD analysis procedures remained essentially the same as described in Appendix A of the earlier paper by Mehta and Klein (10).

The ingredients after thorough mixing with water were cast in plastic vials which were properly covered to prevent access of atmospheric carbon dioxide. After six hours, a small sample of the hydrating material was taken for XRD analysis while the rest

of the hardened specimen was exposed to moist curing in airtight plastic containers lined with cotton pads soaked in distilled water. Samples were regularly withdrawn for XRD analysis at 24, 72 and 168 hours.

For XRD analysis, a Philips Norelco XR generator with Cu target (40 KV, 35 mA) and 0.0007″ nickel filter was used in conjunction with a Philips Norelco Diffractometer scanning at 0.5 deg. 2θ/min. The diffraction pattern was recorded at 1000 counts per second full scale deflection by a Bristol recorder.

Identification of anhydrous compounds as well as of hydrated phases presented no difficulty by XRD analysis technique except for AH_3 which, due probably to very poor crystallinity, yielded broad peaks in the diffration patterns of the specimens. The presence of AH_3 was, therefore, confirmed by solubity test in dilute HCI (1: 5). The solutions exhibiting turbidity in this test were assumed to contain AH_3.

Results and Discussion

The predicted hydration products from the theoretical molar compositions as well as the hydration products actually determined at 168 hours are shown against the respective anhydrous mixtures listed in Tables 1, 2 and 3. The XRD data for earlier ages of hydration are not given in this paper because its inclusion is not considered necessary for the purposes of this report. The reuslts shown in Tables 1, 2 and 3 are plotted in Fig. 1. The following abbreviations are used in the Figure and Tables:

E —Ettringite

M_{18}—Monosulfate hydrate with 18 moles of water (10)

M_{12}—Monosulfate hydrate with 12 moles of water

M_x —Monosulfate hydrate with unknown moles of water. The basal spacing on the XRD pattern indicates that the number of moles of water should be somewhere between 12 and 18 (perhaps 15)

$C_xA_yH_z$—Calcium aluminate hydrates

S. S. Phases—Solid solution phases present probably as a result of interaction of monosulfate hydrates, calcium aluminate hydrates, and calcium hydroxide.

In the Figure at point E which represents "Ettringite", the molar ratio of $C/\bar{S}$ is 2.0 and $A/\bar{S}$ is 0.33. Point M which represents "Monosulfate hydrate" corresponds to a $C/\bar{S}$ ratio of 4.0 and $A/\bar{S}$ ratio of 1.0.

Since unconsumed $C\bar{S}$ is present in all compositions

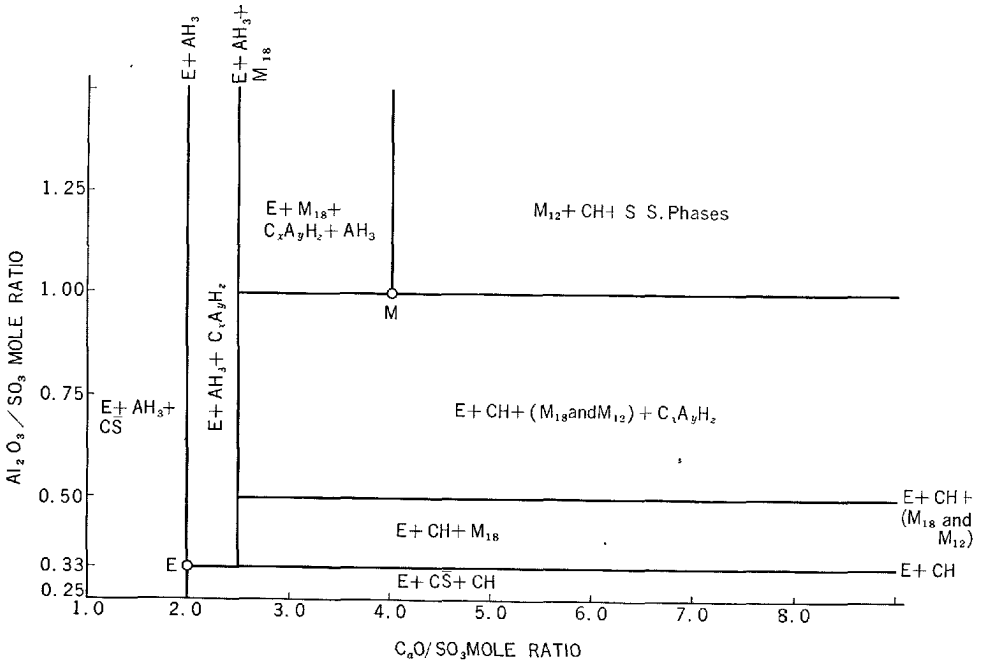

Fig. 1. *Nature of final hydralion products obtained from hydration of mixtures containing* $C_4A_3\bar{S}$, *and* $C\bar{S}$ *lime*

having 0.25 $A/\bar{S}$ mole ratio (regardless of C/S ratio), on theoretical grounds it can be concluded that for all composition below 0.33 $A/\bar{S}$ mole ratio, the alumina content is too low and the sulfate content is too high for depletion of all the available $C\bar{S}$. Similarly from theoretical calculations it can be proved that for compositions below 2.0 $C/\bar{S}$ mole ratio, the lime content is too low and the sulfate content is too high for depletion of all the available $C\bar{S}$, hence there will always be unconsumed $C\bar{S}$ for compositions with $C/\bar{S}$ less than 2.0 (regardless of $A/\bar{S}$ mole ratio).

Regarding compositions having less than 2.0 $C/\bar{S}$ mole ratio, the hydration products always contain ettringite, $C\bar{S}$ and AH_3, the proportion of the latter being increasingly more as the $A/\bar{S}$ ratio is raised in the original mix. At 2.0 $C/\bar{S}$, only ettringite and AH_3 are present in the hydration products except in compositions with lower than 0.33 $A/\bar{S}$. Similarly at 0.33 $A/\bar{S}$, only ettringite and $Ca(OH)_2$ are present in the hydration products except compositions with lower than 2.0 $C/\bar{S}$.

For compositions with $C/\bar{S}$ between 2.5 and 8.0, it can be observed that M_{18} appears in hydration products as soon as $A/\bar{S}$ mole ratio of the mix crosses 0.33. At 0.50 $A/\bar{S}$, M_{12} begins to exist side by side with M_{18}. Beyond 0.5 $A/\bar{S}$, the alumina content becomes high enough to form $C_xA_yH_z$ phases in addition to ettringite and monosulfate hydrates.

Regarding compositions with 0.33 and higher $A/\bar{S}$, $C/\bar{S}$ is raised slightly above 2.0 (but below 2.5) it is observed that $C_xA_yH_z$ phases begin to exist along with ettringite and AH_3. At 2.5 $C/\bar{S}$, the conditions become favourable for the appearance of M_{18} in the system, therefore here M_{18} exists along with ettringite and AH_3.

It can be seen from the Figure that corresponding to A/S ratios of 1.0 and 1.25, and $C/\bar{S}$ ratios between 2.5 and 4.0, the $C_xA_yH_z$ phases again co-exist with ettringite, M_{18} and AH_3. Comparison of theoretically predicted results with actually determined products of hydration shows that $C_xA_yH_z$ phases were readily detectable when CH/AH_3 ratio in the reaction products was between 1.0 and 8.0. When CH/AH_3 was 1.0 or less, (as in the case of the last two mixes in Table 1), free AH_3 was invariably present in the products. Furthermore, at 1.25 $A/\bar{S}$, and 5.0 and above $C/\bar{S}$, when formatoin of $C_xA_yH_z$ phases could be expected on the basis of theoretical equations, no such phases were actually detected due probably to formation of solid solution phases with the monosulfate hydrate.

At 4.0 $C/\bar{S}$ and 1.0 $A/\bar{S}$ (point M) where the theoretical equation predicts the presence of monosulfate hydrate only, both types of the monosulfate hydrate i.e., M_{18} and M_{12} were detected along with a trace of ettringite. At 4.0 $C/\bar{S}$ and 1.25 $A/\bar{S}$, however, no M_{12} and ettringite were detected, only M_{18} and AH_3 being present. On the other hand, at 1.0 $A/\bar{S}$ and greater than 4.0 $C/\bar{S}$, both types of the monosulfate hydrate (M_{18} and M_{12}) along with traces of ettringite continued to exist, CH being an additional product formed in accordance with the theoretical expectations. But as soon as the $A/\bar{S}$ ratio is raised above 1.0 and $C/\bar{S}$ ratio above 4.0, ettringite and M_{18} ceased to be stable phases. Only M_{12}, CH and certain solid solution phases (probably M_{12}—$C_xA_yH_z$—CH) were found capable of existing in this region. This shows that for $C/\bar{S}$ ratios of 4.0 and less, the stability of M_{18} in compositions having 1.0 and more $A/\bar{S}$ may be associated with the presence of ettringite or AH_3 in the hydrated system. Similarly in low alumina mixes, i.e. between 0.33 and 0.5 $A/\bar{S}$ (and corresponding to 2.5 and above $C/\bar{S}$), the stability of M_{18} took place in presence of ettringite and CH. From both the above mentioned cases, ettringite being the common denominator, appears to be the stabilizing influence on the monosulfate hydrate having 18 moles of water.

For compositions above 5.0 $C/\bar{S}$ and between 0.33 — 1.0 $A/\bar{S}$, another monosulfate hydrate M_x (strong peak at 9.6° 2θ) was suspected to be present along with M_{18} and M_{12}. On the basis of basal d-spacing, the number of water moles in M_x are probably 15. The occurrence of M_x is shown in the tabulated data, but is not shown in the Figure.

Conclusions

It can be concluded from the results of this investigation that theoretical equations alone are not adequate to deal with the products of hydration actually formed in the system $C_4A_3\bar{S}$-$C\bar{S}$-C-H.

Among the calcium sulfoaluminate hydrates present, in addition to the trisulfate hydrate at least three types of monosulfate hydrates were found to exist in hydration products, namely, $C_4A\bar{S}H_{12}$, $C_4A\bar{S}H_{18}$ and C_4ASH_x. The hydrate with 12 water moles is well known. The nomosulfate hydrate having 18 moles of water was discussed in an earlier paper by the authors. It appears that the stability of this hydrate is dependent on the presence of the trisulfate hydrate in the system.

Regarding $C_4A\bar{S}H$, it was found present along with other monosulfate hydrates in compositions having greater than 5.0 $C/\bar{S}$ and corresponding to 0.33 – 1.0 $A/\bar{S}$. On the basis of basal d-spacing, the number of water moles in this hydrate are suspected to be 15.

The trisulfate hydrate as well as the monosulfate hydrates having 18 and 15 moles of water were not stable when $A/\bar{S}$ exceed 1.0 and $C/\bar{S}$ exceeded 4.0, hence anhydrous mixes corresponding to these compositions are not expected to be useful in making expansive cements.

It may be pointed out here that the results of this investigation are not adequate for the purpose of designing Type K expansive cements having desired properties. The present investigation has been confined to the study of hydration products in the expansive complex system alone, whereas the expansive cements contain constitutens of the expansive complex as well as of the portland cement (C_3S, C_2S etc). Integration of knowledge of the two independently hydrating systems, namely, the portland cement—water system and the expansive complex—water system will not be appropriate because of the possible interaction caused by simultaneous presence of both the systems in the hydration process.

Acknowledgement

The research was sponsored by the National Science Foundation under grant No. S-21361 for which Professor D. Pirtz of the University of California was the faculty investigator. The research work was conducted at the Laboratories of the Structural Engineering and Structural Mechanics Division of the University of California at Berkeley.

References

1. V. V. Mikhailov, "Stressing cement and the mechanism of selfstressing concrete regulations." Fourth Internat. Symposium on Chem of Cement, Washington, 1960. Proc., Vol. II, 927–955, 1962.
2. V. V. Mikhailov, "New development in selfstressed concrete." World Conf. on Prestressed Concrete, San Francisco, 1957.
3. A. Klein and G. E. Troxell, "Studies of calcium sulfoaluminate admixtures for expansive cements." Proc. ASTM Vol. 58. pp. 986–1008, 1958.
4. A. Klein, T. Karby and M. Polivka, "Properties of an expansive cement for chemical prestressing." Jour. ACI (Proc.), Vol. 58, 59–82, 1961.
5. T. Y. Lin and A. Klein, "Chemical prestressing of concrete elements using expanding cement." Jour. ACI (Proc.) Vol. 60, 1137–1216, 1963.
6. A. Klein and V. Bertero, "Effect of curing temperature and creep characteristics of expansive concrete." Proc. ASTM, Vol. 65, 1008–1025, 1963.
7. G. L. Kalousek, "Sulfoaluminates of calcium as stable and metastable phases." Thesis, Univ. of Maryland, 1941.
8. F. E. Jones, "The quaternary system CaO-Al_2O_3-$CaSO_4$-H_2O at 25°C." Jour Phys. Chem., Vol. 48, 311–356, 1944.
8. J. D'Ans and H. Eick, "The system CaO-Al_2O_3-$CaSO_4$-H_2O at 20°C." (in German) Zement-Kalk-Gips, Vol. 6, 302–311, 1953.
10. P. K. Mehta and A. Klein, "Investigation on the hydration products in the system 4 $CaO \cdot 3Al_2O_3 \cdot SO_3$ – $CaSO_4$-CaO-H_2O." Symp. on Structure of Portland Cement Paste and Concrete, Highway Research Board, Spl. Report 90, 328–352, 1966.

Oral Discussion

Kozo Sugiura

Plotting the chemical composition of the expansive cement being manufactured in the U.S.A. under your guidance on Fig. 1, most of them will be slightly above the line for $Al_2O_3/SO_3 = 1$. Supposed the value were lowered, more trisulfate is made to be produced, I think. Is there any special reason for selecting the composition described above?

Authors' Closure

Alexander Klein and Povindar K. Mehta

The research reported in our paper deals with the nature of hydration products corresponding to different $A/\bar{S}$ and $C/\bar{S}$ molar ratios in the expansive *component* system only. The discusser's question relates to expansive *cements*, and is therefore, beyond the scope of this paper. The information on compositions of Type K commercial expansive cements is of a proprietary nature, and cannot be discussed here. However, it may be pointed out that our phase diagram regarding nature of hydration products in the expansive component system will not hold good for similarly computed $A/\bar{S}$ and $C/\bar{S}$ values from chemical composition of integral expansive cements, because the distribution of aluminate and sulphate ions amongst compounds present there is of a more complex character.

Supplementary Paper IV-69 Fundamental Studies on the Expansive Cement

Nobue Fukuda*

Synopsis

Fundamental studies have been made on Lossier's expansive cement.

The constitution of sulphoaluminate clinker, was investigated by experiments of system CaO-Al_2O_3-SO_3. From the results it was made known that the existence of a ternary compound $3CaO \cdot 3Al_2O_3 \cdot CaSO_4$ (or $3C \cdot 3A \cdot CaSO_4$) was certain. In usual sulphoaluminate clinker, the formation of $3C \cdot 3A \cdot CaSO_4$ is considered to be completed practically, and excess of $CaSO_4$ remains as free $CaSO_4$. And the compound composition is to be calculated, for example, that of a sulphoaluminate clinker prepared by similar method to Lossier's became as follows.

$3CaO \cdot 3Al_2O_3 \cdot CaSO_4$	43.5%
free $CaSO_4$	28.2%
C_2S	20.3%
free CaO, ferrite, etc	8.0%

In order to make clear the hydration mechanism of expansive cement, the author made a basic hydrating experiment of $3C \cdot 3A \cdot CaSO_4$ to which $CaSO_4 \cdot 2H_2O$, calcined $CaSO_4$, and $Ca(OH)_2$ was added. According to the results, without additives, $3C \cdot 3A \cdot CaSO_4$ formed low sulphate hydrate $C_3A \cdot CaSO_4 \cdot 12H_2O$ but no high sulphate $C_3A \cdot 3CaSO_4 \cdot 30\text{-}32H_2O$. In order to form high sulphate, addition of gypsum is necessary.

$3C \cdot 3A \cdot CaSO_4 + 2CaSO_4 \cdot 2H_2O + xH_2O = C_3A \cdot 3CaSO_4 \cdot 30-32H_2O + 2Al_2O_3$ hydrate. In order to increase further the yield of high-sulphate greater amount of gypsum must be given with addition of CaO. The components, i.e. $3C \cdot 3A \cdot CaSO_4$, free $CaSO_4$ and free CaO, contained in the clinkers might possess more effective nature or condition, than that of simple mixtures of these components. When the system is rich in CaO and lacking in $CaSO_4$ for Al_2O_3 to change into high sulphate completely, the formation of $C_2A \cdot 8H_2O$ occurs, besides high- or low-sulphate hydrate. The formation of $C_2A \cdot 8H_2O$ seems to be closely related to the setting.

Introduction

Lossier's expansive cement (1) of sulphoaluminate type has received much attention. Following applications have been studied and carried out; manufacture of non-shrinking cement; production of self-stressed concrete; and other practical uses. But the industry of this sort of cements is still in the course of development, there remains many unsolved problems about the manufacturing process and the properties. And in laboratory, the rate and extent of expansion have been often irregular and unpredictable. Thus, for practical use, fundamental studies should be advanced.

In this paper, following problems have been investigated; the constituents of clinkers obtained by burning the raw mixture of system CaO–Al_2O_3–SO_3; the hydrating behaviors of the constituents of the clinkers; and the relations between these items and the characters of expansion and setting of the cements.

*Cement Division, Tokuyama Soda Co., Ltd., Tokuyama, Japan.

$3CaO \cdot 3Al_2O_3 \cdot CaSO_4 (3C \cdot 3A \cdot CaSO_4)$

Ternary Compound of System $CaO-Al_2O_3-SO_3$

In another experiment (2), replacing the various amount of $CaCO_3$ of portland cement raw mixtures with $CaSO_4$, the clinkers shown in Table 1 were prepared. It has been reported (3) that SO_3 in portland cement clinker forms alkali-sulphate and that excess SO_3 enters into combination with CaO to form $CaSO_4$. Also in this experiment, these reactions were observed. In these clinkers, assuming that all the alkalies formed sulphates and that excess SO_3 formed $CaSO_4$, the mineral composition was calculated by Bogue's method as in Table-1. The contents of C_3A and C_4AF were about 8.0 and 9.6%, and that of $CaSO_4$ was 0.6–5.5%. But X-ray powder diffraction of the clinkers revealed following remarkable facts. When SO_3 content was small just as in clinker So, the formation of C_3A and C_4AF was clear. As SO_3 content increased, the diffraction patterns of C_3A and C_4AF became weak. In the clinkers S_3 and S_4, the patterns could not be observed any longer. As for $CaSO_4$ in clinkers, only when SO_3 content was excessively large as in clinker S_8, the pattern of $CaSO_4$ could be detected. These facts suggested that, in the course of burning, $CaSO_4$ might be lost by the reaction with Al_2O_3 forming a compound (probably ternary compound) and that, on account of the lack of Al_2O_3, C_3A and C_4AF could not be formed.

From the above results, the presence of a ternary compound of system $CaO-Al_2O_3-SO_3$ was predicted.

Experiments of System $CaO-Al_2O_3-SO_3$

If an anhydrous ternary compound could be formed in the system $CaO-Al_2O_3-SO_3$, it might be the main compound of Lossier's sulphoaluminate clinker prepared from the system $CaO-Al_2O_3-SO_3$. In order to confirm the presence of the compound, following experiments of system $CaO-Al_2O_3-SO_3$ were made.

For the solid phase reaction, six series of mixtures were devised from synthesized C_3A and chemical reagents.

i) $C_3A-nCaSO_4$, $n = 0.1, 0.3, 0.5, 1.0, 3.0$
Mixtures were burned at 1,400°C for 10 min.

ii) $3CaO-3Al_2O_3-CaSO_4$
The mixture was burned at 900°C—6 hrs, 1000°C—6 hrs, 1,100°C—3 hrs—3 hrs (repeatedly), 1,200°C—3 hrs, 1,350°C—6 hrs, and 1,400°C—4.5 hrs.

iii) $3Al_2O_3-4CaSO_4$
The mixture was burned at 1,300°C for 3 hrs. Decomposition of $CaSO_4$ was measured.

iv) $5CaO-3Al_2O_3-CaSO_4$
The mixture contained excessively large amount of CaO. It was burned at 1,350°C for (3 + 3) hrs, repeatedly.

v) $4CaO-3Al_2O_3-SO_2$ (gas)
Instead of using $CaSO_4 \cdot 2H_2O$, the mixture $4CaO-3Al_2O_3$ was burned at 1,200°C for 3 hrs in air current containing 5% SO_2 gas.

vi) $n(CaO-Al_2O_3)-CaSO_4$ $n = 1 - 5$
In order to determine the mol ratio $CaO \cdot Al_2O_3/CaSO_4$, the mixtures were burned at 1,350°C for 6 hrs.

The ground and blended mixtures were burned in an electric furnace. After burning they were quenched in air. The products were examined by chemical analysis and X-ray powder diffraction. The contents of free CaO and free Al_2O_3 were determined by chemical analysis, and the contents of the ternary compound and free $CaSO_4$ were measured by X-ray quantitative analysis (internal standard method). And the reaction at high temperature was observed with high temperature X-ray diffractometer.

By X-ray diffraction, all the products showed the same unknown pattern. Products of series ii), showed weak peaks of this pattern at 900°C, and remarkable peaks in coexistence of those of $CaO \cdot Al_2O_3$ at

Table 1. *Composition of clinkers obtained by replacing various amount of $CaCO_3$ of portland cement raw mixtures with $CaSO_4$*

Clinker samples	SO_3 content wt. %	Calculated composition wt. %			X-ray powder diffraction		
		C_3A	C_4AF	$CaCO_3$	C_3A d = 2.691Å int.	C_4AF d = 2.645Å int.	$CaSO_4$ d = 3.49Å int.
S_0	0.1	8.2	9.8	—	w	m	—
S_1	0.9	8.1	9.8	0.6	w	m	—
S_2	1.8	8.1	9.7	2.1	w	w	—
S_3	2.7	8.1	9.5	3.7	—	w	—
S_4	3.9	7.9	9.4	5.5	—	—	—
S_8	10.0			15.8			S

1,000°C. The patterns of $CaO \cdot Al_2O_3$ and uncombined material became weak at 1,100°C. At 1,200°C, only the pattern of the unknown compound was observed distinctly. At 1,300°C the formation seemed to finish, but small amount of Al_2O_3 remained. At 1,400°C, the formation seemed to have already been completed. The calculated composition of the unknown compound became nearly equal to $3CaO \cdot 3Al_2O_3 \cdot CaSO_4$, in all the products of this series. Products of series iii), (mixture of $3Al_2O_3$–$4CaSO_4$) showed the decomposition of $CaSO_4$ in accordance with the formation of the compound $3CaO \cdot 3Al_2O_3 \cdot CaSO_4$. Products of series v), (mixture of $4CaO$–$3Al_2O_3$ burned in SO_2 containing current) showed the formation of $CaSO_4$ and remarkable amount of the above ternary compound. Products of series iv) ($5CaO$–$3Al_2O_3$–$CaSO_4$) contained small amount of C_3A due to excess of CaO and Al_2O_3. The excess of Al_2O_3 was caused by the decomposition of $CaSO_4$. Of course, the main compound was the above ternary compound. Products of series vi) gave the results shown in Table 2. Besides the ternary compound, the products of n = 1 and 2 contained 23% and 6% of free $CaSO_4$ respectively, and the products of n = 4 and 5 contained 22.3% and 35.6% of $CaO \cdot Al_2O_3$ respectively. As for free CaO, the content was small in n = 1 and 2 and extremely small in n = 4 and 5. No free CaO was found in n = 3. The product of n = 3, had remarkable amount of the ternay compound and only 0.2% of free Al_2O_3 was detected. The mixture n = 3 gave maximum yield of the ternary compound, namely 94.8%.

The obtained results are summerized as follows: A sole ternary compound with definite crystalline form exists in the system CaO–Al_2O_3–SO_3. This ternary compound begins to form at about 900°C and is stable at least up to 1,400°C. At the initial stage of this reaction, the formation of $CaO \cdot Al_2O_3$ was often observed. From the results of chemical analysis and X-ray diffraction, the composition of this ternary compound is estimated as $3CaO \cdot 3Al_2O_3 \cdot CaSO_4$.

The compound gives following X-ray powder diffration data.

dÅ	3.75	3.24	2.91	2.65	2.46	2.30	2.17	1.62	1.58
int.	100	7	6	29	7	4	24	7	4

Halstead and Moore (4) made an advanced study of the synthesis and the crystallography of the above ternary compound. They have reported that $3CaO \cdot 3Al_2O_2 \cdot CaSO_4 (4CaO \cdot 3Al_2O_3 \cdot SO_3)$ is the only ternary compound occurring in the system CaO–Al_2O_3–SO_3 below 1,350°C, and the above formula is reasonable and correct judging from the results of chemical analysis and X-ray diffraction. And from the crystallographic investigation, they showed that the compound is an end member of sodalite-noselite-haüynite series with all the Si replaced by Al and all Na by Ca. R. Kondo (5) also described that the above ternary compound is one of the compounds belonging to haüyne type structure and could be obtained by substitution of all of Na and Si of haüyne by Ca and Al.

Table 2. *Burnt products of mixtures,* $n(CaO$–$Al_2O_3)$–$CaSO_4$

		n = 1	n = 2	n = 3	n = 4	n = 5
		Relative intensity				
X-ray diffraction						
$3C \cdot 3A \cdot CaSO_4$	d,Å 3.75	59	76	91	80	62
	2.65	11	27	25	24	18
	2.17	13	17	19	15	14
$CaSO_4$	d,Å 3.50	24	5	—	—	—
	2.85	7	1	—	—	—
	2.33	4	—	—	—	—
$CaO \cdot Al_2O_3$	d,Å 2.97	—	—	—	7	11
	2.52	—	—	—	3	6
	2.41	—	—	—	1	3
X-ray diffractometric quantitative analysis approx. %	$3C \cdot 3A \cdot CaSO_4$			92	75	63
	free $CaSO_4$	23	6			
Chemical analysis, %						
	SO_3	23.1	14.4	12.4	10.1	8.5
	free CaO	4.2	3.1	0.0	0.5	0.2
	free Al_2O_3	0.0	0.1	0.2	0.1	0.2
Calculated amount %						
	$3C \cdot 3A \cdot CaSO_4$	71.4	84.8	94.8	77.2	64.7
	$CaO \cdot Al_2O_3$	—	—	6.3	22.3	35.6

Constitution of Sulpho-Aluminate Clinker

The Experiments on Sulphoaluminate Clinker

Presuming that $3CaO \cdot 3Al_2O_3 \cdot CaSO_4 (3C \cdot 3A \cdot CaSO_4)$ should occur in Lossier's sulphoaluminate clinker, following experiments were made.

Changing the amount of gypsum, raw mixtures of gypsum-bauxite-lime were prepared. They were ground to the fineness of minus 88μ, and after burning at 1,300°C for 30 min, they were quenched in air. Thus six clinkers with various mol ratio Al_2O_3/SO_3 were obtained (Table 3). In all of them, the formation of $3C \cdot 3A \cdot CaSO_4$ was made clear by X-ray diffraction. The content of $3C \cdot 3A \cdot CaSO_4$ was calculated on the base of SO_3 in the case of $Al_2O_3/SO_3 > 3$, and on the base of Al_2O_3 in the case of $Al_2O_3/SO_3 < 3$. On the other hand, the content was determined by X-ray internal standard method. Both of the values were nearly equal, so that the calculated value could be useful. On the change of Al_2O_3/SO_3 mol ratio from 8.2 to 6.0, the content of $3C \cdot 3A \cdot CaSO_4$ increased, reached maximum at $Al_2O_3/SO_3 = 3.5$–2.0, and decreased at $Al_2O_3/SO_3 = 2.0 - 0.8$. The clinker of

Table 3. *Analysis of sulphoaluminate clinkers of various mol ratio of* Al_2O_3/SO_3

Clinkers	1	2	3	4	5	6
Chemical analysis						
Al_2O_3 %	35.6	35.3	34.3	30.8	28.4	21.8
CaO %	42.6	41.9	42.1	42.8	43.4	43.1
SO_3 %	—	3.4	4.5	7.0	11.0	21.1
Mol ratio Al_2O_3/SO_3	—	8.2	6.0	3.5	2.0	0.8
Calculated amount						
$3C\cdot3A\cdot CaSO_4$ %	—	25.6	34.2	53.5	56.7	43.5
Residual Al_2O_3	35.6	22.4	17.1	4.0	—	—
" SO_3	—	—	—	—	3.5	15.5
X-ray diffractometric quantitative analysis						
approx % $3C\cdot3A\cdot CaSO_4$	—	28	34	57	56	41

Table 4. *Sulphoaluminate clinkers, prepared in large quantities*

Chemical analysis %		X-ray diffraction spacing dÅ	int.	remark
Insol.	0.0	3.75	100	$3C\cdot3A\cdot CaSO_4$
SiO_2	7.1	3.49	59	$CaSO_4$
Al_2O_3	21.8	3.24	10	$3C\cdot3A\cdot CaSO_4$
TiO_2	0.4	2.91	6	"
Fe_2O_3	5.4	2.85	12	$CaSO_4$
CaO	42.6	2.79	20	βC_2S
MgO	0.0	2.71	4	"
SO_3	22.3	2.65	30	$3C\cdot3A\cdot CaSO_4$
Ffree CaO	0.0	2.46	11	"
		2.34	w	$CaSO_4$
		2.17	37	$3C\cdot3A\cdot CaSO_4$
		1.63	13	"

Table 5. *Burnt products of mixtures,*
(*A*) $3CaO-3Al_2O_3-CaSO_4-nSiO_2$,
(*B*) $(m+3)CaO-3Al_2O_3-CaSO_4-nSiO_2$

	A			B		
Chemical analyses	n = 0	n = 1	n = 2	m = 1 n = 1	m = 2 n = 1	m = 4 n = 2
SiO_2 %	0.0	11.0	18.6	8.3	7.4	12.1
Al_2O_3 %	49.6	48.1	46.0	42.4	37.8	30.8
CaO %	37.4	36.9	34.3	40.3	42.9	48.3
SO_3 %	13.2	4.4	0.9	8.6	11.8	9.0
free CaO %	0.0	0.0	0.0	0.3	1.0	5.3
Calculated compound composition						
$3C\cdot3A\cdot CaSO_4$ %	100.7	33.5	6.9	65.6	75.4	61.4
C_2S %	—	—	—	7.8	21.2	34.7
C_2AS %	—	50.2	58.1	25.5	—	—
C_3A_5 %	—	16.8	21.0	—	—	—
free $CaSO_4$ %	—	—	—	—	3.5	1.5
X-ray diffractometric analysis, approx. %						
$3C\cdot3A\cdot CaSO_4$	99	49	—	65	73	65
X-ray diffraction			int.			
$3C\cdot3A\cdot CaSO_4$ dÅ 3.75	vs	vs	w	vs	vs	vs
2.65	s	s	w	s	s	s
2.17	s	s	w	s	s	s
βC_2S dÅ 2.779	—	—	—	m	m	m
2.748	—	—	—	w	w	m
2.189	—	—	—	mw	mw	mw
C_2AS dÅ 3.070	—	m	s	w	—	—
2.846	—	vs	vs	m	—	—
1.754	—	m	s	w	—	—
C_3A_5 dÅ 3.505	—	m	m	—	—	—
2.972	—	m	—	—	—	—
2.605	—	m	mw	—	—	—

$Al_2O_3/SO_3 = 0.8$ is the most similar one to the sulphoaluminate clinker reported by Lafuma. (1)

Then, considerable amount of the clinker having similar composition to Lafuma's, was prepared by the above method (Table 4), and examined. X-ray diffraction revealed that this clinker was mainly composed of $3C\cdot3A\cdot CaSO_4$ and free $CaSO_4$, and that $\beta-C_2S$ was formed clearly. The compound composition was calculated; $3C\cdot3A\cdot CaSO_4$ from Al_2O_3, free $CaSO_4$ from excess SO_3 and C_2S from SiO_2. The calculated composition became as follows.

$3CaO\cdot3Al_2O_3\cdot CaSO_4$ 43.5%
free $CaSO_4$ 28.2%
$\beta-C_2S$ 20.3%
free CaO, Fe_2O_3, TiO_2 etc..... 8.0%

Lossier's sulphoaluminate clinker burned at 1,300°C for 30 min, contains $3C\cdot3A\cdot CaSO_4$ as the principal constituent and comparable amount of free $CaSO_4$, which play an important role in expanding reaction. And SiO_2 seemed to form $\beta-C_2S$. In industrial products, calcium aluminate and considerable amount of free CaO may be contained besides the above constituents.

Lafuma reported that his sulphoaluminate clinker was a mixture of free $CaSO_4$, calcium aluminate probably C_5A_3 and $\gamma-C_2S$, and not a ternary compound. Probably, the burning temperature might be too low to form the ternary compound, as Halstead and Moore (4) have described.

Klein and Troxell (6) propared clinkers by burning the mixture of $Ca(OH)_2$ or $CaCO_3$, gypsum and bauxite or aluminium sulphate at 1,350°C. They deduced that they had synthesized two ternary compounds, estimating composition as $5CaO\cdot2Al_2O_3\cdot SO_3$ and $9CaO\cdot4Al_2O_3\cdot3SO_3$. But it seems that the composition reported by Klein and Troxell must be the composition of a mixture of $3C\cdot3A\cdot CaSO_4$ and free $CaSO_4$ or calcium aluminate. In the experiment of the present auther, only $3C\cdot3A\cdot CaSO_4$ was detected as stable ternary compound.

The Effect of SiO_2 on the Formation of $3C\cdot3A\cdot CaSO_4$

In the manufacture of expanding cement, raw materials of Al_2O_3-source often contain considerable amount of SiO_2. In order to make clear the effect of SiO_2 on the formation of $3C\cdot3A\cdot CaSO_4$, following fundamental experiments were made. Raw mixtures were prepared from chemical reagents.

Series (1) $3CaO-3Al_2O_3-CaSO_4-nSiO_2$

Sample No.	S-0	S-0.5	S-1	S-2	S-3
n	0	0.5	1	2	3

Series (2) $(3+m)CaO-3Al_2O_3-CaSO_4-nSiO_2$

Sample No.	CS	2CS	3CS	2C2S	4C2S	6C2S	7.5C2S
m	1	2	3	2	4	6	7.5
n	1	1	1	2	2	2	2

Series (1) was made by changing the amount of SiO_2, while series (2) was made by changing the amount of SiO_2 and CaO. After moulding, the mixtures were burned at 1,300°C or 1,350°C for 30 min. The products were examined by chemical analysis and X-ray diffraction. The results are shown in Table 5 and summerized as follows. Series (1); when the mixtures were burned, the decomposition of $CaSO_4$ occurred depending upon the amount of SiO_2, therefore the content of $3C\cdot3A\cdot CaSO_4$ was reduced. SiO_2 formed C_2AS($2CaO\cdot Al_2O_3\cdot SiO_2$, gehlenite) in the reaction with CaO and Al_2O_3. With the increase of SiO_2, the formation of C_3A_5 and probably of CAS_2 was observed. Series (2); when CaO content was enough to form C_2S, i.e. in the case of molar ratio of extra $CaO/SiO_2 > 2$, no decomposition of $CaSO_4$ occurred, and SiO_2 had no effect on the formation of $3C\cdot3A\cdot CaSO_4$. But in the case of extra $CaO/SiO_2 < 2$, decomposition of $CaSO_4$ occurred and the content of $3C\cdot3A\cdot CaSO_4$ decreased. It can be concluded that SiO_2 has no effect on the formation of $3C\cdot3A\cdot CaSO_4$, only when the mol ratio extra CaO/SiO_2 is greater than 2.

Hydration of Sulphoaluminous Cement

Hydration of $3CaO\cdot3Al_2O_4\cdot CaSO_4$

In order to study the expanding properties of sulphoaluminate type expansive cement, examination was made on the hydrating behaviors of expansive material and sulphoaluminous cement. It has been confirmed that the main constituent of sulphoaluminous cement is $3C\cdot3A\cdot CaSO_4$. The hydration mechanism of this compound has not yet been made clear, and there have been some different points of view about $3C\cdot3A\cdot CaSO_4$ and its hydrated product i.e. $C_3A\cdot3CaSO_4\cdot30\text{-}32H_2O$ which is said to cause expansion. In order to investigate the hydration of sulphoaluminous cement, the basic hydration experiments (7) were made about the following four systems.

(1) $3C\cdot3A\cdot CaSO_4-H_2O$
(2) $3C\cdot3A\cdot CaSO_4-CaSO_4\cdot2H_2O-H_2O$
(3) $3C\cdot3A\cdot CaSO_4-CaSO_4$(calcined)$-H_2O$
(4) $3C\cdot3A\cdot CaSO_4-Ca(OH)_2-H_2O$

System (1)—represents the hydration of only $3C\cdot3A\cdot CaSO_4$, namely hydration with pure water, system (2)—the hydration with coexistence of gypsum, system (3)—the hydration with coexistence of calcined $CaSO_4$ corresponding to free $CaSO_4$ in sulphoaluminate clinker, and system (4)—the hydration with coexistence of free CaO. Varying the amount, the additives i.e. $CaSO_4\cdot2H_2O$, $Ca(OH)_2$ and $CaSO_4$ (calcined at 1,300°C) were mixed with $3C\cdot3A\cdot CaSO_4$. The hydration was carried out in a rotating porcelain pot mill with mixing water (five times in weight of the solid sample) at 20±1°C for 6, 24 and 48 hrs. Then the slurry was filtered rapidly. After washing with absolute alcohol and drying, the solid phase was examined by chemical analysis and X-ray diffraction. At the same time, the extracted substances in the liquid phase were analysed. The results are shown in Fig. 1 and Table 6, and summerized as follows.

In the hydration of $3C\cdot3A\cdot CaSO_4$ and H_2O the

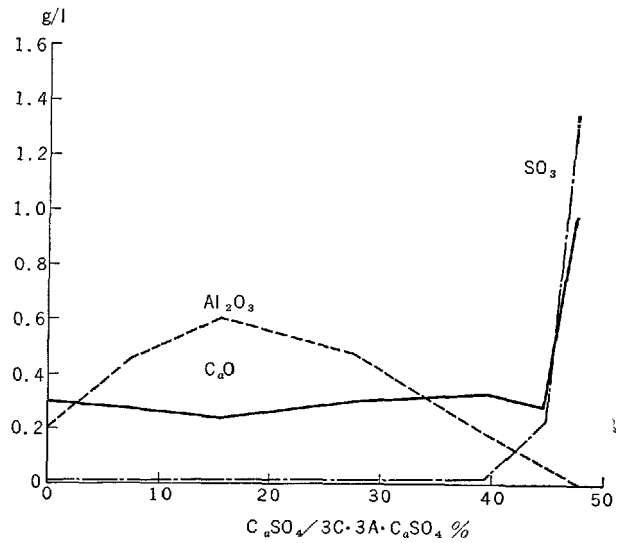

Fig. 1. *Relation of concentrations of solutes and* $CaSO_4/3C\cdot3A\cdot CaSO_4$ *ratios, in hydration of* $3C\cdot3A\cdot CaSO_4-CaSO_42H_2O-H_2O$.

Table 6. *X-ray diffraction of various hydration products of* $3C\cdot3A\cdot CaSO_4$

Hydrate with pure H_2O dÅ	int.	With $CaSO_4\cdot2H_2O$ dÅ	int.	With calcined $CaSO_4$ dÅ	int.	With $Ca(OH)_2$ dÅ	int.	Remark
						10.65	s	$C_2A\cdot8H_2O$
		9.73	100	9.73	88			high s.
8.92	vs	8.92	17	8.92	100	8.92	vs	low s.
						5.34	m	$C_2A\cdot8H_2O$
		5.61	100	5.60	61			high s.
		4.69	52	4.69	19			〃
4.46	s			4.46	31	4.46	s	low s.
4.00	m	4.00	—	4.00	11	4.00	m	〃
		3.88	74	3.88	23			high s.
				3.75	19			$3C\cdot3A\cdot CaSO_4$
		3.48	48	3.48	19			$CaSO_4$, high s.
2.876	s	2.885	15	2.885	80	2.876	s	low s.
		2.780	60	2.780	23			high s.
		2.564	60	2.564	19			〃
2.455	s			2.455	23	2.449	s	low s.
2.417	m			2.417	23	2.417	s	〃
		2.212	65	2.212	23			high s.
1.667	m	1.667	—	1.667	10	1.664	m	low s.

high s. = $C_3A\cdot3CaSO_4\cdot30$–$32H_2O$ low s. = $C_3A\cdot CaSO_4\cdot12H_2O$

low sulphate of calcium aluminium sulphate hydrate, $C_3A\cdot CaSO_4\cdot12H_2O$ was formed, and high sulphate was hardly observed. The reaction seems as follows.

$$3C\cdot3A\cdot CaSO_4 + xH_2O = C_2A\cdot CaSO_4\cdot12H_2O + 2Al_2O_3 \text{ hydrate}$$

In the hydration of $3C\cdot3A\cdot CaSO_4$, gypsum and H_2O, high sulphate of calcium aluminium sulphate hydrate $C_3A\cdot3CaSO_4\cdot30$–$32H_2O$ was formed and low sulphate was hardly observed. Fig. 1 shows the relation between the amount of added $CaSO_4$ and the concentration of Al_2O_3, CaO and SO_3 in the liquid phase. At the amount of added $CaSO_4$ 44.6%, Al_2O_3 in the liquid phase began to decrease, on the contrary SO_3 and CaO began to increase sharply. It indicates that, until the added $CaSO_4$ reaches this point (44.6%), it takes part in the formation of high sulphate hydrate, beyond this point excess of $CaSO_4$ dissolves according to its solubility, and remains in the liquid phase. The value 44.6% corresponds to the mol ratio $CaSO_4/3C\cdot3A\cdot CaSO_4 = 2$.

The reaction seems as follows.

$$3C\cdot3A\cdot CaSO_4 + 2CaSO_4\cdot2H_2O + xH_2O = C_3A\cdot3CaSO_4\cdot30\text{-}32H_2O + 2Al_2O_3 \text{ hydrate}$$

In the hydration of $3C\cdot3A\cdot CaSO_4$ with calcined $CaSO_4$ (corresponding to free $CaSO_4$ in the clinker) both low-and high-sulphate hydrates were formed, probably because of low solubility of calcined $CaSO_4$. The reaction seems as follows.

$$3C\cdot3A\cdot CaSO_4 + CaSO_4 \text{ (calcined)} + xH_2O \longrightarrow \begin{cases} C_3A\cdot CaSO_4\cdot12H_2O + 2Al_2O_3 \text{ hydrate} \\ C_3A\cdot3CaSO_4\cdot30\text{–}32H_2O + 2Al_2O_3 \text{ hydrate} \end{cases}$$

From the results, it seems that calcined $CaSO_4$ or free $CaSO_4$ in the clinker is less available than gypsum.

In the hydration of expansive cement, $3C\cdot3A\cdot CaSO_4$ is in contact with considerable amount of free lime, i.e. free CaO in the clinker, and $Ca(OH)_2$ separated by the hydration of portland cement. When $3C\cdot3A\cdot CaSO_4$ was hydrated under the coexistence of $Ca(OH)_2$, the low sulphate hydrate was formed, while high sulphate was not observed. Besides, small amount of $2CaO\cdot Al_2O_3\cdot8H_2O$ was formed. The reaction is considered as follows.

$$3C\cdot3A\cdot CaSO_4 + 4Ca(OH)_2 + 24H_2O = C_3A\cdot CaSO_4\cdot12H_2O + 2(C_2A\cdot8H_2O)$$

When $3C\cdot3A\cdot CaSO_4$ reacts on H_2O only, low sulphate hydrate and probably Al_2O_3 hydrate are formed. By addition of gypsum to this system, high sulphate is formed. Until the mol ratio $CaSO_4/3C\cdot3A\cdot CaSO_4$ reaches 2, $CaSO_4$ is useful to form high sulphate, beyond this point, the excess of $CaSO_4$ is not useful because of the lack of CaO. Beside high sulphate, Al_2O_3 separates probably as hydrate. With addition of more than 8 and 6 mol of $CaSO_4$ and CaO against one mol of $3C\cdot3A\cdot CaSO_4$, the formation of high sulphate can be completed. Calcined $CaSO_4$ is not so useful as $CaSO_4\cdot2H_2O$ to form high sulphate, because of its low solubility. But this fact does not mean that free $CaSO_4$ in clinker is not so useful as mixed gypsum. Compared with simply mixed gypsum, free $CaSO_4$ contained in clinker often shows favorable results in expansion. When the system is poor in $CaSO_4$ and rich in CaO, low sulphate is formed, and Al_2O_3 separates as $C_2A\cdot8H_2O$. This reaction should be paid attention, because it has something to do with the setting.

Hydration of Expansive Cement

Samples

$3C\cdot3A\cdot CaSO_4$ was synthesized from reagents, and sulphoaluminous cement was prepared from bauxite, lime and gypsum. They were mixed with portland cement, gypsum and blast-furnace slag in the proportion shown in Table 7 and ground to the specific surface of 3,150–3,200 cm^2/g. These cement samples were examined as follows.

Length Change

Cement mortar specimens were prepared in the mixing ratio, cement: sand: water = 1: 2: 0.60 (0.64 or 0.68). The specimens were demolded 2 days after molding. After curing in water (20±1°C) for 0, 3, and 7 days, they were stored in air (20±1°C, RH

Table 7. *Expansive cement samples, mixed with (A) synthesized* $3C \cdot 3A \cdot CaSO_4$, *and with (B) prepared sulphoaluminous cement.*

	Mixing ratio							
A	A_4G_0	A_4G_3	A_4G_6	A_4G_{6S}	A_6G_0	A_6G_0	A_8G_6	A_8S_{20}
Portland cement	96	96	96	96	94	92	92	92
3C 3A $CaSO_4$	4	4	4	4	6	8	8	8
Gypsum	0	3	6	0	0	0	6	0
Slag	0	0	0	10	0	0	0	20
B	$B_{10}G_0$	$B_{10}G_1$	$B_{20}G_0$	$B_{20}G_{05}$	$B_{20}G_1$	$B_{20}G_3$	$B_{20}G_6$	$B_{20}G_{6S}$
Portland cement	90	90	80	80	80	80	80	80
Sulpho-aluminous cement	10	10	20	20	20	20	20	20
Gypsum	0	1	0	0.5	1	3	6	6
Slag	0	0	0	0	0	0	0	10

76%). The length at each period was measured with comparator of JCEA, TYPE II. The results are shown in Fig. 2, 3, and summerized as follows:

Expansive cement containing 10% of sulphoaluminous cement, did not show any expansion, and the addition of 1.0% gypsum had no effect. Expansive cement containing 20% of sulphoaluminous cement continued to expand for the first 2 weeks, then the expansion began to decrease. But the addition of 0.5 or 1.0% gypsum caused remarkable expansion during the first week of curing, and the expansion was kept up to the end of this test, i.e. for 13 weeks after demolding. A similar tendency was observed, also in the case of curing only in air. When the added gypsum reached 6.0%, the specimen expanded extremely and cracked. But when 1.0% gypsum was added to cement sample containing 10% of sulphoaluminous cement, the effect did not appear. There should be a definite range for useful addition of sulphoaluminous cement.

The cement, prepared by mixing synthesized $3C \cdot 3A \cdot CaSO_4$ and portland cement, showed shrinkage instead of expansion. With increased $3C \cdot 3A \cdot CaSO_4$ content, the degree of shrinkage increased. Addition of 3 or 6% gypsum caused a slight decrease in shrinkage but no expansion. When more slag was added, the shrinkage decreased remarkably, but no expansion occurred. Paste specimens also had a similar tendency in the length change at early age of curing.

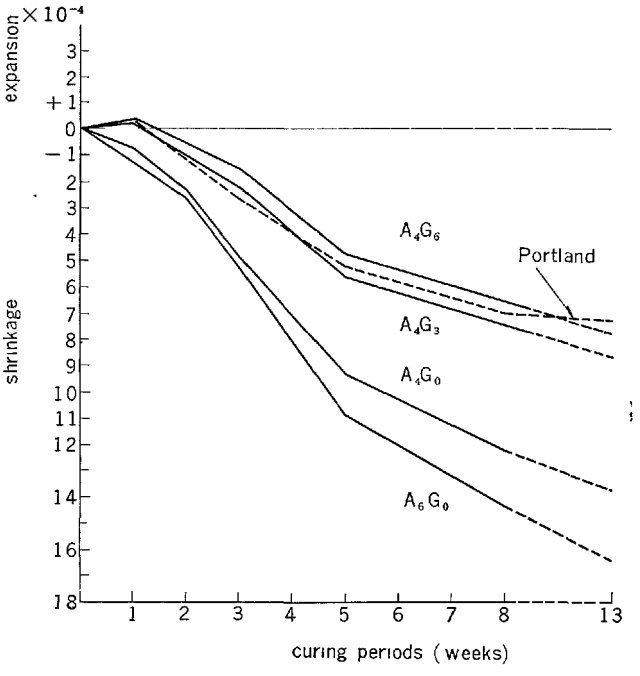

Fig. 2. *Length change of mortars of cement samples, mixed with* $3C \cdot 3A \cdot CaSO_4$. *Initial curing 3 days in water.*

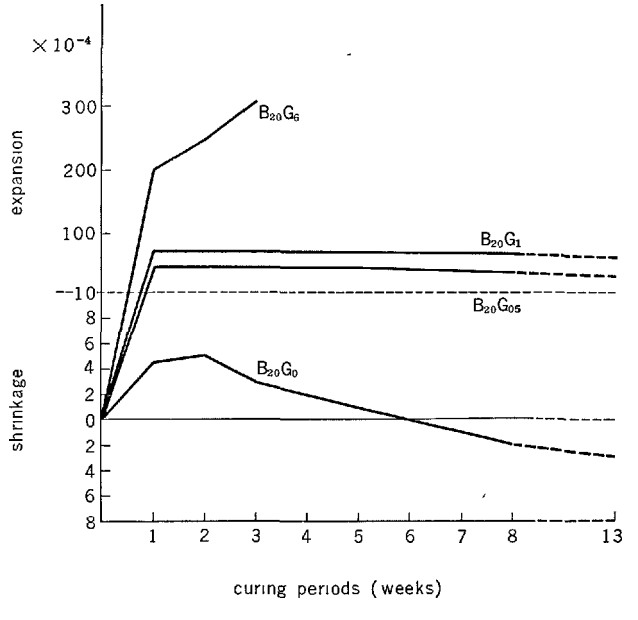

Fig. 3. *Length change of mortars of cement samples, mixed with sulpho aluminous cement. Initial curing 3 days in water.*

Hydrated Products in Paste Specimens

Paste specimens (water/cement = 27%) were cured up to 8 weeks. Samples for each period were pulverized and washed with absolute alcohol. After drying at low temperature, they were examined by X-ray diffraction. The results are shown in Table 8, and summerized as follows:

Paste specimen of expansive cement containing sulphoaluminous cement, cured in air for 2 days and in water for a week, showed obviously the formation of high sulphate hydrate. With the increase of mixed sulphoaluminous cement, the content of high sulphate increased. Expansive cement mixed with 20% of

Table 8. *X-ray diffraction of hydration products of paste specimens.*

d-spacing Å	A_4G_0	A_1G_6	A_6G_0 relative int.	$B_{20}G_0$	$B_{20}G_{05}$	$B_{20}G_6$ relative int.	Remark
9.73	11	28	—	42	40	48	high s.
8.92	22	16	18	24	—	—	low s.
5.61	11	24	—	34	34	38	high s.
4.92	70	90	36	92	68	68	$Ca(OH)_2$
4.46	14	—	—	12	—	—	low s.
3.99	—	—	—	—	—	—	low s.
3.88	—	22	—	30	30	32	high s.
3.03	48	34	44	48	36	44	silicate
2.885	16	16	22	20	12	12	low s.
2.797	100	96	110	80	80	70	silicate
2.629	70	70	50	65	70	55	$Ca(OH)_2$
2.564	—	22	—	22	20	28	high s.
2.455	16	16	18	12	12	12	low s.
2.411	12	12	12	12	12	—	low s.

high s. = $C_3A \cdot 3CaSO_4 \cdot 30\text{–}32H_2O$, low s. = $C_3A \cdot CaSO_4 \cdot 12H_2O$

Table 9. *Setting examinations of cement samples, mixed* $3C \cdot 3A \cdot CaSO_4$ *to portland cement.*

Mixing ratio				Setting time			
$3C \cdot 3A \cdot CaSO_4$	Portland cement	Gypsum	Slag	Mixing water %	Initial setting hrs. min.	Final setting hrs. min.	Remark
100	0	0	0	40.0	3—00	3—35	normal
0	100	0	0	26.4	2—32	3—24	〃
5	95	0	0	26.5	2—10	2—50	〃
10	90	0	0	26.6	0—50	0—55	quick
20	70	0	10	26.5	0—46	0—55	〃
10	70	0	20	26.0	1—20	1—32	normal
10	90	3	0	27.8	0—40	0—50	quick
10	70	3	20	27.0	1—52	2—32	normal
20	80	6	0	27.8	0—23	0—39	quick
20	80	12	0	30.5	0—42	0—59	〃
100	$Ca(OH)_2$ 10	0	0	45.0	0—04	0—10	flash

sulphoaluminous cement, is estimated to contain 8.3% $3C \cdot 3A \cdot CaSO_4$ and 8.0% free $CaSO_4$. It is considered that the free $CaSO_4$ is effective to form high sulphate hydrate.

Paste specimen of cement sample containing synthesized $3C \cdot 3A \cdot CaSO_4$, showed the formation of low sulphate but high sulphate was scarcely observed. Even with addition of 6% gypsum, the formation of high sulphate was not clearly observed. It seems that, much greater amount of gypsum is necessary to form high sulphate. Even with curing of longer age, there was not any appreciable change in the hydrates.

Hydrating Characters

Expansive cement prepared by mixing with sulphoaluminous cement, contained sufficient amount of $3C \cdot 3A \cdot CaSO_4$ and free $CaSO_4$, from which considerable amount of high sulphate was formed in the hydration. From the hydrating experiment of system $3C \cdot 3A \cdot CaSO_4$–$CaSO_4$ (calcined)–H_2O, it was clarified that calcined $CaSO_4$ was not so effective as ordinary gypsum in the formation of high sulphate. Nevertheless, in the hydration of the above expansive cement, the content of high sulphate was observed to be sufficient. Therefore, it seems that $3C \cdot 3A \cdot CaSO_4$ and free $CaSO_4$ contained in sulphoaluminate clinker must be in a particularly activated state.

In the case of cement sample, prepared by mixing with synthesized $3C \cdot 3A \cdot CaSO_4$, its paste showed the formation of low sulphate hydrate, but high sulphate was scarcely observed, and its mortar specimen showed shrinkage. With addition of 6% gypsum (or 4.7% $CaSO_4$) to the cement sample containing 6% of synthesized $3C \cdot 3A \cdot CaSO_4$, high sulphate could hardly be observed, and its mortar specimen did not show any expansion. Addition of much greater amount of gypsum would be necessary to cause the formation of high sulphate and expansion. On the other hand, from the hydrating experiment of system $3C \cdot 3A \cdot CaSO_4$–$CaSO_4 \cdot 2H_2O$–H_2O, the effect of gypsum to form high sulphate has been confirmed. These facts indicate that expansive cement prepared by mixing with sulphoaluminous cement is much more reactive, compared with cement sample prepared by mixing with synthesized $3C \cdot 3A \cdot CaSO_4$ and $CaSO_4$ (gypsum or calcined). It will be necessary to make further studies on the dispersion of components and the effect of portland cement, etc. R. Kondo and N. Nawata (8) also described that a simple mixture of $3C \cdot 3A \cdot CaSO_4$, CaO and $CaSO_4$ could not hydrate or expand so rapidly as the sulphoaluminate clinker, in which $3C \cdot 3A \cdot CaSO_4$ crystals were surrounded by a matrix containing free lime with or without $CaSO_4$.

Setting of the Cements Containing $3C \cdot 3A \cdot CaSO_4$

By J.I.S. method, setting test was made for the mixtures, prepared from $3C \cdot 3A \cdot CaSO_4$, gypsum, blastfurnace slag, $Ca(OH)_2$, and portland cement in the proportion shown in Table 9. The results are summerized as folllws:

$3C \cdot 3A \cdot CaSO_4$ itself showed normal setting. When it was mixed with normal portland cement, the mixture showed quick setting. And addition of 6% gypsum could not retard the setting. When 20% slag was further added, the setting became normal at last. The mixture of $3C \cdot 3A \cdot CaSO_4$ and $Ca(OH)_2$, showed flash setting. Under the presence of $Ca(OH)_2$, the hydration of $3C \cdot 3A \cdot CaSO_4$ seemed to proceed as follows:

$$3C \cdot 3A \cdot CaSO_4 + 4Ca(OH)_2 + 24H_2O = C_3A \cdot CaSO_4 \cdot 12H_2O + 2(C_2A \cdot 8H_2O)$$

Besides low sulphate, $C_2A \cdot 8H_2O$ was formed. With

addition of gypsum to this system, high sulphate is formed. But, when the amount of gypsum is not enough for Al_2O_3 to change into high sulphate completely, the formation of $C_2A \cdot 8H_2O$ should continue. In the hydration of $3C \cdot 3A \cdot CaSO_4$, as in the experiment of system $3C \cdot 3A \cdot CaSO_4 - H_2O$, $C_2A \cdot 8H_2O$ could not be formed because of the lack of CaO, though the system contained considerable amount of Al_2O_3 separated from $3C \cdot 3A \cdot CaSO_4$. When $C_2A \cdot 8H_2O$ was not formed in the hydration, the setting became normal, on the other hand, when $C_2A \cdot 8H_2O$ was formed, quick or flash setting occurred under other conditions. In this way, the setting may be changeable depending upon the extent of formation of $C_2A \cdot 8H_2O$ and other conditions. Thus, the formation of $C_2A \cdot 8H_2O$ is considered to be related closely to setting.

Summary

By the solid phase reaction of system $CaO-Al_2O_3-SO_3$, the author confirmed the presence of a sole ternary compound, which is stable at high temperature. The composition was estimated as $3CaO \cdot 3Al_2O_3 \cdot CaSO_4$. The formation begins at 900–1,000°C, and this compound is stable up to 1,400°C at least. According to Halstead and Moore, the melting point of the compound was indicated between 1,590°C and 1,600°C by a rough differential thermal analysis. The compound gives following X-ray powder diffraction data.

dÅ	3.75	3.24	2.91	2.65	2.46	2.30	2.17	1.62	1.58
int.	100	7	6	29	7	4	24	7	4

In the industrial sulphoaluminate clinker, apart from the variation attributable to manufacturing process, the formation of $3CaO \cdot 3Al_2O_3 \cdot CaSO_4$ is considered to be completed practically. The excess SO_3 in the clinkers can be considered to exist as free $CaSO_4$. Thus, the compound composition of the clinkers can be calculated; the content of $3C \cdot 3A \cdot CaSO_4$ from Al_2O_3, because the mol ratio Al_2O_3/SO_3 is usually less than 3, free $CaSO_4$ from excess of SO_3, and C_2S from SiO_2. The calculated value is thought to be practical.

When the raw mixture contains sufficient amount of CaO, SiO_2 has probably no effect on the formation of $3C \cdot 3A \cdot CaSO_4$.

In the hydration of $3C \cdot 3A \cdot CaSO_4$ by itself or with insufficient amount of $CaSO_4$, low sulphate hydrate $C_3A \cdot CaSO_4 \cdot 12H_2O$ is formed. In the experiment, the low sulphate does not cause any expansion but shrinkage. Without the formation of high sulphate $C_3A \cdot 3CaSO_4 \cdot 30-32H_2O$, expansion can not occur. In the hydration of $3C \cdot 3A \cdot CaSO_4$ with $CaSO_4$ (gypsum), high sulphate is formed and excess of Al_2O_3 is considered to separate as hydrate. In this case, the limit of useful amount of $CaSO_4$ is 2 mol for one mol of $3C \cdot 3A \cdot CaSO_4$.

$$3C \cdot 3A \cdot CaSO_4 + 2CaSO_4 + H_2O = C_3A \cdot 3CaSO_4 \cdot 30-32H_2O + 2Al_2O_3 \text{ hydrate}$$

In order to further increase the yield of high sulphate greater amount of gypsum must be used with CaO added thereto. For one mol of $3C \cdot 3A \cdot CaSO_4$ to change into high sulphate completely, addition of 8 mol $CaSO_4$ and 6 mol CaO is necessary in theory. Lossier's sulphoaluminous cement, usually contains sufficient amount of $3C \cdot 3A \cdot CaSO_4$ and free $CaSO_4$, and some free CaO. In the reaction with sufficient amount of $Ca(OH)_2$ separated from portland cement, those constituents could form enough amount of high sulphate to cause expansion. Probably, free $CaSO_4$ in the sulphoaluminate clinker, is not so reactive, like the gypsum calcined at high temperature, and shows less effect to form high sulphate in the hydration of $3C \cdot 3A \cdot CaSO_4$, compared with ordinary gypsum. But as above mentioned, free $CaSO_4$ in the sulphoaluminous cement is effective in the formation of high sulphate. On the other hand, cement sample prepared by simply mixing synthesized $3C \cdot 3A \cdot CaSO_4$ and gypsum with portland cement, forms low sulphate but scarcely high sulphate. From these facts, it is gathered that, the components, i.e. $3C \cdot 3A \cdot CaSO_4$, free $CaSO_4$ and free CaO contained in sulphoaluminate clinker might possess very effective nature or condition for the hydration. After all, $3C \cdot 3A \cdot CaSO_4$ and free $CaSO_4$ are the principal components of Lossier's sulphoaluminous cement and should play an important role in expansion.

In the hydration with paste state, synthesized $3C \cdot 3A \cdot CaSO_4$ showed normal setting. However, the mixture of pure $3C \cdot 3A \cdot CaSO_4$ and normal portland cement showed quick setting. Even when gypsum was (6%) added, the setting could not be retarded. Sulphoaluminous cement which contains free CaO in some degree, shows quick setting sometimes. In the paste of synthesized $3C \cdot 3A \cdot CaSO_4$, the reaction is considered as follows:

$$3C \cdot 3A \cdot CaSO_4 + xH_2O = C_3A \cdot CaSO_4 \cdot 12H_2O + 2Al_2O_3 \text{ hydrate}$$

And in the paste of the mixture of $3C \cdot 3A \cdot CaSO_4$ and portland cement, the reaction is considered as follows:

$$3C \cdot 3A \cdot CaSO_4 + 4Ca(OH)_2 + 24H_2O = C_3A \cdot CaSO_4 \cdot 12H_2O + 2(C_2A \cdot 8H_2O)$$

With addition of gypsum to this system, the formation of high sulphate begins. But when the amount of gypsum is not enough for Al_2O_3 to change into high sulphate completely, the formation of $C_2A \cdot 8H_2O$ should continue. In the paste specimen of synthesized $3C \cdot 3A \cdot CaSO_4$, because of absence of free CaO or $Ca(OH)_2$, $C_2A \cdot 8H_2O$ is not formed, and the setting is normal. In the pastes of the mixtures of $3C \cdot 3A \cdot CaSO_4$ and portland cement containing $CaSO_4$ (gypsum) or not, $C_2A \cdot 8H_2O$ is formed besides low- or high-sulphate, on account of the presence of $Ca(OH)_2$ separated from portland cement and the paste specimen shows quick or flash setting. Thus, the formation of $C_2A \cdot 8H_2O$, is considered to be related closely to the setting.

References

1. H. Lafuma, "Expansive cement", proc. 3rd. International Symposium on the Chemistry of Cement, London, p. 581–592 (1952).
2. N. Fukuda and M. Yamada, "Experiments on the mixing of gypsum to portland cement raw mixture", Proc. Japan Cement Eng. Assoc. 14th, Tokyo, p. 124–128 (1960).
3. T. F. Newkirk "Effect of SO_3 on the alkali compounds of portland cement clinker." J. Res. Nat. Bur. St. A. **47** 349–352 (1951).
4. P. E. Halstead and A. E. Moor. "Composition and crystallography of an anhydrous Ca-aluminosulphate", J. Appl. Chem., **12** 413–417 (1962).
5. R. Kondo, "Synthesis and crystallography of the compounds belonging to haüyne type structure", J. Ceram. Assoc. Japan, **73** 101–108 (1965)
6. A. Klein and G. E. Troxell, "Studies of calcium sulph-aluminate admixture for expansive cements", Proc. Am. Soc. Testing Material, **58** 986–1008 (1958).
7. N. Fukuda and H. Umeyama, "On the setting of a cement, mixed sulpho-aluminous cement to portland cement", Proc. Japan Cement Eng. Assoc. 18th, Tokyo p. 93–97 (1964).
8. R. Kondo and N. Nawata, "Characteristics of expansive cement affected by the properties of calcium sulpho-aluminate clinker", Proc. Japan Cement Eng. Assoc. 19th, Tokyo, p 54–59 (1965).

Supplementary Paper IV-74 Mineralogical Composition of Expansive Cement Clinker Rich in SiO_2 and Its Expansibility

Takanori Nakamura, Giichi Sudoh and Shigeo Akaiwa*

Synopsis

The authors experimented on the manufacture of expansive cement clinker by the use of kaolin clay as an aluminous material to be mixed with lime-stone and gypsum.

The mineralogical composition of the burned clinker varied with the mixing ratio of limestone, clay and gypsum, but it was roughly divided into the following three cases; 1) as the principal mineral, anorthite CAS_2 is formed, 2) gehlenite C_2AS is formed, 3) $C_4A_3(SO_3)$ is formed. Conditions of mixing raw materials for good expansive cement clinker were presented. In this case, SiO_2 occurred as $2(C_2S)\cdot CaSO_4$ or β-C_2S; Al_2O_3 entered $C_4A_3(SO_3)$ and ferrite phase. When the raw material contained P_2O_5, wilkeite was occasionally produced.

$2(C_2S)\cdot CaSO_4$ is a prismatic crystal, and was decomposed into C_2S and $CaSO_4$ at 1285°C. This compound showed poor hydraulicity and contributed very little to the initial expansion. Appropriate temperature for burning clinker was determined as 1150–1200°C. The rate of expansion became slow with a rise in the burning temperature.

For good expansion behavior due to hydration, the most desirable mineralogical composition of the clinker was as follows: The quantity of $C_4A_3(SO_3)$ should be large enough; free CaO should be 6 moles or more, and free $CaSO_4$ around 8 moles, per 1 mole of $C_4A_3(SO_3)$. Setting of the experimentally prepared expansive cement was retarded by adding gypsum to it. Additional gypsum was apt to cause abnormal expansion and lowering of strength, but these defects were solved by intermixing blast-furance slag.

It was revealed that the expansion of $C_4A_3(SO_3)$ was controlled by the type of formation of ettringite, rather than by the total amount of produced ettringite. The ettringite produced under high concentration of lime caused expansion, whereas the ettringite produced under low lime concentration did not contribute to expansion.

Introduction

This paper is a report of the results of experiments carried out for the purpose of utilizing the widely distributed kaolin clay as an aluminous material for the manufacture of expansive cement clinker.

When an alumina-rich material, such as bauxite, is used, the burning of expansive cement clinker is generally understood as a reaction of the CaO–Al_2O_3–SO_3 system. But, if the material used was comparatively rich in SiO_2, the behavior of the SiO_2 would present a problem, causing difficulties in manufacturing expansive cement clinker. Information is scarce on reactions of the CaO–SiO_2–Al_2O_3–SO_3 system, and reports on the effects of SiO_2 upon the formation of $C_4A_3(SO_3)$, a compound of the CaO–Al_2O_3–SO_3 system, are very few, except those by the present authors, (1) Fukuda and Kiyoku (2) and Budnikov et al (3). Thus, the knowledge pertaining to the use of clay as raw material has hitherto been very poor.

The authors pursued the behavior of SiO_2 in the clinker during the burning of limestone-clay-gypsum mixture, and established the optimum condition, such as the mixing ratio of raw materials and the burning temperature, for manufacturing expanisve cement clinker.

*Chichibu Cement Co., Ltd., Tokyo, Japan.

In the present paper, following notations are used:
E. C. clinker = Expansive cement clinker rich in SiO_2.
O. P. C. clinker = Ordinary portland cement clinker.

Experimental Procedures and Results

Raw Materials, Burning of Clinker and Measurement of Basic Length

In the present experiments, widely distributed kaolin clay, containing 40–45% SiO_2 and 24–30% Al_2O_3, was used as an aluminous material. As a limy material, limestone of a high purity was used, and chemical by-product gypsum was used as an SO_3 material. The gypsum contained about 0.5% P_2O_5. Clay, limestone and gypsum were mixed in the given proportion; the mixture was made into pellets of 10–15 mmϕ, which were burned in a small test rotary kiln at 1050–1300°C. The best temperature for burning varied with the mixing ratio of raw materials. The clinker for each test was pulverized into 3000–4000 cm^2/g of Blaine specific surface area. The clinker was more easily pulverized than the O.P.C. clinker. Chemical properties of the typical clays and the burned clinkers are given in Table 1.

The measurements of starting basic lengths in the expansion tests were all carried out on the test pieces immediately when they were demolded after one and half hours of their molding.

Mixing Ratio of Raw Materials and Mineralogical Composition of Clinker

The minerals formed in the clinker were identified by means of X-ray diffraction analysis. In the lime-rich mix proportion of raw materials, Al_2O_3 of the clinker occurred as $C_4A_3(SO_3)$ and calcium aluminoferrite, even when a large quantity of SiO_2 existed. In the lime-poor mix proportion, however, gehlenite C_2AS or anorthite CAS_2, both being unhydraulic compound, was formed, but occurrence of $C_4A_3(SO_3)$ was not recognized, in spite of the presence of abundant $CaSO_4$, as shown in Fig.1. In other words, E.C. cliker containing $C_4A_3(SO_3)$ was obtained when the chemical composition of the raw mix was more than 1.0 in the $CaCO_3/(Al_2O_3 + 2SiO_2 + 3Fe_2O_3)$ molar ratio; when the molar ratio was below 1.0, C_2AS or CAS_2 was formed and the obtained clinker was not expansive.

It was revealed that the SiO_2 component in the E.C. clinker, in which $C_4A_3(SO_3)$ is formed, occurs as β-C_2S or calcium silicosulphate, *i. e.*, a double salt of dicalcium silicate and $CaSO_4$. As will be mentioned later, the stable temperature range of calcium silicosulphate varies more or less with the condition of raw material mixing, but it was normally found that calcium silicosulphate is formed in the E.C. clinker burned at lower than 1150–1250°C, an when the burning temperature was higher than this, β-C_2S occurs. The chemical composition of this calcium silicosulphate was determined as $2(C_2S)\cdot CaSO_4$.

The calcium aluminoferrite that was formed in the E.C. clinker had the composition of $C_{10}A_2F_3$ which is somewhat Fe_2O_3-rich. Lime and gypsum, which did not contribute to the formation of $C_4A_3(SO_3)$, calcium aluminoferrite, β-C_2S or $2(C_2S)\cdot CaSO_4$, existed as free and unreacted CaO and β-$CaSO_4$. In the use of chemical by-product gypsum, containing a small quantity of P_2O_5, wilkeite $Ca_{10}O[(Si, S, P)O_4]_6$ was occasionally produced. Any aluminate phase, such as C_3A, $C_{12}A_7$ and CA, was not observed to form, and all Al_2O_3 was fixed as $C_4A_3(SO_3)$ and calcium

Table 1. *Chemical analyses of clays and clinkers.*

Analytical or calculated items (%)	Clay		Clinker*							
	1.	2.	1a.	1c.	2a.	2c.	3a.	3b.	4a.	4b.
SiO_2	41.7	44 1	12.0		11.1		11.1		10.5	
Al_2O_3	30.7	25.8	8.8		8.6		8.1		7 7	
Fe_2O_3	11.4	10.4	3.3		3.2		3.1		2.9	
Total CaO	0 6	0.9	48.8		50.1		52.3		54.3	
MgO	0.9	2.0	0.6		0 6		0.7		0.7	
SO_3	tr	tr	25.6		24.9		23.5		22.3	
$Na_2O + K_2O$	—	—	0.18		0.18		0.12		0.10	
ig. loss	14.8	16.1	0 2		0.2		0.4		0.6	
Total	100.1	99.3	99.5		99.5		99 3		99.1	
$C_4A_3(SO_3)$			9	9	8	8	8	8	8	8
$C_{10}A_2F_3$			15	15	14	14	14	14	13	13
$2(C_2S)\ CaSO_4$			48	0	47	0	44	0	42	0
β-C_2S			0	34	0	34	0	32	0	30
Free-CaO			0	0	3	3	8	8	12	12
Free-$CaSO_4$			27	40	26	39	24	37	23	35
Free $CaO/C_4A_3(SO_3)$ mol. ratio (n)			0	0	2	2	6	6	10	10
Free $CaSO_4/C_4A_3(SO_3)$ mol. ratio (m)			8	12	8	12	8	12	8	12

*Letters a, b and c represent the burning temperature of 1200, 1250 and 1300°C, respectively.

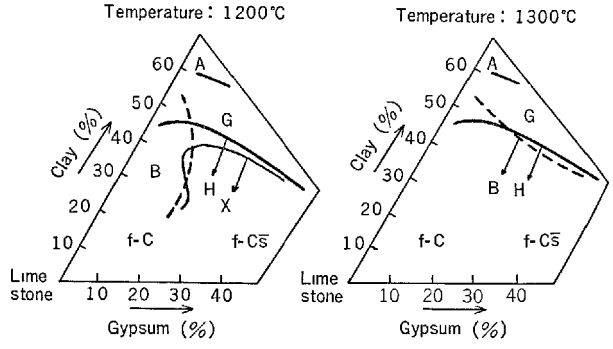

Fig. 1. *Mix proportion of raw materials and minerals formed in clinker. Abbreviation:* $A = CAS_2$; $G = C_2AS$; $H = C_4A_3(SO_3)$; $X = 2(C_2S)\cdot CaSO_4$; $B = \beta - C_2S$; $f-C =$ *free CaO;* $f-C\bar{s} =$ *free* $CaSO_4$.

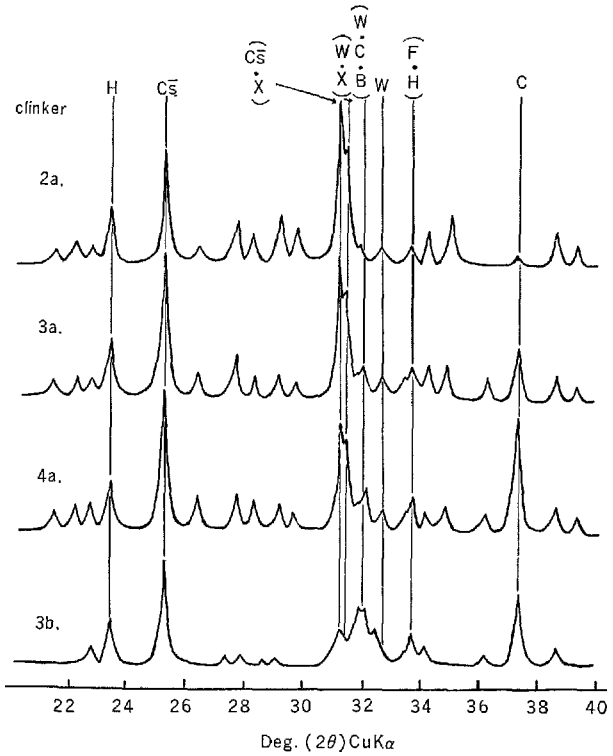

Fig. 2. *X-ray diffraction patterns of typical E.C. clinkers. Abbreviation: $H = C_4A_3(SO_3)$; $B = \beta - C_2S$; $C\bar{S} = CaSO_4$; $C = CaO$; $F = C_{10}A_2F_3$; $W =$ wilkeite $Ca_{10}O\cdot[(Si, S, P)O_4]_6$; $X = 2(C_2S)\cdot CaSO_4$.*

aluminoferrite.

Mixing Condition of Raw Materials for E.C. Clinker

As stated above, the constituent minerals of the E.C. clinker were chiefly $C_4A_3(SO_3)$, $2(C_2S)\cdot CaSO_4$ or β-C_2S, $C_{10}A_2F_3$ solid solution phase, free $CaSO_4$ and free CaO. Quantities of these minerals to be formed were dependent upon the chemical composition of clay and the consequent ratios of limestone, clay and gypsum, as well as upon the burning temperature. Quantities of the principal minerals to be fomed can be expressed by the following equations, taking the formation process of each mineral into consideration:

$$\%\, C_{10}A_2F_3 = 2.60 \times \%\,\overline{Fe_2O_3}$$

$$\%\, C_4A_3(SO_3) = 2.00 \times (\%\,\overline{Al_2O_3} - 0.426 \times \%\,\overline{Fe_2O_3})$$

$$\%\, 2(C_2S)\cdot CaSO_4 = 4.00 \times \%\,\overline{SiO_2}$$

$$\%\, \beta\text{-}C_2S = 2.87 \times \%\,\overline{SiO_2}$$

In the above, the mean chemical composition of the ferrite phase is represented by $C_{10}A_2F_3$; $\%\,\overline{SiO_2}$, $\%\,\overline{Al_2O_3}$ and $\%\,\overline{Fe_2O_3}$ are the contents of the respective components of the raw mix on the ignited base.

Based on these equation, the proportion of raw materials to be mixed, in order to obtain E.C. clinker having the aimed mineralogical composition, can be calculated by the equations given below. Assuming that the weight of clay is 100 on the dry base, $\%\,SiO_2$, $\%\,Al_2O_3$ and $\%\,Fe_2O_3$ as the respective contents in the clay, and the purity of limestone and gypsum as 100%, the following calculation is made:

$$\text{Clay (dry base)} = 100 \quad \ldots\ldots(1)$$

$$\text{Limestone (dry base)} = 1.78\{0.550(\%\,Al_2O_3 - 0.426 \times \%\,Fe_2O_3) + 1.17 \times \%\,Fe_2O_3 + 1.87 \times \%\,SiO_2 + n \times 0.183 \times (\%\,Al_2O_3 - 0.426 \times \%\,Fe_2O_3)\} \quad \ldots\ldots(2)$$

$$\text{Gypsum (dry base)} = 1.13\{0.445(\%\,Al_2O_3 - 0.426 \times \%\,Fe_2O_3) + 1.13 \times \%\,SiO_2^* \times m \times 0.445(\%\,Al_2O_3 - 0.426 \times \%\,Fe_2O_3)\} \quad \ldots\ldots(3)$$

The term marked with asterisk is the quantity of gypsum consumed in formaton of $2(C_2S)\cdot CaSO_4$. Since the SiO_2 in the E.C. clinker burned at high temperature occurs as β-C_2S. the quantity of consumed gypsum was unnecessary to consider. Coefficients m and n represent the molar ratio of free $CaSO_4$ and free CaO, which are to be retained in the E.C. clinker to the quantity of $C_4A_3(SO_3)$ to be formed. As will be mentioned later, the molar ratio is an important factor to control the expansibility of E.C. clinker.

This calculation of the proportion of raw materials to be mixed was an approximate calculation, ignoring SiO_2, Al_2O_3, Fe_2O_3 and P_2O_3 of small quantities existing in limestone and gypsum, and also ignoring TiO_2 and other components contained in clay. It was revealed that in the use of a SiO_2-rich clay, careful attention should be paid to the mixing ratio of raw materials, since an inadequate proportion would cause formation of C_2AS or CAS_2, resulting in unexpansive, poorly hydraulic clinker.

Properties of $2(C_2S)\cdot CaSO_4$

The result of synthesis test on pure chemicals showed that calcium silicosulphate which is formed in E.C. clinker is a double salt of dicalcium silicate and calcium sulphate, having the chemical composition of $2(C_2S)\cdot CaSO_4$. In preparing the synthetic, the prescribed mixture of chemicals was placed in the air-tight platinum capsule, and was heated in the electric furnace at 1170°C for 300 hours. The synthe-

sized material took the form of light green prismatic crystals, the growth of which was slow and the maximum length attained to only 30–40μ. The result of X-ray diffraction analysis showed that this synthetic smaple was identical with the $2(C_2S)\cdot CaSO_4$ phase to be formed in E.C. clinker, without any great differences in X-ray patterns. Table 2 is X-ray powder data of the purely synthetic $2(C_2S)\cdot CaSO_4$.

In the pure synthesis from $CaCO_3$, SiO_2 and $CaSO_4$, this compound was formed in the region of $CaCO_3/2SiO_2$ molar ratio ≥ 1. In the region of $CaCO_3/2SiO_2$ molar ratio < 1, volatilization of SO_3 occurred and formation of rankinite C_3S_2 or pseudowollastonite α-CS was observed. In the case of $CaCO_3/2SiO_2$ molar ratio ≥ 1, volatilization of SO_3 was scarce at temperature below 1250°C, and decomposition of excessive $CaSO_4$, which remained after the formation of $2(C_2S)\cdot CaSO_4$, was not particularly accelerated.

The results of DTA and high-temperature X-ray analysis revealed that pure $2(C_2S)\cdot CaSO_4$ was decomposed at about 1285°C, and after cooling down to room temperature it was recognized as β-C_2S and β-$CaSO_4$. When β-C_2S and β-$CaSO_4$, which are the products of decomposition, were heated they combined with each other again and formed $2C_2S\cdot CaSO_4$. The DTA curve of $2(C_2S)\cdot CaSO_4$ showed a large endothermic peak starting at about 1285°C and a small endothermic peak above 1300°C, as illustrated in Fig. 3. In synthesizing $2(C_2S)\cdot CaSO_4$ from $CaCO_3$, SiO_2 and $CaSO_4$, formation of $2(C_2S)\cdot CaSO_4$ progressed rapidly from about 1220°C and large endothermic peak starting at this temperature was observed in DTA.

The heat of hydration of purely synthetic $2(C_2S)\cdot CaSO_4$ was measured with a twin type conduction calorimeter and by the heat of solution method. The obtained value was somewhat lower than that of β-C_2S and slightly higher than that of a $2(\beta\text{-}C_2S) + CaSO_4$ mixture. $2(C_2S)\cdot CaSO_4$ is slow in the rate of hydration and is poorly hydraulic. It was noticed that extrication of SO_4^{2-} into liquid phase due to hydration is difficult to take place. Table 3 shows the heats of hydration of $2(C_2S)\cdot CaSO_4$ and β-C_2S.

Table 2. *X-ray powder data of synthetic* $2(C_2S)\cdot CaSO_4$

d(Å)	Int.	d(Å)	Int.	d(Å)	Int.	d(Å)	Int.
8.60	5	2.998	15	2.204	5	1.775	5
8.49	10	2.984	15	2.173	15	1.756	10
7.87	5	2.952	3	2.139	3	1.745	3
7.70	10	2.898	3	2.12	3(b)	1.742	3
5.68	5	2.848	100	2.08	3(b)	1.711	3
5.34	5	2.827	100	2.062	5	1.699	15
4.60	1	2.802	3	2.024	5	1.678	3
4.57	15	2.774	5	2.018	10	1.671	5
4.24	5	2.743	5	1.962	15	1.617	5
4.08	15	2.706	5	1.952	5	1.613	5
3.94	20	2.618	30	1.927	5(b)	1.598	3
3.84	5	2.568	50	1.897	15	1.593	3
3.61	5	2.546	3	1.893	30	1.579	3
3.36	3(b)	2.486	5	1.880	3	1.565	3
3.34	20	2.406	15	1.851	3	1.554	3
3.31	5	2.386	5	1.846	3		
3.19	40	2.356	5	1.839	5		
3.15	3	2.290	10	1.824	5		
3.12	20	2.286	10	1.807	5		
3.04	20	2.234	5	1.783	5		

Burning Temperature and Fusibility of E.C. Clinker

The degree of sintering was found to be dependent upon the mixing ratio of raw materials as well as upon the burning temperature. In a mixture where free CaO and free $CaSO_4$ remain abundantly, the E.C. clinker began to fuse at a relatively low temperature. The temperature of decomposition of $2(C_2S)\cdot CaSO_4$ in the clinker was lower than that of a purely synthetic sample, and the decomosing temperature was dependent upon the value of n in equation (2).

From the measurement by DTA, the following result was obtained: When $n = 0$ the decomposing temperature of $2(C_2S)\cdot CaSO_4$ was 1250–1260°C, whereas in the case of $n = 3 - 8$ the decomposing temperature lowered by 20–30°C. Fig. 3 shows the relation between the value of n and the temperature of endothermic peak due to decomposition of $2(C_2S)\cdot CaSO_4$. When the temperature was high, $CaSO_4$ was extricated due to decomposition of $2(C_2S)\cdot CaSO_4$. Therefore, the content of free $CaSO_4$ in the E.C. clinker increased, and SiO_2 occurred as β-C_2S.

Fusibility of E.C. clinker in burning process became a problem from about 1220°C. When the raw mix is such that enables much of free CaO and free $CaSO_4$ to remain in the E.C. clinker, fusion occurs easily even if the burning temperature is low, so that the E.C. clinker is apt to agglutinate during the burning. The variations of raw mix during the burning were studied by means of DTA and TGA, and an endothermic reaction was observed to start at about 1120–1150°C. The quantity of endothermal heat at this temperature increased when the value of m in equation (3) became larger. During this endothermic period the E.C. clinker was sintered, and the degree of

Table 3. *Heat of hydration of* $2(C_2S)\cdot CaSO_4$ *and* $\beta - C_2S$.

Time (day)	Heat of hydration (cal/g)		
	$2(C_2S)\cdot CaSO_4$	β-C_2S	$2(\beta\text{-}C_2S) + CaSO_4$
1	1.8	3.0	2.8
3	2.5	8.6	9.3
7	6.5	9.6	12.2
28	16.2	25.9	20.2
91	29.6	36.5	30.0
150	39.0	41.7	34.8

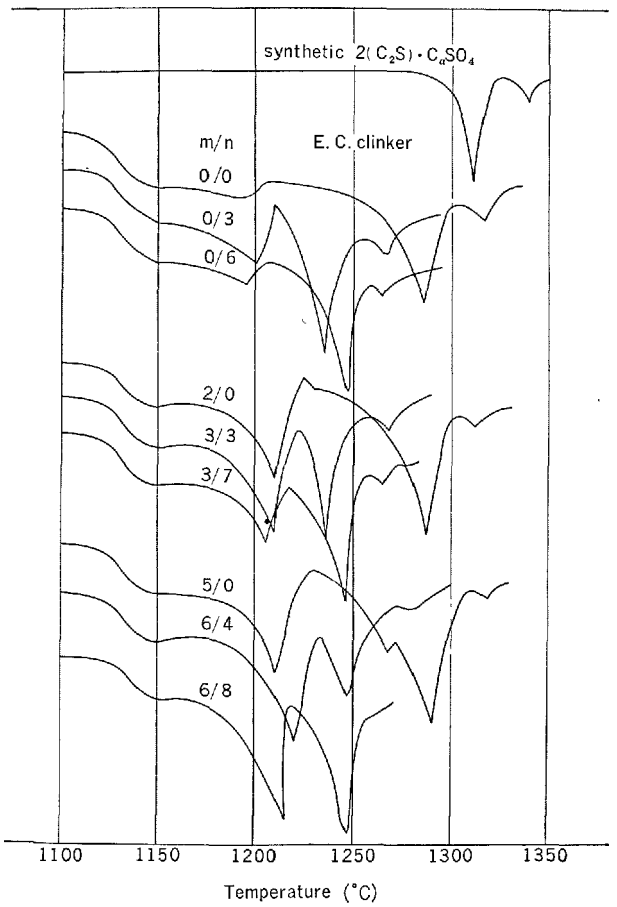

Fig. 3. *Thermograms of synthetic $2(C_2S)\cdot CaSO_4$ and E.C. clinkers.*

sintering was higher with larger quantity of endothermal heat. When later endothermic reactions took place accompanying decomposition of $2(C_2S)\cdot CaSO_4$, the E.C. clinker became much better sintered, and especially when the value of n was large the clinker began to fuse.

Microstructure of E.C. Clinker

The internal structure of E.C. clinker was examined with the optical microscope and the electron probe X-ray microanalyzer. The E.C. clinker burned at temperatures lower than 1100°C was low in the degree of sintering, and the minerals formed in burning were so fine-grained that it was difficult to identify them under the optical microscope.

In the E.C. clinker which was sintered better at 1150–1200°C, the principal minerals $C_4A_3(SO_3)$ and $2(C_2S)\cdot CaSO_4$ were recognized, but the size of crystals was still small, about 5–10μ. $C_4A_3(SO_3)$ was enclosed by $2(C_2S)\cdot CaSO_4$ of the small prismatic crystals

Table 4. *Relation between mix proportion of raw materials and degree of sintering.*

Sample No.	m	n	Burning temperature (°C) 1100	1150	1200	1250	1300
1	0	0	x	x	x	o	o
2	0	3	x	x	o	o	◎
3	0	6	x	x	o	o	F
4	2	0	x	x	o	o	◎
5	3	3	x	x	o	◎	F
6	3	7	x	x	o	◎	F
7	5	0	x	o	o	o	F
8	6	4	x	o	o	F	F
9	6	8	x	o	o	F	F

Note. The degrees of sintering are as follows: X, insufficiently sintered, o, well-sintered; ◎, partly fused, F, completely fused.

and both were included in $CaSO_4$ which, under crossed niclos, could be seen to exist as large crystals of euhedral. However, by observation with reflected light on the polished surface etched with a solution of HNO_3 in alcohol, $CaSO_4$ was recognized as an irregular-shaped phase, without showing any distinct outline of crystals. In the case of fused clinker, in particular, $CaSO_4$ was found to enclose more tightly the $C_4A_3(SO_3)$ and other compounds. In the E.C. clinker burned at temperatures below 1200°C, the ferrite phase had the appearance of groups of minute crystals, but in the fused clinker it was dispersed chiefly in irregular shapes.

In the E.C. clinker sintered well or in the fused clikner, CaO occurs as groups of relatively large crystals. The CaO is surrounded chiefly by $CaSO_4$, and in many cases it does not contact directly with $C_4A_3(SO_3)$, $2(C_2S)\cdot CaSO_4$ or β-C_2S. β-C_2S, produced by decomposition of $2(C_2S)\cdot CaSO_4$, occurred as fine grains at the outset, but it gradually grew larger and finally became globular. As the $2(C_2S)\cdot CaSO_4$ in the E.C. clinker can be colored blue or reddish brown with HNO_3, its identification was easy.

Expansibility of $C_4A_3(SO_3)$

In order to know the characteristic of expansion of SiO_2–rich E.C. clinker, the expansion behavior of mixtures of $C_4A_3(SO_3)$, $Ca(OH)_2$ and $CaSO_4$ was examined as a first step, by making them into paste of W/solid = 0.5, which was kept under air-tight condition at 20°C, and were measured the changes in length. Expansion of $C_4A_3(SO_3)$ occurred only when ettringite was formed, and shrinkage was noticed when other calcium aluminate hydrates, such as calcium monosulphoaluminate hydrate and $C_4A_3\cdot CaSO_4\cdot 18H_2O$ (M phase) (5), were formed. The condition of formation of ettringite from $C_4A_3(SO_3)$ in hydration of pure mixture of $C_4A_3(SO_3)$–$Ca(OH)_2$–$CaSO_4$ system seemed to be dependent upon concentration of SO_4^{2-}

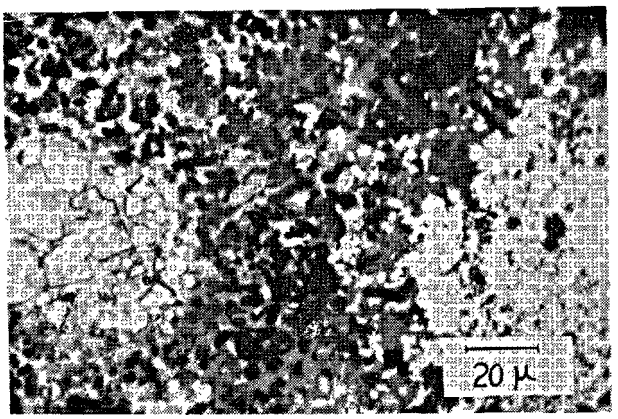

(1)

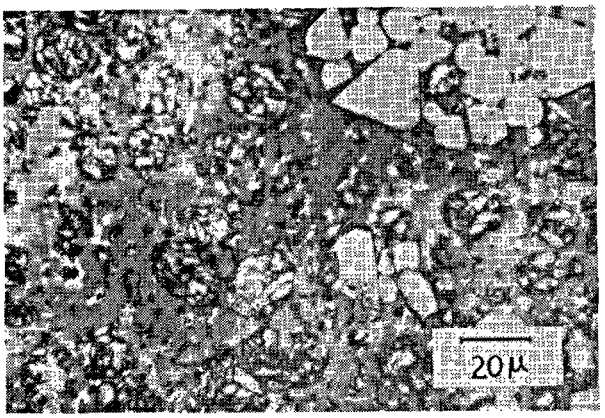

(2)

Fig. 4-1. *Microstructure of E.C. clinkers. Etched with 2% HNO_3 in alcohol. Reflected light. (1) E.C. clinker-4a; (2) E.C. clinker-4b.*

ions around $C_4A_3(SO_3)$, irrespective of existence or absence of $Ca(OH)_2$. With the presence of sufficient SO_4^{2-} ions, ettringite was readily formed and remained stable. When unhydrated $C_4A_3(SO_3)$ remained and SO_4^{2-} ion concentration lowered below a certain value, calcium monosulphoaluminate hydrate, M phase and other calcium aluminate hydrates were formed.

The reaction by which ettringite is formed out of $C_4A_3(SO_3)$ can be expressed stoichiometrically as follows:

$$C_4A_3(SO_3) + 2CaSO_4 \xrightarrow{aq} C_3A \cdot 3CaSO_4 \cdot 32H_2O + 2AH_3 \quad \ldots\ldots(4)$$

$$C_4A_3(SO_3) + 6Ca(OH)_2 + 8CaSO_4 \xrightarrow{aq} 3C_3A \cdot 3CaSO_4 \cdot 32H_2O \quad \ldots\ldots(5)$$

Owing to the presence of $Ca(OH)_2$, the reaction of (5) proceeds in $C_4A_3(SO_3)$, prior to the reaction of (4). The reaction of (5) was active for several hours after water-pouring, and a large quantity of ettringite was crystallized out rapidly, thus giving rise to quick setting and exothermal phenomenon. When $Ca(OH)_2$ was absent, as exemplified by equation (4), there was a tendency that, after the dormant period of several hours after water-pouring, the reaction progressed rapidly and ettringite crystallized out.

It was revealed, however, that the expansion of pure mixture of the $C_4A_3(SO_3)$–$Ca(OH)_2$–$CaSO_4$ system was not necessarily dependent upon the amount of ettringite that was formed. Under the condition shown in Fig. 5-1, where $CaSO_4$ is sufficient ($m = 8$) and only ettringite is formed, the volume of expansion increased with increasing amount of $Ca(OH)_2$ existing simultaneously. When $Ca(OH)_2$ was not added ($n = 0$), formation of ettringite was observed but it was not accompained by expansion.

Successive processes of expansion of $C_4A_3(SO_3)$–$Ca(OH)_2$–$CaSO_4$ system (W/solid = 5.0) at 20°C were studied under the optical microscope, and it was noticed that ettringite was largely developed in the form of acicular crystals when Ca^{2+} ions were relatively scarce. Especially in the case of low concentration of Ca^{2+} ions, as represented by equation (4), formation of ettringite occurred following the solution of unhydrated particles, and ettringite took the form of relatively large crystals in the liquid phase (Fig. 6-(1), (2)). Under high concentration of Ca^{2+} ions, ettringite crystallized as fine grians, coating the surface of $C_4A_3(SO_3)$ particles. This coating develops with progress of hydration, and begins to act on the adjacent particles (Fig. 6-(3), (4)).

The pure mixture of $C_4A_3(SO_3)$–$Ca(OH)_2$–$CaSO_4$ was intermixed with powder of O.P.C. clinker and made into neat paste of expansive cement (W/C = 0.25). Then, the paste was shut off from the air by a vinyl sheet, and its expansion behavior under the sealed condition was studied. It was recognized that, within an hour after water-pouring and kneading, the paste began to set and harden, and continued to expand for more than ten hours. In this early stage reaction, however, the expansion of the pure mixture of $C_4A_3(SO_3)$–$Ca(OH)_2$–$CaSO_4$ was different from that of the pure mixture of ($C_4A_3(SO_3)$–$Ca(OH)_2$–$CaSO_4$) + O.P.C. clinker powder. In the former, expansion attained to maximum when $n = 6$ or larger, whereas the latter's expansion was larger when $n = 2$ than when $n = 6$, and even when $n = 0$ it continued to expand for several hours after hardening. The result is shown in Fig. 5-2.

Expansibility of E.C. Clinker

The rate of expansion of E.C. clinker powder due to

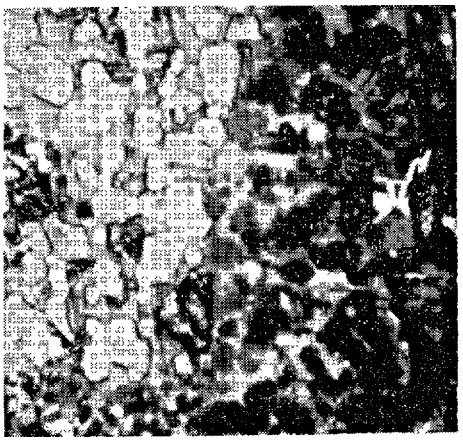

(1)

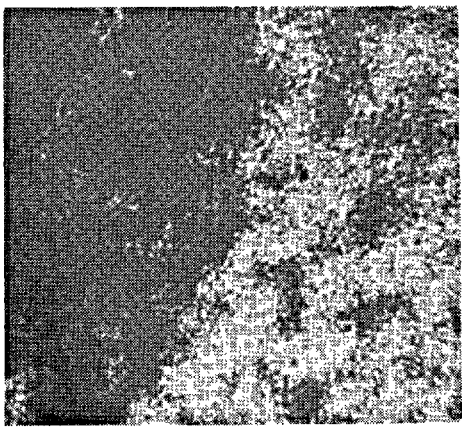

(4)

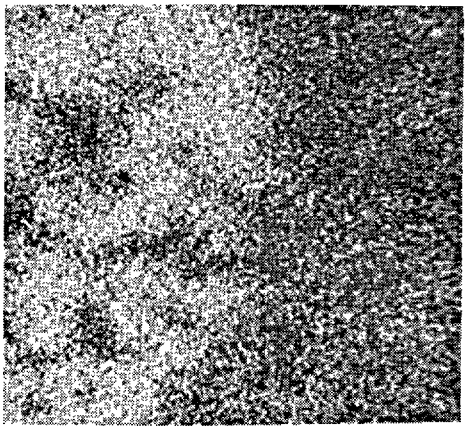

(2)

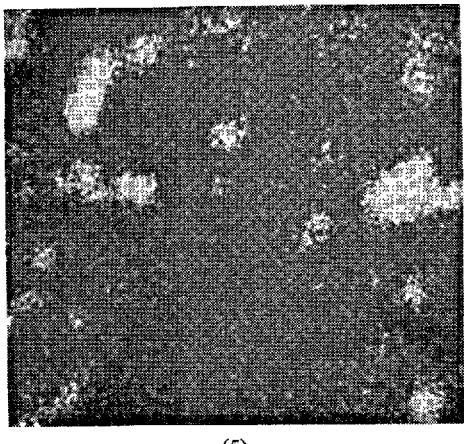

(5)

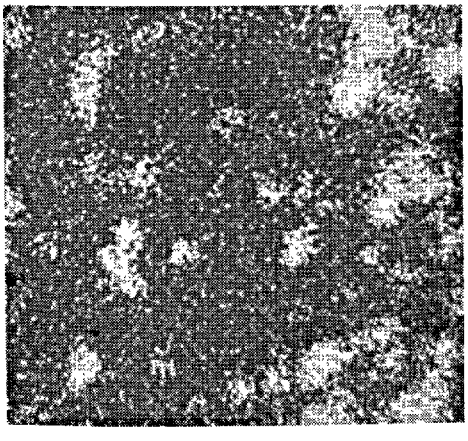

(3)

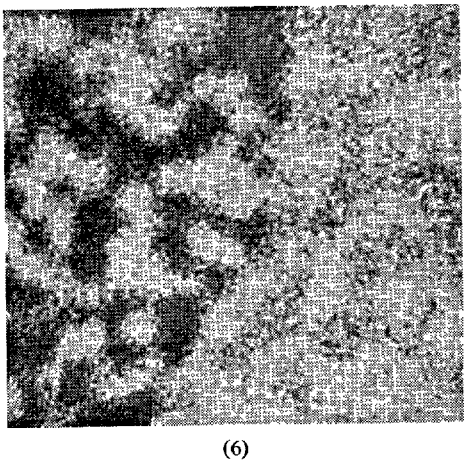

(6)

Fig. 4-2. *Electron probe results for a polished surface of E.C. clinker-4a. (1) Optical micrograph; (2)–(6) Characteristic X-ray images for (2) CaKα, (3) AlKα (4) SiKα, (5) FeKα (6) SKα.*

(1)

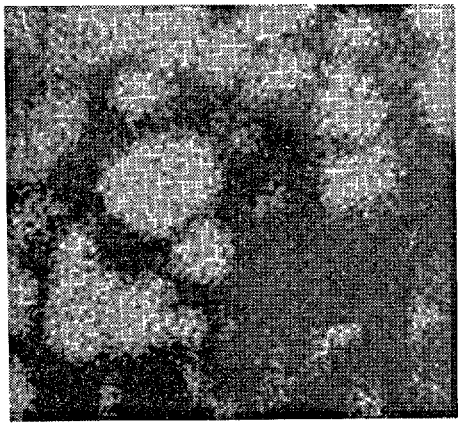

(4)

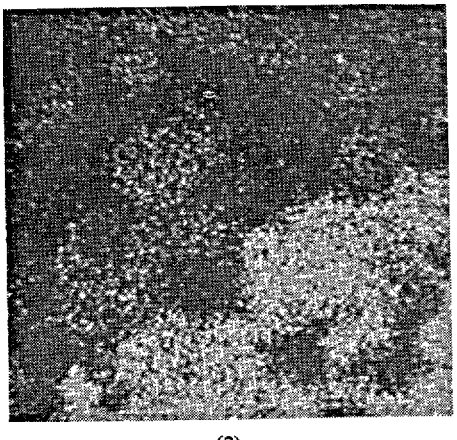

(2)

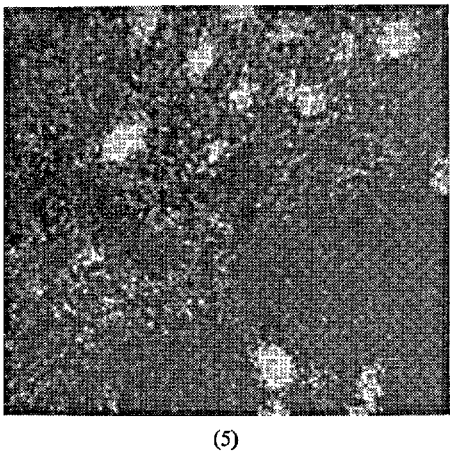

(5)

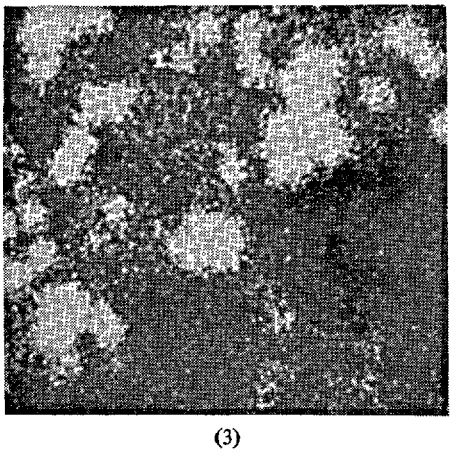

(3)

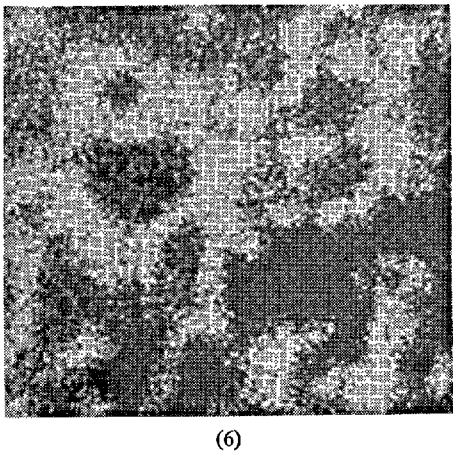

(6)

Fig. 4-3. *Electron proble results for a polished surface of E.C. clinker-4b. (1) Optical micrograph; (2)–(6) Characteristic X-ray images for (2) CaKα, (3) AlKα, (4) SiKα, (5) FeKα, (6) SKα.*

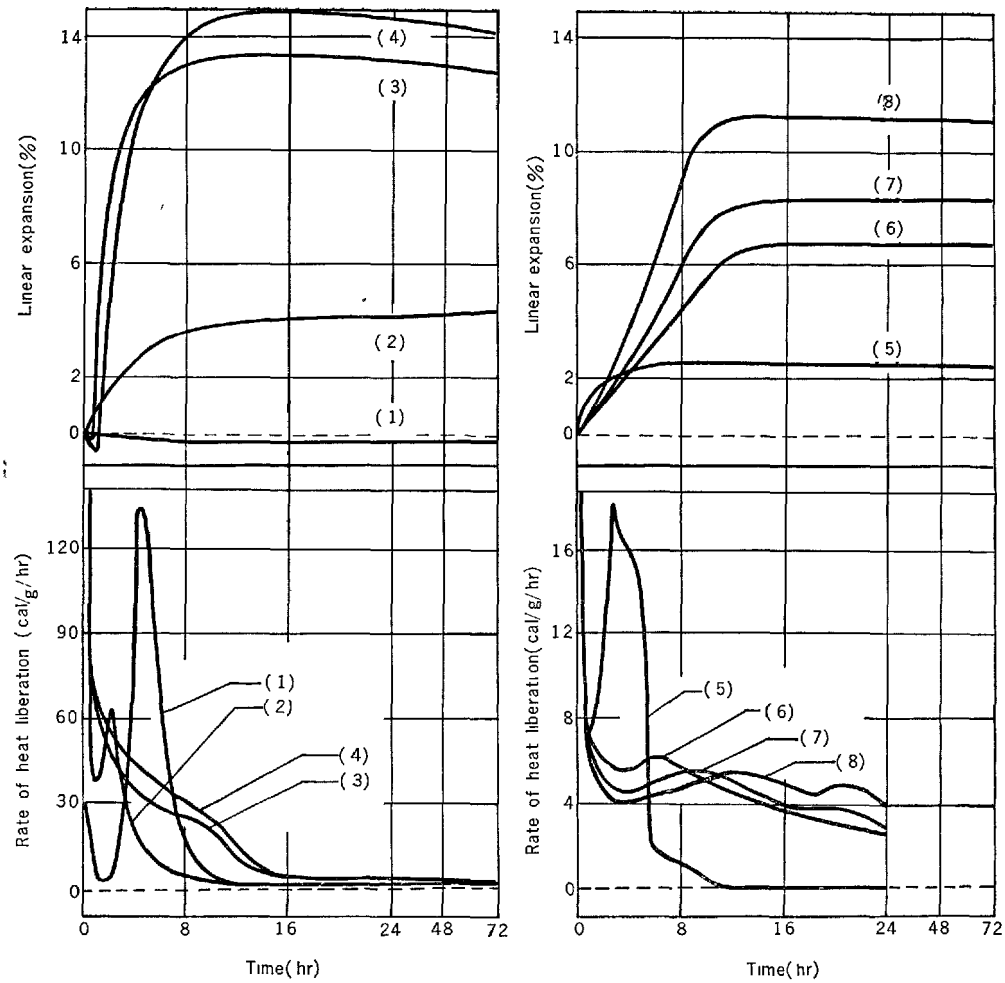

Fig. 5. *Expansibility and rate of hydration of pure $C_4A_3(SO_3)$–$CaSO_4$–$Ca(OH)_2$ mixture as a function of $Ca(OH)_2$ content. (1) $C_4A_3(SO_3) + 8CaSO_4$; (2) $C_4A_3(SO_3) + 8CaSO_4 + 2Ca(OH)_2$; (3) $C_4A_3(SO_3) + 8CaSO_4 + 6Ca(OH)_2$; (4) $C_4A_3(SO_3) + 8CaSO_4 + 10Ca(OH)_2$; (5)–(8) Prepared expansive cements containing 30% of (1)–(4), respectively.*

hydration was considerably slower than that of pure mixture of the $C_4A_3(SO_3)$–$Ca(OH)_2$–$CaSO_4$ system. But, the relation between the expansibility and the quantitative proportion of $C_4A_3(SO_3)$, free CaO and free $CaSO_4$ in the E.C. clinker was similar to that of the pure mixture shown in Fig. 5-1. In general, the expansibility of E.C. clinker was better when a large quantity of $C_4A_3(SO_3)$ was poduced, with $m = 8$ and $n \geq 6$. As indicated by Fig. 8, the SO_3 component in $2(C_2S)\cdot CaSO_4$ contributed very little to the initial expansion.

Using the paste (W/C = 0.25) of a powder mixture of E.C. clinker + O.P.C. clinker, its unrestrained expansion under sealed condition at 20°C was measured (Fig. 7-2), and it was noticed that the expansion started at about the time the paste began to set and harden. The expansibility after hardening was chiefly influenced by the mineralogical composition and hydration behavior of the E.C. clinker, the amount of added E.C. clinker, the amount of mixing water, the curing condition, and by other materials that were added.

The hydration behavior of the clinker was influenced not only by the fineness but also by the amount of free CaO (n-value) against $C_4A_3(SO_3)$ in the clinker, so that the rate of expansion increased as the value of n became larger. In the case of free CaO = 0 (n = 0), expansion was also due to the presence of $Ca(OH)_2$, which was formed by hydration of the O.P.C. clinker, after the paste had set and hardened.

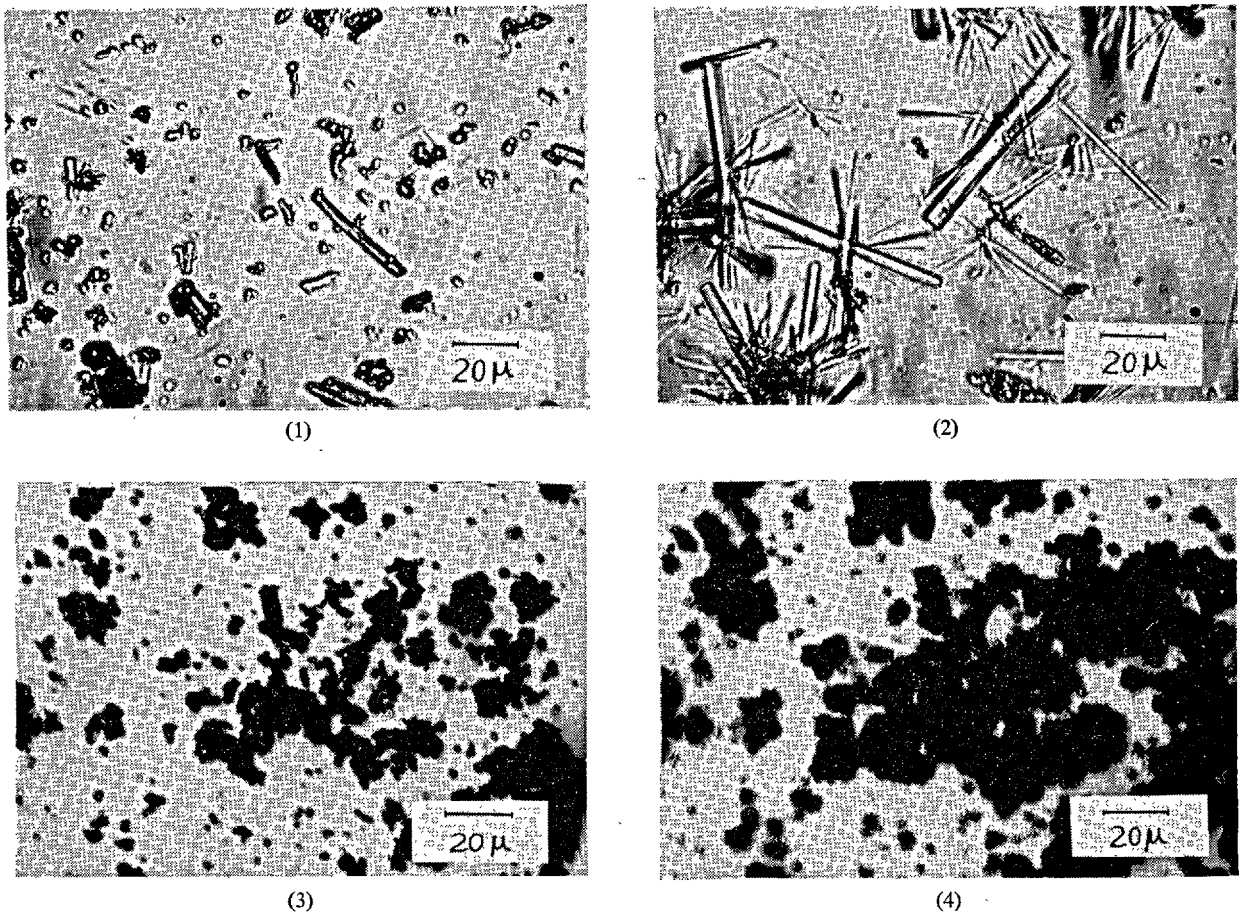

(1) (2)

(3) (4)

Fig. 6. *Types of ettringite formation due to hydration of* $C_4A_3(SO_3)$. *Hydration at 20°C. Ordinary transmitted light. (1)* $C_4A_3(SO_3) + 3CaSO_4$, *hydrated for 1 hr; (2) Same field as (1), hydrated for 7 hrs; (3)* $C_4A_3(SO_3) + 8CaSO_4 + 6Ca(OH)_2$, *hydrated for 10 min; (4) Same field as (3), hydrated for 7 hrs.*

But, the effect diminished as the hardening of the paste advanced, and after two days it contributed very little to expansion, even in the water curing.

Compared with the sealed curing, the water curing showed better expansion after one to two days, and the larger the value of n the more effective. With increasing fineness of E.C. clinker, the hydraion reaction became intense right after the kneading, and expansion was remarkable for 24 hours after setting and hardening, but after one day the expansibility became somewhat lower. Fig. 9 shows an example of the relation between the expansibility and the amount of intermixed E.C. clinker.

Effects of Burning Temperature on the Expansibility of E.C. Clinker

Degree of sintering of E.C. clinker at any temperature was dependent upon the value of m and n, if the materials used were identical, as mentioned already. In the E.C. clinker made of the same materials and with definite values of m and n, the expansibility due to hydration was influenced by the degree of sintering, *i.e.*, burning temperature. The relation is shown in Fig. 10, taking an example of clinker-4. Hydration of the E.C. clinker with the same fineness became lower as the burning temperature rose. In the fused clinker (corresponding to a clinker in which $2(C_2S)\cdot CaSO_4$ was decomposed, when n is large), the rate of expansion was much slower.

By the apparent degree of sintering, the E.C. clinker was divided into three stages; (a) insufficient-sintered clinker (clinker burned at about 1050–1100°C), (b) well-sintered clinker (clinker burned at about 1150–1200°C), and (c) fused clinker (burned above 1220°C). The E.C. clinker of stage (a) began to expand imme-

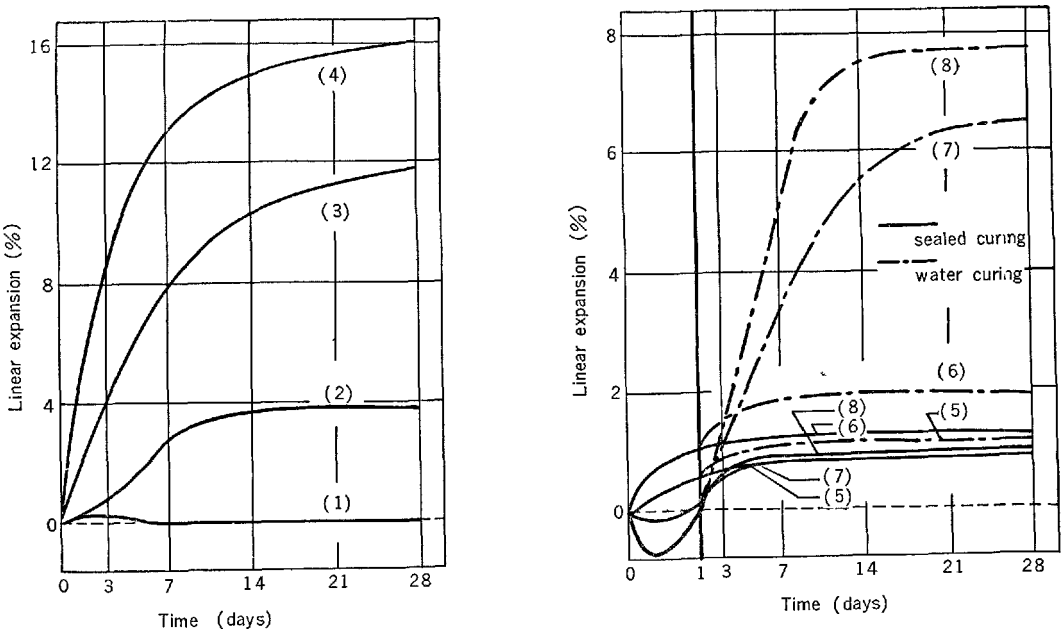

Fig. 7. *Expansibilities of E.C. clinkers and prepared expansive cements. W/C = 0.25, 20°C curing. (1) E.C. clinker-1a; (2) E.C. clinker-2a; (3) E.C. clinker-3a; (4) E.C. clinker-4a; (5)–(8) Prepared expansive cements containing 25% of (1)–(4), respectively.*

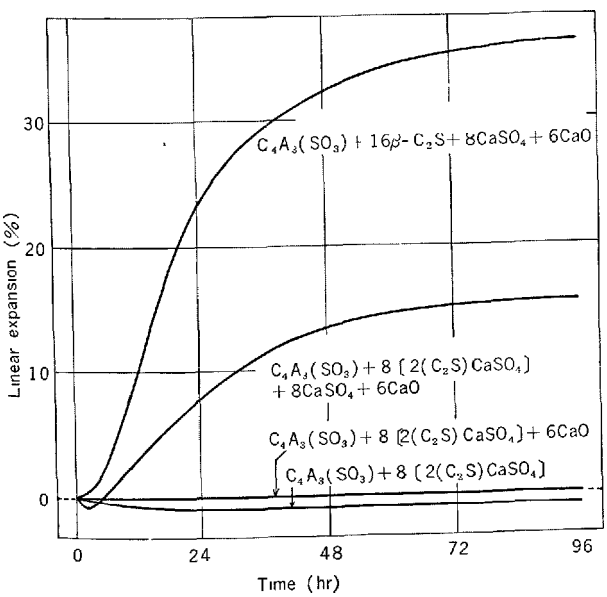

Fig. 8. *Effect of $2(C_2S)\cdot CaSO_4$ on expansion due to hydration of $C_4A_3(SO_3)$.*

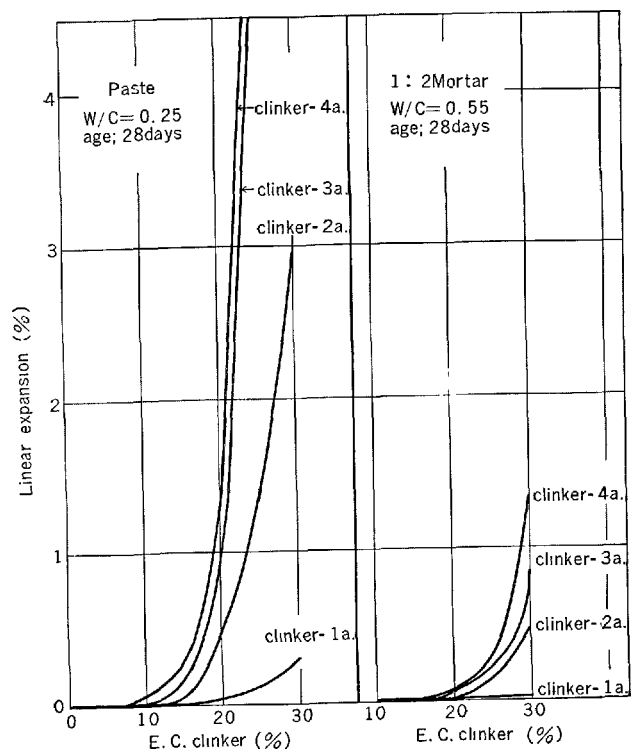

Fig. 9. *Amount of E.C. clinker intermixed and expansibility of prepared cement.*

diately after setting and hardening, and the expansion was almost completed within 24 hours in the sealed curing. After that, it showed little expansion even in the water curing. The E.C. clinker of (b) began to expand gradually after several hours since setting and hardening. After 24 hours the rate of expansion in the sealed curing was slow, but in the water curing the

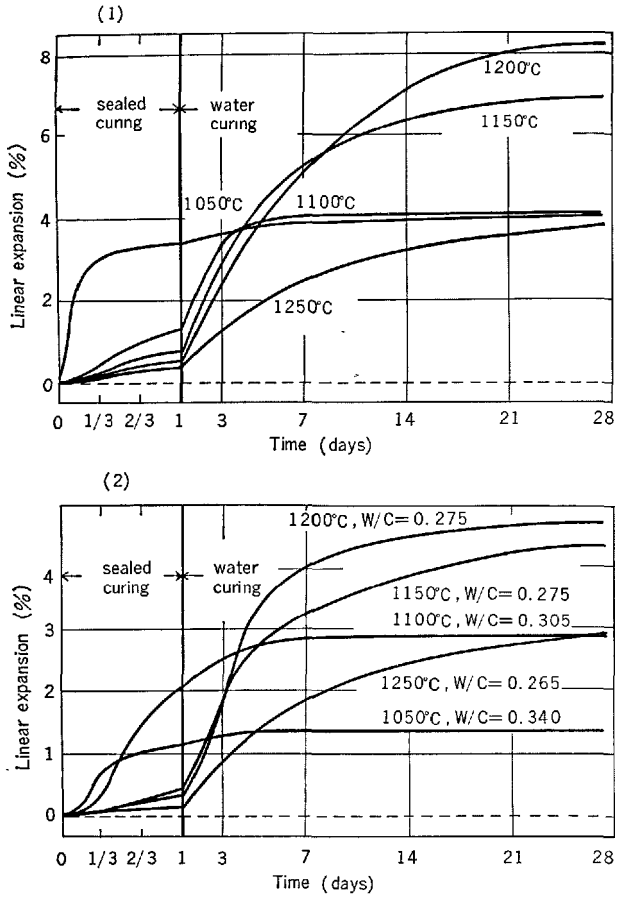

Fig. 10. *Burning temperatures of E.C. clinker and expansibility of prepared cements. E.C. clinker-4, 20°C curing. (1) W/C = 0.25; (2) Normal consistency.*

expansion became much better and was completed in a relatively short time. In the E.C. clinker of (c), the rate of expansion even in the water curing was slower than (b), and it took a long time to complete the expansion.

In the clinker of (a), the grains of produced minerals were very fine on account of the low degree of sintering, and the clinker was porous or fragile. In (b), the sintering is better so that relatively well developed crystals of $C_4A_3(SO_3)$ and $2(C_2S)\cdot CaSO_4$ were seen. The clinker of (c) was in a fused state as decomposition of $2(C_2S)\cdot CaSO_4$ occurred, and the clinker was characteristically dense in texture.

Effects of Gypsum and Blast-Furnace Slag Added to Prepared Expansive Cement

Setting of the experimentally prepared expansive cement was fairly quick, and the setting became quicker with increase in the added amount of E.C. clinker.

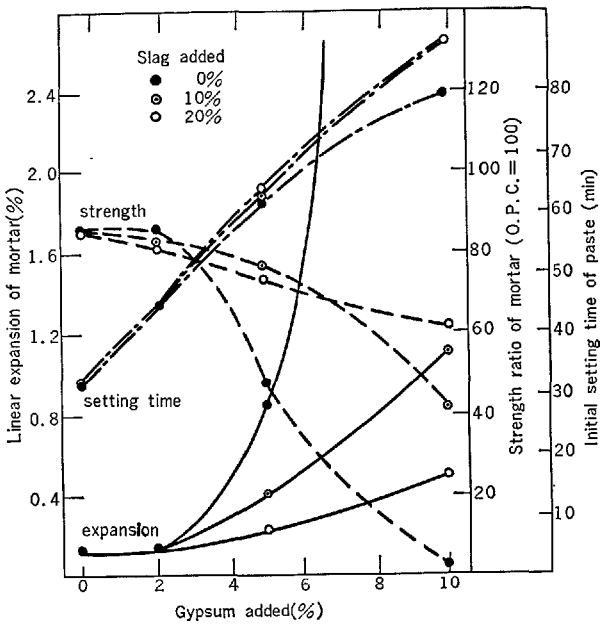

Fig. 11. *Effects of gypsum and blast-furnace slag on property of prepared cement. Mortar: 1: 2 cement-sand, W/C = 0.65, mold storage 24 hrs, 20°C water curing. Paste: normal consistency.*

To retard the setting, addition of gypsum proved effective. However, more than 2% addition of gypsum caused abnormal expansion and, at the same time, the cement strength was lowered. This enormous expansion and the lowering of cement strength were prevented by adding the blast furnace slag, without obstructing the setting retardation effect of gypsum. These cases are illustrated in Fig. 11.

Relation Between the Amount of Absorbed Water and Expansion of the Prepared Expansive Cement

In general, the expansibility of expansive cement after hardening was larger in the water curing or moist curing than in the dry curing. The characteristic of such expansion was that the volume expansion of the test piece was in a linear relation with the amount of water absorbed, as expressed by the following equation, denoting the increased volume by $(1 + \Delta l)^3$ and the total amount of absorbed water by ΔW (%):

$$(1 + \Delta l)^3 = a(\Delta W - \mu) \quad \ldots\ldots\ldots (6)$$

where Δl is the change in length (m/m) and μ is the amount (%) of absorbed water unrelated to the expansion. Using the paste in the range of W/C = 0.23 – 0.32, which was molded under restraining condition in the moist curing for one day, the expansion in the

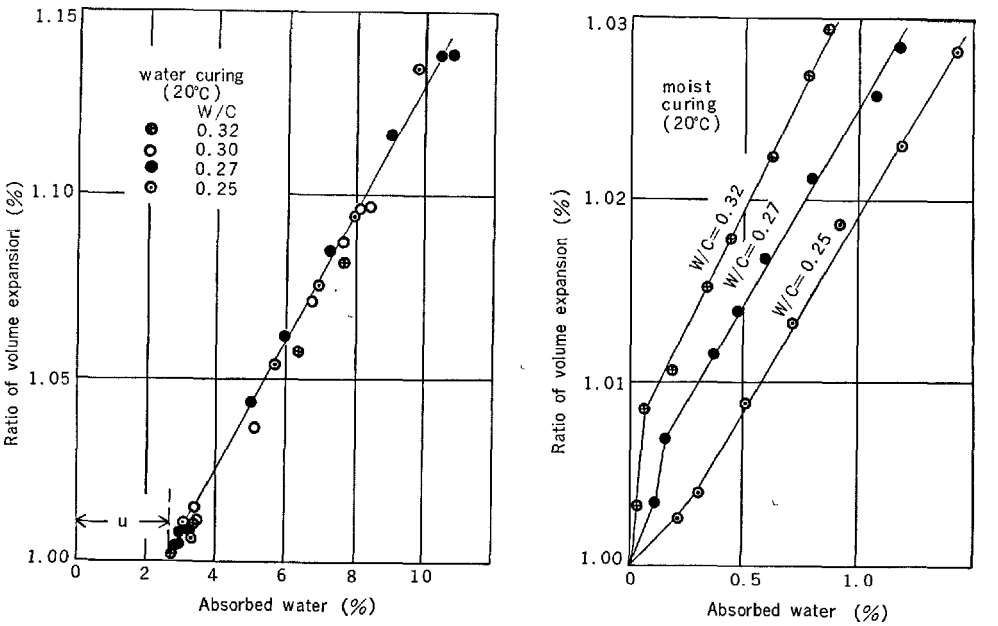

Fig. 12. *Amount of absorbed water and ratio of volume expansion.*

later water curing was measured and a linear relation as expressed by (6) was obtained, irrespective of the amount of water used in kneading.

In the moist curing with 90% in relative humidity, the paste absorbed moisture also from the air and showed expansion, but the mode of expansion varied with the amount of water used in kneading. In the case of the sealed curing or dry curing, where moisture cannot be supplied from outside, the paste expanded for one or two days, but later the expansion became very small even by the use of the E.C. clinker having a large value of n.

Discussion

Mineralogical Composition of E.C. Clinker

Even when the SiO_2-rich aluminous material was used, there was a region in which $C_4A_3(SO_3)$ can be formed stably if the mixing ratio of limestone and gypsum was appropriate. Within this region no other calcium aluminates, such as C_3A, $C_{12}A_7$ and CA, are coexistent. This is probably on account of the presence of gypsum. C_3S, too, is not produced on account of the presence of a large quantity of gypsum.

$2(C_2S)\cdot CaSO_4$ was the only compound of the CaO–SiO_2–SO_3 system, and no other three-component compounds were found to exist at normal temperature. Gutt and Smith (4) also synthesized this compound and reported its X-ray diffraction data. In the E.C. clinker, $C_4A_3(SO_3)$ is easier to form than $2(C_2S)\cdot CaSO_4$, so that the formation of the former seems not to be obstructed by the latter.

Expansibility of E.C. Clinker

The initial hydration of E.C. clinker is controlled chiefly by the content of $C_4A_3(SO_3)$ and by the ratios of $CaSO_4$ and CaO to the former. $2(C_2S)\cdot CaSO_4$ contributes very little to expansion. This was becuse SO_4^{2-} ions were not liberated into liquid phase in the early stage, on account of the slow rate of hydration of $2(C_2S)\cdot CaSO_4$. Accordingly, by raising the burning temperature to let the SiO_2 component occur as β-C_2S, without fixing it as $2(C_2S)\cdot CaSO_4$, an E.C. clinker having the same value of m can be obtained even when the amount of $CaSO_4$ was small in mixing the raw materials at the outset. Thus, the relative content of $C_4A_3(SO_3)$ would become larger and the expansibility should turn better. However, in high temperature burning, which allows β-C_2S to exist, the E.C. clinker is easy to fuse, and the internal structure of the

clinker becomes dense, retarding the rate of expansion.

Expansion of $C_4A_3(SO_3)$ due to hydration depends upon the type of formation of ettringite. The variance of the type of formation of ettringite according to the concentration of Ca^{2+} ions is not discontinuous; the type is considered to change successively, depending on the degree of concentration of Ca^{2+} ions around the unhydrated particles.

When the pure mixture of the $C_4A_3(SO_3)$–$Ca(OH)_2$–$CaSO_4$ system is intermixed with the portland cement, the paste expands rapidly within several hours after kneading and the expansion is completed in a short time, because of the better hydration of the pure synthetic system than the E.C. clinker. In such expansion within a day after kneading, the $Ca(OH)_2$, which is liberated from the cement, accelerates the expansion. Therefore, rather by lessening the amount of $Ca(OH)_2$, which would result in a relative increase in the amount of $C_4A_3(SO_3)$, the volume of expansion can be enlarged. however, a dormant period of O.P.C. clinker occurs at two to three hours after water was poured into the expansive cement, and in and around this dormant period the liveration of $Ca(OH)_2$ is not sufficient, so that the reaction of (4) would progress rapidly in the case of absence of $Ca(OH)_2$ added, unabling further expansion. Therefore, in order to obtain large expansion it wold be necessary to add a small amount of $Ca(OH)_2$ in advance.

On the other hand, E.C. clinker is slow in the rate of expansion, probably because $C_4A_3(SO_3)$ in the clinker is enclosed by other compounds. The expansive cement, composed of portland cement added with powder of E.C. clinker, expands larger when the value of n is large, unlike the case of the pure mixture system. In the sealed curing or dry cruing, where little or no moisture can be supplied from the outside, the expansibility of the cement lowers remarkably within one or two days after kneading, even when the n-value is large, and the expansion comes almost to a standstill. If the n-value is small, or when the E.C. clinker powder is coarse, the cement even shrinks though slightly. It is considered that in the sealed curing the hardening of the cement progresses, and the expansibility lowers with a decrease in the amount of free water. The expansibility is improved by the water cruing, and the difference in the value of n begins to appear. If the value of n is small, for example $n = 2$, the water curing cannot improve the expansibility of the cement in one or two days after its hardening. In other words, the expansion-accelerating effect of $Ca(OH)_2$, which is liberated from the hardened cement, is small in this case.

The fact that free CaO in the E.C. clinker is effective to improve the expansibility may be explained by breakdown of the $C_4A_3(SO_3)$-bearing matrix of the structure, caused by hydration of CaO, as was maintained by Kondo and Nawada (6). But, it can be considered also that the proportion of CaO around $C_4A_3(SO_3)$ particles becomes larger with increasing value of n, so that the expansion is still effective after the hardening.

In the experimentally prepared expansive cement, which was added with gypsum later, fine grains of ettringite began to form on the surface of unhydrated particles of $C_4A_3(SO_3)$ right after the water-pouring, differing from the case of only $CaSO_4$. It is presumed that by this coating of ettringite the later reaction was restrained and setting was retaded.

That the hydration behavior of E.C. clinker varies with brning condition is attributable to the clinker's structure, because the structure becomes harder with rising temperature of burning and the breakdown of the matrix due to hydration would be retarded. In the clinker burned at temperatures below 1100°C, the grains of the respective minerals are minute and the structure is easily broken in water, so that the hydration advances.

Acknowledgements

One of the present authors (G.S.) expresses his sincere gratitude to Professor G. Yamaguchi of Tokyo University, for the kind and continuous guidance. The authors are indebted to President T. Otomo and Vice-president M. Horiguchi of the Chichibu Cement Co., Ltd., for pemritting the publication of this paper.

References

1. S. Akaiwa, T. Nakamura and K. Ozone, "Clinker of limestone-clay-gypsum type and its expansion due to hydration" (in Japanese), Cement Gijutsu Nenpo XX, 92–96 (1966).

2. N. Fukuda and N. Kiyoku, "Effects of SiO_2 on the formation of anhydrous calcium sulphoaluminate" (in Japanese), Cement Gijutsu Nenpo XX, 46–48 (1966).

3. P. P. Budnikov, I. P. Kusnezowa and W. G. Saweljew, "Characteristic of $3CaO \cdot 3Al_2O_3 \cdot CaSO_4$ and its effects on the strength of clinker minerals and cement" (in German), Silikattechnik **16**, 414–417 (1965).
4. W. Gutt and H. A. Smith, "A new calcium silicosulphate", Nature **210**, No. 5034, 408–409 (1966).
5. P. K. Mehta and A. Klein, "Investigations on the hydration products in the system $4CaO \cdot 3Al_2O_3 \cdot SO_3$–$CaSO_4$–$CaO$–$H_2O$", Symposium on the Structure of Portland Cement Paste and Concrete, Highway Research Board, Special Report No. 90, Washington, D. C., P. 378–352 (1966).
6. R. Kondo and N. Nawada, "Characteristics of expansive cement affected by the properties of sulphoaluminous clinker" (in Japanese), Cement Gijutsu Nenpo XIX, 54–59 (1965).

Supplementary Paper IV-83 Prevention of Drying Shrinkage Crack by Use of the Expansive Cement with Calciumsulphoaluminous Cement Clinker

Kazuo Ohmo*, Sin Nakamura** and Taiji Saji***

Introduction

Cement mortar or concrete is liable to cause crack due to its drying shrinkage. In this paper, are presented some results of experiments on the problem of how far the shrinkage crack can be prevented by use of the expansive cement which is blended Calciumsulphoaluminous Cement Clinker (CSA) to ordinary cement clinker. The first half deals with mortar while the latter half with concrete.

Takashige Hattori, Assistant of Hokkaido Univ. Kohichi Yano, Assistant of Tokyo Metropolitan Univ.; Tohei Horishima, Hirokazu Hashimoto, Eiichi Tazawa, and Kuniomi Suzuki, Research members of Taisei Construction Co., Ltd.'s Technical Research Division. Yoshizo Ono, Tsutomu Mizunuma, and Satoru Furui, Research members of Denkikagaku-Kogyo Co. Ltd. All these persons cooperated in the studies.

In the Case of Mortar

Restricted Cracking Test

Expansive cement was prepared by mixing C.S.A. cement with normal portland cement by weight ratios of 0%, 3%, 5%, 7%, 11%, 13%, 15% and, to make test pieces for restricted cracking test, which are shown in Fig. 1 was used using mortar, cement: sand: water = 1: 2: 0.65 by weight, and the occurrence of shrinkage created in those test pieces was observed. The restricted cracking test pieces of Fig. 1 are, $4 \times 4\ cm^2$ in section at the center part and 18 cm in length, tapered toward both ends to enlarge their section and anchored to the steel frame with screw bolts and supported between two sheets of steel plate, $1.2 \times 4\ cm^2$ in section to restricted them from expansion or shrinkage.

Other test pieces were prepared with the same kinds of mortar to be used for measurement of free length change as well as the tests of compressive and flexural strength.

All tests were performed in a curing room, where the temperature was kept approximately at 20°C and the humidity about 70 ~ 80%. None of the test pieces were subjected to cure in water, while the sand used for mortar was Toyoura standard sand f.m. ≒ 1.60. The results are given in Fig. 2 and Fig. 3, occurrence of crack and change of crack width in Fig. 2 and rate of free expansion and shrinkage in Fig. 3. The cracking test results show that the time elapsed from the occurrence of crack was gradually prolonged with the increase of the mixing rate of expansive admixture, as shown in Fig. 2. That is the 0% test piece cracked at the 16th day, and that of 3% addition at the 36th day, 5% at the 63rd day, 7% at the 84th day and addition of 11%, 13% and 15% almost at the same time, that is at the 175th day, 182nd day, 185th day respectively.

It is appreciated from the above-mentioned results, that the occurrence of crack is considerably delayed by the addition of expansive admixture, but in the case of calcium sulfoaluminate adopted in the present experiment, the author could not completely prevent shrinkage cracks from occurring in every kinds of mortar.

What is noteworthy is that, in the case of test pieces, which was mixed with more than 7% expansive admixture, shrinkage cracks developed even when the measured value of free length change was still on the

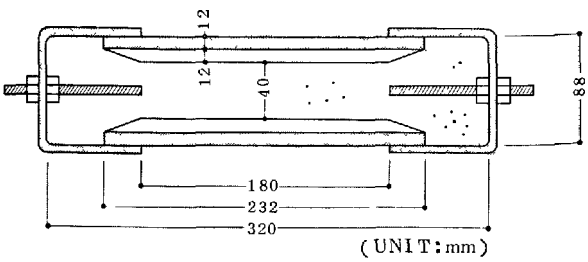

Fig. 1. *Shrinkage crack apparatus*

*Hokkaido University, Sapporo, **Tokyo Metropolitan University, Tokyo and ***Kyushu University, Fukuoka Japan.

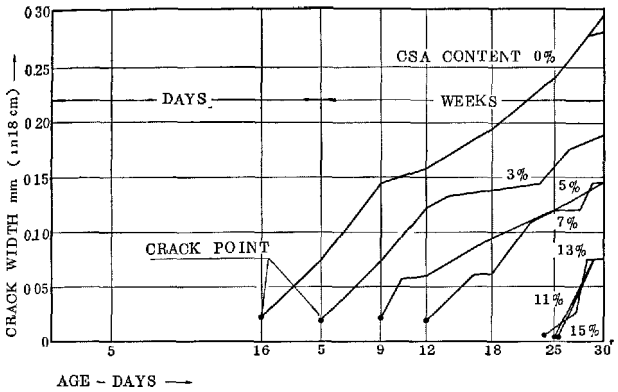

Fig. 2. *Occurrence of crack time and crack width*

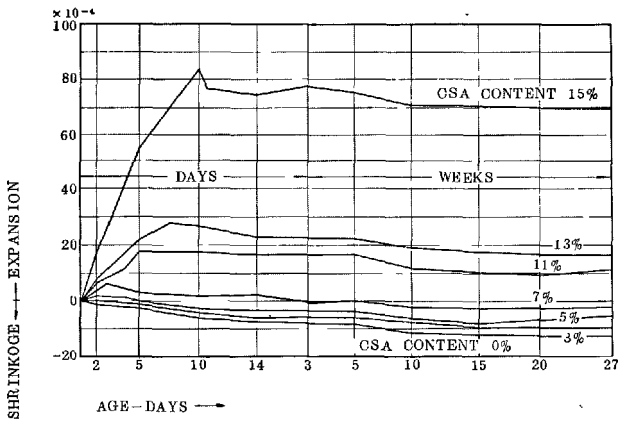

Fig. 3. *Free expansion and shrinkage*

expansion side. This can be explained from the fact the expansion comes to an end rather early time, and thereafter shifts to drying shrinkage.

Even in case of 15% admixture being added, expansion lasts only about the 10 days, thereafter occurs shrinkage, and with the decrease of the amount of addition of admixture, expansion comes to terminate gradually earlier.

Now, tentatively, if the shrinkage rate is calculated for a duration from the time of maximum expansion to the crack occurring time, the result will be about as follows; with 10^{-4} as unit, 0% = 5.44, 3% = 6.25, 5% = 7.00, 7% = 8.14, 11% = 8.10, 13% = 8.52, and 15% = 10.00.

The above values show that the larger the rate of expansion is, the larger the rate of shrinkage becomes and show the effect of expansion to a certain extent.

In the case of more than 11% addition, crack has occurred after about the same number of days had elapsed, which is associated with the decrease of strength due to the increase of addition of expansive admixture.

Reconsidering the effect of expansion at this stage, it is probable that a greater part of expansion has disappeared as compressive creep due to the comparatively earlier expansion as stated before, and besides that the expansion may escape simultaneously in horizontal direction because of the restriction of lengthwise expansion. Dr. K. Shirayama has measured the expansion pressure of concrete under a uniaxial restriction, and reported that the expansion pressure diminishes about the time when the expansion is replaced by shrinkage.

It has been observed that, by the expansive admixture used in this experiment, we cannot prevent shrinkage cracking to the perfection when it is completely restricted in the lengthwise direction. However, with a real structure, restricting force is not so completely effective that the shrinkage crack is expected to be considerably prevented by the use of expansive admixture (C.S.A.)

Application to Plastering Mortar, for Wall

Since portland cement mortar for the use of plaster is liable to crack when it is richly mixed, so that as a method of preventing crack usually considerable amounts of sand mixing in mortar is generally followed. Accordingly, if we can prevent drying shrinkage crack by use of expansive cement, we shall be able to finish up nearly as well as plaster by reducing mixing amount of sand in mortar.

The authors have carried out an experiment here to find out whether comparatively rich mixed mortar is practically applicable to plastering by expansive cement.

As the first test, preliminary experiments were carried out using thirty kinds of mortars with several ratios of sand mixing, and the ratios of water to the whole mixtures added with some % of expansive admixture (C.S.A.) in portland cement, and then on the basis of these experiments, the possibility for plastering was investigated by applying expansive cement mortar to an actually erected building.

The physical properties of tested mortar, are given in the later table Table 1, and an outline of the wall used for the plastering experiment are given in Fig. 4.

For each mix in Table 1 about 10 ± 1 mm consistency was chosen, as the appropriate consistency for plastering. While the consistency adopted was obtained from the Vicat apparatus of JIS R5201, for physical test of cement 9-4, with necessary modifications, penetration-needle was using a 19mmϕ steel bar, and adjusting the total weight of its descending part to 400 gr. Then the value of 100 mm penetrated by this method will be called as consistency of 10 mm.

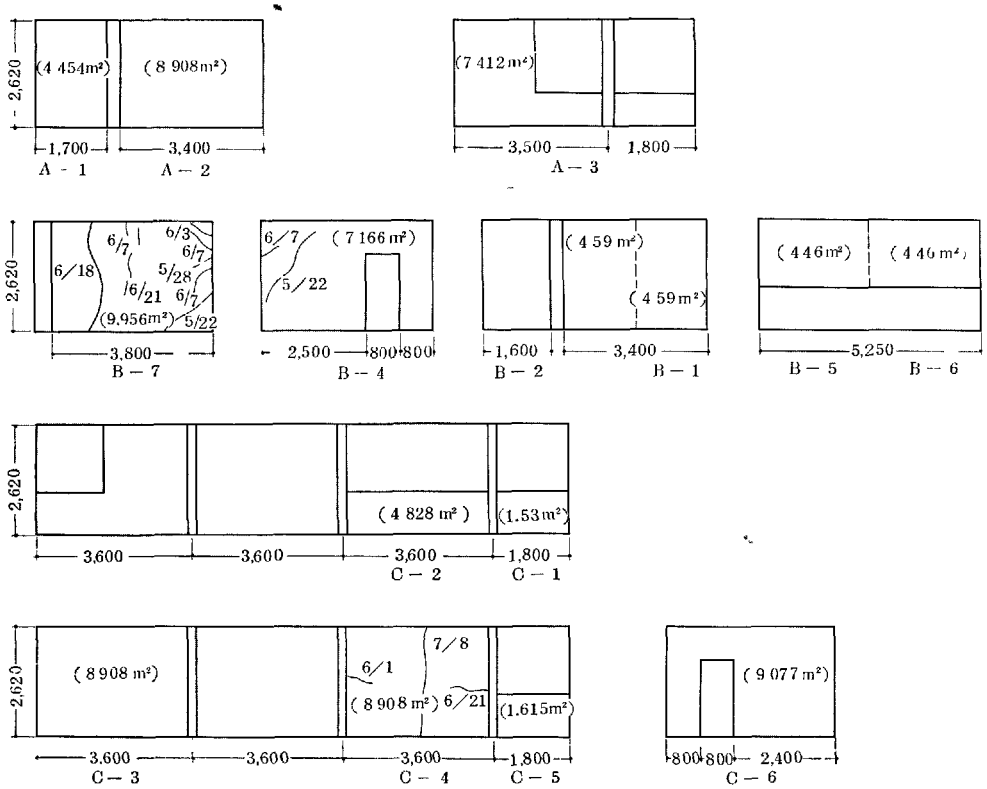

Fig. 4. *Field test of plastering wall and cracking map*

Table 1. *Mixproportion of plastering mortar*

Symbol No.	Kinds of cement	Mixproportion			Flow (mm)	Penertration (mm)	Unit weight (kg/l)
		Cement	Sand	Water			
1	Normal portland cement	1	1	0.339	183	9	2.192
2	〃	1	2	0.430	194	10	2.161
3	10%CSA + 90%P.C.	1	0.5	0.314	196	10	2.168
4	〃	1	1	0.350	185	9	2.180
5	〃	1	1.5	0.384	195	10	2.160
6	〃	1	2	0.457	191	9	2.135
7	3%CSA + 97%P.C.	1	2	0.444	200	11	2.125
8	5%CSA + 95%P.C.	1	2	0.452	195	10	2.157
9	7%CSA + 93%P.C.	1	2	0.454	212	11	2.155
10	Gypsum plaster	1	2	0.564	198	9	1.661
11	10%CSA + 30%D.P. + 60%P.C.	1	2	0.560	182	9	2.105
12	10%CSA + 50%D.P. + 40%P.C.	1	2	0.575	207	10	2.044
13	50%D.P. + 50%P.C.	1	2	0.570	204	10	2.049

P.C. = Normal portland cement
D.P. = Dolomite plaster
CSA = Calcium sulphoaluminous cement clinker

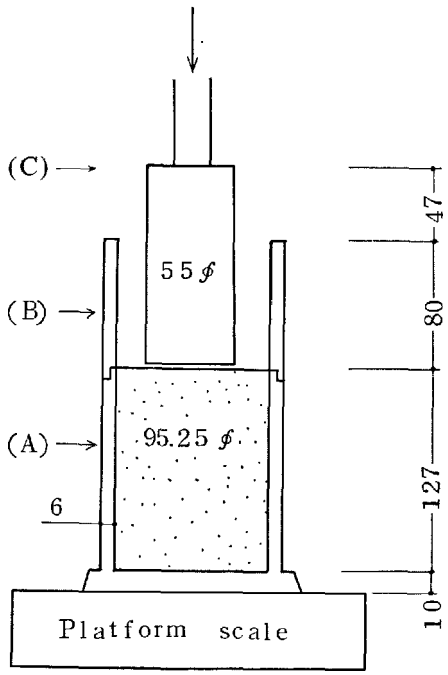

Fig. 5. *Penetration resistance test apparatus*

In the next place, as the method of estimating the suitability of plastering mortar, penetration-resistance test was carried out on each kind of mortars.

Above-mentioned test method is shown in the later Figure (Fig. 5), the mortar being filled in two layers in (A) vessel. The process of filling mortar was to set the vessel (A) on the flow table of cement and move the flow table 5 times for each layer. After the two layers were filled up the collar (B) was set and by penetrating the plunger (C) into the mortar at a constant speed (20 mm/sec), then the penetration resistance corresponding to the depth was measured.

There are shown Fig. 6 and Fig. 7 the values of some typical figures of penetration resistance measured at each depth.

Where the two straight lines represent the range of appropriate values of plastering work, the sand used for this experiment was approximately f.m., 2.09, and the sieve test result is given in Table 2.

Next water holding capacity test was performed. The test was based upon A.S.T.M. with force of absorption set at 50 mm Hg, the water-holding rate was calculated at each elapsed time by the following equation:

$$\text{Water holding rate} = \frac{\text{water ratio after test}}{\text{water ratio before test}} \times 100\%$$

The water holding capacity was apt to decrease when the expansive admixture C.S.A. was added, while that of the material tested with dolomite plaster

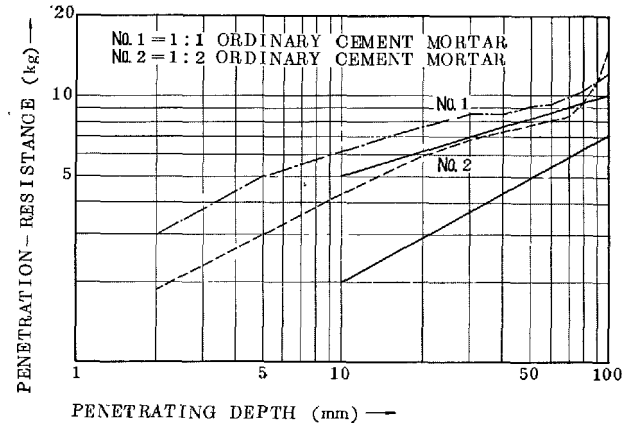

Fig. 6. *Penetration-resistance at each depth*

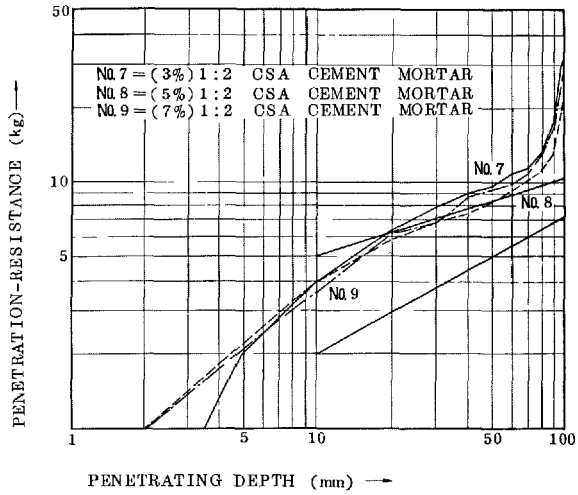

Fig. 7. *Penetration-resistance at each depth*

Table 2. *The sieve analysis of sand*

Sieve (mm)	5.0	2.5	1.2	0.6	0.3	0.15	f.m.
Pass-ratio (%)	100	98.9	94.6	73.5	27.7	0.4	2.09

brought about exceedingly good result. Furthermore, weight decrease rate, drying shrinkage rate Fig. 8 and Fig. 9, and flexural strength were tested. The shrinkage rate showed the minimum in case of (No. 10) gypsum plaster. In the case of C.S.A. cement mortar, shrinkage rate was less than that of ordinary portland cement mortar, but all measured values remained on the shrinkage side. However, the test piece was cured in a curing room where the temperature was 20°C and humidity 50%.

Based on the above-mentioned preliminary experiments each kind of materials given in the foregoing

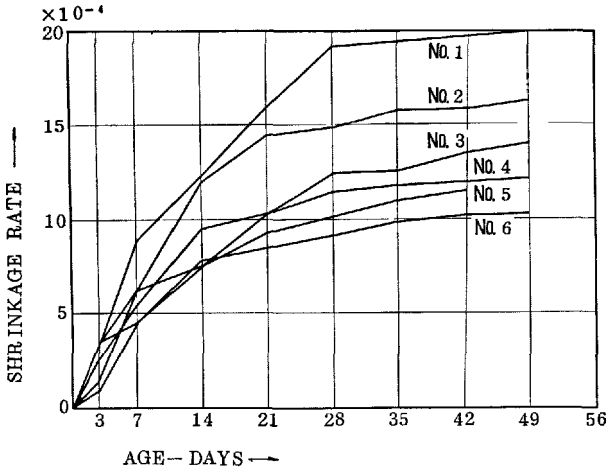

Fig. 8. *Shrinkage rate*

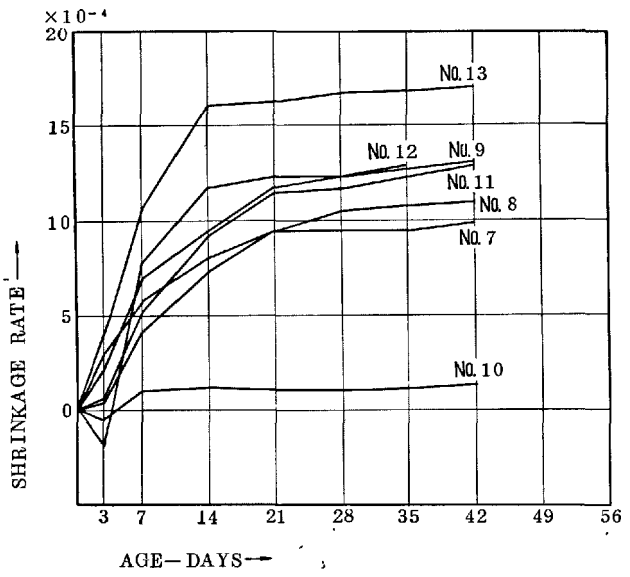

Fig. 9. *Shrinkage rate*

Table 1 was subjected to the field test, in which the thickness of test plastering was about 1.5 cm and the base concrete surface was painted with cement paste, containing 0.2% methyl-cellulose. The finishing up of plastering was also done on the same day. The plan of test house, and the observed crack pattern is shown in Fig. 4.

In this field test, cracks occurred in portland cement mortar of No. 1 and No. 2 in Table 1, the former appearing at the 5th day, and the latter at the 10th day.

As for the expansive cement, crack was found in No. 7 of 3% mixing rate after 23 days, but the surfaces of wall plastered with other expansive cement mortar caused no cracks. Judging from this field experiment,

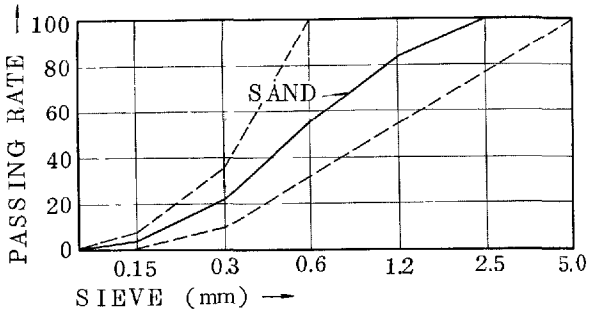

Fig. 10. *Sieve analysis of sand*

it is safe to estimate that mortar mixed with 7% expansive admixture (C.S.A.) will not so easily yield shrinkage cracks.

Application to Plastering Mortar for Floor

It is essential for floor mortar to be endowed with a quality to stand abrasion, since rather high strength of mortar is required, hence rich mixed mortar is to be used, and this fact naturally involves the condition leading to shrinkage crack more easily. Then the authors tried to find out by use of expansive cement (C.S.A.) floor mortar, abrasion-proof and free from shrinkage-cracking.

The experiment is carried out by changing the rate of cement and sand in referred to in the foregoing chapter (for wall), while the amount of water to be added was chosen by the penetration resistance test, and consistency was measured by 19 mmϕ needle penetration test. The sand used in this experiment was passed through 2.5 mm sieve, the result of sieve test being given in (Fig. 10).

The notation of each kind of mortars and the mixing tables are shown in the Table 3. In the next place, water-holding capacity test was performed based on "JIS A6904 Gypsum plaster". It has been clarified from this water holding test and penetration test that there is little difference in quality between expansive cement and ordinary portland cement, provided that mixing rate is the same. Also with a viscosity improving agent such as methyl-cellulose, its effect was found to be very little in the case of rich-mixed mortar.

Flexural strength was also evaluated using $2 \times 4 \times 16$ cm^3 test piece at 10 cm span and by center loading. The results of this test showed nearly the same values in strength between A-3 and P-3, but in the case of A-2 and P-2, A-2 decreased strength as 70% of P-2. Therefore, in the case of expansive cement, we cannot obtain abrasion-proof mortar unless we make cement ratio richer than 1: 1.5 as shown in Fig. 11.

In the next place, the rate of expansion and shrin-

Table 3. *Mix proportion of floor mortar (by weight)*

Kind of cement	Symbol of mortar	Mix proportion			Penetration (mm) (400g-19φncedle)	Flow (mm)	Unit weight (kg/l)
		Cement	Sand	Water			
Normal portland cement	P-2	1	2	0.410	14.0	186	2.18
	P-3	1	3	0.600	15.5	192	2.11
	P-4	1	4	0.840	15.0	203	2.07
	PM-3	1	3	0.535	9.5	171	2.02
	PM-4	1	4	0.725	15.5	178	1.97
CSA11% + 89% Normal portland cement	A-0	1	0	0.250	12.0	176	2.13
	A-0.5	1	0.5	0.265	13.0	181	2.20
	A-1	1	1	0.300	10.5	174	2.23
	A-1.5	1	1.5	0.340	11.5	179	2.20
	A-2	1	2	0.405	10.5	181	2.14
	A-3	1	3	0.575	18.5	189	2.04
	AM-0	1	0	0.265	16.0	176	2.09
	AM-1.5	1	1.5	0.350	10.0	170	2.13
	AM-3	1	3	0.525	17.5	171	1.96
	AC-0	1	0	0.265	24.5	187	2.12
	AC-1.5	1	1.5	0.350	12.5	178	2.17
	AC-3	1	3	0.535	13.0	176	2.00

C and M = Consistency improving agent. (Methyl-cellulose) adding this agent 0.1% of cement. +AC − 3 = 0.2%.

kage was measured, using a test piece of 1 × 4 × 16cm³. For comparison two cases of tests, i.e. The one at temperature of 20 ± 3°C and humidity of 80~85%, the other in water curing of 20 ± 3°C, were partly carried out simultaneously.

According to Fig. 12 the rate of drying shrinkage expansive cement mortar is invariably less than that of portland cement mortar, which is however on the shrinkage side when cured in the air, but the one subjected to water curing shows considerable expansion and the richer the mixing, the more conspicuous the expansion.

With reference to the above-mentioned fundamental experiments, field tests were carried out on the plastering of the floor of a real building. The sketch of field plastering test is shown in Fig. 13 while mix of mortar is as shown in Table 3.

On August 24, 1966 the plastering works of P-3, A-05, A-1 and A-1.5 were performed, of which A-0.5 was replaced afterward by A-1, the formers viscosity being too large for plastering. The expansive cement mortar showed considerable expansion corresponding to the condition of water curing or water sprinkling for a week after its placement, and caused expansion fracture. The swollen-up amount was about to 4 cm at the maximum on the floor line.

As indicated in Fig. 13 plastering work was applied several times, on September 29 (5th time), November 18 (6th time) and November 28 (7th time). At the 5th time ratios of cement to sand 1: 2 and 1: 3 were used, and at the 6th time and 7th time expansive admixture (C.S.A.) added in cement was only 5% in cement. After recoating, no conspicuous cracks occurred except for small hair cracks at several portions. The main results obtained from these experiments on floor

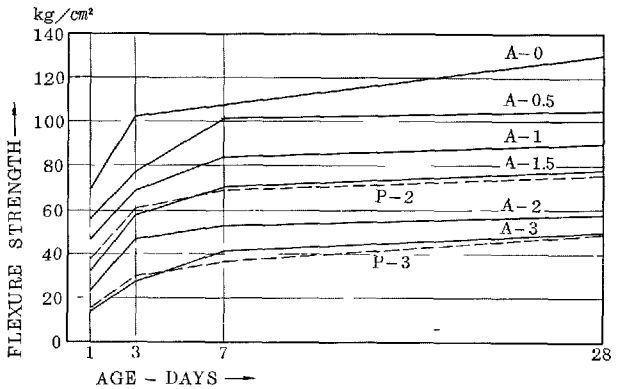

Fig. 11. *Flexural strength*

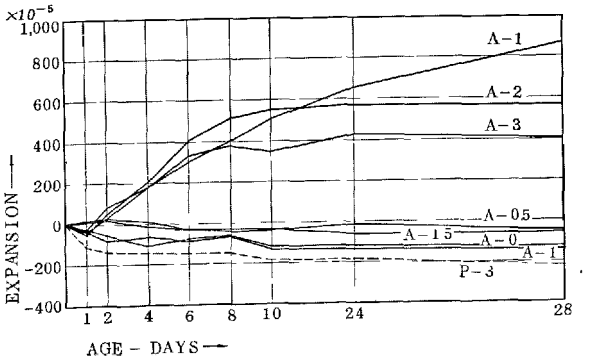

Fig. 12. *Change in length on non-constraint*

mortar are;

*There is little difference in workability between expansive cement and portland cement.

*In order to obtain abrasion-proof mortar, rich mixing mortar more than (1: 1.5) should be chosen in the case of expansive cement (5% C.S.A. mixed).

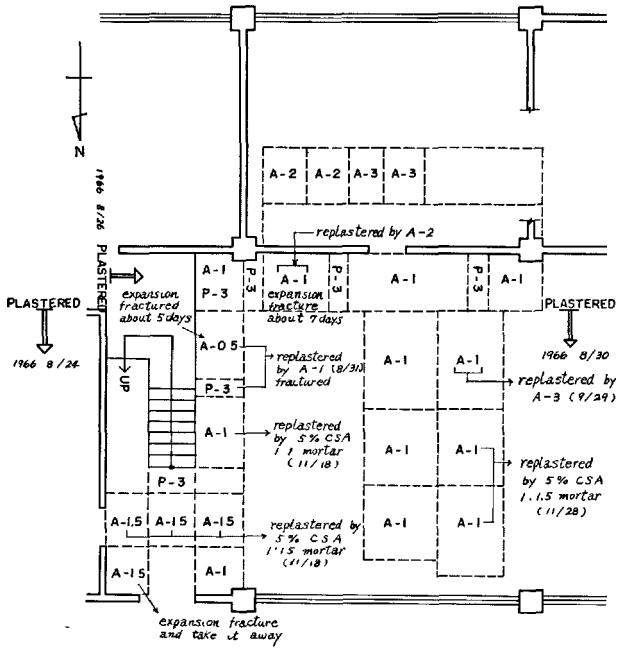

Fig. 13. *Field plastering test*

It is, however, important not to mix too much expansive admixture, for there are some points yet to be thoroughly investigated.

*The fact that this expansive cement considerably varies in its rate of expansion in curing in water or in the air is a problem of great importance in the plastering work, since the damage due to expansion is much worse than that of shrinkage. We have to study further, the mixed amount of expansive admixture (C.S.A.) in portland cement, by use of plastering work.

Mortar Lining for Steel Pipe and Cast Iron Pipe

There is a construction use for which expansive cement consisting of C.S.A. as expansive agent is particularly advantageous.

It is mortar lining for steel pipe and cast iron pipe. There have been considerable troubles with cracking and separation in the lining mortar.

They were due to drying shrinkage of the cement, generally ordinary portland cement used.

As drying shrinkage introduces tensile stress to the lining mortar, the cement that would shrink on hydration cannot be used for mortar lining.

Success in precluding the formation of shrinkage crack and separation was achieved by blending C.S.A. with ordinary portland cement, slag cement or flyash cement.

The proportion in which C.S.A. is mixed with cement is different with the kind of the base cements.

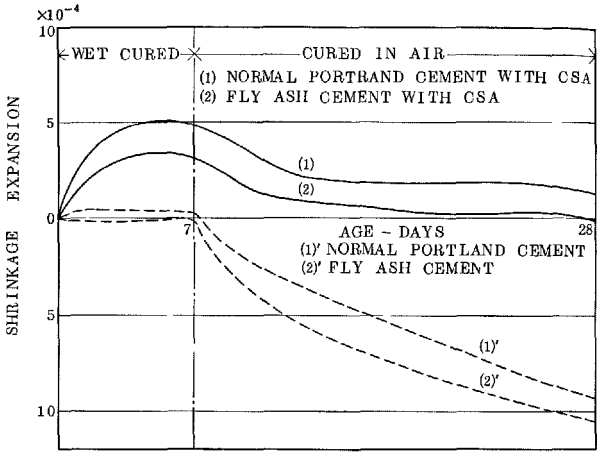

Fig. 14. *Free expansion of non steam curing*

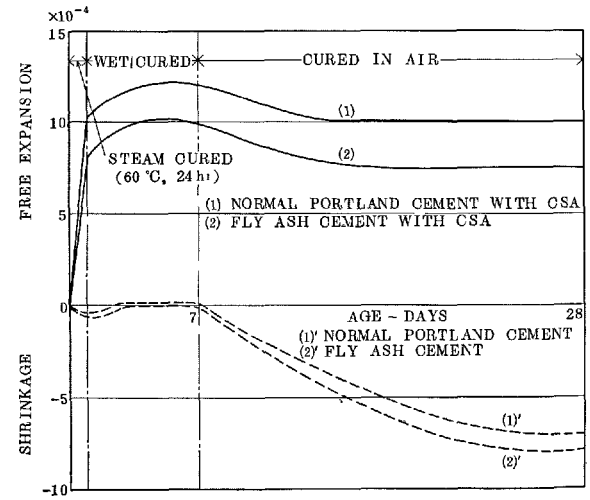

Fig. 15. *Free expansion of the water steam curing*

For instance, C.S.A. has been used by a company for mortar lining in a mix proportion of 8:92 by weight to flyash cement and by another company in a mix proportion of 11:89 by weight to ordinary portland cement. Free expansion of these mortar is shown in Fig. 14. From Fig. 14, it can be seen that free expansion of flyash cement mortar mixed with C.S.A. is less than that of ordinary portland cement with C.S.A. However, these mortar shrinkages after maximum free expansion which occurred at an early age of mortar are the same and enough to prevent the shrinkage crack and separation formation.

The mortar-lined pipe is cured in water or steam on the manufacturing process.

As the expansion of lining mortar is larger in steam curing than in water, and mortar shrinkage is smaller after maximum free expansion, the effect of preventing crack and separation is larger. These facts are shown in Fig. 15.

Table 4. *Chemical analysis of water*

Kind of water*	Smell	pH	M. O. alkalinity ppm	Total hardness ppm	Evaporated residue ppm
Normal portland cement mortar	Normal	11.7	143.5	68.0	180.0
Normal portland cement with CSA mortar	Normal	9.7	45.1	68.0	119.0
Non-immersed	Normal	7.1	39.0	68.0	104.0

*Immersed water of each mortars

On the other hand, researches in the influence of lining mortar containing C.S.A. on soundness and solubility to water were prosecuted by immersing a piece lining mortar vertically in water (60°C) for 1000 hrs. From this test, we could get satisfactory results shown as follows:

*The soundness of the cement with C.S.A. is equivalent to ordinary portland cement.

*Chemical analytic results of the water in which each living mortar is immersed (Table 4) indicate that in the case of the cement with C.S.A. it has lower alkalinity as compared with normal portland cement but almost the same content in other elements.

In the Case of Concrete

Dry Shringkage of Reinforced Concrete Mixed with CSA-Cements

Here are presented the result of two series of observations on the change in length and crack distribution of reinforced concrete mixed with CSA-cements and usual aggregates.

In the first series, a CSA-cement of 13% CSA was tested with the specimens of rectangular plates for the convenience of observing cracks which would be caused by dry shrinkage.

The second series was a test of a CSA-cement with 10% CSA consisting of two parts. The first part was the repetition of the foregoing test with this cement and the second part was a study on the change in length by beam type specimens which enabled to observe the change in length from the first stage of hardening of of concrete. Each series of tests included some comparisons of CSA-cement concrete with the ordinary portland cement concrete.

Test Series I

The purpose of this study was to observe the influence of steel reinforcements on the change in length and the crack distributions for reinforced concrete mixed with a CSA-cement.

Specimens

Type and size. A rectangular plates of 50 × 50 × 10 cm³ was adopted as the specimen.

Reinforcements. Four kinds of double meshes made of deformed bars of 10mm in diameter were applied, as shown in Fig. 16.

Cements. Three kinds of cements were tested—that is, which contained 13% CSA (noted by C), a portland-cement made by the same plant (noted by P) and a certain other manufacturer's portland cement (noted by A). (Table 5)

Aggregates. Sand and gravel from the same river were used. Their physical properties are shown in Table 6.

Mixtures. The mixtures were selected as described in Table 7, where w/c was 0.6 and the slump was controlled to be about 21 cm.

Concrete form. Wooden forms were used. Vinylchloride plates of 1 mm in thickness were lined inside the forms, which gave so smooth surfaces to the specimens that inspection of hair cracks on the surfaces

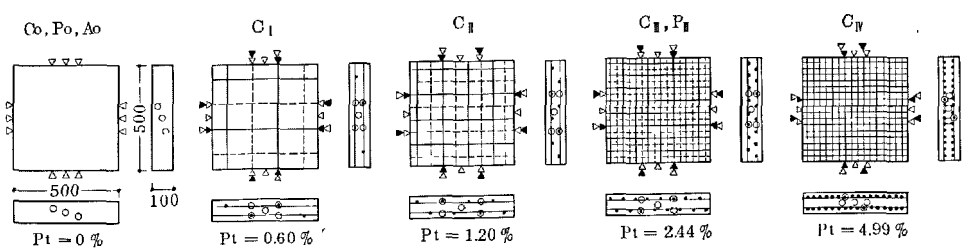

▽ shows the position of the measuring point for concrete
▼ shows the position of the measuring point for bars

Fig. 16. *Kinds of reinforcements*

Table 5a. *Chemical analysis of cements*

Kind of cement	ig. loss	insol.	SiO_2	Al_2O_3	Fe_2O_3	CaO	MgO	SO_3	total	Specific weight	Fineness Blaine specific surface (cm^2/g)
CSA-cement	0.7	0.9	20.0	6.1	3.0	61.6	1.1	6.2	99.6	3.11	3100
Normal portland cement "P"	0.7	0.8	22.0	5.3	3.2	63.9	1.3	1.9	99.1	3.15	3160
Normal portland cement "A"	0.5	0.6	22.6	5.0	2.9	64.3	1.4	1.9	99.2	3.16	3120

Data were supplied from the manufacturers

Table 5b. *Physical test of cements*

Kind of cement	Flexure strength kg/cm^2			Compressive strength kg/cm^2		
	3 days	7 days	28 days	3 days	7 days	28 days
CSA-cement	17.9	22.0	46.5	76	113	208
Normal portland cement "P"	31.2	41.0	57.9	119	182	324
Normal portland cement "A"	24.3	30.4	54.5	93	153	305

Table 6. *Physical properties of aggregates*

Item	Specific gravity	Unit weight kg/l	Size	Fineness modulus
Sand	2.57	1.65	less than 2.5 mm	2.43
Gravel	2.53	1.67	15~5 mm	6.53

Table 7. *Mix proportion of concrete*

Kind of cement	w/c	Cement kg/m^3	Sand kg/m^3	Gravel kg/m^3	Water kg/m^3	Compressive strength kg/cm^2	
						Water curing	Air curing
CSA-cement	0.60	305	820	985	183	185	148
Normal portland cement P	0.60	300	835	985	180	256	162
Normal portland cement A	0.60	295	844	985	177	250	170

was very easy.

Casting of concrete and curing. The wooden forms were set up edgewise like the walls, and the concrete was casted in the upper edge and covered with polyethylene films. The forms were removed after 48 hours and the specimens were also set up edgewise in the room air of about 18°C and 70% R. H. for one week. Then, R.H. was dropped to 45% for three weeks. After 4 weeks the temperature was controlled to be 16°C, but the relative humidity gradually rose to 70%.

Measurement of the Change in Length

Small steel screws were inserted to the concrete surface and on the ends of reinforcement bars, as are pointed in Fig. 16. The distance between a pair of screw heads, which were placed on the contrary edges of the specimen, was measured by a simple apparatus with a couple of 1/1000 mm dialgages. The accuracy of measurement was calculated to be about 2×10^{-6} mm/mm.

The measurement was started immediately after removing the wooden form, and was continued for 15 weeks.

Change in Length of Plain Concrete

The CSA-cement concrete C_0 expanded remarkably in its early age, although the ordinary concrete P_0 and A_0 showed almost no expansion, as shown in Fig. 17. The maximum expansion of C_0 reached over 45×10^{-5} mm/mm at the ninth day. Then, C_0 showed dry shrinkage similar as the ordinary concrete. The magnitude of these shrinkage reached about 50×10^{-5} mm/mm after 15 weeks. Consequently, the amount of change in length became nearly zero compared with the initial length observed in this test.

There can be seen some difference between the change in length of the CSA-cement concrete in the vertical direction and that in the horizontal direction; the former was smaller than the latter. The reason for this phenomenon would be attributed to the constraint against expansion of young concrete by its own weight.

On the other hand, the magnitudes of dry shrinkage of P_0 and A_0 were $54 \sim 61 \times 10^{-5}$ mm/mm compared with their initial length.

Change in Length of Reinforced Concrete

There were some troubles with the measurement of

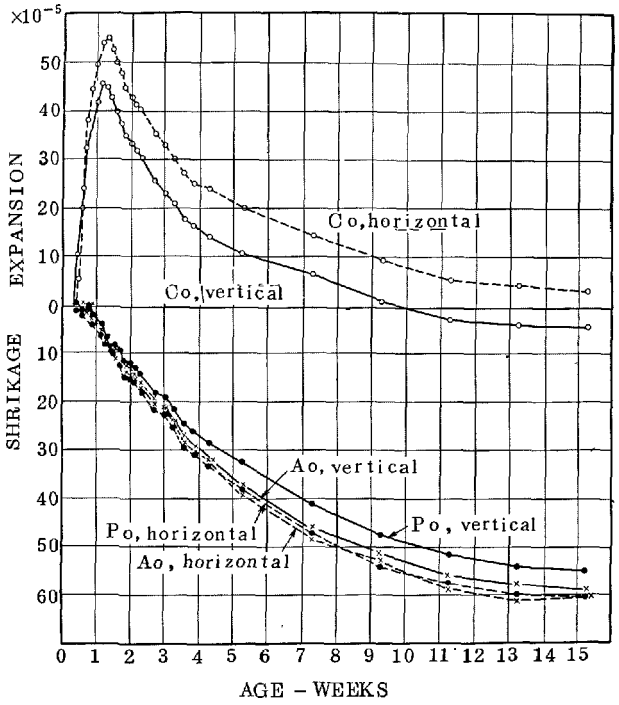

Fig. 17. *The change in length of non-reinforced concrete*

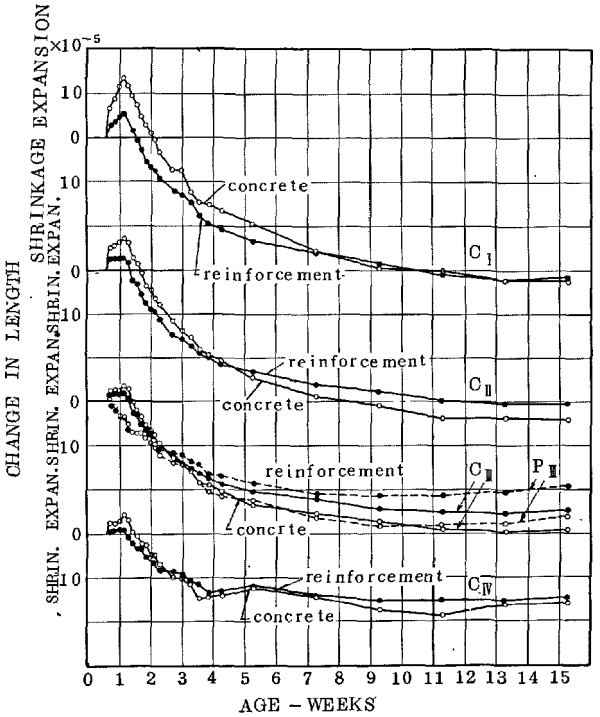

Fig. 18. *The change in length of reinforced concrete*

change in length for the first two days. Therefore, the data were conveniently arranged by taking the length at the fourth day after casting concrete as the standard. The test result are plotted in Fig. 18.

There were some differences between the change in length of reinforcing bars and those of concrete body. The former was less than the latter in both cases of expansion and contraction. It may be supposed that these differences would be caused by the plastic deformation of bond between the concrete and bars, and perhaps by the warp of concrete surface constrained by the bars.

Speaking of the change in length of concrete body, the tendency of expansion was also observed in the early stage of hardening of concrete. However, the magnitudes were considerably smaller than those of plain concrete and the maximum expansion decreased when the reinforcement ratio increased.

As the dry shrinkage of concrete was also constrained by the existence of reinforcement bars, the specimens which had a higher reinforcement showed a smaller shrinkage and the magnitudes of shrinkage after the primary expansion at a certain age decreased almost linearly with the increase of reinforcement ratios.

Fig. 19 shows the relation between the reinforcement ratios and the amount of change in length, when the length at the 4th day after casting concrete

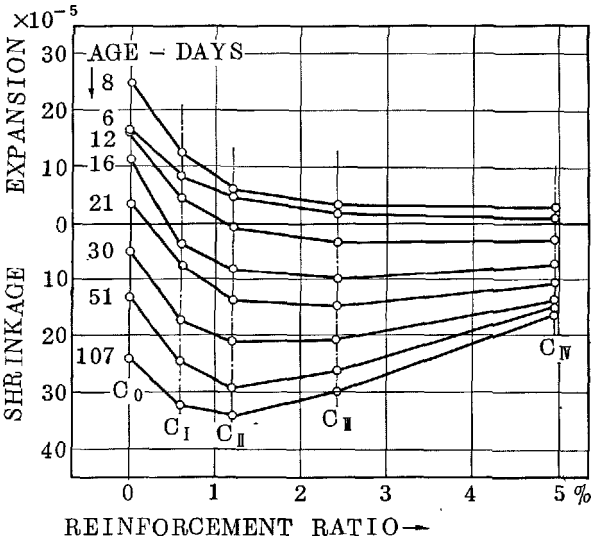

Fig. 19. *The relation between the change in length and the reinforcement ratio*

was taken as the standard. It is very interesting that the specimens with moderate reinforcement ratio showed the largest shrinkage at the 15th week.

Observation of Cracks

An observation of cracks on the surfraces of specimens was proceeded by a magnifying glass.

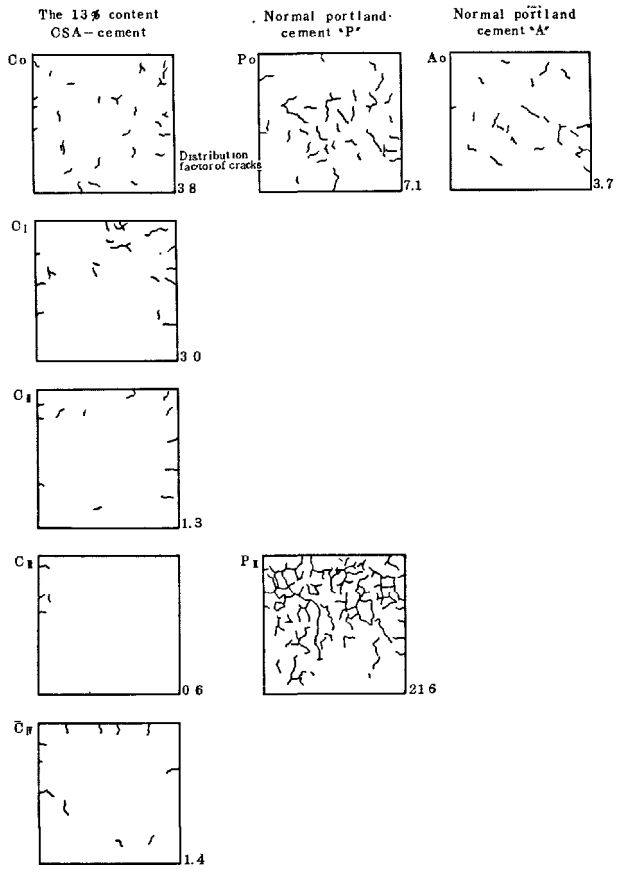

Fig. 20. *Cracking map at the age of 3 weeks*

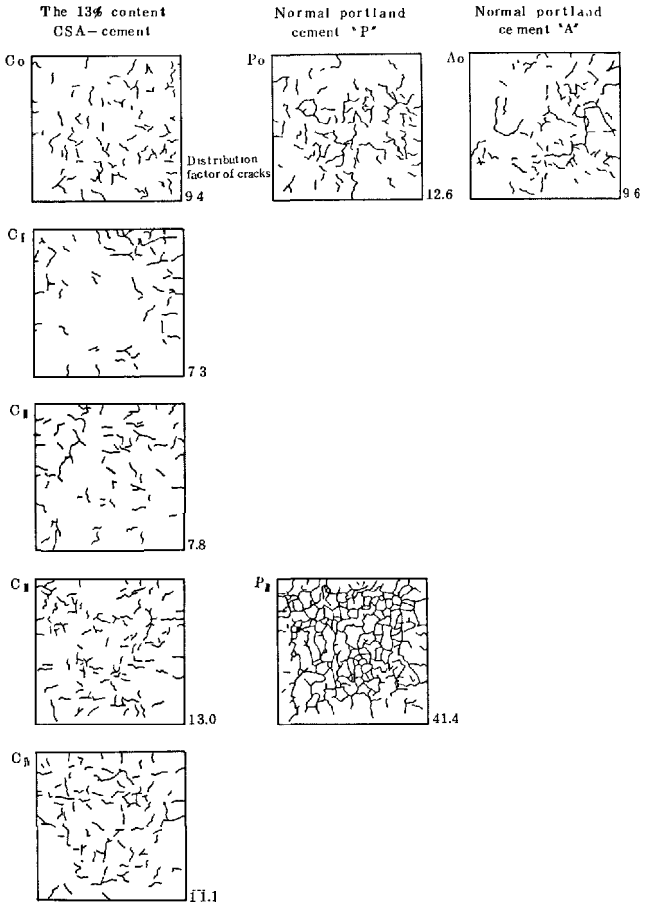

Fig. 21. *Cracking map at the age of 15 weeks*

Table 8. *Distribution factors of cracks*

Symbol	Kind of cement	Reinforcement ratio %	Distribution factor of cracks ($\times 10^{-2}$ cm/cm^2)						
			No. 1		No. 2		No. 3		mean
C_0	CSA-cement	0	9.4	12.6	5.6	6.3	12.4	13.3	10.0
C_I	〃	0.60	7.3	6.2	7.2	6.9	—	11.2	7.8
C_{II}	〃	1.20	7.8	12.8	7.8	3.4	7.5	8.2	8.0
C_{III}	〃	2.44	9.7	13.0	11.9	12.5	16.6	17.5	13.5
C_{IV}	〃	4.99	6.9	11.6	14.8	11.1	13.4	8.2	11.0
P_0	Normal portland cement P	0	14.8	13.4	11.8	8.0	13.5	12.6	12.4
P_{III}	〃	2.44	31.6	32.0	45.4	34.4	47.2	41.4	38.7
A_0	Normal portland cement A	0	6.5	7.0	10.6	10.1	9.6	10.7	9.1

The first hair cracks were observed on every specimen at the age of 16 days, when the relative humidity of test room was about 42%. It looks likely that there was no difference between the age of initial cracking of concrete and the kinds of cements as well as the quantity of reinforcement, in the range of such a low humidity. Fig. 20 and Fig. 21 show the sketch of crack distribution at the age of 3 weeks and 15 weeks respectively, and Table 8 shows the distribution factors of cracks, i.e., the mean length of crack per unit area. Both data indicate that there were not so much difference on the crack distribution for every specimen, in spite of the variation of cement, mixtures and reinforcement ratios, excepting the specimens of P_{III} hardly cracked notwithstanding the same grade of shrinkage. If the crack distributions were the same, the width of crack should theoretically increase with the increase of reinforcement, but any remarkable

difference could not be found in this CSA-cement concrete. Every crack had the width of 0.02–0.04 mm. It was very difficult to distinguish the deep cracks from hair cracks on the surfaces of specimens.

Test Series II-1

The purpose of this test was to compare a CSA-cement with an ordinary portland cement from the viewpoint of crack distribution of reinforced concrete. The testing method of Series 1 was followed in this study by using a CSA-cement with 10% CSA and the portland cement "A".

Specimens

Type and Size, Aggregates, and *Concrete Forms.* These were the same as the foregoing test.

Reinforcements. Two kinds of double meshes, as shown in Fig. 22

Cements. Two kinds of cements, above-mentioned.

Mixtures. The mixtures were selected as shown in Table 9, where w/c was 0.7 and the slump was controlled to be about 18 cm.

Curing. The wooden forms were removed 48 hours after casting concrete and the specimens were cured in the room air of 16°C and 75% R. H. for three weeks, and then of 16°C and 55% R. H.

Measurement of Change in Length

The results of measurement are plotted in Fig. 23.

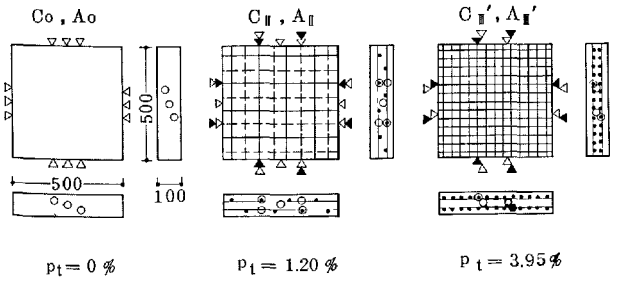

▽ shows the position of the measuring point for concrete.
▼ shows the position of the measuring point for bars

Fig. 22. *Kinds of reinforcements*

Table 9. *Mix proportion of concrete*

Kind of cement	w/c	Slump cm	Cement kg/m³	Sand kg/m³	Gravel kg/m³	Water kg/m³	Compressive strength kg/cm²
CSA-cement	0.70	18.3	275	990	850	193	179
Normal portland cement A	〃	16.8	〃	〃	〃	〃	255
CSA-cement*	0.55	17.6	335	900	911	184	269

*This mixture was used in test series II-2.

The expansions of CSA-cement were very little, even in the case of plain concrete C_0, and there was not so much difference of change in length between C_0 and the ordinary concrete A_0 for the first week. However, A_0 showed thereafter somewhat larger shrinkage than C_0. The magnitudes of dry shrinkage are given in Table 10. It shows that the shrinkage of reinforced concrete at the end of the 7th week almost linearly decreased with the increase of reinforcement ratio for both kinds of cements.

Observation of Cracks

The crack distributions on the surfaces of specimens which were sketched in the 7th week and after 50 weeks are shown in Fig. 24 and Fig. 25 respectively, and their distribution factors are calculated in Table 11.

These results were somewhat different from those in test series I. Both figures show that few cracks were observed on the specimens of plain concrete C_0 and A_0, even after 50 weeks, and that cracks of reinforced concrete mixed with the CSA-cement increased considerably after 7th weeks, although the cracks did not extend so much in the earlier age.

It would be notable that the dry shrinkage of ordinary reinforced concrete with the high reinforcement ratio showed some relaxation after a certain age. It means that some deep cracks reached to the reinforcement bars and the compressive stress of steel bar

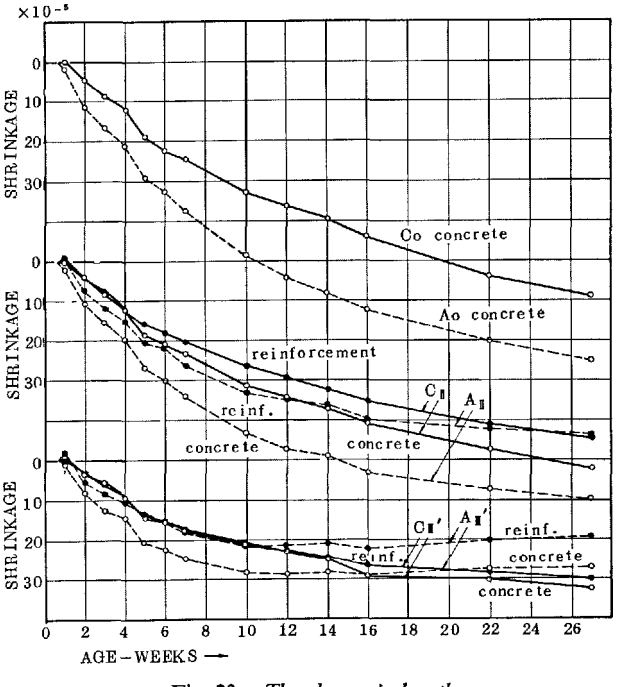

Fig. 23. *The change in length*

Table 10. *The Influence of reinforcements on the shrinkage*

× 10^{-5} mm/mm

Symbol	Kind of cement	Reinf. ratio %	28 days		49 days		70 days		189 days	
C_0	CSA-cement	0	12.0	1.00	24.5	1.00	32.8	1.00	59.0	1.00
C_{II}	CSA-cement	1.20	12.5	1.04	23.7	0.97	31.4	0.96	52.2	0.89
C_{III}'	CSA-cement	3.95	9.6	0.80	17.8	0.73	21.2	0.65	32.8	0.56
A_0	Normal portland cement "A"	0	21.1	1.00	37.5	1.00	48.8	1.00	75.6	1.00
A_{II}	Normal portland cement "A"	1.20	19.9	0.94	34.2	0.91	43.3	0.89	60.0	0.80
A_{III}'	Normal portland cement "A"	3.95	14.8	0.70	24.8	0.66	28.5	0.58	27.2	0.36

Table 11. *The distribution factor of cracks*

× 10^{-2} cm/cm²

Symbol	5th week	7th week	14th week	27th week	50th week
C_0	max. min. 0.30–0.00 0.20	max. min. 0.30–0.00 0.21	max. min. 1.24–0.22 0.71	max. min. 1.80–0.42 1.22	max. min. 3.26–1.12 1.96
C_{II}	0.16–0.00 0.04	0.20–0.00 0.09	2.64 0.52 1.11	3.72–0.80 1.89	5.12–1.78 3.47
C_{III}'	0.58–0.00 0.18	1.12–0.00 0.51	7.26–1.34 3.08	13.26–3.44 6.18	16.78–4.42 8.22
A_0	0.40–0.00 0.17	0.66–0.00 0.34	1.68–0.00 0.84	1.80–0.16 0.99	3.66–0.24 1.62
A_{II}	1.14–0.36 0.73	2.26–0.60 1.30	5.12–0.76 3.17	5.96–1.76 4.82	9.58–1.96 5.79
A_{III}'	7.30–1.26 2.52	9.74–1.62 4.13	15.36–3.46 7.99	19.82–7.32 12.87	21.06–8.36 13.82

Each figures in lower rows show the mean value of six data.

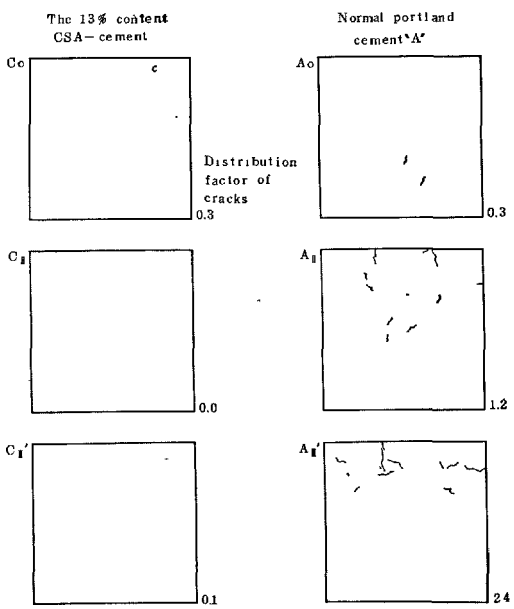

Fig. 24. *Cracking map at the age of 7 weeks*

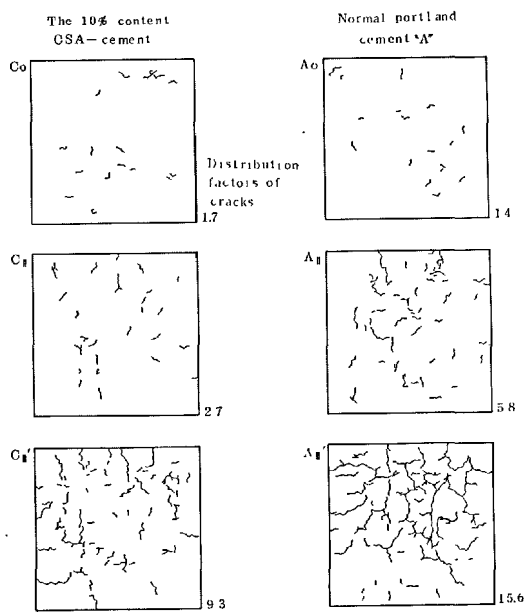

Fig. 25. *Cracking map at the age of 50 weeks*

had partly been released.

Test Series II-2

The aim of this test was to start the measurement of change in length immediately after casting concrete because the CSA-cement concrete in the foregoing test did not show a remarkable expansion.

Specimens

Type and size. A modified beam with the cross section of 20 × 20 cm² and the length of 200 cm was adopted for the specimens of reinforced concrete, as shown in Fig. 26. A beam with the same cross section and the length of 50 cm was adopted for the specimens of plain concrete. Each beam had steel end plates of 9 mm in thickness, where the measuring points made of small screws were installed. These end plates would serve to prevent the drying of concrete from the ends of beams.

For the specimens of reinforced concrete, the end plates were previously welded to the both ends of reinforcement bars; four deformed bars of 16 mm in diameter. The reinforcement ratio became 1.96%. For the specimens of plain concrete, four small bolts were attached to the inside of the end plates in order to secure the bond strength between the plate and concrete body.

Wooden forms were used for manufacturing the specimens. The above-mentioned end plates were fitted as the parts of form.

Aggregates, Cements. These were the same as those referred to in the first part of this test series.

Mixtures. For CSA-cement concrete, two kinds of w/c were applied, i.e., 0.70 and 0.55. For ordinary concrete w/c was 0.70. The mixtures were selected as shown in Table 5 by controlling their slumps to be about 18 cm.

Curing. The wooden forms were removed at the age of 5 days. Then, the specimens were cured in the room air of 18°C and 70% R. H.

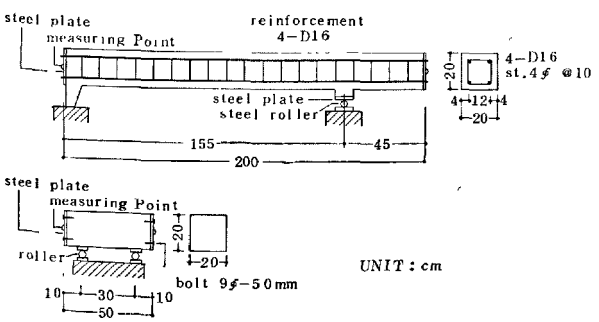

Fig. 26. *The specimens of beam type*

Measurement of Change in Length

The measurement was started at 6–8 hours after casting the concrete. Similar measuring apparatuses as used in Series I were used by providing exclusively one apparatus to one specimen. The results are shown in Fig. 27.

Change in Length in Young Age

All of the specimens of CSA-cement concrete showed a tendency of expansion in the period of one or two days after casting concrete, although the specimens of the ordinary concrete did not show any expansion nor contraction in this period. The magnitudes of expansion in the plain concrete were about 60% of the test results in Series I. The reason could mainly be attributed to the difference of CSA content of 13% and 10%. Besides, the forms would constrain the concrete against free expansion as the reinforcement bars do.

According to Table 12 which indicates the magnitude of the maximum expansion of each specimen, C_5(w/c = 0.55) showed somewhat larger expansion than C_7(w/c = 0.70), in both cases of plain concrete and reinforced concrete. And the expansion of reinforced concrete was only 37 and 38% compared with plain concrete for corresponding w/c of 0.7 and 0.55 respectively.

Dry Shrinkage and Crack

After the primary expansion, both of plain concrete and reinforced concrete mixed with CSA-cement showed dry shrinkage. The behaviors of these dry shrinkage were not so much affected by the difference

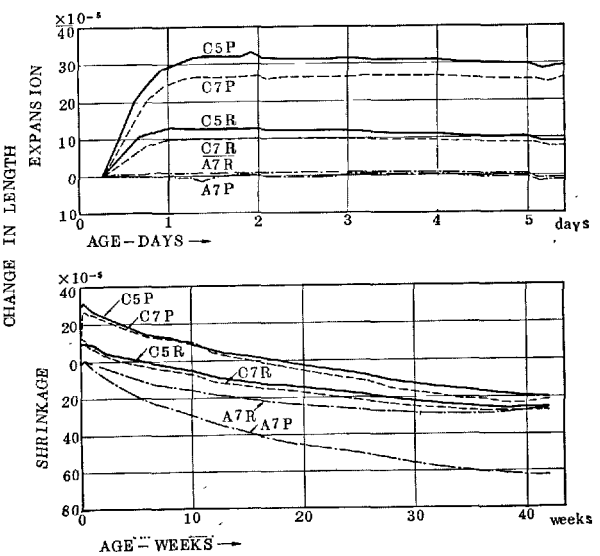

Fig. 27. *The change in length*

Table 12. *The influence of reinforcements on the shrinkage*

× 10^{-5} mm/mm

Symbol	Kind of cement	w/c	Reinforcements ratio %	Max. expansion	Ratio	Max. shrinkage	Ratio
C5P	CSA-cement	0.55	0	33.1	1.00	52.8	1.00
C5R	CSA-cement	〃	1.96	12.6	0.38	37.7	0.71
C7P	CSA-cement	0.70	0	27.0	1.00	48.2	1.00
C7R	CSA-cement	〃	1.96	10.0	0.37	37.0	0.77
A7P	Normal portland cement	〃	0	—	—	61.9	1.00
A7R	Normal portland cement	〃	1.96	—	—	25.9	0.44

of water-cement-ratios.

According to the observations on the cracks of the specimens many cracks transverse to the longitudinal axis of the specimens were found in the pitch of about 10 cm for the ordinary concrete, but very few cracks were found on the CSA-cement concrete.

Summary of this Section

The change in length and crack distribution of plain concrete and reinforced concrete mixed with CSA-cement were studied. Two kinds of CSA-cements which contained 13% and 10% of CSA were used in the separate test series.

In the case of CSA-cement with 13% CSA (w/c = 0.6)

*The plain concrete expanded remarkably in the first week after manufacturing the specimens. The maximum expansion was observed at the 9th day and the magnitude reached over 45×10^{-5} mm/mm. However, after these primary expansion, the CSA-cement concrete showed a large dry shrinkage similar to that of the ordinary concrete. Consequently, the amount of change in length became nearly zero after 15 weeks, when the length at 48 hours after casting concrete was taken as the standard.

*The reinforced concrete showed a similar tendency of primary expansion and successive shrinkage. However, the magnitudes were considerably small and the magnitude of dry shrinkage after the primary expansion decreased almost proportionally with the increase of reinforcement ratio.

*According to the observation of crack distribution on the surfaces of specimens, very little difference could be found between the plain concrete and the reinforced concrete with various kinds of reinforcement ratios. It is uncertain whether this phenomenon was proper to the CSA-cement with 13% CSA or it would be attributed to the low humidity of testing room.

In the case of CSA-cement with 10% CSA (w/c = 0.7)

*Any expansion was hardly observed after removing the concrete form. The observation of crack showed that plain concrete mixed with CSA-cement and the ordinary portland cement had a few cracks in a similar degree, and that the crack distribution increased with the increase of reinforcement ratio for both concrete, less cracks being found in the CSA-cement concrete than in the ordinary concrete.

A study on the CSA-cement concrete with 10% CSA by a special testing method gave the following results.

*For plain concrete, a considerable expansion was observed in the first one or two days and the magnitude of maximum expansion was about 60% of the CSA- cement concrete with 13% CSA. There was not so much difference of the primary expansion and successive shrinkage between two kinds of water-cement-ratios (w/c = 0.55 and 0.70), although the smaller water-cement-ratio gave somewhat larger expansion. The magnitude of dry shrinkage after the primary expansion was about 50×10^{-5} mm/mm at the age of 42 weeks. The corresponding shrinkage of the ordinary concrete was about 60×10^{-5} mm/mm.

*In the case of the reinforced concrete (reinforcement ratio = 1.96%), the magnitude of the primary expansion was less than 40% of the plain concrete for both water-cement-ratios. The shrinkage after the primary expansion was about 70% of the plain concrete at the age of 42 weeks and the amount of the change in length became almost equal to that of the ordinary reinforced concrete. However, very few cracks were observed on the specimens of the CSA-cement concrete, although considerably much cracks were found on the ordinary concrete.

Application to Field Concrete

Up to the present, CSA has been applied in some construction works, including the experimental building (Aug. to Dec. 1964), Nagano Prefectural Office (Apr. 1966 to Mar. 1967), the experimental

paving (Mar. to Apr. 1964) and Noheji By-pass, Aomori Prefecture (Nov. to Dec. 1966), etc. From the above examples, CSA-cement concrete decreased cracks in building and made it possible to perform 60 meters long paving without expansion joints. Also, many other desirable results were obtained. The experimental building and paving that has been metnioned above will be briefly reported hereinafter.

Test 1. Example of Application to Building Works (Experimental Building)

The experimental building and dummy slabs were prepared for measurement of the difference between the 13% content CSA-cement concrete and normal portland cement concrete. The experimental building was composed of two one-storied buildings connected by expansion joint at the central part as shown in Fig. 28.

Dummy slabs were comprised with or without reinforcement. The effects due to expansion of CSA were observed by making comparative studies of inner stresses caused in roof slabs and dummy slabs, and cracks occurred in roof slabs and wall panels. Mixing-ratio of concrete used is shown in Table 13.

Measurement of change in length of roof slabs and dummy slabs was made by using Carlson type extensometer and that of constrained deformation by Carlson type strainmeter. The location of measurement of roof slabs are shown in Fig. 29.

Temperature and humidity during measuring period are shown in Fig. 30. The condition of weather involving rain, snow or sleet during the first 3 months was similar to that in case of wet curing, and the slow appearance of compressive strength seemed due to the effect of low temperature at the beginning of that period.

The compressive strength of concrete is shown in Table 14. Addition of CSA has not a tendency to reduce compressive strength in case of field curing.

Fig. 31 shows the change in length of dummy slabs, and also clearly indicates expansive effect due to CSA.

Fig. 32 shows the inner stresses of concrete. It is clear that there exists inner compressive stresses due to reinforcement constraint. On the other hand, tensile stresses occurr in normal portland cement

Table 13. *Mix proportion of concrete*

Ingredient / Kinds of concrete	Cement kg/m³	CSA kg/m³	Water kg/m³	Sand kg/m³	Gravel kg/m³
Normal portland cement concrete	350.0	0	200	805	1061
The 13% content CSA-cement concrete	304.4	45.6	200	805	1061

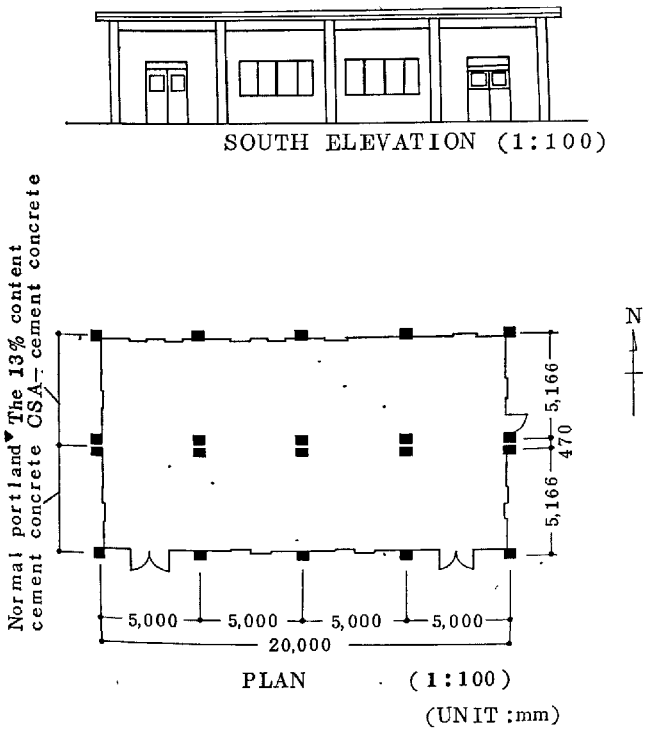

Fig. 28. *Plan and south elevation*

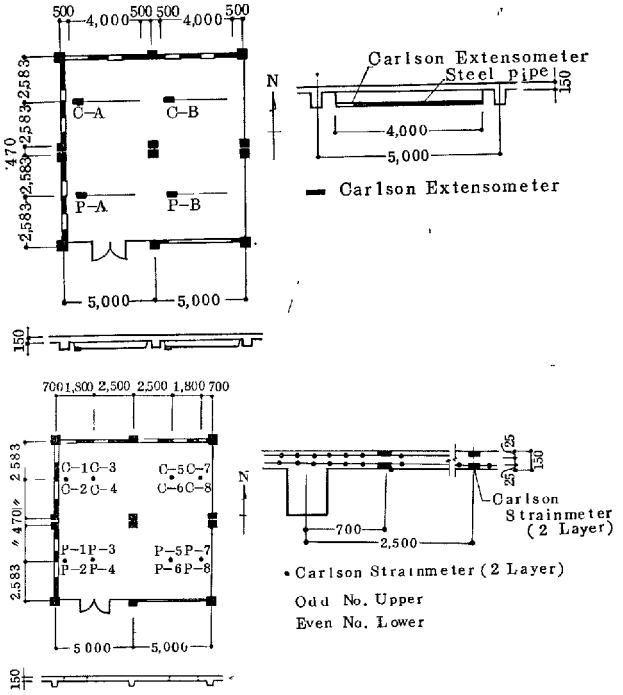

Fig. 29. *The location of measurement of roof slabs (Unit: mm)*

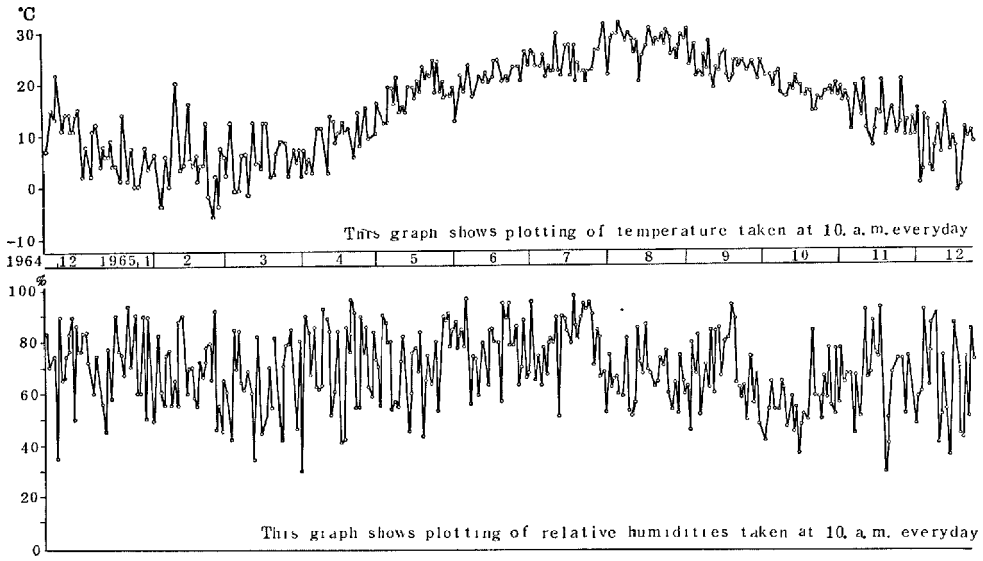

Fig. 30. *Temperature and relative humidity during measuring period*

Table 14. *Compressive strength of concrete*

Kind of concrete / Method of curing	Age-days	Compressive strength kg/cm²			
		7 days	28 days	270 days	400 days
Normal portland cement concrete	Air curing	—	327.1	—	—
	Field curing	86.2	181.2	278.5	398.7
The 13% content CSA-cement concrete	Air curing	—	278.1	—	—
	Field curing	99.9	185.9	303.1	341.3

Air Curing = Air curing (20°C 80% R.H.) after 3 days water curing (20°C)

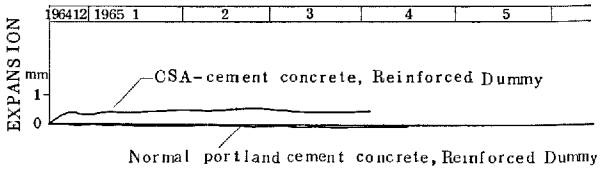

Fig. 31. *Change in length of dummy slab by carlson extensometer*

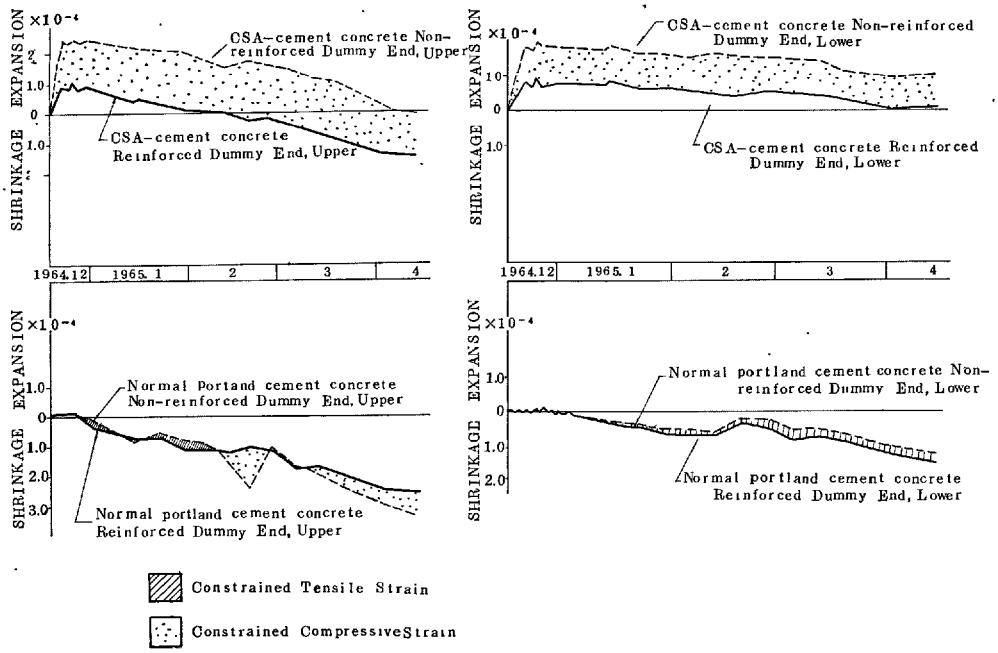

Fig. 32. *Camparison of inner stresses of concrete due to reinforcement constraint by carlson strainmeter*

concrete.

Fig. 33 shows change in length of roof slab at end span, and the 13% content CSA-cement concrete expands by approximately 0.5 mm (1.0×10^{-4}) and is restored to the original length after 1 year. Normal portland cement concrete shrinks by approximately 0.6 mm (1.2×10^{-4}) after 1 year.

Fig. 34 shows the results of the inner stresses of roof slab at end span. It is noted from these results that the 13% content CSA-cement concrete shows larger expansion rate on the upper side and normal portland cement concrete always shows larger shrinkage rate on the upper side.

Fig. 35 shows the condition of cracks that occurred on wall surface after 1 year. Cracks began to occur at the 5th month. During the period from 5th to the 8th month, the occurrence and growth of cracks were prominent probably because of the summer season, However, any change was hardly observed during the following 4 months.

No distinct cracks, however, were observed on the roof slabs.

By the use of CSA, it is possible to create compressive stresses, although in small amounts, within concrete through constraint due to reinforcement, and therefore, it is considered advantageous to use it for building. And, it is also considered to have distinct effect in decreasing shrinkages and cracks. However, the occurrence of a crack as large as 1.2 mm at a certain spot yet remains for us to be studied.

Test 2. Example of Use in Paving (Experimental Paving)

The experimental paving and dummy pavement were prepared for measurement of the difference with the 10%, 13% content CSA-cement concrete and normal portland cement concrete. And, the possibility of increasing the distance between expansion joints and decreasing the thickness of paving were studied. Dummy pavement that avoid surface friction from botton were placed on grease coated steel plate. The experimental paving was approximately 50 meters long and 2 lanes wide as shown in Fig. 36. Mixing-ratio of concretes are shown in Table 15.

On experimental paving, changes of joints width were measured by Carlson type extensometer, con-

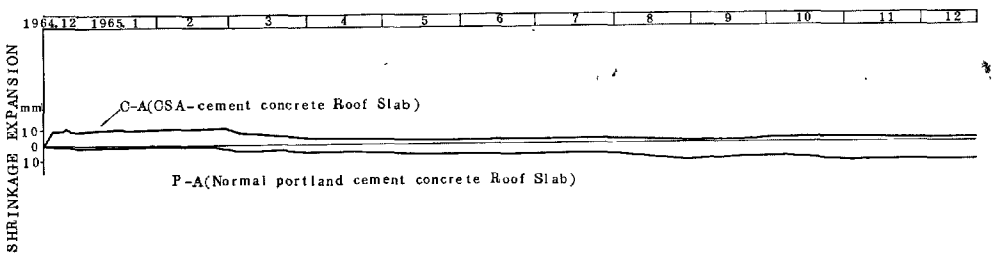

Fig. 33. *Change in length of roof slab at the end span by carlson extensometer*

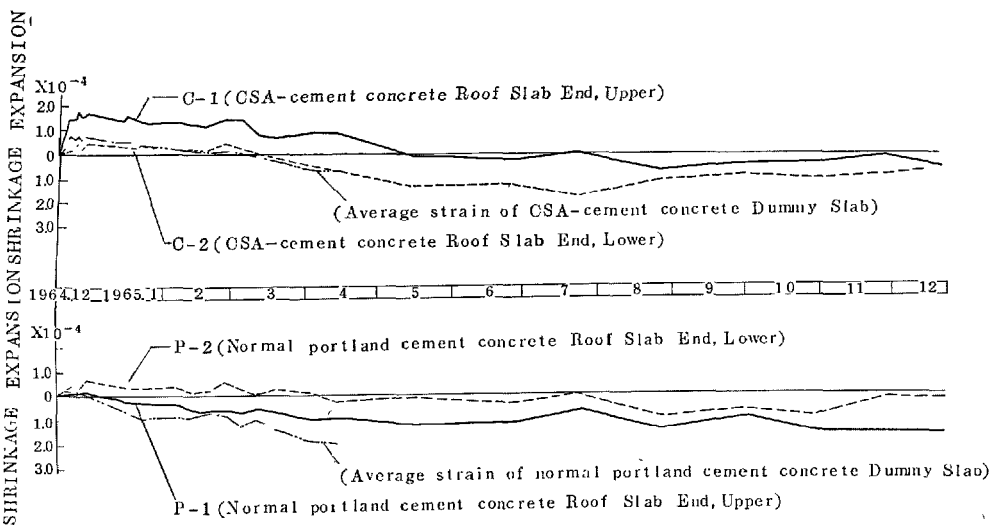

Fig. 34. *The results of measurement by carlson strainmeter on roof slabs*

strained strain by Carlson type strain meter, warping deformation by dial gage and inner temperature of concrete by thermocouple. And on dummy pavement, the changes in length were measured by contact strain meter, and inner temperature of concrete was measured.

Temperature and humidity during measuring period are shown in Fig. 37.

Table 15. *Mixproportion of concrete*

Ingredient / Kind of concrete	Cement kg/m³	CSA kg/m³	Water kg/m³	Sand kg/m³	Gravel kg/m³	Pozzolith No. 8 kg/m³
Normal portland cement concrete	325.0	0	146.5	668	1,285	0.812
The 10% content CSA-cement concrete	292.5	32.5	〃	〃	〃	〃
The 13% content CSA-cement concrete	282.7	42.3	〃	〃	〃	〃

Compressive and flexural strengths of concrete are shown in Table 16. In case of water curing, there is no difference in compressive strength at 28 days be-

Table 16. *Compressive and flexural strengths of concrete*

Kind of concrete / Method of curing	Age-days	Compressive strength kg/cm²		Flexural strength kg/cm²
		7 days	28 days	28 days
Normal portland cement concrete	Water curing	291	430	49.4
	Air curing	230	320	33.0
The 10% content CSA-cement concrete	Water curing	300	396	58.2
	Air curing	265	356	28.8
The 13% content CSA-cement concrete	Water curing	337	423	51.7
	Air curing	287	409	44.5

Water curing (20°C)
Air curing = Air curing (20°C 80% R.H.) after 3 days water curing (20°C)

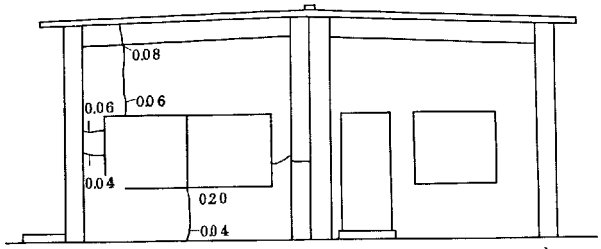

(Normal portland cement concrete) (CSA-cement concrete)

EAST ELEVATION

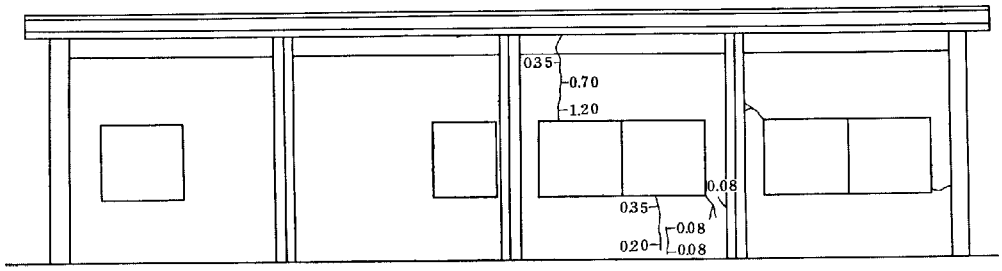

NORTH ELEVATION (CSA-cement concrete)

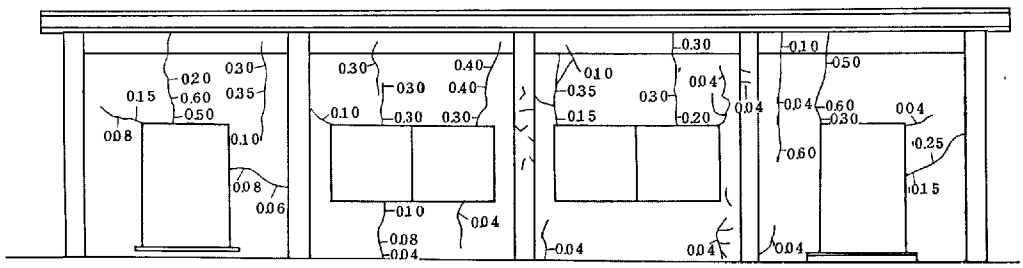

SOUTH ELEVATION (Normal portland cement concrete)

—61—

Fig. 35. *Cracking map on wall crack width . . . unit: mm*

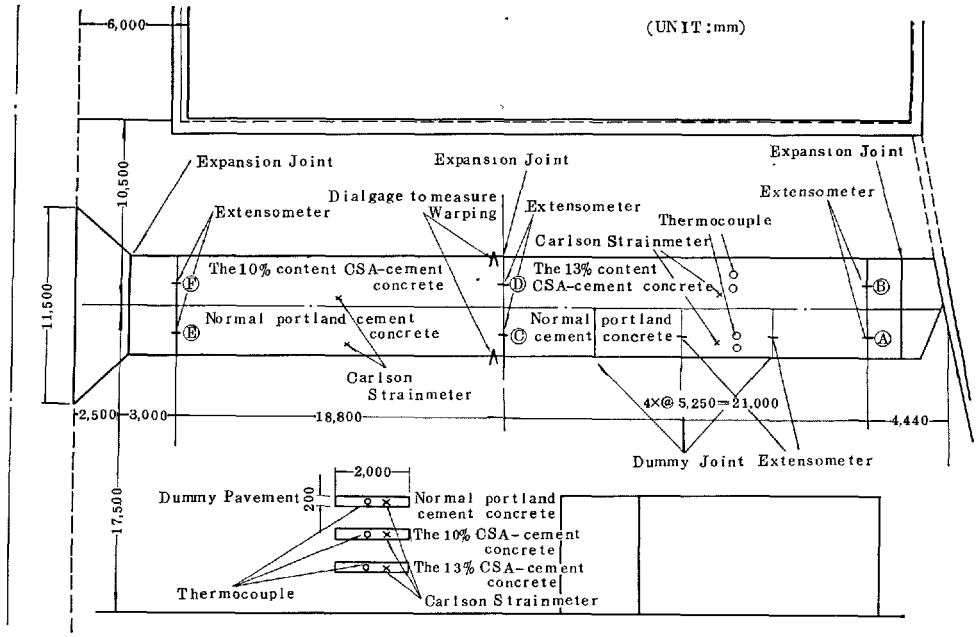

Fig. 36. *Plan of experimental paving and dummy pavement (Unit: mm)*

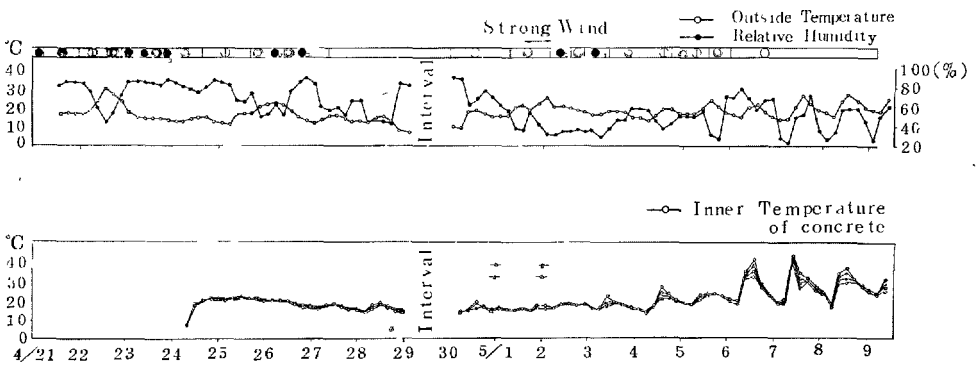

Fig. 37. *Outside temperature and relative humidity and inner temperature of concrete*

tween normal portland cement concrete and the 10%, 13% content CSA- cement concrete. However, in case of field curing, addition of CSA increases compressive strength at 28 days.

Fig. 38 shows the comparison of changes in length of dummy pavement for the 10%, 13% content CSA-cement concrete and normal portland cement concrete. It was found that the maximum change in length is about 0.4 mm due to temperature change in a day in every cases.

An example of change in width of expansion joint of experimental paving is shown in Fig. 39. The difference between CSA- cement concrete and normal portland cement concrete is clearly observed. The results of measurement in central parts of paving by Carlson type strain meter are shown in Fig. 40. The average strain that is calculated in Fig. 39 and the strain in Fig. 40 do not correspond. This suggests a reason why the constrain at central part of paving should have been very large as compared with that of the end. The strain in opposite directions on upper and lower surfaces of paving were shown with mark "0" in Fig. 40. These phenomena are presumed to have happened due to constrained deformation. Strains were 0.5×10^{-4} or around.

Average strain is obtained by dividing the movements of paving ends measured with joint extensometer by the distance between expansion joints, and it is plotted together with the strain of dummy pavement in Fig. 41. According to Fig. 41, the maximum

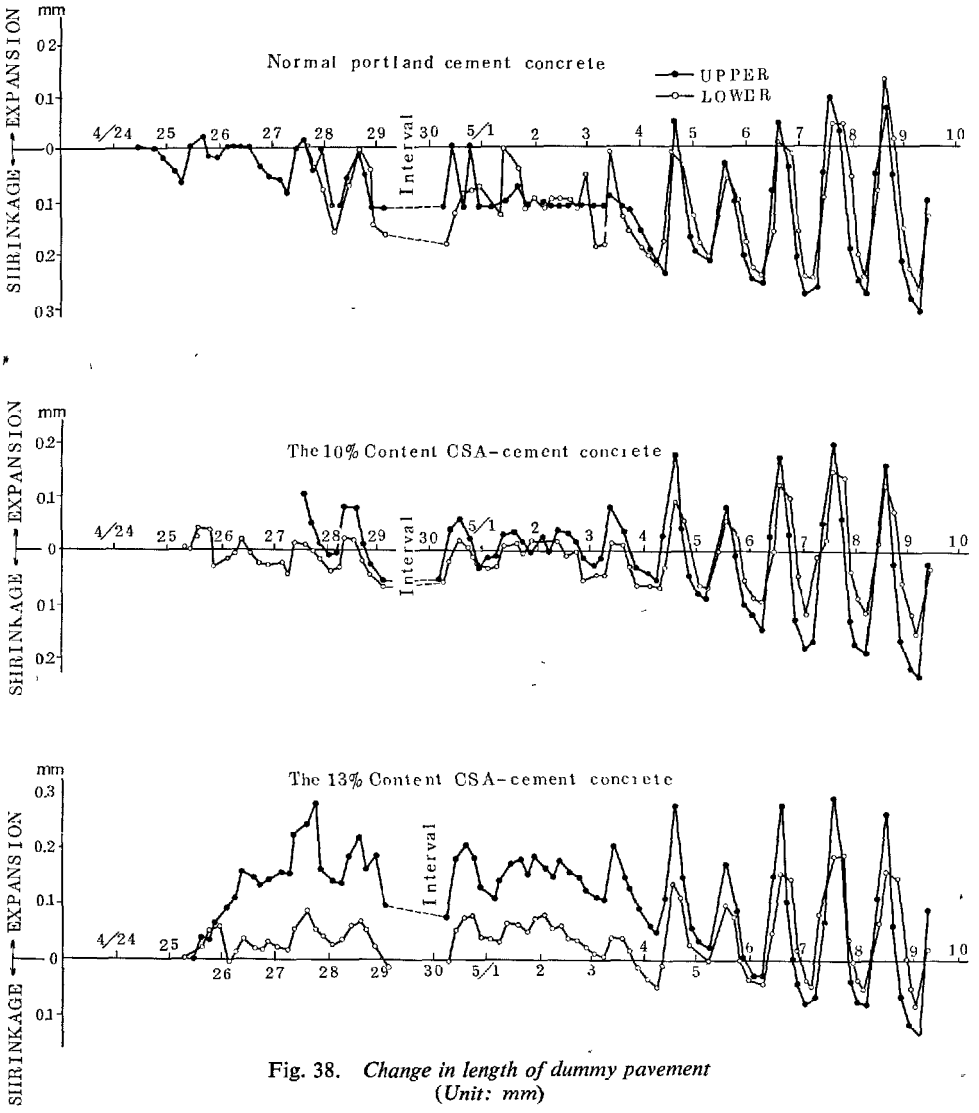

Fig. 38. *Change in length of dummy pavement*
(Unit: mm)

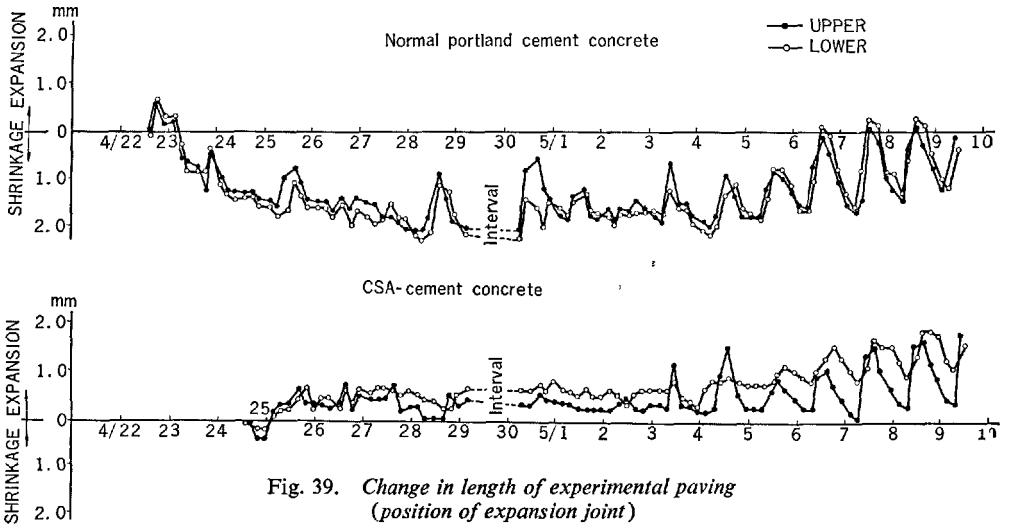

Fig. 39. *Change in length of experimental paving*
(position of expansion joint)

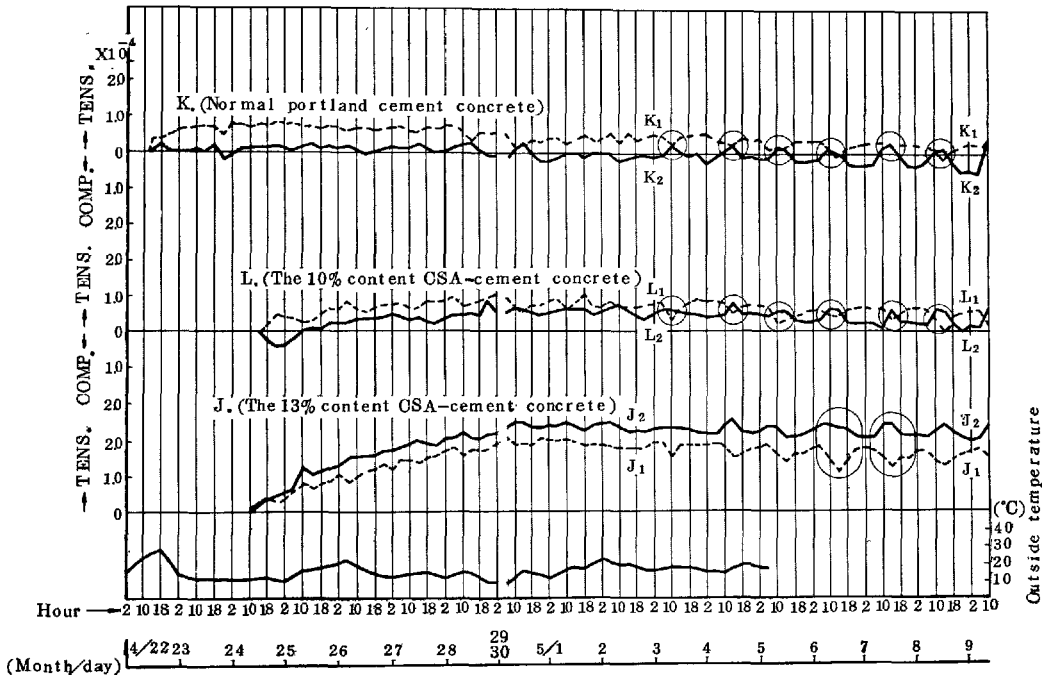

Fig. 40. *Strain of experimental paving by carlson strainmeter*

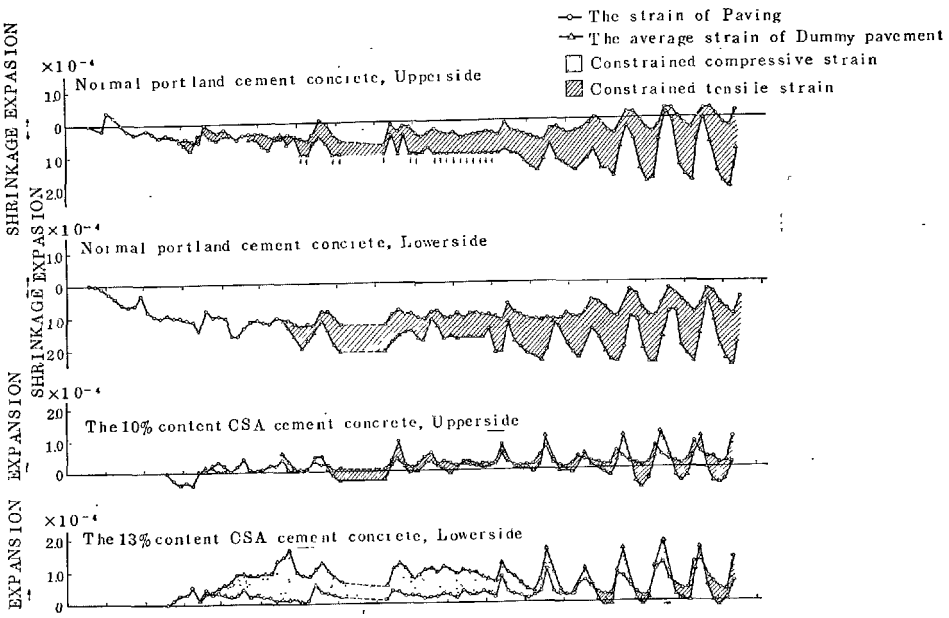

Fig. 41. *Inner constrained stresses*

constrained tensile strain of normal portland cement concrete is 1.6×10^{-4}. If "3/4 of constrained shrinkage deformation remains to be creep and 1/4 as tensile stress"*, then it must be considered that, by taking modulus of elasticity for 2.5×10^{6} kg/cm² along its total length, and in view of this value being an average one, there are some local parts where the value are higher than the average one.

No crack has so far been observed in any of paving, although there were differences in inner stresses as mentioned above. It is common practice to provide a construction joint in every 8 to 10 meters in ordinary

*N.B. Opinion of Mr. Taiji Saji, Kyushu University.

concrete paving. The reason for observing no crack in this experiment may be that the job site was in rainy area and that traffic over the road was not so busy. However, as far as the use of expansive concrete was able to decrease greatly the inner stresses that had occurred within the paving, and with the use of 13% content CSA cement concrete, it was possible to decrease tensile side constrained deformation down to 1/10 approximately.

Supplementary Paper IV-85 General Behavior of Mortar and Concrete Made of Expansive Cement with Calcium Sulphoaluminous Cement Clinker

Tadao Nishi,* Tamotsu Harada and Yoshiro Koh*****

Synopsis

In this paper are reported the results of various experiments which were carried out for the purpose of checking inspection on general behaviors of the expansive cement mortar and concrete, on length change effects, strength, creep, modulus of elasticity, effect of steam curing, effect of resistance to rusting of steel, carbonation (neutralization) of concrete using the expansive cement, thermal properties of the expansive cement concrete, resistance to chemical attack (containing sea water attack) and resistance of the concrete to its frost action, and so on.

These tests for check were carried out with concrete or mortar which used cement containing various contents of calcium sulphoaluminous cement clinker, and the main results obtained were as follows:

Concrete of cement with about 10% content of the expansive agent showed good effects on compressive strength, bond strength and showed that the tendency of carbonation and steel rusting of the concrete with expansive cement of this content was a little larger than that of ordinary cement concrete, but it will be reduced to the same rate as that of ordinary concrete by adding dispersion admixture.

Intensity of expanding pressure reached to maximum at 7 days after reaction and decreased when cured in water.

Effect of steam curing on expansive cement concrete was recognized.

Thermal properties such as effect of high temperature on strength, or thermal conductivity of the expansive cement concrete were observed.

The strength of the expansive cement concrete was rather promoted in alkali solution, but in the solution containing dilute sulphuric acid solution, its strength was reduced as much as the ordinary portland cement concrete.

The sea water resistance of the expansive cement concrete was good.

The result of freezing and thawing test showed that there was not much difference between the expansive cement mortar and the ordinary cement mortar.

This paper is based on a number of test results carried out by Tadao Nishi*, Tamotsu Harada**, Yoshiro Koh***, Kazuo Gotoh[1], Kazuyoshi Hirai[2], Touhei Horishima[3], Kyubei Kizawa[4], Hiroshi Kuriyama[5], Hiroshi Muruguma[6], Syoichi Okushima[7], Yoshizo Ono[8], Taiji Saji[9], Toyokazu Shiire[10], Kazuhisa Shirayama[11] and Eiichi Tazawa[12].

*The University of Tokyo, Tokyo, **Kanagawa University, Yokohama and ***Hokkaido University, Sapporo, Japan.
*Professor, The University of Tokyo, Japan.
**Professor, Kanagawa University, Japan.
***Professor, Hokkaido University, Japan.
[1]Professor, Industrial Materials Research, Tokyo Institute of Technology, Japan.
[2]Assistant Professor, Tohoku University, Japan.
[3]Chief Engineer, Technical Laboratory, Taisei Construction Co., Ltd., Japan.
[4]Professor, Nagoya Institute of Technology, Japan.
[5]Professor, Tohoku University, Japan.
[6]Professor, Kyoto University, Japan.
[7]Professor, Osaka University, Japan.
[8]Chief Researcher, Technical Laboratory, Denki Kagaku Kogyo Co., Ltd., Japan.
[9]Professor, Kyushu University, Japan.
[10]Associate Professor, Tokyo Institute of Technology, Japan.
[11]Chief Researcher, Building Research Institute, Ministry of Construction, Japanese Government.
[12]Researcher, Technical Laboratory, Taisei Construction Co., Ltd., Japan.

Introduction

The purpose of this paper is to clarify the general behavior of CSA-cement mortar and concrete, among others the effects of the contents of CSA and the curing conditions on the physical properties of mortar and concrete compared with ordinary mortars and concretes.

The durability and thermal properties were also tested in the light of every possible usage of the cements.

Two types of expansive cements with different calcium sulphoaluminous cement clinker were used in our experiments. The molar-ratios CaO: Al_2O_3: $CaSO_4$ of calcium sulphoaluminous cement clinkers were adjusted to 3: 1: 3 and 4: 1: 3.

The meanings of following abbreviations used in this paper are as follows.

CSA:	Calcium sulphoaluminous cement clinker
CSA-cement:	Expansive cement with calcium sulphoaluminous cement clinker
CSA-cement mortar:	Mortar made of CSA-cement
CSA-cement concrete:	Concrete made of CSA-cement
3–1–3 CSA:	The molar-ratio CaO: Al_2O_3: $CaSO_4$ of CSA is 3: 1: 3
4–1–3 CSA:	The molar-ratio CaO: Al_2O_3: $CaSO_4$ of CSA is 4–1–3
10% CSA:	Expansive cement with 10% content of CSA

Effects of Mixing Contents and Curing Conditions on the Expansion-Shrinkage Characteristics

Influence of Various Factors

Procedure and Results

In the factorial experiment shown in Table 1, the effects of a number of different factors on the expansion-shrinkage characteristics are investigated simultaneously.

The concretes were made with the normal portland cement and 3–1–3 CSA and were cast in 10 × 10 × 40 cm prisms. Results of the experiment with all factors were shown in Table 2.

In the analyses of variance for the expansion-shrinkage values at the age of 180 days, the relative efficiency of all factors were estimated in Table 3.

Table 1. *Factors and levels*

Factor	Level			
	1	2	3	4
CSA content*	0%	13%	—	—
Cement paste content	30%	25%	—	—
W/C-ratio	70%	50%	—	—
Coarse aggregate	River gravel	A.L.A.**	—	—
Admixture	none	A.E. agent	Dispersing agent	Retarder
Fine aggregate ratio	45~50%	35~40%		
Initial curing	stored in room	cured in water	—	—
Relative humidity	70%	80%	—	—

* Normal porltand cement + CSA
**Artificial light-weight aggregate

Concluding Remarks

Concluding remarks obtained are as follows.

(1) Among these factors which affect the expansion-shrinkage of concrete, the mixing content of CSA is most significant.
(2) The effect of admixtures is great following the mixing contents of CSA.
(3) As the conditions of the initial curing differ, the difference of the expansion-shrinkage of concrete is recognized.
(4) The effect of cement paste contents can be found, but is relatively low.

Effects of another factors have the same tendency as in the case of the ordinary concrete.

Effect of CSA-Contents

Prodedure and Results

A. The effect of variation in the CSA-content on the expansion-shrinkage of CSA-cement mortar was investigated. The normal portland cement and standard sand were used as cementing material and aggregate respectively. The specimens were cast in 25 × 25 × 280 cm prisms, and cured in water at the age of 3 days, and then placed in air at 20°C and 80% R. H.

Table 2. *Results (by T. Shiire)*

No.	Conditions							Expansion-shrinkage value* $\times 10^{-5}$	
	CSA content %	Cement paste content %	W/C-ratio %	Coarse aggregate	Fine aggregate ratio %	Initial curing	Relative humidity %	30 days	180 days
1	0	30	70	River gravel	45	in room	70	−35	−65
2	0	30	70	A.L.A.	50	in water	70	−20	−64
3	13	30	70	River gravel	35	in room	80	+10	−38
4	13	30	70	A.L.A.	40	in water	80	+66	+34
5	0	30	50	River gravel	35	in water	80	−24	−80
6	0	30	50	A.L.A.	40	in room	80	−1	−46
7	13	30	50	River gravel	45	in water	70	+32	−4
8	13	30	50	A.L.A	50	in room	70	−17	−48
9	0	25	70	River gravel	35	in water	70	−39	−78
10	0	25	70	A.L.A	40	in room	70	−18	−45
11	13	25	70	River gravel	45	in water	80	+88	+32
12	13	25	70	A.L.A	50	in room	80	+48	+6
13	0	25	50	River gravel	45	in room	80	−17	−54
14	0	25	50	A.L.A	50	in water	80	+3	−48
15	13	25	50	River gravel	35	in room	70	−21	−45
16	13	25	50	A.L.A	40	in water	70	+94	+54

*+: expansion
−: shrinkage

Table 3. *Efficiency of factors*

Factor	Efficiency of factor %
CSA content	52.7
Cement paste content	3.9
Coarse aggregate	7.0
Admixture	22.1
Initial curing	7.5
Relative humidity	2.1
Error	4.7
Total	100

Table 4. *Mix-proportion of CSA and expansion-shrinkage of CSA cement mortar (by T. Saji)*

3-1-3 CSA content %	Rate of expansion-shrinkage $\times 10^{-5}$*				
	3 days	7 days	28 days	63 days	118 days
0	0	0	−38	−22	−43
5	+18	+14	−25	−5	−29
10	+102	+145	+116	+127	+105
13	+159	+213	+272	+386	+508
20	+539	+1171	+1940	+2620	—
30	+1900	(4 days) +2520	—	—	—

*+: Expansion
−: Shrinkage

Table 4 shows the results measured. Note that additions of 20 and 30% CSA-contents to the mortar resulted in the expansive cracks.

B. And the effect of variation in the CSA-content on expansion-shrinkage of the CSA-cement concrete was investigated, too. Normal portland cement, portland blast-furnace cement and fly ash cement were used as cementing material, and natural river sand and gravel were used as aggregates. W/C-ratio was about 0.6, and the slump was expected to be 18 to 20 cm. The specimens were cast in 10 × 10 × 50 cm prisms, and were removed from the molds at the age of 24 hours, and then stored in a room. The results obtained are shown in Table 5.

Concluding Remarks

The following conclusion will be gained.

Table 5. *Mix-proportion of CSA and expansion-shrinkage of CSA cement concrete (by T. Nishi)*

Cement type	3-1-3 CSA content %	Rate of expansion-shrinkage* $\times 10^{-5}$				
		3 days	7 days	28 days	63 days	105 days
Normal portland cement	0	+5	−2	−21	−51	−60
	10	+5	+2	−13	−40	−48
	13	+18	+13	−2	−24	−33
Portland blast-furnace cement (Type-B)	0	+15	+11	−3	−20	−33
	10	+12	+8	+4	−8	−16
	13	+18	+12	+6	−8	−16
Fly-ash cement (Type-B)	0	+1	+2	−12	−39	−48
	10	+6	+8	0	−21	−31
	13	+24	+33	+20	−1	−11

*+: Expansion
−: Shrinkage

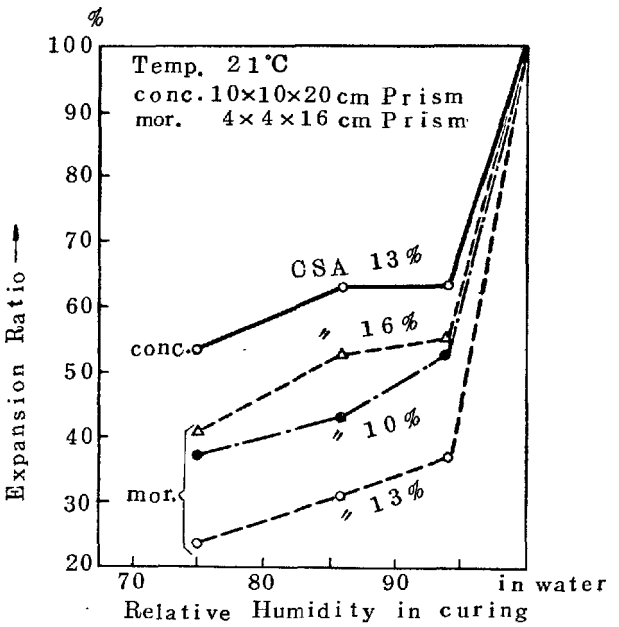

Fig. 1. *Relation between initial curing condition and the maximum expansion of the respective CSA-cement mortar and concrete (by T. Shiire)*

(1) If the CSA- content is less than 5%, the apparent effect of CSA-mixture on compensation of shrinkage is not observed.
(2) If the CSA-content is more than 20%, even expansion cracks are markedly observed.
(3) The rate of drying shrinkage after finishing the initial expansion of CSA-cement mortar and concrete is little different from that of the ordinary cement mortar and concrete.

Effect of Curing Condition

Procedure and Results

A. The relation between the initial curing humidity and the expansion of CSA-cement mortar and concrete is shown in Fig. 1.

In this experiment, the normal portland cement, 3–1–3 CSA and natural river sand and gravel were used as the mixing materials of the concrete. The mixing ratio of cement to fine aggregate and W/C-ratio for the mortar specimens were 1: 3.75 and 0.65 by weight respectively. For the concrete specimens, the proportion of cement: fine aggregate: coarse aggregate and W/C-ratio were 1: 2.58: 2.44 and 0.6 by weight respectively. All specimens reached to arbitrarily constant expansion value at the age of around 7 days.

B. The expansion value of 13% CSA-cement mortar which was, prior to water curing, dried in air at 70% R. H. at the various ages is shown in Fig. 2. The mixing proportion of cement: fine aggregate and W/C-ratio were 1: 1.5 and 0.45 by weight respectively.

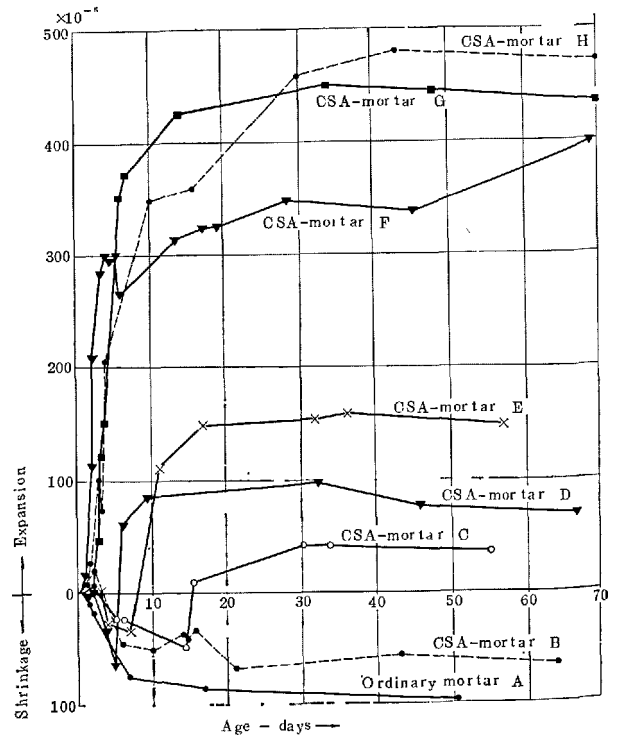

Fig. 2. *Expansion-shrinkage value of CSA-cement (3-1-3, 13% CSA) mortars effected by various initial curing conditions (by H. Muguruma)*

Notes of Fig. 2

A, B: Curing in room, temp. 20°C, R.H. 70%
C: Curing in water after 15 days curing in temp. 20°C, R.H. 70%
D: Curing in water after 4 days curing in temp. 20°C, R.H. 70%
E: Curing in water after 8 days curing in temp. 20°C, R.H. 70%
F: Curing in water temp. 40°C
G: Curing in water after 2 days in temp. 20°C, R.H. 70%
H: Curing in water temp. 20°C

Table 6. *Curing method and expansion-shrinkage of concrete (by K. Shirayama)*

CSA-content %	Curing Condition	Rate of expansion-shrinkage* $\times 10^{-5}$				
		1 week	2 weeks	4 weeks	13 weeks	1 year
0	in water	−5	−5	−6	−7	−21
	in polyethylene bag	+5	−7	−4	−10	—
	indoor	—	−27	−39	−64	−91
	outdoor	—	−21	−26	−19	−16
13	in water	+146	+161	+162	+146	+188
	in polyethylene bag	+88	+92	+90	+82	—
	indoor	+55	+42	+32	+14	−1
	outdoor	—	+128	+111	+136	+130

*+: Expansion
−: Shrinkage

C. The concrete specimens were cured in either of four ways for a long time. Some were placed in water, some in a room, some in the open air, and the others were placed in polyethylene bags. The expansion data in these cases were shown in Table 6.

In this experiment, the ordinary portland cement, 3-1-3 CSA and natural river sand and gravel were used as cementing materials and aggregate respectively. The cement contents of concrete specimens were 340 kg per cubic meter, and slump was 21–23 cm. W/C-ratio was 0.60. The specimens were cast in 15 × 30 cm cylindrical mold.

D. The expansion values of mortars cured in water at 20°C and 40°C were shown in Fig. 2. And the expansion values of mortars cured in water at 20°C and 5°C were shown in Table 7.

In this experiment the ordinary portland cement, 4-1-3 CSA and the standard sand (Japanese standard sand conforming to JIS R5201) were used as cementing material, expansive admixture and aggregate respectively, the mixing proportion of cement to fine aggregate was 1:2 by weight. The specimens were cast in 4 × 4 × 16 cm prisms.

Table 7. *Curing temperature and expansion of concrete (by K. Kuriyama)*

4-1-3- CSA content %	Temperature of curing water, °C	Expansion value $\times 10^{-5}$		
		3 days	7 days	19 days
0	20	21	42	102
	5	5	−6*	69
10	20	105	138	204
	5	36	54	161

*Minus sign indicates shrinkage

Concluding Remarks

The concluding remarks obtained from this experiment are as follows.

(1) The expansion value of CSA-cement mortar and concrete cured in drying air was about 1/2 or less than that of the mortar and concrete cured in water.
(2) The expansion, when cured in water, ceased to grow by one or two weeks.
(3) The longer a curing in drying air was conducted before water curing, the less expansion value was obtained after water curing. In order to get the expansion of about 30×10^{-4} which might be necessary for the chemical prestressing, the concrete should be cured in air for less than 3 days.
(4) If the temperature of curing in water is 5°C or 40°C, little effective expansion is obtained as compared with 20°C.

Summary and Conclusion

(1) Effects of CSA on the expansion of mortar and concrete are produced. However, the drying shrinkage from the maximum free expansion is little different from that of ordinary mortar and concrete. The effective and stable expansion depends on the mix content of CSA.
(2) To produce the effective expansion, it is necessary to supply the sufficient water at the early age. The sooner the water supply, the better the effect is produced.
(3) If the temperature of water curing is too high or too low, the effective expansion of CSA-cement mortar or concrete does not grow.

Mechanical Properties of Mortar and Concrete Made of CSA-Cement

Mechanical Properties of CSA-Cement Mortar

A number of flexural and compressive strengths tests were made on CSA-cement mortar specimens. Following six test series mainly on the effect of curing conditions were carried out by four research institutions.

M 1: Effect of curing conditions on flexural and compressive strength of mortars (Ono).

M 2: Effect of curing conditions on flexural and compressive strength of mortar (Shirayama).

M 3: Effect of curing temperature on compressive strength of mortars using diluvial sand and 3–1–3 13% CSA-cement (Koh and Gotoh).

M 4: Effect of curing temperature and content of CSA on compressive strength of mortars using diluvial sand and 3–1–3 CSA-cement, made in 1964 and 1965 (Koh and Gotoh).

M 5: Effect of curing temperature on compressive strength of mortars using diluvial sand and 4–1–3 10% CSA-cement (Koh and Gotoh).

M 6: Effect of proportion and flow of mortars on flexural and compressive strength of mortars using river sand and 4–1–3 10% CSA-cement (Kuriyama and Hirai).

Series M1

This is a part of fundamental test series to decide the amount of addition of CSA to normal portland cement. Three curing conditions, water curing, air dry conditions and air dry after 3 days water curing, were compared with each other, from the viewpoint of the drying condition at building site which causes the drying shrinkage.

Specimens in this series were 4 × 4 × 16 cm beam according to JIS for testing the strength of cement. Standard and a river sand were used for making mortars and their water cement ratios were 0.65 and 0.45 respectively. The mixing proportion of cement and sand was fixed to 1: 2 by weight. Both 3–1–3 and 4–1–3 CSA were tested and the content of CSA were varied from 0 to 15%.

Series M2

In the test for measuring creep of mortar, the flexural and compressive strengths were tested after curing in water or air for 7 days to 1 year. 4 × 4 × 16 cm beam were made of 3–1–3 13% CSA-cement and standard sand (w/c = 0.60).

Series M3, M4 and M5

Four kinds of mortar mix, with their water cement ratio varied over arange of 0.45, 0.55, 0.65 and 0.75, were tested after curing at 5 and 20°C for planned periods varying from 3 days to 1 year as shown in Table 8. Curing at 0°C was also applied only in M 3 series. The mortar mixes, in which definite diluvial sand was used, were always fixed to compare the effect of low temperature with that of definite ordinary portland cement of Hokkaido district, which is selected as a standard for making our chart[1] for selecting water cement ratio to get required strength, established by Koh by using maturity according to Saul-Bergström.

The specimens were 4 × 4 × 8 cm square column, and most of them were wrapped with polyethylene sheet and cured in air. Curing in water or air is also carried out. The compressive strength was tested at definite ages from 3 days to 1 year as shown in Table 8. The results obtained are shown in Figs. 3 and 4 the series M 3 and M 5 respectively.

Series M6

Nine kinds of river sand mortar were used for the tests of flexural and compressive strength by using 4 × 4 × 16 cm beam specimens made of 4–1–3 10% CSA-cement. The results obtained are shown in Fig. 5.

Table 8. *Experimental scheme of series M3-M5 (by Y. Koh, T. Gotoh)*

Test Series	M3	M4	M5
Specimen	4 × 4 × 8 cm square column		
Mortar mixture (without admixture)	W/C: 0.45, 0.55, 0.65, 0.75	Cement : Sand: 1 : 2.13, 1 : 2.75, 1 : 3.40, 1 : 4.13	Flow: 200 mm
Cement	Normal portland cement		
	3-1-3 CSA-cement (1964)	3-1-3 CSA-cement (1964 & 1965)	4-1-3 CSA-cement (1966)
CSA content	13	5, 10, 13	10
Curing of specimens °C	In air (wrapped in plastic sheet) 0, 5, 20	in air (wrapped in plastic sheet)	5, 20
	In air 0, 5		
	In water 20		
Age	3, 7, 14, 28, 56, 91, 182, 365 days		

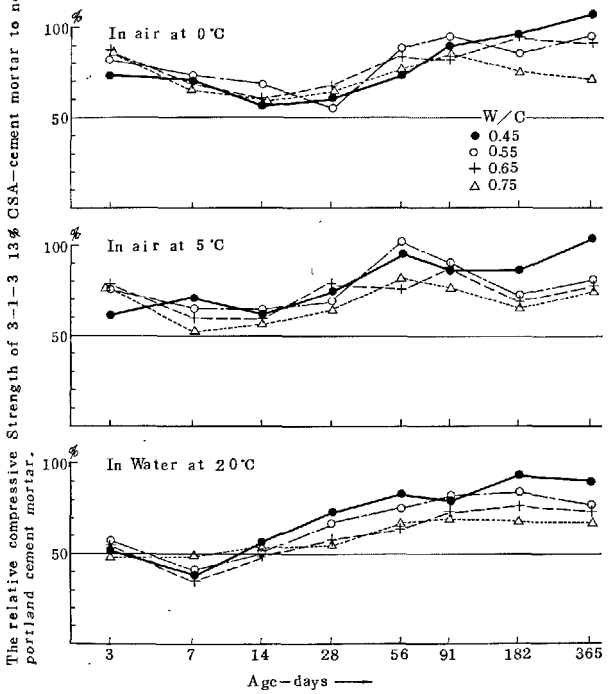

Fig. 3. *Part of test results in series M3 (by Y. Koh, T. Gotoh)*

Mechanical Properties of CSA-Cement Concrete

Nine series of compressive strength tests and two series of tensile strength tests were carried out and elastic moduli were measured by four different research institutions to learn mainly on the effects of curing conditions on the mechanical properties of concrete.

Compressive Strength and Elastic Modulus of CSA-Cement Concrete

Followings are main object of test series.

CC 1: Effect of curing condition and content of 3–1–3 or 4–1–3 CSA as compared with that of normal portland cement (Ono).

CC 2: Effect of curing and testing condition in view of moisture conditions (Tazawa).

CC 3: Gain of strength at building site (Horishima).

CC 4: Effect of moisture condition, as supplementary test for drying shrinkage (Shirayama).

CC 5: Effect of curing temperature (Koh).

CC 6: Long term test to study the effect of curing condition (1) (Shiire and Kawase).

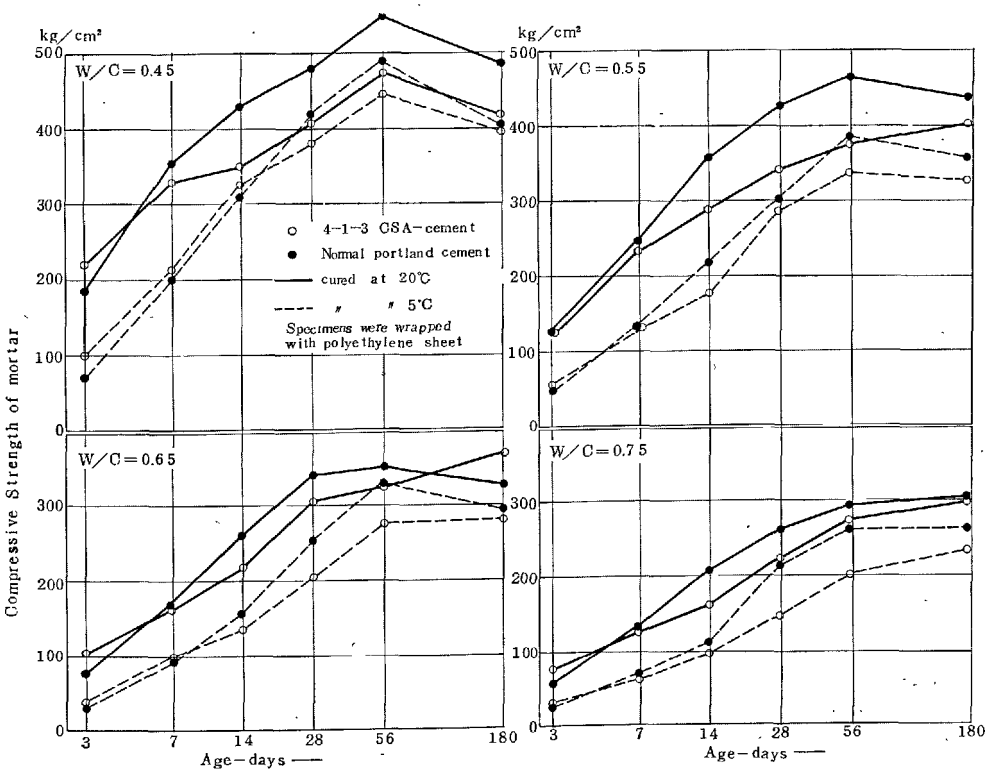

Fig. 4. *Test results of series M5 (by Y. Koh, T. Gotoh)*

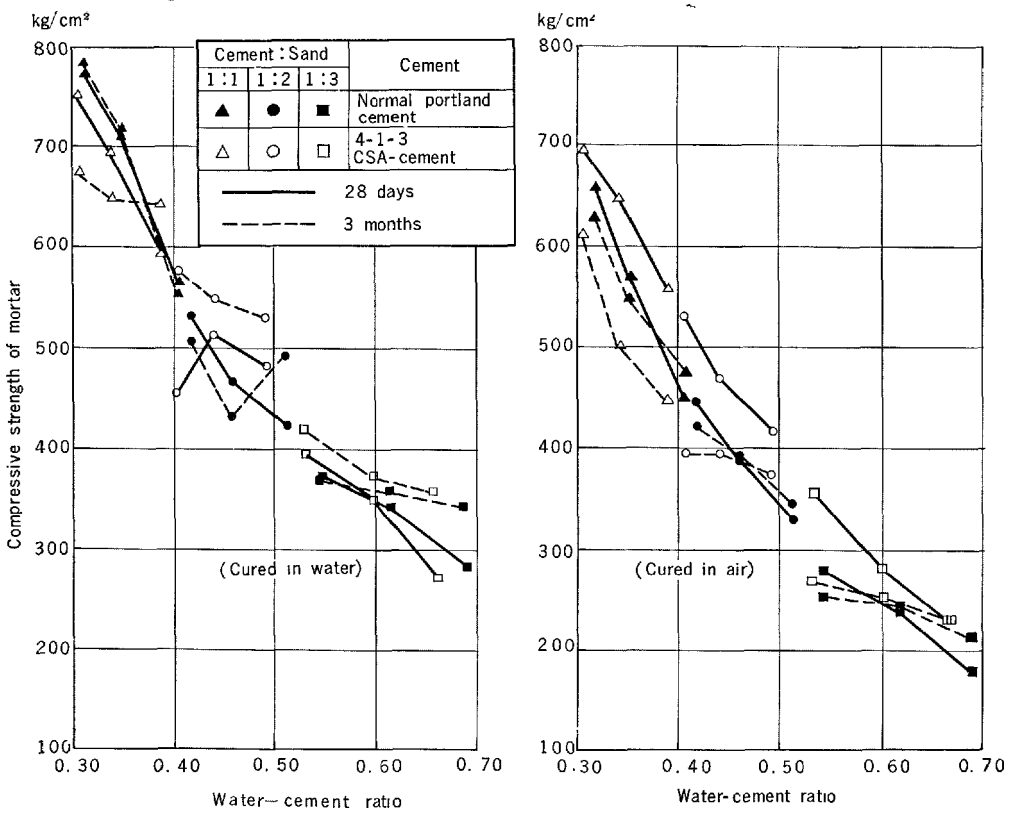

Fig. 5. *Compressive strength of mortars made of 4-1-3 10% CSA-cement and river sand (by H. Kuriyama, K. Hirai)*

CC 7: Long term test to study the effect of curing condition (2) (Koh, Gotoh and Kamada).

CC 8: Effect of curing temperature (1); differences between concrete mixes (Koh, Gotoh and Kamada).

CC 9: Effect of curing temperature (2); differences between two consistency grades (Koh, Gotoh and Kamada).

In the series CC 2–7, 3–1–3 CSA-cement, mainly 13% content of CSA, was used for test, however, 4–1–3 10% CSA-cement was used in series CC 8 and 9.

Series CC 1

This is a part of fundamental test series to decide the amount of addition of CSA to normal portland cement. Three curing conditions, the same with mortar test, were applied to $10\phi \times 20$ cm cylinder specimens made of a definite concrete mix, in which the cement content was maintained at 317 kg/m³ and water cement ratio was fixed to 0.60. River sand (<5 mm, F.M. = 2.65) and river gravel (<25 mm, F.M. = 6.65) were used as aggregates. A part of results is shown in Fig. 6.

Series CC 2

To learn the effect of moisture conditions in curing and testing of concrete, $15\phi \times 30$ cm cylinder specimens were stored and tested under four conditions, i.e., water curing and testing in a saturated condition, water curing but dry test (3 days in air before test), exposed to dry air (20°C and 50% R.H.) and dry test, and exposed to dry air but saturated prior to test. Content of CSA was 0, 6 and 12% by weight.

Series CC 3

3–1–3 13% CSA-cement was used and $10\phi \times 20$ cm cylinder concrete specimens were tested after curing in water or storage at building site.

Series CC 4

Strength and elastic modulus were tested by 3–1–3 13% CSA-cement or portland cement.

Series CC 5

Effect of curing temperature on concrete strength were compared with each other by using 4 kinds of concrete mix. Cylinder specimens measuring $10\phi \times$

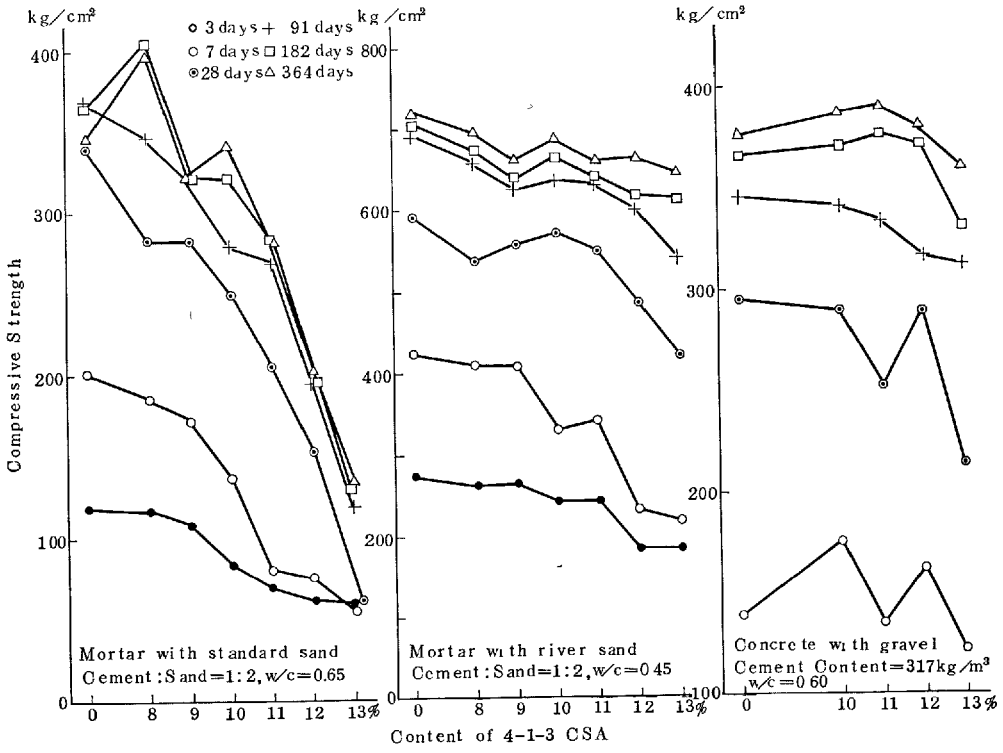

Fig. 6. *Compressive strength of mortar and concrete made of 4-1-3 CSA-cement (water curing) (by Y. Ono)*

20 cm and 15 $\phi \times 30$ cm respectively were made from 3–1–3 13% CSA-cement or normal portland cement with or without air-entraining agent and cured at 20 and 5°C. Test results obtained are shown in Figs. 7 and 8.

Series CC 6 and CC 7

In these series, we intended to clarify long term behavior of concrete strength. In the former, 3–1–3 13% CSA-cement were used and the test was carried out in Tokyo, while the latter was carried out in Sapporo and used cement was changed to 3–1–3 10% CSA-cement, in view of rather large decrease of strength by the former cement, based on the results of other series, e.g., CC 1 and CC 5. Static and dynamic moduli of elasticity were measured in the latter series.

Series CC 8 and CC 9

Effect of temperature and its difference between various mix proportions were compared with each other. 10 $\phi \times 20$ cm cylinder specimens were mainly used. Concrete mixes of these series are shown in Table 9 and results are shown in Fig. 9.

Tensile Strength and Elastic Modulus of Concrete

Direct tensile test and splitting tensile test methods were applied in following two series.

CT 1: 3–1–3 CSA-cement concrete. Content of CSA was varied as 0, 7, 13 and 16% (Shiire).

CT 2: 4–1–3 10% CSA-cement concrete (Shiire).

Table 9. *Experimental scheme of series CC8 and CC9 (by Y. Koh, T. Gotoh, E. Kamada)*

Series	Cement	W/C	Cement kg/m³	Water kg/m³	Slump cm	
					Planned	Measured
CC8	Normal portland cement	0.45	458	206	21	21
		0.55	360	198		21
		0.70	281	197		22
	The 10% 4-1-3 CSA-cement	0.45	476	213		22
		0.55	372	204		23
		0.70	291	203		22
CC9	Normal portland cement	0.563	320	180	18	17
		0.544	300	163	8	8
	The 10% 4-1-3 CSA-cement	0.572	320	183	18	19
		0.544	300	163	8	8

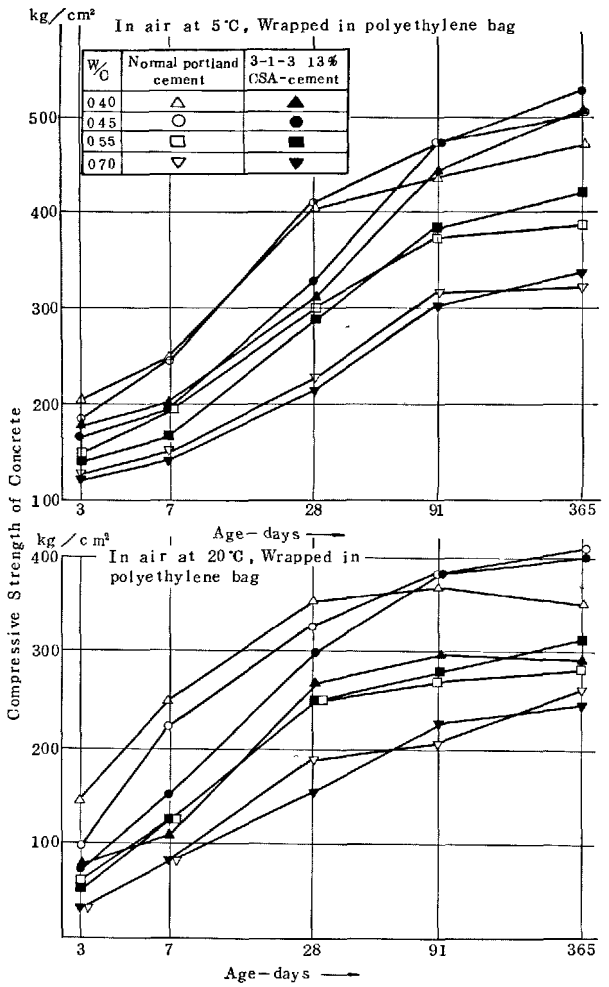

Fig. 7. *Test results of series CC5. Compressive strength tested by using 10φ × 20cm cylinder. Non-AE concrete (by Y. Koh, T. Gotoh)*

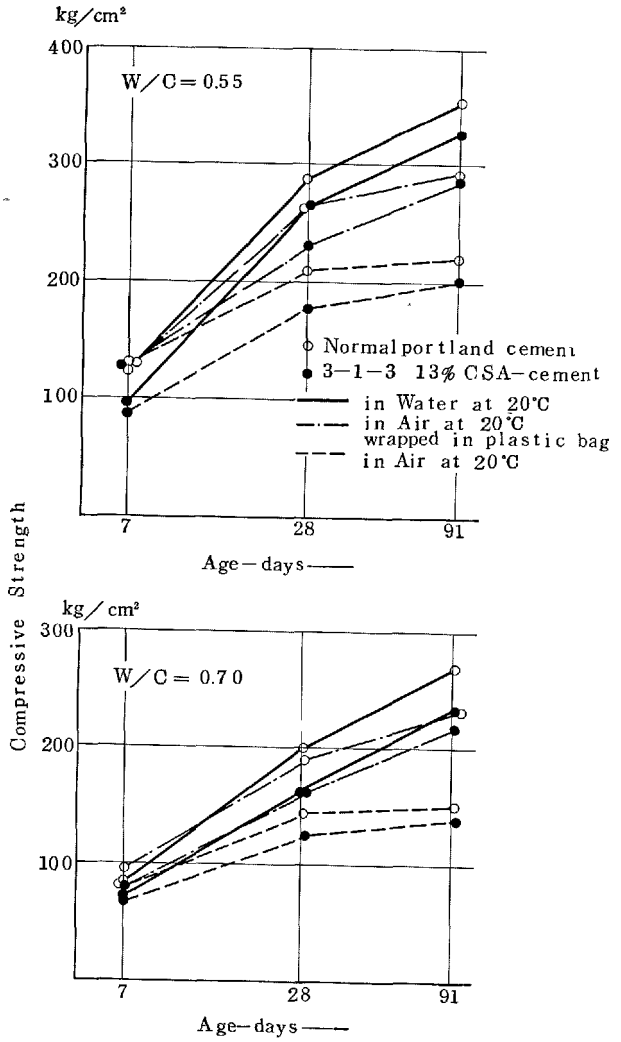

Fig. 8. *Test results of series CC5. Compressive strength tested by using 15φ × 30cm cylinder after curing at 20°C (by Y. Koh, T. Gotoh)*

A part of test results are shown in Fig. 10 and Table 10.

Conclusion on Mechanical Properties of Mortar and Concrete

From all the test above mentioned, it seems that 13% content of CSA is rather excess as the loss of strength is comparatively large, however, 10% addition of CSA, either 3–1–3 or 4–1–3, will be suitable without considerable sacrifice of strength either compressive or flexural strength of both mortar and concrete, because 10% CSA- cement gives nearly the same result as ordinary portland cement either cured at 20°C or 5°C.

In case of tensile strength of CSA-concrete, however, the strength will be little affected when cured in water, and the more the content of CSA, the less the modulus of elasticity.

Creep and Expansive Force of Expansive Cement Mixture

For practical application of expansive cement, it is essential to characterize the expansive force of the cement mixture. Earlier results have shown that mechanical behavior of expansive cement mixture depends to a large degree on the availability of water. Therefore, effect of storage conditions on the expansive force was mainly investigated and other mechanical behaviors related to it, such as creep, volume change, strength etc. were also tested. This report consists of two experiments, that is, mortar test carri-

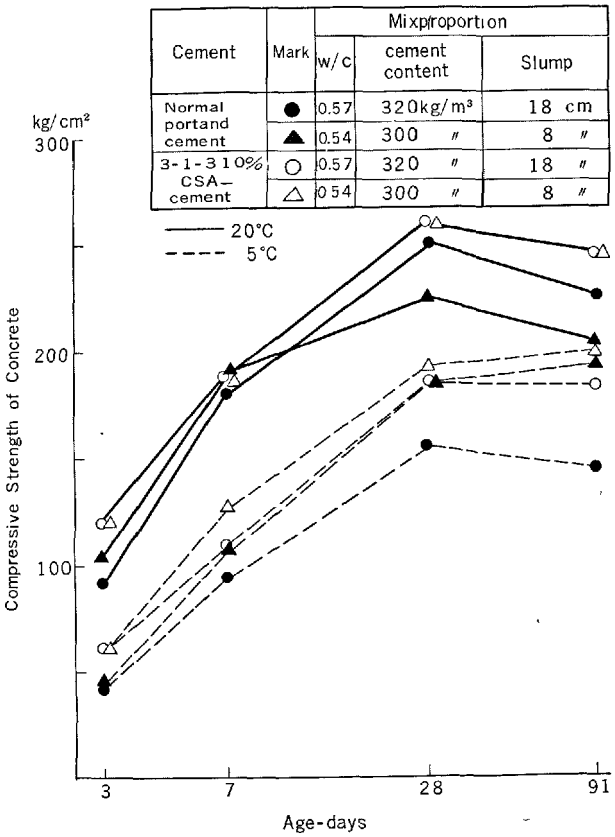

Fig. 9. *Test results of series CC9. Specimens were wrapped by polyethylene sheet and stored in air (by Y. Koh, E. Kamada)*

ed out by K. Kizawa's group, and concrete test carried out by K. Shirayama's group.

Expansive Force of Expansive Cement Mortar

Scope

The principal objective of this study is to find out how advantageous the expansive cement with calcium sulphoaluminous cement clinker (CSA-cement) is, when applied to grouting materials for embedding the anchor of pier.

For this purpose, the expansive force and other mechanical properties, such as strength and volume change were determined for the mortar with CSA-cement and for the mortars with other cementing materials for comparison.

Materials

Cementing materials: As the base of cementing materials, ordinatry portland cement was used. The expansive cements were composed by adding the

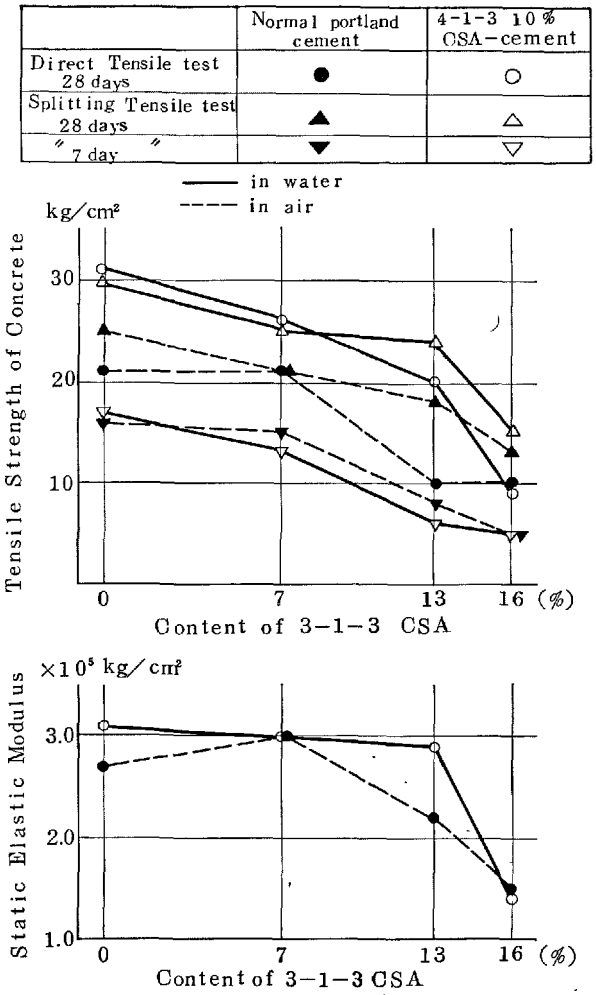

Fig. 10. *Test results of series CT 1. (by T. Shiire)*

Table 10. *Results of series CT2 (by T. Shiire, K. Kawase)*

Cement	Curing	Direct tensile strength (Ft) kg/cm²	Compressive strength (Fc) kg/cm²	Ft/Fc %	Max. strain ×10⁻⁵	Elastic part of strain ×10⁻⁵
The 10% 4-1-3-CSA-cement	Air after 9 days in water	17.3	291	5.9	33	5
	Air after 9 days in wet (92% R.H.)	13.3	230	5.8	28	4
	Air	10.3	107	9.6	26	4
Normal portland cement	Air after 9 days in water	17.2	241	7.1	19	4
	Air	7.0	122	5.7	20	5

Cement content: 300 kg/m³
W/C = 0.60 Slump 16~17 cm

following expansive agents to the base cement; a calcium sulphoaluminous cement clinker (4–1–3 CSA), a compound of gypsum and pulverized limestone: two compounds of iron powder and chemicals. Aggregate: The aggregate was natural sand having the fineness modulus of 2.78. Mortar: The mixing proportion of mortar is shown in Table 11.

Specimens and Measurement

Mortar was placed in 75-by 500 mm cylindrical mold, and the expansive force was determined based on the strain of the mold. Longitudinal expansion of each specimen was also restrained by the end plate set up and fastened to the cylindrical mold after placing concrete, by tightening the nuts at the end of the rods, fixed to the bottom plate at another ends.

Two types of molds were prepared, the one being air-tight to prevent the water evaporation from mortar and the other being not air-tight having many small holes to allow the mortar to dry.

Test Results

Test results were shown in Fig. 11 and it demonstrates the following:

(1) The expansive force of CSA mortars was much larger than that of other mortars. CSA mortar No. 4 casted in the air-tight mold showed the highest expansive force, i.e. 49.5 kg/cm² at the age of about 4 days.

(2) The expansive forces of CSA mortars casted in perforated molds were not determined accurately after the age of 38 hours, because the molds were broken, but it seemed that about half or one-third of the expansive force developed in the air-tight mold.

Table 11. *Mix-proportion of mortar*

Mix number	Expansive agent	Mix-proportion by weight			Water	Flow* mm
		Cement	Expansive agent	Sand		
1	None	1	0	1	0.473	248
2	CSA	1	0.124	1	0.508	256
3		1	0.150	1	0.500	258
4		1	0.176	1	0.491	260
5	Compound of gypsum and pulverized limestone	1	0.0548	1	0.428	269
6	Compound of iron powder and chemicals (A)	1	1	1	0.531	260
7	(B)	1	1	1	0.518	248

*Determined according to JIS R 5201: "Method of Test for Physical Properties of Cement."

Creep and Expansive Force of CSA-Cement Concrete

Scope

The program of the test was concerned with determining creep and expansive force of CSA-cement concrete kept in different storage conditions, that is, under water, in the wrapping of plastic sheet, and in the laboratory air. Compressive strength and volume change of concrete were also determined.

Materials

Cement: Ordinary portland cement and expansive cement with 10% content of 3–1–3 CSA both delivered as common sample to the laboratories concerned, were used. Aggregate: The aggregates were ordinary river sand and river gravel having the maximum size of 20 cm. Concrete: The mix proportion was exactly the same for portland cement concrete and CSA-cement concrete. Both concretes had the cement content of 340 kg/m³, W/C-ratio of 0.6, and their consistensies measured by slump were also nearly the same.

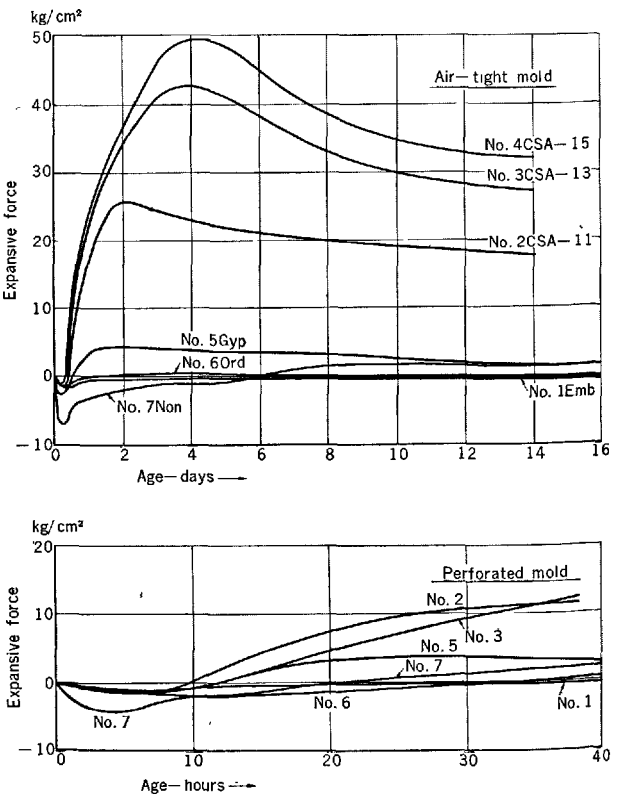

Fig. 11. *Expansive force development of mortar as affected by addition of expansive agent (by K. Kizawa)*

Specimens and Measurement

The concrete specimens were cylinders 15 by 30 cm. They were removed from the mold one day after casting, and then initial readings of the longitudinal length were taken by means of Whittmore gauge. After that, the specimens were stored in different conditions as follows:

(1) Curing in water: The specimens were placed in the sacks of plastic sheet, filled with water.

(2) Air-tight sealing: The specimens were wrapped by plastics sheets.

(3) Exposing to laboratory air: All specimens were stored and tested in the laboratory, maintained at the temperature of 20 ± 3°C and relative humidity of 60 ± 3%. The longitudinal expansive forces of concretes without restraint of transverse expansions, were determined by measuring the load need to maintain the concrete length between the gauge points equal to the initial reading.

At the age of 28 days, the specimens destined for creep tests were subjected to compressive stress of 30 percent of the 28 day compressive strength, and maintained under a constant stress from 2 to 22 months.

Test Results

Test results are shown in Fig. 12, Fig. 13, Fig. 14 and Table 12. The expansive force was highest and lasted for longest time in case of the specimen cured in water, as expected from its large expansion, that is, it attained to more than 27 kg/cm² (about 15% of 28-day compressive strength) at the age of 7 days, and 9.5 kg/cm² of expansive force was still remained at the age of 60 days.

Expansive forces of the specimens wrapped by

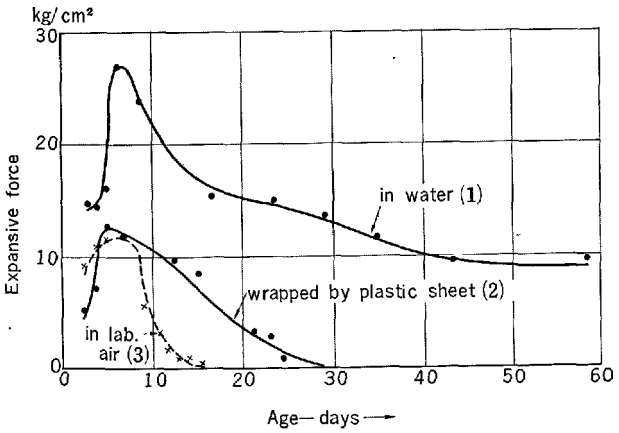

Fig. 12. *Expansive force development of CSA cement concrete affected by storage condition (by K. Shirayama)*

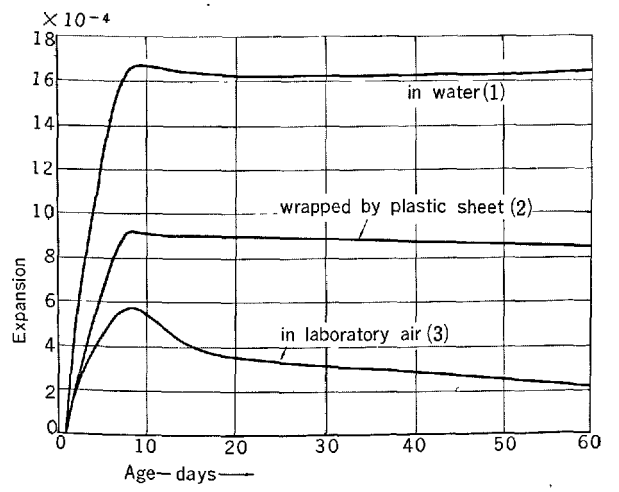

Fig. 13. *Expansion of CSA cement concrete affected by storage condition (by K. Shirayama)*

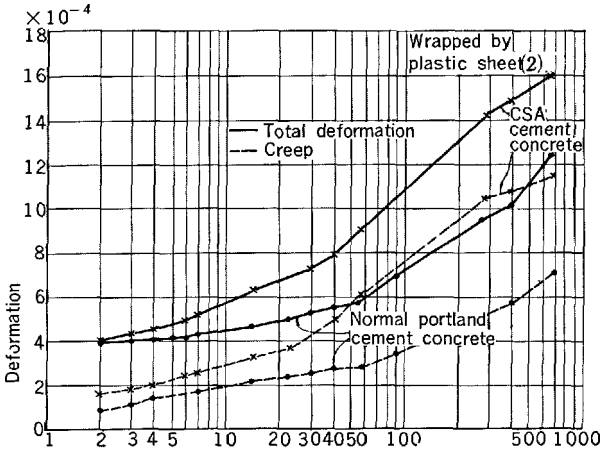

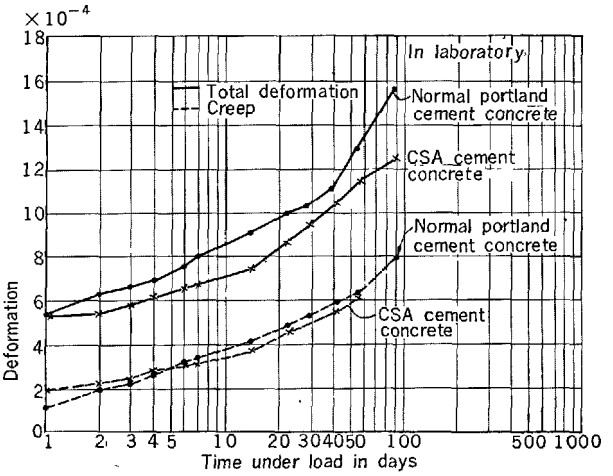

Fig. 14. *Relation between creep and logarithm of time under load for portland cement concrete and CSA cement concrete (by K. Shirayama)*

Table 12. *Summary of creep data (by K. Shirayama)*

Type of cement		Normal portland cement		CSA cement	
Storage condition		Wrapped by plastic sheet	In laboratory air	Wrapped by plastic sheet	In laboratory air
Sustained load, kg/cm²		95	107	51	60
Compressive strength, kg/cm²	28 days	319	358	171	200
	12 months	—	356	—	255
	33 months	471	—	350	—
Initial elastic deformation $\times 10^{-4}$		3.2	4.2	2.4	3.0
At time under load in 8 weeks	Total deformation $\times 10^{-4}$	5.8	13.0	9.2	11.6
	Creep $\times 10^{-4}$	2.7	6.3	6.1	6.3
	Creep function	0.84	1.50	2.54	2.10
At time under load in 22 months	Total deformation $\times 10^{-4}$	12.6	—	16.0	—
	Creep $\times 10^{-4}$	7.1	—	11.4	—
	Creep function	3.94	—	4.75	—

plastic sheet or in the laboratory air were about 12kg/cm² at their maxima, and disappeared in 30 days.

The CSA-cement concrete showed higher creep values than the portland cement concrete, perhaps owing to their lower strengths. However, the differences in creep values get smaller with the time, for the increase of strengths of the CSA-cement concretes was larger than the portland cement concretes.

Conclusions

These two experiments again showed the importance of curing conditions of CSA cement mixture. It seems possible to keep the expansive force of CSA-cement mixture for a considerably long period, if the curing condition is carefully taken.

Bond Strength between Concrete and Reinforcement

Pull out Bond Test

Pull out bond tests were carried out by T. Shiire. Round reinforcing bar, 13 mm in diameter, was embedded vertically in center of 15 × 15 × 15 cm concrete specimens. Concrete mix and the results obtained are shown in Table 13. Specimens cured in air show better values than that cured in water.

Beam Type Bond Test

M. Okushima investigated the effect of CSA-cement on the bond strength of reinforcement by

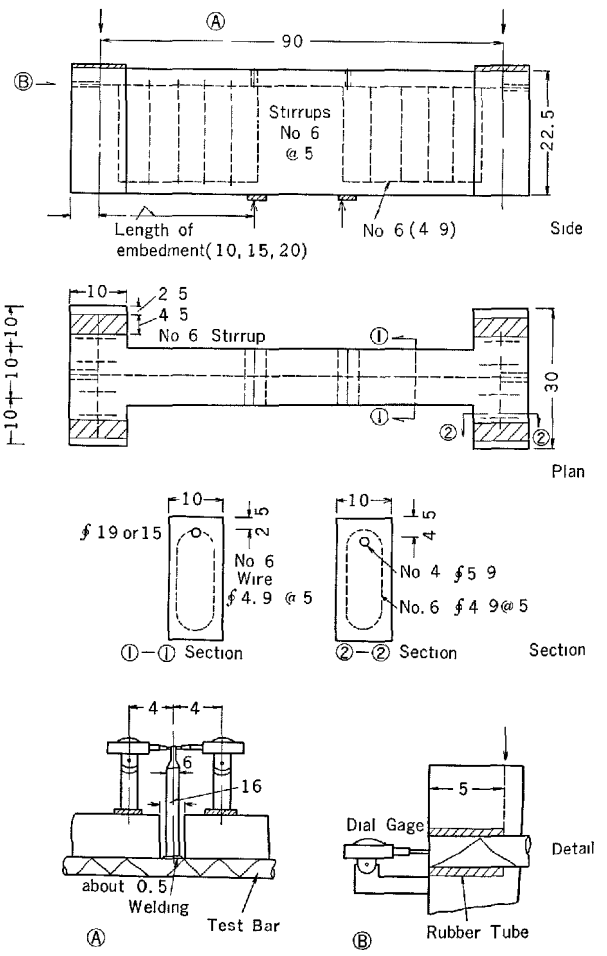

Fig. 15. *Beam type bond strength specimens (Unit: cm)*

beam type bond test shown in Fig. 15 from the viewpoint of factors such as the length of embedment of bars, use of the deformed bars and horizontally placed top or bottom bars.

Concrete mixes are shown in Table 14.

Table 13. *Pull-out test (by T. Shiire)*

Content of 3-1-3 CSA %	W/C	Cement content kg/m³	Slump cm	Unit weight kg/l	Compressive strength at 28 days kg/cm²	Pull-out bond strength kg/cm²	
						Curing	
						in water	in air
0	0.60	356 ~ 358	21	2.34	330	56	59
7			22	2.33	271	—	—
13			21	2.35	194	11	19
16			22	2.33	133	7	9

Table 14. *Concrete mixes for beam type bond strength test (by S. Okushima)*

Cement	Water cement ratio	Slump cm	Sand percent by weight %	Water kg/m³	Cement kg/m³	Sand kg/m³	Gravel kg/m³
The 13% 3-1-3 CSA-cement	0.58	18	46.3	174	300	852	1006
Normal portland cement	0.63	18	45.9	180	285	845	1014

Specimens with 16 mm diameter reinforcement of round and deformed respectively, and length of embedment of 10, 15 and 20 cm, were tested at age of 28 days.

The results are shown in Table 15 and Fig. 16, 17, that can be summarized as follows:

(1) Bond strength of reinforcement in 4–1–3 CSA-cement concrete is generally larger than that of normal portland-cement concrete.

(2) Both in CSA-cement concrete and ordinary concrete, the bond strength decreases as increasing the length of embedment of bars.

(3) Deformed bar is also effective in bond strength for CSA-cement concrete as for ordinary concrete.

(4) Bond strength of the bottom reinforcement is larger than that of the top reinforcement in both CSA-cement concrete and the ordinary concrete, and it is especially remarkable that in

Table 16. *Tested CSA-cement mortar mixes (by K. Gotoh)*

No.	Mortar mix	Water cement ratio	Content of CSA %	Compressive strength at 28 days restricted in steel moulds kg/cm²
A,A′	1:1.5	0.50	0	208
B,B′			10	203
C,C′			20	199
D,D′			40	106

Table 15. *Bond stress of concrete with 4-1-3 CSA-cement and normal portland cement (by S. Okushima)*

Steel bar	Position of bar in beam	Length of embedment cm	$\tau_{0.01}/Fc$		$\tau_{0.01}/Fc$		τ_{max}/Fc		(1)/(2)	(3)/(4)	(5)/(6)
			In case of E.C. (1)	In case of P.C. (2)	In case of E.C. (3)	In case of P.C. (4)	In case of E.C. (5)	In case of P.C. (6)			
Plain	Top	S-10 U	0.168	0.120	0.113	0.069	0.174	0.120	1.40	1.64	1.45
		15	0.087	0.105	0.053	0.042	0.112	0.109	0.83	1.26	1.03
		20	0.082	0.083	0.047	0.035	0.086	0.091	0.99	1.34	0.95
								Mean	1.07	1.41	1.14
	Bottom	S-10 L	0.181	0.132	0.140	0.080	0.202	0.142	1.37	1.75	1.42
		15	0.138	0.148	0.061	0.064	0.168	0.169	0.93	0.95	0.99
		20	0.141	0.110	0.031	0.040	0.164	0.128	1.28	0.78	1.28
								Mean	1.19	1.16	1.23
Deformed	Top	D-10 U	0.221	0.202	0.139	0.061	0.383	0.280	1.09	2.28	1.37
		15	0.168	0.156	0.052	0.039	0.237	0.253	1.08	1.33	0.94
		20	0.168	0.181	0.045	0.044	0.216	0.222	0.93	1.02	0.97
								Mean	1.03	1.54	1.09
	Bottom	D-10 L	0.229	0.210	0.107	0.073	0.281	0.340	1.09	1.47	0.83
		15	0.198	0.217	0.060	0.075	0.236	0.356	0.91	0.80	0.66
		20	0.159	0.160	0.049	0.046	0.229	0.226	0.99	1.07	1.01
								Mean	1.00	1.11	0.83
								Total mean	1.07	1.31	1.08

E.C.: Expansive cement (The 10% content 4-1-3 CSA-cement)
P.C.: Normal portland cement
Fc: Compressive strength of concrete

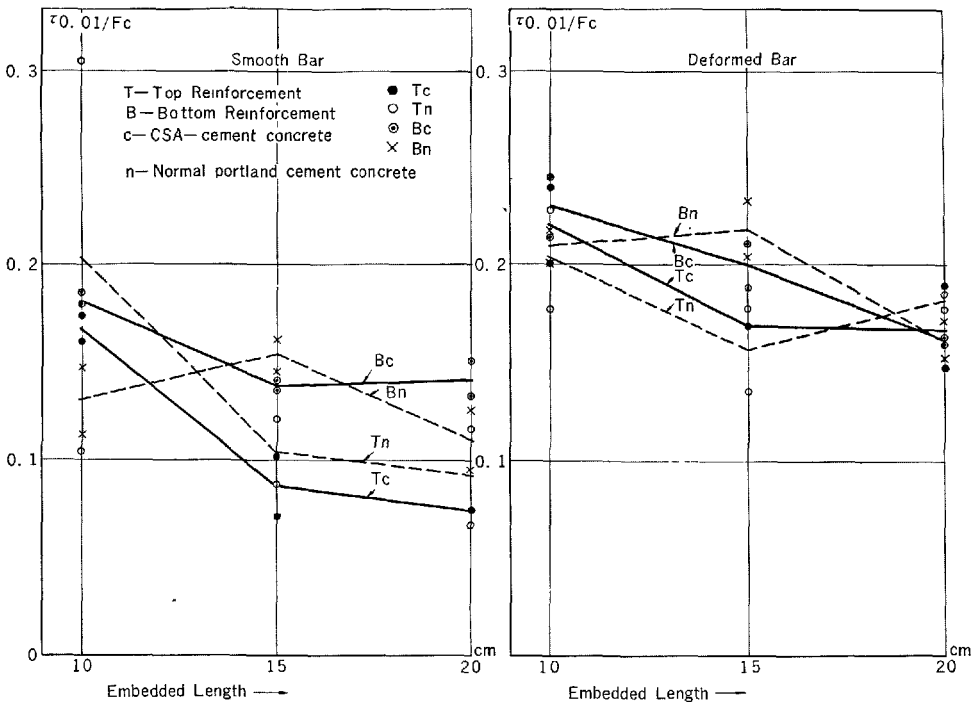

Fig. 16. *Test results of beam type bond strength (by S. Okushima)*

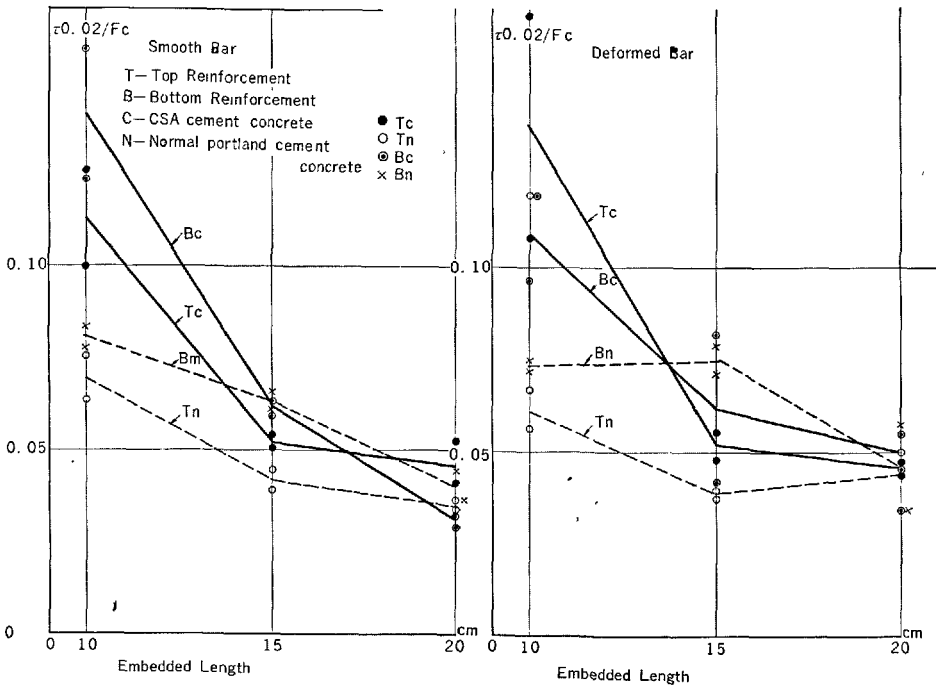

Fig. 17. *Test results of beam type bond strength (by S. Okushima)*

CSA-cement concrete there is a little difference of bond strength between top and bottom.

Bond Test under Restriction

K. Gotoh investigated the bond strength of reinforcement in CSA-cement mortars under restriction for the purpose of jointing precast concrete panels. The round bars, 16 mm in diameter, were vertically placed in a steel pipe, 48.6 mm in diameter and 2.3 mm in thickness, and CSA-cement mortars were grouted into the pipe (Fig. 18).

The length of embedment of bars were 320 and 480 mm. Mortar mix and strength are shown in Table 16.

Pull out test results of specimens at 28 days are shown in Table 17 and Fig. 19.

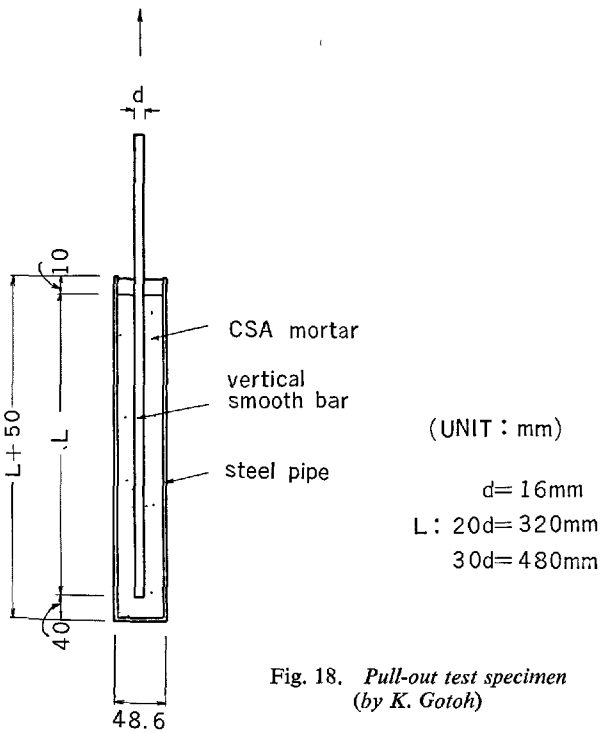

Fig. 18. *Pull-out test specimen (by K. Gotoh)*

Table 17. *Pull-out test results (by K. Gotoh)*

No.	Length of embedment mm	Content of CSA %	Maximum load Kg
A	320 (20 d)	0	2500 3000 2780
B		10	6700 6700 6450
C		20	6550 6950 6400
D		40	6300 6800 6570
A′	480 (30 d)	0	3000 3400 3400
B′		10	7300 6800 6830
C′		20	6700 6900 6900
D′		40	6650 6800 6930

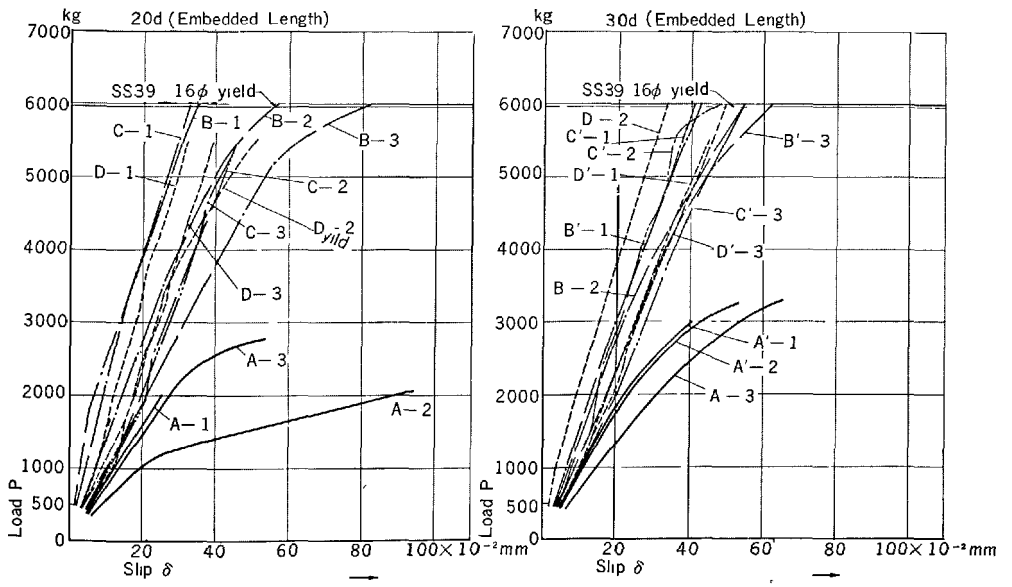

Fig. 19. *Bond slip at loaded end for 20d and 30d length of embedment (by K. Gotoh)*

The results show that the bond strength of round bars in CSA-cement mortars under restriction are much the same value of yield point of steel, and about twice of the bond strength in plain mortars.

Effects of Steam Curing upon the General Behavior of Calcium Sulphoaluminous Cement Mortar and Concrete

Procedure of Experiment

Materials

The expansive cement used for this study carried out by Y. Ono, is composed of blended cement that is mixed with content of 0–17% calcium sulphoaluminous cement clinker.

Aggregates used are river sand and gravel produced in Himekawa River, and they are as shown in Table 18.

Procedure

Table 19 shows measuring items, varieties of specimen and curing conditions.

Results Obtained

Results obtained are shown in Figs. 20–25: Fig. 20 shows that when contents of calcium sulphoaluminous cement clinker in portland cement is less than 13% by weight, the higher the steam curing temperature goes, the larger the expansion grows. When concrete

Table 18. *Physical properties of aggregates (by Ono)*

Aggregate	Name of river	Specific gravity	Absorption coefficient %	Maximum size mm	Fineness modulus
Sand	Himekawa	2.59	1.7	5	2.7
Gravel	Himekawa	2.62	0.8	20	6.7

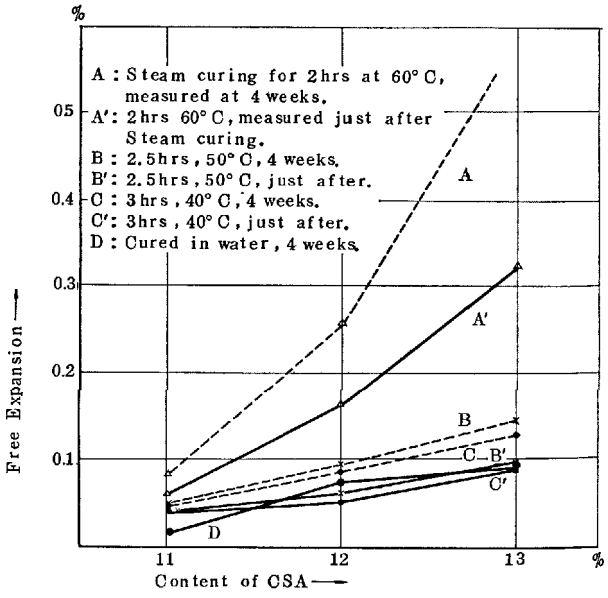

Fig. 20. *Effect of contents of CSA on expansion when cured by steam at various temperatures. (by Y. Ono)*

Table 19. *Conditions of specimens and measurement*

Specimen	Reinforcement	Curing	CSA content %	Measurement
mortar C: S = 1: 2 w/c = 0.45 flow: 180~200	none	a) Short period steam curing. Demolded at 24 hrs. after molding in test room, and cured at: 40°C ... 3 hrs 50°C ... 2.5 hrs 60°C ... 1.3 hrs and cured in nature after out door sprinkling for one week.	0 11 12 13	expansion coefficient Compressive strength tensile strength (split test)
concrete C = 400kg/m³, max. size of gravel: 25mm w/c = 0.476 Slump: 6~8cm S/A = 0.376	none	a) Short period steam curing.	0, 11, 12, and 13	do
	reinforced (Steel ratio: 2.6%)	a) Short period steam curing.	11, 13, 15, and 17	expansion coefficient
		b) Long period steam curing. Demolded at 24 hrs. after molding in test room, and cured at: 40°C ... 32 hrs 60°C ... 19 hrs 70°C ... 11 hrs and cured in water (20°C)	13 15 17	do

1) Initial gauge length was measured by comparator when demolded at 24 hrs. after moulding.
2) Dimension of specimen for compresive strength is ϕ10 × 20cm
3) Dimension of specimen for tensile strength is ϕ15 × 20cm
4) Steel bar used for reinforcement is SS41 (ϕ18mm, conformed to JIS G 3101).

is restrained by reinforcement bars, the maximum expansion coefficient reaches to 11×10^{-4} at temperature of 70°C, 7×10^{-4} at temperature of 60°C, and 4×10^{-4} at temperature of 40°C.

The general tendency of this result is akin to that of non-reinforced concrete. This fact will be seen in Figs. 20, 21 and 22.

Fig. 22 shows length change curves of reinforced concretes cured by steam for a comparatively long period.

Effect of steam curing times and temperatures on CSA-cement concrete will be seen in Fig. 23.

Fig. 24 and 25 show compressive strength and tensile strength respectively.

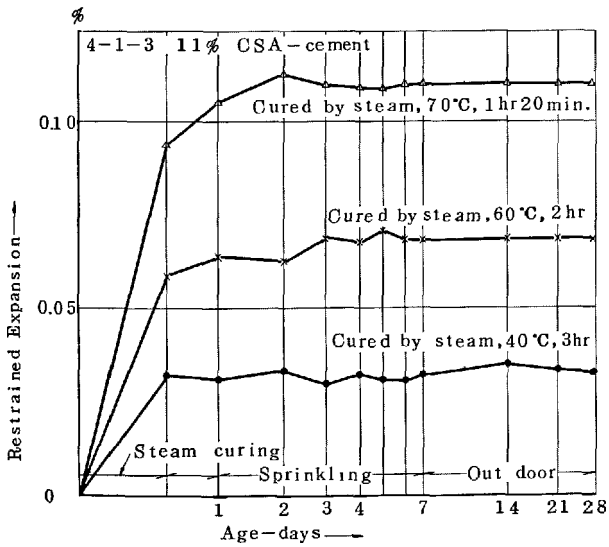

Fig. 21. *Restrained expansion of CSA-cement concrete (short period steam curing) (by Y. Ono)*

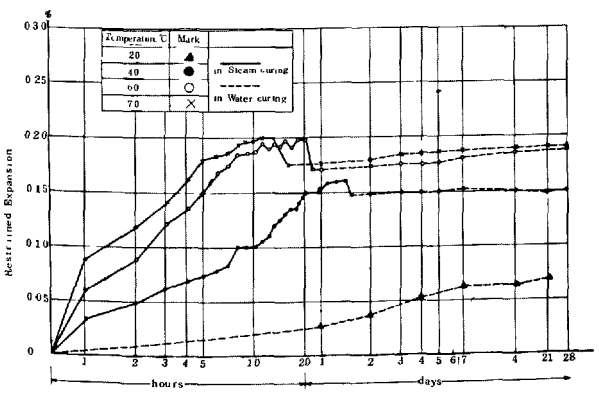

Fig. 22. *Restrained expansion of 4-1-3 11% CSA-cement concrete (long period steam curing) (by Y. Ono)*

Summary and Conclusion

(1) Expanding behavior of calcium sulphoaluminous cement mortar and concrete shows that the higher the curing temperature goes, the swifter the ascending coefficient of expansion ratio becomes and the more rapidly it reaches to the maximum expansion.

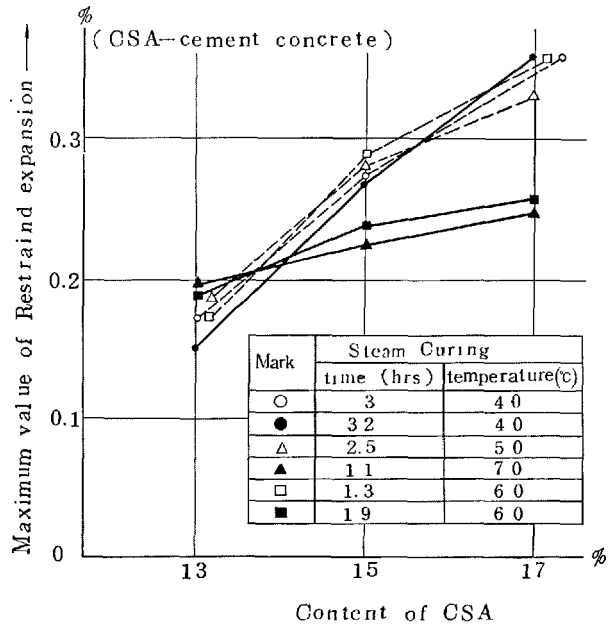

Fig. 23. *Effect of steam curing times and temperatures at different contents of CSA (by Y. Ono)*

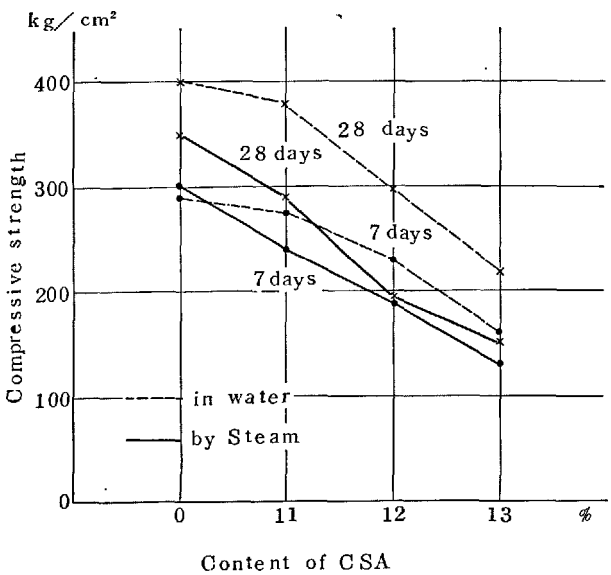

Fig. 24. *Compressive strength of CSA-cement mortar cured in water or by steam (by Y. Ono)*

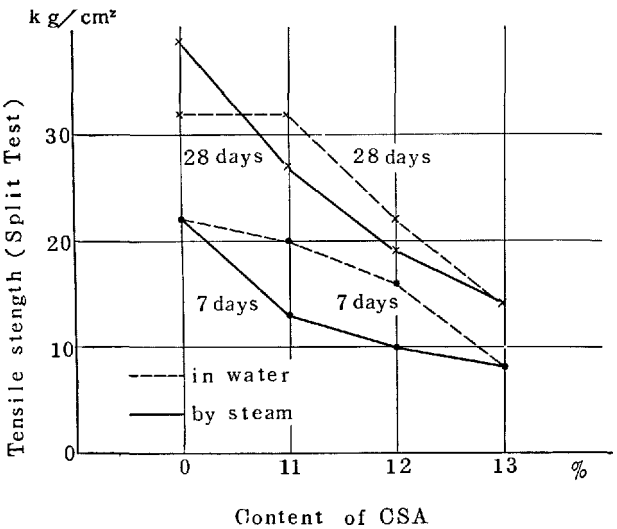

Fig. 25. *Tensile strength of CSA-cement mortar cured in water or by steam (by. Y. Ono)*

(2) Eventhough the curing period is short, if water sprinkling would be done after curing, expansive cement concrete will expand more effectively than in the case of long period steam curing.

(3) The relation between strength and expansion is in inverse proportion independently of their curing temperatures.

Durability

Carbonation of CSA-Cement Concrete and Corrosion of Reinforcing Steel

A. Carbonation of CSA-Cement and Rust of Embedded Steel Reinforcement

Procedure

In this study carried out by T. Horishima et al, the 5, 10 and 13% CSA-cement concrete and normal portland cement concrete were used. Kinds of concrete, their mixing-ratio and dimension of specimens are shown in Table 20 and Fig. 26.

Test specimens were cured in water (20°C) for 3 days and then in dry room (20°C R. H. 50%) for 12–15 months. And then, specimens were cut off by a quarter, and the depth of carbonation was measured by means of spraying phenolphthalein alcoholic liquid on the cut surface. Measuring method of carbonation are shown in Fig. 27.

Next, the remaining specimens were placed in a CO_2 gas chamber (gas concentration 10%, 25°C, R.H. 50%). After 24 days the depth of carbonation was measured again, and the embedded steel bar was observed.

Results Obtained

The results of test are shown in Fig. 28.

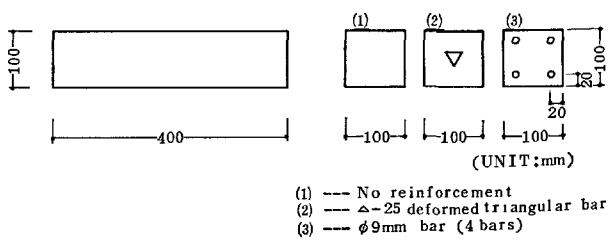

Fig. 26. *Dimension of specimens (by T. Horishima)*

Table 20. *Kinds of concrete and mixing-ratio*

	CSA content %	Materials (per m³)						Slump cm	Unit weight kg/l	Air content %	Compressive strength kg/cm²	Reinforcement
		Cement kg	CSA kg	Water l	Sand kg	Coarse aggregate kg	Pozzolith No. 8 %, cwt					
1	0	325	0	193	840	952	0	21.0	2.307	—	198	△-25
2	5	308	16.2	199	838	950	0	20.9	2.314	—	247	△-25
3	10	293	32.5	210	841	953	0	20.3	2.305	—	216	△-25
4	0	290	0	202	824	941	0.25	22.3	2.170	5.7	—	4-9φ
5	13	252.3	37.7	202	824	941	0.25	21.9	2.160	5.7	—	4-9φ

The depth of carbonation of all specimens reached to 5–15 mm after 15 months. There was no significant difference in the depth of carbonation between normal portland cement concrete and the 5% CSA-cement concrete, but in case of the 10% CSA-cement concrete it was slightly deeper than that of the former. The depth of carbonation after accelerated test reached to 15–25 mm and this tendency was the same as that in the previous case. Also, it was found that the depth of carbonation could be reduced considerably by using water reducing agent.

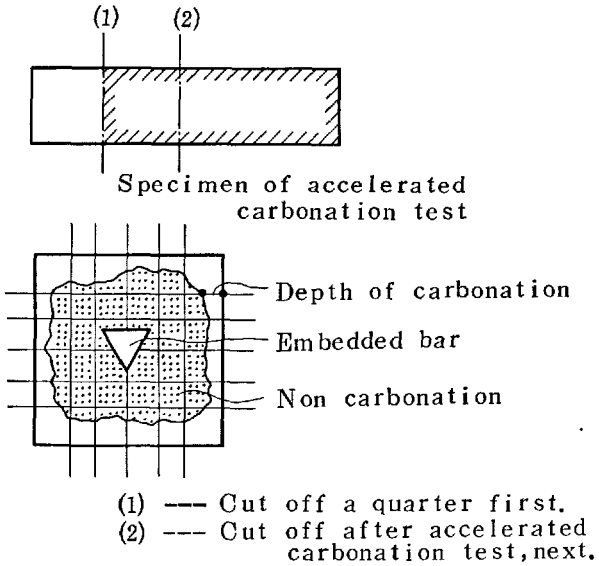

Fig. 27. *Measuring method of carbonation (by T. Horishima)*

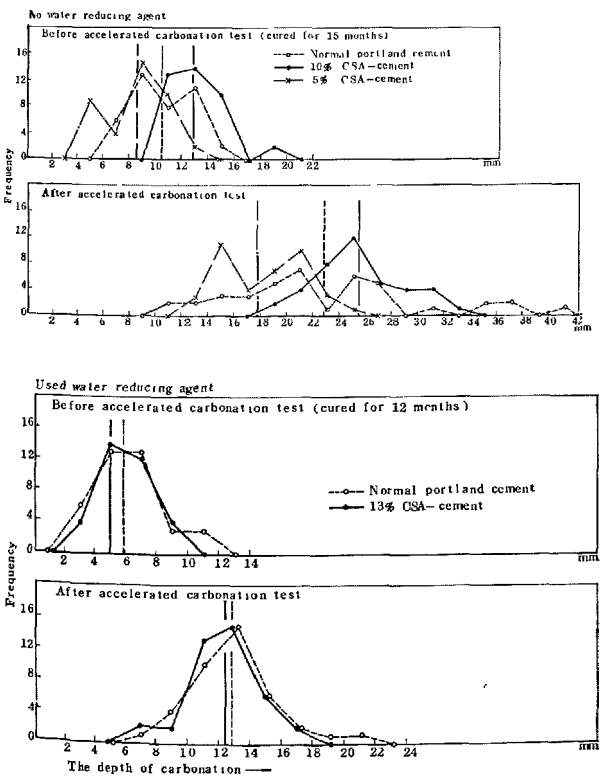

Fig. 28. *Frequency of the measured depth of carbonation (by T. Horishima)*

B. Corrosion of Steel Plates

This study was carried out by Y. Ono.

Procedure

The solutions of CSA, the 10% and 13% CSA-cement, normal portland cement and lime were prepared, and in each of these solution, polished steel plates were dipped and were kept in conditions of 10, 20 and 30°C. A change of pH value of solutions and increase of corrosion on steel plates (by weight) were measured for a month.

Results Obtained

The results of these tests are shown in Fig. 29 and Fig. 30.

pH value of CSA solution changed from 12 to 9 after a month, whereas the others were remained equally 12. The tendency was same in every tempera-

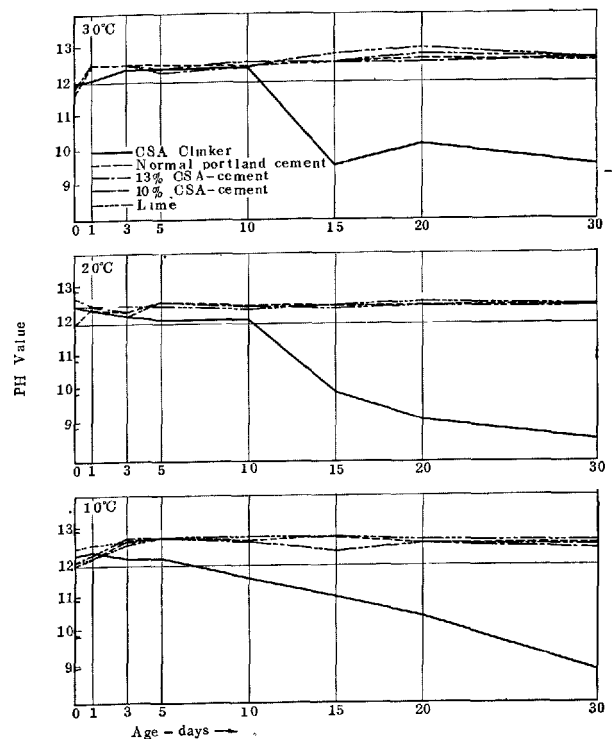

Fig. 29. *pH value change (by T. Horishima)*

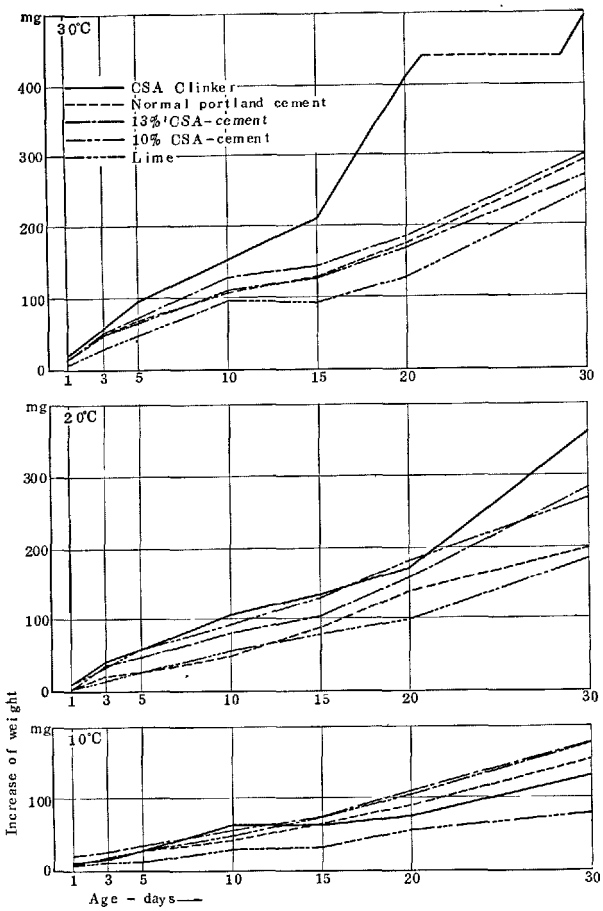

Fig. 30. *Increase of corrosion (by T. Horishima)*

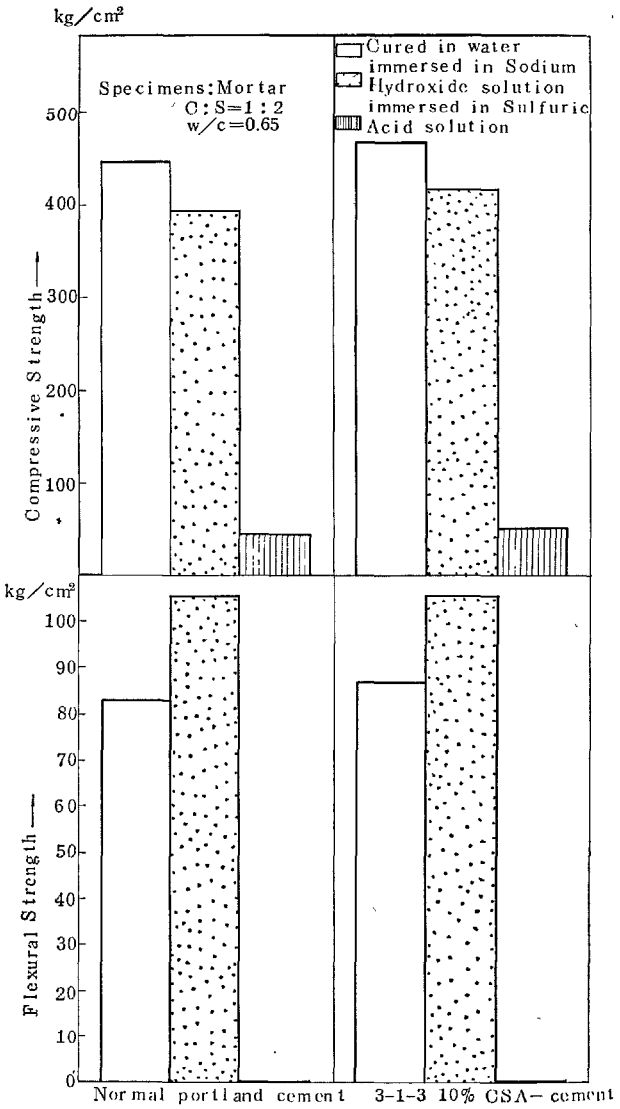

Fig. 31. *Test results of mortar specimens at age of 1 year (by Y. Ono)*

ture. With regard to the corrosion of steel plate, rust began to form at the boundary line between the solution and the air. And the increase of weight by rusting was measured in the order of lime<normal portland cement<the 10% CSA-cement<the 13% CSA-cement <CSA only. This tendency became larger in high temperature.

Resistance of CSA-Cement Mortars and Concretes to Sulphuric Acid Solution, Sodium Hydroxide Solution and Sea Water

Procedure

For the purpose of studying the resistance of CSA-cement to sulphuric acid solution, sodium hydroxide solution and sea water, mortar and concrete specimens were made. These studies were carried out by Y. Ono et al.

After curing for 28 days in water, these specimens were immersed in different solution of 0.2% sulphuric acid solution, 0.2% sodium hydroxide solution and sea water. The change in compressive and flexural strengths of these immersed specimens were measured at the ages of from 4 weeks to 2 years, to estimate the rate of attack by these solutions against water curing strength.

Results Obtained

The results obtained are shown in Fig. 31—Fig. 34.

The test results are summarized as follows.

(1) When immersed in 0.2% solution of sodium

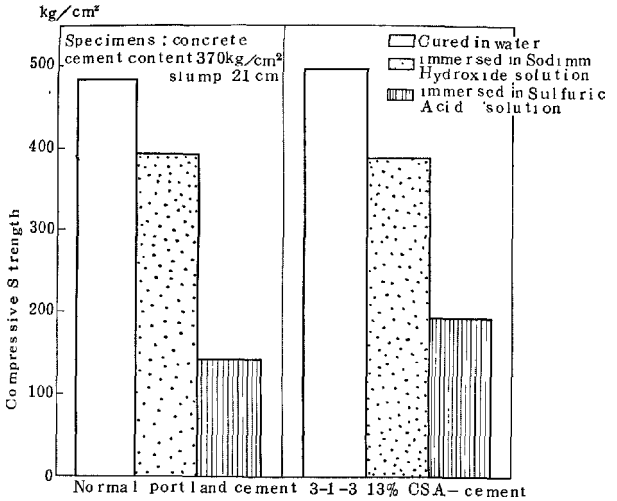

Fig. 32. *Test results of concrete specimens at age of 1 year (by. Y. Ono)*

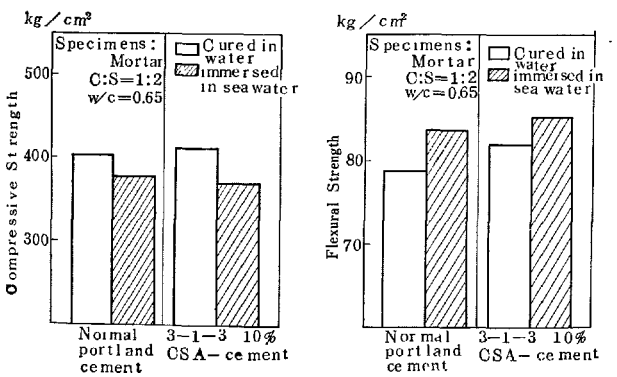

Fig. 33. *Test results of mortar specimens at age of 2 years (by Y. Ono)*

hydroxide, the compressive and flexural strengths of CSA-cement mortar and concrete were as same as the case of ordinary portland cement.

And either specimens reduced slightly the compressive strengths comparing with that of water cured specimens, but the case of flexural strengths were vice versa.

(2) The compressive and flexural strength of mortar and concrete specimens immersed in sulphuric acid solution were very low comparing with the case of water curing.

(3) When immersed in sea water, the flexural strength of the CSA-cement mortar and concrete increased largely as those immersed in 0.2% solution of sodium hydroxide.

(4) Hardly any mark of change was observed in strength of mortar and concrete by replacement

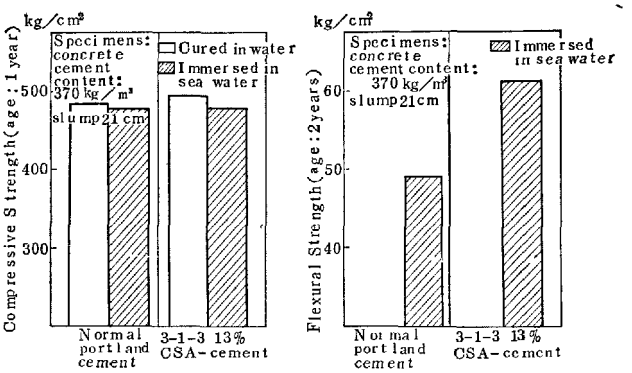

Fig. 34. *Test results of concrete specimens at age of 1 year or 2 years (by Y. Ono)*

Table 21. *Conditions of freezing-thawing test and factors of mortar applied to the test. (by H. Kuriyama, K. Hirai)*

Series	Freezing	Thawing	
FTM 1	−16～−18°C × 22 hours	20°C × 2 hours	Slow
FTM 2	−15 ± 1.5°C	5 ± 1.5°C	Rapid (8 cycles per day)
Factor			
Mortar mix Cement: Sand (by weight)	1 : 1	1 : 2	1 : 3
Flow of mortar tested by JIS (mm)	160	200	240
3-1-3 CSA content (%)	0	10	13

For both test series, 27 kinds of mortar mixes altogether were used.

of ordinary portland cement by 10–13% of CSA.

Durability to Frost Action

Freezing-Thawing Test of Mortar

Following two series of freezing-thawing tests were carried out by Kuriyama and Hirai on mortars made of 3–1–3 CSA-cement and river sand.

Series FTM 1: slow freezing in air and thawing in water.

Series FTM 2: rapid freezing-thawing in water.

The specimens were 4 × 4 × 16 cm beam and were cured in water for 90 days at 20°C or stored in air (20 ± 1°C, 70 ± 10% R. H.) after 3 days water curing and stored in water for 9 months at 20°C, for series FTM 1 and FTM 2 respectively. Results obtained are shown in Table 21–24.

Freezing-Thawing Test of Concrete

Following two test series were carried out by Koh, Gotoh and Kamada on concrete made of 3–1–3 and

Table 22. *Decrease of relative dynamic modulus of elasticity by slow freezing in air and thawing in water after curing in water for 90 days (by H. Kuriyama, K. Hirai)*

Mortar mix cement: sand	Flow of mortar mm	3-1-3 CSA content %	Compressive strength at 90 days kg/cm²	Relative dynamic modulus of elasticity %					
				Number of freezing-thawing cycles					
				0	5	11	17	28	41
1:1	160	0	717	100	99.7	99.5	99.6	101.4	99.9
		10	809	100	98.6	96.8	96.4	96.7	96.0
		13	609	100	98.1	98.9	98.1	99.2	98.1
	200	0	677	100	98.1	94.4	94.4	95.8	95.0
		10	730	100	97.0	96.3	96.6	97.3	97.3
		13	649	100	94.8	92.6	92.6	95.0	92.5
	240	0	644	100	95.8	94.2	93.8	92.4	87.6
		10	691	100	86.3	84.2	81.5	71.8	66.8
		13	549	100	85.1	70.5	40.2	—	—
1:2	160	0	569	100	99.3	97.7	97.7	99.2	99.2
		10	630	100	96.7	96.3	96.1	98.0	96.9
		13	637	100	99.2	99.6	98.8	100.2	100.2
	200	0	689	100	98.0	95.0	94.6	96.3	95.5
		10	649	100	99.5	96.6	97.3	97.9	97.2
		13	569	100	98.8	96.9	97.0	96.1	95.3
	240	0	454	100	94.9	92.2	89.5	90.2	88.6
		10	498	100	79.8	63.6	34.8	—	—
		13	397	100	67.7	34.6	16.6	—	—
1:3	160	0	454	100	96.4	96.8	95.9	96.6	96.2
		10	462	100	99.2	97.6	98.3	99.6	98.4
		13	423	100	95.7	95.6	91.3	90.2	87.5
	200	0	409	100	96.9	90.6	88.6	90.9	88.5
		10	403	100	88.5	78.4	—	—	—
		13	385	100	72.9	48.9	36.6	—	—
	240	0	342	100	78.4	62.9	32.9	—	—
		10	348	100	65.1	25.9	11.8	—	—
		13	236	100	13.7	4.2	—	—	—

4–1–3 CSA-cement and diluvial aggregates.

Series FTC 1: 3–1–3 13% CSA-cement concrete.

Series FTC 2: 4–1–3 10% CSA-cement concrete.

After 28 days curing in water at 20°C, the freezing-thawing tests were started by using 7.5 × 7.5 × 40 cm beams. Eight kinds of concrete mixes were compared with ordinary cement concretes, i.e. four water cement ratios and with or without air-entraining agent (Table 25), by applying the slow freezing-thawing in water to all test series, however, the rapid freezing-thawing in water was also applied to series FTC 1.

The decrease of relative dynamic modulus of elasticity was shown in Figs. 35–38.

Bond Strength of Mortar Rendering as a Reference to Winter Work

Considering the mortar rendering of walls in winter, the bond strength between base mortar and rendering was tested after freezing for 24 hours in early age.

The bond strength at normal temperature is affected mainly by the content of CSA, however, when damaged by freezing in early age the mortar mix or the time of start to freeze has large effect on the bond strength between rendering and base mortar. It seems that there is no significant differences of effect on bond strength between 10 or 13% CSA-cement and normal portland cement.

Conclusion

The following conclusion will be gained.

(1) The result of freezing-thawing test showed that there was not so much difference between the CSA-cement mortar and normal portland cement mortar having rich proportion and small flow, however, the CSA-cement mortar having poor proportion and large flow was a little weaker in its property, except excess content of CSA.

(2) Considering the bad results on mortar and concrete obtained by using 3–1–3 13% CSA-cement, it seems that 13% content of CSA is excess.

(3) For general use 10% content of CSA should be recommended, as the resistance against freez-

Table 23. *Decrease of relative dynamic modulus of elasticity by slow freezing in air and thawing in water after 3 days curing in water succeeded by storage in air for 87 days (by H. Kuriyama, K. Hirai)*

Mortar mix cement: sand	Flow of mortar mm	3-1-3 CSA content %	Compressive strength at 90 days kg/cm²	Relative dynamic modulus of elasticity %					
				Number of freezing-thawing cycles					
				0	5	11	17	28	41
1:1	160	0	755	100	100.3	99.3	99.2	100.7	100.7
		10	735	100	97.1	97.1	94.5	97.4	96.1
		13	460	100	94.3	93.9	93.5	95.1	95.0
	200	0	725	100	98.1	96.2	96.6	99.1	98.3
		10	716	100	97.4	97.0	95.6	97.7	96.7
		13	569	100	97.5	96.1	95.8	98.0	95.8
	240	0	663	100	98.1	96.1	—	—	—
		10	633	100	98.1	95.8	94.2	94.2	90.9
		13	450	100	81.4	63.8	52.9	—	—
1:2	160	0	669	100	98.5	98.4	96.6	98.8	98.7
		10	685	100	98.2	95.3	94.9	96.6	97.0
		13	511	100	100.0	98.4	98.6	99.1	96.5
	200	0	618	100	98.0	95.7	95.7	97.5	95.5
		10	520	100	98.8	96.8	97.1	98.3	97.5
		13	512	100	92.8	90.6	88.3	85.6	86.3
	240	0	567	100	99.1	98.7	97.2	98.7	95.9
		10	421	100	91.8	87.3	85.0	—	—
		13	349	100	72.4	52.9	38.3	—	—
1:3	160	0	481	100	98.3	97.5	95.5	95.7	96.3
		10	434	100	99.2	98.8	97.2	98.6	98.2
		13	309	100	98.3	97.1	95.1	95.0	93.8
	200	0	392	100	98.4	94.4	94.1	92.5	93.6
		10	362	100	94.7	91.5	88.6	90.8	85.4
		13	293	100	90.2	82.8	—	—	—
	240	0	371	100	98.4	93.8	—	—	—
		10	255	100	77.1	16.5	—	—	—
		13	207	100	63.6	—	—	—	—

Table 25. *Concrete mixes for freezing-thawing test (by Y. Koh, T. Gotoh, E. Kamada)*

	Cement	Water-cement ratio	Cement content kg/m³	Water content kg/m³	FTC 1			FTC 2		
					Content of CSA	Air percent	Compressive strength at 28 days kg/cm²	Content of CSA	Air percent	Compressive strength at 28 days kg/cm²*
Non AE concrete	Normal portland cement	0.55	360	198	—	—	299	—	1.4	282
	CSA-cement	0.40	573	228	3-1-3 13%	**		4-1-3 10%	2.1	—
		0.45	475	213		—	259		2.3	363
		0.55	372	204		—	203		1.4	263
		0.70	291	203		—	109		1.8	187
AE concrete	Normal portland cement	0.55	342	188	—	5.8	244	—	3.2	—
	CSA-cement	0.40	541	217	3-1-3 13%	**		4-1-3 10%	3.7	—
		0.45	450	202		—	214		3.3	—
		0.55	355	194		—	169		3.3	—
		0.70	278	193		—	98		4.0	—

*Values for reference in other series. Wrapped in polyethylene sheet and stored in air at 20°C.
**Not tested.

ing-thawing of 10% CSA-cement concrete was about the same or a little larger than that of the normal portland cement.

Table 24. *Decrease of relative dynamic modulus of elasticity by rapid freezing-thawing in water after 9 months curing in water (by H. Kuriyama, K. Hirai)*

Mortar mix cement: sand	Flow of mortar mm	3-1-3 CSA content %	Linear expansion after 9 months in water %	Relative dynamic modulus of elasticity %				
				Number of freezing-thawing cycles				
				0	20	30	40	50
1:1	160	0	0.024	100	97.3	96.4	95.1	94.9
		10	0.497	100	93.9	62.2	24.8	24.6
		13	*	100	95.5	54.1	40.3	30.4
	200	0	0.024	100	98.6	98.4	97.7	97.7
		10	0.389	100	88.6	44.4	26.2	25.2
		13	*	100	95.3	40.1	28.3	8.9
	240	0	0.024	100	94.9	66.4	55.5	55.2
		10	0.343	100	83.3	50.0	41.8	33.0
		13	*	100	82.1	37.9	25.7	5.2
1:2	160	0	0.016	100	44.0	36.9	20.8	16.1
		10	0.247	100	33.5	31.4	29.5	24.8
		13	*	100	34.1	18.3	7.7	—
	200	0	0.021	100	35.7	29.1	19.8	14.1
		10	0.276	100	35.1	33.1	25.5	24.9
		13	*	100	15.7	8.6	3.1	—
	240	0	0.013	100	18.9	13.6	7.9	6.3
		10	0.174	100	24.2	21.7	9.0	4.9
		13	*	100	4.3	—	—	—
1:3	160	0	0.012	100	29.9	22.8	11.8	5.9
		10	0.199	100	24.2	10.6	3.1	—
		13	*	100	13.3	4.7	—	—
	200	0	0.013	100	13.6	13.0	10.8	10.1
		10	0.207	100	18.4	11.6	—	—
		13	*	100	9.5	2.4	—	—
	240	0	0.012	100	4.1	—	—	—
		10	0.244	100	20.4	9.1	—	—
		13	*	100	7.8	—	—	—

*Impossible to measure.

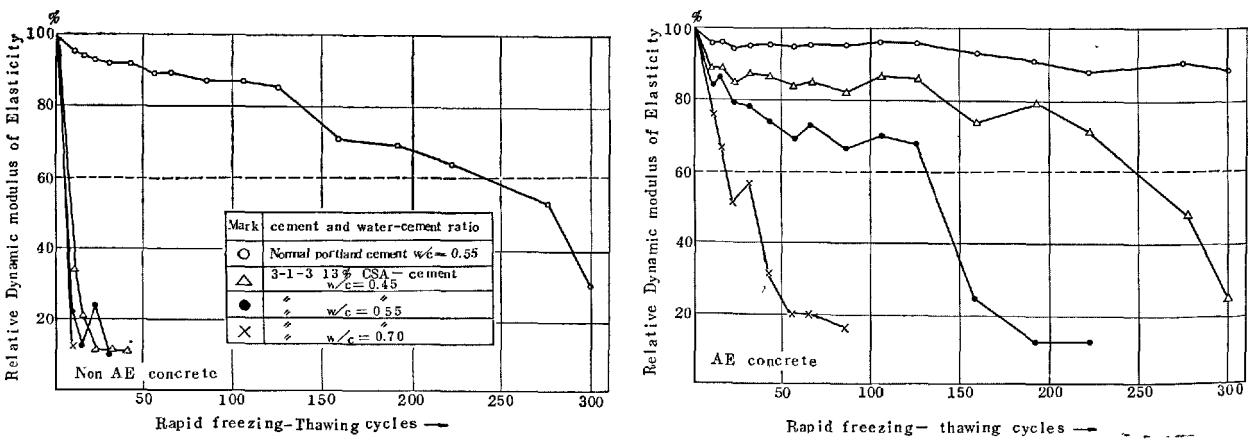

Fig. 35. *Decrease of relative dynamic modulus of elasticity of series FTC1. Tested by rapid freezing-thawing in water. 3-1-3 13% CSA-cement and normal portland cement were used (by Y. Koh, T. Gotoh)*

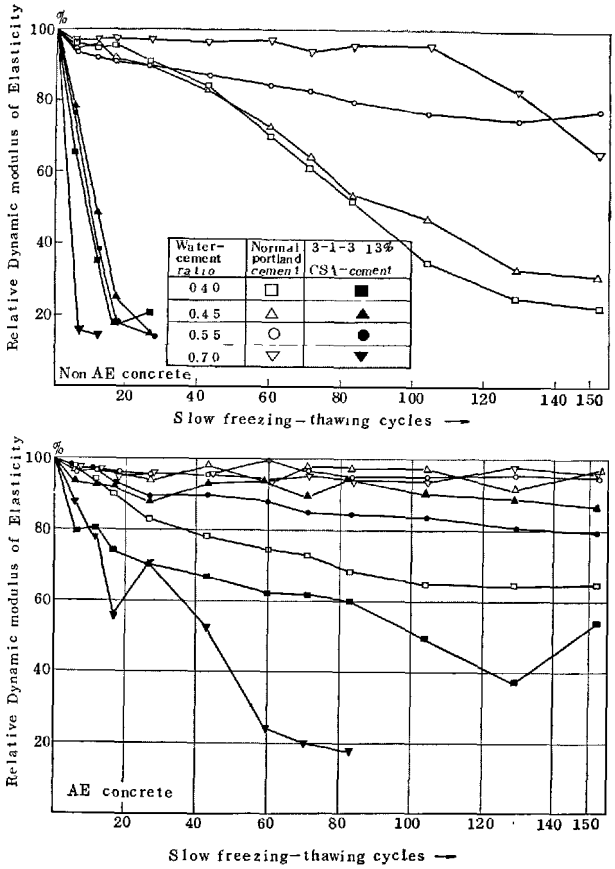

Fig. 36. *Decrease of relative dynamic modulus of elasticity of series FTC1. Tested by slow freezing-thawing in water 3-1-3 13% CSA-cement and normal portland cement were used (by. Y. Koh, T. Gotoh)*

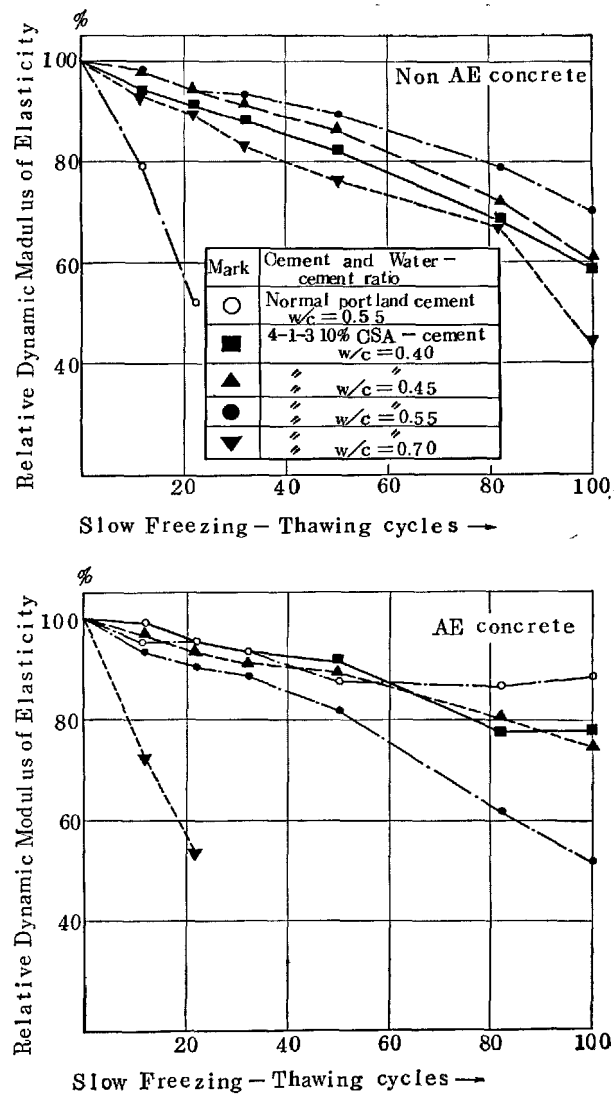

Fig. 37. *Results of series FTC 2: 4-1-3 10% CSA-cement, tested by slow freezing-thawing in water (by Y. Koh, E. Kamada)*

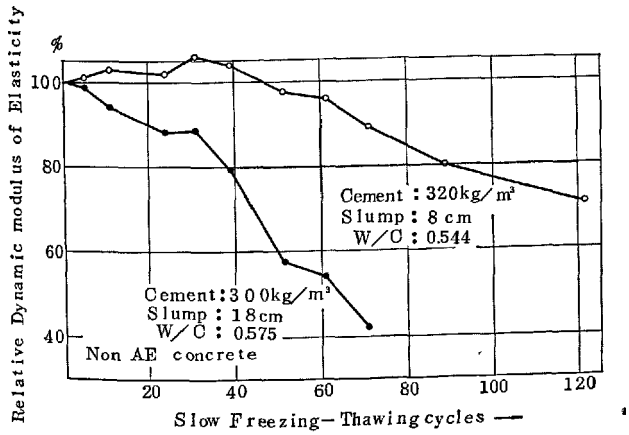

Fig. 38. *Results of series FTC 2: 4-1-3 10% CSA-cement concrete, tested by slow freezing-thawing in water. Difference between two consistencies (by Y. Koh, E. Kamada)*

Thermal Properties

Fire Resistance

The compressive strength and the modulus of elasticity of concrete vary with the temperature. Effects of heating on properties of CSA-cement concrete and in comparison with them, those of the ordinary concrete were described in this paper.

Procedure

CSA-content of the expansive cement was 13% by weight. Aggregates were natural river sand and gravel. The mix of concrete is shown in Table 26.

The specimens of these concretes, prior to the test, were cured in water for 4 weeks and then placed in a room for a month. They were heated to a temperature up to 600°C at the rate of 1.0°C–1.5°C per minute and kept at the same temperature for about an hour. They were then cooled in air gradually to the room temperature. Further 4 weeks after cooling, compression tests were conducted. Numerous specimens heated at 500°C and 600°C showed marked cracks. Figs. 39 and 40 show variations in the strength and in the modulus of elasticity with the temperature.

Results Obtained

The results obtained are as follows.

Table 26. *Mix-proportion of concrete (by Harada)*

No.	Cement	Mix-proportion (by weight)				Slump cm
		Cement	Sand	Gravel	W/C	
F-7	CSA-cement (13%)	1	2.6	2.7	65	15.3
F-8		1	2.3	2.3	55	15.3
F-9	Normal portland cement	1	2.6	2.7	65	16.8
F-10		1	2.3	2.3	55	16.9

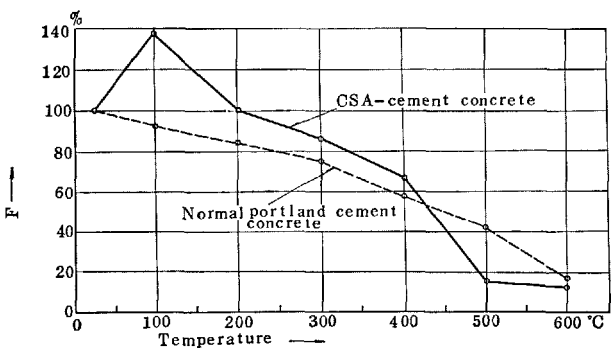

Fig. 39. *Temperature and residual strength, F*

(1) In general, strength changes of the two different type concrete are about the same. The rates of their residual moduli of elasticity change also similarly with the temperature.

(2) Fig. 41 shows the effect of temperature on the stress-strain curve of CSA-cement concrete. As the temperature rises, the elasticity of concrete decreases, indicating the increase of the plasticity of concrete.

Heat Insulation

Procedure

Values of the heat conductivity of CSA-cement mortar and concrete and of their thermal diffusivity at high temperature were measured. As compared with these values, those of ordinary portland cement concrete were also measured.

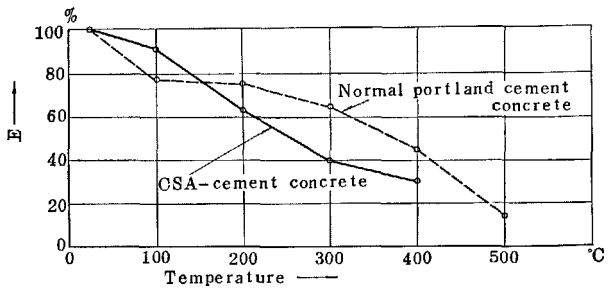

Fig. 40. Temperature and residual elasticity, E

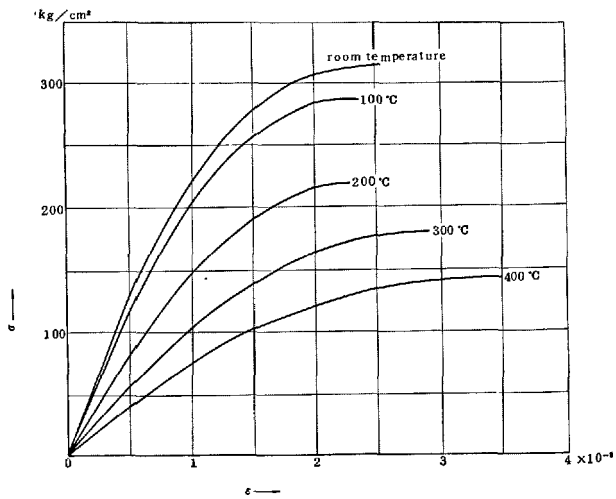

Fig. 41. *Characteristic stress-strain curves of CSA-cement concrete in the temperature range from room temperature to 400°C.*

The content of the expansive material to CSA-cement was 10%. Mix proportion of the CSA-cement concrete was 1: 2: 2.5 by weight, as well as the ordinary concrete. W/C-ratio of the CSA-cement concrete was 0.75, and that of the ordinary concrete was 0.55. As to CSA-cement mortar, the cement sand ratio was 1: 3 by weight. Aggregates used in the two type concretes and the mortar were also natural river sand and gravel. The thermal coefficients were measured in the temperature range up to 600°C. (see Fig. 42 and 43)

Results Obtained

The results obtained are as follows.

(1) Variations in the coefficients of the CSA-cement mortar and concrete with temperature are quite similar to those of the ordinary concrete. As the temperature rises, especially from 100°C to 150°C, these values are markedly reduced. However, it is inclined to somewhat increase in the temperature range to 600°C. This tendency of the variable coefficients with the temperature differs slightly from the common informations.

(2) In general, the thermal properties of the CSA-cement concrete are almost the same as those of the CSA-cement mortar, just as the relation of the ordinary concrete to the ordinary portland cement mortar; mortar is just a little superior to concrete in its insulating property.

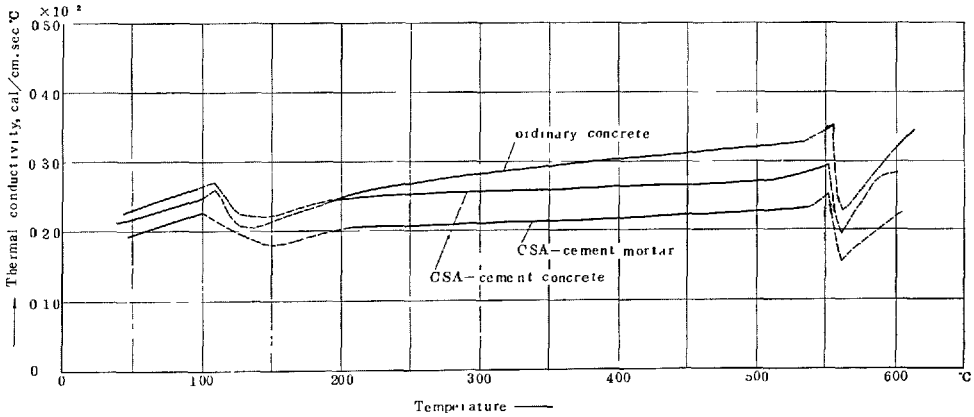

Fig. 42. *Variations of the thermal conductivity according to temperature change*

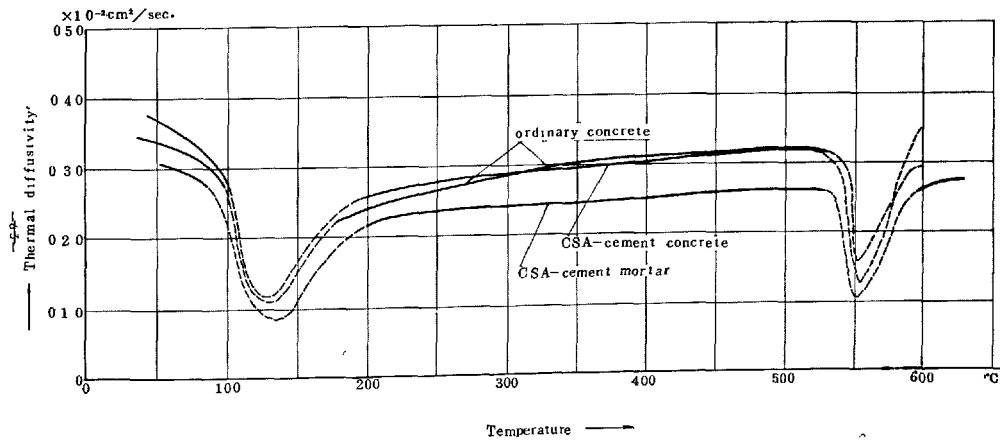

Fig. 43. *Variations of the thermal diffusivity according to temperature change*

Summary and Conclusion

Following conclusion was gained.

1. Calcium sulphoaluminous cement clinker will work for effective expansion by being mixed in cement mortar and concrete, and then it can compensate for their shrinkage of early time.
2. The content of calcium sulphoaluminous cement clinker is in a well mixed condition at about 10% by weight. In this case, final shrinkage of the cement mortar and concrete will be decreased less than the case of ordinary cement ones without sacrificing strength.
3. Wet curing condition is necessary, especially at initial period, for calcium sulphoaluminous cement mortar and concrete.
4. As the molar-ratio, $CaO: Al_2O_3: CaSO_4$ of CSA raw materials, it seems that 4–1–3 is generally better than 3–1–3 for CSA mortar and concrete uses.

References

1. Y. Koh, "Three charts for the estimation of concrete strength for various types of cement" (in Japanese), Review of the Sixteenth General Meeting of JCEA., XVI, 109–114 (1962).

Supplementary Paper IV-86 Development of Expansive Cement with Calcium Sulphoaluminous Cement Clinker

Masaichi Okushima* Renichi Kondo,** Hiroshi Muguruma*** and Yoshizo Ono****

Synopsis

Expansive cement is generally used for two purposes; for preventing the shrinkage cracks of mortar or structural concrete and for chemical prestressing of concrete elements. In the first part of this paper, the fundamental expansion-shrinkage characteristics required for expansive cement will be generally discussed from the viewpoint of shrinkage crack prevention. The results show that crack prevention directly depends on the reduction of drying shrinkage after finishing the expansion and not always on the intial expansion.

Several fundamental problems concerning chemical prestressing are also discussed and the fact that limitations for the economical use of materials, especially the prestressing steels, should be considered in comparison with ordinary prestressed concrete elements is pointed out.

Expansive cement with unique characteristics fulfilling the requirements of concrete engineering has been successfully developed in Japan because of chemical research on synthesis, phase equilibrium, crystallography and chemical engineering data analysis.

The above-mentioned expansive cement is composed of portland cement with an amount of special expansive cement clinker limited to 10%. This clinker has characteristics that allow the composition to be adjusted to a ratio of $CaO: Al_2O_3: CaSO_4 = 4:1:3$, to be heated sufficiently in a rotary kiln under such conditions that the grain size of the crystals is as large as possible, and to be very coarsely ground.

Expansive cement composed of such a clinker makes it possible to minimize the drying shrinkage after finishing the expansion without the sacrifice of mechanical strength.

In order to elucidate the mechanisms of the hydration, hardening, expansion and shrinkage of mortar and concrete, physicochemical investigations are also carried on by means of optics, electron microscopy, X-ray diffraction, determination of capillary pressure, pore size distribution, and so on.

Introduction

One of the greatest disadvantages in concrete structure is shrinkage cracking under drying conditions. The development of the expansive cement, which shows the expansion to overcome or to exceed the shrinkage of portland cement, has theoretically enabled to prevent the shrinkage crack formations. Research on the practical use of expansive cement was mainly carried out in Europe and the U.S.A., especially by H. Lossier (1), H. Lafuma (2), M. E. Perre (3), V. V. Mikhailov (4) and A. Klein (5). However, concerning the expansion-shrinkage characteristics of expanisve cement, basic study (for example, studies on how expansion-shrinkage curves are the most suitable or most appreciable for preventing the shrinkage cracks) has been quite insufficient to this date.

Another active use of expansive cement is to produce prestressed concrete by chemical prestressing. Although at present sufficient data are available for chemical prestressing (5–7), the important thing is to find a reasonable limitation for the economical use of materials, especially from the viewpoint of making the best of concrete and steel strengths.

In the first part of this paper, the fundamental expansion-shrinkage characteristics of expansive cement that are reasonable for the prevention of shrinkage cracks as well as for the economical use of materials for chemical prestressing with expansive concrete were theoretically discussed with reference to some test results.

Much research on expansive cement has been carried out in Japan as in other countries since Lafuma's (2)

*Osaka University, Osaka.
**Tokyo Institute of Technology, Tokyo.
***Kyoto University, Kyoto.
****Denki Kagaku Kogyo Kabushiki Kaisha, Tokyo, Japan.

report.

The expansive cement developed in France was composed of portland cement, calcium sulphoaluminous cement clinker (abbreviated as CSA in this paper) as the expansive agent and granulated blastfurnace slag as the stabilizer.

At that time, the mineral composition of CSA was not very well known, but it has been elucidated by degrees (10). The crystal structure (11 ,12) of the main component of CSA and the hydration mechanism (13, 14) of expansive cement have also been clarified. As a result, the expansive agent has been improved, so that it is now possible to produce an expansive cement of high quality by the addition of an amount of CSA that is only 10% of the cement (expansive cement composed of portland cement and CSA is abbreviated as CSA cement in this paper).

The investigation of expansive cement has been rapidly promoted by mutual exchanges of information between specialists both in basic research and engineering since the CSA Research Group was orgainzed in 1964.

Expansion-Shrinkage Behaviours to be Required to Expansive Cement

Current Concept for Shrinkage Crack Prevention by Expansive Cement

The expansive cements recently used in practice generally consist of mixtures of portland cement and sulphoaluminate additives as the expansion ingredient. Fig. 1 shows the typical expansion-shrinkage curves of expansive cement paste in comparison with that of portland cement. (1) As shown in Fig. 1, the expansive cement shrinks upon drying, just like ordinary portland cement, but by undergoing an initial free expansion of a controlled amount before drying begins, the net free expansion after drying may be any desired amount within limits. That is, it has been considered so far in much research that the formation of shrinkage cracks can be prevented by using expansive cement when the net strain of initial free expansion and the subsequent drying shrinkage becomes sufficiently smaller than the shrinkage strain of ordinary cement.

However, in practice the shrinkage crack formation can not be prevented even if the net free strain of expansive cement remains in expansion even after drying. This fact has been showed by many laboratory or field tests. Fig. 2 shows typical test results on free expansion-shrinkage strains of lining mortars for steel water pipe, where the calcium sulphoaluminous cement clinker (simple substitute CSA) as the expansive agent is blended with Type B blast-furnace slag cement in a mix proportion of 11: 89 by weight. Also Fig. 3 shows the test results on reinforced concrete slabs made of normal portland cement concrete and expan-

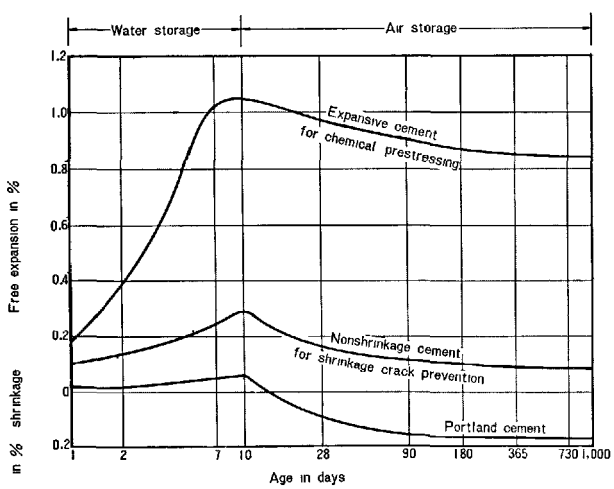

Fig. 1. *Volume changes of neat cement pastes*

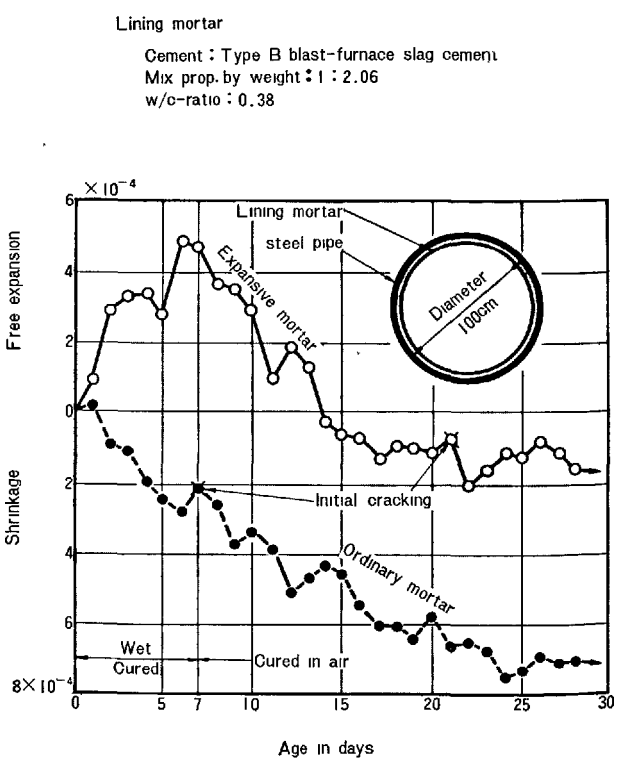

Fig. 2. *Example of shrinkage crack tests on expansive lining mortar of steel pipe (tested by H. Muguruma and Y. Ono)*

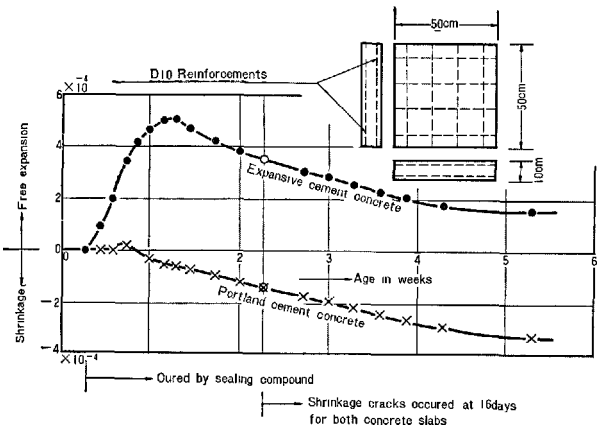

Fig. 3. *Example of shrinkage crack tests on reinforced concrete slabs made of expansive concrete (tested by K. Ohno, Hokkaido University).*

sive cement with calcium sulphoaluminous cement clinker (simple substitute CSA-cement concrete). Thus, from these results it seems that the absolute conditions for the purpose of preventing shrinkage crack formation are not to compensate the shrinkage by initial free expansion, in order words, not to keep the net free strain after drying in expansion.

Ideal Expansion-Shrinkage Curve for Shrinkage Crack Prevention

Considering that the shrinkage cracks do not really take place without the external restraint of free shrinkage of mortar or concrete and also that the easiness of crack formation will be goverened by the degree of restraining, the problem of shrinkage crack prevention can not be discussed without respect to the effects of external restraint. When the initial expansion of expansive mortar or concrete is externally restrained, the inner compressive stress is induced according to the degree of restraint. And, with the lapse of time after finishing the expansion, it is reduced due to creep and shrinkage. Although the larger restraint results in a larger inner compressive stress, the reduction of stress also becomes larger with an increase in the degree of restraining.

To discuss the ideal expansion-shrinkage characteristics for shrinkage crack prevention, the model with elastic restraint shown in the upper part of Fig. 4 is considered by H. Muguruma (8, 9). When the maximum free expansion takes place at an early age in concrete, the corresponding inner compressive stress σ_e induced in the concrete element due to the longitudinal elastic restraint can be written as

$$\sigma_e = \alpha' \frac{E_c S_e}{2} \tag{1}$$

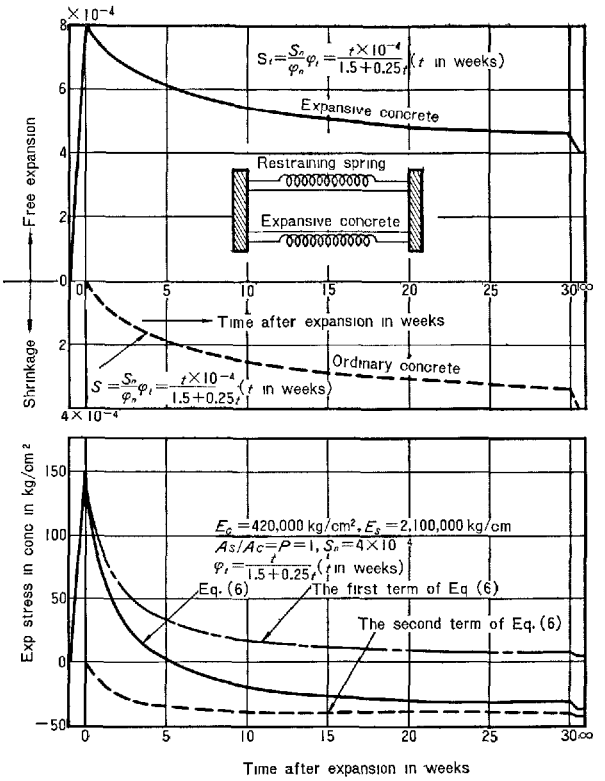

Fig. 4. *Numerical example of expansion-shrinkage stress in concrete due to external restraint of free expansion-shrinkage strain (calculated by H. Muguruma)*

$$\alpha' = \frac{2E_s A_s}{2E_s A_s + E_c A_c} \tag{2}$$

where

E_c and A_c: Elastic modulus and sectional area of concrete specimen,

E_s and A_s: Apparent elastic modulus and sectional area per unit length of elastic spring restraint.

In eq. (1), taking the reduction of stress due to creep during the expansion of the concrete into consideration, the apparent elastic modulus of concrete is assumed to be half that at the age of maximum expansion. After finishing the expansion, the inner compressive stress is released due to creep and shrinkage. Assuming the creep strain of concrete proportional to the applied stress (Davis-Glanville's law), the superposition of creep strains (Whitney's law) and the increase of shrinkage strain linear to creep strain, the following equation concerning stress reduction $\Delta\sigma_t$ can be obtained:

$$\frac{\sigma_e}{E_c}\varphi_t - \frac{\Delta\sigma_t}{E_c} - \int_0^t \frac{\Delta\sigma_t}{E_c} d\varphi_t + \frac{S_n}{\varphi_n}\varphi_t = \frac{A_c \Delta\sigma_t}{E_s A_s}, \quad (3)\,(8, 9)$$

where

φ_t: Creep factor of concrete,
φ_n: Final value of creep factor,
S_n: Final value of shrinkage strain measured from the maximum expansion strain.

Solving eq. (3) under the initial condition of $\Delta\sigma_t = 0$ at the time $t = 0$ (the time when the expansion strain reaches its maximum), we obtain

$$\Delta\sigma_t = \left(\sigma_e + E_c\frac{S_n}{\varphi_n}\right)(1 - e^{-\alpha\varphi_t}), \tag{4}$$

where

$$\alpha = \frac{E_s A_s}{E_c A_c + E_s A_s}. \tag{5}$$

Thus, the remaining stress becomes

$$\sigma_t = \sigma_e - \Delta\sigma_t = \sigma_e e^{-\alpha\varphi_t} - E_c\frac{S_n}{\varphi_n}(1 - e^{-\alpha\varphi_t}), \tag{6}$$

where the compressive stress of σ_t is assigned positive.

The first term of the right hand side in eq. (6) presents the reduction of expansive stress due to creep. Considering that the value of α is nearly unitary under such a stiff restraint as absolute rigidity and also that the final value of φ_t will be 4 for usual concrete, it vanishes rapidly to almost null. As a result, only the tensile streess due to the shrinkage strain subtracted from the maximum expansion given by the second term of eq. (6) finally remains in the concrete. Therefore, if the dropping difference between the maximum expanding strain and the shrinkage strain of expansive concrete is quite the same as that of ordinary concrete, the tensile stress similar to that induced in ordinary concrete could result, even in expansive concrete. That is, the initial expansion does not contribute to the prevention of shrinkage cracking, excepting the possible role of delaying the age of crack formation. This can be seen more evidently from Fig. 4, where the expansion-shrinkage stresses corresponding to the free expansion-shrinkage curves shown in the upper part of this figure are obtained from eqs. (1) and (6) for a concrete specimen having a restraining of $\alpha' = 0.909$ and $\alpha = 0.833$.

Consequently, the necessity for preventing the shrinkage crack formation is not always to compensate the drying shrinkage by initial expansion, but also to reduce the shrinkage strain after finishing the expansion. The net free expansion or the remaining free expansion defined as the sum of initial expansion and subsequential shrinkage has no direct effect on the prevention of shrinkage cracks, excepting the closure of some voids in concrete or mortar by external restraint, which results in superior quality with respect to permeability and strength.

Expansion for Chemical Prestressing

Another use of expansive cement is for chemical prestressing. Much of the past research showed the possibility for the expansion of concrete to produce automatically the prestressed concrete element (3–7). However, no discussions have been given on such a fundamental problem as whether the prestress as required in ordinary prestressed concrete members can be simultaneously induced or not in concrete and embedded steels of the element having an ordinary percentage of prestressing steels. Assuming that the apparent elastic modulus of concrete is half that at the age of maximum expansion, the prestressing force P induced in the concrete section by free expansion S_e can be obtained from

$$P = \frac{E_s \cdot A_s \cdot S_e}{1 - 2np(1 + e^2 A_c/I_c)} \tag{7}$$ (8, 9)

where

n: Modular ratio ($= E_s/E_c$),
p: Percentage of prestressing steels ($= A_s/A_c$),
e: Eccentricity with respect to the center of gravity of the section,
A_c and A_s: Sectional areas of concrete and prestressing steels, respectively,
I_c: Moment of inertia of the concrete section with respect to the center of gravity of the section,
E_c and E_s: Elastic moduli of concrete and prestressing steels, respectively.

Numerical example was made on the rectangular section having elastic moduli of $E_c = 420{,}000$ kg/cm² and $E_s = 2{,}100{,}000$ kg/cm², respectively, and an eccentricity of $e = D/6$ (where D denotes the height of the section). The results obtained for the various percentages of embedded steels are shown in Fig. 5.

From Fig. 5 it can be seen that the steel stress created by initial expansion varies only a little with the increase of steel percentage, while the compressive stress induced in the concrete section becomes larger approximately in proportion to the percentage of steel. In ordinary prestressed concrete members, the average compressive stress (P/A_c) that must be introduced into a rectangular concrete section is from 50 kg/cm² to 75 kg/cm², which corresponds to concrete strengths of 300 kg/cm² to 450 kg/cm². On the other hand, the ordinary percentage of prestressing steels is 0.5 to 1%. Thus, from Fig. 5 it can be seen that the prestressing steels adequate for producing the average concrete stress of 50 to 75 kg/cm² with a steel percentage of 0.5 to 1% are of a type having the allow-

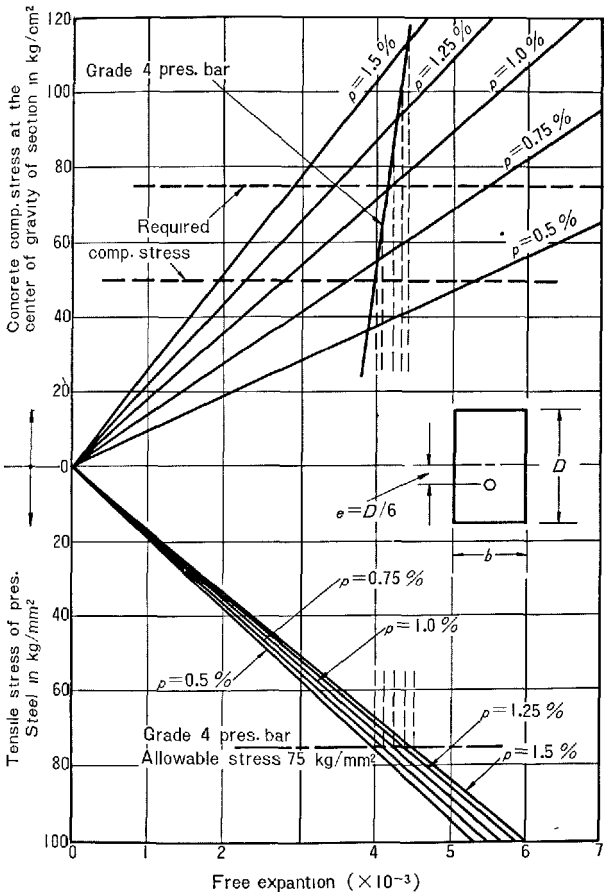

Fig. 5. *Relations between free expansion of concrete and stresses induced in concrete and embedded steels by chemical prestressing (calculated by H. Muguruma)*

able tensile stress of approximately 50 kg/mm² to 90 kg/mm². The corresponding expansion of concrete effective enough to produce such prestressing stresses thus becomes 2.75×10^{-3} to 5×10^{-3}. These results can also be approximately applicable to T or I-section concrete members. (8, 9)

Consequently, it can be stated that prestressing steels satisfying the above requirements are the so-called high tensile prestressing steel bars with relatively lower strength, and the use of piano wires or 7-wire strands having strengths of 150 kg/mm² or more would not always be economical from the viewpoint of the utilization of their higher strengths.

Possibility of Chemical Prestressing by Using CSA-Cement

As can be seen from Fig. 5, the concrete expansion effective for the production of adequate prestressed concrete members by chemical prestressing is from 0.275% to 0.5%. While the free expansion of concrete can be controlled within some limits by increasing the contents of the expansive agent in ordinary cement, the entire amount of free expanding strain is not always effective in creating the tensile stress in steels and the corresponding compressive stress in concrete under the restraining conditions of embedded prestressing steels. Therefore, for the purpose of discussing the possibility of chemical prestressing, the expanding strain effective for the creation of prestress in concrete should be predicted from test on restrained expansive concrete specimens. In this report, such expanding strain is called the effective expansion.

Fig. 6 shows typical results for the expanding strains of CSA-cement concrete specimens restrained longitudinally by embedded prestressing steel bars. Three different mix proportions of CSA and normal portland cement, that is, 10: 90, 13: 87 and 15: 85 by weight, respectively, were used. The degrees of restraining were 0, 0.46, 0.93 and 1.61%, respecitvely, in the percentage of embedded prestressing steel bar. After casting and curing the specimens were removed to the storage room with 100% relative humidity and 20°C room temperature to measure the longitudinal expanding strains. The strain measurements were made for 28 days, while the expansion reached its steady state by 7 days.

From Fig. 6, it can be seen that, although the free expansions (expansions of no restraining specimen) of the concrete having 13% and 15% CSA content were very large, those of restrained specimens were considerably smaller. The effective expansions predicted from Fig. 6 are as follows:

Age	CSA-contents	Free expansion	Predicted effective expansion
	10%	0.03%	0.03%
3 days	13%	0.30%	0.15%
	15%	0.59%	0.18%
7 days	13%	0.54%	0.23%
	15%	3.0 %	0.35%

From the above results, it can be stated that 15% CSA content is not always adequate for chemical prestressing because of the larger decrease in the 28 day compressive strength, as shown on the right side of Fig. 6. 13% weight content seems to be a reasonable limit within the test results reported here. However, as can be seen from Fig. 7, such a content is evidently insufficient to get the adequate effective expansion mentioned in this section (or to induce the adequate prestress of 50 kg/cm² or more in concrete). That is,

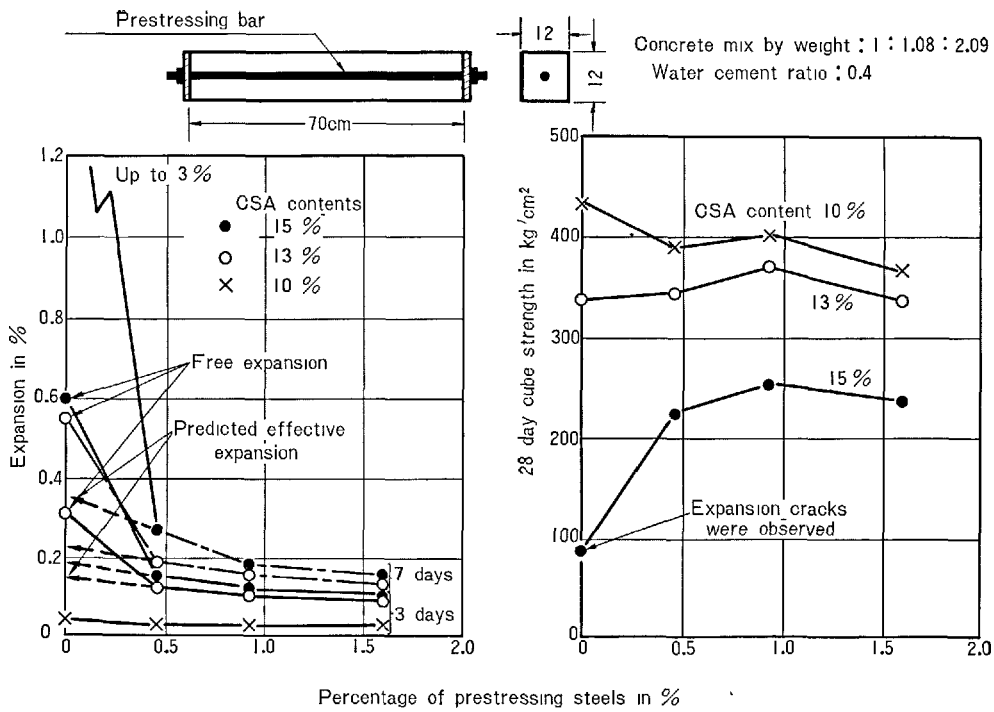

Fig. 6. *Effective expansion and compressive strength of expansive cement concrete with various calcium sulphoaluminate contents (tested by H. Muguruma).*

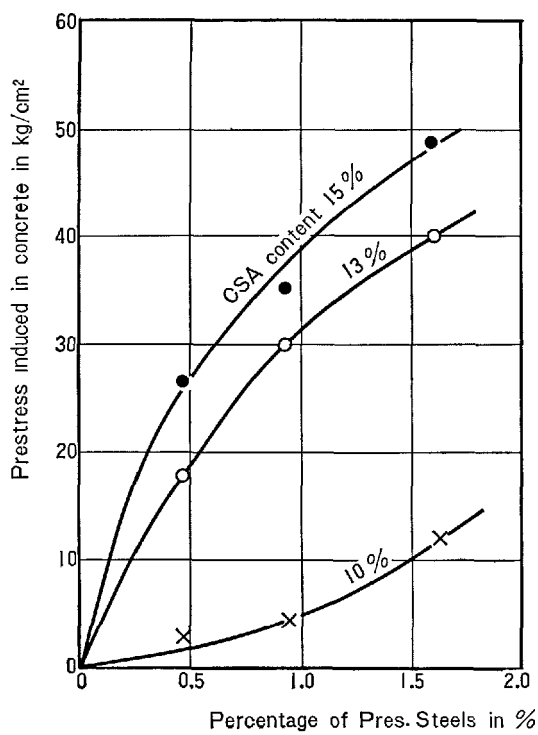

Fig. 7. *Prestress induced in concrete specimen by chemical prestressing (Tested by H. Muguruma)*

in the specimen of 13 % CSA content only 30 kg/cm² prestress was induced in the concrete section having 1 % prestressing steels.

In practice, even if only 30 kg/cm² prestress is induced in the concrete by chemical prestressing, it will be very valuable for increasing the cracking capacity of concrete members. For instance, when applying the chemical prestress in the ordinary reinforced concrete piles, which have quite insufficient flexural cracking capacity, the prestress of 30 kg/cm² in concrete is enough to increase their cracking capacity to more than twice that of ordinary piles and consequently the formation of cracks during transportation or driving in the field would be avoided entirely. (M. Okushima and H. Muguruma)

Basic Studies on Production and Properties of Expansive Cement

Calcium Sulphoaluminous Cement Clinker

The composition of CSA was originally designed to have a molar ratio of $CaO: Al_2O_3: CaSO_4 = 3:1:3$ for the purpose of forming ettringite (trisulphate hydrate TSH) as much as possible by hydration of CSA cement. It was then improved to a ratio of 4:1:3, after the beneficial effect of CaO on expansion—shrinkage characteristics was found.

The CSA is approximately composed of 50% $CaSO_4$, 30% $C_4A_3\bar{S}$, and 20% CaO. In addition, it contains a small amount of glassy phase.

According to Kondo (11), a group of new compounds of the haüyne structure type, $(Ca_2Na_6)Si_6Al_6O_{24}(SO_4)_2$, can be synthesized by the substitution of Ca and Na by Ca, Sr or Cd, Al by Be, all of Al and Si by Al, as well as SO_4 by CrO_4, MoO_4 or WO_4. $C_4A_3\bar{S}$ is a typical member of this group. Furthermore, the hydraulic property of $C_4A_3\bar{S}$ can be explained by the existence of 4-fold coordinated Al^{+++}, asymmetrically coordinated Ca^{++}, and isolated SO_4^{--} in the structure.

The crystal structure of $C_4A_3\bar{S}$ (11) is shown in Fig. 8, and the infrared absorption spectra in Fig. 18.

$C_4A_3\bar{S}$ is formed by either a solid state reaction between $CaSO_4$ and mixtures or compounds composed of CaO and Al_2O_3, or an SO_3 gas reaction with the above-mentioned mixtures. The $C_4A_3\bar{S}$ crystal is well grown in the presence of a melt containing $CaSO_4$.

By means of the Griffine hot-stage microscope, it was found that eutectics exist between $C_4A_3\bar{S}$ and CA or $CaSO_4$. However, $C_4A_3\bar{S}$ and $CaSO_4$, and especially a mixture of them, decomposes rather rapidly to give SO_3 gas when heated in open air. It was also found that CSA began to melt at 1180–1230°C. The higher the heating temperature, the greater the crystal size of either produced $C_4A_3\bar{S}$ or of residual CaO and $CaSO_4$.

Necessity of developing a high level of technology confronted at the outset in order to fulfill the requirements for the characteristics that would permit the growth of the crystal components of CSA, even though the heating temperature range of CSA is very small. In addition, it was improved to reduce the loss of SO_3 vaporization during the heating stage of production to a negligibly small amount. The CSA is heated in a rotary kiln these days, it can also be produced by electric furnaces, etc. (15) Fig. 9 shows a microphotograph of CSA industrially produced.

$CaSO_4$ is a colorless anisotropic crystal. CaO is an isotropic spherical pale yellow particle with a distinctive outline because of its high refractive index. $C_4A_3\bar{S}$ is a colorless isotropic crystal having a little

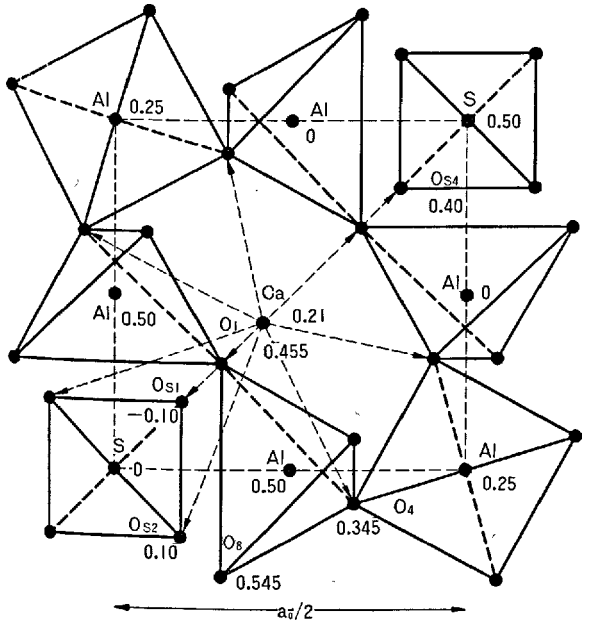

Fig. 8. *Positions of atoms in $a_0/2$ cube of $Ca_8Al_{12}O_{24}(SO_4)_2$, projected on (001) plane.*

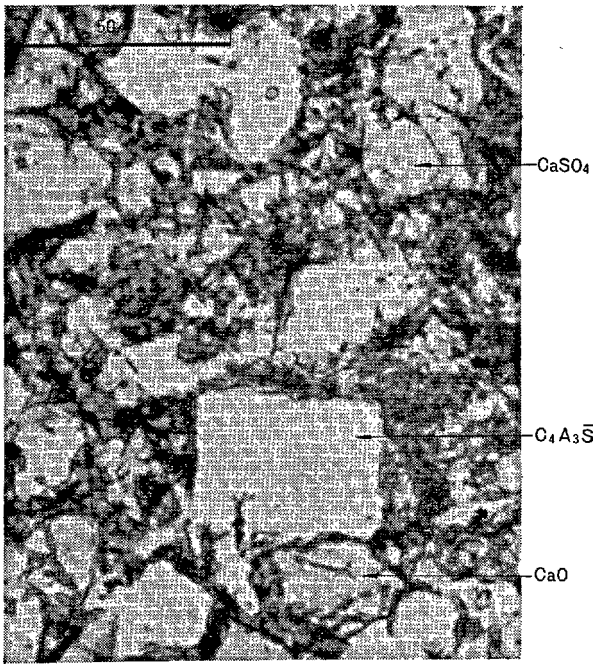

Fig. 9. *Micrography showing the main components of CSA clinker (open nicol)*

lower index than $CaSO_4$. The mean diameter of $C_4A_3\bar{S}$, CaO, and $CaSO_4$ is 50, 15 and 8μ each in the clinker produced by the sintering process, and 120, 40 and 20μ by the melting process.

Silicates and ferrites are scarcely detected among the interstitial materials, but these materials are generally in a glassy phase. By means of a Shimazu electron micro-probe analyzer, the composition of these materials was found to be rich in Al_2O_3, Fe_2O_3, SiO_2 and TiO_2 were also present, but the amount of CaO was comparatively low and there was almost no SO_3. During the cooling of the CSA, a part of $C_4A_3\bar{S}$ crystallizes out of the melted state at the periphery of the glassy material to form a fringed layer, as shown in Fig. 10.

The rate of hydration of CSA powder with a diameter of 15–43μ in the paste form was quantified by X-ray diffraction. It was found that CaO is consumed within 2 days, and the fraction of hydration of $CaSO_4$ and $C_4A_3\bar{S}$ is as shown in Table 1. The reaction of $CaSO_4$ is slower than that of $C_4A_3\bar{S}$, which is similar to the results of the case of J and S described in the paper presented by Mehta and Klein (14).

To preserve the potential force of expansion for an extended period of time by gradual hydration, the crystal growth of CSA must not only proceed properly, but the CSA must also be ground in such a way that the range of particle size is small and the particles are remarkably coarser than those of ordinary cement (16).

Hydration Process of $C_4A_3\bar{S}$ and Morphology of Hydrates

The hydration process of $C_4A_3\bar{S}$ alone, or with $Ca(OH)_2$ and/or $CaSO_4$, were observed by optical and electron microscopes. For comparison, the hydration processes of C_3A were also observed in the same way (17).

Each component used in these experiments was a powder of 5–10μ in diameter.

When the mixture of C_3A and 3 moles of $CaSO_4$ is hydrated, the surface of C_3A begins to be covered with needle-shaped crystals of TSH, after which they will coexist with monosulphate hydrate(MSH or $C_3A\cdot C\bar{S}\cdot H_{12}$) or a solid solution of the latter and C_4AH_{13}.

Fig. 11 shows the electron diffraction pattern of the solid solution. Grudemo (18) has described the formation of hexagonal plate crystals under similar conditions.

TSH is formed either on the surface of C_3A particles or in the solution, but scarcely on the surface of $CaSO_4\cdot 2H_2O$ particles.

In the case of $C_4A_3\bar{S}$ alone, a complex layer of $C_3A\cdot C\bar{S}\cdot H_{12}$ and $Al(OH)_3$ form as the inner product of

Table 1. *Percentage of hydration of* $CaSO_4$ *and* $C_4A_3\bar{S}$ *in CSA clinker* (%)

	Process	1 day	2 days	7 days
$CaSO_4$	sintering	42	53	58
	melting	15	20	30
$C_4A_3\bar{S}$	sintering	75	72	85
	melting	27	42	55

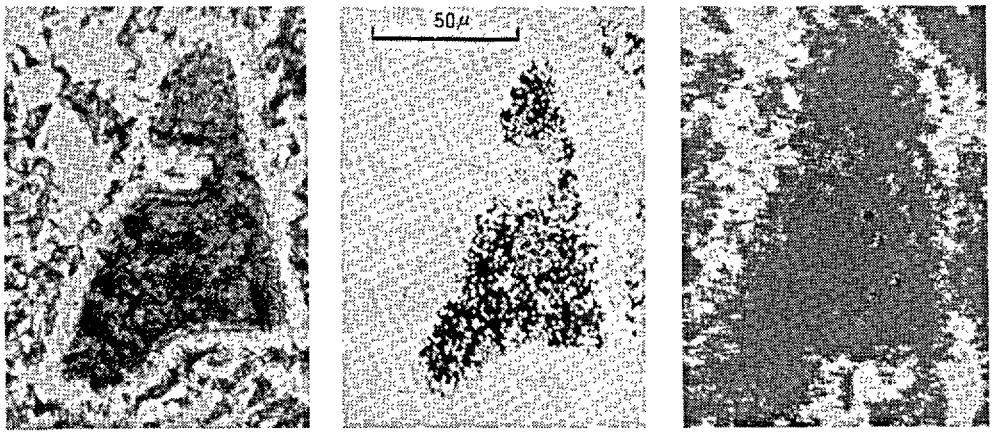

(a) (b) (c)

Fig. 10. *Micrography and characteristic X-ray images of CSA cement clinker with thin section*
(a) Micrography showing espccially the glassy phasc. (open nicol)
(b) Characteristic X-ray image of CaK_α.
(c) Characteristic X-ray image of S: K_α.

$C_4A_3\bar{S}$, and this reaction is completed in 12–24 hrs. As shown in Fig. 12, it is remarkable that the outer shape and dimensions of each grain are almost unchanged throughout this hydration, and TSH, as an outer product, crystallizes out of the solution.

$C_4A_3\bar{S}$ hydrates quickly in the presence of CaO, and the outer shape of its grain is almost unchanged. When $C_4A_3\bar{S}$ is hydrated with $CaSO_4$, the particles of the former are rapidly covered with needly-shaped crystals of TSH.

On the one hand, when a mixture of $C_4A_3\bar{S}$, $CaSO_4$, and CaO adjusted to a molar ratio of $CaO: Al_2O_3: CaSO_4 = 4:1:3$ is hydrated, $C_4A_3\bar{S}$ particles are covered with a thick coating composed of fine crystals of TSH. This coating begins to expand after about 6–8 hrs., and becomes 2–3 times larger than at the beginning at about 24 hrs., as shown in Fig. 13.

On the other hand, when the molar ratio of $CaO: Al_2O_3: CaSO_4$ is 4:1.25:1, a solid solution of $C_3A \cdot C\bar{S} \cdot H_{12}$–$C_4AH_{13}$ crystallizes into a hexagonal plate.

It seems that the expansion due to hydration of $C_4A_3\bar{S}$ in the presence of much $CaSO_4$ and CaO is closely related to the formation of TSH by the reaction between SO_4^{--}, permeating from outside, and

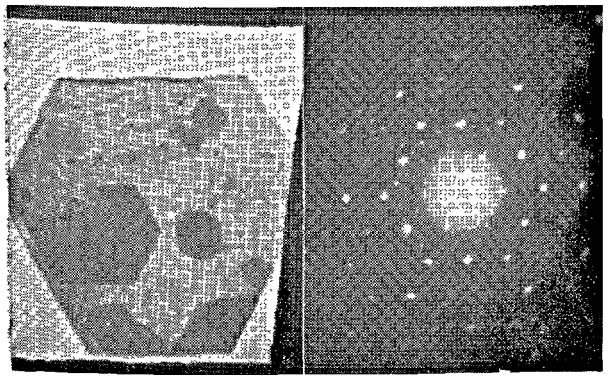

Fig. 11. *Single-crystal diffraction pattern of* $C_3AC\bar{S}H_{12}$–C_4AH_{13} *solid solution*

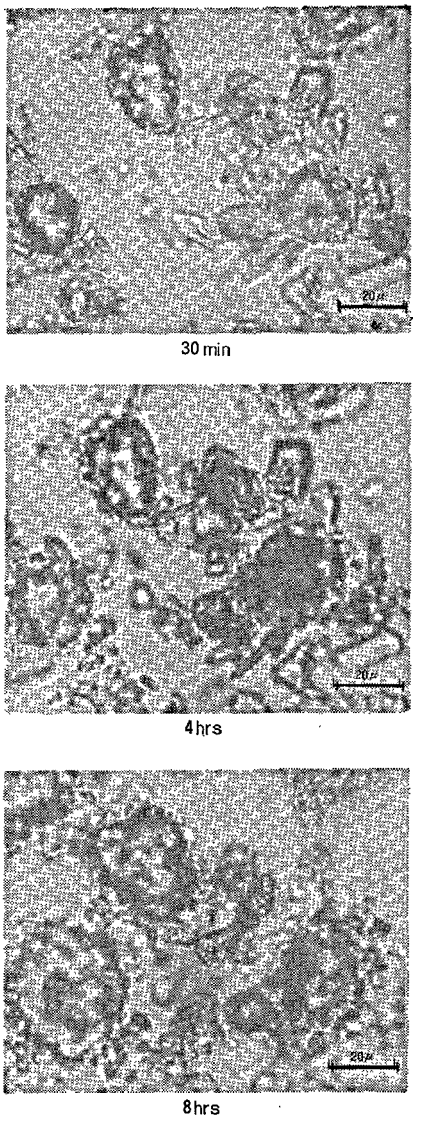

Fig. 13. *Expansion of reacted layer in hydration of* $C_4A_3\bar{S}$ *grain with water in the presence of* CaO *and* $CaSO_4$.

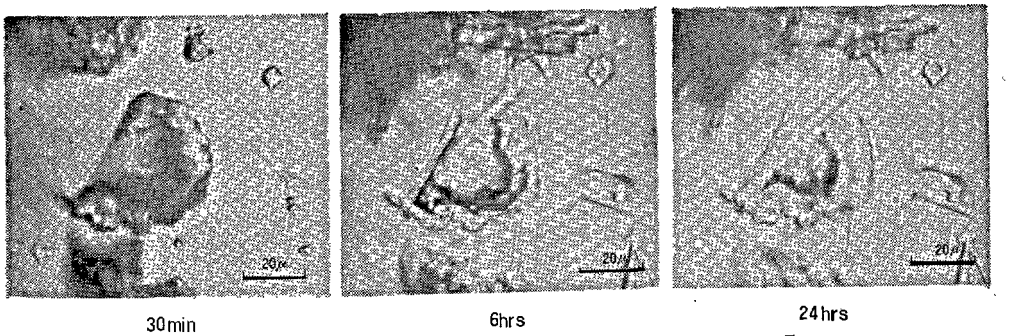

Fig. 12. *Formation of inner products in hydration of* $C_4A_3\bar{S}$ *grain with water*

$C_3A \cdot C\bar{S} \cdot H_{12}$ or its solid solution formed on the interface of each particle of $C_4A_3\bar{S}$.

If we assume that the hydration of CSA powder produces TSH alone, $CaSO_4$ and $C_4A_3\bar{S}$ should decrease accordingly, but the consumption of $CaSO_4$ is delayed as shown in Table 1. This suggests the possibility of the formation of at least a part of MSH.

Fig. 14 shows the results of a semi-quantitative analysis (by means of X-ray diffraction) of the hydration process of CSA cement paste in comparison with that of portland cement.

In this experiment the W/C ratio of paste was 0.4 and the curing temperature was 20°C.

In the case of portland cement, C_3A is eliminated within 7 days, In consumption of $CaSO_4 \cdot 2H_2O$, and at the very early stage it forms TSH, which then converts into MSH after about 3 dyas.

The hydration of C_3S, C_3A, and C_6A_2F in CSA cement is slower than that of C_3S, C_3A, and C_6A_2F in portland cement. After $C_4A_3\bar{S}$ is consumed in 1 day to form large amounts of TSH, C_3A reacts gradually.

$CaSO_4$ is not only expended in the reaction, but independently hydrated to form $CaSO_4 \cdot 2H_2O$. When the CSA cement clinker content is low, TSH partially changes into MSH after 3 days.

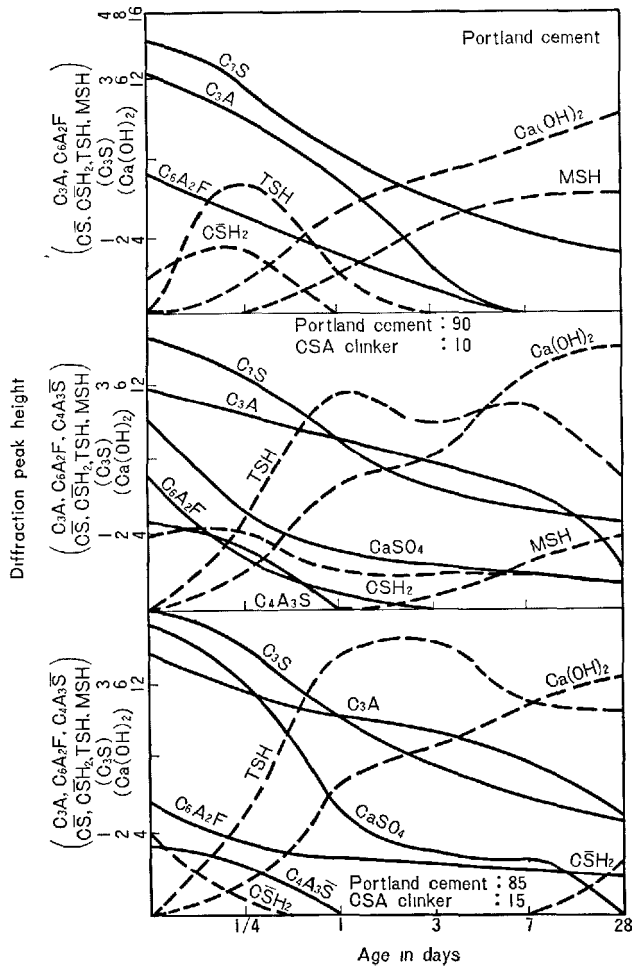

Fig. 14. *Variation of quantity in progress of hydration of CSA cement and portland cement*

The Location of the Deposition of Hydrates in the Hydration of $C_4A_3\bar{S}$ or C_3A

The location of the deposition of hydrates in the hydration of $C_4A_3\bar{S}$ or C_3A with CaO and/or $CaSO_4$ should be closely related to the hydration velocity and the irreversible expansion due to hydration.

First of all, a couple of pastes with different components, such as $C_4A_3\bar{S}$ and $CaSO_4$, were put together with 17 sheets of filter paper between them. The consistency of the pastes was kept constant at about W/C = 0.5–0.6, and they were hydrated for 3, 7, and 28 days at 20°C. On the above days, the filter papers were peeled off to measure the pH of each piece and to be dried for 12 hrs. at R.H. 4 % for examination by X-ray diffration, etc.

Furthermore, the surface of the hardened paste containing $C_4A_3\bar{S}$ or C_3A was repeatedly ground to remove the top 0.2–0.3 millimeters at one time. The surfaces and powders of each paste were examined by X-ray diffraction, and the powders were also analyzed by DTA and TGA.

In addition, the expansion was measured for compacts composed of either $C_4A_3\bar{S}$ or C_3A with CaO and/or $CaSO_4$ after moistening at 20°C and then being immersed in saturated solutions of CaO and/or $CaSO_4$.

The series shown in Table 2 were examined for hydration and expansion (19). The particles of each component here were adjusted by the BAHCO microparticle classifier to be $r = 11 - 22\mu$.

The peaks (2θ, CuK_α) selected for detection of hydrates by X-ray diffraction are as follows:

$C_3A \cdot 3C\bar{S} \cdot H_{32}$ (TSH) 9.0°,

Table 2. *Interaction between $C_4A_3\bar{S}$ or C_3A and additional components in hydration*

Series	Main component	Additional component
1	$C_4A_3\bar{S}$	$CaSO_4$
2	$C_4A_3\bar{S}$ + $CaSO_4$	CaO
3	$C_4A_3\bar{S}$ + CaO	$CaSO_4$
4	$C_4A_3\bar{S}$	$CaSO_4$ + CaO
5	$C_4A_3\bar{S}$ + $CaSO_4$ + CaO	
11	C_3A	$CaSO_4$
12	C_3A + $CaSO_4$	CaO
13	C_3A + 1.5CaO	$CaSO_4$
14	C_3A	$CaSO_4$ + CaO

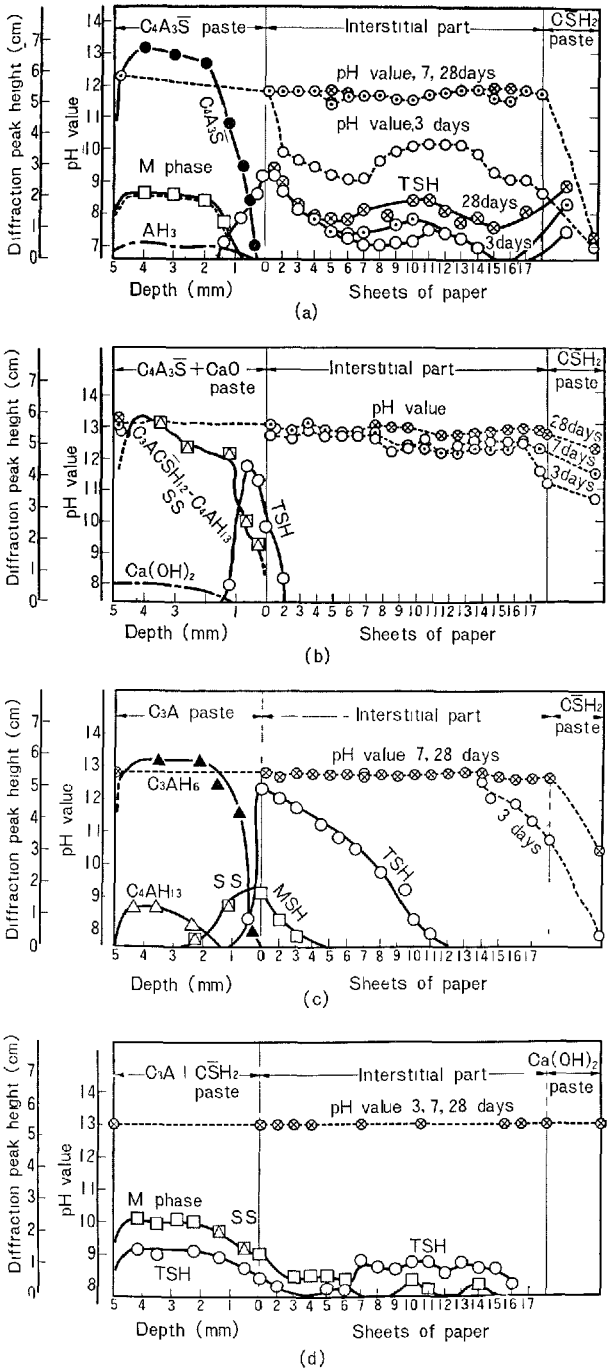

Fig. 15. *Variation of quantity and location of reactants and products in progress of hydrations*

(a) Results after 28 days in paste part and after 3, 7 and 28 days in interstitial part of series 1.

(b) Results after 28 days in paste part and interstitial part of series 3.

(c) Results after 28 days in paste part and interstitial part of series 11.

(d) Results after 28 days in paste part and interstitial part of series 12.

$C_3A \cdot C\bar{S} \cdot H_{12}$ (MSH)	9.9°,
$C_3A \cdot C\bar{S} \cdot H_{12}$–$C_4AH_{13}$ (solid solution)	10.5°,
$C_3A \cdot C\bar{S} \cdot H_{19}$ (*M* phase)	9.3°,
C_4AH_{13}	11.5°,
C_3AH_6	31.8°,
$Al(OH)_3$	20.3°,
$Ca(OH)_2$	34.1°.

Some of the experimental results for hydration are illustrated in Fig. 15. Some results of the expansion measurements are shown in Figs. 16 and 17.

Series 1 and 4: components which dissolve into the filter paper from both pastes form TSH in the pores

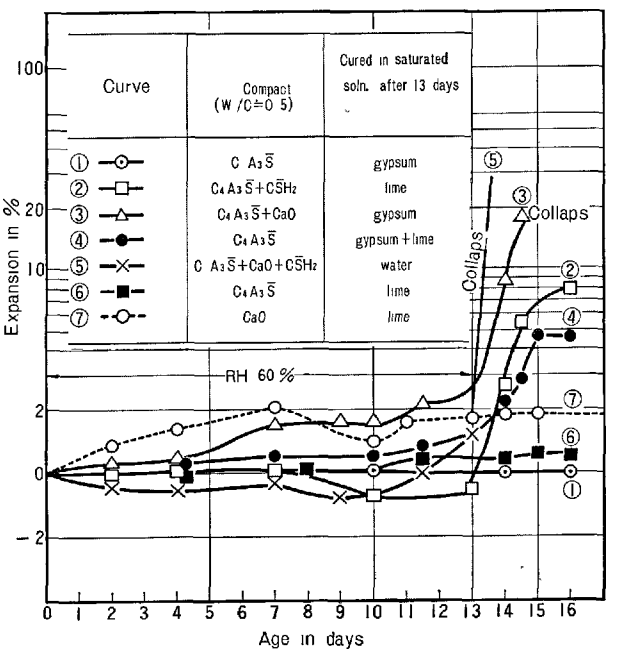

Fig. 16. *Expansion of compacts containing* $C_4A_3\bar{S}$

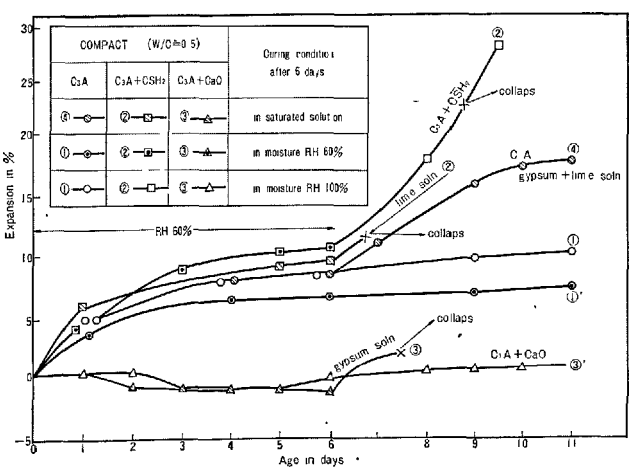

Fig. 17. *Expansion of compacts containing* C_3A.

of the filter paper. Fig. 15 (a) shows the results in the case of Series 1.

Series 2: TSH forms rapidly inside the paste of $C_4A_3\bar{S}$ and $CaSO_4$, but the expansion was very slight.

Series 3: a dense layer of TSH is finally formed along with the remarkable expansion due to the reaction between the permeated $CaSO_4$ and the $C_3A \cdot C\bar{S} \cdot H_{12}$–$C_4AH_{13}$ solid solution which has formed in the paste of $C_4A_3\bar{S}$ and CaO.

Series 5: TSH gradually forms with time and increases in the paste of $C_4A_3\bar{S}$, CaO and $CaSO_4$ along with remarkble expansion, similar to the case of Series 3. But the deposition of hydrates in the filter paper is negligible in this case.

Series 11: in C_3A paste, C_3AH_6 and C_4AH_{13} are detected, but no TSH. The latter is deposited in the filter papers, and MSH appears on the interface between the filter paper and the C_3A paste. In such a case, there is very little expansion.

Series 12: in the first stage, C_3A hydrates with $CaSO_4$ to form TSH, which reacts afterwards with the unreacted C_3A to form C_3A–$C\bar{S} \cdot H_{12}$ or a solid solution of it. In this case there is remarkable expansion.

Series 13: TSH forms only on the interface between the filter paper and paste, while C_4AH_{13}, C_3AH_6, and $Ca(OH)_2$ form on the back surface of the paste, and the solid solution forms in the paste near the filter paper. In this case there is no expansion.

Series 14: C_3A hydrates with CaO and $CaSO_4$ to form C_3AH_6 thoughout the paste, but the above mentioned solid solution in the paste is limited to the area near the filter paper. A condiderable degree of expansion occurs in spite of the limited formation of TSH in this case.

These experimental results led us to the conclusion that the hydration of $C_4A_3\bar{S}$ proceeds stepwise as follows:

$$C_4A_3\bar{S} + 8Ca(OH)_2 + 30H_2O \longrightarrow (C_3A \cdot C\bar{S} \cdot H_{12}\text{–}2C_4AH_{13}),$$

$$(C_3A \cdot C\bar{S} \cdot H_{12}\text{–}2C_4AH_{13}) + 6Ca^{++} + 8SO_4^{--} + 58H_2O \longrightarrow 3(C_3A \cdot 3C\bar{S} \cdot H_{32}).$$

Many investigators acknowledge that very little expansion occurs, regardless of the formation of TSH, if the concentration of CaO in the solution is low (13, 14, 20, 21). On the contrary, the grains of $C_4A_3\bar{S}$ are coated with hydrates at an early stage of reaction as a consequence of the lowering of the solubility of the hydrates if the concentration of CaO is high. Consequently, $C_4A_3\bar{S}$ reacts with H_2O permeated through pores to form $C_3A \cdot C\bar{S} \cdot H_{12}$ or solid solution of it with low crystallinity on the interface of $C_4A_3\bar{S}$. Remarkable expansion would take place as the result of a secondary reaction if the above hydrates with SO_4^{--} ion come from the liquid phase by diffusion to form fine crystalline TSH.

At the same time, expansion due to the formation of MSH was also confirmed when C_3A hydrates at an early stage with a limited amount of $CaSO_4$ to form crystalline TSH, which then reacts with lime to form fine crystalline MSH in the product layer.

Properties of Ettringite (TSH)

We have obtained several additional results (24) concerning the properties of TSH, especially for the state of combined water,which was investigated previously by Berman and Newman (22), and also by Takemoto and Saiki (23).

TSH was synthesized for our study by titration of $Al_2(SO_4)_3$ solution into a saturated solution of CaO and $CaSO_4 \cdot 2H_2O$ at 25°C. The precipitate was filtered by suction, and dried over 70% H_2SO_4. The resulting TSH contained 31.2 moles of combined water. It was found to dehydrate to 10.3 moles of H_2O by drying over CaO, and 6.9 moles of H_2O in the case of $MgClO_4$. TSH is however not dehydrated by portland cement used as a drying agent.

The changes in the amount of combined water of TSH with heating are as follows:

heating temp. (°C)	20	40	65	100	300	400	600	800	1000
H_2O (mole)	31.2	28.0	13.3	6.5	1.8	0.6	0.6	0.8	0.0

Fig. 18 shows the infrared absorption spectra of compounds related to TSH or CSA-cement.

The absorption of OH radical of TSH due to stretching and bending vibration appears at 3400 cm^{-1} and 1650 cm^{-1} each when caused by polymeric intermolecular hydration bond, and at 3640 cm^{-1} and 1620 cm^{-1} each when caused by monomeric OH radical. TSH changs into the amorphous state when heated above 80°C due to the dehydration of interlayer polymeric water, and the monomeric structural water is lost above 200°C. In addition, the spectrum of TSH heated above 600°C shows the existence of $CaSO_4$ and $C_4A_3\bar{S}$.

The specific surface area of TSH is slightly increased by the dehydration of interlayer water, and decreased when it becomes amorphous. Furthermore, the specific surface area of TSH increased rapidly with the destruction of the outer shape of the original crystal, and $CaSO_4$ was deposited by heating above 500°C.

The specific surface area decreased remarkably in relation to the crystallization of $C_4A_3\bar{S}$, CaO, and $C_{12}A_7$ and sintering by heating above 700°C (Fig. 19).

When the heated specimen is wetted, TSH is easily

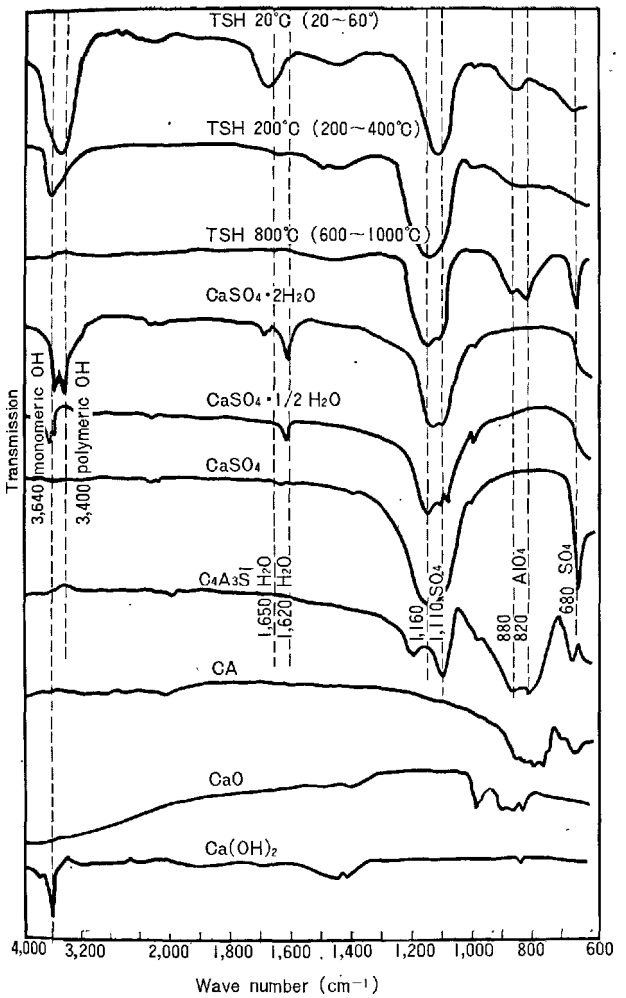

Fig. 18. *Infrared absorption curves*

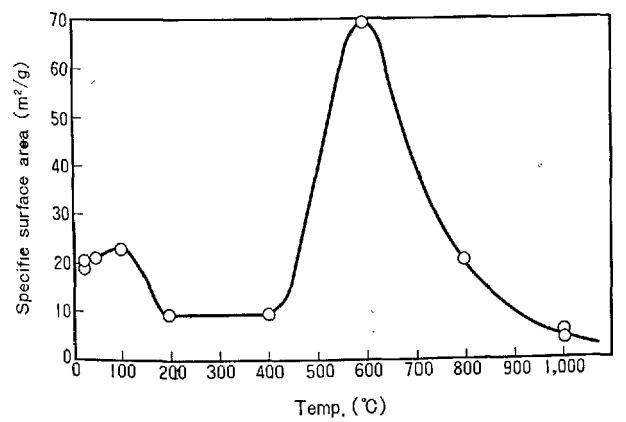

Fig. 19. *Surface area of heated ettringite measured by* N_2 *adsorption (Kept 30 min. at each temp.)*

reproduced, and the higher the heating temperature, the greater the expansion.

Pore Structure of Hardened CSA Cement

The relationship between the pore structure of hardened CSA cement and characteristics such as the expansion or drying shrinkage of CSA cement was investigated (25).

The proportion of mortar was 1:2, W/C = 0.45, and the cements used were 9–13% CSA cement and portland cement as the contrast. It was cured at 20°C in water and in the air with R.H. = 50%.

In this paper, only the results obtained with specimens cured for 18 months will be described.

The mechanical strength is not affected very much by the CSA in the case of water curing, but it decreases gradually with air curing. The strength of the mortar cured in air is about 85% for portland cement and 75% for expansive cement comprised of 13% of the amount of CSA of that in water curing. The degree of neutralization of specimens cured in air increases slightly with the addition of CSA.

According to the X-ray diffraction, the amount of TSH increases with the addition of CSA in the specimens cured in water, while a small amount of $CaCO_3$ was detected, instead of TSH and $Ca(OH)_2$, in specimens cured in air.

In order to examine the pore structure of mortar specimens, measurement of the adsorption and desorption of N_2 gas was carried out.

It was found that the hysteresis of the isotherm is more remarkable for the specimens cured in water than in air. The existence of hysteresis is related to the complexity of the pore structure.

The specific surface area of the specimens cured in water was about 15 m^2/g, while that of those cured in air was only about 4 m^2/g. in comparison, the specific surface area of portland cement and CSA cement were nearly the same for the specimens cured in water, but the latter had a slightly larger value than the former in the case of specimens cured in air.

In regard to the specific surface area, a value about 20% larger than the results obtained by the BET method is given by calculating under the assumption that the pore shape is a circular cylinder in the case of specimens cured in water, while in the case of air curing almost the same values are obtained by both methods.

The pore size distributions calculated by means of a digital computer are shown in Fig. 20. A large peak appears at about 15Å (in diameter) in the case of water curing. In air curing, it is shifted to about 20Å, and the total pore volume falls to lower than 30% of that of the specimens cured in water. This tendency is remarkable in the case of portland cement.

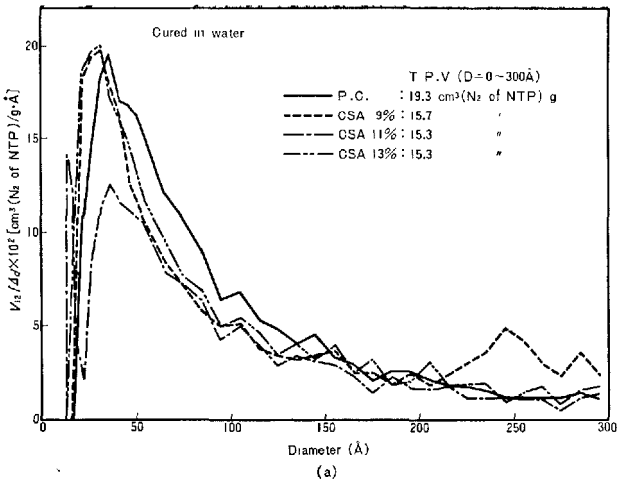

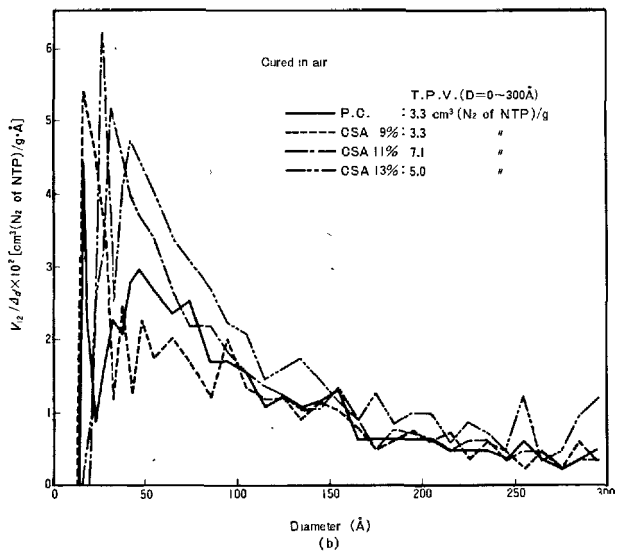

Fig. 20. *Pore size distribution curves calculated by Cranston-Inkley method*

(a) Results of the mortars cured in water for 18 months
(b) Results of the mortars cured in air for 18 months

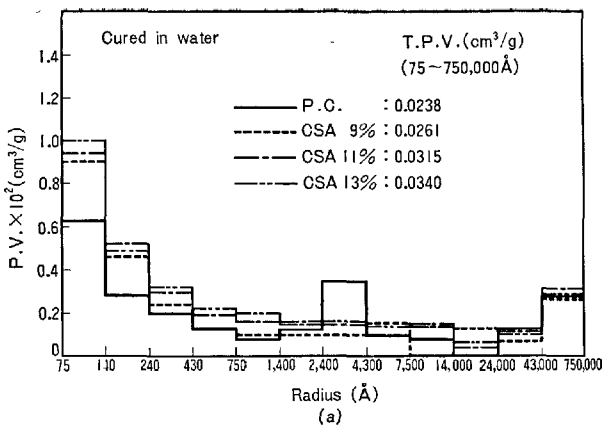

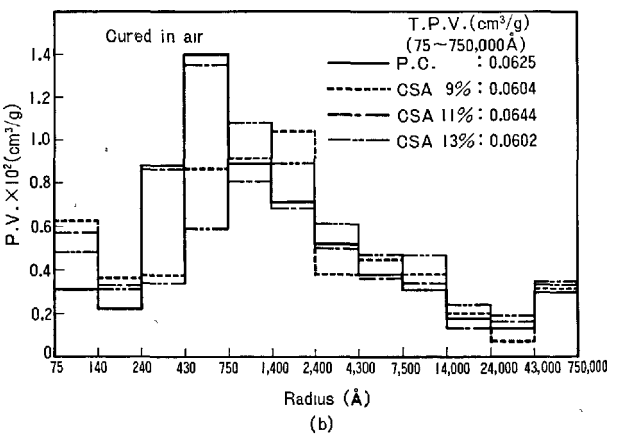

Fig. 21. *Pore size distribution curves measured by mercury pressure porosimeter*

(a) Results of the mortars cured in water for 18 months
(b) Results of the mortars cured in air for 18 months

The position of the peak is not affected by the curing conditions, but it is shifted toward a finer pore size in the case of CSA cement, compared to portland cement. This seems to be related to the formaton of TSH.

In addition, the distribution of pore sizes greater than 75Å in radius was measured by the Carlo Erba mercury pressure porosimeter, with the results shown in Fig. 21.

A peak in pore radius at 75–140Å appeared for the specimens cured in water, and the pore volume corresponding to this range of radius decreased to 60% for the specimens cured in air, for which the peak is broadened and shifted to 430–2400Å.

The pore volume in the range of 75–140Å is the lowest in the case of portland cement and increased with the amount of CSA content, but there is no relation to curing.

Since the pores are not perfectly saturated by water in the specimens cured in air, large pores remain because the pores are not completely filled up by the outer hydration product.

Furthermore, the expansion due to the hydration of CSA cement seems to be mainly accompanied by an increase in the volume of pores with a radius of 75–240Å judging from the results for the specimens at an early curing age.

The peak for the pore size is shifted towards the finer side with the progress of hydration. Also, it seems that the reason for the much lower degree of expansion in the case of curing in open air and even in moisture, compared to the case of water curing, is related to the surface tension or capillary force.

Although the above description gives a fairly clear picture, more precise analysis is being carried out to

determine more accurately the relationship between the pore structure of hardened CSA cement and such characteristics as expansion, drying shrinkage, and the rate of neutralization.

Mechanisms of Irreversible Expansion due to Hydration

When cement reacts with water, the total volume decreases but the solid volume increases. Also, the volume increases when a super-saturated solution deposits crystals. It is not exceptional for the reaction to form TSH. Therefore the expansion in CSA cement can not be explained by an increase in the specific volume due to the formation of TSH.

The reaction of C_3S, CA, C_3A, and $C_4A_3\bar{S}$, for example, with water is not accompained by remarkable expansion. In the case of such a reaction, besides the formation of an inner product, an outer product is also formed at the same time by outward diffusion owing to the high solubility of the reactant surrounded by the product layer. For instance, $Ca(OH)_2$ formed in the hydration of C_3S can only be deposited as an outer product because its solubility is not low enough for it to be deposited in the gel pores as an inner product.

However, very slight expansion occurs in the induction period because of the permeation of water into the surface of the cement grain. Also, a small amount of shrinkage is detected in the acceleratory period because of remarkable effluence.

On the other hand, in respect to the irreversible expansion of expansive cement, there is much discussion, (14, 20, 26) but many physico-chemical factors should be considered and experiments along this line should be carried out. On the remarkable irreversible expansion of expansive cement, it can be explained according to the present state of knowledge as follows (19).

In the hydration of CSA-cement, CaO and $CaSO_4$ are considered the outer reactants because their rate of dissolution is larger than that of aluminates such as C_3A or $C_4A_3\bar{S}$, and the surface of aluminate grain is covered with a less permeable layer of coating. The outer reactants permeate through this layer to the interface of the inner reactant. The inner product is rapidly formed by interaction between the diffused materials and the inner reactant, which also has a large rate of dissolution. The accumulation of hydrates begins inside of the grain because of the low solubility of the aluminate sulphate hydrates formed.

The essential problem is to decide what is the driving force of expansion in which the crystals of products can be grown under compressive stress and the structure of the product previously formed can be deformed.

As for the driving force, to be considered are (1) expansion of the crystal lattice of the hydrate by means of ion exchange, (2) the osmotic pressure produced in aluminate solution, (3) crystal growth pressure occuring at the apex of the crystal undergrowing, and (4) the surface tension which is expected on the interface between the crystal apex to be grown and another solid face.

If the first assumption is true, the conversion of C_4AH_{13} into $C_3A\cdot C\bar{S}\cdot H_{12}$ must take place by ion exchange without dissolution when the former comes in contact with calcium sulphate solution. This is believed very difficult, since the diffusion coefficients within the solid are so small.

Next, we have tried to measure the osmotic pressure in relation to the hydration of CSA cement, and found that it is not likely to be the main cause of expansion because the hydrates formed are mainly crystalline and do not form a semi-permeable membrance. However, the osmotic pressure was formerly regarded to be attributable to the expansion accompanied by the alkali-aggregate reaction.

In consideration of the crystal growth pressure, Jorgensen (27) tried to explain hydration expansion. He found, countrary to his expectation, that the degree of expansion is bigger when small crystals are formed. Nevertheless, the peripherical length was assumed as an assisting factor to effect the crystal growth pressure.

On the other hand, uniaxial pressure appears when crystal growth continues after the apex comes in contact with another fixed solid face. In order for crystal growth to continue, however, it is necessary to allow the liquid to penetrate against the pressure into the interface between the crystal apex and the other solid face.

Correns and Steinborn (28) pointed out the requisite conditions: $\gamma_{cs} > \gamma_{cl} + \gamma_{ls}$, where γ is the surface energy and C,S, and l mean the growing crystal, the other solid and the liquid, respectively. The uniaxial pressure is a function of the degree of super-saturation and also equated by them: $P = (RT/v)\ln (C_{ss}/C_s)$, where C represents the concentration and ss and s mean super-saturation and saturation.

In respect to the hydration of CSA cement, beside high concentration of SO_4^{--} ion at the outer space of aluminate grain, the concentraton of the liquid phase at the interface of unreacted $C_4A_3\bar{S}$ or C_3A should be very high in respect to the solubility of TSH, which is especially lowered by an increasing concentration

of lime. Moreover, it is probable tht TSH possesses a comparatively high surface energy and heat of wetting. Under these conditions, it is expected that significant expansion or compressive stress appears due to the formation of TSH at or near the interface of anhydrous aluminates (R. Kondo).

The Manufacturing Process and Characteristics of CSA Cement

The Manufacture of CSA Cement

Responding to the progressive requirements of concrete technology, basic research on expansive cement has been carried out, with the result that an expansive cement possessing unique characteristics was developed in Japan several years ago. CSA cement, a mixture of CSA and portland cement, can be used both for preventing shrinkage cracks and for self-stressing by means of changing the mixing ratio of CSA and portland cement.

The CSA is manufactured by a process similar to that of ordinary portland cement. Raw materials for preparing CSA are material that contain CaO,Al_2O_3, and SO_3 individually or together. Impurities such as SiO_2, Fe_2O_3, etc., are undesirable because they react with CaO and Al_2O_3 to produce less expansive components. Ordinarily, we use limestone for CaO, white bauxite for Al_2O_3 and chemically produced anhydrous gypsum for CaO and SO_3. An example of the chemical composition of the raw materials is shown in Table 3.

These raw materials are mixed in a proportion to make the ratio $CaO: Al_2O_3: CaSO_4 = 4:1:3$ in mole (CSA 4-1-3). A molar ratio of 3:1:3, which corresponds to a dehydrated TSH, was also tried (CSA 3-1-3). Weighed raw materials are ground together by a mill. The rotary kiln with a cooler is used for heating. Since the sintering degree of clinker has a great influence on the expansion characteristics of CSA, the heating temperture and cooling rate should be carefully controlled. The clinker contains three principal phases: calcium sulphoaluminate, quick lime, and anhydrous gypsum. Closed circuit type ball milling is used for grinding.

As the fineness of CSA has a remarkable influence on the expansion characteristics, two air separators are used for strict adjustment of grain size distribution. Ground CSA is mixed with portland cement at an optional ratio by an ordinary rotary mixer. The normal mixing ratio of CSA: portland cement is 10:90 for drying shrinkage prevention, and 13–17: 87–83 for selfstressing.

Table 3. *Chemical composition of raw materials* (wt. %)

	Ig. loss	SiO_2	Al_2O_3	Fe_2O_3	CaO	MgO	SO_3	Total
Lime stone	41.8	1.3	0.1	0.1	56.1	0.2	trace	99.6
White bauxite	0.3	7.3	86.3	1.9	trace	trace	trace	95.8
Anhydrous gypsum	4.3	0.3	trace	trace	38.3	trace	57.4	100.3

Characteristics of CSA and CSA Cement

Measuring Method

All the measurement described in this section were made according to the Japanese Industrial Standards (JIS) R5201, R5202, and A1125. The expansion of mortar and concrete was measured as follows.

The dimensions of the specimens were $4 \times 4 \times 16$ cm for mortar and $10 \times 10 \times 40$ cm for concrete. They were cast in the mold and cured for 24 hrs., after which the mold was removed and a lined piece of glass was affixed to both ends of the specimens.

Chemical and Physical Properties of CSA

Table 4 and Table 5 show the chemical composition and some physical properties of CSA.

Aeration of CSA Cement

The 10% CSA cement was packed in a sack made of three-fold craft paper and exposed to a temperature of 35°C and a relative humidity of 85%. The weight change of the cement, the expansion and the strength of mortar were measured for aerated CSA cement. The results are shown in Table 6. The results show that the aeration of CSA is more rapid than that of portland cement. Thus CSA cement should be tightly packed in a four-fold sack.

Table 4. *Chemical composition of CSA*

Ig. loss	Insol.	SiO_2	Al_2O_3	Fe_2O_3	CaO	MgO	SO_3	Free lime	Total
0.9	1.4	1.4	13.1	0.6	47.8	0.5	32.2	19.4	97.9

Table 5. *Physical properties of CSA*

Specific gravity	Specific surface area (Blaine method)	Sieving test	
		Residue on 297μ	Residue on 88μ
2.93	1,510 cm^2/g	0.1%	61.4%

Table 6. *Results of aeration test*

Length of exposure in air (day)	weight increase	Expansion (%)	Bending strength (kg/cm²)	Compressive strength (kg/cm²)
0	0	0.087	41.8	161
10	3.2	0.049	44.9	187
20	5.5	0.029	45.6	186
30	7.8	0.021	40.0	161
40	9.0	0.020	41.2	162

Mixing: c/s = 1:2 W/C = 0.65
Curing: 7 days in water (20°C)

Table 7. *Results of setting test (JIS)*

Fraction of CSA (wt. %)	Mixing water (%)	Initial setting (hr-min)	Final setting (hr-min)
0	26.4	2—52	3—52
8	26.4	2—57	3—49
9	26.1	2—45	3—46
10	26.3	2—40	3—37
11	26.0	2—40	3—40
12	26.0	2—50	3—40
13	26.0	2—31	3—35

Setting of CSA Cement

In general, expansive cement has the disadvantage that it begins setting at a relatively early period. This disadvantage, however, can be overcome by proper chemical composition and the fineness of the CSA. From the data shown in Table 7, it is apparent that mixing of CSA gives little effect upon setting.

The Fluidity of CSA Cement Mortar

Fig. 22 shows the relation between the fluidity and W/C ratio of 10% CSA cement mortar. The ordinary flow test method was used. It is apparent that the fluidity of CSA cement mortar is almost the same as that of portland cement mortar. The proportion of mortar or concrete can be set in the same manner as in portland cement.

Expansion Characteristics of CSA Cement Mortar

Fig. 23 shows the curve that represents the relation between expansion and mixing amount of CSA. The curve is not linear and is rather similar to an ordinary stress-strain curve, supposing that the expansive force is proportional to the quantity of CSA. In the case of no restraint, the use of 14% or more CSA cement causes expansion cracking and destruction. If some restraint exists, it is expected that the curve will become linear one.

Fig. 24 shows relation between expansion and curing age for 10% CSA cement mortar. The expansive reaction seems to end at a relatively early age of 4–7 days. As it dries, CSA cement mortar shrinks, but the amount of shrinkage is much smaller.

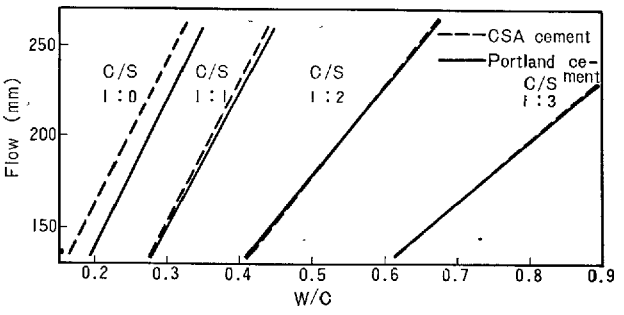

Fig. 22. *Results of flow test of 10% CSA cement*

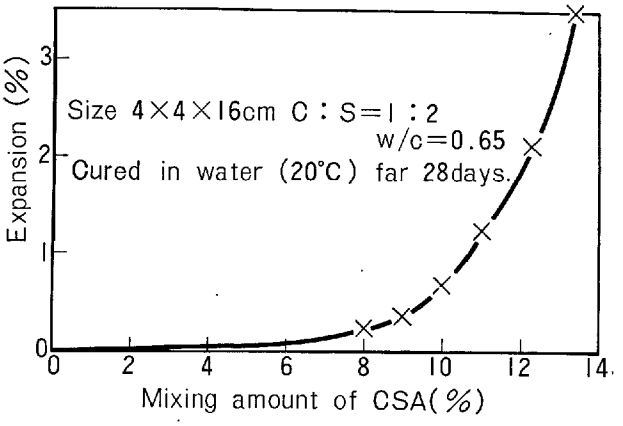

Fig. 23. *Relations between expansion and the amount of CSA*

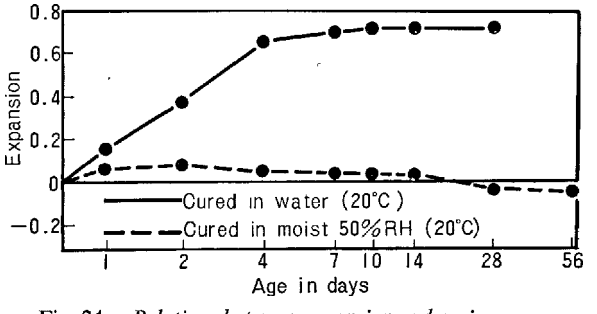

Fig. 24. *Relations between expansion and curing age*

Table 8. *Results of strength test (JIS)*

Fraction of CSA (wt. %)	Bending strength (kg/cm²)			Compressive strength (kg/cm²)		
	3 days	7 days	28 days	3 days	7 days	28 days
0	33.4	48.7	64.0	121	220	393
8	28.5	42.8	57.2	118	184	283
9	23.0	41.6	63.7	109	173	283
10	19.0	31.2	57.3	84	138	250
11	14.9	18.9	51.1	71	79	204
12	12.5	14.9	39.7	62	75	153
13	12.8	14.8	19.7	59	55	60

Compressive and Bending Strength of CSA Cement Mortar

Table 8 shows the results of a strength test on CSA

cement mortar. Owing to the large free expansion, the compressive strength of CSA cement mortar is much lower than that of portland cement. The bending strength is also less than that of portland cement, especially 10% or more CSA cement. But the degree of decrease is not as much as that of its compressive strength. It can be considered that a little selfstress caused by internal restraint makes some contribution. If some external restraint exists, as in the general case in practical use, a certain amount of self-stress appears and the bending stength will be increased to the value of portland cement.

Expansion and Strength of CSA Cement Concrete

The mixing of the concrete is shown in Table 9. Table 10 and Table 11 show the results of the measurement of expansion and compressive strength respectively both in the case of water curing and drying condition.

Since the ratio of cement to aggregates is less than that of mortar, internal restraint is more. Consequently, the expansion is less and the compressive strength is no less than that of portland cement. Apparently, the drying shrinkage is smallest, so the resistance to cracking due to drying shrinkage is naturally great.

Table 9. *Proportions of concrete*

Portland cement + CSA	310 kg/m³
W/C	0.65
Slump	20 ± 1 cm
Sand	F.M = 2.70
Gravel	Top size 20 mm
Proportion of sand to aggregate	47%

Table 10. *Results of free expansion test for concrete*

Fraction of CSA (wt.%)	Expansion (10^{-4})													
	Cured in water (20°C)							Drying (20°C 50% RH)						
	day 1	2	4	7	28	184	365	1	2	4	7	28	184	365
0	(—) 0.1	0.0	(—) 0.1	0.1	0.1	0.6	0.3	(—) 0.2	(—) 0.7	(—) 1.0	(—) 1.2	(—) 3.5	(—) 6.0	(—) 7.0
10	3.2	3.7	4.2	4.3	4.7	5.5	5.5	1.5	1.9	1.5	0.4	(—) 1.2	(—) 2.1	(—) 2.8
11	3.3	3.7	4.5	5.0	5.7	6.4	6.4	1.4	2.4	2.2	1.4	(—) 0.7	(—) 1.5	(—) 1.6
12	5.4	5.5	5.8	6.3	7.7	8.3	7.9	2.1	3.1	3.5	3.2	0.9	0.2	0.5
13	7.3	14.0	20.0	21.0	20.9	20.9	21.0	2.8	4.5	5.0	4.3	2.4	0.4	0.3

Specimen size 10 × 10 × 40 cm

Table 11. *Results of strength test for concrete*

Fraction of CSA (%)	Compressive strength (kg/cm²)					
	Cured in water (20°C)			Drying (20°C 50% RH)		
	7 days	28 days	365 days	7 days	28 days	365 days
0	138	292	370	124	176	225
10	175	289	388	124	183	235
11	134	252	390	142	212	238
12	161	289	381	119	179	235
13	121	212	359	127	173	224

Specimen ϕ10 × 20cm cylinder

The Effect of Reinforcement on the Expansion of CSA Cement

An ordinal steel rod (SS41) was buried in the center of a CSA cement concrete specimen. Both ends of the specimen were restrained by two steel plates, which were connected to the internal rod. The relation between expansion and the degree of reinforcement is shown in Fig. 25. The proportion of concrete is the same as that in Table 9. The specimen was cured in

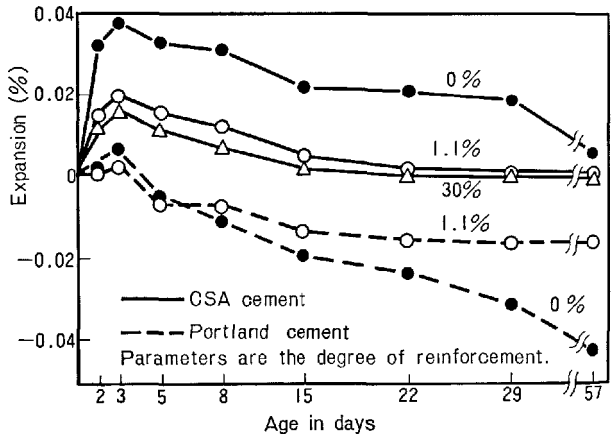

Fig. 25. *Effect of the degree of reinforcement on expansion*

Table 12. *Proportions of concrete*

W/C	Slump	Gravel top size	Quantities per m³ of concrete (kg)			
			Water	Cement	Sand	Gravel
0.44	3~7cm	10mm	185	420	746	949

Table 13. *Dimensions of concrete pipe*

Longitude	Diameter		Arrangement of reinforcement	
	Outside	Inside	Parallel	Spiral
2,000 mm	414 mm	350 mm	ϕ4.96mm × 12	ϕ2.9 mm pitch 20 mm

Table 14. *Results of loading test*

Fraction of CSA (%)	Load T/m			
	Initial cracking	0.1mm crack	0.25mm crack	Break point
0	1.66	1.97	3.37	7.51
13	3.02	3.43	4.68	8.16
17	3.94	4.43	5.12	6.92

water for three days and after that at drying condition of 20°C and a relative humidity of 50%. Apparently the expansion decreased, but the drying shinkage also decreased.

Chemical Prestressing of Concrete Elements by CSA

The introduction of chemical prestress was tried with a pressure pipe. The proportions of the concrete and dimensions of the pipe are shown in Table 12, and Table 13. After about five minutes of mixing, the concrete was cast in a rotating mold. Revolution of the mold was stopped after ten minutes and the concrete pipe was left in the mold for about 24 hrs., after which the mold was removed and reinforcement bars were anchored at the end by nuts. The specimen was cured at 65°C for 2 hrs., in moisture for 7 days, and then in the open air. At the age of 15 days, the pressure pipe was subjected to an outside load ranging over the entire length. The results are shown in Table 14. The larger load required to crack the CSA cement concrete pipe suggests a contribution of chemical prestress. (Y. Ono)

Conclusions

From this study, the following conclusions were obtained.

(1) The initial free expansion of expansive cement mortar or concrete which compensates subsequent drying shrinkage is not as important for the prevention of shrinkage crack formation as was formerly thought. It is necessary to reduce the drying shrinkage after finishing the intitial expansion.

(2) Concerning the chemical prestressing of concrete elements, the limitations for the economical use of the mechanical properties of materials, especially the strength of prestressing steels, should be considered in designing the elements. In this study it can be predicted that the use of high tensile prestressing bars having the allowable stresses of 50 to 90 kg/mm² is most desirable for this purpose.

(3) In the test results on chemical prestressing by CSA-cement reported in this paper, 13% CSA content in normal portland cement is most adequate for chemical prestressing, although only about 30 kg/cm² prestress is expected to be introduced into the concrete section having 1% prestressing steels.

(4) In the manufacture of CSA cement clinker, raw materials in which the molar ratio of $CaO: Al_2O_3: CaSO_4$ equals 4: 1: 3 are heated to produce $C_4A_3\bar{S}$ crystals of the proper size at about 1200°C. Then the clinker is ground rather coarsely so that the particle size distribution is limited. The optimum mixing ratio of portland and CSA for expansive cement was found to be 90: 10 by weight.

(5) In the hydration of $C_4A_3\bar{S}$ in the presence of CaO and $CaSO_4$. the grain of $C_4A_3\bar{S}$ is at first coated with hydrates, through which the liquid phase permeates to the interface of unreacted $C_4A_3\bar{S}$ to form monosulfate hydrat or its solid solution. Irreversible expansion then takes place by the reaction of SO_4^{--} ion diffused from outside and either anhydrous or hydrated aluminates to form TSH. Remarkable expansion also occurs when C_3A reacts secondarily with the previously formed TSH that coats the C_3A grains to produce MSH.

(6) The mechanism of irreversible expansion due to the hydration of CSA cement are regarded as being related to the lack of balance of inward and outward diffusion through the product layer, the degree of super saturation of TSH, especially in the presence of lime, and the surface energy of TSH when adequate. These are most likely the essential factors in making possible the crystal growth of TSH, even under compressive stress, and in giving rise to the remarkable expansion.

(7) The manufacture of CSA cement in Japan was initially undertaken on the basis of the above-mentioned investigations, which made possible a product whose characteristics were very satisfactory. Further research will be carried out on the properties of mortar and concrete.

References

1. H. Lossier, "L'Autocontrainte des Betons par les Ciments Expansifs", Mémoires, Société des Ingenieurs Civils de France, 3–4, 189 (1948).
2. H. Lafuma, "Expansive cements", Proc. of the Third International Symposium on the Chemistry of Cement. 587 (1952).
3. M. E. Perre, "Ciments sans Retraint, Cements Expansifs", Cement and Lime Manufacture, **24,** 75 (1947).

4. V. V. Mikhailov, "New developments in self-stressed concrete", Proc. of the World Conference on Prestressed Concrete, 25 (1957).
5. A. Klein and G. E. Troxell, "Studies of calcium sulfoaluminate admixtures for expansive cements", Proc. of the ASTM, **58,** 986 (1958).
6. A. Klein, T. Karby & M. Polivka, "Properties of an expansive cement for chemical prestressing", J. of the ACI, **58,** 39 (1961).
7. T. Y. Lin and A. Klein, "Chemical prestressing of concrete elements using expanding cements", J. of the ACI, **60,** 1187 (1963).
8. H. Muguruma, "On the expansion-shrinkage characteristics of expansive cement", Proc. of the 10th Japan Congress on Materials Research (1968) (Not yet published).
9. H. Muguruma, "Expansion-shrinkage characteristics to be required to the expansive cements", Transactions of the Architectural Institute of Japan, Extra Summaries of Technical Papers of Annual Meeting of AIJ, 1967, 29 (1967).
10. N. Fukuda, "Investigation of compound compositions of sulpho-aluminous cement", J. Ceram. Assoc. Japan **69,** 187–191 (1961) (in Japanese).
11. R. Kondo, "The synthesis and crystallography of a group of new compounds belonging to the Haüyne Type structure", J. Ceram. Assoc. Japan **73,** 1–8 (1965) (in Japanese).
12. P.E. Halstead and A.E. Moore, "The composition and crystallography of an anhydrous calcium alumino sulphate occuring in expanding cement", Jour. of Appl. Chem. **12,** 413–417 (1962).
13. R. Kondo and N. Nawata, "Characteristics of expansive cement affected by the properties of calcium sulfoaluminous clinker", JCEA Review of 19th General Meeting **19,** 52–55 (1965).
14. R. K. Mehta and A. Klein, "Investigation on the products in the system $C_4A_3\bar{S}$–$CaSO_4$–CaO–H_2O", Annual Meeting of the Highway Research Board, 328–352 (1965).
15. K. Nakagawa and T. Sugimori "On the nonshrinking and expansive cement clinker, and its manufacture", Japanese Patent Application Nr. S42–84441 (in Japanese).
16. M. Miki, "Shrinkage compensated cement", Japanese Patent Nr. 514199 (1968).
17. N. Sera and M. Tsuchiya, "Hydration process of $C_4A_3\bar{S}$ and morphology of hydrates", JCEA Review of 22nd General Meeting **22,** 68～70 (1968).
18. A. Grudemo, "The microstructures of cement gel phases", p. 109 (Elanders Boktryckeri Aktiebolag, Göteborg, Stockholm, Sweden, 1965).
19. R. Kondo and K. Nakagawa, "Hydration mechanisms of calcium sulfoaluminate and tricalcium aluminate" (To be published).
20. S. Chatterji and J. W. Jeffery, "A new hypothesis of sulphate expansion", Magazine of Concrete Research **15,** No. 44, 83–86 (1963).
21. S. Akaiwa, G. Sudoh and T. Nakamura, "Study on the expansion due to hydration of $C_4A_3(SO_3)$", JCEA Review of 21st General Meeting **21,** 156–161 (1967).
22. H. A. Berman and E. S. Newman, "Heat of formation of calcium trisulfoaluminate at 25°C", Chemistry of Cement Proceeding of the Fourth International Symposium, Washington, 247–257 (1960).
23. K. Takemoto and Y. Saiki, "Dehydration of high sulfate form of cement bacillus", JCEA Review of 18th General Meeting **18,** 37–38 (1964).
24. H. Bannai and K. Nakagawa, "Properties of ettringite", Gypsum and Lime No 97, 11–17 (1968–11).
25. R. Kondo, K. Nakagawa and J. Isogai, "Discassions on the porestructure of hardened cement mortar and the mechanism of expansion due to its hydration", J. Ceram. Assoc. Japan **71.** 238～248 (1969) (in Japanese).
26. H. E. Schwiete, U. Ludwig and P. Jäger, "Investigation in the system $3CaO \cdot Al_2O_3$–$CaSO_4$–CaO–H_2O", Symposium on the Structure of Portland Cement Paste and Concrete, 353, Highway Research Board (1966).
27. K. D. Jorgensen, "Setting expansion of gypsum", Reactivity of Solids, 638–642 (Elsevier Pub. Co., Amsterdam, Netherlands, 1961).
28. Carl W. Correns and W. Steinborn, "Experimente zur Messung und Erklärung der sogenannten Kristallisationskraft", Zeitshrift für Kristallography **101,** 117–133 (1939) (in German).

Supplementary Paper IV-132 Properties of Expansive Cement Concretes

Paul Klieger and Nathan R. Greening*

Synopsis

These studies provide information useful in determining the utility of expansive cement systems under a variety of conditions, thus contributing to proper engineering usage.

Earlier work at the PCA Laboratories evaluated the expansive properties of various mixtures of portland cement, calcium aluminate cement, and gypsum in mortars. This was followed by an extensive series of tests, using a particular mixture of portland cement-calcium aluminate cement-gypsum, a Klein-type shrinkage-compensating cement, and Klein expansive cement, which included an evaluation of expansive characteristics and freeze-thaw durability of relatively high cement content (729 to 752 lb/cu yd—approximately 8 U.S. bags) concretes typical of those used in the precasting industry.

The present study was directed to the evaluation of a wider range of concrete properties for air-entrained concretes typical in proportions to those used in cast-in-place structures and pavements (approximately 564 lb of cement/cu yd—6 U.S. bags). These properties include the development of compressive and flexural strength for ages from one day to one year, including the effect of initial and curing temperature; volume change in moist storage and in air, including alternations of wetting and drying; creep under sustained stress; resistance to freezing and thawing and de-icer scaling; resistance to sulphate exposure; abrasion resistance; and other aspects. With respect to durability, sulphate resistance, and abrasion, the data obtained is for both non-reinforced and reinforced (restrained) systems.

Cement formulations included in this study are: (1) portland, ASTM Types I, II, and V: (2) two shrinkage-compensating cements manufactured by intergrinding the expansive component with the portland cement clinker; (3) a shrinkage-compensating cement manufactured as an integral-burn clinker; (4) a portland cement-calcium aluminate cement-gypsum mixture; and (5) a very high C_3A portland cement-gypsum combination.

Included also is information relative to certain use aspects of such cements, including the effect of mixing time and temperature on the expansive potential.

KEY WORDS: Abrasion resistance; air-entrained concrete; aluminous cements and concretes; chemical composition; compressive strength; creep (materials); curing; deicing; durability; expansion; expansive cements; flexural strength; freeze-thaw durability; mixing time; portland cements; restraints; scaling; shrinkage; stresses; sulflate resistance

Introduction

Most studies of concretes made with expansive cement formulations have been concerned with properties such as expansive potential and strength development. Recent work in our laboratories(1)** presented the results of an extensive series of freeze-thaw and surface scaling tests of relatively high cement content concretes (729 to 752 lb/cu yd—approximately 8 U.S. bags). An earlier paper (2) reported tests on properties of mortars and concretes made with portland cement-calcium aluminate cement-gypsum blends.

This present and more comprehensive series of tests was undertaken to develop data on a wider range of concrete properties, using concretes typical in proportions of those used in cast-in-place structures, pavements, and general concrete construction (approximately 564 lb of cement/cu yd—6 U.S. bags).

**Portland Cement Association, Skokie, Illinois, U.S.A.

*Numbers in parentheses refer to list of references at end of paper.

Scope

The concretes used in this study had nominal cement contents (including the expansive materials) of 564 lb (6 U.S. bags) per cubic yard. One 752 lb of cement (8 U.S. bags) per cubic yard concrete was included to provide a comparison of performance with respect to certain properties. Slumps were of the order of 2 to 3 inches and air contents 5 to 6 percent. The maximum size of aggregate used was 3/4 inches.

Specimens were both of the unrestrained and restrained variety. In the case of the prisms, restraint to expansive force was provided by an embedded 1/4 inch diameter threaded steel rod, providing a longitudinal reinforcement percentage of 0.30. The restrained slabs contained welded wire fabric in an amount providing a reinforcement percentage of 0.89 in both directions.

A variety of curing conditions were used. These included curing at temperatures of 40, 73, and 100°F, either in a moist-room at 100% R. H. or in water. Some concretes were subjected to simulated steam curing at 160°F and atmospheric pressure, with subsequent curing at 73°F and 100% R. H. Specific details on curing procedures used are presented in subsequent discussion of various phases of the program.

These tests included (1) the effect of mixing time on unrestrained expansion, (2) the effect of curing environment on strength development of unrestrained concretes, (3) volume change of unrestrained concrete as influenced by curing history, including the effect of alternate cycles of wetting and drying, (4) freeze-thaw and de-icer scale resistance for both unrestrained and restrained concretes, (5) creep of unrestrained concretes under sustained load, (6) sulphate resistance of unrestrained and restrained concretes, (7) abrasion resistance of unrestrained and restrained concretes, and (8) the influence of amount of cementing material on unrestrained expansion in moist and water storage.

Materials

Cementing Materials

Table 1 shows the chemical analyses and finenesses of the portland cements, the calcium aluminate cement, and the various expansive (shrinkage-compensating) cements used in this study. Table 2 provides a brief description of the cements or cement formulations used in the concretes, together with a letter or letter-number designation which will be used in subsequent discussions for identification.

The American Concrete Institute's "Cement & Concrete Terminology" (SP-19) defines expansive

Table 1. *Chemical composition and fineness of cements and expansive materials*

Item	P-I Type I portland cement	P-II Type II portland cement	P-V Type V Portland cement	Calcium aluminate cement	K-1 Shrinkage-compensating cement (blend)	K-2 Shrinkage-compensating cement (integral burn)	K-3 Shrinkage-compensating cement (blend)	S-1 Shrinkage-compensating cement (high C_3A clinker)
PCA Lot No.	20497[c]	LTS 23[d]	20342[a]	19753	20596	20626	20794	20779[e]
SiO_2, %	20.90	21.4	23.40	8.5	18.53	17.96	18.15	18.41
Al_2O_3, %	5.42	4.3	3.16	41.2	6.99	5.33	6.18	7.97
Fe_2O_3, %	2.64	5.4	2.92	11.4[b]	4.10	1.83	4.28	2.35
CaO, %	63.06	63.9	64.60	36.1	62.72	62.93	62.06	62.40
MgO, %	2.87	0.9	3.33	1.3	1.24	3.35	1.19	2.70
SO_3, %	2.18	1.5	1.44	0.4	4.44	5.58	5.68	4.48
Ign. loss, %	1.56	0.7	1.07	0.8	1.77	2.30	1.53	1.36
Insol. res. %	0.12	0.10	0.11	—	0.06	0.11	0.17	0.24
Free CaO, %	1.20	0.4	0.35	0.0	3.11	4.04	2.64	1.19
Na_2O, %	0.35	0.59	0.08	0.06	0.08	0.25	0.14	0.04
K_2O, %	0.69	0.14	0.17	0.12	0.34	0.47	0.53	0.05
Specific gravity	—	—	—	3.11	3.11	3.03	3.00	3.09
Fineness (Blaine)[f] cm^2/g	3470	3110	3520	2970	3540	3980	3370	3925

[a] C_3A content = 3.4%, $C_4AF + 2(C_3A) = 15.7\%$.
[b] Any Fe or FeO is here calculated as Fe_2O_3.
[c] Blend of 4 brands of Type I cement purchased in the Chicago, Ill. area.
[d] Calculated potential C_3A content = 3.7%, $C_4AF + 2(C_3A) = 24.0\%$.
[e] Calculated potential C_3A content = 17.1%
[f] Blaine values for cements other than portland corrected for specific gravity.

cements as follows:

"*Expansive cement (general)*—A cement which when mixed with water forms a paste that, after setting, tends to increase in volume to a significantly greater degree than portland cement paste; used to compensate for volume decrease due to shrinkage or to induce tensile stress in reinforcement (post-tensioning).

"*Expansive cement, Type K*—An expansive cement containing anhydrous aluminosulfate (4 $CaO \cdot 3Al_2O_3 \cdot SO_3$), burned simultaneously with a portland cement composition, or burned separately when it is to be interground with portland cement clinker or blended with portland cement, calcium sulphate ($CaSO_4$), and free lime (CaO).

"*Expansive cement, Type M*—A mixture of portland cement, calcium-aluminate cement, and calcium sulphate.

"*Expansive cement, Type S*—A portland cement containing a large computed C_3A content and modified by an excess of calcium sulphate above usual optimum content."

Referring to Table 2, Cements K-1, K-2, and K-3 are, by these definitions, Type K; Cement M-1 is Type M; and Cement S-1 is Type S.

The amount of expansive component in Cements K-1, K-2, and K-3 is not known. These are samples of commercially available shrinkage-compensating cements. The formulation for Cement M-1 is shown in Table 2. Cement S-1 was prepared in our laboratories by intergrinding a high C_3A portland cement clinker with gypsum and anhydrite to produce the composition shown in Table 1. The oxide analysis of the clinker used is shown in Table 3. Note that the computed potential C_3A content is just over 20 per cent.

Table 2. *Identification of cements*

Designation	Description
P-I	Type I portland cement
P-V	Type V portland cement
P-II	Type II portland cement
M-1	78.33% Type V portland cement 15.00% Calcium aluminate cement 6.67% Gypsum
K-1	Shrinkage-compensating cement (blend)
K-2	Shrinkage-compensating cement (integral burn)
K-3	Shrinkage-compensating cement (blend)
S-1	Shrinkage-compensating cement (intergrind of high C_3A portland cement clinker with gypsum and natural anhydrite)

Table 3. *Oxide analysis of clinker used in preparing S-1*

		% by weight
SiO_2	—	20.28
Al_2O_2	—	8.87
Fe_2O_3	—	1.95
CaO	—	65.40
MgO	—	2.97
SO_3	—	0.14
Na_2O	—	0.04
K_2O	—	0.05
Mn_2O_3	—	0.04
Free CaO	—	1.16
Insol. res.	—	0.13
C_3A content	—	20.2

Table 4. *Aggregate grading*

Elgin sand		Eau Claire gravel	
Sieve No.	Percent passing	Sieve No.	Percent passing
4	100	3/4 in.	100
8	82	3/8 in.	50
16	67	No. 4	0
30	43		
50	13	Fineness modulus	
100	5	of sand = 2.90	

Aggregates

Table 4 shows the grading of the aggregates. The sand from Elgin, Illinois is a partly siliceous and partly calcareous natural sand. The 3/4-inch maximum size natural coarse aggregate from Eau Claire, Wisconsin, is principally siliceous and contains a small percentage of crushed over-size.

Admixture

Neutralized Vinsol resin in solution, added at the mixer, was the air-entraining admixture. The solution contained 22.7 g. NVX per liter. No other admixtures were used in these tests.

Concretes

Concretes were designed to contain 564 lb of cement per cubic yard (6 U.S. bags). A few mixes made with Cement K-1 also contained 752 lb of cement per cubic yard (8 U.S. bags). Sand percentage used was 40 percent by weight of total aggregate. All concretes were air-entrained, with air contents generally in the range of 5 to 6 percent by volume. Most of the slumps were in the range of 2–1/4 to 3–1/2 inches. In those tests involving different mixing times, there were expected changes in slump and air contents.

Detailed concrete mix data are presented in Tables 5 and 15.

Table 5. *Concrete mix data for:*

Strength and volume change tests

Item	Cement designation					
	P-I	M-1	K-1	K-2	K-3	S-1
Slump, in.	2.7	2.3	2.6	2.2	3.4	2.3
Unit wt., lb/cu ft	146.6	146.2	146.6	146.7	146.4	146.7
Air content, %	5.60	5.45	5.90	5.57	5.60	5.70
Cement content[a]						
lb/cu yd	561	565	569	565	565	567
bag/cu yd (U.S.)	5.97	6.01	6.05	6.01	6.01	6.03
Water content,						
lb/cu yd	236	247	230	262	240	230
Water-cement ratio,						
by wt.	0.42	0.44	0.40	0.46	0.42	0.40
A/E admixture,						
ml/lb cement	3.1	5.1	1.7	1.1	1.1	1.9

Creep tests

Item	Cement designation					
	P-I	M-1	K-1	K-2	K-3	S-1
Slump, in.	2.8	2.0	3.6	2.8	2.9	2.3
Unit wt., lb/cu ft	145.8	147.2	145.8	144.1	147.8	146.9
Air content, %	6.20	5.30	6.40	6.30	4.60	5.70
Cement content[a]						
lb/cu yd	565	574	565	569	570	569
bag/cu yd (U.S.)	6.01	6.11	6.01	6.05	6.07	6.05
Water content,						
lb/cu yd	232	235	227	257	243	228
Water-cement ratio,						
by wt.	0.41	0.41	0.40	0.45	0.42	0.40
A/E admixture,						
ml/lb cement	2.9	4.3	1.6	3.8	1.0	2.0

Freezing and thawing and de-icer scaling tests

Item	Cement designation					
	P-1	M-1	K-1	K-2	K-3	S-1
Slump, in.	2.3	2.8	2.2	2.5	3.8	2.6
Unit wt., lb/cu ft	146.0	145.1	146.9	144.7	146.6	146 4
Air content, %	5.83	5.95	5.73	5.77	5.50	6.03
Cement content[a]						
lb/cu yd	558	567	564	564	565	566
bag/cu yd (U.S.)	5.94	6.03	6.00	6.00	6.01	6.02
Water content,						
lb/cu yd	238	249	227	264	237	228
Water-cement ratio,	0.43	0.44	0.40	0.47	0.42	0.40
by wt.						
A/E admixture,						
ml/lb cement	3.2	5.2	1.7	4.3	1.1	1.9

[a]Includes expansive components.

Sulphate resistance tests

Item	Cement designation						
	P-V	P-II	M-1	K-1	K-2	K-3	S-1
Slump, in.	1.9	2.8	2.6	3.0	1.9	2.9	2.8
Unit wt., lb/cu ft	147.8	146.0	145.8	146.8	145.0	147.0	145.9
Air content, %	4.80	5.92	5.50	5.60	5.50	5.00	5.90
Cement content[a]							
lb/cu yd	577	570	568	574	563	573	570
bag/cu yd (U.S.)	6.14	6.07	6.04	6.11	5.99	6.10	6.06
Water content,							
lb/cu yd	238	235	250	232	262	244	237
Water-cement ratio,							
by wt.	0.41	0.41	0.44	0.40	0.46	0.42	0.42
A/E admixture,							
ml/lb cement	4.0	3.4	4.3	1.5	3.9	1.0	1.9

[a]Includes expansive components.

Fabrication and Testing

Concrete Mixing and Fabrication of Specimens

All materials were stored at the temperature at which the concrete was produced: 40, 73, or 100°F. Most of the concretes were cast at a temperature of 73°F. Aggregates were weighed in the air-dried condition (moisture content known) and inundated with a known amount of water 18 to 20 hours prior to use. Excess water was drawn off and weighed immediately prior to mixing.

Concrete batches were mixed for 2–1/2 minutes in a 1–3/4 cu. ft. capacity Lancirick mixer (horizontal open tub), except when mixing time was a variable. Unit weight, slump, and air content by the pressure method were determined immediately after mixing.

All specimens were cast in watertight steel molds, except for the abrasion specimens which were cast in watertight plastic-coated plywood molds. Consolidation of concrete in the molds was accomplished by hand rodding or on a vibrating table operating at a frequency of 4000 cycles per minute for low slump mixes and the slabs with two-way steel. Generally, specimens were made from duplicate batches, each mixed on different days.

Unrestrained prisms, 3 by 3 by $11\frac{1}{4}$-in. in size, contained stainless steel end plugs for length change measurements. Restraint in prisms was provided by a 1/4-inch diameter mild steel rod, threaded over its entire length, and embedded along the longitudinal axis of the prism. The modulus of elasticity of the steel was 27,500,000 psi. yield strength was 55,000 psi. The ends of the rod passed through 3/8-in. thick 3 × 3-inch metal end plates and protruded from the specimen ends. The rod ends were provided with stainless steel acorn nuts, in contact with the steel end plates, which served as reference points for length change measurements. The steel percentage amounted to 0.30 percent. This calculation was based on a root diameter of 0.185 inches. Restraint in the slab specimens, which were 3 by 6 by 15-in. in size, was provided by a double layer of $4 \times 4\ ^{4}/_{4}$ w.w.f. (welded-wire fabric) placed at mid-depth of the specimens. The reinforcement in the longitudinal and in the transverse directions amounted to 0.89 percent. All slabs also were equipped with stainless steel end plugs

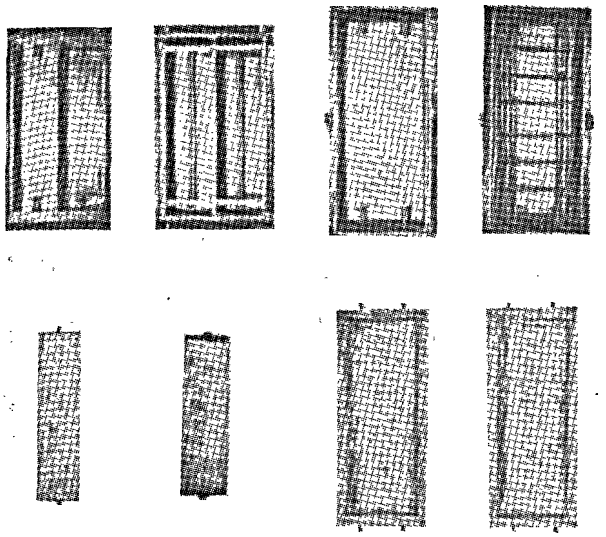

Fig. 1. *Specimen molds and arrangement of reinforcement for unrestrained and restrained prisms and slabs*

for length change measurements. Fig. 1 shows the molds, arrangement of reinforcement and specimens. Restraint in the abrasion specimens was provided by one layer at mid-depth of criss-crossed (at right angles) 1/4-in. diameter threaded rods, providing reinforcement percentages of 0.30 percent in each 12-inch direction.

Curing

Immediately after casting, specimens were covered with damp burlap kept slightly above the finished surfaces. The burlap was covered with polyethylene to retain moisture. The molds containing concretes made with portland cements were stripped at 24 hours. Those containing the various shrinkage-compensating cements were stripped at times ranging from 5 to 12 hours, depending upon the strength gain characteristics of the concrete, thus utilizing as much of the expansive potential as possible under these circumstances.

Most specimens were then cured moist at 100% R.H. at either 40, 73 or 100°F. Some were cured in water at these temperatures. Specimens for strength tests were cured continuously moist until test. Volume change specimens were made for both moist curing and water curing for 7 days at the three temperatures, followed by one day of equilibrating at 73°F in the same environment before being subjected to wetting and drying cycles. One group of volume change specimens was moist cured continuously for 6 months, while a companion set was subjected to drying at 50% R.H. after 7 days of moist curing. Specimens for freeze-thaw and de-icer scaling tests were cured 14 days moist, then 14 days in air at 50% R.H., followed by 3 days immersion in water for the prisms and 3 days with water on the top surface for the slabs, always at 73°F. Creep specimens were cured 7 days moist at 73°F prior to test, as were the specimens for sulphate resistance and abrasion tests.

The simulated steam curing cycle was essentially as follows:

1. Preset period of 6 hours after casting at 73°F. Specimens made with shrinkage-compensating cements removed from molds and measured for initial length. Specimens made with portland cement remained in molds during whole cycle, while the others were exposed directly to the curing atmosphere.
2. Heating period of about 5 hours to reach 160°F.
3. Holding period of about 11 hours at 160°F.
4. Cooling period of about 4 hours to reach 73°F. Portland cement concretes removed from molds for initial length measurement. Other specimens measured to determine expansion during curing.

Test Methods

Strength

Concrete prisms were tested in flexure, with the load applied at the third-points of a 10-inch span, as per ASTM Designation: C78–64. Prism ends were tested in compression as 3-inch modified cubes, as per ASTM Designation: C116–65T. No capping of cubes was required as the loads were applied to surfaces cast against the flat steel surfaces of the mold.

Freezing and Thawing

Concrete prisms were frozen and thawed while continuously immersed in water. Two complete cycles of freezing and thawing were obtained every 24 hours. The rate of cooling at the center of the specimens was approximately 20°F per hour. The minimum and maximum specimen temperatures attained were approximately −10°F and +55°F, respectively. Periodically during the tests, determinations were made of changes in length, weight and fundamental transverse frequency. This test method is equivalent in severity to ASTM Designation: C290–67.

De-Icer Scaling

The de-icer scaling test consisted of freezing a 1/4-inch layer of water on the top surface of the slab in a

room maintained at 0°F and then thawing the ice at about 70°F applying flake calcium chloride in an amount equivalent to 2.4 lb per sq yd of surface area. The slabs were subjected to one cycle of this procedure per day. The amount of scaling was determined by visual examination rated numerically as follows:

0 = no scale	3 = moderate
1 = slight	4 = moderate to severe
2 = slight to moderate	5 = severe

Sulphate Resistsnce

Concrete prisms were stored continuously immersed in a 10 percent sodium sulphate solution at 73°F. Exapansion was used as a criterion of performance.

Creep

Concrete cylinders were subjected to a sustained stress of 1600 psi (1200 psi for those made with Cement M-1) in a loading frame which met the requirements of ASTM Designation: C512–66T. Length change measurements were made using a 10-inch Whittemore strain gage. Companion cylinders were provided for drying shrinkage measurements. Testing was performed in a room maintained at 73°F and 50% R.H.

Abrasion Tests

Twelve-inch square by 3-inch deep slabs, restrained and unrestrained, were subjected to abrasion tests following 7 days of moist curing at 73°F and a period of at least one year of air-drying at 50% R.H. The troweled surfaces were subjected to 20 minutes of abrasion by three assemblies of dressing wheel units revolving about a horizontal axis at a speed of 170 rpm.

Discussion of Results

Table 5 shows the concrete mix data for the unrestrained specimens made for evaluating strength development and volume change characteristics. Note that the water requirements for the different cements did not vary greatly, hence the water-cement ratios are quite similar. There were, however, significant differences in air-entraining admixture requirements, with some of the shrinkage-compensating cements requiring more and some less than the portland cement.

The strength data are shown in Table 6 and are also illustrated in graphical form. Some of the 1-year data are not as yet available.

Figs. 2 and 3 show the compressive and flexural strengths of the unrestrained concretes cured continuously moist at 73°F for ages from 1 day to 1 year (1-year data not as yet available for Cements K-3 and S-1). With the exception of Cement M-1 (the portland cement-aluminate cement-gypsum blend), the strengths of the concretes made with the shrinkage-compensating cements are quite comparable to those for the protland cement concretes (Cement P-I). At 1 year, however, the difference between Cement M-1 and the others is relatively minor.

Curing temperature influences the strength development characteristics of the concretes made with the shrinkage-compensating cements in much the same manner as for the portland cement concretes. Figs. 4 and 5 show the compressive and flexural strength data for all of the concretes cast at 73°F and then stored immediately in a moist-room at temperatures of 40, 73, and 100°F for the first 7 days. After 7 days, all of the concretes were stored moist at 73°F until test. As other studies have shown, the lower the initial curing temperature, the lower the 1- and 7-day strengths. Subsequent curing at 73°F resulted in a reversal at the later ages, with the concretes cured initially at low temperatures generally showing higher strengths at 1 year. The reversal is often apparent as early as 28 days, as can be noted in Figs. 4 and 5.

In addition, Cement K-1 was used in concretes which were cast and cured moist during the first 7 days at 40, 73, and 100°F, with subsequent moist storage at 73°F. Strength data are shown in Table 6 and in Figs. 6 and 7. These changes in initial temperature of the concrete did not materially influence the strength development in comparison with the 73°F initial concrete temperature Cement K-1 strength data shown in Figs. 4 and 5.

The strength data for these same concretes subjected to steam curing at 160°F and atmospheric pressure are shown in Table 6. Again, the 1- and 7-day compressive strengths of the concretes made with Cement M-1 are significantly lower than for the other cements, but the difference is relatively small at 28 days. Flexural strengths of the Cement M-1 concretes were essentially equal, however, with the others at all ages.

These strength data indicate that concretes made with the shrinkage-compensated cements respond to curing environment in much the same manner as portland cement.

Table 6. *Strength development of concretes*

Unrestrained 3 × 3 × 11¼-in. prisms cured continuously moist at 73°F after first 7-day history shown, unless otherwise indicated. Comp. Str.—3-in. mod. cubes. Flexure—1/3 point loading, 10-in. span.

Mix designation	Temperature °F		Compressive str., psi				Flexural str., psi			
	As cast	First 7 days	1d.	7d.	28d.	1 yr.	1d.	7d.	28d.	1 yr.
P-I	73	73	1540	4760	6720	8370	285	620	760	905
	73	100	2620	5100	5480		440	680	660	
	73	40	480	3600	6750	8500	100	530	870	880
	73	(a)	4170	4860	5320	7860	550	650	760	830
M-1	73	73	860	3330	4730	7400	160	465	650	925
	73	100	1340	3520	4370	6870	245	485	540	830
	73	40	190	1870	4880	7960	30	270	555	1020
	73	(a)	2900	3770	5180	7060	490	570	685	850
K-1	73	73	1580	4970	6710	8180	235	650	700	910
	73	100	2730	5260	6120	7940	370	540	635	925
	73	40	450	3370	6580	7740	80	500	685	890
	100	100	3230	5400	6500	7870	400	590	635	980
	40	40	140	2870	6410	7290	20	465	715	940
	73	(a)	4000	5020	6570	6610	500	620	720	760
K-2	73	73	2260	5420	6540	7680	330	630	710	780
	73	100	2970	4840	5700	7080	400	540	590	760
	73	40	920	4280	7140	—	170	500	685	925
	73	(a)	3920	4280	5250	5580	570	525	605	705
K-3	73	73	1790	4850	6750		260	590	775	
	73	100	2720	5560	6040		460	720	740	
	73	40	320	3460	6860		45	480	800	
	73	(a)	4040	5190	6350		480	575	685	
S-1	73	73	1170	4560	6520		185	610	890	
	73	100	3050	5860	6740		350	690	870	
	73	40	300	1750	6320		35	245	760	
	73	(a)	4140	5150	6800		570	620	760	

(a) Steam-cured: 6 hrs. at 73° F, 18 hrs. at 160° F, then to 73° F curing.

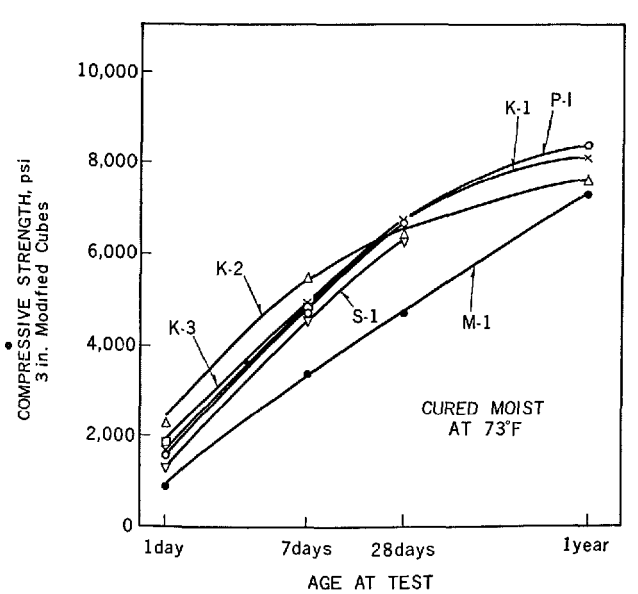

Fig. 2. *Compressive strengths of concrete cured at* 73°F

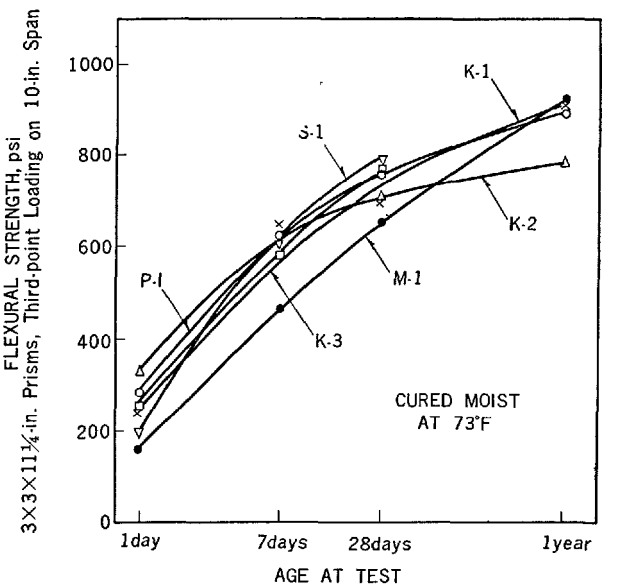

Fig. 3. *Flexural strengths of concrete cured at* 73°F

Volume Change

Effect of Mixing Time

Earlier work (1) reported that extended periods of mixing resulted in reduction of expansive potential of mortars which were wet-screened from concretes mixed for either 45 seconds or 10 minutes. It was felt that this reduction was due both to grinding and abrasion

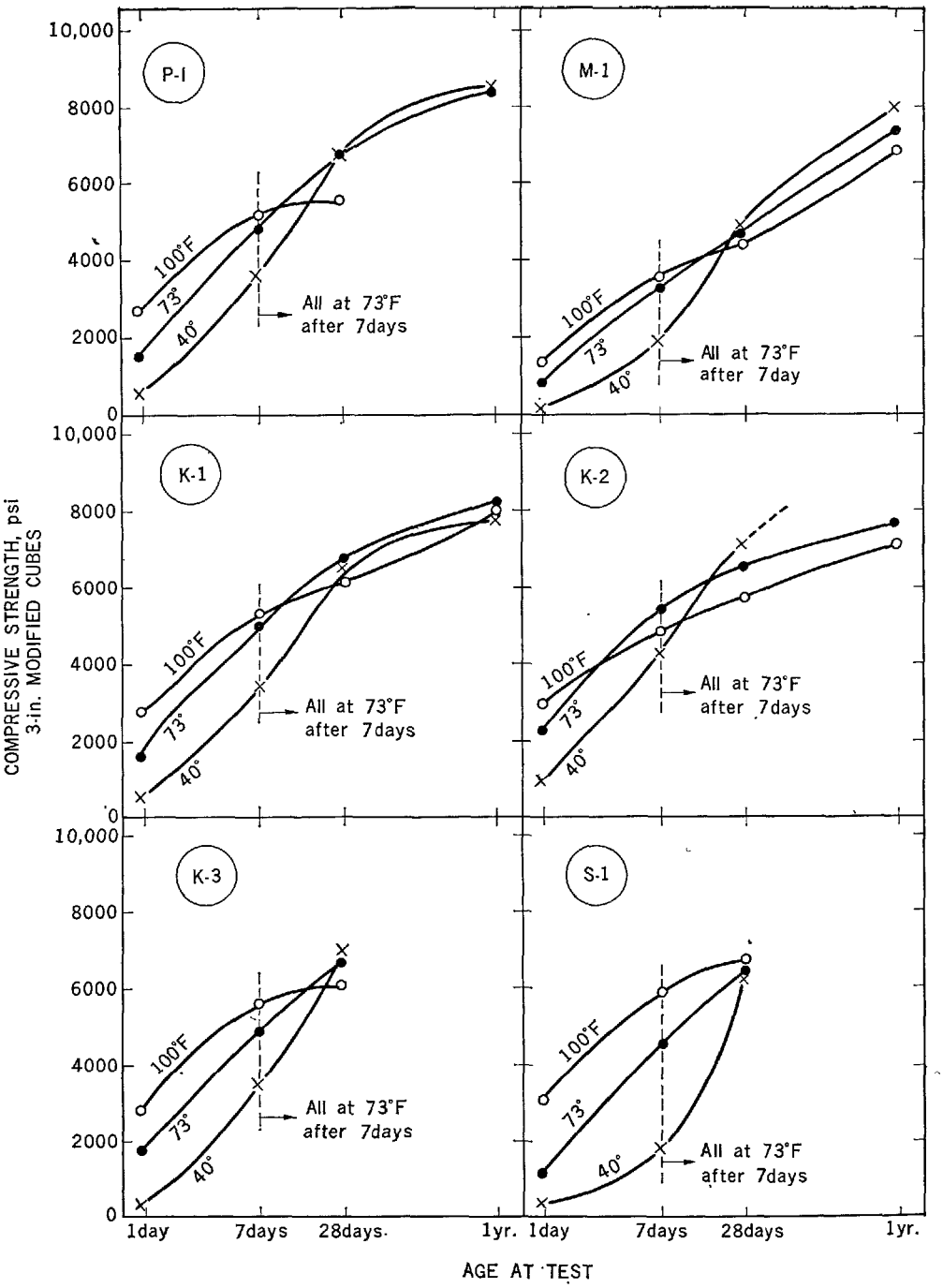

Fig. 4. *Effect of curing temperature on compressive strength*
Concretes cast at 73°F, then immediately to temperature shown for first 7 days

of hydrate coatings, thus accelerating the reaction between sulphates and aluminates (the expansive mechanism in the hardened concrete) before the concrete sets. All of the shrinkage-compensated cements were used in repeat batches which were mixed continuously for different periods of time: 1, 2-1/2, 10 and 30 minutes. Table 7 shows data on resulting slumps and air contents, on the unrestrained expansion during 28 days of moist curing at 73°F, on shrinkage on drying for the next 28 days, and on strengths at 56 days.

Fig. 8 shows the unrestrained expansions as a function of mixing time. Extension of mixing time beyond 2-1/2 minutes significantly reduces the expansive potential. In some cases, the expansions for the 2-1/2 minute mixing times were less than for the 1-minute

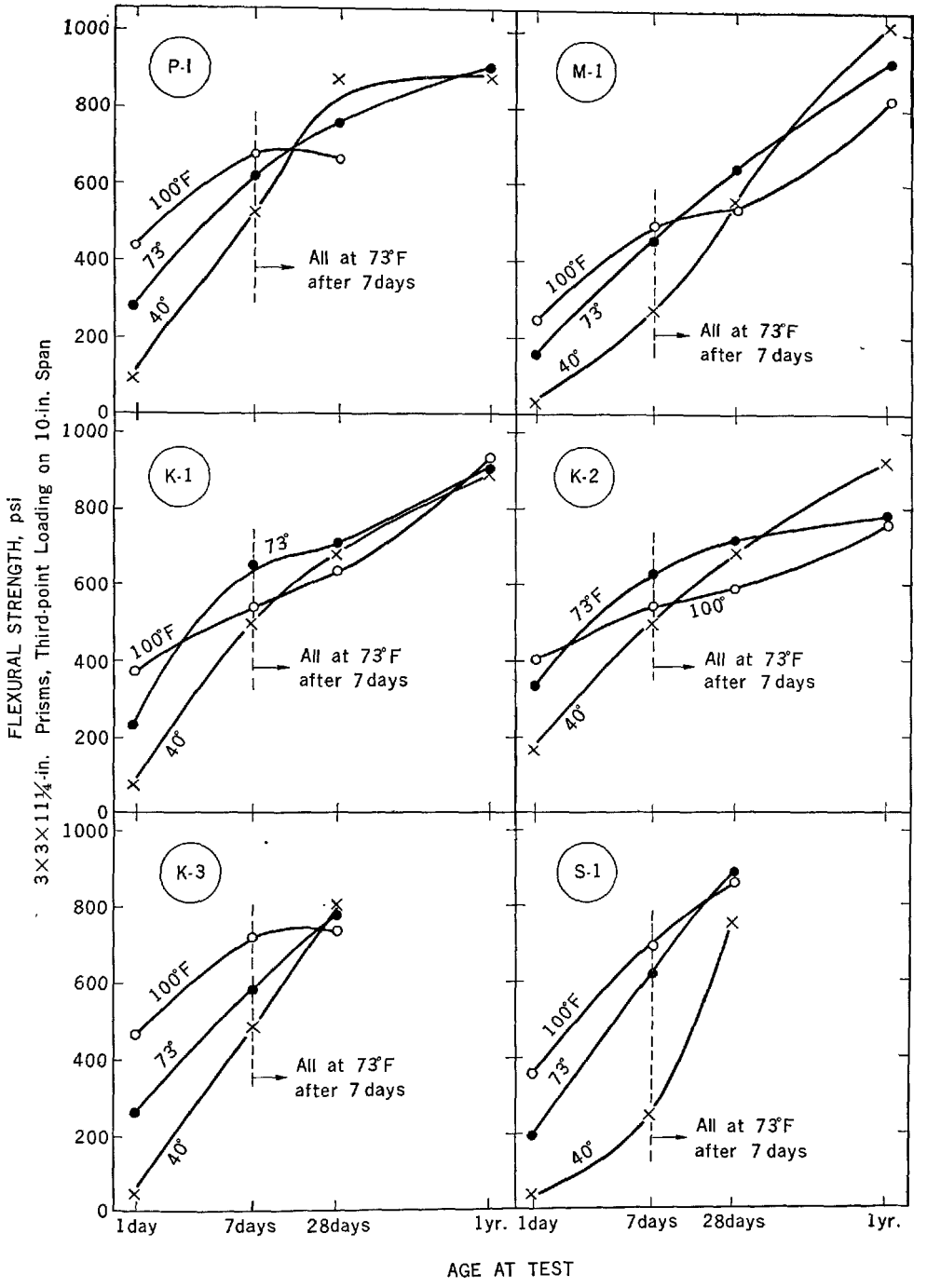

Fig. 5. *Effect of curing temperature on flexural strength*
Concretes cast at 73°F, then immediately to temperature shown for first 7 days

mixing time, in other cases the reverse was true. This latter situation might be attributable to differences in mold stripping time, since the 1-minute mix for Cement M-1 and Cement S-1 required a little more mold time to enable handling without damage, thus possibly losing some of the expansive potential. Verification of this effect is shown for Cement K-1 at 10-minute mixing time, for which two different mold times were used. Those specimens stripped at 5 hours showed significantly more expansion than those stripped at 6 hours. In the case of Cement M-1, which was a blend made at the mixer, the 1-minute mixing time may have been inadequate for uniform distribution of the ingredients.

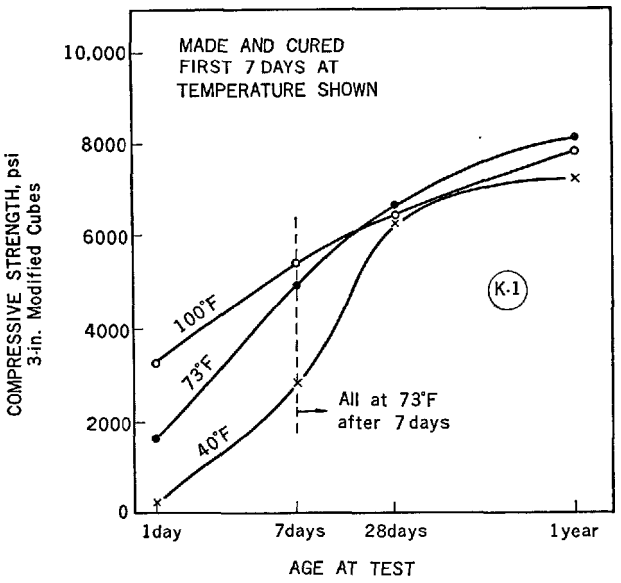

Fig. 6. *Effect of casting and curing temperature on compressive strength*

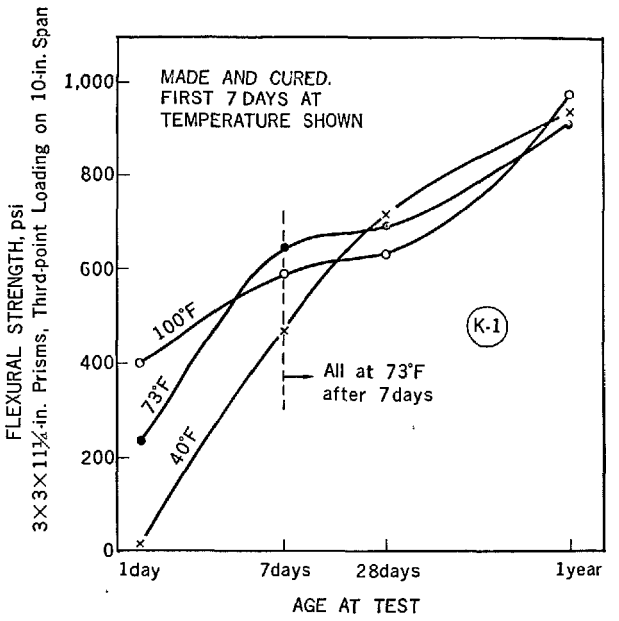

Fig. 7. *Effect of casting and curing temperature on flexural strength*

Table 7. *Effect of mixing time on expansion, drying shrinkage, and strength*
Unrestrained concrete prisms, 3 × 3 × 11¼ in., cured continuously moist at 73° F for 28 days after removal from molds, then to drying in air at 73° F and 50% R.H. for 28 days

Mix designation	Mixing time, min.	Slump, in.	Air content, %	Time in molds, hr.	Expansion, millionths				Shrinkage, millionths	56-day strength, psi	
					1d.	3d.	7d.	28d.	28 days of drying after moist curing	Comp. str.	Flex. str.
M-1	1	1.7	4.0	7	400	670	780	770	360	7400	705
	2½	2.6	5.7	6	560	1010	1110	1080	400	5270	680
	10	1.5	5.6	6	370	610	590	580	390	5750	680
	30	0.2	3.1	4	200	210	230	250	390	8060	865
K-1	1	3.5	4.9	6	930	1000	1040	1080	390	9460	815
	2½	2.9	5.7	6	820	880	920	960	400	8540	775
	10	0.6	3.9	6	440	460	510	560	400	10,600	825
	30	0.2	2.7	6	160	190	230	270	440	9950	960
	10	1.1	4.6	5	660	690	720	800	430	8840	870
K-2	1	1.6	4.2	6	740	1190	1260	1370	460	7300	775
	2½	2.7	5.9	6	710	1040	1110	1210	470	5560	790
	10	1.9	6.6	6	560	750	830	930	470	4930	790
	30	0.7	4.4	4	350	370	470	540	420	8000	890
K-3	1	3.3	5.0	6	700	1210	1430	1470	370(1)	9700(2)	935(2)
	2½	2.9	5.2	6	590	1100	1260	1310	370(1)	9140(2)	925(2)
	10	1.6	3.6	5	490	710	750	780	370(1)	9300(2)	915(2)
	30	0.2	2.7	4	200	260	300	320	390(1)	11,040(2)	940(2)
S-1	1	2.1	4.4	8	340	1180	1420	1410	390	7900	860
	2½	2.3	5.0	8	400	1290	1360	1370	410	7690	815
	10	1.2	4.3	7	390	850	900	930	410	7440	790
	30	0.2	2.6	6	380	390	390	420	420	9180	1035

(1)35 days.
(2)63 days.

The data indicate further that for any particular continuous mixing time, expansion reached a maximum at about 3 days, with only additional small increments at 7 days and essentially none at 28 days.

The 28-day drying shrinkages are essentially equal, showing no effect of mixing time. Strengths appeared to be influenced primarily by changes in air content which resulted from the different mixing times, i.e. increases in air volume resulted in lower strengths, and vice versa.

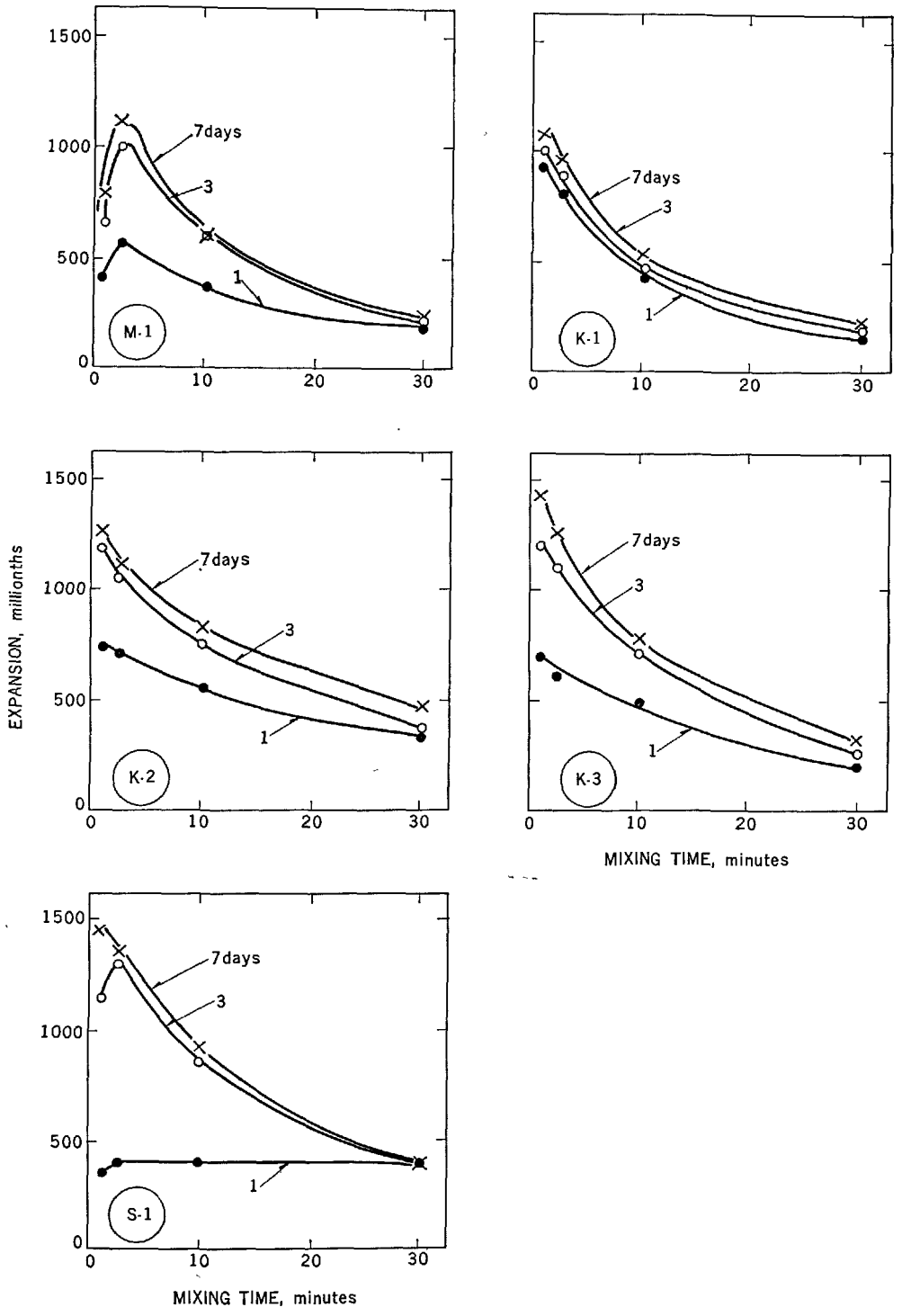

Fig. 8. *Effect of mixing time on unrestrained expansion* $3 \times 3 \times 11^1/_4$-in. *prisms*

Effect of Continuous Moist Storage and Air Drying

Fig. 9 shows the expansions of unrestrained prisms cured continuously moist at 73°F and the shrinkages of companion concretes subjected to drying at 50% R.H. after an initial 7-day moist curing period. Concrete mix data are shown in Table 5. Note that expansions during continued moist storage remain constant after 7 days, with different maxima obtained for the different shrinkage-compensating cements. The

Table 8. *Effect of curing and storage temperature on expansion and stability in wetting and drying*
Specimens are 3 × 3 × 11¼-in. unrestrained concrete prisms all cast at 73° F, cured in molds at temperatures shown, then stored in moist room or water at temperatures shown for 7 days. After an additional day to equilibrate at 73° F where required, all prisms subjected to cycles of 14 days wetting and 14 days of drying at 73° F.

Mix designation	Time in molds, hr.	Mold storage temp, °F	Storage temp. rest of 7 days, °F	Expansion, millionths[c]				
				1d.	3d.	7d.	28d.[b]	After indicated period of wetting and drying
Storage in moist room first 8 days								
P-I	24	40	40	—	30	30	200	−60 at 1 yr.
	24	73	73	—	40	40	40	−180 at 1 yr.
	24	100	100	—	10	−20	−140	−280 at 6 mo.
	24	160[a]	73	—	—	20	20	−160 at 1 yr.
M-1	12	40	40	1210	1620	1810	2180	1960 at 1 yr.
	6	73	73	780	1200	1220	1220	1080 at 1 yr.
	6	100	100	530	580	590	520	410 at 1 yr.
	6	160[a]	73	370	—	420	420	280 at 1 yr.
K-1	9	40	40	660	840	880	1110	950 at 1 yr.
	6	73	73	670	740	780	780	700 at 1 yr.
	6	100	100	610	640	660	560	520 at 1 yr.
	6	160[a]	73	520	600	620	630	490 at 1 yr.
K-2	9	40	40	500	780	940	1180	1080 at 1 yr.
	6	73	73	480	850	940	950	900 at 1 yr.
	6	100	100	560	650	720	650	630 at 1 yr.
	6	160[a]	73	800	1020	1060	1060	970 at 1 yr.
K-3	10	40	40	720	1180	1260	1440	1310 at 6 mo.
	6	73	73	420	900	1040	1040	920 at 6 mo.
	5	100	100	1000	1170	1180	1110	950 at 6 mo.
	6	160[a]	73	720	820	870	880	690 at 6 mo.
S-1	12	40	40	160	530	970	1800	1560 at 6 mo.
	8	73	73	270	1110	1420	1440	1270 at 6 mo.
	5	100	100	730	720	720	620	570 at 6 mo.
	8	160[a]	73	460	480	500	500	380 at 6 mo.

[a]Preset at 73° F for hours shown, 16 hrs. at 160° F, then to 73°F.
[b]Expansion after 1 day conditioning at 73°F.
[c]Based on length after removal from mold.

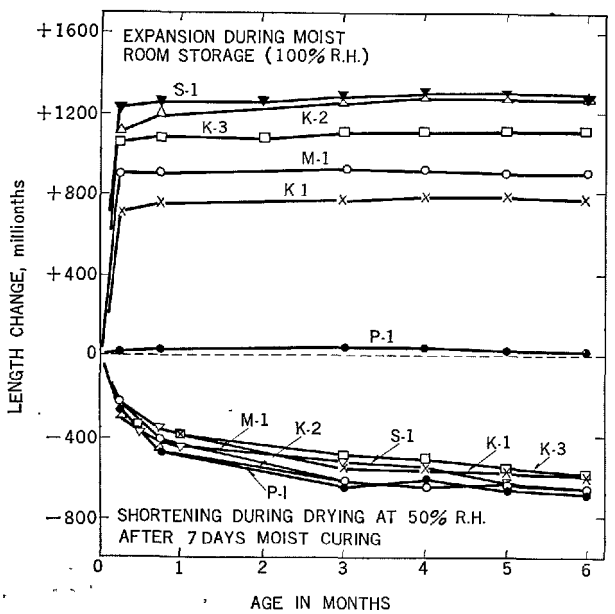

Fig. 9. *Length changes during moist storage and air drying for extended periods*
Unrestrained prisms

concretes made with Cement P-I (ASTM Type I) show the usual very low expansions during moist storage.

The magnitude of drying shrinkages for all of the concretes, including Cement P-I, are quite similar.

Volume Stability on Wetting and Drying as Influenced by Prior Curing

Unrestrained concrete prisms were cast at 73°F, kept in molds at temperatures and for times shown in Table 8, and then subjected to moist curing and to water curing at 40, 73 and 100°F for 7 days. One group was also sujected to steam curing at 160°F, followed by moist curing and water curing at 73°F. All specimens were equilibrated to 73°F on the 8th day, for both the moist and water curing environments and then subjected to alternate cycles of wetting and drying (14 days immersion in 73°F water followed by 14 days of drying at 73°F and 50% R. H.).

Table 8 shows the expansions which took place during the 8-day period described above for these concretes and the residual expansion after cycles of

Table 8. *Effect of curing and storage temperature of expansion and stability in wetting and drying (Cont'd.)*

Mix designation	Time in molds, hr.	Mold storage temp, °F	Storage temp. rest of 7 days, °F	Expansion, millionths[c] 1d.	3d.	7d.	28d.[b]	After indicated period of wetting and drying
Storage in water first 8 days								
P-I	24	40	40	—	60	50	220	−20 at 1 yr.
	24	73	73	—	60	70	70	−120 at 1 yr.
	24	100	100	—	20	30	−100	−280 at 6 mo.
	24	160[a]	73	—	—	60	60	−80 at 1 yr.
M-1	12	40	40	1320	2280	2650	3070	2820 at 1 yr.
	6	73	73	1300	1740	1740	1740	1610 at 1 yr.
	6	100	1000	980	1020	1030	930	830 at 1 yr.
	6	160[a]	73	280	—	350	340	270 at 1 yr.
K-1	9	40	40	1240	1500	1540	1780	1660 at 1 yr.
	6	73	73	800	860	900	900	800 at 1 yr.
	6	100	100	860	920	930	840	760 at 1 yr.
	6	160[a]	73	640	720	740	750	580 at 1 yr.
K-2	9	40	40	470	720	940	1190	1130 at 1 yr.
	6	73	73	590	940	1020	1020	960 at 1 yr.
	6	100	100	900	1080	1040	980	940 at 1 yr.
	6	160[a]	73	870	1110	1140	1140	1060 at 1 yr.
K-3	10	40	40	930	1440	1540	1730	1580 at 6 mo.
	6	73	73	450	1060	1200	1200	1070 at 6 mo.
	5	100	100	1280	1670	1690	1580	1430 at 6 mo.
	6	160[a]	73	960	1110	1120	1130	960 at 6 mo.
S-1	12	40	40	200	600	1040	1980	1730 at 6 mo.
	8	73	73	320	1260	1460	1460	1320 at 6 mo.
	5	100	100	850	870	880	750	640 at 6 mo.
	8	160[a]	73	440	530	540	520	480 at 6 mo.

[a]Preset at 73° F for hours shown, 16 hrs. at 160° F, then to 73° F.
[b]Expansion after 1 day conditioning at 73° F.
[c]Based on length after removal from mold.

wetting and drying for, in most cases, as long as 1 year. Note that all of the concretes show excellent stability to these alternate cycles of wetting and drying.

The effect of curing temperature on the level of expansions is somewhat variable. For Cements M-1, K-1, and K-2, the 7-day expansion level attained generally decreased as curing temperature increased. For Cement K-3, the 7-day expansions at 40 and 100°F were similar, but at 73°F the expansions were significantly lower. For Cement S-1, the 7-day expansions were greater at 73°F than at either 40 or 100°F. There seems to be no consistent effect attributable to the time the specimens were in the mold prior to stripping. After equilibration to 73°F on the 8th day, the residual expansions as a function of initial 7-day curing temperature show excellent correlation except for Cement K-3, with the residual expansion increasing as curing temperature decreased. This is in line with the lower strengths at lower temperatures, i.e. less "internal restraint" in these unrestrained prisms.

Resistance to Freezing and Thawing and De-Icer Scaling

Table 5 shows the mix data for the concretes used in this portion of the program. Concretes for these durability tests were cast and cured moist at 73°F for 14 days, followed by 14 days of air-drying at 50% R.H. The prisms were then soaked in water at 73°F prior to the start of freezing and thawing and the top surfaces of the slabs were covered with water for 3 days prior to the start of de-icer scaling tests.

Tables 9 and 10 show the length change data for the unrestrained and restrained prisms and slabs at various stages of this prior curing treatment. In addition, the tables show the calculated stresses in both the reinforcing steel and the concrete of the restrained specimens. At maximum expansions during moist storage (7 or 14 days), the restrained expansions of the prisms ranged from 52 percent to 72 percent of the unrestrained prism expansions. For the slabs, the range was 45 percent to 56 percent. These percentages did not appear to be influenced by the level of unrestrained expansion. Drying shrinkage during the following 14-day drying period were essentially similar for all concretes and the two types of specimens. On rewetting for 3 days, the prisms regained about two-thirds of the expansion lost during drying. The slabs regained only about 15 to 20 percent of the expansion during the 3 days with water on the top surface.

Table 9. *Length change of concrete prisms prior to freezing and thawing and stresses in restrained prisms*
Curing: 14 days moist, 14 days in air, then 3 days in water.

Mix designation	Restraint (b)	Length change during storage indicated, millionths						Calculated stress—psi[a] at time indicated					
		In moist room				In air at 50% R.H. 14 days (−)	In water for next 3 days (+)	4 day		28 day		31 day	
		1d. (+)	3d. (+)	7d. (+)	14d. (+)			f_s	f_c	f_s	f_c	f_s	f_c
P-I	U	—	20	40	60	350	210	—	—	—	—	—	—
	R	—	20	50	50	250	170	1500	5	−6000	−18	−900	−3
M-1	U	610	1130	1150	1150	340	220	—	—	—	—	—	—
	R	270	590	600	600	340	210	18,000	54	7800	23	14,100	42
K-1	U	460	560	620	660	340	240	—	—	—	—	—	—
	R	340	400	450	480	300	200	14,400	43	5400	16	11,400	34
K-2	U	560	1010	1070	1120	400	270	—	—	—	—	—	—
	R	350	630	690	730	360	230	21,900	66	11,100	33	18,000	54
K-3	U	310	880	1150	1170	290	220	—	—	—	—	—	—
	R	190	520	660	660	220	200	19,800	59	13,200	40	19,200	58
S-1	U	330	1060	1290	1310	340	230	—	—	—	—	—	—
	R	230	670	750	750	280	200	22,500	68	14,100	42	20,100	60

[a] Minus indicates compression in steel and tension in concrete.
[b] U = unrestrained, R = restrained, 0.3% steel—single threaded rod.

Table 10. *Length change of de-icer slabs prior to de-icer scaling test and stresses in restrained slabs*
Curing: 14 days moist, 14 days air, then 3 days with water on top surface.

Mix designation	Restraint[b]	Length change during storage indicated, millionths						Calculated stress—psi[a] at time indicated					
		In moist room				In air at 50% R.H. for next 14 days (−)	Water on top surface for next 3 days (+)	14 day		28 day		31 day	
		1d. (+)	3d. (+)	7d. (+)	14d. (+)			f_s	f_c	f_s	f_c	f_s	f_c
P-I	U	—	30	40	30	300	40	—	—	—	—	—	—
	R	—	20	30	40	280	40	1200	11	−7200	−64	−6000	−53
M-1	U	300	820	830	800	300	60	—	—	—	—	—	—
	R	180	400	370	360	250	40	10,800	96	3300	29	4500	40
K-1	U	400	500	530	570	320	40	—	—	—	—	—	—
	R	210	260	290	310	270	30	9300	83	1200	11	2100	19
K-2	U	540	940	1010	1060	350	50	—	—	—	—	—	—
	R	300	490	540	560	310	40	16,800	149	7500	67	8700	77
K-3	U	230	640	860	860	260	70	—	—	—	—	—	—
	R	120	360	470	480	250	50	14,400	128	6900	61	8400	75
S-1	U	250	860	920	940	310	60	—	—	—	—	—	—
	R	150	450	410	420	280	40	12,600	112	4200	37	5400	48

[a] Minus indicates compression in steel and tension in concrete.
[b] U = unrestrained, R = restrained, 0.89% steel, welded-wire-fabric.

The compressive stresses in the restrained concrete prisms (0.3% steel) and slabs (0.89%) were quite similar at the end of the 14-day moist curing period, ranging from 43 to 68 psi for the prisms and 83 to 149 psi for the slabs. The concrete stresses in the restrained slabs were higher than those in the restrained prisms by about 90 percent. Earlier work (1) with slab specimens and different amounts of steel ranging from 0.7% to 1.8% showed that concrete stress was relatively independent of the amount of reinforcement, at least at these percentages of reinforcement. During the 14-day drying period, a substantial proportion of this compressive stress was lost due to drying shrinkage, but for the prisms at least most of this loss was recovered on subsequent wetting.

Table 11 shows the expansion of concrete prisms, based on the 31-day length, at 100, 300, and 500 cycles of freezing and thawing in water, along with the durability factors calculated from changes in fundamental transverse frequency at 300 cycles. In addition, the weight changes of prisms after 300 cycles are shown.

The concretes made with Cement K-3 did not

Table 11. *Results of freezing and thawing and de-icer scaling tests*

Mix designation	Restraint[a]	3 × 3 × 11¼-in. prisms: Expansion after cycles shown, millionths			Durability factor at 300 Cy.	Weight change after 300 cycles, %	3 × 6 × 15-in. slabs: Scale rating after 300 cycles
		100	300	500			
P-I	U	90	170	240	102	+0.3	0+
	R	70	120	280	105	+0.3	0+
M-1	U	70	140	160	104	−1.9	1−
	R	60	80	170	104	−0.4	1−
K-1	U	120	220	270	102	+0.4	0+
	R	110	190	250	103	+0.4	0+
K-2	U	190	310	380	100	−0.1	0+
	R	110	150	280	103	+0.2	0+
K-3	U	80	140	170 at 400	96	−10.5	2 at 200
	R	30	110	140 at 400	82	−7.8	2+ " "
S-1	U	90	130	150 at 400	105	0	0+ " "
	R	50	130	160 at 400	104	+0.1	0 " "

[a]U = unrestrained, R = restrained (0.3% for prisms, 0.89% for slabs).

Table 12. *Creep of concretes*

Nominal cement content—564 lb/cu yd (6 U.S. bags)
Specimens: 6 × 12-in. cylinders—no reinforcement.
Cured 7 days moist at 73 F.
Loaded at 7 days age, companions to drying environment (50% R.H.) and to compressive strength tests at that age.
Elgin sand and Eau Claire gravel (3/4 in. max. size)

Mix designation	Net w/c, by wt.	Slump, in.	Air content, %	7-day comp. str., psi	Sustained stress, psi	Secant E, million psi	Creep strain, millionths/psi		
							28d.	9 mo.	1 yr.
P-I	0.41	2.8	6.20	4120	1600	4.29	0.323	0.579	.598
M-1	0.41	2.0	5.30	3080	1200	3.75	0.444	0.707	.740
K-1	0.40	3.6	6.40	4020	1600	4.12	0.323	0.502	.516
K-2	0.45	2.8	6.30	3880	1600	3.80	0.473	0.711	.734
K-3	0.42	2.9	4.60	3990	1600	3.43	0.397	.566[a]	
S-1	0.40	2.3	5.70	3920	1600	3.85	0.395	.596[a]	

[a]8-month value.

perform as well as the others. Durability factors were somewhat lower, but still excellent. Weight loss, however, was quite high and de-icer scaling resistance significantly lower. All of the other air-entrained concretes, restrained or unrestrained, show excellent resistance to freezing and thawing and de-icer scaling.

Creep of Unrestrained Concretes

The mix data for the concretes used in casting 6 × 12-in. cylinders for creep and supplementary drying shrinkage tests are shown in Table 5. These cylinders were cured 7 days moist at 73°F and then loaded to a stress level of 1600 psi, except for those made with Cement M-1 which were loaded to 1200 psi due to somewhat lower 7-day strength. Creep tests were conducted at 73°F and 50% R. H.

Table 12 shows the modulus of elasticity for these concretes calculated from the immediate strain on loading and the creep strain per psi after 28 days, 9 months and 1 year of sustained loading (9-month and 1-year data for Cements K-3 and S-1 not yet available). Moduli and creep strain values are reasonably similar. Fig. 10 shows the creep strains and drying shrinkages plotted as a function of time. Concretes made with Cements K-2 and M-1 show significantly greater creep strain per psi than the other concretes. The K-2 concrete required more water and hence had a higher water-cement ratio than the others, however the 7-day strength was about equal to those for Cements K-1,

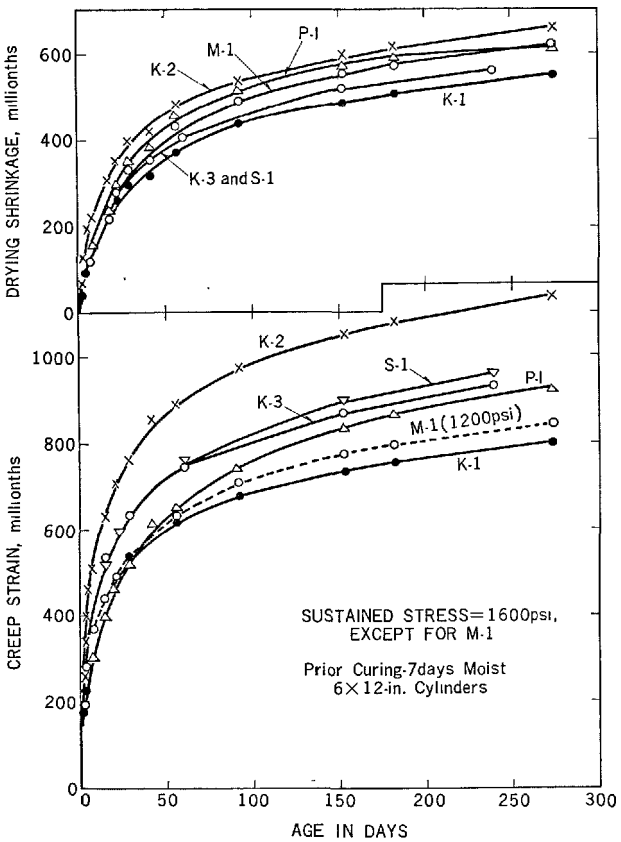

Fig. 10. *Creep and drying shrinkage of concretes*

K-3 and S-1. The 7-day strength of the concrete made with Cement M-1 was significantly lower. All of the concretes showed similar drying shrinkages, as were the case in the prism and slab tests.

Resistance to Sulphate Solution

In these tests, the performance of the shrinkage-compensated concretes was compared with concretes made with Cement P-II (ASTM Type II) and Cement P-V (ASTM Type V). Mix data for these air-entrained concretes are shown in Table 5. Concretes were cured moist at 73°F for 7 days and then kept continuously immersed in a 10 percent sodium sulphate solution at the same temperature.

Table 13 shows the expansions of unrestrained and restrained prisms during the initial 7 days of moist curing and additional expansions which occurred during immersion in the sulphate solutions. Concretes made with Cements P-II and P-V (ASTM Type II and V) showed exceedingly small expansions after 16 months' exposure. All of the shrinkage-compensated concretes show large additional expansions considerably earlier, particularly the unrestrained

Table 13. *Sulphate resistance of concrete prisms*
3 × 3 × 11¼-in. concrete prisms, cured 7 days moist at 73 F, then continuously immersed in 10% Na_2SO_4 solution.

Mix designation	Restraint (a)	Expansion in millionths during 7-day moist storage	Months of immersion in sulfate solution 1	3	4	5	6	7	9	16
P-V	U	20	0	30	40	10	40	40	60	40
	R	0	0	0	30	0	40	70	60	110
P-II	U	50	−20	10	30	0	20	−20	0	0
	R	10	−40	0	30	10	60	100	80	120
M-1	U	1120	100	440	730	1140	2030	3420	D(b)	
	R	340	40	210	320	540	660	760	880	1420
K-1	U	780	150	620	1000	3110	D(b)			
	R	350	100	320	440	740	900	1100	1340	2390
K-2	U	1060	280	880	1220	1920	3140	D(b)		
	R	710	200	550	660	730	900	1060	1210	1890
K-3	U	1160	160	620	1190	2150	3970	D(b)		
	R	640	130	360	460	490	570	660		
S-1	U	1120	160	560	1020	D(b)				
	R	620	200	500	640	740	870	1000		

(a) U = unrestrained.
R = restrained w/threaded steel rod, 0.30% steel.
(b) D = discontinued at time shown.

concretes. Although the restraint provided by the steel reinforcement afforded marked improvement in performance, the level of additional expansions would indicate that these shrinkage-compensated concretes are not able to resist this continuous exposure to concentrated sulphate solutions. Higher percentages of steel reinforcement than that used, 0.30 percent, would probably be helpful in such exposures. In addition, a lower water-cement ratio, richer mix would also be helpful, since numerous studies of sulphate attack have shown the importance of low water-cement ratio in such exposures. Additional work in this area is planned, including also exposure to seawater.

Resistance to Abrasion

Four of the Cements (P-I, M-1, K-1, and K-2) were used in making unrestrained and restrained concrete slabs for evaluating resistance to abrasion. Table 14 shows pertinent mix data, compressive strengths at 28 days and 1 year, and the average abrasion loss for these slabs. Note that the abrasion specimens were given only 7 days of moist curing and were dried at 50% R.H. at least 1 year before being subjected to test.

Although the repeatability and accuracy of the abrasion test requires more than duplicate test specimens, the results indicate that the shrinkage-compensated concretes made with Cements K-1 and K-2 may be somewhat more resistant to abrasion than the

Table 14. *Abrasion resistance of concretes*

Specimens for abrasion tests (2 per mixture) were 12-in. square by 3-in. deep, with steel-troweled surfaces.
Curing for abrasion specimens was 7 days moist at 73°F, then to air of laboratory at 73°F and 50% R.H. until test at ages of 12 to 15 months.
Strength specimens were 3-in. modified cubes, cured continuously moist.
Restrained abrasion specimens reinforced with 1/4 in. diameter continuously threaded rods in both 12-inch directions. Percentage reinforcement in each direction = 0.30%.
Abrasion machine used dressing wheel units.

Mix designation	Net w/c, by wt.	Slump, in.	Air content, %	Comp. str., psi		Average abrasion loss after 20 minutes, mils	
				28d.	1 yr.	U(1)	R(1)
P-I	0.42	3.0	5.85	6720	8370	293	286
M-1	0.44	2.7	6.00	4730	7400	359	266
K-1	0.40	2.6	5.90	6710	8180	146	114
K-2	0.46	2.7	5.65	6540	7680	192	187

(1)U = unrestrained.
R = restrained.

concrete made with Cement P-I. The Cement M-1 shrinkage-compensated concrete showed less resistance to abrasion than the Cement P-I concrete, probably a reflection of its lower 28-day strength. In this instance, restraint was helpful in reducing abrasion loss. For Cements K-1, K-2 and P-I, restraint appeared to have little influence on abrasion loss.

Influence of Cement Content on Strength and Volume Stability

Using Cement K-1, concretes containing 564 lb (6 U.S. bags) and 752 lb (8 U.S. bags) of cement per cubic yard were prepared to compare strength and volume stability. The mix data for these concretes are shown in Table 15. Specimens were unrestrained prisms. For both cement contents, a mold stripping time of 6 hours was observed. In addition, for the 752 lb of cement/cu yd mix a mold stripping time of 18 hours was used. Those for strength tests were cured continuously moist at 73°F. Volume stability prisms were cured 7 days moist or 7 days in water at 73°F, then subjected to the wetting and drying cycles described earlier.

Table 16 shows the compressive and flexural strength data for these concretes. The 752 lb of cement/cu yd concretes showed somewhat higher strengths than the 564 lb of cement/cu yd concretes, except for the 1-year compressive strengths. The effect of mold stripping time on the higher cement content concrete

Table 15. *Concrete mix data for comparison of effect of cement content*
Cement designation: K-1

Item	Nominal cement content, lb/cu yd	
	564	752
Slump, in.	2.6	2.7
Unit wt., lb/cu ft	146.6	146.2
Air content, %	5.90	6.02
Cement content,(a)		
lb/cu yd	569	756
bag/cu yd (U.S.)	6.05	8.04
Water content, lb/cu yd	230	249
Water-cement ratio, by wt.	0.40	0.33
A/E admixture, ml/lb cement	1.7	2.3

(a)Includes expansive components.

Table 16. *Influence of cement content on strength of concretes made with shrinkage-compensating cement K-1*
Unrestrained prisms, 3 × 3 × 11¼ in.
Strength specimens cured continuously moist at 73°F.
Compressive strength—3-in. modified cubes.
Flexural strength—1/3 point loading, 10-in. span.

Item	Test age	Mold stripping time		
		6 hr.		18 hr.
		564(a)	752(a)	752(a)
Compressive strength, psi	1 day	1580	2260	2510
	7 days	4970	6210	6010
	28 days	6710	7620	7050
	1 yr.	8180	7160	7240
Flexural strength, psi	1 day	235	310	315
	7 days	650	705	645
	28 days	700	780	795
	1 yr.	910	1110	1055

(a)lb of cement/cu yd.

Table 17. *Influence of cement content on expansion and stability in wetting and drying of concretes made with shrinkage-compensating cement K-1*
Unrestrained prisms, 3 × 3 × 11¼ in., cured 7 days moist or in water at 73°F, then subjected to cycles of 14 days of wetting and 14 days of drying (50% R.H.) at 73°F for one year.

Item	Mold strippnig time,		
	6 hr.		18 hr.
	564(a)	752(a)	752(a)
Moist storage			
Expansion, millionths:			
1 day	670	570	140
3 days	740	740	300
7 days	780	820	380
Residual, 1 year of wetting and drying	700	740	300
Water storage			
Expansion, millionths:			
1 day	800	1060	280
3 days	860	1240	440
7 days	900	1300	510
Residual, 1 year of wetting and drying	800	1180	430

(a)lb of cement/cu yd.

strengths did not appear to be significant.

Table 17 shows the expansions during 7 days of moist storage or water storage and the residual expansions after 1 year of wetting and drying. The expansions in water storage were significantly greater than those in moist storage. For the higher cement content, the 18-hour mold stripping time resulted in large reductions in expansion. Longer time in the mold results in less total expansion remaining. This lower remaining expansion must also operate against a stronger concrete at 18 hours than one at 6 hours.

Residual expansions after 1 year of wetting and drying cycles indicate concretes of both cement contents to be quite volume stable.

Summary

This report presents data on a variety of engineering properties of air-entrained concretes made with expansive cements of the shrinkage-compensating type. These cements were used in concretes having 564 lb (6 U.S. bags) of cement per cubic yard and suitable for general cast-in-place construction work, for pavements, for precast concrete units, and for other uses of concrete as a construction material. Both unrestrained concretes and restrained concretes (internal steel reinforcement, etc.) were included in these tests.

The shrinkage-compensating cements used included three Type K cements, one Type M cement, and one Type S cement, as they are defined in the American Concrete Institute's "Cement & Concrete Terminology" (SP-19). For comparison purposes, the tests included one each of ASTM Types I, II, and V portland cements.

The tests included an evaluation of strength development as influenced by curing history, the effect of mixing time on expansive potential, the volume stability in continuous moist or air storage and after numerous wetting and drying cycles, the creep under sustained stress, the resistance to freezing and thawing and de-icer scaling, the resistance to sulphate exposure, and the resistance to abrasion.

The results of these tests showed that the strength development characteristics of these concretes in response to curing environment are similar to normal portland cement concretes, that their volumes change and creep characteristics after attaining their designed maximum expansion are comparable to those of portland cement concretes, that they are equally resistant to freezing and thawing and de-icer scaling. Where abrasion tests were conducted, abrasion resistance of restrained specimens was at least comparable to normal portland cement concrete. There was significantly less resistance to sulphate attack, however, than for the concretes made with the ASTM Type II and V portland cements. This defect might be offset by the use of a lower water-cement ratio, richer concrete and a greater percentage of steel reinforcement to provide more restraint to expansion resulting from sulphate attack.

With respect to expansive potential, the data indicate that higher curing temperatures generally resulted in lower expansions and that increased continuous mixing time markedly reduced the level of expansion.

Acknowledgement

The authors wish to acknowledge the valuable assistance of Fletcher Klouthis, Senior Technician in the Concrete Research Section.

References

1. A. H. Gustaferro N. Greening and P. Klieger, "Expansive concrete—laboratory tests of freeze-thaw and surface scaling resistance," Journal of the PCA Research and Development Laboratories, Vol. 8, No. 1, 10–36 (January 1966). Reprinted as PCA Research Department Bulletin 190.
2. G. E. Monfore, "Properties of expansive cement made with portland cement, gypsum, and calcium aluminate cement," Journal of the PCA Research and Development Laboratories, Vol. 6, No. 2, 2–9 (May 1964). Reprinted as PCA Research Department Bulletin 170.

SESSION IV-5 BY-PRODUCT GYPSUM FROM VARIOUS CHEMICAL INDUSTRIES, AS A RETARDER FOR THE SETTING OF CEMENT

Principal Paper Utilization of Chemical Gypsum for Portland Cement

Keiichi Murakami*

Synopsis

Chemical gypsums, the by-products from various industries, are regarded as a main source of gypsum for control of the setting time of portland cement and portland blastfurnace slag cement in Japan. Phosphogypsum is a by-product of phosphoric acid manufacture. The quantity of its production is the largest among chemical gypsums. Therefore, phosphogypsum is now the most important among chemical gypsums. However, it is well known that the impurities usually included in phosphogypsum injuriously affect the hydration of portland cement. The object of this paper is to clarify the characters of impurities in phosphogypsum as well as to understand the effects of impurities on the hydration of cements.

The impurities which mainly affect the hydration of portland cement are P_2O_5 substituted in the crystal lattice of gypsum, the water-soluble P_2O_5 and the water-soluble F which adhered to the surface of gypsum crystals. The analytical procedures for these impurities have been proposed and proved to be useful and successful. The impurities in phosphogypsum generally retard the setting of portland cement, but do not affect the development of three day strength of mortar.

The large quantities of phosphogypsum are now produced from the hemihydrate-dihydrate process in Japan. Since the phosphogypsum produced from the dihydrate process has a relatively large amount of impurities, it is neutralized with milk of lime after dehydration of phosphogypsum.

The grinding of portland cement clinker together with natural gypsum of a higher grade or chemical gypsum requires a larger power consumption than with natural gypsum of a lower grade. The power consumption in grinding, in particular, at a temperature of over 130°C, increases more markedly than at ordinary temperature. The clay minerals included in natural gypsum of the lower grade tend to improve the grindability at a higher as well as lower temperature.

The retarding action of the impurities in phosphogypsum was investigated by measuring the rate of heat liberation of cement hydration with calorimeter and the specific surface area of the hydration products as well as the electron microscopic observation of the hydration products. It has been consequently suggested that the insoluble compounds produced by the reaction between the impurities in phosphogypsum and the high-lime surface of cement grains or lime in the liquid phase of paste form the protective coatings on the surface of cement grains and that they retard temporarily the hydration of portland cement.

The advantages brought by the utilization of the waste products such as chemical gypsum are so great that the present success in Japan will surely become a valuable example.

*Faculty of Engineering, Tohoku University, Sendai, Japan.

Introduction

Generally, the by-product gypsum made from various industries is called "chemical gypsum" in Japan. These chemical gypsums are regarded as the valuable sources of raw material in making gypsum board, gypsum plaster, and of gypsum for control of the setting time of portland cement because the abundant sources of natural gypsum have not been found in Japan.

By the recent development of the gypsum production technique, most types of chemical gypsum have the specific properties satisfying the requirment.

Since the production of phosphogypsum is the largest among the chemical gypsums, it is regarded as a valuable source of gypsum for the portland cement industry which requires the largest amounts of gypsum. It has been demonstrated that phosphogypsum containing the impurities of over some quantities injuriously affects the early stage of the hydration of protland cement.

The purpose of this paper is to clarify the characteristics of impurities in phosphogypsum and the intrinsic features of its influence on the hydration of portland cement. The author believes that the results of these studies will be useful in the various applications of chemical gypsum.

The author expresses his gratitude to
Dr. Y. Suzukawa of Ube Industries, Ltd.
Dr. M. Hanada of Yawata Chemical Industry Co. Ltd.
Dr. K. Miyazawa of Sumitomto Cement Co. Ltd.
Dr. Prof. M. Sekiya of Kogakuin University.
Dr. Prof. T. Kusano of Kogakuin University.
Mr. Assist. Prof. H.Tanaka of Tohoku University
for their invaluable assistance in carrying out the investigation.

Recent Features of Chemical Gypsums in Japan

The Kinds, Productions, Production Reactions, Consumption and Chemical Compositions of Chemical Gypsums

Chemical gypsum is by-produced from various industries. Table 1 shows the most of representative chemical gypsums and their production reactions (1–4). The content of SO_3 of natural gypsum in Japan is approximately 30% to 40%. The grade is generally poor. On the contrary, chemical gypsum has a higher content of SO_3 as shown in Table 2 (5). Table 3 shows the history of the production, the estimation of the production of natural gypsum and their consumptions respectively in Japan for the period from 1965 to 1968 (6). These data also indicate that phosphogypsum, which is the largest in production, is the most valuable source for the set control of portland cement above other chemcial gypsums.

Phosphogypsum and Wet Process in Making Phosphoric Acid

Operations of the wet process in making phosphoric acid ate closely related to the compatibility of hosphogypsum for controlling the setting time of portland cement because phosphogypsum is a by-product in making phosphoric acid. Photo 1_{-i} shows a optical microphotograph of the agglomerated phosphogypsum produced from the conventional dihydrate process. This agglomerated phosphogypsum includes the relatively large amounts of impurities in the interstice among the crystals and in the lattice of phosphogypsum crystals. It will be later clarified that the agglomerated phosphogypsum must be regenerated by the special chemical treatments to be used for controlling the setting time.

There are many reports on the dihydrate process in making phosphoric acid (7–10). Murakami and Hori (11, 12) established the hemihydrate-dihydrate process, by which the recovery of phosphoric acid is higher than by dihydrate process and the quantity of impurities in the by-produced phosphogypsum is less than that in phosphogypsum produced from dihydrate process.

At the present time many plants using this hemihydrate-dihydrate process are operating industrially in Japan (13–26) and also a plant in China. Recently, some new processes directly producing the concentrated phosphoric acid and hemihydrate or anhydrite have been investigated (27, 28).

Qualities of Chemical Gypsum as Gypsum for Control of the Setting Time of Portland Cement

It has been well known that phosphogypsum and fluorogypsum contain some amounts of impurities which unfavorably affect the hydration of portland cement. Most of the previous works have reported

Table 1. *Various chemical gypsums and their production reactions*

No. A	Chemical gypsum by reaction phosphate rock and sulfuric acid. "Phosphogypsum" $Ca_3(PO_4)_2 + 3H_2SO_4 + 6H_2O = 3CaSO_4 2H_2O + 2H_3PO_4$ (Dihydrate Process) $Ca_3(PO_4)_2 + 3H_2SO_4 + 3H_2O = 3CaSO_4 \cdot 1/2H_2O + 2H_3PO_4 + 3/2H_2O$ $CaSO_4 \cdot 1/2H_2O + 3/2H_2O = CaSO_4 \cdot 2H_2O$ (Hemihydrate-dihydrate process)
No. B	Chemical gypsum by reaction of calcium compound with sulfate in making NaCl from sea water. "Saltgypsum" $MgSO_4 + CaCl_2 + 2H_2O = MgCl_2 + CaSO_4 \cdot 2H_2O$
No. C	Chemical gypsum by reaction of fluorite and sulfuric acid in making HF. "Fluorogypsum" $CaF_2 + H_2SO_4 = 2HF + CaSO_4$ (Anhydrite) $CaSO_4 + 2H_2O = CaSO_4 \cdot 2H_2O$
No. D	Chemical gypsum by neutralization reaction of waste sulfuric acid in making TiO_2 from ilmenite. "Titangypsum" $FeOTiO_2 + 2H_2SO_4 = TiOSO_4 + FeSO_4 + 2H_2O$ $TiOSO_4 + 2H_2O = TiO(OH)_2 + H_2SO_4$ $FeSO_4$ or $H_2SO_4 + CaCO_3$ or $Ca(OH)_2 \longrightarrow CaSO_4 2H_2O$
No. E	Chemical gypsum by neutralization reaction of $CaCO_3$ and $Ca(OH)_2$ with waste sulfuric acid in pickling process of iron making. $H_2SO_4 + CaCO_3 + H_2O = CaSO_4 2H_2O + CO_2$ $FeSO_4 + Ca(OH)_2 + 2H_2O = CaSO_4 2H_2O + Fe(OH)_2$
No. F	Chemical gypsum by neutralization reaction with calcium compounds to waste sulfuric acid in refining of cuporus sulfate and zink sulfate. $H_2SO_4 + CaCO_3 + H_2O = CaSO_4 2H_2O + CO_2$
No. G	Chemical gypsum by oxidation and neutralization reaction of SO_2 in combustion gas, exhaust gas from various industries or power plant. $SO_2 + Ca(OH)_2 = CaSO_3 1/2H_2O$ $2CaSO_3 \cdot 1/2H_2O + O_2 + 3H_2O = 2CaSO_4 2H_2O$
No. H	Chemical gypsum by reaction of $CaCl_2$ with Na_2SO_4, from soda ash industry and rayon industry, respectively. "Soda-gypsum" $CaCl_2 + Na_2SO_4 + 2H_2O = CaSO_4 2H_2O + 2NaCl$
No. I	Chemical gypsum by reaction of $CaCO_3$ with aluminum sulfate from activation process of Japanese acid clay. $Al_2O_3 4SiO_2 2H_2O + 3H_2SO_4 = Al_2(SO_4)_3 + 4SiO_2 + 5H_2O$ $Al_2(SO_4)_3 + m_1CaCO_3 + H_2O = m'Al_2(SO_4)_3Al(OH)_3 + CO_2 + CaSO_4 2H_2O$ $m'Al_2(SO_4)_3Al(OH)_3 + m_2CaCO_3 = m''Al_2(SO_4)_3Al(OH)_3 + CO_2 + CaSO_4 \cdot 2H_2O$
No. J	Chemical gypsum in making phenol and humic acid. $(COO)_2Ca + H_2SO_4 + 2H_2O = (COOH)_2 + CaSO_4 2H_2O$
No. K	Chemical gypsum by reaction of ammonium sulfate with $Ca(OH)_2$. $(NH_4)_2SO_4 + Ca(OH)_2 = 2NH_3 + CaSO_4 2H_2O$

In this paper, each chemical gypsum is described as special name or numbered chemical gypsum as shown in this table.

that the impurities of phosphogypsum are the reaction products in the wet process and the impurities in phosphate rock, such as phosphoric acid, alkali silico-fluoride, monocalcium phosphate, dicalcium phosphate, some organic substances, undecomposed phosphate rock, quartz and other inorganic oxides (29–34).

The water-soluble compounds among them are likely to affect injuriously the hydration of portland cement. A large portion of impurity is found on the surface of gypsum crystals and in the interstice of

Table 2. *Chemical compositions of chemical gypsum.*

C.G.		C.W.	SO_3	CaO	$CaSO_4 2H_2O$*
No. A	1	18.0%	40.3%	34.5%	86.6%
	2	20.2	44.4	33.1	95.5
No. B	1	20.5	46.0	31.7	98.9
No. C	1	19.2	42.6	29.6	91.6
	2	18.4	41.1	29.1	88.4
	3	19.4	44.3	32.1	95.2
	4	18.8	41.1	28.9	88.4
	5	19.2	42.4	31.1	91.2
No. F	1	18.6	41.3	32.7	88.8
	2	19.4	43.8	32.7	94.2
	3	19.1	42.4	32.9	91.2
No. H	1	18.3	44.4	31.8	95.5
	2	20.5	46.9	32.9	100.8
No. K	1	19.9	44.2	32.5	95.0
	2	20.2	45.0	32.8	96.8
Others	1	19.1	42.5	33.3	91.4
	2	20.3	45.9	32.4	98.7
	3	18.9	43.8	33.0	94.2

C.W.: combined water.
*: gypsum content calculated from SO_3.
C.G.: chemical gypsum.

Table 3. *Production and consumption of various gypsums*

(Metric ton)

Production		1965	1966	1967	1968
Natural gypsum	Japan	615,041	63,000		
	Import	51,981	50,000		
	total	667,022	680,000		
Chemical gypsum	Phospho-gypsum	1,448,212	1,592,000		
	Others	294,000	300,000		
	total	1,742,212	1,892,000		
Total		2,409,000	2,572,000		
Consumption					
Portland cement	Natural gypsum	620,153			
	Phospho-gypsum	339,569			
	Others	230,374			
	total	1,190,093	1,275,000	1,360,000*	1,445,000*
Plaster board	Phospho-gypsum	654,025			
	Others	34,001			
	total	688,026	741,060	1,230,000*	1,364,000*
Plaster	Phospho-gypsum	308,087			
	Others	12,973			
	Natural gypsum	3,243			
	total	402,000			

*estimated value

agglomerated crystals. Some portions of phosphate enter into solid solution with gypsum by the substitution of HPO_4^{--} for SO_4^{--}, because the both crystals have the similar lattice parameters and belong to the analogous space group.

Optical microphotographs of several phosphogypsums are shown in Photograph 1 by Murakami, Tanaka and Sato (35). The appearances of phosphogypsum HDS-1, 2 and 3 produced from the hemihydrate-dihydrate process show the unagglomerated single crystal or twin crystal with the smooth surface, that the impurities which adhered to the surface are easily removed by a single washing with water. Phosphogypsum HD shown in Photo 1 is also a by-product from the hemihydrate-dihydrate process. Except for phosphogypsum HD-2, however, other phosphogypsums-HD have a large amount of the agglomerated crystals which are resulted from the incomplete decomposition of phosphate rock in the digestion step of the wet process. All phosphogypsum D-1 by-produced from the dihydrate process are agglomerated crystal, the impurities of which

(a) HDS-1

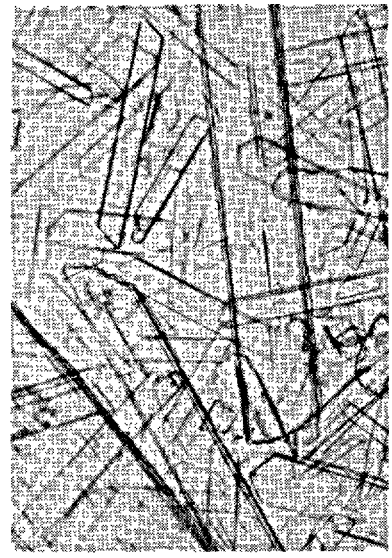

(c) HDS-3

(b) HDS-2

(d) HDS-4

Photo 1. ***Optical microphotographs of phosphogypsum.*** **(×125).**

are impossible to be removed by a single washing with water or lime water.

Table 4 shows the both lattice parameters of dicalcium phosphate dihydrate ($CaHPO_4 2H_2O$) and gypsum ($CaSO_4 2H_2O$) (36). Maki and Suzukawa (37), using infrared spectroscopy, reported that phosphogypsum showed, besides the absorption spectrum of gypsum, weak absorption at 1015 cm^{-1} and 837 cm^{-1} in the related characteristic absorption bands of HPO_4^{--} (Fig. 1). From the study on the absorption of the system $CaSO_4 2H_2O$–$CaHPO_4 2H_2O$, these displacements can be ascribed to the formation of the solid solution of gypsum with dicalcium phosphate dihydrate equivalent to the amount of P_2O_5 in the

Table 4. *Lattice constant and space group of gypsum and dicalcium phosphate dihydrate.*

	$CaSO_4 2H_2O$	$CaHPO_4 2H_2O$
a	5.68 Å	5.812 Å
b	15.18 Å	15.180 Å
c	6.52 Å	6.239 Å
β	118°23′	116°25′
S.G.	I2/a	I2/a, 1a

(e) HD–1

(g) HD–4

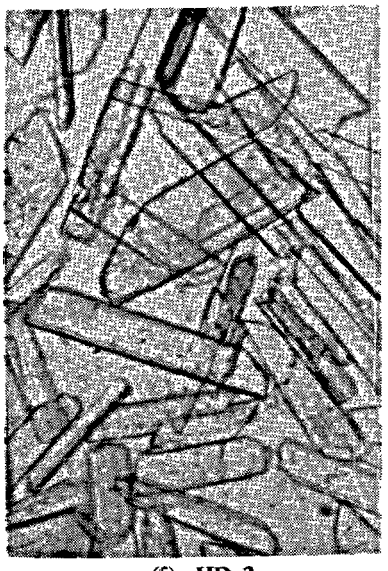

(f) HD–2

(h) HD–3

Photo 1. *Optical microphotographs of phosphogypsum.* (×125).

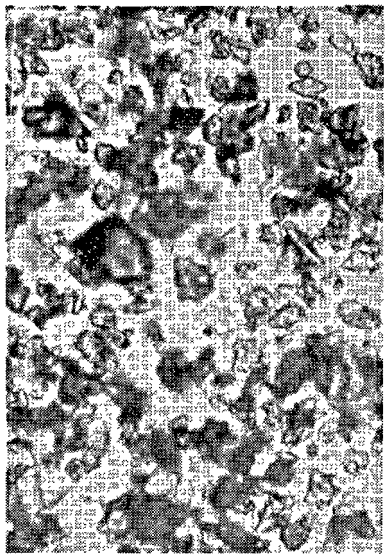

(i) D–1

Photo 1. *Optical microphotographs of phosphogypsum* (×125).

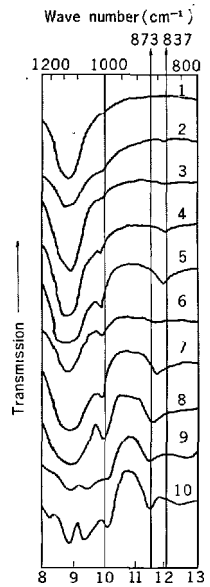

Fig. 1. *Infrared spectra of the solid solutions of system* $CaSO_4 \cdot 2H_2O$–$CaHPO_4 \cdot 2H_2O$.
(1) $CaSO_4 \cdot 2H_2O$ (2) By-product gypsum. (3) $CaSO_4 \cdot 2H_2O$ (95mol%)–$CaHPO_4 \cdot 2H_2O$ (5mol%) solid solution. (4) 90–10 (mol%) ss. (5) 80–20 (mol%) ss. (6) 70–30 (mol%) ss. (7) 60–40 (mol%) ss. (8) 50–50 (mol%) ss. (9) 20–80 (mol%) ss. (10) $CaHPO_4 \cdot 2H_2O$.
ss.: solid solution.

crystal lattice of phosphogypsum. Recent work by Dahlgren (38) also indicates that the amounts of HPO_4^{--} substituted in the crystal lattice of phosphogypsum vary with changing the concentrations of phosphoric acid and sulfuric acid during the operation of the wet process.

Kusano (33, 34, 39), through the measurement of average molecular weight, the infrared abosrption spectra, the detection of functional radicals and the spot test proposed the chemical structure of organic substance in phosphogypsum. Namely, he got the acidic and neutral substance by treating with sodium hydroxide the matters extracted from phosphogypsum by ether and ethanol. The former is a family of carbonic acids. The latter is a family of aliphatic ketons. The number of carbon atoms in a molecule of each compound is approximately from ten to thirty-five. Fig. 2 shows the infrared absorption curve of organic matter extracted from phosphogypsum by ether. The absorptions at 1710 cm^{-1} and 2900 cm^{-1} indicate that $>C=O$ or $-\underset{\underset{OH}{|}}{C}=C$ and $-\underset{|}{CH}$ is respectively included in the structure of above substance.

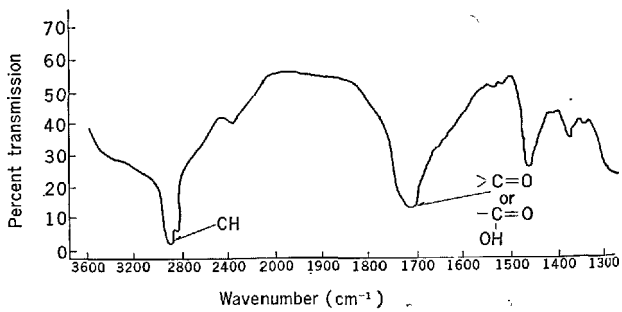

Fig. 2. *Infrared absorption curve of organic substance extracted from phosphogypsum by ether.*

Analytical Procedure of the Impurities in Phosphogypsum

Gypsum contained in cement enters into water immediately after cement comes contact with water and then reacts with the components of cement. How the impurities of chemical gypsum affect the hydration of portland cement varies with the kinds, amounts and locations of impurities presenting in chemical gypsum. In order to estimate the effect of impurities on the hydration of portland cement, the appropriate analytical procedure for the impurities in phosphogypsum must be established.

The existing analytical procedure specified in JIS (40) lay some emphasis on the quantitative analysis of the main component of gypsum, such as CaO, SO_3, H_2O etc., but does not refer to the analysis of the impurities.

In large user of chemical gypsum, such as manufacturer of portland cement, gypsum plaster and

gypsum board, the arbitrary procedures devised by themselves have been used for analysis of the impurities in phosphogypsum. Some results obtained by these procedures indicated that the exact distribution of the impurities in phosphogypsum is not shown frequently and that the analytical procedures are also unfavorable.

In order to improve the existing analytical procedure of the impurities in phosphogypsum, Murakami (35), considering the varieties of crystals of phosphogypsum as illustrated in Photo 1, assumed that the impurities are in the following states; adhering to the surface of crystals of phosphogypsum, settling in the space among crystals of the agglomerated phosphogypsum, solid-soluting in the crystal lattice of phosphogypsum, and remaining in undecomposed phosphate rocks. Then the items of analysis to be accomplished are shown as follows;

1) The water-soluble P_2O_5 adhered to the surface of phosphogypsum—Aw.P_2O_5
2) The water-insoluble F adhered to the surface of phosphogypsum—Ai.F
3) The water-soluble P_2O_5 substituted in the crystal lattice of phosphogypsum —Ss.P_2O_5
4) Total P_2O_5—T.P_2O_5
5) Total F—T.F

Analytical Procedure

Samples of phosphogypsum must be previously pulverized under 325 mesh.

Aw.P_2O_5 (Sum of the water-soluble phosphates, such as phosphoric acid, monocalcium phosphate and dicalcium phosphate).

The pulverized phosphogypsum (10 g) is boiled for thirty minutes with stirring in distilled water (300 ml) saturated with pure gypsum. Then, the resultant suspension is filtered. The soluble P_2O_5 in the filtrate is determined colorimetrically by the molybdovanadophosphoric acid method.

Ss.P_2O_5 (Phosphate in the crystal lattice of phosphogypsum).

The pulverized phosphogypsum (20 g) is boiled for thirty minutes with stirring in distilled water (200 ml) with acid mixture (5 ml) consisted of one volume of concd.HNO_3 and three volumes of concd.-HCl. The resultant suspension is filtered. The residual gypsum crystals are washed with distilled water and then dried. Gypsum (1 g: accurately weighed to mg unit.) with the crystal surface which was cleaned by the aforementioned treatment is completely dissolved in distilled water (200 ml) with concd.HCl (5 ml). Then, P_2O_5 in solution is determined colorimetrically, as in the case of Aw.P_2O_5.

Ai.F (Sum of the water-insoluble F, such as calcium fluoride and undecomposed phosphate rock).

The pulverized gypsum (10 g) is boiled for thirty minutes with stirring in distilled water (500 ml to 700 ml). Then, the resultant suspension is filtered. The residual gypsum is washed and dried. The water-soluble impurities adhered to the surface of crystals of phosphogypsum will be completely removed by these treatment. The resultant gypsum (0.1 g to 0.5 g: accurately weighed to mg unit) with cleaned surface is steam-distilled in the presence of sulfuric acid and the finely powdered silica.

The vaporized silicon fluoride enters into the sodium hydroxide solution and forms sodium silicofluoride. The water-soluble F in sodium silicofluoride is determined colorimetrically by the Th-alizaline or Th-neothorine method (41–49).

T.P_2O_5 (Sum of the water-soluble and water-insoluble phosphates, such as phosphoric acid, monocalcium phosphate, dicalcium phosphate and undecomposed phosphate rock).

The pulverized gypsum is dissolved in mixed acid solution consisted of one volume of concd.HNO_3 and three volumes of concd.HCl. The solution is completely evaporated on a water both or sand bath. The residual substance is dried until the residual HCl is removed completely. This substance is dissolved again in dilute HCl. P_2O_5 in the solution is determined colorimetrically as in the case of Aw. P_2O_5 (50–52).

T.F (Sum of the water-soluble and water-insoluble F, such as fluoric acid, sodium silicofluoride and undecomposed phosphate rock).

The pulverized gypsum (0.1g to 0.5g: accurately weighed to mg unit) is steam-distilled in the presence of sulfuric acid and finely powdered silica. The subsequent procedures are similar to those of the analysis of Ai.F.

The results of chemical analysis of phosphogypsum using the aforementioned procedures are shown in Table 5. Each crystal of phosphogypsum HDS-1, 2 and 4 illustrated in Photograph 1 has the unagglomerated and relatively regular form. Therefore, when the filter cake which has been discharged from the filtration step of the wet process is simply washed again with water, the quantity of the impurities in the washed cake is reduced to under Aw.P_2O_5 0.05% and Ss.P_2O_5 0.2%. Furthermore, the thermal differential analysis of phosphogypsum was studied and its results are illustrated in Fig. 3. The endothermic curves of the first dehydration of phosphogypsums HDS-1 and 2 show a relatively regular profile which is

Table 5. *Chemical compositions of phosphogypsum*

(%)

								P_2O_5		F
	CaO	SO_3	T. P_2O_5	T.F.	H_2O	I.M.	Total	Aw.	Ss.	Ai.
HDS-1	31.52	43.85	0.20	0.15	20.35	2.48	98.55	0.05	0.16	0.05
HDS-2	31.10	43.88	0.19	0.19	20.79	2.90	98.86	0.05	0.15	0.13
HDS-3	31.31	43.48	0.52	1.09	21.32	2.17	99.86	0.32	0.17	0.65
HDS-4	33.55	45.17	0.18	0.06	20.82	0.88	100.66	0.02	0.11	0.01
HDS-5	34.86	43.97	0.28	0.65	20.77	0.29	100.82	0.00	0.20	0.60
HDS-7	33.31	46.94	0.21	0.01	—	0.75	—	0.03	0.19	—
HD -1	30.98	41.95	0.76	0.49	21.82	4.10	101.00	0.17	0.54	0.38
HD -2	32.45	43.93	0.28	0.36	20.46	1.16	98.64	0.06	0.16	0.18
HD -4	31.43	42.70	0.66	0.92	21.81	2.04	99.56	0.18	0.47	0.30
HD -5	31.81	45.42	0.46	0.46	—	5.72	—	0.05	0.40	—
D -1	30.74	42.50	0.89	0.88	21.77	2.63	99.41	0.18	0.60	0.54

I.M.: insoluble matters

Proposed procedure was used for analysis of impurities.

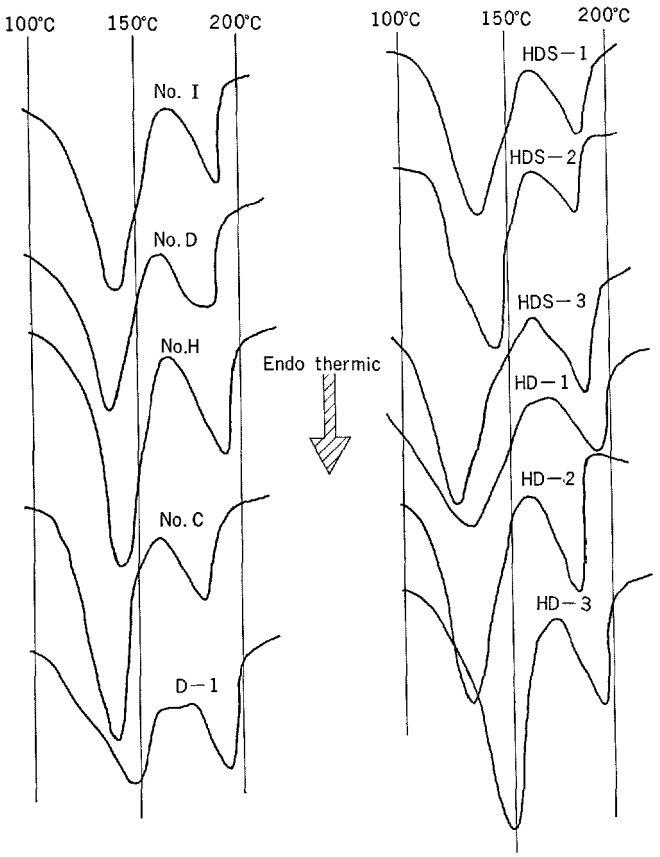

Fig. 3. *Differential thermal analysis of various chemical gypsums.*
Rate of heating : 2° C/min.
Weight of sample : about 0.7 g.
Thermo-couple : Pt-PtRh 13%.
Standard substance: α-Al_2O_3.

very similar to that of chemical gypsums No. I and H without impurities. On the contrary, major portions of crystals of phosphogypsums HD-1 and D-1 are agglomerated and, in which a large quantity of impurities is included. The quantities of their Aw.P_2O_5 and

Table 6. *Chemical compositions of some of fluorogypsums*

(%)

	CaO	SO_3	Total F	Insoluble F	H_2O	Insoluble residue
F-1	36.40	46.74	3.07	0.92	14.81	0.43
F-2	41.35	55.12	—	1.44	1.51	0.33
F-3	33.25	45.12	2.91	0.62	20.04	0.26

F-1: mixture of anhydrite and dihydrate
F-2: anhydrite
F-3: dihydrate

Ss.P_2O_5 are larger than those of phosphogypsums HDS-1, 2 and 4. The endothermic curves of their first dehydration are also broad and anomalous. In the results shown in Table 5, a value of "T.F minus Ai.F" means the water-soluble F, the amount of which is small in phosphogypsum HDS-1, 2 and 4 and large in phosphogypsum D-1. Phosphogypsum HDS-3, which was not washed once with water after removing from the filter step in the wet process, contains the large amounts of impurities. But, in HDS-3 made from the hemihydrate-dihydrate process, the amount of Ss.P_2O_5 is amsll as in the case of HDS-1. Phosphogypsum HDS-5 is the chemically treated HDS-3, in which the large portions of the water-soluble impurities have been neutralized and inactivated with milk of lime. The quantity of Aw. P_2O_5 and "T.F minus Ai.F" in HDS-5 is markedly small.

The results shown in Table 5 indicate evidently that there is a large difference among the wet processes of phosphoric acid manufacture and that the appearances of various phosphogypsums in optical microphotograph and the features of their first endothermic curves in differential thermal analysis are closely related to the quatity of impurities in phosphogypsum. Therefore, the author believes that the proposed procedure is suitable for analysis of the impurities in phosphogypsum.

Table 6 obtained by Murakami (41) shows the chemical compositions of fluorogypsums. Fluorogypsum is produced usually as an anhydrite by the production reaction shown in Table 1. Some portions of the original fluorogypsum are converted into a dihydrate by the hydration reaction while anhydrite is kept standing in the settling pond. Usually, fluorogypsum used for portland cement industry is the mixture of anhydrite and dihydrate. F-3 in Table 6 is a dihydrate which was industrially produced by the hydration of anhydrite in dilute sulfuric acid solution. The water-soluble F originated from the residual fluoric acid in fluorogypsum is different from that originated from sodium silicofluoride including in phosphogypsum. The influence of fluorogypsum on the hydration of portland cement will be later demonstrated.

Utilization of Chemical Gypsum for Portland Cement

Introduction

It has been about long years since phosphogypsum was first used for the manufacture of gypsum plaster and gypsum board in Japan. The first study of phosphogypsum for control of the setting of portland cement was attempted in 1956 by Takemoto, Ito and Suzuki. They examined the false set and the setting time of paste and the strength development of mortar. These paste and mortar were made from portland cement with each of such chemical gypsums as phosphogypsum, fluorogypsum, titangypsum and sodagypsum. When phosphogypsum produced from the dihydrate process was used, the impurities in phosphogypsum markedly retarded the set of paste and slightly lowered the strength of mortar at early stage on the hydration of portland cement. Consequently, they suggested that the setting period of portland cement can be prolonged by the retarding action of impurities into what is normally the hardening period. In addition, they also reported that the false set of paste caused by the dehydration of gypsum in cement and the aeration of cement is scarcely developed from protland cement containing phosphogypsum and sodagypsum.

The water-soluble P_2O_5 of phosphogypsum adheres to the surface of gypsum crystals and also subsitutes for SO_3 in the lattice of gypsum crystals. These water-soluble impurities enter gradually into aqueous phase of cement paste with dissolution of phosphogypsum and affect the hydration of portland cement. The water-soluble F tends to more markedly retard the setting of paste than in the case without it. Except for phosphogypsum, the effect of other chemical gypsums on the hydration of portland cement is similar to that of pure gypsum.

Takemoto, Kataoka and Suzuki (53, 54) and Yamaguchi (54) have deviced the special chemical treatment for regeneration of phosphogypsum containing a large quantity of the impurities. Phosphogypsum regenerated by this treatment did not injuriously affect the hydration of portland cement because all of the water-soluble impurities were turned into the insoluble and inactive compounds. Since this treatment pelletizes the powdered phosphogypsum, the supply of phosphogypsum to cement mill becomes easy (55). Kuzumi and Murasugi (56), in actual use of the regenerated phosphogypsum, reported that, in spite of the complete inactivation of the water-soluble impurities, the delayed set of paste accidentally occurred. The author suggests that this fact is probably due either to the residual impurities that are not neutralized or to the lime added over required for the neutralization of impurities. The results obtained by Yamaguchi (55) and Takemoto (54) et al. on the use of the regenerated phosphogypsum are shown in Table 7.

Yamaguchi, Kobayashi (57), Mori and Sudo (58) have used monocalcium phosphate, dicalcium phosphate and sodium silicofluoride as the representative water-soluble impurities in phosphogypsum and examined the influence of each impurity on the setting and the strength development of portland cement. In their experiments, each of chemical reagents corresponding to each impurity was added to portland cement in eqiuvalent quantity as found in phosphogypsum. The setting of paste is retarded markedly in proportion to the amount of reagent in cement. However, the three day-strength of mortar is not so affected, even when each chemical reagent is added to cement at relatively high concentrations. If a very large amount of each chemical reagent is added to portland cement, the development of three day-strength may be retarded. Kobayashi prepared four kinds of so called "artificial gypsum" containing water-soluble P_2O_5 in substitution for SO_3 in the crystal lattice of gypsum. The quantities of P_2O_5 in them are 0.2%, 0.5%, 1.0% and 2.0%. The retarding action of these artificial gypsum with P_2O_5 substituted in the lattice is stronger than that of gypsum with P_2O_5 which adhered to the crystal surface.

As mentioned above, hitherto, phosphogypsum

Table 7. *Setting time and mortar strength of cements containing the reproduced phosphogypsum*

Gypsum used for cement				Setting of cement			Mortar strength of cement					
		Method of treatment for gypsum		W/C %	Initial hr.-min.	Final hr.-min.	Bending strength (kg/cm²) 1d.	3d.	7d.	Compressive strength (kg/cm²) 1d.	3d.	7d.
Phosphogypsum	Original	Untreated		23.2	6.25	7.45	10.1	32.0	44.8	29	129	245
		Washing with water		23.5	2.30	3.50	10.0	33.2	45.0	30	130	244
		Mixing with 4% $Ca(OH)_2$ milk		23.4	3.00	4.20	9.9	32.4	46.2	28	129	240
	Reproduced	Temp. of calcination (°C)	Matter mixed with gypsum after calcination									
		150	4% $Ca(OH)_2$ milk	23.4	1.52	2.53	—	—	—	—	—	—
		200	4% $Ca(OH)_2$ milk	23.4	1.53	2.52	14.0	23.0	46.3	36	130	245
		150	4% $Ca(OH)_2$ milk with 0.4% NaOH	23.4	1.51	2.50	—	—	—	—	—	—
		200		23.5	1.50	2.43	—	—	—	—	—	—
		300	4% $Ca(OH)_2$ milk	23.3	1.45	2.45	—	—	—	—	—	—
Natural gypsum		—		23.5	1.45	2.40	13.8	33.8	44.5	35	131	241

has been used for control of the setting time of portland cement only in Japan. Recently, Lejsek (59) in Czeckoslovakia has reported a similar results with Japanese investigator's on his study of the utilization of phosphogypsum.

In view of above results, only phosphogypsum among chemical gypsums has some amounts of the impurities harmfully affected the hydration of portland cement. Other chemical gypsums do not have any impurities which are likely to cause trouble on their utilization. However, their productions are far less than phosphogypsum.

A patent about making the super-sulfate cement in which phosphogypsum is used as a main component has been licenced in Germany (60).

In this chapter, the mechanism and the effective protection methods of the retarding action of phosphogypsum on the hydration of portland cement will be investigated.

It is now well known that the setting retardation is the most characteristics action of phosphogypsum and largely dependent upon the amounts, kinds and locations of impurities in phosphogypsum. If it is assumed that the retarding action is caused by the temporary suppression of the hydration with the formation of the insoluble compounds as protective coatings on the surface of cement grains, the setting time will be shortened by agitation for a longer time than specified in JIS. Namely, the protective coatings are probably consist of the reaction products between the impurities of phosphogypsum and the compounds of cement. Therefore, it is suggested that the prolonged agitation of paste or mortar is a suitable method for destroying the coatings.

Assuming that the hydration of portland cement at early stage is a chemical process predominatingly, it will be expected that the retarding action may be increased at lower temperature.

Natural gypsum produced in Japan contain, in general, a relatively large amount of clay minerals and their average SO_3 content are about 30%. On the other hand, the SO_3 content of most of chemical gypsums is usually 40% to 45%. However, chemical gypsum is generally produced in a state of powder. Such discrepancies in the feature between natural and chemical gypsum indicate that there are many important problems which should be newly investigated for the use of chemical gypsums. These problems are the grindability of cement together with chemical gypsum, the fineness of the resultant cement, the dehydration characteristics of chemical gypsum and the setting character of the resultant cement.

On the study of mechanism of the setting retardation caused by the impurities of phosphogypsum, it should be noted that phosphogypsum usually contains several impurities at the same time. Therefore, on understanding the retarding action, it is necessary to investigate the effect of each single impurity on the hydration of cement in order to exclude the complexity resulted from the multiple impurities.

Little has also been demonstrated that which of cement clinker minerals is attacked by the impurities and causes the setting retardation of portland cement.

In the last section of this chapter, the mechanism

retarding action on the hydration of portland cement will be explained with referencing to the results of the studies on the heat liberation during the hydration, the change of specific surface area of the hydration products measured by the adsorption of water vapor and on the elecrton microscopic observation of the hydrating particles of cement.

Practical Methods for Removal of the Impurities in Phosphogypsum

When phosphogypsum is used as gypsum for control of the setting time, it is necessary that the impurities of phosphogypsum are reduced as much as possible. In other words, phosphogypsum used for this purpose should be such that the impurities included in phosphogypsum are easily removed by a simple washing with water. In view of aforementioned fact, it can be said that the industrial success of the hemihydrate-dihydrate process and the utilization of phosphogypsum by-produced from that process is very significant in Japan. Phosphogypsum by-produced from the dihydrate process must be chemically treated in order to be used for control of the setting. The chemical treatment proposed by Yamaguchi and Takemoto is an appropriate one for this purpose. There are two suitable treatments for removing or inactivating the impurities of phosphogypsum produced from the hemihydrate-dihydrate process. One method is to obtain phosphogypsum, such as HDS-1, containing only the small amounts of impurities through vigoruos washing of the filter-cake of phosphogypsum which was discharged from the filter step of the wet process, while it is transported to the storage tank by the water stream. The other method is practiced at place where the sufficient quantity of water cannot be provided for washing the filter cake. Namely, Hanada (61) neutralized the water-soluble impurities in filter-cake of phosphogypsum, such as HDS-3, with milk of lime and consequently got phosphogypsum containing less amounts of impurities, such as HDS-5. When it is indispensable to minimize the effects of even small amounts of the impurities in phosphogypsum, or when it is allowed for using only a small quantity of phosphogypsum containing a large amount of impurities, the mixture containing a large amount of natural or chemical gypsums which do not contain the harmful impurities are usually used by Hanada (61).

Physical Properties of Portland Cement Containing Phosphogypsum

Setting Time and Strength Development of Portland Cement Containing Phosphogypsum

The results of the studies by Miyazawa (62), using two normal portland cement A and B (total SO_3 content 1.6%) which were mixed with each of phosphogypsums listed in Table 8, indicate that the setting time of paste is markedly retarded when portland cement is mixed with phosphogypsum No. 2 containing a larger quantity of water-soluble F than with other phosphogypsums in Table 8 (Table 9). Table 10 shows that the three day-strength of mortar containing these phosphogypsums is slightly lowered in proportion to the amount of impurities in phosphogypsum. Tables 12 and 13 are the results of tests on the setting and the development of mortar strength that was undertaken by Hanada (63) with three kinds of blast-furnace slag cement (total SO_3 content 1.8%) cntaining each kind of phosphogypsums which were neutralized with milk of lime and not. Table 11 shows the chemical compositions of the both phosphogypsums. Table 12 shows that, using the mixture of natural gypsum and

Table 8. *Chemical compositions of phosphogypsum*

(%)

No.	H_2O	c.w.	CaO	SO_3	P_2O_5				F	
					a	b	c	total	d	e
1	4.0	19.2	31.9	45.6	0.015	0.189	0.051	0.255	0.032	0.019
2	4.5	19.0	32.3	45.6	0.038	0.259	0.028	0.325	0.304	0.265
3	5.0	19.0	32.5	45.9	0.016	0.261	0.063	0.340	0.058	0.020
4	4.0	18.6	32.5	46.0	0.016	0.124	0.020	0.160	0.028	0.014

c.w.: combined water.
a : water-soluble P_2O_5 adhered to surface of gypsum crystals.
b : substituting P_2O_5 in crystal lattice of gypsum.
c : insoluble P_2O_5.
d : total F.
e : water-soluble F adhered to surface of gypsum crystals.

phosphogypsum, the retarding action of the untreated phosphogypsum is effectively alleviated. The results on the development of mortar strength given in Table 13 emphasizes that the appreciable reduction in the three day-strength is not observed as far as the quantity of impurities remains in the range of that contained in phosphogypsum used.

Table 9. *Setting time of portland cement containing natural gypsum and phosphogypsum*

Cement—A			Cement—B		
	Initial	Final		Initial	Final
Natural gypsum	100 (3–00)	100 (4–15)	Natural gypsum	100 (2–20)	100 (3–50)
P.G. No. 1	106	122	P.G. No. 1	118	104
P.G. No. 2	186	175	P.G. No. 2	164	152
P.G. No. 3	125	142	P.G. No. 3	132	115
P.G. No. 4	127	139	P.G. No. 4	136	111

P.G.: phosphogypsum.

In this table, numbers without parentheses are relative value of that of other paste when the setting time of paste with natural gypsum is described as 100. Also, numbers in parentheses are real value of setting time.

Effect of Prolonged Mechanical Agitation over Three Minutes with Hand Mixing

Since the hydration of portland cement tends to be accelerated by agitation, it is suggested that the prolonged agitation will tend to prevent the retarding action on the setting of paste with posphogypsum. In transportation of the ready mixed concrete, the prolonged agitation of concrete has already been in practice. Hanada (63) prepared nine kinds of portland

Table 11. *Chemical compositions of phosphogypsum*

(%)

	SO_3	T.P.	W.P.	T.F.	W.F.
P.G.	45.4	0.27	0.15	0.93	0.12
P'.G.	44.3	0.28	0.02	0.94	0.008

P.G. : phosphogypsum.
P'.G.: phosphogypsum neutralized with milk of lime
T.P. : total P_2O_5.
W.P.: water-soluble P_2O_5.
T.F. : total F.
W.F.: water-soluble F.

Table 10. *Physical properties of two cements containing natural gypsum and phosphogypsum*

		Bending strength (kg/cm²)			Compressive strength (kg/cm²)		
Cement	Gypsum	3 days	7 days	28 days	3 days	7 days	28 days
A	Natural gypsum	100 (32.9)	100 (49.0)	100 (69.6)	100 (126)	100 (232)	100 (392)
	No. 1	101	100	104	100	99	102
	No. 2	95	103	108	96	102	108
	No. 3	93	102	104	94	96	104
	No. 4	92	104	108	92	98	100
B	Natural gypsum	100 (33.2)	100 (49.3)	100 (70.1)	100 (140)	100 (245)	100 (403)
	No. 1	90	99	101	92	94	99
	No. 2	94	98	103	91	94	99
	No. 3	100	106	98	99	98	98
	No. 4	103	104	100	101	98	100

In this table, numbers in parentheses are real value of mortar strength. Numbers without parenthesis are relative value.

Table 12. *Setting time of three blastfurnace slag cements containing natural gypsum and phosphogypsum*

Blastfurnace slag cement	Setting	P.G. hr.-min.	N.G. hr.-min.	25P'.G. 75N.G.	50P'.G. 50N.G.	P'.G.
Slag (20)	Initial	3–50	(100) 2–30	(103)	(110)	(147)
Cement (80)	Final	4–45	(100) 3–20	(105)	(105)	(141)
Slag (45)	Initial	4–45	(100) 3–10	(108)	(111)	(150)
Cement (55)	Final	5–45	(100) 4–10	(108)	(112)	(144)
Slag (35)	Initial	5–25	(100) 3–40	(115)	(124)	(167)
Cement (65)	Final	7–00	(100) 4–50	(107)	(115)	(163)

N.G.: natural gypsum.

Numbers without parentheses are real value of the setting time of pastes. Numbers in parenthesis are relative value. Numbers in parentheses in the first column are the proportion of each component of blastfurnace slag cements.

Table 13. *Development of mortar strength of blastfurnace slag cement with natural gypsum and phosphogypsum*

	N.G.	P.G.	Bending strength 3 days	Bending strength 7 days	Bending strength 28 days	Compressive strength 3 days	Compressive strength 7 days	Compressive strength 28 days
Slag (20) Cement (80)	10	0	100 (32)	100 (49)	100 (72)	100 (125)	100 (230)	100 (420)
	7.5	2.5	106	98	103	103	100	100
	5	5	106	100	101	102	101	100
	0	10	116	106	99	106	101	98
Slag (45) Cement (55)	10	0	100 (27)	100 (41)	100 (73)	100 (95)	100 (190)	100 (421)
	7.5	2.5	104	98	100	98	95	100
	5	5	96	98	96	95	97	102
	0	10	100	100	96	100	96	103
Slag (35) Cement (65)	10	0	100 (24)	100 (39)	100 (68)	100 (80)	100 (178)	100 (380)
	7.5	2.5	88	98	100	98	99	99
	5	5	96	100	99	104	104	100
	0	10	92	95	99	98	100	99

In this table, numbers in parentheses in the first column are the proportion of each component of blastfurnace slag cements.
Numbers in other parentheses are real value of mortar strength.
Numbers without parentheses are relative value.
Unit of mortar strength is kg/cm².
Numbers in the second column are the proportions of each component of the gypsum mixture contained in cements.

Table 14–1. *Chemical compositions of various gypsums*

(%)

	H_2O	C.W.	SiO_2	Al_2O_3	Fe_2O_3	CaO	MgO	SO_3	Total
N.G.	0.02	16.85	13.48	2.62	0.54	25.64	5.21	34.76	99.12
P.G.	0.01	20.15	4.00	0.01	0.27	29.73	0.04	45.70	99.91
P'.G.	0.02	20.30	2.30	0.07	0.21	31.87	0	45.47	100.24
W.G.	0.06	18.33	6.46	0.74	0.18	29.48	0.11	44.74	100.10
A.G.	0.15	19.80	2.96	0.14	0.24	31.80	0.44	44.32	100.20

C.W.: combined water.
N.G.: natural gypsum.
P.G.: phosphogypsum.
P'.G.: phosphogypsum neutralized with milk of lime.
W.G.: chemical gypsum by reaction of lime with waste sulfuric acid.
A.G.: chemical gypsum No. K in table 1.

Table 14–2. *Impurities of phosphogypsum*

(%)

	T.P.	W.P.	T.F.	W.F.
P.G.	0.30	0.11	0.72	0.20
P'.G.	0.31	0.02	0.80	0.03

T.P.: total P_2O_5
W.P.: water-soluble P_2O_5
T.F.: total F
W.F.: water-soluble F

cement as well as nine kinds of blastfurnace slag cement containing five kinds of gypsums shown in Table 14 and measured the setting time of paste which was mechanically agitated by Hobert mixer for longer time, such as 3, 5, 7, 10 and 15 minutes, than specified in JIS. The results shown in Tables 15 and 16, indicate that the mechanical agitation, even for three minutes, tends to more accelerate the setting than the agitation with hand, and that also the longer the mechanical agitation the shorter the setting time. Similarly, Miyazawa (64) studied the influence of the agitation time on the flow and strength development of mortar containing several phosphogypsums as shown in Table 17. The SO_3 content in the prepared protland cement was 1.5%, 3.0% and 5.0% and the duration of mechanical agitation was 3, 5 and 30 minutes. The results illustrated in Fig. 4 reveal that, except for the case of a relatively high SO_3 content, such as 5.0%, the mechanical agitation within thirty minutes is independent of the strength development of mortar. But, the fluidity of mortar is considerably reduced by the prolonged agitation. Murakami (65) reported that the strength development of mortar containing phosphogypsum or even pure natural gypsum is markedly lowered by the prolonged agitation over thirty minutes. This results seem to support the Verbeck's hypothesis that the excess agitation of a partially hydrated concrete mixture leads to a weak product.

Effect of Increased Addition of Phosphogypsum

Aside from phosphogypsum, an attempt of adding a

Table 15. *Setting time of paste of portland cement with various gypsums (Mechanical agitation by Hobert mixer)*

Gypsum	W/C (%)	Initial time (hr.-min.)						Final time (hr.-min.)					
		JIS	Mechanical mixing					JIS	Mechanical mixing				
		3 min.	3 min.	5 min.	7 min.	10 min.	15 min.	3 min.	3 min.	5 min.	7 min.	10 min.	15 min.
N.G.	25.4	1–50	1–39	1–37	1–40	1–29	1–33	3–00	2–48	2–42	2–42	2–07	2–31
P.G.	24.8	3–15	3–22	3–15	3–01	3–00	3–00	5–35	4–21	4–15	4–11	4–10	4–07
P'.G.	24.3	2–30	2–29	2–32	2–23	2–13	2–11	3–35	3–18	3–15	3–23	3–14	3–02
W.G.	24.0	1–50	1–39	1–34	1–30	1–30	1–20	3–05	2–42	2–33	2–20	2–23	2–15
A.G.	24.0	1–35	1–43	1–36	1–32	1–32	1–32	2–50	2–55	2–48	2–40	2–32	2–19
P.G. N.G. (1:1)	25.0	2–30	2–34	2–31	2–31	2–27	2–23	4–05	3–43	3–35	3–31	3–30	3–28
P'.G. N.G. (1:1)	24.5	1–50	1–56	1–56	1–51	1–44	1–32	3–05	2–55	2–49	2–44	2–41	2–50
W.G. N.G. (1:1)	24.6	1–40	1–43	1–37	1–35	1–35	1–38	2–50	2–33	2–29	2–25	2–25	2–25
A.G. N.G. (1:1)	24.6	1–25	1–25	1–19	1–21	1–21	1–15	2–45	2–24	2–18	2–17	2–17	2–10

W/C: water-cement ratio
JIS: JIS R 5201 (1953)., agitation with hand for three minutes

Numbers in parenthesis of the first column are the proportions of each component of the gypsum mixture contained in cement.

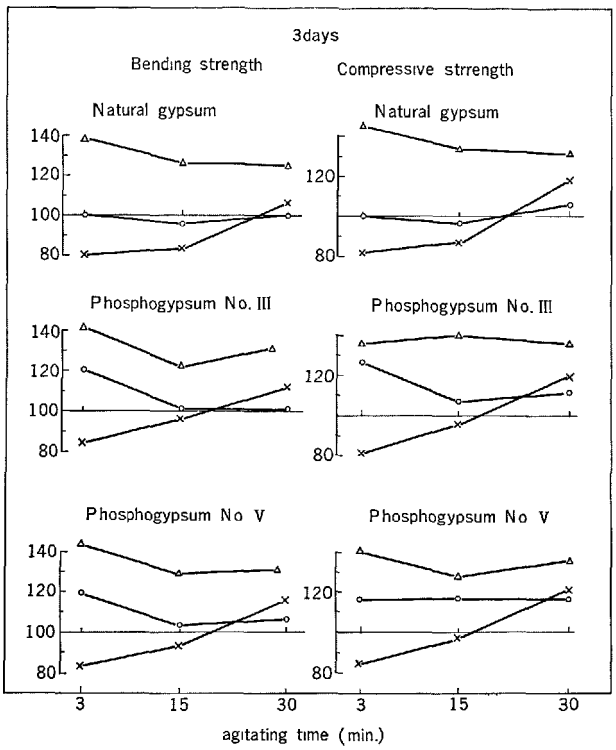

Fig. 4-1. *Three day-strength of mortar agitated over three minutes.*
—○—: SO_3 1.5%.
—△—: SO_3 3.0%.
—×—: SO_3 5.0%.
Ordinate is ratio of mortar strength, in which the strength of mortar (agitating for 3 minutes) containing natural gypsum 1.5% was written as 100.

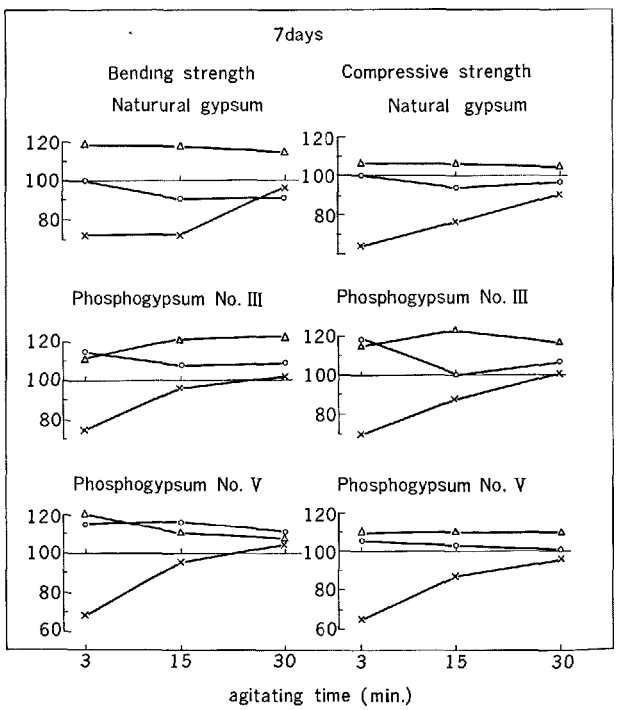

Fig. 4-2. *Seven day-strength of mortar agitated over three minutes.*
—○—: SO_3 1.5%.
—△—: SO_3 3.0%.
—×—: SO_3 5.0%.
Ordinate is ratio of mortar strength, in which the strength of mortar (agitating for 3 minutes) containing natural gypsum 1.5% was written as 100.

larger amount than the present amount of gypsum in portland cement (under total SO_3 content 2.5%) has been discussed in relation to the optimum quantity of gypsum, the false set caused by plaster set, the development of strength, the reduction of contraction and the supply-demand relationship of gypsum. In this chapter, the influence of impurities, which increase in portland cement in proportion to the quantity of

Table 16. *Setting time of paste of blastfurnace cement with various gypsums (Mechanical agitation by Hobert mixer)*

Gypsum	W/C (%)	Initial time (hr.-min.)						Final time (hr.-min.)					
		JIS	Mechanical mixing					JIS	Mechanical mixing				
		3 min.	3 min.	5 min.	7 min.	10 min.	15 min.	3 min.	3 min.	5 min.	7 min.	10 min.	15 min.
N.G.	28.8	2–50	2–25	2–16	2–21	2–20	2–19	4–10	3–51	3–28	3–31	3–29	3–29
P.G.	28.0	5–10	4–40	4–35	4–39	4–38	4–26	6–45	6–07	6–10	6–17	6–10	6–08
P'.G.	27.0	4–30	4–22	4–18	4–15	4–06	4–00	5–40	5–39	5–34	5–38	5–21	5–17
W.G.	27.2	2–45	2–55	2–49	2–44	2–32	2–43	4–30	4–03	4–18	3–59	3–56	4–00
A.G.	28.0	3–10	2–36	2–36	2–43	2–35	2–36	4–35	4–27	4–23	4–29	4–18	4–09
P.G. N.G. (1:1)	28.1	4–05	3–55	3–46	3–40	3–39	3–28	5–55	5–14	5–10	5–05	4–56	4–52
P'.G. N.G. (1:1)	28.0	2–55	3–05	2–59	2–55	2–49	2–45	4–50	4–27	4–20	4–15	4–06	4–04
W.G. N.G. (1:1)	27.9	2–35	2–41	2–23	2–23	2–20	2–18	4–35	3–58	3–51	3–42	3–40	3–46
A.G. N.G. (1:1)	28.0	2–25	2–23	2–12	2–05	2–00	1–58	4–25	3–58	3–47	3–38	3–29	3–26

W/C: water-cement ratio
JIS: JIS R 5201 (1953)., agitation with hand for three minutes

Numbers in parentheses of the first column are the proportion of each component of the gypsum mixture contained in cement.

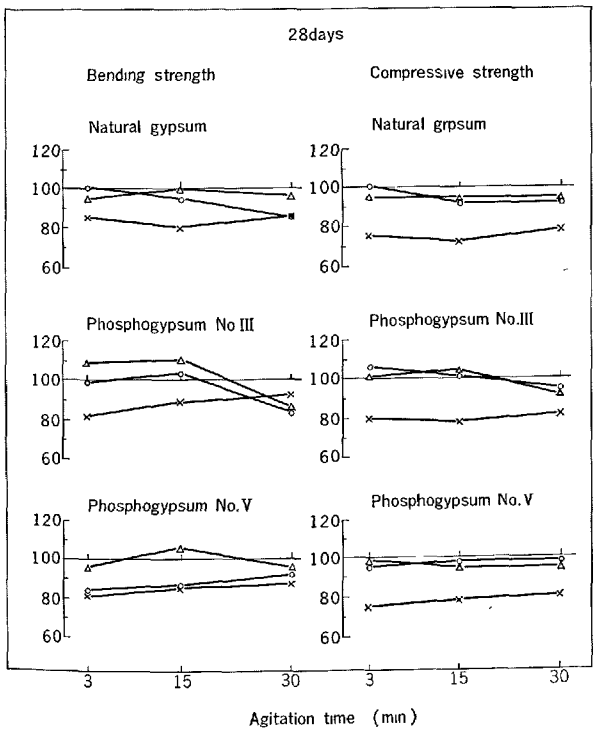

Fig. 4–3. *Twenty-eight day-strength of mortar agitated over three minutes.*
—○—: SO_3 1.5%.
—△—: SO_3 3.0%.
—×—: SO_3 5.0%.
Ordinate is ratio of mortar strength, in which the strength of mortar (agitating for 3 minutes) containing natural gypsum 1.5% was written as 100.

phosphogypsum, on the setting and the strength developmentof portland cement will be investigated.

Miyazawa (64) prepared several portland cements containing phosphogypsum with the impurities as

Table 18. *Setting time of paste with various quantities of gypsum*

	SO_3%	w/c%	Initial hr.-min.	Final hr.-min.
Natural gypsum	1.6	25.2	2–45 (100)	3–50 (100)
	2.0	25.2	2–15 (82)	3–30 (91)
	2.9	25.4	2–20 (85)	3–30 (96)
	3.9	26.6	2–30 (90)	3–40 (96)
	4.9	25.6	2–40 (97)	3–55 (102)
Phospho-gypsum No. I	1.5	25.2	2–30 (91)	3–40 (96)
	1.9	25.2	3–00 (109)	4–10 (109)
	2.9	25.2	2–40 (97)	3–45 (98)
	3.9	25.2	4–00 (145)	5–25 (141)
	4.8	25.0	4–20 (158)	6–15 (163)
Phospho-gypsum No. II	1.5	25.2	3–50 (139)	5–20 (139)
	2.0	25.2	3–35 (135)	5–05 (133)
	3.0	25.2	4–10 (152)	6–05 (133)
	4.0	24.8	4–53 (178)	6–23 (167)
	5.0	25.0	4–25 (161)	6–05 (159)
Phospho-gypsum No. III	1.6	25.6	3–20 (121)	4–30 (117)
	2.0	25.2	4–02 (147)	5–35 (146)
	3.0	25.2	5–30 (200)	7–05 (185)
	4.0	25.2	5–45 (209)	7–30 (196)
	4.8	25.2	5–50 (212)	8–30 (222)
Phospho-gypsum No. IV	1.5	24.8	5–45 (209)	7–55 (206)
	2.0	24.6	7–00 (254)	9–20 (244)
	3.0	24.6	9–50 (358)	14–10 (370)
	4.0	24.8	10–40 (388)	15–10 (396)
	5.0	24.8	10–30 (382)	15–15 (398)

w/c: water-cement ratio

In this table, setting time without parentheses is real value. Numbers in parentheses are relative value, when the setting time of paste with natural gypsum (SO_3 content 1.6%) is described as 100.

in Table 17. The SO_3 contents in the prepared cements are 1.5%, 2.0%, 3.0%, 4.0% and 5.0%. The results shown in Table 18 indicate that, for example, the setting ime in the case of SO_3 content of 2% is prolonged in comparison to natural gypsum and that the degree of prolongation is in the order of phosphogypsum No. IV > III > II > I. Therefore, it can be said that the larger the quantity of phosphogypsum

Table 17–1. *Chemical compositions of phosphogypsum*

	C.W.	CaO	SO_3	Total	$\frac{C.W.}{SO_3}$	$\frac{CaO}{SO_3}$	f. CaO
Phospho-gypsum No. I	18.14%	32.33%	45.66%	96.13%	0.397	0.708	0 %
Phospho-gypsum No. II	17.15	34.07	40.71	91.93	0.421	0.831	0.60
Phospho-gypsum No. III	17.60	32.39	44.25	94.24	0.398	0.732	0
Phospho-gypsum No. IV	18.31	31.83	42.64	92.76	0.430	0.747	0
Phospho-gypsum No. V	18.80	32.39	44.19	95.38	0.425	0.733	0
Natural gypsum	17.88	31.31	44.07	93.26	0.406	0.710	0

C.W.: combined water
f. CaO: free lime

Table 17–2. *Impurities of phosphogypsum*

	P_2O_5 (%)				F (%)	
	a	b	c	Total	d	e
Phosphogypsum No. I	0.012	0.223	0.037	0.272	0.10	0.05
Phosphogypsum No. II	0.002	0.007	0.647	0.656	1.05	0.08
Phosphogypsum No. III	0.051	0.129	0.175	0.355	1.06	0.19
Phosphogypsum No. IV	0.029	0.438	0.095	0.563	0.85	0.39
Phosphogypsum No. V	0.084	0.068	0.128	0.280	0.57	0.20
Natural gypsum	0.001	0.000	0.003	0.004	0.07	0.00

a: water-soluble P_2O_5 adhered to surface of gypsum crystals
b: substituting P_2O_5 in crystal lattice of gypsum
c: insoluble P_2O_5
d: total F
e: water-soluble F adhered to surface of gypsum crystals

in cement, the longer is the setting time of cement. Phosphogypsum No. IV containing the largest quantity of impurities of all the other phosphogypsums in Table 17 shows a strong retarding action on the setting of cement. The results given in Table 19 show that the three day-strength of mortar containing phosphogypsum, the total SO_3 content of which is in the range of 1.5% to 3.0%, is not less than that of the mortar containing natural gypsum. The addition of a large quantity of gypsum, such as total SO_3 content 5.0%, causes the expansion of the hydrating cement to result in markedly lowered mortar strength regardless of using phosphogypsum or not. Furthermore, Miyazawa reported that the length change of the mortar after drying is reduced as the quantity of gypsum in cement increases and that the length change of the mortar is not closely related to the quantity of impurities of phosphogypsum within the limit of his experiment. The expansion-contraction test of mortar was made using the test procedure J.C.E.A.S.H (1962) under the following conditions: curing for five days in water at 20°C followed by standing for thirteen weeks in air with the relative humidity of 44%.

Mixing and Curing at Relatively Higher and Lower Temperature Than 20°C

Assuming that the hydration of portland cement at its early stage is predominated by chemical reaction, it is expected that the time of set is markedly affected by temperature during the mixing or curing of paste and mortar. In practice in cold seasons, it is feared that, on account of the decreased rate of the hydration reaction at lower temperature, the setting period of cement containing phosphogypsum can be prolonged into what is normally the hardening period. Hanada (63) prepared nine kinds of portland cements and nine kinds of blastfurnace cements containing various gypsums, namely, a natural gypsum, two kings of phosphogypsums, two kinds of chemical gypsums and four kinds of the mixtures of two of them. Then, he measured the time of set of pastes and the strength develoment of mortars at each temperature of 5, 10, 20, 30 and 40°C. Tables 20 and 21 show the results of the time of set, in which the time of set of paste containing natural gypsum is written as 100 and those of paste containing other gypsums are shown with a

Table 19. *Mortar strength of portland cement containing various quantities of natural gypsum and phosphogypsum*

	SO_3 (%)	Flow	Bending strength kg/cm²				Compressive strength kg/cm²			
			3 days	7 days	28 days	91 days	3 days	7 days	28 days	91 days
Natural gypsum	1.5	100	100 (35.9)	100 (50.9)	100 (66.1)	100 (69.3)	100 (139)	100 (225)	100 (385)	100 (416)
	2.0	100	107	100	105	103	107	101	95	98
	3.0	100	125	107	95	98	118	103	92	95
	4.0	95	113	97	96	99	113	98	83	90
	5.0	94	71	64	86	96	71	62	74	88
Phospho-gypsum No. I	1.5	100	100 (35.0)	100 (51.2)	100 (64.0)	100 (67.5)	100 (134)	100 (237)	100 (381)	100 (412)
	2.0	100	107	103	103	100	110	100	96	96
	3.0	100	117	108	105	105	118	102	96	96
	4.0	96	110	104	98	102	118	96	88	90
	5.0	92	74	73	87	99	77	68	79	94
Phospho-gypsum No. II	1.5	100	100 (33.1)	100 (47.3)	100 (62.4)	100 (64.1)	100 (131)	100 (229)	100 (373)	100 (415)
	2.0	104	121	111	102	108	120	105	101	100
	3.0	102	129	124	109	108	128	107	95	94
	4.0	101	93	100	99	108	98	91	85	91
	5.0	98	73	64	83	95	71	52	70	84
Phospho-gypsum No. III	1.5	100	100 (31.9)	100 (48.7)	100 (65.5)	100 (67.5)	100 (122)	100 (221)	100 (370)	100 (403)
	2.0	97	108	102	101	100	106	102	99	99
	3.0	98	133	114	108	106	134	108	100	99
	4.0	95	113	106	98	96	120	99	91	95
	5.0	95	76	71	84	94	77	65	76	91
Phospho-gypsum No. IV	1.5	100	100 (28.9)	100 (42.7)	100 (62.2)	100 (63.8)	100 (116)	100 (194)	100 (368)	100 (405)
	2.0	101	128	116	106	102	125	107	99	99
	3.0	98	140	117	109	106	132	114	94	96
	4.0	97	90	92	84	99	94	92	79	89
	5.0	94	69	61	80	91	67	55	69	79

In this table, flow is written as relative value for that of paste with total SO_3 content 1.5%.
Numbers in parentheses are real value of mortar strength.
Numbers without parentheses are relative value of that of cement with other contents when mortar strength of cement with SO_3 1.5% is written as 100.

Table 20. *Setting time of paste of portland cement containing various gypsums*

	5°C			10°C			20°C			30°C			40°C		
	W/C	Initial	Final	W/C	Initial	Final	W/C	Initial	Final	W/C	Initial	Final	W/C	Initial	Final
N.G.	26.5	100 (3-05)	100 (5-30)	26.0	100 (1-30)	100 (2-20)	26.2	100 (1-30)	100 (2-45)	26.9	100 (1-00)	100 (1-45)	27.8	100 (1-00)	100 (1-30)
P.G.	23.8	206	199	24.0	283	254	24.5	300	236	25.2	284	248	25.9	234	239
P'.G.	23.8	100	117	23.8	150	157	24.2	167	145	25.0	158	152	25.6	150	150
W.G.	23.9	76	76	23.6	106	103	23.9	96	97	24.6	100	100	25.1	100	106
A.G.	25.0	103	109	25.0	133	118	25.2	133	130	25.8	125	129	26.6	142	128
N.G. + P.G. (1:1)	25.0	152	155	25.0	156	168	24.1	178	152	26.2	183	156	26.9	167	161
N.G. + P'.G. (1:1)	24.2	89	106	24.6	134	129	24.8	122	127	25.5	150	129	26.2	117	125
N.G. + W.G. (1:1)	24.6	81	85	24.8	106	107	24.8	95	103	25.8	117	109	26.5	100	106
N.G. + A.G. (1:1)	24.6	81	83	25.0	100	111	24.8	89	100	25.5	108	109	25.2	100	115

W/C: water-cement ratio (%)

Setting time (hr.-min.); Numbers in parentheses are real value of setting time.
Numbers without parentheses are relative value of that of paste containing various gypsums for the setting time (100) of paste with natural gypsum.
Numbers in parentheses of the first column are the proportions of each component of the gypsum mixture contained in cement.

relative value to the former. Both time for the initial and final set of paste with natural gypsum at 5°C tend to be two times as longer as the setting time at 20°C. However, it is not observed that, at lower temperature, the setting of paste containing phosphogypsum is more markedly retarded than that of paste without phosphogypsum. Such a tendency is observed in the case of blastfurnace slag cement as well as portland

cement. Table 22 shows the strength development of mortars made from the both cement at each temperature. In view of his results, regardless of whether natural gypsum is contained in cement or not, the strength development of mortar is relatively reduced by lowering the temperature, although the tendency that the lowering in curing temperature increases the retarding action of impurities on the strength development is not observed, even on the three day-strength.

Influence of Phosphogypsum on Properties of Concrete

In view of practical point, the properties of concrete made from portland cement containing phosphogypsum should be investigated in order to be related to those of pastes and mortars obtained by laboratory test. Hanada (63) prepared concrete from portland cement and blastfurnace slag cement containing various gypsums in Table 14 and showed, as in Tables 23 and 24, the change of slump of concrete from the time just after mixing concrete up to 150 minutes. The change of slump of concrete is scarcely affected by the quantity and the kind of impurities in gypsum. Consequently, it can be said that, within the limit of his experiment, the impurities in phosphogypsum do not exert any unfavorable effects on properties of

Table 21. *Setting time of paste of blastfurnace slag cement containing various gypsums*

	5°C			10°C			20°C			30°C			40°C		
	W/C	Initial	Final	W/C	Initial	Final	W/C	Initial	Final	W/C	Initial	Final	W/C	Initial	Final
N.G.	27.5	100 (5–00)	100 (8–50)	28.6	100 (2–20)	100 (3–40)	28.6	100 (2–25)	100 (4–05)	29.5	100 (1–55)	100 (2–55)	30.2	100 (1–40)	100 (2–35)
P.G.	26.5	168	172	26.8	231	193	28.1	194	177	28.2	196	174	29.0	180	158
P'.G.	26.8	165	164	27.0	208	173	27.2	184	172	28.1	187	157	28.6	165	155
W.G.	26.6	128	135	27.0	129	125	27.4	116	117	28.1	117	114	28.6	115	100
A.G.	26.4	105	123	27.0	121	118	27.4	106	114	27.8	100	103	28.2	105	94
N.G. + P.G. (1:1)	27.8	190	166	28.2	182	152	28.2	161	157	29.0	157	152	29.5	165	145
N.G. + P'.G. (1:1)	27.0	152	144	28.2	163	148	28.2	123	135	28.8	126	126	29.2	115	126
N.G. + W.G. (1:1)	26.8	99	115	28.1	129	125	28.1	103	115	28.9	113	109	29.2	100	97
N.G. + A.G. (1:1)	27.0	105	109	28.1	125	112	28.2	100	110	28.8	104	106	29.1	95	100

W/C: water-cement ratio (%)

Setting time (hr.-min.); Numbers in parentheses are real value of setting time.
Numbers without parentheses are relative value of that of paste containing various gypsums for the setting time (100) of paste with natural gypsum.

Numbers in parentheses of the first column are the proportions of each component of the gypsum mixture contained in cement.

Table 23. *Slump of concrete (Portland cement with various gypsums)*

	Slump (cm)						Ratio					
	3 min.	30 min.	60 min.	90 min.	120 min.	150 min.	3 min.	30 min.	60 min.	90 min.	120 min.	150 min.
N.G.	16.0	11.5	11.1	9.4	7.2	7.2	100	72	69	59	45	45
P.G.	17.1	9.0	8.5	5.5	5.5	5.0	100	53	50	32	32	29
P'.G.	16.5	13.8	12.0	9.7	8.1	6.7	100	84	73	59	49	41
W.G.	16.0	11.8	8.2	6.6	4.2	3.7	100	74	51	41	26	23
A.G.	16.7	14.1	7.1	4.8	3.7	3.3	100	84	43	29	22	20
P.G. + N.G. (1:1)	16.5	11.9	7.8	6.0	4.0	3.3	100	72	47	36	24	20
P'.G. + N.G. (1:1)	16.7	13.7	11.1	9.7	6.9	6.6	100	82	66	58	41	40
W.G. + N.G. (1:1)	16.5	14.0	7.6	7.2	5.6	5.3	100	85	46	44	34	32
A.G. + N.G. (1:1)	15.0	12.2	8.6	7.5	5.7	5.5	100	81	57	50	38	37

Numbers in parentheses of the first column are the proportion of each component in the mixture of natural gypsum and chemical gypsum added to cement.

The concrete in this table was prepared from portland cement with various gypsums 4%.

The proportion of aggregate and cement in the concrete mixture is as follows;

water-cement ratio 60%
sand-aggregate ratio 41.1%

Weight of each component of concrete (per $1m^3$)

cement	305 kg
sand	741 kg
aggregate	1106 kg
water	183 kg
total	2335 kg

Table 22. *Bending strength and compressive strength of portland cement and blastfurnace slag cement containing various gypsums*

(kg/cm²)

		3 days		7 days		28 days	
		Bending strength	Compressive strength	Bending strength	Compressive strength	Bending strength	Compressive strength
		5°C					
Portland cement	N.G.	14.6	45	32.2	124	52.6	333
	P.G.	12.1	34	30.2	118	66.5	336
	P'.G.	10.0	37	25.7	121	64.0	345
	W.G.	12.5	45	31.6	132	66.5	351
	A.G.	14.8	46	30.6	132	64.0	338
	P.G. + N.G. (1 : 1)	12.3	35	33.9	132	65	340
	P'G. + N.G. (1 : 1)	13.3	39	35.8	139	65	343
	W.G. + N.G. (1 : 1)	14.2	42	35.1	134	64	320
	A.G. + N.G. (1 : 1)	14.4	42	33.9	138	62	330
Blastfurnace slag cement	N.G.	8.8	25	23.4	74	48	212
	P.G.	7.8	23	19.5	68	47	212
	P'.G.	7.2	23	21.8	67	45	211
	W.G.	6.8	23	18.9	72	49	227
	A.G.	9.9	26	24.8	74	49	211
	P.G. + N.G. (1 : 1)	8.6	24	23.8	70	49	205
	P'.G. + N.G. (1 : 1)	6.1	24	21.0	71	51	201
	W.G. + N.G. (1 : 1)	9.7	28	24.9	78	53	212
	A.G. + N.G. (1 : 1)	9.6	27	22.8	72	50	202
		10°C					
Portland cement	N.G.	18.7	69	42.7	187	57	325
	P.G.	16.0	54	40.2	158	65	348
	P'.G.	12.1	59	40.2	180	66	366
	W.G.	21.3	79	46.4	198	63	354
	A.G.	20.5	75	43.1	188	63	340
	P.G. + N.G. (1 : 1)	17.6	65	41.0	185	65	352
	P'.G. + N.G. (1 : 1)	20.1	73	40.2	180	66	381
	W.G. + N.G. (1 : 1)	27.3	106	40.2	196	63	353
	A.G. + N.G. (1 : 1)	27.9	115	43.3	190	67	364
Blastfurnace slag cement	N.G.	13.7	40	28.7	100	57	262
	P.G.	8.6	31	23.2	87	52	206
	P'.G.	12.1	38	25.5	93	55	254
	W.G.	15.2	41	21.6	94	50	259
	A.G.	14.8	45	29.6	105	53	262
	P.G. + N.G. (1 : 1)	14.2	40	27.5	104	52	258
	P'.G. + N.G. (1 : 1)	16.8	44	29.2	106	53	261
	W.G. + N.G. (1 : 1)	16.2	48	30.3	108	52	267
	A.G. + N.G. (1 : 1)	17.6	48	29.5	112	54	268
		20°C					
Portland cement	N.G.	33.5	134	48.0	229	68.1	401
	P.G.	32.6	131	43.1	207	63.4	379
	P'.G.	32.2	134	46.0	237	70.4	422
	W.G.	35.9	148	49.4	245	68.1	417
	A.G.	32.8	130	46.0	242	71.4	434
	P.G. + N.G. (1 : 1)	29.8	132	47.4	238	69.1	417
	P'.G. + N.G. (1 : 1)	31.0	128	48.3	233	68.9	428
	W.G. + N.G. (1 : 1)	31.8	131	46.4	238	70.0	433
	A.G. + N.G. (1 : 1)	30.0	129	47.0	226	65.5	404
Blastfurnace slag cement	N.G.	25.2	85	36.8	160	64	404
	P.G.	23.4	79	37.9	163	66	401
	P'.G.	23.4	79	42.3	187	71	452
	W.G.	24.4	85	39.6	175	70	420
	A.G.	25.2	87	40.8	184	72	427
	P.G. + N.G. (1 : 1)	24.2	82	40.2	189	70	452
	P'.G. + N.G. (1 : 1)	25.0	82	38.0	152	70	409
	W.G. + N.G. (1 : 1)	24.6	90	39.0	171	67	421
	A.G. + N.G. (1 : 1)	23.6	87	38.4	165	67	420
		30°C					
Portland cement	N.G.	42.1	193	53.6	295	67.1	385
	P.G.	42.2	187	51.9	297	67.9	393
	P'.G.	42.5	198	54.6	304	66.9	398
	W.G.	47.0	210	56.0	322	65.4	413
	A.G.	43.5	196	56.0	311	66.1	410
	P.G. + N.G. (1 : 1)	43.1	199	51.7	314	68.1	407
	P'.G. + N.G. (1 : 1)	42.7	194	54.6	291	65.0	393
	W.G. + N.G. (1 : 1)	42.1	202	58.3	307	66.5	402
	A.G. + N.G. (1 : 1)	42.7	205	54.0	308	67.5	403
Blastfurnace slag cement	N.G.	35.7	148	51.7	273	62.6	399
	P.G.	34.1	147	55.4	275	61.7	406
	P'.G.	34.5	145	54.8	282	68.4	408
	W.G.	34.9	158	57.6	301	65.9	445
	A.G.	36.8	150	57.5	282	68.3	402
	P.G. + N.G. (1 : 1)	33.3	157	56.0	287	65.6	417
	P'.G. + N.G. (1 : 1	35.9	154	58.9	290	65	438
	W.G. + N.G. (1 : 1)	36.5	159	56.0	293	60	455
	A.G. + N.G. (1 : 1)	37.2	157	57.8	296	63	441
		40°C					
Portland cement	N.G.	48.6	267	64.4	346	62	389
	P.G.	49.1	254	53.5	339	62	402
	P'.G.	47.8	258	59.9	349	69	398
	W.G.	50.0	285	58.7	375	66	424
	A.G.	48.0	273	59.3	360	66	412
	P.G. + N.G. (1 : 1)	45.4	239	56.5	318	63	383
	P'.G. + N.G. (1 : 1)	45.8	236	54.5	303	58	396
	W.G. + N.G. (1 : 1)	50.5	272	61.2	352	70	414
	A.G. + N.G. (1 : 1)	47.6	265	60.5	345	66	401
Blastfurnace slag cement	N.G.	39.2	221	43.7	323	59	348
	P.G.	47.2	222	57.2	324	61	374
	P'.G.	46.8	221	54.6	330	65	378
	W.G.	48.0	247	52.9	323	61	390
	A.G.	47.2	245	53.9	312	60	367
	P.G. + N.G. (1:1)	45.4	235	51.5	313	61	356
	P'.G. + N.G. (1 : 1)	48.4	245	54.1	327	52	361
	W.G. + N.G. (1 : 1)	48.4	231	57.4	321	62	349
	A.G. + N.G. (1 : 1)	43.5	232	55.6	317	59	353

Numbers in parentheses of the second column are the proportions of each component of the gypsum mixture contained in cement.

Table 24. *Slump of concrete (Blastfurnace slag cement with various gypsums)*

	Slump (cm)						Ratio					
	3 min.	30 min.	60 min.	90 min.	120 min.	150 min.	3 min.	30 min.	60 min.	90 min.	120 min.	150 min.
N.G.	15.9	12.9	8.4	7.0	6.2	5.5	100	81	53	44	39	35
P.G.	17.6	14.3	10.2	7.2	5.8	4.8	100	81	58	41	33	27
P'.G.	18.8	14.7	13.3	10.6	7.9	7.0	100	78	71	56	42	41
W.G.	16.8	12.3	9.2	6.2	5.1	3.7	100	73	55	37	30	22
A.G.	16.3	10.6	7.3	5.0	4.0	3.0	100	65	45	31	25	18
P.G. + N.G. (1:1)	15.8	9.3	7.5	5.7	4.5	3.6	100	59	47	36	28	23
P'.G. + N.G. (1:1)	17.0	11.0	10.8	6.5	6.3	4.8	100	65	64	38	37	28
W.G. + N.G. (1:1)	16.4	10.6	7.8	5.5	5.5	4.2	100	65	48	34	34	26
A.G. + N.G. (1:1)	15.7	10.0	7.8	6.2	4.4	4.2	100	64	50	39	28	27

Numbers in parentheses of the first column are the proportion of each component in the mixture of natural gypsum and chemical gypsum added to cement.

The concrete in this table was prepared from blastfurnace cement with various gypsums 4%.

The proportion of aggregate and cement in the concrete mixture is as follows;

water-cement ratio 60%
sand-aggregate ratio 41.1%

Weight of each component of concrete (per 1m³)

cement	305 kg
sand	741 kg
aggregate	1106 kg
water	183 kg
total	2335 kg

concrete. The results given in Table 25 indicate that the development of compressive strength of concrete is independent of the impurities of phosphogypsum in concrete, as mentioned previously.

Furthermore, Hanada (63), through ASTM Designation: C403-63T, measured the time of set of concrete prepared from portland cement with various gypsums. The results given in Figs. 5-1 and 5-2 show that the time of set of concrete is not considerably affected by the impurities of phosphogypsum.

Utilization of Other Chemical Gypsums for Portland Cement

There are many kinds of chemical gypsum in Japan, as in Table 1. But phosphogypsum alone is very important for portland cement industry at the stand point of the quantity and property of gypsum. The major part of this paper has been givn for the discussion on the utilization of phosphogypsum. But, some of chemical gypsums are also frequently useful for portland cement. In this chapter, the utilization of other chemical gypsums in making portland cement and the hydration of the prepared cement will be treated.

Fluorogypsum, as in Table 1, is usually produced in the form of anhydrite. After standing in storage ponds, some portions of anhydrite are converted to dihydrate through the hydration reaction. Therefore, fluorogypsum usually used in making portland cement is a mixutre of anhydrite and dihydrate. Generally,

Table 25. *Compressive strength of concrete (Blastfurnace slag cement with various gypsums)*

	Compressive strength (kg/cm²)		
	3 days	7 days	28 days
N.G.	86	138	319
P.G.	70	122	279
P'.G.	72	122	303
W.G.	69	136	275
A.G.	71	140	303
P.G. + N.G. (1:1)	78	146	346
P'.G. + N.G. (1:1)	74	136	331
W.G. + N.G. (1:1)	72	145	304
A.G. + N.G. (1:1)	71	133	286

Numbers in parenthesis of the first column are the proportion of each component in the mixture of natural gypsum and chemical gypsum added to cement.

The concrete in this table was prepared from blastfurnace cement with various gypsums 4%.

The proportion of aggregate and cement in the concrete mixture is as follows;

water-cement ratio 60%
sand-aggregate ratio 41.1%

Weight of each component of concrete (per 1 m³)

cement	305 kg
sand	741 kg
aggregate	1106 kg
water	183 kg
total	2335 kg

fluorogypsum have some amounts of the water-soluble impurities, such as residual hydrofluoric acid, unreacted sulfuric acid and other inorganic salts. Table 6 shows the chemical compositions of

Table 26. *Influence of fluorogypsum on setting time and strength development of portland cement*

	SO_3 (%)	W/C (%)	Initial hr.-min.	Final hr.-min.	Compressive strength		
					3 days	7 days	28 days
Fluorogypsum	1.4	25.0	2–50	4–25	111	108	111
	2.1	25.0	3–20	5–05	120	118	119
Mixture of natural gypsum and waste plaster mold	1.4	25.4	2–35	4–10	100	100	100
	2.1	25.4	2–55	4–25	100	100	100

In this table, compressive strength of portland cement with fluorogypsum is expressed as relative value for that (assuming as 100) of portland cement with the mixture of natural gypsum and waste plaster mold.

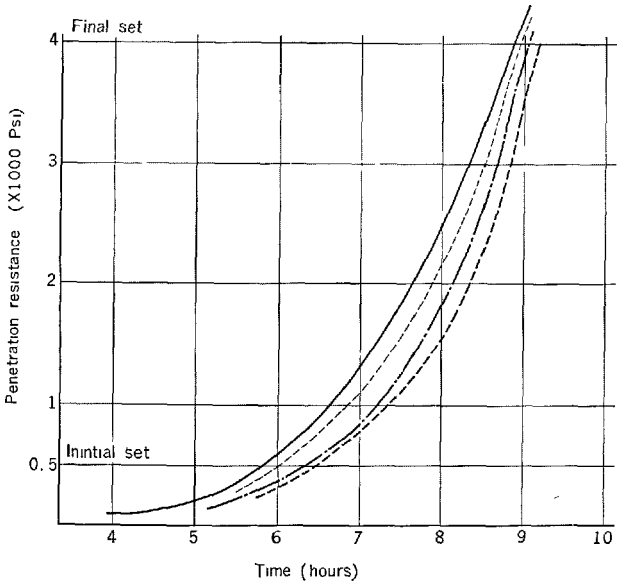

Fig. 5–1. *Setting time of concrete with various gypsums (By ASTM Designation 403–63T).*
———: Natural gypsum.
– – – –: Chemical gypsum No. E.
— - —: HDS–5.
— — —: HDS–3.

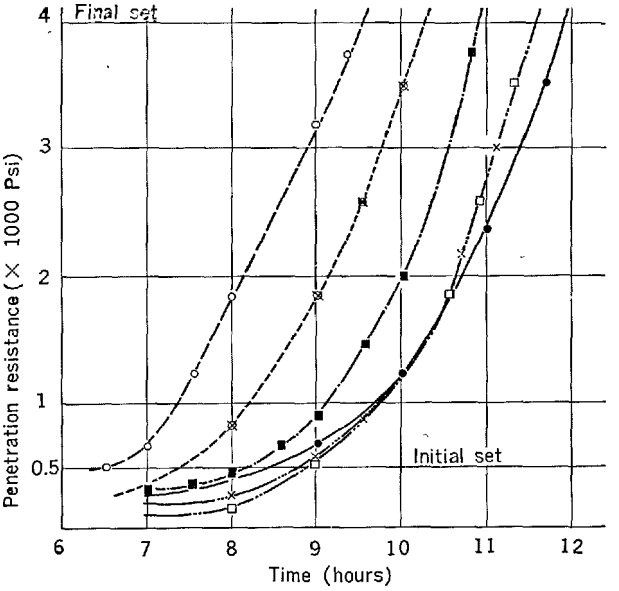

Fig. 5–2. *Setting time of concrete with various gypsums (By ASTM Designation 403–63T).*
—●—: Sodagypsum.
—○—: Pure gypsum.
—⊠—: Ss.P_2O_5 0.1%.
—■—: Ss.P_2O_5 0.5%.
—□—: Ss.P_2O_5 1.0%.
—×—: Ss.P_2O_5 2.0%.

fluorogypsums.

Miyazawa (64) prepared portland cement (total SO_3 content; 1.7% and 2.4%) containing fluorogypsum and the mixture of natural gypsum and the waste Paris mold. The results given in Table 26 show that the retarding action caused by the impurities of fluorogypsum is relatively smaller than that by the impurities of phosphogypsum. Form these results, it is supposed that there is a distinct difference in the reaction mechanism on the hydration of cement between the water-soluble F originated from hydrofluoric acid and that from sodium silicofluoride. The three day-strength of mortar containing fluorogypsum is greater than that containing natural gypsum. Mochizuki (67), using another fluorogypsum obtained from the same source, prepared portland cements containing total SO_3 contents 1.7% and 2.4% and measured the time of set of pastes and the strength development of mortars. The results obtained by him showed that the time for initial and final set is longer when the content of SO_3 was 2.4% than when it was 1.2%. In both cases, however, the strength development of mortar was not affected by the impurities of fluorogypsum.

A characteristic phenomenon in using fluorogypsum for cement is a marked increase of the power consumption for grinding of cement clinker together with fluorogypsum. Comparing with natural gypsum in Japan, the increments of the power consumption are 13% to 18% with the coarse powder of fluorogypsum and 30% to 40% with fine powder. The great increase in power consumption in grinding may be caused by the lack of clay minerals in fluorogypsum.

Takemoto (68) also prepared portland cement containing each of fifteen kinds of fluorogypsums and measured the setting time of its paste and the strength development of its mortar. The amount of the water-soluble F contained in fluorogypsum was 0.003% to 0.05% and the amount of total F was 1.00% to 1.50%. His results indicate that the amount of the water-soluble F and iron salt as well as the acidity of fluorogypsum affected the strength development of mortar. In other words, the increase of the water-soluble F results in the increase of iron salts and the lowering of the strength development of mortar.

The utilization of chemical gypsum No. D for control of the setting time of portland cement was studied by Hanada (63). Table 27 shows the chemical compositions of two kinds of chemical gypsums No. D produced from the first and second neutralization reaction in their production process. The latter has about 6% iron oxide as an impurity. The setting time of paste and the strength devlopment of mortar with these chemical gypsums is given in Tables 28 and 29. The results indicate that the both chemical gypsums do not have any adverse effects on the setting and the strength development. The properties of portland cement with two kinds of chemical gypsums No. D are similar to that of portland cement with a commercial chemical gypsum.

Table 27. *Chemical compositions of chemical gypsum No. E*

(%)

	Water	Combined water	Fe_2O_3	CaO	SO_3
Gypsum by first reaction	13	19.6	0.5	31.8	44.7
Gypsum by second reaction	25	19.2	5.7	30.8	43.1

In Tables 20–25 of last chapter, Hanada, comparing with the setting time of paste and the strength development of mortar containing phosphogypsum and natural gypsum, showed the setting time of paste and the strength development of mortar with two kinds of other chemical gypsums (63).

The work by Takemoto, Ito and Suzuki (53) on the properties of portland cement containing fluorogypsum, titangypsum and sodagypsum indicates that, except that sodagypsum slightly lowers the utilmate development of mortar strength, these chemical gypsums have scarcely the different effect from natural gypsum on the propetties of portland cement. Nakamori and Mizoguchi (69) examined the compatibility of phosphogypsum, saltgypsum, sodagypsum and chemical gypsum No. J for control of the setting time and said that these chemical gypsums can be used if they contain only a small amount of impurities.

Table 28. *Setting time of cement containing chemical gypsum No. E*

		W/C (%)	Initial hr.-min.	Final hr.-min.
Portland cement	Gypsum by first reaction	24.1	2–20	3–35
	Gypsum by second reaction	24.2	2–20	3–35
	Commerical artificial gypsum	24.2	2–20	3–35
Blastfurnace slag cement	Gypsum by first reaction	26.7	3–15	4–20
	Gypsum by second reaction	26.5	3–15	4–30
	Commerical artificial gypsum	27.0	3–15	4–40

The quantity of gypsum added to the both cements is 4%

Table 29. *Strength development of mortar containing chemical gypsum No. E*

		Bending strength (kg/cm²)			Compressive strength (kg/cm²)		
		3 days	7 days	28 days	3 days	7 days	28 days
Portland cement	Gypsum by first reaction	31.6	42.4	74.0	116	201	404
	Gypsum by second reaction 1	30.2	40.8	73.2	119	205	401
	Gypsum by second reaction 2	31.8	42.1	75.0	118	206	402
	Commerical artificial gypsum	32.1	42.5	74.0	118	205	404
Blastfurnace slag cement	Gypsum by first reaction	27.2	39.6	73.0	96	182	410
	Gypsum by second reaction 1	27.0	39.0	73.3	95	180	399
	Gypsum by second reaction 2	28.0	40.2	74.0	98	185	403
	Commercial artificial gypsum	27.0	41.0	73.1	95	180	400

The quantity of gypsum added to the both cements is 4%

Grindability of Clinker together with Chemical Gypsum

While natural gypsums are usually produced in the form of lump, most of chemical gypsums are by-produced in state of powder, unless it is pelletized. The SO_3 content of chemical gypsum is as high as that of pure natural gypsum. Natural gypsum used generally in Japan for making portland cement contains a relatively large amount of clay minerals which may give a favorable effect on the grinding efficiency of cement.

Miyazawa, in preceding chapter, showed that the power consumption in grinding of cement markedly increases when fluorogypsum is used. He also reported that, when pure natural gypsum, pelletized phosphogypsum and powdered chemical gypsum are used, the power consumption required to obtain the cement with a definite fineness was 5% to 19% larger than that in using the relatively poorer grade natural gypsum containing some quantities of clay minerals.

Suzukawa and Kobayashi (70, 71) investigated systematically a group of problems on the grindability of cement with chemical gypsum in connection with the dehydration of gypsum caused by the temperature elevation during the grinding process and the resultant false set. They used some natural gypsums and phosphogypsums having the chemical compositions listed in Table 30.

The results of grinding tests at ordinary temperature and 160°C are given in Table 31. It is evident that at each temperature there are some differences in the grindability of cement caused by the grade of gypsums. In grinding at ordinary temperature, the grinding time required to obtain the cement with a definite fineness is minimum when the lower grade natural gypsum is used, and it is more when the ordinary natural gypsum is used and is longest when pure natural gypsum or phosphogypsum is used.

When grinding is carried out at 160°C, it is generally observed that the amount of ball coatings and the grinding time as well as the quantity of coarse particle in the sieving residue increase markedly. In particular, the grade of gypsum is closely related to the length of grinding time. Namely, using the lower grade natural gypsum, even in grinding at 160°C, it is apparently observed that the amount of ball coatings is greatly decreased, that the grinding time is relatively shortened than grinding at ordinary temperature and, however, that the amount of coarse particle in the sieving residue is unusually increased. Since the cement which is ground together with the lower grade natual gypsum has the size distribution different from that of cement ground with other gypsums, it is suggested that the abnormal acceleration of grinding has been happened only during the milling with natural gypsum of the lower grade. In view of the aforementioned results, the most reasonable conclusion is that the mineral impurities naturally included in natural gypsum are markedly effective to the improvement of grindability of cement.

Some portions of works undertaken by Suzukawa and Kabayashi in order to reconfirm the above results and to solve the problem on grinding of the cement with chemical gypsum are shown in Table 32. In this experiment, they investigated the grindability of

Table 30. *Chemical compositions of cement clinker and various gypsums*

	H_2O	I.L.	I.M.	SiO_2	Al_2O_3	Fe_2O_3	CaO	MgO	SO_3	Crystal size (μ)
Cement clinker	—%	0.2%	0.2%	22.3%	5.4%	3.7%	65.8%	1.1%	0.5%	
Natural gypsum–1	0.2	13.0	18.4		3.5		25.1	4.0	35.5	
Natural gypsum–2	0.5	21.0	1.4		0.3		31.7	0.3	44.7	
Natural gypsum–3	0.0	20.9	0.1		0.1		32.3	0.1	46.0	
Natural gypsum–4	0.2	4.3	6.9		1.1		35.6	1.5	50.1	
Natural gypsum–5	0.3	1.7	38.2		4.5		14.6	6.0	20.4	
Phosphogypsum–1	0.0	20.4	—	—	—	—	—	—	44.2	(100 − 150) × (50 − 70)
Phosphogypsum–2	0.3	20.9	1.9		1.8		31.0	0.0	44.2	(30 − 50) × (20 − 30)
Phosphogypsum–3	0.0	20.6	—	—	—	—	—	—	45.0	(20 − 30) × (10 − 20)
Chemical gypsum–1	0.0	22.5	0.1		0.1		32.6	0.0	44.5	(100 − 150) × (20 − 30)
Chemical gypsum–2	0.0	16.5	2.5				33.5	0.0	48.6	

I.L.: loss on ignition
I.M.: insoluble matters

Table 31. *Grinding tests of cement clinker together with various gypsums at ordinary temperature and at* 160°C

		Grindability		Fineness			Flake	Ball coating
		G.T. min.	T.R. %	Blaine cm^2/g	>88μ %	>44μ %	%	%
Grinding at ordinary temperature	N.G.–1	40	100	3260	0.4	10.4	0.20	0.5
	N.G.–2	45	113	3240	0.4	10.0	0.22	0.5
	N.G.–3	46	115	3250	0.5	10.2	0.26	0.5
	N.G.–4	57	143	3260	0.9	11.8	0.50	0.9
	N.G.–5	35	88	3280	0.5	11.4	0.20	0.5
	P.G.–1	46	115	3270	0.4	9.8	0.20	0.2
	P.G.–2	46	115	3240	0.5	10.8	0.22	0.5
	P.G.–3	48	120	3260	0.5	10.4	0.28	0.5
	C.G.–1	46	115	3260	0.4	9.8	0.22	0.5
	C.G.–2	44	110	3250	0.4	9.0	0.24	0.2
Grinding at 160°C	N.G.–1	43	108	3230	1.1	14.2	0.44	3.4
	N.G.–2	50	125	3290	1.2	14.8	0.74	6.4
	N.G.–3	50	125	3280	1.3	14.8	0.70	5.9
	N.G.–4	57	143	3250	1.2	12.0	0.62	1.8
	N.G.–5	32	80	3270	1.4	15.6	0.34	0.7
	P.G.–1	50	125	3290	1.4	14.4	0.80	5.0
	P.G.–2	50	125	3300	1.6	16.2	0.76	6.8
	P.G.–3	50	125	3300	1.3	13.4	0.74	6.1
	C.G.–1	50	125	3280	1.3	13.8	0.82	4.3
	C.G.–2	50	125	3280	0.8	11.6	0.68	2.7

G.T.: grinding time
T.R.: time ratio
N.G.: natural gypsum
P.G.: phosphogypsum
C.G.: chemical gypsum

Quantity of gypsum used in grinding is as follows., N.G.–1 3.8%, N.G.–2 and 3, P.G.–1, 2 and 3, C.G.–1 3.0%, N.G.–5, C.G.–2 2.7%

All the quantity of gypsum are written as wt.% to clinker.

Table 32. *Grinding tests of cement clinker together with various gypsums at ordinary temperature and at* 160°C

		Grindability		Fineness			Flake	Ball coating
		G.T. min.	T.R. (%)	Blaine cm/g	>88μ (%)	>44μ (%)	(%)	(%)
Grinding at ordinary temperature	N.G.–2 + N.G.–5 (2.4: 1.4)	42	105	3250	0.6	10.4	0.28	0.5
	N.G.–3 + N.G.–5 (2.4: 1.4)	42	105	3240	0.6	11.0	0.28	0.5
	N.G.–4 + N.G.–5 (2.0: 1.8)	43	108	3280	0.5	10.4	0.28	0.5
	P.G.–2 + N.G.–5 (2.4: 1.4)	42	105	3250	0.6	10.6	0.26	0.5
	C.G.–2 + N.G.–5 (2.0: 1.8)	40	100	3260	0.5	10.0	0.18	0.2
Grinding at 160°C	N.G.–2 + N.G.–5 (2.4: 1.4)	40	100	3240	1.0	14.2	0.34	0.9
	N.G.–3 + N.G.–5 (2.4: 1.4)	40	100	3260	0.9	14.0	0.36	1.1
	N.G.–4 + N.G.–5 (2.0: 1.8)	43	108	3240	1.1	14.2	0.46	1.1
	P.G.–2 + N.G.–5 (2.4: 1.4)	40	100	3250	1.3	16.0	0.44	1.6
	C.G.–2 + N.G.–5 (2.0: 1.8)	39	98	3240	1.2	14.0	0.30	1.1

Numbers in parentheses of second column are the proportions of each component in the gypsum mixture added to clinker.

cements containing the mixture of the lower grade natural gypsum and one of other various gypsums at ordinary temperature and 160°C. Before the mixture of each gypsum and the lower grade natural gypsum is ground together with cement clinker, the quantity of the lower grade natural gypsum in the mixture is adjusted so as the quantity of the insoluble substance in the mixture is equal to that in the ordinary natural gypsum in order to avoid the discrepancy on the amount of insoluble substance in the resultant portland cement. These results show that the presence of the mineral impurities is effective to the remarkable reduction of the time of grinding without disturbing the distribution of particle size of the resultant cement. Moreover, the similar tendencies are observed in grinding at 160°C. Fig. 6 illustrates the grindability

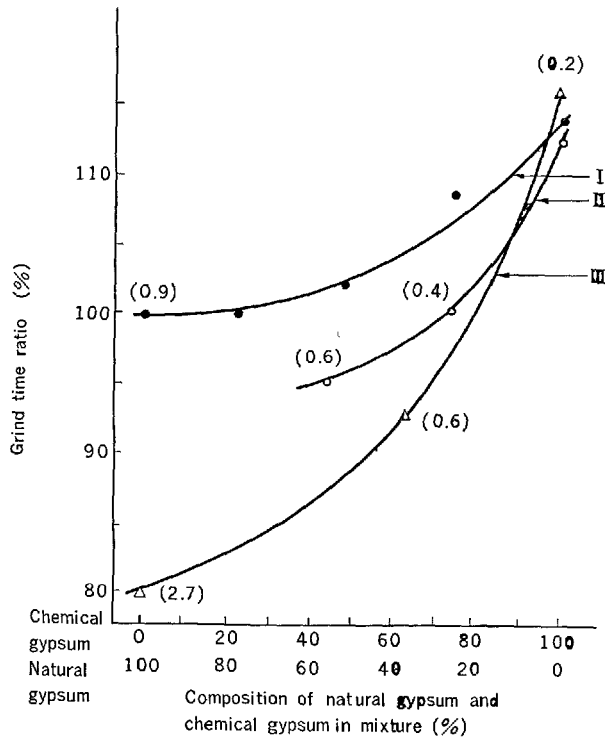

Fig. 6. *Grindability of cement with various gypsums.*
I: Natural gypsum (SO_3 35.5%)—Chemicalgypsum-mixture.
II: Natural gypsum (SO_3 28.5%)—Chemical gypsum-mixture.
III: Natural gypsum (SO_3 20.4%)—Chemical gypsum-mixture.
Grind temperature 160°C.
Grinding time of cement with only natural gypsum (SO_3 35.5%) is a assumed as 100%.
Values in parentheses are the amount of insoluble substance in cement. (wt.% to cement)

of cements containing the mixture of each of chemical gypsums and the different grade natural gypsums. It is apparent that the lower the grade of natural gypsum used by them, the shorter is the time of grinding.

The setting time of paste of portland cement which was ground together with ecah chemical gypsum alone or with the mixture of each chemical gypsum and the lower grade natural gypsum is given in Tables 33 and 34. These results show that the mineral impuritiess

Table 33. *Setting time of portland cement containing various gypsums*

		Setting			Ratio	
		W/C (%)	Initial hr.-min.	Final hr.-min.	Initial	Final
Grinding at ordinary temperature	N.G.–1	25.8	2–02	3–10	100	100
	N.G.–2	24.5	2–00	3–02	98	96
	N.G.–3	24.3	2–02	3–00	100	95
	N.G.–4	24.8	1–34	2–47	77	88
	N.G.–5	28.3	2–05	3–22	102	106
	P.G.–1	24.8	3–55	5–22	193	169
	P.G.–2	24.3	2–27	3–47	120	119
	P.G.–3	24.0	2–05	3–07	102	98
	C.G.–1	24.8	2–21	3–19	116	105
	C.G.–2	24.8	2–37	3–33	129	112
Grinding at 160°C	N.G.–1	23.8	2–09	3–15	106	103
	N.G.–2	25.0	1–45	2–45	86	87
	N.G.–3	25.5	1–46	2–36	87	82
	N.G.–4	24.8	1–31	2–51	75	90
	N.G.–5	28.3	2–15	3–25	111	108
	P.G.–1	24.0	3–00	4–25	148	139
	P.G.–2	24.5	2–15	3–25	111	108
	P.G.–3	25.0	1–43	2–34	84	81
	C.G.–1	25.3	1–47	2–45	88	87
	C.G.–2	23.8	1–54	2–55	93	92

Quantity of gypsum added to cement is as follows; N.G.–1 3.8%, N.G.–2 and 3, P.G.–1, 2 and 3, C.G.–1 3.0%, N.G.–5, C.G.–2 2.7%, N.G.–4 2.7% All the quantity of gypsum are written as wt.% to clinker.

Table 34. *Setting time of portland cements containing various gypsums*

		W/C (%)	Setting		Ratio	
			Initial hr.-min.	Final hr.-min.	Initial	Final
Grinding at ordinary temperature	N.G.–2 + N.G.–5 (2.4: 1.4)	25.5	2–13	3–16	109	103
	N.G.–3 + N.G.–5 (2.4: 1.4)	24.8	2–06	3–07	103	98
	N.G.–4 + N.G.–5 (2.0: 1.8)	26.3	2–25	3–28	119	109
	P.G.–2 + N.G.–5 (2.4: 1.4)	25.3	2–29	3–41	122	116
	C.G.–2 + N.G.–5 (2.0: 1.8)	26.5	2–31	3–54	124	123
Grinding at 160°C	N.G.–2 + N.G.–5 (2.4: 1.4)	26.3	2–01	3–02	99	96
	N.G.–3 + N.G.–5 (2.4: 1.4)	26.0	1–56	3–00	95	95
	N.G.–4 + N.G.–5 (2.0: 1.8)	24.3	2–08	3–10	105	100
	P.G.–2 + N.G.–5 (2.4: 1.4)	25.5	2–22	3–35	116	113
	C.G.–2 + N.G.–5 (2.0: 1.8)	25.0	2–11	3–25	107	108

In this table, ratio of setting time is relative value of the setting time of cement with other gypsum for setting time (assuming as 100) of cement with natural gypsum-No. 1 in Table 33.

Numbers in parentheses of the second column are the proportions of each component of the gypsum mixtures added to cement clinker.

scarcely affect the setting and even the development of the strength of mortar. The results shown in Table 35 indicate that the weight loss of cement on heating and the amount of SO_3 of each section of particle size of the cement ground at 160°C are approximately independent of the change of gyspum grade and, that most of gypsum in the ground cement are present as the particle under 15μ. In a previous paper, Nakamori and Mizoguchi (69) have reported that all the gypsum contained in a commercial portland cement are as fine as the particle under 15μ.

Relation between Chemical Gypsum and False Set

The purpose of this chapter is to investigate whether or not the use of chemical gypsum for portland cement is responsible for the development of a false set of fresh cement. Takemoto, Ito and Suzuki (53) reported that the false set which was caused by aeration scarcely happened in cement containing phosphogypsum or sodagypsum.

Table 35. *Loss on ignition of cements and distribution of* SO_3 *in cements ground together with various gypsums.*

	Cement			Cement under 15μ	
	Ig-loss (%)		SO_3 (%)	Ig-loss 950°C (%)	SO_3 (%)
	350°C	950°C			
N.G. 1	0.03	0.31	1.65	1.34	2.75
N.G. 3	0.06	0.35	1.68	1.81	3.01
N.G. 4	0.05	0.33	1.74	1.98	3.27
N.G. 5	(+)	0.10	1.69	1.17	2.83
P. G. 2	0.03	0.30	1.64	1.37	2.77

Quantities of gypsums added to cement is as follows: N.G.–13.8%, N.G.–3, P.G.–23.0%, N.G.–4 and 52.7%.
All the quantity of gypsum are written as wt.% to clinker.

Suzukawa and Kobayashi studied in detail the relations between the false set of fresh cement and the addition of phosphogypsum (70, 71). Table 36 shows the chemical compositions of various gypsums used in their experiments, namely: three kinds each of natural gypsums, phosphogypsums and artificial gypsums. In two of the three kinds of artificial gypsums, some portions of SO_3 in their crystal lattice are substituted by HPO_4^{--}. Each kind of gypsums was dehydrated and mixed in the cement. False set is examined by J.A.S.S method after paste was agitated for 1.5, 3 and 5 minutes. The relation between the time of hydration versus the penetration of paste is illustrated in Figs. 7–1 and 7–2. These results show that the development of false set is not only affected by the change of grade of gypsum, but also the amount of gypsum in cement. The cement containing phosphogypsum No. 3 that is chemically untreated shows a frequent anomalous set which may be caused by the large amounts of impurities of phosphogypsum. Therefore, in cement containing natural gypsum and even phosphogypsum, a false set is a likely possibility.

False set of the cement made from two clinkers is examined in order to investigate the anomalous set mentioned above under two conditions: one of them is of a constant consistency and the other is of a constant water cement ratio. The chemical compositions of clinkers used in this experiment are given in Table 37. In both cases, the SO_3 content in the prepared cement containing phosphogypsum and natural gypsum is from 0.25% to 2.0%. From the results illustrated in Figs. 8 and 9, the optimum amount of gypsum required for normal set seems to depend on the kind or grade of gypsum. In regard to the devlopment of false set, the influence of the chemically treated phosphogypsum on settting is analogous to that of pure gypsum. It is naturally suggested that the

Table 36. *Chemical compositions of various gypsums used for the test of false set*

	Gypsum						Dehydrated gypsum		
	C.W. (%)	SO_3 (%)	T-P_2O_5 (%)	W-P_2O_5 (%)	F (%)	Specific surface area (m^2/g)	C.W. (%)	SO_3 (%)	Specific surface area (m^2/g)
N.G. 1	20.6	46.3	0.00	0.00	0.00	0.81	6.4	54.7	4.41
N.G. 3	9.5	35.8	0.03	0.01	0.04	0.56	3.1	38.6	9.58
N.G. 4	13.2	27.9	—	—	—	0.76	5.1	30.7	8.78
P.G. 1	20.6	46.2	0.03	0.02	0.01	0.85	6.5	54.2	4.86
P.G. 2	20.4	43.5	1.11	—	0.10	—	6.9	51.1	—
P.G. 3	20.5	44.4	1.12	0.92	0.12	0.46	6.8	52.2	3.70
A.G. 1	20.8	46.4	0.00	0.00	0.00	1.34	6.2	54.2	7.69
A.G. 2	20.7	45.1	1.02	0.81	0.00	2.68	6.2	52.6	6.08
A.G. 3	20.7	40.5	5.04	4.02	0.00	2.99	6.2	46.9	6.93

N.G.: natural gypsum
P.G.: phosphogypsum
A.G.: artificial gypsum
C.W.: combined water
T-P_2O_5: total P_2O_5
W-P_2O_5: water-soluble P_2O_5

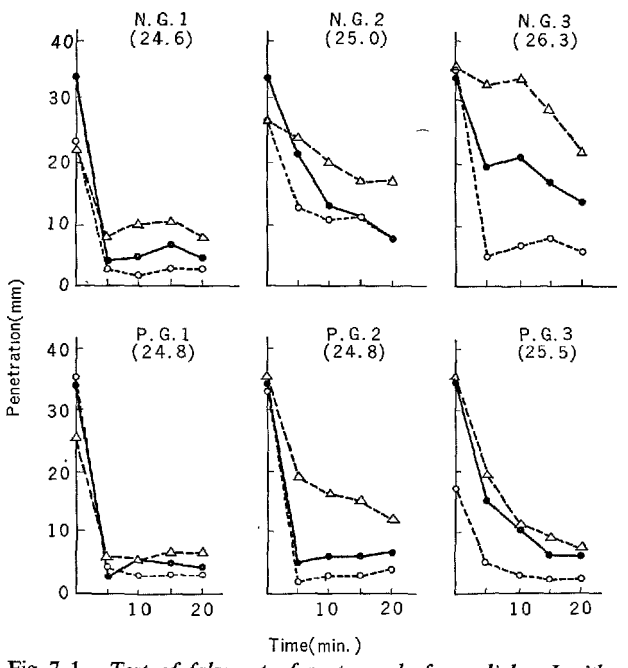

Fig. 7–1. *Test of false set of paste made from clinker I with natural gypsum and phosphogypsum.*
Numbers in parentheses are water-cement ratio required for a definite consistency.
—○—: agitation for 1.5 minutes.
—●—: agitation for 3 minutes.
--△--: agitation for 5 minutes.

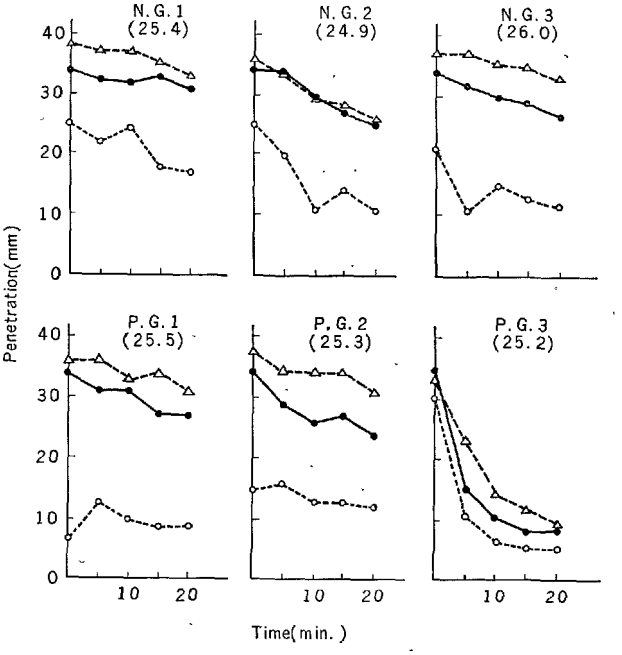

Fig. 7–2. *Test of false set of paste made from clinker II with natural gypsum and phosphogypsum.*
Numbers in parenthesis are water-cement ratio required for a definite consistency.
—○— : agitation for 1.5 minutes.
—●—: agitation for 3 minutes.
--△--: agitation for 5 minutes.

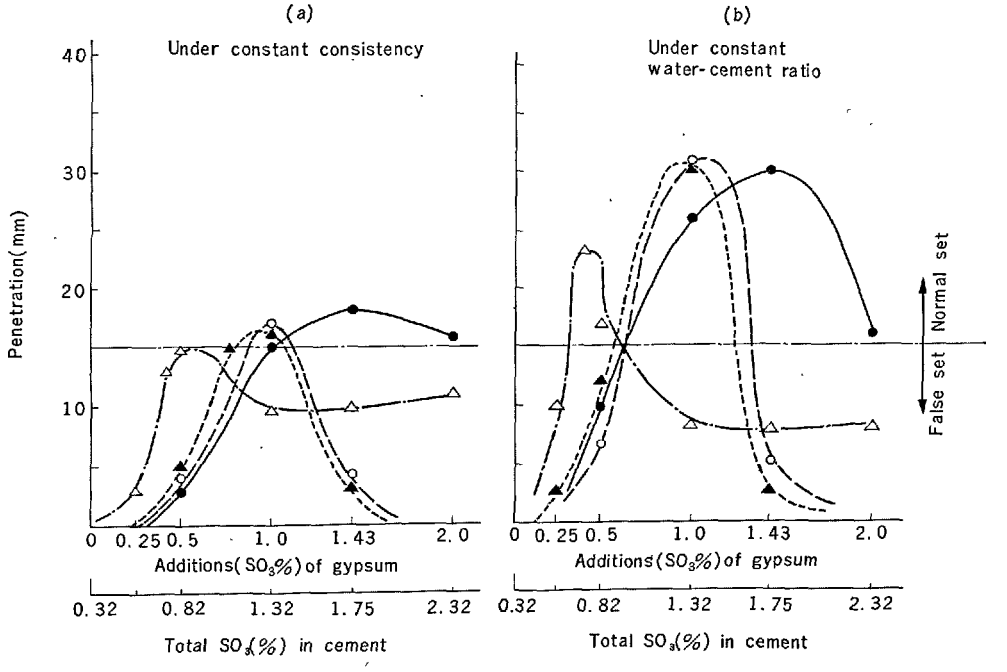

Fig. 8. *Relations between various gypsums and false set (Using clinker I).*
—●—: high grade natural gypsum. (N.G.–1).
--○--: ordinary natural gypsum. (N.G.–2).
---▲---: treated phosphogypsum. (P.G.–1).
--△--: untreated phosphogypsum. (P.G.–3).

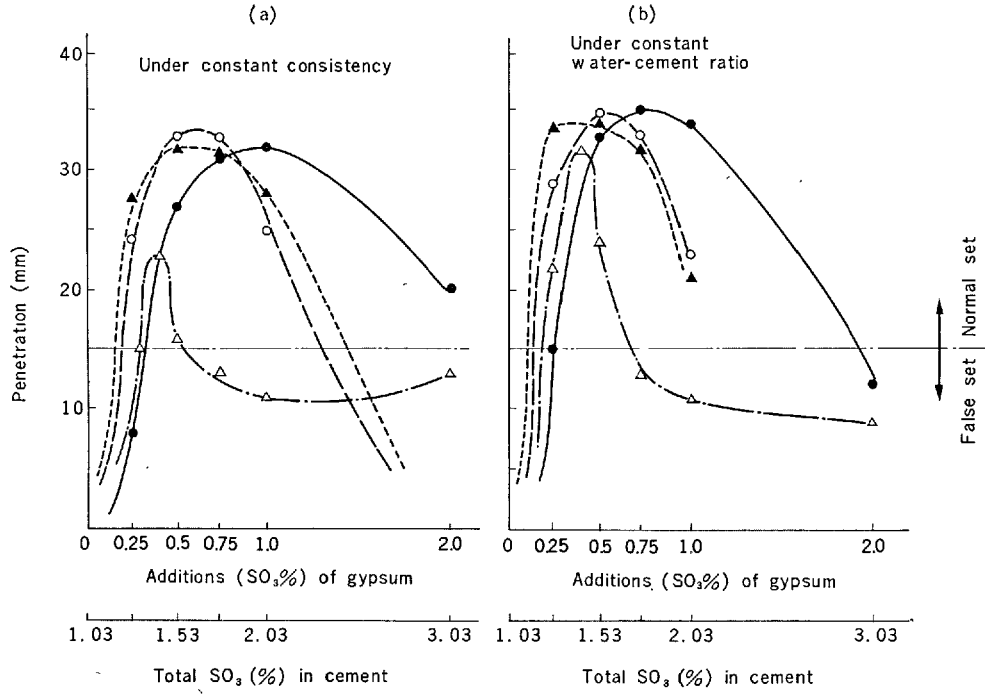

Fig. 9. *Relations between various gypsums and false set.*
(Using clinker II).
—●—: high grade natural gypsum (N.G.–1).
--○--: ordinary natural gypsum (N.G.–2).
▲···: treated phosphogypsum (P.G.–1).
--△--: untreated phosphogypsum (P.G.–3).

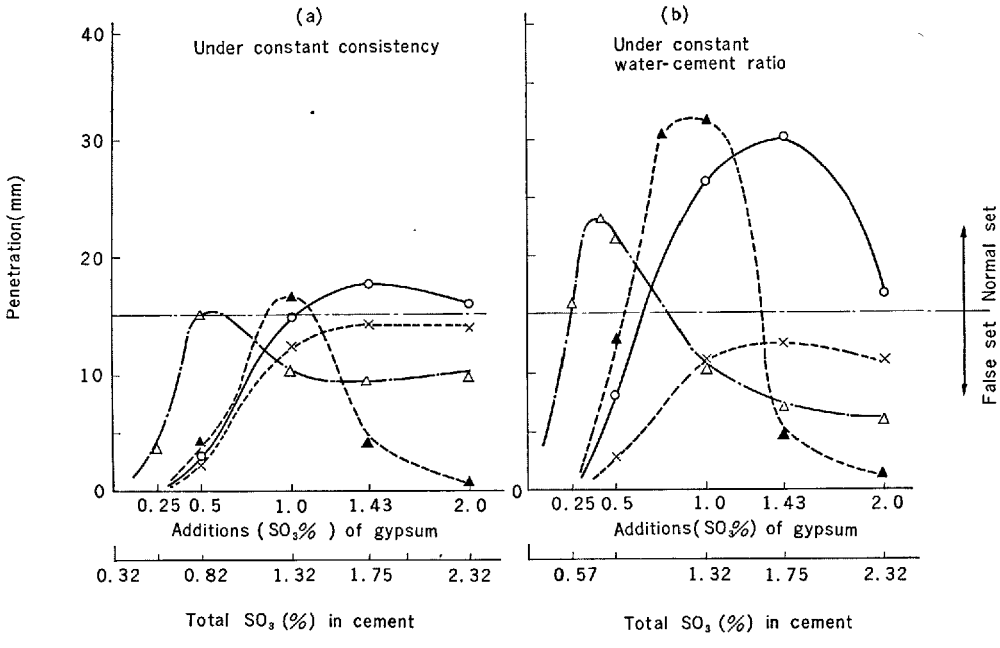

Fig. 10. *Relations between various gypsums and false set.*
(Using clinker I).
--▲--: pure artificial gypsum.
--△--: articial gypsum substituting 1% P_2O_5.
····×···: artificial gypsum substituting 5% P_2O_5.
—○—: ordinary natural gypsum (N.G.–2).

Table 37. *Chemical compositions of clinkers I and II*

(%)

	Ig. loss	Insol.	SiO_2	Al_2O_3	Fe_2O_3	CaO	MgO	SO_2	Na_2O	K_2O	Total	Free-CaO
I	0.2	0.2	22.8	5.0	3.0	66.7	1.1	0.32	0.28	0.63	100.21	0.6
II	0.3	0.1	22.5	4.9	2.9	66.3	1.1	1.03	0.30	0.79	100.19	0.5

Ig. loss: loss on ignition
Insol.: insoluble matters

behavior of cement with phosphogypsum which is not chemically treated differs from that of cement with other gypsums. In addition, they prepared some cements containing various gypsums and then, examined a false set, analysed the soluble components in the liquid phase of paste and measured the solubility of gypsums.

The curves in Fig. 10 show the relation between the time of hydration and the penetration of pastes with artificial gypsums. These results indicate that the tendency to develop false set of fresh cement with artificial gypsum substituting 1.0% P_2O_5 is similar to that in the cement with phosphogypsum No. 3 in Table 36. Also, it was reported that the solubilities of SO_4^{--}, Ca^{++} and OH^- in the liquid phase of paste are obtained as the anomalous curves corresponding to the development of the false set.

Consequently, it may be generally concluded that the dehydration of gypsum during the grinding and subsequent "plaster set" caused by the dehydrated gypsum during the hydration are likely to predominate the development of a false set.

However, the mechanism mentioned above may not be supported, because the present experimental results show that a false set is scarcely developed in cement containing the ordinary or the lower grade natural gypsum. Therefore, it is natural that the false set phenomenon of fresh cement should be investigated on such many factors as the grade of gypsum, the amount of added gypsum and the quantity of impurities.

Influence of Impurities of Phosphogypsum on Hydration of Portland Cement and Its Clinker Minerals

Introduction

It is now generally accepted that the impurities of phosphogypsum have some adverse effects on the hydration of portland cement. Hitherto, the results obtained by Takemoto, Ito and Suzuki (53) showed that the several impurities picked out by them act as a retarder at concentrations 0.1% to 1.0% to gypsum in cement. These impurities are sodium silicofluoride and phosphoric acid as an inorganic substance, and humic acid and sugar as an organic substance. Also, these impurities were used respectively as a single mixture and compound mixture. The retarding action markedly increases, when the compound mixture is used. These results are given in Table 38. Kobayashi also has undertaken a similar experiment and observed the marked retarding action resulted from these compound additives. Mori and Sudo (58) prepared portland cement and blastfurnace slag cement containing monocalcium phosphate and dicalcium phosphate and they reported that the time of set was markedly prolonged with increasing concentration of each impurity in cement. Murakami has also studied the influence of phosphoric acid, monocalcium phosphate, dicalcium phosphate and sodium silicofluoride at relatively higher concentrations and, as in Table 39, he has obtained the same results with those of the preceding investigators.

Each impurity of phosphogypsum, when it is contained in the cement as a chemical reagent, does not give a slightly negative effect on the development of three day strength. These results are shown in Table 40 by Murakami and also are well identical with the previous works (53, 57, 58).

The experiments mentioned above were undertaken to clarify the influence of impurities which adhered to the surface of the crystals of phosphogypsum. However these impurities are likely to turn insoluble rapidly, owing to the neutralization reaction of lime in its liquid phase of cement paste or mortar, immediately after the cement comes into contact with water. Therefore, the retarding action may be relatively weaker than that of the impurities in phosphogypsum even if it is subjected to the same concentrations.

Consequently, it can be said that the retarding action markedly depends upon the rate of dissolution of impurities from inside or outside of the gypsum crystals. Kobayashi has already reported that the

Table 38. *Influence of additions on setting time of cement*

	Percentage of additions to gypsum in cement (%)				Setting time	
	P_2O_5 (%)	F (%)	Organic substance	W/C (%)	Initial setting	Final setting
——	0.0	0.0	0	24.2	2.07	3.11
Sodium silicofluoride (Na_2SiF_6)	0.0	0.25	0	24.2	3.02	3.57
	0.0	0.5	0	24.2	3.23	4.21
	0.0	1.0	0	24.2	3.30	4.30
	0.0	1.5	0	24.2	3.43	4.53
Phosphoric acid (H_3PO_4)	0.5	0.0	0	24.2	2.30	3.25
	1.0	0.0	0	24.2	2.38	3.33
Humic acid	0.0	0.0	0.1	24.2	2.06	3.10
Sugar	0.0	0.0	0.1	24.2	2.10	3.12
$\{Na_2SiF_6\}$ $\{H_3PO_4\}$ mixed	0.5	0.5	0	24.2	4.05	5.25
	0.5	1.0	0	24.2	4.15	5.50
	1.0	0.5	0	24.2	4.20	6.13
	1.0	1.0	0	24.2	4.30	6.25
$\{Na_2SiF_6\}$ $\{H_3PO_4\}$ $\{$Organic-substance$\}$ mixed — Humic acid	0.5	0.5	0.1	24.2	4.40	6.00
	1.0	1.0	0.1	24.2	5.30	6.40
$\{Na_2SiF_6\}$ $\{H_3PO_4\}$ $\{$Organic-substance$\}$ mixed — Sugar	0.5	0.5	0.1	24.2	4.40	5.50
	1.0	1.0	0.1	24.2	5.20	6.40

Table 39. *Setting time of portland cement with chemical reagent corresponded to the impurities of phosphogypsum*

Phosphoric acid				Monocalcium phosphate			
P_2O_5 in cement	w/c	Initial set	Final set	P_2O_5 in cement	w/c	Initial set	Final set
%	%	hr.-min.	hr.-min.	%	%	hr.-min.	hr.-min.
0.00	27.5	2–14	3–24	0.00	27.0	2–28	3–26
0.01	28.0	2–28	3–53	0.01	27.0	2–58	3–53
0.05	28.5	3–11	4–16	0.05	27.5	3–30	4–28
0.10	29.0	3–32	4–46	0.10	28.0	4–05	5–06
0.50	32.5	5–41	7–52	0.50	28.5	5–00	6–21
1.00	40.5	6–52	9–32	1.00	30.0	5–26	7–24
Dicalcium phosphate				Sodium silico-fluoride			
P_2O_5 in cement	w/c	Initial set	Final set	F in cement	w/c	Initial set	Final set
%	%	hr.-min.	hr.-min.	%	%	hr.-min.	hr.-min.
0.000	27.5	2–23	3–18	0.00	28.5	2–40	3–35
0.013	27.5	2–35	3–03	0.01	28.5	3–30	4–27
0.016	27.5	2–35	3–07	0.05	28.5	6–31	8–23
0.126	27.5	2–58	3–48	0.10	28.0	8–25	10–39
0.633	28.0	2–50	3–47	0.50	28.0	8–17	11–41
1.265	28.5	3–18	4–38	1.00	28.8	8–35	14–07

In this table, each chemical reagent is expressed as the concentration of that in cement. The concentrations of chemical reagent to gypsum in cement is written as follows; (concentration in cement) × (33). Therefore, some portions of this experiment were undertaken at extremely high concentrations of chemical reagent.

retarding action of the P_2O_5 substituted in the crystal lattice is stronger than that of the P_2O_5 which adhered to the surface. Murakami also prepared the artificial gypsums with substituted P_2O_5 using calcium chloride, sodium sulfate and disodium phosphate. Their chemical compositions are given in Table 41. Hanada (63) prepared some portland cement containing four kinds of artificial gypsums substituting P_2O_5 and measured the time of set and the development of mortar strength at the three varied temperatures of 10°C, 20°C and 40°C. The total SO_3 content in the prepared cement is 1.0%, 2.0%, and 3.0%. The results are illustrated in Fig. 11. The cement with 1.0% SO_3 content shows a flash set, however, the retarding action in the other hand is strengthened proportionally by increasing the amount of the gypsum substituting P_2O_5 or by increasing the quantity of P_2O_5 substituted in the crystal lattice of gypsum.

Table 40. *Strength development of portland cement with various chemical reagents*

(20 ± 2°C)

P_2O_5 in cemen (%)	Bending strength (kg/cm²)			Compressive strength (kg/cm²)		
	3 days	7 days	28 days	3 days	7 days	28 days
Phosphoric acid						
0	35.2	54.1	73.3	116	219	388
0.01	34.8	53.3	74.7	117	211	407
0.05	35.8	54.1	75.2	134	233	438
0.10	33.1	52.3	76.4	133	258	421
0.50	30.1	55.0	68.0	114	275	382
1.00	20.0	44.1	63.2	62	180	340
Monocalcium phosphate						
0	27.9	47.4	76.1	116	211	388
0.01	31.0	43.9	76.9	144	198	391
0.50	34.8	45.2	77.0	140	181	424
0.10	35.0	44.9	79.2	161	204	396
0.50	37.6	46.1	74.7	158	227	399
1.00	30.1	44.9	73.3	99	197	400
Dicalcium phosphate						
0	35.0	47.4	77.4	126	205	404
0.013	31.5	44.3	71.5	126	188	368
0.016	31.7	43.8	70.6	118	204	376
0.126	29.2	43.6	80.2	121	224	420
0.633	31.6	44.1	79.2	117	203	422
1.265	31.5	44.0	75.3	123	188	351
F in cement	Sodium silico-fluoride					
0 (%)	24	48	81	126	230	426
0.01	27	49	81	124	225	434
0.05	27	52	83	123	235	436
0.10	28	59	82	123	250	421
0.50	30	53	76	147	246	409
1.00	31	60	78	140	241	436

Table 41. *Chemical compositions of artificial phosphogypsum substituting P_2O_5 in the crystal lattice of gypsum*

(%)

NO.	1	2	3	4
CaO	32.6	32.7	33.0	33.5
SO_3	45.3	45.1	44.3	43.9
H_2O	21.4	21.6	21.8	21.5
HPO_3	0.06	0.16	0.44	0.94
Total	99.36	99.56	99.54	99.84
P_2O_5*	0.05	0.13	0.35	0.74
HPO_3/SO_3	0.13	0.35	0.99	2.14

*Quantity of P_2O_5 substituted in crystal lattice

Their action are relatively severe at a lower temperature, and especially a final set is characteristically retarded. In spite of the above retarding action, as in Table 42, the development of mortar strength even at early stage of the hydration is hardly lowered by the prolonged set.

In order to systematically investigate the compound action of impurities in phosphogypsum, Murakami (65) prepared the artificial pure gypsum and artificial gypsum with the water-soluble F which adhered

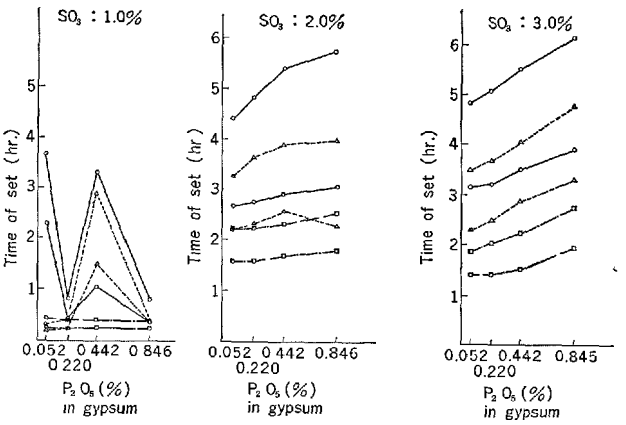

Fig. 11. *Setting time of portland cement paste with artificial gypsums substituting P_2O_5.*
—○—: curing at 10°C.
---△---: curing at 20°C.
-·-□-·-: curing at 40°C.

to the surface of crystal containing to substituted P_2O_5 in the crystal lattice. The quantity of water-soluble F added to artificial gypsum is 0.5% and 1.0%. The water-soluble F represents a fluorine content in sodium silicofluoride which adhered additionally to the surface of gypsum crystals. Hanada, again using these aritficial gypsums, prepared some portland cements with three varied SO_3 contents, such as 1.0%, 2.0% and 3.0% and he measured the time of set and the development of mortar strength at 20°C and 40°C. At 20°C, the setting is generally retarded in proportion to the amount of these gypsum. Furthermore, it is found that the development of mortar strength, in spite of the accumulation of impurities, is increased as the quantity of gypsum increases. Namely, the development of mortar strength is more closely related to the quantity of gypsum in the cement than the quantity of impurities. From the results in Tables 42 and 43, it is apparent that at 40°C the time of set is also progressively delayed in proportion to the quantity of impurities in gypsum. Consequently, the increase of impurities in the cement, resulted from the increase of either quantity of impurities in gypsum or quantity of the added gypsum with impurities, strengthens the retardation of set at 20°C and even at 40°C. But, the retardation at 40°C is less than that at 20°C. The addition of gypsum containing the substituted P_2O_5 in the gypsum lattice or the P_2O_5 which adhered to the surface of gypsum crystals does not give any adverse effect on the development of mortar strength at 40°C, within the limit of this experiment.

Sekiya (75) suggested that major part of an organic impurity in phosphogypsum may be originated from

Table 42. *Setting time and strength development of portland cement containing artificial gypsum with the substituting* P_2O_5

A.G.	SO_3 (%)	Setting			Bending strength (kg/cm²)			Compressive strength (kg/cm²)		
		w/c (%)	Initial set hr.-min.	Final set hr.-min.	3 days	7 days	28 days	3 days	7 days	28 days
Curing at 10°C										
No. 1	1.0	24.4	2–15	3–40	20.3	39.8	58.1	67	165	318
No. 2	1.0	23.9	0–20	0–48	19.1	36.5	55.6	72	141	280
No. 3	1.0	23.6	1–05	3–20	18.3	36.5	57.2	69	161	290
No. 4	1.0	23.6	0–22	0–50	18.3	37.8	54.6	66	149	289
No. 1	2.0	23.6	2–40	4–25	28.7	41.0	64.4	101	167	314
No. 2	1.9	24.0	2–45	4–50	28.3	42.3	63.6	100	176	312
No. 3	1.9	23.8	2–55	5–25	29.2	47.8	63.2	98	185	323
No. 4	2.0	24.1	3–05	5–45	27.9	43.1	61.7	95	181	305
No. 1	3.0	24.1	3–10	4–50	31.8	46.4	62.6	108	201	313
No. 2	3.0	24.0	3–15	5–05	34.1	44.0	61.5	121	186	287
No. 3	2.9	24.1	3–35	5–30	31.6	47.4	67.5	112	181	300
No. 4	2.9	24.3	4–00	6–10	32.6	44.7	64.0	117	178	299
Curing at 20°C										
No. 1	1.0	24.4	0–10	0–20	27.5	43.5	63.0	118	203	384
No. 2	1.0	23.9	0–10	0–25	25.1	40.6	59.3	110	194	361
No. 3	1.0	23.6	1–30	2–55	25.4	41.3	57.2	106	199	358
No. 4	1.0	23.6	0–17	0–23	24.6	37.8	57.0	102	174	350
No. 1	2.0	23.5	2–15	3–15	31.0	45.3	66.9	130	214	382
No. 2	1.9	24.0	2–20	3–40	32.4	47.4	67.7	135	220	387
No. 3	1.9	23.8	2–35	3–55	32.3	48.0	66.3	140	229	391
No. 4	2.0	24.1	2–20	4–00	34.1	49.6	66.0	133	217	374
No. 1	3.0	24.1	2–20	3–30	35.1	46.6	64.2	145	212	367
No. 2	3.0	24.1	2–35	3–45	36.9	50.5	68.1	143	225	382
No. 3	2.9	24.1	2–55	4–05	35.3	50.1	67.1	136	216	375
No. 4	2.9	24.3	3–25	4–50	37.7	51.1	64.9	140	223	366
Curing at 40°C										
No. 1	1.0	24.5	0–13	0–25	44.5	56.6	62.8	211	301	373
No. 2	1.0	24.0	0–12	0–20	37.8	55.8	57.5	202	288	343
No. 3	1.0	23.8	0–15	0–23	41.2	55.6	59.7	206	302	347
No. 4	1.0	23.8	0–13	0–20	38.8	50.8	52.6	207	296	343
No. 1	2.0	24.1	1–35	2–15	45.4	56.2	60.9	221	310	364
No. 2	1.9	24.1	1–35	2–15	45.3	52.1	59.3	214	309	366
No. 3	1.9	24.3	1–45	2–20	45.0	55.1	57.5	227	306	368
No. 4	2.0	24.3	1–50	2–35	43.7	56.2	59.7	224	306	365
No. 1	3.0	24.3	1–25	1–55	44.1	52.9	59.3	200	271	337
No. 2	3.0	24.1	1–30	2–05	46.0	54.0	59.9	211	297	373
No. 3	2.9	24.3	1–35	2–20	43.5	54.8	65.9	213	292	368
No. 4	2.9	24.3	2–00	2–45	42.5	56.6	62.0	198	290	347

Artificial gypsums No. 1, 2, 3 and 4 are similar to those in Table 41.
The time of set of paste and mortar made from portland cement with natural gypsum is as follows: (curing at 20°C)

	Initial set (hr.-min.)	Final set (hr.-min.)
Paste (JIS)	1–45	3–15
Mortar (ASTM)	5–50	8–45

(The quantity of SO_3 in cement is 2%)

chemical reagents which were used for the floatation of phosphate rock. In order to examine the influence of this organic impurities on the hydration of portland cement, he measured the time of set and the strength development of the cement containing oleic acid and diethylen triamine which are regarded as floating agent. But, both chemical reagents did not affect the set and strength development.

Investigation of the Retarding Action of Impurities of Phosphogypsum

Considering the various results obtained in preceding chapters, we are likely to obtain the practical evidence that most of chemical gypsums, especially even phosphogypsum, can be safely used for control of the time of set of portland cement. When a large

Table 43–1 *Setting time and strength development of portland cement containing pure gypsum.*

		SO_3 (%)	W/C	Setting		Bending strength (kg/cm²)			Compressive strength (kg/cm²)		
				Initial hr.-min.	Final hr.-min.	3 days	7 days	28 days	3 days	7days	28 days
Blastfurnace slag cement	20°C	1.0	25.2	2–30	3–50				84	190	340
		1.9	25.0	3–20	4–25				108	198	328
		3.0	24.7	3–50	4–50				129	189	320
	40°C	1.0	25.3	1–50	2–20				156	249	350
		1.9	25.0	1–50	2–30				188	298	375
		3.0	25.3	2–40	3–20				167	250	365
Portland Cement	10°C	1.0	24.3	2–10	3–20	20.5	41.8	58.6	62	159	321
		1.9	23.5	2–50	4–00	28.9	41.2	65.5	100	166	319
		3.0	24.3	3–00	4–20	31.2	46.0	63.0	110	210	313
	20°C	1.0	24.2	0–10	0–20	27.0	40.5	64.0	118	205	380
		2.0	23.5	1–45	2–45	32.4	48.2	62.6	130	230	389
		3.0	24.3	1–50	3–10	34.1	49.2	65.2	148	220	377
	40°C	1.0	24.5	0–15	0–26	43.9	57.1	62.5	215	303	371
		2.0	24.2	1–25	2–10	45.0	55.9	61.8	222	316	364
		3.0	24.2	1–20	1–40	44.3	53.9	59.5	205	273	339

W/C: water cement ratio

Table 43–2. *Setting time and strength development of portland cement containing various artificial gypsums*

			20°C						40°C					
A.G.	SO_3 (%)	Blaine cm²/g	W/C (%)	Setting		Compressive strength (kg/cm²)			W/C (%)	Setting		Comoressive strength (kg/cm²)		
				Initial hr.-min.	Final hr.-min.	3d.	7d.	28d.		Initial hr.-min.	Final hr.-min.	3d.	7d.	28d.
G. + 0.5F	1.0	3170	25.0	3–05	4–45	84	184	331	25.4	2–00	2–50	158	253	352
G. + 1.0F	1.0	3240	24.8	4–05	5–35	55	184	323	25.1	2–05	3–25	169	196	371
Ps.G. + 0.5F	1.0	3200	24.8	3–00	4–40	73	179	319	25.0	1–50	2–50	161	248	351
Ps.G. + 1.0F	1.0	3260	25.0	4–40	6–20	73	169	320	25.4	3–05	4–05	174	283	351
G. + 0.5F	1.9	3200	24.7	4–20	5–55	109	196	326	25.3	2–20	3–00	187	297	364
G. + 1.0F	1.9	3240	25.0	4–35	6–05	88	174	309	25.3	2–35	3–25	168	270	353
Ps.G. + 0.5F	1.9	3280	24.8	4–45	6–50	111	192	325	25.0	2–50	3–30	186	278	345
Ps.G. + 1.0F	2.0	3300	25.0	5–30	7–00	113	194	317	25.3	3–15	4–15	179	271	338
G. + 0.5F	2.9	3160	24.7	4–50	6–35	128	194	318	25.3	3–10	4–15	166	237	310
G. + 1.0F	3.0	3170	24.7	4–00	5–55	123	184	304	25.4	3–00	4–00	176	257	321
Ps.G. + 0.5F	2.9	3170	25.0	5–25	6–55	124	187	313	25.3	3–30	4–10	179	271	346
Ps.G. + 1.0F	2.9	3160	24.8	5–35	7–10	117	183	310	25.3	4–00	5–00	167	242	332

A.G.: artificial gypsum
G.: pure artificial gypsum
Ps.G.: artificial gypsum substituting 0.35% P_2O_5
Ps.G. + 1.0F (for example): Ps.G. adhered 1.0%F to its surface
Ps.G. with water-soluble F1.0% adhered to its surface

quantity of impurities is contained unfortunately in these gypsums, they will be inactivated by the chemical treatments mentioned above. Furthermore, in view of the character of impurities, it will be worth emphasizing that the impurities of phosphogypsum should rather be utilized than be avoided. Before reaching such conclsuion, however, it is necessary to clarify the detailed mechanism of retarding action of the impurities.

In this chapter, the influence of impurities on the hydration of tricalcium aluminate and tricalcium silicate is also studied.

The samples used in this study are the eleven varied phosphogypsums produced from the wet process in many places in Japan and some artificial gypsums containing the impurities corresponding to the quantity of that of phosphogypsum. Table 44 obtained by Murakami shows the time of set of pastes containing each kind of eleven varied phosphogypsums. Total SO_3 content of these cements is 2.0%. The chemical compositions of phosphogypsums have been shown in Table 5. When phosphogypsum containing a small amount of the water-soluble impurities is used, such as HDS-1, 2 and 4, a normal set is given as in the case of pure gypsum. When phosphogypsum containing a large amount of the water-soluble impurities is used, such as HDS-3, HD-1, 4 and D-1, the setting of cement is retarded. Especially, when D-1 is used, it is char-

Table 44. *Setting time of portland cement containing various gypsums*

	Water cement ratio %	Initial set hr.-min.	Final set hr.-min.
Pure gypsum	25.7	2–10	3–20
HDS–1	25.5	2–12	3–39
HDS–2	25.5	2–15	3–30
HDS–3	25.7	2–45	4–25
HDS–4	25.6	2–15	3–25
HDS–5	25.5	2–20	3–35
HD–1	25.5	2–49	4–06
HD–2	25.5	2–10	3–28
HD–4	25.5	2–40	4–00
HD–5	25.7	2–40	4–25
D–1	25.6	5–46	7–05
F–1	25.5	2–21	3–41
org–1	26.1	3–15	4–30
org–0.5	25.6	2–30	3–50

F–1: fluorogypsum in Table 6
org–1: artificial gypsum with 1% organic substance adhered to its surface (Organic substance was collected from crude phosphoric acid.)

acteristically retarded.

Since the tendency of setting is identical with that predicted by the results of the chemical analysis of the impurities of phosphogypsum, it is possible to conclude that the proposed procedures for the chemical analysis of the impurities of phosphogypsum are very appropriate. Murakami prepared some early strength portland cements containing phosphogypsum and artificial gypsum and measured the one day-strength of mortar. His results shown in Table 45 are closely related to the chemical compositions of the impurities given in Table 5. In other words, the one day-strength is sensitively influenced by the amount of impurities.

Heat Liberation during Hydration of Portland Cement and Clinker Minerals with Phosphogypsum

Since the hydration of portland cement and its clinker minerals is generally an exothermic reaction, the mesurement of the heat liberation process during hydration has helped in understanding the nature of various changes in the normal hydration or the prolonged hydration caused by the impurities in phosphogypsum.

For this purpose, various calorimeters have been developed by many investigators. Calorimeter is generally classified into adiabatic and conduction types (approximately "isothermal"). In the field of cement hydration, one of the former was developed by Carlson and Forblich (72) and the first of the conduction calorimeter was devised by Carlson and Lerch (72). Recently, various modifications of the conduction calorimeter have been devised and used for the studies of the cement hydration by Stein (73), Danielson (74), Portland Cement Association in

Table 45. *One-day strength of early strength portland cement containing phosphogypsum and artificial gypsum*

	Bending		Compressive	
	kg/cm²	Ratio	kg/cm²	Ratio
Pure gypsum	26.3	100	79	100
HDS–1	28.9	110	79	99
2	27.3	104	79	99
3	24.5	93	69	84
4	25.2	96	80	101
5	25.2	96	71	90
6	28.2	107	92	116
HD –1	23.6	90	77	97
2	21.6	82	69	87
3	22.2	84	66	83
4	20.8	79	61	77
5	21.6	82	61	76
D –1	20.5	78	63	80
3	22.6	86	68	86
P 0.8	20.7	79	68	86
1.8	20.8	79	68	86
F 0.1	21.6	82	70	88
0.3	19.5	75	61	76
0.5	18.3	70	61	76
1.0	16.8	64	53	66

P 1.8: artificial gypsum substituting 1.8%P_2O_5 in crystal lattice
F 1.0: artificial gypsum adhering 1.0%F to surface of crystals

U.S.A. (75) and Amaya (76). In the present study, both types of the calorimeter devised in the author's laboratory are used. The cross sections of these two calorimeters are schematically shown in Figures 12 and 15, respectively. The detailed operating procedure of the adiabatic calorimeter has already reported (77).

The valuable characteristic of this device is that the heat liberation developed immediately after cement comes into contact with water can be easily measured. Therefore, it is better than the conduction calorimeter in order to study such rapid reaction as a hydration of tricalcium aluminate. It has been well known that the hydration process of tricalcium aluminate is intricately affected by the temperature of hydration and the co-existing other material in the hydration (77–79). Therefore, for the purpose of studying the role of tricalcium aluminate on the hydration of portland cement, the system required for measuring the hydration process of tricalcium aluminate should be corresponded to the condition of hydration of portland cement.

However, there are some unsolved phenomena which may be caused by the complicated matrix structure of cement clinker or alkali in clinker in the hydration of portland cement. It is still difficult to understand completely the hydration behavior of tricalcium aluminate.

In spite of the features mentioned above, some relatively simple systems are used to study the effects of impurities of phosphogypsum on the hydration of

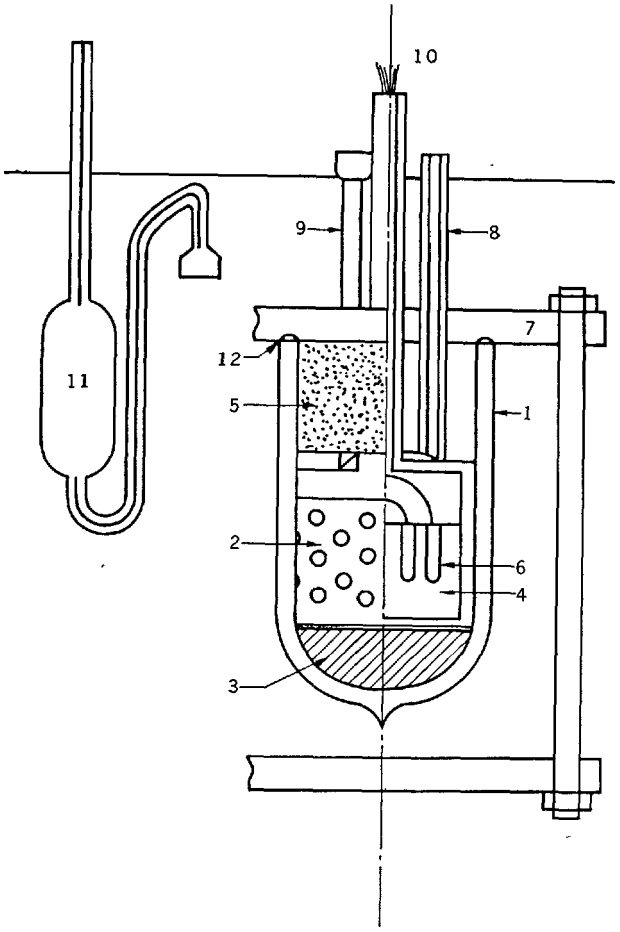

Fig. 12. *Construction of devised adiabatic calorimeter.*

1. Vacuum bottle, 100cc.
2. Bakelite cell.
3. Paraffin ground.
4. Powder sample.
5. Wood stopper.
6. Thermocouple holder.
7. Bakelite plate to keep wood stopper.
8. Air stack.
9. Water stack.
10. Thermopile.
11. Water holder.
12. Rubber packing.

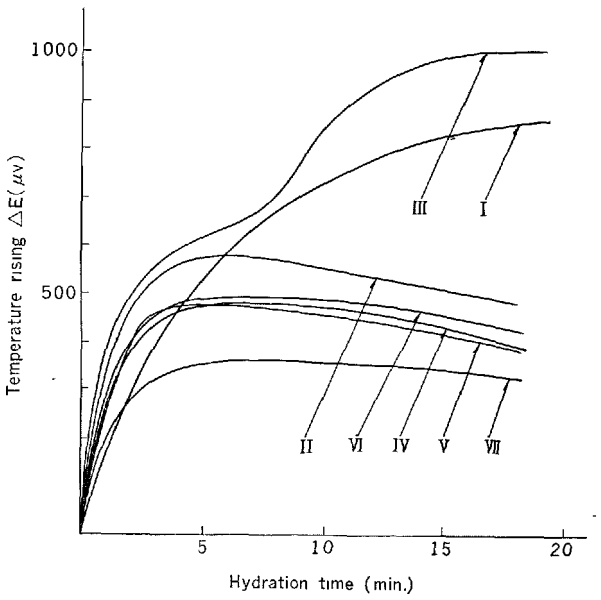

Fig. 13. *Heat liberation curves on hydration of C_3A in various systems.*

I: C_3A–H_2O.
II: C_3A–Pure gypsum–C_3S–H_2O.
III: C_3A–Pure gypsum-H_2O.
IV: C_3A–HDS–1–C_3S–H_2O.
V: C_3A–D–1–C_3S–H_2O.
VI: C_3A–0.3% Ss.P_2O_5, 1.0% F Gypsum–C_3S–H_2O.
VII: C_3A–1.8% Ss.P_2O_5, 0.3% F Gypsum–C_3S–H_2O.
Preparation
C_3A(3 g) + C_3S(1 g) + Gypsum(1 g) + H_2O(13 cc)
+ diluent — Al_2O_3(19 g).
Temperature 20°C ± 0.01°C.

tricalcium aluminate, namely: C_3A–H_2O system, C_3A–C_3S–$CaSO_4 2H_2O$–H_2O system and C_3A–$CaSO_4 2H_2O$–H_2O system. The curves illustrated in Figure 13 show the heat liberation process of the hydration of tricalcium aluminate in various systems at 20°C. Curve I shows that the hydration of tricalcium aluminate alone in water consists, first, of the rapid rising on heat liberation indicating the first formation of hexagonal plate-like crystals (C_4AH_x and C_2AH_8) on the surface of tricalcium aluminate grains immediately after they come into contact with water and, second, of the subsequently slow rising on the heat liberation indicating probably the termination of the initial rapid hydration by the formation of protective coating on the surface of tricalcium aluminate grains. Also, it has been suggested that the conversion from C_4AH_x and C_2AH_8 to cubic C_3AH_6 as well as the direct formation of C_3AH_6 in the hydration of tricalcium aluminate occures in the latter half of curve I. Curve II shows that the combination of calcium hydroxide produced from the hydration of tricalcium silicate and gyspum is very effective on retarding the hydration of tricalcium aluminate. Some investigators have emphasized that the tight protective coatings of trisulfate formed on the surface of tricalcium aluminate grains suppress the subsequent hydration of tricalcium aluminate (78, 79). Curve III shows that the addition of only gypsum accelerates the rapid formation of trisulfate, and does not give an available suppression on the hydration of tricalcium aluminate. Curves IV, V, VI and VII show that, when tricalcium aluminate is mixed with phosphogypsum and aritficial gypsum containing impurities, the suppressing action

to the heat liberation is a little more strengthened than when it is mixed with pure gypsum. This tendency is also observed on the heat liberation process immediately after portland cement comes into contact with water. The early stage of hydration of tricalcium aluminate and portland cement is considerably different from that of tricalcium silicate, moreover, their hydration processes are not markedly affected by the impurities of phosphogypsum, even when a large amount of phosphogypsum is used.

Especially, it has frequently been said that "immediate heat" in early stage of the hydration of portland cement is not mainly caused by the hydration of tricalcium aluminate and calcium aluminoferrite, but that it may be partly caused by such complex exothermic reaction as the hydration of clinker minerals containing alkali or the hydration of defect in all the clinker minerals. Therefore, it is consequently considered that the influence of tricalcium aluminate on a initial heat liberation of the hydration of portland cement may be relatively small. The results illustrated in Fig. 14 show that the initial heat liberation of portland cement is only slightly lowered by phosphogypsum D-1 and aritficial gypsum with the large amounts of impurities.

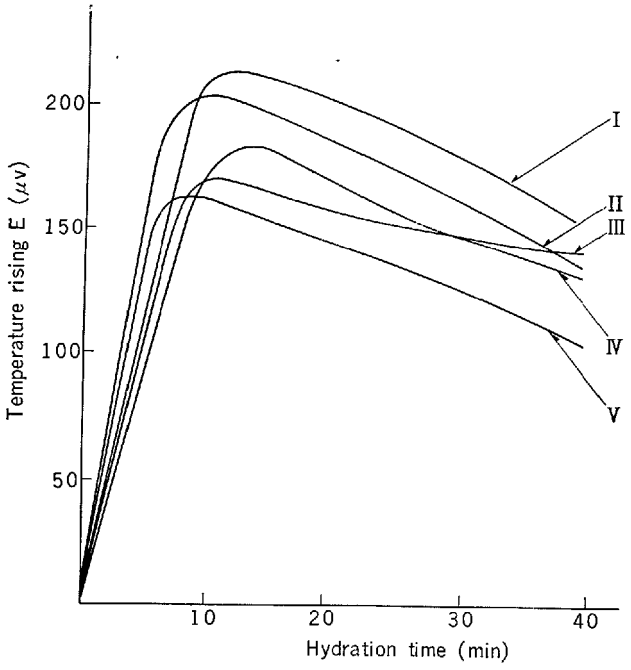

Fig. 14. *Curves of "immediate heat" of portland cement with various gypsums.*
I: Synthetic pure gypsum 4%.
II: Synthetic pure gypsum 8%.
III: D-1.
IV: 0.05%P_2O_5, Ss-gypsum.
V: 0.74%P_2O_5, Ss-gypsum.
Temperature 25°C ± 0.01°C.

Since the calorimeter, as illustrated in Fig. 15, is not capable of determining the rate of the hydration reaction immediately after cement comes into contact with water, it is not suitable for measuring the rapid hydration of tricalcium aluminate. On the other hand, such device is very appropriate for the slow and long continued hydration of tricalcium silicate and portland cement, because the rate of their hydration can be determined by using the paste and mortar prepared with a practical water-cement ratio and a definite agitation. The conduction calorimeter used in this experiment consists of three parts, namely: sample holder (4, 5, 7), heat flow meter (6) aluminum base and block (2, 1). The heat flow meter is made of a polyvinylchloride round plate (thickness 3 mm, diameter 50 mm), on each of both surfaces of which thirty-eight thermocouples [chromel (diameter 0.1mm)—constantan (diameter 0.1mm)] are arranged in series. The sample holder is a double layered container, consisting of the inner tray being made of 18-8 stainless steel and the outer tray being made of copper. They directly contact together for good thermal conduction and the inner tray can be easily removed from the outers. The former directly holds the cement paste and mortar owing to its resistance to the strong alkali solution in cement paste. The outer tray does not directly holds the paste for fear that it may be ruined by the strong alkali solution in the cement paste.

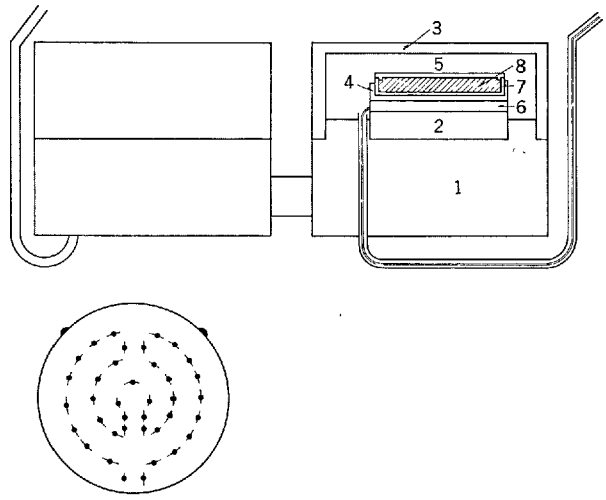

Fig. 15. *Construction of devised conduction calorimeter.*
1. Aluminum block
2. Aluminum base
3. Aluminum cap
4. Copper vessel (Outer tray)
5. Steel cap
6. Polyvinylchloride heat flow meter
7. Sample holder (Inner tray)
8. Cement paste

The bottom surface of the outer tray is tightly bound to the upper surface of the heat flow meter with a thin layer of epoxy resin in order to provide for a good electric insulation and a thermal conduction between the both surfaces. Similarly, the under surface of the heat flow meter is tightly bound to the upper surface of aluminum base. Moreover, the lower half of aluminum base is tightly set in a cavity made on the surface of aluminum block. Aluminum has a good thermal conductivity and the outer surface of the block always comes into contact with water in the both which is kept at constant temperature (20 ± 0.005°C) during the runs. Though the construction of the present device is approximately analogous to that of Stein's calorimeter, it is dum-bell type and is capable of measuring the heat liberation of two paste simultaneously.

In the case of this device, the rate of heat liberation of paste (cal/g.hr.) is shown by the following equation:

$$q = A\Delta E + B \cdot d(\Delta E)/dt$$

where ΔE is the temperature difference or voltage difference between the two surfaces of heat flow meter (mV), t is the time (hr.), A is the thermal conductivity (cal./g.hr.mV) of the heat flow meter and B is the total heat capacity (cal./g.mV) of sample holder, cap and paste.

A_I 9.83×10^{-1} B_I 15.83×10^{-1}

A_{II} 10.73×10^{-1} B_{II} 15.97×10^{-1}

Murakami measured the rate of heat liberation on the hydration of pastes made from portland cement containing phosphogypsum given in Table 5. Tables 46-1 and 46-2 show the chemical compositions of portland cement clinker, tricalcium aluminate and tricalcium silicate. The curves shown in Figs. 16-24 indicate that the time when the apex on the second cycle corresponding to a period of the most rapid hydration of tricalcium siliate phase in cement clinker appears is delayed as the amount of impurities of phosphogyspum increases. In other words, "dormant period" from the end of the first cycle to the beginning of the second cycle is markedly lengthened with increasing the amount of impurities. The development of the second cycle with phosphogypsum with less impurities, such as HDS-1, 2, 4 and 5 and HD-2, is approximately similar to that with pure gypsum (Figs. 16 and 17). This tendency closely relates to the results When the artificial gypsums containing such water-soluble phosphates as phosphoric acid, monocalcium phosphate and dicalcium phosphate which adhered to the surface of gypsum crystals with the substituted P_2O_5 are used, their retarding actions increase as the acidity of phosphates which adhered to the surface increases, namely; its degree is strengthened in the order of phosphoric acid > monocalcium phosphate > dicalcuim phosphate. In this case, the retarding action of the setting time of cement paste and the strength development of early strength cement mortar in reference to the quantity of impurities. The retarding action of artificial gypsum with only P_2O_5 substituted in the crystal lattice is relatively weak (Fig. 18).

Table 46–1. *Chemical compositions and mineral compositions of portland cement clinker*

(%)

Blaine 3250 ± 20 cm²/g								
Ig. loss	SiO_2	Al_2O_3	Fe_2O_3	CaO	MgO	SO_3	Total	f. CaO
0.8	20.8	5.3	3.2	64.4	2.6	0.5	97.6	1.6

C_3S	βC_2S	C_3A	C_4AF	f. CaO	MgO	$CaSO_4$
56.0	17.4	8.6	9.7	1.6	2.6	0.8

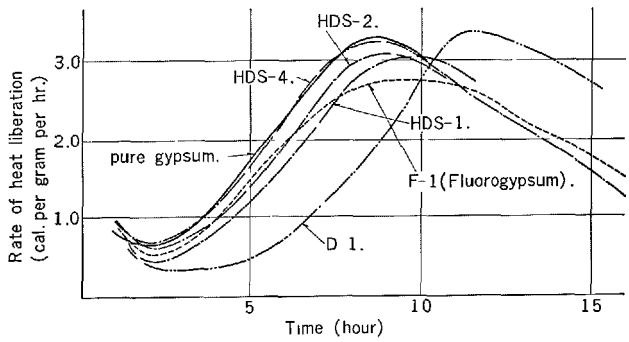

Fig. 16. *Effect of phosphogypsums on rate of hydration of portland cement. (Powder of ordinary portland cement clinker 50 g + gypsum 1.5 g + H_2O 14 cc.) (Water-cement ratio 27%.) (Agitation 3 minutes)*

———: pure gypsum. —·—1: HDS-1.
– – – –: F-1 (Fluorogypsum) —·—2: HDS-2.
—·—·—: D-1. —·—3: HDS-4.

Table 46–2. *Chemical compositions of* C_3A *and* C_3S

(%)

	Ig. loss	CaO	SiO_2	Al_2O_3	MgO	Fe_2O_3	f. CaO	Total
C_3A	0.03	62.34	—	37.50	—	0.04	0.3	99.91
C_3S	—	73.81	26.01	0.01	0.03	0.02	0.5	99.88

also increases in proportion to the quantity of the substituted P_2O_5 in the crystal lattice (Figs. 19-22). Figure 23 shows the effect of artificial gypsum with the water-soluble F which adhered to the surface of the pure gypsum crystals and the gypsum crystals substituting P_2O_5. From these results, it is apparent that the retarding action of the water-soluble F is stronger than that of the water-soluble P_2O_5. Also, the retarding action is progressively strengthened as the quantity of the water-soluble F and of the substituted P_2O_5 in gypsum increase (Figs. 23 and 24).

The curves illustrated above on the rate of the heat liberation process show that there is no appreciable difference between the tangent of the ascending curve of the second peak that is normally developed and that of the ascending curve of the second peak that is considerably retarded. Therefore, the mechanism of retardation is likely that the impurities of phosphogypsum do not directly relate to the hydration reaction of tricalcium silicate, but that the hydration products connected with the impurities are formed as the protective coatings on the surface of cement particle, thus, those suppress temporarily the hydration reaction of tricalcium silicate.

In order to confirm whether the hydration of tricalcium silicate is mainly retarded by the impurities in phosphogypsum or not, the rate of the heat liberation is measured on the hydration of pastes made from the mixture of tricalcium silicate and tricalcium aluminate

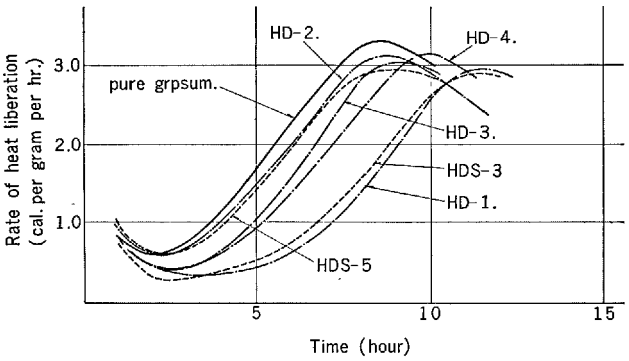

Fig. 17. *Effect of phosphogypsums rate of hydration of portland cement. (Powder of ordinary portland cement clinker 50 g + gypsum 1.5 g + H_2O 14 cc) (Water-cement ratio 27%) (Agitation for 3 minutes.)*

——— : pure gypsum.
-----1: HDS-3.
·····2: HDS-5.
—·—1: HD-1.
—·—2: HD-2.
—·—3: HD-4.
—·—4: HD-3.

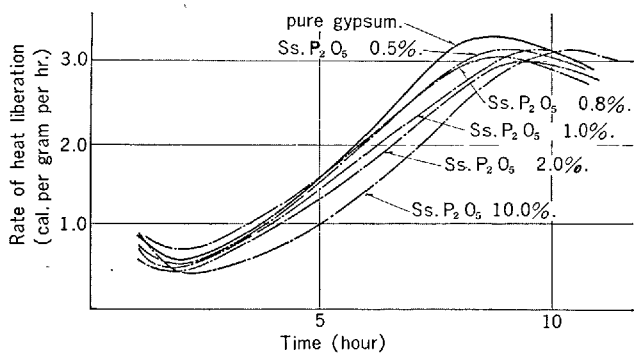

Fig. 18. *Effect of artificial gypsums with P_2O_5 substituted in the crystal lattice. (Powder of ordinary portland cement clinker 50 g + gypsum 1.5 g + H_2O 14 cc.) (Water-cement ratio 27%.) (Agitation for 3 minutes.)*

——— : pure gypsum.
—·—1: $Ss.P_2O_5$ 0.5%.
—·—2: $Ss.P_2O_5$ 0.8%.
—·—3: $Ss.P_2O_5$ 1.0%.
—·—4: $Ss.P_2O_5$ 2.0%.
—·—5: $Ss.P_2O_5$ 10.0%.

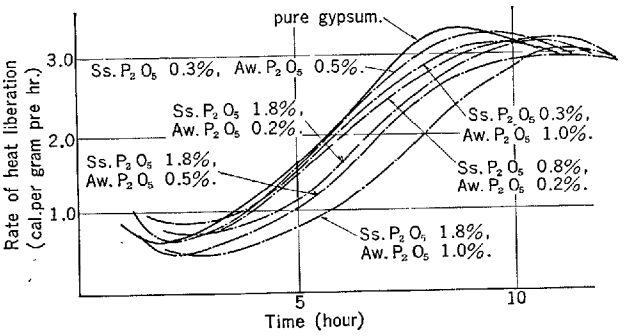

Fig. 19. *Effect of artificial gypsums with H_3PO_4 adhered to the crystal surface and P_2O_5 substituted in the crystal lattice. (Powder of ordinary portland cement clinker 50 g + gypsum 1.5 g + H_2O 14 cc.) (Water-cement ratio 27%.) (Agitation for 3 minutes.)*

——— : pure gypsum.
—·—1: $Ss.P_2O_5$ 0.3%, $Aw.P_2O_5$ 0.5%.
—·—2: $Ss.P_2O_5$ 0.3%, $Aw.P_2O_5$ 1.0%.
—·—3: $Ss.P_2O_5$ 0.8%, $Aw.P_2O_5$ 0.2%.
—·—4: $Ss.P_2O_5$ 1.8%, $Aw.P_2O_5$ 0.2%.
—·—5: $Ss.P_2O_5$ 1.8%, $Aw.P_2O_5$ 0.5%.
—·—6: $Ss.P_2O_5$ 1.8%, $Aw.P_2O_5$ 1.0%.

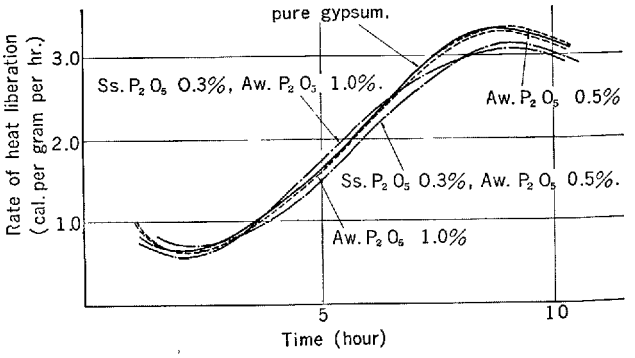

Fig. 20. *Effect of artificial gypsums with $Ca(H_2PO_4)_2 \cdot H_2O$ adhered to the crystal surface and P_2O_5 substituted in the crystal lattice. (Powder of ordinary portland cement clinker 50 g + gypsum 1.5 g + H_2O 14 cc.) (Water-cement ratio 27%.) (Agitation for 3 minutes.)*

——— : pure gypsum.
-----1: Aw. P_2O_5 0.5%.
·····2: Aw. P_2O_5 1.0%.
—·—1: $Ss.P_2O_5$ 0.3%, Aw. P_2O_5 0.5%.
—·—2: $Ss.P_2O_5$ 0.3%, Aw. P_2O_5 1.0%.

with phosphogypsum and artificial gypsum as illustrated in Fig. 25. These results show that the change caused by the impurities in the development of the second peak is more apparently observed in experiments using the mixture of the both clinker minerals than those using portland cement. Consequently, it may be concluded that only the hydration reaction of tricalcium silicate is predominantly delayed by the impurities of phosphogypsum.

Another interesting phenomenon concerned with the retarding action is also observed in Fig. 25. It has been well known that the third peak in the heat liberation curve is caused by the rapid hydration of tricalcium aluminate occurring immediately after the protective coatings of trisulfate produced on the surface of tricalcium aluminate grains at early stage of the hydration were broken. The development of the third peak on the hydration of the mixture of

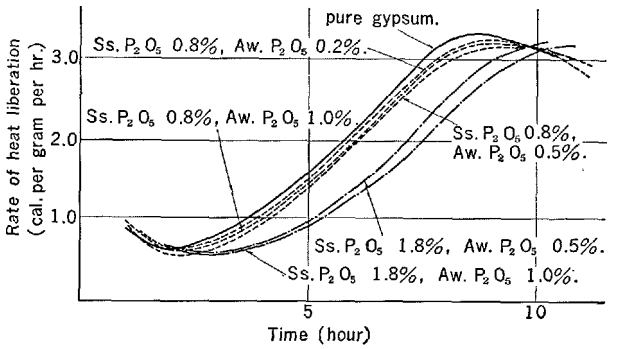

Fig. 21. *Effect of artificial gypsums with* $Ca(H_2PO_4)_2 \cdot H_2O$ *adhered to the crystal surface and* P_2O_5 *substituted in the crystal lattice. (Powder of ordinary portland cement clinker 50 g + gypsum 1.5 g +* H_2O *14 cc) (Water-cement ratio 27%.). (Agitation for 3 minutes.)*

——— : pure gypsum.
—·—1: Ss.P_2O_5 1.8%, Aw. P_2O_5 0.5%.
—·—2: Ss.P_2O_5 1.8%, Aw. P_2O_5 1.0%.
------1: Ss.P_2O_5 0.8%, Aw. P_2O_5 0.2%.
------2: Ss.P_2O_5 0.8%, Aw. P_2O_5 0.5%.
------3: Ss.P_2O_5 0.8%, Aw. P_2O_5 1.0%.

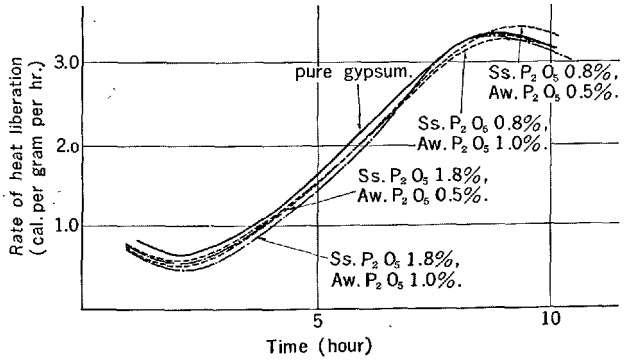

Fig. 22. *Effect of artificial gypsums with* $CaHPO_4 \cdot 2H_2O$ *adhered to the crystal surface and* P_2O_5 *substituted in the crystal lattice. (Powder of ordinary portland cement clinker 50 g + gypsum 1.5 g +* H_2O *14 cc.) (Water-cement ratio 27%.) (Agitation for 3 minutes.)*

——— : pure gypsum.
—·— : Ss.P_2O_5 1.8%, Aw. P_2O_5 1.0%.
------1: Ss.P_2O_5 0.8%, Aw. P_2O_5 0.5%.
------2: Ss.P_2O_5 0.8%, Aw. P_2O_5 1.0%.
------3: Ss.P_2O_5 1.8%, Aw. P_2O_5 0.5%.

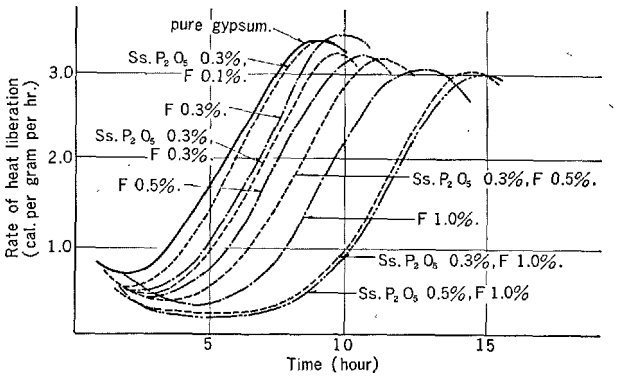

Fig. 23. *Effect of artificial gypsums with the water-soluble F adhered to the crystal surface and* P_2O_5 *substituted in the crystal lattice,* (C_3A–C_3S *mixture 35 g + gypsum 1.5 g +* H_2O *14 cc.) (Water-cement ratio 37%.) (Agitation for 3 minutes.)*

——— : pure gypsum.
------1: Ss.P_2O_5 0.3%, F 0.1%.
------2: Ss.P_2O_5 0.3%, F 0.3%.
------3: Ss.P_2O_5 0.3%, F 0.5%.
------4: Ss.P_2O_5 0.3%, F 1.0%.
—·—1: F 0.3%.
—·—2: F 0.5%.
—·—3: F 1.0%.
—··— : Ss.P_2O_5 0.5%, F 1.0%.

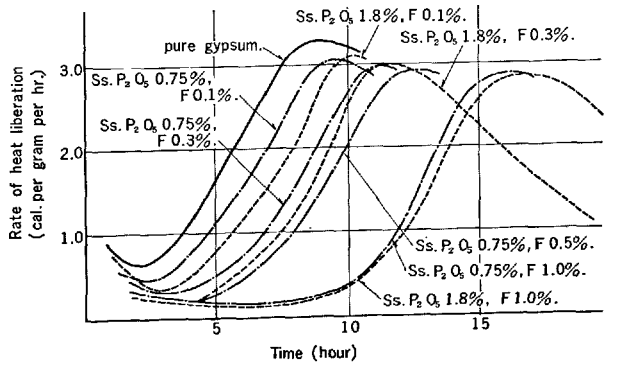

Fig. 24. *Effect of artificial gypsums with the water-soluble F adhered to the crystal surface and* P_2O_5 *substituted in the crystal lattice. (Powder of ordinary portland cement clinker 50 g + gypsum 1.5 g +* H_2O *14 cc.) (Water-cement ratio 27%.) (Agitation for 3 minutes.)*

——— : pure gypsum.
------1: Ss.P_2O_5 1.8%, F 0.1%.
------2: Ss.P_2O_5 1.8%, F 0.3%.
------3: Ss.P_2O_5 1.8%, F 1.0%.
—·—1: Ss.P_2O_5 0.75%, F 0.1%.
—·—2: Ss.P_2O_5 0.75%, F 0.3%.
—·—3: Ss.P_2O_5 0.75%, F 0.5%.
—·—4: Ss.P_2O_5 0.75%, F 1.0%.

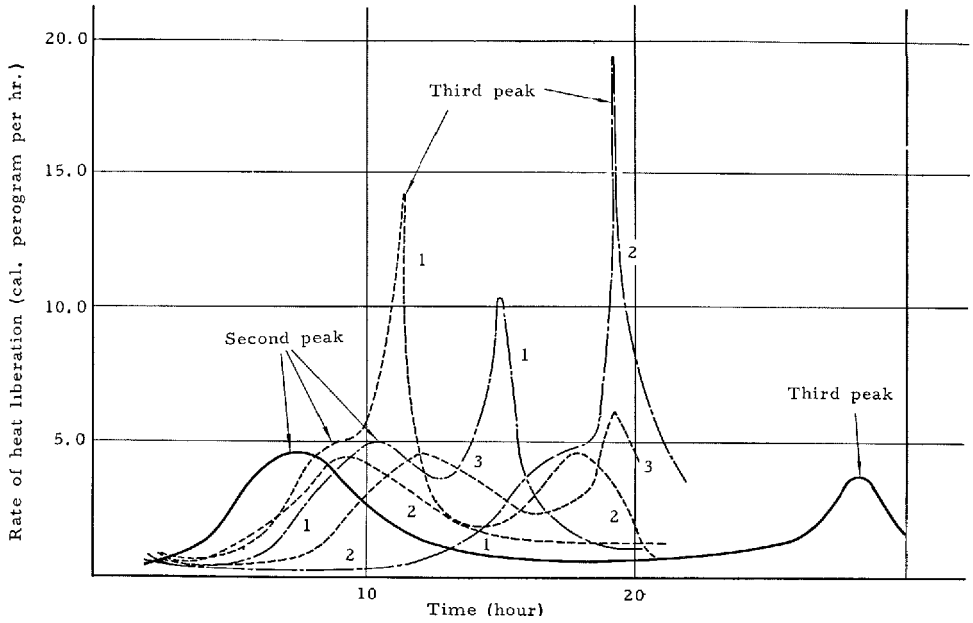

Fig. 25. *Effect of phosphogypsums and artificial gypsums with the adhered water-soluble F and the substituted* P_2O_5 *on the rate of hydration of* C_3A–C_3S *mixture.* (C_3A–C_3S *mixture 35 g + gypsum 1.5 g +* H_2O *13 cc.*) (*Water-cement ratio 37%.*) (*Agitation for 3 minutes.*) *Composition of the mixture is* C_3S (*30 g*) *and* C_3A (*5 g*).

——— : pure gypsum.
—·—1: phosphogypsum HD–4
—·—2: phosphogypsum D–1.
- - - - -1: artificial gypsum F 0.3%.
- - - - -2: artificial gypsum Ss. P_2O_5 0.3%.
- - - - -3: artificial gypsum Ss. P_2O_5 0.3%, F 0.3%.

tricalcium aluminate and tricalcium silicate is observed after approximate thirty hours, when pure gypsum is used. However, when phosphogypsum with a large amount of impurities such as D-1 and some artificial gypsums is used, the development of the third peak is markedly accelerated and is characteristically found on the apex of the second peak in the heat liberation curve.

A resonable explanation for the accelerated third peak is probably that the protective coatings suppressing the first rapid hydration of tricalcium aluminate are not only made of trisulfate, but also structurally strengthened by calcium silicate hydrates produced from the hydration of tricalcium silicate. Because, when the hydration of tricalcium silicate is extremely delayed by the impurities, the development of third peak is more markedly accelerated than that without impurities.

Measurement of Specific Surface Area by Water Vapor Adsorption

It is suggested that the thermal measurement alone on the hydration process of portland cement or clinker minerals is still insufficient for understanding the mechanism of the retardation of set and the development of the strength at early stage by the impurities. In addition to this, the quality and morphology of the hydration products formed in the presence of impurities should be studied. For this purpose, the measurement of the specific surface area of hydration products is considered to be meaningful. On the measurement of specific surface area, it has been frequently discussed about the kinds of adsorbed gas. Powers (81), using water vapor, has reported the details of the structure of cement paste hardened under various conditions. Recently, Hunt and Mikhail (82, 83) studied the structure of the hardening psate by using water vapor, nitrogen, methanol vapor, isopropanol vapor and cyclohexan vapor. They reported that the fine structure of the hardening paste is so sensitive to the polarity and the molecular cross area of adsorbed gas that the change of fine structure of paste with varying the water-cement ratio could be evidently detected.

Since the molecular cross area of water vapor is

Table 47. *Specific surface areas of hydration products of portland cement and the mixture of* C_3A *and* C_3S

	Portland cement (m^2/g)						Mixture of C_3A–C_3S (m^2/g)					
	30 min.	3 hr.	6 hr.	14 hr.	24 hr.	48 hr.	30 min.	3 hr.	6 hr.	14 hr.	24 hr.	48 hr.
No gypsum	3.0	5.9	7.0	20.9	35.6	76.1	6.2	11.9	21.1	58.6	93.9	119
Pure gypsum	3.4	13.6	16.5	38.3	74.4	99.9	4.0	5.5	21.0	59.7	94.8	110
HDS-4	4.1	11.0	15.7	38.5	64.5	89.4	4.8	5.1	12.4	60.3	87.9	105
HDS-3	5.1	—	13.2	—	—	—	—	—	—	—	—	—
D-1	3.4	8.0	12.2	14.1	48.2	81.8	4.2	4.7	9.0	35.9	43.2	112
Ss.P_2O_5 −0.05%	5.4	8.7	16.0	32.4	61.1	83.5	3.9	4.8	9.6	52.9	96.9	105
Ss.P_2O_5 −0.74%	7.3	9.3	12.1	28.6	60.4	84.0	4.1	4.6	9.5	43.1	96.4	116
F −0.5%	5.9	6.9	9.7	27.1	51.9	80.2	4.1	4.9	9.5	49.0	94.7	101
F −1.0%	5.8	6.1	9.2	28.3	52.8	77.6	4.2	4.0	9.3	38.6	98.7	101
Ss.P_2O_5 −0.05% F −0.5%	4.6	5.9	8.6	25.3	57.8	85.2	4.2	4.7	9.2	34.3	93.5	119
Ss.P_2O_5 −0.05% F −1.0%	4.8	6.0	7.7	27.9	57.2	85.6	4.3	4.7	9.3	32.5	90.4	96.7

Adsorbent: water vapor
Hydration temperature: 20°C
Preparation: powdered portland cement clinker 5 g + gypsum 0.2 g + H_2O 2.5 g
C_3A 1 g + C_3S 7 g + gypsum 0.3 g + H_2O 4 g
Ss.P_2O_5: artificial gypsum with P_2O_5 substituted in the crystal lattice
F: artificial gypsum with water-soluble F adhered to the crystal surface

smaller than any one of the aforementioned gases, it is favorable to measure total surface area of the hydration products of cement independent of the water-cement ratio. Table 47 obtained by Murakami shows the specific surface area of pastes made from portland cement and the mixture of tricalcium aluminate and tricalcium silicate with various gypsums listed in the first column of Table 47. Since there is no difference caused by the kinds of gypsum in the specific surface area of plastic paste after thirty minutes, it can be also said that the hydration of tricalcium aluminate or the early stage of hydraion of portland cement is not relatively affected by the impurities of phosphogypsum. The increase of specific surface area of the paste of portland cement during the period from three hours to twenty-four hours or that of the mixture from six hours to twenty-four hours, namely, corresponding to the setting period, is markedly lowered as the amount of impurities increases. Accordingly, it is natural that the development of one day-strength of mortar becomes insufficient when the increase in specific surface area is delayed into what is normally the hardening period. A similar results has also been obtained in the case of one day-strength of mortar of the early strength portland cement.

Since the lag caused by the impurities in specific surface area of the hydration products in setting period, as shown in Table 47, is gradually restored from twenty-four hours to fourty-eight hours, even when the retarding action is relatively strong, it is true that development of three day-strength is scarcely affected.

Consequently, it is again confirmed that the impurities of phosphogypsum effectively retard the hydration of tricalcium silicate. However, phosphogypsum containing less impurities, such as HDS-1, 2, and 4 as well as pure gypsum, does not seriously affect the hydration of portland cement and the cement clinker minerals.

Retarding Mechanism of Water-Soluble F and Water-Soluble P_2O_5

The author has already suggested that the mechanism of the retarding action may be that the impurities of phosphogypsum probably form the protective coatings on the grains of the cement and tricalcium silicate to suppress temporarily the hydration of cement. The study for ascertaining the proposed explanation has been undertaken by Murakami (65), Suzukawa and Kobayashi (71). The former reported that only little amount of P_2O_5 is detected in the liquid phase extracted from the paste from one minute to eight hours after the preparation of paste. Since the liquid phase in paste of portland cement has generally the high pH value due to the high concentration of lime and alkali, it is naturally suggested that the insoluble calcium salts are produced near the cement particles immediately after P_2O_5 enters into the liquid phase and subsequently they cover the surface of the cement grains. Suzukawa and Kobayashi, quoting the explanation proposed by Jones and Forsen, said that the P_2O_5 in gypsum may be settled consequently near cement particle in the paste as the compounds of C_3A–$CaSO_4$–P_2O_5 system.

Furthermore, Murakami, considering such phenomenon that sodium silicofluoride usually produces silica gel or alkali silicates by the reaction with strong alkali, proposed the following equations on the

retarding action of the water-soluble F originated from sodium silicofluoride;

$$Na_2SiF_6 + CaO + H_2O \text{ (or } Ca(OH)_2) \rightarrow CaF_2 + SiO_2 + NaOH \quad \ldots\ldots(1)$$

$$\text{or} \rightarrow CaF_2 + \text{Calcium Silicate Hydrates} + NaOH \quad \ldots\ldots(2)$$

$$\text{or} \rightarrow CaF_2 + \text{Calcium Silicate Hydrates} + \text{Sodium Silicates} \quad \ldots\ldots(3)$$

In spite of the incomplete reaction, the reaction products corresponded to the right side of the above equations have a larger specific surface area (115 $m^2/g.$) than the algebraical sum of those of each component, namely; CaO–H_2O (16.2 $m^2/g.$) and Na_2SiF_6 (1.3 $m^2/g.$). Additionally, X-ray diffraction pattern of the reaction products showed the formation of calcium silicate hydrates. These results indicate that the reaction between the water-soluble F and the lime in high alkaline solution of the cement paste is available.

It may be confirmed by explanation that the high-lime surface of the cement particle is attacked by the water-soluble F and that the protective coatings consisted of silica gel or calcium silicate hydrates are produced on the surface of cement grains. However, the chemical compositions of these coatings have essentially the isomeric relations to the hydration products of portland cement. Therefore, the author suggested that they do not injuriously act on the hydration of portland cement, but may cause only the temporary retardation.

The water-soluble F of fluorogypsum does not so markedly retard the hydration of cement as the water-soluble F of phosphogypsum, because most of them originate from fluoric acid.

Electronmicroscopic Observation on the Surface of Hydrating Tricalcium Silicate Grains

Murakami, using electron microscope, observed directly the influence of impurities on the hydration of tricalcium silicate. He prepared some pastes from tricalcium silicate and the mixture of tricalcium silicate and tricalcium aluminate with artificial gypsum containing the watersoluble F 1.0% and the water-solbule P_2O_5 1.0% and phosphogypsum D-1. Then, the carbon replica of the hydration products at 15 minutes, 30 minutes, 120 minutes and 300 minutes were made by the dispersion method.

Electronmicrophotographs illustrated in Photo 2 show that the formation of CSH-like products is increasingly developed with time on the hydration of tricalcium silicate containing pure gypsum. In the three cases using gypsums with impurities, it is apparent that a small amount of the CSH-like products is produced only at the latter stage of the hydration and that the hydration is markedly retarded.

Closure

The present investigations have been undertaken at the time when various gypsums in Japan are being utilized progressively in cement industry. It has been recognized that phosphogypsum among chemical gypsums is valuable as a main source of gypsum for cement industry. However, there have been many problems to be solved on the impurities included in phosphogypsum. The results obtained in the present study show significantly that a prediction that the impurities of phosphogypsum injuriously affect the hydration of portland cement should be converted to a view that the impurities of phosphogypsum can be useful as the suitable retarder for portland cement.

If, however, the presence of impurities is still undesirable, they can be removed or inactivated by applying the chemical treatment shown in this paper.

Considering the great advantages which are brought by the utilization of waste products such as chemical gypsum, the present success in Japan will certainly become a valuable example.

Acknowledgment

The author is indebted to
Yoshino Sekko Kabushiki Kaisha
Tohoku Hiryo Kabushiki Kaisha
Japan Steel & Tube Corp.
Toyo Koatsu Industries, Inc.
for supplying the chemical gypsums.

The research was supported in part by financial assistance from the Cement Association of Japan.

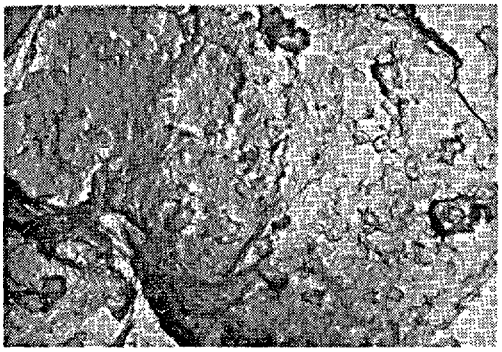

15 mins.

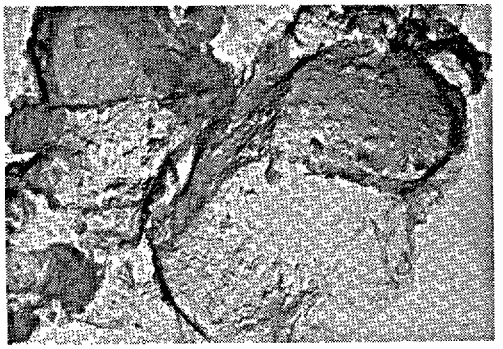

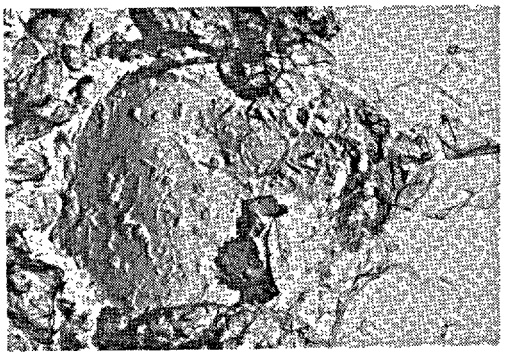

30 mins.

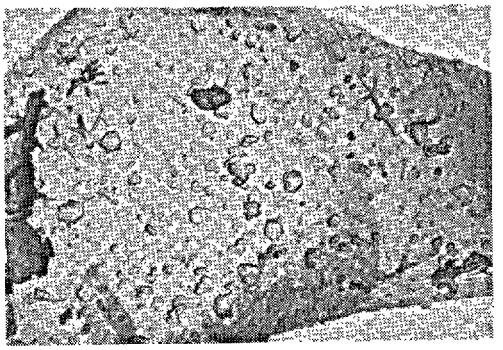

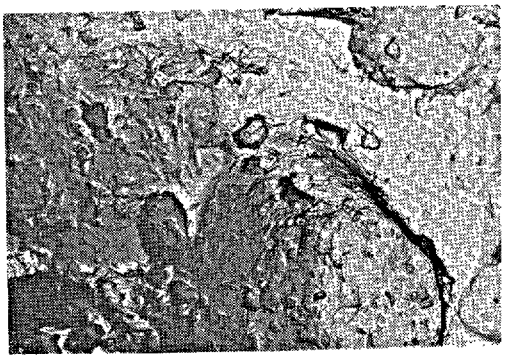

2 hrs.

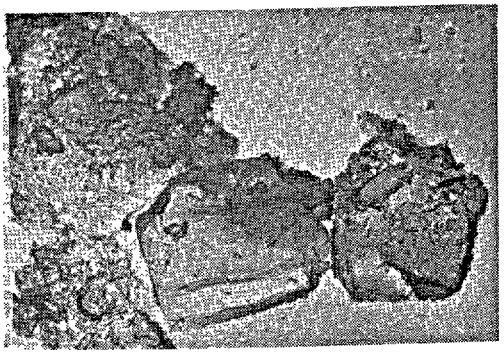

5 hrs.

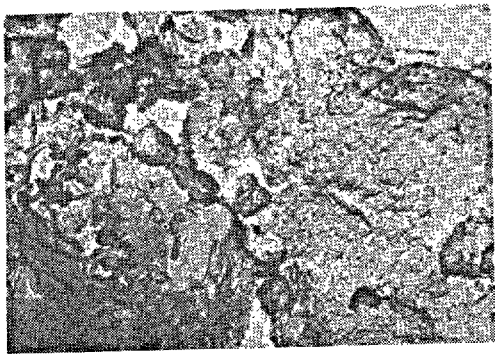

C_3S-pure artificial gypsum

C_3S-artificial gypsum with 1%F

Photo 2. *Electronmicroscopic photographs of surface of the hydrating* C_3S *and* C_3A *in presence of impurities* (×600)

15 mins.

15 mins.

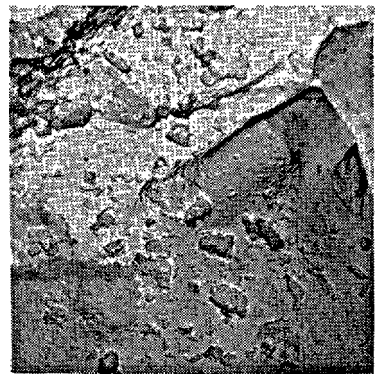

30 mins.

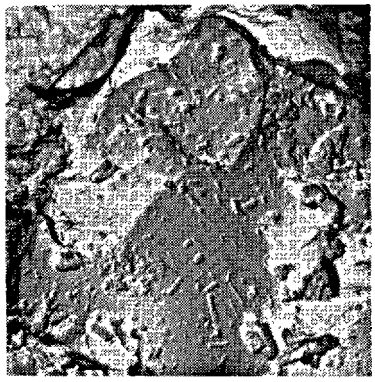

30 mins.

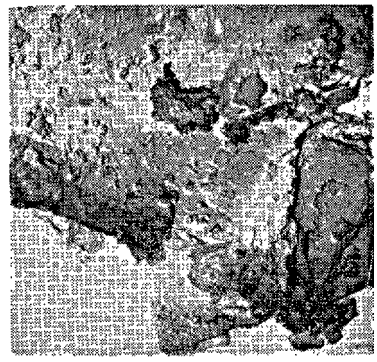

2 hr.

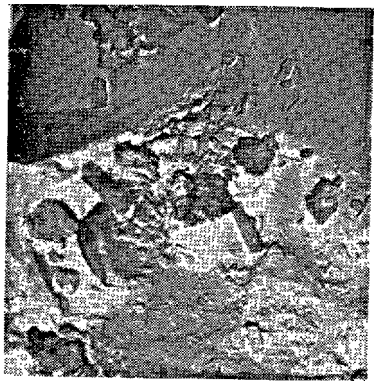

2 hrs.

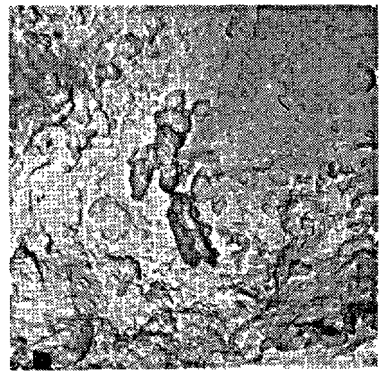

5 hrs.

5 hrs.

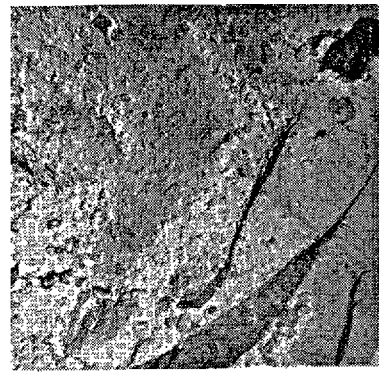

C_3S–C_3A–artificial gypsum with substituting P_2O_5

C_3S–C_3A–phosphogypsum D-1

Photo 3. *Electronmicroscopic photographs of surface of the hydrating* C_3S *and* C_3A *in presence of impurities* ($\times 600$)

References

1. M. Sekiya, Sekko, p. 143–174, (Gihodo, Tokyo, Japan, 1965).
2. Sekko Sekkai Kenkyukai, Sekko Sekkai Binran, p. 97–106, (Gihodo, Tokyo, Japan, 1961).
3. M. Nakahara and K. Murakami, Semento Sekko Sekkai, p. 136–141, (Nikkan Kogyo Shinbun Sha, Tokyo, Japan, 1959).
4. The Cement Association of Japan, "Material test of various chemical gypsums", Technical Report No. 65-4-A, (1965).
5. S. Hirano, K. Nogi and K. Murahashi, "Recent feature of gypsum for portland cement industry in Japan", Sekko Sekkai, **69**, 71–78, (1964).
6. By courtesty of Dr. S. Nagai,: Emeritus Prof. of Tokyo Univ.
7. W. H. Waggaman, Phosphoric Acid, Phosphate and Phosphatic Fertilizers, 2nd ed, p. 158–207, (Reinhold Publishing Corp. N. Y. 1952).
8. P. Parrish and A. OGilvie, Calcium Superphosphate and Compound Fertilizer: Their Chemistry and Manufacture, p. 150–166, (Hutchinson's Scientific and Technical Publications, London: N. Y.: Melbourne: Sydney, 1946).
9. Van. Wazer, Phosphorus and its Compounds, Vol. II,: Technology, Biological Functions, and Applications, p. 1025–1069, (Interscience Publisher, Inc., New York and London, 1961).
10. S. Hori and K. Murakami, Rinsan, p. 111–160, (Seibundo Shinkosha, Tokyo, 1965).
11. S. Hori, K. Murakami and H. Tanaka, Sekko Seizoho, Japan Patent No. 305845.
12. S. Hori and K. Murakami, Toshiki Rinsan Seizoho, Japan Patent No. 247142.
13. K. Murakami and H. Tanaka, "By-product gypsum from phosphoric acid manufacture," Sekko Sekkai, **18**, 841, (1955).
14. K. Murakami and H. Tanaka, "By-produced gypsum in strong phosphoric acid manufacture(II)", Sekko Sekkai, **54**, 207, (1961).
15. K. Murakami, "Wet process in phosphoric acid manufacture and by-product gypsum," Sekko Sekkai, **44**, 25, (1960).
16. K. Murakami, "Phosphoric acid and gypsum", Ryusan, **16**, (8), 165, (1961).
17. K. Murakami and H. Tanaka, "Properties of by-product gypsum", Sekko Sekkai, **61**, 273, (1962).
18. Y. Arai and S. Nagai, "The problem of wet-process phosphoric acid manufacture in the United States of America", Ryusan, 12–21, (1965).
19. R. Ikeno and K. Kaji, "Wet-process with alkylbenzensulfonic acid in phosphoric acid manufacture", Kogyo Kagaku Zasshi, **62**, (1), 47, (1959).
20. K. Murakami, Y. Iijima et. al., "Effects of fluorine on the growth of gypsum crystal and its counterplot", Sekko Sekkai, **62**, 7, (1963).
21. K. Kaji, "Reacting condition of wet-process of phosphoric acid manufacture with Alkylbenzensulfonic Acid", Kogyo Kagaku Zasshi, **63**, (8), 202, (1960).
22. K. Kaji, "Reacting condition of wet-process of phosphoric acid manufacture", Kogyo Kagaku Zasshi, **63**, 1479, (1960).
23. K. Kaji, "Metastability of hemihydrate in phosphoric acid—sulfuric acid", Kogyo Kagaku Zasshi, **64**, (1), 124, (1961).
24. I. Moriyama and T. Abe, "Rate of crystal growth of dihydrate in phosphoric acid-sulfuric acid", Kogyo Kagaku Zasshi, **66**, (12), 14, (1963).
25. I. Moriyama and T. Abe, "Rate of transformation of hemihydrate to dihydrate in phosphoric acid-sulfuric acid", Kogyo Kagaku Zasshi, **66**, (12), 14, (1963).
26. J. Murata and H. Noriyama, "Studies on wet-process in phosphoric acid manufacture by indirect dihydrate method (1)", Sekko Sekkai, **68**, 9, (1964).
27. J. E. Davenport, J. G. Getsinger and F. Carrol, "Foam process and fuming acid process", Ind. Eng. Chem., **4**, 84–88, (1965). New Developments in Fertilizer Technology, TVA, 5th, Demonstration, Oct, 6–7, (1964).
28. K. Murakami, H. Tanaka, M. Narita and U. Mitsuka, "The properties of hemihydrate obtained from Kola phosphate rock", Sekko Sekkai, **84**, 163–169, (1966).
29. T. Yamada, K. Kamata and S. Nagai, "Gypsum by-produced on phosphoric acid process (VI), distribution of P_2O_5 in gypsum crystal", Sekko Sekkai, **53**, 164–168, (1961).
30. K. Kaji and T. Tsuda, "Fluoride and phosphate present in by-produced gypsum of phosphoric acid process," Sekko Sekkai, **48**, 162–167, (1960).
31. H. Amatsu, T. Ishihara and I. Seki, "Chemical gypsum produced from phosphoric acid process for gypsum boards", Sekko Sekkai, **24**, 21–27, (1957).
32. K. Murakami and H. Tanaka, "Dehydration temperature of chemical gypsum", Sekko Sekkai, **24**, 6, (1956).
33. M. Sekiya, G. Yamaguchi et al., "Investigation on the poorer hardening property of by-product gypsum from wet-process phosphoric acid manufacturing and on the improvement thereof", Sekko Sekkai, **83**, 125–129, (1966).
34. M. Sekiya, G. Yamaguchi et al., "Investigation on the poorer hardening property of by-product gypsum from wet-process phosphoric acid manufacture and on the improvement thereof", Sekko Sekkai, **71**, 167–172, (1964).
35. K. Murakami, H. Tanaka and K. Sato, "Chemical analysis of the impurities of phosphogypsum", Sekko Sekkai, **91**, 249–255, (1967).
36. R. Kiriyama and H. Kiriyama, Kozo Muki Kagaku, 2nd ed., II, p. (Kyoritsu Shuppan Sha, Tokyo, Japan, 1965).
37. I. Maki and U. Suzukawa, "Infrared study on the by-product gypsum from the phosphoric acid process", J. Ceram. Association of Japan, **71**, 80–85, (1963).
38. S. E. Dahlgren, "Phosphate substitution in calcium sulfate in phosphoric acid manufacture," Brit. Chem. Eng., **10**, (11), 776, (1965).
39. T. Kusano, Report in Meeting for Study on "Utilization of chemical gypsum for portland cement",

(1967).
40. JIS R 5101, UDC 666, 913–543.
41. K. Murakami Report in Meeting for Study on "Utilization of chemical gypsum for portland cement", (1966).
42. M. Hanada, Unpublished data of Yahata Kagaku Kogyo Kabushiki Kaisha, (1965).
43. K. Emi and R. Hayami, "Spectrophotometric determination of small quantity of fluorine with neo thorin", Nippon Kagaku Zasshi, **76,** 1291, (1955).
44. K. Emi and R. Hayami, "Determination of fluorine in organs of animals", Nippon Kagaku Zasshi, **80,** 735, (1959).
45. R. J. Rowley and J. G. Grier, "Determination of fluoride in vegetation", Anal. Chem., **25.,** 106, (1955).
46. M. Kamada, T. Onishi and M. Ota, "New colorimetric determination of small quantities of fluoride by using p-dimethylaminoazo-phenylarsenic acid Zr lake", Bull. Chem. Soc. Japan., **28,** 148, (1955).
47. F. S. Grimaldi and B. Ingrm, "Determination of small and large amounts of fluorine in rocks", Anal. Chem., **27,** 918, (1953).
48. J. M. Token and B. M. Blank, "Determination of fluoride", Anal. Chem., **25,** 1741, (1953).
49. J. M. Token, "Differential spectrophotometric determination of fluoride", Anal. Chem., **28,** 949, (1956).
50. H. Minato and T. Kato, "Rapid method for analysis of silicate minerals as raw material for ceramic industry", J. Ceram. Association of Japan, **68,** (5), C–145, (1958).
51. G. L. Bridger, "Colorimetric determination of phosphorus pentoxide in fertilizers)" Anal. Chem., **25,** 336–339, (1953).
52. K. P. Quinlan etc., "Spectrophotometric determination of phosphorus as molybdovanadophosphoric acid", Anal. Chem., **27,** 1626–1629, (1955).
53. K. Takemoto, I. Ito and S. Suzuki, "Influence of chemical by-product gypsum on the quality of portland cement", Semento Gijutsu Nenpo, **XI,** 55–61, (1957).
54. K. Takemoto, M. Kataoka and S. Suzuki, "Utilization of by-product gypsum for portland cement", Sekko Sekkai, **33,** 1627–1636, (1958).
55. T, Yamaguchi, "On the making the gypsum by-product in the phosphoric acid process to be suitable for a regulator of the setting time of portland cement", Sekko Sekkai, **58,** 149–154, (1962).
56. Kuzumi and Murasugi, "The use of regenerated phosphogypsum for portland cement", Onoda Kenkyu Iho, **10,** 174–182, (1958).
57. K. Kobayashi, "Influence of the impurities of phosphogypsum on the development of strength and the setting time of portland cement", Semento Gijutsu Nenpo, **XVIII,** 79–85, (1963).
58. H. Mori and G. Sudo, "Influence of phosphates on the hardening of portland cement and blast-furnace slag cement", Semento Gijutsu Nenpo, **XIV,** 67, (1960).
59. L. Lejsek, Study on the use of phosphogysum in czecko-slovakia", Tonind-Ztg., **91,** Nr. 1, (1967).
60. J. Wehmer, "The use of synthetic gypsum", German Patent, 1224190, 1, Sept., 1966., RIGIPS, Baustoffwerke, G.m.b.H.
61. M. Hanada, Report in meeting for study on "Utilization of chemical gypsum for portland cement", (1966).
62. K. Miyazawa, Report in meeting for study on "Utilization of chemical gypsum for portland cement", (1966).
63. M. Hanada, Report in meeting for study on "Utilization of chemical gypsum for portland cement", (1967).
64. K. Miyazawa, Report in meeting for study on "Utilization of chemical gypsum for portland Cement", (1967).
65. K. Murakami, Report in meeting for study on "Utilization of Chemical Gypsum for Portland cement", (1967).
66. G. Verbeck, A private communication to S. A. Greenberg. Chemistry of Cement, Proceedings of the Fourth International Symposium, Washington 1960, p. 791, National Bureau of Standards Monograph 43. U.S. Department of Commerce.
67. M. Mochizuki, Report in meeting for study on "Utilization of chemical gypsum for portland cement", (1967).
68. K. Takemoto, Unpublished data of Onoda Cement Kabushiki Kaisha, (1966).
69. S. Nakamori and Y. Mizoguchi, "Properties of several kinds of chemical gypsum", Semento Gijutsu Nenpo, **XXI,** 33–42, (1966).
70. Y. Suzukawa and K. Kobayashi, "Relations between the grinding temperature and quality of cement", Sekko Sekkai, **82,** 2, (1966).
71. Y. Suzukawa and K. Kobayashi, Report in meeting for study on "Utilization of chemical gypsum for portland cement", (1967).
72. R. Carlson and L. Forblich, "Correlation of methods for measuring heat of hydration of cement", Ind. Eng. Chem., Anal. Ed., **10,** 382, (1938).
73. H. Stein, "Influence of some additives on the hydration of portland cement—I, non ionic organic additives", J. appl. Chem. **11,** 474–482, (1961).
74. U. Danielson, "Heat of hydration of cement as affected by water-cement ratio", Chemistry of Cement, Proceedings of the Fourth International Symposium, Washington 1960, p. 519, National Bureau of Standard Monograph 43. U. S. Department of Commerce.
75. M. Sekiya, Report in meeting for study on "Utilization of chemical gypsum for portland cement", (1967).
76. K. Amaya, "Micro-calorimeter", Bussei, 588, (1963).
77. H. Tanaka, K. Murakami, I. Monna and T. Karaki, "Studies on hydration of $3CaOAl_2O_3$ with calorimeter", J. Ceram. Association of Japan, **70,** 302–326, (1962).
78. H. F. Taylor, The Chemistry of Cements, Volume I, p. 318, (Academic Press, London and New York, 1964).
79. R. F. Feldman and V. S. Ramachandran, "Character of hydration of $3CaOAl_2O_3$", J. Am. Ceram. Soc., **49,** 268–272, (1966).
80. H. N. Stein, "The reaction of $3CaOAl_2O_3$ with water in the Presence of $CaSO_42H_2O$", J. appl. Chem., **15,** 314–325, (1965).

81. T. C. Powers, "Studies of the physical properties of hardened portland cement paste", J. Am. Concrete Inst., (1946 and 1947).
82. C. M. Hunt, "Nitrogen sorption measurement and surface area of hardened cement pastes", Symposium on Structure of Portland Cement Paste and Concrete Highway Resarch Board, 112, (1967).
83. R. S. Mikheil and S. A. Selim, "Adsorption of organic vapors in relation to the pore structure of hardened portland cement pastes", Symposium on Structure of Portland Cement Paste and Concrete Highway Research Board, p. 123, (1967).

Written Discussion

Richard A. Kuntze and Peter Hawkins

The false set of portland cement is attributed to the dehydration of gypsum to hemihydrate during the grinding of the cement clinker and the subsequent reprecipitation of gypsum in the cement paste. The relationship between the stiffening of the cement paste and the crystallization of gypsum has been studied mainly by determining the changes in the SO_3 concentration of the liquid phase of the cement. These studies have shown that the false set is affected by nuclei present in the cement which accelerate the crystallization of gypsum. The effect of impurities and additives which delay the crystallization of gypsum have been examined to a lesser extent.

However, it is well known that various types of hemihydrate, particularly those prepared from phosphogypsum, have different hydration properties and form gypsum at different rates. For this reason the effects of some of these properties on the false set of portland cement have been studied and the results are discussed in the present paper. In this study, various types and amounts of retarders for the hydration of hemihydrate have been added to the cement to delay the crystallization of gypsum. The quantities of gypsum and ettringite formed during the first 30 minutes after mixing cement and water have been determined by differential thermal analyses and compared with the rate of stiffening of the cement paste.

The relationship between different retarders and the quantity of unconverted gypsum, which provides nuclei and accelerates the recrystallization of hemihydrate to gypsum, has been studied also. Mixtures of gypsum and hemihydrate in various proportions have been added to the cement and the time and magnitude of a small temperature rise indicative of gypsum precipitation has been measured by a method developed for this purpose. Retarders have been added in conjunction with the gypsum-hemihydrate mixtures to demonstrate the effect of both retardation and acceleration on the crystallization of gypsum. This procedure provides information about the quantity of gypsum which must crystallize under certain conditions before false set is obtained.

The severity or degree of the stiffening of cement paste cannot be determined adequately with standard penetration methods. Therefore, a cone penetrometer has been developed with which it is possible to study the normal setting process and deviations from it, such as false set.

The results of these studies indicate that the occurrence of false set in portland cement depends not only on the quantity of gypsum crystallizing but also on the time and the rate of crystallization. These factors are influenced by additives and impurities such as phosphates that may be present in dehydrated phosphogypsum. Ettringite appears to contribute to the false set, probably because it forms crystals with a needle-like habit and has a tendency to form crystal clusters similar to gypsum.

Introduction

K. Murakami reported data by Suzukawa and Kobayashi (1) which indicate that dehydrated phosphogypsum behaves differently from natural gypsum with respect to the formation of false set in portland cement. These data show that the development of false set is affected not only by the quantity and the grade of dehydrated gypsum, but also by the type and amount of impurities present. He concluded that the anomalous setting behaviour of cement containing chemically untreated phosphogypsum may be caused by the large amounts of phosphate impurities.

Considering our own data, we would like to suggest that the differences observed may be due to the effect of phosphate impurities on the hydration or setting characteristics of dehydrated phosphogypsum. It is well known that some hemihydrates prepared from phosphogypsum hydrate at a different rate and respond to accelerators to a lesser extent than hemihydrates obtained from natural gypsum. Also, the setting behaviour of natural hemihydrates can be mod-

ified to resemble that of dehydrated phosphogypsum by the addition of polyphosphates or polycarboxylic acids which are known to retard the crystallization of gypsum. Using various types of retarders, we have found that the time and the rate at which the gypsum crystallizes in the cement paste substantially affects the false set phenomenon.

At the Fourth International Symposium on the Chemistry of Cement in Washington in 1960, it was the consensus of opinion that false set is the result of the dehydration of gypsum to hemihydrate during grinding or storage, and the subsequent reprecipitation of gypsum in the cement paste. Hansen (2) states that the crystallization of gypsum is demonstrated by the reduction of the SO_3 concentration in the liquid phase of the cement paste at the time when false set is determined by penetration measurements. It is also generally agreed that the crystallization of gypsum is accelerated by the cement particles and undehydrated gypsum present in the cement. Consequently, false set is not observed when the crystallization of gypsum is accelerated sufficiently to take place during the mixing period. In contrast, false set may be observed after aeration of the cement, which apparently delays crystallization until the mixing is completed.

The above statements are based to a large extent on the correlation between the changes in SO_3 concentration and penetration measurement during the early stages of the setting process. Direct determination of gypsum in the cement paste has not been carried out except by X-ray diffraction which is capable of detecting only changes on the surface of the paste. Also no attempt has been made to examine the role of calcium sulphoaluminates, particularly ettringite. For this reason we have studied the relationship between the stiffening of the cement paste and the concentration of gypsum and ettringite as determined by a direct analytical method (DTA) and a method by which small temperature changes during the setting process can be detected.

Differential Thermal Analysis of Hydrates Formed in Cement Paste

A sample of false setting cement was obtained by the addition of 4 percent hemihydrate to a commercial portland cement. Another sample was prepared by adding, in addition to the hemihydrate, 0.25 percent of an aminopolycarboxylic acid, which was known to delay the crystallization of gypsum without directly affecting the setting behaviour of the cement.

The rate of stiffening of mortars prepared from

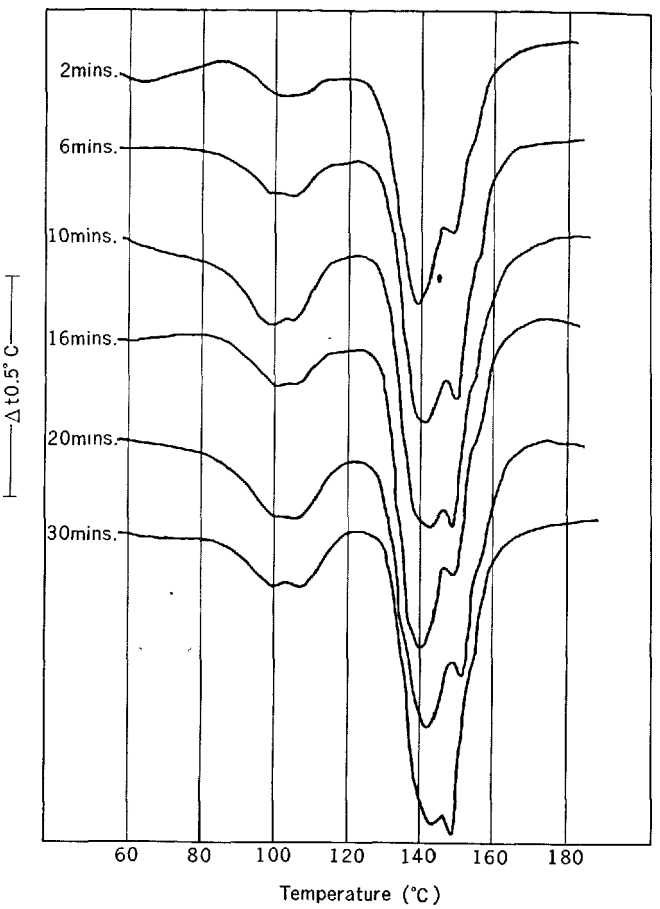

Fig. 1. *Differential thermograms for cements hydrated in the absence of retarder heating rate 4°C/min.*

both samples was determined by penetration measurements (3) over a period of 30 minutes. During this period samples were taken at regular intervals and dispersed in ethanol to prevent further hydration. Differential thermal analyses were carried out on these samples using a procedure and an apparatus described in detail elsewhere (4, 5). The areas under the peaks in the thermograms (Fig. 1 and 2) were used to determine the amounts of ettringite (first endotherm) and gypsum (second endotherm).

As shown in Fig. 3, the cement containing hemihydrate only exhibited false set approximately 6 minutes after addition of water. The false set of the cement containing both hemihydrate and the retarder was delayed to about 10 minutes and was more severe.

The rates of formation of gypsum and ettringite are shown in Fig. 4. These results indicate that the crystallization of gypsum is delayed in the presence of retarder and less gypsum is precipitated even after 30 minutes hydration time. However, ettringite is formed at a considerably faster rate when retarder is present,

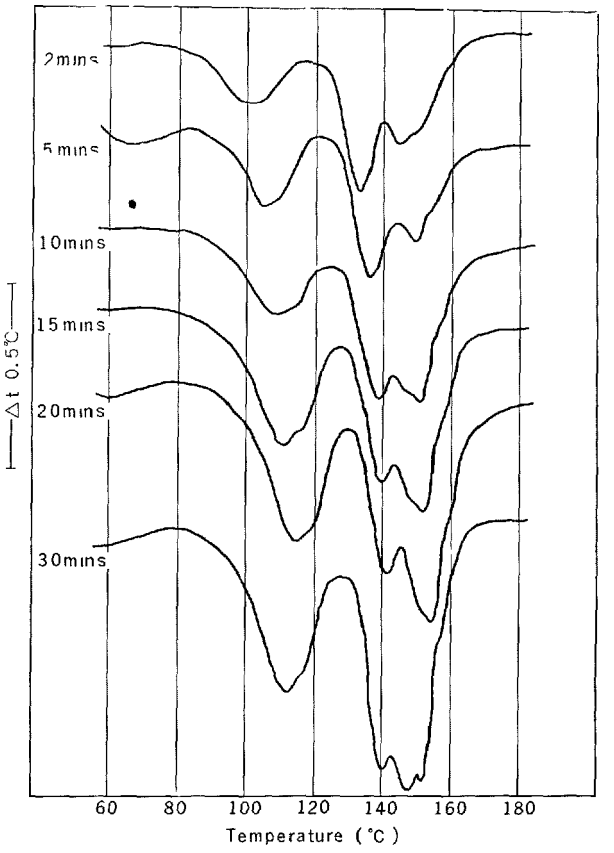

Fig. 2. *Differential thermograms for cements hydrated in the presence of retarder heating rate 4°C/min.*

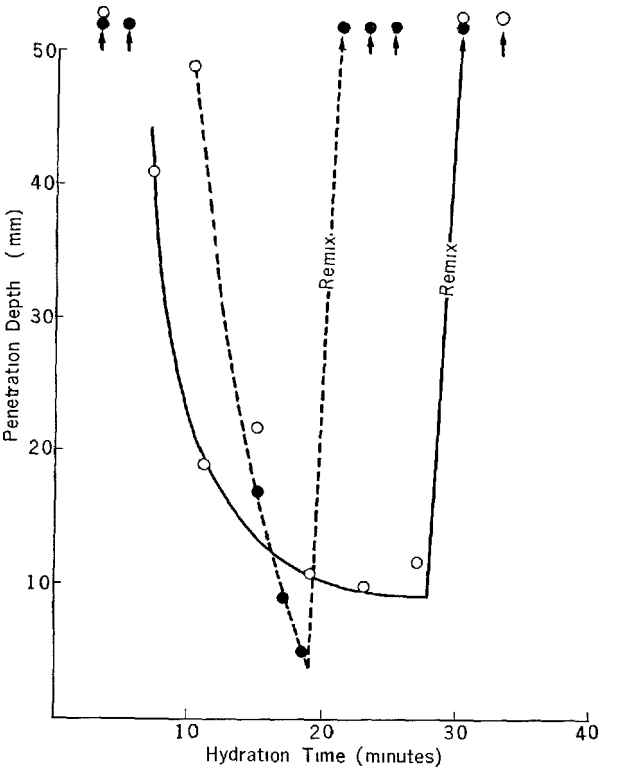

Fig. 3. *Stiffening of cements hydrated in the presence or absence of retarder*

—○— Cement hydrated without retarder.
--● - Cement hydrated with retarder.
↑ Denotes 50+ mm penetration.

probably due to a longer period of supersaturation with respect to gypsum (high concentration of SO_3) in the cement paste during the initial stages of the hydration.

The crystallization of gypsum coincides with the beginning of the rapid stiffening when only hemihydrate is present. In the presence of retarder the stiffening takes place before the maximum amount of gypsum has crystallized. The difference in the behaviour between the two samples may be due to the contribution of ettringite to the stiffening of the cement, since both ettringite and gypsum have a similar needle-like crystal habit and a tendency to form crystal stellates. Therefore, less gypsum is required to produce a false set when the ettringite content is high.

The Effect of the Hemihydrate-Gypsum Ratio on the False Set

It has been suggested that the gypsum added to the cement is often incompletely converted to hemihydrate during grinding. The remaining gypsum particles act as nuclei and therefore accelerate the recrystallization of hemihydrate to gypsum. If the crystallization of gypsum is accelerated sufficiently to fall within the mixing time false set is not obtained because stiffening is destroyed by the mixing.

However, some impurities or additives which delay the crystallization are particularly effective in reducing the accelerating capacity of the gypsum. To study this effect, several samples of cement were prepared by adding mixtures of gypsum and hemihydrate in various ratios maintaining a constant concentration of 2.5 percent SO_3. The temperature variations occurring in mortars prepared from these cements were measured continuously by a differential thermocouple in conjunction with a preamplified recording potentiometer. The data obtained were compared with the rates of stiffening of the mortars as determined by standard penetration methods (3).

As shown in Table 1, a hemihydrate concentration of less than 60 per cent does not produce a stiffening of the cement mortar because the quantity of crystal-

lizing gypsum is insufficient and the crystallization takes place during mixing. At a concentration of 60 to 80 percent of hemihydrate some stiffening is obtained, particularly at the initial penetration. This indicates that part of the crystallization takes place after the mixing is completed. However, the stiffness is relatively weak since most of it is destroyed by slight vibration on handling during the initial test. At a concentration of 90 and 100 percent hemihydrate sufficient gypsum crystallizes after mixing to produce a more severe stiffening which can only be destroyed by remixing.

Fig. 5 shows the corresponding temperature rise curves of the same cement samples, beginning immediately after mixing. All curves show a single peak which increases in size with increasing hemihydrate content. These peaks are due to the exothermic effect of gypsum crystallization superimposed on another but unidentified exothermic effect. This can be demon-

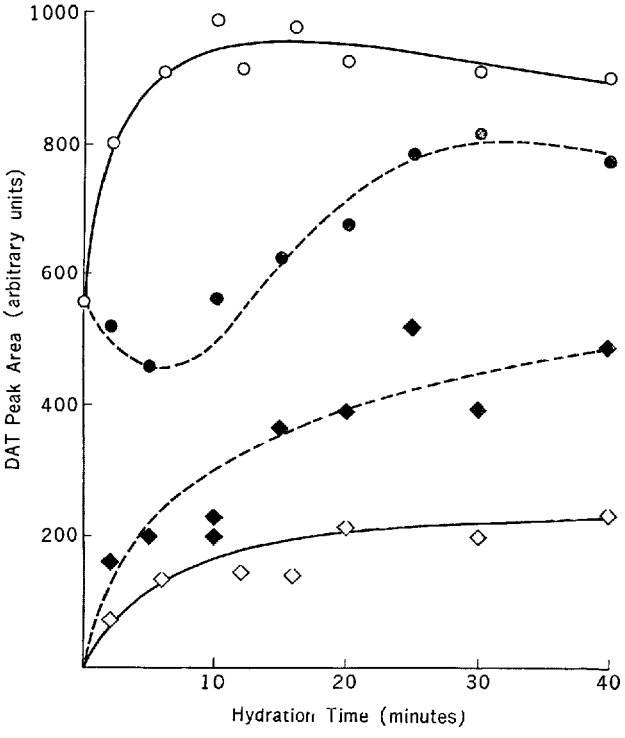

Fig. 4. *Formation of gypsum and ettringite in cements hydrated in the presence or absence of retarder*

—○— Gypsum content of cement hydrated without retarder.
--●-- Gypsum content of cement hydrated with retarder.
—◇— Ettringite content of cement hydrated without retarder.
--◆-- Ettringite content of cement hydrated with retarder.

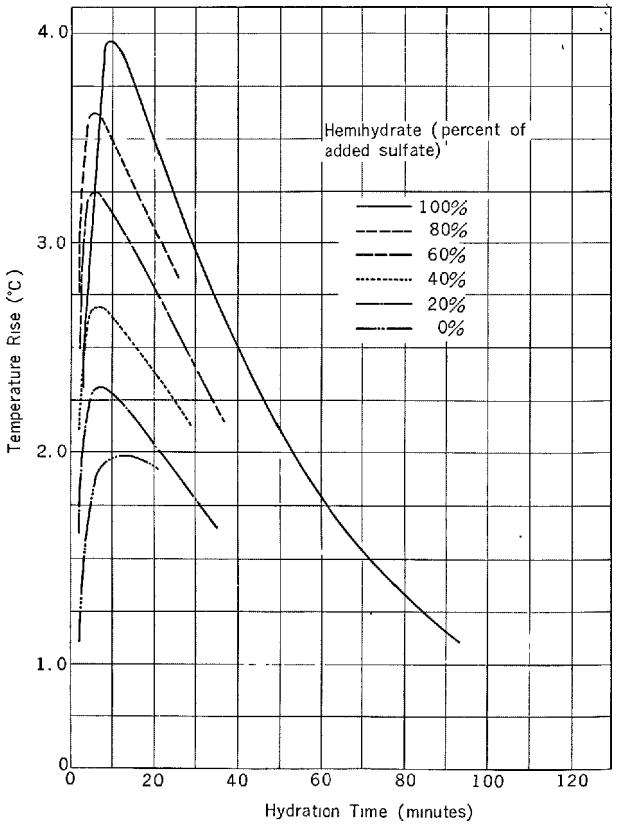

Fig. 5. *Temperature rise of cement hydrating in the absence of retarder*

Table 1.

Compound added		Penetration depth (mm)				
$CaSO_4 \cdot 2H_2O$ percent	$CaSO_4 \cdot 1/2H_2O$ percent	Initial	5 mins.	8 mins.	11 mins.	Remix
100	0	48	48	44	37	48
90	10	46	46 1/2	42	35	48
80	20	48	47	44	37 1/2	48
70	30	48	47	45	39	49
60	40	48	47	42	38	48
50	50	47	47	40 1/2	35 1/2	48
40	60	37	44	41 1/2	38	48
30	70	25	45	44 1/2	45	49
20	80	11 1/2	35	33	34	49
10	90	7 1/2	2 1/2	7	12	49
0	100	10	8	1	1	49

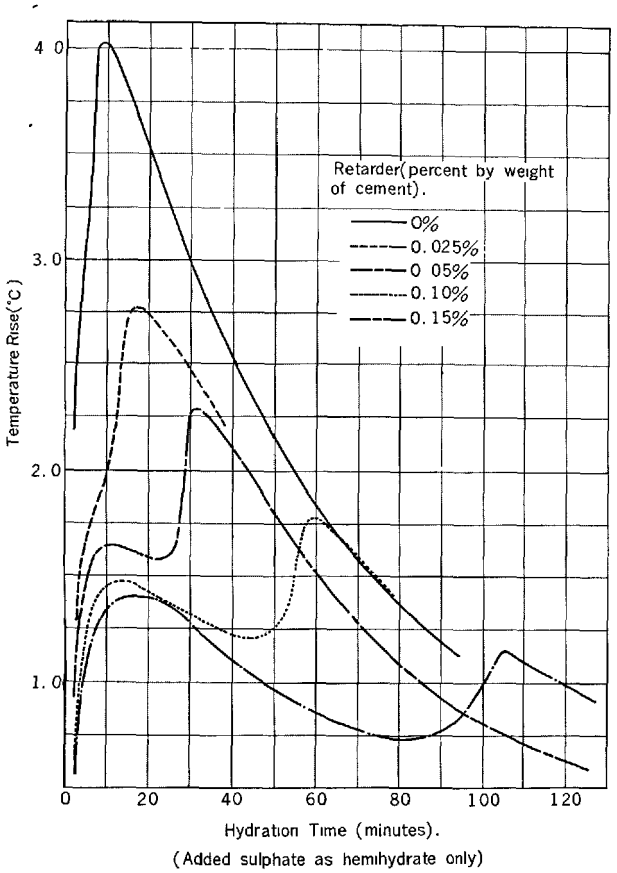

Fig. 6. *Temperature rise of a cement hydrating in the presence of various amounts of retarder*

strated by adding retarder (amino polycarboxylic acid) to cements containing hemihydrate and gypsum in various proportions. As shwon in Fig. 6 the exothermic effect due to the crystallization of gypsum is progressively delayed by the retarder. This indicates that the stiffening of the cement mortar will be postponed also. The extent to which gypsum crystallization is delayed depends on the type of retarder and the concentration of the unconverted gypsum available for nucleation. With some retarders the effect is considerable (Fig. 7) and with others which behave similarly to phosphates, the effect is relatively small (Fig. 8).

The Effect of Phosphates on the False Set of Portland Cement

The standard penetration methods are often not sufficiently sensitive to distinguish between false sets with various degrees of stiffening. However, the determination of the severity of the false set is important, since it is indicative of a variety of factors which influence false set, particularly the hydration behaviour of the dehydrated gypsum. For this reason a more sensitive penetration method has been developed using a blunted cone with an apex angle of 20° and a weight of 250 grams.

The effect of polyphosphate on the false set of cement is demonstrated in Fig. 9. A mild false set was

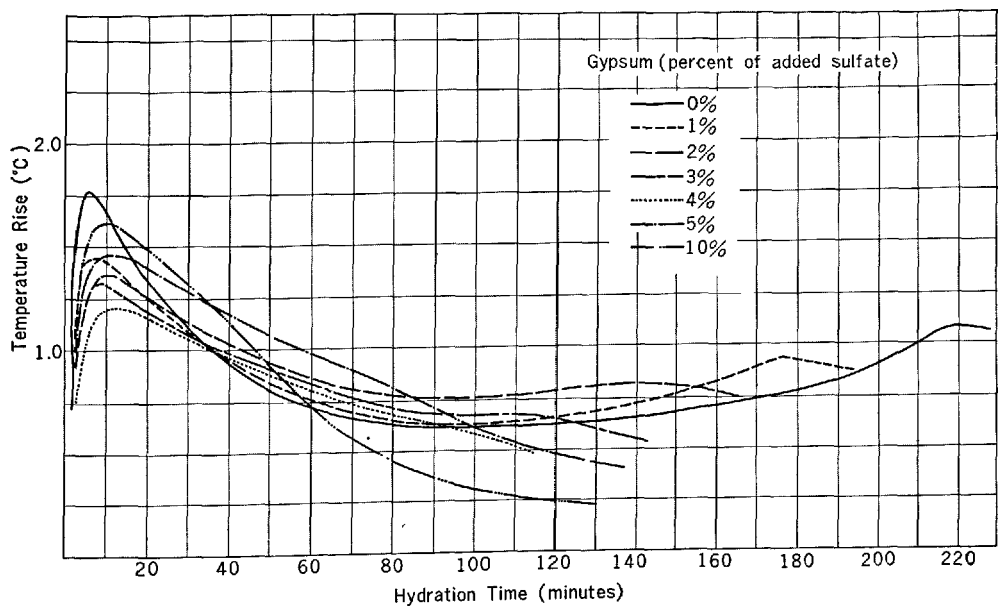

Fig. 7. *Acceleration of the precipitation of gypsum in cement hydrated with 0.2% amino polycarboxylic acid retarder*

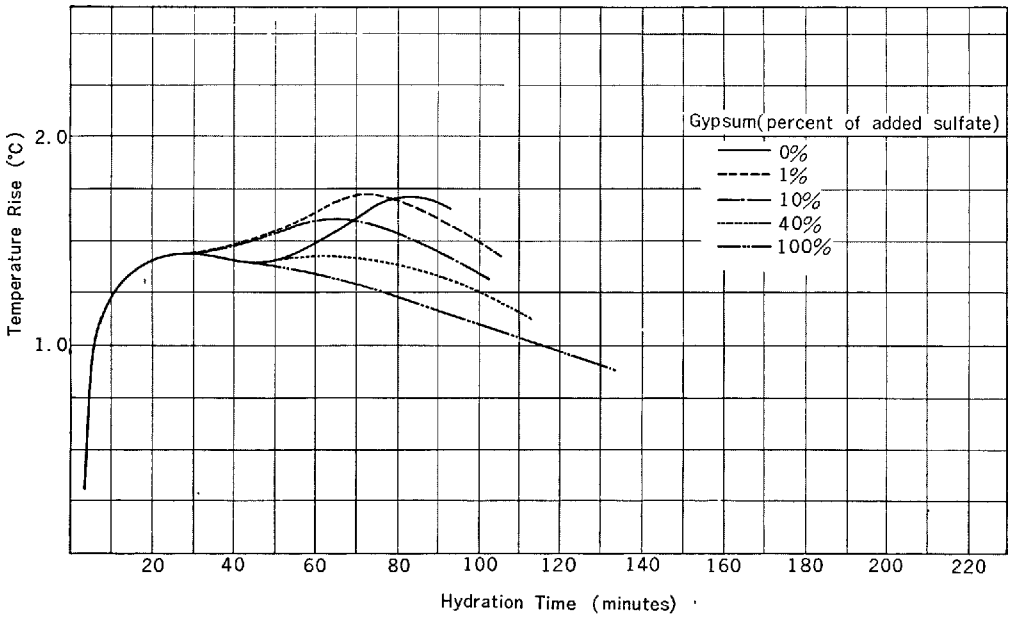

Fig. 8. *Acceleration of the precipitation of gypsum in cement hydrated with 0.2% polycarboxylic acid retarder*

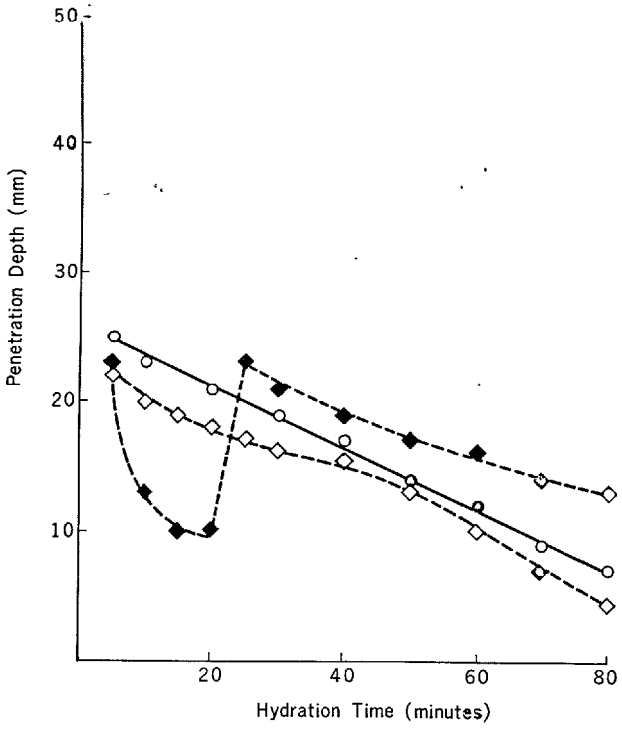

Fig. 9. *Effect of polyphosphate on the severity of the false set*

—○— Normal setting cement.
--◇-- Cement containing 4% hemihydrate.
-◆-- Cement containing 4% hemihydrate and 0.5% polyphosphate.

obtained by adding hemihydrate to portland cement to a total of 4 percent. The relatively small deviation from the setting pattern of normal portland cement is considered to be due to the fact that part of the gypsum crystallizes during the mixing period. This is a borderline case which may not be detected by the usual false set method. The addition of polyphosphate delays the crystallization sufficiently to take place largely after the mixing is completed. Consequently, the false set is somewhat more severe. This type of set will be detected by standard methods to determine false set.

These results indicate that impurities which interfere with the precipitation of gypsum have a considerable effect on the false set of cement. It is felt that the properties of dehydrated phosphogypsum should be examined from that point of view.

Conclusions

The false set behaviour of portland cement may be affected by the type of impurities present in the gypsum which is added to the cement clinker and forms hemihydrate during grinding. If these impurities are capable of retarding the hydration of hemihydrate, e.g. phosphates in phosphogypsum, the reprecipitation of gypsum in the cement paste is delayed until the mixing is completed. Therefore, false set is observed since the gypsum crystals are no longer broken up during the mixing.

Impurities that retard the hydration of hemihydrate also increase the rate of ettringite formation becuse

they maintain a high SO_3 concentration (supersaturation with respect to gypsum) for a longer time, Ettringite appears to contribute to the false set possibly because of a needle-like crystal habit similar to that of gypsum and a greater tendency to form crystal stellates. Consequently, less gypsum is necessary to produce false set at a high ettringite content and the false set tends to be more severe even before all gypsum has crystallized.

Acknowledgement

This work was carried out with a research grant to the Ontario Research Foundation received from the Department of Trade and Development, Province of Ontario. The authors also wish to thank Mr. A. Adami for his contribution to the development of the cone penetrometer.

References

1. Y. Suzukawa and K. Kobayashi, "Relations between the grinding temperature and the quality of cement", Sekko Sekkai **82,** 2 (1966).
2. W. C. Hansen, "The false set of portland cement", Chemistry of Cement, Proceedings of the Fourth International Symposium, Washington, 1960, U. S. Department of Commerce, National Bureau of Standards, Monograph 43–Volume I.
3. "Tentative method for false set of portland cement (Mortar method)", ASTM C 359–64T, Book of ASTM Standards, Part 9, June 1967.
4. R. A. Kuntze, "The determination of small amounts of gypsum in calcium sulfate hemihydrate by differential analysis", Materials Research & Standards 2, 640 (1962).
5. R. A. Kuntze, "Effect of water vapor on the formation of $CaSO_4 \cdot 1/2H_2O$" Can. J. Chem. **43,** 2522 (1965).

Author's Closure

Keiichi Murakami

Here, I would like to introduce the written discussion proposed by Dr. Kuntze and Mr. Hawkins to my principal paper and subsequently to tell you a new data by us about the false set which is attributed to the impurities in phosphogypsum.

In my principal paper, I have concluded, by quoting the experimental results obtained by Dr.Suzukawa and Mr. Kobayashi, that the anomalous setting of cement containing untreated phosphogypsum may be caused by the large amounts of impurities.

In respect to the false set caused by the dehydration of gypsum to hemihydrate occured during grinding, Hansen has stated at last symposium that the crystallization of gypsum is demonstrated by the reduction of the SO_3 concentration in the liquid phase of the cement paste at the time when false set is determined by penetration measurement.

And the false set is not observed when the crystalliza tion of gypsum is accelerated sufficiently to take place during the mixing period.

In contrast, false set may be observed after introduction of CO_2 into the cement by areation, which delays the crystallization until the mixing is completed.

However, Dr. Kuntze and Mr. Hawkins has pointed out some of lacks in the Hansen's statement as follow; Hansen's statement are based to a large extent on the correlation between the changes in SO_3 concentration and penetration measurement during the initial stages of the setting process.

But, the direct determination of gypsum in the cement has not been carried out and also no attempt has been made to examine the role of ettringite.

Then Dr. Kuntze and Mr. Hawkins have studied the relationship between the stiffening of the cement paste and the concentration of gypsum and ettringite by using DTA and a standard penetration method and by measuring small temperature changes of the cement mortar during the setting process.

They have prepared the cement samples containing hemihydrate and both of hemihydrate and retarder such as aminopolyoxylic acid.

Initially, the rate of stiffening of mortars prepared from both samples was determined by penetration measurement.

Then it was reconfirmed that the false set of portland cement does not occur if the crystallization of gypsum which converted to hemihydrate during grinding takes place during the mixing.

But, if the crystallization is delayed by retarder until after the mixing, the false set occures.

Fig. 3 shows the above relationship in penetration measurement.

Fig. 6 shows that the exothermic effect due to the crystallization of gypsum is progressively delayed by the retarder, such as aminopolycarboxylic acid.

Secondary, they have suggested that the ettringite which produced in initial stage of hydration of portland cement contributes to the stiffening of the cement because both ettringite and gypsum have a similar needle-like crystal habit and the former will be act as neuclei in the crystallization of gypsum.

Besides, ettringite is formed at considerable faster rate when retarder is present.

Finally, they have developed a new penetration method which is capable of detecting the weak stiffening impossible to determine with the standard penetration method.

Fig.9 shows the results obtained by using the new method.

Author Index

For Volume IV

Subject Index

For Volume IV

D

E

F

DAINIPPON PRINTING CO., LTD. TOKYO 1969

V — ISCC

GENERAL REPORT

CONTENTS

GENERAL REPORT
OF
SESSION I-1: STRUCTURE OF PORTLAND CEMENT MINERALS

T. Hahn (West Germany)

The following Supplementary Papers are summarized in this report.

Paper No. I-10

SYNTHESIS AND CRYSTALLOGRAPHIC INVESTIGATION OF SOME BELITES

M. Regourd, M. Bigaré, J. Forest & A. Guinier (France)

Paper No. I-36

CATION AND ANION REPLACEMENTS IN THE STRUCTURE OF TRICALCIUM SILICATE

N. A. Toropov (U.S.S.R.)

Paper No. I-54

POLYMORPHISM AND SOLID SOLUTION OF THE FERRITE PHASE

E. Woermann, W. Eysel & T. Hahn (West Germany)

Paper No. I-55

CRYSTAL CHEMISTRY OF TRICALCIUM SILICATE SOLID SOLUTIONS

T. Hahn, W. Eysel & E. Woermann (West Germany)

Paper No. I-92

A STRUCTURAL STUDY ON α'-Ca_2SiO_4

K. Suzuki & G. Yamaguchi (Japan)

Paper No. 127

NEW CRYSTALLOGRAPHIC DATA OF SOME CALCIUM SILICATE PHASES

F. K. F. Liebau (West Germany)

This report deals with six papers on the structure and the crystal chemistry of three major mineral constituents of cements: Tricalciumsilicate (C_3S, alite), dicalciumsilicate (C_2S, belite) and ferrite (C_2F, C_4AF). One paper treats in addition some other Ca-silicates. Accordingly, the contributions are treated in three groups:

GROUP I: TRICALCIUMSILICATE AND ALITES

(1) N.A. Toropov, Leningrad, USSR
"Cation and Anion Replacement in the Structure of Tricalciumsilicate"

(2) Th. Hahn, W. Eysel and E. Woermann, Aachen, Germany
"Crystal Chemistry of Tricalciumsilicate Solid Solutions"

GROUP II: DICALCIUMSILICATE (BELITES) AND OTHER Ca-SILICATES

(3) M. Regourd, M. Bigaré, J. Forest and A. Guinier, Paris, France
"Synthesis and Crystallographic Investigations of some Belites"

(4) K. Suzuki and G. Yamaguchi, Tokyo, Japan
"A Structural Study on α'-Ca_2SiO_4"

(5) F.K.F. Liebau, Kiel, Germany
"New Crystallographic data of some Calcium Silicate Phases"

GROUP III: FERRITES

(6) E. Woermann, W. Eysel and Th. Hahn, Aachen, Germany
"Polymorphism and Solid Solution of the Ferrite Phase"

GROUP I: TRICALCIUMSILICATE AND ALITES

In both contributions solid solutions of Ca_3SiO_5 are discussed with respect to types and limits of substitution as well as effects of polymorphism.

Two problems have been investigated independently by both authors (Toropov; Hahn, Eysel & Woermann): Polymorphism and solid solution in the system Ca_3SiO_5-Ca_3GeO_5 and the stoichiometry of pure Ca_3SiO_5.

System Ca_3SiO_5-Ca_3GeO_5: The two investigations are in good accord and confirm each other. This is the only case known in which Ca_3SiO_5 forms a complete solid solution series, in contrast to the very limited solution ranges observed for other oxides.

[Table I] [Figure 1]

This solid solution corresponds to the substitution formula

$$Ca_3(Si_{1-x}Ge_x)O_5 \quad \text{with} \quad 0 \leq x \leq 1 \quad (Ca/Ge = 3.0)$$

The polymorphism of Ca_3GeO_5, as obtained by both authors, is demonstrated in Table I and compared with that of Ca_3SiO_5. The DTA results of the system Ca_3SiO_5-Ca_3GeO_5 are shown in Figure 1. Throughout the series, modification T_I occurs at room temperature.

The similarity of the silicate and the germanate extends even further: Hahn et al. report, that foreign atoms (Al, Zn, Mg etc.) can be incorporated into Ca_3GeO_5 with similar stabilization effects as in Ca_3SiO_5. Thus, there exist germanate alites analogous to the silicate alites. Ca_3GeO_5 also is metastable at low temperatures (below 1335°C), the decomposition rate being much higher than that of Ca_3SiO_5.

Stoichiometry of Ca_3SiO_5: Here the two authors disagree: Toropov has found an excess of CaO (between 0.5 and 1.0 wt.% CaO, error of the analysis $\pm$ 0.3% CaO) in the strucuture, corresponding to $CaO:SiO_2$ ratios between 3.02 and 3.04. He reports a similar excess for Ca_3GeO_5 (up to 1.5 wt.% CaO). This effect is interpreted as additional incorporation of CaO into vacancies of the structure.

Hahn, Woermann and Eysel, on the other hand, could find neither a composition range for C_3S nor a significant deviation from the stoichiometric composition $3CaO \cdot SiO_2$. They attribute a small excess of CaO which lies within their limit of error ($\pm$ 0.2 wt.% CaO) to the effect of introducing additional SiO_2 by fining the samples in an agate mortar.

Solid Solution Ca_3SiO_5-Y_2SiO_5: Toropov discusses this solid solution series, which involves the substitution $3Ca \rightarrow 2Y$, producing vacancies in the Ca lattice of Ca_3SiO_5. Analogous results have been obtained for La_2SiO_5.

[Figure 2]

The phase diagram Ca_3SiO_5-Y_2SiO_5 (Figure 2) shows a temperature-dependent solubility of Y_2SiO_5 in Ca_3SiO_5, e.g. 8 wt.% at 900°C. Beyond the solubility limit Y_2SiO_5 occurs as a second phase. Throughout the range modification T_I appears at room temperature.

All samples within the solid solution range contained ß- and

γ-Ca_2SiO_4. The amount of C_2S (up to 10-15% Ca_2SiO_4) increased with the Y_2SiO_5-concentration. As second surprising effect is that the excess of CaO increases with the Y-content, ranging from 0.5 wt.% CaO in pure C_3S to 2.5 - 3.0% CaO at the solubility limit for Y_2SiO_5 (corresponding to an increase in the $CaO:SiO_2$ ratio from 3.02 to 3.13). According to Toropov this additional incorporation of CaO is caused by the vacancies produced by the 3Ca → 2Y replacement. Thus, the solid solution must have a ratio Ca/Y smaller than 1.5, the value for pure 3Ca → 2Y substitution.

Combined substitution of MgO, Al_2O_3 and Fe_2O_3 in Ca_3SiO_5

Hahn, Eysel and Woermann have investigated the substution of the most important minor components of clinker - MgO, Al_2O_3 and Fe_2O_3 - in Ca_3SiO_5, i.e. the alite phase in the three quaternary systems $CaO-MgO-Al_2O_3-SiO_2$, $CaO-MgO-Fe_2O_3-SiO_2$ and $CaO-Al_2O_3-Fe_2O_3-SiO_2$ and in the quinary system $CaO-MgO-Al_2O_3-Fe_2O_3-SiO_2$.

For the three quaternary systems it was found, that the C_3S-phase must be represented by three-dimensional bodies of solid solution. The shapes and extensions of the bodies are given in Figures 3, 4 and 5.

[Figures 3 to 5]

The fact that bodies occur implies that the C_3S solid solutions in these systems have 3 degrees of freedom: Two are the concentrations of foreign oxides, the third is the concentration of CaO. All bodies, therefore, possess a "CaO-width", i.e. solid solutions with constant concentrations of foreign oxides may still vary in CaO-content. This result is of interest for the preparation of cement mixtures and for the evaluation of "lime-standard" formulae. The shapes of the bodies indicate that MgO and Al_2O_3 as well as MgO and Fe_2O_3 do not influence each other upon substitution in C_3S, while there exists an

interaction between the trivalent atoms Al and Fe (curved face in Figure 5).

In the solid solution characteristic composition regions occur in which the modifications T_I, T_{II} and M_I are stabilized at room temperature. These regions are indicated in Figures 3, 4 and 5.

The combined substitution of the various atoms essentially is a superposition of the individual substitution types:

Mg replaces Ca
Fe replaces Ca and Si
Al replaces Ca and Si and occupies 6-coordinated voids in the structure.

From this viewpoint the "CaO-width" of the solid solutions appears as a variation of the distribution scheme of Al in the three structural sites. Therefore, it is predominantly Al, which is responsible for the "CaO-width".

The results in the quaternary systems permit conclusions to be drawn about the alite phase in the quinary system $CaO-MgO-Al_2O_3-Fe_2O_3-SiO_2$ and in cement clinker.

GROUP II: DICALCIUMSILICATE AND OTHER Ca-SILICATES

Ca_2SiO_4 occurs in four principal forms: γ, β, α' and α. Two of the papers to be reported here are concerned with the forms α' and β, both of which occur as belites in cement clinker. The third paper by Liebau treats some other newly discovered Ca-silicates.

β-Ca_2SiO_4

Regourd, Bigaré, Forester and Guinier have determined accurate lattice constants of pure β-Ca_2SiO_4:

$a = 5.506$ Å
$b = 6.749$ Å (Space group $P2_1/n$)
$c = 9.304$ Å
$\beta = 94.62^{\circ}$

Different belites have been prepared by incorporation of various foreign atoms. According to the authors, these substances correspond to the formula

$$Ca_2[Me_x^{3+}Si_{1-x}]O_{4-\frac{x}{2}} .$$

with $Me = B^{3+}$: $0 \leq x \leq 0.10$
$Me = Fe^{3+}$: $0 \leq x \leq 0.02$
$Me = Al^{3+}$: $0 \leq x \leq 0.06$

(The solubility limits, i.e. the maximal values of x, have been obtained by DTA investigations of the α'- α - C_2S transformation.)

This formula involves the exchange

$$2Si^{4+} + O^{2-} \rightarrow 2Me^{3+}$$

which is particularly interesting because it implies vacancies in the oxygen framework of β-C_2S.

The authors distinguish two forms of β-Ca_2SiO_4: β_1 is the variety in which the lattice of pure β-C_2S is not significantly modified and which also occurs in technical clinkers; β_2 is a belite (e.g. $Ca_2Fe_{0.05}Al_{0.05}Si_{0.90}O_{3.95}$) in which the powder lines are very broad and where larger variations in the cell parameters c and β are observed.

Two forms of α'-Ca_2SiO_4

In the extant literature, two different cells and several space

groups have been reported for the α'-modification of Ca_2SiO_4 (Table II).

[Table II]

Recently it has been shown, that two different α'-Ca_2SiO_4 forms exist: a "high" form (α'_H) and a "low" form (α'_L). The transformation $\alpha'_L \longleftrightarrow \alpha'_H$ occurs at 1170°C and is reversible. The first indications for these forms were given by Smith, Majumdar and Ordway and by Niesel and Thormann.

Regourd et al. have confirmed these two forms by careful high-temperature powder investigations and by indexing the patterns (Figure 6).

[Figure 6]

The transition $\alpha'_L \rightarrow \alpha'_H$ is characteristed by the disappearance, by discontinuities and by merging of some lines in the powder patterns.

For the α'_H form the simple orthorhombic cell, first suggested by Bredig, was established. The structure is very similar to low-K_2SO_4. The extinctions in the powder pattern clearly establish Pmcn as space group (the non-centrosymmetric space group $P2_1cn$ being excluded due to the analogy with the centrosymmetric low-K_2SO_4 structure).

The α'_L-form, on the other hand, is characterized by a doubling of the a- and b-axes caused by some additional weak lines in the powder pattern. It corresponds to a superstructure of α'_H-Ca_2SiO_4. Regourd et al. have chosen the same space group for this larger cell as for α'_H-Ca_2SiO_4, Pmcn. It should be noted, however, that the extinctions in the powder pattern are equally compatable with Pmnn (obtained by Douglas for bredigite) and even better with Pbcn (the okl reflections with k = 2n are absent in the pattern). Excluded, however, is a

C-centered cell (obtained by Suzuki and Yamaguchi, see below).

The "weak" superstructure of α_L' and the fact that the transition $\alpha_L' \longleftrightarrow \alpha_H'$ is accompanied by a very small reversible DTA signal at 1170°C indicate that both structures are closely related and that α_L' represents a small displacive deformation of the low-K_2SO_4 structure (see structure determination below). It should be noted that all stabilized crystals in Table II are of the α_L'-type.

Suzuki and Yamaguchi have grown single crystals of α'-Ca_2SiO_4, which are stabilized by BaO (11.2 wt.%), SrO (8.6 wt.%) and B_2O_3 (0.9 wt.%). The authors make the reasonable assumption that Ba and Sr substitute for Ca while B replaces Si. The lattice constants are contained in Table II. They fit well into the system of the α_L'-forms. The space group of all 3 crystals is given as $Cmc2_1$. [This is not unique since C2cm and Cmcm have the same extinctions; in view of the successful structure determination (see below), however, this non-centrosymmetric space group must be accepted.] It should be noted that this space group differs from the two space groups reported above for α_L': Pmcn (Regourd et al.) and Pmnn (Douglas, obtained from single crystals of bredigite).

Suzuki and Yamaguchi stress the fact that a high-temperature X-ray diagram (152 lines) of pure α'-Ca_2SiO_4 at 1000°C is completely compatible with the large cell, derived from the single crystals. Since 1000°C lies within the temperature range of α_L', the stabilized α'-forms are α_L' too. It is noteworthy that the Ca_2SiO_4-powder patterns of Regourd et al. and of Suzuki et al. - both obtained at 1000°C - indicate different space groups.

Suzuki and Yamaguchi have determined the crystal structure of α_L'-Ca_2SiO_4, using the BaO-stabilized crystals. This is the first structure determination of α'-Ca_2SiO_4. The intensities were measured by the multiple film technique. The structure was

refined by two- and three-dimensional Fourier series to an R-factor of 0.11. (Figure 7).

[Figure 7]

The structure shows that the doubling of the a- and b-axes is caused by small shifts of the atoms with respect to the low-K_2SO_4 structure.

The authors list only some of the bond lengths (Table III).

[Table III]

There appear to be large deviations in the Si-O distances from the accepted value (1.60 Å) as well as rather different O-O distances within the tetrahedra. No errors of atomic positions are given, however. The authors state that three of the six different Ca-atoms show 8-fold, the other three Ca 6-fold coordination.

Further Ca-silicates

Liebau has obtained single crystals of several new Ca-silicate phases. These materials were obtained during experiments to grow Ca_3SiO_5 and Ca_2SiO_4 single crystals under various conditions.

(1) A new stacking modification of high-Ca_3SiO_3 (pseudowollastonite, Si_3O_9-ring structure) was obtained by heating Ca_3SiO_5 + small amounts of $Ca(OH)_2$ and CaF_2 at 1300°C. The crystals are disordered and represent analogues to the disordered forms of $SrSiO_3$ and $BaSiO_3$. The various forms of pseudowollastonite, known so far, are characteristed in Table IV.

[Table IV]

(2) In mixtures of Ca_2SiO_4 + CaO with excess of $CaCl_2$ needle-like single crystals of two related forms were found. The composition of these crystals is still unknown and their cell dimensions (Table V) show no simple relations to any known Ca-silicate.

[Table V]

(3) In mixtures of Ca_3SiO_5 + Ca_2SiO_4 with large excess of $CaCl_2$, heated to 1500°C, plate-like single crystals were obtained, most of which were twinned. First it was thought, that they were α'-Ca_2SiO_4. Untwinned crystals gave the following cell dimensions:

a = 9.89 Å
b = 6.77 Å
c = 10.91 Å
ß = 106.0°

Space group $P2_1/c$

The chemical composition of this phase probably is $Ca_2SiO_4 \cdot CaCl_2$.

GROUP III: FERRITES

The last paper by Woermann, Eysel and Hahn deals with the ferrite solid solution series $Ca_2(Fe_{1-p}Al_p)_2O_5$.

Substitution of Mg in ferrite

The types and limits of incorporation of Mg atoms in the ferrite structure were analyzed by the lime deviation method.

Two types of substitution have been found, none of them representing the simple replacement Ca/Mg (Table VI).

[Table VI]

The first type implies that two of three Mg atoms substitute for R(Fe+Al), while the third Mg occupies interstitial sites. The second type involves replacement of Ca and R atoms by Mg in addition to occupation of interstitial positions by Mg.

The change in the mode of Mg-incorporation near p = 0.50 indicates that at this composition a discontinuity in the ferrite series occurs.

Discontinuities and polymorphism of the ferrite solid solution series

Smith has described a small structural change at $p \approx 0.30$, involving a gradual transition from space group Pnma to Imma and explained by a change in the distribution of Al over the tetrahedral and octahedral sites.

The cell dimensions of the ferrite series as a function of p, both for MgO-free and MgO-saturated samples, exhibit weak but distinct changes of slope at $p = 0.30$ and $p = 0.50$ (Figure 8), thus confirming the two discontinuities.

[Figure 8]

$Ca_2Fe_2O_5$ shows two weak reversible DTA signals at 430°C and 690°C resp. High-temperature X-ray patterns reveal no change of symmetry, especially no transition from space group Pnma to Imma, in either of these transitions.

The variation of the DTA signals as a function of temperature in the ferrite series, again both for MgO-free and MgO-saturated samples offers further evidence for the discontinuities at $p = 0.30$ and at $p = 0.50$ (Figure 9).

[Figure 9]

At $p = 0.30$ the two signals, mentioned above, disappear, but a new weak signal occurs in the region 780-800°C. At $p = 0.50$ this signal disappears also and for $p > 0.50$ there is no indication of any phase change.

The investigation has revealed several small discontinuities and phase changes in the ferrite series, the structural nature of which still remains to be elucidated.

TABLE I: PHASE TRANSFORMATION IN Ca_3GeO_5 AND Ca_3SiO_5

(Toropov; Hahn, Eysel, Woermann)

Transformation	Ca_3SiO_5 (Bigaré et al.)	Ca_3GeO_5 (Toropov)	Ca_3GeO_5 (Hahn, Eysel, Woermann)
T_I - T_{II}	~600°C	750°C	745°C
T_{II} - T_{III}	920°C	1020°C	1040°C
T_{III} - M_I	980°C	1150°C	1160°C
M_I - M_{II}	990°C		Unobservable because of rapid decomposition
M_{II} - R	1050°C		
Lower stability temperature	~1250°C		1335°C
Melting point (incongruent)	2070°C	1880°C	

TABLE II: LATTICE CONSTANTS AND SPACE GROUPS OF α'-Ca_2SiO_4

(Various authors)

Author	Type	a(Å)	b(Å)	c(Å)	Space group	Temperature of pattern	Material
Bredig	α'	5.30	9.55	6.78	Pmcn	700°C	Powder, pure Ca_2SiO_4
Eysel	α'	5.507	9.293	6.823	Pmcn	20°C	Powder, $Ca_2Si_{0.75}Ge_{0.25}O_4$
Regourd et al.	α'_L	11.184	18.952	6.837	Pmcn, Pbcn, Pmnn	1000°C	Powder, pure Ca_2SiO_4
Douglas	α'_L	11.08	18.55	6.76	Pmnn (?)	750°C	Powder, pure Ca_2SiO_4
"	α'_L	10.91	18.41	6.76	Pmnn	20°C	Single crystals, bredigite
Suzuki and Yamaguchi	α'_L	11.07	18.80	6.85	$Cmc2_1$	20°C	Single crystals, stabilized with CaO
" " "	α'_L	11.02	18.69	6.83	$Cmc2_1$	20°C	Single crystals, stabilized with SrO
" " "	α'_L	10.96	18.43	6.86	$Cmc2_1$	20°C	Single crystals, stabilized with B_2O_3
" " "	α'_L	Cell similar to stabilized crystals				1000°C	Powder, pure Ca_2SiO_4
Regourd et al.	α'_H	5.593	9.535	6.860	Pmcn	1250°C	Powder, pure Ca_2SiO_4
Yamaguchi et al.	α'_H	5.605	9.543	6.883	Pmcn	1300°C	Powder, pure Ca_2SiO_4

TABLE III: SOME BOND LENGTH IN THE STRUCTURE OF α'_L - Ca_2SiO_4

(Suzuki and Yamaguchi)

Si_1 - O_1	1.77 Å	Ca_1 - O_1	2.42
Si_1 - O_2	1.77	Ca_1 - O_3	2.81
Si_1 - O_3	1.67	Ca_1 - O_5	2.40
Si_1 - O_4	1.75	Ca_1 - O_6	2.56
Average	1.74 Å	Ca_1 - O_7	2.32
O_1 - O_2	2.78	Ca_6 - O_3	2.47
O_1 - O_3	2.64	Ca_6 - O_3'	2.23
O_1 - O_4	3.02	Ca_6 - O_5	2.79
O_3 - O_4	2.86	Ca_6 - O_8	2.40
Average	2.82		

TABLE IV: CELL DIMENSIONS OF THE POLYTYPES OF PSEUDOWOLLASTONITE

(Liebau)

Author	a(Å)	b(Å)	d_{001}(Å)	
Liebau	6.90	11.95	9.72	(disordered)
Mc Geachin	~6.9	~11.8	~9.8	(ordered)
Jeffery and Heller	6.90	11.78	2 x 9.83 = 19.65	(ordered)
Smith	~6.9	~11.8	~3 x 9.8 ≈29.4	(ordered)

TABLE V: CELL DIMENSIONS OF TWO NEW CALCIUM SILICATE PHASES OF UNKNOWN COMPOSITIONS

(Liebau)

	Phase I	Phase II
a(Å)	16.08	18.36
b(Å)	7.56	7.75
c(Å)	7.62	12.63
α(o)	90.0	90
β(o)	104.4	90.0
γ(o)	~90	90
V($Å^3$)	897	1797
Symmetry	Triclinic	Orthorhombic or Monoclinic

TABLE VI: SUBSTITUTION OF Mg IN THE FERRITE SERIES

(Woermann, Eysel, Hahn)

Ferrites: $Ca_2(Fe_{1-p}\ Al_p)_2O_5$

(1) For $0 \leq p \leq 0.48$:

$$[Ca_2]Mg_{\frac{x}{3}}[Fe_{1-\frac{x}{3}}Mg_{\frac{x}{3}}]_2O_5 \qquad (Ca/Mg = 2/3)$$

with $0 \leq x \leq 0.045$ at 1300°C

Hypothetical end-member: $Ca_2Mg_3O_5$

(2) For $0.50 \leq p \leq 0.52$:

$$[Ca_{1-\frac{x}{10}}\ Mg_{\frac{x}{10}}]_2\ Mg_{\frac{4}{15}x}\ [R_{1-\frac{4}{15}x}\ Mg_{\frac{4}{15}x}]_2O_5 \qquad (Ca/Mg = 1/3)$$

with $0 \leq x \leq 0.100$ at 1300°C

and $R \approx 1/2\ Al + 1/2\ Fe$

Hypothetical end-member: $Ca_{1\frac{1}{4}}\ Mg_{3\frac{3}{4}}\ O_5 = Ca\ Mg_3O_4$

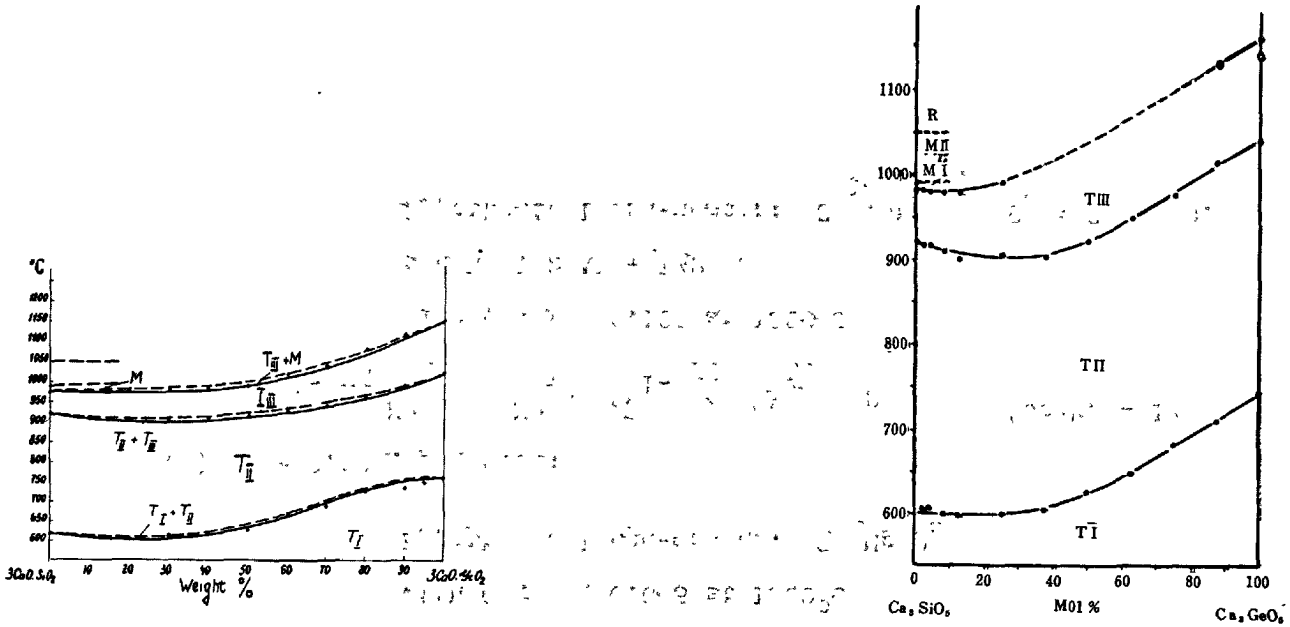

(Toropov) (Eysel)

Figure 1 : Phase diagrams of the system Ca_3SiO_5-Ca_3GeO_5

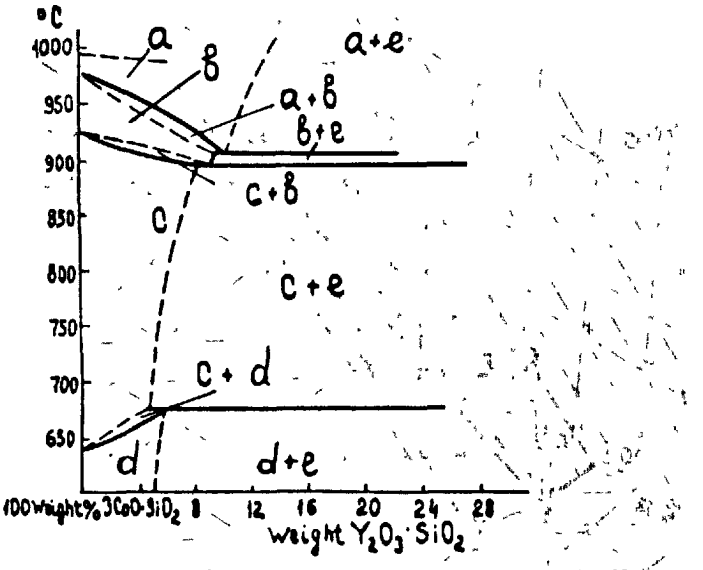

Figure 2 : **Phase diagram of the system Ca_3SiO_5-Y_2SiO_5**

a - Monoclinic
b - Triclinic III
c - Triclinic II
d - Triclinic I
e - Ca_3SiO_5 ss + Y_2SiO_5

(Toropov)

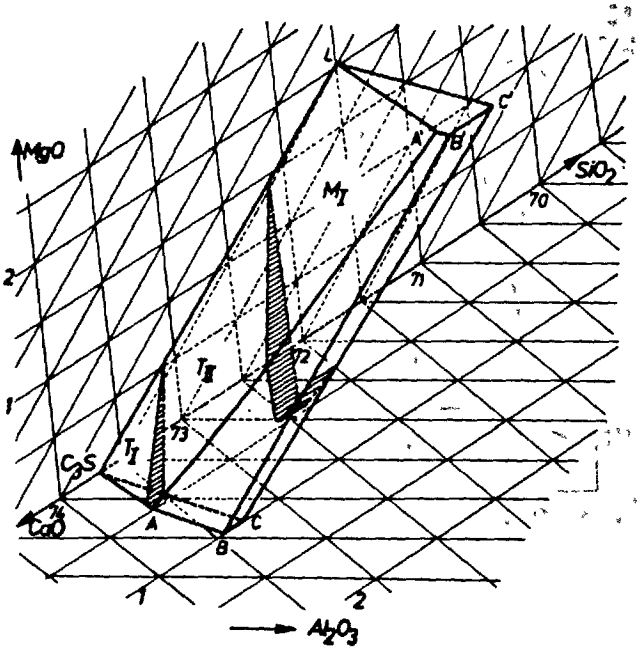

Figure 3 : Body of Ca_3SiO_5 solid solution in the quaternary system CaO-MgO-Al_2O_3-SiO_2 at 1550°C (wt.%). The regions of the modifications T_I, T_{II} and M_I apply to room temperature.

(Hahn, Eysel, Woermann)

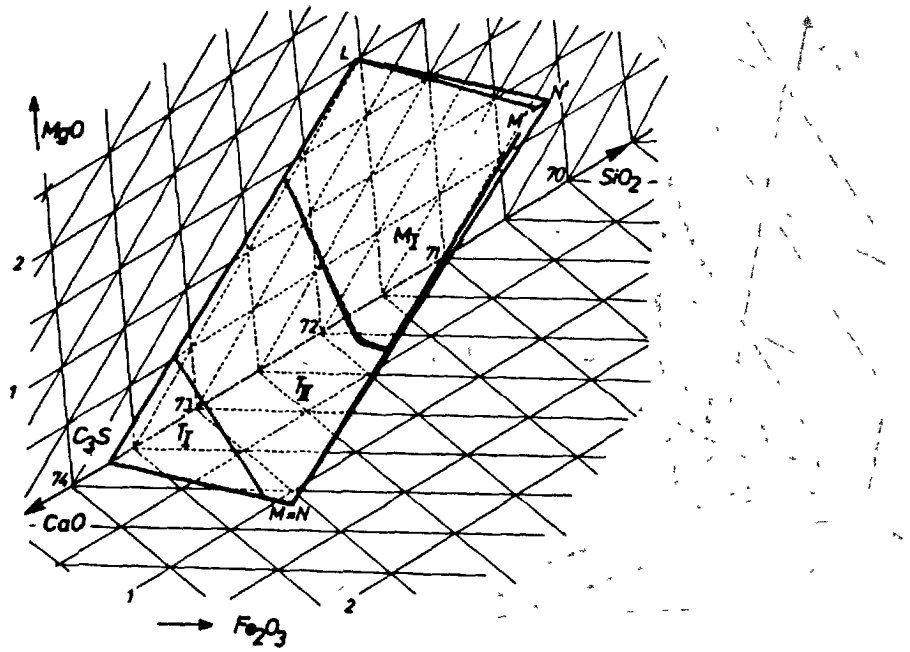

Figure 4 : Body of Ca_3SiO_5 solid solution in the quaternary system $CaO-MgO-Fe_2O_3-SiO_2$ at 1550°C (wt.%). The regions of the modifications T_I, T_{II} and M_I apply to room temperature.

(Hahn, Eysel, Woermann)

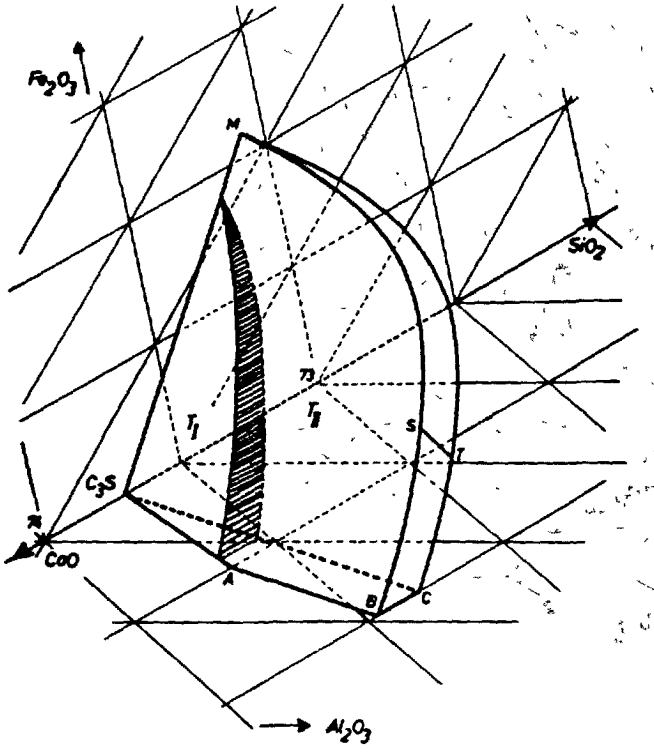

Figure 5 : Body of Ca_3SiO_5 solid solution in the quaternary system $CaO-Al_2O_3-Fe_2O_3-SiO_2$ at 1550^o (wt.%). The regions of the modifications T_I and T_{II} apply to room temperature.

(Hahn, Eysel, Woermann)

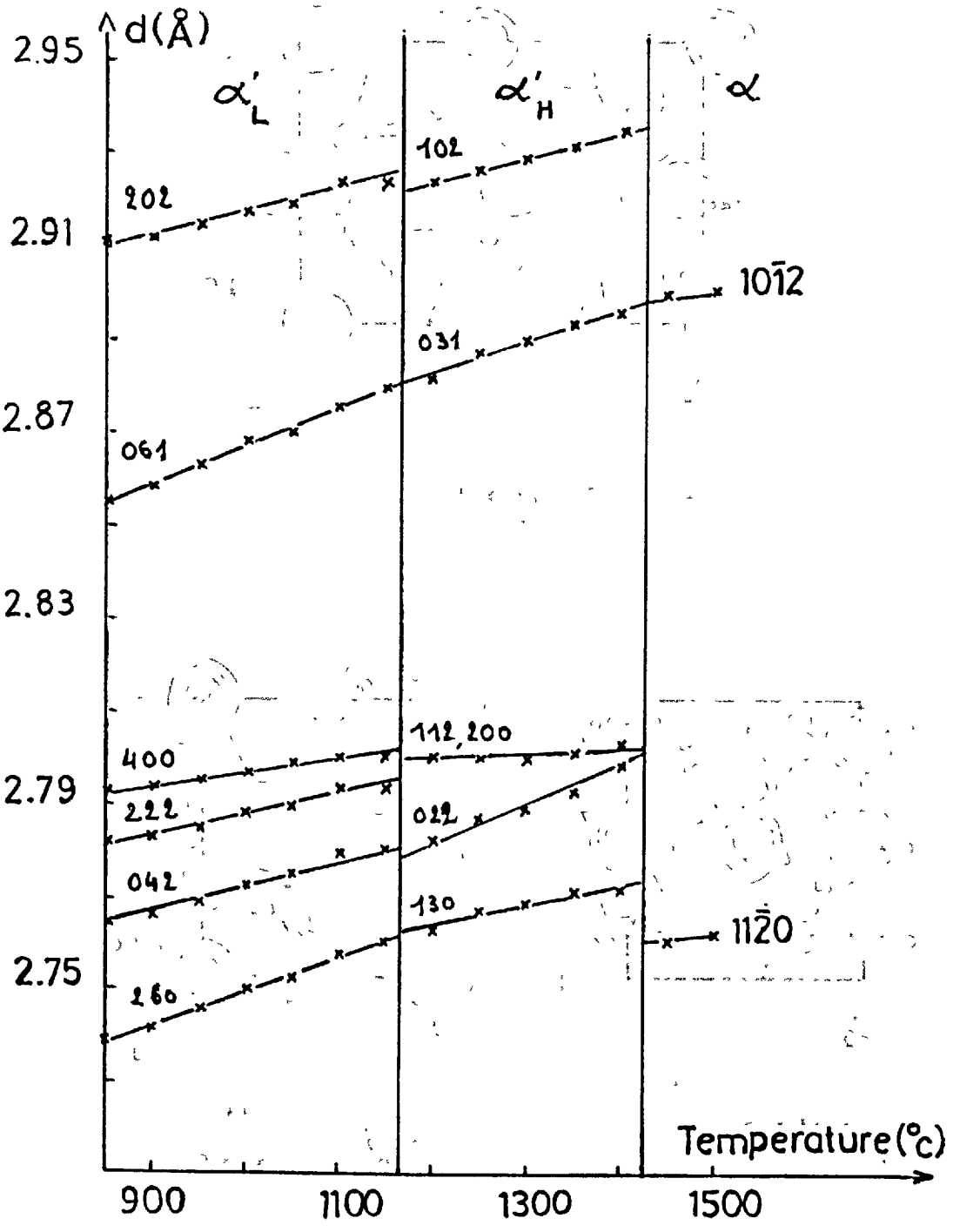

Figure 6 : Variation of some characteristic d-spacings with temperature for α'_L-, α'_H- and α-Ca_2SiO_4

(Regourd, Bigare, Forest, Guinier)

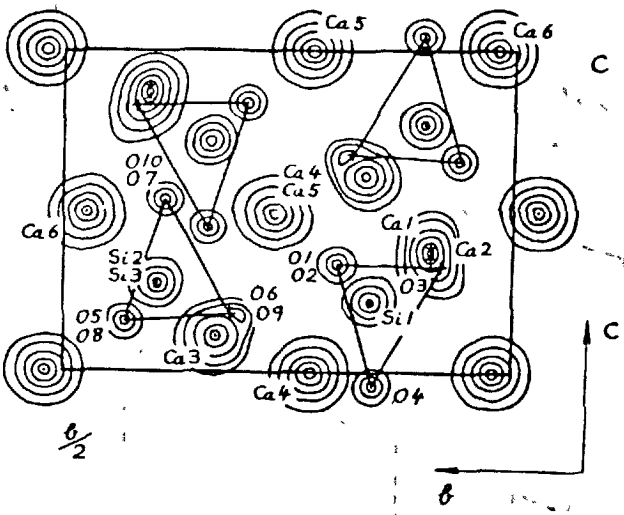

Projection ρ(oyz)

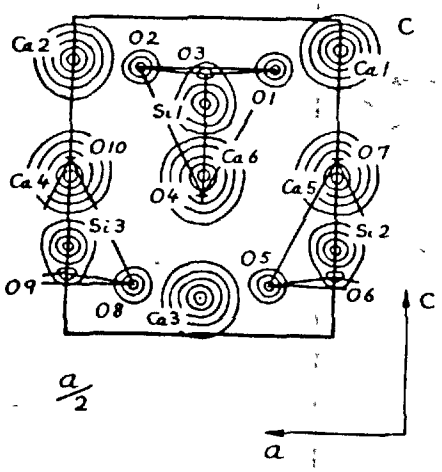

Bounded projection
ρ(xoz) between
y = 0.25 and y = 0.50

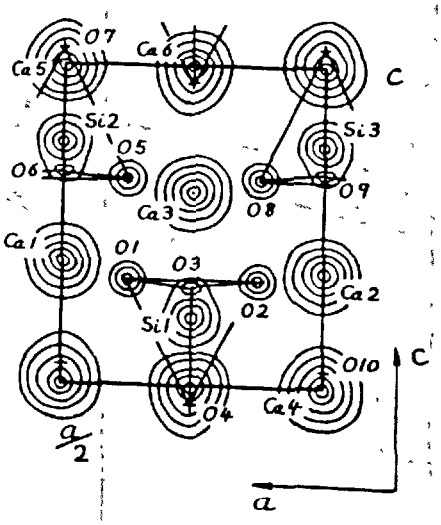

Bounded projection
ρ(xoz) between
y = 0.00 and y = 0.25

Figure 7 : Fourier syntheses of α_L'-Ca_2SiO_4

(Suzuki, Yamaguchi)

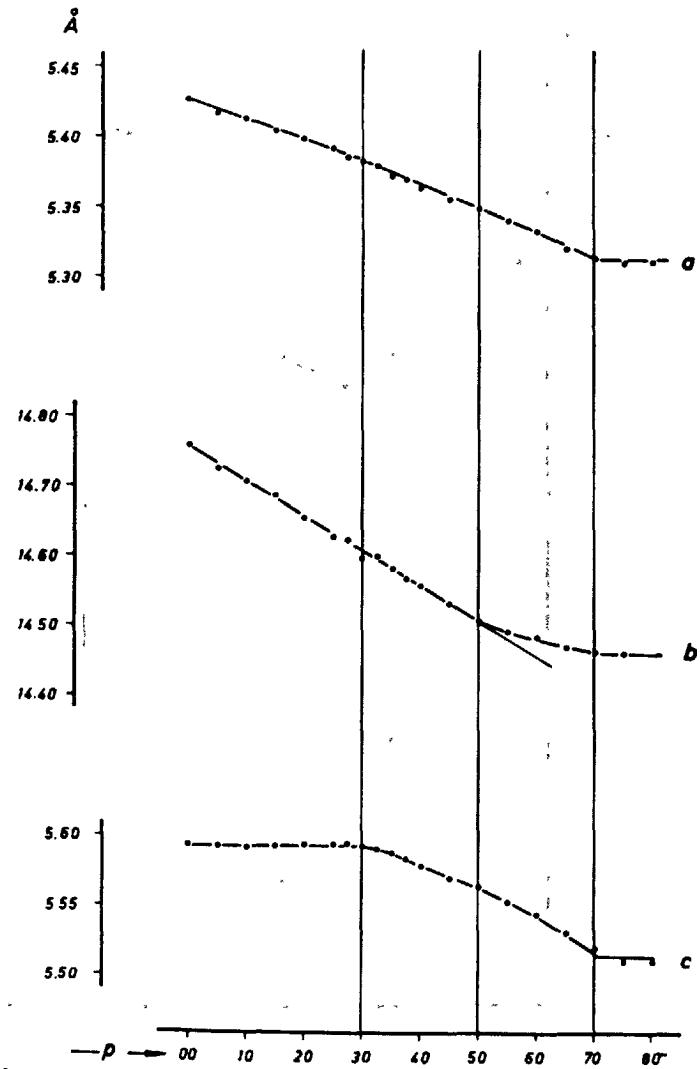

Figure 8 : Variation of lattice parameters of the ferrites series $Ca_2(Fe_{1-p}Al_p)_2O_5$ as a function of the Al-content (p).

(Woermann, Eysel, Hahn)

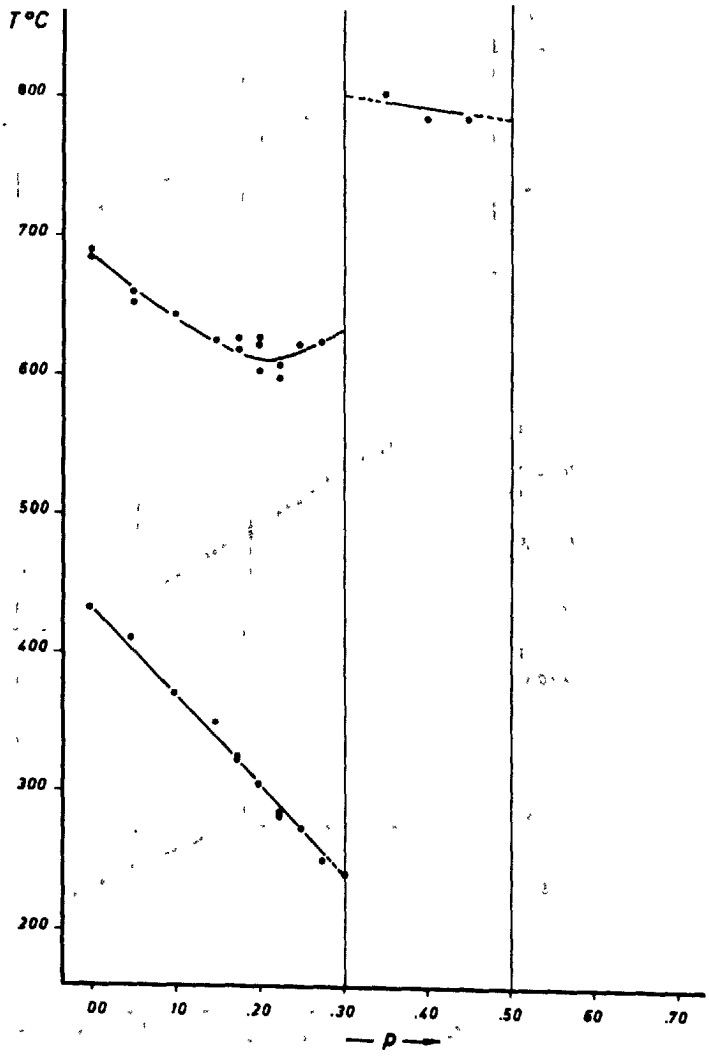

Figure 9 : Variation of transition temperatures of the ferrite series $Ca_2(Fe_{1-p}Al_p)_2O_5$ as determined by DTA.

(Woermann, Eysel, Hahn)

GENERAL REPORT
OF
SESSION I-2: PHASE EQUILIBRIA AND FORMATION OF PORTLAND CEMENT MINERALS

Y. Suzukawa (Japan)

The following Supplementary Papers are summarized in this report.

Paper No. I-9

MANUFACTURE OF PORTLAND CEMENT FROM PHOSPHATIC RAW MATERIALS

W. Gutt (United Kingdom)

Paper No. I-18

BURNABILITY OF RAW MIXES

J. P. Sulikowski (Poland)

Paper No. I-38

ON KINETICS OF FORMATION OF PORTLAND CEMENT CLINKER

P. F. Rumyantsev (U.S.S.R.)

Paper No. I-49

CLINKER BURNING IN FLUIDIZED BED

Y. Suzukawa, H. Kono, H. Miyazaki & S. Nakai (Japan)

Paper No. I-75

NEW COMPOUND $Ca_{12}Si_4O_{19}F_2$ IN THE SYSTEM CaO-SiO_2-CaF_2 AND THE ROLE OF CaF_2 IN THE BURNING OF CEMENT CLINKER

M. Tanaka, G. Sudoh & S. Akaiwa (Japan)

Paper No. I-82

FORMATION OF DOUBLE SALTS IN CEMENT BURNING

M. Amafuji & A. Tsumagari (Japan)

Paper No. I-94

PROBLEM OF ADMIXTURES

M. M. Sichov (U.S.S.R.)

Paper No. I-98

MECHANISMS AND KINETICS OF PORTLAND CEMENT CLINKER FORMATION FOR AN EXAMPLE OF THE SOLID-STATE REACTION IN THE PRESENCE OF A LIQUID PHASE

R. Kondo & S. Choi (Japan)

Paper No. I-133

A REFINEMENT OF THE LIME STANDARD FORMULA

E. Spohn, E. Woermann & D. Knoefel (West Germany)

Among nine Supplementary Papers of this Session, Nos. 9, 75, 82, and 94 presented by Gutt, Tanaka, et al., Amafuji and Tsumagari, and Sichov, respectively, are on the minor components or admixtures in portland cement clinker.

In No. 133 SP, an improved new lime standard formula of cement raw mix is presented by Spohn, et al.

Nos. 18, 38, and 98 SP presented by Sulikowski, Rumyantsev, and Kondo and Choi, respectively, are on the burnability of cement raw mix or on the kinetics of cement clinker formation.

The last one No. 49 presented by Suzukawa, et al. is on the clinker burning in fluidized bed which has already been known as the Pyzel process.

SP No. 9 by W. Gutt

To utilize phosphatic limestone for cement manufacture in Uganda, Africa, studies have been made by Nurse, et al. at the Building Research Station since 1950. This work was further extended by the author to detailed studies in the ternary system $2CaO \cdot SiO_2$-$3CaO \cdot P_2O_5$-CaO as shown in Fig. 1. Tricalcium silicate has a primary crystallization field extending to 13 per cent P_2O_5, and there are two reaction points R_1 and R_2. Compatibility relations were established that apply at 1500°C, and the existing solid solutions defined in the phase diagram were identified. The practical significance of the phase data for this ternary system to the cement making process is discussed.

Since fluorides are sometimes added to the raw mix to improve the

quality of phosphatic cement, the role of fluorine has been explored by investigations of the ternary system $CaO-SiO_2-CaF_2$. Two new calcium silicofluorides were found; $(C_2S)_2 \cdot CaF_2$ and a compound of the approximate composition $(C_3S)_3 \cdot CaF_2$ which correspond to Phase B and A reported by Breczky, respectively. A calcium silicofluoride which differs slightly in composition from the latter compound was reported by Tanaka, et al. as described in SP No. 75, but their X-ray diffraction pattern is identical with each other. Based on the results, the following reaction sequences have been identified as shown in Tab. 1. Further, existing knowledge of the quaternary system containing P_2O_5 is discussed.

As the amount of SO_3 in the clinker influences the quality of phosphatic cement, the ternary system $CaO-SiO_2-SO_3$ and to a limited degree the quaternary system containing fluorine are being studied. A new calcium silicosulfate $(C_2S)_2 \cdot CaSO_4$ was found. Moreover, compositions on the join C_3S-SO_3 with and without 0.5 per cent fluorine have been tested for strength.

Finally, the properties of the phosphatic cements made in Uganda are described, especially, on the low early strength of "Spot" samples of clinkers taken from the plant.

This paper is very valuable not only to the manufacture of portland cement from phosphatic limestone but also to the possible utilization of industrial by-products containing phosphates and fluorides.

SP No. 75 by M. Tanaka, G. Sudoh, and S. Akaiwa

The authors studied the role of CaF_2 in the burning of cement clinker by investigations of the ternary system $CaO-SiO_2-CaF_2$. They found a new ternary compound $11CaO \cdot 4SiO_2 \cdot CaF_2$ and further an unknown phase designated tentatively as Phase II. Optical, crystallographic, and thermal properties

of this ternary compound are given in detail. The results obtained by Breczky, Gutt and Osborne, and the authors, respectively, are comparatively shown in Tab. 2. This ternary compound melts incongruently at 1185°C into trigonal C_3S and α'-C_2S, together with a liquid phase. Further, primary crystallization field in the ternary system $2CaO \cdot SiO_2$-SiO_2-CaF_2 was determined.

When cement raw mix containing CaF_2 was heated, the formation of this compound was conspicuous at about 1050°C, and at 1100 to 1150°C it melted incongruently. Accordingly, the addition of CaF_2 decreases the temperature of formation of alite at 150 to 200°C in comparison with that in a raw mix containing no CaF_2. During cooling, this compound is again formed by peritectic reaction with covering alite. This peritectic structure is considered to be a cause of decrease in the strength of cement. Further, the addition of CaF_2 increases the amount of ferrite phase, and its composition becomes rich in Al_2O_3. On the other hand, the the amount of aluminate phase is decreased.

SP No. 82 by M. Amafuji and A. Tsumagari

The ring formation in cement rotary kiln is related not only to the operating condition of the kiln but also to the mineral composition and texture of the ring. In this paper the authors studied the mineral composition of the ring and found that $CaCO_3$, $CaSO_4$, and $(K \cdot Na)_2SO_4$ and double salts, such as $2C_2S \cdot CaCO_3$, $3C_2S \cdot 2CaSO_4$, and $2CaSO_4 \cdot K_2SO_4$, are formed. The composition of this calcium silicosulfate is assigned tentatively. However, its X-ray diffraction pattern is identical with that of $(C_2S)_2 \cdot CaSO_4$ reported by Gutt and Smith.

Laboratory experiments in an electric furnace showed that the above compounds are formed by gas-solid reaction between CO_2 or SO_2 and cement

raw mix or clinker. Further, when mixed gas having a composition similar to that of the exit gas in rotary kiln was used, the reaction of clinker and SO_2 preferred to that of clinker and CO_2.

The coagulation force of the double salts at high temperatures was also measured with an improved Vicker's apparatus and expressed by penetration degree.

This paper is valuable for elucidating the ring formation and also for evaluation of the temperature of the kiln lining.

SP No. 94 by M. M. Sichov

The author studied the effects of minor components or a small amount of admixtures on sintering and properties of cement. At first the presence of P_2O_5 or B_2O_3 on the synthesis of C_3S is described. When their amount is larger than their solubility limit in C_3S, respectively, the dissociation of C_3S and simultaneously the passivity of CaO and SiO_2 occur. The addition of TiO_2, Mn_2O_3, and Cr_2O_3 decreases the mechanical strength of sintered C_3S, thus the grindability being improved. Hydraulic activity of C_3S increases by the addition of P_2O_5, Cr_2O_3, and TiO_2, etc. The upper allowable amount of these additions has been studied.

Further, it is shown that the increase in hydraulic activity of cement by the addition of admixtures is due not only to the formation of solid solution but also to the modification of microstructure of clinker. Typical modifiers of microstructure are Cr_2O_3 and P_2O_5 because their addition decreases the surface tension of clinker liquid phase. Finally, the effects of MgO and alkali oxides are described on the viscosity of the eutectic melt in the quaternary system and also on the crystallization and microstructure of clinker minerals.

Based on the results, it is concluded that when the amount of admixtures is within a certain limit, their addition is desirable but when the amount exceeds this limit, it has a harmful effect on the sintering and properties of the resulting cement.

SP No. 133 by E. Spohn, E. Woermann, and D. Knoefel

Lime standard formulas suggested by Kuehl and later modified by Lea and Parker are well known. Both formulas, however, are functions of four major components, and minor components, such as MgO, alkali oxide, and SO_3, are not being considered. In this paper the authors modified the formula by including a factor for MgO.

To a series of laboratory-prepared clinkers having a different chemical composition, various amounts of MgO were added, and after reheating at 1500°C, free CaO was determined by the Franke method. An example of the results is shown in Fig. 2. Temperature dependence of the amount of MgO combined was also determined. This value can be assumed as 0.6 per cent MgO per 100°C.

In order to apply successfully to commercial clinker manufacture, the results obtained may be simplified as follows: a maximum 2.0 per cent MgO can be combined in clinker at a CaO/MgO ratio of 0.75. Accordingly, the new formula by the authors will be as follows (Tab. 3):

$$\frac{100(CaO + 0.75\ MgO)}{2.80\ SiO_2 + 1.18\ Al_2O_3 + 0.65\ Fe_2O_3}, \text{ where } MgO \leq 2.0\% \text{ and}$$

$$\frac{100(CaO + 1.50)}{2.80\ SiO_2 + 1.18\ Al_2O_3 + 0.65\ Fe_2O_3}, \text{ where } MgO > 2.0\%.$$

To check the validity of this formula, commercial clinkers from nine different plants were tested, and for the greater part of the tested clinkers, the results were satisfactory.

SP No. 18 by J. P. Sulikowski

The author suggests a laboratory method which makes it possible to estimate comparatively the burnability of cement raw mix in rotary kiln. This method consists of two series tests: the first is the determination of free lime after heating at 800-1400°C and the second is the measurement of the deformation of cylindrical specimens during heating under a constant load of 0.02 kg/cm^2.

From the test results, the following three values characterizing the burnability are obtained:

"K" is the ratio of the lime content of ignited cement raw mix to the maximum free lime content which occurs during heating;

"L" is the temperature range at which the content of free lime is over 10 per cent as shown in Fig. 3; and

"M" is the temperature at which the height of cylindrical specimens contracts by 5 per cent.

Long time observations were made on the behavior of cement raw mix in the burning zone of rotary kiln at four cement plants from which the tested cement raw mixes were sampled. It was found that the above three values "K", "L", and "M" are effective to estimate comparatively the behavior of cement raw mix during burning. The actual meaning of each value as regards the behavior during burning in rotary kiln is also shown.

SP No. 38 by P. F. Rumyantsev

Investigation of portland cement clinker burning as a single process and derivation of a general kinetic equation are inconceivably difficult. Therefore, the author considered the sintering of clinker as a complex of the following three interdependent processes:

(1) dissolution of the minerals in raw mix and the solid-state reaction products in the liquid phase of clinker;

(2) diffusion of Ca^{2+} and SiO_4^{4-} ; and

(3) crystallization of new phases.

As these processes are connected with each other and have a chain character, the process which proceeds with a minimum rate has a determining role in the sintering of clinker. From the analysis of previous reports, it is assumed that the dissolution process has a minimum rate. Observations under high-temperature microscope showed that the crystallyzation of clinker liquid phase at above 800°C occurs very quickly.

Therefore, the formula which describes the dependence of the dissolution time on temperature and diameter of the dissolving particles may be used in reciprocal expression as the kinetic equation for clinker formation.

SP No. 98 by R. Kondo and S. Choi

The authors assumed that in the presence of the melt the reaction of CaO with C_2S to form C_3S is controlled mainly by the diffusion of each component in the liquid phase. Specimens made with two compact disks consisting of CaO and β-C_2S, respectively, were used, the two disks being sandwiched with powdered glassy phase. After heating the specimens, the boundary surface of the formation of C_3S and the concentration distribution of four major elements, i.e., Ca, Si, Al, and Fe were determined. The viscosity of the liquid phase containing various amounts of CaO, γ-C_2S, and C_3S was measured by the ball pulling-up method.

Time does not permit to explain the mathematical derivation of the kinetic equation in detail, and so let me just show you the final result as shown in Tab. 4. From Equation (3), a curve is obtained on α versus

$t/t_{0.5}$. This curve showed a good agreement with experimental results.

Further, the activation energy calculated by the Arrhenius equation increased with increasing the amount of the melt. Finally, the diffusion coefficient calculated from Equation (1) in Tab. 4 and from the viscosity measurement, respectively, was compared with that obtained by the tracer diffusion results reported by Towers and Chipman. All these results show that the assumption on the kinetics described in this paper seems to be reasonable.

SP No. 49 by Y. Suzukawa, H. Kono, H. Miyazaki and S. Nakai

The authors established the basic chemical process designs of the burning of clinker in fluidized bed through the operation of the pilot plant, especially on the combustion of fuel oil in the bed, control of the size distribution of solid particles in the bed, and heat-recovery devices of the exit gas and of the red hot clinker from the bed.

Fig. 4 shows the schematic diagram of the pilot plant. Fuel oil was injected into the bed through injection nozzle (6), and by means of the hot-air jet stream which does not pass through gas distributor, complete combustion of the fuel oil was attained, thus the bed being held at a high temperature required for sintering of clinker. The size distribution of solid particles in the bed was controlled by the following two parameters: (I) the gas velocity for use to discharge selectively coarse clinker particles through discharge pipe opening (12); (II) the size and feed amount of seed pellets made with cement raw mix. The enthalpy of high-temperature exit gas from the bed was recovered by using cyclones in which calcareous and argillaceous components are preheated separately and also the former component is calcined partially, thus the inside wall of cyclone being prevented from the adhesion of cement raw mix.

The resulting clinker showed a low value in free lime and alkalis and also superior quality. However, it is indispensable to obtain superior clinker that cement raw mix fed into the bed is partially calcined.

Fig. 1. PHASE DIAGRAM OF THE SYSTEM C_2S-C_3P-CaO

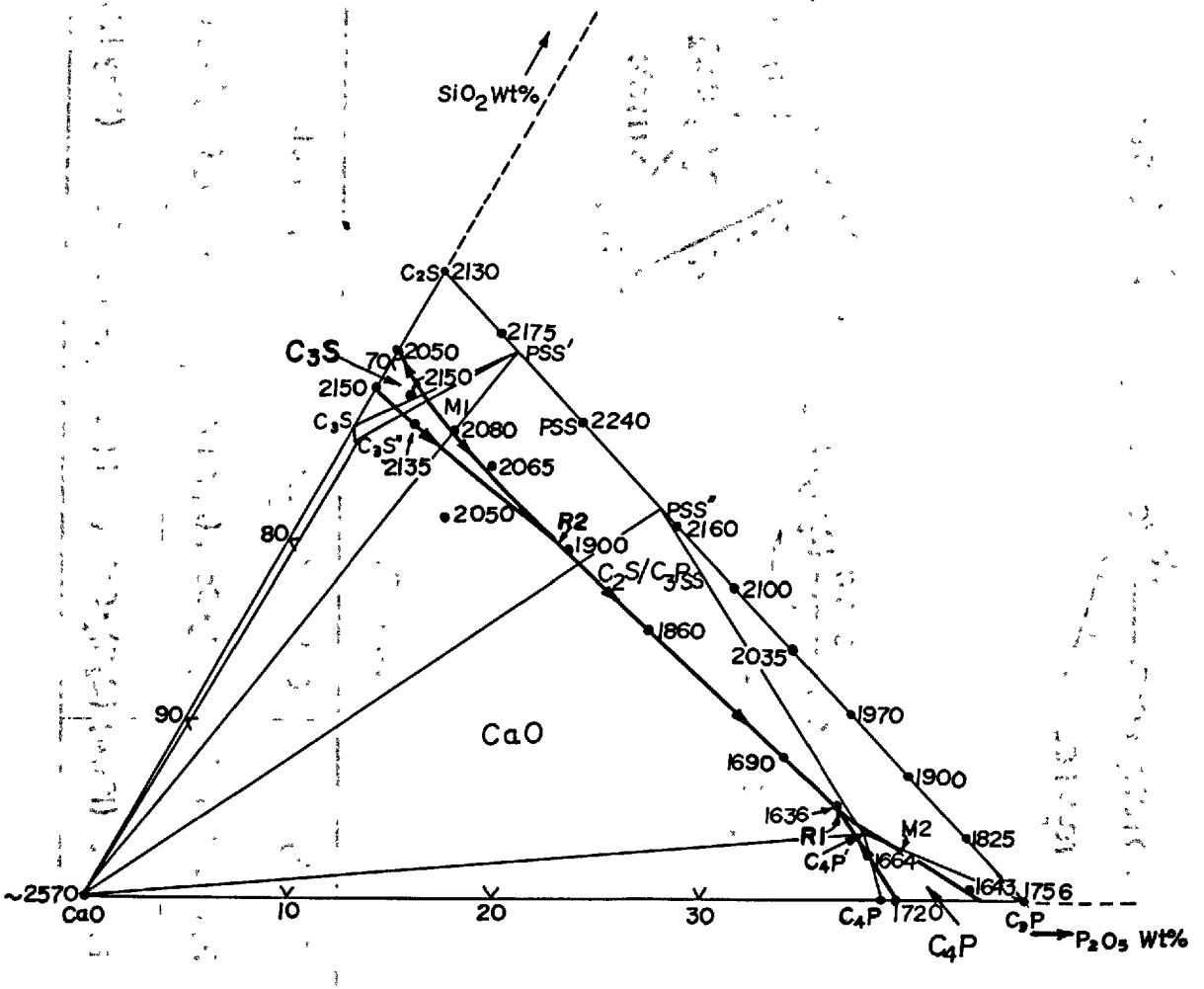

Tab. 1.

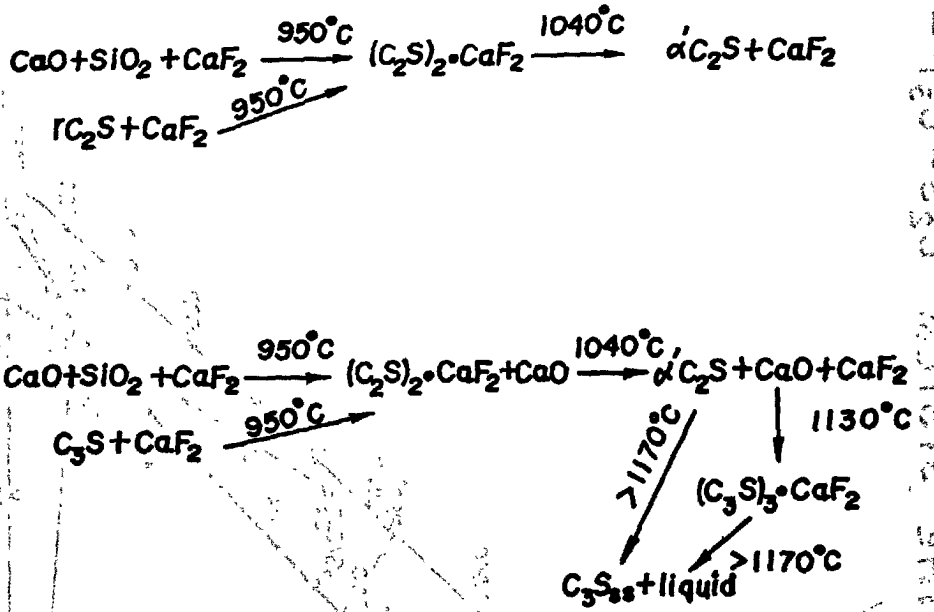

Tab. 2.

Breczky	Gutt & Osborne	Tanaka, et al.
Phase A (1964)	$(C_3S)_3 \cdot CaF_2$ (Apr. 1968)	$11CaO \cdot 4SiO_2 \cdot CaF_2$ (May 1966)
Phase B (1964)	$(C_2S)_2 \cdot CaF_2$ (Sept. 1966)	Phase II (May 1967)

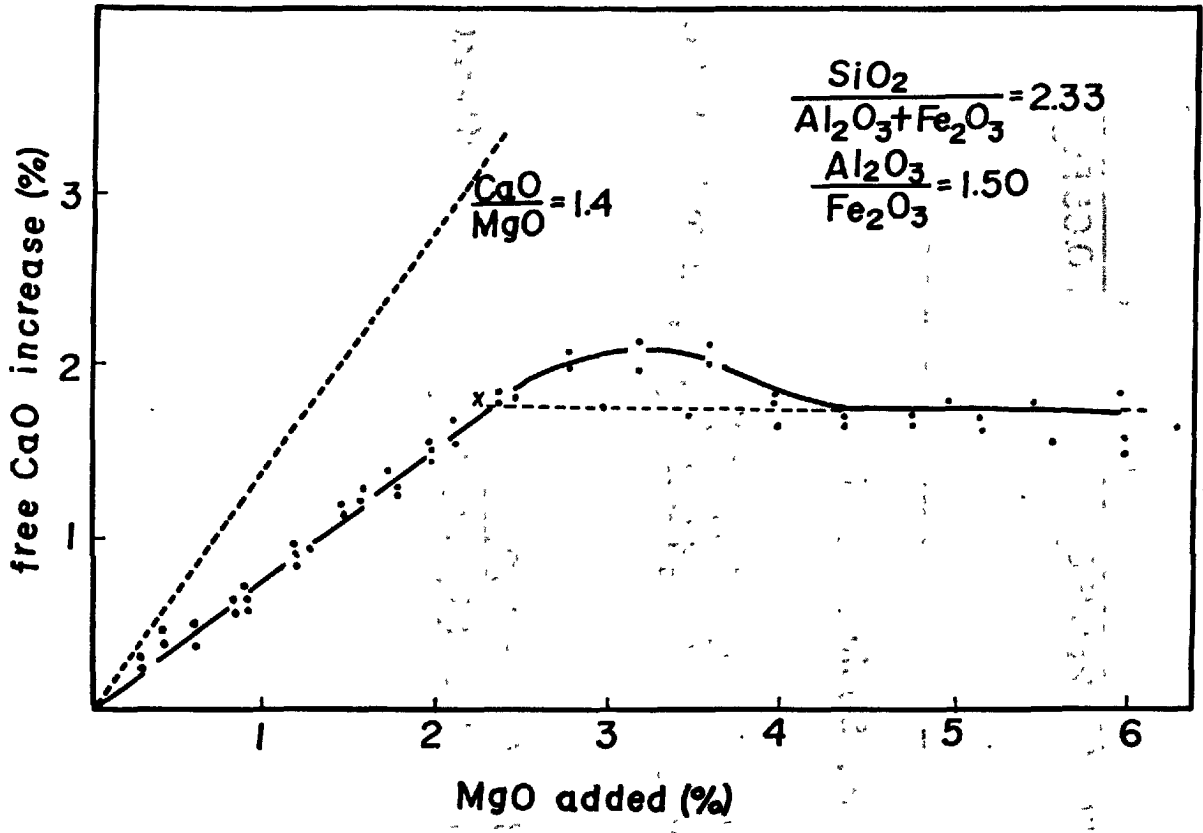

Fig.2. Increase in free CaO by additions of MgO to a laboratory -prepared clinker with "normal" chemical composition.

Tab. 3.

$$LS_t \text{ (Kuehl)} = \frac{100\ CaO}{2.8\ SiO_2 + 1.1\ Al_2O_3 + 0.7\ Fe_2O_3}$$

$$LS_t \text{ (Lea \& Parker)} = \frac{100 \cdot CaO}{2.80\ SiO_2 + 1.18\ Al_2O_3 + 0.65\ Fe_2O_3}$$

E. Spohn, et al.

$$LS_t = \frac{100\ (CaO + 0.75\ MgO)}{2.80 SiO_2 + 1.18 Al_2O_3 + 0.65\ Fe_2O_3}, \text{ where } MgO \leqq 2.0\%$$

$$LS_t = \frac{100\ (CaO + 1.50)}{2.80 SiO_2 + 1.18 Al_2O_3 + 0.65 Fe_2O_3}, \text{ where } MgO > 2.0\%$$

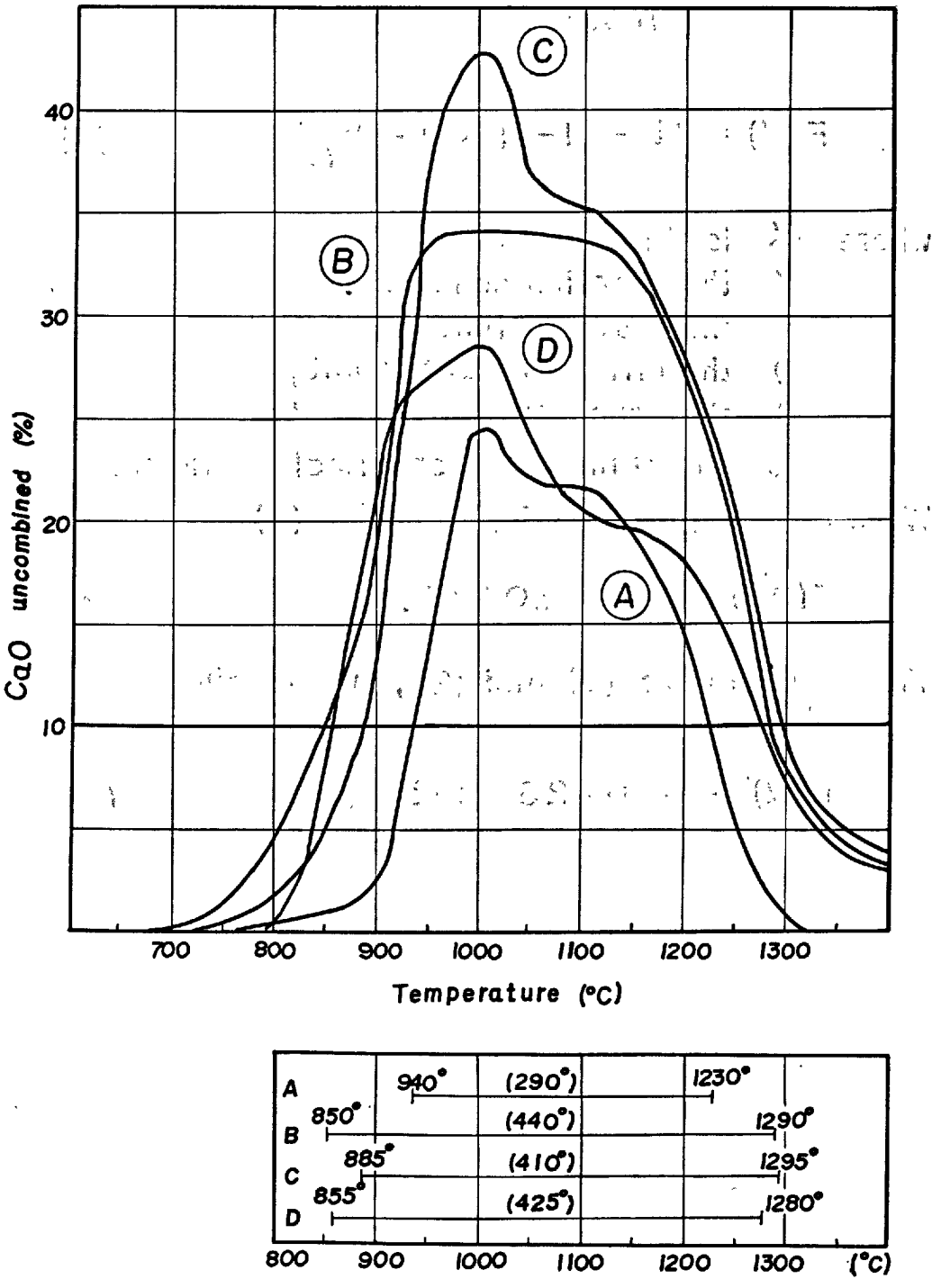

Fig.3. Changes of free CaO.

Tab.4.

$$F(\alpha) = Kt = (1-\sqrt[3]{1-\alpha})^2 = \frac{2D \cdot \Delta C}{r_0^2} \qquad (1)$$

where α is the reaction ratio,
K the reaction constant,
t the reaction time,
D the diffusion coefficient,
C the concentration, and
r_0 the diameter of spherical particles.

When α is equal to 0.5, Equation (1) becomes

$$F(0.5) = Kt_{0.5} = 0.0426. \qquad (2)$$

From Equations (1) and (2), we obtain

$$F(\alpha) = 0.0426\ (t/t_{0.5}). \qquad (3)$$

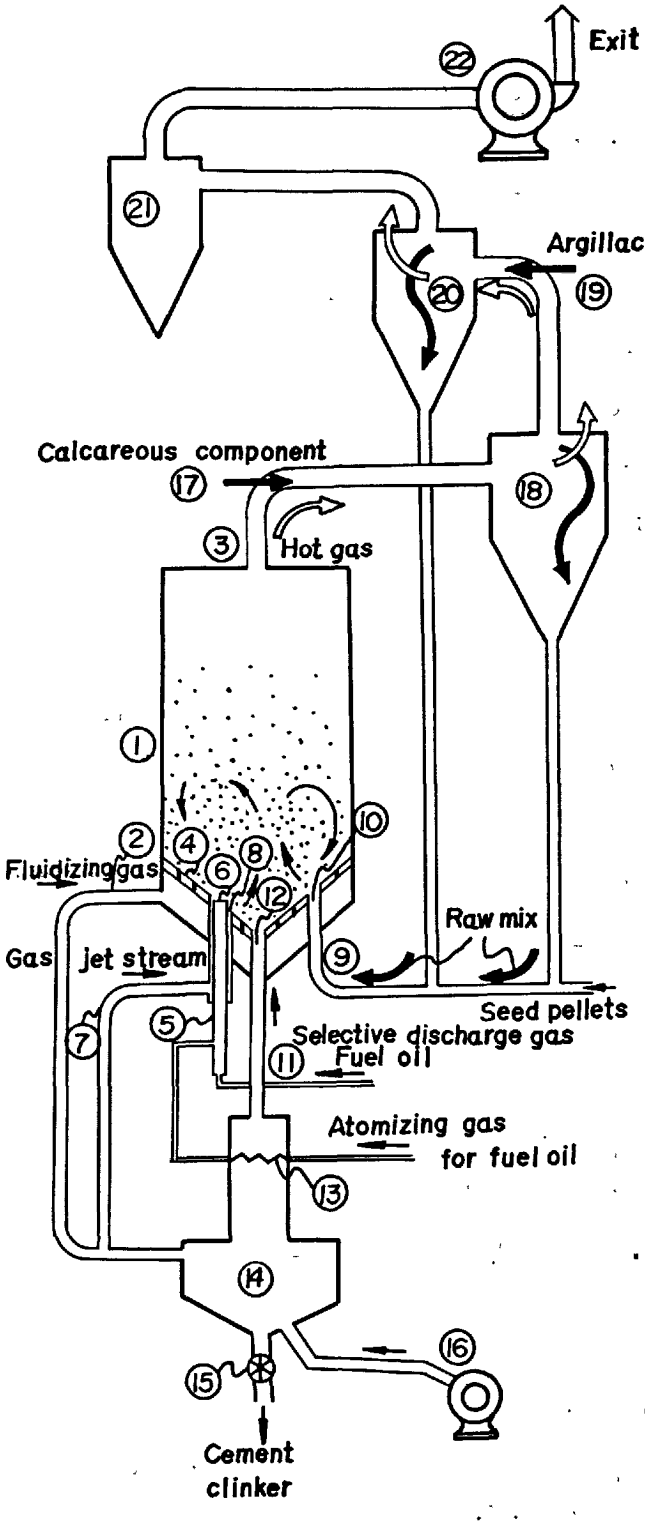

1 : Fluidized-bed reactor
2 : Fluidizing gas inlet
3 : Exhaust port
4 : Gas distributor
5 : Feed pipe of fuel oil
6 : Injection nozzle of fuel oil
7 : Feed pipe of gas jet stream
8 : Injection opening of gas jet stream
9 : Feed pipe of solid material
10 : Injection opening of solid material
11 : Selective discharge pipe
12 : Selective discharge pipe opening
13 : Heat exchanger
14 : Cooler
15 : Discharge gate
16 : Blower
17 : Inlet of calcareous component
18 : Hot cyclone for heating calcareous component
19 : Inlet of argillaceous component
20 : Hot cyclone for heating argillaceous component
21 : Dust collector
22 : Suction blower

Fig.4. Schematic diagram of the pilot plant.

GENERAL REPORT
OF
SESSION I-5: ANALYSIS OF PORTLAND CEMENT CLINKER

A. E. Moore (United Kingdom)

The following Supplementary Papers are summarized in this report.

Paper No. I-12

THE MINOR ELEMENTS IN ALITE (TRICALCIUM SILICATE) AND BELITE (DICALCIUM SILICATE) FROM SOME PORTLAND CEMENT CLINKERS AS DETERMINED BY ELECTRON PROBE X-RAY MICRO-ANALYSIS

H. G. Midgley (United Kingdom)

Paper No. I-57

THE EFFECT OF CHROMIUM OXIDE ON THE STRUCTURAL TRANSFORMATIONS IN TRICALCIUM SILICATE

A. I. Boikova (U.S.S.R.)

Paper No. I-42

THE USE OF THERMOGRAVIMETRIC MEASUREMENTS IN CEMENT CHEMISTRY

P. Longuet (France)

Paper No. I-64

ON THE COLOR OF PORTLAND CEMENT

K. Miyazawa & K. Tomita (Japan)

Paper No. I-76

MISCIBILITIES OF SPECIAL ELEMENTS IN TRICALCIUM SILICATE AND ALITE AND THE HYDRATION PROPERTIES OF RESULTED SOLID SOLUTIONS

R. Kondo & K. Yoshida (Japan)

Paper No. I-79

MICROSCOPIC OBSERVATIONS OF ALITE AND BELITE AND HYDRAULIC STRENGTH OF CEMENT

Y. Ono, S. Kawamura & Y. Soda (Japan)

Paper No. I-95

THERMAL STABILIZATION OF β-$2CaO.SiO_2$

V. I. Korneev & E. B. Bygalina (U.S.S.R.)

Paper No. I-101

PROPERTIES OF SUBSTITUTED DICALCIUM SILICATE AND ALUMINO-FERRITE

M. K. Gharpurey & V. N. Pai (India)

Paper No. I-105

THE EFFECT OF MINOR COMPONENTS ON THE EARLY HYDRAULIC ACTIVITY OF THE MAJOR PHASES OF PORTLAND CEMENT CLINKER

T. Sakurai, T. Sato & A. Yoshinaga (Japan)

Paper No. I-126

THE DISTRIBUTION OF ALKALIS IN PORTLAND CEMENT CLINKER

H. W. W. Pollitt & A. W. Brown (United Kingdom)

Paper No. I-131

CEMENT SURFACE AREA DETERMINATION BY GAS ADSORPTION NEAR ROOM TEMPERATURE

A. A. Tabikh (U.S.A.)

Paper No. I-136

THE CRYSTALLIZATION OF COMPOUNDS IN THE PRESENCE OF Cr_2O_3, P_2O_5 OR SO_3 AND THE PROPERTIES OF THE CEMENT RESULTED

Yu. M. Butt, V. V. Timashev & L. I. Malozhon (U.S.S.R.)

Of the twelve papers presented to this session only two deal mainly with a single analytical technique; the remainder all report work using a number of different techniques, on aspects of the problem of the role of minor elements in modifying the major phases. This problem has already been discussed in Session I, but I think the majority of the papers in this session deal not only with crystallographic modification but also with effects on reactivity. This leads to a question on which I hope we shall hear discussion; to what extent is the reactivity affected by crystallographic modification, and to what extent is the effect purely chemical, or due to the presence of the modifying oxide in solution.

I will deal first with the two purely analytical papers; first "Cement surface area determination by gas adsorption near room temperature" by TABIKH describes a method of specific surface measurement which is applicable both to anhydrous and to hydrated cements. The method is based upon the adsorption of nitrogen or organic vapours at known partial pressure from a gas stream, followed by desorption of the adsorbate into an inert carrier gas stream whose thermal conductivity may be compared with that of the pure carrier gas by means of a thermistor bridge. This gives a d.c. voltage output which is integrated to give a calibration for each adsorbate in terms of samples of known specific surface.

Alternatively, measurements can be made at several partial vapour pressures and the BET equation used to calculate the specific surface.

Dr Tabikh's Table 1 shows results for 5 anhydrous cements and three different organic liquids, as well as measurements of specific surface from adsorption of nitrogen or benzene using the BET calculation determinations. These show that a single point determination can give sufficiently satisfactory agreement with nitrogen/BET to be a useful laboratory method, although the specific surface is about 10 times that measured by the Blaine method.

The technique when used for hydrated cements may be open to some criticism: the sample is oven dried, then heated to 200°C in a helium stream with presumably a very low water content. This must surely change the nature of some of the hydration products (e.g. ettringite, if no other). However, this is a reflexion of the need to choose a sample condition which can be accurately reproduced, before and after the adsorption-desorption cycle. The curves shown for two hydrated cements suggest that the technique at least offers a useful method for comparison of hydration rates.

The next paper - "The use of thermogravimetric measurements in cement chemistry" by LONGUET - presents an exhaustive review of the technique and literature of thermogravimetry.

He draws attention to a number of experimental details which require particular care such as heating rate, sample size, buoyancy correction, thermocouple materials, and control of atmosphere, especially water vapour pressure. Techniques employed in conjunction with thermogravimetry such as DTA or evolved gas analysis are discussed.

Two reactions of interest to the Portland cement field are dealt with in detail; decarbonation, of both $CaCO_3$ and $MgCO_3$, and de-hydration of $Ca(OH)_2$ and $CaSO_4.2H_2O$. Other processes dealt with include oxidation-reduction and adsorption-desorption. Also in the cement field, the use of TGA for a study of reactivity is described, where additions of calcium fluoride are shown to promote the early loss of CO_2 from $CaCO_3$. A point of particular interest is the use of thermogravimetry in a CO_2 atmosphere to determine the C_3S content of clinker. C_3S reacts with CO_2 at between 600 and 800°C to form a mixture of spurrite and $CaCO_3$ in variable proportions; yet in the presence of fluoride, the reaction proceeds more rapidly and quantitatively:

$$2\ C_3S + 2\ CO_2 \longrightarrow CaCO_3 + (C_2S)_2\ CaCO_3$$

and the two different forms of combined CO_2 are released at two distinct temperatures in equal steps (Fig. 8). It is not quite clear to me how the fluoride is combined during this reaction, one would expect the formation of $(C_2S)_2\ CaF_2$.

The next group of four papers deals with studies of single compounds in the anhydrous cement field, modified by the addition of usually only one or two other oxides. These studies make use of a number of techniques, some well-known such as optical and electron microscopy, XRD and DTA, some less well-known such as conductivity and colour measurement.

Starting with the simplest system, we have "Thermal stabilization of β $2CaO.SiO_2$" by KORNEEV and BYGALINA. These authors show that use of a carefully controlled annealing treatment, 30 mins at 1000°C, will permit 85% stabilization of pure β C_2S. This material has the habit of γ C_2S but the birefringence and reactivity of β, as well as X-ray and DTA properties characteristic of β.

The authors further show that the presence of 10% excess CaO over that required to form C_2S will permit the stabilization of β C_2S over a wide range of temperature, as is well known, but in addition gives a material having apparently much improved hydraulic properties in terms of strength at 91 days or later. The authors suggest that the improved reactivity is due to irregular Ca co-ordination in the β C_2S, but it is unfortunately not clear how much of the excess lime is disposed in the β C_2S lattice and how much remains as free CaO, or even possibly forms C_3S.

Another comparatively simple system is described by BOIKOVA in "The effect of chromium oxide on the structural transformations in tricalcium silicate". Mixtures of C_3S and chromium oxide were fired at 1500°C in air and using optical and X-ray methods, DTA and free CaO determination, it was found that the limit of solid solution was 1.5% Cr_2O_3; this solid solution was light green with higher refractive indices than C_3S. The system is unusual in that above 2% Cr_2O_3, the solid solutions decompose to C_2S and free lime, and above 5% Cr_2O_3, no solid solution occurs.

Mixtures of C_3S with MgO as well as Cr_2O_3 show that MgO prevents this decomposition. This presumably indicates stabilization of one of the higher symmetry polymorphs of C_3S.

The colour of chromium-substituted C_3S can be changed by the conditions of heat treatment. Annealing at 600°C in air gives yellow; at 1500°C in air green; and 16-1800°C in argon gives blue coloration.

Chemical analysis shows the valence state of the Cr in these preparations to be mainly Cr^{6+}, mixed Cr^{6+} and Cr^{3+} and mainly Cr^{3+}, respectively.

Boikova suggests that Cr^{6+} replaces Si^{4+} with production of holes:

$$3\ Si^{4+} \rightleftharpoons 2\ Cr^{6+} + \square$$

but that Cr^{3+} replaces Ca:

$$3\ Ca^{2+} \rightleftharpoons 2\ Cr^{3+} + \square$$

also with production of a vacancy.

The next paper - "The effect of minor components on the early hydraulic activity of the major phases of Portland cement clinker" by SAKURAI, SATO and YOSHINAGA also deals with the effect of chromium oxide additions to C_3S.

These authors consider that, at 1550°C in air, the limit of Cr_2O_3 solubility in C_3S is 1.7% wt. (This should be compared with 1.4% at 1550°C found by Woermann, Hahn and Eysel (1) and 1.5% at 1500°C by Boikova (paper in this session).) They find that up to 1.4% the modification remains triclinic (T_I), with decreasing lattice parameters, but between 1.4 and 1.7% Cr_2O_3; T_{II} is formed. The discontinuity $T_I - T_{II}$ is both larger and in the opposite sense from that produced by Al_2O_3. The average valency of the chromium is 4.6 throughout this series, suggesting that there is no change in the replacement at the transition. The average valency for Boikova's three green mixes, which are comparable, is 5.15, 4.71, 5.14; this is perhaps due to the slightly lower firing temperature of Boikova's mixes, 1500°C against 1550°C.

For their next series of mixes, the authors made a series of high-lime C-S-A-F-Cr_2O_3 mixes with graduated Cr_2O_3 content, designed to give C_3S, C_3A and Fss but no C_2S. They then dissolved the C_3S to analyse its A, F and Cr content, and re-synthesized these C_3S compositions, which are saturated with A and F, for a given Cr_2O_3 content. The limit of Cr_2O_3 content was again found to be 1.7%, the modification T_{II} and average chromium valency 4.6 as before. The authors suggest that both Cr and Al

are substituting for Si, but that even so, it is impossible to balance the charges on the basis of this simple replacement. Using conduction calorimetry, they also show that (Fig. 3) increased Cr content both increases the maximum rate of heat production on hydration and shortens the time for this maximum rate to be attained, although it does not affect the total heat production. They go on therefore to a study of the dc conductivity of these compositions, which show (Fig.4) a considerable increase in conductivity for increasing Cr content. The activation energy of the conductivity calculated from these measurements is slightly greater than that for Cr^{3+} - Cr^{4+} and the authors suggest that the conduction mechanism is due to a combination of Cr^{3+} - Cr^{4+}, Cr^{4+} - Cr^{5+} and Cr^{3+} - Cr^{5+}.

Electron microscopy of fractured and etched surfaces in these samples confirms that etch-pit density increases with Cr content, both screw dislocations and grain boundary dislocations being observed. A series of electron micrographs illustrates the way in which reaction is initiated at these dislocations and at the surfaces of contact with interstitial phases.

The authors describe a further series of C_3S compositions in which chromium is replaced by fluorine and phosphorus while maintaining saturation with respect to Al and Fe. The compositions found are tabulated in Fig. 23.

The effects in this system are by no means as clear-cut as in the C-S-A-F-Cr_2O_3 system.

A further study is reported by the same authors on the effects of chromium oxide additions to the ferrite phases. The limits of Cr_2O_3 stability in both C_2F and C_4AF are found to be about 5% (wt.) but the authors feel that the changes in lattice parameters are anomalous. I would suggest that these changes are most interesting and merit further study as they must reflect a preference of chromium atoms for either the tetrahedral or the octahedral sites, which overrides the normal preference for the aluminium to occupy the tetrahedral sites first. The valence state of the chromium is obviously of great importance here.

The authors feel that the XRD intensities are also anomalous but I suggest that this is simply a preferred orientation effect, which occurs also with ferrites containing SO_3. The crystal growth along the b axis is inhibited and thin platelets are formed with faces parallel to h0l; the tendency to preferred orientation can be removed by fine grinding as is seen in Fig. 34. The analogy with sulphur may indicate that the chromium atoms have a preference for the tetrahedral sites.

Because it also deals with the effects of chrome oxide additions, I think that "The crystallization of compounds in the presence of Cr_2O_3, P_2O_5 or SO_3 and the properties of the cement resulted" by BUTT, TIMASHEV and MALOZHON should be considered next.

These authors prepared clinkers designed to contain either C_3S or C_2S and an interstitial phase calculated as 6% of C_3A and 14% of C_4AF with Cr_2O_3, P_2O_5 and SO_3 added singly at levels of 0.5, 1.0, 1.5, 2.0 and 3% by weight as the oxide. Table 1 shows the amount of each oxide retained after firing but for chrome oxide only Cr_2O_3 is reported; in the light of the previous papers, it would be interesting to know if CrO_3 was present. The clinkers were examined by both reflected and transmitted light microscopy and the refractive indices and crystal development are tabulated. It is interesting that although no SO_3 was retained in the belite series, the refractive indices were still lower than those of β C_2S in the zero SO_3 mix. Possibly the fluxing action of the SO_3 introduces additional Al_2O_3 and Fe_2O_3 into the lattice.

These clinkers were than ground with 5% $CaSO_4$ to a specific surface of 3000 cm^2/g and made into paste cubes 1.41 cm side. These were tested in compression at ages from 0.5 days to 6 months and examined by XRD to determine the rate of reaction of the compounds, at 0.5, 3 and 28 days. The results are shown in Table 3 (XRD) and Figures 3, 4 and 5.

The X-ray measurements suggest that both SO_3 and Cr_2O_3 give increased reactivity in C_3S at one day and this is partially borne out by the strength measurements; but at later ages, there is no marked increase in strength and the X-ray measurements show that at 28 days the cements with Cr_2O_3 and SO_3 are very comparable to the cement with no additions; only the P_2O_5 cement is still less reactive and weaker at 28 days. In this case, there is a tendency to show increased strength at 6 months, presumably due to the slow reaction of the C_2S-C_3P solid solution.

The last paper in the group dealing with single compounds and a single added oxide is "Miscibilities of special elements in tricalcium silicate and the hydraulic properties of the resulted solid solutions" by KONDO and YOSHIDA, which studies the effect of titanium or manganese oxide additions to C_3S or Alite. These authors made four series of compositions: C_3S - "$3CaO.TiO_2$", C_3S - "$3CaO.MnO_2$", Alite - "$3CaO.TiO_2$" and Alite - "$3CaO.MnO_2$". By both free lime determination and lattice parameter measurement, they found the limits of titania solid solution to be 13 mol % at 1500°C and 14% at 1600°C, with the transformation to T_{II} occurring at 5 mol % TiO_2. With Alite, the limit of titania solid solution is the same as with C_3S, 13 mol %, even though the alite is already saturated with respect to Al^{3+} and Mg^{2+}; the monoclinic II form transforms to rhombohedral (R) at about 6 mol %. The authors feel that in both cases this is a true solid solution with Ti^{4+} replacing only Si^{4+}.

In the case of manganese, the picture is rather different; for both C_3S and alite, free-lime is detected at 1% replacement and free-lime curve (see Figures 1 and 2) shows an inflection at 6% replacement. For C_3S, the symmetry transformations are $T_I \rightarrow T_{II}$ and 1% and $T_{II} \rightarrow T_{III}$

at 6% replacement. For alite however, there is a decrease in symmetry from M_{II} to M_I at 6%. I feel some reserve about the authors interpretation of this system; surely the valency of manganese is likely to be reduced to 2 at 1600°C, and possibly at 1500°C; and replacement of CaO by MnO is most likely together with formation of a (CaMn)O solid solution.

For the hydration studies the author used one composition from each series, C_3S and alite with 7 mol % Ti, or 5 mol % Mn. These samples were ground to 3220 cm^2/g (C_3S) and 3420 cm^2/g (alite) and formed into both neat-paste samples and mortar bars. The progress of hydration was followed by free $Ca(OH)_2$ determination, XRD of anhydrous phases, conduction calorimetry and strength development. These studies present a consistent picture, typified by Fig. 11. Both Mn and Ti retard reaction between 0 and 24 hours but at this point there is a rapid acceleration in Ti-containing pastes and by 3 days they have overtaken the unmodified C_3S or alite. By 28 days the Mn-containing materials have also caught up or overtaken the unmodified materials. The mortar strength measurements show a very similar picture.

The authors use the measurements of initial particle size and degree of hydration to calculate the thickness of the hydrated layer, assuming all particles spherical, and show that this can be represented by two straight lines on log thickness/log time scales (Fig. 15). They suggest that this indicates a three-stage reaction process, first an induction period, then an accelerating period in which hydration is auto-catalytic, and finally, a third stage where the rate is diffusion controlled and therefore proportional to the density of the hydration product. This part of the paper is due for discussion in the session on kinetics, but I hope that the question of the relative effect of the

chemical composition and the crystallographic modification will be ventilated, either in this session or later.

We come now to papers dealing with systems closer to commercial cements, containing both several phases and several modifying oxides.

"Properties of substituted dicalcium silicate and alumino-ferrite", by GHARPUREY and PAI deals first with an attempt to prepare a C_2S in which $\frac{1}{16}$, $\frac{1}{8}$ or $\frac{1}{4}$ of the Si^{4+} are replaced by Al^{3+}, using felspars (bytownite or microcline) as the source of tetrahedrally co-ordinated alumina. Unfortunately, no chemical analyses are given for the compositions so it is not clear if they were designed as C_2S -"C_2A", C_2S-C_3A or even C_2S - A series. It seems probable that the first was the case and the formation of C_3A from excess alumina has resulted in a shortage of lime for complete reaction of the silica to C_2S and hence the formation of γC_2S which is notoriously favoured by excess silica. The X-ray diffraction diagrams given for the bytownite series certainly suggest that C_3A has formed to an extent which makes it difficult to separate the effects of this during hydration from those due to alumina substitution in C_2S.

The second part of the paper deals with the hydration reactions of some compositions in the system C-A-F-M-M' (M' = Mn_2O_3).

A number of authors[2, 3] have indicated that in the "C_2A"-C_2F series, greater reactivity in solution is correlated with higher aluminium content. The figures which the present authors gave for combined water indicate that the C_6AF_2 in this series was unduly reactive; the unit cell dimensions found for this compound are much closer to those of C_2F than those usually reported for C_6AF_2 and it seems probable that equilibrium was not reached during firing and the sample therefore contained CA, $C_{12}A_7$, or C_3A, any of which would have

shown increased ractivity. (The unit cell dimensions quoted for C_6A_2F are qrong, possibly due to incorrect indexing in the original publication; they should read a = 5.32, b = 14.48, c = 5.53.)

The compositions C_4AF, $C_4AF_{0.85}M'_{0.15}$, $C_4AF_{.5}M'_{.5}$, C_4AM' were also prepared; since these have constant aluminium content, any differences in reactivity should be due to the effect of manganese-iron replacement only, and would be expected to be comparatively small. The combined water measurements for $C_4AF_{0.85}M'_{0.15}$ indicate such a marked increase in reactivity compared with those for C_4AF, while higher manganese contents show much less reactivity, that it seems almost certain that equilibrium was not reached in the preparation of this series.

The next paper in this group, which also deals with the ferrite phase is by MIYAZAWA and TOMITA "On the color change of Portland cement". These authors prepared synthetic cements of three compositions, normal, high C_3S and high C_2S, with graduated additions of MgO, 0, 0.5, 1.0, 1.5, 2.0, 2.5 and 3% (wt.). The colours of these cements were measured photoelectrically for L (luminance), a (+ = red, - = green) and b (+ = yellow, - = blue) component. In all three types there was a marked darkening with increasing MgO content to a minimum L at about 1.5%, b also decreased (i.e. the colour became less yellow) and a was approximately constant.

A series of ferrite phases was prepared in which MgO replaced CaO in C_4AF at levels 0, 1.5, 3.0, 4.5, 6.0 and 9.0 molar %. These compositions were examined both for colour and resistivity and Fig. 5 shows that luminance and specific resistance show very similar relations with MgO content. Because they find very little change in the XRD patterns of this series, the authors suggest that the resistivity

change is not related to structure but to replacement of Fe^{3+} by Mg^{2+} with consequent production of positive holes.

A further series of experiments was made to study the effect of cooling conditions on colour and reactivity of industrial clinkers. Two industrial clinkers were re-heated and cooled in five different ways. All ten samples were then made into cement with added gypsum (1.6% as SO_3) and examined for colour, heat of hydration and strength of mortar bars (in compression and bending). Early strength does appear to be inversely correlated with luminance but at later ages the slowly cooled clinker which is not the lightest shows least strength development.

From the XRD patterns in Fig. 6 I would suggest that it is the effect of cooling on the C_3A which has had the marked effect on early strength. The sample quenched in water shows a micro-crystalline ferrite phase (broad diffraction lines) with a cubic C_3A; all the other patterns show a well-crystallized ferrite and an orthorhombic C_3A. Forrester and Skalny[5] have shown that orthorhombic C_3A is more reactive than cubic at early ages; so apparently, even though a glassy ferrite is considered to be more reactive than a crystalline one, it is not enough to counteract the effect of the cubic C_3A.

The next paper "Microscopic observations of alite and belite and hydraulic strength of cement" by ONO, KAWAMURA and SODA, correlates microscopic and crystallographic properties of clinker minerals in commercial cements and laboratory preparations; it shows how these properties are affected by burning and cooling conditions and hence how they may be used to predict strength of cements.

The authors point out that the presence of impurities in alite (especially alkalis and sulphate) raises the birefringence, that

slow cooling may allow exsolution of these impurities and that an alite slowly cooling in the range 1250 - 1300°C may show low birefringence and mosaic structure; XRD shows it to be monoclinic alite, not C_2S + CaO, but it is possibly disordered.

In belite, impurities are absorbed by the α form but not by α' and are exsolved according to the cooling rate; if they are fully exsolved, the colour of the belite goes to muddy yellow.

The α and α' polymorphs of C_2S have been reported to be weakly- or non-hydraulic but these authors show that this is not always so; three synthetic belites stabilised in the α, α' and β forms are described, with strengths as follows:-

	7 days	28 days	91 days	
α	47	80	169	(kg/cm^2)
α'	11	41	86	
β	11	38	51	

Furthermore, using only one composition but varying the proportions of the C_2S polymorphs (excluding γ) by the burning and cooling conditions, strength (of 1 x 1 x 7 cm mortar bars) at 91 days is shown to be correlated with α content (as determined by XRD).

Similar experiments on plant raw mixes show that conditions which favour high α content, and therefore high later-age strength, need not be incompatible with high alite strength. Finally, a survey of 45 Japanese commercial cements shows that high strength correlates with (1) high α C_2S content, (2) colourless belite, and (3) high birefringence alite. The authors therefore suggest that a fairly long high temperature burn, followed by quick cooling from a moderately high temperature, is desirable.

The remaining two papers deal mainly with analyses of commercial cements in order to estimate true chemical compositions of the clinker phases.

The paper by POLLITT and BROWN on "The distribution of alkalis in Portland cement clinker" is based mainly on chemical analyses of commercial cements separated into fractions by selective solvent extraction and hydrolysis.

These authors show that the alkali sulphates may occur as members of the range of K_2/Na_2SO_4 solid solutions or as the double sulphate, calcium langbeinite, $2CaSO_4.K_2SO_4$ (see Fig. 2). I think that this is the first time this compound has been reported in Portland cement, although it is known to occur in kiln rings. It seems likely that it occurs only in high K_2O/Na_2O ratio cements.

Most interesting also are Table 2 and Fig. 3 which show clearly what I take to be a partition coefficient for potassium and sodium, between sulphate and clinker minerals of two to one. The authors deduce that this reflects the greater affinity of potash for sulphate but I would like to suggest that the similar ionic radii of Na and Ca favours retention of Na in the clinker minerals.

The authors tabulate the distribution of K and Na in sulphates, silicates, aluminate and ferrite phases in Table 4, and show that several correlations can be extracted.

The K/K + N ratio seems to be the same for the ferrite and the C_3A, and the silicates, but there is also a correlation between the potassium/alumina ratio of the C_3A and that of the ferrite phase. There is not much evidence to support Newkirk's suggestion that potash goes preferentially into belite. The authors show also that both potassium and sodium are capable of inducing the cubic-to-orthorhombic transformation of C_3A, at 2.8% equivalent potash or 1.8% equivalent soda.

The last paper, by MIDGLEY, reports "The minor elements in alite and belite from some Portland cement clinkers as determined by electron probe X-ray micro-analysis". It contains analyses for N, K, M, A, F, Ti and Mn. The main problem in obtaining quantitative estimates from the electron-probe lies in the inter-element absorption effect. Midgley has surmounted this by using as standards synthetic materials made to compositions very close to those being analysed. He reports partition coefficients for these elements between the silicate phases, which have not appeared in print before, to my knowledge.

In Table 9 (the last column) values >1 indicate enrichment in belite with respect to alite; thus only MgO is higher in alite than in belite; even Al_2O_3, usually considered to be the essential stabilising oxide in alite, is in fact enriched 3:2 in belite. It seems possible that the alite was not saturated with respect to MgO, as none of these cements contained more than 1.34%; this possibility seems to be borne out by Yamaguchi's EPMA figures for MgO (page 67 of the Principal paper) which indicate that in two cements with MgO contents of about 1.4%, the belite has the higher MgO content. Belite is also shown to be very considerably enriched in potash (in contradiction of Pollitt and Brown's findings) with a higher partition coefficient than any of the other oxides measured. The figures Midgley gives for average molar composition of belite (p.7) correspond to 3.3% replacement of the cations (and only 3% of the oxygen, i.e. an 0.3% oxygen defect).

One of the uses which we hope to make of this kind of measurement is to predict the composition of the phases in a given clinker and hence possibly to arrive at a better calculated composition. A number of the previous papers have made it clear that burning and cooling conditions may have as much effect on reactivity as does composition but it is still tempting to see what correlations exist between total chemical analysis and concentrations in the phases. For Fe_2O_3 and Al_2O_3, using measurements

by Peterson[6], Midgley[7], Fletcher[8], Terrier and Hornain[9] one obtains the relation shown in Slide no. 1 for alite and belite. This seems to indicate a fairly promising correlation for Fe_2O_3, but considerable scatter for Al_2O_3.

REFERENCES

1. E. Woermann, Th. Hahn and W. Eysel, "Chemical and Structural Studies of the Solid Solutions of Tricalcium Silicate", 16, No. 9, pp. 370-375 (1963).

2. W.L. de Keyser and N. Tenoutasse, "Contribution a l'etude du Mecanisme de l'hydration du Ciment et de ses Constituants en Presence du Chlorure de Calcium", Colloque International sur les Adjuvants des Mortiers et Betons, Bruxelles, 30 August-1 September 1967, Rapport II/8, Rilem ABEM, pp 115-141 (1967).

3. E.T. Carlson, "Some Properties of the Calcium Aluminoferrite Hydrates", National Bureau of Standards, Building Science Series, No. 6 (1966), (11 pp.)

4. E.T. Carlson, "Action of Water on Calcium Aluminoferrites", Journal of Research of the National Bureau of Standards - A. Physics and Chemistry, 68A, No. 5, pp. 453-463, (September-October 1964).

5. J.A. Forrester and J. Skalny, "Hydration of Cement: Study of Factors Affecting Rate", Presented at the meeting of Second International Conference on Thermal Analysis, at Worcester, Mass., (August 1968).

6. O. Peterson, "Untersuchung von Portland-Klinker mit der Mikrosonde", Zement-Kalk-Gips, Nr 2, pp 61-64 (1967), and Private Communication.

7. H.G. Midgley, "The Composition of Alite (tricalcium silicate) in a Portland Cement Clinker", Magazine of Concrete Research, 20, No. 62, pp. 41-44, (March 1968).

8. K.E. Fletcher, "The Analysis of Belite in Portland Cement Clinkers by use of an Electron Probe Microanalyser", Magazine of Concrete Research, 20, No. 64, (September 1968).

9. P. Terrier, H. Hornain and G. Socroun, "Quelques application de l'analyse par Microsonde Electronique a l'etude des Mineraux du Clinker, Revue des Materiaux de Construction, No. 630, pp 109-115, (March 1968).

GENERAL REPORT

OF

SESSION I-4: CHEMISTRY OF CALCIUM ALUMINATES AND THEIR RELATING COMPOUNDS

P. H. Halstead (United Kingdom)

The following Supplementary Papers are summarized in this report.

Paper No. I-78

THE CRYSTAL STRUCTURE OF $11CaO.7Al_2O_3.CaF_2$

P. P. Williams (New Zealand)

Paper No. I-90

THE SOLID-SOLUTION IN THE SYSTEM C_2AS (GEHLENITE)-CA_2 AND A NEW TERNARY PHASE

K. Sugiura & T. Yoshioka (Japan)

Paper: "The Crystal structure of $11CaO.7Al_2O_3.CaF_2$" by P.P. WILLIAMS

This paper is of particular interest in that it provides a convincing explanation of the peculiar zeolitic behaviour of $C_{12}A_7$ first reported by Roy and Roy, and Nurse, in 1960 and subsequently investigated in more detail by Majumdar and reported this year[1].

Briefly, at temperatures up to 1100°C '$C_{12}A_7$' can retain water, even in an environment of low partial water vapour-pressure and indeed as normally prepared '$C_{12}A_7$' must be regarded as a ternary compound in the system $CaO-Al_2O_3-H_2O$ and not a binary compound. In equilibrium conditions $C_{12}A_7H$ appears to be the composition of this substance. Dr Williams has obtained a specimen of a compound apparently isomorphous with $C_{12}A_7H$ in which the water, as $Ca(OH)_2$ has been substituted by CaF_2. This compound is not only more stable than $C_{12}A_7H$ but also lends itself more readily to crystal structure analysis and Dr Williams has presented in convincing detail a structure which agrees well with observed x-ray diffraction data.

A further merit of the proposed structure is that it offers an acceptable explanation of the reactivity of '$C_{12}A_7$' toward water and for the close similarity of the structure of anhydrous $C_{12}A_7$, $C_{12}A_7H$ and the halogen substituted analogues.

The proposed structure of $C_{11}A_7.CaF_2$ is a three dimensional network of linked AlO_4 tetrahedra in which the Ca-O and Ca-F coordination is

very iregular. To quote Dr Williams: "the anions which cannot be accommodated in a fully ordered structure are randomly distributed on a 12-fold equipoint of point symmetry $\bar{4}$. These anions contribute to a modified octahedral coordination of up to one-third of the calcium atoms. Large holes occur in the structure where sites in this equipoint remain unfilled, and adjacent calcium atoms have an unbalanced coordination shell".

The compound $C_{12}A_7$ contains one more oxygen atom per formula unit than can easily be accommodated in a simple fashion in its unit cell and no doubt the presence of this excess atom is associated with the reactivity of the anhydrous compound towards water and equally with the close similarity of the X-ray diffraction pattern of the anhydrous compound and $C_{12}A_7H$.

The majority of the paper is devoted to a lucid exposition of the reasoning which has led to the definition of the proposed structure of $C_{11}A_7CaF_2$ and of compounds generally of the composition $C_{11}A_7CaX_2$ where X can be OH^-, F^- or Cl^- and calls for no further comment from me.

What, however, is of some interest is the stability of the compound $C_{12}A_7H$. There are very few substances which are capable of retaining water at temperatures above 1000°C and one might justifiably speculate upon the reasons for the greater stability of the O-H bonds in $C_{12}A_7H$ compound with, say $Ca(OH)_2$ or the hydrates which are formed when portland or aluminous cements react with water. Dr Williams has given an expalanation of the manner in which the $\overline{OH}$ (or F^- or Cl^-) is incorporated in the structure of these compounds. Perhaps the thermodynamicists would come to offer an explanation for their stability?

Paper: "The Solid Solution in the System C_2AS (Gehlenite) - CA_2 and a new Ternary Phase by K. SUGIURA and T. YOSHIDA

This interesting paper describes a detailed investigation of a small region of the ternary system $CaO-Al_2O_3-SiO_2$ bounded by CAS_2 (anorthite), CA_2 and C_2AS (gehlenite).

The authors show clear evidence that a metastable ternary phase can be formed in melts having compositions represented by a zone in the $CAS_2-CA_2-C_2AS$ triangle and that this phase can have the compositions C_3A_3S and $C_3A_3S_2$ as well as other compositions. It appears that this ternary solid solution phase can exist as a monophase without much change in optical properties or cell dimensions in compositions represented by a considerable area of the phase diagram and if my interpretation of the authors' explanation for this is correct, this implies that:-

(i) A continuous series of solid solutions exists of composition represented by a portion of the line C_3A_3S - CAS_2 (anorthite) starting at C_3A_3S.

(ii) A continuous series of solid solutions exists of composition represented by a portion of the line CA_2- CAS_2 (anorthite).

(iii) Solid solutions can apparently be formed between any member of the solid solutions mentioned above as (i) and (ii), thus giving a wide range of compositions in which monophase production is possible.

(iv) The area of the phase diagram which represents this wide range of compositions cannot be regarded as homogeneous because when the properties of solid solutions represented by lines running from CAS_2 (anorthite) towards the $CaO - Al_2O_3$ boundary are studied, there are inflexions in the refractive index v composition graph as one passes the compositions represented approximately by the line $C_3A_3S_2$ - $C_5A_6S_4$ - $C_2A_3S_2$. There are thus perhaps two zones of

composition which represent similar but not identical kinds of solid solution.

The composition of the compound C_3A_3S lies on the edge of one of the zones mentioned above and is also on the line C_2AS (gehlenite) - CA_2.

It is shown that C_3A_3S clearly exists as a monophase when equimolar proportions of C_2AS and CA_2 are heated to 1000-1100°C, and the authors have passed on from this to study the phase composition of mixtures with compositions represented by other points along the C_2AS - CA_2 line to discover whether solid solutions can be formed between C_2AS and CA_2 over a limited range of proportions.

The authors show that when such mixtures are heated to temperatures in the range 950 - 1530°, the sole identifiable phases are a melilite, a glass, CA_2 and phase "X", a ternary phase. They argue that phase "X" is C_3A_3S but do not appear to support this contention by experimental evidence.

As the ratio CA_2/C_2AS in the mixtures is increased at temperatures of 1000-1100 and with compositions having a CA_2 content up to 15 per cent, there is a corresponding increase in a_o cell dimension of the melilite as the CA_2 content increases. This the authors take to indicate that there is a small range of compositions which form solid solutions of CA_2 in C_2AS giving a melilite in which aluminium atoms substitute equally for calcium atoms in the "A" sites of the melilite structure and aluminium atoms substitute for silicon atoms in "C" sites. The latter substitution was foreshadowed by Christie[1] as possible but the former substitution seems unlikely because of the great difference in size of aluminium and calcium atoms. If such substitution does take place, it ought to give rise to a considerable decrease in the c_o cell dimension from that found in gehlenite but the authors do not say whether this change was observed.

If, as the authors claim, phase "X" has truly the composition C_3A_3S, then the claim that CA_2 is entering into solid solution with C_2AS is well founded. If, on the other hand, phase "X" is not C_3A_3S but has some other composition, for example, one represented by the large area mentioned earlier in (iv) or lying along the line C_3A_3S-$C_3A_3S_2$, then the melilite composition must, in the case of the preparations which contained only melilite and phase "X", be silica deficient and lie off the C_2AS - CA_2 line towards the CaO - Al_2O_3 boundary.

To summarise, the authors have clearly demonstrated the existence of a new metastable phase in the CAS_2 - CA_2 - C_2AS region and have offered strong but not completely convincing evidence that C_2AS can absorb up to 15 per cent CA_2 to form a continuous solid solution series.

(1) OLAF, H.J. and CHRISTIE. Norsk Geologisk Tidskrift, 1962, 42, 1-29.

P.E. Halstead
Cement and Concrete Association
Slough, UNITED KINGDOM

GENERAL REPORT

OF

SESSION II-2: CRYSTAL STRUCTURES AND PROPERTIES OF CEMENT HYDRATION PRODUCTS (HYDRATED CALCIUM ALUMINATES AND FERRITES)

(a) Papers regarding Structures

W. Locher (West Germany)

The following Supplementary Papers are summarized in this report.

Paper No. II-14

QUATERNARY CALCIUM ALUMINATE HYDRATES: CRYSTAL STRUCTURE OF CALCIUM ALUMINATE MONOBROMIDE HYDRATE

F. Le Bel & G. Grasland (France)

Paper No. II-15

CONTRIBUTION TO THE STUDY OF COMPLEX ALUMINATES: HYDRATED CALCIUM AND MAGNESIUM MONOCARBOALUMINATES

G. Sadran & B. Cottin (France)

Paper No. II-19

X-RAY INVESTIGATIONS OF SOME COMPLEX CALCIUM ALUMINATE HYDRATES AND RELATED COMPOUNDS

H.-J. Kuzel (West Germany)

Paper No. II-27

PROTON MAGNETIC RESONANCE STUDIES OF C_3AH_6

R. Kiriyama, H. Kiriyama & M. Takagawa (Japan)

Paper No. II-29

CALCIUM ALUMINATE HYDRATES AND RELATED BASIC SALT SOLID SOLUTIONS

M. H. Roberts (United Kingdom)

Paper No. II-77

CRYSTAL STRUCTURES AND REACTIONS OF C_4AH_{12} AND DERIVED BASIC SALTS

S. J. Ahmed, L.S.D. Glasser & H. F. W. Taylor (United Kingdom)

Paper No. II-137

THE ALTERATION OF SILICATE ANIONS IN TOBERMORITE GELS

H. Funk (West Germany)

SYNOPSIS

The degree of condensation of silicate anions in tobermorite gel has been investigated by H. Funk. A criterion for the degree of condensation is the rate of formation of molybdato silicic acid, which occurs after addition of paramolybdate to the sample dissolved in methanolic hydrochloric acid. The results show that the hydration products of tricalcium silicate and dicalcium silicate contain as well monosilicate as higher condensed silicates. The degree of condensation increases with decreasing CaO/SiO_2 ratio in the tobermorite gel and with aging. H. Funk assumes that the coexistence of various silicate anions is the cause for the low degree of crystallisation of tobermorite gel.

The crystal structure of tricalcium aluminate hexahydrate $3CaO.Al_2O_3.6H_2O$, especially the positions of the hydrogen ions, was determined by R. Kiriyama, H. Kiriyama and M. Takagawa with proton magnetic resonance studies. Accordingly the structure consists of $[Al(OH)_6]^{3-}$ anions, which form a ionic lattice of the garnet type together with the Ca^{2+} cations. Inside the oxygen tetrahedrons there are no discrete H_4 clusters.

According to recent investigations of M. H. Roberts the tetracalcium aluminate hydrate $4CaO.Al_2O_3.aq$ occurs in 4 stages of hydration with 19, 13, 11 and 7 H_2O depending on the drying conditions.

The hydrates with 13, 11 and 7 H_2O can dehydrate and rehydrate reversibly. X-ray investigations of S. J. Ahmed, L. S. Dent Glasser and H. F. W. Taylor have shown that the crystal structure of tetracalcium aluminate hydrate consists of principal layers of the composition $[Ca_2Al(OH)_6]^+$, each combined with an interlayer containing one OH ion per unit cell and the water molecules. The principal layer is composed of $Al(OH)_6$ and $Ca(OH)_6$ octahedrons connected with one another by common edges.

The composition of the complex compounds of tetracalcium aluminate hydrate corresponds to the general formula $3CaO.R_2O_3.Ca(X,Y_2).aq$ with R representing Al^{3+}, Cr^{3+}, Ga^{3+} und Fe^{3+}, with X representing a divalent anion such as CO_3^{2-}, SO_4^{2-}, CrO_4^{2-}, and Y representing a monovalent anion such as Cl^-, Br^-, J^-, NO_3^- or BrO_3^- respectively. X-ray investigations of H.-J. Kuzel and of F. Le Bel and G. Grasland confirm that the complex compounds have the same crystal structure as tetracalcium aluminate hydrate and that the anions replace the OH^- ions in the interlayers. Furthermore H.-J. Kuzel describes double salts of the composition $3CaO.Al_2O_3.1/2CaSO_4.1/2CaCl_2.12H_2O$ and $3CaO.Al_2O_3.1/2Ca(NO_3)_2.1/2CaCl_2.10H_2O$, in which sulfate and chloride containing interlayers alternate in the unit cell.

There is a continuous series of solid solution between the monosulfate $3CaO.Al_2O_3.CaSO_4.12H_2O$ and the compound $3CaO.Al_2O_3.1/2Ca(OH)_2.1/2CaSO_4.12H_2O$, which probably belongs to the double salts described by H.-J. Kuzel. The investigations of M. H. Roberts indicate that in the adequate systems hydroxide-carbonate and hydroxide-chloride exist similar series of solid solution.

A complete solid solution series also occurs between the compounds $3CaO.Al_2O_3.CaCO_3.11H_2O$ and $3MgO.Al_2O_3.MgCO_3.11H_2O$. According to G. Sadran and B. Cottin the phases of this series can be prepared by addition of hydromagnesite $3MgCO_3.Mg(OH)_2.3H_2O$ to a metastable calcium aluminate solution with a molar ratio $CaO/Al_2O_3 = 3$. They also occur when high alumina cement hydrates in presence of hydromagnesite and when various calcium aluminate hydrates react with hydromagnesite in a paste.

1. INTRODUCTION

This general report is concerned with the structural composition of tobermorite gel, with the crystal structure of tricalcium aluminate hexahydrate and with equilibrium relations and crystal structure of tetracalcium aluminate hydrate and the related complex compounds. It is based on the following supplementary papers:

Tobermorite gel

H. Funk: The alteration of silicate anions in tobermorite gel.
Arrival No. 137

Tricalcium aluminate hexahydrate

R. Kiriyama, H. Kiriyama, M. Takagawa: Proton magnetic resonance studies of C_3AH_6.
Arrival No. 27

Tetracalcium aluminate hydrate and related complex hydrates

M. H. Roberts: Calcium aluminate hydrates and related basic salt solid solutions.
Arrival No. 29

S. J. Ahmed, L. S. Dent Glasser, H. F. W. Taylor: Crystal structures and reactions of C_4AH_{12} and derived basic salts.
Arrival No. 77

H.-J. Kuzel: X-ray investigations of some complex calcium aluminate hydrates and related compounds.
Arrival No. 19

F. Le Bel, G. Grasland: Quaternary calcium aluminate hydrates. Crystal structure of calcium aluminate monobromide hydrate.
Arrival Nr. 14

G. Sadran, B. Cottin: Contributions to the study of complex aluminates: Hydrated calcium and magnesium monocarbo-aluminates.
Arrival No. 15

2. TOBERMORITE GEL

The paper of H. Funk is concerned with the degree of condensation of silicate anions in calcium silicate hydrate formed by hydration of tricalcium silicate and β-dicalcium silicate at 25 °C. To determine the degree of condensation, a weighed sample is dissolved in methanolic HCl and then a paramolybdate solution is added, which forms a complex compound together with the silicic acid. Under standardized conditions the rate of reaction only depends on the degree of condensation of the silicic acid in the solution which corresponds to the condensation of the silicate anions in the tobermorite gel.

The increase in content of molybdato silicic acid $H_4SiMo_{12}O_{40}$ plotted against reaction time on a logarithmic scale yields a straight line, the slope of which is a criterion for the rate of reaction and consequently for the degree of condensation, too (1)(2)(3)(4). Using this method the monosilicic acid of β-Ca_2SiO_4, the disilicic acid of $Na_6Si_2O_7$, the tricyclosilicic acid of α-$CaSiO_3$,

the tetracyclosilicic acid of $K_4H_4Si_4O_{12}$, and hexacyclosilicic acid of $Cu_6Si_6O_{18}.6H_2O$ can be significantly distinguished (fig. 1a). Mixtures of silicic acids with different degrees of condensation yield a curve instead of a straight line. From the profile of the curve the type and the amount of silicate components in the mixture can be estimated.

The results of adequate investigations on hydration products of tricalcium silicate and β-dicalcium silicate show that both substances contain monosilicate and higher condensed silicates, too. Compounds with more that 6 SiO_4 tetrahedrons are produced by tricalcium silicate to less than 4o %, by β-dicalcium silicate to about 5o %. The degree of condensation of silicate anions in tobermorite gel does not depend on the kind of the basic material only, but on the conditions of hydration, too. Tricalcium silicate hydrated for 9o days at 25 °C in a saturated calcium hydroxide solution yields a calcium silicate hydrate with a molar ratio CaO/SiO_2 of 1.76, consisting of mono-, di-, tri-, and tetrasilicates.

Hydrating tricalcium silicate under same conditions but in water calcium silicate hydrates with a CaO/SiO_2 ratio of 1.54 are formed, 4o % of which have a degree of condensation of 6 or more. Still higher condensed calcium silicate hydrates with about the same CaO/SiO_2 ratio of 1.51 arise from paste hydration of tricalcium silicate after 5 years.

Furthermore the influence of CaO/SiO_2 ratio on the degree of condensation was investigated on calcium silicate hydrates produced by reaction of a o.1 molar solution of $Na_2H_2SiO_4$ with a solution of $Ca(ClO_4)_2$. The CaO/SiO_2 ratio was gradually raised

from o.89 to 1.41 by addition of increasing amounts of NaOH. The degree of condensation in the calcium silicate hydrates increases intensely with decreasing CaO/SiO_2 ratio. There is an increase of condensation, too, when the calcium silicate hydrates remain in contact with the mother liquor for a longer period or when they were dried after filtration (fig. 1b).

The investigations show that the SiOH groups in the tobermorite gel can react to larger units. The degree of condensation mainly depends on the content of CaO in the tobermorite gel and on the method of preparation, especially on aging. Consequently in tobermorite gel silicate anions of various degrees of condensation are present. H. Funk assumes, that the occurence of different silicate anions in the tobermorite gel is the cause for the low degree of crystallization of the calcium silicate hydrates.

3. CRYSTAL STRUCTURE OF TRICALCIUM ALUMINATE HEXAHYDRATE

The crystal structure of tricalcium aluminate hexahydrate with the formula $3CaO.Al_2O_3.6H_2O$ or $Ca_3Al_2(OH)_{12}$ was investigated by R. Weiss and D. Grandjean (5) using X-ray diffraction. Accordingly the space group is Ia3d and the lattice constant at room temperature is 12.573 Å.

The positions of the heavy atoms are:

16 al in (a) (o, o, o)

24 Ca in (c) (1/8, o, 1/4)

96 O in (h) (x_o, y_o, z_o)

where $x_o = o.o3o$

$y_o = o.o52$ and

$z_o = o.64o$

The positions of the hydrogen atoms are not yet known. They are

of special interest with regard to the isomorphism with grossularite $Ca_3Al_2(SiO_4)_3$, which requires a substitution of 1 Si^{4+} by 4 H^+. Therefore R. Kiriyama, H. Kiriyama and M. Takagawa used the proton magnetic resonance method to determine the position of hydrogen atoms.

Tricalcium aluminate hexahydrate was prepared by slow addition of aluminium powder to a saturated solution of calcium hydroxide. The exact X-ray investigations showed a lattice constant of 12.566 Å at 24 °C and 12.536 Å at -170 °C respectively.

The infrared absorption indicated that the sample contained no adsorbed water and that the hydroxyl group was free from any hydrogen bond. The measurements by proton magnetic resonance were carried out in a temperature range between -186 ° and +25 °C. From 20 measurements at low temperature and 15 measurements at room temperature for the second moment ΔH_2^2 mean values resulted of

$$22.7 \pm 0.3 \text{ gauss}^2 \text{ at } -186\,^{\circ}\text{C and}$$

$$19.6 \pm 0.5 \text{ gauss}^2 \text{ at } +25\,^{\circ}\text{C}$$

respectively.

From considerations of symmetry the hydrogen atoms must occupy the 96 (h) positions with the parameters x_H, y_H, and z_H. Since only one value of the second moment is available from the proton magnetic resonance, the three parameters cannot be determined independently. So for the various model structures theoretically possible the second moments were calculated by the method of J. H. van Vleck (6) and compared with the measured moments. For the positions of the hydrogen atoms following parameters resulted:

$$x_H = 0.093;\ y_H = 0.074;\ z_H = 0.681$$

These values differ from those of C. Cohen-Addad, P. Ducros and G. F. Bartaut (7), who found the following positions for the

hydrogen atoms, resulting from neutron diffraction at 4 °K:

$$x_H = 0.101; \; y_H = 0.049; \; z_H = 0.662$$

For this static model the calculated second moment is 26.9 gauss^2 compared with the experimental value of 22.7 gauss^2 at -186 °C. However both investigations showed that there are no discrete H_4 clusters inside the oxygen tetrahedrons.

The distances between two hydrogen atoms of the same $(OH)_4$ tetrahedron are 1.96 Å and 2.56 Å, the shortest H-H distance between adjacent tetrahedrons is 2.02 Å. This arrangement of the hydrogen atoms confirms that the structure is composed of $[Al(OH)_6]^{3-}$ anions, which together with the Ca^{2+} cations form a ionic lattice of the garnet type. The Al-O-H bond is not linear as in a free $[Al(OH)_6]^{3-}$ complex owing to electrostatic interactions but forms an angle of 138 ° caused by the approach of the other ions.

4. TETRACALCIUM ALUMINATE HYDRATE

4.1 Composition, Water Content

The composition of the tetracalcium aluminate hydrates, especially their water content was studied again by M. H. Roberts. As all phases of tetracalcium aluminate hydrate react with CO_2 very quickly, any contact with atmospheric CO_2 during preparation and investigation had to be avoided strictly. The tetracalcium aluminate hydrate with the composition $4CaO.Al_2O_3.19H_2O$ is only formed as a metastable phase in an aluminate solution with a high content of lime under atmospheric pressure at temperatures in the range from 1 ° to 50 °C. There are two polymorphs α_1 and α_2 which have the same longest basal spacing d_B = 10.7 Å but slight differences in the position of the non-basal reflections.

At relative humidities in the range from 81 to 11 % the $4CaO.Al_2O_3.19H_2O$ dehydrates to $4CaO.Al_2O_3.13H_2O$ with a longest basal spacing of 7.9 Å. Rehydration of the 13 H_2O hydrate to 19 H_2O hydrate is not possible. In earlier publications M. H. Roberts (8) and F. E. Jones and M. H. Roberts (9) assumed that $4CaO.Al_2O_3.13H_2O$ exists in two polymorphs α and β with d_B = 8.2 Å und 7.9 Å respectively. But recent X-ray investigations showed that the α-modification with d_B = 8.2 Å is a CO_2 containing phase of the composition $3CaO.Al_2O_3.1/2Ca(OH)_2.1/2CaCO_3.12H_2O$ (chapter 6.2). So $4CaO.Al_2O_3.13H_2O$ only exists in one modification with d_B = 7.9 Å, the water content of which - 13 H_2O - was confirmed by exact chemical determinations.

The investigations of P. Seligmann and N. R. Greening (10)(11) gave the same results. In contrast to this view R. Alègre (12), F. Lavanant (13) and W. Dosch and H. zur Strassen (14) suggested that there exist a $4CaO.Al_2O_3.12H_2O$ with d_B = 7.9 Å and a $4CaO.Al_2O_3.13H_2O$ with d_B = 8.2 Å. According to W. Dosch and H. zur Strassen this 8.2 Å spacing likewise is derived from a compound of composition $3CaO.Al_2O_3.3/4Ca(OH)_2.1/4CaCO_3.aq$. These differences M. H. Roberts attributes to an inadvertent carbonation which can hardly be avoided during preparation and X-ray investigations.

$4CaO.Al_2O_3.11H_2O$ with d_B = 7.4 Å is formed by drying $4CaO.Al_2O_3.13H_2O$ over anhydrous $CaCl_2$ or solid NaOH. When exposed to a moist atmosphere, $4CaO.Al_2O_3.11H_2O$ rehydrates very easily giving the 13 H_2O hydrate. When dried over P_2O_5, $4CaO.Al_2O_3.7H_2O$ with a weak basal reflection with d_B = 5.5 Å is formed. Higher

values for the longest basal spacing found by other authors (12)(13)(14), M. H. Roberts attributes to rehydration which occurs very readily, or to carbonation.

4.2 Crystal Structure

The crystal structure of various stages of hydration of tetracalcium aluminate hydrate is described in the supplementary paper of S. J. Ahmed, L. S. Dent Glasser and H. F. W. Taylor based on recently published results (15)(16). The X-ray investigations were carried out on single crystals of the approximate composition $4CaO.Al_2O_3.12\text{-}13H_2O$, containing some structural carbonate. The crystals are trigonal, space group R $\bar{3}$ c, the unit cell with a = 5.73 Å, c = 47.16 Å (referred to trigonal axes), contains 6 formula units of mean composition $Ca_2Al(OH)_{6\ 3/4}(CO_3)_{1/8}.2\ 1/2H_2O$ or in the carbonate-free compound $Ca_2Al(OH)_7.2\ 1/2H_2O$.

The structure (fig. 2) consists of 6 "principal layers" of the composition $[Ca_2Al(OH)_6]^+$ perpendicular to c with a distance of 7.86 Å in c-direction. The layers are formed by $Al(OH)_6$ and $Ca(OH)_6$ octahedrons which are connected with one another by common edges. The Ca^{2+} ions, however, are shifted along the c-axes for $\pm$ o.5 to o.6 Å out of the plane of the Al^{3+} ions at z = o. Accordingly the $Ca(OH)_6$ octahedrons are distorted. Each principal layer is combined with an interlayer containing one further $(OH)^-$ ion and the water molecules. Two of the water molecules occupy sites marked P in fig. 2, raising the Ca-coordination to 7. The OH ion and eventually one further H_2O molecule occupy the cavities designated by X. The layer complexes, each of them composed of principal and interlayer, are displaced to each other by 2/3 a and 2/3 b.

Including the results of M. H. Roberts the principal layers and interlayers of tetracalcium aluminate hydrates have the following composition and c distances:

$4CaO.Al_2O_3.19H_2O$	$[Ca_2Al(OH)_6.2H_2O]OH.4H_2O$	1o.7 Å
$4CaO.Al_2O_3.13H_2O$	$[Ca_2Al(OH)_6.2H_2O]OH.H_2O$	7.9 Å
$4CaO.Al_2O_3.11H_2O$	$[Ca_2Al(OH)_6.2H_2O]OH$	7.4 Å
$4CaO.Al_2O_3.7H_2O$	$[Ca_2Al(OH)_6]OH$	5.5 Å

According to S. J. Ahmed, L. S. Dent Glasser and H. F. W. Taylor the great diminuation of the layer distance of $4CaO.Al_2O_3.7H_2O$ is caused by a small changing of the arrangement of the $Al(OH)_6^{3-}$ octahedrons and the Ca^{2+} ions. The $4CaO.Al_2O_3.19H_2O$ contains one additional layer of water molecules between the principal layers.

5. COMPLEX COMPOUNDS OF TETRACALCIUM ALUMINATE HYDRATE

5.1 Composition

The composition of the complex tetracalcium aluminate hydrates corresponds to the formulas $3CaO.Al_2O_3.CaX.nH_2O$ or $3CaO.Al_2O_3.CaY_2.nH_2O$ with X representing a divalent and Y representing a monovalent anion respectively. At relative humidities of about 35 % the compounds contain 1o-12 water molecules per formula unit.

The supplementary paper of H.-J. Kuzel describes the crystal structure of compounds containing Cl^-, Br^-, J^-, NO_3^-, and BrO_3^- as monovalent and SO_4^{2-} and CrO_4^{2-} as divalent anions. The compounds with Cl^-, Br^-, and NO_3^- were investigated by S. J. Ahmed, L. S. Dent Glasser and H. F. W. Taylor, too, the compound with Br^- by F. Le Bel and G. Grasland.

From these complex salts series of similar compounds can be derived replacing Al^{3+} by other trivalent cations. G. Malquori and V. Cirilli (17) already reported about the corresponding ferrite hydrates. New results about the substitution of Al^{3+} by Ga^{3+} or Cr^{3+} are communicated here by H.-J. Kuzel.

According to the supplementary paper of G. Sadran and B. Cottin it is moreover possible to replace the Ca^{2+} in the monocarbonate $3CaO.Al_2O_3.CaCO_3.11H_2O$ by Mg^{2+} gradually. These results will be reported in the last chapter about the formation of solid solutions between tetracalcium aluminate hydrate and the related complex compounds.

5.2 Preparation

Bulk preparations of complex compounds can be made by mixing adequate solutions of calcium and aluminium salts with addition of calcium hydroxide solution. Instead of aluminium salt solution often a metastable solution of calcium aluminate is used. Complex salts are also formed when a suspension of $4CaO.Al_2O_3.19H_2O$ in mother liquor is treated with a sufficient addition of corresponding calcium salt.

F. Le Bel and G. Grasland prepared single crystals of monobromide, $3CaO.Al_2O_3.CaBr_2.10H_2O$ with a diameter up to 0.4 mm involving the slow diffusion of a basic alkali aluminate solution or of a calcium bromide solution into water or into a bromide containing solution. H.-J. Kuzel obtained single crystals of monosulfate, $3CaO.Al_2O_3.CaSO_4.12H_2O$ and monochromate, $3CaO.Al_2O_3.CaCrO_4.12H_2O$ with diameters up to 1 cm by reaction of $3CaO.Al_2O_3.6H_2O$ with calcium sulfate or

calcium chromate solutions respectively. Smaller single crystals of compounds which are stable at temperatures above 100 °C can be prepared by heating CaO and $Al(OH)_3$ with adequate solutions of calcium salts at about 150 °C in autoclaves for several weeks. X-ray inspections showed that crystals prepared under hydrothermal conditions were ordered completely, but crystals precipitated from metastable aluminate solutions often showed considerable disorder.

5.3 Crystal Structure

The results of H.-J. Kuzel's X-ray investigations are listed in tables 1 and 2. For the unit cell of the monobromide, $3CaO.Al_2O_3.CaBr_2.10H_2O$, F. Le Bel and G. Grasland found the same value as H.-J. Kuzel for a_o (5.76 Å), but half the value for c_o (24.45 Å) and the space group R 3 or R $\bar{3}$ instead of R 3 c or R $\bar{3}$ c.

According to a former investigation of H.-J. Kuzel (18) the monochloride, $3CaO.Al_2O_3.CaCl_2.10H_2O$ occurs in two polymorphic modifications with the transition point at about 28 °C. The crystals of both polymorphs are small pseudohexagonal plates, but the α-phase stable at lower temperature is monoclinic with d_B = 7.89 Å, the β-modification is trigonal with d_B = 7.81 Å.

The new compound, $3CaO.Al_2O_3.1/2Ca(NO_3)_2.1/2CaCl_2.10H_2O$ is very similar to the compound $3CaO.Al_2O_3.1/2CaSO_4.1/2CaCl_2.12H_2O$ already described earlier (19). Single crystals were prepared under hydrothermal conditions.

H.-J. Kuzel assumes that in the crystal structures of these compounds interlayers containing Cl^- alternate with interlayers containing SO_4^{2-} or NO_3^- respectively. Thus double layers result with composition $[Ca_4Al_2(OH)_{12}]^{2+}.Cl^-.1/2SO_4^{2-}.6H_2O$ or

$[Ca_4Al_2(OH)_{12}]^{2+}.Cl^-.NO_3^-.6H_2O$. The unit cell of these complex salts contains six double layers. According to H.-J. Kuzel compounds of this type are to be expected in similar systems with anions of considerably different sizes. Probably the compounds $3CaO.Al_2O_3.1/2Ca(OH)_2.1/2CaSO_4.12H_2O$ and $3CaO.Al_2O_3.1/2Ca(OH)_2.1/2CaCO_3.12H_2O$ described by M. H. Roberts (chapter 6.1 and 6.2) belong to this type, too.

The values in table 1 show that with increasing size of the anions the lattice constant c_o grows, but a_o remains nearly constant. But when Al^{3+} is replaced by the larger cations Cr^{3+}, Fe^{3+} or Ga^{3+} a_o increases and c_o decreases.

Further information about the crystal structures of these complex compounds give the dehydration reactions of monochloride, monobromide and mononitrate observed with thermal analysis, X-ray investigations and infrared absorption measurements by S. J. Ahmed, L. S. Dent Glasser and H. F. W. Taylor. After longer heating at 100 °C the reaction products showed the composition $3CaO.Al_2O_3.CaY_2.6H_2O$ with a basal spacing of 6.8 Å for monochloride, 7.1 Å for monobromide and 7.9 Å for mononitrate respectively. These infrared absorption spectra compared with those of the initial materials are nearly unchanged. On further heating the residual water is expelled and the crystal lattice is destroyed.

All present results agree with the crystal structure proposed by S. J. Ahmed and H. F. W. Taylor (16), which is especially confirmed by the preliminary Fourier synthesis of monojodide by H.-J. Kuzel. Accordingly the complex compounds of the type $3CaO.R_2O_3.Ca(X,Y_2).aq$ have unit cells similar to those of the various phases of tetracalcium aluminate hydrate (fig. 2). Each

principal layer with the composition $[Ca_2R(OH)_6]^+$ consisting of $R(OH)_6$ and $Ca(OH)_6$ octahedrons is combined with one interlayer containing the anions ($1/2X^{2-}$ or Y^-) and 2 or 3 H_2O molecules. Two of these H_2O molecules occupy regular sites marked P (fig. 2), the monovalent all and the divalent anions half of the cavities of the type marked X, which eventually can take up further H_2O molecules.

6. SOLID SOLUTION BETWEEN TETRACALCIUM ALUMINATE HYDRATE AND THE VARIOUS COMPLEX COMPOUNDS

6.1 Tetracalcium Aluminate Hydrate - Monosulfate

The formation of solid solution between $4CaO.Al_2O_3.mH_2O$ and $3CaO.Al_2O_3.CaSO_4.nH_2O$ was investigated by M. H. Roberts. The various solid solution phases were prepared by treating a suspension of $4CaO.Al_2O_3.19H_2O$ in mother liquor with increasing additions of gypsum.

The results of the X-ray investigations are shown in fig. 3. The indexing of these particular reflections was based on the hexagonal pseudocell with a_o = 5.76 Å and c_o = 26.79 Å determined by H.-J. Kuzel (19). Fig. 3 shows that for $CaSO_4/Al_2O_3$ molar ratios from o.5 to 1 the values for 1/3 c, corresponding to the longest basal spacing (oo3), increase continuously from 8.77 Å to 8.96 Å with increasing $CaSO_4$ content, but a_o with 5.75 Å remains constant. These results indicated that there is a solid-solution series between the compounds $3CaO.Al_2O_3.1/2Ca(OH)_2.1/2CaSO_4.12H_2O$ and $3CaO.Al_2O_3.CaSO_4.12H_2O$. Solids of $CaSO_4/Al_2O_3$ ratios below o.5 consist of mixtures of $4CaO.Al_2O_3.19H_2O$ and the limiting solid-

solution compound with the lowest sulfate content, for ratios over 1 the mixtures consist of monosulfate and $3CaO.Al_2O_3.3CaSO_4.32H_2O$.

The compound $3CaO.Al_2O_3.1/2Ca(OH)_2.1/2CaSO_4.12H_2O$ probably belongs to the type of double salts described by H.-J. Kuzel (chapter 5.3) just as the corresponding carbonate compound, mentioned in the next chapter. It may be assumed that interlayers with hydroxyl ions alternate with interlayers containing sulfate ions in the unit cell and that in the hydroxyl interlayer the OH^- ions can be replaced by sulfate ions continuously.

6.2 Tetracalcium Aluminate Hydrate - Monocarbonate

To prepare carbonate containing tetracalcium aluminate hydrates M. H. Roberts treated suspensions of $4CaO.Al_2O_3.19H_2O$ in mother liquor with different amounts of carbon dioxide. With increasing content of carbonate increasing amounts of a carbonate containing phase with d_B = 8.2 Å occured. When the molar ratio CO_2/Al_2O_3 of 0.5 was reached only this compound was present. Hence it follows that the composition of the 8.2 Å compound corresponds to the formula $3CaO.Al_2O_3.1/2Ca(OH)_2.1/2CaCO_3.12H_2O$. With still larger amounts of CO_2 the monocarbonate, $3CaO.Al_2O_3.CaCO_3.11H_2O$ with d_B = 7.6 Å was also formed while the 8.2 Å compound diminished.

So in this way it was not possible to detect any solid solutions between $3CaO.Al_2O_3.1/2Ca(OH)_2.1/2CaCO_3.12H_2O$ and $3CaO.Al_2O_3.CaCO_3.11H_2O$. But when samples of $3CaO.Al_2O_3.1/2Ca(OH)_2.1/2CaCO_3.12H_2O$ were treated with dilute solution of calcium hydroxide, part of the Al_2O_3 is dissolved from the solid phase and thus the CaO/Al_2O_3 ratio increased. X-ray investigations showed that the basal spacings decrease continuously from 8.15 Å to 7.8 Å.

Already on drying at 33 % relative humidity the compound $3CaO.Al_2O_3.1/2Ca(OH)_2.1/2CaCO_3.12H_2O$ loses two water molecules. The new lo H_2O hydrate with a longest basal spacing of 7.7 Å is even stable over waterfree calcium chloride. When dried over phosphorus pentoxide it loses two more H_2O molecules and the basal spacing decreases to 7.3 Å. On the other hand the monocarbonate $3CaO.Al_2O_3.CaCO_3.11H_2O$ is essentially more stable. Even when dried over waterfree calcium chloride it loses no water.

6.3 Tetracalcium Aluminate Hydrate - Monochloride

Some preliminary investigations of M. H. Roberts obtained on suspensions of $4CaO.Al_2O_3.19H_2O$ with increasing additions of calcium chloride, suggest that there exists a limited solid solution series between $4CaO.Al_2O_3.13H_2O$ and $4CaO.Al_2O_3.CaCl_2.1oH_2O$, similar to the series between $4CaO.Al_2O_3.1/2Ca(OH)_2.1/2CaSO_4.12H_2O$ and $4CaO.Al_2O_3.CaSO_4.12H_2O$. The basal spacing of the solid solution phases decreases from about 8.o Å to 7.8 Å, when the $CaCl_2/Al_2O_3$ molar ratio increases from o.5 to 1.o. A solid solution series between monosulfate and monochloride was not yet observed. The phase $3CaO.Al_2O_3.1/2CaSO_4.1/2CaCl_2.12H_2O$ found by H.-J. Kuzel (18) is a stoichiometric compound.

6.4 Substitution of Calcium by Magnesium in Monocarbonate

Possibilities for the replacement of calcium in monocarbonate, $3CaO.Al_2O_3.CaCO_3.11H_2O$ by magnesium were examined by G. Sadran and B. Cottin. At first they treated a calcium aluminate solution with a CaO/Al_2O_3 ratio of 3 with increasing amounts of hydromagnesite $3MgCO_3.Mg(OH)_2.3H_2O$.

The X-ray investigations showed that without addition of hydromagnesite only dicalcium aluminate hydrate $2CaO.Al_2O_3.8H_2O$ with a longest basal spacing of d_B = 1o.8 Å was formed. With low additions of hydromagnesite also monocarbonate with d_B = 7.6 Å and (according to M. H. Roberts) $3CaO.Al_2O_3.1/2Ca(OH)_2.1/2CaCO_3.12H_2O$ with d_B = 8.2 Å occured. At hydromagnesite contents just required for the formation of $3CaO.Al_2O_3.MgCO_3.aq$ the solid consisted of monocarbonate only. For still higher hydromagnesite additions corresponding to CO_2/Al_2O_3 ratios above 1, monocarbonate coexisted with calcite and aragonite.

Differential thermal analysis showed that the magnesium hydroxide present in hydromagnesite, did not react and occured unchanged in the precipitates. From the chemical composition of the solid including the results of the thermal and X-ray analysis the phase composition of the solid and the chemical composition of the monocarbonate were calculated with the assumption that the molar ratio CO_2/Al_2O_3 of the monocarbonate is 1 and that the magnesium hydroxide of the hydromagnesite did not react. The results indicate that a substitution of Ca^{2+} by Mg^{2+} in monocarbonate is possible. With increasing addition of hydromagnesite the CaO/Al_2O_3 ratio in monocarbonate decreases from 4.5 to o.2 and the MgO/Al_2O_3 ratio increases from o.6 to 4.1. Thus the composition of the monocarbonates corresponds to the general formula $[Ca_{2-x}Mg_xAl(OH)_6]CO_3.5\text{-}6H_2O$, where x can vary from o to 2. The solid solution phases show the same X-ray patterns as $3CaO.Al_2O_3.CaCO_3.11H_2O$, but if more than half the Ca^{2+} ions are replaced by Mg^{2+} ions only the considerably broadened main reflections of monocarbonate occur.

When mixtures of high alumina cement and hydromagnesite hydrated in suspensions with a water/solid ratio of lo or in pastes with a

water/solid ratio of o.5 at first monocalcium aluminate hydrate $CaO.Al_2O_3.10H_2O$ was formed, at higher temperatures dicalcium aluminate hydrate $2CaO.Al_2O_3.8H_2O$ and the cubic tricalcium aluminate hydrate $3CaO.Al_2O_3.6H_2O$. But afterwards all aluminate hydrates reacted with the hydromagnesite forming monocarbonate solid solutions. Pastes prepared from the pure aluminate hydrates with addition of hydromagnesite showed a similar behaviour. In any case the monocarbonate solid solutions were formed very quickly, especially from the cubic tricalcium aluminate hydrate.

REFERENCES

(1) H. Funk and R. Frydrych, "The degrees of anion condensation in silicic acids and silicates", Sympos. on Structure of Portland Cement Paste and Concrete, Special Report 90, Highway Research Board, Washington D. C., 284-290 (1966)

(2) E. Thilo, W. Wieker and H. Stade, "On the relations between the degree of polymerization of silicate anions and their reactivity with molybdic acid" (in German), Zeitschr. anorg. allgem. Chemie 340, 261-276 (1965)

(3) G. B. Alexander, "The reaction of low molecule weight silicic acids with molybdic acids", Journ. Amer. Chem. Soc. 75, 5655-5657 (1953)

(4) E. Weitz, H. Franck and M. Giller, "Investigations on silicic acids" (in German), Zeitschr. anorg. allgem. Chemie 331, 249-255 (1964)

(5) R. Weiss and D. Grandjean, "Structure of tricalcium aluminate hydrate, $3CaO.Al_2O_3.6H_2O$" (in French), Acta Cryst. 17, 1329-1330 (1964)

(6) J. H. van Vleck, "The dipolar broadening of magnetic resonance lines in crystals", Phys. Rev. 74, 1168-1183 (1948)

(7) C. Cohen-Addad, P. Ducros and E. F. Bartaut, "Studies on the substitution of SiO_4 group by $(OH)_4$ in the garnet type compounds, $Al_2Ca_3(OH)_{12}$ and $Al_2Ca_3(SiO_4)_{2.16}(OH)_{3.36}$" (in French), Acta Cryst. 23, 220-230 (1967)

(8) M. H. Roberts, "New calcium aluminate hydrates", J. appl. Chem. 7, 543-546 (1957)

(9) F. G. Jones and M. H. Roberts, "The system $CaO.Al_2O_3.H_2O$ at 25 °C", Building Res. Current papers, Res. Ser. 1 (1962)

(10) P. Seligmann and N. R. Greening, "New techniques for temperature and humidity control in X-ray diffractometry", Journ. PCA Res. Dev. Lab. 4, Nr. 2, 2-9 (1962)

(11) P. Seligmann and N. R. Greening, "Studies of early hydration reactions of portland cement by X-ray diffraction", Highway Res. Rec. No. 62, 89-105 (1964)

(12) R. Alègre, "Investigations on the hexagonal hydrated tetracalcium aluminate" (in French), Rev. Mater. Contr. No. 566, 301-314 (1962)

(13) F. Lavanant, "Contribution to the study of some calcium aluminate hydrates" (in French), Rev. Mater. Constr., No. 592, 1-10; No. 593, 76-87; No. 595, 193-207; No. 596, 251-261; No. 597, 298-304 (1965)

(14) W. Dosch and H. zur Strassen, "Investigation of tetracalcium aluminate hydrate I. The various hydrate stages and the effect of carbonic acid" (in German), Zement-Kalk-Gips 18, 233-237 (1965)

(15) F. G. Buttler, L. S. Dent Glasser and H. F. W. Taylor, "Studies on $4CaO.Al_2O_3.13H_2O$ and the related mineral hydrocalumite", J. Amer. Ceram. Soc. 42, 121-126 (1959)

(16) S. J. Ahmed and H. F. W. Taylor, "Crystal structures of the lamellar calcium aluminate hydrates", Natura 215, 622-623 (1967)

(17) G. Malquori and V. Cirilli, "The calcium ferrite complex salts", Proc. III Intern. Sympos. Chem. Cem., London (1952), 321-328

(18) H.-J. Kuzel, "X-ray investigations in the system $3CaO.Al_2O_3.CaSO_4.nH_2O$-$3CaO.Al_2O_3.CaCl_2.nH_2O$" (in German), Neues Jahrb. Mineral., Monatsh. Nr. 7, 193-2oo (1966)

(19) H.-J. Kuzel, "Synthesis and X-ray investigations of $3CaO.Al_2O_3.CaSO_4.12H_2O$" (in German), Neues Jahrb. Mineral., Monatsh. Nr. 7, 193-197 (1965)

Table 1: Unit cells and space groups of compounds $3CaO.Al_2O_3.Ca(X,Y_2).nH_2O$

Composition	Lattice constants in Å				Pseudo-cell in Å	Number of principle layers	Space groups
	a_o	b_o	c_o	β	c'		
α-$3CaO.Al_2O_3.CaCl_2.10H_2O$	9,962	5,735	16,836	110,49	-	2	C2/c,Cc
β-$3CaO.Al_2O_3.CaCl_2.10H_2O$	5,739	-	46,87	-	7,811	6	R3c,R$\bar{3}$c
$3CaO.Al_2O_3.CaBr_2.10H_2O$	5,761	-	49,06	-	8,177	6	R3c,R$\bar{3}$c
$3CaO.Al_2O_3.CaJ_2.10H_2O$	5,771	-	26,572	-	8,857	3	R3,R$\bar{3}$
$3CaO.Al_2O_3.Ca(NO_3)_2.10H_2O$	5,743	-	8,623	-	-	1	P3,P$\bar{3}$
$3CaO.Al_2O_3.Ca(BrO_3)_2.10H_2O$	5,7532	-	29,425	-	9,808	3	R3,R$\bar{3}$,R32,R3m, R$\bar{3}$m
$3CaO.Al_2O_3.CaSO_4.12H_2O$	5,756	-	26,811	-	8,937	3	R3,R$\bar{3}$
$3CaO.Al_2O_3.CaSO_4.16H_2O$	5,751	-	28,672	-	9,557	3	R3,R$\bar{3}$,R32,R3m, R$\bar{3}$m
$3CaO.Al_2O_3.CaCrO_4.12H_2O$	5,75	-	26,91	-	8,97	3	R3,R$\bar{3}$
$3CaO.Al_2O_3.1/2CaSO_4.1/2CaCl_2.12H_2O$	5,7502	-	100,62	-	16,770	12	R3c,R$\bar{3}$c
$3CaO.Al_2O_3.1/2Ca(NO_3)_2.1/2CaCl_2.10H_2O$	5,744	-	98,28	-	16,380	12	R3c,R$\bar{3}$c

Table 2: Unit cells and space groups of compounds $3CaO.R_2O_3.Ca(X,Y_2).nH_2O$

Composition	Lattice constants in Å		Pseudocell in Å	Number of principle layers	Space groups
	a_o	c_o	c'		
$3CaO.Al_2O_3.CaSO_4.12H_2O$	5,756	26,811	8,937	3	R3,R$\bar{3}$
$3CaO.Cr_2O_3.CaSO_4.12H_2O$	5,831	26,585	8,862	3	R3,R$\bar{3}$,R32,R3m,R$\bar{3}$m
$3CaO.Fe_2O_3.CaSO_4.12H_2O$	5,888	26,625	8,875	3	R3,R$\bar{3}$,R32,R3m,R$\bar{3}$m
β-$3CaO.Al_2O_3.CaCl_2.10H_2O$	5,739	46,87	7,811	6	R3c,R$\bar{3}$c
$3CaO.Cr_2O_3.CaCl_2.10H_2O$	5,8164	23,291	7,764	3	R3,R$\bar{3}$,R32,R3m,R$\bar{3}$m
$3CaO.Fe_2O_3.CaCl_2.10H_2O$	5,858	23,267	7,756	3	R3,R$\bar{3}$,R32,R3m,R$\bar{3}$m
$3CaO.Al_2O_3.CaBr_2.10H_2O$	5,761	49,06	8,177	6	R3c,R$\bar{3}$c
$3CaO.Ga_2O_3.CaBr_2.10H_2O$	5,8358	24,386	8,129	3	R3,R$\bar{3}$

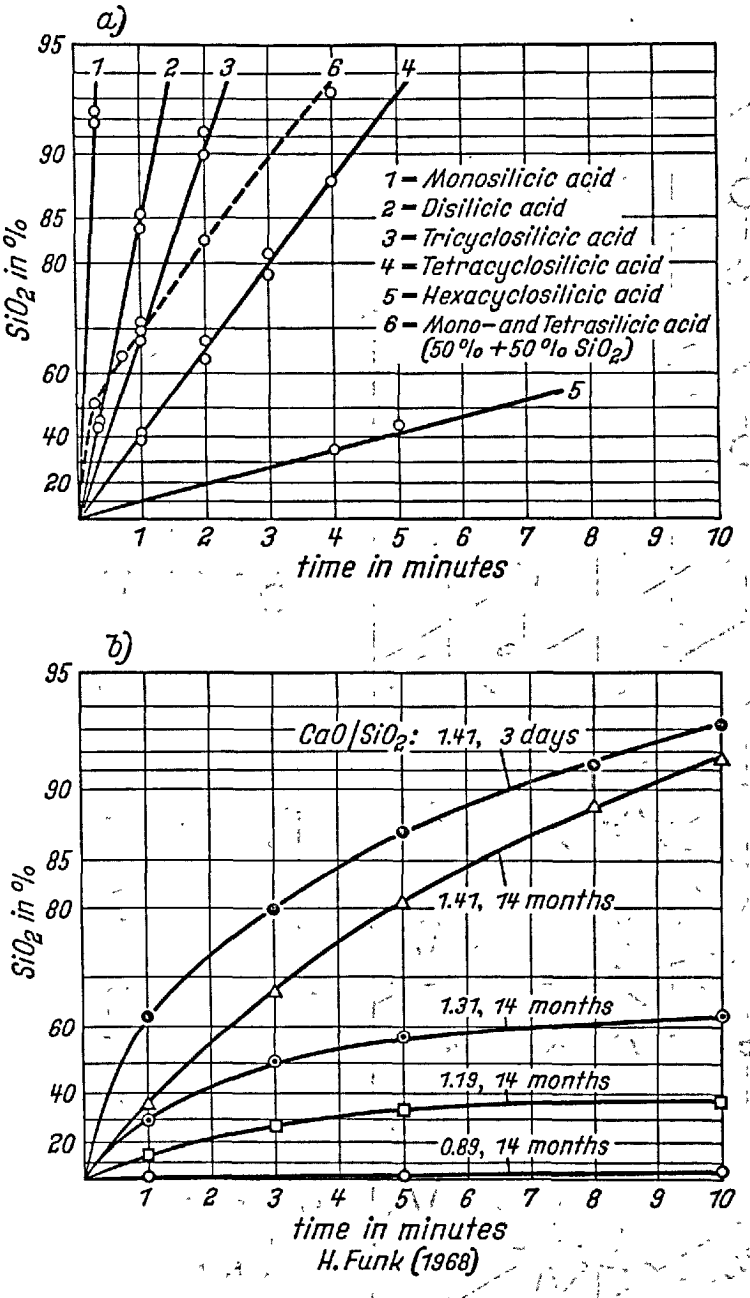

Figure 1: a. Rate of the complexing reaction for silicic acids of known degree of condensation in methanolic hydrochloric acid

b. Condensation degree of anions of silicic acid in tobermorite gel depending on CaO/SiO_2 ratio and on aging

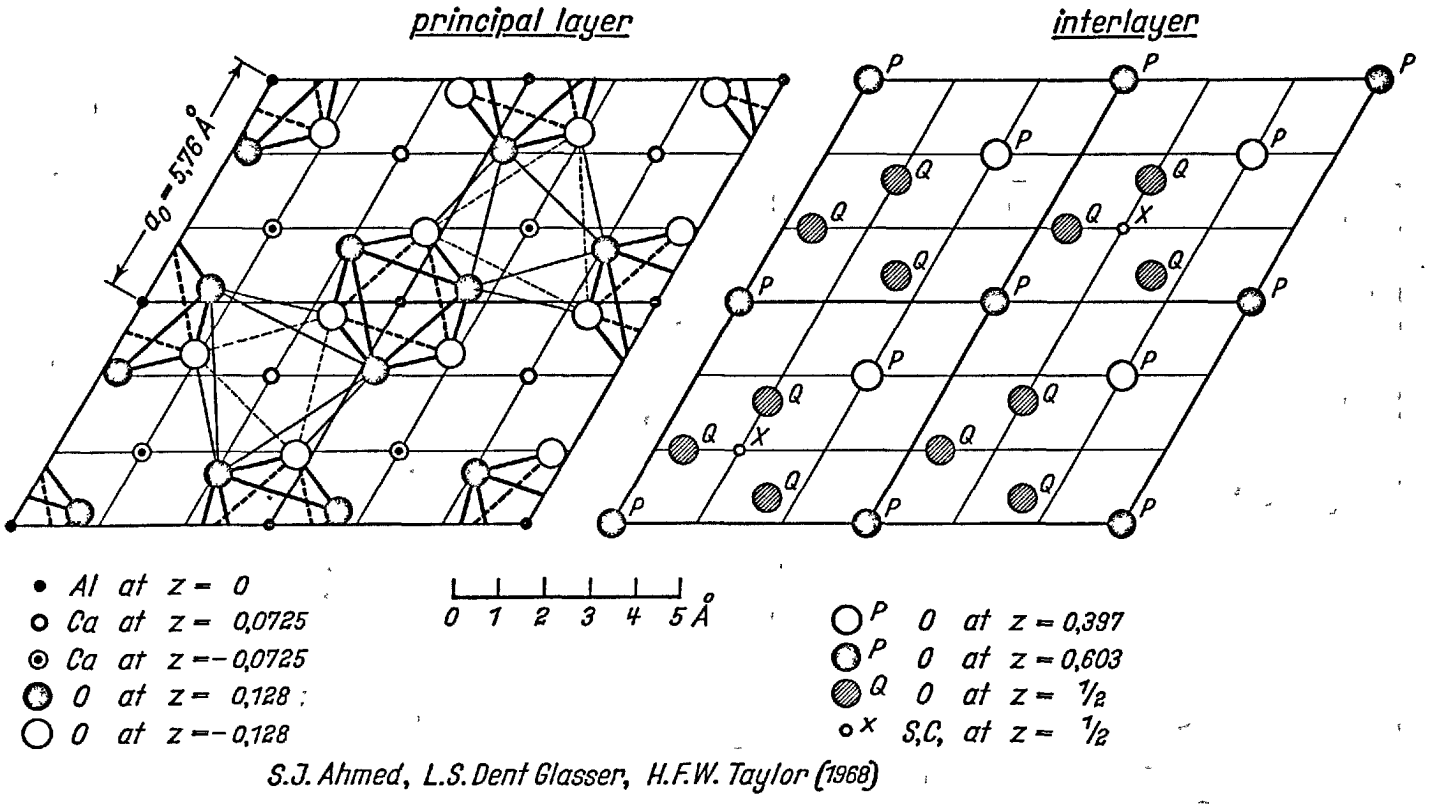

Figure 2: Crystal structure of tetracalcium aluminate hydrate, projection along the c-axis. The z-coordinates are given as fractions of c' = 7.86 Å.

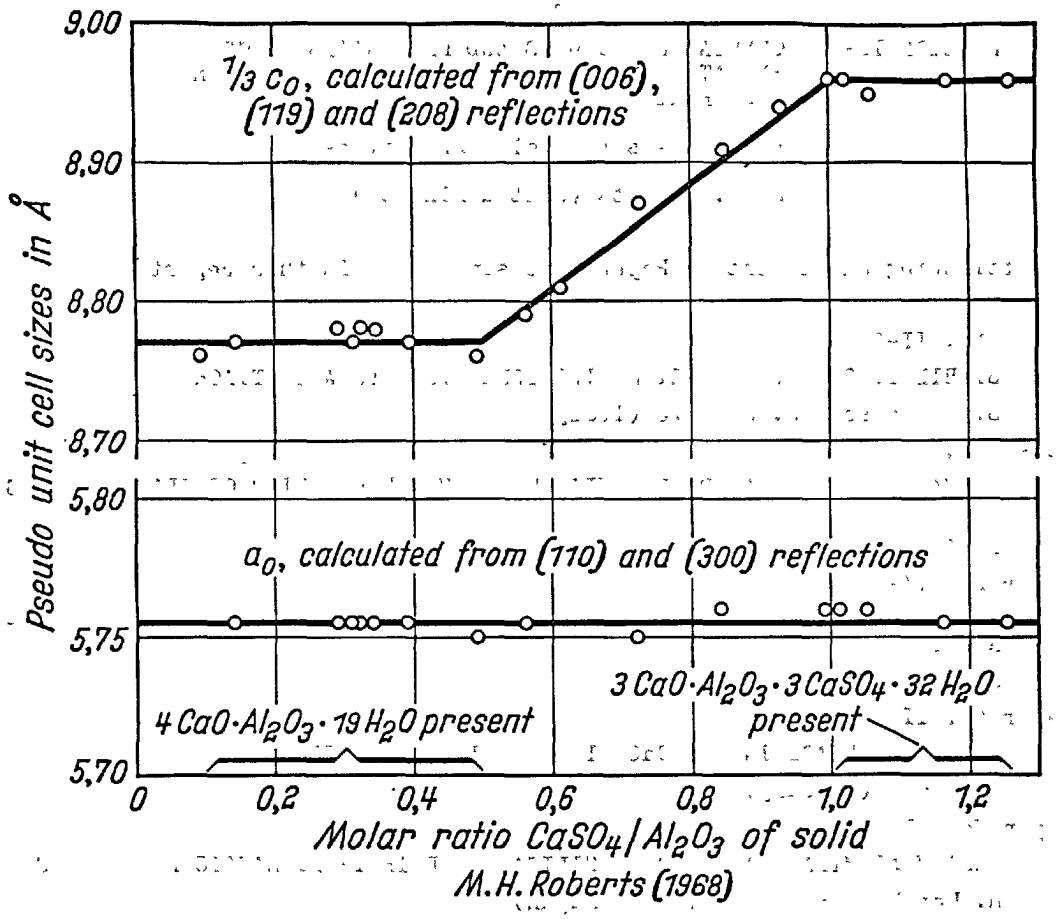

Figure 3: Pseudocell sizes of solid solutions in the system $3CaO.Al_2O_3.1/2Ca(OH)_2.1/2CaSO_4.12H_2O$ $-3CaO.Al_2O_3.CaSO_4.12H_2O$

GENERAL REPORT

OF

SESSION II-2: CRYSTAL STRUCTURES AND PROPERTIES OF CEMENT HYDRATION PRODUCTS (HYDRATED CALCIUM ALUMINATES AND FERRITES)

(b) Papers regarding Properties

M. H. Roberts (United Kingdom)

The following Supplementary Papers are summarized in this report.

Paper No. II-6

STABILITY OF HYDROGARNET SERIES TERMS TO SULPHATE ATTACK

B. Marchese & R. Sersale (Italy)

Paper No. II-40

FORMATION OF HYDRATED GEHLENITE THROUGH THE REACTION OF CLAY MINERALS AND LIME

A. Ariizumi (Japan)

Paper No. II-67

SUCCESSFUL PREVENTION OF LOSS OF STRENGTH IN CONCRETE MADE WITH HIGH-ALUMINA CEMENT

P. K. Mehta (India)

Paper No. II-68

AMORPHOUS PHASE IN THE $CaO-Al_2O_3-CaCl_2-H_2O$ SYSTEM

F. Tamás (Hungary)

Paper No. II-81

BARIUM ALUMINATE AND BARIUM SILICATE AND THEIR HYDRAULIC PROPERTIES

H. Uchikawa & K. Tsukiyama (Japan)

SUMMARY

The contents of five Supplementary Papers to be presented at the Fifth International Symposium on the Chemistry of Cement, Tokyo, October 1968 are summarised and discussed. Two of the papers deal with particular aspects of specific hydrated compounds, and are respectively concerned with the precipitation of different calcium chloroaluminate hydrates by mixing calcium chloride and monocalcium aluminate solutions, and with the reaction of silica-containing hydrogarnets related to $3CaO.Al_2O_3.6H_2O$ with lime-calcium sulphate solutions. Of the remaining papers, one is devoted to an attempt to prevent the loss in strength of high-alumina cement concrete under warm and wet conditions, another paper discusses the reaction of certain clay minerals with lime solutions to form the so-called 'hydrated gehlenite' ($2CaO.Al_2O_3.SiO_2.8\ H_2O$), and the final paper describes the properties and crystal structures of barium hydroxide monohydrate and particular anhydrous and hydrated barium aluminates and silicates.

Building Research Station, Ministry of Public Building and Works

Five Supplementary Papers have been assigned to a theme devoted to the properties of hydrated calcium aluminates and ferrites and related more complex hydrates. Two of the papers deal with particular aspects of specific hydrated compounds, and are respectively concerned with the precipitation of different calcium chloroaluminate hydrates by mixing calcium chloride and monocalcium aluminate solutions, and with the reaction of silica-containing hydrogarnets related to C_3AH_6 with lime-calcium sulphate solutions. Of the remaining papers, one is devoted to an attempt to prevent the loss in strength of high-alumina cement concrete under warm and wet conditions, another paper discusses the reaction of certain clay minerals with lime solutions to form the so-called 'hydrated gehlenite' (C_2ASH_8), and the final paper describes the properties and crystal structures of particular anhydrous and hydrated barium aluminates and silicates. In view of the widely varying nature of the topics covered in these Supplementary Papers, it is therefore proposed in this General Report to separately summarise and discuss the more essential details of each paper.

1. F. Tamas, "Amorphous Phase in the $CaO-Al_2O_3-CaCl_2-H_2O$ System"

A study is made of the solids precipitated when supersaturated monocalcium aluminate solutions are mixed with calcium chloride solutions at temperatures in the range 0°-70°C, but mainly at 22°-25°C. The concentration of the $CaCl_2$ solution varied from 0.125 molar to 2.0 molar, but that of the calcium aluminate solution is not given. The precipitates were separated from the reaction mixtures after 1 hour, and investigated by chemical and X-ray analysis, infra-red spectroscopy and electron microscopy.

It is concluded that the concentration of the $CaCl_2$ solution has a marked effect on the nature of the precipitated solid. While crystalline precipitates are obtained at $CaCl_2$ concentrations of 0.4 molar and below, higher concentrations of 0.5 molar and above resulted in the formation of amorphous solids giving X-ray patterns with only a broad band in the region 3.6-4.4Å. The crystalline solids gave X-ray patterns very similar to that reported for the calcium monochloroaluminate decahydrate ($C_3A.CaCl_2.10H_2O$), but their chemical compositions varied considerably, the alumina content always being higher than that of this formula while the calcium content is lower, and it is inferred that they are members of a $C_4AH_{13}-C_3A.CaCl_2.10H_2O$ solid-solution series. The reported transition from a crystalline to an amorphous solid appeared to be a gradual change, and it is not markedly affected by temperature in the range 0°-70°C. The crystalline and amorphous phases are also said to differ under the electron microscope and in their infra-red spectra, but few details are given.

It is of interest to compare these results with those obtained in previous studies on the system $CaO-Al_2O_3-CaCl_2-H_2O$ by other investigators[1-4]. On the

one hand, provided that sufficient free $Ca(OH)_2$ is present in solution, it has been established that pure crystalline $C_3A.CaCl_2.10H_2O$ is obtained when the $CaCl_2$ concentration in the equilibrium solution is about 3per cent (or 0.27 molar), but lower $CaCl_2$ concentrations in solution resulted in the formation of a solid-solution series between C_4AH_{13} and $C_3A.CaCl_2.10H_2O$, probably only over a restricted range of compositions. On the other hand, when insufficient $Ca(OH)_2$ is present in the reaction mixture, it has been shown[1] that hydrated alumina is also precipitated. The composition of the product obtained by mixing $CaCl_2$ solutions and calcium aluminate solutions will therefore depend not only on the $CaCl_2$ concentration but also on the composition of the calcium aluminate solution and on the amount, if any, of added lime.

Since a monocalcium aluminate solution was used in the experiments by Tamas, it seems probable that the results were influenced by the lack of free $Ca(OH)_2$, together with the progressive reduction in pH caused by increasing $CaCl_2$ concentrations, and the consequent precipitation of alumina gel. It could be suggested that the broad band in the X-ray patterns of 'amorphous' solids may really arise from alumina gel. Similarly, the weak spacings at about 4.8Å and 4.35Å which are included in the X-ray patterns of 'crystalline' solids may also be attributed to hydrated alumina. It is noteworthy that the latter spacings are more intense in the preparation made at 70°C (Table 1, column 5), and this could be explained by better recrystallisation of the hydrated alumina to bayerite and/or gibbsite at the higher temperature. Furthermore, the reported partial solubility of the precipitates in nitric acid may also be an indication of the presence of more difficultly soluble hydrated alumina. The 'crystalline' precipitates may therefore really consist of mixtures of hydrated alumina and $C_3A.CaCl_2.10H_2O$, at any rate at the higher $CaCl_2$

concentrations. The presence of varying amounts of hydrated alumina, probably with some occluded and/or adsorbed Ca and Cl ions, could well account for the widely varying chemical compositions which are indicated. It is clear therefore that further work is needed before the conclusions made by Tamas with regard to the reaction products from $CaCl_2$ and monocalcium aluminate solutions can be accepted.

2. B. Marchese and R. Sersale, 'Stability of Hydrogarnet Series Terms to Sulphate Attack'

An investigation is made of the reactivity at ordinary temperatures of particular hydrogarnet compositions in contact with calcium sulphate solutions saturated with respect to $Ca(OH)_2$ for periods up to 4 months. The four hydrogarnets studied were members of the solid-solution series C_3AH_6-$C_3A.3SiO_2$ (grossularite). These compounds were prepared hydrothermally at 150°C from glasses of appropriate compositions to give respective molar ratios of SiO_2/Al_2O_3 of 0.22, 0.28, 0.35 and 0.43, and a corresponding increasing shrinkage of the crystal lattice relative to that of C_3AH_6.

After treatment with calcium sulphate solution, X-ray analysis and optical and electron microscopy showed the formation of $C_3A.3CaSO_4.31H_2O$ in each case. The extent and rate of this reaction was followed by chemical and X-ray analysis and by differential calorimetry. Similar results were obtained with each method, and these showed that both the rate and the extent of reaction with sulphate progressively decreased with increasing SiO_2 content of the original hydrogarnet.

The diminished reactivity of silica-containing hydrogarnets with calcium sulphate solution indicated by these results may therefore partly account

for the improvement in sulphate resistance obtained by high-pressure steam curing of cements. In this connection, it may be noted that it has also been established[5] that in the case of the hydrogarnet solid solutions formed at room temperature in which Fe_2O_3 replaces Al_2O_3 the relative reactivity towards calcium sulphate solution decreased with increasing Fe_2O_3 content, and the behaviour is thus very similar to that of the silica-containing hydrogarnets.

3. P.K. Mehta, 'Successful Prevention of Loss of Strength in Concrete Made with High-Alumina Cement'

This paper describes an attempt to develop a suitable additive for high-alumina cement to prevent the loss in strength which occurs especially in concretes exposed to warm and wet conditions, and is accompanied by the conversion of the initial main hydration product CAH_{10} into C_3AH_6 and γ-$Al_2O_3\ 3H_2O$ (gibbsite). Recent investigations[6,7] have established that the diminution in strength is associated with an increase in internal porosity in high-alumina cement samples of normal or high water/cement ratio, arising from the conversion of the constituent hydrates, and high strengths and low porosities can be obtained at low water/cement ratios even when C_3AH_6 and gibbsite are formed.

In the described investigation, 2 in. x 4 in. (50 mm x 100 mm) concrete cylinders were prepared at 4°-10°C, using a water/cement ratio of 0.60, standard sand and crushed quartz aggregate, and a laboratory-prepared high-alumina cement composed essentially of monocalcium aluminate, both without and with 5 per cent (by weight of total cementitious material) of an additive consisting of a synthetic anhydrous calcium sulphoaluminate

of composition $C_3A_3.CaSO_4$. The concrete cylinders were cured in cold water (4°-10°C) up to an age of 28 days, and tests were then made on some of the cylinders, while the remaining cylinders were stored in water at 38°C and similarly tested periodically up to an age of 24 weeks. The tests included determinations of the compressive strength and modulus of elasticity of the various concretes, and X-ray analysis of the separated hydrated cement fractions to establish the proportions of the hydrated compounds present.

The compressive strength data showed that comparable strengths of about 8000 lb/in.^{2} (55.2 N/mm^2) are obtained from concretes with and without the sulphoaluminate additive after 28 days at low temperature. On storage at 38°C, the strength of both concretes initially increased during the first 28 days to about 11,000 lb/in.^{2} (75.8 N/mm^2), probably caused by further hydration of the cement, but subsequently the strength of the plain concrete progressively diminished to about 2,000 lb/in.^{2} (13.8 N/mm^2) at an age of 24 weeks, whereas only a slight decrease in strength to about 10,000 lb/in.^{2} (68.9 N/mm^2) occurred over the same period in the concrete with the sulphoaluminate additive. Similar trends are also observed in the values of the modulus of elasticity of the different concretes.

The X-ray diffraction analysis of the hydrated cement fractions from the different concretes confirmed the findings of many previous studies, and established that while CAH_{10} is the main hydration product in the concretes cured at low temperatures, changes in the mineralogical composition occurred in the concrete without any additive and the loss in compressive strength at 38°C is accompanied by the formation of increasing amounts of C_3AH_6 relative to CAH_{10}. Only a small amount of C_3AH_6 appeared

to be formed at 38°C in the concrete containing the sulphoaluminate additive. It is therefore concluded that the $C_3A_3 \cdot CaSO_4$ additive is capable of stabilising the CAH_{10} hydrate, thereby maintaining a high compressive strength and preventing the usual loss in strength of high-alumina cement concretes when these are exposed to warm and wet conditions.

The mechanism of the action of the sulphoaluminate additive in preventing the conversion of CAH_{10} into C_3AH_6 and gibbsite seems to be rather obscure. This $C_3A_3 \cdot CaSO_4$ compound would be expected to react with water to produce alumina gel and calcium monosulphoaluminate hydrate, and it is possible that these hydrates precipitate as protective coatings on the CAH_{10} produced during the hydration of high-alumina cement and prevent its subsequent dissolution to form C_3AH_6. Alternatively, the solution composition may be changed in the presence of the monosulphoaluminate hydrate so that the formation and growth of C_3AH_6 nuclei from the aqueous phase is decreased. Further work is needed to investigate these possibilities, and it also appears to be desirable to carry out additional experiments with commercial high-alumina cements, and at longer duration, in order to confirm the effectiveness of the $C_3A_3 \cdot CaSO_4$ additive in preventing the conversion reaction and the associated loss in strength in high-alumina cement concretes.

4. A. Ariizumi, 'Formation of Hydrated Gehlenite through the Reaction of Clay Minerals with Lime

A review is made of studies on the reaction of saturated lime solution with co-precipitated alumina-silica gels and with hydrated aluminium silicate clay minerals, such as allophane, halloysite and kaolinite, and on the so-called 'hydrated gehlenite' C_2ASH_8 that is thereby formed. The extent

of the reaction was followed by determining the amount of lime removed from solution, and the reaction products were characterised by X-ray diffraction, differential thermal analysis and other methods.

Treatment of allophane with saturated lime solution produced C_2ASH_8, C_3AH_6 (or eventually a silica-containing hydrogarnet), 'C_4AH_{13}' and $C_3A.CaCO_3.11H_2O$, depending upon the lime concentration and the temperature. The C_2ASH_8 hydrate is obtained at temperatures below 50°C, and also at low lime concentrations at 60°C, but C_3AH_6 is formed with high lime concentrations at 60°C and at all concentrations at 80°C. A certain minimum lime concentration is necessary to form C_2ASH_8, while it is unstable in the presence of excess lime. Preliminary heat treatment of the allophane resulted in higher reactivity with lime solutions. In addition, allophane reacted with lime-calcium sulphate solutions to form calcium sulphoaluminate hydrates, either the monosulphate or the trisulphate depending upon the temperature and the amount of calcium sulphate present. On the basis of this type of reaction, it has been established that treatment with lime and gypsum is effective and economical for soil-stabilisation purposes.

Hydrated halloysite showed a similar reaction course to allophane in lime solutions, and absorption of lime from solution is followed by the formation of 'C_4AH_{13}' and $C_3A.CaCO_3.11H_2O$, and eventually C_2ASH_8 is obtained at longer reaction times. The better-crystallised halloysite samples absorbed larger amounts of lime and showed increased reactivity, but dehydration of the halloysite by heating at 150°C decreased its reactivity. Finely-ground kaolinite also reacted easily with lime solutions to form C_2ASH_8.

The reaction of co-precipitated alumina-silica gels of varying Al_2O_3/SiO_2 ratios with saturated lime solution showed a similar behaviour to that observed with natural allophane. In particular, the treatment of a gel with an Al_2O_3/SiO_2 ratio of 1.0 with saturated lime solution at 20°C for 1 year resulted in a product of composition $2.50\ CaO.1Al_2O_3\ 1.08SiO_2.0.18CO_2.8.69H_2O$, after drying over $CaCl_2$. This preparation consisted predominantly of C_2ASH_8, together with small amounts of calcite and hydrogarnet, and possibly also traces of a calcium silicate hydrate. Apart from calcite, the latter compounds are not observable in the DTA curve, which showed an endotherm at 210°C owing to the loss of hydrate water and an exotherm at 940°C arising from the formation of C_2AS. The thermal dehydration curve showed no definite steps, but loss of water started at 50°C, became intensified at about 150°C and all water is practically completely removed at 350-400°C. The X-ray powder diffraction data and the electron microscopical observations showed broad agreement with previously published data for hexagonal C_2ASH_8.

It may be noted that the C_2ASH_8 preparation described above contained 1.7 per cent CO_2, and while this is attributed to the presence of calcite it is possible that some $C_3A.CaCO_3.11H_2O$ is also present. Indeed, the formation of this monocarboaluminate hydrate with a basal spacing of 7.6Å was also observed during the reaction of the various clay minerals with lime solution. Furthermore, the 'C_4AH_{13}' which was frequently present was apparently identified by a 8.2Å basal spacing in the X-ray powder patterns, and this hydrate probably really corresponds to the quaternary carbonate hydrate $C_4A.\frac{1}{2}CO_2.12H_2O$. Unintentional carbonation may therefore have had some influence on the reactions studied by Ariizumi, as also seems to be

the case in previous work[8] on the reaction of montmorillonite with lime solution, where $C_3A.CaCO_3.11H_2O$ was evidently formed.

5. H. Uchikawa and K. Tsukiyama, 'Barium Aluminate and Barium Silicate and their Hydraulic Properties'

The final paper gives an account of investigations on the properties and crystal structures of barium hydroxide monohydrate and particular anhydrous and hydrated barium aluminates and silicates.

Anhydrous monobarium aluminate and dibarium silicate were synthesised by heating stoichiometric mixtures of $BaCO_3$ and α-Al_2O_3 or silica powder at 1500°C. The crystal lattice constants and atomic co-ordinates of the respective hexagonal and orthorhombic compounds were determined from X-ray powder diffraction data. It is also shown that Fe_2O_3 can replace Al_2O_3 in $BaO.Al_2O_3$ with expansion of the crystal lattice to form a solid-solution series.

Hydration of the dibarium silicate at room temperature resulted in the initial precipitation of a fibrous dibarium silicate hydrate ($2BaO.SiO_2.n\ H_2O$), but this hydrate later converted into thin plates of a monobarium hydrate, $BaO.SiO_2.6H_2O$, together with hydrated barium hydroxide. The latter hydrate is referred to as the monohydrate $Ba(OH)_2.H_2O$, but it evidently should occur as the octahydrate $Ba(OH)_2.8H_2O$ in contact with solution. X-ray studies on the $BaO.SiO_2.6H_2O$ hydrate showed it to be orthorhombic, and its X-ray pattern remained essentially unchanged in dry and wet nitrogen, but an orthorhombic basic barium carbonate hydrate ($BaCO_3.m\ Ba(OH)_2.n\ H_2O$) is readily formed on exposure to moist CO_2.

Both barium hydroxide and hydrated alumina are liberated when $BaO.Al_2O_3$ is treated with water at room temperature, and initial precipitation of alumina gel and rectangular plates of a monobarium aluminate hydrate of composition $BaO.Al_2O_3.6.5H_2O$ is followed by the additional formation of polyhedral plates of a hexagonal dibarium aluminate hydrate, $2BaO.Al_2O_3.9H_2O$. The rate of hydration, as measured by quantitative X-ray analysis, increased as the water/solid ratio is raised from 0.4 to 0.6 and then to 1.0. Measurements of heat liberation with a conduction calorimeter showed the presence of a second peak after 3-4 hours, and this is considered to arise from the later formation of the dibarium aluminate hydrate. However, the hydration product obtained after a long period of hydration at a water/solid ratio of 0.6 apparently consisted essentially of $BaO.Al_2O_3.6.5H_2O$, while it appears that a different compound of composition $BaO.Al_2O_3.4H_2O$ is produced at a water/solid ratio of 0.4. The difference in properties and relationship between the different barium aluminate hydrates is not clearly established, and the drying conditions used to obtain the stated water contents are not given.

From a study of the X-ray and electron diffraction patterns, it is concluded that the crystal structure of the monoclinic $BaO.Al_2O_3.6.5H_2O$ compound contains the structural framework of that established for orthorhombic $Ba(OH)_2.H_2O$, with a linkage of two AlO_4 tetrahedra extending along the c-axis and water molecules also stacked along this axis. The latter water molecules can be removed without destruction of the crystal structure, since a reversible transformation is observed under different drying conditions, the longest spacing in the X-ray powder patterns changing from about 7.4Å in dry nitrogen to about 8.2Å in wet nitrogen. Exposure to moist CO_2 resulted in the gradual appearance of the X-ray pattern of a basic barium carbonate hydrate.

The behaviour of hydrated barium aluminate samples at elevated temperatures varied somewhat, depending upon the initial water/solid ratio, and hence upon the particular hydrates present. X-ray, DTA and thermal dehydration studies showed in some cases the formation of an apparently amorphous phase at temperatures up to about 200°C, though the external form of the original crystals is retained, and at higher temperatures a cubic monohydrate, $BaO \cdot Al_2O_3 \cdot H_2O$ is first obtained, followed by the formation of anhydrous $BaO \cdot Al_2O_3$. Associated with these changes, the compressive strength of 1:2 $BaO.Al_2O_3$: sand mortars first increased by drying of the specimens at temperatures up to about 250°C, then decreased slightly with increasing temperature up to about 700°C, followed by a marked increase in strength up to 1300°C accompanied by the formation of anhydrous $BaO \cdot Al_2O_3$. Except at the highest temperature, higher strengths are obtained with mortars of initial water/solid ratio of 0.4 as compared with 0.6. A similar relation between water/solid ratio and compressive and bending strengths of 1:2 mortars is also obtained at ordinary temperatures. The strength values decreased with age from 3 to 28 days, and this is attributed to carbonation and the consequent formation of the basic barium carbonate hydrate $BaCO_3 . m\ Ba(OH)_2 . n\ H_2O$ which can be identified in the X-ray powder patterns of moist-cured mortar specimens at 28 days.

It is evident from these results that the hydration reactions and products of these barium compounds bear some analogies to those of the corresponding calcium silicate and aluminate. However, in contrast to the hydration products of the latter, the barium-containing hydrates are highly water soluble, and they appear to harden mainly by processes of drying and possibly carbonation. The behaviour of $BaO.Al_2O_3.6.5H_2O$ on dehydration in

dry nitrogen, resulting in changes in the X-ray powder pattern, resembles that of the hexagonal-plate dicalcium and tetracalcium aluminate hydrates, though CAH_{10} behaves differently in that loss of water from this compound occurs without marked changes in the X-ray pattern apart from its deterioration. The possibility of the existence of different states of hydration in other barium aluminate hydrates seems to warrant further investigation, as well as the possibility of the formation of complex quaternary carbonate hydrates similar to the calcium carboaluminate hydrates.

However, despite the apparent similarities in composition between some calcium and barium aluminate hydrates, the view has been expressed[9,10] that the various barium aluminate hydrates are in no way analogous to the calcium aluminate hydrates, since they show distinct differences in crystal habit, refractive indices, binefringence and X-ray powder patterns. On the other hand, it has been established[11,12] that the two strontium aluminate hydrates, $3SrO.Al_2O_3.6H_2O$ and $SrO.Al_2O_3.10H_2O$, show properties very similar to those of C_3AH_6 and CAH_{10}, and the corresponding hydrates are isomorphous.

REFERENCES

1. L.S. Wells, 'Reaction of Water on Calcium Aluminates', J. Res. Nat. Bur. Stand., 1, 951-1009 (1928).

2. R. Turrriziani and G. Schippa, 'Contribution to the Knowledge of the Hydrated Alumino-Chloro-Complexes of Calcium' (in Italian), Ricerca Sci., 25, 3102-3106 (1955).

3. M.H. Roberts, 'Effect of Calcium Chloride on the Durability of Pre-tensioned Wire in Prestressed Concrete', Magazine of Concrete Research, 14 (42), 143-154 (1962).

4. M.H. Roberts, 'Calcium Aluminate Hydrates and Related Basic Salt Solid Solutions', This Symposium, Supplementary Paper to Session II-2.

5. E.T. Carlson, 'Some Properties of the Calcium Aluminoferrite Hydrates', U.S. Dept. of Commerce, Nat. Bur. Stand., Building Science Series 6 (1966).

6. H.G. Midgley, 'The Mineralogy of Set High-Alumina Cement', Trans. Brit. Ceram. Soc., 66, 161-187 (1967).

7. R. Alègre, 'Study of the Effects on Hydrated Alumina Cements of the Conversion of $CaO.Al_2O_3.10H_2O$ under the Action of Heat', Rev. Mat. Constr., No. 630, 101-108 (1968).

8. G.H. Hilt and D.T. Davidson, 'Isolation and Investigation of a Lime-Montmorillonite Crystalline Reaction Product', Highway Res. Board Bull., No.304, 51-64 (1961).

9. E.T. Carlson and L.S. Wells, 'Barium Aluminate Hydrates', J. Res. Nat. Bur. Stand., 41, 103-109 (1948).

10. E.T. Carlson, T.J. Chaconas and L.S. Wells, 'Study of the System Barium Oxide - Aluminium Oxide - Water at 30°C', J. Res. Nat. Bur. Stand., 45, 381-398 (1950).

11. E.T. Carlson, 'A Study of Some Strontium Aluminates and Calcium-Strontium Aluminate Solid Solutions', J. Res. Nat. Bur. Stand., 54, 329-334 (1955).

12. E.T. Carlson, 'Some Observations on Hydrated Monocalcium Aluminate and Monostrontium Aluminate', J. Res. Nat. Bur. Stand., 59, 107-111 (1957).

GENERAL REPORT
OF
SESSION II-4: KINETICS OF HYDRATION OF CEMENTS

(a) Papers regarding Mechanism

H. Mori (Japan)

The following Supplementary Papers are summarized in this report.

Paper No. II-26

THE INFLUENCE OF SUGARS ON THE HYDRATION OF TRICALCIUM ALUMINATE

J. F. Young (New Zealand)

Paper No. II-41

SOME PRINCIPLES IN CEMENT HYDRATION

A. Joisel (France)

Paper No. II-43

CONTRIBUTION OF ANALYSIS BY MEANS OF AN ELECTRON MICROPROBE TO THE CEMENT CHEMISTRY

P. Terrier (France)

Paper No. II-62

THE BEHAVIOR OF ALUMINATE-FERRITE PHASE DURING HYDRATION

P. Jäger, U. Ludwig & H. E. Schwiete (West Germany)

Paper No. II-96

SYNTHESIS OF THE ANALOGUES OF PORTLAND CEMENT AND OTHER BINDING MATERIALS ON THE BASIS OF ACIDIC-BASIC REACTIONS

N. F. Fedorov (U.S.S.R.)

Paper No. II-122

ELECTRON MICROPROBE STUDIES OF CEMENT PHASES

D. M. Roy & M. W. Grutzeck (U.S.A.)

Among the Supplementary Papers presented to topic II-4, Nos. 122, 43, 62, 26, 41 and 96 deal with the mechanism of hydration of cements.

The first two show that the electron microprobe is a useful instrument for the study of portland cement hydration. The third one is concerned with the behavior of aluminate-ferrite phase during hydration. The fourth one deals with the influence of sugars on the hydration of C_3A, and the fifth one presents some principles in cement hydration. The last one deals with the development of new binding materials in the solid-liquid system.

This report summarizes these papers.

I. ELECTRON MICROPROBE STUDIES OF CEMENT PHASES (SP No. 122)

by D.M. Roy and M.W. Grutzeck

This study was undertaken in order to explore the possibility of obtaining direct analytical information on hydration products of C_3S, C_2S, C_3A, and their mixtures at various stages by using an electron microprobe.

After the allocated reaction time the hydrated sample was mounted in polyester resin, polished, and examined by the electron microprobe. Visual cathode-ray tube displays of characteristic elemental emission, and electron back scatter displays were used to follow the progress of hydration. Further, counting techniques of characteristic elemental emission were employed to obtain quantitative analytical data. In order to eliminate the effect of many non-random sources of error in quantitative measurements, empirical correction was made by use of calibration standards.

X-ray intensities of the sample were measured at 1 μ intervals taken from the central portion of the crystal through the rim into the plastic. Figure 1 shows an example of the actual data obtained

on a C_3A sample hydrated for one day. This figure gives measured X-ray intensities and shows the electron back scatter photograph. The latter shows the sharp boundaries of the crystal and the distinct hydration rims. The vertical lines seen in the curves of the X-ray intensities also show these boundaries. The points of first break in the slope of these curves represent a CaO/Al_2O_3 molar ratio of approximately 2.8. Although X-ray diffraction data identify the hydration product as C_4AH_{13}, it is postulated on the basis of the microprobe and other microscopic data, to further consist of a crystalline solution of C_4AH_{13} with C_2AH_8 or a 1:1 mixture of them.

Furthermore, such data were obtained on the hydration products of C_3S and of a mixture of C_3S, βC_2S, and C_3A. It appears that the relatively slow rate of hydration of C_3S prevents sufficient buildup of the hydration rim for the accurate analysis.

The authors conclude that existing electron microprobe techniques have been successfully modified to cope with the specialized problems inherent in portland cement hydration studies. They also conclude that the use of electron back scatter display data and elemental display data offer a physical description of the grain-hydrate relationships during the progress of hydration and the use of the elemental analysis data make it possible to follow the progress of hydration in a quantitative manner.

II. CONTRIBUTION OF ANALYSIS BY MEANS OF AN ELECTRON MICROPROBE TO THE CEMENT CHEMISTRY (SP No. 43)

by P. Terrier

In this study an electron microprobe analysis was also applied to the study of the composition of the minerals of cement clinker, the composition of fly ashes, the hydration of portland cement, and

the pozzolanicity of the fly ash. The quantitative analysis is carried out by comparing the intensities of the radiation emitted by the sample with those emitted by standard samples.

Compositions of alite and belite of portland cement clinker as determined by the electron microprobe are shown in Table 1. It appears that alite contains about 3 % minor oxides and belite as much as 5 % minor oxides. On the other hand, the C_3A phase contains about 3 % SiO_2, 5 % Fe_2O_3, 0.6 % MgO, 0.9 % K_2O, etc., and the C_4AF phase about 2 % SiO_2, 2 % MgO, and 1.8 % TiO_2.

The chemical composition of fly ashes is relatively constant. However some heterogeneity is observed between the grains in the same fly ash as the result of the rapid passage of the coal leavings through the flame.

In portland cement pastes the hydration of aluminates takes place with fixation of the sulfate ion and produces acicular crystals which are grouped in discrete sites in the intergranular interstices. The hydration of tricalcium silicate occurs with the penetration of water which transforms the anhydrous silicate into hydrated silicate, while a part of the lime diffuses outside the grain and crystallizes in the hydroxide form: portlandite. The measurements obtained by electron microprobe analysis have shown that the hydrated silicate had a mean ratio CaO/SiO_2 of 1.65 for a duration up to 90 days.

Furthermore, the portlandite crystals have the following composition at the end of three years: 74.2 % CaO, 2.5 % SiO_2, 1.7 % Al_2O_3, 0.7 % K_2O.

The reaction of the ash grains in cement or lime pastes takes place with formation of a hydrated envelope with a low silica content.

The author points out that the electron microprobe is a basic research instrument which is unique for the punctual analysis by comparison with standards placed in the same geometry and detected by the same radiation.

III. THE BEHAVIOR OF ALUMINATE-FERRITE PHASE DURING HYDRATION (SP No.62

by H.E. Schwiete, U. Ludwing and P. Jäger

In this paper, the mechanism of hydration of C_3A, C_6A_2F, C_4AF and C_2F in the presence of $Ca(OH)_2$ and gypsum or anhydrite has been investigated by chemical means, infrared spectroscopy, X-ray diffraction, and electron microscopy.

In the system C_3A-$CaSO_4$-CaO-H_2O, ettringite was formed immediately after the addition of water and the formation of monosulfate hydrate was retarded by gypsum: that is, the amount and the stability of ettringite increases with the rising content of gypsum. When all the sulfate ions have been used to form ettringite or the concentration of sulfate ion becomes insufficient to allow this mineral to crystallize, ettringite reacts with the remaining C_3A to form monosulfate hydrate and mixed crystals of monosulfate hydrate and tetracalcium aluminate hydrate.

In the system calcium aluminoferrite-$CaSO_4$-CaO-H_2O, similar reactions take place. With increasing alumina content of calcium aluminoferrite, the trisulfate hydrate ($C_3(A,F)3CaSO_4.H_{32}$) is altered faster into monosulfate hydrate and mixed crystals of monosulfate hydrate and tetracalcium aluminate hydrate by using up the remaining aluminoferrite. Weight increase of the solid substance in the hydration of aluminate and aluminoferrite is shown in Figure 2. Furthermore, the kind of calcium sulfate used has a great influence

on the hydration of aluminoferrite. The reaction is much faster in the presence of anhydrite than in the presence of gypsum.

Principal hydration products of calcium aluminate and aluminoferrite in portland cement clinker are trisulfate hydrate, monosulfate hydrate and mixed crystals of monosulfate hydrate and tetracalcium aluminate hydrate.

The trisulfate hydrate first formed is more or less completely altered to monosulfate hydrate after a few hours depending upon the amount of sulfate present.

These results lead to the authors to conclude that the amount and the kind of calcium sulfate used is of prime importance for the rate and course of initial hydration of C_3A and calcium aluminoferrite. Particularly, the accelerative effect of anhydrite as compared to gypsum is of great importance in the production of portland cement low in, or free of C_3A.

IV. THE INFLUENCE OF SUGARS ON HYDRATION OF TRICALCIUM ALUMINATE

(SP No. 26)

by J. F. Young

This paper presents results of studies on the influences of monosaccharides and polysaccharides on the paste hydration of C_3A with or without gypsum for periods up to 90 days by means of X-ray diffraction, thermal analysis, and electron microscopy.

Each of nine kinds of the sugars used was found to retard the hydration of tricalcium aluminate paste. According to the results of quantitative X-ray diffraction analyses of the C_3A remaining in pastes after different times of hydration, sucrose and raffinose strongly retarded the hydration of C_3A at all ages. Xylose, ribose, and trehalose were the weakest retarders. The other sugars studied gave

intermediate results.

In pastes without additives the main hydration product is C_3AH_6, and in pastes containing sugars C_4AH_{13} is the predominant phase while C_2AH_8 is often present.

In C_3A-gypsum pastes with a C_3A: gypsum ratio of 2, ettringite is the only product detected up to 14 days. By 28 days monosulfate hydrate is forming in pastes without sugars. However, its appearance is delayed to after 60 days in pastes containing lactose, trehalose, and raffinose, and beyond 90 days with other sugars.

The amount of ettringite formed in C_3A-gypsum pastes which was calculated from TGA is shown in Table 2. Sucrose also retarded strongly at all ages, and lactose, trehalose, and raffinose were initially strong retarders. On the other hand, xylose, glucose, and fructose accelerated the hydration of C_3A-gypsum pastes at early ages, but retarded strongly later. As described above, sugars retarded the formation of ettringite and its subsequent conversion to low-sulfate. Furthermore, morphology of ettringite was modified by sugars.

From the results of these experiments, no definite correlation between the effects of different sugars and their structural differences was observed, as sugars are structurally labile and can exist in several different forms.

Mechanism of retarding by sugars may be explained by complexing, adsorption, and solubility change. The author suggests that complexing of sugars with metals, especially calcium, aluminum, and iron, may be the main factor underlying their behavior as retarders.

V. SOME PRINCIPLES IN CEMENT HYDRATION (SP No. 41)

by A. Joisel

The paper presents some principles extracted inductively in the hydration of calcium silicate and aluminate and the reaction mechanism of retarders and accelerators.

The hydraulic components of the cement grains go into solution in water, and this dissolution is accompanied by a hydrolysis, that is to say that the acids (particularly silica and alumina) and the bases (mainly lime), which constitute cement, regain a certain individuality at the time of dissolution.

Calcium silicates have an incongruent dissolution, i.e. lime passes into solution much faster than silica, and their hydration occurs as shown in schematizing in Figure 3a. The initial surface of each silicate grain keeps a solution of continuity in the hydrated paste during hydration, and the bonds which are formed in the interstices of the grains are growing in number. When recovering a certain individuality during hydration, the lime has a tendency to make its concentration roughly uniform in the whole paste. Therefore, the hydrated silicate has a total composition roughly situated between CSH and $C_{1.5}SH_{1.5}$.

Calcium aluminates pass into solution in their stoichiometric ratio, the faster the richer they are in lime. The hydration of C_3A takes place as indicated in Figure 3b. The surface of the grains in contact with the solution is progressively dissolved by water. It results that the hardening occurs immediately after the moment in which the first bonds are established. Thus this hardening is always rapid and the most stable hydrated aluminate is C_3AH_6.

The products which accelerate or retard the dissolution of the hydraulic components of cement are accelerators or retarders. The acid anions which accelerate the dissolution of the lime are Cl^-, NO_3^-, and SO_4^{--}. On the other hand, the basic cations which accelerate the dissolution of alumina and silica are Na^+, K^+, and NH_4^+, etc.

Retarders are classified into two groups. One is reducers of solubility and the other is coaters. Representative of the reducers is $Ca(OH)_2$, and those of the coaters are alkaline tetraborates and fluorides, etc.

Calcium sulfate is amphoteric and it behave as an accelerator for silicates and aluminates low in calcium and as a retarder for highly calcic aluminates.

The author emphasizes that future researches will formulate more precise knowledge concerning hydration, particularly from the point of view of the development of more quantitative data.

VI. SYNTHESIS OF THE ANALOGUES OF PORTLAND CEMENT AND OTHER MATERIALS ON THE BASIS OF ACIDIC-BASIC REACTIONS (SP No. 96)

by N. F. Fedorov

This study was undertaken to search for new binding materials in the solid-liquid systems where the acid-base reactions take place, because the hardening of portland cement, alumina cement and other most widely distributed binding materials is the result of the chemical reactions in which acid radicals and metal cations interact.

Four groups of materials including less distributed and even rare elements have been investigated in this paper. A great number of combinations in each group have been examined mainly from the

aspect of compressive strength.

First: in the mineral-water system, plumbates, stannates, titanates, and zirconates of the alkali earths have been synthesized and examples of those binding properties are shown in Table 3. These minerals show pronounced binding properties, and autoclaving intensifies the process of hardening of these minerals.

To determine the character of the hydration process of the analogous minerals of calcium silicate, the hydration of calcium stannate has been investigated by means of X-ray, infrared and chemical analyses. As a result, it is shown that calcium orthostannate is hydrolyzed giving off calcium hydroxide and forming hydrostannates, while metastannate is hydrated.

Second: in the metal oxide-acid system, HNO_3, H_2SO_4, HCl, $H_2C_2O_4$, etc., have been used as acid and combined with oxides of different groups of the periodic table. It is shown that on the basis of metal oxide-acid system many kinds of cements may be synthesized, their strength characteristics being similar to those of portland cement and sometimes even much greater.

Third: in the base oxide-acid oxide-water system, oxide of elements of group II are used as base oxides and ones of group IV are used as acid oxides. Prepared mixtures of these materials are ground, molded under pressure, and autoclaved. In this system high strength artificial stones have also been produced.

Fourth: in the metal oxide-polyatomic alcohol system, calcium, strontium, barium and lead oxides when mixed with glycerine or glycol form high strength materials.

The author concludes that it is theoretically possible to obtain new binding materials having much greater strength or having more specific properties than existing cements. He also concludes that the combination of solid inorganic powders and organic liquids will lead to the development of many new binding materials.

GENERAL REPORT
OF
SESSION II-4: KINETICS OF HYDRATION OF CEMENTS

(b) Paper regarding Kinetics

H. N. Stein (Netherlands)

The following Supplementary Papers are summarized in this report.

Paper No. II-35

MUTUAL INTERACTION OF C_3A AND C_3S DURING HYDRATION

J.G.M. de Jong, H. N. Stein & J. M. Stevels (Netherlands)

Paper No. II-44

THE MATHEMATICAL SIMULATION OF CHEMICAL, PHYSICAL AND MECHANICAL CHANGES ACCOMPANYING THE HYDRATION OF CEMENT

G.J.C. Frohnsdorff, W.G. Fryer & P.D. Johnson (U.S.A.)

Paper No. II-53

STUDY ON HYDRATION OF ALUMINA CEMENT BY ULTRASONIC METHOD

S. Koide & K. Okada (Japan)

Paper No. II-70

ON THE HYDRATION KINETICS OF HYDRAULIC CEMENTS

J. H. Taplin (Australia)

Paper No. II-73

EFFECT OF THE TEMPERATURE ON THE EARLY HYDRATION OF THE SYSTEM

$3CaO.Al_2O_3-CaSO_4.2H_2O-Ca(OH)_2-H_2O$

H. Mori & K. Minegishi (Japan)

Paper No. II-93

HYDRATION OF TRICALCIUM SILICATE IN A VERY EARLY STAGE

K. Fujii & W. Kondo (Japan)

Paper No. II-118

THE HYDRATION MECHANISM OF C3A AND C_3S IN THE PRESENCE OF CALCIUM CHLORIDE AND CALCIUM SULPHATE

N. Tenoutasse (Belgium)

Paper No. II-120

THE HYDRATION OF THE FERRITE PHASE OF CEMENTS

W. L. de Keyser & N. Tenoutasse (Belgium)

Kinetic data on the very early stages of the paste hydration of C_3S (liquid/solid ratio 0.7 to 1.0) are reported by K. Fujii and W. Kondo. By isothermal calorimetry, in the main the same heat evolution rate vs. time curve is found as that reported earlier [1)2)], showing an increasing heat evolution rate in the beginning. Fujii and Kondo, however, are able to discern various stages before the heat evolution rises: During the first five minutes, some heat evolution is observed (stage 1) followed by a dormant period (about 30 minutes). After that, the reaction proceeds sluggishly for about three hours (stage 2), and then the heat evolution rate rises rapidly (stage 3).

During stage 1 C_3S starts to dissolve congruently; soon, however, the molar CaO/SiO_2 ratio in solution becomes higher than 3. The amount of combined water at the end of stage 1 corresponds to a layer of 3 to 4 moles on the surface; the authors conclude that stage 1 corresponds to the dissolution of one mole of C_3S throughout the surface. They have to assume, however, that the hydrate formed during stage 1 has the composition CSH_2, (which means that it is the equilibrium product formed in the solution concerned), and that "adsorbed water" is a principal constituent of combined water (which means that it cannot be removed by organic solvents; it is regarded as a "compensation" for the C_3S dissolved). Assuming further that per mole of C_3S reacting during stage 2 as much Ca^{2+} ions are given off to the water phase as during stage 1, it is remarked that about 4 mole layers of C_3S react during stage 2. During stage 2, heat of hydration per mole of combined water is high; this is ascribed to a rearrangement of "adsorbed water" to the formation of hydrates.
The onset of stage 3 is thought to be connected with incipient precipitation

of $Ca(OH)_2$, but no other argument is adduced for that apart from the simultaneity of the phenomena.

No explanation is offered by Fujii and Kondo for the retardation of the hydration reaction near the end of stage 1, and for the sluggish character of the subsequent reaction during stage 2. For this dormant stage of the hydration of C_3S, de Jong, Stein and Stevels[2)3)], basing themselves partly on results obtained by Kantro et alii [4)], had postulated earlier the formation of a metastable hydrate called "First Hydrate" by these authors. They report now data on the interaction of C_3A and C_3S during their hydration, obtained in pastes of water/solid ratio 1:1, and varying C_3A/C_3S ratio. The heat evolution peak due to C_3S hydration is shifted towards later hydration times by small amounts of C_3A, but not by greater amounts of C_3A. This is explained as follows: In suspensions of C_3A in water, small amounts of C_3S accelerate C_3AH_6 precipitation, presumably because silicate ions are built into C_3AH_6 crystals and accelerate therefore C_3AH_6 nucleation; the concentrations in the water phase adjust themselves ultimately to the C_3AH_6 solubility line. However, at high C_3S/C_3A ratio the crystallization of C_3AH_6 is suppressed, and the concentrations, after leaving the point of metastable coexistence of C_2AH_8 and C_4AH_{19} with solution, follow the C_4AH_{19} solubility line; the solution continues to contain considerable amounts of aluminate ions. Heat evolution rate and X ray analyses of the hydration products indicate that the same phenomena occur in pastes, though the time scale may be different: small amounts of C_3S accelerate C_3AH_6 formation, large amounts retard it. The strong retardation, exerted on C_3S hydration by small amounts of C_3A, may then be understood by the retarding action of aluminate ions, such as found also in pastes $C_3S + Al(OH)_3 + H_2O$[5)]. This has been ascribed to aluminate ions being built into "First hydrate" stabilizing the latter toward conversion, as reported by Kalousek[6)] for the case of tobermorite. The absence of this strong retarding action in pastes of high C_3A/C_3S ratio can then be understood by the formation of C_3AH_6, lowering the aluminate ion concentration in the water phase. It might be objected that C_3AH_6 formation is expected at later times only, such as to make this mechanism operative only after some hours'hydration; however, X ray data indicate in mixed $C_3A + C_3S$ + water pastes of high C_3A/C_3S ratio

the presence of C_3AH_6 and the absence of hexagonal calcium aluminate hydrates at very early stages. A confirmation of these ideas will be found in the results of Tenoutasse on pastes $C_3S + C_3A + CaSO_4.2H_2O$ + water, to be discussed later.

A mathematical simulation of processes during the hydration of C_3S by Frohnsdorff, Fryer and Jonhson indicates that an induction period alone cannot be regarded as a proof for the existence of the First Hydrate as postulated by Stein and Stevels. The authors postulate equations describing the rate of dissolution of C_3S as a function of ion concentrations in solution, and the rate of precipitation of hydrates to be governed in addition by the surface area of nuclei. By suitable choice of parameters in these equations, Frohnsdorff et alii are able to obtain a heat liberation vs. time curve resembling experimental data (fig. 2). The course of events suggested is:

a. solution of the anhydrous C_3S untill the aqueous phase is close to saturation with respect to C_3S.
b. nucleation of the products of hydration,
c. growth of the nuclei to form larger particles,
d. as the surface area of particles increases, the rate of product formation increases and the concentrations of the ions in solution fall. This can be considered as an autocatalytic reaction in which the rate-determining step is the deposition of the products of hydration on the growing particles.
e. At a still later stage, as the surface area of the anhydrous C_3S falls, its rate of solution appears to become rate controlling.

The authors emphasize that they regard these calculations as crude first approximations, intended to illustrate how simulation can be used. Such considerations cannot prove or disprove any mechanism proposed on independent evidence. The model is not yet able to take into account different retarding effects of hydrates on the hydration, but such effects could easily be included.

The kinetics of hydration reaction of cement compounds in a more restricted sense are the subject of an investigation by Taplin. This author distinguishes "linear kinetics" (reaction rate proportional to the surface area of cores of unreacted cement) and "quadratic kinetics" (reaction rate inversely proportional to the resistance to diffusion provided by a coherent coating of

reaction products, with special attention to the case where the resistance of the outer products is negligible compared to that of the inner products). It is easily seen that for a reaction characterized by quadratic kinetics the rate decays more rapidly than for a reaction characterized by linear kinetics. Taplin compares the kinetics of various hydration reactions (MgO in $MgCl_2$ or $MgSO_4$ solution; $CaSO_4$ in potassium alum solution; β-C_2S, alite and C_3S in water) with those calculated on the basis of either "linear" or quadratic kinetics, giving due regard to particle size distributions.

In stirred suspensions or slurries, linear or quadratic kinetics are found except for β-C_2S, where the rate decays too slowly for even linear kinetics. This is explained by assuming a process accelerating the reaction (as evidenced by an induction period) counteracting the retarding effects of hydrates. In hardening pastes, the rate tends to decay more rapidly than in stirred suspensions or slurries, for C_3S especially in the later stages.

The data are consistent with a model where the reactions start linear but may become diffusion controlled if the resistance of the diffusion process exceeds that of the surface decomposition. At least the outer products are thought to form a coherent network [7]) and to minimise the generation of disruptive stress; it is assumed that these products must be precipitated from material which has diffused away from the cement grains. Nucleation and precipitation of hydrates near the grain surface is thought to be inhibited by the narrow pore size at those places.

However, then the outward diffusion process must always keep pace with the rate of mineral decomposition; and if we suppose that the hydration rate is controlled by the inward diffusion of water, then the outward diffusion of hydrated material should occur more readily than the inward diffusion of water. But this seems difficult to accept, in view of the higher concentration and greater mobility of water compared to say divalent cations.

In the case where the solubility difference between cement mineral and hydration product is small (e.g., $CaSO_4$ - $CaSO_4.2H_2O$) a mechanism is possible

where the dissolution rate of the anhydrous material is retarded because the concentrations rise towards the solubility of $CaSO_4$. For thermodynamically unstable materials such as C_3S, it is assumed that a stable surface is produced by the adsorption of an outward diffusing chemical species which in this way poisons the reaction if its concentration rises. Joint control by the surface decomposition and by the outward diffusion of the poisoning species is possible too. The experiments indicate that such joint kinetics can exist only in those regions where the kinetics are affected by merging outer products.

Turning to C_3A hydration, we direct our attention first to an investigation by H. Mori and K. Minegishi on the effect of temperature on the early hydration of the system $C_3A + CaSO_4.2H_2O + Ca(OH)_2 + H_2O$.

Again, isothermal calorimetry is used to classify the reaction into stages; two heat evolution peaks are observed. The interpretation follows in the main that given by Stein [8]: gypsum retards C_3A hydration by formation of an ettringite layer, the second heat evolution peak occurs when the gypsum content in the system is insufficient for ettringite formation. However, an important difference with earlier interpretations is that the ettringite layer, previously considered to be removed by scaling off [9][10] is now thought to be removed by a chemical reaction: the amount of ettringite decreases during the rising branch of heat peak II, in marked contrast to the situation in pastes $C_4AF + CaSO_4.2H_2O$ to be discussed later. By direct experiment it is shown that ettringite is converted by C_3A in $Ca(OH)_2$ solution. Similar ideas have been put forward previously [11] for the reaction of C_3A with $CaSO_4.2H_2O$ in water.

Temperature differences in the range 5 - 70°C do not greatly influence the reaction during the first heat evolution peak, but in the "dormant" period between the two peaks the reaction rate is considerably increased by an increase in temperature [12]. This is ascribed to differences in properties of the ettringite layer: at lower hydration temperatures finer ettringite crystals are formed and the ettringite coating of the C_3A is more compact. This interpretation is supported by microscopical observations. At 70°C, no protective layer is formed. Addition of $Ca(OH)_2$ acts similarly as lowering of the temperature.

Kinetically the reaction is discussed on the basis of the equation

$$(1 - \sqrt[3]{1 - \alpha})^N = KT$$

with α = degree of hydration, t = time, N and K = constants. During the dormant period between the two heat evolution peaks, N is rather high (=4) at 5°C, indicating that the coating becomes more compact as the reaction proceeds. With increasing temperature, N decreases, it is equal to 2 at 40°C : at this temperature an increase in the amount of ettringite during the progress of the reaction increases the thickness of the surface layer but brings no change in its structure.

After the second heat evolution peak, N is higher than 2, at all temperatures investigated, indicating that the hydrates form a new barrier around the C_3A grains in this stage.

Similar phenomena are described by Tenoutasse for pastes $C_3A + CaSO_4 . 2H_2O + H_2O$: two heat evolution peaks are found. This stands in contrast with results published previously by Stein [11]) showing a more complicated heat evolution ascribed to successive formation of ettringite, amorphous $Al(OH)_3$, monosulphate and C_4AH_{19}. The difference between the results obtained by Tenoutasse and those reported by Stein may be due to differences in particle size (the sample employed by Tenoutasse contained smaller particles than that used by Stein) in water/C_3A ratio, and to the presence of quartz employed as a filler by Stein. The interpretation is in the main along the same lines as that discussed already for pastes $C_3A + CaSO_4 . 2H_2O + Ca(OH)_2$ solution, but gypsum is considered to be consumed at the top of the second peak. Kinetically, the reaction is described by the same equation as that used by Mori and Minegishi, but N is now found to be = 2. From the temperature dependence of the reaction, an activation energy of 12 Kcal.mole^{-1} is calculated.

Pastes $C_3A + CaCl_2$ + water show a similar behaviour, but in combined pastes $C_3A + CaSO_4 . 2H_2O + CaCl_2$ + water more complicated phenomena are observed: At the beginning a small amount of $CaCl_2$ reacts to give chloroaluminate, but sulphate ions react more extensively to give ettringite. Consumption of Cl^- ions starts again after the sulphate ions have been used up.

Tenoutasse reports also some results on the hydration of C_3S (agreeing with previously published data [2)3)]) and finds that it is accelerated by $CaCl_2$. No hydrate containing Cl^- is formed except at very high $CaCl_2$ contents.

Results on combined pastes C_3S + C_3A + water agree with the results of de Jong, Stein and Stevels mentioned earlier: C_3A slows down the hydration of C_3S (C_3A/C_3S ratio = 0.25). The additional presence of $CaSO_4.2H_2O$ modifies the results as follows: when the second heat peak attributed to the hydration of C_3A + $CaSO_4.2H_2O$ + water lies before the peak due to the hydration of C_3S, the latter peak is greatly retarded. If, however, the second heat peak attributed to C_3A hydration lies after the peak due to the hydration of C_3S, the latter peak is practically unchanged. Tenoutasse does not offer an explanation for these observations; it should be remarked however that they can be explained by the mechanism proposed by de Jong, Stein and Stevels: aluminate ions retard the start of the C_3S heat evolution peak, but in order to do so their concentration must be reasonably high, i.e. sulphate ion concentrations should not be such as to precipitate ettringite.

Analogous phenomena are reported on hydrating calcium aluminoferrites by de Keyser and Tenoutasse. C_2F hydrates very slowly, but the hydration velocity increases with replacement of iron by aluminium. Hexagonal hydrates are found first, and are ultimately converted into cubic $C_3(A,F)H_6$. $Ca(OH)_2$ accelerates the hydration of C_2F, and retards the conversion of hexagonal hydrates in the case of C_6A_2F and C_4AF.

Addition of $CaSO_4.2H_2O$ exerts an influence similar to that observed in the case of C_3A. $CaCl_2$ however reacts so fast with calcium aluminoferrites that it is very difficult to analyse the reaction; the hydrate $C_3(AF).3CaCl_2.30H_2O$ is formed under certain conditions but easily converted into $C_3(AF).CaCl_2.12H_2O$. Replacement of H_2O by D_2O greatly reduces the rate of hydration.

In mixed pastes C_4AF + $CaSO_4.2H_2O$ + $CaCl_2$ + water, three heat peaks are seen. Between the first and second peaks, gypsum reacts forming calcium-trisulphoaluminoferrite; all gypsum is consumed when the top of the second peak has been reached. During the rising branch of the second peak, the

trisulphoaluminoferrite X ray diffraction lines still increase in intensity; this is an interesting difference with the observations of Mori and Minegishi in pastes $C_3A + CaSO_4.2H_2O + Ca(OH)_2 + H_2O$. When the gypsum has been consumed, the hydrates rich in sulphate are converted into hydrates poor in sulphate, but this transformation does not occur as long as Cl^- ions are present. Instead, monochloroaluminoferrite is formed. This is explained by assuming that trisulphoaluminoferrite reacts above all with the hydrated aluminoferrites, $C_4(AF)H_{13}$ and $C_2(AF)H_{17}$.

S. Koide and K. Okada studied the hydration of alumina cement by ultrasonics. Much attention is paid to the development of apparatus that can be used to investigate muddy samples or slurries by ultrasonics. The ultimate apparatus works well at W/C ratios 0.28-0.30, but when W/C ratio drops below 0.28 it becomes difficult to obtain sharp modes of the sonic wave on the oxilloscope by lack of homogeneity of the sample.

Use of the apparatus is exemplified by sound velocity vs. time curves at different hydration temperatures. Sound velocity is found to rise sharply, simultaneously with a drop in electrical conductivity. An increase of the temperature from 20 to 30°C retards this effect, but still higher temperatures accelerate it.

From the sound velocity of the hardened specimen, Young's modulus is calculated and Mechanical strength is predicted, on the basis of a relationship previously established [13].

1. L.R. Forbich, J. Amer. Concr. Inst. Proc. 1940, 37, 161
2. H.N. Stein and J.M. Stevels, J. Appl. Chem. (London) 14, 338 (1964)
3. J.G.M. de Jong, H.N. Stein and J.M. Stevels, J. Appl. Chem. (London) 17, 246 (1967).
4. D.L. Kantro, S. Brunauer and C.H. Weise, J. Phys. Chem. 66, 1804 (1962).
5. J.G.M. de Jong, H.N. Stein and J.M. Stevels, J. Appl. Chem. (London) 18, 9 (1968).
6. G.L. Kalousek, J. Amer. Ceram. Soc 40, 74 (1957).
7. J.H. Taplin, Austr. J. Appl. Sci. 10, 329 - 345 (1959)
8. H.N. Stein, Rec. trav. chim. Pays-Bas 81, 881 (1962)
9. H.N. Stein, J. Appl. Chem. (London) 11, 474 - 482 (1961).
10. H.E. Schwiete, U. Ludwig and P. Jäger, Symposium on Structure of Portland Cement Paste and Concrete, Highway Research Board, Special Report 90, Washington D.C., p. 353 - 367 (1966)
11. H.N. Stein, J. Appl. Chem. (London) 15, 314 - 325 (1965)
12. H. Mori + K. Minegishi, Semento Gijutsu Nenpo 21, 71-76 (1967)
13. S. Koide, K. Kaiden, M. Kawano, Asahi Glass Co. Res. Lab. Rep. 8 (2) 83 - 95 (1958).

GENERAL REPORT
OF
SESSION II-5: HYDRATION OF PORTLAND CEMENT

H. zur Strassen (West Germany)

The following Supplementary Papers are summarized in this report.

Paper No. II-2

CONTRIBUTION OF CALCIUM THIOSULFATE TO THE ACCELERATION OF THE HYDRATION OF PORTLAND CEMENT AND COMPARISON WITH OTHER SOLUBLE INORGANIC SALTS

H. Tanaka & K. Murakami (Japan)

Paper No. II-4

SIGNIFICANCE OF TOTAL AND WATER SOLUBLE ALKALI CONTENTS OF CEMENT

W. J. McCoy & O. L. Eshenour (U.S.A.)

Paper No. II-22

THE INFLUENCE OF LEAD AND ZINC COMPOUNDS ON THE HYDRATION OF PORTLAND CEMENT

W. Lieber (West Germany)

Paper No. II-47

SOME OBSERVATIONS UPON THE DETERMINATION OF HEAT OF HYDRATION OF SLAG AND PORTLAND CEMENTS BY THE METHOD OF DIFFERENTIAL HEAT OF SOLUTION

G. A. Toubeau (Belgium)

Paper No. II-117

THE INFLUENCE OF ALKALI-CARBONATE ON THE HYDRATION OF CEMENT

E.M.M.G. Niël (Netherlands)

Paper No. II-129

AQUEOUS PHASE IN PORTLAND CEMENT PASTES CONTAINING SOLUBLE CHLORIDE ION

K. T. Greene & K. E. Palmer (U.S.A.)

Paper No. II-134

THE EFFECT OF TRICALCIUM ALUMINATE ON THE HYDRATION OF TRICALCIUM SILICATE AND PORTLAND CEMENT

A. Celani, P. A. Moggi & A. Rio (Italy)

This General Report deals with the following Supplementary Papers:

1. G.A. Toubeau: Some observations upon the determination of heat of hydration of slag and Portland cements by the method of differential heat of solution.

2. K.T. Greene, K.E. Palmer: Aqueous phase in Portland cement pastes containing soluble chloride ion.

3. A. Celani, P.A. Moggi, A. Rio: The effect of tricalcium aluminate on the hydration of tricalcium silicate and Portland cement.

4. W.J. McCoy, O.L. Eshenour: Significance of total and water soluble alkali contents of Portland cement.

5. E.M.M.G. Niël: The influence of alkali-carbonate on the hydration of cement.

6. H. Tanaka, K. Murakami: Contribution of calcium thiosulfate to the acceleration of the hydration of Portland cement and comparison with other soluble inorganic salts.

7. W. Lieber: The influence of lead and zinc compounds on the hydration of Portland cement.

The Papers are ordered in such a manner, that the first two deal with measuring of properties of the cement paste - heat of hydration (No.1) and supersaturation of the aqueous phase (No.2) - the other ones with the influence of variation of cement composition on the setting and hardening and other properties - variations of C_3A content (No.3) and alkali content (No.4) in the clinker, addition of potash (No.5), calcium thiosulfate (No.6), lead and zinc (No.7) to the paste.

HEAT OF HYDRATION

For the purpose of winter concreting, the Belgian cement industry intended to classify the cements according to heat development after curing for 3 days at + 5°C. In a first series of comparative determinations, the original ASTM heat of solution method was used, but the results were not satisfactory (Table 1, first column). When using the modified solution method by Santarelli and Goggi, however, the results of the participating laboratories agreed well (second column).and allowed a classification of Belgian cements into 6 classes (third column).

Table 1

Later on, however, a repetition of these comparisons showed marked differences up to 15 calories between the results of the various laboratories; it appeared that some laboratories had modified the mode of procedure. The present work, therefore, was undertaken to clarify and eliminate the possible causes of error.

Among other factors, the most important sources of error were found the determination of the loss on ignition and the grinding of the hydrated sample. The loss on ignition requires a calcination temperature of 1050 ± 50°C. For blast-furnace cements, too, the direct determination - instead of analyzing the CaO-content - is the best method and must be carried out in a nitrogen or argon atmosphere.

The best conditions for grinding the hydrated sample, however, are still a problem. After curing for three days at + 5°C, the hardened paste is still relatively humid; it is not possible, therefore, to grind the paste in the dry state, but only in an organic liquid, alcohol - according to Goggi - or acetone being used. The resulting heats of hydration are dependent both on the nature of the liquid used and on the conditions of washing and drying the sample.

The Author prefers the use of alcohol because it is easier to eliminate this liquid without alterating the paste structure. He questions if it would be advisable to use a liquid for grinding of samples which are cured for longer periods at + 20°C.

The work done by Dr. Toubeau is of high value for the heat of solution method. But it should be considered if this method may yield exact values when the sample is grond in an organic liquid because the hydration stage after drying is not the same as in the original paste.

AQUEOUS PHASE CONTAINING CHLORIDE ION

The results of the equilibrium study by Greene and Palmer on the aqueous system containing the ions K^++ Na^+, Ca^{++}, SO_4^{--}, OH^-, Cl^- are reproduced in 3 diagrams in the Abstract. These diagrams show the equilibrium values of Ca^{++}, SO_4^{--}, and OH^- when the solutions are saturated with $CaSO_4 \cdot 2H_2O$ and $Ca(OH)_2$ at different levels of K^+- and Cl^-- content. The Ca^{++}- content increases with increasing Cl^- and decreasing K^+, SO_4^{--} and OH^- increase with decreasing Cl^- and increasing K^+.

Table 2 shows the compositions of some extracts of cement pastes. With the aid of the solubility diagrams, the ion products in these extracts are calculated and compared with the analytical values (Table 3). From this comparison is shown that some supersaturation with gypsum exists in cement pastes

containing calcium chloride up to 15 minutes after mixing, and that supersaturation with calcium hydroxide is sometimes very high.

Table 2

Table 3

THE EFFECT OF C_3A ON THE HYDRAULIC PROPERTIES

In a comprehensive work Celani, Moggi and Rio studied the influence of various contents of C_3A in the clinker, upon strength development, rate of hydration and development of specific surface, combined with the additional influence of gypsum and calcium chloride. The C_3S and C_2S content of the clinkers were kept constant at about 50 and 25 %, respectively. the C_3A content varied from 3 to 15 %, the rest being the ferrite phase. The correlations between C_3A content, compressive strength and specific surface are represented in Figures 1 and 2.

Figure 1

In Figure 1 a slightly different connection is chosen than given by the Authors, the compressive strength being represented as function of the C_3A content. This figure shows clearly, that the compressive strength - determined on ISO mortar 1 : 3, w/c ratio 0.5 - has in each series at every age - except the 1 day values of cement without added

gypsum - an optimum value shifting from the third cement (- 10 % C_3A) at the early ages to the second one (5.5 % C_3A) at the later ages. At the age of 28 days, the strengths fall off considerably if the C_3A content is raised markedly over the optimum value.

In the series containing gypsum, the gypsum content was adapted to the C_3A content so that the ratio $C_3A/CaSO_4$ was ~1,75. The addition of calcium chloride was constant 2 % by weight of cement, dissolved in the mixing water. The addition of gypsum + calcium chloride results in the highest strengths in any case.

Similar representations are possible for the other parameters studied, but it seemed more informative to show in Figure 2 the strong correlation between strength and specific surface, the only exception being two points at the age of 28 days. If the revealed correlation is not accidental, the deviations of these two points would result with high probability from a false determination of the specific surface.

Figure 2

A close relation, too, exists between strength and the extent of hydrolisis, but the dependence is not linear as in the case of specific surface.

The Authors propose the theory that the presence of C_3A promotes the penetration of water into the clinker grain, so that more water becomes available for the hydration of tricalcium silicate. Successively the aluminate would crystallize without contribution to the specific surface and to the strengths.

TOTAL AND WATER SOLUBLE ALKALI OF PORTLAND CEMENT

The study of McCoy and Eshenour was carried out to clarify the effects of total and water soluble alkali. The solubility was found to vary between 10 and 60 % of total alkali. Potassium and sodium sulfate are the most soluble compounds. Then follows sodium as contained in the NC_8A_3 phase. The most insoluble is potassium as contained in the $KC_{23}S_{12}$ phase.

To obtain information about the influence of alkalis on strength development from a commercial clinker three lots of cement were prepared: the one by reburning the clinker in a laboratory kiln (0,57 % alkali as Na_2O), the second by reburning the clinker with addition of NH_4Cl to eliminate the alkalis (0 % alkali), the third with addition of KOH to the alkali free cement. Table 4 shows the compressive strength of these 3 cements. The strength of the

Table 4

alkali free cement is abnormally low, but can be raised by the addition of KOH.

The effect of total and water soluble alkali on alkali - reactive aggregates was studied with 3 cements with equal total but different soluble alkali content. Table 5 shows that the expansion of the mortar bars is dependent on the content of soluble alkali.

Table 5

INFLUENCE OF ALKALI CARBONATE

The work of Niël had the aim to clarify the irregularities on setting and hardening by addition of potash.

Potash is known as a rapid accelerator of setting. But Figure 3 which shows the setting properties of a Portland cement in function of the K_2CO_3 content reveals that at very little amounts potash acts as retarder. There are three extreme points at approximately 0.25 %, 2.5 %, and 20 % K_2CO_3. The properties of these distinguished compositions are studied in detail.

Figure 3

In Figure 4 are represented the temperature curves during setting which reflect the changes in setting properties. Also the hardening in the first hours shows characteristic differences (Figure 5).

Figure 4

Figure 5

The most detailed research is done in analyzing the rate of hydration by X-ray and infrared measurements. The results of the X-ray study are represented in Figures 6 and 7. For better comparing, the curves are somewhat otherwise ordered than it was done by the Author.

Figure 6

Figure 7

In Figure 6 the decrease of C_3S, C_3A and gypsum and the formation of $Ca(OH)_2$ as caused by different amounts of admixture are compared. Neglecting the - possibly accidental - differences in the first hour, by the addition of 0.25 % K_2CO_3 the decompositions of C_3S and C_3A are markedly delayed during the first day, whereas the reaction of gypsum is accelerated.

At higher amounts of K_2CO_3, the gypsum seems to be decomposed instantly. The reactions of C_3S and C_3A are accelerated during the first hours, but at the end of 28 days the decomposition of C_3S is very incomplete. In the case of 2.5 % addition, the decomposition of C_3A is incomplete, too, the X-ray intensities not being changed from 16 hours to 28 days.

From Figure 7 it is seen that by addition of 0.25 % K_2CO_3 the formation of ettringite, $C_6A\bar{S}H_{31}$, is accelerated and its amount augmented. At higher amounts of K_2CO_3, the sulphate exists as K_2CO_3, only at the 2.5 % level there remains a rest of ettringite for two hours.

The CO_2 content of the pastes is found as monocarbonate $C_4A\bar{C}H_{11}$ at 0, 2.5 and 20 % K_2CO_3 in increasing amounts, at the highest level as $3K_2CO_3 \cdot 2CaCO_3 \cdot 6H_2O$ and $CaCO_3$, too. At 0.25 % addition no carbonate containing phase is recorded, but one can assume that the so - called C_4AH_{13} phase - as well as the same in the paste without admixture - is in reality the quater - or semi - carbonate phase. The "ups and downs" of several curves are not easy to be explained; in the case of the monocarbonate $C_4A\bar{C}H_{11}$, the decrease in X-ray intensity during the first hour at 20 % K_2CO_3 cannot be ascribed to decomposition of this phase at higher temperatures because such a decomposition is only described at the tricarbonate phase $C_6A\bar{C}_3H_{31}$.

In general, the phases as observed by X-rays are in accordance with the changing chemical composition of the pastes and with their setting behaviour. Especially the observed retardation of setting by addition of 0.25 % K_2CO_3 is well to be explained: by conversion of some $CaSO_4$ to $CaCO_3$ and K_2SO_4, the SO_3 content of the aqueous phase is increased and the formation of ettringite augmented; the larger coat of ettringite causes a delayed setting.

CALCIUM THIOSULPHATE AS ACCELERATOR

Tanaka and Murakami have detected that calcium thiosulphate $CaS_2O_3 \cdot 6H_2O$ can be used as accelerator for setting and hardening of cement pastes. In Figure 8 heat liberation curves

of Portland cement containing admixtures of calcium chloride and of various amounts of thiosulphate are represented. It is shown that both salts cause at about the same acceleration of setting time but that the intensity is higher in the case of chloride. By larger additions of thiosulphate, the effect can be improved.

Figure 8

In accordance with this, the gain of early strength is slightly poorer than caused by calcium chloride. In blast furnace slag cement, calcium thiosulphate is used very advantageously because it acts only on the Portland clinker part of the cement. The early strength is improved, therefore, according to the ratio admixture / clinker, whereas the development of strength in the later ages is caused by hydration of the slag part and is not affected by the admixture.

The specific advantage of the thiosulphate admixture compared with calcium chloride is that it is not corrosive on steel. Test pieces of mild steel embedded in mortar with 3 and 6 % admixture of thiosulphate were scarcely corroded after 6 months, whereas the same steel embedded in mortar containing 2 % of chloride showed considerable corrosion after one month.

INFLUENCE OF LEAD AND ZINC

Lead and zinc were known as strong retarders of the setting time, even in very small quantities. The rules of retardation as revealed by Lieber are illustrated by the following figures.

Figure 9

Figure 9 shows the influence of various amounts of PbO on the setting time of two Portland cements, as measured by the rise of temperature in the paste. The influence differs considerably for different cements. The heat evolution is about the same or larger then in the unretarded cement. After the retardation period has finished the cements harden quite normally and attain even better final strength.

When ground to different finenesses the retardation changes in inverse sense as the specific surface (Figure 10).

Figure 10

By experiments on pure cement minerals, it was shown that lead oxide has only an influence on tricalcium silicate, the other phases being not retarded. During the retardation period of a C_3S paste, no water is bound and no lime split off, but with the setting a very rapid hydration takes place.

The technological behaviour of zinc oxide is identically the same as that of lead oxide, but with regard to chemical reactions a deviation was found. During the retardation period, the formation of an intermediate phase was detected which proved to be calcium hydroxo zincate, according to the equation

$$2\ ZnO + Ca(OH)_2 + 4\ H_2O \longrightarrow Ca[Zn(OH)_3H_2O]_2$$

This compound begins to disappear at about the same time when the hydration of tricalcium silicate starts. Consequently, the behaviour of cement pastes was studied in which the admixture of zinc oxide was replaced by the equivalent amount of zincate. From Figure 11 it is seen that the retardation caused by calcium hydroxo zincate is very short as compared with the effect of zinc oxide.

Figure 11

In a last diagram (Figure 12) the influence of the various admixtures on the reactions of added gypsum is represented. In the presence of calcium zincate, gypsum reacts with the aluminates and ferrites in approximately the same way as if no admixture were present. Lead and zinc oxide, however, retard the combination of about half of the SO_3 for several days.

Figure 12

By admixture of calcium zincate, in spite of a slight retardation of setting, the initial and final strengths are markedly increased.

A satisfactory explanation for the mechanism of retardation by lead and zinc is not yet to be given. The retardation is caused obviously by a blocking up of the C_3S surface. With the beginning of the hydration period, the retarding elements probably enter the crystal lattice of the calcium silicate hydrates. But it is still obscure which factor causes the hydration to start.

	A S T M			ASTM modified			Classification
	N	$\bar{x}$	2 s	N	$\bar{x}$	2 s	
PN	3	36,3 ±	3,7	6	34,8 ±	3,9	35 ± 5
PHR	3	36,6 ±	8,2	5	41,5 ±	8,5	45 ± 5
PDR	2	6o,6 ±	8,2	6	57,8 ±	12,2	55 ± 5
HFN	3	31,7 ±	14,9	3	23,8 ±	4,1	25 ± 5
HFHR	4	24,1 ±	12,1	3	3o,2 ±	4,4	3o ± 5
HFDR	2	46,9 ±	7,0	3	49,0 ±	6,5	5o ± 5
	17	±	10,5	26	±	8,0	

Table 1: Comparison of original and modified ASTM heat of hydration methods

P = Portland cement HF = slag cement

N = normal HR = high strength DR = rapid hardening

The original values are transformed in terms of statistics.

About 95 % of measured values are lying in the range $\bar{x} \pm 2$ s

Table 2 Compositions of solutions extracted from cement pastes containing calcium chloride.

Extract No.	Cement Alkalies (%) K_2O	Cement Alkalies (%) Na_2O	W/C	$CaCl_2 \cdot 2H_2O$ Added	Approximate Time After H_2O Contact	Solution Composition (moles per liter) $(K^+)_2$	$(Na^+)_2$	$(Cl^-)_2$	Ca^{++}	SO_4^{--}	$(OH^-)_2$	CO_3^{--}
1	0.91	0.25	0.50	2%	7-10 Min.	0.129	0.011	0.285	0.184	0.013	0.023	0.003
2	.22	.11	.50	1%	7-10 Min.	.009	.002	.137	.166	.012	.022	.003
3a	.52	.07	.50	1%	7-15 Min.	.049	.005	.126	.115	.014	.019	.005
3b	.52	.07	.50	2%	7-15 Min.	.049	.005	.265	.241	.012	.017	.005
4a	.03	.52	.50	1%	7-15 Min.	.001	.016	.126	.145	.012	.020	.002
4b	.03	.52	.50	2%	7-15 Min.	.001	.016	.265	.275	.011	.020	.003

Table 3 Comparison of equilibrium and analytical ion products in cement extracts.

Extract No.	Total $(K^+)_2 + (Na^+)_2$ moles/liter	$(Cl^-)_2$ moles/liter	Estimated Equilibrium Concentrations moles/liter Ca^{++}	SO_4^{--}	$(OH^-)_2$	$(Ca^{++})(SO_4^{--})$ Equilibrium	$(Ca^{++})(SO_4^{--})$ Analytical	$(Ca^{++})(OH^-)^2$ Equilibrium	$(Ca^{++})(OH^-)^2$ Analytical	Conclusions
1	0.140	0.285	0.180	0.013	0.014	234×10^{-5}	239×10^{-5}	141×10^{-6}	389×10^{-6}	Approximately saturated with $CaSO_4 \cdot 2H_2O$. Highly supersaturated with $Ca(OH)_2$.
2	.011	.137	.152	.009	.016	137×10^{-5}	199×10^{-5}	156×10^{-6}	321×10^{-6}	Moderately supersaturated with $CaSO_4 \cdot 2H_2O$. Highly supersaturated with $Ca(OH)_2$.
3a	.054	.126	.096	.012	.016	115×10^{-5}	161×10^{-5}	98×10^{-6}	166×10^{-6}	Somewhat supersaturated with $CaSO_4 \cdot 2H_2O$. Moderately supersaturated with $Ca(OH)_2$.
3b	.054	.265	.236	.009	.014	212×10^{-5}	289×10^{-5}	185×10^{-6}	279×10^{-6}	Somewhat supersaturated with $CaSO_4 \cdot 2H_2O$. Moderately supersaturated with $Ca(OH)_2$.
4a	.017	.126	.132	.009	.016	119×10^{-5}	174×10^{-5}	135×10^{-6}	232×10^{-6}	Moderately supersaturated with $CaSO_4 \cdot 2H_2O$. Moderately supersaturated with $Ca(OH)_2$.
4b	.017	.265	.272	.009	.014	245×10^{-5}	303×10^{-5}	213×10^{-6}	440×10^{-6}	Somewhat supersaturated with $CaSO_4 \cdot 2H_2O$. Highly supersaturated with $Ca(OH)_2$.

cement sample	1 day	3 day	7 day	28 day
alkali = 0.57 %	660	1750	2670	4250
no alkali	160	300	2150	3650
no alkali + KOH	540	1410	2410	3830

Table 4: Effect of the absence of alkali in Portland cement on compressive strength (psi)

	Cement % Na_2O Equiv.		% Expansion			
	Total	Water-Sol.	1 mo.	3 mo.	6 mo.	1 yr.
Reactive Dolomite	.83	.48	.026	.040	.054	.068
	.83	.32	.024	.037	.049	.062
	.84	.14	.018	.028	.034	.048
Watertown Sand	.83	.48	.013	.022	.028	.036
	.83	.32	.008	.014	.015	.022
	.84	.14	.002	.005	.005	.010

Table 5: Effect of water soluble alkali on expansion of alkali - reactive aggregates

Fig.1 : Strength development in Portland cement with different C_3A content

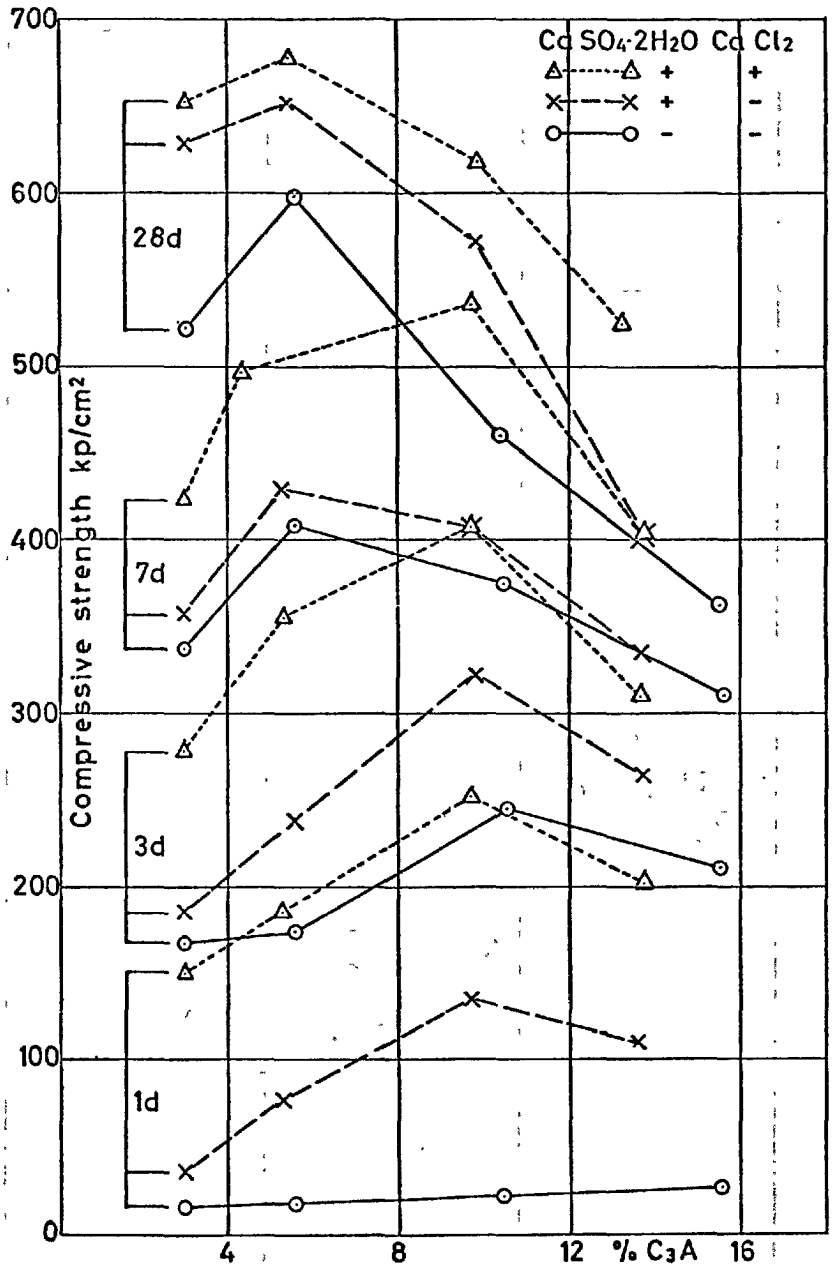

Fig.2 : Correlation between specific surface (nitrogen adsorption) and compressive strength in the cement series containing gypsum

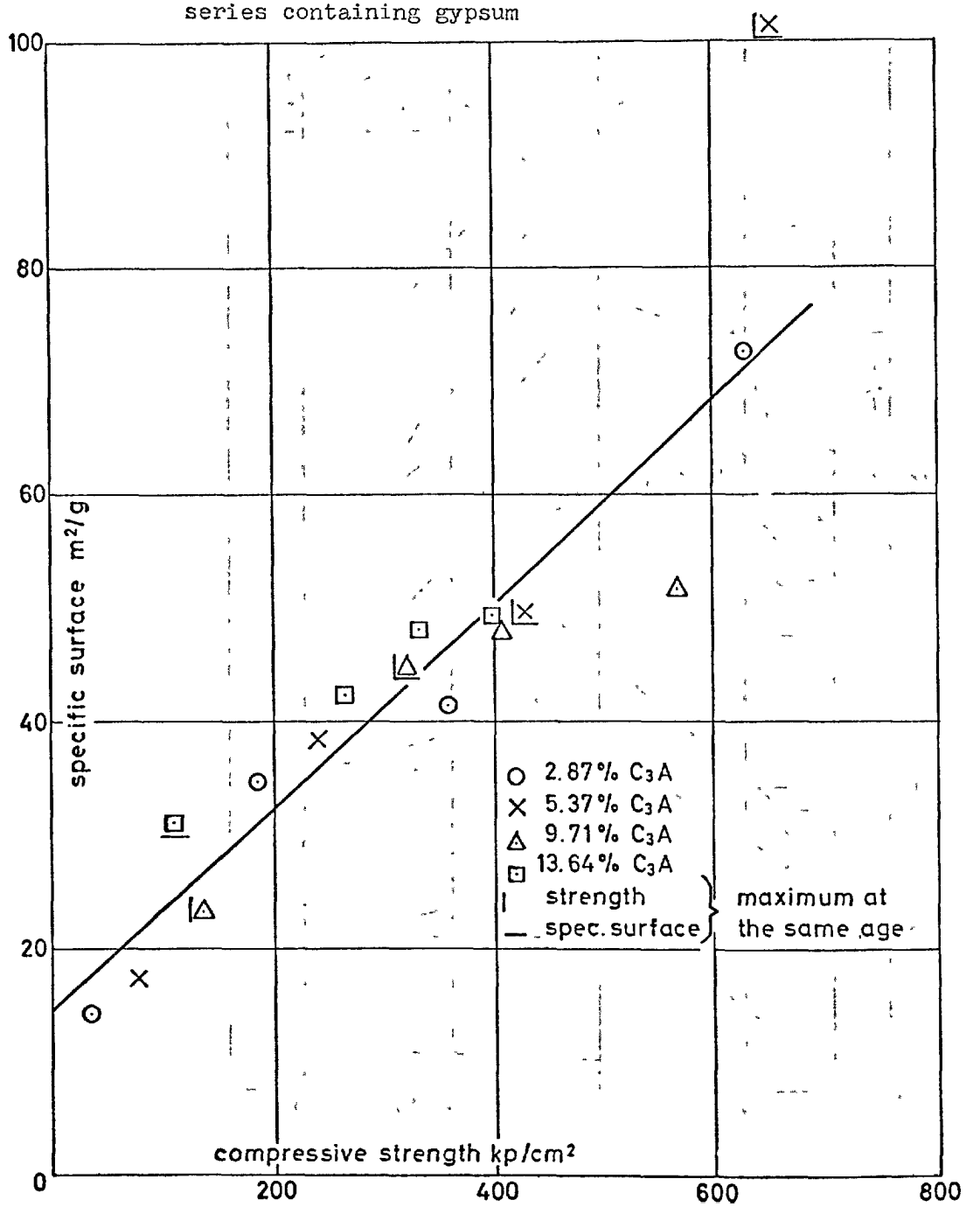

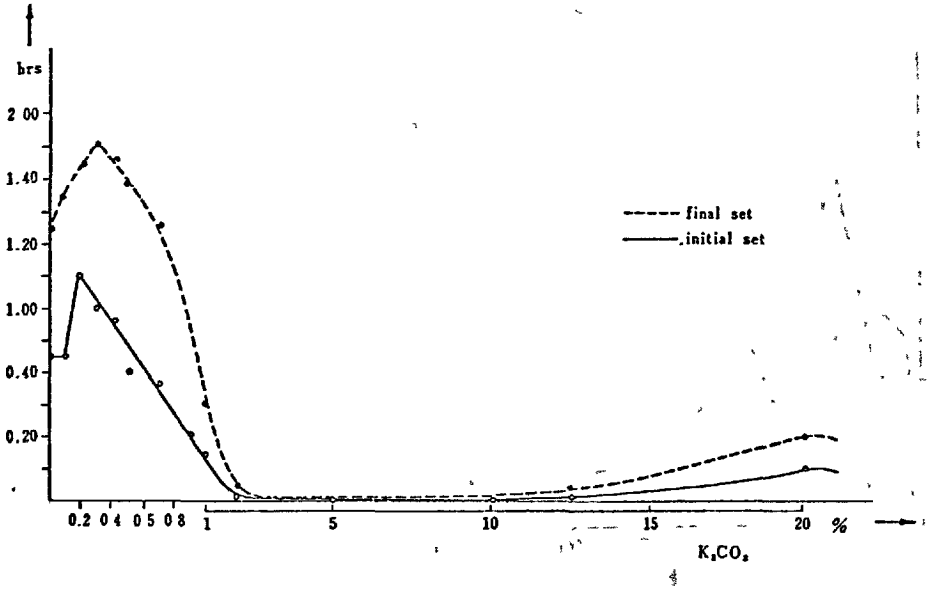

Fig.3 : Setting time of Portland cement depending upon the amount of K_2CO_3 added

Fig.4 : Development of temperature in a Portland cement paste (w/c = 0,3) at different amounts of K_2CO_3 addition

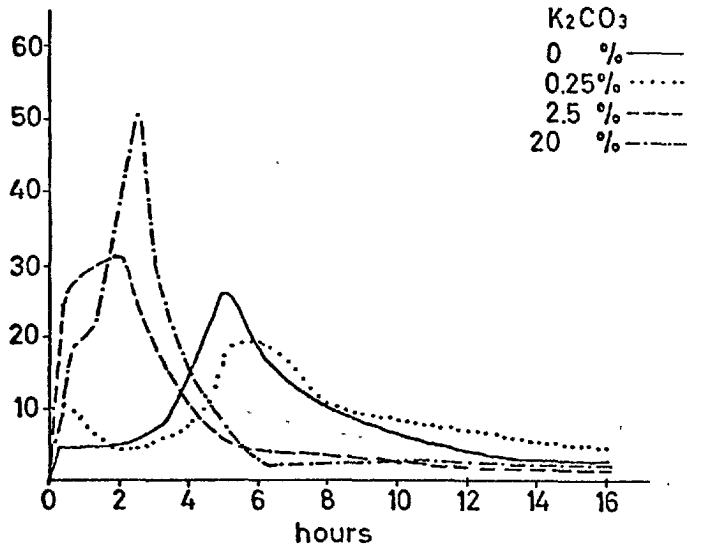

Fig.5 : Development of early strength in mortars of Portland cement at different amounts of K_2CO_3 addition

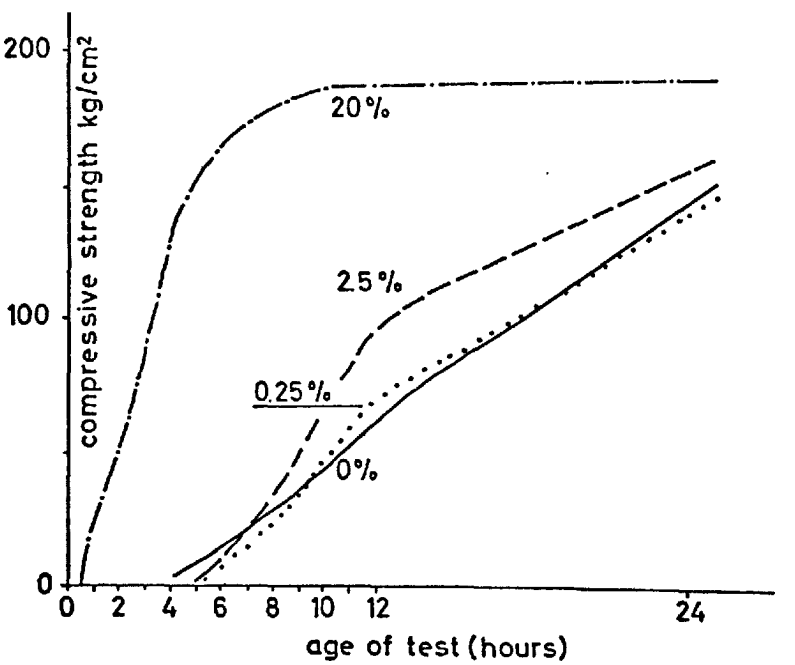

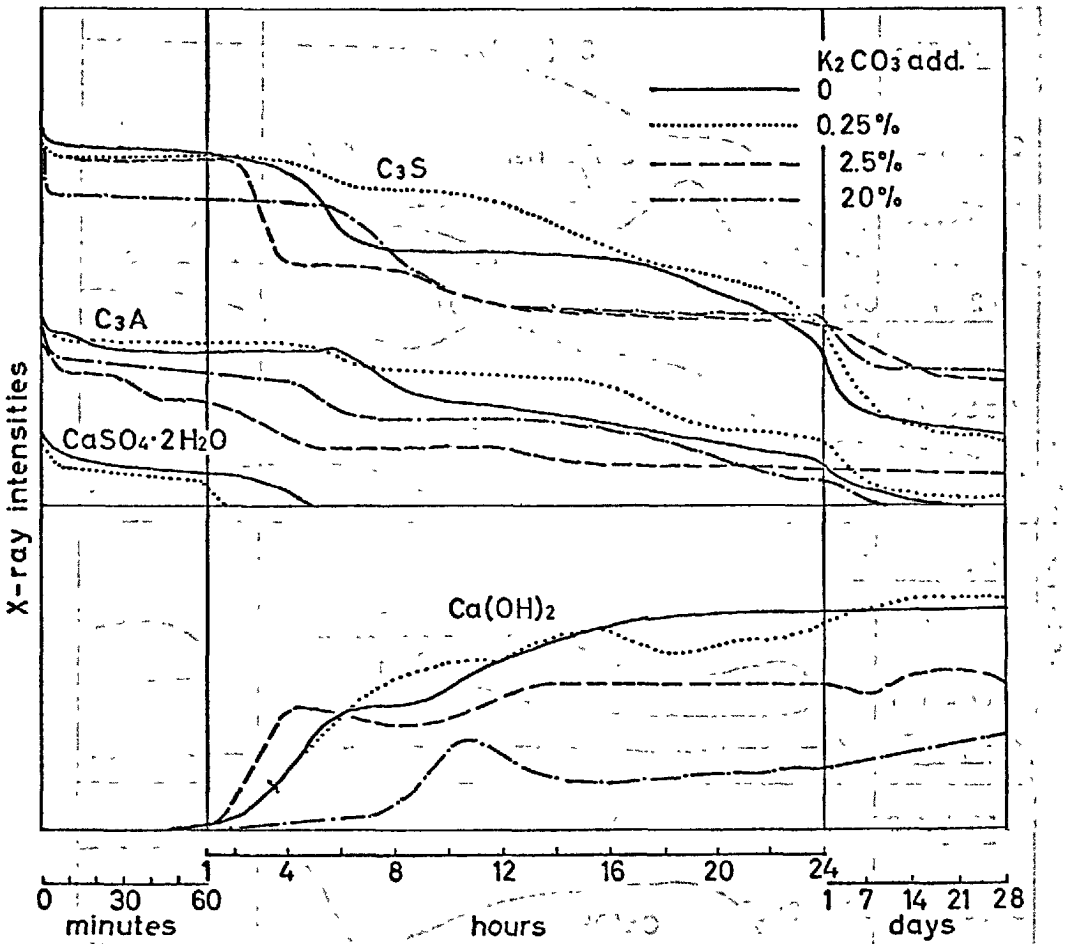

Figure 6: Comparative curves on the influence of various additions of K_2CO_3 on decrease of C_3S, C_3A and gypsum and increase of $Ca(OH)_2$

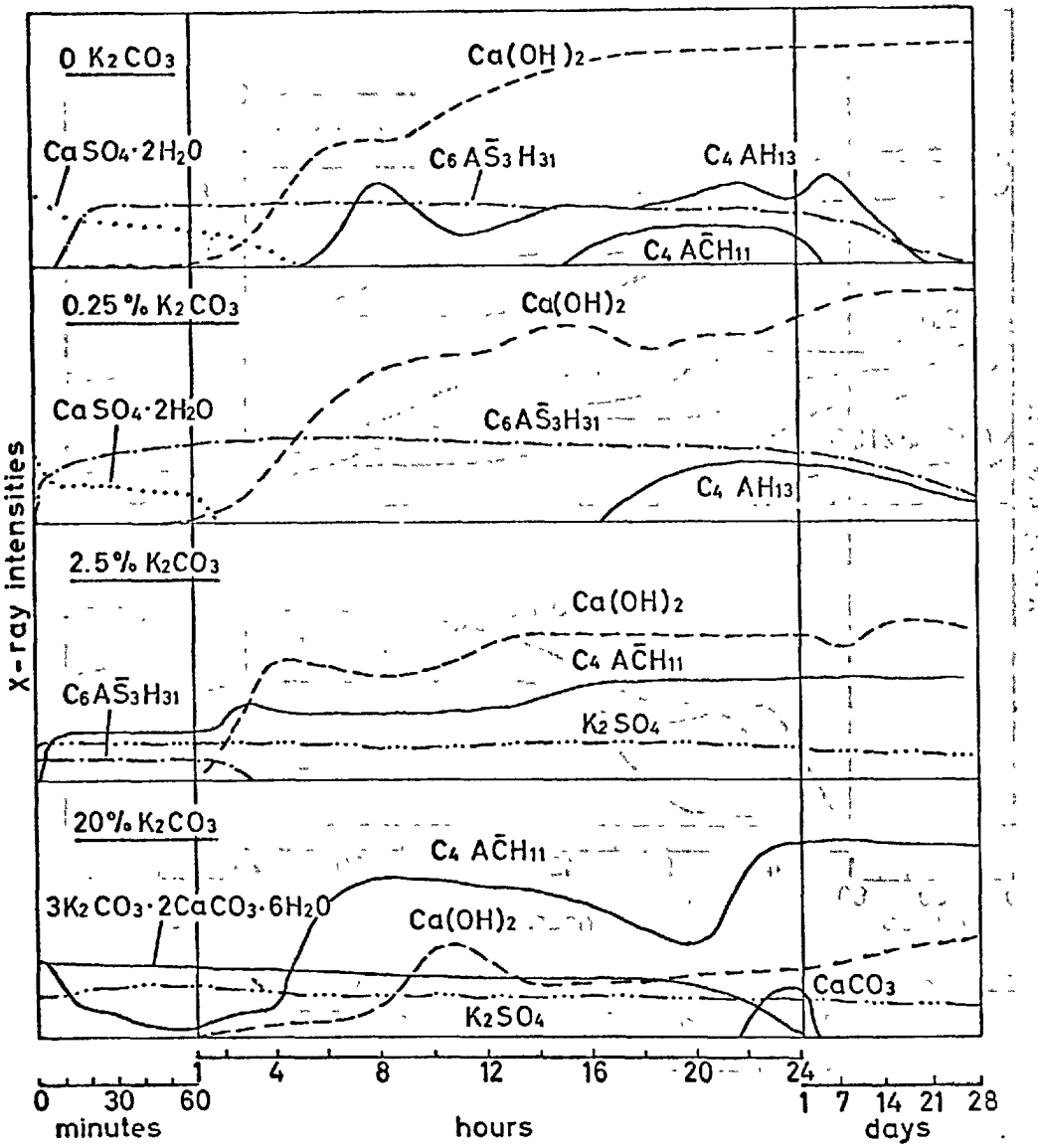

Figure 7: Hydration products of Portland cement pastes (w/c = 0.3) with various additions of K_2CO_3.

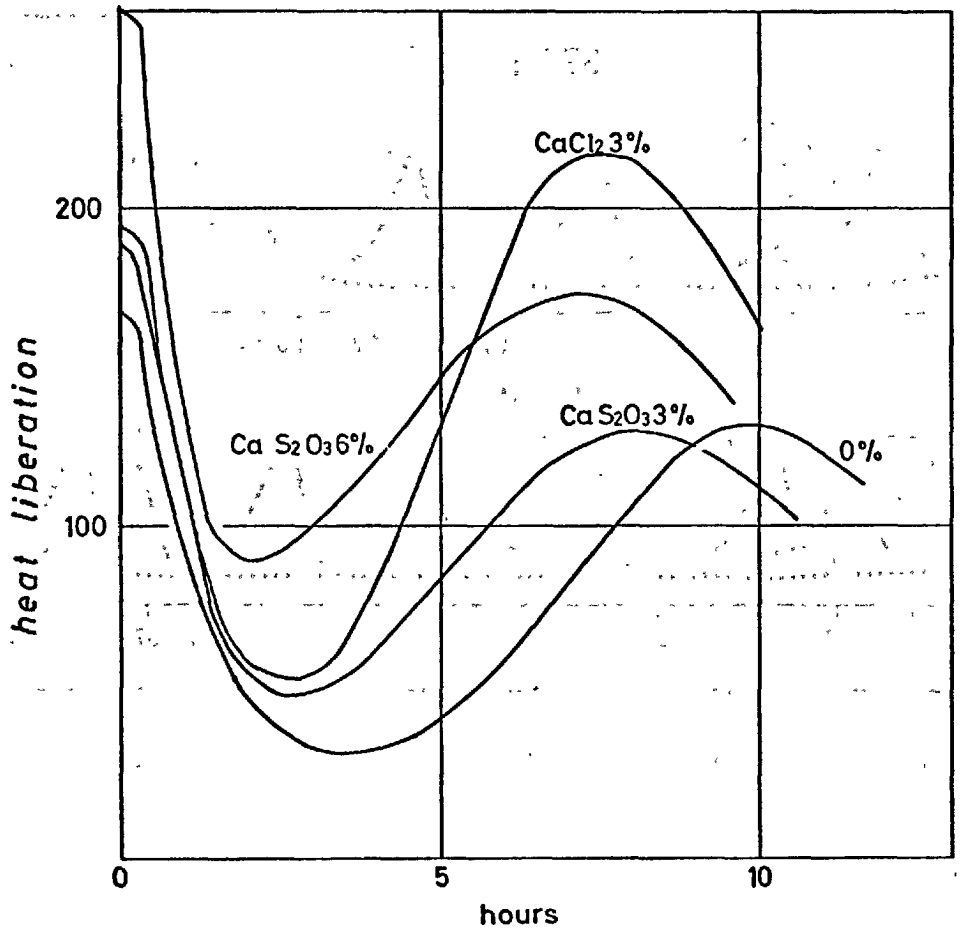

Figure 8: Influence of calcium chloride and calcium thiosulphate on the heat liberation of a Portland cement paste (w/c = 1.6)

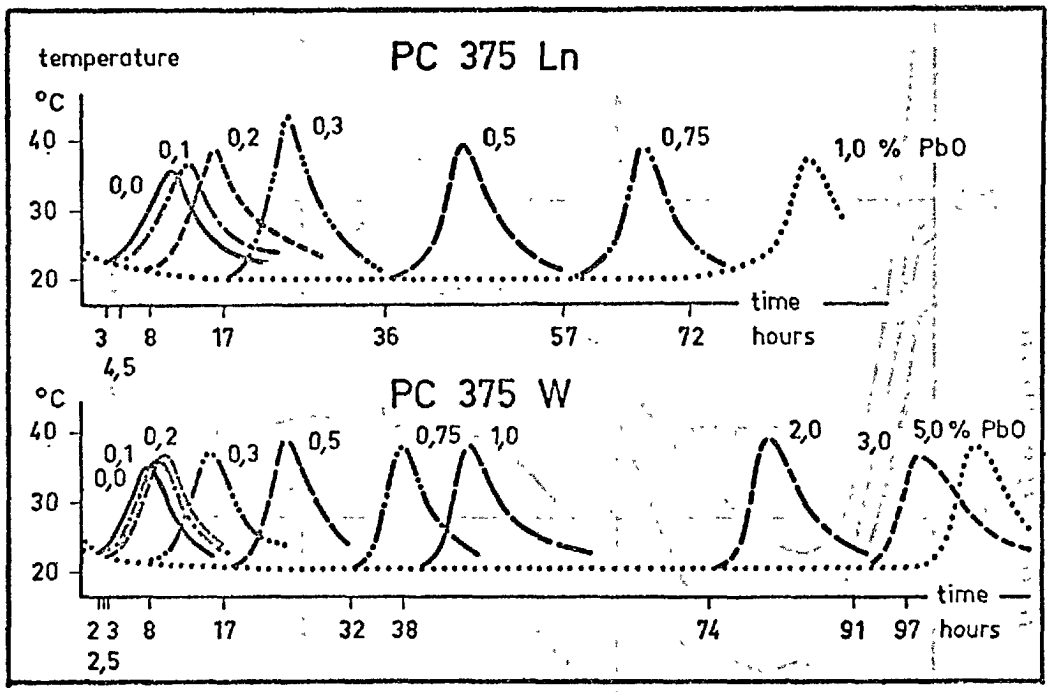

Figure 9: Influence of various admixtures of lead oxide on the setting time of two Portland cement pastes (w/c = 0.35)

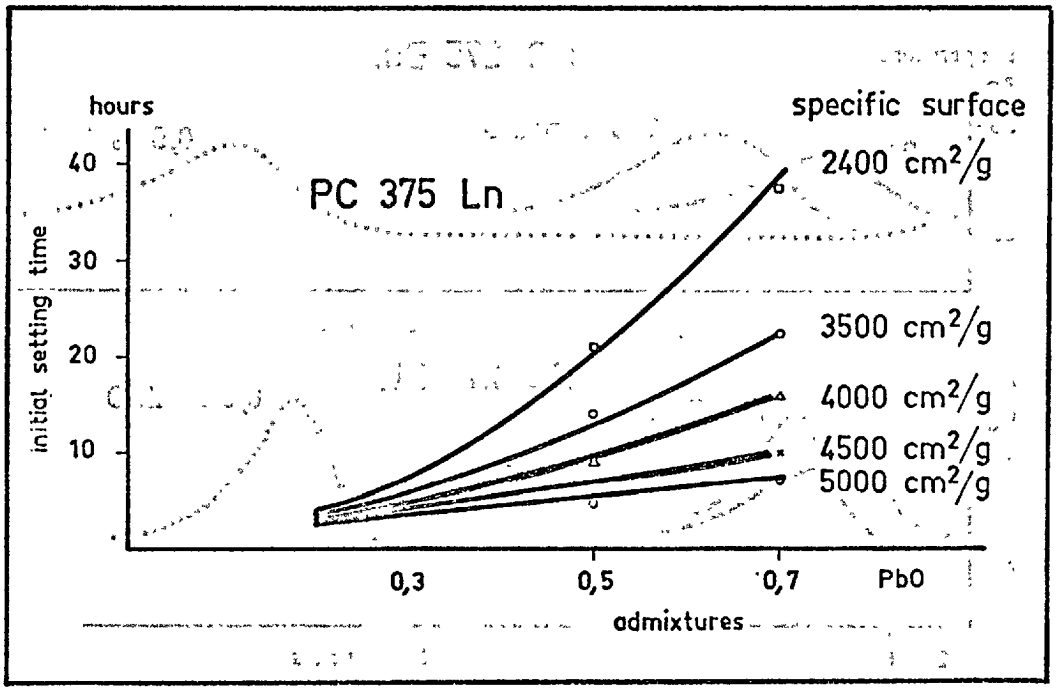

Figure 10: Influence of cement fineness on the retarding effect of lead oxide

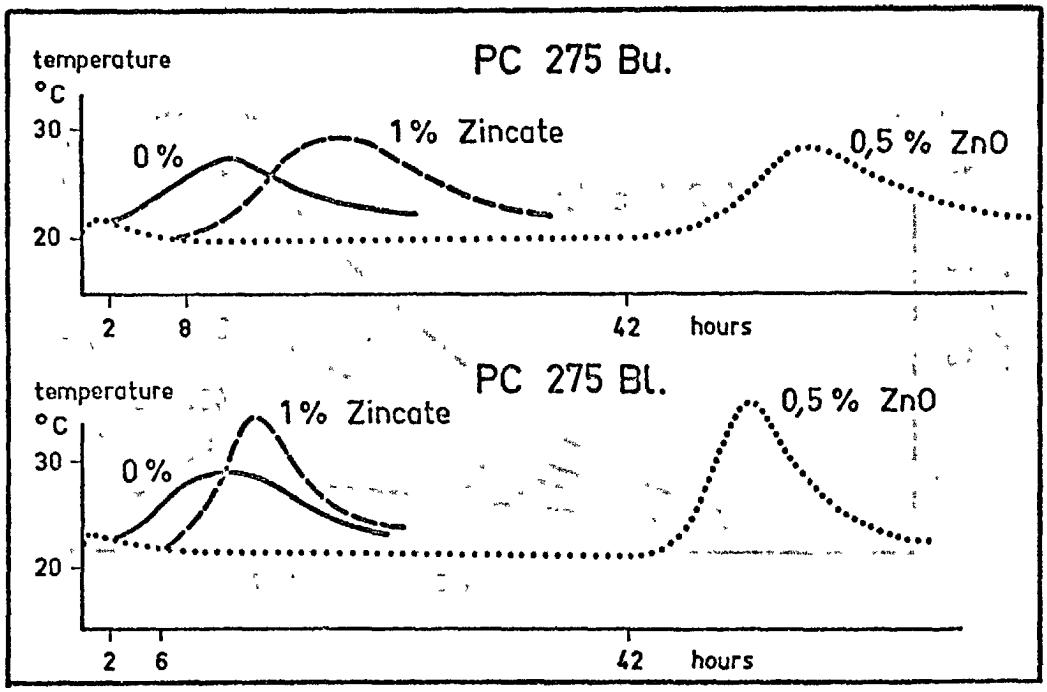

Figure 11: Influence of calcium hydroxo zincate on the setting of Portland cement pastes

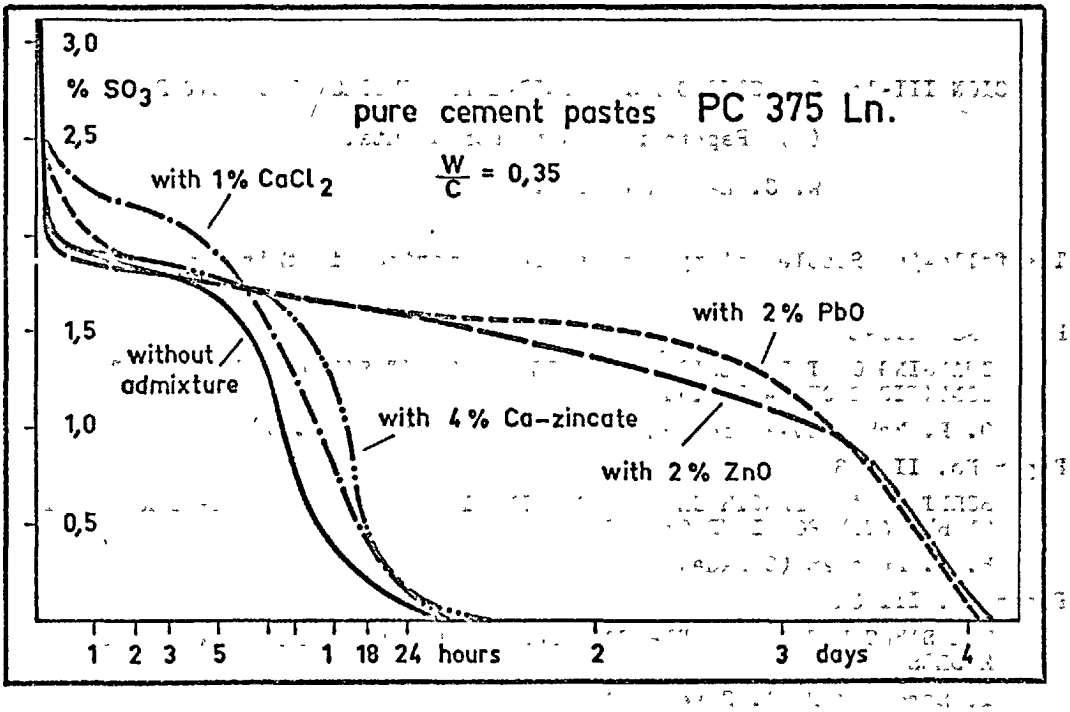

Figure 12: Fixation of SO_3 during hydration in presence of lead and zinc compounds

GENERAL REPORT
OF
SESSION III-1: STRUCTURES AND PHYSICAL PROPERTIES OF CEMENT PASTE

(a) Papers regarding Fundamental

W. C. Hansen (U.S.A.)

The following Supplementary Papers are summarized in this report.

Paper No. III-8

CHANGING OF THE SPECIFIC SURFACE OF CEMENT STONE IN DIFFERENT CONDITIONS OF HARDENING

O. P. Mchedlov-Petrosyan & D. A. Uginčius (U.S.S.R.)

Paper No. III-23

SORPTION AND LENGTH-CHANGE SCANNING ISOTHERMS OF METHANOL AND WATER ON HYDRATED PORTLAND CEMENT

R. F. Feldman (Canada)

Paper No. III-34

THE STRUCTURE OF CEMENT-STONE AND THE USE OF COMPACTS AS STRUCTURAL MODELS

I. Soroka & P. J. Sereda (Canada)

Paper No. III-46

MOLECULAR SIEVE EFFECT IN CONCRETE

R. H. Mills (Canada)

Paper No. III-50

A STATISTICAL STUDY OF THE EFFECTS OF TRACE ELEMENTS ON THE PROPERTIES OF PORTLAND CEMENTS

R. L. Blaine (U.S.A.)

Paper No. III-71

CEMENT PASTE SHRINKAGE--RELATIONSHIPS TO HYDRATION, YOUNG'S MODULUS AND CONCRETE SHRINKAGE

H. Roper (Australia)

Paper No. III-115

ABOUT THE SOME BASIC TENDENCY OF THEORY HARDNESS AND FORMING STRENGTH PROPERTIES CEMENT STONE AND CONCRETE

I. P. Vyrodov (U.S.S.R.)

Paper No. III-125

ELECTRON MICROSCOPIC INVESTIGATIONS ABOUT THE RELATIONS BETWEEN STRUCTURE AND STRENGTH OF HARDENED CEMENT PASTE

W. Richartz (West Germany)

"CHANGING OF THE SPECIFIC SURFACE OF CEMENT-STONE IN DIFFERENT CONDITIONS OF HARDENING" O. P. Mchedlov-Petrosian & D. A. Uginčius.

These investigators studied the development of the specific surface of cement-stone under different temperatures of curing and in the presence of chemical additives. The surface was calculated in accordance with the BET theory. Fig. 3 of the paper shows the influence of water-cement ratio on the surface obtained with a Type II cement. Curves 1, 2, 3 and 4 represent respectively the surfaces at 1, 3, 7 and 28 days at 20°C.

Fig. 4 shows the influence of heating on a Type I cement. Specimens were heated in closed molds at the rate of 40°C per hour. Curves 1, 2, and 3 respectively represent the data for temperatures of 40, 60 and 90°C. After the temperature reached the prescribed value, the specimens were maintained at that temperature for from 1 to 9 hours and then at 20°C for 28 days. These data show that the surfaces of the specimens cured at 40 were much greater than were those of the specimens cured at 60 and 90. Also that the surfaces generally decreased with time after the initial heating for 1 hour and became constant at 3 hours of heating at 40, at 5 hours at 60 and at 6 hours at 90. The authors point out that heating accelerates the rate of hydrolysis and solution but causes the formation of dense hydrate films on the cement grains which retard the diffusion of water and formation of new nuclei. All of these result in a gel with a coarser texture and less specific volume.

Fig. V represents data for a Type III cement. Curve 1 represents

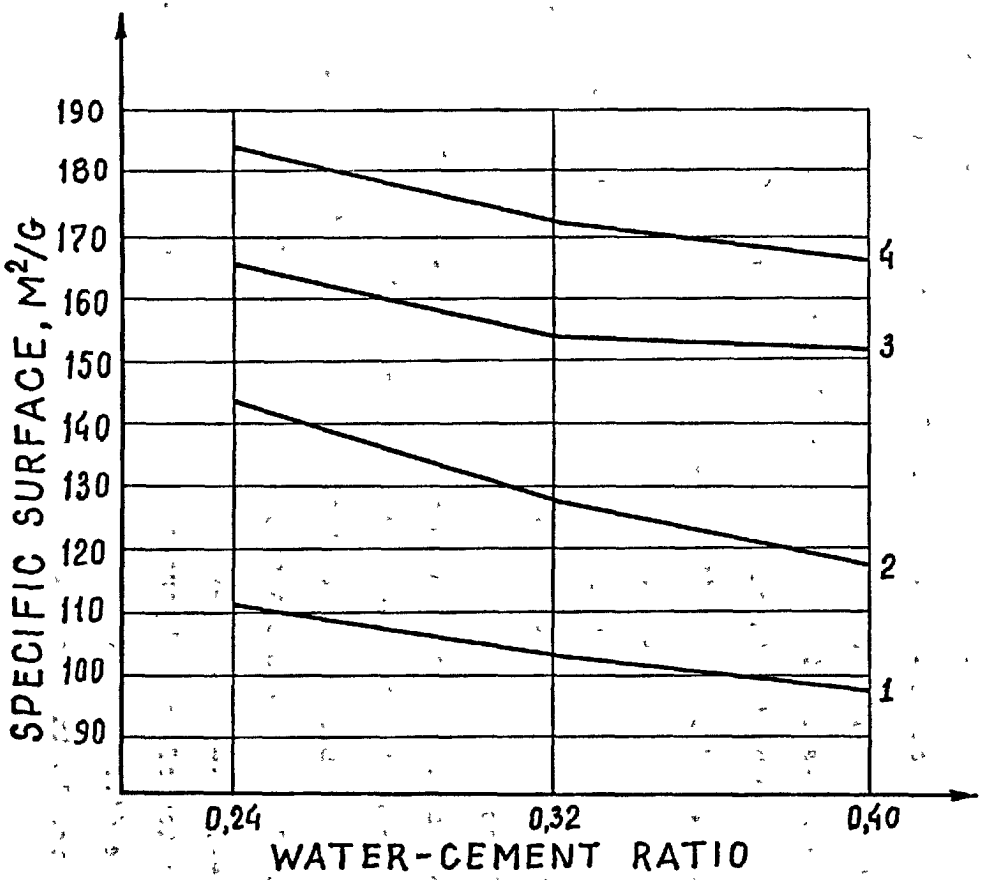

FIGURE 3 (by Otar P. Mechedlov-Petrosyan and Dmitrijs A. Uginčius)

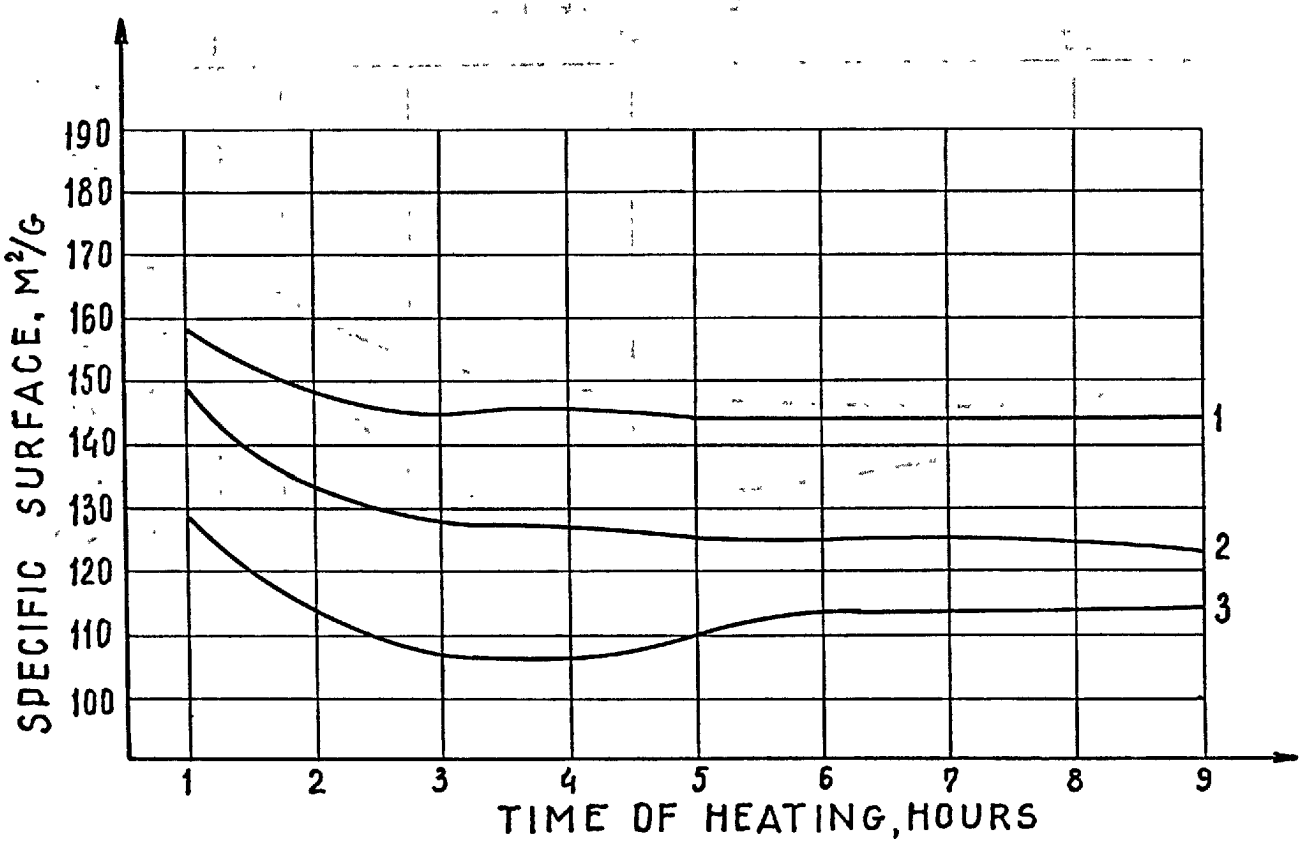

FIGURE 4 (by Otar P. Mechedlov-Petrosyan and Dmitrijs A. Uginčius)

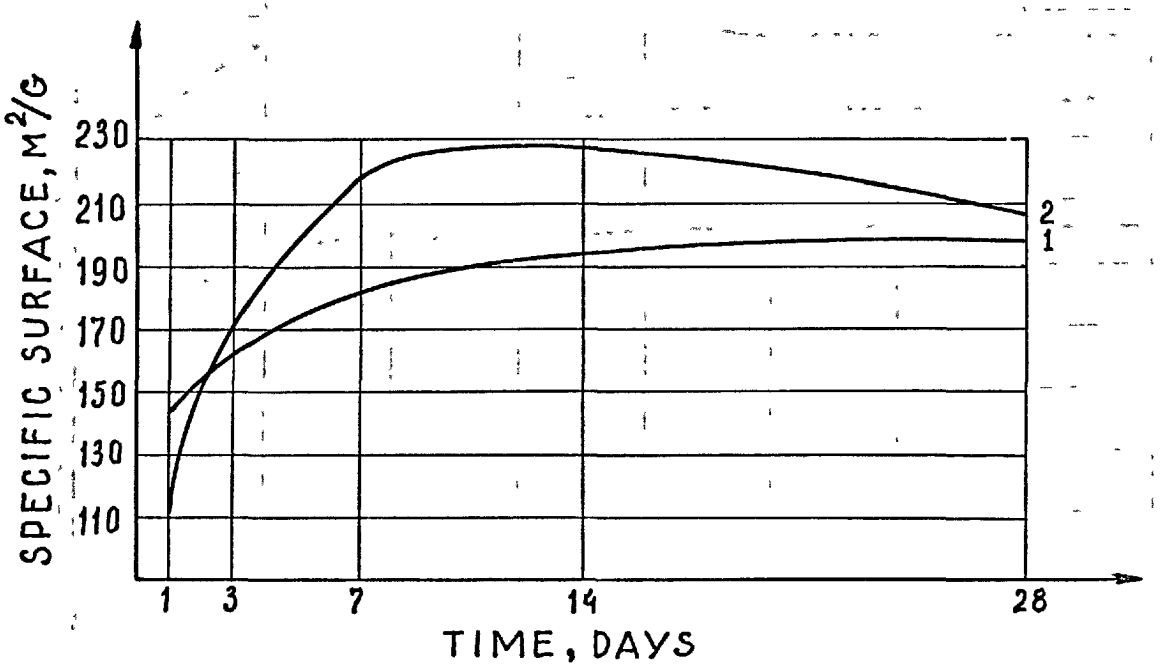

FIGURE 5 (by Otar P. Mechedlov-Petrosyan and Dmitrijs A. Uginčius)

the control sample cured at 20°C. Curve 2 a specimen which immediately after molding was placed in a freezer at minus 20° for 1 day and which after demolding was cured at 20°. Surface measurements were begun after 1 day at 20°.

The author points out that the solubility of the silicate minerals decreases with decreasing temperature but that the probability of the appearance of more basic hydrosilicates increase because the solubility of calciumhydroxide increases. These favorable conditions created in the primary cooling period greatly influences the hardening of the paste at normal temperatures.

"SORPTION AND LENGTH-CHANGE SCANNING ISOTHERMS OF METHANOL AND WATER ON HYDRATED PORTLAND CEMENT" R. F. Feldman

Detailed studies of sorption and desorption isotherms led to the conclusion that the surface area of hydrated portland cement was considerably less than the value of approximately 200m^2/g obtained from determinations by the BET equation for adsorbed water. This is based on the fact that the BET equation, which is valid for the low pressure region of the adsorption isotherm, implicitly assumes reversibility and a constant surface area and the fact that detailed studies of the adsorption and desorption isotherms at low pressures show that irreversible changes occur when hydrated portland cement is dried at low vapor pressures.

The author made detailed studies, by means of scanning loops, of hydrated cement and compacts of bottle-hydrated cement. His Fig. 1 shows weight changes vs vapor pressure for I. compact degassed in a vacuum at 80°C and II. compact degassed in a vacuum at 96°C. The scanning loops show that the isotherm is irreversible even at as

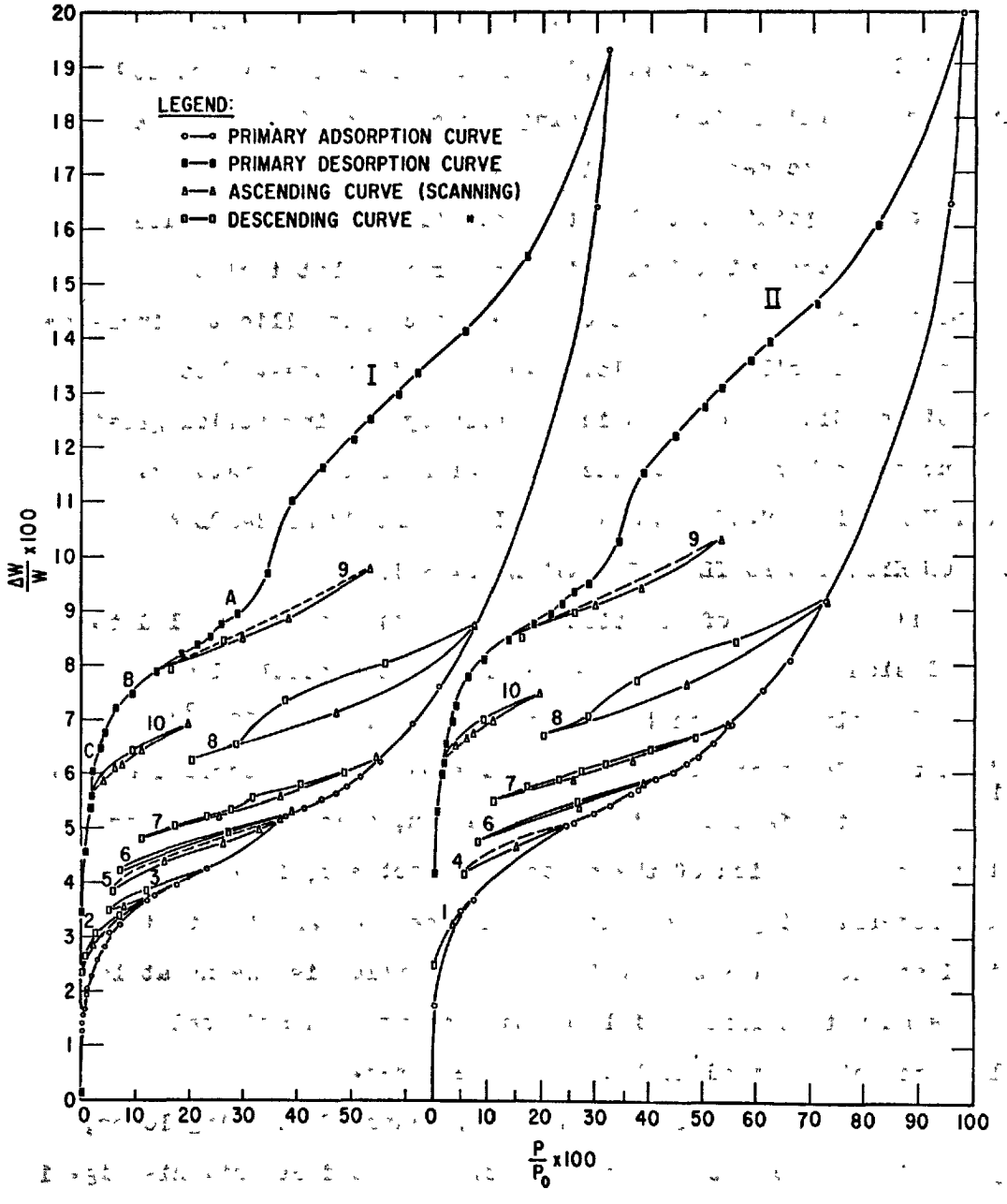

FIGURE 1 (by Rolf F. Feldman)

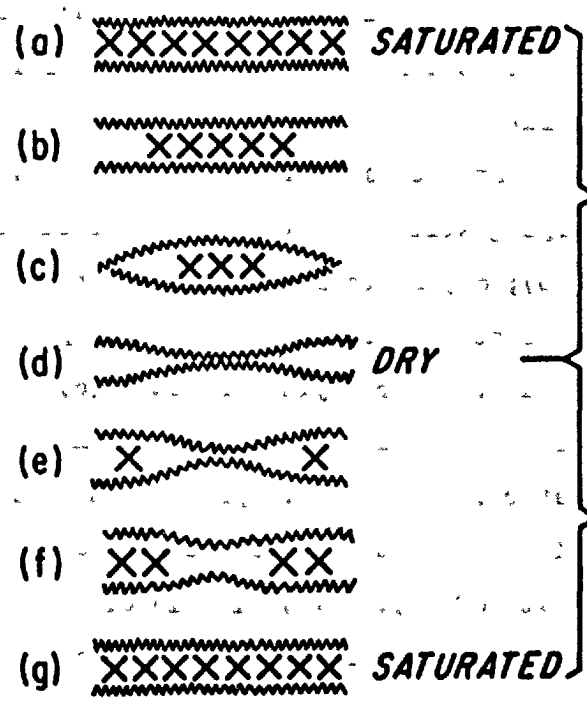

FIGURE 7 (by Rolf F. Feldman)

low a p/p_o of 0.05 and that much of the irreversibly sorbed water is sorbed below p/p_o of 0.35. Calculations based on the scanning loops lead to the conclusion that irreversibly sorbed water is interlayer water in tobermorite.

The process of exit and entry of interlayer water is illustrated in his Fig. 7. Initially drying will take place from the edges with little contraction (a) to (b); drying to state (c) will provide some collpase and large contraction; drying at the edges probably occurs below p/p_o of 0.30 and stronger drying of state (c) below p/p_o of 0.07. Final removal of water in the middle will not occur above p/p_o of 0.09. This water is believed to provide the main bracing for a higher rigidity and removal decreases the modulus as his results show. The state of drying (d) also involves possible reorientation of the plates to produce irreversible contraction. Resorption occurs at the edges, states (c) and (f) being initiated by physical adsorption and resultant surface free energy change on the external surfaces.

The author believes that the surface areas based on nitrogen adsorption probably are nearer correct than those based on water adsorption.

"ON SOME ASPECTS OF THEORY OF SOLIDIFICATION AND STRENGTH FORMATION OF CEMENT-STONE AND CONCRETE" I. P. Vyrodov.

The author divides his paper into three chapters as follows:

I. On the possibility of applying the main principles of molecular physics and thermodynamics for the study of the character of change of mineral binders.

II. Role of diffusion kinetics of reactions in the process of hardening of mineral binders.

III. On some principal aspects of the theory of solidification and strength formation of cement-stone and concrete.

Time does not permit any meaningful review of the highly mathematical material covered in chapters I and II. In chapter III the author points out that (a) some foreign workers consider the modern point of view of Soviet workers to be that of Rebinder and coworkers and (b) that some foreign and Soviet scientitists also share the false impression that Rebinder and coworkers continue the main hypothesis of Baikov in their through-solution theory of the solidification of mineral binders. The theory of Baikov was based on a topochemical mechanism and was divided into three periods.

1. Dissolving of the original mineral binder with the formation of a supersaturated solution.

2. Colloidation, that is the formation by chemical reaction on the surfaces of the binder the small particles of the final product sponsoring the formation of high supersaturation.

3. Crystallization of amorphous gels.

According to the author these concepts seem to be accepted by many Soviet and foreign scientists except for the main point of Baikov's theory regarding the solidification of mineral binders. According to Baikov solidification occurred primarily because of the topochemical reactions of step 2 and not from the crystallization which occurs in step 3. The author restates the three steps of the Baikov theory as follows:

1. Dissolving of hydrates formed by the interaction of cement grains with water.

2. Formation of solid crystalline products or semicrystalline products

on the surfaces of the cement grains after the liquid becomes saturated.

3. Crystallization of the semicrystalline products.

These processes may occur simultaneously. The author has found from X-ray studies that crystalline products are formed at the very beginning of the reaction with water. However the topochemical reactions of step 2 are responsible for the solidification and development of strength.

"CEMENT PASTE SHRINKAGE-RELATIONSHIPS TO HYDRATION, YOUNG'S MODULUS AND CONCRETE SHRINKAGE" Harold Roper.

The paper presents paste shrinkage, hydration and Youngs's modulus data for sixteen cements. It also presents shrinkage data for concrete specimens

Linear regression analyses relating paste shrinkage at constant w/c to cement composition were calculated using an equation of the form

$$dl = a(C_3S) + b(C_2S) + c(C_3A) + d(C_4AF) + e(SO_3)$$

where dl = paste shrinkage.

The only regression coefficient which was consistently significant was that for C_3A. The most significant equation for predicting shrinkage is of the form,

$$1/dl = f - g(C_3A)$$

The constant f remains the same for all w/c ratios, whereas the coefficient g changes systematically. Up to 80 per cent of the variations of paste shrinkage is explicable by the variation in C_3A. It was concluded from the results of all these analyses that the role of C_3A was dominant in explaining the variance in shrinkage.

It was considered that the effects of differences in hydration rates were influencing the shrinkage results significantly hence the non-evaporable water contents of the various pastes were determined. By means of an emperical approach the following equation was found to apply for each individual cement.

$$1/dl = a - b(W_n)$$

dl is the paste shrinkage expressed as a percentage, W_n is the non-evaporable water and a and b are constants. "a" in physical terms is interpreted as representing the reciprocal of the percentage shrinkage which an unhydrated cement compact undergoes from a saturated state to the experimental drying condition. Treating the results as a series of endependent variables gives the following equation.

$$1/dl = 10.844 - 37.035W_n$$

Including Young's modulus gives the following equation.

$$1/dl = 7.620 - 27.301W_n + 0.485E$$

Regression analyses were conducted on data for paste shrinkage and concrete shrinkage for fifteen cements. Paste shrinkage at 28 days was used. The correlation coefficients for 13 degrees of freedom were 0.962; 0.966; 0.886 and 0.841 for shrinkages of concrete at 7, 28, 90 and 365 days. A value of "r" greater than 0.760 indicates a significant relationship at the 0.001 level. It is concluded that highly significant correlation exists between the paste and concrete shrinkage even for drying periods up to one year.

"THE STRUCTURE OF CEMENT-STONE AND THE USE OF COMPACTS AS STRUCTURAL MODELS", I. Soroka and P. J. Serada.

This study was undertaken to obtain data on the structure of

cement-stone, particularly with regards the nature of the interparticle bonds. The specimens were discs of the following.

I. Cement pastes porosity 73 to 98 per cent.

II. Compacted cement paste porosity 25 to 60 per cent.

III. Compacts of bottle-hydrated pastes porosity 20 to 55 per cent.

Some believe that the limited swelling of cement-stone in water is evidence for the existence of some chemical (primary) bonds between the gel particles although they believe that secondary bonds account for most of the strength. The authors interpret primary and secondary bonds as follows: Chemical bonds between particles are solid to solid contacts similiar to that of a grain boundary in a polycrystalline material where some atoms approach the spacing arrangement in the crystal. Secondary bonds assume that adsorbed water is a constituent part of the interparticle bond; hence the general term of van der Waals forces is considered appropriate.

The authors' Fig. 2 is a plot of modulus of elasticity vs porosity together with the regression lines calculated to fit the data. It is seen that the modulus vs porosity relation is the same for the cement paste as for cement paste compacted from a porosity range of 40 to 70 per cent to a porosity range of 25 to 60 per cent. This is taken as strong evidence for the absence of chemical bonds because it is likely that these bonds would be broken (if they were present) when the pore volume is reduced by half during compaction. Also the fact that the values for the modulus of the compacts of bottle-hydrated cement fit so closely to those of the paste and compacted paste lends further support to the idea that the system has none or very few chemical bonds. The results of their Fig. 3 in which hardness is plotted against porosity lead to the same conclusion.

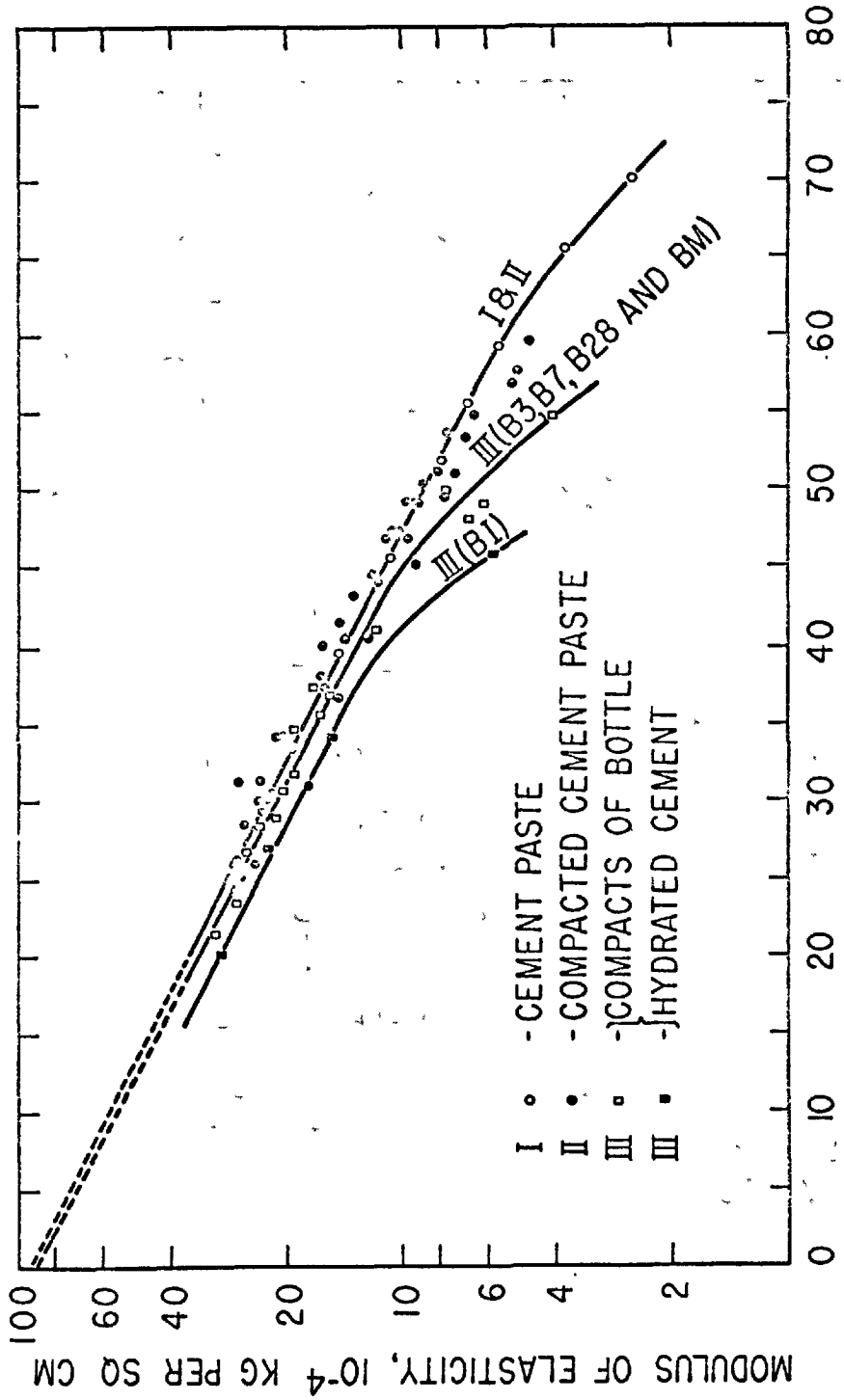

FIGURE 2 (by I. Soroka and P. J. Sereda)
MODULUS OF ELASTICITY VS POROSITY FOR THE CEMENT SYSTEMS

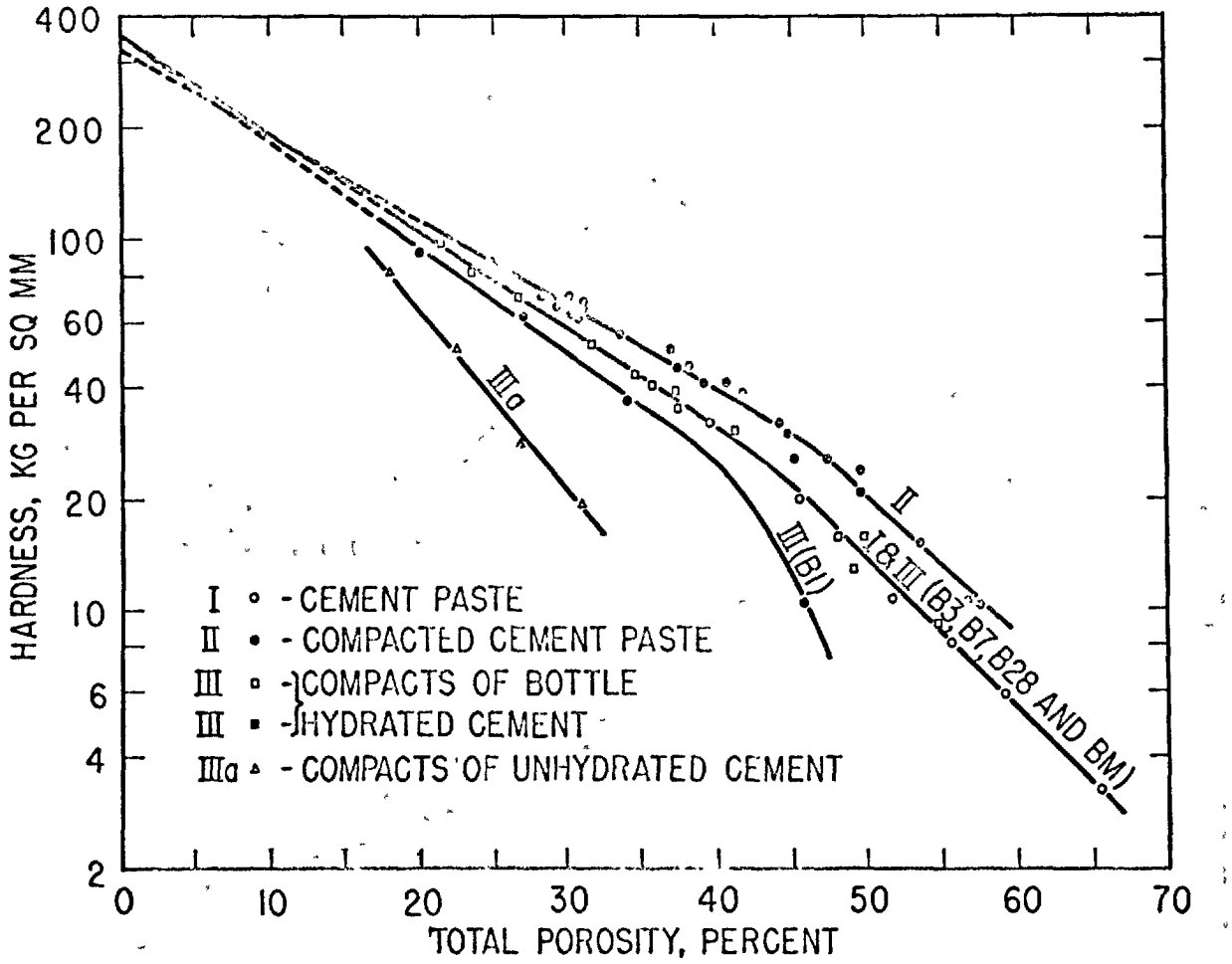

FIGURE 3 (by I. Soroka and P. J. Sereda)
HARDNESS VS POROSITY FOR THE CEMENT SYSTEMS

These results lead the authors to the conclusion that the strength of cement-stone is mainly derived from a particular type of interparticle bond. It is further concluded that this bond is a solid to solid contact resulting from the bringing together of surfaces and that it is essentially the same in compacts as in cement pastes.

"MOLECULAR SIEVE EFFECT IN CONCRETE." R. H. Mills

Investigators have shown that hardened cement pastes act as molecular sieves in that the quantity of fluid adsorbed is a function of the size of the molecules of the fluid. Water is capable of greater penetration than other fluids but it is not capable of complete penetration of the finer pores.

Oven dried specimens were vacuum saturated with an organic fluid, such as kerosene, and then resaturated with water. A "k" factor was calculated by the equation $k = (V_w - V_f)/V_w$ in which V_w and V_f represent respectively the volumes of water and organic fluid at saturation. This ratio represents the fraction of water which has access to space which excludes the organic fluid. To a first approximation, kV_w is a measure of the pore water strongly adsorbed in the micro-cellular structure of the cement hydrate. It is that portion of the pore water which is active in the sense of applying swelling or drying pressure tending to separate primary particles of the paste.

The author's model for the structure of the paste is based on electron microphotographs which show hydrated calcium silicate flowers growing on a grain of cement. The author concludes that the space separating primary particles is unlikely to have parallel

sides and judging from the microphotographs may be described as wedge shaped with the sharp end of the edge pointing in random directions. In terms of this model, water is excluded from the apex of the wedge where interparticle cohesion is provided by primary bonds.

Strength is a linear function of k. Volume changes due to creep and shrinkage appeared to increase with increase in k but values of kV_w after shrinkage and creep had taken place were less than at the start of the test. This suggests a collapse of structure in the cement hydrate. The volume kV_w was found to represent between 1 and 3 monolayers of water and corresponds to the water held at relative humidities between 0 and 28 per cent. Shrinkage varies linearly with weight of water gained or lost within this range of relative humidities.

The author concludes that the parameter $k = (V_w - V_f)/V_w$ is related to the degree of hydration, surface area and strength. And that further research may show a close dependence of creep and shrinkage characteristics on this parameter.

"ELECTRON MICROSCOPIC INVESTIGATION ABOUT THE RELATION BETWEEN STRUCTURE AND STRENGTH OF HARDENED CEMENT." Werner Richartz.

According to the author, electron microscopy shows that the hardening of cement may be divided into three stages. In stage I ettringite crystals form as a thin layer on the cement grains and calcium hydroxide forms as thin plates in the liquid phase. These phases are visible within minutes after the paste is prepared. After about an hour a thin layer of hydrated calcium silicates can be observed on the cement grains. As hydration continues, ettringite and hydrated calcium silicate crystals grow as interlocking fibers

and extend across the large pores and divide them into smaller pores. After hydration is completed these fibers act as a micro-reinforcement of the structure and will increase the ultimate strength. Following this stage II, which requires about twenty four hours, the remaining pores are filled with new hydration products. During this stage hydrated tetracalcium aluminoferrite is formed instead of ettringite and the latter is converted to the monosulfate. Hence the contribution of ettringite to the total strength is doubtful, but it influences the setting of the cement and the early strength.

Low temperatures retard hardening but generally result in higher ultimate strengths. Extension of stage II results in increased formation of long fibrous calcium silicate hydrate crystals and increases strength. Retardation of hardening also results in the formation of long fibers of the calcium silicate crystals and in higher strengths.

When hardening is accelerated either by finer grinding, higher temperatures or accelerators, the surfaces of the cement grains are activated so that the solution in the pores is always supersaturated. This favors spontaneous nuclei formation and increased crystal growth. Accordingly only a few crystals can grow as long fibers in stage II. During about the first 28 days the strength of the accelerated cement exceeds that of the unaccelerated cement but after that the strengths are reversed. These results show that a strict relationship exists between the development of structure and strength. The author gives sixteen electron photomicrographs in support of the conclusions given in the paper.

"A STATISTICAL STUDY OF THE EFFECTS OF TRACE ELEMENTS ON THE PROPERTIES OF PORTLAND CEMENTS." RAYMOND L. BLAINE

A digital computer was used to evaluate significant relationships between the properties of 199 commercial cements. The tests were hydration, autoclave expansion, potential sulfate resistance, compressive strengths of mortars and concretes, and nonrestrained and restrained shrinkage. The computer was used to find and evaluate significant relationships between the results of tests (dependent variables) and variuous independent variables which included chemical composition, minor constituents and trace elements. Multivariable regression equations were calculated by a least-squares method using only commonly determined variables, including sodium and potassium oxides, and these variables together with trace elements. Numerous trial equations were required to determine independent variables which were significantly related to the dependent variable, and the combination of variables which resulted in the lowest estiamted deviation for the equation.

Up to 13 dependent variables could be accomodated in an equation with the computer program used. The output of the computer included the estimated coefficient of each of the endependent variables as well as the estimated standard deviation of each of the coefficients. An independent variable was retained in an equation if the ratio of the estimated coefficient to the estimated standard deviation (coef./s.d.) was greater than 1.0. Although this represents a very low probability of significance, such independent variables were retained primarily because these studies were exploratory. Values between 1.0 and 2.0 may also be considered of doubtful significance.

Values of 2.0 or greater would occur by chance with a probability of 0.05 and therefore independent variables having values of coef/s. d between 2 and 3 are referred to as probably having a significant relationship to thedependent variable. When used as independent variables in multivariable equations, the coefficients of sodium and potassium oxides, in some tests, were highly significant and in other tests variations in one or both of these alkalies had no apparent effect on the property measured. Trace elements that were found to have coef./s. d. greater than 1.0 were Sr., Ba, Cu, and Rb most often, second were Zn, V, P, and Cr and third were Co, Ni, Mn, Li, Pb and Ti. Mo detected in a few cements did not appear in any of the equations.

GENERAL REPORT

OF

SESSION III-1: STRUCTURES AND PHYSICAL PROPERTIES OF CEMENT PASTE

(b) Papers regarding Application

W. L. Dolch (U.S.A.)

The following Supplementary Papers are summarized in this report.

Paper No. III-1

COMPARISON OF VARIOUS MEASUREMENTS CONCERNING THE KINETICS OF HYDRATION OF PORTLAND CEMENTS

S. Popovics (U.S.A.)

Paper No. III-5

MECHANICAL PROPERTIES OF PRECOMPRESSED MORTAR SPECIMENS

O. Ishai (U.S.A.)

Paper No. III-33

DEFORMATIONS OF PLAIN CONCRETE

F. O. Slate & B. L. Meyers (U.S.A.)

Paper No. III-72

CORRELATION OF STRENGTH AND HYDRATION WITH THE COMPOSITION OF PORTLAND CEMENT

K. M. Alexander, H. Taplin & J. Wardlaw (Australia)

Paper No. III-88

RELATION BETWEEN THE HYDRATION OF ALUMINA CEMENT MORTARS AND THEIR STRENGTH IN THE EARLY STAGES

K. Mishima (Japan)

Paper No. III-97

EFFECTS OF HYDRATION OF CEMENT ON COMPRESSIVE STRENGTH, MODULUS OF ELASTICITY, AND CREEP OF CONCRETE

S. Seki, K. Kasahara, T. Kuriyama & M. Kawasumi (Japan)

Paper No. III-119

SOME RECENT ADVANCES IN THE STUDY OF CEMENT AND CONCRETE

H. E. Vivian (Australia)

This is a condensation and summary of seven supplementary papers on the general relationships between the nature and structure of cement pastes and the engineering properties of concretes and mortars made therewith.

The seven papers can be divided logically into three groups: 1) a general review of deformation processes (Slate and Meyers), 2) the influence of composition and other properties of the cement on engineering properties of concrete (Alexander et al, Popovics, Vivian) and 3) the influence of chemical and physical properties of the paste on these same engineering properties (Ishai, Mishima, Seki et al). Categories 2 and 3 are, of course, a separation based on emphasis rather than on the fundamental difference.

The present author has, in his reportorial function, deliberately not taken the part of critic, but has tried merely to summarize the main aspects of the papers assigned to him.

Slate and Meyers discuss in turn the various components of a concrete that are subject to deformation, called deformees, and the various influences that bring about deformation, called deformers. The former comprise all the phases of the concrete: the aggregate pieces, the larger crystals and small crytallites of the paste, the free, capillary, adsorbed, and chemically-combined water, and any air-filled spaces such as bubbles, voids and cracks in the paste or at the paste-aggregate interface.

The deformers considered are the forces attributable to chemical reaction, such as hydration and carbonation, stress and pressure, and changes in moisture content.

The processes that are brought about by interactions of these forces and objects are elastic strain, fracture, flow, diffusion, solution, and reprecipitation.

The authors evaluate these processes in terms of the magnitude of the resulting deformations. Important distinctions are made between deformations from short term loads that result in elastic strain and fracture and those from long term loads that result in creep.

Particular emphasis is placed on the aggregate-paste interface and on the effects that result from cracks at this place. In general, important distinctions are drawn between generalized and localized deformations, and the conclusion is made that the engineering behavior of concrete is determined by and limited by the localized changes that take place at crack tips, water filled voids, and aggregate-paste interfaces.

The paper of Popovics is an attempt to describe the changes in important engineering parameters of concrete by a model that has simple properties. The most important ones are that the cement is composed of only two active components, the C_3S and everthing else, and that the decelerations in the values of any properties associated with the hydration are, at any time, proportional to the magnitude of the property yet to be developed. For example, at any time the deceleration of the strength change would be proportional to the difference between the strength at that time and the ultimate strength to be obtained. This proposition has previously been tested with respect to strength development. In this paper, in

addition to a review of the strength results, the model is tested against two other indexes of cement hydration, the non-evaporable water content and the specific surface of the gel formed. A further assumption was made that the C_3S component is responsible for the generation of three times the non-evaporable water of "other" component.

The test was made by a comparison of the experimental values of others with the values predicted by the model. In addition, effects of curing temperatures are included by combining the model with the Arrhenius equation.

The results are that the model provides a reasonable prediction of the parameters in question, with the agreement for strength being the best and that for specific surface the poorest. The coefficients of deceleration were found to be linear functions of the C_3A content of the cement in the cases of strength and non-evaporable water development.

The considerations of temperature gave a result similar to the well-known maturity rule.

One of the interesting empirical aspects of Popovic's model is that it seems to include the consequence, often observed, that any condition that increases the early strength of concrete will result in a decreased final strength and vice versa. Such conditions as temperature, the presence of accelerators or retarders, and cement fineness seem to follow this generality.

Alexander, Taplin and Wardlaw present data showing the relationships between composition and certain other properties of thirty

cements and the strength and degree of hydration of pastes made therewith. The conditions of hydration include a wide range of water-cement ratios, 0.35-0.80, and temperatures from 5 to 75 C. The duration of hydration of the pastes was from a few hours to six months. The compound compositions of the cements varied from about 40-62 percent for C_3S and from practically nil to 11 percent for C_3A.

The resulting data were analyzed by means of mutiple regression analysis. The most significant general result is the very great dependence of the strength differences on the C_3A contents of the cements. This influence was predominant at ages from 7 days to three months and most important at intermediate ages and water-cement ratios, i.e. at just those conditions under which the strength of concrete is most often determined as an index of its quality, water cement ratios of about one-half and an age of 28 days. This influence of the C_3A seems to be in accord with the findings of Popovics, mentioned earlier. The relatively large differences in C_3S content proved to be comparatively unimportant.

Since the influence of C_3A left a relatively small but significant residual variation unaccounted for, the influence of other compositional and physical property variables was examined. Particle size, free lime, and potassium were the only ones that correlated significantly with strength. The influence of the reciprocal of the mean particle size on strength was positive and appreciable in magnitude at intermediate ages. The influence of free lime was negative and greatest at later ages and lower water-cement ratios. It was also found that the influence of the

manganese content on strength variation was significant at very early ages.

The data seem to show that the silicates are hydrating faster in cements with higher C_3A contents. Speculation is advanced for the possible reasons for this effect.

The data on hydration and on the influence of temperature showed the influence of C_3A content on hydration to be even greater then for strength and to be most important at intermediate temperatures.

Vivian examines certain properties of cement that may be of considerable importance to the workability, strength, and durability of concrete and that are not adequately controlled or measured in current cement production practice.

It is pointed out that the particle size distribution of the finished cement is influenced by the particle size distribution of the raw meal as well as by the final grinding. Inadequate control of these features of the meal can result in variability of the cement that is significant in its performance in concrete. An important aspect is the difference in grindability between the clinker and the gypsum, which results in the presence of the gypsum in predominantly the finer fractions of the cement. Further differences in the cement can be introduced during grinding if the mills are air-swept and the cement is subject to variable amounts of aeration.

Vivian advocates a reduction in the amount and temperature of the air stream, closed circuitry of the air system and increased

separator efficiency to minimize the time the finer particles stay in the circuit.

The paper describes the problems the author states arise when gypsum particles are occluded by the hydration products of the cement and thereby become prevented from going into solution for perhaps long periods of time. This condition can result in insufficient gypsum for normal retardation and a consequent lack of workability of the concrete. At much later times a further problem can exist when some influence, perhaps the volume changes associated with wetting and drying, disrupts the encapsulation of the still-unreacted gypsum and liberates it to undergo possibly expansive reaction with aluminate components of the paste. It is stated that this may be the cause of surface crazing of concrete subjected to temperature and moisture-content cycles.

The author discusses also the influence of particle size and particle size distribution of the cement on the strength and shrinkage of concrete. The main differences seem to be in the distances hydration products may travel during their deposition as well as in the more obvious matters of degree of hydration at any given time.

The paper by Seki, Kasahara, Kuriyama, and Kawasumi examines the relationships between the degree of hydration of cement and several mechanical properties of concrete.

Experiments were conducted with a moderate heat cement in a concrete designed to be typical of mass concrete construction, although the largest size aggregate was screened out prior to the casting of samples. The concrete was then cured under water.

Bound water was determined on pastes by vacuum drying at 5mm Hg over silica gel for three days. The resulting value of 0.37 of the cement weight for complete hydration means the "bound" water in this study includes more than the non-evaporable water of other studies. Values of bound water were used to determine the degree of hydration of the concrete at any given time.

The compressive strengths showed a linear relationship to the ratio of hydrated cement to original water content ratio, both for the laboratory concretes and for samples taken from various dams in Japan. This relation is similar to the well-known gel-space ratio relationship, which is discussed in the principal paper of this session.

Elastic moduli were determined by measurement of the longitudinal wave velocity in the concrete samples. The wave velocity was found to be a linear inverse function of the volume of water in the sample that was not "bound", i.e. the greater the extent of hydration, the higher the velocity and therefore, the elastic modulus, which is normal.

Comparisons were also made between the static and dynamic Young's moduli of elasticity, and the empirical relationship obtained was that the dynamic modulus was about 37 percent greater than the static.

The creep studies resulted in a linear relationship between the creep factor, which is proportional to the creep strain, and the volume of "uncombined" water present. Such results are an additional

confirmation of the seepage theory of creep behavior of concrete.

In general, these studies show, once again, the commanding importance of the amount of hydrated cement in determining the mechanical properties of concrete.

Ishai investigated the strength, elastic modulus, shrinkage, and creep of mortars that had either been cured in the usual fashion or had been subjected to preconsolidation by an applied pressure of about 2400 psi at various times early in their lives.

The preconsolidation always brought about changes in the measured properties. Since the compaction squeezed out a considerable portion of the mixing water and resulted in a lower water-cement ratio, it is understandable that such changes in mechanical properties should occur. It is possible, of course, that the compaction also resulted in a changed structure including more bonding points of contact between the solid phases than are present in normally-cured materials.

When the mortar was preconsolidated about 3 hours after casting the strength was over twice that of normally-cured specimens. The elastic modulus difference was smaller and not nearly proportional to the strength change, which probably in itself is an indication of microstructural change. Precompressed specimens exhibited smaller volume changes on wetting and drying and somewhat less creep strain than their counterparts. Further, specimens that were oven-dried showed no creep strain at all, a result that confirms earlier work.

All the foregoing papers were concerned with problems of portland cements. The paper by Mishima turns to problems of high-alumina cement.

He examines the relationships between the compound composition of the hydration products of high-alumina cement and the strengths of their mortars. The conditions included water-cement ratios of 0.4-0.7, curing temperatures of 10-40 C, and curing times up to 7 days.

The compound compositions were determined by semi-quantitative x-ray diffraction methods. The predominant hydrates formed at 10 and 20 C were CAH_{10} and C_2AH_8, there being relatively more of the former at the lower temperature. At 40 C no CAH_{10} was found and the larger amount of C_2AH_8 initally formed progressively converted to the stable cubic C_3AH_6 and gibbsite, AH_3, in the well-known reaction that brings about important engineering problems in the use of these cements.

At 30 C the formation of significant amounts of any hydrate was delayed until about 12 hours and the conversion to C_3AH_6 began only after several days.

Strengths roughly followed the amounts of hydrates produced except that the conversion to C_3AH_6 resulted in the usual strength decrease. Strengths attributable to the presence of CAH_{10} seemed to be greater than those attributable to the presence of C_2AH_8. The influence of the water-cement ratio was about the same as with portland cements.

At 30 C, which temperature seems to represent the onset of the conversion reaction, the lesser reactivity was reflected in longer setting times and lower strengths.

GENERAL REPORT
OF
SESSION III-2: DURABILITY OF CONCRETE

I. Biczok (Hungary)

The following Supplementary Papers are summarized in this report.

Paper No. III-24

BEHAVIOUR OF MORTARS AND CONCRETES IN THE TEMPERATURE RANGE FROM +20° TO -196°C

G. Tognon (Italy)

Paper No. III-25

THE INFLUENCE OF TEMPERATURE ON SULPHATE ATTACK ON PORTLAND CEMENT MORTARS

J. H. P. van Aardt (South Africa)

Paper No. III-30

THE FROST RESISTANCE OF CEMENT GROUTS FOR PRESTRESSED CONCRETE APPLICATIONS

C. MacInnis (Canada)

Paper No. III-31

CHEMICAL REACTIONS OF STRONG CHLORIDE-SOLUTIONS WITH CONCRETE

H.-G. Smolczyk (West Germany)

Paper No. III-39

A DURABILITY STUDY OF CONCRETE USING MONTE CARLO SIMULATION

K. R. Lauer & C. W. Gray (U.S.A.)

Paper No. III-59

MEASURING OF GAS DIFFUSION FOR THE VALUATION OF OPEN POROSITY ON MORTARS AND CONCRETES

H. J. Böhme, U. Ludwig & H. E. Schwiete (West Germany)

Paper No. III-99

THE BEHAVIOR OF CONCRETE SUBJECTED TO FREEZING AND THAWING AS A REFERENCE FOR FROST RESISTIVITY OF CONCRETE

Y. Koh & E. Kamada (Japan)

Paper No. III-123

EFFECT OF CONVERSION ON PROPERTIES OF CONCRETE USING HIGH-ALUMINOUS CEMENT

R. Tsukayama (Japan)

Paper No. III-124

THE INFLUENCE OF CHLORIDE AND HYDROCARBONATE ON THE SULFATE ATTACK

F. W. Locher (West Germany)

Paper No. III-138

MECHANISMS OF SULPHATE EXPANSION OF HARDENED CEMENT PASTES

S. Chatterji (United Kingdom)

The resistance of the concrete respectively of the cement stone against external aggression is a constant subject of international conferences. On the occasion of the III. International Symposium on the Chemistry of Cement, Washington, 1960, the VI. Section /Destructive Process in Concrete/ dealt with questions of corrosion, but during the deliberations of other sections questions related to the corrosion of concrete were breached as well. Since then, in 1961 the RILEM had a Colloquium in Prague on the durability of concrete. - In 1966 an international conference on silicates was held in Weimar; its III. Section discussed problems of the corrosion of concrete. In 1967 a conference in the same field of interest was organized in Leipzig. Representatives of 37 states participated in the three last mentioned gatherings and more than 90 papers were read, concerned directly or indirectly with problems of concrete corrosion.

It must be mentioned here that among several states, in Japan the Cement Association of Japan organizes General Meetings, where papers are read in this subject matter, and are published in the yearly Reviews.

After such antecedents it may be appropriate to consider, what

kind of phenomena should be included in the scope of concrete corrosion problems. In first concept we mean by the term 'corrosion processes of concrete' damages of concrete caused by the penetration of liquid or gaseous substances into the solidified concrete.

Thus we may speak about corrosion by carbonic acid, by nitrogen oxide, hydrogen sulphide, by gases or by sulphatic, chloridic or other salt solutions of natural origin or occurring as industrial by-products. I would term these as external corrosive effects. Nevertheless the internal transformations of the cement stone, and the recrystallization of the hydrated compounds, produced during the binding of the cement, can cause also structural changes which may initiate or accelerate the start of corrosive processes.

In my German book - Betonkorrosion - Betonschutz, i.e. Concrete corrosion - Concrete Protection; 1968 - I termed these processes as processes of internal origin, shortly as internal corrosive processes. Properly speaking, the destruction of the cement stone caused by the free lime and magnesia and accompanied by expansion, comes also under this heading, although it is not usual to discuss these occurrences within the scope of corrosive effects.

Nevertheless the expansion induced by an excessive quantity of gypsum interground to the clinker, or the destruction effected by the recrystallization of the hydrate compounds of aluminate cements, had appeared in the discussions also as a corrosion phenomenon since a longer time. These latter typical phenomena of internal corrosion were considered always as belonging to this subject matter.

The occurrences of external corrosion are effected by solutions diffunding into the cement stone. Any occurrences promoting diffu-

sion, i.e. increasing the porosity of the concrete, accelerate the proceeding of corrosion. Therefore phenomena having a bearing on the porosity of the cement respectively cement stone can not be separated from the investigation of concrete corrosion. Many observations and theoretical considerations lead to the assumption, that the increasing of the pore volume is brought about by the transformation of the unstable hydrate compounds, developed primarily during the hydratation, or of hydrate compounds getting unstable due to the changes of the surrounding to stable compounds. If the filling of the space by this stable formation is diminishing, fine cracks appear which facilitate the penetration of aggressive solutions and gases.

The study of the corrosive phenomena within the concrete necessitates therefore the examination of the internal corrosive phenomena as well as the exploration of the pertaining research results. It follows from this statement that I deem it necessary to take into consideration the thermodynamical investigations concerning the stability of the products appearing during the setting of cement. On the occasion of the Washington Symposium Brunauer and Greenberg rendered account of such investigations. /Monography, Vol.I. p.155: Free Energies and Entropies of Hydratation/ as well as Mchedlov-Petrosyan and Babushkine /Monography, Vol.I. p.533: Thermodynamics of the hardening processes of cement/. In 1962 a book edited by Mchedlov-Petrosyan appeared in Russian, later in 1965 in German, discussing the thermodynamics of silicates /Thermodynamik der Silikate/. – The same authors have read a very important paper in the next year at the Weimar conference

with the heading: "Die Thermodynamik der Korrosionsreaktionen des Zementsteins" /The Thermodynamics of the Corrosion reactions of the Cement Stone/.

According to these theoretical investigations and estimations, during the hydratation of the tricalcium silicate /C_3S/ and of the beta-dicalcium silicate /C_2S/, any of the known calcium hydrosilicates may be produced. The values of free reaction enthalpies of the development of hillebrandite, phosphagite, tobermorite, riversideite and xonotlite are so near to each other that from a thermodynamical point of view the production of any named hydrate compounds is possible. However only the hillebrandite possesses a stable material structure up to 200 centigrades. In its elementar cell films of xenotlite /$Ca_6[Si_6O_{17}](OH)_2$/ and portlandite occur stratified alternately, yet its $Ca(OH)_2$-content may be more or less. – Thus the proportion CaO/SiO_2 can vary without a change of the basic structure /see e.g. Kantro, Brunauer and Weise, Portland Cement Ass. Bulletin 1961 and 1962, – further Locher: Zement-Kalk-Gips, 1964/.

Although several research workers term this product tobermorite, instead of hillebrandite, in accordance with thermodynamical investigations the stable product constitutes hillebrandite. /I do not consider it as my task to discuss this contradiction./ Due to the variable proportion of Ca/Si, deformations occur, wherefore the hydrate changes its original uniform structure and appears sometimes in a lamellar structure, or in a coiled habit, similar to halloysite. This stable phase is represented in the technical literature by the formula C_2SH and the different morpho-

logies are differentiated by the three capital letters A, B, C. Influenced by various outer factors the hydrosilicates may transform or recrystallize, however this process is accompanied on the one hand by more or less swelling, mostly by volume decrease and the generation of structural discontinuities, which contribute to the shrinkage consequent upon the removal of the gel-water, – on the other hand hair cracks develop easing the diffusion as a consequence of the transformed structure.

From X-ray photographs one must conclude that neither of the mentioned appearances possesses a good stable lattice structure, which fact renders their identification difficult.

These symptoms, the kinetics of the transformations, are influenced by the rate of hydratation, the water-cement ratio and the temperature, – thus the rate of stabilization depends on the mineral composition of the clinker, the grinding fineness of the cement, moreover on the technology of concreting. As the shrinkage of the mortar is somewhat slowed down due to mechanical and physical facts – by the sand blended to the cement paste, and this is veryfied by the fact that the mortar shrinkage estimated on the base of the shrinkage of the cement paste, measured in laboratories, surpasses essentially the actually measured value, – it is apparent that the occurrence of cracks promoting the corrosion is dependent also on the ratio of the cement/fine sand. /Under the term "fine sand" an aggregate finer as a grain size of 0,2 mm is meant./

Here already I want to indicate that, contrarily to the above mentioned proceedings, the self-sealing processes – in most

cases occurrences of calcite /which is a result of carbonization caused by the carbonic dioxyde content of the air/ or of its modifications – may occlude in the case of a Portland-cement binding agent the capillaries carrying water, still with concretes in which the formation of calcium carbonate is not probable or is lacking a possibility, this process – increasing greatly the durability of concrete – does not develop. – It is to be noted that in a moist air the hillebrandite reacts with the carbonic-dioxide content of the air, and some modification of calcium carbonate comes to being, accompanied by a segregation of a silica-gel contributing also to the self-sealing.

It is a known fact that during long-time studies of concrete, fluctuations can be observed, with investigations of strength as well as with measurements of dilatations. It is deplorable that these observations were not cross checked until now by mineralogical investigations and by tests of stability.

The thermodynamical studying of the aluminate hydrates needs yet completions. According to the present computations in the temperature range of 20 to 120° C, the C_4AH_{19} is the stable hydrate compound /which is mentioned mostly as C_4AH_{13} in the technical literature/, whereas at a higher temperature the hydrate compound C_3AH_6 – appearing in the cubic system of crystallization – is stable. Hence it follows that tetracalcium aluminate hydrate ought to originate equally from C_3A, from $C_{11}A_7$, C_2A and CA.

However the experimental results contradict this statement in some respects. The tesseral modification arises already at a lower temperature than 120° C, while below 25° C if C_4AH_{19} or CA

is hydrating the monocalcium aluminate hydrate is the dominating product. As for the calcium aluminate hydrates, I will deal with them in connexion with the dissertation of van Aardt.

Two types of sulphatic aluminate hydrates are known; their formation is equally possible according thermodynamical computations, yet the stable crystallizing compound up to 70° C is the trisulphate, the so called ettringite; above this temperature the formation of a monosulphate is more probable.

Although the classic opinion – evolved already at the end of the past century – was accepted generally for a long while, and was in accordance with the practical experiences, – recently different misgivings arose, as our knowledge was deepened by the development of new instrumental investigations and new theories have been published. For a long time the begin of crystallization of the ettringite could not be observed by microscopic examination, by means of the latest instrumental analytics it could have been proved that the ettringite crystallizes in the cement stone after a delay of some minutes following its getting mixed with water. /Schwiete, H.E.; Ludwig, U.; Jaeger, P. – Zement-Kalk-Gips. 17, 1964. p. 103/. – Nevertheless this statement is contradicted by the observation that at a temperature of about 20° C also a monosulphate may come into being, further that ettringite can be found in a concrete strengthened by steam curing and autoclave treatment.

Some research workers furnished data referring to the possibility that ettringite may decompose at a temperature of about 20° C. Thus Koyanagi showed on the occasion of the 1952 London

Symposium a microphotograph which enabled readily the observation of disintegrated crystalline ettringite needles. /Report ... 1952. p. 252./ Schwiete and Niel /see Zement-Kalk-Gips, 18, 1965. p. 157./ established by means of infra-red absorption photographs that the aluminate-sulphate hydrates issuing from the first minutes of the binding process, disintegrate partly and that gypsum separates out. It has been verified that this disintegration is due to the change of concentration of the cement water.

The calcium-sulpho-aluminate formed on occasion of the binding of cement may be characterized by two features. Investigations conducted up to now show that within a pH-value margin of 11,5 - 11,8, minute rods precipitate from the solution into the dispersed pores, yet their formation does not endanger by any means the stability of the cement stone, on the contrary, their intergrowth increases its strength. /It is an established fact that the hardening of the sulphatic blast-furnace slag cement is due in the first place to the ettringite./

However with a pH-value of the cement water between 12,5 - 12,9, spherically protruding crystal agglomerations arise from the tricalcium-aluminate grains – probably by some topochemical effect – which produce a swelling by their crystallization pressure. Therefore if the CaO-concentration of the cement water is high, /in this case it is usual but perhaps not justified to speak of supersaturation/ a swelling may issue. Not many electron-microphotographs are available, showing a cement structure which has produced in the practice a swelling by gypsum, nevertheless from the few photographs we obtained, the same structure can be

identified which was verified in the case of the ettringite produced by a topochemical process. A difference may be established perhaps by the fact that the ettringite needles do not radiate from a single point, but they appear also in bundles. /See e.g. Dreizler, Zement-Kalk-Gips, 19, 1966. p. 221./ This harmful crystallization of the ettringite can be diminished by the same measure by which we are able to decrease the Ca-ion-content of the cement water, respectively its pH-value. – No ulterior recrystallization is to be feared, as this process can not take place except through a solution, but in this case only an ettringite can be produced which is harmless from a morphological view. While the swelling phenomena caused by the ettringite are proven by microscopic, and in exceptional cases also by macroscopic observations, in recent times – as I mentioned it already – other explanations became known too, which will be discussed in my report referring to the individual papers.

We consider it a necessity to pay further great attention to the elucidation of the formerly outlined phenomena. Before fifty years a dosage of more than 3% of gypsum was not permitted; today there exist cement norms which do not object to a dosage of 9% gypsum stone, if during the grinding of cement a specified fineness or a specific surface area expressed in "Blaine" value can be attained. As a result of an intensive mechanical exploration it is expected that the transformation of calcium aluminates accompanied by a volume increase takes place already prior to the solidification of the cement stone. By this way on the one hand the initial strengthening effect of the ettringite crystal-inter-

growth is fully exploited, on the other hand – and this is of importance from the viewpoint of resistance against corrosion – there remains hardly any tricalcium aluminate as anhydrite in the cement stone, therefore no ulterior sulphate-effect can appear.

Following our opinion the development of the processes can not be clarified so readily, as the change of concentration of the solution must be taken also in consideration, as well as the chemical potemtial of different clinker-minerals and the accessory processes, which increase or decrease the Ca-ion content of the solution. There await many uncleared questions their elucidation till the introducement of increased gypsum quantities ensuring the enhancement of the initial strength could be recommended with responsibility. This remark refers to the formulas also, which were proposed by some research workers for the permissible gypsum dosage.

The sulphatic corrosion and the products appearing at the hydratation of the calcium-aluminates in presence of gypsum, are dealt with by the dissertations of J.H.P. Aardt and S. Chatterji. These two papers represent the continuation of the discussion arisen by the publication in 1963 of the "New Hypothesis of Sulphate Expansion" – a theory of S. Chatterji and J.W. Jefferey.

In his present treatise Chatterji introduces this hypothesis; he starts from the fact that on occasion of the hydratation of calcium aluminates the primary product is the C_4AH_{13}, which reacts with the $CaSO_4$ being in solution, and forms the complex salt termed monosulphate. This formation of crystals is one cause of the sulphatic corrosion, vulgarly of the gypsum swelling. In the

last years several research workers /M.H. Robert, P.K. Mechta, A. Klein/ expressed their opinions on this theory.

Van Aardt does not agree completely with this theory. In the first part of his paper presented on "The Influence of Temperature on Sulphate Attack on Portland Cement Mortars" he furnishes new data, completing the knowledge of the hydrate compounds originating from the hydratation of the tricalcium aluminate. These compounds are characterized by the basal spacing of the lattice in the crystal phases, thus the cubic C_3AH_6 by 5,14 Å; the hexagonal tricalcium-aluminate hydrate by 7 Å; the C_4AH_{19} by 10,6 and 5,3 Å; the C_2AH_8 by 10,7 Å. Those are all known hydrates, but he has found an other, which he terms by 8,2 and 4,1 Å. As there exist some differences between the literary publications, it is to be noted that the C_4AH_{13} is identic with a C_4AH_{19} dehydrated in a small degree.

Among the sulphatic complexes Aardt has detected beside of the known ettringite /9,7 and 5,6 Å/ and the monosulphate compounds /8,9 and 4,4 Å/ 3 intermediary products, which he characterizes by the d-spacing data 10,3 Å, /9,6 and 4,77 Å/ and last by /8,5 and 4,23 Å/.

Though the limited space of such a summarizing report does not permit digressions and the approach of special details, I feel it justified to stress the observation of the intermediary products, because the instrumental analytical methods at our disposal make it already possible to control the views and opinions accepted up to now and considered almost as classic. It turns out in nearly every case that the endproducts develop through instable

intermediary products, nevertheless those intermediary products get in many times stabilized.

Van Aardt published his observations of reactions at 5° respectively 25° C.

At 5° C the aluminate-hydrate substance 10,6 Å forms from the tricalcium aluminate, which produces with 1 mole $CaSO_4$ the intermediary product 9,6 Å; in the course of time the monosulphate develops from this substance.

Similarly at 5° C with 3 moles $CaSO_4$ ettringite forms, which disintegrates after 10 days producing an instable product characterized by 10,3 Å.

At 25° C different transitions lead ultimately to ettringite, but a transitory product 9,6 Å comes into being too. Thus the temperature of hardening influences the set up of the hydrates forming during the hydratation, as well as the composition of the complex compounds forming under the influence of the gypsum.

The author deals with the favourable influence of autoclaving. The autoclaved concretes – as established by other research stations also – are in a great measure sulphate resistent. Without intending to predict the results of future research works, I may remark that any heat treatment, in consequence the autoclaving too, increases the rate of recrystallization; the solubility of the rough-grained calcium hydroxyde lessens, the pH-value of the cement water decreases, what all has a bearing on the composition of the complex sulphate compounds.

By those means we obtain about the same effect as when we diminish the quantity of the Ca-ions dissolved in the cement

water by acidic additions or by intergrinding of blast-furnace slag.

S. Chatterji proposes in his thesis on "Mechanisms of sulphate expansion of hardened cement pastes" to add fineground calcite to the cement and transform this way the C_4AH_{13} into a well known product containing $CaCO_3$, which is unable to transform into a sulpho-compound causing swelling. The author deals further with the specific effect of cations which he classifies into three groups.

The treatise of Dr.Ing. Heinz G. Smolczyk "Einige Beobachtungen und neue Gesichtspunkte zur Einwirkung von Meerwasser auf Beton in der Wasserwechselzone" /Some observations and new viewpoints on the effect of sea-water on concrete in the zone of tidal fluctuations/ /RILEM Bulletin, Nr. 32. 1966./ can be considered as an introduction to his paper presented here on the Chemical Reactions of Strong Salt-Solutions with Concrete. The author surveys the present state of the Helgoland experiments carried out since fifty years concerning the action of sea-water on concrete.

He states that the sea-water having a relatively high chloride content causes on a compact concrete but a slow sulphatic corrosion. /This statement will yet come up in this report later./ However the salt solutions get concentrated in the tidal zone by evaporation. This necessitates the study of the corroding effects of concentrated salt solutions. In his later paper, before our Symposium, he describes the preparation of the test specimens with a water-cement ratio of 0,4, which were stored in a salt solution containing 1,3 mol/liter, further in concentrated salt

solutions. His research results which were not concluded till the spring of 1968, can be harmonized in general with other research results.

The most intensive corrosion was brought about by the solution of magnesium chloride. /We know that this type of corrosion is due not only to the chlorine-ion, effecting chemical decomposition, but also to the ability of the magnesium-ion to replace the chlorine-ion. – To a lesser degree the calcium chloride causes corrosion too, and the sodium chloride was proved harmful to a least extent. It is surprising that the Portland cement possessing but a small saturation by lime, supported the attack of saturated solutions better than expected. For the sake of completeness we may remark that the American Concrete Institue Committee Report 515 declares all chlorides as aggressive, strongly aggressive the calcium-, magnesium-, sodium- and potassium-chlorides, and infers with the ferrous-, copper- and zincum-chlorides a slow concrete destructing effect.

During the last eight years many treatises appeared on aggressive effect of de-iceing solutions. As no paper concerning this theme was submitted to our symposium, I do not want to discuss this most important question in detail. Nevertheless it is evident that against the influence of these solutions containing magnesium-, sodium-, calcium- and often potassium-chlorides, the floorplates of pavements and road surfaces must be protected. One method of protection is the maintaining of the fines-content of the dry concrete mix above a minimum value /of 500 kg/m^3/, further the production of an air-entraining concrete.

It must be stated that the question of sulphate-resisting concrete was discussed by very many authors in the last eight years. The participation of the individual clinker minerals in the sulphate-resistance of the concretes was cleared, except the specific behaviour against sulphatic solutions of the products proceeding from the hydratation of the brownmillerite; this latter problem awaits yet its full elucidation. It has been established what quantity of blast-furnace slag ensures the sulphate resistance of cement, further a light was thrown on the fact that not every metallurgical slag behaves the same way.

The adopting of the rapid testing method by Koch and Steinegger /Zement-Kalk-Gips, 13, 1960, p. 317./ facilitated largely the performing of these examinations, further other investigation methods were employed, which had not been at disposal in the earlier years, e.g. the infra-red spectroscopy, the frequency distribution of the resonance and the electron microscopy. It is but natural that routine tests of strength, of the relative bending-strength value, and measurements of dilatation are used further on, and even the old needle-test of Le Chatelier is employed again.

F.W. Locher /"Influence of Chloride and Hydrogen carbonate on the sulfate attack"/ carried out experiments with small prismatic specimens to study the influence of chloride and hydrocarbonate on sulphatic attack. His dissertation submitted to our Symposium has the purpose to clear the problem, why a concrete shows a greater resistance in sea-water than in solutions of identical concentration prepared in various laboratories. It was supposed till now that this differential behaviour is due to the presence

of sodium chloride. – The work of Professor Locher does not verify this assumption, as he found out that the hydrocarbonate content of the sea-water attenuates the aggressivity of the salt solution. – The formation of a calcite stratum protects the interior of the concrete from the diffusion of the aggressive solution. He proved further that the sodium chloride alone does not diminish the amount of ettringite and that the occurring monochloride originates from the C_3A unconsumed up to then. The determination of these facts will enforce the revision of our present knowledge. The remaining conclusions of the dissertation verify prior research results.

This work proves once more how important a water-insoluble finegrained coating, precipitated on the surface of the concrete is. The fine precipitates seal the microchannels promoting the inflow of the salt solution, as well as the fine cracks originating from the water loss of concretes containing excess water for easier workability, or cracks due to the stabilization of hydrate compounds. The different physical processes and phenomena overlap each other and it is often most difficult to analyse the sometimes uncommunicative descriptions of the research symptoms and to harmonize them with the practical experience.

From among the pores of the cement stone those are important from the view-point of resistivity, which enable the throughflow of gases and solutions in particular. This "apparent porosity", its determination and interdependence with corrosion phenomena, were the objects of several investigators. Thus Schwiete and Ludwig published methods for the measurement of pore sizes /Tonindu-

strie-Zeitung, 90, 1966. p. 562./ Žagar introduced the unit of measurement for the specific permeability, the "perm". – Schwiete and Ludwig show most valuable diagrams demonstrating the frequency distribution of the different pore radii and the variation of this distribution during the hardening of the concrete resp. the cement stone.

It would have been most interesting to compare these research results with our knowledge concerning the stabilization of the hydrate compounds in dependance of time and the pertinent role of different hydraulic additives. /This has been done partly, though in the form of a short reference, in the case of changes taking place in the structure of aluminous cements./

Schwiete, Ludwig and Böhme submitted to this Symposium a dissertation on this subject matter. Their paper on "Measuring of gas diffusion for the valuation of open porosity on mortars and concretes" discloses the determination theory of specific permeability and comes from experimental results to the conclusion that beside the volume diffusion into the cement stone, surface diffusion must also be taken into account. The authors deduce an interdependence between the specific permeability, the carbonization, the compressive strength and the freeze proofness.

I have to mention here that Schwiete and Ludwig presented also a second and very important study with the heading "Influence of open porosity on the stability of concrete and mortar against aggressive solutions" which can be considered as a continuation of the former and contributes by a most valuable item to the clarifying of this very important problem. – The authors performed

their experiments in solutions of sodium-, magnesium- and calcium-sulphates, and of sodium-phormiate and acetic acid. They layed down the fact that a low permeability renders the cement stone corrosion resistant to a greater extent, than could be expected on the basis of the mineral composition of the cement, and of its hydraulite- or blast-furnace-slag-content. In order to ensure the sulphate resistance of the concrete by chemical means, the corrosivity-limit value mut be below 0,8. /Under corrosivity-limit value the following fraction of mol-values is meant: $\frac{CaO}{SiO_2 + Al_2O_3}$ ./

It is an interesting statement that the composition of the cement stone undergoes after a time a change by the influence of a sulphatic corrosive attack. Not only SO_4^{-2} diffuses into the cement stone, but there takes place a migration of material also in the opposite direction. – If the Ca-content of the system is reduced to a certain extent, the further sulphatic corrosion slows down or may cease completely.

This dissertation contains extremely many interesting and important observations. Nevertheless one could want an answer to the question: if ettringite is produced subsequently, what conditions make possible the development of the harmless type of ettringite, – taking into consideration that the sulphatic slag cements contain even after a delay of several months some anhydrite. Moreover in the brownmillerite cements the rate of hydratation of this ferrite phase is so small that a hydratation of aluminates can occur even in the cement stone hardened already. – I consider the the compilation reporting on the results of the more important

seventeen corrosion tests as a particularly valuable item of the treatise.

Concerning the high-aluminous cement, this time a self-contained dissertation comes before the Symposium: Ryuichi Tsukayama's "Effect of Conversion on Properties of Concrete Using High-Aluminous Cement".

Questions in connection with aluminate cements were handled at the Washington Symposium by L'Hopitalier /Paper VIII.-4/, who summarized the research results since 1938, particularly stressing the hydratation of the different calcium aluminates. – He introduces in his report the table of Wells and Carlson, according to which under 24° C the monocalcium aluminate hydrate is the dominating product, whereas at a higher temperature the C_3AH_6, crystallizing in the cubic system, dominates. This result compares fairly with the statements of other researchers, yet there exists a research result, according to which hexahydrate can be found already at 10 centigrades in case of a higher water-cement ratio.

All these results verify in general the thermodynamical computations, and as the differences of free enthalpy are in the case of different hydratation phases not significant, at least temporarily unstable hydrate compounds may arise, which transform at a higher temperature, or after a longer period, or influenced by both, to a stable hydrate. This transformation is accompanied by a 40% diminution of the solid matter volume.

This stabilization process increases greatly the porosity, which fact implies – according to the formerly discussed papers – a lessening of strength and the deterioration of the corrosion

resistance. Research Eng. Talabér reported on the experiments concerning the loss of strength, conducted for 25 years approx., at the RILEM colloquium /Report II. 1962. p. 109/. – This diminishing of strength starts in general after a delay of six months, and no settling of this process at some lower strength level can be determined. With the parallel series of Portland cement fabricates, the increase of strength continues in average for a year, and from this time on the strength remains stable. – It could be recommended to perform on occasion of such well defined experiments complete crystal-chemical investigations.

Now the treatise of Tsukayama brings new data pertaining to this question. The curing of the samples was done at 50 centigrades, at which temperature the hexahydrate should be already the dominating product. As at the time of setting also the formation of unstable mono- and dicalcium-hydrate is possible, the researcher could state a loss of strength. However the apparition of the stable product in a greater quantity could have slackened the extent of transformation and the attendant structural decomposition. It would be of interest to compare these research results with the formerly treated items. – One must agree fully with the author stating that the transformation and the accompanying growth of the pores is interdependent with the loss of strength.

The author raises the idea too, whether the destruction of the high-aluminous cement could be avoided by enforcing initially the formation of stable products. However this technological approach would imply the loss of the great initial strengths.

The durability problem of high-aluminous cements is not only

a scientific question but one of great economic consequence. Biczók summarized at the Leipzig conference in 1967 the damages of conretes made with aluminous cements, come out in the last decade in several countries, which necessitated e.g. in Hungary and Bavaria costly reconstruction works.

In this connexion I show a diagram /see the figure in the Annex/, which is the result of many years of research and practical data collection, and appeared in the Hungarian Cement Handbook, published in 1967.

This diagram enables the designer to predict the development of the strength of an aluminous cement mortar under the influence of the temperature in function of time.

I can't omit to mention here that the cement stone made of a high-aluminous cement shows various changes of colour due to its intrinsic transformations. An oxydizing firing produces a brownish-rosy shade, a reducing one a dark grey or light gray shade; whereas cements produced from iron-free raw materials — by burning in a metallurgical/blast furnace — show a discolouration of white into gray. These discolourations enable the technicians in a certain measure to draw conclusions concerning a qualitative change. In the course of the reconstruction works mentioned formerly, the grade of the decomposition of concretes is established by means of diffraction radiograms, and recently also by the thermographic determination of the $Al/OH/_3$ proceeding from the CAH.

The frost resistance of the concretes is the subject of three papers; one of them investigates the behaviour of the concrete at an extremely low temperature of -180° C. Yoshiro Koh and Eiji

Kamada judge /in their paper on "The Behaviour of Concrete Subjected to Freezing and Thawing as a Reference for Frost Resistivity of Concrete"/ the freeze proofness of concrete on the basis of its freezing and thawing characteristics. The researchers controlled the length change of the 25 cm high test cylinders with recording dilatometers. Part of the test specimens were first dried cautiously and then exposed to alternate thermal effects, part of them were saturated at the start of the experiments by storage in water. There have been prepared test specimens also with differently absorptive aggregates.

The specimens water saturated in a different measure behaved – as expected – in a different manner during, respectively after, the 13 freezing and thawing cycles. The specimens marked by the author with an "s" showed in the course of experiments no greater volume change than corresponding to the temperature change. On the other hand the saturated specimens expanded at freezing and following the experimental cycles a residual volume increase up to 0,3% was observed.

In connection with this treatise some former experimental and theoretical research results deserve mentioning. – In the cement stone – as a result of the occurring chemical proceedings – an internal dewatering ensues, because the fill by the substances of hydrate compounds requires less volume than the volume of the reacting clinker minerals and the necessary hydrating water together. At hardening uniformly distributed pores develop in the cement stone, possessing enough volume to take up the volume increase caused by the freezing of the residual water in the air-dry concrete.

I may refer here to the computations of Czernin /Zement-Kalk-Gips, 9, 1956. p. 525/.

This extraction of water proceeds in parallel with the hydratation, therefore a period exists when the necessary porosity is already developed; from this point the concrete attains the grade of curing where it can be considered as freeze resistant. /RILEM recommendation, see BETON, 14, 1964. p. 411./ The desirable pore volume estimated on this train of ideas obtains only 1%, whereas we aim with air-entraining cements at a pore content of 3-5%. This is explained by the fact that it is impossible to ensure such an uniformity of pore distribution in the air-entraining concretes which comes about automatically in the cement stone as a result of the processes taking place automatically. This question was handled in theory by Powers in 1956 on occasion of a Symposium dealing with the concreting in winter.

G. Tognon controls by his treatise on "Behaviour of mortars and concretes in the temperature range from +20 to -180° C" the effect of freezing on the three strength characteristics and on the modulus of elasticity. – It is somewhat surprising that by the decrease of the treating temperature the strength of the specimens increased, yet this increase halted in the temperature range of -35° and -60° C.

For being able to value such experiments, the structure of the specimens, their pore distribution and their grade of saturation ought to be known. One can not disregard that the cement stone contains a certain quantity of water which – absorbed by the surface of the hydrated products – does not freeze, respective-

ly remains in such a state that it may be nearly considered as a solid, even at +20 centigrades. Consequently the experimental determination of the water distribution should belong to the valuation of the experimental results.

Professor C. MacInnis is occupied by the "Frost Resistance of Cement Grouts for Prestressed Concrete Applications". – He reports on three experimental programs and comes to the conclusion that even with prestressed concrete in a restrained condition /under pressure/ the curing period is the most important factor determining the frost resistance. – His statement that the utilization of air-entrained concrete has also good results, coincides with the results of other workers and with the practice.

K.R. Lauer and C.W. Gray deal in their paper "A Durability Study of Concrete Using Monte Carlo Simulation" with an investigation of the durability of a hypothetical bridge deck. They accomplish their study by employing a calculus of probability known as Monte Carlo simulation method. This work can be considered also as a comparative study of the ordinary dense concrete and of the air-entrained concrete.

This mathematical method, employed formerly on other fields of scientific research, studies by the consideration of the stochastic variables the probability of material qualities. The method termed formerly "model sampling" would be impractical without a high-speed /digital/ computer.

In order to judge the durability of a concrete bridge deck the following influencing factors concerning the material were considered:

the probability of occurrence for compressive strength,

the probability of occurrence for air content, if air-entrained concrete is employed,

the probability of compressive strength loss, due to air-entrainment,

the time and temperature effects /that is the effects of curing/ on the gain in strength, studies by a half-year experiment conducted between −8 and +38 centigrades,

dynamic modulus of elasticity and freeze-thaw cycles, and

de-icing salt scale rating and the number of scale cycles.

The experiments were conducted in a climatic environment comparable to that of South Bend, Indiana /near Lake Michigan/. The results were summarized in 10 diagrams, the computations in 7 tables.

According to the computations the air-entrained deck will be in service for about five times as long /16 years/ as the non air-entrained concrete /3,1 years/. It would be of interest to compare the results of these computations with the experiences obtained with the practical concrete decks in the chosen climatic environment.

- o -

The aforesaid summarizing remarks accentuate the fact that in the last years a very considerable development of the research on concrete corrosion can be recorded. Several phenomena of corrosion were put in a new light.

- o -

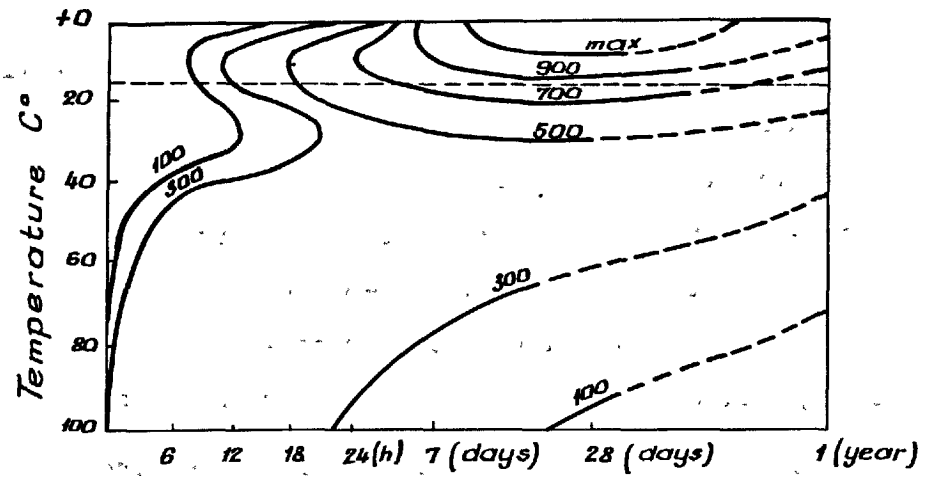

Configuration of the standard compression strength of aluminous cements depending from the temperature and the time. After Bereczky.

GENERAL REPORT
OF
SESSION III-3: CARBONATION OF CONCRETE

H. G. Smolczyk (West Germany)

The following Supplementary Papers are summarized in this report.

Paper No. III-16

VARIATION IN STRENGTH OF MORTARS MADE OF DIFFERENT CEMENTS DUE TO CARBONATION

W. Manns & K. Wesche (West Germany)

Paper No. III-52

INVESTIGATIONS ON THE CARBONATION OF CONCRETE

A. Meyer (West Germany)

Paper No. III-116

MECHANISMS AND KINETICS ON CARBONATION OF HARDENED CEMENT

R. Kondo, M. Daimon & T. Akiba (Japan)

Contents:

G E N E R A L R E P O R T

1. Introduction

It is a great honour for me to give a summarizing report of the three very interesting papers by Professor K.H. Wesche and Mr. W. Manns, by Professor A. Meyer and by Professor R. Kondo, Mr. M. Daimon and Mr. T. Akiba.

These very extensive works reveal an abundance of experimental results concerning the carbonation of concrete under quite different test conditions.

It gives me great pleasure, indeed, to be able to indicate that the experimental results without exception show a surprisingly good conformity. Furthermore there is additional proof given by the test results of other authors and also by our own comprehensive studies.

On the other hand I am afraid that I cannot extend this statement as far as the theoretical evaluations and conclusions are concerned. In few cases, moreover, I could not see the relation between experimental results and final conclusions.

Therefore - to overcome this difficulty - it proved useful to differentiate strictly between the measured test results and the conclusions of the authors.

The following abbreviations have been chosen:

x = depth of carbonation
t = time of carbonation

PZ = Portland cement (Portland Zement)
HOZ = blastfurnace slag cement in general (Hochofenzement allgemein)
EPZ = blastfurnace slag cement with less than 30 % of slag (Eisenportlandzement)

All the other abbreviations are explained in text, figures and tables.

2. The Work of R. Kondo, M. Daimon and T. Akiba

"MECHANISMS AND KINETICS ON CARBONATION OF HARDENED CEMENT"

a) Experimental results

Mortar prisms 2 x 2 x 8 cm with 1 PZ (65 % CaO) and 1 HOZ (55 % CaO) are carbonated in CO_2-gas of 44 % RH. After 7 days' respective 28 days' curing in saturated $Ca(OH)_2$ solution and before carbonation the prisms are stored at 44 % RH to approach equilibrium. Their surfaces are sealed with epoxi-resin in such a manner that only one surface 2 x 2 cm remains free for CO_2-penetration. Part of the mortars are made with an additive (0,3 cm^3 vinsol resin / 1 kg cement).

The pore size distribution of 7 specimens (75 to 75000 Å) is measured. A surview on the total pore volume of the 6 best comparable specimens is shown in Table 1.

The chemical analysis of fixed CO_2 after complete carbonation does not correspond with the content of free $Ca(OH)_2$ before carbonation. On the contrary the amount of fixed CO_2 is equivalent to the total content of CaO in the specimen. The amount of produced calcite - as tested by X-ray analysis - is lower because the certainly also produced vaterite has not been taken into account in the calculation.

The carbonation strongly depends on the curing conditions before carbonation and on the w/c ratio, and the HOZ carbonates at a faster rate than the PZ. The carbonation curves - expressed as $x = f(\sqrt{t})$ - do not start from the origin. After a short period of induction they increase at a markedly faster rate than a function

$$x \sim \sqrt{t}$$

would permit.

b) Evaluations and conclusions

The authors evaluate a carbonation formula for concretes and mortars on the supposition that the approximation

$$x^2 = k_e \cdot t$$

is applicable to further calculation, and taking into consideration the diffusion of CO_2 and of H_2O.

The calculation itself is to be seen in Table 2. The connection between the experimental constant k_e and the calculated theoretical constant k_t is given by introducing the "tortuosity" f. By taking into consideration the order of magnitude of "f" it is possible to decide when the rate of neutralization was controlled by diffusion of CO_2 into the specimen and when by diffusion of H_2O out of the specimen.

The comparison of the rate of neutralization measured by M. Hamada and the new formula of the authors results in the empirically expected value $f = 10$.

3. The Work of W. Manns and K. Wesche

"VARIATION IN STRENGTH OF MORTARS MADE OF DIFFERENT CEMENTS DUE TO CARBONATION"

a) Experimental results

Cores taken from concrete structures with supersulfated slag cement had shown a lower compressive strength in the carbonated layer near the surface than in the deeper located alkaline parts.

For further investigation of this phenomena mortar prisms 4 x 4 x 16 cm, w/c 0,6 with 6 very different cements after 28 days' watercuring are completely dried at 40 °C and then completely carbonated with 9 % CO_2 at 25 °C. During the whole carbonation period a great number of strength tests are performed.

The final result is clearly recognizable on one diagram of the authors which is copied in Figure 1.

First of all it proves clearly that the supersulfated slag cement shows a behaviour quite different from all the other cements. With this cement the drying has resulted only in a very little increase in strength of 16 % and the carbonation effects a genuine loss in strength.

The five other cements - on the contrary - have gained strength increases between 27 % (PC) and 48 % (TBFC I) as a result of the drying process.

(Remark: These strength increases are comparable with the normal afterhardening of concretes during the very slow longtime process of carbonation in practice.)

Furtheron there is to be seen that under these practice-like conditions (afterhardening and carbonation = full marks) all the tested cements show an increase in strength which is largest with the PZ and small with the two cements with 25 % clinker and 18 % clinker.

Taking the strength after the drying procedure as starting point (carbonation without afterhardening = open marks) all the strengths are lower in exact equivalence to the missing afterhardening, naturally.

It is remarkable that in both the forms of representation the PZ and the two trass-blastfurnace cements form a straight line corresponding to the clinker content, whereas the two HOZ show 10 - 20 % higher strengths with respect to their clinker contents. Under the chosen experimental conditions the strengths obviously increase most with regard to the clinker content and least with respect to the trass content of the five cements.

The tensile strengths (F) change in a similar way as the compressive strengths (B). On the other hand the fact has to be emphasized that the well-known relation [1] for mortar prisms 4 x 4 x 16 cm

$$F \simeq B^{0,7}$$

which has proved valid for all cements, so far, (also for supersulfated cements and high alumina cements, and also for completely carbonated mortars) does not prove to be valid any more after the applied drying procedure and also after the carbonation.

Furthermore, the change in weight of the prisms are measured during carbonation. An increase in strength is accompanied by an increase in weight and with decreasing strength also a decrease in weight is measured.

The carbonation is slowest with the HOZ with 60 % clinker and fastest with the trass-blastfurnace cement with 25 % clinker. The HOZ with 60 % clinker carbonates approximately according to the function

$$x \sim \sqrt{t}$$

The carbonation curves of the other cements increase at a faster rate after a short period of induction.

b) Evaluations and conclusions

The authors come to the conclusion, that not only with supersulfated cements but also with all other cements containing less than 40 % clinker the strengths of concretes would decrease with progressing carbonation.

Further they state: "... it cannot be expected, in general, that a building may loose its stability. This statement can, however, be considered as secured only by profound investigations in all questions, ...".

4. The Work of A. Meyer

"INVESTIGATIONS ON THE CARBONATION OF CONCRETE"

a) Experimental results

Numerous tests on old constructions and on test specimens in the laboratory are carried out because the carbonation is suspected to have a very negative effect upon the corrosion of reinforcement.

In a forty-year-old dairy the carbonation of the concrete had reached a depth of 26 mm. In places where the concrete cover of the reinforcement was only 15 mm, the steel was severely corroded, where, however, the cover increased to about 60 mm, the steel showed no sign of corrosion.

The change in compressive strength is tested with tiny mortar cylinders of 11,3 mm in diameter which - after 28 days' water curing - are carbonated in 10 % CO_2 within 21 days. Three PZ, two EPZ, two HOZ, and one high alumina cement show increases in strength, two HOZ with 75 % slag come up to the same average strength after the carbonation as they have after 56 days' water curing, and one supersulfated cement shows a loss in strength of more than 40 %.

On cores from old constructions the permeability and the moisture movement is measured. The permeability is about the same in the carbonated part and in the noncarbonated part. The drying rate at the beginning, however, is much higher in the carbonated part than in the noncarbonated part.

The majority of the tests deal with the parameters of carbonation. The experimental conditions of the five test series carried out in the laboratory are shown in Table 3. As the test conditions listed in the supplementary paper differ slightly from the ones given in the corresponding German publication, I took the test values in the identical diagrams for granted and made use of the already published information (2).

Four parameters are investigated:

Type of cement
Water/cement ratio
Storage conditions during carbonation
Effect of age.

Not investigated are the influences of

Hydraulic capacity of the cement
Chemical composition of the cement and its hydration products
Curing condition before carbonation.

In all the test series all the PZ carbonate less than all the HOZ and all the pozzolanic cements. In the upper part of Figure 2 the results of the test series 4 are shown as a typical sample.

The carbonation increases gradually with growing w/c ratio (Test series 2, 3, 4 and 5). The carbonation ratio of HOZ to PZ on the average decreases with increasing w/c. This gets particularly evident in the test series 3 with concrete.

The moister the storage conditions are, the slower gets

the carbonation. (Test series 2 and 5)

In any case (Test series 1, 2, 3, and 5) the carbonation increases faster than is corresponding to the function

$$x \sim \sqrt{t} \quad .$$

In general this deviation is worse with the PZ than with the HOZ.

In addition a so-called "test series 6" with 60 concretes is mentioned. This, however, brings nothing new, because it includes 12 chosen specimens of test series 3, furthermore, 15 of the remaining 48 specimens are not older than two years. As these specimens are not defined by far as well as those of the test series 2 - 5, an only very indistinct connection of the carbonation with the w/c is to be seen. The main result of this test series, I presume, consists of the reference that here again the average carbonation of the PZ is about half as strong as the average carbonation of all the other cements.

The also mentioned numerous tests on old and very old concrete structures are far more informative. Here the exact conditions of the three types of storage "indoors", "outdoors" and "outdoors protected from rain" can also not be defined accurately, but at least the older concretes with the storage of the type "outdoors protected from rain" should be rather comparable. Furthermore this study includes a great number of tests, and the mean age of the specimens is 5 times greater than the one of the "test series 6".

The carbonation depths and the compressive strengths were measured. To calculate the w/c ratios of these old concretes it was necessary, however, first to estimate the mixing water content of the fresh concrete mix and its porosity. Therefore these values are not given here as measured test results. The curing conditions before carbonation are unknown. Assuming that the general usability "indoors" and "outdoors" is the same for PZ as well as for HOZ and that the specimens are fairly comparable, I calculated the average values of all test results in Table 4.

The difference in compressive strength between the concretes with PZ and the concretes with HOZ after about 23 years amounts to 49 kp/cm^2. The measured difference in carbonation depth of 4 mm to 5 mm corresponds exactly to the theoretical value which is to be expected with this difference in compressive strength.

Taking into consideration that all storage conditions and many other unknown influences have been included, this result proves an excellent experimental technic.

b) Evaluations and conclusions

Mr. Meyer draws the conclusion that the carbonation of concrete can be characterized satisfactorily and also be predicted up to 50 years by using the following parameters:

Age

The carbonation at all events obeys the equation

$$x = \text{const} \cdot \sqrt{t}$$

which is evaluated with the application of Fick's first diffusion law.

Water/cement ratio

The carbonation of all concretes increases linear with increasing w/c ratios, and with w/c 0.80 it will be twice as deep as with w/c 0.50 (see Fig. 2).

Type of cement

The resistance against carbonation is largely due to the content of free $Ca(OH)_2$ in the paste. Therefore the carbonation depths in concretes with slag cements and with pozzolanic cements are always expected to be deeper than those in concretes with Portland cement, all other conditions being identical. The relative ratio of the carbonation depths remains constant in all storage conditions, all carbonation periods, all w/c ratios, and all curing conditions of the young concretes.

S t o r a g e c o n d i t i o n

Concrete with PZ and w/c 0.50 will have a carbonation depth of 10 - 15 mm after 50 years if it is stored outdoors protected from rain. In case it is unsheltered from rain, less carbonation will occur. Stored in a closed dry room, the carbonation will be deepest.

Mr. Meyer's final statement is: "The carbonation resistance of a fully compacted and normally cured concrete is essentially determined by its water/cement ratio and by the type of cement used."

5. Comparison of Results being in Complete Accordance

Comparing all the carbonation tests known to me - the published as well as the unpublished ones - I discovered two empirical relations which have been proved by all tests results very nearly without exception, so far. Therefore, I think, they have the significance of universal rules. They are once again demonstrated by these three reported papers in a surprisingly distinct way.

T h e c a r b o n a t i o n i n c r e a s e s n e a r l y a l w a y s a t a f a s t e r r a t e t h a n a f u n c t i o n $x \sim \sqrt{t}$ w o u l d p e r m i t .

This can distinctly be observed if - drawing carbonation depth x and carbonation time t to double logarithmic scale - the gradient 1/v of the curves is greater than 1/2.

Figure 3 shows the carbonation of the specimens A_{1-4} of R. Kondo, M. Daimon and T. Akiba and also the carbonation curves published by W. Manns and K. Wesche. In both cases the function appears to be

$$X \simeq \text{const.} \cdot \sqrt[v]{t - t_o}$$

The values of v are calculated without taking into account the induction period t_o. Therefore they are even a little bit too high.

Figure 4 shows the mean results of the test series 3 of A. Meyer. The slope of the curves is extremely strong in this case - especially with the PZ - though the concretes carbonated in normal room atmosphere only. The test series 1 likewise resulted in an average v-value $\bar{v} \tilde{=} 1{,}7$, and the test series 2 in $\bar{v} \tilde{=} 1{,}6$. Both the test series 1 and 2 show short induction periods. The test values are taken from the original German paper[2].

Many authors calculate with the approximation $x \sim \sqrt{t}$. This can lead to bad mistakes as far as extrapolations over long-time periods are concerned, as is to be seen in Figure 5. The thick curves represent the genuine experimental carbonation functions of the two cements Z 1 and Z 9 of our own mortar carbonation studies:

$$x_1 \sim \sqrt[2{,}15]{t}$$

$$x_9 \sim \sqrt[1{,}74]{t} \quad \text{(typical for PZ)}$$

Among the three possibilities of a linear $\sqrt{t}$ -approximation, the simple linear extrapolation of the one-year-old carbonation curves (thin lines) leads to unbearable deviations after 10 years.

The second general conformity of test results has even more consequences for practice:

The carbonation of concretes and mortars with increasing time becomes closely proportional to the factor $1/\sqrt{\text{compressive strength}}$.

This fact is proved by all experimental carbonation studies which include strength tests. Probably the permeability - as reported by R. Kondo and several other authors - is the essential factor, which is only represented by the far better measurable strength.

This relation includes the influences of w/c ratio, type of cement, and precuring condition, and has been proved to be valid for cements of most different compositions. The only exceptions are the supersulfated cements and the high alumina cements, so far.

This relation, moreover, is apt to interpret the fact that the slow-hardening PZs (e. g. C_3A-free PZs) carbonate at a markedly faster rate than quick-hardening cements, and that HOZs with higher strengths, if sufficiently cured, often carbonate less than normal PZs.

Therefore, in the results of W. Manns and K. Wesche - see Figure 6 - it is not the PZ that shows the least carbonation depth but the mortar which had the highest strength at the beginning carbonation. Consequently it is not the cement with the lowest clinker content that shows strongest carbonation but the mortar with the lowest compressive strength. The test values are taken from the original German paper [3].

This relation is also valid for very different w/c ratios, as is to be seen in Figure 7, in which the results of the test series 4 of A. Meyer are evaluated. Because of the still very steep strength increase at the beginning of the carbonation (7 days), in this case the 14 days' strengths had to be taken into account. The test values are taken from the original German paper [2].

The studies on old and very old concrete structures by A. Meyer and by two other authors reveal the same tendency [2], [4] and [5]. The concretes being best comparable must be those which had been stored outdoors sheltered from rain and which are old enough for a statistical surview without inaccurate extrapolation of carbonation depths. In Figure 8 all the specimens (without exception) are shown which firstly met this storage condition, secondly were older than 20 years, and thirdly were published with strength datas. (The dotted line is calculated according to results of another very comprehensive German longtime study including more than 15 cements and 3 w/c ratios.) In the case of the old structures, only the final strengths are known. A calculation with the initial strengths and with the certainly very different afterhardenings would surely have brought about a more accurate diagram.

6. Final Conclusions for Practice

The empirical relation $x \sim 1/\sqrt{B}$ is proved by so many test results - also by our own laboratory studies - that a rule can be taken for granted. Before estimating the carbonation behaviour of a concrete with given strength, its afterhardening must be taken into consideration, which possibly can result in remarkable strength increases, especially if slow-hardening cements are concerned. Naturally, this process takes much more time in air than it would take in water, but the carbonation is a longtime process, too.

Provided that also the slow afterhardening in air corresponds to Sadran's formula [6]

$$\frac{1}{B} \sim \frac{1}{t}$$

- which must be slightly altered for this purpose - I calculated the diagram of Figure 9, which takes into consideration all the carbonation studies known to me so far. It is valid for concretes with dense aggregates, which are carbonated outdoors sheltered from rain in average German air conditions. It does neither require the knowledge of the w/c ratio nor the type of cement, with exception of supersulfated cements and high alumina cements.

This diagram contains quite a number of statements and evaluating possibilities. Only two of them shall be pointed out here:

Figure 9 gives an explanation for the fact that a strength difference from 335 to 384 kp/cm^2 after ~ 23 years must result in a carbonation difference of about 5 mm. (See Table 4)

Then Figure 9 shows that in short time tests, i. e. without the effect of afterhardening, a greater carbonation difference must be taken into account, comparing slow-hardening and quick-hardening cements, especially in case of small specimens and short precuring periods [7]. In longtime studies, however, these differences will be compensated or diminished, at least, by the higher afterhardening of the slower cements. This explains the fact that by a statistical evaluation of numerous tests on old and very old concrete structures only very little if any differences in the carbonation behaviour of different cements could be observed [8] and [9].

SUMMARIZING SURVIEW

The three reported papers reveal a number of corresponding test results and observations which enable us to enlarge our present knowledge and to recognize new aspects of carbonation. At this not the type of cement or the amount of free $Ca(OH)_2$, but the permeability and the quality of the concrete and the special storage condition proved to be the decisive factors.

Unfortunately there have been reported no experimental studies on steel corrosion itself, which does not depend on carbonation only, but also on the durability of the concrete in other aggressive media. To complete this surview I just want to mention the comprehensive longtime studies on seawater action on reinforced concretes, carried out in England, Belgium, France, and Norway [10], [11], [12] and [13]. In these studies especially those cements which are often reported of as carbonating faster than Portland cements, provided the better protection of reinforcement against steel corrosion.

REFERENCES

1. A. Hummel: "Das Beton-ABC", 11th edition, p. 13, Ed. W. Ernst & Sohn, Berlin (1951)

2. A. Meyer, H.-J. Wierig, K. Husmann: "Carbonatisierung von Schwerbeton", Beckum 1964, Deutscher Ausschuß für Stahlbeton, Heft 182/I, 1-32, Berlin (1967) (und Heft 170, 40-58, Berlin 1965

3. W. Manns, O. Schatz: "Über die Beeinflussung der Festigkeit von Zementmörteln durch die Karbonatisation" Betonsteinzeitung 33, 148-156 (1967)

4. G. Rehm und H. Moll: "Beobachtungen an alten Stahlbetonteilen hinsichtlich Carbonatisierung des Betons und Rostbildung an der Bewehrung." Deutscher Ausschuß für Stahlbeton, Heft 170, 6-20, Berlin (1965)

5. H.-J. Kleinschmidt: "Untersuchungen über das Fortschreiten der Carbonatisierung an Betonbauwerken" Deutscher Ausschuß für Stahlbeton, Heft 170, 24-36, Berlin (1965)

6. G. Sadran et R. Dellyes: "Representation lineaire de la resistance mecanique des ciments en fonction du temps." Revue Mater. Constr. No. 606, 93-106 (1966)

7. H.-G. Smolczyk: "Diskussion zum Thema 'Korrosionsfragen beim Spannbeton' V. FIP-Kongress, Paris 1966" Kongressbericht, p. 104-105, Ed. Cement and Concrete Assn., London 1968

8. B. Wedler: "Vorwort" zu diversen Arbeiten über Karbonatisierung alter Betone (Zusammenfassung), Deutscher Ausschuß für Stahlbeton, Heft 170, 3-4 und 59, Berlin (1965)

9. F. Schröder, H.-G. Smolczyk, K. Grade, R. Vinkeloe und R. Roth: "Über den Einfluß von Luftkohlensäure und Feuchtigkeit auf die Beschaffenheit der Betone als Korrosionsschutz für Stahleinlagen" Rheinhausen 1964, Deutscher Ausschuß für Stahlbeton, Heft 182/II, 1-28, Berlin (1967)

10. F. M. Lea and C.M. Watkins: "The durability of reinforced concrete in sea-water" National Building Studies Technical Paper 30; HMSO, London 1960

11. F. Campus, R. Dantienne et M. Dzulynski: "Constatations effectuées après trente années d'immersion marine d'eprouvettes de mortier, des bétons et des bétons armés dans la mer du Nord" International Symposium on the "Behaviour of Concretes Exposed to Sea Water" in Palermo, Mai 1965

12. L. Duhoux and A. Tessier: "Usine marémotrice de la Rance. Composition des bétons." RILEM-Bulletin No. 32, 268-278 (1966)

13. O. E. Gjoerv, I. Gukild and H.P. Sundh: "Investigation of concrete piles under varying conditions in sea water" RILEM-Bulletin No. 32, 305-322 (1966)

Tab.1 Total Pore Volume of Mortars in cm^3/g (75-75000 Å)

Test results by R. Kondo, M. Daimon, T. Akiba

Binder	w/c 0,50 watercuring 28 d	w/c 0,50 watercuring 7 d	w/c 0,65 watercuring 28 d	w/c 0,65 watercuring 7 d
PZ without additive		0,038	0,051 (0,037)*	
PZ with additive	0,038 (0,032)*			0,062
HOZ with additive		0,061	0,047	

* carbonated part

Tab. 2
Carbonation Rate of Mortars and Concretes

by Renichi Kondo, Masaki Daimon and Tokuji Akiba

Experimental approximation :

$$x^2 = k_e \cdot t$$

Calculated formula :

$$k_t = \frac{2D}{R \cdot 273^{1,75}} \cdot \frac{T^{1,75} \cdot \Delta P \cdot \xi}{C \cdot \varrho}$$

Introduction of tortuosity f :

$$k_t = k_e \cdot f$$

Carbonation formula :

$$x = const \cdot \sqrt[2]{\frac{T^{1,75} \cdot \Delta P \cdot \xi}{C \cdot \varrho \cdot f}} \cdot \sqrt[2]{t}$$

x : carbonation depth [cm] — t : carbonation period [sec]

D : diffusion constant [cm^2/sec] — R : gas constant = 82,1

T : abs. temperature [°K] — ΔP: difference of pressure [atm]

ξ : porosity of specimen [cm^3/cm^3] — ϱ : density of specimen [g/cm^3]

C : maximum amount of fixed CO_2 or produced H_2O [mole/g specimen]

Tab. 3 Test Series about Progress of Carbonation

by A. Meyer, H.-J. Wierig and K. Husmann

series	specimens	w/c	cements	curing conditions	storage conditions	carbon. tests after
1	concrete bars 10x15x50 cm	0,53	4 PZ 3 HOZ 1 Puzzolanic cement	4 weeks moist	half immerged in H_2O	10 months 19 " 55 " 76 " 86 "
2	concrete cubes 10x10x10 cm	0,4 and 0,8	1 PZ	1 day moist and 6 days in H_2O	a) norm. room atmosph b) twice a week 1 hour in H_2O	1/2 year 1 " 3 " 4 "
3	concrete bars 10x15x70 cm	0,4 0,5	1 PZ	1 day in the mould and 6 days in H_2O	aircond. room, 18°C, 15% RH	1 year 2 1/2 years
4	mortar prisms 4x4x16 cm	0,6 0,8	3 HOZ			
5		1,0	1 Puzzolanic cement		once a week 2 min. in H_2O	

Tab.4 Jnvestigations on Building Constructions

Average results of carbonation, age and compressive strength according to test results of A. Meyer, H.J.Wierig and K.Husmann

type of cement	number of specimens	mean age [years]	mean carbonation [mm]	mean compressive strength [kp/cm²]	mean carbonation after 20 years [mm]
PZ	27	25	10,8	384	9,7
HOZ and EPZ	36	21	14,6	335	14,2
experimental difference				49	4,5

theoretical difference according to the difference in compressive strength from 335 to 384 kp/cm² } ≙ 5 ± 1mm

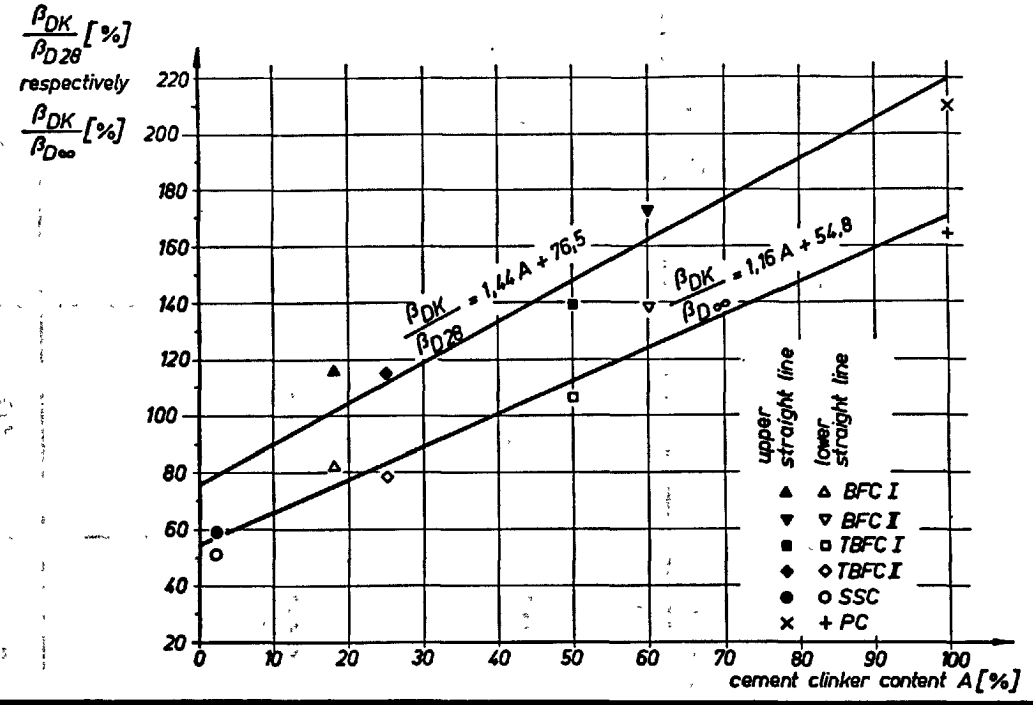

Fig. 1

FJ
Rheinhausen

"Relation between Carbonation and Cement Clinker Content"
by K. Wesche

β = compressive strength of mortars (4x4x16 cm) in kp/cm²
D28 = after 28 days' watercuring before drying
D∞ = after complete drying before carbonation
DK = after carbonation in 9% CO_2

BFC = blastfurnace slag cements
TBFC = trass blastfurnace slag cements
SSC = supersulfated slag cement *PC = Portland cement*

(68/14)

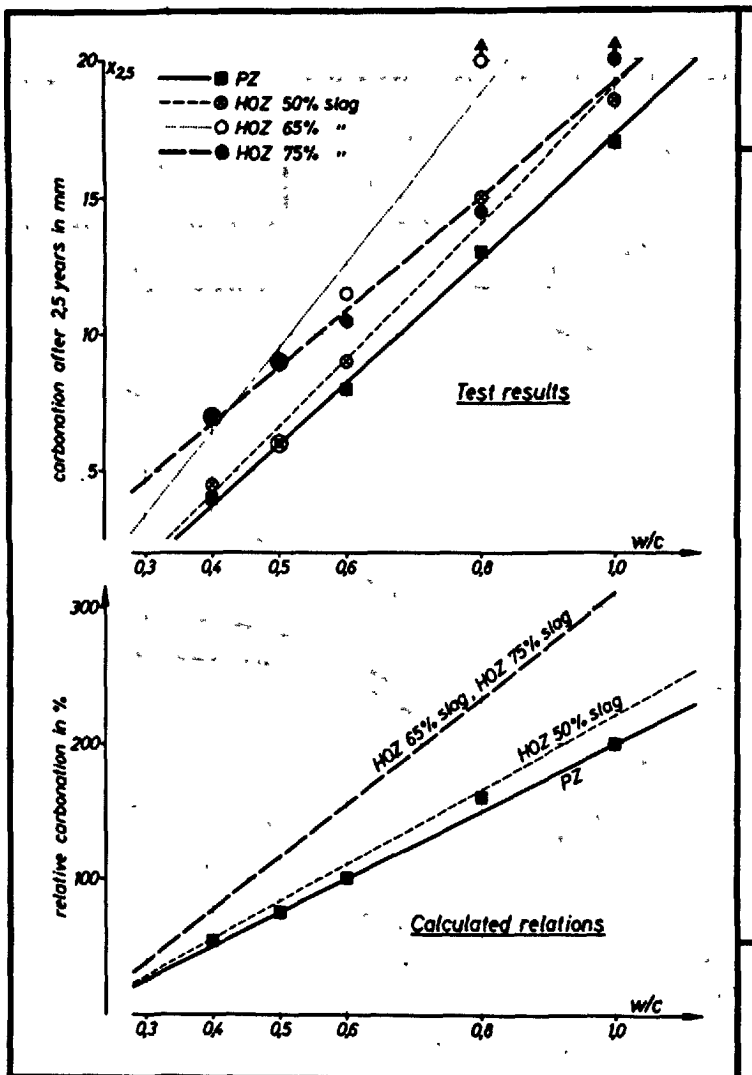

FJ
Rheinhausen

Fig. 2

Carbonation of Mortar Prisms 4 × 4 × 16 cm

Influence of w/c and type of cement according to A. Meyer.

Test results and calculated relations by A. Meyer, H.-J. Wierig and K. Husmann.

(68/13)

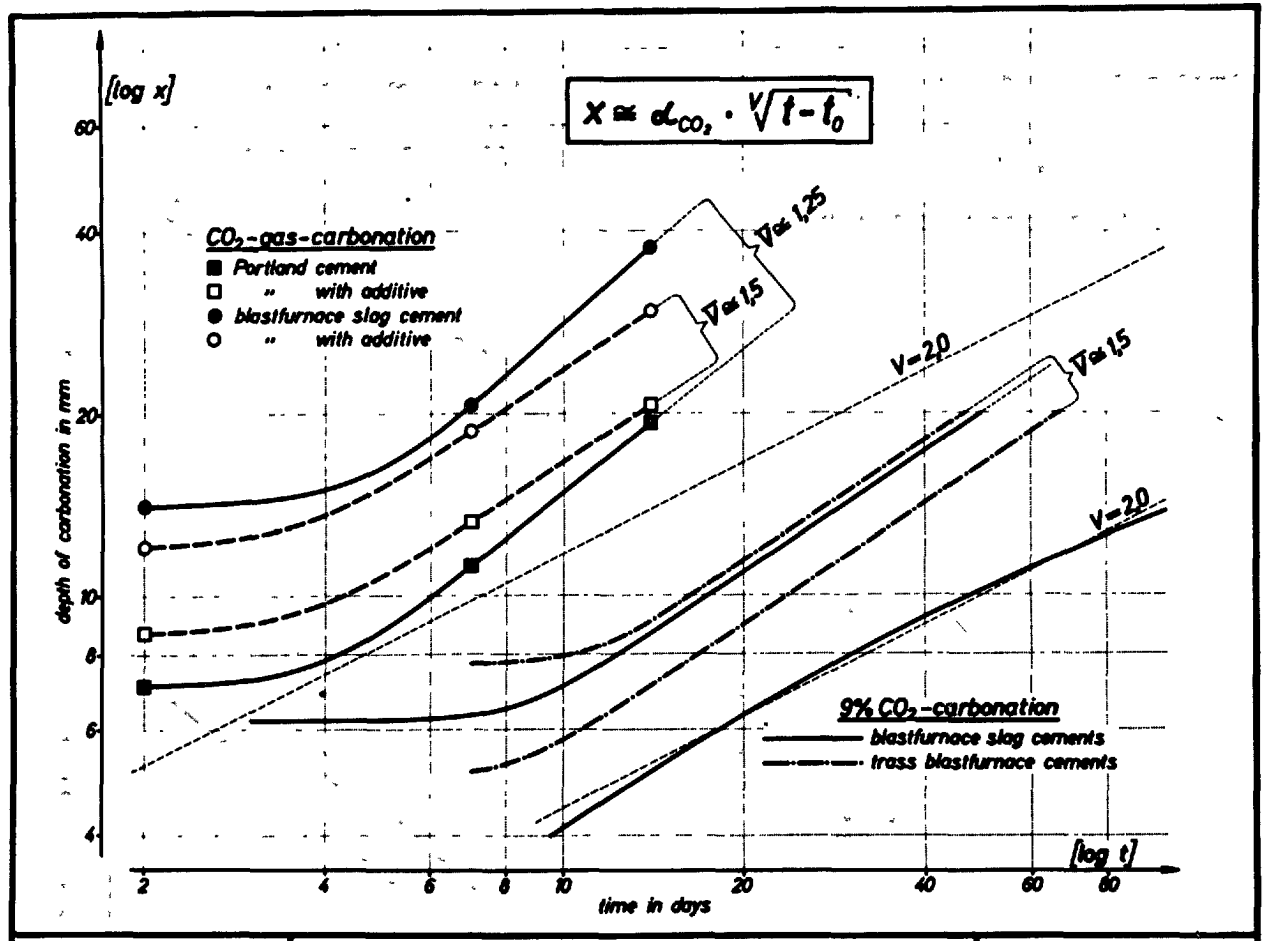

FJ Rheinhausen	**CO_2-Carbonation of Dried Mortars** CO_2-gas according to R. Kondo, M. Daimon and T. Akiba 9% CO_2 according to K. Wesche	(68/11)

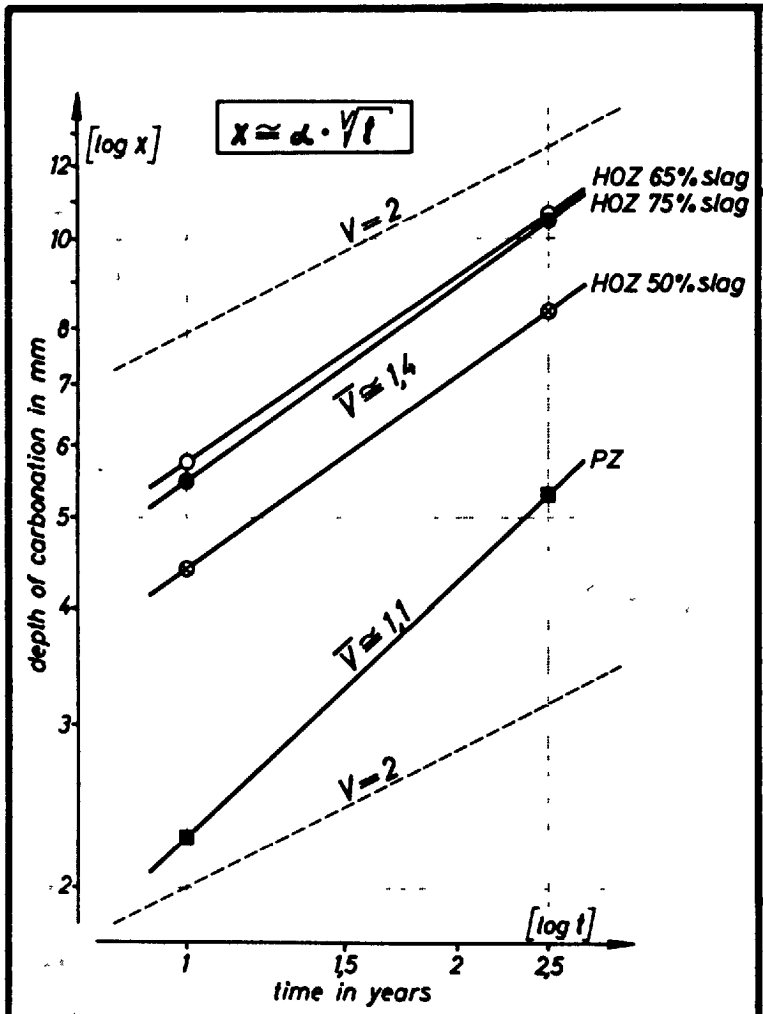

F J
Rheinhausen

Fig. 4

Mean Carbonation Progress of Concrete Bars 10 x 15 x 70 cm

The carbonation slope of each cement is the average of 5 logarithmic carbonation slopes with 5 different w/c ratios

Test results by A. Meyer
H.-J. Wierig
K. Husmann

(68 / 15)

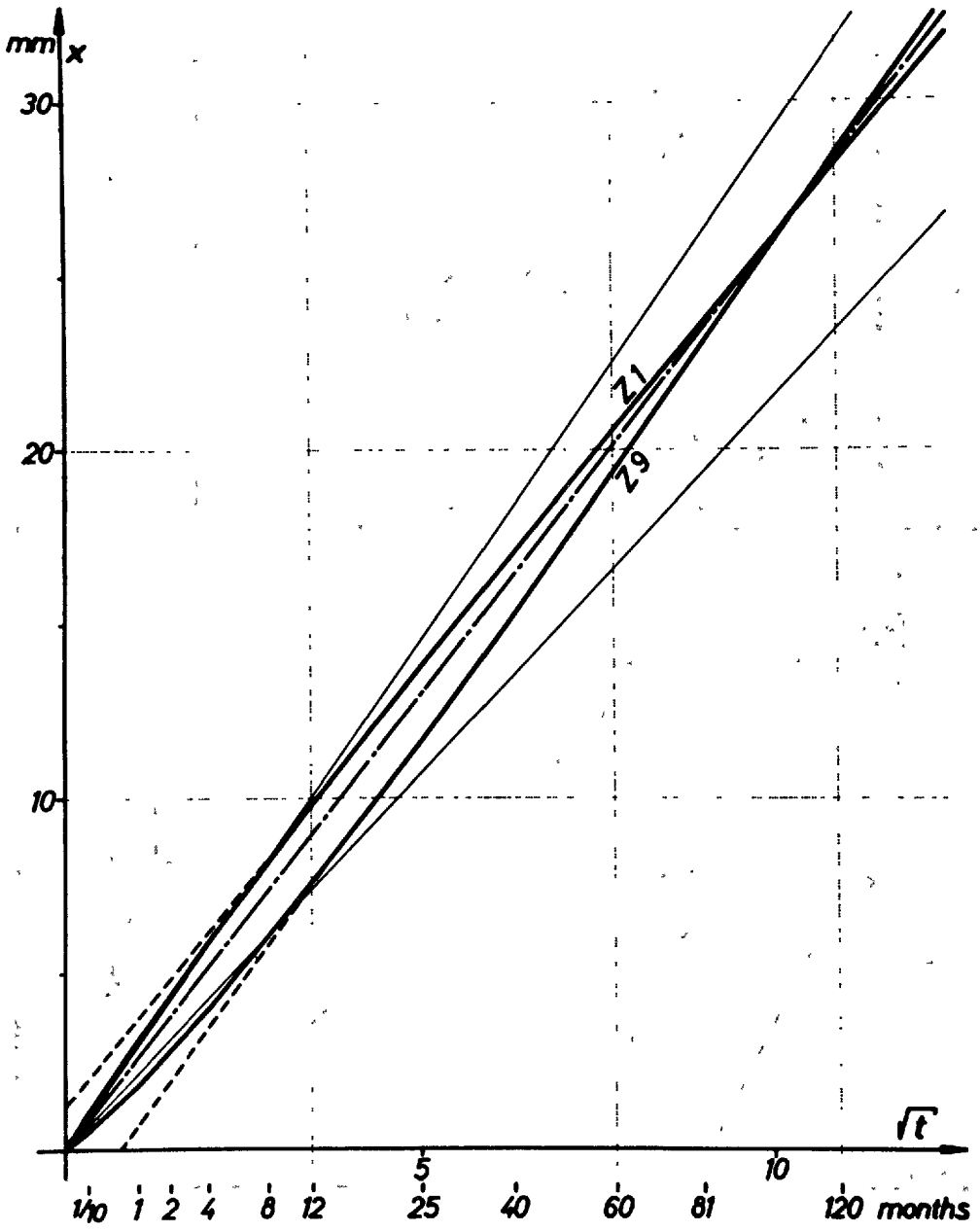

Fig. 5: Genuine Carbonation Progresses of Z1 and Z9 and Trend Lines of $\sqrt[2]{t}$ -Approximation.

- - - - - - - best approximation
——·——·— good long-time approximation
——————— wrong approximation

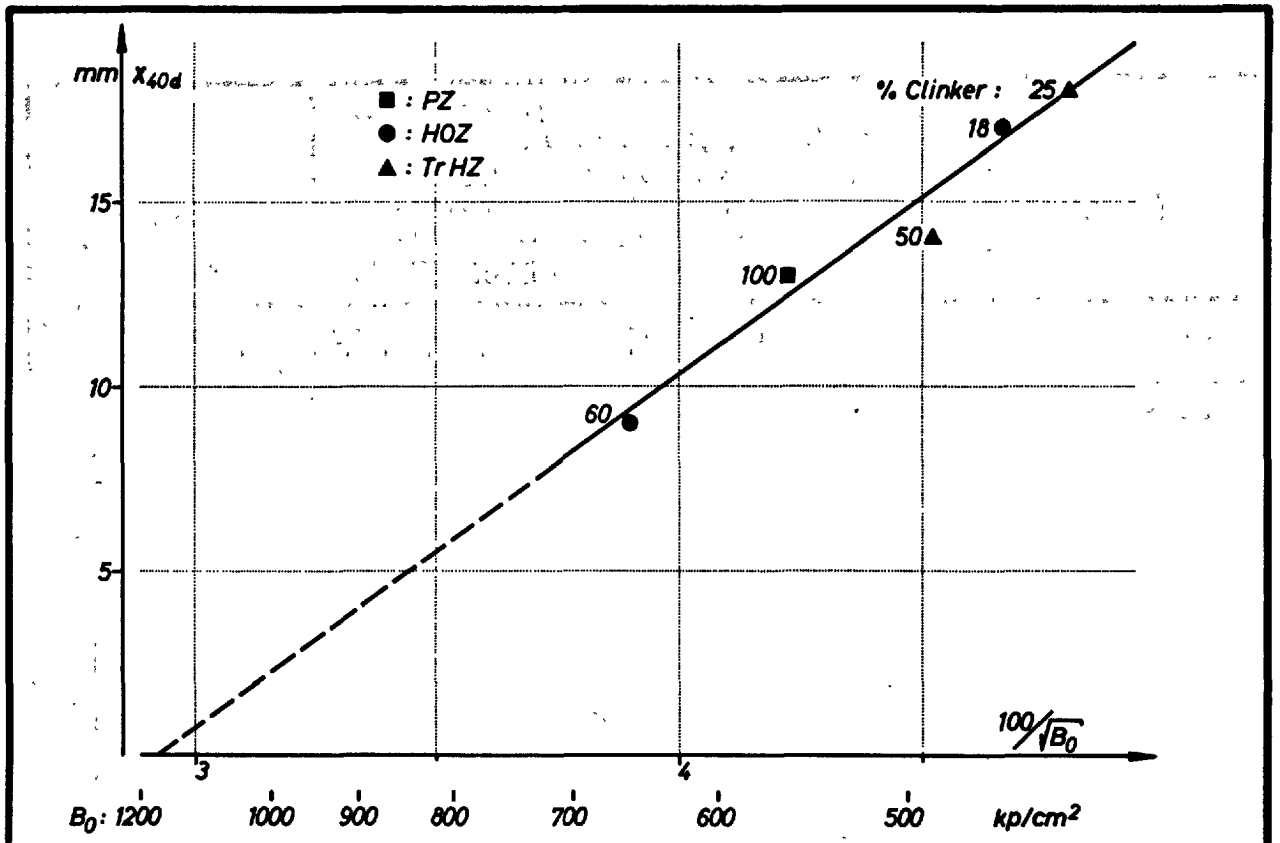

Fig. 6

FJ
Rheinhausen

Carbonation of Completely Dried Mortars after 40 days' storage in 9 % CO_2.

B_0 = compressive strength after heat-treatment (40°C or 105°C)
x_{40d} = carbonation depth

(According to test results of K. Wesche)

(68/10)

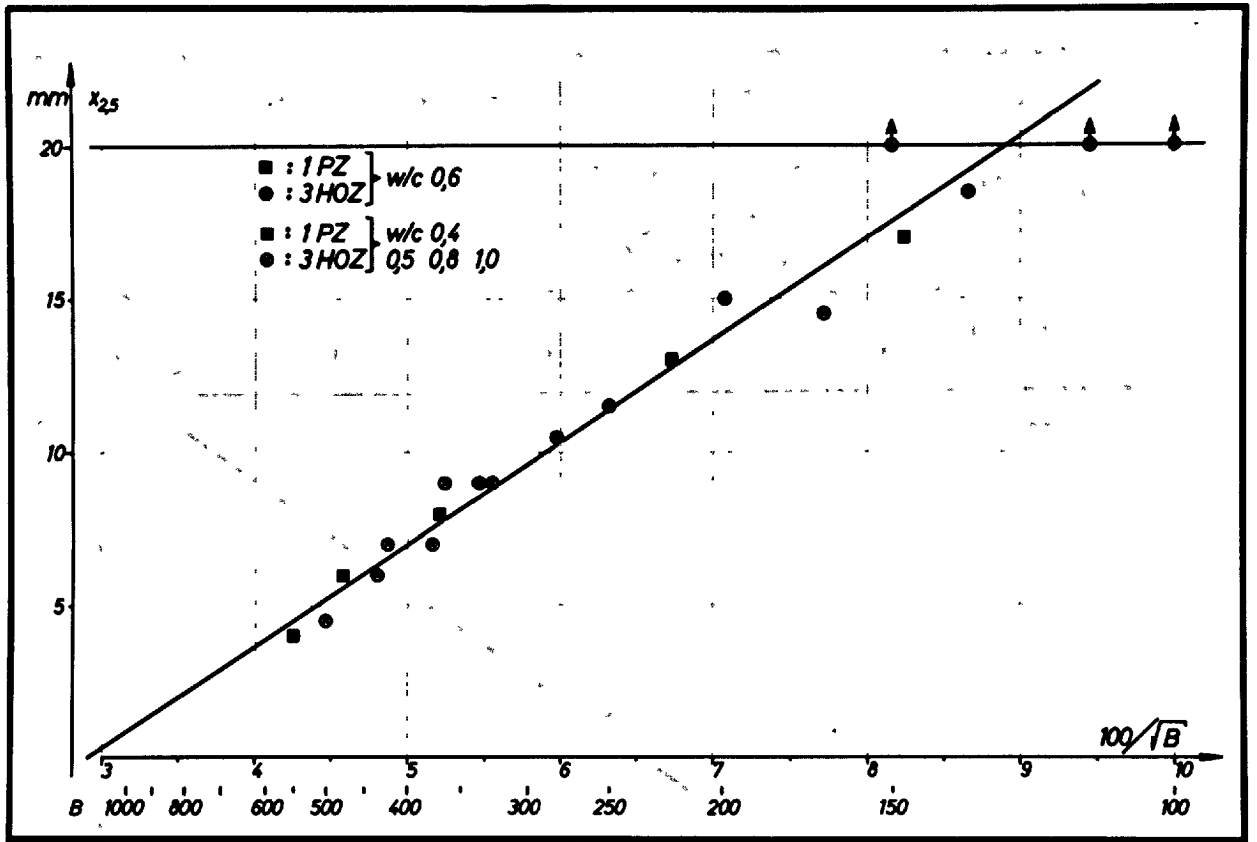

Fig. 7

FJ
Rheinhausen

Carbonation of Mortars "Indoors"

$x_{2,5}$ = carbonation after 2,5 years in mm (published)
B = compressive strength after 14 days' watercuring
(w/c 0,6 published, the other w/c calculated)
(Calculated with test results of A. Meyer, H.-J. Wierig and K. Husmann)

(68/8)

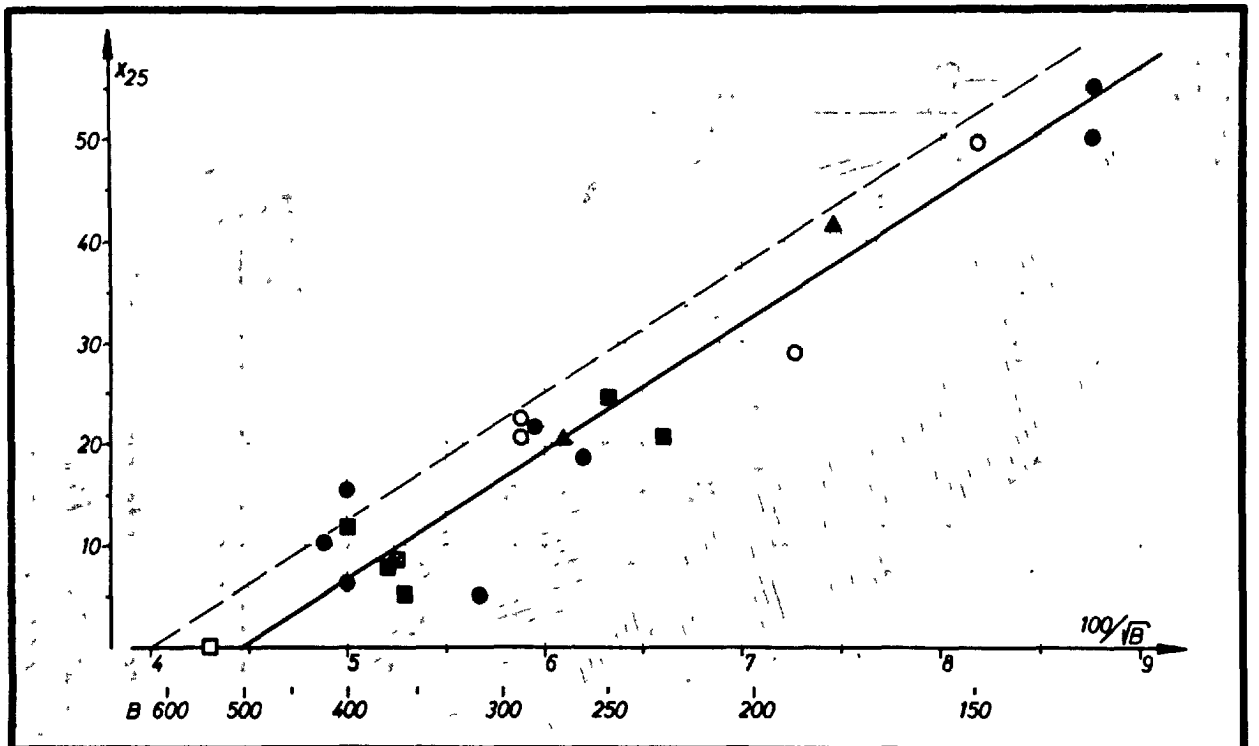

Fig. 8

F.J. Rheinhausen

Carbonation of Old Concrete Structures

"Outdoors Sheltered from Rain" (Age >20 years)

x_{25} = reduced carbonation after 25 years in mm

B = published compressive strength in kp/cm²

■ ■ □ = PZ ● ○ = HOZ ▲ = Cement unknown

(According to A. Meyer, H.-J. Wierig, K. Husmann ■ ● ▲, G. Rehm, H. Moll □ ○ and H.-J. Kleinschmidt ■)

(68/7)

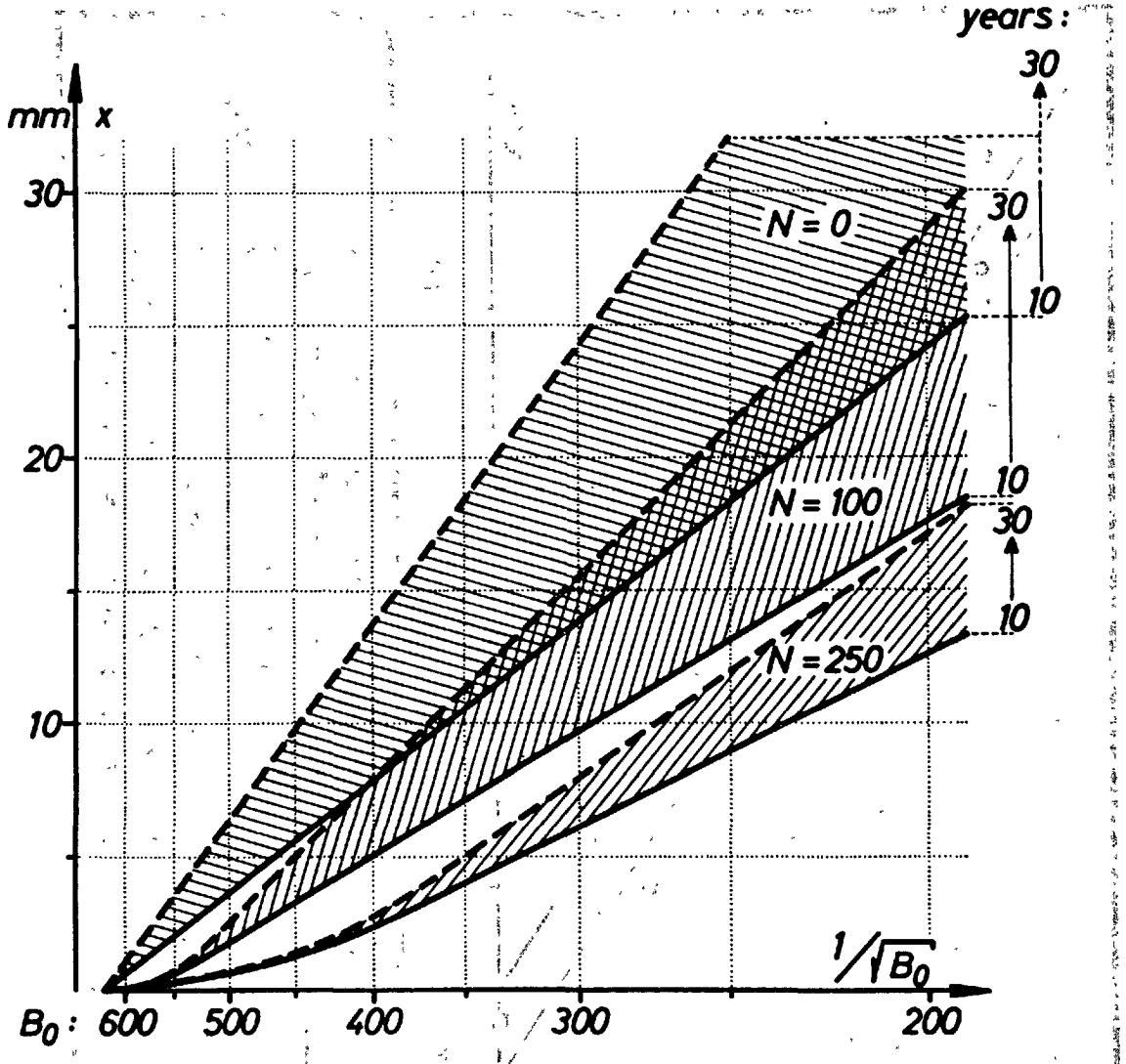

B_0 = initial compressive strength in kp/cm²
N = slow afterhardening in kp/cm²
x = carbonation depth in mm

Fig. 9: Approximative Carbonation of Concretes

"Outdoors Sheltered from Rain"

GENERAL REPORT
OF

SESSION III-4-a: HYDRATION OF PORTLAND CEMENT PASTE AT HIGH-TEMPERATURE UNDER ATMOSPHERIC PRESSURE

and

SESSION III-4-b: HIGH-TEMPERATURE CURING OF CONCRETE UNDER ATMOSPHERIC PRESSURE

P. J. Sereda (Canada)

The following Supplementary Papers are summarized in this report.

Paper No. III-65

INFLUENCE OF CEMENT CHARACTERISTICS ON MIX PROPORTION FOR STEAM-CURED PRESTRESSED CONCRETE

R. K. Lewis & F. A. Blakey (Australia)

Paper No. III-91

HEAT OF HYDRATION OF PORTLAND CEMENT DURING STEAM CURING UNDER ATMOSPHERIC PRESSURE

H. Teramoto & N. Kawada (Japan)

Paper No. III-108

PHYSICAL AND CHEMICAL PROPERTIES OF CEMENT MORTAR CURED AT ELEVATED TEMPERATURES

P. Freiesleben Hansen, J. Jessing, K. Mønsted & E. Trudsø (Denmark)

These papers present results of a number of the physical and chemical changes that occur during curing of cements and their constituents at elevated temperatures. These studies were carried out for the purpose of explaining the complex processes involved in hydration of cement with the hope that such understanding will enable the prediction of the useful properties, such as strength.

Paper No. 65 - INFLUENCE OF CEMENT CHARACTERISTICS ON MIX PROPORTIONS FOR STEAM CURED PRESTRESSED CONCRETE by F. A. Blakey and R. K. Lewis

The Australian Code for Prestressed Concrete requires that a compressive strength of 4000 p. s. i. on cylinders be obtained before transfer of prestress is permitted.

The authors set themselves the goal of establishing relations to enable the prediction of the strength of concrete at any age, given the chemical composition of the cement, the cement factor, and water/cement ratio, after fog curing and following the steam-curing cycle.

Six cements were used with the phase composition shown in Table I.

TABLE I

PHASE COMPOSITION OF THE CEMENTS TESTED, %

Cement No.	Phase Composition			
	C_4AF	C_3A	C_2S	C_3S
1	10	12	12	59
2	13	9	19	53
3	16	4	36	39
4	13	5	14	48
5	11.2	4.4	18.6	58
6	13.1	2.2	27.7	50.6

The slump of all mixes was maintained at approximately 2 in. Samples were compacted for 10 sec. on a vibrator table. When steam curing was used, a delay time of 4 hr was followed by a temperature-time gradient of 10 deg. C/hr and an isothermal period of 6 hr at 80° C.

Typical curves for strength development for fog-cured concrete and steam-cured concrete followed by fog curing is shown in Fig. (2).

The plot for fog-cured samples can be represented by two straight lines on a semi-log plot. The authors made use of the slopes of these two curves naming them as the Initial Gradient Constant (L) and Second Gradient Constant (M) and succeeded in obtaining empirical relations where:

$$L = 50(C_3S + (X)\,C_3A + 0.75C_2S)\sqrt{\frac{S}{3500}}$$

where (X) is a function of the ratio of SO_3 to C_3A and

S is the specific surface area.

$$M = 50(0.64C_3S + 4.23C_2S - 2.36\,(X)\,C_3A\,\sqrt{\frac{S}{3500}}$$

The authors also obtained an equation relating the Initial Gradient Constant and the cement factor.

The success attained by the authors in predicting concrete properties is shown in Table V, part of which is included in this report.

TABLE V

CALCULATED VALUES OF COMPRESSIVE STRENGTH OF CONCRETE

Cement No.	Compressive Strength (Fog Cured), lb/sq. in.			
	1 day		91 day	
	Theoretical	Error, %	Theoretical	Error, %
1	1700	+ 1.8	9020	+ 0.1
2	1690	- 6.1	9610	- 1.2
3	1770	0	13100	- 0.6
4	1680	+11.2	9140	+ 7.1
5	1720	+ 4.2	9460	0
6	1690	- 4.6	9650	- 4.8

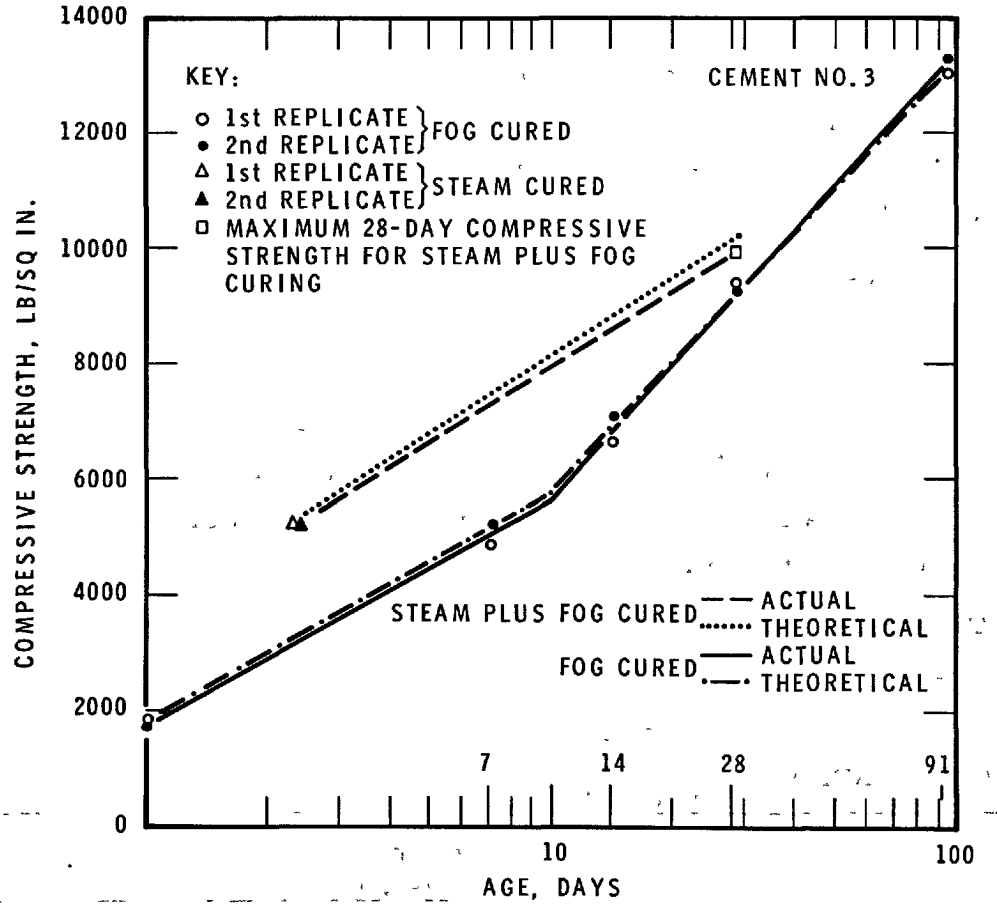

Figure 2 Relationship Between Compressive Strength and Age (from Blakey and Lewis)

The cement factor was predicted to within ±5 per cent, the 1-day compressive strength to within +11.2, -6.1 per cent and the 91-day compressive strength to within +7.1, -4.8 per cent.

The authors state that the results apply only to concrete mixes having the same type of ingredients. Variations in the grading of the sand aggregate, the maximum particle size of the stone, the strength level after steam curing and the workability desired will all affect the relationship. They suspect that a cement which produces rapid early strength in the first 24 hr followed by a lower rate of strength growth thereafter, will give different relationship from the one found in this investigation.

Conclusions

Thus the authors claim to have found a relationship that enables the prediction of strength-age characteristics of fog-cured concrete, proportioned to give a compressive strength of 5100 p.s.i. after a steam cycle giving a maturity of about 1200 deg. C. hr. Such concrete need not necessarily have a strength less than the normal 28-day fog-cured strength. Prediction can also be made of the development of strength of steam-cured concrete with subsequent fog curing to 28 days. The cement factor necessary to produce this strength can be predicted from the chemical characteristics of the cement. The important characteristics of the cement, from the standpoint of these predictions, were found to be the proportions of C_3S, C_3A, C_2S, the specific surface area, and the SO_3/C_3A ratio.

Paper No. 91 - HEAT OF HYDRATION OF PORTLAND CEMENT DURING STEAM CURING UNDER ATMOSPHERIC PRESSURE by Hideo Teramoto and Naoya Kawada

To understand the hydration process of cement during steam curing under atmospheric pressure the authors measured a number of parameters.

These included the rate of heat liberation, volume change, non-evaporable water and uncombined SO_3 as sulfoaluminate in the paste of samples of pure constituents of cement as well as normal portland cement.

By measuring the rate of heat liberation with a twin-type conduction calorimeter the authors were able to follow the progress of the hydration reactions especially, as these were compared for the different conditions of presteaming and different temperatures of isothermal heating.

The authors describe the principal features of several twin-conduction calorimeters and show comparable results obtained with several different types. Using two conduction calorimeters, one having a dummy sample, enables the measurement of rate of heat evolution during a heating period.

Volume change measurements were made by placing the sample in a rubber container and weighing it in water during the progress of the reaction. Volume change was obtained by multiplying the density of water by the change in weight of sample in water.

In Figure 7 the authors show the effect of gypsum on the hydration of normal portland cement for 5 hr at 25°C then heated at the rate of 20°C/hr up to 75°C at which temperature it was cured for 16 hr. The maximum rate of heat liberation at 75°C was 5 to 6 times higher than at 20°C. The two peaks observed are considered to be due, first, to aluminate hydration and second, to the hydration of alite. At SO_3 content of 2.8 per cent, the two occurred together.

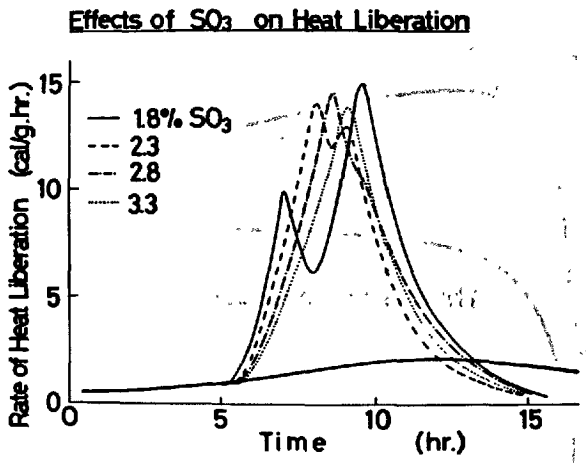

Figure 7 (from Teramoto and Kawada)

In Figure 8 the authors show the strength that developed in cement mortar when different times of presteaming were used. All samples were cured for 5 hr at 85°C and followed the same cycle of rate of heating and cooling. Figure 9 shows the rate of heat liberation for the same series of samples. The fact that maximum strength when measured 1 hr after cooling is obtained at a different presteaming time than that for 28-day cured specimens leads to the conclusion that presteaming time must be determined according to conditions necessary for practical performance and not from heat liberation curves.

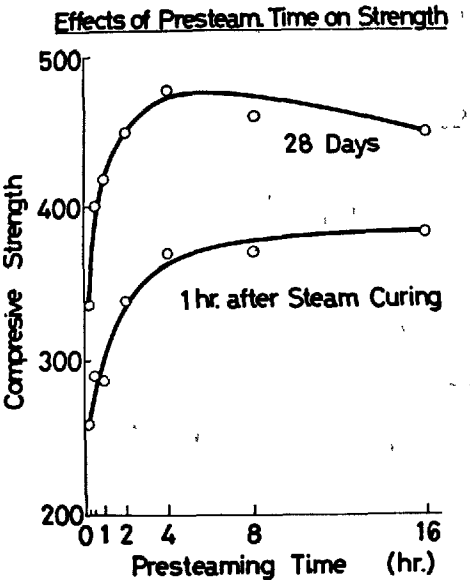

Figure 8 (from Teramoto and Kawada)

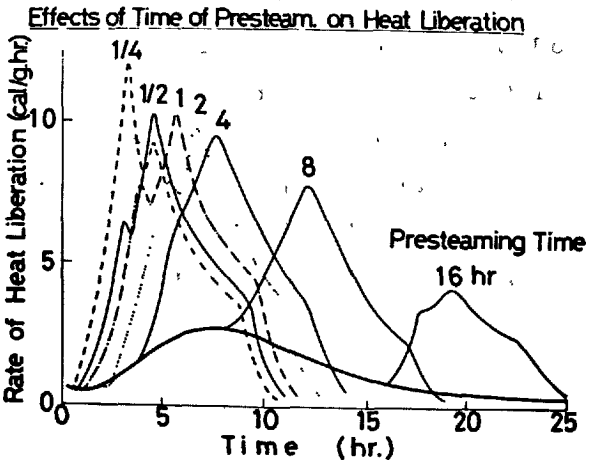

Figure 9 (from Teramoto and Kawada)

Figure 26 shows, for normal portland cement, typical results of rate of volume change, rate of heat liberation, increase of combined water and the SO_3 content obtained during the curing cycle of presteaming time of 2 hr, and curing temperature of 60°C. A large number of similar results are presented by the authors for normal portland cement and pure constituents of cement at different temperatures and different presteaming times.

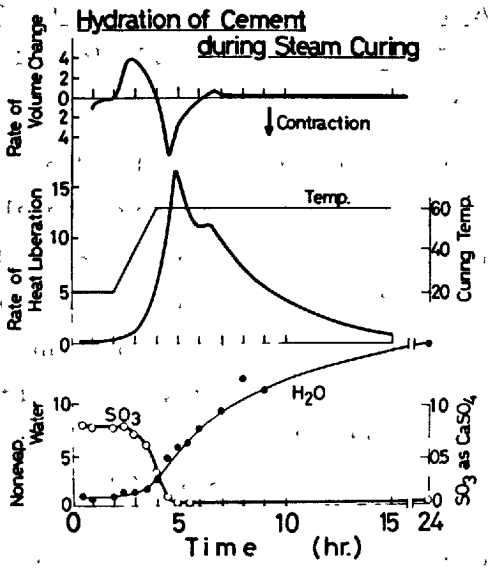

Figure 26 (from Teramoto and Kawada)

A large number of D. T. A. curves are included to indicate the changes in composition that occur during hydration reactions.

Conclusions

The results of physical and chemical changes occurring during accelerated curing of cement and its constituents seem to give a fairly informative picture of the hydration processes. Especially significant are the simultaneous measurements of the various parameters so that interrelations of different effects such as heat liberation and volume change could be assessed.

Paper No.108-PHYSICAL AND CHEMICAL PROPERTIES OF CEMENT MORTAR CURED AT ELEVATED TEMPERATURE by P. F. Hansen, J. Jessing, K. Mønsted and E. Trudsø.

The purpose of the investigation was to explain the effect of the curing temperature by the changes it produces in the chemical and physical processes during hydration. The basic variable was the curing temperatures of 25, 45, 60, and 80°C. A standard cement mortar, made from a rapid-hardening portland-type cement having a fineness of 3930 cm^2/g. (Blaine) was used. The ratio of water to cement was 0.5 and the ratio of paste to sand was also 0.5 (by weight). Two types of specimens were used: cylinders 4 by 8 cm. and a rectangular prism 5 by 10 by 20 cm.

Measurements of compressive strength, dynamic modulus, volume contraction, sound velocity, internal damping, electrical resistance, alkalinity, and content of non-evaporable water were determined intermittently or continuously at the four levels of temperature at ages from 1/2 to 24 hr.

The results for the various physical and chemical changes obtained by the authors are too voluminous to include in this short summary. Some of the more common properties were selected to illustrate the nature of the results and indicate the behaviour of the mortar at the different levels of temperature.

Mechanical Properties

The authors show in Figure 7 that the compressive strength in the early stages of the hardening process may be represented by exponential growth curves which are parallel until a certain level of strength is reached. When this level is reached, specimens at 60 and 80°C begin to develop strength at a lower rate than those at 25 and 45°C. Similar results were obtained for dynamic modulus of elasticity as shown in Figure 8 and obtained by the pulse velocity method. The same apparatus and method were used to measure the internal friction which was expressed as $\log \frac{1}{V}$ where the assumption was made that V (the voltage) was proportional to the amplitude of the pulsed wave. The correspondence of the changes in E (dynamic) and the internal friction parameter were made apparent in plots of the type shown in Figure 11b.

Chemical Reactions and Mechanical Properties

To indicate regions of different reactions or changes in rates of reactions the authors plotted the parameters of dynamic modulus of elasticity, electrical resistivity, temperature, pH and volume contraction

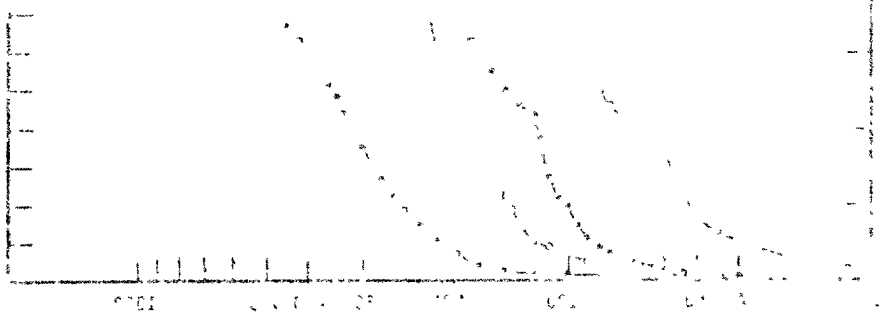

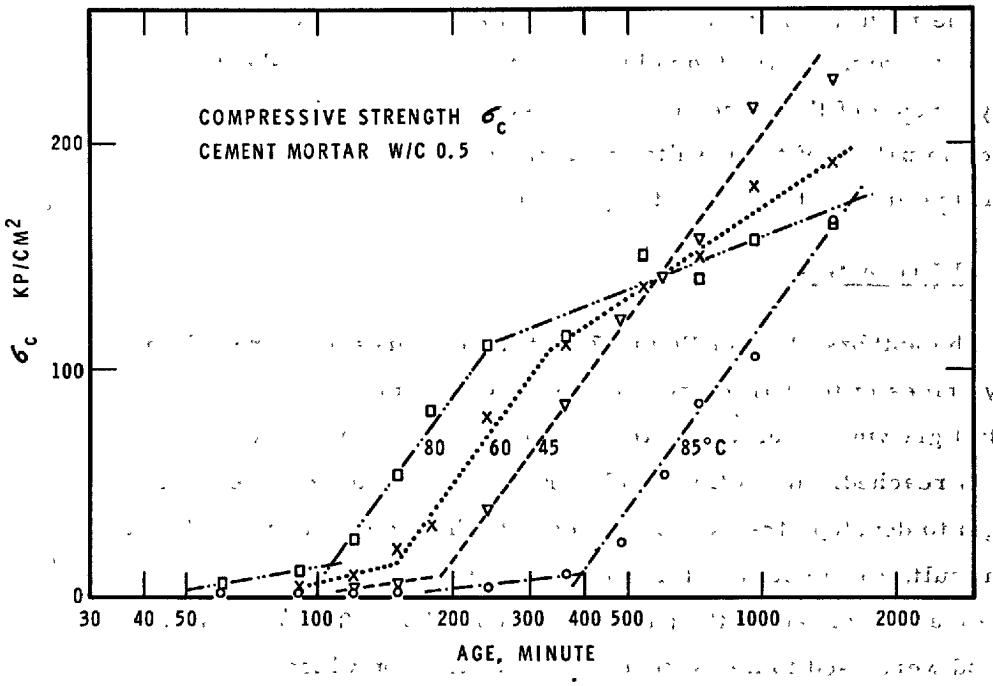

Figure 7 (from Hansen, Jessing, Mønsted and Trudsø)

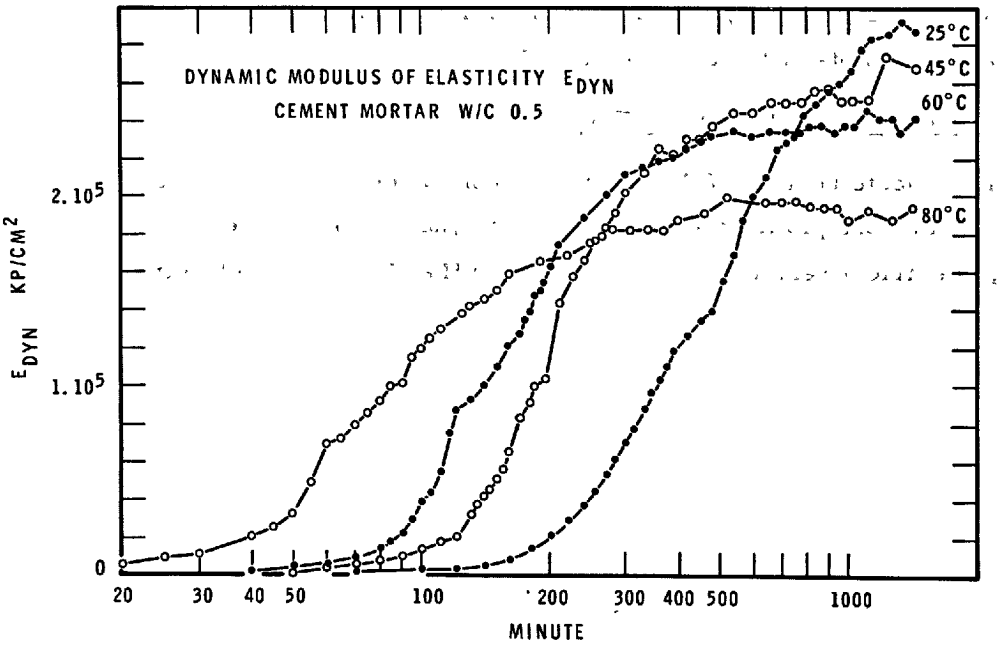

Figure 8 (from Hansen, Jessing, Mønsted and Trudsø)

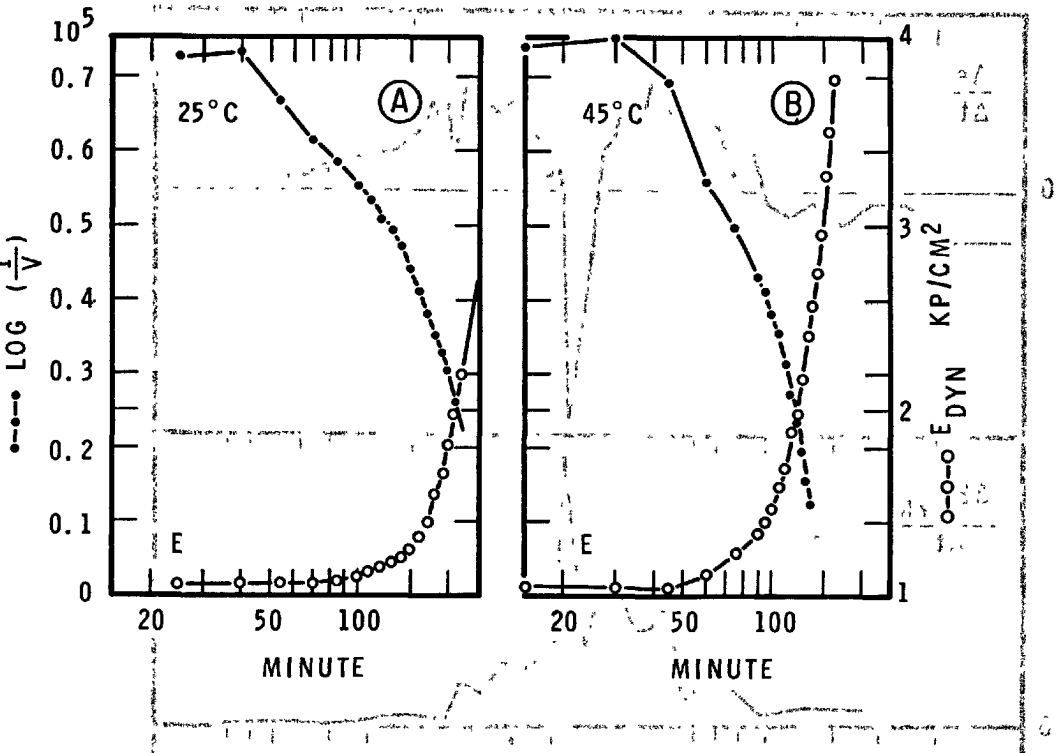

Figure 11 (a and b) (From Hansen, Jessing, Mønsted and Trudsø)

as differentials with respect to time. Thus maxima and minima on the differentiated curves correspond to inflection points on the basic curves. These appeared quite reproducible as shown in Figure 17 for changes in resistance, E_{dyn}, ΔV, temperature, and pH with time. The various maxima and minima are explained as representing different reactions and different stages of hydration beginning with hydration of C_3A then followed by hydration of C_3S.

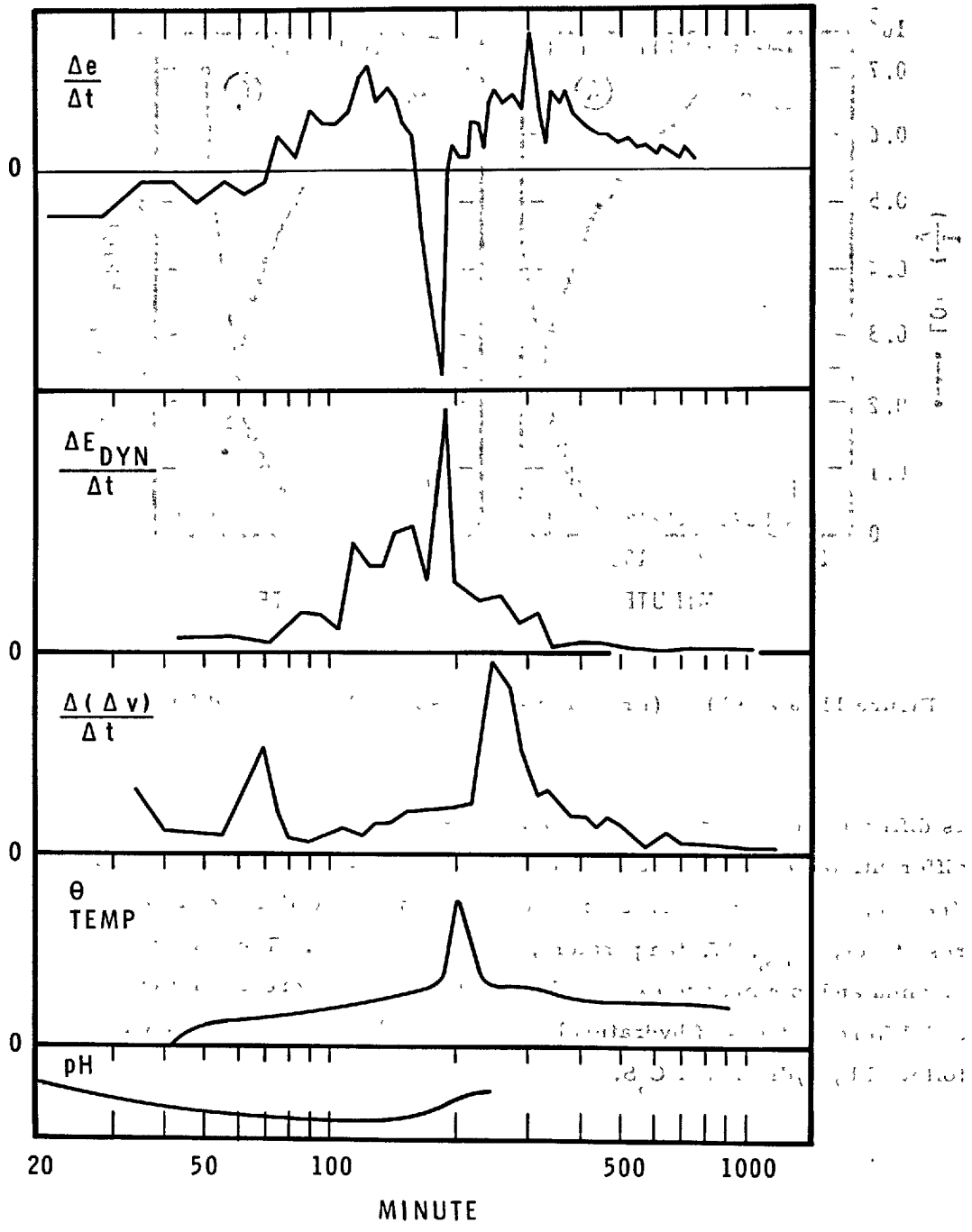

Figure 17 (from Hansen, Jessing, Mønsted and Trudsø)

The authors show that the plot of the log of the rate of the reactions, as indicated by various measured parameters, versus the inverse of the absolute temperature give fairly straight lines thus indicating a fairly good agreement with the Arrhenius equation. Activation energy corresponds to the reaction energy of C_3S.

Conclusions

The authors conclude the following:

1. Curing at elevated temperatures below 100°C accelerates the development of mechanical properties. The acceleration can be accounted for by the concrete maturity, but at ages above 24 hr the quality obtained by curing above 45°C may be impaired due to other influences.

2. By curing at temperatures above 45°C it seems that the hydration of C_3S is accelerated in particular; in cases where this process starts before the hydration of C_3A, the mechanical properties may be impaired.

GENERAL CONCLUSIONS

These papers have indeed advanced the understanding of cement curing at elevated temperature and have given some possibility of predicting the useful properties and the optimum conditions for curing. Perhaps the most useful results of these investigations are the techniques that were developed for the measurement of a number of physical properties during the progress of the curing. These can be used for evaluation of different cements.

GENERAL REPORT
OF
SESSION III-5: HIGH-TEMPERATURE CURING OF CONCRETE UNDER HIGH PRESSURE

H. E. Vivian (Australia)

The following Supplementary Papers are summarized in this report.

Paper No. III-80

HYDROXYL ELLESTADITE PRODUCED BY HYDROTHERMAL REACTION CONTAINING CALCIUM SULFATE

K. Takemoto & H. Kato (Japan)

Paper No. III-87

SOME PHYSICAL PROPERTIES OF AERATED CONCRETE UNDER AUTOCLAVE PROCESS

K. Ono & K. Ojiri (Japan)

Paper No. III-111

INFLUENCE OF MINOR COMPONENTS ON THE STRENGTH OF CALCIUM SILICATE HYDRATE SYNTHESIZED BY HYDROTHERMAL REACTION

G. Shikami (Japan)

These three papers, which are concerned with rather different aspects of hydrothermal reactions of clinker compounds and raw materials, are not closely interconnected. Consequently this summary may appear to be somewhat disjointed. All these papers discuss reactions that occur at elevated temperatures and steam pressures, the compounds formed under these conditions and the effects of various admixture compounds on the chemical reactions and the mechanical properties of the reaction products. Some conclusions drawn from these studies may be usefully applied in the manufacture of concrete products and could have some significance in other fields.

Paper No. 111 by G. Shikami is concerned with the effects on the hydrothermal reaction rates of calcium hydroxide and silica of small additions of beryllium, zinc and alkali metal oxides and with the strength of the resultant calcium silicate hydrate. The results obtained indicate that additions of beryllium and zinc oxides in quantities up to 0.4 per cent retard, but do not inhibit, the rate of hydrothermal reaction. The chemical composition of the reaction products formed in the presence of beryllium and zinc oxides is comparable with that of products formed in the absence of these compounds even though their degree of crystallization is generally poorer. Higher temperatures and longer reaction times tend to correct these defects.

In contrast to the depressing effects of beryllium and zinc oxides, small additions of alkali metal oxides promote the calcium hydroxide-silica reaction and improve the strength

developed by the reaction product. Additions in excess of 0.3 per cent appear to retard the calcium hydroxide-silica reaction and reduce the mechanical strength of the reaction product. It is considered that the progressive lowering in the calcium hydroxide solubility, as the alkali concentration is increased, accounts for the reduced reaction product strength. The physical properties of the hydrothermal reaction products suggest that for autoclaved products the bulk density should increase and the water absorbency and permeability should decrease.

It can be indicated briefly that small alkali additions improve the reaction characteristics and physical properties of lime-pozzoloma mixtures even when cured at atmospheric temperature. It would appear that the presence of the more common alkali metal hydroxides (e.g. sodium and potassium) can increase the rate of lime-silica reaction by acting as a catalyst. Other work has indicated that lithium hydroxide behaves very differently from sodium and potassium hydroxides and under some circumstances may inhibit silica reaction.

Paper No. 80 by K. Takemoto and H. Kato is concerned with the effect of calcium sulphate on the strength of hydrothermally-formed calcium silicate hydrate. The formation of hydroxyl ellestadite, $Ca_{10}(SiO_4)_3(SO_4)_3(OH)_2$, has been demonstrated in mixtures with CaO/SiO_2 molar ratios exceeding 1 while in mixtures of lower CaO/SiO_2 molar ratios anhydrite was the only observed sulphate-bearing phase.

Various properties of synthetically prepared hydroxyl ellestadite were measured and the strength of hydrothermally

produced paste specimens determined. It was observed that, as the SO_3 content of the raw material increased to 2 per cent, the measured specimen strengths increased. At greater SO_3 contents however the measured strengths decreased. It is suggested that the formation of hydroxyl ellestadite could reduce the strength of these pastes.

The actual mechanism of strength improvement in pastes made from materials containing up to 2% SO_3 followed by strength decline when the raw material SO_3 content exceeds 2 per cent has not yet been studied. Such a study would have very wide implications for specifications for cement used in autoclaved products and may help to account for some of the anomalous behaviour observed in such products. The authors also suggest that hydroxyl ellestadite or some of its thermal decomposition products can be observed in sulphate ring deposits in rotary kilns. The effect of these ring deposits on burning and kiln performance is economically significant especially in oil fired kilns and consequently further studies of the formation, composition changes and properties of these products would be desirable.

Paper No. 87 by K. Ono and K. Ojiri is concerned with the physical properties of autoclaved aerated or light-weight concrete specimens. These authors have recognized the difficulty in obtaining suitable test measurements and consequently have discussed equipment and experimental techniques as well as product properties and changes.

Although this paper contains a considerable amount of discussion on the dimensions of specimens, heating and cooling

treatments and heat and moisture distributions in specimens, the most interesting part of this paper is concerned with the linear measurements of specimens during the autoclaving process. An apparatus using an "optical differential lever method" has been described and its use discussed.

It was concluded that the observed expansion-temperature relationship was mainly dependent on the thermal expansion of the solid phase of the specimen and that moisture movements and changes in the amount of hydrated material could also affect the overall measured movements. It is of interest to note that the thermal expansion of specimens is virtually independent of density.

Additions of increasing amounts of hard burnt magnesia to specimens caused expansion, severe cracking and ultimately disintegration. The expansion-contraction performance of specimens indicates that two separate and distinct mechanisms can operate simultaneously in a specimen and affect the observed movements. Even though a specimen is expanded by the hydration of magnesia, shrinkage can occur under appropriate conditions due to the shrinkage characteristics of the hydrated cement and the magnitude of the shrinkage is largely unaffected by the magnitude of the expansion.

This paper points out the significance of thermal stressing and cracking in specimens and emphasises the need to determine specimen requirements and autoclaving procedures in relation to the physical performance of concrete specimens.

As a group these papers, while acknowledging the importance of chemical composition of cements raw materials and hydrothermally-prepared specimens, place a somewhat greater than usual emphasis on physical characteristics and changes in specimens. The reviewer commends these authors for taking up this view since it is considered that the performance of cement and concrete is very largely dependent on the physical properties of the materials and the physical changes that occur in specimens as a result of changes in the environmental conditions.

GENERAL REPORT
OF
SESSION IV-1: USE OF SURFACE ACTIVE AGENTS IN CONCRETE

K. Okada (Japan)

The following Supplementary Papers are summarized in this report.

Paper No. IV-5

INFLUENCE OF SOME ADMIXTURES ON CREEP OF CONCRETE

E. L. Jessop, M. A. Ward & A. M. Neville (Canada)

Paper No. IV-45

EFFECTS OF ORGANIC COMPOUNDS ON THE HYDRATION REACTIONS OF TRICALCIUM ALUMINATE

K. E. Daugherty & M. J. Kowalewski, Jr. (U.S.A.)

Paper No. IV-51

ABNORMALLY DELAYED SETTING OF A LOW-HEAT PORTLAND CEMENT WITH CALCIUM LIGNOSULPHONATE ADMIXTURES

R. Bauset (Canada)

Paper No. IV-89

INVESTIGATIONS ON THE METHOD OF TEST FOR SETTING TIME OF CONCRETE ESPECIALLY FOR CONCRETE CONTAINING WATER REDUCING ADMIXTURE

J. Okabe, K. Nakajima & T. Yoshihara (Japan)

Paper No. IV-107

STUDY ON THE ADMIXTURE FOR AERATED CONCRETES INCLUDING ANHYDRIDE MODIFIED RESIN

K. Akutsu (Japan)

Five papers concerned with the theme of Section IV-1 have been studied for this reports, and the following account is the reporter's summary of their contents.

Four of the papers are essensially related to the water-reducing admixtures, two papers (IV-45, 51) dealing with the effects of additives on the phase composition of hardening cement water paste, one (IV-5) on the creep of concrete and one (IV-89) discussing the testing method of setting time of concrete when additive has been used. Remaining one paper (IV-107) is devoted to the research on using an organic resin as foam-forming agent in foamed cellular concrete.

Two kinds of admixtures as dealt with in the papers - water reducing admixtures and foaming admixtures - are to be classified to different groups, although both being the surface active agents.

IV-45 Effects of Organic Compounds on the Hydration Reaction of Tricalcium Aluminate

Kenneth E. Daugherty

Milton J. Kowalewski

This paper describes the investigation on reaction of organic compounds containing various types and number of hydroxyl groups and carbonyl groups with C_3A. Reviewing literatures reveals that the α-hydroxyl carbonyl group HO - C - C = O adsorbed on C_3A is thought to play a major role in

retarding hydration of portland cement, and this investigation aimed at determining the relationships of carbonyl and hydroxyl groups relative to the set-retardation of C_3A hydration in the absence of sulfate and calcium ions.

Possible mechanism for hydration of tricalcium aluminate in the presence of organic compound is believed to pass through the metastable hexagonal hydroaluminates (C_2AH_8, and C_4AH_n, n = 13 or 19) and transformed to the more stable C_3AH_6 under normal conditions.

Some organic compounds delay the conversion of C_2AH_8 and C_4AH_n to C_3AH_6 while others permit the C_3AH_6 to be formed readily.

Thirteen well-characterized, interrelated, water-soluble organic compounds including acetic acid, glycolic acid, glyceric acid, sucrose, fructose, manitol, sorbibol etc. were selected and used in this study.

The method of investigation is to observe the disappearance of tricalcium aluminate and the appearance of new hydrated phases in the course of the hydration of C_3A in the presence and absense of organic compound by x-ray diffraction using a C_3A-C_3AH_6 calibration curve.

Mixtures having a H_2O/C_3A ratio of 0.6 and containing 1 % by weight of organic compound to C_3A were stored at 20°C for 22 minutes to 64 days. These samples were ground and analysed by x-ray diffraction. Special emphasis was placed on sucrose and the effect of varying concentration of sucrose on the hydration of C_3A was examined. Effects of the blocking action of organic compounds preventing the hexagonal hydroaluminates from forming C_3AH_6 are also discussed.

Principal conclusions derived from the investigation are

(1) Organic compounds containing hydroxyl, carboxyl or carbonyl groups act as either accelerators or retarders for the hydration of C_3A depending upon their concentration levels and composition.

(2) The α-hydroxyl carbonyl group does not appear to be especially important in the hydration of C_3A.

(3) A simple organic compound containing a carboxylic acid group and zero or one hydroxyl group accelerates C_3A hydration and a simple organic compound containing two or more hydroxyl groups retards C_3A hydration. In this test mandelic acid is a strong accelerator and sorbitol a strong retarder.

IV-51 Abnormally Delayed Setting of a Low-heat Portland Cement with Calcium Lignosulfonate Admixture

R. Bauset

This paper reports abnormally long setting time which occurred in the dam concrete at one of the sites of hydro-electric power project in Canada.

Low heat cements were used in the concrete combined with lignosulfonate type of water-reducing agent, and cements from one supplyer showed excessive delay in setting time.

Chemical composition and compressive strength development of the cement compared with other normally-set cements show that the slow setting of the particular cement with calcium lignosulfonate additive was probably due to low C_3A and low SO_3 content in cement.

A similar case of slow-hardening concrete were reported in tunnel lining construction in California[1] and Milenz[2] pointed out that it might be caused due to the low-alkali cement of high C_4AF and low C_3A content in that case.

Table 4 in the paper shows that the cements designated as "A" and causing the slow setting have higher C_3S content (44, 40 %), lower C_3A content (4.4, 5.3 %) and lower SO_3 content (1.27, 1.31 %) than the other low-heat

cements, and appear to belong rather to type II (ASTM) cement, actually corresponding to the moderate heat cement of Japan when judged from only the chemical compounds.

The retarding effect of the admixture on the concrete containing cements supplied by the particular manufacturer "A" was very pronounced when cement contained 1.1 % SO_3. Therefore it appeared that addition of normal dosage of the lignin-base water reducing agent to cement "A" might cause excessive retardation of setting when higher percentage of SO_3 than the value described above was present. Thus, "Having discounted possibility of a high sugar content lignosulfonate being used and the possibility of overdosage of the mixture and delayed addition of the admixture", the dosage of the admixture was regulated to dependending upon the SO_3 content of the cement as follows.

for < 1.6 % SO_3 ..... dosage < 0.2 %

for ~ 2 % SO_3 ..... dosage ~ 0.3 % (normal)

Author also suggests that lower alkali content of $0.5 \sim 0.6$ % for cements "A" may be a contributory factor in this case.

IV-5 Influence of Some Admixtures on Creep of Concrete

E. L. Jessop, M. A. Ward

A. M. Neville

Authors reported before that larger creep was observed in concrete containing water-reducing and set-retarding admixtures than in the corresponding plain mixes having the same workability and the same compressive strength at the time of application of sustained loading.

This paper describes the experimental study done to find the mode of influence of admixtures on creep, on the less of water from hydrated paste

at higher temperatures, density of hydrated paste, surface tension of the solution of admixture in water, and morphology of the hydrated paste and therefore the shape of stress-strain curve.

Tests were done using neat cement pastes of w/c = 0.5 with and without admixture. Type III high early strength portland cement and two admixtures (one belonging to hydroxylated carboxylic acid and one to lignosulfonic acid) were used.

Results of test show that no possible correlations between the surface tension of water or density of hydrated paste and creep exist, and that some relation between the ease with which water can move within and out of the paste and creep is shown to exist.

Several workers observed change of crystal size and shape of hydration products of tricalcium aluminate and of calcium aluminoferrite and changes in the morphology of hydration products of C_3S and C_2S when the admixture is added.

Although the electromicrographs, of which the magnification is 15,000 times, was inadequate in this test to show significant morphological difference between the mixes with and without an admixture, it may be imaginable that the modifications described above as well as the possible modification of boundary relationship among the hydration products undoubtedly affect the creep of hydrated cement.

More important effects of admixtures on physical properties of cement paste are change of pore size distribution and porosity.

Stupachenko's observation[3] using absorption method of benzol and the mercury porosimeter revealed that use of a lignosulfonate admixture at the rate of 0.25 % did not significantly change the total porosity but the volume portion of pores with smaller radius of 500 to 1000 Å was decreased 3 % in mortar and 30 % in paste with admixture.

Hence theoretically the cement paste with the admixture should be more permeable, and therefore more easily loss water from the gel than that without the admixture.

This conclusion, however, would not necessarily relate to the practical concrete as a whole which involves various other factors.

In this investigation moist loss of cement paste was measured in an over at 105°C on specimens cured in fog at RH 100 % for 28 days. Considering this result and the measured value of surface tension in parallel, the authors concluded that some relationship between the ease with which water in paste can move and creep may exist.

IV-89 Investigations on the Method of Test for Setting Time of Concrete Especially for Concrete Containing Water Reducing Admixtures

Jiro Okabe, Koji Nakajima
Takuji Yoshihara

The term "setting of concrete" is used to describe the comparative hardening of concrete with and without set-controlling agents, although the definition is somewhat arbitrary. Easily available methods for measuring the time of setting of concrete are

(1) determination of resistance to the penetration of a needle according to ASTM Standard C 403, and

(2) determination at various intervals of time of the resistance to pulling out of a series of pins[4].

And the penetration resistance method (ASTM C 403) is being used more widely. This method requires wet-screened concrete mortar in order to obtain information more closely related to the hardening characteristics of

concrete to be used in site.

However, in the penetration test, which is essentially more suitable for mortar than for concrete, additional handling and compaction of wet-screened mortar are needed. Hence, use of mortar instead of wet-screened mortar from concrete is sometimes tried in the laboratory.

Authors investigate the effects of mix-proportion, kind of lignosulfonate water-reducing admixtures, mixing sequence and time and temperature on the time of setting by using the mortar method as well as ASTM method, and clarified that the mortar method can give satisfactory information on setting time of practical concrete and obtain more accurate and more reproducible results than ASTM C 403 method.

In the mortar method, test should be performed as follows.

(1) The proportion of mortar shall be theoretically indentical that of the screened mortar from concrete, that is, shall have the same water cement ratio and sand-cement ratio.

(2) The same materials as in the concrete shall be used.

(3) Similar mixing sequence as in the concrete shall be adopted.

Mixing sequence has remarkable effect on the setting time as already pointed out by V. H. Dodson and E. Farkas[5] who discussed on the effect of delayed addition of set-retarding admixture to concrete.

When cement and surface dry saturated aggregates are premixed before the admixture solution is added, the setting time of concrete delays by two to five hours depending upon the kind of admixtures compared with when the mixing starts after the whole materials are introduced into the mixer.

The above delayed setting due to change of mixing sequence was caused probably by quick reaction of cement with a small amount of water absorbed in aggregates prior to addition of admixtures as illustrates by Bruer[6].

The retarding or accelerating effect of the water-reducing and set-retarding or set-accelerating admixture on the setting time of concrete also varies with the change in proportion, mixing sequence, mixing period and temperature.

It seems that the accelerating affect of the water-reducing and set-accelerating admixture decreases with increase in consistency of the concrete and that the prolonged mixing alleviates the retarding effect of the water-reducing and set-retarding admixture.

The above findings indicate that due considerations should be taken of the various factors described above in establishing the standard testing method for setting time of concrete.

IV-107 Study on the Admixture for Aerated Concrete Including Anhydride Modified Resin

Kenji Akutsu

Some surface-active agents used in structural sand-gravel air-entrained concrete may be used as foaming agent for foamed cellular concrete.

Foaming agent is required to introduce stable, and uniformly distributed minute foams into the slurry concrete and consequently to reduce bleeding.

Author tested the basic properties, to be required as foaming agent, of a maleic anhydride modified resin and compared with those of surface active agents such as salt of resin, salt of sulfonated lignin, alkylbenzene sulfonate, and non-ionic compounds.

Maleic anhydride modified resin which is processed by adding maleic anhydride to abietic acid, has totally three carboxyl groups, and so the negative charge may be increased much. The admixture was finaly produced

by saponifying the said maleic acid copolymer and emulsifying it with synthetic foam stabilizers, thus the superior stability of quality and storability being obtained.

Addition of 0 to 0.2 % concentration of the maleic resin admixture decreases surface tension so much in the saturated lime solution with increasing concentration successively to nonionic agent and alkylbenzene sulfonate.

The least bleeding was obtained by using the maleic resin foaming agent in cement paste of w/c = 0.65. It is inferred that the carboxyl groups introduced into the molecule of the maleic anhydride modified resin, may be combined with calcium ions to form an insoluble salts.

All foaming agents except lignosulfonate had little effect on the setting time of cement paste, so far the dosages of admixtures ranged from 0.05 to 1.0 % by cement weight. When adding accelerating or retarding agents to the maleic resin foaming agent, the normal acceleration or delay of setting time was obtained.

In the tests of mortars having mix proportion of 1 : 2 (w/c = 0.60) to 1 : 4 (w/c = 1.00) and containing the maleic resin foaming agent, maximum air content (10 to 20 %) as well as maximum flow was obtained when the dosage of the foaming agent was 0.1 to 0.2 %, almost corresponding to the critical micells concentration.

Strength of mortar decreased with increasing air content, and the compressive strength at 28 days being 90 to 250 kg/cm^2 for around 15 % air content depending upon the mix-proportions.

Drying shrinkage also varied with mix proportions and was 0.09 to 0.17 % at 28 days. Another test revealed that mortar of 1 : 3 mix proportion containing the foaming agent of not less than 0.5 % by weight and so containing about 10 % air showed good waterproofness comparable to the non-foamed

plain mortar.

Author concluded that the maleic anhydride modified resin used in this study may be approved as an effective foaming agent.

References

1. L. H. Tuthill; R. F. Adams, S. H. Bailey and R. W. Smith; A Case of Abnormally Slow Hardening Concrete, Proc. ACI., 32, 1091-1109, 1961

2. R. O. Mielenz ; Use of Surface-Active Agent in Concrete, 5th Intern. Sym. on Chemistry of Cement, Tokyo, Part IV. Session I, Principal Paper, 1968

3. P. P. Stupachenko ; The Influence of Admixtures SSB, GKZh and $Ca(NO_3)_2$ on Structural Porosity of a Mortar Portion of Concrete, RILEM Intern. Sym. on Admixtures for Mortar and Concrete, Brussels, Topic IV/8, 95-107, 1967

4. T. M. Kelly and D. E. Bryant ; Measuring the Rate of Hardening of Concrete by Bond Pullout Pins, Proc. ASTM, 57, 1029-1040, 1957

5. V. H. Dadson and E. Farkas ; Delayed Addition of Set Retarding Admixtures to Portland Cement Concrete, Proc. ASTM, 64, 816-826, 1964

6. G. M. Bruese ; Importance of Mixing Sequence When Using Set-Retarding Agents with Portland Cement, Nature 1999, No. 4888, 32-33, 1963

GENERAL REPORT
OF
SESSION IV-2: FLY ASH AND FLY ASH CEMENT

A. Joisel (France)

The following Supplementary Papers are summarized in this report.

Paper No. IV-7

HYDRATED PHASES AFTER REACTION OF LIME WITH "POZZOLANIC" MATERIALS OR WITH BLAST FURNACE SLAGS

R. Sersale & P. G. Orsini (Italy)

Paper No. IV-17

STUDY OF REACTIONS BETWEEN CaO OR $3CaO.SiO_2$ AND β-$2CaO.SiO_2$ AND POWER STATION FLY ASHES UNDER HYDROTHERMAL CONDITIONS

Z. Šauman (Czechoslovakia)

Paper No. IV-63

INVESTIGATIONS ON THE BEHAVIOUR OF NATURAL AND ARTIFICIAL PUZZOLANAS

H. E. Schwiete, P. Kastanja, U. Ludwig & P. Otto (West Germany)

Paper No. IV-135

THE DIFFERENT ACTION MECHANISM OF POZZOLANIC MATERIALS AND SLAGS IN THE HYDRAULIC BINDERS

A. Celani, P. A. Moggi & A. Rio (Italy)

INTRODUCTION

Among the supplementary papers on Topic IV - 2, Sauman's paper relates to fly ash and those by Celani - Moggo - Rio , Schwiete - Kastanja - Ludwig - Otto , and Sersale - Orsini relate to puzzolanas. Fly ash is a special artificial puzzolana which can be distinguished from other puzzolanas (natural or artificial) by the form of the grains or by a given carbon content, for example. This topic could therefore be entitled "Puzzolanas and Puzzolanic Cements".

I am going to endeavour to compile a survey of these papers which is not a repetition of the synopses prepared by the Authors and which takes account of all the principal papers read at the Symposium which I have received and in particular the paper by Masatane Kokubu on the same topic.

RAW MATERIALS

The substances studied by the Authors are varied. Their chemical compositions by weight are plotted on figure 1 in which the apices of the triangle correspond respectively to SiO_2, to the sum $Al_2O_3 + Fe_2O_3 + TiO_2 + SO_3$, and to the sum $CaO + MgO + Na_2O + K_2O$. (Figures 1 and 3 have been drawn under these conditions for simplification. It is known that many constituents are only interchangeable molecularly , and not without some reservations which are mentioned in the study by Sersale - Orsini in particular).

These raw materials comprise:

- natural "puzzolanas": Italian puzzolanas, trass, tufa, molererde, zeolites: zone (a) of fig.1
- fly ashes (b)
- one acid slag (c)
- basic slags (d)
- artificial glasses (e)

- one clinker (in the triangle C_3S - C_2S - C_3A) (f).
- one silica sand (g)

The overall chemical composition is not enough to characterise the substance for a variety of reasons. For example, a given composition may correspond to a complex mass of grains of very different chemical and mineralogical compositions, and in particular the vitreous nature has a most important influence. A vitreous substance, at the molecular scale, always involves local arrangements analogous to those of glass, and in addition a crystalline substance may be amorphous in part, particularly at the surface since the atoms are not regularly surrounded by their neighbours at the surface like they are within the body of the substance. This may explain, at least partially, why a siliceous sand, which is habitually considered to be inert,"fixes" a small quantity of lime as has been shown by Celani - Moggi - Rio.
However, a substance is not truly puzzolanic unless it is vitreous, in part at least. This is why these Authors indicate a considerable difference between the behaviour of sand and that of "puzzolana 2" in spite of the close similarity of their chemical compositions, (fig. 1).

"Puzzolana", by definition, combines with lime at ordinary temperatures in the presence of water to give bonding products. Sauman reports reactions at 175°C. The other papers relate to the reactions at ordinary temperatures or at 40°C.

The combination with lime has been studied in several ways:

- the development of the concentration of a solution of lime,
- X rays,
- differential thermal analysis,
- electron microscope,
- B.E.T. surface adsorption,
- leaching of the lime,
- mechanical strength.

FIXING OF LIME

The development of the concentration of a solution of lime in the presence of puzzolana has been traced by all the Authors by means of acidimetry, complexometry, and weighing methods. Maintaining a temperature of 40°C as practised by Celani - Moggi - Rio, accelerates the fixation of lime without modifying the process qualitatively. Naturally increasing the fineness of the substance is favourable to combination. But this substance has also an intrinsic puzzolanity in this respect.

Celani - Moggi - Rio, classified the puzzolanity of the substances they studied in the following descending order:-

- "puzzolana 2", "puzzolana 1", "slag 1", "slag 2", sand.

Their fineness is classified by the residue on a 40 micron sieve:-

25 % for the puzzolanas, 14 % for the slags, 21 % for the sand.

Schwiete - Kastanja - Ludwig - Otto, classified their substances in the following order:-

- molererde, Austrian trass, Rheinland trass, Italian puzzolanas and acid slags, Bavarian trass.

But their fineness may be considerably different; the Blaine specific area in particular, which is so important in all the hydration reactions (as pointed out by the Authors) above all at the early stages (as found by Sauman). The fineness of the molererde, for example, is three times greater than that of the trasses and the Italian puzzolanas. These are overall classifications therefore and they do not necessarily affect the intrinsic puzzolanity of these subatances.

Bersale - Orsini, have used substances "powdered to 230 mesh" and they obtained the values reproduced in figure 2.

It will be seen from figure 1 therefore, in accordance with the several papers, that in general the fixing of lime increases as the ratio $A + F + T + SO_3 / C + M + N + K$ of the substance increases.

The basic slags (which almost conform in figure 1 to the simplified potential formula $C_{4.5} AS_{2.5}$) fix little lime. The same applies to glass $C_{3.5} AS_{0.6}$. Furthermore it is known that clinker (which in figure 1 conforms to the simplified formula $C_{16} AS_5$) does not fix lime but liberates it instead during hydration.

The substances which are capable of fixing lime, and which are volcanic substances (puzzolanas, trasses, tufas, molererde) or artificial substances of similar chemical composition (calcined clays, fly ashes, acid slags, artificial glasses) are more "acid" than the slags known as "basic slag". A limiting composition between substances which liberate lime and those which fix it, is given approximately by compositions situated on the $CS - C_3A$ line, (for example those corresponding to the simplified formula $C_6 AS_3$). That may thus be made out: hydrated substances, the most stable, may be considered as formed of silicate which is designated C - S - H (I) (the molecular ratio C/S of which is more often about 1) and of tricalcium aluminate in the hydrated condition $C_3 AH_6$.

Thus Celani - Moggi - Rio, have found that in a mix consisting of 75 % puzzolana and 25 % calcium hydroxide at 40°C all the hydroxide disappeared. Šauman found the same thing at 175°C for 75 % of fly ash and 25 % of CaO or C_3S.

HYDRATED SUBSTANCES

All the papers gave data regarding the X-ray analysis of hydrated substances.

During the hydration of puzzolanas in the presence of lime at 40°C, Celani - Moggi - Rio, found C - S - H (I). They did not find C - S - H (II) (with a high C/S ratio), $C_4 AH_n$ and $C_2 ASH_n$, which they obtained during the hydration of basic slags.

Schwiete - Kastanja - Ludwig - Otto, only found "CSH",(which may contain small amounts of aluminate) as a hydration product of molererde at ordinary temperatures. With all other puzzolanas which they hydrated in the presence of lime they found in addition hydrogarnets C_3 (A,F) H_6 - C_3 (A,F) S_3 which we will write C_3 (A,F) S_pH_n. With volcanic puzzolanas they found C_4AH_n. C_2 ASH_n only appeared occasionally. With Austrian trass containing 2 % of SO_3 , or by adding calcium sulphate during the hydration, they obtained mono-sulphoaluminate, and also tri-sulphoaluminate in the case of adding sulphate.

Sersale - Orsini found by the hydration of puzzolanic and zeolite substances of the (a) zone in figure 1 and of slags in the (d) zone, in the presence of lime: "CSH", C_2ASH_n, C_3AH_n, or C_4AH_n or $C_3ACaCO_3H_n$ and hydrogarnets $C_3AS_pH_n$. At times some hydrates were missing: C_2ASH_n or C_4AH_n or $C_3AS_pH_n$.

With the artificial glasses viz. CAS, $C_2AS_{0.4}$ and $C_{3.5}AS_{0.6}$ they obtained $C_3AS_pH_n$, and with CAS glass they found "CSH" and C_2ASH_n. $C_{3.5}AS_{0.6}$ glass may give $C_3AS_pH_n$ even without the addition of lime. The C/A ratio of the hydrate therefore follows the ratio of the anhydrous substance.

Sauman working on fly ash at 175°C obtained "CSH" and $C_3(A,F)S_pH_n$ as hydrated substances in the presence of lime or of C_3S (the hydration of which releases a high proportion of lime). On the other hand there is scarcely any reaction with the ash in the presence of βC_2S and even the hydration of βC_2S is retarded unless from 1 to 3 % of lime is added. The Author attributes the cause to a coating of the grains of βC_2S by a silica gel from the ash, even when the ash is only present in small amounts (8 to 10 %). The hydrogarnet is also formed from mullite, S_2A_3 and from $Ca(OH)_2$ principally when the two compounds are present in equal proportions, and from mullite and C_3S principally when the ratio between the two compounds is 2/1 by weight.
The composition of these hydrogarnets is approximately, with CaO : C_3ASH_n and with C_3S or βC_2S : $C_3AS_{1.5}H_n$.

The studies carried out by differential thermal analysis, by electron microscope and by surface adsorption have only confirmed the results obtained by R-ray diffractometry.

Thus a summary of the principles which can be derived from the four papers can be seen in figure 3:

- The "basic" slags have compositions which are intermediate between the clinkers and the puzzolanic substances. (The areas of the puzzolanas, basic slags and clinkers shown on figure 3 are the most usual ones. They correspond to molecular ratios $S/A + F + T + SO_3$ of the order of 3 and weight ratios of the order of 2).

- Substances the hydration of which tends to fix lime are situated to the right of the CS - C_3A line. The further they are from this line the more "puzzolanic" they are providing they are vitreous.

- The hydration of clinkers situated to the left of the CS - C_3A line is accompanied by the liberation of lime (portlandite).

- Hydrated substances defined as the most stable are mainly (CS, C_3AS_3, C_2AS, $C_3A)H_n$.

- Some of these hydrates since they are situated to the right of the CS - C_3A line may be thought to be capable of "fixing" (in a manner which has not been explained perfectly) a certain amount of hydrated lime.

This may explain why Celani - Moggi - Rio found an essential difference, during leaching experiments, between puzzolanas and basic slags which are situated on either side of the broken line CS - C_3AS_3 - C_2AS - C_3A . They hydrated both substances at 40°C in the presence of saturated lime water. They then found on subjecting the hydrated substances to leaching with diluted lime water that the slags gave up lime while the puzzolanas continued to fix it.

MECHANICAL STRENGTH

Combination with lime is an essential condition of puzzolanity, but it is not a sufficient condition: it is also essential that bonds should result from this combination from which mechanical strength results ipso facto. Mullite which, according to Sauman, combines with lime but does not give practically any strength, even at 175°C is not a puzzolana therefore.

Sauman considers that there is a certain proportion between the vitreous silica content of puzzolana and the mechanical strength it can develope.

Schwiete - Kastanja - Ludwig - Otto have observed that the mechanical strength confered by puzzolanic substances depends not only on their intrinsic puzzonality but on the fineness and then on the amount of water required for mixing.

CONCLUSIONS

The papers given at the symposium relating to puzzolanas and fly ashes constitute a coherent whole. The results presented in them are not at variance with those which had been obtained previously and they provide very useful information on puzzolanic substances and their hydration products.

Substances richer in lime than the compositions corresponding to line CS - C_3A (figure 3) liberate lime during hydration. Substances which are capable of fixing lime are vitreous substances less rich in lime. They then give the hydrated products, C - S - H, $C_3AS_3(H_n)$, C_2ASH_n, C_3AH_6, some of which fix a small quantity of lime themselves which can be said to be adsorbed. This lime is not revealed by X-rays but it can be leached out more easily than the lime from well defined hydrates.

Fig. 1

Materials

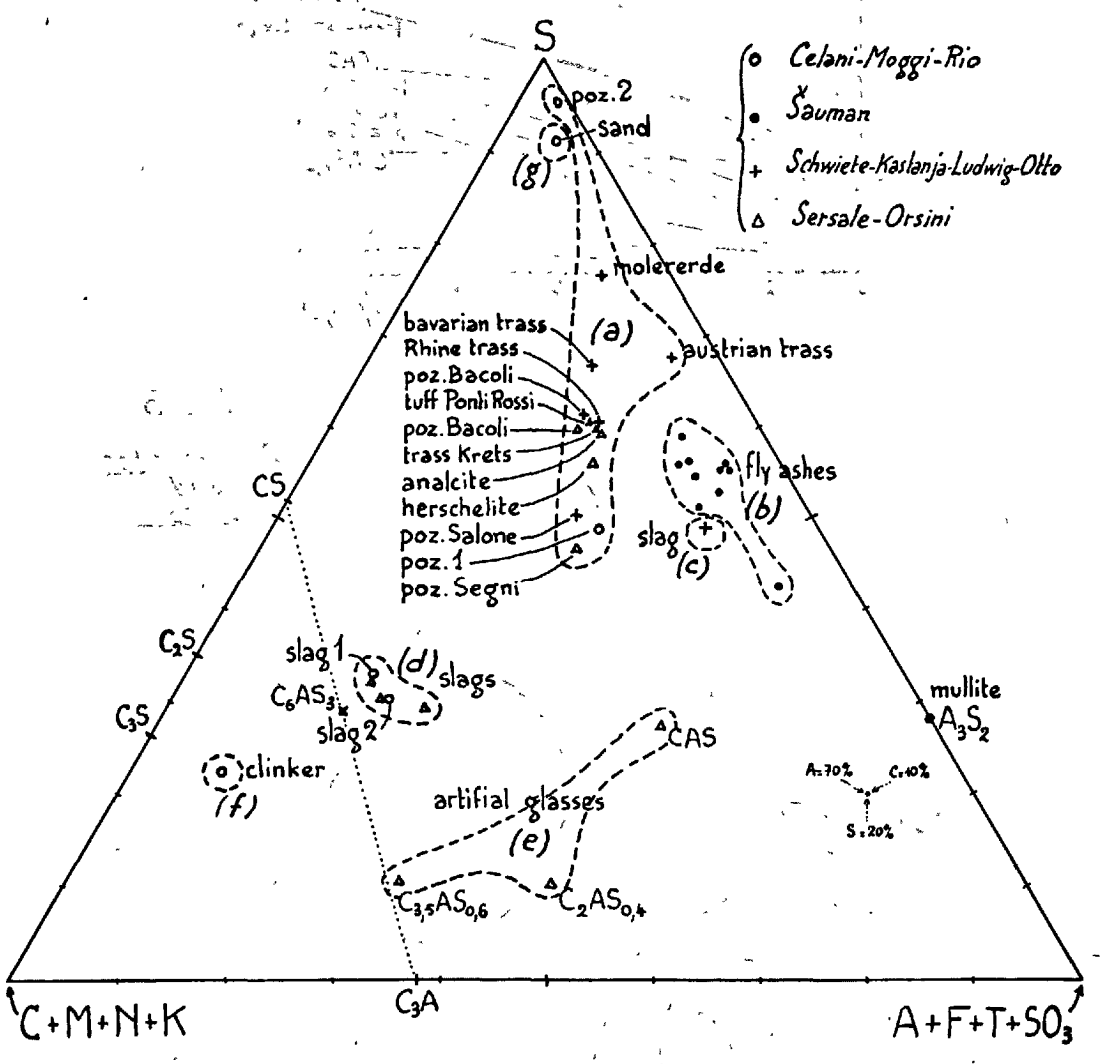

Fig. 2

after Sersale-Orsini

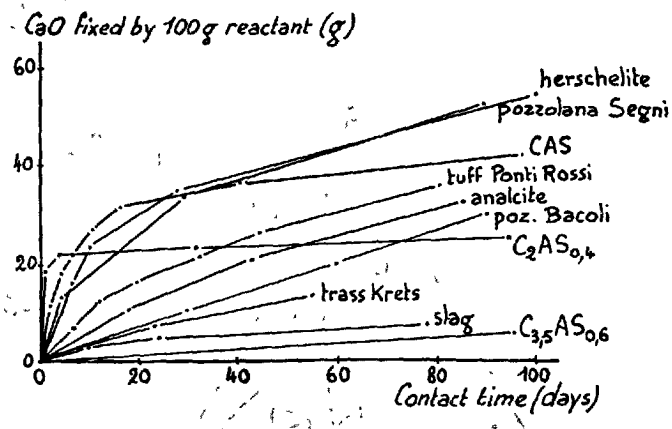

Fig. 3

Anhydrates and hydrates

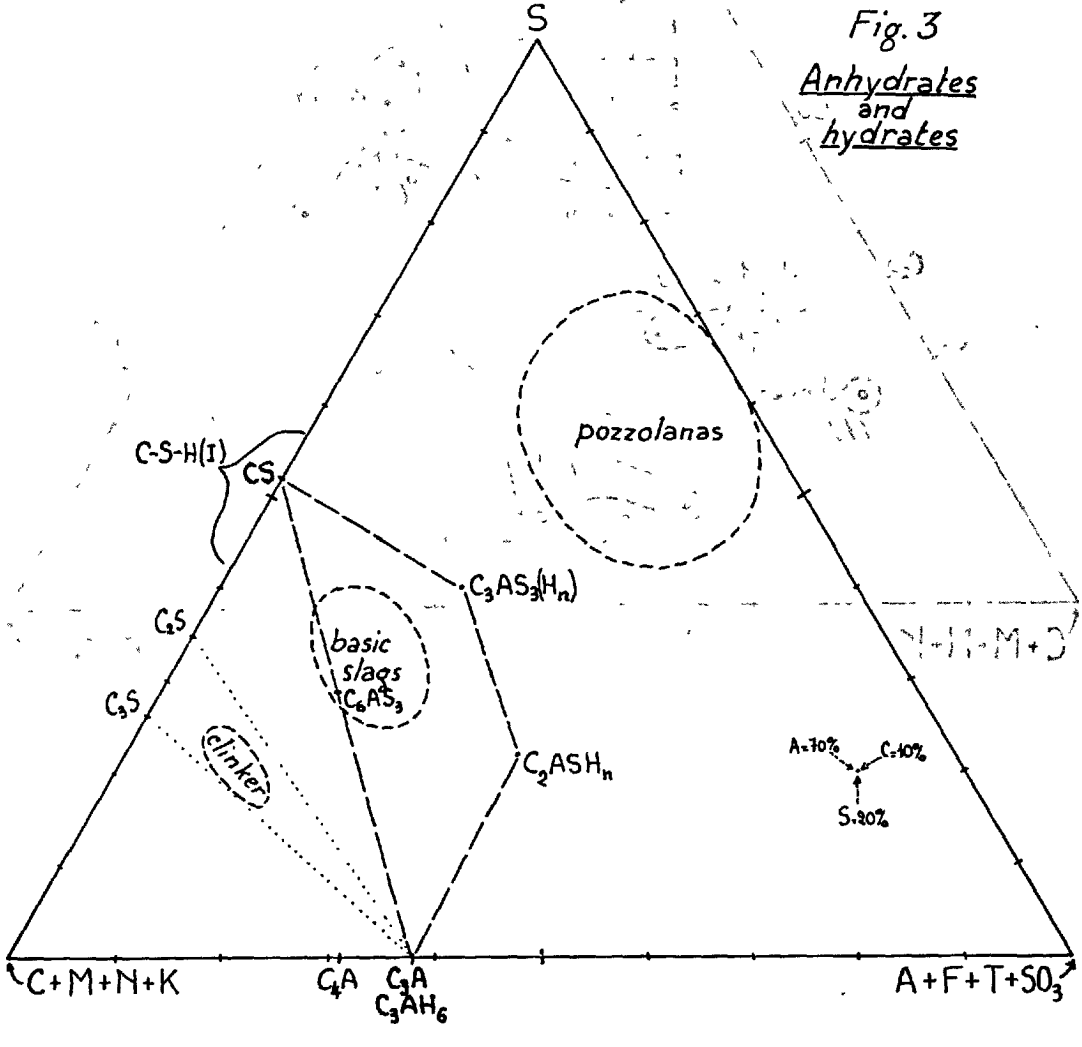

GENERAL REPORT
OF
SESSION IV-3: SLAGS AND SLAG CEMENTS
(a) Papers regarding Slag

R. Sersale (Italy)

The following Supplementary Papers are summarized in this report.

Paper No. IV-11

A METHOD OF UTILIZING BLAST-FURNACE SLAG AS A STRENGTH-IMPROVING AGENT FOR CONCRETE

T. Iwai, T. Mori, A Yoda & M. Oshima (Japan)

Paper No. IV-28

INVESTIGATION OF THE PHYSICOCHEMICAL PROCESSES OF HARDENING OF SLAG PORTLAND CEMENT

V. I. Satarin & Y. M. Syrkin (U.S.S.R.)

Paper No. IV-48

CO-ORDINATION STATE OF ALUMINIUM, MAGNESIUM AND MANGANESE IONS IN SYNTHETIC SLAG GLASSES

S. K. Chopra & C. A. Taneja (India)

Paper No. IV-100

A CONTRIBUTION TO THE STUDY OF THE PHYSICAL PROPERTIES OF HARDENED PASTES OF PORTLAND CEMENTS CONTAINING GRANULATED BLAST-FURNACE SLAG

C. Cesareni & G. Frigione (Italy)

Paper No. IV-102

REACTIVE SLAG-LIKE GLASSES OF THE S-A-F-C-M SYSTEM

V. N. Pai & R. R. Hattiangadi (India)

Paper No. IV-106

STUDIES ON A METHOD TO DETERMINE THE AMOUNT OF GRANULATED BLAST-FURNACE SLAG AND THE RATE OF HYDRATION OF SLAG IN CEMENTS

R. Kondo & S. Ohsawa (Japan)

Paper No. IV-110

MINERAL COMPOSITION OF BLAST-FURNACE SLAG

H. Minato (Japan)

Paper No. IV-113

PORTLAND BLAST-FURNACE CEMENTS--A CASE FOR SEPARATE GRINDING OF SLAG

N. Stutterheim (South Africa)

Paper No. IV-121

THE ROLE OF MAGNESIA AND ALUMINA IN THE HYDRAULIC PROPERTIES OF GRANULATED BLAST-FURNACE SLAGS

M. Cheron & C. Lardinois (Belgium)

In the session "Slag and Slag Cements" nine valuable papers have been devoted to investigate the different aspects of the effects of the composition, the constitution, the way of activation, the nature of the hydration products, on the properties of blastfurnace slags and blastfurnace cements.

Three papers have in fact investigated the influence of different slag treatments on the hydration process and on the properties of the slag cements.

Two papers have investigated the rate of slag hydration and the related physico-chemical phenomena in the slag cements.

Three papers have investigated the composition or the structure of natural or synthetic slags in relation to the pratical behaviour.

One paper has shown the possibility of employing melted and granulated raw materials (unsuitable for portland cement) for cementious products manufacture.

Hydration and hardening processes of rapid-hardening slag portland cement, in comparison to portland cement and ordinary slag portland cement, have been studied by Satarin and Syrkin (1), by means of diffe-

rent experimental facilities.

Rapid-hardening slag portland cement, widely produced in U.R.S.S., is manufactured by mixing clinker, at a Blaine fineness of 5000 cm^2/gr, with slag, at a fineness of 3000 cm^2/gr, in the ratio 60:40 and 50:50, with 4-5% gypsum addition. Such a binder is characterized by mechanical strenght values very similar, at early stages, to those of portland cement.

The Authors have systematically followed the course of hydration and hardening processes by means of chemical, as well as electron microscopy and diffraction, X-ray and thermal investigations.

Samples were prepared by mixing cement with water (water:cement ratio = 0,5) and the composition of the liquid phase, isolated at different time intervals by means of a special pressform under very high pressure, determined. Composition changes in $Ca(OH)_2$, $CaSO_4$ and alkalies content were examined.

It has been ascertained that after 4 minutes hydration, calcium hydroxide content of liquid phase, isolated from ordinary slag portland cement samples (prepared both with basic and with acid granulated respectively slag), is much lower than for portland cement and for rapid hardening slag portland cement. Calcium hydroxide concentration in portland cement and in rapid-hardening slag portland cement liquid phases overpasses, on the other hand, saturation. Lime saturation of liquid phase, reached after 4 hours and maintained during 24 hours, falls down after three days for all cement types. Gypsum content of the liquid phase after 4 minutes hydration does not reach saturation value for all type of cements. The disappearence of gypsum from the liquid phase, which indicate the completeness of the reaction leading to hydrated calcium sulphoaluminate

of ettringite type, has been observed after 24 hours in the liquid phase isolated from portland cement and from rapid-hardening slag portland cement, but only after 3 days for ordinary slag portland cement.

Hydration and hardening processes seem therefore to be somewhat inhibited in slag portland cement in comparison to portland cement and rapid-hardening slag portland cement. Moreover liquid phase isolated from all samples show an alkalies concentration increasing with the time and lower for ordinary slag portland cement.

The kinetic of the hydration process has been evaluated by determining the chemically bound water, too. It has been ascertained that chemical water content, which increase with the age of the sample, is higher for portland cement and for rapid-hardening slag portland cement than for ordinary slag cement, manufactured with the same slag, according with the higher hardening rate of the rapid hardening slag portland cement.

Electronographic examinations have definitely confirmed the results of chemical investigations and showed that at early stages the newly formed hydration products are similar for portland cement and for rapid hardening slag portland cement. Mechanical strenght which caracterizes rapid hardening slag portland cements depend therefore from a more intensive production of high sulphate form of hydrated calcium sulphoaluminate, together with low basic hydrated calcium silicates.

The formation of hydrated compounds goes on in the same way for portland cement as well for rapid hardening slag portland cement, but at early stages the high sulphate form of hydrated calcium sulphoaluminate plays a role of great importance. In the rapid-hardening slag portland

cement samples, cured for one year, hydrated calcium silicates have the main role, while ettringite crystals are quite rare. Thus, particularly at early stages, when it is necessary to stimulate the output from the slag of newly formed compounds, the fineness of the clinker positively affects the properties of slag cements.

Rapid-hardening slag portland cement is to be considered a binding material which share alike the rapid hardening of portland cement with the tendency of slag cements to form hydrated calcium silicates.

The results of electronographic investigations have been confirmed by X-ray and thermal examination.

The first stage of slag cement hydration seems therefore to be the hydrolysis of the clinker. In consequence of this fact, calcium hydroxide and alkalies pass into the liquid phase, thus exciting the hydraulic activity of the slag. The newly formed products are hydrated calcium sulphoaluminate and hydrated calcium silicates similar to tobermorite.

Mori, Iwai, Yoda and Oshima (2) have investigated the possibilities of increasing one-day strenght of portland cement, by employing high-alumina latent hydraulic admixtures.

The rapid strenght development of alumina cement depends upon the prompt monocalcium aluminate hydration, while tricalcium aluminate is the (secondary) component responsible of initial strenght in the portland cement.

It's well known that the alumina content of the slags and fly ashes is higher than that of portland cement. Such admixtures increase therefore the alumina content of portland cement but hydrate slowly and the strenght development is likewise slow.

The study of Mori and Coll. deals with a method of activating the slags by employing a mechanical and chemical treatment.

Unprocessed slag with 50 microns maximum particle size and processed one (namely 25 minutes wet ground slag in a vibrating ball mill) with ten to fifteen microns maximum particle size, were respectively added to rapid hardening portland cement. Strenght development was found to be grater after a week when mortars made with processed slag were used, and smaller for portland cement mortars. This result was notyet satisfactory for having high strenght development in 1-3 days.

Slag was then activated by a mechanical chemical treatment. Samples were prepared by wet grinding slag, calcium sulphate (and sometimes sodium sulphate) and successively addition of such a slurry to portland cement clinker.

Strenght of mortars with milled admixtures varies with slag:sulphate ratio. One-day strenght of mortars made with 80 parts cement and 20 parts admixtures attained in fact maximum point (140 Kg/cm^2) when slag:sulphate ratio was about 15:5.

Partial replacing calcium sulphate by sodium sulphate increases one-day strenght (196 Kg/cm^2) when clinker:slag:calcium sulphate:sodium sulphate ratio equals 80:16:1:3. Sodium sulphate does not however exceed 2% in order to prevent efflorescences.

With reference to grinding time of slurry, a milling time longer than 25 minutes gave a negligible improvement of mortar strenght.

With reference to the slag and anhydrite (or sodium sulphate) mortar content (for a constant amount of sulphates), the optimum slag amount was found to be about 15%, when 4% sulphates is present.

Water:cement ratio higher than 0.5 decreases strenght for samples prepared with clinker:slag:anhydrite:sodium sulphate ratio 81:15:2:2, while strenght ratio for mortar specimens with and without admixtures increases with water:cement ratio.

The opportunity of a separate grinding of blast furnace slags and of portland cement has been emphasized by Stutterheim too, (3) in comparison to the integral one.

It's known that slag tends to vary considerably in grindability, depending upon composition and granulation conditions. Moreover slag is generally much harder to grind than portland cement clinker, so that slag component of an integrally ground cement tends to be coarser than the clinker component. Slag is besides much easier storable than portand cement.

In order to improve quality, reduce costs and produce more uniform materials, the use of separately ground slag, successfully adopted in South Africa, appears to be profitable.

Separate grinding in fact gives control over fineness and uniformity of quality. Slags and clinker can be ground in geographically separated plants in the environs of the production sites and the mixtures prepared on the construction site with different slag:clinker ratio, and with slags of different specific surface. Concretes with properties variable in a pretty large range are therefore obtainable at the discretion of the consulting engineer. The resultant product compares favourably with portland cements for civil engineering works.

With finely-ground slag available at the construction site, concrete workability can be significantly improved. It's therefore possible

to reduce water content compared to the case for portland cement and gain higher strenghts at long stages and lower shrinkage.

The ex-factory cost of ground granulated slag is finally appreciable lower than that of portland cements.

The problem of evaluating slag hydration rate in slag cements has been tackled by Kondo and Ohsawa (4). The possibilities of determining the amount of unreacted slag on the hydration process of slag and slag portland cement pastes, prepared by mixing granulated slag (Blaine 4000 cm^2/g) and portland cement (Blaine 3100 cm^2/g) in the ratio 40:60 and 70:30, respectively, hydrated at 20°C with water:cement ratio 0.4 for different time intervals, have been thoroughly investigated.

Super sulphate slag cement pastes, composed of granulated slag, calcium sulphate and tricalcium silicate in the weight ratio:80:15:5 and tricalcium silicate-slag pastes, prepared in the weight ratio:50:50, with water:cement ratio 0.5, were also examined.

Conditions in which unhydrated slag of slag portland cement hydrated pastes is pratically undissolved, while most of the hydrated slag, clinker minerals and their hydrates are dissolved, have been determined, by adopting a method established by Takashima and improved by the authors.

This method bases itself on the following principle: in a salicylic acid and aceton-methanol solution, slag is pratically insoluble, while most of the hydrated slag, some clinker components and their hydration products dissolve. The method accuracy can be exalted by making some corrections concerning the insoluble or less soluble constituents of the examined cements (aluminate, ferrites, etc.) in the above mentioned solution.

Is therefore possible to determine both the slag content of a cement and the hydration rate of the slag.

The Authors have moreover investigated the chemical composition of the hydration products and the reaction rate of each component: slag, tricalcium silicate etc., as well as the thickness of the reacted layer on the slag and on C_3S particles.

The graphics obtained from experimental data show the unreacted slag percentage in the different type of cement examined, versus hydration time, as well as the reacted slag percentage (in respect of the amount of total slag contenened in the samples) versus hydration time.

Those graphics showed that hydration rate of the slag contained in every type of slag cement is unexpectedly slow.

For all type of cement the experimental results showed that the proposed method is satisfactory and reproducible, particularly by making corrections owing to the fact that a fraction of unreacted slag dissolves into solution (0.7%); a fraction of C_3S is insoluble as well C_3A, C_4AF and the high sulphate form of calcium sulphoaluminate.

Referring to a cement manufactured with slag and clinker, it is necessary to make the following corrections concerning the slag soluble fraction and the clinker components, according to the relation:

Unreacted slag = Insoluble part - clinker x 0,211.

It's to be noticed that the treatment of portland cement with the solvent solution leaves off an insoluble part equal to 21.1%.

Considering that the treatment of ettringite with the solvent solution leaves off an insoluble fraction equal to 61.5%, the unreacted slag amount in the supersulphate cement can be obtained from the follo-

wing relation:

Unreacted slag = Insoluble part - formed ettringite x 0.615.

The formed ettringite amount can be in turn obtained by determining the free calcium sulphate in the cement by the Forsen method and subtracting the reacted calcium sulphate amount (assuming that calcium sulphate forms ettringite only).

The determinations of non evaporable water, free lime, $Ca(OH)_2$ crystals size, free $CaSO_4$ in the above mentioned cements and the x-ray patterns of the newly formed products in the pastes have been also reported by the Authors, together with the connections between the thickness of the layer formed around C_3S (and unreacted slag particles, and the hydration rate of cement pastes. The slowing down of hydration reactions has been after all ascribed to the formation of a sheat around the unhydrated particles.

Cesareni and Frigione (5) have thrown light at the physico-chemical phenomena which occur during hydration of slag portland cement. Hydration process of slag portland cement, in comparison to portland cement, has been investigated by means of experimental methods proposed by Powers and collaborators, namely:
fresch pastes sedimentation; non evaporable water content, surface area and porosity of hardened pastes. Slag cements were prepared by mixing different amount of three types of slags with three types of industrial clinkers, rich in tricalcium silicate and containing different amounts of tricalcium aluminate, with 4% gypsum addition. Wagner specific surface values were about 1850 cm^2/g.

It has been pointed out that a small amount of non-evaporable water

caracterizes hydrated pastes containing slag, though they give place to a gel production similar to that of portland cement pastes. For mixtures containing up to 50% slag, this fact can be interpretated both on the basis of a lower content of $Ca(OH)_2$ and $3CaO.SiO_2$, and with reference to pozzolanic activity of the slag. For mixtures richer in slag, the lower content of non evaporable water attributable to gel, is rather difficult to explane.

It is Author's opinion that the lower content of lime gives place to a more impermeable gel which retard the hydration process and interfere with pozzolanic activity, owing to the a topochemical absence of lime.

Lower basicity of the newly formed products also must be taken into consideration, because of the lower water demand.

Chemical composition of the clinker, particularly tricalcium aluminate content, affects hydration phenomena of the slag, rather indipendently of the type of the slag. The higher content of C_3A seems to influence positively slag hydration. Bleeding capacity and velocity of fresch pastes increase with slag content. The porosity of there pastes is moreover lower in comparison to portland cement.

Physico-chemical phenomena which caracterize hardening process of slag portland cement pastes appear therefore very similar to those concerning portland cement pastes, at least up to 50% slag content.

Portland cement containing more than 50% slag seems to be somewhat different both for the amount of fixed lime and for physico-chemical caracteristic of the pastes.

With reference to the connections between slag chemical composi-

tion and the properties of the corresponding cements, Cheron and Lardinois (6) have studied the influence of magnesium oxide and alumina on the hydraulic properties of granulated industrial slags.

Industrial slags as well as synthetic slag samples obtained by melting and granulating industrial slags and pure oxide mixtures were examined. Slags hydraulic activity was evaluated by determining mechanical strengths (according to the Rilem Cembureau method) of cements obtained by mixing 20;50 or 70% slags separately ground, with 3% gypsum to a 3500 or 4500 Blaine finesses, with standard portland cement containing 3% gypsum to a 3300 Blaine finesses.

Slags and clinker have been separately ground in order to prevent differences in the specific surface due to different chemical composition of the slags. Considering that a partial crystalline state affects hydraulic values, slags vitrosity was checked by X-ray diffraction.

Mechanical tests data obtained after 3 and 7 days were tabulated and plotted in ternary diagrams which showed the beneficial influence of the Al_2O_3 and MgO on the compressive strengths. Such an influence has been also confirmed by 28-days strengths.

Ternary diagrams result from quaternary $CaO-MgO-Al_2O_3-SiO_2$ diagram, by maintaining constant at the levels 9;12 or 15% the Al_2O_3 content.

A linear relation between slags chemical composition and the mechanical strenght of the corresponding cements has been also experimentally deduced, and expressed by the formula:

$$I_h = \frac{CaO + 1,4\ MgO + 0,56\ Al_2O_3}{SiO_2} ,$$

which is in good agreement with the one proposed by Tetmayer. For I_h

values lower than 1,4 a better correlation is obtained when the coefficient 0,56 for Al_2O_3 is replaced by the 0,70 value.

The states of coordination of Al, Mg and Mn ions in synthetic slag glasses corresponding to compositions of the Indian slags which are characterized by comparative lower $CaO:SiO_2$ and higher $Al_2O_3:SiO_2$ ratios, have been determined by Chopra and Taneja (7).

It's known that hydraulicity of granulated blast furnace slags, used for the manufacture of slag cements, is influenced primarly by $CaO:SiO_2$ ratio and by the content of each of the oxides of aluminium, magnesium, manganese etc. Since the stability and the rate of solution of slag glasses, which are foundamental for hydraulic hardening, are dependent upon glass constitution, it is important to know how aluminium, magnesium and manganese oxides are present in the glassy structure.

Six different series of glasses with molecular formulae given below were prepared

Series	Glass composition	n (in moles)
A	$10CaO.8SiO_2.nAl_2O_3$	1 to 7
B	$10CaO.nSiO_2.3Al_2O_3$	7 to 10
C	$10CaO.(10-n)SiO_2.nAl_2O_3$	1 to 4
D	$10CaO.8SiO_2.4Al_2O_3.nMgO$	1 to 4
E	$(12-n)CaO.8SiO_2.4Al_2O_3.nMgO$	
F	$9CaO.8SiO_2.3,5Al_2O_3.nMnO$	0,5 to 1,5

The coordination state was determined by a combination of techniques such as specific volume, molar refractivity, fluorescence in U.V. light, differential thermal analysis. Density determinations were performed by the displacement method (samples weighed in air and in xilene at 27°C,

referred to water at 4°C). Refractive index of powdered glass (passing at No 100 B.S. sieve) was measured by the immersion method, employing liquids of known refractivity indices and examining the Becke line under a microscope.

The total molecular refractivity of a glass was calculated with Lorentz-Lorenz equation. Differential thermal analysis were performed on glass powdered samples diluted with an equal amount of periclase of the same fineness, with heating rate of 10°C per minute up to 1100°C. For magnetic susceptibility measurement a semi-micro aperiodic balance was used; change of weight of the sample (powdered glass) before and after exciting the electromagnet with a 3 amp. current was observed, ferrous ammonium sulphate being used for calibration purposes.

The state of coordination of Al ions was studied by determining the effect of varying Al_2O_3 content on the density and refractive indices of series A, B glasses. The partial molar refractivity of Al_2O_3 indicated that Al ions are always present in four-fold co-ordination. This was also supported by the value of partial specific volume of Al_2O_3 and the rise in temperature of the exothermic peak due to devetrification on substituting increasing amounts of alumina in place of silica in series C glasses. Similarly, partial molar refractivity of magnesia in series D, E indicated a four-fold state of coordination of Mg ions. This was also confirmed by the purple fluorescence of Ni ions in glasses where part of MgO was substituted by NiO. The average value of partial molar refractivity of manganese oxide in series F glasses showed that manganese ions were present in six-fold co-ordination. This was also indicated by the red fluorescence of manganese glasses. The partial molar

refractivity data however indicated further that a part of manganese was present in a higher state of valence and the magnetic susceptibility measurement confirmed that about 18 ÷ 24% of Mn was present in trivalent state.

The connections between cooling rate and mineral composition of blast furnace slags have been investigated by Hideo Minato (8), by means of chemical analysis, X-ray diffraction, optical and electron microscopy. Composition of slags examined ranges as follows:

SiO_2 30 ÷ 35; Al_2O_3 13 ÷ 20; MgO 2 ÷ 6; CaO 40 ÷ 50%.

Six different water quenched slags, examined by X-ray powder method, showed essentially glassy structure with presence of small amounts of melilite (faint 2.8 Å peak). This result is confirmed by the observation of thin sections under polarizing microscope.

Three different slow cooled slags were examined. A stalactitic body spontaneously grown in a cavity inside one of them, and two melilite single crystals isolated in two different slags, have been also studied.

The former shows enrichment of manganese, alkalies and sulphur in comparison with the corresponding slag. Melilite single crystals showed a characteristic zonal structure under the polarizing microscope; its nucleus appeared to be highest in gehlenite while the rim lower.

General constituents of slow cooled slag are melilite, dicalcium silicate and pseudowollastonite.

As it concerns raw materials, Pai and Hattiangadi (9) have investigated the possibility of manufacturing a cementitious product from low grade limestone (unsuitable for portland cement manufacture because the high silica and magnesia content) and from alumina rich materials (such

as bauxite and laterite). These raw materials, after being activated by portland cement, hydrate to give a strenght producing compound.

The process consist in grinding the low $CaCO_3$ stone with bauxite to the same fineness as cement raw materials, melting it and quenching the melt in a manner analogous to the granulation of blast furnace slag. Using the results of previous investigation in the $CaO.Al_2O_3.SiO_2$ and $CaO.MgO.Al_2O_3.SiO_2$ systems as a basis, composition were chosen to have "liquidus" temperature below 1350°C; the melts were fired to 1450 ÷ 1500°C in order to preserve the vitreous state during the quenching with water.

It is now generally agreed that a Ca:Si ratio between 1,5 ad 2,0 in the tobermorite gel obtained by hydration of C_3S and C_2S, is desiderable from the point of view of the mechanical strenght of the hardened paste. Considering this, C_3S alone must be regarded as a too basic component of anhydrous cement, even if reacts with acceptable speed at earlv stages of hydration and if the excess of lime, not combined in tobermorite, forms plates of $Ca(OH)_2$ which give a high pH environment for protecting the reinforcing steel. In the same time this lime is a source of weakness when sulphates are present. The use of a less basic anhydrous material could be, therefore, an advantage; since it is not possible with cristalline solids, the use of materials in the vitreous state offers a possible solution.

A furnace employing butane gas as fuel and developing 1550°C in three hours was used. Nodules of precalcined raw mix were molten in the furnace and quenched in water. The glass content was estimated with the optical microscope and was generally well above 90%. The quenched melt

was ground with portland cement clinker and 5% gypsum. The clinker had a potential C_3S content of about 35%.

The compressive strenghts were tested on 2" mortar cubes prepared according ASTM method of test n° C 109-64 when small quantities of glass were available. When larger quantities of glass were prepared, 4" concrete cubes made according to the British Standard 12-1958 were tested in addition to the mortar cubes above.

The products of hydration were identified by D.T.A. and X-ray diffraction. Cement low in Al_2O_3 and high in Fe_2O_3 showed ettringite up to 7 days in addition to tobermorite. They gave poor strenght, larger exothermic effect due to unreacted glass as well as a fair amount of $Ca(OH)_2$ which has not been taken up by the melt due to its slow hydration.

Those higher in Al_2O_3 gave monosulphates at same ages, and showed traces of lime indicating that lime released by portland clinker has been immediately fixed up by the reactive melt.

Suitable compositions with "liquidus" temperature and compressive strenght have been thoroughly investigated.

References

(1) V.I. Satarin, Y.M. Syrkin. Investigation of the physicochemical processes of hardening of slag portland cement. V-ISCC.

(2) T. Iwai, T. Mori, A. Yoda, M. Oshima. A method of utilizing blast-furnace slag as a strenght-improving agent for concrete. V-ISCC.

(3) N. Stutterheim. Portland blast-furnace cements. A case for separate grinding of slag. V-ISCC.

(4) R. Kondo, S. Ohsawa. Studies on a method to determine the amount of granulated blast-furnace slag and the rate of hydration of slag in cement. V-ISCC.

(5) C. Cesareni, G. Frigione. A contribution to the study of the physical properties of hardened pastes of portland cements containing granulated blast-furnace slag. V-ISCC.

(6) M. Cheron, C. Lardinois. The role of magnesia and alumina in the hydraulic properties of granulated blast-furnace slag. V-ISCC.

(7) S.K. Chopra, C.A. Taneja. Co-ordination state of aluminium, magnesium and manganese ions in synthetic slag glasses. V-ISCC.

(8) H. Minato. Mineral composition of blast-furnace slag. V-ISCC.

(9) Y.N. Pai, R.R. Hattiangadi. Reactive slag-like glasses of the S-A-F-C-M system. V-ISCC.

GENERAL REPORT
OF
SESSION IV-3: SLAGS AND SLAG CEMENTS
(b) Papers regarding High-Sulphate Slag

S. K. Chopra (India)

The following Supplementary Papers are summarized in this report.

Paper No. IV-21

ANHYDRITECEMENT

A. A. van Haute (Belgium)

Paper No. IV-128

CHEMISTRY OF SLAG-RICH CEMENTS

J. C. Yang (U.S.S.R.)

Paper No. IV-130

A COMPARATIVE ASSESSMENT OF THE RESISTANCE OF SUPERSULPHATED, SULPHATE RESISTANT PORTLAND, AND ORDINARY PORTLAND CEMENTS TO SOLUTIONS OF VARIOUS SULPHATES AND DILUE MINERAL ACIDS

G. H. Thomas (United Kingdom)

Of the three papers in the subgroup of Session IV-3, the first paper entitled 'Anhydritecement' by Prof. Hute reports in main the findings of an investigation on the development of a synthetic cement composed of mainly blast furnace slag and the anhydrite obtained by calcining waste gypsum from the phosphoric industry. The basic approach in this investigation is the search for an optimum composition of the anhydritecement which will result not only in highest possible mechanical strengths but also possess other physical properties comparable to those of portland cement.

The anhydrite cement reported to have been used sucessfully in Asiatic Russia and Germany consists of ground gypsum anhydrite ($CaSO_4$) and a catalyser (1,2). The anhydrite cements under report additionally contain ground blast furnace slag as the third component and are akin to anhydrite-slag binders of Grimme (1). In this investigation anhydrite was prepared by calcining waste gypsum (76% $CaSO_4$, 1.15% total P_2O_5 and 1% Fe etc.) at 850-900°C. "Quenched" blast furnace slag having CaO from 35 to 45 per cent, SiO_2 preferably 30 to 33 per cent but not more than 35 per cent, Al_2O_3 not less than 15 per cent, and S not more than 1.5 - 1.8 per cent is recommended for use. The third component is a new catalyst and consists of a mixture of K_2SO_4, $Ca(OH)_2$ and the Lafarge

*Central Building Research Institute, Roorkee (U.P.) INDIA.

aluminous cement. Each of the components of the anhydritecement was ground to a fineness of less than 63 microns.

The physical and mechanical properties of the experimental anhydritecement were tested as per the Belgian Specifications and compositional limits of the catalyst for anhydrite/slag ratio between 45/45 and 50/40 were established as 1.0 to 1.5% per cent $Ca(OH)_2$, 0.9 to 1.2 per cent K_2SO_4 and 5 to 9 per cent aluminous cement. In order to determine more precise limits for the optimum composition, the author carried out a systematic investigation on the influence of the relative quantities of the dirrerent components on the flexural and compressive strengths of the experimental cements at 3, 7 and 28 days. The author reports on more than 100 cement blends and concludes that the strongest anhydrite cement is obtained with a 50/40 anhydrite/slag ratio and the optimum composition of the catalyst for the anhydrite-cement to be strong at 3 days are aluminous cement 6-7%, $Ca(OH)_2$ 1.5% and K_2SO_4-1.2%. For anhydritecement to be strong at 28 days a higher proportionof aluminous cement (8 per cent) and lower proportion of lime (1.1%) are to be used. Such cements show compressive strengths in the range of 400 to 550 Kg/cm^2 at 28 days and satisfy the requirements specified for ordinary portland cement except that initial set takes longer time. Although full information on long-term performance and scope of application of this class of cement under different environments is lacking, this piece of work is of great interest as byproduct gypsum or anhydrite is available in many countries for disposal and utilization, and production of a cement from it is an attractive and profitable proposition.

In the second paper entitled "Chemistry of Slag-rich Cements" Dr. Yang reports and discusses the setting and hardening characteristics of slag-rich cements and evaluates their scope of application. The slag-rich cements are defined as those consisting mainly of 65 to 95 per cent of slag and the balance of portland cement or anhydrite or both. This study pertains to five different American slags and one high magnesia slag from South Africa. Hydration of slag cement under normal curing conditions was studied on pastes at a water/solid ratio of 0.60. A water suspension of of 2 grams of slag cement in 40 distilled water was used for studying hydration under hydrothermal conditions.

Ettringite and tobermorite like CSH-I are reported as the main binders in a supersulphated cement composed of 83% slag, 12% gypsum anhydrite and 5% portland cement and hydrated at atmospheric pressure and temperatures below 75°C. Hydration at 95°C was found to result in the formation of tobermorite and a poorly defined hydrogarnet. Under hydrothermal conditions, i.e. at 100 psi. and higher, ettringite decomposed to fine crystalline $CaSO_4$ which recrystallized during hydration process and grew to crystals upto 20 microns. In view of this and likelihood of delayed expansions due to the action of free CaSO4 with slag constituents in a set product supersulphated cement is recommended for use only for air cured products requiring good sulphate resistance and not for autoclave cured products.

The main hydration products identified in a slag cement containing 25 per cent of portland cement are CSH-1 and $C_4A\ H_{13}$ or its solid solution with $3\ CaO.\ Al_2O_3.\ CaCO_3.\ 12H_2O$. These findings are in general agreement with the main conclusions

of the hydration studies reviewed in the principal paper by Schroder (3). However, it is noteworthy that the slag cement prepared from a slag containing about 15% magnesia does not show upon hydration any detectable free MgO or $Mg(OH)_2$. It will be interesting to know how magnesia is consumed and how it affects the properties of the set cement products.

Under hydrothermal conditions of curing, blast furnace slag cement yielded tobermorite and hydrogarnets, the latter bestowing sulfate resistance and high resistance to carbonation. As autoclaving temperatures approached 225°C the reaction rims around slag grains were found to thicken and a hydrogarnet resembling plazolite was formed. At still higher autoclaving temperature of 300°C, the hydrogarnet formed resembled hibschite.

Addition of silica flour to the slag rich cements in amounts more than 30 per cent was found to check the formation of hydrogarnets and produce greater quantities of CSH compounds and consequently higher strengths. Another advantage mentioned by the author is the lowering of production costs.

The scope of application of slag cement in producing autoclaved asbestos-cement building products was also investigated upon by the author. Flexural strengths of autoclaved specimens consisting of 20 per cent chrysotile fibre blend, 40 per cent silica flour and 40 per cent slag-rich cements are reported and compared with the strengths of a blend of 20 per cent asbestos fibre, 30 per cent silica and 50 per cent Type I portland cement. The data show that optimum strength is achieved with a cement consisting of 75 per cent slag and 25 per cent portland cement at autoclaving pressure of 100 to 125 psi. The slag-rich cements

were further evaluated in a pilot plant and the setting properties and mechanical strengths of asbestos cement pipe products show that satisfactory autoclaved formulation can also be achieved when portland cement is replaced by a blast furnace slag cement. The results of corrosion tests for soft water and dilute sulfuric acid also point out to the soundness of using blast furnace slag cement in producing asbestos cement products.

The last paper in this group by Mr. George H. Thomas reports the results of a specific investigation on the relative merits of a supersulphated cement for use under aggressive environments. The comparative assessment has been based on the results of three different groups of tests carried out on the commercial brands of a supersulphated cement, a sulphate-resisting protland and ordinary portland cement.

In the first group of tests 28 days old specimens of a rich concrete mix were immersed separately in six solutions of sulphates of sodium, magnesium and ammonium, each having two levels of SO_3 concentration as 0.35 and 3.5 per cent, and also in 0.25 and 2.0% W/V of H_2SO_4 solutions. The sulphate resistance was assessed mainly by determining compressive strengths of the specimens after 8 to 10 years storage in aggressive waters versus storage in ordinary water, and statistical methods were employed for analysing the data. The temperatures of storage of specimens in different solutions are not mentioned, it is presumed that tests were done under controlled temperature in view of storage temperature being one of the variables (4).

In the second group of tests the comparative assessment of the acidic resistance of the supersulphated cement was made by

subjecting three different batches of the supersulphated cement concrete to attack in an experimental section of the sewer at Burton-on-Trent. The basis of evaluation were the same as for the tests in the first group.

The third group of tests aims to assess aggressive solution resistance of cement rapidly by immersing ½ inch micro-concrete cubes, prepared from a mix consisting of graded washed silica sand, cement and water adjusted to a constant workability, in sulphate solutions. The curing and testing procedures of the specimens were the same as for tests in the first group.

The results and conclusions of each group of tests are reported in the paper. The statistical techniques have helped undoubtedly in differentiating between the real effects of the different aggressive solutions and the experimental variations. But the author has rightly cautioned that statistical superiority or inferiority should not be taken to imply satisfactory or unsatisfactory performance or life. His other recommendation is that, apart from the general trends of attack of aggressive solution, the rate of deterioration and the residual strength of a cement must also be taken into account. Finally, the important conclusions of this investigation are as follows:

(1) In sodium sulphate solutions supersulphated cement gives by far the best performance. No significant attack was registered in 3.5% SO_3 solution even after eight years. As against this even sulphate-resisting portland cement did not show satisfactory performance. However, in the 0.35% SO_3 sodium sulphate solution the advantage for supersulphated cement is less marked.

(2) Although the sulphate-resisting portland cement gave a statistically better performance in 3.5% SO_3 solution of magnesium

sulphate, in real terms neither this nor supersulphated cement appear to be suitable for use in such high concentrations of this salt. But both of these cements resist the attach of weaker solution of 0.35% SO_3 concentration and the supersulphated cement shows somewhat better resistance.

(3) All the three cements e.g. sulphate-resisting portland, ordinary portland and supersulphated are attacked by ammonium sulphate solutions with 0.35 and 3.5% SO_3 concentration, but again supersulphated cement shows better performance.

(4) The results of both the first and second group of tests in this study confirm the earlier reports about the superiority of supersulphated cement in weak sulphuric acid concentrations.

REFERENCES

1. H. Grimme, "Anhydrite Binding Agents developed in Central Germany", (In German). Zement-Kalk-Gips, 15 (7), 255-298 (1962).

2. M. Tenny and M. Ben.Yair, "Anhydrite Cement in Hot Climates", Cement & Lime Manufacture, Vol. XXXVIII No.3, 49-53 (1965).

3. Fritz Schröder, "Slags and Slag Cement", - this Symposium.

4. John D. Rechards, "The Effect of various Sulphate solutions on the Strength and other properties of Cement mortars at temperatures up to 80°C", Magazine of Concrete Research, 17, No. 51, 69-76 (June, 1965).

GENERAL REPORT
OF
SESSION IV-4: EXPANSIVE CEMENT

G. J. Verbeck (U.S.A.)

The following Supplementary Papers are summarized in this report.

Paper No. IV-66

NATURE OF HYDRATION PRODUCTS IN THE SYSTEM $4CaO.3Al_2O_3.SO_3$--$CaSO_4$-CaO-H_2O

A. Klein & P. K. Mehta (U.S.A.)

Paper No. IV-69

FUNDAMENTAL STUDIES ON THE EXPANSIVE CEMENT

N. Fukuda (Japan)

Paper No. IV-74

MINERALOGICAL COMPOSITION OF EXPANSIVE CEMENT CLINKER RICH IN SiO_2 AND ITS EXPANSIBILITY

T. Nakamura, G. Sudoh & S. Akaiwa (Japan)

Paper No. IV-83

PREVENTION OF DRYING SHRINKAGE CRACK BY USE OF THE EXPANSIVE CEMENT WITH CALCIUMSULFOALUMINOUS CEMENT CLINKER

K. Ohno, S. Nakamura & T. Saji (Japan)

Paper No. IV-85

GENERAL BEHAVIOR OF MORTAR AND CONCRETE MADE OF EXPANSIVE CEMENT WITH CALCIUM SULFOALUMINOUS CEMENT CLINKER

T. Nishi, T. Harada & Y. Koh (Japan)

Paper No. IV-86

DEVELOPMENT OF EXPANSIVE CEMENT WITH CALCIUM SULFOALUMINOUS CEMENT CLINKER

M. Okushima, R. Kondo, H. Muguruma & Y. Ono (Japan)

Paper No. IV-132

UTILITY OF EXPANSIVE CEMENT

P. Klieger & N. R. Greening (U.S.A.)

Note: Text undelivered.

Wal

GENERAL REPORT
OF
SESSION IV-4: EXPANSIVE CEMENT

G. J. Verbeck (U.S.A.)

The following Supplementary Papers are summarized in this report.

Paper No. IV-66

NATURE OF HYDRATION PRODUCTS IN THE SYSTEM $4CaO.3Al_2O_3.SO_3$--$CaSO_4$-CaO-H_2O

A. Klein & P. K. Mehta (U.S.A.)

Paper No. IV-69

FUNDAMENTAL STUDIES ON THE EXPANSIVE CEMENT

N. Fukuda (Japan)

Paper No. IV-74

MINERALOGICAL COMPOSITION OF EXPANSIVE CEMENT CLINKER RICH IN SiO_2 AND ITS EXPANSIBILITY

T. Nakamura, G. Sudoh & S. Akaiwa (Japan)

Paper No. IV-83

PREVENTION OF DRYING SHRINKAGE CRACK BY USE OF THE EXPANSIVE CEMENT WITH CALCIUMSULFOALUMINOUS CEMENT CLINKER

K. Ohno, S. Nakamura & T. Saji (Japan)

Paper No. IV-85

GENERAL BEHAVIOR OF MORTAR AND CONCRETE MADE OF EXPANSIVE CEMENT WITH CALCIUM SULFOALUMINOUS CEMENT CLINKER

T. Nishi, T. Harada & Y. Koh (Japan)

Paper No. IV-86

DEVELOPMENT OF EXPANSIVE CEMENT WITH CALCIUM SULFOALUMINOUS CEMENT CLINKER

M. Okushima, R. Kondo, H. Muguruma & Y. Ono (Japan)

Paper No. IV-132

UTILITY OF EXPANSIVE CEMENT

P. Klieger & N. R. Greening (U.S.A.)

General Report on Supplementary Papers

Part IV - 4 - "Expansive Cements"

by George Verbeck*

The authors of each of the seven Supplementary Papers on Expansive Cement are to be complimented for their contributions to the subject. In addition, and most fortunately, the papers encompass a broad range of areas of interest concerning such cements and their uses.

These papers total 152 pages of text, 92 tables, and 145 figures. Needless to say, it will not be possible to present more than a few of the significant contributions contained in these papers.

Broadly speaking, and for convenience of discussion, the papers may be separated into three general categories:

(1) Four papers primarily concerning clinker phase formations in the C-A-$\overline{S}$ system and the influence of phase composition on the hydration process, and the study of the nature of the hydration products using a variety of techniques,

(2) Two papers primarily on laboratory studies of concretes including those made with all three types of expansive cements; the factors affecting expansivity and cracking tendency and the various engineering properties of such concretes, and

(3) A paper describing practical field experience with an expansive cement in wall plastering, floor topping, pipe lining, reinforced concrete beams, roof slabs, and a pavement.

Regarding the papers on clinker phase compositions in the C-A-$\overline{S}$ system and the nature of the hydration products, Klein and Mehta prepared

*Director of Materials Research Department, Research and Development Division, Portland Cement Association, Skokie, Illinois

mixtures of high-purity $C_4A_3\overline{S}$, calcium sulfate, and calcium oxide at A to $\overline{S}$ molar ratios from 0.25 to 1.25 and C to $\overline{S}$ molar ratios from 2.0 to 8.0. The products of hydration of 45 such mixtures were determined by X-ray diffraction techniques. The formation of ettringite, considered to be required for expansivity was observed in varying amounts except for mixes having A to $\overline{S}$ ratios greater than 1 along with C to $\overline{S}$ ratios greater than 4. A phase diagram was presented to show the nature of the final hydration products in the over-all system. Monosulfate hydrates with 18 and 12 moles of water were also observed and a third monosulfate hydrate, perhaps having 15 moles of water was postulated.

Fukada prepared a wide range of clinker compositions in the C-A-$\overline{S}$ system and identified $C_4A_3\overline{S}$ as the only ternary compound formed. With the addition of silica the clinker may contain C_2AS. When the raw mixture contains sufficient calcium and sulfate the silica appears to have no effect on the formation of $C_4A_3\overline{S}$. When $C_4A_3\overline{S}$ is mixed with normal portland cement and hydrated, ettringite will not be formed and expansivity not observed unless sufficient additional sulfate is present to compensate for the alumina in the portland cement fraction. Quick setting was attributed to the formation of C_2AH_8 the formation of which can be controlled by the addition of gypsum.

Nakamura, Sudoh, and Akaiwa studied the clinkering of mixes of a kaolin clay (containing about 40% S and 30% A), limestone, and gypsum and showed that the mole ratio of C to (A + 2S + 3F) must be greater than 1 to form $C_4A_3\overline{S}$ which was, under such circumstances, the only alumina-containing compound except for $C_{10}A_2F_3$. By means of X-ray diffraction they also showed that below 1285°C a ternary silicate compound $C_5S_2\overline{S}$; forms and above 1285°C this is decomposed

into β-C_2S and $C\bar{S}$. The heat of hydration of $C_6S_2\bar{S}$ was shown to be very similar to that of β-C_2S. Differential thermal analysis, electron probe, electron microscopic, and calorimetric techniques were used to study the clinkers produced and the hydration products. X-ray diffraction and microscopic studies revealed that ettringite formation is necessary for expansion and that only the ettringite formed in the presence of a high lime concentration is effective. Quick setting with this experimental cement could be controlled by adding gypsum, and the resultant increase in expansion was controlled by the addition of blast-furnace slag.

Okushima, Kondo, Muguruma, and Ono also showed a high lime concentration to be necessary for expansion and studied the hydration reactions of pure materials using X-ray diffraction, light microscopy, differential thermal analysis and thermogravimetric analysis. They concluded on the basis of a special experimental technique that the hydration product forms directly on the surface of the $C_4A_3\bar{S}$ or C_3A grains and proceeds from the initial formation of the monosulfate to ettringite at that location. Clinkering studies indicated that relatively large crystallite size and particle size of the $C_4A_3\bar{S}$ produced the best expansivity. The relationships between pore size and expansion and shrinkage characteristics were studied. The authors described the manufacture of expansive cements of the $C_4A_3\bar{S}$ type and discussed those general characteristics of a sulfoaluminate-containing cement necessary to reduce shrinkage cracking in concrete and the need for residual compressive stress in the concrete after shrinkage. They also discussed the role of creep in restrained concretes and the factors of importance to the use of this cement for chemical prestressing. They showed that high expansions tend to give low compressive strengths. Data showing the effect of restraint (up to 1.6% steel) on expansion and strength were

included.

As previously mentioned, two of the papers primarily concerned laboratory studies of mortars and concretes made with expansive cements and the engineering properties of such concretes. These two papers generally confirm and supplement each other.

The paper by Nishi, Harada, and Koh, as with the other previously discussed papers, dealt only with expansive cement made with the calcium sulfoaluminate type clinkers, sometimes referred to as Lossier or Klein type expansive cement. In reality this paper is an extensive collection of the works of 15 different investigators representing 12 different universities, institutes, or organizations and the many important results cannot be adequately summarized briefly.

The study of factors influencing the expansion and shrinkage of mortars and concretes included the effect of

- the composition and amount of the calcium sulfoaluminate clinker used
- the paste content and water-cement ratio of the concrete
- the use of normal weight or lightweight aggregate
- the moisture condition, temperature, and duration of curing, and the use of different steam curing cycles, and
- the use of admixtures (an air-entraining agent, a water-reducing agent and a set-retarder).

In addition to these broad studies regarding expansivity under various conditions, many test results were reported on the engineering properties of mortars and concretes produced under various conditions. These studies included the determination and the comparison with normal portland cement concretes of

- the compressive, flexural and tensile strength properties of such concretes
- the elastic modulus and creep properties
- pull out bond tests of reinforcement
- the rate of carbonation and rusting of embedded steel
- the chemical resistance (to acid, to alkali, and to seawater)
- the resistance to freezing and thawing, and
- the fire resistance and thermal conductivity of such concretes.

Broadly speaking, if the expansion of the concrete was not excessive, the engineering properties would be considered essentially normal for the quality of concrete evaluated in comparison with non-expansive concretes. It should be noted that most of these studies involved the use of non-restrained concretes.

I have enumerated these various factors to demonstrate the breadth of the paper and the wealth of information the paper contains.

The paper by Klieger and Greening also concerned factors influencing expansivity and the properties of shrinkage-compensating and self-stressing concretes. However, the paper differed from the other supplemental papers in that it compared results obtained with all three types of expansive cements as currently recognized and defined by the American Concrete Institute as follows:

(1) Type K, the Klein or Lossier type, the essential ingredient of which is an anhydrous aluminosulfate such as has been discussed in the previous papers. (Currently this general type of cement is being produced in the U.S.A. in three different ways, as an enriched clinker subsequently

blended with portland cement, in a single integral clinkering operation, and as an enriched clinker having, unlike the aforementioned clinkers, a low free lime content).

(2) Type M, the Mikhailov type, which is a mixture of portland cement, calcium aluminate cement, and calcium sulfate, and

(3) Type S, sulfated cement, which is made from a high C_3A clinker (about 20% calculated C_3A content for shrinkage-compensated cement) and calcium sulfate in a quantity above the usual optimum for portland cement.

It is shown that each of these types of cements, adjusted to the same level of expansive potential, will perform in an approximately similar manner and produce concretes having essentially similar engineering properties.

As in the previous paper, many of the factors influencing expansivity and the physical properties of the resulting concretes were studied, but for concretes made with all three basic types of expansive cement, and in addition, comparisons were made with similar concretes made with ASTM Types I, II and V cements.

The effect of degree of restraint was studied in some detail and for many of the concretes evaluated the expansion had been partially restrained. Additional factors studied include the effects of duration of mixing and the evaluation of the long-time volume stability of concretes subjected to alternate wetting and drying, and resistance to de-icer scaling and surface abrasion.

The last paper by Ohno, Nakamura, and Saji summarizes the work of 14 individuals and 5 different universities or organizations. It is largely devoted to description of practical field experiences in the use of the calcium sulfoaluminate type of expansive cement.

The usefulness of expansive mortars was evaluated in wall plastering, floor topping and pipe lining. If the expansive level was sufficiently high, the cracking of wall plaster was avoided. This may be attributable to the modest degree of restraint offered by the concrete subbase wall and perhaps to the expansive tendency of the mortar during the early period during which the mortar was subjected to drying and drying shrinkage. These two effects could offset each other during the early and most critical stages of drying when the mortar has not developed sufficient tensile strength to resist the shrinkage stresses that would otherwise normally occur. As a floor topping, excessive expansion was observed -- this is attributed to the extended period of water curing used and an excessively high level of expansive component. Satisfactory performances as a pipe lining was observed. This is presumed related to the high degree of restraint afforded by the confining pipe.

The authors report encouraging results with the use of shrinkage-compensating cements in large-scale reinforced concrete specimens, slabs and beams, the results depending upon the inherent expansivity of the cement and the amount and type of reinforcement. The authors used this shrinkage-compensating cement in construction of an instrumented, reinforced concrete building and reported distinct benefits in decreasing shrinkages and cracks. In addition they reported lack of cracking (to date) in instrumented experimental concrete pavements made with shrinkage-compensating and normal portland cement concrete.

In summary, these papers demonstrate that the chemistry of the expansive sulfoaluminate type of cements and their hydration products is well advanced. Many factors that influence the expansivity have been elucidated and many of the practical engineering properties of such concretes

determined. There appears to be further need for suitable engineering design criteria for the use of such cements in various types of applications. With proper design criteria the construction of suitably engineered structures will permit proper evaluation of the technologic and economic aspects related to the use of expansive cements.